one is above the Li_3 prismane base, and three bridge the three BaLi prismane edges. The tetrahydrofuran oxygen centers are coordinated to the Ba centers that are not part of the prismane. If the O^{2-} inner centers are also considered, each polyhedron face is at least singly O-capped.

The polyion aggregate $\{[Ba_6Li_3O_2][OC(CH_3)_3]_{11}(O_3C_4H_8)\}$ contains 204 centers and 932 electrons. A model $\{[Ba_6Li_3O_2](OH)_{11}\}$, simplified by the substitution $(H_3C)_3 \rightarrow H$ and removal of the THF ligands still contains 33 centers and 460 electrons; nevertheless, calculations on this molecule are possible with the presently best-suited LCGTO-DF (Linear Combinations of Gaussian Type Orbitals Density Functional) method[4, 5] and a CRAY YMP. A more severely simplified model accentuating, however, the polyion character of the title compound is $\{[Ba_6Li_3O_2]^{11+}(e^-)_{11}\}$, in which the anions are represented by point charges, and which reduces the problem to 11 centers and (still) 350 electrons. The Kohn–Sham eigenvalue spectra calculated for both models (Fig. 2) provide essential information.

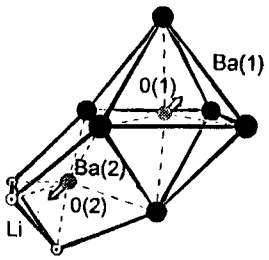

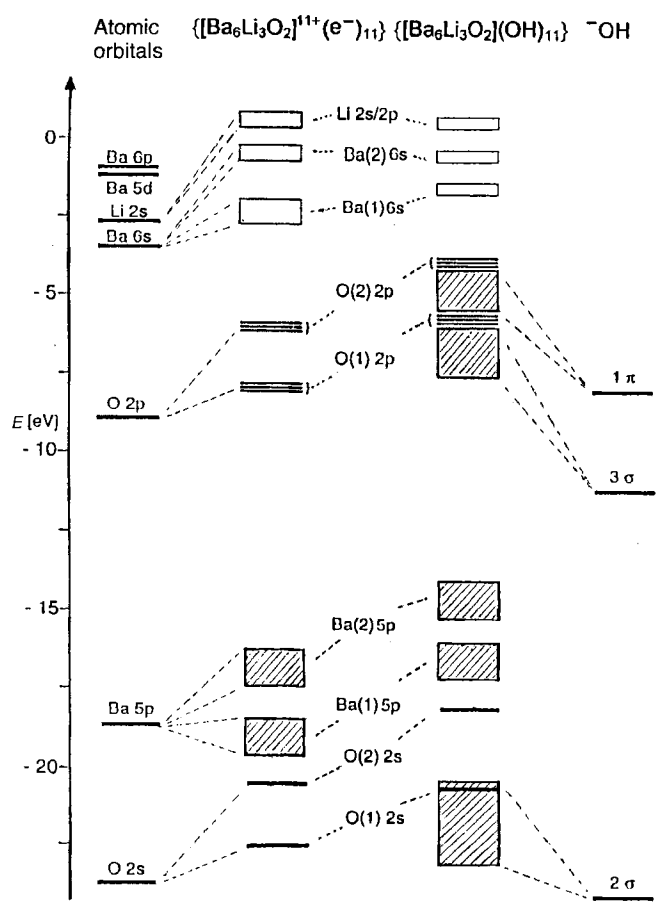

Fig. 2. Kohn–Sham eigenvalue spectra of LCGTO-DF-calculated valence orbitals [5] for both cluster models $\{[Ba_6Li_3O_2]^{11+}(e^-)_{11}\}$, and $\{[Ba_6Li_3O_2](OH)_{11}\}$ based on the spin-averaged Ba, Li, O atomic orbitals and OH molecular orbitals (filled and empty levels for Ba without spin/orbit splitting are represented by shaded and unshaded boxes, respectively).

The eigenvalues can be classified according to the basis orbital contributions Ba(1) for the centers of the outer Ba_3 triangle of the octahedron and Ba(2) for the shared Ba_3 face between octahedron and prismane, and in addition, the O^{-2} oxygen centers O(1) of the octahedron and O(2) of the prismane. Because of the O contacts on both sides, the contributions of Ba(2) to the molecular orbital energies are smaller than those of Ba(1). Furthermore, due to the smaller ionic character of the adjacent Li contacts, O(2) > O(1). In the $(OH)_{11}$ model the diversity of the 2σ, 3σ and 1π orbitals has to be taken into account. The electrostatic field of $(OH)_{11}$ predominantly shifts the occupied levels to higher energies and thereby reduces the HOMO–LUMO energy difference of 3.17 eV (102 a′ – 74 a″) in the $(e^-)_{11}$ model to 1.82 eV (137′ a′ – 138 a′). The bond energy of the individual OH ligands is calculated to be −25.1 eV for ionic dissociation to $^-$OH and −5.8 eV for homolytic clearage to $^\bullet$OH; comparable values for water are −18.1 eV ($H^+ + {}^-OH$) and −5.4 eV ($H^\bullet + {}^\bullet OH$). With respect to the electrostatic interaction in the $(e^-)_{11}$ model, each $^-$OH ligand stabilizes the cluster by 1 eV.

Special attention was focused on the two O^{2-} cluster oxygens. Hypersurface calculations within the $(e^-)_{11}$ model allow estimation of force constants[5] and vibrational frequencies and predict a weak O(1)···O(2) coupling of about 40 cm^{-1}. For the different charge distribution, a numerical integration over atomic lattice cells[5] yields −1.95 for O(1) and −1.68 for O(2). In the point charge approximation, satisfactory agreement is achieved by calculating the potential −24.2 eV at O(1) and −22.3 eV at O(2). The charges at the metal centers[5] obtained on numerical integration further confirm that the ionic contributions are more pronounced in the $Ba_o^{(2.1-2.2)+}$ octahedron than in the $Ba^{2.2+}Li^{0.8+}$ prismane. The analysis of the charge density distribution, therefore, supports the assignment as a polyion aggregate.

Despite of the information gathered both from crystallization and structure determination (Fig. 1) as well as from the LCGTO density functional calculations (Fig. 2), there are still numerous unanswered questions such as whether barium metal after dissolution in *tert*-butyl alcohol accompanied by H_2 evolution is already present as a $[Ba_6O]^{10+}$ octahedron.[6] Above all, it is of interest how the oxygen centers are incorporated. One possibility is, for instance, that it occurs as investigated almost 30 years ago[7] in the formation of the copper complexes $[Cu_4OL_4X_6]$ (L = amine, X = halide) containing an O^{2-} center in the Cu_4^{2+} tetrahedron. These and other facets of the intriguing novel lipophilically wrapped polyion aggregates are presently being explored.

Received: December 19, 1994 [Z 7559 IE]
German version: *Angew. Chem.* **1995**, *107*, 1439–1441

Keywords: barium compounds · density functional calculations · lithium compounds · polyion aggregates · structure elucidation

[1] The crystals of $\{[Ba_6Li_3O_2]^{11+}(^-OC(CH_3)_3)_{11}(OC_4H_8)_3\}$, which are grown under aprotic conditions [$c(H^+) < 0.1$ ppm], decompose violently in air. All operations, therefore, have to be carried out under purified argon. The mounting of a crystal (0.4 × 0.4 × 0.5 mm), covered with perfluorinated oil, to the needle of the goniometer is performed in a stream of N_2 cooled to 150 K. Crystal data: colorless prisms, $M_r = 1969.51$, $a = 1505.7(1)$, $b = 1746.3(1)$, $c = 1850.5(1)$ pm, $\beta = 104.17(1)^\circ$, $V = 4717.7(7) \times 10^6$ pm^3 ($T = 150$ K), $\rho_{calcd} = 1.387$ g cm^{-3}, monoclinic, $P2_1/m$ (no. 4), $Z = 2$, Siemens P4 four-circle diffractometer, $Mo_{K\alpha}$ irradiation, empirical absorption correction, $\mu = 2.51$ mm^{-1}, 9525 measured reflections which $3^\circ \le 2\theta \le 50^\circ$, of which 8437 were independent, and 8437 were used for refinement. Structure solution with direct methods and difference-Fourier-technique (SHELXS-86), structure refinement versus F^2 (SHELXL-93), 404 parameters, $w = 1/[\sigma^2(F_o^2) + (0.0747P)^2 + 17.52P]$, R for 6113 $F_o > 4\sigma(F_o) = 0.0463$, $wR2$ for all 8430 data = 0.1454, GOF = 1.043, residual electron density 0.95/−0.87 e Å^{-3} (adjacent to Ba3). The Li, O, Ba, and C atoms, except the carbon atoms of three disordered THF molecules, were refined anisotropically. All hydrogens were placed in ideal positions and refined

 © VCH Verlagsgesellschaft mbH, D-69451 Weinheim, 1995 0570-0833/95/1212-1354 $ 10.00+.25/0

isotropically with a riding model using individual displacement parameters ([U(H) = 1.5 U_{eq}(C-methyl)], [U(H) = 1.2 U_{eq}(C-methylene]). Three THF molecules were disordered and refined according to a split model. In one of these THF molecules the oxygen could not be localized unequivocally and was therefore refined as carbon. Further details of the crystal structure investigation are available on request from Fachinformationszentrum Karlsruhe, D-76344 Eggenstein-Leopoldshafen (Germany) on quoting the deposition number CSD-58880.

[2] The following "lipophilically wrapped polyion aggregates" have been crystallized and characterized by structure: a) the hexameric sodium imido(tetraphenoxydiphosphate), a hydrocarbon ellipsoid $\{H_{120}C_{144}O_{24}[OP\text{-}N^-PONa^+]_6\}$ containing a Na_6O_{12} core (H. Bock, H. Schödel, Z. Havlas, E. Herrmann, *Angew. Chem.* **1995**, *107*, 1441; *Angew. Chem. Int. Ed. Engl.* **1995**, *34*, 1355); b) $\{(H_{52}C_{44}O_4)^{3-}[Li_6^+(NH_3)_2]^{6+}(O_4C_{44}H_{52})^{3-}\}$, an edge-shared Li_6^+ double tetrahedron between calix[4]arene trianion half-shells (H. Bock, A. John, C. Näther, Z. Havlas, *J. Am. Chem. Soc.* **1995**, *117*, in press); c) $\{(H_8C_{12}C{=}NO_2)_6^{6-}K_6(OC_4H_8)_2(O_2C_4H_8)\}$, a hexameric aci-9-nitrofluorene potassium salt containing the coordination cluster K_6O_{12} (H. Bock, R. Dienelt, H. Schödel, Z. Havlas, *J. Chem. Soc. Chem. Commun.* **1995**, submitted); d) aluminumlithium-bis(catecholate)-penta(dimethoxyethane), a $C_{48}H_{76}$-wrapped infinite chain of $[O_3Li^+(O_4^-Al^{2+})(O_2Li^+O_2)(Al^{2+}O_4^-)Li^+O_3]$ links (H. Bock, R. Beck, H. Schödel, Z. Havlas, unpublished results); cf. R. Beck, Masters thesis, Universität Frankfurt, **1995**.

[3] The search through the Cambridge Crystallographic Data Bank for already known lipophilically wrapped polyion aggregates cannot be carried out in a single approach. The following isolated details were uncovered: a) D. Fenske, G. Longoni, G. Schmid summarized information on S- and Se-containing transition metal clusters ("Clusters and Colloids – From Theory to Applications" (Ed.: G. Schmid), VCH, Weinheim, **1994**, pp. 89–298); b) clusters of alkali metal oxides such as Rb_9O_2 or $Cs_{12}O_3$ consisting of O-filled Rb_6 or Cs_6 octahedra have been known since 1971 (A. Simon, *Struct. Bonding* **1979**, *36*, 81); c) isolated reports concern lithium-3,3-dimethyl-1-buten-2-olate-tetrahydrofuran (**A**; R. Amstutz, W. B. Schweizer, D. Seebach, J. D. Dunitz, *Helv. Chim. Acta* **1981**, *64*, 2617) and nonameric sodium-*tert*-butanolate (**B**; J. E. Davies, J. Kopf, E. Weiss, *Acta Crystallogr. Sect. B* **1982**, *38*, 2251; see also E. Weiss, *Angew. Chem.* **1993**, *105*, 1565; *Angew. Chem. Int. Ed. Engl.* **1993**, *32*, 1501. As the space-filling representations of **A** and **B** show, the $(Na^+O^-)_9$ double hexagon is less lipophilically wrapped than the $(Li^+O^-)_4$ cubane.

$[(H_3C)_3C\text{-}C(=CH_2)O^{\ominus}Li^{\oplus}(OC_4H_8)]_4$ $[(H_3C)_3CO^{\ominus}Na^{\oplus}]_9$

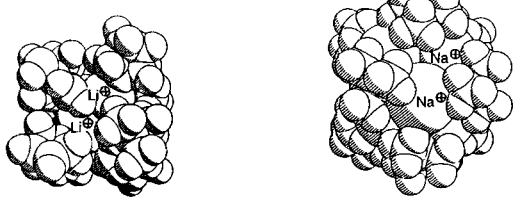

A **B**

[4] Cf. B. I. Dunlap, N. Rösch, *Adv. Quantum Chem.* **1990**, *21*, 317; see also "Electronic Structure of Metal Clusters and Clusters Compounds": N. Rösch, G. Pacchioni in *Clusters and Colloids – From Theory to Applications* (Ed.: G. Schmid), VCH, Weinheim, **1994**, pp. 5–88. A quasi-relativistic variant (O. D. Häberlen, N. Rösch, *Chem. Phys. Lett.* **1992**, *199*, 491) is applied together with a local density approximation of the exchange correlation energy functional (S. H. Vosko, L. Wilk, M. Nusair, *Can. J. Phys.* **1980**, *58*, 1200) or of the gradient-corrected exchange and correlation energy functionals (A. D. Becke, *Phys. Rev. A* **1988**, *38*, 3098 and C. Lee, W. Yang, R. Parr, *Phys. Rev. B* **1988**, *37*, 785).

[5] Details of the LCGTO-DF-calculations: Basis sets Ba (18s, 13p, 8d, 1f), Li (9s, 4p), O^{2-} (11s, 7p, 1d), O (9s, 5p, 1d), H (6s, 1p) with generalized atom contractions of TZVP quality; the additional charge density and exchange correlation potential basis sets were designed according to standard procedures [4]. The three-dimensional numerical integration to determine the exchange correlation contributions to the total energy were performed using a cell grid of the ionic radii $r(Ba^{2+}) = 135$ pm, $r(Li^+) = 76$ pm, $r(O^{2-}) = 140$ pm, and $r(H) = 37$ pm. The eigenvalue scheme (Fig. 2) was supplemented by the calculated dipole moments of 29 D in the $(e^-)_{11}$ model and of 21 D in the $(^-OH)_{11}$ model, as well as by the different 1s-shifts relative to the atomic value of +7.7 eV for O(1) and of +9.2 eV for O(2) in the $(^-OH)_{11}$ model, which are predominantly due to the electrostatic potential difference of −1.9 eV between the centers O(1) and O(2). The force constants for the O(1)/O(2)-coupling are $f_{11} \approx f_{22} \approx 1.2$ and $f_{12} \approx 0.1$ mdyn Å^{-3}.

[6] K. G. Caulton, M. H. Chisholm, S. R. Drake, J. C. Huffman, *J. Chem. Soc. Chem. Commun.* **1990**, 1349, 1498.

[7] H. Bock, H. tom Dieck, H. Pyttlick, M. Schnöller, *Z. Anorg. Allg. Chem.* **1968**, 357, 54.

The Lipophilically Wrapped Polyion Aggregate $\{H_{120}C_{144}O_{24}(OP)_2N^-Na_6^+\}$, a Hexameric Sodium Tetraphenyl Imidodiphosphate Containing an $[Na_6O_{12}]$ Core in a Hydrocarbon Ellipsoid**

Hans Bock*, Holger Schödel, Zdenek Havlas, and Eckhard Herrmann*

Dedicated to Professor Peter Schuster

Tetraphenyl imidodiphosphate $HN[PO(OC_6H_5)_2]_2$[2a] with its $[OP\text{-}N\text{-}PO]^-$ chelate pincer is a Brønsted acid with advantages for complexation[2b] and extraction[2c] of metal ions. If salts are formed, not in water or alcohols[2] but in dry benzene, with sodium hydride, instead of the well-known[2d] monomeric chelate complexes $[Me^nL_n]$ a novel hexamer results [Eq. (a)].

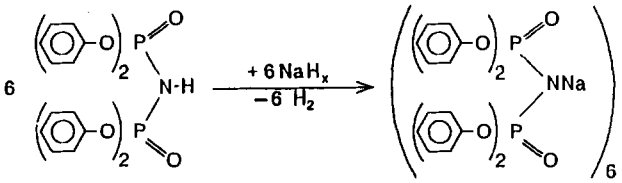

(a)

The structure determination on the colorless prisms of the hexamer[3] (Fig. 1) reveals a "hydrocarbon skin" $H_{120}C_{144}$ composed of 24 phenyl rings (Fig. 1, top right), which lipophilically wraps a polyion aggregate with an $[Na_6O_{12}]^{6+}$ core within a circle of four imidodiphosphate ions (Fig. 1, bottom left), capped above and below by two others (Fig. 1, bottom right).

In the three-dimensional cluster core $[Na_6O_{12}]^{6+}$, the distances between the Na^+ ions and the deprotonated nitrogen centers of the anions are, on average, 370 pm; the complexation, therefore, is accomplished through the 223 to 250 pm long $Na\cdots O{=}P$ contacts (Fig. 1, bottom right). Every Na^+ ion is surrounded by four close O centers and is coordinated in addition to another at a larger distance (see legend of Fig. 1; values in brackets between 265 and 305 pm). The Na_6O_{12} network contains a center of inversion and a total of 24 stronger and 6 weaker $Na^+\cdots O^{\delta-}$ interactions. Of the stronger ones, 14 are located in the tetramer circle (dashed lines in Fig. 1, bottom left) and the other 10 connect the two capping tetraphenyl imido disphosphate ligands which bridge the metal centers Na1, Na2, Na3, Na1′, Na2′, and Na3′ (Fig. 1, bottom right, O50P5N3P6O60).

According to ab initio calculations with a "double zeta" basis set, the $Na^+\cdots O^{\delta-}$ interactions are largely ionic[4a] and support the designation of the compound as a polyion aggregate.

[*] Prof. Dr. H. Bock, Dipl.-Chem. H. Schödel
Chemische Institute der Universität
Marie-Curie-Strasse 11, D-60439 Frankfurt am Main (Germany)
Telefax: Int. code + (69)5800-9188
Dr. Z. Havlas
Institute of Organic Chemistry and Biochemistry
of the Czech Academy of Sciences, Prag (Czech Republic)
Prof. Dr. E. Herrmann
Hochschule für Technik und Wirtschaft
Josephinen-Strasse 1, D-01069 Dresden (Germany)
Telefax: Int. code + (351)4622230

[**] Lipophilically Wrapped Polyion Aggregates, Part 2, and Interactions in Crystals, Part 70. The research project was supported by the Adolf-Messer-Foundation, the Deutsche Forschungsgemeinschaft, the State of Hesse, and the Fonds der Chemischen Industrie. Part 1 and Part 69: ref. [1].

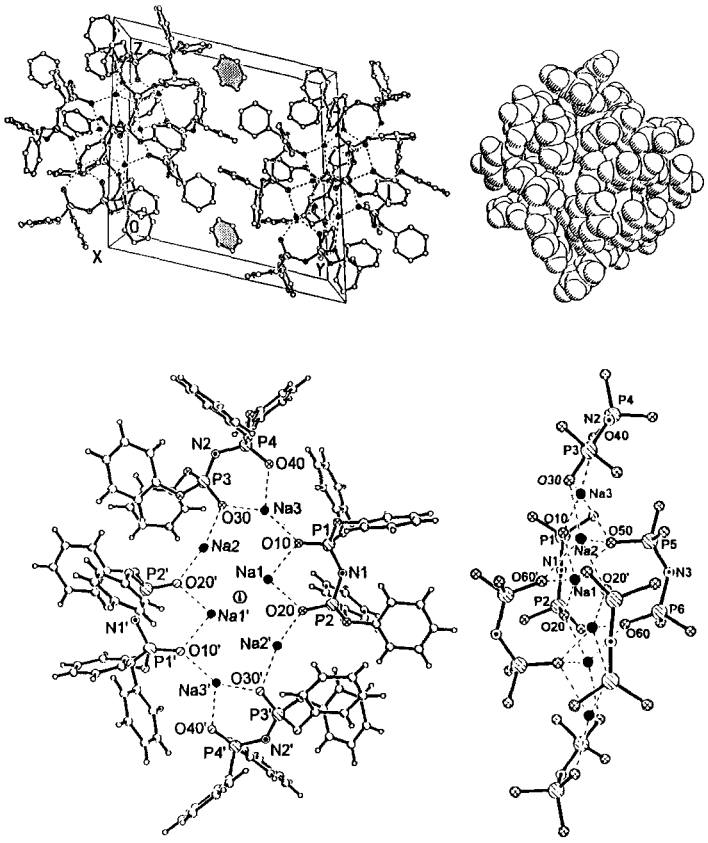

Fig. 1. Single-crystal structure of hexameric sodium tetraphenyl imidodiposphate at 200 K [3]. Top left: unit cell (triclinic $P\bar{1}$, $Z = 2$) viewed along the x direction with two molecules of benzene in crystal cavities per three formula units shaded; shortest non-bonded C···C distance to the phenyl substituents 360 pm). Top right: space-filling representation of the hexamer. Bottom left: View of a cut through the $[Na_6O_{12}]^{6+}$ core showing four of the six tetraphenyl imidodiphosphate ions encircling the cluster (ⓘ: center of inversion). Bottom right: side view of the polyion aggregate $[\{O_2(O)PN\text{-}P(O)O_2\}^-Na]_6$, without phenyl groups, around the three types of centers, Na1, Na2, and Na3. Selected bond lengths [pm] and angles [°]: Na1O10 234, Na1O20 223, Na1O50 226, Na1O60′ 230, Na1O60 (265), Na2O20′ 230, Na2O30 231, Na2O50 238, Na2O60′ 249, Na2O31 (284), Na3O10 228, Na3O30 229, Na3O40 223, Na3O50 238, Na3O52 (305), O10Na1O20 92, O10Na1O50 86, O10Na1O60 145, O20Na1O50 154, O20Na1O60 87, PN 156, P=O 148, P–O 160 PNP 132, OPO 105, 110, OPN 105, 120.

The formal charge separation $Na^+\cdots OPN^-$ impedes MNDO calculations of enthalpies of formation: Relative to $[\{(HO)_2OP\}_2N^-Na^+]_n$ with $n = 1$, for hexamerization ($n = 6$) a lower limit of $\Delta\Delta H_f^{MNDO} = -146\ kJ\,mol^{-1}$ per monomer is estimated, which on consideration of all contacts $Na^+\cdots O^{\delta-}$, increases to an average of $\Delta\Delta H_f^{MNDO} = -200\ kJ\,mol^{-1}$.[4c] The total enthalpy of formation calculated from the structural data (Fig. 1) of $\Delta H_f^{MNDO} = -9021\ kJ\,mol^{-1}$ includes a Coulomb repulsion contribution within the Na_6^+ network of $\Delta\Delta H_f^{MNDO} = 3942\ kJ\,mol^{-1}$.

The lipophilic $H_{120}C_{144}$ hydrocarbon skin of the hexameric tetraphenyl imidodiphosphate is composed of 24 phenyl rings whose interactions can be estimated. The starting point is the statistical structure analysis of 34 phenyl-containing proteins from the database of the Cambridge Crystallographic Data Centre,[5] which traces the formation of "phenyl clusters" to CH/π interactions: according to this analysis, two phenyl rings with an average centroid/centroid distance of 505 pm and a dihedral angle between their planes of 70° should contribute about $-5\ kJ\,mol^{-1}$ to the enthalpy of formation.[5a] In crystals of aromatic compounds with six-membered rings, these interactions can generate the known herringbone patterns. For benzene dimers in the gas phase, calculations with highly correlated wavefunctions predict a stabilization of at least $-9\ kJ\,mol^{-1}$[5c] for a parallel-shifted arrangement of C_6 rings 385 pm apart. For the "phenyl skin" of the polyion aggregate presented here (Fig. 1), an analysis of the structural data (Fig. 2) yields a distribution of the total of 62 ring intercentroid distances and angles between the planes of the 24 phenyl rings. The histograms show 44 intercentroid distances smaller than 600 pm and 29 arrangements with interplanar angles smaller than 60°. The average values are $\bar{d}_{R\cdots R} = 534$ pm and $\bar{\omega} = 35°$. Fitting the correlated calculation results for benzene dimers[5c] to a Morse potential curve yields an estimated $-1\ kJ\,mol^{-1}$ for parallel phenyl rings 500 pm apart and thus an overall cluster stabilization contribution by the phenyl wrapping of at most $-50\ kJ\,mol^{-1}$.[6]

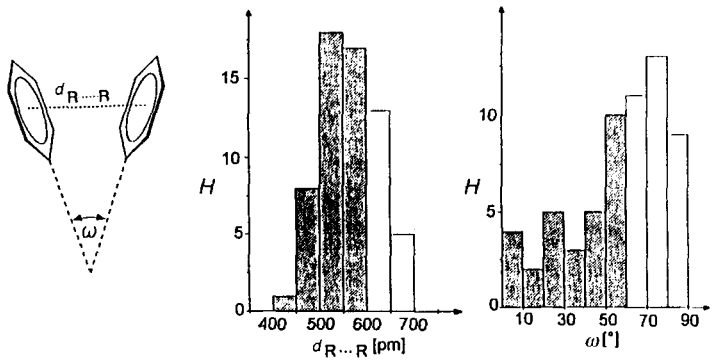

Fig. 2. Abundances H of distances d and angles ω between phenyl rings in the title compound.

Lipophilically wrapped polyion aggregates are characterized[1] by a cluster core of cations and anions that provides thermodynamic stability, and by a largely impenetrable hydrocarbon skin, which adds kinetic stability. A generalizable crystallization (self-organization) principle[1] now emerges. Within a few months, we succeeded in crystallizing and structurally characterizing the following polyion aggregates:

- $\{[Ba_6Li_3O_2]^{11+}[^-OC(CH_3)_3]_{11}(OC_4H_8)_3\}$, an (octahedron + prismane) polyhedron,[1]
- $\{(H_{52}C_{44}O_4)^{3-}[Li_6^+(NH_3)_2](O_4C_{44}H_{52})^{3-}\}$, an edge-sharing double tetrahedron between calix[4]arene trianions,[7a]
- $\{[(H_8C_{12}C{=}NO_2)^-K^+]_6(OC_4H_8)_2(O_2C_4H_8)\}$, a hexameric aci-9-nitrofluorene potassium with a K_6O_{12} core,[7b] and
- $\{(H_{76}C_{48})[Li_4^+Al_2^{2+}O_8^-O_{10}]\}_\infty$, an aluminumlithium-bis(catecholate)-penta(dimethoxyethane) chain.[7c]

In the hexameric sodium tetraphenylimidodiphosphate presented here, the thermodynamic stability is analogously dominated by the energetically favorable ionic contacts ($Na^+\cdots O^{\delta-}$).[3] The lipophilic wrapping determines on one hand the selective crystallization of the hexamer because of the spatial demands of the 24 phenyl substituents, and on the other the kinetic stability because of its impermeability at least to larger molecules.

Received: December 20, 1994
Revised: February 27, 1995 [Z 7560 IE]
German version: *Angew. Chem.* **1995**, *107*, 1441–1443

Keywords: polyion aggregates · sodium compounds · structure elucidation

 © VCH Verlagsgesellschaft mbH, D-69451 Weinheim, 1995 0570-0833/95/1212-1356 $ 10.00+.25/0

[1] H. Bock, T. Hauck, C. Näther, M. Rösch, M. Staufer, O. Häberlein, *Angew. Chem.* **1995**, *107*, 1439; *Angew. Chem. Int. Ed. Engl.* **1995**, *34*, 1353: See also the definition for "lipophilically wrapped polyion aggregates" given therein.

[2] a) S. Kulpe, I. Seidel, E. Herrmann, *Cryst. Res. Technol.* **1984**, *19*, 661; b) M. L. Nielsen, *Inorg. Chem.* **1964**, *3*, 1760; H. Richler, E. Fluck, H. Riffel, H. Hess, *Z. Anorg. Allg. Chem.* **1983**, *496*, 109; E. Herrmann, H. Nang, R. Dreyer, *Z. Chem.* **1979**, *19*, 187; c) O. Navratil, E. Herrmann, *Collect. Czech. Chem. Commun.* **1992**, *57*, 1655, and references therein; d) see, for example, $[Yb_3^+\{(H_5C_6O)_2OP\text{-}N\text{-}PO(OC_6H_5)_2\}_3^-]$: S. Kulpe, I. Seidel, E. Herrmann, *Z. Chem.* **1981**, *24*, 333.

[3] The crystalline powder from reaction (a) was recrystallized from dry benzene at room temperature under argon. Crystal structure determination: $(C_{24}H_{20}NP_2O_6Na)_3(C_6H_6)_2$, $M_r = 1666.2$, crystal dimensions $0.66 \times 0.52 \times 0.40$ mm, colorless prisms, temperature 200 ± 1 K, $a = 1398.4(1)$, $b = 1758.5(1)$, $c = 1788.9(1)$ pm, $\alpha = 101.74(1)$, $\beta = 107.06(1)$, $\gamma = 95.37(1)^\circ$, $V = 4061.9(6)$, 10^6 pm^3, $Z = 2$, $\rho_{calcd} = 1.362$ g cm^{-3}, $\mu(Mo_{K\alpha}) = 71.07$ pm, triclinic, space group $P\bar{1}$ (no. 2), Siemens P4 four-circle diffractometer, 14256 measured reflections within $3^\circ \leq 2\theta \leq 50^\circ$, 13631 independent reflections of which 10459 with $I > 2\sigma(I)$, structure solution by direct methods (SHELXS), 1043 parameters refined on F (SHELXTL PC), $R = 0.038$, $R_w = 0.039$, residual electron density $+0.27/-0.32$ e Å^{-3}, $S = 1.608$. C, N, O, P positions anisotropically refined, hydrogens in ideal positions (d(C-H) = 96 pm) and refined isotropically using a riding model with a temperature factor common to the phenyl rings. One molecule benzene is 33% disordered; its main position was refined anisotropically and minor positions refined isotropically as idealized hexagons. Further details for the crystal structure determination can be requested from the Fachinformationszentrum Karlsruhe, D-76344 Eggenstein-Leopoldshafen (Germany), on quoting the depository number CSD-58881.

[4] The calculations were performed with the programs GAMESS (M. W. Schmidt, K. K. Baldridge, J. A. Boatz, J. H. Jensen, S. Koseki, M. S. Gordon, K. A. Nguyen, T. L. Windus, S. T. Elbert, *QCPE Bull.* **1990**, *10*, 52) and MOPAC 6.00 (J. J. P. Stewart, QCPE Programm 455, Indiana University, Bloomington) on our work station IBM RISC 6000. The storage limit of 252 atoms required the replacement of the phenyl groups by hydrogen, because the hexamer contains 324 centers. a) The ab initio calculations started from the structural data and employed a "double zeta" basis set (S. Huzinaga, J. Andzelm, M. Klobukowski, E. Radzio-Andzelm, Y. Sakai, H. Tatewaki, *Gaussian Basis Sets for Molecular Orbital Calculations*, Elsevier, Amsterdam, **1984**). A potential energy plot yielded two preferred positions for Na^+ at the $[O(HO)_2P\text{-}N'\text{-}P(OH)_2O]^-$ anion: in the center of the chelate pincer with Na1 $\cdots$ O distances of 233 and 234 pm, and outside them with a distance of 228 pm between Na3 and each oxygen atom. The total energy differences amounted to -603 (Na1) and -462 kJ mol^{-1} (Na3), and the charges to $+0.94$ (Na1) and $+0.96$ (Na3); b) based on the structural data (Fig. 1) the following MNDO-enthalpies of formation (kJ mol^{-1}) were calculated: $[(HO)_2OP\text{-}N\text{-}PO(OH)_2Na]_n$ for $n = 1$ -1358 and for $n = 6$ -9021; for the difference $\Delta\Delta H_f^{MNDO}$ -873, for each monomer -146 and for 6 Na^+ $+4515$ and for $(Na^+)_6$ $+7835$; c) with the individual contributions of the fragments O10Na1O20, O30Na2O40, and O50Na3O60 of -1262, -1261, and -1251, respectively, an enthalpy difference $\Delta\Delta H_f^{MNDO}$ of 8734 kJ mol^{-1} for the complexation $(Na^+)_6 \rightarrow$ hexamer and -4792 for 6 $Na^+ \rightarrow$ hexamer (without Coulomb repulsion is calculated, that is, an average stabilization of -200 for each $Na^+ \cdots O^\delta$ contact.

[5] a) S. K. Burley, G. A. Petsko, *Science* **1985**, *229*, 23; *J. Am. Chem. Soc.* **1986**, *108*, 7955. Cf. also C. A. Hunter, J. Singh, J. Thornton, *J. Mol. Biol.* **1991**, *218*, 837, C. A. Hunter, J. K. Sanders, *J. Am. Chem. Soc.* **1990**, *112*, 5525; b) J. Bernstein, J. A. R. P. Sarma, A. Gavezzotti, *Chem. Phys. Lett.* **1990**, *174*, 361; c) P. Hobza, H. L. Selzle, E. W. Schlag, *J. Am. Chem. Soc.* **1994**, *116*, 3500, and references therein.

[6] Based on the minimum of the Morse curve at $R_0 = 3.848$ and $D_0 = -2.276$ [4c] variation yields a parameter α 2.7 for the optimum fit. Approximate distance-dependent interaction energies (kJ mol^{-1}) can thus be calculated: for 400 pm -8.09, for 500 pm -0.85, and for 600 pm -0.06.

[7] a) H. Bock, A. John, C. Näther, Z. Havlas, *J. Am. Chem. Soc.* **1995**, *117*, in press; b) H. Bock, R. Dienelt, H. Schödel, Z. Havlas, *J. Chem. Soc. Chem. Commun.* submitted; c) H. Bock, R. Beck, H. Schödel, Z. Havlas, unpublished results; cf. R. Beck, Diplomarbeit, Universität Frankfurt, **1995**.

Aromatic Gallium Heterocycles: Synthesis of the First Gallatabenzene**

Arthur J. Ashe III,* Saleem Al-Ahmad, and Jeff W. Kampf

Dedicated to Professor Herbert Schumann on the occasion of his 60th birthday

Boratabenzene derivatives (**1**) have been intensely investigated for 25 years.[1-4] The high acidity of the precursor boracyclohexadienes (**2**),[5] and the close resemblance of boratabenzene metal complexes such as **3** with the corresponding cyclopentadienyl metal complexes[3, 4, 6] convincingly demonstrate that **1** is an anionic aromatic ring with six π electrons. Recent research suggests that boron's heavier congener gallium may also be able to form π bonds with carbon;[7, 8] thus an exploration of the chemistry of gallatabenzene should be of interest. We report here on the first synthesis of an arylgallatabenzene (**6**) and structural data for its $Mn(CO)_3$ complex (**7**).

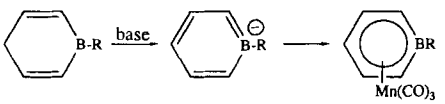

2 **1** **3**

In order to inhibit the Lewis acidity of the gallium atom we chose the highly hindered arylgallatabenzene **6** (Ar = tBu$_3$C$_6$H$_2$) as our target. The precursor gallacyclohexadiene **5** may be prepared by an adaption of the method used by Jutzi et al. to prepare silacyclohexadiene.[9] The reaction of (1*Z*,4*Z*)-1,5-dilithio-1,4-pentadiene (**4**) with 2,4,6-tri(*tert*-butyl)phenylgallium dichloride[10] gives **5** as air- and moisture-sensitive white crystals in 80% yield. The spectroscopic properties are completely consistent with the assigned structure. Compound **5** may be deprotonated with bases (tBuLi, Ph_3CLi, lithium diisopropylamide, or fluorenyllithium) in THF to afford yellow solutions of **6**. Treatment of **5** with one equivalent of indenyllithium in THF initially gives **6** and indene; however, on standing indenyllithium is reformed along with the conjugated gallacyclohexadiene **8**. Quenching **6** with excess cyclopentadiene affords a 1:1 mixture of **5** and **8**. Alternatively **5** may be completely converted to **8** by treatment with a trace of indenylithium in THF.

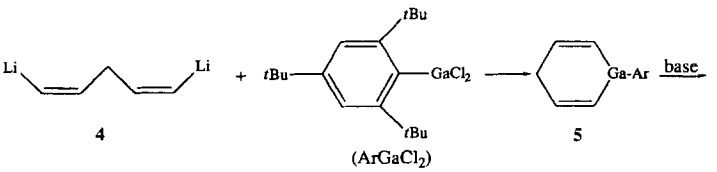

4 (ArGaCl$_2$) **5**

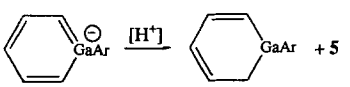

6 **8**

Thus, the acidity of **5** is bracketed between that of cyclopentadiene ($pK_a \approx 16$)[11] and that of indene ($pK_a \approx 21$),[11] while the more stable **8** is less acidic than indene. Since **5** is considerably

[*] Prof. Dr. A. J. Ashe III, Dr. S. Al-Ahmad, Dr. J. W. Kampf
Department of Chemistry, The University of Michigan
Ann Arbor, MI 48109-1055 (USA)
Telefax: Int. code +(313) 747-4865

[**] This work was supported by the National Science Foundation.

more acidic than acyclic 1,4-dienes ($pK_a \approx 31$),[11, 12] there is a strong presumption that the gallium atom of **6** accepts π-electron density from the carbon atoms to form an aromatic ring with six π electrons. However under similar conditions **2** (R = Me) is more acidic than cyclopentadiene.[1b, 5] Thus the driving force for aromatization must be smaller for gallatabenzene than for boratabenzene.

The ^{1}H NMR spectrum of **6** in [D$_8$]THF shows a characteristic first-order [*AA'BB'C*] pattern for the signals of the five gallatabenzene ring protons, while the signals in the ^{13}C NMR spectrum can be unambiguously assigned by using selective ^{1}H-^{13}C decoupling. The ^{1}H and ^{13}C NMR chemical shift values of **1** (R = Me) and **6** are compared with those of the nonaromatic cyclohexadienide **9**[13] in Scheme 1. ^{13}C NMR chemical shift

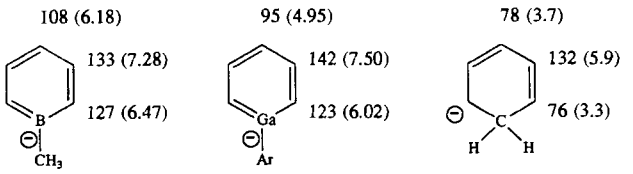

1 6 9

Scheme 1. Comparison of the ^{13}C NMR and the ^{1}H NMR (in parentheses) chemical shift values for anions **1** (R = Me), **6**, and **9** in [D$_8$]THF.

values have been used extensively to evaluate π-charge densities of carbanions[13, 14] and heterocarbanions.[15] The spectrum of cyclohexadienide (**9**) is typical for π-delocalized carbanions.[13] The signals for the negatively charged carbon atoms C1, C3, and C5 occur approximately 50 ppm higher field than those for the uncharged carbon atoms C2 and C4. The spectra of **1** (R = Me) and **6** deviate from this pattern in that the upfield shifts of the corresponding nuclei are much smaller, which is consistent with diminished negative charge at these carbon centers due to π-electron donation to the respective heteroatoms. In the same manner the ^{1}H NMR chemical shifts of the ring protons of **1** (R = Me) and **6** are shifted substantially downfield from the corresponding signals for **9**. This effect is consistent with ring current effects and/or diminished negative charge at carbon.[2] Thus the NMR spectra suggest that gallatabenzene **6** has aromatic character.

In order to explore further the chemistry of **6** we have prepared the Mn(CO)$_3$ complex **7**. The reaction of **6** with [Mn(CO)$_3$(CH$_3$CN)$_3$]PF$_6$ affords **7** in 46% yield as yellow air-

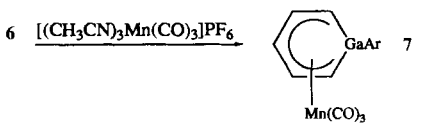

and moisture-sensitive crystals. An X-ray structural analysis allowed determination of the molecular structure of **7** as illustrated in Figure 1.[16] The structure of **7** shows that the gallatabenzene ring is η^5 coordinated through its planar pentadienyl moiety to the Mn(CO)$_3$ group. The ring is folded so that the C4-C5-C6-C7-C8 and C4-Ga-C8 planes intersect at 34.5°. While the five C–Mn bonds are of normal length (2.12–2.30 Å),[17] the Ga–Mn distance of 3.03 Å is much longer than the 2.50 Å reported for a Ga–Mn bond of a related complex.[18] The three C–Ga bond lengths of the trigonally surrounded Ga atom are not significantly different and fall in the expected range (1.94–1.96 Å) for single bonds. The plane of the aryl substituents is perpendicular to the C4-Ga-C8 plane. Thus the structure of **7** provides no evidence for Ga–C π bonding.

Table 1. Spectroscopic data for **5**–**8**.

5: ^{1}H NMR (360 MHz, C$_6$D$_6$): δ = 1.37 (s, *p*-*t*Bu), 1.40 (s, *o*-*t*Bu), 2.93 (m, CH$_2$), 6.73 (dt, *J* = 14, 1.7, CH(2,6)), 7.08 (dt, *J* = 14, 3.7, CH(3,5)), 7.52 (s, *m*-CH); ^{13}C NMR (90.6 MHz, C$_6$D$_6$): δ = 32.0 (*p*-*t*Bu, CH$_3$), 33.8 (*o*-*t*Bu, CH$_3$), 35.3 (*p*-*t*Bu, C), 36.2 (CH$_2$), 38.4 (*o*-*t*Bu, C), 120.9 (*m*-CH), 136.1 (*ipso*-C), 138.4 (CH(2,6)), 149.3 (CH(3.5)), 150.3 (*p*-C), 157.7 (*o*-C); HRMS (EI): $C_{23}H_{35}{}^{69}Ga$: calcd.: 380.1995; found: 380.2003

6: ^{1}H NMR (360 MHz, [D$_8$]THF): δ = 1.42 (s, *p*-*t*Bu), 1.51 (s, *o*-*t*Bu), 4.95 (t, *J* = 9, H4), 6.02 (d, *J* = 12, H2,6), 7.30 (s, *m*-CH), 7.50 (dd, *J* = 12, 9, H3,5); ^{13}C NMR (90.6 MHz, [D$_8$]THF): δ = 30.7 (*p*-*t*Bu-C), 31.9 (*o*-*t*Bu, CH$_3$), 35.8 (*p*-*t*Bu, CH$_3$), 38.9 (*o*-*t*Bu-C), 94.5 (C4), 119.5 (*m*-CH), 123 (C2,6), 141.5 (C3,5), 145.0 (*ipso*-C), 147.5 (*p*-C), 157.8 (*o*-C)

7: ^{1}H NMR (360 MHz, C$_6$D$_6$): δ = 1.32 (s, *p*-*t*Bu), 1.39 (s, *o*-*t*Bu), 2.82 (d, *J* = 11.8, H2), 4.49 (t, *J* = 6.6, H4), 6.6 (dd, *J* = 11.8, 6.6, H3), 7.47 (s, *m*-H); ^{13}C NMR (90.6 MHz, C$_6$D$_6$): δ = 31.9 (*p*-*t*Bu-Me), 34.4 (*o*-*t*Bu-Me), *p*-*t*Bu(C)), 37.8 (*o*-*t*Bu(C)), 77.2 (C4), 77.5 (C2), 114.5 (C3), 120.8 (*m*-CH), 135.2 (*ipso*-C), 151.0 (*p*-C), 157.4 (*o*-C); IR (KBr): ν̃ = 2011, 1937, 1914 cm^{-1}; HRMS (EI): $C_{26}H_{34}{}^{69}GaMnO_3$: calcd.: 518.1144, found: 518.1147

8: ^{1}H-NMR (360 MHz, [D$_8$]THF): δ = 1.32 (s, *p*-*t*Bu), 1.43 (s, *o*-*t*Bu), 1.69 (dd, *J* = 5, 1.6, H6), 5.91 (m, H4), 6.30 (dt, *J* = 5, 2.5, H5), 6.61 (d, *J* = 14, H2), 7.01 (dd, *J* = 14, 6.3, H3), 7.37 (s, *m*-CH); ^{13}C-NMR (90.6 MHz, [D$_8$]THF): δ = 157.7 (*o*-C), 150.3 (*p*-C), 134.6 (*ipso*-C), 145.7, 134.6, 120.0, 115.9 (C2-C5), 121.2 (*m*-CH), 38.7 (*o*-*t*Bu(C)), 35.6 (*p*-*t*Bu(C)), 33.8 (*o*-*t*Bu-CH$_3$), 31.9 (*p*-*t*Bu-CH$_3$), C6 not observed; HRMS (EI): $C_{25}H_{35}{}^{69}Ga$: calcd.: 380.1995, found: 380.1999

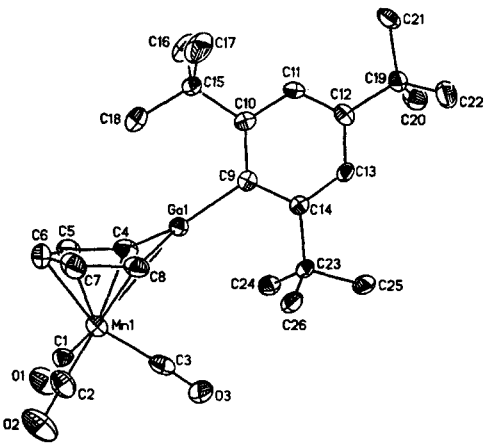

Fig. 1. Solid-state structure of **7** (ORTEP). Selected distances [Å] and angles [°]: Ga1-C8 1.936(3), Ga1-C4 1.942(4), Ga1-C9 1.961(3), Ga1-Mn1 3.0290(7), Mn1-C4 2.303(3), Mn1-C5 2.161(4), Mn1-C6 2.121(4), Mn1-C7 2.152(4), Mn1-C8 2.291(3), C4-C5 1.396(5), C5-C6 1.416(5), C6-C7 1.434(6), C7-C8 1.387(5); C9-Ga1-C4 132.75(15), C9-Ga1-C8 133.78(14), C4-Ga1-C8 93.5(2).

However, the electronic isolation of the Ga atom in **7** is a probable consequence of steric effects. A displacement of the Ga atom towards the ring plane, which is necessary to achieve η^6 coordination, would involve severe steric compression of the *ortho tert*-butyl group (C24, C26) and the carbonyl (C303). In a relevant related study Cowley et al. have found that the planar 1-(2,4,6-tri-*tert*-butylphenyl)-2,3,4,5-tetramethylgallole distorts on complexation to a CpCo group to form **10** by folding the Ga atom away from the metal.[8] We intend to prepare derivatives of **7** with smaller substituents on gallium which may show η^6 coordination.

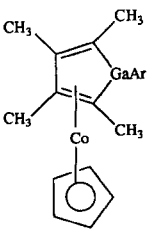

10

Experimental Procedure

5: A solution of **4**, prepared from 5.25 mmol butyllithium in hexane (2.1 mL) and (1*Z*,4*Z*)-1,5-diiodohexa-1,4-diene (0.84 g, 2.63 mmol) in diethyl ether (30 mL), was added dropwise with stirring to a solution of ArGaCl$_2$ (1.01 g, 2.63 mmol) in diethyl ether (20 mL) at −78 °C. The reaction mixture was allowed to warm to 25 °C over 90 min, after which the solvent was removed under vacuum. The residue was extracted with pentane (40 mL). The volume of the extracts was reduced under re-

 © VCH Verlagsgesellschaft mbH, D-69451 Weinheim, 1995 0570-0833/95/1212-1358 $ 10.00+.25/0 Angew. Chem. Int. Ed. Engl. 1995, 34, No. 12

duced pressure to 15 mL. Cooling to −78 °C afforded 0.8 g (80%) of **5** as white crystals; m.p. 127 °C.

6: To a solution of **5** (20 mg, 0.051 mmol) in [D$_8$]THF (0.5 mL) at −78 °C was added a solution of *tert*-butyllithium (0.051 mmol) in pentane (30 μL). On warming to 25 °C the solution became yellow. The NMR spectrum was consistent with the formation of **6**. It showed only signals of **6**, the solvent, and the conjugate acid of the base. An identical spectrum was recorded for **6** prepared from **5** and fluorenyllithium. Compound **6** did not react with excess fluorene but was quenched to a 1:1 mixture of **5** and **8** by treatment with excess cyclopentadiene.

8: A solution of **5** (50 mg, 0.13 mmol) in THF (5 mL) was treated with a trace of indenyllithium (3 mg) for 24 h. Removal of solvent left a waxy solid which was recrystallized from pentane to give 42 mg (84%) of **8**; m.p. 159 °C.

7: A solution containing one equivalent of lithium diisopropylamide in diethyl ether (10 mL) was added dropwise to a stirred solution of **5** (0.4 g, 1.05 mmol) in diethyl ether (15 mL) at −78 °C. The reaction solution was allowed to warm to 25 °C affording a yellow solution, which was cooled to −78 °C and added dropwise to a suspension of [Mn(CO)$_3$(CH$_3$CN)$_3$]PF$_6$ (0.43 g, 1.05 mmol) in diethyl ether (10 mL) at −78 °C. The reaction mixture was allowed to warm to 25 °C and stirred for 3 h. The solvent was removed under reduced pressure, and the residue was extracted with pentane (40 mL). Reduction of the volume to 20 mL and cooling at −20 °C for 24 h afforded 0.25 g (46% yield) of yellow crystals of **7**; m.p. 189 °C.

Received: December 13, 1994
Revised version: February 21, 1995 [Z 7544 IE]
German version: *Angew. Chem.* **1995**, *107*, 1479–1481

Keywords: arene complexes · gallium compounds · heterocycles · manganese compounds

[1] a) G. E. Herberich, G. Greiss, H. F. Heil, *Angew. Chem.* **1970**, *82*, 838; *Angew. Chem. Int. Ed. Engl.* **1970**, *9*, 805; b) G. E. Herberich, B. Schmidt, U. Englert, *Organometallics* **1995**, *14*, 471.
[2] A. J. Ashe III, P. Shu, *J. Am. Chem. Soc.* **1971**, *93*, 1804.
[3] G. E. Herberich, H. Ohst, *Adv. Organomet. Chem.* **1986**, *25*, 199.
[4] G. E. Herberich in *Comprehensive Organometallic Chemistry, Vol. 1* (Eds.: G. Wilkinson, F. G. A. Stone, E. W. Abel), Pergamon, Oxford, **1982**, p. 381.
[5] S. A. Sullivan, H. Sandford, J. L. Beauchamp, A. J. Ashe III, *J. Am. Chem. Soc.* **1978**, *100*, 3737; H. Sandford, Dissertation, University of Michigan, **1979**.
[6] A. J. Ashe III, E. Meyers, P. Shu, T. Von Lehmann, J. Bastide, *J. Am. Chem. Soc.* **1975**, *97*, 6865.
[7] A. H. Cowley, F. P. Gabbaï, C. J. Carraño, L. M. Mokry, M. R. Bond, G. Bertrand, *Angew. Chem.* **1994**, *106*, 584; *Angew. Chem. Int. Ed. Engl.* **1994**, *33*, 578.
[8] A. H. Cowley, F. P. Gabbaï, A. Decken, *Angew. Chem.* **1994**, *106*, 1429; *Angew. Chem. Int. Ed. Engl.* **1994**, *33*, 1370.
[9] P. Jutzi, J. Baumgärtner, W. Schraut, *J. Organomet. Chem.* **1977**, *132*, 333.
[10] M. A. Petrie, P. P. Power, H. V. Rasika Dias, K. Ruhlandt-Senge, K. M. Waggoner, R. J. Wehmschulte, *Organometallics* **1993**, *12*, 1086; S. Schulz, S. Pusch, E. Pohl, S. Dielkus, R. Herbst-Irmer, A. Meller, H. W. Roesky, *Inorg. Chem.* **1993**, *32*, 3343.
[11] The pK_a values in ethers are not thermodynamic values but are reasonably comparable with pK_a values determined in cyclohexylamine or DMSO: A. Streitweiser, Jr., E. Juaristi, L. L. Nebenzahl in *Comprehensive Carbanion Chemistry, Part A* (Eds.: E. Buncel, T. Durst), Elsevier, Amsterdam, **1980**, p. 323.
[12] F. G. Bordwell, G. E. Drucker, H. E. Fried, *J. Org. Chem.* **1981**, *46*, 632; T. B. McMahon, P. Kebarle, *J. Am. Chem. Soc.* **1974**, *96*, 5940.
[13] G. A. Olah, G. Asensio, H. Mayr, P. von R. Schleyer, *J. Am. Chem. Soc.* **1978**, *100*, 4347.
[14] a) D. H. O'Brien in *Comprehensive Carbanion Chemistry, Part A* (Eds.: E. Buncel, T. Durst), Elsevier, Amsterdam, **1980**, pp. 271–322; b) D. H. O'Brien, A. J. Hart, C. R. Russell, *J. Am. Chem. Soc.* **1975**, *97*, 4410; c) H. Spiesecke, W. G. Schneider, *Tetrahedron Lett.* **1961**, 468.
[15] P. Jutzi, M. Meyer, H. V. Rasika Dias, P. P. Power, *J. Am. Chem. Soc.* **1990**, *112*, 4841.
[16] **7**: Monoclinic, space group *C*2/*c* (No. 15) with $a = 14.222(2)$, $b = 18.206(2)$, $c = 20.364(2)$ Å, $\beta = 110.08(1)°$, $V = 4952(1)$ Å^3, $Z = 8$ ($\rho_{calcd.} = 1.393\,g\,cm^{-3}$), $T = 178$ K, (Mo$_{K\alpha}$, $\lambda = 0.71073$ Å, $\mu = 16.22\,cm^{-1}$; 4872 unique reflections were used in refinement (SHELXTL-93); R ($I \geq 2\sigma(I)$): $R_1 = 0.0352$, $wR_2 = 0.0638$, GOF = 0.804 (all data); $R_1 = 0.0715$, $wR_2 = 0.0692$. Further details of the crystal structure investigation are available on request from the Director of the Cambridge Crystallography Data Centre, 12 Union Road, GB-Cambridge CB21EZ (UK) on quoting the full journal citation.
[17] M. R. Churchill, F. R. Scholer, *Inorg. Chem.* **1969**, *8*, 1950.
[18] A. H. Cowley, A. Decken, C. A. Olazábal, N. C. Norman, *Inorg. Chem.* **1994**, *33*, 3435.

Metal Oxo Cation Receptors: Multimode Coordination to the Dioxoosmium(VI) Cation**

A. S. Borovik, Justin Du Bois, and Kenneth N. Raymond*

The selective recognition of metal ions conventially has been achieved by using a host with an appropriately sized spherical cavity that matches the ionic radius of the metal guest.[1, 2] In contrast, the selective binding of nonspherical species often relies on combinations of weak and strong bonding interactions between a molecular host and its nonspherical guest.[3–6] Successful binding requires proper spatial alignment of recognition sites between the host and guest.

We are developing new molecular systems that utilize multimode coordination to bind nonspherical metal oxo cations.[7–9] The approach takes advantage of the chemical and morphological properties of the metal oxo cations by using ligands that can simultaneously stabilize the highly oxidized metal center through coordinate-covalent bonds, while interacting with the oxo moieties through intramolecular hydrogen bonds. To examine the requisite structural features for multimode binding to metal oxo cations, we have synthesized a series of tetraamidato ligands with appendages containing hydrogen bond donors. In this report we present electrochemical evidence showing that these ligands provide significant stabilization of the dioxoosmium(VI) cation. Furthermore, X-ray crystallographic results show that the orientation of the appended hydrogen bond donors can be varied and positioned toward the oxo moieties of a bound osmyl cation to achieve multimode binding.

The multimode bonding approach has proven successful for the selection and stabilization of metal–ligand adducts. Recent examples of molecular systems that combine covalent and intramolecular hydrogen bonds include an Fe^{II} porphyrin system that stabilizes an O_2 adduct,[10] uranyl Schiff base complexes that recognize $H_2PO_4^-$,[11] and a Pd^{II} macrocyclic species that selectively binds nucleobases.[12] The ligands described here have been constructed with a binding pocket composed of two *N*-acylated 1,2-diaminobenzene units fastened together with a diethyl malonyl strap. The strongly basic nitrogen atoms of the amidato ligands effectively stabilize highly oxidized metal centers, as has been shown by the elegant work of Collins et al.[13–16] The nitrogen atoms opposite the malonyl strap in the H_6-**1** and H_6-**2** ligands used here (Scheme 1) are components of urea groups whose function is twofold: the urea nitrogen atoms attached to the aryl supports can be deprotonated to complete the tetraamidato metal ion binding pocket, while the tethered C(O)NHR moieties provide hydrogen bond donors to the oxygen atoms of the oxo ligands of the osmyl cation. CPK models suggest that hexadentate chelate formation with intramolecular hydrogen bonds is energetically favored through a side-on approach of the appended ureas to the oxo oxygen atoms. To test these design concepts the osmyl complexes of H_6-**1** and H_6-**2** have been synthesized. These complexes have been used to examine both the oxidative stability of a high valent metal center in a tetraamidato pocket as well as the extent of intramolecular hydrogen bonding between the urea moieties

[*] Prof. K. N. Raymond, Dr. A. S. Borovik, J. Du Bois
Department of Chemistry
University of California
Berkeley, CA 94720 (USA)
Telefax: Int. code + (510)486-5283

[**] Stereognostic Coordination Chemistry, Part 4 – Part 3: [9]. This research was supported by the United States National Science Foundation Grant no. CHE-8919207. We thank Dr. Fred Hollander and Dr. Sonya J. Franklin for their help in determining the solid-state structures.

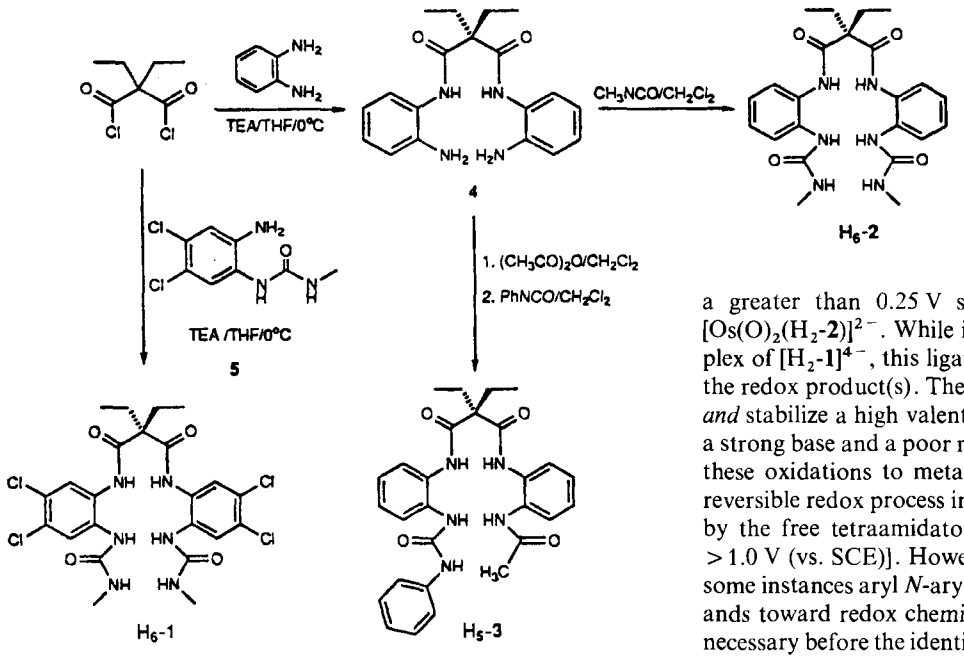

Scheme 1. Synthesis of the ligands used. TEA = triethylamine.

and the oxo oxygen atoms. Additionally, an unsymmetrical complex, $[Os(O)_2(H\text{-}3)]^{2-}$, has been prepared which allows for analysis of the influence of adjacent groups (which lack hydrogen bond donors) on the orientation of the remaining urea moiety.

Ligand H_6-**1** was synthesized in a stepwise manner by treating 1,2-diamino-4,5-dichlorobenzene with one equivalent of methyl isocyanate to afford the urea species **5**, which was then treated with 2,2-diethyl malonyl dichloride to give the desired ligand in 21% yield (based on the starting diamine) (Scheme 1). H_6-**2** and H_5-**3** were synthesized in yields of 91 and 26%, respectively, from the diamide–diamine intermediate **4** (Scheme 1). Treatment of the ligands with a methanolic slurry of $K_2[Os(O)_2(OH)_4]$ afforded the osmyl complexes $[Os(O)_2(H_2\text{-}1)]^{2-}$ and $[Os(O)_2(H_2\text{-}2)]^{2-}$, which were further purified by metathesis with Ph_4P^+, and $K_2[Os(O)_2(H\text{-}3)]$, which was obtained in pure form after recrystallization. All of the dioxoosmium(VI) complexes are stable in air, both in solution and the solid state.

Cyclic voltammetry (CV) was used to assess the ability of the ligands to stabilize the oxidized forms of the osmyl cation: $[Os(O)_2(H_2\text{-}1)]^{2-}$ and $[Os(O)_2(H_2\text{-}2)]^{2-}$ exhibit two redox processes at potentials above zero volts. A one-electron redox wave is found for $[Os(O)_2(H_2\text{-}1)]^{2-}$ at 0.461 V (vs. SCE), while the corresponding couple for $[Os(O)_2(H_2\text{-}2)]^{2-}$ occurs at 0.206 V (vs. SCE) (Fig. 1a). For $[Os(O)_2(H_2\text{-}2)]^{2-}$, this couple only approaches reversibility at scan rates $>0.75\ Vs^{-1}$; at lower speeds there is significant loss of current for the return cathodic scan, which is characteristic of an electron transfer chemical reaction (EC) process. In contrast, this redox process in $[Os(O)_2(H_2\text{-}1)]^{2-}$ is reversible throughout the scan range studied (0.010 to $2.0\ Vs^{-1}$). The higher potential events are significantly less stable: a one-electron couple at 0.840 V (vs. SCE) is observed for $[Os(O)_2(H_2\text{-}1)]^{2-}$ that is only quasi-reversible at scan rates $>1.0\ Vs^{-1}$, whereas $[Os(O)_2(H_2\text{-}2)]^{2-}$ has an irreversible oxidation at 0.650 V (vs. SCE) (Fig. 1b). Finally, $[Os(O)_2(H_2\text{-}3)]^{2-}$, with one appended acetamido group, is the most unstable of the complexes when oxidized, having an irreversible oxidation at 0.385 V (vs. SCE).

$[Os(O)_2(H_2\text{-}2)]^{2-}$ is oxidized at relatively modest potentials; yet the oxidized product(s) are prone to decomposition under the conditions of the CV experiment. This suggests that $[H_2\text{-}2]^{4-}$ provides sufficient electron density to allow for the formation of highly oxidized metal species, but that the ligand itself can not stabilize the resulting products. Placing chloro substituents on each aryl ring of the ligand, as is done in $[Os(O)_2(H_2\text{-}1)]^{2-}$, causes a greater than 0.25 V shift in the oxidation compared to $[Os(O)_2(H_2\text{-}2)]^{2-}$. While it is harder to oxidize the osmyl complex of $[H_2\text{-}1]^{4-}$, this ligand is significantly better at stabilizing the redox product(s). These results show that in order to access *and* stabilize a high valent metal species, a ligand must be both a strong base and a poor reducing agent. It is tempting to assign these oxidations to metal-centered processes, particularly the reversible redox process in $[Os(O)_2(H_2\text{-}1)]^{2-}$. [This is supported by the free tetraamidato ligands having oxidation potentials >1.0 V (vs. SCE)]. However, Collins et al. have shown that in some instances aryl *N*-arylamidato donors are non-innocent ligands toward redox chemistry;[17] thus further experiments are necessary before the identity of these redox couples can be determined unambiguously.

The solid-state molecular structures of the osmyl complexes of $[H_6\text{-}1]$ and $[H_5\text{-}3]$ were determined by X-ray diffraction.[18] In $(Ph_4P)_2[Os(O)_2(H_2\text{-}1)]$ (Fig. 2A), the Os^{VI} center lies in the plane formed by the four N donor centers of the amidato ligands of the binding pocket. The average Os–N bond length is 2.058(11) Å.[18] The primary coordination sphere of the osmium center is completed by the two oxo oxygen atoms which are in the expected *trans* configuration (O1-Os-O2 angle is 179.5(5)°). The X-ray structural analysis of $[Os(O)_2(H_2\text{-}1)]^{2-}$ also reveals the near-symmetrical disposition of the appended C(O)NHMe fragments to opposite faces of the equatorial coordination plane. The twisting of these fragments by approximately 34° relative to the coordination plane results in the appropriate conformations for intramolecular hydrogen bonding between the appended HN moieties and the oxo ligands of the osmyl cation. The heavy atom N1–O1 and N2–O2 distances of 3.00 and 3.01 Å are within van der Waals contacts; approach angles,

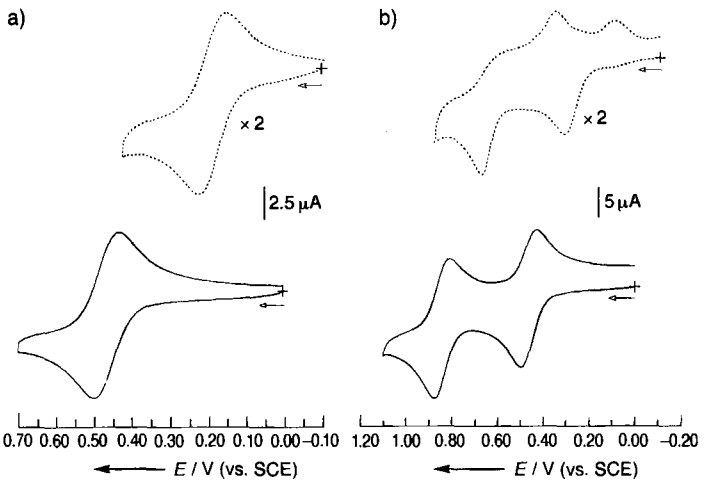

Fig. 1. a) Cyclic voltammograms of the first oxidative process for $[Os(O)_2(H_2\text{-}1)]^{2-}$ (—) and $[Os(O)_2(H_2\text{-}2)]^{2-}$ (---) at a scan rate of $0.75\ Vs^{-1}$. b) Cyclic voltammograms of $[Os(O)_2(H_2\text{-}1)]^{2-}$ (—) and $[Os(O)_2(H_2\text{-}2)]^{2-}$ (---) at a scan rate of $2.0\ Vs^{-1}$. Conditions: glassy carbon working electrode, platinum wire auxiliary electrode, SCE reference electrode, 0.1 M NBu_4PF_6 in CH_3CN. $E^{0'}$ for the ferrocinium/ferrocene couple was +0.42 mV under these conditions.

 © VCH Verlagsgesellschaft mbH, D-69451 Weinheim, 1995 0570-0833/95/1212-1360 $ 10.00+.25/0 Angew. Chem. Int. Ed. Engl. 1995, 34, No. 12

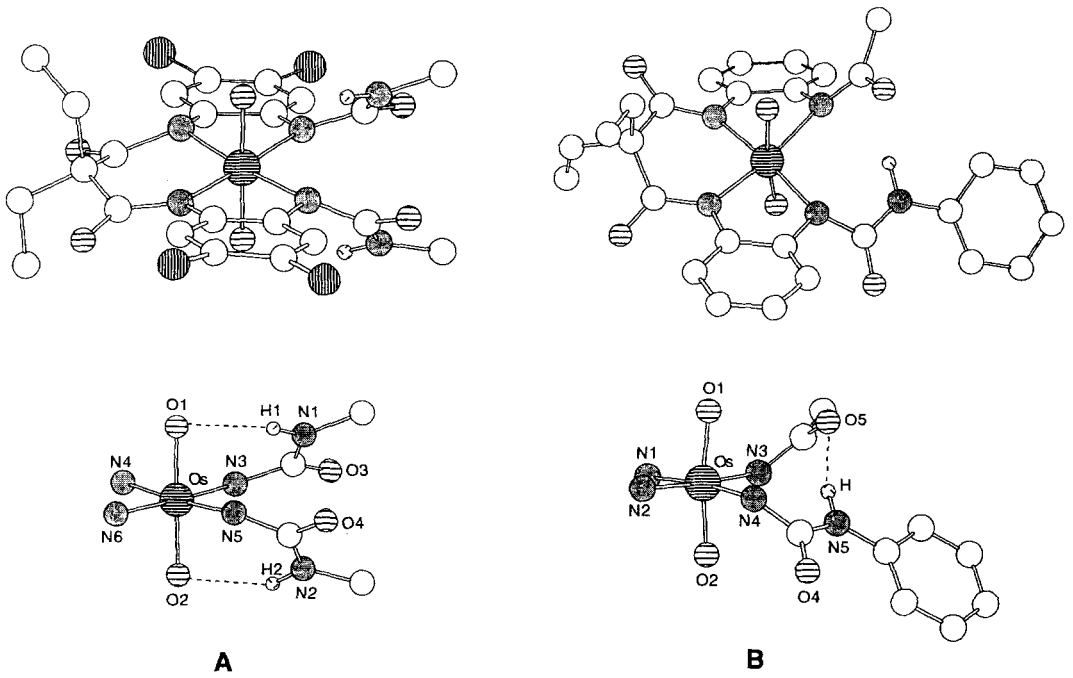

Fig. 2. Molecular structures of $[Os(O)_2(H_2\text{-}\mathbf{1})]^{2-}$ (**A**) and $[Os(O)_2(H\text{-}\mathbf{3})]^{2-}$ (**B**). The solvent molecules, counterions, and non-amide hydrogen atoms are removed for clarity.

Table 1. Spectroscopic and analytical data for osmyl complexes.

$(Ph_4P)_2[Os(O)_2(H_2\text{-}\mathbf{1})]$: ^{1}H NMR (250 MHz, [D$_6$]DMSO, 25 °C, TMS, dipotassium salt): δ = 8.58 (s, 2H; ArH), 8.50 (s, 2H; ArH), 6.36 (q, ^3J(H,H) = 4.7 Hz, 2H; C(O)-NH), 2.63 (d, ^3J(H,H) = 4.7 Hz, 6H; C(O)-NH(CH_3), 1.99 (q, ^3J(H,H) = 7.4 Hz, 4H; $-CH_2-$), 0.69 (t, ^3J(H,H)=7.3 Hz, 6H; $-CH_3$). FT-IR (KBr): $\tilde{\nu}$[cm^{-1}] = 3395 (s, br) (N-H, urea); 808 (s) ($Os(O)_2$ asym). Elemental analysis for ($C_{71}H_{66}N_6P_2O_6O_s$): calcd.: C 63.10, H 4.92, N 6.22; found: C 63.03, H 5.17, N 6.16.

$(Ph_4P)_2[Os(O)_2(H_2\text{-}\mathbf{2})]$: ^{1}H NMR (500 MHz, [D$_6$]DMSO, 25 °C, TMS): δ = 8.24 (d, ^3J(H,H) = 8.0 Hz, 2H; ArH), 8.20 (d, ^3J(H,H) = 8.0 Hz, 2H; ArH), 7.95 (t, ^3J(H,H) = 6.5 Hz, 8H; ArH), 7.80 (m, 16H; ArH), 7.72 (m, 16H; ArH), 6.53 (t, ^3J(H,H)=7.8 Hz, 2H; ArH), 6.46 (q, ^3J(H,H) = 4.7 Hz, 2H; C(O)-NH), 6.40 (t, ^3J(H,H) =7.8 Hz, 2H; ArH), 2.60 (d, ^3J(H,H) = 4.5 Hz, 6H; C(O)-NH(CH_3), 2.00 (q, ^3J(H,H) = 8.6 Hz, 4H; $-CH_2-$), 0.67(t, ^3J(H,H) = 9.1 Hz, 6H; $-CH_3$). FT-IR (KBr): $\tilde{\nu}$[cm^{-1}] = 3388 (s, br) (N-H, urea), 817 (s) ($Os(O)_2$ asym.). Elemental analysis for ($C_{71}H_{66}N_6P_2O_6Os$): calcd.: C 63.10, H 4.92, N 6.22; found: C 63.03, H 5.17, N 6.16.

$K_2[Os(O)_2(H_2\text{-}\mathbf{3})]$: ^{1}H NMR (250 MHz, [D$_6$]DMSO, 25 °C, TMS): δ = 9.58 (s, 1H; C(O)-NH), 8.20 (m, 3H; ArH), 7.74 (m, 2H; ArH), 7.43 (d, 2H; ArH), 7.20 (t, 2H; ArH), 6.70 (m, 4H; ArH), 2.39 (s, 3H; C(O)-(CH_3), 2.05 (unresolved q, 4H; $-CH_2-$), 0.73 (t, 6H; $-CH_3$). FT-IR (Nujol): $\tilde{\nu}$[cm^{-1}] = 823 (s), 842 (w) ($Os(O)_2$ asym.). Elemental analysis for ($[C_{28}H_{27}K_2N_5O_6Os] \cdot 3.0\ H_2O$): calcd.: C 39.47, H 3.91, N 8.22; found: C 39.69, H 3.99, N 7.88.The water solvates were corroborated by ^{1}H NMR spectroscopy.

N-H-O_{oxo} and Os-O_{oxo}-N_{urea}, range between 135–140° and 88–93°, respectively. These data indicate weak, side-on intramolecular hydrogen bonds and constitute structural evidence that multimode binding can be achieved between a metal oxo cation and a single molecular species.

To maximize the affinity of these ligands for metal oxo cations the interactions between the appendages must be taken into account. In particular, how does an appended group influence the orientation(s) of a neighboring hydrogen bond donor? To investigate these orientational effects the unsymmetrical complex $[Os(O)_2(H_2\text{-}\mathbf{3})]^{2-}$ has been synthesized in which one urea group has been replaced with an acetamido group. The molecular structure of $[Os(O)_2(H_2\text{-}\mathbf{3})]^{2-}$ shows that the lone urea appendage is not oriented toward either oxo ligand of the bound osmyl cation; rather it is interacting with the appended acetamido ligand through an intramolecular hydrogen bond (Fig. 2B).[21] The preference of the urea of form hydrogen bonds to the more basic carbonyl oxygen produces an eight-membered ring with a N5–O5 distance of 2.781 Å and a N5–H–O5 angle of 160.9°.[21] ^{1}H NMR studies show that this conformation remains intact in solution. The signal for the urea hydrogen in $[Os(O)_2(H_2\text{-}\mathbf{3})]^{2-}$ is shifted significantly downfield compared to that in H_5-**3** [$\Delta\delta$ = 1.74 (CD_3CN) and $\Delta\delta$ = 0.575 in [D$_6$]DMSO], which is indicative of an urea hydrogen bond.[22]

In summary the strong σ bonds between metal centers and nitrogen atoms of deprotonated amides have been combined with weak hydrogen bonds to develop systems that stabilize the osmyl cation. Since the electronic and structural features of these systems can be readily tuned, a variety of different systems can be tailored to fit a given metal oxo cation. In addition, the system provides access to a variety of appended groups, allowing us to analyze structurally different hydrogen bond donors.

Received: November 7, 1994 [Z 7453 IE]
German version: *Angew. Chem.* **1995**, *107*, 1473–1476

Keywords: chelate ligands · complexes with nitrogen ligands · hydrogen bonds · osmium compounds

[1] D. J. Cram, *Angew. Chem.* **1988**, *100*, 1041–1052; *Angew. Chem. Int. Ed. Engl.* **1988**, *27*, 1009–1020.
[2] J. M. Lehn, *Angew. Chem.* **1988**, *100*, 91–116; *Angew. Chem. Int. Ed. Engl.* **1988**, *27*, 89–112.
[3] A. Hamilton, *J. Chem. Educ.* **1990**, *67*, 821.
[4] F. Diederich, *J. Chem. Educ.* **1990**, *67*, 813.
[5] T. Tjivikua, P. Ballester, J. Rebek, Jr., *J. Am. Chem. Soc.* **1990**, *112*, 1249.
[6] K.-S. Jeong, A. V. Muehldorf, J. Rebek, Jr., *J. Am. Chem. Soc.* **1990**, *112*, 6144.
[7] T. S. Franczyk, K. R. Czerwinski, K. N. Raymond, *J. Am. Chem. Soc.* **1992**, *114*, 8138.
[8] A. S. Borovik, T. M. Dewey, K. N. Raymond, *Inorg. Chem.* **1993**, *32*, 413.
[9] T. M. Dewey, J. Du Bois, K. N. Raymond, *Inorg. Chem.* **1993**, *32*, 1729.
[10] G. E. Wuenschell, C. Tetreau, D. Lavalette, C. Reed, *J. Am. Chem. Soc.* **1992**, *114*, 3346.
[11] D. M. Rudkevich, W. Verboom, Z. Brzozka, M. J. Palys, W. P. R. V. Stauthamer, G. J. Van Hummel, S. M. Franken, S. Harkema, J. F. J. Engbersen, D. N. Reinhoudt, *J. Am. Chem. Soc.* **1994**, *116*, 4341.
[12] J. E. Kickham, S. J. Loeb, S. L. Murphy, *J. Am. Chem. Soc.* **1993**, *115*, 7031.
[13] F. C. Anson, J. A. Christie, T. J. Collins, R. J. Coots, J. J. Furutani, S. L. Gipson, J. T. Keech, T. E. Krafft, B. D. Santarsiero, G. H. Spies, *J. Am. Chem. Soc.* **1984**, *106*, 4460–4472.

 © VCH Verlagsgesellschaft mbH, D-69451 Weinheim, 1995 0570-0833/95/1212-1361 $ 10.00+.25/0

[14] T. J. Collins, K. L. Kostka, E. Münck, E. S. Uffelman, *J. Am. Chem. Soc.* **1990**, *112*, 5637–5639.
[15] T. J. Collins, T. R. Nichols, E. S. Uffelman, *J. Am. Chem. Soc.* **1991**, *113*, 4708–4709.
[16] T. J. Collins, B. G. Fox, Z. G. Hu, K. L. Kostka, E. Münck, C. E. F. Rickard, L. J. Wright, *J. Am. Chem. Soc.* **1992**, *114*, 8724.
[17] T. J. Collins, K. L. Kostka, E. S. Uffelman, T. L. Weinberger, *Inorg. Chem.* **1991**, *30*, 4204–4210.
[18] Crystal data for $(Ph_4P)_2[Os(O)_2(H_2\text{-}\mathbf{1})] \cdot 2DMF$: dark red crystals were isolated from DMF/ether in the space group $P\bar{1}$ with the following cell constants: $a = 12.268(2)$, $b = 13.053(3)$, $c = 13.953(3)$ Å; $\alpha = 116.41(2)$, $\beta = 110.34(2)$, $\gamma = 92.91(2)°$; $V = 1819.3(8)$ Å^3, $Z = 1$. Of 8326 reflections collected ($Mo_{K\alpha}$, $2\theta(max) = 55°$, $T = -102\,°C$) 8326 were independent and 8187 were observed ($F_{obs} > 3.0\,\sigma(F)$). The structure was solved by Patterson map and refined to an $R = 0.025$ and $R_w = 0.031$ with a GOF = 1.416 [20].
[19] Crystal data for $K_2[Os(O)_2(H_2\text{-}\mathbf{3})] \cdot 2DMF \cdot H_2O$: dark red crystals were isolated from DMF/ether in the space group *Pbca* with the following cell constants: $a = 11.405(3)$, $b = 13.928(4)$, $c = 49.358(8)$ Å; $V = 7840(5)$ Å^3, $Z = 8$. Of 5759 reflections collected ($Mo_{K\alpha}$, $2\theta(max) = 45°$, $T = -98\,°C$) 5107 were independent and 3022 were observed ($F_{obs} > 3.0\,\sigma(F)$). The structure was solved by Patterson map and refined anisotropically to an $R = 0.037$ and $R_w = 0.039$ with a GOF = 1.163 [20].
[20] Further details of the crystal structures are available on request from the Director of the Cambridge Crystallographic Data Centre, 12 Union Road, GB-Cambridge CB2 1EZ (UK), on quoting the full journal citation.
[21] In the solid-state structure of $[Os(O)_2(H\text{-}\mathbf{3})]^{2-}$ O2, O5, and N5 also interact with one potassium counterion.
[22] T. N. Sorrell, *Interpreting Spectra of Organic Molecules*; University Science Books: Mill Valley, CA, **1988**, p. 24.

$S(NPMe_3)_4^{2+}$: The First Structure Determination of a Dication of Hexavalent Sulfur**

Hella Folkerts, Wolfgang Hiller, Martin Herker, Sergei F. Vyboishchikov, Gernot Frenking, and Kurt Dehnicke*

Cationic species of hexavalent sulfur like $H_3SO_4^+$ and $H_2SO_3F^+$ are important as "super acids" and "magic acids" and are employed as protonating agents for weak bases.[1, 2] However, compounds containing these cations have not been isolated to date.[2] Using the super acid systems HF/SbF_5, pentafluoro-λ^6-sulfanylamines can be converted to the sulfanylammonium salts **1** (n = 1, 2).[3] Several other monocations of hexavalent sulfur containing sulfur atoms with a coordination number 3, 4, or 5 are known,[4, 5] which usually are derived from dialkylamido and monoalkylamido derivatives. The oxo derivatives $OSF_3^+AsF_6^-$[6] and $OSF_2Cl^+AsF_6^-$[7] have been characterized by structure determinations. A dication of hexavalent sulfur, $SF_2(NMe_2)_2^{2+}$, characterized by NMR spectroscopy, was first reported in 1984.[8] No confirmed data are available for the S^{VI}-phosphorane iminato derivative $[S(NPPh_3)_3]Cl_3$.[9] Numerous examples of cations of tetravalent sulfur are known. They include cations of the general formula SX_3^+ with X = organic group, halide, CN, and other ligand atoms[10] as well as the monomeric SN^+ ion.[11]

$[Me_{3-n}H_nNSF_5]^+AsF_6^-$ **1**

Investigations of phosphorane iminato complexes of transition metals, [M] = N = PR_3, have shown that the ligand NPR_3^- can stabilize the elements M in high oxidation states, due to the large M–N bond orders.[12] We have now confirmed this observation for the reaction of disulfur dichloride with the silylated phosphorane imine $Me_3SiNPMe_3$. The reaction proceeds in boiling acetonitrile and leads to a disproportion according to Equation (a).

$$3S_2Cl_2 + 4Me_3SiNPMe_3 \longrightarrow \underset{\mathbf{2}}{[S(NPMe_3)_4]Cl_2} + {}^5/_8S_8 + 4ClSiMe_3 \quad (a)$$

Compound **2** · 4 CH_3CN was isolated as colorless needles after removal of the precipitated sulfur by filtration. If kept under vacuum the crystals loose the coordinated acetonitrile. The IR spectrum of **2** shows two intensive stretching vibrations of the symmetry species *E* at 1128 and 985 cm^{-1}, which can be assigned to ν_{as}(PN) and ν_{as}(SN). This is in agreement with the S_4 symmetry of the cation[13] as determined by X-ray crystallography. The related deformation vibrations are found at 480 and 413 cm^{-1}. The less intensive, IR-active vibrations of the symmetry species *B* are presumably hidden underneath the strong bands of the symmetry species *E*. The IR spectrum shows no evidence of a S–Cl stretching vibration. This is in agreement with the results of the crystal structure analysis[14] which suggests an ionic structure for **2**. In the dication $S(NPMe_3)_4^{2+}$ (Fig. 1) the sulfur atoms are surrounded by the N atoms of the phosphorane iminato ligands in a tetrahedral fashion. The S–N interatomic distances are 156.5 pm and correspond to double bonds; similar values are observed in cyclic sulfur–nitrogen cations[15] like $S_4N_3^+$[16] and $S_4N_4^{2+}$.[17] The S–N interatomic distances in tris(imino) derivatives **3** are even shorter (150.4 pm (E = Si) and 151.1 pm (E = C)[18]), which is due to the low coordination number (CN = 3) of the sulfur atom. In contrast, the S–N interatomic distances in $[S(NPPh_3)_3]Cl$, which contains tetravalent sulfur, are 163.5 pm[9b] and therefore considerably longer than those in **2**. The P–N interatomic distances in **2** are 162.1 pm corresponding to double bonds,[19] while the bond angles of 122.3° at the N atoms are indicative of sp^2 hybridization.

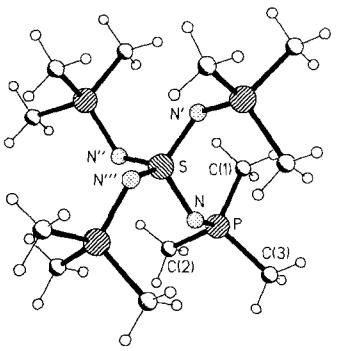

Fig. 1. View of the structure of the cation in **2** · 4 CH_3CN.

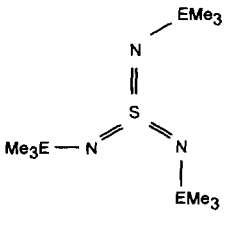

3, E = C, Si

The geometry of the parent compound $S(NPH_3)_4^{2+}$ (**2'**), which was derived from **2**, was optimized with an ab initio calculation at the Hartree–Fock level.[20] The calculation results in a structure possessing S_4 symmetry (Fig. 2) for **2'**, which is essentially identical with the skeleton geometry of **2**. The calculated interatomic distances and bond angles of **2'** are in good agreement with the values found for **2** (Table 1). A NBO analysis of **2'**[21] reveals a strongly positive partial charge at the

[*] Prof. Dr. K. Dehnicke, Dr. H. Folkerts, Dipl.-Chem. S. F. Vyboishchikov, Prof. Dr. G. Frenking
Fachbereich Chemie der Universität
Hans-Meerwein-Strasse, D-35032 Marburg (Germany)
Telefax: Int. code + (6421)288917
Prof. Dr. W. Hiller, Dipl.-Chem. M. Herker
Anorganisch-chemisches Institut der Technischen Universität München (Germany)

[**] This work was supported by the Deutsche Forschungsgemeinschaft, the Fonds der Chemischen Industrie, and by Hewlett Packard. We gratefully acknowledge Prof. Dr. R. Mews, University of Bremen, Germany, for valuable comments.

Table 1. Calculated structure data and results of the NBO analysis of $S(NPH_3)_4^{2+}$ (**2'**) and $S(NH_2)_4^{2+}$ (**4**) [a].

Quantity [a]	Variable	**2'** (S_4)	**4** (D_{2d})
r	N-S	156.7	157.5
r	N-P	163.7	–
ϑ	N-S-N	109.5	102.4; 124.7
ϑ	S-N-P	122.6	–
q	S	+2.64	+2.53
q	N	−1.47	−1.15
q	P	+1.27	–
%N	N-S	64.2	61.9
Hybr. (N)	N-S	$sp^{2.20}d^{0.01}$	$sp^{2.43}d^{0.01}$
Hybr. (S)	N-S	$sp^{2.91}d^{0.09}$	$sp^{2.90}d^{0.01}$
%N	N-P	71.0	–
Hybr. (N)	N-P	$sp^{2.11}d^{0.01}$	–
Hybr. (P)	N-P	$sp^{2.76}d^{0.07}$	–

[a] Interatomic distances r [pm], bond angles ϑ [°], partial charges q, %N-orbital share of the N–S and N–P bonds, hybridization of the bonding orbitals of N, S, and P in the N–S and N–P bonds.

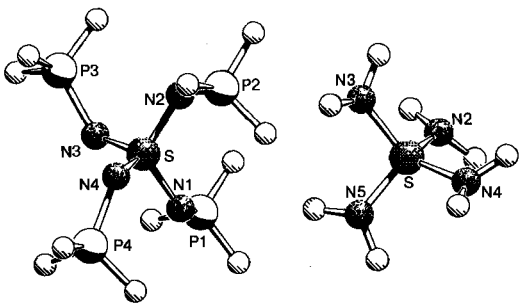

2' **4**

Fig. 2. Calculated structures of **2'** and **4**.

sulfur atom (+2.64) and at the phosphorus atoms (+1.27) and a strongly negative partial charge at the nitrogen atoms (−1.47). According to the calculation, the N–S and the N–P bonds each correspond to single bonds which are strongly polarized towards the more electronegative nitrogen atom (Table 1). The hybridization of the N orbitals is close to sp^2 for both bonds, while approximate sp^3 hybridization with a minor contribution of the d orbitals to the bonds is found for S and P. Two lone-pair orbitals are calculated for each nitrogen atom. The results of the NBO analysis of **2'** are in agreement with the classical ideas of the bonding situation, which is suggested by the experimentally determined geometry of **2**. The $S(NPMe_3)_4^{2+}$ ion contains polar covalent N–S and N–P single bonds, which as a result of strong charge attraction between the negatively charged nitrogen atom and the positively charged phosphorus and sulfur atoms, respectively, tend towards double bonds.

We have also calculated the structure of the parent compound $S(NH_2)_4^{2+}$ **4**. There is some evidence that **4** exists; however, its isolation and the determination of its geometry has not been reported to date. The calculated structure of **4** shows D_{2d} symmetry (Fig. 2). The recently isolated, isoelectronic $P(NH_2)_4^+$ ion also has D_{2d} symmetry as determined by X-ray structure analysis.[22] The calculated N-S-N bond angles of **4** are 102.4 and 124.7°, the analogous N-P-N bond angles of the $P(NH_2)_4^+$ ion are 102.7 and 124.2°[22]. The S–N interatomic distances of **4** are slightly longer (157.5 pm) than those of **2'**.

Received: February 8, 1995
Revised version: March 3, 1995 [Z 7700 IE]
German version: *Angew. Chem.* **1995**, *107*, 1469–1470

Keywords: ab initio calculations · imines · phosphorus compounds · sulfur compounds

[1] G. A. Olah, A. M. White, D. H. O'Brien, *Chem. Rev.* **1970**, *70*, 561.
[2] T. A. O'Donnell, *Super-Acids and Acidic Melts as Inorganic Chemical Reaction Media*, VCH, Weinheim, **1993**.
[3] T. Meier, R. Hoppenheit, R. Mews, *Z. Anorg. Allg. Chem.* **1993**, *619*, 1241.
[4] Review: R. Mews, *Adv. Inorg. Chem. Radiochem.* **1976**, *19*, 185.
[5] R. Mews, *Angew. Chem.* **1978**, *90*, 561; *Angew. Chem. Int. Ed. Engl.* **1978**, *17*, 530; R. Mews, H. Henle, *J. Fluorine Chem.* **1979**, *14*, 495; T. Meier, R. Mews, *Angew. Chem.* **1985**, *97*, 349; *Angew. Chem. Int. Ed. Engl.* **1985**, *24*, 344; R. Bartsch, H. Henle, T. Meier, R. Mews, *Chem. Ber.* **1988**, *121*, 451; T. Meier, R. Mews, *J. Fluorine Chem.* **1994**, *66*, 141; E. Lindner, H. Weber, *Chem. Ber.* **1968**, *101*, 2832; J. Wessel, G. Kleemann, K. Seppelt, *ibid.* **1983**, *116*, 2399; R. S. Michalak, J. C. Martin, *J. Am. Chem. Soc.* **1982**, *104*, 1683; D. D. Desmarteau, W. Y. Lam, B. A. O'Brien, S.-C. Chang, *J. Fluorine Chem.* **1984**, *25*, 387.
[6] C. Lau, H. Lynton, J. Passmore, P.-Y. Siew, *J. Chem. Soc. Dalton Trans.* **1973**, 2535.
[7] C. Lau, J. Passmore, *Chem. Commun.* **1971**, 950.
[8] H. Henle, R. Hoppenheit, R. Mews, *Angew. Chem.* **1984**, *96*, 509; *Angew. Chem. Int. Ed. Engl.* **1984**, *23*, 507.
[9] a) H. Prakash, H. H. Sisler, *Inorg. Chem.* **1968**, *7*, 2200; b) J. Bojes, T. Chivers, G. McLean, R. T. Oakley, A. W. Cordes, *Can. J. Chem.* **1979**, *57*, 3171.
[10] T. M. Klapötke, I. C. Tornieporth-Oetting, *Nichtmetallchemie*, VCH, Weinheim, **1994**; N. N. Greenwood, A. Earnshaw, *Chemistry of the Elements*, Pergamon, Oxford, **1985**.
[11] W. Clegg, O. Glemser, K. Harms, G. Hartmann, R. Mews, M. Noltemeyer, G. M. Sheldrick, *Acta Crystallogr. Sect. B* **1981**, *37*, 548.
[12] K. Dehnicke, J. Strähle, *Polyhedron* **1989**, *8*, 707.
[13] J. Weidlein, U. Müller, K. Dehnicke, *Schwingungsspektroskopie*, Thieme, Stuttgart, **1988**.
[14] Crystallographic data of $2 \cdot 4CH_3CN$ (−60 °C): space group $I4_1/a$, a = 1098.1(1), c = 3579.1(3) pm, Z = 4. Four-circle diffractometer Enraf-Nonius CAD4, $Mo_{K\alpha}$ radiation, graphite monochromator, ω-scan, θ = 3–27°, 2335 independent reflections [R_{int} = 0.0397], 1876 with $F > 4\sigma(F)$, empirical absorption correction, $\mu(Mo_{K\alpha})$ = 3.66 cm^{-1}. All H atoms were localized and refined with the "riding model". This resulted in $wR2$ = 0.2495 for all data corresponding to a conventional R = 0.066 for reflections with $F > 4\sigma(F)$, goodness of fit: 1.131 (F^2, 84 refined parameters), residual electron density: max 1575 and min −410 enm^{-3}. Further details of the crystal structure investigation may be obtained from the Fachinformationszentrum Karlsruhe, D-76344 Eggenstein-Leopoldshafen (Germany), on quoting the depository number CSD-58924.
[15] Reviews: H. W. Roesky, *Adv. Inorg. Chem. Radiochem.* **1979**, *22*, 239; *Angew. Chem.* **1979**, *91*, 112; *Angew. Chem. Int. Ed. Engl.* **1979**, *18*, 91.
[16] J. Weiss, *Angew. Chem.* **1962**, *74*, 216; *Angew. Chem. Int. Ed. Engl.* **1962**, *1*, 214; *Z. Anorg. Allg. Chem.* **1964**, *333*, 314.
[17] R. J. Gillespie, J. P. Kent, J. F. Sawyer, D. R. Slim, J. D. Tyrer, *Inorg. Chem.* **1981**, *20*, 3799.
[18] O. Glemser, S. Pohl, F.-M. Tesky, R. Mews, *Angew. Chem.* **1977**, *89*, 829; *Angew. Chem. Int. Ed. Engl.* **1977**, *16*, 789; S. Pohl, B. Krebs, U. Seger, G. Henkel, *Chem. Ber.* **1979**, *112*, 1751.
[19] A. F. Wells, *Structural Inorganic Chemistry*, Clarendon, Oxford, **1984**.
[20] The calculations were carried out using the program Gaussian 92 [23]. For N and H a 6-31G(d) basis set was used. For S and P a pseudo potential for the $1s^22s^22p^6$ electrons and a (31/31/1) valence basis set was applied [24]. The calculations of the Hesse matrix of **2'** and **4** revealed that the optimized structures are minima on the potential energy hypersurface.
[21] A. E. Reed, L. A. Curtiss, F. Weinhold, *Chem. Rev.* **1988**, *88*, 899.
[22] W. Schnick, S. Horstmann, A. Schmidpeter, *Angew. Chem.* **1994**, *106*, 818; *Angew. Chem. Int. Ed. Engl.* **1994**, *33*, 785.
[23] Gaussian 92: M. J. Frisch, G. W. Trucks, M. Head-Gordon, P. M. W. Gill, M. W. Wong, J. B. Foresman, H. B. Schlegel, K. Raghavachari, M. A. Robb, J. S. Binkley, C. Gonzalez, R. Martin, D. J. Fox, D. J. DeFrees, J. Baker, J. J. P. Stewart, J. A. Pople, Gaussian Inc., Pittsburgh, PA, USA, **1992**.
[24] A. Bergner, M. Dolg, W. Küchle, H. Stoll, H. Preuss, *Mol. Phys.* **1993**, *80*, 1431.

 © *VCH Verlagsgesellschaft mbH, D-69451 Weinheim, 1995* *0570-0833/95/1212-1363 $ 10.00+.25/0*

"Cation-π Interactions" Detected by Mass Spectrometry; Selective Recognition of Alkali Metal Cations by a π-Basic Molecular Cavity

Fumiaki Inokuchi, Yuji Miyahara, Takahiko Inazu, and Seiji Shinkai*

Recently, the "cation–π interaction" has been of interest as a new type of secondary valence force, which is thought to play a crucial role in biological systems.[1] Complementary results have been accumulated with several artificial systems.[2–6] Kebarle et al. showed for the first time by mass spectrometry that K^+ binds to benzene in the gas phase.[7] This finding stimulated the study of cation–π interactions between benzene and metal cations.[8–12] We report here on our studies with cyclophanes that complex metal cations in their π-basic cavities.[13–17] We recently noticed that appropriately charged host–guest-type complexes, the concentration of which is very low in solution, can be easily detected by mass spectrometry.[18] We tested three conformationally rigid conformers of 25,26,27,28-tetrapropoxycalix[4]arene (**1**) (cone-**1**, partial-cone-**1**, and 1,3-alternate-**1**),[16, 17] conformationally mobile 5,11,17,23-tetra-*tert*-butylcalix[4]arene (**2**),[19] and [1.1.1.1]paracyclophane (**3**).[20] We have found that the cation–π interaction is conveniently and selectively detectable by mass spectrometry (particularly, with **3**). Compounds **1**–**3** and the complexes with alkali metal and silver cations were analyzed by positive secondary ion mass spectrometry (positive SIMS), in which the sample is "dissolved" in a matrix, and by positive electrospray ionization mass spectrometry (positive ESI-MS), for which no matrix is needed.

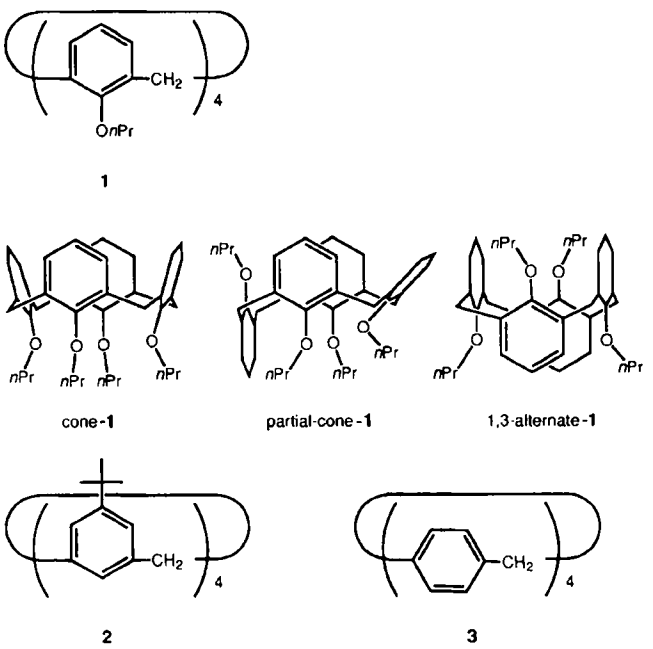

1 **2** **3**

We have found that in solution the affinity of the conformers of **1** with K^+ and Ag^+ appears in the order of 1,3-alternate-**1** > partial-cone-**1** ≫ cone-**1**.[16, 17] The Ag^+ complexes provided clear evidence that the high affinity of 1,3-alternate-**1** and partial-cone-**1** to Ag^+ is ascribable to π-donor participation. The distance between two distal benzene rings in these conformers is very close to the diameter of the Ag^+ ion, and therefore they can sandwich Ag^+ without changing their structure.[16, 17] The signal intensity of $(\mathbf{1} + M)^+$ in the SI mass spectra (normalized relative to $(NBA + H)^+$; NBA = *m*-nitrobenzyl alcohol) for alkali metal cations appears in the order of $K^+ > Rb^+ > Cs^+ \gg Na^+ > Li^+$ and that for the conformers of **1** appears in the order of 1,3-alternate-**1** > partial-cone-**1** ≫ cone-**1** (Fig. 1).[21] These orders are completely consistent with those observed in solution.[16, 17] Since signals for the starting compounds and the solvent, which are useful for normalization, could not be detected, we used the absolute intensity of the signals of each metal complex. In the ESI mass spectra the trend in the signal intensities of $(\mathbf{1} + M)^+$ is very similar to that for SIMS (Fig. 1). The reproducibility is excellent (±5%) when the same measurement conditions are used. However, we found one significant difference between the two sets of experiments: the signal intensity for $(\text{cone-}\mathbf{1} + M)^+$ is much greater in the ESI mass spectra and the difference among three conformers is relatively small. This result implies that although the metal affinity of cone-**1** is weak in solution, it can compete with that of 1,3-alternate-**1** and partial-cone-**1** in a matrix-free system. Consistent with this proposal, the signal intensities in ESI mass spectra decrease with increasing NBA concentration. These results suggest the significant contribution of the cation-π interaction, but the propoxy groups may also be involved in the metal binding.

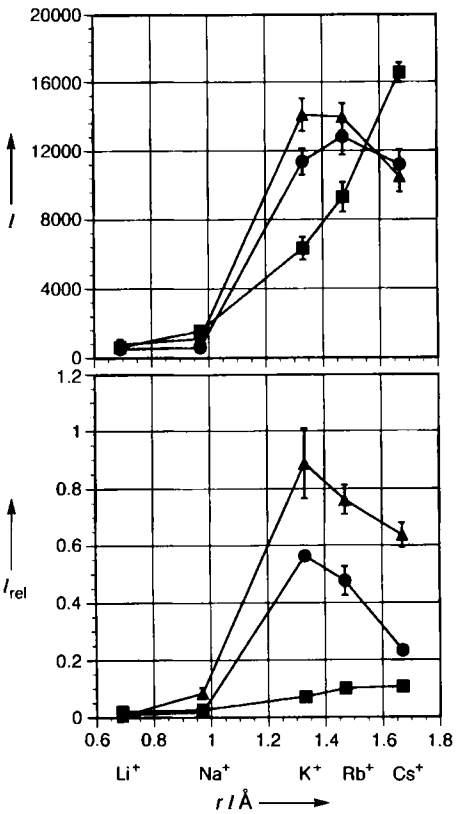

Fig. 1. Absolute signal intensities $I((1 + M)^+)$ in ESI mass spectra (top) and relative signal intensities $I_{rel}((1 + M)^+/(NBA + H)^+)$ in SI mass spectra (bottom) plotted versus the ionic radii *r* [Å] of M^+. ▲: $(\text{1,3-alternate-}\mathbf{1} + M)^+$; ●: $(\text{partial-cone-}\mathbf{1} + M)^+$; ■: $(\text{cone-}\mathbf{1} + M)^+$.

[*] Prof. Dr. S. Shinkai, F. Inokuchi
Chemirecognics Project, ERATO
Research Development Corporation of Japan
Aikawa 2432-3, Kurume, Fukuoka 830 (Japan)
Telefax: Int. code + (942)37-6125
Dr. Y. Miyahara, Prof. Dr. T. Inazu
Department of Chemistry, Faculty of Science
Kyushu University, Fukuoka (Japan)

To exclude this possibility we used calix[4]arene without propoxy groups (**2**).[19] This molecule is conformationally mobile. Although the signals assignable to $(2 + M)^+$ ions could be detected in the SI mass spectra, the intensities were about two orders of magnitude less than those for $(1 + M)^+$, and significant metal ion selectivity was not observed (Fig. 2).[21] The result indicates that the freezing of the conformation is indispensable to efficient detection of the complex. In the ESI mass spectrum a strong peak was observed for $(2 + Cs)^+$. This could be expected based on the results with cone-**1**. Conceivably, when metal ions are not "solvated" in a matrix, the large, soft Cs^+ ion can be bound selectively to the π-basic cavity of **2**.

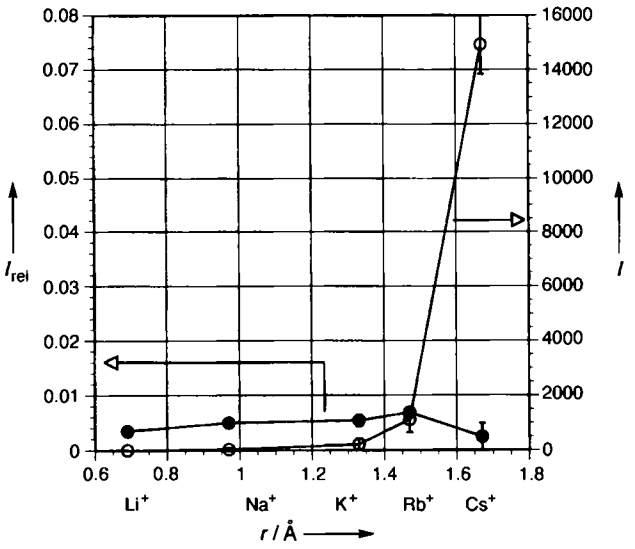

Fig. 2. Absolute signal intensities $I((2 + M)^+)$ in ESI mass spectra (○) and relative signal intensities $I_{rel}((2 + M)^+/(NBA + H)^+)$ in SI mass spectra (●) plotted versus the ionic radii r [Å] of M^+.

We also examined compound **3**, which has a well-defined cavity formed by four benzene rings and which is conformationally fixed.[20] The signals for $(3 + Li)^+$, $(3 + Na)^+$, and $(3 + K)^+$ were scarcely detectable by SIMS, whereas the signals due to $[3 + Rb]^+$ and $[3 + Cs]^+$ were very intense (Fig. 3).[21, 22] Very similar results were also obtained from ESI-MS. From semiempirical molecular orbital calculations (MOPAC version 6.0 PM3 Hamiltonian) on calixarene **3** we estimate that the distance from the center of a bridgehead carbon atom to the center of the cavity is 3.44 Å. This is very close to the sum of the ionic radius of Cs^+ (1.67 Å)[24] and the van der Waals radius of an aryl carbon atom (1.70 Å)[23]. For Rb^+ (1.47 Å)[24] this sum is slightly less, and for Li^+ (0.69 Å), Na^+ (0.97 Å), and K^+ (1.33 Å)[24] much less than 3.44 Å. Li^+, Na^+, and K^+ ions cannot interact with all four benzene rings in **3**, but the size of Rb^+ and Cs^+ ions is comparable with the size of the cavity in **3**. Cs^+, in particular, can nest exactly in the cavity and interact with the four benzene walls simultaneously. This finding can be rationalized only by the presence of the cation–π interaction.[25]

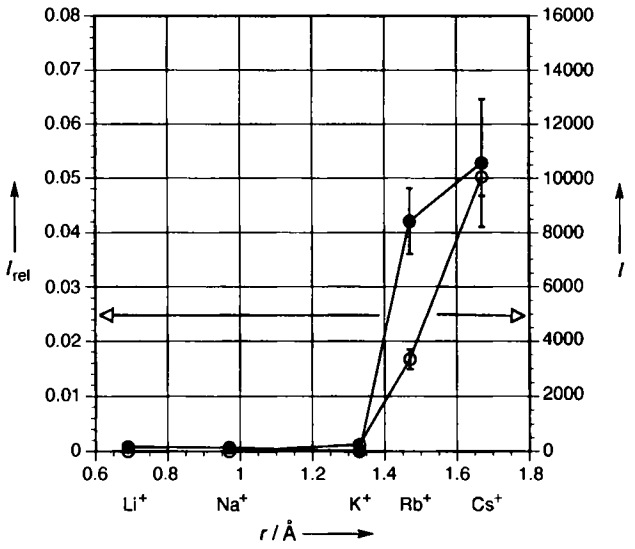

Fig. 3. Absolute signal intensities $I((3 + M)^+)$ in ESI mass spectra (○) and relative signal intensities $I_{rel}((3 + M)^+/(NBA + H)^+)$ in SI mass spectra (●) plotted versus the ionic radii r [Å] of M^+.

To further confirm the contribution of the cation–π interaction we examined the Ag^+ complexes of **1** and **3** by mass spectrometry. As expected from the data obtained in solution,[16, 17] the $[1 \cdot Ag]^+$ complexes gave very intense signals assignable to each conformer complex ($(1 + Ag)^+/(NBA + H)^+ = 0.16$ for 1,3-alternate-**1**, 0.25 for partial-cone-**1**, and 0.21 for cone-**1**). In contrast, the signal attributed to the $[3 \cdot Ag]^+$ complex could not be detected. Although the Ag^+ ion has a special affinity for carbon–carbon double bonds,[13–16] it is comparable in size to K^+ and smaller than the cavity in **3**. Thus Ag^+ cannot form a complex with **3**. In contrast, Cs^+ has no special affinity but fits into the cavity of **3** and forms a complex. These findings support the view that the metal ion selectivity in the present system is governed by the host–guest-type "hole-size selectivity".

By mass spectrometry it is very difficult to detect a complex that forms in solution through weak secondary valence forces. In fact, we could not obtain any sign of the complexes formed between **3** and alkali metal cations in solution. The difficulty is attributed firstly to competition between inclusion of the guest in the host molecule and solvation of the guest molecules, and secondly to competition between the enthalpy gain caused by the host–guest interaction and the entropy loss caused by the organization of the host molecule induced upon guest inclusion. Hence, weak host–guest-type complexation should be detectable when the solvation terms are eliminated and when the host molecule is well-preorganized. These requirements are satisfied in the by $[3 \cdot M]^+$ complexes in the gas phase.

Experimental Procedure

For the SIMS experiments (Hitachi M-2500 mass spectrometer) the host compound (0.01 M in 5 μL chloroform), *m*-nitrobenzyl alcohol (NBA) as matrix (15 μL), and the alkali metal chloride or silver nitrate (0.01 M in 5 μL methanol) were mixed. Then 1 μL of the mixture was loaded on the silver target. Xe^+ was employed as a primary ion and accelerated at 6.0 kV. Secondary ions were accelerated at 3.0 kV. The signal intensities were averaged over ten scans. ESI-MS experiments were performed on the same apparatus with an ESI ion source (M-2517). A chloroform solution (50 μL) containing the host compound (0.001 M) and a methanol solution (50 μL) containing a mixture of alkali metal chlorides (0.001 M each LiCl, NaCl, KCl, RbCl, and CsCl) were mixed. A portion of the solution (20 μL) was injected directly into the ESI source by syringe pump (Hitachi L-6200). General instrument settings: vaporization temperature 180 °C, mobile phase chloroform/methanol 1/1, flow rate 0.06 mL min^{-1}, N_2 gas pressure 1.0 kg cm^{-2} (Pneumatically Assisted ESI). The signal intensities were averaged over five scans and recorded as the sum of the corresponding isotopic peaks.

Received: October 19, 1994
Revised version: March 7, 1995 [Z 7413 IE]
German version: *Angew. Chem.* **1995**, *107*, 1459–1462

Keywords: alkali metal compounds · calixarenes · cyclophanes · host–guest chemistry · mass spectrometry

[1] a) J. L. Sussman, M. Harel, F. Frolow, C. Oefner, A. Goldman, L. Toker, I. Silman, *Science* **1991**, *253*, 872; b) M. Harel, I. Schalk, L. Ehret-Sabatier, F. Bouet, M. Goeldner, C. Hirth, P. H. Axelsen, I. Silman, J. L. Sussman, *Proc. Natl. Acad. Sci. USA* **1993**, *90*, 9031.

[2] a) M. A. Petti, T. J. Shepodd, R. E. Barrans, Jr., D. A. Dougherty, *J. Am. Chem. Soc.* **1988**, *110*, 6825; b) D. A. Stauffer, R. E. Barrans, Jr., D. A. Dougherty, *Angew. Chem.* **1990**, *102*, 953; *Angew. Chem. Int. Ed. Engl.* **1990**, *29*, 915.

[3] P. C. Kearney, L. S. Mizoue, R. A. Kumpf, J. E. Forman, A. McCurdy, D. A. Dougherty, *J. Am. Chem. Soc.* **1993**, *115*, 9907.

[4] H.-J. Schneider, D. Güttes, U. Schneider, *J. Am. Chem. Soc.* **1988**, *110*, 6449.

[5] a) S. Shinkai, K. Araki, T. Matsuda, N. Nishiyama, H. Ikeda, I. Takasu, M. Iwamoto, *J. Am. Chem. Soc.* **1990**, *112*, 9053; b) K. Araki, H. Shimizu, S. Shinkai, *Chem. Lett.* **1993**, 205.

[6] K. S. Kim, J. Y. Lee, S. J. Lee, T.-K. Ha, D. H. Kim, *J. Am. Chem. Soc.* **1994**, *116*, 7399.

[7] J. Sunner, K. Nishizawa, P. Kebarle, *J. Phys. Chem.* **1981**, *85*, 1814.

[8] a) R. W. Taft, F. Anvia, J.-F. Gal, S. Walsh, M. Capon, M. C. Holmes, K. Hosn, G. Oloumi, R. Vasanwala, S. Yazdani, *Pure Appl. Chem.* **1990**, *62*, 17; b) B. C. Guo, J. W. Purnell, A. W. Castleman Jr., *Chem. Phys. Lett.* **1990**, *168*, 155.

[9] H. Bock, K. Ruppert, Z. Havlas, D. Fenske, *Angew. Chem.* **1990**, *102*, 1095; *Angew. Chem. Int. Ed. Engl.* **1990**, *29*, 1042.

[10] a) C. Lambert, P. von R. Schleyer, *Angew. Chem.* **1994**, *106*, 1187; *Angew. Chem. Int. Ed. Engl.* **1994**, *33*, 1129; b) D. Hoffmann, W. Bauer, P. von R. Schleyer, U. Pieper, D. Stalke, *Organometallics* **1993**, *12*, 1193.

[11] L. Heginbotham, R. MacKinnon, *Neuron* **1992**, *8*, 483.

[12] R. A. Kumpf, D. A. Dougherty, *Science* **1993**, *261*, 1708.

[13] R. Leppkes, F. Vögtle, *Chem. Ber.* **1983**, *116*, 215.

[14] J.-L. Pierre, P. Baret, P. Chautemps, M. Armand, *J. Am. Chem. Soc.* **1981**, *103*, 2986.

[15] H. C. Kang, A. W. Hanson, B. Eaton, V. Boekelheide, *J. Am. Chem. Soc.* **1985**, *107*, 1979.

[16] a) A. Ikeda, S. Shinkai, *Tetrahedron Lett.* **1992**, *33*, 7385; b) *J. Am. Chem. Soc.* **1994**, *116*, 3102, and references therein.

[17] a) K. Iwamoto, A. Ikeda, K. Araki, T. Harada, S. Shinkai, *Tetrahedron* **1993**, *49*, 9937; b) A. Ikeda, H. Tsuzuki, S. Shinkai, *J. Chem. Soc. Perkin Trans. 2* **1994**, 2073.

[18] a) F. Inokuchi, Y. Shiomi, H. Kawabata, T. Sakaki, S. Shinkai, *Chem. Lett.* **1993**, 1595; b) F. Inokuchi, K. Araki, S. Shinkai, *ibid.* **1994**, 1383; c) H.-F. Wu, J. S. Brodbelt, *J. Am. Chem. Soc.* **1994**, *116*, 6418; d) S. R. Wilson, Y. Wu, *Supramolec. Chem.* **1994**, *3*, 273.

[19] a) Z. Goren, S. E. Biali, *J. Chem. Soc. Perkin Trans. 1* **1990**, 1484; b) F. Grynszpan, Z. Goren, S. E. Biali, *J. Org. Chem.* **1991**, *56*, 532.

[20] Y. Miyahara, T. Inazu, T. Yoshino, *Tetrahedron Lett.* **1983**, *24*, 5277.

[21] Even when the signal intensities of $(1 + M)^+$ or $(1 + M)^+/1^+$ are plotted versus the ionic radius very similar plots are obtained. When an equimolar mixture of **1**, **2**, and **3** was analyzed in the absence of metal cations, the ratio of the signal intensities was $1^+:2^+:3^+ = 2.81:7.13:1.00$, indicating the relatively stability of the host cations.

[22] The attempt to detect $[3 \cdot Cs]^+$ in solution by ^1H NMR spectroscopy and solvent extraction failed.

[23] A. Bondi, *J. Phys. Chem.* **1964**, *68*, 441.

[24] C. Schade, P. von R. Schleyer, *Adv. Organomet. Chem.* **1987**, *27*, 169.

[25] Very recently, Ungaro et al. reported on cation-π interactions in a [calix[4]arene-crown-6 $\cdot$ Cs]$^+$ complex (R. Ungaro, A. Casnati, F. Ugozzoli, A. Pochini, J.-F. Dozol, C. Hill, H. Rouquette, *Angew. Chem.* **1994**, *106*, 1551; *Angew. Chem. Int. Ed. Engl.* **1994**, *33*, 1506). Although the X-ray crystal structure shows that the distance between benzene rings and Cs^+ is short, the presence of cation-interactions is doubtful due to the presence of many metal-coordinating oxygen atoms (as in the complexes $[1 \cdot M]^+$.

Efficient Total Synthesis of the Pharmacophore of the Anticancer Antibiotic CC-1065 by Zirconocene- and Palladium-Initiated Cyclizations**

Lutz F. Tietze* and Wilm Buhr

Dedicated to Professor Richard R. Schmidt on the occasion of his 60th birthday

The antibiotic CC-1065 (**1**), which was first isolated from *Streptomyces zelensis* in 1978, is one of the most potent antitumor agents known at present.[1] It contains three pyrrolo-[3,2-*e*]dihydroindole moieties; the A-unit with an unusual spirocyclopropyl group is the pharmacophore, whereas the B- and C-units are responsible for the strong binding to DNA. It has been shown that the A-unit of **1**, called CPI, selectively alkylates

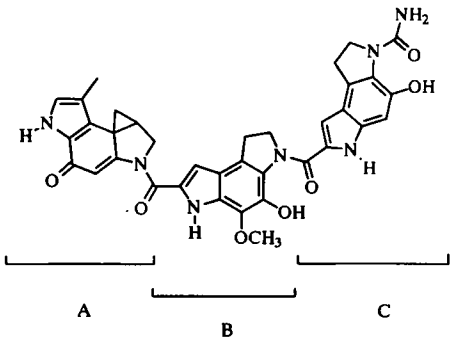

CC-1065 1

AT-rich regions of the minor groove of double-stranded DNA.[2] However, **1** cannot be used as a drug because of delayed fatal hepatotoxicity. In contrast, derivatives of the CPI unit having similar antitumor activity do not show this negative property.[3]

For the design of selective anticancer agents[4] we have developed a new and highly efficient synthesis of the (N^2-benzenesulfonyl)-CPI derivative **2**. This synthesis is superior to the known procedures and is distinguished by its short reaction sequence. The key steps are two consecutive cyclizations mediated by organo transition metal complexes which allow the formation of first the pyrroline and then the pyrrole ring in **2**.

Retrosynthetically, **2** can be traced back to the N^2-benzenesulfonyl-*seco*-CPI **3**, which via **5** leads to the starting material **4**. The special feature of this synthesis is that not only is the pyrroline ring constructed in the first cyclization with zirconocene methyl chloride,[5f, 5g, 6a, b] but during the quenching with iodine, in addition to the formation of a iodomethyl group, a second iodine atom is simultaneously introduced at the arene. This can be used for the construction of the pyrrole ring in the subsequent Heck reaction.[7a-c]

Substrate **4** was synthesized in 66% yield in four steps starting from the commercially available 2-methoxy-4-nitroaniline through Pt-catalyzed hydrogenation in dioxane, twofold *N*-ben-

[*] Prof. Dr. L. F. Tietze, Dipl.-Chem. W. Buhr
Institut für Organische Chemie der Universität
Tammannstrasse 2, D-37077 Göttingen (Germany)
Telefax: Int. code + (551)39-9476

[**] Anticancer Agents, Part 22. This work was supported by the Fonds der Chemischen Industrie. We wish to thank the Degussa AG for their generous gifts of noble metal compounds. Part 21: ref. [4b].

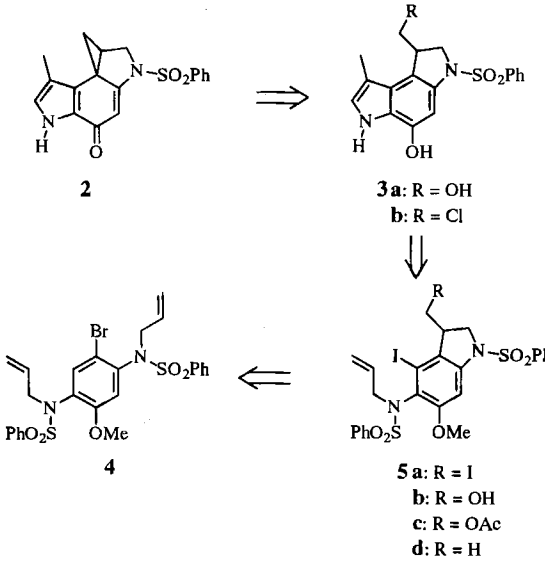

zenesulfonization with benzenesulfonyl chloride in pyridine,[8] bromination with *N*-bromosuccinimide in tetrahydrofuran, and double allylation with allyl bromide in the presence of tetrabutylammonium iodide also in tetrahydrofuran. Halogen–metal exchange in **4** with *t*BuLi in tetrahydrofuran and subsequent metal exchange with $[Cp_2ZrCl(CH_3)]$ proceeded supposedly through a zirconium–didehydrobenzene complex **6** to the zirconacyclopentene derivative **7**,[6c] which gave **5a** in 60% yield as a single product after quenching with two equivalents of iodine in dichloromethane. In the reaction of **7** with iodine, first the aryl–zirconium bond and then the alkyl–zirconium bond was cleaved. This was deduced from the reaction of **7** with only one equivalent of iodine followed by aqueous workup, which gave **5d** exclusively. Somewhat surprising is the high regioselectivity of the cyclization of **4**; the insertion of the alkene group in complex **6** occurs exclusively *para* to the methoxy group.[9]

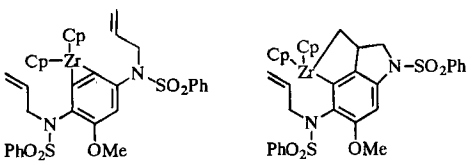

Compound **5a** could not be used directly in the Heck reaction since both the iodobenzene moiety and the iodomethylpyrroline group react to form a methylpyrrole unit. For this reason **5a** was first converted into the hydroxymethyl derivative **5b** with silver oxide on silica gel in 90% yield (acetone/water, 20 °C, 24 h). The transformation of the iodomethyl group in **5a** caused many problems at the beginning since all attempts at nucleophilic substitution, for example with acetate, failed; instead elimination with partial isomerization of the formed double bond occurred.

The Heck reaction for the preparation of **3** can be carried out with **5b** as well as with **5c**, which is obtained quantitively from **5b** by acetylation with sodium acetate in acetic anhydride. With catalytic amounts of tetrakis(triphenylphosphane)palladium **5b** gave a 17:1 mixture of **8a** and **9a** in 90% yield (2 mol% $[Pd(PPh_3)_4]$, CH_3CN/Et_3N, 60 °C, 18 h). In contrast, reaction of **5c** with palladium acetate in the presence of silver carbonate led in 90% yield exclusively to **8b** (2 mol% $Pd(OAc)_2$, 1.5 equiv Ag_2CO_3, DMF, 20 °C, 2 h). Without further workup the respective mixtures of **8a**/**9a** and **8b** were isomerized with camphorsulfonic acid quantitively to give **9a** and **9b** (CH_2Cl_2, 20 °C, 1 h). The cleavage of the aryl methyl ether in **9b** to give **9c** was achieved with boron tribromide in 80% yield (CH_2Cl_2, −10 °C, 1 h); under these conditions **9a** provided only a mixture of products.

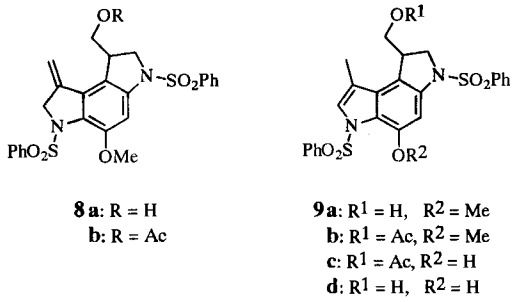

Solvolysis of **9c** in methanol in the presence of potassium carbonate afforded **9d**, and successive cleavage of the benzenesulfonyl group at the indole nitrogen with sodium bis(2-methoxyethoxy)dihydroaluminate (Red-Al) led to the desired *seco*-CPI **3a** with an overall yield of 70%. The conversion of **3a** to **2** is known[10] and was carried out not only by means of Mitsunobu's method[11] with diethyl azodicarboxylate, but also via the chloride **3b** with a subsequent base-induced cyclization.

In summary, the pharmacologically important CPI derivative **2** was prepared in 11 steps with an overall yield of 12% starting from commercially available 2-methoxy-4-nitroaniline. The double cyclization mediated by zirconocene and palladium complexes is of general synthetic value, and we are currently testing it for the construction of other complex bis-*ortho*-annelated arenes.

Experimental Procedure

To a solution of **4** (0.34 mmol) and $[Cp_2ZrCH_3Cl]$ (0.35 mmol) in dry THF (10 mL) was added slowly with stirring at −78 °C a solution of *tert*-butyllithium in hexane (0.70 mmol). Stirring was continued for 1 h at −78 °C and 18 h at 20 °C. The solvent was evaporated in vacuo and the residue dissolved in dry CH_2Cl_2 (20 mL) and cooled to 0 °C. To this solution was slowly added a suspension of iodine (0.72 mmol) in dry CH_2Cl_2 (20 mL), and the mixture was stirred for 1 h at 0 °C and 36 h at 20 °C. The reaction mixture was filtered through celite, washed with saturated Na_2SO_3 solution, water, and brine (10 mL each), dried over $MgSO_4$, and concentrated to dryness. After chromatography (petroleum ether/ethyl acetate 3:1) **5a** was obtained in 60% yield. Recrystallization from ethyl acetate gave colorless needles.

5a: M.p. 206.9 °C; ^{1}H NMR (300 MHz, $CDCl_3$): δ = 2.34 (dd, J = 10, 9.0 Hz, 1H, 3-CH_a), 3.32 (s, 3H, O-CH_3), 3.34–3.46 (m, 2H, 3-H, 3-CH_a), 3.85–4.00 (m, 2H, 2-H_a, 1'-H_a), 4.10 (d, J = 12 Hz, 1H, 2-H_b), 4.49 (dd, J = 13.5, 6.0 Hz, 1H, 1'-H_b), 4.93 (d, J = 6 Hz, 1H, *trans*-CH=CH_2), 4.98 (s, 1H, *cis*-CH=CH_2), 5.83–5.97 (cm, 1H, CH=CH_2), 7.14 (s, 1H, 7-H), 7.48–7.69 (m, 6H, Ph-H), 7.72–7.79 (m, 2H, Ph-H), 7.82 (d, J = 8.0 Hz, Ph-H).

9c: ^{1}H NMR (200 MHz, $CDCl_3$): δ = 2.01 (s, 3H, OAc), 2.21 (s, 3H, 8-CH_3), 3.10 (dd, J = 10, 9.0 Hz, 1H, 1-CH_a), 3.52–3.78 (m, 2H, 1-H, 1-CH_b), 4.06 (dd, J = 11.5, 3.5 Hz, 1H, 2-H_a) 4.16 (d, J = 11.5 Hz, 2-H_b), 7.15 (s, 1H, 7-H), 7.37 (s, 1H, 4-H), 7.38–7.63 (m, 6H, Ph-H), 7.76 (d, J = 8.0 Hz, 2H, Ph-H), 7.85 (d, J = 8.0 Hz, 2H, Ph-H), 8.85 (s, 1H, Ph-OH).

Received: November 10, 1994 [Z 7469 IE]
German version: *Angew. Chem.* **1995**, *107*, 1485–1487

Keywords: antibiotics · antitumor agents · cyclizations · Heck reactions · zirconium compounds

 © VCH Verlagsgesellschaft mbH, D-69451 Weinheim, 1995 0570-0833/95/1212-1367 $ 10.00+.25/0

[1] L. J. Hanka, A. Dietz, S. A. Gerpheide, S. L. Kuentzel, D. G. Martin, *J. Antibiot.* **1978**, *31*, 1211.
[2] a) D. L. Boger, S. M. Sakya, *J. Org. Chem.* **1992**, *57*, 1277; b) M. A. Warpehosky, L. H. Hurley, *Chem. Res. Toxicol.* **1988**, *1*, 315; c) V. L. Reynolds, I. Molineux, D. J. Kaplan, D. H. Swenson, L. H. Hurley, *Biochemistry* **1985**, *24*, 6228; d) D. L. Boger, W. Yun, *J. Am. Chem. Soc.* **1994**, *116*, 5523.
[3] J. P. Gorren, G. L. Clarke, E. A. Prutt, *J. Antibiot.* **1984**, *37*, 63.
[4] a) Reviews: L. F. Tietze in *Molecular Aspects of Chemotherapy* (Eds.: E. Borowski, D. Shugar), Pergamon, New York, **1990**, pp. 55–70; b) L. F. Tietze, A. Fischer-Beller, *Carbohydr. Res.* **1994**, *254*, 169, and references therein.
[5] a) W. Wierenga, *J. Am. Chem. Soc.* **1981**, *103*, 5621; b) P. Magnus, Y. S. Or, *J. Chem. Soc. Chem. Commun.* **1983**, 26; c) G. A. Kraus, S. Yue, *ibid.* **1983**, 1198; d) D. L. Boger, R. S. Coleman, *J. Am. Chem. Soc.* **1988**, *110*, 4796; e) *ibid.* **1988**, *110*, 1321; f) L. F. Tietze, T. Grote, *Chem. Ber.* **1993**, *126*, 2733; g) *J. Org. Chem.* **1994**, *59*, 192; h) N. Uesaka, M. Mori, K. Okamura, T. Date, *ibid.* **1994**, *59*, 4542.
[6] a) J. H. Tidwell, D. R. Senn, S. L. Buchwald, *J. Am. Chem. Soc.* **1991**, *113*, 4685; b) J. H. Tidwell, S. L. Buchwald, *J. Org. Chem.* **1992**, *57*, 6380; c) G. Erker, *Angew. Chem.* **1989**, *101*, 411; *Angew. Chem. Int. Ed. Engl.* **1989**, *28*, 397.
[7] a) T. Jeffery, *J. Chem. Soc. Chem. Commun.* **1984**, 1287; b) *Synthesis* **1987**, 70; c) R. C. Larock, B. E. Baker, *Tetrahedron Lett.* **1988**, *29*, 905.
[8] R. Adams, T. E. Young, *J. Am. Chem. Soc.* **1951**, *75*, 3235.
[9] Based on the NMR data of **5a** the two possible regioisomeric cyclization products cannot be differentiated. The assignment relied on a comparison of the product **3b** with authentic material.
[10] P. Magnus, T. Gallagher, *J. Chem. Soc. Chem. Commun.* **1984**, 289.
[11] O. Mitsunobu, *Synthesis* **1981**, 1.

Corrigendum

Several literature citations should be corrected in the review "Stereospecific Olefin Polymerization with Chiral Metallocene Catalysts" by H. H. Brintzinger et al. (*Angew. Chem. Int. Ed. Engl.* **1955**, *34*, 1143–1170). On p. 1162, in the left-hand column, third paragraph, last line, reference [95b] should be reference [125]; three lines below [140, 141b, 143b] should be [142, 143b, 147]; in the right-hand column five lines from the top [213, 217] should be [214, 217].

Troubleshooting...

with VCH books!

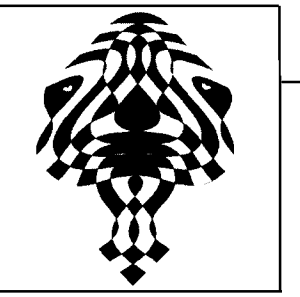

Neuhoff, V.
Scientists in Conference
The Congress Organizer's Handbook
1987. X, 223 pages.
Hardcover. DM 68.00
ISBN 3-527-26579-1

Do you have to organize a conference? Well, sometimes, this can't be avoided. But you don't want to get crushed by the wheels of paperwork? And you want to stay in your budget? Then this handy little book is your survival kit!

Schoenfeld, R.
The Chemist's English
Third, revised edition with Say It in English, Please!
1990. XII, 195 pages with 9 figures.
Hardcover. DM 48.00
ISBN 3-527-28003-0

"Recommended without qualification; and a suitable gift for friends."
Chemical and Engineering News

"The book might well serve as a prescribed text for PhD students."
Nature

Ebel, H.F. /Bliefert, C. / Russey, W.
The Art of Scientific Writing
From Student Reports to Professional Publications in Chemistry and Related Fields
1990. XIX, 493 pages with 27 figures and 16 tables.
Softcover. DM 48.00
ISBN 3-527-26677-1

First of all, here we have a highly readable text on scientific communication - with all its ramifications from writing the most effective text to getting it published. Never before has so much information on scientific writing been assembled in a single book.

To order please contact your bookseller or:
VCH, P.O. Box 10 11 61,
D-69451 Weinheim,
Telefax (0) 62 01 - 60 61 84
VCH, Hardstrasse 10, P.O. Box,
CH-4020 Basel
VCH, 8 Wellington Court,
Cambridge CB1 1HZ, UK
VCH, 303 N.W. 12th Avenue,
Deerfield Beach, FL 33442-1788,
USA
toll-free: 1-800-367-8249 or
fax: 1-800-367-8247
VCH, Eikow Building,
10-9 Hongo 1-chome, Bunkyo-ku,
Tokyo 113

VCH

 © VCH Verlagsgesellschaft mbH, D-69451 Weinheim, 1995 0570-0833/95/1212-1368 $ 10.00+.25/0

Protection Rackets?

Tactics of Organic Synthesis. By *Tse-Lok Ho.* Wiley, Chichester, Great Britain, 1994. 450 pp., hardcover £ 49.50.—ISBN 0-471-59896-8

As the most recent offshoot of a series on modern organic synthesis, containing up to now five monographs, Tse-Lok Ho presents his most recent work "Tactics in Organic Synthesis". His self-declared aim is to provide a standardized overview on synthetic tactics based on selected examples. The term "tactics" can be understood as the skillful application of one or more individual reactions within the framework of an overall concept ("strategy"). The book consists of nine chapters, which deal successively with the topics of convergency, protective groups ("Activity Modulation, Group Protection, and Latent Functionalities"), Umpolung, tandem reactions, cyclic compounds ("Cyclic Arrays for Structural and Stereochemical Manipulations"), execution of intramolecular reactions, template and chelation effects, symmetry considerations, and various others ("Miscellaneous Tactics").

A wide range of tactics and methods is discussed in the individual chapters, in such a compressed form that can hardly be found anywhere else. Almost every class of natural product appears once in some connection or other, and almost every important fact on the regio- and stereoselective control of a reaction is treated somewhere. In spite of the division into chapters, the content nevertheless remains heterogeneous, and on reading the text one is occasionally unaware in which section one currently is. In view of the extensive amount of material (ca. 1400 literature references) it is difficult to criticize the choice, although almost inevitably one may occasionally regard another example as more important or more instructive. The almost exclusive restriction to references from the primary literature appears to me to be unfortunate, with the result that numerous important reviews can only be found after a long search or even not at all. The references in the text follow the general system [surname of the first named author, year], and correspond with an appropriate appendix to the complete list of citations at the end of the book. An author index is unfortunately not provided. Based on about 150 randomly selected references, the details were found to be predominantly reliable. The year of publication was found to be incorrect for only three examples. A reference given in the text (p. 264) as [B. A. Anderson, 1992] could not be found in the appendix, another was incorrectly cited (p. 14) as [J. Davies, 1981]. In a few cases references in the text were missing, for example, the work of Nicolaou's group on the endiandrinic acids (p. 97). I could not find the example shown on p. 78 for chelate control in the source given, [Masuyama, 1988]. Printing errors are kept within limits and are rarely so meaningful as the "wild intermediate" on p. 244 ("animal" rather than "aminal"). German-speaking authors are almost inevitably not spared the mutilation of their names (Hoffman, p. 416; Oppenaur, p. 81; Kauffman, p. 419; Vorbrügen, p. 206). Sentences such as "reactions... are under chelation control in THF, but not in THF" (p. 309) should have been eliminated on reading the proofs.

In terms of content, the book is based on a uniform pattern. The author first describes in a couple of sentences a tactical manoeuver on one molecule, and this is followed by a reaction scheme illustrating the reaction concerned. Such schemes (ca. 800) make up a large part of the book and are reproduced uniformly, largely based on those in the original publications. Those explanations that are not accompanied by the appropriate schemes are difficult to comprehend, as one can rarely understand, without visual aids, what it is actually all about. Generally, I found the text wooden and dry, sometimes long-winded. I found it distracting that reference was frequently made in the text to numbering (D-ring, C-14, etc.) that was not indicated in the formulas. One also wonders why schemes appear in identical form in two distinct places in the book (pp. 97/388, 98/191, 126/380, 192/388, 246/272, 255/395) and not simply cross-referenced on the corresponding page. The reaction schemes are so constructed that a key intermediate is presented, beginning with the starting material, without any indication of reaction conditions (double arrow), for which the tactical measures under discussion are being carried out. In the ideal case, the result of this procedure is that a single reaction arrow, inscribed with reagents and reaction conditions, leads to a product that is also displayed graphically. From there one manages to reach the target molecule of the synthesis via reactions conducted without further detail (double arrow). Unfortunately, the author frequently deviates from this ideal position. The key reaction arrow frequently covers several steps, and the reagents are not specified at all or only incompletely. Retrosynthetic arrows, which should be superfluous, sometimes appear within the schemes. As a result of these deficiencies, the diagrams are often difficult to grasp or ambiguous. The process of comprehension is interrupted, because one is forced to engage in speculation. This is exacerbated by the fact that a comparatively high percentage of the reaction equations contain errors. These include transposed symbols or groups (in 19 schemes, e.g., on p. 127, where a methyl ether erroneously undergoes a fragmentation in place of an alcohol), missing or superfluous groups (in 25 schemes, e.g., on p. 319, where a methylene group is forgotten in two equations), the wrong reagents (in 10 schemes, e.g., p. 377, where NaOMe is used for an isomerization in place of the NaHMDS used in the original publication) or wrong configurations (in 6 schemes, e.g., on p. 30, where the Mitsunobu reaction is erroneously shown as not leading to inversion), and factual discrepancies (in 10 schemes, e.g., on p. 293, where the course of the Heck reaction is not given correctly). Neverthe-

This section contains book reviews and a list of new books received by the editor. Book reviews are written by invitation from the editor. Suggestions for books to be reviewed and for book reviewers are welcome. Publishers should send brochures or (better) books to Dr. Ralf Baumann, Redaktion Angewandte Chemie, Postfach 101161, D-69451 Weinheim, Federal Republic of Germany. The editor reserves the right of selecting which books will be reviewed. Uninvited books not chosen for review will not be returned.

less, the impression should not be created that the overall graphical presentation is poor. Many of the drawings are decidedly effective and show stereochemical relationships especially well. Statistically, however, every tenth figure is afflicted with a blemish. The book loses much of its charm as a consequence of the lack of attention paid to production of the figures.

In summary, I regard this book as a useful purchase, if one regards it as a hotch-potch of various, highly interesting key steps in organic synthesis and uses it as such. The use of individual chapters for graduate courses in organic synthesis can be considered after careful reworking. The book could serve as a textbook only in rare cases. For this purpose the wealth of material presented is too large and the presentation too condensed.

Thorsten Bach
Organisch-chemisches Institut
der Universität Münster (Germany)

Protecting Groups. By *P. J. Kocienski.* Thieme, Stuttgart, 1994. 265 pp., paperback DM 60.00.—ISBN 3-13-135601-4

"Protection is not a principle, but an expedient." With this very apt comment Philip Kocienski begins his book on protecting groups in organic synthesis. Synthetic chemists would dearly like to be able to work without protecting groups, but are very glad that they exist. Without protecting groups there would be no syntheses of taxol, calicheamicin, Saragossa acid, or erythronolide, to name just a few recent highlights of synthetic chemistry.

The standard work on the subject up to now has been Theodora Greene's *Protective Groups in Organic Synthesis*, first published in 1981, followed in 1991 by an updated version (Greene and Wuts). Whereas the book by Greene and Wuts is set out rather in the form of an encyclopedia, treating over 700 different protecting groups, Kocienski limits his coverage to the 50 or so protecting groups that have been most proven in practice. In the author's words: "We felt the need for a critical survey of the subject, that focuses on the widely most protecting groups, for the most common functional groups, used by most organic chemists most of the time." Measured against these aims, Kocienski has done an excellent job in writing this book.

It begins with an introductory chapter on general aspects of the use of protecting groups. First Kocienski states the conditions that must be fulfilled by a good protecting group: it must be cheap, easy to introduce, stable over a wide range of conditions, capable of being detached selectively, and should not interfere unnecessarily with the analysis of the host molecule. The selective removal of a protecting group is more important than the conditions for introducing it. Many synthetic chemists are familiar with examples in which a total synthesis failed in its last stage because the protecting groups, whose importance is often underestimated, could not be detached in the desired way. Ideally one would like to be able to choose a set of protecting groups, each one of which can be selectively removed in the presence of all the other groups. Kocienski calls this an orthogonal set of protecting groups. Even though it is never possible in practice to fully realize the aim of choosing such a set, Kocienski names twelve deprotecting conditions which together come very close to achieving it. These twelve ways of detaching a protecting group are: basic solvolysis, action of acids, action of transition metals, action of fluorides, reductive elimination using zinc, β-elimination, hydrogenolysis, oxidation, action of Na/NH_3, use of S_N2 conditions, removal of allyl groups, and photochemical action. All these twelve conditions are described in the introductory chapter and illustrated by examples. Next the author discusses temporary protection (for example, of aldehydes in the form of α-amino-alkoxides), and the effects of neighboring groups on protecting groups; in particular it is pointed out that an apparently harmless protecting group can be transformed by the effects of neighboring groups into a highly reactive functional group.

This introductory chapter is followed by five separate chapters on protecting groups for alcohol, diol, carboxyl, carbonyl, and amino functions. In each case the most important and commonly used protecting groups are discussed, beginning with the methods for detaching these groups, followed by methods for preparing them. The use of each protecting group is illustrated by several recent examples, with clearly set out reaction schemes. These schemes are superior to those in the book by Greene and Wuts, both in their information content and in their clarity. NMR data are also given for each protecting group, information that will be of particular value for the practical user.

Reading the book is made more enjoyable by the author's peculiarly British brand of humor. An example of this is the introductory remarks to the chapter on amino-protecting groups: "Nitrogen is the element of faction neatly dividing organic chemists into camps. Those who have mastered its vagaries are undaunted by the prospect of contending with its reactivity. Then there are those in the minority antipodal camp (like the author) who respect that nitrogen is best confined to a cylinder and used to shield precious reactions and reagents from the ravages of air and moisture!"

Chapter 7 is in the form of an epilogue, in which the progress achieved in the chemistry of protecting groups is illustrated by describing the total synthesis of erythronolide. Also, as an outstanding example of the art of achieving a synthesis with as few protecting group stages as possible, Kocienski describes the synthesis of (9*S*)-dihydroerythronolide A, as reported in *Angewandte Chemie* by Hoffmann and Stürmer.

Each chapter ends with a comprehensive list of references. A detailed list of contents and a glossary of abbreviations are provided to help the reader.

Who should read this book? Certainly the advanced student who is already, or about to begin, working for a higher degree or doctorate in a research group using synthetic methods. Then every practicing chemist in industry or university who needs to know about protecting groups. The book should also be available in every chemistry library. The economical price of this paperback version will certainly not be an obstacle to buying it.

Ulrich Koert
Fachbereich Chemie
der Universität Marburg (Germany)

Der große Schwindel. By *F. DiTrocchio.* Campus, Frankfurt/New York, 1994. 221 pp., hardcover DM 48.00.—ISBN 3-593-35116-1

Like the Biblical deadly sins, dishonesty in science is officially condemned with a vehemence very like that with which in practice "in real life" it is tolerated and pursued. The "wink-of-an-eye" expression employed in the title of this book (translated: *The Great Swindle*; the harsher terms fraud and 'falsification' are reserved for the subtitle) speaks a language every bit as eloquent as certain international laboratory jargon that touches on the same theme, whether it be in English (When in doubt, throw it out; fudge factor), German ("π mal Daumen" and "eh er noch den Schmelzpunkt kannte, sand ers an die *Angewandte*") or French ("corriger la fortune"). To put it another way, science's exalted demands cannot

 © VCH Verlagsgesellschaft mbH, D-69451 Weinheim, 1995 0570-0833/95/1212-1370 $ 10.00+.25/0

always be met by (occasionally) weak mortals. Has this always been the case? Or has scientific fraud been increasing of late? If so, why? What causes scientists to practice fraud in the first place? What in fact *is* scientific fraud? Where does it begin and where does it end? Does it include the "cleaning up" of a set of data or providing inaccurate yield information (cf. yield, isolated yield, Swiss yield), summarizing a publication one has only skimmed, reviewing a book one has scarcely read? All questions worthy of academic consideration, ones the author logically proposes to address through establishment of the independent scientific discipline Defraudistics (something that heretofore has always been more akin to an art). *The Great Swindle* would admittedly not be the first monograph devoted to this discipline, but it would certainly soon join the ranks of the standard works, and for several reasons.

In the first place, the book represents a collection of examples of famous instances of falsification and fraud, including both authentic cases and others one might more properly define as borderline situations.

Among the authentic illustrations one would assuredly cite the case of Moewus (who proved that certain green algae exchange genetic material through copulation), that of Burt (who through his legendary investigation of twins decided once and for all the question of whether intelligence can be inherited), or the famous Piltdown case, to which is devoted an extensive chapter ("Improper Fossils and Missing Limbs") because of its great significance in the controversy surrounding Darwinian evolution. This chapter introduces in a critical way, one after another, all the relevant suspects including famous authors like Teilhard de Chardin and Sir Arthur Conan Doyle. Such clear-cut cases of fraud, even though the true guilty party in the Piltdown episode remains unidentified to this day, could easily be supplemented by chemists: starting with the Kögl case, proceeding with polywater and cold fusion, and perhaps culminating in the recently perpetrated fraud involving stereoselective synthesis in an NMR spectrometer.

I would characterize as "borderline cases" those described in the opening chapter ("Even Nobel Prize Winners Commit Fraud"), most of which more nearly resemble a scientific ride across Lake Constance than a calculated attempt at deceit. Newton provides a good example. Not only the present author but various other historians and theoreticians of science have accused Newton of "playing loose" with the accuracy required in his experiments and measurements in an attempt to substantiate his theoretical models, even adjusting his measured variables until he achieved the values prescribed by the models. This may well be the case, although it is not easily proven in specific instances; nonetheless, Newton's actual achievement is the fact that he managed to reach the shores of safety and thereby discover a new law of nature, one that has subsequently stood up to repeated testing. The situation is similar with E. Haeckel, who in the context of establishing the law of species also stands accused of perpetrating falsehoods (documented in *The Great Swindle*). The significance of Haeckel's research into the principles of the general morphology of organisms may thus be somewhat diminished, but it is certainly not negated. (Although from our current perspective a title like *Sandalion. An Open Response to the Falsification Claims by the Jesuits*, Frankfurt 1910, does leave one a bit skeptical.)

These particular frauds and others cited by DiTrocchio, which include Galileo, Millikan, and Einstein, differ quite drastically from the true falsifiers discussed at the outset. As Brecht observed in his powerful drama *Galileo*: Not everything a great man does is itself great.

DiTrocchio deals especially in the chapter entitled "Big Science or Big Fraud?" with the question of whether instances of fraud in science are on the increase. Reduced to a single sentence, the thesis he offers is that present-day fraud [is related to] the financing of research as introduced after World War II in the United States and subsequently [propagated] throughout the Western world. In other words: The science of falsification was essentially born when science was transformed from a calling into a profession. Put yet another way: Whereas Galileo practiced deceit in order to verify and disseminate a theory, Bruening [an American psychologist and notorious fraud] practiced deceit as a way of justifying in the eyes of the responsible agency [the National Institutes of Health] his receipt of financial support. In other words, on one hand a scientific Titan (with minor weaknesses), on the other a scientific mercenary for whom any means are regarded as legitimate. I do not believe this thesis is tenable. A gentleman scientist of the English leisure class, or a private scholar enjoying the patronage of an Italian prince, certainly appears more likely to have a "calling" than a modern-day professional scientist, who is obliged simultaneously to engage in the profane pursuit of a living. But the latter is not necessarily more inclined toward fraud. The actual number of fraud cases is of course unknown, but it may well be presumed to have risen in recent years; after all, the incidence of scientific fraud should be proportional in a general way to the number of active scientists. What is it, therefore, that motivates some (few) scientists to present falsified, improved, or freely invented results? The reasons are certainly very diverse, ranging from the humorous (cultivated particularly in Britain in the form of the hoax), through attempts to damage the reputations of others and cases of pathological ambition, all the way to megalomania and obsession with an *idée fixe*. Notwithstanding the above reservations, there may also be certain societal factors today that have the effect of stimulating fraud. An era like the present, so obsessed with individual success and being someone special, would presumably be more conducive to engendering fraud out of the (self-)recognition that one is in fact *not* particularly special than an era in which doubts about one's personal worth were less widespread. One of the remarkable facts associated especially with the most recent examples of fraud is the lack of attention on the part of the perpetrator to the question: Is this piece of deception worthwhile? Indeed, it is likely that this question was never even posed. The corresponding answer is quite straightforward: Fraud does not pay. There is no way to extract financial gain from scientific fraud because it cannot be marketed, certainly not over any prolonged period. The scientific fame one might perhaps be seeking will also not be achieved, because a spectacular experiment is certain to be repeated throughout the world, at which point the deception becomes obvious. Could fraud be motivated by the joy of having beaten the system through smuggling a piece of false data into the body of scientific wisdom? If so the victory would be a cheap one, because only the perpetrator of the fraud will be in a position to enjoy it, unless he or she invokes a kind of Rumpelstiltskin effect and plays an active role in disclosure of the deceit. Moreover, such a victory, especially in chemistry, is exceedingly easy to achieve. Thanks to modern methods of numerical calculation and the plethora of existing experimental data (e.g., spectral and structural data bases) it would be child's play today, for example, to describe a first synthesis of some new substance in such a convincing way that even a competent reviewer would be unlikely to recommend against publication of the work. But is that really falsification? Has it not always been an important

 © VCH Verlagsgesellschaft mbH, D-69451 Weinheim, 1995 0570-0833/95/1212-1371 $ 10.00+.25/0

goal to develop theoretical methods that permit one to predict physical and chemical properties with such precision that a real experiment leading to the same result becomes unnecessary?

DiTrocchio raises questions of this type in the last chapter of his book, entitled The Scientist as Deceiver, where he explicitly dismisses any interest in small-time fraud or simple falsification. In this intellectually stimulating discourse the author promotes the thesis that all scientists, but especially those not engaged in normal science according to Kuhn's use of the term, *must* engage in deception. In DiTrocchio's own words: "[Ever since Popper we know] that it is possible to provide proof only for that which is false, whereas one can never prove absolutely that something is true. This means that all the scientific theories we hold to be true cannot be regarded as true because their truth has actually been proven, but only because the scientists who formulated them succeeded in making such truth plausible to their colleagues and to us. This ordinarily includes the use of more or less serious falsifications or tricks, albeit ones that are not apparent, or only become apparent after a long period of time. In the end, scientists thus perpetrate fraud in the name of truth, because they are in no position to prove truth itself." In this particular quote I find the words falsification, tricks, and fraud somewhat disturbing. Scientists are in fact very much aware of the limits of their abilities. They know they are dealing with images, analogies, and metaphors (DiTrocchio speaks of science as a great illusion), which they formulate as accurately as possible within the confines of the knowledge available, their own personal creativity, and their imagination. The claim is never made (at least not any more) that one is presenting a comprehensive exposition of truth. Science remains an open endeavor and thus occasionally open to fraud and deceit, at least as defined in a court of law, but open also to the sort of high-level manoevering noted above, which one might better describe as un-deceiving in the sense of destroying an illusion. Otherwise the public is too likely to gain the impression that even science amounts to nothing but a big swindle. This may be precisely the message many of our contemporaries wish to hear, but it is not the case, nor is it the message the author wished to convey—or is he attempting to deceive us?

Henning Hopf
Institut für Organische Chemie
der Technischen Universität Braunschweig (Germany)

Stereoselective Synthesis. 2nd Edition. By *M. Nógrádi*. VCH Verlagsgesellschaft, Weinheim/VCH Publishers, New York, 1994. 368 pp., paperback DM 68.00, $ 45.00.—ISBN 3-527-29243-8/1-56081-895-6

Like its first edition published in 1986, this enlarged and revised second edition of *Stereoselective Synthesis* has two purposes. Firstly it is intended for chemists involved in the synthesis of enantiomerically pure chiral natural products and active agents. Secondly it aims to provide advanced students and postgraduates with a clearly understandable account of basic principles and progress in the ever growing field of asymmetric synthesis.

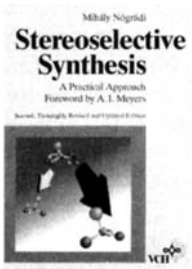

Nógrádi's book describes the impressive developments that have occurred in stereoselective synthesis during the past 20 years. The earlier chapters contain a detailed account of the theoretical basis of methods for regio- and stereoselective synthesis. Recent discoveries and theories, such as the isoinversion principle, have been included in this new edition. The aspects treated in the following chapters include classical variants of methods for stereoselective functionalization, for example using chiral auxiliaries. The types of reactions discussed include such varied examples as stereoselective non-catalytic reductions, oxidations, nucleophilic additions, electrophilic additions, cycloadditions, and pericyclic reactions. The most recent published work (up to December 1992), such as the development of chiral reagents and innovations in the use of chiral auxiliaries, e.g. for 1,3-dipolar cycloadditions, is only partly covered in this new edition. Advances and new applications in the area of enantioselective catalysis are covered in greater detail. The trend away from stoichiometric methods to catalytic methods is impressively described, with examples from the areas of catalytic hydrogenations, epoxidations, and the *cis*-hydroxylation of olefins. The wide-ranging uses of chiral ligands and chiral Lewis acids are also discussed, as applied, for example, to enantioselective additions (the increasing success of organozinc reagents, and the catalysis of aldol reactions and ene reactions by chiral boron or aluminum Lewis acids). The reader wishing to study topics in greater depth has access in this edition to more than 1800 literature references, of which 831 are more recent (although these extend only up to December 1992!).

The choice of topics covered sometimes seems a little arbitrary and turns out to be incomplete, and the results reported are heavily concentrated on the best known research groups. Consequently the advanced reader who wants to avoid missing important recent developments will often need to refer to the original papers and follow up other references that these bring to light. However, since there have been so many new developments in asymmetric synthesis it is understandable that the author has not been able to include all the new work of the last few years.

To summarize, the appearance of a new edition of this book is well justified in view of the immense amount of published work and new developments in asymmetric synthesis in recent years, and this edition continues to give a good overall insight into this highly topical field of organic synthesis. The availability of a paperback version now means that students can afford to buy it, and it undoubtedly offers them welcome additional reading to accompany lecture courses on the subject.

Karola Rück
Institut für Organische Chemie
der Universität Mainz (Germany)

 © VCH Verlagsgesellschaft mbH, D-69451 Weinheim, 1995 0570-0833/95/1212-1372 $ 10.00+.25/0

My Search for Carbocations and Their Role in Chemistry (Nobel Lecture)**

George A. Olah*

Every generation of scientific men (i.e., scientists) starts where the previous generation left off, and the most advanced discoveries of one age constitute elementary axioms of the next.
Aldous Huxley

Introduction

Hydrocarbons are compounds of the elements carbon and hydrogen. They make up natural gas and oil and thus are essential for our modern life. Burning of hydrocarbons generates energy in our power plants and heats our homes. Derived gasoline and diesel oil propel our cars, trucks, airplanes. Hydrocarbons are also the feedstock for practically every synthetic material from plastics to pharmaceuticals. What nature gives us needs, however, to be processed and modified. We will eventually also need to make hydrocarbons ourselves, as our natural resources are depleted. Many of the processes used are acid-catalyzed, and the chemical reactions involved proceed through positive ion intermediates. Consequently, the knowledge of these intermediates and their chemistry is of substantial significance in both fundamental research and practical science.

Carbocations are the positive ions of carbon compounds. In 1901 Norris[1a] and Kehrmann and Wentzel[1b] independently discovered that colorless triphenylmethyl alcohol gave deep yellow solutions in concentrated sulfuric acid. Triphenylmethyl chloride similarly formed orange complexes with aluminum and tin chlorides. Adolf von Baeyer (Nobel laureate, 1905) should be credited for having recognized in 1902 the saltlike character of the products [Eq. (1)].[1c]

$$Ar_3C{-}X \rightleftharpoons Ar_3C^+ + X^- \qquad (1)$$

He then suggested a correlation between the appearance of color and salt formation—the so-called "halochromy". Gomberg[1d] (who had shortly before discovered the stable triphenylmethyl radical) as well as Walden[1e] contributed to the evolving understanding of the structure of related cationic dyes, such as malachite green **1**.

[*] Prof. Dr. G. A. Olah
Loker Hydrocarbon Research Institute and Department of Chemistry
University of Southern California
Los Angeles, CA 90089-1661 (USA)
Telefax: Int. code +(213) 740-6679

[**] Copyright: The Nobel Foundation 1995. We thank the Nobel Foundation, Stockholm, for permission to print this lecture.

Stable carbocationic dyes were soon found to be present even in nature. The color of red wine as well as of many flowers, fruits, leaves, etc. is due in part to flavylium and anthocyanin compounds formed upon cleavage of their respective glycosides.

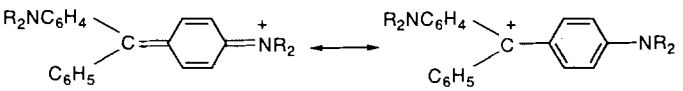

1

The elucidation of the constitution of flavylium and anthocyanin compounds developed from Robinson's and Willstätter's pioneering studies. Werner[1f] formulated the parent benzopyrilium or xanthylium salts **2** and **3** as oxonium salts, while Baeyer[1g] emphasized their great similarity to triarylmethylium salts and considered them carbenium salts. Time has indeed justified both points of view with the realization of the significance of the contribution of both oxonium and carbenium ion resonance forms.

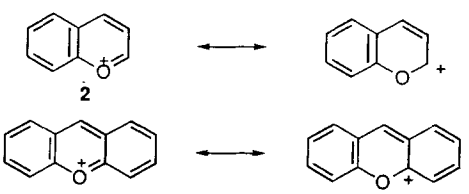

2

3

Whereas the existence of ionic triarylmethyl and related dyes was established at around the turn of the 20th century, the more general significance of carbocations in chemistry was long unrecognized. Triarylmethyl cations were considered as an isolated curiosity of chemistry, not unlike Gomberg's triarylmethyl radicals. Not only were simple hydrocarbon cations believed to be unstable, their fleeting existence was even doubted.

One of the most original and significant ideas in organic chemistry was the suggestion that carbocations (as we now call all the positive ions of carbon compounds) might be intermediates in the course of reactions that start from nonionic reactants and lead to nonionic covalent products.

It was Hans Meerwein[2] who, while studying the Wagner rearrangement of camphene hydrochloride to isobornyl chloride together with van Emster in 1922, found that the rate of the reaction increased with the dielectric constant of the solvent. Further, he found that certain Lewis acid chlorides such as $SbCl_5$, $SnCl_4$, $FeCl_3$, $AlCl_3$, and $SbCl_3$ (but not BCl_3 or $SiCl_4$)

as well as dry HCl, which promote the ionization of triphenylmethyl chloride by formation of carbocationic complexes, also considerably accelerated the rearrangement of camphene hydrochloride (**4**) to isobornyl chloride (**5**). Meerwein concluded that the isomerization actually does not proceed by way of migration of the chlorine atom but by a rearrangement of a cationic intermediate. Hence, the modern concept of carbocationic intermediates was born. Meerwein's views were, however, greeted with much skepticism by his peers in Germany, and he was discouraged from following up on these studies.

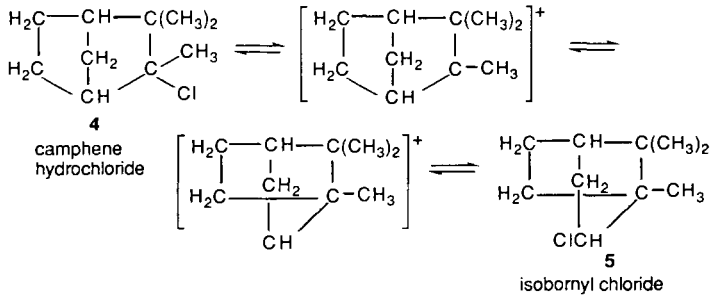

C. K. Ingold, E. H. Hughes, and their collaborators in England started in the late 1920s to carry out detailed kinetic and stereochemical investigations on what became known as nucleophilic substitution at saturated carbon and as polar elimination reactions.[3] Their work relating to unimolecular nucleophilic substitution and elimination called S_N1 and E1 reactions [Eq. (2) and (3)] laid the foundation for the role of electron-deficient carbocationic intermediates in organic reactions.

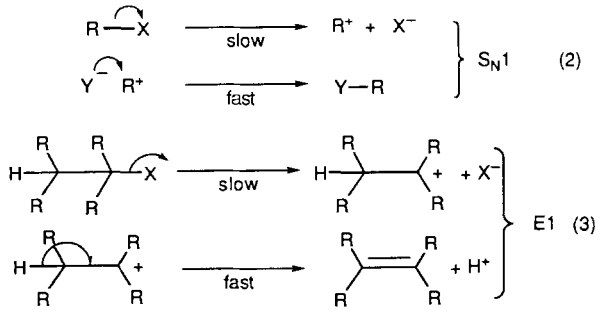

F. C. Whitmore[4] in the US in the thirties generalized these concepts to include many other organic reactions in a series of papers. Carbocations, however, were generally considered to be unstable and transient (short-lived), as they could not be directly observed. Many leading chemists, including Roger Adams, determinedly doubted their existence as real intermediates and strongly opposed even mentioning them. Whitmore consequently never was able in any of his publications in the prestigeous Journal of the American Chemical Society to use the notation of ionic R_3C^+. The concept of carbocations, however, slowly grew to maturity through kinetic, stereochemical, and product studies of a wide variety of reactions. Leading investigators such as P. D. Bartlett, C. D. Nenitzescu, S. Winstein, D. J. Cram, M. J. S. Dewar, J. D. Roberts, P. v. R. Schleyer, and others have contributed fundamentally to the development of modern carbocation chemistry. The role of carbocations as one of the basic concepts of modern chemistry was firmly established and is well reviewed.[5-7] With the advancement of mass spectrometry the existence of gaseous cations was proven, but this could give no indication of their structure or allow extrapolation to solution chemistry. Direct observation and study of stable, long-lived carbocations, such as of alkyl cations in the condensed state remained an elusive goal.

My involvement with the study of carbocations dates back to the fifties and resulted in the first direct observation of alkyl cations and subsequently the whole spectrum of carbocations as long-lived species in highly acidic (superacidic) solutions.[5, 8, 9] The low nucleophilicity of the counteranions (SbF_6^-, $Sb_2F_{11}^-$ etc.) greatly contributed to the stability of the carbocationic salts, which could in some instances even be isolated as crystalline salts. The techniques we developed with superacids to generate stable ions also gained wide application in the preparation of other ionic intermediates (nitronium, halonium, oxonium ions, etc.). At the same time the preparation and study of an ever increasing number of carbocations allowed a general concept of carbocations, which I suggested in a 1972 paper, to evolve. In the same paper I suggested that the cations of carbon compounds be termed "carbocations".[10] "Carbocations" is now the approved[11] (IUPAC) generic name for all cationic carbon compounds. Similarly, the anionic compounds are called "carbanions".

George A. Olah was born in 1927 and educated in Budapest, Hungary. He moved in 1957 first to Canada and then to the USA with the Dow Chemical Company. Since 1977 he has been Director of the Loker Hydrocarbon Research Institute and Distinguished Professor of Organic Chemistry at the University of Southern California, Los Angeles. He is a member of the US National Academy of Sciences, a Foreign Member of the Italian Academia dei Lincei, and an Honorary Member of the Hungarian Academy of Sciences. He received Honorary Doctorates from the University of Durham (England), the University of Munich, the University of Crete (Greece), and his alma mater, the Technical University of Budapest. He is the recipient of many awards including the American Chemical Society Awards in Petroleum Chemistry, Creative Work in Synthetic Organic Chemistry, the Roger Adams Award, and the Nobel Prize in Chemistry, 1994. His research interests are in the area of synthetic and mechanistic organic chemistry, reactive intermediates (carbocations), superacids, and hydrocarbon chemistry. He has published more than 1000 scientific papers, holds 100 patents, and authored or co-authored 15 monographs.

From Acyl Cations to Alkyl Cations

The transient nature of carbocations arises from their high reactivity towards reactive nucleophiles present in the system. The use of counterions with relatively low nucleophilicity, particularly tetrafluoroborate (BF_4^-), enabled Meerwein in the forties to prepare a series of oxonium and carboxonium ion salts, like $R_3O^+BF_4^-$ and $HC(OR)_2^+BF_4^-$, respectively.[12] These Meerwein salts are efficient alkylating agents; they transfer alkyl groups in S_N2-type reactions. However, no acyl ($RCO^+BF_4^-$) or alkyl cation salts ($R^+BF_4^-$) were obtained in Meerwein's studies.

Acetic acid and acetic anhydride were shown to form complexes with Lewis acids such as boron trifluoride. The behavior of acetic acid and acetic anhydride in strong protic acids (sulfuric acid, oleum, perchloric acid, etc.) was also extensively studied. None of these resulted, however, in the isolation or unequivocal characterization of the acetyl cation (or other related homologous acyl cations). F. Seel prepared acetylium tetrafluoroborate[13] for the first time in 1943 by treating acetyl fluoride with boron trifluoride [Eq. (4)].

$$CH_3COF + BF_3 \rightleftharpoons CH_3CO^+BF_4^- \quad (4)$$

In the early fifties, I became interested in organic fluorine compounds while working at the Organic Chemical Institute of the Technical University in Budapest led by the late Professor G. Zemplén, a noted carbohydrate chemist and former student of Emil Fischer (Nobel laureate, 1902) whose "scientific grandson" I can thus consider myself. Zemplén was not very impressed by my ideas, as he thought attempts to study fluorine compounds which necessitated "outrageous" reagents such as hydrogen fluoride to be extremely foolish. Eventually, however, I prevailed and was allowed to convert an open balcony at the rear of the top floor of the chemistry building into a small laboratory, where together with some of my early dedicated associates, A. Pavlath, S. Kuhn, we started up the study of organic fluorides as reagents. Seel's previous work particularly fascinated me. As Zemplén's interest was in glycoside synthesis and related carbohydrate chemistry, I thought that selective α- or β-glycoside synthesis could be achieved by treating either acetofluoroglucose (and other fluorinated carbohydrates) or their relatively stable, deacetylated fluorohydrins with the appropriate aglucons. In the course of the project -COF compounds were needed. As Seel did not seem to have followed up his earlier study, I became interested in exploring acylation with acyl fluorides in general. The work was subsequently extended to alkylation with alkyl fluorides with boron trifluoride as catalyst for Friedel-Crafts type reactions. These studies also aroused my interest in the mechanistic aspects of the reactions, including the complexes of RCOF and RF with BF_3 and subsequently with other Lewis acid fluorides [Eq. (5) and (6)]. Thus, my long fascination with the chemistry of carbocationic complexes began.

$$ArH + RCOF \overset{BF_3}{\rightleftharpoons} ArCOR + HF \quad (5)$$

$$ArH + RF \overset{BF_3}{\rightleftharpoons} ArR + HF \quad (6)$$

Carrying out such research in post-war Hungary was not easy. There was no access to such chemicals as anhydrous HF, FSO_3H, or BF_3, and we had to prepare them ourselves. HF was prepared from fluorspar (CaF_2) and sulfuric acid, and its reaction with SO_3 (generated from oleum) gave FSO_3H. By treating boric acid with fluorosulfuric acid we made BF_3. Handling these reagents and performing this chemistry in a laboratory equipped with the barest of necessities was indeed a challenge. It was only around 1955 through Meerwein, who read some of my early publications, started corresponding with me, and offered his help, that we received a cyclinder of BF_3 gas. What a precious gift it was![14]

My early work with acyl fluorides also involved formyl fluoride, HCOF,[15] which was first prepared by Nesmejanov and Kahn in the thirties,[16] but they did not pursue its use in synthesis. We also prepared a series of higher homologous acyl fluorides and studied their chemistry.[15]

In Friedel-Crafts chemistry when pivaloyl chloride is treated with aromatics in the presence of aluminum chloride, *tert*-butylated products were obtained besides the expected ketones [Eq. (7)].[17]

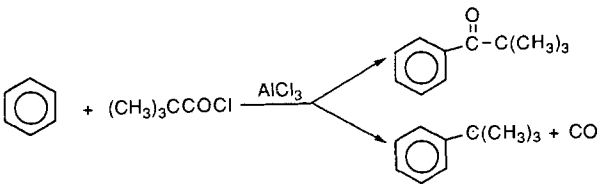

(7)

These were assumed to be formed by decarbonylation of the intermediate pivaloyl complex or cation. In the late fifties, now working at the Dow Chemical Company laboratory in Sarnia, Ontario (Canada), I was able to return to my investigations and extend them by using IR and NMR spectroscopy to study isolable complexes between acyl fluoride and Lewis acid fluoride, including those higher valency Lewis acid fluorides such as SbF_5, AsF_5, PF_5. Consequently, it was not unexpected that the $(CH_3)_3CCOF-SbF_5$ complex we generated showed substantial tendency toward decarbonylation.[18] What was exciting, however, was that we could follow this process by NMR spectroscopy and observe what turned out to be the first stable, long-lived alkyl cation salt, namely, *tert*-butyl hexafluoroantimonate.[18-20]

$$(CH_3)_3CCOF + SbF_5 \longrightarrow (CH_3)_3CCO^+SbF_6 \overset{-CO}{\longrightarrow} (CH_3)_3C^+SbF_6^- \quad (8)$$

This breakthrough was first reported in my 1962 papers[18-19] and was followed by studies that led to methods yielding long-lived alkyl cations in solution.[20] Before recollecting some of this exciting development, however, a brief review of the long quest for these elusive alkyl cations is in order.

Earlier Unsuccessful Attempts To Observe Alkyl Cations in Solution

Until the early sixties alkyl cations were considered only as transient species. Their existence had been indirectly inferred from kinetic and stereochemical studies.[3] No reliable spectro-

scopic or other physical measurements of simple alkyl cations in solution or in the solid state were reported despite decades of extensive studies (including conductivity and cryoscopic measurements). Gaseous alkyl cations had been investigated since the fifties by electron bombardment of alkanes, haloalkanes, and other precursors in mass spectrometric studies, but these investigations, of course, did not provide structural information.[21]

The existence of complexes between Friedel–Crafts alkyl halides and Lewis acid halides had been established from observations, such as Brown's study of the vapor pressure depression of CH_3Cl and C_2H_5Cl in the presence of gallium chloride.[22] The conductivity of aluminum chloride in alkyl chlorides[23] and of alkyl fluorides in boron trifluoride was measured,[24] and the effect of ethyl bromide on the dipole moment of aluminum bromide was studied.[25] However, in no case could well-defined, stable alkyl cation complexes be detected, even at very low temperatures.

Electronic spectra of alcohols and olefins in strong protic acids such as sulfuric acid were obtained by Rosenbaum and Symons.[26] They observed that several simple aliphatic alcohols and olefins give an absorption maximum around 290 nm and ascribed this characteristic absorption to the corresponding alkyl cations. Finch and Symons,[27a] on reinvestigation, however, showed that condensation products, formed with acetic acid (used as solvent for the precursor alcohols and olefins), were responsible for the spectra and not the simple alkyl cations. Moreover, protonated mesityl oxide was also identified as the absorbing species in the isobutylene/acetic acid/sulfuric acid system.

Deno and his coworkers[27b] carried out an extensive study of the fate of alkyl cations formed from alcohols or olefins in undiluted H_2SO_4 and oleum, and showed that equal amounts of a saturated hydrocarbon mixture (C_4 to C_{18}) insoluble in H_2SO_4 and a mixture of cyclopentenyl cations (C_9 to C_{20}) in the H_2SO_4 layer formed. These cations exhibit strong ultraviolet absorption around 300 nm. Olah, Pittman, and Symons subsequently reviewed and clarified the question of electronic spectra of carbocationic systems and the fate of various precursors in different acids.[27c]

At this stage it was clear that all earlier attempts to prove the existence of long-lived, well-defined alkyl cations were unsuccessful in acids such as sulfuric acid, perchloric acid, etc. and at best inconclusive in case of the interaction of alkyl halides with Lewis acid halides. Proton elimination from any alkyl cation formed as intermediate gives an olefin, which then reacts further and can lead to complex systems affecting conductivity, as well as other chemical and physical studies.

It was not realized till the breakthrough in superacid chemistry (see below) that in order to suppress the deprotonation of alkyl cations to olefins [Eq. (9)] and the subsequent formation of very complex systems by reactions such as alkylation, oligomerization, polymerization, and cyclization of olefins with alkyl cations, acids much stronger than those known and used at the time were needed.

$$(CH_3)_3C^+ \rightleftharpoons H^+ + (CH_3)_2C{=}CH_2 \qquad (9)$$

Finding such acids (called "superacids") turned out to be the key to obtaining stable, long-lived alkyl cations and carbocations in general. If any deprotonation were still to take place, however, the alkyl cation (a strong acid) would immediately react with the olefin (a good π-base) to give the multitude of mentioned reactions.

Long-Lived Alkyl Cations from Alkyl Fluorides in Antimony Pentafluoride and Related Conjugate Superacids

The idea that ionization of alkyl fluorides to stable alkyl cations could be possible with an excess of strong Lewis acid fluorides that serve as solvents first came to me while I was working in Hungary in the early fifties and studying the boron trifluoride catalyzed alkylation of aromatics with alkyl fluorides. In the course of these studies I attempted to isolate $RF{:}BF_3$ complexes. Realizing the difficulty to find suitable solvents that would allow ionization but at the same not react with developing, potentially highly reactive alkyl cations, we condensed neat alkyl fluorides with boron trifluoride at low temperatures. At the time I had no access to spectroscopic methods such as IR or NMR, which were still in their infancy. I remember a visit by Costin Nenitzescu (an outstanding but never fully recognized Rumanian chemist, who carried out much pioneering research on acid-catalyzed reactions). We commiserated our lack of access even to an IR spectrometer. (Nenitzescu later recalled sending a cyclobutadiene–Ag^+ complex on the Orient Express to a colleague in Vienna for IR studies, but it decomposed en route.) All we could do at the time on our $RF-BF_3$ systems were conductivity measurements. The results showed that methyl fluoride and ethyl fluoride gave only low conductivity complexes, whereas the isopropyl fluoride and *tert*-butyl fluoride complexes were highly conducting [Eq. (10)]. The latter systems, however, also showed some polymerization (from deprotonation of the involved carbocations to give olefins). Thus, the conductivity data must have been affected by acid formation.[24]

$$R{-}F + BF_3 \rightleftharpoons \overset{\delta+}{R}{-}F \rightarrow \overset{\delta-}{BF_3} \rightleftharpoons R^+BF_4^- \qquad (10)$$

After the defeat of the 1956 Hungarian revolution I escaped with my family and spent some months in London before moving to Canada, where I was able to continue my research at the Dow Chemical Company Research Laboratory in Sarnia, Ontario. After a prolonged, comprehensive search of many Lewis acid halides I finally hit on antimony pentafluoride.[18–20] It turned out to be an extremely strong Lewis acid and for the first time enabled the ionization of alkyl fluorides in solution to stable, long-lived alkyl cations. Neat SbF_5 solutions of alkyl fluorides are viscous, but diluted with liquid sulfur dioxide the solutions could be cooled and studied at $-78\,^{\circ}C$. Subsequently, I also introduced even lower nucleophilicity solvents such as SO_2ClF or SO_2F_2 which allowed studies at much lower temperatures. As sequel to the observation of the decarbonylation of the pivaloyl cation that gave the first spectral evidence for the tertiary butyl cation, *tert*-butyl fluoride was ionized in excess antimony pentafluoride. The solution of the *tert*-butyl cation turned out to be remarkably stable, allowing chemical and spectroscopic studies alike.[28, 29]

In the late fifties the research director of the Canadian Dow laboratories was not yet convinced about the usefulness of NMR spectroscopy. Consequently we had no such instrumentation of our own. Fortunately the Dow laboratories in Midland (Michigan) just 100 miles across the border had excellent facilities run by E. B. Baker, a pioneer of NMR spectroscopy, who offered his help. To probe whether our SbF_5 solution of alkyl fluorides indeed contained alkyl cations, we routinely drove with our samples in the early morning to Midland and watched Ned Baker obtain their NMR spectra. *tert*-Butyl fluoride itself shows a characteristic doublet in its ^1H NMR spectrum due to the fluorine–hydrogen coupling of $J_{H,F} = 20$ Hz. In SbF_5 solution the doublet disappeared and the methyl protons became significantly deshielded from about $\delta = 1.5$ to $\delta = 4.3$. This was very encouraging but not yet entirely conclusive to prove the presence of the *tert*-butyl cation. If one assumes that with SbF_5 *tert*-butyl fluoride forms only a polarized donor–acceptor complex, which undergoes fast fluorine exchange (on the NMR time scale), the fluorine–hydrogen coupling would be "washed out", while still a significant deshielding of the methyl protons would be expected. The differentiation of a rapidly exchanging, polarized donor–acceptor complex from the long sought-after, really ionic $t\text{-}C_4H_9^+SbF_6^-$ thus became a major challenge [Eq. (11)].

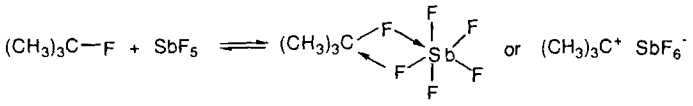

(11)

Ned Baker, despite being himself a physicist, showed great interest in our chemical problem. To solve it, he devised a means to obtain the ^{13}C NMR spectra of our dilute solutions, an extremely difficult task before the advent of Fourier transform NMR techniques. Labeling with carbon-13 was generally possible at the time only to about 50% level (from $Ba^{13}CO_3$). When we prepared 50% ^{13}C-labeled *tert*-butyl fluoride, we could obtain at best only 5% solutions in SbF_5. Thus, the ^{13}C content of the solution was highly diluted. Baker, however, undaunted devised an INDOR (INDOR = internuclear double resonance) method. Using the high sensitivity of the proton signal, he was able by the double resonance technique to observe the ^{13}C shifts of our dilute solutions—a remarkable achievement around 1960! To our great joy the tertiary carbon atom [$\delta(^{13}C) = 335.2$] in $(CH_3)_3CF–SbF_5$ turned out to be more than $\Delta\delta = 300$ deshielded from that of the covalent starting material! Such very large chemical deshielding (the most deshielded ^{13}C signal at the time) could not be reconciled with a donor–acceptor complex. It indicated rehybridization from sp^3 to sp^2 and at the same time showed the effect of significant positive charge on the carbocationic carbon center. For simplicity I am not discussing here the nature of the counterion, which can be a dimer ($Sb_2F_{11}^-$) or even an oligomer, or questions of ion-pairing and separation (concepts developed by Winstein).

Besides the *tert*-butyl cation we also succeeded in preparing and studying the related *sec*-isopropyl and the *tert*-amyl cations [Eq. (12) and (13)]. The isopropyl cation was of particular interest. Whereas in the *tert*-butyl cation the methyl protons are attached to carbons that are adjacent only to the carbocationic center, in the isopropyl cation a proton is directly attached to it. When we obtained the proton NMR spectrum of the $i\text{-}C_3H_7F–SbF_5$ system, the CH proton showed up as an enormously deshielded septet at $\delta = 13.5$, ruling out the possibility of a polarized donor–acceptor complex and indicating the formation of $(CH_3)_2CH^+$ ion. The ^{13}C NMR spectrum was also conclusive showing a very highly deshielded (by $\Delta\delta > 300$) ^+C atom (chemical shift: $\delta(^{13}C) = 320.6$). The spectrum of the *tert*-amyl cation showed an additional interesting feature in the strong long-range H–H coupling of the methyl protons adjacent to the carbocationic center with the methylene protons. If only the donor–acceptor complex were involved, such long range coupling through an sp^3 carbon would be small (1–2 Hz). Instead the observed significant coupling ($J_{H,H} = 10$ Hz) indicated that the species studied indeed had an sp^2 center through which the long-range H–H coupling became effective. Figure 1 reproduces the ^1H NMR spectra of the *tert*-butyl, *tert*-amyl, and isopropyl cations. These original spectra are framed and hung in my office as a momento, as is the ESCA spectrum of the norbornyl cation (see below).

$$(CH_3)_2CHF + SbF_5 \longrightarrow (CH_3)_2CH^+SbF_6^- \quad (12)$$

$$(CH_3)_2CFCH_2CH_3 + SbF_5 \longrightarrow (CH_3)_2\overset{+}{C}CH_2CH_3SbF_6^- \quad (13)$$

Our studies also included an IR spectroscopic investigation of the observed ions (Fig. 2).[29] John Evans, at the time a spectroscopist at the Midland Dow laboratories, offered his cooperation and was able to obtain and analyze the vibrational spectra of our alkyl cations. It is rewarding to see that some thirty years later FTIR spectra obtained by Denis Sunko and his colleagues in Zagreb with low-temperature matrix-deposition techniques and Schleyer's calculations of the spectra show good agreement with

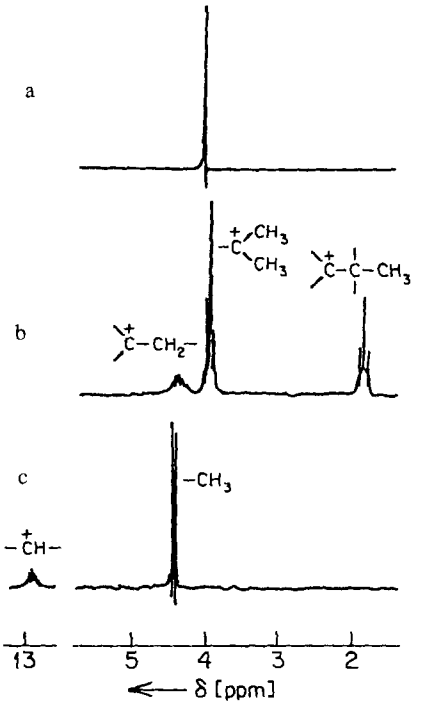

Fig. 1. ^1H NMR spectra (60 MHz, in SbF_5/SO_2ClF solution, −60 °C) of a) the *tert*-butyl cation [trimethylcarbenium ion, $(CH_3)_3C^+$], b) the *tert*-amyl cation [ethyldimethylcarbenium ion, $(CH_3)_2C^+–C_2H_5$], and c) the isopropyl cation [dimethylcarbenium ion, $(CH_3)_2C^+–H$].

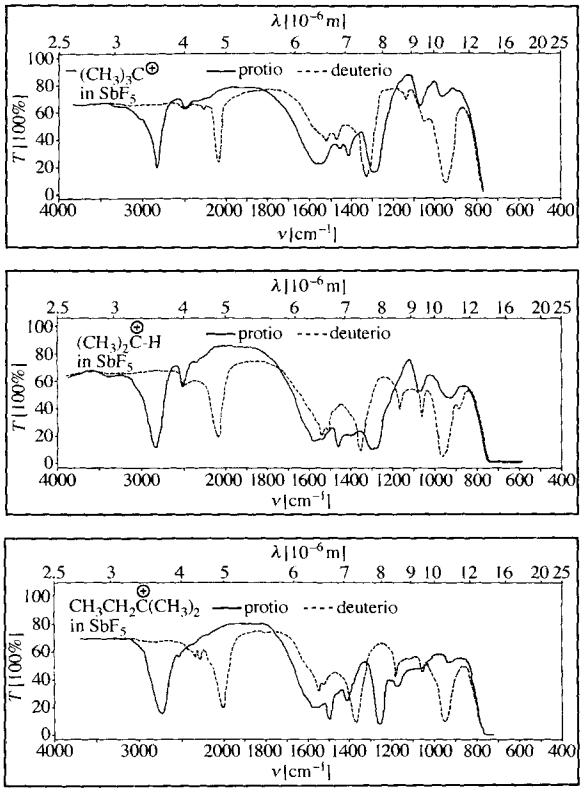

Fig. 2. IR spectra of *tert*-butyl (top), isopropyl (center), and *tert*-amyl (bottom) cations. T = transmission.

our early work, even though our work was carried out in neat SbF_5 at room temperature long before the advent of the FTIR methods.[30]

Subsequently in 1968–1970 with Jack DeMember and August Commeyras[31] we were able to carry out more detailed IR and laser Raman spectroscopic studies of alkyl cations. Comparison of the data of unlabeled and deuterium-labeled *tert*-butyl cations (**6**) with those of isoelectronic trimethylboron (**7**) proved the planar structure of carbocation **6** (Table 1).

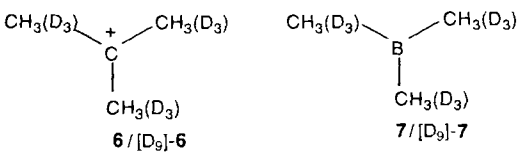

6 / [D9]-**6** **7** / [D9]-**7**

This was also an early example of the realization that for nearly all carbocations there exist neutral isoelectronic isostructural boron analogues, which later in the hands of R. E. Williams and others proved so useful.

When in the summer of 1962 I was able for the first time to present our work in public at the Brookhaven Organic Reaction Mechanism Conference[28a] and subsequently in a number of other presentations and publications,[28b–e, 29] I had convincing evidence to substantiate that after a long and frequently frustrating search stable, long-lived alkyl cations had finally been obtained in superacidic solutions.

The chemistry of stable, long-lived carbocations as they became known, began and its progress became fast and wide spread. In an industrial laboratory, publication of research is not always easy. I would therefore like to thank the Dow Chemical Company for allowing me not only to carry out the work, but also to publish the results.

After successful preparation of long-lived, stable carbocations in antimony pentafluoride solutions, the work was extended to a variety of other superacids. Protic superacids such as FSO_3H (fluorosulfuric acid) and CF_3SO_3H (triflic acid) as well as conjugate acids such as $HF–SbF_5$, $FSO_3H–SbF_5$ (Magic Acid), $CF_3SO_3H–SbF_5$, and $CF_3SO_3H–B(O_3SCF_3)_3$, were extensively used to ionize precursors, including alcohols. Superacids based on fluorides such as AsF_5, TaF_5, and NbF_5, and other strong Lewis acids such as $B(O_3SCF_3)_3$ were also successfully introduced. The name Magic Acid for the $FSO_3H–SbF_5$ system was given by J. Lukas, a German post-doctoral fellow working with me in Cleveland in the sixties, who after a laboratory party put remainders of a Christmas candle into the acid. The candle dissolved and the resulting solution gave an excellent NMR spectrum of the *tert*-butyl cation. This observation understandably evoked much interest, and hence he termed the acid "Magic". The name stuck in our laboratory. I think it was Ned Arnett who subsequently introduced the name into the literature where it increasingly became used. When a former graduate student of mine, J. Svoboda, started a small company (Cationics) to make some of our ionic reagents commercially, he obtained trade name protection for Magic Acid, and it has been marketed as such since.

Many contributed to the study of long-lived carbocations. The field rapidly expanded and allowed successful study of practically any carbocationic system. Time does not allow crediting here all my former associates and the many researchers around the world who contributed so much to the development of the field. Their work can be found in the extensive literature. I would like, however, to specifically mention the pioneering work of D. M. Brouwer and H. Hogeveen, as well as their colleagues at the Shell Laboratories in Amsterdam in the sixties and seventies. They contributed fundamentally to the study of long-lived carbocations and related superacidic hydrocarbon chemistry. The first publication from the Shell laboratories on alkyl cations appeared in *Chemical Communications* in 1964,[32] following closely my initial reports of 1962–1964. Similarly,

Table 1. Raman and IR frequencies $\tilde{\nu}$[cm^{-1}] of **6**/[D_9]-**6** and **7**/[D_9]-**7**.

Species	$\nu_1,\nu_{12},\nu_7,\nu_{19}$	ν_2,ν_{13}	ν_{21}	ν_{14}	ν_{15}	ν_{17}	ν_5	ν_{16}	ν_6	ν_9	ν_{10}	ν_{18}
$(CH_3)_3C^+$ **6**	2947	2850		1450		1295			667		347	306
$(CH_3)_3B$ **7**	2975	2875	1060	1440	1300	1150	906	866	675	973 (486?)	336 [a]	320
$(CD_3)_3C^+$ [D_9]-**6**	2187	2090		1075		980			720		347	300
$(CD_3)_3B$ [D_9]-**7**	2230	2185		1033	1018	1205			620	870	(289) [b]	(276) [b]

[a] IR frequency. [b] Calculated.

I would like to emphasize the fundamental contributions of R. J. Gillespie to strong acid (superacid) chemistry[33] and also his generous help while I was working at the Dow Laboratories in Canada. I reestablished contact with him during this time after we first met in the winter of 1956 at University College in London where he worked with C. K. Ingold. Subsequently, he moved to McMaster University in Hamilton, Ontario. In the late fifties he already had an NMR spectrometer and in our study of SbF_5 containing highly acidic systems of carbocations we were gratified by his help to run some of our spectra on his instrument. His long-standing interest in fluorosulfuric acid and our studies in SbF_5-containing systems found common ground in studies of FSO_3H–SbF_5 systems.[34] It was also Gillespie who suggested calling protic acids stronger than 100% sulfuric acid as superacids.[33] This arbitrary, but most useful definition is now generally used. It should be pointed out, however, that the name "superacid" goes back to J. B. Conant of Harvard who used it in 1927 to denote acids such as perchloric acid, which he found stronger than conventional mineral acids and capable of protonating even such weak bases as carbonyl compounds.[35] Our book "Superacids" published in 1985 with Surya Prakash and Jean Sommer[33c] was appropriately dedicated to the memory of Conant. Few of today's chemists are aware of his contributions to this field.

My memories of the already mentioned 1962 Brookhaven Mechanism Conference,[28a] where I first reported on long-lived carbocations in public, are still clear in my mind. The scheduled "main event" of the meeting was the continuing debate between Saul Winstein and Herbert C. Brown (the pioneer of hydroboration chemistry, Nobel laureate, 1979) on the classical or nonclassical nature of some carbocations (or carbonium ions as they were still called at the time).[36] It must have come to them and others in the audience as quite a surprise that a young chemist from an unknown industrial laboratory was invited to give a major lecture and claimed to have obtained and studied stable, long-lived "carbonium" ions (i.e., carbocations) by the simple new method of using a highly acidic (superacidic) system. I remember being called aside separately by both Winstein and Brown during the conference and cautioned that a young chemist should be exceedingly careful making such claims. Each pointed out that most probably I was mistaken and could not have obtained long-lived carbonium ions. Just in case, however, my method should turn out to be real, I certainly would obtain evidence for the "nonclassical" or "classical" nature, of the much disputed 2-norbornyl cation (**8**, see Scheme 1). Their much heralded controversy[36b, c] centered around the question whether the experimentally observed, significant rate enhancement of the hydrolysis of 2-*exo*- over 2-*endo*-norbornyl esters and high *exo* selectivity in the system were caused, as suggested by Winstein, by σ participation of the C_1–C_6 single bond with delocalization to a bridged nonclassical ion or only by steric hindrance in the *endo* system and involving equilibrating classical trivalent ions. Nonclassical ions, a term first used by J. D. Roberts,[37] were suggested by P. D. Bartlett to contain too few electrons to allow a pair for each "bond", that is, in the ground state they must contain delocalized σ electrons.[36a] As my method allowed us to prepare carbocations as long-lived species, clearly the opportunity was given to decide the question experimentally through direct observation of the ion. At the time I had obtained only the proton spectrum of 2-norbornyl fluoride in SbF_5 at room temperature, which displayed a single, broad peak indicating complete equilibration through hydride shifts and Wagner–Meerwein rearrangement (well-known in solvolysis reactions and related transformations of 2-norbornyl systems). However, my curiosity was aroused and subsequently when in 1964 I transferred to Dow's Eastern Research Laboratory (established under Fred McLafferty as laboratory director first in Framingham, MA, and then moved to Weyland, MA), the work was further pursued in cooperation with Paul Schleyer from Princeton University and Marty Saunders from Yale University.[38a] Paul, who became a life-long friend, had, even at that time, a knack of acting as the catalyst to initiate cooperative efforts. Using SO_2 as solvent, we were able to lower the temperature of our solution to $-78\,^{\circ}C$ and also prepared the ion by ionization of cyclopentenylethyl fluorides or by protonation of nortricyclene in $FSO_3H/SbF_5/SO_2ClF$ (Scheme 1).

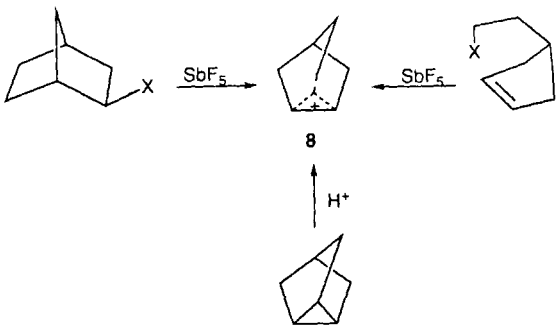

Scheme 1.

I still did not have access to suitable low temperature instrumentation to carry out needed NMR studies, but Marty Saunders did. Thus, our samples now traveled the Massachusetts turnpike to New Haven, where Saunders was able to study solutions of the norbornyl cation at increasingly low temperatures using his own home-built NMR instrumentation housed in the basement of the Yale chemistry building. We were able to obtain NMR spectra of the ion at $-70\,^{\circ}C$, where the 3,2-hydride shift was frozen out. It took, however, till 1969 following my move to Cleveland to Case Western Reserve University to develop efficient low-temperature techniques with solvents such as SO_2ClF and SO_2F_2, to obtain high resolution ^1H and ^{13}C NMR spectra of the 2-norbornyl cation eventually down to $-159\,^{\circ}C$ in supercooled solutions.[38b, c] Both 1,2,6-hydride shifts and the Wagner–Meerwein rearrangement could be frozen out at such a low temperature and the static, bridged ion was observed (Figs. 3a and 3b).[38c]

The differentiation of bridged, nonclassical from rapidly equilibrating classical carbocations based on NMR spectroscopy is difficult, since NMR is a relatively slow physical method with a limited time scale. We addressed this question in some detail in our work by comparing estimated shifts of the two systems with model systems.[38b, c] Of course these days this task is greatly simplified by highly efficient theoretical methods such as IGLO and GIAO to calculate NMR shifts of ions and comparing them with the experimental data.[38d] It is rewarding

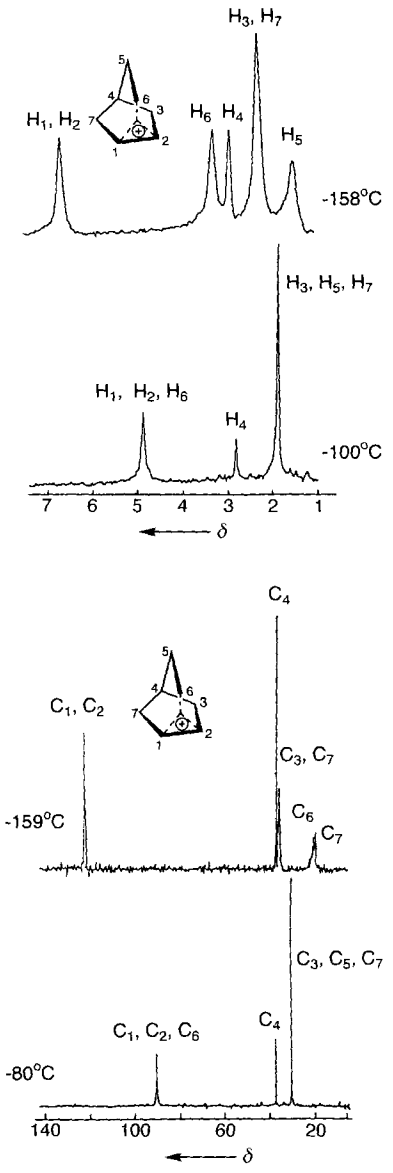

Fig. 3. Top: 395 MHz ^{1}H NMR spectra of the 2-norbornyl cation in $SbF_5/SO_2ClF/SO_2F_2$ solution. Bottom: 50 MHz, proton-decoupled ^{13}C NMR spectra of 2-norbornyl cation (^{13}C enriched) in $SbF_5/SO_2ClF/SO_2F_2$ solution.

to see that our results and conclusions stood up well to comparison with all the more recent studies.

As mentioned, we carried out IR studies (using fast vibrational spectroscopy) early in our work on carbocations. In our studies of the norbornyl cation we also obtained Raman spectra,[38b] and although at the time it was not possible to calculate the spectra theoretically, comparison with model compounds (2-norbornyl system and notricyclene) indicated the symmetrical, bridged nature of the ion. Sunko and Schleyer recently were able to obtain the FTIR spectrum in elegant studies and compare it with theoretical calculations.[30]

Kai Siegbahn's (Nobel laureate in Physics, 1981) core electron spectroscopy (ESCA) was another fast physical method we applied to resolve the question of bridged vs. rapidly equilibrating ions. We were able to study carbocations in the late sixties by this method, adapting it to superacidic matrixes. George Mateescu and Louise Riemenschneider in my Cleveland laboratory established ESCA instrumentation and the needed methodology for obtaining the ESCA spectra of a number of carbocations, including the *tert*-butyl and the 2-norbornyl cation in SbF_5-based superacidic matrixes (Fig. 4).[39] These studies again convincingly showed the nonclassical nature of the 2-norbornyl cation, because no trivalent carbenium ion center was observed in the ESCA spectrum characteristic of a classical ion, such as is the case for the *tert*-butyl cation. Although again some criticism was leveled at our work by proponents of the equilibrating classical-ion concept, subsequent studies by Dave Clark fully justified our results and conclusions.[39c] So did a comparison of theoretical calculations with the experimental data.

It is proper to mention here some significant, more recent studies. Saunders's studies showed the absence of deuterium

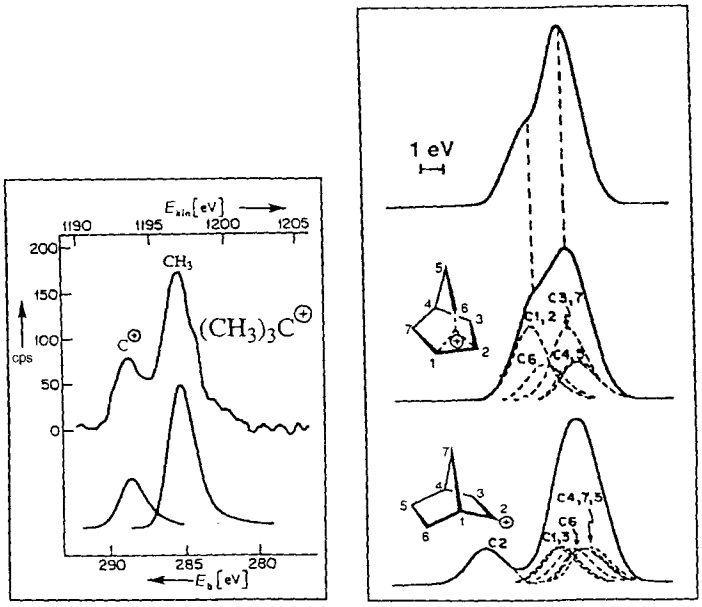

Fig. 4. Left: Carbon 1s photoelectron spectrum of the *tert*-butyl cation (top curve from experiment; bottom curve calculated). Right: 1s core-hole-state spectra for the 2-norbornyl cation (top), and Clark's simulated spectra for the classical (center) and nonclassical ions (bottom).

isotopic perturbation, as anticipated for a classical equilibrating system.[40] Myhre and Yannoni[41] at very low (5 K!) temperatures were able to obtain solid state ^{13}C NMR spectra that showed no indication of freezing out any equilibrating classical ions; the barriers at this temperature should be as low as 200 cal mol^{-1} (the energy of a vibrational transition). Laube was able to carry out single crystal X-ray structural studies on substituted 2-norbornyl cations.[42] Schleyer's theoretical studies,[38d] includng IGLO and related calculation of NMR shifts and their comparison with experimental data, contributed further to the understanding of σ-bridged carbonium ion nature of the 2-norbornyl cation. (The classical 2-norbornyl cation was not even found to be an energetically high-lying intermediate!) So did Arnett's calorimetric studies.[43] In a 1983 paper entitled "Conclusion of the Norbornyl Ion Controversy" with Prakash and Saunders we were able to state[44] that "all these studies unequivocally ended the so-called nonclassical-ion controversy". Winstein's original views were fully justified by the extensive structural studies made possible through my "stable ion" chemistry.

Although many believe that too much effort was expended on this problem, in my view the norbornyl ion controversy had significant consequences for chemistry. It not only helped to extend the limits of available techniques for structural studies and theoretical calculations, but also laid the foundation for the chemistry of C–H and C–C single bonds with electrophiles and thus of saturated hydrocarbons (see below).

Intensive, critical studies of a controversial topic always help to eliminate the possibility of any errors. One of my favorite quotations is that by Georg von Békésy (Nobel laureate in Physiology and Medicine, 1961).[45]

> "[One] way of dealing with errors is to have friends who are willing to spend the time necessary to carry out a critical examination of the experimental design beforehand and the

results after the experiments have been completed. An even better way is to have an enemy. An enemy is willing to devote a vast amount of time and brain power to ferreting out errors both large and small, and this without any compensation. The trouble is that really capable enemies are scarce; most of them are only ordinary. Another trouble with enemies is that they sometimes develop into friends and lose a good deal of their zeal. It was in this way the writer lost his three best enemies. Everyone, not just scientists, need a few good enemies!"

Clearly there was no lack of devoted adversaries (perhaps a more proper term than enemies) on both sides of the norbornyl controversy. It is to their credit that we know probably more today about the structure of carbocations such as the norbornyl cation than of any other chemical species. Their efforts resulted in the most rigorous studies and the development or improvement of many techniques.

To me the most significant consequence of the norbornyl cation studies was the realization that C–H and C–C single bonds can act as two-electron σ donors not only in intramolecular but also in intermolecular transformations and electrophilic reactions. Two-electron, three-center (2e–3c) bonding (familiar in boron and organometallic chemistry) is the key for these reactions. Much new chemistry rapidly evolved, and the broad scope and significance of the chemistry of hypercoordinated carbon compounds (in short hypercarbon) was recognized.[46]

The General Concept of Carbocations

The study of carbocations by direct observation of long-lived species and related superacid chemistry made it apparent that the carbocation concept is wider than previously thought and needed a more general definition, which I offered in a 1972 paper.[10] The definition takes into account the existence of two major limiting classes of carbocations with a continuum of species with different degrees of delocalization bridging them.

a) Trivalent "classical" carbenium ions contain an sp^2-hybridized electron-deficient carbon atom, which tends to be planar in the absence of constraining skeletal rigidity or steric interference. (It should be noted that sp-hybridized, linear oxocarbonium ions and vinyl cations also show substantial electron deficiency on carbon). The carbenium carbon center contains six valence electrons and is thus highly electron deficient. The structure of trivalent carbocations can always be adequately described by using only two-electron, two-center bonds (Lewis valence bond structures). CH_3^+ is the parent trivalent ion.

b) Pentacoordinated (or higher coordinated) "nonclassical" carbonium ions, which contain five (or more coordinated carbon atoms. They cannot be described by two-electron, two-center single bonds alone, but also necessitate the use of two-electron, three- (or multi-) center bonding. The carbocation center is always surrounded by eight electrons, but overall the carbonium ions are electron-deficient because two electrons are shared between three (or more) atoms. CH_5^+ can be considered the parent for carbonium ions.

Subsequently in 1977 Brown and Schleyer offered a related definition:[36c]

"A nonclassical carbonium ion is a positively charged species which cannot be represented adequately by a single Lewis structure. Such a cation contains one or more carbon or hydrogen bridges joining the two electron-deficient centers. The bridging atoms have coordination numbers higher than usual, typically five or more for carbon and two or more for hydrogen. Such ions contain two-electron, three- (or multiple-) center bonds including a carbon or hydrogen bridge."

Lewis's concept that a covalent chemical bond consists of a pair of electrons shared between the two atoms became a cornerstone of structural chemistry. Chemists tend to brand compounds as anomalous if their structures cannot be depicted in terms of such bonds alone. Carbocations with too few electrons to allow a pair for each "bond" came to be referred to as nonclassical, a name first used by J. D. Roberts[37] for the cyclopropylcarbinyl cation and adapted by Winstein to the norbornyl cation.[47] The name is still used even though it is now recognized that like other compounds, they adopt the structures appropriate for the number of electrons they contain with two-electron, two- or three- (even multi-) center bonding (not unlike the bonding principles for boron compounds established by Lipscomb, Nobel laureate, 1976). The terms classical and nonclassical are expected, however, to fade away gradually as the general nature of bonding becomes recognized.

Whereas the differentiation of trivalent carbenium, and pentacoordinated carbonium ions serves a useful purpose to define them as limiting ions, it should be clear that in carbocationic systems varying degrees of delocalization always exist. This can involve participation by neighboring n-donor atoms, π-donor groups, or σ-donor C–H or C–C bonds.

Carbocations

trivalent "classical" ions (carbenium ions) CH_3^+ is parent	pentacoordinated (or higher) "nonclassical" ions (carbonium ions) CH_5^+ is parent

Trivalent carbenium ions are the key intermediates in reactions of unsaturated π-donor hydrocarbons with electrophiles. At the same time pentacoordinated carbonium ions are the key to reactions of saturated σ-donor hydrocarbons with electrophiles. The ability of single bonds to act as electron donors lies in their ability to form carbonium ions by two-electron, three-center (2e–3c) bond formation.

Expansion of the carbon octet through 3d orbital participation does not seem possible; there can be only eight valence electrons in the outer shell of carbon, a small, first row element.[46] The valency of carbon cannot exceed four. Kekulé's concept of the tetravalency of carbon in bonding terms represents attachment of four atoms (or groups) involving 2e–2c Lewis-type bonding. There is, however, nothing that prevents carbon from also participating in multicenter bonding. Pentacoordination (or higher) of carbon implies five (or more) atoms or ligands simultaneously attached to it within reasonable bonding distance.[46]

Neighboring group participation with the vacant p orbital of a carbenium ion center contribute to its stabilization through

delocalization, which can involve atoms with unshared electron pairs (n-donors), π-electron systems (direct conjugative or allylic stabilization), bent σ-bonds (as in cyclopropylcarbinyl cations), and C–H and C–C σ-bond hyperconjugation. Trivalent carbenium ions, with the exception of the parent CH_3^+, therefore always show varying degrees of delocalization without becoming pentacoordinated carbonium ions. The limiting cases define the extremes of the spectrum of carbocations (Scheme 2).

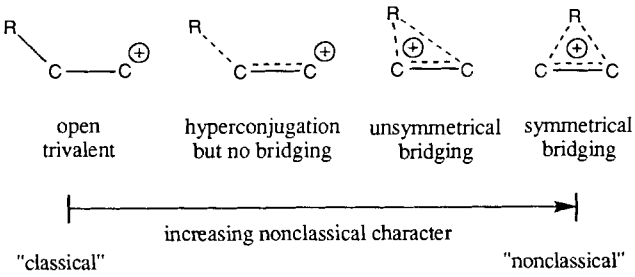

Scheme 2.

The Role of Carbocations in Electrophilic Reactions

Acid-catalyzed electrophilic reactions and transformations such as isomerization, alkylation, substitution, addition, elimination, rearrangements, etc. involve carbocationic intermediates. Many of these reactions also gained significance in industrial applications. Aromatic hydrocarbon chemistry and that based on acetylene laid the foundation for industrial organic chemistry a century ago. Subsequently olefin-based chemistry took on great significance. In all this chemistry reactive π-bonded systems are the electron donor substrates. In electrophilic reactions they readily form trivalent carbocationic intermediates [Eq. (14) and (15)].

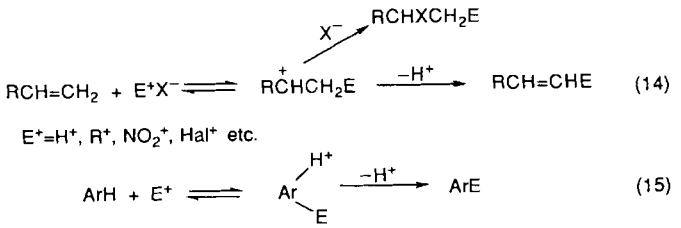

The discovery of pentacoordinate carbonium ions discussed previously led to the realization that they play an important role not only in understanding the structure of nonclassical ions, but more importantly as the key to electrophilic reactions at single bonds, for example, of saturated aliphatic hydrocarbons (alkanes and cycloalkanes). Such reactions include not only acid-catalyzed hydrocarbon isomerizations, fragmentations, cyclizations, but also substitutions and related electrophilic reactions and transformations.

In ionization of β-phenylethyl systems, neighboring π-orbital participation with the carbocationic center occurs, which can be considered as intramolecular π-alkylation giving Cram's phenonium ions. The corresponding ionization of 2-norbornyl systems involves participation of a properly oriented C–C single bond (that is, intramolecular σ-alkylation) giving the bridged ion (Scheme 3).

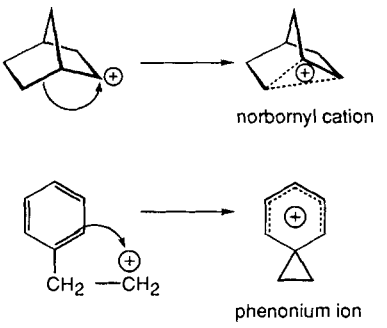

Scheme 3.

Alkylation of π systems in Friedel–Crafts type reactions (either by an inter- or intramolecular route) has long been widely known and well studied. To extend these relationships it was logical to ask why intermolecular alkylation (and other electrophilic reactions) of σ-donor hydrocarbons could not be affected (Scheme 4).

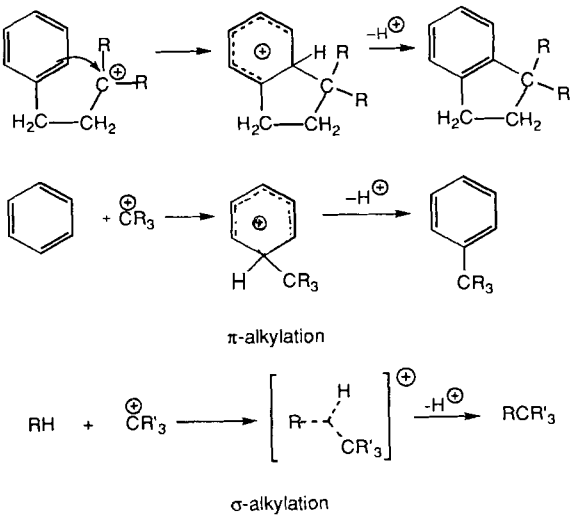

Scheme 4.

Our studies in the late sixties and early seventies for the first time provided evidence for the general reactivity of covalent C–H and C–C single bonds of alkanes and cycloalkanes in various protolytic processes as well as in hydrogen–deuterium exchange, alkylation, nitration, halogenation, etc. [Eq. (16) and (17)]. This reactivity is due to the σ-donor ability (σ basicity) of single bonds, which allows bonds to share their bonded electron pairs with an electron-deficient reagent in two-electron, three-center bond formation. The reactivity of single bonds thus stems from their ability to participate in the formation of pentacoordinate carbonium ions. Subsequent cleavage of the three-center

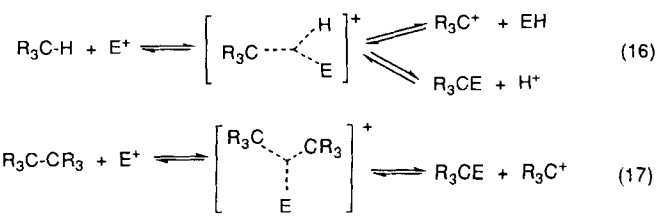

bond in a C H reaction results in formation of substitution products, whereas C–C reaction results in bond cleavage and formation of a fragment carbenium ion, which then can react further.

As bond-to-bond shifts can readily take place through the low barriers within five coordinate carbonium ions, the intermediates can be more complex but always involve interconverting carbonium ions.

Superacidic hydrocarbon chemistry under conditions favoring carbocationic intermediates is also gaining in significance in practical applications. Isomerization of alkanes at relatively low temperature, a much improved and environmentally adaptable alkylation, new approaches to the functionalization of methane and possibilities in its utilization as a building block for higher hydrocarbons and their derivatives, as well as moderate conditions for coal liquefaction are just a few examples to be mentioned here.[48]

Protosolvolytic Activation of Carbocationic Systems

Carbocations are electrophiles, that is, electron-deficient compounds. In electrophilic reactions of unsaturated, π-donor hydrocarbons and their derivatives (such as acetylenes, olefins, aromatics) the reaction with the electrophilic reagents is facilitated by the nucleophilic assistance of the substrates. In reactions with increasingly weaker (deactivated) π-donors and even more so with only weakly electron-donating saturated hydrocarbons (σ-donors), the electrophile itself must provide the driving force for the reactions. Hence the need for very strongly electron-demanding electrophiles and comparably low nucleophilicity reaction media (such as superacidic systems).

It was only more recently realized[49] that electrophiles capable of further interaction (coordination, solvation) with strong Brønsted or Lewis acids can be greatly activated. The resulting enhancement of reactivity can be very significant compared to that of the parent electrophiles under conventional conditions and indicates *superelectrophile* formation, that is, electrophiles with greatly enhanced electron deficiency (frequently of dipositive nature). I have reviewed[49] elsewhere the superelectrophilic activation of various electrophiles and will not discuss it here, except for some superelectrophilic activation which can also affect the reactivity of carbocations.

In carboxonium ions, originally studied by Meerwein, alkyl groups of an alkyl cation, such as the *tert*-butyl cation, are replaced by alkoxy, such as methoxy groups. The methoxy groups delocalize charge (by neighboring oxygen participation) and thus make these ions increasingly more stable:

$$(CH_3)_3C^+ < (CH_3)_2\overset{+}{C}OCH_3 < CH_3\overset{+}{C}(OCH_3)_2 < {}^+C(OCH_3)_3$$

At the same time their reactivity as carbon electrophiles decreases. For example, they do not alkylate aromatics or other hydrocarbons. Strong oxygen participation thus greatly diminishes the carbocationic nature.

Neighboring oxygen participation, however, can be decreased if a strong acid protosolvates (or protonates) the nonbonded oxygen electron pairs [Eq. (18)]. Consequently, carboxonium ions (and related ions such as acyl cations) in superacidic media

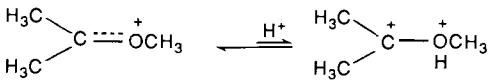

(18)

show greatly enhanced carbon electrophilic reactivity indicative of dicationic nature.

Similarly halogen-substituted carbocations, such as the trichloromethyl cation Cl_3C^+,[50] are greatly stabilized by n–p back donation (not unlike BCl_3). They can also be greatly activated by superacidic media, which protosolvate (protonate) the nonbonded halogen electron pairs, thus diminishing neighboring halogen participation [Eq. (19)].

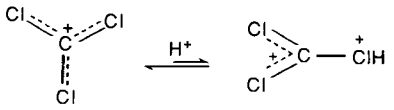

(19)

This explains for example why carbon tetrachloride highly enhances the reactivity of protic superacids for alkane transformations. Lewis acids have similar activating effect.[49]

Alkyl cations themselves, in which only hyperconjugative C–H or C–C single bond interactions stabilize the electron-deficient center, are activated by superacidic solvation. Results of theoretical calculations and hydrogen–deuterium exchange of long-lived alkyl cations in deuterated superacids, under conditions where no deprotonation–reprotonation can take place substantiate the existence of these protoalkyl dications as real intermediates [Eq. (20)].[51]

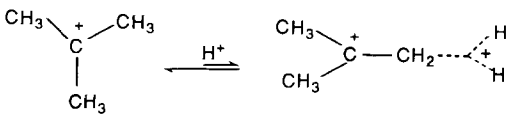

(20)

The widely recognized high reactivity of alkanes for isomerization alkylation reactions in strongly acidic media is very probably assisted by protosolvation of the intermediate alkyl cations. Similar activation can be involved in other acid-catalyzed hydrocarbon transformations, which are preferentially carried out in solutions containing excess acid.

Activation by Solid Superacids and Possible Relevance to Enzymatic Systems

The chemistry of carbocations and their activation was discussed so far in superacidic solutions. However, superacidic systems are not limited to solution chemistry. Solid superacids, possessing both Brønsted and Lewis acid sites, are of increasing significance. They range from supported or intercalated systems, to highly acidic perfluorinated resinsulfonic acids (such as Nafion-H and its analogues) to certain zeolites (such as H-ZSM-5).

To explain why their remarkable activity, for example in catalytic transformations of alkanes (even methane), an appraisal of the de facto activity at the acid sites of such solid acids is called for.[49]

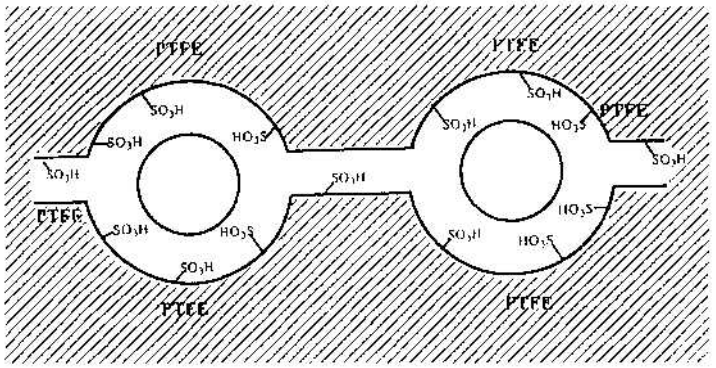

Fig. 5. Clustered SO_3H acid sites in a perfluorinated resinsulfonic acid.

Nafion-H is known to contain acidic SO_3H groups clustered together (Fig. 5).

H-ZSM-5, which also displays superacidic activity, was found by Haag et al.[52] to isomerize and alkylate alkanes readily (H_2 was observed as the protolytic by-product in stoichiometric amounts). In this zeolite, active Brønsted and Lewis acid sites are again in close proximity, approximately 2.5 Å apart (Fig. 6).

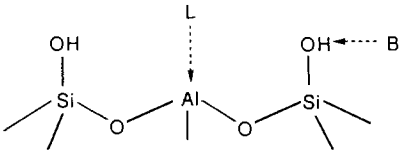

Fig. 6. Brønsted (B) and Lewis acid sites (L) in zeolites.

It is reasonable that in these (and other) solid superacid catalyst systems, bi- or multidentate interactions forming highly reactive intermediates is possible. This amounts to the solid-state equivalent of protosolvation (protonation).[49]

Nature is able to perform its own transformations in ways which chemists have only begun to understand and cannot yet come close to duplicating. At enzymatic sites many significant transformations take place which are acid-catalyzed (including electron-deficient metal-ion-catalyzed processes). Because of the unique structure at enzymatic sites bi- and multidentate interactions must be possible; the concepts discussed here thus may also have relevance to our understanding of some enzymatic processes.[49]

Conclusions

The chemistry of long-lived carbocations became a very active and fast developing field with contributions by researchers from all around the world. It is with understandable satisfaction that I look back at the progress achieved and the possibilities ahead. What started out as a for one of the most significant class of chemical reaction intermediates, the carbocations, as long-lived species and a study of their structure, led subsequently to the development of the general concept of the reactivity of single bonds, such as C–H and C–C bonds, with electrophiles and related superacidic hydrocarbon chemistry.

Despite all the progress that has been made I believe that most exciting chemistry in the field still lies ahead for future generations to explore. I wish them as much excitement and satisfaction in their work as I had.

The concept of the tetravalency of carbon stated by Kekulé well over a century ago remains an essential foundation of organic chemistry. Carbon, as a small first row element, cannot extend its valance shell, and the octet rule allows formation of only four two-electron, two-center (2e–2c) Lewis-type bonds (or their equivalent multiple bonds). It is, however, possible for one (or more) electron pair of carbon to be involved in two-electron, three-center (2e–3c) bonding.[46] This allows carbon to simultaneously bond five (or even six) atoms or groups. This is the case in carbonium ions which contain hypercarbon (hypercoordinate carbon). It also provides the key to understanding the rapidly emerging chemistry of saturated hydrocarbons with electrophiles, including that of the parent methane and of C–H and C–C bonds in general. Whereas hypercoordinate carbocations are 8e carbon systems that do not violate the octet rule, carbanionic S_N2 transition states $[Y\cdots CR_3\cdots X]^-$ are 10e systems and thus cannot be intermediates.

I wrote more than twenty years ago[9] "The realization of the electron donor ability of shared (bonded) electron pairs (single bonds) could one day rank equal in importance with G. N. Lewis' realization of the electron donor unshared (nonbonded) electron pairs (or for this reason I could add the electron pairs involved in multiple bonding). We can now not only explain the reactivity of saturated hydrocarbons and single bonds in general electrophilic reactions, but indeed use this understanding to explore new areas and reactions of carbocation chemistry." It is with some satisfaction that I feel this promise is being fulfilled.

I was fortunate to be able to build on the foundations laid by many. I would like to acknowledge particularly the fundamental contributions of Hans Meerwein (1879–1965) and Christopher Kelk Ingold (1893–1970), who recognized the role of carbocations in some chemical reactions, and Frank Whitmore (1887–1947), who generalized it to many others. I am also greatly indebted to all my former students and associates, whose dedication, hard work, and major scientific contributions made our joint effort possible. My wife Judy till her retirement was not only an integral part of our scientific effort. All those who ever worked in the Olah group appreciated greatly her warmth, caring, and concern for our "scientific family". In our 20 years of association from brilliant graduate student to trusted friend and colleague, G. K. Surya Prakash made invaluable contributions. The Loker Hydrocarbon Research Institute of the University of Southern California provided a wonderful home and support for our work in the last 15 years. The board of the Institute, particularly Mrs. Katherine Loker, Harold Moulton, and Carl Franklin are thanked for their support and friendship over the years. I also cherish close association with such wonderful colleagues and friends as Ned Arnett, Joseph Casanova, Paul Schleyer, Jean Sommer, Peter Stang, Ken Wade, and Robert Williams, who are senior distinguished fellows of the Loker Institute. The National Institutes of Health and the National Science Foundation gave support over the years to our studies of carbocations, and the Loker Institute mainly supported the work on hydrocarbon chemistry.

Received: December 5, 1994 [A 97 IE]
German version: *Angew. Chem.* **1995**, *107*, 1517

Keywords: carbocations · hydrocarbons · Nobel lecture · reactive intermediates

[1] a) J. F. Norris, *Am. Chem. J.* **1901**, *25*, 117; b) F. Kehrmann, F. Wentzel, *Ber. Dtsch. Chem. Ges.* **1901**, *34*, 3815; c) A. Baeyer, V. Villiger, *ibid.* **1902**, *35*, 1189, 3013; d) M. Gomberg, *ibid.* **1902**, *35*, 2397; e) P. Walden, *ibid.* **1902**, *35*, 2018; f) A. Werner, *ibid.* **1901**, *34*, 3300; g) A. Baeyer, *ibid.* **1905**, *38*, 569.

[2] H. Meerwein, K. van Emster, *Ber. Dtsch. Chem. Ges.* **1922**, *55*, 2500.

[3] C. K. Ingold, *Structure and Mechanism in Organic Chemistry*, Cornell University Press, Ithaca, NY, **1953**, and references therein, 2nd ed., **1969**.

[4] F. C. Whitmore, *J. Am. Chem. Soc.* **1932**, *54*, 3274, 3276; *Annu. Rep. Prog. Chem.* **1933**, 177; *Chem. Eng. News* **1948**, *26*, 668.

[5] *Carbonium Ions, Vols. I–V* (Eds.: G. A. Olah, P. von R. Schleyer), Wiley-Interscience, New York, **1968–1976**, and reviews cited therein.

[6] D. Bethell, V. Gold, *Carbonium Ions*, Academic Press, London, **1967**.

[7] P. Vogel, *Carbocation Chemistry*, Elsevier, Amsterdam, **1985**.

[8] G. A. Olah, *Chem. Eng. News* **1967**, *45*, 76 (March 27, 1967); *Science* **1970**, *168*, 1798.

[9] G. A. Olah, *Angew. Chem.* **1973**, *85*, 183; *Angew. Chem. Int. Ed. Engl.* **1973**, *12*, 173; *Carbocations and Electrophilic Reactions*, Verlag Chemie, Weinheim, Wiley, New York, **1974**.

[10] G. A. Olah, *J. Am. Chem. Soc.* **1972**, *94*, 808.

[11] *Compendium of Chemical Terminology: IUPAC Recommendations*, Blackwell Scientific Publication, Oxford, **1987**.

[12] H. Meerwein, *Methoden Org. Chem. (Houben-Weyl) 4th ed. 1952–*, Vol. VI/3, **1965**, and references therein.

[13] F. Seel, *Z. Anorg. Allg. Chem.* **1943**, *250*, 331; *ibid.* **1943**, *252*, 24.

[14] For my reminiscences, see: In Memory of H. L. Meerwein (*Top. Curr. Chem.* **1979**, *80*, 21).

[15] G. A. Olah, S. Kuhn, *Acta Chim. Acad. Sci. Hung.* **1956**, *10*, 233; *Chem. Ber.* **1956**, *89*, 866; *J. Am. Chem. Soc.* **1960**, *82*, 2380.

[16] A. N. Nesmejanov, E. J. Kahn, *Ber. Dtsch. Chem. Ges.* **1934**, *67*, 370.

[17] D. E. Pearson, *J. Am. Chem. Soc.* **1950**, *72*, 4169.

[18] G. A. Olah, S. J. Kuhn, W. S. Tolgyesi, E. B. Baker, *J. Am. Chem. Soc.* **1962**, *84*, 2733.

[19] G. A. Olah, *Rev. Chim. (Bucharest)* **1962**, *7*, 1139 (Nenitzescu issue).

[20] G. A. Olah, W. S. Tolgyesi, S. J. Kuhn, M. E. Moffatt, I. J. Bastien, E. B. Baker, *J. Am. Chem. Soc.* **1963**, *85*, 1328.

[21] *Mass Spectrometry of Organic Ions* (Ed.: F. W. McLafferty), Academic Press, New York, **1963**.

[22] H. C. Brown, H. Pearsall, L. P. Eddy, *J. Am. Chem. Soc.* **1950**, *72*, 5347.

[23] E. Wertyporoch, T. Firla, *Justus Liebigs Ann. Chem.* **1933**, *500*, 287.

[24] G. A. Olah, S. J. Kuhn, J. A. Olah, *J. Chem. Soc.* **1957**, 2174.

[25] F. Fairbrother, *J. Chem. Soc.* **1945**, 503.

[26] J. Rosenbaum, M. C. R. Symons, *Proc. Chem. Soc. London* **1959**, 92; J. Rosenbaum, M. Rosenbaum, M. C. R. Symons, *Mol. Phys.* **1960**, *3*, 205; J. Rosenbaum, M. C. R. Symons, *J. Chem. Soc. London* **1961**, 1.

[27] a) A. C. M. Finch, M. C. R. Symons, *J. Chem. Soc. London* **1965**, 378. b) For a summary, see M. C. Deno, *Prog. Phys. Org. Chem.* **1964**, *2*, 129; c) G. A. Olah, C. U. Pittman, Jr., M. C. R. Symons in *Carbonium Ions, Vol. I* (Eds.: G. A. Olah, P. von R. Schleyer), Wiley Interscience, New York, **1968**, p. 153.

[28] Preliminary communications and lectures: a) G. A. Olah, Conference Lecture at 9th Reaction Mechanism Conference, Brookhaven, New York, August **1962**; b) G. A. Olah, Abstract 142nd National Meeting of the American Chemical Society, Atlantic City, NJ, September **1962**, p. 45; c) G. A. Olah, W. S. Tolgyesi, J. S. MacIntyre, I. J. Bastien, M. W. Meyer, E. B. Baker, Abstracts A, XIX International Congress of Pure and Applied Chemistry, London, June **1963**, p. 121; d) G. A. Olah, *Angew. Chem.* **1963**, *75*, 800; *Angew. Chem. Int. Ed. Engl.* **1963**, *2*, 629; e) *C. D. Nenitzescu's 60th Birthday Issue* (*Rev. Chim (Bucharest)* **1962** *7*, 1139); f) *Repr. Am. Chem. Soc. Div. Pet. Chem.* **1964**, *9(7)*, C31; g) Intermediate Complexes and Their Role in Electrophilic Aromatic Substituents, Conference Lecture at Organic Reaction Mechanism Conference, Cork, Ireland, June **1964** (*Spec. Publ. Chem. Soc.* **1965**, 19); h) G. A. Olah, C. U. Pittman, Jr., *Adv. Phys. Org. Chem.* **1966**, *4*, pp. 305.

[29] G. A. Olah, E. B. Baker, J. C. Evans, W. S. Tolgyesi, J. S. McIntyre, I. J. Bastien, *J. Am. Chem. Soc.* **1964**, *86*, 1360.

[30] a) H. Vancik, D. E. Sunko, *J. Am. Chem. Soc.* **1989**, *111*, 3742; b) S. Sieber, P. Buzek, P. von R. Schleyer, W. Koch, J. W. de M. Carneiro, *J. Am. Chem. Soc.* **1993**, *115*, 25.

[31] G. A. Olah, J. R. DeMember, A. Commeyras, J. L. Bribes, *J. Am. Chem. Soc.* **1971**, *93*, 459, and references therein.

[32] D. M. Brouwer, E. L. Mackor, *Proc. Chem. Soc. London* **1964**, 147.

[33] a) R. J. Gillespie, *Acc. Chem. Res.* **1968**, *1*, 202; b) R. J. Gillespie, T. E. Peel, *Adv. Phys. Org. Chem.* **1972**, *9*, 1; *J. Am. Chem. Soc.* **1973**, *95*, 5173; c) G. A. Olah, G. K. S. Prakash, J. Sommer, *Superacids*, Wiley, New York, **1985**; d) R. J. Gillespie, *Can. Chem. News* **1991**, May issue, 20.

[34] a) J. Bacon, P. A. W. Dean, R. J. Gillespie, *Can. J. Chem.* **1969**, *47*, 1655; b) G. A. Olah, M. Calin, *J. Am. Chem. Soc.* **1968**, *90*, 938.

[35] N. F. Hall, J. B. Conant, *J. Am. Chem. Soc.* **1927**, *49*, 3047.

[36] a) P. D. Bartlett, *Nonclassical Ions*, Benjamin, New York, **1965**; b) S. Winstein, *Q. Rev. Chem. Soc.* **1969**, *23*, 1411; c) H. C. Brown (with commentary by P. von R. Schleyer), *The Nonclassical Ion Problem*, Plenum, New York, **1977**.

[37] J. D. Roberts, R. H. Mazur, *J. Am. Chem. Soc.* **1951**, *73*, 3542.

[38] a) M. Saunders, P. von R. Schleyer, G. A. Olah, *J. Am. Chem. Soc.* **1964**, *86*, 5680; b) G. A. Olah, A. M. White, J. R. DeMember, A. Commeyras, C. Y. Lui, *ibid.* **1970**, *92*, 4627; c) G. A. Olah, G. K. S. Prakash, M. Arvanaghi, F. A. L. Anet, *ibid.* **1982**, *104*, 7105; d) P. von R. Schleyer, S. Sieber, *Angew. Chem.* **1993**, *105*, 1676; *Angew. Chem. Int. Ed. Engl.* **1993**, *32*, 1606, and references therein.

[39] a) G. A. Olah, G. D. Mateescu, L. A. Wilson, M. H. Gross, *J. Am. Chem. Soc.* **1970**, *92*, 7231; b) G. A. Olah, G. D. Mateescu, J. L. Riemenschneider, *ibid.* **1972**, *94*, 2529; c) S. A. Johnson, D. T. Clark, *ibid.* **1988**, *110*, 4112.

[40] M. Saunders, M. R. Kates, *J. Am. Chem. Soc.* **1980**, *102*, 6867.

[41] C. S. Yannoni, V. Macho, P. C. Myhre, *J. Am. Chem. Soc.* **1982**, *104*, 7380.

[42] T. Laube, *Angew. Chem.* **1987**, *99*, 580; *Angew. Chem. Int. Ed. Engl.* **1987**, *26*, 560.

[43] E. M. Arnett, N. Pienta, C. Petro, *J. Am. Chem. Soc.* **1980**, *102*, 398.

[44] G. A. Olah, G. K. S. Prakash, M. Saunders, *Acc. Chem. Res.* **1983**, *16*, 440.

[45] G. von Békésy, *Experiments in Hearing*, McGraw Hill, New York, **1960**, p. 8.

[46] G. A. Olah, G. K. S. Prakash, R. E. Williams, L. D. Field, K. Wade, *Hypercarbon Chemistry*, Wiley, New York, **1987**.

[47] S. Winstein, D. Trifan, *J. Am. Chem. Soc.* **1952**, *74*, 1154.

[48] a) G. A. Olah, A. Molnár, *Hydrocarbon Chemistry*, Wiley, New York, **1995**, and references therein; b) I. Bucsi, G. A. Olah, *Catal. Lett.* **1992**, *16*, 27; c) G. A. Olah, *Acc. Chem. Res.* **1987**, *20*, 422; d) G. A. Olah, M. Bruce, E. H. Edelson, *Fuel* **1984**, *63*, 1130.

[49] G. A. Olah, *Angew. Chem.* **1993**, *105*, 805; *Angew. Chem. Int. Ed. Engl.* **1993**, *32*, 767, and references therein.

[50] G. A. Olah, L. Heiliger, G. K. S. Prakash, *J. Am. Chem. Soc.* **1989**, *111*, 8020.

[51] a) G. A. Olah, N. Hartz, G. Rasul, G. K. S. Prakash, *J. Am. Chem. Soc.* **1993**, *115*, 6985; b) G. A. Olah, N. Hartz, G. Rasul, G. K. S. Prakash, M. Burkhart, K. Lammertsma, *ibid.* **1994**, *116*, 3187.

[52] W. O. Haag, R. H. Dessau, *Int. Catal. Congr. Proc. 8th 1984* **1984**, *II*, 105.

G Proteins and Regulation of Adenylate Cyclase (Nobel Lecture)**

Alfred G. Gilman*

Introduction

Earl Sutherland, a friend of my father, wrote to me in the spring of 1961 with a proposal to participate in what was then an educational adventure—a combined M.D.–Ph.D. training program that he had devised at Western Reserve University (now Case Western Reserve University) in Ohio. My reaction was entirely negative. I thanked him, politely I think, but the idea of spending seven years in Cleveland had little appeal. Happily, Sutherland was persistent. He wrote again in the fall of 1961 (the beginning of my last year in college), I decided the idea was worth a visit, and I had my first glimpse of cyclic AMP, for whose discovery, in 1957, Sutherland was later awarded the Nobel Prize (in 1971). Cyclic AMP, Sutherland, and the M.D.–Ph.D. Program all looked rather appealing. Thus, on my arrival in September, 1962, I was disappointed to learn that Sutherland was about to depart for Vanderbilt University. However, there was an attractive opportunity to work with Theodore Rall, Sutherland's younger collaborator, who had played a pivotal role in the crucial experiments of 1957. I entered the Rall lab, and in over 30 subsequent years have never escaped the lure of cyclic nucleotide research, despite occasional attempts to try. The most determined of these efforts came with my choice of Marshall Nirenberg's newly proclaimed neurobiology laboratory for postdoctoral training. However, in our first conversation after my arrival at the National Institutes of Health in Bethesda, Marshall asked me to establish an assay for cyclic AMP in his laboratory. I was trapped again, but I didn't fight back very vigorously.

Rall and Sutherland's discovery of cyclic AMP and adenylate cyclase (or adenylyl cyclase), the hormone-sensitive enzyme that synthesizes the cyclic nucleotide from ATP, gave birth to the concepts of transmembrane signaling and of hormone-regulated synthesis of intracellular second messengers (Fig. 1). Both men were trained as biochemists (Sutherland with Carl Cori, Rall with Albert Lehninger), and together they initiated a classical reductionistic approach to deciphering hormone action. In the 1950s, hormones could almost be defined as regulatory molecules that would act only on intact cells. Sutherland and Rall's

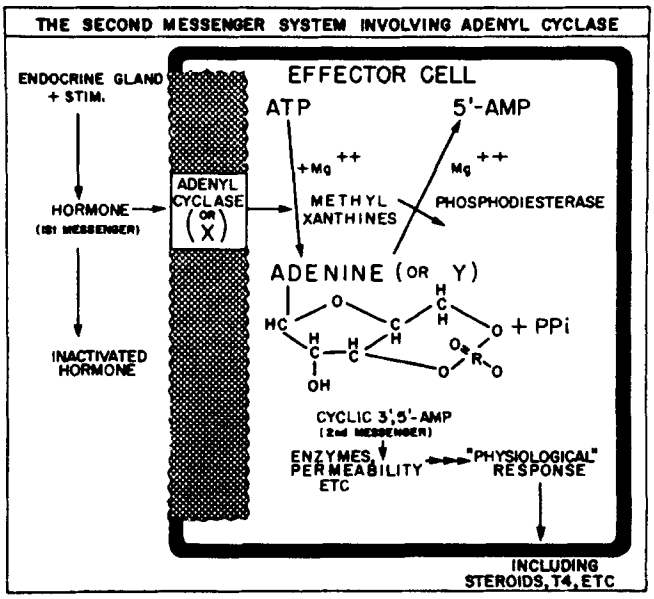

Fig. 1. An early pictorial formulation of Sutherland's second messenger concept.

coup was to assemble a system in which a characteristic effect of epinephrine and glucagon (activation of phosphorylase) could be observed in homogenates and then to dissect the system into its major components—hormone-stimulated synthesis of a factor, cyclic AMP, by the particulate fraction and subsequent action of the factor in the cytosol to activate phosphorylase.[1] An assay (albeit torturous) for adenylate cyclase was in hand, and hormone action could then be studied by adding ATP to plasma membranes.

Although the concept of receptors for endogenous regulatory molecules and drugs arose with the pharmacological experiments of Langley and Ehrlich in the late nineteenth and early twentieth centuries, the word evoked only metaphysical associations in many at the time of the discovery of cyclic AMP. The term receptor does not appear in the index of the 1955 edition of *The Pharmacological Basis of Therapeutics*, the standard textbook of pharmacology, but the following sentence is there: "Years ago, Langley named the differentiating substance the 'receptive substance'; this term is still widely employed, but it must be realized that the 'receptor' may not be a morphologically demonstrable structure." Rall and Sutherland's experiments provided test-tube assays for receptors, and the assays demonstrated that the receptors were authentic. The effects of epinephrine and congeners on adenylate cyclase were shown to

[*] Prof. A. G. Gilman
Department of Pharmacology
The University of Texas Southwestern
Medical Center at Dallas
Dallas, TX 75235 (USA)
Telefax: Int. code +(214) 648-8812

[**] Copyright© The Nobel Foundation 1995. We thank the Nobel Foundation, Stockholm, for permission to print this lecture.

conform to Ahlquist's new conceptualization of β-adrenergic receptors (as distinguished from α receptors), and the effects were blocked with the first, newly discovered β-adrenergic antagonist.[2] Biochemical approaches to receptors were thus born, and the question arose of the relationship of the β-adrenergic receptor to adenylate cyclase. Could the enzyme be the receptor? Perhaps, but this model would demand the existence of a family of adenylate cyclases with distinct regulatory sites, because regulation of the enzyme was shown not to be restricted to epinephrine and glucagon; adrenocorticotropic hormone (ACTH), thyrotropin (TSH), lutinizing hormone (LH), alcohol dehydrogenase (ADH), and other stimulators were soon in evidence, as was inhibition of adenylate cyclase activity by cholinergic agonists.[3]

Over a decade after the discovery of adenylate cyclase, Martin Rodbell and colleagues provided reasonably compelling, although indirect, evidence that receptors and adenylate cyclases were distinct molecular entities. The adenylate cyclase of adipocytes is stimulated by a myriad of hormones. If there were distinct cyclases that each also served as a receptor, responses to maximally effective concentrations of hormones would be additive. They were not, implying that distinct receptors could interact with a common pool of adenylate cyclase.[4] The issue was resolved definitively in the 1970s with the advent of ligand binding assays for receptors. Receptors could finally be examined by methods that did not rely on detection of a functional response. It was then possible to solubilize and resolve adenylate cyclases from β-adrenergic receptors, proving that they were distinct macromolecules[5, 6]

Early Times for G Proteins

The question of the moment thus became the mechanism of interaction or "coupling" between receptors and adenylate cyclase. The relatively simple notion that an agonist–receptor complex could act as an allosteric regulator of the enzyme was also challenged by Rodbell, who first promulgated the notion of a "transducer" acting as an intermediary between receptors and adenylate cyclase.[7] Although this notion was at first based predominantly on excellent instinct and the lipid bilayer was named as a candidate transducer, supportive data for something more specific were soon forthcoming. Rodbell, Birnbaumer, and their colleagues made the surprising discovery that one regulatory ligand (the receptor agonist) was not sufficient to activate adenylate cyclase. A hormone could not activate the enzyme unless guanosine triphosphate (GTP) was also present.[8] This crucial observation had been missed for over a decade because of contamination of both membrane preparations and substrate ATP with sufficient (μM) concentrations of GTP to meet the requirement. It was subsequently determined that hormonal inhibition of adenylate cyclase activity was similarly dependent on GTP.[9] I will leave it to Rodbell to describe these observations in more detail.[*] However, it should be noted that there was considerable skepticism about the significance of the findings (Fig. 2), in part generated by difficulties in reproduction of the result; most biochemists were not working with the very nice membrane preparations available in the Rodbell laboratory.

Fig. 2. A cartoon from the 1970s, drawn by Dr. Pierre DeMeytes, suggested that not all investigators could readily observe the requirement for GTP in transmembrane signaling. (Printed with permission from Dr. DeMeytes.)

Several observations of the mid-1970s spoke to the undeniable importance of GTP in regulation of hormone-sensitive adenylate cyclase activity. Most significantly, Cassel and Selinger detected a hormone-stimulated GTPase activity that appeared to be associated with activation of adenylate cyclase, and, despite enormous technical difficulties, they correctly deduced (from kinetic analysis) the significance of the GTPase in terminating a hormonally mediated signal.[10] Consistent with

[*] See the following Nobel Lecture by M. Rodbell.

Alfred G. Gilman was born in New Haven, CT (USA) in 1941. He received his B.S. in biochemistry from Yale University in 1962 and his M.D./Ph.D. in pharmacology in 1969 from Case Western Reserve University in Cleveland, OH. He completed his postdoctoral training in the Laboratory of Biochemical Genetics at the National Institutes of Health in Bethesda, MD. In 1971 Gilman moved to the Department of Pharmacology at the University of Virgina, where he rose through the ranks (Assistant Professor 1971–1973, Associate Professor 1973–1977, Professor 1977–1981). Since 1981 he has been Chairman of Pharmacology at the University of Texas Southwestern Medical Center at Dallas. Gilman discovered, characterized, and purified a set of guanine nucleotide binding regulatory proteins (G proteins). His observations provided a firm molecular basis for understanding certain signal transduction processes present throughout nature. He has received a number of honors and awards for this work including the 1994 Nobel Prize for Medicine and Physiology.

these thoughts, Londos and Schramm and co-workers had noted that nonhydrolyzable analogs of GTP, such as Gpp(NH)p, activated adenylate cyclase dramatically and without the need for hormone.[11, 12] Michael Maguire, my first postdoctoral fellow, discovered that GTP decreased the affinity of receptors selectively for agonists, but not for antagonists.[13] The interpretation of this counterintuitive observation was not clear, but it surely appeared to be significant.

Throughout this time a few brave souls had attempted to solubilize and purify components of hormone-sensitive adenylate cyclase systems. All encountered great difficulties. Hormonal responsiveness was quickly lost on solubilization with detergents, and adenylate cyclase itself appeared to be remarkably labile. Eva Neer was perhaps the first to treat the enzyme as an approachable biochemical object, with a careful exploration of its hydrodynamic properties.[14] Despite this, a conventional biochemical approach to the system looked difficult indeed.

The turning point, for us, started with the description by Daniel et al. of the cytocidal effect of cyclic AMP on clonal S49 lymphoma cells.[15] Bourne and associates were soon able to isolate a variant (cyc$^-$) of these cells that appeared to lack adenylate cyclase,[16] despite continued expression of a normal number of β-adrenergic receptors.[17] We were able to select another S49 cell variant that intrigued us even more—an uncoupled (UNC) mutant that appeared to have normal receptors and adenylate cyclase but that failed to generate a cyclic AMP signal in response to appropriate hormones (β-adrenergic agonists or prostaglandins).[18] The availability of these genetic variants made the biochemistry appear more approachable, particularly to Elliott Ross, an extremely talented and well-trained membrane biochemist who joined my lab in 1975. Ross sought to reconstitute the cyc$^-$ mutant in vitro, first by extracting adenylate cyclase from cells that lacked β-adrenergic receptors and then by somehow coaxing the protein back into fruitful interactions with the receptors present in cyc$^-$ membranes. The experiment eventually worked; cyc$^-$ membranes were reconstituted to display catecholamine-sensitive adenylate cyclase activity.[19] We were pleased that we had taken the first step in resolution and reconstitution of the system, but we had little idea how quickly the investment would pay dividends. The reconstitution had not worked for the anticipated reasons. When we inactivated the adenylate cyclase in the detergent extract used for the reconstitution, we still observed undiminished levels of hormone-stimulated adenylate cyclase activity. That is, addition of a detergent extract devoid of adenylate cyclase activity to receptor-containing cyc$^-$ membranes (which also had no adenylate cyclase activity) led to restoration of the complete response (Fig. 3). Treatments with proteases quickly revealed that both the detergent extract and the cyc$^-$ membranes contained proteins that were necessary for observation of *any* adenylate cyclase activity—basal or that stimulated by hormones, fluoride, or guanine nucleotides. (We now know that the specific isoforms of adenylate cyclase that predominate in S49 cells have notably low basal activity.) Thus two proteins were required—the catalyst or adenylate cyclase itself, which in fact was present in so-called cyc$^-$ membranes, and a stimulatory protein, deficient in cyc$^-$ membranes, that had survived the mild conditions used to inactivate adenylate cyclase in the extract used for reconstitution. We proposed that the role of the hormone receptor

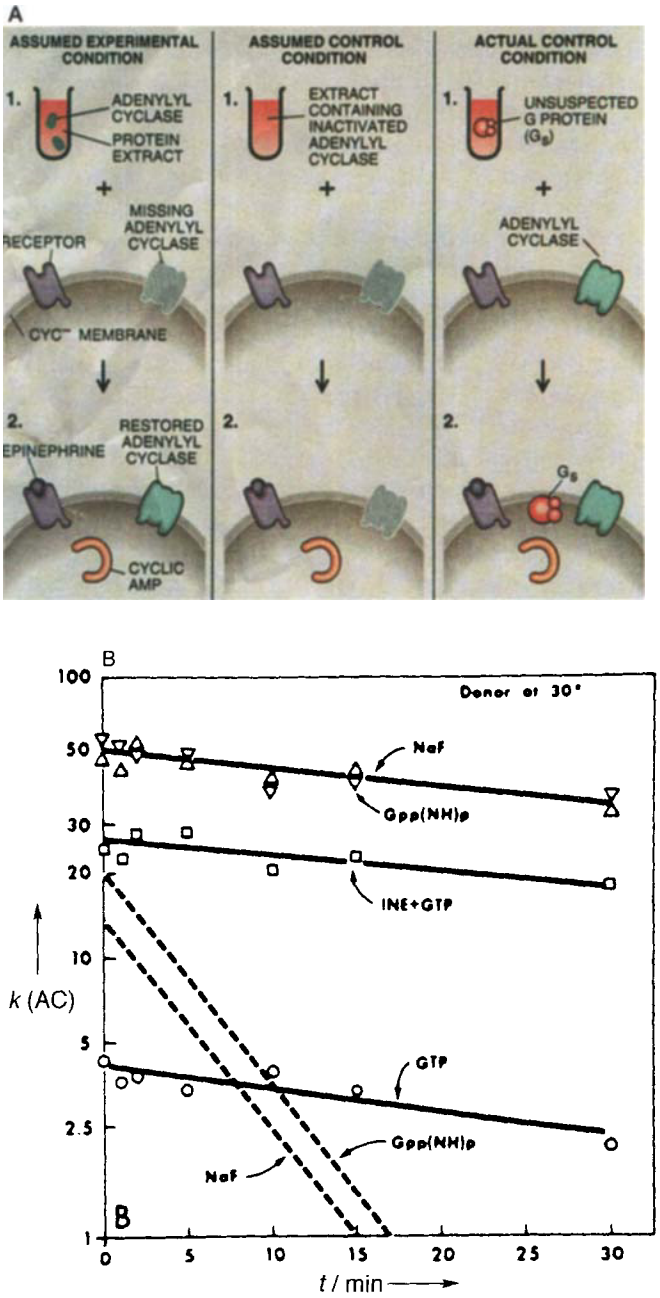

Fig. 3. Experiments leading to the discovery of G_s. A) Cartoon of the protocols. Left: 1. In the first experiments, Elliott M. Ross added a detergent extract of membrane proteins to so-called cyc$^-$ membranes, which were thought to lack adenylate cyclase. 2. Epinephrine stimulated cyclic AMP production, which seemed to indicate that adenylate cyclase had been inserted into the deficient membranes. Middle: In the control experiment, the adenylate cyclase in the extract was inactivated. Even without it, epinephrine caused the cyc$^-$ membranes to make cyclic AMP. Right: 1. This puzzling finding led to the discovery that the cyc$^-$ membranes did contain adenylate cyclase but lacked a third component necessary to activate it—a G protein that persisted in the extract after adenylate cyclase had been inactivated. Restoration of the G protein to the membranes enabled adenylate cyclase to synthesize cyclic AMP. (Reprinted with permission from ref. [154].) B) Data from these experiments. Reconstitution of hormone-sensitive adenylate cyclase by mixture of cyc$^-$ membranes with heat-inactivated wild-type membrane extracts. Detergent extracts of wild-type membranes were heated at 30 °C for the times indicated on the abscissa, chilled, and mixed with cyc$^-$ membranes. The NaF- and Gpp(NH)p-stimulated adenylate cyclase activities, k(AC) [pmol min^{-1} mL^{-1}] of the incubated extracts are shown by the dashed lines. Aliquots of the reconstituted mixtures, prepared with these incubated extracts, were assayed with GTP, isoproterenol (a congener of epinephrine) plus GTP, NaF, or Gpp(NH)p, as indicated. (Reprinted with permission from ref. [21].)

was to regulate the interaction between these two components.[20, 21] Coincidentally, Pfeuffer achieved partial resolution between adenylate cyclase and an activating protein that bound selectively to a guanine nucleotide based affinity resin.[22]

The novel protein became the object of our attentions, in part because of its more mysterious nature and in part because it was not as labile as adenylate cyclase. Additional experiments by Ross implied that the protein (at the time termed G/F, but eventually named G_s) was the site of action of guanine nucleotides (and fluoride),[21] and these hypotheses were strengthened by hydrodynamic characterization of the activity by Allyn Howlett; she detected Gpp(NH)p- and fluoride-induced alterations suggestive of subunit dissociation upon activation by these ligands.[23] The really hard work fell to Paul Sternweis and John Northup, who together undertook the task of purification. The good luck of G_s was its revelation by mutation in S49 cells and the existence of an easy assay for the protein by activation of adenylate cyclase. The bad luck, unknown at the time, was that G_s is among the least abundant of the G proteins. Nevertheless, perseverance (by all involved) and skill (by those doing the experiments) paid off, and G_s, with its unsuspected 35-kDa β subunit, finally emerged as a homogeneous guanine nucleotide binding protein, capable of activating adenylate cyclase in its Gpp(NH)p- or fluoride-activated forms (Fig. 4).[24, 25] The third, 8-kDa (γ) subunit went unnoticed at the time.

Further studies of G_s performed shortly thereafter revealed that one equivalent of guanine nucleotide bound to the α subunit of the oligomer, that activation by Gpp(NH)p or fluoride was in fact accompanied by subunit dissociation, and that the resolved Gpp(NH)p-bound α subunit was necessary and sufficient for activation of adenylate cyclase (Fig. 5).[26, 27] Additional work on the mechanism of activation of G_s by fluoride provided surprises and even amusement. The effect of fluoride, observable when experiments were performed in glass test tubes

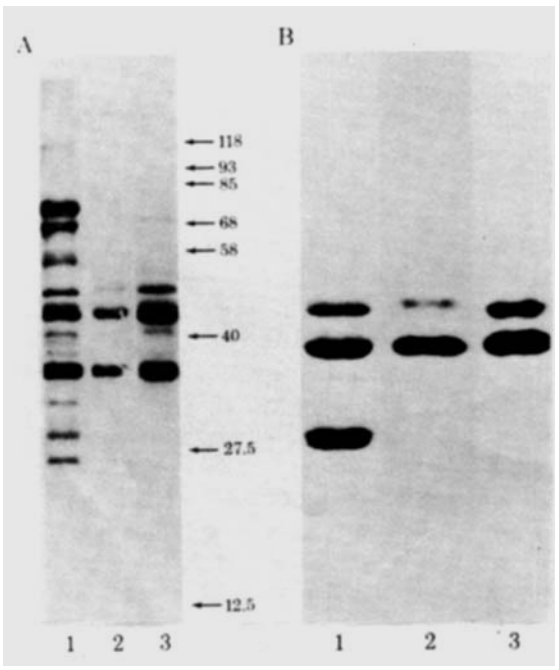

Fig. 4. A) Polyacrylamide gel electrophoresis of purified fractions of G_s. Lane 1: Protein from an intermediate step of purification. Lanes 2 and 3: Purified protein, 3 µg and 8 µg, respectively. B) Labeling of purified G_s with cholera toxin and [^{32}P]NAD. Lane 1: Purified protein stained with Coomassie blue. Lanes 2 and 3: Autoradiograms of the cholera toxin labeled protein, exposed for 16 and 48 h, respectively. The two higher molecular weight bands in the purified preparation, both of which are labeled with cholera toxin, are alternatively spliced forms of $G_{s\alpha}$. The lower molecular weight band is the β subunit. (Reprinted with permission from ref. [24].)

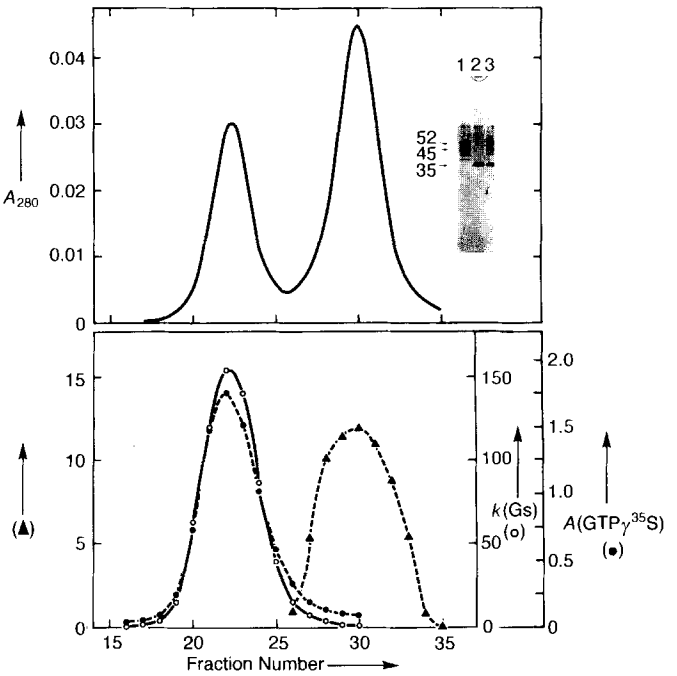

Fig. 5. Separation of the subunits of G_s by gel filtration. Purified G_s was labeled by incubation with [^{35}S]GTPγS. After removal of free nucleotide, the protein was subjected to high-performance gel filtration. The top panel shows the absorbance A (280 nm) of the eluted protein. The inset shows the silver staining pattern for sodium dodecylsulfate/polyacrylamide gel electrophoresis of the pooled peaks of protein (lane 1 = first peak, lane 2 = second peak) and of the protein applied (lane 3). The lower panel shows the activities assayed. G_s activity, $k(G_s)$ [nmol min^{-1}] (o), is quantified by activation of adenylate cyclase. The radioactivity A (GTPγ^{35}S) [10^6 counts min^{-1} mL^{-1}] (•) indicates high-affinity binding of the radioactive nucleotide. 35 K Activity A (35 K) at 14 min $- t_{1/2}$ (▲) is a measure of the activity of the $\beta\gamma$ subunit complex. Nucleotide binding activity and the capacity to activate adenylate cyclase were exclusively associated with the resolved α subunit of G_s, which dissociated from $\beta\gamma$ on activation with GTPγS. (Reprinted with permission from ref. [27].)

or in the presence of components of the adenylate cyclase assay (i.e. ATP), was lost in the absence of ATP when experiments were done in plastic test tubes.[28, 29] Another mystery factor was skillfully pursued by Paul Sternweis, who purified the coactivator from both ATP and from aqueous extracts of disposable glass test tubes. A metal seemed to be involved, and neutron-activation analysis revealed Al^{3+} as the culprit.[29] The significance and value of that observation has become particularly apparent a decade later.

An interesting side activity at this time was study of the ADP-ribosylation of G_s by cholera toxin. That this occurred was very strongly implied by the work of Gill,[30] Vaughan,[31] and Bourne,[32] and was proven with purification of the protein. However, as purification proceeded, the capacity of cholera toxin to ADP-ribosylate G_s was lost. This could be restored by addition of a protein factor[33] that was eventually purified, named ADP-ribosylation factor or ARF, and found to be a low-molecular-weight GTP binding protein.[34, 35] ARF is, of course, now leading a happy existence as an important regulator

of protein trafficking[36] and as an activator of phospholipase D.[37] Its association with cholera toxin and/or G_s remains to be explained.

Work in Japan in the late 1970s and early 1980s by Michio Ui and his colleagues resulted in characterization of islet-activating protein (IAP), a toxin from *Bordetella pertussis*. Treatment of cells or membranes with this toxin resulted in loss of hormonal inhibition of adenylate cyclase (and in some cases enhancement of hormonal stimulation of the enzyme).[38] Coincidentally, the toxin appeared to catalyze the incorporation of the ADP-ribosyl moiety of NAD into a 41-kDa membrane protein.[39] The parallel with cholera toxin was remarkable. Toshiaki Katada, Professor Ui's student, applied for a postdoctoral position in my lab and was quickly accepted. As Gary Bokoch, another newly arrived postdoc, and Katada began to work with Professor Ui's toxin, John Northup realized that he had frequently been plagued with a 41-kDa contaminant during purification of G_s. He even had fractions in the freezer that were enriched in this contaminant. Moral: never throw anything away! (This contaminant can be seen in Fig. 4). The obvious experiment worked beautifully on the first try; Northup's contaminant was a superb substrate for ADP-ribosylation by IAP. Our relatively tortuous experience with the purification of G_s then paid off, and purification of the true IAP substrate proceeded quickly,[40] aided by the fact that it is substantially more abundant than G_s. The hypothesis that the IAP substrate represented G_i, a homologous G protein responsible for inhibition of adenylate cyclase, was obvious, and its validity was established a year later with thorough characterization of G_i.[41-44] Nevertheless, the actual mechanisms (plural intended) of inhibition of adenylate cyclase by G_i remained elusive.

Throughout much of this time, Bitensky, who had detected a light-activated cyclic GMP phosphodiesterase in the retina,[45] called attention to parallels between the visual transduction pathway and hormone-sensitive adenylate cyclases. Particularly notable were descriptions of a light-activated GTPase[46] and a guanine nucleotide requirement for activation of the phosphodiesterase. These observations led to purification of transducin (G_t)[47,48] and appreciation that G_s, G_i, and G_t represented a family of structurally homologous guanine nucleotide binding proteins with related α subunits and very similar (or identical) β subunits[49] (Fig. 6). The existence of the γ subunit of the transducin heterotrimer was recognized early because of its great abundance. Poor avidity for stain delayed its recognition as a component of G_s and G_i.[41,50]

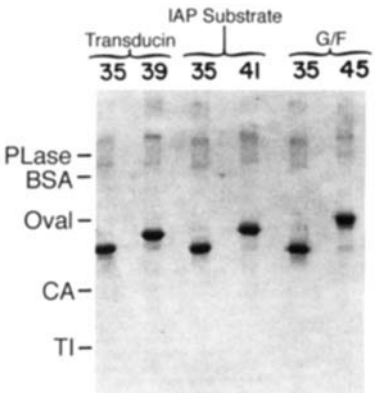

Fig. 6. Electrophoretic profile of the purified subunits of transducin (G_t), the IAP substrate (G_i), and G/F (G_s). The α subunits of the three G proteins have different molecular weights, while the β subunits appeared to be the same. Peptide mapping and analysis of amino acid compositions of the subunits indicated that the α subunits were distinct but related, while the β subunits were very similar or identical. PLase = pig liver esterase, BSA = bovine serum albumin, Oval = ovalbumin, CA = carboanhydrase, TI = soybean trypsin inhibitor. (Reprinted from ref. [49].)

For a brief period of time in the early 1980s it seemed that things might calm down. Guanine nucleotide mediated stimulation and inhibition of adenylate cyclase was in the hands of G_s and G_i, while transducin explained the observations in the visual system. In collaboration with Ross, we were able to observe hormonal stimulation of adenylate cyclase using three purified proteins—the β-adrenergic receptor, G_s, and adenylate cyclase—reconstituted into phospholipid vesicles.[51] What more was there? Major clues came quickly. Paul Sternweis,[52] now independently, and Eva Neer[53] discovered G_o as a startlingly abundant protein in brain; Fain[54] and Gomperts[55] observed hormone- and GTP-dependent stimulation of inositol trisphosphate synthesis; amino acid sequence homologies were detected between signal-transducing G proteins and the $p21^{ras}$ gene products;[56] and the cloners arrived.[57,58] It was clearly time to add some new technology to the repertoire and welcome many new people to the party.

G Proteins from Pheromones to Photons

It now seems appropriate to abandon the historical, storytelling approach and attempt to describe the current level of understanding of G protein mediated transmembrane signaling. It has become abundantly clear, particularly over the past decade, that this relatively large family of heterotrimeric GTP-binding and -hydrolyzing proteins plays an essential transducing role in linking hundreds of cell surface receptors to effector proteins at the plasma membrane. These systems are widely utilized in nature, controlling processes ranging from mating in yeast to cognition in man. Receptors that activate G proteins are correspondingly diverse and encompass proteins that interact with hormones, neurotransmitters, autacoids, odorants, tastants, pheromones, and photons. Several reviews of this area are recommended[59-70] and should also be consulted for references to the original literature.

Overview of G Protein Function and Structure

Although G proteins are structural heterotrimers, they function as dissociable dimers. The β and γ subunits exist as tightly associated complexes that function as a unit. The identity of the α subunit is currently used to define a given G protein oligomer. Although a number of different $\beta\gamma$ subunit complexes can apparently associate fruitfully and promiscuously with a variety of α subunits, it is unknown to what extent this occurs in vivo.

Sixteen distinct genes encode G protein α subunits in mammals; 20 or more proteins are synthesized, including the products that arise as a result of alternative splicing of mRNA. The commonly recognized subclassification of the α subunit family is based on structural relationships, but this scheme does reasonable justice to functional relationships as well[66] (Fig. 7). Four subfamilies are usually discussed: 1) the small G_s group (G_s and G_{olf}), best recognized as activators of adenylate cyclases; 2) the large and functionally diverse G_i group, whose members are pertussis toxin substrates with one exception (G_z); 3) the G_q group, activators of the several isoforms of phospholipase Cβ; and 4) the most recently recognized G_{12} group, whose

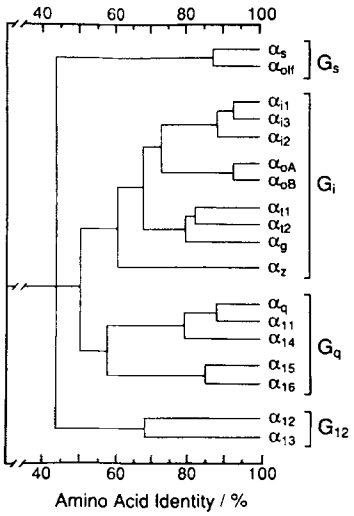

Fig. 7. Sequence relationships between α subunits of mammalian G proteins and family groupings. (Modified with permission from refs. [65, 66].)

functions are unknown. There are five known genes encoding β subunits and six for γ subunits. If all possible combinations of α, β, and γ subunits were allowed, we would need to consider at least 600 G protein oligomers. Although some combinations of β and γ subunits appear to be forbidden and there are some preferences of α subunits for specific $\beta\gamma$ dimers, the number is still likely to be very large.

Each G protein α subunit has a single high-affinity binding site for guanine nucleotide. The GDP-bound form of α is relatively inactive and has high affinity for $\beta\gamma$. Thus, GDP-$\alpha\beta\gamma$ constitutes the inactive oligomer. Receptor-catalyzed guanine nucleotide exchange results in formation of GTP-α, and resultant conformational changes cause dissociation of α from $\beta\gamma$ (see Fig. 8). Two regulators of downstream effectors, GTP-α and $\beta\gamma$, are thus liberated. G protein α subunits are themselves enzymes, albeit poor ones, with intrinsic GTPase activity. After a period of time characteristic of individual α subunits, GTP is hydrolyzed to GDP, subunits associate, and the basal state is restored. G proteins thus function as switches and timers. The high affinity of α (and particularly of the oligomer) for GDP holds the switch off; nucleotide exchange turns the switch on; hydrolysis of GTP turns it off again with a characteristic delay (seconds to perhaps minutes) as a result of slow catalysis; this constitutes the timer, which is an important element of signal amplification.

G protein subunits are subjected to a number of covalent modifications, both physiologically and pathologically. Lipid covalent modifications are particularly evident. Members of the G_i subfamily are myristoylated, with the C14 fatty acid incorporated in amide linkage to amino-terminal glycine residues.[71-73] This modification is an important determinant of the affinity of these α subunits for $\beta\gamma$ and of the affinity of the $G_{i\alpha}$ proteins for adenylate cyclase (see below).[74, 75] All α subunits with the exception of $G_{t\alpha}$ are palmitoylated, in some cases doubly so, and the C16 fatty acid is bound in thioester linkage to cysteine residues near the amino terminus.[76] In the case of members of the G_i family, the palmitoylated cysteine residue is immediately adjacent to the myristoylated glycine. While myristoylation presumably occurs cotranslationally and the modification is irreversible, palmitate is incorporated post-translationally and the bound fatty acid turns over relatively rapidly. Of particular interest, turnover of palmitate is a receptor-regulated phenomenon, with control apparently exerted at the level of removal of palmitate from the α subunit.[77, 78] The significance of this phenomenon is not yet fully appreciated, but it could represent part of a pathway for attenuation of transmembrane signaling. Finally, for the lipids, γ subunits contain typical CAAX boxes at their carboxyl termini and are prenylated; the γ_1 subunit, found in the retina, is farnesylated,[79] while the other γ subunits appear to be geranylgeranylated.[80, 81] Although prenylation is not essential for the formation of high-affinity $\beta\gamma$ dimers, it is crucial for the interactions of $\beta\gamma$ with α and with at least certain effectors (e.g. adenylate cyclases).[82] All of the lipid modifications may play important roles in localization of G protein subunits to membranes, although the mechanisms that dictate the specificities of these protein–membrane interactions remain to be discovered. We suspect that $G_{s\alpha}$ contains an as yet unidentified covalent modification. The natural protein (purified from liver or brain) has a substantially higher affinity for adenylate cyclase than does recombinant $G_{s\alpha}$ synthesized in bacteria.[83]

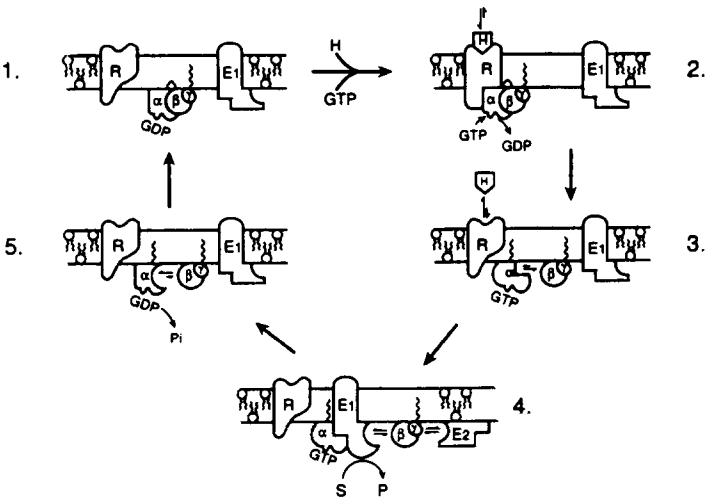

Fig. 8. G protein mediated transmembrane signaling. 1) In the basal state G proteins exist as heterotrimers with GDP bound tightly to the α subunit. The hormone receptor R is unoccupied, and the effector E is unregulated. 2) Upon binding of hormone H and receptor activation, the receptor interacts with the heterotrimer to promote a conformational change and dissociation of GDP from the guanine nucleotide binding site; at normal cellular concentrations of guanine nucleotides, GTP fills the site immediately. (Under experimental conditions where GTP is absent, the hormone has high affinity for the receptor and the H–R–G complex is stable.) 3) Binding of GTP to G_α induces a conformational change with two consequences. First, the G protein dissociates from the H–R complex, reducing the affinity of hormone for receptor and, in turn, freeing the receptor for another liaison with a neighboring quiescent G protein. Second, GTP binding also reduces the affinity of G_α for $G_{\beta\gamma}$, and subunit dissociation occurs. 4) This frees G_α–GTP to fulfill its primary role as a regulator of effectors and activate the enzymatic transformation of substrate S into product P. At least in some systems, the free $G_{\beta\gamma}$ complex also interacts directly with effectors (E_1) and modulates the activity of the active complex, or it acts independently at distinct effectors (E_2). 5) G_α possesses an intrinsic GTPase activity. The rate of this GTPase determines the lifetime of the active species and the associated physiological response. The G_α-catalyzed hydrolysis of GTP leaves GDP in the binding site and causes dissociation and deactivation of the active complex G_α–E_1. G_α–GDP has high affinity for $G_{\beta\gamma}$; subsequent reassociation of G_α–GDP with $G_{\beta\gamma}$ returns the system to the basal state (a). (Reprinted with permission from ref. [68].)

ADP-ribosylation of G protein α subunits by bacterial toxins is a particularly interesting, irreversible covalent modification of pathological significance. The diarrheagenic enterotoxin produced by *Vibrio cholerae* and the heat-labile toxin synthesized by certain strains of *E. coli* are ADP-ribosyltransferases with great specificity for $G_{s\alpha}$. NAD is the donor of the ADP-ribosyl moiety, which is attached to an active site arginine residue of the substrate.[84] The resultant inhibition of the GTPase activity of $G_{s\alpha}$ causes persistent activation of both $G_{s\alpha}$ and adenylate cyclase. Diarrhea is the dominant sign of disease because of the

local, enteric nature of the infection. A toxin (islet-activating protein) produced by *Bordetella pertussis* catalyzes ADP-ribosylation of a cysteine residue near the carboxyl-terminus of members of the G_i family of α subunits.[85] This results in inhibition of interactions between G proteins and receptors, effectively blocking the affected pathways, including those that cause inhibition of adenylate cyclase. As a sidelight, it is interesting to note that other microorganisms have developed different strategies for elevation of host cell concentrations of cyclic AMP. A toxin elaborated by *Bacillus anthacis* and a distinct *Bordetella pertussis* toxin are themselves calmodulin-activated adenylate cyclases that permeate mammalian cells.

High-resolution crystal structures of two G protein α subunits, $G_{t\alpha}$ and $G_{i\alpha 1}$, in different liganded states have been described recently.[86-88] We have been pleased to collaborate with Stephen Sprang in these efforts. The general architecture of these closely related proteins is essentially identical (Fig. 9).

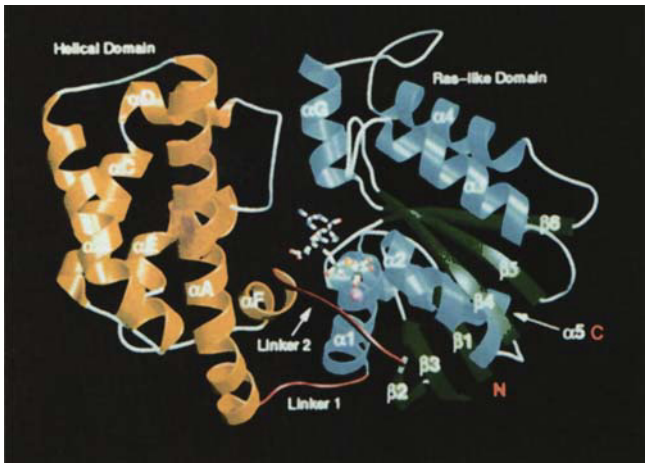

Fig. 9. Ribbon and coil representation of $G_{i\alpha 1}$ subunit. The helical domain is colored yellow, and the $p21^{ras}$-like domain is green and cyan. Linker-1 and linker-2 strands are colored red. The GTPγS is shown as a ball-and-stick model, and the magnesium ion is depicted as a magenta sphere. Secondary structure elements are labeled. The red letters N and C mark the positions of the first ordered residues at the N and C termini of the molecule. (Reprinted with permission from ref. [88].)

Each is constructed of two very distinct domains: a $p21^{ras}$-like $\alpha\beta$ domain that is flanked by a unique (to G proteins) α-helical domain. The two structures are connected by a pair of linker strands. Although all of the direct contacts between the protein and guanine nucleotide are formed with either the $p21^{ras}$-like domain or the linker-2 peptide, the nucleotide is virtually buried in the cleft between the two major domains. It is hypothesized that receptor-mediated conformational changes sufficient to permit guanine nucleotide exchange result in substantial separation of the helical and $p21^{ras}$-like structures.

Despite the existence of several superb crystal structures of $p21^{ras}$ proteins and of GTPase-deficient mutants of $p21^{ras}$, it has been difficult to deduce the mechanism of GTP hydrolysis, perhaps in large part because the proteins are such poor catalysts in the absence of activators (GTPase activating proteins or GAPS). The same is true of the structures of the GTPγS-bound forms of $G_{t\alpha}$ and $G_{i\alpha 1}$. Happily, however, the AlF_4^--bound conformations of these proteins are more illuminating. As noted above, Al^{3+} was unexpectedly found to be a cofactor necessary for activation of G proteins by F^-, and it had been deduced that AlF_4^- probably binds to G_α proteins in proximity to GDP, mimicking the γ-phosphoryl moiety of GTP.[29, 89, 90] The X-ray structure revealed this hypothesis to be nearly correct.[88] However, rather than simply mimicking GTP, GDP–AlF_4^- appears to be acting as a transition state analog, revealing critical roles played by active-site amino acid residues.

Two residues, Arg^{178} ($G_{i\alpha 1}$ numbering) and Gln^{204}, had been implicated in catalysis as the result of isolation or construction of GTPase-deficient proteins with mutations at these sites.[91-94] In addition, this Arg residue corresponds to the Arg in $G_{s\alpha}$ that is ADP-ribosylated by cholera toxin, and the Gln corresponds to Gln^{61} in $p21^{ras}$, a residue known to be critical for catalysis. (There is no homolog of Arg^{178} in $p21^{ras}$; Arg^{178} is in the linker-2 peptide.) Rearrangement of the positions of these two residues in the GDP–AlF_4^- structure (relative to their positions in the GTPγS-bound protein) reveals their roles in catalysis (Fig. 10). Gln^{204} appears to be stabilizing and orienting the hydrolytic water molecule in the trigonal–bipyramidal transition state, while Arg^{178} stabilizes the negative charge at the equatorial oxygen atoms of the pentacoordinate phosphate intermediate. Since this Arg residue is unique to G_α proteins, its presence may explain the higher hydrolytic activity of G_α proteins relative to those of members of the $p21^{ras}$ family.

Hydrolysis of GTP by $G_{i\alpha 1}$ is accompanied by relaxation of both the linker-2 strand and a twenty-residue segment that contains Gln^{204}. The loss of any ordered conformation in these residues (which are invisible in the electron density map) accounts for alterations in properties known to be characteristic of the GDP-bound form of the protein: loss of the Mg^{2+} binding site, a somewhat reduced affinity for guanine nucleotide, enhanced susceptibility to proteolysis in this region, and quenching of tryptophan fluorescence.

A surprising consequence of GTP hydrolysis is the assembly of the amino and carboxyl termini into a distinct, organized α-helical domain. This structural change occurs nearly 30 Å from the catalytic site, and it is difficult to discern an intramolecular pathway of conformational transition between these sites. Even more surprising is the discovery that the newly formed domain forms an exceedingly complimentary and extensive packing interface with the α-helical domain and the linker-2 strand of the neighboring molecule in the crystal lattice (Fig. 11). Thus, the transmission of structural changes between the GTP binding site and the amino and carboxyl terminii (which form part of the presumptive binding surface for the $\beta\gamma$ subunit complex) might be by means of intermolecular contacts.[95] Interestingly, these observations could be pertinent to recent speculations by Rodbell on the possibility of G protein oligomerization.[96]

Functions of α Subunits of G Proteins

Almost all known G protein α subunits and many distinct $\beta\gamma$ subunit complexes have been purified to homogeneity from tissue sources or purified after expression in heterologous systems (either *E. coli* or Sf9 cells) (Table 1). Properties of several subunits have also been inferred by application of new-wave bio-

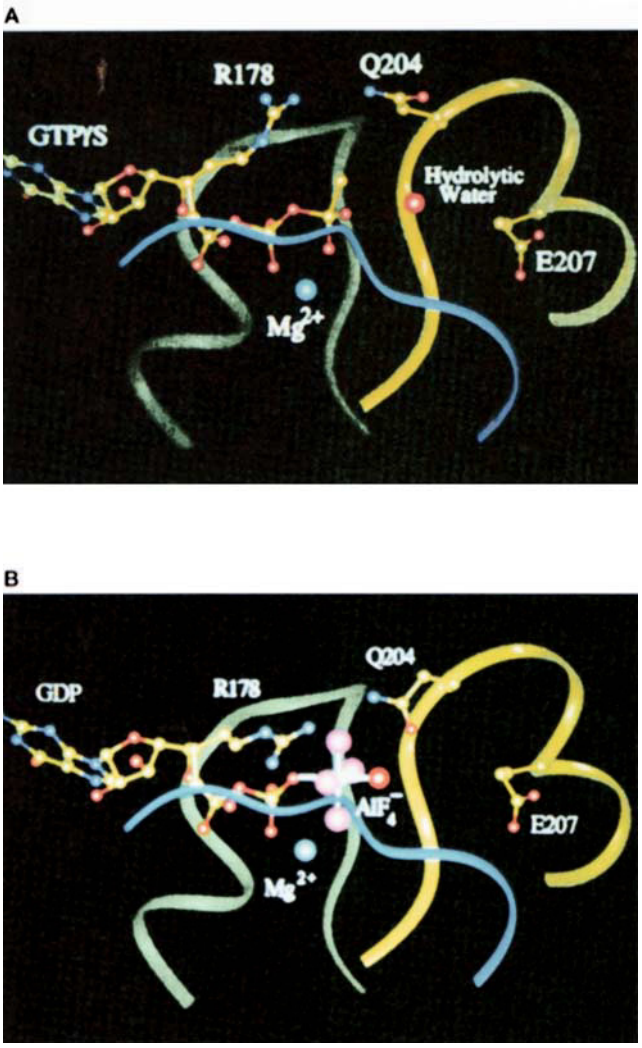

Fig. 10. A) A representation of the active site in the GTPγS–$G_{i\alpha 1}$ complex, showing the disposition of Arg^{178} and Gln^{204}; these residues are not within hydrogen-bonding distance of the nucleotide. The nucleophilic water molecule is *trans* axial to the O atom of the P–O–P bridge, and the O(H_2O)–P distance is 3.85 Å. The β_1–α_1 loop is colored green, the $\beta 2$–$\alpha 3$ switch peptide yellow, and the linker-2 strand blue. B) The GDP–AlF_4^- complex shown from the same perspective. Arg^{178} and Gln^{204} have rotated to contact the AlF_4^- cluster, and the nucleophilic water molecule has moved into the ligand field of the aluminum ion. C) Model of the active site of $G_{i\alpha 1}$ at the transition state of the phosphorolysis reaction, based on the structure of the GDP–AlF_4^- complex. (Reprinted with permission from ref. [88].)

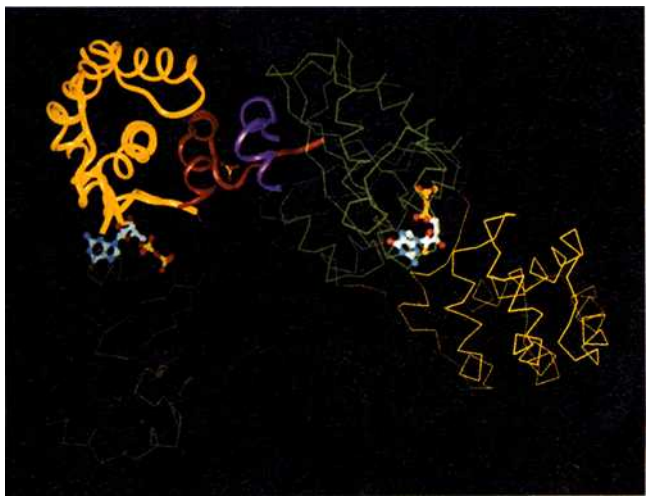

Fig. 11. Symmetry-related molecules of GDP–$G_{i\alpha 1}$ form a helical array in the crystalline state. The C- and N-termini of $G_{i\alpha 1}$ are disordered in the GTP complex but fold into a discrete protein microdomain comprising nearly 40 residues upon hydrolysis of the nucleoside triphosphate. A phosphate ion, which contacts three arginine residues from the amino terminus and lysine 180 from the linker-2 strand, may act as a nucleation center for the microdomain. (A sulfate ion serves this role in crystals of GDP–$G_{i\alpha 1}$.) This microdomain forms an extensive and complementary interface with the α-helical domain and the linker-2 strand of the neighboring molecule. The contact buries more than 1800 $Å^2$ of solvent-accessible surface, an area equivalent to that encompassed by many protein antigen–immunoglobulin complexes.

chemistry—experiments performed "in transfecto". Each system has advantages and disadvantages. While the *E. coli*-derived proteins may be missing certain covalent modifications (although myristoylation can be accomplished by coexpression of protein N-myristoyl transferase), they have the distinct advantage of being unambiguously free of other G protein subunits. This can be difficult to prove with G proteins isolated from other sources.

The members of the $G_{s\alpha}$ subfamily (α_s, α_{olf}) activate various adenylate cyclases, and they do so by direct interactions with these proteins. All known isoforms of membrane-bound mammalian adenylate cyclase are activated by $G_{s\alpha}$. $G_{s\alpha}$ is expressed as four distinct polypeptides (± residues encoded in exon 3; ± a serine residue at the splice junction) as a result of alternative splicing of a single precursor mRNA, but these variants have not been well distinguished functionally.[97–99] The α subunit of G_{olf} is expressed predominantly in olfactory neuroepithelium, where it presumably couples odorant receptors with a largely olfactory-specific isoform of adenylate cyclase (type III).[100] Purified $G_{s\alpha}$ also activates dihydropyridine-sensitive, voltage-gated Ca^{2+} channels in patches excised from skeletal and cardiac muscle[101] and inhibits cardiac Na^+ channels.[102] The physiological significance of these last two effects is difficult to judge. G_s is activated by receptors that stimulate adenylate cyclase activity; β-adrenergic receptors are prototypical.

Members of the G_i subfamily were first encountered as retinal transducins and then as substrates for islet-activating protein. The two isoforms of transducin are selectively expressed in retinal rods and cones.[103] They are activated by photolyzed rhodopsin or the cone opsins, and each stimulates a cyclic GMP specific phosphodiesterase, resulting in lowered intracellular concentrations of cyclic GMP on illumination. A transducin-like G protein, gusducin, is expressed selectively in taste

Table 1. Properties of mammalian G protein α subunits.

Family/ subunit	M_r [kDa]	Amino acid identity [%] [a]	Toxin [b]	Lipid [c]	Distribution in tissue	Representative receptors [d]	Effector/Role [f]
G_s							
$\alpha_{s(S)}$ (2×) [e]	44.2	100	CT	P	ubiquitous	βAR,	↑ adenylate cyclase
$\alpha_{s(L)}$ (2×) [e]	45.7	–	CT	P	ubiquitous	glucagon,	↑ Ca^{2+} channels
						TSH, others	↓ Na^+ channels
α_{olf}	44.7	88	CT	P?	olfactory, neuroepithelium	odorant	↑ adenylate cyclase
G_i							
α_{i1}	40.3	100	PT	M, P	nearly ubiquitous		↓ adenylate cyclase
α_{i2}	40.5	88	PT	M, P	ubiquitous	M_2Cho, α_2AR,	↑ K^+ channels (?)
α_{i3}	40.5	94	PT	M, P	nearly ubiquitous	others	↑ phospholipase A_2 (?)
α_{oA}	40.0	73	PT	M, P	brain, others	Met-Enk,	↓ Ca^{2+} channels
α_{oB}	40.1	73	PT	M, P	brain, others	α_2AR, others	↓ adenylate cyclase, others?
α_{t1}	40.0	68	CT, PT	M	retinal rods	rhodopsin	↑ cGMP-specific
α_{t2}	40.1	68	CT, PT	M	retinal cones	cone opsins	phosphodiesterase
α_g	40.5	67	CT (?), PX	?	taste buds	taste (?)	?
α_z	40.9	60	–	M, P	brain, adrenal, platelets	M_2Cho (?), others (?)	↓ adenylate cyclase, others(?)
G_q							
α_q	42	100	–	P	nearly ubiquitous	M_1Cho, α_1AR, others	
α_{11}	42	88	–	P	nearly ubiquitous		
α_{14}	41.5	79	–	P	lung, kidney, liver	C5a, IL-8, others	↑ phospholipase Cβ's, others (?)
α_{15}	43	57	–	P?	B-cells, myeloid cells	IL-8, others (?)	
α_{16}	43.5	58	–	P	T-cells, myeloid cells	IL-8, others (?)	
G_{12}							
α_{12}	44	100	–	P	ubiquitous	?	?
α_{13}	44	67	–	P	ubiquitous	?	?

[a] Comparison is with the first-listed member of each family. [b] Cholera toxin (CT) and pertussis toxin (PT) catalyze the ADP-ribosylation of an arginine residue (CT) and a cysteine residue (PT) of the indicated α subunits. [c] Modifications by linkage to palmitic acid (P) and/or myristic acid (M). [d] Receptor abbreviations: βAR, β-adrenergic; M_2Cho, M_2-muscarinic cholinergic; α_2AR, α_2-adrenergic; Met-Enk, methionine-enkephalin; M_1Cho, M_1-muscarinic cholinergic; α_1AR, α_1-adrenergic. [e] Splice variations: $\alpha_{s(S)}$ = short forms of α_s; $\alpha_{s(L)}$ = long forms of α_s. [f] ↑ = activation; ↓ = inhibition.

buds.[104] The relationship of gusducin to the transducins is sufficiently close that a cyclic nucleotide phosphodiesterase is hypothesized to be the effector in a pathway mediating response to certain tastants.

Three closely related genes encode the three $G_{i\alpha}$ subunits. These proteins are functionally very similar in vitro, although they differ in both their cellular and subcellular distribution. Demonstration of the direct involvement of these α subunits as inhibitors of adenylate cyclases was long delayed for several technical reasons, including a requirement for comparatively high concentrations, the need for myristoylation of the α subunit, and differential responses of different isoforms of adenylate cyclase.[75, 105] This role is now well established. Although the $G_{i\alpha}$ proteins were originally thought to activate K^+ channels in cardiac myocytes and neural tissue,[106] their role in this pathway is now more controversial and may be secondary to that played by the βγ subunit complex.[107] Evidence has also accumulated for a role of at least certain $G_{i\alpha}$ proteins in membrane trafficking.[108–110] Participation of these proteins in such apparently distinct cellular pathways is confusing.

$G_{z\alpha}$ differs substantially from the $G_{i\alpha}$ proteins, but it also inhibits adenylate cyclase activity in transfected cells[111] and in vitro.[112] Notably, $G_{z\alpha}$ is not a substrate for pertussis toxin and has a very slow rate of GTP hydrolysis.[113]

As mentioned previously, the discovery of G_o was an eye-opener because of its abundance in brain (1–2% of brain membrane protein) and apparent lack of involvement with known guanine nucleotide regulated systems. Although $G_{o\alpha}$ appears to play a major role as an inhibitor of voltage-sensitive Ca^{2+} channels,[114] I assume it has other extremely important roles. Hints are supplied by its high concentration in neural growth cones[115] and apparent interactions with GAP-43, a Ca^{2+}-binding protein that is also concentrated in these structures.[116]

Compelling evidence for regulation of phosphoinositide-specific phospholipase C activities was in hand well before the relevant G proteins could be identified.[54, 55] This is a pertussis toxin insensitive process in most cells, and the PCR-based cloning of members of the $G_{q\alpha}$ subfamily provided candidates for this role.[117] Nearly simultaneously, G proteins that serve this function were identified by classical reconstitutive techniques[118, 119] and by purification of novel α subunits using clever subunit affinity and exchange techniques.[120] All three paths merged with the identification of $G_{q\alpha}$ and then $G_{11\alpha}$, $G_{14\alpha}$, and $G_{15/16\alpha}$ as activators of the various isoforms of phospholipase Cβ. Purification of the relevant proteins proved that interactions of $G_{q\alpha}$ family members with the phospholipases are direct, and these appear to occur at carboxyl-terminal domains of the enzymes. Particularly interesting is the observation that the phospholipase Cβ subunits act as GAPs or GTPase-activating proteins towards $G_{q\alpha}$.[121] In the absence of the effector, the k_{cat} value for hydrolysis of GTP by these proteins is very low, but it is increased over 50-fold by the effector. The simplest interpretation of this effect is that phospholipase Cβ should block its own activation. However, kinetic analyses of these interactions suggest that receptor, G_q, and the phospholipase associate in a complex that binds and hydrolyzes GTP rapidly, such that there is substantial steady-state activation of phospholipase C associated with particularly rapid responses.

The roles of $G_{12\alpha}$ and $G_{13\alpha}$ are unknown. Both of these proteins are structurally related to the product of the *Drosophila*

concertina gene, which appears to play a role in gastrulation.[122] Transfection of NIH 3T3 cells with $G_{12\alpha}$ cDNA results in cellular transformation.[123, 124]

Functions of $\beta\gamma$ Subunits of G Proteins

General acceptance of downstream regulation of effectors by the $\beta\gamma$ subunit complex (Table 2) is relatively recent.[69, 70] These subunits were first assigned less glamorous roles. The binding of GDP and $\beta\gamma$ to α is positively cooperative. $\beta\gamma$ thus stabilizes the inactive GDP-bound form of α by markedly reducing the rate of dissociation of nucleotide.[125] As a result, $\beta\gamma$ acts as a noise suppressor.[126] By contrast, interactions of GTP and $\beta\gamma$ with α are negatively cooperative, and it was hypothesized that $\beta\gamma$ could speed deactivation of α and thereby cause inhibition of relevant downstream responses.[127] The significance of this possibility remains ill-defined, but the eventual observation of inhibitory effects of $G_{i\alpha}$ proteins on adenylate cyclase has obviated the "need" for this hypothesis. Receptor-catalyzed exchange of GDP for GTP on G_s requires $\beta\gamma$,[128] and $\beta\gamma$ can act catalytically in this role. The G protein heterotrimer is thus the form that is recognized by receptor, and reassociation of subunits is a requisite for activation.

The first strong evidence for interaction of $\beta\gamma$ with effectors came from Logothetis et al.,[107] who detected activation of K^+ channels in cardiac atrial myocytes with $\beta\gamma$ but not with $G_{i\alpha}$. Controversy about the interpretation of these observations kept $\beta\gamma$ at least partially in the closet for a few years, despite genetic evidence that $\beta\gamma$ was the primary mediator of downstream signaling in the pheromone response pathway of budding yeast.[129] Interesting and direct interactions between $\beta\gamma$ and effectors such as adenylate cyclases[130–132] and phospholipases[133, 134] have now been observed using simple biochemical assays that have been widely reproduced; the issue thus now seems to be settled. Effects of $\beta\gamma$ on different adenylate cyclases will be discussed below.

The issue of specificity among different species of $\beta\gamma$ subunits remains vexing. Other than observations that nonretinal α subunits and effectors appear to discriminate against retinal $\beta\gamma$ ($\beta_1\gamma_1$), little specificity is observed in examination of the interactions of a number of $\beta\gamma$ subunit complexes with a variety of α subunits and effectors.[82, 135, 136] These observations, made in vitro, fly in the face of striking observations of specificity made in intact cells by Kleuss and associates.[82, 135–139] Voltage-sensitive Ca^{2+} channels in GH_3 cells are inhibited by both M_4-muscarinic and somatostatin receptors. Selective suppression of either of the two splice variants of $G_{o\alpha}$ with antisense oligonucleotides demonstrates that the muscarinic response depends on the expression of $G_{o1\alpha}$ but not $G_{o2\alpha}$, while the response to somatostatin is selectively dependent on $G_{o2\alpha}$. Similar suppression of individual β or γ subunits also yielded striking results, consistent with muscarinic signaling through $\alpha_{o1}\beta_3\gamma_4$ and somatostatin signaling through $\alpha_{o2}\beta_1\gamma_3$. The best current guess is that this specificity is exerted at the level of receptor/G protein interactions, but demonstrations of such by reconstitution of purified components in vitro remains less than convincing.

Adenylate Cyclases

We have maintained our interest in adenylate cyclases throughout the "diversion" into G proteins, although "the job" of adenylate cyclase was for some time the domain of only one individualistic lab member. This situation changed and improved substantially in 1989.

Mammalian adenylate cyclases are activated by forskolin, a diterpene found in the roots of the plant *Coleus forskolii*. The development of a forskolin-affinity matrix by Pfeuffer and Metzger[140] made purification of the enzyme possible, but not simple. Smigel was the first in our laboratory to purify a calmodulin-sensitive form of adenylate cyclase from bovine brain by adapting Pfeuffer's techniques,[141] and Krupinski and coworkers[142] finally purified a sufficient amount of protein to obtain amino acid sequence. With the invaluable help of Randall Reed at Johns Hopkins, whose collaborative efforts we sought because of the abundance of adenylate cyclase in olfactory neuroepithelium, cDNAs encoding type I (by definition) adenylate cyclase were obtained from a bovine brain library. Several labs have now contributed to the isolation of six additional full-length clones (types II–VI and VIII) by application of low-stringency hybridization and PCR techniques; all of these proteins have been expressed, and their regulatory properties are being defined.[143–145]

Table 2. Properties of mammalian G protein β and γ subunits.

Subunit	M_r [kDa]	Amino acid identity [%] [a]	Tissue distribution	Effector/Role [b]
β				support of agonist-induced receptor phosphorylation and desensitization
β_1	37.3	100	ubiquitous	
β_2	37.3	90	nearly ubiquitous	required for G_s-receptor interaction
β_3	37.2	83	nearly ubiquitous	
β_4	37.2	89	nearly ubiquitous	inhibiton of G_t activation
β_5	38.7	52	brain	
γ				↑ or ↓ adenylate cyclase (isoform-specific responses)
γ_1	8.4	100	retinal rods	↑ phospholipase Cβ_2, β_3
γ_2	7.9	38	brain, adrenal	
γ_3	8.5	36	brain, testis	↑ K^+ channels
γ_4	(?partial)	(34)	(kidney, retina (?))	
γ_5	7.3	25	ubiquitous	↑ phospholipase A_2 (?)
γ_7	7.5	35	ubiquitous	

[a] Comparison is with the first-listed member of each family. [b] ↑ = activation; ↓ = inhibition.

Mammalian, membrane-bound adenylate cyclases have a complex (deduced) structure that is reminiscent of a variety of transporters and channels (Fig. 12). Their topographical relationship to the P glycoprotein and the cystic fibrosis transmembrane conductance regulator is striking, although they share no amino acid sequence homologies with these proteins. A short

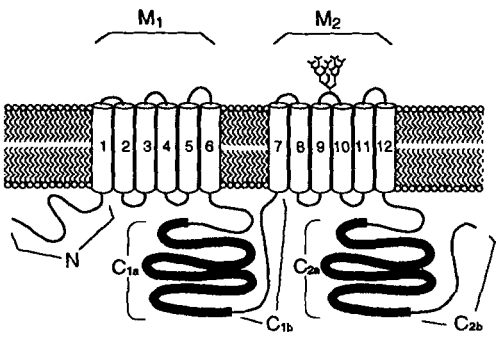

Fig. 12. Predicted topology of membrane-bound adenylate cyclases. Cylinders represent membrane-spanning regions, while bold lines indicate regions of high amino acid similarity among all members of the family. N: N-terminal domain; M_1, M_2: sets of membrane-spanning regions; C_{1a}, C_{1b}, C_{2a}, C_{2b}: large intracellular cytoplasmic domains. (Reprinted with permission from ref. [145].)

cytoplasmic amino terminus is followed by six putative transmembrane spans (designated M_1) and a roughly 40-kDa cytoplasmic domain (C_1). This apparent structural unit is then repeated: a second set of six transmembrane spans (M_2) is again followed by a second large cytoplasmic domain (C_2). Although this structure is unique for a "simple" enzyme, its significance is elusive. I find it fascinating that the regulatory motif for adenylate cyclases—activation by a GTP binding protein—is apparent in *Saccharomyces cerevisiae*. Although this mode of regulation is conserved from yeast to mammals, the molecular players are not. The adenylate cyclase of *Saccharomyces* is a very large peripheral membrane protein with little resemblance to its mammalian counterpart.[146] The GTP-binding protein in yeast responsible for stimulation of cyclic AMP synthesis is the resident homolog of mammalian $p21^{ras}$,[147] even though yeast has heterotrimeric G proteins. Evolution works in strange ways.

Two regions of roughly 200 amino acid residues each (C_{1a} and C_{2a}) are highly conserved among the mammalian adenylate cyclases, and this relationship also extends to the topographically similar enzymes of *Drosophila* and *Dictyostelium*. The C_{1a} and C_{2a} domains are also quite similar to each other and to the catalytic domains of both membrane-bound and soluble guanylate cyclases. These relationships indicate that one or both of these domains is a site of catalysis.

Unfortunately, it has not been possible to detect significant adenylate cyclase activity following expression of either of these putative catalytic domains as discrete proteins; the same is true if individual halves of the molecule are expressed in Sf9 cells. Nevertheless, concurrent expression of M_1C_1 and M_2C_2 results in appearance of a substantial level of adenylate cyclase activity that can be regulated characteristically by G protein subunits and, in the case of the type I enzyme, by calmodulin.[130] We tentatively assume that interaction between the C_1 and C_2 domains is necessary for catalysis. This is consistent with the facts that both subunits of heterodimeric, soluble guanylate cyclases are required for catalysis (each subunit contains sequences homologous to C_{1a} and C_{2a})[148] and that the membrane-bound guanylate cyclases are homo-oligomers.[149] It is also interesting that point mutations in either C_{1a} or C_{2a} can impair adenylate cyclase activity severely and that mutations in either domain can elevate the K_m value for ATP. Both domains may bind ATP; both might also catalyze cyclic AMP synthesis, or one may be the dominant catalyst while the other serves a regulatory role.

Regulation of Adenylate Cyclases by G Protein Subunits

All seven of the isoforms of adenylate cyclase identified to date are activated by $G_{s\alpha}$ (and forskolin). Surprisingly, these features (and so-called P-site inhibition by adenosine analogs) are the only shared regulatory motifs. The type I isoform is also activated by calmodulin, while it is strongly inhibited by the G protein $\beta\gamma$ subunit complex. Although this effect was originally attributed to sequestering of calmodulin by $\beta\gamma$, purification of the expressed cyclase has permitted demonstration of its direct interaction with $\beta\gamma$.[132] The three isoforms of $G_{i\alpha}$ and $G_{o\alpha}$ can also inhibit type I adenylate cyclase, but the effect is much less prominent than that of $\beta\gamma$ when calmodulin is the activator of the enzyme, and it nearly disappears when the cyclase is activated by $G_{s\alpha}$.[105]

Type I adenylate cyclase is the only isoform found to date that is inhibited by $\beta\gamma$. When we looked for such interactions with other isoforms, we were very surprised to find strong stimulation of enzymatic activity with the type II and type IV proteins.[131, 150] Particularly interesting, these stimulatory effects of $\beta\gamma$ are highly conditional. The subunits have little or no effect on adenylate cyclase activity when added alone, but the complex stimulates enzymatic activity five- to tenfold when $G_{s\alpha}$ is also present. Stimulation of type II and IV adenylate cyclases by $\beta\gamma$ requires substantially higher concentrations of $\beta\gamma$ than of $G_{s\alpha}$, and we presume that effective concentrations of both activators cannot arise by dissociation of oligomeric G_s. The source of $\beta\gamma$ is believed to be the G_i or G_o oligomers, both of which are present in high concentrations in brain. We thus envision type II and IV adenylate cyclases as molecules designed to detect coincidental activation of two regulatory pathways, marking such events with a distinctive signal. The biochemical properties of these adenylate cyclases provide an excellent explanation for phenomena described in the 1970s by Rall and associates,[151] who observed highly synergistic stimulation of cyclic AMP accumulation in brain slices after application of pairs of neurotransmitters now known to work through G_s- and G_i-regulated pathways. Given activation of type II adenylate cyclase by $\beta\gamma$, which presumably arises from G_i, it would be problematic if $G_{i\alpha}$ were to inhibit the enzyme; gratifyingly, it does not.

The first really believable demonstrations of inhibition of adenylate cyclases by $G_{i\alpha}$ were observed with the type V and type VI isoforms, where the effect is prominent.[75, 105] As noted above, it is dependent on myristoylation of these α subunits and requires fairly high, but we believe quite reasonable, concentrations of the proteins (high nM–μM). Type V and VI adenylate cyclases are thus regulated in the relatively simple way that was envisioned to be the general rule—activation by $G_{s\alpha}$ and inhibi-

tion by $G_{i\alpha}$. But even these isoforms provided surprises, in that they are inhibited by low (μM) concentrations of Ca^{2+}.

Three distinct patterns of regulation of mammalian adenylate cyclases are thus evident (Fig. 13). All isoforms are activated by $G_{s\alpha}$, and two other subclasses of G proteins, G_i and G_q, are implicated as well, either directly or indirectly. The effects of G_q family members are exerted through Ca^{2+}, either acting alone, with calmodulin, or with protein kinase C. G_i- and G_q-mediated pathways can both activate an adenylate cyclase (types II and probably IV) in concert with $G_{s\alpha}$, or they can both oppose such activation (types V and VI). The effects of G_i and G_q are antagonistic to each other with the type I enzyme. Even at this relatively early stage of investigation of the regulatory complexities of adenylate cyclases, it is clear that these enzymes have evolved to permit extensive integration and cross-talk between signaling pathways. The adenylate cyclases are focal points for the convergence of a great deal of regulatory information.

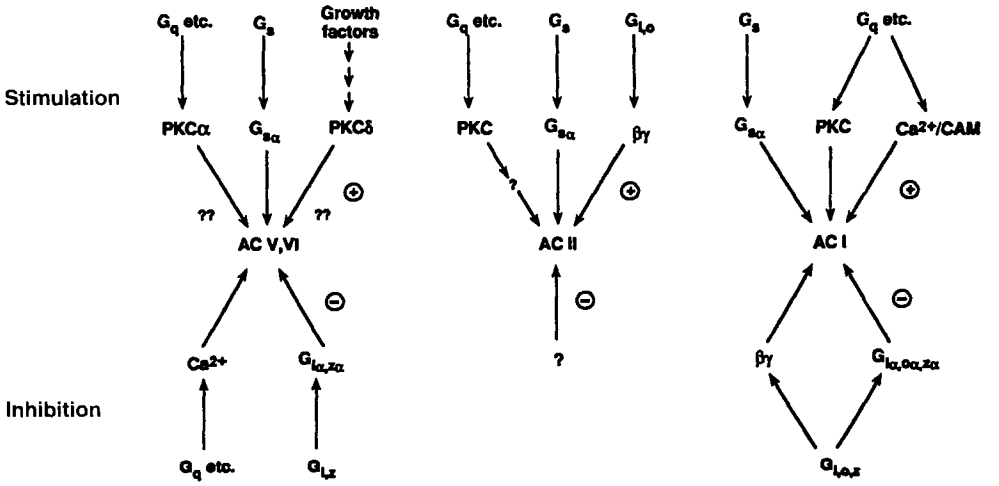

Fig. 13. Patterns of regulation of adenylate cyclase activity. PKC = protein kinase C; CAM = calmodulin; AC = adenylate cyclase. See text for discussion. (Reprinted with permission from ref. [145].)

Future Directions for Research on Adenylate Cyclase

Adenylate cyclases are labile intrinsic membrane proteins; their level of expression is low, even under artificial conditions. New tools are needed to probe their structures and mechanisms of regulation. With these thoughts in mind, Wei-Jen Tang has attempted to construct a soluble adenylate cyclase that would retain characteristic regulatory properties, be synthesized in large quantities, and be amenable to genetic analysis. He has recently succeeded in designing and synthesizing a molecule that may have all of these properties.[152] The current product is a chimera of the C_{1a} domain of type I adenylate cyclase, joined by a linker to the C_2 domain of type II adenylate cyclase. The molecule is synthesized by *E. coli*, where it accumulates in the cytoplasm. It is activated dramatically (from an extremely low basal activity) by $G_{s\alpha}$ and, surprisingly, forskolin. Cyclase-deficient strains of *E. coli* are dependent on expression and activation of the adenylate cyclase for growth on maltose. Genetic selection of mutants with informative phenotypes thus seems possible, as does purification, detailed characterization, and, hopefully, structural analysis. We hope that this approach will open the door for true understanding of these important proteins.

Why G Proteins?

One might well ask why G proteins are included in signaling pathways, and why the systems are so complex structurally. Transmembrane signaling is clearly accomplished with simpler (although usually oligomeric) molecular assemblages such as tyrosine kinases, ligand-gated ion channels, and receptor guanylate cyclases. I believe there are several reasons for the evolution of complex signaling systems. At a relatively simple level, the existence of these molecular switches and timers permits enormous amplification in the signaling process. A single agonist–receptor complex can catalyze the activation of many G proteins during the time that a single G protein α subunit remains active;[153] delayed deactivation of the α subunit permits further amplification at the level of catalytic effector molecules. There is also the possibility of substantial regulatory complexity, with opportunities to modulate both the quantitative and qualitative aspects of signaling by alterations in rates of synthesis and degradation of many gene products, as well as more acute regulation by covalent modification of these molecules. Most importantly, perhaps, the tripartite nature of these signaling systems permits enormous diversity of outputs. G protein regulated signaling pathways are characterized by both convergence and divergence at each step. Many different kinds of receptors can converge to activate a single type of G protein, while a single type of receptor can interact with more than one species of G protein to initiate several events. Similarly, different G proteins may converge on a single effector to alter its activity, either additively, synergistically, or antagonistically, while a single G protein may also interact with more than one effector. G proteins can also exert effects through either their α or βγ subunits. The complexity of the cellular switchboard thus appears sufficiently vast to permit each cell to design a highly customized signaling repertoire by expression of a relatively modest number of modular components. Identification of all of these components seems certain in the next decade or so. With this information in hand, we will be able to complete our understanding of the wiring diagram of the signaling switchboard in each type of cell. Such knowledge, coupled with both increasing sophistication in rational drug design and increasingly clever approaches to screen huge chemical libraries, will revolutionize both pharmacology and therapeutics.

There are many who have earned my most profound gratitude. My father encouraged a love of science by example, and it was carefully nurtured by my doctoral and postdoctoral mentors, Theodore W. Rall, who perhaps should have won a Nobel Prize, and Marshall W. Nirenberg, who did. All of the students and postdoctoral fellows who have worked in our laboratory have made substantial contributions. These individuals are (in alphabetical order): David Berman, Gary Bokoch, Lawrence Brunton, Patrick Casey, Francoise Coussen, Carmen Dessauer, Alex Duncan, Kenneth Ferguson, Michael Freissmuth, Boning Gao, Michael Graziano, Tatsuya Haga, Emanuel Hanski, Bruce Harris, John Hepler, Tsutomu Higashijima, Allyn Howlett, Jorge Iñiguez-Lluhi, Hiroshi Itoh, Richard Kahn, Toshiaki Katada, Christiane Kleuss, Tohru Kozasa, John Krupinski, Ethan Lee, Hsin Chieh (Calvin) Lin, Maurine Linder, Michael Maguire, David Manning, Pamela Middleton, Susanne Mumby, John Northup, Bruce Posner, Lynn Quarmby, Andre Raw, Janet Robishaw, Elliott Ross, Leonard Schleifer, Joseph Schwarzmeier, Murray Smigel, Paul Sternweis, Roger Sunahara, Wei-Jen Tang, Ronald Taussig, and Natsuo Ueda. Many members of our staff have also played crucial roles, but two long-term employees truly stand out—Pamela Sternweis and Wendy Deaner. Collaborations with others on our faculty and elsewhere have been invaluable. Particularly notable roles have been played by Susanne Mumby, Elliott Ross, Stephen Sprang, and Paul Sternweis. Our research has been supported continuously since 1972 by grants from the National Institutes of Health (first the National Institute of Neurological Disorders and Stroke and then the National Institute of General Medical Sciences) and, since 1977, by the American Cancer Society. Other invaluable sources of support have included Mr. and Mrs. Peter O'Donnell, the Lucille P. Markey Charitable Trust, the Raymond Willie Chair of Molecular Neuropharmacology, the Perot Family Foundation, the Meadows Foundation, and the Robert A. Welch Foundation.

Received: January 16, 1995 [A 102 IE]
German version: *Angew. Chem.* **1995**, *107*, 1533–1548

Keywords: adenylate cyclases · G proteins · Nobel lecture

[1] T. W. Rall, E. W. Sutherland, J. Berthet, *J. Biol. Chem.* **1957**, *224*, 463–475.
[2] F. Murad, Y.-M. Chi, T. W. Rall, E. W. Sutherland, *J. Biol. Chem.* **1962**, *237*, 1233–1238.
[3] T. W. Rall, E. W. Sutherland, *Cold Spring Harbor Symp. Quant. Biol.* **1961**, *26*, 347–354.
[4] L. Birnbaumer, M. Rodbell, *J. Biol. Chem.* **1969**, *244*, 3477–3482.
[5] L. E. Limbird, R. J. Lefkowitz, *J. Biol. Chem.* **1977**, *252*, 799–802.
[6] T. Haga, K. Haga, A. G. Gilman, *J. Biol. Chem.* **1977**, *252*, 5776–5782.
[7] M. Rodbell, L. Birnbaumer, S. L. Pohl in *The Role of Adenyl Cyclase and Cyclic 3',5'-AMP in Biological Systems* (Eds.: T. W. Rall, M. Rodbell, P. Condliffe) (*Fogarty Int. Cent. Proc. n4*), National Institutes of Health, Bethesda, MD, **1969**, pp. 59–76.
[8] M. Rodbell, L. Birnbaumer, S. L. Pohl, H. M. J. Krans, *J. Biol. Chem.* **1971**, *246*, 1877–1882.
[9] K. H. Jakobs, K. Aktories, G. Schultz, *Arch. Pharm. (Weinheim Ger.)* **1979** *310*, 113–119.
[10] D. Cassel, Z. Selinger, *Biochem. Biophys. Acta* **1976**, *452*, 538–551.
[11] C. Londos, Y. Salomon, M. C. Lin, J. P. Harwood, M. Schramm, J. Wolff, M. Rodbell, *Proc. Natl. Acad. Sci. USA* **1974**, *71*, 3087–3090.
[12] M. Schramm, M. Rodbell, *J. Biol. Chem.* **1975**, *250*, 2232–2237.
[13] M. E. Maguire, P. M. Van Arsdale, A. G. Gilman, *Mol. Pharmacol.* **1976**, *12*, 335–339.
[14] E. J. Neer, *J. Biol. Chem.* **1974**, *249*, 6527–6531.
[15] V. Daniel, G. Litwack, G. M. Tomkins, *Proc. Natl. Acad. Sci. USA* **1973**, *70*, 76–79.
[16] H. R. Bourne, P. Coffino, G. M. Tomkins, *Science* **1975**, *187*, 750–752.
[17] P. A. Insel, M. Maguire, A. G. Gilman, H. R. Bourne, P. Coffino, K. L. Melmon, *Mol. Pharmacol.* **1976**, *12*, 1062–1069.
[18] T. Haga, E. M. Ross, H. J. Anderson, A. G. Gilman, *Proc. Natl. Acad. Sci. USA* **1977**, *74*, 2016–2020.
[19] E. M. Ross, A. G. Gilman, *Proc. Natl. Acad. Sci. USA* **1977**, *74*, 3715–3719.
[20] E. M. Ross, A. G. Gilman, *J. Biol. Chem.* **1977**, *252*, 6966–6969.
[21] E. M. Ross, A. C. Howlett, K. M. Ferguson, A. G. Gilman, *J. Biol. Chem.* **1978**, *253*, 6401–6412.
[22] T. Pfeuffer, *J. Biol. Chem.* **1977**, *252*, 7224–7234.
[23] A. C. Howlett, A. G. Gilman, *J. Biol. Chem.* **1980**, *255*, 2861–2866.
[24] J. K. Northup, P. C. Sternweis, M. D. Smigel, L. S. Schleifer, E. M. Ross, A. G. Gilman, *Proc. Natl. Acad. Sci. USA* **1980**, *77*, 6516–6520.
[25] P. C. Sternweis, J. K. Northup, M. D. Smigel, A. G. Gilman, *J. Biol. Chem.* **1981**, *256*, 11517–11526.
[26] J. K. Northup, M. D. Smigel, A. G. Gilman, *J. Biol. Chem.* **1982**, *257*, 11416–11423.
[27] J. K. Northup, M. D. Smigel, P. C. Sternweis, A. G. Gilman, *J. Biol. Chem.* **1983**, *258*, 11369–11376.
[28] A. C. Howlett, P. C. Sternweis, B. A. Macik, P. M. Van Arsdale, A. G. Gilman, *J. Biol. Chem.* **1979**, *254*, 2287–2295.
[29] P. C. Sternweis, A. G. Gilman, *Proc. Natl. Acad. Sci. USA* **1982**, *79*, 4888–4891.
[30] D. M. Gill, R. Meren, *Proc. Natl. Acad. Sci. USA* **1978**, *75*, 3050–3054.
[31] J. Moss, M. Vaughan, *J. Biol. Chem.* **1977**, *252*, 2455–2457.
[32] H. R. Kaslow, Z. Farfel, G. L. Johnson, H. R. Bourne, *Mol. Pharmacol.* **1979**, *15*, 472–483.
[33] L. S. Schleifer, R. A. Kahn, E. Hanski, J. K. Northup, P. C. Sternweis, A. G. Gilman, *J. Biol. Chem.* **1982**, *257*, 20–23.
[34] R. A. Kahn, A. G. Gilman, *J. Biol. Chem.* **1984**, *259*, 6228–6234.
[35] R. A. Kahn, A. G. Gilman, *J. Biol. Chem.* **1986**, *261*, 7906–7911.
[36] J. E. Rothman, *Nature (London)* **1994**, *372*, 55–63.
[37] H. A. Brown, S. Gutowski, C. R. Moomaw, C. Slaughter, P. C. Sternweis, *Cell* **1993**, *75*, 1137–1144.
[38] O. Hazeki, M. Ui, *J. Biol. Chem.* **1981**, *256*, 2856–2862.
[39] T. Katada, M. Ui, *J. Biol. Chem.* **1982**, *257*, 7210–7216.
[40] G. M. Bokoch, T. Katada, J. K. Northup, E. L. Hewlett, A. G. Gilman, *J. Biol. Chem.* **1983**, *258*, 2072–2075.
[41] G. M. Bokoch, T. Katada, J. K. Northup, M. Ui, A. G. Gilman, *J. Biol. Chem.* **1984**, *259*, 3560–3567.
[42] T. Katada, G. M. Bokoch, J. K. Northup, M. Ui, A. G. Gilman, *J. Biol. Chem.* **1984**, *259*, 3568–3577.
[43] T. Katada, J. K. Northup, G. M. Bokoch, M. Ui, A. G. Gilman, *J. Biol. Chem.* **1984**, *259*, 3578–3585.
[44] T. Katada, G. M. Bokoch, M. D. Smigel, M. Ui, A. G. Gilman, *J. Biol. Chem.* **1984**, *259*, 3586–3595.
[45] N. Miki, J. J. Keirns, F. R. Marcus, J. Freeman, M. W. Bitensky, *Proc. Natl. Acad. Sci. USA* **1973**, *70*, 3820–3824.
[46] G. L. Wheeler, M. W. Bitensky, *Proc. Natl. Acad. Sci. USA* **1977**, *74*, 4238–4242.
[47] H. Kuhn, *Nature (London)* **1980**, *283*, 587–589.
[48] B. K.-K. Fung, J. B. Hurley, L. Stryer, *Proc. Natl. Acad. Sci. USA* **1981**, *78*, 152–156.
[49] D. R. Manning, A. G. Gilman, *J. Biol. Chem.* **1983**, *258*, 7059–7063.
[50] J. D. Hildebrandt, J. Codina, R. Risinger, L. Birnbaumer, *J. Biol. Chem.* **1984**, *259*, 2039–2042.
[51] D. C. May, E. M. Ross, A. G. Gilman, M. D. Smigel, *J. Biol. Chem.* **1985**, *260*, 15829–15833.
[52] P. C. Sternweis, J. D. Robishaw, *J. Biol. Chem.* **1984**, *259*, 13806–13813.
[53] E. J. Neer, J. M. Lok, L. G. Wolf, *J. Biol. Chem.* **1984**, *259*, 14222–14229.
[54] I. Litosch, C. Wallis, J. N. Fain, *J. Biol. Chem.* **1985**, *260*, 5464–5471.
[55] S. Cockcroft, B. D. Gomperts, *Nature (London)* **1985**, *314*, 534–536.
[56] J. B. Hurley, M. I. Simon, D. B. Teplow, J. D. Robishaw, A. G. Gilman, *Science* **1984**, *226*, 860–862.
[57] M. A. Lochrie, J. B. Hurley, M. I. Simon, *Science* **1985**, *228*, 96–99.
[58] K. Yatsunami, H. G. Khorana, *Proc. Natl. Acad. Sci. USA* **1985**, *82*, 4316–4320.
[59] A. G. Gilman, *Annu. Rev. Biochem.* **1987**, *56*, 615–649.
[60] E. M. Ross, *Neuron* **1989**, *3*, 141–152.
[61] A. M. Brown, L. Birnbaumer, *Annu. Rev. Physiol.* **1990**, *52*, 197–213.
[62] H. R. Bourne, D. A. Snaders, F. McCormick, *Nature (London)* **1990**, *348*, 125–132.
[63] H. R. Bourne, D. A. Sanders, F. McCormick, *Nature (London)* **1991**, *349*, 117–127.
[64] H. G. Dohlman, J. Thorner, M. G. Caron, R. J. Lefkowitz, *Annu. Rev. Biochem.* **1991**, *60*, 653–688.
[65] Y. Kaziro, H. Itoh, T. Kozasa, M. Nakafuku, T. Satoh, *Annu. Rev. Biochem.* **1991**, *60*, 349–400.
[66] M. I. Simon, M. P. Strathmann, N. Gautam, *Science* **1991**, *252*, 802–808.
[67] A. M. Spiegel, P. S. Backlund, Jr., J. E. Butrynski, T. L. Z. Jones, W. F. Simonds, *Trends Biochem. Sci.* **1991**, *16*, 338–341.
[68] J. R. Hepler, A. G. Gilman, *Trends Biochem. Sci.* **1992**, *17*, 383–387.
[69] D. E. Clapham, E. J. Neer, *Nature (London)* **1993**, *365*, 403–406.
[70] J. Iñiguez-Lluhi, C. Kleuss, A. G. Gilman, *Trends Cell Biol.* **1993**, *3*, 230–236.
[71] J. E. Buss, S. M. Mumby, P. J. Casey, A. G. Gilman, B. M. Sefton, *Proc. Natl. Acad. Sci. USA* **1987**, *84*, 7493–7497.

[72] S. M. Mumby, R. O. Heuckeroth, J. I. Gordon, A. G. Gilman, *Proc. Natl. Acad. Sci. USA* **1990**, *87*, 728–732.
[73] T. L. Z. Jones, W. F. Simonds, J. J. Merendino, Jr., M. R. Brann, A. M. Spiegel, *Proc. Natl. Acad. Sci. USA* **1990**, *87*, 568–572.
[74] M. E. Linder, I.-H. Pang, R. J. Duronio, J. I. Gordon, P. C. Sternweis, A. G. Gilman, *J. Biol. Chem.* **1991**, *266*, 4654–4659.
[75] R. Taussig, J. Iñiguez-Lluhi, A. G. Gilman, *Science* **1993**, *261*, 218–221.
[76] M. E. Linder, P. Middleton, J. R. Hepler, R. Taussig, A. G. Gilman, S. M. Mumby, *Proc. Natl. Acad. Sci. USA* **1993**, *90*, 3675–3679.
[77] S. M. Mumby, C. Kleuss, A. G. Gilman, *Proc. Natl. Acad. Sci. USA* **1994**, *91*, 2800–2804.
[78] P. B. Wedegaertner, H. R. Bourne, *Cell* **1994**, *77*, 1063–1070.
[79] Y. Fukada, T. Takao, H. Ohguro, T. Yoshizawa, T. Akino, Y. Shimonishi, *Nature (London)* **1990**, *346*, 658–660.
[80] H. K. Yamane, C. C. Farnsworth, H. Xie, W. Howald, B. K.-K. Fung, S. Clarke, M. H. Gelb, J. A. Glomset, *Proc. Natl. Acad. Sci. USA* **1990**, *87*, 5868–5872.
[81] S. M. Mumby, P. J. Casey, A. G. Gilman, S. Gutowski, P. C. Sternweis, *Proc. Natl. Acad. Sci. USA* **1990**, *87*, 5873–5877.
[82] J. A. Iñiguez-Lluhi, M. I. Simon, J. D. Robishaw, A. G. Gilman, *J. Biol. Chem.* **1992**, *267*, 23409–23417.
[83] M. P. Graziano, M. Freissmuth, A. G. Gilman, *J. Biol. Chem.* **1989**, *264*, 409–418.
[84] C. Van Dop, M. Tsubokawa, H. R. Bourne, J. Ramachandran, *J. Biol. Chem.* **1984**, *259*, 696–698.
[85] R. E. West, Jr., J. Moss, M. Vaughan, T. Liu, T.-Y. Liu, *J. Biol. Chem.* **1985**, *260*, 14428–14430.
[86] J. P. Noel, H. E. Hamm, P. B. Sigler, *Nature (London)* **1993**, *366*, 654–663.
[87] D. G. Lambright, J. P. Noel, H. E. Hamm, P. B. Sigler, *Nature (London)* **1994**, *369*, 621–628.
[88] D. E. Coleman, A. M. Berghuis, E. Lee, M. E. Linder, A. G. Gilman, S. R. Sprang, *Science* **1994**, *265*, 1405–1412.
[89] J. Bigay, P. Deterre, C. Pfister, M. Chabre, *FEBS Lett.* **1985**, *191*, 181–185.
[90] T. Higashijima, M. P. Graziano, H. Suga, M. Kainosho, A. G. Gilman, *J. Biol. Chem.* **1991**, *266*, 3396–3401.
[91] M. P. Graziano, A. G. Gilman, *J. Biol. Chem.* **1989**, *264*, 15475–15482.
[92] C. A. Landis, S. B. Masters, A. Spada, A. M. Pace, H. R. Bourne, L. Vallar, *Nature (London)* **1989**, *340*, 692–696.
[93] M. Freissmuth, A. G. Gilman, *J. Biol. Chem.* **1989**, *264*, 21907–21914.
[94] S. B. Masters, R. T. Miller, M.-H. Chi, F.-H. Chang, B. Beiderman, N. G. Lopez, H. R. Bourne, *J. Biol. Chem.* **1989**, *264*, 15467–15474.
[95] M. Mixon, D. E. Coleman, A. M. Berghuis, E. Lee, A. G. Gilman, S. R. Sprang, unpublished.
[96] S. Coulter, M. Rodbell, *Proc. Natl. Acad. Sci. USA* **1992**, *89*, 5842–5846.
[97] J. D. Robishaw, M. D. Smigel, A. G. Gilman, *J. Biol. Chem.* **1986**, *261*, 9587–9590.
[98] P. Bray, A. Carter, C. Simons, V. Guo, C. Puckett, J. Kamholz, A. Spiegel, M. Nirenberg, *Proc. Natl. Acad. Sci. USA* **1986**, *83*, 8893–8897.
[99] T. Kozasa, H. Itoh, T. Tsukamoto, Y. Kaziro, *Proc. Natl. Acad. Sci. USA* **1988**, *85*, 2081–2085.
[100] D. T. Jones, R. R. Reed, *Science* **1989**, *244*, 790–795.
[101] A. Yatani, J. Codina, Y. Imoto, J. P. Reeves, L. Birnbaumer, A.M. Brown, *Science* **1987**, *238*, 1288–1292.
[102] B. Schubert, A. M. J. VanDongen, G. E. Kirsch, A. M. Brown, *Science* **1989**, *245*, 516–519.
[103] C. L. Lerea, D. E. Somers, J. B. Hurley, I. B. Klock, A. H. Bunt-Milam, *Science* **1986**, *234*, 77–80.
[104] S. K. McLaughlin, P. J. McKinnon, R. F. Margolskee, *Nature (London)* **1992**, *357*, 563–569.
[105] R. Taussig, W.-J. Tang, J. R. Hepler, A. G. Gilman, *J. Biol. Chem.* **1994**, *269*, 6093–6100.
[106] J. Codina, A. Yatani, D. Grenet, A. M. Brown, L. Birnbaumer, *Science* **1987**, *236*, 442–444.
[107] D. E. Logothetis, Y. Kurachi, J. Galper, E. J. Neer, D. E. Clapham, *Nature (London)* **1987**, *325*, 321–326.
[108] J. L. Stow, J. B. de Almeida, N. Narula, E. J. Holtzman, L. Ercolani, D. A. Ausiello, *J. Cell. Biol.* **1991**, *114*, 1113–1124.
[109] J. G. Donaldson, R. A. Kahn, J. Lippincott-Schwartz, R. D. Klausner, *Science* **1991**, *254*, 1197–1199.
[110] N. T. Ktistakis, M. E. Linder, M. G. Roth, *Nature (London)* **1992**, *356*, 344–346.
[111] Y. H. Wong, B. R. Conklin, H. R. Bourne, *Science* **1992**, *255*, 339–341.
[112] T. Kozasa, A. G. Gilman, *J. Biol. Chem.* **1995**, *270*, 1734–1741.
[113] P. J. Casey, H. K. W. Fong, M. I. Simon, A. G. Gilman, *J. Biol. Chem.* **1990**, *265*, 2383–2390.
[114] J. Hescheler, W. Rosenthal, W. Trautwein, G. Schultz, *Nature (London)* **1987**, *325*, 445–447.
[115] S. M. Strittmatter, D. Valenzuela, T. E. Kennedy, E. J. Neer, M. C. Fishman, *Nature (London)* **1990**, *344*, 836–841.
[116] S. M. Strittmatter, D. Valenzuela, Y. Sudo, M. E. Linder, M. C. Fishman, *J. Biol. Chem.* **1991**, *266*, 22465–22471.
[117] M. Strathmann, T. M. Wilkie, M. I. Simon, *Proc. Natl. Acad. Sci. USA* **1989**, *86*, 7407–7409.
[118] S. J. Taylor, J. A. Smith, J. H. Exton, *J. Biol. Chem.* **1990**, *265*, 17150–17156.
[119] G. L. Waldo, J. L. Boyer, A. J. Morris, T. K. Harden, *J. Biol. Chem.* **1991**, *266*, 14217–14225.
[120] A. V. Smrcka, J. R. Hepler, K. O. Brown, P. C. Sternweis, *Science* **1991**, *251*, 804–807.
[121] G. Berstein, J. L. Blank, D. Y. Jhon, J. H. Exton, S. G. Rhee, E. M. Ross, *Cell* **1992**, *70*, 411–418.
[122] S. Parks, E. Wieschaus, *Cell* **1991**, *64*, 447–458.
[123] A. M. L. Chan, T. P. Fleming, E. S. Mcgovern, M. Chedid, T. Miki, S. A. Aaronson, *Mol. Cell. Biol.* **1993**, *13*, 762–768.
[124] N. Z. Xu, L. Bradley, I. Ambdukar, J. S. Gutkind, *Proc. Natl. Acad. Sci. USA* **1993**, *90*, 6741–6745.
[125] T. Higashijima, K. M. Ferguson, P. C. Sternweis, M. D. Smigel, A. G. Gilman, *J. Biol. Chem.* **1987**, *262*, 762–766.
[126] R. A. Cerione, C. Staniszewski, M. G. Caron, R. J. Lefkowitz, J. Codina, L. Birnbaumer, *Nature (London)* **1985**, *318*, 293–295.
[127] A. G. Gilman, *Cell* **1984**, *36*, 577–579.
[128] V. A. Florio, P. C. Sternweis, *J. Biol. Chem.* **1985**, *260*, 3477–3483.
[129] C. Dietzel, J. Kurjan, *Cell* **1987**, *50*, 1001–1010.
[130] W.-J. Tang, J. Krupinski, A. G. Gilman, *J. Biol. Chem.* **1991**, *266*, 8595–8603.
[131] W.-J. Tang, A. G. Gilman, *Science* **1991**, *254*, 1500–1503.
[132] R. Taussig, L. M. Quarmby, A. G. Gilman, *J. Biol. Chem.* **1993**, *268*, 9–12.
[133] M. Camps, C. Hou, D. Sidiropoulos, J. B. Stock, K. H. Jakobs, P. Gierschik, *Eur. J. Biochem.* **1992**, *206*, 821–831.
[134] M. Camps, A. Carozzi, P. Schnabel, A. Scheer, P. J. Parker, P. Gierschik, *Nature (London)* **1992**, *360*, 684–686.
[135] N. Ueda, J. A. Iñiguez-Lluhi, E. Lee, A. V. Smrcka, J. D. Robshaw, A. G. Gilman, *J. Biol. Chem.* **1994**, *269*, 4388–4395.
[136] O. Kisselev, N. Gautam, *J. Biol. Chem.* **1993**, *268*, 24519–24522.
[137] C. Kleuss, J. Hescheler, C. Ewel, W. Rosenthal, G. Schultz, B. Wittig, *Nature (London)* **1991**, *353*, 43–48.
[138] C. Kleuss, H. Scherubl, J. Hescheler, G. Schultz, B. Wittig, *Nature (London)* **1992**, *358*, 424–426.
[139] C. Kleuss, H. Scherubl, J. Hescheler, G. Schultz, B. Wittig, *Science* **1993**, *259*, 832–834.
[140] T. Pfeuffer, H. Metzger, *FEBS Lett.* **1982**, *146*, 369–375.
[141] M. D. Smigel, *J. Biol. Chem.* **1986**, *261*, 1976–1982.
[142] J. Krupinski, F. Coussen, H. A. Bakalyar, W.-J. Tang, P. G. Feinstein, K. Orth, C. Slaughter, R. R. Reed, A. G. Gilman, *Science* **1989**, *244*, 1558–1564.
[143] W.-J. Tang, A. G. Gilman, *Cell* **1992**, *70*, 869–872.
[144] R. Iyengar, *FASEB J.* **1993**, *7*, 768–775.
[145] R. Taussig, A. G. Gilman, *J. Biol. Chem.* **1995**, *270*, 1–4.
[146] T. Kataoka, D. Broek, M. Wigler, *Cell* **1985**, *43*, 493–505.
[147] T. Toda, I. Uno, T. Ishikawa, S. Powers, T. Kataoka, D. Broek, S. Cameron, J. Broach, K. Matsumoto, M. Wigler, *Cell* **1985**, *40*, 27–36.
[148] M. Nakane, K. Arai, S. Saheki, T. Kuno, W. Buechler, F. Murad, *J. Biol. Chem.* **1990**, *265*, 16841–16845.
[149] M. Chinkers, E. M. Wilson, *J. Biol. Chem.* **1992**, *267*, 18589–18597.
[150] B. Gao, A. G. Gilman, *Proc. Natl. Acad. Sci. USA* **1991**, *88*, 10178–10182.
[151] A. Sattin, T. W. Rall, J. Zanella, *J. Pharmacol. Exp. Ther.* **1975**, *192*, 22–32.
[152] W.-J. Tang, A. G. Gilman, *Science*, **1995**, in press.
[153] D. R. Brandt, E. M. Ross, *J. Biol. Chem.* **1986**, *261*, 1656–1664.
[154] M. E. Linder, A. G. Gilman, *Sci. Am.* **1992**, *267(1)*, 56–65.

Signal Transduction: Evolution of an Idea (Nobel Lecture)**

Martin Rodbell*

In general there is no set of observations conceivable which can give enough information about the past of a system to give complete information as to its future.
Norbert Wiener

Think simplicity; then discard it.
Alfred North Whitehead

Introduction

I was born in 1925, a time when there were no talking movies, when radio was just emerging as a popular listening device, newspapers printed important information, and libraries were sources of both pleasure and learning. My father's grocery store (above which we lived) was a community center where people from blocks away would come for their groceries and to gossip. We knew or knew about everyone in our neighborhood. In that atmosphere I grew up as a young man feeling the warmth of this community. Retrospectively, I have come to realize how important this long-gone community and the intense human relationships have been to my development as a scientist. My scientific neighborhood encompasses a place where cultural and language differences have been melded seamlessly and with synergy to promote communication, to expand knowledge with a kinship of purpose, and to create new thought. Nature, which we often equate with our genetic make up, and Nurture, which symbolizes our environment, interact mutually and synergistically in this community. These are the forces that have given meaning to life; the question of which comes first, the chicken or the egg, is not of biological importance.

My lecture reflects my interest in societal/cellular relationships and concerns the broad issues of biological communication. The first half will deal with the development of the concept of transducers and their role in cell signaling. Since this concept is still at an evolutionary phase, I will conclude with an hypothesis which in its simplest message argues that biological communication consists of a complex meshwork of structures in which G proteins, surface receptors, the extracellular matrix, and the vast cytoskeletal network within cells are joined in a community of effort, for which my life and those of my colleagues is a metaphor.

[*] Prof. M. Rodbell
National Institute of Environmental Health Sciences
Building 18-01
P.O. Box 12333
Research Triangle Park, NC 27709 (USA)
Telefax: Int. code +(919) 541-0669

[**] Copyright © The Nobel Foundation 1995. We thank the Nobel Foundation, Stockholm, for permission to print this lecture.

Receptors, Allostery, and the Second-Messenger Theory

The concept of receptors as sensory elements in biology has a long history. Early in this century Paul Ehrlich realized the importance of surface receptors and postulated a "lock-and-key" theory to explain their interactions with antigenic materials and drugs. Today, it is understood that receptors are proteins with the patterns of design and malleability of structure required for discriminating between an extraordinary variety of chemical signals. My interest in receptors began in the early 1960s, when I uncorked the means of freeing adipocytes from their tissue matrix by collagenase treatment and found that insulin at physiological concentrations stimulated glucose uptake.[1] Searching for the possible site of action of the hormone, I tested the effects of treating adipocytes with phospholipases and proteases on the assumption that, if the surface or plasma membrane contains insulin receptors, these digestive enzymes might prevent insulin action. Surprisingly, phospholipases mimicked the known actions of insulin on glucose utilization and protein synthesis.[2, 3] Based on such observations, I postulated that insulin might act by stimulating phospholipases,[4] not a bad hypothesis in view of the accumulated evidence of the importance of phospholipases in mediating the actions of a variety of hormones.[5]

During the 1960s two major theories influenced the course of my research on hormone receptors. One was the "second-messenger" theory.[6, 7] This theory suggested that extracellular or primary messengers in the form of hormones or neurotransmitters act through receptors that regulate the production of adenosine-3′,5′-monophosphate (cyclic AMP), considered to be the intracellular messenger that mediates the actions of hormones on all aspects of cellular metabolism, growth, and differentiation. The perceptions of Monod and colleagues that led to their incisive theory of allosteric regulation[8] blended beautifully with Sutherland's theory that receptors are structurally and functionally linked to the regulation of cyclic AMP production. Overwhelmingly persuasive was the notion that adenyl (now adenylate or adenylyl cyclase) is an allosterically regulated enzyme system containing two distinct sites for binding receptors and for triggering catalytic action. Located at the surface or plasma membrane of cells, the asymmetric positioning of these sites—the allosteric hormone-sensing sites on the exterior and ATP-utilizing catalytic sites at the interior surfaces of the membrane—provided a logical framework for investigating the molecular basis for hormone action. My attention shifted from

insulin to those hormones known to stimulate the production of cyclic AMP in fat cells.

The Multireceptor Adenylate Cyclase System in Adipocytes

At the time, the only specific assay for cyclic AMP production relied on a complicated, time-consuming bioassay. Krishna[9] and later Salomon[10] developed relatively simple chromatographic assays which for the first time allowed rapid, multiple assays of adenylate cyclase. When Lutz Birnbaumer arrived in my laboratory in 1967, that assay literally danced under his extraordinary prowess, yielding information that laid the foundation for the concept of transducers. Prior to his coming, I had developed a rapid method for obtaining fat cell membranes (called "ghosts") responsive not only to insulin but also to various hormones that stimulate cyclic AMP production and resultant lipolysis in fat cells.[11] These hormones included epinephrine, adrenocorticotropic hormone (ACTH), thyrotropin (TSH), lutinizing hormone (LH), and secretin, as well as glucagon and fluoride ions. The latter, shown previously to stimulate adenylate cyclase in a variety of cell membranes,[6] activated the fat cell system by a Mg^{2+}-dependent process displaying a Hill coefficient of 2.0, suggesting that the system may contain at least two sites of action for Mg ions, one certainly a Mg–ATP complex at the catalytic site. That a regulatory site for Mg ions exists was suggested by the finding that both ACTH and fluoride ions markedly reduced the concentration of Mg ions necessary for stimulation of activity.[12] The kinetics of ATP action proved too complicated for interpretation at the time. Not realizing that ATP was contaminated with GTP, we couldn't interpret what later proved to be the stimulatory and inhibitory actions of GTP on adenylate cyclase systems. The lesson is clear to me today: never attempt to interpret a hyperbolic curve; it describes the behavior of the entire universe!

Demonstration of Distinct Hormone Receptors

Much of our energy and time was devoted to delineating the receptors for the hormones that stimulated the cyclase system. The pharmacology of the peptide hormones receptor was essentially unknown and necessitated a variety of indirect tests, including the effects of proteases, inhibitory analogs, and differential ion dependencies, which in combination suggested that each of the hormones stimulated cyclase through distinct receptor types. Since the enzyme system and the receptors were contained in the same cell, these findings allowed us to test a fundamental question: do all of the hormones operate on the same enzyme or, as depicted in the Sutherland model, is each hormone receptor coupled to separate cyclase models? The various hormones were tested at maximal and submaximal concentrations alone or combined with the other hormones. Synergy was seen with some combinations but, most importantly, additivity of response was not obtained with maximal concentrations of the hormones.[13] Similar findings were reported simultaneously.[14] Although not proof, we argued that the fat cell cyclase system most likely consists of multiple receptors interacting with a common catalytic unit. Conceptually, the picture that emerged is that each receptor contains specific binding regions and some common structural element that interacts with the catalytic component to stimulate conversion of MgATP to cAMP. At that time we considered that the catalytic component contains the regulatory site for Mg ions and is the site of action of fluoride ion. Lipids were somehow involved in the structural interactions between receptors and catalytic unit, because, unlike fluoride action, hormone action was exquisitely sensitive to agents (phospholipases, detergents) that affect membrane structure.[15] It was clear that hormone action involved a more complex structural and regulatory enzyme system than originally thought. It was inconceivable to me that several hormone receptors could be structurally annealed to the same enzyme (I referred to this problem as "too many angels on a pinhead"). A new concept of hormone action had to be considered.

Martin Rodbell was born in 1925 in Baltimore, MD (USA) and studied biology and chemistry at Johns Hopkins University. He earned his PhD in biochemistry in 1954 at the University of Washington in Seattle for his research on the biosynthesis of lecithin in rat liver conducted under the direction of Prof. D. Hanaken. During subsequent postdoctoral studies with Dr. H. E. Carter at the University of Illinois in Urbana he examined the biosynthesis of chloramphenicol. He then worked with Dr. Anfinsen at the National Heart Institute in Bethesda, MD, where he studied lipoproteins. In 1960 he joined Prof. J. Brachet's research group at the Free University of Brussels, Belgium, and then moved to the laboratory headed by Dr. P. Gaillard in Leiden, The Netherlands. He returned to the U.S. in 1961 and was offered a position in the Laboratory of Nutrition and Endocrinology at the Institute of Arthritis and Metabolic Diseases in Bethesda, MD. Here he conducted research on lipoprotein lipases and insulin action on the utilization of glucose in fat cells. In the mid-1960s Rodbell's research interests were redirected by Earl Sutherland's "second-messenger" theory of hormone action and the role of cyclic AMP. In the next few years Rodbell and Lutz Birnbaumer developed the concept of transducers and principles of signal transduction. During the period 1967–1968 Rodbell focused his research efforts on the effect of hormones on ion and amino acid transport in fat cells. He served as interim Director of the Institut de Biochimie Clinique in Geneva, Switzerland, and was later appointed Professor at the Laboratory of Biochemistry at the University of Geneva (1981–1983), during which time he conducted research on the structure and function of glucagon.

Informational Processing: The Concept of Transduction

At that time my thinking on the subject of how hormonal information is transferred across the cell membrane and translated into action was greatly influenced by the theories of informational processing proposed by Norbert Wiener,[16] the originator of cybernetic theory. This subject was introduced to me by Oscar Hechter, who had previously proposed several important theoretical considerations concerning hormone action. He was the first to question the proposition that hormones act directly on the adenylate cyclase enzyme.[17] Through lengthy discussions at a downtown hotel bar in Washington D.C. prior to a meeting that I had organized at NIH to honor Sutherland, we arrived at the concept of transduction as a means of coupling information between signal-activated receptor and regulation of adenylate cyclase. Given the paucity of knowledge at that time, the concept of informational processing was put in abstract cybernetic terms: a discriminator representing the receptor, a transducer, and an amplifier representing adenylate cyclase because of the large increase in cyclic AMP generated when converted to its activated state. The transducer is a coupling device designed to allow communication between discriminator and amplifier. At the meeting I presented this idea, illustrated (but without participation of Mg ions and GTP at that time) in Figure 1. We considered the possibility that Mg ions and lipids participate in the transduction process, but we realized that the transducer concept required fleshing out with more evidence on the structure/functional relationships between receptor and enzyme.

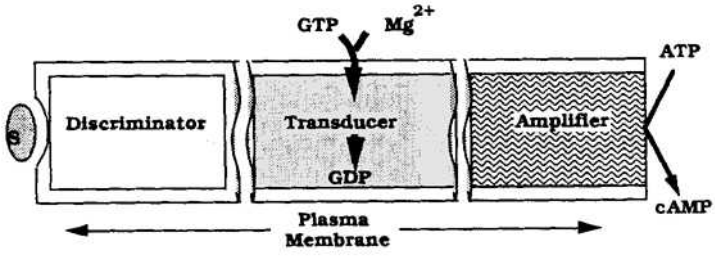

Fig. 1. Cybernetic description of signal transduction. S = signal.

The Actions of GTP and Glucagon on Liver Cyclase

Because of the experimental complexity of studying the multireceptor adenylate cyclase system in rat adipocytes, my colleagues (Birnbaumer, Pohl, Krans) and I turned our attention to the glucagon-sensitive adenylate cyclase system in liver. To some extent this change was made because of the historical significance of the hepatic system in hormone action and, coincidentally, because David Neville[18] at NIH had reported purification of rat liver plasma membranes by a relatively simple procedure. As importantly, we radio-labeled glucagon with ^{125}I making it possible to investigate both the nature of the glucagon receptor and the relationship between hormone binding and hormonal activation of adenylate cyclase.

Michiel Krans began the glucagon-binding studies with our findings that hormonal activation of adenylate cyclase in liver membranes rises within seconds and falls rapidly when the hormone is displaced by an antagonist such as des-his-glucagon, which proved later to be a weak partial agonist. Our expectations were that binding of ^{125}I-labeled glucagon would proceed rapidly (within seconds) and would be reversed easily by washing the membranes free of medium containing the hormone. Instead, Krans observed that binding was extremely slow requiring at least 20 minutes before reaching a plateau. Extensive washing under a variety of conditions failed to remove the bound material. None of the binding characteristics fit with the kinetics of hormone action. However, the medium used for binding contained nothing but salt and buffer, whereas the cyclase assay medium contained multiple components including the substrate, MgATP. A dramatic change resulted when all of the cyclase ingredients were added to the hormone-binding medium. The level of bound hormone at "steady state" was drastically reduced; maximal binding was attained within seconds. We subsequently found that ATP was the principal culprit. Realizing from painful experience as a graduate student that commercial preparations of ATP contain a variety of contaminating nucleotides, I tested many types of purine and pyrimidine nucleotides. GTP, GDP, and ITP were the only nucleotides that mimicked the effects of ATP. Most importantly, the guanine nucleotides acted at concentrations much lower (two to three orders of magnitude) than ATP. GppCp, a poorly hydrolyzable analog, also acted, although its effects required much higher concentrations than those of GTP or GDP. Each of the nucleotides induced rapid release of prebound glucagon from its receptor. We established that guanine nucleotides act by lowering the affinity of receptor for the hormone.[19]

At that point the central question was the possible relationship of this effect of GTP on hormone binding to the actions of glucagon on adenylate cyclase activity. To avoid the problem of contaminating GTP in the assay for the enzyme, we prepared [^{32}P]APP(NH)p as substrate using a biosynthetic method. This analog proved stable to degradation by ATPases in the membrane. Under these conditions, glucagon did not stimulate adenylate cyclase unless GTP was present in approximately the same concentrations as those that affected the affinity of the receptor.[20] Subsequently, Michael Lin and Yoram Salomon[21] demonstrated that hormone and GTP concertedly and rapidly induced the active form of the enzyme. Glucagon, moreover, reduced the small lag in activation given by activating nucleotide alone. The die was cast; logically GTP acts at the transduction process along with Mg ions (Fig. 1). Although the components of the informational processing system remained unknown, there was little doubt in our minds that a transducer exists and that this crucial component mediates the transfer of information between receptor and enzyme.

GTP Hydrolysis

Because GTP was susceptible to hydrolysis by nucleotidases in membranes, our next objective was to substitute GTP with a nonhydrolyzable derivative. Taking a cue from our experience with App(NH)p, Gpp(NH)p was synthesized. A few months later, we found that Gpp(NH)p caused the enzyme's activity to "take off" to an extent not even seen with fluoride ions. To our

amazement, the normally unstable cyclase system remained fully active even after three days at room temperature. We then tested Gpp(NH)p on a variety of cyclase systems using every cell membrane preparation we could obtain. All showed the same phenomenon.[22] Gpp(NH)p, unlike hormone plus GTP, stimulated activity following a rather lengthy lag period which was shortened considerably when hormone was added.[21] Yoram Salomon investigated the binding of [^{32}P]Gpp(NH)p to liver membranes and found substantial guanine nucleotide-specific binding, far in excess of the number of glucagon receptors.[23] These findings were discounted by others because of the seeming disparity in the levels of glucagon receptor and guanine nucleotide binding sites. However, it was not understood at the time that multiple types of receptors interact with several types of GTP-binding proteins; that story evolved nearly ten years later. The key elements of signal transduction gained from these findings were that Gpp(NH)p binds to the liver membranes in the absence of hormone, whereas glucagon accelerated the ability of the nucleotide to activate adenylate cyclase, not vice versa. These findings plus modeling of the kinetics of Gpp(NH)p/Mg[24] gave rise to a three-state model in which hormones act by promoting the conversion of the nucleotide-bound E′ state to the activated E* state [Eq. (1)]. However, as this model had 21 parameters and only two variables (Mg^{2+} and Gpp(NH)p concentrations), we realized that this yielded only an approximation of what must be a very complicated system.

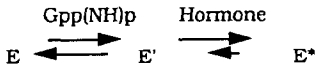

(1)

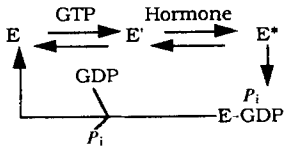

(2)

At about the same time Michael Schramm, in a series of beautifully executed experiments, demonstrated that Gpp(NH)p acts in a pseudo-irreversible fashion; in other words, removal of the nucleotide from the medium after incubation resulted in retention of the high level of cyclase activity.[25] Based on this finding with Gpp(NH)p taken together with the inability of GTP alone to stimulate activity, we proposed that the transducer must have the capacity to hydrolyze GTP. When GTP was substituted for Gpp(NH)p in the modeling of the liver system's kinetics [Eq. (2)], the data fit with the hypothesis that the activated state E* is the state in which GTP was converted to GDP + P_i. In this fashion, it could be understood why activation by GTP and hormone involved essentially no lag period whereas with Gpp(NH)p + hormone, the lag was shortened but persisted. GTP turnover, in this model, is required for the rapid, reversible actions of the hormone. A few years later, Cassel and Selinger, in a brilliant set of experiments, showed conclusively that hormones stimulated the hydrolysis of GTP to GDP + P_i. From these findings, they elaborated the theory that hydrolysis of GTP to GDP is the "turn-off" reaction and the resultant bound GDP converts the transducer to its inhibitory state.[26] Hormones promote the displacement of GDP and its exchange with GTP; this exchange reaction is the key to hormonal activation of G proteins. Nucleotide exchange and GTP hydrolysis are fundamental to the regulation of all types of G proteins that have been examined to date. Not considered in this theory, however, is that the overall turnover of GTP is a complex set of reactions including hydrolysis and subsequent release of phosphate from a bound state. In a detailed study of the light-activated rhodopsin system,[27] it was suggested that hydrolysis of GTP is a very rapid process, whereas the rate-limiting step is the release of inorganic phosphate from its binding sites on transducin, the G protein responsible for activation of phosphodiesterase in outer segments of retinal rod cells. This proposal fits with the prolonged activation by fluoride ions (complexed with aluminum or magnesium ions) which most likely act by binding to the same Mg–phosphate binding sites on transducin.

Dual Stimulatory and Inhibitory Actions of GTP and Fluoride Ions

The multireceptor fat cell system proved invaluable not only for investigating the multiple actions of hormones. It provided the first insight that adenylate cyclase is both inhibited and stimulated by two independent processes involving GTP and fluoride ions. Hans Löw and Jim Harwood found that fluoride ions and both GTP and Gpp(NH)p induced stimulation and inhibition of the enzyme as the concentrations of these agents were increased.[28, 29] The mechanism was elusive until Hirohei Yamamura[30] noted marked differences in the properties of the stimulatory and inhibitory phases. Subsequent characterization of the dual process[31] and the discovery[32] that the fat cells contained adenosine receptors that induce inhibition of adenylate cyclase by means of a GTP-dependent process finally placed the inhibitory role of guanine nucleotides on the same level of importance as the stimulatory process. From these studies arose the new concept of dual regulation of adenylate cyclase by hormones, guanine nucleotides, and fluoride ions.[33] Implicit in the argument was the understanding that transduction involving stimulation and inhibition must be exercised through distinct GTP-binding proteins. We called them nucleotide regulatory proteins (abbreviated N) because ITP was also active. Thus arose the nomenclature N_s and N_i, now commonly known as G_s and G_i. One logical consequence of these findings is that G proteins are independent of both receptors and adenylate cyclase. Pfeuffer's purification of a 42 kDa protein that he could label by incubating membranes with [^{32}P]NAD and cholera toxin[34, 35] provided the first tangible evidence for the existence of G_s, the cyclase stimulatory transducer. It had been discovered earlier that cholera toxin greatly increased the production of cAMP in intestinal cells, suggesting that the toxin acts on the adenylate cyclase system (reviewed in ref. [36]). Later, pertussis toxin[37] provided the means for detecting and purifying G_i and G_o. Meanwhile, in the laboratory of Gordon Tompkins it was found that treatment of cultured lymphoma cells (rat S49) with cyclic AMP resulted in their death.[38] Based on this phenomenon they isolated surviving mutant forms; in one of these the enzyme could not be stimulated by Gpp(NH)p and fluoride ions, and

epinephrine action was also abolished.[39] Using the mutant called AC^- (because it was mistakenly thought to lack adenylate cyclase). Gilman and his colleagues[40,41] subsequently demonstrated that supplementation with extracts from wild-type cells restored both hormonal action in a GTP-dependent fashion and the actions of Gpp(NH)p and fluoride ions. This assay proved useful for the first purification of what was then called G/F factor, now known as G_s, the transduction protein(s) responsible for stimulating adenylate cyclase.

During this period, studies in the lab[42,43] showed that hormone receptors linked with G_s displayed very different physical and kinetic properties from those observed when adenylate cyclase was linked (after activation) with G_s, suggesting either different states or different forms of the GTP regulatory process. Finally, and perhaps most critical for our work was the discovery by Bitensky and colleagues[44] that light-activation of a cyclic GMP phosphodiesterase in outer segments of rod cells is mediated by a guanine nucleotide dependent process, similar to the actions of guanine nucleotides on adenylate cyclase. By 1980 it was clear that the actions of guanine nucleotides are not confined to the adenylate cyclase system. In a brief overview[33] I proposed that there must be several types of GTP-binding proteins, which I called N_s, N_i, N_t (now transducin), and N_x, that mediate the actions of hormones on a number of effector systems. N_x was postulated when I learned that GTP affected the binding of agonists to receptors known to alter calcium uptake in liver cells.[45] By 1990 those predictions were proven correct. However, the number and variety of GTP-binding proteins involved in signal transduction are now greater than I had imagined.

General Characteristics of Guanine Nucleotide Action

During the 1970s some of the fundamental characteristics of receptor systems coupled through GTP-binding proteins had been delineated. What followed in the ensuing 20 years was the elaboration of the types of G proteins, now numbering about 20. Beginning with transducin,[46] it emerged that G proteins are constructed of three types of subunits, an α subunit uniquely capable of binding and degrading GTP and a tightly knit complex of β and γ subunits. This discovery, eventually established for all G proteins coupled to receptors,[47] opened up a new chapter in signal transduction which, in recent years, has helped to explain the pleiotropic actions of hormones.

Dr. Gilman will present much of the work on detailed structures of G proteins, including the recent X-ray crystallographic studies of $G_{s\alpha}$.[*] I will now turn to a subject that has dominated my efforts for the past 15 years.

Topological Disposition of Components

One of the most difficult problems in membrane biology is to understand how components are organized or structured within the plane of the membrane. The topological relationship of membrane proteins to the exterior and interior components of the cell presents another major problem. The "mobile receptor" concept introduced the notion that receptor proteins are free to move rapidly within the membrane. In the case of receptors linked to G proteins, this concept gave rise to the hypothesis that hormones act by stimulating the engagement between receptors and G proteins. The "collision-coupling" model[48] attributes the rate of cyclase activation to the frequency and efficiency of collisions between agonist-bound receptors and G proteins. In this manner any one receptor can activate a number of G proteins due to the free mobility of each component. The rate of activation of G proteins (and adenylate cyclase) are directly proportional to the number of agonist-occupied receptors.

Although kinetic analysis can provide important insights into mechanism, in reality the fundamental question is how the different components are constructed and distributed in the plane of the membrane so that they interact with the observed efficiency and rapidity. The logistics of the encounters are obviously better if the membrane is packed with receptors, as in the case of rhodopsin in rods or cones, where the number of receptors is in large excess of G proteins and effectors. However, in most cells hormone receptors are present at relatively low concentrations.

For this reason, I thought that receptors and G proteins may be precoupled and that hormones act by altering the nature of the coupling process. This notion now seems justified based on biophysical studies which reveal that receptors are complexed with G proteins, and that such complexes are confined within matrix-like, specialized domains.[49] In fact, the structures involved in receptor-coupled signaling processes in general now seem more Buddha-like, both in their stationary setting and their multicomponent structures, which appear to interact in a flickering fashion more in keeping with the ephemeral relationship between action and inaction, between life and death.

The major concern in my laboratory starting in the late 1970s was the structure of the hormone-sensitive cyclase systems as they exist in their native membrane environment. I had learned of target or irradiation analysis from a report that target analysis might be useful for discerning the nature of the interactions between the components of the glucagon-sensitive system in liver membranes.[50] The interpretations of the data were based on the mobile receptor theory. Of major concern to us was the fact that irradiation studies were carried out with freeze-dried material. We had learned that freeze-drying of liver membranes, for example, leads to drastic reductions in hormonal regulation of adenylate cyclase. We decided to use this technique employing a different protocol not involving freeze-drying.

Fortunately, on the floor above my lab dwelled a scientist with the necessary credentials. Ellis Kempner had conducted his graduate thesis on the usage of irradiation analysis, knew both its promises and its faults, and became interested in our problem. As importantly, a young scientist from Switzerland trained in biophysics had just arrived in the lab looking for a suitable research problem. Werner Schlegel and Kempner began a project that became the focal point of our research for the next 15 years.

[*] See Nobel Lecture by A. G. Gilman.

Target Analysis

Schlegel and Kempner ultimately worked out procedures that fully preserved activity and, indeed, provided the first detailed "functional structure" of each component of the glucagon-sensitive system in liver membranes and the hormone-sensitive, stimulatory and inhibitory structures in rat adipocytes.[51, 52] I emphasize the phrase "functional structure" since the analysis measures the exponential decay in activity in relation to the energy input of electrons that bombard the system; this relationship provides the "functional mass". As reviewed recently by Kempner,[53] irradiation of complex, multicomponent enzyme systems does not cause disruption of complexes, but introduces breakages in the protein backbone along each chain of the complex. Thus, although activity is lost, the decrease in activity accurately reflects the loss in functional mass.

Most surprising and initially puzzling were the findings that irradiation of both the liver and adipocyte systems prior to exposure to regulatory ligands—hormones, fluoride ions, guanine nucleotides—gave functional target masses of about 1500 kDa for the stimulatory processes involving glucagon and GTP; an even larger functional mass was exhibited by the inhibitory phase of the adipocyte adenosine receptor mediated process. Such large sizes did not fit with the estimated masses of receptors, G proteins and adenylate cyclase. When the systems were exposed first to activating ligands and then analyzed for their target masses, dramatic reductions in functional mass were observed. For example, in the presence of glucagon and GTP, the functional mass was reduced to about 350 kDa. In the presence of fluoride ions or Gpp(NH)p, the mass was reduced to about 250 kDa. The mass of adenylate cyclase as measured with MnATP as substrate was about 120 kDa, and has now been confirmed by the structure of cloned cyclases.

Disaggregation Theory of Hormone/GTP Action

Out of these findings arose the postulate that the hormone-sensitive cyclase system is composed of an oligomeric complex of receptors and G proteins which, upon interaction with hormone and GTP, disaggregate into the receptor and G protein monomers.[33] Most importantly, target analysis led me to the conclusion that the primary signal emanating from the actions of hormones must be a protein, which had to consist, minimally, of a GTP-binding protein. Not knowing that G proteins were heterotrimers, we estimated the size of the monomer to range from about 120 kDa (fluoride or Gpp(NH)p activation) to about 220 kDa after glucagon treatment (correcting for the estimated mass of cyclase). The estimated values obtained after fluoride or Gpp(NH)p treatment were much larger than that of $G_{s\alpha}$ (43–50 kDa). The larger value obtained after glucagon treatment I conjectured as the combination of the receptor complexed with a monomer of G_s. The monomer complex, considered to be the true "messenger" of hormone action, reacts with adenylate cyclase resulting in either stimulation (by G_s) or inhibition (by G_i). This theory I termed the "Disaggregation Theory of Hormone Action".[33] Incorporated are the fundamental ideas that the structure of the receptor/G protein complex is a multimer of these components, that adenylate cyclase exists separately from the complex, and that a "monomeric" structure derived from the disaggregation is the messenger that communicates information from the hormone-bound receptor/G protein complex to the effector or enzyme.

In this model, I had assumed that receptors and G proteins exist in about equal amounts and are coupled stoichiometrically. Much later when accurate methods became available for measuring the concentrations of receptors and G proteins in cells, it became clear that in most cells, G proteins are present in excess of receptors, possibly in a ratio of as much as 10:1. Given this information, clearly the model must be altered; such that the largest portion of the mass of the glucagon-sensitive adenylate cyclase (or the adenosine-sensitive, inhibitory system in adipocytes) is attributed to G proteins; in other words, G proteins are most likely multimeric structures.

The disaggregation theory soon fell into disfavor because of the findings that heterotrimeric G proteins treated with Gpp(NH)p or the later more popular GTPγS dissociated into free α subunits and $\beta\gamma$ complexes.[54, 55] From this arose Gilman's "dissociation" theory in 1988. The disaggregation theory clearly needed biochemical evidence for the existence of multimeric forms of G proteins. We began the odyssey in this direction with two approaches: cross-linking experiments with synaptoneurosomes from rat brain and extraction of G proteins with various detergents followed by sucrose-gradient analysis of the hydrodynamic properties of the extracted material.

Cross-Linking Studies

Synaptoneurosome membranes were chosen for most of the studies because brain tissue contains the bulk of all known types of G proteins. We were greatly aided in these studies by generous contributions from several colleagues in the field (principally, Dr. Alan Spiegel at NIH) who had prepared polyclonal antibodies against peptide sequences of the α and β subunits of several types of G proteins (G_s, G_i, G_o, and G_q), including subspecies of these proteins.

We tested a variety of cross-linking agents for both their efficacy and selectivity of action at low concentrations. *N,N'*-(1,4-phenylene)dimaleimide (1,4-dimaleimidobenzene) proved the most satisfactory. In addition to all of the G proteins tested, multimeric tubulin and F actin were the only two types of membrane-associated proteins that were detectably cross-linked.[56] After cross-linking in their membrane environment, the G proteins were extracted with sodium dodecylsulfate and chromatographed on sieving columns that allow separation of proteins over a large range of sizes. In this manner it was found that both α and β subunits of G_s, G_i, G_o, and G_q were cross-linked to form structures comparable in size to cross-linked tubulin or actin. We concluded from these studies that G proteins, most likely intact heterotrimers, are multimeric structures in association with the plasma membrane. Such evidence provided substantial credence to our basic arguments for the disaggregation theory. Most importantly, it appeared that multimeric G proteins are responsible for the large ground state structures observed with target analysis.

Detergent Studies

The next stage necessitated some means of isolating the multimeric G proteins, a process requiring the use of detergents. Aware of the fact that detergents such as sodium cholate and Lubrol extract intact heterotrimeric structures,[57] in other words monomers of the putative multimers, we considered the possibility that these detergents may disrupt the multimeric structure. Accordingly, we tested a variety of detergents and determined the sizes of G protein structures extracted by using hydrodynamic properties on sucrose gradients as our assay. Of the seven detergents tested, octyl-β-glucoside (OG), tween 20, and digitonin yielded structures behaving hydrodynamically larger than those obtained with sodium cholate or Lubrol, after correction for the possible contributions of micellar forms of the detergents.[58] OG extracted from liver membranes gave structures that were heterodisperse; about 10% sedimented through sucrose gradients and the bulk remained soluble. When membranes were treated with cholera toxin in the presence of [^{32}P]NAD (the means of specifically labeling $G_{s\alpha}$, the majority of the labeled material appeared in the insoluble fraction.[59, 60] When such labeled material in the membranes was subjected to the combined actions of glucagon and low concentrations of GTPγS, a large portion of the insoluble material became soluble and appeared in a fraction similar to that of purified heterotrimeric G_s.

Based on the cross-linking and hydrodynamic studies we deduced that G_s is likely multimeric in liver and synaptoneurosome membranes, that only multimeric structures are altered by glucagon and low concentrations of GTPγS in liver membranes, and that one of the primary results of their action is the disaggregation of multimers to monomers, as predicted in the disaggregation theory. In synaptoneurosomes high concentrations of GTPγS caused the heterotrimeric G proteins to dissociate into free α and $\beta\gamma$ subunits when dissolved in Lubrol or sodium cholate but not in digitonin.[58] Hence, our suspicions were confirmed that the native structures of G proteins are not preserved with detergents used for purifying heterotrimeric forms of G proteins.

An Extended Disaggregation Theory of Hormone Action

Target analysis provided the initial impetus for the development of the disaggregation theory. However, it has become clear that the theory as originally presented has to be modified to account for the fact that G proteins are the major contributor to the large functional mass; that is, G proteins form multimeric structures. We had also established that there are marked differences between the regulation of G proteins by the coupled receptors and the regulation of adenylate cyclase by G proteins.[42, 43] When the structures and regulatory properties of adenylate cyclases became known,[61] particularly the fact that these are transmembrane proteins that have a two-cassette structure (i.e. two distinct domains on a 12 membrane-spanning structure), it became possible to construct a more coherent theory to explain the regulation of the cyclase system.[62] Regulatory cycles A for regulation of multimer to monomer G proteins and B for regulation of cyclase by a monomeric G protein (G_s) are illustrated in Figure 2.

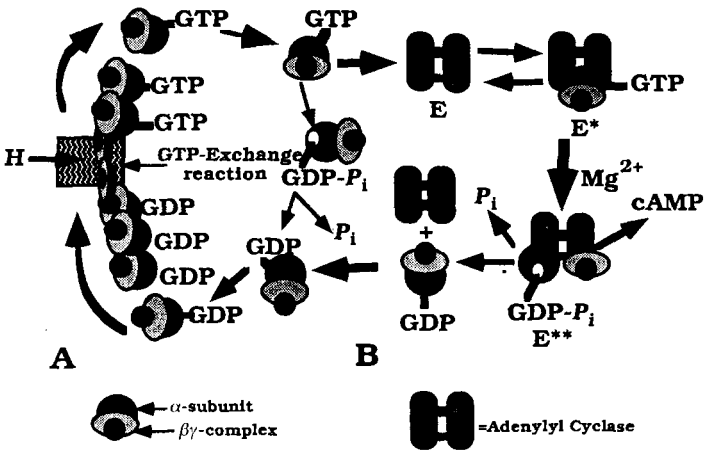

Fig. 2. Regulatory cycles for signal transduction. A) Receptor activation of G proteins. B) G_s-mediated activation of adenylate cyclase. H = hormone, E = enzyme (adenylate cyclase), E* = enzyme/G protein/GTP complex, E** = enzyme/G protein/GDP-P_i complex.

The excursion of receptor along the multimeric G protein chain is governed by the hormone-induced exchange of GTP and GDP. The GTP-occupied monomer at one end is released, allowing it either to interact with adenylate cyclase or to return (after hydrolysis of GTP to GDP) to the other terminus of the multimer. In cycle B the GTP-occupied monomer interacts with the enzyme E without necessarily inducing significant changes in enzyme activity (E*). Activity is governed by Mg^{2+}-dependent hydrolysis of bound GTP to GDP + P_i. In this scenario hydrolysis induces dissociation of the α subunit from the $\beta\gamma$ complex; the resultant separated subunits interact distinctively with the two cassettes or domains of adenylate cyclase (E**). Depending on the type of adenylate cyclase associated with the G protein, activity is governed solely by the α_s subunit, synergistically by the combination of α_s and $\beta\gamma$ subunits, or by inhibition of α_s stimulation by the $\beta\gamma$ subunit. Release of P_i from its binding site on α_s results in reassociation of α_s with $\beta\gamma$. The GDP-bound G_s protein then reassociates with the multimer to become part of the hormone-regulated cycle. It should be emphasized that both cycles occur in association with the surface membrane. The principal element that differs from other theories of hormone-regulated cyclase systems is that the concerted interactions of enzyme, Mg^{2+}, and GTPase are responsible for separation of the α_s and $\beta\gamma$ subunits. The extent and duration of enzyme stimulation are controlled by the independent actions of the separated subunits and the rate at which P_i is released following hydrolysis.

Most people in the field will argue that hydrolysis is not necessary for activation because nonhydrolyzable analogs of GTP are fully capable of stimulating cyclase activity. However, my view is that allosteric regulation by Gpp(NH)p, a slow, hysteretic process, may involve stabilization of a Mg^{2+}-induced disassociation of G_s that normally exists transiently and which does not require any participation by adenylate cyclase in the dissociative process. In this sense, the nonhydrolyzable analogs of GTP may have misguided many in the G protein field into thinking that energy derived from the splitting of GTP is not involved in signal transduction.

It should be noted in this extension of the disaggregation theory that disaggregation of multimers and dissociation of monomers are separate but interrelated phenomena, both contributing to the overall dynamics of signal transduction.

The Similar Structure and Regulation of G Proteins and Cytoskeletal Proteins

During these studies, my attention was drawn to the striking similarities of the properties of G proteins to those of tubulin and actin, the major cytoskeletal elements in cells (reviewed in ref. [63]). For example, G proteins, like actin and tubulin, are associated with the inner aspect of the surface membrane, adhering possibly both through intrinsic membrane proteins such as receptors and to membrane lipids. Of particular interest is the fact that all three types of multimeric proteins are subject to regulation by either GTP (G proteins and tubulin) or ATP (actin) and their hydrolytic products (dinucleotides and P_i). Receptors regulate exchange of bound nucleotides (GDP with GTP) and act catalytically in the process. Similarly, the excursion of a single myosin molecule during muscle contraction along the chain of actin multimers is governed by the exchange of bound ADP with ATP and the hydrolysis of ATP to ADP and P_i. As stated previously, GTP turnover (production of GDP + P_i) is essential for the rapid and sustained actions of hormones; release of P_i is the crucial rate-limiting process in the overall dynamics of signaling. The same is true for myosin/actin interactions.[64]

With these similarities in structure and regulation, G proteins can be classified as part of the cytoskeletal matrix. The primary functional difference is that G proteins serve as chemical signaling devices, whereas tubulin and actin serve as mechanical signaling devices. The release of monomers from multimers is the basis for chemical signaling by G proteins. Dynamic changes in the disaggregation–aggregation cycle of actin and tubulin multimers are also regulatory devices designed for regulating the interactions or movement between specialized components of cells. Based on evidence accumulated over the past decade,[63] all three types of cytoskeletal proteins are connected in some manner to a variety of signaling systems that adhere to the cytoskeletal matrix. These include heterotrimeric G proteins, so-called low molecular weight G proteins, protein kinases and phosphatases, and other proteins or systems that communicate between the surface membrane and the interior of cells. These components form weblike structures that possibly interact in a flickering manner in response to activation of membrane receptors, including those that are growth promoting.

Given the extraordinary complexity of signaling processes at the biochemical level, new investigatory tools are clearly needed. Already promising are the microscopic imaging techniques with immunofluorescent molecules for specifically tagging and viewing structures in their living environment. I suspect that the reductionists with their prowess in molecular biology and X-ray crystallography and those of us attempting to view the living process at the cellular level will merge with our assemblages of ideas and experiences. When this larger, multiplex community of effort finally is consummated, a bright new era in scientific discovery will certainly emerge.

This article and the following "poem" are dedicated to all my colleagues, former and present, who contributed heavily to the concept of signal transduction. Without their efforts, the field of G proteins would not have existed.

To My Friends: Thoughts from "On High"

Life on a roller coaster, oscillating from hither to yon,
no respite for the iconoclast, wandering from dusk to dawn.
Conjuring strange thoughts foreign and twice forbidden,
like Prometheus unbound, this Nobelist climbs in vain
to Andean peaks, seeking what most would proclaim insane.
Why, he ponders, are there no answers to protean questions
when others thinking cleanly and simply with Occam's sharp razor
proclaim what seems obvious given the beam of their unerring laser.
Nature, happily unfettered with philosophy, or with cunning, or with intent
moves relentlessly onward or even backward with energy unspent
while we mortals test and probe with twinkling machines
blinking precisely at each movement, striving to unravel
its irresolute randomness, its fathomless, unlimited, meaningless rush into spiraling chaos,
oblivious of its multitudinous trials & errors which we pontifically believe must be unerring truth & resolution.
The laugh is on those who, burdened with pretensions of truth, believe they can fathom within 15 minutes of human existence what has transpired over eons of space and time in this Universe.
So, I extol the intuitions encapsulated in the folds of my mind from whence occasionally they hurtle to the forebrain and in a twinkling of a proton's discharge bring to fruition a thought, an idea borne on the feathery appendages of teeming neurons wedded in a seamless synergy. Those fleeting moments are cherished, as are those precious impulses imparted by the innumerable individuals who nurtured and instilled unknowingly their encrypted thoughts in mine.
So, with these fanciful thoughts in mind I give praise to you—my friends, my colleagues, my soul-mates, my loved ones for letting my soul and thoughts meander hither and yonder in this attempt at philosophy and poetry. We now belong to the gods on high who praise us for our frailties and our achievements.

Received: January 16, 1995 [A 101 IE]
German version: *Angew. Chem.* **1995**, *107*, 1549–1558

Keywords: G proteins · Nobel lecture · signal transduction

[1] M. Rodbell, *J. Biol. Chem.* **1964**, *239*, 375–380.
[2] M. Rodbell, *J. Biol. Chem.* **1966**, *241*, 130–139.
[3] M. Rodbell, A. B. Jones, *J. Biol. Chem.* **1966**, *241*, 140–143.
[4] M. Rodbell, A. B. Jones, E. E. Chiappe de Cingolani, L. Birnbaumer, *Recent Progr. Horm. Res.* **1968**, *24*, 215.
[5] M. J. Berridge, R. F. Irvine, *Nature (London)* **1984**, *312*, 315–321.
[6] E. W. Sutherland, T. W. Rall, T. Menon, *J. Biol. Chem.* **1962**, *237*, 1220–1227.
[7] E. W. Sutherland, G. A. Robison, *Pharmacol. Rev.* **1966**, *18*, 145–161.
[8] J. Monod, J. P. Changeux, F. Jacob, *J. Mol. Biol.* **1963**, *6*, 306–329.
[9] G. Krishna, B. Weiss, B. B. Brodie, *J. Pharmacol. Exp. Ther.* **1968**, *163*, 379–386.
[10] Y. Salomon, C. Londos, M. Rodbell, *Anal. Biochem.* **1974**, *58*, 541–548.
[11] M. Rodbell, *J. Biol. Chem.* **1967**, *242*, 5757.
[12] L. Birnbaumer, S. L. Pohl, M. Rodbell, *J. Biol. Chem.* **1969**, *244*, 3468–3476.
[13] L. Birnbaumer, M. Rodbell, *J. Biol. Chem.* **1969**, *244*, 3477–3482.
[14] H. P. Bär, O. Hechter, *Proc. Natl. Acad. Sci. USA* **1969**, *63*, 350–356.
[15] L. Birnbaumer, S. L. Pohl, H. M. J. Krans, M. Rodbell, *Biochem. Psychopharmacol.* **1970**, *3*, 85–106.

[16] N. Wiener, *Cybernetics*, MIT, Cambridge, MA, **1961**.
[17] O. Hechter, I. D. K. Halkerston in *The Hormones, Vol. V*, (Eds.: G. Pincus, K. V. Thiman, E. B. Astwood), Academic Press, New York, **1964**, pp. 697–825.
[18] D. Neville, *Biochim. Biophys. Acta* **1968**, *154*, 540–546.
[19] M. Rodbell, H. M. J. Krans, S. L. Pohl, L. Birnbaumer, *J. Biol. Chem.* **1971**, *246*, 1872–1876.
[20] M. Rodbell, L. Birnbaumer, S. L. Pohl, H. M. J. Krans, *J. Biol. Chem.* **1971**, *246*, 1877–1882.
[21] M. Rodbell, M. C. Lin, Y. Salomon, *J. Biol. Chem.* **1974**, *249*, 59–65.
[22] C. Londos, Y. Salomon, M. C. Lin, J. P. Harwood, M. Schramm, J. Wolff, M. Rodbell, *Proc. Natl. Acad. Sci. USA* **1974**, *71*, 3087–3090.
[23] Y. Salomon, M. Rodbell, *J. Biol. Chem.* **1975**, *250*, 7245–7250.
[24] M. S. Rendell, M. Rodbell, M. Berman, *J. Biol. Chem.* **1977**, *252*, 7909–7912.
[25] M. Schramm, M. Rodbell, *J. Biol. Chem.* **1975**, *250*, 2233–2237.
[26] D. Cassel, H. Levkovitz, Z. Selinger, *J. Cyclic Nucleotide Res.* **1977**, *3*, 393–406.
[27] T. D. Ting, Y. K. Ho, *Biochemistry* **1991**, *30*, 8996–9007.
[28] J. P. Harwood, H. Low, M. Rodbell, *J. Biol. Chem.* **1973**, *254*, 6239–6245.
[29] J. P. Harwood, M. Rodbell, *J. Biol. Chem.* **1973**, *248*, 4901–4904.
[30] H. Yamamura, P. M. Lad, M. Rodbell, *J. Biol. Chem.* **1977**, *252*, 7964–7966.
[31] D. M. F. Cooper, W. Schlegel, M. C. Lin, M. Rodbell, *J. Biol. Chem.* **1979**, *254*, 8927–8931.
[32] C. Londos, J. Wolff, *Proc. Natl. Acad. Sci. USA* **1977**, *74*, 5482–5486.
[33] M. Rodbell, *Nature (London)* **1980**, *284*, 17–22.
[34] T. Pfeuffer, *J. Biol. Chem.* **1977**, *252*, 7224–7234.
[35] T. Pfeuffer, J. M. Helmreich, *J. Biol. Chem.* **1975**, *250*, 867–876.
[36] D. M. Gill, *Adv. Cyclic Nucleotide Res.* **1977**, *8*, 85–118.
[37] T. Katada, M. Ui, *Proc. Natl. Acad. Sci. USA* **1982**, *79*, 3129–3133.
[38] V. Daniel, G. Litwack, G. M. Tomkins, *Proc. Natl. Acad. Sci. USA* **1973**, *70*, 76–79.
[39] H. R. Bourne, P. Coffino, G. M. Tomkins, *Science* **1975**, *187*, 750–752.
[40] E. M. Ross, A. G. Gilman, *J. Biol. Chem.* **1977**, *252*, 6966–6969.
[41] E. M. Ross, A. C. Howlett, A. G. Gilman, *J. Biol. Chem.* **1978**, *253*, 6401–6412.
[42] P. M. Lad, A. F. Welton, M. Rodbell, *J. Biol. Chem.* **1977**, *252*, 5942–5946.
[43] A. E. Welton, P. M. Lad, A. C. Newby, H. Yamamura, S. Nicosia, M. Rodbell, *J. Biol. Chem.* **1977**, *252*, 5947–5950.
[44] M. W. Bitensky, G. L. Wheeler, B. Aloni, S. Vetury, Y. Matuo, *Adv. Cyclic Nucleotide Res.* **1978**, *9*, 553–572.
[45] M. Goodhardt, N. Ferry, P. Geynet, J. Hanoune, *J. Biol. Chem.* **1982**, *257*, 11577–11582.
[46] B. K. K. Fung, *J. Biol. Chem.* **1983**, *258*, 10495–10502.
[47] A. G. Gilman, *Annu. Rev. Biochem.* **1987**, *56*, 615–650.
[48] A. M. Tolkovsky, A. Levitzki, *Biochemistry* **1978**, *17*, 3795–3810.
[49] R. R. Neubig, *FASEB J.* **1994**, *8*, 939–946.
[50] G. A. Houslay, J. C. Ellory, G. A. Smith, T. R. Hesketh, J. M. Stein, G. B. Warren, J. C. Metcalfe, *Biochim. Biophys. Acta* **1977**, *467*, 208–219.
[51] W. Schlegel, E. Kempner, M. Rodbell, *J. Biol. Chem.* **1979**, *254*, 5168–5176.
[52] W. Schlegel, D. M. F. Cooper, M. Rodbell, *Arch. Biochem. Biophys.* **1980**, *2011*, 678–682.
[53] E. S. Kempner, *Trends Biochem. Sci.* **1993**, *18*, 236–239.
[54] J. Codina, J. D. Hildebrandt, L. Birnbaumer, R. D. Sekura, *J. Biol. Chem.* **1984**, *259*, 22408–11418.
[55] J. K. Northup, P. C. Sternweiss, A. G. Gilman, *J. Biol. Chem.* **1983**, *258*, 11369–11376.
[56] S. Coulter, M. Rodbell, *Proc. Natl. Acad. Sci. USA* **1992**, *89*, 5842–5846.
[57] P. C. Sternweis, J. K. Northup, M. D. Smigel, A. G. Gilman, *J. Biol. Chem.* **1981**, *256*, 11517–11527.
[58] S. Jahangeer, M. Rodbell, *Proc. Natl. Acad. Sci. USA* **1993**, *90*, 8782–8786.
[59] S. Nakamura, M. Rodbell, *Proc. Natl. Acad. Sci. USA* **1990**, *87*, 6413–6417.
[60] S. Nakamura, M. Rodbell, *Proc. Natl. Acad. Sci. USA* **1991**, *88*, 7150–7154.
[61] W. J. Tang, A. G. Gilman, *Science* **1991**, *254*, 1500–1503.
[62] M. Rodbell, S. Jahangeer, S. Coulter in *GTPases in Biology II* (Eds.: B. F. Dickey, L. Birnbaumer), Springer, Berlin, **1993**, pp. 3–14.
[63] M. Rodbell, *Curr. Top. Cell. Regul.* **1992**, *32*, 1–47.
[64] M. F. Carlier, *Adv. Biophys.* **1990**, *26*, 51–73.

Fullerene Model Compounds: Bowl-Shaped Aromatic Hydrocarbons and Cyclophane-Based Cage Molecules

Rüdiger Faust*

Despite the continuous stream of exciting reports about the chemistry of buckminsterfullerene C_{60},[1, 2] a classical total synthesis of this spherical molecular carbon allotrope remains a great intellectual and preparative challenge.[3] Meanwhile, the curved "aromatic" surface of the fullerene and the cavity it encapsulates have stimulated the investigation of model compounds that, besides being interesting in their own right, may ultimately prove to be suitable starting points for a flexible assembly of carbon spheres. Bowl-shaped aromatic hydrocarbons and cyclophane-based cage compounds are among the promising candidates, and some of the more recent results in these fields are highlighted in the following.

Corannulene **1**,[4] the archetypical bowl-shaped aromatic hydrocarbon (Fig. 1), was first synthesized by Barth and Lawton

1

Fig. 1. Corannulene **1**, the archetypical bowl-shaped aromatic hydrocarbon.

in the pre-fullerene era almost thirty years ago in a tedious, seventeen-step procedure. It was not until 1991 that Scott and co-workers[5] followed up on this milestone effort and reported a convenient access to **1** from simple fluoranthene precursors by flash vacuum pyrolysis techniques.[6] In addition to the attractive brevity of this protocol it proved to be of great generality (vide infra) and, furthermore, it is easily modified to provide substituted derivatives of **1**. Thus, starting from 7,10-bis(2,2-dibromovinyl)fluoranthene (**2**) (readily prepared from acenaphthenequinone and dimethyl 3-oxoglutarate), bromocorannulene **3** could be obtained in reasonable but variable yields (around 29% in one case) along with **1** and 1,6-dibromocorannulene (Scheme 1).[7] Reaction of the lithiated derivative of **3** with acetone resulted in the formation of the corresponding racemic 2-corannulenyl-2-propanol (**4**), whose diastereotopic methyl groups were used as probes to determine the equilibrium

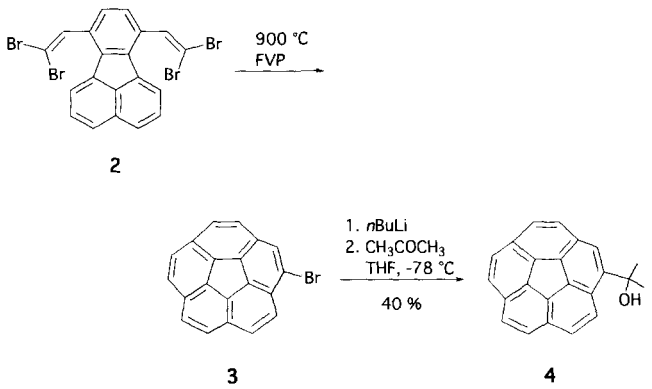

Scheme 1. Pyrolytic synthesis of bromocorannulene **3** by flash vacuum pyrolysis (FVP) and its conversion to **4**.

of bowl-to-bowl inversion by dynamic NMR methods. Truly remarkable for a seemingly rigid framework as that of **1** consisting solely of sp^2-hybridized carbon atoms, the barrier to bowl inversion of **4** was determined to be $\Delta G^{\neq} = 10.2 \pm 0.2$ kcal mol^{-1} at $-64\,^{\circ}C$, indicating that at room temperature cup-shaped corannulene inverts more than 200000 times per second! Even greater flexibility was demonstrated for the 1,2-dihydro- and 1,2,5,6-tetrahydrocorannulene derivatives with $\Delta G^{\neq}$ values of 8.5 ± 0.5 and 6–7 kcal mol^{-1}, respectively.[6a]

The first metal complex of corannulene was obtained by treating it with excess lithium metal in [D_8]THF.[8] In agreement with theoretical predictions **1** was slowly converted into a stable, diamagnetic tetraanion in which the negative charge is distributed on the internal as well as on the peripheral carbons. One can therefore speculate that $\mathbf{1}^{4-}$ is best represented electronically as an aromatic cyclopentadienyl anion embedded in an aromatic 18 π electron [15]annulene trianion. Evidence for supramolecular phenomena of corannulene tetraanions and their counterions in solution was first detected when alkylated derivatives of **1** were treated with lithium metal.[9] Aggregation of the resulting monosubstituted corannulene tetraanions led to stereoisomeric dimers that were readily distinguished by ^{1}H NMR spectroscopy. It was therefore proposed that $\mathbf{1}^{4-}$ occurs as $[\{(Li^+)_4 \cdot \mathbf{1}^{4-}\}_2]$ in analogy. An elegant ^{7}Li NMR study further revealed that four of the eight Li cations are sandwiched between the two charged corannulenes, while two of the remaining four reside on each of the outer sides of the hydrocarbons (Fig. 2). Variable-temperature NMR experiments demonstrat-

[*] Dr. R. Faust
Pharmazeutisch-chemisches Institut der Universität
Im Neuenheimer Feld 364, D-61920 Heidelberg (Germany)
Telefax: Int. code + (6221) 56-3430

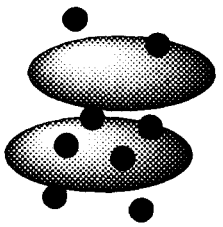

Fig. 2. Schematic representation of dimeric tetralithiocorannulene in solution.

ed a rapid exchange between the exterior and the interior lithium cations at room temperature ($\Delta G^{\neq}$ = 13.2 kcal mol^{-1} at 265 K) and indicated that this process occurs without dissociation of the dimeric complex. MNDO calculations suggest that the two bowls prefer a convex–concave spatial relationship, like stacked cups in a cupboard. However, the magnetic equivalence of the two arenes and the four exterior lithium cations even at 190 K led to the conclusion that a rapid concerted bowl-to-bowl inversion process of the two corannulenes must occur.

An interesting comparison to the lithiated corannulenes is provided by the recent report of de Meijere, Stalke, and coworkers on the crystal structure of dilithiated acepentalene (**5**),[10] whose curved carbon framework constitutes a fragment

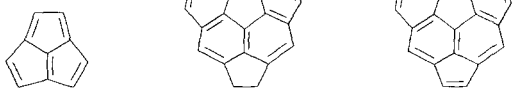

5 **6** **7**

of the smallest theoretically possible fullerene C_{20}. Similar to the corannulene tetraanions, acepentalenediide forms a dimeric aggregate in the solid state in which two dianionic hydrocarbon moieties are bridged by two lithium cations and one of the remaining two Li^+ ions resides on each of the two exterior sides of the dimer (Fig. 3). In contrast to the stacking pattern proposed for dimeric tetralithiocorannulene, the acepentalenediide units show a convex–convex spatial relationship in which the bottoms of the bowls are directed towards each other. This arrangement, however, does not seem to prevail in solution, where apparently either rapid fluctuation processes (e.g. bowl inversion, monomer–dimer equilibrium) occur or distinct monomers of dilithioacepentalenediide exist.

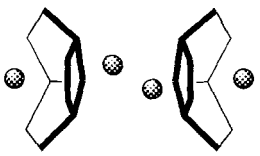

Fig. 3. Schematic representation of dimeric dilithioacepentalenediide in the solid state. The DME solvent molecules coordinated to the lithium cations are omitted for clarity.

The rate of inversion in bowl-shaped aromatic hydrocarbons can be effectively reduced by increasing the curvature of the bowl and/or deepening its cavity. This concept was explored by Rabideau et al. who showed that the ^{1}H NMR resonances of the ethano bridge hydrogens in dihydrocyclopenta[*bc*]corannulene **6** do not coalesce up to the observable temperature limit of 135 °C.[11] Spin polarization transfer experiments at 127 °C allowed the estimation of $\Delta G^{\neq}$ = 26 kcal mol^{-1} as the lower limit for the inversion barrier of **6**. This means that the molecule is essentially locked into one conformation of the cup even at elevated temperatures with a barrier to inversion that is more than twice as high as that of non-annelated **4** and hence **1**. The rigid structures of **6** and cyclopentacorannulene **7** also lead to interesting long-range packing effects in the solid state.[12] X-ray crystallographic analysis of **7** reveals that the molecules are stacked together in a concave–convex fashion as depicted schematically in Figure 4. The presence of weak π-stacking interac-

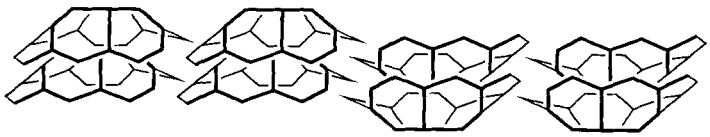

Fig. 4. Idealized representation of the stacking pattern of **7** in the solid state.

tions between the arenes is suggested by 24 intermolecular C–C distances that are shorter than the sum of the van der Waals radii of two carbon atoms. Such a regular stacking pattern is absent in the solid-state structure of **1**,[4c] where presumably rapid fluxional processes prevent a higher degree of orientation. In the gas phase, on the other hand, **1** seems to interact with curved aromatic surfaces, as implied by reactions between **1** and its radical cation, and between **1** and $C_{60}^{\cdot+}$.[13] Electrostatic considerations point to a dominantly concave–convex arrangement in $[\mathbf{1}\cdot\mathbf{1}]^{\cdot+}$, while some ambiguity remains about the structure of the $[\mathbf{1}\cdot C_{60}]^{\cdot+}$ complex.

With respect to a possible total synthesis of buckminsterfullerene, bowl-shaped aromatic hydrocarbons whose carbon skeletons constitute half of the C_{60} surface are particularly relevant as potential synthetic intermediates. These so-called semibuckminsterfullerenes[14] have recently attracted considerable attention, both from a synthetic and a theoretical point of view. Starting from 1,2,5,6-tetraoxopyracene and relying on pyrolytic methodology developed by Stang and co-workers, Rabideau et al. were able to synthesize **8** as the first member of this class of compounds.[15] Although the yellow needles of **8** (decomp. > 300 °C) were not suitable for X-ray diffraction studies, the bowl-shaped topology of **8** is convincingly supported by computational structure optimizations at the ab initio HF/3-21G level. Compared to smaller fullerene fragments, the depth of the bowl is significantly increased, leading to an estimated (computed) barrier of bowl-to-bowl inversion of 57 kcal mol^{-1}. The degree of curvature on the surface of **8** is predicted to be very close to that of C_{60}, suggesting that topologically **8** is indeed a good model for the fullerene. As a direct precursor for carbon spheres, however, **8** is of little value, since dimerization

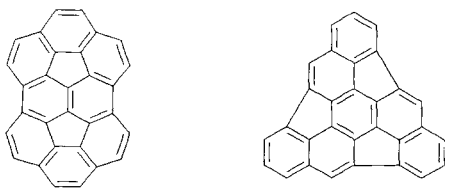

8 **9**

of this C_{30} unit would lead to a carbon cage with four pairs of adjacent five-membered rings, a structure that would violate the "pentagon rule" for stable fullerenes.

Another member of this class of semibuckminsterfullerenes is triindenotriphenylene **9**, a molecule whose carbon skeleton was

already suggested in 1987 by McKee and Herndon[16] as a possible intermediate in the formation of C_{60}. Although **9** is still elusive experimentally, it has received keen interest recently,[14, 17–19] partly because the rigidity of the bowl-shaped carbon frame should give rise to a large inversion barrier[17] (calculated to be 74 kcal mol^{-1}), rendering **9** a test case for competitive concave or convex metal complexation.[14, 18] While semiempirical calculations favor coordination of some cations (e.g. Li^+, Tl^+, and Pb^+) to the outside of the bowl, other metals (e.g. Na^+, K^+, Ga^+) are predicted to bind preferentially to the concave side of **9**. Ab initio calculations with the HF/6-31G*//3-21G basis set, on the other hand, suggest that the electron density inside the bowl is significantly greater than on the outside, but also indicate that the bias for binding most metal cations on either face of **9** is rather small and amounts to an energy difference of only 1–2 kcal mol^{-1}.[18b] Clearly, the true value of metal ion complexed, bowl-shaped aromatic hydrocarbons as models of exo- or endohedral fullerene derivatives will only be evident after much needed experimentation.

A different approach to fullerene model compounds was recently presented by Vögtle and co-workers.[20] They realized that certain cyclophane-based hydrocarbon cages define an almost spherical cavity which, in contrast to the inside of the fullerenes, can be accessed through custom-tailored openings on the surface of these "spheriphanes". In light of the finding that pyrolysis of simple aromatic compounds such as naphthalene leads to the formation of fullerenes,[21] concave cyclophane hosts with an appropriate number of carbon centers can be envisioned to serve as direct precursors for endohedral fullerene complexes[22] that are currently obtained by arc-discharge vaporization of doped graphite.

While this concept is still far from being practical, first steps in this direction have now been made with the synthesis of two "spherical" hydrocarbons, namely **10** (molecular formula $C_{60}H_{60}$) and the smaller, more rigid hydrocarbon cage **11**

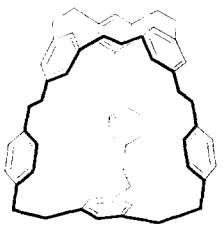

10

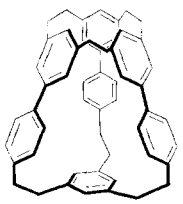

11

($C_{54}H_{48}$). Both compounds were obtained from simple benzene derivatives by established cyclophane methodology. Semiempirical structure optimizations predict that the cavity of **10** should be large enough to accommodate a variety of neutral, organic guests such as adamantylamine and *tert*-butylamine. Although cocrystallization experiments have proved to be unsuccessful so far, preliminary studies at high pressure indicate that such supramolecular inclusion complexes can indeed be obtained.

Quite remarkable is the complexation behavior of **10** towards silver cations. Extraction experiments show that 10^{-3} M chloroform solutions of **10** are able to extract 10% of the silver cations from aqueous $AgNO_3$ solutions. In comparison to other π-spherands like **12**[23] and **13**,[24] both of which are known to form stable inclusion complexes with Ag^+, the extracting power of **10** under these conditions is at least two times higher than that of **13** and exceeds those of the smaller cyclophane **11** and of **12** by one order of magnitude. In addition, the hydrocarbon cage **10** shows high selectivity for Ag^+ and almost ignores other metal ions like Na^+, Ca^{2+}, and Zn^{2+}, as well as Tl^+ and Hg^{2+}, which have ionic radii similar to that of Ag^+.

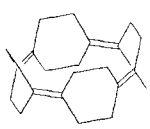

12

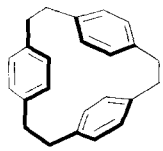

13

It is tempting to assume that the silver ion resides inside the deep cavity of **10**, but neither the exact composition of the complex nor the location of the metal ion could as yet be determined experimentally. However, the characterization of endohedral cyclophane complexes of **10** is clearly only a matter of time and will mark another step towards a rational assembly of "filled" fullerenes.[25]

German version: *Angew. Chem.* **1995**, *107*, 1562–1564

Keywords: arenes · cage compounds · cyclophanes · fullerenes

[1] W. Krätschmer, L. D. Lamb, K. Fostiropoulos, D. R. Huffmann, *Nature (London)* **1990**, *347*, 354–358.

[2] a) R. Taylor, D. R. M. Walton, *Nature (London)* **1993**, *363*, 685–693; b) A. Hirsch, *Angew. Chem.* **1993**, *105*, 1189–1192; *Angew. Chem. Int. Ed. Engl.* **1993**, *32*, 1138–1141; c) *Chem. Unserer Zeit* **1994**, *28*, 79–87; d) *The Chemistry of the Fullerenes*, Thieme, Stuttgart, **1994**.

[3] Some early attempts to synthesize C_{60} are reported in: a) F. Diederich, Y. Rubin, *Angew. Chem.* **1992**, *104*, 1123–1146; *Angew. Chem. Int. Ed. Engl.* **1992**, *31*, 1101–1123. For the synthesis of potential non-graphitic precursors to C_{60} see for example: b) P. Magnus, D. Witty, A. Stamford, *Tetrahedron Lett.* **1993**, *34*, 23–26; c) S. Hagen, U. Nuechter, M. Nuechter, G. Zimmermann, *ibid.* **1994**, *35*, 7013–7014; d) M. J. Plater, *Synlett* **1993**, 405–406; e) F. Sbrogiò, F. Fabris, O. De Lucchi, *ibid.* **1994**, 761–762; f) G. Mehta, K. V. Rao, *ibid.* **1995**, 319–320; g) J. S. Siegel, T. J. Seiders, *Chem. Br.* **1995**, 313–316.

[4] a) W. E. Barth, R. G. Lawton, *J. Am. Chem. Soc.* **1966**, *88*, 380–381; b) R. G. Lawton, W. E. Barth, *ibid.* **1971**, *93*, 1730–1745; c) J. C. Hanson, C. E. Nordman, *Acta Crystallogr. Sect. B* **1976**, *32*, 1147–1153.

[5] L. T. Scott, M. M. Hashemi, D. T. Meyer, H. B. Warren, *J. Am. Chem. Soc.* **1991**, *113*, 7082–7084. This procedure has been improved further, see: L. T. Scott, P.-C. Cheng, M. S. Bratcher, *Seventh International Symposium on Novel Aromatic Compounds*, Victoria, BC, Canada, July 19–24, 1992, Abstract 64.

[6] For alternative pyrolytic routes to **1** see: a) A. Borchardt, A. Fuchicello, K. V. Kilway, K. K. Baldridge, J. S. Siegel, *J. Am. Chem. Soc.* **1992**, *114*, 1921–1923; b) G. Zimmermann, U. Nuechter, S. Hagen, M. Nuechter, *Tetrahedron Lett.* **1994**, *35*, 4747–4750.

[7] L. T. Scott, M. M. Hashemi, M. S. Bratcher, *J. Am. Chem. Soc.* **1992**, *114*, 1920–1921.

[8] A. Ayalon, M. Rabinovitz, P.-C. Cheng, L. T. Scott, *Angew. Chem.* **1992**, *104*, 1691–1692; *Angew. Chem. Int. Ed. Engl.* **1992**, *31*, 1636–1637.

[9] A. Ayalon, A. Sygula, P.-C. Cheng, M. Rabinovitz, P. W. Rabideau, L. T. Scott, *Science* **1994**, *265*, 1065–1067.

[10] R. Haag, R. Fleischer, D. Stalke, A. de Meijere, *Angew. Chem.* **1995**, *107*, 1642–1644; *Angew. Chem. Int. Ed. Engl.* **1995**, *34*, 1492–1495.

[11] A. H. Abdourazak, A. Sygula, P. W. Rabideau, *J. Am. Chem. Soc.* **1993**, *115*, 3010–3011.

[12] A. Sygula, H. E. Folsom, R. Sygula, A. H. Abdourazak, Z. Marcinow, F. R. Fronczek, P. W. Rabideau, *J. Chem. Soc. Chem. Commun.* **1994**, 2571–2572.

[13] H. Becker, G. Javahery, S. Petrie, P.-C. Cheng, H. Schwartz, L. T. Scott, D. K. Bohme, *J. Am. Chem. Soc.* **1993**, *115*, 11636–11637.

[14] R. Faust, K. P. C. Vollhardt, *J. Chem. Soc. Chem. Commun.* **1993**, 1471–1473.
[15] P. W. Rabideau, A. H. Abdourazak, H. E. Folsom, Z. Marcinow, A. Sygula, R. Sygula, *J. Am. Chem. Soc.* **1994**, *116*, 7891–7892. For an unsuccessful attempt to synthesize **8**, see ref. [3c].
[16] M. L. McKee, W. C. Herndon, *J. Mol. Struct. (THEOCHEM)* **1987**, *153*, 75–84.
[17] A. Sygula, P. W. Rabideau, *J. Chem. Soc. Chem. Commun.* **1994**, 1497–1499.
[18] a) J. Plater, H. S. Rzepa, F. Stoppa, S. Stossel, *J. Chem. Soc. Perkin Trans. 2* **1994**, 399–400; b) A. Sygula, P. W. Rabideau, *J. Chem. Soc. Chem. Commun.* **1994**, 2271–2272.
[19] M. J. Plater, H. S. Rzepa, S. Stossel, *J. Chem. Soc. Chem. Commun.* **1994**, 1567–1568.
[20] J. Gross, G. Harder, F. Vögtle, H. Stephan, K. Gloe, *Angew. Chem.* **1995**, *107*, 523–526; *Angew. Chem. Int. Ed. Engl.* **1995**, *34*, 481–484.
[21] R. Taylor, G. J. Langley, H. W. Kroto, D. R. M. Walton, *Nature (London)* **1993**, *366*, 728–731, and references therein.
[22] F. T. Edelmann, *Angew. Chem.* **1995**, *107*, 1071–1075; *Angew. Chem. Int. Ed. Engl.* **1995**, *34*, 981–985, and references therein.
[23] a) J. E. McMurry, G. J. Haley, J. R. Matz, J. C. Clardy, J. Mitchell, *J. Am. Chem. Soc.* **1986**, *108*, 515–516; b) A. Schröder, H.-B. Mekelburger, F. Vögtle, *Top. Curr. Chem.* **1994**, *172*, 179–201.
[24] a) J. L. Pierre, P. Baret, P. Chautemps, M. Armand, *J. Am. Chem. Soc.* **1981**, *103*, 2986–2988; b) C. Cohen-Addad, P. Baret, P. Chautemps, J. L. Pierre, *Acta Crystallogr. Sect. C* **1983**, *39*, 1346–1349; c) H. C. Kang, A. W. Hanson, B. Eaton, V. Boekelheide, *J. Am. Chem. Soc.* **1985**, *107*, 1979–1985. For main group metal complexes of **13**, see: d) H. Schmidbaur, R. Hager, B. Huber, G. Müller, *Angew. Chem.* **1987**, *99*, 354–365; *Angew. Chem. Int. Ed. Engl.* **1987**, 26, 338–340; e) T. Probst, O. Steigelmann, J. Riede, H. Schmidbaur, *ibid.* **1990**, *102*, 1471–1473 and **1990**, 29, 1397–1398.
[25] **Note added in proof** (June 6, 1995): The heat of formation of corannulene has been determined recently to be $\Delta H_f^\circ = 342.3 \pm 5.6$ kJ mol^{-1}. See T. Kobayashi, M. Sakiyama, K. Yamamoto, P.-C. Cheng, L. T. Scott, *J. Am. Chem. Soc.* **1995**, *117*, 3270–3721.

Progress in Oligosaccharide Synthesis through a New Orthogonal Glycosylation Strategy**

Hans Paulsen*

Glycoconjugates have numerous important biological functions.[1, 2] For a better understanding of these functions, defined natural and modified glycoconjugates are needed. To this end, intensive efforts in the last few years have been aimed at the synthesis of glycoconjugates, resulting in remarkable progress in oligosaccharide synthesis. New glycosylation methods have been developed with efficient leaving groups, which lead to good yields and high stereoselectivity under mild conditions. The halide, thioglycoside, and trichloroacetimidate methods,[3–5] in modified forms, have proved to be especially effective. Chemical and enzymatic reactions can also be combined, as long as the glycosyl transferases and the activated nucleotide sugar are available.[6]

The most effective methods for the construction of larger oligosaccharides is block synthesis, in which blocks of di- or trisaccharides are coupled. The configuration of the anomeric centers is already fixed in the nonreducing block sequences.[7] One drawback here is that the anomeric center at the reducing unit of a block must be reactivated for subsequent coupling. Activation of the anomeric center should not require many steps or, better yet, should be direct. Thus 2-(trimethylsilyl)ethyl-glycosides, for example, have been prepared from blocks,[8] which are readily deprotected and converted into activated trichloroacetimidates.[5, 9] Glycal-type structures can also be activated by epoxidation, making renewed coupling possible.[10] However, use of stable thioglycosides at the anomeric center of the block is best, since a wide variety of structures and promoters is possible.

For the construction of an oligosaccharide building block a glycosylation reaction is also necessary. The synthesis of a thioglycoside-containing unit, for example, requires a different glycosylation procedure with a different leaving group for the donor, since the potentially activatable thioglycoside would be destroyed otherwise. Numerous strategies are available, which involve several or more additional reaction steps, depending on the blocking pattern. The coupling of donors activated by benzyl substituents with acceptors deactivated by acetyl groups has also been suggested.[11, 12] Ogawa et al. recently described an interesting and provocative strategy that starts with a set of two donors, which can be extended in an orthogonal glycosylation reaction.[13]

The approach was demonstrated with a model reaction sequence leading to long-chain $\beta(1 \rightarrow 4)$-glycosidically linked 2-acetamido-2-deoxy-D-glucose units (Scheme 1). Thioglycoside **1** and glycosyl fluoride **4** serve as the two building blocks. Thioglycoside **1** can be coupled with the deactylated glycosyl fluoride **3** without affecting fluorine at the anomeric center, and the resulting disaccharide **5** with the activated anomeric center can be used directly for further glycoside synthesis. Inversely, the reaction of glycosyl fluoride **4** with the deacetylated thioglycoside **2** yields disaccharide **7** in which the thioglycoside is unchanged. This disaccharide can also be employed directly in further glycosidation without any additional steps. This flexible method thus enables glycosidation without destruction of the active anomeric center at the acceptor. This promising strategy can be applied to other systems.

The phenylthioglycosides employed are activated with *N*-iodosuccinimide trifluoromethanesulfonic acid (NIS-TfOH) (or NIS-AgOTf), and the phenylthiogroup acts as a leaving group. In reactions with the glycosyl fluorides the promotor is the reagent Cp_2HfCl_2–$AgClO_4$. Thus larger oligosaccharide blocks can be constructed from the two monosaccharides **1** and **4** with these two reagents. Compounds **1** and **4** contain an *N*-phthaloyl group at C-2, which induces uniform β-glycosidic linkage.

[*] Prof. Dr. H. Paulsen
Institut für Organische Chemie der Universität
Martin-Luther-King-Platz 6, D-20146 Hamburg (Germany)
Telefax: Int. code + (40)4123-3834

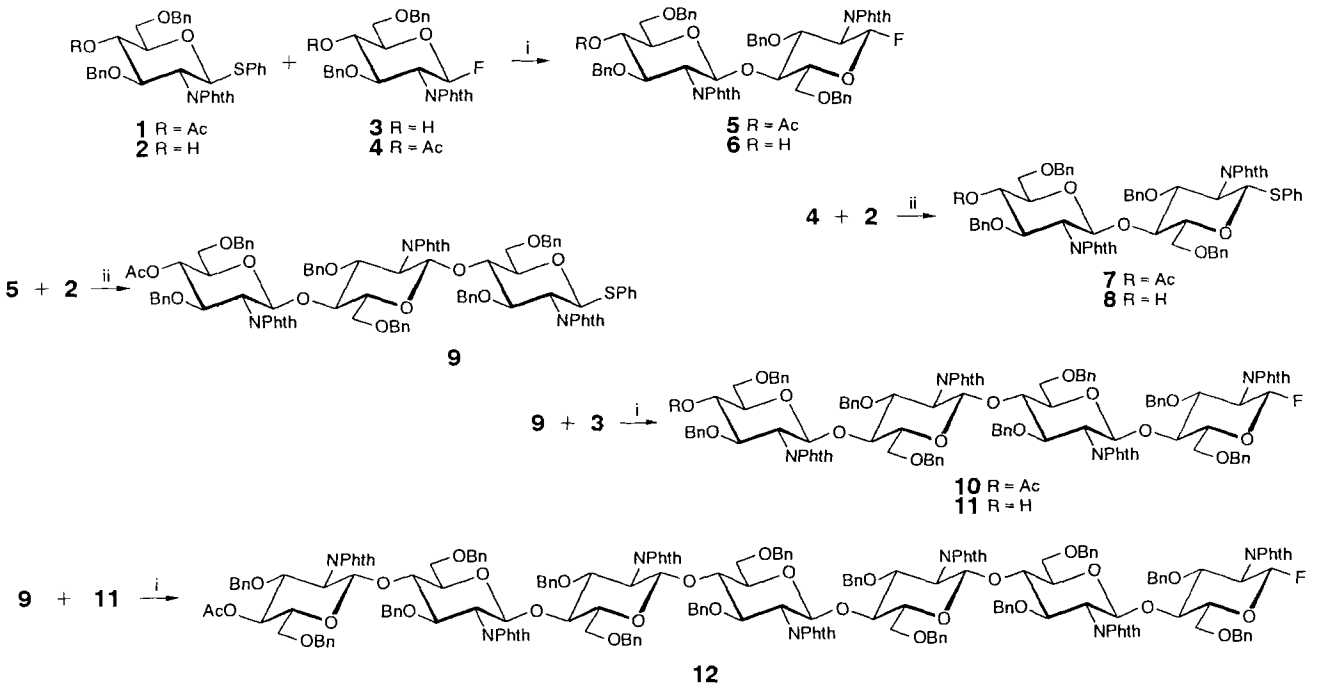

Scheme 1. i) NIS, TfOH (AgOTf); ii) Cp_2HfCl_2, $AgClO_4$.

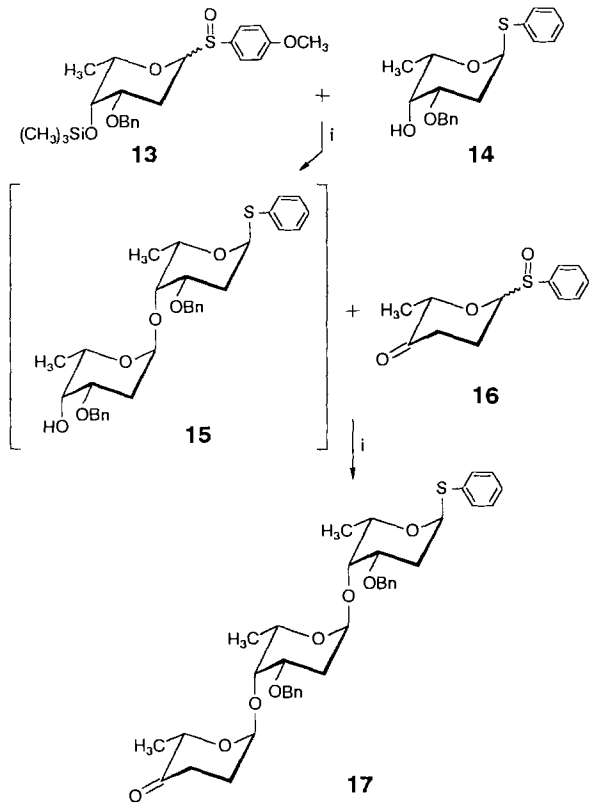

Scheme 2. i) TfOH, $HC{\equiv}CCO_2CH_3$, −78 °C.

The approach was demonstrated with the following synthesis. Coupling of **1** and **3** affords disaccharide **5** (85%), whereas the reaction of donor **4** with **2** gives the disaccharide **7** (81%). Disaccharide **5** is treated with **2** to furnish trisaccharide **9** (72%). The subsequent coupling of **9** with **3** yields tetrasaccharide **10** (65%). Deacetylation of **10** to **11** can be followed by block condensation of trisaccharide **9** with **11**, which yields heptasaccharide **12** (67%). Phenylthioglycosides and glycosyl fluorides are used both as donors and as acceptors, and additional steps for activation of the anomeric center are not required in either case.

Kahne et al.[14] used a similar strategy in a very elegant synthesis of a trisaccharide in practically one step. The building blocks they used, the S-glycosides **13**, **14**, and **16**, have considerably different reactivities at the anomeric center (Scheme 2). Phenylthioglycoside **14** is definitely the least reactive, while phenyl sulfoxide **16** is considerably more reactive. The reactivity of **16** can be increased yet further by introduction of a methoxy substituent on the phenyl group, thus giving the highly reactive *p*-methoxyphenylsulfoxide **13**.

A solution of building blocks **13**, **14**, and **16** in Et_2O/CH_2Cl_2 is simply mixed in the presence of TfOH and $HC{\equiv}CCO_2CH_3$ at −78 to −70 °C, and trisaccharide **17** is isolated in 25% after 45 min. It is assumed that the modestly reactive **14** reacts first with the highly reactive **13** to give disaccharide **15**; the silyl ether is cleaved simultaneously, and **15** reacts with the moderately reactive **16** to provide **17**.

In view of the available arsenal of glycosylation reactions,[15, 16] these two examples should point the way for the development of similar strategies.

German version: *Angew. Chem.* **1995**, *107*, 1562–1564

Keywords: glycosyl fluorides · oligosaccharide syntheses · thioglycosides

[1] A. Varki, *Glycobiology* **1993**, *3*, 97.
[2] R. A. Dwek, *Biochem. Soc. Trans.* **1995**, *23*, 1.
[3] O. Lockhoff, *Houben-Weyl: Methoden der Organischen Chemie, Vol. E14a/3*, Thieme, Stuttgart, **1992**, 621.
[4] K. Toshima, K. Tatsuda, *Chem. Rev.* **1993**, *93*, 1503.
[5] R. R. Schmidt, W. Kinzy, *Adv. Carbohydr. Chem. Biochem.* **1994**, *50*, 21.

[6] C.-H. Wong, R. L. Halcomb, Y. Ichikawa, T. Kajimoto, *Angew. Chem.* **1995**, *107*, 569; *Angew. Chem. Int. Ed. Engl.* **1995**, *34*, 521.
[7] H. Paulsen, *Angew. Chem.* **1990**, *102*, 851; *Angew. Chem. Int. Ed. Engl.* **1990**, *29*, 823.
[8] J. Jansson, G. Naori, G. Magnusson, *J. Org. Chem.* **1990**, *55*, 3181.
[9] H. Paulsen, M. Pries, J. P. Lorentzen, *Liebigs Ann. Chem.* **1994**, 389.
[10] S. J. Danishefsky, K. F. McClure, J. T. Randolph, R. B. Ruggeri, *Science* **1993**, *260*, 1307; J. T. Randolph, S. J. Danishefsky, *Angew. Chem.* **1994**, *106*, 1538; *Angew. Chem. Int. Ed. Engl.* **1994**, *33*, 1470.
[11] D. R. Mootoo, P. Konradsson, U. Udodong, B. Fraser-Reid, *J. Am. Chem. Soc.* **1988**, *110*, 5583.
[12] L. A. J. M. Sliedregt, K. Zegelaar-Jaarsveld, G. A. van der Marel, J. H. van Boom, *Synlett* **1993**, 335.
[13] O. Kanie, Y. Ito, T. Ogawa, *J. Am. Chem. Soc.* **1994**, *116*, 12073.
[14] S. Raghavan, D. Kahne, *J. Am. Chem. Soc.* **1993**, *115*, 1580.
[15] G.-J. Boons, S. Isles, *Tetrahedron Lett.* **1994**, *35*, 3593.
[16] *Modern Methods in Carbohydrate Synthesis* (Eds.: S. E. Khan, R. A. O'Neill), Harwood Academic Publisher, Chur, Switzerland, in press.

 © VCH Verlagsgesellschaft mbH, D-69451 Weinheim, 1995 0570-0833/95/1313-1434 $ 10.00+.25/0

[WL(NO)(O)(CH$_3$)]—An Unusual Nitrosyltungsten Complex**

Jochen Böhmer, Karl Wieghardt,* and Bernhard Nuber

Recently we reported[1] the first example of a mononuclear nitrosyl(oxo)molybdenum(II) complex, [MoL(NO)(O)(OH)] (L = 1,4,7-triisopropyl-1,4,7-triazacyclononane), in which the strong π-acceptor ligand NO and the strong π-donor ligand O^{2-} are bound to the same metal ion in a *cis* arrangement. This 18e complex is of the $\{M\text{-}NO\}^4$ type; the terminal Mo=O and Mo=NO bonds are short and both have double-bond character. A synergistic bonding model has been proposed in which electron density is transferred from the filled p orbitals of the oxo ligands to the empty π* orbitals of the nitrosyl ligand thus weakening the N–O bond.[1] We report here on an unusual organometallic variant of this class of compound.[2]

Nitrosylation of [WL(CO)$_3$][3] with $NaNO_2$ and concentrated HCl in methanol, followed by addition of KPF_6, gave yellow air-stable crystals of [WL(NO)(CO)$_2$]PF$_6$ (**1**). Reduction of **1** with $LiAlH_4$ in dry THF under anaerobic conditions (Scheme 1) results in a blue solution from which, following hydrolysis with H_2O and filtration, blue crystals of [WL(NO)(CO)(CH$_3$)] (**2**) were isolated.[4] Complex **2** reacts quantitatively in CH_3CN with concentrated HCl in the absence of oxygen to yield one equivalent each of methane and [WL(NO)(CO)(NCCH$_3$)]Cl. The latter is converted with $NaClO_4$ to the perchlorate salt **3**, which is air stable in solution and in the solid state. The 18e complexes **1**–**3** are of the $\{W\text{-}NO\}^6$ type.[5]

Complex **2** reacts in acetone with oxygen within seconds at room temperature, as evidenced by a change in the color of the solution from blue to red. After removal of the solvent we obtained red microcrystals of [WL(NO)(O)(CH$_3$)] (**4**) in almost quantitative yield; this compound represents a complex of $\{W\text{-}NO\}^4$ type. In the IR spectrum, the NO and W=O stretching frequencies are observed at 1433 cm^{-1} (!) and 835 cm^{-1}, respectively. If the reaction is carried out in the presence of $^{18}O_2$ only the latter band shifts to lower wavenumbers (796 cm^{-1}), whereas the band attributable to NO does not shift. The observed value for the ν(NO) stretching frequency of **4** constitutes, to the best of our knowledge, the lowest wavenumber ever reported for a linear M–NO group.

The gaseous products that form when **2** is allowed to react with O_2 were analyzed quantitatively (GC, MS) and identified as CO_2 and CO; the combined amount of these two gases corresponds exactly to the one equivalent of CO ligand that has been displaced from **2** [Eqs. (a) and (b)]. The CO_2/CO ratio is

$$2[WL(NO)(CO)(CH_3)] + O_2 \xrightarrow{2} 2[WL(NO)(O)(CH_3)] + 2CO \quad (a)$$

$$[WL(NO)(CO)(CH_3)] + O_2 \rightarrow [WL(NO)(O)(CH_3)] + CO_2 \quad (b)$$

[*] Prof. Dr. K. Wieghardt, Dr. J. Böhmer
Max-Planck-Institut für Strahlenchemie
Stiftstrasse 34–36, D-45470 Mülheim an der Ruhr (Germany)
Telefax: Int. code + (208)3063951
Dr. B. Nuber
Anorganisch-chemisches Institut der Universität Heidelberg (Germany)

[**] This work was supported by the Fonds der Chemischen Industrie.

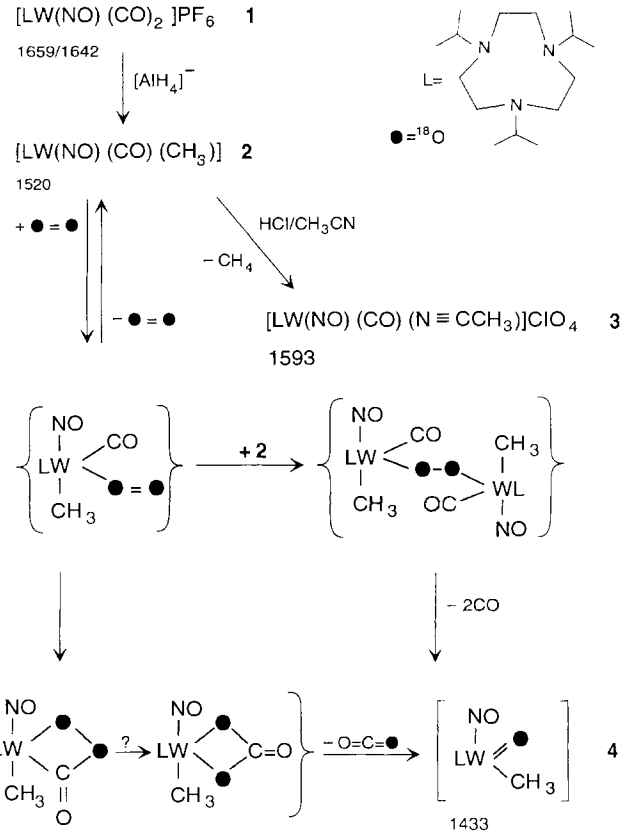

Scheme 1. Synthesis and labeling of the complexes. The numbers refer to the wavenumbers for the ν(NO) stretching frequency in cm^{-1} (KBr).

Table 1. Selected physical data for **1**–**4**.

1: ^{1}H NMR (CD_3CN, 400 MHz): δ = 3.59 (sep, 2H), 3.26 (sep, 1H), 3.20–2.87 (m, 12H), 1.34 (d, 6H), 1.33 (d, 6H), 1.21 (d, 6H); $^{13}C\{^1H\}$ NMR (CD_3CN, 106.22 MHz): δ = 221.21, 65.19, 63.05, 54.04, 53.43, 52.97, 18.82, 18.68, 18.43; IR: ν_{as}(CO) 2002, ν_s(CO) 1905, 1892, ν(NO) 1659, 1642 cm^{-1}; FAB-MS: *m/z* 525.1 $[M - PF_6]^+$; UV Vis (CH_3CN): λ_{max} (ε, L mol^{-1} cm^{-1}) = 240 (sh) (9000), 260 (8350), 338 (310), 391 (200), 460 (sh) nm (90)

2: ^{1}H NMR (CD_2Cl_2, 400 MHz): δ = 3.76 (sep, 1H), 3.67 (sep, 1H), 3.36 (sep, 1H), 3.15–2.42 (m, 12H), 1.43 (d, 3H), 1.38 (d, 6H), 1.30 (d, 3H), 1.14 (d, 3H), 1.02 (d, 3H), 0.06 (s/d, ^2J(W,H) = 7.32 Hz, 3H); IR: ν(CO) 1805, ν(NO) 1520 cm^{-1}; UV/Vis (CH_3CN): λ_{max} (ε, L mol^{-1} cm^{-1}) = 232 (4660), 319 (1050), 395 (140), 593 nm (60)

3: ^{1}H NMR (CD_3CN, 400 MHz): δ = 3.57 (sep, 1H), 3.47 (sep, 1H), 3.29 (sep, 1H), 3.19–2.79 (m, 12H), 2.67 (s, 3H), 1.41 (d, 3H), 1.30 (d, 3H), 1.29 (d, 3H), 1.28 (d, 3H), 1.21 (d, 3H), 1.16 (d, 3H); $^{13}C\{^1H\}$ NMR (CD_3CN, 106.22 MHz): δ = 206.29, 142.39, 67.13, 61.14, 60.56, 55.12, 54.04, 53.48, 52.13, 50.42, 19.92, 19.18, 18.72, 17.27, 15.97, 4.57; IR: ν(CO) 1871, 1863; ν(NO) 1593 cm^{-1}; FAB-MS: *m/z* 538.2 $[M - ClO_4]^+$; UV/Vis (CH_3CN): λ_{max} (ε, L mol^{-1} cm^{-1}) = 230 (8840), 274 (7380), 335 (1100), 396 (160), 522 (125)

4: ^{1}H NMR (CD_3OD, 400 MHz): δ = 4.13 (sep, 1H), 3.68 (sep, 1H), 3.29 (sep, 1H), 3.20–2.58 (m, 12H), 1.41 (d, 3H), 1.34 (d, 3H), 1.27 (d, 3H), 1.10 (d, 3H), 1.03 (d, 3H), 1.00 (d, 3H), 0.27 (s/d, ^2J(W,H) = 7.80 Hz, 3H); $^{13}C\{^1H\}$ NMR (CD_3OD, 106.22 MHz): δ = 62.21, 60.53, 60.38, 59.49, 59.22, 58.39, 46.15, 45.03, 44.39, 21.31, 21.17, 21.04, 19.49, 15.81, 15.48, 14.91; IR: ν(NO) 1433, ν(W^{16}O) 835, ν(W^{18}O) 796 cm^{-1}; FAB-MS: *m/z* 500.1 $[M^+]$; UV/Vis (CH_3CN) λ_{max} (ε, L mol^{-1} cm^{-1}) = 228 (4500), 330 (sh) (500), 385 (sh) (160), 548 (70)

dependent on the initial concentration of **2**: at 0.023 M [**2**] this ratio is approximately 80:20; whereas at [**2**] $< 10^{-3}$ M the only detectable gaseous reaction product is CO_2. When the reaction was carried with $^{18}O_2$, the isotopically labeled products $[WL(N^{16}O)(^{18}O)(CH_3)]$, $C^{18}O^{16}O$, and $C^{16}O$ could be identified by IR spectroscopy and mass spectrometry. The mechanistic interpretation of these results is shown in Scheme 1.[6] Kinetic studies aimed at the elucidation of the mechanism of the oxidation of **2** with O_2 are in progress.

The results of single-crystal X-ray diffraction analyses[7] of **2**·acetone and **4**·$C_2H_5OH \cdot 2H_2O$ confirm the mononuclear nature of these complexes (Figs. 1 and 2, respectively). The W=O bond in **4** is relatively short (1.826(9) Å) and has substantial double-bond character; it is slightly longer than those in octahedral oxotungsten(VI) complexes (1.67–1.76 Å).[8] The W–NO bond is also rather short (1.71 Å), whereas the N–O bond appears to be weak at 1.24(2) Å. In the solid state, the W=O group in **4** forms a strong hydrogen bond to one ethanol molecule ($O(1)\cdots O_{EtOH}$ 2.567(8) Å), whereas the oxygen atom of the nitrosyl ligand is bound to one molecule of water of crystallization ($O(4)\cdots O_{H_2O}$ 2.533 Å). The presence of O–H···O hydrogen bonds confirms the increased electron density and, therefore, the basicity of the two oxygen atoms in the neutral molecule of **4**.

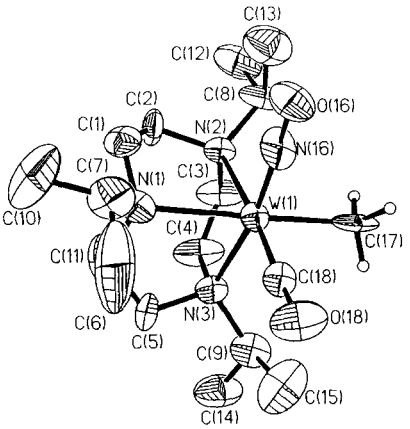

Fig. 1. Structure of the neutral complex in crystals of **2**·acetone. Selected bond lengths [Å] and angles [°]: W(1)-N(1) 2.35(2), W(1)-N(2) 2.38(2), W(1)-N(3) 2.34(2), W(1)-N(16) 1.80(2), W(1)-C(17) 2.29(2), W(1)-C(18) 1.87(2), N(16)-O(16) 1.21(3), C(18)-O(18) 1.21(3); N(16)-W(1)-C(18) 86.8(10), W(1)-N(16)-O(16) 173.6(22), W(1)-C(18)-O(18) 177.2(19).

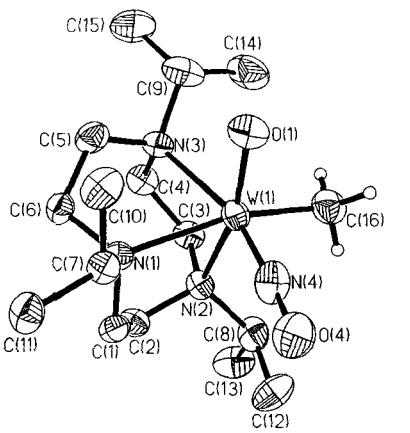

Fig. 2. Structure of the neutral complex in crystals of **4**·$C_2H_5OH \cdot 2H_2O$. Selected bond lengths [Å] and angles [°]: W(1)-N(1) 2.297(8), W(1)-N(2) 2.422(9), W(1)-N(3) 2.417(11), W(1)-N(4) 1.708(14), W(1)-O(1) 1.826(9), W(1)-C(16) 2.15(1), N(4)-O(4) 1.24(2); O(1)-W(1)-N(4) 101.5(5), O(1)-W(1)-C(16) 98.2(4), N(4)-W(1)-C(16) 93.9(5), W(1)-N(4)-O(4) 174.0(10).

Interestingly, ^{183}W satellite peaks are discernible in the 400 MHz ^1H NMR spectra of **2** (in CD_2Cl_2) and **4** (in CD_3OD); these satellite peaks are characteristic for $W-CH_3$ groups. The $^2J(W,H)$ coupling constants for **2** and **4** are 7.32 Hz and 7.80 Hz, respectively. For comparison, a coupling constant of 9.5 Hz has been reported for $[Tp^*W^{VI}(O)_2(CH_3)]$ (Tp* = tris(3,5-dimethyl-1-pyrazolyl)borate).[9] A correlation exists between the $^2J(W,H)$ coupling constant and the formal oxidation state of the tungsten center, which increases from zero in **2**, to two in **4**, and to six in $[Tp^*W(O)_2(CH_3)]$.

Complex **4** comprises the strong π-acceptor ligand NO, the very strong π-donor ligand O^{2-}, *and* one very strong σ-donor ligand, CH_3^-. All of these ligands are coordinated to the same metal ion in a *cis* arrangement. This shows once again the marked tendency of nitrosyl ligands to undergo (M–NO) π-backbonding with concurrent weakening of the N–O bond (ν(NO) at 1433 cm^{-1}). Compound **4** can be regarded as an 18e complex if one assumes the presence of a W=O double bond with the 4e donor O^{2-} as ligand. Alternatively, the electronic structure of **4** can be described in terms of an octahedrally coordinated W^{IV} center (d^2), an antiferromagnetically coupled NO ligand ($S = 1$), and one oxo and one methyl anion.[10] The presence of an oxophilic W^{IV} center in this formulation readily explains the remarkable stability of **4**.

Experimental Procedure

1: Concentrated HCl (10 mL) was slowly added (effervescence!) to a suspension of $[LW(CO)_3]$ (1 g, 1.9 mmol) and $NaNO_2$ (0.3 g, 4.3 mmol) in methanol (100 mL) resulting in a yellow solution. Insoluble material was removed by filtration, and the filtrate was evaporated to dryness under reduced pressure. The residue was dissolved in water (100 mL) and the solution was filtered. The yellow product **1** was precipitated by adding a solution of KPF_6 (0.5 g, 2.7 mmol) in water (50 mL) to the filtrate. Yield: 1.15 g (90%).

2: A solution of **1** (1 g, 1.5 mmol) in THF (200 mL) was purged with argon, and $LiAlH_4$ (0.3 g, 7.9 mmol) was added in small portions. The mixture was stirred at room temperature until the solution had turned blue, whereupon unreacted $LiAlH_4$ was removed by filtration. Degassed water (30 mL) was slowly added to the filtrate and the resulting precipitate was collected by filtration under an inert argon atmosphere. The THF was removed under vacuum and the blue product **2** precipitated as a microcrystalline powder from water. Yield: 0.46 g (60%).

3: Under an inert argon atmosphere, **2** (0.3 g, 0.6 mmol) was dissolved in a solvent mixture of HCl/CH_3CN (1:3) (the solvent mixture was purged with argon prior to use) resulting in effervescence and a red solution. The solvent was removed under vacuum and the residue was dissolved in methanol (10 mL). Upon addition of $NaClO_4$ (0.1 g), the product **3** precipitated as a red, microcrystalline solid. Yield: 0.33 g (90%).

4: **2** (1.0 g, 2.0 mmol) was dissolved in CH_2Cl_2 (15 mL) in air. The color of the solution changed from blue to red. After removal of the solvent the red product **4** was obtained quantitatively. Yield: 0.95 g (95%).

All compounds gave satisfactory elemental analyses (C, H, N). Selected physical data for these complexes is summarized in Table 1.

Received: January 26, 1995 [Z 7661 IE]
German version: *Angew. Chem.* **1995**, *107*, 1603–1605

Keywords: complexes with nitrogen ligands · complexes with oxygen ligands · hydrogen bonds · tungsten compounds

[1] J. Böhmer, G. Haselhorst, K. Wieghardt, B. Nuber, *Angew. Chem.* **1994**, *106*, 1556; *Angew. Chem. Int. Ed. Engl.* **1994**, *33*, 1473.
[2] a) G. B. Richter-Addo, P. Legzdins, *Metal Nitrosyls*, Oxford University Press, New York, **1992**; b) P. Legzdins, J. E. Veltheer, *Acc. Chem. Res.* **1993**, *26*, 41.
[3] G. Haselhorst, S. Stoetzel, A. Strassburger, W. Walz, K. Wieghardt, B. Nuber, *J. Chem. Soc. Dalton Trans.* **1993**, 83.
[4] This reaction is reminiscent of the analogous chemistry of $[CpRe(NO)(CO)_2]$, for example: a) R. P. Stewart, N. Okamoto, W. A. G. Graham, *J. Organomet. Chem.* **1972**, *42*, C32; b) J. R. Sweet, W. A. G. Graham, *ibid.* **1979**, *173*, C9;

c) *J. Am. Chem. Soc.* **1982**, *104*, 2811; d) C. P. Casey, M. A. Andrews, J. E. Riuz, *ibid.* **1979**, *101*, 741; e) W. Tam, W. Wong, J. A. Gladysz, *ibid.* **1979**, *101*, 1589; f) C. P. Casey, M. A. Andrews, D. R. McAllister, *ibid.* **1979**, *101*, 3371; g) W. Tam, G. Y. Lin, W.-K. Wong, W. A. Kiel, V. K. Wong, J. A. Gladysz, *ibid.* **1982**, *104*, 141. h) We were subsequently able to show that this reaction can be applied to amine rhenium(I) complexes and have prepared [Re(tacn)(NO)(CO)(CH_3)] (tacn = 1,4,7-triazacyclononane) which was found to be stable toward oxygen: C. Pomp, K. Wieghardt, *Inorg. Chem.* **1988**, *27*, 3796.

[5] J. H. Enemark, R. D. Feltham, *Coord. Chem. Rev.* **1974**, *13*, 339.

[6] The proposed mechanism for the formation of **4** and $C^{16}O^{18}O$ involves the intramolecular rearrangement of a coordinated peracid ester and is formulated in analogy to mechanisms for the reaction of [IrCl(CO)(tdpme)] or [Os(NO)(CO)Cl(PPh_3)$_2$] with O_2 (tdpme = 1,1,1-tris(diphenylphosphanomethyl)-ethane). In both of these reactions an intermediate comprising a bidentate carbonato ligand has been identified. In the present reaction such a carbonato complex is also conceivable as an intermediate which subsequently decomposes to give **4** and CO_2. W. O. Siegl, S. J. Lapporte, J. P. Collman, *Inorg. Chem.* **1971**, *10*, 2158; K. R. Laing, W. R. Roper, *J. Chem. Soc. Chem. Commun.* **1968**, 1556; A. F. Hill, W. R. Roper, J. M. Waters, A. H. Wright, *J. Am. Chem. Soc.* **1983**, *105*, 5939.

[7] **2**·acetone: $C_{30}H_{42}N_4O_3W$, crystals from acetone; orthorhombic, space group *Pbca* (no. 61), $a = 12.86(1)$, $b = 16.589(6)$, $c = 22.45(2)$ Å, $V = 4789(8)$ Å^3, $Z = 8$, $\rho_{calcd} = 1.57$ g cm^{-3}, $\mu Mo_{K\alpha} = 4.95$ mm^{-1}; 1845 observed reflections ($I \geq 2.5\sigma(I)$); absorption correction: empirical, Ψ scans, $2\theta_{max} = 50°$, $R = 0.066$; $R_w = 0.051$; residual electron density = 1.2 e Å^{-3}. **4**·$C_2H_5OH \cdot 2H_2O$: $C_{18}H_{40}N_4O_5W$, crystals from $CH_3CN/C_2H_5OH(H_2O)$; monoclinic, space group $P2_1/c$ (no. 14), $a = 9.915(4)$, $b = 16.080(4)$, $c = 14.980(5)$ Å, $\beta = 106.61(3)°$, $V = 2289(4)$ Å^3, $Z = 4$, $\rho_{calcd} = 1.68$ g cm^{-3}, $\mu Mo_{K\alpha} = 5.19$ mm^{-1}; 2905 observed reflections ($I \geq 2.5\sigma(I)$); absorption correction: empirical, Ψ scans, $2\theta_{max} = 52.5°$, $R = 0.060$; $R_w = 0.051$; residual electron density = 2.1 e Å^{-3}. Reflection intensities were measured on a Syntex-R3 diffractometer at 293 K with monochromated $Mo_{K\alpha}$ radiation. The structures were solved by the Patterson method and difference-Fourier syntheses; refinement on F for all independently observed reflections (heavy atoms isotropically, H atoms (calculated) with isotropic temperature factors). Structure determination and refinement employing the program Siemens-SHELXTL-PLUS (PC version) by G. M. Sheldrick (Universität Göttingen). Further details of the crystal structure investigations may be obtained from the Fachinformationszentrum Karlsruhe, D-76344 Eggenstein-Leopoldshafen (Germany), on quoting the depository number CSD-58933.

[8] W. A. Nugent, J. M. Mayer in *Metal-Ligand Multiple Bonds*, Wiley, New York, **1988**.

[9] J. Sundermeyer, J. Putterlik, H. Pritzkow, *Chem. Ber.* **1993**, *126*, 289.

[10] C. A. Brown, M. A. Pavlosky, T. E. Westre, Y. Zhang, B. Hedman, K. O. Hodgson, E. I. Solomon, *J. Am. Chem. Soc.* **1995**, *117*, 715.

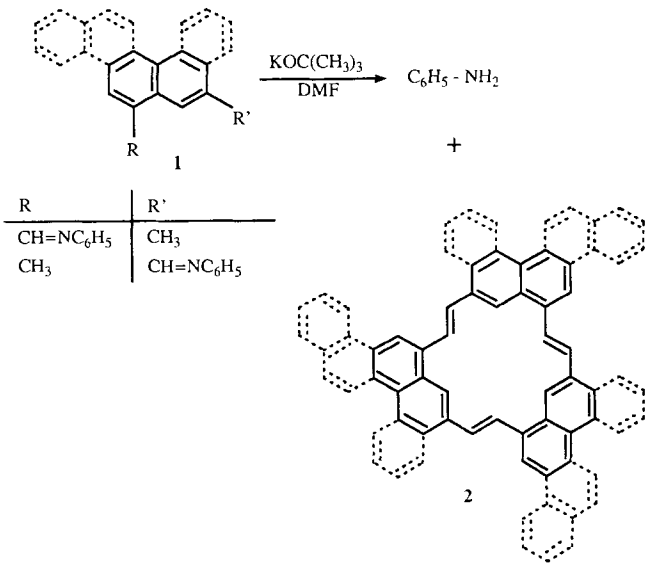

R	R'
$CH{=}NC_6H_5$	CH_3
CH_3	$CH{=}NC_6H_5$

Scheme 1.

The introduction of alkoxy side chains not only improves the solubility but also frequently allows the formation of nematic or columnar discotic liquid crystals (LC). For example, compounds **2c**, **e**–**h**, **i**, **k** form thermotropic LC phases.

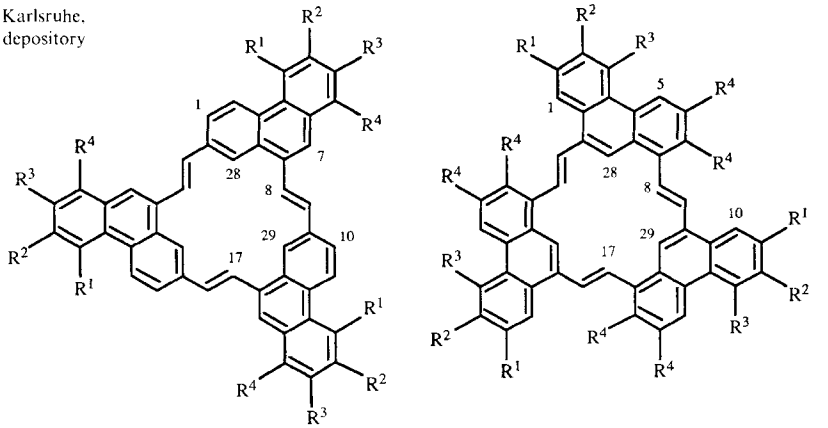

2a-h **2i-k**

2	R^1	R^2	R^3	R^4
a	H	OC_6H_{13}	H	H
b	H	$OC_{12}H_{25}$	$OC_{12}H_{25}$	H
c	H	OC_6H_{13}	OC_6H_{13}	OC_6H_{13}
d	OCH_3	OCH_3	OCH_3	H
e	OC_6H_{13}	OC_6H_{13}	OC_6H_{13}	H
f	OC_8H_{17}	OC_8H_{17}	OC_8H_{17}	H
g	$OC_{10}H_{21}$	$OC_{10}H_{21}$	$OC_{10}H_{21}$	H
h	$OC_{12}H_{25}$	$OC_{12}H_{25}$	$OC_{12}H_{25}$	H
i	H	H	H	OC_6H_{13}
j	H	OC_6H_{13}	H	OC_6H_{13}
k	$OC_{12}H_{25}$	$OC_{12}H_{25}$	$OC_{12}H_{25}$	H

Synthesis of Belt Cyclophanes**

Herbert Meier* and Klaus Müller

Dedicated to Professor Manfred Regitz on the occasion of his 60th birthday

Cyclophanes[1, 2] and compounds with beltlike structures[3] are important themes in organic chemistry. We report here on the synthesis of novel belt cyclophanes. Their molecular basis is an [18]annulene anellated with arenes. The preparatively simple approach to these compounds is based on a highly stereoselective triple cyclocondensation of azomethines.[4, 5] The naphthalene, phenanthrene, and chrysene derivatives **1** are transformed by elimination of aniline under alkaline conditions into compounds **2** (Scheme 1).

[*] Prof. Dr. H. Meier, Dipl.-Chem. K. Müller
Institut für Organische Chemie der Universität
J.-J.-Becher-Weg 18–22, D-55099 Mainz (Germany)
Telefax: Int. code + (6131)39-5396

[**] This work was supported by the Deutsche Forschungsgemeinschaft and the Fonds der Chemischen Industrie.

In contrast to unsubstituted [18]annulene,[6] the areno-condensed [18]annulenes **2** are not planar but have a pyramidal structure with C_3 symmetry.[4] In this case the lowest energy structure corresponds to a compromise between the increased resonance stabilization in the planar structure and the simultaneously increased steric interaction of the six inner H atoms. Force field calculations (MMX, PC Model 4.0 Serena)[7] for $R^i = H$ ($i = 1...4$) indicated that the anellated compounds **2a–h** should be more planar than **2i–k**. Characteristic parameters are the torsion angles θ (C_8-C_9-C_{9a}-C_{29}), which are 25.1° in the first case and 33.2° in the second. The enthalpy of formation ΔH_f is correspondingly lower for the first set of compounds than for the second (208.7 versus 216.5 kcal mol^{-1}, $R^i = H$).

Compounds **2** have chromophores with interesting photochemical characteristics. The longest wavelength absorption maximum lies between 330 and 360 nm for the phenanthro-condensed systems, whereas for the more planarized naphtho-anellated systems it is red-shifted to 370–400 nm. The nature of the anellation also plays an important role, as the spectra of the isomeric tris(dodecyloxy) compounds **2h** and **2k** show. The long-wavelength maximum is bathochromically shifted in the more planar compound **2h** compared to that of **2k**.

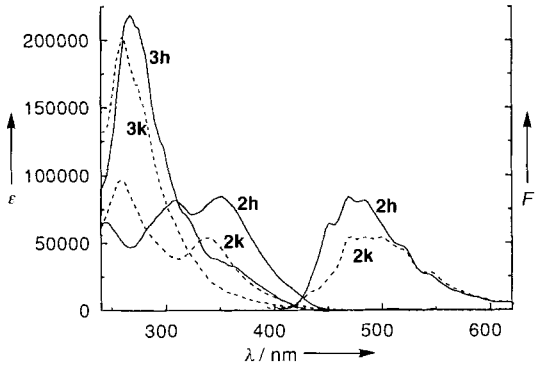

Fig. 1. UV/Vis spectra of compounds **2h** (—) and **2k** (- - -), as well as of the irradiation products **3h** (—) and **3k** (- - -), in *n*-hexane. Fluorescence spectra of **2h** and **2k** in *n*-hexane (intensities *F* in arbitrary units).

Irradiation ($\lambda \geq 290$ nm) of **2h** and **2k** in oxygen-free benzene (freeze-pump-thaw technique) leads to dimers **3h**[8] and **3k**[9] in 56 and 68% yield, respectively. These represent new cyclophane types. The belt structure shown in Scheme 2 results from a highly regio- and stereoselective triple [2π + 2π]cycloaddition. The phenanthrene systems are arranged opposite each other on each edge of the belt.

In comparison to the flexible 18-membered rings in the annulenes **2h,k**, the dimers are completely rigid. In the UV/Vis spectra the "phenanthrene transitions" (β-bands) are retained with a maximum at roughly 265 nm. It must be taken into account that the molar concentration of chromophores is doubled in **3h,k** compared to **2h,k**. The long-wavelength maxima of **2h,k** disappear after the dimerization; however, the long-wavelength absorption edges remain because electronic transitions typical for cyclophanes occur in this region.

An interesting structural question arises from considerations of whether **3** is formed from the preferred conformation or a higher energy conformation of **2**, in which the inner and outer protons 8-H/9-H, 17-H/18-H, 26-H/27-H have exchanged places. This can be determined by using isotopic labeling and NOE difference spectroscopy. With this in mind we synthesized (9-D,18-D,27-D)**2h** from the corresponding compound **1** with a deuterated phenyl imino group -CD=NC_6H_5. Irradiation of the ^{1}H NMR signal of the 8-H protons in the 18-membered ring in **3h,k** gave a positive NOE effect at 28-H, while irradiation of the signal of 9-H gave a positive NOE effect at 10-H and 7-H. This indicates that the preferred conformation of **2** also determines the stereochemistry of **3**. The S_1 state responsible for the photoreaction exerts no additional stereochemical changes. Analogous photodimerizations are observed with the other annulenes **2** irrespective of anellation mode; exceptions to this are compounds **2i,j**, which are photostable. R^4 Residues in **2i,j** cause a still stronger deviation from the planar arrangement. The torsion angle θ (C_{28a}-C_{7a}-C_8-C_9) is 129.1° in **2i** according to MMX calculations; that is, the olefinic bond is twisted out of the phenanthrene plane by 50.9°. This inhibits the formation of excimers, which are responsible for the regio- and stereospecific course of the photodimerization.[10]

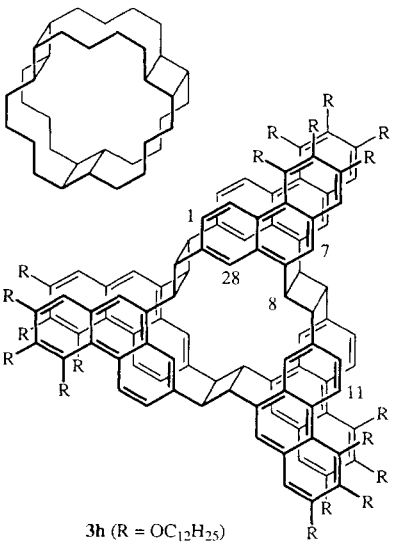

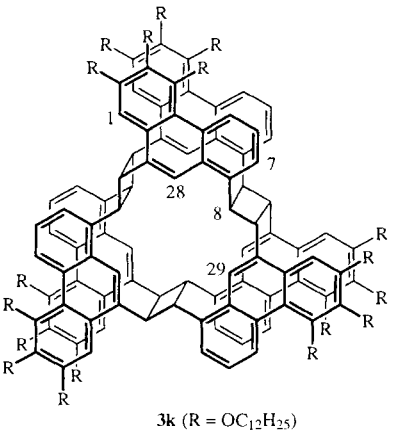

Scheme 2.

In general, photodimerizations from electronically excited singlet states become inefficient below a concentration of 10^{-2} to 10^{-3} M, because the average lifetime of the S_1 state is not sufficient for dimerization partners to come together simply by diffusion.[10] Surprisingly, the dimerization of **2h,k** proceeds even in a 10^{-5} M solution. According to diffusion theory this would require an unrealistic lifetime for the singlet state of $\tau > 10^{-6}$ s. Due to the unusually strong concentration effect on the ^{1}H NMR shifts in **2h,k** ($\Delta\delta$ of up to 1), we assume that in the ground state these large disc-shaped molecules associate in solution.

The association of the discotic mesogens is crucial for the formation of columnar liquid crystals, which we have proved for **2h,k** by X-ray small-angle diffraction, differential scanning calorimetry (DSC), and polarization microscopy. The DSC measurements for **2k** are shown in Figure 2. The cooling and heating curves indicate an extremely wide range for the LC phase. Irradiation ($\lambda \geq 300$ nm) at 230 °C leads to a quantitative

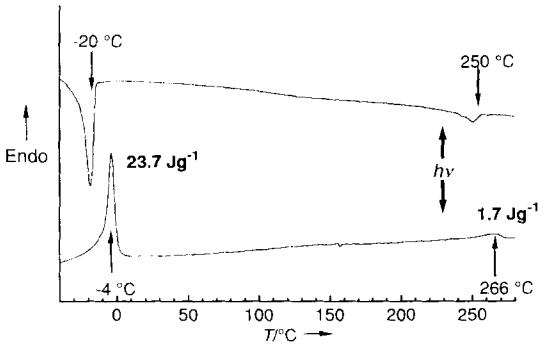

Fig. 2. DSC measurement of **2k** (upper cooling curve, lower heating curve, 20 K min^{-1} in each case).

formation of the belt cyclophane **3k**. The LC properties are irreversibly lost in the process. At lower temperatures the quantum yield drops to zero. At room temperature the LC phase is photostable. Compound **2h** shows analogous behavior. The large temperature effect on the photoreactivity cannot be explained by a thermal activation barrier in the S_1 state, since then the temperature dependence would also appear in the solution photolysis. We explain this effect by the temperature-dependent mobility. The photocyclodimerization requires not only a parallel orientation of the large discoid mesogens, but also a small separation of the olefinic centers. Only with the increased molecular mobility at higher temperatures and the thereby increased rotation about the column axis can a photodimerization take place in the LC phase. Under the described conditions this is even more efficient than in solution.

Received: February 1, 1995 [Z 7679 IE]
German version: *Angew. Chem.* **1995**, *107*, 1598–1600

Keywords: annulenes · cyclophanes · dimerizations · liquid crystals · photochemistry

[1] W. Kiggen, F. Vögtle, *Prog. Macrocyclic Chem.* **1987**, *3*, 309.
[2] F. Vögtle, *Cyclophanes I, II* (Ed.: *Top. Curr. Chem.* **1983**, *113*, *115*).
[3] See for example P. R. Ashton, G. R. Brown, N. S. Isaacs, D. Giuffrida, F. H. Kohnke, J. P. Mathias, A. M. Z. Slawin, D. R. Smith, J. F. Stoddart, D. J. Williams, *J. Am. Chem. Soc.* **1992**, *114*, 6330; J. F. Stoddart, F. H. Kohnke, *Angew. Chem.* **1988**, *100*, 981; *Angew. Chem. Int. Ed. Engl.* **1988**, *27*, 966.
[4] H. Kretzschmann, K. Müller, H. Kolshorn, D. Schollmeyer, H. Meier, *Chem. Ber.* **1994**, *127*, 1735.
[5] H. Meier, H. Kretzschmann, H. Kolshorn, *J. Org. Chem.* **1992**, *57*, 6847.
[6] F. Sondheimer, R. Wolovsky, Y. J. Amiel, *J. Am. Chem. Soc.* **1962**, *84*, 274.
[7] U. Burkert, N. L. Allinger, *Molecular Mechanics*, American Chemical Society, Washington, DC, **1982**.
[8] **3h**: Oil which forms a glass on cooling. ^{1}H NMR (400 MHz, $CDCl_3$): δ = 0.86 (t, 54H, CH_3), 1.15–1.31 (m, 288H, CH_2), 1.50 (m, 36H, γ-CH_2), 1.60–1.95 (m, 36H, β-CH_2), 3.71/3.80 (m, 12H, OCH_2), 3.97/4.04 (m, 12H, OCH_2), 4.11 (m, 12H, OCH_2, overlapping diastereotopic protons), 5.42 (m, 6H, 9-H), 6.79 (m, 6H, 8-H), 7.05 (s, 6H, 6-H), 7.14 (d, 6H, 1-H), 7.79 (s, 6H, 7-H), 9.00 (d, 6H, 2-H), 9.79 (s, 6H, 28-H); ^{13}C NMR (100 MHz, $CDCl_3$): δ = 14.0 (CH_3), 22.7–31.8 (CH_2), 43.4 (C-8), 45.2 (C-9), 68.6/73.2/74.0 (OCH_2), 106.1 (C-6), 118.2 (C-2b), 125.5/126.4/126.7/127.6 (C-1, C-2, C-7, C-28), 128.8/129.3/129.6/132.8/134.9 (C-2a, C-6a, C-7a, C-27a, C-28a), 142.0 (C-4), 151.2/151.9 (C-3, C-5).
[9] **3k**: Oil: ^{1}H NMR (400 MHz, $CDCl_3$): δ = 0.86 (t, 54H, CH_3), 1.15–1.37 (m, 288H, CH_2), 1.50 (m, 36H, γ-CH_2), 1.60–2.05 (m, 36H, β-CH_2), 3.63 (m, 12H, OCH_2), 3.90/4.03 (m, 12H, OCH_2), 4.13/4.30 (m, 12H, OCH_2), 6.10 (m, 6H, 9-H), 6.81 (m, 6H, 8-H), 7.37 (t, 6H, 6-H), 7.49 (s, 6H, 1-H), 7.96 (d, 6H, 7-H), 9.02 (d, 6H, 5-H), 9.48 (s, 6H, 28-H); ^{13}C NMR (100 MHz, $CDCl_3$): δ = 14.0 (CH_3), 22.7–31.8 (CH_2), 40.8/43.9 (C-8, C-9), 69.3/73.6/74.0 (OCH_2), 101.6 (C-1), 120.2 (C-4a), 123.9/124.5/125.2/125.6 (C-5, C-6, C-7, C-28), 128.5/128.7/129.2/130.9/134.3 (C-4b, C-7a, C-9a, C-9b, C-28a), 142.2 (C-3), 151.7/151.8 (C-2, C-4).
[10] H. Meier, *Angew. Chem.* **1992**, *104*, 1425; *Angew. Chem. Int. Ed. Engl.* **1992**, *31*, 1399, and references therein.

Silacyclopropene: Generation by High-Vacuum Flash Pyrolysis and Matrix-Spectroscopic Identification **

Günther Maier,* Harald Pacl, and Hans Peter Reisenauer

Dedicated to Professor Manfred Regitz on the occasion of his 60th birthday

In 1961 Vol'pin et al. reported the synthesis of a compound with a silacyclopropene structure.[1] However, it was shown soon afterwards that the structure assignment was incorrect and that the isolated product was a 1,4-disilacyclohexa-2,5-diene.[2] This resulted in renewed attempts to produce silacyclopropenes.[3] These proved unsuccessful until 1976, when Gaspar et al. succeeded for the first time in preparing a substituted silacyclopropene.[4] Shortly afterwards the synthesis of further silacyclopropenes was reported.[5–7] At that time two methods were available for the synthesis of this class of substances. One enabled the formation of silacyclopropenes by the addition of substituted silanediyls (silylenes) to disubstituted alkynes,[4, 5] and the other by the photolysis of alkynyldisilanes.[6, 7] Recently silacyclopropene chemistry has experienced an upswing: the first stable silacyclopropenes monosubstituted at the double bond were prepared.[8] Sander et al. came close to the synthesis of the unsubstituted parent compound with the generation of 1,1-dimethylsilacyclopropene[9] by the photolysis of a bis(diazomethyl)silane. The first silacyclopropene not substituted at the double bond was obtained in this way.

Here we report on the first generation of the long-sought parent substance, the unsubstituted silacyclopropene **4**. At the same time a new route to this class of substances is presented. Silacyclopropene **4** is formed in the high-vacuum flash pyrolysis of 1,1,1-trimethyl-2-vinyldisilane **1** by elimination of trimethylsilane. This method, in which trimethylsilane is eliminated by pyrolysis leading to the generation of reactive species, has already been applied successfully in our group to the production of 1-silacyclopropenylidene as well as other C_2H_2Si isomers.[10] The precursor **1** can be obtained from 1,1,1-trimethyl-2-phenyldisilane:[11] the latter reacts with trifluoromethanesulfonic acid (pentane, 1 h, 0 °C) to give the corresponding triflate; treating this with vinylmagnesium chloride in THF yields **1**, which can be distilled and then isolated by preparative gas chromatography (silicone phase OV 101, 175 °C) in 70% yield.[12]

[*] Prof. Dr. G. Maier, Dipl.-Chem. H. Pacl, Dr. H. P. Reisenauer
Institut für Organische Chemie der Universität
Heinrich-Buff-Ring 58, D-35392 Giessen (Germany)
Telefax: Int. code + (641)702-5712

[**] Hetero π Systems, Part 21. This work was supported by the Fonds der Chemischen Industrie and by the Deutsche Forschungsgemeinschaft. – Part 20: ref. [10].

The association of the discotic mesogens is crucial for the formation of columnar liquid crystals, which we have proved for **2h,k** by X-ray small-angle diffraction, differential scanning calorimetry (DSC), and polarization microscopy. The DSC measurements for **2k** are shown in Figure 2. The cooling and heating curves indicate an extremely wide range for the LC phase. Irradiation ($\lambda \geq 300$ nm) at 230 °C leads to a quantitative

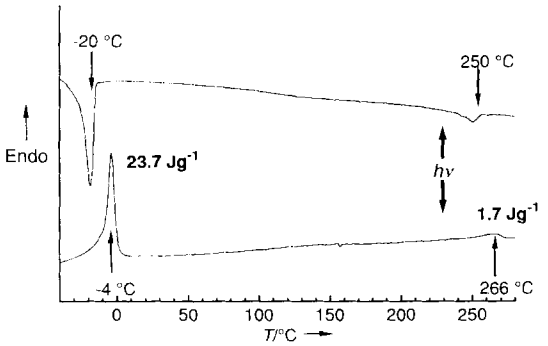

Fig. 2. DSC measurement of **2k** (upper cooling curve, lower heating curve, 20 K min^{-1} in each case).

formation of the belt cyclophane **3k**. The LC properties are irreversibly lost in the process. At lower temperatures the quantum yield drops to zero. At room temperature the LC phase is photostable. Compound **2h** shows analogous behavior. The large temperature effect on the photoreactivity cannot be explained by a thermal activation barrier in the S_1 state, since then the temperature dependence would also appear in the solution photolysis. We explain this effect by the temperature-dependent mobility. The photocyclodimerization requires not only a parallel orientation of the large discoid mesogens, but also a small separation of the olefinic centers. Only with the increased molecular mobility at higher temperatures and the thereby increased rotation about the column axis can a photodimerization take place in the LC phase. Under the described conditions this is even more efficient than in solution.

Received: February 1, 1995 [Z 7679 IE]
German version: *Angew. Chem.* **1995**, *107*, 1598–1600

Keywords: annulenes · cyclophanes · dimerizations · liquid crystals · photochemistry

[1] W. Kiggen, F. Vögtle, *Prog. Macrocyclic Chem.* **1987**, *3*, 309.
[2] F. Vögtle, *Cyclophanes I, II* (Ed.: *Top. Curr. Chem.* **1983**, *113*, *115*).
[3] See for example P. R. Ashton, G. R. Brown, N. S. Isaacs, D. Giuffrida, F. H. Kohnke, J. P. Mathias, A. M. Z. Slawin, D. R. Smith, J. F. Stoddart, D. J. Williams, *J. Am. Chem. Soc.* **1992**, *114*, 6330; J. F. Stoddart, F. H. Kohnke, *Angew. Chem.* **1988**, *100*, 981; *Angew. Chem. Int. Ed. Engl.* **1988**, *27*, 966.
[4] H. Kretzschmann, K. Müller, H. Kolshorn, D. Schollmeyer, H. Meier, *Chem. Ber.* **1994**, *127*, 1735.
[5] H. Meier, H. Kretzschmann, H. Kolshorn, *J. Org. Chem.* **1992**, *57*, 6847.
[6] F. Sondheimer, R. Wolovsky, Y. J. Amiel, *J. Am. Chem. Soc.* **1962**, *84*, 274.
[7] U. Burkert, N. L. Allinger, *Molecular Mechanics*, American Chemical Society, Washington, DC, **1982**.
[8] **3h**: Oil which forms a glass on cooling. ^{1}H NMR (400 MHz, $CDCl_3$): δ = 0.86 (t, 54H, CH_3), 1.15–1.31 (m, 288H, CH_2), 1.50 (m, 36H, γ-CH_2), 1.60–1.95 (m, 36H, β-CH_2), 3.71/3.80 (m, 12H, OCH_2), 3.97/4.04 (m, 12H, OCH_2), 4.11 (m, 12H, OCH_2, overlapping diastereotopic protons), 5.42 (m, 6H, 9-H), 6.79 (m, 6H, 8-H), 7.05 (s, 6H, 6-H), 7.14 (d, 6H, 1-H), 7.79 (s, 6H, 7-H), 9.00 (d, 6H, 2-H), 9.79 (s, 6H, 28-H); ^{13}C NMR (100 MHz, $CDCl_3$): δ = 14.0 (CH_3), 22.7–31.8 (CH_2), 43.4 (C-8), 45.2 (C-9), 68.6/73.2/74.0 (OCH_2), 106.1 (C-6), 118.2 (C-2b), 125.5/126.4/126.7/127.6 (C-1, C-2, C-7, C-28), 128.8/129.3/129.6/132.8/134.9 (C-2a, C-6a, C-7a, C-27a, C-28a), 142.0 (C-4), 151.2/151.9 (C-3, C-5).
[9] **3k**: Oil: ^{1}H NMR (400 MHz, $CDCl_3$): δ = 0.86 (t, 54H, CH_3), 1.15–1.37 (m, 288H, CH_2), 1.50 (m, 36H, γ-CH_2), 1.60–2.05 (m, 36H, β-CH_2), 3.63 (m, 12H, OCH_2), 3.90/4.03 (m, 12H, OCH_2), 4.13/4.30 (m, 12H, OCH_2), 6.10 (m, 6H, 9-H), 6.81 (m, 6H, 8-H), 7.37 (t, 6H, 6-H), 7.49 (s, 6H, 1-H), 7.96 (d, 6H, 7-H), 9.02 (d, 6H, 5-H), 9.48 (s, 6H, 28-H); ^{13}C NMR (100 MHz, $CDCl_3$): δ = 14.0 (CH_3), 22.7–31.8 (CH_2), 40.8/43.9 (C-8, C-9), 69.3/73.6/74.0 (OCH_2), 101.6 (C-1), 120.2 (C-4a), 123.9/124.5/125.2/125.6 (C-5, C-6, C-7, C-28), 128.5/128.7/129.2/130.9/134.3 (C-4b, C-7a, C-9a, C-9b, C-28a), 142.2 (C-3), 151.7/151.8 (C-2, C-4).
[10] H. Meier, *Angew. Chem.* **1992**, *104*, 1425; *Angew. Chem. Int. Ed. Engl.* **1992**, *31*, 1399, and references therein.

Silacyclopropene: Generation by High-Vacuum Flash Pyrolysis and Matrix-Spectroscopic Identification **

Günther Maier,* Harald Pacl, and Hans Peter Reisenauer

Dedicated to Professor Manfred Regitz on the occasion of his 60th birthday

In 1961 Vol'pin et al. reported the synthesis of a compound with a silacyclopropene structure.[1] However, it was shown soon afterwards that the structure assignment was incorrect and that the isolated product was a 1,4-disilacyclohexa-2,5-diene.[2] This resulted in renewed attempts to produce silacyclopropenes.[3] These proved unsuccessful until 1976, when Gaspar et al. succeeded for the first time in preparing a substituted silacyclopropene.[4] Shortly afterwards the synthesis of further silacyclopropenes was reported.[5–7] At that time two methods were available for the synthesis of this class of substances. One enabled the formation of silacyclopropenes by the addition of substituted silanediyls (silylenes) to disubstituted alkynes,[4, 5] and the other by the photolysis of alkynyldisilanes.[6, 7] Recently silacyclopropene chemistry has experienced an upswing: the first stable silacyclopropenes monosubstituted at the double bond were prepared.[8] Sander et al. came close to the synthesis of the unsubstituted parent compound with the generation of 1,1-dimethylsilacyclopropene[9] by the photolysis of a bis(diazomethyl)silane. The first silacyclopropene not substituted at the double bond was obtained in this way.

Here we report on the first generation of the long-sought parent substance, the unsubstituted silacyclopropene **4**. At the same time a new route to this class of substances is presented. Silacyclopropene **4** is formed in the high-vacuum flash pyrolysis of 1,1,1-trimethyl-2-vinyldisilane **1** by elimination of trimethylsilane. This method, in which trimethylsilane is eliminated by pyrolysis leading to the generation of reactive species, has already been applied successfully in our group to the production of 1-silacyclopropenylidene as well as other C_2H_2Si isomers.[10] The precursor **1** can be obtained from 1,1,1-trimethyl-2-phenyldisilane:[11] the latter reacts with trifluoromethanesulfonic acid (pentane, 1 h, 0 °C) to give the corresponding triflate; treating this with vinylmagnesium chloride in THF yields **1**, which can be distilled and then isolated by preparative gas chromatography (silicone phase OV 101, 175 °C) in 70% yield.[12]

[*] Prof. Dr. G. Maier, Dipl.-Chem. H. Pacl, Dr. H. P. Reisenauer
Institut für Organische Chemie der Universität
Heinrich-Buff-Ring 58, D-35392 Giessen (Germany)
Telefax: Int. code + (641)702-5712

[**] Hetero π Systems, Part 21. This work was supported by the Fonds der Chemischen Industrie and by the Deutsche Forschungsgemeinschaft. – Part 20: ref. [10].

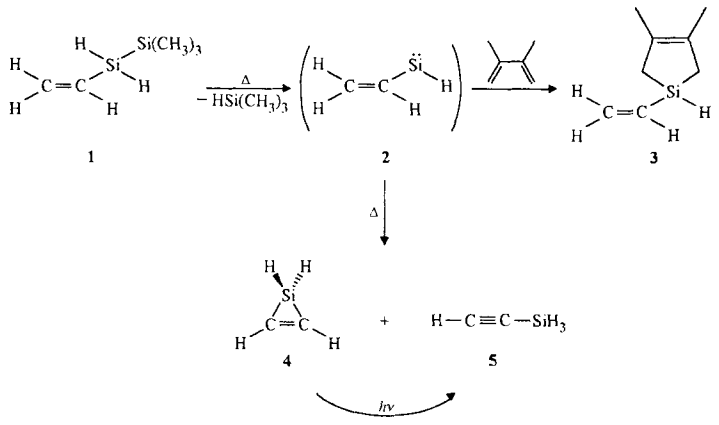

A high-vacuum flash pyrolysis (quartz tube: diameter 8 mm, length of heated zone 5 cm; ca. 10^{-3} mbar; 650 °C) was carried out on a gas mixture comprising disilane **1** and argon (1:1000). After leaving the hot zone the reaction products were directly condensed onto a CsI window at 10 K. Subsequently the matrix-isolated products were studied by IR and UV/Vis spectroscopy. The C_2H_4Si isomers ethynylsilane **5** and silacyclopropene **4** (Table 1) were detected in addition to trimethylsilane, acetylene, and small amounts of ethylene. Vinylsilanediyl **2** was not deposited onto the matrix holder, although its formation was expected in view of the structure of the precursor **1**. Indeed **2** is the primary product of the pyrolysis, since silacyclopentene **3** is obtained in 50 % yield as a trapping product from **2** in the copyrolysis of **1** with 2,3-dimethylbutadiene (quartz tube: length 33 cm, length of heated zone 25 cm, diameter 15 mm, filled with quartz Raschig rings; 450 °C; nitrogen as carrier gas).[13] Trapping products of the other C_2H_4Si isomers have not been detected. Evidently **4** and **5** are formed from the vinylsilanediyl **2** under the conditions used in the high-vacuum flash pyrolysis; presumably **5** does not arise directly from **2** but from the silacyclopropene **4** formed from **2**.

To explain the reaction mechanism and identify the C_2H_4Si species formed apart from **5**, we carried out a geometry optimization and a calculation of the vibrational spectra at the MP2/6-31G** level[14] for the C_2H_4Si isomers **2** and **4**–**9**. The resulting energy levels of the C_2H_4Si isomers increase in the order ethynylsilane **5** (global minimum) < silacyclopropene **4** < 1-silacyclopropylidene **6** < ethylidenesilanediyl **7** < *anti*- < *syn*-vinylsilanediyl **2** < 1-silaallene **8**. Particularly noteworthy is that the energy levels of all the isomers considered are extremely close to one another (Scheme 1). Compared with older calculations,[15] in which frequency calculations were not carried out, the relatively high energy content of **2** is particularly notable. As expected from the calculations, only the two lowest energy isomers, **4** and **5**, are actually formed in significant quantities in the pyrolysis.

Table 1. IR data of silacyclopropene **4** (experimental (Ar matrix, 10 K) as well as calculated (MP2/6-31G**) and corrected wavelengths [cm^{-1}]); integrated intensities (relative to the strongest band) are given in parentheses.

Vibration		Assignment	D compound	$\tilde{\nu}_{calc.}$	$\tilde{\nu}_{corr.}$ [a]	$\tilde{\nu}_{exp.}$
ν_1 [b]	a_1 [b]	CH str [b]		3304.7(3)		3061.2(5)
ν_{12}	b_2	CH str		3281.7(3)		3041.6(8)
ν_9	b_1	SiH str		2345.3(100) [c]		2176.3(68)
			[1-D]**4**	2341.8	2171.5 [d]	2171.7
			[2-D]**4**	2345.2	2176.2	2175.7
ν_2	a_1	SiH str		2338.4(57)		2166.7(97)
			[1-D]**4**	1686.8	1564.1 [d]	1582.2
			[2-D]**4**	2338.2	2166.5	2166.8
ν_3	a_1	CC str		1544.1(10)		1467.2(25)
			[1-D]**4**	1541.5	1464.7	1464.1
			[2-D]**4**	1513.5	1438.1	1441.3
ν_{13}	b_2	CH def		1169.9(11)		1105.1(21)
			[1-D]**4**	1168.4	1103.7	1103.4
			[2-D]**4**	1120.0	1057.9	1058.4
ν_4	a_1	SiH_2 def		1053.4(66)		975.9(100)
			[2-D]**4**	1046.7	969.7	969.6
ν_7	a_2	CH/SiH def		959.7(0)		
ν_5	a_1	CH def		957.5(4)		900.6(4)
ν_6	a_1	SiC str		805.7(7)		778.5(18)
			[1-D]**4**	802.7	775.6	773.4
ν_{14}	b_2	SiC str		721.3(24)		707.4(35)
			[1-D]**4**	721.3	707.4	707.1
ν_{10}	b_1	SiH/CH def		717.5(76)		695.1(51)
ν_{15}	b_2	SiH_2 def		706.7(24)		655.4(25)
ν_8	a_2	SiH/CH def		605.6(0)		
ν_{11}	b_1	SiH/CH def		589.8(9)		589.2(11)

[a] $\tilde{\nu}_{corr.} = \tilde{\nu}_{exp.}(\mathbf{4}) / \tilde{\nu}_{calc.}(\mathbf{4}) \times \tilde{\nu}_{calc.}$(isotopomer). [b] The figures in these columns refer only to the nonlabeled silacyclopropene **4**. [c] Absolute intensity 182 km mol^{-1}. [d] The arithmetic mean of the two SiH stretching vibrations was used as the reference.

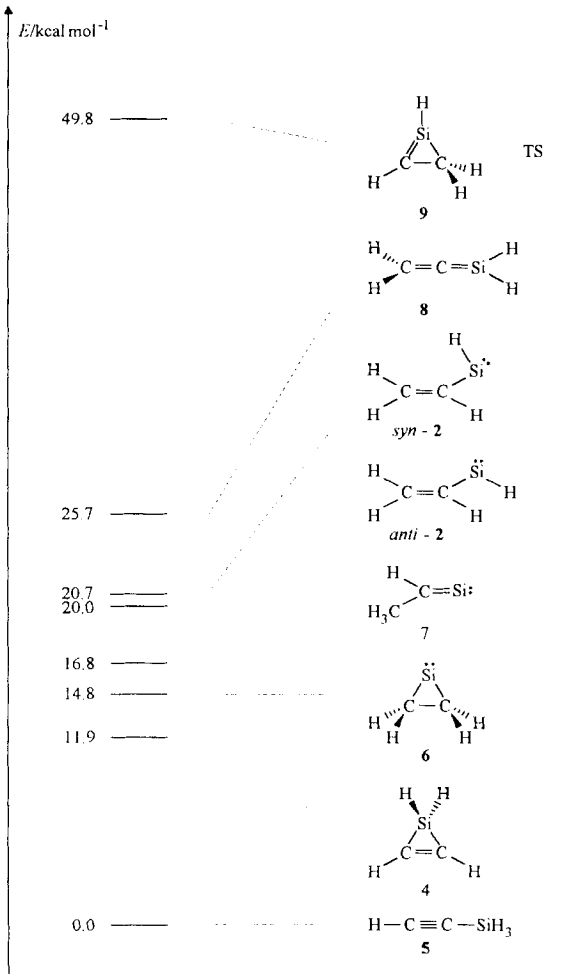

Scheme 1. Relative energies E [kcal mol^{-1}] of the C_2H_4Si isomers **2**, **4**–**8** (energy minima), and **9** (transition state TS) calculated at the MP2/6-31G** level taking into account the zero point vibrational energy.

Good agreement between the experimental and calculated IR spectra is found only for silacyclopropene **4** (Fig. 1, Table 1).[16] Thus, in accordance with the calculation, its IR spectrum shows two bands for the CH stretching vibrations (3061.2 and 3041.6 cm^{-1}), two for the SiH stretching vibrations (2176.3

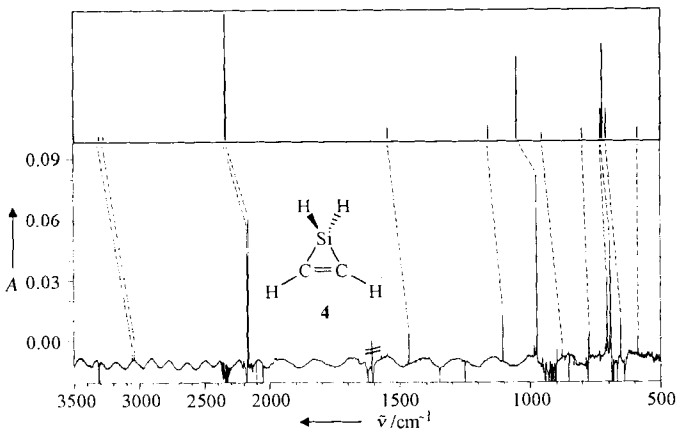

Fig. 1. Comparison of the experimental (bottom) and calculated IR spectra (MP2/6-31G**, top) of silacyclopropene **4**. The experimental spectrum (Ar matrix, 10 K) is the difference spectrum for the photoreaction **4** → **5**. The bands due to water have been crossed.

and 2166.7 cm^{-1}), and one for the CC stretching vibration (1467.2 cm^{-1}). In addition the pattern of the remaining eight lower lying absorption bands corresponds to the calculated ones. Particularly characteristic is the strong band arising from the SiH_2 deformation at 975.9 cm^{-1}. Irradiation of **4** with light of wavelength $\lambda = 254$ nm results in the selective rearrangement to **5**, even though **4** shows no UV maximum above 250 nm. 1,1-Dimethylsilacyclopropene behaves in a similar way.[9] Ethynylsilane **5** is photostable.

In addition to the unmarked precursor we have also investigated the deuterated analogue [2,2-D_2]**1**. This can be obtained from 1,1-dibromo-2,2,2-trimethyl-1-phenyldisilane[11b] by reduction with $LiAlD_4$ and subsequent conversion with trifluoromethanesulfonic acid and vinylmagnesium chloride as described above. The high-vacuum flash pyrolysis of [2,2-D_2]**1** led to two important findings: Firstly, the observed band shifts (see Table 1) confirm the reliability of the present structure assignment of **4**. Secondly, the results give an insight into the reaction mechanism. In the pyrolysis of [2,2-D_2]**1** the silacyclopropene isotopomers [1-D]**4** and [2-D]**4** are formed approximately in the ratio 1:1. The two ethynylsilanes [1-D]**5** and [3-D]**5** are also formed, but here the former predominates.

To explain these results we suggest the following mechanism: Pyrolysis results initially in the formation of vinylsilanediyl [1-D]**2** as confirmed by the trapping studies. This is in equilibrium with its isotopomer [2-D]**2** through the 1-silaallene intermediate [1-D]**8**. The energetically more favorable silacyclopropene isotopomers [1-D]**4** and [2-D]**4** are then formed in equal amounts from [1-D]**2** and [2-D]**2**.

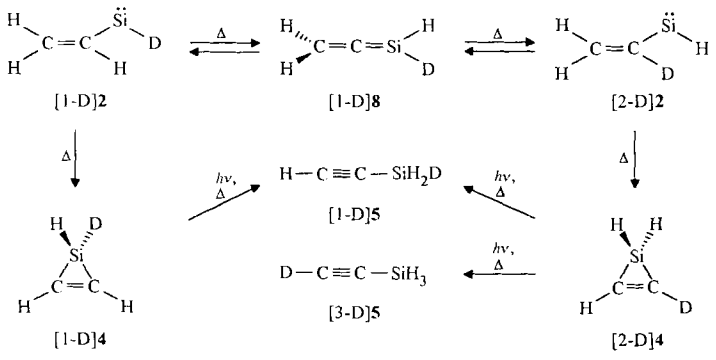

The rearrangement **2** → **4** could be initiated by the addition of the silanediyl center to the C–C double bond. This reaction would be analogous to the well-known formation of cyclopropenes from vinylcarbenes. In our case, the 1-silacycloprop-1-ene **9** would have to be formed first under this assumption, followed by a 1,2-hydrogen shift. However, the structure of **9** does not represent an energy minimum according to the calculation, but rather **9** is a transition state with a relative energy of 49.8 kcal mol^{-1}. In principle the formation of **4** from **2** can also occur quite differently by the insertion of the silanediyl center in the C–H bond of the olefinic CH_2 group in **2**.

Under pyrolysis conditions the silacyclopropenes [1-D]**4** and [2-D]**4** are already partly opened to give the ethynylsilane isotopomers [1-D]**5** and [3-D]**5**, so that the global minimum is reached. The same ring-opening can also be photochemically induced.

Received: March 6, 1995 [Z7765IE]
German version: *Angew. Chem.* **1995**, *107*, 1627–1629

Keywords: flash pyrolysis · photochemistry · silicon compounds · strained rings

[1] a) M. E. Vol'pin, Yu. D. Koreshkov, D. N. Kursanov, *Izv. Akad. Nauk SSSR, Otd. Khim. Nauk* **1961**, 1355–1356; b) M. E. Vol'pin, Yu. D. Koreshkov, V. G. Dulova, D. N. Kursanov, *Tetrahedron* **1962**, *18*, 107–122.

[2] a) R. West, R. E. Bailey, *J. Am. Chem. Soc.* **1963**, *85*, 2871–2872; b) F. Johnson, R. S. Gohlke, W. H. Nasutavicus, *J. Organomet. Chem.* **1965**, *3*, 233–244; c) N. G. Bokii, Yu. T. Stuchkow, *Zh. Strukt. Khim.* **1965**, *6*, 751–758. d) For a theoretical analysis of the dimerization of silacyclopropenes at higher temperatures refer to E. A. Halevi, R. West, *J. Organomet. Chem.* **1982**, *240*, 129–141.

[3] W. H. Atwell, D. R. Weyenberg, *Angew. Chem.* **1969**, *81*, 485–493; *Angew. Chem. Int. Ed. Engl.* **1969**, *8*, 469–477.

[4] R. T. Conlin, P. P. Gaspar, *J. Am. Chem. Soc.* **1976**, *98*, 3715–3716.

[5] D. Seyferth, D. C. Annarelli, S. C. Vick, *J. Am. Chem. Soc.* **1976**, *98*, 6382–6384.

[6] M. Ishikawa, T. Fuchikami, M. Kumada, *J. Am. Chem. Soc.* **1977**, *99*, 245–247.

[7] H. Sakurai, Y. Kamiyama, Y. Nakadaira, *J. Am. Chem. Soc.* **1977**, *99*, 3879–3880.

[8] J. Belzner, H. Ihmels, *Tetrahedron Lett.* **1993**, *34*, 6541–6544.

[9] M. Trommer, W. Sander, C. Marquard, *Angew. Chem.* **1994**, *106*, 816–818; *Angew. Chem. Int. Ed. Engl.* **1994**, *33*, 766–769.

[10] G. Maier, H. P. Reisenauer, H. Pacl, *Angew. Chem.* **1994**, *106*, 1347–1349; *Angew. Chem. Int. Ed. Engl.* **1994**, *33*, 1248–1250.

[11] a) E. Hengge, G. Bauer, H. Marketz, *Z. Anorg. Allg. Chem.* **1972**, *394*, 93–100; b) D. Littmann, Dissertation, Universität Gießen, **1985**.

[12] **1**: ^{1}H NMR (capillary): $\delta = 0.44$ (s, 9H, $Si(CH_3)_3$), 3.97 (d, ^3J(H,H) = 3.4 Hz, 2H, SiH), 6.03–6.17 (m, 1H, =CHSi), 6.21–6.35 (m, 2H, $=CH_2$); ^{13}C NMR (capillary): $\delta = -0.8$ ($Si(CH_3)_3$), 129.8 (=CHSi), 135.5 ($=CH_2$); ^{29}Si NMR ([D_6]benzene): $\delta = -63.0$ (SiH_2), -18.2 ($Si(CH_3)_3$).

[13] **3**: ^{1}H NMR (capillary): $\delta = 1.65$–1.74 (m, 2H, CH_2), 1.80–1.88 (m, 2H, CH_2), 1.95 (m, 6H, CH_3), 4.53–4.58 (m, 1H, SiH), 6.05–6.48 (m, 3H, $HC=CH_2$); ^{13}C NMR: $\delta = 19.3$ (CH_3), 21.9 ($SiCH_2$), 130.7, 134.3, 134.9; ^{29}Si NMR: $\delta = -12.7$.

[14] Gaussian 92, Revision B: M. J. Frisch, G. W. Trucks, M. Head-Gordon, P. M. W. Gill, M. W. Wong, J. B. Foresman, B. G. Johnson, H. B. Schlegel, M. A. Robb, E. S. Replogle, R. Gomperts, J. L. Andres, K. Raghavachari, J. S. Binkley, C. Gonzales, R. L. Martin, D. J. Fox, D. J. Defrees, J. Baker, J. J. P. Stewart, J. A. Pople, Gaussian, Inc., Pittsburgh PA, **1992**.

[15] a) M. S. Gordon, R. D. Koob, *J. Am. Chem. Soc.* **1981**, *103*, 2939–2944; b) M. H. Lien, A. C. Hopkinson, *Chem. Phys. Lett.* **1981**, *80*, 114–118; c) J.-C. Barthelat, G. Trinquier, G. Bertrand, *J. Am. Chem. Soc.* **1979**, *101*, 3785–3789; d) K. Krogh-Jespersen, *J. Comput. Chem.* **1982**, *3*, 571–579. e) See also the calculation on the triplet energy hypersurface: M.-D. Su, R. D. Amos, N. C. Handy, *J. Am. Chem. Soc.* **1990**, *112*, 1499–1504. f) For details on the aromatic character of silacyclopropenes refer to P. Jones, D. D. White, *J. Organomet. Chem.* **1978**, *154*, C33–C36.

[16] An older calculation of the IR spectrum of **4**, but without details of the intensities, is given by M. S. Gordon, *J. Am. Chem. Soc.* **1980**, *102*, 7419–7422.

First Steps Towards Ordered Monolayers of Ligand-Stabilized Gold Clusters**

Stefanie Peschel and Günter Schmid*

Dedicated to Professor Peter Paetzold on the occasion of his 60th birthday

The achievement of an ordered arrangement of chemically produced quantum dots is very important in the light of future applications in nanotechnology. Most of the work carried out in this field concerns the use of semiconductor quantum dots, since it is hoped that the transition of a semiconductor from the bulk state to the nanometer region, will give rise to novel physical properties, particularly in the field of electrooptics.[1] Apart from the difficulty of synthesizing semiconductor clusters with largely uniform size and defined structure, the main problem is to achieve a two- or three-dimensional arrangement of the particles, without them touching. Numerous attempts have been made to use zeolites or porous materials as host lattices.[2] Polymers have also been used to prevent a coalescence of the semiconductor particles. To date there has been no recognizable breakthrough in the practical effectiveness of these types of systems.

With the synthesis of ligand-stabilized transition metal clusters a different kind of approach to quantum dots has become possible, which has advantages over conventional systems: 1. uniform particle size, 2. the stabilization by largely inert ligand shells, 3. the equidistant arrangement as a result of defined ligand shells, 4. the avoidance of coalescence processes, 5. the possibility of varying the separation between the clusters by chemical modification of the ligand shell. Figure 1 illustrates these possibilities which are decisive for the utilization of quantum properties.

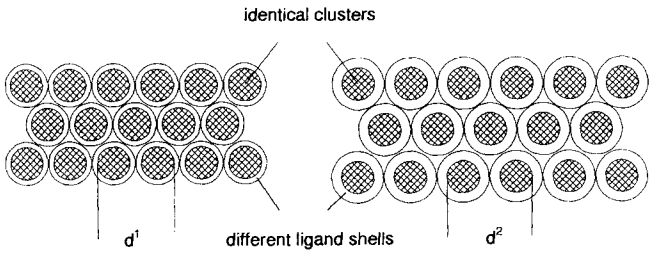

Fig. 1. The intermolecular distances and therefore the Coulomb barriers between the clusters can be modified by varying the ligand shell.

Recently, we were able to answer unequivocally the question of whether besides semiconductor clusters also metal clusters could be applied as quantum dots. Gold clusters of composition $[Au_{55}(PPh_3)_{12}Cl_6]$ are composed of a cluster core about 1.4 nm in diameter and a ligand shell 0.35 nm thick, which results in an approximately spherical particle with a total diameter of about 2.1 nm. In a close packed three-dimensional arrangement these clusters show conductivity, which is characterized by single-electron tunneling (SET) processes between the cluster cores separated by the ligand shells.[3] Investigations of clusters on the surface of pellets using scanning tunnel microscopy (STM) and scanning tunneling spectroscopy (STS) produce images which show that the ligand shells of the individual clusters are in contact, and in the current/voltage diagram there is not only the expected Coulomb barrier[4] but also, for the first time, energy fine line splitting of the electronic states in individual clusters at room temperature.[5] Therefore, ligand-stabilized metal clusters seem to fulfill the requirements for their application in the nanometer range.

In contrast to the readily synthesized, but complicated workings of three-dimensional cluster arrangements in crystals and pellets, ordered monolayers on suitable substrates should facilitate electronic investigations. This applies to an even greater extent to one-dimensional cluster arrangements (quantum wires), which we are currently trying to produce.

We were able to synthesize largely ordered monolayers of ligand-stabilized Au_{55} clusters for the first time. In order to accomplish this we used the established principle of self-assembly with the help of poly-electrolytes.[6] However, we could not use the $[Au_{55}(PPh_3)_{12}Cl_6]$ cluster itself but had to synthesize a derivative in which the PPh_3 was replaced by a $PPh_2(m\text{-}C_6H_4SO_3H)$ ligand. To this end we used the previously reported sodium salt $[Au_{55}\{PPh_2(m\text{-}C_6H_4SO_3Na)_{12}\}Cl_6]$[7] and converted it into the free acid by ion exchange. When a freshly prepared thin layer of poly(ethylenimine) (PEI) on a mica surface is immersed into a solution of the cluster there is a strongly attractive interaction between the sulfonic groups and the imino groups.

The coating is carried out by immersion of a mica platelet for 24 hours in a 10^{-4} molar aqueous solution of PEI. After intensive washing with distilled water and drying in vacuo, the coated platelet was then immersed in a 3×10^{-6} molar aqueous solution of the Au cluster. In order to remove any additional cluster molecules sticking to the surface, the platelet was washed with a total of 0.5 L of distilled water and dried in vacuo. Because of the ready solubility of the cluster, this procedure ensures that only the strongly adhesive monolayer produced by the acid–base interaction remains. Figure 2 is a simplified illustration of the principle of the cluster/PEI interaction.

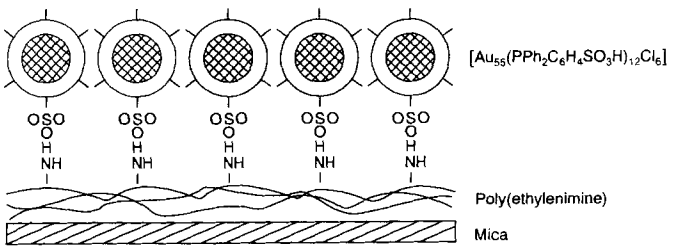

Fig. 2. Schematic illustration of the interaction between cluster molecules and poly(ethylenimine). A mica platelet (ca. 1 cm^2) coated with PEI, was immersed for 24 h in a 3×10^{-6} M aqueous cluster solution. As a consequence the sulfonic groups of the cluster ligands interact with the imino groups of the polymer.

Figure 3 (top) shows a three-dimensional atomic force microscopic (AFM) image[8] of a section of the cluster monolayer. Sections of comparable quality can be obtained from all areas of the approximately 1 cm^2 surface. Shorter reaction times between the PEI layer and the cluster solution, for example six or twelve hours, gave a relatively closely packed occupation, however, the level shown in Figure 3 top occurs only after 24 hours. Numerous cross-sections show that less than 5% of the surface is disordered or uncovered.

[*] Prof. Dr. G. Schmid, Dipl.-Chem. S. Peschel
Institut für Anorganische Chemie der Universität
Universitätsstrasse 5–7, D-45117 Essen (Germany)
Telefax: Int. code + (201) 183-2402

[**] This work was supported by the Deutsche Forschungsgemeinschaft. We would like to thank the Förderverein der Stadt Essen for their generous donations. We are grateful for the valuable discussions with Prof. H. Ringsdorf.

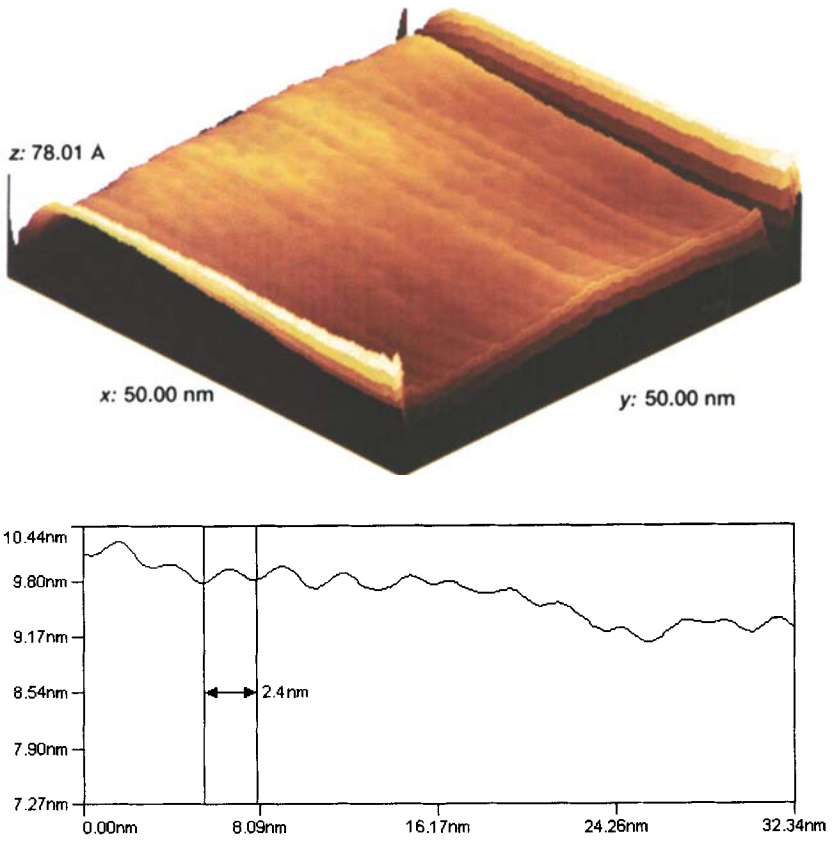

Fig. 3. Top: Three-dimensional representation of a largely ordered monolayer of $[Au_{55}\{PPh_2(m\text{-}C_6H_4SO_3H)_{12}\}Cl_6]$ on poly(ethylenimine). Bottom: Cross-section of a single cluster row. The separation between the clusters is 2.4 nm, which is in agreement with the calculated cluster size.

The equidistance of the clusters within a row and the resulting organization can be seen at the bottom of Figure 3 which shows a typical cross-section. The average distances of 2.4 $\pm$ 0.2 nm are in very good agreement with those expected for SO_3H-substituted clusters. These easily synthesized cluster monolayers can now be used to study electronic transitions in two-dimensional arrangements of quantum dots (cluster cores) separated by the ligand shells and spaced 1.4 nm apart, a distance which cannot be obtained either by the usual semiconductor technology or by the semiconductor clusters described above. Furthermore, this principle can be used for the formation of sandwich structures because the cluster monolayer can, in turn, be coated with PEI. Since it should be possible to synthesize the corresponding cluster monolayers with clusters from other metals, additional possibilities are available for the generation of multilayer systems with different metals.

Received: November 30, 1994
Revised version: February 2, 1995 [Z 7513 IE]
German version: *Angew. Chem.* **1995**, *107*, 1568–1569

Keywords: clusters · gold compounds · monolayers · nanostructures

[1] H. Weller, *Angew. Chem.* **1993**, *105*, 43; *Angew. Chem. Int. Ed. Engl.* **1993**, *32*, 41; *Adv. Mater.* **1993**, *5*, 88; J. N. Fendler, *Chem. Rev.* **1987**, *87*, 877; A. Henglein, *Top. Curr. Chem.* **1988**, *143*, 115; M. C. Steigerwald, L. E. Brus, *Ann. Rev. Mater. Sci.* **1989**, *19*, 471; O. V. Salata, P. J. Dobson, P. J. Hull, J. L. Hutchison, *Adv. Mater.* **1994**, *6*, 772; J. E. B. Katari, V. L. Colvin, A. P. Alivisatos, *J. Phys. Chem.* **1994**, *98*, 4109.

[2] Y. Wang, N. Herron, *J. Phys. Chem.* **1988**, *92*, 4988; *ibid.* **1987**, *91*, 257; G. A. Ozin, S. Özkar, *Adv. Mater.* **1992**, *4*, 111; J. Kuczyuski, J. K. Thomas, *Chem. Phys. Lett.* **1985**, *89*, 2720.

[3] U. Simon, G. Schön, G. Schmid, *Angew. Chem.* **1993**, *105*, 264; *Angew. Chem. Int. Ed. Engl.* **1993**, *32*, 250; U. Simon, G. Schmid, G. Schön, *Mater. Res. Soc. Symp. Proc.* **1992**, *272*, 167; G. Schmid in *Clusters and Colloids – From Theory to Applications* (Ed.: G. Schmid), VCH, Weinheim, **1994**.

[4] R. Houbertz, T. Feigenspan, F. Mielke, U. Memmert, U. Hartmann, U. Simon, G. Schön, G. Schmid, *Europhys. Lett.* **1994**, *28*, 641.

[5] U. Hartmann, unpublished.

[6] G. Mao, Y. Tsao, M. Tirrell, H. T. Davis, V. Hessel, H. Ringsdorf, *Langmuir* **1993**, *9*, 3461; L. F. Chi, R. R. Johnston, H. Ringsdorf, N. Kimizuka, T. Kunitake, *Thin Solid Films* **1992**, *210/211*, 111; G. Decher, *Nachr. Chem. Techn. Lab.* **1993**, *41*, 793; G. Decher, J. D. Hong, J. Schmitt, *Thin Solid Films* **1992**, *210/211*, 831; G. Decher, J. D. Hong, *Ber. Bunsenges. Phys. Chem.* **1991**, *95*, 1430.

[7] G. Schmid, N. Klein, L. Korste, U. Kreibig, D. Schönauer, *Polyhedron* **1988**, *7*, 605.

[8] ARIS 3300, Burleigh Instruments.

Self-Assembly of a Ferromagnetically Coupled Manganese(II) Tetramer**

Angelo J. Amoroso, John C. Jeffery, Peter L. Jones, Jon A. McCleverty,* Peter Thornton, and Michael D. Ward*

We recently described the preparation of the podand ligand tris[3-(2′-pyridyl)pyrazol-1-yl]hydroborate, L^-.[1] This ligand contains three *N*,*N*-bidentate chelating arms linked at the apical boron atom and is the first example of a podand ligand based on the tris(pyrazol-1-yl)hydroborate core. The cavity size was found to be appropriate for lanthanide(III) ions (ionic radius ≈ 1 Å), and some 1:1 nine-coordinate complexes such as $[Eu(L)F(MeOH)_2]PF_6$ were prepared in which the lanthanide ion was located in the hexadentate ligand cavity.[1] We thought it would be of interest to see how the ligand behaved with first-row transition-metal dications (ionic radius ≈ 0.7–0.8 Å), which are both smaller than lanthanides and prefer lower coordination numbers. Molecular modeling studies indicated that 1:1 complexes with sensible metal–ligand bond lengths would involve considerable strain on the ligand; conversely if the ligand were allowed to adopt a strain-free conformation then the metal–pyridyl bond lengths would be unrealistically long (> 3 Å).

[*] Prof. J. A. McCleverty, Dr. M. D. Ward, Dr. A. J. Amoroso, Dr. J. C. Jeffery, P. L. Jones
School of Chemistry, University of Bristol
Cantock's Close, Bristol BS8 1TS (UK)
Telefax: Int. code + (117) 929-0509
e-mail: wardmd@siva.bristol.ac.uk
Dr. P. Thornton
Department of Chemistry, Queen Mary and Westfield College, London (UK)

[**] This work was partly funded by the EPSRC and Unilever Research. We thank Dr. J. P. Maher for recording the EPR spectrum, Dr. J. Crosby and Miss Kate Byrom for recording the electrospray mass spectra, and Dr. S. G. Carling and Prof. P. Day of the Royal Institution for assistance with recording the magnetic data.

Reaction of KL with one equivalent of $Mn(CH_3CO_2)_2 \cdot 4H_2O$ in methanol followed by treatment with KPF_6 afforded a yellow solid **1**.[2] Elemental analysis and fast-atom bombardment mass spectrometry (FAB-MS) both indicated the formulation $[MnL]PF_6$ for **1**. However an electrospray mass spectrum (ES-MS: solvent: $MeCN/H_2O$ (1/1); capillary voltage, 3.48 kV; cone voltage, 25 V; source temperature, 80 °C) gave an intense peak at 1996.4 Daltons, whose position and isotopic pattern were consistent with formation of a tetrameric species $[Mn_4L_4]^{4+}$. The crystal structure determination confirmed this,[3] and three views of the structure of the cation are in Figures 1–3. There is no crystallographically imposed symmetry within the tetrameric unit. The complex contains four crystallographically independent Mn^{II} ions which are arrayed approximately in a tetrahedron with Mn–Mn separations (all different) of between 6.218 and 6.293 Å. Each ligand L^- sits "above" one triangular face of this tetrahedron and donates one bidentate arm to each of the three metal ions on that face. Each ligand therefore interacts with three different metal ions (see Fig. 4a), and each metal ion is coordinated by one bidentate arm from each of three different ligands. The Mn–N distances lie in the range 2.17–2.38 Å and are typical of Mn^{II}–N(pyridyl) and Mn^{II}–N(pyrazolyl) bonds in high-spin complexes.[5] The coordination geometries of the metal ions are highly distorted octahedra (Fig. 3): the N-Mn-N angles lie in the range 72–110°; the bite angles of the bidentate chelating fragments are 72–73°. It is apparent from Figure 2 that aromatic π-stacking interactions between pyrazolyl rings are present, which may help to stabilize the structure of **1**. The interaction between the pyrazolyl rings from different ligands and attached to adjacent metals is shown in Figure 4b; the average separation between the overlapping areas is about 3.4 Å.

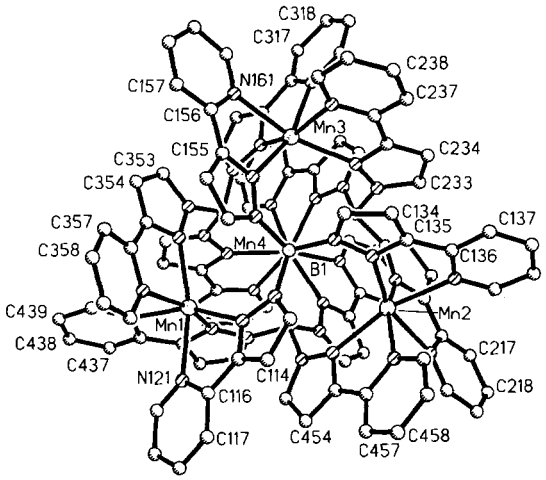

Fig. 1. Crystal structure of the cation of **1** with the numbering scheme. The Mn–N distances lie in the range 2.17–2.38 Å, N-Mn-N angles in the range 72–110°.

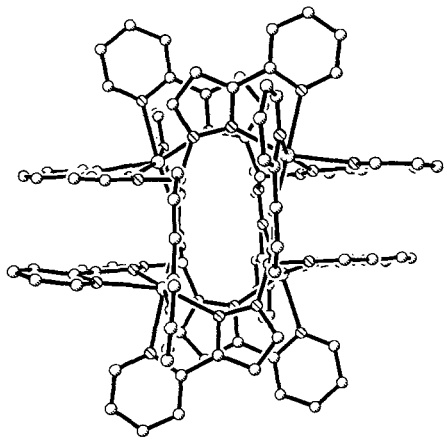

Fig. 2. Alternative view of the crystal structure of the cation of **1**.

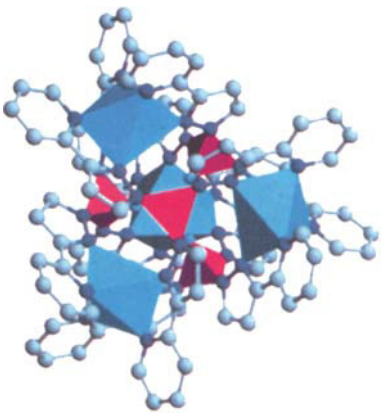

Fig. 3. Representation of the structure of **1** emphasizing the coordination polyhedra. The octahedra represent the coordination spheres of Mn^{II} centers, the smaller tetrahedra those of boron atoms, which have the B–H bonds directed inwards.

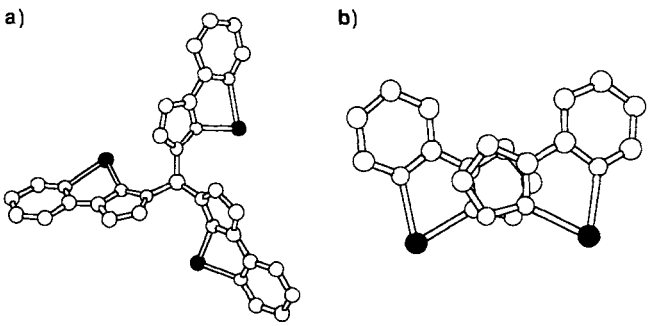

Fig. 4. Fragments of the crystal structure of **1** showing a) the disposition of a single ligand, and b) the π stacking of the pyrazolyl rings attached to adjacent metals.

The formation of this tetramer in high yield by assembly of eight components, involving formation of 24 metal–ligand bonds as well as additional noncovalent interactions, is an interesting example of how a relatively complicated molecule can form from simple components when there is an appropriate degree of complementarity between the properties of the metal (size, preference for a particular coordination geometry) and those of the ligand (number, arrangement and type of binding sites, steric limitations).[6] Appropriate combinations of carefully designed ligands with particular metal ions therefore can be considered to be "pre-programmed" to self-assemble in a specific and unique way, and such methods have resulted in the formation of complicated molecular architectures such as double[7] and triple[8] helices, cylinders,[9] capped cylinders,[10] and grids.[11] Ligand L^- is particularly versatile in that it can behave in quite different ways according to the properties of the metal ions it reacts with (lanthanide or first-row transition metal).

The EPR spectrum of **1** in MeCN at room temperature showed a single, featureless, very broad resonance at $g = 2.008$ with a peak–peak separation of 650 G. The lack of the usual hyperfine coupling and the breadth of the signal are consistent

with the presence of magnetic exchange effects. Low-temperature magnetic susceptibility measurements on **1** (5–300 K) confirm the presence of a weak ferromagnetic interaction. A plot of $1/\chi$ versus T is exactly linear over the whole range (correlation coefficient with best-fit straight line = 1.000) with a ferromagnetic θ value of 1.5 K. The magnetic moment μ per Mn^{II} center (Fig. 5) rises steadily from 5.83 μ_B at 300 K to 5.93 μ_B at 40 K.

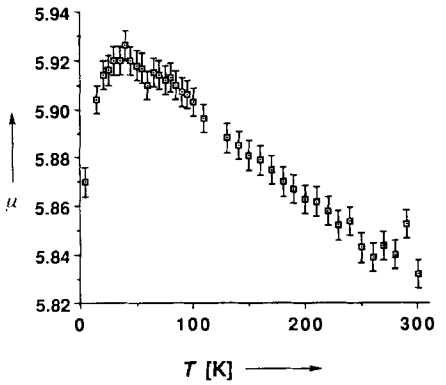

Fig. 5. Low-temperature magnetic data for **1**: a plot of μ per Mn^{II} center vs T.

The origin of the decrease in the value of μ at temperatures below 40 K is not clear and a fuller analysis will have to await field-dependency studies. That the limiting high-temperature value of μ is fractionally less than the spin-only value despite ferromagnetic exchange may be ascribed to trace diamagnetic impurities, but the overall trend is clear.

The presence of ferromagnetic exchange is surprising, as the Mn^{II} centers are too far apart to have any direct orbital overlap between them and there are no direct bridges linking pairs of Mn^{II} ions; magnetic exchange is commonly associated with, for example, phenolate bridges.[12] The shortest pathway linking each Mn^{II} ion to its neighbors is via the aromatic stacking interaction depicted in Figure 4b, and we suggest that this $\pi-\pi$ interaction offers a route for the transmission of magnetic effects, possibly by a McConnell spin-polarization mechanism, especially as the pyridyl and pyrazolyl groups are π-acidic and some of the unpaired electron density in the metal d(π) orbitals will therefore be delocalized onto the ligand fragments involved in the π stacking. Intermolecular exchange can be ruled out since the shortest intermolecular Mn–Mn contact is 12.00 Å and there is no bridging pathway comparable to that within the tetramer; in addition the EPR spectrum showed that the exchange interaction was maintained even in dilute solutions. Recently very weak ferromagnetic exchange between separate complex units in a crystal was ascribed solely to intramolecular $\pi-\pi$ overlap of terminal aromatic ligands;[13] thus, complex **1** represents the second example of this phenomenon. The ability to transmit magnetic exchange interactions through noncovalent interactions such as hydrogen bonding,[14] nonbonding van der Waals interactions,[13] and now π stacking is of considerable importance to the design and synthesis of bulk ferromagnets,[15, 16] particularly as these noncovalent interactions play important roles both in self-assembly of supramolecular complexes and the three-dimensional ordering in crystal structures.

Similar complexes of L^- have been obtained with Fe^{II}, Co^{II}, Ni^{II}, and Zn^{II}. In every case ES-MS indicated formation of tetrameric $[M_4L_4]^{4+}$ species. We have also determined the crystal structure of $[Zn_4L_4](PF_6)_4$, which, apart from small changes in bond lengths and angles and the presence of a threefold symmetry axis in the tetrameric cation, is the same as that of **1**.[17] Full details of this structure and of the magnetic properties of the other complexes will be the subject of a full paper in due course.

Received: March 6, 1995 [Z 7764 IE]
German version: *Angew. Chem.* **1995**, *107*, 1577–1580

Keywords: complexes with nitrogen ligands · magnetic properties · manganese compounds · self-assembly · structure elucidation

[1] A. J. Amoroso, A. M. Cargill Thompson, J. C. Jeffery, P. L. Jones, J. A. McCleverty, M. D. Ward, *J. Chem. Soc. Chem. Commun.* **1994**, 2751.

[2] A mixture of KL (0.241 g, 0.5 mmol) and $Mn(CH_3CO_2)_2 \cdot 4H_2O$ (0.123 g, 0.5 mmol) was dissolved in MeOH (20 mL) to give a pale yellow solution. Dropwise addition of excess aqueous KPF_6 precipitated an off-white solid which was filtered off and dried to give 0.28 g of **1** (87%). X-ray quality crystals were grown from $MeCN/Et_2O$. A satisfactory elemental analysis was obtained.

[3] Crystal data for $[Mn_4L_4](PF_6)_4 \cdot (MeCN)_4 \cdot (Et_2O)$: $C_{108}H_{98}B_4F_{24}Mn_4N_{40}OP_4$, $M = 2815.14$, pale yellow blocks, monoclinic, space group $P2_1/n$, $a = 21.778(8)$, $b = 20.352(6)$, $c = 28.898(9)$ Å, $\beta = 103.83(3)°$, $V = 12437(7)$ Å^3, $Z = 4$, $\rho_{calcd} = 1.503$ g cm^{-3}, $\mu = 5.50$ cm^{-1}, $F(000) = 5720$. The crystal selected (0.75 × 0.75 × 0.6 mm) was mounted in a glass capillary tube in some of the recrystallization solvent as a precaution against facile solvent loss. Using a Siemens SMART diffractometer with a CCD area detector (graphite-monochromated $Mo_{K\alpha}$ radiation, $\lambda = 0.71073$ Å, $T = 293$ K) 42954 reflections were collected ($2\theta_{max} = 46.5°$, $-24 \le h \le 24$; $-21 \le k \le 22$; $-32 \le l \le 13$) of which 17194 were unique. Data were corrected for Lorentz and polarization effects, and an empirical absorption correction was applied (XEMP) based on multiple measurements of equivalent data. The structure was solved by direct methods using SHELXTL and refined (1673 parameters with 46 restraints) using SHELX93 by full-matrix least-squares on all F^2 data [4]. All non-hydrogen atoms were refined anisotropically; hydrogen atoms were included in calculated positions and refined with fixed isotropic thermal parameters. Refinement converged at R_1 [$F > 4\sigma(F)$] = 0.064, wR_2 (all data) = 0.169. Maximum/minimum residual electron density: +0.652/−0.522 e Å^{-3}. The asymmetric unit contains four molecules of MeCN and one of Et_2O in addition to one tetrameric cation and four PF_6^- ions. Full details of the crystal structure determination are available on request from the Cambridge Crystallographic Data Centre, 12 Union Road, GB-Cambridge, CB2 1EZ, on quoting the full journal citation.

[4] a) G. M. Sheldrick, SHELXTL-PLUS, Siemens Analytical X-ray Instruments Inc., Madison, WI, USA, **1989**; b) G. M. Sheldrick, SHELX-93, program for the refinement of crystal structures, Göttingen, **1993**.

[5] a) S. C. Shoner, P. P. Power, *Inorg. Chem.* **1992**, *31*, 1001; b) D. J. Hodgson, B. J. Schwartz, T. N. Sorrell, *ibid.* **1989**, *28*, 2226.

[6] a) J.-M. Lehn, *Angew. Chem.* **1990**, *102*, 1347; *Angew. Chem. Int. Ed. Engl.* **1990**, *29*, 1304; b) J.-M. Lehn in *Perspectives in Coordination Chemistry* (Eds.: A. F. Williams, C. Floriani, A. E. Merbach), Verlag Helvetica Chimica Acta/VCH, Basel/Weinheim, **1992**, p. 447.

[7] a) R. F. Carina, G. Bernardinelli, A. F. Williams, *Angew. Chem.* **1993**, *105*, 1483; *Angew. Chem. Int. Ed. Engl.* **1993**, *32*, 1463; b) E. C. Constable, A. J. Edwards, P. R. Raithby, J. V. Walker, *ibid.* **1993**, *105*, 1486 and **1993**, *32*, 1465; c) T. M. Garrett, U. Koert, J.-M. Lehn, A. Rigault, D. Meyer, J. Fischer, *J. Chem. Soc. Chem. Commun.* **1990**, 557; d) C. Piguet, G. Bernardinelli, B. Boquet, A. Quattropani, A. F. Williams, *J. Am. Chem. Soc.* **1992**, *114*, 7440.

[8] a) R. Krämer, J.-M. Lehn, A. DeCian, J. Fischer, *Angew. Chem.* **1993**, *105*, 764; *Angew. Chem. Int. Ed. Engl.* **1993**, *32*, 703; b) G. Bernardinelli, C. Piguet, A. F. Williams, *ibid.* **1992**, *104*, 1626 and **1992**, *31*, 1622.

[9] P. Baxter, J.-M. Lehn, A. DeCian, J. Fischer, *Angew. Chem.* **1993**, *105*, 92; *Angew. Chem. Int. Ed. Engl.* **1993**, *32*, 69.

[10] E. Leize, A. Van Dorsselaer, R. Krämer, J.-M. Lehn, *J. Chem. Soc. Chem. Commun.* **1993**, 990.

[11] P. N. W. Baxter, J.-M. Lehn, J. Fischer, M.-T. Youinou, *Angew. Chem.* **1994**, *106*, 2432; *Angew. Chem. Int. Ed. Engl.* **1994**, *33*, 2284.

[12] a) J. C. Jeffery, P. Thornton, M. D. Ward, *Inorg. Chem.* **1994**, *33*, 3612; b) Y. Gultneh, A. Farooq, S. Liu, K. D. Karlin, J. Zubieta, *ibid.* **1992**, *31*, 3607; c) R. A. Bartlett, J. J. Ellison, P. P. Power, S. C. Shoner, *ibid.* **1991**, *30*, 2888; d) M. Mikuriya, K. Nakadera, T. Tokii, *Inorg. Chim. Acta*, **1992**, *194*, 129; e) H.-R. Chang, S. K. Larsen, P. D. W. Boyd, C. G. Pierpont, D. N. Hendrickson, *J. Am. Chem. Soc.* **1988**, *110*, 4565; f) D. Luneau, J.-M. Savariault, P. Cassoux, J.-P. Tuchagues, *J. Chem. Soc. Dalton Trans.* **1988**, 1225; g) A. Caneschi, D. Gatteschi, R. Sessoli, P. Rey, *Acc. Chem. Res.* **1989**, *22*, 392.

[13] M. Wesolek, D. Meyer, J. A. Osborn, A. De Cian, J. Fischer, A. Derory, P. Legoll, M. Drillon, *Angew. Chem.* **1994**, *106*, 1660; *Angew. Chem. Int. Ed. Engl.* **1994**, *33*, 1592.

[14] a) J. M. Moreno, J. Ruiz, J. M. Dominguez-Vera, E. Colacio, *Inorg. Chim. Acta*, **1993**, *208*, 111; b) E. Colacio, J. P. Costes, R. Kivekäs, J. P. Laurent, J. Ruiz, M. Sundberg, *Inorg. Chem.* **1991**, *30*, 1475; c) P. A. Goodson, J. Glerup, D. J. Hodgson, K. Michelsen, U. Rychlewska, *Inorg. Chem.* **1994**, *33*, 359; d) M. C. Morón, F. Palacio, J. Pons, J. Casabó, X. Solans, K. E. Merabet, D. Huang, X. Shi, B. K. Teo, R. L. Carlin, *Inorg. Chem.* **1994**, *33*, 746.

[15] For recent reviews see: a) J. S. Miller, A. J. Epstein, W. M. Reiff, *Chem. Rev.* **1988**, *88*, 201; b) J. S. Miller, A. J. Epstein, *Angew. Chem.* **1994**, *106*, 399; *Angew. Chem. Int. Ed. Engl.* **1994**, *33*, 385; c) C. Kollmar, O. Kahn, *Acc. Chem. Res.* **1993**, *26*, 259; d) O. Kahn, Y. Pei, Y. Journaux in *Inorganic Materials* (Eds.: D. W. Bruce, D. O'Hare), Wiley, Chichester, **1992**, p59.

[16] Some recent examples based on manganese: a) P. D. W. Boyd, Q. Li, J. B. Vincent, K. Folting, H.-R. Chang, W. E. Streib, J. C. Huffman, G. Christou, D. N. Hendrickson, *J. Am. Chem. Soc.* **1988**, *110*, 8537; b) D. P. Goldberg, A. Caneschi, S. J. Lippard, *ibid.* **1993**, *115*, 9299; c) H.-L. Tsai, H. J. Eppley, N. de Vries, K. Folting, G. Christou, D. N. Hendrickson, *J. Chem. Soc. Chem. Commun.* **1994**, 1745.

[17] A. J. Amoroso, J. C. Jeffery, P. L. Jones, J. A. McCleverty, L. Rees, M. D. Ward, unpublished results.

The Two-Dimensional Network Structure and Metamagnetic Properties of the 2:1 Complex of $[Mn(3\text{-MeOsalen})(H_2O)]ClO_4$ and $K_3[Fe(CN)_6]$**

Hitoshi Miyasaka, Naohide Matsumoto,* Hisashi Ōkawa, Nazzareno Re, Emma Gallo, and Carlo Floriani*

The field of molecular magnetism has shown quite spectacular advances in the last decade.[1] In particular ferro- and ferrimagnetic one-dimensional chain compounds based upon metal complexes have brought noteworthy success in the field of molecular design and synthesis, magnetism, and theoretical studies.[1] However, although it is easier to design the structure and synthesis of one-dimensional rather than two- or three-dimensional compounds, recent efforts have been directed at molecular design of multidimensional magnetic compounds, since the ferromagnetism itself is a three-dimensional property.[1, 2]

The cyanide system based on the Prussian blue family $CA^{II}[B^{III}(CN)_6]$ ($C = Cs^+$; A = Ni, Mn, Cr; B = Cr, Fe) exhibits an excellent basis for the molecular design of ferri- and ferromagnets, in which the $[B^{III}(CN)_6]^{3-}$ ion acts as a multidentate complex ligand and the A^{II} ion receives the donor atoms.[3] These cyanide compounds have rigid three-dimensional structures in which two magnetic centers alternate, and the CN^- ion bridges the two metal ions as a simple magnetic mediator. However, because of difficulties in obtaining single crystals, the details of the correlation between the magnetism and the crystal structure remain uncertain.

Manganese Schiff base complexes possess a high degree of structural versatility; variation in coordination geometry, nuclearity, and metal oxidation state are all possible.[4] Since manganese(III) complexes of salen analogs (H_2salen = *N*,*N*′-bis(salicylidene)ethylenediamine) can receive donor atoms at the apical sites, it was anticipated that the coupling of the manganese Schiff base complex to $[B^{III}(CN)_6]^{3-}$ ion might enable the formation of a novel family of magnetic compounds with potential control over the structure of the crystal lattice. We therefore examined the reaction of $[MnL(H_2O)]ClO_4$ (L = salen analogs) and $K_3[Fe(CN)_6]$. The products are easily crystallized and display a remarkable variety of magnetic behavior and a rich structural chemistry. One such compound, $K[Mn(3\text{-MeOsalen})]_2[Fe(CN)_6]$, has a unique two-dimensional structure and exhibits a spontaneous three-dimensional magnetic ordering.

An ORTEP drawing of this trinuclear molecule with the atom numbering scheme is given in Figure 1.[5] Since the space group

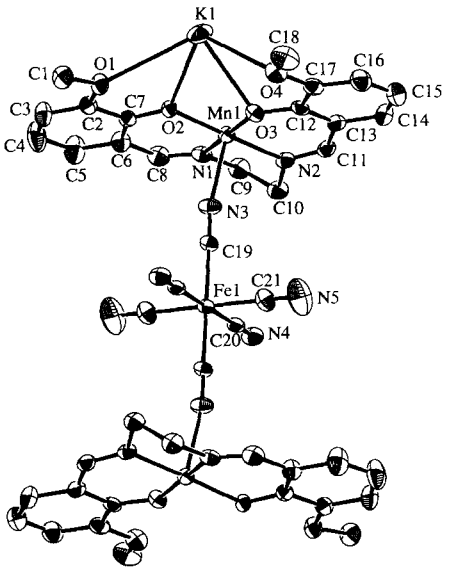

Fig. 1. Structure of the trinuclear unit of $K[Mn(3\text{-MeOsalen})]_2[Fe(CN)_6] \cdot 2DMF$ (ORTEP drawing) with the numbering scheme of the unique atoms (50% probability ellipsoids).

is $P2_1/c$ and the unit cell contains two trinuclear molecular units, the unsymmetrical unit is one half of the trinuclear molecular unit, and the Fe and K ions must occupy the special positions. The Fe ion is positioned at a center of symmetry (1/2,0,1/2) and surrounded octahedrally by six CN^- groups. Two CN^- groups of the $[Fe(CN)_6]^{3-}$ moiety bridge to the Mn ions to give a linear bridging unit of (3-MeOsalen)Mn-NC-Fe-CN-Mn(3-MeOsalen) with bond lengths of Fe–C19 = 1.932(5) Å, Mn–N3 = 2.290(5) Å, and C19–N3 = 1.150(7) Å and angles of Fe-C19-N3 = 177.2(5)° and C19-N3-Mn = 169.5(5)°. The Fe–C19 bond length of 1.932(5) Å within this bridging fragment is rather shorter than the other two iron–cyanide bonds [Fe–C20 of 1.943(6) Å and Fe–C21 of 1.941(7) Å]. A projection of the trinuclear complex along the Fe–Mn vector shows that the Fe–C20 and Fe–C21 bonds bisect the N1-Mn-N2 and N1-Mn-O2 angles, respectively. The K^+ ion positioned at the inversion center (1/2,0,0) interacts with eight oxygen atoms of the two Mn(3-MeOsalen) moieties of adjacent trinuclear units. The two methoxy groups at the 3-position of the (3-MeOsalen) ligand contribute to the formation of the sandwich structure and form a crown-ether-like sandwich structure around the K^+ ion, which produces a one-dimensional chain. The sandwich structure around K^+ and the dimensions of K–O [K–O2 of 2.721(4) and K–O3 of

[*] Prof. N. Matsumoto, H. Miyasaka, Prof. H. Ōkawa
Department of Chemistry, Faculty of Science, Kyushu University
Hakozaki, Higashi-ku, Fukuoka 812 (Japan)
Telefax: Int. code + (926)32-2734
Prof. C. Floriani, Dr. E. Gallo
Institut de Chimie Minérale et Analytique
Université de Lausanne (Switzerland)
Dr. N. Re
Dipartimento di Chimica, Perugia (Italy)

[**] We thank the referees for their valuable suggestion for interpreting the magnetic behavior. N. M. thanks the Ministry of Education, Science, and Culture of Japan for giving him a Grant-in-Aid for Scientific Research (No. 04453048).
(3-MeOsalen)$^{2-}$ = dianion of bis(3-methoxysalicylidene)ethylenediamine.

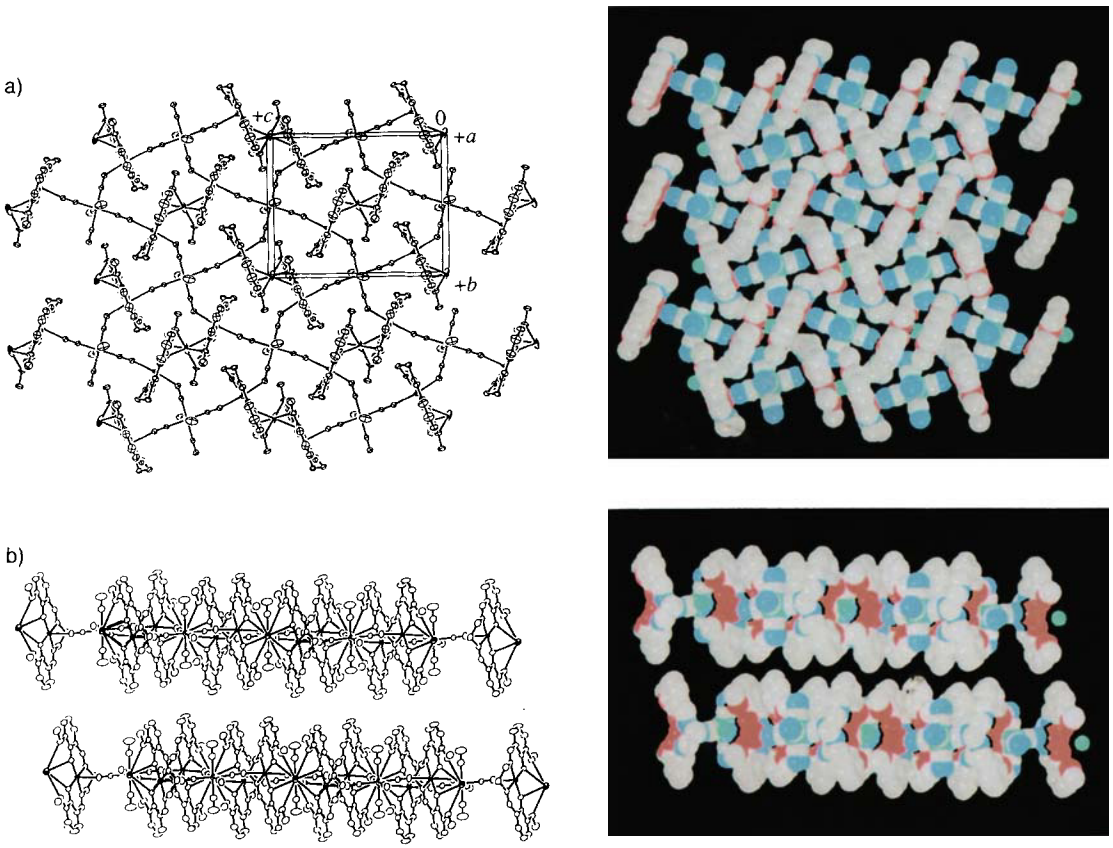

Fig. 2. a) Projection along the a axis, showing a two-dimensional network structure, in which a net unit is composed of a cyclic, octanuclear structure ($\cdots$Mn-NC-Fe-CN$\cdots)_4$ and involves a sandwich structure. b) Projection perpendicular to the a axis, showing stacking of the sheet structure by van der Waals contacts. In each case on the right are the corresponding space-filling representations of the two-dimensional network structure.

2.789(4) Å for the K-phenoxy oxygen atoms and K–O1 of 3.211(4) and K–O4 of 3.109(4) Å for K-methoxy oxygen atoms] are compatible with those of [K(benzo[15]crown-5)$_2$] and related crown ether compounds.[6]

The crystal structure projected onto the bc plane showing the two-dimensional structure is given in Figure 2a. Another two CN^- groups of the $Fe(CN)_6^{3-}$ moiety are bound to the Mn atoms of the adjacent chains with a Mn–N4 distance of 2.415(5) Å, which creates a two-dimensional network in which a net unit is composed of a cyclic octanuclear structure ($\cdots$Mn-NC-Fe-CN$\cdots)_4$ and internally bridged by a sandwich structure (see Fig. 2a). The interchain bridging unit Fe-C20-N4$\cdots$Mn*, where * indicates a symmetry operation of $(x, 1/2 - y, 1/2 + z)$, has bond lengths of Fe–C20 = 1.943(6), C20–N4 = 1.157(7), and N4$\cdots$Mn* = 2.415(5) Å, with angles of Fe-C20-N4 = 178.4(6) and C20-N4-Mn* = 137.2(4)°, indicating a large bending of the C–N$\cdots$Mn interaction. Because of the coordination of the CN^- group of the adjacent chain, the Mn ion is six-coordinate, assuming a square-bipyramidal geometry in which the two apical sites are occupied by nitrogen atoms N3 of the chain and N4 of the adjacent chain, and the equatorial sites by the N_2O_2 donor atoms of the quadridentate ligand (average bond lengths: (Mn–N) = 1.970(5), (Mn–O) = 1.873(4) Å). The two-dimensional sheet structure stacks along the a axis by a transformation, and on the basis of the interlayer distances, the interaction between the layers is attributable to van der Waals contacts.

The magnetic behaviors of the two samples prepared by Method A and Method B (see Experimental Procedure) are very similar, but they show a slight difference below about 250 G. In this communication, the magnetic behavior of the Method B sample is described.

The magnetic susceptibility was measured from 1.9 K to 300 K by a SQUID magnetometer (SQUID = superconducting quantum interference device) under the applied magnetic field of 800 G, and the plot of μ_{eff} vs. T is depicted in Figure 3. The effective magnetic moment per trinuclear unit is 7.33 μ_B at room temperature, which is slightly larger than the spin-only value 7.14 μ_B for the magnetically dilute, three-spin system (S_{Mn}, S_{Fe}, S_{Mn}) = (2, 1/2, 2). On lowering the temperature, μ_{eff} increases gradually and then sharply without a minimum, reaches the maximum value of 32.1 μ_B at 9 K, and finally decreases abruptly to 17.4 μ_B at 1.9 K.[7] The maximum value of μ_{eff} is very much larger than the spin-only value of the possible largest spin-state S_T = 9/2 for (S_{Mn}, S_{Fe}, S_{Mn}) = (2, 1/2, 2), μ_{so} = 9.95 μ_B.

The FCM curve (field-cooled magnetization M vs. T) was obtained by cooling the sample under a weak magnetic field of 0.5 G. On lowering the temperature, the magnetization shows a

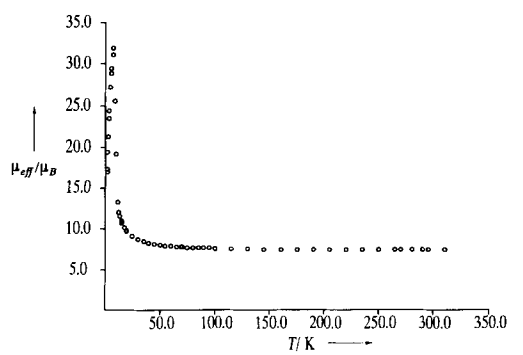

Fig. 3. Plot of the effective magnetic moments of K[Mn(3-MeOsalen)]$_2$[Fe(CN)$_6$] per Mn_2Fe unit against temperature.

 © VCH Verlagsgesellschaft mbH, D-69451 Weinheim, 1995 0570-0833/95/1313-1447 $ 10.00+.25/0

rapid increase below about 10 K till the maximum at 9.2 K, and then a decrease. The abrupt increase of the magnetization indicates the on-set of long-range magnetic ordering due to the ferromagnetic coupling within each layer. The decrease below 9.2 K indicates the presence of interlayer antiferromagnetic interaction. The FCM curves were also measured under 100 G and 300 G. The M vs. T curve at 100 G still shows a sharp peak, whereas the curve at 300 G has no peak and remains constant after the abrupt increase at 9 K. This result is also indicative of interlayer antiferromagnetic interaction. The hysteresis loop at 4.5 K is shown in Figure 4, where the initial magnetization pro-

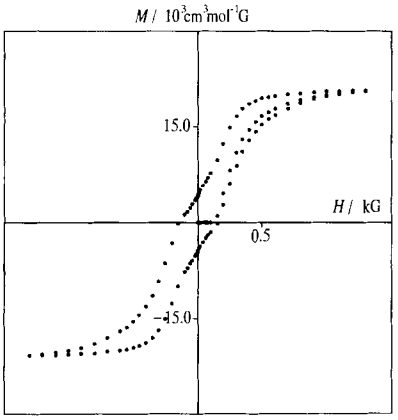

Fig. 4. Hysteresis loop (M vs. H) at 4.5 K.

cedure from 0 G to 300 G shows a metamagnetic character. The field dependence of the magnetization up to 5.5 T on a powder sample was measured at 4.2, 6.0, and 7.5 K. On increasing the applied magnetic field at 4.2 K, the magnetization value is close to zero below about 250 G, increases rapidly reaching the plateau region (about $M = 3\,N\mu_B$) around 1500 G, and then increases linearly to 6 $N\mu_B$ at 5.5 T. Since the saturation magnetization M_s is expected to be 9 $N\mu_B$ for this system (S_{Mn}, S_{Fe}, S_{Mn}) = (2, 1/2, 2) according to the equation $M_s = Ng\mu_B S$, the higher magnetic field than 5.5 T is necessary for the magnetic saturation of this compound. It can be also seen that the magnetization saturates more easily as the temperature increases. This behavior shows a metamagnetic character,[9] in which the coupling between magnetic metal ions is ferromagnetic within each layer, but the layers are antiferromagnetically coupled. The interlayer antiferromagnetic interaction of the compound prepared according to Method B is expected to be very weak as a result of the van der Waals contacts where DMF molecules of crystallization are positioned between the layers. Therefore, the magnetic difference below 250 G between the samples prepared by Method A and Method B can be ascribed to the slight difference in the interlayer interaction.

The compound in question possesses two favorable characteristics imparted by the component iron–cyanide and manganese Schiff base complexes. The cyanide system assumes a rigid cubic structure whose three-dimensional arrangement is essential for three-dimensional magnetic ordering, but the poor quality of the crystal has prevented a single-crystal X-ray analysis of the structure. The manganese(III) complex with the salen analogs can accommodate bridging ligands such as the CN^- ion at its axial sites, and the structure is sufficiently flexibile. As anticipated, the coupling of these two compounds gives a magnetic material with high crystallinity and multidimensional structure. Further studies are now in progress.

Experimental Procedure

Caution! Perchlorate salts are potentially explosive and should only be handled in small quantities.

The complex can be prepared by two methods, Method A and Method B.

Method A: To the solution of [Mn(3-MeOsalen)(H_2O)]ClO_4 (294 mg, 0.5 mmol) in methanol (50 mL) was added a solution of $K_3[Fe(CN)_6]$ (165 mg, 0.5 mmol) in water (5 mL) at room temperature. The resulting solution was left to stand for 1 h, and the reddish brown precipitate thus produced was collected by suction filtration, washed with 1:1 v/v methanol/water, and dried in vacuo. Anal.: calcd for $C_{42}H_{36}N_{10}O_8KFeMn_2$: C 49.77, H 3.58, N 13.18, Mn 10.84, Fe 5.51; found: C 49.63, H 3.68, N 13.57, Mn 10.63, Fe 5.03. IR(KBr): ν = 1601, 1624 (C=N), 2097, 2114 cm^{-1} (C≡N); m.p. > 300 °C.

Method B: A solution of $K_3[Fe(CN)_6]$ in 2-propanol/water (1:1 v/v, 0.25 mmol in 30 mL mixed solution) was allowed to diffuse into a solution of [Mn(3-MeOsalen)(H_2O)]ClO_4 (0.25 mmol) in *N*,*N*-dimethylformamide (30 mL). After one week at room temperature in the dark, thin, brown platelets were obtained. The crystals contain two *N*,*N*-dimethylformamide molecules per trinuclear unit as solvent of crystallization.

Received: November 29, 1994
Revised version: February 25, 1995 [Z 7510IE]
German version: *Angew. Chem.* **1995**, *107*, 1565–1568

Keywords: magnetic properties · manganese compounds · Prussian blue · salen complexes

[1] O. Kahn, *Molecular Magnetism*, VCH, Weinheim, Germany, **1993**; *Magnetic Molecular Materials* (Eds.: D. Gatteschi, O. Kahn, J. S. Miller, F. Palacio) (NATO ASI Ser. Ser. E, **1990**, *198*); Proceedings of the Symposium on the Chemistry and Physics of Molecular Based Magnetic Materials: H. Iwamura, J. S. Miller, *Mol. Cryst. Liq. Cryst.* **1994**, *33*, 232; J. S. Miller, A. J. Epstein, *Angew. Chem.* **1994**, *106*, 399; *Angew. Chem. Int. Ed. Engl.* **1994**, *33*, 385.

[2] H. Tamaki, Z. J. Zhong, N. Matsumoto, S. Kida, M. Koikawa, N. Achiwa, Y. Hashimoto, H. Ōkawa, *J. Am. Chem. Soc.* **1992**, *114*, 6974; M. C. Moron, F. Palacio, J. Pons, J. Casabo, X. Solans, K. E. Merabet, D. Huang, X. Shi, B. K. Teo, R. L. Carlin, *Inorg. Chem.* **1994**, *33*, 746; H. O. Stumpf, L. Ouahab, Y. Pei, D. Grandjean, O. Kahn, *Science* **1993**, *261*, 447.

[3] W. D. Grieber, D. Babel, *Z. Naturforsch. B* **1982**, *87*, 832; T. Mallah, S. Thiebault, M. Verdaguer, P. Veillet, *Science* **1993**, *262*, 1555; V. Gadet, T. Mallah, I. Castro, P. Veillet, M. Verdaguer, *J. Am. Chem. Soc.* **1992**, *114*, 9213.

[4] V. L. Pecoraro, *Manganese Redox Enzymes*, VCH, Weinheim, **1992**; K. Wieghardt, *Angew. Chem.* **1989**, *101*, 1179; *Angew. Chem. Int. Ed. Engl.* **1989**, *28*, 1153; J. E. Penner-Hahn, R. M. Fronko, V. L. Pecoraro, C. F. Yocum, S. D. Betts, N. R. Bowlby, *J. Am. Chem. Soc.* **1990**, *112*, 2549; E. Gallo, E. Solari, S. D. Angelis, C. Floriani, N. Re, A. Chiesi-Villa, C. Rizzoli, *ibid.* **1993**, *115*, 9850; J. W. Gohdes, W. H. Armstrong, *Inorg. Chem.* **1992**, *31*, 368; W. Chiang, D. M. Ho, D. V. Engen, M. E. Thompson, *ibid.* **1993**, *32*, 2886.

[5] X-ray structure analysis: Rigaku AFC7R diffractometer with graphite monochromator, $Mo_{K\alpha}$ radiation (λ = 0.71069 Å) and a 12 kW rotating anode generator at 298 K, Lorentz polarization and Ψ scan absorption correction. The structure was solved by direct methods and expanded with Fourier techniques. Full-matrix, least-squares refinement based on observed reflections ($I > 3.00\sigma(I)$) were employed. The computer program was teXsan (Crystal Structure Analysis Package, Molecular Structure Corporation (**1985** and **1992**)). Crystal data for K[Mn(3-MeOsalen)]$_2$[Fe(CN)$_6$] · 2 DMF, $Mn_2O_{10}N_{12}C_{48}KFeH_{50}$: M_r = 1159.82, brown thin platelets, monoclinic, space group $P2_1/c$, a = 13.750(4), b = 12.456(2), c = 15.646(2) Å, β = 102.91(1)°, V = 2612.0(8) Å^3, Z = 2, $\rho_{measured}$ = 1.49 g cm^{-3}, flotation method in benzene/tetrachloromethane, ρ_{calcd} = 1.475 g cm^{-3}, $\mu(Mo_{K\alpha})$ = 8.97 cm^{-1}, no. of reflections = 3221, crystal size 0.5 × 0.3 × 0.1 mm, R = 0.049, R_w = 0.050, $R = \sum||F_o| - |F_c||/\sum|F_o|$; $R_w = \{\sum[w(|F_o| - |F_c|)^2]/\sum[w|F_o|^2]\}^{1/2}$, $w = 1/\sigma(F_o)^2$ [10].

[6] *Synthetic Multidentate Macrocyclic Compounds* (Eds.: R. M. Izatt, J. J. Christensen), Academic Press, New York, **1978**.

[7] A net unit in the two-dimensional structure is composed of a cyclic octanuclear structure $(\cdots Mn\text{-}NC\text{-}Fe\text{-}CN\cdots)_4$ involving a sandwich structure. In the cyclic tetramer there are two kind of magnetic paths between Mn^{III} and Fe^{III} ions through the CN^- group, that is, intratrimer (linear unit) and intertrimer paths, both exhibiting ferromagnetic interaction. The magnetic interaction through the K^+ ion between two manganese ions is negligible [8].

[8] J. A. Bonadies, M. L. Kirk, M. S. Lah, D. P. Kessissoglou, W. E. Hatfield, V. L. Pecoraro, *Inorg. Chem.* **1989**, *28*, 2037.

[9] R. L. Carlin, *Magnetochemistry*, Springer, Berlin, **1986**.

[10] Further details of the crystal structure investigations may be obtained from the Fachinformationzentrum Karlsruhe, D-76344 Eggenstein-Leopoldshafen (Germany), on quoting the depository number CSD-58932.

Macrobicyclic Titanium(IV) Complexes with C_3-Symmetric Synthetic Peptides**

Kay Severin, Wolfgang Beck,* Gunter Trojandt, Kurt Polborn, and Wolfgang Steglich*

Dedicated to Professor Rolf Huisgen on the occasion of his 75th birthday

The synthesis of C_3-symmetric pseudo-peptides[1] has been achieved during studies related to the chemistry of electrophilic glycine equivalents. The tricarboxylic acid 2,2',2''-nitrilotris-[2-(benzoylamino)acetic acid], N(BzGly*OH)$_3$ **1** is accessible in a few further steps from the coupling of methyl α-bromohippurate with ammonia. This compound, which is stabilized by three intramolecular hydrogen bonds, has proven to be a suitable template for the synthesis of C_3-symmetric pseudo-peptides with defined geometry.[1] The coordination properties of this class of compound are of interest for several reasons. Firstly, applications as chiral ligands for stereoselective synthesis seem possible;[2] and secondly, peptides with a well-defined metal coordination site are model compounds for metalloenzymes.[3] The reaction of $[(\eta^5\text{-}C_5H_5)TiCl_3]$ or $[(\eta^5\text{-}C_5Me_5)TiCl_3]$[4] with the trianion of **1** (*RRR*/*SSS*) yields the complexes **2** and **3**. The

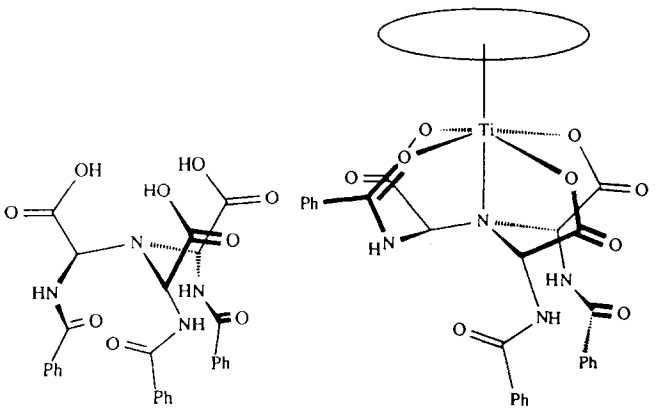

1
RRR/SSS

$[(\eta^5\text{-}C_5H_5)Ti(1)]$ **2**

$[(\eta^5\text{-}C_5Me_5)Ti(1)]$ **3**

X-ray structural analysis[5] of **3** (Fig. 1) shows the pseudo-amino acid functions as a pentadentate ligand: besides the titanatrane-like complexation,[6] coordination of a benzoyl O atom occurs.

If the Cp* ring is regarded as an unidentate ligand, the environment around the titanium atom can be described as distorted octahedral. The Ti atom resides slightly above the plane formed from the O atoms O1, O3, O4, and O7. The molecular structure also provides an explanation for the remarkable stability[7] of the complexes **2** and **3**: the ligand causes the complete sterical shielding of the Ti atom.

[*] Prof. Dr. W. Beck, Dipl.-Chem. K. Severin
Institut für Anorganische Chemie der Universität
Meiserstrasse 1, D-80333 München (Germany)
Telefax: Int code +(89) 5902 451

Prof. Dr. W. Steglich, Dipl.-Chem. G. Trojandt, Dr. K. Polborn
Institut für Organische Chemie der Universität München (Germany)

[**] Generous support by the Deutsche Forschungsgemeinschaft, the Fonds der Chemischen Industrie, and Studienstiftung des Deutschen Volkes is gratefully acknowledged.

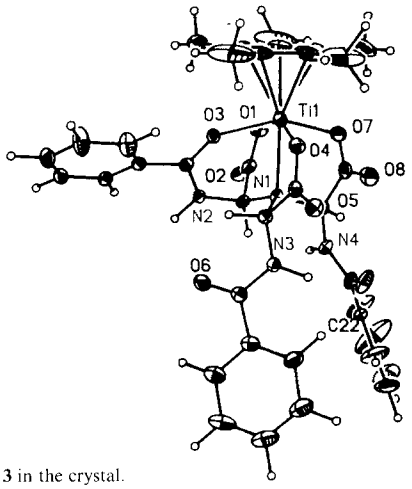

Fig. 1. Molecular structure of **3** in the crystal.

An important aspect of the structure of **3** is the stabilization by inter- and intramolecular hydrogen bonds. By coordination of the benzoyl group two of—in the free ligand three—intramolecular hydrogen bonds between the amide-N and -O atoms are broken. The amide N atoms N2 and N4 "released" by this coordination now form intermolecular hydrogen bonds: N2–H to a water molecule present in the crystal (not shown in Fig. 1), N4–H to the carboxylate-O atom of an adjacent molecule. This leads to a dimerization of the complex in the crystal (Fig. 2). Interestingly both enantiomers (*RRR* and *SSS*) are linked through hydrogen bonds.[8]

This structural type is consistent with the spectroscopic data also for **2**. The lowering of the ligand symmetry is manifested in the NMR spectra. They show separate signals for the three hippuric acid residues. The ^{1}H NMR signals of the amino acid ligand of **3** in [D$_6$]DMSO are substantially broadened at elevated temperatures. This coalescence phenomenon is presumably a consequence of an exchange between coordinated and free benzoyl groups. Treatment of the disodium salt of **1** with $[(\eta^5\text{-}C_5H_5)TiCl_2]$ in methanol also affords **2** as the major product (NMR-spectroscopic proof). Presumably a double substitution of carboxylato for chloro ligands occurs first, followed by an

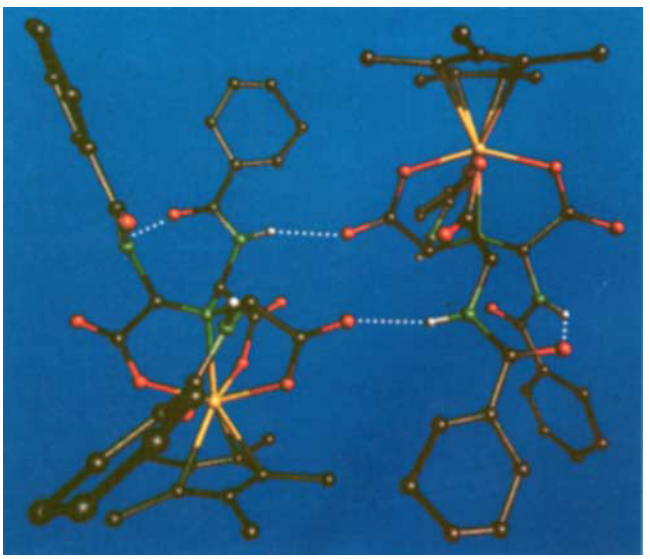

Fig. 2. Dimerization of **3** through hydrogen bonds.

intramolecular protolysis of a cyclopentadienyl ligand by the remaining acid function.

Pseudo-peptides, prepared starting from **1**, exhibit a uniform basic structure stabilized by hydrogen bonds in the crystalline state.[1] Hence they should be ideally preorganized for the formation of macrobicycles. Amino acids with sterically demanding side chains were chosen deliberately for the C-terminii; these shield the titanium atom, and consequently stabilize the complexes and prevent a di- or oligomerization through intermolecular coordination of the metal atom.

The reaction of the pseudo-nonapeptides $N(BzGly*GlyLeuOH)_3$, $N(BzGly*GlyPheOH)_3$, and $N(BzGly*LeuPheOH)_3$ with three equivalents of sodium methoxide in dichloromethane and subsequent treatment with $[Cp*TiCl_3]$ gives the complexes **4**–**6**, respectively (depicted schematically in Fig. 3). These complexes can be isolated by extraction with dichloromethane/ether (**4** and **5**) or dichloromethane/pentane (**6**). In this way, side products can be separated quantitatively. The yields of the reactions are above 50%. The pseudo-nonapeptides used for the synthesis of compounds **4** and **6** were purified by fractional crystallization before saponification. One of the two diastereoisomers is thereby separated. The absolute configuration of the ligands in these compounds (*RRR* in **4**; *SSS* in **6**) can be determined by recording the CD spectra.[11] A mixture of isomers (ca. 2.5:1) was used for the synthesis of **5**. During complexation and/or the subsequent workup procedures for **5** one diastereomer (*SSS*) becomes enriched (ca. 5:1).

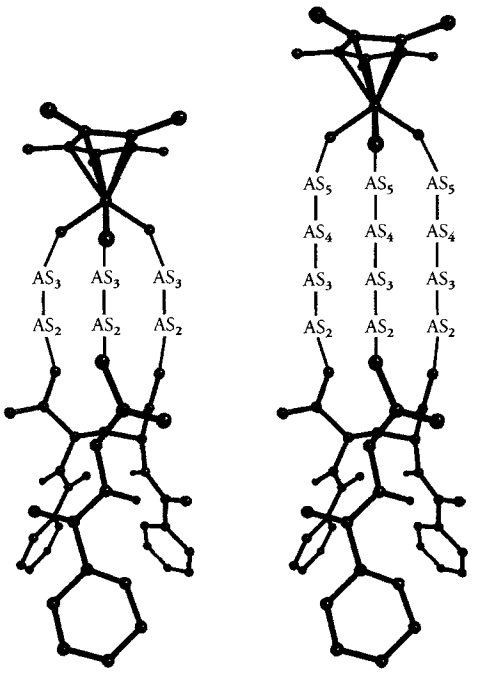

4-6 7,8

	AS_2	AS_3	AS_4	AS_5
4	Gly	Leu		
5	Gly	Phe		
6	Leu	Phe		
7	Val	Val	Gly	Val
8	Val	Leu	Gly	Phe

Fig. 3. Schematic representation of the macrobicyclic $Cp*Ti^{IV}$ complexes **4**–**8** (AS = α-amino acid).

To record the NMR spectra of compounds **4**–**6**, low concentrations of the samples are required (below 0.8 mM), since at higher concentrations, considerable line broadening is observed, presumably due to aggregation. The spectra show one set of signals for the three peptide chains in each case. This proves that in solution the C_3 symmetry of the peptide ligands remains intact after complexation. An exact assignment of the ^1H NMR signals was achieved with the help of H-H-COSY spectra. The shifts of the amide protons of AS_1 and AS_2 indicate the presence of six intramolecular hydrogen bonds in **4**–**6**, similar to the situation in the uncomplexed pseudo-peptides. Only the amide protons of the C-terminal amino acids (AS_3) apparently do not form hydrogen bonds. The "Cp*Ti-lid" provides additional rigidity for the peptide frame. This becomes noticeable in the ^1H NMR spectra by the difference between the chemical shifts of diastereotopic protons.[9] Thus, the signals of the glycine methylene protons (AS_2) in the free ligand are separated by 0.6 ppm, those in **5** by 1.1 ppm. This effect is less marked for the diastereotopic methylene protons of the phenylalanine or leucine side chains.

Figure 4 shows a simulation of the molecular structure of **4**.[10] This was performed on the basis of structural data of $N(BzGly*GlyLeuOMe)_3$.[1] The basic framework fixed by hydrogen bonds was used unchanged, the carboxylate groups of the leucine residues were rotated (without change of symmetry) into a position favorable for complexation, and the methyl ester functions replaced by the Cp*Ti fragment. The lipophilic leucine side chains point away from the molecular axis and are an important reason for the good solubility of **4** in organic solvents. The same holds for the phenylalanine and leucine side chains of compounds **5** and **6**. As the three peptide chains are bound relatively close to each other through hydrogen bonds, the space inside the molecules appears too small for a hypothetical guest molecule.

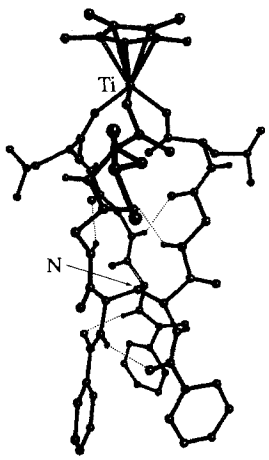

Fig. 4. Simulation of the molecular structure of **4**.

In Figures 3 and 4, the carboxylate groups are shown as unidentate ligands; however, an η^2-coordination with formation of four-membered chelate rings cannot be ruled out either on the basis of NMR or IR spectroscopic data. This holds for compounds **4**–**6** as well as for the following compounds **7** and **8**.

In order to explore the limitations of this synthetic concept, two pseudo-pentadecapeptides, $[N(BzGly*ValValGlyValOMe)_3$ and $N(BzGly*ValLeuGlyPheOMe)_3]$, were prepared. Also here amino acids with lipophilic side chains were chosen deliberately to increase the solubility. The synthesis of the macrobicyclic complexes **7** and **8** (ring size 32 atoms) was achieved analogously to that for **4**–**6**; however as expected the yields are lower (13% for **7**; 6% for **8**), the solubility in dichloromethane likewise. The molecular structures of **7** and **8** are shown schematically in Figure 3.

The cyclopentadienyl–Ti^{IV} complexes presented here are examples for the use of C_3-symmetric peptide bundles as ligands. We are currently investigating whether by suitable functionalization of the peptide chains it is possible to introduce other metal fragments into the peptide bundles.

Experimental Procedure

The pseudo-amino acid and peptide esters used were prepared as described in ref. [1], and subsequently saponified with LiOH in THF/water. The synthesis of complexes **2**–**8** was performed under argon with dry purified solvents. FAB mass

spectra were obtained for all complexes. The isotopic distribution corresponded to the calculated values within the precision limits of the experiment. All compounds gave satisfactory elemental analyses.

2: A solution of **1** (219 mg, 0.40 mmol) in methanol (10 mL) was treated with a methanolic NaOMe solution (1.20 mmol) and stirred for 45 min at room temperature. After addition of $[CpTiCl_3]$ (86 mg, 0.39 mmol) and 2.5 h stirring, a yellow precipitate formed from the originally clear solution. The suspension was concentrated in vacuo to 5 mL and stirred for 30 min at 0 °C. The precipitate was isolated by centrifugation and recrystallized from dichloromethane/hexane. Yellow crystals were obtained by layering an ethyl acetate solution with hexane. Yield 176 mg (66%), m.p. >175 °C (decomp).-IR (KBr): $\tilde{\nu} = 1673\ cm^{-1}$ vs and br. (CO_2 and CON), 1602 s, 1563 s and 1525 s (CON). – ^1H NMR (400 MHz, $CDCl_3$): $\delta = 4.87$ (d, $^3J = 6$ Hz, 1H, NHCH), 5.28 (d, $^3J = 7$ Hz, 1H, NHCH), 5.79 (d, $^3J = 9$ Hz, 1H, NHCH), 6.94 (s, 5H, Cp), 7.23–7.63 (m, 11H, Ph), 7.74 (d, $^2J = 9$ Hz, 1H, NHCH), 7.78 (dd, $^3J = 7$, $^4J = 1$ Hz, 2H, *o*-Ph), 7.95 (d, $^3J = 7$ Hz, 1H, NHCH), 7.99 (dd, $^3J = 8$, $^4J = 1$ Hz, 2H, *o*-Ph), 9.38 (d, $^3J = 6$ Hz, 1H, NHCH). – ^{13}C NMR (100.5 MHz, $CDCl_3$): $\delta = 66.24$, 69.63 and 77.81 (NHCH), 127.84, 127.88, 128.16, 128.43, 128.61, 129.91, 131.85, 132.05, 132.68, 132.73 and 135.65 (Cp and Ph), 168.24, 169.27, 169.49, 169.73, 170.55 and 170.70 (CO_2 and CON).

3: Synthesis analogous to that for **2** in methanol (20 h, room temperature). Purification by extraction with dichloromethane and recrystallization from ethyl acetate/hexane. Red crystals, yield 198 mg (68%), m.p. >197 °C (decomp).-IR (Nujol): $\tilde{\nu} = 1714\ cm^{-1}$ s (CON, coord.), 1670 s and 1647 s (CO_2 and CON), 1597 s, 1560 s and 1525 s (CON). ^1H NMR (400 MHz, $CDCl_3$): $\delta = 2.21$ (s, 15H, Cp*), 4.79 (d, $^3J = 7$ Hz, 1H, NHCH), 5.11 (d, $^3J = 7$ Hz, 1H, NHCH), 5.64 (d, $^3J = 9$ Hz, 1H, NHCH), 6.82 (d, $^3J = 9$ Hz, 1H, NHCH), 7.22–7.62 (m, 11H, Ph), 7.73 (dd, $^3J = 8$, $^4J = 1$ Hz, 2H, *o*-Ph), 7.83 (d, $^3J = 7$ Hz, 1H, NHCH), 7.95 (dd, $^3J = 8$, $^4J = 1$ Hz, 2H, *o*-Ph), 8.77 (d, $^3J = 7$ Hz, 1H, NHCH). – ^{13}C NMR (100.5 MHz, CD_3OD): $\delta = 13.01$ [$C_5(CH_3)_5$], 67.05, 67.96 and 71.03 (NHCH), 128.63, 129.05, 129.10, 129.38, 129.50, 129.70, 130.46, 132.90, 133.22, 133.45, 134.11, 135.61 and 137.86 [$C_5(CH_3)_5$ and Ph], 170.56, 171.25, 172.50, 172.70, 173.50 and 173.91 (CO_2 and CON).

4: A solution of N(BzGly*GlyLeuOH)$_3$ (159 mg, 0.15 mmol) in dichloromethane (20 mL) was treated with a methanolic NaOMe solution (0.41 mmol) and stirred for 2 h at room temperature. Then a solution of $[Cp^*TiCl_3]$ (39 mg, 0.14 mmol) in dichloromethane (5 mL) was added slowly, the solution stirred for another 2 h and the solvent was evaporated in vacuo. The residue was extracted with a 1:1 mixture of dichloromethane and ether (15 mL). The resulting solution was concentrated in vacuo to about 1 mL. The product precipitated after addition of pentane (20 mL) and was washed with pentane (20 mL). Orange powder. Yield 104 mg (56%), m.p. >196 °C (decomp).-IR (KBr): IR (KBr): $\tilde{\nu} = 1659\ cm^{-1}$ vs (CO_2 and CON), 1525 vs (CON). ^1H NMR (400 MHz, $CDCl_3$): $\delta = 0.95$ [d, $^3J = 6$ Hz, 9H, CH(CH_3)$_2$], 1.00 [d, $^3J = 7$ Hz, 9H, CH(CH_3)$_2$], 1.43–1.78 [m, 9H, CH(CH$_3$)$_2$ and CH$_2$-Leu], 2.12 (s, 15H, Cp*), 3.54 (dd, $^2J = 16$, $^3J = 3$ Hz, 3H, CH$_2$-Gly), 4.50 (dt, $^3J = 10$, $^3J = 10$, $^3J' = 5$ Hz, 3H, NHCH-Leu), 4.68 (dd, $^2J = 16$, $^3J = 9$ Hz, 3H, CH$_2$-Gly), 5.65 (d, $^3J = 10$ Hz, 3H, NH-Leu), 5.84 (d, $^3J = 10$ Hz, 3H, NHCHN), 7.11 (t, $^3J = 8$ Hz, 6H, *m*-Ph), 7.29 (t, $^3J = 8$ Hz, 3H, *p*-Ph), 7.37 (d, $^3J = 8$ Hz, 6H, *o*-Ph), 8.61 (d, $^3J = 10$ Hz, 3H, NHCHN), 8.70 (m, 3H, NHCH$_2$). – ^{13}C NMR (100.5 MHz, $CDCl_3$): $\delta = 12.05$ [$C_5(CH_3)_5$], 21.72, 23.16 and 24.72 [CH(CH$_3$)$_2$ and CH(CH_3)$_2$], 40.27, 42.50, 51.39 (CH$_2$-Leu, NHCH-Leu and CH$_2$-Gly), 62.85 (NHCHN), 127.47, 127.90, 131.13, 133.53 and 135.15 [$C_5(CH_3)_5$ and Ph], 166.94, 168.51 and 169.93 (CO_2 and CON).

5: Synthesis analogous to that for **4**; extraction with dichloromethane/ether (2:3) (20 mL). Orange powder. Yield 128 mg (53%), m.p. >194 °C (decomp).-IR (KBr): $\tilde{\nu} = 1658\ cm^{-1}$ vs (CO_2 and CON), 1524 vs (CON). – ^1H NMR (400 MHz, $CDCl_3$): $\delta = 2.04$ (s, 15H, Cp*), 2.80 (dd, $^2J = 15$, $^3J = 10$ Hz, 3H, CH$_2$-Phe), 3.14 (dd, $^2J = 15$, $^3J = 5$ Hz, 3H, CH$_2$-Phe), 3.33 (dd, $^2J = 16$, $^3J = 4$ Hz, 3H, CH$_2$-Gly), 4.41 (dd, $^2J = 16$, $^3J = 10$ Hz, 3H, CH$_2$-Gly), 4.66 (m, 3H, NHCH-Phe), 5.57 (d, $^3J = 9$ Hz, 3H, NH-Phe), 5.61 (d, $^3J = 9$ Hz, 3H, NHCHN), 6.98–7.24 (m, 30H, C_6H_5), 8.20 (m, 6H, NHCHN and NHCH$_2$). – ^{13}C NMR (100.5 MHz, $CDCl_3$): $\delta = 12.19$ [$C_5(CH_3)_5$], 37.18, 42.35 and 53.40 (CH$_2$-Gly, CH$_2$-Phe and NHCH-Phe), 62.84 (NHCHN), 127.33, 127.41, 127.88, 128.53, 128.75, 128.87, 131.16, 133.41 and 135.73 [$C_5(CH_3)_5$ and Ph], 166.94, 168.30 and 169.80 (CO_2 and CON).

6: Synthesis analogous to that for **4**; extraction with dichloromethane/pentane (20 mL) (1:1). Orange powder. Yield 110 mg (49%), m.p. >189 °C (decomp).-IR (KBr): $\tilde{\nu} = 1664\ cm^{-1}$ vs (CO_2 and CON), 1518 vs (CON). – ^1H NMR (400 MHz, $CDCl_3$): $\delta = 0.89$ [d, $^3J = 6$ Hz, 9H, CH(CH_3)$_2$], 0.94 [d, $^3J = 7$ Hz, 9H, CH(CH_3)$_2$], 1.37 [m, 3H, CH(CH$_3$)$_2$], 2.04 (m, 6H, CH$_2$-Leu), 2.13 (s, 15H, Cp*), 2.94 (dd, $^2J = 15$, $^3J = 10$ Hz, 3H, CH$_2$-Phe), 3.29 (dd, $^2J = 15$, $^3J = 5$ Hz, 3H, CH$_2$-Phe), 4.63–4.68 (m, 3H, NHCH-Phe), 4.69–4.75 (m, 3H, NHCH-Leu), 5.75 (d, $^3J = 9$ Hz, 3H, CH-Gly), 5.83 (d, $^3J = 8$ Hz, 3H, NH-Phe), 7.02–7.54 (m, 30H, Ph), 8.39 (d, $^3J = 9$ Hz, 3H, NH-Leu), 8.60 (d, $^3J = 9$ Hz, 3H, NH-Gly). – ^{13}C NMR (100.5 MHz, $CDCl_3$): $\delta = 12.10$ [$C_5(CH_3)_5$], 21.51, 23.53 and 24.84 [CH(CH$_3$)$_2$ and CH(CH_3)$_2$], 36.99 and 40.38 (CH$_2$-Leu and CH$_2$-Phe), 50.46 and 54.15 (NHCH-Phe and NHCH-Leu), 63.20 (NHCHN), 127.34, 127.52, 127.74, 127.86, 128.56, 128.94, 131.02, 133.42 and 135.34 [$C_5(CH_3)_5$ and Ph], 166.65, 167.70 and 171.92 (CO_2 and CON).

7: Synthesis analogous to that for **4**; extraction with dichloromethane/acetone (2:1) (30 mL). The slight difficulties in obtaining high-resolution spectra of complexes **4**–**6** became more dominant in compounds **7** and **8**; even at low concentrations only poorly resolved signals can be obtained. Orange powder. Yield 35 mg (13%), m.p. >203 °C (decomp). IR (KBr): $\tilde{\nu} = 1657\ cm^{-1}$ vs (CO_2 and CON), 1523 vs (CON).

8: Synthesis analogous to that for **4**; extraction with dichloromethane/ether (3:1) (20 mL). Orange powder. Yield 32 mg (6%), m.p. >189 °C (decomp).-IR (KBr): $\tilde{\nu} = 1657\ cm^{-1}$ vs (CO_2 and CON), 1523 vs (CON).

Received: February 15, 1995 [Z 7714 IE]
German version: *Angew. Chem.* **1995**, *107*, 1570–1572

Keywords: cyclopentadienyl complexes · macrocycles · pseudopeptides · titanium compounds

[1] G. Trojandt, K. Polborn, W. Steglich, M. Schmidt, H. Nöth, *Tetrahedron Lett.* **1995**, *36*, 857–860. Another type of tripodal peptides was reported by Y. Tor, J. Libman, A. Shanzer, C. E. Felder, S. Lifson, *J. Am. Chem. Soc.* **1992**, *114*, 6653–6661.

[2] Examples for chiral tripodal and C_3-symmetric ligands: C. Bolm, K. B. Sharpless, *Tetrahedron Lett.* **1988**, *29*, 5101–5104; C. Bolm, W. M. Davis, R. L. Halterman, K. B. Sharpless, *Angew. Chem.* **1988**, *100*, 882–883; *Angew. Chem. Int. Ed. Engl.* **1988**, *27*, 835–837; M. J. Burk, R. L. Harlow, *ibid.* **1990**, *102*, 1511–1513 bzw. **1990**, *29*, 1462–1464; M. J. Burk, J. E. Feaster, R. L. Harlow, *Tetrahedron: Asymmetry* **1991**, *2*, 569–592; C. J. Tokar, P. B. Kettler, W. B. Tolman, *Organometallics* **1992**, *11*, 2737–2739; H. Lütjens, P. Knochel, *Tetrahedron: Asymmetry* **1994**, *5*, 1161–1162.

[3] H.-B. Kraatz, *Angew. Chem.* **1994**, *106*, 2143–2144; *Angew. Chem. Int. Ed. Engl.* **1994**, *33*, 2055–2056, and references therein.

[4] Cyclopentadienyl-Ti^{IV} complexes of carboxylate ligands: Y. Dang, *Coord. Chem. Rev.* **1994**, *135/136*, 93–128; Cp_2Ti^{IV} complexes of α-aminocarboxylates: C. J. Cardin, A. Roy, *Inorg. Chim. Acta* **1985**, *107*, L33–L35; A. Schäfer, E. Karl, L. Zsolnai, G. Huttner, H. Brintzinger, *J. Organomet. Chem.* **1987**, *328*, 87–99; I. Recht, B. I. Cohen, A. S. Goldman, J. Kohn, *Tetrahedron Lett.* **1990**, *31*, 7281–7284; T. M. Klapötke, H. Köpf, I. C. Tornieporth-Oetting, P. S. White, *Organometallics* **1994**, *13*, 3628–3633; T. M. Klapötke, H. Köpf, I. C. Tornieporth-Oetting, P. S. White, *Angew. Chem.* **1994**, *106*, 1587–1589; *Angew. Chem. Int. Ed. Engl.* **1994**, *33*, 1518–1519; E. Schuhmann, C. Robl, W. Beck, *Z. Naturforsch. B* **1994**, *49*, 1569–1579.

[5] Suitable single crystals of **3** were obtained by layering an ethyl acetate solution with hexane. $C_{39}H_{36}N_4O_9Ti \cdot H_2O$; $M = 746.64$; red fragment; monoclinic; only crystals of relatively poor quality could be found. One phenyl group and the Cp* ring are severely disordered—the disorder could not be resolved; space group $C2/c$ (no. 15); $a = 2.3493(2)$; $b = 1.4973(3)$; $c = 2.0238(4)$ Å; $\beta = 94.879(12)°$; $V = 7.093(2)\ nm^3$; $Z = 8$; $\mu(Mo_{K\alpha}) = 2.989\ cm^{-1}$; $\rho_{calcd} = 1.401\ g\,cm^{-3}$. Diffractometer Enraf-Nonius CAD4; 291 K; graphite monochromator; scan range (θ): 2–23°; $\pm h$, $-k$, $-l$; scan width: $(0.54 + 0.35 \tan\theta)°$; max. measurement time 15 s per reflection; negligible crystal decomposition; empirical absorption correction (psi-scan) T_{min}/T_{max}: 0.92/0.99; 5313 reflections measured/4147 symmetry independent/3450 "observed" for $|F| > 2\sigma(|F|)$; structure solution with SIR; refinement with SHELXTL-PLUS; H atoms geometrically positioned and refined using the "riding" model; 469 parameters; max./min. residual electron density 0.73/−0.35 e Å^{-3}; $R = 0.0689$; $R_w = 0.0705$ [$w^{-1} = \sigma^2(F_0)$]. Further details of the crystal structure determination can be obtained from the Fachinformationszentrum Karlsruhe, D-76344 Eggenstein-Leopoldshafen (Germany), on quoting the depository number CSD-401635.

[6] A. A. Naiini, S. L. Ringrose, Y. Su, R. A. Jacobson, J. G. Verkade, *Inorg. Chem.* **1993**, *32*, 1290–1296; J. G. Verkade, *Acc. Chem. Res.* **1993**, *26*, 483–489; W. M. P. B. Menge, J. G. Verkade, *Inorg. Chem.* **1991**, *30*, 4628–4631; R. Taube, P. Knoth, *Z. Anorg. Allg. Chem.* **1990**, *581*, 89–98.

[7] Compounds **2** and **3** are insensitive to protic solvents. Thus, **3** can be washed with water or refluxed in 2-propanol without decomposition.

[8] The importance of pair formation in solution was examined by molecular mass determination. The value obtained for **2** is slightly, but not significantly higher than the one calculated for a monomeric complex.

[9] W. B. Jennings, *Chem. Rev.* **1975**, *75*, 307–322.

[10] The simulation was performed with the program "UniChem 2.0" from Cray Research, Inc., on an Indigo workstation from Silicon Graphics.

Rapid Water Diffusion in a Cage-Type Crystal Lattice: β-Cyclodextrin Dodecahydrate**

Thomas Steiner, Aida M. Moreira da Silva, José J. C. Teixeira-Dias, Jörn Müller, and Wolfram Saenger*

Crystalline β-cyclodextrin-dodecahydrate (β-CD · 12 H_2O) is an excellent model for research on hydrogen bonding and on water clusters.[1–6] In the crystal lattice, the β-CD molecules form molecular cages that host seven water molecules. These are statistically and dynamically distributed over eleven positions, between which they move with jump rates of around 10^{10}–10^{11} s^{-1}.[4–6] There is no direct connection between the cages, so that water diffusion through the crystal lattice should occur only slowly (or not at all) (for further structural information see ref. [7]). Recently, however, we have shown that the water content of β-CD hydrate adjusts itself to humidity changes in the atmosphere within minutes.[8] This requires exchange of water molecules with the surroundings and water diffusion within the crystals with a rate of about 1/1000 of that in pure water,[9] although the crystal structure is apparently densely packed (Fig. 1, see also legend). This rapid diffusion through the crystal lattice must be associated with structural fluctuations of the β-CD molecules, which temporarily open suitable diffusion paths. In the following, we investigate these phenomena by using a combination of H_2O/D_2O and $H_2{}^{16}O/H_2{}^{18}O$ exchange experiments.

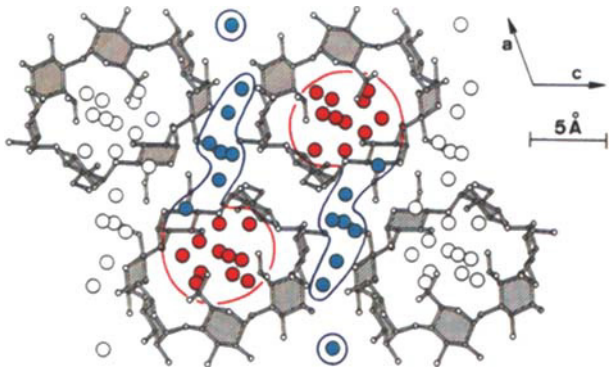

Fig. 1. Crystal structure of β-CD · 12 H_2O, projected along the monoclinic b axis (using coordinates from [3]). The eleven partially occupied water sites in the β-CD cavity are drawn red, and the eight water sites between the β-CD molecules are drawn blue. Red and blue envelope lines show the approximate "surface" of the water arrangement. The β-CD pyranose rings are shaded. The water cluster in the β-CD cavity is connected with a water chain between the β-CD molecules, but neither this chain nor the β-CD cavities are connected between neighboring crystal asymmetric units. In each asymmetric unit, one "solitary" water molecule is isolated from all other water molecules, and forms hydrogen bonds only to C–OH groups.

[*] Prof. Dr. W. Saenger, Dr. T. Steiner
Institut für Kristallographie der Freien Universität
Takustrasse 6, D-14195 Berlin (Germany)
Telefax: Int. code +(30) 838-6702
A. M. Moreira da Silva, M. Sc.
Polytechnical Institute, School of Agriculture, Coimbra (Portugal)
Prof. Dr. J. J. C. Teixeira-Dias
Molecular Physical Chemistry, University of Coimbra (Portugal)
Prof. Dr. J. Müller
Institut für Anorganische und Analytische Chemie der
Technischen Universität Berlin (Germany)

[**] This study was supported by the Deutsche Forschungsgemeinschaft (Sa 196/25-1), the Fonds der Chemischen Industrie, the Deutscher Akademischer Austauschdienst (322-inida-dr), and the Junta Nacional de Investigação Cientifica e Tecnológica (Lisboa). T. S. is on leave from Max-Delbrück-Centrum für Molekulare Medizin, Forschungsgruppe Kristallographie, Robert-Rössle-Strasse 10, D-13122 Berlin (Germany).

If crystalline β-CD · 12 H_2O is exposed to an atmosphere containing D_2O or $H_2{}^{18}O$, these "markers" diffuse into the sample. This can be followed by Raman spectroscopy and mass spectrometry, respectively. In the first experiment, microcrystalline β-CD hydrate[10] was exposed at room temperature to the atmosphere over a reservoir of D_2O, without having contact to the bulk liquid. After defined time periods, samples were quickly sealed in glass capillaries and the Raman spectra were recorded.[11] The bands of O–H and O–D stretching vibrations are very broad, but they are distinctly separated from all other bands[12] (ν_{OH} centered near 3400 cm^{-1}, ν_{OD} centered near 2500 cm^{-1}), and from their integrated intensities, the O–H/O–D ratio in the sample can be obtained. A typical series of spectra is shown in Figure 2: the H(O) concentration falls exponentially

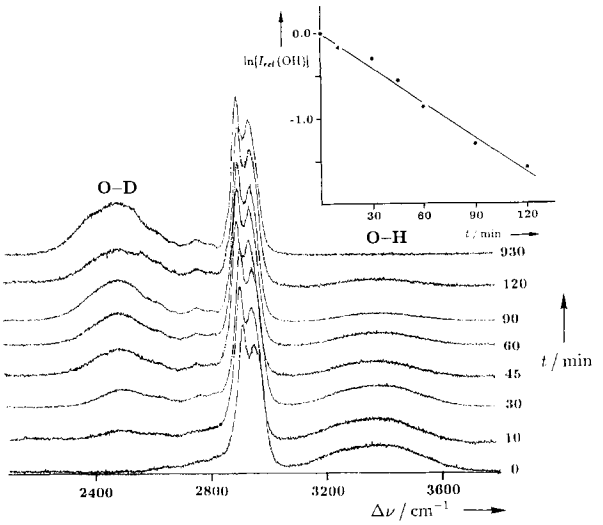

Fig. 2. H(O) → D(O) exchange. β-CD · 12 H_2O was exposed to D_2O vapor for defined time periods, and Raman spectra were then recorded. Typical series of spectra for hydrated commercial β-CD [10], sample ≈ 20 mg, only the relevant spectral region 2300–370 cm^{-1} is shown (invariable central peak: ν_{CH}). Drawn on a semi-logarithmic scale, the integrated relative intensity of the ν_{OH} band decreases linearly.

according to first order kinetics $c_H = c_{H,0}\, e^{-kt}$ (see the inset in Fig. 2 showing linearity of the semi-logarithmic plot). After few hours, *no*[13] H(O) is left in the sample. This kinetics is invariably observed for samples of different origin, and with different experimental arrangements. It must be stressed, however, that the macroscopic rate constant k is not an absolute value: due to shorter diffusion paths, the exchange is faster in small than in large samples (in Fig. 2: $k = 1.4 \times 10^{-2}$ min^{-1}; i.e. 50% exchange within 50 min). If deuterated samples are exposed to H_2O atmosphere, the back-exchange is equally rapid and complete.

The above experiment shows that D atoms diffuse into the sample and H atoms out, but it does not show the mechanism of transport: D and H atoms could be transported by diffusion of intact water molecules, but also by chains of proton (or deuteron) transfer processes. This question was answered by a complementary experiment, in which crystalline β-CD · 12 $H_2{}^{16}O$ was exposed to the atmosphere over a reservoir of $H_2{}^{18}O$.[14] After defined time periods, small samples were transferred into a mass spectrometer,[15] and gradually heated to 110 °C to expel the crystal water. The intensities of the mass signals m/z 18 for $H_2{}^{16}O$ and m/z 20 for $H_2{}^{18}O$ were continuously recorded, until all water was removed from the sample. After background subtraction, the integrated intensities

of these signals measure the relative $H_2{}^{16}O$ and $H_2{}^{18}O$ contents in the sample. The quantity $I_{18}/(I_{18}+I_{20})$ gives the percentage $H_2{}^{16}O$ of the total water content and falls exponentially with exposure time (Fig. 3). This shows that $H_2{}^{16}O$ is actually replaced by $H_2{}^{18}O$ from the atmosphere. For comparable sample dimensions, the exchange rates are similar to those for the H/D exchange experiment (for the example in Fig. 3: $k = 1.2\times10^{-2}\ min^{-1}$, corresponding to 50% exchange within 60 min). This exchange is also (almost[16]) complete, that is, it affects *all* water sites in the crystal.

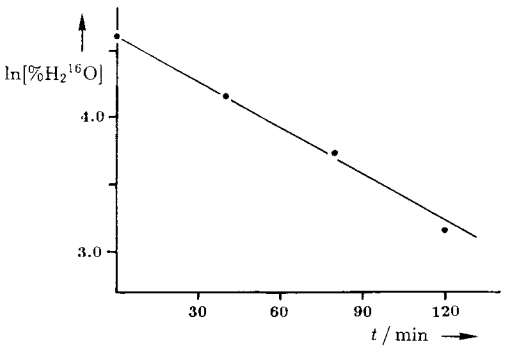

Fig. 3. $H_2{}^{16}O \rightarrow H_2{}^{18}O$ exchange. β-CD $\cdot 12H_2{}^{16}O$ samples were exposed to an $H_2{}^{18}O$ atmosphere for defined time periods, and the percentage of $H_2{}^{16}O$ in the crystal water was determined by mass spectrometry. To show the exponential behavior, the percentage $H_2{}^{16}O$ is drawn on a semi-logarithmic scale.

Since D and ^{18}O markers diffuse with comparable rates, these experiments indicate that intact water molecules diffuse through the crystal lattice. Although there are no continuous water channels, the diffusion is fast with macroscopic walks of $\approx$0.1 mm within minutes. This would be only in conflict with the crystal structure if the β-CD molecules are regarded as rigid objects. In fact, however, it is known from crystallographic displacement parameters[2] and from a molecular dynamics simulation study[4] that the C and O atoms in β-CD hydrate vibrate with amplitudes around 0.4 Å. These fluctuations are sufficient to transiently open passages through which water molecules can travel between adjacent crystal asymmetric units.

In the H/D exchange experiment, D is carried by intact water molecules over "long"[17] distances. Locally, D is transferred also to hydroxyl groups. The observation that the H/D exchange is complete has two important implications: 1) There is no H(O) atom in the crystal that is fixed in a "permanent" O–H $\cdots$ O hydrogen bond, and 2) since the H/D exchange also reaches those C–OH groups that are not sterically accessible for water molecules, there must be local chains of H/D transfer processes between hydroxyl groups. These involve *all* 21 O–H groups of the β-CD molecule, including those which appear to be ordered in the crystal structure determined by neutron diffraction.[2] This means that in the crystal lattice of β-CD $\cdot 12H_2O$, there is permanent internal transfer of protons and of water molecules.

The above dynamic processes are certainly associated with the structural disorder of hydroxyl groups and water molecules.[2] In crystalline α-CD $\cdot 6H_2O$ where all H_2O and C–OH groups are well ordered,[18] the H/D exchange is several orders of magnitude slower.

Received: February 27, 1995 [Z 7741 IE]
German version: *Angew. Chem.* **1995**, *107*, 1573–1575

Keywords: cyclodextrins · diffusion · H/D exchange · Raman spectroscopy · solid-state structures

[1] G. A. Jeffrey, W. Saenger, *Hydrogen Bonding in Biological Structures*, Springer, Berlin, **1991**.
[2] C. Betzel, W. Saenger, B. E. Hingerty, G. M. Brown, *J. Am. Chem. Soc.* **1984**, *106*, 7545–7557.
[3] T. Steiner, G. Koellner, *J. Am. Chem. Soc.* **1994**, *116*, 5122–5128.
[4] J. E. H. Koehler, W. Saenger, W. F. van Gunsteren, *Eur. Biophys. J.* **1987**, *15*, 211–224; *ibid.* **1988**, *16*, 153–168.
[5] T. Steiner, W. Saenger, R. E. Lechner, *Mol. Phys.* **1991**, *72*, 1211–1232.
[6] M. G. Usha, R. J. Wittebort, *J. Mol. Biol.* **1989**, *208*, 669–678; M. G. Usha, R. J. Wittebort, *J. Am. Chem. Soc.* **1992**, *114*, 1541–1548.
[7] β-CD is a macrocyclic oligosaccharide consisting of seven $\alpha(1\rightarrow4)$ linked D-glucopyranose units. From aqueous solution, it crystallizes as a dodecahydrate, β-CD $\cdot 12H_2O$, space group monoclinic $P2_1$. X-ray [3] and neutron [2] crystal structures show that *all* twelve H_2O are disordered to some degree. About seven H_2O are distributed over eleven partially occupied sites in the β-CD cavity; the other five H_2O molecules are distributed over eight sites in interstices. The β-CD molecules are packed in a herringbone arrangement, so that the H_2O molecules in neighboring crystal asymmetric units are sterically isolated from each other [3]. The β-CD molecule carries 21 O–H groups, of which only five have an ordered H position. The other 16 exhibit dynamic orientational disorder ("flip-flop" disorder [2]). Of these 16 disordered O–H groups, four are hydrogen-bonded only to other O–H groups and are consequently not directly accessible to water molecules.
[8] The water content varies continuously between 12.3 H_2O per β-CD at 100% ambient humidity (and crystals under mother liquor), $\approx$11.6 H_2O per β-CD at $\approx$60%, and $\approx$9.4 H_2O per β-CD at 15% humidity. This affects the water molecules enclosed in the β-CD cavity to a larger extent than those in interstitial sites. Commercially available β-CD hydrate has similar water content (if hydrated at humid atmosphere). Complete dehydration (for example in a desiccator) leads to collapse of the crystalline structure. The obtained substance fully re-hydrates at humid atmosphere; in the X-ray beam it shows a diffuse diffraction pattern indicating some residual crystalline order (Y. Nakai, K. Yamamoto, K. Terada, A. Kajiyama, I. Sasaki, *Chem. Pharm. Bull.* **1986**, *34*, 2178–2182).
[9] For a β-CD $\cdot 12H_2O$ crystal of $0.4\times0.3\times0.2\ mm^3$, dehydration was observed to follow e^{-kt} with $k = 0.33\ min^{-1}$, and was completed after $\approx$15 min [3]. This can serve to estimate an isotropic diffusion constant (which is only a very rough estimate because crystals are anisotropic): in isotropic diffusion, the mean square distance of random walks in a time period t is $\langle r^2\rangle = 6Dt$. Assuming that in the above experiment, most water molecules must have walked distances $\approx$0.1 mm within $t < 10$ min, a diffusion constant $D \approx 3\times10^{-8}\ cm^2s^{-1}$ is required (D in pure water: $2.2\times10^{-5}\ cm^2s^{-1}$ [19]).
[10] Samples for Raman spectroscopy: a) commercially available β-CD (Wacker-Chemie, München), hydrated by contact with the atmosphere. b) Ground crystals of β-CD $\cdot 12H_2O$ grown from solutions in H_2O.
[11] Jobin-Yvon T64000 Raman spectrometer (with software for determining band intensities), Coherent-Innova 300-05 Ar^+ laser, $\lambda = 514.5$ nm, 100 mW at the sample position, standard errors of measured wavenumbers $\approx 1\ cm^{-1}$. Samples sealed in capillary tubes with 0.8 mm inner diameter.
[12] O. Egyed, *Vibrational Spectroscopy* **1990**, *1*, 225–227.
[13] In Figure 2, the ν_{OH} band for $t = 0$ min exposure corresponds to $\approx$45 H(O) atoms per β-CD (21 C–OH, 12 H_2O). As estimated from the integrated intensities, the ν_{OH} band at 120 min represents 9.0 ± 1.0 H(O) atoms per β-CD ($=80\%$ exchange), and the flat spectrum (around 3400 cm^{-1}) for 930 min is compatible with less than 1.0 H(O) atom per β-CD.
[14] $H_2{}^{18}O$ from Isotec Inc., Miamisburg (Ohio), labeled as 97 atom %.
[15] Varian MAT311A mass spectrometer, modified by AMD Intectra, Kratos DS90 data system, EI (70 eV), ion accelerating voltage 5 kV, direct inlet probe, sample heating rate $\approx 5°\ min^{-1}$. Sample transfer into the spectrometer requires 1–2 minutes, in which slight back-exchange with atmospheric $H_2{}^{16}O$ cannot be avoided. Background intensity from contamination with atmospheric water in the sample crucible and in the spectrometer also cannot be completely avoided.
[16] The sample with longest exposure to $H_2{}^{18}O$, eight days, still contained 10% $H_2{}^{16}O$ (i.e. only 90% $H_2{}^{18}O$). For the water reservoir producing the vapor, a content of $\approx$8% $H_2{}^{16}O$ was measured. As the $^{16}O/^{18}O$ ratios in the water reservoir and in the sample were barely different, the exchange in the sample is actually better than 90%.
[17] This means that a given water molecule on the average performs many diffusion jumps between two H-(or D)-transfer processes. The distance walked between two such processes is therefore large compared to the jump distance. However, this distance need not be "macroscopic": it is assumed that during its journey from the surface to the interior of the crystal, a water molecule experiences many H-(or D)-transfer processes.
[18] P. C. Manor, W. Saenger, *J. Am. Chem. Soc.* **1974**, *96*, 3630–3639.
[19] D. Eisenberg, W. Kauzmann, *The Structure and Properties of Water*, Clarendon, Oxford, **1969**.

X-Ray Diffraction Evidence for a Cyclohexatriene Motif in the Molecular Structure of Tris(bicyclo[2.1.1]hexeno)benzene: Bond Alternation after the Refutation of the Mills–Nixon Theory**

Hans-Beat Bürgi,* Kim K. Baldridge, Kenneth Hardcastle, Natia L. Frank, Peter Gantzel, Jay S. Siegel,* and Joseph Ziller

For over 60 years, chemists have attributed bond length alternation in various types of benzenoid structures to the Mills–Nixon effect.[1] Originally, this theory was an attempt to account in structural terms for the observed regioselectivity of electrophilic substitution in tetralin and indan. A historical analysis of the development of this effect has shown that Mills and Nixon based their proposal on the incorrect Kekulé oscillation model for benzene, in which two D_{3h}-symmetric cyclohexatrienes are presumed to be in equilibrium; appropriate substitutions could then, in principle, shift the equilibrium to one side. Because the bond lengths and angles in this model are assumed to be dictated by van't Hoff tetrahedra, and the strain energy is thought to be described by Baeyer's theory,[2] the Mills–Nixon postulate has strong structural implications. Specifically, indan and related annelated benzenes are predicted to be cyclohexatriene-like, with double bonds positioned exocyclic to the five-membered ring; however, experimental structural data has never been available to support such speculations.

Given the postulate's faulty premises, it is wholly incorrect to interpret bond alternation in benzenoids in terms of the "theory" of Mills and Nixon. Nonetheless, the notion of angle-strain induced bond alternation in benzene has persisted even without experimental structural proof.[3] Semiempirical[4] and minimal basis set[5] calculations have predicted bond alternation to be common among trisannelated benzenes with exocyclic bond angles deviating significantly from 120°, and extreme for tri(cyclobuteno)benzene (**1**); however, experimental structure determinations of strained monocyclic annelated benzenes like **1**[6] have provided no evidence for this effect. Indeed, except for molecules like starphenylene **2**[7] where strong π effects are at play,[8] significant bond alternation in benzenoids has not been documented experimentally.[9] Ab initio computations at the Restricted Hartree–Fock 6-31G(D) level and higher predict a uniquely large bond alternation to be present in tris(bicyclo-[2.1.1]hexeno)benzene (**3**).[10] The present X-ray crystallographic analysis of **3** produces a molecular structure consistent with the computational predictions, and suggests a "bicyclic-strain" effect that is distinctly *not* a legacy of Mills and Nixon.

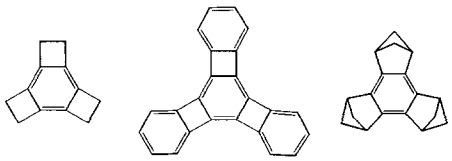

1 2 3

Wittig trimerization of 2-chlorobicyclo[2.1.1]hex-2-ene gave **3** in poor yield, but isolable quantity. Single crystals of **3** were grown by slow evaporation from benzene at room temperature.[11] The crystal lattice is built from molecular layers showing translational symmetry. The stacking of the layers manifests deviations from translational symmetry leading to an order–disorder crystal structure,[12] such that the molecular structure of **3** and its nearest neighbor relationships can be obtained from the diffraction data, but the crystal packing as a whole remains uncertain.

Compound **3** is the first bona fide mononuclear benzenoid hydrocarbon with a cyclohexatriene-like geometry. The central ring is planar and the internal angles are all 120° (Fig. 1); however, the two inequivalent bonds in the benzene ring differ

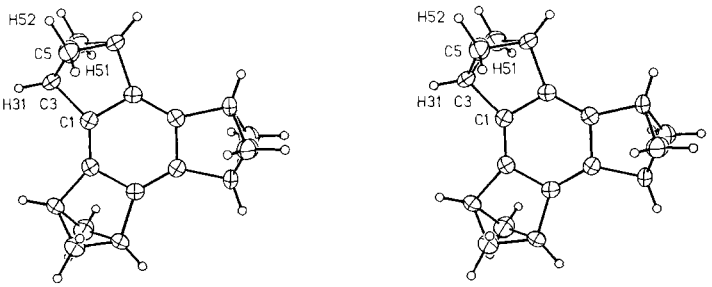

Fig. 1. Stereoview of **3** down the threefold symmetry axis.

by 0.089 Å (1.438(5)–1.349(6) Å). These lengths correspond to Pauling bond orders of 1.86 and 1.39 for the shorter and longer bond, respectively,[13] giving a bond order difference of roughly 0.5. In comparison, the difference in the bond order for the bonds in the central ring of **2** is 0.75, and in **1** it is less than 0.1. Although the average bond length in the benzene ring in **3** is "normal" compared to the average bond length for a hexasubstituted benzene (1.397 ± 0.009 Å),[9, 14] the *endo* bond is more than 4σ longer, and the *exo* bond is more than 4σ shorter.[9] Thus, either length alone would be remarkable. The radial bond from C(arom.) to C(methine) is quite normal (1.514(3) Å), as is the C(methine)–C(methylene) bond of the four-membered ring (1.558(8) Å).[15] The bicyclic annelation strongly constricts the C(arom.)-C(arom.)-C(methine) angle down to 102.3(2)°, and this angle distortion is presumed to be correlated to the manifestation of bond alternation.[16]

Ab initio computations at the Hartree–Fock 6-31G(D) level and higher, as well as Density Functional Theory (DFT) have predicted significant bond alternation in **3** (Fig. 2, Table 1).[17–23] Reasonable structures are obtained with gradient-corrected density functional methods, which inherently account for electron correlation, as well as from the Restricted Hartree–Fock 6-31G(D) basis set. Smaller basis sets or semiempirical quantum mechanical methods overestimate the degree of

[*] Prof. Dr. H.-B. Bürgi
Laboratorium für Chemische und Mineralogische Kristallographie der Universität
CH-3012 Bern (Switzerland)
Prof. J. S. Siegel, N. L. Frank, Dr. P. Gantzel
Department of Chemistry, University of California-San Diego
La Jolla, CA 92093-0358 (USA)
Telefax: Int. code + (619) 534-5383
Dr. K. K. Baldridge
San Diego Supercomputer Center, San Diego, CA (USA)
Prof. K. Hardcastle
Department of Chemistry, California State University-Northridge
Northridge, CA (USA)
Dr. J. Ziller
Department of Chemistry, University of California-Irvine
Irvine, CA (USA)

[**] This work was supported by the National Science Foundation (CHE-9307582, ASC-8902827), the Alfred P. Sloan Foundation (J. S. S), and the Schweizerischen Nationalfonds zur Förderung der wissenschaftlichen Forschung (H. B. B). The San Diego Supercomputer Center provided a grant for computing time.

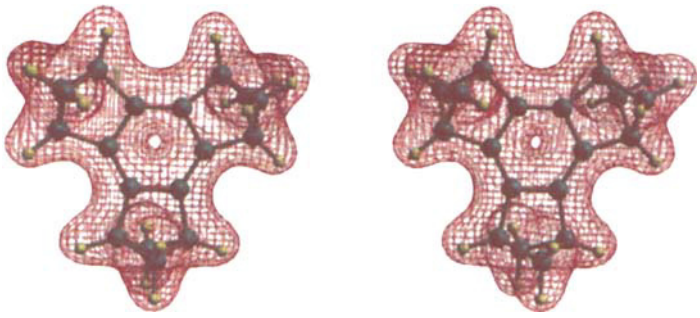

Fig. 2. Stereoview of the computed structure of **3** (non-local density functional theory). The net represents the electron density contour 0.3 e Å^{-3}.

Table 1. Selected experimental and calculated bond lengths and angles for **3**.

Method	C(1)-C(1')[*endo*]	C(1)-C(1')[*exo*]	C(1')-C(1)-C(3)[*endo*]
X-ray diffraction	1.438(5)	1.349(6)	102.3(2)
6-31G(D)	1.440	1.344	101.8
TZV(D)	1.442	1.340	101.8
MP2/6-31G(D)	1.430	1.373	102.1
LDF (local)	1.433	1.356	101.8
LDF (non-local)	1.431	1.353	102.5

bond localization. This preference for bond localization in lower basis set calculations has been noted in a computational study of the hypothetical all-*cis* conformation of cyclodecapentaene.[24]

Consecutive layers of **3** are related by local centers of symmetry leading to a nearest neighbor relationship in which the center of a molecule in one layer is situated over a hydrogen atom in the wing of a molecule in a neighboring layer (Fig. 3). This juxtaposition evokes thoughts of the polar/π interactions between benzenes with hydrogens.[25]

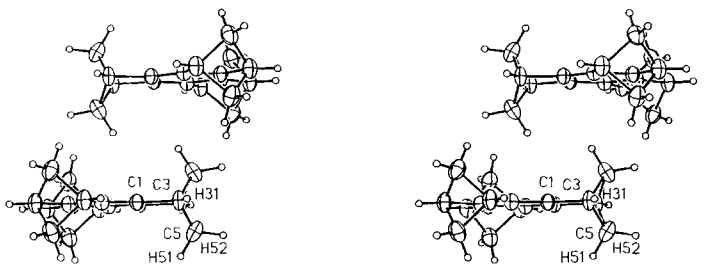

Fig. 3. Stereoview of nearest neighbor relationship between two molecules of **3** showing CH π interactions.

Received: February 27, 1994 [Z 7744 IE]
German version: *Angew. Chem.* **1995**, *107*, 1575–1577

Keywords: bond length alternation · cyclohexatriene · Mills–Nixon effect

[1] W. H. Mills, I. G. Nixon, *J. Chem. Soc.* **1930**, 2510–2524.

[2] a) J. S. Siegel, *Angew. Chem.* **1994**, *106*, 1908; *Angew. Chem. Int. Ed. Engl.* **1994**, *33*, 1721. b) Indeed, the coincidental overlap of the structural theories of van't Hoff, Kekulé, and Baeyer (ring strain), and the lack of pertinent structural data from diffraction experiments and/or molecular orbital theory, makes the prediction seem reasonable.

[3] a) M. J. Collins, J. E. Gready, S. Sternhell, C. W. Tansey, *Aust. J. Chem.* **1990**, *43*, 1547; b) R. H. Mitchell, P. D. Slowey, T. Kamada, R. V. Williams, P. J. Garratt, *J. Am. Chem. Soc.* **1984**, *106*, 2431; c) Y. Apeloig, D. Arad, *ibid.* **1986**, *108*, 3241; d) R. Faust, E. D. Glendening, A. Streitweiser, K. P. C. Vollhardt, *ibid.* **1992**, *114*, 8263; e) P. C. Hiberty, G. Ohanessian, F. Delbecq, *ibid.* **1985**, *107*, 3095; f) A. Stanger, *ibid.* **1991**, *113*, 8277.

[4] K. K. Baldridge, J. S. Siegel, unpublished results.

[5] a) M. Eckert-Maksic, D. Kovacek, M. Hodoscek, D. Mitic, K. Poljanec, Z. B. Maksic, *J. Mol. Struct. (THEOCHEM)* **1990**, *206*, 89–98; b) Z. B. Maksic, M. Eckert-Maksic, D. Kovacek, M. Hodoscek, K. Poljanec, J. Kudnig, *ibid.* **1991**, *234*, 201–212.

[6] a) 1,2,3,4,5,6-Hexahydrotricyclobuta[*a,c,e*]benzene (**1**) displayed a bond alternation of 0.023 Å at 125 K: R. Boese, D. Bläser, W. E. Billups, M. M. Haley, A. H. Maulitz, D. L. Mohler, K. P. C. Vollhardt, *Angew. Chem.* **1994**, *106*, 321–325; *Angew. Chem. Int. Ed. Eng.* **1994**, *33*, 313–316. b) For the synthesis, see W. Natakul, R. P. Thummel, A. D. Taggart, *J. Am. Chem. Soc.* **1979**, *101*, 770–771.

[7] a) R. Diercks, K. P. C. Vollhardt, *J. Am. Chem. Soc.* **1986**, *108*, 3150; b) D. L. Mohler, K. P. C. Vollhardt, S. Wolff, *Angew. Chem.* **1990**, *102*, 1200; *Angew. Chem. Int. Ed. Engl.* **1990**, *29*, 1151. c) Similar but less dramatic bond alternation is seen in angular terphenylene. See: d) R. Diercks, K. P. C. Vollhardt, *Angew. Chem.* **1986**, *98*, 268; *Angew. Chem. Int. Ed. Engl.* **1986**, *25*, 266 (X-ray); e) M. Nambu, K. Hardcastle, K. K. Baldridge, J. S. Siegel, *J. Am. Chem. Soc.* **1992**, *114*, 369 (ab initio, DFT calculations).

[8] K. K. Baldridge, J. S. Siegel, *J. Am.. Chem. Soc.* **1992**, *114*, 9583–9587.

[9] In this context, significance is defined as follows: The length of a C(arom.)–C(arom.) bond for a hexasubstituted benzene is 1.397 Å, with $\sigma = 0.009$ Å; σ for all benzene derivatives is 0.013 Å. A value of $\pm 3\sigma$ (i.e. ± 0.027–0.039 Å) or greater is considered significant. The values for σ are taken from the Cambridge Crystallographic Database (F. H. Allen, O. Kennard, D. G. Watson, L. Brammer, A. G. Orpen, R. Taylor, *J. Chem. Soc. Perkin Trans. 2* **1987**, S1–S19).

[10] N. L. Frank, K. K. Baldridge, J. S. Siegel, *J. Am. Chem. Soc.* **1995**, *117*, 2102.

[11] Crystallographic details for **3**: Precession photographs taken at room temperature showed a diffraction pattern with Laue symmetry 6/*mmm* but with diffuse diffraction streaks along c^* for $h - k + 3n$. The streaks are more intense around l odd than around l even. Reciprocal lattice lines along c^*, for which $h - k = 3n$, show sharp reflections for l even and systematic absences for l odd. These diffraction characteristics indicate an order–disorder structure [12]. Three sets of diffraction data had been collected before photographs were taken, one on an Enraf-Nonius CAD4 diffractometer equipped with a molybdenum tube, the second on a Siemens P4RA diffractometer equipped with a rotating Mo-anode, both at room temperature (hexagonal unit cell constants, $a = 9.007(5)$, $c = 17.802(11)$ Å, $V = 1250.7(21)$ Å^3) and the third at ca. 140 K on a Siemens P3 diffractometer with a molybdenum tube ($a = 8.74(4)$, $c = 17.736(8)$ Å, $V = 1237.0(16)$ Å^3). All three data sets show the following characteristics: reflections with $h - k = 3n$, $l = 2m$ are strong and show reasonable to excellent internal R-values when averaged with respect to 6/*mmm* symmetry; reflections with $h - k = 3n$, $l = 2m + 1$ are essentially absent; measurements with $h - k + 3n$ show poor internal R-values. The last observation is consistent with the fact that intensities measured by scanning across continuous diffraction streaks depend critically on the orientation of the crystal axes relative to the goniometer axes and on the unavoidable errors in the corresponding orientation matrix. As a consequence, measurements in symmetry-equivalent parts of reciprocal space may differ significantly. Sharp reflections are far less affected by these problems. The structure may be solved by first considering only the sharp reflections with $h - k = 3n$, $l = 2m$. These define a reduced hexagonal unit cell with $a' = (2a + b)/3$, $b' = (-a + b)/3$, $c' = c/2$ ($a' = b' = 5.200(3)$, $c' = 8.901(6)$ Å, $V = 208.4(4)$ Å^3). There are 1147 sharp reflections in the layers $-3 \le h' \le 6$, $-6 \le k' \le 3$, $-11 \le l' \le 11$. Averaging the second data set in 6/*mmm* symmetry leads to 114 uniques reflections with $R(\mathrm{int}) = 0.033$. The systematic absences of the reduced cell are $(00l')$, $l' = 2n + 1$ and $(h'h'l')$, $l' = 2n + 1$, thus indicating space group $P6_3/mmc$ for the reduced cell. Use of direct methods shows two molecules centered at 2/3, 1/3, 1/4 and 1/3, 2/3, 3/4 with site symmetry D_{3h} and related by a center of symmetry at 1/2, 1/2, 1/2. There are three carbon and three hydrogen atoms in the molecular asymmetric unit. Carbon atoms were refined anisotropically; C–H vectors were fixed in chemically meaningful directions. The C–H distances at C5 (see Fig. 1 for numbering) refined to 1.00(3) Å; the C–H distance at C3 was fixed at 0.95 Å. An isotropic displacement parameter, common to all hydrogen atoms, refined to 0.043(6) Å^2. The number of refined parameters is 22, including a scale and an extinction factor. Refinement converged smoothly at $R(|F|) = 0.028$, $wR(F^2) = 0.076$ and GOF = 1.222 for all 114 observations. All calculations were performed with the programs SHELX93 and XP. Treating the other two data sets in the same way leads to essentially the same, but less accurate results. In the original unit cell the molecular centers would be at 1/3, 1/3, z; $-1/3$, 0, z; 0, $-1/3$, z; 1/3, 0, $z + 1/4$; 0, 1/3, $z + 1/4$; $-1/3$, $-1/3$, $z + 1/4$ (with $z = 1/8$ and 5/8). For steric reasons and because the translational symmetry perpendicular to the threefold axis is a,b rather than a',b', only one of the three alternative positions can be occupied for a given value of z. The basic building blocks of the crystal structure are thus well-ordered layers of **3**, one per unit mesh in a,b, with their threefold axes perpendicular to the a,b-plane. The layer symmetry group is $p\bar{6}2m$. The layers above and below any given layer each have a choice governed by probability rules between three alternative, but well-defined positions; this will be elaborated elsewhere. However, no matter which alternative is chosen, the nearest neighbor relationship between molecules in adjacent layers is always as shown in Figure 2. Since the

 © VCH Verlagsgesellschaft mbH, D-69451 Weinheim, 1995 0570-0833/95/1313-1455 $ 10.00+.25/0

stacking of consecutive layers is governed by a combination of probability rules and well-defined nearest neighbor relationships, the crystal shows the observed combination of diffuse and sharp scattering.

[12] a) J. D. Dunitz in *X-ray Analysis and the Structure of Organic Molecules*, Cornell University Press, Ithaca, NY, **1979**, pp. 58–59; b) K. Dornberger-Schiff in *Lehrgang über OD-Strukturen*, Akademie, Berlin, **1966**.

[13] L. Pauling, *The Nature of the Chemical Bond*, 3rd ed., Cornell University Press, Ithaca, NY, **1961**, pp. 239–40.

[14] Alternatively, the total bond order in **3** is 9.75, less than the bond order in benzene (10) but greater than that in hexasubstituted benzenes (9.54) based on the average bond lengths.

[15] The mean values and their estimated standard deviations listed in ref. [9] are 1.554(21) Å for cyclobutane (any substitution) and 1.510(14) Å for $R_2CH-C=C$.

[16] The angle distortion effect seems to be nullified in benzenes with monocyclic annelations, like **1**, perhaps due to "bent bonds" in those systems; the angular effect for bicyclics appears to be more effective. For an example of a related distortion in the norbornyne trimer, see: N. L. Frank, K. K. Baldridge, P. Gantzel, J. S. Siegel *Tetrahedron Lett.* **1995**, in press.

[17] Computational details: The molecular structure of **3** was determined at a variety of theoretical methods to determine self-consistency. Reported here are the split-valence 6-31G(D) [18] and triple-zeta valence TZV(D) [19] basis sets, employed at the restricted Hartree–Fock (RHF) self-consistent field (SCF) level of theory. These basis sets include a set of six d polarization functions on all heavy atoms. These calculations were performed with the aid of the analytically analytically determined gradients and search algorithms contained in GAMESS [20]. Additional calculations at the MP2/6-31G(D) and Density Functional Theory levels were performed to determine the effects of dynamical correlation. Calculations using the former method, a post-RHF method that incorporates correlation in terms of Møller-Plesset theory of order 2 (MP2) [21], were performed using the GAUSSIAN 92 suite of programs [22]. Calculations using Density Functional Theory (DFT) Methods, which inherently incorporate effects of correlation in their development, were performed with the aid of the numerical methods within Dmol [23]. A double numerical basis set augmented by polarization functions, comparable in size to the 6-31G(D) basis set of the traditional Hartree–Fock methods, was chosen for the DFT calculations.

[18] a) P. C. Hariharan, J. A. Pople, *Theor. Chim. Acta* **1973**, *28*, 213; b) M. S. Gordon, *Chem. Phys. Lett.* **1980**, *76*, 163.

[19] a) T. H. Dunning, *J. Chem. Phys.* **1971**, *55*, 716; b) A. D. McLean, G. S. Chandler, *J. Chem. Phys.* **1980**, *72*, 5639; c) A. J. H. Wachters, *J. Chem. Phys.* **1970**, *52*, 1033.

[20] M. W. Schmidt, K. K. Baldridge, J. A. Boatz, J. H. Jensen, S. Koseki, M. S. Gordon, K. A. Nguyen, T. L. Windus, S. T. Elbert, *QCPE Bull.* **1990**, *10*, 52.

[21] J. A. Pople, J. S. Binkley, R. Seeger, *Int. J. Quantum Chem. Symp.* **1976**, *10*, 1.

[22] Gaussian 92, Revision C: M. J. Frisch, G. W. Trucks, M. Head-Gordon, P. M. W. Gill, M. W. Wong, J. B. Foresman, B. G. Johnson, H. B. Schlegel, M. A. Robb, E. S. Replogle, R. Gomperts, J. L. Andres, K. Raghavachari, J. S. Binkley, C. Gonzalez, R. L. Martin, D. J. Fox, D. J. Defrees, J. Baker, J. J. P. Stewart, J. A. Pople, Gaussian Inc., Pittsburgh, PA, **1992**.

[23] a) B. Delley, *J. Chem. Phys.* **1990**, *92*, 508. DMol is available commerically from BIOSYM Technologies, San Diego, CA. b) B. Delley, *J. Chem. Phys.* **1991**, *94*, 7245.

[24] a) R. C. Haddon, K. Raghavachari, *J. Am. Chem. Soc.* **1982**, *104*, 3516–3518; b) *J. Am. Chem. Soc.* **1985**, *107*, 289–297; c) Y. Xie, H. F. Schaefer III, G. Liang, J. P. Bowen, *J. Am. Chem. Soc.* **1994**, *116*, 1442–1449.

[25] a) M. Nishio, M. Hirota, *Tetrahedron* **1989**, *45*, 7201–7245; b) F. Cozzi, J. S. Siegel, *Pure Appl. Chem.* **1995**, *67*, 683.

Architectural Control in "Living" Free Radical Polymerizations: Preparation of Star and Graft Polymers**

Craig J. Hawker*

The ability to accurately control macromolecular architecture is becoming an increasingly important theme in polymer science with the interest being driven by the desire to prepare materials with new and/or improved properties.[1] One way to achieve these goals is to introduce branches into the polymer backbone. For example, graft and star systems have been shown to be useful as rheology control agents, compatabilizers for polymer blends, and emulsifiers.[2] Traditionally, graft and star polymers have been prepared by anionic[3] and cationic polymerization,[4] or by group transfer techniques.[5] However these techniques suffer from rigorous synthetic conditions, an inability to form many random copolymer systems, and incompatibility with a wide range of monomer units. One goal of synthetic polymer chemistry is to devise a free radical approach to the preparation of graft and star systems which has the same degree of macromolecular control as the above techniques but does not suffer from their synthetic drawbacks. Previous attempts at using free radical methods have not been entirely successful due to a lack of macromolecular control and combination reactions, which result in network formation.[6] In this report we describe a novel "living" free radical methodology which overcomes these problems and allows the synthesis of star and graft copolymers with controlled molecular weights and low polydispersities under mild conditions.

This new polymerization method is based on the use of novel initiators containing a covalent adduct of styrene and 2,2,6,6-tetramethylpiperidinyloxy (TEMPO).[7] Previously we have demonstrated that the molecular weight and chain ends of polystyrene can be accurately controlled by the use of **1** as an initiator.[8] These results, coupled with the pioneering work by Georges et al.[9] and Rizzardo et al.[10] suggest that the polymerization proceeds with little or no termination and may be considered living in nature. It is this lack of termination reactions, coupled with a high degree of macromolecular control, which may allow the synthesis of well-defined star and graft polymer systems using TEMPO-based initiators.

To investigate this question we examined the synthesis of a trifunctional initiator, **2**, which contains three initiating styrene-TEMPO groups. It was hoped that each of the three styrene-TEMPO groups of **2** would independently initiate a growing polymer chain and that these individual polymer chains would grow at approximately the same rate to give well-defined star macromolecules. It was found that the benzyl ester group of the starting material **1** could be hydrolyzed with potassium hydroxide to give the alcohol **3** in excellent yields. Reaction of **3** with 1,3,5-benzenetricarbonyl chloride (**4**) in the presence of 4-dimethylaminopyridine proceeded smoothly to give the desired trifunctional initiator **2** in 71% yield after purification (Scheme 1). Under the conditions developed previously,[7, 9] bulk polymerization of 200 equivalents of deuterated styrene with **2** at 130 °C for 72 h was found to give the polystyrene **5** in 84% yield with no detectable amounts of crosslinked or insoluble material (Scheme 2). Analysis of **5** revealed a molecular

[*] Dr. C. J. Hawker
IBM Research Center, Almaden Research Center
650 Harry Road, San Jose, CA 95120-6099 (USA)
Telefax: Int. code +(408)927-3310

[**] Financial support of this work was provided by National Institute of Standards and Technology through ATP contract No. 70 NANB-3H-365.

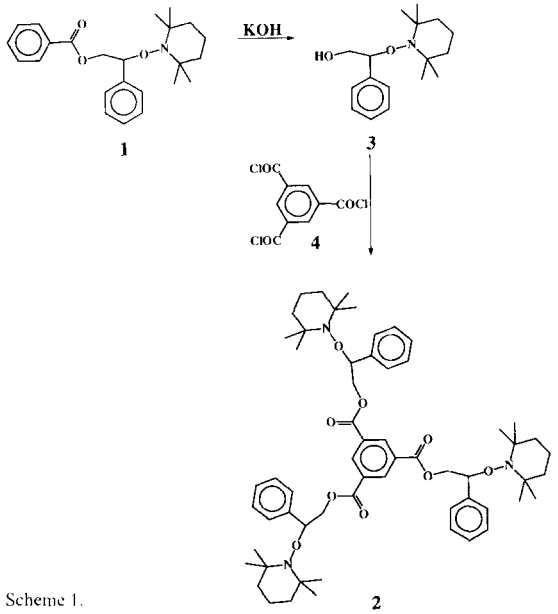

Scheme 1.

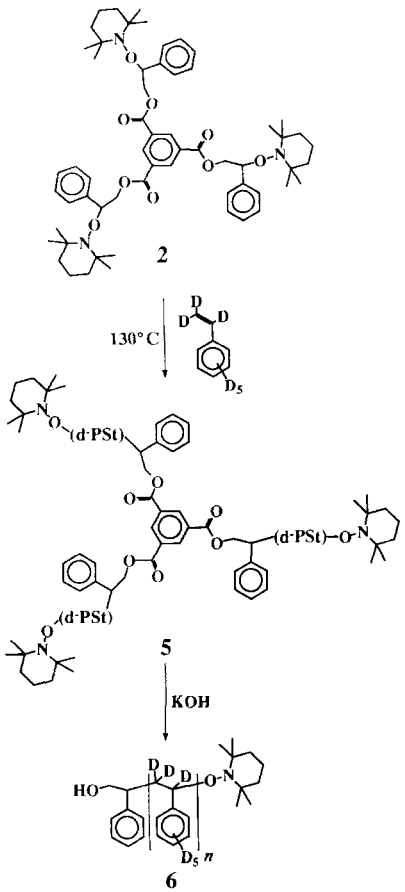

Scheme 2.

weight M_n of 16500 amu and a polydispersity (PD) of 1.20.[11] From the feed ratio, and assuming a three-arm star polymer is formed, the theoretical molecular weight M_n of **5** should be 21000 with each arm having a number average molecular weight of 7000. This discrepancy in molecular weights is, however, fully consistent with the proposed structure since the hydrodynamic volume of a star polymer is less than that of a comparable linear polymer. To determine the molecular weights of the individual arms of the star polystyrene, **5** was hydrolyzed with potassium hydroxide (Scheme 2). Significantly, the hydrolyzed product **6** was found to have a molecular weight M_n of 7600 (PD = 1.12) which agrees closely with the theoretical value for one arm of the star polymer ($M_n = 7000$). These results support the formation of a well-defined three-arm star macromolecule from **2**, the molecular weight of which can be accurately controlled by the initial feed ratio.

Further evidence for the proposed structures was obtained by comparing the ^{1}H NMR spectra of the trifunctional initiator **2** with that of the deuterated star polystyrene **5** and its hydrolyzed product **6**. As can be seen in Figure 1, the signals of the protons

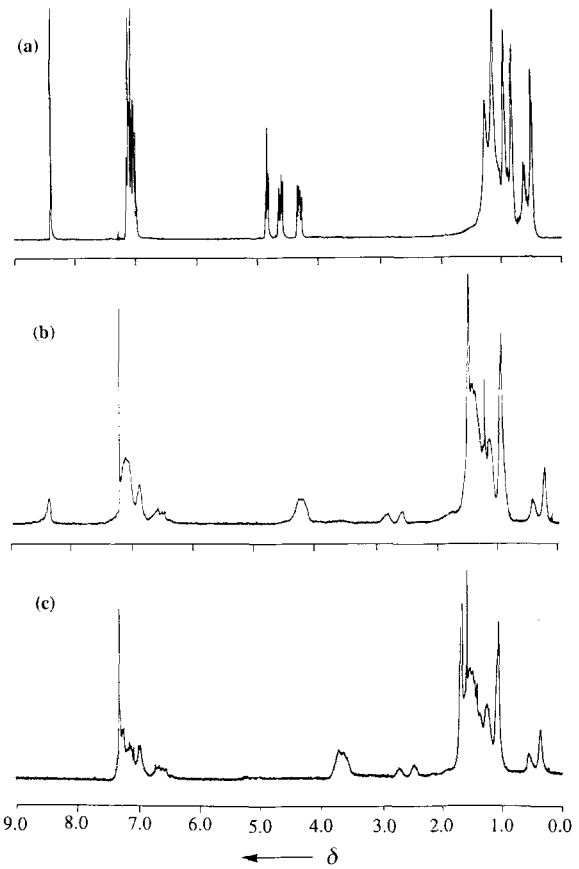

Fig. 1. a) ^{1}H NMR spectrum (300 MHz, $CDCl_3$) of the trifunctional initiator **2**; b) ^{1}H NMR spectrum (300 MHz, $CDCl_3$) of the three-arm deuterated polystyrene star **5**; c) ^{1}H NMR spectrum (300 MHz, $CDCl_3$) of the hydrolysis product **6**.

H_a, H_b, and H_c, which stem from the styrene unit in **2**, appear as three AB quartets at $\delta = 4.30-5.10$, and the protons of the symmetrically substituted core unit appear as a singlet at $\delta = 8.20$. On reaction with [D_8]styrene the resonances for H_a, H_b, and H_c undergo upfield shifts which correlate with the insertion of deuterated styrene units between the TEMPO and styrenic units of **2**, while the resonance for the core unit remains as a singlet at $\delta = 8.16$. On hydrolysis the resonance for the core unit at about $\delta = 8.20$ disappears, and the resonances for H_a, H_b, and H_c undergo shifts which are consistent with the generation of a hydroxy end group. In fact the spectrum of **6** is identical to that obtained when the alcohol **3** is used to initiate the polymerization of deuterated styrene.[8] In all three spectra the resonances for the TEMPO group are observed at $\delta = 0.0-1.5$ which demonstrates the stability of the TEMPO linkage to hydrolysis conditions.

Repetition of the above polymerization/hydrolysis reactions with up to 1000 equivalents of styrene was found to give similar results and illustrates the usefulness of this technique for the preparation of high molecular weight materials. For example, reaction of **2** with 700 equivalents of styrene was found to give a three-arm star polystyrene in 88% yield which had a M_n of 53000 and a PD of 1.19. While this value is again less than the theoretical number average molecular weight of 73000, hydrolysis to give the individual arms resulted in much closer agreement ($M_n = 22000$; PD = 1.09) with the theoretical number average molecular weight of 24000. This high degree of macromolecular control coupled with a lack of crosslinked material supports a "living" nature for this novel polymerization process with no termination due to combination or disproportionation. The versatility and usefulness of this "living" free radical chemistry is also demonstrated by the ability to use monomers such as *p*-chloromethylstyrene as well as acrylates and methacrylates. For example, previously unreported star polymers containing narrow dispersity arms which are random copolymers of styrene and butyl acrylate can be prepared from **2**.

This lack of termination steps also opens up the possibility of using this polymerization process to prepare graft systems. In an effort to also investigate the compatibility of the styrene-TEMPO group with standard free radical procedures the synthetic strategy for preparation of the graft systems involved initial synthesis of a monomer unit incorporating the styrene-TEMPO group, copolymerization with styrene under normal free radical conditions, followed by a "living" free radical polymerization with a second feed of styrene. The synthesis of the polymeric initiator is outlined in Scheme 3. Reaction of **2** with *p*-chloromethylstyrene in the presence of sodium hydride was found to give the desired monomeric derivative **7** in 71% yield after purification. Copolymerization of **7** with styrene was conducted under normal conditions using azobisisobutyronitrile (AIBN) as an initiator in refluxing tetrahydrofuran. Significantly the polymerization proceeded smoothly to give the desired copolymer **8** ($M_n = 12000$; PD = 1.80) in 72% yield after purification. Analysis of the copolymer by ^1H and ^{13}C NMR spectroscopy showed the expected resonances for the styrene-TEMPO group, and comparison with the aromatic styrenic resonances for the backbone polymer permitted the ratio of monomer units to be determined. The experimentally determined value of 1:19 agrees with the feed ratio and shows that the styrene-TEMPO group has little effect on reactivity ratios. Bulk polymerization of a mixture of the copolymer **8** and 200 equivalents of styrene at 130 °C for 72 h resulted in polymerization of the added styrene to give the proposed graft system **9**. Comparison of the gel permeation chromatographic (GPC) traces for the starting polymer **8** and the graft system **9** clearly shows an increase in molecular weight for **9** and the absence of unreacted starting polymer (Fig. 2). In this case the nature of the grafted polymer chain **10** could not be probed by hydrolysis due to the stability of the ether linkage, and cleavage of this group was therefore accomplished by treatment of **9** with an excess of trimethylsilyl iodide (Scheme 4). This results in a dramatic change in the GPC trace for the isolated product, no peak for the starting graft system is observed, and the polydispersity of the sample is lowered from 2.01 to 1.26. Interestingly, the number average molecular weight for **10** was determined to be 23000, which agrees closely with the theoretical M_n for the grafted chains of 21000. These results demonstrate that a graft system is produced and that the TEMPO groups attached to the polystyrene backbone of **8** are capable of initiating the polymerization of styrene to give grafts of controlled molecular weight and low polydispersity. The small shoulder at lower molecular weight in the GPC trace for **10** correlates with the molecular weight of the starting polymer **8**, and is due to the cleaved backbone polymer, whose signal underlies the main peak for the grafted chain. This ability to conduct one free radical polymerization and then by simply increasing the temperature and adding new monomer, to conduct a second "living" free radical polymerization is intriguing and may open up new paths to unusual macromolecular architectures. As for the star polymers unusual graft copolymers can be readily prepared by this "living" free radical technique from monomers which cannot be polymerized by better known anionic or cationic techniques.

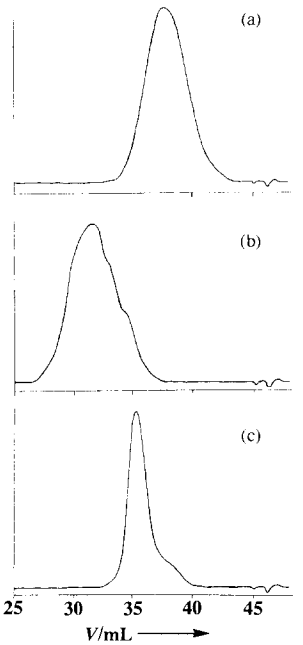

Fig. 2. a) Gel permeation chromatogram of the starting copolymer **8**; b) gel permeation chromatograph of the graft polymer **9**; c) gel permeation chromatogram of the cleaved graft polymer **10**.

In conclusion we have demonstrated that "living" free radical polymerizations based on TEMPO derivatives allow for the accurate control of macromolecular architecture. Star and graft copolymers can be prepared from the appropriate multifunctional initiators with no observation of crosslinking or termination by combination even under melt conditions. The molecular weights of the arms, or grafts, can be controlled by varying the equivalents of monomer added while maintaining very low polydispersities. We believe that this novel polymerization process offers the architectural control previously obtainable only under synthetically more rigorous anionic or cationic conditions.

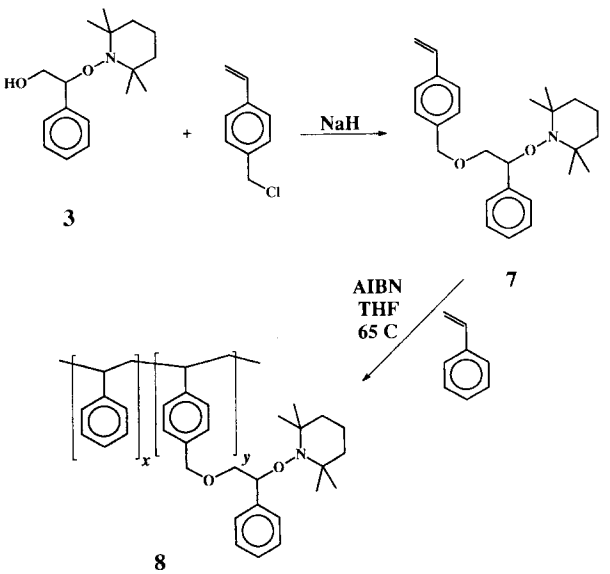

Scheme 3.

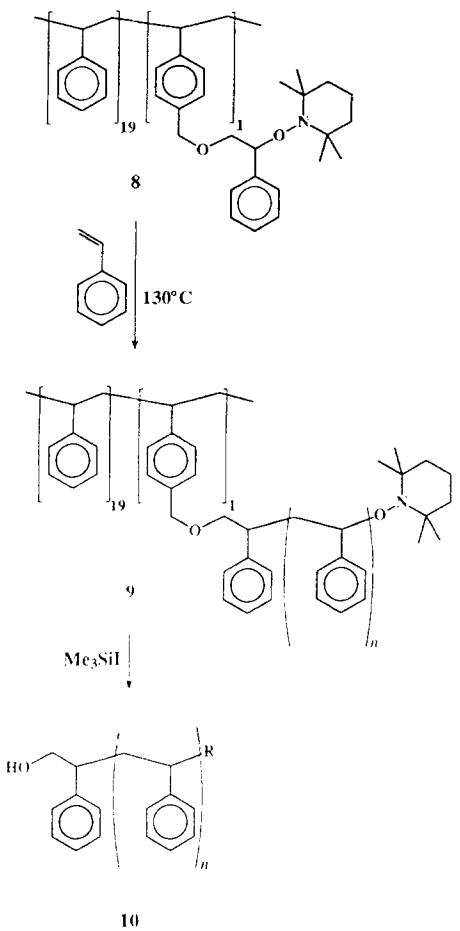

Scheme 4.

Experimental Procedure

2: To a solution of the alcohol **3** (1.0 g, 3.6 mmol) and **4** (290 mg, 1.1 mmol) in dry tetrahydrofuran (20 mL) was added dropwise a solution of 4-dimethylaminopyridine (50 mg, 0.4 mmol) and pyridine (300 mg, 3.8 mmol) in tetrahydrofuran (2.0 mL). The reaction mixture was stirred at room temperature under argon for 16 h and then evaporated to dryness. The residue was partitioned between dichloromethane (50 mL) and water (50 mL), and the aqueous layer extracted with dichloromethane (2 × 50 mL). The combined organic layers were dried, evaporated to dryness, and purified by flash chromatography eluting with 1:2 hexane/dichloromethane increasing to dichloromethane. This gave the trifunctional initiator **2** as a pale yellow oil. Yield 71%; ^{1}H NMR ($CDCl_3$): δ = 0.79, 1.03, 1.25, 1.62 (each brs, 12H, CH_3), 1.34 – 1.58 (m, 6H, CH_2), 4.60 (ABq, J = 6 Hz, 1H, C*H*H), 4.91 (ABq, J = 6 Hz, 1H, CH*H*), 5.14 (t, J = 3 Hz, 1H, C*H*), 7.25 – 7.52 (m, 5H, ArH), 8.20 (s, 3H, ArH); ^{13}C NMR ($CDCl_3$): δ = 17.17, 20.38, 34.12, 40.47, 60.15, 67.30, 83.89, 127.74, 128.18, 128.85, 130.92, 131.55, 134.53, 140.33, and 164.54; mass spectrum (EI) *m/z* 987; anal. calcd. for $C_{60}H_{81}N_3O_9$: C 72.9, H 8.26, N 4.25; found: C 73.2, H 7.99, N 4.43.

Preparation of three-arm polystyrene **5** from **2**: A solution of the trifunctional TEMPO initiator **2** (150 mg, 0.152 mmol) in [D_8]styrene (3.40 g, 30.4 mmol, 200 equiv) was heated at 130 °C with stirring under argon for 72 h. During this time the viscosity of the solution was observed to gradually increase and the clear reaction mixture eventually solidified. The reaction mixture was then dissolved in dichloromethane (25 mL) and precipitated into hexane (1 L) followed by re-precipitation into methanol (1 L). The three-arm polystyrene **5** was isolated as a white solid after drying. Yield 84%; M_n = 16500 and PD = 1.20; ^{1}H NMR ($CDCl_3$): δ = 0.40 (br d), 0.90 – 1.70 (br m), 2.65 and 2.90 (br d, H_c), 4.35 (m, 2H, H_a and H_b), 6.40 – 7.25 (br m), 8.40 (s, core H's); ^{13}C NMR ($CDCl_3$): δ = 17.10, 20.90, 39.4–43.8, 125.0 (br), 127.34 (br), 128.22, 129.42, 132.73, 144.8–145.8 (a number of resonances were too small to observe).

7: To a solution of the alcohol **3** (1.0 g, 3.6 mmol) in dry tetrahydrofuran (20 mL) was added sodium hydride (200 mg, 5.0 mmol) and the mixture stirred at room temperature for 10 min. A solution of *p*-vinylbenzyl chloride (1.52 g, 10.0 mmol, 3.0 equiv) was added and the mixture stirred at room temperature for 1 h, then heated at reflux for 16 h. The reaction mixture was then evaporated to dryness and partitioned between dichloromethane (50 mL) and water (50 mL) and the aqueous layer extracted with dichloromethane (2 × 50 mL). The combined organic layers were dried, evaporated to dryness and purified by flash chromatography eluting with 1:1 hexane/dichloromethane increasing to dichloromethane. This gave the styrene derivative **7** as a pale yellow oil. Yield 71%; ^{1}H NMR ($CDCl_3$): δ = 0.63, 1.01 (each brs, 6H, CH_3), 1.15 – 1.55 (m, 12H, 3 × CH_2 and 2 × CH_3), 3.65 (ABq, J = 6 Hz, 1H, C*H*H), 3.95 (ABq, J = 6 Hz, 1H, CH*H*), 4.41 (s, 2H, CH_2), 4.84 (d of d, J = 2 and 6 Hz, 1H, C*H*H), 5.20 (d of d, J = 2 and 7 Hz, 1H, =CH*H*), 5.71 (d of d, J = 2 and 6 Hz, 1H, =CH*H*), 6.66 (d of d, J = 6 and 7 Hz, 1H, =CH), 7.08 (d, 2H, Ar*H*), 7.25–7.52 (m, 7H, Ar*H*); ^{13}C NMR ($CDCl_3$): δ = 17.17, 20.56, 33.87, 40.48, 59.36, 72.74, 72.83, 85.41, 113.52, 126.04, 127.24, 127.53, 127.82, 127.88, 136.62, 138.14, and 141.79; mass spectrum (EI) *m/z* 393.

Copolymerization of **7** with styrene: A solution of the styrene-TEMPO monomer **7** (450 mg, 1.15 mmol), styrene (2.40 g, 23.0 mmol, 20 equiv), and AIBN (40 mg, 0.23 mmol) in dry tetrahydrofuran (20 mL) was heated at reflux under argon for 24 h. The reaction mixture was evaporated to dryness, redissolved in dichloromethane (10 mL) and precipitated into methanol (500 mL) followed by hexane (500 mL). The copolymer **8** was isolated as a white powder. Yield 72%; M_n = 12000 and PD = 1.80; ^{1}H NMR ($CDCl_3$): δ = 0.65, 0.90 – 1.70, 3.65, 3.95, 4.30, 4.82, 6.40 – 7.25 (br m); ^{13}C NMR ($CDCl_3$): δ = 17.25, 39.0 – 43.5, 125.3 (br), 127.5 (br), 128.30, 144.7 – 145.8 (a number of resonances were too small to observe).

Preparation of graft polystyrene **9**: A solution of the polymeric initiator **8** (200 mg, 0.085 mmol, 1.0 equiv) in styrene (1.82 g, 17.5 mmol, 200 equiv) was heated at 130 °C with stirring under argon for 72 h. During this time the viscosity of the solution was observed to gradually increase and the clear reaction mixture eventually solidified. The reaction mixture was then dissolved in dichloromethane (25 mL) and precipitated into hexane (1 L) followed by re-precipitation into methanol (1 L). The graft polystyrene **9** was isolated as a white solid after drying. Yield 80%; M_n = 86000 and PD = 2.01; ^{1}H NMR ($CDCl_3$): δ = 0.90 – 1.70 (br m), 6.40 – 7.25; ^{13}C NMR ($CDCl_3$): δ = 39.0 – 44.5, 125.0 (br), 127.5 (br), 144.5 – 146.0.

Received: January 13, 1995
Revised version: March 17, 1995 [Z 7634 IE]
German version: *Angew. Chem.* **1995**, *107*, 1623 – 1627

Keywords: graft polymers · polymers · radical polymerization · star polymers

[1] J. M. J. Fréchet, *Science* **1994**, *263*, 1710.
[2] P. F. Rempp, P. J. Lutz in *Comprehensive Polymer Chemistry, Vol. 7* (Ed.: S. V. Aggarwal), Pergamon, Oxford, **1988**, Chapter 12.
[3] P. J. Lutz, G. Beinert, P. F. Rempp, *Macromol. Chem.* **1982**, *183*, 2787.
[4] H. A. Nguyen, J. P. Kennedy, *Polym. Bull.* **1983**, *10*, 74.
[5] D. Y. Sogah, W. R. Hertler, O. W. Webster, G. M. Cohen, *Macromolecules* **1987**, *20*, 1473.
[6] G. C. Eastmond, L. W. Harvey, *Polymer* **1985**, *17*, 275.
[7] C. J. Hawker, *J. Am. Chem. Soc.* **1994**, *116*, 11185.
[8] C. J. Hawker, J. L. Hedrick, *Macromolecules* **1995**, *28*, 2993.
[9] M. K. Georges, R. P. N. Veregin, P. M. Kazmaier, G. K. Hamer, *Macromolecules* **1993**, *26*, 2987; *Trends Polym. Sci. (Trivandrum India)* **1994**, *2*, 66.
[10] E. Rizzardo, *Chem. Aust.* **1987**, *54*, 32; D. H. Solomon, E. Rizzardo, P. Cacioli CSIRO, US-A 4581429, **1985**.
[11] Number average molecular weights were determined experimentally by gel permeation chromatography using commercially available narrow molecular polystyrene sample as standards.

 © VCH Verlagsgesellschaft mbH, D-69451 Weinheim, 1995 0570-0833/95/1313-1459 $ 10.00+.25/0

A Novel Chainlike Heteropolyanion Formed by Keggin Units: Synthesis and Structure of $(ET)_{8n}[PMnW_{11}O_{39}]_n \cdot 2nH_2O$**

José Ramón Galán-Mascarós, Carlos Giménez-Saiz, Smaïl Triki, Carlos J. Gómez-García, Eugenio Coronado,* and Lahcène Ouahab

Heteropolyanions with the general formula $[X_xM_mO_y]^{-q}$ (M = W, Mo, Nb, V etc.; X = Si, P, B, Co, Fe, Cu etc.), have been known for well over a century and constitute a large fundamental class of inorganic compounds[1] that in recent years have aroused increasing interest because of their relevance to several disciplines due to their topological and electronic versatilities.[2] In spite of the vast number of known polyoxoanions, the number of different structural types is relatively low. Most of them present discrete clusterlike structures of definite sizes and shapes. In fact, they can be viewed as molecular fragments of metal oxides formed by closed and highly symmetrical networks of MO_x polyhedra (usually octahedra and tetrahedra) sharing corners, edges, or faces.

The first characterized, and the best known, of these structural types is the Keggin polyoxoanion.[3] It consists of four M_3O_{13} groups (M = Mo, W) surrounding a central heteroatom in a tetrahedral cavity. Each M_3O_{13} group is formed by three octahedra sharing edges and having a common oxygen atom which is also shared with the central heteroatom. By removing one, two, or three M atoms in the Keggin structure it is possible to obtain the mono-, di-, and trivacant Keggin polyoxometalates.[4] These lacunary species can, generally, be reconstituted with ease by using their ability to form stable complexes with d-transition metals. The resulting mono-,[5] di-,[6] and trisubstituted[7] Keggin polyoxoanions, however, have shown discrete structures in all cases.

Structures of extended heteropolyanions have been observed very rarely. In these structures the metal heteroatoms (mainly rare earth metals) are linked to the external oxygen atoms of the polyoxoanion ligand to give chain structures in which the metal cation and the polyoxoanion alternate. Examples of this kind are the complexes formed from $[UMo_{12}O_{42}]^{8-}$ and Th^{4+} ions,[8] $[Mo_8O_{27}]^{6-}$ and Eu^{3+} ions,[9] and $[H_2W_{12}O_{42}]^{10-}$ and Co^{2+} ions.[10] However, none of the structures reported for Keggin anions or their derivatives has shown the existence of polymeric species.[11]

In this communication we report the synthesis and structure of the first characterized compound containing a chain of Keggin polyoxoanions: $(ET)_8[PMnW_{11}O_{39}] \cdot 2H_2O$, where ET is the organic donor bis(ethylenedithio)tetrathiafulvalene. This compound has been obtained as a part of our investigation on hybrid radical materials formed by conducting organic donors and magnetic inorganic polyoxoanions.[12, 14b] Single-crystals of the title compound **1** have been prepared by electro-oxidation of ET in presence of the monosubstituted Keggin anion

$(ET)_{8n}[PMnW_{11}O_{39}]_n \cdot 2nH_2O$ **1**

$[PMn(H_2O)W_{11}O_{39}]^{5-}$ (abbreviated to $PMnW_{11}$). Its structure[13] is related to those found in the α_1 and α_2 phases of radical salts $(ET)_8[XW_{12}O_{40}] \cdot (solv.)_n$ ($X = Co^{2+}$, Cu^{2+}, Fe^{3+}, $(H^+)_2$, B^{3+}, Si^{4+}).[14] It consists of alternate layers of the organic donor with the α packing mode[15] and the inorganic Keggin polyoxometalates. Nevertheless, the unit cell parameters and the molecular packing of the inorganic layers of **1** are different, so we prefer to call this new structure an α_3 phase.

The most striking feature of this new α_3 phase **1** lies in the fact that the undecatungsto complex of Mn^{2+} is connected by a common oxygen atom forming chains that run along the *c* axis (Fig. 1). This bridging oxygen atom connects two opposite positions of the Keggin unit occupied by Mn^{2+} and W^{6+} ions with an occupancy factor of one half (we name this position as Z).[16] From the structural point of view, it is important to note that the localization of the Mn atom over two of the twelve metal sites is quite unusual for this type of heteropolyanion. In many crystalline salts of the monosubstituted Keggin anions XMW_{11}, the metal atom M positions are fully disordered as a consequence of the cubic crystal structure.[17] The lower symmetry of **1** (monoclinic) has allowed the Mn atom to be located and distortions in the polyanion to be determined. In fact, the structure of the Keggin ion in **1** is elongated along the *c* axis as can be seen from the P–metal distances, which increase from 3.54–3.57 Å (for P–W) to 3.63 Å (for P–Z) (see Fig. 1). From the chemical point of view, the existence of this polymer involves a displacement of the molecule of H_2O coordinated to Mn in one Keggin unit by a terminal O atom on W in another unit. In this context, we have found that the Mn compound is the only

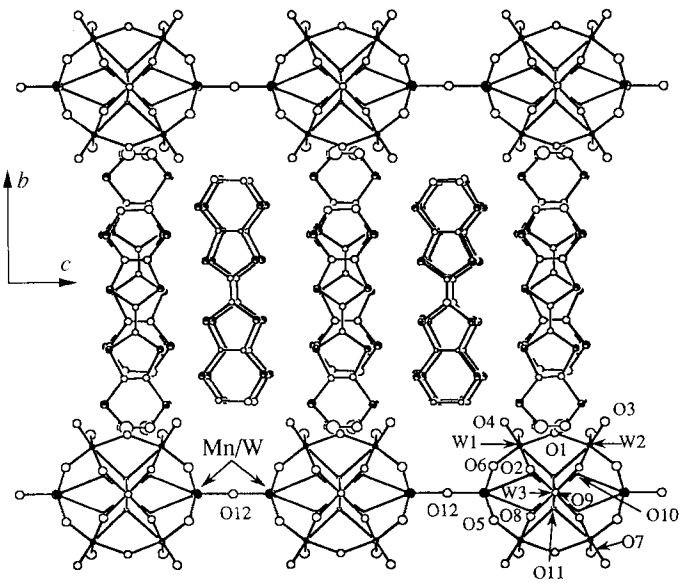

Fig. 1. Structure of the radical salt **1** showing the eclipsed and dimerized ET chains as well as the chains of Keggin polyoxometalates. Selected bond lengths [Å]: W1-O1 1.92(2), W1-O2 1.90(1), W1-O4 1.69(2), W1-O6 1.84(2), W1-O7 1.88(2), W1-O10 2.40(2), W1-O11 2.56(3), W2-O1 1.92(2), W2-O3 1.71(2), W2-O5 1.84(2), W2-O7 1.92(2), W2-O8 1.91(2), W2-O10 2.38(2), W2-O11 2.53(2), Z-O5 2.02(2), Z-O6 2.02(2), Z-O10 2.60(2), Z-O12 1.969(2), W3-O2 1.88(2), W3-O8 1.88(2), W3-O9 1.76(2), W3-O11 2.41(2), W1-W2 3.612(1), W1-W2 3.541(1) [symmetry code $-x, y, -z$], W1-W3 3.573(1), W1-Z 3.576(1), W2-W3 3.569(1), W2-Z 3.581(2) [symmetry code $-x, -y, -z$], Z-Z 3.939(3) [symmetry code $-x, -y, -z-1$], W1-P 3.567(1), W2-P 3.572(1), W3-P 3.544(1), Z-P 3.631(2); Z = 0.5 Mn + 0.5 W.

[*] Prof. Dr. E. Coronado, J. R. Galán-Mascarós, C. Giménez-Saiz, Dr. S. Triki, Dr. C. J. Gómez-García
Departamento de Química Inorgánica
Universidad de Valencia
Dr. Moliner 50, E-46100 Burjasot (Spain)
Telefax: Int. code +(6)-3864322

Dr. L. Ouahab
Laboratoire de Chimie du Solide et Inorganique Moléculaire
Université de Rennes (France)

[**] This work was supported by the Ministerio de Educación y Ciencia (CICYT) and the Generalitat de Cataluña (CIRIT) (Grant QFN93-4510), the European Union (Network on New Molecular Conductors and post-doctoral grant to C. J. G.), the Caja de Ahorros del Mediterráneo, and the CNRS. S. T. thanks the CICYT for a post-doctoral grant. ET = bis(ethylenedithio)tetrathiafulvalene.

member of the series $(ET)_8[XMW_{11}]$ ($XM = PMn^{2+}$, PNi^{2+}, PCo^{2+}, $SiCr^{3+}$, $SiFe^{3+}$) that gives rise to the polymeric chain anion. The other compounds belong to the α_2 phase, showing discrete Keggin anions.[18] A possible reason for this difference may be related with the larger size of Mn^{2+} compared with that of the other ions. In the case of manganese, the bridge can be formed with a smaller variation in the lattice parameters (c is reduced by ca. 1 Å when passing from α_2 to α_3 phases).

The structure of the organic layers in **1** exhibits the α mode of packing in the ET molecules. As in other α_1 and α_2 phases, these layers are formed by two kinds of ET chains (I and II in Fig. 2) that run along the [101] direction and alternate in the [$\bar{1}$01] direction. Three crystallographically independent molecules

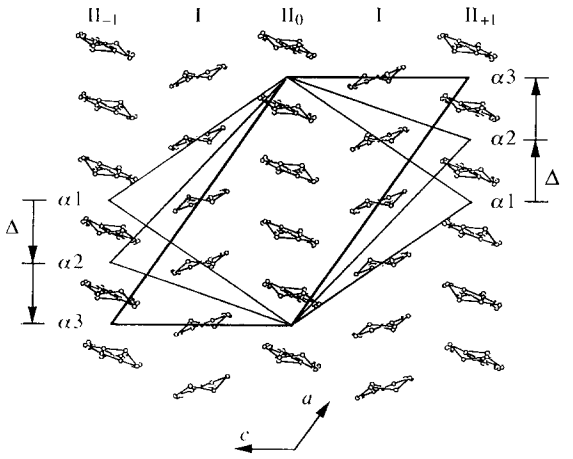

Fig. 2. Structure of the organic layer in the ac plane showing the α mode of packing and the structural relationship existing between this α phase (α_3) and the other two related phases (α_1 and α_2).

noted A, B, and C are present in the α_3 phase. Type I chains comprise alternating B and C molecules packed in an eclipsed way with intrachain S···S distances of 4.02 Å, whereas type II chains are formed by zigzag dimers of A molecules with similar intra- and inter-dimer S–S distances (3.79 Å and 3.90 Å, respectively). Each dimer is displaced by about 3.12 Å along the [010] direction (i.e., the direction of the central C=C bond) in such a way that six S atoms are eclipsed with the neighboring dimers. The shortest interchain S···S distances (3.41(2)–3.55(2) Å) are significantly shorter than the intrachain ones, emphasizing the bidimensional character of the packing. The ET molecules are tilted with respect to the axis of the chain giving rise to dihedral angles between ET molecules of neighboring chains of about 49° (in the other two α phases these angles are about 46°). A structural relationship exists between the three α modifications: Starting from a given α_i structure, the opposite displacements of two type II chains (II_{+1} and II_{-1}) with respect to a central chain (II_0) in the [101] direction by a distance of about 4 Å (which is the intrastack ET–ET separation), gives rise to the α_{i+1} structure (Fig. 2). These displacements are accompanied by the corresponding displacements in the inorganic sublattice, which give rise to a shortening in the distances between terminal oxygen atoms (Ot and Ot′ in Fig. 3) of neighboring Keggin units. Thus, the Ot–Ot′ distance decreases from 7.95 Å in α_1 to 3.70 in α_2, and to 0 Å in α_3 where neighboring Keggin anions are linked through an oxygen bridge (O12).

The nature of this new salt adds to the recent interest of polyoxometalates as inorganic components of organic–inorganic hybrid materials with interesting solid-state properties. In fact, preliminary physical characterization[19] has shown that

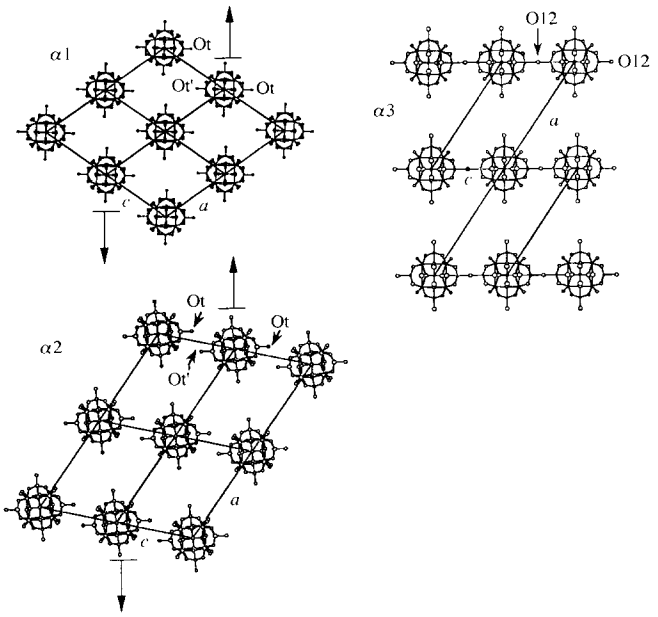

Fig. 3. Structure of the inorganic sublattice in the ac plane for the three α phases.

the compound is a magnetic semiconductor ($\sigma \approx 0.1$ S cm^{-1} at room temperature) which exhibits weak antiferromagnetic interactions between Mn^{2+} ions and the organic spin sublattice.[20] In this context it is to be noted that **1** represents the first member of a wide series of materials formed by monosubstituted Keggin anions and the organic radical; the Keggin anions show localized magnetic moments on their surface, the ET molecules delocalized electrons. The complete structural and physical characterization of this series of radical salts is under way.

Experimental Procedure

$[PM(H_2O)W_{11}O_{39}]$: All Keggin monosubstituted polyoxometalates $[PM(H_2O)W_{11}O_{39}]$ were synthesized by the following method: To a solution of $Na_8H[PW_9O_{34}] \cdot 19H_2O$[21] (3.6 mmol) in water (100 mL) was added glacial acetic acid (2 mL) and about a twofold excess of the transition metal salt (acetate, nitrate, or sulfate) as a solid. The pH of these solutions was set to approximately 5 by addition of small amounts of glacial acetic acid when necessary. These colored solutions were refluxed for at least two hours and filtered hot through paper to remove any insoluble material. An excess of solid Bu_4NBr was added with stirring to the clear solutions resulting in the immediate precipitation of a colored solid which was filtered, washed with water, and air dried overnight. These solids were recrystallized in acetonitrile and allowed to crystallize at room temperature. After about two days, the well-formed polyhedral-shaped single crystals were collected and air dried. The presence of the anion, as well as that of the Bu_4N^+ ion was confirmed by single-crystal X-ray studies and by the IR spectra, which were very similar for all compounds.

1: Single crystals of **1** were obtained by the electrochemical oxidation of ET (2.5×10^{-3} M in a mixture of wet $CHCl_2CH_2Cl/CH_3CN$ 1:1) in the presence of the Bu_4N^+ salt of the polyoxoanion (3×10^{-3} M in a mixture of wet $CHCl_2CH_2Cl/CH_3CN$ 1:1) in a U-shaped cell with Pt electrodes (1 mm in diameter) separated by a sintered-glass frit. The intensity of the current was fixed at 0.6 μA and after two weeks at 1.25 μA. After five weeks, shiny black prismatic single crystals of **1** were collected carefully, washed with CH_3CN, and air dried. The purity of the single crystals was checked by chemical analysis; this showed a Mn:W ratio of 1/11.

Received: January 3, 1995
Revised version: March 18, 1995 [Z 7602IE]
German version: *Angew. Chem.* **1995**, *107*, 1601–1603

Keywords: fulvalenes · Keggin anions · polyoxometalates · solid-state structures

[1] a) M. T. Pope, *Heteropoly and Isopoly Oxometalates*, Springer, Berlin, **1983**; b) M. T. Pope, A. Müller, *Angew. Chem.* **1991**, *103*, 56; *Angew. Chem. Int. Ed. Engl.* **1991**, *30*, 34.

[2] *Polyoxometalates: from Platonic Solids to Anti-Retroviral Activity* (Eds.: M. T. Pope, A. Müller), Kluwer, Dordrecht, **1994**.

[3] a) J. F. Keggin, *Nature* **1933**, *131*, 908; b) *Proc. R. Soc. London, A* **1934**, *144*, 75.

[4] a) P. Souchay, *Ann. Chim.* **1945**, *20*, 73; b) J. Fuchs, A. Thiele, R. Palm, *Z. Naturforsch. B* **1981**, *36*, 544.

[5] a) L. C. W. Baker, V. S. Baker, K. Eriks, M. T. Pope, M. Shibata, O. W. Rollins, J. H. Fang, L. L. Koh, *J. Am. Chem. Soc.* **1966**, *88*, 2329; b) C. Tourné, G. Tourné, *Bull. Soc. Chim. Fr.* **1969**, *4*, 1124; c) T. J. R. Weakley, *J. Chem. Soc. Dalton Trans.* **1973**, 341; d) F. Zonnevijlle, C. M. Tourné, G. M. Tourné, *Inorg. Chem.* **1982**, *21*, 2742; *ibid.* **1982**, *21*, 2750; e) T. J. R. Weakley, *Acta Crystallogr. Sect. C* **1984**, *40*, 16.

[6] C. J. Gómez-García, E. Coronado, P. Gómez-Romero, N. Casañ-Pasor, *Inorg. Chem.* **1993**, *32*, 89.

[7] a) Q. Lun-yu, Z. Bao-jian, P. Jun, L. Jing-fu, *Transition Met. Chem. (London)* **1988**, *13*, 183; b) P. Jun, Q. Lun-yu, C. Ya-guang, *Inorg. Chim. Acta* **1991**, *183*, 157; c) L. Jingfu, F. Ortega, P. Sethuraman, D. E. Katsoulis, C. E. Costello, M. T. Pope, *J. Chem. Soc. Dalton Trans.* **1992**, 1901; d) K. Wassermann, H. J. Lunk, *Acta Crystallogr. Sect. C* **1994**, *50*, 348.

[8] V. N. Molchanov, I. C. Tatjanina, E. A. Torchenkova, L. P. Kazansky, *J. Chem. Soc. Chem. Commun.* **1981**, 93.

[9] T. Yamase, H. Naruke, *J. Chem. Soc. Dalton Trans.* **1991**, 285.

[10] We have obtained the chain $([H_2W_{12}O_{42}\{Co(H_2O)_4\}_2]^{6-})_\infty$, where the polyanion $[H_2W_{12}O_{42}]^{10-}$ is connected by two Co^{2+} atoms. C. Giménez-Saiz, J. R. Galán-Mascarós, S. Triki, E. Coronado, L. Ouahab, *Inorg. Chem.* **1995**, *34*, 524.

[11] We have very recently found out that T. J. R. Weakley and H. T. Evans obtained a polymeric structure for the Et_3NH^+ salts of the anions $PCoW_{11}$ and $AsCoW_{11}$. However, in their case the precision in the structure determinations has been limited by gross disorder of the Et_3NH^+ and H_2O, and also partial disorder of the W and Co atoms involved in the bridges (personal communication).

[12] a) See E. Coronado, C. J. Gómez-García in ref. [2]; b) E. Coronado, C. J. Gómez-García, *Comments Inorg. Chem.*, in press.

[13] $(ET)_8[PMnW_{11}O_{39}]\cdot 2H_2O$: black shiny prismatic crystal: $0.15\times0.15\times0.35\ mm^3$, Enraf-Nonius CAD4 diffractometer, $M = 5845.77$, monoclinic, space group $I2/m$ with $a = 19.927(5)$, $b = 43.384(7)$, $c = 11.199(5)$ Å, $\beta = 123.06(3)^\circ$, $V = 8114$ Å^3, $Z = 2$, ($\rho_{calcd} = 2.392\ g\,cm^{-3}$; $Mo_{K\alpha}$ radiation $\lambda = 0.71069$ Å, $\mu = 88.71\ cm^{-1}$), structure solved by direct methods and successive Fourier difference synthesis, refinement of 309 variables with anisotropic thermal parameters (for Z, W, and P atoms) gave $R(F) = 0.046$ and $R_w(F) = 0.064$ by using 3165 absorption corrected reflections with $I \geq 5\sigma(I)$. Statistic disorder was observed between Mn and W atoms on two metallic sites. The refinements of the occupancy factors converge to a a value of 0.5. Then, a fictitious atom called Z corresponding to 50% contribution of Mn and 50% of W was introduced in the refinements. It will be noted that this disorder was observed when the refinements were conducted in the noncentrosymmetric space group Im. Further details of the crystal structure determination may be obtained from the Fachinformationszentrum Karlsruhe, D-76344 Eggenstein-Leopoldshafen (Germany), on quoting the depository number CSD-58931.

[14] a) A. Davidson, K. Boubekeur, A. Pénicaud, P. Auban, C. Lenoir, P. Batail, G. Hervé, *J. Chem. Soc. Chem. Commun.* **1989**, 1373; b) C. J. Gómez-García, L. Ouahab, C. Giménez-Saiz, S. Triki, E. Coronado, P. Delhaes, *Angew. Chem.* **1994**, *106*, 234; *Angew. Chem. Int. Ed. Engl.* **1994**, *33*, 223; c) C. J. Gómez-García, C. Giménez-Saiz, S. Triki, E. Coronado, P. Le Magueres, L. Ouahab, L. Ducasse, C. Sourisseau, P. Delhaes, *Inorg. Chem.* in press.

[15] J. M. Williams, J. R. Ferraro, R. J. Thorn, K. D. Carlson, U. Geiser, H. H. Wang, A. M. Kini, M. H. Whangbo, *Organic Superconductors. Synthesis, Structure, Properties and Theory* (Ed.: R. N. Grimes), Prentice Hall, Englewood Cliffs, NJ, USA, **1992**.

[16] This partial disorder is not due to the symmetry center of the group $I2/m$. In fact, this disorder remains when the structure is refined in the noncentrosymmetric group Im, in which the two metal sites are not equivalent.

[17] H. T. Evans, Jr., *Perspect. Struct. Chem.* **1971**, *4*, 1.

[18] The difference between the Mn undecatungsto complex and the other Keggin polyanions is only observed in the solid-state radical salts. In the precursor Bu_4N^+ salts of these polyanions, the substituted Keggin anions of Mn are present as discrete units as in the other members of the series XMW_{11}. In fact, all these Bu_4N^+ salts are isostructural exhibiting a cubic lattice with $a = 17.6$ 17.7 Å. Probably in nonaqueous solution the polyanions are also present as discrete species, and only when the lattice is formed the Mn complex polymerizes.

[19] E. Coronado, J. R. Galán-Mascarós, C. Giménez-Saiz, C. J. Gómez-García, S. Triki, P. Delhaes, *Mol. Cryst. Liq. Cryst.*, in press.

[20] The magnetic moment of **1** (6.6 BM at 300 K) shows a gradual decrease upon cooling down, approaching the value of one isolated Mn^{II} ion at low temperatures (4.92 BM at 6 K). These results support the presence of an ordered sequence Mn-O-W in the chain since no magnetic Mn Mn interaction is detected, thus eliminating the possibility of Mn-O-Mn bridges. Below 6 K the magnetic moment of the $(ET)_8[PMnW_{11}]$ radical salt crosses the curve of the $Bu_4N[PMnW_{11}]$ Keggin salt, suggesting the presence of very weak antiferromagnetic interactions between the two sublattices.

[21] R. G. Finke, M. W. Droege, P. J. Domaille, *Inorg. Chem.* **1987**, *26*, 3886.

A Silicon Strand of More than 7 Å in Diameter in $Ba_2Eu_3Si_7$**

Christina Häußermann and Reinhard Nesper*

Dedicated to Professor Gerhard Fritz on the occasion of his 75th birthday

The binary compounds formed by silicon with alkaline-earth and rare-earth metals differ substantially in their crystal structures, as well as in their stoichiometries and physical properties. Barium forms the five stable silicides $BaSi_2$,[1] Ba_3Si_4,[2] BaSi,[3] Ba_5Si_3,[4] and Ba_2Si,[5] whereas only two europium compounds, $EuSi_2$[6] and EuSi[3], are yet known. Except for BaSi and EuSi, both of which crystallize in the CrB structural type with planar, one-dimensional zigzag chains $^1_\infty[Si^{2-}]$, there are no other direct structural relationships between Eu and Ba silicides. $BaSi_2$ contains isolated Si^{4-}_4 tetrahedra, whereas a three-dimensional Si skeleton of three-bonded (3b), trigonal-planar Si atoms is present in $EuSi_2$. A Si^{6-}_4 butterfly anion occurs in Ba_3Si_4, which according to the Zintl–Klemm concept is a reduced form of the tetrahedron.

Only a small number of ternary silicides $M_xM'_ySi$ have been reported.[7, 8] For our studies of magnetic interactions in diluted spin systems, we have begun to synthesize such three-component compounds. During investigations of the phase width of $Ba_xEu_{1-x}Si_2$, the title compound $Ba_2Eu_3Si_7$ was found and characterized. It is not a direct derivative of the binary silicides, because in these neither the stoichiometry nor the crystal structure is represented. $Ba_2Eu_3Si_7$ forms as gray metallic needles.[10] It decomposes peritectically at 1260 K, which makes it difficult to obtain a pure phase.

The crystal structure determination was performed on a single crystal by X-ray diffraction. $Ba_2Eu_3Si_7$ crystallizes hexagonally in the space group $P\bar{6}2m$-D^3_{3h} with one formula unit in the unit cell.[11] The structural type is new, and it contains a novel Zintl anion of silicon. The silicon atoms constitute one-dimensional infinite strands $^1_\infty[(Si(Si_3)Si_3)^{10-}]$ (Fig. 1). Corresponding to the charge transfer of ten electrons per formula unit, two-(2b) and three-bonded (3b) silicon atoms are present. Without exception the latter have trigonal-planar coordination and act as central Si–Si links, whereas the (2b)Si belong to the

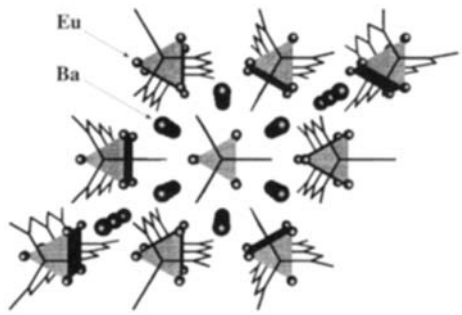

Fig. 1. Perspective view of the crystal structure of $Ba_2Eu_3Si_7$ in the [001] direction. The black lines represent Si Si bonds and the filled polyhedra Eu prisms. Ba atoms (large spheres) occupy the space between the $^1_\infty[(Eu_3Si_7)^{4-}]$ strands.

[*] Prof. Dr. R. Nesper, C. Häußermann
Laboratorium für Anorganische Chemie der Eidgenössischen Technischen Hochschule
CH-8092 Zürich (Switzerland)
Telefax: Int. code + (1)632-1149

[**] This work was supported by the Schweizerische Nationalfonds zur Förderung der wissenschaftlichen Forschung. We would like acknowledge the scientific support of Dipl.-Chem. A. Currao for this investigation.

boundary, as can be seen in Figure 2a–c. Together, the (2b)Si and (3b)Si atoms also form planar arrangements.[12] The Si–Si bonds are slightly longer than expected for uncharged single bonds (2.409 and 2.437 Å). We know, however, that bond lengths in solids are significantly affected by charge repulsion and cation influences.[13–15] Strong variations have also been reported for Si–Si single bonds in molecules. These are explained in terms of influences of the ligands.[16]

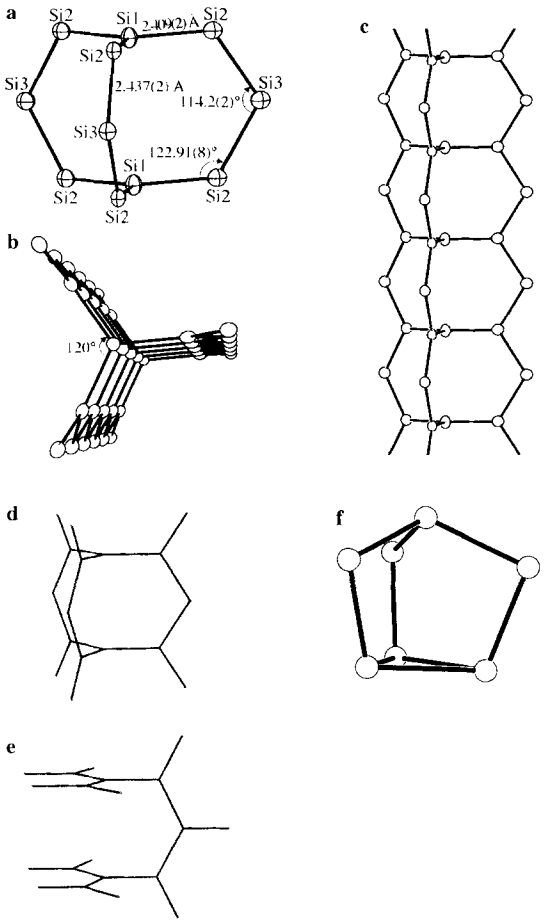

Fig. 2. a) Bicyclic Si_7 fragment (3,3,3-barrelane) from the one-dimensional Si chain in $Ba_3Eu_3Si_7$ (bond lengths and angles are given); b) perspective view along the chain; c) side view; d) section of the polyanion $^1_\infty[Si_7^{10-}]$; and e) corresponding section of the Si substructure in $EuSi_2$ for comparison; f) structure of P_7^{3-} and X_4Y_3 with X = P, As and Y = S, Se.

The angle at the three-bonded Si2 atom is not restricted by symmetry, yet deviates by less than three degrees from threefold symmetry, while an angle of 114° on the two-bonded Si3 appears to be somewhat large for an atom with two free electron pairs. We assume that the cation's influence is of importance also in this case.

This silicon strand with a diameter of approximately 7.5 Å is not very compact, if the silicon atoms alone are considered (Fig. 2c). Actually, it is the largest one-dimensional, polymeric strand of silicon ever synthesized in a well-defined compound.

The lone pairs on Si3 do not point directly at barium or europium atoms, but are directed toward regions between them. The barium atoms surround the central strand like an internal surface and are clearly separated from the europium sites (Fig. 1). The latter form trigonal prisms about the central Si atoms of the strand, whereas Ba atoms coordinate the terminal Si atoms (Fig. 1). Trigonal prismatic arrangements are rather typical for transition-metal and rare-earth-metal atoms in silicides, though several variants are possible. $EuSi_2$, for instance, crystallizes under normal conditions with the α-$ThSi_2$ structure,[6, 18] with prisms twisted by 90 degrees relative to one another along the c direction. The ternary compounds of the $Eu(Cu_xSi_{2-x})$ type, on the other hand, crystallize with the AlB_2 structure, in which all prisms are parallel.[18] The Zintl anions of silicon are particularly suitable for studying and, to some extent, controlling the various functional influences of cations upon the silicon substructure.[15]

The chemical reactivities and melting points indicate that Ba-silicides are distinctly more stable than Eu-silicides. This can be interpreted in terms of stronger interactions between the rare-earth metal and the silicon atoms, which makes the distribution of Eu atoms in the central strand plausible. Ba atoms evidently form a positively charged envelope for the $^1_\infty[(Eu_3Si_7)^{4-}]$ polymer. The Si-polyanion could be understood as part of the $EuSi_2$ structure in which two of the three (2b)Si atoms are twisted and joined to form end groups (compare Figures 2d and e). The third silicon atom remains unchanged. The impression on examining Figure 1 and 2 is of a $EuSi_2$-structure that is partly dissolved and coordinated by barium ligands. Attempts to isolate the silicon substructure are in progress.

Isoelectronic relatives to the Zintl anion Si_7^{10-} have been found among the pnictogen compounds X_7^{3-} and X_4Y_3 phases (X = P, As; Y = S, Se).[17] The connectivity in these compounds, however, is different; only two of the (3b)X atoms are linked to each other (Fig. 2f).

Received: March 2, 1995 [Z 7755 IE]
German version: *Angew. Chem.* **1995**, *107*, 1593–1594

Keywords: lanthanide compounds · silicon compounds · solid-state structures · Zintl anions

[1] H. Schäfer, K. H. Janzon, A. Weiss, *Angew. Chem.* **1963**, *75*, 451; *Angew. Chem. Int. Ed. Engl.* **1963**, *2*, 393.
[2] B. Eisenmann, K. H. Janzon, H. Schäfer, A. Weiss, *Z. Naturforsch. B* **1969**, *24*, 457.
[3] F. Merlo, M. L. Fornasini, *J. Less-Common Met.* **1967**, *13*, 603.
[4] K. H. Janzon, H. Schäfer, A. Weiss, *Z. Naturforsch. B* **1966**, *21*, 287.
[5] G. Bruzzone, E. Francheschi, *J. Less-Common Met.* **1978**, *57*, 201; A. Widera, H. Schäfer, *Z. Naturforsch. B* **1976**, *31*, 1434.
[6] J. Evers, G. Oehlinger, A. Weiss, F. Hulliger, *J. Less-Common Met.* **1983**, *90*, L19.
[7] J. Evers, G. Oehlinger, A. Weiss, *J. Less-Common Met.* **1980**, *69*, 399.
[8] Nakano-Hideyuki, Yamanaka-Shoji, *J. Solid State Chem.* **1994**, *108*, 260.
[9] E. Zintl, *Angew. Chem.* **1939**, *52*, 1; E. Zintl, G. Brauer, *Z. Phys. Chem. B* **1933**, *20*, 245; E. Zintl, W. Dullenkopf, *Z. Phys. Chem. A* **1931**, *154*, 1; *Z. Phys. Chem. B* **1932**, *16*, 183; W. Klemm, FIAT-Review of German Science, Naturforschung und Medizin in Deutschland 1939–1946, Anorganische Chemie Teil IV, Vol. 103; *Trab. Reun. Int. React. So'lidos 3rd* **1956**, *1*, 447; *Proc. Chem. Soc. London* **1959**, 329; E. Mooser, W. B. Pearson, *Phys. Rev.* **1956**, *101*, 1608; in *Progress in Semiconductors, Vol. 5* (Eds.: A. F. Gibson, R. E. Burgess, P. Aigrain, F. A. Kröger), Wiley, New York, **1960**, p. 103; W. Klemm, *Festkörperprobleme*, Vieweg, Braunschweig, **1963**; E. Busmann, *Z. Anorg. Allg. Chem.* **1961**, *313*, 90; H. Schäfer, *Angew. Chem.* **1973**, *85*, 742; *Angew. Chem. Int. Ed. Engl.* **1973**, *12*, 694.
[10] According to differential-thermoanalytical investigations, $Ba_3Eu_3Si_7$ does not melt congruently, but undergoes peritectical decomposition at 1260 K. We have therefore obtained this phase in only approximately 50% yields. The synthesis was carried out from the pure elements (Ba rods, 99.5%, Eu rods, 99.5%; Si powder, 99.99%) in a 1:3:7 molar ratio in welded Nb ampoules under an argon atmosphere. In typical synthesis about 1 g of reactant is heated to 1570 K, and then cooled to room temperature at a rate of 50 K h^{-1}.
[11] Crystal structure of $Ba_3Eu_3Si_7$: single crystal, $M = 927.19$ g mol^{-1}; $a = 927.42(5)$, $c = 409.12(7)$ pm; space group $P\bar{6}2m$-D^1_{3h} (no. 189); $Z = 1$; $V = 183.51$ cm^3 mol^{-1}; $\rho_{calcd} = 5.052$ g cm^{-3}; $N(hkl) = 452$ including 436 with $F \geq 2\sigma(F)$, $R_{int} = 0.041$; $R_{aniso} = 0.020$; data collection: STOE STADI4 four-circle diffractometer, graphite monochromator, scintillation counter, $Mo_{K\alpha}$ radiation, ω scan $5 \leq 65°$, 293 K; empirical absorption correction with Ψ scan;

 © VCH Verlagsgesellschaft mbH, D-69451 Weinheim, 1995 0570-0833/95/1313-1463 $ 10.00+.25/0

structure refinement: solution by SHELXS (combination of Patterson and direct methods), refinement by SHELX93 (least squares). Further details of the crystal structure investigation can be ordered from the Fachinformationszentrum Karlsruhe, D-75344 Eggenstein-Leopoldshafen (Germany), on quoting the depository number CSD-58983.

[12] The coplanar Si coordination in transition-metal and rare-earth-metal compounds is understood to be a result of d-orbital influences. However, silicides of heavy alkaline-earth metals have recently been found that also contain trigonal planar Si atoms (compare ref. [15]). There is at present no satisfactory explanation to this.

[13] H. G. von Schnering in *Homoatomic Rings, Chains and Makromolecules of Main-Group Elements* (Ed.: A. L. Rheingold), Elsevier, New York, **1977**, Chap. 14, p. 317.

[14] R. Nesper, Habilitation dissertation, Universität Stuttgart, **1988**.

[15] R. Nesper, A. Currao, S. Wengert, in *Organosilicon Chemistry, Vol. II*, in press.

[16] H. Bock, *Angew. Chem.* **1993**, *105*, 413; *Angew. Chem. Int. Ed. Engl.* **1993**, *32*, 414.

[17] H. G. von Schnering, W. Hönle, *Chem. Rev.* **1988**, *88*, 243.

[18] R. Nesper, H. G. von Schnering, J. Curda, VIth Int. Conf. on Solid Compounds of Transition Elements, Stuttgart, **1979**, Abstracts volume, p. 150.

The Role of Dehydroalanine in Catalysis by Histidine Ammonia Lyase**

Martin Langer, Andrea Pauling, and János Rétey*

The conversion of L-histidine into urocanic acid, catalyzed by histidine ammonia lyase (HAL), is an unusual elimination reaction and poses a mechanistic challenge for chemists.[1] The stepwise and the concerted[1] reaction modes either lead to unlikely, energetically disfavored intermediates or are based on implausible assumptions. HAL catalyzes the first step in histidine degradation in most organisms, and its failure in humans causes histidinemia.[2] HAL and the important plant enzyme phenylalanine ammonia lyase are the only enzymes known to contain a catalytically essential dehydroalanine,[3, 4] which has been shown to arise posttranslationally from serine 143[5] and serine 202,[6] respectively. Because of the electrophilicity[3, 7] of this prosthetic group it has been suggested[1, 3] that the α-amino group of histidine attacks it as a nucleophile thus enhancing the leaving ability of the amino group. But such a mechanism is unsatisfactory for the following reasons:

1) It does not answer the question of how the β-H_{Re} atom[3, 8] is activated.
2) The leaving ability of the α-amino group could be also enhanced by simple protonation.
3) It does not explain the finding of Furuta et al.[9, 10] that HAL catalyzes not only the exchange of β-H_{Re} but also that of 5-H in the imidazole ring.
4) It does not explain why L-cysteine and L-homocysteine strongly inhibit HAL, while other amino acids do not.[11, 12]

Klee at al.[13] found that L-5-nitrohistidine is a moderately good substrate of HAL. While [β-$^2H_2$]histidine exhibits a kinetic deuterium isotope effect of $k_H/k_D \approx 1.5-2.0$,[13, 14] no such effect is observed with L-5-nitro[β-$^2H_2$]histidine. The obvious explanation for this finding is the activation of the β-H atoms by the nitro group (Scheme 1). As a consequence, proton abstraction by a basic group of the enzyme is no longer rate-limiting for the overall reaction.

[*] Prof. Dr. J. Rétey, Dr. M. Langer, Dr. A. Pauling
Institut für Organische Chemie der Universität
Richard-Willstätter-Allee, D-76128 Karlsruhe (Germany)
Telefax: Int. code + (721) 608-4823

[**] This work was supported by the Deutsche Forschungsgemeinschaft and the Fonds der Chemischen Industrie.

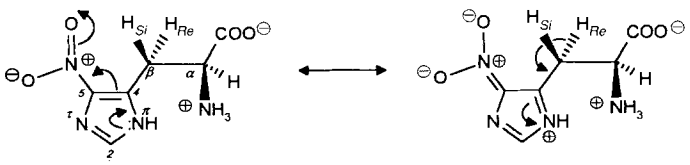

Scheme 1. Activation of the β-H atom by the nitro group in 5-nitrohistidine.

Recently we prepared mutants of HAL in which the codon for Ser 143 is exchanged with the codons of Ala and Thr.[5, 15] These mutants showed almost no activity with L-histidine as substrate. Here we report the results of experiments in which the activity of our HAL mutants, S143A and S143T, as well as of the sodium borohydride-treated wild-type histidase (HAL_{red}) was examined with both histidine and L-5-nitrohistidine as substrates and which suggest a novel mechanism for the HAL reaction.

First we compared the activities using L-5-nitrohistidine as substrate. The corresponding kinetic constants, K_m and V_{max}, are listed in Table 1. Surprisingly, the "inactive" mutants readily

Table 1. Michaelis constants K_m and V_{max} of wild-type, S143A, S143T, and HAL_{red} histidine ammonia lyases with L-5-nitrohistidine as substrate [a].

HAL	V_{max} [IU mg^{-1}] [b]	K_m [mM]
wild-type	0.85 ± 0.1	7.7 ± 1.5
S143A	0.87 ± 0.2	9.8 ± 3.0
S143T	0.87 ± 0.1	12.8 ± 2.9
HAL_{red}	0.79 ± 0.1	13.6 ± 3.9

[a] For the determination of K_m and V_{max} the substrate concentration in the enzyme assay was varied between 1 and 15 mM, and the increase of absorption was monitored at 400 nm [13]. The values were determined using Lineweaver-Burk diagrams. [b] IU = international enzyme unit.

accept L-5-nitrohistidine as substrate to the same extent that wild-type HAL does. Their kinetic constants differ only insignificantly. The slight increase of K_m for the S143T mutant may be due to unfavorable steric interactions between the methyl group of threonine and the nitro group of the substrate. Similarly, the slight impairment of both K_m and V_{max} in the case of the sodium borohydride-treated enzyme may arise from unspecific reactions by the reagent.

At this point it was necessary to reexamine the "inactivity" of our mutants with the natural substrate L-histidine. Using a much larger amount of HAL in the assay mixture (relative to the amount of 5-nitrohistidine used previously), we could determine the kinetic constants (Table 2). Whereas the K_m values of the mutants are on the same order of magnitude as those for wild-type HAL, the V_{max} values are about 1000 and 50000 times less.

Table 2. Michaelis constants K_m and V_{max} of wild-type, S143A, S143T, and HAL_{red} histidine ammonia lyases with L-histidine as substrate [a].

HAL	V_{max} [IU mg^{-1}] [b]	K_m [mM]	$\frac{V_{wild\text{-}type}}{V_{mutant}}$
wild-type	25	5.2 ± 0.8	1
S143A	0.0214	7.5 ± 0.9	1170
S143T	0.00047	3.1 ± 0.6	53100
HAL_{red}	<0.1	–	–

[a] For the determination of the K_m and V_{max} values the substrate concentration in the enzyme assay was varied between 0.5 and 34 mM, and the increase of absorption monitored at 277 nm. The values were determined using Lineweaver-Burk diagrams. [b] IU = international enzyme unit.

Two explanations could account for the slight activity of our mutants with L-histidine: 1) An error in the expression; in other words, misreading the GCC or ACC codons for the TCC codon (serine) could occasionally produce wild-type HAL.[16] 2) The mutants could catalyze a slow deamination of histidine even though they lack the prosthetic group. In the first case the unaltered K_m value would be obvious; in the second case one must postulate that the prosthetic dehydroalanine residue is not involved in the formation of the initial Michaelis complex.

Our conclusions rely on the more dramatic differences in the V_{max} values. While the absence of the dehydroalanine prosthetic group results in almost no activity with L-histidine as substrate, virtually no effect is seen when L-5-nitrohistidine is used as substrate. To make sure that the spectrophotometric enzyme assay does not simulate a conversion, the progress of the reaction was also monitored by ^{1}H NMR spectroscopy. All four HALs catalyzed the conversion of L-5-nitrohistidine into 5-nitrourocanate at a similar rate. However, the reaction slowed down with time and stopped when 5-nitrourocanate reached a concentration of about 1 mM. This product inhibition was verified by kinetic experiments using wild-type HAL as a catalyst and L-histidine as a substrate. 5-Nitrourocanate inhibited the reaction with a K_i value of 0.6 mM, which is about ten times lower than the K_m value for the substrate.

The conversion of L-5-nitrohistidine was also confirmed by preparative experiments with both the wild-type and the mutant histidine ammonia lyases. After denaturation and removal of the protein, the pH of the reaction mixture was adjusted to 1.0. In all three experiments about the same amount of 5-nitrourocanic acid crystallized as orange-brown cubes.[17]

The reactivity of the mutants lacking dehydroalanine and the sodium borohydride-treated enzyme with L-5-nitrohistidine as substrate rules out the mechanism in which the α-amino group of histidine attacks this electrophilic group.[1] The results of Klee et al.,[13] together with ours, suggest that the only function of the dehydroalanine prosthetic group lies in enhancing the acidity of the β-H_{Re} atom and hence facilitating the formation of the corresponding carbanion.

Besides its α-amino group histidine has still another nucleophilic site, namely the imidazole nucleus, which could react with the electrophilic dehydroalanine. The nucleophilic reactivity of imidazole in an enzymatic reaction was discovered several years ago.[18] In Scheme 2 a mechanism is shown starting with an electrophilic substitution at the 5-imidazole position by the dehydroalanine side chain. This leads to the immonium intermediate **1** in which the H atoms at the two carbon centers are activated. Abstraction of the β-H_{Re} proton by a basic group of the enzyme is followed by elimination of ammonia. In the last step (indicated only by arrows) the dehydroalanine–urocanate adduct fragments to urocanate and HAL under regeneration of the prosthetic group. Reversible abstraction of the likewise acidified 5-H atom in the immonium intermediate **1** could account for the exchange of this atom with solvent deuterium.[9, 10]

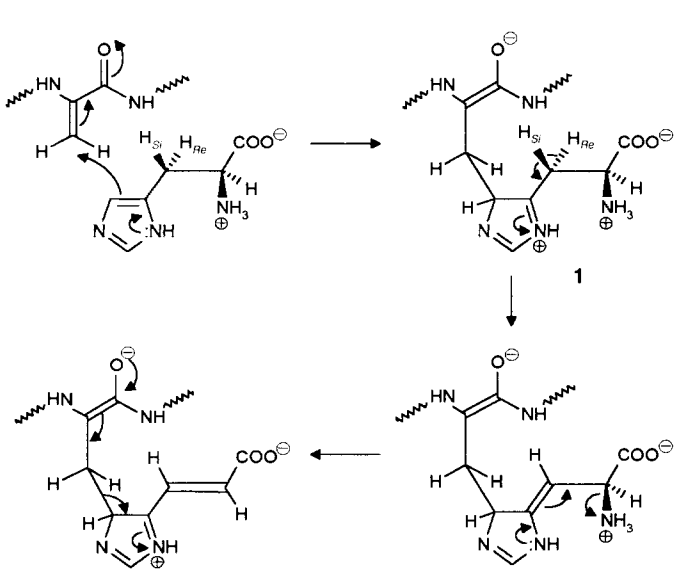

Scheme 2. Proposed mechanism of the HAL-catalyzed transformation of L-histidine into urocanic acid.

As mentioned earlier the activity of the imidazole 5-position is precedented in the urocanase reaction in which the electrophile is a prosthetic NAD^+ molecule.[18] Although in the case of HAL the postulated covalent adduct has not yet been observed directly, the indirect evidence and the chemical plausibility are very convincing. Such a mechanism is also in accord with the strong inhibition of HAL by L-cysteine and L-homocysteine.[11, 12] In these amino acids the sulfur nucleophile is positioned at the correct distance (compared with the imidazole 5-position of histidine) to attack the electrophilic dehydroalanine center. Recently we proposed a mechanism for the irreversible inhibition by these amino acids in the presence of oxygen.[15]

Since circular dichroism measurements indicate that the three-dimensional structure is not changed in our S143A and S143T mutants relative to that of wild-type HAL,[5, 15] their reactivity with L-5-nitrohistidine is readily explained by the more acidic nature of the β-H_{Re} proton in this substrate. Thus the nitro group fulfills the same task as the dehydroalanine prosthetic group and renders it unnecessary.

Received: March 18, 1995 [Z 7807 IE]
German version: *Angew. Chem.* **1995**, *107*, 1585–1587

Keywords: dehydroalanine · enzyme catalysis · histidine · reaction mechanisms

[1] K. R. Hanson, E. A. Havir, *Enzymes 3rd Ed. 1970*– **1972**, 7, 75, 166.
[2] R. G. Taylor, H. L. Levy, R. R. McInnes, *Mol. Biol. Med.* **1991**, *8*, 101.
[3] I. L. Givot, T. A. Smith, R. H. Abeles, *J. Biol. Chem.* **1969**, *244*, 6341.
[4] R. B. Wickner, *J. Biol. Chem.* **1969**, *244*, 6550.
[5] M. Langer, G. Reck, J. Reed, J. Rétey, *Biochemistry* **1994**, *33*, 6462.
[6] B. Schuster, J. Rétey, *FEBS Lett.* **1994**, *349*, 252.
[7] T. A. Smith, F. H. Cordelle, R. H. Abeles, *Arch. Biochem. Biophys.* **1967**, *120*, 724.
[8] J. Rétey, H. Fierz, W. P. Zeylemaker, *FEBS Lett.* **1970**, *6*, 203.
[9] T. Furuta, H. Takahashi, Y. Kasuya, *J. Am. Chem. Soc.* **1990**, *112*, 3633.
[10] T. Furuta, H. Takahashi, H. Shibasaki, Y. Kasuya, *J. Biol. Chem.* **1992**, *267*, 12600.
[11] C. B. Klee, *Biochemistry*, **1974**, *13*, 4501.
[12] D. Hernandez, J. G. Stroh, A. T. Phillips, *Arch. Biochem. Biophys.* **1993**, *307*, 126.
[13] C. B. Klee, K. L. Kirk, L. A. Cohen, *Biochem. Biophys. Res. Commun.* **1979**, *87*, 343.
[14] C. B. Klee, K. L. Kirk, P. McPhie, L. A. Cohen, *J. Biol. Chem.* **1975**, *250*, 5033.
[15] M. Langer, A. Lieber, J. Rétey, *Biochemistry* **1994**, *33*, 14034.
[16] P. Schimmel, *Acc. Chem. Res.* **1989**, *22*, 232–233.
[17] ^{1}H NMR data for 5-nitrourocanic acid: (^2H_2O, $p^2H = 11.2$, 250 MHz): $\delta = 7.85$ (d, $J = 21$ Hz, 1H, β-H), 7.4 (s, 1H, 2-H), 6.6 (d, $J = 21$ Hz, 1H, α-H).
[18] J. Klepp, A. Fallert-Müller, K. Grimm, W. E. Hull, J. Rétey, *Eur. J. Biochem.* **1990**, *192*, 669.

 © VCH Verlagsgesellschaft mbH, D-69451 Weinheim, 1995 0570-0833/95/1313-1465 $ 10.00+.25/0

Solubilized Derivatives of C_{195} and C_{260}: The First Members of a New Class of Carbon Allotropes $C_{n(60+5)}$**

Lyle Isaacs, Paul Seiler, and François Diederich*

Dedicated to Professor Hans-Jürgen Bestmann on the occasion of his 70th birthday

As part of our program on the synthesis, chemistry, and material properties of new carbon allotropes,[1] we became interested in fullerene–acetylene hybrid systems.[2] As first targets we chose members of the family of allotropes with the molecular formula $C_{n(60+5)}$, which can be viewed as adducts of *cyclo*-C_n[3] and C_{60}, and synthesized by the oxidative cyclization of a diethynylmethanofullerene..[2] Thus, the smallest member in this family, C_{195} (**1**), consists of a *cyclo*-C_{15} core surrounded by three peripheral fullerenes, whereas C_{260} (**2**) is a *cyclo*-C_{20} derivative with four fullerenes attached. Structures related to the proposed carbon allotropes, in which the fullerene end-capping groups are exchanged for C_2H_4 fragments, have recently been reported by Scott, de Meijere, and coworkers.[4]

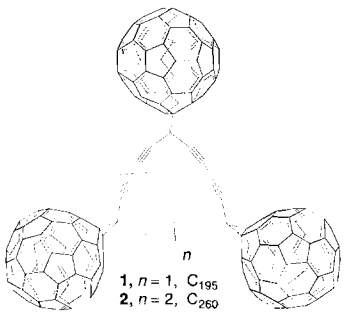

Although **1** and **2** were expected to be stable compounds, their synthesis by oxidative coupling of 61,61-diethynylmethanofullerene[60] failed, and resulted in an intractable mixture of insoluble compounds.[2] Therefore, we decided to prepare derivatives of **1** and **2** bearing solubilizing groups on the fullerene spheres. In order to avoid a mixture of diastereomeric macrocycles, solubilizing functional groups in the diethynylmethanofullerene cyclization component needed to be attached so that the two free ethynyl groups were chemically equivalent. Taking advantage of our recently developed tether-directed remote functionalization methodology,[5] we targeted a C_{2v}-symmetrical diethynylmethanofullerene, which would give isomerically pure derivatives of **1** and **2** upon oxidative cyclization. By this methodology we had previously prepared the hexaadduct **3**, whose X-ray crystal structure has now been solved. Here we give preliminary information on the solid-state structure of **3**, and report the preparation of **4** and **5**, the first derivatives of the carbon allotropes C_{195} (**1**) and C_{260} (**2**), as well as matrix-assisted laser-desorption-ionization time-of-flight (MALDI-TOF) mass spectrometric studies, which suggest that **4** and **5** may be direct precursors to the cyclocarbons *cyclo*-C_{15} (**6**) and *cyclo*-C_{20} (**7**).

A stereoview of the X-ray structure of **3** with its six addends, one of which is disordered, is shown in Figure 1.[6] The largest deformations on the C_{60} surface occur within the six-bridged pyracylene subunits, as expected. Bridgehead 6–6 bond lengths of the cyclopropane rings range from 1.591(3) Å to 1.617(3) Å; those of the cyclohexene rings amount to 1.596(3) Å. They are in good agreement with corresponding bond lengths between bridgehead atoms reported for other methanofullerenes[7] and fullerene Diels–Alder adducts.[8] Significant deformations also occur in the remaining part of the C_{60} skeleton. The eight six-

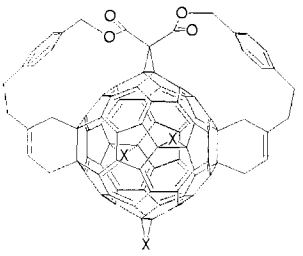

3, X = EtO_2CCCO_2Et

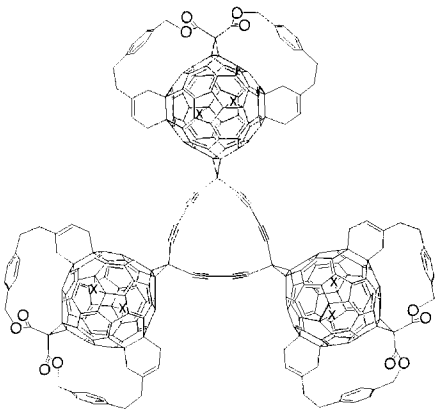

4, X = $(EtO_2CCH_2O_2C)_2C$

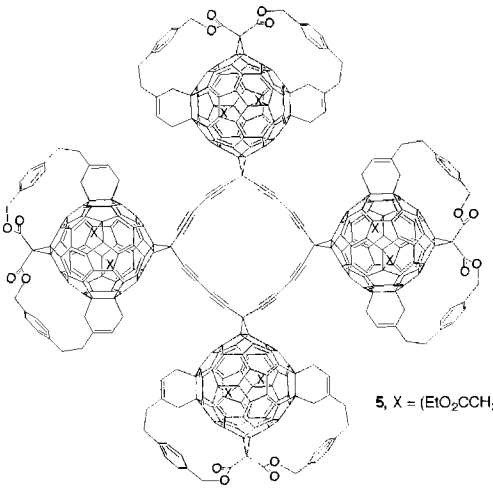

5, X = $(EtO_2CCH_2O_2C)_2C$

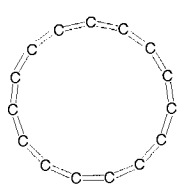

6, *cyclo*-C_{15}

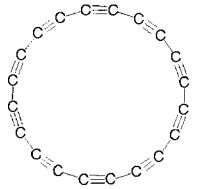

7, *cyclo*-C_{20}

[*] Prof. F. Diederich, L. Isaacs, P. Seiler
Laboratorium für Organische Chemie, ETH Zentrum
Universitätstrasse 16, CH-8092 Zürich (Switzerland)
Telefax: Int. code + (1)632-1109

[**] This work was supported by the Schweizerische Nationalfonds zur Förderung der wissenschaftlichen Forschung. We thank Dr. W. Amrein and H.-U. Hediger for the MALDI-TOF mass spectra.

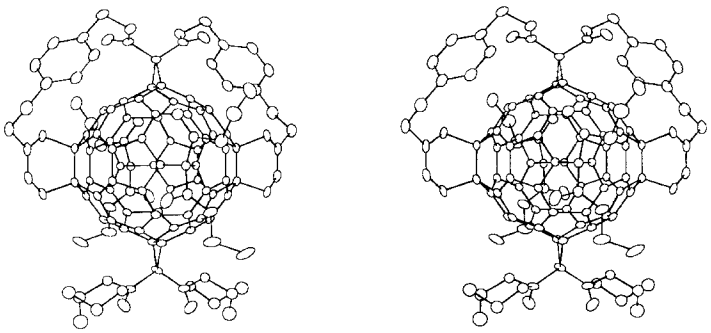

Fig. 1. Stereoview of the X-ray crystal structure of **3**.

membered rings not bridged to any of the functional groups are located at the corners of a cubic cyclophane-type network. The average length of 6–6 and 6–5 bonds within these rings is 1.386 and 1.426 Å, respectively, and the inter-ring, biphenyl-type bond length averages 1.471 Å. With respect to an I_h C_{60}-skeleton, the bond length alternation in these six-membered rings is reduced from about 0.07 (in C_{60}) to 0.04 Å. The same trend has been observed in the crystal structures of two analogous hexaadducts[7d, 9] and interpreted as an indication that these six-membered rings have become more benzene-like.

As a starting material for the synthesis of solubilized derivatives of **1** and **2**, we initially chose the C_s-symmetrical tetraadduct **9**.[5] Its precursor, trisadduct **8**,[5] is now available in 1.3 g batches (60% yield) by performing the tether-directed double Diels–Alder reaction at about 0.6 mM concentration, a sixfold increase over the previously reported concentration. To prepare a C_{2v}-symmetrical pentaadduct for the subsequent introduction of a diethynylmethano group, **9** was treated with diethyl α-bromomalonate in PhCl at 20 °C in the presence of 1,8-diazabicyclo[5.4.0]undec-7-ene (DBU)[5, 10] to give a mixture of two fullerene pentaadducts C_{2v} **11** and C_s **12** in a ratio of 80:20 (70%, Scheme 1). In CH_2Cl_2 at −40 °C a ratio of 75:25 was obtained, while in CCl_4 at 20 °C the selectivity was increased to 91:9.

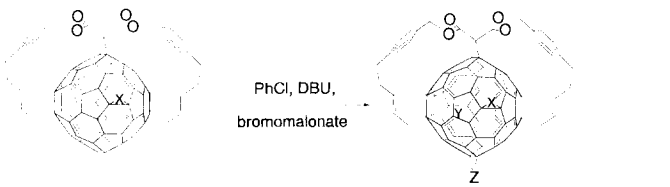

Scheme 1. Synthesis of pentaadducts of C_{60}.

These results were relatively surprising since, to a first approximation, each of the two reactive 6–6 bonds has three addends located in equatorial positions, which were expected to exert similar activating effects.[11] Close examination of the molecular structure of **9** (Scheme 1) revealed that the more reactive bond is doubly e_{face} and singly e_{edge} while the less reactive bond is doubly e_{edge} and singly e_{face} with regard to the addends already in place (Fig. 2). This is the first experimental evidence for the enhanced reactivity of e_{face} bonds over e_{edge} bonds, which had been predicted in computational studies.[7d] Unfortunately, the R_f values of **11** and **12** were identical, and their chromatographic separation on SiO_2 was not possible.

We therefore decided to add the more polar bromomalonate **16**, prepared from **15** (Scheme 2), to trisadduct **8**, hoping to generate a larger difference in the R_f values of the isomeric C_{2v}- and C_s-symmetrical pentaadducts. Reaction of **16** with **8** following the reported procedure[5, 10] gave tetraadduct **10** in 70% yield. Also formed were trace quantities of three isomeric products which could be separated easily by chromatography on silica gel H (CH_2Cl_2). Further reaction of **10** with **16** (Scheme 1) gave the C_{2v}- and C_s-symmetrical pentaadducts **13** and **14** in a relative ratio of 71:29 along with trace quantities of a third product. Satisfyingly, separation of the isomeric mixture was readily achieved by column chromatography on silica gel H (CH_2Cl_2/AcOEt 100:1.5). The structures of C_{2v} **13** and C_s **14** are supported by the presence of 16 (17 expected) and 30 (32 expected) ^{13}C NMR resonances for the fullerene C atoms, as well as the presence of two chemically nonequivalent CH_2CO_2Et groups (in a 1:1 ratio) for **13** and three (in a 1:1:2 ratio) for **14** in the ^1H NMR spectra. In the MALDI-TOF spectrum of both compounds, the molecular ion appeared as the base peak at $m/z = 1712$ along with weaker peaks resulting from fragmentation of the malonate groups. The C_{2v} isomer **13** is pale orange, while the C_s isomer **14** is orange-red in CH_2Cl_2 solution; accordingly, the UV/Vis spectra of the two compounds are quite different: the end-absorption of **13** occurs at $\lambda = 550$ nm and of **14** at $\lambda = 590$ nm.[12]

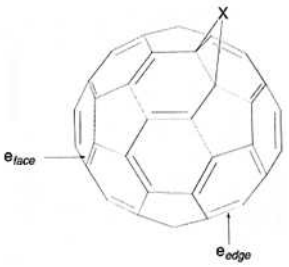

Fig. 2. Depiction of the difference between e_{face} and e_{edge} bonds in a hypothetical monoadduct $C_{60}X$. The e_{face} bond sees the face of the bridging addend, whereas the e_{edge} bond sees its edge.

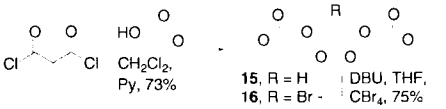

Scheme 2. Synthesis of a polar bromomalonate for the Bingel reaction.

The introduction of the diethynylmethano group was achieved by the reported ionic route[2a] via nucleophilic addition/elimination of 1,5-bis(trimethylsilyl)-3-bromopenta-1,4-diyne (Scheme 3). The reaction was found to be quite solvent dependent: under the conditions used for the monoaddition to C_{60} (toluene, 20 °C), no significant conversion of **13** occurred, and only partial conversion was achieved in THF as solvent. When the reaction was conducted in Me_2SO, however, a very

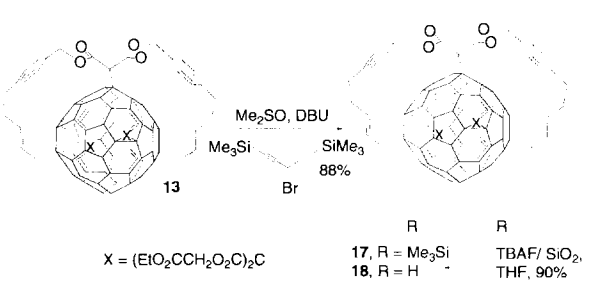

Scheme 3. Synthesis of the C_{2v}-symmetrical diethynylmethanofullerene **18**.

clean conversion was achieved, and the desired dialkynylmethanofullerene hexaadduct **17** was obtained in 88% yield (Scheme 3).

The ^{1}H NMR spectrum of **17** in $CDCl_3$ showed only a single Me_3Si resonance, and the presence of 17 fullerene C-atom resonances in the ^{13}C NMR spectrum provided conclusive proof of the depicted C_{2v} symmetry. The MALDI-TOF mass spectrum showed the expected molecular ion at $m/z = 1918$, but the base peak was the fragment at $m/z = 1711$ resulting from loss of the diethynylmethylene group from the molecule, which regenerates the pentaadduct ion **13**$^+$. Attempts to deprotect **17** under basic conditions (K_2CO_3, MeOH/THF) led to products resulting from cleavage of the ester groups. However, reaction of **17** with tetrabutylammonium fluoride (TBAF, 2.75 equiv) on SiO_2 in anhydrous THF gave the free diethynyl derivative **18** in 90% yield (Table 1) after chromatography on silica gel H (CH_2Cl_2/AcOEt 100:1.5). The successful use of TBAF illustrates that hexaadducts of C_{60} have dramatically reduced reactivity towards nucleophilic attack by fluoride anions, relative to the unsubstituted carbon sphere.

Oxidative cyclization of **18** ($c = 0.3$ mM) under Glaser–Hay conditions (CuCl, *N,N,N′,N′*-tetramethylethylenediamine (TMEDA), air, CH_2Cl_2) failed to produce isolable amounts of cyclic oligomers. However, when a solution of **18** ($c = 0.16$ mM) was subjected to the Eglinton–Glaser coupling conditions[13] (200 equiv of anhydrous $Cu(OAc)_2$, dry pyridine, under Ar), two major products were detected by TLC (SiO_2, $R_f = 0.28$ and 0.15 in CH_2Cl_2/AcOEt 100:5). Isolation of the two yellow compounds was achieved by chromatography on silica gel H (CH_2Cl_2/AcOEt 100:5 then 100:8.5), and their structures were established as cyclic trimeric D_{3h}-**4** and cyclic tetrameric D_{4h}-**5**, based on their spectroscopic properties. The ^{1}H NMR spectra of both oligomers showed no peaks for terminal acetylenic H atoms, two independant sets of CH_2CO_2Et peaks, and one set of peaks for the tether-cyclohexene moiety. In the ^{13}C NMR spectrum, 17 resonances were visible for the fullerene C atoms. This implies local C_{2v} symmetry, which, when combined with a single peak for the bridging methano C atom and only two acetylenic carbon resonances, indicated overall D_{nh} symmetry. The shapes of the UV/Vis spectra of **4** and **5** are almost identical and very similar to those reported previously for fullerene hexaadducts[5, 7d] with the exception of the molar extinction coefficients, which increase as the number of fullerene moieties per molecule increases.

The size of the cyclic oligomers was determined by MALDI-TOF mass spectrometry. In the spectrum of **4** (Fig. 3) the expected molecular ion appeared at $m/z = 5317$ ($C_{348}H_{174}O_{60}$ requires 5314)[14] along with weaker peaks at higher masses, which can be ascribed to matrix adducts of the cyclic oligomer.

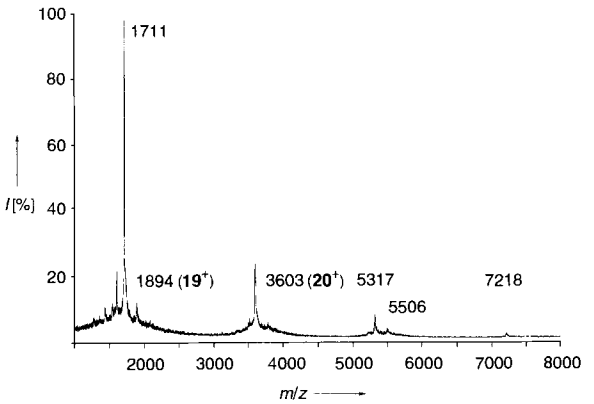

Fig. 3. MALDI-TOF mass spectrum of **4** measured in the linear positive ion mode at 25 kV acceleration voltage with α-cyano-4-hydroxycinnamic acid as the matrix. The peak at $m/z = 5506$ corresponds to a matrix adduct of **4** ($C_{359}H_{181}O_{63}N$ requires 5503), the peak at $m/z = 7218$ to an adduct of **4** with the matrix and fragment **13** ($C_{469}H_{239}O_{83}N$ requires 7214).

Strong fragment ions confirmed the large propensity of dialkynylmethanofullerenes to undergo retroaddition with loss of the fullerene, which was already noted for **17** and **18**. The base peak in the spectrum of **4** appeared at $m/z = 1711$, which corresponds to the fullerene pentaadduct ion **13**$^+$. This very interesting fragmentation also explains the relatively intense fragment ions at $m/z = 3603$ ($C_{237}H_{116}O_{40}$ requires 3602) and 1894 ($C_{126}H_{58}O_{20}$ requires 1891), which arise from the loss of one and two fullerene pentaadducts **13** to generate ions corresponding to bis- and monofullerene adducts of *cyclo*-C_{15}, respectively. Unfortunately, it was not possible to observe a peak for *cyclo*-C_{15}^+ itself, because matrix peaks severely obscured the spectrum in the mass region around $m/z = 180$. The corresponding spectrum recorded without matrix assistance did not yield further information since, at the required higher laser power, significant fragmentation of the solubilizing groups occurred, once again obscuring the mass region around $m/z = 180$.

The mass spectrum of the cyclization product with the lower R_f value did not give a molecular ion peak at masses expected for tetrameric, pentameric, or hexameric cyclic oligomers. However, a very weak peak was observed at $m/z = 5385$ ($C_{353}H_{174}O_{60}$ requires 5374) and a relatively strong one at

Table 1. Selected physical data of compounds **18**, **4**, and **5** [a, b].

4: Yellow solid; m.p. > 250 °C. $R_f = 0.28$ (silica gel, CH_2Cl_2/AcOEt 100:5); IR (KBr): 1751 (C=O) cm^{-1}; ^{1}H NMR ($CDCl_3$, 300 MHz): $\delta = 7.16$ (br s, 24H), 6.19 (t, $J = 5.4$, 6H), 5.22 (br s, 12H), 4.77 (s, 12H), 4.71 (s, 12H), 4.24 (q, $J = 7.2$, 12H), 4.20 (q, $J = 7.2$, 12H), 3.25 (d, $J = 5.4$, 12H), 3.10–2.85 (br m, 12H), 1.28 (t, $J = 7.2$, 18H), 1.26 (t, $J = 7.2$, 18H); ^{13}C NMR ($CDCl_3$, 125 MHz): $\delta = 166.45$, 166.43, 162.82, 162.75, 162.57, 155.97, 155.25, 145.81, 145.43, 145.39, 144.59 (br), 144.18, 143.30 (br), 143.15 (br), 142.49, 139.71, 139.49, 139.12 (br), 138.66, 131.66, 130.29, 128.32 (br), 125.17, 88.41, 71.77, 70.42, 68.64, 67.77, 65.99, 62.26, 62.22, 61.74, 61.69, 61.63, 61.61, 45.20, 44.77, 42.34 (br), 39.17 (br), 34.84 (br), 34.09 (br), 21.19, 14.13; UV/Vis (CH_2Cl_2): λ_{max} (ε) = 337 sh (155000), 312 sh (201000), 291 (209000), 250 nm sh (227000); MALDI-TOF MS: m/z 5317 (7%, M^+), 3603 (21, $[M-13]^+$), 1894 (11, $[M-213]^+$), 1711 (100, [**13**$^+$]).

5: Yellow solid; m.p. > 250 °C. $R_f = 0.15$ (silica gel, CH_2Cl_2/AcOEt 100:5). IR (KBr): 1752 (C=O) cm^{-1}; ^{1}H NMR ($CDCl_3$, 300 MHz): $\delta = 7.18$ (br s, 32H), 6.17 (t, $J = 5.0$, 8H), 5.23 (br s, 16H), 4.78 (s, 16H), 4.68 (s, 16H), 4.24 (q, $J = 7.2$, 16H), 4.17 (q, $J = 7.2$, 16H), 3.21 (d, $J = 5.0$, 16H), 3.10–2.90 (br m, 16H), 1.29 (t, $J = 7.2$, 24H), 1.24 (t, $J = 7.2$, 24H); ^{13}C NMR ($CDCl_3$, 75 MHz): $\delta = 166.47$, 166.43, 162.80, 162.67, 155.78, 155.24, 145.84, 145.78, 145.55, 145.02, 144.23, 143.30, 143.22, 142.50, 139.76, 139.45, 139.11, 138.51, 131.69, 130.33, 128.36 (br), 124.80, 75.77, 70.39, 69.49, 68.66, 68.52, 66.01, 62.32, 62.23, 61.74, 61.68, 61.63, 45.18, 44.84, 42.37, 39.26, 34.84, 34.24, 19.84, 14.14, 14.09; UV/Vis: (CH_2Cl_2): λ_{max} (ε) = 337 sh (202000), 311 (280000), 291 (292000), 250 nm sh (322000); MALDI-TOF MS: m/z 5385 (1%, $[M-13]^+$), 3666 (17, $[M-213]^+$), 1952 (10, $[M-313]^+$), 1734 (48, [**13** + Na]$^+$), 1711 (100, [**13**$^+$]).

18: Yellow solid; m.p. > 270 °C. $R_f = 0.21$ (silica gel, CH_2Cl_2). IR (KBr): 2119 (C≡C), 1751 (C=O) cm^{-1}; ^{1}H NMR ($CDCl_3$, 200 MHz): $\delta = 7.15$ (br s, 8H), 6.16 (t, $J = 5.2$, 2H), 5.21 (br s, 4H), 4.77 (s, 4H), 4.71 (s, 4H), 4.24 (q, $J = 7.2$, 4H), 4.18 (q, $J = 7.2$, 4H), 3.21 (d, $J = 5.2$, 4H), 3.10 - 2.85 (br m, 12H), 2.42 (s, 2H), 1.28 (t, $J = 7.2$, 6H), 1.23 (t, $J = 7.2$, 6H); ^{13}C NMR ($CDCl_3$, 125 MHz): $\delta = 166.53$, 166.48, 162.87, 162.80, 162.66, 155.88, 155.22, 145.84, 145.52, 145.49, 144.04, 143.35 (br), 143.21 (br), 142.49, 139.56, 139.51, 139.10 (br), 139.03, 131.67, 130.29, 128.36 (br), 125.02, 76.89, 71.84, 70.34, 68.63, 65.99, 62.27, 62.23, 61.71, 61.64, 61.63, 61.60, 45.20, 44.67, 42.34, 39.46, 34.83, 34.12, 18.37, 14.14, 14.06; UV/Vis (CH_2Cl_2): λ_{max} (ε) = 353 sh (18700), 308 sh (53400), 286 nm (65600); MALDI-TOF MS m/z 1772 (100%, M^+), 1711 (87, [**13**$^+$]).

[a] MALDI-TOF MS spectra were measured using 2,5-dihydroxybenzoic acid or α-cyano-4-hydroxycinnamic acid as the matrix. [b] New compounds in Schemes 1 and 2 were fully characterized by ^{1}H and ^{13}C NMR, FT-IR, EI-MS, and correct elemental analysis or high-resolution MS.

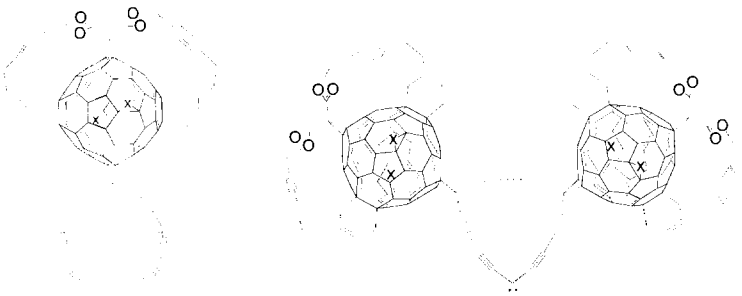

$m/z = 3666$ ($C_{242}H_{116}O_{40}$ requires 3662). In analogy to the fragmentation pattern observed in the spectrum of cyclic trimeric **4**, these peaks correspond to ions formed by the loss of one and two molecules of pentaadduct **13** from cyclic tetrameric **5**. The peak at $m/z = 1952$ ($C_{131}H_{58}O_{20}$ requires 1951) results from the loss of a third equivalent of **13** and corresponds to the ion of an adduct between the fullerene derivative **13** and *cyclo*-C_{20}. These characteristic fragment peaks provide strong support for the cyclic tetrameric structure **5** assigned to the oligomer with the lower R_f value. Just as in the spectrum of the cyclic trimeric **4**, matrix peaks prevented the unambiguous observation of a peak for free *cyclo*-C_{20}^+. The formation and observation of free *cyclo*-C_{15} and *cyclo*-C_{20} ions, starting from **4** and **5** respectively, and their gas phase ion–molecule coalescence reactions are now being further investigated by Fourier-transform mass spectrometry (FT-MS), a technique that had previously been successfully applied to the study of other cyclocarbon molecules.[3b, 15] Continuing studies are also directed toward the synthesis of less highly and reversibly functionalized derivatives of C_{195} and C_{260} and, ultimately, target the preparation of the free carbon allotropes C_{195} (**1**) and C_{260} (**2**).

Experimental Procedure

4 and **5**: To a suspension of 4 Å molecular sieves (8 g) in pyridine (380 mL) containing anhydrous $Cu(OAc)_2$ (2.345 g, 12.91 mmol) under Ar was added **18** (114.4 mg, 0.065 mmol) in pyridine (20 mL) over 3.75 h by syringe pump. After 20 h the reaction mixture was poured into toluene (300 mL), washed with aqueous $CuSO_4$ and saturated aqueous NaCl, and dried ($MgSO_4$). Column chromatography (silica gel H) eluted with CH_2Cl_2/AcOEt 100:5 gave a yellow fraction of **4**, while elution with CH_2Cl_2/AcOEt 100:8.5 afforded a yellow fraction of **5**. Upon addition of cyclohexane and concentration, the products precipitated. Washing with cyclohexane gave **4** (37.1 mg, 32%), and **5** (23.8 mg, 21%), both as yellow solids.

Received: March 8, 1995 [Z 7773 IE]
German version: *Angew. Chem.* **1995**, *107*, 1636–1639

Keywords: carbon allotropes · *cyclo*-C_n compounds · fullerenes

[1] a) F. Diederich, Y. Rubin, *Angew. Chem.* **1992**, *31*, 1123–1146; *Angew. Chem. Int. Ed. Engl.* **1992**, *31*, 1101–1123; b) F. Diederich, *Nature (London)* **1994**, *369*, 199–207.

[2] a) H. L. Anderson, R. Faust, Y. Rubin, F. Diederich, *Angew. Chem.* **1994**, *106*, 1427–1429; *Angew. Chem. Int. Ed. Engl.* **1994**, *33*, 1366–1368; b) Y.-Z. An, Y. Rubin, C. Schaller, S. W. McElvany, *J. Org. Chem.*, **1994**, *59*, 2927–2929.

[3] a) F. Diederich, Y. Rubin, C. B. Knobler, R. L. Whetten, K. E. Schriver, K. N. Houk, Y. Li, *Science* **1989**, *245*, 1088–1090; b) S. W. McElvany, M. M. Ross, N. S. Goroff, F. Diederich, *ibid.* **1993**, *259*, 1594–1596; c) F. Diederich, Y. Rubin, O. L. Chapman, N. S. Goroff, *Helv. Chim. Acta* **1994**, *77*, 1441–1457.

[4] a) L. T. Scott, M. J. Cooney, C. Otte, C. Puls, T. Haumann, R. Boese, P. J. Carroll, A. B. Smith III, A. de Meijere, *J. Am. Chem. Soc.* **1994**, *116*, 10275–10283; b) A. de Meijere, S. Kozhushkov, C. Puls, T. Haumann, R. Boese, M. J. Cooney, L. T. Scott, *Angew. Chem.* **1994**, *106*, 934–936; *Angew. Chem. Int. Ed. Engl.* **1994**, *33*, 869–871.

[5] L. Isaacs, R. F. Haldimann, F. Diederich, *Angew. Chem.* **1994**, *106*, 2434–2437; *Angew. Chem. Int. Ed. Engl.* **1994**, *33*, 2339–2342.

[6] X-ray crystal data of **3** ($C_{110}H_{60}O_{16}$)·2(C_6H_6), $M_r = 1793.8$): monoclinic space group $C2/c$ (No. 15), $\rho_{calcd} = 1.47\ g\,cm^{-3}$, $Z = 4$, $a = 17.680(4)$, $b = 21.164(4)$, $c = 21.740(4)$ Å, $\beta = 93.63(2)°$, $V = 8118(3)$ Å^3, Enraf–Nonius CAD diffractometer, $Cu_{K\alpha}$ radiation, $\lambda = 1.5418$ Å, $T = 233$ K. Single crystals were obtained by very slow evaporation of a benzene–acetonitrile solution. The structure was solved by direct methods (SHELXTL PLUS) and refined by full-matrix least-squares analysis using an isotropic extinction correction and an exponentially modified weight factor with $r = 5$ Å^2. One of the malonic acid diethyl ester groups is disordered (see Fig. 1). Final $R(F) = 0.049$, $wR(F) = 0.063$ for 663 variables and 6061 observed reflections with $F > 4\sigma(F)$ and $\theta \leq 70°$ (ordered heavy atoms anisotropic, disordered atoms isotropic). Full details of the X-ray crystal structure will be published elsewhere.

[7] a) H. L. Anderson, C. Boudon, F. Diederich, J.-P. Gisselbrecht, M. Gross, P. Seiler, *Angew. Chem.* **1994**, *106*, 1691–1694; *Angew. Chem. Int. Ed. Engl.* **1994**, *33*, 1628–1631; b) J. Osterodt, M. Nieger, F. Vögtle, *J. Chem. Soc. Chem. Commun.* **1994**, 1607–1608; c) E. F. Paulus, C. Bingel, *Acta Crystallogr. Sect. C* **1995**, *51*, 143–146; d) I. Lamparth, C. Maichle-Mössmer, A. Hirsch, personal communication on the X-ray crystal structure of a hexakis[bis(ethoxycarbonyl)methano] adduct of C_{60}; see A. Hirsch, I. Lamparth, T. Grösser, H. R. Karfunkel, *J. Am. Chem. Soc.* **1994**, *116*, 9385–9386.

[8] a) Y. Rubin, S. Khan, D. I. Freedberg, C. Yeretzian, *J. Am. Chem. Soc.* **1993**, *115*, 344–345; b) F. Diederich, U. Jonas, V. Gramlich, A. Herrmann, H. Ringsdorf, C. Thilgen, *Helv. Chim. Acta* **1993**, *76*, 2445–2553; c) P. Belik, A. Gügel, A. Kraus, J. Spickermann, V. Enkelmann, G. Frank, K. Müllen, *Adv. Mater.* **1993**, *5*, 854–856; d) P. Seiler, A. Herrmann, F. Diederich, *Helv. Chim. Acta* **1995**, *78*, 344–354.

[9] P. J. Fagan, J. C. Calabrese, B. Malone, *J. Am. Chem. Soc.* **1991**, *113*, 9408–9409; for a hexaadduct of C_{60} with 2,3-dimethyl-1,3-butadiene, see B. Kräutler, J. Maynollo, *Angew. Chem.* **1995**, *107*, 69–71; *Angew. Chem. Int. Ed. Engl.* **1995**, *34*, 87–88.

[10] C. Bingel, *Chem. Ber.* **1993**, *126*, 1957–1959.

[11] a) A. Hirsch, I. Lamparth, H. R. Karfunkel, *Angew. Chem.* **1994**, *106*, 453–455; *Angew. Chem. Int. Ed. Engl.* **1994**, *33*, 437–438; b) A. Hirsch, *The Chemistry of the Fullerenes*, Thieme, Stuttgart, New York, **1994**.

[12] L. Isaacs, F. Diederich, unpublished.

[13] O. M. Behr, G. Eglinton, A. R. Galbraith, R. A. Raphael, *J. Chem. Soc.* **1960**, 3614–3625.

[14] The calculated highest peak of the molecular ion cluster is given.

[15] Y. Rubin, M. Kahr, C. B. Knobler, F. Diederich, C. L. Wilkins, *J. Am. Chem. Soc.* **1991**, *113*, 495–500.

First Synthesis of 2*H*-Azepine**

Dieter Hamprecht, Kurt Polborn, and Wolfgang Steglich*

Dedicated to Professor Rolf Huisgen on the occasion of his 75th birthday

Of the four possible azepine isomers only 1*H*-azepine **1** and 3*H*-azepine **2** are known so far, from pioneering work by Hafner[1] and Vogel et al.[2] Stimulated by the natural occurrence of 2*H*-azepines,[3] we have now developed a general synthesis for this type of heterocycle, which has led to the preparation of the previously unknown 2*H*-azepine **3**.

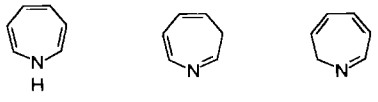

1 **2** **3**

[*] Prof. Dr. W. Steglich, Dipl.-Chem. D. Hamprecht, Dr. K. Polborn
Institut für Organische Chemie der Universität
Karlstrasse 23, D-80333 München (Germany)
Telefax: Int. code + (89)5902-604
e-mail: wos@org-chemie.uni-muenchen.de

[**] We thank Dr. B. Steffan for carrying out the NMR experiments. D. H. thanks the Fonds der Chemischen Industrie for a Doktorandenstipendium.

Hitherto, substituted 2*H*-azepines have been obtained only in some special cases.[4] The pungent 2*H*-azepine alkaloid chalciporone **4** was isolated from the mushroom *Chalciporus piperatus*.[3] In solution **4** readily rearranges at room temperature to the 3*H*-azepine **5** (Scheme 1).

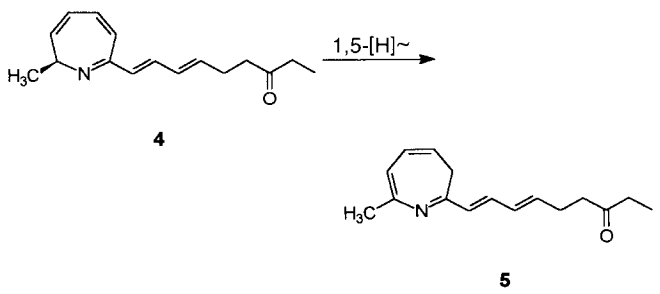

Scheme 1. Formation of the 3*H*-azepine isochalciporone **5** by rearrangement of the 2*H*-azepine chalciporone **4**.

The 2*H*-azepine **3** was synthesized starting from the *N*-Boc-glycine methoxymethylamide **6**,[5] which, according to Weinreb et al.,[6] reacts with 2.7 equivalents of lithiated 4-tetrahydropyranyloxy-1-butyne **7**[7] to give the alkynone **8** (Scheme 2); excess **7** can be recovered. Reduction of the carbonyl group and acetylation of the resulting alcohol gives a high yield of the protected diol **9**, which is then hydrogenated (Lindlar catalyst) to the (*Z*)-alkene. Cleavage of the tetrahydropyranyl ether by pyridinium *para*-toluenesulfonate (PPTS) catalyzed transacetalization with ethylene glycol yields the alcohol **10**.[8] The oxidation of **10** to the β,γ-unsaturated aldehyde **11** presented unexpected difficulties. For instance, the oxidation with pyridinium chlorochromate (PCC), PCC/NaOAc, DMSO/oxalyl chloride/NEt_3, or catalytic quantities of tetrapropylammonium perruthenate/*N*-methylmorpholine-*N*-oxide was unsuccessful; however, the problem of the oxidation was overcome by treating **10** with Dess–Martin periodinane.[9] Attempts to purify **11** by chromatography on silica gel or neutral alumina led to the formation of the (*E*,*E*)-dienal **12** by elimination of acetic acid. According to the ^{1}H NMR spectrum the crude oxidation product contains about 80% **11**. Treatment of this material with trifluoroacetic acid in dichloromethane at low temperature, followed by addition of a base [1,4-diazabicyclo[2.2.2]octane (DABCO) or 4-dimethylamino pyridine (DMAP)] leads to 2*H*-azepine **3** (Scheme 2). Under acidic reaction conditions, the Boc group is cleaved, and condensation to give the cyclic imine and the 1,4-elimination of acetic acid takes place. The cyclization of **11** is favored by the (*Z*)-configuration of the double bond. This is supported by the fact that under the above reaction conditions in the presence of a catalytic amount of iodine the (*E*,*E*)-dienal **12** forms only traces of **3**.

The 2*H*-azepin **3** is difficult to isolate because of its high volatility and instability in pure form. On careful evaporation of an ethereal solution of **3** at 0 °C, we observed a severe loss of product and rapid yellowing of the residue together with a pyridine-like odor. Thus, the yield of **3** is difficult to determine and amounts to approximately 1%, according to the ^{1}H NMR spectrum. For the NMR experiments a solution of **3** in deuterochloroform was obtained by condensation of the volatiles in a cold trap at −78 °C/2 mbar. In contrast to chalciporone **4** and other 2,7-disubstituted 2*H*-azepines, **3** is surprisingly stable in solution. After 48 h at room temperature or 30 min at 60 °C no trace of the thermodynamically favored[4d] 3*H*-azepine **2** could be detected. After standing at room temperature for one week the solution turned yellow. The structure of **3** was confirmed by NMR spectroscopy (^{1}H NMR: Fig. 1 and Table 1,

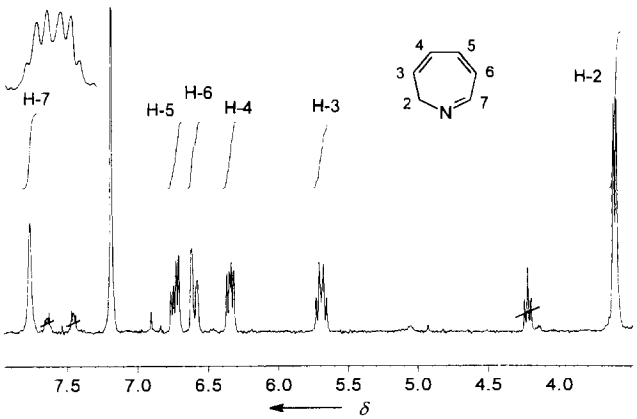

Fig. 1. ^{1}H NMR spectrum of **3** (300 MHz, $CDCl_3$). The signal of H-7, showing the complex coupling pattern, is enlarged (600 MHz, CD_2Cl_2, 270 K).

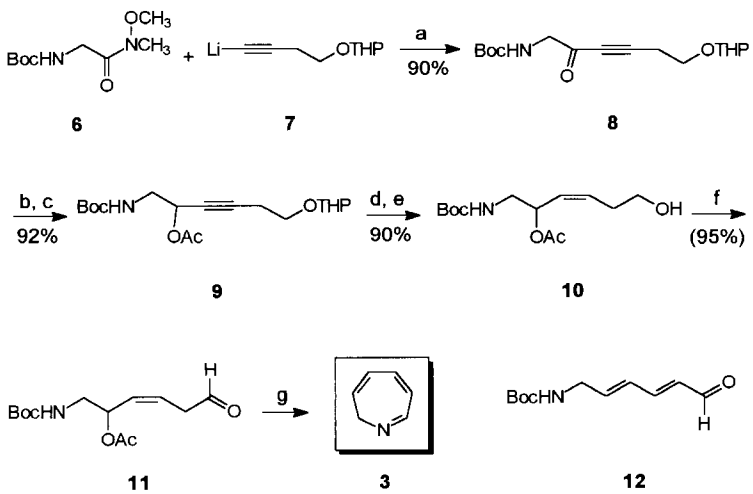

Scheme 2. Synthesis of 2*H*-azepine **3**. a) THF, −78 °C → −50 °C, 90 min, then dilute acetic acid; b) $NaBH_4$, MeOH, 0 °C, 1 h; c) Ac_2O, pyridine, cat. DMAP, CH_2Cl_2, 25 °C, 50 min; d) glycol, DME, cat. PPTS, 70 °C, 135 min (94% conversion); e) quinoline poisoned Lindlar catalyst, C_6H_6, H_2 (1 bar), 25 °C, 3 h; f) Dess–Martin periodinane, CH_2Cl_2, 25 °C, 30 min; g) trifluoroacetic acid, CH_2Cl_2 or $CDCl_3$, −10 °C, 4 h, then DMAP or DABCO.

Table 1. ^{1}H NMR data (300 MHz, $CDCl_3$; coupling constants *J* determined at 600 MHz in CD_2Cl_2) and ^{13}C NMR data (151 MHz, $CDCl_3$) of 2*H*-azepine **3**.

H	δ	Pattern	*J* [Hz]	C	δ
2	3.61	dd	6.6, 1.2	2	50.92
3	5.69	dtdd	9.3, 6.6, 0.9, 0.9	3	126.74
4	6.35	ddd	9.3, 5.4, 1.3	4	129.25
5	6.74	dddd	11.2, 5.4, 1.1, 1.1	5	136.73
6	6.60	dddd	11.2, 3.0, 1.1, 1.1	6	130.76
7	7.84	ddt	3.0, 1.2, 1.2	7	158.53

^{13}C NMR: Table 1, H-H-COSY, C-H-COSY, NOESY) and GC-MS. The signal of the atom H-7 is remarkable, resembling a broadened singlet; however, the coupling pattern of the signal is revealed upon observation of the ^{1}H NMR spectrum (600 MHz) of **3** at 270 K in dichlorodideuteromethane at higher resolution (Fig. 1).

From the nonvolatile residue of the reaction mixture 3,4,4a,9-tetrahydro-3,3-dimethyl-1*H*-[1,3]oxazino-[3,4-*a*]azepin-1-one **13** (Scheme 3) can be isolated in 5 to

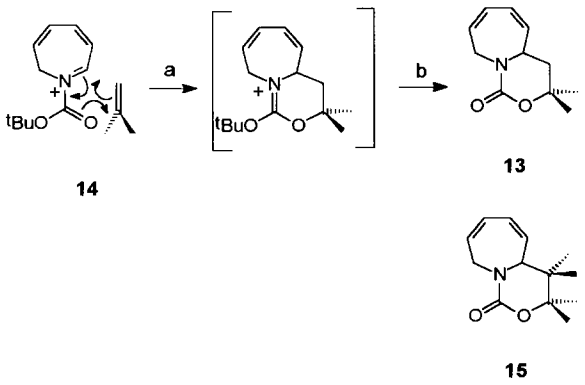

Scheme 3. Proposed mechanism of the formation of **13**: a) [2 + 4]cycloaddition; b) liberation of isobutene and deprotonation.

10% yield from **11**. The structure of **13** was assigned by NMR spectroscopy (^{1}H NMR, ^{13}C NMR, H-H-COSY, DEPT) and mass spectrometry and confirmed by crystal structure analysis[10] (Fig. 2). It seems plausible that **13** results from a [2 + 4]cycloaddition between the isobutene formed in situ and

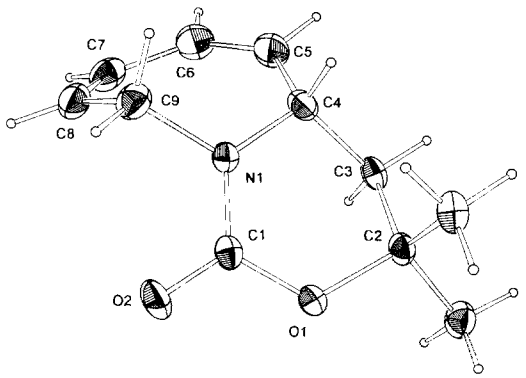

Fig. 2. ORTEP representation of the crystal structure of **13**.

the immonium ion **14** (Scheme 3). Similar Diels–Alder reactions of *N*-acylimmonium compounds are well known.[11] On addition of excess 2,3-dimethyl-2-butene to the reaction mixture, besides some **13** (**15**:**13** ≙ 7:1), 3,4,4a,9-tetrahydro-3,3,4,4-tetramethyl-1*H*-[1,3]oxazino[3,4-*a*]azepin-1-one **15** is formed in 11% yield. Surprisingly, the seven-membered ring can be formed prior to deprotection of the amino group.

Our synthetic route offers a flexible access to a variety of substituted 2*H*-azepines, including the natural product **4**, which will be reported at a later date.

Experimental Procedure

3: In a dry Schlenk flask **11** (0.16 g, 0.50 mmol; about 85% pure) in $CDCl_3$ (2.0 mL) was cooled to −11 °C. Trifluoroacetic acid (0.24 mL) and molecular sieves 4 Å (0.09 g) were added, and the red solution was stirred for 3.5 h at −11 °C (TLC control). Then the solution was cooled to −20 °C and DABCO (0.42 g, 3.7 mmol) was added, which caused the solution to turn yellow. The volatile components were distilled in vacuo (2 mbar) at room temperature and collected in a cold trap (−78 °C). The solution containing **3** was dried for a short time over $MgSO_4$ and used directly to determine the physical data. ^{1}H and ^{13}C NMR: Table 1; UV/Vis (Et_2O): λ_{max} = 306, 247, 214 nm; GC-MS: retention time = 5.1 min (column: Fissons DB 1701, 15 m × 0.25 mm, 30 °C, 15 psi He), *m/z* (%): 94.1 (7), 93.1 (100) [M^+], 92.1 (20), 78.1 (6), 67.1 (10), 66.1 (42), 65.1 (37), 63.1 (8), 51.0 (5), 41.0 (6), 40.0 (20), 39.0 (32), 38.0 (9).

13: The nonvolatile residue of the reaction mixture of **3** was dissolved in *tert*-butylmethyl ether, washed with water and brine, dried ($MgSO_4$), and the solvent was removed in vacuo. Flash-chromatography (silica gel) afforded **13** as a colorless solid (8 mg, 8%). Crystals suitable for crystal structure analysis (colorless needles) were obtained by slow crystallization from CH_2Cl_2/hexane. M.p. 79–81 °C; ^{1}H NMR (300 MHz, $CDCl_3$): δ = 6.27–6.34 (m, 1H; CH), 5.89–6.07 (m, 2H; 2 CH), 5.74–5.80 (m, 1H; CH), 4.38–4.47 (m, 1H; CH), 4.29 (dd, ^3J(H,H) = 14.6, 6.7 Hz, 1H, CH_2), 3.61 (dd, ^3J(H,H) = 14.6, 4.9 Hz, 1H; CH_2), 2.02 (dd, ^3J(H,H) = 13.8, 5.7 Hz, 1H; CH_2), 1.74 (dd, ^3J(H,H) = 13.8, 11.0 Hz, 1H; CH_2), 1.40 (s, 3H; CH_3), 1.37 (s, 3H; CH_3); ^{13}C NMR (75 MHz, $CDCl_3$): δ = 152.90, 135.57, 132.01, 126.49, 126.89, 76.41, 56.10, 45.24, 39.43, 28.99, 24.97; IR (film): $\tilde{\nu}$ = 2980, 1690, 1370, 1170 cm^{-1}; FAB-MS: *m/z*: 194 [M + H$^+$].

Received: March 10, 1995 [Z 7787 IE]
German version: *Angew. Chem.* **1995**, *107*, 1639–1641

Keywords: azepines · Diels–Alder reactions · heterocycles

[1] K. Hafner, *Angew. Chem.* **1963**, *75*, 1041–1050.
[2] E. Vogel, H.-J. Altenbach, J.-M. Drossard, H. Schmickler, H. Stegelmeier, *Angew. Chem.* **1980**, *92*, 1053–1054; *Angew. Chem. Int. Ed. Engl.* **1980**, *19*, 1015.
[3] O. Sterner, B. Steffan, W. Steglich, *Tetrahedron* **1987**, *43*, 1075–1082; W. Steglich, H. Bauer, M. Grosse-Bley, R. Jeschke, J. Josten, J. Klein, *J. Heterocycl. Chem.* **1990**, *27*, 107–110.
[4] a) K. Narasimhan, P. R. Kumar, T. Selvi, *Heterocycles* **1984**, *22*, 2751–2755; b) A. Albini, G. Bettinetti, G. Minoli, *J. Am. Chem. Soc.* **1991**, *113*, 6928–6934; c) K. Satake, R. Okuda, M. Hashimoto, Y. Fujiwara, I. Watadani, H. Okamoto, M. Kimura, S. Morosawa, *J. Chem. Soc. Chem. Commun.* **1991**, 1154–1156; d) K. Satake, R. Okuda, M. Hashimoto, Y. Fujiwara, H. Okamoto, M. Kimura, S. Morosawa, *J. Chem. Soc. Perkin Trans. 1* **1994**, 1753–1757; e) The 2*H*-azepine published by A. Krebs, H. Colberg, U. Höpfner, H. Kimling, J. Odenthal, *Heterocycles* **1979**, *12*, 1153–1156 is the 3*H*-isomer. We thank Prof. Dr. A. Krebs, Hamburg, for this information.
[5] D. T. Davies, P. J. O'Hanlon, *Synth. Commun.* **1988**, *18*, 1173–1180.
[6] S. Nahm, S. M. Weinreb, *Tetrahedron Lett.* **1981**, *22*, 3815–3818.
[7] M. V. Sargent, S. Wangchareontrakul, *J. Chem. Soc. Perkin Trans. 1* **1990**, 1429–1434.
[8] Compounds **8**–**10** and the isolated intermediates were fully characterized and gave satisfactory elemental analyses.
[9] D. B. Dess, J. C. Martin, *J. Am. Chem. Soc.* **1991**, *113*, 7277–7287.
[10] Crystal structure analysis of **13**: 0.16 × 0.20 × 0.93 mm, monoclinic, space group *Cc*, a = 1764.8(8), b = 728.0 (3), c = 814.7 (3) pm, V = 1.0466 nm^3, Z = 4, ρ_{calcd} = 1.223 g cm^{-3}, 4° < 2θ < 46°, λ ($Mo_{K\alpha}$) = 0.71073 Å, 23 °C, ω data collection, 1455 independant reflections, 1292 [$I > 3\sigma(I)$] reflections observed, Lp-correction, structure solution: SHELXS-86, refinement: MolEN, 125 free parameters, hydrogen atoms were allowed to ride on their parent atoms, U = 1.3 × binding atom, R = 0.0345, R_w = 0.0413, refined against |F|, residual electron density = −0.324 × 10^6 to 0.245 × 10^6 e$^-$ pm^{-3}. Further details of the crystal structure investigation may be obtained from the Director of the Cambridge Crystallographic Data Centre, 12 Union Road, GB-Cambridge CB2 1EZ, on quoting the full journal citation.
[11] For a review see: S. M. Weinreb, P. M. Scola, *Chem. Rev.* **1989**, *89*, 1525–1534.

 © VCH Verlagsgesellschaft mbH, D-69451 Weinheim, 1995 0570-0833/95/1313-1471 $ 10.00+.25/0

Lyotropic Phases Formed by "Molecular Bottlebrushes"**

Matthias Wintermantel, Karl Fischer, Markus Gerle, Roland Ries, Manfred Schmidt,* Kanji Kajiwara, Hiroshi Urakawa, and Isao Wataoka

The polymerization of macromonomers (that is, end-functionalized oligomers, Scheme 1) has been a matter of extensive research in order to prepare well-defined comblike polymers.[1]

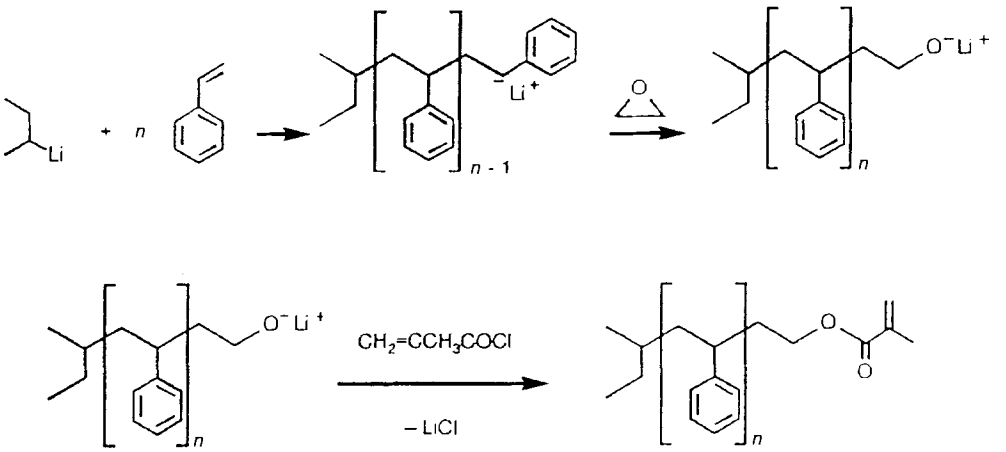

Scheme 1. Reaction scheme for the preparation of the macromonomers.

However, the homopolymerization of macromonomers did not yield degrees of polymerization significantly exceeding the length of a macromonomer itself, unless copolymerized with conventional small monomers. A major breakthrough was achieved by Tsukahara et al., who in a radical mechanism homopolymerized anionically prepared oligostyrenes with molar masses between 10^3 and 10^4 g mol^{-1} that were end-functionalized with methacryloyl groups and obtained degrees of polymerization (weight average) P_w of up to 1000.[2] Recent structure characterization of such long-chain polymacromonomers revealed that the main chain exhibits an almost rodlike conformation as measured by the Kuhn statistical segment length of $l_k > 1000$ Å.[3] Apparently, the extended structure of the polymethacrylate (PMA) main chain is caused by the strong overcrowding of the oligostyrene side chains, which are only separated by a contour distance $l = 2.5$ Å at the polymer backbone. Also, because of the length of the side chains, the diameter or cross-section of this curved cylindrical macromolecule or "bottlebrush" is quite large ($d \approx 70-150$ Å for a side chain of molar mass $M_n = 3950$ g mol^{-1}, dependent on whether hydrodynamic data or X-ray investigations of the cross-sectional radius of gyration were used for the determination of diameter).[3] Still, the aspect ratio L_w/d (L_w is the weight-averaged contour length, $L_w = P_w \cdot l$, and d the diameter of the chain) is of the order of 10–50 for most of the samples, and accordingly, such polymers should form liquid-crystalline phases.

Here we report on X-ray scattering measurements of the polymacromonomers in toluene performed at the synchroton source in Tsukuba, Japan, which indeed show the formation of lyotropic phases, probably nematic, in semi-concentrated solution. The investigated polymacromonomer sample had a molar mass of $M_w = (2.2 \cdot 10^6)$ g mol^{-1} corresponding to a contour length $L_w = 1400$ Å. The polydispersity index determined by gel permeation chromatography (GPC) was $M_w/M_n \approx 1.5$, and the Kuhn statistical segment length (as measure of chain stiffness) $l_k = 1250$ Å.[3]

Figure 1 shows the X-ray scattering intensity $I(q)$ as a function of the scattering vector q [$q = (4\pi/\lambda \sin(\theta/2)$, where λ is the wavelength in the medium and θ the scattering angle) for polymacromonomer concentrations $0.2 \le c \le 30\%$ (w/w). In the dilute regime $c < 0.5\%$ the form factor $P(q)$ of a single chain is measured: the intensity is seen to decrease monotonically with increasing q. However, the q regime investigated here reflects the scattering pattern of the chain cross-section. With increasing concentrations a shoulder develops into a clearly resolved scattering peak.

Particularly at the highest measured concentration of 31.5%, the width of the scattering peak narrows drastically. The scattering peaks observed at higher concentrations cannot be explained by single-particle scattering but rather reflect the interparticle structure factor $S(q)$ originating from the intermolecular order of the molecules.

On application of Bragg's relation, a mean distance d_B between the scattering planes (100) of hexagonal order is obtained from the scattering peak at q_{max} [Eq. (a)]. The mean par-ticle distance d_2 is then derived from Equation (b). In order to

$$d_B = 2\pi/q_{max} \quad \text{(a)}$$

$$d_2 = 2d_B/\sqrt{3} \quad \text{(b)}$$

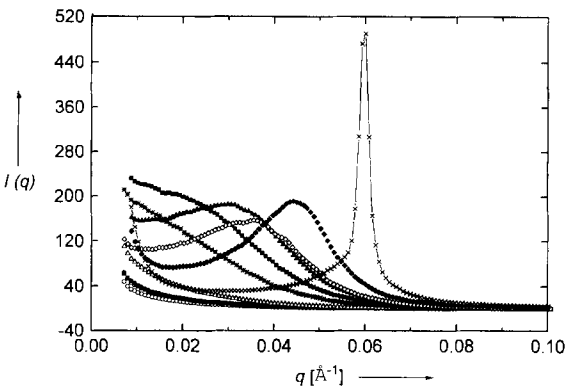

Fig. 1. X-ray scattering intensity $I(q)$ in arbitrary units as a function of the scattering vector q for different polymacromonomer concentrations in wt%: ○ 0.306%, □ 0.393%, ● 0.481%, △ 0.964%, * 4.93%, ■ 8.0%, ▲ 10.7%, ◇ 12.3%, ◆ 19.8%, × 31.5%.

[*] Prof. Dr. M. Schmidt, Dr. M. Wintermantel, Dr. K. Fischer, M. Gerle, Dr. R. Ries
Makromolekulare Chemie II der Universität
D-95440 Bayreuth (Germany)
Telefax: Int. code + (921) 55-3393
Prof. Dr. K. Kajiwara, Dr. H. Urakawa, Dr. I. Wataoka
Kyoto Institute of Technology
Kyoto 606 (Japan)

[**] Financial support by the Deutsche Forschungsgemeinschaft and by the Fonds der Chemischen Industrie is gratefully acknowledged (M. W. and M. S.).

compare the present results with earlier investigations on the tabacco mosaic virus (TMV)[4] and on poly-γ-benzylglutamate (PBG),[5] a reduced plot of d_2/d_0 (d_2 is the mean distance between the particles and d_0 their "hard-core" diameter) versus the volume fraction of solute is shown in Figure 2. Since a hard-core

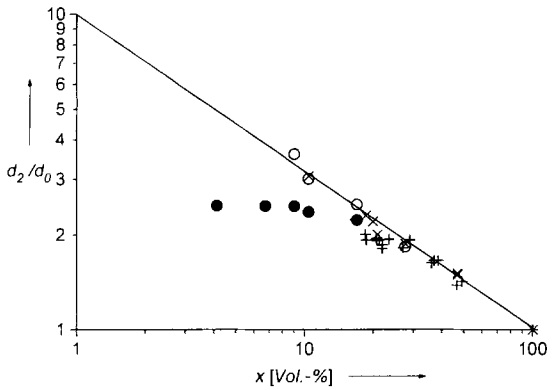

Fig. 2. Reduced interparticle distance d_2/d_0 vs. the volume fraction of polymer: × TMV [4], + PBG [5], ●, ○ polymacromonomer. The mean distance $\bar{d}_2$ is derived from $I(q)$ (×, +, ○) or from $S(q)$ (●) as explained in the text.

diameter for the polymacromonomer is impossible to define (because of the radially decaying segment density), a value of d_0 of 67 Å is assumed in order to obtain an approximate superposition with the other curves. This value of d_0 compares well with the cross-sectional radius of gyration $R_{g,c} = 36.4$ Å as determined by X-ray scattering ($d_{g,c} = 72.8$ Å[3]). For comparison, the hypothetical "hard-core" diameter of a molecule with the bulk density $\rho = 1.05\ g\,cm^{-3}$ of polystyrene would amount to $d_2 = 57$ Å, and the hydrodynamically effective cross-section as determined by diffusion measurements to $d_h = 150$ Å. The solid line shows the expected scaling relation for the packing of parallel cylinders [Eq. (c)].

$$d_2/d_0 \approx c^{-1/2} \qquad \text{(c)}$$

The observed agreement of the relative spacing as a function of the volume fraction for the polymacromonomer (PBG and TMV) is expected, because the aspect ratio L/d of all three systems is of the order of 15. Surprisingly, the data evaluation as described above does not give any evidence for the occurrence of a biphasic (isotropic/anisotropic) regime, which is theoretically predicted by Onsager[6] and Flory[7] at volume fractions between 10–20%, because in the biphasic region the mean distance is expected to be independent of the concentration of polymers.

Although the influence of the decaying single-particle form factor $P(q)$ might seriously influence the position of the maximum intensity, particularly at the lower q values, this has been ignored in the presentation of the data so far. For spherically symmetric particles, the total intensity $I(q)$ is expressed by the product of the particle scattering factor and the structure factor [Eq. (d)]. Equation (d) breaks down for anisotropic particles,

$$I(q) = P(q)\,S(q) \qquad \text{(d)}$$

because the structure factor $S(q)$ becomes a function of $P(q)$ as now the interparticle interference depends on the shape of the single particles, that is, on the spatial distribution of the scattering centers within one macromolecule. Unfortunately, there is no unique solution to this problem except to assume, a priori, a certain density distribution of the molecules and calculate the Fourier transform into q space.

For a preliminary treatment of more detailed data analysis we assume Equation (d) to be approximately valid for our system. Accordingly, the structure factor $S(q) = I(q)/P(q)$ is shown in Figure 3 for the concentrations $c \geq 4.93\%$. To reduce the noise

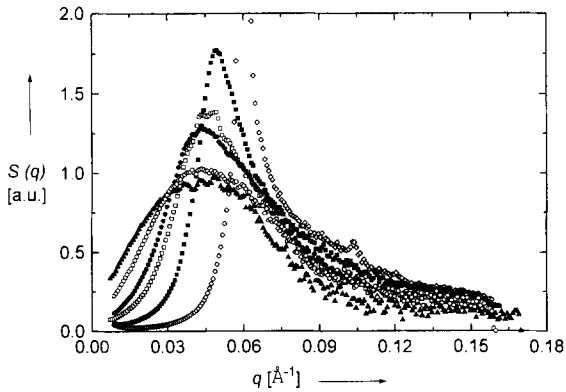

Fig. 3. The static structure factor $S(q)$ in arbitrary units as a function of the scattering vector q for different polymacromonomer concentrations in wt%: △ 4.93%, ○ 8.0%, ● 10.7%, □ 12.3%, ■ 19.8%, ◇ 31.5%. For the highest concentration even higher order peaks are observed with a relative spacing of $d_1:d_2:d_3 = 1:\sqrt{3}:2$, which supports the hexagonal packing.

in the data the single-particle form factor $P(q)$ was evaluated from the average intensities of the concentrations $c = 0.306\%$, 0.393%, and 0.481%. For $c < 12.3\%$ the maximum of the observed broad structure peaks remains approximately constant and increases in intensity with increasing concentration. This is exactly the result expected from the biphasic regime where the volume fraction of the anisotropic phase increases with increasing concentration but the interparticle distance within the ordered phase remains constant. From the position of the maximum, a mean distance of $d_2 = 156$ Å is calculated from Equations (a) and (b), which is interpreted as the mean distance of the cylinders in the ordered part of the biphasic region, that is, between the A and B points. The solution becomes fully anisotropic at concentrations above 12.8% (B point) as now the interparticle separation starts to decrease with increasing concentration as expected ($d_2 \approx c^{-1/2}$, solid line in Fig. 2).

The formation of lyotropic liquid crystals by polymacromonomers is also detected by polarized light microscopy on thin films that were prepared by slow evaporation of the solvent. The resulting pictures shown in Figure 4 (bottom) were developed by exposing the film for 10 min. This documentation of the small optical anisotropy of the particles is explained by an expanded, but still random conformation of the polystyrene side chains, which hardly contribute to the birefringence. Upon heating (see thermal history, Fig. 4 top), the birefringence of the film disappears at 140 °C, which lies significantly above the glass transition temperature of $T_g \approx 100$ °C and does not reappear on slow cooling (which may be due to kinetic effects).

We have reported on a new concept for preparing stiff polymers that form liquid crystals and consist of "commodity" monomers such as styrene and methacrylate. This concept is simply based on the overcrowding of bulky side chains

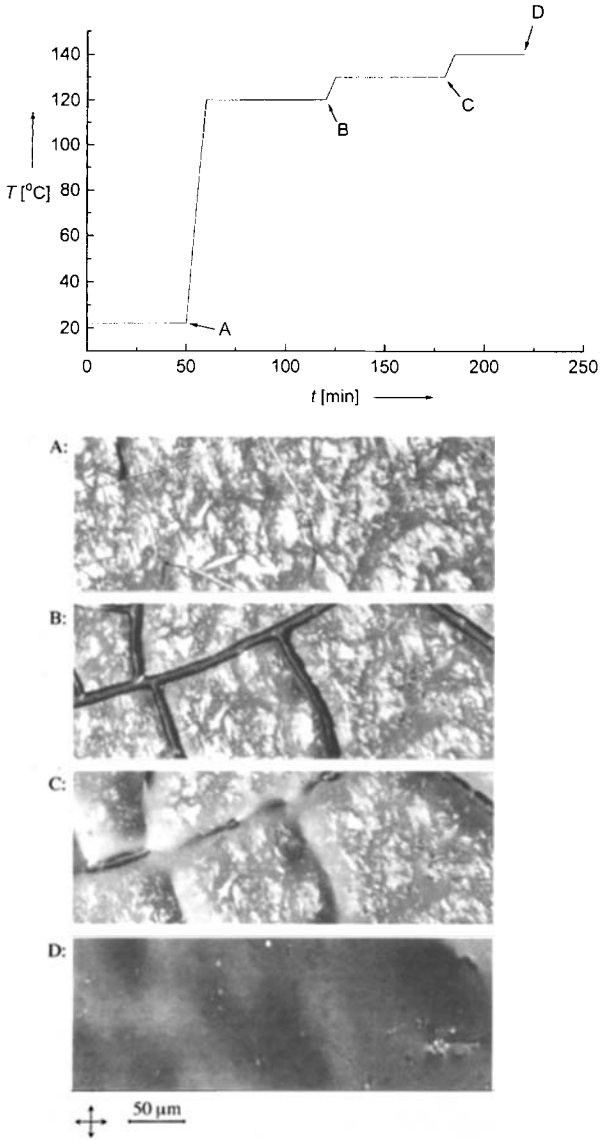

Fig. 4. Top: Thermal history of the anisotropic polymacromonomer film. Bottom: Polarization microscopy pictures at temperatures A–D as depicted above.

which forces the otherwise flexible main chain into a stretched conformation with significantly reduced degrees of freedom.

Received: February 17, 1995 [Z 7724IE]
German version: *Angew. Chem.* **1995**, *107*, 1606–1608

Keywords: liquid crystals · polymacromonomers · polymers · X-ray scattering

[1] P. Chaumont, J. Herz, P. Rempp, *Eur. Polym. J.* **1979**, *15*, 459; Y. Yamashita, *J. Appl. Polym. Sci. Appl. Polym. Symp.* **1981**, *36*, 193; P. Rempp, E. Franta, P. Masson, P. Lutz, *Prog. Colloid Polym. Sci.* **1986**, *72*, 112.
[2] Y. Tsukahara, K. Tsutsumi, S. Yamashita, S. Shimada, *Macromolecules* **1990**, *23*, 5201; Y. Tsukahara, K. Mikano, A. Segawa, Y. Yamashita, *ibid.* **1989**, *22*, 1546; Y. Tsukahara, K. Tsutsumi, Y. Ukamoto, *Macromol. Chem. Rapid. Commun.* **1992**, *13*, 409.
[3] M. Wintermantel, M. Schmidt, Y. Tsukahara, K. Kajiwara, S. Kohjiya, *Macromol. Rapid Commun.* **1994**, *15*, 279; M. Wintermantel, Dissertation, Universität Bayreuth, **1994**; M. Wintermantel, M. Gerle, K. Fischer, M. Schmidt, I. Wataoka, H. Urakawa, K. Kajiwara, Y. Tsukahara, S. Kohjiya, *Macromolecules*, submitted.
[4] J. D. Bernal, I. Fankuchen, *J. Gen. Physiol.* **1941**, *25*, 111.
[5] C. Robinson, *Tetrahedron* **1961**, *13*, 219.
[6] L. Onsager, *Ann. N.Y. Acad. Sci.* **1949**, *51*, 627.
[7] P. J. Flory, *Proc. R. Soc. London Ser. A* **1956**, *234*, 73.

Enhancement of Catalytic Activity for Hydroformylation of Methyl Acrylate by Using Biphasic and "Supported Aqueous Phase" Systems**

Georges Fremy, Eric Monflier, Jean-François Carpentier, Yves Castanet, and André Mortreux*

Among the numerous hydroformylation reactions, those of α,β-unsaturated esters are of particular interest. In this area, much attention has been focused on the hydroformylation of acrylate esters to give 2-formylpropanoate esters, since the latter are used extensively for the synthesis of pharmaceuticals[1] and may also be considered a potential source of the extremely important methacrylate esters (Scheme 1).[2] Generally, rhodium-based homogeneous catalytic systems show good catalytic activities as well as high *iso*/*n* regioselectivities for acrylate esters, and

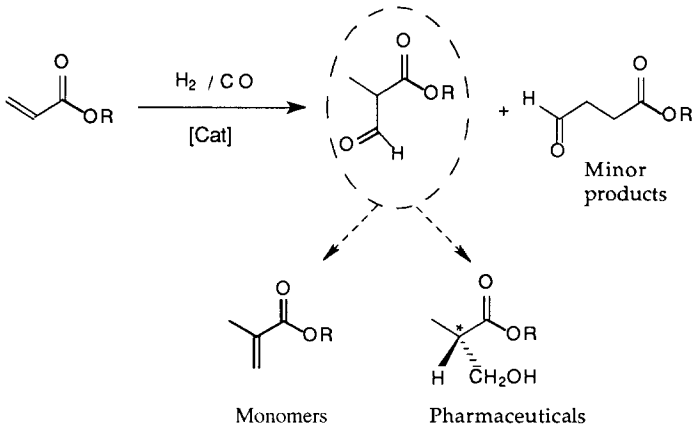

Scheme 1.

many examples have been reported.[3] However, due to the high cost of rhodium, alternative ways for recovering the catalyst have been developed for many hydroformylation reactions, for example through the use of biphasic[4] and "supported aqueous phase" (SAP)[5] systems using water-soluble phosphanes. Despite their advantages, these catalytic systems almost always suffer from poor activities; put simply, they are always far slower than analogous reactions in the homogeneous phase. However, very recently, an acceleration effect on the rhodium-based biphasic hydroformylation of 1-octene using trisulfonated triphenylphosphane (TPPTS) in the presence of triphenylphosphane (TPP) was reported.[6] Under these biphasic conditions, turnover frequencies (TOFs) were almost comparable to those obtained with homogeneous systems.[5e, 6] In this paper, we describe biphasic and heterogeneous catalytic systems for the hydroformylation of methyl acrylate which have much higher activities than the homogeneous variant.

[*] Prof. Dr. A. Mortreux, Dipl.-Chem. G. Fremy, Dr. J.-F. Carpentier, Prof. Dr. Y. Castanet
Laboratoire de Catalyse Hétérogène et Homogène
Université des Sciences et Technologies de Lille, BP 108
F-59652 Villeneuve d'Ascq Cedex (France)
Telefax: Int. code + 20436585
Dr. E. Monflier
Université d'Artois, Faculté des Sciences Jean Perrin, Lens (France)

[**] This work was supported by ELF-ATO Co.

Table 1. Catalytic hydroformylation of methyl acrylate with various systems [a].

Entry	Phosphane	Toluene/Water [mL/mL]	[min] [b]	Yield Methyl propionate [mol %]	Yield Aldehydes [mol %]	α/β ratio [c]	Initial TOF [h^{-1}] [d]
1	TPP	40/0	140	4.6	95.4	> 200	225
2	DPPB	40/0	90	1.5	98.5	102	350
3	TPPMS	40/30	420	12.3	87.7	10	150
4	TPPTS	40/30	120	3.4	96.6	128	545
5 [e]	TPPTS	40/30	120	3.6	96.4	115	583
6	DPPBTS	40/30	180	68.3	31.7	> 200	220
7 [f]	TPPTS/SiO_2	40/0.9	120	3.0	97.0	149	870
8 [f]	TPPTS/SiO_2	40/6	12	5.1	94.9	136	4300
9 [f]	TPPTS/SiO_2	40/10	120	6.6	93.4	148	570

[a] Reaction conditions: 0.2 mmol of $[Rh(acac)(CO)_2]$, 2 mmol (equiv P) of phosphane, 100 mmol of methyl acrylate; $T = 50\,^{\circ}C$; $p = 50$ bar ($CO/H_2 = 1$). [b] Optimized time for total conversion of methyl acrylate. [c] Ratio α-aldehyde/β-aldehyde. [d] Defined as mole of initially converted methyl acrylate per mole of rhodium per hour. [e] $[HRh(CO)(TPPTS)_3]$ was used as catalyst. [f] SiO_2 (60 Å, 490 $m^2 g^{-1}$, 70–230 mesh): 9 g.

We first compared the activities and selectivities obtained with sulfonated phosphanes in the hydroformylation of methyl acrylate under conventional biphasic conditions with those obtained with triphenylphosphane (TPP) and 1,4-bis(diphenylphosphino)butane (DPPB), the ligands typically used under homogeneous conditions (Table 1). The (DPPB)Rh system is the most active and selective (entry 2),[3a] and served as a comparison.

The respective mono- and tetrasulfonated analogues (TPPMS and DPPBTS, respectively) gave lower activities and very poor chemo- and/or regioselectivities for the desired branched aldehyde (entries 3 and 6). This was particularly the case for DPPBTS which led to the predominant formation of the hydrogenated product. Surprisingly, when the trisulfonated triphenylphosphane (TPPTS) was used, we observed a significant increase in the reaction rate relative to that of the homogeneous reaction (cf. entries 1 and 4).[7] Selectivities for the hydroformylated products were similar, and both ligands led almost exclusively to the branched aldehyde. The hydridorhodium(I) species $[HRh(CO)(TPPTS)_3]$ gave comparable results (cf. entries 4 and 5). This indicated the rapid formation of the catalytic species from the precursors under our conditions. To our knowledge, such an increase in activity from the transposition of an homogeneous reaction to aqueous biphasic conditions has never been reported. In fact, catalytic rates under biphasic conditions, even with TPP as promoter ligand,[5e, 6] are almost always lower than those in a homogeneous medium.[4a, 8]

The above findings led us to examine the behavior of SAP systems, in which the catalyst precursors—a rhodium complex and a water-soluble phosphane—are deposited on silica gel with a variable amount of water. Under these conditions, the catalytic rates could be greatly improved. Methyl acrylate could be hydroformylated with an exceptionally high TOF of 2370 h^{-1} (entry 9) compared to 330 h^{-1} for DPPB (entry 2). Typical kinetic data for systems based on TPP derivatives are illustrated in Figure 1.

The results obtained with silica gel supported catalysts were strikingly dependent on the water content (entries 7–9, Fig. 2). The maximum initial activity (4300 h^{-1}) was obtained for a water content of 37% by weight[9] (entry 8); even slight deviations from this water content led to decreased activities. When larger amounts of water were present, the catalytic rates observed were similar to those found under classical biphasic conditions (cf. entries 4 and 9). These results are in sharp contrast with the previously reported examples in which these techniques were employed with higher α-olefins (e.g. heptene, tetradecene).[5] In these studies the activities of heterogeneous catalytic systems were much lower than the corresponding homogeneous systems. We assume that in our case, polar interactions between methyl acrylate and silica gel and/or the water phase supported on the silica gel surface may be responsible for the high catalytic rates observed. In line with this hypothesis, several hydroformylation experiments conducted with propylene, a nonpolar substrate, did not show increased rates of reaction on transposition from biphasic to SAP conditions. Further experiments to confirm the above hypothesis and extend the range of substrates are currently under way.

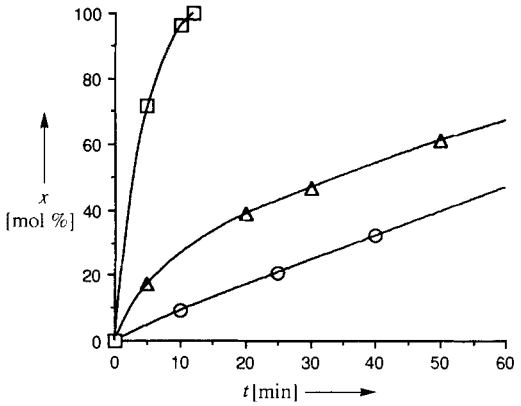

Fig. 1. Conversion x of methyl acrylate as a function of time for TPP (○), TPPTS (△), and TPPTS/SiO_2 (□) rhodium catalyst systems. See Experimental Procedure for reaction conditions.

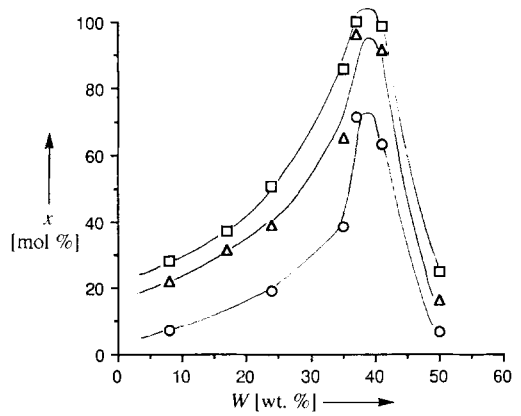

Fig. 2. Conversion x of methyl acrylate as a function of water content W for supported aqueous phase Rh/TPPTS/SiO_2 systems. Reaction times: 5 min (○), 10 min (△), and 15 min (□). See Experimental Procedure for reaction conditions.

Experimental Procedure

Preparation of the reaction mixtures. a) Homogeneous systems: Under an atmosphere of N_2, 0.2 mmol of the rhodium precursor [Rh(acac)$(CO)_2$], 2 mmol (equiv P) of phosphane, and 100 mmol of methyl acrylate were dissolved in 40 mL of toluene. b) Biphasic systems: 0.2 mmol of the rhodium precursor and 2 mmol (equiv P) of phosphane were stirred in 30 mL of water until total dissolution, and then 100 mmol of methyl acrylate in 40 mL of toluene was added. c) Silica gel supported systems: 0.2 mmol of the rhodium precursor and 2 mmol of TPPTS were stirred in 20 mL of water until total dissolution, and then added to 9 g of freshly dried silica. Water was then partially removed under vacuum until the desired water content was reached; this was precisely determined by gravimetric thermal analysis of an aliquot. The resulting powder was mixed with a solution of 100 mmol of methyl acrylate in 40 mL of toluene.

Catalytic reactions: A 100 mL stainless steel autoclave was charged under an atmosphere of N_2 with the reaction mixture, then heated at 50 °C, and pressurised with 50 bar of CO/H_2 (1/1). Mechanical stirring (1000 rpm) with a multipaddle unit was then started. The pressure was kept constant throughout the whole reaction by using a gas reservoir along with a pressure regulator. The reaction was monitored by quantitative gas chromatographic analysis (CP Si 5-CB, 25 m × 0.32 mm).

Received: February 7, 1995 [Z 7698 IE]
German version: *Angew. Chem.* **1995**, *105*, 1608–1610

Keywords: biphasic catalysis · catalysis · hydroformylation · methyl acrylate · rhodium catalysts

[1] a) M. F. Züger, F. Giovannini, D. Seebach, *Angew. Chem.* **1983**, *95*, 1024; *Angew. Chem. Int. Ed. Engl.* **1983**, *22*, 1012; b) K. Nakamura, T. Miyai, K. Ushio, S. Oka, A. Ohno, *Bull. Chem. Soc. Jpn.* **1988**, *61*, 2089.

[2] K. Schwirten, H. W. Schneider, R. Kummer (BASF AG), DE-B 2643205, **1978** [*Chem. Abstr.* **1978**, *89*, 005946].

[3] a) M. Tanaka, T. Hayashi, I. Ogata, *Bull. Chem. Soc. Jpn.* **1977**, *50*, 2351; b) D. Neibecker, R. Réau, *Angew. Chem.* **1989**, *101*, 479; *Angew. Chem. Int. Ed. Engl.* **1989**, *28*, 500; c) E. Drent, A. J. M. Breed (Shell Co.), EP-B 306094, **1989** [*Chem. Abstract* **1989**, *111*, 099367]; d) H. Alper, J.-Q. Zhou, *J. Org. Chem.* **1992**, *57*, 3729; e) H. Yamashita, B. L. Roan, T. Sakakura, M. Tanaka, *J. Mol. Catal.* **1993**, *81*, 255.

[4] a) Review: W. A. Herrmann, C. W. Kohlpaintner, *Angew. Chem.* **1993**, *105*, 1588; *Angew. Chem. Int. Ed. Engl.* **1993**, *32*, 1524; b) B. Fell, G. Papadogianakis, *J. Prakt. Chem.* **1994**, *336*, 591; c) H. Ding, B. E. Hanson, T. Bartik, B. Bartik, *Organometallics* **1994**, *13*, 3761.

[5] a) J. P. Arhancet, M. E. Davis, J. S. Merola, B. E. Hanson, *Nature (London)* **1989**, *339*, 454; b) I. T. Horvath, *Catal. Lett.* **1990**, *6*, 43; c) J. P. Arhancet, M. E. Davis, B. E. Hanson, *J. Catal.* **1991**, *129*, 94; d) *ibid.* **1991**, *129*, 100; e) M. E. Davis, Chemtech **1992**, 498; f) B. B. Bunn, T. Bartik, B. Bartik, W. R. Bebout, T. E. Glass, B. E. Hanson, *J. Mol. Catal.* **1994**, *94*, 157; g) Y. Z. Yuan, J. L. Xu, H. . B. Zhang, K. R. Tsai, *Catal . Lett.* **1994**, *29*, 387.

[6] R. V. Chaudari, B. M. Bhanage, R. M. Deshpande, H. Delmas, *Nature (London)* **1995**, *373*, 501.

[7] The purity of the TPPTS used was carefully controlled. In particular, ^{31}P NMR spectroscopy indicated that this product was not contaminated by unsulfonated ligand (TPP).

[8] P. Kalck, F. Monteil, *Adv. Organomet. Chem.* **1992**, *34*, 219.

[9] Amount of water defined as weight of water in the solid, including silica gel, water, TPPTS, and rhodium precursor.

A Remarkable Effect of Silyl Substitution on Electrocyclization of Vinylallenes

Masahiro Murakami,* Hideki Amii, Kenichiro Itami, and Yoshihiko Ito*

Considerable attention has been directed toward the effects of silyl substituents,[1] which are now widely utilized in a variety of organic reactions.[2] Of these, β-cation stabilization in electrophilic reactions of organosilicon compounds is one of the most exploited. We now report a remarkable effect of silyl substitution on the kinetics and the thermodynamics of the thermal electrocyclization of vinylallenes.

[*] Prof. M. Murakami, H. Amii, K. Itami, Prof. Y. Ito
Department of Synthetic Chemistry, Faculty of Engineering
Kyoto University, Yoshida, Kyoto 606-01 (Japan)
Telefax: Int. code + (75)753-5668

The electrocyclic ring closure of conjugated dienes has been a source of continuing interest from the viewpoints of both organic and theoretical chemistry. 1,3-Butadiene (**1**), an open-chain compound, is thermodynamically favored over cyclobutene (**2**).[3] In contrast, 3,4-bis(alkylidene)cyclobutene (**4**), a ring-closed compound, is favored over bis(allene) (**3**) despite the ring strain (Scheme 1).[4]

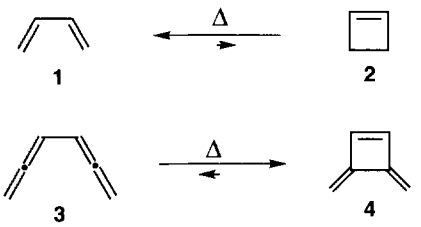

Scheme 1. The equilibrium of thermal electrocyclization of conjugated diene systems.

Interestingly vinylallene, which is structurally intermediate between **1** and **3**, also has an intermediate equilibrium position for the ring closure, and relatively high temperature is required for electrocyclization;[5] Pasto et al. reported that heating of vinylallene **5** produced an equilibrium mixture of **5**:**6** = 19:81 at 360 °C, and of **5**:**6** = 30:70 at 435 °C (Scheme 2).

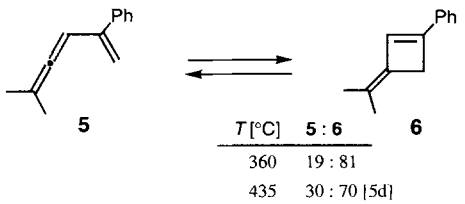

Scheme 2. The thermal electrocyclization of non-silyl-substituted vinylallene **5**.

During the course of our study on the use of the silastannation reaction in synthesis,[6] we found that in marked contrast to **5**, the vinylallene **7a** that differs from **5** only in the silyl substituent at C5 underwent unidirectional electrocyclization[7] at about 145 °C to give (alkylidene)cyclobutene **8a** in 95% isolated yield (Scheme 3). None of **7a** remained after heating for 3 h.

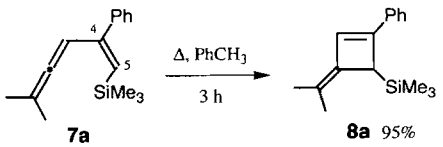

Scheme 3. The facile and unidirectional electrocyclization of silyl-substituted vinylallene **7a**.

This result shows that the ring-closed product **8a** is thermodynamically much more stable than **7a**. Furthermore, the activation energy for electrocyclization is much smaller than that of non-silyl-substituted vinylallene **5**.

Other examples of facile and unidirectional electrocyclization of silyl-substituted vinylallenes are given in Table 1.[8] At reflux in xylene, both *cis* and *trans*-5-silyl-substituted vinylallenes **7** yield (alkylidene)cyclobutenes **8** in high yield.

Table 1. Unidirectional electrocyclization of vinylallenes **7** in xylene at reflux (ca. 145 °).

7	t [h]	8	Yield [%]
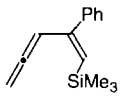 **7b**	2	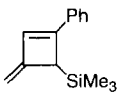 **8b**	99
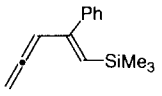 **7c**	2	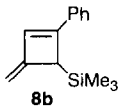 **8b**	90
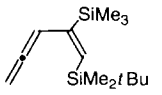 **7d**	15	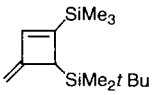 **8d**	95
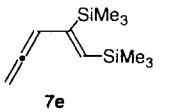 **7e**	12	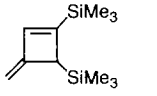 **8e**	98
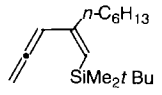 **7f**	21	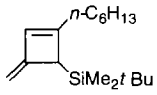 **8f**	85

The trimethylsilyl group of **8a** was removed on treatment with Bu_4NF to produce, in overall high yield from **7a**, (alkylidene)cyclobutene **6**, which was fairly stable up to at least 160 °C[5d] (Scheme 4). The direct electrocyclization of **5** failed to complete conversion.

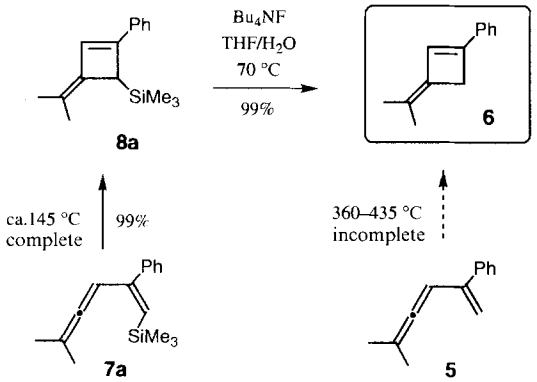

Scheme 4. Efficient synthesis of **6** by electrocyclization of **7a** followed by desilylation.

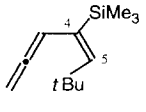
9

The origin of this effect of silyl-substitution is of much interest. For comparison with **7d** and **7e**, vinylallene **9**, having a tertiary butyl group instead of a silyl group at C5, was heated at reflux in xylene. As no (alkylidene)cyclobutene was obtained after heating for 17 h, it is unlikely that electrocyclization is promoted by the steric factor of a silyl group. Besides, the silyl group at C4 does not promote the electrocyclization. Silyl-substituted (alkylidene)cyclobutene **8** has two C–C double bonds. The silyl group is located at the allylic position of both of them. Since hyperconjugation ($\sigma-\pi$ conjugation) is thought to raise the energy of the π system of an allylsilane,[9] it is also difficult to explain the stabilization of **8** in terms of the electronic effect of the silyl group.

Although the origin is equivocal, the present experimental finding exemplifies the significant effect of the introduction of silicon on the thermal electrocyclicization of vinylallenes. Precise theoretical studies on the origin of this effect are currently underway.

Experimental Procedure

7a,b,d, f: See ref. [6].

8a: A solution of **7a** (200 mg, 0.83 mmol) in xylene (3 mL) was heated at reflux for 12 h. The reaction mixture was cooled, reduced in volume, and purified by chromatography on silica gel (hexane) to afford **8a** (190 mg, 95%) as an oil. ^{1}H NMR (200 MHz, $CDCl_3$): $\delta = 0.00$ (s, 9H), 1.71 (s, 3H), 1.79 (s, 3H), 3.19 (s, 1H), 6.60 (s, 1H), 7.15–7.40 (m, 5H); ^{13}C NMR (50 MHz, $CDCl_3$): $\delta = -1.2$, 19.6, 20.3, 38.9, 117.2, 123.9, 125.5, 127.2, 128.1, 133.5, 135.0, 147.6; $C_{16}H_{22}Si$: calcd C 79.27, H 9.15; found C 79.53, H 9.14.

Received: February 16, 1995 [Z 7720 IE]
German version: *Angew. Chem.* **1995**, *107*, 1649–1650

Keywords: cyclobutenes · electrocyclic reactions · silyl effect · vinylallenes

[1] A. R. Bassindale, P. G. Taylor in *The Chemistry of Organic Silicon Compounds, Vol. 2* (Eds.: S. Patai, Z. Rappoport), Wiley Interscience, Chichester, **1989**, p. 893.
[2] E. W. Colvin, *Silicon Reagents in Organic Synthesis*, Academic Press, London, **1989**.
[3] a) T. Durst, L. Breau in *Comprehensive Organic Synthesis, Vol. 5* (Eds.: B. M. Trost, I. Fleming), Pergamon, Oxford, **1991**, p. 675; b) S. Niwayama, K. N. Houk, *Tetrahedron Lett.* **1993**, *34*, 1251, and references therein.
[4] a) H. Hopf, *Angew. Chem.* **1970**, *82*, 703; *Angew. Chem. Int. Ed. Engl.* **1970**, *9*, 732; b) H. Hopf, F. T. Lenich, *Chem. Ber.* **1973**, *106*, 3461; c) D. J. Pasto, S.-H. Yang, *J. Org. Chem.* **1989**, *54*, 3544; d) F. Toda, P. Garratt, *Chem. Rev.* **1992**, *92*, 1685, and references therein.
[5] a) E. Gil-Av, J. Herling, *Tetrahedron Lett.* **1967**, 1; b) H. Hopf, *Nachr. Chem. Tech.* **1975**, *23*, 235; c) R. Schneider, H. Siegel, H. Hopf, *Liebigs Ann. Chem.* **1981**, 1812; d) D. J. Pasto, W. Kong, *J. Org. Chem.* **1989**, *54*, 4028.
[6] M. Murakami, H. Amii, N. Takizawa, Y. Ito, *Organometallics* **1993**, *12*, 4223.
[7] Another facile and unidirectional cyclization of vinylallene has recently been found in a retinoids: J. G. Rey, J. Rodríguez, A. R. de Lera, *Tetrahedron Lett.* **1993**, *34*, 6293.
[8] Vinylallenes unsubstituted at C4 afforded complex mixtures of intractable compounds.
[9] a) C. G. Pitt, *J. Organomet. Chem.* **1973**, *61*, 49; b) J. C. Giordan, *J. Am. Chem. Soc.* **1983**, *105*, 6544; c) J. Yoshida, T. Murata, S. Isoe, *Tetrahedron Lett.* **1986**, *27*, 3373; d) H. Bock, *Angew. Chem.* **1989**, *101*, 1659; *Angew. Chem. Int. Ed. Engl.* **1989**, *28*, 1627.

 © VCH Verlagsgesellschaft mbH, D-69451 Weinheim, 1995 0570-0833/95/1313-1477 $ 10.00+.25/0

C_3-Symmetric Hexakis(trimethylsilyl)[7]phenylene ["Tris(biphenylenocyclobutadieno)cyclohexatriene"], a Polycyclic Benzenoid Hydrocarbon with Slightly Curved Topology**

Roland Boese,* Adam J. Matzger, Debra L. Mohler, and K. Peter C. Vollhardt*

Dedicated to Professor Ivar Ugi on the occasion of his 65th birthday

The phenylenes constitute a new class of [4*n*]annuleno[4*n* + 2]-annulenes composed of alternating fused benzene and cyclobutadiene rings.[1] Several topologies may be envisaged, the simplest being represented by the purely linear, angular, and trigonal frames of **1**,[2] **2**,[3] and **3**.[4] Such π systems activated by

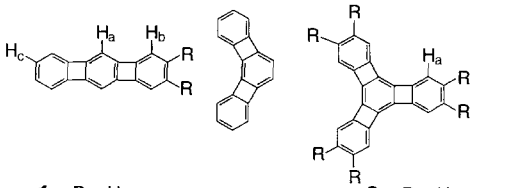

1a, R = H
1b, R = $Si(CH_3)_3$

2

3a, R = H
3b, R = $Si(CH_3)_3$

strain and electronic features are of intrinsic theoretical interest as unique subjects on which to study the relative contributions of σ and π electrons to the structure and reactivity of the "aromatic" benzene ring,[5] and as potential organic molecular magnetic and/or conducting materials.[6] While the linear[7] and angular[8] homologous series of **1** and **2** have been extended up to the [5]phenylenes, **3** is so far the only member with trigonal geometry. Yet, the symmetry of the latter is of particular interest because it leads to orbital degeneracy that, under certain conditions, may provide molecules with a stable triplet ground state, which, if correctly juxtaposed, could impart ferromagnetism on the bulk material.[9]

We present here the total synthesis of the hexasilylated trigonal [7]phenylene **9**, a comparison of its physical properties with those of **1**, **3**, and the unilaterally extended **6** and **7**, and its highly unusual bowed structure. The title compound **9** is the largest phenylene yet known, and model **7** represents a new isomer in the [5]phenylene series (the third of 12 possible structures). The syntheses of both necessitated the use of 1,6-bis(triisopropylsilyl)-1,3,5-hexatriyne (**4**) as the cocyclization partner in the crucial CpCo-catalyzed chain-extension steps,[7b] thus avoiding stepwise elaboration of **3b** in which the central ring is subject to electrophilic attack.

$iPr_3Si-C\equiv C-C\equiv C-C\equiv C-Si iPr_3$ **4**

[*] Prof. Dr. K. P. C. Vollhardt, A. J. Matzger, Dr. D. L. Mohler
Department of Chemistry, University of California at Berkeley
and
The Chemical Sciences Division, Lawrence Berkeley Laboratory
Berkeley, CA 94720 (USA)
Telefax: Int. code + (510)643-5208
Prof. R. Boese
Institut für Anorganische Chemie der Universität-Gesamthochschule
Universitätsstrasse 5–7, D-45117 Essen (Germany)

[**] This work was supported by the National Science Foundation (CHE-9202152), the National Institutes of Health (instrumentation grant S10RR5651A), and the Fonds der Chemischen Industrie. A. J. Matzger acknowledges a Syntex predoctoral fellowship (1994–1995). We thank Prof. A. Streitwieser for helpful discussions.

Schemes 1 and 2 detail the synthetic strategies toward **7** and **9**,[10] starting with the known precursors **5**[4] and **8**, respectively.[11] Noteworthy are the excellent yields in the transformation of **8** to **9** (equivalent to about 73% for each CpCo-catalyzed [2 + 2 + 2]cycloaddition) and the fact that of the thirteen rings in **9**, twelve are made by cobalt catalysis. No sign of the CpCo complexes[7] of **6** and **9** was detected in the cyclizations.

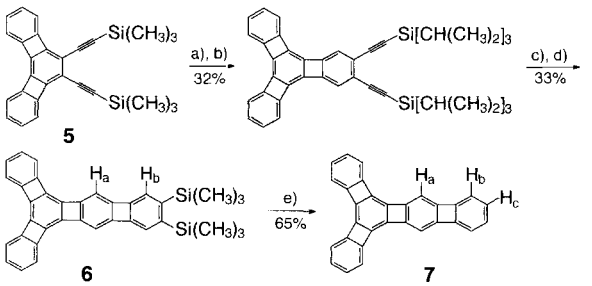

Scheme 1. a) $Bu_4N^+F^-$, THF, toluene, 23 °C, 2h; b) **4** (5 equiv), $[CpCo(CO)_2]$, toluene, Δ, *hv*, 16h; c) $Bu_4N^+F^-$, THF, 23 °C; d) $(CH_3)_3SiC\equiv CSi(CH_3)_3$, $[CpCo(CO_2)]$, THF, Δ, *hv*, 16 h; e) CF_3COOH, CH_2Cl_2, 23 °C, 16 h.

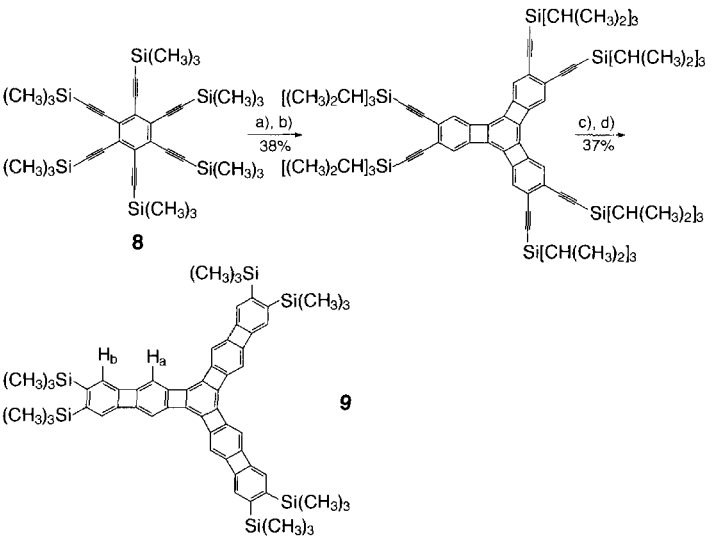

Scheme 2. a) $KF\cdot 2H_2O$, [18]crown-6, DME, 23 °C; b) **4** (7 equiv), $[CpCo(CO)_2]$, toluene, Δ, *hv*, 16 h; c) $Bu_4N^+F^-$, THF, 23 °C, 30 min; d) $(CH_3)_3SiC\equiv CSi(CH_3)_3$, $[CpCo(CO_2)]$, THF, Δ, *hv*, 16 h.

The comparison of the physical properties of the moderately air-stable [5]- and [7]phenylenes (Table 1) with each other and related substructures of the individual systems, in particular **3**, are of interest. It becomes immediately evident that the presence of one linear [3]phenylene unit (for example, **3a** → **7**) induces a relatively large bathochromic shift in the electronic spectrum [$\Delta\lambda_{max}$ (highest wavelength band) = 107 nm], whereas subsequent benzocyclobutadiene annelation causes a relatively attenuated change [for example, **3b** → **9**, corresponding $\Delta\lambda_{max}$ = 133 nm, or **6** → **9**, $\Delta\lambda_{max}$ = 37 nm; the slight incongruence is a consequence of the different degree of silyl substitution]. Similarly, the diagnostic proton chemical shifts for H_a ($CDCl_3$) from **3a** through **6** to **9** decrease by greatly differing increments (δ = 7.18, 6.68, 6.56, respectively), though the corresponding values for H_b in **6** and **9** are almost identical. The observations suggest that there is only a relatively small interaction of the three "outside" biphenylene units in **9** across the central cyclo-

Table 1. Selected physical data for **6**, **7**, and **9**.

6: orange-red flakes (from ethyl acetate), m.p. > 280 °C; UV/Vis (hexanes): λ_{max} (lg ε) = 229 (4.08), 238 (4.11), 258sh (4.27), 268 (4.31), 288sh (4.29), 299 (4.43), 317 (4.27), 331sh (4.24), 351 (4.04), 371sh (4.11), 379 (4.14), 395 (4.29), 430 (3.54), 458 (3.64), 490 (3.65) nm; IR (KBr): $\tilde{\nu}$ = 2965, 2935, 1403, 1250, 1095, 1030, 1013, 848, 797, 739, 679 cm^{-1}; MS (70 eV): *m/z* (%): 518 (M^+, 100), 503 (6), 488 (6), 487 (8), 473 (4), 446 (14), 431 (11), 430 (12), 429 (8), 415 (9); ^{1}H NMR (300 MHz, $CDCl_3$): δ = 7.09–7.22 (ABCDm, 8H), 6.90 (s, 2H), 6.68 (s, 2H), 0.32 (s, 18H); $^{13}C\{^1H\}$ NMR (75 MHz, $CDCl_3$): δ = 153.68, 149.43, 148.86, 148.69, 148.44, 148.11, 128.91, 128.55, 128.42, 128.36, 127.17, 122.22, 119.90, 119.65, 111.40, 2.14. High resolution MS Calcd for $C_{36}H_{30}Si_2$: 518.18861; found: 518.18970.

7: orange-red flakes (from hexanes), m.p. > 270 °C; UV/Vis (CH_2Cl_2): λ_{max} (lg ε) = 224 (4.49), 238sh (4.41), 260sh (4.63), 264 (4.64), 297 (4.68), 313 (4.59), 346 (4.36), 377 (4.45), 392 (4.57), 428 (3.80), 456 (3.94), 486 (3.94) nm; IR (KBr): = 2862, 2828, 1466, 1403, 1348, 1307, 1151, 1099, 961, 856, 735, 618 cm^{-1}; MS (70 eV): *m/z* (%): 374 (M^+, 100), 373 (11), 372 (31), 371 (34), 187 (16), 186 (13), 185 (10), 111 (11), 97 (16), 85 (14), 83 (14), 71 (20), 57 (30); ^{1}H NMR (200 MHz, $CDCl_3$): δ = 7.15–7.21 (ABCDm, 8H), 6.71–6.75 (AA'm, 2H), 6.65 (s, 2H), 6.55–6.59 (BB'm, 2H); ^{1}H NMR (200 MHz, CD_2Cl_2): δ = 7.18–7.28 (ABCDm, 8H), 6.74–6.81 (AA'm, 2H), 6.72 (s, 2H), 6.62–6.67 (BB'm, 2H).

9: red crystals (from THF), m.p. > 250 °C; UV/Vis (hexanes): λ_{max} (lg ε) = 279sh (4.57), 298 (4.69), 332 (4.30), 392sh (4.64), 410 (4.81), 448sh (4.48), 527sh (3.72) nm; IR ($CHCl_3$): $\tilde{\nu}$ = 2953, 2905, 1351, 1311, 1267, 1093, 1039, 1021, 961, 865, 650, 636 cm^{-1}; MS (FAB$^+$): *m/z* (%): 955 (M^+, 41), 401 (36), 326 (43), 281 (55), 221 (100), 207 (68); ^{1}H NMR (300 MHz, $CDCl_3$): δ = 6.92 (s, 6H), 6.56 (s, 6H), 0.34 (s, 54H); $^{13}C\{^1H\}$ NMR (75 MHz, $CDCl_3$): δ = 153.24, 149.53, 148.62, 148.57, 124.66, 122.37, 111.20, 2.18. High resolution FAB-MS Calcd for $C_{60}H_{66}Si_6$: 954.37803; found: 954.37925.

hexatriene, not unlike the situation encountered in **3**.[4] Alternatively, one could interpret the topologies of **6**, **7**, and **9** essentially as perturbed linear [3]phenylenes in which one of the terminal benzene rings (namely that representing the internal core of the **3**-subunit) has been forced into complete bond alternation (as indicated in the resonance structures chosen to depict **6**, **7**, and **9**; see also the X-ray data below). This model leads to the prediction of reduced paratropism in the cyclobutadienoid rings and the expectation that H_a–H_c would be significantly deshielded relative to the corresponding hydrogens in **1a** or **1b** (as references for **7** or **6** and **9**, respectively).[2] Such an effect is indeed observed ($\Delta\delta$ values in $CDCl_3$): (**7**–**1a**) for H_a: 0.41, H_b: about 0.15, H_c: about 0.10; (**6**–**1b**) for H_a: 0.37, H_b: about −0.04; (**9**–**1b**) for H_a: 0.25, H_b: about −0.02. Consistent with this view, the actual chemical shifts of H_a–H_c in **6**, **7**, and **9** are the same as or very close to those in biphenylene and 2,3-bis(trimethylsilyl)biphenylene.[2]

As expected, such subtle trends are not reflected in the ^{13}C NMR data, which are less diagnostic of the presence of ring current effects. Rather, the ^{13}C chemical shifts are readily computed by taking into account cumulative incremental changes along the series of phenylenes **1**–**3**. As exceptions, the central cyclohexatriene carbon atoms in **3b** (δ = 131.23) experience a "long-range shielding effect" of increasing benzocyclobutadiene annelation to **6** (δ = 128) and **9** (δ = 122.37). Considering that the cyclobutadienoid carbon atoms in biphenylene resonate at δ = 151.9, these smaller chemical shifts are remarkable and most likely the result of unusual hybridization at these positions to accommodate σ strain and minimize antiaromatic π contributions.[5a–c]

To gain further insight into how the strain is accommodated in the molecules reported, X-ray structural investigations were performed. Unfortunately in the case of **6**, severe twinning prevented a refinement of the structure beyond its gross features. Gratifyingly, better data were obtained on the more important **9** (Fig. 1).[12] In the unit cell, two molecules stack in a staggered cofacial arrangement with offset centers, seemingly to enable π–π interactions[13] between two internal biphenylene units. The distance between the atoms C12A and C21B of the symmetry related (inversion center) molecules is 3.39 Å, the corresponding value between the two planes of the four-membered rings C5, C6, C19, C24 (ring I) is 3.52 Å, comparable to related separations in biphenylene[14a] and its charge transfer complexes.[14b] There is one molecule of THF associated with (but not contacting) each molecule of **9**.

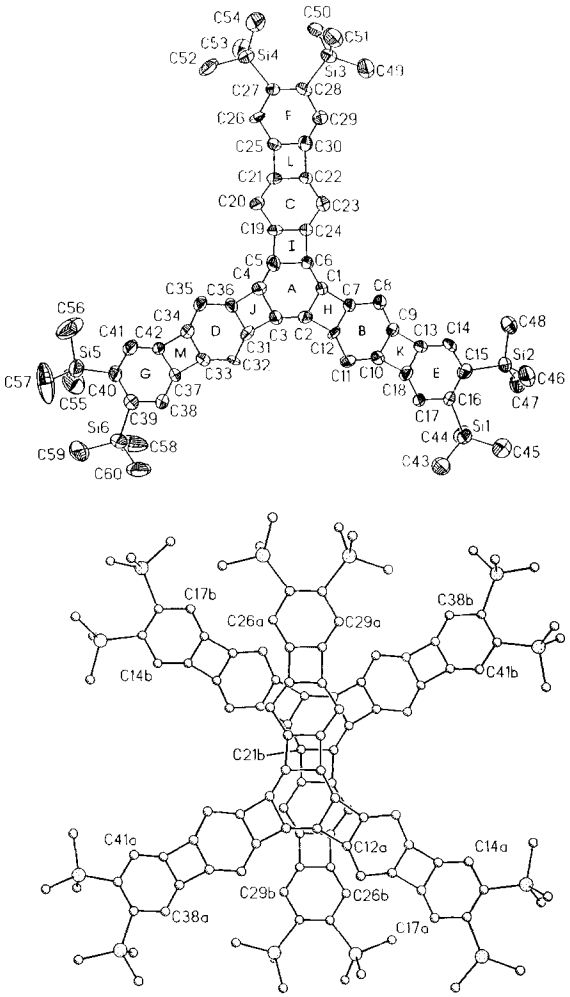

Fig. 1. Molecular structure of **9** (top) and arrangement of the two molecules in the unit cell (bottom).

Most instructive is Figure 2 which depicts the changes that occur on trisbenzocyclobutadiene annelation of **3b** or, alternatively, enforcing bond alternation at one of the terminal benzene rings of **1** by bisbenzocyclobutadiene annelation. In the first comparison, it is immediately apparent that the central six-membered ring in **9** is completely bond localized (1.326, 1.509 Å), arguably (from standard deviations) even more so than that in **3b** (1.335, 1.494 Å).[22] Moreover, the rectangular nature of rings H, I, J is slightly reduced (1.419, 1.485 Å vs. 1.408, 1.501 Å), and the order of bond alternation of the non-fused bonds in rings B, C, D inverted (1.405, 1.377 Å vs. 1.368, 1.417 Å). The terminal benzene rings adopt a geometry close to those of the two reference compounds and even biphenylene itself[15] [when one corrects for the effect of *ortho*-bis(trimethylsilyl) substitution].[16] Taking the tetrasilyl[3]phenylene as a reference point, conversion to the framework of **9** causes a structural alteration in the direction that might be expected from a biphenylene attached to a cyclobutacyclohexatriene. Bearing the caveat of standard deviations and the relatively qualitative nature of such comparisons in mind, but encouraged

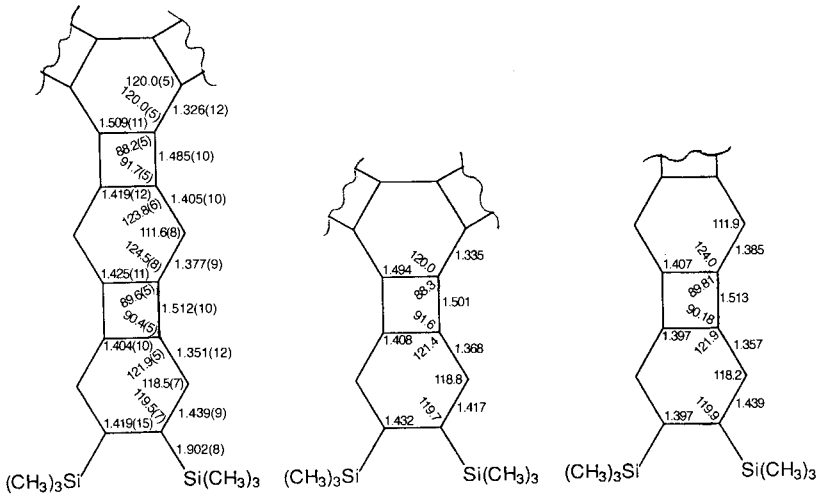

Fig. 2. Averaged (for idealized symmetry) selected bond distances [Å] and angles [°] of **9** (left), **3b** (middle)[4], and **1b** with two additional silyl substituents (2,3,7,8-tetrakis(trimethylsilyl)[3]phenylene [2], right).

by the internal consistency with the ^{1}H NMR data, we feel that **9** can be loosely described as a tris(biphenylenocyclobutadieno)cyclohexatriene.

Perhaps most striking is the observation that **9** is not planar, but (slightly) bowl-shaped, and that the two molecules in the unit cell are stacked in a concave–concave manner (Fig. 3). It is

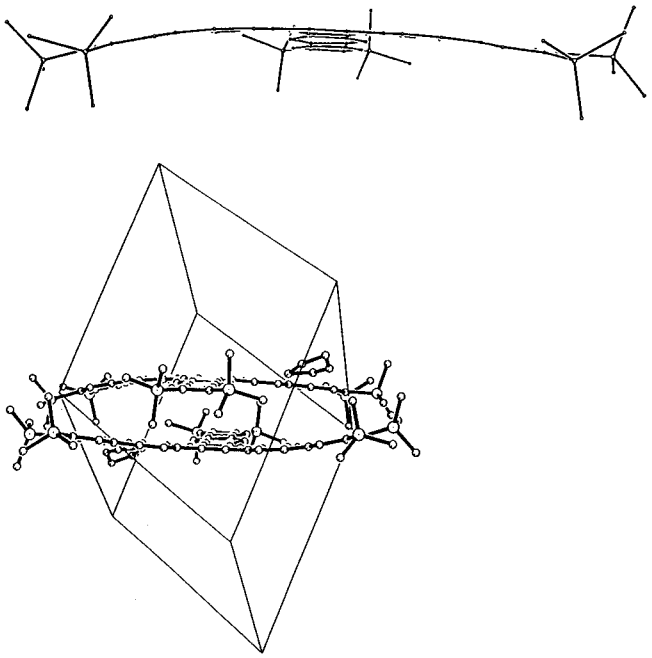

Fig. 3. Side view of a single molecule of **9** (top) and of the unit cell with THF molecules of crystallization (bottom).

difficult to quantitate the extent of deplanarization in **9** in a simple manner, because the planes of neighboring rings are not only bent with respect to each other but also twisted.[12] A best attempt at specifying the degree of curvature is the deviation of the perimeter atoms C15, C16, C27, C28, C39, and C40 from the plane of the central ring A, which varies from 0.20 to 1.08 Å, with a mean value of 0.63 Å. The "arm" A–F is bent the least, very likely because the two molecules are mutually offset along this axis (see Fig. 1). As there are no obvious crystal packing reasons for the observed curving of **9**, it appears that the molecule "voluntarily" adopts a non-flat conformation. Indeed, it is possible that this phenomenon may be general for (some of) the (higher) phenylenes. Thus, while **2** is completely planar,[3] its linear analog appears sinusoidal,[2] and, more significantly, the trigonal **3b** distorts in exactly the same manner as **9**,[4] although crystal packing forces were invoked at the time to explain these observations.

Calculations at the highest level (6-31G*) that can be reasonably performed on **3a** show that symmetrical bending of the planes of the fused cyclobutadienes and benzene rings with respect to the central core is energetically remarkably inexpensive.[17] It is noteworthy in this connection that: 1) one of the molecules in the unit cell of biphenylene is slightly nonplanar, bent by 1.9° (interplanar angle);[14a] 2) the biphenylene nucleus can be forced to deplanarize by [*d*,*e*,*f*]-fusion[18a] and incorporation into a cyclophane framework;[18b] 3) fused benzenoid hydrocarbons are flat, unless forced to exist otherwise by nonbonding interactions[19] or specific annelation as (most dramatically) exemplified by the buckybowls corannulene and semibuckminsterfullerene;[20] 4) there may be a driving force towards deplanarization in phenylenes on enthalpic (accommodation of ring strain and decrease in antiaromatic overlap) and entropic (degrees of freedom) grounds; and 5) should point 4) be borne out by further experiments, it may have ramifications for the stability and hence synthetic accessibility of cyclobutadienoid fullerenes,[21a,b] in particular the spherical phenylenes described by a truncated cuboctahedron, C_{48}, and a truncated icosidodecahedron, C_{120} ("archimedene").[21c]

Received: February 1, 1995 [Z7678IE]
German version: *Angew. Chem.* **1995**, *107*, 1630–1633

Keywords: antiaromaticity · strained rings · oligophenylenes

[1] K. P. C. Vollhardt, *Pure Appl. Chem.* **1993**, *65*, 153; D. L. Mohler, K. P. C. Vollhardt in *Advances in Strain in Organic Chemistry*, Vol. 5 (Ed.: B. Halton), JAI Press, London, **1995**; M. K. Shepherd, *Cyclobutarenes*, Elsevier, Amsterdam, **1991**.

[2] B. C. Berris, G. H. Hovakeemian, Y.-H. Lai, H. Mestdagh, K. P. C. Vollhardt, *J. Am. Chem. Soc.* **1985**, *107*, 5670.

[3] R. Diercks, K. P. C. Vollhardt, *Angew. Chem.* **1986**, *98*, 268; *Angew. Chem. Int. Ed. Engl.* **1986**, *25*, 266.

[4] R. Diercks, K. P. C. Vollhardt, *J. Am. Chem. Soc.* **1986**, *108*, 3150.

[5] See a) R. Boese, D. Bläser, W. E. Billups, M. M. Haley, A. H. Maulitz, D. L. Mohler, K. P. C. Vollhardt, *Angew. Chem.* **1994**, *106*, 321; *Angew. Chem. Int. Ed. Engl.* **1994**, *33*, 313; b) E. D. Glendening, R. Faust, A. Streitwieser, K. P. C. Vollhardt, F. Weinhold, *J. Am. Chem. Soc.* **1993**, *115*, 10952; c) R. Faust, E. D. Glendening, A. Streitwieser, K. P. C. Vollhardt, *ibid.* **1992**, *114*, 8263; d) N. Trinajstic, T. G. Schmalz, T. P. Živković, S. Nikolić, G. E. Hite, D. J. Klein, W. A. Seitz, *New J. Chem.* **1991**, *15*, 27; e) I. Gutman, S. J. Cyvin, J. Brunvol, *Monatsh. Chem.* **1994**, *125*, 887 and references therein.

[6] a) J. S. Miller, A. J. Epstein, *Angew. Chem.* **1994**, *106*, 399; *Angew. Chem. Int. Ed. Engl.* **1994**, *33*, 385; b) U. Scherf, K. Müllen, *Synthesis* **1992**, *23*; c) R. H. Baughman, H. Eckhardt, M. Kertesz, *J. Chem. Phys.* **1987**, *87*, 6687; d) J. L. Brédas, R. H. Baughman, *J. Polym. Sci. Polym. Lett. Ed.* **1983**, *21*, 475.

[7] a) M. Hirthammer, K. P. C. Vollhardt, *J. Am. Chem. Soc.* **1986**, *108*, 2481; b) L. Blanco, H. E. Helson, M. Hirthammer, H. Mestdagh, S. Spiroudis, K. P. C. Vollhardt, *Angew. Chem.* **1987**, *99*, 1276; *Angew. Chem. Int. Ed. Engl.* **1987**, *26*, 1246.

[8] R. H. Schmidt-Radde, K. P. C. Vollhardt, *J. Am. Chem. Soc.* **1992**, *114*, 9713.

[9] a) J. S. Miller, A. J. Epstein, W. M. Reiff, *Chem. Rev.* **1988**, *88*, 201; b) R. Breslow, *Mol. Cryst. Liq. Cryst.* **1989**, *176*, 199, and the following papers in this issue; c) J. Thomaides, P. Maslak, R. Breslow, *J. Am. Chem. Soc.* **1988**, *110*, 3970, and references therein; d) for **3** and **9** a stack of radical cations $[M^{+}M^{+}\leftrightarrow M^{0}M^{2+}]$ may provide the conditions for this effect: J. B. Torrance, S. Oostra, A. Nazzal, *Synth. Met.* **1987**, *19*, 709. See, however, also C. Kollmar, O. Kahn, *J. Am. Chem. Soc.* **1991**, *113*, 7987.

[10] All new compounds gave satisfactory analytical and spectral data (see Table 1).

[11] R. Diercks, J. C. Armstrong, R. Boese, K. P. C. Vollhardt, *Angew. Chem.* **1986**, *98*, 270; *Angew. Chem. Int. Ed. Engl.* **1986**, *25*, 268.

[12] Crystal size $0.13\times0.10\times0.04$ mm^3, space group $P\bar{1}$, scan range $3\leq2\theta\leq45^\circ$, $a=14.059(6)$, $b=14.996(8)$, $c=16.593$ (8) Å, $\alpha=103.75$ (4), $\beta=104.14(4)$, $\gamma=107.28$ (4)°, $V=3146$ (3) Å^3, $Z=2$, $\rho_{calcd}=1.291$ g cm^{-3}, $\mu=0.19$ mm^{-1}, 4783 unique reflections at room temperature, of which 2823 were taken as observed $[I_o\geq3\sigma(F)]$, $R=0.0790$, $R_w=0.0786$. Further details of the crystal structure analysis may be obtained from the Fachinformationszentrum Karlsruhe, D-76344 Eggenstein-Leopoldshafen (Germany), on quoting the depository number CSD-49155.

[13] a) C. A. Hunter, J. K. M. Sanders, *J. Am. Chem. Soc.* **1990**, *112*, 5525; b) C. A. Hunter, *Angew. Chem.* **1993**, *105*, 1653; *Angew. Chem. Int. Ed. Engl.* **1993**, *32*, 1584; *Chem. Soc. Rev.* **1994**, 101.

[14] a) J. K. Fawcett, J. Trotter, *Acta Crystallogr.* **1966**, *20*, 87; R. Boese, unpublished work; b) J. J. Stezowski, R.-D. Stigler, N. Karl, *J. Chem. Phys.* **1986**, *84*, 5162; G. Agostini, C. Corvaja, G. Giacometti, L. Pasimeni, D. A. Clemente, G. Bandoli, *Mol. Cryst. Liq. Cryst.* **1986**, *141*, 165.

[15] A. Yokozeki, C. F. Wilcox, Jr., S. H. Bauer, *J. Am. Chem. Soc.* **1974**, *96*, 1026.

[16] Compare R. Boese, D. Bläser, *Angew. Chem.* **1988**, *100*, 293; *Angew. Chem. Int. Ed. Engl.* **1988**, *27*, 304; K. P. Moder, E. N. Duesler, N. J. Leonard, *Acta Crystallogr. Sect. B* **1981**, *37*, 1524.

[17] ΔE in kcal mol^{-1} (in parentheses the degrees of bending for each of the two component rings of the attached benzocyclobutadienes): 0.59 (3), 2.36 (6), 5.31 (9), 9.43 (12). Calculations were performed with Gaussian 92, Revision E.2, M. J. Frisch, G. W. Trucks, M. Head-Gordon, P. M. W. Gill, M. W. Wong, J. B. Foresman, B. G. Johnson, H. B. Schlegel, M. A. Robb, E. S. Replogle, R. Gomperts, J. L. Andres, K. Raghavachari, J. S. Binkley, C. Gonzalez, R. L. Martin, D. J. Fox, D. J. Defrees, J. Baker, J. J. P. Stewart, J. A. Pople, Gaussian, Inc., Pittsburgh, PA, **1992**. An extensive theoretical analysis of this problem will be the subject of a full paper: A. J. Matzger, A. Streitwieser, K. P. C. Vollhardt, in preparation.

[18] a) F. Vögtle, J. E. Schulz, K. Rissanen, *J. Chem. Soc. Chem. Commun.* **1992**, 120; b) K. Saitmacher, J. E. Schulz, M. Nieger, F. Vögtle, *ibid.* **1992**, 175.

[19] W. C. Herndon, P. C. Nowak in *Advances in Theoretically Interesting Molecules, Vol. 2* (Ed.: R. P. Thummel), JAI Press, London, **1992**, p. 113; W. C. Herndon, P. C. Nowak, D. A. Connor, P. Lin, *J. Am. Chem. Soc.* **1992**, *114*, 41.

[20] For recent work, see: a) A. Ayalon, A. Sygula, P.-C. Cheng, M. Rabinovitz, P. W. Rabideau, L. T. Scott, *Science* **1994**, *265*, 1065; b) P. W. Rabideau, A. H. Abdourazak, H. E. Folsom, Z. Marcinow, A. Sygula, R. Sygula, *J. Am. Chem. Soc.* **1994**, *116*, 7891; c) A. Sygula, P. W. Rabideau, *J. Chem. Soc. Chem. Commun.* **1994**, 1497; d) A. Sygula, H. E. Folsom, R. Sygula, A. H. Abdourazak, Z. Marcinow, F. R. Fronczek, P. W. Rabideau, *ibid.* **1994**, 2571; e) R. Faust, K. P. C. Vollhardt, *ibid.* **1993**, 1471.

[21] a) R. Taylor, *J. Chem. Soc. Chem. Commun.* **1994**, 1629; b) Y.-D. Gao, W. C. Herndon, *J. Am. Chem. Soc.* **1993**, *115*, 8459; c) A. D. J. Haymet, *Chem. Phys. Lett.* **1985**, *122*, 421.

[22] On the question of bond localization in benzene see also J. S. Siegel, *Angew. Chem.* **1994**, *106*, 1808; *Angew. Chem. Int. Ed. Engl.* **1994**, *33*, 1721.

Photoinduced Valence Tautomerism in Cobalt Complexes Containing Semiquinone Anion as Ligand: Dynamics of the High-Spin $[Co^{II}(3,5\text{-dtbsq})_2]$ to Low-Spin $[Co^{III}(3,5\text{-dtbsq})(3,5\text{-dtbcat})]$ Interconversion **

David M. Adams, Bulang Li, John D. Simon,* and David N. Hendrickson*

Cobalt complexes with two semiquinone-derived ligands have been shown[1-3] to undergo a valence tautomeric interconversion between high-spin $[Co^{II}(\overset{\frown}{N\ N})(sq)_2]$ and low-spin $[Co^{III}(\overset{\frown}{N\ N})(sq)(cat)]$ forms, where $\overset{\frown}{N\ N}$ is a chelating diiminium ligand such as 2,2′-bipyridine (bpy). In these molecules, an intramolecular electron transfer converts the high-spin Co^{II} ion to a low-spin Co^{III} ion, and one of the ligands is reduced by one electron from a semiquinone anion ligand (sq^-) to a catecholato (cat^{2-}) ligand. There are two different mixed-valence isomers of the Co^{III} complex. The dynamical processes that are possible for such a valence-tautomeric complex are summarized in Scheme 1.

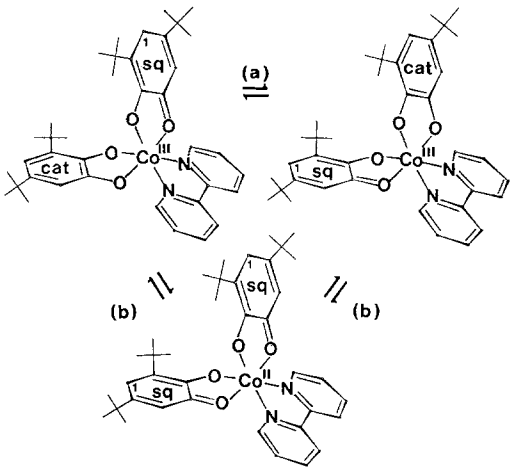

Scheme 1. Possible intramolecular electron transfer processes present in a cobalt complex with two semiquinone anion ligands.

The valence tautomeric interconversion (process b) can be thermally driven. In solution[1, 3, 4] it occurs gradually over a large temperature range of about 100 K, whereas in the solid state[1, 2] the interconversion can occur abruptly in a range of about 10 K. The valence tautomeric transformation is accompanied by structural changes (bond lengths between the cobalt ion and the ligands) and large changes in the optical and magnetic properties of the complexes. There are two important motivations for studying these cobalt complexes. First, they are excellent model systems for elucidating factors that control intramolecular electron transfer. In particular, the influence of the spin change (low-spin vs. high-spin Co) on electron transfer (Scheme 1, process b) can be explored. Second, these valence

[*] Prof. J. D. Simon, Prof. D. N. Hendrickson, D. M. Adams, B. Li
Department of Chemistry-0358
University of California at San Diego
La Jolla, CA 92093-0358 (USA)
Telefax: Int. code + (619)534-5383

[**] This work was supported by the U. S. National Science Foundation (CHE-9306485 (J. D. S.), CHE-9115286 and CHE-9420322 (D. N. H.)) and the National Institutes of Health (HL13652 (D. N. H.)). 3,5-dtbsq = 3,5-di-*tert*-butylbenzosemiquinone; 3,5-dtbcat = 3,5-di-*tert*-butylcatecholate.

tautomeric complexes could serve as fast optical switching devices.[5, 6]

In this communication we report results of the first picosecond time-resolved optical experiments on valence-tautomeric cobalt complexes. We have studied the Co^{III} complexes **1** and **2**,

[Co(dpbpy)(3,5-dtbsq)(3,5-dtbcat)] **1**

[Co(dmbpy)(3,5-dtbsq)(3,5-dtbcat)] **2**

where dpbpy is 4,4'-diphenyl-2,2'-bipyridine, dmbpy is 4,4'-dimethyl-2,2'-bipyridine, and 3,5-dtbsq$^-$ and 3,5-dtbcat^{2-} are the semiquinone anion and catecholate forms of 3,5-di-*tert*-butyl-1,2-benzoquinone, respectively. Valence tautomeric complexes, like spin-crossover complexes,[7] are particularly suitable for photophysical investigations since the electronic absorption spectra of the ground and the lowest energy excited state can be obtained by varying the temperature. Figure 1 shows the temperature dependence of the spectrum of the dpbpy complex **1** in tetrahydrofuran over the temperature range 298–348 K. The ligand-to-metal charge transfer (LMCT) band at 600 nm, characteristic of the low-spin Co^{III} species, decreases at elevated temperatures and is replaced by the two transitions at 540 nm and 770 nm which are associated with the high-spin Co^{II} species. The transient picosecond "pump/probe" apparatus has been described elsewhere.[8] A pump pulse in the visible range (532 nm, $\approx$70 ps pulse width, 0.2 mJ per pulse) into the LMCT band of the Co^{III} tautomer results in a transient absorption monitored at 720 nm and a corresponding transient bleach monitored at 600 nm. Figure 2 displays the transient curves obtained for a solution of complex **1** in toluene (1.63×10^{-3} M) at 298 K. Least-squares fitting (solid lines) shows that these transients are well described by single-exponential functions with the same time constant, $\tau_{obs}=1.15$ ns. The observation of a bleach and absorption with identical kinetics around an isosbestic point indicates that we are looking at a light-induced population of the high-spin $[Co^{II}(\overset{\frown}{N}\,\overset{\frown}{N})(sq)_2]$ state, followed by relaxation back to equilibrium. It should be noted that valence tautomers are in thermal equilibrium in solution according to Equation (a). Thus the

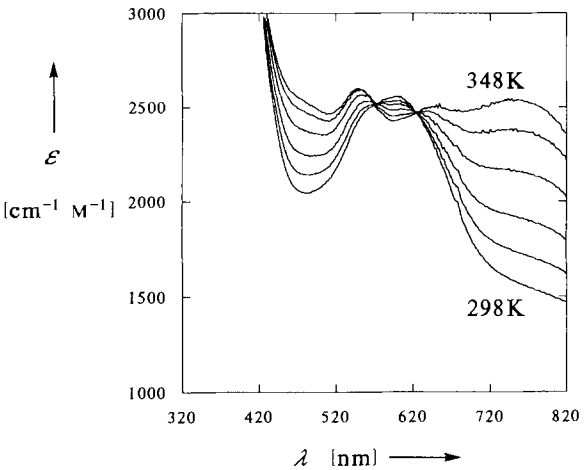

Fig. 1. Temperature dependence of the electronic absorption spectrum of a solution of **1** in tetrahydrofuran at $T=298$, 308, 318, 328, 338, and 348 K. The molar extinction coefficent ε is plotted versus wavelength λ.

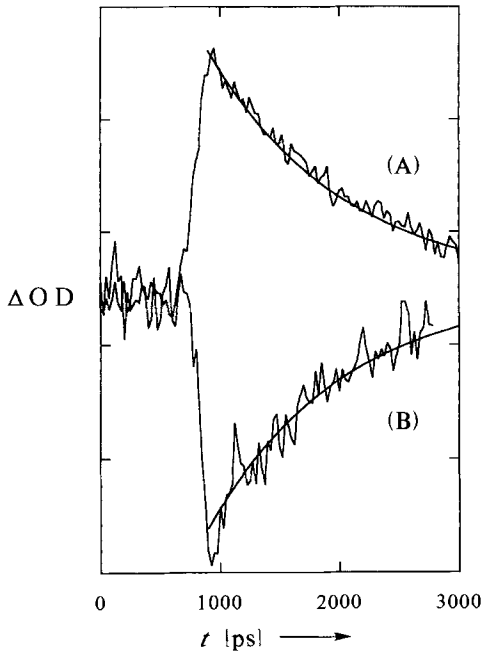

Fig. 2. A) Changes in the transient absorption (ΔOD = difference in absorption) of **1** in toluene at 298 K monitored at 720 nm after excitation at 532 nm. B) Transient bleach monitored at 600 nm after excitation at 532 nm. The solid line represents a least-squares fit to single exponential and gives the value of $\tau_{obs}=1.1$ ns for both data sets.

tautomerization involves a reversible first-order reaction, where $K_{eq}=k_1/k_{-1}$ and $\tau_{obs}=1/k_1+1/k_{-1}$. Since we see no indication of a rise time, the high-spin Co^{II} state is formed within the experimental resolution (70 ps).

The solvent dependence of the valence tautomeric relaxation has been examined. For the dpbpy complex the observed lifetimes of the excited state are 1.1 (toluene), $\approx$2.0 (tetrahydrofuran), and $\approx$10 ns (dichloromethane). Figure 3 shows the traces obtained after photoperturbation ($\lambda_{pump}=532$ nm and $\lambda_{probe}=720$ nm) of solutions of the dpbpy complex in THF (1.09×10^{-3} M) and in CH_2Cl_2 (1.64×10^{-3} M). Variable-temperature UV/Vis spectroscopy of this complex in various solvents suggests that the critical temperature (T_c) of the valence

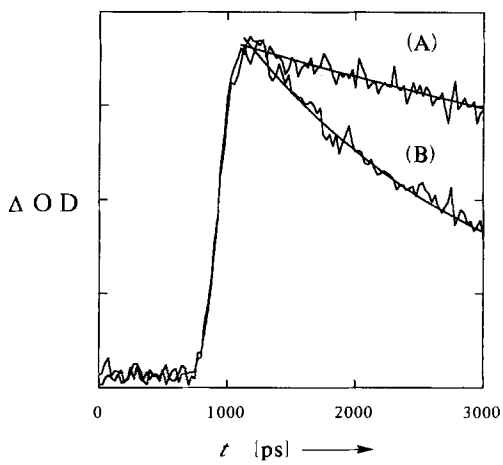

Fig. 3. Changes in the transient absorption of **1** in different solvents at 298 K, monitored at 720 nm after excitation at 532 nm. A) CH_2Cl_2. B) tetrahydrofuran. The solid line represents a least-squares fit to a single exponential and gives $\tau_{obs}=2.0$ ns.

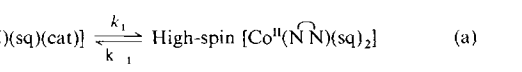

(a)

tautomeric conversion shifts to lower temperatures in polar solvents.[9] This implies that the zero-point energy difference between tautomers decreases when changing to more polar solvents. The T_c decreases by about 25 K on changing from toluene to THF. Since τ_{obs} in these solvents increases from 1.1 ns to 2 ns, respectively, it would appear that as the driving force decreases the rate decreases. However, it must be kept in mind that τ_{obs} is the sum of $1/k_1$ and $1/k_{-1}$. In order to make quantitative correlations between the driving force and the rate of back valence tautomerization k_{-1}, it is necessary to determine K_{eq}.[10] Solution magnetic susceptibility determinations of K_{eq} are currently in progress.

It has been previously established that the counter-ligand provides a subtle handle for controlling the zero-point energy differences between valence tautomers.[1, 3] We have also investigated the rate of the valence tautomerization of the dmpby complex **2**. This complex is known to have a smaller energy gap between tautomers than the dpbpy complex **1**.[1] The observed lifetime of the excited state for a solution of the dmbpy complex **2** in toluene (1.10×10^{-3} M) at 298 K following photoexcitation ($\lambda_{pump} = 532$ nm and $\lambda_{probe} = 720$ nm) is ≈ 8 ns. Furthermore, we have investigated the kinetics of the dmbpy complex doped into a polystyrene polymer film ($M_w = 250000$) g mol^{-1}).[11] Relative to toluene, the polymer provides a less polar environment for the complex and thus tends to increase the energy separation between the tautomers. Consequently, the observed lifetime of the excited state decreases to about 2 ns. Since similar relaxation behavior is observed in doped polymer films and in solution, it is likely that we are observing a single molecule process.

A relaxation time of 1–10 ns for the valence tautomerization (process b in Scheme 1) is interesting in view of the fact that this process involves separate or concomitant metal-to-ligand electron transfer and a spin change at the cobalt ion. $\Delta S = 2$ spin-crossover relaxation times in solution at room temperature are on the order of 30–150 ns for Fe^{II} complexes and 2–10 ns for Fe^{III} complexes.[12] The spin-crossover transformation for a Co^{II} complex is a $\Delta S = 1$ process where the high- and low-spin states interact through a first-order spin-orbit interaction and short relaxation times are expected. Spin-crossover relaxation times for $[Co(terpy)_2]^{2+}$ (terpy = 2,2′:6′,2″-terpyridine) are reported[13] to be on the order of 0.1 ns. The valence-tautomeric conversion is from a high-spin $Co^{II}(sq)_2$ to a low-spin $Co^{III}(sq)(cat)$ complex, where the latter has an $S = 1/2$ ground state resulting from the single unpaired electron on the one sq^- ligand. There is a very weak[14] magnetic exchange interaction between the sq^- ligands and the $S = 3/2$ high-spin Co^{II} ion. Thus, the $Co^{II}(sq)_2$ complexes have one $S = 1/2$, two $S = 3/2$, and one $S = 5/2$ states in close energy proximity. Since the valence-tautomerization (process b in Scheme 1) is slow relative to spin-crossover in simple Co^{II} complexes, it must be that the intramolecular electron transfer also affects the rate of reaction.

Further studies aimed at understanding the way in which factors such as the driving force, ligands, temperature, and solvent influence the excited state dynamics of these valence tautomeric complexes are currently in progress.

Received: January 3, 1995 [Z 7603 IE]
German version: *Angew. Chem.* **1995**, *107*, 1580–1582

Keywords: cobalt compounds · complexes with semiquinone ligands · electron transfer · spin crossover · tautomerism

[1] a) D. M. Adams, A. Dei, A. L. Rheingold, D. N. Hendrickson, *Angew. Chem.* **1993**, *105*, 954; *Angew. Chem. Int. Ed. Engl.* **1993**, *32*, 880; b) D. M. Adams, A. Dei, A. L. Rheingold, D. N. Hendrickson, D. N. *J. Am. Chem. Soc.* **1993**, *115*, 8221.

[2] G. A. Abakumov, V. K. Cherkasov, M. P. Bubnov, O. G. Ellert, Z. B. Dobrokhotova, L. N. Zakaharov, Y. T. Struchov, *Dokl. Akad. Nauk. SSSR* **1993**, *328*, 12.

[3] a) O. S. Jung, C. G. Pierpont, *Inorg. Chem.* **1994**, *33*, 2227; b) O. S. Jung, C. G. Pierpont, *J. Am. Chem. Soc.* **1994**, *116*, 127.

[4] R. M. Buchanan, C. G. Pierpont, *J. Am. Chem. Soc.* **1980**, *102*, 4951.

[5] a) O. Kahn, J. Kröber, C. Jay, *Adv. Mater.* **1992**, *4*, 778; b) N. S. Hush, A. T. Wong, G. B. Backsay, J. R. Reimers, *J. Am. Chem. Soc.* **1990**, *112*, 4192; c) J. P. Launay in *Molecular Electronic Devices II* (Ed.: F. L. Carter), Dekker, New York, **1987**.

[6] A. Hauser, *Chem. Phys. Lett.* **1993**, *202*, 173.

[7] a) J. K. McCusker, K. N. Walda, R. C. Dunn, J. D. Simon, D. Magde, D. N. Hendrickson, *J. Am. Chem. Soc.* **1993**, *115*, 298. b) J. K. McCusker, K. N. Walda, R. C. Dunn, J. D. Simon, D. Magde, D. N. Hendrickson, *ibid.* **1992**, *114*, 6919; c) S. Schenker, A. Hauser, *ibid.* **1994**, *116*, 5497; d) A. Hauser, A. Vef. P. Adler, *J. Chem. Phys.* **1991**, *95*, 8710; e) A. Hauser, *Coord. Chem. Rev.* **1991**, *111*, 275; f) J. J. McGarvey, H. Toftlund, A. H. R. Al-Obaidi, K. P. Taylor, S. E. J. Bell, *Inorg. Chem.* **1993**, *32*, 2469; g) A. H. R. Al-Obaidi, J. J. McGarvey, K. P. Taylor, S. E. J. Bell, K. B. Jensen, H. Toftlund, *J. Chem. Soc. Chem. Commun.* **1993**, 536.

[8] Sub-nanosecond pump/probe experiments were carried out by using a mode-locked Q-switched and cavity-dumped Nd-YAG Laser and synchronously pumped dye laser. See X. Xie, J. D. Simon, *Opt. Commun.* **1989**, *69*, 303.

[9] T_c is defined as the temperature at which $K_{eq} = 1$. The dielectric constants ε at 20 °C for toluene, tetrahydrofuran, and dichloromethane are 2.57, 7.58, and 9.08 respectively.

[10] From UV/Vis spectra it can be estimated that $K_{eq} \approx 0$ for the dpbpy complex **1** in toluene at 298 K. Thus, $\tau_{obs} \approx 1/k_1$. For the dmbpy complex in toluene at 298 K the value of K_{eq} may be as high as 1.0.

[11] Polystyrene films were made by dissolving complex and polystyrene in CH_2Cl_2 followed by solution casting onto glass dishes.

[12] J. K. Beattie, *Adv. Inorg. Chem.* **1988**, *32*, 1.

[13] J. K. Beattie, N. Sutin, D. H. Turner, G. W. Flynn, *J. Am. Chem. Soc.* **1993**, *75*, 2052.

[14] M. W. Lynch, R. B. Buchanan, D. N. Hendrickson, C. G. Pierpont, *Inorg. Chem.* **1981**, *20*, 1038.

Burial of Hydrocarbon Causes Cooperative Enhancement of Electrostatic Binding**

Gary J. Sharman, Mark S. Searle, Bellinda Benhamu, Patrick Groves, and Dudley H. Williams*

The hydrophobic effect, involving the burial of hydrocarbon formerly exposed to water, provides a major driving force in molecular recognition, and is fundamental to our understanding of the structure and function of biological systems. The desire to rationalize the forces involved in molecular complexation[1, 2] and the stabilization of highly ordered molecular assemblies[3, 4] has led to attempts to correlate the magnitude of the hydrophobic free energy with the nonpolar surface area no longer accessible to solvent.[5] This approach potentially provides a useful

[*] Dr. D. H. Williams, G. J. Sharman, Dr. M. S. Searle, Dr. P. Groves[+]
Cambridge Centre for Molecular Recognition
University Chemical Laboratories
Lensfield Road, GB-Cambridge CB2 1EW (UK)
Telefax: Int. code + (1223) 336362

B. Benhamu
Dpto. de Quimica Organica, Facultad de Ciencias Quimicas
Universidad Complutense de Madrid (Spain)

[+] Current address:
Physical Chemistry 2, University of Lund (Sweden)

[**] We thank GLAXO, The Wellcome Trust, and BBSRC for financial support, and the NMR Center of the MRC National Institute for Medical Research, Mill Hill, London, for access to NMR facilities.

numerical estimate for assessing binding contributions in molecular recognition studies.[2, 4, 6] However, data from protein engineering experiments[4, 6] and ligand binding studies[2] suggest that the hydrophobic effect promotes binding in aqueous solution to a larger extent than is estimated from solvent transfer measurements.[7] An explanation for this discrepancy has been sought, at least partially, in terms of changes in volume entropy in the two sets of experiments.[7] In the present work we show that burial of hydrocarbon in a molecular recognition site can lead to the strengthening of adjacent electrostatic interactions.

The electrostatic binding of a peptide C-terminal carboxylate group, an interaction crucial to cell wall recognition by glycopeptide antibiotics, is conveniently monitored through the ^{1}H NMR chemical shifts of several glycopeptide backbone NH groups (w_2 and w_3 in Fig. 1), which undergo large downfield

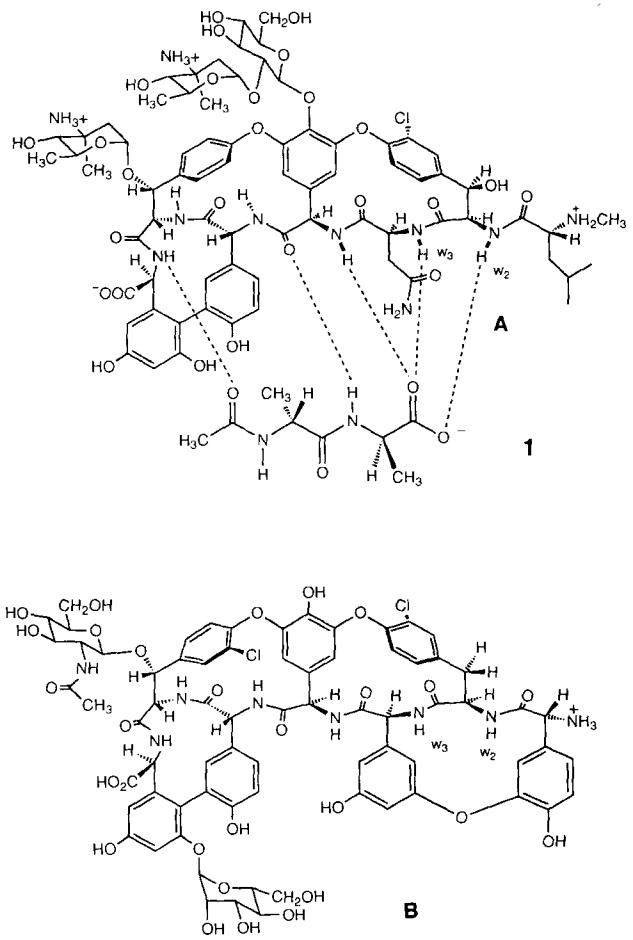

Fig. 1. Structures of eremomycin (**A**) and teicoplanin A_3-1 (**B**). An exploded view of the complex of eremomycin with the dipeptide cell wall analogue *N*-Ac-D-Ala-D-Ala is shown. Dotted lines represent hydrogen bonds.

shifts in the presence of cell wall peptides (up to $\Delta\delta \approx 3.5$ for w_2). In studies with the antibiotics eremomycin (**A**) and teicoplanin A_3-1 (**B**) (Fig. 1),[8] we have systematically deleted ligand methyl interactions through the synthesis of a series of Gly- and D-Ala-containing dipeptides (Fig. 2) and measured their binding properties.[9] Each alanine methyl group buries hydrocarbon surface area from solvent;[10] the increase in dipeptide binding affinity can be accounted for in terms of contributions from the classical hydrophobic effect and possibly van der Waals interactions that are stronger in the complex than

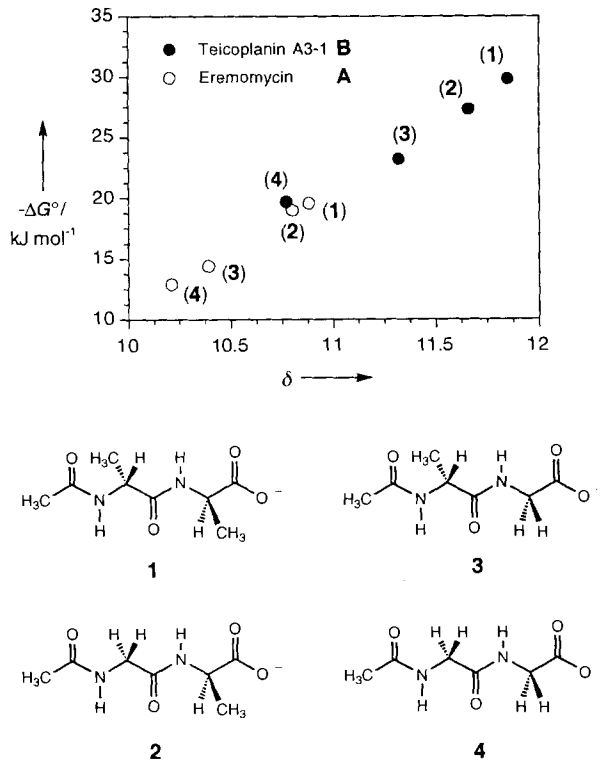

Fig. 2. Dipeptide ligands considered in this study. Plot of ligand binding energy ΔG° (pH 4.5, 298 K) to eremomycin (**A**) and teicoplanin A_3-1 (**B**) versus limiting ^{1}H NMR chemical shift of amide NH group w_2. For eremomycin the limiting chemical shift represents the average of the w_2 shifts in the two nonequivalent dimer binding sites that differ by $\Delta\delta < 0.1$. Errors in ΔG° values are less than reflected in the size of the data points.

with solvent. Each dipeptide in the series (Fig. 2) shares a completely analogous set of hydrogen bonding interactions with the glycopeptide. Molecular modeling studies of all the complexes, based upon NOE data, establish that the hydrogen bonding arrangements of the bound ligands do not vary significantly, nor do the structures of the antibiotics, which are relatively inflexible on account of extensive cross-linking of aromatic amino acid side chains (Fig. 1). Thus, there are no clear changes in binding geometries or antibiotic structure that are likely to result in significant differences in the observed ^{1}H NMR chemical shifts of w_2 amongst the various ligands. Indeed ^{13}C NMR data have recently been used to show that a wide range of ligands bearing carboxylate groups all bind with similar arrangements.[11] We conclude that the strength of the carboxylate binding interaction is reflected in the limiting NMR chemical shift of w_2 (at ligand concentrations in which <95% of the antibiotic is bound), and this has been monitored as a function of the overall ligand binding energy ΔG° (Fig. 2). It is evident that as ΔG° becomes more negative, through the introduction of alanine methyl groups, the limiting shift of w_2 (and w_3, not shown) also increases. We interpret the change in limiting shift of w_2 as reflecting a structure with binding interactions over shorter distances,[12] such that a cooperative enhancement of the electrostatic binding energy of the carboxylate group arises through the burial of hydrocarbon in an adjacent site. Thus, when the restriction of motion of the carboxylate group is aided by the burial of hydrocarbon, or through other electrostatic interactions such as hydrogen bonds, as previously described,[13] then on average the carboxylate group will occupy a deeper position in its electrostatic (enthalpic) well corresponding to a greater binding exothermicity.[14]

These observations may account for the fact that the burial of hydrocarbon appears to give a larger free energy change when measured in systems in which the hydrocarbon is "anchored" into a molecular recognition site than in the solvent transfer model, where translational and rotational freedom is unaffected.[7] While protein engineering experiments[4, 6] and ligand binding studies[2] have indicated surface area dependent free energy contributions from burial of hydrocarbon of 0.19–0.25 kJ mol^{-1} Å^{-2}, the value from the solvent transfer model is approximately half this value, 0.08–0.13 kJ mol^{-1} Å^{-2}.[7, 15] One possible explanation for this discrepancy is suggested by the above results: the introduction of the hydrocarbon entity may strengthen adjacent polar interactions, such that the burial of hydrocarbon in experiments with proteins[4, 6] and antibiotics[2] may derive some favorable free energy increment (over that of the solvent transfer model) through an electrostatic (enthalpic) term, whereas the solvent transfer portion (the classical hydrophobic effect) is essentially entropy-driven at room temperature.[15] We have shown that this is the case for one specific neighboring interaction, but the extra binding energy is likely to arise from a cooperative enhancement of all interactions.

The results presented suggest that the assignment of enthalpic contributions to specific interactions (implied through changes in ^{1}H NMR chemical shifts) are subject to cooperative enhancement. By monitoring a specific binding interaction, we have illustrated a cooperative interplay between hydrophobic and electrostatic contributions to binding in a molecular recognition site.

Received: February 4, 1995 [Z 7693 IE]
German version: *Angew. Chem.* **1995**, *107*, 1644–1646

Keywords: electrostatic binding · hydrophobic effect · molecular recognition · peptides

[1] P. R. Andrews, D. C. Craik, J. L. Martin, *J. Med. Chem.* **1984**, *27*, 1648; A. R. Fersht, *Trends Biochem. Sci.* **1987**, *12*, 301.
[2] M. S. Searle, D. H. Williams, U. Gerhard, *J. Am. Chem. Soc.* **1992**, *114*, 10697.
[3] K. A. Dill, *Biochemistry* **1990**, *29*, 7134; A. R. Fersht, *Enzyme Structure and Function*, 2nd ed., Freeman, New York, **1985**; L. Serrano, A. Horovitz, B. Avron, M. Bycroft, A. R. Fersht, *Biochemistry* **1992**, *29*, 9343; B. A. Shirley, P. Stanssens, U. Hahn, C. N. Pace, *ibid.* **1992**, *31*, 725.
[4] L. Serrano, J.-L. Neira, J. Sancho, A. R. Fersht, *Nature (London)* **1992**, *356*, 453.
[5] R. B. Herman, *Proc. Natl. Acad. Sci. USA* **1977**, *74*, 4144; C. H. Tanford, *The Hydrophobic Effect*, Wiley, New York, **1980**.
[6] J. T. Kellis, K. Nyberg, A. R. Fersht, *Biochemistry* **1989**, *28*, 4914; D. Shortle, W. E. Stites, A. K. Mecker, *ibid.* **1990**, *29*, 8033.
[7] K. A. Sharp, A. Nicholls, R. Friedman, B. Honig, *Biochemistry* **1991**, *30*, 9686.
[8] Glycopeptide antibiotics have been shown to dimerize in aqueous solution: J. P. Waltho, D. H. Williams, *J. Am. Chem. Soc.* **1989**, *111*, 2475; U. Gerhard, J. P. Mackay, R. A. Maplestone, D. H. Williams, *ibid.* **1993**, *115*, 232; J. P. Mackay, U. Gerhard, D. A. Beauregard, R. A. Maplestone, D. H. Williams, *ibid.* **1994**, *116*, 4573. This dimerization has been proposed to play an important role in mediating biological activity: J. P. Mackay, U. Gerhard, D. A. Beauregard, M. S. Westwell, M. S. Searle, D. H. Williams, *ibid.* **1994**, *116*, 4581. To show that the observed trends in w_2 ^{1}H NMR chemical shifts are independent of the ability of the antibiotics to dimerize, we present results for both eremomycin (**A**) and teicoplanin A_3-1 (**B**). The former has a large dimerization constant ($K_{dim} \approx 10^6$ M^{-1}), while the latter shows no measurable tendency to dimerize. In addition, dimerization of eremomycin and ligand binding are cooperative phenomena; K_{dim} is roughly a factor of 100 greater in the presence of ligands.
[9] Binding constants were measured in triplicate by UV difference spectroscopy at antibiotic concentrations between 50 and 200 μM at pH 4.5 and 298 K in 100 mM sodium phosphate/1 M NaCl buffer. NMR spectra were recorded in 90% H_2O/10% D_2O solution using a 1-1 binomial solvent suppression sequence; exchangeable protons were assigned in all cases using 2D NOE experiments.
[10] Cell wall analogues are bound within a shallow surface cleft on the antibiotic such that the deletion of methyl groups (Ala → Gly) results in exposure of the previously buried hydrocarbon of the antibiotic to solvent, rather than creating a vacant cavity.
[11] C. M. Pearce, U. Gerhard, D. H. Williams, *J. Chem. Soc. Perkin Trans. 2* **1994**, *159*.
[12] U. Sternberg, E. Brunner, *J. Magn. Reson. Ser. A* **1994**, *108*, 142.
[13] P. Groves, M. S. Searle, M. S. Westwell, D. H. Williams, *J. Chem. Soc. Chem. Commun.* **1994**, 1519; M. P. Williamson, D. H. Williams, *Eur. J. Biochem.* **1984**, *138*, 345.
[14] It is of course also true that the peptide ligands containing one or more methyl groups will be less flexible than those containing only Gly residues. However, the term "burial of hydrocarbon" must include changes in flexibility in the bound state as well as the classical hydrophobic effect since the variables are inseparable.
[15] C. Chothia, *Nature (London)* **1974**, *248*, 338; R. L. Baldwin, *Natl. Acad. Sci. USA* **1986**, *83*, 8069.

Novel, Blue-Transparent Frequency Doublers Based on 1,8-Di(hetero)arylnaphthalenes**

André Bahl, Walter Grahn,* Stefan Stadler, Franz Feiner, Grant Bourhill, Christoph Bräuchle, Axel Reisner, and Peter G. Jones

Dedicated to Professor Wolfgang Lüttke on the occasion of his 75th birthday

Nonlinear optics (NLO)[1] has become a focus of attention for material scientists in the expectation that revolutionary progress will be associated with the transition from electronics to photonics.[2] The preparation of many photonic devices requires materials with high non-linear optical susceptibilities χ[2], which on the molecular level depend on the first hyperpolarizability β. A series of organic compounds have shown themselves to be particularly suitable in terms of their high β values, and other positive properties such as low optical loss and facile handling.[1c, 3]

A technically important application of NLO is frequency doubling, [second harmonic generation (SHG)] for example, of light of wavelengths 800–830 nm (working wavelengths of diode lasers).[4] Materials that are to exploit this process effectively must simultaneously be transparent at 830 (λ) and 415 nm ($\lambda/2$) and display high NLO activity.[5] However, the necessary high β values—consistent with predictions based on the usual models[6]—have so far only been observed for NLO-(chromo)phores of the charge transfer (CT)-type **1**, which ab-

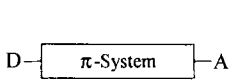

1

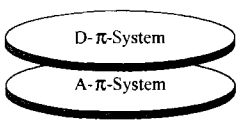

2

[*] Priv.-Doz. Dr. W. Grahn, Dipl.-Chem. A. Bahl, Dipl.-Chem. A. Reisner
Institut für Organische Chemie der Technischen Universität
Hagenring 30, D-38106 Braunschweig (Germany)
Telefax: Int. code + (531) 391-5388
Dipl.-Chem. S. Stadler, Dipl.-Phys. F. Feiner, Dr. G. Bourhill,
Prof. Dr. C. Bräuchle
Institut für Physikalische Chemie der Universität München (Germany)
Prof. Dr. P. G. Jones
Institut für Anorganische und Analytische Chemie der Technischen Universität Braunschweig (Germany)

[**] This work forms part of the doctoral thesis of A. B. It was financially supported by the Volkswagen-Stiftung and the Fonds der Chemischen Industrie.

sorb at long wavelengths.[7] Despite many promising developments[5a, 8] it has not yet proved possible to find an optimal compromise between the linear and nonlinear optical properties for the conventional NLO-phores (**1**).

We have decided on a fundamentally different approach to the improvement of the efficiency–transparency trade-off,[5b] by choosing the basic structure **2**, thus avoiding a direct conjugation between the donor (D) and acceptor (A). Compounds of this type are distinguished by higher energy electronic transitions and offer potential noncovalent interactions between the opposing surfaces of the D/A π-electron systems.[9] Through-space interactions have scarcely been investigated or realised as a basis for NLO activity,[10] although quantum-chemical calculations by Ratner, Marks, et al. indicate that CT complexes should be NLO-active.[11]

As the subject of our investigations we have chosen the 1,8-di(hetero)arylnaphthalenes **3**–**5** in which one aryl substituent is rendered electron-rich by an electron donor and/or heteroarene,

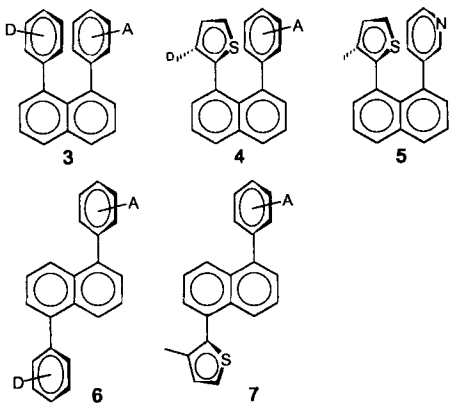

while the other has reduced electron density as a result of an electron-withdrawing group or heteroarene. The 1,5-di(hetero)-arylnaphthalenes **6** and **7** are suitable reference compounds, since like **1** they may display conjugative CT through the π-electron system, which is not possible with a 1,8 substitution pattern of naphthalene (Scheme 1).

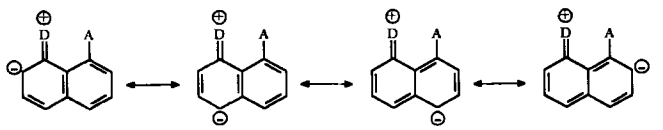

Scheme 1. Resonance structures of 1,8-disubstituted naphthalenes.

Few 1,8-di(hetero)arylnaphthalenes are known, consistent with the lack of a general synthesis. The preparation of known derivatives[12] cannot be generalized, because the methods either do not allow an unsymmetrical functionalization and/or greatly restrict the range of substituents.

The Suzuki reaction[13] provides a method of aryl–aryl cross-coupling with a wide range of applications. 1,8-Diiodonaphthalene (**8**)[12g] can be selectively transformed into the corresponding 8-aryl-1-iodonaphthalenes such as **9** by Pd-catalyzed coupling with an aryldihydroxyborane (Scheme 2 reaction a). These, and their bromo analogues, react smoothly with another (different) arylboronic acid (in spite of considerable steric hindrance) to form **3** (Scheme 2 reaction b and Scheme 3 reaction b). Such consecutive Suzuki couplings were used to synthesize

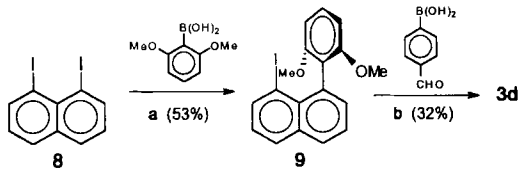

Scheme 2. Synthesis of **3d**: a) [Pd(PPh$_3$)$_4$], NaHCO$_3$, benzene/EtOH/H$_2$O, reflux; b) as a), but Na$_2$CO$_3$ as base in toluene/EtOH/H$_2$O.

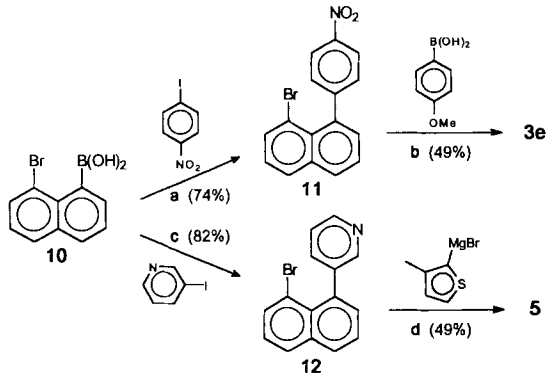

Scheme 3. Synthesis of **3e** and **5**: a–c) [Pd(PPh$_3$)$_4$], Na$_2$CO$_3$, toluene/EtOH/H$_2$O, reflux; d) [NiCl$_2$(dppp)] (dppp = 1,3-bis(diphenylphosphano)propane), Et$_2$O/THF, 0 °C, then heated at reflux.

most of the unsymmetrically substituted diarylnaphthalenes such as **3a**–**d**.

Problems with the preparation and stability of some arylboronic acids led us to incorporate the organometallic function into the naphthalene coupling component. This "Umpolung" is typified by the synthesis of 1-(8-bromonaphthyl)dihydroxyborane (**10**),[14] a key compound in the general synthesis of 1,8-di(hetero)arylnaphthalenes. As an example, **10** can be monoarylated with 1-iodo-4-nitrobenzene or 3-iodopyridine to form **11** or **12** in good yield (Scheme 3 reaction a or c).

Compound **5** is best prepared by Grignard cross-coupling of **11** with 2-(3-methylthienyl)magnesium bromide (Scheme 3 reaction d), since in this case no functional groups restrict the use of organomagnesium compounds.

The X-ray structure analysis of **3e**[15] (Fig. 1) shows that both phenyl rings subtend an angle of 62.6° with the plane of the naphthalene. Similarly high torsion angles are observed in other diarylnaphthalenes[16] and lead to the face-to-face arrangement of the π-electron systems indicated in general structure **2**. The very close approach of the two phenyl rings in 1,8 arrangement is noteworthy: the value of 298.5 pm (C9–C18) is smaller than in 1,8-diphenylnaphthalene (299.3 pm) and markedly smaller than the van der Waals distance for parallel aromatic systems (about 340 pm).[16b]

Characteristic for this arrangement of the aryl rings are the significant high-field shifts ($\Delta\delta$ = 0.5–0.6 for various **3**) of the ^{1}H NMR signals of both 1,8-aryl substituents relative to those for corresponding 1-arylnaphthalenes. This effect, which has been attributed to an electronic interaction, is also observed for the paracyclophanes, with analogous arrangement of aryl rings (stereological[17a] molecules),[17b] and similar compounds.[12]

The lack of D/A conjugation means that compounds of the type **3**–**5** have relatively small dipole moments. This property, together with possible D–A/D–A stacking, tends to favor the formation of acentric structures. Thus **3e** crystallizes in the noncentrosymmetric space group $P2_1$,[15] which confers a

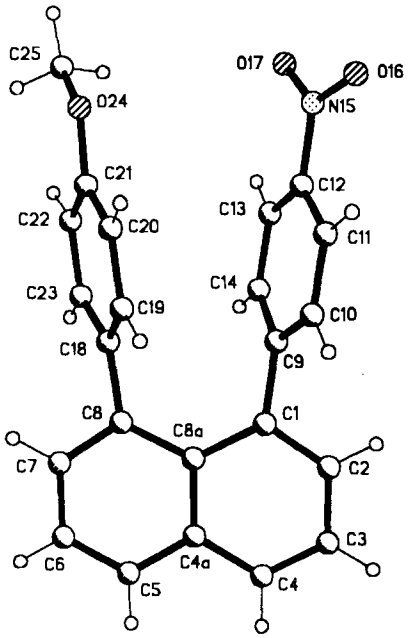

Fig 1. Crystal structure of **3e** [15]. Selected distances [pm]: C1–C8 257.7(5), C4–C5 243.1(5), C9–C18 298.5(4), C12–C21 377.9(5). Interplanar angles [°]: C1–C8a/C9–C14 62.56(10), C1–C8a/C18–C23 62.65(9).

macroscopic nonlinearity upon the crystals and renders them candidates for a frequency-doubling function.

The β values of compounds **3**–**7**[18] (presented in Table 1) were measured by means of hyper-Rayleigh-scattering (HRS),[19] since this method covers all components of the β tensor.

Table 1. Longest wavelength absorption maxima λ_{max} with extinction coefficients ε_{max} and transparency limits ($\lambda_{cut\ off}$) in $CHCl_3$, and first hyperpolarizibilities β (HRS measurements at 1064 nm in $CHCl_3$) for **3**–**7**.

No.	A [a]	D [a]	λ_{max} [nm]	$\lambda_{cut\ off}$ [nm]	ε_{max}	$10^{30} \times \beta_{HRS}$ [c] [esu]
3a	CF_3	OMe	320	360	8700	35
3b	CN	OMe	298	375	10100	26
3c	CN	SMe	304	378	16800	32
3d	CHO	2,6-OMe	304	380	13100	27
3e	NO_2	OMe	308	428	14100	32
4a	CF_3	H	304	364	10000	44
4b	CF_3	Me	300	366	9600	-
4c	CN	H	292	374	14100	42
4d	CN	Me	296	372	13300	38
5			298	374	8100	23
6	CN	OMe	312	372	15400	18
7a	CF_3	Me	306	358	12700	22
7b	CN	Me	310	370	14800	23
	PNA [b]		350	428	14200	17

[a] In the 4-position, if not otherwise indicated. [b] Paranitroaniline (PNA) served as external reference. [c] Error limits approximately ± 15%.

Apart from the nitroarene **3e**, all 1,8-diarylnaphthalenes **3**–**5** display the necessary transparency ($\lambda_{cut-off} < 380$ nm) and are markedly more NLO-active than the colored *p*-nitroaniline (PNA). Compounds **4a** and **4c** display the highest β values (44 and 42×10^{-30} esu, respectively), which are those of the highly active blue-transparent representatives of the conventional NLO-systems **1** (40,[8a] 60[5a] and $80^{[8c]} \times 10^{-30}$ esu).

In order to increase the molecular hyperpolarizability β of **3** and **4**, the most promising D/A combinations according to the "two-level" model[6] were tested: the linear optical properties show the expected dependency on the D/A strength. The methoxy derivatives **3b** and **3e** show that a stronger acceptor (**3b**: CN, **3e**: NO_2) leads, as expected, to bathochromism and increased extinction. In contradiction of the accepted structure–property relations[17] for NLO-phores of type **1** and of the two-level model, the nonlinear optical properties are, however, scarcely affected.

In this context it is remarkable that the CT bands in the UV/Vis spectra of **3**–**5** are always overlapped, never isolated. If a transannular $\pi-\pi$ interaction of the two 1,8-aryl rings is nevertheless (partly) responsible for the observed NLO activity, the 1,8-diarylnaphthalenes should be more NLO-active than the comparably substituted 1,5-isomers! Despite a clear hypso- and hypochromism of their light absorption, compounds **3b** and **4d** do indeed display considerably higher β values than their *conjugated* analogues **6** and **7b**.

Because of their high nonlinearity, transparency, and thermal stability, the novel NLO-phores **3**, **4**, and **5** represent fascinating alternatives to the conventional extended conjugated systems **1** for the development of blue-transparent frequency-doubling devices. We hope that our newly won knowledge of these chromophores and the corresponding models will enable us to achieve still higher efficiencies β without reducing transparency.

Experimental Procedure

All reactions were carried out under a N_2 atmosphere [18].

10: A solution of **9** (1.25 g, 5.00 mmol) [14], 1-iodo-4-nitrobenzene (1.49 g, 6.00 mmol), Na_2CO_3 (1.27 g, 12.00 mmol), and $[Pd(PPh_3)_4]$ (173 mg, 0.17 mmol) in a mixture of toluene (15 mL), ethanol (15 mL), and water (10 mL) was heated at reflux for 48 h. The mixture was then freed from solvent, taken up in $CHCl_3$, washed three times with 1 M NaOH and once with water, and dried over Na_2SO_4. Chromatography on 180 g silica gel (Merck KG-60 Art. No. 7734, $CHCl_3$) gave **10** as the second fraction; it was recrystallized analytically pure from *n*-hexane. Yield 1.21 g (74%). M.p. 124 °C.

11: As for **10**, starting from **9** (1.25 g, 5.00 mmol) and 3-iodopyridine (1.23 g, 6.00 mmol), but taken up in Et_2O and extracted with 1 M HCl. The aqueous phase was made alkaline with 2 M NaOH, taken up again in Et_2O, dried over K_2CO_3, and the solvent was removed in vacuo. Kugelrohr distillation (180 °C/0.3 mbar) yields **11** (82%) as a colorless, viscous oil (1.17 g).

3e: A solution of **10** (0.64 g, 2.00 mmol), (4-methoxyphenyl)dihydroxyborane (0.47 g, 3.00 mmol), Na_2CO_3 (0.64 g, 6.00 mmol), and $[Pd(PPh_3)_4]$ (69 mg, 0.06 mmol), in a mixture of toluene (6 mL), ethanol (6 mL), and water (4 mL) was heated at reflux for 48 h. Workup as for **10** gave, after TLC (silica gel KG-60, $CHCl_3$, third fraction) and recrystallization (*n*-hexane with a little ethyl acetate), 0.35 g (49%) of yellow crystals, m.p. 183–184 °C; ^{1}H NMR: δ = 8.90 (dd, ^3J = 8.2, ^4J = 1.4 Hz, 1H; 4-H), 7.95 (dd, ^3J = 8.2, ^4J = 1.4 Hz, 1H; 5-H), 7.73 (AA'XX', N = 8.8 Hz, 2H; 17/19-H), 7.58 (m, 1H; 6-H), 7.56 (m, 1H; 3-H), 7.44 (dd, ^3J = 7.1, ^4J = 1.4 Hz, 1H; 7-H), 7.37 (dd, ^3J = 7.1, ^4J = 1.4 Hz, 1H; 2-H), 7.07 (AA'XX', N = 8.8 Hz, 2H; 16/20-H), 6.84 (AA'XX', N = 8.7 Hz, 2H; 10/14-H), 6.47 (AA'XX', N = 8.7 Hz, 2H; 11/13-H), 3.63 (s, 3H; OCH_3); ^{13}C NMR: δ = 158.4 (C-12), 150.3 (C-15), 145.5 (C-18), 139.5 (C-8), 138.0 (C-1), 135.4 (C-4a), 131.0 (C-10/14) 131.0 (C-7), 130.9 (C-2), 130.4 (C-16/20), 130.0 (C-4), 129.3 (C-8a), 128.5 (C-5), 125.7 (C-6), 125.0 (C-3), 122.1 (C-17/19), 113.1 (C-11/13), 55.3 (OCH_3).

6: A solution of 2-(3-methylthienyl)magnesium bromide (from Mg turnings (0.15 g, 6.3 mmol) and 2-bromo-3-methylthiophene (1.02 g, 5.7 mmol) in diethyl ether (12 mL)) was added at 0 °C over 15 min to a suspension of **11** (0.82 g, 2.9 mmol) and $[NiCl_2(dppp)]$ (31.2 mg, dppp = 1,3-bis(diphenylphosphano)propane) in Et_2O/THF (1:1, 20 mL). After 1 h at room temperature with constant stirring, the mixture was heated at reflux for 4 h. After hydrolysis with NH_3/NH_4Cl and removal of solvent by distillation, the residue was taken up in Et_2O, washed with NH_3/NH_4Cl solution and water, dried over K_2CO_3, and the solvent again removed by distillation. Column chromatography (80 g basic Al_2O_3 Act. 1; $CHCl_3$) gave **6** as the third fraction; it was recrystallized from *n*-hexane. Yield 430 mg (49%) of yellowish crystals, m.p. 125.5 °C; ^{1}H NMR ($CDCl_3$): δ = 8.53 (m), 8.31 (m), 8.27 (m), 7.97 (m), 7.95 (m), 7.55–7.51 (m), 7.47 (m), 7.30 (m), 7.25 6.86 (m), 6.32 (m), 6.31 (m), 1.76 (s), 1.69 (s); ^{13}C NMR ($CDCl_3$): 24 signals in the range δ = 150.5–121.1.

Received: February 28, 1995 [Z 7745 IE]
German version: *Angew. Chem.* **1995**, *107*, 1587–1590

Keywords: naphthalenes · nonlinear optics · $\pi-\pi$ interactions · Suzuki coupling

 © VCH Verlagsgesellschaft mbH, D-69451 Weinheim, 1995 0570-0833/95/1313-1487 $ 10.00+.25/0

[1] a) W. Nie, *Adv. Mater.* **1993**, *5*, 520–545; b) R. W. Munn, C. N. Ironside, *Principles and Application of Nonlinear Optical Materials*, Chapman & Hall, London, **1993**; c) P. N. Prasad, D. J. Williams, *Introduction to Nonlinear Optical Effects in Molecules and Polymers*, Wiley, New York, **1991**; d) D. J. Williams, *Angew. Chem.* **1984**, *96*, 637–651; *Angew. Chem. Int. Ed. Engl.* **1984**, *23*, 690–703.
[2] D. F. Eaton, G. R. Meredith, J. S. Miller, *Adv. Mater.* **1991**, *3*, 564–565.
[3] A. Ulman, C. S. Willand, W. Köhler, D. R. Robello, D. J. Williams, L. Handley, *J. Am. Chem. Soc.* **1990**, *112*, 7083–7090.
[4] E. G. J. Staring, *Recl. Trav. Chim. Pays-Bas* **1991**, *110*, 492–506.
[5] a) I. Cabrera, A. Mayer, D. Lupo, U. Falk, U. Scheunemann, W. Hickel, *Nonlinear Opt.* **1995**, *9*, 161–169; b) I. Ledoux, J. Zyss, A. Jutand, C. Amatore, *Chem. Phys.* **1991**, *150*, 117–123.
[6] J. L. Oudar, D. S. Chemla, *J. Chem. Phys.* **1977**, *66*, 2664–2668.
[7] a) S. R. Marder, J. W. Perry, *Adv. Mater.* **1993**, *5*, 804–815; b) L.-T. Cheng, W. Tam, S. H. Stevenson, G. R. Meredith, G. Rikken, S. R. Marder, *J. Phys. Chem.* **1991**, *95*, 10631–10643; c) L.-T. Cheng, W. Tam, S. R. Marder, A. E. Stiegman, G. Rikken, C. W. Spangler, ibid. **1991**, *95*, 10643–10652.
[8] a) P. Boldt, M. Blenkle, I. Cabrera, D. Lupo, W. Hickel, *Nonlinear Opt.* **1994**, *8*, 173–182; b) E. Kelderman, G. J. T. Heesink, L. Derhaeg, T. Verbiest, P. T. A. Klaase, W. Verboom, J. F. J. Engbersen, N. F. van Hulst, K. Clays, A. Persoons, D. N. Reinhoudt, *Adv. Mater.* **1993**, *5*, 925–930; c) P. Walther, R. Gompper, W. Hickel, D. Lupo, H. Anneser, R. Dietrich, F. Feiner, C. Bräuchle, *Nonlinear Opt.* **1994**, *8*, 15–23.
[9] Recently the subject of controversial discussions in: C. A. Hunter, *Angew. Chem.* **1993**, *105*, 1653–1655; *Angew. Chem. Int. Ed. Engl.* **1993**, *32*, 1584–1586.
[10] a) Y. Mori, H. Nakanishi (Toshiba Corp.) JP-B 01059222, **1989** [Chem. Abstr. **1989**, *111*, 105457t]; b) S. Norvez, M. Barzoukas, *Chem. Phys. Lett.* **1990**, *165*, 41–44; c) E. Kelderman, W. A. J. Starmans, J. P. M. van Duynhoven, W. Verboom, J. F. J. Engbersen, D. N. Reinhoudt, *Chem. Mater.* **1994**, *6*, 412–417.
[11] S. Di Bella, I. L. Fragalá, M. A. Ratner, T. J. Marks, *J. Am. Chem. Soc.* **1993**, *115*, 682–686.
[12] a) F. Cozzi, M. Cinquini, R. Annunziata, J. S. Siegel, *J. Am. Chem. Soc.* **1993**, *115*, 5330–5331; b) B. M. Foxman, D. A. Gronbeck, N. Khruschova, M. Rosenblum, *J. Org. Chem.* **1993**, *58*, 4078–4082; c) K. Komatsu, R. Tsuji, Y. Inoue, K. Takeuchi, *Tetrahedron Lett.* **1993**, *34*, 99–102; d) M. Kuroda, J. Nakayama, M. Hoshino, N. Furusho, T. Kawata, S. Ohba, *Tetrahedron* **1993**, *49*, 3735–3748; e) E. Ibuki, S. Ozasa, Y. Fujioka, H. Mitzutani, *Bull. Chem. Soc. Jpn.* **1982**, *55*, 845–851; f) R. L. Clough, P. Mison, J. D. Roberts, *J. Org. Chem.* **1976**, *41*, 2252–2255. g) H. O. House, D. G. Koepsell, W. J. Campbell, *ibid.* **1972**, *37*, 1003–1011.
[13] N. Miyaura, T. Yanagi, A. Suzuki, *Synth. Commun.* **1981**, *11*, 513–519.
[14] Synthesis of **10** starting from 1,8-dibromonaphthalene (D. Seyferth, S. C. Vick, *J. Organomet. Chem.* **1977**, *141*, 173–187) by treatment with 1 equiv of *n*BuLi at −60 °C, subsequent reaction with $B(OMe)_3$ and hydrolysis with saturated NH_4Cl solution.
[15] Crystal data for **3e**: monoclinic, $P2_1$, $a = 845.93(10)$, $b = 1435.1(2)$, $c = 1465.5(2)$ pm, $\beta = 90.207(10)°$, $V = 1.7791$ nm^3, $Z = 4$ (two independent molecules), $T = -100$ °C. Yellow prism $0.9 \times 0.8 \times 0.8$ mm, Siemens P4 diffractometer, 3479 intensities to $2\theta_{max}$ 50°, 3250 independent. Structure solution: direct methods. Structure refinement: anisotropic on F^2 (program SHELXL-93, G. M. Sheldrick, University of Göttingen); H atoms with riding model; $wR(F^2)$ 0.094, with conventional $R(F)$ 0.042, for 489 parameters and 505 restraints; max. $\Delta\rho$ 163 e nm^{-3}. The structure could also be solved and refined in the orthorhombic space group $P2_12_12_1$; the apparent higher symmetry must, however, be regarded as pseudosymmetry, because the β angle deviates too far from 90° (in general, maximum deviations from genuine 90° angles are about 0.02°). To check the cell constants, those of another crystal were measured on a different diffractometer at −130 °C: β was 90.14(2)°. The assumption of a genuine deviation from orthorhombic symmetry was thus strengthened, but routine diffractometer measurements will probably not give unambiguous proof. Further details can be obtained from the Fachinformationszentrum Karlsruhe, D-76344 Eggenstein-Leopoldshafen, on quoting the depository number CSD-401564.
[16] X-ray structure analyses of other 1,8-diarylnaphthalenes: a) P. G. Jones, W. Grahn, A. Bahl, A. Reisner (né Chrapkowski), *Z. Kristallogr.* **1995**, *210*, 229–230; b) R. L. Clough, W. J. Kung, R. E. Marsh, J. D. Roberts, *J. Org. Chem.* **1976**, *41*, 3603–3609.
[17] a) R. Leppkes, F. Vögtle, *Angew. Chem.* **1981**, *93*, 404–405; *Angew. Chem. Int. Ed. Engl.* **1981**, *20*, 396–397; b) T. Otsubo, S. Mizogami, Y. Sakata, S. Misumi, *Bull. Chem. Soc. Jpn.* **1973**, *46*, 3831–3835.
[18] The structures of the new compounds **3a–e**, **4a–d**, **5**, **6** and **7a–b** are indicated by the spectroscopic data [^{1}H NMR (400 MHz, $CDCl_3$, TMS), ^{13}C NMR (101 MHz, $CDCl_3$; $\delta = 77.05$), EI-MS (70 eV), IR, UV/Vis] and correct elemental analyses.
[19] K. Clays, A. Persoons, *Phys. Rev. Lett.* **1991**, *66*, 2980–2983.

The Active Sites of the Native Cytochrome-c Oxidase from Bovine Heart Mitochondria: EXAFS-Spectroscopic Characterization of a Novel Homobinuclear Copper Center (Cu_A) and of the Heterobinuclear Fe_{a3}-Cu_B Center**

Gerald Henkel,* Arnd Müller, Stefan Weissgräber, Gerhard Buse, Tewfik Soulimane, Guy C. M. Steffens, and Hans-Friedrich Nolting

Cytochrome-c oxidase [E. C. 1.9.3.1] catalyzes the reduction of molecular oxygen to water in the respiratory chain and converts the redox energy to an electrochemical proton potential across the plasma or mitochondrial membrane. Owing to its important function, the metalloenzyme has been the subject of numerous investigations. The membrane-spanning protein is composed of 13 subunits and contains in addition to two heme-A groups (Fe_a and Fe_{a3}) two copper centers (Cu_A and Cu_B) as well as a zinc and a magnesium ion. While the Cu_A center has been shown to act as the primary electron acceptor, the catalytic reduction of oxygen takes place at the binuclear center Fe_{a3}-Cu_B.[1]

According to the results of homologous classifications of numerous sequences from subunit II and molecular biological studies of the expressed soluble Cu_A domain from *Paracoccus denitrificans*, the amino acid ligands for the Cu_A center are most probably two histidine and two cysteine residues. In addition, one methionine residue is also conserved.[2, 3] The precise copper content of the protein was not established until quite recently. Whereas earlier assumptions proposed that the native enzyme contained two copper ions, Buse and co-workers were recently able to demonstrate the presence of a third, specifically bound copper ion.[4] After a short and somewhat controversial discussion in the literature (see e.g. ref. [5]), the existence of the third copper ion is now considered to be correct.[6] EPR studies indicate its presence as an integral constituent of the Cu_A center.[7, 12] On the basis of the results of a recent EXAFS (EXAFS = extended X-ray absorption fine structure) investigation on the expressed soluble Cu_A domain from subunit II of the caa_3-cytochrome-c oxidase from *Bacillus subtilis* and on a mixed-valence reference complex, the authors proposed a binuclear center containing a direct copper–copper bond without any bridging ligands.[8, 9]

In an attempt to characterize the metal centers, we performed high-resolution X-ray absorption measurements in the K edge regions of copper, iron, and zinc by using intact preparations of cytochrome-c oxidase from bovine heart mitochondria. They were shown to contain three copper and two iron atoms as well as one zinc and one magnesium atom by precise metal content analyses (ICP-AES). In this paper we report the analysis of the EXAFS regions of the copper and iron edges. The experimentally determined EXAFS functions are shown in Figure 1.

[*] Prof. Dr. G. Henkel, Dipl.-Chem. A. Müller, Dr. S. Weissgräber
Fachgebiet Anorganische Chemie der Universität
Lotharstrasse 1, D-47048 Duisburg (Germany)
Telefax: Int. code + (203)-3792110
Prof. Dr. G. Buse, Dr. T. Soulimane, Dr. G. C. M. Steffens
Institut für Biochemie der Technischen Hochschule,
Klinikum, Aachen (Germany)
Dr. H.-F. Nolting
European Molecular Biology Laboratory
Outstation Hamburg, c/o DESY (Germany)

[**] Financial support from the Deutsche Forschungsgemeinschaft, the Bundesministerium für Forschung und Technologie, the European Union, and the Fonds der chemischen Industrie is gratefully acknowledged.

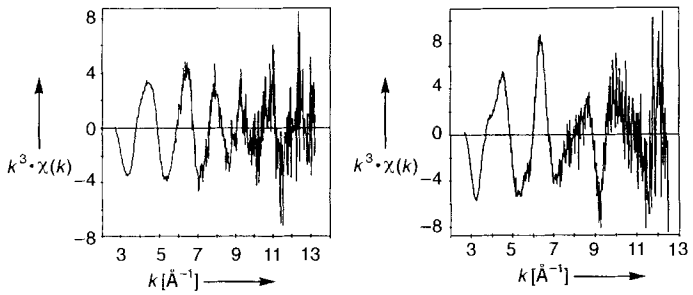

Fig. 1. Left: Experimental copper EXAFS (k^3-weighted); right: Experimental iron EXAFS (k^3-weighted).

Based on the results of the curve fitting procedure, the Cu_A center of the intact cytochrome-c oxidase from bovine heart mitochondria is a novel homobinuclear complex with a copper–copper distance of 2.46 Å. Though the enzyme has already been the subject of several EXAFS investigations,[10] a backscatterer contribution in the range between 2.4 and 2.7 Å has only been reported in connection with measurements on membrane-oriented layers.[10k] This contribution was assigned to a copper–methionine interaction; at the time the Cu_A center was thought to be mononuclear.

In order to evaluate the data, the copper EXAFS (Fig. 1, left) was Fourier-filtered in the distance range between 1.45 and 4.35 Å. The characteristic Fourier transform observed in this region could be modeled with an appropriate set of ligand atoms taking multiple scattering effects into account (see Fig. 2c and 2d).

During the initial steps of the structure refinement based on the Fourier-filtered EXAFS function, the first coordination sphere of Cu was modeled with a ligand set composed of nitrogen and sulfur donor atoms at distances of about 1.98 and 2.30 Å, respectively. Inspection of the Fourier transform, revealed an additional significant backscatterer at a distance of about 2.5 Å. The backscattering contributions at about 3 and 4 Å (see Fig. 2) were also not covered by this model. They are characteristic features of complexes with coordinated five-membered imidazole-type rings, representing the backscattering contributions of the α-carbon atoms (at ca. 3 Å) and the sum of the contributions of the atoms in β-positions (carbon and nitrogen atoms) and of multiple scattering effects within the five-membered ring (at ca. 4 Å).[11] The introduction of a total of three coordinating histidine groups in the structural model led to a distinct improvement of the fitting result. However, the deficiency in the backscattering density at 2.5 Å in the Fourier transform remains (Fig. 2a and 2b). The modeling of this contribution is best achieved with the phase and amplitude functions of a scatterer from the series of electron-rich 3d metals. Since in our opinion the metal–metal distance within the binuclear Fe_{a3}–Cu_B center must be at least 1 Å longer than 2.5 Å due to the steric shielding of the iron atom by the porphyrin ring, only copper is suitable as the backscatter atom in this case. A further convincing argument for this interpretation can be derived from the occupation numbers, which clearly favor a total of two copper–copper interactions (fit-index 0.234) over only one copper–iron contact. The refinement of the complete structural model results in a copper–copper distance of 2.46 Å.

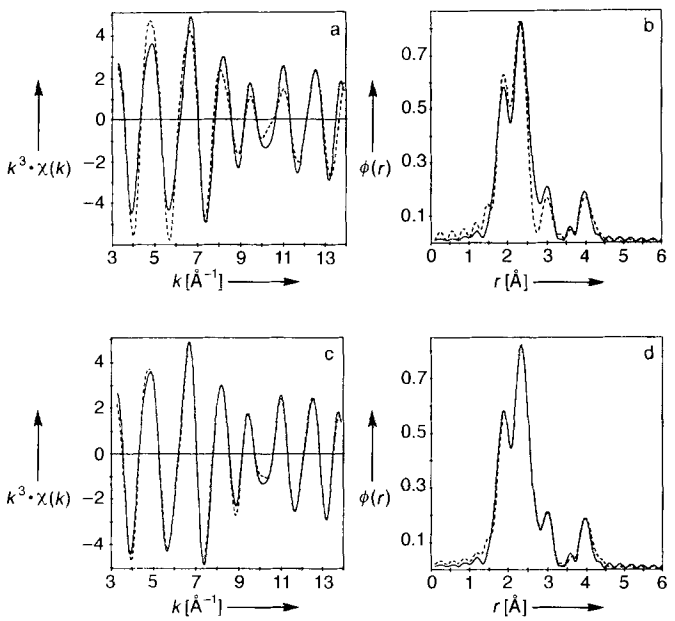

Fig. 2. a) Fourier-filtered copper EXAFS (solid line) and theoretically fitted curve (three histidine residues, four N/O and five S/Cl donor functions, dashed line) and b) corresponding Fourier transform (solid line: experiment; dashed line: model); fit-index: 1.262; c) Fourier-filtered copper EXAFS and theoretically fitted curve as in Fig. 2a, but including additional copper and iron backscatterer contributions (complete model, see Table 1) and d) corresponding Fourier transform; fit-index: 0.176.

Attempts to fit this contribution with an additional sulfur instead of a nitrogen atom led to a negative Debye–Waller factor (Cu–S = 2.60 Å, $2\sigma^2 = -0.004$ Å^2). Combined with the slightly worse fit-index of 0.255, the physically not meaningful value clearly supports a model with an electron-rich 3d transition metal backscatterer in accordance with our interpretation as copper atom. However, the existence of an additional, weakly bonded methionine residue in a distance range from about 2.6 to 3.1 Å cannot be ruled out completely as its contribution would be masked by the copper in this constellation.

In order to account for a backscattering contribution to the peak at 4 Å not yet considered, the structural model was completed by addition of an iron atom at a distance of about 3.9 Å from the copper atom. The final structural model consists of a set of backscatterers of the type O and/or N, a set of imidazole fragments from the histidine residues, a set of sulfur atoms from the cysteine residues as well as a set of copper and iron atoms in the local environment of the copper atoms. It should be mentioned that possible backscattering contributions of chloro ligands are modeled by the sulfur ligand shell due to very similar amplitude and phase functions (Fig. 2c and 2d).

During the final cycles of the structure refinement, the occupation numbers of the individual coordination spheres were varied in integral units under preservation of the coordination number four. For each set of possible occupation numbers generated, a common value for E_0, the distances of the individual shells from the central atom as well as their averaged Debye–Waller factors were refined taking multiple scattering effects into account. During the refinements, the imidazole rings were treated as rigid groups. The results for the set with the best fit index are listed in Table 1.

The interpretation of the results is complicated by the fact that the Cu EXAFS is a superposition of the contributions from all three copper atoms. On average, each copper atom has four directly bonded ligands, and a total of five copper–sulfur(chlorine) interactions is observed.

According to sequence classifications[2] and investigations by Lappalainen and Saraste,[3] two cysteine and two histidine residues are available to bind to copper in the homobinuclear center Cu_A. The conserved methionine residue probably does not belong to the first coordination sphere of copper.[3] Since

Table 1. Results of the curve fitting procedure for the Fourier-filtered EXAFS data of the copper K edge [a].

Shell	Occupation number	Distance [Å]	Debye–Waller factor [Å^2]
N/O	1.33 (4/3)	2.03	0.013
N_{His}	1.00 (3/3)	1.96	0.003
S/Cl	1.67 (5/3)	2.29	0.014
Cu	0.67 (2/3)	2.46	0.008
C_{His}	1.00 (3/3)	2.94	0.003
	1.00 (3/3)	2.98	0.019
Fe	0.33 (1/3)	3.89	0.003
N_{His}	1.00 (3/3)	4.11	0.015
C_{His}	1.00 (3/3)	4.21	0.034

[a] The occupation number is normalized to one copper atom (total coordination number four); the atoms of the histidine residues are refined as a rigid unit; estimated error in distances: 0.03 Å.

five Cu–S(Cl) bonds are detected in this study, both cysteine residues within the Cu_A center must be present as bridging ligands, because the coordination of Cu_B is dominated by N and/or O donor ligands in accordance with its redox properties as a high-potential center ($E_{1/2}$ ca. 0.34 V). As the Cu_A center is the primary electron acceptor which transfers an electron to the active site, the native enzyme could contain mixed-valence $Cu^{1.5+}$ centers. Evidence for this hypothesis was recently found by comparative EPR investigations of N_2O reductase and cytochrome-c oxidase,[12] thus a tetrahedral ligand environment of both copper atoms is assumed to be most likely.

The surprisingly short Cu···Cu distance within the binuclear Cu_A center raises the question of a plausible structural model for the complete homobinuclear complex. In fact, synthetic binuclear copper compounds with mixed tetrahedral sulfur–nitrogen ligand spheres and comparably short copper–copper distances are unknown to date.[9] To our knowledge there is only one binuclear complex of a 3d metal with tetrahedral coordination and alkanethiolato bridges known so far, where the metal–metal distance is shorter than 2.5 Å. This is the complex ion $[Co_2(SC_3H_7)_5]^-$, in which the two MS_4 tetrahedra share a common face.[13] Since the metal–metal distances in similar complexes with coordination tetrahedra sharing common edges are invariably longer,[14] we propose a structural unit that contains a third bridging function in addition to the two cysteine bridges as the model for the homobinuclear Cu_A center of cytochrome-c oxidase. This third bridge could be the oxygen atom of a water molecule or of an aspartic acid residue, which invariably occurs in the peptide sequence at a suitable position. The tetrahedral coordination of each copper atom is completed by two terminally bonded histidine residues leading to an ideally linear N–Cu···Cu–N chain. The proposed structural model is shown in Figure 3. The short Cu···Cu distance does of course not rule out a direct metal–metal bond. However, magnetic investigations on $[Co_2(SC_3H_7)_5]^-$ and on its selenium-substituted counterpart, $[Co_2(SeC_3H_7)_5]^-$, indicate that the unpaired 3d electrons are coupled through superexchange mechanisms and not through direct metal–metal bonds.[15]

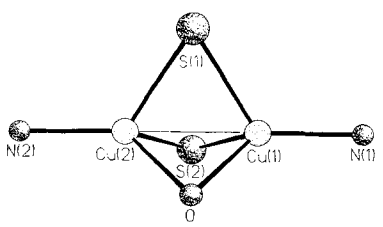

Fig. 3. Model for the homobinuclear Cu_A center of the cytochrome-c oxidase from bovine heart mitochondria (ball and stick model).

Accordingly, one histidine residue, one sulfur or chlorine, and two nitrogen and/or oxygen donor functions remain available for the coordination of copper within the Cu_B center. However, we cannot rule out the possibility that one of the remaining nitrogen or oxygen donor functions belongs to another histidine residue. The interpretation is not completely conclusive in this respect, since similar fit indices result for the alternative structural models. We favor the model with a total of three imidazole residues because the Debye–Waller factors of the ring atoms in β positions are of an order comparable to those of the α carbon atoms.

The Cu EXAFS yields a copper–iron distance of 3.89 Å. This value corresponds to that one expected for a tetrahedrally coordinated copper site linked to a heme unit through a ligand bridge. The bridge most probably is a sulfur or chlorine atom, since a corresponding iron–sulfur or iron–chlorine contact could be identified on evaluating the fine structure of the iron edge.

Different interpretations of the copper EXAFS have led to contradictory descriptions in the literature about the copper–iron distance within the Fe_{a3}-Cu_B center of cytochrome-c oxidase. The value derived by Powers et al. is 3.8 Å,[10a] while the distance found by Scott et al. (3.0 Å) is considerably shorter.[10f] A similar short distance was also described by George et al.[10k] These values are rather uncertain, because in the evaluation of the EXAFS data no attempts were made to model the multiple scattering pathways within the imidazole fragments. In a recent EXAFS investigation of a aa_3-quinol oxidase from *Bacillus subtilis* containing a Fe_{a3}-Cu_B center but no Cu_A center, a copper–iron distance of 3.7 Å was described.[16]

In analogy to Cu, the Fe EXAFS analysis was carried out by using a Fourier-filtered function (Fig. 4, left) which accounts for

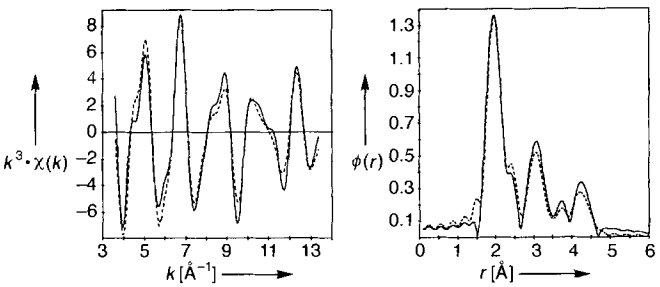

Fig. 4. Left: Fourier-filtered iron EXAFS (solid line) and theoretically fitted curve (complete model, dashed line); right: Corresponding Fourier transform.

all backscattering contributions in a distance range between 1.50 and 4.65 Å (Fig. 4, right). The first coordination sphere can be modeled quite well with a ligand set of nitrogen and sulfur donor atoms. The backscattering contributions with peaks at about 3.0 and 4.2 Å (Fig. 4 right) are essentially caused by the non-coordinated ring atoms of the tetrapyrrole and imidazole fragments. These contributions were taken into account by considering multiple scattering effects during the subsequent curve-fitting procedure. The contribution of a copper atom to the fine structure of the iron K edge becomes apparent in a destructive interference at about 3.9 Å. The complete structural model consists of a set of imidazole fragments from the histidine residues, a set of tetrapyrrole fragments, a set of bridging methine-C atoms, a set of sulfur or chlorine atoms as well as a set of copper atoms in the local environment of the iron atoms.

During the final cycles of the structure refinement, the occupation numbers of the individual coordination spheres were

varied in integral units under preservation of the coordination number six. For each set of possible occupation numbers generated, a common value for E_0, the distances of the individual shells from the central atom as well as their averaged Debye–Waller factors were refined taking multiple scattering effects into account. During the refinements, the imidazole rings and the tetrapyrrole fragments were treated as rigid groups. The results for the set with the best fit-index are listed in Table 2. The

Table 2. Results of the curve fitting procedure for the Fourier-filtered EXAFS data of the iron K edge [a].

Shell	Occupation number	Distance [Å]	Debye–Waller factor [Å^2]
N_{His}	1.50 (3/2)	1.99	0.002
N_{por}	4.00 (8/2)	2.03	0.009
S/Cl	0.50 (1/2)	2.32	0.002
C_{His}	1.50 (3/2)	2.94	0.005
	1.50 (3/2)	3.06	0.005
C_{por}	4.00 (8/2)	3.04	0.004
	4.00 (8/2)	3.09	0.028
C_{por}	4.00 (8/2)	3.36	0.023
Cu	0.50 (1/2)	4.04	0.006
N_{His}	1.50 (3/2)	4.10	0.014
C_{His}	1.50 (3/2)	4.19	0.014
N_{por}	4.00 (8/2)	4.29	0.042
N_{por}	4.00 (8/2)	4.27	0.022

[a] The occupation number is normalized to one iron atom (total coordination number six); the atoms of the histidine and porphine residues are refined as rigid units; estimated error in distances: 0.03 Å

iron–copper distance within the Fe_{a3}-Cu_B center derived from the Fe EXAFS is 4.04 Å and thus slighly longer than the corresponding distance derived from the Cu EXAFS. The deviation can be explained by uncertainties in modeling the five-membered rings and the multiple scattering effects within the ligand frameworks, which arise from the application of averaged geometries for the five-membered ring systems of the imidazole and tetrapyrrole residues. Here we appear to have reached the limits of the method, which demonstrates that the iron–copper distance determined has a relatively high error. The backscattering contribution at 2.31 Å is the result of a sulfur or chlorine donor function, which has to be formulated as a bridge between Cu_B and Fe_{a3}. Further statements, for example about the separation between the metal centers in different subunits of the enzyme, are not possible due to the limited range of the method, which usually does not exceed 4 to 5 Å in biomolecules.

While the work described in this paper was in the last stages of evaluation,[17] the results of an EXAFS investigation on the soluble Cu_A domain from subunit II of the caa_3-cytochrome-c oxidase from *Bacillus subtilis* expressed in *Escherichia coli* were published.[8] They confirm the results of this work with regard to the distance between the copper atoms within the homobinuclear center. Despite this fact, there are significant differences, especially with respect to the total number of copper–sulfur contacts. Whereas the interpretation of the EXAFS data of the intact cytochrome-c oxidase from bovine heart mitochondria requires the assumption of two cysteine bridges, the number of copper–sulfur bonds for the soluble Cu_A domain of the bacterial cytochrome-c oxidase was determined with only two (i.e. bridging ligands excluded).[8] It should also be mentioned that the characteristic imidazole backscattering contributions found in the Cu EXAFS of the complete mitochondrial cytochrome-c oxidase are almost completely lacking in the spectrum of the soluble Cu_A domain. Because it is highly unlikely that the Cu_A centers of the bacterial cytochrome-c oxidases differ characteristically from the Cu_A centers of the corresponding oxidases in mammals, there might be significant differences between the domain reconstructed by gene technology and the native enzyme. The structural model proposed by Blackburn et al.[8] is based on measurements on samples with excess copper contents and contains a copper–copper bond without any bridging ligands. This model, however, refers to the reconstructed domain and is hence not readily transferable to the Cu_A center of the intact cytochrome-c oxidase from bovine heart mitochondria.

The structural models for the homobinuclear Cu_A as well as for the heterobinuclear Fe_{a3}-Cu_B center derived from our EXAFS experiments are depicted schematically in Figure 5.

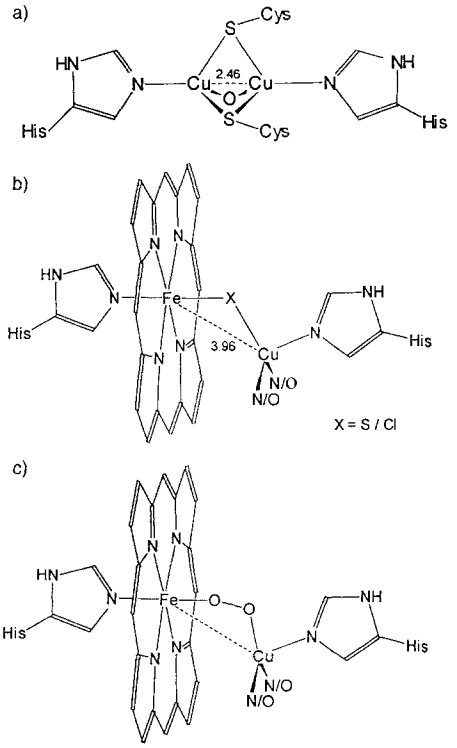

Fig. 5. Models for the metal centers of cytochrome-c oxidase in schematic representation: the homobinuclear center Cu_A (a), the heterobinuclear center Fe_{a3}-Cu_B (b), and the proposed binding situation of the O_2 molecule (c).

Since the enzyme in its examined form readily reacts with oxygen without any activation phase, the metal atoms of the Fe_{a3}-Cu_B center should already be in the catalytically relevant position. Based on this assumption, we propose a model for the binding of the O_2 molecule which is shown in Figure 5c. In this model, the O_2 molecule is bound in a *cis*-μ-1,2 arrangement to both the iron and the copper atom.

Experimental Procedure

Cytochrome-c oxidase was isolated from bovine heart mitochondria as described and purified on Q-Sepharose FF (Pharmacia) in 0.1% Triton TX-100, 10 mM Tris/HCl (pH 7.6) in the final step [18]. The enzyme exists as a monodisperse dimer under these conditions and reacts rapidly and monophasically with cyanide; the maximal activity corresponds to the activity in situ, that is, in its membranous environment. The chemical purity of the protein was checked by SDS-polyacrylamide gel electrophoresis, amino acid analysis, and quantitative determination of the N-terminal amino acids by Edman degradation. The metal content was determined by ICP-AES [18].

The enzyme solution used for X-ray absorption spectroscopy was concentrated by ultrafiltration in Centricon-100 (Amicon) to 800 µM. The samples were filled in polystyrene cuvettes with Kapton windows (layer thickness 1 mm, volume 150 µL), shock frozen in a cryogenic bath with ethanol/dry ice (195 K), and subsequently

cooled down to 77 K. During the measurements the samples were kept in a helium cryostate at 20 K.

The X-ray absorption spectra in the region of the iron, copper, and zinc K edges were recorded with the EXAFS spectrometer of the European Molecular Biology Laboratory (EMBL) in the Hamburger Synchrotronstrahlungslabor (HASYLAB) at the Deutsches Elektronen-Synchrotron (DESY, Hamburg) center using the synchrotron radiation from the storage ring DORIS II (4.5 GeV; average beam current 50 mA) [19]. The optical system of the EXAFS spectrometer consists of a Si(111) double crystal monochromator and a focussing toroidal mirror. Selected Bragg reflections of a suitably mounted Si crystal simultaneously recorded with the spectrum are used for the absolute calibration of the energy axis [20].

The spectra were recorded by measuring the fluorescence radiation in a range from 6915 to 7780 eV (Fe) and from 8725 to 9710 eV (Cu) with a 13-element solid-state detector (Canberra). The measuring time was 1–2 s per point with about 1400 points per spectrum. A total of 34 (Fe edge) and 23 (Cu edge) single scans, repectively, were averaged after individual energy calibration. The EXAFS functions were isolated from these spectra by literature procedures [21], and the determination of the background was achieved with a spline function. The data evaluation was carried out with the program packages EXPROG (energy calibration and data reduction) [22] and EXCURV88 (curve fitting procedures employing theoretical amplitude and phase functions) [23].

Received: February 23, 1995 [Z 7732IE]
German version: *Angew. Chem.* **1995**, *107*, 1615–1619

Keywords: cytochrome-c oxidase · metalloenzymes · X-ray absorption spectroscopy

[1] B. C. Hill, *J. Biol. Chem.* **1994**, *269*, 2419.
[2] G. C. M. Steffens, T. Soulimane, G. Wolff, G. Buse, *Eur. J. Biochem.* **1993**, *213*, 1149.
[3] P. Lappalainen, M. Saraste, *Biochim. Biophys. Acta* **1994**, *1187*, 222.
[4] G. C. M. Steffens, R. Biewald, G. Buse, *Eur. J. Biochem.* **1987**, *164*, 295.
[5] a) B. G. Malmström, R. Aasa, *FEBS Lett.* **1993**, *325*, 49, and references therein; b) R. J. Gurbiel, Y.-C. Fann, K. K. Surerus, M. M. Werst, S. M. Musser, P. E. Doan, S. I. Chan, J. A. Fee, B. M. Hoffman, *J. Am. Chem. Soc.* **1993**, *115*, 10888.
[6] M. Kelly, P. Lappalainen, G. Talbo, T. Haltia, J. van der Oost, M. Saraste, *J. Biol. Chem.* **1993**, *268*, 16781.
[7] P. M. H. Kroneck, W. E. Antholine, D. H. W. Kastrau, G. Buse, G. C. M. Steffens, W. G. Zumft, *FEBS Lett.* **1990**, *268*, 274.
[8] N. J. Blackburn, M. E. Barr, W. H. Woodruff, J. van der Oost, S. de Vries, *Biochemistry* **1994**, *22*, 10401.
[9] H. Bertagnolli, W. Kaim, *Angew. Chem.* **1995**, *107*, 847; *Angew. Chem. Int. Ed. Engl.* **1995**, *34*, 771.
[10] a) L. Powers, W. Blumberg, B. Chance, C. Barlow, J. S. Leigh, J. Smith, T. Yonetani, S. Vik, J. Peisach, *Biochim. Biophys. Acta* **1979**, *546*, 520; b) R. A. Scott, S. P. Cramer, R. W. Shaw, H. Beinert, H. B. Gray, *Proc. Natl. Acad. Sci. USA.* **1981**, *78*, 664; c) L. Powers, B. Chance, Y. Ching, P. Angiolillo, *Biophys. J.* **1981**, *34*, 465; d) A. Naqui, C. Kumar, Y.-C. Ching, L. Powers, B. Chance, *Biochemistry* **1984**, *23*, 6222; e) L. Powers, B. Chance, *J. Inorg. Biochem.* **1985**, *23*, 207; f) R. A. Scott, J. R. Schwartz, S. P. Cramer, *Biochemistry* **1986**, *25*, 5546; g) P. M. Li, J. Gelles, S. I. Chan, R. J. Sullivan, R. A. Scott, *ibid.* **1987**, *26*, 2091; h) L. Powers, B. Chance, Y.-C. Ching, C.-P. Lee, *J. Biol. Chem.* **1987**, *262*, 3160; i) C. Kumar, A. Naqui, L. Powers, Y.-C. Ching, B. Chance, *ibid.* **1988**, *263*, 7159; j) R. A. Scott, *Annu. Rev. Biophys. Biophys. Chem.* **1989**, *18*, 137; k) G. N. George, S. P. Cramer, T. G. Frey, R. C. Prince, *Biochim. Biophys. Acta* **1993**, *1142*, 240.
[11] a) R. W. Strange, S. S. Hasnain, N. J. Blackburn, P. F. Knowles, *J. Phys C Solid State Phys.* **1986**, *8*, 593; b) N. Binsted, R. W. Strange, S. S. Hasnain, *Biochemistry* **1992**, *31*, 12117.
[12] W. E. Antholine, D. H. W. Kastrau, G. C. M. Steffens, G. Buse, W. Zumft, P. M. H. Kroneck, *Eur. J. Biochem.* **1992**, *209*, 875.
[13] G. Henkel, S. Weissgräber, *Angew. Chem.* **1992**, *104*, 1382; *Angew. Chem. Int. Ed. Engl.* **1992**, *31*, 1368.
[14] G. Henkel, C. Chen, *Inorg. Chem.* **1993**, *32*, 1064.
[15] G. Henkel, S. Weissgräber, unpublished.
[16] L. Powers, M. Lauraeus, K. S. Reddy, B. Chance, M. Wikström, *Biochim. Biophys. Acta* **1994**, *1183*, 504.
[17] S. Weissgräber, A. Müller, G. Henkel, G. C. M. Steffens, G. Buse, H.-F. Nolting, C. Hermes, *Jahresbericht HASYLAB*, Hamburg 1992, p. 493.
[18] T. Soulimane, G. Buse, *Eur. J. Biochem.* **1995**, *227*, 588.
[19] C. Hermes, E. Gilberg, M. H. J. Koch, *Nucl. Instrum. Methods Phys. Res. Sect. A* **1984**, *222*, 207.
[20] R. F. Pettifer, C. Hermes, *J. Appl. Crystallogr.* **1985**, *18*, 404.
[21] B. K. Teo, *EXAFS: Basic Principles and Data Analysis*, Springer, Berlin, **1986**.
[22] H.-F. Nolting, C. Hermes, *EXPROG: EMBL EXAFS data analysis and evaluation Program Package*, **1992**
[23] N. Binsted, S. J. Gurman, J. W. Campbell, *SERC Daresbury Laboratory EXCURV88 Programm*, **1986**.

Dilithium Acepentalenediide: An Unusual Dimer of Contact Ion Triplets with Bowl-Shaped Dianions**

Rainer Haag, Roland Fleischer, Dietmar Stalke,* and Armin de Meijere*

Dedicated to Professor Paul von Ragué Schleyer on the occasion of his 65th birthday

New allotropic forms of carbon like C_{60} **1** and higher fullerenes are currently a popular research topic.[1] Alkali metal doped C_{60}-fullerenes, in particular, have attracted considerable attention due to their superconductivity at low temperatures.[2] Corannulene **2**,[3] the smallest complete subunit of C_{60} with a curved molecular surface, consists of a five-membered ring fully surrounded by six-membered rings. Its alkali metal derivatives have also been studied extensively.[4]

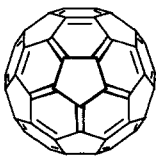

1

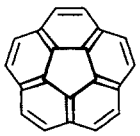

2

3

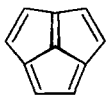

4

The smallest conceivable fullerene is C_{20} **3**, which is made up of five-membered rings only. Both dodecahedradecaene **3**[5] and acepentalene **4**,[6] the smallest curved subunit of **3**, have been targets for synthesis in spite of their obviously exceedingly high strain. The $C_{10}H_6$ hydrocarbon **4** is even more strained than the $C_{20}H_{10}$ corannulene **2** and has been predicted to be a triplet diradical in the ground state.[7] However, this electronic destabilization can be overcome, and the corresponding closed-shell dianion **6** has been obtained with remarkable ease by treating triquinacene **5** with a superbasic mixture[8] of *n*-butyllithium, potassium *tert*-pentoxide, and TMEDA[9] (Scheme 1). Although **6** has been characterized unequivocally by its spectroscopic data and trapping reactions with electrophiles, its structure remained unknown, because the dipotassium salt **6a** initially formed from **5** could not be purified sufficiently.

[*] Prof. Dr. A. de Meijere, Dipl.-Chem. R. Haag
Institut für Organische Chemie der Universität
Tammannstrasse 2, D-37077 Göttingen (Germany)
Telefax: Int. code + (551)39-9475
Priv.-Doz. Dr. D. Stalke, Dipl.-Chem. R. Fleischer
Institut für Anorganische Chemie der Universität
Tammannstrasse 4, D-37077 Göttingen (Germany)
Telefax: Int. code + (551)39-2582

[**] This work was supported by the Volkswagen-Stiftung, the Deutsche Forschungsgemeinschaft, and the Fonds der Chemischen Industrie, as well as by BASF, Bayer, and Hüls AG through generous gifts of chemicals. We are grateful to Mr. W. Zolke, Göttingen, for recording the ^{7}Li CP-MAS NMR spectra and Prof. M. Rabinovitz, Jerusalem, for helpful discussions. R. H. is indebted to the Gottlieb-Daimler and Karl-Benz-Stiftung for a travel grant.

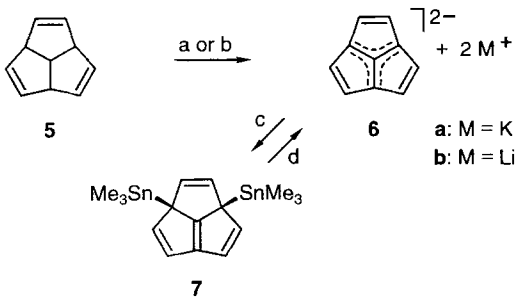

Scheme 1.

We have now succeeded in preparing and purifying 4,7-bis(trimethylstannyl)dihydroacepentalene **7** by sublimation. From **7**, pure dilithium acepentalenediide **6b** can be obtained by a cleanly proceeding transmetalation with methyllithium in dimethoxyethane (DME) at −60 °C. Compound **6b** crystallized very well from a solution in DME at low temperatures (−30 °C), and a single-crystal structure analysis was performed at 153 K.[10] In the crystal, **6b** forms dimers consisting of two bowl-shaped $C_{10}H_6$ dianions whose convex surfaces face each other (Fig. 1). Two lithium counterions, Li2 and Li2A, each of

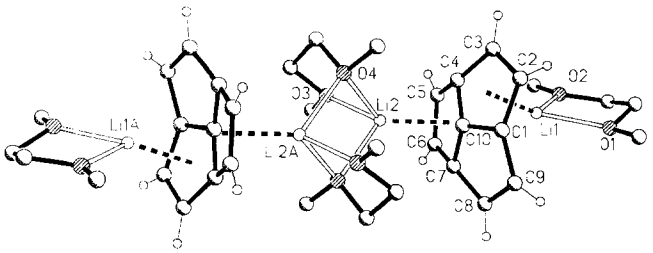

Fig. 1. The solid-state structure of **6b**; selected bond lengths [pm]: Li1-C 232.9(4), Li2-C 237.2(4), Li1-O1 204.1(4), Li1-O2 202.1(4), Li2-O3 200.8(4), Li2-O4 213.2(4), Li2A-O4 223.5(4), Li1-C_5(center) 198.9, Li2-C_5(center) 203.9. For averaged structural parameters of the CH skeleton see Fig. 2.

which coordinate one molecule of dme, are sandwiched between the two convex surfaces, but with different distances to each of them. The remaining two lithium counterions are located on the outward pointing concave faces of the bowl-shaped dianions (Li1 and Li1A in Fig. 1). These cations each coordinate one of the three angularly fused five-membered rings in an almost ideal η^5 fashion; the Li–C distances range from 225.9 (Li–C1) to 238.9 pm (Li–C3). The coordination spheres of Li1 and Li1A are also completed by dme donor molecules with average Li–O distances of 203.1 pm.

The lithium ions on the convex faces of the dianions also have ideal η^5 coordination, but each one to a second five-membered ring (C4, C5, C6, C7, C10) with distances between 227.0 (Li2–C10) and 241.7 pm (Li2–C4). In addition, the inner lithium atoms Li2 and Li2A each coordinate one dme molecule, but not in the same fashion as the coordination of dme by Li1 and Li1A. Both oxygen atoms chelate the same lithium atom, and one oxygen atom (O4) forms an μ_2 bridge between the two inner metal atoms, resulting in a four-membered, central Li_2O_2 ring. The crystallographic inversion center is located in the middle of that ring. Because of the different bonding modes, the Li–O distances in this ring are not equal. While Li2–O3 is 200.8 pm, the bonds to O4 are longer (Li2–O4 213.2, Li2–O4A 223.5 pm) due to unequal electron distribution between both electropositive lithium atoms. Because Li2 gets electron density from three oxygen atoms and Li1 only from two, the carbanionic fragment is more attractive to Li1, resulting in a shorter distance between the Li1 atom and the center of the five-membered ring (198.9 pm) than that between Li2 and the corresponding five-membered ring (203.9 pm).[13]

Although the structure of **6b** should be regarded as a contact ion triplet with all the implications of ion pairing phenomena,[14] the $C_{10}H_6$ dianion adopts almost ideal local C_3 symmetry with C10 on the threefold axis. The coordination sphere of C10 is considerably pyramidalized (26.3 pm out of the plane of the three neighboring atoms; sum of the three bond angles: 349.7°). The three central C–C bonds are of equal length (140.4 pm)[15] within error limits, and despite the negative charges in the molecule they are only marginally shorter than those in the central five-membered ring of corannulene **2** (141.1 pm[16]). The six C–C(H) bonds in **6b** are 5 pm longer (av. 145.5 pm) and the three peripheral C(H)–C(H) about the same length (av. 141.1 pm) as those in **2**. Unlike corannulene **2**, in which the central five-membered ring is completely regular with all bond angles equal to 108°, in **6b** the endocyclic bond angles range from 101.9° (average) for the C-C-C(H) angles and 109.6° (average) for C-C(H)-C(H) to 116.6° (average) for C-C-C angles at the central carbon C10 (Fig. 2). Yet all three five-membered rings in **6b** are almost ideally planar with a maximum deviation of only 2.8 pm from the best plane in each case.

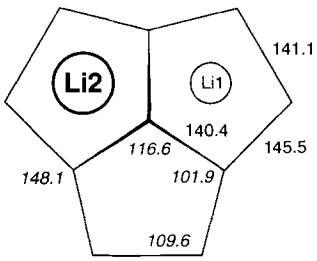

Fig. 2. Structural parameters of the CH skeleton of **6b**. Geometrically equivalent bond lengths [pm] and angles [°] are averaged; angles are in italics.

Unexpectedly, the structural parameters of the single five-membered ring of the $C_{10}H_6$ unit not coordinated to a lithium ion are basically the same as those of the other two. Like in Ph_3CM (M = Li, Na)[17] contact ion pairs, the two lithium ions in **6b** do not affect the bonding parameters in the carbon skeleton. It would be interesting to see whether structural distortion would be more pronounced in higher alkali metal derivatives of acepentalene, since in such derivatives of Ph_3CM (M = K, Rb, Cs)[18] with η^6 coordination of one of the three phenyl rings by the metal, the bond between this ring and the central carbon atom is considerably shorter than that to the other two.[19]

An analogous dimeric assembly, in solution however, has also been deduced from NMR spectroscopic studies of the tetraanion of corannulene, $C_{20}H_{10}^{4-}$ **2**$^{4-}$, with lithium counterions.[4] In contrast to the arrangement of the two $C_{10}H_6Li_2$ units in the crystal of **6b**, the two $C_{20}H_{10}$ subunits in the dimer of $C_{20}H_{10}Li_4$ are postulated to face each other with one convex and one concave side ("stacked-bowl" arrangement) with rapid inversions of both.[4] Another remarkable difference between $(C_{20}H_{10}Li_4)_2$ **2**$^{4-}$ and $(C_{10}H_6Li_2)_2$ **6b** is that the solid-state structure of the latter could not be verified in solution. The ^7Li and ^1H NMR spectra of **6b** in solution ([D$_8$]THF, −60 °C) show single signals at $\delta_{LiBr} = -8.2$ and $\delta_{TMS} = 6.16$, respectively. The three different types of carbon atoms in **6b** give rise to three signals [δ_{TMS} = 108.5 (d, C-2(3,5,6,8,9), 116.2 (s, C-1(4,7), 151.8 (s, C-10)] in the ^{13}C NMR spectrum ([D$_8$]THF, −60 °C).[20] This indicates C_3 symmetry of the molecules of **6b** in solution, which may either be caused by fluxional behavior in the dimer (rapid exchange of inside and outside positions, e.g. by inversion), by a rapid dimer–monomer equilibrium, or by the sole occurrence of a stable monomer of **6b** in solution. Even

at $-110\,^{\circ}C$ it was not possible to resolve the signals of different ^{1}H, ^{7}Li, and ^{13}C nuclei in the respective NMR spectra in solution. However, in the ^{7}Li CP-MAS NMR spectrum of solid **6b**, two different resonances were observed at $\delta = -4.9$ and -9.8 (ext. LiCl), similar to that reported for other oligolithio compounds in the solid state.[21] Because of its chemical shift and shape, the broad signal at lower field is tentatively assigned to the outer lithium ions Li1/Li1A in the dimer, and the other to the inner ones (Li2/Li2A). This is in line with the observed ^{7}Li chemical shifts of the tetralithium corannulene $\mathbf{2}^{4-}$ in solution.[4e] Unfortunately, different signals for the carbon atoms could not be resolved in the ^{13}C CP-MAS NMR spectrum of **6b**, possibly due to the relatively high quadrupole moment of the coordinated ^{7}Li nuclei or a dynamic process of the lithium counterions even in the solid state. This difficulty might be overcome by studying the corresponding ^{6}Li-enriched derivative, which is currently being prepared.

It is also noteworthy that unlike $\mathbf{2}^{4-}$ and **6b**, the dilithium pentalenediide, which can be considered a subunit of dilithium acepentalenediide **6b**, does not form a dimer.[22] Instead it is a monomeric "ion triplet" with the two lithium ions on opposite sides of the planar hydrocarbon skeleton. Such ion triplets are known for a number of lithium derivatives of conjugated hydrocarbons.[23] Also, "reverse" ion triplets with a single lithium ion between two organic anions are known.[24] But aggregates larger than the one reported here for **6b** and for corannulene tetraanion $\mathbf{2}^{4-}$,[4] in which several lithium ions are sandwiched between two hydrocarbon polyanions, are relatively rare.[25, 26] It remains to be seen whether the curved shape of acepentalenediide **6b** is static or easily inverted like the corannulene molecule **2**[3c] and its tetraanion $\mathbf{2}^{4-}$.[4]

Received: December 10, 1994 [Z 7537 IE]
German version: *Angew. Chem.* **1995**, *107*, 1642–1644

Keywords: acepentalenes · fullerenes · pentalenes · structure elucidation

[1] a) W. Kraetschmer, L. D. Lamb, D. R. Huffmann, *Nature* **1990**, *347*, 345; b) R. E. Smalley, *Acc. Chem. Res.* **1992**, *25*, 98; c) H. W. Kroto, *Angew. Chem.* **1992**, *104*, 113; *Angew. Chem. Int. Ed. Engl.* **1992**, *31*, 111; d) F. Diederich, Y. Rubin, *ibid.* **1992**, *104*, 1123 and **1992**, *31*, 1101; e) Y. Elemes, S. K. Silverman, C. Sheu, M. Kao, C. S. Foote, M. M. Alvarez, R. L. Whetten, *ibid.* **1992**, *104*, 364 and **1992**, *31*, 351; f) H. Schwarz, *ibid.* **1992**, *104*, 301 and **1992**, *31*, 293; g) A. Hirsch, *The Chemistry of the Fullerenes*, Thieme, Stuttgart, **1994**, and references therein.

[2] a) A. F. Hebard, M. J. Rosseinsky, R. C. Haddon, D. W. Murphy, S. H. Glarum, T. T. M. Palstra, A. P. Ramirez, A. R. Kortan, *Nature* **1991**, *350*, 600; b) R. M. Flemming, A. P. Ramirez, M. J. Rosseinsky, D. W. Murphy, R. C. Haddon, S. M. Zahurak, A. V. Makhija, *ibid.* **1991**, *352*, 787; c) K. Tanigaki, I. Hirosawa, T. W. Ebbesen, J. Mizuki, Y. Shimakawa, Y. Kubo, J. S. Tsai, S. Kuroshima, *ibid.* **1992**, *356*, 419; d) K. Tanigaki, *Advances in Superconductivity IV* (Eds.: H. Hyakawa, N. Koshizuka), Springer, Tokyo, **1991**, p. 203, and references therein.

[3] a) L. T. Scott, M. M. Hashemi, D. T. Meyer, H. B. Warren, *J. Am. Chem. Soc.* **1991**, *113*, 7082; b) A. Borchard, A. Fuchicello, K. V. Kilway, K. K. Baldridge, J. S. Siegel, *ibid.* **1992**, *114*, 1921; c) L. T. Scott, M. M. Hashemi, M. S. Bratcher, *ibid.* **1992**, *114*, 1920; d) H. Becker, G. Petrie, P.-C. Cheng, H. Schwarz, L. T. Scott, D. K. Bohme, *ibid.* **1993**, *115*, 11636; e) G. Javahery, H. Becker, S. Petrie, P.-C. Cheng, H. Schwarz, L. T. Scott, *Org. Mass Spectrom.* **1993**, *28*, 1005.

[4] a) A. Ayalon, M. Rabinovitz, P.-C. Cheng, L. T. Scott, *Angew. Chem.* **1992**, *104*, 1691; *Angew. Chem. Int. Ed. Engl.* **1992**, *31*, 1636; b) A. Ayalon, A. Sygula, P.-C. Cheng, M. Rabinovitz, P. W. Rabideau, L. T. Scott, *Science* **1994**, *265*, 1065. c) Y. Cohen, A. Ayalon, *Angew. Chem.* **1995**, *107*, 888–891; *Angew. Chem. Int. Ed. Engl.* **1995**, *34*, 816.

[5] a) J.-P. Melder, R. Pinkos, H. Fritz, H. Prinzbach, *Angew. Chem.* **1990**, *102*, 105; *Angew. Chem. Int. Ed. Engl.* **1990**, *29*, 95; b) J.-P. Melder, R. Pinkos, H. Fritz, J. Woerth, H. Prinzbach, *J. Am. Chem. Soc.* **1992**, *114*, 10213; c) K. Weber, H. Prinzbach, R. Schmidlin, F. Gerson, G. Gescheidt, *Angew. Chem.* **1994**, *105*, 907; *Angew. Chem. Int. Ed. Engl.* **1994**, *32*, 875; d) F. Wahl, J. Wörth, H. Prinzbach, *Angew. Chem.* **1993**, *104*, 1788–1791; *Angew. Chem. Int. Ed. Engl.* **1993**, *32*, 1722–1726; e) Review: H. Prinzbach, K. Weber, *ibid.* **1994**, *106*, 2329 and **1994**, *33*, 2239.

[6] a) H. Butenschön, A. de Meijere, *Angew. Chem.* **1984**, *96*, 722; *Angew. Chem. Int. Ed. Engl.* **1984**, *23*, 707; b) *Helv. Chim. Acta* **1985**, *68*, 1658; c) *Tetrahedron* **1986**, *42*, 1721; d) G. Schröder, H. Butenschön, R. Boese, T. Lendvai, A. de Meijere, *Chem. Ber.* **1991**, *124*, 2423.

[7] a) A. Streitwieser, Jr., *Molecular Orbital Theory for Organic Chemists*, Wiley, New York, **1961**; b) R. Zahradnik, J. Michl, J. Koutecký, *Collect. Czech. Chem. Commun.* **1964**, *29*, 1932; c) R. Zahradnik, J. Michl, *ibid.* **1965**, *30*, 3529; d) V. Bonačić-Koutecký, J. Koutecký, J. Michl, *Angew. Chem.* **1987**, *99*, 216; *Angew. Chem. Int. Ed. Engl.* **1987**, *26*, 170.

[8] T. Lendvai, T. Friedel, H. Butenschön, T. Clark, A. de Meijere, *Angew. Chem.* **1986**, *98*, 734; *Angew. Chem. Int. Ed. Engl.* **1986**, *25*, 719. We prefer to call dianion **6** "acepentalenediide" to reflect its preparation from the neutral hydrocarbon acepentalene **4** by twofold electron transfer rather than from dihydroacepentalene by twofold deprotonation, which would lead to the somewhat misleading name "dihydroacepentalenediide".

[9] a) L. Lochmann, J. Pospisil, D. Lim, *Tetrahedron Lett.* **1966**, 257; b) M. Schlosser, S. Strunk, *ibid.* **1984**, *25*, 741; c) M. Schlosser, *Pure Appl. Chem.* **1988**, *60*, 1627; d) L. Lochmann, W. Bauer, *J. Am. Chem. Soc.* **1992**, *114*, 7482, and references therein.

[10] Crystal data of **6b**: $C_{18}H_{20}Li_2O_4$, $M = 320.3$, monoclinic, space group $P2_1/c$, $a = 1333.5(3)$, $b = 847.3(2)$, $c = 1578.9(3)$ pm, $\beta = 91.57(3)^{\circ}$, $V = 1.7833(6)$ nm^3, $Z = 4$, $\rho_{calcd} = 1.193$ Mg m^{-3}, $F(000) = 688$, $\lambda = 71.073$ pm, $T = 153$ K, $\mu(Mo_{K\alpha}) = 0.080$ mm^{-1}. Data were collected on a Stoe-AED diffractometer. A suitable crystal ($0.6 \times 0.4 \times 0.4$ mm) in a drop of oil [11] was cooled rapidly and mounted at $-80\,^{\circ}C$. Intensities were collected by the $2\theta/\omega$ methods in the range $5 < 2\theta < 50^{\circ}$. Of a total of 5666 reflections 3097 were independent; largest difference peak and hole: 643 and -288 e nm^{-3}, $R1(I > 2\sigma(I)) = \Sigma \, ||F_o| - |F_c|| / \Sigma \, |F_o| = 0.065$ und $wR2 = \{\Sigma \, [w(F_o^2 - F_c^2)^2] / \Sigma \, [w(F_o^2)^2]\}^{0.5} = 0.211$ based on F^2 for all data. The structure was solved by direct methods (SHELXS92) [12a] and refined by full-matrix least squares on F^2 (SHELXL93) [12b]. The hydrogen atom positions were refined with a riding model with the CH_3 groups free to rotate about their local threefold axes. Further details of the crystal structure investigation may be obtained from the Director of the Cambridge Crystallographic Data Centre, 12 Union Road, GB-Cambridge CB21EZ (UK), on quoting the full journal citation.

[11] T. Kottke, D. Stalke, *J. Appl. Crystallogr.* **1994**, *26*, 615.

[12] a) G. M. Sheldrick, *Acta Crystallogr. Sect. A* **1990**, *46*, 467; b) G. M. Sheldrick, Program for Crystal Structure Refinement, University of Göttingen, **1993**.

[13] D. Stalke, *Angew. Chem.* **1994**, *106*, 2256; *Angew. Chem. Int. Ed. Engl.* **1994**, *33*, 2168.

[14] C. Lambert, P. von R. Schleyer, *Angew. Chem.* **1994**, *106*, 1187; *Angew. Chem. Int. Ed. Engl.* **1994**, *33*, 1129.

[15] This is consistent with, but not necessarily a proof for Y-type conjugation as suggested for the trimethylenemethane dianion and related systems: a) P. Gund, *J. Chem. Educ.* **1972**, *49*, 100; b) J. Klein, A. Medlik, *J. Chem. Soc. Chem. Commun.* **1973**, 275; c) J. Klein, *Tetrahedron* **1988**, *44*, 503.

[16] The crystal structure analysis of **2** referred to was carried out at 203 K: J. C. Hanson, C. E. Nordman, *Acta Crystallogr. Sect. B.* **1976**, 1147.

[17] a) J. J. Brooks, G. D. Stucky, *J. Am. Chem. Soc.* **1972**, *94*, 7333; b) R. A. Bartlett, H. V. R. Dias, P. P. Power, *J. Organomet. Chem.* **1988**, *341*, 1; c) H. Köster, E. Weiss, *ibid.* **1979**, *168*, 273.

[18] D. Hoffmann, W. Bauer, P. von R. Schleyer, U. Pieper, D. Stalke, *Organometallics* **1993**, *12*, 1193.

[19] This bond shortening is even more pronounced in (diphenylpyridylmethyl)metal derivatives $Ph_2(2\text{-}NC_5H_4)CM$ (M = Li, Na, K), because the delocalization of the negative charge is distorted by the introduction of a nitrogen atom into a six-membered ring. U. Pieper, D. Stalke, *Organometallics* **1993**, *12*, 1201.

[20] The previously reported (ref. [8]) ^{1}H and ^{13}C NMR chemical shifts for dipotassium acepentalenediide **6a** were recorded at $-40\,^{\circ}C$ with impure and highly dilute samples. Despite the influence of a different counterion, different temperature, different concentration, and possible association with impurities these values are remarkably close to those of **6b**.

[21] a) F. Pauer, J. Rocha, D. Stalke, *J. Chem. Soc. Chem. Commun.* **1991**, 1477; b) S. Freitag, W. Kolodziejski, F. Pauer, D. Stalke, *J. Chem. Soc. Dalton Trans* **1993**, 3479; c) H. Gornitzka, D. Stalke, *Angew. Chem.* **1994**, *106*, 695; *Angew. Chem. Int. Ed. Engl.* **1994**, *33*, 693.

[22] a) D. Wilhelm, J. L. Courtneidge, T. Clark, A. G. Davies, *J. Chem. Soc. Chem. Commun.* **1984**, 810; b) J. J. Stezowski, H. Hoier, D. Wilhelm, T. Clark, P. von R. Schleyer, *ibid.* **1985**, 1263.

[23] a) A. Streitwieser, Jr., J. T. Swanson, *J. Am. Chem. Soc.* **1983**, *105*, 2502; b) A. Streitwieser, Jr., *Acc. Chem. Res.* **1984**, *17*, 353; c) Y. Cohen, J. Klein, M. Rabinovitz, *J. Chem. Soc. Chem. Commun.* **1986**, 1071; d) A. Sygula, K. Lipkowitz, P. W. Rabideau, *J. Am. Chem. Soc.* **1987**, *109*, 6602; e) J. W. Bausch, P. S. Gregory, G. A. Olah, G. K. S. Prakash, P. von R. Schleyer, G. A. Segal, *ibid.* **1989**, *111*, 3633; f) B. Wind, A. Sygula, U. Govindarajan, U. Edlund, I. Sethson, P. W. Rabideau, *J. Org. Chem.* **1991**, *56*, 618; g) I. Sethson, D. Johnels, T. Lejon, U. Edlund, B. Wind, A. Sygula, P. W. Rabideau, *J. Am. Chem. Soc.* **1992**, *114*, 953.

[24] a) G. Fraenkel, M. P. Hallden-Abberton, *J. Am. Chem. Soc.* **1981**, *103*, 5657; b) L. M. Jackman, L. M. Scarmoutzos, W. Porter, *ibid.* **1987**, *109*, 6524; c) A. S. Galiano-Roth, D. B. Collum, *ibid.* **1988**, *110*, 3546; d) L. A. Paquette, W. Bauer, M. R. Sivik, M. Bühl, M. Feigel, P. von R. Schleyer, *ibid.* **1990**, *112*, 8776; e) W. Bauer, G. A. O'Doherty, P. von R. Schleyer, L. A. Paquette, *ibid.* **1991**, *113*, 7093; f) M. Eiermann, K. Hafner, *ibid.* **1992**, *114*, 135; g) S. Harder, M. H. Prosenc, *Angew. Chem.* **1994**, *106*, 1830; *Angew. Chem. Int. Ed. Engl.* **1994**, *33*, 1744; h) F. Zaegel, J. C. Gallucci, P. Mennier, B. Gautheron, M. R. Sirik, L. A. Paquette, *J. Am. Chem. Soc.* **1994**, *116*, 6466.

[25] Examples of dimers in solution: a) M. J. Goldstein, T. T. Wenzel, G. Whittaker, S. F. Yates, *J. Am. Chem. Soc.* **1982**, *104*, 2669; b) M. J. Goldstein, T. T. Wenzel, *J. Chem. Soc. Chem. Commun.* **1984**, 1654, 1655.

[26] Examples of dimers in the solid state: a) D. Bladauski, H. Dietrich, H.-J. Hecht, D. Rewicki, *Angew. Chem.* **1977**, *89*, 490; *Angew. Chem. Int. Ed. Engl.* **1977**, *16*, 474; b) D. Bladauski, W. Broser, H.-J. Hecht, D. Rewicki, H. Dietrich, *Chem. Ber.* **1979**, *112*, 1380.

Electron Transfer and Polar Reactions of Cyclizable Anion Radicals: Structural Consequences of Orbital Selection Rules and Chain-Length Constraints**

G. Narahari Sastry, A. Chandrasekhar Reddy, and Sason Shaik*

To be or not to be bonded is a fundamental question for the transition state (TS) of an electron transfer (ET) reaction of an electrophile nucleophile combination that also has a classical polar (bond-forming) pathway available to it.[1] Valence bond configuration mixing (VBCM) analysis predicts that when either the nucleophile or the electrophile is an ion radical, both the ET and polar pathways may have TS structures with strong bonding interactions governed by reaction-specific orbital selection rules.[2, 3] These orbital selection rules determine the resonance energies of the respective transition states and thereby exert stereo- and regiospecific requirements. According to the VBCM analysis,[2] when the reactive fragments involve a carbonyl anion radical moiety and a carbon–halide moiety (C–X), the orbital selection rule for the ET-TS dictates a structure that optimizes the overlap between the singly occupied π^* orbital of the anion radical moiety and the σ^* orbital of the C–X moiety. In contrast, the TS structure for the polar (substitution) mechanism requires the optimum overlap between the doubly occupied oxygen lone-pair orbital of the anion radical and the σ^* orbital of C–X. The reaction-specific orbital interactions provide structural rules for the dichotomy of ET and polar mechanisms in ion radical chemistry. The role of the orbital selection rules has been corroborated in a recent ab initio study[4] of the intermolecular ET and substitution (SUB) reactions in a simple model system: the formaldehyde anion radical and methyl chloride. It was found that the structures of both the ET and SUB transition states have strong bonding interactions and possess distinct regio- and orientational selectivity in accord with the selection rules.

What is still missing for establishing the dichotomy of ET and polar mechanisms on solid structural foundations is a clear demonstration that the orbital selection rules are indeed at work in systems or models thereof that are known to display both ET and polar mechanisms, and in which the selection rules pose stringent structural constraints for the ET-TS. The opportunity is provided by recent elegant studies of Kimura et al.,[5, 6] who showed that the anion radicals of ω-haloalkyl phenyl ketone undergo competitive ET and SUB reactions and exhibit intriguing trends such as a common activation driving force law and a alternating dependence of the relative efficiency on the chain length. We report on ab initio computational studies of the intramolecular ET and SUB reactions of ω-chloroalkanal anion radicals (Scheme 1), models of compounds used by Kimura et al. The computational results provide structural and energetic evidence for the dominating influence of reaction-specific orbital selection rules and for the specific bonding features that are established in the ET-TS even when the anion radicals have adverse structural constraints.

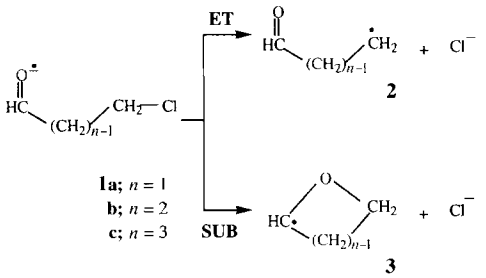

Scheme 1.

The ab initio MO computations used the split-valence plus polarization (6-31G*) basis set at the unrestricted Hartree–Fock level, and employed standard geometry optimization and characterization procedures.[7–9] This level was chosen after the ET and SUB processes for **1b** had been tested at UHF and UMP2 levels of theory with the 6-31G* and 6-31 + G* basis sets. Calculations at all of these levels showed identical mechanistic details and also the same trends in the relative energies. Moreover, previous studies for the reactions between formaldehyde anion radical and methyl chloride had shown an identical mechanistic dichotomy at the UHF, ROHF, and post-HF levels up to CCSD(T).[4, 10] The invariance of the trends indicates that the mechanistic conclusions reached at the UHF level of theory are very unlikely to change at higher levels, and this allows us to study the computationally more demanding system **1c**.

The calculations reported are at UHF/6-31G* level, which is the highest common level employed here for **1a**–**1c**. Anion radical **1a** ($n = 1$) is unstable and dissociates without an activation barrier to give exclusively the ET product **2a**. An experimental study on a substituted analogue of **1a** arrived at an identical result.[6] In contrast, **1b** ($n = 2$) and **1c** ($n = 3$) are stable and react according to ET and SUB mechanisms to yield corresponding products as shown in Scheme 1. The optimized structures of reactants (**1b**, **1c**), ET transition states (**4b**, **4c**), and SUB transition states (**5b**, **5c**), for for both reactions (with $n = 2$ and $n = 3$) are depicted in Figure 1, and are seen to exhibit an identical mechanistic dichotomy. In all cases both the ET and SUB transition states involve backside attack on the C–Cl bond. However, while for all systems the C–C–Cl unit in the ET-TS is oriented preferentially perpendicular to the plane of the HC=O unit, in the twin SUB-TS the O–C–Cl group is in the same plane as the carbonyl group. It is intriguing that the

[*] Prof. Dr. S. Shaik, G. N. Sastry, Dr. A. C. Reddy
Department of Organic Chemistry
and the Fritz Haber Centre of Molecular Dynamics
The Hebrew University, Jerusalem 91904 (Israel)
Telefax: Int. code + (2) 6585345

[**] This research was sponsored by the Volkswagen-Stiftung.

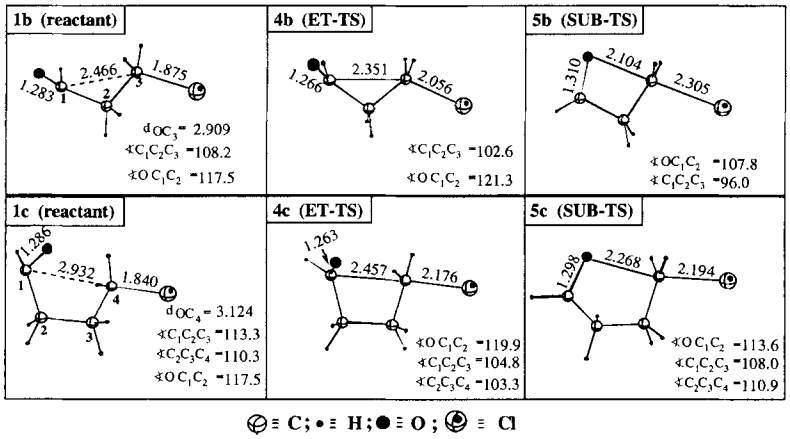

Fig. 1. UHF/6-31G*-optimized structures of the reactants (**1b**, **1c**) and the ET (**4b**, **4c**) and SUB transition states (**5b**, **5c**) for $n = 2$ and 3 (Scheme 1). Only important structural parameters are specified (angles in [°], distances in [Å]).

ET process takes place through the C end of the carbonyl group despite the fact that the extra negative charge is on oxygen![11] Attempts to find alternative pathways for the ET process starting from **1b** and **1c**, for example through the O end or in different trajectories, have either failed or resulted in the C-oriented ET-TS structures in Figure 1. No direct C-alkylation pathway could be found from the reactant, which is in full agreement with the experimental observation of only the O-alkylation product besides the ET product.[5, 6] As seen in Figure 2, these findings all follow the VBCM orbital selection rules, which dictate that the structure of the ET-TS is determined by optimizing the overlap between the π^* (CO) and the σ^* (CCl) orbitals, whereas the structure of the SUB-TS is determined by the overlap requirements between oxygen's lone pair n(O) and the σ^* (CCl) orbitals.

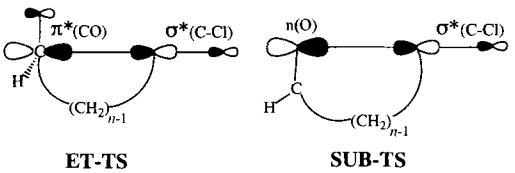

Fig. 2. Sketch of overlapping orbitals showing the resonance interactions in the ET-TS (left) and SUB-TS (right), as predicted by VBCM analysis [2]. Note the different orientations of the HCO moiety in the two transition states.

Table 1 lists the computed energies and isotope effects for the SUB and ET pathways. The activation barriers are dramatically different for the two systems, reflecting the effect of the orbital selection rules imposed on the chain-length constraints. Thus, for **1b** with $n = 2$ the ET barrier is smaller than that for the SUB process. In contrast, for **1c** with $n = 3$ the exact opposite is found. While the first trend (entries 1, 2) follows the relative thermodynamics of the ET and SUB pathways, the second trend (entries 3, 4) does not. Therefore the trends in Table 1 reflect very specific structural effects on the twin transition states, which are independent of the thermodynamic effect.

A close look at the optimized structures of reactant **1b** and the corresponding ET and SUB transition states (**4b** and **5b**) reveals why ET is the favored pathway (Fig. 1). The C–C distance between the carbonyl carbon and the terminal carbon is already short in reactant **1b**. Consequently, ET-TS **4b** requires only a little reorganization for achieving the necessary C–C bonding in the carbonyl π plane, since the carbonyl moiety is already appropriately oriented in reactant **1b** with respect to the C–Cl bond. The shortening of the C–C distance in the ET-TS (from 2.466 Å in **1b** to 2.351 Å in **4b**) is an indication that the ET-TS tries to achieve π^*(CO)–σ^*(CCl) bonding as strong as possible. In contrast, the SUB-TS **5b** requires major reorganization to achieve the requisite bonding via a strained four-membered ring. Thus, due to the constraints of the $n = 2$ chain, the orbital selection rule requirement is easily met for ET process of **1b** ($n = 2$), while for the corresponding SUB-TS the bonding requirement is met at the expense of high ring strain.

An increase in the length of the methylene chain by one unit to **1c** ($n = 3$) dramatically reverses the barrier for the ET and SUB mechanisms (Table 1, entries 3, 4), because chain-length constraints now operate against the orbital selection rule for the ET pathway. Thus, the π^*(CO)–σ^*(CCl) bonding for the ET pathway requires ET-TS **4c** to assume a strained four-membered ring structure with very small C-C-C angles (Fig. 1). On the other hand, the n(O)–σ^*(CCl) selection rule for the SUB-TS requires an almost strain-free five-membered ring structure (with close to normal bond angles; Fig. 1).[5] As already mentioned, it is intriguing that although the extra electron resides on oxygen,[11] the ET process takes place through the C end of the carbonyl group; the seemingly available, favorable five-membered ring arrangement that would be expected if ET were to proceed at the O end is avoided. The computed strained C orientation is therefore a strong indication that the ET-TS has a specific bonding requirement that has to be met despite structural constraints imposed by the intervening chain.

Table 1. Computed energies [a] and kinetic isotope effects [b] at the UHF/6-31G* level.

Reaction	$\Delta E^{\neq}$	ΔE_{rxn} [c]	$\alpha(CH_2/CD_2)$	$\alpha(C^{12/13})$
(1) ET ($n = 2$)	2.0	−34.9 (−46.9)	1.059	1.030
(2) SUB ($n = 2$)	12.6	−12.7 (−21.3)	0.996	1.040
(3) ET ($n = 3$)	8.2	−37.9 (−50.5)	1.141	1.045
(4) SUB ($n = 3$)	3.4	−38.6 (−46.9)	0.992	1.046

[a] All values are in kcal mol^{-1}. [b] Using the Eyring equation at the UHF/6-31G* level with frequencies scaled by 0.8929. The α position is designated with respect to Cl. [c] ΔE values refer to the conversion of particular reactant to give the respective products. The values in parentheses correspond to conversion of reactants to clusters of products.

Kinetic isotope effects can be used to distinguish the two mechanisms and to unravel their bonding properties. As shown in Table 1, the $\alpha(CH_2/CD_2)$ isotope effects, which are inverse for SUB mechanism and normal for ET pathway, may be used as criteria.[12] The $\alpha(C^{12/13})$ isotope effect, which is a measure of the tightness of a transition state,[13] is seen to be normal for both mechanisms. The calculated normal and large $\alpha(C^{12/13})$ isotope effect indicates that the ET transition states for $n = 2$ and $n = 3$ have strong bonding interactions much like their twin SUB transition states.

The present computational study demonstrates that the dichotomy between ET and polar mechanisms in ion radical chemistry can be explained by bonding principles derived from

mechanism-specific orbital selection rules. It is demonstrated that the orbital selection rules set stringent structural requirements on the geometries of both the ET-TS and the twin SUB-TS, and determine all of their stereochemical information—stereospecificity, regiospecificity, orientational specificity—and the consequent activation barriers. Thus, the ET-TS is found to possess a robust stereochemistry that follows the maximum bonding principle allowed by the selection rule. The existence of kinetic isotope effects for the ET-TS may help establish or challenge the structured ET-TS presented here, and put it in perspective with the traditional notion of weak bonding in the outer sphere model.[14–17]

Received: February 2, 1995 [Z 7686 IE]
German version: *Angew. Chem.* **1995**, *107*, 1619–1621

Keywords: ab initio calculations · electron transfer · substitution reactions · transition states

[1] L. Eberson, *Electron Transfer Reactions in Organic Chemistry*, Springer, Heidelberg, **1987**; J. K. Kochi, *Angew. Chem.* **1988**, *100*, 1331; *Angew. Chem. Int. Ed. Engl.* **1988**, *27*, 1227; A. Pross, *Acc. Chem. Res.* **1985**, *18*, 212; J. K. Cho, S. S. Shaik, *J. Am. Chem. Soc.* **1991**, *113*, 9890; C. J. Schlesener, C. Amatore, J. K. Kochi, *J. Phys. Chem.* **1986**, *90*, 3747; M. Juliard, J. P. Scagliarini, M. Rajzmann, M. Chanon, *Chimia* **1986**, *40*, 16; K. Daasberg, S. U. Pedersen, H. Lund, *Acta Chem. Scand.* **1991**, *45*, 424; R. D. Busli, H. Schwarz, *Chem. Ber.* **1990**, *123*, 535.

[2] L. Eberson, S. S. Shaik, *J. Am. Chem. Soc.* **1990**, *112*, 4484.

[3] S. S Shaik, *Acta Chem. Scand.* **1990**, *44*, 205; Y. Apeloig, O. M. Aharoni, D. Danovich, A. Ioffe, S. Shaik, *Isr. J. Chem.* **1993**, *33*, 387. For closed-shell electrophile nucleophile combinations a single bonding mechanism exists that can mix the reactant state with the electron transfer transition state. This mechanism is the basis of the polar reaction, and by default the ET-TS has only weak bonding interactions.

[4] G. N. Sastry, S. Shaik, *J. Am. Chem. Soc.* **1995**, *117*, 3290.

[5] N. Kimura, S. Takamuku, *J. Am. Chem. Soc.* **1994**, *116*, 4087.

[6] N. Kimura, S. Takamuku, *Bull. Chem. Soc. Jpn.* **1991**, *64*, 2433.

[7] All calculations were performed with the Gaussian 92 program package [8]. Geometries were optimized with gradients and characterized by frequency analysis. Reaction pathways were ascertained by IRC calculations [9]. The spin contamination of all the critical species for the ET and polar mechanisms are small; $\langle s^2 \rangle$ values are between 0.76 and 0.77. Isotope effects were computed with the Eyring equation at the UHF/6-31G* level using frequencies scaled by 0.8929.

[8] M. J. Frisch, G. W. Trucks, M. Head-Gordon, P. M. W. Gill, M. W. Wong, J. B. Foresman, B. G. Johnson, H. B. Schlegel, M. A. Robb, E. S. Replogle, R. Gomperts, J. L. Andres, K. Raghavachari, J. S. Binkley, C. Gonzalez, R. L. Martin, D. J. Fox, D. J. Defrees, J. Baker, J. J. P. Stewart, J. A. Pople, Gaussian 92, Revision C3, Gaussian, Inc., Pittsburgh PA, **1992**.

[9] C. Gonzalez, H. B. Schlegel, *J. Chem. Phys.* **1989**, *90*, 2154.

[10] Currently available tests (S. Shaik, G. N. Sastry, unpublished) include ROHF optimization, and single-point calculations on the UMP2/6-31 + G* and UMP2/6-31G* optimized geometries at levels up to CCSD(T). All tests give identical mechanistic schemes.

[11] The structure of formaldehyde anion radical is mostly described by $^{\bullet}CH_2O:^{-}$. Even though the spin is localized on C, the extra electron is on O.

[12] S. Wolfe, C.-K. Kim, *J. Am. Chem. Soc.* **1991**, *113*, 8056.

[13] B. S. Axelsson, B. Langström, O. Matsson, *J. Am. Chem. Soc.* **1987**, *109*, 7233.

[14] R. A. Marcus, *Ann. Rev. Phys. Chem.* **1964**, *15*, 155.

[15] N. S. Hush, *J. Chem. Phys.* **1958**, *28*, 962.

[16] J.-M. Savéant, *Adv. Phys. Org. Chem.* **1990**, *26*, 1.

[17] L. Eberson, *New J. Chem.* **1992**, *16*, 151.

New Nonlinear Optical Materials: Expedient Topotactic Self-Assembly of Acentric Chromophoric Superlattices**

Wenbin Lin, Shlomo Yitzchaik, Weiping Lin, Amit Malik, Mary K. Durbin, Andrew G. Richter, George K. Wong, Pulak Dutta, and Tobin J. Marks*

Although molecule-based assemblies offer many attractions for the construction of efficient second-order nonlinear optical materials (large nonresonant response, ultrafast response times, low dielectric constants/losses, and intrinsic tailorability), significant synthetic challenges have impeded the realization of optimum materials.[1, 2] These challenges include maximizing chromophore hyperpolarizability and number density as well as maximizing the degree and thermal/temporal stability of induced microstructural acentricity. An attractive alternative to electric field poled glassy polymers[2, 3] and Langmuir–Blodgett films[4] is a self-assembly[5] approach in which acentric chromophoric superlattices[6] are built up in a layer-by-layer fashion through the formation of covalent bonds.[6, 7] In the past, the efficiency of this approach has been limited by the slow rate (days) at which the large hyperpolarizability stilbazolium chromophore layers[6] could be assembled and the resulting, less than optimum superlattice structural regularity. We report here a new topotactic "molecular layer assembly approach in which the key assembly step is effected in either a solvent-free solid state or chemical vapor deposition mode, which in combination with other building block modifications, allows the expedient assembly of robust chromophoric architectures with high structural regularity and with very large nonlinear optical response. The results suggest that other self-assembly routes to multilayer structures could be achieved in a similar manner.

The present approach to acentric chromophoric superlattices utilizes the sequential repetition of three layer-building steps (Fig. 1), beginning upon a clean, hydroxylated surface (e.g., SiO_2 or single-crystal silicon). The progress of the assembly process is monitored by X-ray photoelectron spectroscopy (XPS), advancing aqueous contact angle (θ_a) measurements,

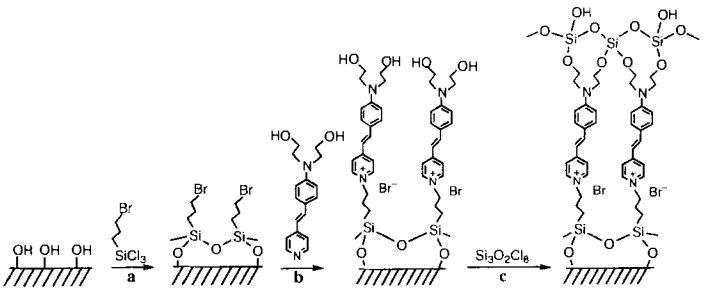

Fig. 1. Schematic representation of the self-assembly of covalent chromophoric superlattices. Conditions: see Experimental Procedure. The steps **a**–**c** can be repeated.

[*] Prof. T. J. Marks, Dr. Wenbin Lin, Dr. S. Yitzchaik
Department of Chemistry and the Materials Research Center
Northwestern University, Evanston, IL 60208-3113 (USA)
Telefax: Int. code + (708)-491-2990
e-mail: tjmarks@casbah.acns.nwu.edu

Weiping Lin, A. Malik, M. K. Durbin, Prof. G. K. Wong, Prof. P. Dutta, A. G. Richter
Department of Physics and Astronomy and the Materials Research Center
Northwestern University, Evanston, IL 60208-3112 (USA)

[**] This research was supported by the NSF through the Northwestern University Materials Research Center (grant DMR9120521) and by the AFOSR (contract 93-1-0114). We thank Stephen Roscoe for helpful discussions.

transmission optical spectroscopy, polarized second harmonic generation (SHG; $\lambda_0 = 1064$ nm), and specular X-ray reflectivity (XRR).[8]

Step **a** introduces a bromoalkyl functionality, the presence of which is evident from Br 3d XPS (peak at 70.4 eV, characteristic of a bromoalkane),[9] an appropriate hydrophobic change in θ_a (increases from 15° for SiO_2 to 75°), and an XRR monolayer thickness of about 10 Å. The cure component of this step is designed to achieve maximum intrafilm and film–substrate crosslinking.

Step **b** can be effected in either of two efficient modes. 1) A thin layer (≈ 1000 Å) of the stilbazolium chromophore precursor, 4-(*N*,*N*-dihydroxyethylamino)stilbazole,[6] is spin-coated onto the bromoalkyl-functionalized surface, followed by brief heating in vacuo to effect quaternization and removal of excess reagent (130 °C/0.4 Torr). 2) The precursor vapor can be passed over the heated substrate in a chemical vapor deposition (CVD) process. The course of the quaternization/assembly is verified by quantitative formation of Br^- in the Br 3d XPS (68.0 eV), the appearance of amine and pyridinium N1s XPS signals (399.5, 401.6 eV; 1:1 intensity ratio), an appropriate hydrophilic change in θ_a (75° → 50°), an increased film thickness to about 30 Å in the XRR (consistent with molecular models), and an extremely large SHG response from the anchored, high-hyperpolarizability[10] stilbazolium chromophore, $\chi^{(2)}_{zzz} = 7 \times 10^{-7}$ esu. Angular-dependent SHG measurements reveal an average tilt angle of the chromophore β_{zzz} direction of $40 \pm 3°$ away from the surface normal, in good agreement with earlier results.[6]

The course of step **b**, as monitored by in situ SHG measurements (Fig. 2) reveals the onset of chromophore formation at about 120 °C, far below the melting point of 4-(*N*,*N*-dihydroxyethylamino)stilbazole (194 °C), and suggestive of an interfacial

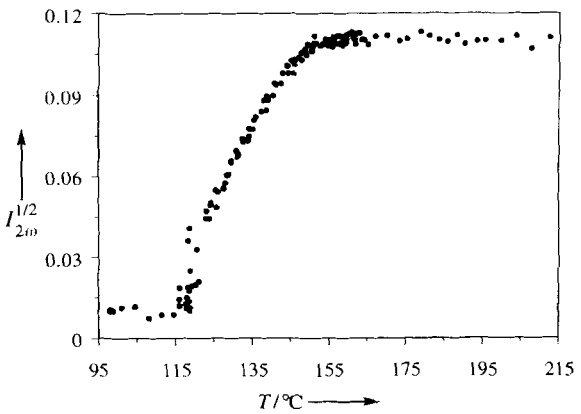

Fig. 2. In situ monitoring of the quaternization/chromophore formation step **b** in Fig. 1 by transmission second harmonic generation ($\lambda_0 = 1064$ mn). Temperature ramp rate: 25–160 °C, 1 °C min^{-1}; 160-215 °C, 3 °C min^{-1}. $I^{1/2}_{2\omega}$ data are in arbitrary units.

solid-state reaction. The quaternization process is complete by about 150 °C. It can also be seen by the persistence of the SHG response that the monolayer is stable under these conditions to 215 °C.

Step **c** is designed to provide lateral structural stabilization/planarization through interchromophore crosslinking and to provide a substrate for the subsequent iterative superlattice assembly process. The course can be ascertained from the expected hydrophilic change in θ_a (50° → 17°) and the additional thickness detected in the XRR (≈ 7 Å).

In the present admittedly crude, first-generation embodiment, about three to five complete iterations (trilayer assemblies) of steps **a**–**c** can be achieved per day—an increase in growth efficiency of about 30-fold over earlier work.[6] The degree to which this scheme produces a regular superlattice microstructure without loss of acentricity (deleterious randomization of chromophore orientation) and diminution of SHG efficiency, was investigated as a function of the number of added layers (steps **a**–**c**) by XRR, transmission optical spectroscopy, and SHG. The superlattice thicknesses calculated from the XRR data (Fig. 3a) show a smooth, monotonic increase as a

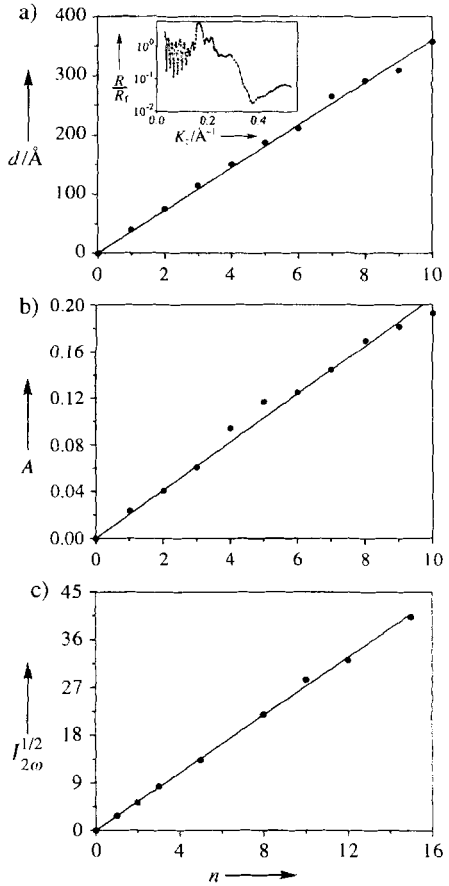

Fig. 3. Dependence of several characteristics of the chromophoric superlattice of Fig. 1 on the number of layers n, each composed of steps **a**–**c**. a) Thickness d derived from specular X-ray reflectivity measurements. Inset: normalized X-ray reflectance plotted versus wave vector for a specimen with 10 layers. b) Transmission optical absorbance A at 480 nm. c) Square root of the 532 nm second harmonic generation intensity (arbitrary units, $\lambda_0 = 1064$ nm).

function of the total number of assembled layers, consistent with a high degree of structural regularity. XRR data for a typical sample are shown in Figure 3a (inset). The maximum at $K_z = 0.17$ Å^{-1} is a "Bragg" peak due to scattering from individual layers; the interlayer spacing calculated from this peak position is 36 ± 1 Å, in good agreement with the thickness data and molecular models. The closely spaced minima in the data are due to interference between reflections from the superlattice–substrate and superlattice–air interfaces.

Further evidence for the buildup of regular superlattice layers with uniform chromophore orientation comes from the linear dependence of the 480 nm stilbazolium chromophore HOMO → LUMO longitudinal charge-transfer excitation[11] ab-

 © VCH Verlagsgesellschaft mbH, D-69451 Weinheim, 1995 0570-0833/95/1313-1498 $ 10.00+.25/0

sorbance on the number of assembled layers (Fig. 3b). A final test of the present superlattice regularity comes from the SHG response as a function of the number of layers. Because the film thicknesses are small compared to the wavelength of the incident light, the intensity of the SHG light from a regular structure should scale quadratically with the number of layers. The observed linear dependence of the square root of the second harmonic response on the number of layers (Fig. 3c) indicates both structural regularity in layer thicknesses as well as uniform alignment of the chromophore molecules. From the slope, $\chi^{(2)}_{zzz} \approx 5 \times 10^{-7}$ esu (≈ 200 pm V^{-1}) can be deduced; this value is slightly lower than the aforementioned monolayer result (see above) due to the added thickness imparted by the siloxane layer introduced in step **c**. Although it is probably resonance-enhanced,[11] this level of frequency doubling efficiency rivals or exceeds those under the same conditions of the most efficient poled polymers and Langmuir–Blodgett films reported to date.[1, 2] In addition to the information in Figure 2, aging studies still in progress indicate complete thermal stability of the SHG response over many months at 25 °C and some decay over the course of several hundred hours at 100 °C.

It is interesting to note that chromophoric superlattices of the present type can also be assembled if siloxane capping step **c** is deleted. Although XRR and optical spectroscopy indicate the buildup of a regular superlattice (as in Figs. 3a and b), the response of SHG intensity with the number of layers is not quadratic (in contrast to Fig. 3c). When the number of layers exceeds three, the SHG intensity begins to fall. This result indicates that in the absence of the lateral stabilization imparted by step **c**, randomization of chromophore alignment, perhaps induced by chromophore dipole–dipole repulsions, destroys the microstructural acentricity. In conclusion, these results demonstrate an expeditious and probably generalizable route to robust, intrinsically acentric (not requiring an electric poling field) and structurally regular, self-assembled superlattices exhibiting very large second-order nonlinear optical responses. Further elaboration of this chemistry and application to device structures[12] is in progress.

Experimental Procedure

All the operations were carried out using standard Schlenck techniques. Pentane and heptane (Fisher Scientific) were distilled from Na/K alloy immediately before use. (3-bromopropyl)trichlorosilane (Lancaster) was purified by vacuum distillation. Octachlorotrisiloxane was prepared by controlled hydrolysis of $SiCl_4$; 4-(*N*,*N*-dihydroxyethylamino)stilbazole was prepared according to the procedures in ref. [6].

Step **a**: Freshly cleaned glass or silicon single-crystal substrates were immersed in a 1:100 (v/v) solution of (3-bromopropyl)trichlorosilane in heptane for 20 min, and then washed with copious amounts of pentane, followed by sonication in acetone for 1 min. The samples were then air-cured at 110 °C for 10 min.

Step **b**: 1) The silylated substrates (after step **a**) were spin-coated with a 4 mM solution of 4-(*N*,*N*-dihydroxyethylamino)stilbazole in methanol at 4000 rpm and then heated at 130 °C in a vacuum oven (0.4 Torr) for 30 min. 2) The silylated substrates were placed directly above a petri dish containing 4-(*N*,*N*-hydroxyethylamino)stilbazole in a vacuum oven (0.4 Torr) at 130 °C for 30 min.

Step **c**: The glass and silicon single-crystal substrates (after step **a** and step **b** treatments) were immersed in a 1:150 (v/v) solution of octachlorotrisiloxane in heptane for 30 min and then washed with copious amounts of pentane, followed by sonication in acetone for 1 min. The samples were then air-cured at 110 °C for 10 min.

The X-ray reflectivity measurements were performed at Beam Line X23B of the National Synchrotron Light Source at Brookhaven National Laboratory in Upton, NY, USA, using the instrumentation and analysis procedures described in ref. [8]. Polarized second harmonic generation measurements were carried out as described in ref. [6b].

Received: February 13, 1995 [Z7711IE]
German version: *Angew. Chem.* **1995**, *107*, 1646–1649

Keywords: NLO materials · nonlinear optics · self-assembly · thin films

[1] Special issue: *Chem. Rev.* **1994**, *94*, and references therein.
[2] T. J. Marks, M. A. Ratner, *Angew. Chem.* **1995**, *107*, 167–187; *Angew. Chem. Int. Ed. Engl.* **1995**, *34*, 155–173 and references therein.
[3] D. M. Burland, R. D. Miller, C. A. Walsh, *Chem. Rev.* **1994**, *94*, 31–75.
[4] a) G. J. Ashwell, P. D. Jackson, W. A. Crossland, *Nature* **1994**, *368*, 438–440; b) T. L. Penner, H. R. Matschmann, N. J. Armstrong, M. C. Ezenyilimba, D. J. Williams, *ibid* **1994**, *367*, 49–51; c) M. Flörsheimer, M. Küpfer, C. Bosshard, H. Looser, P. Günter, *Adv. Mater.* **1992**, *4*, 795–798.
[5] a) A. Ulman, *An Introduction to Ultrathin Organic Films*, Academic Press, New York, **1991**, Part 3; b) S. R. Wasserman, Y.-T. Tao, G. M. Whitesides, *Langmuir* **1989**, *5*, 1074–1087; c) M. Pomerantz, A. Segmuller, L. Netzer, J. Sagiv, *Thin Solid Films* **1985**, *132*, 153–162; d) G. Cao, H.-G. Hong, T. E. Mallouk, *Acc. Chem. Res.* **1992**, *25*, 420–425.
[6] a) D. Li, M. A. Ratner, T. J. Marks, C. Zhang, J. Yang, G. K. Wong, *J. Am. Chem. Soc.* **1990**, *112*, 7389–7390; b) S. Yitzchaik, S. B. Roscoe, A. K. Kakkar, D. S. Allan, T. J. Marks, Z. Xu, T. Zhang, W. Lin, G. K. Wong, *J. Phys. Chem.* **1993**, *97*, 6958–6960; c) S. B. Roscoe, S. Yitzchaik, A. K. Kakkar, T. J. Marks, W. Lin, G. K. Wong, *Langmuir* **1994**, *10*, 1337–1339.
[7] a) H. E. Katz, G. Scheller, T. M. Putvinski, M. L. Schilling, W. L. Wilson, C. E. D. Chidsey, *Science* **1991**, *254*, 1485–1486; b) H. E. Katz, W. L. Wilson, G. Scheller, *J. Am. Chem. Soc.* **1994**, *116*, 6636–6640.
[8] M. C. Shih, J. B. Peng, K. G. Huang, P. Dutta, *Langmuir* **1993**, *9*, 776–782.
[9] J. F. Moulder, W. F. Stickle, P. E. Sobol, K. D. Bomben, *Handbook of X-ray Photoelectron Spectroscopy*, Perkin Elmer, Eden Praire, MN, USA, **1992**.
[10] $\beta^{calc}_{vec} = 946 \times 10^{-30}$ cm^{5}esu^{-1} ($\lambda_0 = 1064$ nm) by the semiempirical ZINDO/SOS formalism.
[11] P. M. Lundquist, S. Yitzchaik, T. Zhang, D. R. Kanis, M. A. Ratner, T. J. Marks, G. K. Wong, *Appl. Phys. Lett.* **1994**, *64*, 2194–2196.
[12] S. Yitzchaik, P. M. Lundquist, W. Lin, T. J. Marks, G. K. Wong, *SPIE Proc.* **1994**, *2285*, 282–289.

Structure Organization of Aluminosilicate Polyanions with Surfactants: Optimization of Al Incorporation in Aluminosilicate Mesostructural Materials

Guoyi Fu, Colin A. Fyfe,* Wilhelm Schwieger, and George T. Kokotailo

Recently a new family of silicate-surfactant mesostructural materials, discovered by researchers at Mobil Corporation, has drawn considerable attention due to their potential applications as either highly ordered mesoporous molecular sieves, organic-inorganic nanocomposites or materials with biomimetic importance.[1–5] One member of this family, designated MCM-41, has highly ordered mesoscopic channels in a hexagonal arrangement, whose size may be engineered to be greater than 100 Å. For this type of mesoporous material to be practically useful as a catalyst, it is essential to incorporate a suitable amount of a metallic element into the silicate framework. The incorporation of vanadium or titanium oxides into the silicate framework of MCM-41 has been reported, and the resulting materials have been found to show promising activities in certain oxidation reactions.[6] For the aluminosilicate MCM-41 materials, efforts have been made to increase the framework Al content by using

[*] Prof. Dr. C. A. Fyfe, Dr. G. Fu, Dr. G. T. Kokotailo
Department of Chemistry, University of British Columbia
2036 Main Mall, Vancouver, B. C., V6T 1Z1 (Canada)
Telefax: Int. code + (604) 822-2847
Dr. W. Schwieger
Institut für Technische Chemie und Makromolekulare Chemie der Universität Halle-Wittenberg
Schloßberg 2, D-06108 Halle (Germany)

[**] G. F. gratefully acknowledges the NSERC of Canada for financial support in the form of a Postdoctoral Fellowship, C. A. F. in the form of Operating and Equipment Grants, W. S. acknowledges the financial support of the Alexander-von-Humboldt Foundation, Germany.

alternative aluminum sources, such as sodium aluminate or aluminum alkoxides, to replace pseudo-boehmite alumina which is commonly used in these syntheses.[7]

In a recent paper,[8] we described a new two-step synthetic approach using well-characterized silicate polyanions, specifically the well-known double four-ring (D4R) silicate, $Si_8O_{20}^{8-}$ (Si_8), as precursors. Firstly, the mutual structure organization of the silicate species and the surfactant molecules, governed by electrostatic interactions, leads to mesophasic precipitates with layer or rod-based structures. Further structure ordering of these precipitates can then be achieved by vapor phase treatment. A critical difference between this procedure and previous syntheses is that the materials are isolated after precipitation in the first step and then treated under quite different conditions in the second. Using this approach, we have cleanly synthesized the hexagonal, the cubic, and the lamellar mesostructures and also, for the first time, observed the phase transformations between these mesophases in a systematic manner. Herein, we extend this new synthetic route to the analogous aluminosilicate system focusing on maximizing the aluminum incorporation in the mesostructural framework by using well-characterized aluminosilicate polyanions as precursors.

The aluminosilicate precursor used was $Al_4Si_4(OH)_8O_{12}^{4-}$ (Al_4Si_4), which has a similar cubelike structure to the D4R silicate, but with four Al replacing four Si atoms in alternating corners of the cube. This has been characterized in solution by NMR spectroscopy and also as the crystalline tetramethylammonium (TMA) salt by NMR spectroscopy and X-ray diffraction techniques.[9, 10] The structure of the Al_4Si_4 anion is shown schematically in Figure 1. Three different surfactants were used in the present work, namely, hexadecyltrimethyl ammonium chloride (C_{16}TACl), dodecyltrimethylammonium bromide (C_{12}TABr) and dodecylammonium chloride (C_{12}AMCl).

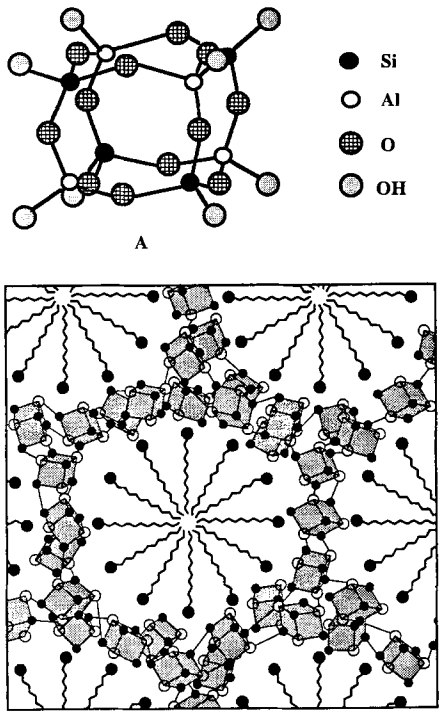

Fig. 1. Top: Schematic representation of the $Al_4Si_4O_{12}(OH)_8^{4-}$ structure; bottom: Schematic representation of the structure of the Al_4Si_4-C_nTA hexagonal phase (AS-H_1) in the plane perpendicular to the cylindrical channels showing the arrangement of templates and precursor cubes. Note that the walls in the real material may be thicker than the single layer of cubes shown here and the cubes themselves may be distorted to differing degrees by the condensation reactions.

The X-ray diffraction pattern (Fig. 2a) of the Al_4Si_4-C_{16}TA precipitate indicates that it is dominated by a rod-based mesophase similar to that observed for the Si_8-C_{16}TA system in acidic media (H_0 phase).[8] As we have rationalized for the Si_8-C_{16}TA system, this precipitate phase is formed by silicate- (aluminosilicate in this case) coated surfactant mesoscopic rods with

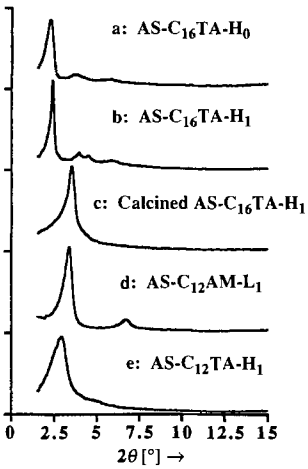

Fig. 2. X-ray diffraction patterns obtained on a Rigaku Rotaflex rotating anode diffractometer using $Cu_{K\alpha}$ radiation of a) the aluminosilicate precipitate phase (AS-H_0) formed by mixing Al_4Si_4 and C_{16}TACl solutions; b) the aluminosilicate hexagonal phase (AS-H_1) obtained from AS-H_0 by vapor phase treatment at 110 °C for 3 days; c) the AS-H_1 phase calcined by slowly increasing the temperature to 500 °C with a stream of N_2 passing through the sample and then maintaining the temperature at 500 °C for 3 h with a stream of air passing through the sample; d) the lamellar phase (AS-L_1) obtained by first precipitating Al_4Si_4 with $C_{12}NH_3^+$ in solution and then treating the precipitate in refluxing isopropyl alcohol for 24 h; and e) the hexagonal phase of Al_4Si_4-C_{12}TA obtained by a similar procedure as for the Al_4Si_4-C_{16}TA system.

poorly ordered hexagonal packing. We denote this aluminosilicate phase here as AS-H_0. From AS-H_0, more ordered hexagonal phases (AS-H_1) can be obtained by vapor phase treatment (Fig. 2b). The schematic structure model of this hexagonal phase is shown in Figure 1 top. The ^{29}Si NMR spectrum of the TMA crystals (Fig. 3a) shows a very strong resonance in the

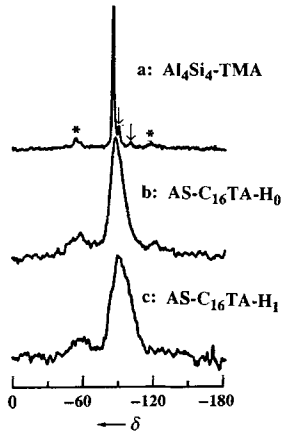

Fig. 3. ^{29}Si MAS NMR spectra obtained with a spinning rate of 3 kHz using a Bruker AM-400 spectrometer and a home-made MAS probe. a) Spectrum of $(NMe_4)_4Al_4Si_4O_{12}(OH)_8 \cdot xH_2O$ (^{29}Si NMR peaks indicated with arrows are thought to be due to a very small amounts of Al_3Si_5); b) and c) the AS-H_0 and AS-H_1 phases described in Fig. 2a and Fig. 2b, respectively. The ^{29}Si NMR chemical shifts are referenced to TMS using Q_8M_8 as an intermediate reference. The peaks indicated with an asterisk are spinning sidebands.

Q^3(3 Al) region ($\delta = -85$) and two very weak peaks in Q^3(2 Al,1 Si) and Q^3(3 Si) regions ($\delta = -90$ and -100, respectively), indicating that the Al_4Si_4 species is dominant with a minimal amount of Al_3Si_5 ($\approx 5\%$) also present. The broadened, unresolved ^{29}Si NMR peaks for the AS-H_0 and AS-H_1 phases (Fig. 3b and c) are due to condensations between Al_4Si_4 cubes, which result in new Si environments, such as Q^4(4 Al) and Q^4(3 Al,1 Si) sites, in addition to uncondensed Q^3 sites, and also to line broadening caused by variable site distortion. Line broadening is also observed for the ^{27}Al resonances of the mesophases (Fig. 4) compared to that of the TMA crystals

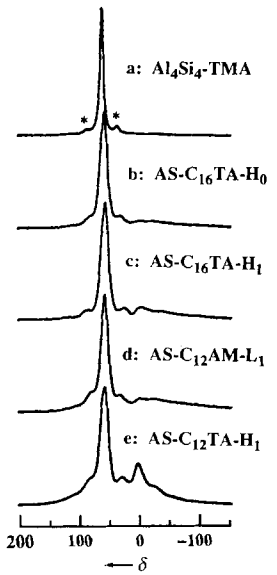

Fig. 4. ^{27}Al MAS NMR spectra obtained with a spinning rate of 3 kHz using a Bruker AM-400 spectrometer and a home-made MAS probe. The spectra in Fig. 4a–c are of the same materials as in Fig. 3a–c; the spectra in Fig. 4d and e are of the same materials as in Fig. 2d and e. The ^{27}Al NMR chemical shifts are referenced to the $Al(H_2O)_6^{3+}$ resonance of a 1 M solution of $Al(NO_3)_3 \cdot 6H_2O$. The peaks indicated with an asterisk are spinning sidebands.

(Fig. 4a) due to similar distribution of T-site geometries. The ^{27}Al NMR spectra (Fig. 4) also show that these mesostructures contain a number of octahedrally (O_h) coordinated Al centers. Janicke et al.[7c] have recently suggested that the resonance for the octahedrally coordinated Al centers in the ^{27}Al NMR spectrum of an aluminosilicate (Si/Al = 16/1) MCM-41 structure obtained from aluminum isopropoxide precursors is due to framework Al, since these Al sites were converted to tetrahedrally coordinated ones after calcination. The small amount of octahedrally coordinated Al observed in our mesophases is possibly from the same kind of framework Al. It has been reported[4] that if Catapal-B alumina is used as the Al source, complete incorporation of Al cannot be achieved even if only a small amount of alumina is used. With sodium aluminate as the Al source, a Si/Al ratio of as low as 8.5/1 without contamination from unreacted alumina has been recently reported for an MCM-41 structure.[7a] Clearly, the nature of the Al source is important in determining the amount of Al incorporated into a mesostructure. Using Al_4Si_4 as precursor, we have achieved a Si/Al ratio very close to 1/1, the lowest ratio possible for an aluminosilicate with tetrahedrally coordinated Al centers without the formation of unstable Al-O-Al linkages. Clearly, in comparison to the commonly used methods based on gel precursors, it is advantageous to incorporate aluminum at the oligomer stage using aluminosilicate polyanions as precursors.

Although Al_4Si_4 has the same cubic structure as Si_8, its charge is only half that of Si_8 according to the single crystal X-ray diffraction results.[10] Also, in the Al_4Si_4 structure all the terminal groups are OH rather than O^- groups as in Si_8. These differences make these two precursors behave differently in both the initial structural organization and the extended mesostructure formation (condensation) processes. It is clear that the charge density balance at the inorganic-surfactant interfaces is one of the important factors that determine the mesophasic structure formed.[2, 3, 8] The lower charged Al_4Si_4 requires a larger head-to-chain volume ratio of the surfactant assembly and therefore promotes the formation of a structure with curved interfaces. As a result, only the rod-based AS-H_0 can be obtained as a major phase for the Al_4Si_4-C_{16}TA system even under basic conditions although, under such conditions, a layer-based mesophase (L_0) is dominant for the more highly charged Si_8 precursor. In addition, the terminal OH groups in Al_4Si_4 condense much more readily than the O^- groups in Si_8, which makes it unnecessary to use acid to promote the condensation during the vapor phase treatment and also makes the time of the treatment much shorter than for the corresponding Si_8-C_{16}TA system. Furthermore, using only water rather than acid in the vapor phase treatment increases the possibility of the Al_4Si_4 precursor remaining intact in the final mesostructural materials. Preliminary results from a dipolar-based ^{27}Al-^{29}Si solid-state NMR connectivity experiment[11] on the Al_4Si_4-C_{16}TA system indicates that the Si-O-Al linkage remains intact in the hexagonal mesophases. It should be noted that Al_4Si_4 is the stable species under the conditions of the initial precipitations, and that they are stable in solution to 90 °C and in the solid state to temperatures above 100 °C as monitored by solid-state NMR spectroscopy.

Interestingly, a lamellar phase is obtained for the Al_4Si_4-C_{12}AM system (Fig. 2d and Fig. 4d) although it cannot be prepared with the surfactants with quaternary ammonium groups. This may be understood by considering that, in contrast to the quaternary ammonium ions, the primary ammonium (C_{12}AM) ions can become partially deprotonated during the precipitation process when they are mixed with the basic TMA-Al_4Si_4 solution (pH ≈ 11). The effective structure organizing agent in this case will be a mixture of charged ammonium ions and neutral amine molecules, which will decrease the head-to-chain volume ratio of the surfactant arrays and make the formation of a layered mesostructure favorable. The existence of amine functionalities, which are basic in aqueous solution, in the precipitated mesophases makes it inappropriate to carry out water vapor treatment because the base could be deleterious for the aluminosilicate framework. Instead, the precipitate can be refluxed with organic solvents (e.g., isopropyl alcohol) to achieve better structure ordering and condensation. The different behavior of surfactants with primary and quaternary ammonium ions in the organization of the Al_4Si_4 polyanions strongly suggests that not only can the charge density of the inorganic precursors be adjusted to achieve a desired mesostructure as we have done for the Si_8-C_{16}TA system,[8] it is also possible to adjust the surfactant component to modify the charge density at the interfaces. This example also provides further evidence that the charge density balance at the interface determines the mesostructure formed.

In addition to the Al_4Si_4 species, aluminosilicate polyanions with the same cubic structure, $AlSi_7$, Al_2Si_6 (two isomers), and Al_3Si_5 have also been reported and characterized[12] and could be used as precursors. Moreover, the incorporation of Al into the cubic Si_8 structure can be achieved with the bulk Si/Al ratio continuously varying from infinity (in the pure Si_8 case) to 1/1 (in the pure Al_4Si_4 case) by the procedure given above starting from TMA silicate and TMA aluminate solutions with an appropriate silicate to aluminate molar ratio. It is also known that other polysilicates such as double three-ring (D3R), double five-ring (D5R) silicates, etc., exist in certain systems with quaternary ammonium groups.[12] Partial substitution of Si in these structures with Al is also possible. Incorporation of other metallic elements in the Si_8 structure should also be possible, and this will considerably enrich the chemistry of these mesostructural materials and extend their possible applications. By selection of appropriate precursor species in terms of both structure and composition, it should be possible to synthesize mesostructural and mesoporous materials with desired properties and a degree of local structure.

Calcination of the AS-H_1 phase by slowly heating the sample under N_2 to 500 °C over a period of five hours, and then heating it in air at 500 °C for another five hours leads to a considerable contraction of the structure. The X-ray diffraction patterns

show that the $d(100)$ value decreases from about 36 Å for AS-C_{16}TA-H_1 (Fig. 2b) to about 25 Å for the calcined material (Fig. 2c). The ^{27}Al NMR spectra of calcined samples indicate some of the tetrahedrally coordinated Al centers are converted to octahedrally coordinated ones. Partial dealumination is not unexpected for an aluminosilicate structure with such a high Al content, but it is also possible that these Al centers are still relatively strongly bound to the framework and the walls have become thicker and the pores smaller. We are currently exploring the structural details of these calcined materials and the possibility of removing the templates by other, less destructive, procedures.

In summary, this work, together with our previous results on the Si_8 precursor demonstrates that it is possible to organize inorganic oligomers with surfactants step by step into mesostructural materials. Incorporation of metallic elements, and other modifications in structure and composition can be carried out more easily and more effectively at the oligomer stage than with gel precursors. It is also possible to achieve true materials design and structure-tailoring through such a synthetic pathway by using suitable structure building blocks (e.g., oligomers) and by effectively controlling the structure assembling processes (e.g., condensation).

Experimental Procedure

Crystalline TMA-Al_4Si_4 was prepared according to the literature procedure by slowly evaporating a solution containing TMA silicate and TMA aluminate in a 1:1 Si/Al ratio [9]. The TMA-silicate solution was prepared by dissolving Ludox silica into a TMAOH solution to obtain a final concentration of 1 M for both Si and TMA. The TMA aluminate solution used was freshly prepared by hydrolyzing aluminum isopropoxide in a TMAOH solution to a final Al concentration of 0.3 M and a TMA/Al ratio of 1.5/1. The precipitation of Al_4Si_4 with surfactants was performed by mixing an Al_4Si_4 solution (typically, TMA-Al_4Si_4 crystals (10 g) dissolved in H_2O(100 g)) and a solution of a surfactant (for example, 12.3% C_{16}TACl (200 mL)). The C_{12}AM solution was prepared by dissolving dodecylamine in an aqueous solution containing an equivalent amount of hydrochloric acid. The precipitate-mother liquor mixtures were aged overnight to equilibrate the condensation, and the precipitates were then isolated by filtration, washed with distilled water at room temperature and air-dried. The vapor phase treatments of the resulting Al_4Si_4-C_nTA ($n = 16$, 12) precipitates were carried out by using the procedure given in reference [8] but water alone was used in the present work rather than the HCl solution used for the Si_8-C_{16}TA systems. The Al_4Si_4-C_{12}AM precipitate was treated in refluxing isopropyl alcohol ($T = 90$ °C) for 24 hours to achieve further condensation.

Received: December 27, 1995 [Z 7585 IE]
German version: *Angew. Chem.* **1995**, *107*, 1582–1585

Keywords: aluminum compounds · mesophases · microporosity · silicon compounds · surfactants

[1] C. T. Kresge, M. E. Leonowicz, W. J. Roth, J. C. Vartuli, J. S. Beck, *Nature* **1992**, *359*, 710–712; J. S. Beck, J. C. Vartuli, W. J. Roth, M. E. Leonowicz, C. T. Kresge, K. D. Schmitt, C. T.-W. Chu, D. H. Olson, E. W. Sheppard, S. B. McCullen, J. B. Higgins, J. L. Schlenker, *J. Am. Chem. Soc.* **1992**, *114*, 10834–10843.

[2] Q. Hou, D. I. Margolese, U. Ciesla, P. Feng, T. E. Gier, P. Sieger, R. Leon, P. M. Petroff, F. Schüth, G. D. Stucky, *Nature* **1994**, *368*, 317–321; Q. Hou, D. I. Margolese, U. Ciesla, D. G. Demuth, P. Feng, T. E. Gier, A. Firouzi, B. F. Chmelka, F. Schüth, G. D. Stucky, *Chem. Mater.* **1994**, *6*, 1176–1191.

[3] A. Monnier, F. Schüth, Q. Hou, D. Kumar, D. Margolese, R. S. Maxwell, G. D. Stucky, M. Krishnamurty, P. Petroff, A. Firouzi, M. Janicke, B. F. Chmelka, *Science* **1993**, *261*, 1299–1303; G. D. Stucky, A. Monnier, F. Schüth, Q. Hou, D. Margolese, D. Kumar, M. Krishnamurty, A. Petroff, A. Firouzi, M. Janicke, B. F. Chmelka, *Mol. Cryst. Liq. Cryst.* **1994**, *240*, 187–200.

[4] C. Y. Chen, H. X. Li, M. E. Davis, *Microporous Mater.* **1993**, *2*, 17–26; C. Y. Chen, S. L. Burkett, H. X. Li, M. E. Davis, *ibid.* **1993**, *2*, 27–34.

[5] P. Behrens, G. D. Stucky, *Angew. Chem.* **1993**, *105*, 729–732; *Angew. Chem. Int. Ed. Engl.* **1993**, *32*, 696–699; S. Man, *Nature* **1993**, *365*, 499.

[6] P. T. Tanev, M. Chibwe, T. J. Pinnavaia, *Nature* **1994**, *368*, 321–323; A. Corma, M. T. Navarro, J. Pérez-Pariente, *J. Chem. Soc. Chem. Commun.* **1994**, 147–148; A. Corma, M. T. Navarro, J. Pérez-Pariente, F. Sánchez, *Stud. Surf. Sci. Catal.* **1994**, *84A*, 69–75; O. Franke, J. Rathousky, G. Schulz-Ekloff, J. Stárek, A. Zukal, *Stud. Surf. Sci. Catal.* **1994**, *84A*, 77–84; K. Reddy, I. Moudrakovski, A. Sayari, *J. Chem. Soc. Chem. Commun.* **1994**, 1059–1060.

[7] a) R. Schmidt, D. Akporiaye, M. Stöcker, O. H. Ellestad, *J. Chem. Soc. Chem. Commun.* **1994**, 1493–1494; b) R. Schmidt, D. Akporiaye, M. Stöcker, O. H. Ellestad, *Stud. Surf. Sci. Catal.* **1994**, *84A*, 61–68; c) M. Janicke, D. Kumar, G. D. Stucky, B. F. Chmelka, *ibid.* **1994**, *84A*, 243–250.

[8] C. A. Fyfe, G. Fu, *J. Am. Chem. Soc.*, submitted.

[9] D. Hoebbel, G. Garzó, K. Ujszaszi, G. Engelhardt, B. Fahlke, A. Vargha, *Z. Anorg. Allg. Chem.* **1982**, *484*, 7–21; G. Engelhardt, D. Hoebbel, M. Tarmak, A. Samoson, E. Lippmaa, *ibid.* **1982**, *484*, 22–32.

[10] Y. I. Smolin, Y. F. Shepelev, A. S. Ershov, D. Hoebbel, *Sov. Phys. Dokl. (Engl. Trans.)* **1987**, *32*, 943–945; M. Grube, M. Wiebcke, J. Felsche, G. Engelhardt, *Z. Anorg. Allg. Chem.* **1993**, *619*, 1098–1104.

[11] C. A. Fyfe, K. T. Mueller, H. Grondey, K. C. Wong-Moon, *J. Phys. Chem.* **1993**, *97*, 13484–13495.

[12] G. Engelhardt, D. Michel, *High Resolution Solid-State NMR of Silicates and Zeolites*, Wiley, Chichester, **1987**, Ch. III, pp. 75–105, and references therein.

One-Electron Redox Reactions of CoASH Esters in Anaerobic Bacteria—A Mechanistic Proposal**

Wolfgang Buckel* and Reinhart Keese

In his seminal work on the structure and function of acetyl-coenzyme A (acetyl-CoA), Feodor Lynen recognized already in 1951 that the thioester moiety of CoASH esters has properties similar to those of aldehydes and ketones.[1] This concept was further developed by Sir John W. Cornforth in 1959[2] and later confirmed by ^{13}C NMR spectroscopy. The chemical shift of the C atom in the thioester functional group was shown to be similar to that of aldehydes ($\delta \approx 195$), whereas signals for C atoms in the carboxyl group of typical oxygen esters are found at a higher field ($\delta \approx 160$). The ketone-like carbon of thioesters is readily attacked by nucleophiles such as amines, alcohols, and enolates. Furthermore, it lowers the pK_a value of a C–H bond of an adjacent carbon atom from roughly 30 (in carboxylate anions) to about 21,[3] thereby enhancing the rate of deprotonation. These two properties are relevant to many of the known reactions of thioesters in biology. The first property is exploited by a variety of enzymes catalyzing the transfer of the acyl groups of CoA esters to water, alcohols, amines, carboxylates, and thiols (thioester hydrolases EC 3.1.2., acyltransferases EC 2.3.1., and CoA-transferases EC 2.8.3.) as well as to hydrides derived from nicotinamide adenine dinucleotide phosphate (NAD(P)H) (aldehyde dehydrogenases, CoA-acylating, EC 1.2.1.). The second property, the enolization, is used by enzymes catalyzing Claisen condensations (e.g. citrate synthases, EC 4.1.3.7/28) and thioester condensations (e.g. thiolase, acetyl-CoA C-acetyltransferase, EC 2.3.1.9), as well as β-eliminations (e.g. acyl-CoA

[*] Prof. Dr. W. Buckel
Laboratorium für Mikrobiologie
Fachbereich Biologie der Universität
D-35032 Marburg (Germany)
Telefax: Int. code + (6421) 28-5833
Prof. Dr. R. Keese
Institut für Organische Chemie der Universität Bern (Switzerland)

[**] This work was supported by grants from the European Community (R. K. and W. B.), the Deutsche Forschungsgemeinschaft (W. B.), the Fonds der Chemischen Industrie (W. B.), and the Schweizerische National Fonds (R. K.). We thank our colleagues Prof. G. Boche (Marburg), Prof. Sir J. W. Cornforth (Brighton), Dr. T. Dabre (Bern), Prof. B. T. Golding (Newcastle upon Tyne), Prof. R. K. Thauer (Marburg), and Dr. P. Willadsen (Brisbane) for valuable advice and helpful discussions.

dehydrogenases such as EC 1.3.99.2/3 and 3-hydroxyacyl-CoA dehydratases such as EC.4.1.2.17).

In recent years, however, five different enzymatic reactions of CoA derivatives have been discovered that do not fit into the generalizations mentioned above. These are dehydrations, reductions, and oxidations that occur only in certain bacteria growing under anaerobic conditions: 1) the reversible *syn*-dehydration of (*R*)-2-hydroxyacyl-CoA **1** to (*E*)-enoyl-CoA **2** (see Fig. 2 and ref. [4]); 2) the reversible dehydration of 4-hydroxybutyryl-CoA **3** to crotonyl-CoA **4** (see Fig. 3);[5, 6] 3) the oxidation of phenylacetyl-CoA **5** to mandelyl-CoA **6** (see Fig. 4);[7] 4) the reduction of benzoyl-CoA **7** to cyclohexa-1,5-diene-1-carboxyl-CoA **8** (see Fig. 5);[8] 5) the reduction of 4-hydroxybenzoyl-CoA **9** to benzoyl-CoA **7** (see Fig. 6).[9]

The dehydration of (*R*)-2-hydroxyacyl-CoA giving (*E*)-enoyl-CoA **2** is of considerable mechanistic interest since it requires the abstraction of a nonactivated β-hydrogen atom with a pK_a of $\geqslant 30$. The (*R*)-lactyl-CoA dehydratase from *Clostridium propionicum* (Fig. 2, R = H, CH_3)[10–14] and the (*R*)-2-hydroxyglutaryl-CoA dehydratases from *Acidaminococcus fermentans* and *Fusobacterium nucleatum* (R = CH_2COO^-)[15–20] have been purified to homogeneity. The enzymes have been characterized as extremely oxygen-sensitive ($t_{1/2}$ in air about 10 s) and contain reduced flavin mononucleotide (FMN) and riboflavin, as well as iron–sulfur clusters. The enzymes require activation by a reducing agent, preferentially titanium(III) citrate ($E' \approx -600$ mV),[21] as well as $MgCl_2$ and catalytic amounts of adenosine triphosphate (ATP), which is hydrolyzed to adenosine diphosphate (ADP) and inorganic phosphate. In the proposed mechanism the nonactivated β-hydrogen is abstracted by the oxidized flavin as a hydride, as in acyl-CoA dehydrogenases.[4, 14, 19] In order to provide oxidized flavin, it was assumed that the hydroxyl group is displaced by a hydride derived from the reduced flavin present in the enzyme. This S_N2 reaction is facilitated by the adjacent electron-withdrawing thioester, similar to the facile nucleophilic substitution of the bromine in phenacylbromide. Furthermore, the nucleofugicity of the hydroxyl group could be enhanced by coordination to the iron–sulfur cluster, which may be regarded as a biological analogue of a tosylation agent, as shown by Beinert and Kennedy[22a] for aconitase (EC 4.2.1.3), an enzyme from the citric acid cycle. Although this mechanism appears to be plausible and explains the presence of flavins and iron–sulfur clusters in the dehydratases, the reduction of (*R*)-2-hydroxyacyl-CoA to acyl-CoA remains problematic. Thus, for S_N2 displacements with hydride, which would be conducted with $NaBH_4$ or even $LiAlH_4$ in organic chemistry, NADH ($E^{\circ\prime} = -320$ mV) would be a much better hydride donor than $FMNH^-$ ($E^{\circ\prime} \geq -200$ mV). In addition, neither (*R*)-lactyl-CoA dehydratase nor (*R*)-2-hydroxyglutaryl-CoA dehydratases are able to function as electron acceptors and catalyze the respective oxidation and dehydration of the putative intermediates propionyl-CoA and glutaryl-CoA, respectively, by ferricenium ion.[22b]

In this paper an alternative mechanism is presented, for which α-hydroxyketones (**10**; Fig. 1) may serve as models for 2-hydroxyacyl-CoA derivatives. There are several examples of reactions in which tosylated or acetylated α-hydroxyketones are reduced to the corresponding unsubstituted ketones (**11**) by single-electron donors such as zinc in acetic acid, chomium(II) and dithionite.[23] Samarium(II) ions are even able to reductively eliminate the hydroxy group of α-hydroxy esters.[24] It is suggested that the carbonyl group in **10** is first reduced by one electron to a ketyl group (**12**; only one resonance structure is shown in Fig. 1). The electron pair at the former carbonyl carbon atom displaces the adjacent hydroxyl group with the formation of a

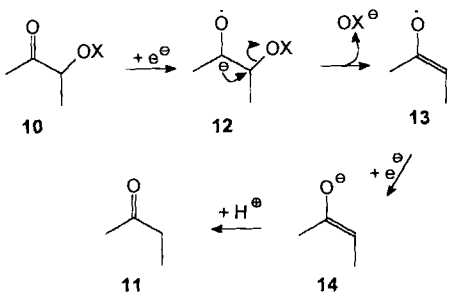

Fig. 1. Reduction of α-hydroxyketones **10** to unsubstituted ketones **11** by one-electron donors. X = H, acetyl, tosyl, etc.

enoxy radical **13**. A second one-electron reduction then leads to enolate **14**, which is protonated to give ketone **11**. Abstraction of a β-hydrogen atom from enolate **14** as a hydride rather than protonation at the enolate α-carbon, however, would yield a vinyl ketone, an analogue of enoyl-CoA **2**. This mechanism proposed for the reversible dehydration of (*R*)-2-hydroxyacyl-CoA **1** to (*E*)-enoyl-CoA **2** is shown in Figure 2.

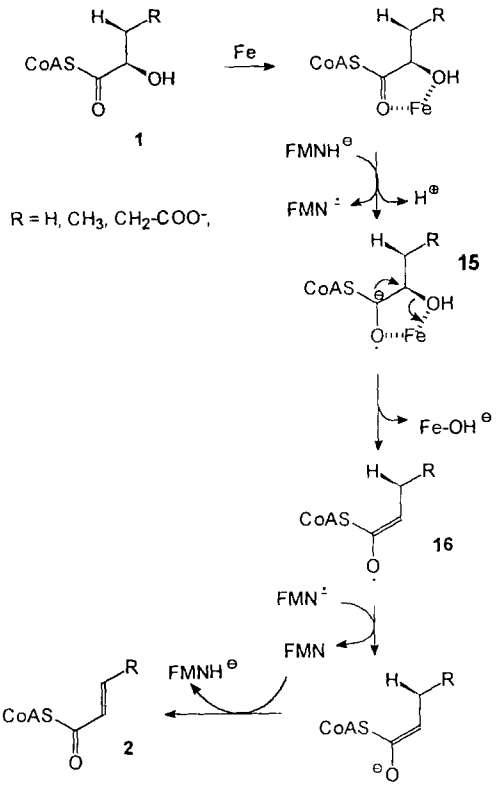

Fig. 2. Reversible *syn*-dehydration of (*R*)-2-hydroxyacyl-CoA **1** to (*E*)-enoyl-CoA **2**. Fe = [4Fe-4S] cluster like that in aconitase [22a] (see also ref. [24]).

The mechanism has following features: 1) It is based on the assumption that thioesters can be regarded as analogues of aldehydes or ketones.[1, 2] 2) It accounts for the ability of flavins not only to accept hydride ions, but also to act as donors and acceptors of single electrons, forming semiquinones.[25] 3) It assumes that ketyls derived from thioesters (**15**, Fig. 2) are as stable as those obtained from ketones. The latter are isoelectronic to the indefinitely stable nitroxyl radicals.[26] 4) The two sequential one-electron reductions of the thioester avoid the accumulation of two negative charges, which would be the case if both elec-

trons were delivered simultaneously. On the other hand, the transfer of two electrons together with a proton, or as a hydride, would lead to the reduction of the thioester to give the aldehyde. 5) It avoids saturated acyl-CoA derivatives as intermediates. 6) It is consistent with stereochemical investigations, which indicate that a freely rotating methylene radical (R = H)[27] or a less freely rotating methine radical (R = CH_3) in the β-position is unfavored.[14]

A probable variant of this mechanism would be the removal of the β-hydrogen as a *proton* already from the enoxy radical **16**, yielding the corresponding ketyl of enoyl-CoA, which is consequently oxidized to the product. Thereby a cycle is formed in which a single, high-energy electron is turned over many times. This would also explain the catalytic activation: Titanium(III) citrate supplies the electron, which is energized by hydrolysis of ATP[28b] as shown for nitrogenase.[28a]

A similar mechanism can be postulated for the reversible dehydration of 4-hydroxybutyryl-CoA **3** to crotonyl-CoA **4** (Fig. 3). Again the C–H bond at the β-carbon is not activated

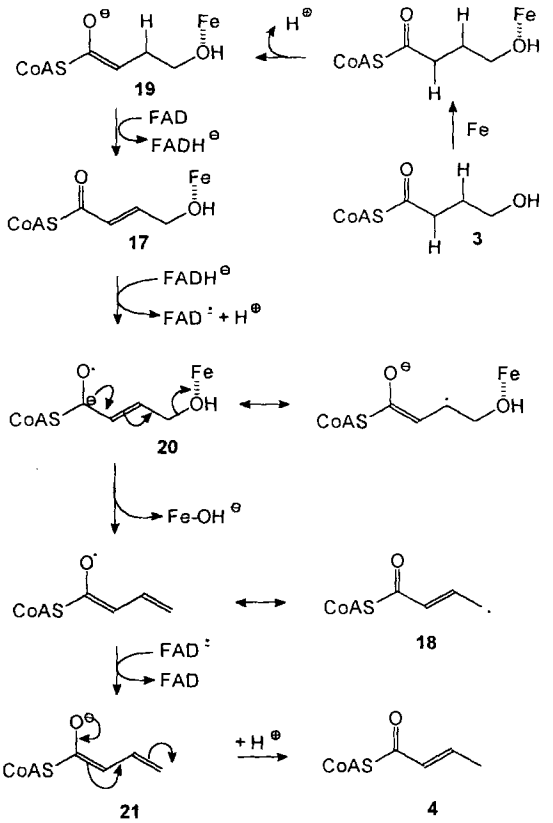

Fig. 3. Reversible dehydration of 4-hydroxybutyryl-CoA **3** to crotonyl-CoA **4**.

and hence cannot be deprotonated. The 4-hydroxybutyryl-CoA dehydratases from *Clostridium aminobutyricum*[5] and *C. kluyveri*[6] contain iron–sulfur clusters and FAD in the oxidized state. Reduction of the flavin inactivates the enzyme, which is reactivated by oxidation with hexacyanoferrate(III). Oxygen, however, irreversibly inactivates the enzyme, probably due to the destruction of the iron–sulfur cluster. The dehydration may be initiated by an FAD-dependent α,β-oxidation of 4-hydroxybutyryl-CoA **3** to 4-hydroxycrotonyl-CoA **17**. In turn, compound **17**, a vinylogous 2-hydroxyacyl-CoA, is reduced to crotonyl-CoA via ketyl intermediates, whereby FAD is regenerated. In the course of this reaction the methylene group at C-4 of 4-hydroxybutyryl-CoA is converted into the methyl group of crotonyl-CoA. Hence, introduction of all three hydrogen isotopes might lead to a "chiral methyl group".[29, 30] In the proposed γ-crotonyl radical intermediate **18** rotation of the methylene group most likely has a substantial barrier. It is expected, therefore, that one enantiomer of the chiral methyl group will be formed preferentially. In analogy to the dehydration of 2-hydroxyacyl-CoA, the dehydration of 4-hydroxybutyryl-CoA could also proceed by a one-electron cycle, in which the removal of a hydride from enolate **19** by FAD is replaced by a one-electron oxidation followed by deprotonation to give ketyl **20**. After elimination of the hydroxide ion, the resulting dienoxy radical **18** would be reduced to dienolate **21** followed by protonation to give crotonyl-CoA **4**. In contrast to the dehydration of 2-hydroxyacyl-CoA, this reverted one-electron cycle should turn over on a much lower energy level due to the conjugated intermediates, which agrees well with its lack of ATP requirement.

The oxidation of phenylacetyl-CoA **5** to phenyl(hydroxyacetyl)-CoA **6** (mandelyl-CoA; Fig. 4) should proceed as the

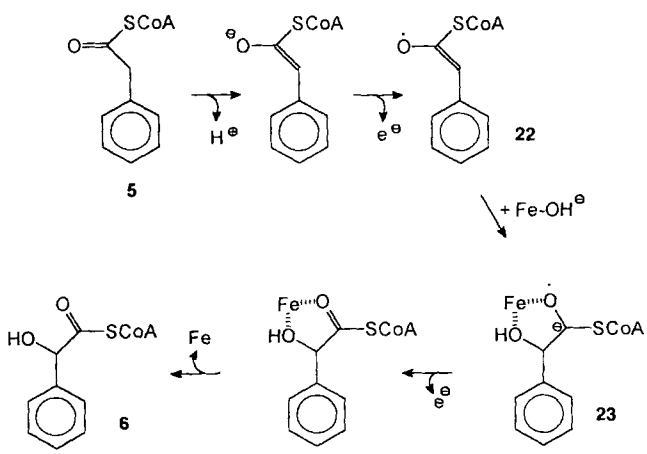

Fig. 4. Oxidation of phenylacetyl-CoA **5** to mandelyl-CoA **6**.

reversal of the reduction of a 2-hydroxyketone (Fig. 1). The mechanism predicts the presence of an iron–sulfur cluster facilitating the addition of the hydroxyl group to the enoxy radical **22**, whereby the ketyl **23** is formed. In contrast to the dehydratases (see Figs. 2 and 3), involvement of a flavin is not necessary, since hydrides are not transferred and other compounds such as ferredoxins could serve as one-electron acceptors.

The recently discovered reduction of benzoyl-CoA **7** to cyclohexa-1,5-diene-1-carboxy-CoA **8** in the bacterium *Thauera aromatica* can also be explained by stepwise addition of two electrons (Fig. 5). This reaction could proceed via radical anions in analogy to the Birch reduction of arenes. Calculations have shown that the *para* position of the radical anion of benzaldehyde, a close analogue of the radical anion of benzoyl-CoA, is the most electron-rich position and thus subject to preferential protonation.[31] A similar mechanism can be proposed for the 1,4- or 2,5- addition of two hydrogens to benzoyl-CoA **7**, which was observed by Gibson and Gibson.[32a] The thioester group thus serves as the entrance for the electrons into the aromatic ring, while the position of protonation is controlled by the enzyme. This new function for the thioester was not considered in an earlier proposal also involving one-electron transfers.[8] The stoichiometric ATP hydrolysis[32b] coupled to this reduction is necessary to reduce the redox potential of unidentified biologi-

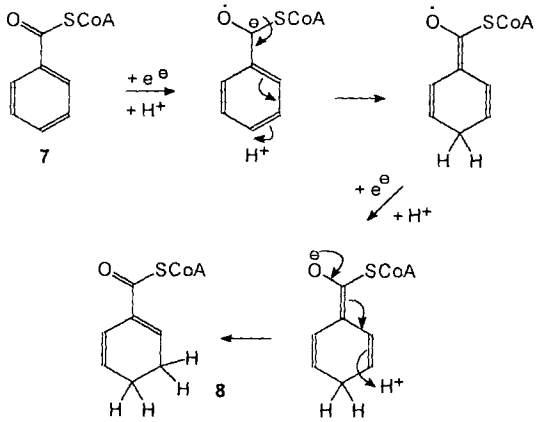

Fig. 5. Reduction of benzoyl-CoA 7 to cyclohexa-1,5-diene-1-carboxyl-CoA 8.

cal electron donors to at least -550 mV (see also 2-hydroxyacyl-CoA dehydratase). As mentioned above, for the same purpose, stoichiometric amounts of ATP are required for the biological fixation of nitrogen.[28]

In a similar way, 4-hydroxybenzoyl-CoA 9 may be reduced to benzoyl-CoA 7 (Fig. 6). The 4-hydroxybenzoyl-CoA reductase

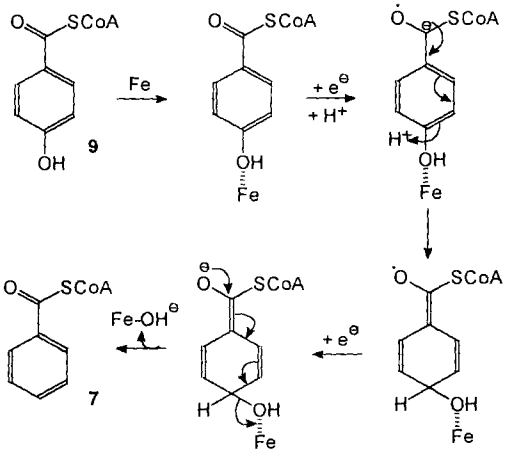

Fig. 6. Reduction of 4-hydroxybenzoyl-CoA 9 to benzoyl-CoA 7.

has been purified to homogeneity and characterized as an iron–sulfur enzyme. Flavin could not be detected.[9] With this type of mechanism the removal of the hydroxyl groups from 2-hydroxybenzoyl-CoA (salicylyl-CoA), and the amino group from 2-aminobenzoyl-CoA (anthranilyl-CoA) may also be explained. It is of interest that the reduction of 3-chlorobenzoate to benzoate does not proceed at the thioester level.[33]

All the five reactions discussed here, for which one-electron transfers have been postulated, are extremely oxygen-sensitive. This can be explained by the high reactivity of oxygen towards single "energy-rich" electrons at low potential. Under aerobic conditions, one-electron transfers are only found at potentials ≥ 0 mV. At lower potentials all reductions are two-electron steps, the lowest being that by NADH ($E^{\circ\prime} = -320$ mV). The research group of W. Buckel is currently investigating these single-electron transfers by EPR spectroscopy.

It has been demonstrated in this paper that the reduction of a ketone to a ketyl results in an umpolung of the electrophilic carbonyl carbon into a nucleophilic one. Another example of an umpolung is the oxidative decarboxylation of pyruvate to acetyl-CoA catalyzed by pyruvate ferredoxin oxidoreductase (pyruvate synthase, EC 1.2.7.1) from *Halobacterium halobium*. In this reaction a free radical, indeed a ketyl, has been detected and characterized by EPR spectroscopy (Fig. 6).[34] The umpolung is achieved by addition of pyruvate to thiamine diphosphate. The addition product reversibly decarboxylates to give hydroxyethyl-thiamine diphosphate. It has been shown that the hydroxyethyl moiety of the latter is oxidized by an iron–sulfur cluster with the removal of one electron to the ketyl (Fig. 6). Further oxidation of the ketyl to acetylthiamine diphosphate,[35] followed by an acetyl transfer to CoASH yields the final product acetyl-CoA (Fig. 7).

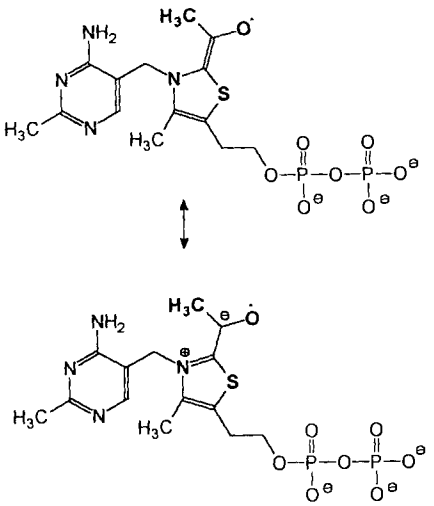

Fig. 7. A ketyl as an intermediate of the pyruvate ferredoxin oxidoreductase.

Received: November 10, 1994 [Z 7465 IE]
German version: *Angew. Chem.* **1995**, *107*, 1595–1598

Keywords: biochemistry · coenzyme A · reaction mechanisms · redox reactions

[1] F. Lynen, E. Reichert, L. Rueff, *Justus Liebigs Ann. Chem.* **1952**, *574*, 1–32.
[2] J. W. Cornforth, *J. Lipid Res.* **1959**, *1*, 3–28.
[3] T. L. Amyes, V. Jagannadham, J. P. Richard in *Organic Reactivity: Physical and Biological Aspects* (Eds.: B. T. Golding, R. J. Griffin, H. Maskill), Royal Society of Chemistry, Cambridge, **1995**, pp. 334–350.
[4] W. Buckel, *FEMS Microbiol. Rev.* **1992**, *88*, 211–232.
[5] U. Scherf, W. Buckel, *Eur. J. Biochem.* **1993**, *215*, 421–429.
[6] U. Scherf, B. Söhling, G. Gottschalk, D. Linder, W. Buckel, *Arch. Microbiol.* **1994**, 161, 239–245.
[7] M. E.-S. Mohamed, B. Seyfried, A. Tschech, G. Fuchs, *Arch. Microbiol.* **1993**, *159*, 563–573.
[8] J. Koch, W. Eisenreich, A. Bacher, G. Fuchs, *Eur. J. Biochem.* **1993**, *211*, 649–661.
[9] R. Brackmann, G. Fuchs, *Eur. J. Biochem.* **1993**, *213*, 563–571.
[10] G. Schweiger, W. Buckel, *FEBS Lett.* **1984**, *171*, 73–78.
[11] G. Schweiger, W. Buckel, *FEBS Lett.* **1985**, *185*, 253–256.
[12] R. D. Kuchta, R. H. Abeles, *J. Biol. Chem.* **1985**, *260*, 13181–13189.
[13] R. D. Kuchta, G. R. Hanson, B. Holmquist, R. H. Abeles, *Biochemistry* **1986**, *25*, 7301–7307.
[14] A. E. M. Hofmeister, S. Berger, W. Buckel, *Eur. J. Biochem.* **1992**, *205*, 743–749.
[15] W. Buckel, *Eur. J. Biochem.* **1980**, *106*, 439–447.
[16] G. Schweiger, W. Buckel, *Arch. Microbiol.* **1984**, *137*, 302–307.
[17] G. Schweiger, R. Dutscho, W. Buckel, *Eur. J. Biochem.* **1987**, *169*, 441–448.
[18] R. Dutscho, G. Wohlfarth, P. Buckel, W. Buckel, *Eur. J. Biochem.* **1989**, *181*, 741–746.
[19] A.-G. Klees, D. Linder, W. Buckel, *Arch. Microbiol.* **1992**, *158*, 294–301.

[20] K. Bendrat, W. Buckel, *Eur. J. Biochem.* **1993**, *211*, 697–702.
[21] D. S. Weiss, P. Gärtner, R. K. Thauer, *Eur. J. Biochem.* **1994**, *226*, 799–809.
[22] a) H. Beinert, A. C. Kennedy, *Eur. J. Biochem.* **1989**, *186*, 5–15; b) A.-G. Klees, A. Hofmeister, U. Müller, W. Buckel, unpublished results.
[23] G. A. Molander, G. Hahn, *J. Org. Chem.* **1986**, *51*, 1135–1138.
[24] K. Kusuda, J. Inanaga, M. Yamaguchi, *Tetrahedron Lett.* **1989**, *30*, 2945–2948.
[25] S. Ghisla, V. Massey, *Eur. J. Biochem.* **1989**, *181*, 1–17.
[26] G. Berthier, J. Serre in *The Chemistry of the Carbonyl Group, Vol. 1* (Ed.: S. Patai), **1966**, pp. 1–77.
[27] S. L. Brunelle, R. H. Abeles, *Bioorg. Chem.* **1993**, *21*, 118–126.
[28] a) W. G. Zumft, L. E. Mortenson, G. Palmer, *Eur. J. Biochem.* **1974**, *46*, 525–535; b) U. Müller, W. Buckel, *ibid.* **1995**, *230*, 698–704.
[29] J. W. Cornforth, J. W. Redmond, H. Eggerer, W. Buckel, V. Gutschow, *Nature* **1969**, *221*, 1212–1213.
[30] J. Lüthy, J. Rétey, D. Arigoni, *Nature* **1969**, *221*, 1213–1214.
[31] A. J. Birch, A. L. Hinde, L. Radom, *J. Am. Chem. Soc.* **1980**, *102*, 3370–3376.
[32] a) K. J. Gibson, J. Gibson, *Appl. Environ. Microbiol.* **1992**, *58*, 696–698; b) G. Fuchs, Universität Ulm, private communication.
[33] G. D. Griffith, J. R. Cole, J. F. Quensen III, J. M. Tiedje, *Appl. Environ. Microbiol.* **1992**, *58*, 409–411.
[34] L. Kerscher, D. Oesterhelt, *Eur. J. Biochem.* **1981**, *116*, 595–600.
[35] K. J. Gruys, C. J. Halkides, P. A. Frey, *Biochemistry* **1987**, *26*, 7575–7585.

Synthesis and Structure of the First Sulfur-Bridged [1]Ferrocenophane**

John K. Pudelski, Derek P. Gates, Ron Rulkens, Alan J. Lough, and Ian Manners*

[1]Ferrocenophanes have attracted attention because of their interesting structures and reactivity,[1] their applications as surface derivatization agents,[2] and very recently as precursors to novel transition-metal-based polymers through ring-opening polymerization (ROP).[3] The first [1]ferrocenophane, **1** ($ER_x = SiPh_2$), was isolated by Osborne et al. in 1975 from the reaction of dilithioferrocene·tmeda (tmeda = tetramethylethylenediamine) and Ph_2SiCl_2.[4] This species was shown to possess an unusual, strained structure in which the planes of the cyclopentadienyl ligands were tilted with respect to one another by about 19°.[5] Germanium-bridged [1]ferrocenophanes **1** (E = Ge) have been subsequently reported and possess slightly less strained structures.[1, 6] Group 15 elements such as phosphorus and arsenic have also been successfully incorporated into the bridge structure,[1, 6–8] and the cyclopentadienyl ring-tilts for species **1** (E = P or As) are greater (about 23–27°).[6, 8] In 1992 we reported the discovery that silicon-bridged [1]ferrocenophanes undergo facile thermally induced ROP reactions to afford high molecular weight ($M_n > 10^5$) poly(ferrocenylsilanes) **2** (E = Si, $R_x = Me_2$, Ph_2) (Scheme 1).[9] We have also observed that related [1]ferrocenophanes with germanium or phosphorus in the bridge polymerize thermally and that ROP can be induced in solution by using anionic initiators.[3, 10–12]

[1]Ferrocenophanes containing Group 16 elements in the bridge are unknown at present, but would be expected to possess even more strained, ring-tilted structures[13] than their Group 14 and 15 analogues and might also function as precursors to novel polymers. Trithio-bridged [3]ferrocenophanes such as **3** have been previously prepared from the reactions of dilithiated ferrocenes with elemental sulfur.[14, 15] Although essentially unstrained (tilt angles smaller than 4.5°),[16, 17] Rauchfuss and co-workers have recently reported an elegant ROP reaction of these species, induced by sulfur atom abstraction with PBu_3, which affords polymers such as **4**.[17–19] Strained dithio-bridged [2]ferrocenophanes **5** have been proposed as possible intermediates in these polymerization reactions but have not been identified or isolated to date. In this paper we report the first example of a sulfur-bridged [1]ferrocenophane.[20]

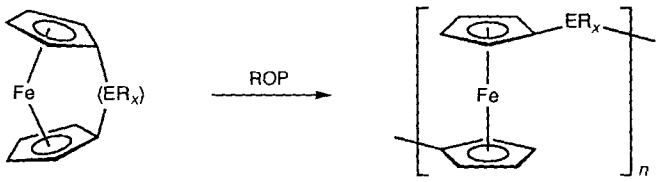

1 **2**

Scheme 1.

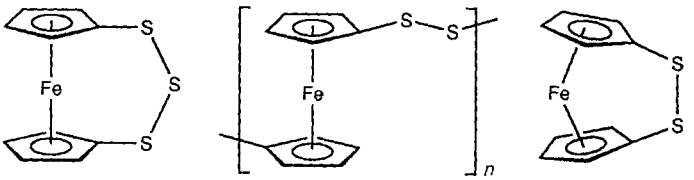

3 **4** **5**

We attempted to prepare the sulfur-bridged [1]ferrocenophane **6** by the low temperature reaction of dilithioferrocene·tmeda with $(PhSO_2)_2S$ in THF.[21, 22] Removal of the $LiSO_2Ph$ by-product followed by vacuum sublimation of the crude product residue afforded a purple sublimate contaminated with a trace quantity of ferrocene. Recrystallization of this sublimate from hexanes at −30 °C afforded **6**, free of ferrocene, as a purple crystalline material in 14% yield.

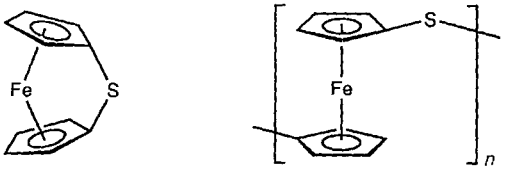

6 **7**

Characterization of **6** by NMR and UV/Vis spectroscopy confirmed the assigned structure and provided interesting insight into the strained nature of this species. For example, the ^1H NMR spectrum (in C_6D_6) of **6** consists only of a pair of widely separated pseudo triplets at $\delta = 3.96$ and 4.61, assigned to the α and β cyclopentadienyl protons. In the ^{13}C NMR spectrum (in C_6D_6) (Fig. 1), the *ipso* cyclopentadienyl carbon atom of **6** resonates at the highest field yet observed ($\delta = 14.3$) for the *ipso* carbons of a [1]ferrocenophane[23] and clearly reflects structural distortion at these sites.[1] In hexanes, **6** exhibits a UV/Vis absorbance at 504 nm, which is considerably red-shifted

[*] Prof. I. Manners, Dr. J. K. Pudelski, D. P. Gates, R. Rulkens, Dr. A. J. Lough
Department of Chemistry
University of Toronto
80 St. George Street, Toronto, Ontario, M5S 1A1 (Canada)
Telefax: Int. code + (416)978-8775
e-mail: imanners@alchemy.chem.utoronto.ca

[**] We thank the donors of the Petroleum Research Fund, administered by the American Chemical Society, for financial support of this work. D. G. also thanks NSERC for a graduate fellowship and I. M. is grateful to the Alfred P. Sloan Foundation for a Research Fellowship (1994–1996).

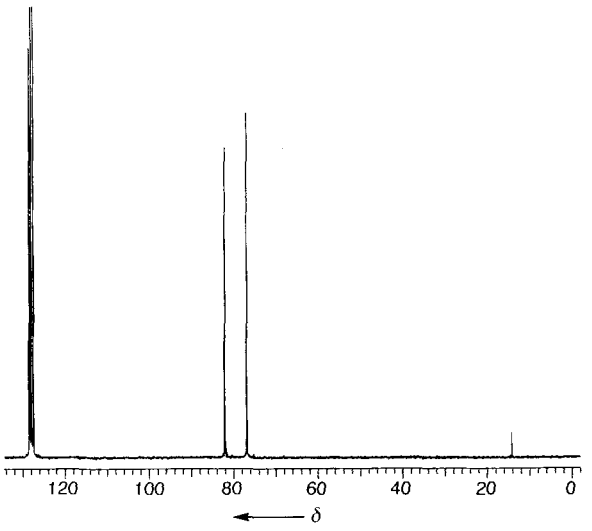

Fig. 1. ^{13}C NMR spectrum of **6** (50.3 MHz, C_6D_6).

relative to the 440 nm absorbance of ferrocene and is indicative of highly tilted cyclopentadienyl rings.[1, 24]

A single crystal X-ray diffraction study of **6** was undertaken in order to probe the structure of this novel species.[25] A suitable crystal was obtained by cooling a solution of **6** in hexanes to −30 °C; the resulting structure diagram is shown in Figure 2.

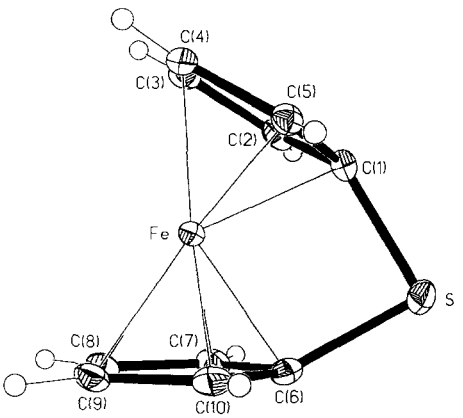

Fig. 2. Crystal structure of **6**. Selected bond lengths [Å] and angles [°]: S–C(1) 1.807(2), S–C(6) 1.805(2), Fe–C(1) 1.969(2), Fe–C(2) 2.005(2), Fe–C(5) 2.018(2), Fe–C(3) 2.074(2), Fe–C(4) 2.082(2), Fe–C(6) 1.967(2), Fe–C(7) 2.021(2), Fe–C(10) 2.010(2), Fe–C(8) 2.091(2), Fe–C(9) 2.083(2), C(1)-S-C(6) 89.03(9).

The most striking structural feature of **6** is the unprecedented 31.05(10)° tilt angle between the planes of the cyclopentadienyl rings. This tilt angle is the largest yet reported for a [1]ferrocenophane and the first over 30° for any Group 8 [*n*]metallocenophane.[26] Cyclopentadienyl ring tilting is accompanied by a RC1-Fe-RC2 angle (RC = ring centroid) of 156.9(1)° compared to 180° in ferrocene and a 0.326(2) Å displacement of the iron atom from the line joining the two ring centroids. The tilted cyclopentadienyl rings maintain an eclipsed conformation with a C1-RC1-RC2-C6 torsion angle of 0.4(3)°. Additional structural distortions include angles of 29.1(1)° and 28.8(1)° between the cyclopentadienyl ring planes and the exocyclic C–S bonds. The C1-S-C6 angle of 89.03(9)° is smaller than the analogous angles in silicon-bridged [1]ferrocenophanes (about 96°–99°) and similar to the angles found in phosphorus-bridged species (about 91°). The S–C bond lengths (average, 1.806(3) Å) are typical of C–S single bonds, although slightly elongated relative to analogous bonds in trithio-bridged [3]ferrocenophanes (about 1.75–1.76 Å).

Despite its highly strained structure, **6** is stable as a solid and in solution (C_6D_6) at room temperature in the absence of air or moisture. Cyclic voltammetric analysis[27] of **6** showed a quasi-reversible oxidation ($I_{red}/I_{ox} = 0.74$) at 500 mVs^{-1} in contrast to silicon-bridged [1]ferrocenophanes, which, under identical conditions, exhibit reversible oxidations.[28] Preliminary studies reveal that when **6** is heated at 150 °C a orange-brown solid product, insoluble in common organic solvents (such as THF, toluene), is obtained. Mass spectrometric analysis of this solid showed peaks that could be assigned to oligomeric $[(\eta\text{-}C_5H_4)Fe(\eta\text{-}C_5H_4)S]_n$ species of up to four repeat units in length, which is consistent with the proposed polymeric structure **7**.[29]

Further studies of the reactivity of **6** and attempts to prepare soluble polymeric materials by ROP are in progress.

Experimental Procedure

To a mixture of dilithioferrocene·tmeda (1.07 g, 3.41 mmol) and $(PhSO_2)_2S$ (1.16 g, 3.69 mmol) cooled to −196 °C by a liquid N_2 bath was added dry THF (30 mL) precooled to −78 °C. The resulting red mixture was allowed to warm slowly to room temperature. Solvent was removed in vacuo, and the resulting residue was extracted with dry hexanes (3 × 10 mL). The extracts were passed through a fritted glass disk, and the red filtrate was concentrated in vacuo. The resulting residue was sublimed at 25 °C (0.01 mm Hg), and 0.15 g of crude **6** was collected on a cold probe (−40 °C). Two successive recrystallizations from hexanes at −30 °C afforded 0.10 g (14 %) of **6** as a dark purple crystalline solid: m.p. 104 °C; ^1H NMR (200 MHz, C_6D_6): $\delta = 4.61$ (ps t, $J = 2$ Hz, 4H), 3.96 (ps t, $J = 2$ Hz, 4H); ^{13}C NMR (50.3 MHz, C_6D_6): $\delta = 82.1$ (cyclopentadienyl), 76.9 (cyclopentadienyl), 14.3 (*ipso*-cyclopentadienyl); UV/Vis (hexanes): λ_{max} (ε) = 504 nm (343 $Lcm^{-1}mol^{-1}$); HR-MS calcd for $C_{10}H_8{}^{56}FeS$ 215.9696, found 215.9689.

Received: February 7, 1995 [Z 7699 IE]
German version: *Angew. Chem.* **1995**, *107*, 1633–1635

Keywords: metallocenophanes · polymerizations · poly(metallocene)s · ring-opening polymerization · sandwich complexes

[1] A. G. Osborne, R. H. Whiteley, R. E. Meads, *J. Organomet. Chem.* **1980**, *193*, 345.
[2] A. B. Fischer, J. B. Kinney, R. H. Staley, M. S. Wrighton, *J. Am. Chem. Soc.* **1979**, *101*, 6501.
[3] I. Manners, *Adv. Organomet. Chem.* **1995**, *37*, 131.
[4] A. G. Osborne, R. H. Whiteley, *J. Organomet. Chem.* **1975**, *101*, C27.
[5] H. Stoeckli-Evans, A. G. Osborne, R. H. Whiteley, *Helv. Chim. Acta* **1976**, *59*, 2402.
[6] H. Stoeckli-Evans, A. G. Osborne, R. H. Whiteley, *J. Organomet. Chem.* **1980**, *194*, 91.
[7] D. Seyferth, H. P. Withers, *Organometallics* **1982**, *1*, 1275.
[8] I. R. Butler, W. R. Cullen, F. W. B. Einstein, S. J. Rettig, A. J. Willis, *Organometallics* **1983**, *2*, 128.
[9] D. A. Foucher, B.-Z. Tang, I. Manners, *J. Am. Chem. Soc.* **1992**, *114*, 6246.
[10] R. Rulkens, A. J. Lough, I. Manners, *J. Am. Chem. Soc.* **1994**, *116*, 797.
[11] R. Rulkens, Y. Ni, I. Manners, *J. Am. Chem. Soc.* **1994**, *116*, 12121.
[12] [2]Metallocenophanes with hydrocarbon bridges also possess strained, ring-tilted structures and also polymerize thermally. See: a) J. M. Nelson, H. Rengel, I. Manners, *J. Am. Chem. Soc.* **1993**, *115*, 7035; b) J. M. Nelson, A. J. Lough, I. Manners, *Angew. Chem.* **1994**, *106*, 1019; *Angew. Chem. Int. Ed. Engl.* **1994**, *33*, 989.
[13] Single-bond covalent radii (Si 1.17 Å, P 1.12 Å, S 1.02 Å) and covalent single-bond distances (Si–C 1.87, P–C 1.84, S–C 1.82 Å) suggest that sulfur would represent the smallest element incorporated into the bridge of a [1]ferrocenophane. See W. L. Jolly, *The Principles of Inorganic Chemistry*, McGraw-Hill, New York, **1976**, Chap. 2.
[14] J. J. Bishop, A. Davison, M. L. Katcher, D. W. Lichtenberg, R. E. Merrill, J. C. Smart, *J. Organomet. Chem.* **1971**, *27*, 241.
[15] Triseleno- and tritelluro- bridged [3]ferrocenophanes have also been prepared by similar routes. See a) A. G. Osborne, R. E. Hollands, J. A. K. Howard, R. F. Bryan, *J. Organomet. Chem.* **1981**, *205*, 395; b) M. Herberhold, P. Leitner, U. Thewalt, *Z. Naturforsch. B* **1990**, *45*, 1503.
[16] B. R. Davis, I. Bernal, *J. Cryst. Mol. Struct.* **1972**, *2*, 107.
[17] D. L. Compton, T. B. Rauchfuss, *Organometallics* **1994**, *13*, 4367.

[18] P. E. Brandt, T. B. Rauchfuss, *J. Am. Chem. Soc.* **1992**, *114*, 1926.
[19] C. P. Galloway, T. B. Rauchfuss, *Angew. Chem.* **1993**, *105*, 1407; *Angew. Chem. Int. Ed. Engl.* **1993**, *32*, 1319.
[20] Alternatively, this compound (**1**, $ER_x = S$) might be termed a 1-thia-[1]ferrocenophane, though this terminology does not conform to IUPAC recommendations.
[21] J. De Jong , M. J. Janssen, *J. Org. Chem.* **1971**, *36*, 1645.
[22] $(PhSO_2)_2S$ has also been used to prepare bis(ferrocenyl)sulfide. See D. C. O. Salazar, D. O. Cowan, *J. Organomet. Chem.* **1991**, *408*, 227.
[23] For example, the following *ipso* cyclopentadienyl ^{13}C NMR shifts were observed for **1**: $ER_x = SiPh_2$, 31.0 ($CDCl_3$); $ER_x = GePh_2$, 28.5 ($CDCl_3$); $ER_x = PPh$, 18.7 (C_6D_6); $ER_x = AsPh$, 18.3 (C_6D_6). See a) ref. [1] and b) D. Seyferth, H. P. Withers, *J. Organomet. Chem.* **1980**, *185*, C1.
[24] In cyclohexane, **1** ($ER_x = PPh$) exhibits a UV/Vis band at 501 nm and **1** ($ER_x = SiPh_2$) a band at 483 nm. See ref. [1].
[25] Crystallographic data for $C_{10}H_8FeS$ **6**: monoclinic $P2_1/c$, $a = 10.429(2)$, $b = 7.334(1)$, $c = 11.125(2)$ Å, $\beta = 106.67(1)°$, $V = 815.1(2)$ Å^3, $Z = 4$, $\mu = 2.033$ mm^{-1}, $Mo_{K\alpha}$ ($\lambda = 0.71073$ Å), $\rho_{calcd} = 1.761$ Mgm^{-3}, 173(2) K, Siemens P4 diffractometer with graphite monochromator, purple crystal ($0.40 \times 0.24 \times 0.36$ mm). Of 2468 reflections collected ($3.37 \le 2\theta \le 29.99°$), 2360 were independent $R_{int} = 0.0177$, and 2049 were observed with $F_0 \ge 4\sigma(F_0)$. Solution by direct methods, with SHELXTL-PC (G. M. Sheldrick, Siemens Analytical X-ray Instruments Inc., Madison, Wisconsin, USA, 1990), refinement on F^2 with SHELXL-93 (G. M. Sheldrick, Program for the Refinement of Crystal Structures, University of Göttingen, Germany, **1994**), non-hydrogen atoms were refined with anisotropic thermal parameters, hydrogen atoms with isotropic thermal parameters, $R1 = 0.0286$, $wR2 = 0.0788$ ($R1 = \Sigma(F_o - F_c)/\Sigma F_o$ observed data, $wR2 = \{\Sigma[w(F_o^2 - F_c^2)^2]/\Sigma[w(F_o^2)^2]\}^{1/2}$ for all data), GOF = 1.101, $N_o/N_v = 16.6$, and $\Delta\rho_{max} = 0.366$ e Å^{-3}. Further details of the crystal structure investigation may be obtained from the Fachinformationszentrum Karlsruhe, D-76344 Eggenstein-Leopoldshafen (Germany), on quoting the depository number CSD-58879.
[26] The largest tilt angle previously reported for a [*n*]ferrocenophane is 28.8° for a bis(hydrocarbon)-bridged [2$_2$]ferrocenophane. See K. Hafner, C. Mink, H. J. Linder, *Angew. Chem.* **1994**, *106*, 1566; *Angew. Chem. Int. Ed. Engl.* **1994**, *33*, 1479. The largest tilt angle of a Group 8 [*n*]metallocenophane is 29.6(5)° for a hydrocarbon-bridged [2]ruthenocenophane. See ref. [12b].
[27] Cyclic voltammetry was performed on a CH_2Cl_2 solution which was 1×10^{-3} M in **6** and 0.1 M in $[Bu_4N][PF_6]$ at 22 °C. At 500 mVs^{-1} an $E_{1/2} = 0.22$ V vs. the ferrocene/ferrocenium couple. At scan rates smaller than 500 mVs^{-1} the oxidation was irreversible indicating that the ferrocenium derivative of **6** is unstable under the conditions of our study.
[28] J. K. Pudelski, D. A. Foucher, C. H. Honeyman, A. J. Lough, I. Manners, S. Barlow , D. O'Hare, *Organometallics* **1995**, *14*, 2470.
[29] Linear oligomers of similar structure have been previously characterized by Herberhold et al. See: M. Herberhold, H.-D. Brendel, O. Nuyken, T. Pöhlmann, *J. Organomet. Chem.* **1991**, *413*, 65.

Synthesis and X-Ray Powder Structure of a Novel Porous Uranyl Phenylphosphonate Containing Unidimensional Channels Flanked by Hydrophobic Regions**

Damodara M. Poojary, Daniel Grohol, and Abraham Clearfield*

A variety of metal phosphonate compounds have been synthesized and examined in view of their applications in catalysis, sorption, ion exchange, intercalation chemistry, etc. These systems generally form mononuclear coordination complexes,[1, 2] linear one-dimensional structures,[3, 4] or layered compounds.[5–7] The layered compounds are of special interest because of the ordered arrangement of organic groups on either side of the metal–phosphonate layers, which provide a highly organized media for specific reactions of the type mentioned above.[7, 8] Metal–phosphonate compounds showed further promise in their diverse applications when porous compounds similar to zeolites were discovered: aluminum methylphosphonate[9] and copper methylphosphonate[10] have inorganic frameworks and unidimensional channels similar to those in zeolites. In these structures the methyl groups are projected towards the center of the channels resulting in hydrophobic channels. In this communication we describe the structure of the uranyl phenylphosphonate $UO_2(O_3PC_6H_5)\cdot 0.7H_2O$,[11] which has similar unidirectional pores; the most remarkable feature of this structure, however, is that the phenyl groups are arranged on the outer periphery of isolated channels and the channel is lined with uranyl oxygen atoms.

Step scanned X-ray powder diffraction data were collected on a Rigaku automated diffractometer ($Cu_{K\alpha}$, 50 kV, and 180 mA), and the pattern was indexed by Ito methods.[12] The systematic absences were consistent with either the space group *P*6/*mcc* or *P*6*cc*. The initial choice of the centric space group was found to be correct from the successful solution and refinement of the structure. Integrated intensities were extracted from the profile, and a Patterson map was computed by using 74 unambiguously indexed reflections. The position of the uranium atom was located from this map. Constrained refinement against this data set and subsequent difference Fourier maps revealed the positions of the P and all the oxygen atoms. This structural model was then entered into GSAS[13] for Rietveld refinement. Subsequent Fourier maps revealed the positions of all the carbon atoms of the phenyl group. Two positions were identified for lattice water molecules. O(W1) is located at the center of the pore and is at hydrogen-bonding distance (2.39 Å) from O(W2). Since symmetry-related O(W2) positions are close to each other (1.6 Å), they cannot exist with full occupancy. The corresponding occupancy refined to about 0.5 thus totally accounting for 0.67 moles of water, which is close to the amount of water loss (2.7%) determined by thermogravimetric analysis. This low water content is probably dictated by the strain energy imposed by the curvature of the channels. The crystallographic data are given in reference [14] and Table 1. The observed and calculated powder patterns are shown in Figure 1.

Table 1. Positional and thermal parameters for $UO_2(O_3PC_6H_5)\cdot 0.7H_2O$.

Atom	*x*	*y*	*z*	U_{iso} [Å^2]
U1	−0.0523(1)	0.2504(1)	0	0.062(2)
P1	0.1093(6)	0.3490(6)	0.0	0.033(8)
O1	−0.067(1)	0.321(1)	0	0.022(7)
O2	−0.036(1)	0.173(1)	0.0	0.022
O3	0.062(1)	0.315(1)	0.177(1)	0.022
O4	0.170(1)	0.332(1)	0.0	0.022
C1	0.145(1)	0.444(1)	0.0	0.035(6)
C2	0.218(1)	0.496(1)	0.0	0.035
C3	0.246(1)	0.568(1)	0.0	0.035
C4	0.200(1)	0.595(1)	0.0	0.035
C5	0.131(1)	0.552(1)	0.0	0.035
C6	0.104(1)	0.479(1)	0.0	0.035
O(W1)	0.0	0.0	0.25	0.05(1)
O(W2)	−0.054	0.03	0.0	0.05

The coordination geometry of the uranium atom and the atom labeling are given in Figure 2 top, and the projection of the structure down the *c* axis is shown in Figure 2 bottom. The structure is porous with one-dimensional channels along the *c* axis. The inorganic framework extends continuously along the

[*] Prof. Dr. A. Clearfield, Dr. D. M. Poojary, D. Grohol
Department of Chemistry, Texas A & M University
College Station, TX 77843 (USA)
Telefax: Int. code + (409)845-2370
e-mail: Clearf@acxrd.tamu.edu

[**] This work was supported by the National Science Foundation (grant no. DMR-907715) and the Robert A. Welch Foundation (grant no. A673), for which grateful acknowledgement is made.

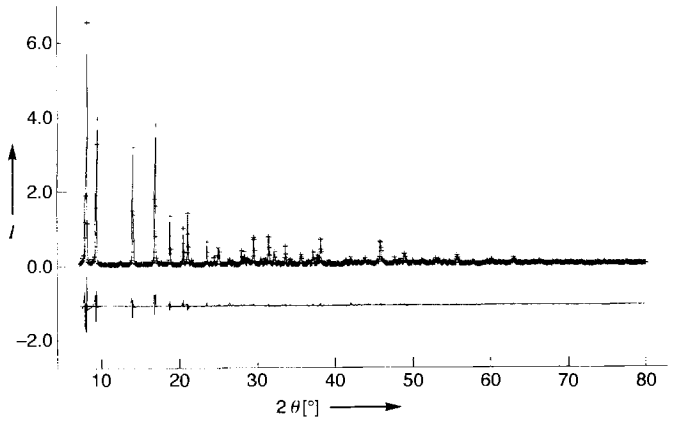

Fig. 1. Observed (+) and calculated (—) profiles (X-ray intensity I in units of 10^4 counts versus 2θ) for the Rietveld refinement. Bottom: the difference plot on the same intensity scale. The first peak (100 reflection) at 18.8 Å was not included in the final Rietveld plot.

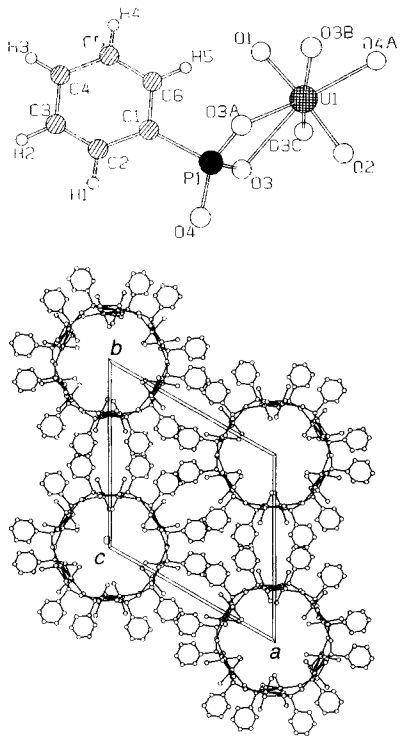

Fig. 2. Top: Structure of $UO_2(O_3PC_6H_5)\cdot 0.7\,H_2O$ showing the coordination about the metal atom and the numbering scheme. Phenyl hydrogen atoms were placed at calculated positions. Selected bond lengths [Å] and angles[°]: U–O(uranyl)$_{mean}$ 1.81(2), U–O3 and U–O3A 2.51(1), U–O3B and U–O3C 2.30(1); U–O4 2.15(1), P–O$_{mean}$ 1.55(1), P–C 1.82(1); O-P-O$_{mean}$ 110(1). Bottom: Projection of the structure down the c axis showing one-dimensional pores separated by the hydrophobic regions. The lattice water positions are not included.

walls of these pores but no such linkages exist between neighboring channels. This structure therefore is different from the copper[10] and aluminum[9] methylphosphonates which contain three-dimensional networks. The pore in the present structure consists of a 12-ring in which six uranium and six phosphorus centers alternate; the distance between the adjacent uranium atoms in this ring is about 6.1 Å (i.e. distance between U atoms in a or b direction). All the atoms except one of the phosphonate oxygens (O3) lie on a mirror plane at $z = 0.0$ and 1/2. The uranium atoms are arranged in the form of a zigzag chain along the wall of the channels with an intermetallic distance of about 4.1 Å (i.e. distance between U atoms in c direction). The oxygen atoms (O3) are involved both in chelation and bridging the metals along the c axis. This leads to double chains with alternating four-membered rings along the wall of the pore; one consisting of two U atoms and two O atoms, the other of two O atoms, a U atom, and a P atom. These double chains are linked together by the phosphonate oxygens O4 along the a (or b) direction (Fig. 3). This type of metal–phosphonate binding is

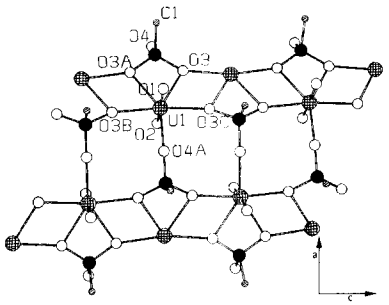

Fig. 3. Arrangement of uranyl phosphonate double chains along the wall of the pore.

strikingly similar to that observed for $UO_2(O_3PCH_2Cl)$,[15] although the latter compound is layered; the organic groups point on either side of the layer. The coordination geometry about the U atom is thus a pentagonal bipyramid, in which the five phosphonate oxygen atoms form the basal plane and the uranyl oxygen atoms (O1 and O2) occupy the axial sites. One of the uranyl oxygen atoms projects towards the center of the pore. The phenyl groups are arranged on the outside of the pore and they are held together by stacking interactions.[16] This grouping of the phenyl groups thus creates isolated channels whose arrangement is dictated by the packing forces.

The distance between the diagonally opposite U atoms in the 12-ring is 12.2 Å. Since one of the uranyl oxygen atoms (O2) is in the same plane of the ring and is directed roughly towards the center of the channel, the diameter of the pore is reduced by a factor equivalent to about two U=O bond lengths. Taking this and the van der Waals radius of O(1.4 Å) into account, the calculated diameter of the available pore is about 7.3 Å. The compound is stable up to about 350 °C. The d spacing of the dehydrated sample is nearly the same as the starting material, indicating the porous structure of the compound. Investigations on intercalation reactions and other physicochemical studies are in progress.

Experimental Procedure

Uranyl nitrate hexahydrate (5.0 g, 10.0 mmol) was dissolved in distilled water (160 mL), filtered, and 50% HF(1.75 mL, 60 mmol) was added. Phenylphosphonic acid (2.37 g, 15.0 mmol) was dissolved in water (160 mL) and added to the uranyl nitrate solution. The total volume of the mixture was then adjusted to 350 mL with distilled water and the temperature was raised to 90 °C. After 1–2 h a yellow powder started to precipitate, which was filtered off after about 5 h, washed with distilled water and air-dried. Thermogravimetric analysis was carried out at a rate of 10 °C min^{-1} under a flow of O_2. The weight loss up to 150 °C was 2.7% and the total weight loss up to 500 °C was 19.5%. Elemental analysis: Found: P 6.13, C 17.51, H 1.67; calc. for $UO_2(O_3PC_6H_5)\cdot 0.67\,H_2O$: P 7.07, C 16.44, H 1.46.

Received: March 1, 1995 [Z7749IE]
German version: *Angew. Chem.* **1995**, *107*, 1650–1652

Keywords: microporosity · phosphonates · structure elucidation · uranyl phenylphosphonates

[1] E. T. Clark, P. R. Rudolf, A. E. Martell, A. Clearfield, *Inorg Chim. Acta* **1989**, *164*, 59.
[2] P. R. Rudolf, E. T. Clark, A. E. Martell, A. Clearfield, *J. Coord. Chem.* **1985**, *14*, 139.
[3] B. Bujoli, P. Palvadeau, J. Rouxel, *Chem. Mater.* **1990**, *2*, 582.
[4] D. M. Poojary, Y. P. Zhang, B. Zhang, A. Clearfield, *Chem. Mater.* **1995**, *7*, 822.
[5] G. Alberti, U. Costantino, S. Allulli, N. Tomassini, *J. Inorg. Nucl. Chem.* **1978**, *40*, 1113; D. M. Poojary, H.-L. Hu, F. L. Campbell, III, A. Clearfield, *Acta Crystallogr. Sect. B* **1993**, *49*, 996; K. J. Martin, P. J. Squattrito, A. Clearfield, *Inorg. Chim. Acta* **1989**, *155*, 1.
[6] G. Cao, H. Hong, T. E. Mallouk, *Acc. Chem. Res.* **1992**, *25*, 420.
[7] A layered zirconium phosphite-diphosphonate pillared compound with interlayer porosity is also known. See G. Alberti, U. Costantino, F. Marmottini, R. Vivani, P. Zappelli, *Angew. Chem.* **1993**, *105*, 1396; *Angew. Chem. Int. Ed. Engl.* **1993**, *32*, 1357.
[8] M. E. Thompson, *Chem. Mater.* **1994**, *6*, 1168.
[9] K. Maeda, Y. Kiyozumi, F. Mizukami, *Angew. Chem* **1994**, *106*, 2427; *Angew. Chem. Int. Ed. Engl.* **1994**, *33*, 2335.
[10] J. L. Bideau, C. Payen, P. Palvadeau, B. Bujoli, *Inorg. Chem.* 1994, *33*, 4885.
[11] Depending upon the reaction conditions (temperature, molar composition of the reactants and solvents) a number of uranyl phenylphosphonate phases have been isolated and characterized. The structures of $UO_2[(HO_3PC_6H_5)_2(H_2O)]\cdot nH_2O$ and that of an ethanol adduct, $UO_2[HO_3PC_6H_5]_2\cdot C_2H_5OH$ consist of linear chains. Structural studies on two orthorhombic phases are also in progress.
[12] J. W. Visser, *J. Appl. Crystallogr.* **1969**, *2*, 89.
[13] A. Larson, R. B. Von Dreele, *GSAS. Generalized Structure Analysis System*, Los Alamos National Laboratory, **1988**.
[14] Crystallographic data: Scan range (2θ) 3–80°, increment 0.01°, time constant 10 s, rotating anode source ($Cu_{K\alpha}$), $C_6H_5O_5UP\cdot 0.7H_2O$, $M_r = 438$, space group *P6/mcc* (no. 192), $a = b = 21.827(2)$, $c = 7.0796(8)$ Å, $V = 2921$ Å^3, $Z = 12$, $\rho_{calcd} = 2.98$ Mg m^{-3}, $T = 23$ °C. No. of contributing reflections ($K_{\alpha 1} + K_{\alpha 2}$) 676, no. of geometric observations $N_{var} = 20$; average distances [Å] used to constrain the bond lengths in the refinement: P–O 1.53(2), $U-O_{uranyl} = 1.80(2)$, O–O (PO_4), 2.55(2), P–C 1.80(2), C–C 1.38; 28 structural parameters, 11 profile parameters, $R_{wp} = 0.177$, $R_p = 0.12$, $R_F = 0.05$, $R_{exp} = 0.04$.(see ref. [13] for definitions).
[15] D. M. Poojary, D. Grohol, A. Clearfield, *J. Phys. Chem. Solids*, in press.
[16] The phenyl rings are grouped about the sixfold axes, in such a way that three rings are in one plane (at $z = 0$) and the other three at a plane with $z = 1/2$ and vice versa. For a given phenyl group, there are two nearest neighboring phenyl groups, both at a plane shifted half along the c axis. The interactions between the groups from the same channel involve C2 and C3 atoms (C2···C2′ 3.78, C3···C3′ 3.9 Å), while that between neighboring channels involve C4 and C5 atoms (C4–C4′ 3.5, C5–C5′ 3.6, C4–C5′ 3.8, and C5–C4′ 3.8 Å). The C6 atoms of the adjacent phenyl rings are separated further apart to accommodate one of the uranyl oxygen atoms O1.

Hydrocarbon Activation with Metal Halides: Catalysis of the Jacobsen Rearrangement by $(ZrCl_4)_n$ in the Presence of Aromatic Hydrocarbons**

Euro Solari, Fabrizio Musso, Richard Ferguson, Carlo Floriani,* Angiola Chiesi-Villa, and Corrado Rizzoli

The metal-promoted rearrangement of hydrocarbons involving C–C bond cleavage and formation is of major interest.[1] Amongst the more interesting approaches, though not frequently employed, is the use of acidic metal electrophiles such as early transition metal halides.[2, 3] This approach has a parallel in organic chemistry—reactions with super acidic compounds.[4] A significant advantage of acidic metals over expensive, low-valent metals in elaborate coordination environments[1] is their straightforward preparation, low cost, and stability towards oxygen.

We report here on a number of observations concerning the interaction of alkylbenzenes with $ZrCl_4$. Although $ZrCl_4$ is extremely insoluble in noncoordinating solvents, it is very soluble in CH_2Cl_2 in the presence of a stoichiometric amount of 1,2,4,5-$Me_4C_6H_2$ (durene). The ^1H NMR spectrum of the reaction mixture in CD_2Cl_2 initially shows the presence of an unshifted singlet for the Me groups of durene, but after some time numerous peaks of increasing intensity appear in its vicinity. Addition of THF to the solution results in $[ZrCl_4(thf)_2]$, in addition to durene and a small amount of other alkylbenzenes. The dissolution of $ZrCl_4$ promoted by durene has been interpreted according to Reaction (a).

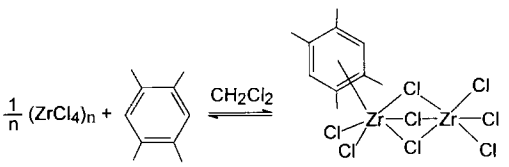

1 (a)

The solubility of $ZrCl_4$ is also increased in the presence of other alkylbenzenes, although the hydrocarbon:$ZrCl_4$ ratio depends on the arene. In the case of mesitylene[5] the dissolution occurs with an arene:$ZrCl_4$ ratio of 2:1, which reflects the lower basicity of mesitylene compared to that of durene. However, this technique cannot be extended to C_6Me_5H and C_6Me_6, because, though they react with $ZrCl_4$, they form insoluble compounds.

When the CH_2Cl_2 solution of $ZrCl_4$–durene was left standing for several weeks, significant amounts of C_6HMe_5, C_6Me_6, $C_6Me_4H_2$, and $C_6Me_3H_3$ formed, along with some insoluble compounds. This conversion continued until the starting durene is completely consumed. Thus the transformation of the $ZrCl_4$–durene system in CH_2Cl_2 solution can be summarized by Scheme 1.

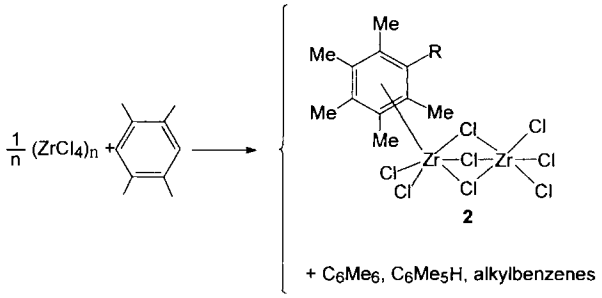

Scheme 1. **2**: R = H (50%), Me (50%).

We isolated compound **2**, $[(\eta^6\text{-}Me_5C_6R)Zr_2Cl_8]$ (R = H, 50%; R = Me, 50%), as a crystalline solid. Its structure, identical to that of **1** and $[(\eta^6\text{-}C_6Me_6)Zr_2Cl_8]$ (**3**), and its composition have been proved by an X-ray analysis and by analysis of the decomposition products arising from the reaction with THF. To avoid the statistical presence of the C_6Me_6 and C_6Me_5H

[*] Prof. Dr. C. Floriani, Dr. E. Solari, F. Musso, Dr. R. Ferguson
Institut de Chimie Minérale et Analytique
Université de Lausanne, BCH 3307
CH-1015 Lausanne (Switzerland)
Telefax: Int. code + 21 692 39 05
e-mail: carlo-floriani@icma.unil.ch
Prof. Dr. A. Chiesi-Villa, Dr. C. Rizzoli
Dipartimento di Chimica, Università di Parma
Viale delle Scienze, I-43100 Parma (Italy)

[**] This work was supported by the Fonds National Suisse de la Recherche Scientifique (grant no. 20-40268.94) and by Ciba-Geigy SA (Basel, Switzerland).

ligands in **2**, we synthesized the analogous complex **3** from pure C_6Me_6 and $ZrCl_4$ in 1,2-$Cl_2C_6H_4$. The ^1H NMR spectrum of **3** in CD_2Cl_2 shows two singlets at $\delta = 2.20$ (low intensity) and $\delta = 2.55$ corresponding to free C_6Me_6 and zirconium-coordinated C_6Me_6, respectively. The structure of **3** is shown in Figure 1[6] with some selected structural parameters. Some distantly related examples of (η^6-arene)zirconium(IV) complexes have been reported recently.[7]

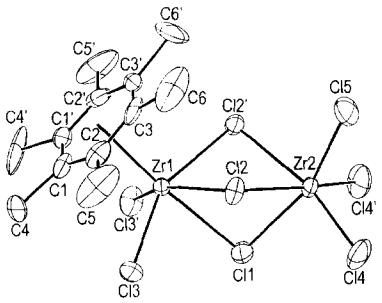

Fig. 1. ORTEP view of complex **3** (ellipsoids at 30% probability). Selected distances [Å]: Zr1 Cl1 2.762(2), Zr1 Cl2 2.587(2), Zr1 Cl3 2.375(2), Zr1 · Cb1 2.367(6), Zr1 C1 2.739(6), Zr1 · C2 2.725(8), Zr1–C3 2.768(7), Zr2–Cl1 2.519(3), Zr2 Cl2 2.609(2), Zr2–Cl4 2.347(3), Zr2–Cl5 2.357(4). Bond angles [°]: Cl3-Zr1-Cl3' 94.0(1), Cl2-Zr1-Cl3 151.4(1), Cl2-Zr1-Cl2' 78.2(1), Cl1-Zr1-Cb1 174.7(2), Cl4'-Zr2-Cl4 99.4(1), Cl2-Zr2-Cl4 91.0(1), Cl1-Zr2-Cl2 76.6(1), Cl1-Zr2-Cl5 161.4(1). Primed atoms denote a transformation of x, $0.5 - y$, z. Cb1 refers to the centroid of the aromatic ring.

Complex **3** has a crystallographic mirror plane passing through both Zr atoms, Cl1, and Cl5. The assignment of an η^6 bonding mode to the hexamethylbenzene fragment is supported by the narrow range of the Zr–C distances [2.725(8)–2.768(7) Å]. The terminal Zr–Cl bonds have an average length of 2.365(9) Å, while significant asymmetry is observed for the bridging chlorine atoms; the longest Zr–Cl distance is to Cl1, which is *trans* to the η^6-C_6Me_6 ligand [Zr1–Cl1 2.762(2) Å].[8] This chlorine atom should therefore be the easiest to ionize. Indeed, complexes **1**–**3** should be considered as models of the precursors for the formation of $[(\eta^6\text{-}C_6Me_6)TiCl_3]^+[Ti_2Cl_9]^-$, which is generated from the reaction of C_6Me_6 with a large excess of $TiCl_4$ in CH_2Cl_2.[9] The large ionic radius and the greater acidity of zirconium versus titanium allow the isolation of the neutral arene complexes **2** and **3** prior to subsequent ionization processes.

We have investigated the possible roles played by CH_2Cl_2, including whether it serves as the source of methyl groups. To rule out this hypothesis, we performed the same durene rearrangement in other solvents such as 1,2-$C_6H_4Cl_2$, $C_2H_2Cl_4$, and *n*-octane.[10] In addition, when the reaction was carried out in CD_2Cl_2 we did not observe incorporation of deuterated methyl groups into the final alkylbenzenes.

The reaction in Scheme 1 is catalytic, albeit to only a limited extent. Furthermore, complexes **2** and **3** dissolved in CH_2Cl_2 are also able to promote the disproportionation of durene. The $ZrCl_4$-assisted rearrangement of C_6Me_5H is quite similar to that discussed for durene. The rates of both reactions can be increased considerably by conducting the reaction in 1,2-$Cl_2C_6H_4$ at 60 °C, or by using a higher $ZrCl_4$:hydrocarbon ratio. We should mention at this stage that the isomerization of durene was observed previously by action of concentrated sulfuric acid, the so-called Jacobsen reaction.[11, 12a, 12b]

The mechanism of the reaction in Scheme 1 is open. Contrary to our results, in the alkylation and dealkylation reactions promoted either by H_2SO_4 or Lewis acids such as H^+, BF_3, and AlX_3, the methyl migration occurs almost exclusively in an intramolecular fashion.[12c] Such reactions are believed to proceed via a carbocation intermediate, as is the case in alkylbenzene rearrangements promoted by the $TaCl_5/CH_2Cl_2$ system[13a] and in alkane isomerization assisted by CX_4/AlX_3.[13b] Unlike these cases, we believe that in our reaction a methyl group is transferred intermolecularly from a methyl donor to a methyl-accepting arene, and this probably does not require a carbocation intermediate. As a matter of fact, when we performed the reaction at 100 °C in 1,2-$Cl_2C_6H_4$ with C_6Me_6, we observed the formation of partially methylated benzenes and alkylated solvent.[14]

Studies in progress are aimed at extending these reactions to the functionalization of hydrocarbons and other kinds of hydrocarbon rearrangements, and to making these reactions catalytic in zirconium. In addition, we should mention that the solution of durene–$ZrCl_4$ in CH_2Cl_2 can be used as a source of a soluble, weakly solvated form of dimeric $ZrCl_4$.

Experimental Procedure

1: A solution of $ZrCl_4$ (40.0 g, 171.7 mmol) and durene (23.05 g, 171.7 mmmol) in CH_2Cl_2 (100 mL) gave a red-violet solution after 15–18 h. THF (5.0 mL) was added to a 5.0 mL aliquot of the solution and $[ZrCl_4(thf)_2]$ was isolated. Durene was identified as the major organic product (by GC-MS) along with significant amounts of C_6Me_5H and C_6Me_6, and all the $C_6H_2Me_4$ isomers. After a reaction time of six months at room temperature, we found that the initial durene was completely converted into C_6Me_5H and C_6Me_6 in a 4:3 molar ratio with an overall yield of 90%; the durene isomers amounted to only 1%, and we did not determine the amounts of the other demethylated species such as the mesitylene isomers and the insoluble products. We indirectly proved that insoluble diarylmethanes containing bridging CD_2 units form from benzene and toluene by the action of CD_2Cl_2 assisted by $ZrCl_4$. The addition of THF to the final solution gave $[ZrCl_4(thf)_2]$ (95%).

2: A $ZrCl_4$–durene solution in CH_2Cl_2 was left standing at room temperature for one month, then concentrated to dryness. The solid was recrystallized from 1,2-$Cl_2C_6H_4$ to give **2** (93%). Anal. calcd for $C_{23}H_{34}Cl_{16}Zr_4$: C 22.23, H 2.76; found: C 23.01, H 2.95. Compound **2** decomposed on treatment with THF giving a 1:1 mixture of C_6Me_5H and C_6Me_6. Crystal data for **2**: $[Zr_2Cl_8(C_{12}H_{18})_{0.5}(C_{11}H_{16})_{0.5}]$, orthorhombic, space group *Pnma*, $a = 19.514(3)$, $b = 13.266(3)$, $c = 8.130(6)$ Å, $V = 2104.6(1.7)$ Å^3, $Z = 4$.

3: A suspension of $ZrCl_4$ (2.50 g, 10.7 mmol) in 1,2-$Cl_2C_6H_4$ (150 mL) and C_6Me_6 (0.865 g, 5.30 mmol) was heated to boiling until it became a clear solution. The solution was then allowed to cool to ambient temperature, affording **3** as a microcrystalline solid (90%). Anal. calcd for $C_{12}H_{18}Cl_8Zr_2$: C 22.94, H 2.89; found: C 23.01, H 2.97.

Isomerization of durene: A moderately catalytic isomerization of durene to C_6Me_6 and C_6Me_5H in CH_2Cl_2 was observed when high durene:$ZrCl_4$ ratios were used. The conversion of durene to C_6Me_6 and C_6Me_5H was roughly 40% complete in one day when a durene:$ZrCl_4$ ratio of 10:1 was used. To accelerate the reaction and demonstrate catalysis, we used a high $ZrCl_4$:substrate ratio. With a $ZrCl_4$:durene ratio of 4:1, durene in CH_2Cl_2 was completely converted in one day. The first addition of durene was followed by several others while maintaining the same ratio, with no noticeable loss in activity. In every case complete conversion required one day. In this way the conversion of durene assisted by $ZrCl_4$ extends to more than 20 times the stoichiometric value.

Received: March 1, 1995 [Z 7751 IE]
German version: *Angew. Chem.* **1005**, *107*, 1621–1623

Keywords: arene complexes · hydrocarbons · isomerizations · Jacobsen rearrangement · Zirconium compounds

[1] a) J. A. Davies, P. L. Watson, J. F. Liebman, A. Greenberg. *Selective Hydrocarbon Activation*, VCH, New York, **1990**; b) *Activation and Functionalization of Alkanes*, (Ed.: C. L. Hill), Wiley, New York, **1989**; c) A. E. Shilov, *Activation of Saturated Hydrocarbons by Transition Metal Complexes*. Reidel, Ingham, MA, **1984**; d) W. D. Jones, F. J. Feher, *Acc. Chem. Res.* **1989**, *2*, 91; e) A. D. Ryabov, *Chem. Rev.* **1990**, *90*, 403; f) A. Sen, *Acc. Chem. Res.* **1988**, *21*, 421; g) R. H. Crabtree, *Chem. Rev.* **1985**, *85*, 245.

[2] a) I. P. Rothwell, *The Homogeneous Activation of Carbon-Hydrogen Bonds by Electrophilic Metal Systems*, Chapter 3 in ref. [1a]; b) P. L. Watson, *C–H Bond Activation with Complexes of Lanthanides and Actinide Elements*, Chapter 4 in ref. [1a]; c) I. P. Rothwell, *The Homogeneous Activation of Carbon-Hydrogen Bonds by High Valent Early d-Block, Lanthanides and Actinide Metal Systems*, Chapter 5 in ref. [1b].

[3] a) J. A. Labinger, A. M. Herring, J. E. Bercaw, *J. Am. Chem. Soc.* **1990**, *112*, 5628; b) G. A. Luinstra, J. A. Labinger, J. E. Bercaw, *ibid.* **1993**, *115*, 3004; c) J. A. Labinger, A. M. Herring, D. K. Lyon, G. A. Luinstra, J. E. Bercaw, I. T. Horváth, K. Eller, *Organometallics* **1993**, *12*, 895; d) A. Sen, M. Lin, L.-C. Kao, A. C. Hutson, *J. Am. Chem. Soc.* **1992**, *114*, 6385.

[4] a) G. A. Olah, G. K. Surya Prakash, J. Sommer, *Super-Acids*, Wiley, New York, **1985**; b) P. Vogel, *Carbocation Chemistry*, Elsevier, Amsterdam, **1985**, and references therein; c) J. Sommer, M. Muller, K. Laali, *New J. Chem.* **1982**, *6*, 3; M. Siskin, J. Porcelli, *J. Am. Chem. Soc.* **1974**, *96*, 3640, and 3641; *ibid.* **1976**, *98*, 5413; *ibid.* **1978**, *100*, 1838.

[5] $ZrCl_4$ (10.0 g, 42.9 mmol) can be dissolved in 100 mL of CH_2Cl_2 in the presence of mesitylene (10.32 g, 85.9 mmol) in 15–20 h.

[6] Crystal data for **3**: $C_{12}H_{18}Cl_8Zr_2$, orthorhombic, space group *Pnma*; $a = 19.524(4)$, $b = 13.218(3)$, $c = 8.355(4)$ Å, $V = 2156.2(12)$ Å^3, $Z = 4$, $\rho_{calcd} = 1.936$ g cm^{-3}; $Mo_{K\alpha}$ radiation ($\lambda = 0.71069$ Å), $\mu_{MoK\alpha} = 19.48$ cm^{-1}; crystal dimensions $0.21 \times 0.30 \times 0.38$ mm. The structure was solved by the heavy-atom method starting from a Patterson map calculated using SHELX-76 and refined anisotropically for all non-hydrogen atoms. The high values of the U_{ij} thermal parameters of the methyl carbons suggested the presence of some disorder due to a possible noncentrosymmetric structure. We tried to refine the structure in the noncentrosymmetric space group $Pna2_1$, but we did not succeed because of strong correlations between pseudosymmetry-related parameters. The centrosymmetric refinement was then considered satisfactory and the high anisotropic thermal parameters attributed to some rotation of the hexamethylbenzene molecule in the plane perpendicular to the Zr–centroid direction. The hydrogen atoms were ignored. The refinement was based on the unique total data and carried out using SHELX-92. For 1948 unique total reflections [$I > 2\sigma(I)$] collected at room temperature ($6 < 2\theta < 50^\circ$) and corrected for absorption, the final *wR2* was 0.092 ($R = 0.042$ for 1098 unique observed reflections). All calculations were done on an Encore 91 computer. Further details of the crystal structure investigation may be obtained from the Director of the Cambridge Crystallographic Data Centre, 12 Union Road, GB-Cambridge CB2 1EZ (UK), on quoting the full journal citation.

[7] G. D. Gillis, M.-J. Tudoret, M. C. Baird, *J. Am. Chem. Soc.* **1993**, *115*, 2543; M. Bochmann, G. Karger, A. J. Jaggar, *J. Chem. Soc. Chem. Commun.* **1990**, 1038; C. Pellecchia, A. Grassi, A. Immirzi, *J. Am. Chem. Soc.* **1993**, *115*, 1160; C. Pellecchia, A. Immirzi, A. Grassi, A. Zambelli, *Organometallics* **1993**, *12*, 4473.

[8] The Zr–Cl distances range from 2.307(2) to 2.655(2) Å in polymeric $(ZrCl_4)_n$: B. Krebs, *Z. Anorg. Allg. Chem.* **1970**, *378*, 263.

[9] a) E. Solari, C. Floriani, A. Chiesi-Villa, C. Guastini, *J. Chem. Soc. Chem. Commun.* **1989**, 1747; b) E. Solari, C. Floriani, K. Schenk, A. Chiesi-Villa, C. Rizzoli, M. Rosi, A. Sgamellotti, *Inorg. Chem.* **1994**, *33*, 2018.

[10] Although the solubility of $ZrCl_4$ in the presence of durene in 1,2-$Cl_2C_6H_4$, $C_2H_2Cl_4$, and octane is far less important than in CH_2Cl_2, we found in all cases that the same rearrangement of durene occurs.

[11] A. Koeberg-Telder, H. Cerfontain, *J. Chem. Soc. Perkin II* **1977**, 717; *Trav. Chim. Pays-Bas* **1987**, *106*, 85; H. Cerfontain, A. Koeberg-Telder, *Can. J. Chem.* **1988**, *66*, 162.

[12] a) J. March, *Advanced Organic Chemistry*, 4th ed., Wiley, New York, **1992**; b) p. 565 in [12a] and references therein; c) pp. 561–563 in [12a] and references therein.

[13] a) E. Solari, C. Floriani, A. Chiesi-Villa, C. Rizzoli, *J. Chem. Soc. Chem. Commun.* **1991**, 841; b) I. Akhrem, A. Orlinkov, M. Vol'pin, *ibid.* **1993**, 671.

[14] Complete transformation of C_6Me_6 (1.73 g, 10.7 mmol) was observed when the reaction was conducted at 100 °C in 1,2-$Cl_2C_6H_4$ (100 mL) for 2–3 days with $ZrCl_4$ (5.0 g, 21.5 mmol). The GC-MS analysis showed the presence of pentamethylbenzene, durene and isodurene, mesitylene isomers, and *o*-dichloro(methyl)benzene isomers, all of them in the same ratio.

Nonheme Iron Centers in Oxygen Activation: Characterization of an Iron(III) Hydroperoxide Intermediate**

Marcel Lubben, Auke Meetsma, Elizabeth C. Wilkinson, Ben Feringa,* and Lawrence Que, Jr.*

Peroxoiron(III) complexes are increasingly being considered as potential intermediates in oxidations catalyzed by nonheme iron centers in biology, because of anticipated difficulties in stabilizing high-valent iron-oxo species in the absence of porphyrins.[1] For example, spectroscopic studies of "activated bleomycin" (BLM[2]), an antitumor drug that effects the oxidative cleavage of DNA and the oxidation of hydrocarbons,[3] cumulatively support its formulation as a low-spin hydroperoxidoiron(III) species.[4] A model for "activated BLM" has been synthesized that mimics its reactivity and gives rise to the same optical and EPR spectra;[5] however, more detailed spectroscopic data is not yet available. In a related area, alkylperoxoiron(III) complexes have been implicated in hydrocarbon oxidations;[6] several have been stabilized at low temperature and spectroscopically characterized.[7] To date, however, "activated BLM" remains the only characterized iron hydroperoxide complex in a nonheme environment. Our own efforts have been directed at generating analogous species in different but related nonheme ligand environments. We thus present here the synthesis and X-ray structure of **1**, an iron(II) complex of a new pentadentate ligand ("N4Py"). Complex **1** reacts with H_2O_2 to generate a transient purple species **2** which is characterized as a low-spin hydroperoxoiron(III) complex. (The compound numbers **1** and **2** are used both for the Fe^{II} and Fe^{III} cations, respectively, and also for their perchlorate salts.)

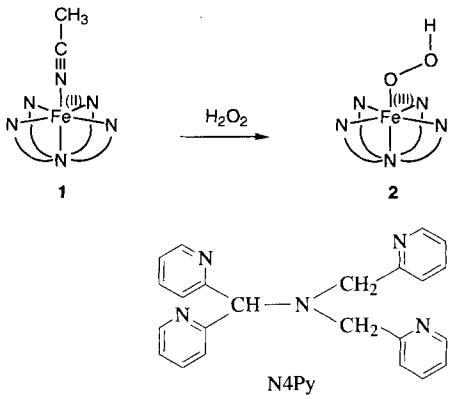

Treatment of N4Py with one equivalent of $Fe(ClO_4)_3 \cdot 10\,H_2O$ in a CH_3OH/CH_3CN mixture followed by vapor diffusion of ethyl acetate yielded dark red crystals of [Fe(N4Py)(CH_3CN)]-

[*] Prof. L. Que, Jr., E. C. Wilkinson
Department of Chemistry, University of Minnesota
Minneapolis, MN 55455 (USA)
Telefax: Int. code + (612)624-7029

Prof. B. Feringa, Dr. M. Lubben, Dr. A. Meetsma
Department of Organic and Molecular Inorganic Chemistry
Groningen Center for Catalysis and Synthesis
University of Groningen
Nijenborgh 4, NL-9747 AG Groningen (The Netherlands)

[**] Financial support of this research by Unilever Research (Vlaardingen, Netherlands) to B. L. F. and the National Institutes of Health (USA) to L. Q. (GM-33162) is gratefully acknowledged. E. C. W. thanks the NIH for a predoctoral traineeship (GM-07323).

$(ClO_4)_2$ (**1**). The structure of **1** shows a six-coordinate iron(II) center surrounded by N atoms from four equatorial pyridine ligands and the apical positions are occupied by the N atom of the tertiary amine and that of acetonitrile (Fig. 1).[8] The four pyridine rings are all positioned *perpendicular* to the basal plane

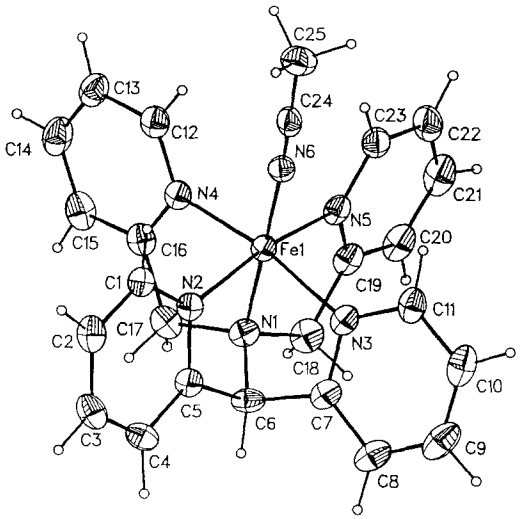

Fig. 1. Structure of the cation of **1** (ORTEP plot) showing 50% probability ellipsoids; hydrogen atoms have been omitted for clarity. Selected distances [Å]: Fe1–N1 1.961(3), Fe1–N2 1.976(3), Fe1–N3 1.967(3), Fe1–N4 1.968(3), Fe–N5 1.975(3), Fe–N6 1.915(3).

of coordination, a situation markedly different from porphyrin systems where the pyrrole groups are within the basal plane. Complex **1** has a low-spin iron(II) center as indicated by the short Fe–N bond lengths of 1.91–1.98 Å.[9] Furthermore all its protons can be accounted for by features in the diamagnetic region of its ^{1}H NMR spectrum, consistent with a low-spin iron(II) complex. The thermodynamic stability of this low-spin iron(II) center is probably the driving force for the reduction of the initially formed iron(III) complex in the synthetic procedure. The ability of the N4Py ligand to stabilize the iron(II) state is supported by the cyclic voltammetry of **1** in CH_3CN which shows a reversible oxidation at 990 mV vs the normal hydrogen electrode (NHE) corresponding to the Fe^{III}/Fe^{II} couple.

Complex **1** exhibits a UV/Vis spectrum with a distinct band at 458 nm ($\varepsilon = 4000\,M^{-1}cm^{-1}$) in acetone (Fig. 2). Treatment of **1** in acetone with an excess (80 equiv) of H_2O_2 at $-8\,^\circ C$ causes the appearance of a purple species ($\lambda_{max} = 530$ nm, $\varepsilon \approx 1100\,M^{-1}cm^{-1}$) with a half-life of 45 min (Fig. 2). At 25 °C however, the purple color disappears within minutes due to disproportionation of H_2O_2, but reappears by the addition of more H_2O_2. A UV/Vis titration of **1** with H_2O_2 shows that the characteristic band for **1** completely disappears with the addition of 0.5 equiv H_2O_2 before the purple color of **2** appears with further addition of H_2O_2, indicating that **1** is first converted to an iron(III) species prior to forming **2**.

The intermediate **2** exhibits an EPR spectrum with g values at 2.17, 2.12, and 1.98 (Fig. 2 inset), indicative of a low-spin iron(III) species. Its signal intensity accounts for as much as 80% of the iron present and correlates directly with the intensity of the purple chromophore. We ascribe the purple color of **2** to a peroxide-to-iron(III) charge transfer transition, but, unlike for high-spin peroxoiron(III) complexes,[10] this assignment could not be corroborated by resonance Raman spectroscopy due to the photoinstability of **2**. Other low-spin peroxoiron(III) species such as "activated BLM" and its Fe(pma) analogue also appear to decompose with laser irradiation.[5]

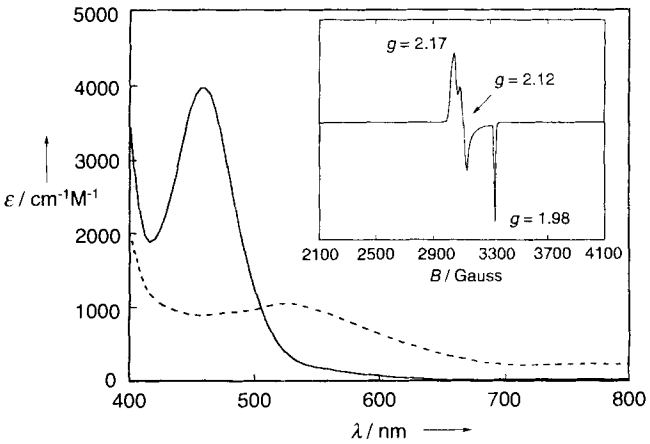

Fig. 2. UV/Vis spectra of **1** (dashed line) and **2** (solid line) in acetone at $-8\,^\circ C$. Inset: X-band EPR spectrum of **2** in acetone at 4 K.

Insight into the nature of **2** has been obtained from electrospray ionization mass spectrometric analysis. Introduction of a cold solution of **2** into a Sciex API III spectrometer affords positive and negative ion mass spectra with the most prominent peak clusters at m/z 555 and 753, respectively. These features correspond to the ions, $\{[(N4Py)FeOOH]ClO_4\}^+$ and $\{[(N4Py)FeOOH](ClO_4)_3\}^-$ and exhibit isotope intensity patterns that match calculated patterns for their formulae (Fig. 3).

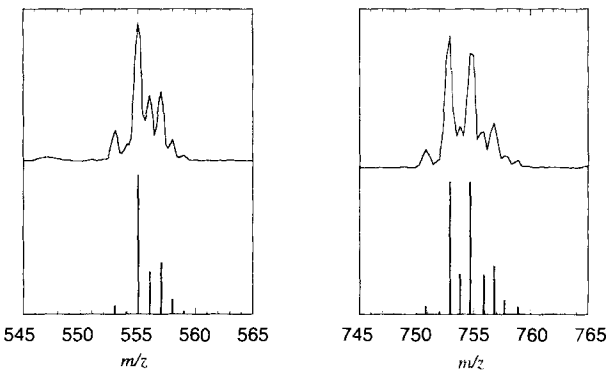

Fig. 3. Electrospray ionization mass spectrometric features of **2** at m/z + 555 and −753, corresponding to the ions $\{[(N4Py)FeOOH]ClO_4\}^+$ and $\{[(N4Py)FeOOH](ClO_4)_3\}^-$, respectively; calculated isotope patterns are represented by bars under each peak cluster.

Furthermore, the intense purple color of **2** is maintained throughout the course of the mass spectrometric experiment, showing that the complex has not decomposed. It is thus clear from these data that **2** is best formulated as $[Fe(N4Py)OOH]^{2+}$; given the pentadentate nature of N4Py and the available coordination site, we favor an end-on coordination mode for the bound hydroperoxide in **2**. This represents the first mass spectrometric evidence for a synthetic hydroperoxoiron(III) intermediate and lends strong support for the formulation of "activated BLM" as $[Fe^{III}(BLM)OOH]^{2+}$.[4, 11]

The intermediate **2** is able to oxidize alkanes. Treatment of **1** with 100 equiv H_2O_2 in the presence of 1000 equiv cyclohexane results in the formation of 13 equiv cyclohexanol and 5 equiv cyclohexanone with respect to **1** within 0.5 h. This corresponds to 36 turnovers per hour and represents an alkane functionaliza-

tion activity comparable to those observed for Fe(tpa) and Fe(bpy) complexes[6] and the "Gif" family of catalysts,[12] which are the best nonheme iron oxidation catalysts reported thus far. Intermediate **2** is observed in the presence of substrate, and cyclohexane oxidation ceases upon disappearance of the purple color, suggesting the involvement of **2** in the catalytic oxidation of cyclohexane. Further experiments to establish the exact role of **2** in catalysis are in progress.

In summary, using the novel pentadentate N4Py ligand we have characterized an air-stable low-spin iron(II) complex that reacts with H_2O_2 to form a transient low-spin iron(III) intermediate **2** in high yield. The intermediate **2** was stable enough to be characterized by electrospray ionization mass spectrometry as $[(N4Py)Fe^{III}OOH]^{2+}$. Furthermore **2** can hydroxylate cyclohexane efficiently. Our studies thus demonstrate that such hydroperoxy complexes can be formed without the participation of an amidate ligand as found in bleomycin and support the notion that an Fe^{III}-OOH moiety can be a viable alternative for high-valent iron-oxo species in mechanisms proposed for nonheme iron oxygenases.[11]

Experimental Procedure

Caution: Complexes with organic ligands and perchlorate anions are potentially **explosive**!

N4Py: Picolyl chloride hydrochloride (6.8 g, 41.5 mmol) was added to an aqueous solution of NaOH (5 M, 8.3 mL) at 0 °C. After stirring for 10 min, this solution was added to bis(2-pyridyl)methylamine (4.13 g, 20.75 mmol) and another portion of aqueous NaOH (5 M, 8.3 mL). This solution was allowed to stir for 48 h at 25 °C, and then concentrated $HClO_4$ was added to precipitate a yellow solid, which was recrystallized from hot water. Treatment of this perchlorate salt with 2.5 M NaOH solution and extraction with dichloromethane yielded the free amine of 4NPy (2.84 g, 37% yield). ^{1}H NMR (300 MHz, $CDCl_3$, 25 °C): δ = 3.97 (s, 4 H, CH_2), 5.35 (s, 1 H, CH), 7.13 (m, 4 H, Py), 7.63 (m, 8 H, Py), 8.51 (d, 2 H, J = 4.8 Hz, Py), 8.57 (d, 2 H, J = 4.7 Hz, Py).

1: $Fe(ClO_4)_3 \cdot 10H_2O$ (0.215 g, 0.403 mmol) was added to a solution of N4Py (0.144 g, 0.392 mmol) in methanol/acetonitrile (1:1). The solution was allowed to stir for 5 min, and then was placed in an ethyl acetate bath. The red crystalline product was collected and washed with ethyl acetate to yield **1** as dark, red crystals (0.178 g, 65% yield). ^{1}H NMR (300 MHz, CD_3CN, 25 °C): δ = 4.27 (d, 2 H, J = 18.1 Hz, CH_2), 4.40 (d, 2 H, J = 18.1 Hz, CH_2), 6.34 (s, 1 H, CH), 7.06 (d, 2 H, J = 7.8 Hz, Py), 7.33 (m, 4 H), 7.68 (m, 2 H, Py), 7.88 (m, 4 H, Py), 8.90 (d, 2 H, J = 5.4 Hz, Py), 9.03 (d, 2 H, J = 5.4 Hz, Py). UV/Vis (acetone): λ_{max} (ε) = 382 (5700), 458 (4000); anal. calcd for $C_{25}H_{28}Cl_2FeN_6O_{10}$: C 42.94, H 4.04, N 12.02; found: C 43.21, H 3.76, N 12.02.

Received: December 12, 1994
Revised version: March 8, 1995 [Z75631E]
German version: *Angew. Chem.* **1995**, *107*, 1610–1612

Keywords: electrospray mass spectrometry · hydroperoxide compounds · nonheme iron compounds · oxygen activation

[1] a) L. Que, Jr. In *Bioinorganic Catalysis*, (Ed.: J. Reedijk), Marcel Dekker, New York, **1993**; pp 347–393; b) A. L. Feig, S. J. Lippard, *Chem. Rev.* **1994**, *94*, 759–805; c) J. S. Valentine, W. Nam, R. Y. N. Ho, in *The Activation of Dioxygen and Homogeneous Catalytic Oxidation* (Eds.: D. H. R. Barton, A. E. Martell, D. T. Sawyer), Plenum: New York, **1993**; pp 183-198.

[2] Abbreviations used: BLM, bleomycin; bpy, 2,2'-bipyridine; N4Py, *N*,*N*-bis(2-pyridylmethyl)-*N*-bis(2-pyridyl)methylamine; pma-H, 2-(2',5'-diazapentyl)-5-bromopyrimidine-6-carboxylic acid N-2-(4'-imidazolyl)ethyl amide; tpa, tris(2-pyridylmethyl)amine.

[3] a) J. Stubbe, J. W. Kozarich, *Chem. Rev.* **1987**, *87*, 1107–1136; b) S. M. Hecht, *Acc. Chem. Res.* **1986**, *19*, 383–391.

[4] a) J. W. Sam, X.-J. Tang, J. Peisach, *J. Am. Chem. Soc.* **1994**, *116*, 5250–5256; b) T. E. Westre, K. E. Loeb, J. M. Zaleski, B. Hedman, K. O. Hodgson, E. I. Solomon, *ibid.* **1995**, *117*, 1309–1313; c) R. M. Burger, T. A. Kent, S. B. Horwitz, E. Münck, J. Peisach, *J. Biol. Chem.* **1983**, *258*, 1559-1564.

[5] R. J. Guajardo, S. E. Hudson, S. J. Brown, P. K. Mascharak, *J. Am. Chem. Soc.* **1993**, *115*, 7971–7977.

[6] a) R. A. Leising, J. Kim, M. A. Pérez, L. Que, Jr., *J. Am. Chem. Soc.* **1993**, *115*, 9524–9530. b) S. Ménage, J.-M. Vincent, C. Lambreaux, G. Chottard, A. Grand, M. Fontecave, *Inorg. Chem.* **1993**, *32*, 4766–4773.

[7] a) Y. Zang, T. E. Elgren, Y. Dong, L. Que, Jr., *J. Am. Chem. Soc.* **1993**, *115*, 811–813; b) S. Ménage, E. C. Wilkinson, L. Que, Jr., M. Fontecave, *Angew. Chem.* **1995**, *107*, 198–200; *Angew. Chem. Int. Ed. Engl.* **1995**, *34*, 203–205.

[8] Crystal data: **1**·CH_3OH ($C_{25}H_{24}Cl_2FeN_6O_8 \cdot CH_3OH$, M_r = 695.30), T = −143 °C, monoclinic space group $P2_1/n$, a = 12.191(1), b = 18.500(1), c = 13.015(1) Å, β = 95.928(8)°, V = 2919.6(4) Å^3, Z = 4. A red block-shaped crystal 0.12 × 0.35 × 0.48 mm was glued to a glass fiber and cooled by using an on-line liquid nitrogen cooling system. 7130 reflections were measured on an Enraf-Nonius CAD-4F diffractometer with $Mo_{K\alpha}$ radiation. For 4543 unique observed reflections with $I > 4.0\sigma(I)$ and 503 refined parameters, the structure was refined to R = 0.046 and R_w = 0.049. Intensity data were corrected for Lorentz and polarization effects and scale variation, but not for absorption. The structure was solved by Patterson methods, and extension of the model was accomplished by direct methods applied to difference structure factors using the program DIRDIF. Further details of the crystal structure may be obtained from the Director of Cambridge Crystallographic Data Centre, 12 Union Road, GB-Cambridge CB2 1EZ (UK) on quoting the full journal citation.

[9] a) P. N. Hawker, M. V. Twigg in *Comprehensive Coordination Chemistry, Vol. IV* (Ed.: G. Wilkinson), Pergamon, Oxford, **1987**, p 1179; b) V. L. Goedken, Y. Park, S.-M. Pong, J. Molin Norris, *J. Am. Chem. Soc.* **1974**, *96*, 7693–7701; c) L. E. McCandlish, B. D. Santarsiero, N. J. Rose, E. C. Lingafelter, *Acta Crystallogr. Sect. B*, **1979**, *35*, 3053–5056.

[10] a) S. Ahmad, J. D. McCallum, A. K. Shiemke, E. H. Appelman, T. M. Loehr, J. Sanders-Loehr, *Inorg. Chem.* **1988**, *27*, 2230–2233; b) B. A. Brennan, Q. Chen, C. Juarez-Garcia, A. E. True, C. J. O'Connor, L. Que, Jr. *Inorg. Chem.* **1991**, *30*, 1937–1943.

[11] The mass spectrometric features associated with $[Fe^{III}(BLM)OOH]^{2+}$ overlap with those of $[Fe^{III}(BLM)Cl]^{2+}$ which is present in significant amounts in the "activated BLM" sample [4a].

[12] D. H. R. Barton, D. Doller, *Acc. Chem. Res.* **1992**, *25*, 504–512, and references therein.

The pH-Dependent Synthesis and Structural Study of Dimer and Cyclic Trimer Complexes of 9-Methyl- or 9-Ethylhypoxanthine Nucleobases with (η^5-Pentamethylcyclopentadienyl)-rhodium Aqua Complexes**

Hong Chen, Marilyn M. Olmstead, David P. Smith, Marcos F. Maestre, and Richard H. Fish*

Recently there has been a dramatic new focus on the reactions of organometallic complexes with biologically important ligands, and interestingly, the majority have been performed in aqueous solution.[1] In our own bioorganometallic chemistry studies, we have been investigating the unique coordination chemistry of Cp*Rh aqua complexes (Cp* = C_5Me_5) with DNA/RNA nucleobases, nucleosides, nucleotides, and oligonucleotides in both organic and aqueous solutions.[1a–e] In one of these studies, we reported on a structure of a monomeric Cp*Rh-9-methylhypoxanthine (9-MH) complex (**1**, OTf = OSO_2CF_3) obtained from the reaction of one equivalent of 9-MH with $[Cp^*Rh(MeOH)_3](OTf)_2$ generated in situ in MeOH.[1d]

$[Cp^*Rh\{\eta^1(N^7)\text{-}9\text{-}MH\}(MeOH)_2](OTf)_2$ **1**

[*] Dr. R. H. Fish, Dr. H. Chen, Dr. D. P. Smith, Dr. M. F. Maestre
Lawrence Berkeley Laboratory, 70-193A, University of California
Berkeley, CA 94720 (USA)
Int. code + (510)486-5401
Dr. M. M. Olmstead
Department of Chemistry, University of California
Davis, CA 95616 (USA)

[**] Bioorganometallic Chemistry, Part 6. The studies at LBL were generously supported by NIH Grant A I 08427 to M. F. M. and by LBL Laboratory Directed Research and Development Funds to M. F. M. and R. H. F., and the U. S. Department of Energy (No. DE-ACO3-76SF00098). Part 5: [1e].

An ^{1}H NMR pH titration profile of **1** in D_2O clearly defined the role of pH in the conversion of this monomer to presumed cyclic trimer and dimer complexes. By observing the H8 and H2 regions of the ^{1}H NMR spectra at various pD values (pD = pH + 0.4), we found that **1** remained unchanged from pD 2.45 to 5.13 (signal broadened slightly at the latter pH); however, an equilibrium process occurred when the pD values were increased to 6.45, 7.96, and 10.50 (Fig. 1). At pD 6.45 the ^{1}H NMR spectrum showed the dramatic chemical shifts diagnostic for the formation of cyclic trimers,[1a, d] while at pD 10.50, a new complex was formed with significant upfield shifts of H8 and H2 that were reminiscent of a $[\{Cp^*Rh(\mu\text{-}OH)(L)\}_2]$ dimer (L = 1-methylcytosine).[1b]

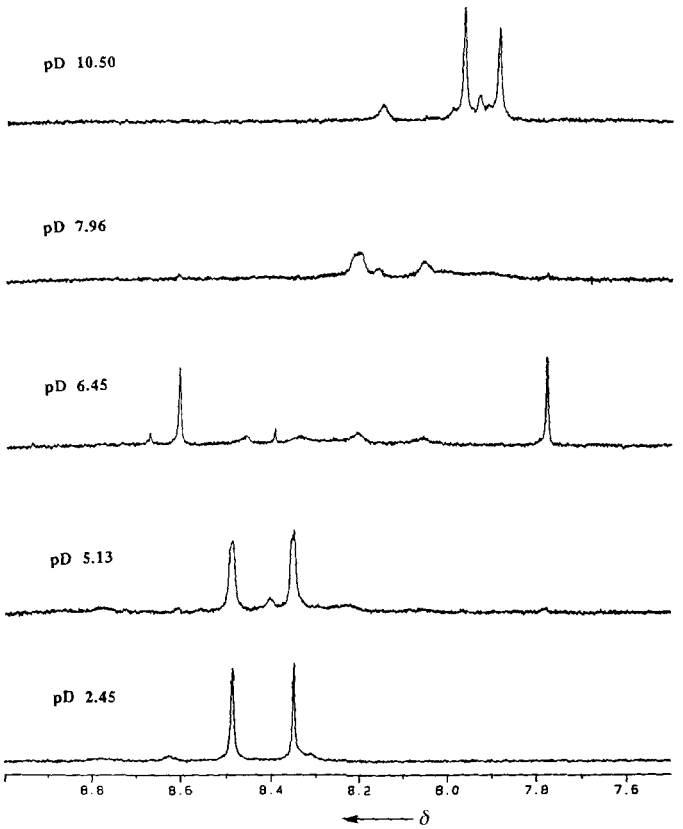

Fig. 1. ^{1}H NMR (400 MHz) spectra of **1** at ambient temperature and different pH values.

In this communication we report on several novel bonding modes of the nucleobase, 9-MH, and an ethyl analogue, 9-ethylhypoxanthine (9-EH), on coordination to Cp*Rh aqua complexes at intermediate and high pH values. Thus, we were able to isolate a new cyclic trimer at a pH of 6.1, the complex **2**,[2] as well as another new complex (**3**)[3] at a pH of 10.2, that were both unequivocally characterized by single-crystal X-ray crystallography studies.

$[\{Cp^*Rh[\mu_2\text{-}\eta^1(N^1)\text{:}\eta^2(N^7,O^6)\text{-}9\text{-}EH]\}_3](OTf)_3$ **2**

$[\{Cp^*Rh[\eta^1(N^1)\text{-}9\text{-}MH](\mu\text{-}OH)\}_2]$ **3**

The cyclic trimer **2**, a racemic mixture, was obtained as yellow crystals from $MeOH/H_2O$, and the cation of one enantiomer of **2** has the X-ray crystal structure shown in Figure 2.[4] A key feature is the simultaneous $\eta^2(N^7,O^6)$ and $\eta^1(N^1)$ ligation of

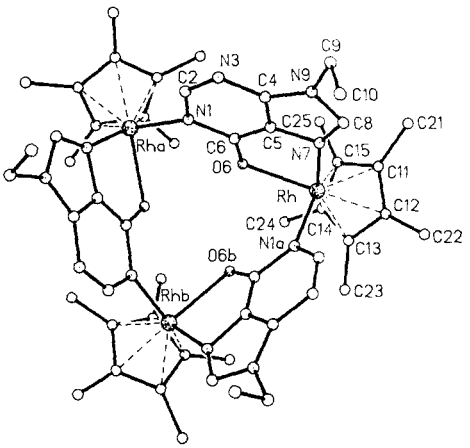

Fig. 2. Structure of $2 \cdot 3.33\,CH_3OH$. Selected bond lengths [Å] and angles [°]: Rh-C15, 2.115(26); Rh-N1a, 2.135(14); Rh-N7, 2.133(16); Rh-O6, 2.240(14); O6-Rh-N7, 80.2(6); O6-Rh-N1a, 88.1(6); N7-Rh-N1a, 85.0(7); Rh-O6-C6, 106.9(14); Rh-N7-C5, 106.0(14); N7-Rh-C15, 116.8(9); O6-C6-C5, 122.3(20); C6-C5-N7, 123.6(17); C2-N1-C6, 114.8(21); N1-C6-C5, 114.1(18); N1-C6-O6, 123.6(22); C5-N7-C8, 102.2(17).

9-EH, which is unprecedented in comparison to a great majority of N7 monodentate complexes,[5] and the few examples of $\eta^2(N^7,O^6)$ binding modes of 9-substituted guanine and hypoxanthine derivatives found in the literature.[6] It is interesting to note, for comparison, the $\eta^2(N^7, N^6)$ and $\eta^1(N^1)$ ligation of 9-methyladenine with [Cp*Rh] that we previously reported.[1a]

Two other structural features of **2** merit comment. First, the cation of **2** has a triangular dome-like cavity; three Cp* groups stretch out from the top of the dome, three ethyl groups point to the bottom, three hypoxanthine planes form the surrounding shell, and three Rh atoms are embedded on the top of the dome. The view shown in Figure 2 is from the bottom of this cavity along the C_3 axis, which passes from the top of the dome to the bottom. Second, the C6–O6 bond distance of 1.296(24) Å falls between the single-bond length of 1.42 Å found in an alcohol,[7] and the double-bond length of 1.233(4) and 1.230(7) Å in inosine,[8] and the $\eta^1(N^7)$ monodentate monomer **1**, respectively. This result suggests that a significant amount of multiple-bond character still exists in the C6–O6 bond of **2**, an argument supported by the long C6–N1 bond (1.401(29) Å) in **2**, relative to a typical C4–N3 double-bond length of 1.358(10) Å that was found in the *trans*-$[\{Cp^*Rh[\eta^1\text{-}(N^3)\text{-}1\text{-methylcytosine}](\mu\text{-}OH)\}_2]^{2+}$ complex.[1b]

The structure of the orange dimer **3**, isolated from its aqueous reaction mixture at pH 10.2, is shown in Figure 3.[4] The main structural features of interest are the unique $\eta^1(N^1)$,[5] rather than $\eta^1(N^7)$ or $\eta^2(N^7,O^6)$ binding mode of 9-MH, and the intramolecular hydrogen bonding between

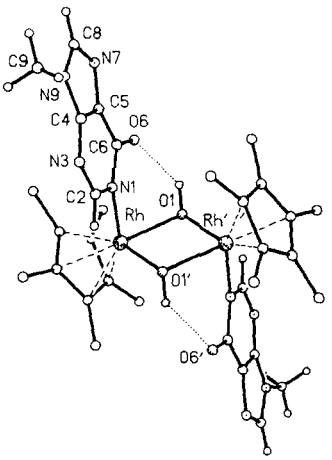

Fig. 3. Structure of **3**, $[\{Cp^*Rh(9\text{-}MH)(OH)\}_2]\cdot 18H_2O$. Selected bond lengths [Å] and angles [°]: Rh-O1, 2.136(4); Rh-N1, 2.148(5); H1···O6, 1.99(1), O1-H1···O6, 140(1); O1-Rh-N1, 86.4(2); Rh-O1-Rh', 102.1(1); Rh-N1-C6, 118.1(4); Rh-N1-C2, 119.8(4); C2-N1-C6, 121.1(5); N1-C6-C5, 113.3(5); N1-C6-O6, 121.3(6); O6-C6-C5, 125.5(5); C6-C5-N7, 130.8(5); C5-N7-C8, 103.1(5).

the μ-OH groups and O6 of this nucleobase. These binding arrangements are in sharp contrast to those in **1** and **2**, as well as other reported metal complexes of 9-substituted guanine and hypoxanthine derivatives,[6] but precedented as shown by the studies of Lippert and co-workers on the $\eta^1(N^1)$ binding of 9-methylguanine to Pt^{II}.[5] However, this $\eta^1(N^1)$-9-methylguanine–Pt^{II} complex was not formed directly, but was prepared via the [μ-$\eta^1(N^7)$:$\eta^1(N^1)$-9-methylguanine]diplatinum(II) complex by selective cleavage of the Pt^{II} atom at N7 with CN^-. We wish to note that guanosine formed a mononuclear [Cp*Rh] complex with $\eta^1(N^7)$ coordination[1a] rather than a cyclic trimer like 9-EH, and thus, unlike Pt^{II}, the [Cp*Rh] group appears to be too sterically demanding to form $\eta^1(N^1)$ complexes with the guanine nucleus; that is, the adjacent NH_2 group at C2 might prevent this type of bonding.

Dimeric complex **3** represents a rare example in which the μ-OH group is involved in intramolecular hydrogen bonding.[1b] The C6–O6 bond of 1.259(7) Å is slightly longer than those observed in inosine (1.233(4) Å), **1** (1.230(7) Å), and a typical aldehyde (1.22 Å),[7] which indicates the primary double-bond character of this C6–O6 group. The elongation of this bond is presumably due to the intramolecular H-bond between O6 and the μ-OH group as well as the intermolecular H-bond between O6 and the H_2O molecules present in the crystal lattice.

The core structure of **3** is similar to the *cis*-[9] and *trans*-$[\{Cp^*Rh(\eta^1\text{-}L)(\mu\text{-}OH)\}_2]^{2+}$[1b] dimeric complexes with heteroaromatic nitrogen ligands (*cis*: L = quinoline, **4**; *trans*: L = 1-methylcytosine, **5**); however, some slight differences merit comment. The planar $Rh_2(\mu\text{-}OH)_2$ fragment of **3** has an O-Rh-O angle of 77.9(1)°, which is in between that of **5** (78.8(2)°), and **4** (75.1(1), 74.8(1)°), and an Rh-O-Rh angle of 102.1(1)°, which is larger than that of **5** (101.2(2)°), yet smaller than that of **4** (105.0(1)°). These structural features are consistent with the intermediate Rh···Rh distance of 3.309(1) Å for **3** relative to those observed for **4** (3.322(1) Å) and **5** (3.290(2) Å). These slight structural differences between **3**, **4**, and **5** are presumably caused by the different numbers of intramolecular H-bonds in these three complexes. Complex **3** has two intramolecular H-bonds in which the $Rh_2(\mu\text{-}OH)_2$ core acts only as H donors, whereas complex **5** has four intramolecular H-bonds in which the $Rh_2(\mu\text{-}OH)_2$ core acts both as a H donor and a H acceptor, and complex **4** has no intramolecular H-bonds. The four intramolecular H-bonds in **5** possibly cause the two μ-OH groups to be further apart, thus providing the largest O-Rh-O angle and shortest Rh···Rh distance amongst these three dimeric complexes.

Although the exact mechanism of the formation of **3** is still not known, it is conceivable that the deprotonation of NH1 ($pK_a = 9.5$)[10] at pH 10.2 makes the N1 site much more nucleophilic than N7 or O6, and in addition, the intramolecular H-bonding between O6 and the μ-OH group stabilizes the dimeric arrangement of **3**. Moreover, at pH 6.1 the construction of the cyclic trimer **2** might emanate from the more favorable $\eta^2(N^7,O^6)$ bidentate five-membered ring complex, since N7 is more nucleophilic at this pH than NH1, and presumably, this $\eta^2(N^7,O^6)$ coordination is more thermodynamically favored. The facile deprotonation of NH1 was followed by formation of the third binding site to an adjacent [Cp*Rh] moiety, a [Cp*Rh{$\eta^2(N^7,O^6)$-9-MH}](OTf) intermediate complex, since the NH1 would be more acidic upon the formation of the $\eta^2(N^7,O^6)$ bidentate five-membered ring.

In conclusion, the novel cyclic trimer **2** and dimer **3** complexes of 9-EH and 9-MH were synthesized in aqueous solution at pH 6.1 and 10.2, respectively, and their structures were verified by single-crystal X-ray crystallography. Finally, the formation of dramatically different structures at various pH values could be explained by the changes in the nucleophilicity of N7, O6, and N1 binding sites. We are pursuing other examples of unique structures for [Cp*Rh]–nucleobase complexes as a function of pH.

Experimental Procedure

2: To a solution of $[Cp^*RhCl_2]_2$ (0.075 g, 0.12 mmol) in H_2O (14 mL, degassed once) was added AgOTf (0.13 g, 0.51 mmol). The reaction mixture was stirred at ambient temperature for 3 h and then filtered. To the filtrate was added 9-EH (0.040 g, 0.24 mmol), and after all the 9-EH had dissolved, the pH was adjusted to 6.1 by the addition of 0.10 N NaOH. The final reaction mixture was degassed and stirred at 25 °C overnight and then at 50 °C for 45 min. The solvent was removed in vacuo, and the yellow residue was taken up in MeOH (5 mL). The product precipitated from MeOH, was collected on a frit, washed with small amounts of MeOH, and dried in vacuo to give 60 mg yellow microcrystals (yield, 45%). FAB-MS, $[M + H-OTf]^+$ (15.2%), $[\{Cp^*Rh(9\text{-}EH)\}_2(OTf)]^+$ (20%), and $[\{Cp^*Rh(9\text{-}EH)\}_2]^+$ (45%). Elemental analysis for $C_{54}H_{66}F_6N_{12}O_{12}Rh_2S_2 \cdot 2H_2O$, calcd C 38.4, H 4.15, N 9.97; found, C 38.1, H 3.97, N 9.71. ^1H NMR (400 MHz, [D$_4$]MeOH, 25 °C): δ = 8.86 (s, 1H, H8), 7.80 (s, 1H, H2), 4.20 (q, ^3J(H,H) = 7 Hz, 2H, CH_2), 1.89 (s, 15H, Cp*), and 1.44 (t, ^3J(H,H) = 7 Hz, 3H, CH_3).

3 was prepared as for **2**, except that the pH was adjusted to 10.2, and the X-ray quality product crystallized on concentration of the aqueous reaction mixture (yield, 60%). FAB/MS, $[M-2CH_3]^+$ (3.3%), $[M-2CH_3-Cp^* + 2H]^+$ (3%), $[M/2-3H]^+$ (3%), and $[M/2-2CH_3-H]^+$ (100%). Elemental analysis for $C_{32}H_{42}N_8O_4Rh_2 \cdot 3H_2O$, calcd C 44.5, H 5.57, N 12.99; found, C 44.3, H 5.29, N 12.56. ^1H NMR (400 MHz, [D$_4$]MeOH, 25 °C) δ = 8.17 (s, 1H, H8), 7.81 (s, 1H, H2), 3.70 (s, 3H, CH_3), 1.76 (s, 15H, Cp*).

Received: March 3, 1995 [Z 7761 IE]
German version: *Angew. Chem.* **1995**, *107*, 1590–1593

Keywords: complexes with nitrogen ligands · coordination · nucleobases · rhodium compounds

[1] a) D. P. Smith, E. Baralt, B. Morales, M. M. Olmstead, M. F. Maestre, R. H. Fish, *J. Am. Chem. Soc.* **1992**, *114*, 10647; b) D. P. Smith, M. M. Olmstead, B. C. Noll, M. F. Maestre, R. H. Fish, *Organometallics* **1993**, *12*, 593; c) D. P. Smith, E. Kohen, M. F. Maestre, R. H. Fish, *Inorg. Chem.* **1993**, *32*, 4119; d) D. P. Smith, M. T. Griffin, M. M. Olmstead, M. F. Maestre, R. H. Fish, *ibid.* **1993**, *32*, 4677; e) H. Chen, M. F. Maestre, R. H. Fish, *J. Am. Chem. Soc.* **1995**, *117*, 3631; f) J. H. Toney, T. J. Marks, *ibid.* **1985**, *107*, 947; g) J. H. Toney, C. P. Brock, T. J. Marks, *ibid.* **1986**, *108*, 7263; h) L. Y. Kuo, M. G. Kanatzidis, T. J. Marks, *ibid.* **1987**, *109*, 7207; i) L. Y. Kuo, M. G. Kanatzidis, M. Sabat, A. L. Tipton, T. J. Marks, *ibid.* **1991**, *113*, 9027; j) A. L. Beauchamp, D. Cozak, A. Mardhy, *Inorg. Chim. Acta* **1984**, *92*, 191; k) D. Cozak, A. Mardhy, M. J. Olivier, A. L. Beauchamp, *Inorg. Chem.* **1986**, *25*, 2600; l) N. H. Agnew, T. G. Appleton, J. R. Hall, G. F. Kilmister, I. J. McMahon, *J. Chem. Soc. Chem. Comm.* **1979**, 324; m) A. D. Ryabov, D. L. Menglet, M. D. Levi, *J. Organomet. Chem.* **1991**, *421*, C16; n) H. Bauer, G. M. Sheldrick, U. Nagel, W. Beck, *Z. Naturforsch. B* **1985**, *46*, 1237; o) J. E. Kickham, S. J. Loeb, *Inorg. Chem.* **1994**, *33*, 4351; p) A. D. Ryabov, *Angew. Chem.* **1991**, *103*, 945; *Angew. Chem. Int. Ed. Engl.* **1991**, *30*, 931; q) G. Jaouen, A. Vessieres, I. S. Butler, *Acc. Chem. Res.* **1993**, *26*, 361; r) R. Kramer, K. Polborn, C. Robl, W. Beck, *Inorg. Chim. Acta* **1992**, *198–200*, 415.

[2] 9-Ethylhypoxanthine deprotonated at N1.

[3] 9-Methylhypoxanthine deprotonated at N1.

[4] Complex **2**, $(C_{56.5}H_{76}F_6N_{12}O_{14.5}Rh_2S_2)$, M_r = 1731.2), crystallizes from MeOH/H_2O at −20 °C; crystal size, 0.08 × 0.08 × 0.10 mm^3, rhombohedral, space group *R*3*c*, a = 22.736(7), c = 24.402(10) Å, Z = 6, V = 10919(8) Å^3, ρ_{calcd} = 1.58 g cm^{-3}, $2\theta_{max}$ = 45.0°, $Mo_{K\alpha}$ radiation, λ = 0.71073 Å, ω scans, 130 K, 3418 measured reflections, 1636 independent reflections, of which 1460 with $|F| > 4.0\sigma(|F|)$ were used for refinement; a Lorentzian polarization correction and an absorption correction (XABS) were applied (program XABS provides an empirical correction based on F_o and F_c differences. H. Hope, B. Moezzi, Chemistry Department, University of California, Davis); μ = 0.85 mm^{-1}, max/min transmission = 0.94/0.92, structure was solved by direct methods using SHELXTL PLUS, and refined by a full-matrix least-squares method based on $|F|$ with 181 parameters, hydrogen atoms were located or added geometrically, and refined by using the riding model with fixed isotropic temperature factors, R = 0.0746, wR = 0.1003, largest difference peak = 0.94 e Å^{-3}.
Complex **3**, $(C_{32}H_{78}N_8O_{22}Rh_2$, M_r = 1132.8), crystallizes from its aqueous reaction mixture at 4 °C; crystal size 0.04 × 0.22 × 0.44 mm^3, monoclinic, space group $P2_1/c$ with a = 11.615(3), b = 13.527(3), c = 16.516(3) Å, β = 103.92(2)°, Z = 2, V = 2518.8(9) Å^3, ρ_{calcd} = 1.49 g cm^{-3}, $2\theta_{max}$ = 112.0°, $Cu_{K\alpha}$ radiation,

$\lambda = 1.54178$ Å, 2θ–ω scans, 130 K, 3632 measured reflections, 3268 independent reflections, of which 2965 with $|F| > 4.0\sigma(|F|)$ were used for refinement, a Lorentzian polarization correction and an absorption correction (XABS) were applied (see above), $\mu = 6.00$ mm^{-1}, max/min transmission = 0.82/0.33; structure was solved by Patterson and difference Fourier methods using SHELXTL PLUS, and refined by a full-matrix least-squares method based on $|F|$ with 244 parameters, hydrogen atoms were located or added geometrically, and refined by using the riding model with fixed isotropic temperature factors. $R = 0.0550$; $wR = 0.0857$, largest difference peak = 1.80 e Å^{-3}. Further details of the crystal structure investigations may be obtained from the Director of the Cambridge Crystallographic Data Centre, 12 Union Road, GB-Cambridge CB21EZ (UK), on quoting the full journal citation.

[5] G. Frommer, I. Mutikainen, F. J. Pesch, E. C. Hillgeris, H. Preut, B. Lippert, *Inorg. Chem.* **1992**, *31*, 2429.

[6] K. R. Dunbar, J. H. Matonic, V. P. Saharan, C. A. Crawford, G. Christou, *J. Am. Chem. Soc.* **1994**, *116*, 2201, and references therein.

[7] D. A. Johnson, *Some Thermodynamic Aspects of Inorganic Chemistry*, Cambridge University Press, Cambridge, **1982**.

[8] A. R. I. Munns, P. Tollin, *Acta Crystallogr. Sect. B* **1970**, *26*, 1101.

[9] R. H. Fish, H.-S. Kim, J. E. Babin, R. D. Adams, *Organometallics* **1988**, *7*, 2250.

[10] J. H. J. Den Hartog, M. L. Salm, J. Reedijk, *Inorg. Chem.* **1984**, *23*, 2001

Single-Crystal X-Ray Structure of the Metastable Aryne Precursor Tetrafluorophenyllithium and of 1,2,3,4-Tetrafluorobenzene**

Thomas Kottke, Kuangsen Sung, and Richard J. Lagow*

Dedicated to Paul von Ragué Schleyer on the occasion of his 65th birthday

The development of a dehydrobenzene concept can be traced back to the studies of the reaction of phenyllithium with fluorobenzene performed by Wittig in 1942.[1] The existence of benzyne (1,2-didehydrobenzene) and related arynes as intermediates was later established by Roberts,[2] Huisgen,[3] and Wittig.[4] Ever since, dehydrobenzene chemistry has played a major part in many laboratories and is well-documented by numerous review articles.[5] The formation of arynes generally involves the β-elimination of appropriately positioned substituents from an aromatic precursor. Suitable synthetic methods are the fragmentation of benzo-fused cyclic systems, the elimination of nitrogen and carbon dioxide from benzenediazonium carboxylates or related compounds, and the elimination of halide ions from "aryl anion"[6] intermediates.

A prime example of the halide-ion elimination is the elimination of metal halides from metalated aryl halides, the classical procedure for the generation of arynes. The reaction mostly proceeds under mild conditions, particularly when organolithium intermediates are involved. Apart from solvent effects, the stability of those intermediates has essentially been attributed to the character of the substituents as well as to the nature of the leaving halogen. Substituents that inductively stabilize the negative charge of the intermediate "aryl anion" reduce the tendency to lose halide.[5b, 7] The ease of aryne formation with respect to the nature of the leaving halide follows the order $F < Cl < Br$.[5b, 8]

Recently, Boche and co-workers introduced geometric parameters which may structurally reflect the reactivity of metalated aryl halides towards β-elimination when they determined the crystal structures of two potential aryne precursors:[9] 3-bromo-2-lithiobenzofuran **1**, and 3-fluoro-2-lithio-1-phenylsulfonylbenzene **2**. Although both compounds contain lithium and halogen on neighboring carbon atoms, only in **2** can elimination of lithium halide be initiated. Based on a comparison with average C_{aryl}–X bond lengths (X = halogen), the authors correlated the difference in reactivity with the extent of the C–X bond lengthening apparent in the solid-state structures. Relative to the C–Br bond in **1**, **2** has an elongated C–F bond, and in addition, a shorter intramolecular Li–X distance. Moreover, ab initio MO calculation of unsolvated *ortho*-fluorophenyllithium revealed a remarkably long C–F bond (142.2 pm vs. 133.8 pm in *para*-fluorophenyllithium) as a consequence of an intramolecular Li–F coordination.[10]

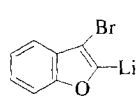

1

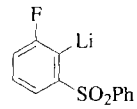

2

To determine the magnitude of C–X bond lengthening accurately and to investigate a possible involvement of solid-state Li···F interactions we have determined the crystal structures[11] of 1,2,3,4-tetrafluorobenzene (**3**) and of THF-solvated tetrafluorophenyllithium (**4**). Because of the low melting point of **3** (−42 °C) and the decomposition of solid **4** at −22 °C (the colorless crystals turn black within seconds), low temperature crystallization and mounting techniques had to be applied to facilitate structural characterization.[12]

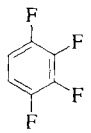

3

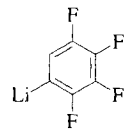

4

As expected, within the standard deviation, the bond lengths and angles of the planar ring system in **3** are symmetrical with respect to the axis bisecting the C2–C3 and the C5–C6 bond (Fig. 1). Minor differences between the geometric parameters along this axis are due to substituent effects (as discussed below): The carbon skeleton of the ring shows slightly alternating bond lengths; the longest is C5–C6 (138.6(2) pm), and the shortest C1–C6 and C4–C5 (136.9(2) pm each). The ring bond angles at C1 and C4 (121.3(1) and 121.4(1)°, respectively) are slightly larger than the others (119.2(1)–119.5(1)°). The molecules are packed in layers, which

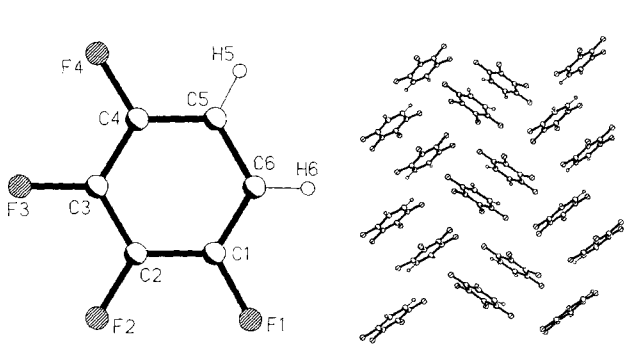

Fig. 1. Molecular structure of **3** (left), and the packing in the crystal (right, one layer is shown). Selected bond lengths [pm] and angles [°]: C1–F1 134.9(2), C1–C2 137.9(2), C2–F2 134.1(2), C2–C3 137.3(2), C3–F3 134.1(2), C3–C4 137.6(2), C4–F4 134.9(2), C4–C5 136.9(2), C5–C6 138.6(2), C6–C1 136.9(2), C6-C1-C2 121.3(1), C1-C2-C3 119.5(1), C2-C3-C4 119.3(1), C3-C4-C5 121.4(1), C4-C5-C6 119.3(1), C5-C6-C1 119.2(1).

[*] Prof. Dr. R. J. Lagow, Dr. T. Kottke, Dr. K. Sung
University of Texas at Austin
Department of Chemistry and Biochemistry
Austin, Texas 78712 (USA)
Telefax: Int. code + (512)471-8648

[**] This work was supported by the National Science Foundation (NSF), grant no. CHE-9106482. T. K. thanks the Alexander von Humboldt Foundation for a Feodor-Lynen scholarship.

resemble a chessboard in which each field is formed by a pair of molecules oriented parallel to each other (Fig. 1, right).

Metalation of **3** with *n*BuLi in THF yields the benzyne precursor **4**. LiF elimination from **4** occurs in solution at temperatures above −40 °C, in contrast to + 60 °C observed in **2**. This is in agreement with the less marked stabilizing effect of the fluorine substituents vs. a phenylsulfonyl group.[5b, 9] The X-ray structure analysis reveals that **4** is a monomer in the solid state (Fig. 2).

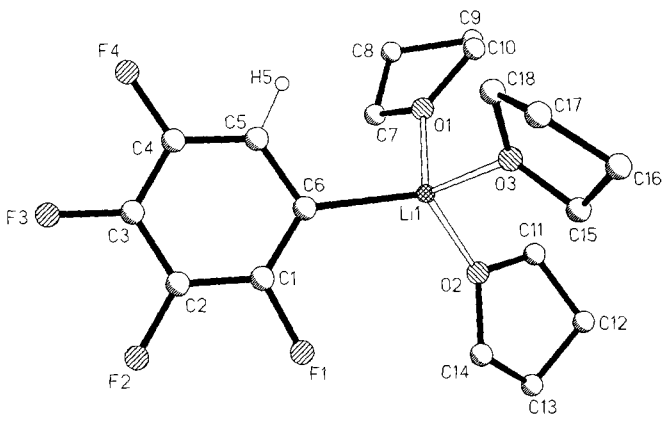

Fig. 2. Molecular structure of **4**. Selected bond lengths [pm] and angles [°]: Li1–C6 213.6(5), Li1–O1 195.6(4), Li1–O2 195.1(4), Li1–O3 196.4(4), C1–F1 138.2(3), C1–C2 136.9(4), C2–F2 136.3(3), C2–C3 136.8(3), C3–F3 134.7(3), C3–C4 137.3(4), C4–F4 136.8(3), C4–C5 136.5(4), C5–C6 141.5(3), C6–C1 136.7(3); C6-C1-C2 125.7(2), C1-C2-C3 119.3(2), C2-C3-C4 118.1(2), C3-C4-C5 121.3(2), C4-C5-C6 122.4(2), C5-C6-C1 113.1(2).

The lithium atom is positioned nearly in the plane defined by the aromatic carbon atoms (torsion angle C2-C1-C6-Li1 = 173.3(3)°). The coordination sphere of Li1 is made up of three THF molecules and the deprotonated carbon atom C6. The Li1–C6 bond length of 213.6(5) pm falls within the range of corresponding Li–C distances observed in the few known examples of monomeric aryllithium structures (207.4–213.5 pm).[13]

The structure of the attached benzene ring shows the typical distortions earlier ascertained in aryllithium structures.[13, 14] The narrowing of the *ipso* angle along with the widening of the *ortho* angles has been explained in terms of a rehybridization of the *ipso*-carbon atom.[14c, 15] While electropositive substituents decrease the corresponding ring angle and slightly elongate the $C_{ipso}-C_{ortho}$ bond lengths, electronegative substituents have the opposite effect. The presence of electropositive and unsymmetrically arranged electronegative substituents make a complex combination of both effects a crucial feature in **4**, causing the remarkably large C_{ortho} angles and different $C_{ipso}-C_{ortho}$ lengths. The nonbonding Li1–F1 distance of 344.8(4) pm is smaller than in **2** (367.2(7) pm[9]). However, it is significantly larger than nonbonding Li–F distances observed in compounds with obvious Li···F interactions (for example, an Li–F distance of 225.2 pm[16] has been observed in dimeric, ether-solvated 2,4,6-tris(trifluoromethyl)phenyllithium). Furthermore, it by far exceeds the Li–F distance in the calculated structure of unsolvated 1-fluoro-2-lithiobenzene (190.1 pm[10]), which could be considered as a lower limit of Li–F distances in related structures.

The longest C–F bond in **4** is 138.2(3) pm (C1–F1), which is indeed the one adjacent to the C–Li bond. However, the difference with respect to the other C–F bond lengths is not very pronounced. In fact, comparison with **3** reveals an elongation of all C–F bonds. This effect becomes less significant at the positions further away from the "anionic" carbon atom. The involvement of all C–F bonds indicates that the "anionic character" of the phenyl group is responsible for the bond lengthening rather than an Li···F interaction affecting per se only one C–F bond. This interpretation is supported by the exterior bond angles at C1 and C6. F1-C1-C6 (119.4(2)°) and Li1-C6-C1 (129.9(2)°) are each larger than their counterparts (F1-C1-C2 = 114.9(2)° and Li1-C6-C5 = 116.7(2)°, respectively), which is probably due to the steric influence of the THF ligands and the short C1–C6 distance (136.7(3) pm vs. 141.5(3) pm for C6–C5). A dominant Li···F interaction in **4** would lead to a somewhat different geometry. A possible explanation for the longer C–F bonds may be a partial distribution of the negative charge over the ring skeleton—enhanced by the electron-withdrawing effect of the fluorine substituents—reducing the polarity of the C–F bonds and consequently resulting in bond elongation.

The structures of **3** and **4** do not suggest a correlation between solid-state Li–F distances and the reactivity of aryne precursors towards LiF elimination. Although the Li–F distance is 313.3(3) pm in the crystal structure of monomeric THF-solvated pentafluorophenyllithium,[17] which is significantly shorter than Li1–F1 in **4**, LiF elimination occurs only above −6 °C in the solid state and slowly at −10 °C[7a] in etheral solution; this is in agreement with the greater number of stabilizing fluorine substituents.

Experimental Procedure

3: A solution of 1,2,3,4-tetrafluorobenzene (2.1 g, 14 mmol) in a mixture of pentane (15 mL) and toluene (5 mL) was maintained at −90 °C for several hours. The initially formed crystals were redissolved leaving only a few crystallites in the solution. After 2–3 days at −78 °C colorless blocks, suitable for X-ray structure analysis, had grown.

4: Following the procedure reported earlier [18], **3** (2 g, 13 mmol) dissolved in THF (50 mL) were treated with *n*BuLi (33 mmol, 13.2 mL, 2.5 M solution in hexane) for 2 h at −70 °C. Within one week single crystals had grown after treatment of the reaction solution as described for **3**.

Received: March 7, 1995 [Z 7767 IE]
German version: *Angew. Chem.* **1995**, *107*, 1612–1614

Keywords: arynes · fluorobenzenes · lithium compounds · structure elucidation

[1] G. Wittig, *Naturwissenschaften* **1942**, *30*, 696.
[2] a) J. D. Roberts, H. E. Simmons Jr., L. A. Carlsmith, C. W. Vaughan, *J. Am. Chem. Soc.* **1953**, *75*, 3290; b) J. D. Roberts, D. A. Semenow, H. E. Simmons Jr., L. A. Carlsmith, *ibid.* **1956**, *78*, 601.
[3] R. Huisgen, H. Rist, *Naturwissenschaften* **1954**, *41*, 358.
[4] a) G. Wittig, L. Pohmer, *Angew. Chem.* **1955**, *67*, 348; b) G. Wittig, L. Pohmer, *Chem. Ber.* **1956**, *89*, 1334.
[5] a) G. Wittig, *Angew. Chem.* **1965**, *77*, 752; *Angew. Chem. Int. Ed. Engl.* **1965**, *4*, 731; b) R. W. Hoffmann, *Dehydrobenzene and Cycloalkynes*, Academic Press, New York, **1967**; c) E. K. Fields in *Organic Reactive Intermediates* (Ed.: S. P. McManus), Academic Press, New York, **1973**, p. 448; d) M. G. Reinecke in *Reactive Intermediates, Volume 2* (Ed.: R. A. Abramovitch), Plenum Press, New York, **1982**, p. 367; e) T. L. Gilchrist in *The Chemistry of Functional Groups, Supplement C: The Chemistry of Triple-Bonded Functional Groups, Part 1* (Eds.: S. Patai, Z. Rappoport), Wiley, New York, **1983**, p. 383; f) M. A. Bennett, H. P. Schwemlein, *Angew. Chem.* **1989**, *101*, 1349; *Angew. Chem. Int. Ed. Engl.* **1989**, *28*, 1296.
[6] As has been emphasized again recently, the term carbanion is inappropriate for such species: C. Lambert, P. von R. Schleyer, *Angew. Chem.* **1994**, *106*, 1187; *Angew. Chem. Int. Ed. Engl.* **1994**, *33*, 1129.
[7] a) P. L. Coe, R. Stephens, J. C. Tatlow, *J. Chem. Soc.* **1962**, 3227; b) K. Grohmann, *Dissertation*, Universität Heidelberg **1965**.
[8] a) H. Gilman, R. D. Gorsich, *J. Am. Chem. Soc.* **1956**, *78*, 2217; b) O. M. Nefedov, A. I. D'yachenko, *Angew. Chem.* **1972**, *84*, 527; *Angew. Chem. Int. Ed. Engl.* **1972**, *11*, 507.

[9] F. Bosold, P. Zulauf, M. Marsch, K. Harms, J. Lohrenz, G. Boche, *Angew. Chem.* **1991**, *103*, 1497; *Angew. Chem. Int. Ed. Engl.* **1991**, *30*, 1455.

[10] N. J. R. van Eikema Hommes, P. von R. Schleyer, *Angew. Chem.* **1992**, *104*, 768; *Angew. Chem. Int. Ed. Engl.* **1992**, *31*, 755.

[11] Crystallographic data: data collection on a Siemens P4 four-circle diffractometer with graphite-monochromated $Mo_{K\alpha}$ radiation ($\lambda = 0.71073$ Å). Structure solution with direct methods (G. M. Sheldrick, *Acta Crystallogr. Sect. A* **1990**, *46*, 467), full-matrix least-squares refinement on F^2 (SHELXL-93). **3**: $C_8H_2F_4$, monoclinic space group $P2_1/n$, crystal dimensions $a = 669.55(6)$, $b = 756.18(6)$, $c = 1110.58(8)$ pm, $\beta = 92.818(6)$°, $V = 0.56161(8)$ nm^3, $\rho_{calcd} = 1.775$ Mg m^{-3}, $\mu = 0.197$ mm^{-1}; 2369 reflections ($6 < 2\theta < 50$), of which 976 are unique ($R_{int} = 0.0232$) and 828 observed ($I > 2\sigma(I)$) were measured at 120 °C in $2\theta/\omega$ scan mode. All non-hydrogen atoms were refined anisotropically, the hydrogen atoms were located by difference Fourier synthesis and refined freely and isotropically. $R1 = 0.0264$, $wR2 = 0.0700$ (all data) for 100 parameters. **4**: $C_{18}H_{25}F_4LiO_3$, monoclinic space group $P2_1/n$, crystal dimensions $a = 984.2(1)$, $b = 1452.3(2)$, $c = 1360.5(2)$ pm, $\beta = 100.754(9)$°, $V = 1.9104(4)$ nm^3, $\rho_{calcd} = 1.294$ Mg m^{-3}, $\mu = 0.111$ mm^{-1}; 6836 reflections ($6 < 2\theta < 50$), of which 3340 unique ($R_{int} = 0.0633$) and 1843 observed ($I > 2\sigma(I)$) were measured at -120 °C in $2\theta/\omega$ scan mode. All non-hydrogen atoms were refined anisotropically; H5 was located by difference Fourier synthesis and refined freely and isotropically, all other hydrogen atoms were geometrically positioned and refined according to a riding model. $R1 = 0.0455$, $wR2 = 0.1239$ (all data) for 249 parameters and 62 restraints. Further details of the crystal structure investigations are available on request from the Director of the Cambridge Crystallographic Data Centre, 12 Union Road, GB-Cambridge CB2 1EZ (UK), on quoting the full journal citation.

[12] a) T. Kottke, D. Stalke, *Angew. Chem.* **1993**, *105*, 619; *Angew. Chem. Int. Ed. Engl.* **1993**, *32*, 580 b) T. Kottke, D. Stalke, *J. Appl. Crystallogr.* **1993**, *26*, 615.

[13] a) U. Schürmann, J. Kopf, E. Weiss, *Angew. Chem.* **1985**, *97*, 222; *Angew. Chem. Int. Ed. Engl.* **1985**, *24*, 215; b) T. Maetzke, D. Seebach, *Helv. Chim. Acta* **1989**, *72*, 624; c) M. M. Olmstead, P. P. Power, *J. Organomet. Chem.* **1991**, *408*, 1; d) G. S. Girolami, M. E. Riehl, K. S. Suslick, S. R. Wilson, *Organometallics* **1992**, *11*, 3907.

[14] a) D. Thoennes, E. Weiss, *Chem. Ber.* **1978**, *111*, 3157; b) A. A. H. van der Zeyden, G. van Koten, *Recl. Trav. Chim. Pays-Bas* **1988**, *107*, 431; c) S. Harder, P. F. Ekhart, L. Brandsma, J. A. Kanters, A. J. M. Duisenberg, P. von R. Schleyer, *Organometallics* **1992**, *11*, 2623.

[15] a) A. Domenicano, A. Vaciago, C. A. Coulson, *Acta Crystallogr.* **1975**, *B31*, 221; b) A. Domenicano, A. Vaciago, C. A. Coulson, *ibid.* **1975**, *B31*, 1630; c) A. Domenicano in *Accurate Molecular Structures* (Eds.: A. Domenicano, J. Hargittai), Oxford University Press, New York, **1992**, p. 437.

[16] D. Stalke, K. H. Whitmire, *J. Chem. Soc. Chem. Commun.* **1990**, 833.

[17] T. Kottke, R. J. Lagow, unpublished results.

[18] a) R. J. Harper Jr., E. J. Soloski, C. Tamborski, *J. Org. Chem.* **1964**, *29*, 2385; b) G. M. Brooke, B. S. Furniss, *J. Chem. Soc.* **1967**, *C*, 869.

 © VCH Verlagsgesellschaft mbH, D-69451 Weinheim, 1995 0570-0833/95/1313-1519 $ 10.00+.25/0

A Nucleus of Modern Chemical Techniques

Advanced Organic Chemistry of Nucleic Acids. By *Z. A. Shabarova* and *A. A. Bogdanov*. VCH Verlagsgesellschaft, Weinheim, 1994. 588 pp., hardcover DM 248.00.—ISBN 3-527-29021-4

Alongside the classical disciplines of organic, inorganic, and physical chemistry, a number of related disciplines are nowadays increasing in importance. One of these is bioorganic chemistry. Whereas it was formerly regarded as just a minor branch of biology, or at best accepted as biochemistry and perhaps tolerated at the periphery of organic chemistry, this field is now, with good reason, being seen as increasingly important. The growth of interest in this interdisciplinary area is gaining further momentum from the rapid advances in research into the molecular mechanisms that determine life. In particular the developments in protein and nucleic acid chemistry are the pacemakers.

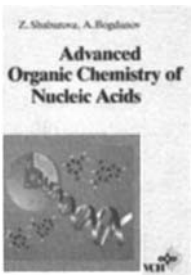

During the last few years several monographs dealing with these topics at a specialist level have appeared. In contrast, the existing textbooks are not up-to-date. The book reviewed here, by the Russian authors Zoe Shabarova and Alexey Bogdanov, is the most recent treatment of nucleic acid chemistry. As indicated by the title, the subject of the book is the organic chemistry of this class of natural compounds. In the preface the authors make it clear that their main aim was to produce a textbook specifically for students.

The book is a completely revised English version of the textbook originally published by the same authors in 1978 in Russian under the title "The Chemistry of Nucleic Acids and their Compounds". Much new material has been added, including a chapter on the highly topical subject of ribozymes.

The book is divided into 11 chapters (588 pages), most of which have been written by Z. Shabarova. First the structure of nucleosides is described (Chapter 1: pyrimidines and purines, importance of the configuration of the anomeric center, nucleoside antibiotics). Their properties are then discussed (Chapter 2: tautomeric structures, reactions with nucleophiles and electrophiles, addition reactions, stability of the glycosidic bond). The following chapters describe the nucleotides which are the building blocks of DNA and RNA (Chapters 3 and 4: acid/base behavior, properties of the phosphate group(s), reactions at the phosphate group). Beginning on page 187, Chapter 5 deals with the primary structure of the nucleic acids DNA and RNA. The nomenclature of nucleic acids is explained, followed by a discussion of the action of nucleases and methods for determining the nucleoside sequence. In Chapter 6 ("Determination of the Primary Structure of Nucleic Acids") the methods of sequencing are treated in greater detail, including DNA-mapping, chemical sequencing, and enzymatic sequencing. Also included here is the method of sequencing on a solid support, as well as the highly topical polymerase chain reaction (PCR) method. Chapter 7 deals with the basic features of the secondary structure of nucleic acids, including the conformational characteristics of nucleotide monomers and single-strand oligonucleotides. The macromolecular structure of DNA and RNA, starting with the Watson–Crick model, is treated in Chapter 8. Supercoiled DNA and other unusual DNA structures such as G-tetrads and "hairpins" are described, followed by the secondary structures of the t-RNAs and high molecular mass RNAs. In the following chapter the student is introduced to the chemical properties of polynucleotides and to modifications of nucleic acids, e.g., involving the carbohydrate or aglycon moieties. The chapter ends with short descriptions of two studies of conformational changes in DNA and four-stranded G4-DNA. As mentioned earlier, Chapter 10 deals with the highly topical field of ribozyme chemistry. This very readable book ends with a chapter on a very "chemical" aspect: the synthesis of nucleic acids. This consists of about 100 pages in which not only chemo-enzymatic methods but also the different chemical strategies of oligonucleotide synthesis are discussed in detail. The chapter is completed by a description of the preparation of synthetic genes and the technique of cloning. Literature references are listed at the end of each chapter.

After reading this well-written book nobody can really doubt that the chemistry of nucleosides and nucleic acids is an intrinsic part of organic chemistry. Although some of the formula schemes are unconventional and take a little time to get used to, the authors are to be congratulated on the quality of their work. As a textbook this is a very successful effort. My only complaint is that the publishers need to introduce a cheaper paperback version as soon as possible, because the price of DM 248 is not affordable to students. I fear that until that is remedied, the high price will limit the distribution of this excellent book.

Chris Meier
Institut für Organische Chemie
der Universität Frankfurt (Germany)

Modern Electroorganic Chemistry. By *D. Kyriacou*. Springer, Heidelberg, 1994. 228 pp., hardcover DM 98.00.—ISBN 3-540-57504-9

During the last twenty years there have been enormous developments in electroorganic chemistry and many books and review articles have appeared. In this book D. Kyriacou has aimed to give a systematic presentation of current knowledge in the area of electroorganic chemistry. There are five chapters: an introduction (17 pp.), followed by chapters on

This section contains book reviews and a list of new books received by the editor. Book reviews are written by invitation from the editor. Suggestions for books to be reviewed and for book reviewers are welcome. Publishers should send brochures or (better) books to Dr. Ralf Baumann, Redaktion Angewandte Chemie, Postfach 101161, D-69451 Weinheim, Federal Republic of Germany. The editor reserves the right of selecting which books will be reviewed. Uninvited books not chosen for review will not be returned.

anodic, cathodic, and indirect electroorganic reactions (92, 56, and 26 pp. respectively), and finally a chapter on various interesting special areas of electrosynthesis (33 pp.).

The introductory chapter presents the fundamental principles needed for an understanding of electroorganic reactions. The basic components required to achieve a successful electrochemical reduction or oxidation are described (the electrodes, the electrolytic cell, the conducting electrolyte, and the potentiostat), and the author explains concepts such as direct and indirect electrochemical reactions, electron transfer, electrode potential, equilibrium potential, and overvoltage.

The anodic reactions discussed in Chapter 2 include oxidation of hydrocarbons, alcohols, phenols, carboxylic acids, amines, amides, ethers, esters, N-heterocycles, and organosulfur compounds. Thus, for example, the author describes the oxidation of alkanes in the presence of acetonitrile (acetamidation), the anodic coupling of arenes, the Kolbe synthesis for preparing ω,ω'-disubstituted alkanes, and the synthesis of poly(2,6-dimethyl-1,4-phenyleneoxide) from 2,6-dimethylphenol. The anodic substitution reactions described include cyanidation, acetoxylation, halogenation, hydroxylation, and alkoxylation.

The cathodic reactions discussed in Chapter 3 are electrochemical hydrogenations and reductions of carbonyl, organohalogen, organonitro, and organosulfur compounds and of N-heterocycles, and also electrocarboxylation. Thus, for example, cyclopropanes are synthesized from alkenes in the presence of methylene bromide at a graphite cathode, which is combined with a zinc sacrificial anode in an unpartitioned cell. The reduction and hydrolysis of purine gives 4-aminomethyl-5-amino-2-imidazoline, and the electrocarboxylation of ethene gives succinic acid. Carbon dioxide is converted to methanol in a photoelectrochemical reduction using leuco-indigo, and the indigo thus generated is then reduced back to leuco-indigo. The latter process forms the basis of a recently developed solar cell.

In cases where the electron exchange in an electrochemical oxidation takes place via a mediator the reaction is said to be indirect. Chapter 4 deals with indirect electroorganic reactions, under the headings of oxidative and reductive indirect reactions. Species that can be used as oxidative mediators are the transition metal ions Ce^{4+} and Ru^{4+}, the halogen cations I^+ and Br^+, and tris(*p*-bromophenyl)-amine. Metal ions in low oxidation states, such as Fe^{2+}, Cr^{2+}, and Sn^{2+}, are effective as reductive mediators. Anthracene is used as an organic reductive mediator.

The final chapter collects together a number of special areas of electroorganic synthesis, such as electropolymerization and the synthesis of natural products.

This book covers all the important modern developments in electroorganic synthesis, and by providing a wealth of literature references enables the reader to study this interesting field in greater depth. The inclusion of laboratory recipes for the electrochemical synthesis of many different compounds is especially useful. Moreover, all the information in the book is very clearly presented. There are few errors, and those that have occurred do not detract from the very high quality of the book. For example, it was undesirable to use the same symbol Q for quantity of charge (p. 14) and for the quotient of the activities in the Nernst equation (p. 8). For consistency the formula chosen for naphthalene on page 95, with five double bonds (ten π-electrons), should also have been used on page 27.

Karlheinz Seifert
Lehrstuhl für Organische Chemie I/2
der Universität Bayreuth (Germany)

Derivative Spectrophotometry. Low and Higher Order. By *G. Talsky*. VCH Verlagsgesellschaft, Weinheim, 1994. 228 pp., hardcover DM 248.00.—ISBN 3-527-28294-7

I approached this book with high expectations, hoping to learn about important applications of derivative methods to spectroscopic interpretation. However, my first impressions were that the publishers had not made a very good job of language-polishing, and also that the text ought have been checked by a proof-reader with a mathematical background. For me there were many small points that rankled. The impression is given that the infrared region ends at 2.5 μm, thus: "Higher energies are necessary though, for electron excitation." Sometimes things are expressed in an awkward way, as in "...the curve is computet", or "...derivative orders contribute only littel..." In stating the Lambert–Beer law the mention of Bouguer as the earlier discoverer is wrongly spelt, and Volkmann is wrongly cited as the author of a book on "infrared spectrophotometry". These printing errors are mildly amusing, but the mistakes in the mathematical formulas are pure carelessness, and several times I had to overcome a strong temptation to abandon the book. Sometimes plus signs, sub- and superscripts are missing, while in other cases a symbol that should be a subscript is printed at normal height. Occasionally the wrong result is given for an elementary operation such as differentiation or calculation of a logarithm—sorry, such mistakes just cannot be tolerated. Proportional is not the same as equals!

The chapter on derivatives, for example those of the Gaussian function, is unnecessarily awkward and labored. I cannot understand why the author has not kept to a consistent nomenclature (there was already a hint of this in the discussion of the various symbols for differentiation). It seems a little strange that extinction coefficients and band distances are given in millimeters. And since when is the Lorentzian band-shape an exponential function? The Savitzky–Golay smoothing equation (Eq. 3–22) contains printing errors. Certain general recursion formulas are cited without mentioning the restrictions stated in the original publications.

I was often reminded of old times when the author referred to cutting out peaks and weighing to determine their areas, and again in the descriptions of instrumentation. Even graphical methods of estimating tangents are included. The literature references too are a little antiquated. What is the purpose of the short digression on the binary system?—It is hardly necessary to point out that modern computers still use it. I certainly did not think that analog and hybrid methods still have an important role in differentiation routines. The literature on digital methods of smoothing and differentiation is well covered. However, references to some recent monographs on this subject area should certainly have been included (e.g., P. Gans, *Data Fitting in the Chemical Sciences*, Wiley, Chichester, **1992**). One would also expect to find a mention of recent publications on the suppression or elimination of "spikes".

The treatment of practical aspects begins with Chapter 4. However, the choice of examples to illustrate the advantages of derivative spectroscopy seems to me unconvincing. With regard to the fundamental question of what is the optimal order of differentiation, the author's answer is that every shoulder and turning point in the original spectrum must appear in the derivative as an extreme value. It would also have been useful to compare the derivative method with alternative procedures that have grown in importance in the last few years, for example resolution enhancement using techniques such as the maximum entropy method or self-deconvolution; these avoid the interference by satellites that can arise in derivative spec-

 © VCH Verlagsgesellschaft mbH, D-69451 Weinheim, 1995 0570-0833/95/1313-1524 $ 10.00+.25/0

troscopy. Regrettably, the literature coverage extends only to 1990. On the other hand, the survey of the applications of derivative spectroscopy, which are summarized in the form of 57 tables, is impressive. Looking through these and noting the order of differentiation, one finds that, with very few exceptions, the derivative spectra are of lower orders with fourth order as the maximum. Even after reading this (very expensive) book, it seems to me that the use of higher orders has little to recommend it.

H. Michael Heise
Institut für Spektrochemie
und Angewandte Spektroskopie
Dortmund (Germany)

Enzymes in Synthetic Organic Chemistry. (Tetrahedron Organic Chemistry Series, Vol. 12.) By *C.-H. Wong* and *G. M. Whitesides*. Elsevier, Oxford, 1994. 370 pp., hardcover £ 55.00/paperback £ 25.00.—ISBN 0-08-035942-6/0-08-035941-8

During the last ten years there has been a great increase in the use of enzymes in organic synthesis; a survey of the wide-ranging areas of application of such methods will therefore be welcomed by everyone interested in using these powerful catalysts to solve problems of synthesis.

This book on the subject contains six chapters: an introductory one explaining the basic general principles of enzymatic catalysis and a further five treating important types of reactions. The first chapter deals with the physicochemical principles whereby enzymatic catalysis increases reaction rates, with the kinetics of such reactions, and with the effects of the solvent, temperature, and pH on the specificity of the enzyme. Further aspects treated here are the important problem of cofactor regeneration, and the behavior of enzymes in organic solvents. The second chapter describes the use of hydrolyzing enzymes for the formation or breaking of carbon–nitrogen and carbon–oxygen bonds in amides, peptides, esters, nitriles, and epoxides; the enzymes used are amidases, proteases, esterases, lipases, phosphatases, nitrilases, and epoxide-hydrolases. The effectiveness of these enzymes, especially for peptide synthesis and for preparing enantiomerically pure carboxylic acid derivatives and hydroxy compounds, is illustrated by describing results from about 400 published studies. Chapter 3 is devoted to the use of enzymes in redox reactions. As such reactions usually depend on nicotinamide cofactors, the question of cofactor regeneration is discussed in detail. The basic principles of stereoselectivity in redox reactions mediated by NAD(P) are also explained. Many of the examples of reductions and oxidations described here involve horse-liver alcohol dehydrogenase, but the discussion also extends to applications of other alcohol dehydrogenases and of numerous keto-acid dehydrogenases, as well as metal-mediated enolate reductases, galactose oxidase, lipooxygenase, arene dioxygenase, and various monooxygenases. Chapter 4 is concerned with carbon–carbon bond formation reactions, a topic of great importance for organic synthesis. In describing typical applications the authors devote special attention to enzyme-catalyzed aldol reactions, but they also explain how cyanohydrins, acyloins, and polycyclic compounds such as isoprenoids and steroids can be prepared using the appropriate enzymes. The current state of knowledge on the use of aldolases for stereoselective syntheses of monosaccharides, neuraminic acid, and related polyhydroxy compounds with many chiral centers is well described with numerous examples.

The growth in understanding of the role of carbohydrates in the functions of the bacterial cell wall and of their importance for cell adhesion, cell differentiation, and cell development has led to a great upsurge of interest in the synthesis of oligo- and polysaccharides. For solving the various regio- and stereochemical problems of such syntheses, enzymatic methods are becoming ever more important. The influence of these developments is evident in Chapter 5, which is concerned with the formation of glycosidic bonds by enzymatic catalysis. Reactions for converting monosaccharides into the reactive nucleoside phosphates needed for glycoside formation, and the use of glycosyl transferases, are described in detail. Here we see that, in this area especially, the use of these enzymes on a preparative scale is still severely handicapped by the difficulty of obtaining them. Chapter 6 deals with enzyme-catalyzed addition and elimination reactions, and the use of enzymes to catalyze the transfer of phosphate, methyl, sulfate, and amino groups. In view of the central importance of phosphoric acid esters in biochemical conversion reactions, much space is devoted to the regeneration of ATP and the synthesis of phosphorylated carbohydrates.

The book does not claim to provide a general introduction to the principles of enzymology or of biochemistry. However, by treating the applications in five chapters devoted to important types of reactions it should enable every synthetic organic chemist to gain a quick overview of the current state of the art in enzymatic catalysis as an aid to organic synthesis. By using this book, with the approximately 1500 literature references provided, the interested reader will be able to discover quickly whether there is a good prospect of solving a particular synthetic problem by such methods. It can therefore be recommended to everyone seeking to exploit the great potential of enzymatic catalysis in his or her work.

Hans Schick
Abteilung Organische Synthese
Institut für Angewandte Chemie
Berlin (Germany)

 © VCH Verlagsgesellschaft mbH, D-69451 Weinheim, 1995 0570-0833/95/1313-1525 $ 10.00+.25/0

Structure and Bonding in Organometallic Anions of Heavy Group 14 and 15 Elements

Michael A. Paver, Christopher A. Russell, and Dominic S. Wright*

Alkali metal organometallic complexes (containing C–metal bonds) and the frequently structurally related alkali metal amides and alkoxides have been investigated extensively both in the solid state and in solution in the past two decades. However, until recently, the related complexes containing the heavier metallic and semi-metallic p block elements and the alkali and alkaline earth metals had rarely been studied in their own right. Recent solid-state structural studies have illustrated the immense structural diversity and bonding modes to be found within these species. One of the principal focuses of recent studies has been complexes containing organometallic anions of p block metals (e.g., triorganostannates, containing R_3Sn^-) in which metal–metal bonds occur between the heavy p block metal and the alkali or alkaline earth metal and the investigation of the nature of this bonding. The development of new synthetic routes has also allowed the preparation of a variety of anionic ligands with p block metal centers which promise new opportunities in coordination chemistry. In addition, the synthesis of a family of homologous anionic π complexes has given a fresh direction in the chemistry of p block metal metallocene complexes.

Keywords: antimony compounds · bismuth compounds · lead compounds · thallium compounds · tin compounds

1. Introduction

In the past twenty years or so there has been a great deal of interest in the structures and reactivity of organometallic reagents used in organic synthesis. This is particularly true of the organolithium compounds (containing C–Li bonds)[1] and of the structurally related amide, imide (with N–Li bonds),[2] and alkoxide complexes (with O–Li bonds).[3] All these compounds are widely employed as potent deprotonation reagents (sterically demanding bases) and as "anion equivalents" (nucleophilic sources of R^-) in standard organic syntheses. Extensive data is now available on the structures in solution and in the solid state of oligomeric (ring, cage, and ladder[1–3]) complexes containing organic anions linked by such *nonmetallic* p block elements (C, N, P, O, S) to alkali and alkaline earth metals.

Complexes containing alkali metals and *metallic* or *semi-metallic* p block elements have been known for many years.[4] For example, triorganostannates, commonly formulated as "$MSnR_3$" or as $M^+SnR_3^-$, are used to promote the formation of Sn–C bonds by their reactions with electrophilic organic substrates.[5] However, few such complexes containing metals or semi-metals have been investigated in their own right in the solid state or in solution, although many of these species are commonly generated in situ as precursors by organic chemists to perform a variety of transformations. Recently, there has been a renewed interest in complexes containing organometallic anions, alkoxides, or amides and low valent p block metals and semi-metals. Such studies have been made possible mainly by modern handling techniques and, particularly, by improved techniques for the low-temperature X-ray characterization of these commonly thermally unstable compounds.[6] Although this is still a relatively under-developed area, recent studies have shown that such compounds exhibit a wealth of novel bonding situations and exciting new structures in the solid state. The work carried out to date provides the basis for a developing new area of coordination chemistry and the fuel for many theoretical studies probing the nature of the bonding in these compounds.

Our interests in this field were stimulated by the lack of structural information on complexes containing bonds between "early" main group metals (groups 1 and 2) and metallic p block elements. Initially, we were interested in probing the nature of the metal–metal interactions (ionic vs. covalent) and of the bonding in the complex anions with p block metal centers. A second, and perhaps more general interest, stemmed from the desire to develop mild synthetic strategies to potentially unstable complexes containing anions of p block metals, utilizing nucleophilic addition reactions to neutral precursors and acid/base reactions. These initial goals have led us to broader investigations of the interaction of a variety of anionic p block metal amides with main group and transition metals and to the synthesis of new organometallic π complexes derived from neutral p block metal cyclopentadienides.

[*] Dr. D. S. Wright, M. A. Paver, C. A. Russell
University Chemical Laboratory
Lensfield Road
Cambridge CB21EW (UK)
Telefax: Int. code + (1223)336-362

 © VCH Verlagsgesellschaft mbH, D-69451 Weinheim, 1995 0570-0833/95/1515-1545 $ 10.00+.25/0

2. Complexes Containing Bonds between Alkali and Alkaline Earth Metal and Heavy p Block Metals

Early work on the reactions of organometallic halides of heavy p block metals with alkali metals in liquid ammonia showed that a variety of salts containing alkali metal cations and p block metal organometallic anions could be prepared. For example, "$NaSnMe_3$" was first prepared by the reaction of Me_3SnBr and Na in liquid ammonia in 1922 as a yellow-tan powder[7] and "$NaSbPh_2$" was synthesized in 1941 by the reaction of Ph_2SbI with Na in liquid ammonia.[8] These species are extremely air- and moisture-sensitive and many, for example the triorganoplumbates, are not stable for prolonged periods at room temperature and are in some cases light sensitive, for example, the dioranostibanes.[4] Organic chemists have made frequent use of these species as "soft" organometallic nucleophiles in syntheses.[5] The favored method of synthesis of these reagents has depended on the particular heavy p block metal involved. The main synthetic strategies to such complexes are 1) the reaction of metal–halogen bonds with an alkali metal [Eq. (a)], 2) the rection of a metal–hydrogen bond with an alkali metal organometallic compound [Eq. (b)], and 3) the cleavage of a p block metal–metal bond with a group 1 or 2 metal organometallic compound [Eq. (c)] or with the metals themselves [Eq. (d)].[4, 5] Additionally, the reaction of a labile metal–carbon bond is valuable in certain circumstances, for example in the in situ synthesis of $NaPbPh_3$ from Ph_4Pb.[4] Evidently for the heaviest elements (Pb and Bi), whose hydrides are unstable or cannot be prepared, cleavage of E–E bonds or E–X bonds are the best approaches.

$$R_nE\text{-}X + 2M \longrightarrow R_nE\text{-}M + MX \quad (a)$$

$$R_nEH + R'M \longrightarrow R_nE\text{-}M + R'H \quad (b)$$

$$R_nE\text{-}ER_n + R'M \longrightarrow R_nE\text{-}M + R_nR'E \quad (c)$$

$$R_nE\text{-}ER_n + 2M \longrightarrow 2R_nE\text{-}M \quad (d)$$

Despite the potential for the formation of metal–metal bonds between the alkali or alkaline earth metals and the p block metals in these compounds, it was not until recently that the existence of such bonding has been unequivocally demonstrated by X-ray analysis. This development has come about by employing aprotic (aromatic and ethereal) solvents as the reaction media and, generally, by making use of Lewis base donor solvation of the alkali and alkaline earth metal cations to solublize complexes and aid crystallization. The area remains one in which a great deal of synthetic and structural work still has to be done. Surprisingly, even for the semi-metal silicon only a few alkali metal bonded complexes have been structurally characterized[9] and there are no examples of such metal–metal bonded complexes of germanium.

The first truly metal–metal bonded complex to be characterized in the solid state, [Ph_3SnLi(pmdeta)] **1** (pmdeta = $MeN(CH_2CH_2NMe_2)_2$) was prepared by the reaction of *n*BuLi with Ph_3SnH and pmdeta (molar ratio 1:1:1) in toluene.[10] The complex (Fig. 1) contains a Sn–Li bond whose length is slightly greater than the sum of the covalent radii of Sn and Li (average over two independent molecules 2.817 Å; the sum of covalent radii of Sn and Li is 2.74 Å).

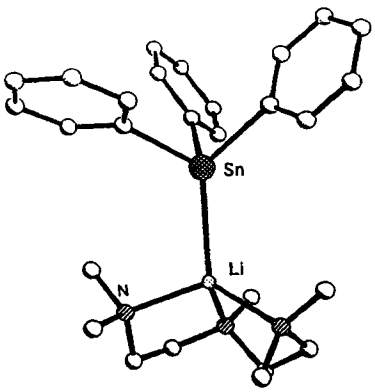

Fig. 1. Crystal structure of the monomeric molecules of **1**.

The Pb complex analogous to **1**, [Ph_3PbLi(pmdeta)] (**2**), is prepared from the reaction of Ph_3Pb–$PbPh_3$ with *n*BuLi and pmdeta (molar ratio 1:1:1).[11] It is stable for only about 12 h under N_2 at room temperature. The thermal decomposition pathway appears to involve the migration of a phenyl group as indicated by the formation of Ph_4Pb and elemental Pb. The essential structural features of **2** are very similar to those of **1**. The Pb–Li distance is slightly greater than the sum of the covalent radii of Pb and Li (average over both independent molecules 2.858 Å; sum of covalent radii of Pb and Li is 2.81 Å). The Ph_3Pb moiety of **2** is, however, more pyramidal than the Ph_3Sn unit of **1** and the Ph_3Si unit of [$Ph_3SiLi(thf)_3$] (**3**) (average

Dominic S. Wright was born in Gosport, Hampshire, England, in 1964. He studied chemistry at the University of Strathclyde in Glasgow (1982–1986), and then moved to Cambridge University where he obtained a Ph.D. in 1989 under the supervision of Dr. Ronald Snaith. He was elected a Research Fellow in Cambridge at Gonville and Caius College (1989) and was made a member of staff at Cambridge University in 1991. In 1993 he received the Meldola Medal, a prize awarded by the Royal Society of Chemistry in conjunction with the Society of Maccabaeans, for developments in the organometallic chemistry of the alkali and alkaline earth metals. His research interests include various aspects of main group organometallic chemistry.

C-Si-C angle in **3** 101.3°,[9f] average C-Sn-C angle in **1** 96.1°,[10] average C-Pb-C angle in **2** 94.3°[11]). The significant distortion in the Ph_3E units of **1**, **2**, and **3** away from a tetrahedral geometry is consistent with the expected increase in effective energetic separation of the s and p orbitals on descending group 14. This results in the metals progressively preferring to use predominantly p orbitals to bond to the C centers and the E–Li bonds largely involving the metal *n*s orbital. The pyramidal geometries of the Ph_3E moieties in **1**–**3** and in the ion-separated complex $[([18]crown-6)]K^+ \cdots Ph_3Sn^-]$ (**4**),[12] contrast with the near planar geometry found for the ion-separated Ph_3C^- ion where, as a result of more energetically favorable orbital mixing, the C atom is sp^2 hybridized.[13]

Concerning the nature of the bonding and the question of which orbitals of the heavy p block metal are used in the bonds between alkali metals and heavy p block metals of **1** and **2**, ab initio MO calculations show that the Sn–Li and Pb–Li bonds of Ph_3SnLi and Ph_3PbLi involve the p_z orbitals of Sn and Pb (which are directed along the metal–metal bonds) as well as their s orbitals (Fig. 2).[11]

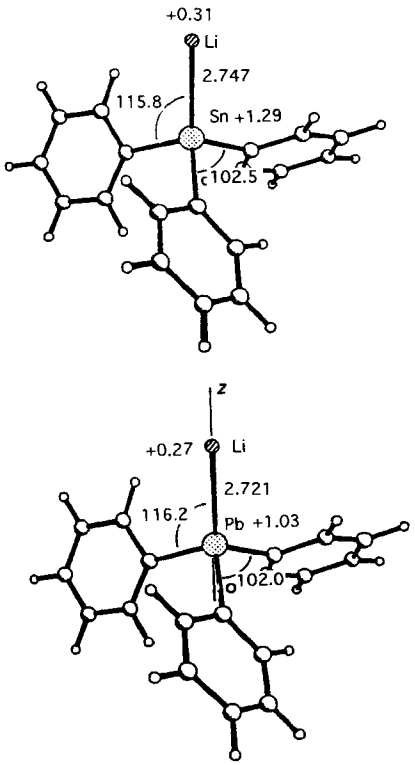

Fig. 2. Structures of Ph_3SnLi (top) and Ph_3PbLi (bottom) optimized by ab initio calculations.

The effect of solvation of the alkali metals in the above models is, not surprisingly, to elongate the E–Li bonds towards those found experimentally. Although limited in terms of mimicking the steric demands present in **1** and **2**, calculations on ion-contacted H_3PbLi and ion-separated H_3Pb^- illustrate that the coordination geometry about the heavy p block metal tends towards pyramidal (i.e. away from tetrahedral) as the contact to the alkali metal is broken (H-Pb-H 101.2° in H_3Pb-Li and 93.2° in H_3Pb^-). Thus the geometry of the p block metal center can be used to gauge the strength of the metal–metal interaction. The distinctly pyramidal geometries of the Sn and Pb anions in **1** and **2**, respectively, imply that such metal–metal bonding is very weak.

The weakness of the bonds between these heavy p block and early main group metals is further emphasized by the outcomes of the reactions of Ph_3SnH with *n*BuLi in the presence of other Lewis base donors. If one equivalent of monodentate HMPA ($O=P(NMe_2)_3$) or bidentate TMEDA ($(Me_2NCH_2)_2$) are present, the ion-separated complexes $[Li_2(hmpa)_5]^{2+}[Ph_3Sn]_2^-$ (**5**)[14] and $[Li(tmeda)_2]^+[Ph_3Sn]^-$ (**6**),[15] respectively, in which more than one equivalent of each donor is incorporated in to the product, are formed favorably. Solvation of the alkali metals by the Lewis base donor ligands clearly competes with the bonding between early main group metals and heavy p block metals. The Ph_3Pb units in transition metal complexes, for example in $[Ph_3PbV(CO)_6]$ (**7**) (C-Pb-C ca. 106.2°)[16] and in *cis*-$[Pt(Ph_3Pb)(PPh_3)_2Ph]$ (**8**) (C-Pb-C average 106.6°),[17] are distinctly more tetrahedral than that in **2**; thus together with the results of the calculations mentioned above on ion-paired and ion-separated H_3Pb^- systems, this illustrates that the interactions between alkali metals and p block metals are weaker than those between alkali metals and transition metals.

Cryoscopic molecular mass measurements in benzene show that **1** is monomeric and that the Sn–Li bond is therefore sustained in solution. Low-temperature ^7Li NMR studies of **1** (−90 °C) exhibit a large combined ^{117}Sn- and ^{119}Sn–Li coupling ($^1J_{Sn-Li}$ = 412 Hz) (Fig. 3).[10] Recently values of ^{119}Sn–^7Li coupling constants as high as 466 Hz have been recorded for

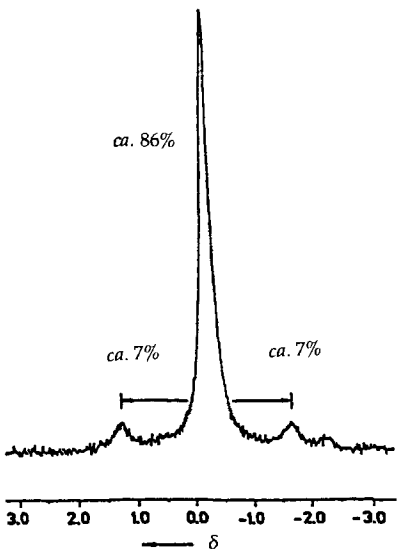

Fig. 3. ^7Li NMR spectrum of **1** at −90 °C in $[D_8]$toluene.

$n Bu_3SnLi$ in HMPA.[18] Rather than implying that there is a significant amount of covalent character in these Sn–Li bonds, the large coupling constants observed are most probably symptomatic of the employment of a predominantly 5s orbital in the Sn–Li bonds. The magnitude of these coupling constants, although significantly greater than the Si–Li coupling constants in covalent silyllithium compounds (ca. 50 Hz[9f, 19]), are in the

range expected on the basis of the trend observed previously for a variety of group 14 triorgano metal complexes in solution.[20]

The stannyl potassium compound $[(Me_3CCH_2)_3SnK(toluene)_3]$ **10**, in which a Sn–K bond is present (Sn–K 3.32–3.72 Å), shows a range of fascinating structural features in the solid-state (Fig. 4).[21] The complex **10** is prepared by the cleavage of the Sn–Sn bond of $(Me_3CCH_2)_3SnSn(CH_2CMe_3)_3$ (**9**)[21] with K metal in THF. Remarkably, the K^+ cation of **10**

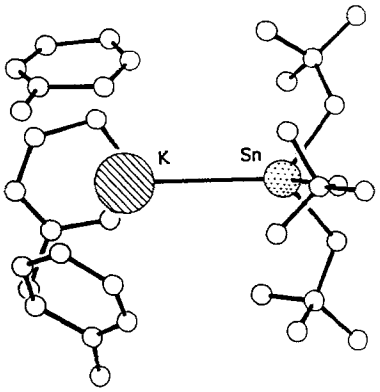

Fig. 4. Crystal structure of the monomeric molecules in **10**.

is solvated by three π-bonded toluene molecules. Thus, complex **10** is the first example of a complex containing a bond between an early main group metal and a heavy p block metal in which the alkali metal ion is not stabilized by heteroatom (O, N, etc.) donors.

The presence of the Sn–K bond in **10** is also manifest in its cross-polarization magic angle spinning (CP-MAS) solid-state ^{119}Sn NMR spectrum in which ^{119}Sn–^{39}K coupling is seen for the first time.[21]

Although the structural work on complexes containing semi-metallic p block elements of group 15 (As) and group 16 (Se, Te) is far less well developed than those containing the nonmetallic elements (N[2] and O[3]), it is clear that the same aggregation principles are observed with these complexes. The occurrence of monomers ($n = 1$),[22–27] dimers ($n = 2$),[22, 28–30] trimers ($n = 3$, i.e., the boat-shaped trimer $[\{Li[\mu\text{-}AsCH(SiMe_3)_2]\}_3]$ **11**[31]), and hexamers ($n = 6$, i.e., $[\{Li\{\mu_3\text{-}TeSi(SiMe_3)_3\}\}_6]$ (**12**)[30]) containing $(AsM)_n$, $(SeM)_n$, and $(TeM)_n$ frameworks illustrates the greater structural diversity of these complexes compared to those of Sn and Pb. The higher degrees of oligomerization attained stem from the apparently greater strengths of the semi-metallic bonds to the early main group metals. This greater tendency for association is manifest in the complexes $[\{(thf)Li[\mu\text{-}As(AstBu_2)(tBu)]\}_2]$ (**13**)[28] and $[\{(dme)Li[\mu\text{-}TeSi(SiMe_3)_3]\}_2]$ (**14**) (dme = $MeOCH_2CH_2OMe$),[32] in which despite solvation of the Li^+ ions by Lewis bases oligomerization into dimers occurs rather than dissociation (in a manner akin to the ion-separated complexes **5** and **6**).

Until recently there were no examples of molecular compounds with Sb–Li or Bi–Li bonds.[33] The structure of the complex $[cy_2SbLi(pm,deta)]$ (**15**) (cy = cyclohexyl) (Fig. 5)[34] was found to contain an Sb–Li bond (2.84 Å) which, like the E–Li bonds in the monomeric complexes **1** and **2** with Sn–Li and Pb–Li bonds is slightly longer than the sum of the covalent

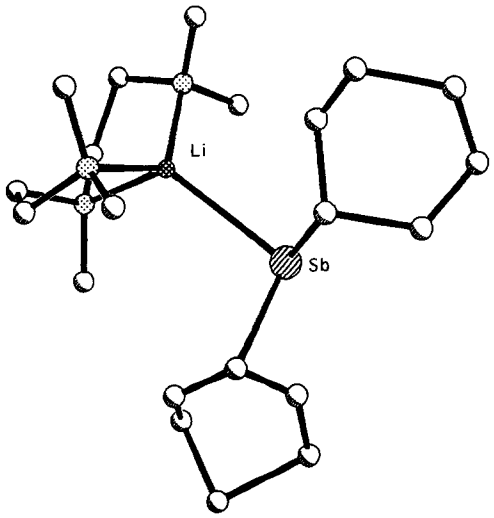

Fig. 5. Crystal structure of the monomeric molecules of **15**.

radii of Sb and Li (2.77 Å). The fact that this bond is sustained even in THF solutons is an indication that Sb–Li bonds are more stable than Sn–Li and Pb–Li bonds.

Perhaps the greatest challenge for the future in this area is the synthesis and characterization of complexes with bonds between metallic p block elements and early main group metals containing larger frameworks (rings and cages, etc.), since all the structurally characterized compounds so far are monomers. As alluded to above, bearing in mind the weakness of E–Li bonds where E is a metallic element, avoiding strong Lewis base solvation will be a key consideration in future investigations. A further area of developing interest is the application of Sn derivatives of alkaline earth metals in the synthesis of alkaline earth metal organometallic complexes. This is exemplified by the recent structural characterization of the monomeric Ca complex *trans*-$[Ca(SnMe_3)_2(thf)_4]$ **16**.[35] The cleavage of the weak Ca–Sn bonds of **16** with organometallic nucleophiles may well provide a key synthetic route in the syntheses of such organometallic compounds.[35]

3. New Anionic Ligands

Amides and alkoxides containing the heavy p block metals of groups 14 and 15 (Sn, Pb, Sb, Bi) exhibit a very diverse coordination chemistry. Such ions are being increasingly employed as novel ligands to a range of main group and transition metals.

Probably the most well-known and most simple examples of alkoxide or amide complexes are those of group 14. These generally have a trigonal bipyramidal structure in which the group 14 elements are linked through bridging heteroatoms to an early main group metal.[36a] Such a design is particularly common for alkoxide cages of Ge, Sn, and Pb.[36–40] The discrete cage complex $[Li(\mu\text{-}2,6\text{-}Ph_2C_6H_3O)_3Sn]$ **17** (Li–Sn 2.784 Å)[37] typifies this structural design and the basic bonding pattern present within these species (Fig. 6). The Li^+ ion and the Sn^{II} center of **17** are held together solely by μ-O alkoxide bridges. Since the lone pair on Sn points away from the Li^+ ion

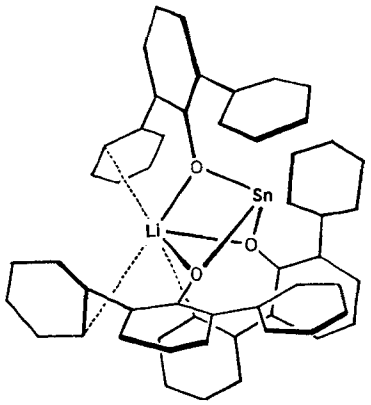

Fig. 6. Crystal structure of the monomers of **17**.

there is little or no Sn–Li bonding present (despite the presence of a close Sn···Li contact in **17**).

The flexibility of alkoxystannates as ligands is evident from the aggregation of the basic trigonal bipyramidal building units upon increasing the metallic radii of the alkali metal ion thus satisfying the increased coordination sphere of the cation. This is seen in the series of complexes $[\{Sn(OtBu)_3M\}]_n$ (M = Li (**18**), Na (**19**), $n = 2$; M = K (**20**), Cs (**21**), Rb (**22**), $n = \infty$)[39] in which structural ammendment occurs from dimers consisting of fused rings with fourfold coordination of Li and Na for **18** and **19** (Fig. 7), to polymeric structures based on SnO_3M trigonal bipyramids which are associated by additional intermonomer M–O bonds for **20**–**22**.[39a,d] Veith et al. have demonstrated that the $(tBu_3O)_3Sn^{:-}$ ion can, by utilizing both the μ-O linkage and the Sn lone pair, act as a bifunctional tripod ligand to main group and transition metals.[36b] Veith has written an extensive review on main group metal cage compounds and their coordination chemistry.[36a]

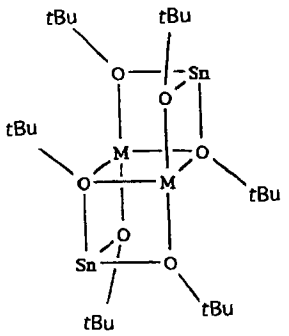

Fig. 7. Schematic structure of the fused dimers of **18** and **19**.

For the anionic tris-pyrazolyltin and -germanium compounds which have recently been investigated,[40,41] an unprecedented alternative to the aggregation noted for **18**–**22** is found. Dimerization rather than polymerization is the result of coordination to Na^+ in the structure of $[\{(Pz)_3SnNa(thf)_2(PzH)\}_2]$ (**23**). Two of the pyrazolyl groups of each $[(Pz)_3Sn]^-$ ion link the alkali metal ions together and the third is uncoordinated (Fig. 8). This bonding mode contrasts with the more conventional tridentate attachment observed in the Ge analogue which has the conventional monomeric trigonal bipyramidal structure. Such "claw" tris-pyrazolyl ligands $(Pz)_3E^-$ (E = Sn, Ge) are very flexible in their coordination to a range of metal ions and promise to be an exciting new area in the future.[41] This study also points the way forward for the design of selective ligands by tailoring the heteroatomic center within such anionic ligands (i.e., by varying the hardness/softness, steric demands of the organic group, and ligand bite) to the coordination environment suitable for a particular metal.

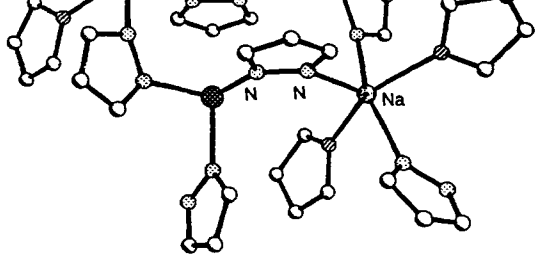

Fig. 8. Cyclic dimer structure of **23**.

The conventional synthesis of amide and alkoxide complexes is by nucleophilic substitution of the metal halides with the appropriate organic anion. However, the development of nucleophilic substitution of Cp_2E (E = Sn, Pb) allows the syntheses of a host of such anions in the absence of potential interference by halide ions.[42–44] In the light of their applications as selective ligands mentioned above, this new approach is of importance in broadening the range of complexes accessible. The reactions of more potent (imino, amido, or organometallic) nucleophiles with Cp_2E appear to occur by an associative (addition–elimination mechanism) rather than by a concerted pathway. This is shown by the isolation of $[Cp(Me_3Si)_2NSn(\mu\text{-}Cp)Li(pmdeta)]$ (**24**) from the 1:1 reaction of Cp_2Sn with $(Me_3Si)_2NLi$ in the presence of PMDETA.[45] The complex is best regarded as a "loose-contact" complex of the neutral components $[Cp(Me_3Si)_2NSn\cdots(\mu\text{-}Cp)Li(pmdeta)]$ as is shown by its dissociation into the neutral fragments in aromatic solvents even at room temperature.[45] As such, complex **24** can be regarded as a model intermediate for such nucleophilic substitution.

In contrast to the development of group 14 alkoxide and amide derivatives as ligands, the derivatives of group 15 have received far less attention. However, very recently a series of polyamidoantimonate complexes have been prepared by stepwise metalation of primary amines employing $(Me_2N)_3Sb$ as a metalating source. An example of this "mixed-metalation" procedure is the reaction of $Li[Sb(NHCy)]_4$ with $(Me_2N)_3Sb$ (molar ratio 1:2) which gives the unusual polynuclear amidoantimonate complex $[LiSb_3(Ncy)_4(NMe_2)_2]$ **25**. This complex contains a Sb_3N_6Li "deck-chair" core (Fig. 9 left).[46] Using a similar method $[\{Li_2Sb_2(Ncy)_4\}_2]$ (**26**),[47] consisting of a core of two interlocked broken cubes (Fig. 9 middle), and $[\{(PhCH_2CH_2NLi)_3Sb(thf)\}_2]$ (**27**),[46] containing a fourteen-membered polyhedral core (Fig. 9 right), can also be synthesized. The polyimidoantimonate ions of **25**, **26**, and **27** are potential ligands to a range of main group and transition metals.

The robust nature of this new type of ligand is confirmed by the recent synthesis of $[Cu_4\{Sb_2(Ncy)_4\}_2]$ (**28**) from the transmetalation of **26** with CuCl (Fig. 10).[48] In contrast to **26** which contains a roughly tetrahedral array of Li atoms in the central portion of the molecule, complex **28** contains an almost ideal square-planar Cu_4 core. The function of the $[Sb_2(Ncy)_4]^{2-}$ ligands of **28** is similar to that observed recently in $[Cu_4\{C_6H_4O_2(Me_2SiNtBu)_2\}_2]$ (**29**), which also contains a square-planar Cu_4 core.[49]

The solution behavior of **26** is of interest. Cryoscopic molecular mass measurements and variable-temperature ^7Li NMR spectroscopy show that the complex is involved in a dissociative

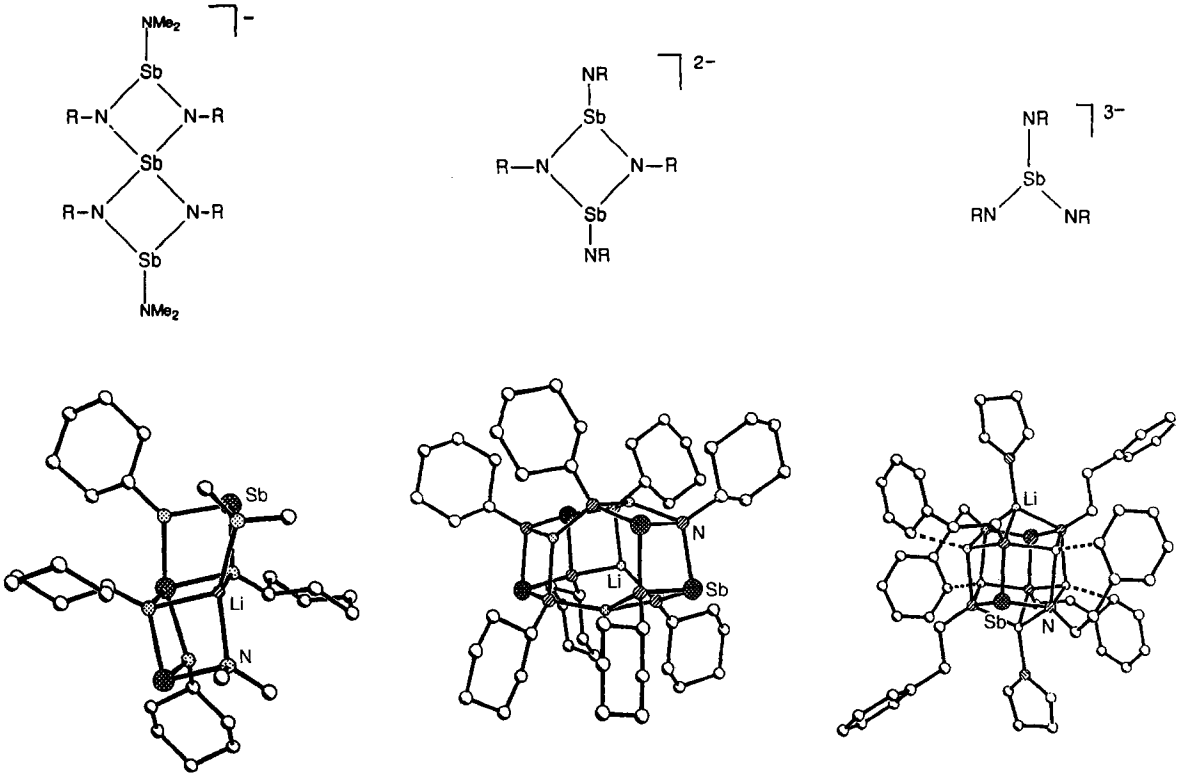

Fig. 9. Polyamidoantimonate ions of **25**–**27** (top) and their cage structures (bottom).

equilibrium in which the cubane halves of the core are formed, that is $[\{Li_2Sb_2(Ncy)_4\}_2] \rightleftarrows 2[Li_2Sb_2(Ncy)_4]$.[47b] Such symmetrical dissociation is relevant to the ability of these polyamido antimonate complexes to capture other metal salts. This is seen in the cage expansion reaction of the fourteen-membered polyhedral complex $[\{(cyNLi)_3Sb\}_2]$ **30**, whose structure is similar to that of **27**, with *t*BuOK (molar ratio 1:3) in toluene. The resulting twenty-membered cage complex is $[\{(cyNLi)_3Sb\}_2(t\text{BuOK})_3(\eta\text{-toluene})_2(\text{toluene})_2]$ (**31**) (Fig. 11 bottom).[50] The formation of **31** can be visualized as occurring by symmetrical cleavage of the precursor cage followed by cocomplexation with a $[K_3(\mu\text{-O})_3]$ ring (Fig. 11 top). The development of the mixed-metalation procedure to other p block metals of group 14 (Sn, Pb) and 15 (Bi, As) provides some exciting new possibilities as regards the coordination chemistry of related anions in the synthesis of bimetallic and trimetallic complexes by transmetalation and cocomplexation reactions.

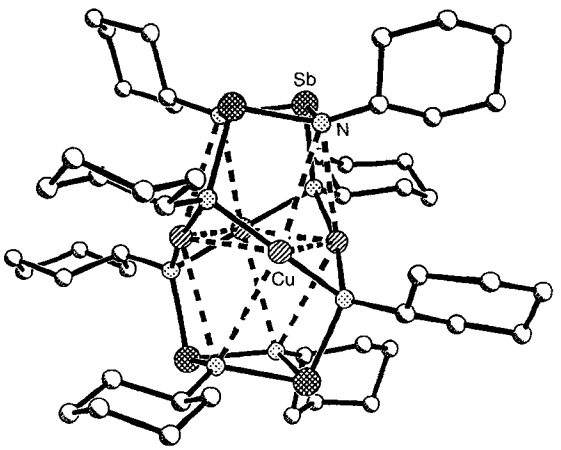

Fig. 10. Crystal structure of **28**.

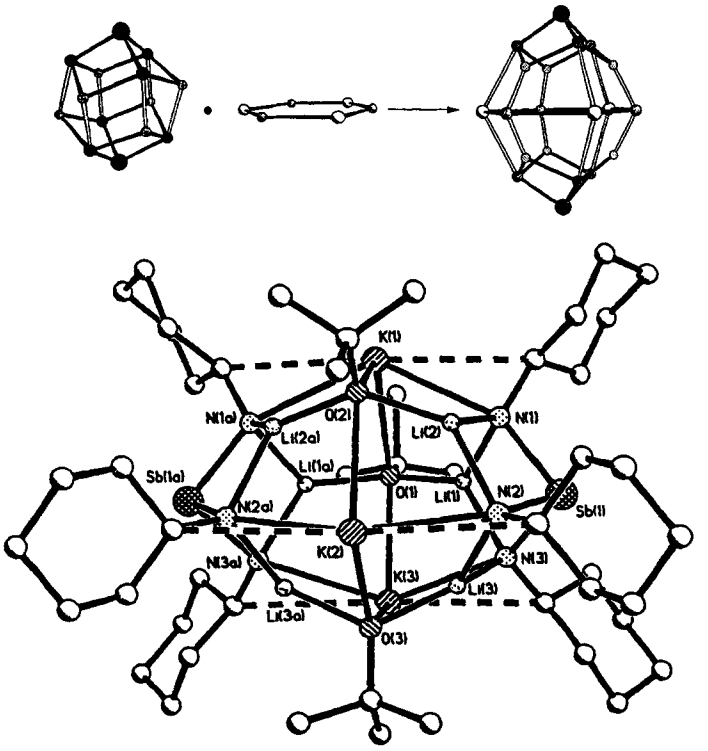

Fig. 11. Top: Schematic representation of the cage expansion reaction of **30** with 3k*O*t*Bu* leading to **31**; bottom: Structure of **31** (π solvation of K^+ by $C_6H_5CH_3$ has been omitted for clarity).

4. Anions from p Block Metals and Cyclopentadienyl Ligands

Cyclopentadienyl derivatives of the heavy p block metals have been investigated extensively in the past thirty years or so.[51] An examination of the solid-state and gas-phase structures and of the formal electron counts of the metals in these complexes [CpE, E = In (**32**), Tl (**33**);[52,53] Cp_2E, E = Si (**34**), Ge (**35**), Sn (**36**);[54-56] Cp_3E, E = Sb (**37**), Bi (**38**)[57]] provides a useful predictive tool in assessing the possible occurrence of anionic and cationic[58,59] species generated from them. As illustrated in Figure 12, nucleophilic addition of Cp^- would potentially produce a family of anionic species which are isolelectronic with the neutral cyclopentadienyl complex of a neighboring group.

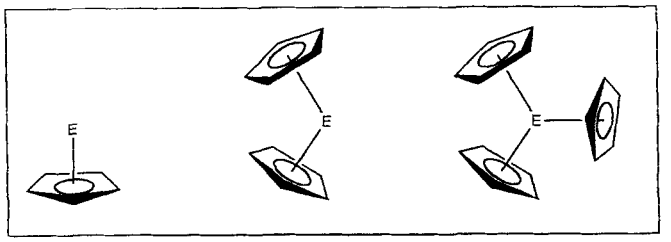

Fig. 12. Isoelectronic and isostructural relationships between neutral, anionic, and cationic cyclopentadienyl species.

Addition of Cp^- to CpE (E = In, Tl) should result in an isolated 14e anion Cp_2E^-, whose electron count corresponds to that of the neutral Cp_2E in group 14 (Fig. 12). In practice addition of CpLi and Cp_2Mg to polymeric $[(\mu\text{-}\eta^5\text{-Cp})Tl]_\infty$ does indeed "extrude" a 14e unit of this lattice.[60] The structures of ion-contacted [CpTl(μ-Cp)Li(pmdeta)] (**39a**) and ion-separated [CpMg(pmdeta)] [Cp_2Tl] (**39b**) (Fig. 13) have been determined in the solid state and contain bent thallocene anions (average $Cp_{centroid}$-Tl-$Cp_{centroid}$ 153.3° in **39a** and 156.7° in **39b**) which are isoelectronic with stannocene.

While the Tl center of $[(\eta^5\text{-Cp})_2Tl]^-$ in **39b** is attached almost equivalently to the η^5-Cp ligands, in **39a** the terminal η^5-Cp contact (Tl–$Cp(a)_{centroid}$ 2.60 Å) is significantly shorter than that made with the Li^+–bridging μ-Cp ligand. In **39a** the Li^+ ion competes with the Tl^I center for the electron density of the bridging Cp ligand and pulls this Cp away from the Tl^I center. There is a compensatory enhancement in the interaction between the terminal η^5-Cp ligand and Tl, and the Tl–$Cp(a)_{centroid}$ distance approaches that found in the gas phase structure of monomeric $[(\eta^5\text{-Cp})Tl]$.[53]

Ab initio MO calculations on various isomers of the discrete $[(\eta^5\text{-Cp})_2Tl]^-$ ion show that the association of Cp^- and CpTl is reasonably favorable (-28.0 kcal mol^{-1} for the ECP-DZ basis set). Furthermore, results at higher levels of calculation (MP2, MP3, MP4) illustrate that the most stable bent structure (with C_s symmetry) is only marginally more favorable than the most stable linear structure (with D_{5d} symmetry) (e.g., only 0.82 kcal mol^{-1} at the MP4 level). These results suggest, contrary to findings of calculations on Cp_2Ge (**40**), where orbital admixing of the antibonding a_{1g}^* MO with the metal p_x atomic orbital leads to a significantly greater stability of the bent structure,[61] that orbital admixing is ineffective in the discrete $[(\eta^5\text{-Cp})_2Tl]^-$ ion. This view is confirmed by the fact that an essentially spherical (s-like) lone pair is present on the Tl center of the bent $[(\eta^5\text{-Cp})_2Tl]^-$ ion. Examination of the electron density in the bent structure also suggests that the interactions of the Tl atom with the two Cp ligands are not equivalent and that the anion is probably best regarded as a "close-contact" complex between CpTl and Cp^-.

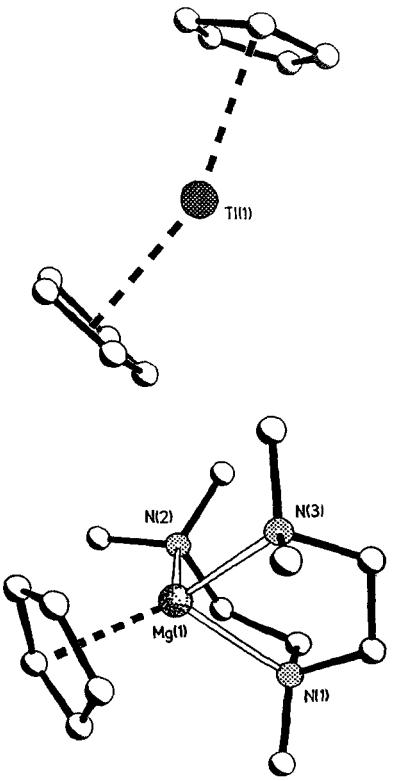

Fig. 13. Crystal structure of **39b**.

The nucleophilic addition of CpNa and Cp_2Mg to Cp_2Sn and $[Cp_2Pb]_\infty$ produce a range of ion-paired $[(\eta^5\text{-Cp})_2E(\mu\text{-}\eta^5\text{-Cp})Na(pmdeta)]$, E = Sn (**41**),[62] Pb (**42**)[63] (Fig. 14 top) and ion-separated $[Mg(thf)_6][(\eta^3\text{-Cp})_3E]_2$, E = Sn (**43**),[43] Pb (**44**),[63] (Fig. 14 bottom) complexes. These species contain highly unusual nearly planar "paddle-wheel" triorganostannate and plumbate ions whose geometries are in marked contrast to the classic pyramidal structures discussed above for ion-separated and ion-paired Ph_3E^- complexes.[10,12,14,15,22] This unique structural modification is of interest with respect to the applications of triorganostannates as reagents in organic synthesis, since it is likely that the nucleophilicity of the Sn center (which now appears to be sp^2-hybridized) will also be modified.

The E(μ-Cp)Na bridges of the ion-contacted complexes **41** and **42** (Fig. 14 top) can be rationalized in a similar way to the Tl(μ-Cp)Li bridge of **39a**. Interestingly, the ion-separated complexes **43** and **44** contain Cp_3E^- ions that are distinctly more pyramidal than the ion-paired species. The latter, and the change in hapticity of the Cp rings from η^5 in **41** and **42** to η^3 in **43** and **44** appears, at least on geometrical grounds, to reflect an increase in Sn and Pb lone pair character upon ion-separation. In respect to the trend outlined earlier for isoelectronic and isostructural species, the Cp_3E^- ions of complexes **41**–**44** can be seen as being related to 20e Cp_3E (E = Sb and Bi[57]), and the

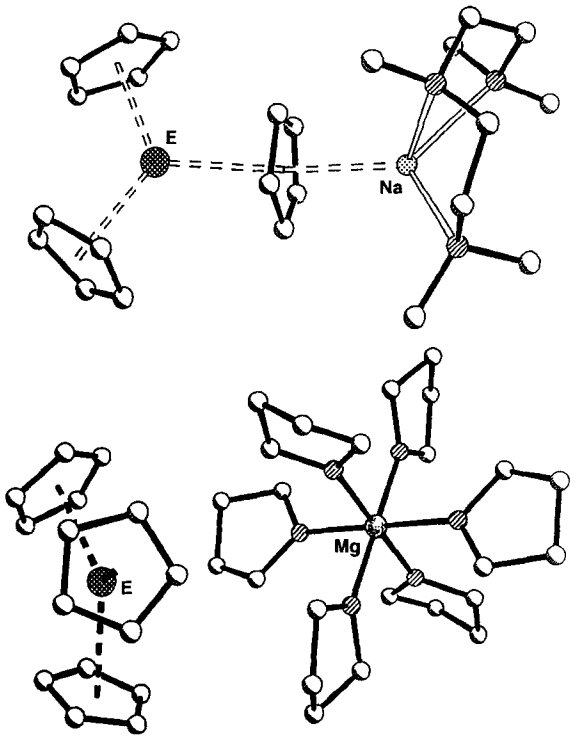

Fig. 14. Top: Structure of **41** and **42**, and bottom: structure of **43** and **44**.

ion-separated and ion-paired Pb complexes (**42** and **44**, respectively) can be regarded as extruded fragments of the $[Cp_2Pb]_\infty$ lattice. The observation of an ion-separated Cp_3Pb^- ion in **44** suggests that the 1:1 electrolyte produced when Cp_2Pb is dissolved in THF is most likely $[CpPb(thf)_x]^+[Cp_3Pb]^-$ (**45**), as opposed to the previously suggested $CpPb^+$ and discrete Cp^- ion.[64]

Ab initio MO calculations show the importance of Na^+ ion solvation in influencing the nature of the ion-contacted species; whether best considered as loose-contact $[Cp_2E\cdots CpNa(pmdeta)]$ or as close-contact complexes $(Cp_2E-Cp^{\delta-}\cdots Na^{\delta+})$.[63] Calculations on $[Cp_2E(\mu\text{-}Cp)Na]$, as models for **41** and **42**, show that in the absence of solvation these species are best regarded as loose-contact complexes. However, solvation of Na^+ diminishes the competition between this cation and the Sn and Pb centers for the electron density of the bridging Cp ligand and tips the balance towards closer and closer interaction of Sn and Pb with the bridging Cp ring. Calculations on Cp_3E^- in ion-separated complexes illustrate, in a similar way to the results on the $[(\eta^5\text{-}Cp)_2Tl]^-$ ion in complexes with separated ions,[60] that even here one of the E–Cp interactions is weaker than the other two. The results of the calculations are largely consistent with those from solid-state ^{119}Sn MAS-NMR studies on the Sn complexes; according to these NMR studies the Cp_2Sn character is more pronounced in the ion-paired complex **41** than in the ion-separated complex **43**.[63]

The view of the $[(\eta^5\text{-}Cp)_2Tl]^-$ ion mentioned above as an extruded fragment of the parent $[(\eta^5\text{-}Cp)Tl]_\infty$ lattice is confirmed by the recent synthesis of $[Li([12]crown\text{-}4)_2]^+[(\eta^5\text{-}Cp)Tl(\mu\text{-}Cp)Tl(\eta^5\text{-}Cp)]^-$ (**46**) (Fig. 15).[65] The complex contains an extended anion which is the next homologue of the bis(cyclopentadienyl)thallate ion, and the first homometallic

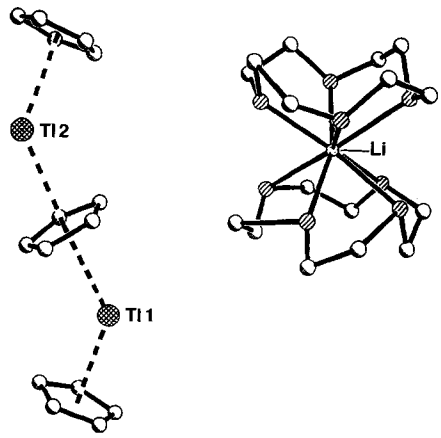

Fig. 15. Crystal structure of **46**.

main group metal triple-decker sandwich complex. This result suggested that yet higher chain homologues of $[(\eta^5\text{-}Cp)_2Tl]^-$ and of $[(\eta^3\text{-}Cp)_3E]^-$ (E = Sn and Pb) should be possible. Very recently this expectation has been confirmed: The reaction of Cp_2Pb with CpLi and [12]crown-4 (2:1:2) was carried out in an attempt to prepare the $[Cp_5Pb_2]^-$ ion (the next highest homologue of the $[Cp_3Pb]^-$ ion).[66] However, the only isolated product has an empirical formula $[Li([12]crown\text{-}4)_2]^+[Cp_7Pb_3]^-$. A subsequent X-ray study showed that the complex has the structural formula $[Li([12]crown\text{-}4)_2]_2^+[Cp_5Pb_2]^-[Cp_9Pb_4]^-$ (**47**) (Fig. 16),[66] containing the second and fourth homologues of the Cp_3Pb^- ion rather than the third (as might have been suggested from the empirical formula).

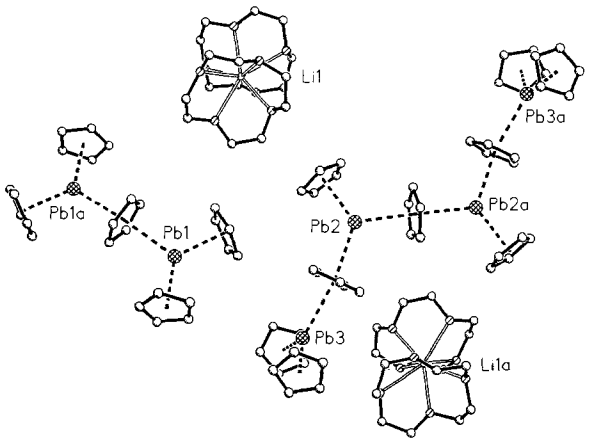

Fig. 16. Crystal structure of **47**.

5. Concluding Remarks and Outlook

Complexes containing p block metal organometallic anions as well as corresponding alkoxides and amides are a highly diverse family of compounds. With the development and greater availability of low-temperature X-ray crystallography and with modern handling procedures, many of these unstable materials can now be structurally characterized. Such investigations have illustrated the exceptionally diverse bonding patterns to be

found in this class of complex and have set the stage for the development of the coordination chemistry and of detailed theoretical investigations of these species.

The unequivocal characterization of monomeric compounds containing bonds between early main group metals and heavy p block metals has laid the foundations for studies of more structurally elaborate oligomers containing frameworks with metal–metal bonds. One problem to be overcome in the synthesis of such compounds is that these metal–metal interactions are weaker than those between non-metallic or semi-metallic elements and early main group metals. The development of new synthetic approaches to anionic p block alkoxides and amides provides the basis for a great deal of future work on selective ligands to a range of metals. Simple derivatives of group 14 [containing R_3E^- units, with R bearing a heteroatom-centered (E) organic group] constitute a highly versatile class of readily prepared ligands in which variation of the metal or hardness and softness of the heteroatom center can be used to change the affinity of the anion for a particular metal. The synthesis of more complicated polyamido anions of group 15 by "mixed-metalation" (employing the Me_2NM derivatives) promises a greater ligand versatility and the potential, by using a similar synthetic route, to prepare a new class of related group 14 anions. Finally, the syntheses of a family of anions by nucleophilic addition of Cp^- to the cyclopentadienyl derivatives of the heavier p block metals gives rise to a variety of new synthetic challenges. Higher linear and cyclic homologues as well as mixed-metal derivatives will be future goals.

We would like to thank Dr. D. R. Armstrong (Strathclyde), Dr. D. Barr and Dr. S. Cook (Associated Octel), Dr. M. G. Davidson (Cambridge), Dr. A. J. Edwards (Cambridge), Dr. D. Moncrieff (Florida State), Dr. P. R. Raithby (Cambridge), Dr. D. Reed (Edingburgh), M.-A. Rennie (Cambridge), Dr. D. Stalke (Göttingen), and Dr. A. Steiner (Göttingen) for their valuable contributions to much of the work discussed in this review. D. S. W. would also like to thank Dr. Ronald Snaith (Cambridge) for his support and guidance throughout his carreer. We would also like to thank The Engineering and Physical Sciences Research Council (UK), The Nuffield Research Council, The Royal Society, Associated Octel (Ellesmere Port, UK), and The Cambridge Crystallographic Data Centre for financial support.

Received: April 13, 1994,
Revised version: February 21, 1995 [A 63 IE]
German version: *Angew. Chem.* **1995**, *107*, 1677–1686

[1] W. N. Setzer, P. von R. Schleyer, *Adv. Organomet. Chem.* **1985**, *24*, 353; E. Weiss, *Angew. Chem.* **1993**, *105*, 1565; *Angew. Chem. Int. Ed. Engl.* **1993**, *32*, 1501; see also a review on the heavier alkali metals: C. Schade, P. von R. Schleyer, *Adv. Organomet. Chem.* **1987**, *27*, 169.

[2] K. Gregory, P. von R. Schleyer, R. Snaith, *Adv. Inorg. Chem.* **1991**, *37*, 47; R. E. Mulvey, *Chem. Soc. Rev.* **1991**, *20*, 167.

[3] D. Seebach, *Angew. Chem.* **1988**, *100*, 1685; *Angew. Chem. Int. Ed. Engl.* **1988**, *27*, 1624; see also a review on sulfones: G. Boche, *ibid.* **1989**, *101* and 286, **1989**, *28*, 277.

[4] B. J. Aylett, *Organometallic Compounds: The Main Group Elements, Vol. 1*, Chapman and Hall, London, **1979**, and references therein.

[5] M. Pereyre, J.-P. Quintard, A. Rahm, *Tin in Organic Synthesis*, Butterworths, London, **1987**; P. G. Harrison, *Chemistry of Tin*, Blackie, Glasgow, **1989**; I. Omae, *Organotin Chemistry*, Elsevier, Amsterdam, **1989**, and references therein.

[6] T. Kottke, D. Stalke, *J. Appl. Crystallogr.* **1993**, *26*, 615.

[7] C. A. Kraus, W. N. Greer, *J. Am. Chem. Soc.* **1922**, *44*, 2629.

[8] L. A. Wood, H. Gilman, *Proc. Iowa Acad. Sci.* **1941**, *48*, 251.

[9] a) T. F. Schaaf, W. Butler, M. D. Glick, J. P. Oliver, *J. Am. Chem. Soc.* **1974**, *96*, 7593; b) W. H. Isley, T. F. Schaaf, M. D. Glick, J. P. Oliver, *ibid.* **1980**, *102*, 3769; c) B. Tecle, W. H. Isley, J. P. Oliver, *Organometallics* **1982**, *1*, 875; d) G. Becker, H.-M. Hartmann, H. Münch, H. Riffel, *Z. Anorg. Allg. Chem.* **1985**, *530*, 29; e) G. Becker, H.-M. Hartmann, E. Hengge, F. Schrank, *ibid.* **1989**, *572*, 63; f) H. V. R. Dais, M. M. Olmstead, K. Ruhlandt-Senge, P. P. Power, *J. Organomet. Chem.* **1993**, *462*, 1.

[10] D. Reed, D. Stalke, D. S. Wright, *Angew. Chem.* **1991**, *103*, 1539; *Angew. Chem. Int. Ed. Engl.* **1991**, *30*, 1459.

[11] D. R. Armstrong, M. G. Davidson, D. Moncrieff, D. Stalke, D. S. Wright, *J. Chem. Soc. Chem. Commun.* **1992**, 1413.

[12] T. Birchall, J. Vetrone, *J. Chem. Soc. Chem. Commun.* **1988**, 877.

[13] J. J. Brooks, G. D. Stucky, *J. Am. Chem. Soc.* **1972**, *94*, 7333; H. Köster, E. Weiss, *J. Organomet. Chem.* **1979**, *168*, 273; R. A. Bartlett, H. V. R. Dias, P. P. Power, *ibid.* **1988**, *341*, 1; M. M. Olmstead, P. P. Power, *J. Am. Chem. Soc.* **1985**, *107*, 2174; D. Hoffmann, P. von R. Schleyer, D. Stalke, $[k(pmdeta)]^+[Ph_3C]^-$, unpublished.

[14] L. Crow, A. J. Edwards, M. A. Paver, P. R. Raithby, M.-A. Rennie, D. Stalke, D. S. Wright, unpublished.

[15] D. R. Armstrong, D. Moncrieff, M. A. Paver, D. Stalke, D. S. Wright, unpublished.

[16] F. Calderazzo, F. Pampaloni, G. Pelizzi, F. Vitali, *Polyhedron* **1988**, *7*, 2039.

[17] B. Crociani, M. Nicolini, D. A. Clemente, G. Bandoli, *J. Organomet. Chem.* **1973**, *49*, 249.

[18] H. J. Reich, J. P. Borst, R. R. Dykstra, *Organometallics* **1994**, *13*, 1.

[19] U. Edlund, T. Lejon, *J. Am. Chem. Soc.* **1985**, *107*, 6408.

[20] U. Edlund, T. Lejon, P. Pyykkö, T. K. Venkatachalam, E. Buncel, *J. Am. Chem. Soc.* **1987**, *109*, 5982.

[21] P. B. Hitchcock, M. F. Lappert, G. A. Lawless, B. Royo, *J. Chem. Soc. Chem. Commun.* **1993**, 554.

[22] R. A. Bartlett, H. V. R. Dias, H. Hope, B. D. Murray, M. M. Olmstead, P. P. Power, *J. Am. Chem. Soc.* **1986**, *108*, 6921; see also G. Becker, C. Witthauer, *Z. Anorg. Allg. Chem.* **1982**, *492*, 28.

[23] M. Driess, H. Pritzkow, *Angew. Chem.* **1992**, *104*, 350; *Angew. Chem. Int. Ed. Engl.* **1992**, *31*, 316.

[24] W.-W. du Mont, S. Kubinick, L. Lange, S. Pohl, W. Saak, I. Wagner, *Chem. Ber.* **1991**, *124*, 1315; K. Ruhlandt-Senge, P. P. Power, *Inorg. Chem.* **1991**, *30*, 3683.

[25] P. J. Bonasia, J. Arnold, *J. Organomet. Chem.* **1993**, *449*, 147.

[26] D. G. Gindelberger, J. Arnold, *J. Am. Chem. Soc.* **1992**, *114*, 6242.

[27] G. Becker, K. W. Klinkhammer, W. Schwarz, M. Westerhausen, *Z. Naturforsch. B* **1992**, *47*, 1225.

[28] A. M. Arif, R. A. Jones, K. B. Kidd, *J. Chem. Soc. Chem. Commun.* **1986**, 1440.

[29] P. J. Bonasia, D. E. Gindelberger, B. O. Dobbousi, J. Arnold, *J. Am. Chem. Soc.* **1992**, *114*, 5209.

[30] G. Becker, K. W. Klinkhammer, S. Lartiges, P. Böttcher, W. Poll, *Z. Anorg. Allg. Chem.* **1992**, *613*, 7.

[31] P. B. Hitchcock, M. F. Lappert, S. J. Smith, *J. Organomet. Chem.* **1987**, *320*, C27.

[32] G. Becker, K. W. Klinkhammer, W. Massa, *Z. Anorg. Allg. Chem.* **1993**, *619*, 628.

[33] $[(MeOCH_2CH_2OMe)LiE\{C(SiMe_3)_3\}_2]_2$ (E = Sb, Bi) have polymeric structures: G. Becker, A. Münch, C. Witthauer, *Z. Anorg. Allg. Chem.* **1982**, *492*, 15; O. Mundt, G. Becker, M. Rössler, C. Witthauer, *ibid.* **1983**, *506*, 42.

[34] A. J. Edwards, D. J. Kane, M. A. Paver, P. R. Raithby, M.-A. Rennie, C. A. Russell, D. S. Wright, unpublished.

[35] M. Westerhausen, *Angew. Chem.* **1994**, *106*, 1585; *Angew. Chem. Int. Ed. Engl.* **1994**, *33*, 1493.

[36] a) M. Veith, *Chem. Rev.* **1990**, *90*, 3; b) see also M. Veith, R. Röseler, *Angew. Chem.* **1982**, *94*, 867; *Angew. Chem. Int. Ed. Engl.* **1982**, *21*, 858.

[37] G. D. Smith, P. E. Fanwick, I. P. Rothwell, *Inorg. Chem.* **1989**, *28*, 618.

[38] M. Veith, C. Ruloff, V. Huch, F. Töllner, *Angew. Chem.* **1988**, *100*, 1418; *Angew. Chem. Int. Ed. Engl.* **1988**, *27*, 1381.

[39] a) M. Veith, R. Rösler, *Z. Naturforsch. B* **1986**, *41*, 1071; b) M. Veith, D. Käfer, D. Huch, *Angew. Chem.* **1986**, *98*, 367; *Angew. Chem. Int. Ed. Engl.* **1986**, *25*, 375; c) M. J. McGreary, R. H. Clayton, K. Folting, J. C. Huffman, K. G. Caulton, *Polyhedron* **1992**, *11*, 1369; d) M. Veith, D. Käfer, L. Stahl, V. Huch, A. Sebald, *Z. Naturforsch. B* **1991**, *46*, 403.

[40] A. Steiner, D. Stalke, *J. Chem. Soc. Chem. Commun.* **1993**, 1702.

[41] A. Steiner, D. Stalke, *Inorg. Chem.*, in press.

[42] A. J. Edwards, M. A. Paver, P. R. Raithby, C. A. Russell, D. S. Wright, *J. Chem. Soc. Chem. Commun.* **1993**, 1086; A. J. Edwards, M. A. Paver, P. R. Raithby, C. A. Russell, D. Stalke, D. S. Wright, *Inorg. Chem.*, in press.

[43] A. J. Edwards, M. A. Paver, P. R. Raithby, C. A. Russell, D. Stalke, A. Steiner, D. S. Wright, *J. Chem. Soc. Dalton Trans.* **1993**, 1465.

[44] D. Stalke, M. A. Paver, D. S. Wright, *Angew. Chem.* **1993**, *105*, 445; *Angew. Chem. Int. Ed. Engl.* **1993**, *32*, 428; A. J. Edwards, M. A. Paver, P. R. Raithby, C. A. Russell, D. S. Wright, unpublished.

[45] M. A. Paver, C. A. Russell, D. Stalke, D. S. Wright, *J. Chem. Soc. Chem. Commun.* **1993**, 1349.

[46] A. J. Edwards, M. A. Paver, P. R. Raithby, M.-A. Rennie, C. A. Russell, D. S. Wright, *Angew. Chem.* **1994**, *106*, 1334; *Angew. Chem. Int. Ed. Engl.* **1994**, *33*, 1277.
[47] (a) R. A. Alton, D. Barr, A. J. Edwards, M. A. Paver, P. R. Raithby, M.-A. Rennie, C. A. Russell, D. S. Wright, *J. Chem. Soc. Chem. Commun.* **1994**, 1481; (b) M. A. Beswick, A. J. Edwards, M. A. Paver, P. R. Raithby, M.-A. Rennie, C. A. Russel, K. L. Verhorevoort, D. S. Wright, unpublished.
[48] D. Barr, A. J. Edwards, M. A. Paver, S. Pullen, P. R. Raithby, M.-A. Rennie, C. A. Russell, D. S. Wright, *Angew. Chem.* **1994**, *106*, 1960; *Angew. Chem. Int. Ed. Engl.* **1994**, *33*, 1875.
[49] M. Veith, K. L. Woll, *Chem. Ber.* **1993**, *126*, 2383.
[50] D. Barr, A. J. Edwards, M. A. Paver, P. P. Raithby, M.-A. Rennie, C. A. Russell, D. S. Wright, *Angew. Chem.* **1995**, *107*, 1088; *Angew. Chem. Int. Ed. Engl.* **1995**, *34*, 1012.
[51] P. Jutzi, *Adv. Organomet. Chem.* **1986**, *26*, 217.
[52] C. Panattoni, E. Frasson, F. Menegus, *Nature (London)* **1963**, *199*, 1087.
[53] J. K. Tyler, A. P. Cox, J. Sheridan, *Nature (London)* **1959**, *183*, 1182.
[54] J. L. Atwood, W. E. Hunter, A. H. Cowley, R. A. Jones, C. A. Stewart, *J. Chem. Soc. Chem. Commun.* **1981**, 925.
[55] A. Almenningen, A. Haaland, T. Motzfeldt, *J. Organomet. Chem.* **1967**, *7*, 97.
[56] C. Panattoni, G. Bombieri, U. Croatto, *Acta Crystallogr. Sect. A* **1966**, *21*, 823.
[57] E. O. Fischer, S. Schreiner, *Chem. Ber.* **1960**, *63*, 1417.
[58] P. Jutzi, F. X. Kohl, P. Hofmann, C. Krüger, Y.-H. Tsay, *Chem. Ber.* **1980**, *113*, 757; P. Jutzi, F. Kohl, C. Krüger, *Angew. Chem.* **1979**, *91*, 81; *Angew. Chem. Int. Ed. Engl.* **1979**, *18*, 59.
[59] P. Jutzi, T. Wippermann, C. Krüger, H.-J. Kraus, *Angew. Chem.* **1983**, *95*, 244; *Angew. Chem. Int. Ed. Engl.* **1983**, *22*, 250.
[60] D. R. Armstrong, R. Herbst-Irmer, A. Kuhn, D. Moncrieff, M. A. Paver, C. A. Russell, D. Stalke, A. Steiner, D. S. Wright, *Angew. Chem.* **1993**, *105*, 1807; *Angew. Chem. Int. Ed. Engl.* **1993**, *32*, 1774.
[61] J. Almlöf, L. Fernholt, K. Faegri, Jr., A. Haaland, B. E. R. Schilling, R. Seip, K. Tauglsøl, *Acta Chem. Scand. Ser. A* **1983**, *37*, 131.
[62] M. G. Davidson, D. Stalke, D. S. Wright, *Angew. Chem.* **1992**, *104*, 1265; *Angew. Chem. Int. Ed. Engl.* **1992**, *31*, 1226.
[63] D. R. Armstrong, M. G. Davidson, M. J. Duer, D. Moncrieff, C. A. Russell, C. Staurton, D. Stalke, A. Steiner, D. S. Wright, unpublished.
[64] W. Strohmeier, H. Landsfeld, F. Gernert, *Z. Elektrochem.* **1962**, *66*, 823.
[65] D. R. Armstrong, A. J. Edwards, D. Moncrieff, M. A. Paver, P. R. Raithby, M.-A. Rennie, C. A. Russell, D. S. Wright, *J. Chem. Soc. Chem. Comm.* **1995**, 927.
[66] M. J. Duer, N. C. Page, M. A. Paver, P. R. Raithby, M.-A. Rennie, C. A. Russell, C. Staurton, A. Steiner, D. S. Wright, *J. Chem. Soc. Chem. Commun.* **1995**, 1141.

26th INTERNATIONAL SYMPOSIUM ON ENVIRONMENTAL ANALYTICAL CHEMISTRY

Vienna, Austria, 9 - 12 April 1996

Organization: Austrian Society for Analytical Chemistry,
Vienna University of Technology,
International Association of Environmental Analytical Chemistry

Chairmen: M. Grasserbauer (Vienna), J. Tarradellas (Lausanne)

The Symposium will cover the following major topics:

- development of new analytical techniques, instrumentation and procedures for environmental studies
- application of analytical techniques to environmental problems

Program highlights covered by invited lectures of leading scientists will include:

• sampling strategies and sample preparation (e.g. SFE, SPE, SPME) • hyphenated techniques (e.g. LC-GC, GC-MS, GC-AES, HPLC-MS) • elemental analysis, inorganic speciation and organic trace analysis • sensors for environmental monitoring • biochemical detection techniques • multiresidue (screening) procedures • quality assurance in environmental analysis • air, water and soil analysis • transnational environmental problems in Europe • environmental pollution in sensitive ecosystems

Scientific contributions on all topics related to environmental analytical chemistry will be considered for oral or poster presentation !

FOR INFORMATION PLEASE CONTACT: Dr. Erwin Rosenberg, Institute of Analytical Chemistry, Vienna University of Technology, Getreidemarkt 9/151, A- 1060 Vienna, Austria; Fax: (+43-1) 586 7813

Patterns in Hydrogen Bonding: Functionality and Graph Set Analysis in Crystals**

Joel Bernstein,* Raymond E. Davis,* Liat Shimoni, and Ning-Leh Chang

Whereas much of organic chemistry has classically dealt with the preparation and study of the properties of *individual* molecules, an increasingly significant portion of the activity in chemical research involves understanding and utilizing the nature of the *interactions between* molecules. Two representative areas of this evolution are supramolecular chemistry and molecular recognition. The interactions between molecules are governed by intermolecular forces whose energetic and geometric properties are much less well understood than those of classical chemical bonds between atoms. Among the strongest of these interactions, however, are hydrogen bonds, whose directional properties are better understood on the local level (that is, for a single hydrogen bond) than many other types of nonbonded interactions. Nevertheless, the means by which to characterize, understand, and predict the consequences of many hydrogen bonds among molecules, and the resulting formation of molecular aggregates (on the microscopic scale) or crystals (on the macroscopic scale) has remained largely enigmatic. One of the most promising systematic approaches to resolving this enigma was initially developed by the late M. C. Etter, who applied graph theory to recognize, and then utilize, patterns of hydrogen bonding for the understanding and design of molecular crystals. In working with Etter's original ideas the power and potential utility of this approach on one hand, and on the other, the need to develop and extend the initial Etter formalism was generally recognized. It with that latter purpose that we originally undertook the present review.

Keywords: hydrogen bonds · self organization · solid-state structures

I perceived that you had acquired some knowledge in those matters from others, and that you were perplexed and bewildered; yet you sought to find out a solution to your difficulty. I urged you to desist from this pursuit, and enjoined you to continue your studies systematically; for my object was that the truth should present itself in connected order, and that you should not hit upon it by mere chance.[1]

1. Introduction

In a number of papers we have advocated the use of graph sets for the analysis of hydrogen-bonding patterns in organic crystals.[2–6] There has been considerable interest in this method,[7] and there appeared to be a need to expand upon our earlier formal presentation of the rules for determining the graph sets. Moreover, during the past few years we gained experience in our own use of graph sets, and as a result of numerous inquiries from others who have attempted to apply these methods, we have become aware of a number of problems, misunderstandings, and ambiguities in the prescriptions we had provided for determining the graph sets.[3, 5] We therefore thought it fitting to review those rules here in more practical terms than those presented earlier, and to present a number of worked examples that might provide additional assistance and guidelines for those who wish to apply the method.

We are particularly aware that for the graph set approach to be of any utility, its language must be straightforward and consistent. Assignments from different research groups must be arrived at according to readily understood and commonly accepted rules, they must be easy to make, and they must be identical. One way to guarantee such a situation is to provide widely available computer programs for use in making the graph set assignments. This is certainly a goal to which we aspire, and we are currently working to design software that will meet these objectives. In the meantime, it is of crucial importance to prevent the spread of misunderstandings and misconceptions about the use and applications of the method, as well as to avoid the proliferation of incorrectly assigned graph sets.

[*] Prof. Dr. J. Bernstein, L. Shimoni
Department of Chemistry
Ben-Gurion University of the Negev
Beer Sheva 84105 (Israel)
Telefax: Int. code + (7)237787
Prof. Dr. R. E. Davis, Dr. N.-L. Chang
Department of Chemistry and Biochemistry
The University of Texas at Austin
Austin, TX 78712-1167 (USA)
Telefax: Int. code + (512)471-8696

[**] This work is the first scientific collaboration of Bernstein and Davis, whose friendship dates to their days as teammates on the Yale University Chemistry Department softball team in the early 1960s.

 © *VCH Verlagsgesellschaft mbH, D-69451 Weinheim, 1995* *0570-0833/95/1515-1555 $ 10.00+.25/0*

With that purpose in mind we undertook the writing of this paper. We will first review briefly the essential features of the graph set approach, recalling that a more formal approach has been given earlier. We then present a number of worked examples of graph set assignments, noting some difficulties and pitfalls and how they may be avoided. Finally, we will discuss the utility of graph set analysis in discovering hydrogen-bond pattern functionalities that cross the traditional boundaries of chemical functionality.

2. Graph Set Definitions

Perhaps the most remarkable feature of the graph set approach to analysis of hydrogen-bond patterns is the fact that even complicated networks can be reduced to combinations of four simple patterns, each specified by a designator: chains (**C**), rings (**R**), intramolecular hydrogen-bonded patterns (**S**), and other finite patterns (**D**). Specification of a pattern is augmented by a subscript designating the number of hydrogen-bond donors **d** (in the most common case covalently bonded hydrogens, but certainly not limited to them), and a superscript giving the number of hydrogen-bond acceptors **a**. In addition, the number of atoms **n** in the pattern is called the degree of the pattern and is specified in parentheses. The graph set descriptor is then given as $\mathbf{G}_{\mathbf{d}}^{\mathbf{a}}(\mathbf{n})$,[*] where **G** represents one of the four possible designators.

These four patterns and their descriptors are best illustrated by examples. A chain whose "link" is composed of four atoms as in **1** would be specified as **C(4)**. When no subscript and superscript are given, one donor and one acceptor are implied. Similarly, the intramolecular hydrogen bond in **2** would be specified as **S(6)**, for the six atoms comprising the intramolecular pattern. When the donor and acceptor are from two (or more) *discrete* entities (molecules or ions), as in **3**, the designation of the hydrogen bond is **D**. The entities, as we will demon-

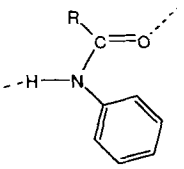

1 C(4)

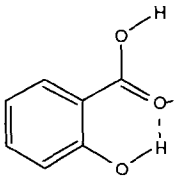

2 S(6)

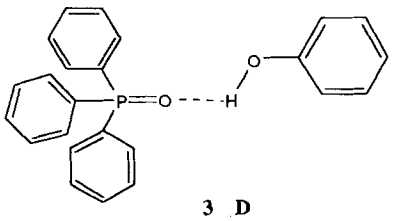

3 D

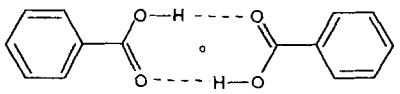

4 $\mathbf{R}_2^2(8)$

[*] Note that some symbols might be confused with formula numbers which are also in boldface.

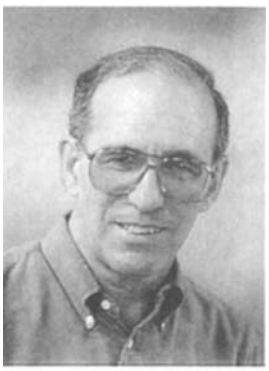

Joel Bernstein was born in Cleveland, Ohio, in 1941. After obtaining a B. A. at Cornell University, he earned a Ph.D. in physical chemistry at Yale University for research on the solid-state spectroscopy of organic compounds. Following two-year postdoctoral stints in X-ray crystallography with Ken Trueblood at UCLA and in organic solid-state chemistry with the late Gerhardt Schmidt at the Weizmann Institute of Science in Rehovoth, Israel, he joined the faculty of the newly established Ben-Gurion University of the Negev, where he is now Professor of Chemistry. His research interests center on the organic solid state, with particular emphasis on understanding and utilizing polymorphism, structure–property relations, and organic conducting materials. His career has been punctuated by visiting professorships at the University of Illinois, Cornell University, and most recently at the University of Minnesota, where he continued a long cooperation with the late Margaret C. Etter.

Raymond E. Davis was born in Hobbs, New Mexico, in 1938. Following his B. S. in Chemistry at the University of Kansas, he obtained a Ph.D. in physical chemistry at Yale University for research in the structures of organic compounds by X-ray crystallography. He then spent two years in the laboratory of David Harker at the Center for Crystallographic Research, Roswell Park Memorial Institute, Buffalo, New York. In 1966, he joined the faculty of the University of Texas at Austin, where is now Professor of Chemistry and Biochemistry. He has received many awards for teaching excellence and is the co-author of a widely used general chemistry textbook. His research has involved structural studies of organic and organometallic compounds, emphasizing π complexes, phosphorus macrocycles, and metal–phosphorus cluster compounds. More recently he has turned his attention to organic solid-state chemistry, especially studies of packing in molecular crystals and methods for crystal engineering.

strate below, may differ on chemical grounds (that is, the molecules or ions involved are two different chemical entities) or on crystallographic grounds (that is, chemically identical molecules not related by a crystallographic symmetry operation). In **3** there is only one donor and one acceptor, and the pattern involves only the hydrogen bond; in this case other atoms need not be counted, and the degree of the pattern **(2)** may be omitted.[8] Finally, the fourth possible pattern is the ring **4**. In the example shown, the two hydrogen atoms in the ring are not different (they are related by the crystallographic inversion center indicated in the diagram), but they could be.[9] The pattern contains a total of eight atoms, two of them donors and two acceptors, and hence is designated $\mathbf{R_2^2(8)}$.

The analysis of hydrogen-bonding patterns into these four simple categories can lead to important insights regarding the patterns of recognition between both like and unlike molecules. Cataloguing these patterns for particular functional groups can lead to a language describing their interaction and self-recognition similar to that of organic chemists for the reactivity of those same functional groups. Just as widely differing chemical groups may exhibit similar reactivities with respect to particular reagents, so differing functional groups may be seen as having similar hydrogen-bonding characteristics based on the patterns recognized through an analysis with these descriptors (Table 1).

Table 1. Glossary of terms

degree (of a pattern)	the number of atoms in the pattern
designator, **G** (of a pattern)	one of four letters designating the fundamental type of pattern: **C** (chain), **R** (ring), **S** (intramolecular pattern), **D** (other finite patterns)
descriptor, $\mathbf{G_d^a(n)}$ (of a pattern)	a notation summarizing the pattern: **G**: the pattern designator; **d**: a subscript describing the number of donors in the pattern; **a**: a superscript describing the number of acceptors in the pattern; **n**: the degree of the pattern
motif	a hydrogen-bonded pattern in which only one type of hydrogen bond is present
unitary graph set, $\mathbf{N_1}$[a]	a listing of the descriptors for all of the motifs in a structure
binary graph set, $\mathbf{N_2}$ [b]	a descriptor of a pattern in which two types of hydrogen bonds are present
basic/complex graph set	(for a *particular set* of hydrogen bonds) basic: the graph set of lowest degree for those hydrogen bonds; complex: any graph set of higher degree involving those hydrogen bonds

[a] Alternative terminology: first-level graph set. [b] Alternative terminology: second-level graph set.

3. Terminology and Notation

A motif is a pattern containing only one type of hydrogen bond.[3] Specifying the motif for each different hydrogen bond in a network according to one of the four pattern descriptors in the preceding section leads to a description of the network in the form of a list of the motifs. In earlier papers we specified this as a first-order graph set ($\mathbf{N_1}$), and followed that specification, when the chemical or structural problem required it, with the definition of higher order graph sets. In retrospect the choice of the term "order" seems to be unfortunate. In theoretical chemistry, "of increasingly higher order" often implies "of increasingly less importance". That implication was by no means intended in the language of graph sets. On the contrary, the intent was to specify "of increasing size or increasing complexity" in terms of the number of atoms and/or hydrogen bonds in the particular pattern. We now feel that the designation *order* should be replaced by *level*, and we will henceforth make use of the latter term exclusively. Hence, specifying the motifs for the different hydrogen bonds according to a prescribed hierarchy[3] defines the *unitary*, or first-level, graph set $\mathbf{N_1}$.

The chemically interesting or topologically characteristic patterns of a system often appear when more than one type of hydrogen bond is included in the description, that is, in higher level graph sets.[5, 6] This will be true for **S**, **D**, and **C** patterns. Suppose a structure contains three distinct hydrogen bonds, designated *a*, *b*, and *c*. There will now be several possible *binary* (or second-level) graph sets, each one describing a pattern formed by two of these H-bonds—that is, $\mathbf{N_2}(ab)$, $\mathbf{N_2}(ac)$, $\mathbf{N_2}(bc)$. Note further that we now advocate the notation $\mathbf{N_2}$ for any binary graph set (that is, a set containing exactly two types of hydrogen bonds); we believe that this is more systematic and thus more readily reproducible by different workers than the previous notation of somewhat arbitrarily assigning subscripts based on the accidental order in which the graph sets were worked out.[6] The *ternary* or third-level graph sets (there might be more than one possible—see Section 12) are those that involve all three H-bonds, that is, $\mathbf{N_3}(abc)$.

Different pathways might also be found that include the same set of H-bonds, but with different degrees (**n**). To describe this situation, we suggest the term *basic* to describe the graph set of *lowest degree* and the term *complex* to describe ones of *higher degree*. Consideration of some of the choices for the binary graph set for α-glycine[10] illustrates this point (Fig. 1). The shortest path involving H-bonds *a* and *b* gives the binary graph set $\mathbf{C_2^2(6)}$; this is the *basic* binary graph set for *a* and *b*. A longer chain, $\mathbf{C_2^2(10)}$, represents a *complex* binary graph set for the same two H-bonds. Neither of these, however, describes the most obvious feature of this array, the ring structure; this is denoted by another complex binary graph set, $\mathbf{R_4^4(16)}$. In addi-

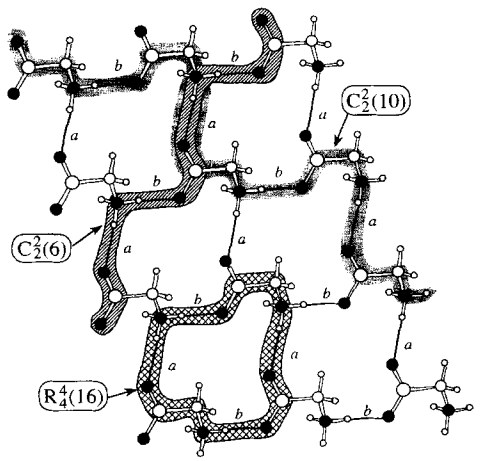

Fig. 1. Graph set assignments for the binary level of α-glycine. In this and many figures that follow, different types of hydrogen bonds (solid lines) are distinguished by labeling with italic lower case letters; carbon and hydrogen atoms are shown as open circles, oxygen atoms as solid circles, and nitrogen atoms as shaded circles.

tion, for extended **R** patterns that contain at least one edge (that is, one bond) in common, it is also possible to define an infinite number of increasingly larger ring systems. It is possible to generate binary graph sets for infinitely higher degrees (additional complex sets) for the two H-bonds in Figure 1, each one representing an increasingly larger pattern (Scheme 1).

$\mathbf{R}_6^6(26)$ with sequence $\overline{\lceil aabaab \rceil}$

$\mathbf{R}_6^6(26)$ with sequence $\overline{\lceil abbabb \rceil}$

$\mathbf{R}_8^8(36)$ with sequence $\overline{\lceil abbaabab \rceil}$

$\mathbf{R}_8^8(36)$ with sequence $\overline{\lceil aabbaabb \rceil}$

Scheme 1. Examples of complex graph sets.

This is the graph set manifestation of the "chicken wire" structure: a two-dimensional network of rings that have at least one bond (valence bond or hydrogen bond) in common.[11] Hence, the general protocol for defining graph sets must also include the possibility of increasing the degree (**n**) of the pattern, as well as the number of different hydrogen bonds (the level). Patterns that might later seem "characteristic" of a series of structures sometimes show up at higher levels or in more complex graph sets (or both). This point will be further exemplified in Sections 8 and 9.

4. The Hydrogen Bond—A Working Definition

The discussion in this section will refer specifically to hydrogen bonds, although in principle, of course, other types of interactions, for example, S···S, C–Cl···O, may be analyzed in precisely the same manner. Graph set analysis of hydrogen-bond networks is generally quite straightforward, and our experience has taught us that confusion can generally be avoided by proceeding in a systematic manner.

Assigning the descriptors to hydrogen-bond patterns requires first isolating the *hydrogen bonds* in the structural unit under study and *not* just the hydrogen atoms that participate in hydrogen bonding. The structural unit in question will generally be the crystallographic asymmetric unit and may be a single molecule, a number of the same molecules, part of a molecule, a complex, more than one molecule in a cocrystal, a molecule plus solvent molecule, etc. For that unit it is necessary to determine how many different hydrogen-bonding hydrogen atoms are to be considered. This is not a trivial question. Commonly recognized hydrogen bonds are those connecting oxygen and nitrogen atoms (for example O–H···N or O–H···O), but certainly C–H···O and C–H···N interactions are now included in hydrogen bonding,[12] and in cases where they play a clear role in the interactions among molecules it may be desirable to incorporate them in the graph set analysis. The decision on which hydrogen atoms are to be considered for inclusion may, in fact, vary from problem to problem, depending again on the chemical or structural questions being asked.

The hydrogen atoms to be considered as participants in hydrogen bonding interactions having been defined, it then becomes necessary to define the hydrogen bonds in which they participate. At this juncture the indication of whether a hydrogen bond exists or not will be based on a geometric (distance) criterion, although later we will definitely want to consider other criteria as well. Determining the geometric criterion for inclusion of an interaction as a hydrogen bond is a crucial, and by no means trivial step in the process. As a result of statistical surveys of the crystallographic literature and of structures in the Cambridge Structural Database, it has been possible to define characteristic values for many kinds of interactions, including hydrogen bonds.[13–15] These geometric characteristics are of immense value as the basis for theoretical calculations of molecular electronic structure, in, for instance, molecular mechanics and molecular dynamics, in modeling studies, protein structure determination, and the derivation of new potential energy functions. However, it has been shown that the application of geometric criteria, in particular that of a DH···A or D···A distance test as the strict test for the presence or absence of a hydrogen bond is not justifiable.[16] For instance, in a survey of amino acids Jeffrey and Maluszynska[17] have demonstrated that there are most probable DH···A and D···A distances for hydrogen bonds, but a smooth decrease in the distribution curve beyond that most probable value to about 3.0 Å for D···A distances. Beyond that distance, H···H van der Waals interactions begin to appear; the most frequent distance for these is 3.5 Å.

Dependence on a strict test for the presence or absence of a hydrogen bond is, in many ways, contrary to the philosophy of the graph set approach and hence fraught with dangers. As noted above, one of the principal advantages of the graph set approach is the facility for recognizing *patterns* of hydrogen bonding. Simply stated, patterns do not always have strict geometrical limitations. Hence, putting a limit of, say, 3.20 Å on the O···O or O···N distance might lead to ignoring a pattern for which the distance is 3.21 Å, but which is of no less importance in the overall scheme of hydrogen bonding. The limit to this reasoning is an infinite distance, but in practice nominal limiting distances can be defined; these are, however, considerably greater than those currently in vogue or based on van der Waals radii. Such distances should be considered as variable, depending on the system under study. Very large interaction distances are not to be expected ("nature abhors a vacuum"), so, as a result of interactions other than hydrogen bonding, other atoms will be present. Moreover, we wish to urge flexibility in setting arbitrary geometric criteria to determine hydrogen-bond interactions to ensure the recognition of patterns.

This interest in recognizing and defining hydrogen-bond patterns leads us to an operational definition of hydrogen bonds that incorporates their organizational consequences[2] rather than exclusively their geometrical characteristics. It is worth repeating here that definition, which parallels Pauling's definition of a chemical bond:[18]

> "A hydrogen bond is an interaction that directs the association of a covalently bound hydrogen atom with one or more other atoms, groups of atoms, or molecules into an aggregate structure that is sufficiently stable to make it convenient for the chemist to consider it as an independent chemical species."

In summary, then, in most cases it will be convenient for the chemist to employ some yes/no geometric criterion to test for hydrogen bonds. However, there is an increasing recognition of the subtlety of intermolecular interactions of many different types,[19] and for the time being at least, the best way to recognize these is to *look for* them and to *look at* them. Fortunately, in the age of desk top computer graphics, the ability to do this is within the reach of an increasingly large segment of the scientific community.

The C–H···O hydrogen bond is particularly illustrative in this regard. In his chapter titled "Selected Topics in Hydrogen Bonding" in the 1968 Festschrift[20] marking Linus Pauling's 65th birthday, Jerry Donohue included a section subheaded "The C–H···O Hydrogen Bond: What Is It?" Following a survey of the admittedly scant crystallographic information then available on such interactions, Donohue rather bluntly concluded the section with the sentence, "It appears to me that the answer to the question in the title of this section is: 'It isn't'". It is perhaps not an exaggeration to suggest that this statement traumatized virtually an entire generation of chemists and crystallographers, who subsequently avoided use of the term "hydrogen bond" when referring to C–H···O interactions. For at least the next decade, discussions of hydrogen bonds were limited to those involving a hydrogen atom bonded to an oxygen or nitrogen atom while the other atom was a hydrogen bond acceptor.

Nevertheless, there was considerable structural evidence for the presence of similar interactions between a hydrogen atom bonded to carbon when oxygen was the acceptor. For instance, in the structure of triclinic quinhydrone[21] (the 1:1 complex between quinone and hydroquinone, Fig. 2) there are clearly

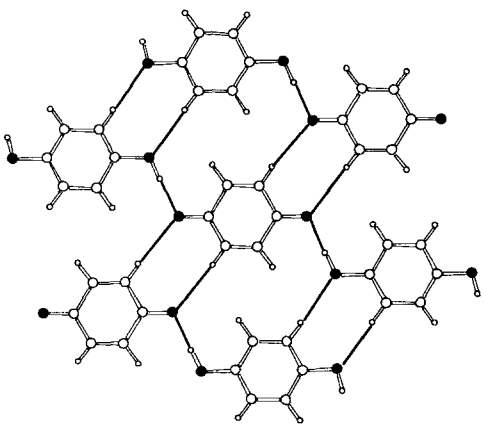

Fig. 2. Triclinic quinhydrone; view of the layer structure normal to the central benzoquinone molecule (based on Sakurai [21]). The figure shows shows C–H···$O_{carbonyl}$, C–H···$O_{hydroxyl}$, and O–H···$O_{carbonyl}$ contacts [22].

interactions between C–H groups and carbonyl or hydroxy groups, in addition to the expected O–H···O interactions. The first form centrosymmetric $\mathbf{R_2^2(8)}$ rings reminiscent of those in benzoic acid (**4**); these rings persist in the structure of 1,4-naphthoquinone[23] (Fig. 3) in which there are no hydroxyl hydrogen atoms. Examination of many more structures of this type confirms beyond any doubt the presence of a C–H···O interaction, which has been geometrically characterized and which is

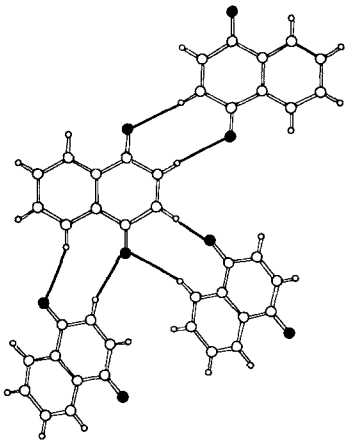

Fig. 3. View of the structure of 1,4-naphthoquinone normal to the molecular plane, showing C–H···O contacts [22]. Based on Gaultier and Hauw [23].

now perfectly acceptable in the growing family of hydrogen bonds.[12] The characteristic H···O distance is in the range 2.16–2.65 Å with a mean value of 2.45 Å.[12, 17] In many cases this centrosymmetric (at least topologically so) $\mathbf{R_2^2(8)}$ ring arrangement is found, which is clearly a hydrogen-bonding *pattern* that is common to this type of interaction. Such a pattern is distinctly recognizable, for instance, in the crystal structure of *meta*-(dithienylquinone) benzene (**5**),[24] as shown in Figure 4,

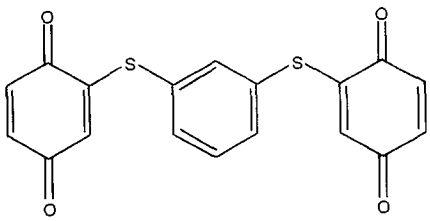

5

even though the O···H distance is 2.8 Å. In fact, there apparently is no other specific interaction in this structure. In looking at crystal structures of hydrogen-bonded systems we will try to recognize patterns with such ideas in mind.

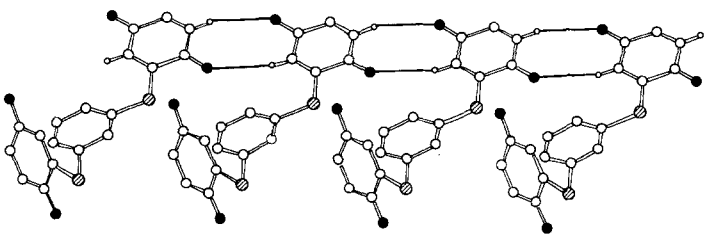

Fig. 4. View of the structure of **5**. Oxygen atoms are shown as solid circles; hydrogen atoms on the benzene ring have been omitted for clarity. The C–H···O distance is 2.8 Å. Taken from ref. [24].

5. A Reminder and a Caveat

Many of the problems in assigning graph sets that have been brought to our attention stem from a lack of adherence to the fundamental definition of a hydrogen-bonding motif. We repeat that definition here and follow with an example.

A motif is a hydrogen-bonded set in which only one type of hydrogen bond is present.

The crucial point in this definition is the presence of only one *type of hydrogen bond*, not one *hydrogen atom*. Thus, in **6a**, if the two hydrogen atoms are not crystallographically equivalent, the unitary level graph set $\mathbf{N}_1$ would be **DD**, and the binary level would be $\mathbf{R}_2^2(6)$. Similarly, the two branches of a three-centered ("bifurcated") hydrogen bond such as **6b** should be treated as

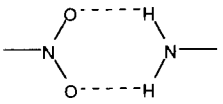

6a

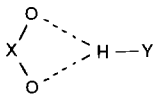

6b

two different hydrogen bonds if the two branches are not crystallographically equivalent; the description of such an arrangement would appear at the binary level as $\mathbf{R}_1^2(4)$. Although this approach may appear at first to complicate the process of assigning graph sets, we believe that the contrary is true. As we will show in a number of examples below, strict adherence to this procedure will remove ambiguities from the process of assigning graph sets. Admittedly, this rigorous approach does sacrifice some of the aesthetic appeal of the whole procedure, in that the characteristic and distinguishing patterns will often appear later on in the formal process of assigning graph sets. However, those characteristic patterns that distinguish and relate different materials and that make the whole method so appealing are by no means lost; they simply appear at higher levels. Put another way, first identifying patterns "by eye" and then assigning their graph sets without regard to issues of crystallographic dependence/independence, level, and so on, limits the utility of the graph set approach to a *descriptive* function; by contrast, following a procedure and allowing the graph set descriptions of the patterns to develop systematically gives the approach a *diagnostic* as well as a descriptive dimension. The rigor advocated here has developed in part as a result of considering the design of algorithms for programming an automatic procedure that can be integrated into existing programs for plotting crystal structures and into structural databases, such as the Cambridge Structural Database.

As one illustration, in the complex **7** the two molecules are chemically different. Considering for the moment only the donors and acceptors involved in forming the ring, the two hydrogen bonds that participate in the ring are different; so in this case the first-level graph set is $\mathbf{N}_1 = \mathbf{DD}$. What will generally be considered the truly interesting chemical and essence-bearing pattern, again $\mathbf{R}_2^2(8)$, is found only at the binary level, which, by definition, contains two types of hydrogen bonds.

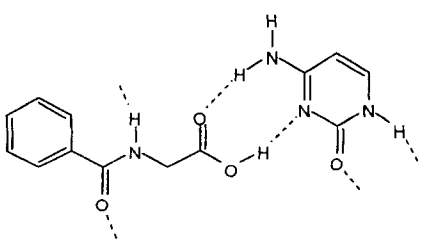

7

6. A Protocol for Assigning Graph Sets

Working independently in Austin and in Beer Sheva we have found that there is a natural protocol for assigning the graph set to a hydrogen-bonded system.[25] All investigators, of course, will find shortcuts and conveniences inherent in their own software, and perhaps even their own scientific background and interests, but the following procedure should make the assignment of hydrogen-bond graph sets relatively straightforward and, more importantly, consistent.

Two computer programs are essential: one that can calculate geometry, including intermolecular distances based on space group symmetry operations and translations, and a second that can plot crystal structures, preferably in stereo, and can easily accommodate addition and removal of molecules related by symmetry and translation, and rotation of the view. We often take our structures for study from the Cambridge Structural Database (CSD), and find it most convenient when the geometry calculation and plotting programs can use CSD entries without further modification.[26]

It is particularly helpful for the remainder of the process if all of the calculations are based on sets of fractional coordinates that define recognizable chemical units; otherwise it is easy to get lost in a maze of symmetry operations. After selection of the hydrogen atoms that are to be considered as possible participants in hydrogen bonding, the first program is used to calculate the possible hydrogen-bonding distances. A decision must then be made about which interactions should be included as hydrogen bonds; the nominal distance values cited above would serve as reasonable starting criteria. At this point intramolecular **S** motifs should be identified.

Through use of the symmetry positions of the calculated acceptor atoms for intermolecular hydrogen bonds, the molecular environment of the hydrogen bonds can be constructed. This is done by first generating on the graphics output both the original reference molecule(s) (whose coordinates were originally stored for computer plotting and geometry calculations) and, if necessary, a neighboring molecule that is connected to the first by a hydrogen bond. The presence of a crystallographic inversion center (or less commonly a $\bar{3}$, $\bar{4}$, or $\bar{6}$ axis) that relates the molecules that are hydrogen-bonded to each other prescribes an **R** motif. An **R** motif could also be generated by a two-fold rotation or by mirror reflection; however, for reasons related to packing efficiency such arrangements are extremely rare in the crystal structures of organic molecules.[27] The absence of inversion symmetry suggests that the motif is probably either a **C** or a **D**; the former is generated by unit cell translations or by symmetry operations of the second kind (screw axis or glide plane), and the latter arises in the absence of any symmetry relating the two molecules. Being finite, first-level **D** motifs are relatively easy to identify. Having determined the pattern designator, the degree of the pattern must be determined by counting the number of atoms. For **C** motifs we generally start at a hydrogen atom, traverse the hydrogen bond, and continue until reaching the same hydrogen atom in a symmetry-related molecule. It is particularly enlightening to carry out this procedure one molecule at a time, carefully labeling each new molecule as it is added to the graphic display. The repetition of a symmetry operation may be necessary to complete or extend a particular

hydrogen-bonding motif. In this way it is possible to generate each motif, one at a time. Generating hard copy and highlighting the motifs in different colors is a convenient way of preserving a permanent record of the graph set analysis.

After the initial assignment of the motifs and then the first-level graph set, higher level graph sets can be determined, if necessary, by systematically taking combinations of the different hydrogen bonds. We denote the motifs as *a*, *b*, *c*, etc. according to the hierarchy specified[3] for the first-level graph set. Binary (that is, pairs of hydrogen-bond types) graph sets, $\mathbf{N_2}(ab)$, $\mathbf{N_2}(ac)$, $\mathbf{N_2}(bc)$, etc. are then generated. For example, for three hydrogen bonds we would generate three basic unitary motif descriptors and three basic binary graph sets; four hydrogen bonds would correspond to four basic motif descriptors and six basic binary graph sets. The bookkeeping for this process is facilitated by use of a summary table in the form of a matrix in which the unitary motif descriptors appear on the diagonal and the second-level graph set descriptors appear off the diagonals. This is illustrated for anthranilic acid (Table 2 in Section 10) and iminodiacetic acid (Table 3 in the appendix). Higher level sets—ternary, quaternary, etc.—can then be generated as desired. As already discussed, the graph set description of complex networks can often yield insight into the characteristic chemical and structural features of the hydrogen bonding.

For the time being, at least, we have not addressed the problem of the directionality of hydrogen-bonding patterns. Even for a pairwise combination of motifs, say **DD**, the possibility of directionality certainly exists. In cyclic systems **R** that are generated by a crystallographic rotation axis, a number of possibilities exist, depending on the nature of the unique unit from which the **R** is generated and the presence or absence of symmetry elements in addition to the rotation axis. The distinction between homodromic and heterodromic patterns in cyclic systems has also been discussed by Jeffrey and Saenger.[16] Specifying the sense of such patterns would require an additional index in the pattern descriptor, and at this point we prefer to keep the notation to a minimum.

7. Structural Aspects As Motivation for Graph Set Analysis

In the remainder of this review, we raise, and attempt to resolve, some questions that have arisen in our attempts to use the graph set formalism to shed light on similarities and differences in packing patterns of related structures. Because many of the examples we cite arise from that work, it might be useful to elaborate briefly on its motivation, by giving but two illustrations of areas in which the graph set approach shows promise.

The focus in Beer Sheva has been on the study of polymorphic systems, with the additional goal of providing some guidelines for understanding the changes in hydrogen-bonding networks that result from the transformation from one polymorphic form to another. Two published examples have established the usefulness of the method of graph set analysis of hydrogen bonding in such systems.[5, 6] One area of work in Austin involves the comparison of hydrogen-bonding patterns for the same substance in enantiomeric and racemic crystalline forms—a relationship similar to that in polymorphism—with an eye to issues of resolution, racemic vs. conglomerate crystallization, etc. A subset of this work deals with amino acids; chemical similarities within this set of structures provide another thread of relationships that we can pursue with graph sets.

Clearly, one raison d'être of polymorphic forms in organic crystals is the possibility of the formation of different patterns of hydrogen bonding, and in many cases this is indeed manifested in differences in the graph sets found for polymorphs of a substance.[28] Similarly, the possibility of different patterns of hydrogen bonding is surely a potential factor in determining relative stabilities of racemic vs. enantiomeric crystals for a substance. However, there are also cases for which the graph sets of a racemate/enantiomer pair or of two polymorphs are identical at all levels. In such cases, the different structures clearly are not attributable directly to differences in hydrogen-bonding *patterns*, but rather to the subtleties of hydrogen-bonding *energetics* within the networks, and to further subtleties of non-hydrogen-bonding energetics between the hydrogen-bonding networks.

As an example of a pair of structures in which the enantiomeric and the racemic structures have identical hydrogen-bonding patterns at all levels, consider the structures of D,L-alanine[29] (Fig. 5, top) and L-alanine[30] (Fig. 5, bottom). A comparison of these diagrams suggests that the hydrogen-bonding patterns for the two structures are identical in all regards, an impression that is reinforced by the unitary graph sets, **C(5)C(5)C(5)**. Higher

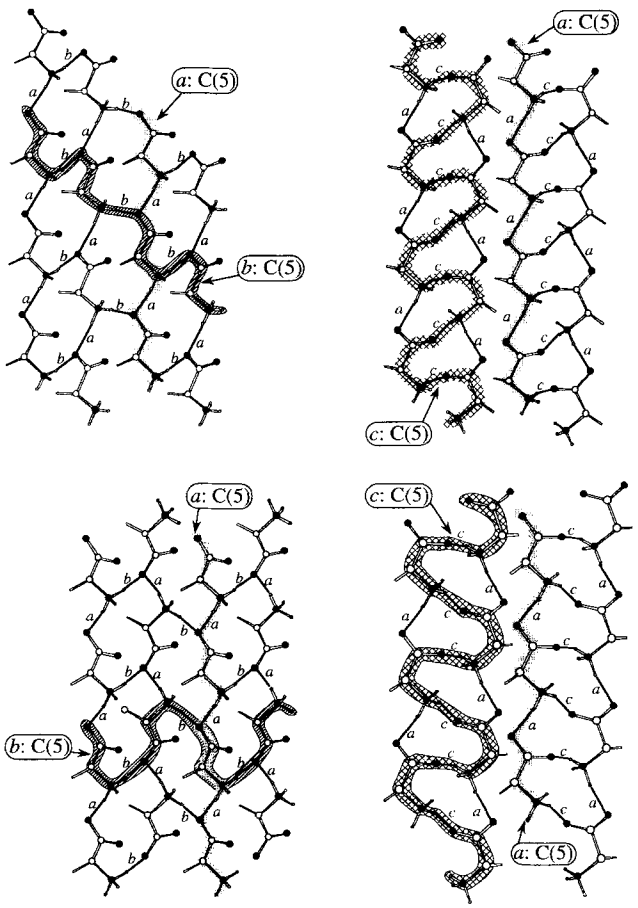

Fig. 5. Hydrogen-bond patterns of the structure of D,L-alanine (top) and L-alanine (bottom), showing the three hydrogen bonds: on the left those labeled *a* and *b*, and on the right those labeled *a* and *c*.

level graph sets, not marked in the figures, also correspond—$\mathbf{C_2^1(4)}$ for the basic (a,b) graph set, $\mathbf{R_4^4(14)}$ and rings of higher degree for complex (a,b) graph sets (analogous to α-glycine, see Fig. 1), $\mathbf{C_2^2(6)}$ for the basic (a,c) graph set, and so on.

A similar situation is seen for the two polymorphic structures α-D,L-methionine[31] (Fig. 6, top) and β-D,L-methionine[31] (Fig. 6, bottom). The unitary graph sets for both are **C(5)C(5)C(5).** The only significant difference between these two structures is in the conformation of the terminal CH_3S group. Higher level graph sets, again not marked in the figures, agree—$\mathbf{C_2^1(4)}$ for the basic (a,b) graph set, $\mathbf{R_4^4(12)}$ and rings of higher degree for complex (a,b) graph sets (again analogous to α-glycine, see Fig. 1), $\mathbf{R_4^4(12)}$ for the basic (a,c) graph set, and so on.

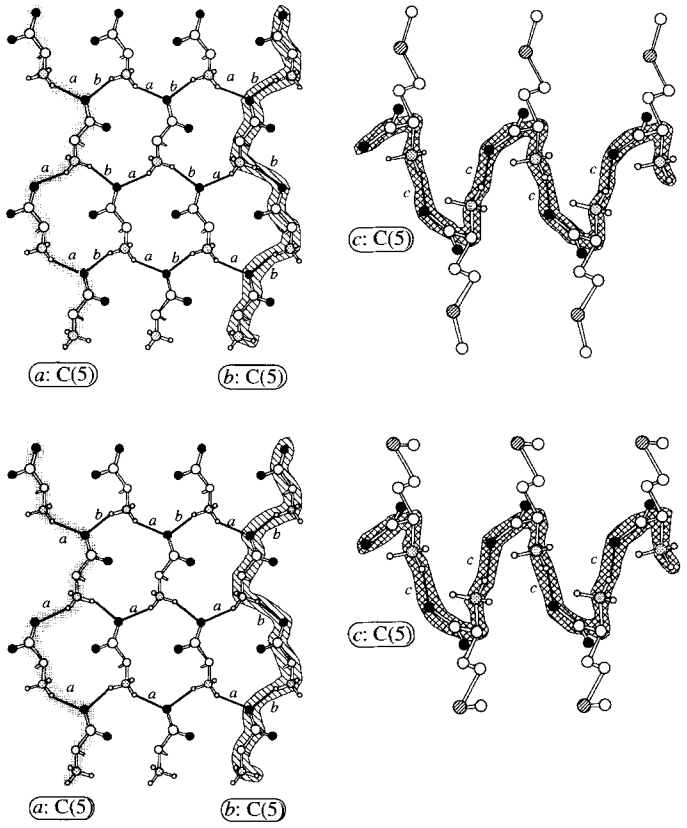

Fig. 6. Hydrogen-bond patterns of the structure of α-D,L-methionine (top) and β-D,L-methionine (bottom), showing the three hydrogen bonds: on the left those labeled *a* and *b*, and on the right those labeled *c*.

Comparison of the four structures just discussed and α-glycine (Fig. 1) exemplifies one essential point: Identical graph set notations at one level—for example, first-level graph sets **C(5)C(5)C(5)** for these five structures—*do not ensure* that the patterns are identical at all levels. The figures and, with even greater certainty, the higher-level graph sets as formally deduced, show clearly that three different structural arrangements are represented in these five structures. If differences in the graph sets of patterns appear, the conclusion that the patterns are different necessarily follows; however, one should conclude that patterns are identical only after establishing that *all graph sets, both basic and complex, at all levels* are the same for the structures.[32] Thus, we must emphasize again that the diagnostic power of the graph set approach would be diminished or lost without a systematic, thorough analysis, probably facilitated by computer algorithms in all but the simplest cases.

8. Rings or Chains or Both?

In many structures the hydrogen-bonding pattern clearly consists of chains whose "links" contain rings. Such a pattern appears in the triclinic form of tetramethyl-β-oxoglutaric acid (TOXGLU10) (Fig. 7a). There is no crystallographic symmetry within the molecule; the hydrogen-bonded rings at the ends of

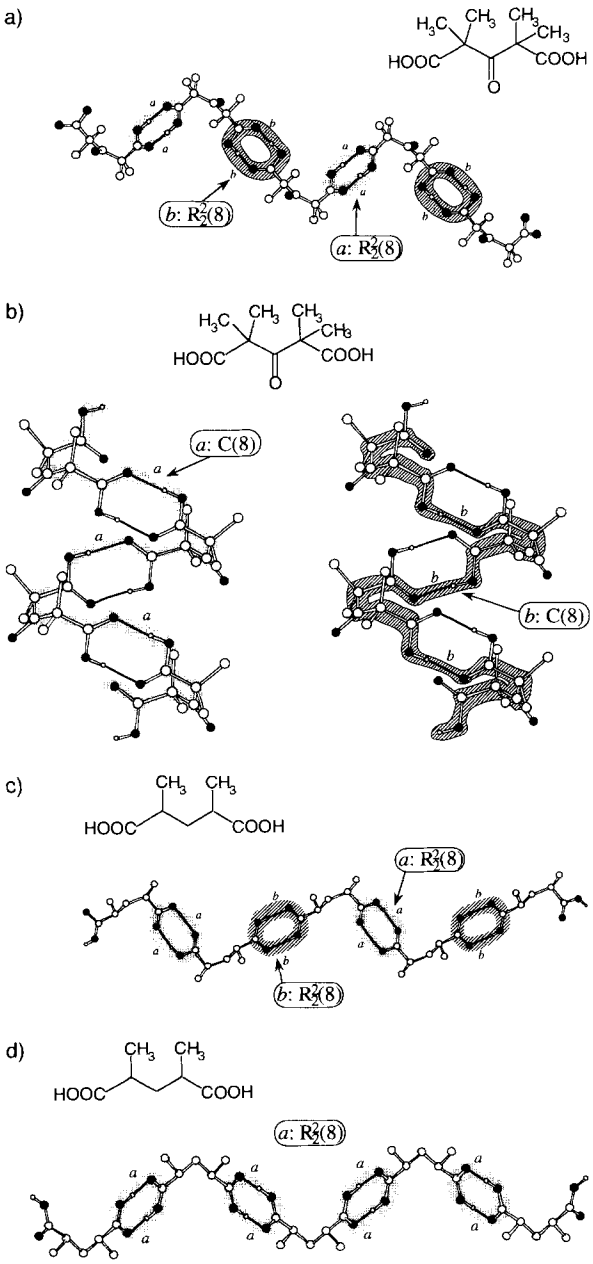

Fig. 7. a), b) Hydrogen-bond patterns for the triclinic form of tetramethyl-β-oxoglutaric acid, showing the two crystallographically independent rings in the chain (a) and the two alternatives for constructing chains (b). c) Hydrogen-bond patterns for *meso*-α,α′-dimethylglutaric acid, showing the two crystallographically independent rings in the chain. d) Hydrogen-bond pattern for *rac*-α,α′-dimethylglutaric acid, showing the effect of symmetry, which makes all $\mathbf{R_2^2(8)}$ equivalent.

the molecule occur around different inversion centers, so each carboxylic acid dimer appears at the unitary level. The motifs are $\mathbf{R_2^2(8)}$ and $\mathbf{R_2^2(8)}$ for the two H-bonds *a* and *b*, giving the *basic* unitary graph set $\mathbf{R_2^2(8)R_2^2(8)}$. The basic binary graph set is $\mathbf{C_2^2(16)}$, counting through only one branch of each dimer ring. However, this basic representation does not adequately point to the presence of the ring as a characteristic topological element that distinguishes this hydrogen bonding pattern from a simple chain pattern; we might term this pattern a "chain of rings". We advocate a notation in which the ring designation is appended in square brackets to the chain designation: the extended notation for this pattern is thus $\mathbf{C_2^2(16)[R_2^2(8)]}$.[3]

Another such case is schematically represented for *N*-methylaniline[33a] in **8**, for which the basic binary graph set is $\mathbf{R_1^2(4)}$.[33b] Designating the chain by the complex binary notation $\mathbf{C_1^2(8)}$ would not be unique, however, because one could imagine a hypothetical (to the best of our knowledge) pattern such as **9** with the same designation. Using the square brackets notation introduced above, the full designation for the structure **8** is $\mathbf{C_1^2(8)[R_1^2(4)]}$.

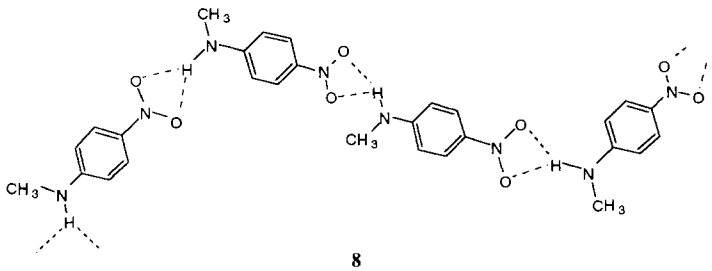

8

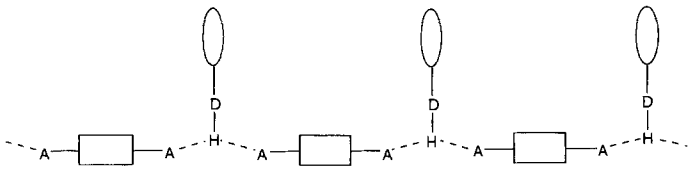

9

Some ways that a chain of rings could arise are shown schematically as **10**–**13**, in which the designations *a* to *d* each represent a hydrogen bond. In **10**, all hydrogen bonds are crystallographically equivalent, which implies symmetry both within and between molecules; thus this chain of rings appears at the unitary level. Examples of such chains are the *β* form of oxalic acid (see Section 9), *rac*-dimethylglutaric acid (RADMGA, Section 9), and *β*-ketoglutaric acid.[34] If the molecule contains no symmetry but each ring is formed around a symmetry element (most commonly an inversion center), pattern **11** arises, in which the chain of rings appears at the binary level. Instances of pattern **11** include *meso*-dimethylglutaric acid (GLUTAC10, Section 9), triclinic tetramethyloxoglutaric acid (TOXGLU10, above), and Form I of amobarbital (Section 10). The absence of symmetry within either the molecule or the ring can give rise to the pattern **12**, again at the binary level, as in, for example, monoclinic tetramethyloxoglutaric acid (TOXGLU11, Section 9). Pattern **13**, would appear only at the quaternary level, because four different hydrogen bonds are involved. This could occur, for instance, when adjacent residues in the chain are crystallographically distinct, for example, in a cocrystal (including solvates), an ionic structure, or a structure with more than one formula unit per asymmetric unit ($Z' > 1$). Form II of amobarbital (Section 10) provides an example of such a pattern.

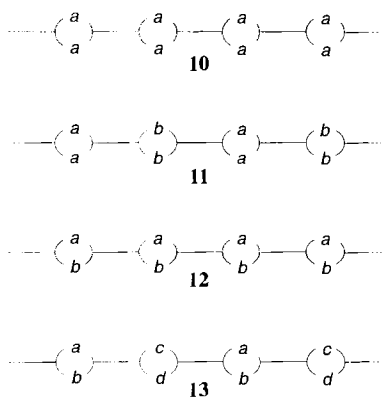

10 **11** **12** **13**

9. Crystallographic Symmetry Within and Between Molecules

In the previous section, we touched on the effects of crystallographic symmetry between and/or within molecules. In a similar vein, we noted above in Section 2 that for benzoic acid (**4**) the ring structure is due to the presence of a crystallographic inversion center. In that case, the two hydrogen bonds are identical, related by the inversion center; this resulted in the now-familiar $\mathbf{R_2^2(8)}$ ring as the basic unitary graph set.

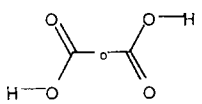

14

In the *β* form of oxalic acid (**14**),[35] the asymmetric unit is composed of only one half of the molecule; the full molecule is generated by a crystallographic inversion center, so there is only *one* crystallographically independent OH group in this structure. An additional inversion center, operating in the same manner as in the benzoic acid structure, generates the $\mathbf{R_2^2(8)}$. The crystal structure, shown in Figure 8, clearly contains chains composed of rings linked through the molecule so the pattern at the unitary level is fully specified as $\mathbf{C(5)[R_2^2(8)]}$.

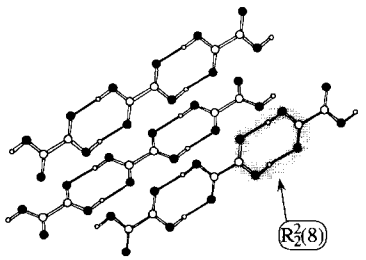

Fig. 8. The structure of the *β* form of oxalic acid, indicating the $\mathbf{R_2^2(8)}$ ring pattern typical of many carboxylic acids. The difunctionality of the molecule leads to a chain structure.

The glutaric acid derivatives shown in Figure 7 further illustrate the ideas of this and preceding sections.

TOXGLU10: As discussed in Section 8, the motifs for the triclinic form of tetramethyl-*β*-oxoglutaric acid (Fig. 7a)[36] are $\mathbf{R_2^2(8)}$ for the two H-bonds *a* and *b*, giving the *basic* unitary graph set $\mathbf{R_2^2(8)R_2^2(8)}$. The basic binary graph set is $\mathbf{C_2^2(16)}$, with the extended notation $\mathbf{C_2^2(16)[R_2^2(8)]}$.

TOXGLU11: The monoclinic form of tetramethyl-*β*-oxoglutaric acid (Fig. 7b)[37] has no crystallographic symmetry within the molecule or relating the two H-bonds per molecule. The motifs are **C(8)** for the two H-bonds *a* and *b*, giving the *basic* unitary graph set **C(8)C(8)**. Because the carboxylic acid dimer

involves two crystallographically independent H-bonds, its familiar notation appears in the basic binary graph set, $\mathbf{R_2^2(8)}$.

GLUTAC10: The triclinic form of *meso*-a,a'-dimethylglutaric acid[38] (Fig. 7c) has the same symmetry and packing pattern as TOXGLU10. The basic unitary graph set is $\mathbf{R_2^2(8)R_2^2(8)}$ and the basic binary graph set $\mathbf{C_2^2(16)}$, with the extended notation $\mathbf{C_2^2(16)[R_2^2(8)]}$.

RADMGA: In *rac*-α,α'-dimethylglutaric acid[39] (Fig. 7d) the molecule lies on a crystallographic symmetry element (a twofold rotation axis), and the hydrogen bonding at each end occurs around an inversion center. Thus there is only one crystallographically independent H-bond. The motif could be described either as $\mathbf{R_2^2(8)}$ to emphasize the ring or **C(8)** to emphasize the chain. At present, the protocol for assigning graph sets does not specify a priority of assignment when two or more alternatives are of the same degree, here 8. We recommend the "chain of rings" notation discussed in the preceding section, $\mathbf{C(8)[R_2^2(8)]}$.

The common pattern in these four glutaric acid derivatives is the chain of rings shown as **15**. This consists of a chain with

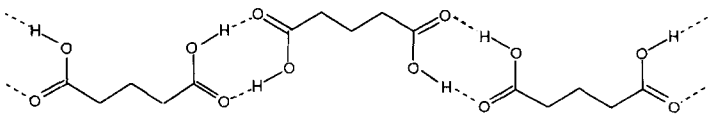

15

periodicity eight, containing an eight-membered ring, or $\mathbf{C(8)[R_2^2(8)]}$. In the formal analysis of RADMGA, this notation appears directly as the unitary graph set. In the other three structures, it would show up in the complex binary graph sets with periodicity 16 and containing *two* $\mathbf{R_2^2(8)}$ rings, or $\mathbf{C_2^2(16)[R_2^2(8)]}$; we recognize this as *twice* the fundamental $\mathbf{C(8)[R_2^2(8)]}$ pattern. This illustrates again that a formal, systematic approach eventually leads to recognizably similar graph set designations when common features are present. It also points up the additional necessity of inspecting the graph sets not just for common features but also for *multiples* of common features.

10. Structures with More than One Molecule in the Asymmetric Unit ($Z' > 1$)

A significant number of crystal structures contain more than one molecule in the asymmetric unit. In such cases, the structural/chemical question is: do the different molecules in the asymmetric unit have identical or different hydrogen-bond patterns? If the patterns differ, and the structure is one of a set of related structures, is there any commonality of patterns between different molecules in the asymmetric unit and the other structures?

Crystallographically, two or more molecules in the asymmetric unit are totally independent. If they have different hydrogen-bonding patterns as revealed from the graph set analysis, then they are exhibiting different properties of molecular recognition. When crystallographically nonequivalent molecules have the same hydrogen-bond environment, is it necessary to define the graph set for each? On the other hand, if they do not have the same environment, what is the prescription for defining the graph set in the general case?

We have recently carried out a survey of polymorphic structures in which at least one of the structures contains more than one molecule in the asymmetric unit. Though this survey was not exhaustive, it did suggest the variety of cases possible. The examples we present here will serve as a prescription for defining the graph sets in many such cases.[40]

Our first encounter with this problem came with the analysis of trimorphic iminodiacetic acid (**16**).[5] In this case Form 2 contains two molecules with identical hydrogen-bond patterns in the asymmetric unit. Hence the two molecules were treated as identical, and the graph set was assigned for one of them. Although the chemical implications of that analysis are not altered, in light of our subsequent experience we realize that each of the molecules in the asymmetric unit should have been treated individually. A reanalysis of the graph sets for iminodiacetic acid Form 2 with the protocols developed here appears in the Appendix.

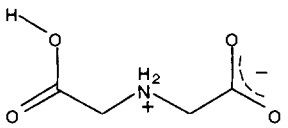

16

The problem and its solution are demonstrated in the two known polymorphic forms of amobarbital (5-ethyl-5-isoamylbarbituric acid) (**17**). Form I contains one molecule in the asymmetric unit, and Form II contains two.[42] The molecule has two hydrogen atoms that can participate in hydrogen bonding and the three potential hydrogen-bond acceptor carbonyl groups. In the unitary graph set for Form I (Fig. 9a), each of these forms a centrosymmetric $\mathbf{R_2^2(8)}$: the unitary graph set is thus simply $\mathbf{N_1 = R_2^2(8)R_2^2(8)}$.

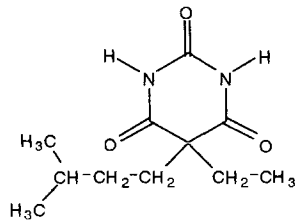

17

For Form II there are now four different hydrogen atoms that must be accounted for in the unitary graph set. The representative part of the structure is shown in Figure 9b. The two hydrogen atoms from molecule A form hydrogen bonds with carbonyl groups from molecule B and vice versa. Each one of these combinations is a **D** motif; hence the unitary graph set for Form II is $\mathbf{N_1 = DDDD}$. Even a cursory comparison of Figures 9a and b indicates a great similarity between the two, which is not reflected so far in the unitary graph sets. Two of the binary graph sets for Form II, (*a*,*b*) and (*c*,*d*), will be $\mathbf{R_2^2(8)}$ (Fig. 9c), which does, of course, reflect the identity with the first level for Form I. These graph set assignments assist in demonstrating the great similarities between the two structures. These similarities will continue at higher levels. For instance, the obvious "chain-of-rings" feature that is described at the binary level in Form I would appear at the quaternary level in Form II. Because of the presence of twice as many hydrogen atoms in Form II as in Form I there will be twice as many possible levels for the former than for the latter, and the formal identities in graph set assignments would never appear at the same level. Nevertheless, a combination of systematic graph set assignment and careful visual inspection will reveal those similarities.

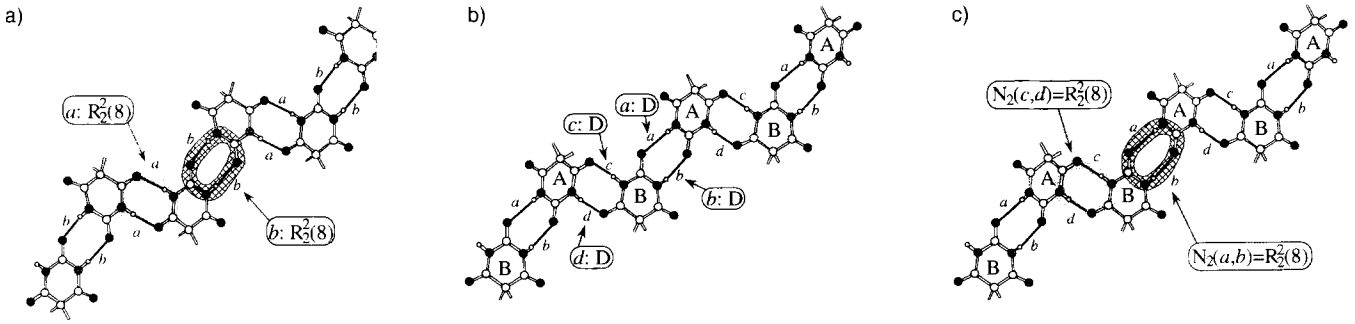

Fig. 9. Graph set assignments for the two polymorphs of amobarbital (**17**). Pendant groups have been omitted for clarity. a) Form I, first-level motifs. b) Form II, first-level motifs; A and B designate the two different molecules in the asymmetric unit. c) Form II, two of the binary graph sets.

Another example is trimorphic 4-methyl-2-nitroacetanilide (**18**).[43-45] Polymorphs 1 and 2 each contain one molecule in the asymmetric unit; polymorph 3 has two. The molecule clearly has one hydrogen that can participate in a hydrogen bond. The most likely acceptor for that hydrogen is the carbonyl oxygen, although those on the nitro group are also somewhat basic in character. Unless the hydrogen participates in two different hydrogen bonds, the first-level graph set should be defined by one motif for Forms 1 and 2 and by two motifs for Form 3. The graph sets are given in Figure 10. Form 1 is distinguished by a **C(4)** motif from an N–H···O=C hydrogen bond, whereas the single molecule in the asymmetric unit in Form 2, and the two molecules in Form 3 all exhibit an **S(6)** motif resulting from an intramolecular N–H···O–N hydrogen bond.[46] In this case the unitary graph sets of the two molecules in the asymmetric unit of Form 3 are identical, and are the same as that for Form 2.

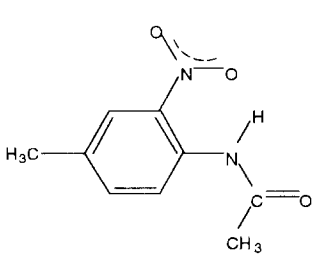

18

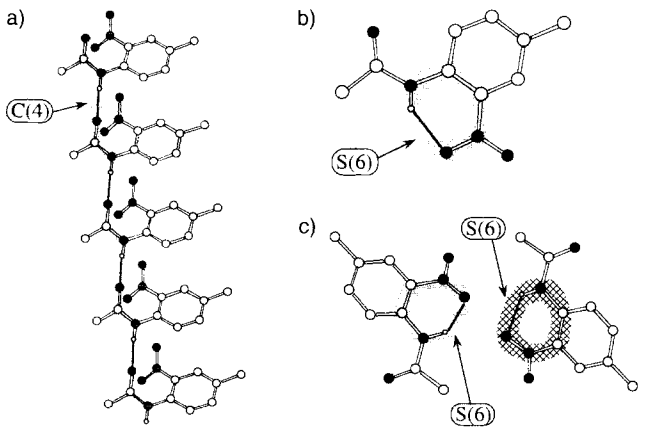

Fig. 10. First-level graph sets for the three polymorphs of 4-methyl-2-nitroacetanilide (**18**). Relevant parts of the crystal structure are shown for Form 1. The two molecules in the asymmetric unit of Form 3 are shown in their true crystallographic relationship to each other (see text). a) Form 1. b) Form 2. c) Form 3.

The situation differs in anthranilic acid (**19**), another trimorphic material whose structural chemistry has been widely studied.[47-54] This case illustrates a number of aspects in the choice of cutoff distance as criterion for defining the hydrogen-bond network. The molecule may exist in either the neutral **19a** or zwitterionic **19b** form. In either case each molecule has three

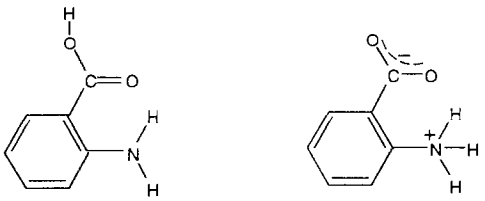

19a **19b**

hydrogen atoms that can participate in hydrogen bonds. For the neutral molecule the carbonyl oxygen atom is the obvious candidate as best hydrogen acceptor; the hydroxyl oxygen atom is considerably less suitable. For the zwitterionic case, both oxygen atoms are equally good acceptors.

These structures and their graph sets are presented in Figure 11. In Forms II and III the one molecule in the asymmetric unit is in the neutral form; in Form I there are two molecules per asymmetric unit, one neutral and one zwitterionic. In Form II (Fig. 11a), the hydrogen atom of the carboxyl group forms the now familiar ring structure $\mathbf{R_2^2(8)}$ about a crystallographic inversion center. One of the amino hydrogen atoms participates in an intramolecular motif **S(6)**. The closest acceptor to the second amino hydrogen is 2.38 Å. Hence by "normal" standards it might not be considered as participating in a hydrogen bond. However, that hydrogen atom clearly points in the direction of a carbonyl oxygen atom, and although the latter must then be counted as participating in three hydrogen bonds, we believe that the pattern exhibited here warrants including this in the hydrogen-bond network description as a chain, **C(6)**. Thus the first-level graph set is $\mathbf{N_1 = C(6)S(6)R_2^2(8)}$ (diagonal terms in Table 2).

In Form III (Fig. 11b) once again the carboxylic acid forms the $\mathbf{R_2^2(8)}$ ring about a crystallographic inversion center. One amino hydrogen atom is intramolecularly hydrogen-bonded to the carboxyl carbonyl oxygen atom to again yield **S(6)**, and the second amino hydrogen atom is hydrogen-bonded, this time to

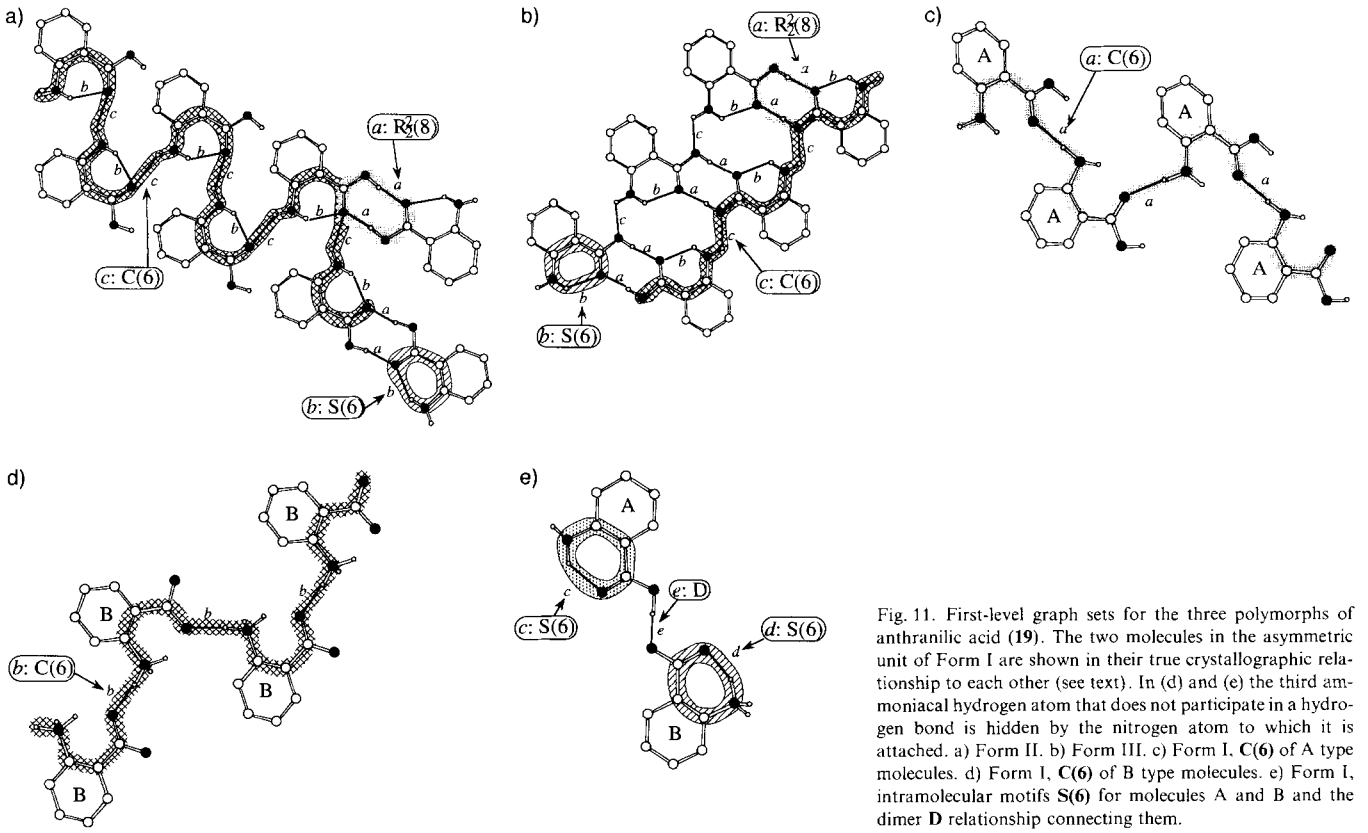

Fig. 11. First-level graph sets for the three polymorphs of anthranilic acid (**19**). The two molecules in the asymmetric unit of Form I are shown in their true crystallographic relationship to each other (see text). In (d) and (e) the third ammoniacal hydrogen atom that does not participate in a hydrogen bond is hidden by the nitrogen atom to which it is attached. a) Form II. b) Form III. c) Form I, **C(6)** of A type molecules. d) Form I, **C(6)** of B type molecules. e) Form I, intramolecular motifs **S(6)** for molecules A and B and the dimer **D** relationship connecting them.

the carboxy hydroxyl oxygen atom to form the chain **C(6)**. In the first level the graph sets are identical: $\mathbf{N_1}$ = **C(6)S(6)R_2^2(8)**.

The two molecules in the asymmetric unit of Form I can be distinguished chemically. Neutral molecule A forms a **C(6)** motif using an amino hydrogen and a carboxyl carbonyl oxygen atom (Fig. 11c); the zwitterion B has the same motif with an ammoniacal hydrogen and a carboxylate oxygen atom (Fig. 11d). As in the other two polymorphs, a second hydrogen atom on the nitrogen leads to an **S(6)** motif for each of the molecules in the asymmetric unit (Fig. 11e). Molecules A and B are linked together through an $O-H\cdots O_{carboxylate}$ bond, a **D** motif. The sixth hydrogen atom (that is, the remaining ammoniacal one on molecule B) is not involved in hydrogen bonding, at least for $O\cdots H$ distances less than 3 Å. Hence the first-level graph set for Form 1 is $\mathbf{N_1}$ = **C(6)C(6)S(6)S(6)D**.

To distinguish between Forms II and III we turn to the binary graph sets. In principle three hydrogen bonds can be combined pairwise in three different ways (that is, the off-diagonal terms in Table 2). The resulting $\mathbf{C_2^1(4)}$ for Form II is shown in Figure 12a, which reflects the fact that the same carbonyl oxygen atom participates in both hydrogen bonds in the chain. For

Table 2. Unitary motifs (on-diagonal) and binary graph sets (off-diagonal) for anthranilic acid, Form II [a].

Type of H-Bond	*a*	*b*	*c*
a	$\mathbf{R_2^2(8)}$		
b	$\mathbf{R_2^2(16)}$	**S(6)**	
c	$\mathbf{C_2^2(8)}$	$\mathbf{C_2^1(4)}$	**C(6)**

[a] See Figs. 11a, 12a.

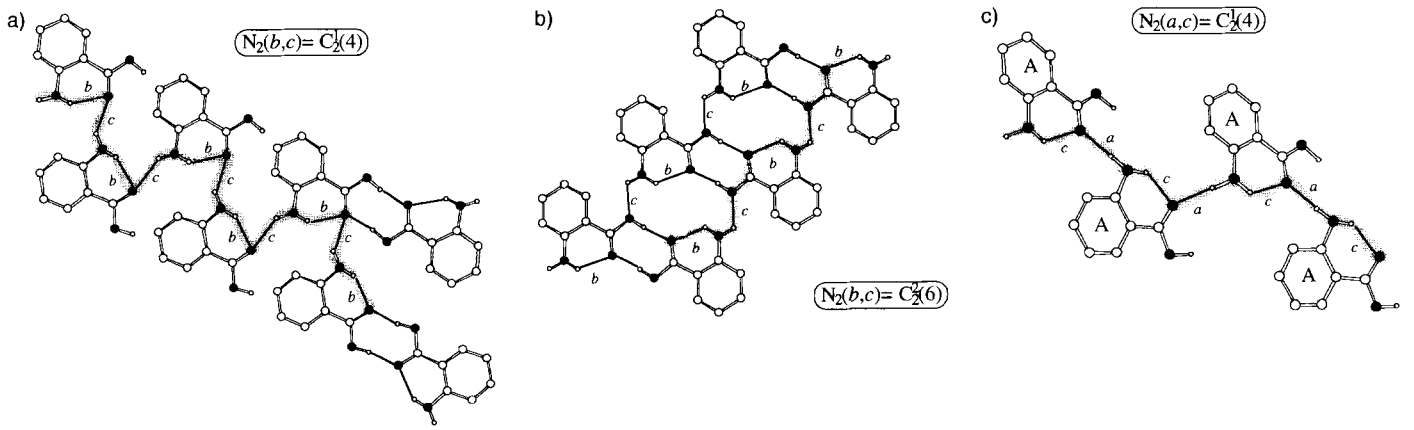

Fig. 12. Second-level graph set for anthranilic acid (**19**). General comments in the legend of Fig. 11 apply here, too. a) Form II. b) Form III. c) Form I, molecule A.

Form III (Fig. 12b) the chain $C_2^2(6)$ goes through both oxygen atoms of the carboxyl group; hence two acceptors and two more atoms in each "link". The binary graph set for Form I, $C_2^1(4)$ (Fig. 12c), is identical to that of Form II, but it is important to note that only A type molecules are present in this pattern.

This example demonstrates some more of the important aspects of graph set analysis of hydrogen-bonding networks: 1) the distance cutoff for the definition of a hydrogen bond must be flexible; 2) the crystal structures must be examined carefully when deciding on the presence or absence of hydrogen bonds in borderline cases; 3) higher level graph sets are needed to distinguish between those that are identical at the first level; 4) different molecules in the asymmetric unit must be clearly distinguished and treated separately; 5) a simple and straightforward analysis leads to readily identifiable similarities and differences among the polymorphs; 6) the resulting representation of the structure is readily comparable with that of other structures.

11. "Cyclic" Systems Generated by a Rotational Symmetry Element

The two forms of acetamide (**20**) demonstrate a number of principles in the assignment of graph sets, and also the simplification in understanding the similarities and differences between them. Acetamide crystallizes in an orthorhombic form with two molecules in the asymmetric unit[55] and a relatively unusual rhombohedral form with one molecule in the asymmetric unit.[56] The presence of two molecules (A and B) in the asymmetric unit in the orthorhombic form means that motifs must be defined for the hydrogen bonds formed by four hydrogen atoms. In the first-level graph set (Fig. 13a) A and B molecules each form a **C(4)** motif, and one A molecule as hydrogen donor is paired with a B molecule as hydrogen acceptor and vice versa in two **D** motifs. The first-level graph set is therefore N_1 = **C(4)C(4)DD**. The first-level graph set of the rhombohedral form (Fig. 13b) is generated by hydrogen bonds formed by the two amido hydrogen atoms, each leading to a **C(4)** motif, and N_1 = **C(4)C(4).**

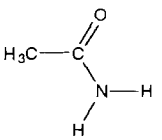

20

The basic binary graph set for the orthorhombic structure is obtained by combining the two **D** motifs, leading to $R_2^2(8)$ (Fig. 13c). In the rhombohedral form, the hydrogen bonds from the two amido hydrogen atoms are arranged around the threefold axis, leading to the binary-level ring pattern $R_6^3(12)$ (Fig. 13d). The generation of an $R_6^3(12)$ ring by the threefold axis is analogous to the generation of an $R_2^2(8)$ ring by the center of symmetry.

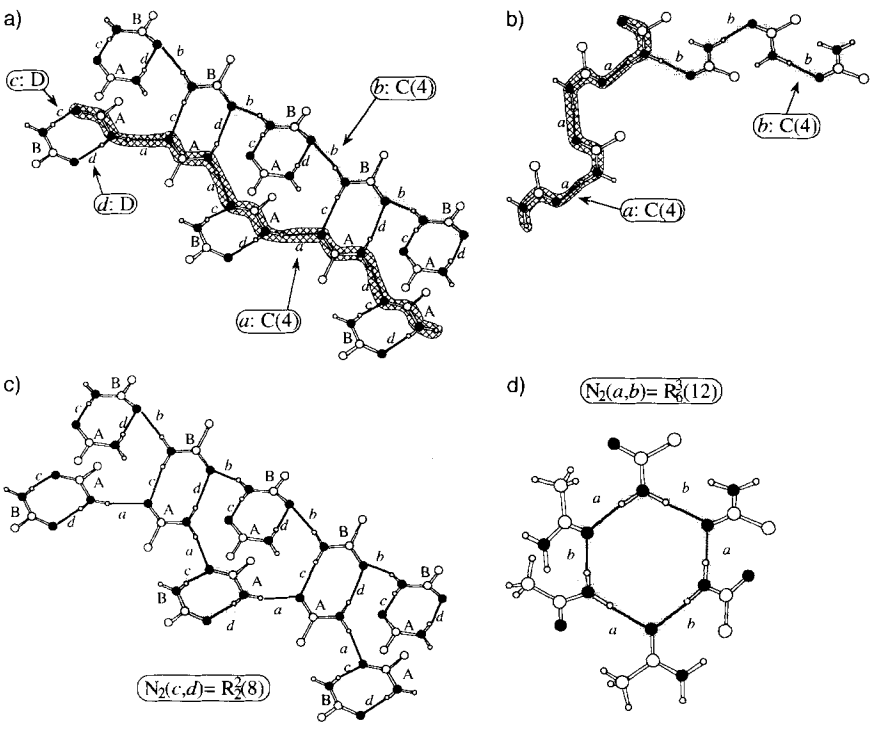

Fig. 13. Graph sets for the two polymorphs of acetamide (**20**). a) Orthorhombic form, first level; A and B designate the two different molecules in the asymmetric unit. b) Rhombohedral form, first level. c) Orthorhombic form, second level. d) Rhombohedral form, second level.

12. Does D Ever Contain More than Two Units? (and Other Curiosities)

All the examples of **D** (or "discrete") patterns we have encountered to this point have included only two molecules. There are however, many cases in which the finite **D** unit contains more than two molecules. Although we have not made any systematic analysis of the saccharides, this class of compounds appears to be particularly rich in patterns of this type.[57] One example of a **D** pattern composed of more than two molecules appears in dimorphic cyanoacetic acid (**21**), which is also of interest because both polymorphs have several molecules in the asymmetric unit: the α form[58] with three molecules per asymmetric unit (A, B, C) and the β form[59] with two (A, B). The presence of one hydrogen-bond donor and two hydrogen-bond acceptors on a single molecule provides various hydrogen-bonding possibilities.

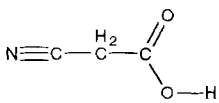

21

The first-level graph set of the α form (Fig. 14a) is composed of a **C(6)** motif of A molecules linked by an O–H···N hydrogen bond; the same motif is observed for B molecules. In the C molecules, on the other hand, the carboxyl groups form the O–H···O hydrogen bond, leading to the common $R_2^2(8)$ motif. The first-level graph set is then N_1 = **C(6)C(6)**$R_2^2(8)$**.** The presence of both of these hydrogen bonds in the same structure suggests a similar basicity for the carboxyl carbonyl and the cyano nitrogen atoms. Additional evidence for this observation is provided in the hydrogen bonding of the β form (Fig. 14b). The A molecules

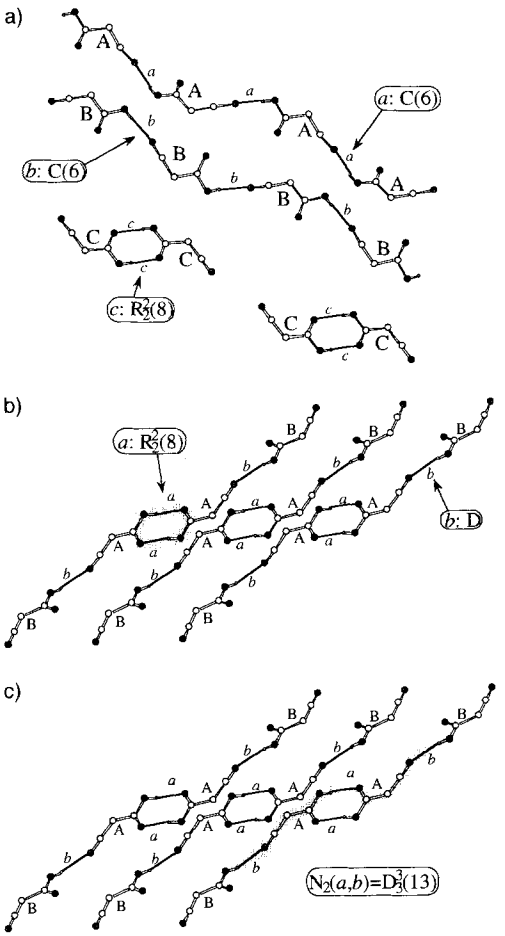

Fig. 14. Graph sets of the two polymorphs of cyanoacetic acid (**21**). a) α form, first level. b) β form, first level. c) β form, second level.

are in an $\mathbf{R_2^2(8)}$ motif typical of carboxylic acids, and the carboxylic hydrogen atom of a B molecule forms a hydrogen bond with the nitrogen atom of an A molecule. The first-level graph set is thus $\mathbf{N_1 = DR_2^2(8)}$.

The α form of **21** provides the first example we have presented here for which there are no graph sets beyond the first level, because no links between motifs exist. In the β form the combination of the two hydrogen bonds described by $\mathbf{N_1}$ leads to a finite pattern at the binary level (hence **D**, Fig. 14c) for which a suitable description is $\mathbf{D_3^3(13)}$.[60] In light of the discussion in Section 8, however, an extended notation would additionally make note of the fact that the $\mathbf{R_2^2(8)}$ ring is present in this pattern by augmenting the pattern descriptor: $\mathbf{D_3^3(13)[R_2^2(8)]}$.

The **D[R]** pattern is not as unusual as we thought at first. In a study of hydrogen-bonding patterns in nine derivatives of trimethoprim (**22**),[61] we have found 21 occurrences of patterns of this type at the binary level. In addition to four more occurrences of $\mathbf{D_3^3(13)[R_2^2(8)]}$, that study yielded multiple occurrences of each of the graph sets listed in Scheme 2.

$\mathbf{D_3^3(9)[R_2^2(8)]}$	$\mathbf{D_3^3(11)[R_2^2(16)]}$	$\mathbf{D_3^3(13)[R_2^2(16)]}$
$\mathbf{D_3^3(13)[R_2^2(18)]}$	$\mathbf{D_3^3(14)[R_2^2(18)]}$	$\mathbf{D_3^3(15)[R_2^2(4)]}$
$\mathbf{D_3^3(15)[R_2^2(8)]}$	$\mathbf{D_3^3(16)[R_2^2(18)]}$	$\mathbf{D_3^3(17)[R_2^2(16)]}$
$\mathbf{D_3^3(20)[R_2^2(18)]}$		

Scheme 2. Examples of **D[R]** patterns for nine derivatives of **22**.

It is clear that hydrogen-bonding patterns in centrosymmetric crystals with crystallographically distinct moieties, for example, ionic structures, solvated structures, and those with $Z' > 1$, will be replete with the **D[R]** binary graph sets.

13. Toward a Hydrogen-Bond Pattern Functionality

We have demonstrated that graph set analysis provides the tools for a systematic analysis of the patterns of hydrogen-bonded networks. Moreover, in principle, the methodology for this analysis is straightforward. The actual process of analysis is still not automated, although efforts in this direction are now under way. However, the potential of such automated analyses is already evident, and we present here some examples.

As a natural consequence of the historical development of chemistry over the last century, in particular organic chemistry, chemists have been taught to think in terms of chemical functional groups or chemical functionality. Virtually every basic organic chemistry text is organized according to this classification. The mention of aldehydes, ketones, amides, amines, or nitriles, for instance, evokes a whole series of mental associations such as group composition, group structure, methods of preparation, types of reactions, and physical properties. Similarly, associations elicited by the use of reaction mechanism notations (SN_1, E_2, etc.) convey a wealth of commonly understood and accepted information about a particular reaction mechanism, such as the types of molecules that can and cannot participate in a reaction type, the limiting conditions, expected products, stereochemistry, and many other characteristics and properties.

Graph set analysis of hydrogen-bonded systems potentially provides a means for analyzing a large number of structures and for seeking systematic correlations between the resultant patterns that demonstrate a *hydrogen bond pattern functionality*. This pattern functionality can be easily recognized in the concept of *isographic* relationships, as originally defined by Etter[2] (that is, chemically different functional groups having the same graph set are described as isographic).

Because hydrogen bonding is perhaps the most dominant mechanism for molecular recognition, such a classification scheme will allow us to define the hydrogen-bonding patterns by which molecules "recognize" each other. Cataloguing the hydrogen-bond graph sets for a wide variety of hydrogen-bonding groups can illuminate hydrogen bond pattern functionality, which can cut across the traditional boundaries of chemical functionality. In the same manner that chemical functionality can be used to predict reaction products and stereochemistry, and to design molecules and synthetic routes, so hydrogen bond pattern functionality might then be employed to predict the three-dimensional structure of a compound or complex, or to design substances with a desired and predetermined structure.

Some of these functionalities have been revealed almost as a matter of course in the preceding discussion. For instance, the homodromic[116] $\mathbf{R_2^2(8)}$ pattern—in a variety of different forms—is pervasive, the best-known example probably being the hydrogen-bonded carboxylic acid dimer. It was the presence of the $\mathbf{R_2^2(8)}$ pattern that prompted our recognition of the C–H $\cdots$ O hydrogen bonding in **5** (Fig. 4). In addition to the many

examples included here, the $\mathbf{R_2^2(8)}$ pattern also appears in Watson–Crick base pairing.[3] Our study[61] of trimethoprim (**22**) has yielded many more instances of this pattern that involve 2,4-diaminopyrimidine hydrogen bonding at the unitary level, arranged either as **23a** or **23b**.[62]

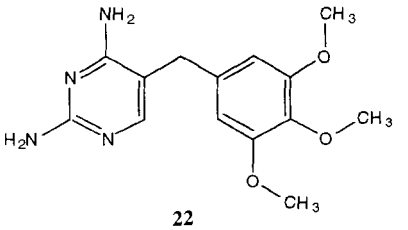

22

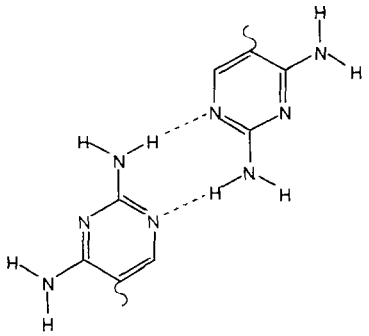

23a

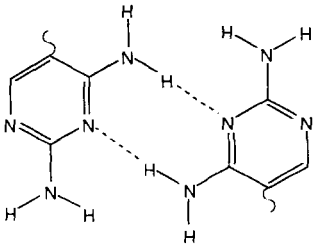

23b

Our curiosity piqued by the frequent occurrences of homodromic $\mathbf{R_2^2(8)}$ just cited, we carried out a preliminary survey of the CSD for the centrosymmetric (or pseudocentrosymmetric) $\mathbf{R_2^2(8)}$ pattern **24**, in which D represents a donor, A represents an acceptor, X is any element, and the X–A and X–D bonds are of any order. This survey revealed more than 2800 occurrences of pattern **24** in more than 2400 structures including more than 80 different element combinations represented by D, X, and A. Though we have just begun to analyze the chemical functional groups represented, it is already clear that dozens of chemical functionalities are represented in this single hydrogen-bond pattern.

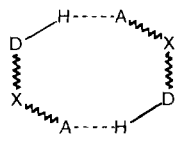

24

In trimethoprim salts, the 2,4-diaminopyrimidinium group is often involved in binary-level heterodromic[116] $\mathbf{R_2^2(8)}$ arrangements in which both donors are on the protonated trimethoprim and both acceptors are on the anion; these are shown schematically as **25a** and **25b**. In the three trimethoprim structures of type **25a**, the anions are all different; A–X–A represents, variously, O–C–O of benzoate or of acetate and O–S–O of ethylsulfonate. Yet another trimethoprim derivative, a cocrystal with barbital,[63] gives a more involved pattern (**26**) but still one based at the binary level on $\mathbf{R_2^2(8)}$.

The potential power of the concept of hydrogen bond pattern functionality is further demonstrated by considering the pattern $\mathbf{R_4^2(8)}$ (**27**), which is a characteristic binary graph of primary amides (Fig. 15a). Because this pattern generally involves four molecules routine searches for the presence of individual hydrogen bonds would not easily reveal it. $\mathbf{R_4^2(8)}$ also appears when primary amides form cocrystals, for example in (*N*-acetyl-

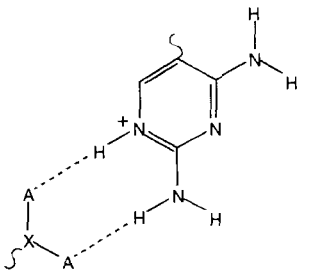

25a

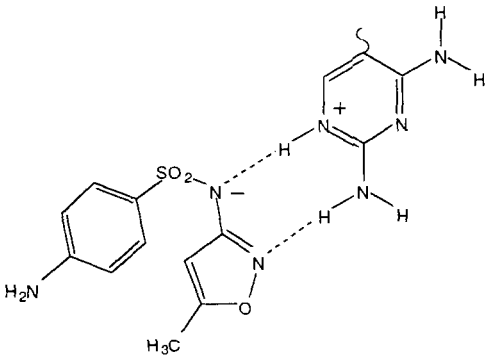

25b

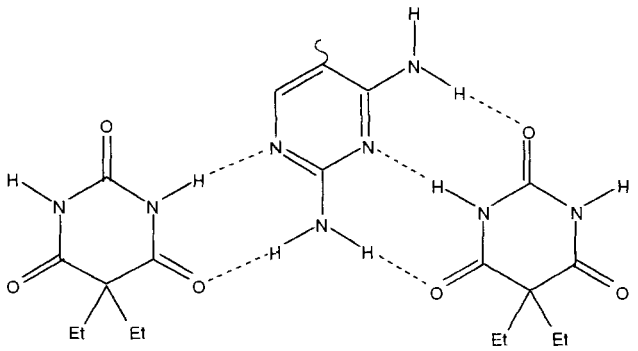

26

acetamide)–(4-hydroxybenzamide) structure (Fig. 15b). We have also seen this in the chemically very different compound, iminodiacetic acid (**16**), in particular in the quaternary graph set of Form 2 (Fig. 15c; also see Appendix). We can go even farther afield chemically with, for example, the complex (1-methylcytosine)–(5-fluorouracil) (Fig. 15d),[64] and with a series of cocrystals between nitroanilines and triphenylphosphine oxide and its derivatives (Fig. 15e).[65] Our exposure to this pattern from these structures made it readily recognizable in α-$Me_4NOH \cdot 2H_2O$, in which D is $O(H_2O)$ and A is OH^-. The same pattern is observed when the hydrogen-bond acceptor is changed from oxygen (neutral or charged) to a halide (D is $O(H_2O)$, and A is X^- in $[Zn(en)_3]F_2 \cdot H_2O$, $Et_4NCl \cdot H_2O$, and $[(CH_2)_6N_4CH_3]Br \cdot H_2O$]).[66–69] In his thorough survey of interactions of water and ionic halides, Rowland has observed the same

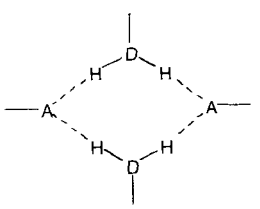

27

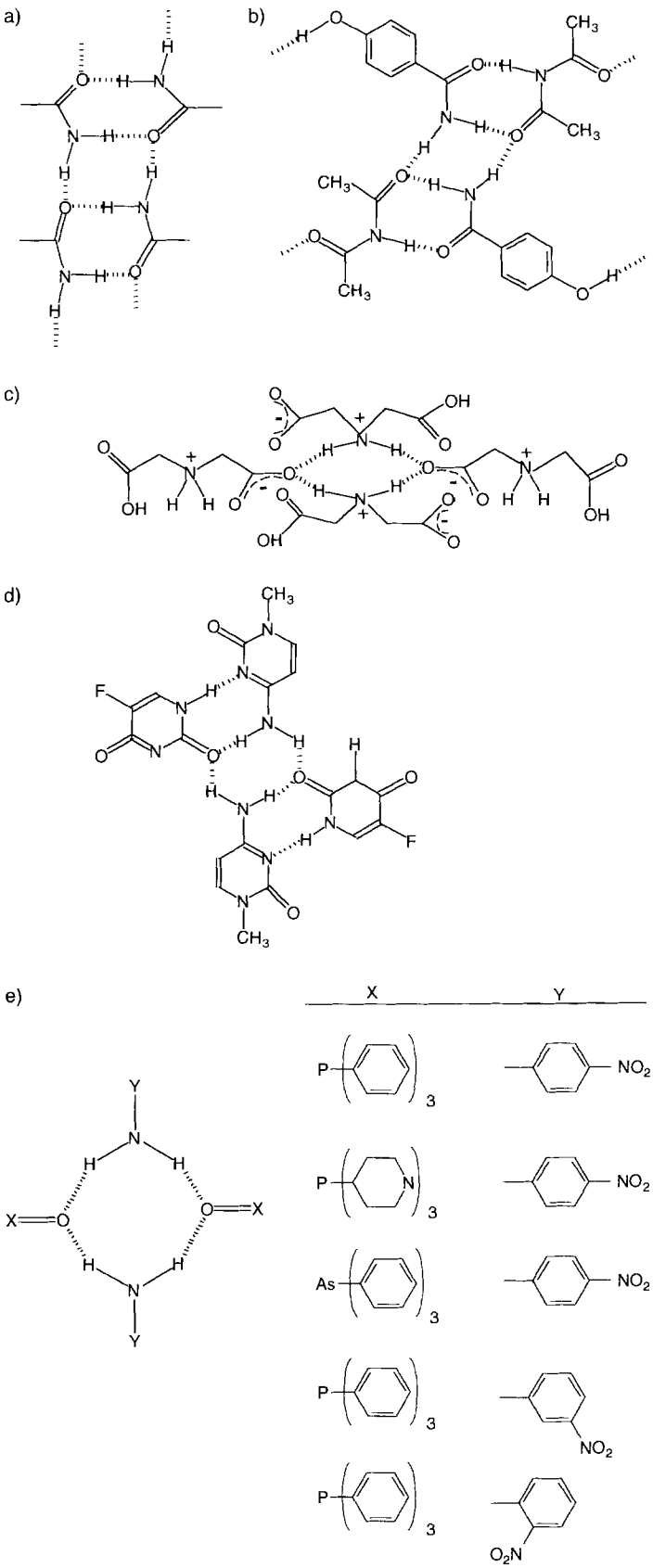

Fig. 15. The $\mathbf{R_4^2(8)}$ hydrogen bond pattern functionality in a variety of compounds. a) The second-level graph set of benzamide (benzene rings have been omitted); b) the fourth-level graph set of the cocrystal of (*N*-acetylacetamide)–(4-hydroxybenzamide); c) the quaternary graph set of iminodiacetic acid (**16**), polymorph 2; d) the cocrystal (1-methylcytosine)–(5-fluorouracil); e) the series of five cocrystals between nitroanilines and some R_3(P,As) oxides.

pattern (D is $O(H_2O)$, A is Cl^-).[70] Salts of trimethoprim[61] in which D is $N(NH_2)$, and A is $-O^-$ (in the benzoate)[71] or $^-O\text{-}SO_2CH_2CH_3$ (in the ethyl sulfonate[72]) further illustrate the pervasiveness of the $\mathbf{R_4^2(8)}$ pattern, even though the anions and the crystal structures are very different. The intramolecular manifestation of $\mathbf{R_4^2(8)}$, denoted as $\mathbf{S_4^2(8)}$, is also seen, for example, at the quaternary level in *trans*-dinitro(1,10-diamino-4,7-diazadecane)cobalt(III) bromide (**28**).[73] Even from this relatively small sampling of structures we can already see that $\mathbf{R_4^2(8)}$, together with its intramolecular analogue $\mathbf{S_4^2(8)}$, is a pattern that includes many traditionally classified chemical functionalities.

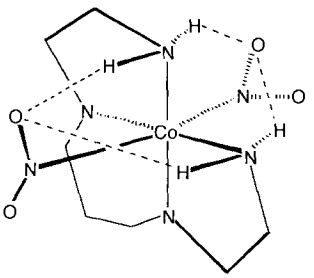

28

Until now, recognition of the patterns of hydrogen bonding has depended a great deal on serendipity: on which structures were being analyzed, usually for other reasons, and the chance possibility of human recognition of some unexpected, but persistent pattern. The steps we are taking to automate and to systematize the process of assigning graph sets will facilitate application of this methodology in a diagnostic as well as a descriptive mode. The incorporation of pattern-recognition software into structural search software should largely obviate the need for the arbitary human intervention and chemical intuition that was previously the order of the day. This will allow chemists more readily to recognize and correlate patterns that characterize hydrogen bond pattern functionality, which we believe holds great promise for analyzing and understanding the way molecules aggregate both in crystals and in solution.

14. Summary and Outlook

This paper reviews much of our current thinking on the use of graph sets in interpreting and understanding hydrogen-bonding patterns. We have demonstrated that it already allows rather complicated networks to be described in an efficient shorthand manner for the comparison and cataloguing of a large variety of structures. Moreover, we have found that the very process of working out the graph sets for any particular structure yields considerable insight into the nature of the hydrogen bonding in particular and the packing in general. We expect that as more specific software becomes available for generating the hydrogen-bond networks and their corresponding graph sets and presenting them in a convenient way, the method will become an even more useful tool for the diagnosis, analysis, understanding, and prediction of supramolecular aggregates dominated by hydrogen bonds.

There is still much to be done to develop this methodology for more complex systems. For instance, there are additional features of molecular and crystal structures in general, and hydrogen-bonded structures in particular, that one would like to include in the shorthand notation described here. These include branched chains, "ladder"-type chains, ribbons, sheets, double layers, and helices. Many of these can indeed be described using

the current nomenclature, but there appear to be distinguishing characteristics between similar structures, say sheets of various kinds, that are not immediately apparent from the graph set description as we have developed it to this point. Just as the work presented here represents progress due to our accumulated experience in working out problems encountered in the recent past, we expect that the solutions to many of the challenges mentioned above will come as we continue to expand the application of the method to increasingly knotty problems.

Appendix - A Reanalysis of Iminodiacetic Acid

At a number of points we have referred here to the graph set analysis of trimorphic iminodiacetic acid (**16**). This comprised one of our early attempts to use the methodology described here to define the differences and similarities among polymorphs characterized by rather complex hydrogen-bond networks.[5] In polymorph Form 2 of this system there are two molecules in the asymmetric unit. At the time we carried out this analysis we were not aware of the importance of considering crystallographically independent hydrogen atoms (and hydrogen bonds) separately as we have prescribed here. This was due in part to the fact that in this system the pairs of chemically equivalent hydrogen atoms on the two independent molecules have the same hydrogen bonding properties (as noted in ref. [5]). We now know that Form 2 must be analyzed in terms of six, rather than three, hydrogen atoms that participate in hydrogen bonds. That analysis and a comparison with the earlier results are presented here.

Each of the six independent hydrogen atoms participates in one hydrogen bond (Fig. 16). Hence the first-level graph set

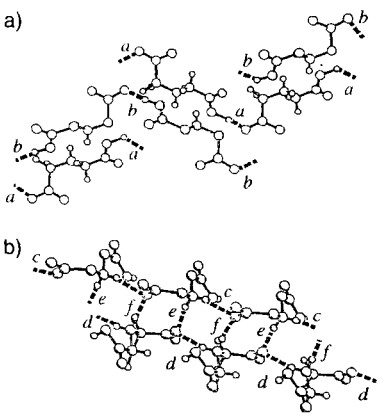

Fig. 16. Hydrogen-bond patterns of Form 2 of iminodiacetic acid (**16**), adapted from ref. [3]. The pattern is best understood from two separate drawings: a) the **C(8)** motifs for the two crystallographically independent carboxylic hydrogen atoms; b) the four motifs for the four amino hydrogen atoms. The six motifs combine to give the unitary network.

contains six motif descriptors, $\mathbf{N_1}$ = **DDC(5)C(5)C(8)C(8).** The identical hydrogen-bonding properties of the chemically equivalent hydrogen atoms on the two molecules are suggested here. At the binary level there are fifteen possible unique, pairwise combinations of the six hydrogen bonds. As indicated in Table 3, four of those are not defined, because all paths connecting the two hydrogen bonds traverse other hydrogen bonds. The chemical equivalency of the hydrogen bonds from the two molecules is reflected in the commutative identity of the graph sets of five pairs of combinations. The remaining binary graph set is $\mathbf{R_2^2(10)}$, which appeared at the unitary level in the earlier analysis that ignored the crystallographic nonequivalence of the two molecules.

Table 3. Unitary motifs (on-diagonal) and binary graph sets (off-diagonal) for iminodiacetic acid, Form 2.

Type of H-Bond Participating atomo	*a* H(1)A···O	*b* H(1)B···O	*c* H(2)A···O	*d* H(2)B···O	*e* H(3)A···O	*f* H(3)B···O
a H(1)A···O	**C(8)**					
b H(1)B···O	[a]	**C(8)**				
c H(2)A···O	$\mathbf{C_2^2(10)}$	[a]	**C(5)**			
d H(2)B···O	[a]	$\mathbf{C_2^2(10)}$	[a]	**C(5)**		
e H(3)A···O	$\mathbf{D_2^2(8)}$	$\mathbf{D_2^2(10)}$	$\mathbf{D_3^3(10)}$	$\mathbf{D_3^3(8)}$	**D**	
f H(3)B···O	$\mathbf{D_2^2(10)}$	$\mathbf{D_2^2(8)}$	$\mathbf{D_3^3(8)}$	$\mathbf{D_3^3(10)}$	$\mathbf{R_2^2(10)}$	**D**

[a] No link at binary level.

It is recalled that for Form 1 $\mathbf{N_1}$ = **C(5)C(8)$\mathbf{R_2^2}$(10)** and for Form 3 $\mathbf{N_1}$ = **C(5)C(5)C(8),** so the earlier analysis of Form 2 as **C(5)C(8)$\mathbf{R_2^2}$(10)** had indicated at the unitary level that Form 1 and Form 2 were equivalent. This is no longer true. Further, the graph set feature that did distinguish between them, $\mathbf{R_4^2(8)}$, now appears at the quaternary level for Form 2 (hydrogen bonds *c*, *e*, *d*, *f*), rather than at the binary level.

I do not presume to think that this treatise settles every doubt in the minds of those who understand it, but I maintain that it settles the greater part of their difficulties. No intelligent man will require and expect that on introducing any subject I shall completely exhaust it; or that on commencing the exposition of a figure, I shall explain all its parts. Such a course could not be followed by a teacher in a viva voce exposition, much less by an author in writing a book, without becoming a target for every foolish conceited person to discharge the arrows of folly at him.[11]

We were introduced to the realm of graph set analysis of hydrogen bonds by the late Margaret C. Etter, whose insight was inspirational and whose enthusiasm was contagious. We had the good fortune to discuss many of the aspects of this work with her prior to her death on June 10, 1992. In some ways this paper is but a very modest attempt to perpetuate a part of her considerable scientific legacy, achieved in a tragically shortened scientific career. While many of the ideas were thrashed out in our discussions and correspondence with her, the full responsibility for this work lies with us. We hope we are true to her spirit. J. B. and R. E. D. thank Dr. Olga Kennard for her hospitality at the Cambridge Crystallographic Data Center where early drafts of this paper were prepared and discussed. J. B. acknowledges a grant from the Israel Academy of Sciences (Jerusalem). Part of the work of L. S. was also supported by the US-Israel Binational Science Foundation (Jerusalem). The work in Austin (R. E. D., N-L. C.) was supported in part by the Robert A. Welch

Foundation (Grant F-233). John MacDonald of Professor Etter's group at the University of Minnesota provided advice, corrections, criticism, and encouragement throughout the development of our ideas and this work; we are indeed grateful to him. Dr. Geoffrey Khan of the Cambridge University Library assisted in locating the preambulary and postscript quotations from Maimonides.

Received: March 22, 1994 [A 571E]
German version: *Angew. Chem.* **1995**, *107*, 1687–1706

[1] From the Introduction to "The Guide of the Perplexed" by the medieval Jewish philosopher/physician, Rabbi Moshe ben Maimon, also known as the Rambam or Maimonides.

[2] M. C. Etter, *Acc. Chem. Res.* **1990**, *23*, 120.
[3] M. C. Etter, J. C. MacDonald, J. Bernstein, *Acta Crystallogr. Sect. B* **1990**, *46*, 256.
[4] M. C. Etter, *J. Phys. Chem.* **1991**, *95*, 4601.
[5] J. Bernstein, M. C. Etter, J. C. MacDonald, *J. Chem. Soc. Perkin Trans. 2* **1990**, 695.
[6] J. Bernstein, *Acta Crystallogr. Sect. B* **1991**, *47*, 1004.
[7] C. Andre, P. Luger, R. Bach, J. H. Fuhrhop, *Carbohydr. Res.* **1995**, *266*, 15; L. Shimoni, J. P. Glusker, C. W. Bock, *J. Phys. Chem.* **1995**, *99*, 1194; J. C. MacDonald, G. M. Whitesides, *Chem. Rev.* **1994**, *94*, 2383; C. B. Aakeroy, M. Nieuwenhuyzen, *J. Am. Chem. Soc.* **1994**, *116*, 10983; L. Shimoni, J. P. Glusker, *Struct. Chem.* **1994**, *5*, 383; G. Ferguson, J. F. Gallagher, C. Glidewell, C. M. Zakaria, *Acta Crystallogr. Sect. B* **1994**, *50*, 146; C. Glidewell, C. M. Zakaria, G. Ferguson, *Acta Crystallogr. Sect. C* **1994**, *50*, 678; C. Glidewell, G. Ferguson, *ibid.* **1994**, *50*, 924; G. Ferguson, C. Glidewell, C. M. Zakaria, *ibid.* **1994**, *50*, 928; J. F. Gallagher, G. Ferguson, C. Glidewell, C. M. Zakaria, *ibid.* **1994**, *50*, 18; G. Ferguson, J. F. Gallagher, C. Glidewell, C. M. Zakaria, *ibid.* **1994**, *50*, 70; C. Glidewell, C. M. Zakaria, G. Ferguson, J. F. Gallagher, *ibid.* **1994**, *50*, 233; C. Glidewell, G. Ferguson, *ibid.* **1994**, *50*, 1362; G. Ferguson, J. F. Gallagher, J. N. Low, R. A. Howie, *ibid.* **1993**, *49*, 2162; C. G. Choo, S. D. Rychnovsky, M. C. Etter, *Chem. Mater.* **1994**, *6*, 1200; V. A. Russell, M. C. Etter, M. D. Ward, *ibid.* **1994**, *6*, 1206; J. H. Loehlin, M. C. Etter, C. Gendreau, E. Cervasio, *ibid.* **1994**, *6*, 1218; M. D. Hollingsworth, M. E. Brown, B. D. Santarsiero, J. C. Huffman, C. R. Goss, *ibid.* **1994**, *6*, 1227; M. Kaftory, M. Kapon, M. Botoshansky, *ibid.* **1994**, *6*, 1245; C. P. Brock, L. L. Duncan, *ibid.* **1994**, *6*, 1307; K. A. Wheeler, B. M. Foxman, *ibid.* **1994**, *6*, 1330; A. Ellern, J. Bernstein, J. Y. Becker, S. Zamir, L. Shahal, S. Cohen, *ibid.* **1994**, *6*, 1378; S. Bhattacharya, P. Dastidar, T. N. G. Row, *ibid.* **1994**, *6*, 531; L. Shimoni, H. L. Carrell, J. P. Glusker, M. M. Coombs, *J. Am. Chem. Soc.* **1994**, *116*, 8162; V. A. Russell, M. C. Etter, M. D. Ward, *ibid.* **1994**, *116*, 1941; C. Glidewell, G. Ferguson, A. J. Lough, C. M. Zakaria, *J. Chem. Soc. Dalton Trans.* **1994**, 1971; P. Lightfoot, C. Glidewell, P. G. Bruce, *J. Organomet. Chem.* **1994**, *466*, 51; A. Gavezzotti, G. Filippini, *J. Phys. Chem.* **1994**, *98*, 4831; D. Braga, F. Grepioni, P. Sabatino, G. R. Desiraju, *Organometallics* **1994**, *13*, 3532 (see also: G. R. Desiraju, *Angew. Chem.* **1995**, *107*; *Angew. Chem. Int. Ed. Engl.* **1995**, *34*, in press); S. R. Byrn, R. R. Pfeiffer, G. Stephenson, D. J. W. Grant, W. B. Gleason, *Chem. Mater.* **1994**, *6*, 1148; E. A. Genkina, *Kristallografiya* **1994**, *39*, 641; G. Ferguson, J. F. Gallagher, C. Glidewell, C. M. Zakaria, *Acta Crystallogr. Sect. B* **1994**, *50*, 146; C. B. Aakeroy, K. R. Seddon, *Chem. Soc. Rev.* **1993**, *22*, 397; J. Yang, E. K. Fan, S. J. Geib, A. D. Hamilton, *J. Am. Chem. Soc.* **1993**, *115*, 5314; G. Gilli, V. Bertolasi, V. Ferretti, P. Gilli, *Acta Crystallogr. Sect. B* **1993**, *49*, 564; T. Steiner, W. Hinrichs, W. Saenger, R. Gigg, *ibid.* **1993**, *49*, 708; G. Ferguson, J. F. Gallagher, C. Glidewell, C. M. Zakaria, *Acta Crystallogr. Sect. C* **1993**, *49*, 967; S. Ianelli, M. Nardelli, D. Belletti, B. Jamartgregoire, N. Brosse, P. Caubere, *ibid.* **1993**, *49*, 1098; P. Lightfoot, M. Tremayne, C. Glidewell, K. D. M. Harris, P. G. Bruce, *J. Chem. Soc. Perkin Trans. 2* **1993**, 1625; K. D. M. Harris, N. M. Stainton, A. M. Callan, R. A. Howie, *J. Mater. Chem.* **1993**, *3*, 947; S. Ghosh, D. A. Adsmond, J. Huotari, D. J. W. Grant, *J. Pharm. Sci.* **1993**, *82*, 901; J. Bernstein, *J. Phys. D* **1993**, *26*, B66; S. Larsen, H. L. Dediego, *Acta Crystallogr. Sect. B* **1993**, *49*, 303; T. Steiner, W. Saenger, *J. Am. Chem. Soc.* **1992**, *114*, 10146; C. B. Aakeroy, G. S. Bahra, P. B. Hitchcock, Y. Patell, K. R. Seddon, *J. Chem. Soc. Chem. Commun.* **1993**, 152; F. Pertlik, W. Mikenda, E. Steinwender, *J. Crystallogr. Spectrosc. Res.* **1993**, *23*, 389; J. G. Stowell, P. H. Toma, S. R. Byrn, *Bioorg. Med. Chem. Lett.* **1992**, *2*, 185; N. M. Stanton, K. D. M. Harris, R. A. Howie, *J. Chem. Soc. Chem. Commun.* **1991**, 1781; S. Arumgam, C. Glidewell, K. D. M. Harris, *ibid.* **1992**, 724; C. B. Aakeroy, P. B. Hitchcock, K. R. Seddon, *ibid.* **1992**, 553; R. G. Ball, M. W. Baum, *J. Org. Chem.* **1992**, *57*, 801; R. M. Reutzel, M. C. Etter, *J. Phys. Org. Chem.* **1992**, *5*, 44; D. Braga, *Chem. Rev.* **1992**, *92*, 633; M. C. Etter, D. Britton, S. M. Reutzel, *Acta Crystallogr. Sect. C* **1991**, *47*, 561; M. C. Etter, S. M. Reutzel, *J. Am. Chem. Soc.* **1991**, *113*, 2586; M. A. Kennedy, R. R. Vold, R. L. Vold, *J. Magn. Reson.* **1991**, *91*, 301; M. C. Etter, Z. Urbanczyklipkowska, M. Zia-Ebrahimi, T. W. Panunto, *J. Am. Chem. Soc.* **1990**, *112*, 8415.
[8] Note that a hydrogen bond from a cation to an anion, or from a molecule to a cocrystallized solvent molecule must be denoted in the first level as **D**. A discrete set that involves more than one hydrogen bond (binary or higher level) would necessarily have more than one donor and/or acceptor and more than two atoms in the pattern, so the subscript, superscript, and parenthetic notation of degree would all be required.
[9] This would correspond to a different *level* of the graph set assignment (see Section 3).
[10] L. F. Power, K. E. Turner, F. H. Moore, *Acta Crystallogr. Sect B.* **1976**, *32*, 11; P.-P. Legros, A. Kvick, *ibid.* **1980**, *36*, 3052.
[11] The appearance of these more complex ring notations in some automatic fashion, for example, in a computerized graph set assignment procedure, would be an indication of such an extended ring pattern. The ring system shown here is a pervasive feature in crystal structures of the amino acids.
[12] R. Taylor, O. Kennard, *J. Am. Chem. Soc.* **1982**, *104*, 5063.
[13] F. H. Allen, J. E. Davis, J. J. Galloy, O. Johnson, O. Kennard, C. F. McCrae, E. M. Mitchell, G. F. Mitchell, J. M. Smith, D. G. Watson, *J. Chem. Inf. Comput. Sci.* **1991**, *31*, 187.
[14] R. Taylor, O. Kennard, W. Versichel, *Acta Crystallogr. Sect. B* **1984**, *40*, 280.
[15] R. Taylor, O. Kennard, W. Versichel, *J. Am. Chem. Soc.* **1984**, *106*, 244.
[16] G. A. Jeffrey, W. Saenger, *Hydrogen Bonding in Biological Structures*, Springer, New York, **1991**, Chapter 2.
[17] G. A. Jeffrey, H. Maluszynska, *Int. J. Biol. Macromol.* **1982**, *4*, 173.
[18] L. Pauling, *The Nature of the Chemical Bond*, 3rd ed.; Cornell University Press, New York, **1960**, p. 6.
[19] a) S. K. Burley, G. A. Petsko, *FEBS Lett.* **1986**, *203*, 139; b) S. K. Burley, G. A. Petsko, *Science*, **1985**, *229*, 23; c) M. Levitt, M. F. Perutz, *J. Molec. Biol.* **1988**, *201*, 751; d) G. A. Jeffrey, W. Saenger, *Hydrogen Bonding in Biological Structures*, Springer, New York, **1991**, Chapters 10 and 11.
[20] J. Donohue in *Structural Chemistry and Molecular Biology* (Eds.: A. Rich, N. Davidson), W. H. Freeman, San Francisco, **1968**, pp. 443–465.
[21] T. Sakurai, *Acta Crystallogr.* **1965**, *19*, 320; *Acta Crystallogr. Sect. B* **1968**, *24*, 403.
[22] This figure has been redrawn from one in J. Bernstein, M. D. Cohen, L. Leiserowitz, in *Chemistry of the Quinones* (Ed.: S. Patai), John Wiley, **1974**, pp. 37–110. The caption used in that chapter is repeated here. Note the use of the term "contacts" rather than "hydrogen bonds".
[23] J. Gaultier, C. Hauw, *Acta Crystallogr.* **1965**, *18*, 179.
[24] J. Bernstein, E. Harlev, unpublished results.
[25] The following discussion is based on the assumption of the availability of rather primitive software for calculating geometry and plotting crystal structures. Surprisingly, very few of the currently available molecular modeling software packages have convenient means for displaying and analyzing *crystal* structures, as opposed to *molecular* structures.
[26] One of the problems in developing the graph sets stems from the necessity in most cases to generate rather extended descriptions of the *crystal structure*, including the hydrogen bonding, rather than simply the *molecular* structure or the "view of the packing" that are sometimes automatically generated. The latter generally does not include sufficient numbers of molecules to portray all the specific intermolecular interactions. In many cases, a single view of the crystal structure, even in stereo, is difficult to interpret. Software for readily generating and rotating crystal structures with a number of unit cells considerably facilitates this task, and will make the examination of crystal structures and the assignment of their hydrogen-bonding graph sets a much more common practice.
[27] A. I. Kitaigorodsky, *Organic Chemical Crystallography*, Consultants' Bureau, New York, **1955**.
[28] L. Shimoni, M. Sc. Thesis, Ben-Gurion University of the Negev, Beer Sheva, Israel, **1992**.
[29] J. Donohue, *J. Am. Chem. Soc.* **1950**, *72*, 949.
[30] M. S. Lehmann, T. F. Koetzle, W. C. Hamilton, *J. Am. Chem. Soc.* **1972**, *94*, 2657.
[31] T. Taniguchi, Y. Takaki, K. Sakura, *Bull. Chem. Soc. Jpn.* **1980**, *53*, 803.
[32] In this admonition, the word "all" must be taken in the light of the infinite number of increasingly larger ring systems that appear in a mesh such as that discussed earlier for α-glycine.
[33] a) T. W. Panunto, Z. Urbanczyk-Lipkowska, R. Johnson, M. C. Etter, *J. Am. Chem. Soc.* **1987**, *109*, 7786; b) The two hydrogen bonds are crystallographically distinct and should be treated separately, as discussed in Section 5.
[34] E. Martuscelli, G. Avitabile, *Ric. Sci.* **1967**, *37*, 102.
[35] J. L. Derissen, P. H. Smit, *Acta Crystallogr. Sect. B* **1974**, *30*, 2240.
[36] G. Avitabile, P. Ganis, E. Martuscelli, *Acta Crystallogr. Sect. B* **1969**, *25*, 2378.
[37] G. Avitabile, P. Ganis, U. Lepore, *Macromolecules* **1971**, *4*, 239.
[38] E. Martuscelli, E. Benedetti, P. Ganis, C. Pedone, *Acta Crystallogr.* **1967**, *23*, 747.
[39] P. Ganis, P. A. Temussi, M. G. Northolt, L. E. Alexander, *J. Phys. Chem.* **1968**, *23*, 747.
[40] The nomenclature for distinguishing polymorphs has never really been standardized [41]. To avoid even further confusion than already exists in the literature we have chosen in the following discussion to use the names of the

polymorphs as they appear in the original literature that is cited here. This has been done at the expense of consistency in style in this paper.
[41] J. Haleblian, W. C. McCrone, *J. Pharm. Sci.* **1969**, *58*, 911.
[42] B. M. Craven, E. A. Vizzini, A. Rodrigues, *Acta Crystallogr. Sect. B* **1969**, *25*, 1978.
[43] J. C. Moore, A. Yeadon, *J. Crystallogr. Spectrosc. Res.* **1983**, *13*, 279.
[44] J. C. Moore, A. Yeadon, *J. Crystallogr. Spectrosc. Res.* **1984**, *14*, 283.
[45] J. C. Moore, R. A. Palmer, A. Yeadon, *Acta Crystallogr. Sect. A* **1978**, *34*, 97.
[46] The relative orientation of the two independent molecules in Form 3 suggested to us the possibility of a previously unrecognized element of symmetry (inversion center or twofold axis); a careful check of relationships among the coordinates revealed that no such relationship exists.
[47] G. E. Hardy, W. C. Kaska, B. P. Chandra, J. I. Zink, *J. Am. Chem. Soc.* **1981**, *103*, 1074.
[48] C. J. Brown, *Proc. R. Soc. London A* **1968**, *302*, 185; C. J. Brown, M. Ehrenberg, *Acta Crystallogr. Sect. C* **1985**, *41*, 441.
[49] Anonymous, *Anal. Chem.* **1949**, *21*, 1016.
[50] P. R. Arnold, F. Jones, *Mol. Crystallogr. Liq. Crystallogr.* **1972**, *19*, 133.
[51] D. A. d'Avignon, T. L. Brown, *J. Phys. Chem.* **1981**, *85*, 4073.
[52] W. H. Ojala, M. C. Etter, *J. Am. Chem. Soc.* **1993**, *114*, 10288.
[53] C. D. G. Boone, J. L. Derissen, J. C. Schoone, *Acta Crystallogr. Sect. B* **1977**, *33*, 3205.
[54] H. Takezawa, S. Ohba, Y. Saito, *Acta Crystallogr. Sect. C* **1986**, *42*, 1880.
[55] W. C. Hamilton, *Acta Crystallogr.* **1965**, *18*, 866; G. A. Jeffrey, G. Ruble, *Acta Crystallogr. Sect. B* **1980**, *36*, 2292; T. Ottersen, *Acta Chem. Scand. Ser. A* **1975**, *29*, 939.
[56] W. A. Deene, R. W. Small, *Acta Crystallogr. Sect. B* **1971**, *27*, 1094; F. Senti, D. Hakker, *J. Am. Chem. Soc.* **1940**, *62*, 2008.
[57] G. A. Jeffrey, W. Saenger, *Hydrogen Bonding in Biological Structures*, Springer, New York, **1991**, Chapter 13.
[58] J. A. Kanters, G. Roelofson, L. H. Straver, *Acta Crystallogr. Sect. B* **1978**, *34*, 1393.
[59] J. A. Kanters, G. Roelofson, L. H. Straver, *ibid.* **1978**, *34*, 1396.
[60] The original graph set specifications [3] prescribed the degree of a **D** motif as "the number of atoms in the entire length of the hydrogen-bonded set starting with the proton of the first hydrogen bond, proceeding along the shortest pathway, and ending with the acceptor atom in the last hydrogen bond of the set". Following those instructions would lead to degree 12 for the binary pattern shown in Fig. 14c; that description would mislead, as it does not encompass all the hydrogen bonds that link the discrete cluster. The guideline should be amended so that the degree **n** includes counting through all hydrogen bonds, that is, including all donors and acceptors. The same conclusion was reached by J. C. MacDonald (Ph.D. Dissertation, University of Minnesota, **1993**).
[61] R. E. Davis, H. Robb, V. Cody, unpublished.
[62] H. Nakai, M. Takasuka, M. Shiro, *J. Chem. Soc. Perkin Trans. 2* **1984**, 1459.
[63] N. Shimizu, S. Nishigaki, Y. Nakai, K. Osaki, *Acta Crystallogr. Sect. B* **1982**, *38*, 2309.
[64] S.-H. Kim, A. Rich, *J. Mol. Biol.* **1969**, *42*, 87.
[65] M. C. Etter, K. S. Huang, G. M. Frankenbach, D. Adsmond in *Materials for Nonlinear Optics, Chemical Perspectives* (Eds.: S. R. Marder, J. E. Sohn, G. C. Stucky) (*ACS Symp. Ser.* **1991**, *455*, 446–455.
[66] D. Mootz, R. Seidel, *J. Inclusion. Phenom. Mol. Recognit. Chem.* **1990**, *8*, 139.
[67] J. Emsley, M. Arif, P. A. Bates, M. B. Hursthouse, *J. Chem. Soc. Chem. Commun.* **1989**, 738; *Inorg. Chim. Acta* **1989**, *165*, 191.
[68] T. C. W. Mak, S. P. So, C. Chieh, K. S. Jasim, *J. Mol. Struct.* **1985**, *127*, 375; J. Gao, S. Boudon, G. Wipff, *J. Am. Chem. Soc.* **1991**, *113*, 9610; E. F. Kleinman, J. Bordner, B. J. Newhouse, K. MacFerrin, *ibid.* **1992**, *114*, 4945.
[69] T. C. W. Mak, *Inorg. Chem.* **1984**, *23*, 620.
[70] R. S. Rowland, Cambridge Crystallographic Data Centre (UK), personal communication.
[71] G. Guiseppetti, C. Tadini, G. P. Bettinetti, F. Giordano, A. La Manna, *Acta Crystallogr. Sect. C* **1984**, *40*, 650.
[72] V. Cody, *Acta Crystallogr. Sect. C* **1984**, *40*, 1000.
[73] N. C. Payne, *Inorg. Chem.* **1972**, *11*, 1376.

Exciting Results from the Field of Homogeneous Two-Phase Catalysis

Boy Cornils*

With the advent of two-phase catalysis, the last and in fact inherent disadvantage of homogeneous catalysis relative to its heterogeneous counterpart appears to have been swept away. This breakthrough has been achieved by arranging the process such that, at least when reaction is complete, the organometallic complex serving as a catalyst on one hand, and the reaction product (and residual starting material) on the other, are located in different phases, so a simple phase separation is sufficient for isolating the product from the catalyst (which may then be introduced immediately into another catalyst cycle).[1] The catalyst is situated in a mobile phase which, because it is confined within the reactor, also serves as an immobilization medium. Interestingly, quite atypically, the principle itself was implemented on a large (ca. 10^6 tonnes per annum) scale in industry in the Shell higher olefins process (SHOP), as well as the Ruhrchemie/Rhône–Poulenc oxo process even prior to the onset of comprehensive scientific investigation, initiated later by a number of academic research groups.[2] An indication of the significance of the process as far as the scientific world is concerned is the fact that the "standard ligand" for aqueous two-phase catalysis, triphenylphosphane trisulfonate (TPPTS), now appears in the Aldrich Catalogue of Fine Chemicals.

This elegant approach to catalyst separation has in turn led to intense preoccupation with possible laboratory and industrial applications of two-phase catalysis, as well as extension of the process into new areas. A series of important contributions to the literature has recently cast a rather bright spotlight in this direction.

Not surprisingly, the ideal form of the process is *aqueous* two-phase catalysis, in which the organometallic two-phase catalyst resides in a stationary aqueous solution in the reaction system. This is not only the most convenient arrangement on both the laboratory and industrial scale, but also the optimal modification with respect to cost and environmental considerations. Use of water as the second phase has its limitations, however, especially when the water solubility of the starting materials proves too low, preventing adequate transfer of organic substrate into the aqueous phase or at the phase boundary, and consequently reducing the reaction rate to such an extent that it becomes unacceptable. Cases like this can be dealt with by introducing a surfactant (or by using ligands that confer surfactant properties), but other alternatives include addition of a solvating agent that produces a quasi "mechanical" effect, or use perhaps of a cosolvent, two measures that presumably increase either the mutual solubility of the components or mobility across the phase boundaries. The effectiveness of additives of this type has been the subject of much controversy in the literature, and it depends heavily on such specific factors as the ligands and their purity, the nature and behavior of the substrate, the presence of miscibility gaps, and precise reaction conditions. From an engineering and economic standpoint it is also important to remember that any "foreign" additive will inevitably increase the difficulty and cost of purification, thereby mitigating the clear advantages associated with two-phase catalysis in its purest form.

Chaudhari et al.[3] were the first to suggest introducing "promoter ligands" soluble exclusively in the organic phase, thus altering the solubility of the complex *internally*. These authors were able to show through hydroformylation of the extremely water-insoluble 1-octene (equilibrium solubility in water at 298 K: 2.408×10^{-5} kmol m^{-3}; cf. propene, with a solubility of ca. 7×10^3 kmol m^{-3}) with $[HRh(CO)(TPPTS)_3]$ as catalyst that addition of triphenylphosphane to the 1-octene increases the reaction rate by a factor of 10–50. Ligand exchange during the course of the reaction leads to the formation of isolable mixed-ligand complexes of the type $[HRh(CO)(TPPTS)_{3-x}(TPP)_x]$ ($x = 0$–3). These display activities somewhat greater than is observed for catalysts modified only with TPPTS, though still inferior to the activity obtained by simple physical addition of TPP alone, a result that indicates the importance of as yet unexplained effects at the boundary surfaces of the two reaction phases (cf. Fig. 1).

With respect to the development of an industrial process for the hydroformylation of higher olefins (a challenge not yet met) it must of course be noted that the suggestion by Chaudhari et al. of adding a promoter ligand once again raises the problem of a "foreign substance," with the resulting need for a costly separation step. Nevertheless, these experiments do suggest that a search for ligands with carefully matched hydrophilic and hydrophobic characteristics may lead to a solution to the problem, provided the electronic characteristics of the oxo catalyst can be optimized simultaneously.

The foreign additive problem is avoided in an approach suggested by Jin, Fell, et al.,[4, 5] who have proposed a two-phase hydroformylation of higher olefins (up to 1-dodecene) based on replacing the ligands in $[HRh(CO)_4]$ with

[*] Prof. Dr. B. Cornils
Hoechst AG
D-65926 Frankfurt am Main (Germany)
Telefax: Int. code +(69)305-301954

 © VCH Verlagsgesellschaft mbH, D-69451 Weinheim, 1995 0570-0833/95/1515-1575 $ 10.00+.25/0

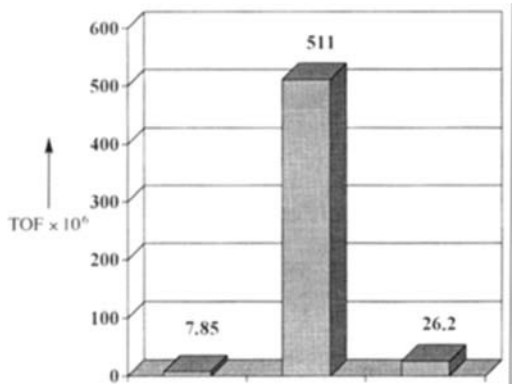

Fig. 1. Two-phase hydroformylation of 1-octene. Turnover frequencies (TOF) obtained under three different operating conditions: Column 1: Hydroformylation with $[HRh(CO)(TPPTS)_3]$. Column 2: Addition to **1** of 3.33×10^3 kmol TPP per m^3 of organic phase. Column 3: $[HRh(CO)(TPPTS)_{3-x}(TPP)_x]$. The TOF values indicate how many kmol of product per kg rhodium are formed per second.

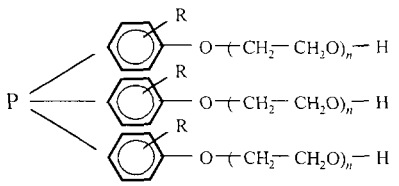

1, $n > 6$-8

ethoxylated tris(*p*-hydroxyphenyl)phosphanes of the structure indicated in **1**.

The corresponding Chemical Abstracts entry fails to provide any indication of the real novelty involved in the Chinese work, but the German version of the paper makes it clear that this particular oxo catalyst takes advantage of a temperature-dependent "cloud point" associated with the phosphorus-bound poly(alkylene glycol ether) ligands. Thus, above the cloud point the ligand (and thus the complex catalyst) loses its hydration shell, just as in the case of other compounds of this type, causing the two-phase reaction mixture normally obtained when olefin is added to the catalyst solution to merge into a single phase, thereby initiating a rapid transformation that is no longer impeded by material-transport problems. Subsequent lowering of the temperature causes the hydration shell to be reversibly restored, inducing the complex catalyst solution once again to separate this time from the reaction product (the desired higher aldehydes) as an independent phase. Since the agent responsible for the merger and subsequent separation of the phases is the appropriately custom-designed ligand itself, there is no call for investing extra effort in the removal and recycling of a foreign additive, and this must therefore be regarded as a promising avenue for further exploration on a commercially realistic scale.

Results reported in two other papers by Bergbreiter et al.[6] and Wan and Davis[7] take advantage of similar effects. Bergbreiter et al. applied the designation "smart ligands" in describing certain phosphorus-bound poly(alkylene oxide) oligomers that together with rhodium precursors form complexes with the structure **2**, complexes that display both hydrogenation and oxo activity. Here again, an inverse temperature dependency of the complex catalyst's solubility leads at high temperature to single-phase behavior and correspondingly increased reaction rates.

$[Rh(Cl)\{Ph_2P(CH_2CH_2O)_nCH_2CH_2PPh_2\}_{1.5}]$ **2**

Wan and Davis combined the possibilities inherent in the supported liquid phase catalysis (SLPC) and supported aqueous phase catalysis (SAPC) techniques with a modified water-soluble (and thus hydrophilic) ruthenium catalyst dissolved in ethylene glycol in their demonstration of an enantioselective hydrogenation of 2-(6′-methoxy-2′-naphthyl)-acrylic acid (**3**). The reaction leads to (*S*)-naproxene (**4**) with *ee* values as high as 96%. Ligand modification was accomplished with tetrasulfonated BINAP [2,2′-bis(diphenylphosphino)-1,1′-binaphthyl], which in conjunction with ruthenium chloride generates the active hydrogenation complex $[Ru(BINAP\text{-}4\text{-}SO_3Na)(C_6H_6)Cl]Cl$ (Scheme 1).

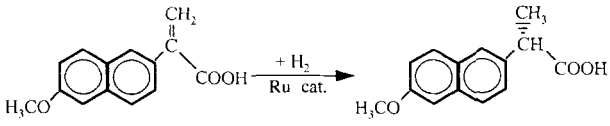

3 **4**

Scheme 1. Homogeneous hydrogenation of the acrylic acid derivative **3** to give (*S*)-naproxene (**4**).

The substrate is dissolved in the hydrophobic solvent mixture cyclohexane/chloroform. This combination forms a second phase in the presence of the highly polar supported-catalyst solution, which is in turn immiscible with organic liquids. Wan and Davis attempted in this way to achieve a double "heterogenization" or "immobilization" of a complex catalyst that would otherwise be homogeneous: Deposition on the selected support CPG (controlled-pore glass) causes the catalyst to become *heterogeneous*, and the two-phase technique results in its further *immobilization*. The success reported in conjunction with this remarkable experiment is quite astounding. It will certainly be worth waiting a bit to see if the success proclaimed[8] can be confirmed with other substrates, and whether the indirect "proofs" cited for localized retention of the ruthenium catalyst in fact withstand closer scrutiny. Given all the previous experience with liquid–solid phase catalysts and their susceptibility to "leaching" this would seem somewhat unlikely.

Another approach to two-phase catalysis and the immobilization of homogeneous catalysts has been suggested by Horváth and Rábai at Exxon. Following preliminary conference reports[9] and an article in *Science*,[10] a corresponding European Patent application has now been published as well.[11] Horváth and Rábai discuss their new "fluorous biphase system" (or "fluorous multiphase system" as it is characterized in the broader set of claims constituting the patent application) also in the context of the hydroformylation reaction as an illustrative example. Thus, a modified oxo catalyst bearing partially fluorinated ligands bound via phosphorus, such as that illustrated in structure **5**, is introduced into certain perfluoro (or partially fluorinated) solvents with which ordinary organic substrates and solvents are immiscible.

$[HRh(CO)\{P[CH_2CH_2(CF_2)_5CF_3]_3\}_3]$ **5**

Proper "tailoring" of the ligands is said to be extraordinarily important. For example, the methylene group located between the phosphorus atom and the perfluoro end group in **5** is alleged

to be responsible for controlling the influence of the electron-withdrawing end groups ("fluorous ponytails"[12]) and fine-tuning their effect to the appropriate level. The two-phase mixture consisting of catalyst phase and olefin becomes homogeneous at higher temperature, causing the catalytic process itself to occur with a correspondingly high rate of reaction in a single phase. The system is subsequently cooled, permitting one to take advantage of a thermally defined miscibility gap in order to separate the reaction product from the catalyst, which then becomes available for immediate reuse.

The practical applicability on an industrial scale of this rather exotic two-phase system remains to be demonstrated. Doing so will require a clarification of such basic issues as activity, cost, catalyst lifetimes (and thus catalyst life and economic feasibility), toxicity, concerns regarding the ozone depletion potential (ODP) and greenhouse warming potential (GWP) values of the corresponding fluorinated compounds, etc. There is also the possibility of competitive extraction of fluorinated hydrocarbons by the aldehyde phase in the oxo reaction (leading to potential problems in subsequent hydrogenation to the plasticizer alcohols that are in fact the desired products).

The professional world will also follow with some interest the future course of the patent application itself and the possibility that there may be appeals, since at least part of the basic idea underlying the Exxon process was described previously in a 1991 dissertation by M. Vogt entitled "Zur Anwendung perfluorierter Polyether bei der Immobilisierung homogener Katalysatoren" (On the Application of Perfluorinated Polyethers in the Immobilization of Homogeneous Catalysts).[13] Vogt was attempting to develop ligands based on hexafluoropropene oxide (HFPO) oligomers for subsequent complexation with appropriate cobalt or nickel precursors, and to exploit the latter for oligomerization or polymerization reactions. It did indeed prove possible in principle to bind HFPO oligomers to homogeneous transition-metal catalysts, conferring upon the modified complexes the solvophobic properties characteristic of this class of compounds. The result was a two-phase reaction procedure conducted in a perfluoropolyether medium facilitating separation of the product from the catalyst.

There now exists evidence for the extension of two-phase catalysis into a new area, suggesting interesting possibilities in an entirely different field of application. Gassner and Leitner[14] have described a hydrogenation of carbon dioxide to formic acid [Eq. (a)] that is accompanied by astonishingly high

$$H_{2(aq)} + CO_2(aq) = HCOOH_{(aq)} \qquad (a)$$

turnover values in aqueous solution in the presence of TPPTS-modified rhodium catalysts. This potentially relevant process will certainly generate considerable interest if it proves feasible to carry out a selective transformation of "technical grade" carbon dioxide (i.e., without prior purification) at "industrial concentrations" (meaning a CO_2 content in the range of a few percent). The high specificity associated with two-phase processes makes rapid progress in this regard appear likely as well.

The specificity of biphase catalyst systems (in conjunction with activities comparable to those anticipated with single-phase systems) has been illustrated in an elegant way by Mortreux et al.[15] In a regioselective hydroformylation of methyl acrylate to give α-formylpropionic acid with the catalyst $[HRh(CO)(TPPTS)_3]$, these authors observed an aldehyde yield comparable to that achieved with TPP, as well as an α/β product ratio of the expected order of magnitude and an even higher turnover frequency (TOF) (Scheme 2).

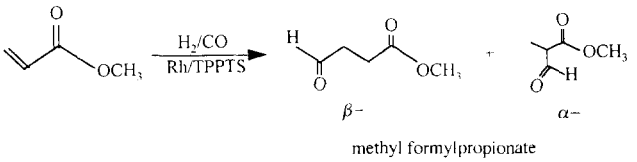

methyl formylpropionate

Scheme 2. Hydroformylation of methyl acrylate.

A $[HRh(CO)(TPPTS)_3]$ catalyst of the SAPC type on SiO_2 led to TOF values that were higher still, exceeding those obtainable with the homogeneous single-phase $[HRh(CO)(TPP)_3]$ system by a factor of 220 depending on experimental conditions. This is impressive evidence of the fact that it is dangerous to make predictions about reaction rates with biphasic catalyst systems, and that the nature of the associated substrate must always be taken into account.

German version: *Angew. Chem.* **1995**, *107*, 1709–1711

Keywords: catalysis · hydrogenations · hydroformylations · two-phase catalysis

[1] Introduction to the topic: W. A. Herrmann, C. W. Kohlpaintner, *Angew. Chem.* **1993**, *105*, 1588; *Angew. Chem. Int. Ed. Engl.* **1993**, *32*, 1524.
[2] Thus, a *NATO Advanced Research Workshop* was held in August/September 1994 on the subject "Aqueous Organometallic Chemistry and Catalysis" (Debrecen, Hungary); at the Spring ACS Meeting in Anaheim (CA) in April 1995, a workshop took place on two-phase catalysis.
[3] R. V. Chaudhari, B. M. Bhanage, R. M. Deshpande, H. Delmas, *Nature* **1995**, *373*, 501.
[4] Y. Yan, H. Zhuo, Z. Jin, *Fenzi Cuihua* **1994**, *8*(2), 147 [*Chem. Abstr.* **1994**, *121*, 111.875a].
[5] Z. Jin, Y. Yan, H. Zuo, B. Fell, *Z. Prakt. Chem./Chem. Ztg.* **1995**, in press.
[6] D. E. Bergbreiter, L. Zhang, V. M. Mariagnanam, *J. Am. Chem. Soc.* **1993**, *115*, 9295.
[7] K. T. Wan, M. E. Davis, *Nature* **1994**, *370*, 449.
[8] J. M. Brown, S. G. Davies, *Nature* **1994**, *370*, 418.
[9] *NATO Advanced Research Workshop* (see ref. [2]), Preprints p. 35.
[10] I. T. Horváth, J. Rábai, *Science* **1994**, *266*, 72.
[11] Exxon Research and Engineering Company (I. T. Horváth, J. Rábai), EP-Appl. 0.633.062 (**1994**).
[12] J. A. Gladysz, *Science* **1994**, *266*, 55.
[13] M. Vogt, Dissertation, Technische Hochschule Aachen, 26. August 1991.
[14] F. Gassner, W. Leitner, *J. Chem. Soc. Chem. Commun.* **1993**, 1465.
[15] G. Fremy, E. Montflier, J.-F. Carpentier, Y. Castanet, A. Mortreux, *Angew. Chem.* **1995**, *107*, 1608–1610; *Angew. Chem. Int. Ed. Engl.* **1995**, *34*, 1474–1476.

 © VCH Verlagsgesellschaft mbH, D-69451 Weinheim, 1995 0570-0833/95/1515-1577 $ 10.00+.25/0

New Dimensions in the Sol–Gel Process

Hans Reuter* and Maria-Theresia Brandherm

One of the characteristics of our modern, fast-moving age is certainly the fact that, as consumers, we take for granted many of the things which we find very practical and useful every day without thinking more deeply about them. It is therefore not surprising that the general public does not realize that chemical processes play a decisive role in the production of many products of everyday life, especially since the press more often than not only publishes articles on the negative aspects of chemistry. However, these critics also appreciate the advantages of a dazzle-free rear-view mirror in a car or of an office which is nicely flooded by daylight but at the same time the temperature inside is still normal because of windows with solar reflecting glass.

How many people are aware that these amenities are the products of high-tech chemistry[1] and are based on a procedure whose underlying principles were already known more than a hundred years ago[2] but whose technological application has achieved its breakthrough only in the last fifteen years.[3] The procedure referred to here is the so-called solution–sol–gel process (SSG process),[4] which involves the hydrolysis of metal alkoxides in solution, followed by formation of a sol and its subsequent gelation. The gel is then converted into the corresponding metal oxide after heat treatment.

The advantages[5] of the SSG process over other methods for the production of ceramics lies in the comparatively low temperatures required for the preparation of the oxide, the high purity of the starting materials, the ease with which the process can be undertaken, and the possibility, in principle, to carry out the shaping already at the solution or sol stage in the fluid phase.

With regard to the shaping, the production of thin oxide films on various substrates in particular has proved successful in technical applications[6] such as those mentioned above. The spreading of the fluid phase takes place either after the so-called dip-coating or after the spin-coating procedure. The course of these procedures is outlined in the steps shown in Scheme 1. Layer thicknesses of between 50 and 100 nm can be achieved in this way, and thicker layers can be readily obtained by repeating the coating procedure several times.

The fact that the technological breakthrough of a procedure does not necessarily mean that the relevant research comes to a standstill is evident from two recent publications which have attracted a great deal of attention. In one of the articles I. Moriguchi et al.[7] describe their studies on—as the authors call it—the two-dimensional sol–gel process.

In the preparation of a film by the SSG process, the solution of the metal alkoxide is usually spread *onto the substrate* and is hydrolyzed only thereafter, whereas in the two-dimensional sol–gel process a solution of the metal alkoxide as a film is spread *onto an aqueous phase*. As shown in Scheme 2 the novelty of this procedure is that the hydrolysis can occur on both the lower and upper side of the film.

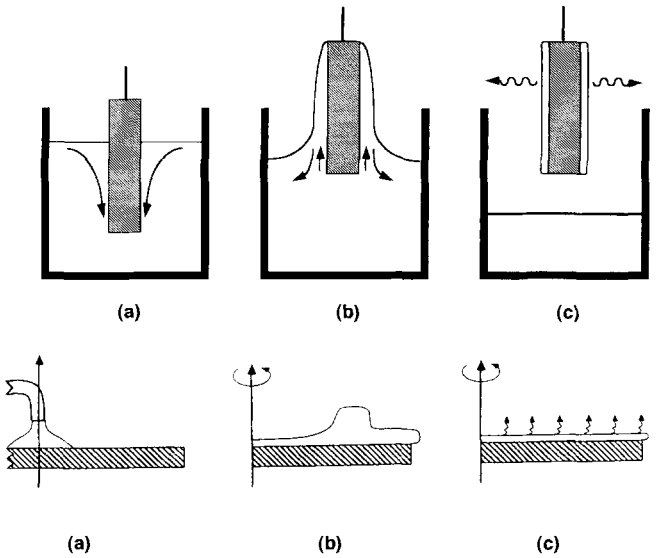

Scheme 1. Flow diagram of the principal course of the dip-coating (top) and spin-coating procedure (bottom) for the spreading of metal alkoxide solutions or sols according to the SSG process. In the dip-coating procedure the substrate initially dipped in the solution of the precursor (a), on removal (b) the solution flows off from the substrate under the influence of gravity until only a thin film remains; in the final step (c) the solvent is evaporated and the metal alkoxide is hydrolyzed to the gel. In the spin-coating procedure the solution of the precursor is spread in the middle of the substrate (a) and subsequently (b) distributed evenly as a thin film by rapid rotation of the substrate; in the final step (c) the solvent is evaporated and the alkoxide is hydrolyzed.

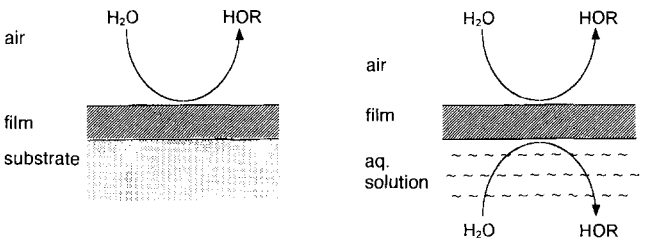

Scheme 2. The direction of attack of the hydrolysis in the preparation of films according to traditional (left) and two-dimensional solution sol–gel process (right).

In the present case a solution of tetrabutoxytitanium in chloroform was spread on a surface of water, and the formation and morphology of the condensate film was studied with fluorescence spectroscopy. It was shown that initially a lot of floating islands made up of solid material were formed on the water surface. These islands later gather together and eventually form a featureless, homogeneous layer. Since the observed apparent molecular area is significantly smaller than that of the precursor, the authors conclude that this condensate film is not the molecular monolayer of the precursor.

In the traditional solution–sol–gel process it is known that acetic acid and acetylacetonate suppress the hydrolysis and condensation of the metal alkoxides in solution because they form chelate complexes with the metal atom.[8] In the present case such a suppression effect is also encountered in the 2D sol–gel process since an increase of the apparent molecular area

[*] Prof. Dr. H. Reuter, M.-T. Brandherm
Institut für Chemie der Universität
Barbarastrasse 7, D-49069 Osnabrück (Germany)
Telefax: Int. code + (541)969-2370

 © VCH Verlagsgesellschaft mbH, D-69451 Weinheim, 1995 0570-0833/95/1515-1578 $ 10.00+.25/0

is observed on addition of these two reagents to the aqueous phase. The condensate films obtained in this way are considerably more stable.

For subsequent application it is important that the resulting nanometer-thick TiO_2 films can be transferred onto substrates such as CaF_2 or quartz. This was achieved by using the Langmuir–Blodgett technique, in which the chelate-stabilized films can be transferred considerably more easily and safer than the films prepared on pure water. According to the authors the original homogeneous state of the condensate film is preserved. The film deposited on CaF_2, also shows C–H and Ti-O-C vibrations in the IR spectrum. However, the C and H contents determined from the elemental analysis of the vacuum-dried film are considerably lower than values expected for the precursor.

These results were interpreted as indicating that the precursor hydrolyzes on the water surface, condenses, and then undergoes two-dimensional aggregation; this process results in some residual butoxy groups. The authors further speculate that the hydrophobicity of the butoxy groups and probably also their moderate reactivity are indispensible in the formation of such floating condensate films.

The films transferrred onto the substrates can be densified by conventional methods by heat treatment. Thermogravimetric measurements on the powders scraped off the surface showed that the conversion of the gel to crystalline TiO_2, that is dehydration and elimination of the remaining butoxy groups, is completed at 723 K. The IR bands of the organic ligands already disappear after heat treatment at 573 K for 30 min. X-ray diffraction (XRD) and scanning electron microscopy (SEM) proved ineffective in characterizing the films. However, the thickness of the TiO_2 layer was determined to be 4.3 nm by depth-profiling X-ray photoelectron spectroscopy (XPS). In the UV spectrum an absorption edge was found at 337 nm, which is significantly blue-shifted compared to quantum-size TiO_2.[9]

The second article by Nakamura and Matsui[10] takes us from two-dimensional layers to one-dimensional *tubes*. The preparation of *fibers* by the SSG process has already been possible for several years;[11] however, the preparation of hollow fibers is described here for the first time. The tubes were formed in a process in which silicon tetraethoxide was hydrolyzed in a mixture of ethanol, ammonia, water, and tartaric acid. The reaction products were washed on a net with fine pores with a large amount of water to remove impurities. Interestingly, most of the tubes had a square cross section with an outer diameter of 0.8–1.0 μm and were 200–300 μm in length; the inner diameter and wall thickness lie in the range 0.02–0.8 and 0.15–0.3 μm, respectively. Only a few tubes had an oval cross section with a circular inner channel. Furthermore, the authors established that the diameter decreased with falling process temperature. Thus, the finest tube had an outer diameter of 0.05–0.1μm.

The authors also report on a remarkable substrate selectivity for the formation of the nanotubes. Only the racemate of the tartaric acid and a mixture of L- and D-tartaric acid yield this product; the L, D, and *meso* isomer alone were ineffective. According to their calculations the authors attribute this to a system of hydrogen bonds, whose relative position to one another is considered to be favorable in the first case and unfavorable in the second. However, the reaction mechanism for the formation is still unkown.

These gel tubes could be converted to glass tubes at 800–1000 °C in air. In the IR spectrum the band of the Si–OH vibration diminishes, whereas the Si–O band adopted the shape and position found for that band in the correspondingly treated SiO_2 glass. The SiO_2 tubes thus obtained proved to be X-ray amorphous.

The two publications show that the solution–sol–gel process still has a few surprises in store even after more than a hundred years of research and development, which only at first sight appear to be alchemistic since we know too little about the "background" chemistry. It remains rewarding and exciting to follow further developments in this highly topical field of research,[12] not least because of the numerous overlaps with other areas of chemistry.

German version: *Angew. Chem.* **1995**, *107*, 1712–1714

Keywords: nanostructures · sol–gel process · thin films

[1] Thin Films from the Sol–Gel Process: H. Disslich in *Sol–Gel Technology for Thin Films, Fibers, Performs, Electronics and Speciality Shapes* (Ed.: L. C. Klein), Noyes Puplications, New Jersey, **1988**, p. 50.
[2] M. Ebelmen, *Ann. Chim. Phys.* **1846**, *16*, 129.
[3] L. C. Klein, *Sol–Gel Technology for Thin Films, Fibers, Performs, Electronics and Speciality Shapes*, Noyes Puplications, New Jersey, **1988**.
[4] R. Roy, *Science* **1987**, *238*, 1664.
[5] H. Schmidt, *J. Non-Cryst. Solids* **1988**, *100*, 51.
[6] C. J. Brinker, G. W. Scherer, *Sol–Gel Science The Physics and Chemistry of Sol–Gel Processing*, Academic Press, San Diego, **1990**.
[7] I. Morguchi, H. Maeda, Y. Teraoka, S. Kagawa, *J. Am. Chem. Soc.* **1995**, *117*, 1139.
[8] J. Livage, M. Henry, C. Sanchez, *Prog. Solid State Chem.* **1988**, *18*, 259.
[9] C. Kormann, D. Bahnemann, M. R. Hoffmann, *J. Phys. Chem.* **1988**, *92*, 5196.
[10] H. Nakamura, Y. Matsui, *J. Am. Chem. Soc.* **1995**, *117*, 2651.
[11] S. Sakka, *J. Non-Cryst. Solids* **1990**, *121*, 417.
[12] D. R. Ulrich, *J. Non-Cryst. Solids* **1990**, *121*, 465.

 © VCH Verlagsgesellschaft mbH, D-69451 Weinheim, 1995 0570-0833/95/1515-1579 $ 10.00+.25/0

Transition Metal Catalyzed Dimerization of Allenyl Ketones**

A. Stephen K. Hashmi*

Furans are present in many natural products and important pharmaceuticals as well as in flavorings and fragrances.[1] Furthermore, they are very popular synthetic building blocks.[2] Therefore a great deal of effort has been devoted to the development of new synthetic methods for the formation of furans.[1-3]

A milestone in the area of transition metal catalyzed syntheses of furans was the discovery by Marshall[4] that the readily available allenyl ketones **1**[5] can be isomerized selectively to furans by using Rh^I or Ag^I catalysts. Several years prior to this discovery, similar rearrangements had been observed by Jullien et al.[6] and Huntsman et al.[7] when allenyl ketones were subjected to flash vacuum thermolysis.

We have found that the terminal allenyl ketones **1** are not only converted into the expected isomerization products **2**, but also into the dimers **3**; the product ratio **2**:**3** is strongly dependent on

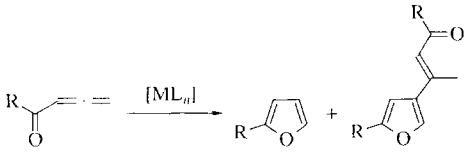

1 **2** **3**

a, R = Me
b, R = Pr
c, R = $CH(CH_2)_4$
d, R = *t*Bu
e, R = Ph
f, R = CH_2Cl
g, R = 2-IC_6H_4
h, R = 3,4-$(MeO)_2C_6H_3$
i, R = OEt

the catalyst used. The most efficient conversion of **1a** into **3a** (Table 1) was achieved by using tetrakis(2,2,2-trifluoroethoxycarbonyl)palladacyclopentadiene ($TCPC^{TFE}$), which was introduced by Trost.[8] When $AgNO_3$, $[Rh_2(OAc)_4]$, or $[RuCl_2(CO)_3]_2$ were employed, **2a** was formed exclusively, whereas the use of Cu^ICl led to the predominant formation of **2a** along with traces of **3a** (see Table 3). The structure of **3a** was elucidated by HETCOR, 1D-INADEQUATE, and NOE NMR experiments.[9] The C,C coupling constants and NOE data are listed in Scheme 1.

The selectivity of the dimerization to **3a** is remarkable. Since the transformation proceeds readily at room temperature, Diels-Alder reactions between the allenyl ketone and a furyl group in one of the products do not occur.[10] Furthermore,

[*] Dr. A. S. K. Hashmi
Institut für Organische Chemie der Freien Universität
Takustrasse 3, D-14195 Berlin (Germany)
Telefax: Int. code + (30)838-5163
e-mail: hashmi@chemie.fu-berlin.de

[**] The author thanks the Fonds der Chemischen Industrie for a Justus-von-Liebig stipend and Prof. Dr. J. Mulzer for his generous support. This work was supported by the Deutsche Forschungsgemeinschaft. Some of the precious metal salts were donated by the Degussa AG.

Table 1. Reactions of **1a** with some transition metal catalysts (1 M **1a** in $[D_6]$acetone at room temperature).

Catalyst (amount [mol %])	**2a**:**3a** [a]	Yield of **3a** [%] [b]
CuCl (1.0)	1.0:traces [c, d]	-
$AgNO_3$ (1.0)	1.0:0 [c, d]	
$[Rh_2(OAc)_4]$ (1.0)	1.0:0 [d]	-
$[Ru(Cl)_2(CO)_3]_2$ (0.5)	1.0:0 [c]	
$Pd(OAc)_2$ (0.5)	1.0:2.4	71
$TCPC^{TFE}$ (0.1)	1.0:8.8	86
$TCPC^{TFE}$ (0.05) [e]	1.0:9.0	76
$TCPC^{TFE}/PPh_3$ (0.1)	- [f]	

[a] Determined by ^1H NMR spectroscopy. [b] Due to its low boiling point, **2a** cannot be separated from the solvent. [c] Some by-products were formed in low amounts. [d] Slow reaction. [e] 20 mmol scale in nondeuterated acetone. [f] No reaction at room temperature, polymerization of the ester at 50 °C.

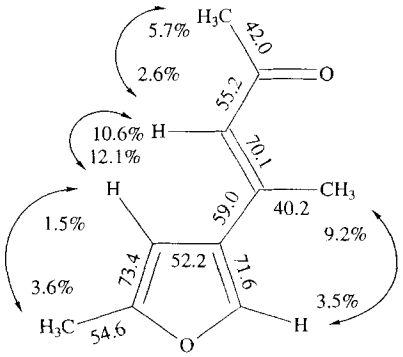

Scheme 1. C,C coupling constants and NOE data for **3a**.

[2 + 2] cycloadducts are not formed as seen in transition metal catalyzed dimerizations of unfunctionalized allenes.[11] The trisubstituted double bond in **3a** is formed selectively with (*E*)-configuration. Moreover, when Pd^{II} catalysts were used with a turnover number (TON) of >1100, the substrate/catalyst ratios (0.05–0.1 mol%) were much higher than with Ag^I (TON = 5.6)[4c, 12] or Rh^I (TON = 8.5)[4a, 12] catalysts. As a result, it was possible to convert multigram quantities of **1a** with the Pd catalyst. The catalytic activity of Pd is inhibited by phosphane ligands.

Similar results were obtained with the allenyl ketones **1b–e** (Table 2). On increasing the bulkiness of the substituent R, the

Table 2. $TCPC^{TFE}$-catalyzed reactions of **1b–e** in $[D_6]$acetone at room temperature.

Allenyl ketone	**2**:**3** [a]	Yield of **3** [%] [b]
1b	1.0:4.7	76
1c	1.0:3.0	67
1d	1.0:1.0	33
1e	1.0:6.1	81
1f	1.0:2.2	60
1g	- [c]	91

[a] Determined by ^1H NMR spectroscopy. [b] Due to its volatility, **2** cannot be separated from the solvent. [c] Not determined.

amount of monomer **2** increases and the yield of **3** decreases. Even compounds such as α-chloroketone **1f** could be cyclized, which is not feasible with Ag catalysts. The reaction of aryl iodide **1g** is an example that exhibits interesting chemoselectivity. We did not observe any products derived from either an oxidative addition followed by an inter- or intramolecular carbometalation of the allene[13] or a deactivation of the catalyst. Therefore it should be possible to perform interesting tandem reactions. Only one additional substituent at the allene, as in **4**, is sufficient to suppress the dimerization completely. Thus, **5** is formed in quantitative yield (NMR spectroscopy) using only 0.1 mol% of the Pd catalyst. Ester **1i** did not react with the Pd catalyst at room temperature; at higher temperatures it polymerized.

4 **5**

The mechanism of the formation of **3** is probably related to the Marshall cycloisomerization of **1** to **2**.[4d] The coordination of the Pd atom by the allene (complex **6**) is presumably followed by an intramolecular oxypalladation of the terminal double bond. In this way the γ-donor substituted vinyl carbene complex **7** would form as an intermediate. In cross-over experiments

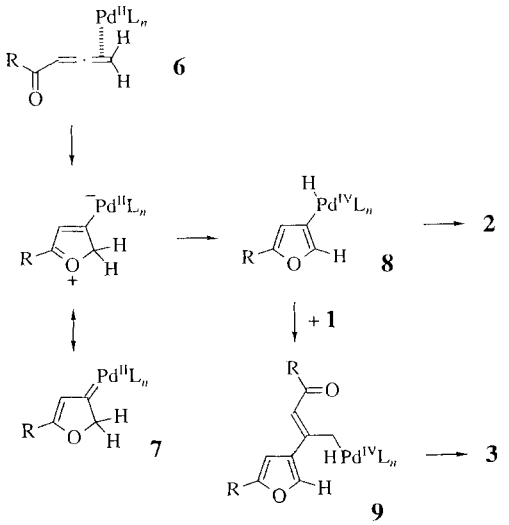

between **1a**, which is monodeuterated at the terminal methylene group of the allene, and nondeuterated **1h** (and between monodeuterated **1h** and nondeuterated **1a**), a statistical mixture was formed that included the monomers **2a** and **2h**, the dimers **3a** and **3h**, as well as both mixed dimers. A deuterium distribution indicating H/D exchange was not obtained; however, we observed a deuterium isotope effect of $k_H/k_D = 3.1$ (22 °C). On the other hand, an H/D exchange with a protic solvent as described by Marshall was observed, but only to a minor extent. The cyclization of **1a** in acetone in the presence of 12 equivalents of D_2O gave rise to only 36% of the product monodeuterated at the desired position and 64% of the nondeuterated product. These findings are consistent with a β-H-elimination, which would lead to the furyl-hydrido species **8**.[14] Because of the low concentration of **8**, only the slow H/D exchange with D_2O, which is present in high concentration, can be observed and not, however, the exchange between deuterated and nondeuterated **8**.

Compound **8** can either form product **2** by a reductive elimination or can be converted to **9** by a carbopalladation of an additional molecule of **1** followed by a reductive elimination to form dimer **3**. The electrophilic character of the Pd^{IV} atom in **8** appears to be crucial for the high selectivity of the carbopalladation at the electron-rich, terminal double bond of the cumulene.[15] The selective formation of the (*E*)-configurated double bond can be explained by an addition of the Pd atom to the side of the double bond pointing away from the acyl substituent.

In conclusion, the cyclization of allenyl ketones to furans is not limited to the use of Rh^I and Ag^I compounds as catalysts, but can also be carried out successfully with Pd compounds, which catalyze these reactions much more efficiently. Furthermore, a novel reaction pathway has been established in the transformation of terminal allenyl ketones with Pd^{II} catalysts, namely the cycloisomerization/dimerization to **3**. Product **3** was formed under mild conditions and in preparatively useful amounts. Since allenyl ketones are readily available, the formation of **3** with its dendralene-like double bond system[16] presents a simple way to starting materials for "diene-transmissive" Diels–Alder reactions.[17]

Table 3. Selected spectroscopic data of compounds **3a**, **e** and **g**.

3a: IR (film): $\tilde{\nu} = 1675$ (C=O) cm^{-1}; UV/Vis (methanol): λ_{max} (lg ε) = 296 nm (2.574); ^{1}H NMR (270 MHz, $CDCl_3$): δ = 2.08 (s, 3H), 2.12 (s, 3H), 2.23 (d, J = 0.8 Hz, 3H), 6.05 (q, J = 0.8 Hz, 1H), 6.25 (s, 1H), 7.39 (s, 1H); ^{13}C NMR (67.9 MHz, $CDCl_3$): δ = 12.9 (q), 16.2 (q), 31.6 (q), 103.0 (d), 120.7 (d), 128.9 (s), 141.1 (d), 144.5 (s), 153.1 (s), 198.1 (s); MS (70 eV): *m/z* (%): 164 (34) [M^+], 149 (19), 121 (24), 93 (20), 91 (60), 78 (18), 77 (70), 65 (24); $C_{10}H_{12}O_2$: calcd. 164.08373; found 164.08370 (MS); elemental analysis for $C_{10}H_{12}O_2$: calcd. C 73.15, H 7.37; found C 73.16, H 7.30

3e: IR (film): $\tilde{\nu} = 1681$ (C=O) cm^{-1}; ^{1}H NMR (270 MHz, $CDCl_3$): δ = 2.53 (d, J = 0.9 Hz, 3H), 6.92 (s, 1H), 7.18 (d, J = 0.9 Hz, 1H), 7.28–7.58 (m, 6H), 7.69–7.23 (m, 2H), 7.76 (s, 1H), 7.97–8.01 (m, 2H); ^{13}C NMR (67.9 MHz, $CDCl_3$): δ = 17.5 (q), 102.3 (d), 119.2 (d), 124.1 (2d), 128.1 (d), 128.1 (2d), 128.5 (2d), 128.8 (2d), 130.2 (s), 130.7 (s), 132.4 (d), 139.7 (s), 142.0 (d), 146.0 (s), 155.5 (s), 191.6 (s); MS (70 eV): *m/z* (%): 288 (35) [M^+], 273 (8), 105 (100), 77 (27); $C_{20}H_{16}O_2$: calcd. 288.11503; found 288.11491 (MS); elemental analysis for $C_{20}H_{16}O_2$: calcd. C 83.31, H 5.59; found C 83.24, H 5.65

3g: IR (film): $\tilde{\nu} = 1658$ (C=O) cm^{-1}; ^{1}H NMR (270 MHz, $CDCl_3$): δ = 2.56 (d, J = 0.8 Hz, 3H), 6.85 (s, 1H), 6.97–7.03 (m, 1H), 7.08–7.14 (m, 1H), 7.25 (s, 1H), 7.35–7.48 (m, 3H), 7.57–7.61 (m, 1H), 7.83 (s, 1H), 7.89–7.96 (m, 2H); ^{13}C NMR (67.9 MHz, $CDCl_3$): δ = 17.5 (q), 92.0 (s), 94.6 (s), 106.9 (d), 121.1 (d), 128.1 (2d), 128.5 (d), 129.3 (d), 129.6 (d), 129.7 (s), 131.3 (d), 134.3 (s), 140.0 (d), 140.7 (d), 142.6 (d), 146.1 (s), 146.9 (s), 155.0 (s), 194.6 (s); MS (70 eV): *m/z* (%): 540 (24) [M^+], 231 (100); $C_{20}H_{14}I_2O_2$: calcd. 539.90808; found 539.90854 (MS); elemental analysis for $C_{20}H_{14}I_2O_2$: calcd. C 44.47, H 2.61; found C 44.47, H 2.57

Experimental Procedure

Typical synthesis: TCPC^{TFE} (6.6 mg, 10 μmol) was added to **1a** (1.64 g, 20.0 mmol) in absolute acetone (20 mL) under an inert gas atmosphere. After complete conversion (NMR monitoring), the solvent was removed in vacuo and the residue was purified by chromatography on silica gel with hexanes/ethyl acetate (6/1) (**3a**: 1.24 g, 76%).

Received: February 14, 1995,
Revised version: April 13, 1995 [Z7712IE]
German version: *Angew. Chem.* **1995**, *107*, 1749–1751

Keywords: allenes · furans · palladium compounds

[1] R. L. Danheiser, E. J. Stoner, H. Koyama, D. S. Yamashita, C. A. Klade, *J. Am. Chem. Soc.* **1989**, *111*, 4407–4413, and references therein.
[2] M. E. Maier, *Nachr. Chem. Tech. Lab.* **1993**, *41*, 696–704.
[3] For recent examples see: a) J. A. Marshall, W. J. DuBay, *J. Am. Chem. Soc.* **1992**, *114*, 1450–1456; b) Y. Yang, H. N. C. Wong, *J. Chem. Soc. Chem. Commun.* **1992**, 1723–1725; c) L. A. Paquette, P. C. Astles, *J. Org. Chem.* **1993**, *58*, 165–169; d) A. R. Katritzky, J. Li, M. F. Gordeev, *ibid.* **1993**, *58*, 3038–3041; e) J. A. Marshall, W. J. DuBay, *ibid.* **1993**, *58*, 3602–3603; f) K. Tani, Y. Sato, S. Okamoto, F. Sato, *Tetrahedron Lett.* **1993**, *34*, 4975–4978; g) T. L. Gilchrist, *Contemp. Org. Synth.* **1994**, 205–217; h) J. A. Marshall, W. J. DuBay, *J. Org. Chem.* **1994**, *59*, 1703–1708; i) J. A. Marshall, C. E. Bennett, *ibid.* **1994**, *59*, 6110–6113.

[4] a) J. A. Marshall, E. D. Robinson, *J. Org. Chem.* **1990**, *55*, 3450–3451; b) J. A. Marshall, X.-j. Wang, *ibid.* **1991**, *56*, 960–969; c) *ibid.* **1992**, *57*, 3387–3396; d) J. A. Marshall, G. S. Bartley, *ibid.* **1994**, *59*, 7169–7171.
[5] a) M. Huché, *Tetrahedron* **1980**, *36*, 331–342; b) H. F. Schuster, G. M. Coppola, *Allenes in Organic Synthesis*, Wiley, New York, **1984**; c) R. C. Larock, M.-S. Chow, S. J. Smith, *J. Org. Chem.* **1986**, *51*, 2623–2624; d) D. Bernard, A. Doutheau, J. Gore, *Tetrahedron* **1987**, *43*, 2721–2732.
[6] J. Jullien, J. M. Pechine, F. Perez, J. J. Piade, *Tetrahedron* **1982**, *38*, 1413–1416.
[7] W. D. Huntsman, T.-K. Yin, *J. Org. Chem.* **1983**, *48*, 3813–3814.
[8] B. M. Trost, M. K. Trost, *J. Am. Chem. Soc.* **1991**, *113*, 1850–1852.
[9] A large number of isomeric products is possible when transition metal catalyzed [2 + 2] and [4 + 2] cycloadditions and subsequent double bond isomerizations or rearrangements are considered.
[10] Both the standard Diels–Alder reaction between the furan as the electron-rich diene and the allenyl ketone as the electron-deficient dienophile as well as an inverse-electron demand Diels–Alder reaction between the allenyl ketone as the 1-oxadiene and a double bond of the furan as the dienophile are possible: a) M. Bertrand, J.-L. Gras, *Bull. Soc. Chim. Fr.* **1967**, 4336–4343; b) J.-L. Gras, B. S. Galledou, M. Bertrand, *ibid.* **1988**, 757–767.
[11] a) G. Wilke, *The Organic Chemistry of Nickel*, Academic Press, New York, **1975**; b) P. W. Jolly in *Comprehensive Organometallic Chemistry, Vol. 8* (Eds.: G. Wilkinson, F. G. A. Stone, E. W. Abel), Pergamon Press, Oxford, **1982**, pp. 613–711; c) B. L. Shaw, A. J. Stringer, *Inorg. Chim. Acta Rev.* **1973**, *7*, 1–10; d) F. L. Bowden, R. Giles, *Coord. Chem. Rev.* **1976**, *20*, 81–106.
[12] In the experiments carried out with Rh^{II} and Ag^{I}, turnover numbers of up to 100 could be achieved (Table 1); however; the reaction time to obtain complete conversion exceeded one week. When the same amount of a Pd catalyst was used, the reaction was complete after about 24 h.
[13] S. Ma, E.-i. Negishi, *J. Org. Chem.* **1994**, *59*, 4730–4732.
[14] For similar Pd^{IV} hydrides see B. M. Trost, *Acc. Chem. Res.* **1990**, *23*, 34–42.
[15] B. M. Trost, G. Kottirsch, *J. Am. Chem. Soc.* **1990**, *112*, 2816–2818.
[16] H. Hopf, *Angew. Chem.* **1984**, *96*, 947–958; *Angew. Chem. Int. Ed. Engl.* **1984**, *23*, 948–960.
[17] For diene transmissive reactions [Eq. (a)] see C. Spino, G. Liu, N. Tu, S. Girard, *J. Org. Chem.* **1994**, *59*, 5596–5608, and references therein.

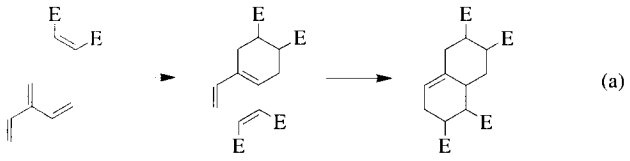

(a)

A Cycloaddition–Cyclodehydrogenation Route from Stilbenoids to Extended Aromatic Hydrocarbons

Markus Müller, Heike Mauermann-Düll, Manfred Wagner, Volker Enkelmann, and Klaus Müllen*

Dedicated to Professor Wolfram Grimme on the occasion of his 65th birthday

The photochemical conversion of 2,2′-distyrylbiphenyl (**1**) both in solution[1] and as a film[2] yields cyclobutane **2** by a stereoselective [2 + 2] cycloaddition. We were interested in preparing a thermally active stilbene derivative analogous to **1** not only for synthetic and mechanistic reasons but also for structuring thin layers. An intramolecular [4 + 2] cycloaddition would require the previously unknown all-*trans*-2(4-phenylbuta-1,3-dienyl)-2′-styrylbiphenyl (**3**). We describe here the synthesis of **3**, its thermal cyclization under mild conditions to give cyclohexene **4**, and the subsequent dehydrogenation affording triphenylene **5** (Scheme 1).

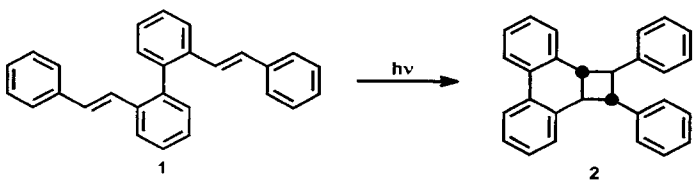

1 **2**

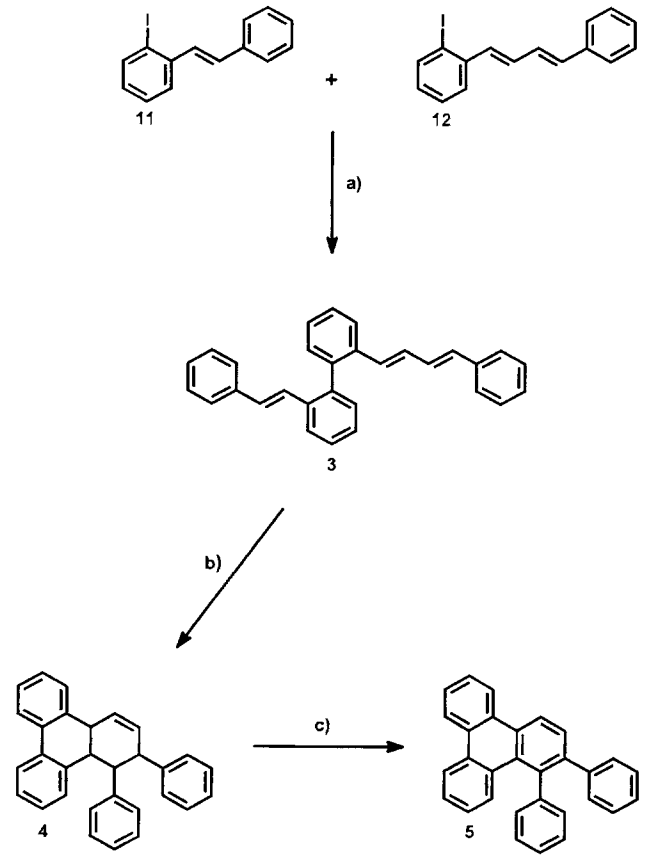

Scheme 1. a) 1. **11**, BuLi, THF, −78 °C; 2. $ZnBr_2$, THF, −78 °C; 3. **12**, tris(dibenzylidenacetone)dipalladium(0) [$Pd_2(dba)_3$], THF, −78 → 25 °C; b) toluene, 100 °C; c) DDQ, benzene, 78 °C.

The general importance of the synthetic scheme described here leading to extended polyaryl compounds is demonstrated by the application of the strategy to a homologue of **3**. The extended phenylenevinylene compound **6** undergoes a double Diels–Alder cycloaddition affording **7**, which in turn can be dehydrogenated to furnish hydrocarbon **8** (Scheme 2).

We show that the most important consequence of the cycloaddition is that the products, triphenylenes **5** and **8**, undergo multiple electron transfer induced cyclodehydrogenations to give extended planar graphitic sections[3] such as **9** and **10** in high yields.

Compound **3** was synthesized from *trans*-2-iodostilbene (**11**) and *trans,trans*-2′-iodo-1,4-diphenylbuta-1,3-diene (**12**) by aryl–aryl coupling via zincates according to the method of Knochel et al.[4] (75% yield). The coupling partners **11** and **12** were constructed readily by Wittig reaction of 2-iodobenzyltriphenylphosphonium chloride with benzaldehyde and *trans*-cinnamaldehyde, respectively. The mixtures of configurational isomers that resulted were converted into the thermodynamically more stable *trans* isomers by heating in toluene at 110 °C with

[*] Prof. Dr. K. Müllen, Dipl.-Chem. M. Müller,
Dipl.-Chem. H. Mauermann-Düll, Dr. M. Wagner, Dr. V. Enkelmann
Max-Planck-Institut für Polymerforschung
Ackermannweg 10, D-55128 Mainz (Germany)
Telefax: Int. code + (6131)379350

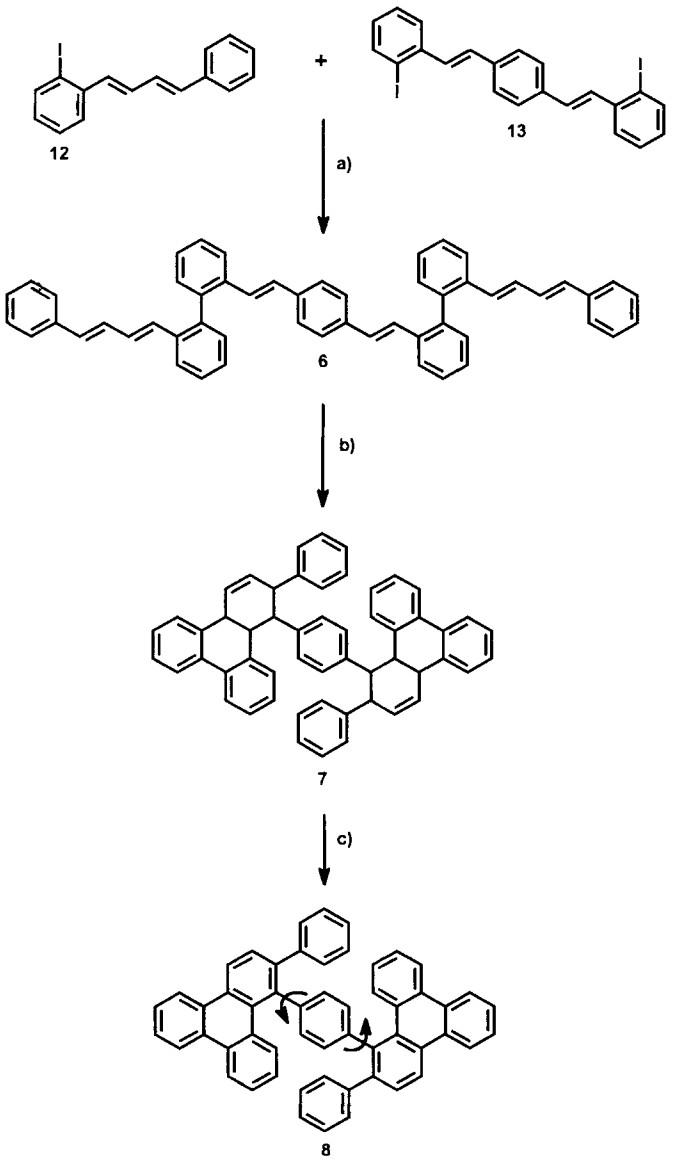

Scheme 2. a) 1. **12**, BuLi, THF, −78 °C; 2. $ZnBr_2$, THF, −78 °C; 3. **13**, $[Pd_2(dba)_3]$, THF, −78 → 25 °C; b) toluene, 100 °C; c) DDQ, 1,1,2,2-tetrachloroethane, 140 °C.

catalytic amounts of iodine in the absence of light. Photocyclization products did not form.

When compound **3**, which contains both a dienophile and a diene, was heated in toluene at 100 °C, an intramolecular Diels–Alder reaction resulted in the quantative formation of 1,2,4a,12b-tetrahydro-1,2-diphenyltriphenylene (**4**) (as a mixture of stereoisomers, see below). When the intermolecular [4 + 2] cyclization of *trans,trans*-1,4-diphenylbuta-1,3-diene and *trans*-stilbene was attempted under the same conditions, no conversion was observed even after reaction times of over 100 h. The cyclohexene ring in compound **4** was dehydrogenated with 2,3-dichloro-5,6-dicyano-1,4-benzoquinone (DDQ) with aromatization to give 1,2-diphenyltriphenylene (**5**) (75% yield). Compound **5** was previously observed as a side product (9% isolated yield) in investigations of the photochemistry of the Diels–Alder product formed from tetraphenylfuran and maleic anhydride.[5]

In the synthesis of **6** the aryl–aryl couplings of two equivalents of the 2′-iodophenylbutadiene component **12** with the central *trans,trans*-1,4-di(2′-iodostyryl)benzene (**13**) also proceed via an activated zinc species; in this case compound **12** undergoes iodine–zinc exchange. The relatively low yield of **6** (32%) in this biscoupling can be explained by the low reaction temperature, which is necessary to avoid premature intramolecular Diels–Alder reactions.

The *para*-distyryl-substituted benzene **13**, the "double" dienophile component in the subsequent thermally induced [4 + 2] cycloaddition, was synthesized by the double Wittig reaction of 2-iodobenzyltriphenylphosphonium chloride and terephthaldialdehyde and, like the Wittig products **11** and **12**, was transformed into the thermodynamically stable all-*trans* isomer. In analogy to the reaction of **3**, heating compound **6** in toluene at 100 °C provided **7** in 94% yield. Because several chiral centers are formed in this reaction, **7** was obtained as a mixture of isomers, which were not separated. The crude mixture of **7** was dehydrogenated by treatment with DDQ, in analogy to the synthesis of **5**, affording 1,4-di(2-phenyltriphenylen-1-yl)benzene (**8**) in 98% yield. Important physical and spectroscopic data for compounds **3**–**10** are listed in Table 1.

Table 1. Physical and spectroscopic data for **3**–**10**.

3: ^{1}H NMR (500 MHz, $CDCl_3$, 30 °C): δ = 7.82, 7.76 (each d, ^3J(H,H) = 9.3 and 9.8 Hz, each 1H; H6, H6′, biphenyl), 7.45–7.36 (m, 2H; H5, H5′, biphenyl), 7.34–7.18 (m, 14H), 7.02, 6.83 (each d, ^3J(H,H) = 16.2 Hz, each 1H; AB, olef. AB system), 6.91–6.86, 6.77–6.72 (each m, each 1H; BC, olef. ABCD system), 6.57, 6.42 (each d, ^3J(H,H) = 15.8 Hz, each 1H; AD, olef. ABCD system); MS (EI, 70 eV): *m/z* (%) = 384(5) [M^+], 206 (100) [$M^+ - C_{14}H_{10}$], 192 (23) [M^{2+}], 178 (47) [$C_{14}H_{10}^+$]; UV/Vis ($CHCl_3$): λ_{max} (ε) = 263 (92000), 269 (104000), 280 (91000), 325 (53000), 339 (52000), 357 nm (31000); m.p. 117–118 °C (decomp.)

4: ^{1}H NMR (500 MHz, $CDCl_3$, 30 °C): δ = 3.83–3.75 (m, 2H), 3.49 (d, ^3J(H,H) = 9.8 Hz, 1H), 3.33 (t, ^3J(H,H) = 14.3 Hz, 1H); the NMR data refer exclusively to the aliphatic signals of the major pair of enantiomers **4c/d**; MS (EI, 70 eV): *m/z* (%) = 384 (3) [M^+], 206 (100) [$M^+ - C_{14}H_{10}$], 178 (42) [$C_{14}H_{10}^+$], 91 (35) [$C_7H_7^+$], 77 (7) [$C_6H_5^+$]; UV/Vis ($CHCl_3$): λ_{max} = 263, 269, 288 nm; m.p. 183 °C (mixture of isomers)

5: ^{1}H NMR (500 MHz, $CDCl_3$, 30 °C): δ = 8.62 (d, ^3J(H,H) = 8.4 Hz, 1H; H4, triphenylene), 8.61–8.59, 8.55–8.53 (each m, each 1H), 7.63–7.61 (m, 3H), 7.53 (d, ^3J(H,H) = 8.6 Hz, 1H), 7.34, 6.93 (each t, ^3J(H,H) = 7.4 Hz, each 1H) (H5–H12, triphenylene), 8.47 (d, ^3J(H,H) = 8.4 Hz, 1H; H3, triphenylene), 7.19–7.15 (m, 6H; *m*-H, *p*-H, phenyl), 7.05–7.03, 7.00–6.98 (each m, each 2H; *o*-H, phenyl); MS (EI, 70 eV): *m/z* (%) = 381 (28) [$M^+ + 1$], 380 (100) [M^+], 303 (30) [$M^+ - C_6H_5$]; UV/Vis ($CHCl_3$): λ_{max} (ε) = 263 (112000), 269 (126000), 288 nm (95000); m.p. 224–225 °C

6: ^{1}H NMR (500 MHz, $CDCl_3$, 30 °C): δ = 7.78, 7.71 (each d, ^3J(H,H) = 7.8 and 7.7 Hz, each 2H; H6, H6′, biphenyl), 7.40–7.34 (m, 4H; H5, H5′, biphenyl), 7.32–7.13 (m, 18H; phenyl, biphenyl), 7.11 (s, 4H; phenyl central), 6.93, 6.74 (each d, ^3J(H,H) = 16.2 Hz, each 2H; AB, olef. AB system), 6.83, 6.69 (each m_c, each 2H; BC, olef. ABCD system), 6.52, 6.36 (each d, ^3J(H,H) = 17.1 Hz, each 2H; AD, olef. ABCD system); MS (FD, 8 kV): *m/z* (%) = 690 (25) [M^+], 512 (100) [$M^+ - C_{14}H_{10}$], 178 (16) [$C_{14}H_{10}^+$]; UV/Vis ($CHCl_3$): λ_{max} = 329, 343, 362, 388 nm; m.p. > 60 °C (decomp.)

7: ^{1}H NMR (500 MHz, [D_2]1,1,2,2-tetrachloroethane, 80 °C): δ = 7.76 (m_c, 2H), 7.65 (m_c, 2H), 7.39 (m_c, 2H), 7.21 (t, ^3J(H,H) = 7.6 Hz, 2H), 7.02 (m_c, 8H), 6.82 (m_c, 2H), 6.55 (d, ^3J(H,H) = 6.5 Hz, 4H), 6.46 (d, ^3J(H,H) = 10.1 Hz, 2H), 6.12–6.08 (m, 2H), 5.99–5.74 (m, 4H), 3.56–3.51 (m, 4H; $H_{aliph.}$), 3.40–3.33 (m, 2H; $H_{aliph.}$), 3.22 (t, ^3J(H,H) = 12.3 Hz, 2H; $H_{aliph.}$); the NMR data refer exclusively to the major Diels–Alder product in the reaction mixture; MS (FD, 8 kV): *m/z* (%) = 690 (6) [M^+], 512 (100) [$M^+ - C_{14}H_{10}$], 178 (32) [$C_{14}H_{10}^+$]; UV/Vis ($CHCl_3$): λ_{max} = 263, 269, 288 nm; m.p. > 300 °C

8: ^{1}H NMR (500 MHz, [D_2]1,1,2,2-tetrachlorethane, 120 °C): δ = 8.64 (d, ^3J(H,H) = 8.4 Hz, 4H), 8.61 (m_c, 2H), 8.54 (d, ^3J(H,H) = 8.0 Hz, 2H), 7.69–7.67 (m, 6H), 7.64 (d, ^3J(H,H) = 7.2 Hz, 2H), 7.33–7.18 (m, 14H), 6.97 (s, 4H; phenyl central); MS (FD, 8 kV): *m/z* (%) = 682 (100) [M^+], 341 (6) [M^{2+}]; UV/Vis ($CHCl_3$): λ_{max} = 263, 269, 286 nm; m.p. > 300 °C

9: ^{1}H NMR (500 MHz, [D_2]1,1,2,2-tetrachloroethane, 120 °C): δ = 9.21 (s, 2H), 9.05 (d, ^3J(H,H) = 7.9 Hz, 2H), 8.96 (d, ^3J(H,H) = 7.4 Hz, 2H), 8.92 (d, ^3J(H,H) = 8.5 Hz, 2H), 8.84 (d, ^3J(H,H) = 8.0 Hz, 2H), 8.09 (t, ^3J(H,H) = 7.8 Hz, 2H), 7.77 (m_c, 4H); MS (FD, 8 kV): *m/z* (%) = 753 (12) [$2M^+$], 376 (100) [M^+], 188 (7) [M^{2+}]; UV/Vis ($CHCl_3$): λ_{max} = 263, 269, 288, 299, 335, 350, 369 nm; m.p. > 300 °C

10: MS (FD, 8 kV): *m/z* (%) = 670 (100) [M^+], 335 (42) [M^{2+}]; MS (LD-TOF): *m/z* (%) = 670 (55) [M^+] (calibrated with C_{60} and C_{70}); UV/Vis ($C_2H_2Cl_4$): λ_{max} = 260, 307, 354, 370, 389, 407 nm; m.p. > 300 °C

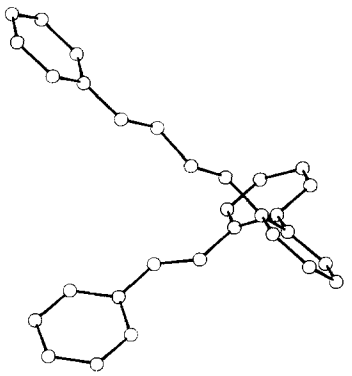

Fig. 1. X-ray structure of **3**.

The X-ray crystal structure of **3** (Fig. 1)[6] reveals that the biphenyl unit is twisted by 69°. The corresponding angle in analogue **1** is considerably greater (115°), such that the two styryl groups in **1** have an *anti* arrangement.[2]

One of the requirements of the intramolecular Diels–Alder reaction of **3** is free rotation about the central σ bond of the biphenyl unit, since the double bonds approach each other only when the interplanar angle within the biphenyl unit is sufficiently small. Another requirement of the reaction is the conversion of the transoid conformation of the *trans,trans*-butadiene unit found in the crystal into a cisoid arrangement. In the concerted Diels–Alder cycloaddition of **3** two diastereomeric pairs of enantiomers **4a/b** and **4c/d** are possible products.[7]

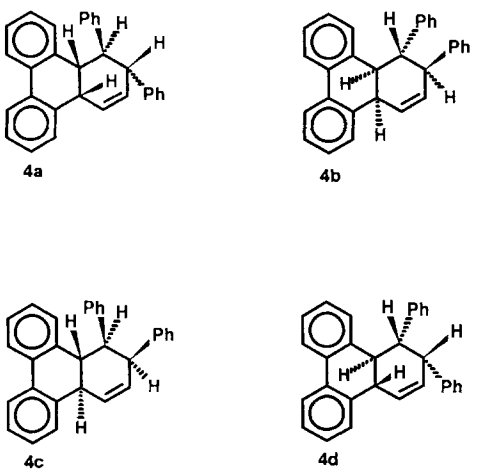

NMR spectroscopic analyses (NOE experiments, ^{1}H,^{1}H-COSY, ^{13}C,^{1}H-COSY measurements) showed that the **4c/d** pair of enantiomers is the main product of the [4 + 2] cyclization (**4a/b**:**4c/d** = 1:5). The relative configuration of **4c** was confirmed by the X-ray structure determined for a single crystal obtained from the reaction mixture (Fig. 2).[6]

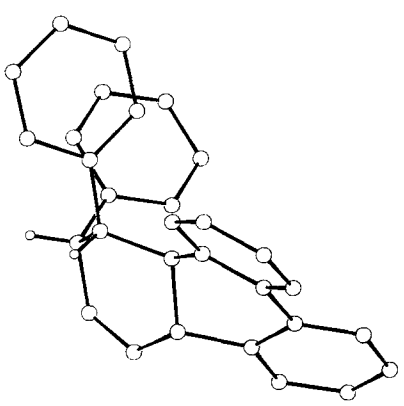

Fig. 2. X-ray structure of **4c**.

The synthesis of graphitic sections described here relies on the cyclodehydrogenation of **5** giving tribenzo[*b,n,pqr*]perylene (**9**)[8] (Scheme 3). This conversion was possible by reduction of a solution of **5** in 1,2-dimethoxyethane at 5 °C with a potassium mirror for several days and subsequent

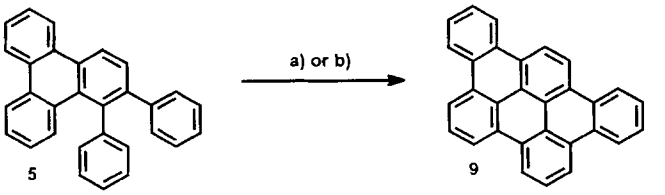

Scheme 3. a) 1. K, 1,2-dimethoxyethane, 5 °C; 2. I_2, toluene; b) $AlCl_3$, $CuCl_2$, CS_2, room temperature.

oxidation with iodine in toluene (yield 47%, after twofold recrystallization from nitrobenzene). Alternatively, oxidation of **5** with copper dichloride and aluminum trichloride in carbon disulfide provided **9** (room temperature, 2 d, 77% yield). The latter procedure can be used for larger scale preparation of **9**.

The oxidative cyclodehydrogenation of **8** was conducted in analogy to the cyclization of triphenylene **5** (99% yield; Scheme 4). The loss of 12 hydrogen atoms, proved by FD- and

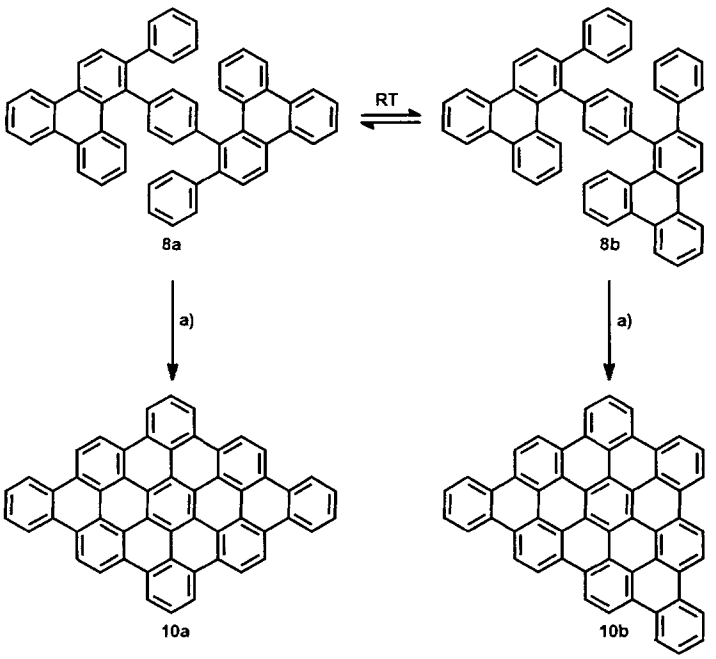

Scheme 4. a) $AlCl_3$, $CuCl_2$, CS_2, room temperature.

LD-TOF mass spectrometry, indicates formation of six new aryl–aryl bonds and complete planarization of the polybenzenoid arene **8**. Since the cyclodehydrogenated, polycyclic arene **10** is extremely insoluble in all standard solvents, more extensive characterization was not possible. Thus we have not yet determined which of the two isomers, **10a** or **10b**, results. The formation of **10a** or **10b** should depend on whether the extremely twisted polyaryl compound **8** assumes the planar conformation **8a** or **8b** in the oxidative cyclodehydrogenation. We will describe an independent synthesis of **10a** shortly as conclusive structural proof.

The cycloaddition–cyclodehydrogenation sequence described here offers a new, surprisingly simple route to extended aromatic hydrocarbons. The application of the Diels–Alder cyclization developed with biphenyl **3** to its homologue **6** suggests that poly(phenylenevinylene) compounds can be employed that contain suitable ene and diene units; such compounds could undergo multiple Diels–Alder reactions and subsequent aroma-

tization and cyclodehydrogenation. This would be an especially attractive approach for the preparation of larger graphitic sections.

Received: March 10, 1995 [Z7786IE]
German version: *Angew. Chem.* **1995**, *107*, 1751–1754

Keywords: cycloadditions · cyclodehydrogenations · Diels–Alder reactions · graphitic sections · polycycles

[1] A. J. W. Tol, W. H. Laarhoven, *J. Org. Chem.* **1986**, *51*, 1663–1668; A. Böhm, K. Meerholz, J. Heinze, K. Müllen, *J. Am. Chem. Soc.* **1992**, *114*, 688–699.
[2] A. Böhm, M. Adam, H. Mauermann, S. Stein, K. Müllen, *Tetrahedron Lett.* **1992**, *33(20)*, 2795–2798.
[3] R. Goddard, M. W. Haenel, W. C. Herndon, C. Krüger, M. Zander, *J. Am. Chem. Soc.* **1995**, *117*, 30–41.
[4] C. Jubert, P. Knochel, *J. Org. Chem.* **1992**, *57*, 5425–5431; A. Sidduri, M. J. Rozema, P. Knochel, *ibid.* **1993**, *58*, 2694–2713.
[5] B. Fuchs, G. Scharf, *J. Org. Chem.* **1981**, *46*, 5395–5398.
[6] Crystal structure analyses were conducted with a Nonius CAD-4 diffractometer with graphite-monochromated $Cu_{K\alpha}$ radiation ($\lambda = 1.5418$ Å) at room temperature. Lattice parameters were obtained from 25 reflections by least squares analysis ($\theta > 25°$). The intensities were measured with $\theta/2\theta$ scans. The structures were solved by direct methods, the C atoms refined with anisotropic deflection parameters, and the H atoms treated with a riding model. Empirical absorption correction; programs used: Molen, SIR, ORTEP. **3** ($C_{30}H_{24}$): monoclinic, $C2/c$, $a = 43.530(9)$, $b = 5.632(3)$, $c = 18.770(3)$ Å, $\beta = 111.232(9)°$, $V = 4289.5$ Å^3, $Z = 8$, $\rho_{calcd} = 1.191$ g cm^{-3}, $\mu = 4.736$ cm^{-1}, 3011 reflections, of which 1799 were observed ($I > 3\sigma(I)$), $R = 0.043$, $R_w = 0.047$. **4c** ($C_{30}H_{24}$): orthorhombic, $P2_12_12_1$, $a = 10.286(1)$, $b = 11.433(1)$, $c = 17.911(1)$ Å, $V = 2106.2(5)$ Å^3, $Z = 4$, $\rho_{calcd} = 1.213$ g cm^{-3}, $\mu = 4.823$ cm^{-1}, 1568 reflections, of which 1330 were observed ($I > 3\sigma(I)$), $R = 0.033$, $R_w = 0.031$. Further details of the crystal structure investigations may be obtained from the Fachinformationszentrum Karlsruhe, D-76344 Eggenstein-Leopoldshafen (Germany) on quoting the depository number CSD-58920.
[7] In the HPLC separation a minor fraction (7 area%) was isolated, whose UV absorption maxima are red-shifted relative to those of the two diastereomeric pairs of enantiomers. This can be explained by a twofold 1,3-hydrogen shift converting the Diels–Alder product **4** into a phenanthrene. This phenanthrene derivative also yields diphenyltriphenylene **5** on dehydrogenation.
[8] E. Clar, M. Zander, *J. Chem. Soc.* **1958**, 1861–1865; H. Hopff, H. R. Schweizer, *Helv. Chim. Acta* **1959**, *42*, 2315–2333; A. H. A. Tinnemans, W. H. Laarhoven, *J. Am. Chem. Soc.* **1974**, *96*, 4617–4622; Y. Fujioka, *Bull. Chem. Soc. Jpn.* **1985**, *58*, 481–489.

$XeOF_5^-$, an Anion with Pentagonal-Pyramidal Structure**

Arkady Ellern and Konrad Seppelt*

$XeOF_4$ and IF_5 have strikingly similar physical, chemical, and structural properties. Both have a square-pyramidal structure[1, 2] and show distinct intermolecular interactions in condensed phase. With fluoride acceptors they form the cations IF_4^+ and $XeOF_3^+$, which have a similar structure.[3, 4] Alkali metal fluorides dissolve in IF_5 and $XeOF_4$ to form the crystalline associates $F^- \cdot 3IF_5$ and $F^- \cdot 3XeOF_4$, which also display almost identical structures in which the three square-pyramidal IF_5 and $XeOF_4$ units solvate the F^- ion, but themselves remain structually virtually unaltered.[5, 6] Removal of IF_5 or $XeOF_4$ from these associates in vacuum yields the anions IF_6^- and $XeOF_5^-$. Because the salts always form as powders, structural investigations were difficult. $(CH_3)_4N^+IF_6^-$ could, however, be obtained in the form of single crystals. The structure of the anion IF_6^- is an octahedron strongly distorted towards C_{3v} symmetry. Because of its steric effect the nonbonding lone electron pair lies on the threefold axis. With the small cation NO^+ as counterion an $I_4F_{24}^{4-}$ cluster is obtained,[7] which resembles the tetramer found in solid XeF_6 and its solutions.[8, 9]

No exact data on the structure of $XeOF_5^-$ have yet been obtained. After analysis of the IR and Raman data, Holloway, Schrobilgen et al. assumed a low-symmetry C_s structure.[6] Christe et al. reported that ab initio calculations and a new analysis of the IR and Raman data showed a pentagonal-pyramidal structure with C_{5v} symmetry.[10]

Initially during studies of the anions XeF_7^- and XeF_8^{2-} we serendipitously obtained crystals of $NO^+XeOF_5^-$, which were apparently formed by hydrolysis. $NO^+XeOF_5^-$ is formed directly from NOF and $XeOF_4$ and crystallizes from the liquid phase below room temperature in millimeter long, colorless crystals. During the study of the NOF/$XeOF_4$ system a long time ago the existence of a 1:1 compound was established.[11]

Our precise single-crystal structural analysis of $NO^+XeOF_5^-$ gave a structure (Fig. 1a) that resembles neither the C_{3v}-symmetric structure of $(CH_3)_4N^+IF_6^-$ nor the cluster structure of

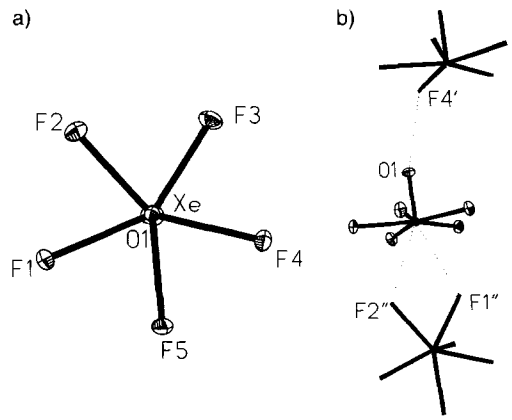

Fig. 1. Structure of the $XeOF_5^-$ ion in crystals of $NO^+XeOF_5^-$ (ORTEP representation, 50% probability). View onto the average plane through the five fluorine atoms. Distances [pm]: Xe–O 171.0(2), Xe–F1 203.2(2), Xe–F2 197.8(2), Xe–F3 195.6(2), Xe–F4 199.9(2), Xe–F5 201.1(2). The oxygen atom lies slightly off the ideal fivefold axis. b) View about perpendicular to the fivefold axis. Interanionic interactions are indicated by dotted lines. Distances [pm]: Xe···F1" 278, Xe···F2" 299, O···F4' 285.

$(NO^+IF_6^-)_4$. The $XeOF_5^-$ ion has a pentagonal-pyramidal structure with the oxygen atom in apical position. This structure is not only exceptionally aesthetic and unique in fluorine chemistry, but is also extremely regular. The lengths of all Xe–F bonds lie between 195.6(2) and 203.2(2) pm. The small variations can be explained by intramolecular interactions (Fig. 1b). The Xe–O bond of 171.0(2) pm is short as anticipated from its apical position. The xenon atom is situated merely 2.5(1) pm above the best plane through the five fluorine atoms; that is, the O-Xe-F angles are, with only one exception (89.1(1)°), slightly larger than 90° (90.6–91.8(1)°). The fluorine atoms, however, deviate up to 2.9(2) pm from this best plane. These slight deviations from ideal C_{5v} symmetry can also be explained by intermolecular interactions. The F-Xe-F angles lie between 71.2(1) and 74.0(1)°, thus showing minimal scatter about the ideal value of 72° for a planar XeF_5 unit.

Why does $XeOF_5^-$ behave so differently from IF_6^-? The oxygen–xenon bond must occupy substantially more space

[*] Prof. Dr. K. Seppelt, Dr. A. Ellern
Institut für Anorganische und Analytische Chemie der Freien Universität Berlin
Fabeckstrasse 34–36, D-14195 Berlin (Germany)
Telefax: Int. code + (30)838-2424
e-mail: seppelt@blume.chemie.fu-berlin.de

[**] This work was supported by the Deutsche Forschungsgemeinschaft and the Fonds der Chemischen Industrie. We thank the Alexander von Humboldt Foundation for scholarship for A. E.

than the fluorine atoms because of its partial double-bond character; the apical position of a pentagonal pyramid is well suited for such particularly large ligands; the nonbonding electron pair can occupy the *trans* apical position. In contrast to the central atom in BrF_6^- and XeF_8^{2-},[12, 13] the xenon atom in $XeOF_5^-$ is coordinatively unsaturated. It forms intermolecular Xe–F contacts (278.4 and 298.5 pm) with two fluorine atoms of adjacent anions. This additional coordination still leaves enough space for the nonbonding lone pair. On the other hand, these intermolecular interactions are comparatively weak and have no strong structure-determining influence. We had not previously found a suitable solvent for high-resolution NMR measurements of $NO^+XeOF_5^-$. $NO^+XeOF_5^-$ dissolves in acetonitrile; in the ^{19}F NMR spectrum at $-40\,^{\circ}C$ a broad signal (600 Hz) is observed at $\delta = 141$; this is explained by an intermolecular fluorine exchange.

Experimental Procedure

$XeOF_4$ and NOF (in the approximate ratio 1:1) were condensed under vacuum (stainless steel vacuum apparatus) into a perfluoroethene–propene (Teflon–FEP) tube, which was then sealed. The liquid phase solidified slightly below room temperature to form large crystals that were partly formed by sublimation as well. Crystal structure analysis: A suitable crystal with dimensions $0.4 \times 0.4 \times 0.4$ mm was mounted at low temperature ($T = -153\,^{\circ}C$) on an Enraf–Nonius CAD4 diffractometer; space group $P2_1/n$ (no. 14), $a = 669.8(1)$, $b = 551.0(1)$, $c = 1425.1(2)$ pm, $\beta = 101.2(2)^{\circ}$, $V = 515.9(1)$ pm^3, $Z = 4$, $2\theta_{max} = 90^{\circ}$, $Mo_{K\alpha}$, 71.069 pm, ω scan, 4275 measured reflections of which 4169 were independent and 4150 used, Lorentz polarization correction, Difabs absorption correction [14], $\mu = 68.3$ mm^{-1}, min./max. correction 0.73/1.10, structure solved with the program SHELXS-86 [15], structure refinement with SHELXL-93 [16], 83 parameters, $R_1 = 0.0296$, $wR_2 = 0.0806$, extinction coefficient 0.0114(9), residual electron density 2.7 e $\times 10^6$ pm^{-3} (80 pm from xenon atom). Further details of the crystal structure investigation may be obtained from the Fachinformationszentrum Karlsruhe, D-76344 Eggenstein-Leopoldshafen (Germany) on quoting the depository number CSD-58969.

Received: March 15, 1995 [Z77981E]
German version: *Angew. Chem.* **1995**, *107*, 1772–1773

Keywords: fluorine compounds · xenon compounds

[1] J. F. Martins, E. B. Wilson, Jr., *J. Mol. Spectr.* **1968**, *26*, 410–417; *J. Chem. Phys.* **1964**, *41*, 570–571; E. J. Jacob, H. B. Thompson, L. S. Bartell, *J. Mol. Struct.* **1971**, *8*, 383–394.
[2] A. G. Robiette, R. H. Bradley, P. N. Brier, *J. Chem. Soc. D* **1971**, 1567–1568.
[3] A. J. Edwards, P. Taylor, *J. Chem. Soc. Dalton Trans.* **1975**, 2174–2177.
[4] H. Selig, *Inorg. Chem.* **1966**, *5*, 183–186; D. E. McKee, C. J. Adams, A. Zalkin, N. Bartlett, *J. Chem. Soc. Chem. Commun.* **1973**, 26–28; D. E. McKee, C. J. Adams, N. Bartlett, *Inorg. Chem.* **1973**, *12*, 1722–1725; R. J. Gillespie, G. J. Schrobilgen, *ibid.* **1974**, *13*, 2370–2374.
[5] K. O. Christe, *Inorg. Chem.* **1972**, *11*, 1215–1219; A. R. Mahjoub, A. Hoser, J. Fuchs, K. Seppelt, *Angew. Chem.* **1989**, *101*, 1528–1529; *Angew. Chem. Int. Ed. Engl.* **1989**, *28*, 1526–1527.
[6] J. H. Holloway, V. Kaucic, D. Martin-Rovet, D. R. Russell, G. J. Schrobilgen, H. Selig, *Inorg. Chem.* **1985**, *24*, 678–683; G. J. Schrobilgen, D. Martin-Rovet, P. Charpin, M. Lance, *J. Chem. Soc. Chem. Commun.* **1980**, 894–897.
[7] A. R. Mahjoub, K. Seppelt, *Angew. Chem.* **1991**, *103*, 309–311; *Angew. Chem. Int. Ed. Engl.* **1991**, *30*, 323–324.
[8] R. D. Burbank, G. R. Jones, *J. Am. Chem. Soc.* **1974**, *96*, 43–48.
[9] H. H. Rupp, K. Seppelt, *Angew. Chem.* **1974**, *86*, 669–670; *Angew. Chem. Int. Ed. Engl.* **1974**, *13*, 612–613; K. Seppelt, H. H. Rupp, *Z. Anorg. Allg. Chem.* **1974**, *409*, 331–337; K. Seppelt, N. Bartlett, *ibid.* **1977**, *436*, 122–126; G. J. Schrobilgen, J. H. Holloway, P. Granger, C. Brevard, *Inorg. Chem.* **1978**, *17*, 980–987.
[10] K. O. Christe, D. A. Dixon, J. C. P. Sanders, G. J. Schrobilgen, S. S. Tsai, W. W. Wilson, *Inorg. Chem.* **1995**, *34*, 1868.
[11] G. J. Moody, H. Selig, *Inorg. Nucl. Chem. Lett.* **1966**, *2*, 319–320.
[12] A. R. Mahjoub, A. Hoser, J. Fuchs, K. Seppelt, *Angew. Chem.* **1989**, *101*, 1528–1529; *Angew. Chem. Int. Ed. Engl.* **1989**, *28*, 1526–1527; A. R. Mahjoub, X. Zhang, K. Seppelt, *Chem. Eur. J.* **1995**, *1*, 261–265.
[13] S. W. Peterson, J. H. Holloway, B. A. Coyle, J. M. Williams, *Science* **1971**, *173*, 1238–1239.
[14] N. Walker, D. Stuart, *Acta Crystallogr. Sect. A* **1983**, *39*, 158–166.
[15] G. M. Sheldrick, *Program for Crystal Structure Solution*, Universität Göttingen, **1986**.
[16] G. M. Sheldrick, Program for Crystal Structure Refinement, Universität Göttingen, **1993**.

Hydroxylation of Alkanes with Molecular Oxygen Catalyzed by a New Ruthenium-Substituted Polyoxometalate, $[WZnRu_2^{III}(OH)(H_2O)(ZnW_9O_{34})_2]^{11-}$**

Ronny Neumann,* Alexander M. Khenkin, and Mazal Dahan

The utilization of dioxygen in liquid-phase oxidation of hydrocarbons is currently an important research goal due to its availibility and its benign effect on the environment. Since dioxygen has a triplet ground state, direct oxidation of organic compounds is not possible. Common modes of dioxygen "activation" thus include a) formation of hydrocarbon radicals leading to formation of reactive hydroperoxides by free-radical autoxidation mechanisms,[1] b) photoexcitation of dioxygen to form highly reactive singlet oxygen,[2] c) use of dioxygen as a secondary oxidant in metal-ion-catalyzed mechanisms as in Wacker-type processes,[3] and d) reductive cleavage of transition-metal dioxygen complexes to form highly active metal–oxo intermediates as in manganese porphyrins[4] and the various Gif systems.[5] A more desirable mode of activation would be the direct use of dioxygen to elicit oxygenation without formation of hydrocarbon radicals, or use of photoexcitation or reducing agents. A few such examples exist including alkene epoxidation with ruthenium porphyrins[6] and alkane hydroxylation with perfluorinated iron porphyrins,[7] although recently evidence has been put forward claiming that the latter is a free-radical autoxidation.[8]

In this paper we report on the preparation of a diruthenium-substituted polyoxometalate **1** and its use as a catalyst for the

$[WZnRu_2^{III}(OH)(H_2O)(ZnW_9O_{34})_2]^{11-}$ **1**

hydroxylation of alkanes such as adamantane with molecular oxygen at atmospheric pressure. Hydroxylation takes place almost *exclusively* at the tertiary carbon positions. This regioselectivity indicates that the oxidaton is not a typical free-radical autoxidation and that the ruthenium-substituted polyoxometalate activates molecular oxygen in a non-radical pathway. Supportive of this conclusion are the findings that adamantane is more reactive than triphenylmethane, that the reaction is not inhibited by the presence of alkyl-radical scavengers such as *tert*-butylcatechol, and that oxidation with hydroperoxides (required intermediates in autoxidations) yield significantly different reaction selectivities.

The polyoxometalate may be viewed as a dimer of a truncated Keggin structure having a "belt" of W, Zn, and Ru cations sandwiched between the two B-XW_9O_{34} trivacant Keggin fragments (Fig. 1). This new ruthenium polyoxometalate is isostructural with other similar transition-metal-substituted compounds reported[9, 10] and used previously.[11] Temperature-dependent magnetic susceptibility measurments[12] and the EPR spectrum[13] of the polycrystalline solid both support the X-ray analysis, indicating that the polyoxometalate should be viewed as a compound with two hexacoordinate ruthenium(III) centers at the designated terminal positions with one labile aqua

[*] Dr. R. Neumann, Dr. A. M. Khenkin, M. Dahan
Casali Institute of Applied Chemistry, Graduate School of Applied Science
The Hebrew University of Jerusalem, Jerusalem 91904 (Israel)
Telefax: Int. code + (26) 528250
e-mail: ronnyta vms.huji.ac.il

[**] This research was supported by the Basic Research Foundation administered by the Israel Academy of Sciences and Humanities. We thank Dr. Shmuel Cohen for the crystallographic analysis.

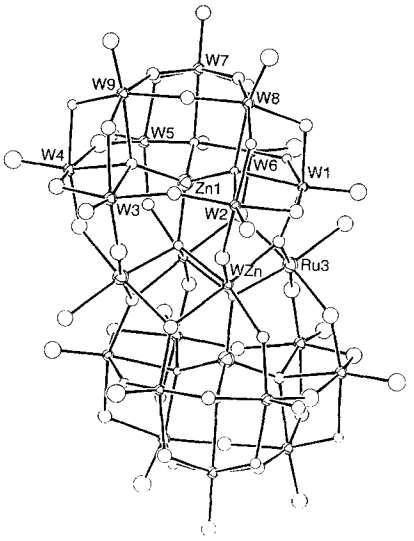

Fig. 1. Ortep drawing of the crystal structure of the anion in Na_{11}-**1**.

and one hydroxy ligand. Cyclic voltammetry shows a reversible Ru^{III}/Ru^{IV} oxidation at + 0.38 V.

The results of the oxidation reactions are summarized in Table 1. Substrates such as adamantane (**1**) and congressane (**2**)

Table 1. Hydroxylation of alkanes catalyzed by ruthenium polyoxometalate [a].

Substrate	Products (mol product/mol catalyst)		
1 [b]	**3** (103–118)	**4** (trace)	**5** (trace)
1 [c]	**3** (369)	**4** (trace)	**5** (3)
1 [d]	**3** (92)	**4** (trace)	**5** (trace)
1 [e]	**3** (trace)	**4** (trace)	**5** (trace)
1 [c, e]	**3** (38)	**4** (2)	**5** (13)
2	**6** (87)	**7** (trace)	**8** (trace)
2 [d]	**6** (78)	**7** (trace)	**8** (trace)
c-C_6H_{12} [f]			
i-C_6H_7Ph [f]			
Ph_3CH	Ph_2CO (5)	Ph_3COH (15)	
PH_3CH [d]	Ph_2CO (11)	Ph_3COH (20)	
Ph_2CH_2 [f]			
1 [g]	**3** (trace)	**4** (trace)	**5** (trace)
1 [h]	**3** (156)	**4** (22)	**5** (37)

[a] See Experimental Procedure. [b] Range for five reactions. [c] Reaction time 7 days. [d] 1 mmol *tert*-butylcatechol added. [e] No catalyst; conversion in % × 10. [f] No reaction. [g] Catalyst $PRuW_{11}O_{39}^{4-}$. [h] Catalyst $PRuMo_{11}O_{39}^{4-}$.

having both tertiary and secondary saturated carbon atoms that bear hydrogen atoms react virtually only at the tertiary position yielding 1-adamantanol (**3**) and 1-congressanol (**6**). Very little alcohol or ketone is formed at the secondary carbon.[14]

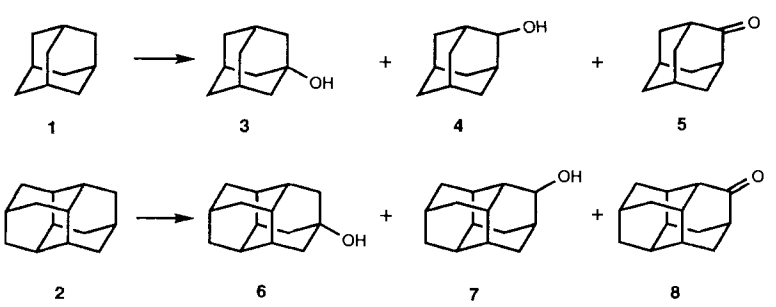

Further confirmation of this trend can be seen in the complete inactivity of alkanes with only secondary carbon centers such as cyclohexane and diphenylmethane. Under free-radical conditions, normal ratios of oxidation at tertiary vs. secondary positions is 3:1. Furthermore, addition of the alkyl-radical scavenger, *tert*-butylcatechol, even at four times the amount of alkane substrate, caused only a very slight decrease in catalytic activity.[15] Additionally, alkylaromatic compounds such as cumene and triphenylmethane, known to be relatively highly reactive to free-radical autoxidations, were inactive or only slightly active in the presence of the disubstituted ruthenium polyoxometalate. Finally, oxidations with of adamantane with *tert*-butylhydroperoxide yielded a ratio of oxidation tertiary/secondary of 6.7:1. Assuming similar regioselectivity of all tertiary hydroperoxides, this result would also seem to indicate that adamantane hydroperoxide, the expected intermediate in an autoxidation pathway, is not an intermediate in the oxidation with molecular oxygen. Other ruthenium-substituted polyoxometalates reported in the literature were inactive ($PRuW_{11}O_{39}^{4-}$,[16] $SiRuW_{11}O_{39}^{5-}$),[17] yielded the usual ratio of autoxidation products ($PRuMo_{11}O_{39}^{4-}$),[18] or are known to form μ-oxo dimers ($(P_2W_{17}O_{61}Ru)_2O^{16-}$).[19] It would presumptuous at this stage to give a mechanistic explanation for our findings; however, a variety of explanations ranging from formation of caged hydrocarbon radicals within **1** to formation of active ruthenium–oxo intermediates is to be explored. The mechanistic uncertainty, however, does not detract from the importance of the discovery of a new mode of dioxygen activation in the hydroxylation of alkanes by use of a novel "oxidatively stable"[20] ruthenium-substituted polyoxometalate.

Experimental Procedure

The ruthenium-disubstituted polyoxometalate Na_{11}-**1**·$42H_2O$ was prepared by adding $Ru[(CH_3)_2SO]_4Cl_2$ (4.0 g, 12.2 mmol) to a solution of $Na_{12}Zn_3(H_2O)_2Zn_2W_{19}O_{68}\cdot 46H_2O$ (23 g, 3.9 mmol) in water (10 mL) at 90 °C under argon. The solution was stirred at this temperature for 18 h, then cooled, and opened to air. When 2 g of KCl was added to the brown solution, 10.9 g of the desired compound precipitated. The product was recrystallized twice from hot water. Overall yield: 24%; anal. calcd for $K_{11}Ru_2Zn_3W_{19}O_{68}\cdot 15H_2O$: K 6.97, Ru 3.60, Zn 3.50, W 62.32, H_2O 4.82; found K 7.06, Ru 3.56, Zn 3.24, W 61.30, H_2O 4.69. Single crystals for X-ray analysis were obtained by recrystallizing 0.12 g of the potassium salt in 10 mL of 0.5 M NaCl solution.

A stock solution of 2.71×10^{-4} M $Q_{11-x}Na_x$-$\mathbf{1}_2$ (Q = tricaprylmethylammonium) was prepared by mixing Na_{11}-$\mathbf{1}_2$·$42H_2O$ (1 g) dissolved in water with tricaprylmethyammonium chloride (1 g) dissolved in 1,2-dichloroethane (10 mL), separating phases, and drying the organic phase with Na_2SO_4. Concentrations were determined by UV-Vis spectroscopy; $\lambda_{max}(\varepsilon) = 306$ nm($50000\,M^{-1}cm^{-1}$).

Hydroxylation reactions were carried out by holding a solution of substrate (0.25 mmol) and ruthenium polyoxometalate (0.25 μmol, 0.1 mol%) in 1,2-dichloroethane (0.5 mL) under dioxygen (10 mL, approximately 0.45 mmol) at atmospheric pressure at 80 °C for 24 h. After cooling, reaction mixtures were analyzed unambiguously by GLC with two different columns using reference samples; the product identity was crosschecked by GLC-MS.

Received: February 1, 1995
Revised version: April 3, 1995 [Z 7677 IE]
German version: *Angew. Chem.* **1995**, *107*, 1740–1742

Keywords: oxygen activation · polyoxometalates · ruthenium compounds

[1] R. A. Sheldon, J. K. Kochi, *Metal Catalysed Oxidation of Organic Compounds*, Academic Press, New York, **1981**.
[2] H. H. Wassermann, R. W. Murray, *Singlet Oxygen*, Academic Press, New York, **1978**.
[3] G. W. Parshall, S. D. Ittel, *Homogeneous Catalysis*, 2. ed., Wiley, New York, **1992**, p. 138.
[4] I. Tabushi, *Coord. Chem. Rev.* **1988**, *86*, 1.
[5] D. H. R. Barton, E. Csuhai, N. Ozbalik, *Tetrahedron* **1990**, *46*, 3743.
[6] J. T. Groves, R. Quinn, *J. Am. Chem. Soc.* **1985**, *107*, 5790.

[7] P. E. Ellis, Jr., J. E. Lyons, *J. Chem. Soc. Chem. Commun.* **1989**, 1315.
[8] M. W. Grinstaff, M. G. Hall, J. A. Labinger, H. B. Gray, *Science* **1994**, *264*, 1311.
[9] The crystallographic analysis yielded a formula of $Na_{11}WZnRu_2(OH)(H_2O)(ZnW_9O_{34})_2 \cdot 42H_2O$. The anion had essentially the same cell dimensions and positional parameters as other analogous polyoxometalates.
[10] C. M. Tourné, F. F. Tourné, F. Zonnevijlle, *J. Chem. Soc. Dalton Trans.* **1991**, 143.
[11] R. Neumann, M. Gara, *J. Am. Chem. Soc.* **1994**, *116*, 5509.
[12] The molecular magnetic moment at 100 K was 4.48 μ_B, indicative of two Ru^{III} centers; the temperature dependence of the molecular moment was due to spin–orbit coupling with no ferromagnetic or antiferromagnetic interactions.
[13] The EPR spectrum was typical of a nonmagnetically coupled Ru^{III} center with $S = 1/2$ in an octahedral coordination with $g_{\parallel} = 1.80$ and $g_{\perp} = 2.30$.
[14] Typically yields were 10% based on the organic substrate on use of 0.1 mol% of **1** within 24 h. Yields of up to 55% could be obtained at 1 mol% catalyst.
[15] *tert*-Butylcatechol has an autoxidizability 10000 times greater than tertiary carbon atoms; cf. N. M. Emmanuel, E. T. Denisov, Z. K. Maizus, *Liquid-Phase Oxidation of Hydrocarbons*, Plenum, New York, **1967**.
[16] C. Rong, M. T. Pope, *J. Am. Chem. Soc.* **1992**, *114*, 2932.
[17] R. Neumann, C. Abu-Gnim, *J. Am. Chem. Soc.* **1990**, *112*, 6025.
[18] R. Neumann, M. Dahan, *J. Chem. Soc. Chem. Commun.* **1995**, 171.
[19] W. J. Randall, T. J. R. Weakley, R. G. Finke, *Inorg. Chem.* **1993**, *32*, 1068.
[20] C. L. Hill, *Activation and Functionalization of Alkanes*, Wiley, New York, **1989**, p. 243.

The Crafts–Friedel Reaction: Aromatic Alkylation within the Complex Formed upon Addition of a Gaseous Arenium Ion to an Olefin**

Massimiliano Aschi, Marina Attinà, and Fulvio Cacace*

Alkylation of arenes with olefins, one of the most important industrial applications of Friedel–Crafts reactions, proceeds by preliminary protonation of the alkenes by Brønsted acids such as $H(BF_3OH)$, $H(AlCl_3OH)$, H_2SO_4, followed by addition of the carbenium ions formed, or their polarized complexes, to the arene [Eq. (a)].[1] An alternative route is conceivable, in which alkylation occurs within a complex formed upon addition of an arenium ion to the olefin [Eq. (b)].

$$C_3H_6 + HA \longrightarrow iC_3H_7^{\delta+} \cdots A^{\delta-} \xrightarrow{+C_6H_6} \mathbf{1} + A^- \quad (a)$$

$$C_6H_7^+ + C_3H_6 \longrightarrow [C_6H_7^+ \cdot C_3H_6] \rightleftharpoons [C_6H_6 \cdot iC_3H_7^+] \rightleftharpoons \mathbf{1} \quad (b)$$

2 **3**

Sequence (b) represents a distinct reaction pathway, with special kinetic and mechanistic features, only if alkylation occurs within the complex, without separation of the reagents. If, on the contrary, the carbenium ion escapes into the medium and reacts with the arene only at some later stage, the whole sequence is tantamount to a conventional Friedel–Crafts alkylation whose only peculiarity is that the acid used to protonate the olefin is an arenium ion.

Aromatic alkylation promoted by the reaction of arenium ions with olefins was envisaged long ago by Olah,[2] but because discrimination between the alternative pathway (b) and the conventional mechanism (a) is extremely difficult in solution, further developments were blocked. We report here the first demonstration that the alkylation mechanism outlined in sequence (b) is actually operative in the gas phase and present a preliminary account of its essential features, deduced from the joint application of mass spectrometry and radiolysis.[3]

To demonstrate operation of sequence (b) in the gas phase, preliminary FT-ICR experiments were performed, where $C_6H_6D^+$ benzenium ions ($m/z = 80$), obtained by chemical ionization of $[^{12}C]C_6H_6$ with CO/D_2 in the external ion source of the spectrometer, were driven into the resonance cell, isolated by multiple ejection techniques, and allowed to react with C_3H_6. As expected, at the low stationary pressure (less than 5×10^{-7} Torr) of the cell, the $C_9H_{12}D^+$ ion from sequence (b) could not be detected, owing to its fast back dissociation under conditions of inefficient collisional stabilization.

However, by using a pulsed valve one can obtain, albeit for a short time (5 ms), C_3H_6 pressures up to 5×10^{-5} Torr, which allows stabilization of a fraction of the $C_9H_{12}D^+$ ions, which can thus be positively identified by accurate mass measurements (Fig. 1). Despite their low relative abundance (< 5%) formation of the $C_9H_{12}D^+$ ions is significant, since it can only occur within the complex formed by the reactants. In fact, no C_6H_6 is introduced into the reaction cell, which excludes the role of any free $iC_3H_6D^+$ as a source of the $C_9H_{12}D^+$ ion observed.[4]

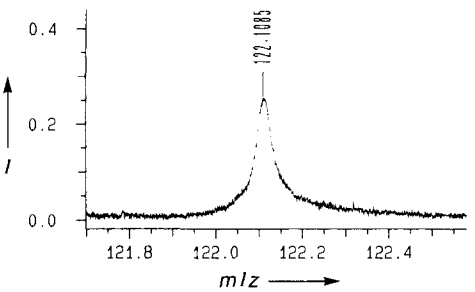

Fig. 1. Exact mass analysis of the $C_9H_{12}D^+$ adduct from the reaction of $C_6H_6D^+$ with C_3H_6 under the conditions given in the text. Relative ionic intensity in arbitrary units.

The FT-ICR results are consistent with, but do not prove the occurrence of sequence (b) since the data give no structural information, and it cannot be excluded that the $C_9H_{12}D^+$ ions observed are noncovalent complexes, like **2** and/or **3**, rather than protonated cumene **1**. More conclusive evidence was obtained from the radiolytic experiments (see Table 1).

In the experiments a bulk gas, for example, CH_3F at atmospheric pressure, containing small amounts of the reactants (C_6D_6 and C_3H_6), a radical scavenger (O_2), and a gaseous base such as $(CH_3)_2O$, is subjected to γ irradiation. According to a well-established reaction sequence,[5] ionization of CH_3F produces stable $(CH_3)_2F^+$ ions that react efficiently with C_6D_6 to give $C_6D_6CH_3^+$ ions,[6] which are largely converted by the base into $C_6D_5CH_3$, a major radiolytic product.[7] Those toluenium ions that escape deprotonation are available to promote iso-

[*] Prof. Dr. F. Cacace, Dr. M. Aschi
Università di Roma "La Sapienza"
Piazzale A. Moro 5, I-00185 Rome (Italy)
Telefax: Int. code + (6)4991-3888
Prof. Dr. M. Attinà
Università di Camerino (Italy)

[**] This work was supported by the Italian Ministero per l'Università e la Ricerca Scientifica e Tecnologica (MURST) and Consiglio Nazionale delle Ricerche (CNR).

Table 1. Alkylated products from the reaction with olefins of the arenium ions from the attack of radiolytically formed cations on C_6D_6.

T [°C]	Gas phase [a]	Olefin	Alkylated products (*o*:*m*:*p*)	Product ratio [b]
42	CH_3F	C_3H_6	$CH_3C_6D_4iC_3H_6D$	ca. 1.4×10^{-3}
80	CH_3F	C_3H_6	$CH_3C_6D_4iC_3H_6D$	6.0×10^{-3}
120	CH_3F	C_3H_6	$CH_3C_6D_4iC_3H_6D$ (50:25:25)	$\frac{CH_3C_6D_4iC_3H_6D}{C_6D_5CH_3} = 3.1\times10^{-2}$
135	CH_3F	C_3H_6	$CH_3C_6D_4iC_3H_6D$	3.6×10^{-2}
120	CH_3F	cC_6H_{10}	$CH_3C_6D_4cC_3H_{10}D$	$\frac{CH_3C_6D_4cC_6H_{10}D}{C_6D_5CH_3} = 5.6\times10^{-2}$
42	CF_4	C_3H_6	$CF_3C_6H_4iC_3H_6D$ (0:74:26)	0.13
80	CF_4	C_3H_6	$CF_3C_6H_4iC_3H_6D$	$\frac{CF_3C_6H_4iC_3H_6D}{C_6D_5CF_3} = 0.11$

[a] All systems contained C_6D_6 (1.5–2.8 Torr), the olefin (5–10 Torr), O_2 (10 Torr), and a gaseous base (Me_2O, 1.1 Torr). Absorbed dose 1.3×10^4 Gy; dose rate 2×10^4 Gy h^{-1}. [b] Standard deviation of the ratio ±10%.

propylation (Scheme 1, X = H). The nature and the isomeric composition of the products, established by GC/MS, correspond exactly to the isomeric $CH_3C_6D_4iC_3H_6D$ cymenes expected from sequence (b). Furthermore, under the conditions prevailing in the radiolytic experiments, isopropylation necessarily occurs within an ion–molecule complex, which excludes a role for free $iC_3H_6D^+$ ions. The efficiency of the process, expressed by the cymenes/toluene ratio (last column of Table 1), undergoes a 26-fold increase as the reaction temperature is raised from 42 to 135 °C, and points to an activation barrier most likely associated with conversion of complex **4** into **5** (X = H), which is endothermic because toluene is more basic than propene. If the deprotonation rate of **4** by B is essentially independent of the temperature, a reasonable assumption for an exothermic proton transfer from an unhindered arenium ion to an n-type base, the activation energy for the conversion of **4** into **5** can be calculated from the dependence of the cymenes/toluene ratio on the temperature. The result ($E_a = 9.1\pm1.0$ kcal mol^{-1}) is significantly close to the difference in proton affinity between toluene and propene of 9.3 kcal mol^{-1}.[8]

It is noteworthy that the isomeric composition of the cymenes from (b) is the same as that in control experiments involving alkylation of toluene by free $iC_3H_7^+$ ions at the same temperature.[9] Replacing C_3H_6 with cC_6H_{10} yields an a isomeric mixture of $CH_3C_6D_4cC_6H_{10}D$ *cyclo*-hexyltoluenes, and it is apparent from Table 1 that the efficiency of the alkylation increases appreciably when the more basic cycloalkene is used.[10] Remarkably, no 1-methyl-cyclopentyl derivative was detected among the products: fast trapping within the [toluene–cyclohexylium ion] complex must prevent rearrangement of the cation, a reaction that is unavoidable in conventional bimolecular reactions even at pressures up to 1470 Torr in the presence of high concentrations of an efficient nucleophile.[11] Significantly, isodurenium ions from the methylation of mesitylene are completely unreactive toward C_3H_6 even at 135 °C. Finally, alkylation of C_6D_6 with CF_3^+ from the radiolysis of CF_4[12] promotes the reaction sequence outlined in Scheme 1, X = F, leading to formation of isomeric $CF_3C_6D_4iC_3H_6D$. This reaction displays a weakly negative temperature dependence and is considerably more efficient than for X = H, consistent with the lower basicity of $CF_3C_6D_5$ compared to that of $CD_3C_6D_5$, which reduces or cancels the endothermicity, and hence lowers the barrier for the conversion of **4** into **5** when X = F.

Despite their preliminary nature, the above results conclusively demonstrate operation of sequence (b) in the gas phase and provide a coherent picture of its peculiar features that allows sharp mechanistic discrimination from conventional Friedel–Crafts alkylation. For example, the seemingly paradoxical observation that the rate of formation of isopropylated trifluorotoluenes exceeds that of cymenes, whereas isopropylation of isodurene does not occur at all, that is, a trend that runs contrary to that prevailing in conventional Friedel–Crafts alkylation, is easily accommodated in the framework of sequence (b). In fact, in those cases where the **4** → **5** conversion is rate determining, the process is favored by a relatively low basicity, and hence by a low nucleophilicity of the arene, whereas this feature depresses the reactivity in conventional electrophilic alkylation (a).

The present results are of relevance to the theory of aromatic substitution, and outline a new class of electrophilic alkylation reactions, whose salient feature is the extremely short lifetime (down to the picosecond scale) of the alkylating cation prior to reaction. This widens the scope of aromatic alkylation by allowing substitution by unstable carbenium ions that would undergo isomerization in conventional bimolecular reactions. This work is also relevant to gas-phase ion chemistry, providing the first demonstration of an aromatic substitution occurring within an ion–molecule complex prepared by assembling ini-

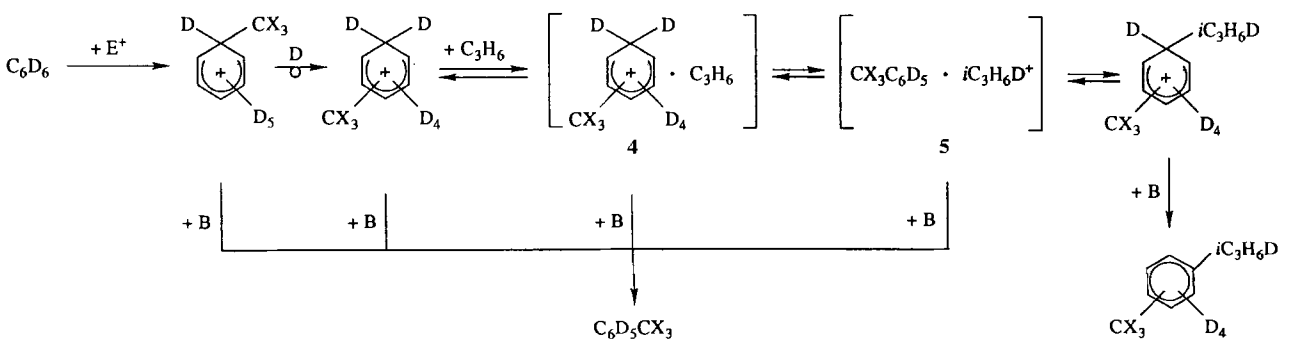

Scheme 1. $E^+ = (CH_3)_2F^+$, X = H; $E^+ = CF_3^+$, X = F.

 © VCH Verlagsgesellschaft mbH, D-69451 Weinheim, 1995 0570-0833/95/1515-1590 $ 10.00+.25/0

tially separate components. The role of ion–molecule complexes has long been postulated in mass spectrometry,[13] but was based, in general, on indirect evidence from the fragmentation pattern of excited species from the ionization of molecules in which the putative components of the complex were initially covalently bound. In the specific case of alkylbenzenes, irrefutable mass spectrometric evidence is lacking for complexes such as **2**; results of molecular orbital calculations[14] do not appear inconsistent with ours.

Experimental Procedure

The gaseous samples for the radiolytic experiments were prepared in sealed 135 mL glass vessels, irradiated in a 220 Gammacell (Nuclear Canada Ltd.), fitted with a thermostat. The gases and the chemicals used were research-grade products from commercial sources. The radiolytic products were analyzed by GC/MS (50 m long, 0.2 mm i.d. fused silica column, coated with a 0.5 μm methylsilicone film; VG Micromass TRIO quadrupole mass spectrometer). The FT-ICR experiments were performed with a Bruker Spectrospin Apex TM 47e spectrometer equipped with an external ion source.

Received: March 1, 1995 [Z 7754 IE]
German version: *Angew. Chem.* **1995**, *107*, 1719–1721

Keywords: alkylations · aromatic substitutions · gas-phase chemistry · kinetics · ICR spectroscopy

[1] C. Friedel, J. M. Crafts, *Bull. Soc. Chim. Fr.* **1877**, *27*, 530; *Friedel–Crafts and Related Reactions* (Ed.: G. A. Olah), Wiley-Interscience, New York, **1963**; G. A. Olah, *Friedel–Crafts Chemistry*, Wiley-Interscience, New York, **1973**; R. M. Roberts, A. A. Khalab, *Friedel–Crafts Alkylation Chemistry*, Dekker, New York, **1984**; R. Taylor, *Electrophilic Aromatic Substitution*, Wiley, New York, **1990**.

[2] G. A. Olah, Abstract of Papers 3P, 138th Meeting of the American Chemical Society, New York, **1960**; see ref. [1].

[3] F. Cacace, *Acc. Chem. Res.* **1988**, *21*, 215.

[4] C_6H_6 leaking from the external source is actually present in traces within the cell, but it cannot be a source of detectable $C_9H_{12}D^+$ because of its low partial pressure (less than 10^{-9} Torr) and the $[C_3H_6]/[C_6H_6]$ ratio greater than 5×10^4.

[5] J. L. Beauchamp, D. Holz, S. D. Woodgate, S. L. Patt, *J. Am. Chem. Soc.* **1972**, *94*, 2718; J. Hollis, J. M. Tedder, G. S. Walker, *J. Chem. Soc. Perkin Trans. 2* **1991**, 1187.

[6] M. Speranza, N. Pepe, R. Cipollini, *J. Chem. Soc. Perkin Trans. 2* **1979**, 1179.

[7] Depending on the composition of the system, the yields of $C_6D_5CH_3$, expressed by the corresponding G_{-M} values (number of molecules formed per 100 eV absorbed) range from 0.2 to 0.4.

[8] J. E. Szulejko, T. B. McMahon, *J. Am. Chem. Soc.* **1993**, *115*, 7839.

[9] The substitution pattern at 37.5 °C in C_3H_8 at 720 Torr is $o:m:p = 43:31:26$; M. Attinà, F. Cacace, G. Ciranni, P. Giacomello, *J. Am. Chem. Soc.* **1977**, *99*, 2611.

[10] The proton affinity of cC_6H_{10} is 189 kcal mol^{-1}: S. G. Lias, J. E. Bartmess, J. F. Liebman, J. L. Holmes, R. D. Levin, W. G. Mallard, *J. Phys. Chem. Ref. Data* **1988**, *17*, Suppl. 1.

[11] M. Attinà, F. Cacace, A. Di Marzio, *J. Am. Chem. Soc.* **1989**, *111*, 6004.

[12] R. Cipollini, G. Lilla, N. Pepe, M. Speranza, *J. Phys. Chem.* **1978**, *82*, 1207.

[13] R. D. Bowen, *Acc. Chem. Res.* **1991**, *24*, 364; A. G. Harrison, *Can. J. Chem.* **1985**, *64*, 1051; R. W. Holman, M. L. Gross, *J. Am. Chem. Soc.* **1989**, *111*, 3560; D. Kuck, *Mass Spectrom. Rev.* **1990**, *9*, 586.

[14] D. Berthomieu, V. Brenner, G. Ohanessian, J. P. Denhez, P. Millié, H. E. Audier, *J. Am. Chem. Soc.* **1993**, *115*, 2505.

Electrochemical Evidence for Through-Space Orbital Interactions in Spiromethanofullerenes**

Matthias Eiermann, Robert C. Haddon, Brian Knight, Q. Chan Li, Michele Maggini, Nazario Martín, Toshinobu Ohno, Maurizio Prato, Toshiyasu Suzuki, and Fred Wudl*

While buckminsterfullerene C_{60}[1] can be converted efficiently into a remarkable number of methanofullerenes and fulleroids,[2] gaining control over its electronic properties still is an interesting and demanding goal[3] which might open up a broad variety of applications similar to achievements in classical benzene chemistry.

The cyclic voltammetry (CV) data of diphenylmethanofullerenes **1** with electron-donating groups (EDGs) and electron-withdrawing groups (EWGs) in the *p,p'* positions of the phenyl groups are independent of the functional groups.[4] In contrast, spiroannelated analogues show remarkable substituent effects which we suggested calling "periconjugation".[5] Here we describe our experimental evidence obtained from 1,1-(4-oxocyclohexa-2,5-dieno)- and 9,9-fluorenofullerenes and present the conclusions derived from the observations.

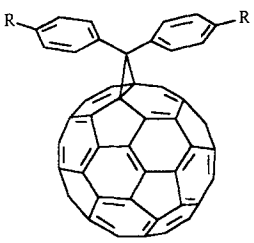

1 (R = EWG, EDG)

The most direct method for studying the influence of addends on the electronic properties of fullerene C_{60} is cyclic voltammetry. The CV measurements were carried out in *o*-dichlorobenzene, because the spiroannelated methanofullerenes are most soluble in this solvent[6] and four reduction waves of C_{60} can be detected. Since various irreversible processes can be observed in some of the cyclic voltammograms, peak potentials rather than the averaged data are given in Table 1 and in the discussion. All compounds described were prepared by known methods.[2, 7]

Since the 5/6- and 6/6-isomers of 1,1-(4-oxocyclohexano)-fullerene, **2a** and **2b**, respectively, can be separated, both could be characterized by CV individually. Their first reductions are fully reversible and occur at −1158 and −1164 mV (peak potentials, vs. ferrocene/ferrocenium), respectively, well within the expected range for "standard" methanofullerenes.[2, 8] In comparison, the reduction is facilitated by more than 70 mV (vs. **2b**)

[*] Prof. Dr. F. Wudl, Dr. M. Eiermann, B. Knight, Q. C. Li, N. Martín, T. Ohno, T. Suzuki
Institute for Polymers and Organic Solids
Departments of Physics and Chemistry, University of California
Santa Barbara, CA 93106 (USA)
Telefax: Int. code + (805)893-4755
e-mail: wudl@physics.ucsb.edu

R. C. Haddon
AT&T Bell Laboratories, Murray Hill, NJ (USA)

M. Maggini
Centro Meccanismi Reazioni Organiche del CNR
Dipartimento di Chimica Organica, Padova (Italy)

M. Prato
Dipartimento di Scienze Farmaceutiche, Trieste (Italy)

[**] This work was partially supported by the MRL Program and the National Science Foundation (award DMR-91-3048 and grants DMR-91-22536, DMR-91-11097, and CHE-89-08323). M. E. is indebted to the Alexander-von-Humboldt-Stiftung, and to Prof. P. C. Ford, UCSB, for support (Feodor-Lynen fellowship). M. P. and F. W. are indebted to NATO for a travel grant. N. M. is indebted to Universidad Complutense de Madrid for a "Del Amo" fellowship.

Table 1. Peak potentials E for reductions (in mV vs. ferrocene/ferrocenium) for C_{60} and compounds **1**–**13** from their cyclic voltammograms.

Cmpd.	$E_{(1,\text{red.})}$	$E_{(2,\text{red.})}$	$E_{(>2,\text{red.})}$
C_{60}	−1123	−1455	−1913, −2383
1 (R = H)	−1151	−1531	−2031
2a	−1158	−1550	−2010, −2379 [d]
2b	−1164	−1554	−2044, −2504
3	−1081 [b, f]	−1559 [f]	
4	−1097 [e]	−1620 [d]	−2037
5	−1042 [a]	−1197 [a]	−1602, −2016
6	−1143	−1501	−1703, −2073
7 [12]	−1176	−1541 [a, b]	−1915, −2070
8	−1070 [a]	−1383 [a]	−1516 [d], −1942 [d], −2092 [d], −2477 [d]
9	−1175	−1479	−1615, −2235
10 [12]	−1249	−1590 [a–c]	−2045, −2311
11	−1040 [a]	−1352 [a]	−1523 [d], −1933 [d], −2045 [d], −2444 [d]
12 [12]	−1150 [a]	−1510 [a]	−1627 [d], −1894 [d], −2063 [d], −2293 [d]
13	−1073 [a]	−1368 [a]	−1573 [d], −2010 [d], −2391 [d]

[a] Irreversible. [b] Peak position depends on scan rate. [c] Structured at low scan rates. [d] Reversibility could not be determined unambiguously. [e] Two-electron process. [f] Scan rate 10 mV s^{-1}.

in the 6/6 adduct **3**, which has two double bonds in the cyclohexane ring. The di-*tert*-butyl and dimethyl derivatives **4** and **5**, respectively, exhibit the same behavior (Table 1); however, the reduction of the latter is irreversible.

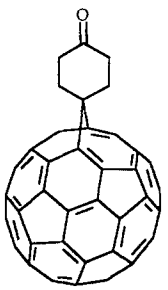

2a

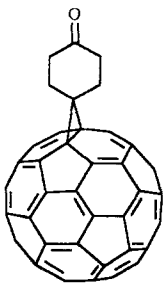

2b

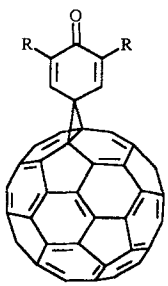

3: R = H
4: R = *t*Bu
5: R = Me

All fluorenofullerenes **6**–**13** described in the following could be isolated exclusively as adducts on 6/6 junctions; no 5/6 isomers were detectable. Assuming that this is a general structural principle of fluorenofullerenes applicable to the conversion of a mono- into a bisadduct, no other regiochemical control besides steric repulsion seems to direct the location of the second addition relative to the first.[9] Thus all bis(fluoreno)fullerenes were obtained as mixtures of five (**12**: six) regioisomers,[10] which could be separated only partially by HPLC (Scheme 1).

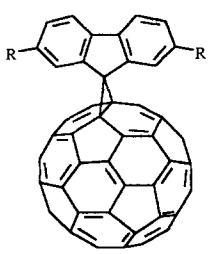

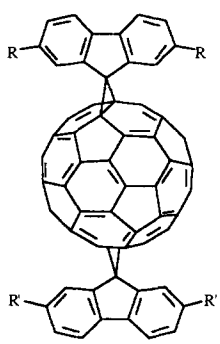

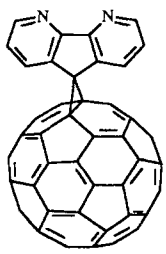

6: R = H
7: R = NBn_2
8: R = NO_2

9: R = H, R' = H
10: R = NBn_2, R' = NBn_2
11: R = NO_2, R' = NO_2
12: R = NBn_2, R' = NO_2

13

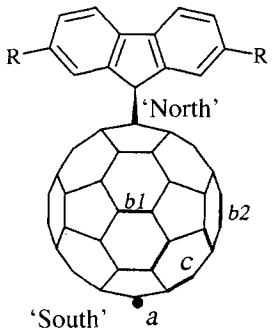

Scheme 1. Possible positions for a second addend on the "south pole" (*a*), on the "equator" (*b*1, *b*2), and in between (*c*, three possible positions)[10]. For clarity, symmetry-equivalent positions have been omitted.

The CV spectra of the spiroannelated methanofullerenes clearly demonstrate the striking influence of the addends on the C_{60} moiety. The positions (Table 1) of the first two reduction waves correlate with the electronic demand of the fluorenyl groups.[11] In the unsubstituted and the exclusively EDG-substituted[12] fluorenofullerenes (**6**, **7**, **9**, **10**), the first and the second reduction waves are strictly electrochemically reversible. The uptake of a third electron is electrochemically irreversible, exhibiting a scan rate dependent gap between reduction and reoxidation (Fig. 1).

The spiroannelated methanofullerenes bearing EWGs (**8**, **11**–**13**) give rise to CV curves that are more difficult to resolve.

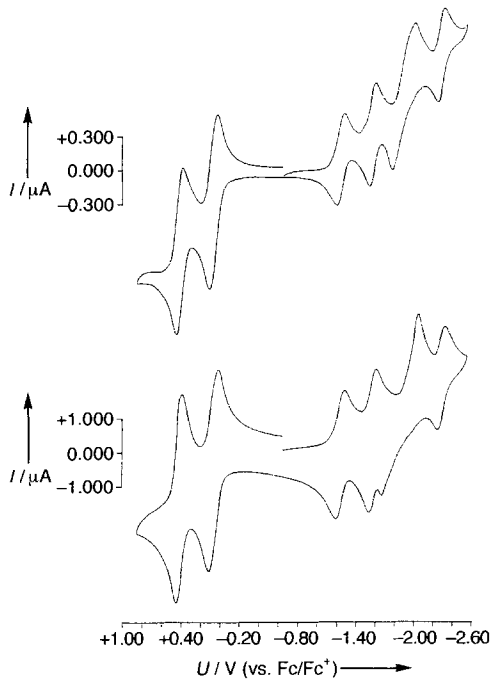

Fig. 1. Cyclic voltammograms of **10** (upper scan: 10 mV s^{-1}; lower scan: 100 mV s^{-1}; potential vs. ferrocene/ferrocenium (Fc/Fc^+)).

 © VCH Verlagsgesellschaft mbH, D-69451 Weinheim, 1995 0570-0833/95/1515-1592 $ 10.00+.25/0

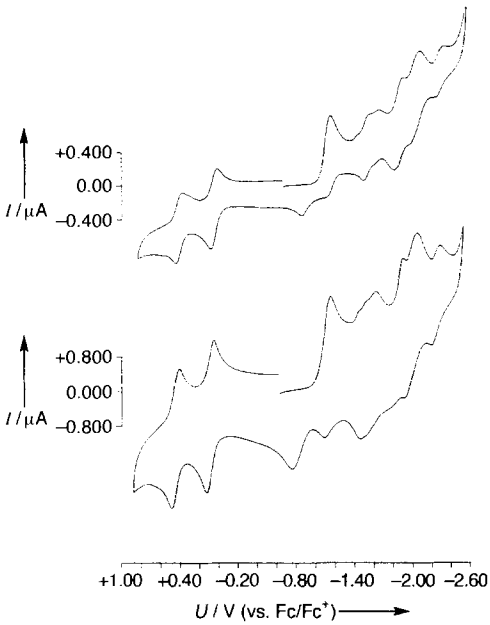

Fig. 2. Cyclic voltammograms of **12** (upper scan: $10\,mVs^{-1}$; lower scan: $100\,mVs^{-1}$; potential vs. Fc/Fc^+).

The first, second, and third reduction peaks are electrochemically irreversible, with complicated multiple reoxidation waves (Fig. 2). This behavior is not yet fully understood and will be the subject of further investigations; however it may be ascribed to the opening of a cyclopropane ring, as shown in Scheme 2.

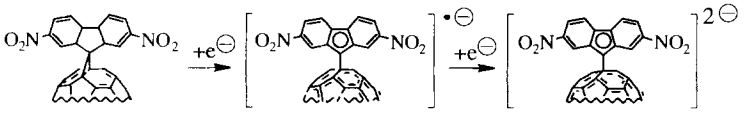

Scheme 2.

The crucial structural difference between 9,9-fluorenofullerenes **6**–**13** and (diphenylmethano)fullerenes **1** is that in the latter the phenyl rings are free to rotate but prefer to lie "parallel" to the fullerene surface, whereas the aromatic rings in **6**–**13** are held rigidly perpendicular to the surface of the spheroid. The cyclohexadienone derivatives **3**–**5** have similar structures. Models show that there is a likelihood of unusual periconjugation, different from spiroconjugation,[13] between the p_z orbitals of the addends and the "p_z" orbitals of the fullerene carbon atoms adjacent to the bridge atom. Even though a spiro atom also separates the π systems in **3**–**13**, the mode of interaction of the corresponding p_z orbitals is geometrically completely different from spiroconjugation. This can be easily seen by looking at the relative orientations of the atomic orbitals involved (Fig. 3).

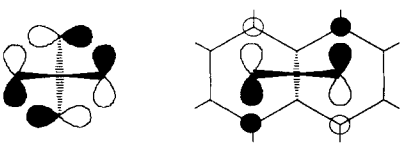

Fig. 3. Modes of orbital interaction in spiroconjugation (left) and periconjugation (right).

MNDO calculations on the spirocyclopentadiene compound **14** were used to model the interaction. In the fully optimized structure, which gives a transannular cyclopropane bond length of 1.602 Å,[14] the HOMO is bonding between the cyclopentadiene and C_{60} residues (Fig. 4). The LUMO has a_1 symmetry and is followed in energy by the b_2 and b_1 orbitals. When the length of the transannular cyclopropane bond is constrained to 2.0 Å, the energy is increased by 13 $kcal\,mol^{-1}$ and the HOMO is no longer bonding between the two moieties. The b_1 orbital then becomes the LUMO followed by the a_1 and b_2 orbitals. Since the b_1 orbital is antibonding with respect to the transannular cyclopropane bond, its population (e.g. by electrochemical reduction) will weaken the bond. These frontier orbital interactions may account for the complex findings in the electrochemical studies of **6**–**13**.

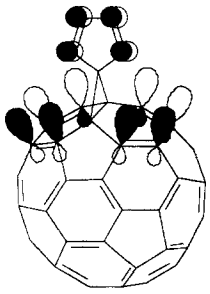

14

Fig. 4. HOMO interaction in cyclopentadienofullerene **14**. The remaining atomic orbitals contributing to the molecular HOMO are left out for clarity.

The ability to control the electron acceptor and donor strength of methanofullerenes—a fine-tuning of the electrochemical properties—opens up more possibilities for fullerene modification. Current research is aimed at an improved theoretical understanding of the effects as well as application of the results described here to the preparation of more electropositive and electronegative methanofullerenes.

Received: February 8, 1995 [Z 7701 IE]
German version: *Angew. Chem.* **1995**, *107*, 1733–1735

Keywords: electrochemistry · fullerenes · through-space interactions

[1] W. Krätschmer, L. D. Lamb, K. Fostiropoulos, D. R. Huffman, *Nature (London)* **1990**, *347*, 354; R. E. Haufler, J. Conceicao, L. P. F. Chibante, Y. Chai, N. E. Byrne, S. Flanagan, M. M. Haley, S. C. O'Brien, C. Pan, Z. Xiao, W. E. Billups, M. A. Ciufolini, R. H. Hauge, J. L. Margrave, L. J. Wilson, R. F. Curl, R. E. Smalley, *J. Phys. Chem.* **1990**, *94*, 8634.

[2] T. Suzuki, Q. Li, K. C. Khemani, F. Wudl, Ö. Almarsson, *Science* **1991**, *254*, 1186; F. Wudl, *Acc. Chem. Res.* **1992**, *25*, 157; M. Prato, V. Lucchini, M. Maggini, E. Stimpfl, G. Scorrano, M. Eiermann, T. Suzuki, F. Wudl, *J. Am. Chem. Soc.* **1993**, *115*, 8479, and references therein.; F. Diederich, L. Isaacs, D. Philp, *Chem. Soc. Rev.* **1994**, 243.

[3] M. Keshavarz-K., B. Knight, F. Wudl, *J. Org. Chem.*, submitted.

[4] However, the waves are shifted by 30–90 mV to more negative potentials relative to those of C_{60}.

[5] F. Wudl, T. Suzuki, M. Prato, *Synth. Met.* **1993**, *59*, 297. The CV data given in this paper were measured in THF.

[6] CV conditions: 0.15 M $(n\text{Bu})_4\text{NBF}_4$ in *o*-dichlorobenzene, 25 °C. Working electrode: Pt disk (2 mm diameter). Counter electrode: Pt wire. Reference electrode: aq. Ag/AgCl (Fc/Fc^+ internal standard). Potentiostat: BAS-100A, scan rate $100\,mVs^{-1}$. Other standard CV solvents (THF, acetonitrile) as well as toluene/acetonitrile (Q. Xie, E. Perez-Cordero, L. Echegoyen, *J. Am. Chem. Soc.* **1992**, *114*, 3978) did not provide sufficient solubity for all compounds of our study.

[7] All compounds gave satisfactory spectroscopic and analytical data. As an example, the data of **10** and **13** are given. **10**: $C_{142}H_{68}N_4$; M_r = 1830.13; ^{1}H NMR (CS_2/[D_{12}]cyclohexane 10:1): δ = 4.30–4.85 (m, 16H, Ph-CH_2-), 6.65–7.55 (m, 48H, phenyl-H, fluorene-H), 7.80–8.50 (10d, J = 2 Hz, 4H, fluorene-1-H, -8-H); ^{13}C NMR (CS_2/[D_{12}]cyclohexane 10:1): δ = 55.0–56.0 (5 peaks), 76.9–79.8 (9 peaks), 110.2–111.6 (9 peaks), 113.1–113.7 (5 peaks), 119.5–119.8 (5 peaks), 126.8–127.8 (10 peaks), 128.7–129.3 (4 peaks), 131.4–132.5 (8 peaks), 137.6–149.0 (77 peaks); FAB MS: *m/z* 1827–1829; FT-IR (KBr): $\tilde{\nu}$ = 1610 (m), 1570 (w), 1495 (m), 1485 (s), 1450 (m), 1355 (w), 1230 (w), 960 (w), 800 (w), 730 (w), 695 (w), 530 (w) cm^{-1}; UV/Vis (cyclohexane): λ_{max} = 221, 245, 324, 344 sh, 430 sh, 470, 569 sh, 623 sh, 692 nm. Anal. calcd. for $C_{142}H_{68}N_4$: C 93.19, H 3.75, N 3.06; found: C 93.11, H 3.78, N 2.99.

13: $C_{71}H_6N_2$; M_r = 886.85; ^{1}H NMR (CS_2/$CDCl_3$): δ = 7.48 (dd, J = 8.1, 4.4 Hz, 2H), 8.92 (dd, J = 4.4, 0.9 Hz, 2H), 9.08 (dd, J = 8.1, 0.9 Hz, 2H); ^{13}C NMR (CS_2/CD_2Cl_2): δ = 123.0, 132.1, 139.2, 141.5, 141.6, 142.4, 143.4, 143.6, 144.1, 144.9, 145.0, 145.3, 145.6, 149.0, 150.7, (too insoluble for detection of the bridge and bridgehead carbons at δ = 70–85); FAB MS: m/z 887, 886; IR (KBr): $\tilde{\nu}$ = 2910 (w), 1565 (w), 1410 (s), 1165 (w), 1035 (w), 815 (w), 750 (s), 745 (vs), 530 (s) cm^{-1}; UV/Vis (cyclohexane): λ_{max} = 200, 211, 256, 308, 327, 433 sh, 470, 695 nm. Anal. calcd. for $C_{71}H_6N_2$: C 96.16, H 0.68, N 3.16; found: C 96.02, H 0.81, N 3.17.

[8] M. Eiermann, F. Wudl, M. Prato, M. Maggini, *J. Am. Chem. Soc.* **1994**, *106*, 8364.

[9] A. Hirsch, I. Lamparth, H. R. Karfunkel, *Angew. Chem.* **1994**, *106*, 453; *Angew. Chem. Int. Ed. Engl.* **1994**, *33*, 437.

[10] The number of isomers was deduced from the ^{1}H NMR spectra. If one designates the location of the first addition as the "north pole" of the fullerene, there are four different types of 6/6 junctions on the "southern" hemisphere including the "south pole", giving rise to four regioisomeric bisadducts. Two further types of 6/6 junctions on the "equator" lead to two additional bisadducts only if the second substituent is different from the first (a total of six regioisomers). Otherwise only one additional regioisomer is formed (a total of five regioisomers).

[11] In the cyclic voltammograms of all isomeric mixtures of bisadducts **9**–**12** the signal shapes are, in general, similar to those of the corresponding monoadducts, indicating that relative positions of the substituents has a surprisingly small effect on the redox potentials.

[12] All compounds with dibenzylamino groups (**7**, **10**, **12**) can be oxidized reversibly in two steps due to a charging of the amino-substituted fluorenyl moieties. Oxidation peak potentials: **7**: +114 mV, +463 mV; **10**: +147 mV, +473 mV (two-electron processes); **12**: +129 mV, +464 mV (see Figs. 1 and 2) (vs. ferrocene/ferrocenium). This behavior was also detected in 2,7-bis(dibenzylamino)-9-fluorenone.

[13] H. Dürr, R. Gleiter, *Angew. Chem.* **1978**, *90*, 591; *Angew. Chem. Int. Ed. Engl.* **1978**, *17*, 559; T. A. Albright, J. K. Burdett, M.-H. Whangbo, *Orbital Interactions in Chemistry*, Wiley, New York, **1985**, p. 226. Spiroconjugation is manifested not only by a bathochromic shift in the UV/Vis spectra but also by substantial changes in the cyclic voltammograms: P. Maslak, M. P. Augustine, J. D. Burkey, *J. Am. Chem. Soc.* **1990**, *112*, 5359.

[14] The first full structure of a methanofullerene was recently published: J. Osterodt, M. Nieger, F. Vögtle, *J. Chem. Soc. Chem. Comm.* **1994**, 1607. More recently a low-temperature X-ray structure analysis of a 6/6-methanofullerene with a cyclopropane base bond length of 1.574(3) Å was reported: H. L. Anderson, C. Boudon, F. Diederich, J.-P. Gisselbrecht, M. Gross, P. Seiler, *Angew. Chem.* **1994**, *106*, 1691–1694; *Angew. Chem. Int. Ed. Engl.* **1994**, *33*, 1628.

α-Ethoxyvinyllithium: An Unexpected Polymeric Structure—Tetrameric Subunits Linked by Li–C π Interactions**

Klas Sorger, Walter Bauer, Paul von Ragué Schleyer,* and Dietmar Stalke

Dedicated to Professor Heinz Viehe on the occasion of his 65th birthday

Serving as an acyl anion equivalent, α-ethoxyvinyllithium (**1**) is a widely used synthetic reagent.[1] We now report the complex X-ray structure of unsolvated **1**, as well as NMR spectroscopic evidence for its nature in THF. In general, organolithium systems with α-halogen or α-oxygen substituents (R^1R^2CXLi) have "carbenoid" character, with bridging lithium and elongated C–X bonds.[2–5]

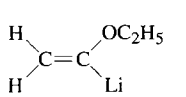

1

Crystals of **1** (synthesized by tin/lithium exchange) were obtained from hexane in the absence of cosolvents. The structure of **1** adopts a self-assembled, polymeric chain in the solid state (Fig. 1).[6] The asymmetric unit contains six $H_2C{=}C(Li)OEt$ molecules. Four of them are aggregated to form a distorted cubic Li_4C_4 tetramer, the remaining two generate a second tetramer by a C_2 axis (Fig. 1a).

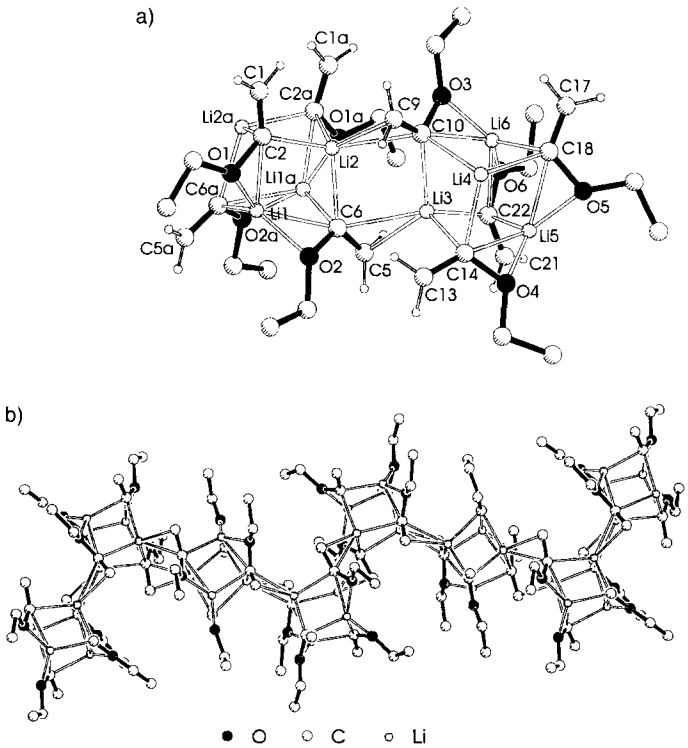

Fig. 1. a) Crystal structure of polymeric **1** showing the monoclinic unit cell. The methylene and methyl hydrogen atoms of the ethoxy groups have been omitted for clarity (the labels with a letter identify atoms which are related by a C_2 axis). b) Chain structure of polymeric **1** showing the tetrameric subunits linked by C–Li π-interactions. Selected bond lengths [pm] and angles [°]: Li1–O1 183.6(9), Li1–O2 189.8(9), Li1–C2 216.8(11), Li1–C6 245.9(10), Li1–C6a 222.1(10), Li2–C2 223.4(10), Li2–C2a 232.1 (10), Li2–C6 227.9(11), Li2–C9 244.6(10), Li2–C10 253.1(10), Li3–C10 225.1(11), Li3–C14 231.3(10), Li3–C22 227.4(10), Li3–C5 244.8(10), Li3–C6 251.8(10), Li4–C10 236.6(10), Li4–C14 223.0 (10), Li4–C18 227.2(11), Li4–C13a 242.5(10), Li4–C14a 251.5(10), Li5–O4 186.0(10), Li5–O5 188.0(10), Li5–C14 234.1(11), Li5–C18 230.1(12), Li5–C22 221.4(11), Li6–O3 187.9(9), Li6–O6 186.6(10), Li6–C10 231.3(11), Li6–C18 214.4(10), Li6–C22 228.3(11), Li bridged C=C (mean) 133.3(8), nonbridged C=C (mean) 131.9(8); C=C O (mean) 117.7, C1-C2-Li1 172.1(5), C5-C6-Li1 149.0(4), C9-C10-Li6 156.5(5), C13-C14-Li5 156.2(5), C17-C18-Li5 163.8(6), C21-C22-Li6 158.0(5).

The Li/oxygen carbenoid character of **1** is shown by the elongated C_α–O bond (142.1(6)–143.6(6) pm, mean: 142.8(7) pm;[3, 5a–d] the C_{vinyl}–O bond length in vinylethers is about 136 pm (Fig. 2 bottom[7]). Similar elongations of 6.8 and 8.5 pm were observed in α-lithiobenzofuran[5d] and 3-bromo-2-lithiobenzofuran,[5b] respectively. The C_α–O bond of monomeric α-methoxyvinyllithium (computed ab initio at the Becke3LYP/6-311 + G**[8] level) is even longer (13 pm, Fig. 2 top) which can be attributed to the absence of other lithium ligands. Due to the unfavorable lone pair repulsions in the s-*cis* form, the α-methoxyvinyl anion favors the *s-trans* conformation (Fig. 2 middle). Both the conformation of α-methoxyvinyllithium and

[*] Prof. Dr. P. von R. Schleyer, Dipl.-Chem. K. Sorger, Dr. W. Bauer
Institut für Organische Chemie der Universität Erlangen-Nürnberg
Henkestrasse 42, D-91054 Erlangen (Germany)
Telefax: Int. code + (9131)85-9132
Priv.-Doz. Dr. D. Stalke,
Institut für Anorganische Chemie der Universität
Tammannstrasse 4, D-37077 Göttingen (Germany)

[**] This work was supported by the Fonds der Chemischen Industrie, the Stiftung Volkswagenwerk, the Convex Computer Corporation, and the Deutsche Forschungsgemeinschaft. K. S. thanks the Freistaat Bayern for a scholarship.

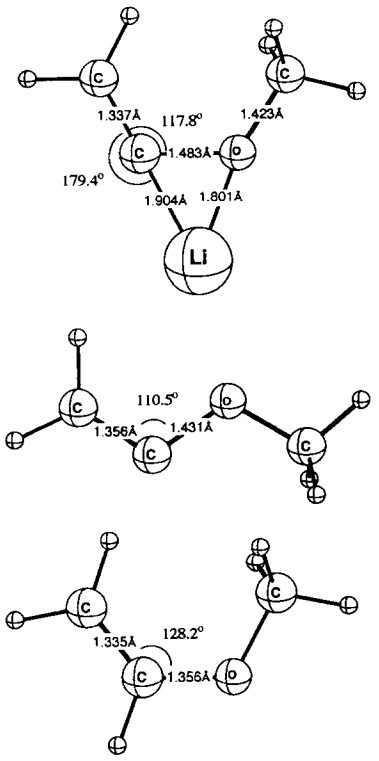

Fig. 2. Becke3LYP/6-311 + G** optimized C_s geometries (energy minima) of monomeric α-methoxyvinyllithium (top), the *s-trans* α-methoxyvinyl anion (middle), and *s-cis* methylvinylether (bottom). The different conformational preferences and the C–O bond lengths are noteworthy.

the *s-cis* form of the methylvinyl ether differ from the conformation of the anion. The C_α–O bond elongation of 7.5 pm in the anion is much less than that computed for the lithium derivative. This emphasizes the effect of ion pairing.[9]

The lithium cations in the polymeric solid-state structure of **1** bridge the C–O bonds in notable ways: two lithium atoms in each tetramer coordinate simultaneously to *two* oxygen atoms, namely, Li1 to O1 and O2, Li1a to O1a and O2a, Li5 to O4 and O5, Li6 to O3 and O6 [Li–O distance: 183.6(9) – 189.8(9), mean: 187.0(10) pm] (Fig. 1a), resulting in pentacoordinate lithium centers. Similar double-coordination of lithium to two heteroatoms is found in 1-lithio-2-methoxybenzene,[10] in which lithium bridges an anionic carbon atom and a β-oxygen atom.

The two other lithium cations in each tetramer, Li2 and Li2a (as well as Li3 and Li4 in the polymeric chain), do *not* have oxygen contacts. Instead, these cations exhibit π interactions to the C=C double bonds of α-ethoxyvinyllithium units in the neighboring tetramer (Fig. 1). Consequently, these lithium atoms are σ-bonded to three vinylic carbon atoms [C–Li distance: 223.4(10)–236.6(10) pm] and are η^2-coordinated to a C–C π bond. Hence, there are two different lithium environments in polymeric **1**: pentacoordination with contacts to two oxygen atoms and pentacoordination to five carbon atoms, two of them π-bound.

The unusual manner in which neighboring tetrameric subunits are connected –through Li–C_{vinyl} η^2-interactions—is intriguing (Fig. 1b).[11] The Li–C π contacts in the solid-state structure of **1** saturate the coordination sphere of the lithium cations and link the tetramers into a polymeric chain. In contrast, the Li_4C_4 tetramers in polymeric [(PhC≡CLi)$_4$(tetramethylhexanediamine)$_2$][12] are linked by the diamine ligands to form helices. Since the π electrons are polarized towards the terminal carbon (C_β) upon lithiation (i.e., ethylvinylether vs **1**),[19] the Li–C_β distances are significantly shorter [242.5(10)–244.8(10) pm] than the Li–C_α distances [251.5(10)–253.1(10) pm]. However, both distances are within the range of Li–C bond lengths observed for π-bonded lithium.[11, 13]

Consistent with computational findings,[14] the lithium-bridged C=C bonds [mean: 133.3(8) pm] are 1.4 pm (marginally but systematically) *longer* than the nonbridged C=C bonds [mean: 131.9(8) pm]. At the Becke3LYP/6-311 + G** level,[8] the C=C bond elongation in the Li^+–ethylene C_{2v} π complex is 1.2 pm.

A low-temperature ^{13}C NMR spectrum of α-ethoxyvinyllithium (**1** – ^{6}Li) reveals that the solid-state structure is not retained in [D$_8$]THF solution. At −90 °C, a well-resolved seven-line ^{13}C multiplet due to ^{13}C-^{6}Li scalar coupling is observed for the lithiated carbon. This is consistent with a static tetramer ($^1J(^{13}C$-$^6Li)$ = 5.0 Hz).[15, 19] The lithiated carbon C_α couples with three *equivalent* lithium cations.[15, 19] A tetramer **2**[16]

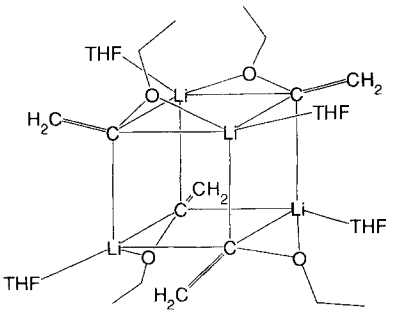

2

with lithium bridging the C–O bond is confirmed by ^{6}Li-^{1}H heteronuclear Overhauser effect spectroscopy (HOESY):[17] under the same conditions, however, in the presence of one equivalent of undeuterated THF per lithium atom, ^{6}Li cross peaks with nearly identical intensities to *all* hydrogens of **1**, as well as to the THF α-hydrogens are found. Close contacts between lithium and the methylene, and even the methyl hydrogen atoms of the ethoxy group, demonstrate the lithium bridging of the C_α–O bond in solution. Close contacts between lithium and the THF α-hydrogens indicate the coordination of THF to lithium.

The downfield shift of the ^{13}C NMR signal of the lithiated carbon in **1** relative to the $\delta(^{13}C(1))$ of H_2C=CHOEt, $\Delta\delta$ = 60.7,[18] is typically large for carbenoids.[4c, 5c, 19, 20] This downfield shift exceeds that of "non-carbenoid" tetrameric vinyllithium[17] ($\Delta\delta$ = 54.4). The C(Li)O carbenoid character of **1** is thus confirmed both by the C–O bond elongation and by the ^{13}C NMR characteristics.

Experimental Procedure

n-Butyllithium (3.30 mmol, 2.06 mL of a 1.6 M solution in hexane) was added to a solution of tributyl(1-ethoxyvinyl)stannane [1.19 g, 3.30 mmol, prepared [1e] by reaction of α-ethoxyvinylpotassium [21] with tributyltin chloride (yield 90%)] in hexane (17.0 mL) at −40 °C. The solution was then stirred for 5 h at 0 °C. The product, a white precipitate, was warmed into solution (50 °C). Cooling to 8 °C yielded the crude product which was recrystallized from *n*-hexane at room temperature. This resulted in the formation of long, but very thin, colorless needles, which, under these conditions, are stable only for about 12 h. After several attempts, a single-crystal suitable for X-ray analysis was obtained. The crystal was selected and transported to the diffractometer at −50 °C [22]. ^{1}H NMR [25] (400 MHz, [D$_8$]THF, c = 3.4, −50 °C): δ = 4.85 (s, 1H, H_{trans}), 3.96 (s, 1H, H_{cis}), 3.58 (q, ^3J(H,H) = 13.4 Hz, 2H, CH_2), 1.29 (t, ^3J(H,H) = 13.4 Hz, 3H, CH_3); ^{13}C NMR see ref. [18]; ^{6}Li NMR ([D$_8$]THF, c = 3.4, −90 °C, referenced to 1 M LiBr in [D$_8$]THF): δ = −0.20 (s).

Received: March 30, 1995 [Z 7849 IE]
German version: *Angew. Chem.* **1995**, *107*, 1766–1768

Keywords: acyl anions·carbenoids·lithium compounds

[1] a) Review: O. W. Lever, *Tetrahedron* **1976**, *32*, 1943 (see p. 1958, and references therein); b) U. Schöllkopf, P. Hänssle, *Justus Liebigs Ann. Chem.* **1972**, *763*, 208; c) I. Hoppe, U. Schöllkopf, *Liebigs Ann. Chem.* **1980**, 1474; d) J. E. Baldwin, G. A. Höfle, O. W. Lever, Jr., *J. Am. Chem. Soc.* **1974**, *96*, 7125; e) J. A. Soderquist, A. Hassner, *ibid.* **1980**, *102*, 1577; f) T. Takahashi, H. Yamada, J. Tsuji, *ibid.* **1981**, *103*, 5259; g) M. Shimano, A. I. Meyers, *ibid.* **1994**, *116*,

10815; h) R. R. Schmidt, R. Betz, *Synthesis* **1982**, 748; i) P. G. McDougal, J. G. Rico, D. VanDerveen, *J. Org. Chem.* **1986**, *51*, 4492; j) R. K. Boeckman, Jr., K. J. Bruza, *Tetrahedron*, **1981**, *37*, 3997; k) S. J. Gould, B. D. Remillard, *Tetrahedron Lett.* **1978**, 4353; l) E. J. Corey, D. L. Boger, *ibid.* **1978**, 13; m) P. Lesimple, J.-M. Beau, G. Jaurand, P. Sinay, *ibid.* **1986**, *27*, 6201.

[2] a) T. Clark, P. von R. Schleyer, *J. Chem. Soc. Chem. Commun.* **1979**, 883; b) *Tetrahedron. Lett.* **1979**, 4963; c) *J. Am. Chem. Soc.* **1979**, *101*, 7747; see also B. Wang, C. Deng, *Chem. Phys. Lett.* **1988**, *147*, 99, and B. Wang, C. Deng, L. Xu, T. Tao, *ibid.* **1989**, *161*, 388.

[3] a) T. Clark, P. von R. Schleyer, K. N. Houk, N. G. Rondan, *J. Chem. Soc. Chem. Commun.* **1981**, 579; b) P. von R. Schleyer, T. Clark, A. J. Kos, G. W. Spitznagel, C. Rohde, D. Arad, K. N. Houk, N. G. Rondan, *J. Am. Chem. Soc.* **1984**, *106*, 6467.

[4] a) G. Boche, M. Marsch, A. Müller, K. Harms, *Angew. Chem.* **1993**, *105*, 1081; *Angew. Chem. Int. Ed. Engl.* **1993**, *32*, 1032, and references therein; b) G. Boche, K. Harms, M. Marsch, A. Müller, *J. Chem. Soc., Chem. Commun.* **1994**, 1393; c) A. Maercker, *Angew. Chem.* **1993**, *105*, 1072; *Angew. Chem. Int. Ed. Engl.* **1993**, *32*, 1023, and references therein.

[5] a) C. Lambert, P. von R. Schleyer, E.-U. Würthwein, *J. Org.* Chem. **1993**, *58*, 6377; b) G. Boche, A. Opel, M. Marsch, K. Harms, F. Haller, J. C. W. Lohrenz, C. Thümmler, W. Koch, *Chem. Ber.* **1992**, *125*, 2265; c) G. Boche, F. Bosold, J. C. W. Lohrenz, A. Opel, P. Zulauf, *ibid.* **1993**, *126*, 1873; d) S. Harder, J. Boersma, L. Brandsma, J. A. Kanters, W. Bauer, R. Pi, P. von R. Schleyer, H. Schöllhorn, U. Thewalt, *Organometallics* **1989**, *8*, 1688; e) G. Boche, M. Marsch, J. Harbach, K. Harms, B. Ledig, F. Schubert, J. C. W. Lohrenz, H. Ahlbrecht, *Chem. Ber.* **1993**, *126*, 1887.

[6] Crystal data of polymeric **1** $[LiC_4H_7O]_6$: $M = 468.22$, monoclinic, space group $C2/c$, $a = 3322(2)$, $b = 976.7(7)$, $c = 2491(2)$ pm, $\beta = 130.47(3)^\circ$, $V = 6.149(8)$ nm^3, $Z = 8$, $\rho_c = 1.011$ Mg m^{-3}, $F(000) = 2016$, $\lambda = 0.71073$ Å, $\mu(Mo_{K\alpha}) = 0.066$ mm^{-1}, $T = 153$ K. data were collected on a Stoe-Siemens-AED. Intensities of a $0.9 \times 0.1 \times 0.05$ mm rapidly cooled crystal in an oil drop [22] were collected by the $2\theta/\omega$ method in the range of $8^\circ \leq 2\theta \leq 45^\circ$. Of a total of 5121 refections, 4028 were independent and 4024 used to refine 368 parameters, largest difference peak and hole: 223 and -195 e nm^{-3}, $R1(F > 4\sigma(F)) = 0.079$ and $wR2 = 0.230$ (all data) with $R1 = \Sigma||F_o| - |F_c||/\Sigma|F_o|$ and $wR2 = (\Sigma\omega(F_o^2 - F_c^2)^2/\Sigma\omega(F_o^2)^2)^{0.5}$. The structure was solved with direct methods (SHELXS-90 [23]) and refined by full-matrix least-squares on F^2 (SHELXL-93 [24]). The hydrogen atom positions of the CH_2 groups were refined freely with the C–H bond length restrained to be the same while a riding model was applied to refine the hydrogen atom positions of the other groups. Further details of the crystal sructure investigations may be obtained from the Director of the Cambridge Crystallographic Data Centre, University Chemical Laboratory, Lensfield Road, GB-Cambridge CB2 1EW (UK), by quoting the full journal citation.

[7] R. Amstutz, W. B. Schweizer, D. Seebach, J. D. Dunitz, *Helv. Chim. Acta* **1981**, *64*, 2617.

[8] a) GAUSSIAN 92/DFT, Revision G.2: M. J. Frisch, G. W. Trucks, H. B. Schlegel, P. M. W. Gill, B. G. Johnson, M. W. Wong, J. B. Foresman, M. A. Robb, M. Head-Gordon, E. S. Replogle, R. Gomberts, J. L. Andres, K. Raghavachari, J. S. Binkley, C. Gonzalez, R. L. Martin, D. J. Fox, D. J. Defrees, J. Baker, J. J. P. Stewart, J. A. Pople, Gaussian Inc., Pittsburgh, PA, **1993**.

[9] a) C. Lambert, P. von. R. Schleyer, *Angew. Chem.* **1994**, *106*, 1187; *Angew. Chem. Int. Ed. Engl.* **1994**, *33*, 1129; b) C. Lambert, P. von R. Schleyer, in *Methoden Org. Chem. (Houben-Weyl) 4th Ed. 1952-, vol. E19d*, **1993**, p. 1.

[10] S. Harder, J. Boersma, L. Brandsma, G. P. M. van Mier, J. A. Kanters, *J. Organomet. Chem.* **1989**, *364*, 1.

[11] Reviews concerning the structures of organolithium compounds: a) E. Weiss, *Angew. Chem.* **1993**, *105*, 1565; *Angew. Chem. Int. Ed. Engl.* **1993**, *32*, 1501; b) W. N. Setzer, P. von R. Schleyer, *Adv. Organomet. Chem.* **1985**, *24*, 353; c) P. von R. Schleyer, *Pure Appl. Chem.* **1983**, *55*, 355; *ibid.* **1984**, *56*, 151; d) D. Stalke, *Angew. Chem.* **1994**, *106*, 2256; *Angew. Chem. Int. Ed. Engl.* **1994**, *33*, 2168; see also R. Haag, R. Fleischer, D. Stalke, A. de Meijere *Angew. Chem.* **1995**, *107*, 1642; *Angew. Chem. Int. Ed. Engl.* **1995**, *34*, 1492.

[12] B. Schubert, E. Weiss, *Angew. Chem.* **1983**, *95*, 499; *Angew. Chem. Int. Ed. Engl.* **1983**, *22*, 496.

[13] R. Amstutz, J. D. Dunitz, T. Laube, W. B. Schweizer, D. Seebach, *Chem. Ber.* **1986**, *119*, 434.

[14] J. E. Del Bene, M. J. Frisch, K. H. Raghavachari, J. A. Pople, P. von R. Schleyer, *J. Phys. Chem.* **1983**, *87*, 73.

[15] W. Bauer, P. von R. Schleyer in *Advances in Carbanion Chemistry, Vol.1* (Ed.: V. Snieckus), JAI Press, Greenwich, CT, **1992**, p. 89.

[16] Li–O_{ethoxy} bond scrambling must be rapid on the NMR time scale.

[17] W. Bauer, F. Hampel, *J. Chem. Soc. Chem. Commun.* **1992**, 903, and references therein.

[18] F. T. Oakes, J. F. Sebastian, *J. Org. Chem.* **1980**, *45*, 4959.

[19] D. Seebach, R. Hässig, J. Gabriel, *Helv. Chim. Acta* **1983**, *66*, 308.

[20] $\Delta\delta$ values of 56.6 and 57.2 have been determined for the closely related α-lithio-2,3-dihydrofuran and α-lithio-2,3-dihydro-4H-pyran, the carbenoid character of which is well established [5c]: see ref. [18].

[21] H. D. Verkruijsse, L. Brandsma, P. von R. Schleyer, *J. Organomet. Chem.* **1987**, *332*, 99.

[22] T. Kottke, D. Stalke, *J. Appl. Crystallogr.* **1993**, *26*, 615.

[23] SHELXS-90: G. M. Sheldrick, *Acta Crystallogr. Sect. A* **1990**, *46*, 467

[24] G. M. Sheldrick, SHELXL-93, program for crystal structure refinement, Göttingen, **1993**.

[25] ^{1}H NMR chemical shifts of the vinylic protons in **1**: R. Knorr, T. von Roman, *Angew. Chem.* **1984**, *96*, 349; *Angew. Chem. Int. Ed. Engl.* **1984**, *23*, 366.

A New Family of Chiral Binaphthyl-Derived Cyclophane Receptors: Complexation of Pyranosides**

Sally Anderson, Ulf Neidlein, Volker Gramlich, and François Diederich*

Dedicated to Professor Dr. Manfred Regitz on occasion of his 60th birthday

Carbohydrate recognition is central to many biological processes, including the transmission of disease and the operation of the immune system.[1] Carbohydrates are suitable molecules for recognition, because they have a much greater capacity to store information than other biopolymers.[2] The study of these recognition processes can be either carried out directly on biological systems, for example by analyzing the interactions in protein–carbohydrate complexes by X-ray crystallography[3] or in enzyme-linked immunosorbent assays,[4] or by synthesizing simpler analogous receptors whose binding properties can be systematically varied and analyzed.[5] We targeted the chiral receptors **1a–d** (Scheme 1), which show a remarkable degree of

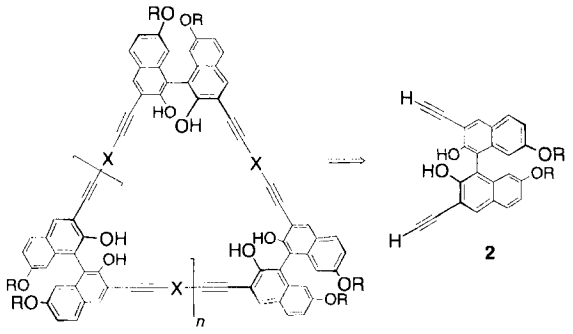

1a-d $n = 1 - 3$
R = CH_2Ph, $CH_2CH_2N^+Me_3$

Scheme 1. Targeted receptors and retrosynthetic disconnection to the chiral cyclization component. **a**, X = –; **b**, X = $Pt(PBu_3)_2$; **c**, X = 1,4-C_6H_4; **d**, X = 1,3-C_6H_4.

[*] Prof. F. Diederich, Dr. S. Anderson,[+] Dipl.-Chem. U. Neidlein
Laboratorium für Organische Chemie, ETH Zentrum
Universitätstrasse 16, CH-8092 Zürich (Switzerland)
Telefax: Int. code + (1) 632-1109
e-mail: Diederich@org.chem.ethz.ch

Dr. V. Gramlich
Institut für Kristallographie und Petrographie, ETH-Zentrum, Zürich (Switzerland)

[+] Current address: Dyson Perrins Laboratory, South Park Road, GB-Oxford OX1 3QY (UK)

[**] This work was supported by the Schweizerische Nationalfonds zur Förderung der wissenschaftlichen Forschung (Chiral 2) and Hoffmann-La Roche. S. A. thanks the Royal Society, London, for a European Science Exchange Programme Postdoctoral Fellowship and Trinity College, Cambridge, for a Research Fellowship. We thank Dipl.-Chem. Jens Cuntze for the NMR titrations.

preorganization: six, eight, or ten OH groups converge upon a central cavity providing a ring of H-bonding sites for carbohydrate recognition.[6] These receptors, derived from the 3,3′-diethynyl-1,1′-binaphthyl-2,2′-diol spacer **2**, allow economy in the synthesis of a wide range of hosts. The introduction of linking groups X between the acetylenes would widen the cavity and provide enough space either to replace the convergent OH groups with other H-bonding residues or to bind di- and higher oligosaccharides. These linking groups could also offer a foundation on which to attach a hydrophobic floor parallel to the plane of H-bonding sites; Lemieux[7] has convincingly shown that hydrophobic desolvation and van der Waals interactions are at least as important for biological carbohydrate binding in aqueous solution as the H-bonding interactions. Varying the divergent R groups at the periphery should lead to receptors soluble in solvents of any desired polarity, including water. Here we report the synthesis of the neutral receptors (*R*,*R*,*R*)-(−)-**3** and (*R*,*R*,*R*,*R*)-(−)-**4**, and of the tetraanionic receptor (*R*,*R*,*R*,*R*)-(−)-**5**, as well as preliminary binding studies with pyranosides.

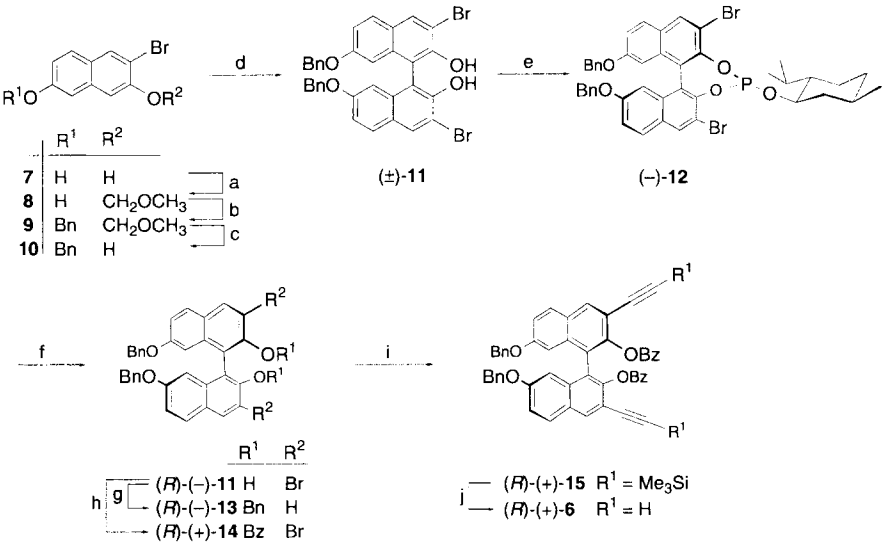

Scheme 2. Synthesis of the cyclization component (*R*)-(+)-**6**. a) CH_3OCH_2Cl, K_2CO_3, DMF, 0 °C, 44%; b) $C_6H_5CH_2Cl$ (BnCl), K_2CO_3, DMF, 80 °C, 91%; c) HCl(g), THF/*i*PrOH 1:1, 20 °C, 88%; d) *t*$BuNH_2$, $CuCl_2$, MeOH, 89%; e) (L)-menthyl phosphorodichloridite [10], Et_3N, THF, 0 °C, then recrystallization (twice) from Et_2O, 29%; f) K_2CO_3, MeOH/$CHCl_3$, 20 °C, 91%; g) Pd/C (10%), $HCOONH_4$, MeOH, 60 °C, then BnCl, K_2CO_3, DMF, 80 °C (yield not determined); h) PhCOCl (BzCl), 4-(dimethylamino)pyridine (DMAP), pyridine/CH_2Cl_2, 20 °C, 90%; i) starting from (*R*)-(+)-**14**: $[Pd(PPh_3)_4]$, Me_3Si-C≡C-$SnMe_3$, 2,6-di-*tert*-butyl-4-methylphenol, toluene, 100 °C, 45%; j) K_2CO_3, MeOH/THF, 85%.

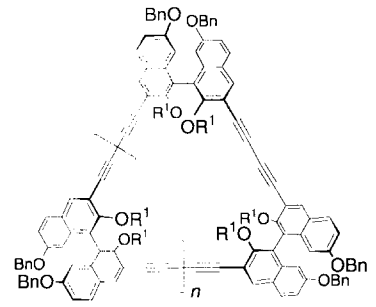

	n	R¹
(*R*,*R*,*R*)-(−)-**3**	1	H
(*R*,*R*,*R*,*R*)-(−)-**4**	2	H
(*R*,*R*,*R*)-(−)-**16**	1	Bz
(*R*,*R*,*R*,*R*)-(−)-**17**	2	Bz
(*R*,*R*,*R*,*R*,*R*)-(−)-**18**	3	Bz

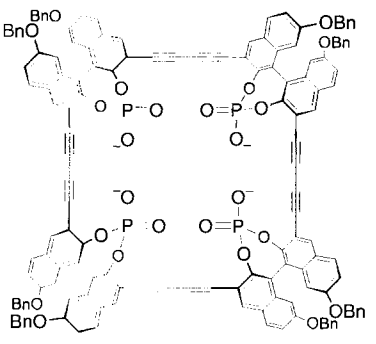

(*R*,*R*,*R*,*R*)-(−)-**5**

The synthesis of the novel receptors started with the preparation of the optically active cyclization component (*R*)-(+)-**6** (Scheme 2). Differential O-protection and O-deprotection of 2-bromo-3,6-naphthalenediol[8] (**7** → **8** → **9** → **10**) followed by oxidative coupling afforded the racemic dibrominated 1,1′-binaphthyl-2,2′-diol **11**, whose constitution was confirmed by single crystal X-ray diffraction.[9] Optical resolution of **11** was accomplished via the (L)-menthyl phosphite **12**: diastereoisomer (−)-**12**[10] (diastereomeric excess > 99.5%)[11] crystallized readily, whereas (+)-**12** failed to crystallize from the filtrate even after concentration. The menthyl phosphite was readily cleaved[10] with K_2CO_3 in MeOH/$CHCl_3$ to give diol (−)-**11**. To show that (−)-**11** was the *R* enantiomer, the diol was debrominated, benzylated to give (−)-**13**, and the optical rotation of (−)-**13** ($[\alpha]_D^{22} = -15.2$, $c = 0.5$, CH_2Cl_2; Table 1) compared with that of (*S*)-(+)-**13** ($[\alpha]_D^{22} = +15.2$, $c = 0.5$, CH_2Cl_2), derived from benzylation of (*S*)-(+)-7,7′-bis(benzyloxy)-1,1′-binaphthyl-2,2′-diol, whose absolute configuration had been previously determined.[12]

Table 1. Optical rotations of nonmacrocyclic precursors.

	$[\alpha]_D^{22}$	*c* (in CH_2Cl_2)
(*R*)-(+)-**6**	+26.6	1.0
(*R*)-(−)-**11**	−79.4	1.0
(*R*)-(−)-**12**	−394.5	1.0
(*R*)-(−)-**13**	−15.2	0.5
(*R*)-(+)-**14**	+8.0	1.0
(*R*)-(+)-**15**	+1.6	1.0

The OH groups in (*R*)-(−)-**11** were benzoylated to give (*R*)-(+)-**14**, and Stille coupling[13] with Me_3Si-C≡C-$SnMe_3$ afforded (*R*)-(+)-**15** containing two silylethynyl groups. Deprotection with K_2CO_3 in MeOH/THF gave, without attack at the ester protecting groups, the cyclization component (*R*)-(+)-**6**. Neither Stille nor Heck coupling[14] with unprotected (*R*)-(−)-**11** gave the desired dialkynylated product.

Oxidative Glaser–Hay coupling (air, CuCl, *N*,*N*,*N*′,*N*′-tetramethylethylenediamine (TMEDA)) of (*R*)-(+)-**6** ($c = 4 \times 10^{-4}$ mol L^{-1}) in CH_2Cl_2 rapidly led to a product mixture from which the cyclic trimeric oligomer (*R*,*R*,*R*)-(−)-**16** (20%), tetrameric (*R*,*R*,*R*,*R*)-(−)-**17** (20%), and pentameric

 © VCH Verlagsgesellschaft mbH, D-69451 Weinheim, 1995 0570-0833/95/1515-1597 $ 10.00+.25/0

(*R,R,R,R,R*)-(−)-**18** (3%) were isolated by flash chromatography (SiO_2, cyclohexane/AcOEt) (Table 2). Fast atom bombardment (FAB) mass spectra with positive ion detection gave strong molecular ions indicating the size of the oligomers, and the ^{13}C NMR spectra showed the required 22 peaks for cyclic oligomers of this type. Importantly, two signals were observed between $\delta = 75$ and 85, corresponding to the C atoms in the butadiyne links. Further confirmation of the butadiyne groups was obtained from the IR spectra, where both symmetric and antisymmetric stretches were observed in the region between 2100 and 2250 cm^{-1}. The ^1H NMR spectra of the three cyclic oligomers were very similar, except for the aromatic signals from the benzoyl protecting groups; presumably the observed differences in the positions of the benzoyl resonances reflect the different degrees of crowdedness in the three cavities.

Benzoyl ester hydrolysis of (*R,R,R*)-(−)-**16** and (*R,R,R,R*)-(−)-**17** proceeded smoothly with KOH in MeOH/THF and yielded the targeted neutral receptors (*R,R,R*)-(−)-**3** (90%) and (*R,R,R,R*)-(−)-**4** (92%). Similarly, (*R*)-(−)-**19** was prepared by deprotection of (*R*)-(+)-**6** as a control for binding experiments.[15] Since ionic hydrogen bonding is known to contribute greatly to strong carbohydrate binding in biological and synthetic receptors,[3, 5a] we have also prepared the tetraphosphate receptor (*R,R,R,R*)-(−)-**5** by treating (*R,R,R,R*)-(−)-**4** for 3 h at 20 °C with $POCl_3$ in dry CH_2Cl_2 in the presence of NEt_3, followed by hydrolysis with THF/H_2O for 12 h at 40 °C and ion exchange chromatography (Dowex 50WX8, Bu_4N^+, $CHCl_3$/CH_3CN 1:1) (67%). As a control for the binding experiments, monophosphate (*R*)-(−)-**20** was obtained in a similar way from (*R*)-(−)-**11**.

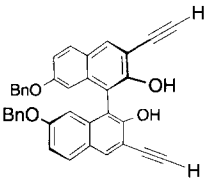

(*R*)-(−)-**19**

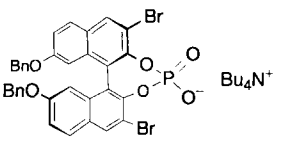

(*R*)-(−)-**20**

CPK models and computer modeling showed that the binding site of (*R,R,R*)-(−)-**3** is complementary in size and shape to a hexopyranose ring. ^1H NMR titration studies with (*R,R,R*)-(−)-**3** and pyranosides in dry $CDCl_3$[16] ($T = 300$ K), in which the change in chemical shift of the receptor OH protons was monitored as a function of the concentration of guest, showed the formation of stable 1:1 complexes. The association constants K_a between 90 and 370 L mol^{-1} (Table 3) for the complexes of 1-*O*-octyl glucopyranosides **21**–**23** were obtained by nonlinear least-squares curve fitting of the titration data.[17] Under the same conditions, no significant complexation of these substrates was observed in control runs with (*R*)-(−)-**19**, which demonstrates that OH groups from more than one of the three

Table 2. Selected physical data of (*R,R,R*)-(−)-**3**, (*R,R,R,R*)-(−)-**4**, (*R,R,R,R*)-(−)-**5**, (*R,R,R*)-(−)-**16**, (*R,R,R,R*)-(−)-**17**, and (*R,R,R,R,R*)-(−)-**18** [a].

(*R,R,R*)-(−)-**3**: m.p. 205 °C (decomp.); $[\alpha]_D^{22} = -1114$ ($c = 1.0$ in CH_2Cl_2); IR ($CHCl_3$): $\tilde{\nu} = 3520$ (OH), 2203, 2129 (C≡C–C≡C) cm^{-1}; ^1H NMR (300 MHz, $CDCl_3$): $\delta = 8.08$ (s, 6H), 7.75 (d, $J = 9.3$ Hz, 6H), 7.23–7.07 (m, 36H), 6.41 (d, $J = 2.4$ Hz, 6H), 5.75 (s, 6H), 4.67 (q, AB, $J = 12.0$ Hz, 12H); ^{13}C NMR (75 MHz, [D$_8$]THF): $\delta = 159.5$, 156.3, 137.9, 137.1, 134.4, 130.6, 129.0, 128.4, 128.2, 124.8, 117.5, 114.1, 111.2, 106.0, 80.6, 79.1, 70.2; FAB$^+$-MS: *m/z*: 1633 (M^+, $^{13}C^{12}C_{113}H_{72}O_{12}$ requires 1633.57)

(*R,R,R,R*)-(−)-**4**: m.p. 199 °C (decomp.); $[\alpha]_D^{22} = -759.6$ ($c = 1.0$ in $CHCl_3$); IR ($CHCl_3$): $\tilde{\nu} = 3522$ (OH), 2211, 2133 (C≡C–C≡C) cm^{-1}; ^1H NMR (300 MHz, $CDCl_3$): $\delta = 8.11$ (s, 8H), 7.75 (d, $J = 8.6$ Hz, 8H), 7.33–7.06 (m, 48H), 6.36 (d, $J = 2.2$ Hz, 8H), 4.74 (q, AB, $J = 13.1$ Hz, 16H); ^{13}C NMR (125.8 MHz, $CDCl_3$): $\delta = 163.7$, 159.0, 136.2, 135.7, 135.0, 130.1, 128.5, 128.0, 127.5, 124.1, 117.7, 112.0, 108.2, 104.9, 79.3, 78.3, 69.8; FAB$^+$-MS: *m/z*: 2178 (MH^+, $^{13}C^{12}C_{151}H_{97}O_{16}$ requires 2178.77)

(*R,R,R,R*)-(−)-**5**: m.p. 252 °C (decomp.); $[\alpha]_D^{22} = -554.9$ ($c = 1.0$ in CH_3CN); IR (CH_3CN): $\tilde{\nu} = 2211$, 2144 (C≡C–C≡C) cm^{-1}; ^1H NMR (500 MHz, CD_3CN): $\delta = 8.26$ (s, 8H), 7.87 (d, $J = 9.2$ Hz, 8H), 7.23–7.04 (m, 48H), 6.62 (s, 8H), 4.64 (q, AB, $J = 12.1$ Hz, 16H), 3.06–3.03 (m, 32H), 1.55–1.41 (m, 32H), 1.26–1.33 (m, 32H), 0.91 (t, $J = 7.3$ Hz, 48H); ^{13}C NMR (50 MHz, CD_3CN): $\delta = 159.6$, 138.2, 136.4, 135.1, 131.5, 129.8, 129.2, 128.5, 127.0, 123.0, 119.7, 116.5, 115.0, 108.4, 80.6, 78.1, 71.1, 59.5, 24.5, 20.5, 14.1; ^{31}P NMR (121.5 MHz, CD_3CN): $\delta = -2.90$; FAB$^+$-MS: *m/z*: 3173 [M^+ + Na−Bu$_4$N], $^{13}C_2{}^{12}C_{198}H_{196}N_3O_{24}P_4Na$ requires 3172.37), 2932 ([M^+ + Na + H−2Bu$_4$N], $^{13}C_2{}^{12}C_{182}H_{161}O_{24}N_2P_4Na$ requires 2931.08), 2690 ([M^+ + Na + 2H−3Bu$_4$N], $^{13}C^{12}C_{167}H_{126}O_{24}NP_4Na$ requires 2688.80), 2448 ([M^+ + Na + 3H−4Bu$_4$N], $^{13}C^{12}C_{151}H_{91}O_{24}P_4Na$ requires 2447.51)

(*R,R,R*)-(−)-**16**: m.p. 168–172 °C; $[\alpha]_D^{22} = -869.5$ ($c = 1.0$ in CH_2Cl_2); IR (CCl_4): $\tilde{\nu} = 2213$, 2140 (C≡C–C≡C), 1745 (C=O) cm^{-1}; ^1H NMR (300 MHz, $CDCl_3$): $\delta = 7.93$ (s, 6H), 7.85 (dd, $J = 1.2$, 8.4 Hz, 12H), 7.61 (d, $J = 9$ Hz, 6H), 7.24–7.12 (m, 36H), 6.99 (m, 6H), 6.78 (dd, $J = 7.8$, 7.8 Hz, 12H), 6.58 (d, $J = 2.4$ Hz, 6H), 4.65 (q, AB, $J = 12.1$ Hz, 12H); ^{13}C NMR (75 MHz, $CDCl_3$): $\delta = 164.3$, 158.5, 148.8, 136.2, 134.2, 134.1, 133.5, 130.3, 129.7, 128.4, 128.3, 127.9, 127.8, 127.4, 126.7, 123.3, 120.2, 113.0, 105.6, 69.9; ^{13}C NMR (75 MHz, [D$_8$]THF)[b]: $\delta = 79.2$, 78.3; FAB$^+$-MS: *m/z*: 2259 (MH^+, $^{13}C^{12}C_{155}H_{97}O_{18}$ requires 2258.76)

(*R,R,R,R*)-(−)-**17**: m.p. 185–188 °C; $[\alpha]_D^{22} = -855.6$ ($c = 1.0$ in CH_2Cl_2); IR ($CHCl_3$): $\tilde{\nu} = 2214$, 2144 (C≡C–C≡C), 1744 (C=O) cm^{-1}; ^1H NMR (300 MHz, $CDCl_3$): $\delta = 7.93$ (s, 8H), 7.71 (m, 16H), 7.65 (d, $J = 9.3$ Hz, 8H), 7.10–7.30 (m, 72H), 6.60 (d, $J = 2.1$ Hz, 8H), 4.79 (q, AB, $J = 12.0$ Hz, 16H); ^{13}C NMR (75 MHz, $CDCl_3$): $\delta = 164.4$, 158.4, 148.3, 136.3, 134.8, 134.6, 133.1, 130.0, 129.5, 129.0, 128.4, 128.2, 127.9, 127.6, 126.5, 123.4, 120.1, 113.0, 106.0, 77.9, 77.8, 69.9; FAB$^+$-MS: *m/z*: 3011 (M^+, $^{13}C_2{}^{12}C_{206}H_{128}O_{24}$ requires 3011.01)

(*R,R,R,R,R*)-(−)-**18**: m.p. 205–210 °C; $[\alpha]_D^{22} = -838.8$ ($c = 0.5$ in CH_2Cl_2); IR ($CHCl_3$): $\tilde{\nu} = 2216$, 2143 (C≡C–C≡C), 1740 (C=O) cm^{-1}; ^1H NMR (200 MHz, $CDCl_3$): $\delta = 7.93$ (s, 10H), 7.64 (m, 30H), 7.50–7.10 (m, 90H), 6.59 (d, $J = 2.4$ Hz, 10H), 4.81 (q, AB, $J = 12.0$ Hz, 20H); ^{13}C NMR (75 MHz, $CDCl_3$): $\delta = 164.2$, 158.4, 148.0, 136.3, 135.0, 134.6, 133.1, 129.9, 129.4, 129.0, 128.4, 128.2, 127.9, 127.6, 126.5, 123.4, 120.0, 113.0, 106.0, 78.1, 77.8, 69.9; FAB$^+$-MS: *m/z*: 3764 (MH^+, $^{13}C_2{}^{12}C_{258}H_{161}O_{30}$ requires 3764.27)

[a] All new compounds described were fully characterized by ^1H and ^{13}C NMR spectroscopy, FT-IR spectroscopy, FAB$^+$ mass spectrometry, and, except for (*R,R,R,R*)-(−)-**4** and (*R,R,R,R*)-(−)-**5**, correct elemental analysis. [b] These butadiyne signals were obscured by the $CDCl_3$ solvent resonance.

Table 3. Binding constants K_a and binding free energies ΔG° from ^1H NMR binding titrations for 1:1 complexes of octyl glucopyranosides with (*R,R,R*)-(−)-**3** in $CDCl_3$ at 300 K [a].

Guest	K_a [L mol^{-1}]	$-\Delta G^0$ [kcal mol^{-1}]	Degree of saturation	$\Delta\delta_{sat}$
21	195	3.1	57	2.0
22	90	2.7	37	2.5
23	370	3.5	60	2.4

[a] [(*R,R,R*)-(−)-**3**] ≈ 0.5 mmol L^{-1}. Reproducibility of K_a values about ±15%. Also shown are the complexation-induced changes in chemical shift at saturation binding of the host OH protons ($\Delta\delta_{sat}$), and the degree of saturation reached. For the preparation of **22**, see ref. [5k].

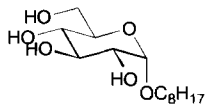

21

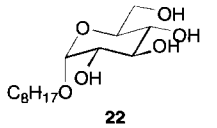

22

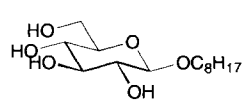

23

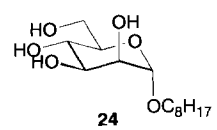

24

binaphthyl spacers in (*R,R,R*)-(−)-**3** participate in the binding to the pyranoside in the macrocyclic cavity. The stronger binding of octyl β-D-glucopyranoside (**23**) compared to its anomer **21** seems to reflect the greater amount of intramolecular H-bonding in the unbound α-anomer.[5n, 18] (*R,R,R*)-(−)-**3** shows a modest selectivity between the two enantiomers of octyl α-glucopyranoside.

Binding between (*R,R,R*)-(−)-**3** and 1-*O*-octyl α-D-mannopyranoside **24**[19] was also investigated, but the receptor OH-signal was too broad at ambient temperature; variable temperature studies on this system showed that the complex formed is in exchange with its free components at an intermediate rate on the NMR time scale at room temperature and can be forced into fast exchange by heating to 330 K. Cooling to 240 K gives rise to a very complicated spectrum in which the signals of bound host and guest are very broad, since the low symmetry of the pyranoside is imposed on the resonances of the trimeric receptor. The surprisingly slow exchange kinetics, relative to those observed for pyranoside binding to cleft-type receptors,[5a, n] supports a complex geometry in which the sugar substrate must fully penetrate into the receptor cavity rather than docking onto one of the two receptor faces.

In preliminary studies we have also explored the complexation between the tetraanionic macrocycle (*R,R,R,R*)-(−)-**5** (with four convergent phosphodiester groups) and octyl β-D-glucopyranoside (**23**). The formation of ionic host–guest hydrogen bonds between the phosphates of the receptor and the OH groups of the substrate dramatically increases the complexation strength, which becomes too large to be evaluated by ^{1}H NMR titrations in pure CD_3CN, a much more competitive solvent than $CDCl_3$ for the H-bonding centers of the binding partners.[5a] Complexation occurred even in the presence of a protic cosolvent, and host–guest binding was observed by ^{1}H NMR in CD_3CN solutions containing up to 20% v/v of CD_3OD. The ^{1}H NMR signals of all sugar protons were considerably shifted upfield on complexation: for example at equal concentrations of host and guest of 1.0 mmol L^{-1}, the anomeric CH signal of **23** moved upfield from $\delta = 4.197$ to $\delta = 3.787$ in pure CD_3CN to $\delta = 3.903$ in CD_3CN/CD_3OD 98:2 (v/v), and to $\delta = 4.116$ in CD_3CN/CD_3OD 90:10 (v/v). Attempts at quantitative binding titrations in CD_3CN/CD_3OD 98:2 (v/v) rapidly showed that the receptor tends to form complexes with higher, presumably 1:2 host–guest stoichiometry. When pyranoside **23** was present in excess over the receptor, higher complexation clearly predominated as indicated by the shape of the titration curves.[5a] A host–guest complexation ratio of 1:2 can be readily rationalized by the eight phosphate ester O atoms forming H-bonds to four OH groups of two sugars that presumably dock from opposite faces onto the receptor. At low concentrations with an excess of host (c = 0.5 to 2 mmol L^{-1}) over guest (c = 0.5 mmol L^{-1}), binding titration curves and Job plots suggested the predominant formation of a stable 1:1 complex, and evaluation of the upfield complexation shifts of the anomeric proton H-C(1) ($\Delta\delta_{sat} = 0.27$) and proton H-C(2) ($\Delta\delta_{sat} = 0.15$) yielded a preliminary association constant of $K_a = 15000 \pm 5000$ L mol^{-1} ($\Delta G^\circ = -5.7$ kcal mol^{-1}, $T = 300$ K). In the presence of CD_3OD as a cosolvent, comparison compound (*R*)-(−)-**20** did not show detectable binding to **23**, whereas a weak 1:1 complex was formed in pure CD_3CN ($K_a = 170 \pm 20$ L mol^{-1}, $\Delta G^0 = -3.1$ kcal mol^{-1}).

The preparation of this first class of receptors from the chiral binaphthyl (*R*)-(+)-**6** illustrates the synthetic potential of the large receptor family shown in Scheme 1, and the preliminary binding studies show their recognition potential. The observed complexation of neutral carbohydrates in the presence of a protic cosolvent suggests that, with appropriately designed receptors from this family, complexation of these substrates in aqueous solutions may be achieved in the near future.

Experimental Procedure

Glaser–Hay coupling to form (*R,R,R*)-(−)-**16**, (*R,R,R,R*)-(−)-**17**, and (*R,R,R,R,R*)-(−)-**18**: CH_2Cl_2 (1.0 L, freshly distilled over CaH_2) was added to a mixture of (*R*)-(+)-**6** (150 mg, 0.4 mmol) and freshly prepared [20] copper(I) chloride (2.71 g, 27 mmol). The mixture was stirred under dry air for 10 min (vigorous stirring at this stage reduces the particle size of the copper(I) chloride, which accelerates the reaction when TMEDA is added). TMEDA (4.21 mL, 3.24 g, 28 mmol) was then added, and the reaction mixture turned dark green. After 20 min, TLC analysis (SiO_2, cyclohexane/AcOEt 80:20) showed that there was no starting material left. The reaction was quenched with H_2O (1.0 L) and exhaustively washed with H_2O (3 × 1.0 L) until the CH_2Cl_2 phase was yellow and most of the copper salts had been removed. After evaporation, the product mixture was separated by flash column chromatography (SiO_2, cyclohexane, then cyclohexane/AcOEt 85:15, then cyclohexane/AcOEt 80:20), to give (*R,R,R*)-(−)-**16** (31 mg, 20%), (*R,R,R,R*)-(−)-**17** (31 mg, 20%), and (*R,R,R,R,R*)-(−)-**18** (5 mg, 3%).

Received: March 8, 1995 [Z 7772 IE]
German version: *Angew. Chem.* **1995**, *107*, 1722–1724

Keywords: biaryls · carbohydrates · cyclophanes · hydrogen bonding · molecular recognition

[1] N. Sharon, H. Lis, *Sci. Am.* **1993**, *268(1)*, 74–81.
[2] C. H. Wong, R. L. Halcomb, Y. Ichikawa, T. Kajimoto, *Angew. Chem.* **1995**, *107*, 453–474; *Angew. Chem. Int. Ed. Engl.* **1995**, *34*, 412–423.
[3] F. A. Quiocho, *Pure Appl. Chem.* **1989**, *61*, 1293–1306.
[4] R. U. Lemieux, M.-H. Du, U. Spohr, *J. Am. Chem. Soc.* **1994**, *116*, 9803–9804.
[5] a) G. Das, A. D. Hamilton, *J. Am. Chem. Soc.* **1994**, *116*, 11139–11140; b) P. B. Savage, S. H. Gellman, *ibid.* **1993**, *115*, 10448–10449; c) L. K. Mohler, A. W. Czarnik, *ibid.* **1993**, *115*, 2998–2999; d) J. M. Coterón, C. Vicent, C. Bosso, S. Penadés, *ibid.* **1993**, *115*, 10066–10076; e) Y. Kikuchi, Y. Tanaka, S. Sutarto, K. Kobayashi, H. Toi, Y. Aoyama, *ibid.* **1992**, *114*, 10302–10306; f) K. Kobayashi, Y. Asakawa, Y. Kato, Y. Aoyama, *ibid.* **1992**, *114*, 10307–10313; g) R. Liu, W. C. Still, *Tetrahedron Lett.* **1993**, *34*, 2573–2576; h) M.-F. Paugam, G. T. Morin, B. D. Smith, *ibid.* **1993**, *34*, 7841–7844; i) H. Murakami, T. Nagasaki, I. Hamachi, S. Shinkai, *ibid.* **1993**, *34*, 6273–6276; j) R. P. Bonar-Law, A. P. Davis, B. A. Murray, *Angew. Chem.* **1990**, *102*, 1497–1499; *Angew. Chem. Int. Ed. Engl.* **1990**, *29*, 1407–1408; k) K. M. Bhattarai, R. P. Bonar-Law, A. P. Davis, B. A. Murray, *J. Chem. Soc. Chem. Commun.* **1992**, 752–754; l) R. P. Bonar-Law, J. K. M. Sanders, *J. Am. Chem. Soc.* **1995**, *117*, 259–271; m) A. V. Eliseev, H. J. Schneider, *ibid.* **1994**, *116*, 6081–6088; n) J. Cuntze, L. Owens, V. Alcázar, P. Seiler, F. Diederich, *Helv. Chim. Acta* **1995**, *78*, 367–390.
[6] J. Rebek, Jr., *Angew. Chem.* **1990**, *102*, 261–272; *Angew. Chem. Int. Ed. Engl.* **1990**, *29*, 245–255.
[7] R. U. Lemieux, *ACS Symp. Ser.* **1991**, *519*, 5–18.
[8] C. F. Koelsch, *Org. Synth. Collect. Vol.* **1955**, *3*, 132–133.
[9] X-ray crystal structure of (±)-**11** ($C_{34}H_{24}Br_2O_4$, $M_r = 656.4$): Orthorhombic space group *Pccn*, $\rho_{calcd} = 1.531$ g cm^{-3}, $Z = 4$, $a = 10.928(6)$, $b = 15.873(11)$, $c = 16.415(11)$ Å, $V = 2847(3)$ Å^3, $Mo_{K\alpha}$ radiation, $2\theta \leq 40^\circ$, 1322 unique reflections. The structure was solved by the Patterson method (SHELXTL PLUS) and refined by full-matrix least-squares analysis using experimental weights (heavy atoms anisotropic; H atoms riding model, fixed isotropic). Final $R(F) = 0.0398$, $wR(F) = 0.0490$ for 181 variables and 915 observed reflections with $F > 4.0\sigma(F)$. Further details of the crystal structure investigations are available on request from the Director of the Cambridge Crystallographic Data Centre, University Chemical Laboratory, 12 Union Road, GB-Cambridge CB2 1EZ (UK), on quoting the full journal citation.
[10] J.-M. Brunel, G. Buono, *J. Org. Chem.* **1993**, *58*, 7313–7314. Addition of PCl_3 to (L)-menthol in THF, as suggested in this reference, led to a product mixture from substitution of one, two, and three Cl atoms by menthol. When menthol was added to PCl_3, the monosubstituted menthyl phosphorodichloridite was the predominant product. In the cited reference, the phosphite was cleaved by conversion into the phosphate, followed by treatment with $LiAlH_4$.
[11] The diastereomeric excess (*de*) was calculated from the proton-decoupled ^{31}P NMR spectrum of recrystallized (−)-**12**; M. Mikolajczyk, J. Omelanczuk, M. Leitloff, J. Drabowicz, A. Ejchart, J. Jurczak, *J. Am. Chem. Soc.* **1978**, *100*, 7003–7008.
[12] J. Reeder, P. P. Castro, C. B. Knobler, E. Martinborough, L. Owens, F. Diederich, *J. Org. Chem.* **1994**, *59*, 3151–3160.
[13] J. K. Stille, J. H. Simpson, *J. Am. Chem. Soc.* **1987**, *109*, 2138–2152.
[14] S. Takahashi, Y. Kuroyama, K. Sonogashira, N. Hagihara, *Synthesis* **1980**, 627–630.

[15] Deprotection was carried out after macrocyclization because of problems with furan formation during Glaser–Hay coupling with (*R*)-(−)-**19**. It seems that 2-alkynylphenols are stable under neutral and mildly basic conditions, but are more likely to form furans under strongly acidic or basic conditions; see: a) C. E. Castro, E. J. Gaughan, D. C. Owsley, *J. Org. Chem.* **1966**, *31*, 4071–4078; b) S. Torii, L. H. Xu, H. Okumoto, *Synlett.* **1992**, 515–516.

[16] $CDCl_3$ was allowed to stand over anhydrous K_2CO_3 for at least 24 h prior to use in titrations. Remaining water was removed by the addition of just enough powdered molecular sieves (4 Å) to the NMR tube to make the water peak at $\delta = 1.54$ disappear; see ref. [5l].

[17] Associate V. 1.6, Blake Peterson, Ph.D. thesis, UCLA **1994**.

[18] C.-Y. Huang, L. A. Cabell, E. V. Anslyn, *J. Am. Chem. Soc.* **1994**, *116*, 2778–2792.

[19] Y. Kikuchi, H. Toi, Y. Aoyama, *Bull. Chem. Soc. Jpn.* **1993**, *66*, 1856–1858.

[20] R. N. Keller, H. D. Wycoff in *Inorganic Syntheses, Vol. 2* (Ed.: W. C. Fernelius), McGraw Hill, New York, **1946**, pp. 1–4.

Jasmonic Acid and Coronatin Induce Odor Production in Plants

Wilhelm Boland,* Jörn Hopke, Jens Donath, Jörg Nüske, and Friedemann Bublitz

Dedicated to Professor Dieter G. Müller on the occasion of his 60th birthday

Jasmonic acid (JA) and certain derivatives (e.g. methyl jasmonate, JA-Me) play a key role as phytohormones, elicitors, and signal transducers.[1] They are formed from linolenic acid through a known sequence of reactions (Scheme 1)[2] and induce the expression of specific genes in the form of proteins (Jasmonate Induced Proteins, JIPs),[3] which are responsible for a number of effects including defoliation, senescence promotion,[4] and emission of ethylene.[5] Similar, adverse results can be induced by application of the structurally related phytotoxin coronatin, which has been previously isolated from culture filtrates of pathogenic strains of *Pseudomonas syringae*[6] and *Xanthomonas campestris*.[7] Again, the typical effects are chlorose, senescence, and enhanced ethylene production.[8]

In recent years JA has been found to stimulate a number of other effects. Among them, tomato tuber induction,[9] tendril coiling,[10] and the induction of secondary metabolite biosynthesis[11] in cell suspension cultures of *Escholtzia californica* and *Rauvolfia canescens* are particularly noteworthy. Again, similar effects can be triggered by coronatin.[12] Moreover, JA and JA-Me appear to be important stress signals, or signal transducers, in plants' defense against herbivores, since both induce the biosynthesis of proteinase inhibitors.[13,14] Plant defense also involves the release of volatile substances which may act inter alia as intra- or interspecific "SOS signals",[15] attracting predators that prey on herbivores.[16,17]

We report here that the biosynthesis and emission of volatiles can be triggered in many plant species by application of JA and coronatin. The effect is demonstrated in Figure 1 for *Nicotiana tabacum*. Leaves from untreated tobacco plants release volatiles at relatively low levels (Fig. 1A). However, following 30 h of incubation with JA (10 $\mu mol\,mL^{-1}$), supplied through the petiole of a freshly detached leaf, a dramatic increase in the production of a number of volatiles is seen (Fig. 1B). The effect can still be triggered with roughly 100 $nmol\,mL^{-1}$ of JA. An overview of the JA-treated plants, the type of volatiles produced, and the extent to which individual compounds or compound classes are triggered is presented in Table 1. As previously shown for *Phaseolus lunatus* (lima bean) and *Zea mays* (maize), the maximum rate of volatile emission is reached within 20–30 h after application of JA.[18] The volatile substances released can be divided into three classes of compounds: 1) mevalogenins,

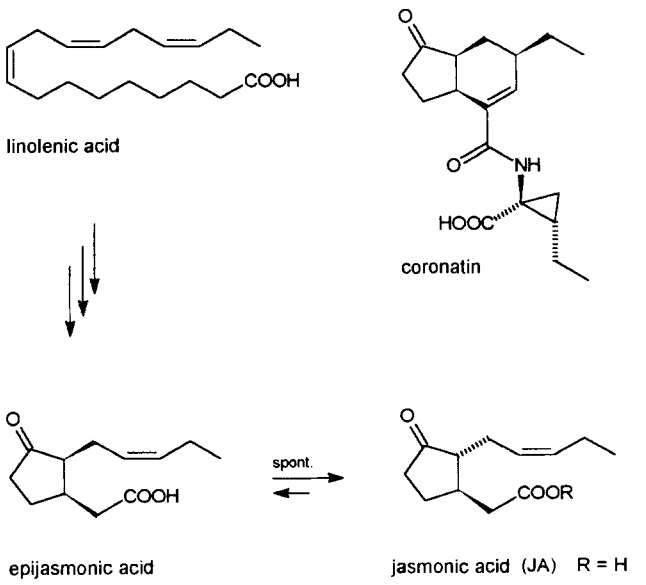

Scheme 1. Synthesis of jasmonic acid and methyl jasmonate from linolenic acid and the structure of coronatin.

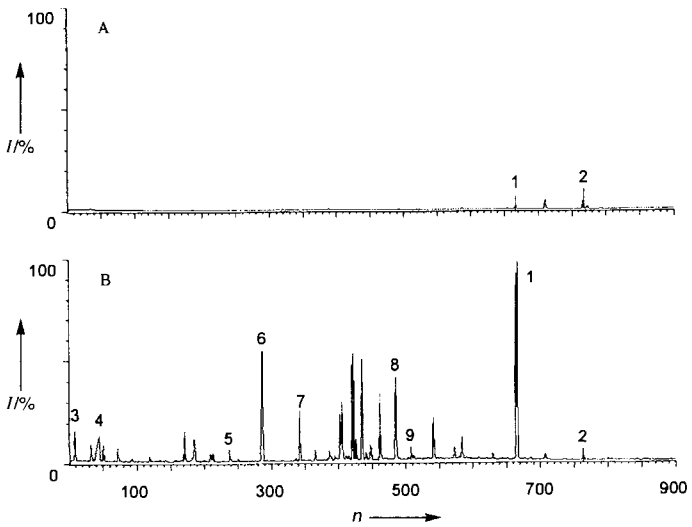

Fig. 1. Gas chromatographic analysis of volatiles from tobacco leaves (*Nicotiana tabacum*) A) untreated, B) after treatment with jasmonic acid. The relative signal intensity *I* is plotted against the number *n* of the scan (1 scan per second). Compounds identified: neophytadiene (**1**), $C_{20}H_{32}$ **2**, (3*Z*)-hex-3-enyl acetate (**3**), oct-1-en-3-ol (**4**), indole (**5**), (3*Z*)-hex-3-enyl tiglate (**6**), β-elemene (**7**), (3*Z*)-hex-3-enyl benzoate (**8**), 4,8,12-trimethyltrideca-1,3,7,11-tetraene (**9**).

[*] Prof. Dr. W. Boland, Dipl.-Chem J. Hopke, Dr. J. Donath
Institut für Organische Chemie und Biochemie der Universität
Gerhard-Domagk-Strasse 1, D-53121 Bonn (Germany)
Telefax: Int. code + (228) 735388
Dr. J. Nüske, Dr. F. Bublitz
Institut für Mikrobiologie der Universität Jena (Germany)

[**] Herbivore-Induced Volatiles, Part 2. This work was supported by the Deutsche Forschungsgemeinschaft and by the Fonds der Chemischen Industrie. We thank Dr. R. Kaiser, Givaudan Company (Dübendorf, Switzerland), for samples of methyl jasmonate. Part 1: ref. [18].

Table 1. Semiquantitative compilation of volatiles from selected plants after treatment with jasmonic acid [a].

	Brassica oleracea	*Dryopteris filix-mas*	*Eucalyptus globulus*	*Gerbera jamesonii*	*Ginkgo biloba*	*Lathyrus vernus*	*Lycopersicon esculentum*	*Nicotiana tabacum*	*Phaseolus lunatus*	*Salix alba*	*Zea mays*
Terpenes											
(*E*)-β-ocimene	-/-	o/o	+/+	o/o	-/-	-/-	-/-	-/+	o/+	o/++	-/-
linalool	-/-	-/o	+/+	o/+	-/++	-/-	-/-	-/o	-/++	o/o	-/-
$C_{11}H_{18}$ [b]	-/-	-/-	+/+	+/+++	-/-	-/-	-/-	-/-	o/+++*	+/+	-/o
$C_{10}H_{14}$ [c]	-/-	-/-	o/+	-/+	-/-	-/-	-/-	-/o	o/++	o/+	-/-
nerolidol	-/-	o/+	-/-	o/++	o/++	-/o	-/-	-/-	o/+	o/+	o/++
$C_{16}H_{26}$ [d]	-/-	o/+	-/-	o/+	-/-	-/o	-/-	-/+	o/++	o/+	o/++
β-caryophyllene	-/-	-/+	+/++	-/+	-/++	-/-	o/o	-/-	-/+	o/o	-/++
additional monoterpenes	+/+	o/o	+++/+++*	o/+	o/o	-/-	++/+++*	o/+	o/+++	o/++	-/-
additional sesquiterpenes	o/o	+/+++*	+++/+++	o/+++*	o/+++*	+/+++*	-/-	+/+++	o/o	o/+++*	-/+++
diterpenes	-/-	o/+	-/-	-/-	o/o	-/-	-/-	+/+++*	-/-	-/-	-/-
Acetogenins											
(3*Z*)-hex-3-enyl acetate	+/+	-/-	-/o	o/+	-/-	-/o	-/++	-/++	-/+++	o/o	-/o
1-octen-3-ol	-/-	o/++	-/-	-/-	-/+	-/-	-/-	-/+++	-/++	-/-	-/-
additional acetogenins	+++/+++*	-/-	-/-	o/o	+/+	-/-	+/+	+/+++	-/+	o/+	+/o
Arenes											
benzyl alcohol	-/-	-/-	-/-	-/-	-/+	-/-	-/-	-/o	-/++	-/-	-/o
methyl salicylate	-/-	-/-	-/-	-/-	-/o	-/-	-/+	-/o	-/+	o/o	-/-
indole	-/++	-/-	-/-	-/++	-/-	-/-	-/-	-/+	-/+	o/+	-/+
additional arenes	o/o	-/-	-/++	-/-	o/+	-/-	-/-	-/++	-/+	-/-	o/+
methyl jasmonate	-/-	-/+++	-/-	-/-	-/++	-/+	-/+++	-/+	-/++	-/-	-/+++*

[a] Designations (untreated/treated with jasmonic acid): -: not present, o: <5%, +: 0.5–5%, ++: 5–25%, +++: >25%, *: main component of the mixture. The percentages are calculated relative to the major component in the chromatogram. [b] 4,8-Dimethylnona-1,3,7-triene. [c] Monoterpene. [d] 4,8,12-Trimethyltrideca-1,3,7,11-tetraene.

mainly mono- and sesquiterpenes; 2) acetogenins, degradation products of fatty acid hydroperoxides (e.g. esters of leaf alcohols and oct-1-ene-3-ol); 3) aromatic compounds (alcohols, esters, and indole).

While the leaves of most plants show significant characteristics of senescence (withering, browning along the vascular bundles) after treatment with JA (>10 μmol mL^{-1}), similar adverse effects failed to appear after treatment with coronatin (50 and 100 nmol mL^{-1}). Experiments were carried out with the lima bean (*P. lunatus*) and maize (*Z. mays*) as two typical representatives of mono- and dicotyledonous plants. In general, coronatin proved to be the superior inducing agent; the threshold concentration for odor induction was roughly 1 nmol mL^{-1}. The pattern of the induced volatiles corresponds to that from treatment with JA, but owing to the low concentrations of coronatin used (50 and 100 nmol mL^{-1}) no senescence promotion was observed.

Strong odor induction by JA in the fern *Dryopteris filixmas* indicates that this signal transduction pathway may be an archetypal development within the phylogeny of plants, which apparently persists even in modern dicotyledonous plants like *N. tabacum* and *P. lunatus*. This is also supported by JA induction of volatiles in the leaves of the pharmacologically interesting gingko tree (*Ginkgo biloba*), the last representative of the genus *Ginkoopsida*. Leaves of the willow tree (*Salix alba*) likewise release volatiles after treatment with JA.

It must be emphasized, however, that the application of JA does not always result in the production and emission of novel compounds; in several cases only the relative composition of the mixture of volatiles is altered (Table 1, *Brassica oleracea*, *Eucalyptus globulus*). It remains to be established whether the production of volatiles is due to activation of the defense genes within the various plants, or if it is a concomitant effect of senescence. Irrespective of the signaling pathway within the plant, it is interesting to see that the JA- or coronatin-induced volatiles from the lima bean (*P. lunatus*) and maize (*Z. mays*) correspond to those typically released in response to an attacking herbivore.[16–18]

The emission of methyl jasmonate (JA-Me) from some of the JA-treated plants (cf. Table 1) appears significant, since gaseous JA-Me has been shown to induce defense reactions in neighboring plants like, for example, the synthesis of proteinase inhibitors[13] and phytoalexins.[10,19] In this respect, the emission of JA-Me may be taken as additional evidence for the involvement of volatile jasmonates in interplant communication. In a similar fashion volatile methyl salicylate (Table 1, *P. lunatus*) may activate defense genes,[20] but this effect still remains to be established.

Odor induction by JA and coronatin provides interesting perspectives. Since the biosynthesis of most of the volatile compounds in Table 1 is known, their detection after JA or coronatin treatment should allow preliminary extrapolations to the enzymatic level and may provide valuable hints for the identification of still unknown JIPs. Other interesting applications may include the attraction of useful insects into crop fields[16,17] threatened by herbivores by preventive induction of volatile synomones and/or resistance genes,[20] and the enhanced production of valuable flavor compounds. Preliminary induction experiments with JA in cell suspension cultures of *N. tabacum* and *P. lunatus* demonstrated, however, that emission of volatiles remains restricted to only a few compounds and does not show the full pattern of compounds from the JA- or coronatin-treated differentiated, intact plant.

Experimental Procedure

Freshly detached plantlets (with 2–5 leaves) of the plants listed in Table 1 were placed in solutions of racemic *trans*-JA (10 μmol mL^{-1}) or coronatin (50 and 100 nmol mL^{-1}) in tap water. Following 10 h of preincubation, the plants were placed in a closed system (ca. 750 mL), and the volatiles were collected on a small charcoal trap (1.5 mg) by air circulation [21] over 20 h. After desorption of the volatiles from the charcoal with dichloromethane (30 μL), the compounds were analyzed by GC-MS (DB1 silica gel capillary column, 10 m × 0.31 mm; temperature program: 50 °C (2 min), then an increase of 10 °C min^{-1} to 200 °C; detection: Fisons MD 800 mass spectrometer, GC interface at 260 °C, scan range: 35–300 Da s^{-1}. The mixture of compounds released from freshly detached plantlets placed in water served as a control. Plants: *P. lunatus* and *Z. mays* were cultivated as described in ref. [18]. *Gerbera jamesonii*, cv. *Sirtaki* was kindly provided by Prof. Dr. M. Dicke, Agricultural University, Wageningen, The Netherlands. All other plants were from the Botanical Garden of the University of Bonn.

Received: December 22, 1994
Revised version: March 6, 1995 [Z 7570 IE]
German version: *Angew. Chem.* **1995**, *107*, 1715–1717

Keywords: induced volatiles · jasmonic acid · phytohormones

[1] G. Sembdner, B. Parthier, *Annu. Rev. Plant Physiol. Plant. Mol. Biol.* **1993**, *44*, 569.
[2] B. A. Vick, D. C. Zimmermann, *Plant Physiol.* **1984**, *75*, 458.
[3] R. A. Weidhase, H. Kramell, J. Lehmann, H. Liebisch, W. Lerbs, B. Parthier, *Plant Sci. (Limerick, Irel.)* **1987**, *51*, 177.
[4] J. Ueda, J. Kato, *Plant Physiol.* **1980**, *66*, 246.
[5] M. Saniewski, J. Czapski, *Experientia* **1985**, *41*, 256.
[6] J. Nüske, F. Bublitz, *J. Basic Microbiol.* **1993**, *33*, 241.
[7] K. Tamura, Y. Takikawa, S. Tsuyumu, M. Goto, M. Watanabe, *Nippon Shokubutsu Byori Gakkaiho* **1992**, *58*, 276.
[8] F. Greulich, T. Yoshihara, H. Toshima, A. Ichihara, *Abstract of the XV. Int. Botanical Congress*, Tokio, **1993**, p. 4152.
[9] Y. Koda, Y. Okazawa, *Plant Cell Physiol.* **1988**, *29*, 969.
[10] E. Falkenstein, B. Groth, A. Mithöfer, E. W. Weiler, *Planta* **1991**, *185*, 316.
[11] H. Gundlach, M. J. Müller, T. M. Kutchan, M. H. Zenk, *Proc. Natl. Acad. Sci. USA* **1992**, *89*, 2389.
[12] E. W. Weiler, T. M. Kutchan, T. Gorba, W. Brodschelm, U. Niesel, F. Bublitz, *FEBS Lett.* **1994**, *345*, 9.
[13] E. E. Farmer, C. A. Ryan, *Proc. Natl. Acad. Sci. USA* **1990**, *87*, 7713.
[14] E. E. Farmer, C. A. Ryan, *Plant Cell* **1992**, *4*, 129.
[15] H. J. Zeringue, *Phytochemistry* **1992**, *31*, 2305.
[16] M. Dicke, M. A. Sabelis, J. Takabayashi, J. Bruin, M. A. Posthumus, *J. Chem. Ecol.* **1990**, *16*, 3091.
[17] T. C. J. Turlings, J. H. Tumlinson, *Proc. Natl. Acad. Sci. USA* **1992**, *89*, 8399.
[18] J. Hopke, J. Donath, S. Blechert, W. Boland, *FEBS Lett.* **1994**, *352*, 146.
[19] H. Dittrich, T. M. Kutchan, M. H. Zenk, *FEBS Lett.* **1992**, *309*, 11462.
[20] J. P. Metraux, H. Signer, J. Ryals, E. Ward, M. Wyss-Benz, J. Gaudin, K. Raschdorf, E. Schmid, W. Blum, *Science* **1990** *250*, 1004.
[21] W. Boland, P. Ney, L. Jaenicke, G. Gassmann in *Analysis of Volatiles* (Ed.: P. Schreier), Walter De Gruyter, Berlin, New York, **1984**, p. 371.

Pericyclic Reactions in Nature: Spontaneous Cope Rearrangement Inactivates Algae Pheromones**

Wilhelm Boland,* Georg Pohnert, and Ingo Maier

Dedicated to Professor Hans-Jürgen Bestmann on the occasion of his 70th birthday

Female gametes of marine brown algae use olefinic C_{11} hydrocarbons as chemical signals to trigger the release of and/or attract conspecific flagellated motile male sex cells.[1, 2] In 1971 Müller et al.[3] isolated ectocarpene (**2a**), the pheromone of the cosmopolitan brown algae *Ectocarpus siliculosus*. It soon proved to be the prototype of a whole series of structurally related 6-substituted cyclohepta-1,4-dienes, which attract male gametes or induce their mass release (release factors). The most frequently occurring compounds include dictyotene (**1**),[4] desmarestene (**3**),[5] and lamoxirene (**4**).[6, 7] The latter is typical for the highly evolved order Laminariales, in which the pheromone induces spermatozoid release prior to attraction. The threshold concentration of male response towards the signal is typically found in the range of 10 nmol L^{-1} to 0.01 nmol L^{-1}, depending upon algae species and pheromone function.

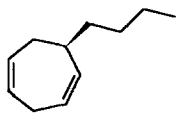

1

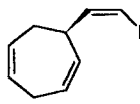

2a, R = C_2H_5
2b, R = H

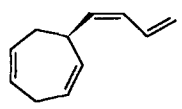

3

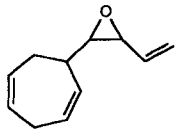

4

Recently we have shown that female gametes of marine brown algae use C_{20} fatty acids as starting materials in the biosynthesis of **1** and **2a** (Scheme 1).[8, 9] The precursor of dictyotene (**1**) was shown to be arachidonic acid, whereas ectocarpene (**2a**) was found to originate from *cis*-eicosa-5,8,11,14,17-pentaenic acid (**5**). The first steps of fatty acid activation remain unknown, but by analogy with the biogenesis of **2** in higher plants,[10] a 9-hydroperoxy fatty acid **6** (9-HPEPE) is implicated as the first O-functionalized intermediate. A hydroperoxide lyase could cleave the reactive intermediate 9-HPEPE **6** directly to give the thermally labile *cis*-disubstituted cyclopropane (1*R*,2*S*)-**7a** (C_{11}) and the C_9 dicarbonyl fragment **8** (Scheme 1). Divinylcyclopropanes of type **7** are thermally labile and rearrange in a spontaneous [3,3] sigmatropic reaction

[*] Prof. Dr. W. Boland, Dipl.-Chem. G. Pohnert
Institut für Organische Chemie und Biochemie der Universität
Gerhard-Domagk-Strasse 1, D-53121 Bonn (Germany)
Telefax: Int. code + (228) 735388

Dr. I. Maier
Fakultät für Biologie der Universität Konstanz (Germany)

[**] Biosynthesis of Algae Pheromones, Part 4. This work was supported by the Deutsche Forschungsgemeinschaft and the Fonds der Chemischen Industrie. We thank Prof. Dr. D. G. Müller (Universität Konstanz) for his support. Part 3: ref. [17].

 © VCH Verlagsgesellschaft mbH, D-69451 Weinheim, 1995 0570-0833/95/1515-1602 $ 10.00+.25/0

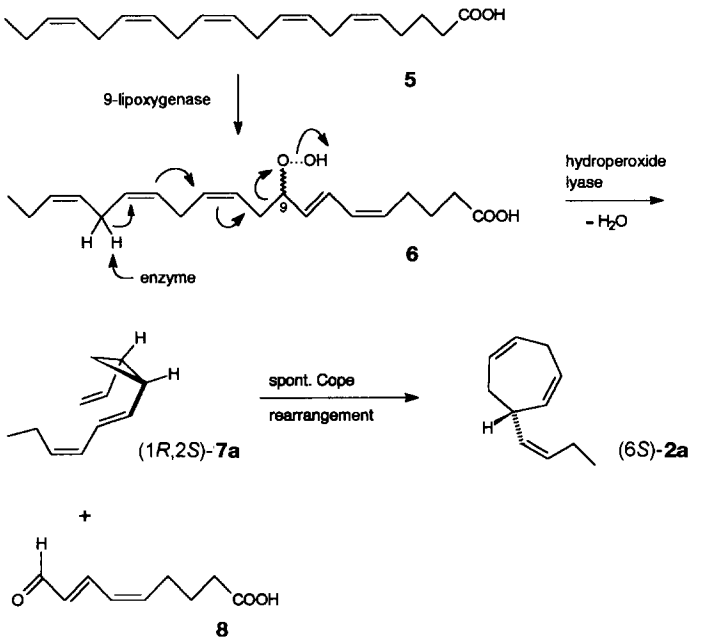

Scheme 1. Postulated mechanism of the biosynthesis of ectocarpene (6*S*)-**2a** from all-*cis*-eicosa-5,8,11,14,17-pentaenic acid (**5**). Activation of **5** by a lipoxygenase yields the 9-hydroperoxide (**6**). Oxidative cleavage of the hydroperoxide by a hydroperoxide lyase is assumed to formally give the C_{11} fragment (1*R*,2*S*)-**7a** and the dicarbonyl compound **8**.

(Cope rearrangement) yielding cyclohepta-1,4-dienes **1**–**4**.[1, 11]

To verify this hypothesis we developed a synthesis of the thermolabile cyclopropanes (1*R*,2*S*)-**7a**, (1*R*,2*S*)-**7b**, and (1*R*,2*S*)-**7c**[12, 13] and determined the activation energies of the Cope rearrangements yielding (6*S*)-**2a**, (6*R*)-**3**, and (6*S*)-**2b**, respectively.[14] Table 1 lists the Arrhenius parameters and half-lives

Table 1. Activation parameters and half-lives for the Cope rearrangement of cyclopropanes (1*R*,2*S*)-**7**.

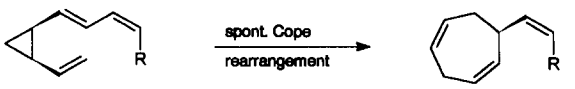

(1*R*,2*S*)-**7**

Cyclopropane	Cycloheptadiene	R	E_a [kJ mol^{-1}]	ln *A*	$t_{1/2}$(8 °C) [min]	$t_{1/2}$(18 °C) [min]
(1*R*,2*S*)-**7a**	(6*S*)-**2a**	C_2H_5	63.8±1.2	18.9±0.4	56	21
(1*R*,2*S*)-**7b**	(6*R*)-**3**	$CH{=}CH_2$	62.6±1.5	18.5±0.5	45	18
(1*R*,2*S*)-**7c**	(6*S*)-**2b**	H	64.9±1.2	19.0±0.4	77	30

for these transformations at two temperatures typical for the surroundings of marine brown algae (spring temperatures in Arctic and Mediterranean regions). The activation energies are in accord with published data for the unsubstituted *cis*-divinylcyclopropane.[15, 16] In light of these relatively long half-lives for the rearrangement of divinylcyclopropane derivatives (18 to 77 min), the actual nature of the pheromone had to be verified. The cyclohepta-1,4-dienes **1**–**4** had been thought to be the signaling agent, but the question arose as to whether thermolabile precursors like (1*R*,2*S*)-**7a** were actually the active pheromones. Comparative bioassays with male gametes of *Ectocarpus siliculosus* (clone PAr 27a) using (1*R*,2*S*)-**7a** and **2a** showed that only the unstable cyclopropane (1*R*,2*S*)-**7a** was an effective pheromone. In previous work a threshold concentration of approximately 10 nmol L^{-1} of (6*S*)-**2a** in seawater was determined.[17, 18] In contrast, that of (1*R*,2*S*)-**7a** was found to be significantly lower, around 5 pmol L^{-1} (Fig. 1). Even the accumulation factor at the highest available concentration Q_{max} (quotient of the number of cells within a standard area on a pheromone-containing droplet and that on a blank control droplet) for (1*R*,2*S*)-**7a** ($Q_{max} \approx 15$) is significantly higher than that reported for (6*S*)-**2a** ($Q_{max} \approx 2.2$).[17] The efficiency is comparable to that of other known thermostable pheromones of marine brown algae.[18–20]

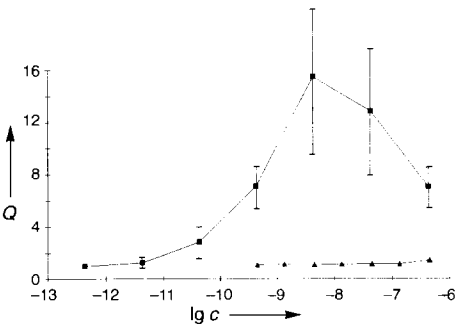

Fig. 1. Biological activity test [21] of (1*R*,2*S*)-**7a** (■) and (6*S*)-**2** (▲) with male gametes of *Ectocarpus siliculosus* (clone PAr-27a♂). The diagram shows a plot of the accumulation factor *Q* against the logarithm of the concentration *c* of (1*R*,2*S*)-**7a** and of (6*S*)-**2** in seawater [19, 22]. Male gametes of the clone used in this test only respond to the highest available concentration of (6*S*)-**2a**.

Pheromone release by female gametes, chemotactic orientation of male gametes, and fusion of the sexual cells all occur within only a few minutes. Thus (6*S*)-**2a**, the rearrangement product of the unstable pheromone (1*R*,2*S*)-**7a**, cannot assume a time-dependent role as a chemical signal; the half-life for the rearrangement of (1*R*,2*S*)-**7a** is significant longer than time required for sexual encounter in algae.

The plot in Figure 1 clearly shows the biological effect of the Cope rearrangement in the rapid, temperature-dependent degradation of the cyclopropyl pheromones. Further (a)biotic degradation to the completely inactive oxygenated products progresses significant slower, taking from hours to days.[1] In their sexual cycle marine brown algae have developed the fastest and most effective mechanism known for spontaneous inactivation of attractant and/or release factors. Furthermore, this is the only known signal system in which deactivation occurs by a [3,3] sigmatropic reaction.

The high biological activity of the disubstituted cyclopropane (1*R*,2*S*)-**7a** provides strong evidence for the proposed model of cycloheptadiene biosynthesis (see Scheme 1) in marine brown algae. In fact, the release of (1*R*,2*S*)-**7a** can even be proved directly by HPLC analysis. An extract from a dense suspension of freshly released female gametes of *E. siliculosus* (ca. 5×10^7 cells) was analyzed by HPLC (RP-18 column). A transient signal was observed, which had the same retention volume and UV absorption (λ_{max} = 246 nm) as the synthetic reference (1*R*,2*S*)-**7a**. In addition, the half-life of the signal given by the natural product corresponded with the decrease in the signal of synthetic (1*R*,2*S*)-**7a** caused by rearrangement to (6*S*)-**2a** (see Table 1).

These results suggest that systems in which cycloheptadienes were identified as pheromones or release factors should be reexamined; thermally labile cyclopropyl precursors of type **7** may be the actual pheromones and have even lower threshold con-

centratons. First results on bioassays with fertile male gametophytes of the North Atlantic brown algae *Desmarestia aculeata*, using a thermally stable analogue of **7b** (CH_2OCH_3 instead of $CH{=}CH_2$ at C(2)[19]), showed high activity. Thus for another algal pheromone, a cyclopropane derivative is implicated as an active substance.

A large variety of pericyclic and electrocyclic rearrangements were shown to occur in the biosynthesis of marine brown algae pheromones. For example, 7-methylcycloocta-1,3,5-triene (**9**), a trace component in the pheromone blend of the Mediterranean brown algae *Cutleria multifida*, is believed to be derived from the linear (1,3*Z*,5*Z*,7*E*)-nonatetraene by means of an 8π electrocyclic ring closure reaction. In addition, thalli of fertile *Giffordia mitchellae* release (2*Z*,4*Z*,6*E*,8*Z*)-undeca-2,4,6,8-tetraene (**10**, giffordene). The unusual geometry of this tetraene is produced by a [1,7]-hydrogen shift, which occures spontaneously at ambient temperatures.[1, 20]

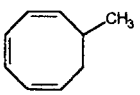

9

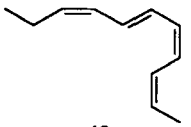

10

Experimental Procedure

Fertile female gametophytes of *Ectocarpus siliculosus* (ca. 2.1 g fresh weight) were kept for ca. 16 h at 2 °C. Gamete release was then induced by increasing the temperature to 18 °C and exposing the sample to light. In order to obtain a significant accumulation of pheromone, the cell suspension (5.2×10^7 cells in 10 mL of seawater) was concentrated by removing excess seawater and kept under light for 4 h at 4 °C (ca. 70 $\mu mol\,m^{-2}\,s^{-1}$). The suspension was treated with 4 mL of MeOH (0 °C) and extracted with 5 mL of CH_2Cl_2 (0 °C). The organic layer was concentrated to 1 mL at 0 °C and analyzed immediately by HPLC (LiChrospher 100, RP 18, 25 × 0.4 cm; eluent: MeOH:H_2O 9:1; flow rate: 0.5 mL min^{-1}; injection volume: 100 μL; detection: 244 nm). The rearrangement of the thermolabile precursor was followed by stopping the flow at the peak maximum. Comparison of the rate of the extinction decay with the synthetic reference leads to the identification of the natural product.

Received: February 4, 1995 [Z 7692 IE]
German version: *Angew. Chem.* **1995**, *107*, 1717–1719

Keywords: biosyntheses · Cope rearrangements · pericyclic reactions · pheromones

[1] W. Boland, *Proc. Natl. Acad. Sci. USA* **1995**, *92*, 31.
[2] I. Maier, *Plant Cell Environ.* **1993**, *16*, 891.
[3] D. G. Müller, L. Jaenicke, M. Donike, T. Akintobi, *Science* **1971**, *171*, 815.
[4] D. G. Müller, G. Gassmann, W. Boland, F.-J. Marner, L. Jaenicke, *Science* **1981**, *212*, 1040.
[5] D. G. Müller, A. Peters, G. Gassmann, W. Boland, F.-J. Marner, L. Jaenicke, *Naturwissenschaften* **1982**, *69*, 290.
[6] D. G. Müller, G. Gassmann, K. Lüning, *Nature (London)* **1979**, *279*, 430.
[7] F.-J. Marner, B. Müller, L. Jaenicke, *Z. Naturforsch. C* **1984**, *39*, 689.
[8] K. Stratmann, W. Boland, D. G. Müller, *Angew. Chem.* **1992**, *104*, 1261; *Angew. Chem. Int. Ed. Engl.* **1992**, *31*, 1246.
[9] K. Stratmann, W. Boland, D. G. Müller, *Tetrahedron* **1993**, *49*, 3755.
[10] C. Neumann, W. Boland, *Eur. J. Biochem.* **1990**, *191*, 453.
[11] R. E. Moore, *Acc. Chem. Res.* **1977**, *10*, 40.
[12] a) D. Wirth, I. Fischer-Lui, W. Boland, D. Icheln, T. Runge, W. A. König, J. Phillips, M. Clayton, *Helv. Chim. Acta* **1992**, *75*, 734; b) S. Pantke, Diplomarbeit, Universität Karlsruhe, **1992**.
[13] G. Pohnert, W. Boland, *Tetrahedron* **1995**, in press.
[14] Kinetic measurements: Dilute solutions of (1*R*,2*S*)-**7a**, (1*R*,2*S*)-**7b**, and (1*R*,2*S*)-**7c** (each ca. 0.01% in *n*-octane) in quartz cuvettes were placed in a thermostated cell holder of a Perkin-Elmer Lamda 2 spectrometer connected to a Haake D1 cryostat (± 0.1 °C). The temperature was continuously recorded as a function of time using NiCr–Ni thermocouple, type K, and a precision digital voltmeter. A run was followed over two to three half-lives. For statistical calculations (standard deviations) each run was conducted three times. The isomerization was monitored by the decrease of the absorption maximum of (1*R*,2*S*)-**7a**: 244 nm; (1*R*,2*S*)-**7b**: 279 nm; (1*R*,2*S*)-**7c**: 241 nm). The raw data was plotted as a function of time to calculate the rate constants according to the method of Swinbourne [23].
[15] J. M. Brown, B. T. Golding, J. J. Stofko, Jr., *J. Chem. Soc. Perkin 2* **1979**, 436.
[16] M. Schneider, Angew. Chem. **1975**, *87*, 717; *Angew. Chem. Int. Ed. Engl.* **1975**, *14*, 707.
[17] W. Boland, L. Jaenicke, D. G. Müller, A. Peters, *Eur. J. Biochem.* **1984**, *144*, 169.
[18] W. Boland, F.-J. Marner, L. Jaenicke, D. G. Müller, E. Fölster, *Eur. J. Biochem.* **1983**, *134*, 97.
[19] W. Boland, K. Jakoby, L. Jaenicke, D. G. Müller, E. Fölster, *Z. Naturforsch. C* **1980**, *36*, 262.
[20] G. Pohnert, W. Boland, *Tetrahedron* **1994**, *50*, 10235.
[21] I. Maier, M. Calenberg, *Bot. Acta* **1994**, *107*, 451.
[22] The actual concentration of the pheromone in seawater is calculated from the concentration of the substance in a biologically inert solvent (perfluorohydrocarbon FC 72, 3M Company, Düsseldorf) and the partition coefficient *K*(FC 72/seawater). The partition coefficient of the unstable (1*R*,2*S*)-**7a** can only be estimated, *K*(FC 72/seawater) ≈ 2000; that of the stable *trans* isomer is 2700. (For comparison: The partition coefficients of the *cis*- and *trans*-disubstituted cyclopentene pheromones [19] are 4800 and 6200, respectively.)
[23] E. S. Swinbourne, *J. Chem. Soc.* **1960**, 473, 2371.

Photoswitchable Electrical Communication of Glucose Oxidase and Glutathione Reductase with Electrode Surfaces through Photoisomerizable Redox Mediators**

Mazzi Lion-Dagan, Sharon Marx-Tibbon, Eugenii Katz, and Itamar Willner*

Reversible photochemical activation and deactivation of biomaterials, especially of enzymes, has recently been a subject of extensive research activity.[1] Photochemical control of enzyme activities was accomplished by chemical modification of the biocatalysts with photoisomerizable components,[2, 3] immobilization of the biocatalysts in photoisomerizable polymers,[4] and by selective association of redox proteins with photoisomerizable monolayer interfaces.[5] Photoswitchable redox enzymes were applied for the amperometric transduction of optical signals and their amplification.[5, 6] Electron transfer communication between redox proteins, for example glucose oxidase or nitrate reductase, and electrode surfaces is mediated by electron relays such as ferrocenes, bipyridinium salts, and quinones.[7–9] The design of photoisomerizable electron mediators could provide a novel means of photochemically controlling redox enzymes, since the photoisomer states of the mediator could be recognized differentially by the biocatalyst. Here we report on the reversible photochemical activation–deactivation of the electrical communication of the redox proteins of glucose oxidase (GOD) and glutathione reductase (GR) with electrode surfaces, using the ferrocene–nitrospiropyran **1a**[10] (for GOD) and *N*,*N*′-bipyridinium-nitrospiropyran **2a**[12] (for GR) as photoisomerizable electron mediators.

The enzymes GOD and GR were organized as multilayer arrays on a base self-assembled monolayer on a rough gold electrode[14] (Scheme 1). The roughness factor corresponded to

[*] Prof. I. Willner, M. Lion-Dagan, S. Marx-Tibbon, Dr. E. Katz
Institute of Chemistry
The Hebrew University of Jerusalem
Jerusalem 91904 (Israel)
Telefax: Int. code + (2)652 7715

[**] This research was supported by the Ministry of Science and Technology, Israel, and by the Commission of the European Community.

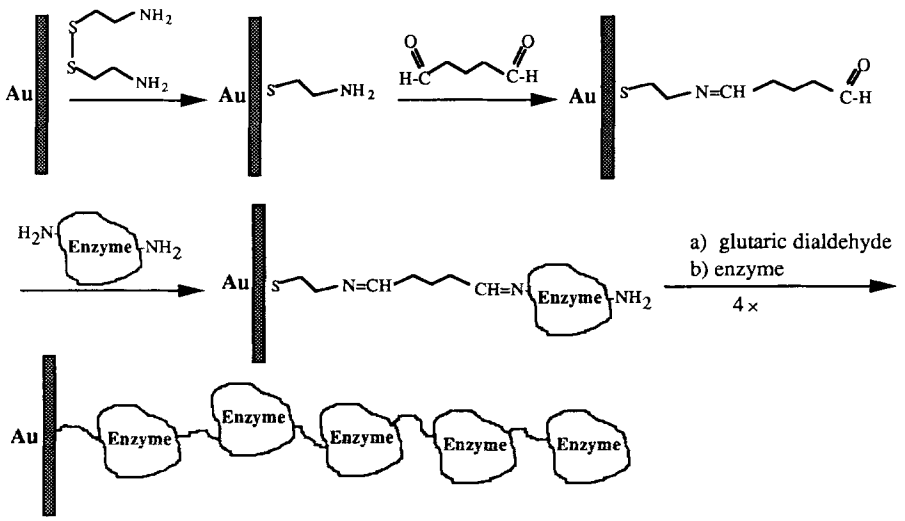

Scheme 1. Organization of enzyme monolayer arrays on the surface of the Au electrode.

20. A cystamine monolayer was assembled on the electrode and subsequently reacted with glutaric dialdehyde. The resulting monolayer was then treated with the respective enzyme. By a two-step procedure involving modification of the enzyme layer with glutaric dialdehyde followed by the reaction with the biocatalyst, a defined number of enzyme layers was constructed onto the base enzyme layer. For the experiments employing GOD and GR, five layers of the respective enzyme were immobilized on the electrodes. It should be noted that this procedure leads to a cross-linked network of the enzyme layers; however, the surface density of the enzyme is similar in each of the assembled layers.[7b]

Ferrocene–nitrospiropyran **1a** and *N,N'*-bipyridinium–nitrospiropyran **2a** can be photoisomerized reversibly. Irradiation of **1a** or **2a** ($360 < \lambda < 380$ nm) results in photoisomerization to the redox-relay merocyanine states **1b** and **2b**, respectively. Further illumination of the merocyanine isomer states with visible light ($\lambda > 475$ nm) restores the ferrocene– and bipyridinium–nitrospiropyrans **1a** and **2a**, respectively. Cyclic voltammetry experiments revealed that the ferrocene–nitrospiropyran **1a** exhibits a reversible oxidation wave at $E^\circ = +0.44$ V (vs. SCE). The bipyridinium–nitrospiropyran **2a** displays a quasi-reversible reduction wave at $E^\circ = -0.535$ V (vs. SCE). The cyclic voltammograms of the ferrocene (Fig. 1) and bipyridinium redox units were unaffected by photoisomerization to **1b** or **2b**, respectively.

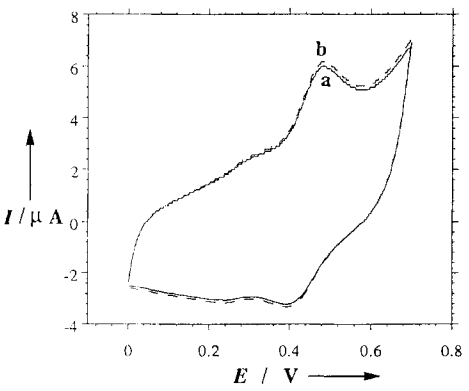

Fig. 1. Cyclic voltammograms of a) ferrocene–nitrospiropyran **1a** (1×10^{-4} M); b) ferrocene–nitromerocyanine **1b** (1×10^{-4} M), Na_2SO_4 (0.05 M), and 0.01 M phosphate buffer, pH 7.0, and 10% v/v ethanol, using the GOD-modified electrode as working electrode. Potential scan rate 100 mV s^{-1}.

Figure 2 shows the steady-state amperometric responses of the GOD multilayer electrode in the presence of the photoisomerizable electron mediator **1** and in the presence of added glucose.[15] In the presence of the electron mediator in the ferrocene–spiropyran state **1a**, addition of 4 mM glucose (addition time indicated by arrow) results in current development in the electrochemical cell (curve a). This implies that electrochemically oxidized **1a** mediates the oxidation of the GOD redox center that biocatalyzes the oxidation of glucose. Irradiation of the electrolyte solution ($360 < \lambda < 380$ nm) followed by isomerization of **1a** to **1b** results in background current (curve b). This result indicates that ferrocene–merocyanine **1b** does not act as electron mediator for GOD, even though it is effectively oxidized to ferrocene–spiropyran cation. Further photoisomerization of **1b** to **1a** by

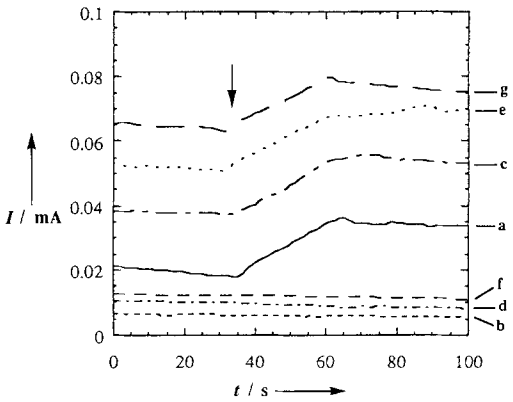

Fig. 2. Amperometric responses of the GOD-modified electrode upon multiple addition of glucose (4 mM; time of addition indicated by arrow). Curves a, c, e, and g correspond to the steady-state currents in the presence of electron mediator **1a** (1×10^{-4} M). Curves b, d, and f correspond to the steady-state currents in the presence of electron mediator **1b** (1×10^{-1} M). Electrolyte solution consists of 0.01 M phosphate buffer, pH 7.0, and 0.1 M Na_2SO_4. Applied potential corresponds to +0.55 V (vs. SCE).

irradiation ($\lambda > 475$ nm) results in the initial amperometric response as a result of electrochemically biocatalyzed oxidation of glucose. Further addition of glucose causes an increase in the current developed in the system (curve c), reconfirming that **1a** acts as electron mediator for the biocatalyst. Subsequent isomerization of **1a** to **1b** restores the background current (curve d). It can be seen that the layered GOD array exhibits electrical communication with the electrode surface when the electron mediator is in the ferrocene–spiropyran state **1a**, whereas electrical interaction is prohibited in the photoisomer state **1b**. The electrical communication of the biocatalyst with the electrode interface can be switched on and off reversibly by photoisomerization of the electron relay. As noted, the redox potential of the ferrocene units in **1a** and **1b** is identical. Hence, only the structural isomerization of the relay units yield the "ON–OFF" electrocatalytic activation and deactivation of GOD.

The activity of glutathione reductase has been photochemically regulated in a similar manner by the application of the

N,N'-bipyridinium–spiropyran **2a** as electron transfer mediator. Previous studies[7c, 16] indicated that the *N,N'*-bipyridinium radical cation acts as an electron transfer mediator for the enzyme that stimulates the reduction of oxidized glutathione [Eq. (a); GSSG = oxidized glutathione, GSH = glutathione, GR = glutathione reductase, V^{2+} = *N,N'*-bipyridinium relay]. The GR multilayered Au electrode (five layers) was used as the working electrode in the electrochemical cell.[15]

$$GSSG + 2V^{\bullet+} + 2H^+ \xrightarrow{GR} 2GSH + 2V^{2+} \quad (a)$$

In the presence of *N,N'*-bipyridinium–nitrospiropyran **2a** in the electrochemical cell, effective electrochemically biocatalyzed reduction of GSSG occurs ($v \approx 6$ mM s^{-1}). Photoisomerization of **2a** to **2b** ($360 < \lambda < 380$ nm) blocks the formation of GSH, implying that the enzyme GR does not electrically communicate with **2b**. Subsequent photoisomerization of **2b** to **2a** restores the electrochemically biocatalyzed reduction of GSSG. Reversible electrical activation–deactivation of the enzyme by photoisomerization of the electron relay through states **2a** and **2b** is feasible (Fig. 3).[17]

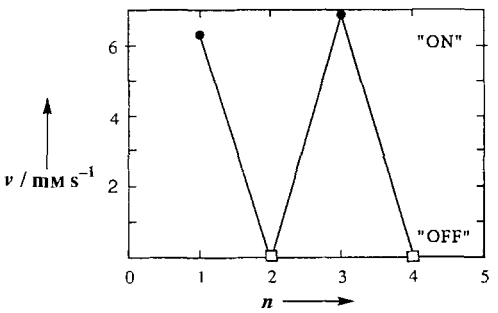

Fig. 3. Cyclic photochemically stimulated formation of GSH by the GR electrode. ●: In the presence of **2a** (1×10^{-4} M); □: in the presence of **2b** (1×10^{-4} M). Applied potential corresponds to −0.62 V (vs. SCE); n = number of cycles; v = rate of GSH formation.

We thus conclude that the application of photoisomerizable redox relays provides a novel means of controlling the electrical communication of redox proteins with electrode surfaces. The photoisomer states linked to the electron mediator control the redox interactions of the charge carrier with the protein (Scheme 2). The specific origin for the lack of electrical interactions between the respective proteins and the redox relay in the merocyanine state is at present unknown. We assume that steric constraints or electrostatic repulsive interactions between the isomers and the proteins or their active-site surroundings prevent the intimate contact of the mediator and the enzyme redox center required for electrical communication.

Received: December 27, 1994 [Z 7578 IE]
German version: *Angew. Chem.* **1995**, *107*, 1730–1733

Keywords: electrochemistry · enzymes · photochemistry · supramolecular chemistry

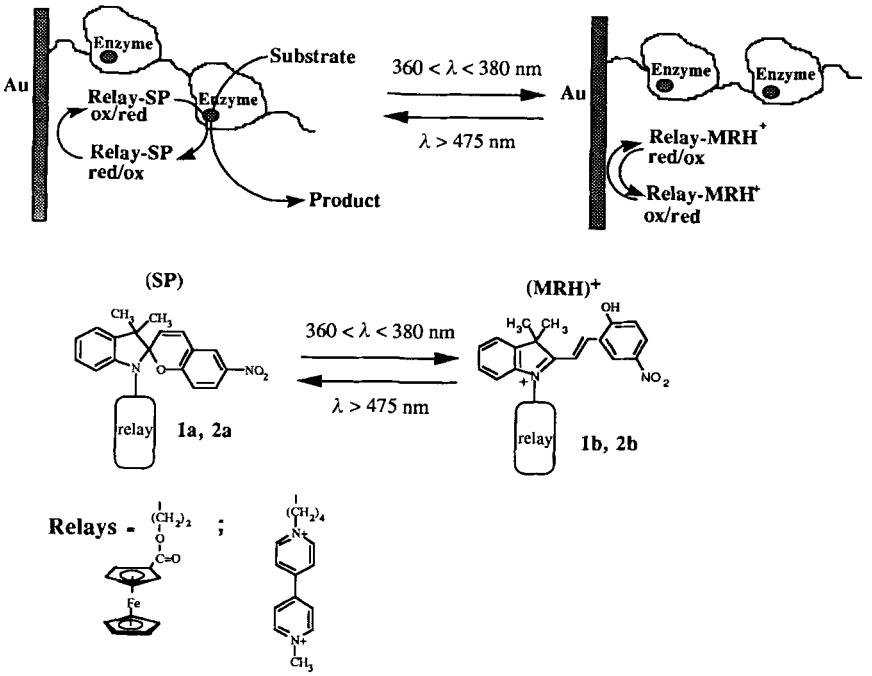

Scheme 2. Reversible photochemical activation–deactivation of enzymes in the presence of photoisomerizable electron relays.

[1] I. Willner, B. Willner in *Bioorganic Photochemistry – Biological Application of Photochemical Switches, Vol. 2* (Ed.: H. Morrison), Wiley, New York, **1993**, p. 1.
[2] I. Willner, S. Rubin, A. Riklin, *J. Am. Chem. Soc.* **1991**, *113*, 3321.
[3] I. Willner, S. Rubin, J. Wonner, F. Effenberger, P. Bäuerle, *J. Am. Chem. Soc.* **1992**, *114*, 3150.
[4] a) I. Willner, S. Rubin, T. Zor, *J. Am. Chem. Soc.* **1991**, *113*, 4013; b) I. Willner, S. Rubin, R. Shatzmiller, T. Zor, *ibid.* **1993**, *115*, 8690.
[5] M. Lion-Dagan, E. Katz, I. Willner, *J. Am. Chem. Soc.* **1994**, *116*, 7913.
[6] M. Lion-Dagan, E. Katz, I. Willner, *J. Chem. Soc. Chem. Commun.* **1994**, 2741.
[7] a) I. Willner, N. Lapidot, A. Riklin, R. Kasher, E. Zahavy, E. Katz, *J. Am. Chem. Soc.* **1994**, *116*, 1428; b) I. Willner, A. Riklin, B. Shoham, D. Rivenzon, E. Katz, *Adv. Mater.* **1993**, *5*, 912; c) I. Willner, E. Katz, N. Lapidot, *Bioelectrochem. Bioenerg.* **1992**, *29*, 29.
[8] a) P. N. Bartlett in *Biosensor Technology, Fundamentals and Applications* (Eds.: R. Buck, W. E. Hatfield, M. Umana, E. F. Bowden), Dekker, New York, **1990**, p. 95; b) W. Schuhmann, H.-L. Schmidt in *Advances in Biosensors, Vol. 2* (Ed.: A. P. F. Turner), JAI Press, London, **1992**, p. 79.
[9] Y. Degani, A. Heller, *J. Am. Chem. Soc.* **1988**, *110*, 2615.
[10] Compound **1a** was synthesized by the reaction of ferrocenecarboxylic acid (0.5 g, 2.5 mmol) with 1-(β-hydroxyethyl)-3,3-dimethyl-6′-nitrospiro-(indoline-2,2′-2H-benzopyran) [11] (0.97 g, 2.75 mmol) in 10 mL of CH_2Cl_2 using *N,N'*-dicyclohexylcarbodiimide (DCC) (0.57 g) and 1-pyrrolidinopyridine (0.037 g) as coupling reagents.
[11] E. L. Zajtseva, A. Prohoda, L. H. Kurkovskaya, R. R. Shifrina, N. S. Kardash, D. A. Drapkina, V. A. Krongaus, *Khim. Geterotsikl. Soedin.* **1973**, *10*, 1362.
[12] Compound **2a** was synthesized by alkylation of *N*-methyl-pyridinium 4-pyridine with 1-(4′-iodobutyl)-3,3-dimethyl-6′-nitrospiro(indoline-2,2′-2H-benzopyran) [13] in DMF at 110 °C.
[13] M. Aizawa, K. Namba, S. Suzuki, *Arch. Biochem. Biophys.* **1977**, *180*, 41.
[14] E. Katz, D. D. Schlereth, H.-L. Schmidt, *J. Electroanal. Chem.* **1994**, *367*, 59.
[15] Electrochemical experiments were performed under Ar using a three-electrode cell configuration where the enzyme monolayer Au electrode was used as working electrode, a carbon electrode was applied as counter electrode, and SCE was used as reference electrode. All experiments were recorded at room temperature (22 °C). Isomerization of the nitrospiropyran electron mediators **1a** and **2a** to **1b** and **2b**, respectively, was accomplished with a 18 W mercury pencil lamp (Oriel-6042) equipped with a long-wave filter ($360 \text{ nm} < \lambda < 380$ nm). Back isomerization of **1b** and **2b** to **1a** and **2a**, respectively, was accomplished by irradiation of the solution with a 150 W xenon lamp equipped with a Schott filter ($\lambda > 475$ nm).
[16] I. Willner, A. Riklin, N. Lapidot, *J. Am. Chem. Soc.* **1990**, *112*, 6438.
[17] It should be noted that photostimulation of GR by **2a** or **2b** could be detected only upon electrochemically biocatalyzed reduction of GSSG over an extended period, due to the substantially lower activity of GR relative to that of GOD.

 © VCH Verlagsgesellschaft mbH, D-69451 Weinheim, 1995 0570-0833/95/1515-1606 $ 10.00+.25/0

Reversible Template-Directed Activation of Equatorial Double Bonds of the Fullerene Framework: Regioselective Direct Synthesis, Crystal Structure, and Aromatic Properties of T_h-$C_{66}(COOEt)_{12}$**

Iris Lamparth, Cäcilia Maichle-Mössmer, and Andreas Hirsch*

Multiple additions to the fullerene core are remarkably regioselective.[1, 2] By successive cyclopropanations of equatorial (*e*) 6–6 double bonds we were able to synthesize the T_h symmetric hexaadduct $C_{66}(COOEt)_{12}$ (**1**).[2, 3] The preferred attack of 6–6 double bonds in *e* positions (Fig. 1) relative to addends already bound to the fullerene core can be explained by a consideration of both the thermodynamic stability of the different regioisomers and the enhanced orbital coefficients of frontier orbitals in *e* positions of the corresponding precursor molecules.[2] Meanwhile, other hexaadducts with an analogous addition pattern were synthesized by Diederich et al.,[4] who used spacer-controlled functionalization, and by Kräutler et al.[5] through six [4 + 2] cycloadditions. The facile access to high yields of stable and highly symmetric oligoadducts of C_{60}, which can be further functionalized, plays a very important role, for example, in the field of material science and biological applications of fullerene derivatives and is still one of the major synthetic challenges in fullerene chemistry. In this work we report for the first time on a new and very simple concept of a template-directed activation of the C_{60} framework, which allows the direct synthesis of **1** with very high regioselectivity and yields of up to 50%, as well as on its crystal structure and enhanced aromatic character relative to C_{60}. Furthermore, we show that the stable compound **1** can be transformed quantitatively into the corresponding hexamalonic acid **2**, which is of great importance with regard to modifications of the side chain.

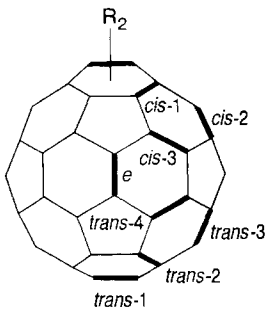

Fig. 1. Positional relationships of the eight different double bonds in a C_{60} monoadduct relative to the 6–6 bond carrying the first addend R_2 (R_2, for example, methylene).

The regioselectivity of attacks to *e* double bonds becomes even more pronounced as the number of addends already bound in *e* positions increases. This is expressed, for example, by further enhanced orbital coefficients in the LUMOs as well as in the HOMOs in these positions.[2] If the formation of adducts is reversible, besides kinetic control, thermodynamic control[6] gains importance. At equilibrium, adducts with incomplete octahedral addition patterns predominate. They can serve as template or matrix for irreversible *e* additions or addend-substitution reactions. Looking for a suitable template intermediate, we found that the reaction of C_{60} and 9,10-dimethylanthracene (DMA) is reversible already at room temperature. Addition of DMA to a solution of C_{60} in toluene causes a slow change in color from purple to chestnut-brown as the corresponding Diels–Alder adducts $C_{60}(DMA)_n$ are formed (Scheme 1). After

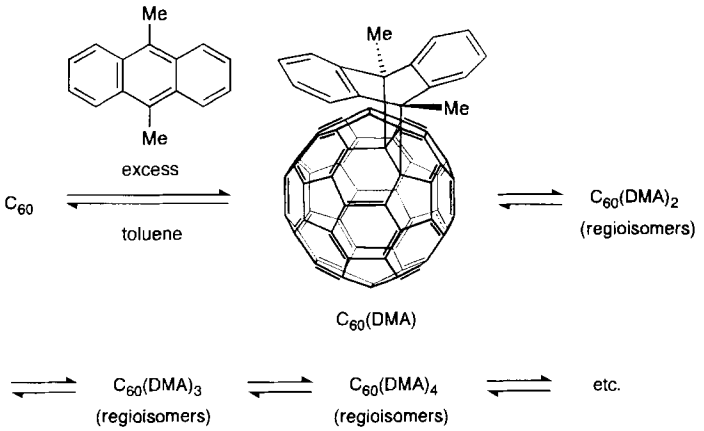

Scheme 1.

the equilibrium was established, the dependence of the distribution of adducts on the concentration of DMA was investigated quantitatively with HPLC. The peaks in the chromatograms can be assigned to particular adducts by their UV/Vis spectra,[1, 2] which were recorded simultaneously by diode array scans. An increasing concentration of DMA causes a shift of the equilibrium towards higher adducts. Whereas the addition of only one equivalent of DMA yields C_{60} (40%) and the monoadduct $C_{60}(DMA)$ (48%) as major components besides traces of $C_{60}(DMA)_2$ (7%), the equilibrium shifts towards the higher adducts $C_{60}(DMA)_2$ (52%) and $C_{60}(DMA)_3$ (24%) when 10 equivalents of DMA are added, and no unmodified C_{60} can be detected. The adducts $C_{60}(DMA)_n$ are mixtures of regioisomers predominantly consisting of adducts with an octahedral addition pattern, for example, the C_3 symmetric *e,e,e* isomer in the case of $C_{60}(DMA)_3$, as UV/Vis spectra show. Elevated reaction temperatures shift the equilibrium towards unmodified C_{60}. DMA can be removed from the equilibrium by the reaction with oxygen in laboratory light or with dimethyl acetylenedicarboxylate under formation of the cycloadducts **3** and **4** and of unmodified C_{60} (Scheme 2). The facile formation of the endo-

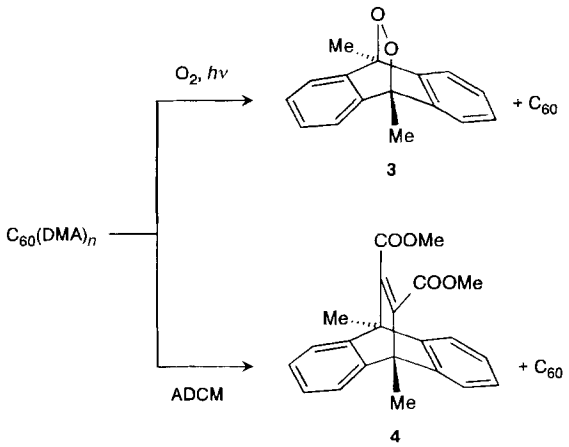

Scheme 2. ADCM = dimethyl acetylenedicarboxylate.

[*] Prof. Dr. A. Hirsch, I. Lamparth
Institut für Organische Chemie der Universität
Richard-Willstätter-Allee 2
D-76131 Karlsruhe (Germany)
Telefax: Int. code + (721)698-305
e-mail: hirsch@ochhades.chemie.uni-karlsruhe.de
Dr. C. Maichle-Mössmer
Institut für Anorganische Chemie der Universität Tübingen (Germany)

[**] This work was supported by the Deutsche Forschungsgemeinschaft (DFG), the Bundesministerium für Forschung und Technologie (BMFT), Hoechst AG, and the Dr. Otto Röhm Gedächtnisstiftung GmbH.

peroxide **3** is promoted by the efficient photosensitizing properties of C_{60} and its derivatives.[7]

The synthesis of **1** by successive cyclopropanation[1,2,8] of C_{60} with diethyl bromomalonate and NaH without template activation, isolating all intermediate products, gives a total yield of 0.2%. After template activation with DBU (DBU = 1,5-diazabicyclo[4.3.0]non-5-ene) as a base and 10 equiv DMA, the one-step reaction (with 8 equiv diethyl bromomalonate) yields 37% (HPLC) of **1** as the only regioisomeric hexaadduct. Thus, the yield is increased by a factor of 120 (Scheme 3). In addition, a

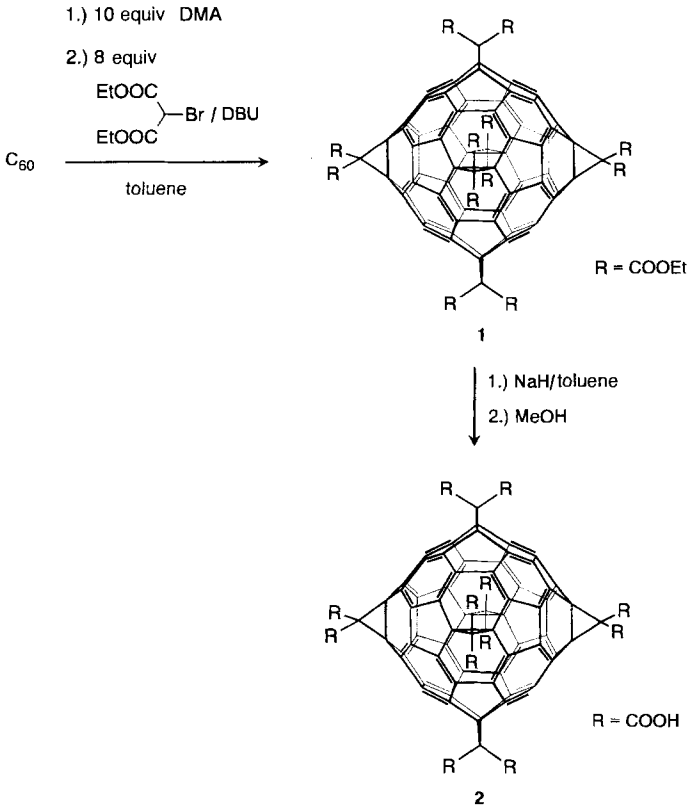

Scheme 3.

considerable amount of C_{2v}-$C_{65}(COOEt)_{10}$[2] and C_s-$C_{64}(COOEt)_8$[2] with an incomplete octahedral addition pattern is obtained, which can undergo further cyclopropanation and yield another 11% of **1** (total yield 48%). Compound **1** can be isolated from the reaction mixture simply by flash chromatography followed by recrystallization from $CHCl_3$/bromobenzene (1:1). The majority of the free DMA can be recovered. This procedure gives an overall yield of **1** of 23% (based on amount of C_{60}) as light yellow rhombic crystals.

The one-step reaction of C_{60} with 8 equiv diethyl bromomalonate/DBU without template activation proceeds with decreased regioselectivity and with a significantly lower yield of **1** (14%). A considerable amount of $C_{65}(COOEt)_{10}$ possessing a "wrong" (that is, not octahedral) addition pattern and of $C_{67}(COOEt)_{14}$ having C_1 symmetry and not being formed from **1**[9] is obtained. Without template activation a pronounced proportion of the successive cyclopropanation of C_{60} proceeds along different channels. This is plausible, as the least regioselective step is the formation of the bisadducts $C_{62}(COOEt)_4$.[1] Among eight possible regioisomers the *e* isomer C_s-$C_{62}(COOEt)_4$, a precursor molecule of **1**, is the main product (relative yield 38%), but 60% of the products are five other isomers from which **1** can not be formed.[10] Thus, the decisive advantage of template activation of C_{60} with DMA is that the reversible formation of adducts guarantees large amounts of *e*-$C_{60}(DMA)_2$ and *e,e,e*-$C_{60}(DMA)_3$ from which **1** can be formed with very high regioselectivity. Furthermore, if, for example, *e,e,e*-$C_{60}(DMA)_3$ is cyclopropanated in a position other than *e*, the DMA addends can rearrange to an isomer with complete octahedral addition pattern because of the reversibility of adduct formation. The principle of template activation offers facile access to the high-yield synthesis of mixed adducts with octahedral addition patterns. For example, the reaction of the monoadduct C_{2v}-$C_{60}(N_2C_4H_8)$[11] (fulleropiperazine) with diethyl bromomalonate/DBU in the presence of 10 equiv DMA gives a 27% yield (according to HPLC) of the mixed hexaadduct **5**.[12]

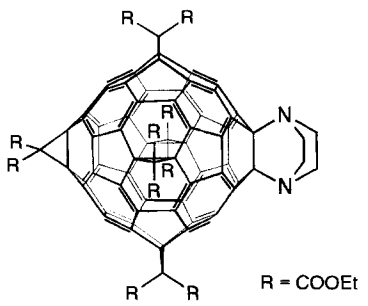

The crystals of **1** grown from a $CHCl_3$/bromobenzene solution are in the triclinic space group $P\bar{1}$ and contain two molecules of bromobenzene in the unit cell.[13] The molecular structure (Fig. 2) confirms the results of NMR investigations[2] of **1** according to which the cyclopropanated bonds of C_{60} are single bonds ($d = 1.59$ Å), and the fullerene core is closed. Very remarkable is the bonding in the remaining π-electron system of

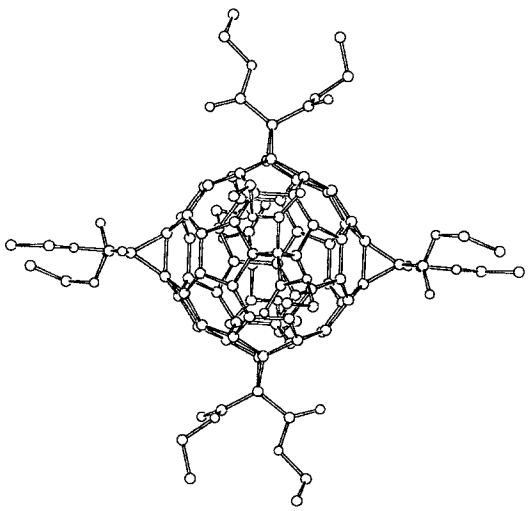

Fig. 2. Crystal sructure of **1**. The two bromobenzene molecules per unit cell are omitted for clarity.

1 which is a new type of an oligocyclophane[2,4-6] (Fig. 3). The alternation of bond lengths between 6–6 bonds and 5–6 bonds characteristic of unmodified C_{60}[14] is reduced by half to approximately 0.03 Å in **1**. A resulting increase of the benzenoid character is manifested in the optical properties of compound **1**. Relative to solutions of C_{60} (purple) or its adducts $C_{61}(COOEt)_2$ to $C_{65}(COOEt)_{10}$ (red to orange) the light yellow solutions of **1** show only weak absorption bands in the visible region of the spectrum ($\varepsilon_{vis} < 2400$). The mixed adduct **5** has

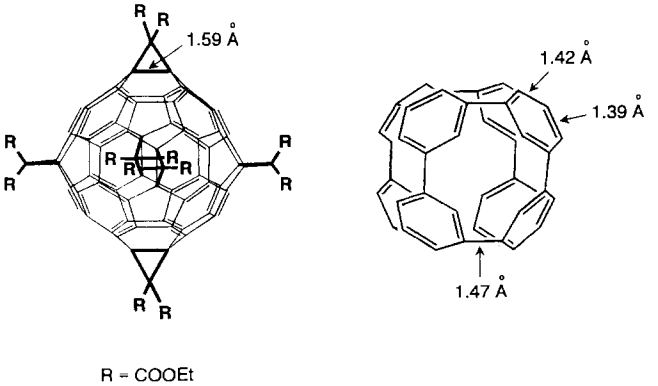

Fig. 3. Schematic illustration of **1** with selected bond lengths and of the remaining benzenoid π-electron system.

similar optical properties. Remarkably, the color of C_1-$C_{67}(COOEt)_{14}$ is again orange, because no truly benzenoid substructures can be formed within the fullerene framework.

The hexamalonate $C_{66}(COOEt)_{12}$ (**1**) is stable towards light, air, and moisture. This is essential for further side-chain chemistry as well as for potential practical applications. In fact, if **1** is treated with NaH and methanol[15] it can be transformed easily and quantitatively into the corresponding highly water-soluble hexamalonic acid derivative **2**[16] (Scheme 3). This compound has ideal features for use as a building block for dendrimers, as a buffer system, or as a starting molecule for the synthesis of biologically active fullerene derivatives.

Received: February 20, 1995 [Z7726IE]
German version: *Angew. Chem.* **1995**, *107*, 1755–1757

Keywords: cyclopropanations · fullerenes · isomerism

[1] A. Hirsch, I. Lamparth, H. R. Karfunkel, *Angew. Chem.* **1994**, *106*, 453; *Angew. Chem. Int. Ed. Engl.* **1994**, *33*, 437.
[2] A. Hirsch, I. Lamparth, T. Grösser, H. R. Karfunkel, *J. Am. Chem. Soc.* **1994**, *116*, 9385.
[3] In **1** all *e* and *trans-1* positions are occupied (complete "octahedral" addition pattern, see Figs. 1–3).
[4] L. Isaacs, R. F. Haldimann, F. Diederich, *Angew. Chem.* **1994**, *106*, 2435; *Angew. Chem. Int. Ed. Engl.* **1994**, *33*, 2339.
[5] B. Kräutler, J. Maynollo, *Angew. Chem.* **1995**, *107*, 66; *Angew. Chem. Int. Ed. Engl.* **1995**, *34*, 87.
[6] P. J. Fagan, J. C. Calabrese, B. Malone, *J. Am. Chem. Soc.* **1991**, *113*, 9408.
[7] a) J. W. Arbogast, A. P. Darmanyan, C. S. Foote, Y. Rubin, F. Diederich, M. M. Alvarez, S. J. Anz, R. L. Whetten, *J. Phys. Chem.* **1991**, *95*, 11; b) Y.-Z. An, J. L. Anderson, Y. Rubin, *J. Org. Chem.* **1993**, *58*, 4799.
[8] C. Bingel, *Chem. Ber.* **1993**, *126*, 1957.
[9] This was proved by further cyclopropanating a mixture of trisadducts that did not contain the C_3-symmetric *e,e,e*-$C_{63}(COOEt)_6$ and only traces of *e,e,trans-1*-$C_{63}(COOEt)_6$ (precursor molecule of **1**). The main component was the C_1-symmetric isomer *trans*-3,*trans*-4,*e*-$C_{63}(COOEt)_6$, from which **1** can not be formed. We obtained C_1-$C_{67}(COOEt)_{14}$ in 17% yield but no isolable amount of **1**.
[10] The *cis-1* isomer is not formed at all and the isomer *trans-1*-$C_{62}(COOEt)_4$, the other potential precursor molecule of **1** besides *e*-$C_{62}(COOEt)_4$, is formed only in traces (2%, see ref. [1]).
[11] K.-D. Kampe, N. Egger, M. Vogel, *Angew. Chem.* **1993**, *105*, 1203; *Angew. Chem. Int. Ed. Engl.* **1993**, *32*, 1174.
[12] **5**: M = 1595.55; MS (FAB): m/z 1595 ([M^+], 59 %), 1510 ([$M^+ - C_4H_8N_2$], 100 %); UV/Vis (CH_2Cl_2): λ_{max} [nm] = 245, 268, 286, 312, 334 sh; IR (KBr): $\tilde{\nu}$ [cm^{-1}] = 2939, 2874, 1738, 1585, 1493, 1452, 1407, 1390, 1327, 1313, 690, 561, 507; ^{1}H NMR (250 MHz, $CDCl_3$, 25 °C): δ = 4.30 (m, 20 H; CH_2), 3.89 (m, 4 H; CH_2), 3.11 (m, 4 H; CH_2), 1.30 (m, 30 H; CH_3); ^{13}C NMR (62.9 MHz, $CDCl_3$, 25 °C): δ = 164.15, 163.92, 163.68, 163.36, 150.16 (4 C), 146.42 (4 C), 146.36 (4 C), 146.19 (4 C), 145.45 (4 C), 145.15 (4 C), 144.86 (4 C), 142.13 (4 C), 142.02 (4 C), 140.04 (4 C), 138.81 (4 C), 138.11 (4 C), 75.38, 69.86, 69.51, 68.95, 67.37, 62.91, 62.82, 62.73, 62.67, 45.96, 45.59, 44.81, 40.05, 14.01.
[13] Crystal structure of **1**: triclinic, space group $P\bar{1}$, a = 13.512(3), b = 14.262(3), c = 14.889(4) Å, α = 116.631(10), β = 96.498(13), γ = 113.841(9)°, V = 2188.6(8) Å^3, Z = 2, ρ_{calcd} = 1.505 g cm^{-3}, data collection at T = 293 K with an Enraf Nonius CAD4 diffractometer, $Cu_{K\alpha}$ radiation, λ = 1.54056, μ = 14.555, $F(000)$ = 1016, 8467 reflections measured, of which 7423 were independent, (R_{int} = 0.043), hkl range $-1 \rightarrow 15$, ± 16, ± 17. Structure solution with direct methods (SHELXS86); absorption correction by PSI scan. Subsequent difference Fourier syntheses showed the whole molecule, H atoms were calculated on ideal positions. The anisotropic temperature parameters were assigned to all except the H atoms, and further refinement gave the final R value of R_1 = 0.066, R_2 = 0.174 (GOF = 1.024, parameters 631) (SHELXL93). The residual electron density is given as $\Delta\rho_{fin}$ = 1.042. Further information can be obtained from the Fachinformationszentrum Karlsruhe, D-76344 Eggenstein-Leopoldshafen (Germany) on quoting the depository number CSD-58937.
[14] A. Hirsch, *The Chemistry of the Fullerenes*, Thieme, Stuttgart, New York, 1994.
[15] I. Lamparth, A. Hirsch, *J. Chem. Soc. Chem. Commun.* **1994**, 1727.
[16] **2**: ^{13}C NMR (62.9 MHz, D_2O, 25 °C): δ = 169.91 (br, 12 C), 141.49 (24 C), 141.25 (24 C), 72.70 (12 C), 47.30 (6 C).

Diodelike Current–Voltage Curves for a Single Molecule—Tunneling Spectroscopy with Submolecular Resolution of an Alkylated, *peri*-Condensed Hexabenzocoronene**

Andreas Stabel, Peter Herwig, Klaus Müllen,* and Jürgen P. Rabe*

The spectroscopy of single molecules in a defined environment is of relevance not only as a tool in future molecular electronics.[1] A single molecule dispersed amongst many others in an amorphous matrix can be selected by laser spectroscopy on account of its specific surroundings.[2] Single molecule detection is achieved by optical spectroscopy in an extremely small sample volume of a highly diluted substance. In the nearfield optical microscope this volume can be as small as 100 nm^3, which is still sufficient for a satisfactory distinction from the background.[3] These methods do, however, not allow for a spatial localization of the molecule. One method that circumvents this shortcoming is the local excitation of luminescence with the help of a scanning tunneling microscope.[4] Another method is tunneling spectroscopy of single molecules. At submolecular resolution this technique offers a way to chemically identify individual molecular moieties. It consists of immobilizing the molecules on a solid surface, imaging them by scanning tunneling *microscopy* (STM), and then performing tunneling *spectroscopy* (STS) at a specific location. While scanning tunneling microscopy of molecules has evolved into a precise and widespread method,[5] few reliable results have been published for spatially resolved tunneling spectroscopy. Most of them concern investigations on Si and GaAs in ultrahigh vacuum, for which detailed spectroscopic data obtained by classical methods of surface science

[*] Prof. Dr. J. P. Rabe
Institut für Physik der Humboldt-Universität zu Berlin
Invalidenstrasse 110, D-10115 Berlin (Germany)
Telefax: Int. code + (030)2803-232
Prof. Dr. K. Müllen, Dr. A. Stabel, Dipl.-Chem. P. Herwig
Max-Planck-Institut für Polymerforschung
Postfach 3148, D-55021 Mainz (Germany)
Telefax: Int. code + (6131)379-100

[**] This work was supported by the BMBF (project "Muster selbstorganisierender Moleküle") as well as by the European Strategic Program for Research and Development in Information Technologies (Long Term Research Projects TOPFIT and PRONANO). A. S. wishes to thank the Fonds der Chemischen Industrie for a Kekulé fellowship.

were already available.[6] Tunneling spectroscopy investigations on molecular systems were commonly presented without concomitant molecular resolution STM imaging.[7, 8] This limitation arises because, in general, the sharpest, highest resolution tips are the most likely to give unreliable tunneling spectra.[9] One possible reason for this behavior is the strong influence that an unusually bound single atom at the very end of the tip has on tunneling spectra. In the case of a blunter tip, the influence of such an atom diminishes. These tips are therefore the most likely to give consistent current–voltage (*IV*) curves. The price for reproducible tunneling spectra is therefore paid in a reduced spatial resolution and, consequently, in the limitation to spatially extended molecular moieties.

We therefore set out to obtain reproducible tunneling spectra of molecules exhibiting two electronically different and spatially extended moieties. We chose alkylated polycyclic arenes. The energy of the molecular electronic states of the alkyl part of these molecules is far from that of the Fermi level of the electrodes, while the energy of the highest occupied molecular orbital (HOMO) of the aromatic core can quite easily come close to it.

1,4-Didodecylbenzene,[10] 1,5-dihexadecyloxynaphthalene,[11] and hexakis(hexadecyloxy)triphenylene[12] had already been shown to adsorb from organic solutions onto the basal plane of graphite in ordered two-dimensional structures. In our search for spatially more extended molecules, we investigated 3,10-didodecylperylene.[13] Tunneling spectroscopic investigations from +1.5 V to −1.5 V reveal that the *IV* curves are asymmetric, with a higher current at positive tip bias. These characteristic curves can be unequivocally and reproducibly distinguished from *IV* curves of simple alkanes. However, we could not unambiguously assign different *IV* curves to the alkyl and the aromatic moieties. This led us to synthesize a spatially even more extended, alkylated polycyclic arene. The alkyl side chains should, on one hand, guarantee the processability of the substance from solution, and on the other, favor the formation of adlayers on graphite. We decided to synthesize an alkyl-substituted, *peri*-condensed hexabenzocoronene (**3**). This substance was until now only known in its unsubstituted, insoluble form.[14]

The synthesis (Scheme 1) begins with 4,4′-di-*n*-dodecyltolane (**1**),[15] which is easily obtainable in four steps.[16] Tolane **1** is then cyclotrimerized[17] under the catalytic action of $[Co_2(CO)_8]$. The resulting hexa(4-dodecylphenyl)benzene (**2**)[18] is readily soluble in organic solvents. In the next step **2** is cyclodehydrated under oxidative conditions ($Cu(CF_3SO_3)_2/AlCl_3$, CS_2, 25 °C).[19] The yield of the target molecule **3** is relatively low (49%), because intermolecular aryl–aryl couplings and dealkylation could not be suppressed. The new substance **3** is soluble in various organic solvents at room temperature already and can therefore be comprehensively characterized (see Experimental). The cyclovoltammetric determination of the first reduction potentials shows the reversible formation of the mono- and dianion ($E^1_{1/2} = -2.12$ V, $E^2_{1/2} = -2.36$ V). Oxidation occurs at $E^1 = +1.01$ V and $E^2 = +1.42$ V and is irreversible, because an insoluble film forms on the electrode.

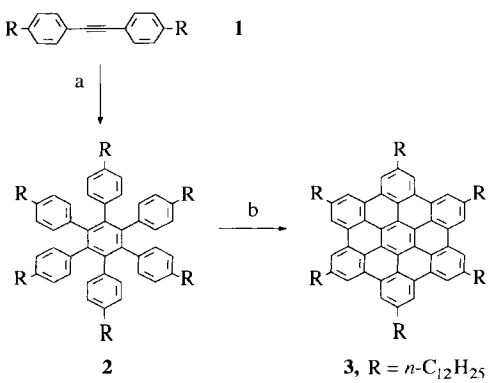

Scheme 1. a) $[Co_2(CO)_8]$, dioxane, 100 °C (92% yield); b) $Cu(CF_3SO_3)_2/AlCl_3$, CS_2, 25 °C (49%).

Structural investigations by electron diffraction experiments (LEED) of monolayers of unsubstituted *peri*-condensed hexabenzocoronene (R = H in **3**) on highly oriented pyrolytic graphite (HOPG) have been reported.[20] Since it lacks an aliphatic moiety, however, this molecule is not suited for locally differentiating tunneling spectroscopy. In the STM images of the alkylated *peri*-condensed hexabenzocoronene **3** (Fig. 1a), the bright areas (high tunneling current) correspond to the aromatic cores, while the dark areas (low tunneling current) correspond to the aliphatic part of the two-dimensional lattice.[5] As indicated in Figure 1b, the adsorbed alkyl chains have a preferential direction parallel to one of the main axes of the underlying graphite lattice. Because the depicted packing results in some free volume, the alkyl chains fill this space dynamically by utilizing the thermal energy kT at room temperature. The unit cell drawn in Figure 1 ($a = 1.94$ nm, $b = 2.64$ nm, $\gamma = 80°$) reveals that the sixfold symmetry of the molecule has been reduced to a twofold symmetry of the adsorbate lattice. This phenomenon of symmetry reduction was previously known from the system hexakis(hexadecyloxy)triphenylene–HOPG.[12] The current–voltage curve **a** in Figure 2 was taken above the aliphatic part marked by A in Figure 1a. The broken black lines show the *IV* curves with the bias values scanned from minus to plus; the grey lines document the backscans. Curve **a** is symmetric with respect to the origin. It can therefore not be distinguished from an *IV* curve taken on pure graphite covered only by a thin film of solvent.[13] The energy of the highest occupied molecular orbitals (HOMO) of alkanes is so far from that of the Fermi level of the electrodes that a coupling of these states during a scan of ±1.5 V to the tunneling current seems extremely unlikely.[21] The curve **b** in Figure 2 was taken above the aromatic core of a molecule of **3** marked by B in Figure 1a. Contrary to curve **a**, it exhibits a strong asymmetry. The diodelike shape reveals a factor of asymmetry of approximately one order of magnitude with respect to the maximal current values.

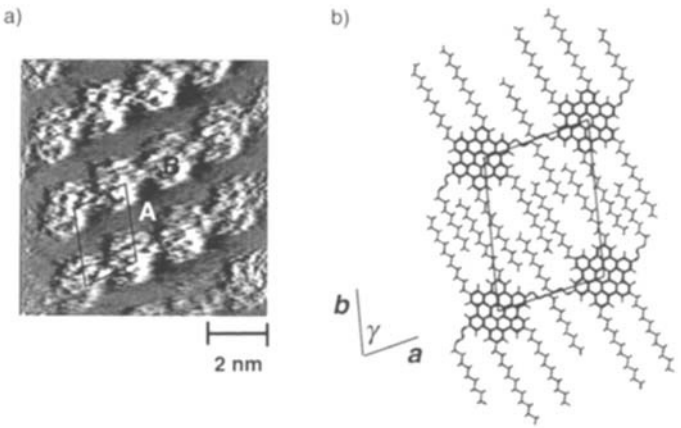

Fig. 1. a) STM image of **3** on HOPG with unit cell depicted. $U_T = 0.9$ V, $I_T = 0.5$ nA. b) Close packed model of a two-dimensional crystal of **3**.

A detailed explanation has still to be elaborated; nevertheless, two factors seem to be responsible for the observed asymmetric

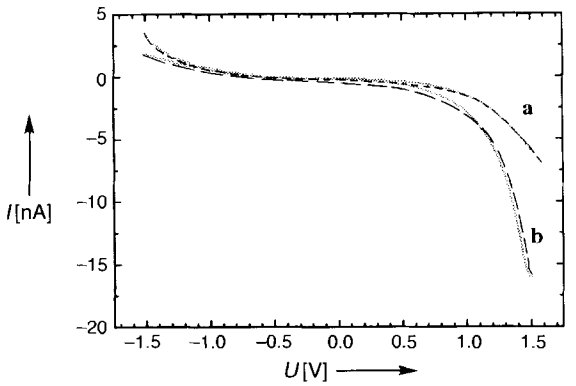

Fig. 2. a) Current–voltage curve of **3**: **a)** symmetric for the alkyl part; **b)** diodelike curve for the aromatic part of the molecule.

behavior.[13] The position of the HOMO within a range of ± 1.5 V about the Fermi level of the electrodes makes a resonant tunneling current possible.[22] This has been demonstrated by Fischer et al. who investigated a Langmuir–Blodgett film consisting of a few monolayers of an octasubstituted palladium–phthalocyanine (PcPd) and a perylene 3,4,9,10-tetracarboxydiimide (PTCDI) sandwiched between two evaporated gold electrodes.[23] The HOMO of **3** lies within a few tenths of an electron volt from the HOMO of PTCDI and PcPd.[23–25] The Fermi level of the employed Pt/Ir electrodes is also close to that of gold (about 5 eV). A resonant amplification of the tunneling current is therefore possible in the present case. Secondly, the asymmetric position of the benzocoronene layer in the tunneling gap plays an important role. At a relatively high tunneling resistance (in our case approx. 650 MΩ before the interruption of the feedback loop), the adsorbate layer is closer to the substrate than to the tip.[26] In contrast with the symmetric experiments of Fischer et al., who obtained symmetric *IV* curves, the break in geometric symmetry in our experiment entails an asymmetric current response of the system.

The observed asymmetry is similar to the one detected by Pomerantz et al. for copper–phthalocyanine on oxidatively modified graphite.[7] They could not, however, image the molecules with STM and were therefore not able to present laterally resolved *IV* spectra on a molecular scale. The present work on the other hand proves that STS can, in principle, be employed for chemical recognition of extended molecular moieties. Furthermore it could be shown that an *IV* curve, caused by the properties of a single molecule of *peri*-condensed hexabenzocoronene in contact with two electrodes, resembles that of a diode.

Experimental Procedure

Spectroscopic data of **3**: ^{1}H NMR (500 MHz, $CDCl_3$): δ = 8.14(s, 12H), 2.90(t, 12H), 1.93(m, 12H), 1.63(m, 12H), 1.54(m, 12H), 1.40(m, 84H), 0.90(t, 18H); ^{13}C NMR(125 MHz, $CDCl_3$): δ = 138.2, 128.1, 121.7, 119.5, 117.8, 36.1, 31.4, 30.9, 29.1, 28.9, 28.88, 28.8, 28.7, 28.3, 21.6, 13.0); UV/Vis: λ_{max} (ε) [nm] = 447 (2930), 440 (3044), 391 (53682), 374 (193444), 352 (101007).

For a tunneling spectroscopic investigation, a monolayer of **3** adsorbed on graphite from solution is first imaged by STM. For this a drop of a saturated solution of **3** in 1,2,4-trichlorobenzene is placed on the basal plane of graphite by means of a Pasteur pipette. The two-dimensional crystallization was induced by a bias pulse between tip and sample (10 V/150 ns). The STM images were obtained with a home-built instrument [27] in the constant height mode under ambient conditions (scan rate: 0.3 Hz/image, tip bias: positive, Pt/Ir tip; cut). They were recorded on videotape in real time and digitalized later. No digital image processing was performed.

In the dynamic scan mode the molecular moiety to be analyzed is brought into the center of the image. The x and y scanning is then reduced stepwise to zero. As a consequence, the tip slides into the center of the image. The feedback loop is then interrupted, and the tip fixed at a constant distance of a few nanometers from the sample. Subsequently a voltage ramp between -1.5 V to $+1.5$ V is applied, and the current response registered on a digital oscilloscope (LeCroy9400). The ramp is repeated between twelve and sixteen times within a time slot of 60 ms to 80 ms. The current signal that has been read out is then subdivided into the individual cycles, which are then used to compute an averaged *IV* curve. After the measurement the feed back loop is reactivated, and scanning in both x and y directions picked up again. An image appears again. A complete cycle image measurement–image takes about eight seconds.

Received: December 27, 1995
Revised version: May 6, 1995 [Z 7581 IE]
German version: *Angew. Chem.* **1995**, *107*, 1768–1770

Keywords: arenes · scanning tunneling microscopy · single molecule spectroscopy

[1] *Introduction to Molecular Electronics* (Ed.: M. C. Petty, M. R. Bryce, D. Bloor), Arnold, London, **1995**.
[2] W. E. Moerner, T. Basché, *Angew. Chem.* **1993**, *105*, 537–557; *Angew. Chem. Int. Ed. Engl.* **1993**, *32*, 457–476.
[3] E. Betzig, R. J. Chichester, *Science* **1993**, *262*, 1422–1425; T. Basché, *Angew. Chem.* **1994**, *106*, 1805–1807; *Angew. Chem. Int. Ed. Engl.* **1994**, *33*, 1723–1725.
[4] R. Berndt, R. Gaisch, B. Reihl, R. R. Schlitter, W. D. Schneider, M. Tschudy, *Science* **1993**, *262*, 1425–1427.
[5] S. Chiang, *Scanning Tunneling Microscopy I* (Ed.: H. J. Güntherodt, R. Wiesendanger) (*Springer Ser. Surf. Sci.* **1992**, *20*, 181–206); J. Frommer, *Angew. Chem.* **1992**, *104*, 1325–1357; *Angew. Chem. Int. Ed. Engl.* **1992**, *31*, 1298–1328; J. P. Rabe, S. Buchholz, L. Askadskaya, *Phys. Scr. T* **1993**, *49*, 260–263.
[6] J. A. Stroscio, R. M. Feenstra, *Methods Exp. Phys.* **1993**, *27*, 95–145.
[7] M. Pomerantz, A. Aviram, R. A. McCorkle, L. Li, A. G. Schrott, *Science* **1992**, *255*, 1115–1118.
[8] T. David, J. K. Gimzewski, D. Purdie, B. Reihl, R. R. Schlittler, *Phys. Rev. B* **1994**, *50*, 5810–5813.
[9] T. Klitsner, R. S. Becker, J. S. Vickers, *Phys. Rev. B* **1990**, *41*, 3837–3840.
[10] J. P. Rabe, S. Buchholz, *Phys. Rev. Lett.* **1991**, *66*, 2096–2099.
[11] J. P. Rabe, S. Buchholz, L. Askadskaya, *Synth. Met.* **1993**, *54*, 339–349.
[12] L. Askadskaya, C. Boeffel, J. P. Rabe, *Ber. Bunsenges. Phys. Chem.* **1993**, *97*, 517–521.
[13] A. Stabel, PhD thesis 1995, Mainz, Germany.
[14] The known dimethyl derivative is not distinctly more soluble: W. Hendel, Z. H. Khan, W. Schmidt, *Tetrahedron* **1986**, *42*, 1127–1134.
[15] **1**: ^{1}H NMR (300 MHz, CD_2Cl_2): δ = 7.42 (m, 4H), 7.18 (m, 4H), 2.62 (t, 4H), 1.60 (m, 4H), 1.31 (m, 36H), 0.89 (t, 6H); ^{13}C NMR (75 MHz, CD_2Cl_2): δ = 143.9, 131.7, 128.9, 120.9, 89.2, 36.2, 32.3, 31.7, 30.1, 29.9, 29.8, 29.7, 23.1, 14.3.
[16] Substitution of the amine group by iodine to yield 4-dodecyliodobenzene ($C_5H_{11}NO_2$/KI (65%)), coupling with trimethylsilylacetylene (Pd^0/piperidine (98%)), removal of the trimethylsilyl group (KF/DMF (100%)), and finally coupling with 4-dodecyliodobenzene (Pd^0/piperidine (92%)).
[17] K. P. C. Vollhardt, *Acc. Chem. Res.* **1977**, *10*, 1–8.
[18] **2**: ^{1}H NMR (300 MHz, $CDCl_3$): δ = 6.61 (q, 24H), 2.32 (t, 12H), 1.37 (m, 12H), 1.24 (m, 108H), 0.87 (t, 18H); ^{13}C NMR (75 MHz, $CDCl_3$): δ = 140.2, 139, 138.3, 131.4, 126.4, 35.3, 31.9, 31.2, 29.8, 29.7, 29.5, 29.3, 28.8, 22.6, 14.1.
[19] P. Kovacic, F. W. Koch, *J. Org. Chem.* **1965**, *30*, 3176–3181.
[20] U. Zimmermann, N. Karl, *Surf. Sci.* **1992**, *268*, 296–306.
[21] G. Lambin, M. H. Delvaux, A. Calderone, R. Lazzaroni, J. L. Brédas, T. C. Clarke, J. P. Rabe, *Mol. Cryst. Liq. Cryst.* **1993**, *235*, 75–82.
[22] W. Mizutani, M. Shigeno, K. Kaijmura, M. Ono, *Ultramicroscopy* **1992**, *42–44*, 236–241.
[23] C. M. Fischer, M. Burghard, S. Roth, K. von Klitzing, *Europhys. Lett.* **1994**, *28* (2), 129–134.
[24] J. Simon, J. J. André, *Molecular Semiconductors*, Springer, Berlin, **1985**.
[25] E. Clar, W. Schmidt, *Tetrahedron* **1977**, *33*, 2093–97; the value of the first ionization potential in the gas phase is given. For direct comparison, a shift between the first ionization potential in the gas phase and that in the solid state has to be taken into account. This shift is due to the polarization energy and is on the order of 1.5–1.9 eV toward less negative values [28, 29].
[26] D. M. Eigler, C. P. Lutz, W. E. Rudge, *Nature (London)* **1991**, *352*, 600–603.
[27] J. P. Rabe, M. Sano, D. Batchelder, A. A. Kalatchev, *J. Microsc. (Oxford)* **1988**, *152*, 573–578.
[28] J. L. Brédas, R. L. Elsenbaumer, R. R. Chance, R. Silbey, *J. Chem. Phys.* **1983**, *78*, 5656–5662.
[29] N. Sato, K. Seki, H. Inokuchi, *J. Chem. Soc. Faraday Trans. 2* **1981**, *77*, 1621.

Reactions of Neopentyl 2,2,2-Trifluoroethanesulfonate (Tresylate) with Nucleophiles: A Model Study for the Coupling of Nucleophiles with Tresyl Agarose**

James F. King* and Manjinder Singh Gill

Recently, Demiroglou et al.[1] presented evidence for the need to revise the previously held picture of the reactions of 2,2,2-trifluoroethanesulfonyl (tresyl) agarose with nucleophiles such as hydroxide, thiolate anions, and primary amines. Though they showed clearly that the reaction does not go by a simple S_N2 displacement at carbon, the revised structures that they proposed for the coupled products, an alkylsulfuric acid, a dialkyl thiosulfate, and a dialkyl sulfamate, respectively, appeared to us to be incorrect, justifiable neither by precedent nor by the well-established principles of reaction mechanisms. It seemed much more likely that the attachment of nucleophiles would occur by way of some form of the β-elimination/Michael-type addition sequence shown by Stirling[2] for compounds of the general structure $-SO_2-\underset{|}{C}H-\underset{|}{C}-Lg$ (Lg = leaving group). Related conversions, for example, of tresyl fluoride into sulfoacetic acid and related products,[3] and a tresylate ester into a mesylate ester have been reported.[4] We now describe experiments with neopentyl tresylate (**1**), a model system chosen to 1) avoid the problems of determining the structures of polymers, 2) be unlikely to show S_N2 reactions at the primary carbon,[5] and hence 3) be well set up to show the coupling reactions of tresyl agarose with amines and thiols.

The reactions of **1** and further interconversions of the products are shown in Schemes 1 and 2; structural assignments of new compounds are supported by ^1H NMR, ^{13}C NMR, and IR spectra and exact mass determinations (Table 1). Structure **2** for the product of the reaction of **1** with hydroxide follows from its decarboxylation to neopentyl mesylate (**4**). Conversion of **2** via the acid chloride **5** into the amides **3a** and **3b** confirm these as the products of the reaction of **1** with butylamine and diethylamine, respectively.

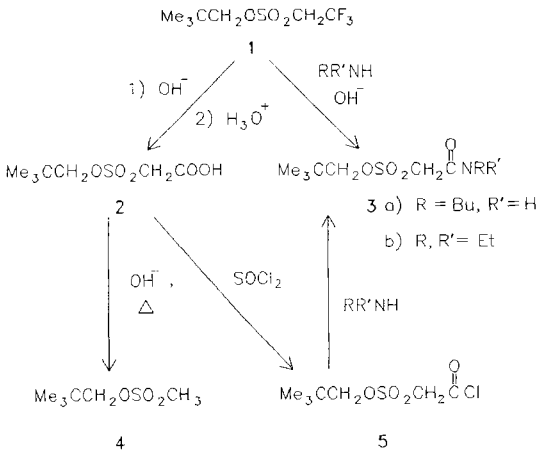

Scheme 1. Reactions of neopentyl tresylate (**1**) with amines and hydroxide, and further transformations.

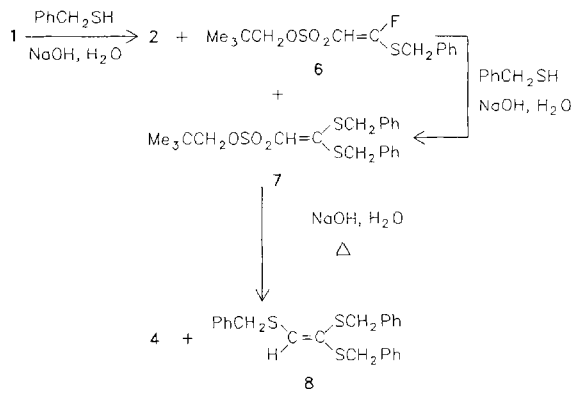

Scheme 2. Reactions of **1** with phenylmethanethiol and hydroxide, and further reactions.

Table 1. Characterization of new compounds.

1 [a]: m.p. 32–33 °C; IR ($CHCl_3$) $\tilde{\nu}$ [cm^{-1}] = 1387 (s), 1369 (s), 1326 (s), 1274 (s), 1258 (s), 1183 (vs), 1138 (s), 1091 (s), 956 (vs), 887 (m); ^1H NMR (300.1 MHz, $CDCl_3$, 25 °C, TMS): δ = 1.00 (s, 9H), 3.89 (q, J = 8.8 Hz, 2H), 4.00 (s, 2H); ^{13}C NMR (75.46 MHz): δ = 25.6, 31.6, 52.1 (q, J = 33 Hz), 81.0, 121.1 (q, J = 277.5 Hz).

2: IR (neat) $\tilde{\nu}$ [cm^{-1}] = 2964 (s), 1734 (vs), 1363 (s), 1177 (s), 969 (s); ^1H NMR: δ = 0.99 (s, 9H), 4.01 (s, 2H), 4.17 (s, 2H), 8.53 (br s, 1H); ^{13}C NMR: δ = 25.9, 31.9, 54.1, 81.3, 166.2; HRMS (CI): calcd. for $C_7H_{14}O_5S$ (M + H) 211.0640, found 211.0635.

3a: m.p. 48–50 °C; IR (neat) $\tilde{\nu}$ [cm^{-1}] = 2961 (s), 1662 (vs), 1557 (m), 1365 (s), 1176 (s), 961 (s), 848 (w); ^1H NMR: δ = 0.91 (t, 3H), 0.97 (s, 9H), 1.28–1.41 (m, 2H), 1.46–1.56 (m, 2H), 3.29 (q, 2H), 3.93 (s, 2H), 3.97 (s, 2H), 6.51 (br s, 1H); ^{13}C NMR: δ = 13.6, 19.9, 25.9, 31.2, 31.9, 39.9, 55.5, 81.0, 160.1; HRMS (EI): calcd. for $C_{11}H_{23}NO_4S$ 265.1348, found: 265.1347.

3b: IR (neat) $\tilde{\nu}$ [cm^{-1}] = 1652 (vs), 1457 (m), 1364 (s), 1174 (s), 966 (s), 845 (w); ^1H NMR: δ = 0.95 (s, 9H), 1.13 (t, 3H), 1.87 (t, 3H), 3.34–3.46 (m, 4H), 4.00 (s, 2H), 4.13 (s, 2H); ^{13}C NMR: δ = 12.6, 14.2, 25.9, 31.8, 40.9, 43.1, 53.7, 81.5, 160.0; HRMS (EI): calcd. $C_{11}H_{23}NO_4S$ 265.1348, found 265.1342.

5: ^1H NMR: δ = 0.98 (s, 9H), 4.01 (s, 2H), 4.53 (s, 2H); ^{13}C NMR: δ = 25.9, 31.9, 63.0, 81.8, 162.6.

(*E*)-**6**: m.p. 38–39 °C; IR ($CHCl_3$) $\tilde{\nu}$ [cm^{-1}] = 1602 (s), 1367 (s), 1271 (w), 1170 (vs), 964 (s), 859 (m); ^1H NMR: δ = 0.91 (s, 9H), 3.66 (s, 2H), 4.09 (s, 2H), 5.81 (d, J = 28.6 Hz, 1H), 7.25–7.37 (m, 5H); ^{13}C NMR: δ = 26.0, 31.6, 35.7, 79.9, 105.2 (d, J = 12.6 Hz), 128.3, 128.7, 129.0, 134.6, 167.2 (d, J = 316.5 Hz); HRMS (EI): calcd. for $C_{14}H_{19}FO_3S_2$ 318.0760, found 318.0767.

(*Z*)-**6**: IR ($CHCl_3$) $\tilde{\nu}$ [cm^{-1}] = 1587 (vs), 1366 (s), 1168 (vs), 965 (s), 836 (w); ^1H NMR: δ = 0.91 (s, 9H), 3.66 (s, 2H), 4.15 (s, 2H), 6.76 (d, J = 16.5 Hz, 1H), 7.26–7.36 (m, 5H); ^{13}C NMR: δ = 26.0, 31.6, 34.6, 79.8, 105.9 (d, J = 31.7 Hz), 128.0, 128.8, 128.9, 135.5, 170.8 (d, J = 319.4 Hz); calcd. exact mass for $C_{14}H_{19}FO_3S_2$ 318.0760, found: 318.0764.

7: m.p. 104–104.5 °C; IR ($CHCl_3$) $\tilde{\nu}$ [cm^{-1}] = 1495 (w), 1352 (s), 1157 (vs), 967 (s), 852 (m); ^1H NMR: δ = 0.91 (s, 9H), 3.57 (s, 2H), 4.06 (s, 2H), 4.27 (s, 2H), 6.02 (s, 1H), 7.25–7.37 (m, 10H); ^{13}C NMR: δ = 26.1, 31.5, 37.5, 38.9, 79.3, 113.7, 127.8, 128.1, 128.6, 128.8, 128.9, 129.2, 133.6, 135.4, 156.8; HRMS (EI): calcd. exact $C_{21}H_{26}O_3S_3$ 422.1044, found: 422.1043.

8: IR (neat) $\tilde{\nu}$ [cm^{-1}] = 1601 (m), 1494 (s), 1452 (s); ^1H NMR: δ = 3.77 (s, 2H), 3.8 (s, 2H), 4.02 (s, 2H), 6.44 (s, 1H), 7.2–7.32 (m, 15H); ^{13}C NMR: δ = 37.5, 38.1, 38.7, 123.7, 126.9, 127.0, 127.2, 128.3, 128.4, 128.6, 128.7, 128.9, 129.0, 137.4, 137.8, 138.1, 138.3; HRMS (EI): calcd. for $C_{23}H_{22}S_3$ 394.0884, found: 394.0880.

[a] Prepared by the general procedure in ref. [7].

The composition of the product from reaction of **1** with NaOH and phenylmethanethiol varied with the relative amounts of the reactants. With one equivalent of the thiol the product mixture consisted of **2**, the stereoisomeric fluoromonosulfides (*E*)-**6** and (*Z*)-**6**, and the ketene dithioacetal **7** in a 3:3:1:3 ratio. With three equivalents of the thiol the product was mainly **7** (80% yield). The structure of **7** follows from its mode of formation and spectra, as well as its slow transformation with NaOH in hot aqueous dioxane into neopentyl

[*] Prof. J. F. King, M. S. Gill
Department of Chemistry
University of Western Ontario
London, Ontario N6A 5B7 (Canada)
Telefax: Int. code + (519)661-3022

[**] This work was supported by the Natural Sciences and Engineering Research Council of Canada

mesylate (**4**); this reaction presumably takes place by way of **2**, which readily yields **4** under these conditions. The structure of **6** is clear from spectra and its ready conversion with the thiolate to **7**; the *trans* orientation ((*E*)-**6**) of the hydrogen and fluorine atoms is assigned to the isomer with the larger H–F coupling. Formation of **8** is readily accounted for by reaction of **7** with $PhCH_2S^-$ (produced along with **4**), presumably by way of **9** formed by addition of $PhCH_2S^-$ to **7**, followed by loss of the alkylsulfite anion. In a separate experiment, **7** on reaction with $PhCH_2SH$ and aqueous NaOH, gave **8** in good yield. The identity of **8** was confirmed by synthesis from trichloroethylene and $PhCH_2S^-$ by a known general method.[8]

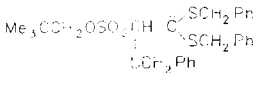

9

The production of **2**, **3**, **6**, and **7** from **1** is easily rationalized by assuming initial conversion of **1** by an E1cB process into **10** (Scheme 3), which may undergo Michael-type addition–elimination as in the sequence **1**→**10**→**11**→**12**; repetition of the addition–elimination and (or) hydrolysis leads to the products.

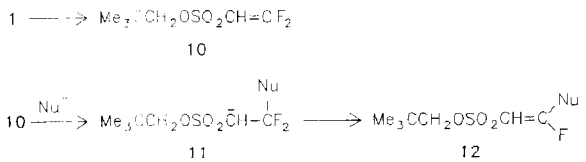

Scheme 3. The initial elimination–addition sequence of the reactions of **1**.

Although any extension of our solution chemistry to the solid phase must be made with caution, we conclude that in the light of our results with neopentyl tresylate the structures proposed by Demiroglou et al.[1] are extremely unlikely. The published information[1] on the products of the reactions of tresyl agarose appears to be consistent with their having the structures $RO\text{-}SO_2CH_2COOH$ (reaction with NaOH), $ROSO_2CH_2CONHBu$ (reaction with $BuNH_2$), and almost equal amounts of $RO\text{-}SO_2CH{=}C(SBu)_2$ and $ROSO_2CH_2COOH$ (reaction with BuSH).[9] These model experiments provide critical information for the understanding of the tresyl agarose reactions and the basis of the chromatographic utility of these products.

Experimental Procedure

Except where otherwise noted the reaction products were characterized by at least ^1H and ^{13}C NMR spectra (see Table 1).

1 → **2**: A mixture of **1** (112 mg, 0.48 mmol), 1 M aqueous NaOH (2 mL), and dioxane (1 mL) was stirred at room temperature for 1 h; workup gave **2** as a white solid (90 mg, 90%).

2 → **4**: A mixture of **2** (13.2 mg, 0.06 mmol), 1 M NaOH (0.3 mL),and dioxane (0.5 mL) was heated at reflux for 2 h. The reaction mixture was cooled and extracted with $CDCl_3$ (1 mL). The ^1H NMR spectrum showed signals due to **4**; comparison of their integrals with those from added toluene (7 μL) showed the yield of **4** to be 60%. Evaporation of the solvent gave a clear liquid; its ^1H NMR spectrum showed only **4** with a trace of unconverted **2**.

1 → **3**: A solution of **1** (255 mg, 1.09 mmol) in dioxane (0.8 mL) was added to a stirred solution of 1 M NaOH (2 mL) and butylamine (0.1 mL, 1.0 mmol) at 0 °C. The mixture was stirred for 1 h and then worked up to give an oil; its ^1H NMR spectrum showed it to be a 1:1 mixture of **2** and **3a**. Preparative thin-layer chromatography (tlc) (silica gel) with elution with a 1:2 mixture of EtOAc and petroleum ether (b.p. 30–60 °C) gave **3a** as a white solid (80 mg, 28%), which was recrystallized from ether/petroleum ether; m.p. 48–50 °C. A similar mixture of **1** (67 mg, 0.29 mmol) 1 M NaOH (0.72 mL), diethylamine (90 μL, 0.87 mmol) in dioxane (0.7 mL), after 40 min reaction, gave a clear liquid, its ^1H NMR spectrum showing the presence of **3a** with traces of **2**; removal of the latter by washing with aqueous NaOH (pH 12–13) gave **3b** (60 mg, 80%).

2 → **5** → **3**. Thionyl chloride (5 mL) containing **2** (288 mg, 1.37 mmol) was heated at 50–55 °C with stirring for 4.5 h. The excess $SOCl_2$ was removed under reduced pressure to leave **5** as a light brown solid (228 mg, 73%). A solution of **5** (100 mg, 0.44 mmol) in CH_2Cl_2 (1 mL) added dropwise with stirring to butylamine (0.22 mL, 2.2 mmol) in CH_2Cl_2 at 0 °C gave, after 3 h, **3a** (81 mg, 75%). Similar reaction of **5** with Et_2NH gave **3b** (75 mg, 65%).

1 → **2** + **6** + **7**: A dioxane solution (1 mL) of **1** (200 mg, 0.85 mmol) was added with stirring to $PhCH_2SH$ (100 μL, 0.85 mmol) in a mixture of 1 M NaOH (1.9 mL) and dioxane (0.5 mL) at room temperature. Workup after 1 h gave an oil (0.30 g); its ^1H NMR spectrum showed it to consist of **2**, (*E*)-**6**, (*Z*)-**6**, and **7** in a 3:3:1:3 ratio. The acid (**2**, 50 mg, 28%) was removed by washing a CH_2Cl_2 solution with 0.25 M NaOH, and the neutral components were separated by preparative tlc; elution with a 1:8 mixture of EtOAc and petroleum ether (b.p. 35–60 °C) gave (*Z*)-**6** (17 mg, 6%) as the faster moving band and a mixture of (*E*)-**6** and **7** as the slower. The latter mixture was separated into (*E*)-**6** (faster) (43 mg, 16%) and **7** (75 mg, 21%) on further tlc (elution three times with CH_2Cl_2/petroleum ether 1:2).

1 → **7**: A dioxane solution (1 mL) of **1** (106 mg, 0.45 mmol) was added to $PhCH_2SH$ (160 μL, 1.36 mmol) in 1 M NaOH (1.14 mL). A white precipitate appeared after 3–5 min; workup after 15 min, and recrystallization from Et_2O gave **7** (154 mg, 80%).

7 → **4** + **8**. A mixture of **7** (36 mg, 0.09 mmol), 6.6 M NaOH (6.5 mL, 43 mmol) and dioxane (3 mL) after 6 h at reflux gave a product identified by its ^1H NMR spectrum as a 1:4:4 mixture of **4**, **7**, and **8**.

7 → **8**. A dioxane solution (1 mL) of **7** (36 mg, 0.09 mmol) was added to a solution of $PhCH_2SH$ (68 μL, 0.58 mmol) in 6.6 M NaOH (1 mL) under N_2, and the mixture was heated at reflux for 2 h; the oily product on tlc (elution with EtOAc/petroleum ether, 1:10) gave **8** as a light yellow oil (25 mg, 74%), identical to that prepared by heating a mixture of trichloroethene (1.37 g, 10 mmol) in absolute EtOH (15 mL) at reflux with $PhCH_2S^-Na^+$ (38 mmol) for 21 h under N_2 [8].

(*Z*)-**6** → **7**. A solution of (*Z*)-**6** (10 mg, 0.03 mmol) in dioxane (50 μL) was added to a mixture of 1 M NaOH (140 μL) and $PhCH_2SH$ (20 μL, 0.15 mmol). Workup after 15 min gave a product (10 mg, 75%) with a ^1H NMR spectrum identical to that of **7**.

(*E*)-**6** → **2** + **7**. A mixture of (*E*)-**6** (14 mg, 0.04 mmol), 1 M NaOH (100 μL), and dioxane (50 μL) was stirred at room temperature for 11 h, giving on workup a product (12 mg) that showed ^1H NMR signals appropriate for unconverted (*E*)-**6**, **2**, and **7** in a 1:1:1 ratio.

Received: October 17, 1994
Revised: April 21, 1995 [Z7409IE]
German version: *Angew. Chem.* **1995**, *107*, 1778–1780

Keywords: carbohydrates · substitutions · sulfonic acids

[1] A. Demiroglou, C. Bandel-Schlesselmann, H. P. Jennissen, *Angew. Chem.* **1994**, *106*, 126; *Angew. Chem. Int. Ed. Engl.* **1994**, *33*, 120–123.
[2] C. J. M. Stirling, *Chem. Ind. (London)* **1960**, 933; A. T. Kader, C. J. M. Stirling, *J. Chem Soc.* **1962**, 3686–3692 and later papers in this series.
[3] A. F. Eleev, G. A. Sokol'skii, I. L. Knunyants, *Izv. Akad. Nauk SSSR, Ser. Khim.* **1978**, 2084–2090; *Bull. Acad. Sci. USSR Div. Chem. (Engl. transl.)* **1978**, *27*, 1837–1842).
[4] Y. S. Choe, J. A. Katzenellenbogen, *Tetrahedron Lett.* **1993**, 1579–1580.
[5] Recently we found that the use of a bulky group to suppress the S_N2 reaction at carbon is unnecessary, and that ethyl, isobutyl, and octyl tresylates give reactions like those in Schemes 1 and 2. Genuine S_N2 reactions at the carbon atom of a primary tresylate with relatively weakly basic nucleophiles (azide anion, thiourea) are known [6].
[6] J. F. King, S. M. Loosmore, M. Aslam, J. D. Lock, M. J. McGarrity, *J. Am. Chem. Soc.* **1982**, *104*, 7108–7122.
[7] R. K. Crossland, W. E. Wells, V. J. Shiner, *J. Am. Chem. Soc.* **1971**, *93*, 4217–4219.
[8] W. E. Truce, R. Kassinger, *J. Am. Chem. Soc.* **1958**, *80*, 1916–1919.
[9] Among other more likely structures for possible components of the thiolate reaction are $ROSO_2CH{=}CF(SBu)$, the analogue of **6** that would account for residual fluorine in the product, and $RSO_2CH_2C(SBu)_3$, the trithioorthoester, an analogue of which is found as a minor product from isobutyl tresylate and the major product (53% vs 41% for the ketene dithioacetal) in the reaction of ethyl tresylate with three equivalents of $PhCH_2S^-$ (cf. ref. [5]); the ^1H NMR spectrum of this last product also indicated the presence of a small amount (about 6%) of the simple thioether, $EtSCH_2Ph$. Prof. H. P. Jennissen has kindly shown us solid phase ^{13}C NMR spectra that he obtained from the *N*-butyl and *S*-butyl agarose materials. The spectrum of the former appears in accord with the amide structure ($ROSO_2CH_2CONHBu$) along with a smaller amount of the acid ($ROSO_2CH_2COOH$). The *S*-butyl agarose spectrum shows fewer well-defined signals, perhaps suggesting (when taken with other information) that the product composition may be complex, including probably $RO\text{-}SO_2CH_2COOH$, and some (or all) of the following: $ROSO_2CH{=}CF(SBu)$, $ROSO_2CH{=}C(SBu)_2$, $ROSO_2CH_2C(SBu)_3$, $ROSO_2CH_2COSBu$, and even possibly the thioether, RSBu.

Diphosphanyl- and Diarsanyl-Substituted Carbene Homologues: Germanediyls, Stannanediyls, and Plumbanediyls with Remarkable Electronic Structures**

Matthias Driess,* Rudolf Janoschek,* Hans Pritzkow, Stefan Rell, and Uwe Winkler

Dedicated to Professor Egon Uhlig on the occasion of his 65th birthday

Compounds with multiple bonds (π-electron systems)[1] and subvalent compounds (carbene analogues)[2] of the heavy main group elements (period > 3) differ fundamentally from those of the elements of the second period with respect to their electronic structure.[3] This is illustrated impressively, for example, by carbene homologues which, in contrast to methanediyl, have a singlet ground state (S_0). The synthesis of thermally stable compounds of the form $:EX_2$ with η^1-bound ligands X (germanediyls,[4] stannanediyls,[5] and plumbanediyls[6]) has enabled extensive preparative and theoretical investigations.[7] The focus of these studies has been the influence of the electronic structure (singlet triplet (S/T) separation) on the reactivity (dimerization and cycloaddition behavior). The results have demonstrated that the carbene homologues are monomeric and show no tendency to oligimerize when they have a relatively large S/T separation and the ligands X are particularly bulky and/or function as intramolecular donor centers. To date, alkyl, aryl, OR, SR, and NR_2 groups have been used as the ligand X, and the structures of several of these colored, diamagnetic carbene homologues have also been characterized.[8] A phosphanyl-substituted monomeric carbene analogue was not known until now. Instead, despite the incorporation of bulky $P(SiMe_3)_2$[9] and $PtBu_2$[10] groups, phosphorus-bridged dimers **A** or ate complexes **B** were formed. The recently reported stannanediyl **C** was characterized by its ^1H and ^{31}P NMR spectroscopy and cryoscopy.[11]

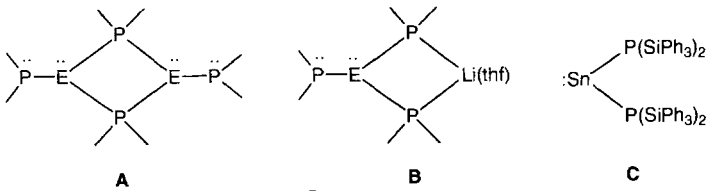

A **B** **C**

E = Ge, Sn, Pb

Herein, we report on the syntheses and crystal and electronic structures of a complete series of thermally stable, homoleptic phosphanyl-substituted carbene analogues of germanium, tin, and lead (**2**–**4**). In addition, we describe the first diarsanyl-substituted stannanediyl **5**, whose structure was also determined by a crystal structure analysis. These compounds were synthesized within the framework of our investigations into P- and As-metalated (fluorosilyl)silylphosphanes and -arsanes, which are suitable precursors for the synthesis of thermally stable Si=P and Si=As compounds.[12] During the transmetalation of the sterically demanding lithium (fluorosilyl)silylphosphanides **1a,b**, we observed that both compounds react with GeI_2, $SnCl_2$, and $PbCl_2$ in toluene at −78 °C. The germanediyl, stannanediyl, and plumbanediyl derivatives **2**–**4** can be obtained in the form of dark green crystals. In contrast to **1a,b**, these compounds are stable in toluene up to 90 °C and decompose at higher temperature with the elimination of Ge, Sn, and Pb metal, respectively.

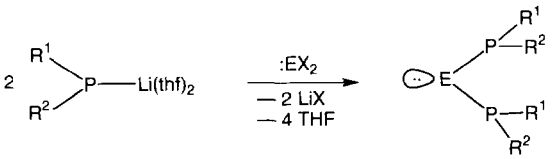

1a: R^1 = Si(Is)$_2$F; R^2 = Si*i*Pr$_3$
1b: R^1 = Si(*t*Bu)(Is)F; R^2 = Si*i*Pr$_3$
Is = 2,4,6-*i*Pr$_3$C$_6$H$_2$

2: E = Ge, R^1 = Si(Is)$_2$F
3a: E = Sn, R^1 = Si(Is)$_2$F
3b: E = Sn, R^1 = Si(*t*Bu)(Is)F
4: E = Pb, R^1 = Si(*t*Bu)(Is)F

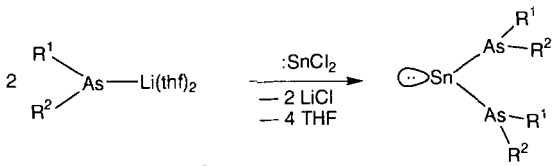

6: R^1 = Si(*t*Bu)(Is)F; R^2 = Si*i*Pr$_3$

5

The compounds were characterized by multinuclear NMR spectroscopy and elemental analysis. In the ^{31}P NMR spectra of **2**, **3a**, and **3b**, singlets are observed at $\delta = -62.1$, −102.5, and −121.3. The resonances for **3a** and **3b** show Sn satellites ($^1J(^{119}Sn,P) = 1682$, 1628 Hz); the positions of the signals are barely influenced by the polarity and donor character of the solvent. The magnitudes of the coupling constants are significantly larger than the values for compounds with Sn^{IV}–P^{III} single bonds (700–1000 Hz)[13] and dimeric carbene analogues **A** and **B** (1250–1360 Hz).[8, 9] By far the largest $^1J(Sn,P)$ coupling constants (2199–2200 Hz) were observed for phosphanylidenestannanes ($R_2Sn{=}PR$).[14] It is still unclear to what extent these larger values for **3a,b** can be interpreted in terms of increased Sn–P π interactions. Because of the limited solubility of **3b**, only **3a** could be characterized by ^{119}Sn NMR spectroscopy. The spectrum of **3a** shows a triplet at comparably low field ($\delta = 1551$ ($^1J(Sn,P) = 1682$ Hz)) which supports the fact that monomeric stannanediyl molecules, without stabilization by a donor, are present in solution. For OR, SR, or NR_2-substituted stannanediyls, the ^{119}Sn NMR signals are shifted to significantly higher field (90–900 ppm).[5, 8]

The ^{31}P NMR spectrum of the plumbanediyl **4** surprisingly shows two broad signals in a 1:1 ratio at $\delta = -88.8$ and −95.6 (298 K) with ^{207}Pb satellites ($^1J(Pb,P) = 1995$, 1979 Hz). This indicates that two diastereomeric forms, which show no coalescence up to 90 °C, are present; however, these chemical shifts are strongly temperature dependent. In contrast, the $^1J(Pb,P)$ coupling constants for dimeric plumbanediyls of forms **A** and **B** have values of 1260–1660 Hz and 1770 Hz, respectively.[10] Both diastereomers are formed when single crystals of **4**, which is present as only one diastereomer (see crystal structure analysis; Fig. 1), are dissolved in toluene. This is presumably attribut-

[*] Priv.-Doz. Dr. M. Driess, Dr. H. Pritzkow, S. Rell, Dr. U. Winkler
Anorganisch-chemisches Institut der Universität
Im Neuenheimer Feld 270, D-69120 Heidelberg (Germany)
Telefax: Int. code + (6221) 56-4197
Prof. Dr. R. Janoschek
Institut für Theoretische Chemie der Universität
Mozartgasse 14, A-8010 Graz (Austria)
Telefax: Int. code + (316) 38-2130

[**] This work was supported by the Deutsche Forschungsgemeinschaft (SFB 247) and the Fonds der Chemischen Industrie. We thank the Messer Griesheim GmbH for the donation of chemicals.

Table 1. UV/Vis spectroscopic data (λ_{max} (hexane) [nm]) for **2**–**5** as well the calculated transitions [nm] for :GeH_2, :GeR_2 [a], :SnH_2, and :SnR_2 [b]. R = $P(SiH_3)_2$.

	2	**3a**	**3b**	**4**	**5**	:GeH_2	:GeR_2	:SnH_2	:SnR_2	Assignment
S_1	626	644	579	645	641	502	526	495	545	HOMO → LUMO
S_2	396	433	438	465	459	241	296	245	319	[HOMO-1] → LUMO
S_3	–	384	–	346	–	198	277	207	285	[HOMO-2] → LUMO

[a] Geometry with experimental Si-P-Ge-P dihedral angle from **2**. [b] Geometry with experimental Si-P-Sn-P diheral angle from **3a**.

ed to the fact that the phosphorus inversion barrier in **4** is higher than that for the tin analogue **3b**.

The colors of the carbene analogues **2**, **3a,b**, and **4** are unusual. With the exception of **3b** (dark yellow-brown), they are intense green in solution (toluene, hexane, CH_2Cl_2, and THF); in the solid state **3b** is also dark green. This finding is reflected in the UV/Vis spectra (λ_{max} values) (Table 1).

Calculations of electronic transitions were carried out at the CIS level with the ab initio Los Alamos pseudopotential method (LANL1DZ),[15] which had been implemented in the Gaussian92 program.[16] The transitions for the parent compound :$E[P(SiH_3)_2]_2$ (E = Ge, Sn) are in very good agreement with the experimental S_1 values (deviations 0.2–0.4 eV). However, the calculations show that the λ_{max} values (S_1) are strongly dependent on the dihedral angle. A rotation of the E–P bond can lead to a signal in the range 300–800 nm. The results for the transitions for :$E[P(SiH_3)_2]_2$ (E = Ge, Sn, (Table 2)) are based on the

Table 2. Orbital energies [eV], Mulliken net atomic charges Q(Sn) [e], and S_1 excitation energies [eV] of several stannanediyls.

	:SnH_2	:$Sn[N(SiH_3)_2]_2$	:$Sn[P(SiH_3)_2]_2$
LUMO	−0.39	0.27	−0.45
HOMO	−8.52	−8.93	−7.51
Q(Sn)	0.507	1.269	0.683
S_1	2.50	4.13	2.27

experimentally determined geometries for **2** and **3**. The calculated S_1 transition for :$Sn[N(SiH_3)_2]_2$ is, in contrast to that for :$Sn[P(SiH_3)_2]_2$, hypochromically shifted by 245 nm. The unusual color of the phosphanyl-substituted carbene analogues **2**–**4** is evidently due to the destabilization of the HOMO. A comparison with :SnH_2 shows that charge depletion at the Sn atom by the ligands also plays a role (Table 2). In fact, all stannanediyls known to date have an absorption at significantly lower wavelength and are, therefore, yellow or red (λ_{max} 380–495 nm).[5]

The three lone pairs of electrons in :$E[P(SiH_3)_2]_2$ (E = Ge, Sn) fill three molecular orbitals which are made up of the 4s, 4p (Ge), 5s, 5p (Sn), and 3s,3p (P) valence orbitals (Scheme 1). We have also calculated (MP2/DZ + POL//RHF/DZ + ZPE)[15, 16] the reaction profile for the isomerization of :$E(PH_2)_2$ (E = Si, Ge, Sn, Pb) **D** via the transition state **E** to the

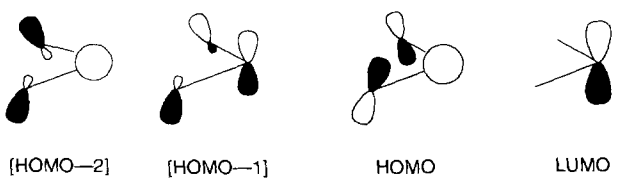

Scheme 1. Selected frontier orbitals for :$E[P(SiH_3)_2]_2$ (E = Ge, Sn).

tautomer **F** with an E=P bond, and observe that the carbene-like form **D** is increasingly preferred over **F** in the series Si, Ge, Sn, Pb (Scheme 2, Table 3).

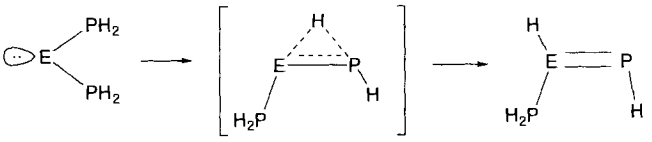

Scheme 2. Calculated reaction pathway for the isomerization of **D** to **F** via the intermediate **E**. E = Si, Ge, Sn, Pb.

Table 3. Relative enthalpies $\Delta H(0)$ [kcal mol^{-1}] for the reaction profile of the **D** → **E** → **F** isomerization; calculated with the ab initio pseudopotential method.

E	**D**	**E** (TS)	**F**
Si	0.0	29.2	−18.2
Ge	0.0	40.4	−2.1
Sn	0.0	54.6	14.8
Pb	0.0	70.6	32.4

Bonding behavior like that in the diphosphanyl compounds **2**–**4** is also observed for the diarsanylstannanediyl **5**, which is obtained in 74% yield by the reaction of lithium arsanide **6** with $SnCl_2$. Green crystals of **6** yield, as with **3b**, a yellow-brown solution, whose signal due to the S_1 transition indicates high dispersion.

The monomeric carbene homologous molecules have a V-shaped P-E-P (E = Ge, Sn, Pb) or a As-Sn-As arrangement, even in the solid state; this was confirmed by X-ray structure analyses for **2**–**5** (Fig. 1).[17] Due to disordering, a discussion of

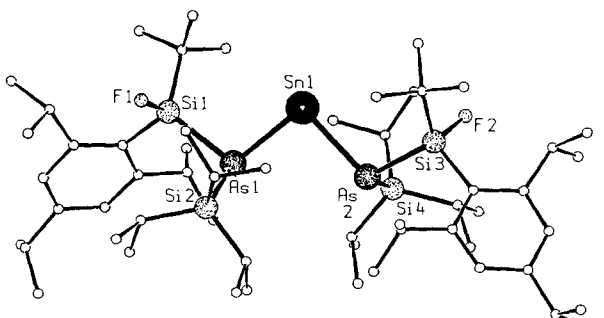

Fig. 1. Molecular structure of **5** in the crystal. The compounds **3b** and **4** are isotypic with **5**. The two crystallographically independent molecules differ only slightly. Selected distances [Å] and angles [°] for **5**: Sn-As 2.652(1), As-Si(F) 2.380(2), As-Si(*i*Pr) 2.388(2), Si-F 1.647(2); As-Sn-As 94.64(4), Sn-As-Si(F) 105.64(5) Sn-As-Si(*i*Pr) 105.62(5). **3b**: Sn-P 2.567(1), P-Si(F) 2.270(2), P-Si(*i*Pr) 2.286(2), Si-F 1.615(2); P-Sn-P 98.78(4), Sn-P-Si(F) 107.05(5), Sn-P-Si(*i*Pr) 108.45(5). **4**: Pb-P 2.654(4), P-Si(F) 2.263(5), P-Si(*i*Pr) 2.278(5), Si-F 1.613(8); P-Pb-P 97.88(4), Pb-P-Si(F) 106.76(5), Pb-P-Si(*i*Pr) 107.89(5).

 © VCH Verlagsgesellschaft mbH, D-69451 Weinheim, 1995 0570-0833/95/1515-1615 $ 10.00+.25/0

the structures of **2** and **3a** is not meaningful. As a result, only the crystal structures of **3b**, **4**, and **5** will be discussed here. These compounds are isotypic; the same enantiomeric form is present in each case.

There is a relatively small angle at tin (**3b**: 98.78(4)°, **5**: 94.64(4)°, average values) and lead (**4** 97.84(4)°) despite the fact that there are bulky phosphanyl and arsanyl substituents present. This is due to the "reluctance to hybridize" which is found among these heavy main group elements.[3] Identical angles have been obtained for the amino analogues.[4] The P and As atoms are pyramidally coordinated (average sum of angles: **3b**: 320.9, **4**: 320.5, and **5**: 315.2°) and the average Sn–P (2.567(1) Å), Pb–P (2.654(4) Å), and Sn–As (2.652(1) Å) distances are significantly shorter than the corresponding values in the dimeric[10] and hypervalent[18] stannanediyls and plumbanediyls. The Sn–P and Pb–P distances in the Sn^{IV}–P^{III} and Pb^{IV}–P^{III} compounds are shorter (2.51 Å vs. 2.61 Å)[19] due to the partial charge at the center.

Experimental Procedure

2: A slurry of GeI_2 (0.60 g, 1.83 mmol) in toluene (50 mL) was treated at −78 °C with **1a** (2.91 g, 3.66 mmol) The reaction mixture was warmed to room temperature over 12 h during which time an intense green solution was formed. After the LiI was removed by filtration, the filtrate was concentrated to about 10 mL and left at 10 °C for crystallization. Yield: 1.1 g (0.8 mmol, 44%) green, cubic crystals; m.p. 110 °C (decomp.).

Compounds **3**–**5** were prepared analogously.

3a: $SnCl_2$ (0.54 g, 2.87 mmol) and **1a** (4.55 g, 5.75 mmol) yielded dark green crystals (3.01 g, 2.15 mmol, 75%); m.p. 131 °C (decomp.).

3b: $SnCl_2$ (0.31 g, 1.61 mmol) and **1b** (2.08 g, 3.22 mmol) yielded green cubes (1.50 g, 1.35 mmol, 84%) after crystallization from hexane; m.p. 158 °C (decomp.).

4: $PbCl_2$ (0.44 g, 1.58 mmol) and **1b** (2.04 g, 3.16 mmol) yielded green cubes (1.10 g, 0.92 mmol, 58%) after crystallization from hexane; m.p. 53 °C (decomp.).

5: $SnCl_2$ (0.19 g, 1.02 mmol) and **6** (1.40 g, 2.04 mmol) yielded green cubes (0.90 g, 0.75 mmol, 74%) after crystallization from hexane at −20 °C; m.p. 136 °C (decomp.).

Received: March 9, 1995 [Z77771E]
German version: *Angew. Chem.* **1995**, *107*, 1746–1749

Keywords: arsenic compounds · carbene analogues · phosphorus compounds · subvalent compounds

[1] Review: A. H. Cowley, *Polyhedron* **1984**, *3*, 389; P. Jutzi, *Chem. Unserer Zeit* **1981**, *15*, 149; M. Driess, *ibid.* **1993**, *27*, 141.

[2] Interesting compounds with elements of group 14: P. Jutzi, D. Kanne, C. Krüger, *Angew. Chem.* **1986**, *98*, 163; *Angew. Chem. Int. Ed. Engl.* **1986**, *25*, 164; M. J. Fink, D. B. Puranik, *Organometallics* **1987**, *6*, 1809; M. Denk, R. Lennon, R. Hayashi, R. West, A. V. Belyakov, H. P. Verne, A. Haaland, M. Wagner, N. Metzler, *J. Am. Chem. Soc.* **1994**, *116*, 2691; see also refs. [3–5].

[3] W. Kutzelnigg, *Angew. Chem.* **1984**, *96*, 262; *Angew. Chem. Int. Ed. Engl.* **1984**, *23*, 272.

[4] D. E. Goldberg, D. H. Harris, M. F. Lappert, K. M. Thomas, *J. Chem. Soc. Chem. Commun.* **1976**, *261*; P. J. Davidson, D. H. Harris, M. F. Lappert, *J. Chem. Soc. Dalton Trans.* **1976**, 2268; P. Jutzi, A. Becker, H. G. Stammler, B. Neumann, *Organometallics* **1991**, *10*, 1647; W. A. Herrmann, M. Denk, J. Behm, W. Scherer, F.-R. Klingan, H. Bock, B. Solouki, M. Wagner, *Angew. Chem.* **1992**, *104*, 1489; *Angew. Chem. Int. Ed. Engl.* **1992**, *31*, 1485; see also ref. [7].

[5] D. H. Harris, M. F. Lappert, *J. Chem. Soc. Chem. Commun.* **1974**, 895; C. D. Schaeffer, J. J. Zuckerman, *J. Am. Chem. Soc.* **1974**, *96*, 7160; M. Veith, *Angew. Chem.* **1975**, *87*, 287; *Angew. Chem. Int. Ed. Engl.* **1975**, *14*, 263; M. Veith, O. Recktenwald, *Top. Curr. Chem.* **1982**, *104*, 1; T. Fjeldberg, H. Hope, M. F. Lappert, P. P. Power, A. J. Thorne, *J. Chem. Soc. Chem. Commun.* **1983**, 639; H. Grützmacher, H. Pritzkow, F. T. Edelmann, *Organometallics* **1991**, *10*, 23; U. Lay, H. Pritzkow, H. Grützmacher, *J. Chem. Soc. Chem. Commun.* **1992**, 260; N. Tokitho, M. Saito, R. Okazaki, *J. Am. Chem. Soc.* **1993**, *115*, 2065; M. Weidenbruch, J. Schlaefke, A. Schäfer, K. Peters, H. G. von Schnering, H. Marsmann, *Angew. Chem.* **1994**, *106*, 1938; *Angew. Chem. Int. Ed. Engl.* **1994**, *33*, 1846.

[6] P. J. Davidson, D. H. Harris, M. F. Lappert, *J. Chem. Soc. Dalton Trans.* **1976**, 2268; S. Brooker, J.-K. Buijink, F. T. Edelmann, *Organometallics* **1991**, *10*, 25.

[7] G. Olbrich, *Chem. Phys. Lett.* **1980**, *73*, 110; P. Bleckmann, H. Maly, R. Minkwitz, G. Olbrich, W. P. Neumann, B. Watta, *Tetrahedron Lett.* **1982**, *23*, 4655; G. Trinquier, *J. Am. Chem. Soc.* **1990**, *112*, 2130, and references therein.

[8] H. Braunschweig, P. B. Hitchcock, M. F. Lappert, L. J.-M. Pierssens, *Angew. Chem.* **1994**, *106*, 1243; *Angew. Chem. Int. Ed. Engl.* **1994**, *33*, 1156, and references therein.

[9] S. C. Goel, M. Y. Chiang, D. J. Rauscher, W. E. Buhro, *J. Am. Chem. Soc.* **1993**, *115*, 160.

[10] A. H. Cowley, D. M. Giolando, R. A. Jones, C. M. Nunn, J. M. Power, *Polyhedron* **1988**, *7*, 1909; A. M. Arif, A. H. Cowley, R. A. Jones, J. M. Power, *J. Chem. Soc. Chem. Commun.* **1986**, 1446; W.-W. du Mont, K. J. Kroth, *Angew. Chem.* **1977**, *89*, 832; *Angew. Chem. Int. Ed. Engl.* **1977**, *16*, 792; W.-W. du Mont, M. Grenz, *Chem. Ber.* **1985**, *118*, 1045.

[11] M. A. Matchett, M. Y. Chang, W. E. Buhro, *Inorg. Chem.* **1994**, *33*, 1109.

[12] M. Driess, U. Winkler, W. Imhof, L. Zsolnai, G. Huttner, *Chem. Ber.* **1994**, *127*, 1031, and references therein; M. Driess, *Adv. Organomet. Chem.* **1995**, in press; M. Driess, S. Rell, H. Pritzkow, *J. Chem. Soc. Chem. Commun.* **1995**, 253.

[13] M. Dräger, B. Mathiasch, *Angew. Chem.* **1981**, *93*, 1079; *Angew. Chem. Int. Ed. Engl.* **1981**, *20*, 1029; C. Couret, J. Escudié, J. Satgé, A. Raharinirina, J. D. Andriamizaka, *J. Am. Chem. Soc.* **1985**, *107*, 8280.

[14] H. Ranaivonjatovo, J. Escudié, C. Couret, J. Satgé, *J. Chem. Soc. Chem. Commun.* **1992**, 1047.

[15] P. J. Hay, W. R. Wadt, *J. Chem. Phys.* **1985**, *82*, 270, 284, 299.

[16] GAUSSIAN 92, Revision C.4: M. J. Frisch, G. W. Trucks, M. Head-Gordon, P. M. W. Gill, M. W. Wong, J. B. Foresman, B. G. Johnson, H. B. Schlegel, M. A. Robb, E. S. Replogle, R. Gomperts, J. L. Andres, K. Raghavachari, J. S. Binkley, C. Gonzalez, R. L. Martin, D. J. Fox, D. J. Defrees, J. Baker, J. J. P. Steward, J. A. Pople, Gaussian Inc., Pittsburgh, PA, **1992**. The standard DZ valence basis was extended for the atoms Ge and Sn with a diffuse sp set (0.03, 0.02) erweitert.

[17] **3b**: triclinic, $P\bar{1}$, $a = 11.565(6)$, $b = 21.304(11)$, $c = 26.443(13)$ Å, $\alpha = 85.46(3)$, $\beta = 82.52(2)$, $\gamma = 81.55(2)$°, $V = 6378$ Å^3, $Z = 4$, four-circle diffractometer ($Mo_{K\alpha}$ radiation, ω scan, $T = 208$ K), $2\theta_{max} = 46$°, 17704 measured reflections, 14049 observed, ($I > 2\sigma(I)$), refinement against F^2 (all data) [20], 1239 parameters. All non-hydrogen atoms were refined anisotropically, the hydrogen atoms in calculated positions. $R1 = 0.034$, $wR2 = 0.095$. **4**: triclinic, $P\bar{1}$, $a = 11.593(7)$, $b = 21.313(16)$, $c = 26.479(15)$ Å, $\alpha = 85.81(5)$, $\beta = 82.59(5)$, $\gamma = 81.54(6)$°, $V = 6407$ Å^3, $Z = 4$, four-circle diffractometer ($Mo_{K\alpha}$ radiation, ω scan, $T = 218$ K), $2\theta_{max} = 45$°, 16749 measured reflections, 11155 observed, ($I > 2\sigma(I)$), refinement against F^2 (all data) [20], 1229 parameters. All non-hydrogen atoms were refined anisotropically, the hydrogen atoms in calculated positions. $R1 = 0.077$, $wR2 = 0.254$. **5**: triclinic, $P\bar{1}$, $a = 11.558(6)$, $b = 21.389(11)$, $c = 26.639(13)$ Å, $\alpha = 86.15(3)$, $\beta = 82.59(4)$, $\gamma = 81.65(4)$°, $V = 6453$ Å^3, $Z = 4$, four-circle diffractometer ($Mo_{K\alpha}$ radiation, ω scan, $T = 203$ K), $2\theta_{max} = 47.5$°, 19174 measured reflections, 15568 observed, ($I > 2\sigma(I)$), refinement against F^2 (all data) [20], 1238 parameters. All non-hydrogen atoms were refined anisotropically, the hydrogen atoms in calculated positions. $R1 = 0.031$, $wR2 = 0.069$. Further details of the crystal structure investigations may be obtained from the Fachinformationszentrum Karlsruhe, D-76344 Eggenstein-Leopoldshafen (Germany) upon quoting the depository numbers CSD-401 771(**5**), 401 772(**3b**), and 401 773(**4**).

[18] H. H. Karsch, A. Appelt, G. Müller, *Angew. Chem.* **1985**, *97*, 404; *Angew. Chem. Int. Ed. Engl.* **1985**, *24*, 402; *Organometallics* **1986**, *5*, 1664; A. L. Balch, D. E. Oram, *ibid.* **1986**, *5*, 2159.

[19] D. Weber, C. Mujica, H. G. von Schnering, *Angew. Chem.* **1982**, *94*, 869; *Angew. Chem. Int. Ed. Engl.* **1982**, *21*, 863.

[20] G. M. Sheldrick, SHELXL-93, Universität Göttingen, **1993**.

 © VCH Verlagsgesellschaft mbH, D-69451 Weinheim, 1995 0570-0833/95/1515-1616 $ 10.00+.25/0

Biosyntheses of Novel Emycins from the Mutant Strain *Streptomyces cellulosae* ssp. *griseoincarnatus* 1114-2**

Martin Gerlitz, Györgyi Udvarnoki, and Jürgen Rohr*

The development of concepts for the search for structurally novel natural products which may eventually serve as lead structures for pharmaceutical or other indications is a permanent challenge, increased by resistance problems. This challenge may be faced in particular in academic research institutions, since sufficient test assays established on the industrial side are waiting for use.[1] Parallel to the concept of creating novel natural products through targeted genetic modifications of polyketide-producing streptomycetes,[2] we also use the often faster approach of arbitrarily genetically modifying selected streptomycetes. In this context we are particularly interested in those polyketide producers whose product spectra are obviously influenced by oxidoreductases. A good example is *Streptomyces cellulosae* ssp. *griseoincarnatus* (FH-S 1114),[4] an angucyclinone[5] producer yielding elmycin D (**1**) as the major product, the known antibiotics ochromycinone (**2**)[5] and deoxyrabelomycin (**3**)[5] as minor products, and, among others, emycin A (**4**) as trace products.[6] From this product spectrum one can assume a biosynthetic relationship between these four metabolites resulting from oxidoreductase activities. Oxygenases are especially able to markedly modify a primary biosynthetic molecular backbone, as known from the biosynthesis of the polyether antibiotic monensin[7a, b] or prostaglandins.[7c] Thus a mutation of a strain showing intense oxidoreductase activities may result in a whole spectrum of novel products.

Indeed, a mutant (strain 1114-2) showing a significantly changed product spectrum (TLC, HPLC)[3] was obtained readily by NTG (NTG = *N*-methyl-*N'*-nitro-*N*-nitrosoguanidine) treatment[3] of the wild-type strain FH-S 1114. Besides the wild-type strain products **1**, **2**, and **4** (major products), the production of four novel metabolites, namely the emycins C (**5**) (small side product), D (**6**), E (**7**), and F (**8**) could be observed, the latter three being also major products of *S. cellulosae* ssp. *griseoincarnatus* 1114-2 (Fig. 1). The structure elucidation of the

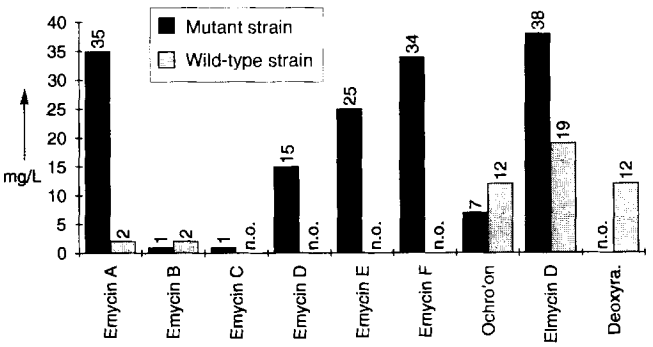

Fig. 1. Comparison of the products of the wild-type strain S-1114 and of the mutant strain 1114-2.

new compounds **5**–**8** by spectroscopic methods[8] (NMR data: see Tables 1 and 2) yielded the surprising result that two of the compounds, namely emycins D (**6**) and E (**7**), each appear as a pair of nonseparable diastereoisomers (see NMR data), which complicated the interpretation of the spectra. The constitution of the novel emycins was mainly established through $^{n}J_{C,H}$

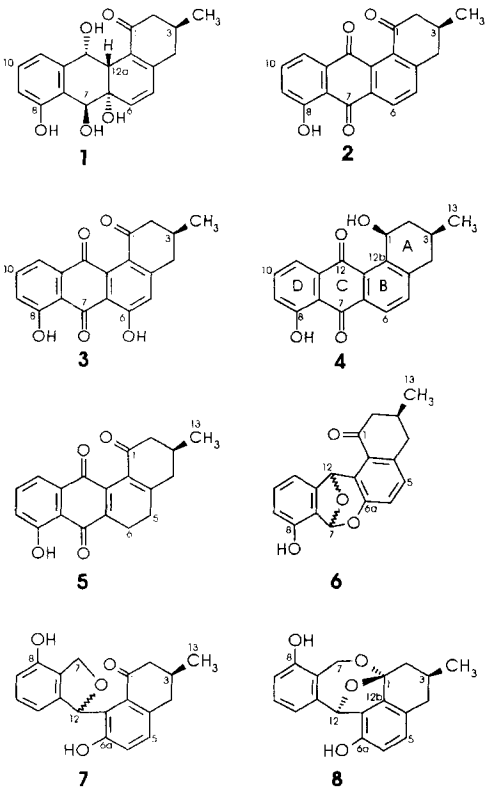

Table 1. ^{1}H NMR data of the novel emycins C (**5**), D (**6**), E (**7**), and F (**8**), (relative to internal TMS, at 500 MHz, *J* in Hz). Additional NMR data of the diastereoisomers of **6** and **7** (Diast.) are given as footnotes.

	5 [a]	**6** [b]	**7** [b]	**8** [c]
2-H_2	2.68 ddd (16, 4, 2) 2.26 dd (16, 13)	2.61 ddd (15, 4, 2) [d] 2.50 dd (15, 12)	2.64 ddd (15, 4, 2) [e] 2.50 dd (15, 12)	2.15 dd (14, 3) 1.45 dd (14, 14)
3-H	2.35 m	2.26 m	2.36 m [f]	2.40 m
3-CH_3	1.11 d (6)	1.08d (6) [g]	1.12 d (7) [h]	1.11 d (6)
4-H_2	2.43 m	2.84 ddd (16, 3.2) [i] 2.64 dd (16, 11)	2.95 ddd (16, 4, 2) [j] 2.64 dd (16,10)	2.93 dd (16, 6) 2.15 dd (16, 16)
5-$H_{(2)}$	2.53 dd (18, 8) 2.34 m	7.09 d (8)	7.19 d (8) [k]	6.95 d (8)
6-$H_{(2)}$	2.83 ddd (18, 8, 7) 2.55 dd (18, 7)	6.82 d (8) [l]	6.90 d (8) [m]	6.70 d (8)
7-$H_{(2)}$	–	6.75 s	5.40 d (12) [n] 5.06 d (12)	3.95 d (15) 5.20 d (15)
8-OH	12.00s [o]	9.10 s [o]	9.00 s [o, p]	–
9-H	7.56 m	6.76 d (8)	6.73 d (8)	6.70 d (8)
10-H	7.29 m	7.08 dd (8, 8)	6.99 dd (8, 8)	7.05 dd (8, 8)
11-H	7.56 m	7.05 d (8)	6.37 d (8) [q]	6.95 d (8)
12-H	–	6.71 s [r]	7.33 s [s]	5.85 s

[a] In $CDCl_3$. [b] In $[D_6]$acetone; [c] In CD_3OD. [d] Diast.: 2.75 ddd and 2.20 dd. [e] Diast.: 2.76 ddd and 3.30 dd. [f] Diast.: 2.27 m. [g] Diast.: 1.04 s. [h] Diast.: 1.11 d. [i] Diast.: 2.87 ddd and 2.52 dd. [j] Diast.: 3.00 ddd and 2.70 dd. [k] Diast.: 7.18 d. [l] Diast.: 6.83 d. [m] Diast.: 6.89 d. [n] Diast.: 5.05 d and 5.40 d. [o] Exchangeable with D_2O. [p] Or 6a-OH, only one was observed. [q] Diast.: 6.36 d. [r] Diast.: 6.70. [s] Diast.: 7.25 s.

[*] Priv.-Doz. Dr. J. Rohr, Dipl.-Chem. M. Gerlitz, Dipl.-Ing. G. Udvarnoki
Institut für Organische Chemie der Universität
Tammannstrasse 2, D-37077 Göttingen (Germany)
Telefax: Int code + (551)39-9660
e-mail: jrohr@gwdg.de

[**] This work was supported by the Deutsche Forschungsgemeinschaft and the Fonds der Chemischen Industrie. We thank the Hoechst AG, Frankfurt/Main, Germany, for the wild-type strain FH-S 1114.

Table 2. ^{13}C NMR data and incorporation of [1-^{13}C]acetate (* = enriched carbons): elmycin D (**1**), ochromycinone (**2**), and emycins A (**4**), D (**6**), E (**7**), and F (**8**) (relative to internal TMS, 125.7 MHz, multiplicities from the APT (*a*ttached *p*roton *t*est) experiment, J_{C-C} in Hz from the incorporation experiment with [1,2-$^{13}C_2$]acetate, assignments by APT, C,H-COSY and HMBC.

C atom	**1** [a]	**2** [b]	**4** [b]	**6** [c]	**7** [c]	**8** [d]
1*	198.1 s (53)	199.1 s (54)	66.6 d (44)	200.0 s (51) 199.5 s (51)	201.2 s (50) 200.6 s (50)	109.6 s (49)
2	46.1 t (−)	47.5 t (−)	39.9 t (−)	48.2 t (−) 47.2 t (−)	49.8 t (−) 48.9 t (−)	42.4 t (−)
3*	28.2 d (35)	30.8 d (35)	27.4 d (36)	30.9 d (36) 29.8 d (36)	31.7 d (36) 31.0 d (36)	29.3 d (36)
4	37.5 t (40)	38.4 t (40)	40.4 t (41)	37.5 t (42) 37.4 t (42)	39.0 t (42)	35.0 t (43)
4a*	149.4 s (40)	150.4 s (40)	146.9 s (41)	136.6 s (42) 136.3 s (42)	137.3 s (42) 137.0 s (42)	125.0 s (43)
5	127.4 d (67)	132.9 d (58)	135.5 d (57)	129.2 d (58) 129.1 d (58)	130.8 d (58) 130.6 d (58)	129.5 d (60)
6*	136.8 d (67)	128.9 d (58)	126.4 d (57)	121.9 d (58)	123.0 d (58)	118.7 d (60)
6a	71.7 s (45)	135.8 s (54)	133.7 s (54)	148.6 s (−)	157.0 s (−) 156.9 s (−)	150.7 s (−)
7*	67.6 d (45)	187.5 s (54)	188.1 s (54)	99.1 d (−) 99.2 d (−)	70.9 t (−)	60.7 t (−)
7a	123.1 s (68)	115.4 s (63)	115.1 s (63)	122.3 s (74)	125.7 s (72) 125.6 s (72)	126.3 s (68)
8*	156.9 s (68)	161.9 s (63)	161.7 s (63)	151.5 s (74)	152.1 s (72)	155.7 s (68)
9	113.5 d (57)	119.5 d (62)	123.9 d (58)	115.6 d (60)	114.9 d (59) 114.8 d (59)	116.0 d (58)
10*	127.8 d (57)	135.0 d (62)	136.6 d (58)	130.7 d (60)	129.6 d (59)	128.9 d (58)
11	120.5 d (58)	123.6 d (58)	120.1 d (62)	110.8 d (63)	114.8 d (63)	120.4 d (59)
11a*	140.8 s (58)	136.9 s (58)	134.4 s (62)	148.9 s (63)	143.6 s (63)	144.2 s (59)
12	67.2 d (37)	182.9 s (54)	186.8 s (54)	77.8 d (44) 77.7 d (44)	84.3 d (48)	86.3 d (44)
12a*	37.6 d (37)	133.4 s (54)	132.2 s (54)	127.0 s (44) 126.8 s (44)	125.2 s (48) 124.8 s (48)	126.3 s (44)
12b	128.8 s (53)	136.5 s (54)	143.4 s (44)	127.4 s (51) 127.3 s (51)	132.4 s (50)	138.7 s (49)
13	20.3 q (35)	21.5 q (35)	21.5 q (36)	20.7q (36) 20.1 q (36)	21.6 q (36) 21.0 q (36)	22.1 q (36)
∅ [e]	2.7%	4.5%	4.6%	1.7%	44.5%	3.1%

[a] In [D_6]DMSO. [b] In $CDCl_3$. [c] In [D_6]acetone. [d] In CD_3OD. [e] Average specific incorporation [14].

long-range couplings from the HMBC NMR experiment (HMBC = *H*etero *M*ultiple *B*ond *C*onnectivity Spectroscopy) and the COLOC NMR experiment (COLOC = *Co*rrelation Spectroscopy via *Lo*ng-Range Couplings) (Fig. 2). The absolute configurations of the structures of **6**–**8** were determined by X-ray analyses.[8, 9]

The molecular frameworks of the emycins D (**6**), E (**7**), and F (**8**) are unprecedented; thus, we attempted to elucidate their

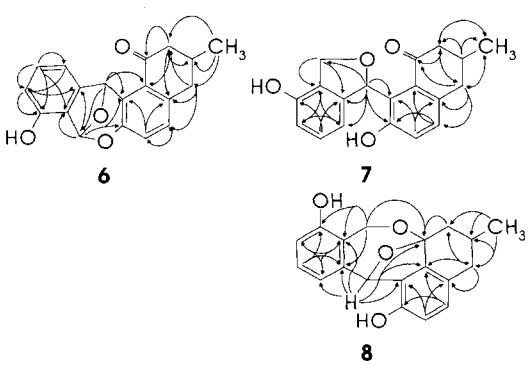

Fig. 2. Observed $^nJ_{C-H}$ long-range couplings of emycins D (**6**), E (**7**), and F (**8**) (HMBC and COLOC spectra, respectively).

generation through biosynthetic investigations. In all three novel structures, rings A, B, and D of the benz[*a*]anthracene framework of the angucyclinones[5] (see emycin A (**4**)) turned out to be largely unchanged in comparison with the wild-type strain products, and thus a biosynthetic relationship to the wild-type strain products seemed evident. Labeling experiments using [1-^{13}C]-, [1,2-$^{13}C_2$]-, and [1-^{13}C,$^{18}O_2$]acetate as well as a fermentation carried out under an ^{18}O-enriched atmosphere revealed the biosynthetic sources of all carbon and oxygen atoms of the major products of mutant strain *S. cellulosae* ssp. *griseoincarnatus* (1114-2). For the typical angucyclinones **1**, **2**, and **4** the expected acetate incorporation pattern was found, namely construction from a single polyketide chain assembled from ten acetate units starting at C-13 and ending at C-2 (under decarboxylation of the last acetate unit).[10] There were also no unexpected results with respect to the biogenetic origin of the oxygen atoms, that is there was no evidence for prearomatic deoxygenation steps as were found recently for some multicyclic aromatic polyketides.[10d, 10e, 11] In the biosyntheses of the novel emycins D (**6**), E (**7**), and F (**8**), the fourth acetate unit is cleaved, since carbons C-6a and C-7 appear as enriched singlets (instead of a coupling pair) in the ^{13}C NMR spectrum after the feeding experiment with the doubly labeled [1,2-$^{13}C_2$]acetate. Thus an oxidative carbon–carbon split between C-6a and C-7 must have occurred. This was supported by the fermentation

Table 3. ^{13}C NMR upfield shifts ($\Delta\delta$) after the incorporation experiments with ^{18}O-labeled precursors: elmycin D (**1**), ochromycinone (**2**), emycins A (**4**), D (**6**), E (**7**), and F (**8**); **A**: incorporation of [1-^{13}C,$^{18}O_2$]acetate (99% ^{13}C, 55% ^{18}O); **B**: fermentation under an $^{18}O_2$ (50% ^{18}O)-enriched atmosphere; (% relative ^{18}O-enrichment [a]).

C atom	1		2		4		6		7		8	
	A	B	A	B	A	B	A	B	A	B	A	B
1	0.04 (35)	–	0.04 (24)	–	0.01 (40)	–	0.05 (30)	–	–	–	0.01 (22	0.03 (11)
6a	–	0.03 (8)	–	–	–	–	–	0.02 (9)	–	0.01 (32)	–	0.01 (19)
7	0.02 (26)	–	0.05 (18)	–	0.03 (22)	–	–	0.02 (8)	–	n.o.	n.o.	–
8	0.01 (38)	–	0.02 (23)	–	0.02 (13)	–	0.02 (34)	–	0.01 (10)	–	0.02	– (45)
12	–	0.02 (17)	–	n.o.	–	n.o.	–	0.03 (9)	–	n.o.	–	0.01 (24)

[a] % Enrichment = ($I^{13}C$-^{18}O/[$I^{13}C$-^{18}O + $I^{13}C$-^{16}O + $I^{13}C$-^{18}O]) × 100%; n.o. = not observed.

experiment in an $^{18}O_2$-enriched atmosphere, in which 6a-O was labeled in all three compounds **6**–**8**, proving its origin from atmospheric oxygen. The results are summarized in Figure 3 (only elmycin D (**1**) is shown as an example of a common angucyclinone) as well as in Tables 2 and 3.

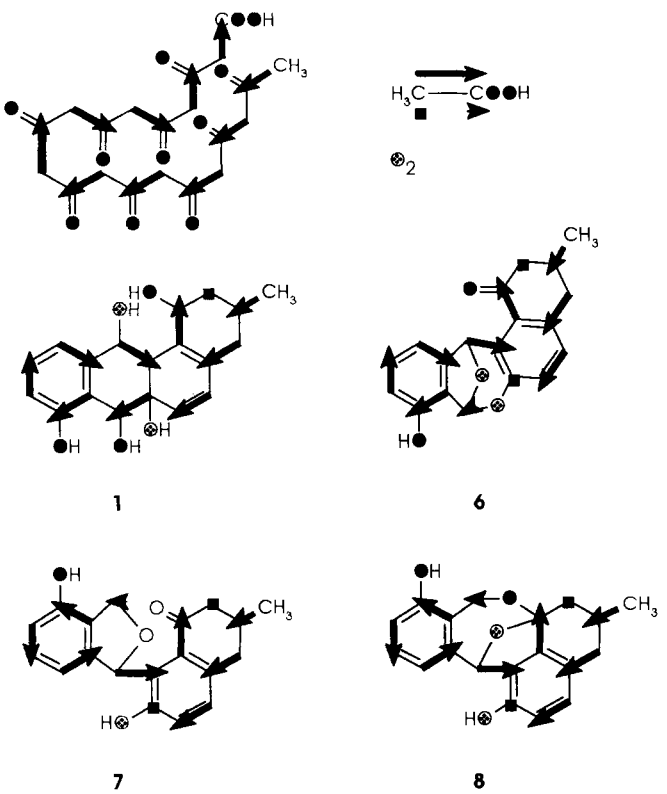

Fig. 3. Results of the incorporation experiments with ^{13}C- and ^{18}O-labeled precursors.

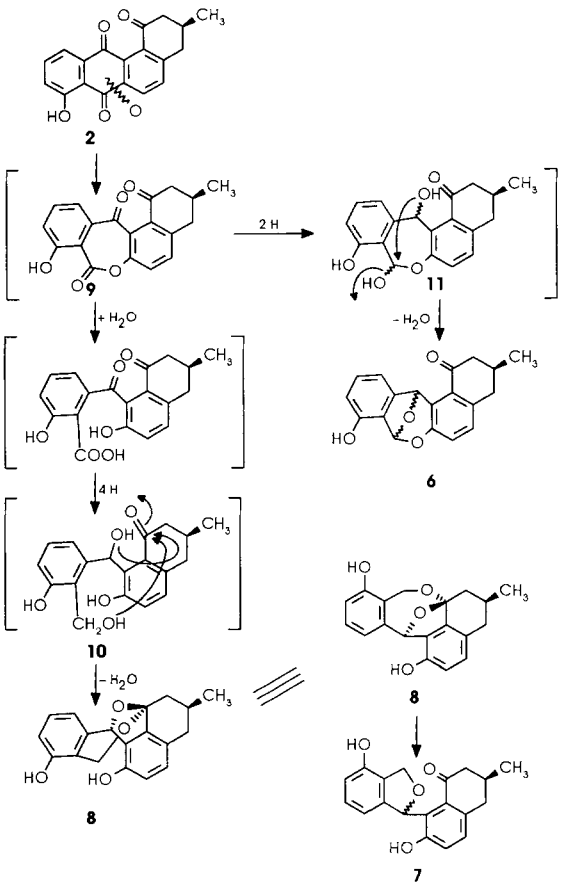

Scheme 1. Hypothetical biosynthesis cascade for the generation of the unusual emycins D (**6**), E (**7**), and F (**8**).

A hypothetical biosynthesis scheme (Scheme 1) was deduced from the results of the biosynthetic investigations that explains the generation of the novel molecular frameworks of emycins D–F (**6**–**8**) in a plausible way: starting with an enzymatic Baeyer–Villiger oxidation on a quinone precursor,[11a] presumably with ochromycinone (**2**), which results in the lactone intermediate **9**, and continues through the opening of the lactone **9** and the subsequent reduction to give the intermediate **10**, an intramolecular ketalization into emycin F (**8**) takes place as a key biosynthetic step. This finally rearranges (under participation of non-enzymatic steps?) into the thermodynamically more stable emycin E (**7**). The intramolecular ketalization of the dialcohol intermediate **10** is possible because of the free rotation about the C-12/C-12a axis after cleavage of the lactone and the reduction. This step must be catalyzed by an enzyme, since **8** appears as a sole diastereoisomer. Emycin D (**6**) is probably a shunt product, whose formation may start at lactone **9**. Both carbonyl carbons C-7 and C-12 of **9** have to be reduced into the hemiacetal and secondary alcohol, respectively, to form intermediate **11** which can be intramolecularly cyclized into the

acetal emycin D (**6**). That **6** emerges as a diastereomeric mixture (with C-7 and C-12 in *R*, or both stereocenters in *S* configuration;[8] *R,R* : *S,S* = 1:1) is unexpected and intriguing, since this has to be caused by an unspecific oxidoreductase (dehydrogenase) reducing the C-12 keto function into a stereochemically inconsistently configurated alcohol (Scheme 1). We are currently investigating the formation of **6**. The last step of the biosynthetic cascade of the emycins is a novel type of rearrangement, initiated by the protonation of 7-O, which eases the cleavage of the C-1/7-O bond. The resulting carbenium ion with the positive charge at C-1 in **12** induces the second necessary scission between C-12 and its adjacent oxygen atom; in this way the C-1 keto function is regenerated and a more stable carbenium ion with the positive charge at C-12 in **13** is formed (Scheme 2). The

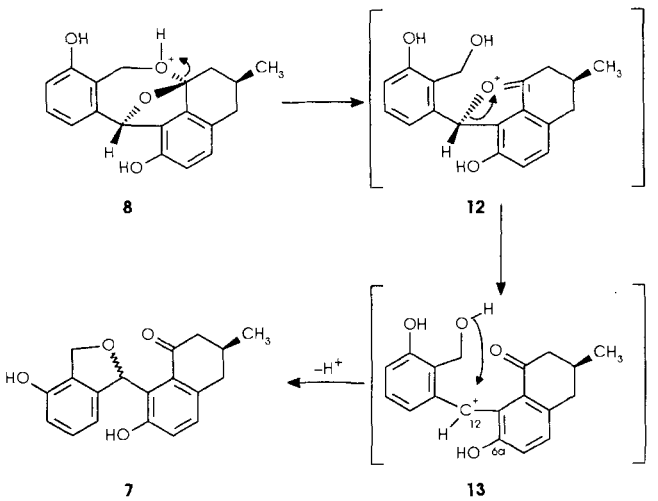

Scheme 2. Rearrangement of emycin F (**8**) into emycin E (**7**).

C atom, which carries the positive charge in **13**, lies in the benzylic position to both neighboring arene units; in this arrangement the 6-OH group in particular contributes a stabilizing neighboring group effect. Therefore the carbenium ion at C-12 can be intramolecularly attacked on both sides by the oxygen atom of the primary alcohol group at C-7 with the formation of the dihydrofuran moiety, leading to emycin E (**7**) as a diastereomeric mixture (Scheme 2). The quantitative rearrangement of emycin F (**8**) into emycin E (**7**) could also be performed in a model reaction, namely stirring **8** at pH 1 for 24 h. Since such a low pH neither occurs during the fermentation of *S. cellulosae* ssp. *griseoincarnatus* (1114-2) nor during the workup procedure, this rearrangement has to be caused by a similar acidic milieu inside the cells, or under the participation of an enzyme. Within the rearrangement of **8** into **7** a hydrate structure (not shown in Scheme 2) at C-1 probably occurs as an intermediate, since the ^{18}O label (from the fermentation in $^{18}O_2$) disappears during the rearrangement, or is introduced, if the reaction is carried out in $H_2{}^{18}O$.

The work described here shows that genetic modifications can cause a significant change in the secondary metabolite spectrum of streptomycetes and lead to the production of considerable quantities of novel compounds (see Fig. 1). Furthermore, oxidoreductases play a significant role in these reactions. Nevertheless, it is not certain whether the mutation effected one or more oxidoreductases directly or whether it caused a regulatory change through which, for example, ochromycinone **2** is produced in higher yields and could thus serve as a substrate for the oxygenase responsible for the Baeyer–Villiger oxidation. The latter alternative is more likely, since we also found the novel emycins D, E, and F in the wild-type strain, but only in traces ($< 1\ mg\ L^{-1}$). Interesting structure modifications of angucyclinones induced by oxidating enzymes were also reported recently by S. Gould et al.[12]

Experimental Procedure

Bacterial strain, cultivation, and isolation of the products: Mutant strain *S. cellulosae* ssp. *griseoincarnatus* (1114-2) was prepared by NTG-mutation [3]. Its cultivation as well as the isolation of the products will be described elsewhere [8].

Instruments/NMR methods: see refs. [2b,3,11a].

Labeled compounds and incorporation experiments: [1-^{13}C]- and [1,2-$^{13}C_2$]acetate (each 99% ^{13}C) was obtained from CIL (Cambridge Isotope Laboratories, Cambridge, MA, USA), $^{18}O_2$ (98% ^{18}O) from Isotec Inc. (Miamisburg, OH, USA), [1-^{13}C,$^{18}O_2$]acetate was synthesized as described before [13]. The labeled acetates were fed in five equal portions (1 g each, H_2O solutions) to a growing culture of strain 1114-2, 45, 53, 61, 69, and 77 h after inoculation of the fermentor. To avoid O-exchange with the solvent, the [1-^{13}C,$^{18}O_2$]acetate was always dissolved immediately before feeding. The $^{18}O_2$ was diluted with $^{16}O_2$ to 50% in our closed system apparatus [13a], which was connected here to a 1 L-fermentor, from 45 h after inoculation to the end of the fermentation (96 h).

Emycin C (**5**): $C_{19}H_{16}O_4$ (308.33); $[\alpha]_D^{20} = +108.1$ ($c = 0.007$, MeOH); EI-MS (70 eV): *m/z* (%) 308 (35, M^+, HR calcd. for $C_{19}H_{16}O_4$ and found: 308.1048), 266 (60), 94 (100); ^{1}H NMR: see Table 1; ^{13}C NMR (125.7 MHz, $CDCl_3$): $\delta = 194.6$ (s, C-1), 46.0 (t, C-2), 29.5 (d, C-3), 39.8 (t, C-4), 129.0 (s, C-4a), 29.1 (t, C-5), 19.0 (t, C-6), 141.6 (s, C-6a), 188.7 (s, C-7), 114.8 (s, C-7a), 161.0 (s, C-8), 119.3 (d, C-9*), 136.2 (d, C-10*), 123.5 (d, C-11*), 133.0 (s, C-11a), 182.0 (s, C-12), 141.9 (s, C-12a), 130.5 (C-12b), 21.0 (q, C-13); * assignments are interchangeable.

Emycin D (**6**): $C_{19}H_{16}O_4$ (308.33); $[\alpha]_D^{20} = -34.9$ ($c = 0.072$, $CHCl_3$); EI-MS (70 eV): *m/z* (%) 308 (60, M^+, HR calcd. for $C_{19}H_{16}O_4$ and found 308.1049), 279 (30), 239 (100); ^{1}H and ^{13}C NMR: see Tables 1 and 2, respectively.

Emycin E (**7**): $C_{19}H_{18}O_4$ (310.35); $[\alpha]_D^{20} = +49.0$ ($c = 0.071$, MeOH); EI-MS (70 eV): *m/z* (%) 310 (100, M^+, HR calcd. for $C_{19}H_{18}O_4$ and found: 310.1207), 295 (85), 239 (70); ^{1}H and ^{13}C NMR: see Tables 1 and 2, respectively.

Emycin F (**8**): $C_{19}H_{18}O_4$ (310.35); $[\alpha]_D^{20} = +209.9$ ($c = 0.016$, MeOH); EI-MS (70 eV): *m/z* (%) 310 (100, M^+, HR calcd. for $C_{19}H_{18}O_4$ and found 310.1205), 295 (85), 239 (30); ^{1}H and ^{13}C NMR: see Tables 1 and 2, respectively.

Received: March 24, 1995 [Z 7831 IE]
German version: *Angew. Chem.* **1995**, *107*, 1757–1761

Keywords: antibiotics · biosynthesis · oxidoreductases · polyketides · rearrangements

[1] a) H. C. Neu. *Science* **1992**, *257*, 1064–1073, and references therein; b) J. Travis, E. Culotta, R. Nowak, S. Kingman, R. Stone, *ibid.* **1994**, *264*, 360–367; c) W.-D. Busse, *Nachr. Chem. Tech. Lab.* **1994**, *42*, 1231.

[2] a) See also the highlight: J. Rohr, *Angew. Chem.* **1995**, *107*, 963-967; *Angew. Chem. Int. Ed. Engl.* **1995**, *34*, 881–885, and references therein; b) H. Decker, S. Haag, G. Udvarnoki, J. Rohr, *Angew. Chem.* **1995**, *107*, 1214–1217; *Angew. Chem. Int. Ed. Engl.* **1995**, *34*, 1107–1110.

[3] a) J. Rohr, M. Schönewolf, G. Udvarnoki, K. Eckardt, G. Schumann, C. Wagner, J. M. Beale, S. D. Sorey, *J. Org. Chem.* **1993**, *58*, 2547–2551, and references therein;

[4] The bacterial strain was classified by Dr. M. Wink, Hoechst AG, Frankfurt, Germany [8].

[5] J. Rohr, R. Thiericke, *Nat. Prod. Rep.* **1992**, *9*, 103–137, and references herein.

[6] a) S. Dobreff, Ph.D. thesis, Universität Göttingen, **1989**; b) S. Dobreff, A. Zecck, M. Wink, S. Grabley, unpublished.

[7] a) D. E. Cane, W. D. Celmer, J. W. Westley, *J. Am. Chem. Soc.* **1983**, *105*, 3594–3600; b) See also the highlight: U. Koert, *Angew. Chem.* **1995**, *107*, 326–328; *Angew. Chem. Int. Ed. Engl.* **1995**, *34*, 298–300, and references therein; c) B. Samuelsson, *J. Am. Chem. Soc.* **1965**, *87*, 3011–3013.

[8] a) J. Rohr, M. Gerlitz, G. Udvarnoki, G. Remberg, J. Machinek, C. Zolke, J. Wink, unpublished; b) M. Walker, E. Pohl, G. M. Sheldrick, M. Gerlitz, J. Rohr, unpublished.

[9] The diastereoisomers behave like enantiomers because of their nearly mirror imaged 3D structure. Even the crystallization of the natural products as well as of the *o*-bromobenzoate of **6** gave no separation, but cocrystals of both diastereomers (1:1) [8b].

[10] a) N. Imamura, K. Kakinuma, N. Ikekawa, H. Tanaka, S. Ōmura, *J. Antibiot.* **1982**, *35*, 602–608; b) J. Rohr, J. M. Beale, H. G. Floss, *ibid.* **1989**, *42*, 1151–1157; c) S. J. Gould, K. A. Halley, *J. Am. Chem. Soc.* **1991**, *113*, 5092–5093; d) S. J. Gould, X.-C. Cheng, C. Melville, *ibid.* **1994**, *116*, 1800–1804; e) S. Weber, C. Zolke, J. Rohr, J. M. Beale, *J. Org. Chem.* **1994**, *59*, 4211–4214.
[11] a) H. Bockholt, G. Udvarnoki, J. Rohr, U. Mocek, J. M. Beale, H. G. Floss, *J. Org. Chem.* **1994**, *59*, 2064–2069, and references therein; b) S. J. Gould, X.-C. Cheng, K. A. Halley, *J. Am. Chem. Soc.* **1992**, *114*, 10066–10068.
[12] S. J. Gould, X. C. Cheng, *J. Org. Chem.* **1994**, *59*, 400–405.
[13] a) G. Udvarnoki, T. Henkel, R. Machinek, J. Rohr, *J. Org. Chem.* **1992**, *57*, 1274–1276; b) P. D. Boyer, O. J. Koeppe, W. W. Luchsinger, *J. Am. Chem. Soc.* **1956**, *78*, 356–357.
[14] A. I. Scott, C. A. Townsend, K. Okada, M. Kajiwara, R. J. Cushley, P. J. Whitman, *J. Am. Chem. Soc.* **1974**, *96*, 8069–8080.

An aqueous solution of per-2,3-anhydro-(2*S*)-β-cyclodextrin (**2**)[5] was refluxed for five days (Scheme 2). The progress of the reaction was monitored by thin-layer chromatography (double elution on silica gel plates (MeOAc/*n*PrOH/H_2O 8/7/6)). The starting material disappeared in favor of only one major

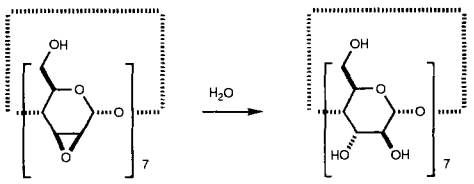

2 **3**

Scheme 2. The preparation of **3** from **2**.

β-Cycloaltrin: A Cyclooligosaccharide Consisting of Seven α(1 → 4)-Linked Altropyranoses**

Kahee Fujita,* Hideaki Shimada, Kazuko Ohta, Yasuyoshi Nogami, Kyoko Nasu, and Toshitaka Koga

Cyclodextrins, for example β-cyclodextrin (**1**) (Scheme 1), are cyclic oligosaccharides made up of 1,4-linked D-glucopyranose units in $^4C_1$ chair conformation. They can include a wide variety of substrates in their hydrophobic cavities. The formation of inclusion complexes and reactions constrained to the cavities have been studied extensively.[1] Several cyclooligosaccharides uniformly composed of sugars other than glucose have been reported such as the inulin-derived α-cyclofructin,[2] α- and β-cyclomannins, synthesized chemically,[3] and α-cyclogalactin, which so far has been characterized by molecular modeling only.[4] In this paper, we report the preparation of a novel cyclooligosaccharide constituted of seven α(1 → 4)-linked altropyranoses, which we designate, in accord with a recent proposal for simplified nomenclature,[4] as β-cycloaltrin (**3**) (Scheme 1).

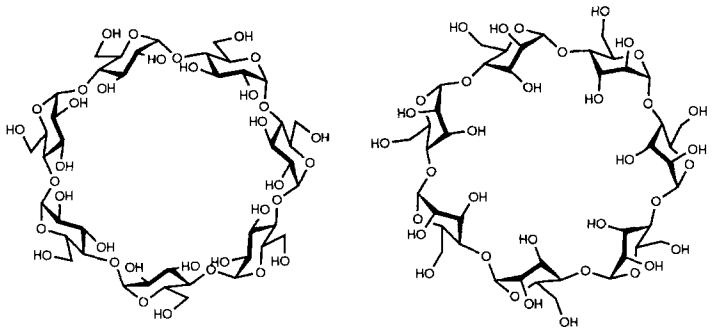

1 **3**

Scheme 1. Structures of **1** and **3** ($^4C_1$ conformation).

product with $R_f = 0.19$, which has distinctly different mobility from that of **1** and **2** ($R_f = 0.32$ and 0.84, respectively). Reversed-phase column chromatography gave the novel cyclooligosaccharide **3** in 72.9% yield. The FAB mass spectrum showed **3** to have the same molecular weight as **1**; however, the NMR data (Fig. 1) are clearly different. The assignment of the

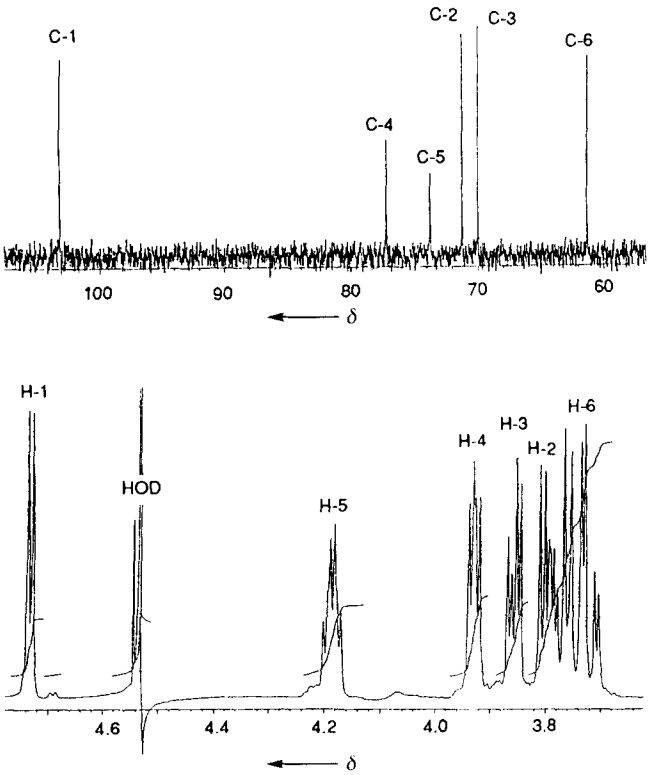

Fig. 1. Top: ^{13}C NMR spectrum of **3** (125 MHz, D_2O, 40 °C, CH_3CN). Bottom: ^1H NMR spectrum of **3** (500 MHz, D_2O, 40 °C, CH_3CN).

signals of **3** relied on ^1H, ^1H- and $^1H,^{13}C$-COSY NMR spectra, and indicates that **3** consists of altropyranoses. The coupling constants (e.g. J(H-1, H-2) = 4.5 Hz) indicate that **3** is a mixture of at least two rapidly interconverting[6] conformations, $^1C_4$ and $^4C_1$ chair conformations (see Scheme 1). Alternatively, **3** assumes a single fixed conformation, for example, in which the altropyranose units have a twist conformation, since the vicinal coupling constant J(H-1, H-2) is intermediate between that of

[*] Prof. K. Fujita, H. Shimada, K. Ohta
Faculty of Pharmaceutical Sciences, Nagasaki University
Bunkyo-machi, Nagasaki 852 (Japan)
Telefax: Int. code + (958)46-5736
Prof. Y. Nogami, K. Nasu, Prof. T. Koga
Daiichi College of Pharmaceutical Sciences (Japan)

[**] We thank Japan Maize Products (Nihon Shokuhin Kako) for a generous gift of β-cyclodextrin.

α-methylaltropyranoside (2.0 Hz; $^4C_1$ chair conformation) and that of the α-altropyranose unit in $2^A(S),3^A(R)$-β-cyclodextrin (6.6 Hz;[7] mainly $^1C_4$ chair conformation).[8]

The major product of acidic hydrolysis of **3** was a mixture of altrose and altrosan (1,6-anhydroaltropyranose), which is produced by acid treatment of altrose.[7] Further studies on the conformation, the inclusion properties, and the chemical modification of **3** are currently in progress.

Experimental Procedure

3: A solution of 100 mg of **2**, prepared according to ref. [5b], in water (50 mL) was refluxed for five days [9]. The mixture was concentrated in vacuo and chromatographed on a reversed-phase column (Merck Lobar column RP18, size B) with water to give **3** (82.0 mg, 72.9%), m.p. 227 °C (decomp.); $[\alpha]_D^{16} = +63.4$ ($c = 0.41$ in H_2O); ^{1}H NMR (500 MHz, D_2O, 40 °C, CH_3CN): $\delta = 4.73$ (d, ^3J(H,H) = 4.5 Hz, 7H; H-1), 4.19 (m, 7H; H-5), 3.93 (dd, ^3J(H,H) = 3.7, 5.8 Hz, 7H; H-4), 3.86 (dd, ^3J(H,H) = 3.7, 7.8 Hz, 7H; H-3), 3.80 (dd, ^3J(H,H) = 4.5, 7.8 Hz, 7H; H-2), 3.77 (dd, ^3J(H,H) = 6.3, 12.5 Hz, 7H; H-6), 3.72 (dd, ^3J(H,H) = 3.6, 12.5 Hz, 7H; H-6); ^{13}C NMR (125 MHz, D_2O, 40 °C, CH_3CN): $\delta = 103.1$ (C-1), 77.2 (C-4), 73.7 (C-5), 71.2 (C-2), 70.0 (C-3), 61.3 (C-6); FAB-MS: *m/z*: 1135 $[M + H^+]$, 1157 $[M + Na^+]$.

Received: December 13, 1994
Revised version: April 27, 1995 [Z 7546 IE]
German version: *Angew. Chem.* **1995**, *107*, 1783–1784

Keywords: altrose · β-cycloaltrin · cyclodextrins · oligosaccharides

[1] G. Wenz, *Angew. Chem.* **1994**, *106*, 851–870; *Angew. Chem. Int. Ed. Engl.* **1994**, *33*, 803–822, and references therein.
[2] M. Sawada, T. Tanaka, Y. Takai, T. Hanafusa, M. Kawamura, T. Uchiyama, *Carbohydr. Res.* **1991**, *217*, 7–17.
[3] M. Mori, Y. Ito, T. Ogawa, *Tetrahedron Lett.* **1989**, *30*, 1273–1276; M. Mori, Y. Ito, J. Uzawa, T. Ogawa, *ibid.* **1990**, *31*, 3191–3194.
[4] F. W. Lichtenthaler, S. Immel, *Tetrahedron: Asymmetry* **1994**, *5*, 2045–2060.
[5] a) A. W. Coleman, P. Zhang, C.-C. Ling, J. Mahuteau, H. Parrot-Lopez, M. Miocque, *Supramol. Chem.* **1992**, *1*, 11–14; b) A. R. Kahn, L. Barton, V. T. D'Souza, *J. Chem. Soc. Chem. Commun.* **1992**, 1112–1114.
[6] The conformational energy of $^1C_4$ conformation of α-altropyranose was reported to be close to that of the $^4C_1$ conformation; S. J. Angyal, *Angew. Chem.* **1969**, *81*, 172–182; *Angew. Chem. Int. Ed. Engl.* **1969**, *8*, 157–166; S. J. Angyal, V. A. Pickles, *Aust. J. Chem.* **1972**, *25*, 1695–1710.
[7] K. Fujita, K. Ohta, Y. Ikegami, H. Shimada, T. Tahara, Y. Nogami, T. Koga, K. Saito, T. Nakajima, *Tetrahedron Lett.* **1994**, *35*, 9577–9580.
[8] For a pyranoid $^1C_4$ conformation $^3J_{1,2}$ should be around 8 Hz. Therefore, the pyranose rings in **3** may be closer to a $^4C_1$ rather than the $^1C_4$ form.
[9] The purity of **2** is very important for the reaction; contamination by even a small amount of benzenesulfonates, which are intermediates in the epoxidation leading to **2**, is very harmful for the present reaction, since **3** is hydrolyzed by sulfonic acid produced during the reaction.

Novel Biological Copper Proteins through Anion Addition to the Mutant Met121Gly of *Pseudomonas aeruginosa* Azurin**

Momcilo Vidakovic and Juris P. Germanas*

Blue copper proteins are widely distributed in nature, where they function as electron-transfer mediators in important biochemical processes such as photosynthesis and metabolism.[1] The unique spectrochemical properties of these proteins have long attracted the attention of bioinorganic chemists.[2] For proteins in the oxidized state [copper(II)], these characteristics include an intense absorption band centered around 600 nm ($\varepsilon = 2000-6000\ M^{-1}cm^{-1}$), an EPR spectrum with an unusually small copper hyperfine splitting ($I = 3/2$, $A_{\parallel} \leq 70 \times 10^{-4}\ cm^{-1}$), and anomalously high redox potentials for the Cu^{II}/Cu^{I} couple [180–680 mV versus the normal hydrogen electrode (NHE)]. Crystallographic analysis has revealed that the copper(II) ion in these proteins is coordinated to two histidine residues and one cysteine residue in an approximately trigonal planar geometry.[3] Besides these three strong interactions, weaker axial interactions between the copper ion and other ligands are generally present. For example, in azurin and plastocyanin, the thioether sulfur atom of a methionine residue interacts with the copper center, while in stellacyanin, a glutamine carboxamide oxygen is thought to coordinate to the metal.[4] The nature of the axial interaction is believed to significantly influence the spectrochemical characteristics of metal centers of the blue copper proteins.[5] To probe the effect of various axial ligands on the spectroscopic and electrochemical properties of these copper sites, we have prepared by site-directed mutagenesis a variant of *Pseudomonas aeruginosa* azurin, Met121Gly,[6] in which the weakly coordinating ($R_{S-Cu} = 3.1$ Å) thioether side chain of Met121 is replaced by a hydrogen atom. This creates a cavity that can be occupied by exogenous ligands.[7] In this communication we report the preparation and characterization of unique biological copper species, obtained through addition of the anions N_3^-, SCN^-, and CN^- to Met121Gly azurin. Their spectroscopic properties are distinct from those of any known naturally occurring copper proteins.[8]

The UV-Vis spectra of blue copper proteins display a characteristic absorption band at about 600 nm, due to a $S_{cys}(\pi)$ to Cu^{II} charge transfer (LMCT) transition, along with another band at about 450 nm from a S_{cys} (pseudo-σ) to Cu^{II} LMCT.[9] The relative intensities of the two bands vary, depending on the protein. A correlation between the relative intensity of the band at 450 nm and the axial displacement of the copper atom from the plane formed by the His_2Cys ligand set has been reported for a number of blue copper proteins.[10] Upon titration of Met121Gly azurin with azide, thiocyanate, or cyanide, the intense absorption band at 614 nm of the uncomplexed protein disappeared, and a new, weaker band at approximately 420 nm arose, along with a feature at about 590 nm (Table 1).[11] The wavelengths of the transitions at 420 nm were dependent on the specific anion, indicating that the anion ligated directly to the

[*] Prof. Juris P. Germanas, Momcilo Vidakovic
Department of Chemistry
University of Houston
Houston, TX 77204-5641 (USA)
Telefax: Int. code + 713-743-2709
e-mail: germanas@uh-edu

[**] This work was supported by the University of Houston and the American Cyanamid (Faculty Research Award to J. P. G.). The authors express their gratitude to Prof. R. S. Czernuszewicz and G. Fraczkiewicz (University of Houston) for the resonance Raman spectra, and Mr. V. Kurchev for assistance in acquiring the EPR spectra.

Table 1. Spectroscopic and electrochemical properties of *P. aeruginosa* Met121Gly (M121G) azurin and its anion adducts

Protein/Anion	$\lambda_{max}(\varepsilon)$ [a] [nm ($M^{-1}cm^{-1}$)]	λ_{max} (ε) [a] [nm ($M^{-1}cm^{-1}$)]	K_a [b] [M^{-1}]	$g_{\parallel}$ [c]	$A_{\parallel}$ [c] (10^{-4} cm^{-1})	E^{w} [d] (mV vs. NHE)	$\Delta\nu$ [e] (cm^{-1})
Wild type azurin	628 (5300)	–	–	2.259	58 [f]	293	408
M121G azurin	614 (3500)	456 (560)	–	2.270	53 [f]	261	408
M121G + N_3^-	590 (950)	420 (2000)	30	2.247	101	239	358
M121G + SCN	582 (1100)	416 (2020)	30	2.205	89	234	353
M121G + CN	580 (950)	432 (1990)	1800	2.216	106	nd [g]	338

[a] Optical absorption maxima and extinction coefficients of S_{cys}-Cu CT bands centered around 600 and 400 nm. [b] Protein–ligand association constant at 23 °C. [c] X-band EPR parameters ($g_z = g_{\parallel}$; $A_z = A_{\parallel}$ for splitting due to copper nuclear spin, $I = 3/2$). [d] Midpoint redox potential at 23 °C, 0.1 M NaCl, 0.3 M ligand, 20 mM Tris · HCl, pH 8.0. [e] Frequency of most intense peak of resonance Raman spectrum. [f] Determined by computer simulation of spectrum. [g] Not determined.

copper(II) ion. From the greater intensities of the 420 nm bands relative to those of the 590 nm bands in the spectra of the protein–ligand adducts, we inferred a larger separation between the copper(II) ion and the plane of the protein's His_2Cys ligand set than in the uncomplexed form.[10] The formation constants of the 1:1 complexes, determined spectrophotometrically, revealed the cyanide adduct to be substantially more stable than the azide or thiocyanate adducts (Table 1).

Resonance Raman spectra of Met121Gly azurin and its anion adducts were recorded with excitation wavelengths of 568 nm (without exogenous ligand) or 413 nm (with exogenous ligand). The set of four strong bands in the spectrum of the uncomplexed protein[12] was replaced in the spectrum of the anion adducts by a pair of peaks at lower energy (Fig. 1). Since the most intense band in the resonance Raman spectra of blue copper proteins results from a predominantly Cu–S stretching vibrational mode,[12] the shift of the intense band in the spectra of the anion adducts to lower wavenumber indicated that the anion complexes possessed weaker, and consequently longer, Cu–S bonds than the uncomplexed protein (Table 1). The appearance of bands attributable to bond-stretching modes of azide and thiocyanate in the spectra of the specific adducts further confirmed that these anions coordinated directly to the copper(II) ion of Met121Gly azurin (Fig. 1).

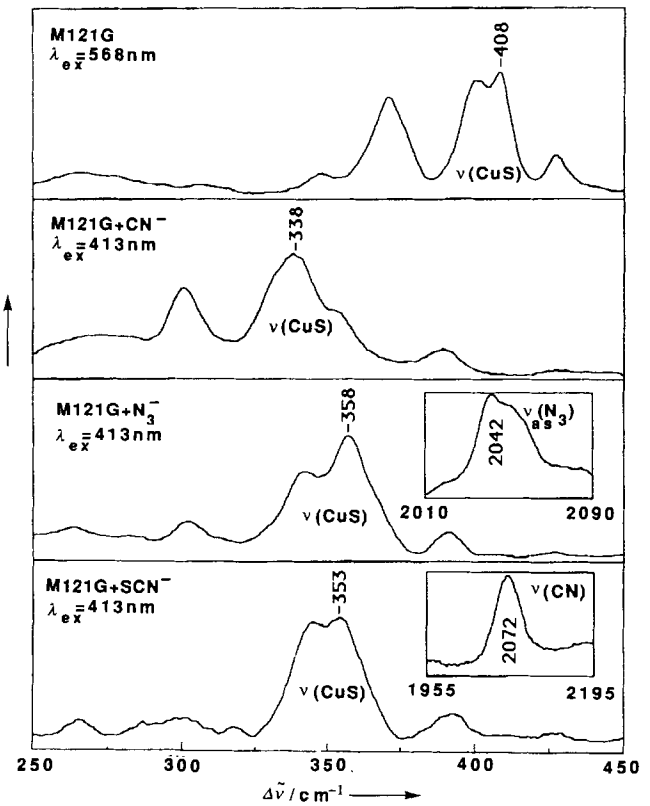

Fig. 1. Resonance Raman spectra of (from top) Met121Gly azurin; Met121Gly azurin + cyanide; Met121Gly azurin + azide; Met121Gly azurin + thiocyanate. Excitation wavelengths λ_{ex} for each protein are given. I = intensity

The EPR data of spectra of the 1:1 complexes also reflected a change in coordination environment at the copper site in the protein–anion adducts. The copper(II) centers of the adducts displayed EPR spectra with axial symmetry, in contrast to the uncomplexed protein, which displayed an EPR spectrum with rhombic symmetry (Fig. 2). Strikingly, the values for the copper

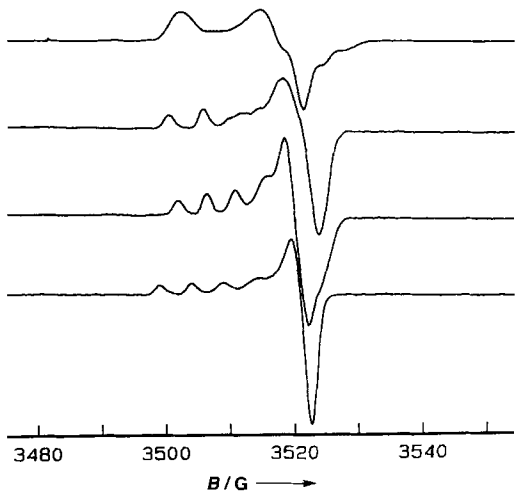

Fig. 2. X-band EPR spectra at 77 K of the Met121Gly mutant of *P. aeruginosa* azurin and its adducts with anions. The spectra are (from top) Met121Gly azurin; Met121Gly azurin + cyanide; Met121Gly azurin + thiocyanate, and Met121Gly azurin + azide.

hyperfine coupling constant ($A_{\parallel}$) of the complexes (Table 1) were well above the range of values observed for typical blue copper sites ($\leq 70 \times 10^{-4}$ cm^{-1}).[2] Furthermore the $A_{\parallel}$ values for the adducts were considerably smaller than those seen for common tetragonal, or type 2, copper compounds ($160-220 \times 10^{-4}$ cm^{-1}).[2] Plots of $g_{\parallel}$ versus $A_{\parallel}$ for copper complexes often produce linear correlations for compounds of similar structural or electronic origin.[13] When the values of $g_{\parallel}$ for the Met121Gly–anion adducts were plotted against the values of $A_{\parallel}$, a linear correlation was obtained ($R = 0.95$), which was distinct from the correlations seen for blue or type 2 (tetragonal) copper centers. Differences in the precise values of the adduct's EPR parameters reflected small structural variations in the ligand environment of the copper atom of each adduct.[13]

The redox potentials of Met121Gly azurin and its anion complexes were determined by potentiometric titration. Binding of thiocyanate or azide to the copper(II) ion of the protein pro-

duced species with lower redox potentials than the free protein (Table 1). The midpoint potential of the cyanide adduct could not be determined by this method because of competitive oxidation of cyanide. The lower potentials of the two anion adducts relative to Met121Gly azurin could be rationalized by inferring electrostatic stabilization of the higher copper oxidation state by the negatively charged ligands.

The spectroscopic properties of the Met121Gly azurin–anion adducts indicate the presence of a novel form of protein-bound copper having spectroscopic properties distinct from those of either blue or type 2 copper proteins. According to a computer-generated model of the Met121Gly active site,[14] coordination of external ligands to the copper(II) ion in the space previously occupied by the Met121 side chain should result in a distorted tetrahedral environment for the metal center. Binding of anionic species to the copper(II) ion should also result in lengthening of the other metal–ligand bonds. Absorption and resonance Raman spectra of the Met121Gly azurin–anion complexes reflect substantial axial displacement of the copper atom from the plane of the His_2Cys ligand set along with elongation of the S_{cys}–Cu bond.[10, 12] The values for the parallel hyperfine splittings in the EPR spectra of the 1:1 complexes are consistent with diminished covalency in the S_{cys}–Cu bond relative to the uncomplexed form, resulting from S–Cu bond lengthening.[15] In natural blue copper proteins with distorted tetrahedral metal centers and short axial interactions with neutral ligating atoms, absorption spectra display intense bands at about 450 nm, and EPR spectra suggest a rhombic g tensor.[2] Absorption spectra with λ_{max} at about 420 nm and EPR spectra with axial symmetry for the Met121Gly azurin–anion adducts signify a unique electronic structure of the copper centers in these proteins as a result of the anionic character of the axial ligands. Further support for the proposed model of the Met121Gly azurin–anion adduct copper centers comes from properties of structurally characterized, pseudo-tetrahedral copper complexes, which display spectroscopic characteristics remarkably similar to those of the adducts reported here.[16]

A variety of unusual copper proteins can be easily created through addition of anions to the azurin mutant Met121Gly. The ability to create ligand-accessible metal centers in coordinatively saturated metalloproteins by directed mutagenesis holds promise for the preparation of metalloproteins with selective ion-sensing capabilities. Further studies aimed at detailed characterization of the electronic and geometric structure, as well as the electron-transfer properties of the active sites of these unusual proteins are in progress.

Received: January 24, 1995 [Z 7656 IE]
German version: *Angew. Chem.* **1995**, *107*, 1773–1776

Keywords: copper compounds · EPR spectroscopy · metalloproteins · mutagenesis · Raman spectroscopy

[1] a) E. T. Adam, *Adv. Protein Chem.* **1991**, *42*, 145–197; b) E. T. Adman in *Topics in Molecular and Structural Biology. Metalloproteins* (Ed.: P. M. Harrison) MacMillan, New York, **1986**, pp. 1–42.

[2] E. I. Solomon, M. J. Baldwin, M. D. Lowery, *Chem. Rev.* **1992**, *92*, 521–542.

[3] a) *P. aeruginosa* azurin: H. Nar, A. Messerschmidt, R. Huber, M. van de Kamp, G. W. Canters, *J. Mol. Biol.* **1991**, *221*, 765–772; E. T. Adam, L. H. Jensen, *Isr. J. Chem.* **1981**, *21*, 8–12; b) *A. denitrificans* azurin: G. E. Norris, B. F. Anderson, E. N. Baker, *J. Mol. Biol.* **1983**, *165*, 501–521; c) poplar plastocyanin: J. M. Guss, H. C. Freeman, *ibid.* **1983**, *169*, 521–563; d) basic blue protein from cucumber: J. M. Guss, E. A. Merritt, R. P. Phizackerley, B. Hedman, M. Murata, K. O. Hodgson, H. C. Freeman, *Science* **1988**, *241*, 806–811; e) ascorbate oxidase: A. Messerschmidt, A. Rossi, R. Ladenstein, R. Huber, M. Bolognesi, G. Gatti, A. Marchesini, R. Petruzzelli, A. Finazzi-Agro, *J. Mol. Biol.* **1989**, *206*, 513–529; f) *A. cycloclastes* nitrite reductase: J. W. Godden, S. Turley, D. C. Teller, E. T. Adman, M. Y. Liu, W. J. Payne, J. LeGall, *Science* **1991**, *253*, 438–442.

[4] a) Three-dimensional model of stellacyanin, B. A. Fields, J. M. Guss, H. C. Freeman, *J. Mol. Biol.* **1991**, *222*, 1053–1065; b) ENDOR evidence of the coordination of Gln in stellacyanin: H. Thomann, M. Bernardo, M. J. Baldwin, M. D. Lowery, E. I. Solomon, *J. Am. Chem. Soc.* **1991**, *113*, 5911–5913; c) *Alcaligenes denitrificans* azurin mutant with spectroscopic similarities with stellacyanin: A. Romero, C. W. G. Hoitink, H. Nar, R. Huber, A. Messerschmidt, G. W. Canters, *J. Mol. Biol.* **1993**, *229*, 1007–1021.

[5] a) A. A. Gewirth, S. L. Cohen, H. J. Schugar, E. I. Solomon, *Inorg. Chem.* **1987**, *26*, 1133–1146; b) H. B. Gray, B. G. Malmstrom, *Comments Inorg. Chem.* **1983**, *2*, 203–209.

[6] a) T. K. Chang, S. A. Iverson, C. N. Kiser, A. N. Lew, C. Rodrigues, J. P. Germanas, J. H. Richards, *Proc. Natl. Acad. Sci. USA* **1991**, *88*, 1325–1329; b) B. G. Karlsson, M. Nordling, T. Pascher, L.-C. Tsai, L. Sjolin, G. Lundberg, *Protein Eng.* **1991**, *4*, 343–349.

[7] Regeneration of copper centers of blue copper proteins through exogenous ligand addition to a type 2 azurin mutant: T. den Blaauwen, G. W. Canters, *J. Am. Chem. Soc.* **1993**, *115*, 1121–1129.

[8] This work was first presented at the Symposium "Copper Coordination Chemistry: Bioinorganic Perspectives", August 3–7, 1992 (presentation P56). As this work was being carried out, Pascher et al. reported UV–Vis and EPR data for forms existing at high pH of two azurin mutants, Met121Glu and Met121Lys (T. Pascher, B. G. Karlsson, M. Nordling, B. G. Malmstrom, T. Vanngard, *Eur. J. Biochem.* **1993**, *212*, 289–296), which resemble those of the Met121Gly anion complexes reported here; the similarities of the spectroscopic data imply that the position 121 side chain in the former proteins coordinates to the copper(II) ion.

[9] A. A. Gewirth, E. I. Solomon, *J. Am. Chem. Soc.* **1988**, *110*, 8311–8320.

[10] a) J. Han, T. M. Loehr, Y. Lu, J. S. Valentine, B. A. Averill, J. Sanders-Loehr, *J. Am. Chem. Soc.* **1993**, *115*, 4256–4263; b) Y. Lu, L. B. LaCroix, M. D. Lowery, E. I. Solomon, C. J. Bender, J. Peisach, J. A. Roe, E. Gralla, J. S. Valentine, *ibid.* **1993**, *115*, 5907–5918.

[11] No changes in the UV-vis spectrum of Met121Gly azurin were detected in the presence of substantial concentrations ($c > 2$ M) of the following anions at pH 8.0: acetate, bromide, chloride, cyanate, fluoride, nitrite, or phosphate.

[12] B. C. Dave, J. P. Germanas, R. S. Czernuszewicz, *J. Am. Chem. Soc.* **1993**, *115*, 12175–12176.

[13] a) A. W. Addison in *Copper Coordination Chemistry: Biochemical and Inorganic Perspectives* (Eds.: K. D. Karlin, J. Zubieta) Adenine, New York, **1985**, pp. 109–128; b) J. Peisach, W. E. Blumberg, *Arch. Biochem. Biophys.* **1974**, *165*, 691–708.

[14] Carried out using the Quanta Package with the structure described by Nar et al. (ref. [3a]) as a framework.

[15] S. E. Shadle, J. E. Penner-Hahn, H. J. Schugar, B. Hedman, K. O. Hodgson, E. I. Solomon, *J. Am. Chem. Soc.* **1993**, *115*, 767–776.

[16] O. P. Anderson, J. Becher, H. Frydendahl, L. F. Taylor, H. Toftlund, *J. Chem. Soc. Chem. Commun.* **1986**, 699–701.

A Redox-Switchable Hemilabile Ligand: Electrochemical Control of the Coordination Environment of a Rh^I Complex**

Elizabeth T. Singewald, Chad A. Mirkin,* and Charlotte L. Stern

We report the synthesis and characterization of a redox-switchable hemilabile ligand (RHL), $FcOCH_2CH_2PPh_2$ (**1**, $Fc = (\eta^5\text{-}C_5H_5)Fe(\eta^5\text{-}C_5H_4)$, and its complexation to Rh^I to form the square-planar, *cis*-phosphane, *cis*-ether Rh^I complex **2** (Scheme 1). This new ligand type can yield electrochemical con-

[*] Prof. C. A. Mirkin, E. T. Singewald, C. L. Stern
Department of Chemistry, Northwestern University
Evanston, Illinois 60208-3113 (USA)
Telefax: Int. code + (708)491-7713

[**] This work was supported in part by the National Science Foundation (NSF, CHE-9121859), the Dow Chemical Company, and Johnson–Matthey (gift of $RhCl_3$). C. A. M. acknowledges a Dreyfus Foundation New Faculty Award (1991–1996), a Beckman Young Investigator Award (1992–1994), a Naval Young Investigator Award (1994–1997), a National Science Foundation Young Investigator Award (1993–1998), and an A. P. Sloan Fellowship (1995–1997) for partial support of this research.

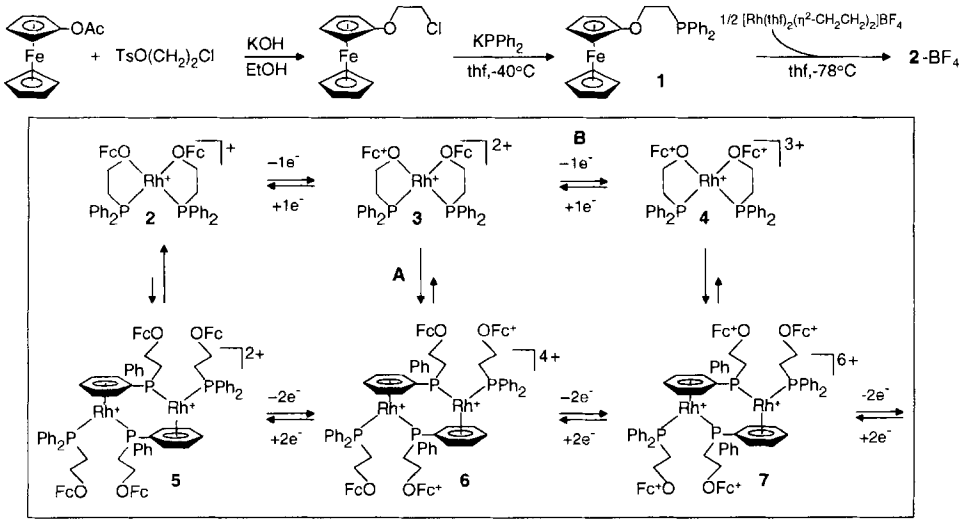

Scheme 1. Synthesis of ligand **1** and complex **2** (top) and proposed electrochemical transformations for **2** (in frame). Formal charges are denoted at appropriate atoms; overall charge is denoted outside the bracket.

trol over the electronic and steric environments of the Rh^I center. Bidentate ligand **1**, which was designed for complexation to late transition metals, has two important characteristics. First, for the example reported herein (**2**), ligand **1** is hemilabile because the phosphane moiety binds strongly to Rh^I to form a substitutionally inert bond, while the ether functionality forms a weak bond to Rh^I, which is substitutionally labile; hemilabile ligands have been studied extensively.[1] Second, the ferrocenyl group in **1** is covalently attached to the ether moiety; therefore, the binding affinity of the O atom for Rh is dependent on the oxidation state of the ferrocenyl group. With this RHL design, coordination sites at the transition-metal center to which **1** is chelated can be labilized selectively by applying a potential that can oxidize the ferrocenyl group, thereby yielding electrochemical control over transition-metal coordination environment. Electrochemical control over the coordination environment of the transition-metal complex controls the reactivity of the complex and in principle, its catalytic properties. To this end, we are designing a series of new electrocatalysts based on the RHL concept. This work complements the work of others involving 1) the design of redox-switchable ligands for sensor probes and ion transport membranes[2] and 2) the use of *substitutionally inert* redox-active ligands to tune the reactivity of transition metals.[3] The approach reported herein is fundamentally different from the latter work, because it focuses on controlling ligand binding characteristics rather than the electronic character of the transition-metal center to which the redox-active ligands are bound.[4]

The synthesis of **2**-BF_4 begins with the reaction between ferrocenylacetate[5] (5.8 mmol), KOH (5.8 mmol), and $TsOCH_2CH_2Cl$ (Ts = *p*-$(CH_3C_6H_4)SO_2$, 23 mmol) in ethanol (30 mL) at reflux for 20 h to form $[(\eta^5\text{-}C_5H_5)Fe(\eta^5\text{-}C_5H_4OCH_2CH_2Cl)]$ in 65% yield (Scheme 1). The reaction of $[(\eta^5\text{-}C_5H_5)Fe(\eta^5\text{-}C_5H_4OCH_2CH_2Cl)]$ (6.9 mmol) with one equivalent of $KPPh_2$ in 60 mL of THF at −40 °C gives ligand **1** in 92% yield. Compound **2** is then formed from the reaction between ligand **1** (0.52 mmol) and $[(\eta^2\text{-}C_2H_4)_2Rh(thf)_2]BF_4$[6] (0.26 mmol) in THF (100 mL) at −78 °C. Compound **2**-BF_4 was isolated in 55% yield as an orange-red crystalline salt by recrystallization from CH_2Cl_2/pentane.

Spectroscopic data for **2**-BF_4 in dilute CD_2Cl_2 solutions (10 mM) are fully consistent with its proposed structure (see Experimental). For example, the ^{31}P NMR resonance signal and Rh–P coupling constant are highly diagnostic of a square-planar *cis*-phosphane, *cis*-ether Rh^I complex[1, 7a] and compare well with the ^{31}P NMR data for crystallographically characterized, isoelectronic $[Rh(\eta^4\text{-}(\{\eta^5\text{-}C_5H_4\}OCH_2CH_2PPh_2)_2Fe)]BF_4$, ($^{31}P\{^1H\}$ NMR: $\delta = 61.2$, d, $J_{Rh,P} = 210.6$ Hz).[7b]

Slow diffusion of pentane into a CH_2Cl_2 solution of **2** (0.9 mM) yielded X-ray quality single crystals. Surprisingly, a single crystal X-ray diffraction study shows that **2** forms a μ_2-η^6-arene dimer (**5**) in the solid state (Fig. 1).[12] Bis(phosphane), η^6-arene pianostool dimers similar to **5** have been reported by others, although all of these examples involve chelating bis(phosphane) ligands.[8] Significantly, upon dissolving 2 mg of crystalline **5** in CD_2Cl_2 (0.5 mL), it cleanly reverts to the monomeric species **2** as shown by its ^{31}P NMR spectrum. Apparently **2** and **5** are in equilibrium (Fig. 1), and at high concentrations (for example, single crystals) the dimer **5** is favored over the monomer **2**.

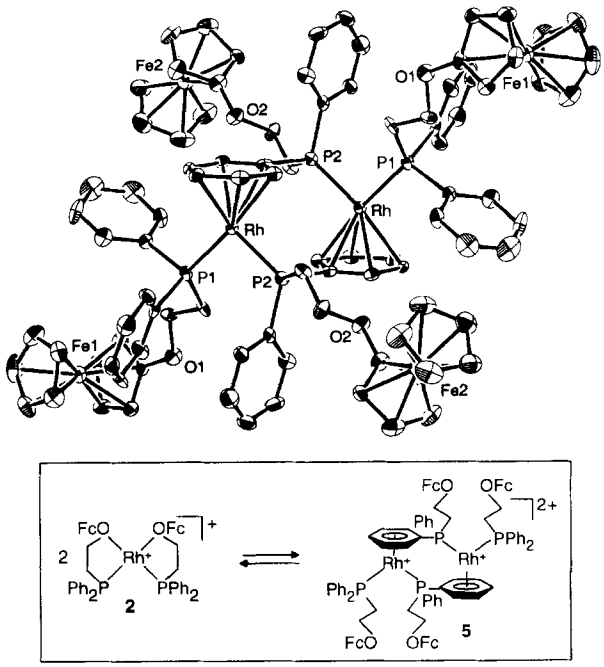

Fig. 1. Structure of **5** (ORTEP drawing; thermal ellipsoids are drawn at 50% probability; BF_4 anions and CH_2Cl_2 molecules are omitted for clarity). Selected distances [Å] and angles [°]: Rh–Rh 4.238(2), Rh–P1 2.260(3), Rh–P2 2.239(3), Rh–C(centroid) 1.423; P1-Rh-P2 95.08(9).

Cyclic voltammetry of complex **2** at concentrations at which only **2** is detected in solution by spectroscopy (1 mM) is dependent on the scan rate (Fig. 2). At a sweep rate of 20 mVs^{-1} the cyclic voltammogram of **2** exhibits two reversible waves at 260 mV and 980 mV vs. Ag wire (Fig. 2A). Initially, one might be inclined to assign the wave at 260 mV, a two-electron transfer

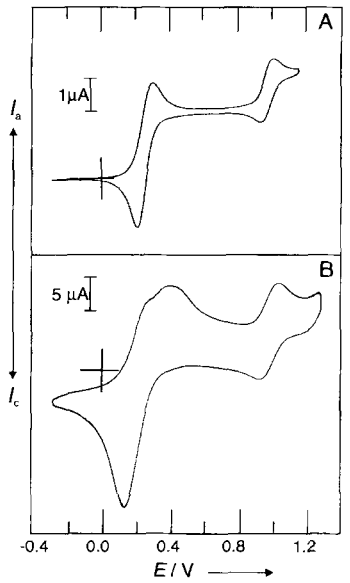

Fig. 2. Cyclic voltammogram for **2**-BF_4 (1 mM) with 0.1 M nBu_4NPF_6 in CH_2Cl_2 as supporting electrolyte, a Au disk as working electrode (0.03 cm^2), and a Ag reference electrode: A) sweep rate 20 mVs^{-1}, B) 1 Vs^{-1}.

process (see below), to the oxidation of the two Fc groups of **2** and the wave at 980 mV to a one-electron, Rh-centered oxidation/reduction of 2^{2+} (that is, **4** in Scheme 1). However, a reversible Rh^I/Rh^{II} redox couple for **4** would be highly unusual since there are only a few examples of mononuclear Rh^{II} complexes. Although some of these compounds have square-planar geometry around Rh, there are no examples of square-planar *cis*-phosphane, *cis*-ether Rh^{II} complexes.[9] In fact, a model Rh^I tetrafluoroborate compound (**8**), which is isoelectronic with **2**, exhibits an *irreversible* Rh-centered oxidation (E_p = 890 mV vs. Ag wire).[10] Therefore, we conclude that the species being oxidized at 980 mV in Figure 2A is *not* a square-planar *cis*-phosphane, *cis*-ether Rh^I complex.

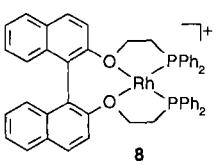

8

For compound **2**, as the scan rate is increased to 1 Vs^{-1}, the oxidative wave assigned to the two Fc-centered oxidations at 20 mVs^{-1} broadens and then splits into two distinct waves (Fig. 2B). On the reverse scan only one cathodic wave is observed for the Fc/Fc^+ couples. At 1 Vs^{-1} the wave assigned to Rh oxidation also appears reversible (Fig. 2B).

The electrochemical response for compound **2** is highly consistent with an electrochemically induced, haptotropic rearrangement and dimerization that ultimately results in the formation of complex **7** (Scheme 1). According to our proposed scheme, at a sweep rate of 20 mVs^{-1}, **2** undergoes a Fc-centered oxidation to form **3**. This weakens the Fc^+O–Rh bond, and on the time scale of the experiment, the Fc^+O group of **3** along with its FcO group are displaced by an arene ligand in a dimerization reaction to form **6** (path A in Scheme 1). Once displaced, the unoxidized FcO groups in **6** are immediately oxidized, which results in the formation of compound **7**. If on the time scale of the electrochemical experiment the dimerization is fast, a single wave associated with oxidation of two Fc groups per Rh center for **2** would be expected (Fig. 2A). The spontaneous oxidation of the uncomplexed FcO groups in **6** is reasonable; they should be more electron-rich than the Rh^+-complexed FcO group in **3** and therefore more easily oxidized. The wave at 980 mV is attributed to a Rh^I/Rh^{II} redox couple for **7** (Fig. 2A). Note that the Rh centers of complex **7** are not square-planar ones but have adopted piano-stool geometries. We have shown that a series of isoelectronic mononuclear *cis*-phosphane, η^6-arene piano-stool complexes exhibit reversible Rh^I/Rh^{II} redox couples.[11] A comparison of the current passed for the oxidation of **7** (Scheme 1 and Fig. 2) and the current associated with the **7** to **5** conversion (1:2) indicates that oxidation of **7** is a two-electron transfer process. The nature of the product formed from the oxidation of **7** is currently under investigation.

At 1 Vs^{-1} (Fig. 2B), the electrochemical reaction sequence for **2** follows a different pathway (path B in Scheme 1), but ultimately yields the same dimer (**7**) that formed in path A. The first step is a Fc-centered oxidation of **2** to form **3**, but before dimerization occurs, a second Fc-centered oxidation forms **4**. Since the Fc^+O group in **3** remains bound to Rh on the time scale of the electrochemical experiment, the FcO group in **3** is oxidized at a more positive potential than the FcO group(s) in **2** (or **6** in path A, Scheme 1). In short, at fast scan rates the second FcO group in **2** is more difficult to oxidize than the first because they are in electronic communication with each other through their interaction with the Rh center. Compound **4** then dimerizes by arene displacement of its labile Fc^+O groups to form **7**. As at a sweep rate of 20 mVs^{-1}, the oxidation of **7** at 1 Vs^{-1} is a reversible process. On the return sweep at both 20 mVs^{-1} and 1 Vs^{-1}, all Fc^+O groups of **7** are reduced at one potential to form **5**, because all are dissociated from the Rh centers and therefore are not in electronic communication with each other. Once **5** is formed, it deoligomerizes to reform **2**, which makes the entire electrochemical sequence a chemically reversible process. This deoligomerization step is analogous to the dissolution of crystals of **5** in CD_2Cl_2 to form **2** (see above).

These experiments clearly show that RHLs may be used to control transition-metal coordination environment (both steric and electronic), and in the case of **2**–**7**, they may be used to control the position of the monomer/dimer equilibrium.

Experimental Procedure

All NMR spectra were recorded on a Varian Gemini 300 MHz spectrometer at 20 °C. For all ^{31}P NMR spectra 85% H_3PO_4 was the external reference.

(2-chloroethyl)ferrocenyl ether: ^1H NMR (C_6D_6): δ = 3.20 (t, J(H,H) = 5.6 Hz, 2H, CH_2Cl), 3.50 (t, J(H,H) = 5.6 Hz, 2H, CH_2O), 3.62 (t, J(H,H) = 1.9 Hz, 2H, Fc protons), 3.89 (t, J(H,H) = 1.9 Hz, 2H, Fc protons), 4.08 (s, 5H, Fc protons); MS(EI) (60 eV, 190 °C): m/z 264 [M^+]. Elemental analysis: calcd for $C_{12}H_{13}ClFeO$: C 54.49, H 4.95; found: C 54.67, H 4.98.

1: ^1H NMR (C_6D_6): δ = 2.43 (t, J(H,H) = 7.5 Hz, 2H, CH_2P), 3.63 (t, J(H,H) = 1.9 Hz, 2H, Fc protons), 3.86 (dt, J(H,H) = J(H,P) = 7.6 Hz, 2H, CH_2O), 3.92 (t, J(H,H) = 1.9 Hz, 2H, Fc protons), 4.02 (s, 5H, Fc protons), 7.00–7.45 (m, 10H, Ph); ^{31}P NMR (C_6D_6): δ = −21.3 (s); FAB-MS: m/z 414 [M^+]. Elemental analysis: calcd for $C_{24}H_{23}FeOP$: C 69.58, H 5.59; found: C 69.78, H 5.67.

2: ^1H NMR (CD_2Cl_2): δ = 2.78 (m, 4H, CH_2P), 3.82 (m, 4H, Fc protons), 3.98 (s, 10H, Fc protons), 4.20 (m, 8H, CH_2O and Fc protons), 7.27–7.42 (m, 20H, Ph); ^{31}P NMR (CD_2Cl_2): δ = 61.0 (d, J(Rh,P) = 211.3 Hz); FAB-HRMS: m/z calcd 931.0727 [M^+], found 931.0703 [M^+].

Received: February 15, 1995
Revised: April 13, 1995 [Z 7715 IE]
German version: *Angew. Chem.* **1995**, *107*, 1725–1728

Keywords: complexes with phosphorus ligands · electrochemistry · rhodium compounds

[1] A. Bader, E. Lindner, *Coord. Chem. Rev.* **1991**, *108*, 27.
[2] a) P. D. Beer, *Chem. Soc. Rev.* **1989**, *18*, 409; b) J. C. Medina, T. T. Goodnow, M. T. Rojas, J. L. Atwood, B. C. Lynn, A. E. Kaifer, G. W. Gokel, *J. Am. Chem. Soc.* **1992**, *114*, 10583.
[3] a) I. M. Lorkovié, M. S. Wrighton, W. M. Davis, *J. Am. Chem. Soc.* **1994**, *116*, 6220; b) J. C. Kotz, C. L. Nivert, J. M. Lieber, R. C. Reed, *J. Organomet. Chem.* **1975**, *91*, 87; c) P. Braunstein, L. Douce, F. Balegroune, D. Grandjean, D. Bayeul, Y. Dusausoy, P. Zanello, *New J. Chem.* **1992**, *16*, 925.
[4] Since the submission of this work, a ligand system that could fit into this category was published: S. B. Sembiring, S. B. Colbran, D. C. Craig, *Inorg. Chem.*, **1995**, *34*, 761.

[5] A. N. Nesmeyanov, V. A. Sazonova, V. N. Drozd, *Dokl. Chem. (Engl. Transl.)* **1959**, *129*, 1113.
[6] Postulated in situ product of the reaction between 2 equiv of $AgBF_4$ and $[(\eta^2\text{-}CH_2CH_2)_4Rh_2(\mu\text{-}Cl)_2]$ in THF, the synthetic procedure for $[(\eta^2\text{-}CH_2CH_2)_4Rh_2(\mu\text{-}Cl)_2]$, see R. Cramer, *Inorg. Chem.* **1962**, *1*, 722.
[7] a) A. M. Allgeier, E. T. Singewald, C. A. Mirkin, C. L. Stern, *Organometallics* **1994**, *13*, 2928; b) M. Alvarez, N. Lugan, R. Mathieu, *J. Organomet. Chem.* **1994**, *468*, 249.
[8] a) J. Halpern, D. P. Riley, A. S. C. Chan, J. J. Pluth, *J. Am. Chem. Soc.* **1977**, *99*, 8055; b) D. P. Riley, *J. Organomet. Chem.* **1982**, *234*, 85; c) D. P. Fairlie, B. Bosnich, *Organometallics* **1987**, *7*, 936; d) A. Miyashita, H. Takaya, T. Souchi, R. Noyori, *Tetrahedron* **1984**, *40*, 1245.
[9] K. K. Pandey, *Coord. Chem. Rev.* **1992**, *121*, 1, and references therein.
[10] T. B. Higgins, E. T. Singewald, C. A. Mirkin, unpublished results.
[11] E. T. Singewald, C. A. Mirkin, A. D. Levy, C. L. Stern, *Angew. Chem.* **1994**, *106*, 2524; *Angew. Chem. Int. Ed. Engl.* **1994**, *33*, 2473.
[12] Crystal data for **5**-$(BF_4)_2$: $C_{96}H_{92}Fe_4B_2F_8O_4P_4Rh_2 \cdot 4CH_2Cl_2$, $M_r = 2206.34$, $0.29 \times 0.14 \times 0.05$ mm, triclinic, space group $P\bar{1}$, $a = 10.934(2)$, $b = 14.322(3)$, $c = 16.956(4)$ Å, $\alpha = 73.29(2)$, $\beta = 83.43(2)$, $\gamma = 81.66(2)$ Å, $V = 2509(2)$ Å^3, $\rho_{calcd} = 1.460$ g cm^{-3}, $Z = 1$, $\theta_{max} = 22.60°$, $\mu(Mo_{K\alpha}) = 11.11$ cm^{-1}, $\lambda = 0.71069$ Å, $F(000) = 1120$. Data were collected on an Enraf-Nonius CAD-4 diffractometer at -120 ± 1 °C using the ω–θ scan technique ($2\theta \leq 45.9°$). The data were corrected for Lorentz and polarization effects. In addition, an analytical absorption correction was applied with transmission factors ranging from 0.84–0.95. The structure was solved by direct methods (SHELXS-86). Of the 6959 reflections, 4065 with $I > 3.00\sigma(I)$ were used in the refinement. Refinement of 589 variable parameters (TEXAN 5.0) converged with the residuals of $R = 0.051$ and $R_w = 0.052$. Four dichloromethane solvent molecules were found in the unit cell; two remained disordered after refinement. The highest peaks left in the final difference map were located in the vicinity of the disordered solvent molecules. Further details of the crystal structure investigation may be obtained from the Director of the Cambridge Crystallographic Data Centre, 12 Union Road, GB-Cambridge CB21EZ (UK), on quoting the full journal citation.

Synthesis and Reactions of Vinyl Isoselenocyanates**

Klaus Banert* and Christoph Toth

Dedicated to Professor Harald Günther on the occasion of his 60th birthday

The existence of isoselenocyanates ("seleno mustard oils") was doubted for a long time,[1] but the synthesis of several aryl and alkyl derivatives has been achieved in recent years.[2] To the best of our knowledge, however, vinyl isoselenocyanates have not yet been prepared. We now report on isomerization reactions that are derived from the known equilibration[3] of allyl selenocyanate **1** and allyl isoselenocyanate **2**, but direct the isoselenocyanato function to a *vinylic* position for the first time. These [3,3]sigmatropic rearrangements provide access to the highly reactive allenyl isoselenocyanates **4** and the isoselenocyanate-substituted 1,3-butadienes **11** and **15**.

An equilibrium of prop-2-ynyl selenocyanates **3** and allenes **4** is established on gas-phase thermolysis[4] of **3**[5] (Scheme 1). Due to their pronounced tendency to polymerize, the isoselenocyanates **4** can only be handled in solution. They can nevertheless be purified by flash chromatography (SiO_2, hexane/Et_2O 10:1; for characterization of **4**, see Table 1). The equilibrium **3a** ⇌ **4a**[6] is verified by renewed gas-phase thermolysis of **4a**.

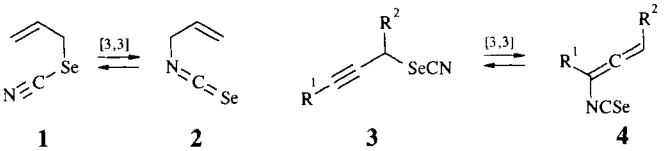

1 **2** **3** **4**

Scheme 1. **3a**, **4a**: $R^1 = R^2 = H$; **3b**, **4b**: $R^1 = H$, $R^2 = Me$; **3c**, **4c**: $R^1 = Me$, $R^2 = H$; yields based on converted **3**: **4a** 80%, **4b** 82%, **4c** 76%; ratios at equilibrium: **3a**/**4a** = 37:63; **3b**/**4b** = 17:83; **3c**/**4c** = 79:21.

Table 1. Selected physical data of compounds **4a–c**, **5**, and **9** [a].

4a: ^{1}H NMR: $\delta = 5.44$ (d, $^4J = 6.4$, 2 H; H-3), 6.16 (t, $^4J = 6.4$, 1 H; H-1); ^{13}C NMR: $\delta = 86.30$ (t; C-3), 89.51 (br. d; C-1), 128.40 (v. br. s; NCSe), 210.88 (s; C-2); GC-MS: *m/z* (%): 145 (82) [M^+], 118 (38) [$M^+ - HCN$], 39 (100) [$C_3H_3^+$]; IR (CCl_4): $\tilde{\nu} = 2080$ (NCSe).

4b: ^{1}H NMR: $\delta = 1.79$ (dd, $^3J = 7.4$, $^5J = 2.7$, 3 H; H-4), 5.80 (dq, $^3J = 7.4$, $^4J = 5.9$, 1 H; H-3), 6.03 (dq, $^4J = 5.9$, $^5J = 2.7$, 1 H; H-1); ^{13}C NMR: $\delta = 13.62$ (q; C-4), 87.94 (br. d; C-1), 97.63 (d; C-3), 126.90 (br. s; NCSe), 206.26 (s; C-2).

4c: ^{1}H NMR: $\delta = 1.96$ (t, $^5J = 3.2$, 3 H; CH_3), 5.24 (q, $^5J = 3.2$, 2 H; CH_2); ^{13}C NMR: $\delta = 18.97$ (q; CH_3), 83.73 (t; CH_2), 98.75 (br. s; *c*-NCSe), 128.18 (br. s; NCSe), 208.03 (s; C-2).

5: yellow crystals: m.p. 128 °C; ^{1}H NMR: $\delta = 1.35$ (t, $^3J = 7.1$, 6 H; CH_2CH_3), 2.37 (d, $^4J = 1.5$, 3 H; 5-CH_3), 4.27 (q, $^3J = 7.1$, 4 H; CH_2), 6.92 (q, $^4J = 1.5$, 1 H; H-4), 12.70 (s, 1 H; NH); ^{13}C NMR: $\delta = 13.68$ (q, 2 C; CH_2CH_3), 14.36 (q; 5-CH_3), 60.10 (t, 2 C; CH_2CH_3), 87.62 (s; $C(CO_2Et)_2$), 122.48 (d; C-4), 128.40 (s; C-5), 168.00 (s), 175.00 (s); IR (CCl_4): $\tilde{\nu} = 1650$ (C=O), 1620 (C=O), 1250 (C–O); correct elemental analysis based on $C_{11}H_{15}NO_4Se$.

9: light-red, viscous liquid: ^{1}H NMR: $\delta = 4.21$ (d, $^4J = 0.9$, 2 H; CH_2), 7.20–7.80 (m, 11 H; 2 × Ph and H-4); ^{13}C NMR: $\delta = 25.35$ (t; CH_2), 127.85 (d; Ph), 128.56 (s; C-5), 129.34 (d; Ph), 129.50 (d; Ph), 129.80 (d; Ph), 133.80 (d; Ph), 135.98 (d; Ph), 142.37 (d; C-4), 143.59 (s; *i*-Ph), 146.15 (s; *i*-Ph), 164.85 (s; C-2); correct elemental analysis of the picrate based on $C_{22}H_{16}N_4O_7Se_2$.

[a] ^{1}H NMR ($CDCl_3$, 300 or 200 MHz, *J* in Hz), ^{13}C NMR ($CDCl_3$, 75 or 50 MHz, *J* in Hz), MS (EI, 70 eV, correct isotopic distribution), IR ($\tilde{\nu}$ in cm^{-1}), elemental analyses (C,H,N).

In contrast to allenyl isocyanates[7] but similar to allenyl isothiocyanates,[8] compounds **4** afford heterocyclic products on treatment with carbon-, nitrogen-, oxygen-, or seleno-containing nucleophiles (Scheme 2). The syntheses of selenazoles[9] **5**–**9** (Table 1) show that **4a** reacts distinctly more slowly with nucleophiles than the unusually reactive allenyl isothiocyanate.[8]

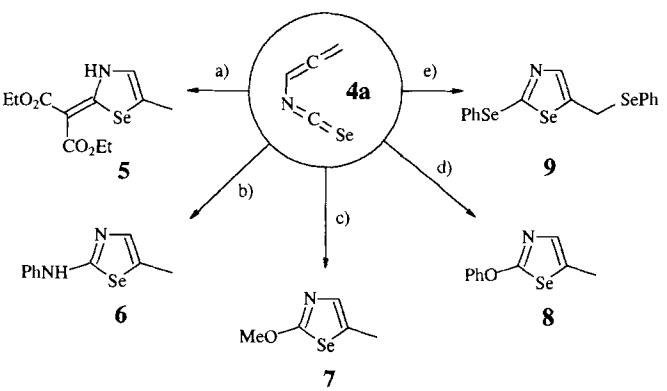

Scheme 2. Reactions of **4a** with nucleophiles to give the selenazoles **5**–**9**; a) NaH, THF, $CH_2(CO_2Et)_2$, then **4a**, 20 °C, 2 h, then NH_4Cl, H_2O (65%); b) $PhNH_2$, Et_2O, hexane, 60 °C, 17 h (60%); c) MeOH, 60 °C, 24 h (50%); d) PhOH, NEt_3, Et_2O, hexane, 60 °C, 48 h (88%); e) NaH, THF, Ph_2Se_2 (excess), 75 °C, 1.5 h, then **4a** 40 °C, 5 h and 20 °C, 16 h, then NH_4Cl, H_2O (50%).

[*] Prof. Dr. K. Banert, Dipl.-Chem. C. Toth
Lehrstuhl für Organische Chemie der Technischen Universität Chemnitz-Zwickau
Strasse der Nationen 62, D-09111 Chemnitz (Germany)
Telefax: Int. code + (371) 531-1839
e-mail: email@chemie.tu-chemnitz.de

[**] Rearrangement Reactions, Part 5. This work was supported by the Deutsche Forschungsgemeinschaft and the Fonds der Chemischen Industrie. Part 4: K. Banert, S. Groth, H. Hückstädt, K. Vrobel, *Phosphorus, Sulfur, Silicon Relat. Elem.* **1994**, *95–96*, 323–324.

Not only the prop-2-ynyl selenocyanates **3** but also the buta-2,3-dienyl selenocyanates **10b** and **10d**, which are easily accessible from the respective precursors **10a**[10] or **10c**[11] and potassium selenocyanate, are suitable reactants for rearrangements that direct an isoselenocyanate function to a vinylic position. The buta-1,3-dienes **11a** and **11b** are formed by gas-phase thermolysis[4] in a virtually irreversible reaction (in the case of **10d** thermolysis is also possible in solution). On treatment with the reactive dienophiles **12**, **11b** undergoes [4 + 2] cycloadditions to give **13** (Scheme 3, Table 2).

Heating of a very dilute solution of **14**[12] in toluene causes a double [3,3]sigmatropic isomerization to produce the bis(isoselenocyanate) **15** (yield 12%, Table 2), which can be separated from unconverted **14** (26%) by flash chromatography (SiO_2, hexane/Et_2O 10:1). In this case, gas-phase thermolysis entails considerable decomposition on attempts to evaporate the precursor and provides unsatisfactory yields (about 1%) due to the low volatility of **14** and the extreme tendency of **15** to polymerize.

The bis(isocyanide) **16a** is produced in a rapid and smooth reaction on treatment of **15** with triethyl phosphite, triphenylphosphane, or polymer-supported triphenylphosphane. This 2,3-diisocyanobuta-1,3-diene constitutes the central structural element of the xanthocillines **16b**,[13] a group of natural antibiotics. Deselenizations **11a** → **17a**, **11b** → **17b**, and **4a** → **18**[14] are performed analogously (Scheme 4, Table 2). Isonitrile **17b** can be distilled under vacuum whereas **17a** possesses a distinctly lower stability; **16a** can be handled only in solution. As yet we have not succeeded in synthesizing the isonitriles on desulfurization of the corresponding isothiocyanates.[8]

Table 2. Selected physical data of compounds **11a,b**, **15**, **16a** and **17a,b** [a].

11a: ^{1}H NMR: δ = 5.17 (br. s, 1 H; H-1), 5.31 (br. s, 1 H; H-1), 5.37 (dd, ^3J = 10.3, ^5J = 1.5, 0.8, 1 H; *E*-H-4), 5.59 (d, ^3J = 16.7, 1 H; *Z*-H-4), 6.27 (dd, ^3J = 16.7, 10.3, 1 H; H-3); ^{13}C NMR: δ = 114.68 (dd; CH_2), 117.97 (dd; CH_2), 128.46 (br. s; NCSe), 131.18 (d; C-3), 134.28 (s; C-2).

11b: ^{1}H NMR: δ = 1.88 (dd, ^4J = 0.7, 1.4, 3 H; CH_3), 5.18 (ddqd, ^5J = 1.7, 0.8, ^4J = 1.4, ^2J = 1.0, 1 H; *E*-H-4), 5.24 (ddd, ^5J = 0.8, 0.7, ^2J = 1.0, 1 H; *E*-H-1), 5.29 (ddd, ^5J = 1.7, 0.7, ^2J = 1.0, 1 H; *Z*-H-1), 5.40 (ddqd, ^5J = 0.7, 0.7, ^4J = 0.7, ^2J = 1.0, 1 H; *Z*-H-4); ^{13}C NMR: δ = 18.95 (q; CH_3), 112.39 (t; CH_2), 116.43 (dd; CH_2), 128.30 (v. br. s; NCSe), 135.83 (br. s; C-2), 136.50 (s; C-3); IR (CCl_4): $\tilde{\nu}$ = 2100 (NCSe).

15: ^{1}H NMR: δ = 5.56 (d, ^2J = 1.2, 2 H), 5.70 (d, ^2J = 1.2, 2 H); ^{13}C NMR: δ = 114.83 (t; CH_2), 130.01 (s), 133.46 (br. s); IR ($CDCl_3$): $\tilde{\nu}$ = 2062 (NCSe).

16a: ^{1}H NMR: δ = 5.82 (br. t, 2 H), 6.09 (v. br. t, 2 H); ^{13}C NMR: δ = 118.30 (t; CH_2), 169.30 (br. s; NC); GC-MS: *m/z* (%): 104 (13) [M^+], 77 (95) [M^+ − HCN], 52 (100); IR ($CDCl_3$): $\tilde{\nu}$ = 2130 (NC).

17a: disagreeable, acrid liquid: ^{1}H NMR: δ = 5.27 (t, ^3J(H,N) = 5.4, 1 H; *E*-H-1), 5.41 (d, ^3J = 10.1, 1 H; *E*-H-4), 5.45 (t, ^3J (H,N) = 2.0, 1 H; *Z*-H-1), 5.67 (d, ^3J = 16.3, 1 H; *Z*-H-4), 6.23 (ddt, ^3J = 16.3, 10.1, ^3J (H,N) = 2.7, 1 H; H-3); ^{13}C NMR: δ = 116.88 (t; CH_2), 118.55 (t; CH_2), 129.53 (d; C-3), 132.19 (t, *J* (C,N) = 5.3; C-2), 164.75 (t, *J* (C,N) = 5.3; NC); GC-MS: *m/z* (%): 79 (42) [M^+], 52 (100) [M^+ − HCN]; IR (CCl_4): $\tilde{\nu}$ = 2130 (NC)

17b: disagreeable, acrid liquid: b.p.: 55 °C/42 Torr; ^{1}H NMR: δ = 1.92 (ddd, ^4J = 1.4, 0.7, ^5J = 0.3, 3 H; CH_3), 5.27 (ddqd, ^5J = 1.6, 0.7, ^4J = 1.4, ^2J = 0.7, 1 H; *E*-H-4), 5.36 (dddt, ^5J = 0.7, 0.7, ^2J = 0.7, *J* (H,N) = 5.5, 1 H; *E*-H-1), 5.50 (ddqdt, ^5J = 1.6, 0.7, 0.3, ^2J = 0.7, *J* (H,N) = 2.7, 1 H; *Z*-H-1), 5.58 (dddq, ^5J = 0.7, 0.7, ^2J = 0.7, ^4J = 0.7, 1 H; *Z*-H-4); ^{13}C NMR: δ = 18.55 (q; CH_3), 114.58 (t; C-1), 117.43 (t; C-4), 134.13 (t, *J* (C,N) = 11.3; C-2), 134.99 (s; C-3), 163.46 (br. s; NC); GC-MS: *m/z* (%): 93 (40) [M^+], 66 (100) [M^+ − HCN], 53 (60) [$C_4H_5^+$]; IR ($CDCl_3$): $\tilde{\nu}$ = 2130 (NC).

[a] ^{1}H NMR ($CDCl_3$, 300 or 200 MHz, *J* in Hz). ^{13}C NMR ($CDCl_3$, 75 or 50 MHz, *J* in Hz). MS (EI, 70 eV, correct isotopic distribution). IR ($\tilde{\nu}$ in cm^{-1}).

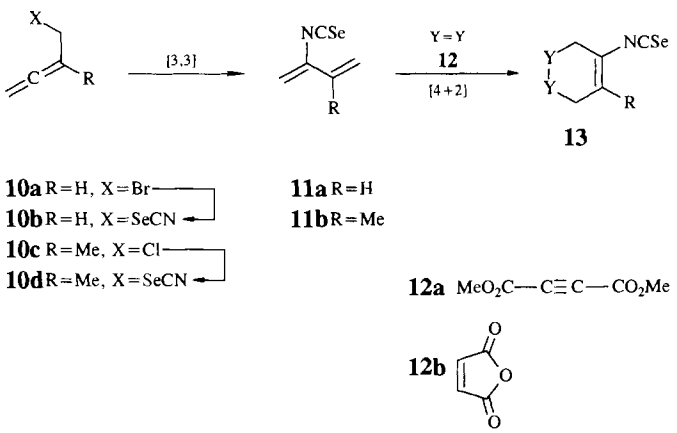

Scheme 3. Yields: **10b**, 92%; **10d**, 88%; **11a**, 90%; **11b**, 90%; **13** based on **11b** and **12a**, 50%; **13** from **11b** and **12b**, 50%.

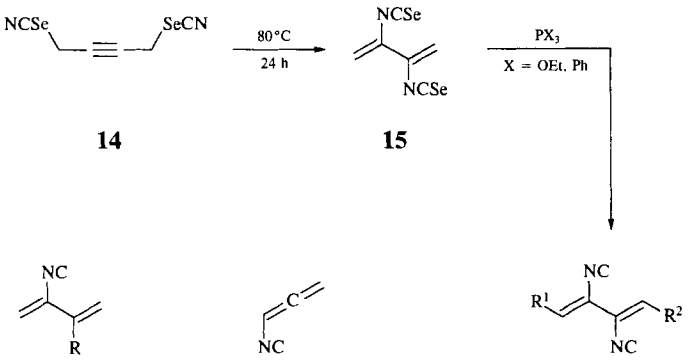

Scheme 4. Yields: **16a** based on **15** and $P(OEt)_3$ (^{1}H NMR), 82%; **16a** from **15** and PPh_3 (^{1}H NMR), quantitative; **17a** based on **11a** and PPh_3, 30%; **17b** from **11b** and PPh_3, 88%; **18** from **4a** and $P(OEt)_3$ (^{1}H NMR), 87%.

At the moment we are trying to get plausible indications of the unknown isotellurocyanates[2b] using similar sigmatropic rearrangements.

Received: March 11, 1995 [Z 7791 IE]
German version: *Angew. Chem.* **1995**, *107*, 1776–1778

Keywords: isocyanides · isoselenocyanates · selenium compounds · rearrangements

[1] H. Rheinboldt, *Methoden Org. Chem. (Houben-Weyl) 4th ed. 1952–, Vol. 9*, **1955**, p. 951.

[2] Reviews: a) C. Paulmier, *Selenium Reagents and Intermediates in Organic Synthesis*, Pergamon, Oxford, **1986**, p. 70–71; b) *The Chemistry of Organic Selenium and Tellurium Compounds, Vol. 2* (Ed.: S. Patai), Wiley, Chichester, **1987**; c) A. Toshimitsu, S. Uemura in [2b], pp. 541–590; c) F. S. Guziec in [2b], pp. 215–273; d) E. Bulka in *The Chemistry of Cyanates and their Thio Derivatives, Part 2* (Ed.: S. Patai), Wiley, Chichester, **1977**, pp. 887–922.

[3] a) T. Tarantelli, D. Leonesi, *Ann. Chim. (Rome)* **1963**, *53*, 1113–1122; b) A. Fava, *Chem. Org. Sulfur Compd.* **1966**, *2*, 73–91.

[4] The selenocyanates were passed at a pressure of about 0.1–0.01 Torr without carrier gas through a glass tube (about 45 × 1.5 cm) filled with Raschig rings and heated to 350–400 °C. To prevent polymerization the products were collected in a cold trap and diluted with an inert solvent before thawing. Gas-phase thermolyses of **3** performed at temperatures lower than 350 °C resulted in incomplete equilibration (increased ratio **3**:**4**), whereas temperatures higher than 400 °C led to a constant **3**:**4** ratio (see Scheme 1) but also to several (volatile) products of successive reactions. With optimized conditions **3** could be evaporated nearly without residue, but it was not possible to avoid the deposition of decomposition products in the pyrolysis tube completely.

[5] All selenocyanates were prepared on treatment of halogen compounds or sulfonates with potassium selenocyanate in DMSO. Under these conditions the

formation of S_N2' products, for example, the reaction of 1-methylprop-2-ynyl tosylate ("3-tosyloxy-1-butyne") to give 1-selenocyanatobuta-1,2-diene, could be repressed to a large extent. Yields: **3a** 80% from the bromide, b.p. 55–60 °C at 2 Torr; **3b** 80% from the tosylate, b.p. 60–61 °C at 3 Torr; **3c** 33% from the tosylate, b.p. 50 °C at 0.1 Torr.

[6] For comparison: The equilibration of the allyl compounds resulted in a **1**:**2** ratio of 73:27 (^{1}H NMR, 80 °C, $CDCl_3$).

[7] K. Banert, S. Groth, *Angew. Chem.* **1992**, *104*, 865–867; *Angew. Chem. Int. Ed. Engl.* **1992**, *31*, 866–868.

[8] K. Banert, H. Hückstädt, K. Vrobel, *Angew. Chem.* **1992**, *104*, 72–74; *Angew. Chem. Int. Ed. Engl.* **1992**, *31*, 90–92.

[9] Alternative synthesis for selenazole **6**: E. Bulka, K.-D. Ahlers, H. Ewert, W. Haase, P. Meier, W. Pilz, *Chem. Ber.* **1968**, *101*, 1910–1916.

[10] J. Pornet, B. Randrianoelina, L. Miginiac, *J. Organomet. Chem.* **1979**, *174*, 1–13.

[11] E. D. Bergmann, D. Herrman, *J. Am. Chem. Soc.* **1951**, *73*, 4013–4015.

[12] R. Gleiter, S. Rittinger, H. Langer, *Chem. Ber.* **1991**, *124*, 357–363.

[13] a) W. Rothe, *Pharmazie* **1950**, *5*, 190; b) I. Hagedorn, H. Tönjes, *ibid.* **1956**, *11*, 409–410; **1957**, *12*, 567–580; c) H. Achenbach, H. Strittmatter, W. Kohl, *Chem. Ber.* **1972**, *105*, 3061–3066.

[14] a) J. W. Zwikker, R. W. Stephany, *Synth. Commun.* **1973**, *3*, 19–23; b) R. W. Stephany, M. J. A. de Bie, W. Drenth, *Org. Magn. Reson.* **1974**, *6*, 45–47.

Photochemically Initiated Protein Splicing**

Sandra N. Cook, William E. Jack, Xiaofeng Xiong, Lora E. Danley, Jonathan A. Ellman, Peter G. Schultz, and Christopher J. Noren*

Protein splicing is a post-translational rearrangement process in which an internal polypeptide segment (intein)[1] is excised from a primary translation product, with concomitant ligation of the flanking polypeptides (exteins).[2] This process results in the production of two protein products from a single precursor polypeptide: the intein (often a homing endonuclease thought to initiate lateral transmission of the intein coding sequence)[3] and the ligated exteins.

A substantially purified precursor protein has been shown to splice in vitro, which indicates that protein splicing is autocatalytic.[4] Expression of intein coding sequences in foreign genetic contexts has demonstrated that all of the residues required for splicing reside within the intein except for the first residue of the C-extein.[4–6] Comparison of seven examples of self-splicing proteins revealed several conserved features, including small nucleophilic residues (Cys, Ser, or Thr) immediately following both splice junctions and the sequence His–Asn immediately preceding the downstream junction.[2] Substitutions for the Ser/Cys/Thr residues at either junction abolished splicing,[2e, i, 5–7] which has led to the proposal of splicing mechanisms in which either or both of these residues play a role analogous to that of the active site nucleophiles of serine and cysteine proteases.[2e, h, i, 4, 8] We have begun to probe the mechanism of this novel biochemical reaction using the method of unnatural amino acid mutagenesis and now report the generation and characterization of a photochemically initiated self-splicing reaction.

Intein-2 from the DNA polymerase of *Thermococcus litoralis* (*Tli pol*, Vent polymerase) was chosen for initial studies. This protein has a serine at the upstream splice junction and a threonine at the downstream junction.[2d] In order to cage the unspliced precursor protein, the 2-nitrobenzyl ether of serine was substituted for the conserved Ser1082 residue at the upstream splice junction (Scheme 1).[9] Upon irradiation at 300–350 nm, 2-nitrobenzyl ethers undergo rapid conversion to the

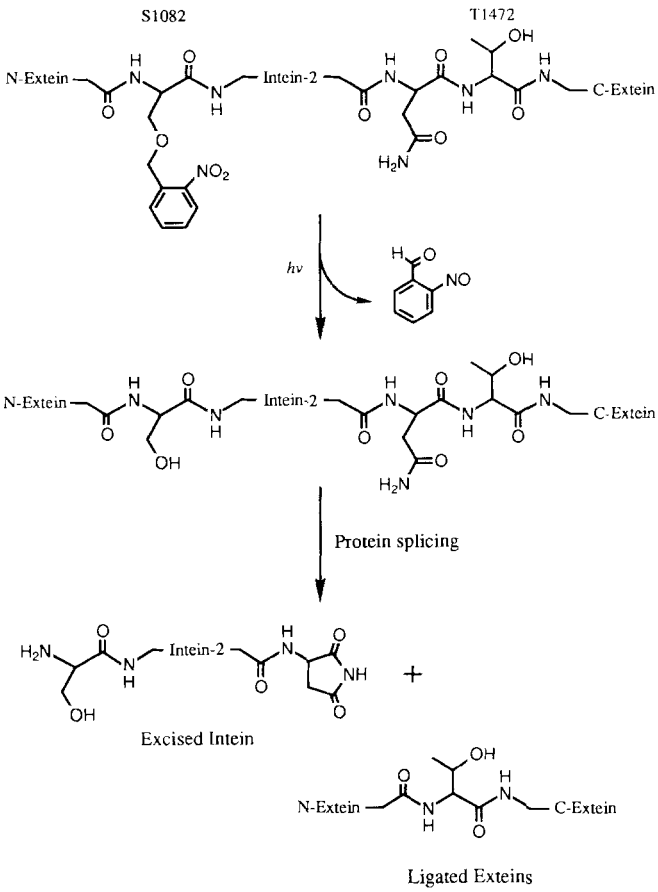

Scheme 1. Initiation of protein splicing of truncated *Thermococcus litoralis* DNA polymerase by photolysis of 2-nitrobenzyl ether at the upstream splice junction.

free alcohol and 2-nitrosobenzaldehyde,[10] so the wild-type sequence should be restored upon photolysis and splicing should proceed normally. Incorporation of the caged serine analog *O*-(2-nitrobenzyl)serine was accomplished by in vitro suppression of the corresponding amber nonsense mutation with a chemically aminoacylated suppressor tRNA.[11, 12] To simplify analysis of splicing products, the Ser1082 → amber (Ser1082*am*) mutation was introduced into a truncated construct (pANY5) in which the 45.3 kDa *Tli pol* intein-2 is flanked by only 2.2 kDa of the N-extein and 8.3 kDa of the C-extein.[13]

When expressed in an *E. coli* coupled transcription/translation system[11, 14] (Fig. 1), the wild-type construct pANY5 yielded the expected 55.8 kDa precursor and the 45.3 kDa excised intein (the endonuclease PI-*Tli*I), which were detected by Western analysis using an anti-PI-*Tli*I antibody.[15] The yield of spliced product was approximately 70%, which is in agreement with reported results for archaea inteins expressed in *E. coli*.[2e, 4] This presumably reflects an incorrectly folded subpop-

[*] Dr. C. J. Noren, S. N. Cook, Dr. W. E. Jack, Dr. X. Xiong
New England Biolabs
32 Tozer Road, Beverly, MA 01915 (USA)
Telefax: Int. code + (508)921-1350
e-mail: noren@neb.com

L. E. Danley, Prof. J. A. Ellman, Prof. P. G. Schultz
College of Chemistry, University of California
Berkeley, CA 94720 (USA)

[**] P. G. S. acknowledges support from the Office of Energy Research, Division of Material Sciences and Division of Energy Biosciences, and the Office of General Life Sciences, Structural Biology Division, of the U. S. Department of Energy under Contract No. DE-AC03-76SF00098. The authors thank Huimin Kong and Sharon Cload for technical assistance, and Francine Perler, Paul Evans, Virginia Cornish, and Don Comb for helpful discussions.

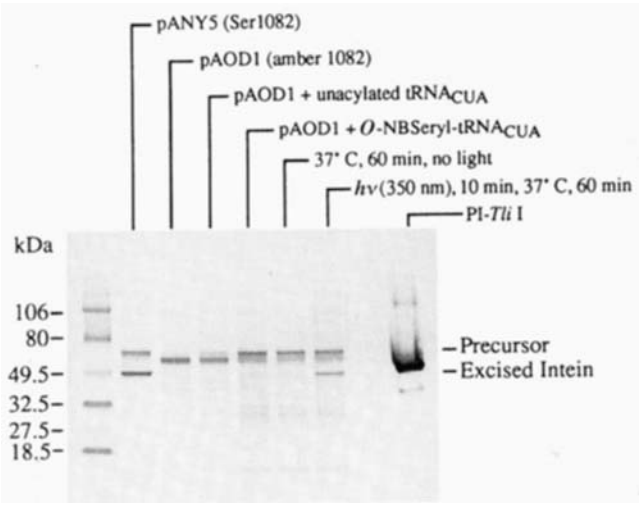

Fig. 1. Western blot analysis of in vitro suppression and photochemically initiated splicing. In vitro transcription/translation reactions [14] (30 μL) contained 3 μg of the expression vector pANY5 (2.2 kDa N-extein/45.3 kDa intein/8.3 kDa C-extein) or the upstream amber mutant pAOD1 (S1082*am*) as indicated, and were supplemented with 8.5 μL of S-30 extract from *E. coli* D-10, 450 units T7 RNA polymerase, 3 μg rifampicin, and, where indicated, 4 μg unacylated $tRNA_{CUA}$ [11c] or 10 μg *O*-NB-seryl-$tRNA_{CUA}$ [11b]. Reactions were incubated 30 min in the dark at 37 °C with shaking. A 5 μL portion of each reaction was withdrawn and precipitated with acetone for later gel analysis. Translation was then arrested in the *O*-NB-Ser-suppressed reactions with RNase A (0.3 mg mL^{-1}), and protein splicing was photoinitiated by irradiating half of each reaction on ice with a 275 watt tungsten lamp equipped with a UV filter (GE model RSK6B) at a distance of 20 cm for 10 min, while the other half was kept in the dark as a control. Both portions were then incubated in the dark for 60 min at 37 °C to allow the splicing reaction to take place, after which 5 μL of each was precipitated with acetone for gel analysis. All samples were denatured and electrophoresed on a 10–20% gradient SDS-tricine gel (NOVEX), transferred to nitrocellulose membrane, and probed with anti-PI-*Tli*I antibody (mouse polyclonal serum, C. Carlow) [2d]. Blots were developed with goat anti-mouse IgG/alkaline phosphatase conjugate, using NBT/BCIP as colorimetric substrate [15]. Purified intein-2 (PI-*Tli*I, NEB) was used as a Western standard.

ulation of precursor molecules due to the lower growth temperature of *E. coli*. Expression of the upstream amber mutant pAOD1 (S1082*am*) in the absence of added suppressor tRNA produced a 53 kDa product, consistent with reinitiation of translation following the amber codon. As expected, the intensity of this band was diminished in the presence of aminoacylated suppressor tRNA. Readthrough of the amber codon by endogenous aminoacyl-tRNA (yielding full-length 56 kDa precursor) was insignificant under the conditions employed.

The dinucleotide pdCpA was acylated with *N*-biphenylisopropyloxycarbonyl (BPOC)-protected *O*-(2-nitrobenzyl) serine (*O*-NB-Ser) and ligated to truncated $tRNA_{CUA}$(-CA)[11c] using T4 RNA ligase.[11d, 12a] In vitro transcription/translation of the Ser1082 amber mutant pAOD1 in the presence of deprotected *O*-NB-seryl-$tRNA_{CUA}$ yielded the 55.8 kDa precursor protein (Fig. 1). No 45.3 kDa product corresponding to the excised intein was observed, which indicates that the 2-nitrobenzyl group on the serine hydroxyl group quantitatively blocked the splicing reaction. Brief irradiation of the blocked precursor, followed by further incubation to allow the splicing reaction to occur, resulted in excision of the 45.3 kDa intein with an efficiency comparable to that of the wild-type construct (about 50%). No excision was observed in a control reaction in which the irradiation step was omitted; the excision process is thus absolutely dependent upon irradiation. Attempts to detect the 10 kDa ligation product were unsuccessful, possibly because of the proteolytic sensitivity of *T. litoralis* DNA polymerase in *E. coli*.[2e] Nonetheless, since the wild-type amino acid sequence is liberated upon photolysis, we know from previous studies that intein excision is coupled to extein ligation.[2e, 4]

These results demonstrate that the *O*-NB-Ser-$tRNA_{CUA}$ efficiently suppresses the Ser1082 amber mutant to produce a full-length precursor protein in which splicing can be initiated by brief photolysis. These experiments should make possible a range of time-resolved studies relevant to dissecting the mechanism of the protein splicing reaction.

Received: March 2, 1995 [Z 7571E]
German version: *Angew. Chem.* **1995**, *107*, 1736–1737

Keywords: biochemistry · photolysis · proteins · splicing · suppressor tRNA

[1] By analogy with RNA introns, the excised protein segment has been termed the intein, while the flanking polypeptides that are ligated following excision of the intein are called exteins. N-extein and C-extein refer to the upstream and downstream flanking exteins, respectively (F. B. Perler, E. O. Davis, G. E. Dean, F. S. Gimble, W. E. Jack, N. Neff, C. J. Noren, J. Thorner, M. Belfort, *Nucleic Acids Res.* **1994**, *22*, 1125-1127).

[2] a) P. M. Kane, C. T. Yamashiro, D. F. Wolczyk, N. Neff, M. Goebl, T. H. Stevens, *Science* **1990**, *250*, 651–657; b) R. Hirata, Y. Ohsumi, A. Nakano, H. Kawasaki, K. Suzuki, Y. Anraku, *J. Biol. Chem.* **1990**, *265*, 6726-6733; c) E. O. Davis, S. G. Sedgwick, M. J. Colston, *J. Bacteriol.* **1991**, *173*, 5653–5662; d) F. B. Perler, D. G. Comb, W. E. Jack, L. S. Moran, R. B. Kucera, J. Benner, B. E. Slatko, S. K. Hempstead, C. K. S. Carlow, H. Jannasch, *Proc. Natl. Acad. Sci. USA* **1992**, *89*, 5577–5581; e) R. A. Hodges, F. B. Perler, C. J. Noren, W. E. Jack, *Nucleic Acids Res.* **1992**, *20*, 6153–6157; f) H. H. Gu, J. Xu, M. Gallagher, G. E. Dean, *J. Biol. Chem.* **1993**, *268*, 7372-7381; g) E. O. Davis, H. S. Thangaraj, P. C. Brooks, M. J. Colston, *EMBO J.* **1994**, *13*, 699–703; h) C. J. A. Wallace, *Protein Sci.* **1993**, *2*, 697–705; i) Y. Anraku, R. Hirata, *J. Biochem.* **1994**, *115*, 175–178.

[3] a) F. S. Gimble, J. Thorner, *Nature* **1992**, *357*, 301–306; b) D. A. Shub, H. Goodrich-Blair, *Cell* **1992**, *71*, 183–186; c) R. F. Doolittle, *Proc. Natl. Acad. Sci. USA* **1993**, *90*, 5379–5381; d) A. M. Lambowitz, M. Belfort, *Annu. Rev. Biochem.* **1993**, *62*, 587–622.

[4] M.-Q. Xu, M. W. Southworth, F. B. Mersha, L. J. Hornstra, F. B. Perler, *Cell* **1993**, *75*, 1371–1377.

[5] E. O. Davis, P. J. Jenner, P. C. Brooks, M. J. Colston, S. G. Sedgwick, *Cell* **1992**, *71*, 201–210.

[6] A. A. Cooper, Y. J. Chen, M. A. Lindorfer, T. H. Stevens, *EMBO J.* **1993**, *12*, 2575–2583.

[7] R. Hirata, Y. Anraku, *Biochem. Biophys. Res. Comm.* **1992**, *188*, 40–47.

[8] M.-Q. Xu, D. G. Comb, H. Paulus, C. J. Noren, Y. Shao, F. B. Perler, *EMBO J.* **1994**, *13*, 5517-5522.

[9] A post-translational modification strategy was employed to photoreversibly inhibit serine proteases with cinnamates: a) I. V. Berezin, S. D. Varfolomeyev, K. Martinek, *FEBS Lett.* **1970**, *8*, 173–175; b) N. A. Porter, J. Bruhnke, *J. Am. Chem. Soc.* **1989**, *111*, 7616–7618; c) B. L. Stoddard, J. Bruhnke, P. Koenigs, N. Porter, D. Ringe, G. A. Petsko, *Biochemistry* **1990**, *29*, 8042–8051.

[10] a) T. W. Greene, *Protective Groups in Organic Chemistry*, Wiley, New York, **1981**, p. 32; b) U. Zehavi, B. Amit, A. Patchornik, *J. Org. Chem.* **1972**, *37*, 2281–2284; c) U. Zehavi, A. Patchornik, *ibid.* **1972**, *37*, 2285.

[11] a) C. J. Noren, S. J. Anthony-Cahill, M. C. Griffith, P. G. Schultz, *Science* **1989**, *244*, 182–188; b) J. Ellman, D. Mendel, S. Anthony-Cahill, C. J. Noren, P. G. Schultz, *Methods Enzymol.* **1991**, *202*, 301–336; c) C. J. Noren, S. J. Anthony-Cahill, K. A. Noren, M. C. Griffith, P. G. Schultz, *Nucleic Acids Res.* **1990**, *18*, 83–88; d) S. A. Robertson, C. J. Noren, S. J. Anthony-Cahill, M. C. Griffith, P. G. Schultz, *ibid.* **1989**, *17*, 9649–9660.

[12] a) D. Mendel, J. A. Ellman, P. G. Schultz, *J. Am. Chem. Soc.* **1991**, *113*, 2758–2760; b) J. A. Ellman, D. Mendel, P. G. Schultz, *Science* **1992**, *255*, 197–200; c) D. Mendel, J. A. Ellman, Z. Chang, D. L. Veenstra, P. A. Kollman, P. G. Schultz, *ibid.* **1992**, *256*, 1798–1802; d) H. Chung, D. Benson, P. G. Schultz, *ibid.* **1993**, *259*, 806–809; e) K. Judice, T. R. Gamble, E. C. Murphy, A. M. de Vos, P. G. Schultz, *ibid.* **1993**, *261*, 1578–1581; f) V. W. Cornish, D. R. Benson, C. A. Altenbach, K. Hideg, W. L. Hubbell, P. G. Schultz, *Proc. Natl. Acad. Sci. USA* **1994**, *91*, 2910–2914.

[13] The truncated construct pANY5 was prepared by PCR deletion mutagenesis of pNEB687 [2d], in which the *Tli pol* gene, with intein-1 deleted, is under T7 promoter control. The amber mutation S1082*am* was introduced into pANY5 by oligonucleotide-directed mutagenesis (T. A. Kunkel, K. Bebenek, J. McClary, *Methods Enzymol.* **1991**, *204*, 125–139), creating pAOD1.

[14] a) G. Zubay, *Annu. Rev. Genet.* **1973**, *7*, 267–287; b) J. Collins, *Gene* **1979**, *6*, 29–42; c) J. Pratt in *Transcription and Translation: A Practical Approach* (Eds.: B. D. Hames, S. J. Higgins), IRL, Oxford, **1984**, pp. 179–209.

[15] J. Sambrook, E. F. Fritsch, T. Maniatis, *Molecular Cloning: A Laboratory Manual*, 2nd ed., Cold Spring Harbor Laboratory Press, Cold Spring Harbor, **1989**, pp. 18.60–18.74

Mesogenic Properties of Amphiphilic Liquid Crystals with an Unusual Head-Group Topology**

Frank Hildebrandt, Jörg Andreas Schröter, Carsten Tschierske,* Reinhard Festag, Ralf Kleppinger, and Joachim Heinz Wendorff

Liquid crystalline phases may be displayed by anisotropic as well as by amphiphilic molecules. Anisotropic (calamitic or discotic) molecules are arranged with their long axes parallel to each other to give thermotropic smectic or columnar liquid-crystalline phases. In contrast, the driving force of the self-organization of amphiphilic molecules is their ability to segregate incompatible (for example, hydrophilic and hydrophobic) parts of the individual molecules. This gives rise to large aggregates which form the basis of lamellar, columnar, or cubic thermotropic and lyotropic mesophases. A combination of these two structural principles can provide new liquid-crystalline materials, consisting of rigid units connected with one, two, or even more hydrophilic groups at the termini of their alkyl chains.[1] The segregation of the different parts of the molecules is facilitated by the parallel arrangement of the rigid cores and visa versa. In amphiphilic polyhydroxy compounds this gives rise to significant mesophase stabilization.[2, 3] The question arose: What happens if a hydrophilic group is not terminally (Fig. 1, A), but laterally (C) attached to a rigid core? The two

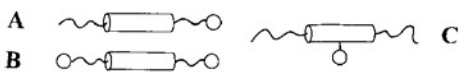

different organizing forces of liquid-crystalline phases would be perpendicularly directed to each other in these compounds, and the parallel arrangement of the calamitic units would disturb the segregation of hydrophilic and hydrophobic parts of the molecules and visa versa. We have therefore synthesized novel amphiphilic compounds with hydrophilic groups laterally attached to a rigid 4,4″-didecyloxy-*p*-terphenyl core.

The glycerol ether **3** (Fig. 2, see also Table 1)[4] is the first compound containing this molecular structure. Polarization microscopy established that it is a liquid-crystalline material. On cooling from the isotropic melt at 114 °C the transition to a liquid-crystalline phase can be seen by the formation of batonnets that rapidly coalesce to a focal conic fan texture with pseudoisotropic areas indicating a mesophase of the smectic A type, which crystallizes at 36 °C. No additional phase transition was detected in this temperature range. Reheating gives a melting point of 83 °C.

Institut für Organische Chemie der Universität
Weinbergweg 16, D-06015 Halle (Germany)
Telefax: Int. code + (345)5511182

R. Festag, Dr. R. Kleppinger, Prof. Dr. J. H. Wendorff
Fachbereich Physikalische Chemie und Wissenschaftliches Zentrum für Materialwissenschaften der Universität Marburg (Germany)

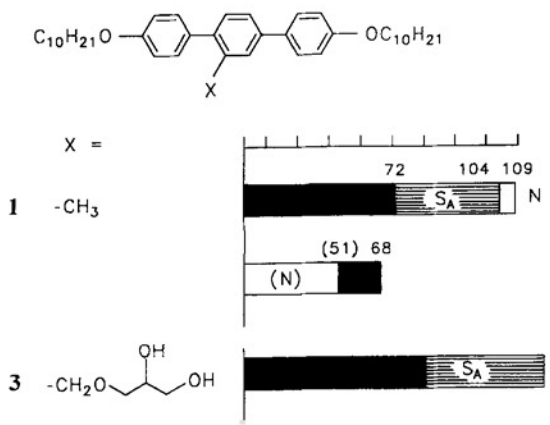

Fig. 2. The influence of lateral substituents on the mesophase behavior of 2′-substituted 4,4″-didecyloxy-terphenyl derivatives. The transition temperatures are displayed as columns: black areas indicate the crystalline state and hatched or blank areas correspond to liquid-crystalline phases (S_A and N, respectively). If the liquid-crystalline phase appears below the melting point, these are metastable (monotropic) mesophases; they were detected by cooling from the isotropic melt. The numbers above the bars indicate that phase-transition temperatures as determined by polarization microscopy. Values in brackets refer to monotropic phase transitions. Abbreviations: N = nematic mesophase, S_A = smectic A Phase. In the case of **1** a monotropic smectic C phase occurs at 70 °C.

In addition the mesophase of compound **3** was investigated with X-ray scattering. The X-ray pattern shows several sharp reflections in the small-angle region, which can be attributed to a layered structure: the peaks can be indexed to the third order. An amorphous halo occurs in the wide-angle region. The compound **3** thus displays a smectic layer structure without long-range order in the layers (S_A phase). A layer thickness of 3.13 nm (at 92 °C) results. Using CPK models and assuming an all-*trans* conformation of the alkyl chains, the molecular length was estimated to be 3.8 nm. The individual molecules are thus arranged parallel to each other in the layers, and the diol groups are placed between the terphenyl groups. The thickness of the smectic layers is significantly smaller than the length of the individual molecules. This can be attributed to a partial intercalation of the terminal alkyl chains. Because the lateral groups are comparatively large, the terphenyl groups are forced apart. The additional free space between the alkyl chains allows a deep interdigitation, which results in a layer distance significantly lower than the molecular length.

A comparison of the diol compound **3** with the 4,4″-didecyloxy-2′-methylterphenyl (**1**, Fig. 2)[5] indicates an influence of the bulky lateral diol group that stabilizes the mesophase. It is indeed very surprising that although the diol **3** has a significantly larger lateral substituent, it displays the greater mesophase stability. This mesophase stabilization is especially evident from the comparison of the diol **3** with compound **2** carrying a lateral substituent of comparable size but without hydroxyl groups; it is contradictory to all previous experience. Until now it was well established that larger substituents in the lateral position of the rigid core of calamitic liquid crystals give rise to a more or less significant destabilization of the liquid-crystalline phases.[6]

We therefore have to assume, that hydrogen bonding between the diol groups is responsible for the unexpected mesophase stabilization of compound **3**.

Although the mesophase stabilization by hydrogen bonding is well documented for amphiphilic diols with terminal diol groups,[2] the mesophase stabilization by lateral diol groups is rather surprising. The formation of a smectic layer structure can only be explained if one assumes a parallel arrangement of the terphenyl units with the diol groups placed between the rigid

cores within the layers. This arrangement contrasts with the usually observed segregation of hydrophilic and hydrophobic parts of amphiphilic molecules and should disturb the hydrogen bonding.

The IR spectra of compound **3** display a broad absorption in the frequency range of the O–H stretching vibrations, indicating the presence of large hydrogen bonding networks. Temperature-dependent measurements of the pure compound show an unusually large shift of its frequency with increasing temperature (Fig. 3). This temperature dependence can be attributed to a successiv collapse of intermolecular hydrogen bonding with increasing temperature. Intermolecular H-bonding is dominant in the crystalline state ($\tilde{\nu}_{max}$ = 3360 cm^{-1}) and also in the liquid-crystalline state. The aggregates are significantly smaller in the liquid state, and an absorption at 3580 cm^{-1} indicates the presence of a substantial number of single molecules with intramolecular hydrogen bonding between the OH groups within the diol unit. The arrangement of the molecules in layers seems to allow the most efficient intermolecular hydrogen bonding and any disturbence of the longitudinal order causes their breakdown.

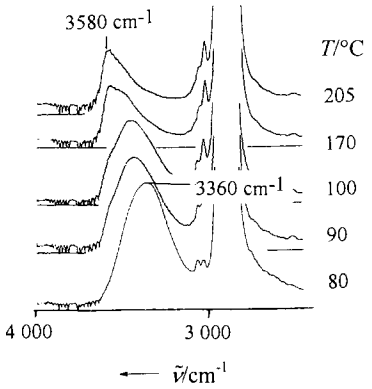

Fig. 3. Sections of the temperature-dependent IR spectra of compound **3** in the range 2500–4000 cm^{-1}, measured with a BIORAD-FTS-40 spectrophotometer, in a heated thermal cell SPECEC P/N 21.500.

In order to estimate the influence of the lateral hydrogen bonding on the molecular order within the smectic mesophase, the nonamphiphilic compound **1** was also investigated by X-ray scattering. In the S_A phase the layer thickness is 3.47 nm (at 85 °C). This is a little bit surprising, because this distance is larger than that of compound **3**. However, the lateral side group of compound **1** is only a methyl group and thus much smaller than the bulky 2-oxa-4,5-dihydroxypentyl group of compound **3**. The possibilities for interdigitation are reduced, and the thickness is consequently much closer to the molecular length. Another remarkable finding is the smaller number of small-angle peaks (three distinct peaks for compound **3** and only two at compound **1**). This indicates a better longitudinal order of the layers built up by the diol derivative **3**. The better ordering is evidently due to the formation of hydrogen bonds between the diol groups. The position of these groups and therefore of the hydrogen bonds between the rigid cores leads to an enhancement of the longitudinal ordering of those cores.

We must conclude that the liquid-crystalline phases of calamitic mesogens can be stabilized by lateral substituents that strongly interact with each other by hydrogen bonding. In order to verify this hypothesis, the chemical structure of these new amphiphilic liquid crystals has been varied by changing the lateral hydrophilic group. The thermotropic liquid crystalline properties of the amides **5**–**8**[7] are compared in Figure 4 (for spectroscopic data of **7** and **8**, see Table 1). It indicates that the mesophase stability of the S_A phase indeed rises with increasing number of hydroxyl groups in the growing lateral chain. The "glucamide" **8** (1-[2,5-bis(4-decyloxyphenyl)benzoylamido]-1-deoxy-D-sorbitol) represents the first example of an entirely novel type of liquid-crystalline carbohydrates.[8] The microscopic texture of the

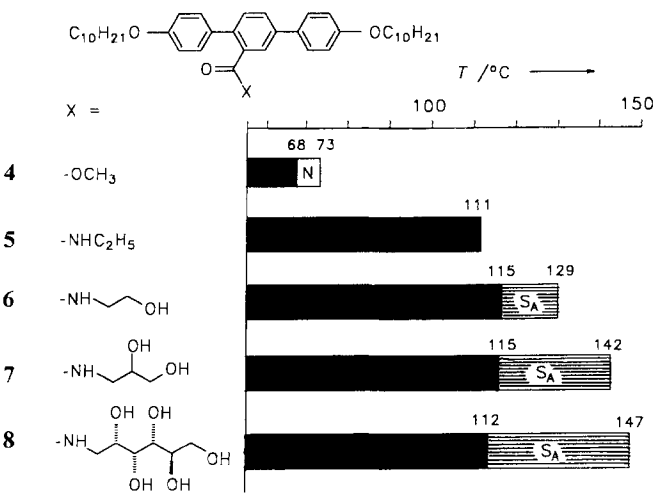

Fig. 4. The influence of the number of hydroxyl groups on the thermotropic mesophase behavior of 2'-substituted 4,4''-didecycloxyterphenyl derivatives. For an explanation see Fig. 2.

Table 1. Spectroscopic data of **3**, **7**, and **8** [a].

3: ^{1}H NMR (200 MHz, $CDCl_3$): δ = 7.64 (d, J = 1.7 Hz, 1H), 7.49–7.57 (m, 4H), 7.24–7.33 (2d, 4H), 6.91–6.99 (2d, 4H), 4.49 (s, 2H), 3.99 (t, J = 6.5 Hz, 4H), 3.81–3.84 (m, 1H), 3.55–3.71 (m, 2H), 3.42–3.56 (m, 2H), 1.80 (m, 4H), 1.27–1.64 (m, 28H), 0.88 (t, J = 6.0 Hz, 6H); MS: m/z 646 ([M]$^+$, 100%)

7: ^{1}H NMR (500 MHz, $CDCl_3$): δ = 7.86 (d, J = 2.0 Hz, 1H), 7.63 (dd, J = 2.0 Hz, J = 8.0 Hz, 1H), 7.54 (d, J = 8.7 Hz, 2H), 7.36 (d, J = 8.0 Hz, 1H), 7.33 (d, J = 8.7 Hz, 2H), 6.93–6.97 (2d, 4H), 5.72 (t, J = 6.0 Hz, 1H), 3.99 (t, J = 6.7 Hz, 2H), 3.98 (t, J = 6.7 Hz, 2H), 3.57 (ddd, 1H), 3.45 (dd, J = 4.5 Hz, J = 11.6 Hz, 1H), 3.40 (dd, J = 5.2 Hz, J = 11.6 Hz, 1H), 3.32–3.38 (m, 1H), 3.21–3.27 (m, 1H), 1.79 (m, 4H), 1.27–1.50 (m, 28H), 0.87 (t, J = 6.5 Hz, 6H); MS: m/z 659 ([M]$^+$, 100%)

8: ^{1}H NMR (500 MHz, [D$_6$]DMSO): δ = 8.13 (t, J = 5.4 Hz, 1H), 7.56–7.71 (m, 4H), 7.38 (d, J = 8.1 Hz, 1H), 7.33 (d, J = 8.6 Hz, 2H), 7.02 (d, J = 8.5 Hz, 2H), 6.93 (d, J = 8.5 Hz, 2H), 4.72 (d, J = 4.8 Hz, 1H), 4.44 (d, J = 5.4 Hz, 1H), 4.34 (d, J = 5.8 Hz, 1H), 4.29 (t, J = 5.6 Hz, 1H), 4.22 (d, J = 6.6 Hz, 1H), 3.96–4.01 (2t, 4H), 3.31–3.69 (m, 7H), 3.16 (m, 1H), 1.72 (m, 4H), 1.26–1.42 (m, 28H), 0.85 (t, J = 6.8 Hz, 6H); MS: m/z 749 ([M]$^+$, 67%).

[a] Correct C,H analyses and ^{1}H NMR spectra are available for all compounds.

mesophase between 112 °C and 147 °C is typical for a smectic A phase. The X-ray pattern exhibits a sharp Bragg reflection and the corresponding reflections of second and third order (Fig. 5). The d value amounts approximately 3.3 nm, which again corresponds to a smectic layer structure in which the terphenyl units are arranged parallel to each other.

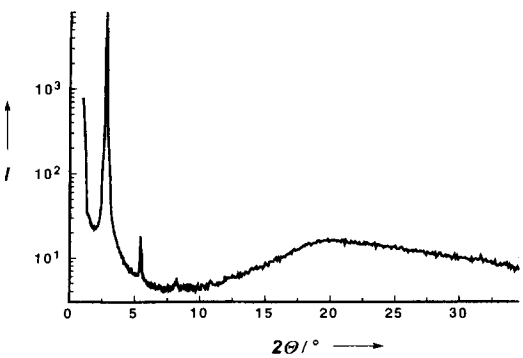

Fig. 5. X-ray scattering of compound **8** in the mesophase at 116 °C. I = intensity in arbitary units.

 © VCH Verlagsgesellschaft mbH, D-69451 Weinheim, 1995 0570-0833/95/1515-1632 $ 10.00+.25/0

Though no detailed miscibility studies have been carried out, preliminary contact preparations suggest that the smectic A phases of compounds **1** and **3** and those of the compounds **3** and **8** are completely miscible.

Intermolecular hydrogen bonding is also found in carboxylic acids that are known to form dimers. In Figure 6 the carboxylic acid **10** is compared with its acid chloride **9** and the methyl carboxylate **4**. Again the carboxylic acid (the compound that

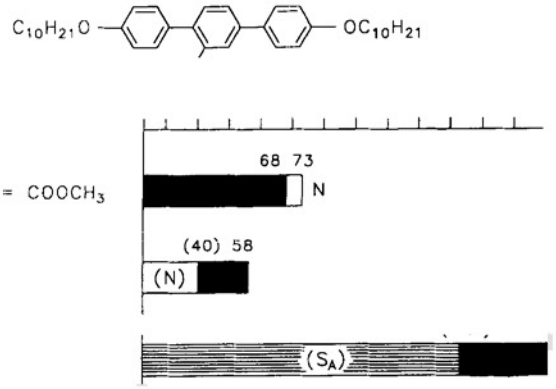

Fig. 6. Comparison of the phase-transition temperatures T/°C of 2,5-bis(4-decyloxyphenyl)benzoic acid (**10**) and the corresponding acid chloride **9** and methyl benzoate **4** (determined by polarization microscopy).

can form hydrogen bonding) displays the higher mesophase stability. The recently described laterally connected siamese twin mesogens[9] and also the covalent, laterally connected trimesogens[5] may be looked upon as examples for covalent, laterally fixed molecules. These compounds also display higher mesophase stabilities compared with structurally related calamitic single mesogens.

If one compares the compounds **1**–**10** it is obvious that lateral fixing of calamitic molecules by hydrogen bonding also increases the structural order, which stabilizes the layered smectic A phase with respect to the nematic phase (N) of the nonamphiphilic compounds. These new compounds also differ in this respect from laterally alkyl substituted calamitic compounds which usually favor the nematic phase.[6]

In summary, we have shown that there is an ambivalent influence of hydrophilic lateral substituents. Their steric requirements tend to separate the rigid cores from each other, which decreases the molecular order and should thus give rise to a significant mesophase destabilization. However, attractive forces between these substituents—such as hydrogen bonding—strongly fix the individual molecules to each other. If these attractive forces exceed the repulsive forces, the longitudinal order of the molecules is increased, and smectic liquid-crystalline phases are stabilized. In this way, lateral fixing of calamitic mesogens by hydrogen bonding is a new approach to smectic materials with broad mesomorphic ranges.

Furthermore, these new amphiphilic diol derivatives resemble an amphiphilic architecture which closely resembles that of the naturally occurring cholic acid salts and some peptides;[10] both consist of rigid stuctures with surfaces of different polarity. The biomimetic potential of these facial amphiphiles makes it exciting to study their ability to form other self-organizing supramolecular systems, such as lyotrophic mesophases, micelles, and thin films. These investigations are under way.

[1] H. Ringsdorf, B. Schlarb, J. Venzmer, *Angew. Chem.* **1988**, *100*, 117–162; *Angew. Chem. Int. Ed. Engl.* **1988**, *27*, 113–158.
[2] D. Joachimi, C. Tschierske, H. Müller, J. H. Wendorff, L. Schneider, R. Kleppinger, *Angew. Chem.* **1993**, *105*, 1205–1207; *Angew. Chem. Int. Ed. Engl.* **1993**, *32*, 1165–1167.
[3] F. Hentrich, C. Tschierske, S. Diele, C. Sauer, *J. Mater. Chem.* **1994**, *4*, 1547–1558.
[4] Compound **3** was obtained by phase-transfer-catalyzed etherification of 2'-bromomethyl-4,4''-didecyloxyterphenyl [5] with 4-hydroxymethyl-2,2-dimethyl-1,3-dioxolane (50% NaOH, cat. Bu_4NHSO_4, 100 °C, 2 h) followed by acid-catalyzed hydrolysis (pyridinium toluene-4-sulfonate (Py · TosOH, MeOH)) of the isopropylidene protective group (yield 30%). For the synthesis of **2** *n*-propanol was used.
[5] J. Andersch, S. Diele, P. Göring, J.-A. Schröter, C. Tschierske, *J. Chem. Soc. Chem. Commun.* **1995**, 107–108.
[6] W. Weissflog, D. Demus, *Cryst. Res. Technol.* **1984**, *19*, 55–64.
[7] Compound **4** was synthesised by Pd-catalyzed cross-coupling of methyl 2,5-dibromobenzoate with two equiv. 4-decyloxyphenyl boronic acid [5] (yield 93%). Saponification gave the carboxylic acid **10**, which was transformed into the acid chloride **9** by treatment with oxalyl chloride (R. Adams, L. H. Ulich, *J. Am. Chem. Soc.* **1920**, *42*, 599). Compounds **6**–**8** were obtained by aminolysis of crude compound **9** with excess 2-aminoethanol, 2,3-dihydroxypropylamine, and D-glucamine, respectively (yields: 76–91%).
[8] Reviews: B. Pfannemüller, *Starch* **1988**, *40*, 476–486; G. A. Jeffrey, *Acc. Chem. Res.* **1986**, *19*, 168; G. A. Jeffrey, L. M. Wingert, *Liq. Cryst.* **1992**, *12*, 179–202.
[9] W. Weissflog, D. Demus, S. Diele, P. Nitschke, W. Wedler, *Liq. Cryst.* **1989**, *5*, 111–122; A. C. Griffin, S. F. Thames, M. S. Bonner, *Mol. Cryst. Liq. Cryst.* **1977**, *34*, 135–139.
[10] M. C. Carey, D. M. Small, *Arch. Intern. Med.* **1972**, *130*, 506, 7319–7320; T. M. Stein, S. H. Gellman, *J. Am. Chem. Soc.* **1992**, *114*, 3943–3950; D. G. Barrett, S. H. Gellman, *ibid.* **1993**, *115*, 9343–9344.

Bromides of Rare Earth Metal Boride Carbides —A System of Building Blocks**

Hansjürgen Mattausch and Arndt Simon*

Only a few metal-rich rare earth metal halides MX_n with $n \leq 2$ are known namely M_2X_3[1–3] and LaI.[4] Other compounds described as binary phases and accessible in low yields, however, finally turned out to be "stabilized" by interstitial atoms.[5] Due to the electropositive nature of the rare earth metals these interstitial atoms have anionic character.

Addition of H, C, N, O in experiments to reduce rare earth trihalides led to numerous new ternary compounds, whose structures could be systematized in terms of a condensation of characteristic building units[6]: M_4O tetrahedra, M_6N_2 double tetrahedra, M_4H tetrahedra, and M_6H_2 octahedra as well as M_6C and M_6C_2 octahedra were repeatedly found. These units can be combined as was demonstrated recently with compounds containing the interstitial atoms C/H,[7] C/O,[8, 9] and C/N[10, 11] simultaneously. Here we report new phases with B/C which particularly well illustrate this building block principle.

$Gd_4Br_3C_2B$, $La_3Br_2C_2B$, and $Ce_6Br_3C_3B_2$ are the first members of a presumably large class of compounds. They can be

[*] Prof. Dr. A. Simon, Dr. H. Mattausch
Max-Planck-Institut für Festkörperforschung
Heisenbergstrasse 1, D-70569 Stuttgart (Germany)
Telefax: Int. code + (711)689-1642

[**] The help of C. Hochrathner, R. Eger, R. Pöttgen, and N. Weishaupt in drawing, preparation, X-ray diffraction and electrical measurements, respectively, is gratefully acknowledged.

obtained as black needles or bars by heating stoichiometric amounts of MBr_3, M, C, and B for several days.[12]

Figure 1 shows the building blocks that occur in the structures of $Gd_4Br_3C_2B$, $La_3Br_2C_2B$, and $Ce_6Br_3C_3B_2$.[13] In these building blocks discrete C atoms are always octahedrally coordinated by M atoms, and B–C units are formed with a trigonal prism around the B atoms connected to a tetragonal pyramid around C. The structure of $Gd_4Br_3C_2B$ contains molecular B–C units with $d_{B-C} = 156$ pm and discrete C atoms (Fig. 1a, 1b).

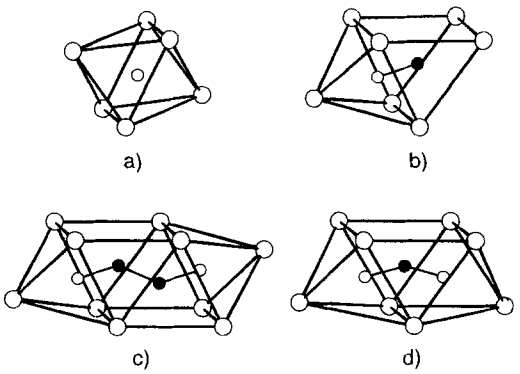

Fig. 1. Monomeric units in the structures of $Gd_4Br_3C_2B$, $La_3Br_2C_2B$, and $Ce_6Br_3C_3B_2$. B: small filled circles, C: small open circles, M: large circles. a) Octahedral coordination of discrete C atoms by M atoms; b) B–C unit with the B atom residing in a trigonal prism and the C atom in a tetragonal pyramid; c) Condensation of two B–C (cf. Fig. 1b) units to form a C-B-B-C group. d) C-B-C unit with the B atom residing in a trigonal prism around and both C atoms in tetragonal pyramids.

In the structure of $Ce_6Br_3C_3B_2$ single C atoms occur together with C-B-B-C groups (Fig. 1a, 1c) which form by condensation of two units of the building blocks shown in Figure 1b through the prism faces. The distances in the B_2C_2 group are $d_{C-B} = 153$ pm and $d_{B-B} = 164$ pm; the C-B-B angle is 139°. The structure of $La_3Br_2C_2B$ contains exclusively BC_2 units characterized by a d_{B-C} distance of 149 pm and C-B-C angle of 148°.

The units shown in Figure 1 are condensed in layers according to Figures 2–4.[15] The space between the layers is filled by Br atoms which belong to a single layer in $Ce_6Br_3C_3B_2$ and $La_3Br_2C_2B$, but some of them interconnect layers in $Gd_4Br_3C_2B$. In the chosen projection of the structure of $Gd_4Br_3C_2B$ the layers are composed of alternating double chains of the building blocks shown in Figures 1a and 1b. The octahedra and prisms are condensed through edges and square faces, respectively. The expansion of these faces leads to long distances between neighboring B–C units ($d_{B-B} = 208$ pm). In the chosen projection for $Ce_6Br_3C_3B_2$ and $La_3Br_2C_2B$ the prisms condensed through their triangular faces are clearly visible. The resulting chains of prisms alternate with chains of octahedra in the case of $Ce_6Br_3C_3B_2$ and are directly coupled in $La_3Br_2C_2B$. The interatomic distances between adjacent B–C groups exceed 380 pm.

The described discrete B-C, C-B-B-C, and C-B-C units are characteristic fragments of the structures of boride carbides of transition metals, lanthanoids, and actinoids. For example, the B_2C_2 units characteristic for $Ce_6Br_3C_3B_2$ are linked to give chains in the structures of UBC[16] and ThBC[17] by the formation of B–B bonds, and the structure of $Th_3B_2C_3$ ($= Th_3C(BC)_2$)[18] contains C-B-B-C units and discrete C atoms. The incorporation of halogen atoms, leads to a breakdown of such three-dimensional networks into layers. The

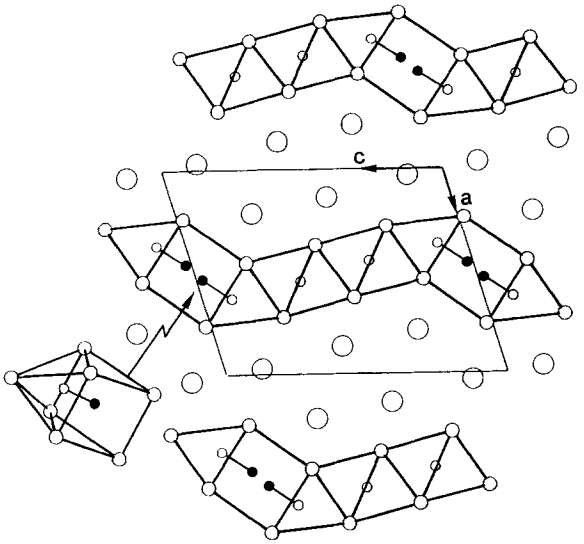

Fig. 2. Projection of the structure of $Gd_4Br_3C_2B$ along [010]. Units (1a) and (1b) (see Fig. 1) are condensed into layers with Br atoms (large circles) arranged between the layers. To illustrate the environment of the B–C unit the prisms and the tetragonal pyramids are drawn separately on the lower left-hand side. The unit cell is outlined.

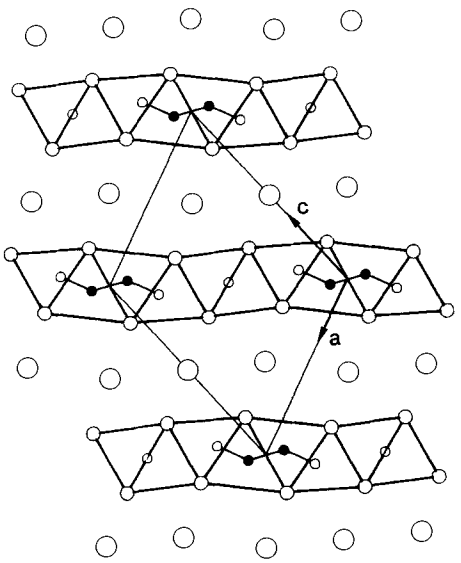

Fig. 3. Projection of the structure of $Ce_6Br_3C_3B_2$ along [010]. Alternating strings of units (1a) and (1c) (see Fig. 1) are condensed into layers which are linked through Br atoms. The unit cell is outlined.

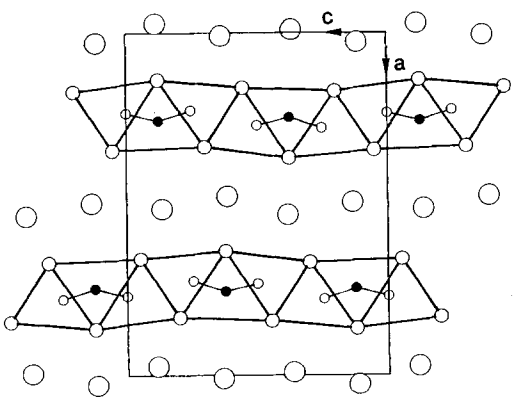

Fig. 4. Projection of the structure of $La_3Br_2C_2B$ along [010]. Slightly corrugated layers, parallel to (001) are composed of unit (1d) (see Fig. 1) and separated by Br atoms. The unit cell is outlined.

 © VCH Verlagsgesellschaft mbH, D-69451 Weinheim, 1995 0570-0833/95/1515-1634 $ 10.00+.25/0

fragmentation gives access to a local description of the complex bonding situation in carbide borides.

The structural units found in $Gd_4Br_3C_2B$ can be discussed within the Zintl–Klemm concept as $(Gd^{3+})_4(Br^-)_3(C^{4-})(CB^{5-})$. The B–C distance of 155 pm is in agreement with that calculated for the "methyl borane"-derived BC^{5-} anion.[19] However, it is clear from the low electrical resistivity (van der Pauw method[20]) of this compound, $\rho = 8$ mΩcm in the range between 50 and 300 K, that the treatment of chemical bonding in terms of localized electrons is only applicable in certain cases. In fact, the distance $d_{B-B} = 208$ pm corresponds to a Pauling bond order of 0.22.[19] The existence of weak bonds between B atoms of adjacent B–C units is verified by COOP (COOP = crystal orbital overlap population) analysis on the basis of extended Hückel calculations.[21] Although the "intermolecular" distances between B_2C_2 units in $Ce_6Br_3C_3B_2$ are sufficiently large to exclude bonding interactions, the question remains, whether $B_2C_2^{11-}$ anions can be formulated or whether electrons are partially delocalized in bands exhibiting metal–metal bonding character. For $La_3Br_2C_2B$ the anionic species BC_2^{7-}, which is isoelectronic with SO_2, can be derived according to the Zintl–Klemm concept $(La^{3+})_3(Br^-)_2(BC_2^{7-})$. The BC_2 unit, however, is less bent than SO_2 ($\sphericalangle$O-S-O = 119°, $\sphericalangle$C-B-C = 148°). In Sc_2BC_2 the BC_2 unit is even linear. Evidently, in agreement with the metallic conductivity[22] and the results of band structure calculations[23] one electron per formula unit is delocalized in bands with M–M bonding character in accordance with the formulation $(Sc^{3+})_2(BC_2^{5-})e^-$. $La_3Br_2C_2B$ also shows metallic conductivity so that a partial delocalization of electrons in bands with La character is also expected in this metallic phase.

In the structures of rare earth metal carbide halides zero-, one- and two-dimensional fragments of the three-dimensional carbide structures are realized. We aim to develop a similar structural chemistry with carbide borides.

Received: April 4, 1995 [Z 7864 IE]
German version: *Angew. Chem.* **1995**, *107*, 1764–1766

Keywords: boron compounds · bromides · carbides · lanthanoids · solid-state structures

[1] D. A. Lokken, J. D. Corbett, *Inorg. Chem.* **1973**, *12*, 556.
[2] A. Simon, N. Holzer, H. Mattausch, *Z. Anorg. Allg. Chem.* **1979**, *456*, 207.
[3] H. Mattausch, J. B. Hendricks, R. Eger, J. D. Corbett, A. Simon, *Inorg. Chem.* **1980**, *19*, 2128.
[4] J. D. Martin, J. D. Corbett, *Angew. Chem.* **1995**, *107*, 234; *Angew. Chem. Int. Ed. Engl.* **1995**, *34*, 233.
[5] A. Simon, *Angew. Chem.* **1981**, *93*, 23; *Angew. Chem. Int. Ed. Engl.* **1981**, *20*, 1.
[6] A. Simon, H. Mattausch, G. J. Miller, W. Bauhofer, R. K. Kremer, *Handbook on the Physics and Chemistry of Rare Earth, Vol. 15* (Eds.: K. A. Gschneidner, Jr, L. Eyring), Elsevier, Amsterdam, **1991**, p. 191.
[7] M. Ruck, A. Simon, *Z. Anorg. Allg. Chem.* **1992**, *617*, 7.
[8] G. Meyer, H. Mattfeld, K. Kraemer, *Z. Anorg. Allg. Chem.* **1993**, *619*, 1384.
[9] H. Mattausch, H. Borrmann, A. Simon, *Z. Naturforsch. B* **1993**, *48*, 1828.
[10] H. Mattausch, H. Borrmann, R. Eger, R. K. Kremer, A. Simon, *Z. Anorg. Allg. Chem.* **1994**, *620*, 1889.
[11] H. Mattausch, H. Borrmann, R. Eger, R. K. Kremer, A. Simon, *Z. Naturforsch. B*, **1995**, *50*, 931.
[12] The starting materials (~2 g) were heated in Ta-containers welded under 1 atm Ar and protected against oxidation by quartz glass ampoules (10 days at 1370 K for $La_3Br_2C_2B$, 12 days at 1320 K for $Gd_4Br_3C_2B$ and 10 days at 1470 K for $Ce_6Br_3C_3B_2$) and quenched to room temperature. For the preparation and purification of the starting materials compare ref. [10].
[13] Measurement of the single-crystal intensities on a four-circle diffractometer (CAD4, Enraf-Nonius), $Ag_{K\alpha}$ radiation. Empirical absorption correction (ψ-scan). Full matrix least-squares refinement on F^2 [14]. $La_3Br_2C_2B$: *Pnma*; $a = 1532.3(1)$, $b = 397.3(1)$, $c = 1156.7(1)$ pm. La(1): 0.3315(1), 1/4, 0.7003(1); La(2): 0.1360(1), 1/4, 0.8775(1); La(3): 0.3411(1), 1/4, 0.0527(1); Br(1): 0.0270(1), 1/4, 0.1151(1), Br(2): 0.0089(1), 1/4, 0.6348(1); C(1): 0.2682(2), 1/4, 0.4997(2); C(2): 0.2760(2), 1/4, 0.2527(2); B(1): 0.2548(2), 3/4, 0.8757(3). $R_1 = 0.027$, $wR_2 = 0.048$ (all 2719 independent reflections). – $Gd_4Br_3C_2B$: $P2_1/m$; $a = 954.7(4)$, $b = 369.3(1)$, $c = 1244.5(3)$ pm, $\beta = 106.68(1)$°. Gd(1): 0.6266(1), 1/4, 0.4596(1); Gd(2): 0.4565(1), 1/4, 0.8058(1); Gd(3): 0.2813(1), 1/4, 0.2664(1); Gd(4): 0.7594(1), 1/4, 0.0207(1); Br(1): 0.9686(1), 1/4, 0.8678(1); Br(2): 0.1358(1), 1/4, 0.4443(1); Br(3): 0.2136(1), 3/4, 0.7238(1); C(1): 0.5491(9), 1/4, 0.6330(2); C(2): 0.3704(10), 1/4, 0.1049(6); B(1): 0.4647(12), 3/4, 0.0217(8). $R_1 = 0.053$, $wR_2 = 0.113$ (all 2775 independent reflections). – $Ce_6Br_3C_3B_2$: $P2/m$; $a = 860.2(2)$, $b = 382.9(1)$, $c = 1022.0(2)$ pm, $\beta = 112.53(3)$°. Ce(1): 0.2867(1), 0, 0.4836(1); Ce(2): 0.9433(1), 1/2, 0.1633(1); Ce(3): 0.3722(1), 1/2, 0.2223(1); Br(1): 0, 1/2, 1/2; Br(2): 0.6505(1), 0, 0.1868(1); C(1): 1/2, 1/2, 1/2; C(2): 0.1673(3), 0, 0.2264(3); B(1): 0.0928(4), 0, 0.0650(3). $R_1 = 0.027$, $wR_2 = 0.049$ (all 2410 independent reflections). The correct assignment of B and C shows up clearly in the *R* values and the displacement parameters. Further details of the crystal structure investigations may be obtained from the Fachinformationszentrum Karlsruhe, D-76344 Eggenstein-Leopoldshafen (Germany, on quoting the depository numbers CSD-401744 ($Ce_6Br_3C_3B_2$), CSD-401745 ($Gd_4Br_3C_2B$), and CSD-401746 ($La_3Br_2C_2B$).
[14] G. M. Sheldrick, *SHELXTL-PLUS, Göttingen*, **1992** und *SHELX-93*, Göttingen, **1993**.
[15] C. K. Johnson, ORTEP-ORNL-3794, Oak Ridge Nat. Lab., Oak Ridge, **1971**.
[16] P. Rogl, B. Rupp, I. Felner, P. Fischer, *J. Solid State Chem.* **1993**, *110*, 377.
[17] P. Rogl, *J. Nucl. Mater.* **1978**, *73*, 198.
[18] P. Rogl, *J. Nucl. Mater.* **1979**, *79*, 154.
[19] L. Pauling, *Die Natur der chemischen Bindung*, Verlag Chemie, Weinheim, **1973**.
[20] L. J. van der Pauw, *Philips Res. Rep.* **1958**, *13*, 1.
[21] J. Köhler, *PC-Version eines Extended-Hückel-Programmes*, unpublished, **1993**.
[22] J. Bauer, M. Potel, P. Gougeon, J. Padiou, H. Noël, *Proc. 9th Int. Conf. on Solid Compounds of Transition Elements, Royal Society of Chemistry, Dalton Division*, Oxford, **1988**.
[23] J. F. Halet, J.-Y. Saillard, J. Bauer, *J. Less-Common Met.* **1990**, *158*, 239.

A New Application of Capillary Zone Electrophoresis: Determination of Energy Barriers of Configurationally Labile Chiral Compounds**

Gerald Weseloh, Christian Wolf, and Wilfried A. König*

Various techniques may be applied in the investigation of configurationally labile compounds. The racemates may be resolved into their enantiomers, and the energy barrier of enantiomerization investigated by chiroptical methods. Alternatives avoiding enantiomeric enrichment or separation are dynamic NMR spectroscopy, HPLC, or GC.[1] Kinetic parameters must, however, be determined by computer simulation of the experimental data.

We describe a new procedure for the determination of energy barriers of enantiomerization reactions based on capillary zone electrophoresis (CZE).[2] With this method enantiomerization reactions may be investigated in the temperature range 25 °C–95 °C by using small amounts of racemic samples, which are typical for CZE. Subsequent computer simulation is unnecessary.

4,4′-Diamino-2,2′-diisopropylbiphenyl **1**, which is present as its diammonium dication in the buffer of pH 3.0, is excellently resolved into its enantiomers by the chiral additive heptakis(2,3,6-tri-*O*-methyl)-β-cyclodextrin in the electrophoretic buffer. Figure 1 shows sche-

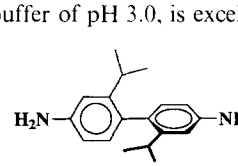

1

[*] Prof. Dr. W. A. König, Dipl.-Chem. G. Weseloh, Dipl.-Chem. C. Wolf
Institut für Organische Chemie der Universität
Martin-Luther-King-Platz 6, D-20146 Hamburg (Germany)
Telefax: Int. code + (40)4123-2893
e-mail: doenneck@chemie.uni-hamburg.de

[**] C.W. thanks the Fonds der Chemischen Industrie for a scholarship.

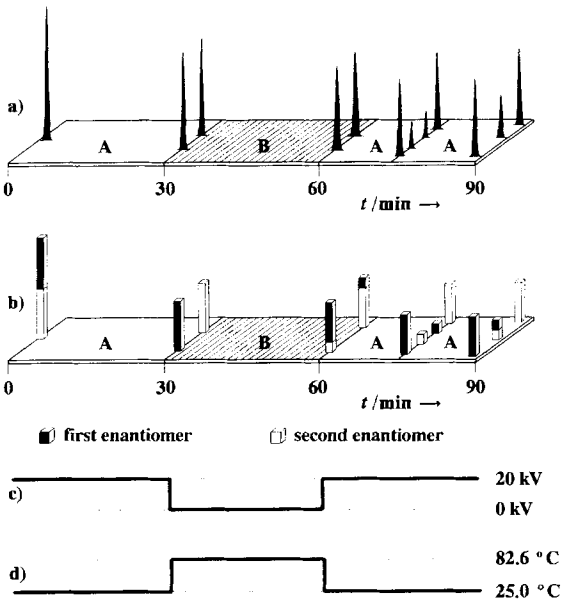

Fig. 1. Schematic illustration of the separation procedure in the capillary over the whole experiment including the enantiomerization time (a) and the enantiomeric composition of each peak (b). In section A the separation proceeds, whereas in section B enantiomerization takes place. The voltage during the experiment is given by (c), and the temperature in the capillary by (d).

matically the analytic method and illustrates the experimental voltage and temperature program. Initially the separation procedes at low temperature to the middle of the capillary. At this point the voltage is switched off. The sample is already completely resolved into the enantiomers. The temperature is increased to a certain value, and the separated enantiomers are left to interconvert for a certain period. The capillary is then cooled to the original temperature, and by switching on the voltage, electrophoresis is continued in the second half of the capillary. In the detector the newly formed racemate is recorded as a new signal located exactly between the signals of the two enantiomers. A correction of the peak area, which is usually indispensable in CZE because of the difference in speed of the sample components is not necessary.[3] Figure 2 shows a typical electropherogram of an enantiomerization experiment.

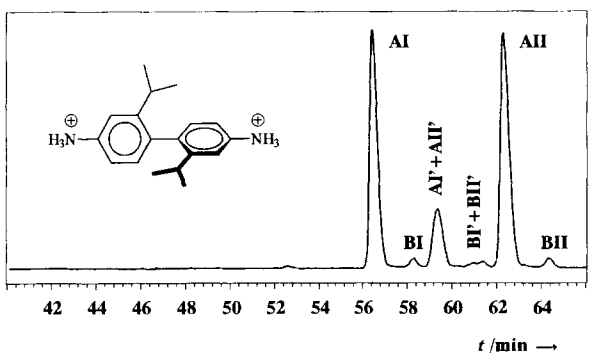

Fig. 2. Electropherogram of an enantiomerization experiment. The duration of enantiomerization is not accounted for in the time axis. AI and AII are the signals of the two enantiomers of **1**. AI' + AII' is the signal corresponding to the interconverted sample. BI, BII, and BI' + BII' are the signals of a structural isomer of **1**. Capillary length: 130 cm; distance to the detector 110 cm; buffer: 30 mM H_3PO_4/NaH_2PO_4 (pH 3.0) to which 0.05% hydroxyethylcellulose had been added as well as heptakis(2,3,6-tri-*O*-methyl)-β-cyclodextrin (30 mM) as a chiral selector; field strength: 154 Vcm^{-1}; separation temperature: 25 °C; temperature of enantiomerization: 82.6 °C. The sample (0.1 mmolar solution) was electrokinetically injected (3 sec at 20 kV).

For the determination of the rotational barriers, experiments with different periods of enantiomerization were performed (Fig. 3). The energy barrier was calculated according to first-order reaction kinetics.

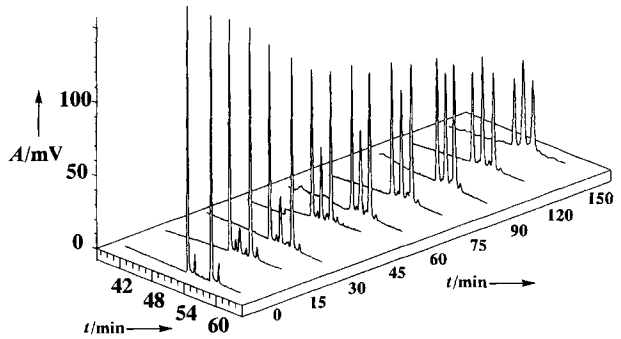

Fig. 3. Comparison of separations with different enantiomerization times.

The rotational energy barrier of the dication of **1** determined by this procedure was 115.2 ± 0.2 $kJmol^{-1}$ at 82.6 °C. Polarimetric investigations of the enantiomerically enriched dication of **1** in ethanol/HCl gave 112.8 ± 0.1 kJ^{-1} at 86.9 °C. Since the energy barrier was determined at comparable temperatures and in similar solvent systems with both methods, the difference of 2.4 $kJmol^{-1}$ may be ascribed to a stabilizing interaction with the cyclodextrin derivative.

The procedure introduced here allows the determination of rotational energy barriers of compounds that cannot be investigated by dynamic GC, HPLC, or NMR spectroscopy. The method can be applied easily on minute sample amounts. No preseparation of the racemate into enantiomers is required. The peak areas are directly correlated with the interconverted sample amount. Thus, in contrast to dynamic methods, a computer simulation is unnecessary.

Experimental Procedure

All experiments were performed with a capillary electrophoresis System 100 (Grom, Herrenberg). The capillary was kept at constant temperature by a water thermostat Julabo Paratherm FT 20B electronic and by a mgw Lauda RC20 cryostat. The sampling system was modified to accommodate sample vials. For recording the detector signals (UV at 210 nm) an Atari-ST computer with a data system from F & A Gibau (Hamburg) was used.

After installation the capillary was rinsed for 10 min each with 1 M NaOH, 0.1 M NaOH, and fully deionized water (Millipore RO_{10}Plus). Before each experiment it was rinsed for 5 min with the buffer used. All solutions were filtered through a 0.45 µm syringe filter (Sartorius RC 15 and Lida 0.45 µm Nylon). To avoid the formation of air bubbles in the capillary during the heating period, the buffer was degassed with helium directly prior to electrophoresis.

Received: February 1, 1995 [Z 7680 IE]
German version: *Angew. Chem.* **1995**, *107*, 1771–1772

Keywords: atropisomerism · biphenyls · capillary zone electrophoresis · chirality · cyclodextrins

[1] a) G. Bott, L. D. Field, S. Sternhell, *J. Am. Chem. Soc.* **1980**, *102*, 5618–5626; b) A. Mannschreck, L. Kießl, *Chromatographia* **1989**, *28*, 263–266; c) M. Jung, M. Fluck, V. Schurig, *Chirality* **1994**, *6*, 510–512.
[2] H. Engelhardt, W. Beck, J. Kohr, T. Schmitt, *Angew. Chem.* **1993**, *105*, 659–680; *Angew. Chem. Int. Ed. Engl.* **1993**, *105*, 629–649.
[3] X. Huang, W. F. Coleman, R. N. Zare, *J. Chromatogr.* **1989**, *480*, 95–110.

Self-Assembling Discotic Mesogens**

Ralf Kleppinger, C. Peter Lillya,* and Changqing Yang

Since their discovery in 1977[1] many varieties of discotic liquid crystals have been described.[2] While there are many examples of calamitic (rod-shaped) mesogens that self-assemble by hydrogen bonding,[3] there are few examples of columnar mesophase formation by well-defined supramolecules. Some neat soaps,[4] diisobutylsilane diol,[5] Lattermann's monoaryl esters of *cis,cis*-1,3,5-cyclohexanetriol,[6] and Praefcke's inositol derivatives[7] form columnar mesophases as a consequence of amphiphilic interactions. Rationally planned association is apparent in examples reported by Malthête et al.[8] (carboxylic acid dimerization), by Lehn et al.[9] (complementary base pairing), and by Matsunaga et al.[10] (hydrogen bonding parallel to the column axes). None of these examples involves a self-assembled supramolecule with a predictable composition and a persistent disklike shape. Malthête's and Lehn's examples come the closest, but their supramolecules must act in pairs to simulate disks, behavior which would not have been predicted on the basis of molecular structure. We report below the first example of rational molecular design of a predictable self-assembled disklike supramolecule that forms a columnar mesophase.

Our strategy takes advantage of the strong tendency of α-pyridones to form hydrogen-bonded dimers, a phenomenon elegantly exploited by Wuest in his design and study of techtons and other self-assembling species.[11] We surmised that suitably substituted 6(5*H*)-phenanthridinones (**1**) would form persistent disklike dimers (Scheme 1) and consequently would behave as discotic mesogens.

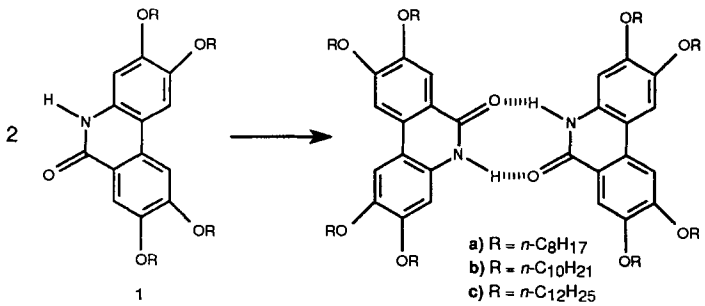

Scheme 1. Dimerization of 6(5*H*)-phenanthridinone derivatives.

To test this hypothesis we synthesized three tetraalkoxy-6(5*H*)-phenanthridinones (**1a–c**, Table 1) via the tetramethoxybiphenylcarboxylate intermediate **2** (Scheme 2), the synthesis of which was previously reported by Dow.[12] Phenanthridinone derivatives **1a–c** exhibited reproducible behavior over multiple DSC heating and cooling cycles[17] (Table 2). The octyl derivative **1a** exhibits several transitions on cooling only, but the decyl (**1b**) and dodecyl (**1c**) derivatives each show two endotherms on heating and two exotherms on cooling. The transitions at the higher temperatures exhibit small enthalpies, consistent with mesophase–isotropic phase transitions.[13] The large enthalpies and supercooling values of the lower temperature transitions are consistent with crystallization.[14]

Table 1. Physical data for compounds **1a–c** [a].

1a: IR (KBr): $\tilde{\nu}$ = 3400 (br., N–H str.), 1670 cm^{-1} (C=O, str.); ^{1}H NMR (200 MHz, $CDCl_3$, TMS): δ = 10.23 (br. s, 1H; N*H*), 7.89 (s, 1H; H_5), 7.50 (s, 1H; H_{10}), 7.42 (s, 1H; H_1), 6.77 (s, 1H; H_4), 4.24–4.07 (m, 8H; OCH_2), 1.90 (m, 8H; OCH_2CH_2), 1.3 (m, 40H; CH_2), 0.89 (t, ^3J = 6.3 Hz, 12H; CH_3); ^{13}C NMR (75 MHz, $CDCl_3$, TMS): δ = 162.2, 153.7, 151.3, 149.0, 145.4, 130.9, 129.8, 118.3, 111.4, 109.9, 108.8, 104.3, 100.7, 71.0, 69.3, 69.2, 31.8, 29.6, 29.4, 29.3, 29.2, 26.1, 22.7, 14.1; MS: *m/z* = 707.5487 [*M*$^+$], 708.5549 [*M*$^+$ + H].

1b: IR (KBr): $\tilde{\nu}$ = 3400 (br., N–H str.), 1670 cm^{-1} (C=O, str.); ^{1}H NMR (200 MHz, $CDCl_3$, TMS): δ = 9.53 (s,1H; N*H*), 7.86 (s, 1H; H_5), 7.49 (s, 1H; H_{10}), 7.41 (s, 1H; H_1), 6.69 (s, 1H; H_4), 4.2–4.0 (m, 8H; OCH_2), 1.9 (m, 8H; OCH_2CH_2), 1.5–1.2 (m, 56H; $(CH_2)_7$), 0.88 (t, ^3J = 6.5 Hz, 12H; CH_3); ^{13}C NMR (75 MHz, $CDCl_3$, TMS): δ = 162.0, 153.7, 151.3, 149.1, 145.4, 130.8, 129.7, 118.4, 111.4, 110.0, 108.9, 104.3, 100.6, 71.0, 69.3, 69.2, 31.9, 29.6, 29.5, 29.2, 26.1, 22.7, 14.1; MS: *m/z* = 819.6741 [*M*$^+$], 820.6797 [*M*$^+$ + H]. Elemental analysis: calcd for $C_{53}H_{80}NO_5$: C 77.60, H 10.96, N 1.71; found: C 77.35, H 11.27, N 2.02.

1c: IR (KBr): $\tilde{\nu}$ = 3400 (br., N–H str.), 1670 cm^{-1} (C=O, str.); ^{1}H NMR (200 MHz, $CDCl_3$, TMS): δ = 9.89 (br. s, 1H; N*H*), 7.88 (s, 1H; H_5), 7.49 (s, 1H; H_{10}), 7.41 (s, 1H; H_1), 6.73 (s, 1H; H_4), 4.24–4.06 (m, 8H; OCH_2), 1.90 (m, 8H; OCH_2CH_2), 1.5–1.3 (m, 72H; CH_2), 0.88 (t, ^3J = 6.3 Hz, 12H; CH_3); ^{13}C NMR (75 MHz, $CDCl_3$, TMS): δ = 162.2, 153.7, 151.3, 149.0, 145.4, 130.8, 129.7, 118.4, 111.4, 110.0, 108.9, 104.3, 100.7, 71.0, 69.3, 69.2, 31.9, 29.72, 29.68, 29.53, 29.46, 29.39, 29.2, 26.1, 22.7, 14.1; MS: *m/z* = 931.8028 [*M*$^+$], 932.8101 [*M*$^+$ + H].

[a] Mass spectrometry results were obtained from the Midwest Center for Mass Spectrometry at the University of Nebraska, Lincoln.

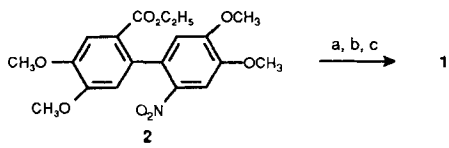

Scheme 2. Synthesis of 6(5*H*)-phenanthridinones **1a–c**. Reagents: a) 1. BBr_3/CH_2Cl_2, −78 °C to room temperature; 2. CH_3OH. b) RBr/KI/K_2CO_3/4-methyl-2-pentanone, reflux, 3 days. c) Fe/AcOH, 100 °C, 12 h. Overall yield: 20–25%.

Table 2. Phase transition temperatures of **1a–c**, determined by DSC [a].

	1a		**1b**		**1c**	
	K–M	M–I	K–M	M–I	K–M	M–I
Heating *T* [°C]	114.2 [b]		98.8	118.4	88.3	108.0
ΔH [J g^{-1}]	68.0 [b]	–	66.7	2.8	40.5	1.8
Cooling *T* [°C]	90.4	111.2	78.8	104.7	69.3	103.1
ΔH (J g^{-1}]	66.0	2.3	69.0	2.7	57.9	2.0

[a] K = crystalline phase; M = mesophase; I = isotropic phase. Heating and cooling at 10 °C min^{-1}. [b] K→*I* transitions.

Examination by polarizing optical microscopy[17] confirmed that **1a** forms a monotropic mesophase on cooling, while **1b** and **1c** form enantiotropic mesophases. In the mesophase **1a–c** exhibit focal conic textures. Cooling all three compounds from the isotropic phase caused the dendritic mesophase growth that is a common feature of columnar phase formation[14] (Fig. 1).

In variable-temperature FT-IR measurements[15] on **1c** over a temperature range from 70 °C to 170 °C only hydrogen-bonded phenanthridinone could be detected. At all temperatures the N–H absorption was broad with no high frequency components, while the carbonyl absorption appeared near 1670 cm^{-1}.

[*] Prof. Dr. C. P. Lillya, Dr. R. Kleppinger, Dr. C. Yang
Department of Chemistry, University of Massachusetts
Amherst, MA 01003-4510 (USA)
Telefax: Int. code + (413) 545-4490

[**] This work was supported by the Material Research Laboratory of the University of Massachusetts and the Petroleum Research Fund of the American Chemical Society. The original ideas were developed while C. P. L. enjoyed the hospitality of Prof. H. Ringsdorff's research group at the Institut für Organische Chemie at the Universität Mainz, Germany. R. K. thanks the Deutsche Forschungsgemeinschaft for a fellowship grant (KL 954/1-1).

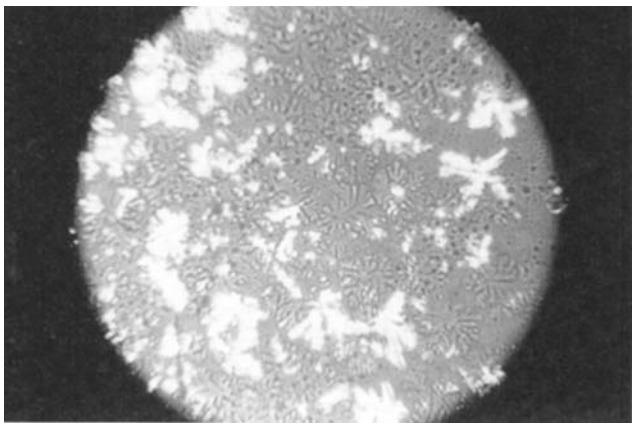

Fig. 1. Photomicrograph of dendritic mesophase growth of **1b**, cooled from isotropic phase to 105 °C. Photo with nearly parallel polarizers, 100×.

X-ray diffraction patterns[16] of the unoriented mesophase of **1b** revealed sharp reflections corresponding to Bragg spacings of 26, 15, and 13 Å, consistent with hexagonal packing of columns. Indeed, small angle diffraction patterns of properly oriented samples resolved into six hexagonally oriented spots on annealing in the mesophase (Fig. 2). The wide-angle region revealed a

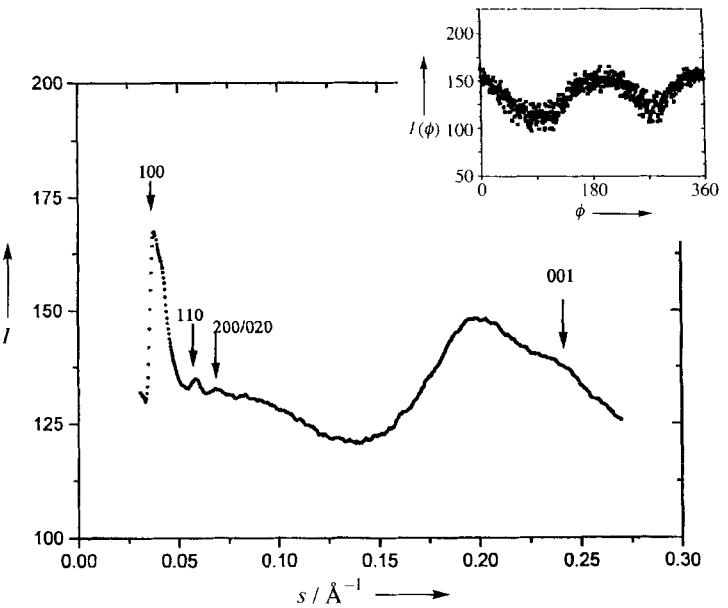

Fig. 2. X-ray scattering diagram of mesophase of **1b**. The radial intensity distribution (I in arbitrary units, $s = (2\sin\theta)/\lambda$ [Å]$^{-1}$) displays reflections from inter- (100, 110, 200/020) and intracolumnar order (001). The insert shows the azimuthal intensity distribution $I(\phi, s = 0.25$ Å$^{-1})$ of the intracolumnar reflection, derived from a densitometer scan performed on a flat-chamber X-ray diagram. The original X-ray pattern was taken from an oriented sample in the mesophase at 110 °C.

halo (max. at 4.5 Å) arising from the liquidlike alkyl side chains, and a broad reflection at 3.6 Å, corresponding to the average distance between disks in the stack. These observations are consistent with a hexagonal columnar phase (D_h), with an intercolumnar distance of 31 Å, and an intracolumnar disk stacking distance of 3.6 Å. Using these lattice parameters, we calculated a mesophase density of 0.45 g cm^{-3} if the mesogenic entity is the monomer but 0.90 g cm^{-3} if the mesogenic entity is a dimer. Only the latter value is tenable; thus phenanthridinone derivatives **1a–c** form the predicted disk-shaped dimers, which, in turn, form hexagonal columnar mesophases.

Received: January 27, 1995
Revised version: April 26, 1995 [Z 7667 IE]
German version: *Angew. Chem.* **1995**, *107*, 1762–1764

Keywords: hydrogen bonding · liquid crystals · phenanthridinones · self-assembly

[1] S. Chandrasekhar, B. K. Sadashiva, K. A. Suresh, *Pramana* **1977**, *9*, 471.
[2] For review, see: a) S. Chandrasekhar in *Advanced Liquid Crystals, Vol. 5* (Ed.: G. H. Brown), Academic Press, **1982**, p. 49; b) S. Chandrasekhar, *Liq. Cryst.* **1993**, *14*, 3; c) S. Chandrasekhar, *Liquid Crystals*, Cambridge University Press, **1977**; d) A. J. Leadbetter in *Thermotropic Liquid Crystals* (Ed.: G. W. Gray), Wiley, New York, **1987**, p. 1; e) N. H. Tinh, H. Gasparoux, C. Destrade, *Mol. Crystal. Liq. Crystal.* **1981**, *68*, 101; f) N. H. Tinh, C. Destrade, H. Gasparoux, *Phys. Lett. A* **1979**, *72*, 251.
[3] a) G. W. Gray, B. Jones, *J. Chem. Soc.* **1953**, 4179; b) G. W. Gray, B. Jones, *ibid.* **1954**, 683; c) J. W. Goodby, *Mol. Cryst. Liq. Cryst.* **1984**, *110*, 205; d) T. Kato, J. M. J. Fréchet, *J. Am. Chem. Soc.* **1989**, *111*, 8533; e) T. Kato, A. Fujishima, J. M. J. Fréchet, *Chem. Lett.* **1990**, 919.
[4] P. A. Segt, A. E. Skoulios, *Acta Crystallogr.* **1966**, *21*, 892, and references therein.
[5] a) *Liquid Crystals of One- and Two-Dimensional Order* (Eds.: W. Helfrich, G. Heppke), Springer, Berlin, **1980**; b) J. D. Bunning, J. W. Goodby, G. W. Gray, J. E. Lydon in ref. [5a], p. 397.
[6] a) G. Lattermann, *Liq. Cryst.* **1987**, *2*, 723; b) G. Lattermann, G. Staufer, *ibid.* **1989**, *4*, 347; c) M. Ebert, R. Kleppinger, M. Soliman, M. Wolf, J. H. Wendorff, G. Lattermann, G. Staufer, *ibid.* **1990**, *7*, 553.
[7] K. Praefcke, P. Marquardt, B. Kohne, W. Stephan, A.-M. Levelut, E. Wachtel, *Mol. Cryst. Liq. Cryst.* **1991**, *203*, 149.
[8] J. Malthête, A. Collet, A.-M. Levelut, *Liq. Cryst.* **1989**, *5*, 123. We thank a referee for calling this case to our attention and pointing out that a single disk, or column slice, contains *two* carboxylic acid dimers. This is deducible from the lattice parameters given in ref. [8].
[9] M.-J. Brienne, J. Gabard, J.-M. Lehn, I. Stibor, *J. Chem. Soc. Chem. Commun.* **1989**, 1868.
[10] a) J. Kawamata, Y. Matsunaga, *Mol. Cryst. Liq. Cryst.* **1993**, *231*, 79, and previous publications; b) J. Malthête, A.-M. Levelut, L. Liébert, *Adv. Mater.* **1992**, *4*, 36.
[11] a) Y. Ducharme, J. D. Wuest, *J. Org. Chem.* **1988**, *53*, 5787; b) M. Gallant, M. T. Phan Viet, J. D. Wuest, *ibid.*, **1991**, *56*, 2284; c) *J. Am. Chem. Soc.* **1991**, *113*, 721; d) M. Simard, D. Su, J. D. Wuest, *ibid.* **1991**, *113*, 4696. Wuest et al. proposed the term techton (Gr.: builder) for compounds whose interactions are determined by associative forces and which self-assemble to a network structure with a particular architecture or function.
[12] R. L. Dow, (Pfizer Inc.), *PCT Int. Appl. WO 92/21660*, (Cl. C07D221/12), **1992**; US Appl. 706 629 29, **1991**. We thank Dr. Dow for communicating the experimental details for related syntheses.
[13] a) C. Destrade, M. C. Mondon, J. Malthete, *J. Phys. (Paris)* **1979**, *40*, C3; b) C. Destrade, N. H. Tinh, H. Gasparoux, J. Malthete, A.-M. Levelut, *Mol. Cryst. Liq. Cryst.* **1981**, *71*, 111; c) S. Kumar, E. J. Wachtel, E. Keinan, *J. Org. Chem.* **1993**, *58*, 3821. The unusually large supercooling of the **1b** I→M transition is reproducible.
[14] a) J. Billard in ref. [5a], p. 383; b) J. Billard, J. C. Dubois, N. H. Tinh, A. Zann, *Nouv. J. Chim.* **1978**, *2*, 535.
[15] We thank Professor S. L. Hsu and his students, Department of Polymer Science and Engineering, University of Massachusetts, for carrying out these measurements.
[16] X-ray diffraction was performed on the X-ray facilities in the Department of Polymer Science and Engineering. Wide-angle X-ray scattering was performed on a Siemens D-500 goniometer ($Cu_{K\alpha}$ radiation, $\lambda = 1.54$ Å) operating in reflection mode. Heating was maintained with a homemade heating stage. Flat-chamber exposures on samples annealed just below the clearing temperature were performed with a Statton camera, with an X-ray beam collimated with a 200 mm pinhole.
[17] We thank Prof. H. Winter, and Prof. R. Porter, Department of Polymer Science and Engineering, University of Massachusetts, for the enabling us to perform the microscopy and calorimetic studies.

Disaccharide Mimetics by Enzymatic Tandem Aldol Additions**

Oliver Eyrisch and Wolf-Dieter Fessner*

Dedicated to Professor R. R. Schmidt on the occasion of his 60th birthday

The increasing amount of detailed knowledge on the mode of action of complex oligosaccharides in biological recognition phenomena and the occurrence of longer chain sugars as the bioactive principle of compounds like the tunicamycins have placed the synthesis of higher homologous sugars containing 8–13 carbons and their derivatives in the focus of modern carbohydrate chemistry.[1] Of particular interest are *C*-disaccharides[2] as nonhydrolyzing antimetabolites, that is, potential inhibitors of glycoside-processing enzymes. Classical synthetic strategies—iterative chain elongation or convergent block condensations on the basis of available pentoses or hexoses—require the free, unmasked carbonyl group of the sugars and thus intensive protecting group manipulations. Limited availability or reactivity of suitably configurated precursors from the "chiral pool" are obvious further restrictions.

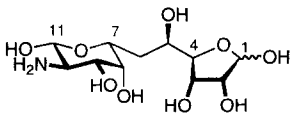

Tunicamine

In the context of the developing enzymatic de novo syntheses of simple sugars[3] and extending their chains by a C_3 unit to form C_8 and C_9 homologues by using aldolases,[4, 5] we present a new procedure: twofold chain elongation ("tandem" aldolization[6]) of simple, readily available dialdehydes afford dodeco-2,11-diuloses of doubly furanoid or pyranoid nature[7]—formally derived from ketohexoses by C-coupling tail to tail—in a highly stereoselective fashion and with deliberately variable substitution patterns.

The enzyme-mediated aldol reaction of dihydroxyacetone phosphate (DHAP) and 2- or 3-hydroxylated aldehydes leads to ketofuranoses or ketopyranoses, respectively, while the absolute and relative configurations of all stereocenters in the products can be controlled by the choice of the aldolase (C-3, C-4)[8] and by adopting a kinetically[9a] or thermodynamically selective[9b] reaction mode (C-5, C-6). In principle, such a process should also be applicable to difunctional aldehydes.[10] A plausible candidate for initial tests was 2,5-dihydroxyhexanedial (**2**). Dial **2** is smoothly formed by ozonolysis of racemic cyclohex-2-ene-1,4-diol (**1**)[11] followed by reductive workup and, according to an NMR analysis, exists in solution as a mixture of several constitutional isomers (hydrates, hemiacetals; mostly **2a**) (Scheme 1). Its FruA-catalyzed[8] coupling with DHAP, generated in situ by retroaldolization of fructose 1,6-bisphosphate (FBP), proceeded at a satisfactory rate (about 10% rel. v_{max}) with transient formation of a monoadduct (**3**; TLC analysis). The secondary addition to form **4a** may be at a certain kinetic disadvantage, because in the equilibrium the pyranose form **3a** with a masked aldehyde group is presumably more stable than **3b**, a furanose having a free aldehyde (hydrate) group, but the intermediate is

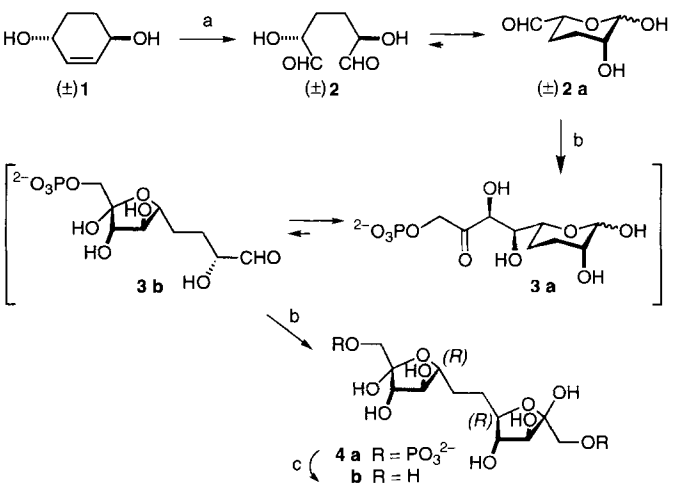

Scheme 1 [8]. a) O_3/MeOH, −78 °C; Me_2S, room temperature (RT). b) 1.3 equiv FBP, FruA (125 U), triosephosphate isomerase (250 U), pH 7.2, 2 days. c) Acid phosphatase (25 U), pH 5.8, 3 days; 37% **4b** from *rac*-**1**.

practically completely consumed in the presence of a slight excess of DHAP (FBP). After enzymatic dephosphorylation of **4a** with acid phosphatase, chromatography on Ca^{2+} ion-exchange resin, and crystallization from water–acetone, a bisadduct was isolated in 37% overall yield (based on *rac*-**1**; 74% based on (*R,R*)-**1**), which according to its spectra is unequivocally the C_2-symmetrical, all-*trans*-configurated **4b**,[12] a 6,6′-linked dimer of D-fructose. In the crude product mixture no significant amounts of the diastereomer stemming from the (*S,S*) antipode of **2** were detectable ($\leq 5\%$), which is expected to be significantly less stable owing to a twofold *cis*-vicinal substitution.

3,4-Dihydroxyhexanedial (**6**) was generated by oxidative ring cleavage of doubly homoallylic diol *rac*-**5**[13] (Scheme 2) and

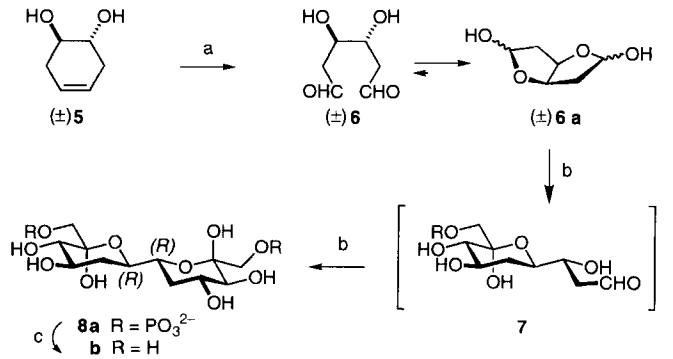

Scheme 2 [8]. a) O_3/MeOH, −78 °C; Me_2S, RT. b) 1.0 equiv FBP, FruA (500 U), triosephosphate isomerase (500 U), pH7.2, 7 days; 40% conversion. c) Acid phosphatase (50 U), pH 5.8, 16 h; 13% **8b** from *rac*-**5**.

shown by NMR spectroscopy to exist in aqueous solution as mixed bicyclic anomers **6a** ($\alpha\alpha$:$\alpha\beta$:$\beta\beta$ = 7:9:2), with no indication of a prevalence of a linear species ($\leq 2\%$). Accordingly, the primary aldolization step with DHAP/FruA proceeded considerably more sluggishly than the addition to **2**. The intermediate (presumably mainly pyranose **7**) was not detectable, and the only bisphosphate product was isolated after 7 days of reaction. Dephosphorylation provided in 13% total yield (based on *rac*-**5**; 26% based on (*R,R*)-**5**; about 60–70% when corrected for conversion) the crystalline bipyranoid diketose **8b**. Its C_2-symmetry and the bisequatorial connection between the rings

[*] Prof. Dr. W.-D. Fessner, Dr. O. Eyrisch
Institut für Organische Chemie der Technischen Hochschule
Professor-Pirlet-Strasse 1, D-52056 Aachen (Germany)
Telefax: Int. code + (241) 8888 127
e-mail: fessner@rwth-aachen.de

[**] Enzymes in Organic Synthesis, Part 10. This work was supported by the Deutsche Forschungsgemeinschaft (Grant Fe 244/2-2) and the Schwerpunktsprogramm "Synthese-Enzyme" from the state of Baden-Württemberg. We thank Christina Schütte for experimental assistance. Part 9: [5].

are conclusively corroborated by the simple NMR spectra[12] and by the typical occurrence of a pseudo-quartet for the axial protons 5-H and 8-H with almost identical geminal and vicinal couplings of approximately 12 Hz. Despite the use of an excess of DHAP (as FBP) no adduct of the (*S,S*) enantiomer of **6** had been formed. Its constitution (demanding a diaxial linkage) thus seems to be thermodynamically highly disadvantageous even relative to the furanoid FBP.

The *meso*-dialdehyde **10** can stabilize itself only by single cyclization (**10a**, Scheme 3) and therefore should display much better substrate qualities. Indeed, relatively rapidly a bisadduct

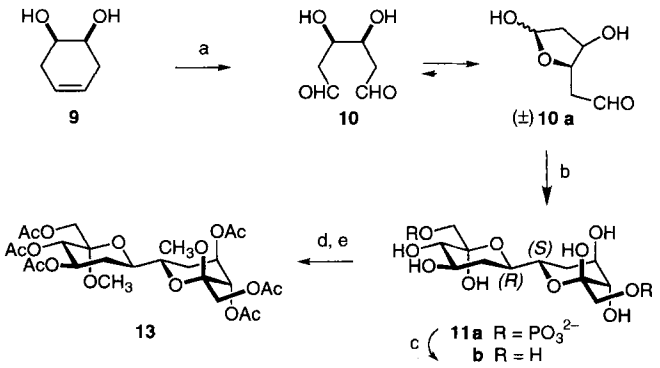

Scheme 3 [8]. a) O_3/MeOH, −78 °C; Me_2S, RT. b) 1.0 equiv FBP, FruA (250 U), triosephosphate isomerase (500 U), pH7.2, 16 h. c) Acid phosphatase (50 U), pH 5.8, 16 h; 71% from **9**. d) **11b** + MeOH, Dowex 50W-X8, reflux; 87% **12** (corresponds to **13**, where H replaces Ac). e) Ac_2O/py, RT; 91% **13**.

accumulated directly from the enzymatic reaction with DHAP/FruA; consequently a potential kinetic preference of the aldolase for the 3-(*S*)- or 3-(*R*)-hydroxyaldehyde moieties within **10** could not be uncovered. Neither phosphate ester **11a**, nor the free syrupy sugar **11b**, obtained in 70% overall yield by conventional processing, allowed a satisfactory NMR analysis to be carried out, because a complex equilibrium of anomers and/or conformers was apparently established, further complicated by the unequivocal participation of partially acyclic forms. Complete signal[12] and conformational analysis was possible for **13**, which was obtained by peracetylation of the sparingly soluble dimethyl glycoside **12** (87%). This revealed that the pyranose subunit stemming from the (*S*)-configurated part of the dialdehyde has to tolerate two axial *O*-acyl substituents at C-3′/C4′ in order to obviate an unfavorable equatorial to axial ring connection.

An application of the RhuA, stereocomplementary to FruA,[8] tested with **6** as example, furnished two rather startling results (Scheme 4): 1) Rapid consumption of DHAP abruptly ceased with formation of a monoadduct **14**, from which a bisadduct (**15a**) could only be obtained upon addition of the FruA enzyme; 2) NMR analysis[12] of **15b** unambiguously established a *cis*-vicinal substitution pattern in one of the two rings, rather than the expected two *trans* forms.

The failure of the RhuA enzyme in the second addition step has to be assigned to the anionic charge of the phosphate ester moiety in the intermediate **14a** (likewise, glyceraldehyde 3-phosphate is not accepted[14]). According to molecular models this charge can be oriented spatially close to the aldehyde group. Since on the other hand the FruA preferentially converts anionic substrates[4] but accepts **6** only reluctantly, the two biocatalysts complement each other almost perfectly for usage in a one-pot synthesis in which **15a** is indeed generated by simulta-

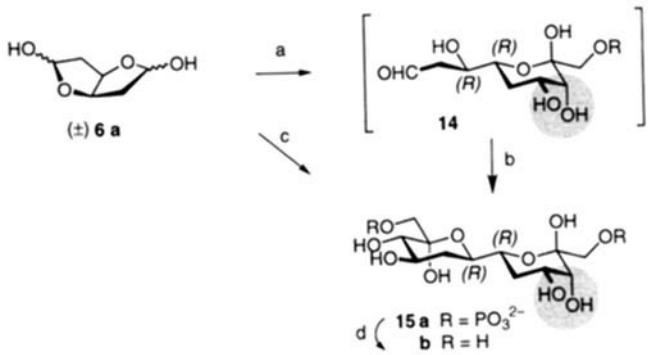

Scheme 4 [8]. a) 2.5 equiv. of DHAP, RhuA, pH 6.8. b) + FruA. c) 0.75 equiv. of FBP, RhuA (150 U), FruA (150 U), triosephosphate isomerase (500 U), pH7.2, 20 h. d) Acid phosphatase (50 U), pH 5.8, 16 h; 46% **15b** from *rac*-**6**.

neous action of both aldolases on **6** and on FBP with high selectivity (≥90% content of **15a** in the crude product; 46% total yield of **15b**). NMR analysis of the adduct and spectral comparison with **8b** substantiated the diequatorial ring connection, an all-equatorially substituted pyranose, and an axially oriented 3-OH group in the second ring ($J_{3,4}$ = 9.4, $J_{3',4'}$ = 3.2 Hz). Because of the employment of *rac*-**6** and "enantiogenic" aldolases, the *cis*-configuration could, in principle, have been created by either of the two enzymes (*epi*-4 OH by RhuA, *epi*-3 OH by FruA; **15** or *ent*-**15**, respectively), but may more plausibly be rationalized merely as the result of an incorrect binding of the aldehyde by the RhuA, since mechanistic arguments suggest enantiospecificity of all DHAP-dependent aldolases for C-3,[15] whereas a limited diastereoselectivity of the RhuA at C-4 for certain types of substrates has been documented.[16] Equilibration at longer reaction times probably allows the erroneously connected *cis*-adduct to accumulate.

The yields of the tandem reactions, some of which need improvement, on one hand reflect the inferior substrate qualities of aldehydes masked as hemiacetals and presumably having high apparent K_m values, and on the other hand the as yet nonoptimized reaction conditions, which, particularly due to the choice of fructose 1,6-bisphosphate as the source for DHAP, may have potential weaknesses in the slow attainment of equilibria of unknown nature; oxidative generation of DHAP in situ[17] seems to be a reasonable alternative. However, the fact that enantiomerically pure complex sugar skeletons of high structural variability can be made from readily accessible, racemic starting materials in a single synthetic step with creation of four new asymmetric centers and differentiation of two more (one of which is independent), makes enzymatic tandem aldolizations highly attractive.

Received: March 23, 1995 [Z 7824 IE]
German version: *Angew. Chem.* **1995**, *107*, 1738–1740

Keywords: aldolases · carbohydrates · disaccharide mimetics · tandem reactions

[1] a) S. J. Danishefsky, M. P. DeNinno, *Angew. Chem.* **1987**, *99*, 15–23; *Angew. Chem. Int. Ed. Engl.* **1987**, *26*, 15–23; b) C.-H. Wong, G. M. Whitesides, *Enzymes in Synthetic Organic Chemistry*, Pergamon, Oxford, **1994**; C.-H. Wong, R. L. Halcomb, Y. Ichikawa, T. Kajimoto, *Angew. Chem.* **1995**, *107*, 453–474; *Angew. Chem. Int. Ed. Engl.* **1995**, *34*, 412–432; **1995**, *107*, 569–593 and **1995**, *34*, 521–546.

[2] R. M. Paton, K. J. Penman, *Tetrahedron Lett.* **1994**, *35*, 3163–3166; R. W. Armstrong, D. P. Sutherlin, *ibid.* **1994**, *35*, 7743–7746; L. Lay, F. Nicotra, C. Pangrazio, L. Panza, G. Russo, *J. Chem. Soc. Perkin Trans. 1*, **1994**, 333–338, and references therein.

[3] W.-D. Fessner, C. Walter, *Angew. Chem.* **1992**, *104*, 643–645; *Angew. Chem. Int. Ed. Engl.* **1992**, *31*, 614–616.

[4] M. D. Bednarski, H. J. Waldmann, G. M. Whitesides, *Tetrahedron Lett.* **1986**, *27*, 5807–5810.

[5] O. Eyrisch, M. Keller, W.-D. Fessner, *Tetrahedron Lett.* **1994**, *35*, 9013–9016.

[6] L. F. Tietze, U. Beifuss, *Angew. Chem.* **1993**, *105*, 137–170; *Angew. Chem. Int. Ed. Engl.* **1993**, *32*, 131–163.

[7] The diketoses presented here (**4**, **8**, **11**–**12**, **15**) are neither carba-sugars nor *C*-glycosides. Their structural relationship to disaccharides suggests biological activities, which are currently under investigation.

[8] W.-D. Fessner in *Microbial Reagents in Organic Synthesis* (Ed.: S. Servi), Kluwer Academic Publishers, Dordrecht, **1992**, pp. 43–55. FruA = fructose 1,6-bisphosphate aldolase [EC 4.1.2.13], commercial enzyme from rabbit muscle (Sigma Type IV); RhuA = rhamnulose 1-phosphate aldolase [EC 4.1.2.19], recombinant enzyme from *E. coli* (purified according to ref. [16]). Amounts of enzyme activities correspond to respective DHAP equivalent.

[9] a) W.-D. Fessner, J. Badia, O. Eyrisch, A. Schneider, G. Sinerius, *Tetrahedron Lett.* **1992**, *33*, 5231–5234; W.-D. Fessner, A. Schneider, O. Eyrisch, G. Sinerius, J. Badia, *Tetrahedron Asymmetry* **1993**, *4*, 1183–1192; b) J. R. Durrwachter, C. H. Wong, *J. Org. Chem.* **1988**, *53*, 4175–4181; M. D. Bednarski, E. S. Simon, N. Bischofberger, W.-D. Fessner, M.-J. Kim, W. Lees, T. Saito, H. Waldmann, G. M. Whitesides, *J. Am. Chem. Soc.* **1989**, *111*, 627–635; W. J. Lees, G. M. Whitesides, *J. Org. Chem.* **1993**, *58*, 1887–1894.

[10] Although several attempts of additions to α,ω-dialdehydes (glyoxal, glutaric dialdehyde) have been reported in the literature, in no case has a product been characterized [18]. Our extensive studies corroborate that enzymatic assays indicate consumption of DHAP, but no defined products result (TLC, NMR analysis). Another problem is the cross-linking by aliphatic dialdehydes, which irreversibly destroys enzymatic activity. We attribute the success of the experiments presented here to the formation of stable hemiacetals by hydroxylated dialdehydes; relative rates of enzyme deactivation, however, have not been determined.

[11] J.-E. Bäckvall, S. E. Byström, R. E. Nordberg, *J. Org. Chem.* **1984**, *49*, 4619–4631.

[12] **4b**: M.p. 164 °C, $[\alpha]_D^{22}$ +11.7° (*c* = 0.3, H_2O), ^1H NMR (400 MHz, D_2O; β,β manomer) δ = 4.08 (d, 3-,10-H), 4.02 (t, 4-,9-H), 3.77 (m, 5-,8-H), 3.59 (d, 1a-,12a-H), 3.52 (d, 1b-,12b-H), 3.82–3.78 (m, 6-,7-H); ^{13}C NMR (100.6 MHz, D_2O; β,β anomer) δ 101.6, 80.2, 78.4, 75.9, 63.3, 29.9. **8b** (monohydrate): m.p. 87 °C, $[\alpha]_D^{22}$ −59.7° (*c* = 1.2, MeOH), ^1H NMR (400 MHz, D_2O) δ = 4.00 (d, 6-,7-H), 3.97 (ddd, 4-,9-H), 3.70 (d, 1a-,12a-H), 3.55 (d, 1b-,12b-H), 3.42 (d 3-,10-H), 1.97 (ddd, 5e-,8e-H), 1.63 (q, 5a-,8a-H); ^{13}C NMR (100.6 MHz, D_2O) δ = 98.4, 72.5, 70.3, 68.9, 64.2, 34.9. **12**: M.p. 228–230 °C (decomp.), $[\alpha]_D^{22}$ −15.8° (*c* = 0.6, H_2O), ^{13}C NMR (100.6 MHz, D_2O) δ = 101.9, 100.8, 73.4, 71.0, 68.7, 68.3, 66.9, 65.8, 61.2, 58.2, 48.5, 48.2, 34.2, 28.3. **13**: M.p. 189 °C, $[\alpha]_D^{22}$ −25.7° (*c* = 0.3, MeOH), ^1H NMR (400 MHz, $CDCl_3$) δ = 5.28 (ddd, 4-H), 5.16 (d, 3-H), 4.95 (d, 10-H), 4.90 (q, 9-H), 4.29, 4.16 (2 d, 1a-,12a-H), 4.07, 4.04 (2 d, 1b-,12b-H), 3.85 (ddd, 7-H), 3.72 (ddd, 6-H), 3.31, 3.26 (2 s, 2 OCH_3), 2.44 (ddd, 5e-H), 2.11, 2.09, 2.08, 2.08, 2.03, 2.02 (6 s, 6 Ac), 1.95 (dm, 8e-H), 1.76 (ddd, 8a-H), 1.57 (q, 5a-H). **15b**: syrup, $[\alpha]_D^{22}$ −15.6° (*c* = 2.4, MeOH), ^1H NMR (400 MHz, D_2O) δ = 4.17 (ddd, 9-H), 3.99 (d, 6-,7-H), 3.97 (m, 4-H), 3.76 (d, 10-H), 3.74, 3.71 (2 d, 1a-,12a-H), 3.54, 3.53 (2 d, 1b-,12b-H), 3.45 (d, 3-H), 1.98 (ddd, 5e-H), 1.80 (q, 8a-H), 1.68 (ddd, 8e-H), 1.63 (q, 5a-H); ^{13}C NMR (100.6 MHz, D_2O) δ = 98.8, 98.4, 72.4, 70.9, 70.6, 68.9, 68.2, 66.2, 64.8, 64.2, 34.8, 29.5.

[13] H. Suemune, M. Hizuka, *Chem. Pharm. Bull.* **1989**, *37*, 1379–1381.

[14] G. Sinerius, Dissertation, University of Freiburg, **1994**.

[15] R. A. Periana, R. Motiu-DeGrood, Y. Chiang, D. J. Hupe, *J. Am. Chem. Soc.* **1980**, *102*, 3923–3927.

[16] W.-D. Fessner, G. Sinerius, A. Schneider, M. Dreyer, G. E. Schulz, J. Badia, J. Aguilar, *Angew. Chem.* **1991**, *103*, 596–599; *Angew. Chem. Int. Ed. Engl.* **1991**, *30*, 555–558.

[17] W.-D. Fessner, G. Sinerius, *Angew. Chem.* **1994**, *106*, 217–220; *Angew. Chem. Int. Ed. Engl.* **1994**, *33*, 209–212.

[18] F. Effenberger, A. Straub, *Tetrahedron Lett.* **1987**, *28*, 1641–1644; H. P. Brockamp, M. R. Kula, *ibid.* **1990**, *31*, 7123–7126.

closo-$[B_5H_4PPh_3\{Fe(CO)_3\}\{Ir(CO)_2PPh_3\}]$: The First Structurally Characterized *closo*-Heterobimetallaheptaborane System**

Jonathan Bould, Nigam P. Rath, and Lawrence Barton*

nido-Metallahexaboranes, that is species in which a metal moiety replaces a BH group in *nido*-B_6H_{10}, are convenient starting materials for reactions of hexaboranes since they are easier to handle than B_6H_{10} itself.[1] Two metallahexaboranes can be easily prepared in high yield: *nido*-$[B_5H_9\{Os(CO)(PPh_3)_2\}]$[2] and *nido*-$[B_5H_8\{Ir(CO)(PPh_3)_2\}]$ (**1**).[2,3] While some reactions with osmahexaborane have been reported,[4] other than recent calculations[5] and our own preliminary report of the preparation of $[B_5H_6\{Ir(CO)(PPh_3)_2\}(\mu\text{-}H)\{PtCl(PMe_2Ph)\}]$,[6] nothing has been published about the reactivity of the iridahexaborane cluster since its synthesis was first reported in 1979.[3] This contrasts with, for example, metalladecaboranes which have been extensively studied and which show great similarities to the parent decaboranes.[7]

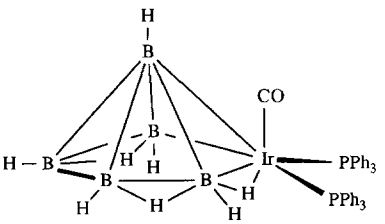

1

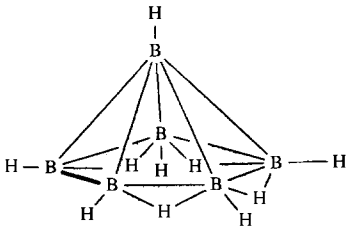

2

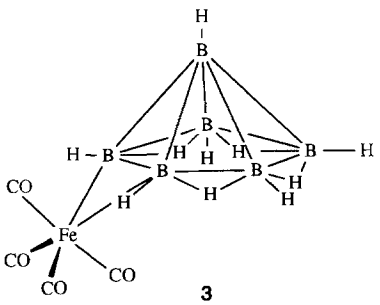

3

The B_6H_{10} cluster **2** contains a basal B–B bond with a high degree of basic character.[8] This is a feature that has been exploited in the formation of a number of compounds with iron,[9a–d] iridium,[9b] rhodium,[9b] and platinum,[9e] in which this bond donates two electrons to the metal. Thus for iron the reaction of B_6H_{10} with $[Fe_2(CO)_9]$ affords $[B_6H_{10}\{\mu\text{-}Fe(CO)_4\}]$ (**3**). It was therefore of interest to see if the iridahexaborane analogue **1**, which has a similar basal B–B bond as determined by single-crystal X-ray diffraction (B–B distance 1.65 Å vs. 1.63 Å in B_6H_{10}),[3,10] would undergo an analogous reaction.

[*] Prof. L. Barton, Dr. J. Bould, Dr. N. P. Rath
Department of Chemistry
University of Missouri-St. Louis
St. Louis, MO 63121 (USA)
Telefax: Int. code + (314)516-5342
e-mail: c4626@slvaxa.umsl.edu

[**] We thank the National Science Foundation, the Missouri Research Board, and the University of Missouri-St. Louis for financial support of this work and the Johnson Mathey Company for a loan of $IrCl_3 \cdot 3H_2O$.

Compound **1** was stirred with $[Fe_2(CO)_9]$ (molar ratio 1:1) in CH_2Cl_2 for 24 h. Thin-layer chromatography of the resultant mixture afforded the title compound **5** in approximately 1% yield. NMR[11] and IR[12] spectroscopic investigations suggested a *closo*-iridapentaborane cluster with iron incorporated, and this was confirmed by a single-crystal X-ray diffraction study.[13] The structure of **5** (Fig. 1) reveals a *closo*-bimetallaheptaborane cluster with an $Fe(CO)_3$ moiety in the axial position and an $[Ir(CO)_2(PPh_3)]$ moiety in an equatorial position. As such, **5** is both the first pentagonal-bipyramidal metallaheptaborane to be structurally characterized (two others, $[B_6H_6Cp^*Ni]^{2-}$ [14] and $[B_5H_7(Cp^*Co)_2]$[15] ($Cp^* = C_5Me_5$) have been proposed from NMR evidence) and also the first iridaferraborane. The presence of both first- and third-row transition elements in a metallaborane cluster is also rare.

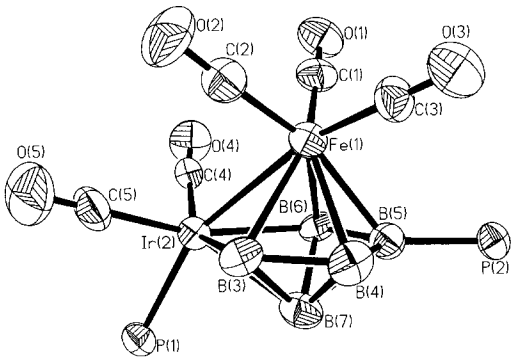

Fig. 1. The molecular structure of **5**. Phenyl rings have been omitted for clarity. There is a terminal hydrogen atom on each boron atom except B(5) as shown by ^1H-{^{11}B} NMR spectroscopy. Selected interatomic distances [Å] and angles [°]: Fe(1)–Ir(2) 2.706(2), Fe(1)–B(3) 2.234(13), Fe(1)–B(4) 2.218(13), Fe(1)–B(5) 2.124(12), Fe(1)–B(6) 2.238(11), Fe(1)–C(1) 1.792(12), Fe(1)–C(2) 1.769(12), Fe(1)–C(3) 1.752(12), Ir(2)–B(3) 2.169(14), Ir(2)–B(6) 2.155(12), Ir(2)–B(7) 2.29(2), Ir(2)–P(1) 2.332(3), Ir(2)–C(4) 1.927(12), Ir(2)–C(5) 1.919(12), B–B 1.57(2)–1.85(2); C-Fe(1)-C 95.5(5)–99.8(5), C(1/2)-Fe(1)-Ir(2) 95.3(3)/88.1(4), C(5)-Ir(2)-C(4) 104.5(5), P(1)-Ir(2)-C(4/5) 92.2(3)/92.4(4).

The Fe–Ir distance in **5** (2.706(2) Å) is slightly longer than the sum of the covalent radii and lies in the center of the range of Ir–Fe distances in iron–iridium metal clusters and bridged binuclear complexes that has been taken in these compounds to indicate a significant bonding interaction.[16] The Fe–B distances of 2.12–2.23 Å, which are similar to or longer than the $Ir-B_{(equatorial)}$ distances of 2.16 and 2.17 Å, perhaps reflect the η^5 coordination of the iron center compared to the η^4 coordination of the iridium center. In line with this, the $Ir-B_{(axial)}$ distance of 2.29 Å is about 0.1 Å longer than the the $Ir-B_{(equatorial)}$ distances. Similarly, the $B_{(axial)}-B_{(equatorial)}$ distances (1.77–1.82 Å) are longer than the distances in the equatorial belt (1.57–1.69 Å). The $[B_5H_4\{Ir(CO)_2(PPh_3)\}]$ portion of the molecule retains much of the overall geometry of a *nido*-$[B_5H_8\{Ir(CO)(PPh_3)_2\}]$ cluster with the $\{Fe(CO)_3\}$ moiety effectively capping the open face of the IrB_5 cluster subunit.

In accordance with skeletal electron counting rules,[17] compound **5** is a 16-electron *closo*-polyhedron with seven vertices; the $[Fe(CO)_3]^{2+}$ vertex capping a formal *nido*-$[B_5H_4(PPh_3)\{Ir(CO)_2(PPh_3)\}]^{2-}$ unit. Although the analogy between BH and $Fe(CO)_3$ has been well documented,[18] as far as we are aware there is only one other metallaborane compound in which an $[Fe(CO)_3]$ moiety is η^5 bonded in a *closo*-borane; this is the recently described metallacarborane *closo*-$[C_2B_9H_{11}\{Fe(CO)_3\}]$.[19] It is possible, even though the yield is low and the reaction must be necessarily complex, that the product is formed by the initial addition of an $Fe(CO)_4$ moiety to the iridaborane, followed by ligand rearrangement in which a carbonyl group migrates to the iridium center, and the PPh_3 moiety migrates to the borane cage together with concurrent loss of hydrogen (Scheme 1). The product **5** is the first structurally characterized metallaheptaborane and is one of very few known heterobimetallaboranes based on a mid-sized borane template.

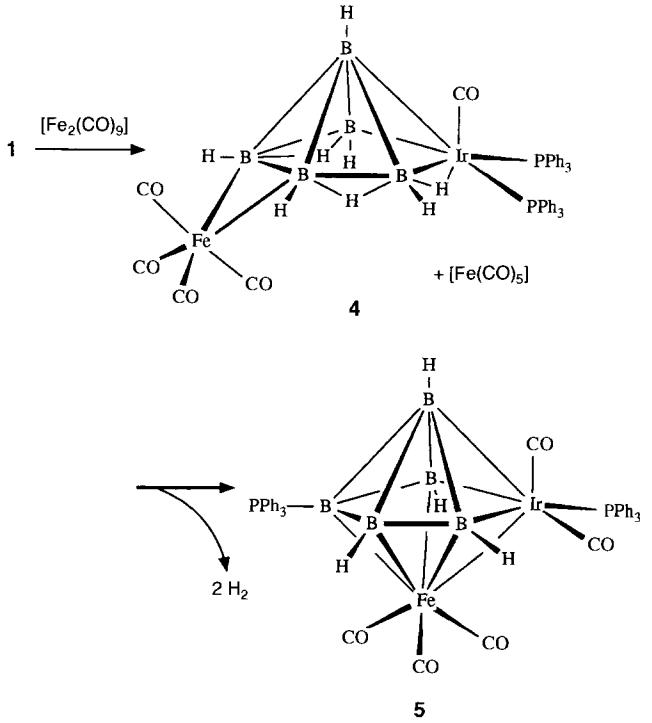

Scheme 1.

Experimental Procedure

A solution of $[B_5H_8\{Ir(CO)(PPh_3)_2\}]$ (200 mg, 0.25 mmol) and $[Fe_2(CO)_9]$ (90 mg, 0.25 mmol) in CH_2Cl_2 was stirred under nitrogen for 24 h. ^{11}B NMR spectra of the solution showed that the initial metallaborane had been completely consumed to give new borane-containing products and also that the title compound was present in the mixture. The solution was concentrated and purified by thin-layer chromatography on silica gel using CH_2Cl_2/pentane as the eluant. A number of bands were observed but only one was sufficiently stable to be isolated by this technique, and this was characterized as the title compound **5** (1.8 mg, 0.8% yield, elemental analysis for $C_{41}H_{34}B_5FeIrO_5P_2$, found (calculated) %: C 50.35 (50.73), H 3.36 (3.53). A crystal suitable for single-crystal X-ray diffraction analysis was obtained by pentane diffusion in to a CH_2Cl_2 solution of the compound.

Received: December 27, 1994
Revised version: March 25, 1995 [Z 7585 IE]
German version: *Angew. Chem.* **1995**, *107*, 1744–1746

Keywords: boron compounds · iridium compounds · iron compounds · metallaboranes

[1] J. D. Kennedy, *Prog. Inorg. Chem.* **1984**, *32*, 519.
[2] J. Bould, N. N. Greenwood, J. D. Kennedy, *J. Organomet. Chem.* **1983**, *11*, 249.
[3] N. N. Greenwood, J. D. Kennedy, W. S McDonald, D. Reed, J. Staves, *J. Chem. Soc. Dalton Trans.* **1979**, 117.
[4] a) J. Bould, J. E. Crook, N. N. Greenwood, J. D. Kennedy, *J. Chem. Soc. Chem. Commun.* **1983**, 951; b) J. D. Kennedy, *Prog. Inorg. Chem.* **1986**, *34*, 211; c) J. D. Kennedy, *Main Group Met. Chem.* **1989**, *12*, 149; d) J. Bould, J. E. Crook, N. N. Greenwood, J. D. Kennedy, *J. Chem. Soc. Dalton Trans.* **1991**, 185.

[5] a) A. M. Mebel, D. G. Musaev, N. Koga, K. Morokuma, *Bull. Chem. Soc. Jpn.* **1993**, *66*, 3239; b) A. M. Mebel, K. Morokuma, D. G. Musaev, *J. Am. Chem. Soc.* **1994**, *116*, 3932.

[6] J. Bould, L. Barton, *Abstr., Fourth Boron-USA Workshop*, Syracuse, NY, July, **1994**, 45.

[7] a) K. B. Gilbert, S. K. Boocock, S. G. Shore, in *Comprehensive Organometallic Chemistry, Part 6*, (Eds.: G. Wilkinson, E. W. Abel, F. G. A. Stone), Pergamon, Oxford, **1982**, Chapter 41, pp. 879–945. b) L. Barton, D. K. Srivastava, *Comprehensive Organometallic Chemistry, II*, (Eds.: G. Wilkinson, E. W. Abel, F. G. A. Stone), Pergamon, **1995**, in press. c) J. D. Kennedy, *Prog. Inorg. Chem.* **1986**, *36*, 211.

[8] a) J. J. Solomon, R. F. Porter, *J. Am. Chem. Soc.* **1972**, *94*, 1443; b) H. D. Johnson, V. T. Brice, G. L. Brubaker, S. G. Shore, *ibid.* **1972**, *94*, 6711.

[9] a) A. Davison, D. D. Traficante, S. S. Wreford, *J. Chem. Soc. Chem. Commun.* **1972**, 1155; b) A. Davison, D. D. Traficante, S. S. Wreford, *J. Am. Chem. Soc.* **1974**, *96*, 2802; c) L. Barton, D. K. Srivastava, *Organometallics* **1991**, *10*, 2982; d) D. K. Srivastava, N. P. Rath, L. Barton, J. D. Ragaini, O. Hollander, R. Godfroid, S. G. Shore, *ibid.* **1993**, *12*, 2017; e) J. P. Brennan, R. Schaeffer, A. Davison, S. S. Wreford, *J. Chem. Soc. Chem. Commun.* **1973**, 354.

[10] L. Barton, T. Onak, S. G. Shore, *Gmelin Handbook of Inorganic Chemistry, Boron Compounds 20 (New supplement Series Vol. 54)*, Springer, Berlin, **1979**, pp. 52–79.

[11] ^{11}B (160.5 MHz), ^{1}H (500.1 MHz), and ^{31}P (122 MHz) NMR data ($CDCl_3$, 25 °C, relative intensities in parentheses): $\delta(^{11}B) = +46.7(1), +46.3(1)$, *ca.* $+12(1), +10.7(1), -3.1(1)$ (resonances too broad to observe proton coupling); $\delta(^{1}H) = +5.12(2), +3.16(1), +3.09(1), +7.0$ to $+7.5$ (phenyl); $\delta(^{31}P) = +20.7$ (1, s), ca. $+20$ (1, v br).

[12] IR data (KBr disc): $\tilde{\nu}$[cm^{-1}] = $\nu_{(BH)}$ 2500 (v br), $\nu_{(CO)}$ 2043(sh), 2001(s) 1953(m).

[13] Crystallographic data for $C_{41}H_{34}FeIrO_5P_2$ (**5**), crystal dimensions $0.20 \times 0.50 \times 0.30$ mm, (298(2) K): $a = 10.675(5)$, $b = 10.736(3)$, $c = 19.221(7)$ Å, $\alpha = 88.90(2)$, $\beta = 78.26(4)$, $\gamma = 71.69(3)°$, $V = 2045.2(13)$ Å^3, $Z = 2$, crystal system triclinic, space group $P\bar{1}$, $\rho_{calcd} = 1.576$ g cm^{-3}, $\mu = 3.762$ mm^{-1}, $T_{max} = 0.7604$, $T_{min} = 0.3470$. Structure solution and refinement were carried out with SHELXTL 5.0 (Siemens analytical X-ray Division Madison, WI, **1994**). Of 11458 reflections collected ($3.00 > 2\theta > 55.0°$) 9424 independent reflections were used in the refinement. Full matrix least squares refinement was carried out by minimizing $S > w(F_o^2 - F_c^2)^2$. The final residual values were $R(F) = 0.0733$ for reflections $F > 2\sigma(F)$, $wR(F^2) = 0.1525$, $s = 1.042$, number of parameters = 491. Further details of the crystal structure investigation may be obtained from the Director of the Cambridge Crystallographic Data Centre, 12 Union Road, GB-Cambridge, CB2 1EZ (UK), on quoting the full journal citation.

[14] D. M. Vinitskii, V. L. Lagun, K. A. Solntsev, N. T. Kuznetsov, K. N. Marushkin, J. Janousek, K. Base, B. Stibr, *Russ. J. Inorg. Chem.* **1984**, *29*, 984.

[15] T. L. Venable, R. N. Grimes, *Inorg. Chem.* **1982**, *21*, 887.

[16] J. T. Mague, *Organometallics* **1990**, *10*, 513 and references therein. From 12 published studies, the known Ir–Fe distances in cluster and binuclear complexes range from 2.960 Å in $[FeIr(\mu\text{-}PPh_2)(CO)_5(PPh_3)_2]$ (D. A. Roberts, G. R. Steinmetz, M. J. Breen, P. M. Shulman, E. D. Morrison, M. R. Dutter, C. W. DeBrosse, R. R. Whittle, G. L. Geoffroy, *Organometallics* **1983**, *2*, 846) to 2.55 Å in $[Cp^*Ir(C(Me)=CHCH=C(Me))\{\mu\text{-}SFe(CO)_4\}Fe(CO)_2]$ (J. Chen, L. M. Daniels, R. J. Angelici, *J. Am. Chem. Soc.* **1991**, *113*, 2544).

[17] a) K. Wade, *Adv. Inorg. Chem. Radiochem.* **1976**, *18*, 1; b) R. E. Williams, *ibid.* **1976**, *18*, 67; c) R. W. Rudolph, *Acc. Chem. Res.* **1976**, *9*, 446; d) D. M. P. Mingos, *ibid.* **1984**, *17*, 311.

[18] a) T. P. Fehlner in *Boron Chemistry 4, Plenary Lectures at the 4th International Meeting on Boron Chemistry, Salt Lake City, 1979*; (Eds.: R. W. Parry, G. J. Kodama), Pergamon, Oxford, **1980**, pp. 95–107; b) C. E. Housecroft, T. P. Fehlner, *Adv. Organomet. Chem.* **1982**, *21*, 57.

[19] S. S. Lee, C. B. Knobler, M. F. Hawthorne, *Organometallics* **1991**, *10*, 670.

Enantiospecific Syntheses of Valiolamine and its (1*R*), (2*R*), (1*R*,2*R*) Diastereomers from (−)-Quinic Acid**

Tony K. M. Shing* and Leong H. Wan

Recently the chemotherapeutic potential of glycosidase inhibitors (for example, as anti-HIV agents) was recognized and is being exploited.[1] Natural product valiolamine (**1**), isolated from the fermentation broth of *Streptomyces hygroscopicus* subsp. *limoneus* IFO12703[2] that produces antibiotic validamycin, is the most potent α-glucosidase inhibitor among the amino pseudosugars (carbasugars)[3] valienamine, validamine, and hydroxyvalidamine obtained from chemical or microbial degradation[4] of validamycin. The structure of valiolamine (**1**) was deduced to be (2*S*)-(1,2,4,5/3)-5-amino-1-*C*-hydroxymethyl-1,2,3,4-cyclohexanetetraol on the basis of spectral studies,[5] and its absolute configuration was confirmed by a stereoselective transformation of valienamine or validamine into valiolamine.[6] The *N*-[2-hydroxy-1-(hydroxymethyl)ethyl]valiolamine, coded as AO-128, displayed higher activities than the parent valiolamine and is undergoing clinical trial for treatment of diabetes.[7] Scheme 1 shows the structural resemblance between **1** and α-D-glucose. Since **1** is a potent α-D-glucosidase inhibitor, its (1*R*) diastereomer **2** (1-*epi*-valiolamine) that possesses a β-amino group might be a β-D-glucosidase inhibitor. Along this line of reasoning, (2*R*) and (1*R*,2*R*) diastereomers of valiolamine (**3** and **4**) may inhibit α-D- or β-D-mannosidase, respectively. Three total syntheses of valiolamine (**1**) were achieved starting from a Diels–Alder (furan–acrylic acid) cycloadduct,[8] from D-glucose by a Ferrier rearrangement,[9] and from 2,3,4,6-tetra-*O*-benzyl-D-glucono-1,5-lactone involving an aldol reaction.[10] The last synthesis[10] can also be used to prepare **2**, but no syntheses of amino pseudosugars **3** and **4** have been reported. Our endeavors in pseudosugar synthesis from (−)-quinic acid (**5**) have already furnished 2-crotonyloxymethyl-(4*R*,5*R*,6*R*)-4,5,6-trihydroxycyclohex-2-enone (COTC),[11] pseudo-β-D-mannopyranose, pseudo-β-D-fructopyranose,[12] pseudo-α-D-

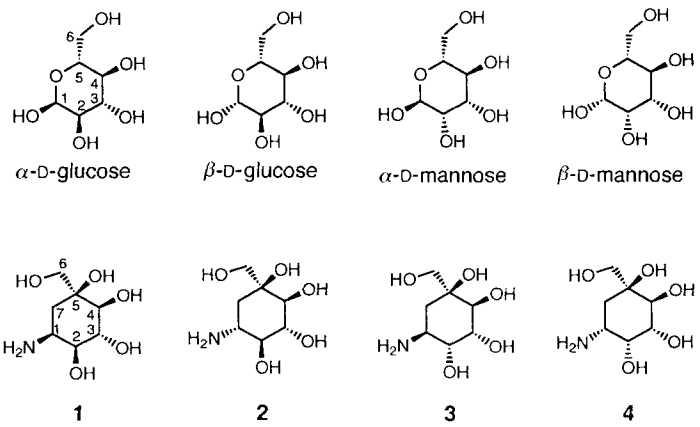

Scheme 1. Structural relationship between hexoses and aminocyclitol inhibitors of glycosidases.

[*] Dr. T. K. M. Shing, L. H. Wan
Department of Chemistry, The Chinese University of Hong Kong
Shatin, Hong Kong
Telefax: Int. code + 2603-5057
e-mail: b094796@mailserv.cuhk.hk

[**] This work was supported by the RGC Earmarked Grant (CUHK69/92E).

glucopyranose, pseudo-α-D-mannopyranose,[13] and cyclophellitol and its diastereomers.[14] This communication further demonstrates the versatility of this approach in facile syntheses of **1**–**4**.

The route to valiolamine **1** and its (2*R*) diastereomer **3** is shown in Scheme 2. Our previous work[14] has indicated that (−)-quinic acid (**5**) could be easily converted into alkene **6** in five

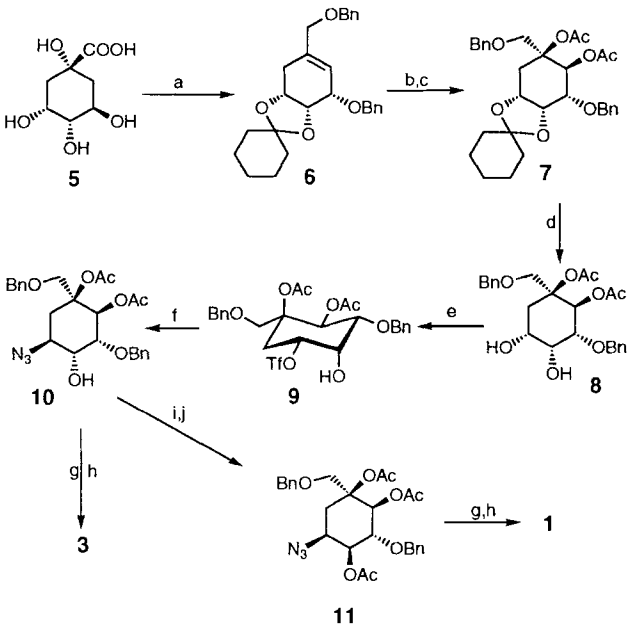

Scheme 2. Syntheses of valiolamine (**1**) and 2-*epi*-valiolamine (**3**): a) 5 steps, 47%, see ref. [13]; b) OsO_4, H_2O, Me_3NO, pyridine, *t*BuOH, reflux, 75%; c) Ac_2O, DMAP, Et_3N, reflux, 90%; d) TFA, H_2O, CH_2Cl_2, 90%; e) Tf_2O (1 equiv), pyridine, CH_2Cl_2, 0 °C, 90%; f) NaN_3, benzo[15]crown-5, DMF, 60%; g) K_2CO_3, MeOH; h) H_2, $Pd(OH)_2$, EtOH, (two steps, 58% for **3**; 73% for **1**); i) Tf_2O, pyridine, CH_2Cl_2, 0 °C, 90%; j) nBu_4NOAc, THF, 80%.

steps with an overall yield of 47%. Catalytic OsO_4 dihydroxylation[15] of alkene **6** from the less hindered β face gave the β-diol, which was protected as diacetate **7**. Acidic removal of the cyclohexylidene acetal in **7** furnished diol **8**, $[\alpha]_D^{25} = -13.5$ ($c = 0.4$ in $CHCl_3$).[16] Selective esterification of the equatorial OH-1 in **8** with one equivalent of triflic anhydride in pyridine gave triflate **9** which reacted with NaN_3 to give azide **10**, $[\alpha]_D^{27} = +9.9$ ($c = 1.6$ in $CHCl_3$).[17] Deprotection of **10** yielded 2-*epi*-valiolamine (**3**) for the first time, $[\alpha]_D^{25} = -11.1$ ($c = 0.4$ in H_2O).[18] On the other hand, triflylation of the alcohol in **10** followed by nucleophilic displacement with nBu_4NOAc in THF provided azido triacetate **11**, $[\alpha]_D^{25} = -14.0$ ($c = 1.5$ in $CHCl_3$). Deprotection of **11** then afforded **1**, $[\alpha]_D^{22} = +15.4$ ($c = 2.2$ in H_2O) [literature value:[5] $[\alpha]_D^{20} = +18.8$ ($c = 1.0$ in H_2O)].

The route to 1-*epi*-valiolamine (**2**) and the ((1*R*,2*R*) diastereomer **4** is illustrated in Scheme 3. Alkene **12** was readily accessible from the diol **8** by a Corey–Winter[19] reaction in 64% overall yield. *cis*-Dihydroxylation of **12** with the catalyst osmium tetraoxide[15] was disappointing and gave 20% yield of β-diol **13**, 10% of the α-diol **8**, and 60% of the starting material **12**. It is noteworthy that our newly developed flash dihydroxylation procedure with catalytic RuO_4[20] afforded the desired β-diol **13**, m.p. 127–128 °C; $[\alpha]_D^{25} = +21.9$ ($c = 1.0$ in $CHCl_3$) in 80% yield! The diol **13** was then converted into the cyclic sulfate **14**, m.p. 61–67 °C; $[\alpha]_D^{21} + 42.2$ ($c = 3.9$ in $CHCl_3$), according to the Sharpless method.[21] Regioselective ring opening of **14** with azide occurred at the C-1 atom to form the desired azido alcohol

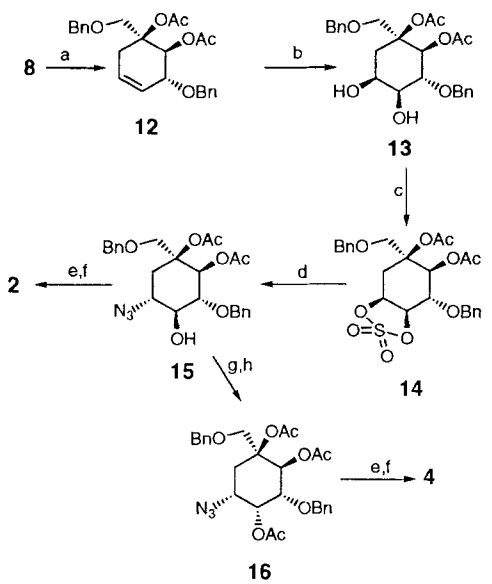

Scheme 3. Syntheses of 1-*epi*-valiolamine (**2**) and the (1*R*,2*R*) diastereomer **4**: a) 1,1′-thiocarbonyldiimidazole, toluene, reflux, then $P(OMe)_3$, reflux, 64% overall; b) $RuCl_3 \cdot H_2O$, $NaIO_4$, EtOAc, CH_3CN, H_2O, 0 °C, 80%; c) $SOCl_2$, Et_3N, CH_2Cl_2, 0 °C, then $RuCl_3$, $NaIO_4$, CCl_4, CH_3CN, H_2O, 0 °C, 74% overall; d) LiN_3, DMF, then 20% aq. H_2SO_4, THF, 50%; e) K_2CO_3, MeOH; f) H_2, $Pd(OH)_2$, EtOH (two steps, 75% for **2**; 68% for **4**; g) Tf_2O, pyridine, CH_2Cl_2, 0 °C, 78%; nBu_4NOAc, THF, 95%.

15, $[\alpha]_D^{27} = -3.4$ ($c = 0.9$ in $CHCl_3$). Deprotection of **15** thus afforded 1-*epi*-valiolamine (**2**), $[\alpha]_D^{20} = -27.9$ ($c = 0.5$ in H_2O) [literature value:[10] $[\alpha]_D^{24} = -23.2$ ($c = 0.5$ in H_2O)]. On the other hand, inversion of the C-2 configuration in **15** by triflylation and subsequent nucleophilic substitution with acetate afforded the azido triacetate **16**, $[\alpha]_D^{29} = -61.5$ ($c = 0.7$ in $CHCl_3$). Deprotection of **16** furnished the target molecule **4**, $[\alpha]_D^{19} = -13.7$ ($c = 0.5$ in H_2O).

In summary, we have described facile syntheses of amino pseudosugars valiolamine and its diastereomers from quinic acid. The application of this flexible strategy to the construction of valienamine, validamine, and hydroxyvalidamine is in progress.

Received: April 1, 1995 [Z 7859 IE]
German version: *Angew. Chem.* **1995**, *107*, 1742–1744

Keywords: aminosugars · asymmetric syntheses · dihydroxylations · quinic acid · valiolamine

[1] G. W. J. Fleet, L. E. Fellows in *Natural Product Isolation* (Eds.: G. H. Wagman, R. Cooper), Elsevier, Amsterdam, **1988**, p. 540; M. J. Humphries, K. Matsumoto, S. L. White, K. Olden, *Proc. Natl. Acad. Sci. USA* **1986**, *83*, 1752; G. W. J. Fleet, A. Karpas, R. A. Dwek, L. E. Fellows, A. S. Tyms, S. Petursson, S. K. Namgoong, N. G. Ramsden, P. W. Smith, J. C. Son, F. Wilson, D. R. Witty, G. S. Jacob, T. W. Rademacher, *FEBS Lett.* **1988**, *237*, 128 and references therein; D. C. Montefoiori, W. E. Robinson, W. M. Mitchell, *Proc. Natl. Acad. Sci. USA* **1988**, *85*, 9248.

[2] Y. Kameda, N. Asano, M. Yoshikawa, M. Takeuchi, T. Yamaguchi, K. Matsui, *J. Antibiot.* **1984**, *37*, 1301.

[3] For a review on pseudosugars, see T. Suami, S. Ogawa, *Adv. in Carbohydr. Chem. Biochem.* **1990**, *48*, 22.

[4] Y. Kameda, S. Horii, *J. Chem. Soc. Chem. Commun.* **1972**, 746; S. Horii, T. Iwasa, E. Mizuta, Y. Kameda, *J. Antibiot.* **1971**, *24*, 59.

[5] Y. Kameda, N. Asano, M. Yoshikawa, M. Takeuchi, T. Yamaguchi, K. Matsui, *J. Antibiot.* **1984**, *37*, 1301.

[6] S. Horii, H. Fukase, Y. Kameda, *Carbohydr. Res.* **1985**, *140*, 185.

[7] S. Horii, H. Fukase, T. Matsuo, Y. Kameda, N. Asano, K. Matsui, *J. Med. Chem.* **1986**, *29*, 1038.

[8] S. Ogawa, Y. Shibata, *Chem. Lett.* **1985**, 1581.

[9] M. Hayashido, N. Sakairi, H. Kuzuhara, *J. Carbohydr. Chem.* **1988**, *7*, 83.

[10] H. Fukase, S. Horii, *J. Org. Chem.* **1992**, *57*, 3642, 3651.
[11] T. K. M. Shing, Y. Tang, *J. Chem. Soc. Chem. Commun.* **1990**, 312; *Tetrahedron* **1990**, *46*, 6575.
[12] T. K. M. Shing, Y. Tang, *J. Chem. Soc. Chem. Commun.* **1990**, 748; *Tetrahedron* **1991**, *47*, 4571.
[13] T. K. M. Shing, Y.-X. Cui, Y. Tang, *J. Chem. Soc. Chem. Commun.* **1991**, 756; *Tetrahedron* **1992**, *48*, 2349.
[14] T. K. M. Shing, V. W.-F. Tai, *J. Chem. Soc. Chem. Commun.* **1993**, 995; *J. Chem. Soc. Perkin Trans. 1* **1994**, 2017.
[15] R. Ray, D. S. Matteson, *Tetrahedron Lett.* **1980**, *21*, 449.
[16] Selected ^{1}H NMR data (250 MHz, $CDCl_3$): for **8**: δ = 1.93 (3H, s, Ac), 2.00–2.01 (1H, br s, OH), 2.04 (3H, s, Ac), 2.23 (1H, m, 7-H), 2.62 (1H, br s, OH), 2.74 (1H, dd, J = 4.8, 13.8, 7'-H), 3.71, 3.92 (2H, ABq, J = 9.0), 3.73 (1H, dd, J = 2.9, 10.0, 3-H), 3.74 (1H, m, 1-H obscured), 4.20 (1H, m, 2-H), 4.37, 4.45 (2H, ABq, J = 11.7, OCH_2Ph), 4.60, 4.66 (2H, ABq, J = 12.1, OCH_2Ph), 5.46 (1H, d, J = 10.0, 4-H), 7.20–7.40 (10H, m, Ph); for **10**: δ = 2.00 (3H, s, Ac), 2.03 (3H, s, Ac), 2.37 (1H, m, 7'H), 2.39 (1H, m, 7-H), 2.57 (1H, br s, OH), 3.6–3.7 (1H, m, 1-H), 3.71, 3.99 (2H, ABq, J = 9.8, 6-H), 3.8–3.9 (2H, m, 2-H, 3-H), 4.36, 4.50 (2H, ABq, J = 11.9, OCH_2Ph), 4.58, 4.69 (2H, ABq, J = 11.5, OCH_2Ph), 5.67 (1H, d, J = 6.7, 4-H), 7.2–7.4 (10H, m, Ph); for **11**: δ = 1.91 (3H, s, Ac), 1.95 (1H, dd, J = 3.7, 15.9, 7'-H), 2.04 (3H, s, Ac), 2.09 (3H, s, Ac), 3.02 (1H, dd, J = 3.3, 15.9, 7-H), 3.44, 3.98 (2H, ABq, J = 8.8, 6-H), 4.13 (1H, t, J = 9.8, 3-H), 4.1–4.2 (1H, m, 1-H), 4.35, 4.44 (2H, ABq, J = 11.6, OCH_2Ph), 4.66, 4.73 (2H, ABq, J = 11.7, OCH_2Ph), 5.03 (1H, dd, J = 4.1, 9.8, 2-H), 5.29 (1H, d, J = 9.8, 4-H), 7.1–7.4 (10H, m, Ph); for **13**: δ = 1.73 (1H, dd, J = 2.8, 16.0, 7-H), 1.96 (3H, s, Ac), 2.03 (3H, s, Ac), 2.54 (1H, br s, OH), 2.75 (1H, br s, OH), 3.13 (1H, dd, J = 5.4, 16.0, 7'-H), 3.48, 3.97 (2H, ABq, J = 8.8, 6-H), 3.62 (1H, dd, J = 3.2, 9.2, 2-H), 4.04 (1H, dd, J = 9.2, 9.9, 3-H), 4.1–4.2 (1H, m, 1-H), 4.36, 4.47 (2H, ABq, J = 11.7, OCH_2Ph), 4.67, 4.77 (2H, ABq, J = 11.5, OCH_2Ph), 5.27 (1H, d, J = 9.9, 4-H), 7.2–7.45 (10H, m, Ph); for **14**: δ = 1.91 (3H, s, Ac), 2.07 (3H, s, Ac), 2.15 (1H, dd, J = 3.8, 17.4, 7-H), 3.43, 4.05 (2H, ABq, J = 8.7, 6-H), 3.52 (1H, dd, J = 1.7, 17.4, 7'-H), 4.33, 4.47 (2H, ABq, J = 11.8, OCH_2Ph), 4.50 (1H, dd, J = 7.8, 10.6, 3-H), 4.64, 4.84 (2H, ABq, J = 11.5, OCH_2Ph), 4.96 (1H, dd, J = 5.4, 7.9, 2-H), 5.17–5.25 (1H, m, 1-H), 5.25 (1H, d, J = 10.6, 4-H), 7.2–7.4 (10H, m, Ph); for **15**: δ = 1.62 (1H, dd, J = 12.3, 14.7, 7-H), 1.92 (3H, s, Ac), 2.12 (3H, s, Ac), 2.62 (1H, br d, J = 2.4, OH), 2.90 (1H, dd, J = 4.4, 14.6, 7'-H), 3.46 (1H, ddd, J = 4.4, 9.0, 12.3, 1-H), 3.59 (1H, dt, J = 2.4, 9.0, 2-H), 3.62, 3.94 (2H, ABq, J = 9.0, 6-H), 3.73 (1H, dd, J = 9.0, 9.9, 3-H), 4.36, 4.44 (1H, ABq, J = 11.6, OCH_2Ph), 4.68, 4.75 (1H, d, J = 11.5, OCH_2Ph), 5.21 (1H, d, J = 9.9, 4-H), 7.1–7.4 (10H, m, Ph); for **16**: δ = 1.93 (3H, s, Ac), 2.05 (3H, s, Ac), 2.18 (3H, s, Ac), 2.18 (1H, dd, J = 13.0, 14.1 Hz, 7-Hax), 2.84 (1H, ddd, J = 1.5, 4.3, 14.1 Hz, 7-Heq), 3.44 (1H, ddd, J = 3.0, 4.3, 13.0 Hz, 1-H), 3.73 (1H, dd, J = 3.0, 10.2 Hz, 3-H), 3.70, 3.98 (2H, ABq, J = 9.1 Hz, 6-H), 4.40, 4.47 (2H, ABq, J = 11.7 Hz, OCH_2Ph), 4.42, 4.71 (2H, ABq, J = 11.8 Hz, OCH_2Ph), 5.40 (1H, d, J = 10.2 Hz, 4-H), 5.75 (1H, m, 2-H), 7.33 (10H, m, Ph).
[17] Ring opening of cyclic sulfate **A** derived from the diol **8** with LiN_3 gave predominantly the undesired C-2 azide **B** (**B**:**C** = 10:1).

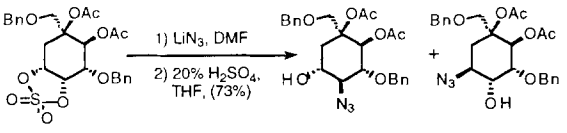

[18] Selected ^{13}C NMR data (62.5 MHz, D_2O; dioxane was used as an internal reference at 67.4): for **1**: δ = 33.34, 51.57, 66.74, 72.42, 74.30, 74.93, 77.06; for **2**: δ = 34.96, 50.76, 66.58, 73.99 74.75, 75.12, 75.77; for **3**: δ = 31.05, 50.90, 66.22, 70.11, 71.42, 71.86, 76.22; for **4**, δ = 31.63, 48.38, 66.40, 67.40 (overlapped with dioxane signal), 70.48, 71.62, 74.20.
[19] E. J. Corey, R. A. E. Winter, *J. Am. Chem. Soc.* **1963**, *85*, 2677.
[20] T. K. M. Shing, V. W.-F. Tai, E. K. W. Tam, *Angew. Chem.* **1994**, *106*, 2408; *Angew. Chem. Int. Ed. Engl.* **1994**, *33*, 2312.
[21] B. M. Kim, K. B. Sharpless, *Tetrahedron Lett.* **1989**, *30*, 655; Y. Gao, K. B. Sharpless, *J. Am. Chem. Soc.* **1988**, *110*, 7538.

Preparation of a Surface-Active Chiral Diphosphane and Its Use in the Hydrogenation of Prochiral Olefins**

Hao Ding, Brian E. Hanson,* and József Bakos

The synthesis of novel water-soluble phosphanes has attracted a great deal of attention recently.[1] Much of the effort has been directed toward the preparation of water-soluble chiral diphosphanes for two-phase asymmetric hydrogenation.[2–5] Syntheses of water-soluble diphosphanes that require sulfonation of phenyl groups directly bound to phosphorus suffer from relatively low yield due, in part, to oxidation of the phosphane.[6] It has recently been reported by Herrmann et al. that oxidation of the phosphane can be virtually eliminated during the sulfonation of phenylphosphanes when the reaction is carried out in the presence of orthoboric acid;[7] however, the new sulfonation conditions still require oleum and long reaction times. We describe here the high yield preparation of a chiral water-soluble diphosphane that contains four sulfonate groups. Furthermore, dynamic light scattering experiments demonstrate that this phosphane aggregates under certain conditions in water, and catalytic reactions in a two-phase system occur faster in the presence of the surface-active phosphane than with similar ligands that contain $P[C_6H_4\text{-}m\text{-}SO_3Na]_2$ groups.

Previously we reported that sulfonation of $P[C_6H_4\text{-}p\text{-}(CH_2)_3\text{-}C_6H_5]_3$ (**1**) occurs in high yield under remarkably mild conditions;[8] this reaction requires concentrated sulfuric acid (no oleum) and takes less than three hours at room temperature to go to completion [Eq. (a)]. The product, **2**, forms aggregates with a hydrodynamic radius of 20 Å in aqueous NaCl solution.[8]

$$\underset{\mathbf{1}}{P[C_6H_4(CH_2)_3C_6H_5]_3} \xrightarrow[\text{2. NaOH}]{\text{1. } H_2SO_4} \underset{\mathbf{2}}{P[C_6H_4(CH_2)_3C_6H_4SO_3Na]_3} \qquad \text{(a)}$$

Triarylphosphanes are readily cleaved by alkali metals under a variety of reaction conditions.[9] Mixed triarylphosphanes $PAr_{3-x}Ar'_x$ are reported to cleave at the most electron-withdrawing aryl group;[10] however, analysis of the cleavage products by NMR spectroscopy shows that in the case of Ar = Ph and Ar' = p-$C_6H_4NMe_2$ cleavage does not take place exclusively at the phenyl ring.[11] For this reason the phosphane **1** rather than a mixed triarylphosphane is used as the precursor to chiral chelating phosphanes that contain $P[C_6H_4\text{-}p\text{-}(CH_2)_3\text{-}C_6H_5]_2$ units. Cleavage of **1** is accomplished with excess lithium metal in THF [Eq. (b)]. The resulting lithium phosphide **3** may be isolated as a red oil upon addition of hexanes. The oil is used directly

[*] Prof. B. E. Hanson, H. Ding
Department of Chemistry
Virginia Polytechnic Institute and State University
Blacksburg, VA 24061-0212 (USA)
Telefax: Int. code + (703)231-3255
e-mail: bhanson@chemserver.chem.vt.edu
Prof. J. Bakos
Organic Chemistry Department
University of Veszprém
Egyetem u. 10, POB. 158
H-8201 Veszprém (Hungary)

[**] This work was supported by the National Science Foundation. We thank Dr. Imre Tóth for discussions on the synthesis of chiral diphosphane ligands. NATO Advanced Research Workshops is gratefully acknowledged for the initiation of collaborative work.

$$P[C_6H_4(CH_2)_3C_6H_5]_3 \xrightarrow[2.\ tBuCl]{1.\ Li} Li\{P[C_6H_4(CH_2)_3C_6H_5]_2\} \quad (b)$$

1 **3**

in reactions with chiral ditosylates. Hydrolysis of an aliquot of **3** with D_2O yields the corresponding deuterated secondary phosphane (^{31}P NMR, $\delta = -43.06$) ($^1J_{D,P} = 32.7$ Hz)).

The reaction of **3** with (*R*,*R*)-2,4-pentanediylditosylate leads to the bis(diphenylphosphino)pentane (BDPP) analog **4** in high yield as an oily pale yellow liquid. Sulfonation of **4** occurs under similar conditions as those for reaction (a). The tetrasulfonated product **5** (shown schematically in Fig. 1), is formed in high

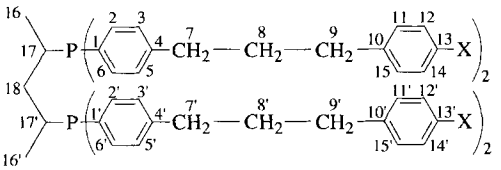

4, X = H
5, X = SO_3Na

yield after six hours. Both the ^1H and ^{13}C NMR spectra are consistent with sulfonation in the *para* position; that is, only the AA'BB' pattern of the signals expected for *para* substitution in an aromatic ring is observed in the ^1H spectrum, and in the ^{13}C NMR spectrum four signals are observed for the ring ω to phosphorus rather than the six required for *ortho* or *meta* substitution.

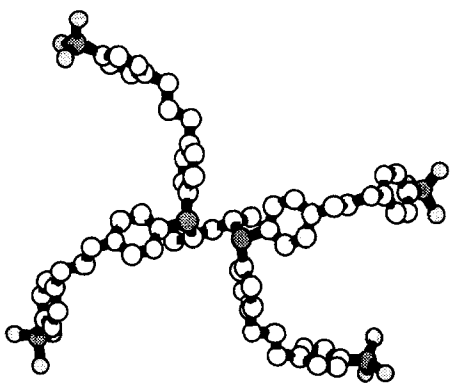

Fig. 1. Schematic representation of the ligand **5**. The ligand is drawn to scale and in the necessary conformation to form a skew chelate ring when bound to a metal.

Dynamic light scattering experiments on **5** show that aggregates with a radius of 25 Å are formed in aqueous solutions that are 0.01 M in **5** and 0.25 M in NaCl.

As a test to see if the surface-active character of **5** influences its catalytic activity in a two-phase reaction, the hydrogenation of the prochiral olefin, (*Z*)-2-(*N*-acetamido)cinnamic acid ester (AACA-Me), was performed in a two-phase reaction medium consisting of either dichloromethane or ethyl acetate and water. The results of several of these reactions are collected in Table 1. For comparison results with BDPP[12] and tetrasulfonated BDPP (BDPPTS)[2] are included in the table.

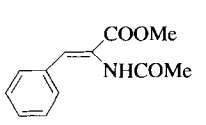

AACA-Me

It is well-known that the BDPP ligand is not the best for the asymmetric hydrogenation of AACA-Me. With BDPP the maximum *ee* value reported is 72% with this substrate, while with diphosphane derivatives of methyl-α-D-glucopyranosides (glup) and related compounds as the ligand, *ee* values of > 95% are obtained in the presence of nonchiral surfactants.[13] The substrate AACA-Me was chosen to determine if a two-phase reaction medium could be modified with surface-active chiral ligands to improve reactivity and selectivity, since potential improvement in selectivity is best observed in a ligand and substrate system that begins with modest selectivity, as was observed with the glup ligands mentioned above.

Table 1. Hydrogenation of AACA-Me under various conditions [a].

Exp.	Ligand	Solvent	Pressure [atm]	Time [h]	Yield [%]	*ee* [%]
1	BDPP [b]	MeOH	1	0.20	100	72
2	**5** [c]	MeOH	1	0.75	100	75
3	BDPPTS	MeOH	15	1	100	72
4	**5** [b]	EtOAc/H_2O	1	1.5	100	69
5	**5** [d]	EtOAc/H_2O	1	1.5	100	66
6	**5** [e]	EtOAc/H_2O	1	20	67	35
7a	BDPPTS [f]	EtOAc/H_2O	15	not reported	100	45
7b	BDPPTS [g]	EtOAc/H_2O	15	1.3	100	44
8	BDPPTS [h]	EtOAc/H_2O	1	20	32	20
9	BDPPTS [i]	EtOAc/H_2O	1	20	36	18

[a] The reactions were carried out as follows: $T = 25$ °C, solvent EtOAc/H_2O = 1/1 (except in experiments 1–3); the catalyst was prepared from $[\{Rh(cod)Cl\}_2]$ and the water-soluble ligand in water. Optical purity was determined by optical rotation as described previously [4b]. [b] See ref. [11]. [c] 0.0025 M Rh, 0.0025 M **5**, AACA-Me/Rh = 100/1. [d] As in [c] + 0.05 M SDS. [e] As in [b] + 0.05 M Na_2HPO_4. [f] See ref. [2]. [g] Repeat of the experiment described in ref. [2]. [h] 0.0025 M Rh, 0.0025 M BDPPTS, AACA-Me/Rh = 1001/1. [i] As in [g] + 0.05 M SDS.

Nearly identical hydrogenation activity and selectivity are obtained with the rhodium complexes of **5** and of BDPP, when the reactions are carried out homogeneously in methanol (experiments 1–3). The selectivity with BDPPTS in a two-phase system is dependent on the nature of the organic phase. In EtOAc/H_2O 45% *ee* is obtained at 15 atm (entry 7 in Table 1). Furthermore, the reactions with BDPPTS in a two-phase system are relatively slow; in EtOAc/H_2O only 32% conversion is observed after 20 h at 1 atm (experiment 8). In contrast, in the same two-phase system, using catalysts based on **5** only 1.5 hours are required to reach 100% conversion and an enantiomeric excess of 69% is obtained (experiment 4). This value approaches that seen in methanol alone as the solvent and is an improvement over the BDPPTS ligand in the same solvent systems; however, all the reactions in two-phase systems are less selective and slower than the homogeneous reactions in methanol.

Addition of a salt, Na_2HPO_4, has the effect of decreasing reactivity of **5** (experiment 6). This result is not surprising in that there is no excess phosphane present to form micelles at high ionic strength. It has been observed in related systems that high ionic strength has the effect of decreasing reactivity in a two-phase system with a poorly water-soluble substrate in the absence of micelles. Addition of Na_2HPO_4 also decreases the selectivity perhaps due to formation of a monohydride species.[13] The selectivity is not improved if sodium dodecylsulfate (SDS) is added to the catalyst (experiment 5). This is somewhat surprising in light of the results of Selke et al.[14] They note that surfactants can induce a modest increase in selectivity as well as improve reactivity in the hydrogenation of cinnamic acid derivatives with the glup ligands in water.

In summary the surface-active ligand **5** gives catalytsts that show improved reactivity and similar selectivity to its nonmod-

 © VCH Verlagsgesellschaft mbH, D-69451 Weinheim, 1995 0570-0833/95/1515-1646 $ 10.00+.25/0

ified analog BDPP. We conclude then that the incorporation of the easily sulfonated pendant group, *p*-(3-phenylpropyl)phenyl, into other diphosphanes will lead generally to chiral catalysts of improved activity in two-phase systems. The selectivity will be set by the parent chiral ligand system.

Experimental Procedure

The phosphanes **4** and **5** were synthesized under nitrogen by standard procedures for organophosphorus chemistry [8]. NMR measurements were done on a Bruker WP 200 at 200.13 MHz for ^{1}H, 50.323 MHz for ^{13}C, and 81.015 MHz for ^{31}P. An asterisk by the multiplicity data stands for pseudo. The numbering of the carbon atoms in the phosphanes can be taken from the formula of **5**.

4: Finely chopped lithium metal (0.14 g, 0.02 mol) was suspended in dry THF (10 mL), and tris-[*p*-(3-phenylpropyl)phenyl]phosphane (6.2 g, 0.01 mol) in THF (100 mL) was added from a dropping funnel over a period of about 10 min with vigorous stirring. The resulting deep red solution was stirred at room temperature for an additional 2 h. *tert*-Butyl chloride (0.93 g, 0.01 mol) was added and the reaction mixture was brought to reflux for 15 min. The volume of the solution was reduced to about 10 mL and dry degassed pentane (80 mL) was added. A dark red viscous residue (**3**) separated at −78 °C. The red oil was redissolved in THF (50 mL) and either (*S,S*)- or (*R,R*)-2,4-pentanediol-ditosylate (2.0 g, 0.0049 mol) in THF (10 mL) was added. After 10 h the solvent was removed to yield a pale yellow oil. The oil was redissolved in diethyl ether (40 mL) and washed three times with water (10 mL). The ether layer was dried over $MgSO_4$ and the volume reduced to about 10 mL; methanol (30 mL) was added to yield a pale yellow oil (**4**). Yield: 3.2 g, 71 %.

^{31}P NMR data for **3** and the deuterated secondary phosphane formed upon deuterolysis in THF: **3**: $\delta = -25.97$ (s); deuterium bis[*p*-(3-phenylpropyl)phenyl]-phosphane: $\delta = -43.06$ (t, ^1J(D,P) = 32.7 Hz).

Physical data for **4**: ^{1}H NMR ($CDCl_3$): $\delta = 0.87$ {dd, ^3J(H,H) = 6.7, ^3J(H,P) = 15.4 Hz, 6H, (16)CH_3 + (16′)CH_3}; 1.31 {* quin., ^3J(H,H) + ^3J(H,P) = 6.9 Hz, 2H, (18)CH_2}, 1.86 {m, 8H, (8)CH_2 + (8′)CH_2}; 2.37 {m, 2H, (17)CH + (17′)CH}; 2.53 {m, 16H, (7)CH_2 + (7′) CH_2 + (9)CH_2 + (9′)CH_2}; 7.01–7.30 (m, 36 H, aromatic protons); ^{13}C NMR ($CDCl_3$): 15.72 {d, ^2J(C,P) = 12.1 Hz, 2C, (16)CH_3 + (16′)CH_3}; 27.49 {*t, 2C, (17)CH + (17′)CH}; 32.64 {s, 4C, (8) CH_2 + (8′)CH_2}; 35.18 {s, 4C, (9) CH_2 + (9′)CH_2}; 35.42 {s, 4C, (7)CH_2 + (7′)CH_2}; 36.54 (br. s, 1C, (18)CH_2}; 125.72 {s, 4C, (13)CH + (13′)CH}; 128.26 {s, 8C, (12)CH + (12′)CH + (14)CH + (14′)CH}; 128.38 {s, 8C, (11)CH + (11′)CH + (15)CH + (15′)CH}; 133.62 {d, ^3J(C,P) = 21.1 Hz, 8C, (3)CH + (3′)CH + (5)CH + (5′)CH}; 142.51 {d, ^2J(C,P) = 50.3 Hz, 8C, (2)CH + (2′)CH + (6)CH + (6′)CH}; the signals for (1)C, (4)C, (10)C are not observed; ^{31}P NMR: δ (in $CDCl_3$) −1.80 (s); δ (in THF) −2.30 (s); MS(FAB$^+$): m/z = 913 (M + 1)

5: Compound **4** (5 g, 5.5 mmol) was placed into a 1000 mL flask, cooled to −78 °C; 96% H_2SO_4 (20 mL) was then added with stirring. The mixture was allowed to come to room temperature. The reaction mixture was neutralized by slow addition of 20% NaOH after 6 h. The pH was adjusted to 9 and the final volume was about 120 mL. Methanol (720 ml) was added and the mixture was heated to reflux for 30 min, filtered, and the precipitate extracted with hot methanol (200 mL). After two extractions, the filtrates were combined and the volume was reduced to about 45 mL. Acetone (270 mL) was added to precipitate **5** as a white solid which was collected and dried. Yield: 6.1 g, 84%.

Physical data for **5**: ^{1}H NMR (CD_3OD): $\delta = 0.82$ {dd, ^3J(H,H) = 6.5, ^3J(H,P) = 15.5 Hz, 6H, (16)CH_3 + (16′)CH_3}; 1.17 {m, 2H, (18)CH_2}; 1.81 {m, 8H, (8)CH_2 + (8′)CH_2} 2.38 {m, 2H (17)CH + (17′) CH}; 2.52 {m, 16 H, (7)CH_2 + (7′)CH_2 + (9)CH_2 + (9′)CH_2}; 7.02 {m, 8H} + 7.24 (m, 8H} {(12)CH + (12′)CH + (14′)CH + (14′)CH + (11)CH + (11′)CH + (15)CH + (15′)CH}; 7.14 {m, 8H} + 7.64 {m, 8H} {(2)CH + (2′)CH + (6)CH + (6′)CH + (3)CH + (3′)CH + (5)CH + (5′)CH}; ^{13}C NMR (CD_3OD): δ = 16.33 {d, ^2J(C,P) = 17.9 Hz, 2C, (16)CH_3 + (16′)CH_3}; 28.50 {*t, ^1J(P,C) + ^3J(P,C) = 8.4 Hz, 2C, (17)CH + (17′)CH}; 33.98 {s, 4C, (8)CH_2 + (8′)CH_2]; 36.10 {br. s, 8C, (9)CH_2 + (9′) CH_2 + (7)CH_2 + (7′)CH_2}; 36.97 {br. s, 1C (18)CH_2}; 127.08 {s, 8C, (11)CH + (11′)CH + (15)CH + (15′)CH}; 129.35 {s, 8C, (12)CH + (12′)CH + (14)CH + (14′)CH}; 129.52 {d, ^3J(C,P) = 7.7 Hz, 8C, (3)CH + (3′)CH + (5)CH + (5′)CH}; 134.78 {dd, ^2J(C,P) = 19.4 Hz, ^6J(C,P) = 10.0 Hz, 8C, (2)CH + (2′)CH + (6)CH + (6′)CH}; 142.09 {s, 4C, (10)C + (10′)C}; 143.89 {s, 4C, (4)C + (4′)C}; 144.38 {d, ^1J(C,P) = 4.2 Hz, 4C, (1)C + (1′)C}; 146.10 {s, 4C, (13)C + (13′)C}; ^{31}P NMR (CD_3OD): $\delta = -1.11$ (s); MS ($C_{65}H_{66}Na_4O_{12}P_2S_4$, R = $C_6H_4(CH_2)_3C_6H_4$; FAB$^+$): m/z: 1343 (M + Na$^+$), 1321 (M + H$^+$), 1241 (M − (SO_3^-)), 967 (MH$^+$ − R − (SO_3^-) − Na$^+$), 718 (M − PR_2 + Na$^+$), 648 (PR_2 + Na$^+$). Elemental analysis, calc. for the tetrahydrate: $C_{65}H_{74}Na_4O_{16}P_2S_4$: C 56.05, H 5.37; found: C 55.63, H 5.53.

Received: March 20, 1995
Revised version: May 5, 1995 [Z 7811 IE]
German version: *Angew. Chem.* **1995**, *107*, 1728–1730

Keywords: asymmetric syntheses · catalysis · chiral auxiliaries · hydrogenations · sulfonations

[1] a) W. A. Herrmann, C. W. Kohlpaintner, *Angew. Chem.*, **1993**, *105*, 1588; *Angew. Chem. Int. Ed. Engl.* **1993**, *32*, 1524; b) B. Cornils, E. Wiebus, *CHEMTECH* **1995**, *25*, 33.
[2] Y. Amrani, L. Lecomte, D. Sinou, F. Bakos, I. Toth, B. Heil, *Organometallics*, **1989**, *8*, 542.
[3] a) C. Lensink, J. G. DeVries, *Tetrahedron: Asymmetry*, **1992**, *3*, 235; b) J. Bakos, A. Orosz, B. Heil, M. Laghmari, P. Lhosta, D. Sinou, *J. Chem. Soc. Chem. Commun.* **1991**, 1684.
[4] a) I. Toth, B. E. Hanson, *Tetrahedron: Asymmetry*, **1990**, *1*, 890; b) I. Toth, B. E. Hanson, M. E. Davis, *ibid.* **1990**, *1*, 913.
[5] K. Wan, M. E. Davis, *J. Chem. Soc. Chem. Commun.* **1993**, 1262.
[6] T. Bartik, B. B. Bunn, B. Bartik, B. E. Hanson, *Inorg. Chem.* **1994**, *33*, 164.
[7] a) W. A. Herrmann, G. A. Albanese, R. Manetsberger, P. Lappe, H. Bahrmann, *Angew. Chem.* **1995**, *107*, 893; *Angew. Chem. Int. Ed. Engl.* **1995**, *34*, 811; b) W. A. Herrmann et al., DE-B 4.435.190.
[8] H. Ding, B. E. Hanson, T. Bartik, B. Bartik, *Organometallics*, **1994**, *13*, 3761.
[9] W. Kosolapoff, L. Maier, *Organic Phosphorus Compounds. Vol.1*, Wiley Interscience, New York, **1972**.
[10] U. Schmidt, K. Kabitzke, K. Markau, A. Muller, *Chem. Ber.* **1966**, *99*, 1497.
[11] I. Toth, B. E. Hanson, M. E. Davis, *Organometallics*, **1990**, *9*, 675.
[12] J. Bakos, I. Toth, B. Heil, L. Marko, *J. Organomet. Chem.* **1985**, *279*, 23.
[13] F. Joó, P. Csiba, A. Bényei, *J. Chem. Soc. Chem. Commun.* **1993**, 1602.
[14] a) A. Kumar, G. Oehme, P. P. Roque, M. Schwarze, R. Selke, *Angew. Chem.* **1994**, *106*, 2272; *Angew. Chem. Int. Ed. Engl.* **1994**, *33*, 2197; b) R. Selke, C Fackiam, H. Foken, D. Heller, *Tetrahedron: Asymmetry* **1993**, *4*, 369; G. Oehme, E. Paetzold, R. Selke, *J. Mol. Catal.* **1992**, *71*, L1; I. Grassert, E. Paetzold, G. Oehme, *Tetrahedron*, **1993**, *49*, 6605.

$(CuI)_3P_{12}$: A Solid Containing a New Polymer of Phosphorus Predicted by Theory**

Arno Pfitzner* and Eva Freudenthaler

Despite numerous investigations on phosphanes and phosphides[1–3] since the determination of the crystal structure of Hittorf's phosphorus only assumptions have been made concerning the existence and especially the structure of further allotropic forms of red phosphorus.[4] A concrete model for this polymorph was put forward very recently by Häser and Böcker based on theoretical methods.[5] They proposed a thermodynamically stable helix consisting of condensed five- and six-membered rings only. Nevertheless, this allotrope has not yet been obtained in a crystalline state, possibly because difficulties associated in the packing of such helices result in amorphous solids.

Systematic investigations on new copper(I) ion conductors consisting of adducts of copper(I) halides and elemental phosphorus have yielded the new solid compound $(CuI)_3P_{12}$. The structure of the above-mentioned neutral phosphorus fragment has not been observed previously by experiment (but was predicted by theory). Evidently, the screws can be crystallized together with CuI which is known to show a large variety of compounds in which the copper atoms are coordinated differently.[6] Investigations on $CuTe_2X$, $CuSe_2X$, and CuSeTeX (X = Cl, Br, I) show the flexibility of the copper(I) halides coordinated to neutral polymeric chalcogen screws.[7–12] Recently

[*] Dr. A. Pfitzner, Dipl.-Chem. E. Freudenthaler
Fachbereich 8 - Anorganische Chemie II der Universität-Gesamthochschule
Adolf-Reichwein-Strasse
D-57068 Siegen (Germany)
Telefax: Int. code + (271)740 2555
e-mail: pfitzner@chemie.uni-siegen.d400.de

[**] We thank Prof. Deiseroth for his continuous support, Prof. von Schnering for helpful discussions, Dr. Schwarz, Universität Stuttgart, for the collection of X-ray data, and the Hoechst AG for a gift of red phosphorus.

 © VCH Verlagsgesellschaft mbH, D-69451 Weinheim, 1995 0570-0833/95/1515-1647 $ 10.00+.25/0

even a helical arrangement of face-sharing tetrahedra in $[(C_6H_5)_4P]^1_\infty[Cu_3I_4]$ has been reported.[13]

Here we present some of the results of experiments on the Cu-X-P (X = Cl, Br, I) systems. The only previously reported examples of this class of compounds are the ternary compound $Cu_2P_3I_2$,[14] which contains polymeric $^1_\infty[P^0_{12}]$ incorporated in CuI and is best expressed by the formula $(CuI)_8P_{12}$, and $Cu_3P_{15}I_2$, a copper(I) iodide phosphide containing $^1_\infty[P^-_{15}]$ ions, which we published recently.[15]

The crystal structure of the hitherto unknown compound $(CuI)_3P_{12}$ was determined by single-crystal X-ray diffraction.[16] It exhibits two crystallographically independent phosphorus strands (strands 1 and 2), which do not differ significantly (Fig. 1). In the crystal these strands are arranged in a rod packing, and are bound together by P-Cu-P interactions to form slabs parallel to (100). Cu-I-Cu bridges link these slabs along [001]. The copper atoms may be divided up into three different groups with respect to their coordination by iodine and phosphorus. The copper atoms are all tetrahedrally coordinated. Cu1 and Cu2 are each bonded to one phosphorus atom of strand 1 and three iodine atoms. The copper atoms Cu3–Cu6 are each bonded to two iodine and two phosphorus atoms; these phosphorus atoms belong to one (Cu3, Cu4) or two strands (Cu5, Cu6). The iodine atoms are bonded to two (I1–I4, $2.526(1) \le d_{Cu-I} \le 2.668(1)$ Å), or to three copper atoms (I5, I6, $2.568(1) \le d_{Cu-I} \le 2.718(1)$ Å).

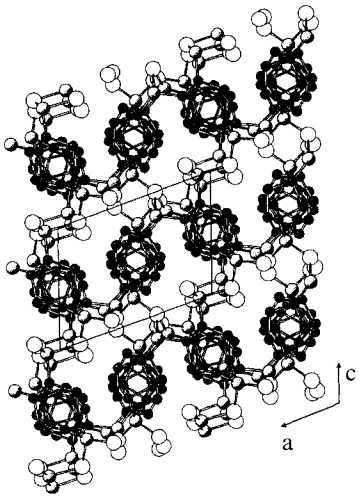

Fig. 1. Section of the crystal structure of $(CuI)_3P_{12}$. P: black, Cu: shaded, I: empty circles. View along [010].

The most remarkable features of the structure of $(CuI)_3P_{12}$ are the one-dimensional infinite strands of phosphorus, which stretch along the needle axis [010] and consist of five- and six-membered rings of phosphorus only. According to the theoretical calculations reported by Böcker and Häser,[5] this arrangement should be more stable than the $^1_\infty[P^0_{12}]$ chains in $Cu_2P_3I_2$, which additionally contain four-membered rings. The difference between the two crystallographically independent strands in $(CuI)_3P_{12}$ is a result of packing in the solid; that is, the strands differ with respect to their interactions to the surrounding copper atoms. In line with the nomenclature proposed by Böcker and Häser[5] the strands are named $^1_\infty([P10]P2[])^0$ (in comparison the $Cu_2P_3I_2$ contains linear $^1_\infty([P8]P4(4)[])^0$ units). The basic [P10] unit in $(CuI)_3P_{12}$ is shown in Figure 2a. Addition of a copper atom attached to the six-membered ring results in CuP_{10} units with pseudo "ufosane" structure. These P_{10} units are linked formally by P_2 fragments (P2 and P5 in strand 1, and P22 and P25 in strand 2), leading to the formation of infinite one-dimensional screws of phosphorus. The length of such a repeating unit ([P10]P2[]) in $(CuI)_3P_{12}$ is $b/2 = 6.93$ Å, which is about 1 Å less than observed for the linear strand ([P8]P4(4)[]) in $Cu_2P_3I_2$. This is in good agreement with the value of about 7.2 Å predicted by theory (SCF/SVP-level).[17] The extent to which the copper atoms contribute to the stabilization of the phosphorus helices $^1_\infty([P10]P2[])^0$ is the subject of theoretical studies. The formation of the phosphorus strands can alternatively be described by the linkage of P_7 norbornane-analogous fragments (Fig. 2b).

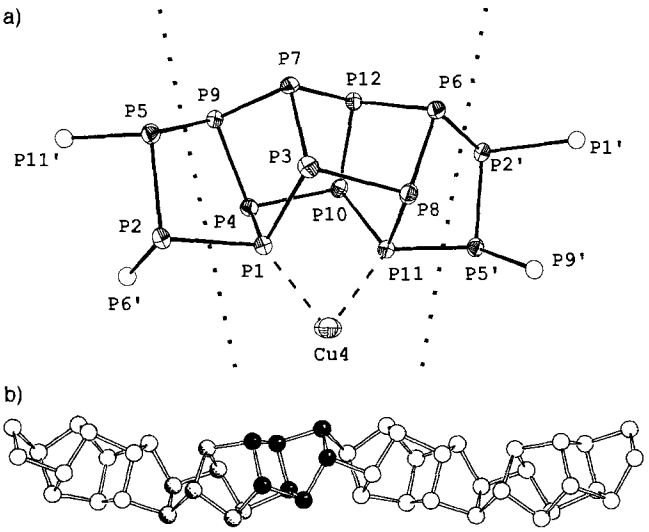

Fig. 2. a) CuP_{10} unit with pseudo "ufosane" structure in $(CuI)_3P_{12}$; these units are linked by P2, P5 in strand 1, and P2′ and P5′ in strand 2. b) Section of a phosphorus strand; two norbornane-analogous P_7 fragments are emphasized.

The phosphorus atoms in the strands each show three covalent bonds to neighboring phosphorus atoms; the d_{P-P} distances range from 2.18 to 2.28 Å. The d_{P-P} bond lengths do not vary significantly with the coordination of additional copper atoms. The distances between copper and phosphorus atoms all lie in the small range $2.27 < d_{Cu-P} < 2.32$ Å, similar to the situation in Cu_2P_7.[18] Our investigations on $Cu_3P_{15}I_2$[15] indicated that the d_{Cu-P} distance is not affected by a formal negative charge on the phosphorus atoms. The different coordination pattern of the two crystallographically independent strands leads to the conclusion that packing effects, which are supported by the great flexibility of the copper iodide substructure, are primarily responsible for the phosphorus structure observed here.

It seems reasonable to assume that the $^1_\infty[P^0_{12}]$ screws described in this work are formed in the reaction of CuI with P, regardless of whether amorphous red or white phosphorus are used as the starting material. The interesting question of whether these phosphorus chains are already present in elemental red phosphorus and may be extracted from it by reaction with copper iodide remains to be answered.

Experimental Procedure

$(CuI)_3P_{12}$ was prepared by reaction of CuI and P in the ratio CuI:P = 1:4 in evacuated silica tubes with an excess volume as small as possible (typical setup: 1 g in total, inner diameter of ampoule 12 mm, ampoule length ca. 3 cm). Depending on the use of white or red phosphorus as starting material the reaction temperature of 500 °C can be reached more or less quickly. No crystalline ternary product was obtained by applying much lower temperatures (e.g. 150 °C, P_4). After a few weeks flat shiny needles of $(CuI)_3P_{12}$, which are very sensitive to mechanical manipulations, can be separated from by products, such as $Cu_3P_{15}I_2$, and others which have not yet been completely characterized. Crystals freed from impurities by cleaning in water are stable in air for some time. Because of strong texture effects it was difficult to obtain X-ray powder patterns with sufficient quality for sample characterization. Up to now it has not been possible to obtain any useful ^{31}P solid-state NMR spectra.

Received: March 25, 1995 [Z 7836 IE]
German version: *Angew. Chem.* **1995**, *107*, 1784–1786

Keywords: copper compounds · phosphorus compounds · solid-state structures

[1] H. G. von Schnering, W. Hönle, *Chem. Rev.* **1988**, 88, 243.
[2] M. Baudler, K. Glinka, *Chem. Rev.* **1993**, *93*, 1623.
[3] M. Baudler, *Angew. Chem.* **1987**, *99*, 429; *Angew. Chem. Int. Ed. Engl.* **1987**, *26*, 419.
[4] H. Thurn, H. Krebs, *Acta Crystallogr. Sect. B* **1969**, *25*, 125.
[5] S. Böcker, M. Häser, *Z. Anorg. Allg. Chem.* **1995**, *621*, 258.
[6] S. Jagner, G. Helgesson, *Adv. Inorg. Chem.* **1991**, *37*, 1.
[7] J. Fenner, *Acta Crystallogr. Sect. B* **1976**, *32*, 3084.
[8] W. Milius, A. Rabenau, *Z. Naturforsch. B* **1988**, *43*, 243.
[9] W. Milius, *Z. Naturforsch. B* **1989**, *44*, 990.
[10] T. Sakuma, T. Kaneko, H. Takahashi, K. Honma, *J. Phys. Soc. Jpn.* **1991**, *60*, 1136.
[11] R. B. Beeken, J. E. Dean, W. L. Jetzer, D. S. Lee, T. Sakuma, *Solid State Ionics* **1992**, *58*, 189.
[12] A. Pfitzner, S. Zimmerer, *Z. Anorg. Allg. Chem.*, **1995**, *621*, 969.
[13] H. Hartl, F. Mahdjour-Hassan-Abadi, *Angew. Chem.* **1994**, *106*, 1929; *Angew. Chem. Int. Ed. Engl.* **1994**, *33*, 1841.
[14] M. H. Möller, W. Jeitschko, *J. Solid State Chem.* **1986**, *65*, 178.
[15] A. Pfitzner, E. Freudenthaler, *Z. Kristallogr.* **1995**, *210*, 59.
[16] Usually crystals of $(CuI)_3P_{12}$ are twinned; thus a double c axis is simulated, resulting in non-space group extinctions (hkl with $h = 2n$ and $l = 2n + 1$ are extinct). Crystal structure of $(CuI)_3P_{12}$ (untwinned crystal): monoclinic, space group $P2_1$ (no. 4), $a = 12.846(4)$, $b = 13.857(3)$, $c = 9.651(3)$ Å, $\beta = 109.43(2)°$, $V = 1620.2(7)$ Å^3, $Z = 4$, $\rho_{calcd} = 3.866$ g cm^{-3}. 6197 reflections, 5757 of which are symmetry independent ($R_{int} = 0.055$), (room temperature, Wykoff scans, $Mo_{K\alpha}$ radiation, $\lambda = 0.71073$ Å, $2\theta_{max} = 56.2°$, crystal size $0.6 \times 0.3 \times 0.1$ mm^3, empirical absorption correction (Ψ scans)). Structure solution: direct methods (NRCVAX [19]), refinement against F^2 (full matrix, SHELXL-93 [20]), 325 free parameters, R(all) = 0.0248, w$R2$(all) = 0.0605. Further details of the crystal structure investigation are available on request from the Fachinformationszentrum Karlsruhe, D-76344 Eggenstein-Leopoldshafen (Germany), on quoting the depository number CSD-401755.
[17] M. Häser, personal communication.
[18] M. H. Möller, W. Jeitschko, *Z. Anorg. Allg. Chem.* **1982**, *491*, 225.
[19] E. J. Gabe, Y. Le Page, J.-P. Charland, F. L. Lee, P. S. White, *J. Appl. Crystallogr.* **1989**, *22*, 384.
[20] G. M. Sheldrick, SHELXL-93, Program for crystal structure refinement, Universität Göttingen (Germany), **1993**.

Corrigendum

In a thorough reinvestigation T. J. Collins, E. Münck, et al. (*Angew. Chem.* **1995**, *34*, 1216–1219) have found that the values for the zero-field splitting parameter D in Table 1 should be corrected to 9 ± 2 for compound **1** and 3 ± 2 for compound **2**. The title of the communication should read "A Stable Aquairon Complex with $S = 1$: Structure and Spectroscopic Properties."

Making Connections: Update on Thin Metal Films

The Chemistry of Metal CVD. Edited by *T. T. Kodas* and *M. J. Hampden-Smith*. VCH Verlagsgesellschaft, Weinheim, 1994. 538 pp., hardcover DM 228.00.—ISBN 3-527-29071-0

Chemical vapor deposition (CVD) is a method of producing pure metal films for a wide variety of applications, and has become increasingly important in recent years. It was at first thought that thin metal films produced by MOCVD (metal organic chemical vapor deposition) would be contaminated by unacceptable levels of carbon (or hydrocarbon fragments) and that coatings obtained by this method would therefore be of only limited value. However, many examples have been found which contradict that view, causing a reassessment of the method. Nevertheless, progress continues to be hampered by poor communication between chemists, process technologists, materials scientists, and electrochemists. To help remedy that problem the editors of this book offer a comprehensive overview of the current state of research (with about 1470 references extending up to 1994), to serve the needs of a heterogeneous readership from different disciplines.

Chapter 1 is a short introduction concerned with aspects of the application of metal contacts to silicon-based semiconductor devices (diffusion barriers, contact between metal and silicon), likely future developments, and the advantages and disadvantages of currently used deposition techniques. Chapters 2–8 then deal in turn with the deposition of individual metals: aluminum (Ch. 2), tungsten (Ch. 3), copper from Cu^{II} precursors (Ch. 4), copper from Cu^{I} precursors (Ch. 5), gold and silver (Ch. 6), platinum, palladium, and nickel (Ch. 7), and lastly (Ch. 8) tantalum, chromium, molybdenum, iron, cobalt, rhodium, iridium, and some less common metals, intermetallic phases, and alloys. The chapters on aluminum CVD (M. G. Simmons and W. L. Gladfelter) and copper CVD (G. L. Griffin, A. W. Maverick, M. J. Hampden-Smith, and T. T. Kodas) are well-rounded, packed with information, and well-written from a learning standpoint, and are therefore suitable as material for incorporating into lecture courses on materials chemistry for students of appropriate disciplines. The concise, succinct, and very competent treatment covers a wealth of topics; to name just a few, it includes the interaction between surfaces and the chemistry of the gas phase, dependence of results on the details of the process (type of reactor, method of supplying energy, etc.), area-selective deposition, prenucleation in the gas phase, purity, and electrical and morphological properties. On the other hand Chapters 3, 6, 7, and 8 are written more in the style of literature surveys which, although thoroughly comprehensive, do not always include critical evaluation. The detailed chemical descriptions of organometallic compounds used as precursors are largely, if not entirely, superfluous for readers with a knowledge of chemistry. It would have helped the reader considerably if the authors had been more careful and selective in their treatment of the literature, as there are long passages of text which merely paraphrase the contents of tables. In this respect the discussions here differ only slightly from several recent review articles by other authors in various journals and progress report series. In Chapter 8 the authors have attempted a critical evaluation of the miscellaneous factual information that is drawn together here, but a few important aspects are missing. For example, there is little discussion of how likely it is that pure metallic films of titanium, chromium, vanadium, niobium, or tantalum can be produced by MOCVD, in view of the fact that all these readily form carbides. On the whole, well-established information about mechanisms is given in only a few cases. However, this is not so much an omission on the part of the authors as a reflection of the fact that the field is still in a state of rapid development, and therefore it is not surprising that many of the sections are of a very speculative nature. Chapter 9, "Overview of Metal CVD", is essentially a summary, in 70 pages, of the whole work, together with a brief outline of some process-orientated aspects (reactor design, precursor transport, kinetics of film growth, etc.). Compared with other treatments (e.g. Hitchman and Jensen, 1993; Vossen and Kern, 1991) this is limited to just the bare essentials. The overall structure of the book, treating individual elements or metals in turn, and the arrangement of the subject matter, has resulted in much repetition. The text could have been tightened up considerably and the factual information arranged more effectively under broad headings such as the incorporation of carbon, nucleation, selectivity, morphology, the influence of process variables, and so on.

The book is very handsomely produced and is virtually free of printing errors. It is certainly a valuable resource, both for the molecular chemist interested in this field and for the practical user, enabling the reader to get a rapid overview of the widely scattered original literature. Parts of it offer a good basis for preparing teaching courses. However, as the first comprehensive treatment in book form of this already well-established field of research, which the title appears to claim, it has some shortcomings. It is also by no means cheap for the information that it contains.

Roland A. Fischer
Anorganisch-chemisches Institut
der Technischen Universität München
(Germany)

Phosphorus-31 NMR Spectral Properties in Compound Characterization and Structural Analysis. Edited by *L. D. Quin* and *J. G. Verkade*. VCH Publishers, New York, 1994. 450 pp., hardcover DM 260.00.—ISBN 1-56081-637-6

This volume on new developments in ^{31}P NMR spectroscopy is in principle

This section contains book reviews and a list of new books received by the editor. Book reviews are written by invitation from the editor. Suggestions for books to be reviewed and for book reviewers are welcome. Publishers should send brochures or (better) books to Dr. Ralf Baumann, Redaktion Angewandte Chemie, Postfach 101161, D-69451 Weinheim, Federal Republic of Germany. The editor reserves the right of selecting which books will be reviewed. Uninvited books not chosen for review will not be returned.

greatly to be welcomed, in view of the rapid growth of information on this and other methods of structure determination. Important new developments in this field include, for example, automation using robotic sample changers, multidimensional NMR experiments with heteronuclear chemical shift correlation (HETCOR), studies of phosphorus compounds of biological interest with multiple isotopic labeling, and solid-state NMR spectroscopy. However, the editors' treatment of the subject is not entirely satisfactory, as becomes especially evident on comparing the book with its predecessor (now no longer to be printed) in the series *Methods in Stereochemical Analysis*. That book began by laying the foundations of a sound understanding of the theory of the method (in several chapters with a comprehensive bibliography) and of the experimental techniques (construction of the spectrometer, etc.), thereby equipping the reader with the necessary knowledge to deal with problems of qualitative, quantitative, and structural analysis. In contrast the present book is unconvincing with regard to its conception and content. The contributors are well-recognized experts (experimentalists in many cases), and the articles treating the chemistry of their specialist areas from an analytical viewpoint are mostly very well illustrated. However, these are presented against a very sketchy and inadequate theoretical background, thus making it difficult for the reader to properly understand their contents and to appreciate the advances in techniques that have been achieved.

The book consists of nine chapters containing 33 individual contributions (each of about 10–18 pages including a bibliography), and has an author index and a subject index. In view of the many abbreviations and acronyms by which the various NMR procedures are known, it is unfortunate that no glossary of these has been provided. The book has been carefully produced, and the quality of the spectra that are reproduced varies from good to very good.

The first article, by D. B. Chesnut and B. E. Rusiloski, is on ab-initio calculations of ^{31}P chemical shifts. Chapter 2 consists of three contributions on the conformational analysis of phosphorus heterocycles. M. Mikolajczyk and P. P. Graczyk give a detailed account of work on 2-chalcogenophosphoranyl-substituted 1,3-dithianes. Next comes an article by R. R. Holmes and coauthors on phosphorus(III) and phosphorus(V) heterocycles (e.g. dibenzo[*d,f*]-1,3,2-dioxaphosphepine) which act as sterically selective phosphane ligands in metal-catalyzed reactions. The chapter ends with a contribution by W. G. Bentrude on the determination of $^{1}H,^{31}P$ coupling constants for the conformational analysis of three-, four-, and fivefold-coordinated 1,3,2-dioxaphosphorinanes. Mono- and polycyclic compounds are also the main theme of Chapter 3, the exception being R. H. Neilson's article on phosphino-substituted allenes, acetylenes, and dienes. The first paper on the main topic is by J.-P. Majoral and coauthors, who describe the unusual spectroscopic properties of 1,3-diaza-2,4-diphosphetidines in both their monomeric and oligomeric forms, including examples such as the phosphorus macrocycles and dendrimers that are currently attracting much interest. E. Fluck and G. Heckmann report on acyclic and cyclic $1\lambda^3,3\lambda^5$-phosphorylides. M. Baudler and coauthors describe the use of ^{31}P NMR spectroscopy to determine the structure of the bicyclic phosphide LiH_5P_8, which is an instructive example of the capabilities of the SPT (selective polarization transfer) experiment. The chapter ends with articles on the determination of the structures of cyclophosphazenes (C. W. Allen) and phosphazenes (M. Pomeranz), in which ^{15}N NMR measurements also play a part.

Chapter 4 is entirely devoted to the chemistry and spectroscopic properties of compounds with phosphorus in low-coordination states. M. Meisel and coauthors describe the use of donor-stabilized metaphosphates in the synthesis of heterocyclic compounds, and M. Regitz and coauthors report on the oligomerization products of *t*-butylphosphaacetylene and their identification by ^{31}P NMR spectroscopy. E. Niecke and D. Gudat discuss configurational and substituent effects on the ^{31}P NMR parameters of iminophosphanes, both in solution and in the solid state. M. Yoshifuji contributes an article on methylenephosphanes and diphosphenes. This chapter is completed by an article by R. W. Reed and G. Bertrand on the wide-ranging uses of the bis(diisopropylamino)-phosphino substituent for the stabilization of reactive compounds. Chapter 5 is concerned with spectroscopic studies of transition metal complexes with phosphane ligands. J. H. Nelson describes work on metal-mediated intramolecular [4 + 2]-cycloadditions of phospholes. E. Lindner and coauthors discuss the dynamic behavior of five-membered etherphosphane ligands and thermodynamic data on these. The article by J. F. Nixon and coauthors is concerned with metal-mediated syntheses of mono- and polycyclic phosphane ligands and the characterization of the products. A. H. Hughes describes work on determining the structures of homo- and heterobinuclear complexes with phosphorus-containing chelate ligands (such as dppm), with particular emphasis on the $^{31}P,^{31}P$ coupling constants.

Chapter 6 reports on advances in the structural analysis of biochemically important phosphorus compounds. G. Lowe discusses the stereochemical analysis of $[^{16}O,^{17}O,^{18}O]$-isotopically labeled chiral inorganic thiophosphates, and the introduction of these as terminal groups in adenosine triphosphate. D. G. Gorenstein describes the use of specific HETCOR and PAC pulse sequence experiments to yield information about the conformation of the phosphodiester backbone in oligonucleotides of moderate chain lengths (12–20 base pairs). T. Glonek describes techniques for obtaining phospholipid extracts, preparing samples from these, and analyzing them by ^{31}P NMR spectroscopy.

Chapter 7 is concerned with the investigation of reaction mechanisms. In the first article E. Vedejs and C. F. Marth describe a careful and thorough analysis of the λ^5-oxaphosphetane intermediate in the synthetically important Wittig reaction. In another very interesting contribution P. M. Cullis describes an investigation of the stereochemistry of the transfer of ^{17}O-labeled phosphoryl and thiophosphoryl groups by ADP. L. N. Markovsky and coauthors report on examples of reversible coordination isomerism involving proto-, halo-, and phosphotropic effects in inorganic compounds. Chapter 8 introduces some new areas of application of ^{31}P NMR spectroscopy and others where recent advances have occurred. First M. Murray gives an introduction to two-dimensional methods as applied to P,P and P,H correlation experiments. This is followed by a well-structured article by J. K. Gard on advances in the automation of such measurements (e.g. by using an automatic sample changer) and on the interpretation of results on oligophosphates of industrial importance. The contribution by J. G. Verkade is also likely to be of industrial interest, dealing with the analysis of coal constituents (alcohols, amines, acids) by first derivatizing these with simple phosphorus-containing reagents. M. J. Gallagher describes the spectroscopic characterization of the parent compounds of various phosphoric acid derivatives. The chapter ends with an interesting article in which G. H. Hägele describes the use of ^{31}P NMR measurements for monitoring titrations. The final chapter is devoted to solid-state ^{31}P NMR spec-

 © VCH Verlagsgesellschaft mbH, D-69451 Weinheim, 1995 0570-0833/95/1515-1652 $ 10.00+.25/0

troscopy, which has advanced greatly in the last ten years, based on the CP/MAS method developed by Schaefer and Stejskal. First M. J. Potrzebowski and J. Michalski give a short introduction to this field. Taking a bis(phosphoryl)disulphide as an example, they compare the information yielded by CP/MAS measurements with that given by X-ray crystallography, and show correlations between the two (e.g. $\Delta\delta$ is correlated with the S–P–S bond angle). L. D. Quin describes how electrophilic compounds containing phosphorus in low-coordination states, supported on silica gel, are used as scavengers to prepare samples which are then analyzed by CP/MAS ^{31}P NMR spectroscopy. This last chapter ends with an introduction to MAS-frequency-dependent NMR spectroscopy by R. E. Wasylishen, illustrated by results on $Cd(PPh_3)(NO_3)_2$.

The book as a whole suffers from the defects already mentioned earlier and from those of conference reports in general, namely heterogeneity across the chapters and a relatively high price due to the short print run. However, it is certainly not redundant, since it collects together for the first time the many analytical capabilities of ^{31}P NMR spectroscopy, which can be used to investigate such widely different substances as highly reactive intermediates, nucleic acids, cyclotriphosphazenes, and derivatized coal constituents. The book can therefore be recommended not only for readers with interests in these topics but for others too.

Rainer Streubel
Institut für Anorganische und
Analytische Chemie
der Technischen Universität
Braunschweig (Germany)

Diazo Chemistry I. By *H. Zollinger*. VCH Verlagsgesellschaft, Weinheim, 1994. 453 pp., hardcover DM 198.00.—ISBN 3-527-29213-6

Heinrich Zollinger, the author of this monograph on the chemistry of aromatic and heteroaromatic diazo compounds, is better qualified than virtually anyone else to write a comprehensive and critical work on the subject. Diazo compounds are of great industrial importance, and their chemistry raises difficult and challenging problems. The work reviewed here incorporates the knowledge gained from the author's experience in the industrial application of diazonium compounds and in research into their modes of reaction. Its predecessors are Zollinger's earlier books *Diazo and Azo Chemistry of Aliphatic and Aromatic Compounds* (1961) and *Color Chemistry* (1987, followed by a second edition in 1991). Part II of the present work, covering aliphatic and inorganic diazonium compounds, is to be published within a year following the first volume.

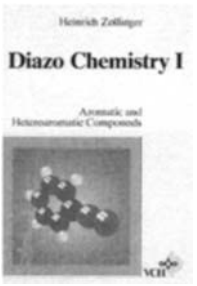

In thirteen chapters *Diazo Chemistry I* deals with all the important concepts and properties that make up the present understanding of the chemistry of aromatic and heteroaromatic diazo compounds. Chapter 1 (9 pp.) describes the historical development of the subject and explains the nomenclature for this group of compounds. Chapter 2 (21 pp.) deals with preparative methods, beginning with the most common procedure, the diazotization of amines by alkali metal nitrites in dilute mineral acids. Aspects of diazotization in concentrated mineral acids and under anhydrous conditions are then discussed. The author also deals briefly with the isolation of diazonium salts and draws attention to the special case of the diazotization of aminophenols, which are readily deprotonated to give diazoketones. Apart from the nitrosation of amines, there are only a few other methods for preparing diazonium salts, and this concludes the chapter. The third chapter (25 pp.) is concerned with the kinetics and mechanisms of diazotization. After critically reviewing the considerable literature on this subject, the author devotes special attention to the effects of different mineral acids and concentrations on the diazotization mechanism. Other aspects treated include the use of nucleophilic catalysis in diazotization, and the conversion of isolated *N*-nitrosamines to diazonium salts. Chapter 4 (23 pp.) deals with the structure of diazonium salts, reviewing the latest results from crystal structure determinations. Spectroscopic observations and the reactive properties of diazonium compounds are discussed and explained in the light of theoretical studies. In Chapters 5 and 6 (48 pp. altogether) the author discusses the addition of nucleophiles to aryldiazonium compounds. The effect of pH on the reaction of diazonium salts with water is treated in detail, followed by discussions of the reactions with O-, S-, N-, P-, and C-nucleophiles. These two chapters are completed by a section on intramolecular coupling reactions, which yield some interesting heterocyclic compounds. Chapter 7 (16 pp.) discusses the mechanism of the addition of nucleophiles to diazonium ions and the structures of the resulting compounds. Mechanistic aspects of the reactions of diazonium compounds involving loss of nitrogen are treated in Chapter 9 (48 pp.), and Chapter 10 (67 pp.) describes the synthetic applications of such reactions as a general method for introducing nucleophiles into non-activated arenes. Chapter 11 (15 pp.) deals briefly with host–guest complexes of arene-diazonium salts, then in Chapter 12 (78 pp.) the author treats what is undoubtedly the most important reaction of aromatic and heterocyclic diazonium compounds, the coupling reaction yielding azo dyes. The last chapter (19 pp.) is concerned with the formation and reactions of triazenes.

The author's comprehensive knowledge of aromatic and heteroaromatic diazonium compounds has resulted in a monograph which contains practically all the information that a specialist working in this field could wish for. The reader approaching the subject from a somewhat greater distance may find that the often very detailed treatment presents a rather formidable "energy barrier". Also many of the formula schemes are not very carefully prepared, in stark contrast to the precision of the text. As well as many errors of stoichiometry, the most serious problem is that in many cases insufficient care has been taken with the layout of the formulas. Better formula schemes presenting the information clearly would have greatly improved the book, especially for the non-specialist.

However, every chemist whose work is concerned with diazonium compounds, whether in industry or academia, will find this book indispensable. Furthermore, those whose research interests lie in other directions but who occasionally have to deal with diazonium compounds, especially in a teaching role, should certainly use this book at such times.

Franz Effenberger
Institut für Organische Chemie
und Isotopenforschung
der Universität Stuttgart (Germany)

Scalar Coupling Constants—Their Analysis and Their Application for the Elucidation of Structures

Matthias Eberstadt, Gerd Gemmecker, Dale F. Mierke, and Horst Kessler*

Dedicated to Professor Richard R. Ernst

Since their discovery in the early fifties, scalar coupling constants have been of great interest to the NMR spectroscopist. Their impact on structure determination by NMR spectroscopy is founded on the fact that the size of the coupling constant is directly related to molecular conformation. Today, for most chemical substances the parameters for the Karplus relationship, which relates the vicinial (3-bond) coupling constant to the dihedral angle, have been determined. In addition to proton–proton distances, the application of coupling constants in modern conformational analysis is indispensable. In the study of larger molecules which are of current interest, more and more involved experiments are necessary in order to overcome signal overlap and increasing line widths. A large number of experimental techniques for the determination of coupling constants has been developed; however, for this reason the choice of the most appropriate experiment to use has become more difficult. This decision must be made carefully to maximize instrument usage and obtain the largest number of couplings with the greatest accuracy possible. Many of the computer programs used in structure calculations can directly apply coupling constant restraints, similar to proton–proton distances developed from NOEs. Therefore, not only is the quality of the structure improved, but the molecular motions (internal dynamics) are better described. In this article, we review the techniques that exist today with particular attention paid to helping the non-expert to choose the appropriate experiment for the problem at hand. In addition, the use of coupling constants in computer simulations are discussed.

Keywords: NMR spectroscopy · structure elucidation

1. Introduction

Since its discovery in the early days of NMR spectroscopy by Gutowsky et al.,[1, 2] as well as independently by Hahn and Maxwell,[3, 4] indirect scalar spin–spin coupling (J coupling) has been realized as an important structural parameter. As the coupling is mediated by bonding electrons, it provides important information about the constitution of molecules in terms of the connectivity of the coupled nuclei. The size of the coupling constant depends not only on the number of bonds that separate the coupled nuclei, but also on the configuration of the electrons and their spatial arrangement.[5, 6] The latter effect can be especially useful in the determination of stereochemistry (configuration and conformation) and will be one of the major points of this article.

Many J coupling constants illustrate a clear dependency on dihedral angles and therefore are an important source of conformational information. This relationship is particularly distinct for ^3J couplings and the so-called Karplus relation, which for example correlates the $^3J_{H^N,H^\alpha}$ coupling in amino acids with the ϕ dihedral angle (cf. Fig. 1a). Such J couplings were employed early on in the study of conformation; however, since that time they have become less important as distance parameters developed from NOE have taken on a dominating role.[7–9] Only recently has a renaissance of sorts been seen in the use of J coupling constants. This has been brought about by the development of a series of new methods which allow for a more exact determination of the size of coupling constants.[10–13] Simultaneously, coupling constants for very large molecules which were previously not accessible, can now be measured with the help of multidimensional methods.[14–16] In addition, new methods to use the value of the J couplings in structure calculations have been developed.[17–20] Thereby a larger set of experimental data is available, so that not only the dependability of structures determined by NMR spectroscopy can be increased but also information about flexibility and internal molecular dynamics becomes accessible. Both play an important part in understanding the interaction between molecules ("molecular recognition").

[*] Prof. Dr. H. Kessler, Dr. M. Eberstadt, Dr. G. Gemmecker Institut für Organische Chemie und Biochemie der Technischen Universität München
Lichtenbergstrasse 4, D-85747 Garching (Germany)
Telefax: Int. code + (89)3209-3210
Prof. Dr. D. F. Mierke
Gustaf H. Carlson School of Chemistry
Clark University
950 Main Street, Worcester, MA 01610 (USA)

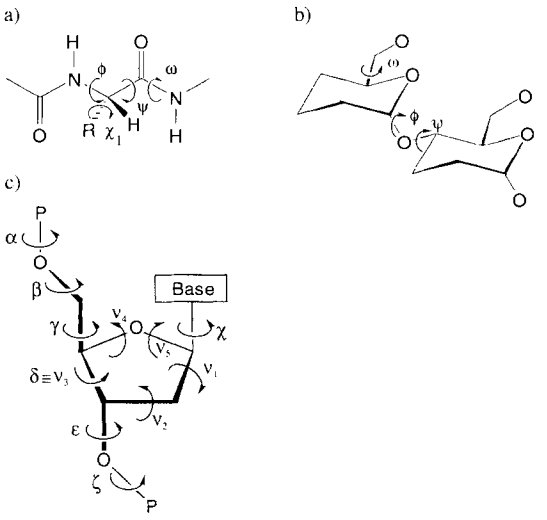

Fig. 1. Definitions of the dihedral angles in peptides, glycosides, and nucleic acids. a) Fragment of a peptide (L-amino acid) with the relevant dihedral angles for the peptide backbone and side chain using the IUPAC-IUB nomenclature. b) The dihedral angles ϕ, ψ, and ω in oligosaccharides: ϕ = H1-C1-O1-C_X, ψ = C1-O1-C_X-H_X, ω = C1-O1-C6-C5. c) Torsion angles of the sugar-phosphate backbone as well as of the glycosidic angle χ used to define the conformation of nucleic acids.

Here, the IUPAC-IUB definitions of the dihedral angles for the most important biopolymers (Fig. 1) are given for future reference.[23] Conformation and dynamics of these substances are at the center of interest in bioorganic chemistry and in this article we will concentrate on the measurement and utilization of the J couplings of these molecules. Based on these couplings (homo- and heteronuclear) the conformational preferences of most of these torsions can be characterized.

In the following we elucidate the fundamental principles which are necessary to understand the various methods to determine coupling constants. The exact procedure to use depends on the size of the molecule, type of coupling to be measured as well as the required precision and the possibility of isotopic enrichment. During the last few years numerous new multidimensional techniques have been developed. Because of the great variety of these experiments, it is not a trivial task to choose the optimal experiment for a specific question. It is our intent with this article to close the gap in the literature regarding this problem. The individual methods will then be combined in separate sections according to the method of determination, simplifying the survey of the existing procedures. After this we will touch upon several conformationally relevant dependencies which influence the size of the coupling constant and close with the employment of J values in distance geometry and molecular dynamics calculations.

2. The Determination of Coupling Constants

Basic Features

The scalar coupling of a nucleus A with nucleus X causes a splitting of the signal for A, a result from the different orienta-

Horst Kessler, born in 1940 in Suhl, Thüringen, studied in Leipzig and Tübingen, and received his doctorate in 1966 under the supervision of Eugen Müller for work on a preparative organic topic. He completed his habilitation in 1969 for work on the detection of inner molecular mobility by NMR spectroscopy. In 1971 he became a Professor for Organic Chemistry at the Unversität Frankfurt. In 1989 he moved to the Technische Universität München. He was awarded the Otto-Bayer-Preis in 1986 and the Max-Bergmann-Medaille for peptide chemistry in 1988. Guest professorships have taken him to Halifax, Tokyo, Madison, and Haifa. His research interests include rational molecule design based on the conformation, synthesis and structure of peptides and peptidomimetica, and the development of NMR techniques and calculational methods for the determination of molecular structures.

Dale F. Mierke, born in 1961 in Sacramento, California, received his Bachelor of Sciences in Physical Chemistry and Biology at the University of California, Irvine, in 1984. He obtained his doctorate under the supervision of Murray Goodman at the University of California, San Diego, for research on the structural properties of peptides. In 1990 he was awarded a Fulbright fellowship to work in the research group of Horst Kessler, where he remained until 1993. Since then he has worked at the Gustav H. Carlson School of Chemistry of Clark University and at the Pharmacology Department at the Medical Center of the University of Massachusetts in Worchester, Massachusetts.

Gerd Gemmecker, born in 1961 in Hanau am Main, studied chemistry from 1981 to 1986 in Frankfurt and received his doctorate in 1989 under the supervision of Horst Kessler for NMR studies of cyclic peptides. 1990/1991 he carried out post doctoral research with S. W. Fesik (Abbot Labs., USA) on the elucidation of the structures of the complexes cyclophilin/cyclosporin A and FKBP/ascomycin by NMR spectroscopy. From 1991 to 1993 he studied protein structures with NMR methods as a Liebig-Stipendiat at the TU München, since 1994 he has continued research there on NMR spectroscopic investigations of protein nucleic acid complexes within the framework of the Sonderforschungsbereich 369 "Grundlagen des Sekundärstoffwechsels".

Matthias Eberstadt, born in 1967 in Hof, Bayern, studied chemistry from 1986 to 1991 at the Technische Universität München, and completed his diploma thesis with work on the determination of coupling constants under the supervision of Horst Kessler. From 1992 to 1995 he carried out work in the same research group toward his doctorate. His interests include experimental and theoretical studies on the structures of proteins with the help of NMR spectroscopy.

tions (spin states) of the coupled spin X in a magnetic field. In the case of 1/2 spin nuclei, two spin states (often denoted α and β) are produced. The spin–spin coupling causes a splitting in the signal producing a doublet separated by the size of the coupling $J_{A,X}$. The size of the coupling constant, in contrast to chemical shifts, is independent of the strength of the external magnetic field. In this article we will deal only with weakly coupled spin systems (i.e. the coupling constant J is small in comparison to the difference in the chemical shifts, $\Delta\nu$, of the coupled atoms). For analysis of higher order spin systems, which is especially prevalent for low magnetic fields, we recommend the following textbooks given in references [24–29].

For first-order spin systems (with weak spin–spin coupling) the single multiplet lines are – in the simplest case – well-separated and the J value can be read directly from the one-dimensional (1D)-spectrum (see Fig. 2 top). If signals in the 1D spectrum overlap, the measurement of a two-dimensional (2D) spectrum is often helpful: as a rule the cross peaks contain the same multiplicity in their fine structure as the corresponding 1D signals. When dealing with well-separated multiplet lines, coupling constants can simply be read from the cross-section of a cross peak (usually in the direct dimension where a sufficient digital resolution can be easily obtained), although there are some 2D experiments whose cross peaks normally do not produce clean phases (e.g. the common TOCSY spectrum). For such occasions the insertion of a z-filter[30, 31] before the detection or the employment of selective pulses is helpful.[32] If one is interested in only a few coupling constants, the modified 1D equivalent of the 2D experiment (i.e. selective 1D experiments,[33, 34] chemical shift selective filters (CSSF) [35, 36]) can be utilized.

Regarding multidimensional spectra *active* and *passive* couplings must be distinguished. If the two nuclei A and X are coupled with each other the coupling constant $J_{A,X}$ makes possible a coherence transfer between the *active* nuclei A and X resulting in a corresponding cross peak (A,X). The coupling constant $J_{A,X}$ is therefore described as an active coupling. All

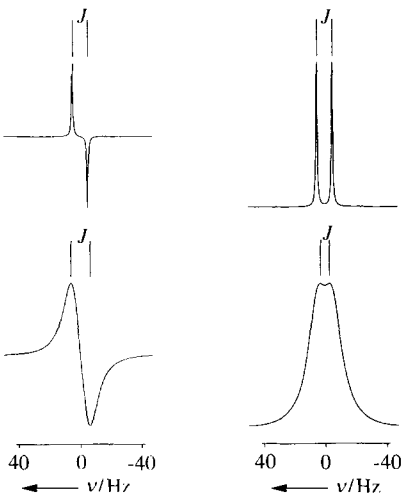

Fig. 2. Comparison of antiphase (left) and in-phase (right) doublets with a coupling constant J of 10.0 Hz and different line widths: width at half-height 1 Hz (top row) and 15 Hz (lower row). In the case with base line separation (top), both spectra lead to the correct coupling constant. In contrast, for larger line widths (below), the apparent coupling constant is too large for the antiphase and too small for the in-phase components.

further couplings involving these nuclei to a third nucleus M (e.g. $J_{A,M}$ or $J_{X,M}$), which are not responsible for the formation of the (A,X) cross signal, are described as passive couplings. Depending on the size of the spin system several passive couplings can come into existence. Active and passive couplings can differ by means of different phase in the spectrum: for example, in the 2D-COSY experiment the active coupling is antiphase, while the passive couplings are in-phase; whereas in the z-filtered 2D-TOCSY experiment all couplings are in-phase.[25] Examples of in-phase and antiphase signals are given in Figure 2.

In this article the most simple case (completely separated multiplet lines) will not be considered, but techniques will be presented which allow for the reliable extraction of coupling constants from signals with nonresolved fine structure.

Coupling constants are often within the range of the natural line widths of the signals. The line width mainly depends on the molecular weight of the substance under examination: small molecules, which reorientate quickly in solution, have relatively sharp lines (1 Hz or less), whereas the spectra of big molecules have broad lines (e.g. 20–30 Hz are common for medium-sized proteins). If the line width in comparison with the coupling constant is significant (i.e. is not small enough to be neglected), the single multiplet lines are no longer base-line separated and the distance between the lines (i.e. the distance between the maxima of the lines) does not exactly correspond to the coupling constant. As shown in Figure 2, the greater the line width the more the coupling constant is overestimated in the case of antiphase signals [37] and underestimated in the case of in-phase couplings. When choosing a technique for the determination of a coupling constant one should therefore pay heed to line width. Of course this is important for larger molecules, but also must be addressed with small molecules when measuring very small coupling constants or if the measurements are carried out at low temperatures or in viscous solvents.

Overview of Techniques for the Determination of Coupling Constants

To provide a better overview of the different experimental methods and the points mentioned above, we have divided the manuscript into three different sections according to the method of determination of the coupling constant. First, procedures which use the form of lines in one- or multidimensional spectra, including reference spectra in the analysis, will be discussed. Secondly, multidimensional methods which produce an E.COSY pattern, from which the passive coupling constant is determined, are developed. Finally methods in which the coupling constant is determined by the signal intensity in correlated spectra are given.

It is impossible to discuss all of the procedures that have been published for the determination of coupling constants, and therefore we will discuss only a few of the most important ones. The experiments, given in Tables 1–3, are organized according to the type of determination as outlined above: 1) form of the signal, 2) E.COSY-signal patterns, and 3) intensity of the signal. We want to state that most of the techniques can be improved by the application of pulsed-field gradients (see e.g. Section 2.3.4). However, for clarity we want to avoid describing all possible variations and instead concentrate on the ideas behind

Table 1. Measurement of coupling constants from line shape.

Name	Short description	Comments [a]	References
Homonulear coupling constants			
A) Coupling constants from 1D spectra			
a) z-filter spectra	pure phase, e.g. 2D-TOCSY	Ad.: 1D and 2D possible Dis.: increased measurement time because of z-filter	[30, 31]
b) selective decoupling [b]	sel. decoupling and spectra simulation	Ad.: exact method Dis.: limited to small molecules, selective decoupling required	[45]
c) J-doubling [b]	manipulation of measured data	Ad.: possible as multidimensional experiments, exact method Dis.: limited to small molecules	[41, 42]
B) Coupling constants from antiphase multiplets			
a) AX coupling constants from COSY [b]	fitting from calculated dispersive and absorptive spectra	Ad.: easy to carry out, also good for medium sized molecules Dis.: good signal-to-noise ratio required, only for AX spin systems	[38]
b) DISCO [b]	combination of antiphase [c] with other in-phase [d] or antiphase signals [c]	Ad.: complicated signal pattens and overlap can be addressed Dis.: interactive calculation of scaling factor	[11, 39, 40]
c) convolution of complementary multiplets [b]	similar to DISCO, but with computer fitting	Ad.: more exact than DISCO	[43]
C) Coupling constants from in-phase multiplets			
a) analysis of phase-multiplets after inverse FT [b]	mathematical manipulation of measured data of inphase multiplets	Ad.: signals from NOESY or HSQC, also good for large molecules Dis.: only for AX spin systems	[15]
b) HMQC with "purge"- pulse	^{15}N-HMQC spectrum	Ad.: sensitivity Dis.: large line widths lead to problems, ^{15}N-labeling required	
Heteronuclear coupling constants			
a) 2D-*J*-spectroscopy	heteronuclear coupling is read from multiplet in F_1	Dis.: only for small molecules, direct detection (sensitivity problems), no pure phase signal	[166-168]
b) selective INEPT	same as a)	Ad.: more sensitive than 2D-*J* Dis.: protons must be well resolved, only for small molecules, direct detection	[169]
c) DEPT-*J*-spectroscopy	same as a)	Ad.: editing of multiplets possible Dis.: same as for 2D-*J*	[170, 171]
d) HMBC with homonuclear reference spectrum [b]	convolution of hetero- and homonuclear multiplets; coupling constants is obtained from fitting procedure	Ad.: coupling constants to quaternary carbons possible, numerous couplings per spectrum, inverse detection Dis.: good signal-to-noise ratio (greater measurement time) required	[12, 48, 51]
e) FIDS-HSQC	heteronuclear coupling e.g. ^3J(C,P), ^3J(H,P) in nucleotides	Ad.: sensitive method Dis.: good signal-to-noise ratio required	[76]

[a] Ad. = advantages, Dis. = disadvantages. The comments are derived from our personal experience and will generally hold true. For special circumstances the disadvantages can be overcome or otherwise addressed. [b] Discussed in detail in the text. [c] For example, obtained from a COSY, P.COSY, E.COSY, P.E.COSY. [d] From a 1D signal or refocused COSY spectra with z-Filter, for example TOCSY spectra with z-Filter.

the methods referring only to the original literature. Therefore, in Sections 2.1 to 2.3 only details of the most important experiments are discussed.

2.1. Determination of Coupling Constants from the Shape of the Signal

In this section procedures which are employed mainly for small molecules and suited for the determination of homonuclear and heteronuclear coupling constants are given. For heteronuclear couplings it is important that the technique be as sensitive as possible and is suitable for samples in natural abundance.

In principle all these techniques attempt to correct or compensate for the partial overlapping of multiplet lines by either using additional parameters which depend on the shape of the signals or by fitting a model to the overlapping experimental signal (most often carried out by using a reference signal). However, this procedure presupposes that the line width is not significantly larger than the coupling constant and furthermore, the signals have a good signal-to-noise ratio, so that enough information for the correction can be obtained from the experimental signal form.

2.1.1. *A-X couplings from COSY Spectra*

As was shown in Figure 2, only a rough approximate value of the coupling constant can be determined from an antiphase (e.g. COSY) cross peak, which in principle is too large because of the reciprocal signal cancellation of the antiphase structure. If the line shape and width is known, it is relatively easy to obtain the actual coupling from simulated spectra that reproduce the experimental measurement (Fig. 3).

Kim and Prestegard[38] have described an especially simple method for the determination of coupling constants from AX spectra in which the line width is not explicitly required. Instead the coupling constant is calculated from two parameters, ν_a and ν_d, the splitting of the absorptive and dispersive signal, respectively, which can usually be easily determined (Fig. 4).

This procedure offers the advantage that no additional spectrum has to be recorded (a COSY spectrum is usually necessary for signal assignment in the study of biomolecules). Furthermore, no mathematical follow-up treatment of the raw data is required.

This method is based on the assumption of a Lorentzian line shape for the multiplet. For a complete description of a doublet, generally only two parameters are needed: the line width at half

Table 2. Experiments that utilize an E.COSY cross peak pattern.

Name	Short description	Comments [a]	References
Homonuclear coupling constants			
A) Coupling constants from homonuclear spectra			
E.COSY	passive coupling constants from combination of multiple quantum spectra	Ad.: homonuclear, good resolution Dis.: at least three coupled spins required	[11, 54, 55]
P.E.COSY	combination from β-COSY with reference spectrum	Ad.: easier and more sensitive than E.COSY Dis.: not as exact as E.COSY, less sensitive than E.COSY and P.E.COSY	[54, 59]
z-COSY	similar pulse sequence as NOESY with small flip angle pulses	Ad.: absorptive diagonal Dis.: complications from NOE cross peaks	[172]
soft-COSY	E.COSY signal produced by application of selective pulses	Ad.: more sensitive than E.COSY, only for small molecules Dis.: selective pulse, for more coupling constants many spectra required	[173, 174]
PICSY	selective pulse in TOCSY, E.COSY with in-phase signal component	Ad.: in-phase multiplets Dis.: selective pulse, only for small molecules	[44]
B) Coupling constants from heteronuclear spectra			
I) In natural abundance			
JHH-TOCSY	E.COSY signals produced with signal components in-phase or antiphase to each other	Ad.: utilization of ^1J(X,H) coupling constant, also good for ^{15}N-labeled proteins Dis.: only good for XH spin systems, does not work for XH_2	[175]
XLOC	uses of selective proton pulse	Ad.: coherence transfer does not depend on J(H,H), no requirements for spin systems	[176]
II) Isotopically enriched materials			
triple resonance experiments	for the determination of $^3J(H^N,H^\alpha)$ coupling constant in proteins or peptides	– first implementation increase in sensitivity – utilization of gradients and further increase in sensitivity	[13] [14] [177]
HCCH-E.COSY techniques	for the determination of ^3J(H,H) coupling constant in proteins and peptides e.g. $^3J(H^\alpha,H^\beta)$	– with β-pulse – with selective pulse – utilization of $^3J(H^\alpha,H^\beta)$ coupling constants in proteins with TOCSY for C,C-transfer	[87] [86] [89, 181] [88, 178]
Heteronuclear coupling constants			
I) In natural abundance			
soft-H, C-COSY	soft heteronuclear pulses to produce E.COSY-multiplet pattern	Dis.: low sensitivity, selective pulse	[179]
HSQC	heteronuclear coupling constants, for example ^3J(C,P) and ^3J(H,P) in nucleic acids		[75]
HETLOC [b]	ω_1-filtered TOCSY-spectrum	Ad.: simple pulse sequence, BIRD-pulse can be used to increase repetition rate Dis.: only coupling to heteroatoms that possess a directly bound proton	[62–65]
BIRD-3D-HSQC-TOCSY	$^3J(H^\beta,C^\delta)$ coupling constants	Ad.: natural abundance or "random labeling"	[180]
II) Isotopically enriched materials [c]			
homonuclear techniques	no heteronuclear decoupling	Ad.: very simple method Dis.: only for resolved heteroatoms (^{15}N)	[60, 61]
band-selective decoupling of homonuclear spectra	selective heteronuclear decoupling	Ad.: very easy method Dis.: selective decoupling	[181]
HYSEL-CH, REPAY-CH, CH_2	heteronuclear ^3J(C,H) coupling constants	Ad.: elimination of diagonal, editing possible	[189]
triple resonances experiments	for the determination of $^3J(H^N,C')$, $^3J(N(i), H^\alpha(i-1)$ or $^3J(H^N,C^\beta)$ coupling in peptides	Ad.: also suitable for large proteins	[4, 177, 183–188, 190, 194]
HCCH-E.COSY techniques	heteronuclear coupling e.g. $^3J(H^\beta,C')$ in peptides	Ad.: exact method, also good for large molecules Dis.: labeling required	[89, 182]

[a] See footnote in Table 1. [b] More detailed description can be found in the literature. [c] Of course, for higher natural abundance spins (for example ^{31}P), enrichment is not necessary.

Table 3. Measurement of coupling constants from signal intensity.

Name	Short description	Comments [a]	References
COLOC	constant-time experiment	Ad.: simple relationship between intensity and coupling constant Dis.: direct detection, sensitivity problems, most often coupling only qualitatively measured	[47]
HMBC	proton detected experiment for measurement of long-range connectivities	Ad.: sensitivity from inverse detection Dis.: consideration of homonuclear coupling necessary	[46]
selective HMBC	similar to HMBC, with selective ^{13}C-pulses	Ad.: better resolution than with HMBC Dis.: selective pulse necessary	[93]
[^{15}N,^{1}H]-COSY $^{3}J(H^{N},H^{\alpha})$	similar to HSQC, for $^{3}J_{H}N_{H}\alpha$ in peptides	Ad.: very precise method Dis.: long measurement time, ^{15}N enrichment required	[94, 95]
LRCC	hetero-hetero coupling constants, for example ^{3}J(C,C) in proteins	Ad.: otherwise very difficult to measure coupling constants Dis.: isotope enrichment required	[98]
LRCH	heteronuclear coupling constants, for example $^{3}J(C^{\gamma},H^{\beta})$ and $^{2}J(C^{\delta},H^{\gamma})$		[99]
CT-HSQC-Difference	constant-time-HSQC, coupled and decoupled spectra recorded; e.g. ^{n}J(C,N)	Ad.: sensitive, otherwise very difficult to measure coupling constants Dis.: possible disturbance from relaxation times	[104]
C-C Correlation	constant-time experiment, coupling constant is measured from ratio of two signals; e.g. ^{n}J(C,C)	Ad.: sensitive, otherwise very difficult to measure coupling constants Dis.: possible disturbance from relaxation times, ^{13}C enrichment required	[97]
$H_{N}NH_{AB}$-COSY	heteronuclear coupling constant; e.g. $^{3}J(N,H^{\beta})$		[191]
HNHA	$^{3}J(H^{N},H^{\alpha})$	Ad.: very sensitive, ^{15}N-labeling required Dis.: possible disturbances for relaxation times, not good for very large molecules	[16]

[a] See footnote in Table 1.

height $v_{1/2}$ and the scalar coupling constant J, which can be determined from two independent experimentally measurable parameters. For this purpose Kim and Prestegard use both the estimated coupling (v_a) (i.e. the distance of the maxima in the absorptive doublet) and the distance v_d of the two outer extremes in the 90° phase-shifted (i.e. dispersive) doublet (instead of the linewidth, which is not easily accessible from the doublet alone). By calculation of the analytical expression for these two values from the theoretical Lorentzian-line shape, an expression for J [Eq. (1)], which contains only the two experimentally available parameters v_a and v_d, can be developed. J can now be calculated from the square root of the only real root of this cubic equation.

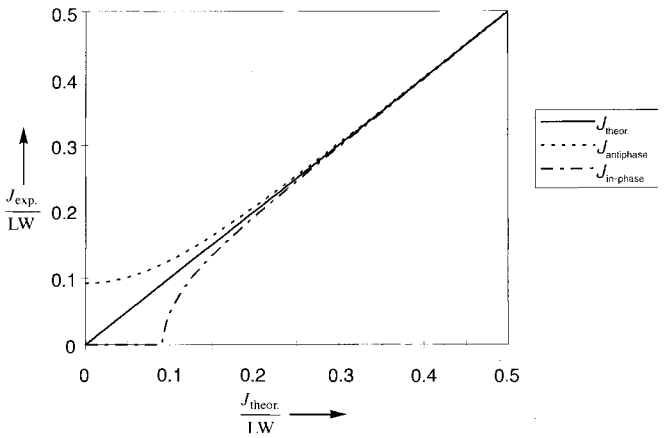

Fig. 3. The correlation of the measured splitting, J_{exp}/LW (LW = line width), with the theoretical coupling constant (J_{theor}/LW) for a Lorentzian doublet is shown for antiphase and in-phase multiplets. In the range of approximately 0.15–0.3 the coupling constant measured from the antiphase and in-phase doublets can be corrected to account for line shape. For values under 0.1, the J_{exp} measured from an antiphase multiplet is only slightly dependent of the measured splitting, while the correlation for couplings measured from in-phase multiplets completely disappears. For these cases, correction of the measured values is not possible.

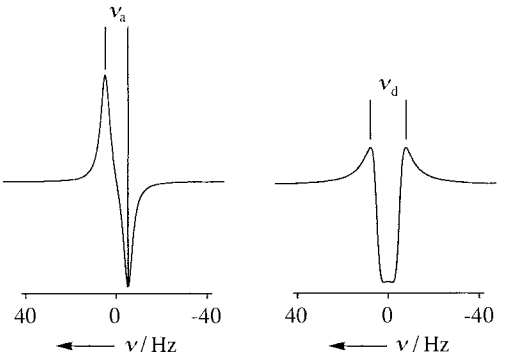

Fig. 4. The measurement of the separation of the signal maxima of an antiphase doublet for the absorptive (v_a) and dispersive (v_d) component. From these two parameters the coupling constant J can be calculated from the cubic Equation (1).

$$J^6 - v_d^2 J^4 - \left(\frac{9}{4}v_a^4 - \frac{3}{2}v_a^2 v_d^2 - \frac{3}{4}v_d^4\right)J^2 + \frac{81}{64}v_a^6 - \frac{9}{16}v_a^4 v_d^2 - \frac{21}{32}v_a^2 v_d^4 - \frac{1}{16}v_d^6 + \frac{v_d^8}{64 v_a^2} = 0 \quad (1)$$

This procedure is straightforward to perform and is recommended for the evaluation of COSY signals, for example, (H^{N},H^{α}) cross signals of peptides and proteins especially if signals in the 1D spectrum overlap. A good signal-to-noise ratio is necessary for the accurate determination of v_d. For signal-to-noise ratios of under 5 inaccuracies of v_a and especially v_d will result in significant errors for the calculated J values. Regarding apodization of the experimental signal, one is limited to the exponential function since the theoretical basis of the method requires a Lorentzian line shape. However, in practice other apodization functions cause only small errors.

2.1.2. The DISCO Procedure

The cross peaks of a nucleus in a COSY spectrum are differentiated by the fact that each time *one* coupling (namely the active coupling) is in antiphase, while all of the other couplings appear in-phase. The overlapping of the latter couplings often produces a complicated multiplet pattern, from which no coupling constants can be easily read. In this instance there is a series of procedures, which combine antiphase splitting with in-phase splitting so that the number of the multiplets diminish and the coupling constant can be read from the simplified fine structure. The required antiphase signals are available through COSY signals (Fig. 5a). The in-phase signals can be obtained in principle from the COSY diagonal signal or a 1D spectrum, or if signal overlap is a problem from the cross peak of a TOCSY experiment, in which phase distortions from dispersive antiphase contributions are minimized by using a z-filter (as discussed above).[30, 31]

By forming the *di*fference or the *s*um of cross signals in *COSY* spectra (DISCO) [11, 39, 40] one obtains a halving of the

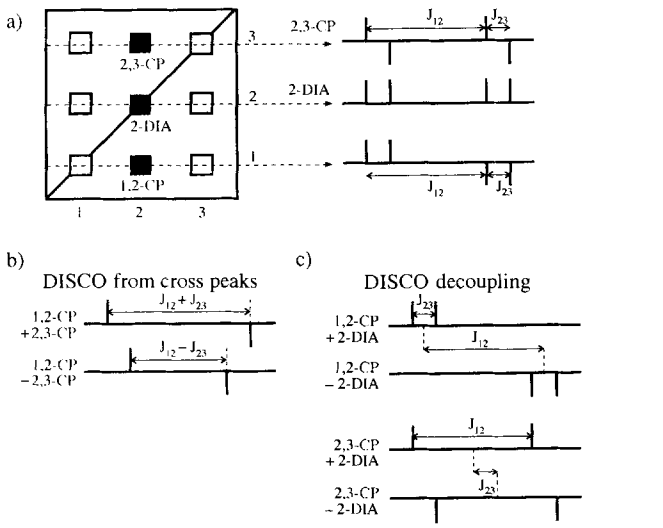

Fig. 5. a) DISCO experiment with cross peaks for spin 2 of a three-spin system. Left: schematic representation of a COSY spectrum; right: slices of the cross peaks between spins 1-2 and 2-3 (1,2-CP, 1,3-CP) along with the diagonal (2-DIA) in ω_2. b) DISCO method from addition and subtraction of the cross peaks. c) DISCO decoupling from addition and subtraction of the cross peak and diagonal signal.

number of multiplet components (Fig. 5b). From the traces of two cross peaks a multiplet can be obtained by addition (with proper weighting) which contains the sum of the two active coupling constants in antiphase. As a rule less overlapping occurs in such additions so that the distances between the lines can be determined more precisely. From the difference (negative combination) of the two traces, the differences between the active couplings of the cross peak can be obtained which is often difficult to measure because of the small size. The DISCO procedure is schematically depicted in Figure 6.

A variation referred to as decoupled-DISCO can be obtained by mixing antiphase multiplets (positive intensity) and in-phase multiplets (negative intensity) resulting in spectra "decoupled" with regard to the active coupling; each component is shifted to the left and right by half the coupling constant (Fig. 5c). Using this procedure coupling constants can be determined from multiplets with broad lines.

However, one problem with the DISCO procedure is that the correct scaling factor for the combination of the two spectra is unknown; this value must be determined interactively. In addition, the evaluation of complicated, strongly coupled spin systems remains difficult.

2.1.3. *J* Doubling

The procedure of *J* doubling[41] is founded on a purely mathematical follow-up treatment of the raw, experimental data. For this treatment, in-phase and antiphase signals have to be differentiated; here the discussion is limited to in-phase multiplets. We refer to the literature for an analogous analysis of antiphase signals.[42]

For this procedure the FID of a freely exposed, in-phase doublet is necessary (i.e. either the FID of the 1D spectrum or—for overlapping signals—a series of slices from a 2D spec-

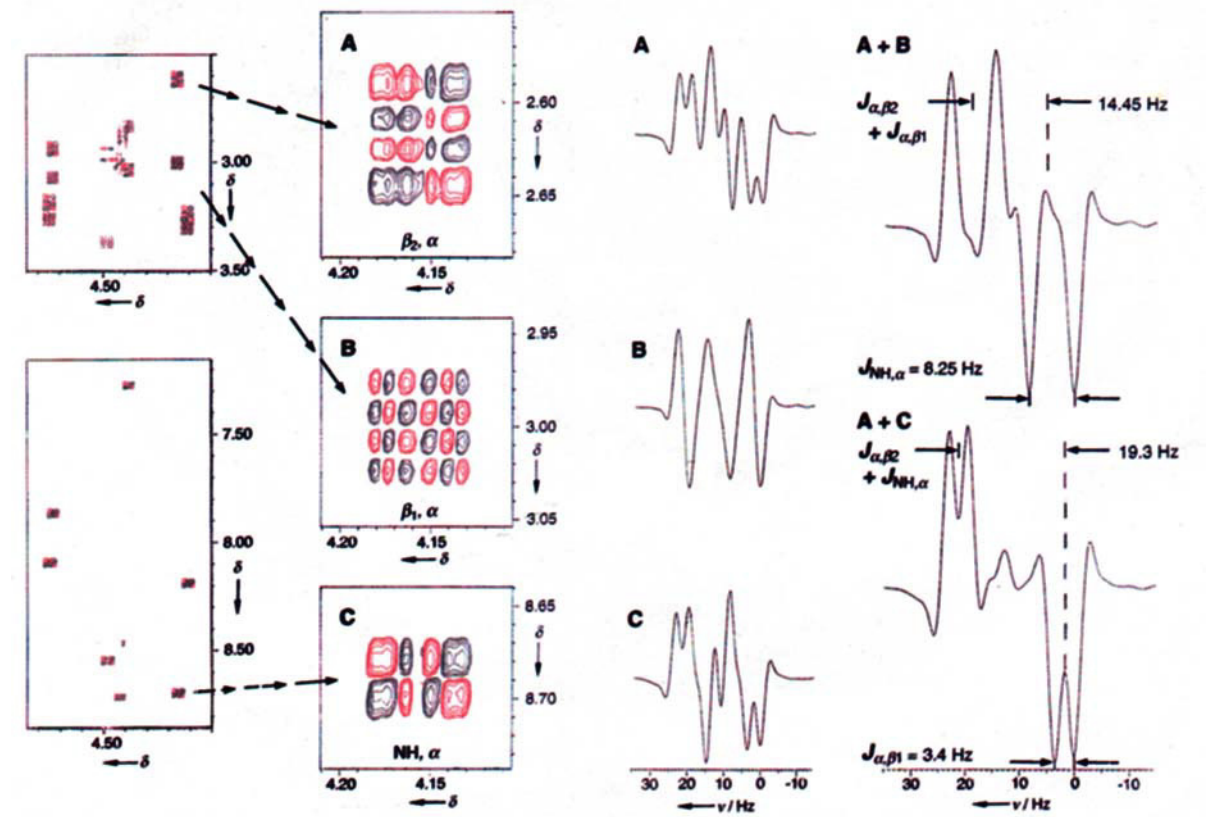

Fig. 6. Illustration of the DISCO method for the $\alpha\beta$ coupling in aromatic amino acids of a cyclic hexapeptide. First column: (H^{α},H^{β}) cross peak (top) and (H^{α},H^{N}) cross peak from a 2D-DQF-COSY spectrum. Second column: expanded portion of the cross peaks H^{α},$H^{\beta2}$ (A), H^{α},$H^{\beta1}$ (B), and H^{α},H^{N} (C). Third column: slice along the F_2 dimension through the corresponding cross peak. Fourth column: slices resulting from the sums of the slices A + B (top) and A + C (below). The sum of the coupling constants ($^3J(H^{\alpha},H^{\beta2})$ + $^3J(H^{\alpha},H^{\beta1})$ and ($^3JH^{\alpha},H^{\beta2}$) + $^3J(H^{\alpha},H^{N})$) can be measured with high accuracy.

trum containing a resolved cross peak which can afterwards be transformed into a corresponding pseudo-FID by inverse Fourier transformation (IFT). In the time domain an in-phase doublet corresponds to a damped harmonic vibration, which is modulated by a $\cos(\pi Jt)$ signal, in which J is the coupling constant to be determined. By multiplying this FID with a function $\sin(\pi J_{test}t)$ one obtains after Fourier transformation an additional antiphase splitting of size J_{test}. The two middle lines of the four resulting lines will exactly cancel out each other because of the antiphase character when $J = J_{test}$ (Fig. 7). The coupling J can therefore be determined by optimizing the parameter J_{test} in the FID modulation function until these multiplet lines disappear. This criterion of optimization is ideal for automated evaluation (e.g. the integral of the complete multiplet in absolute value representation is driven to a minimum).[42]

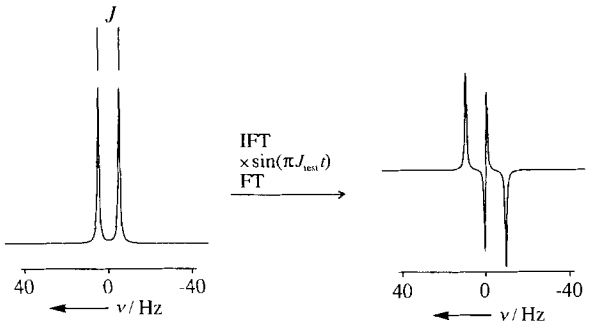

Fig. 7. The doubling of the coupling constant J for an in-phase multiplet. The FID from an IFT is multiplied by the function $\sin(\pi J_{test}t)$, which produces an antiphase doublet with a coupling constant of J_{test}. The value J_{test} is varied until the central antiphase doublet disappears and therefore $J_{test} = J$.

The procedure of J doubling can be performed in many different variations (e.g. the same cancellation of the central pair of lines can be obtained by modulating the FID with $\cos(\pi J_{test}t)$, corresponding to an additional in-phase splitting around J_{test}, starting from an antiphase doublet). By using more complex modulation functions for the FID, more complex line patterns can be generated, which are also greatly simplified by cancellation in the case of $J = J_{test}$. Finally the procedure is not limited to doublets: in the case of more complex multiplets several minima of the signal intensity will be obtained, corresponding to the different coupling constants included in the signal. It must be noted that by multiplication of the signal by the test coupling more lines are created, which can have the negative consequence of even greater signal overlap.

2.1.4. *Simulation of Line Forms with Reference Signals*

The fundamental idea for this technique is founded on the simulation of a complex, nonresolved multiplet starting out from various experimental multiplets. We begin this portion with the discussion of two relatively easy methods for obtaining homonuclear coupling constants and then discuss a very important variation for the measurement of a heteronuclear long-range coupling constant. As given in Section 2.1.3, a signal can be deconvoluted with an additional, in-phase (or antiphase) splitting by modulating the FID with $\cos(\pi J_{test}t)$ (or $\sin(\pi J_{test}t)$) (Fig. 8). By using a J_{test} that corresponds to an antiphase (or in-phase) multiplet the phase properties of the resulting spectrum can be manipulated: each signal then includes an in-phase

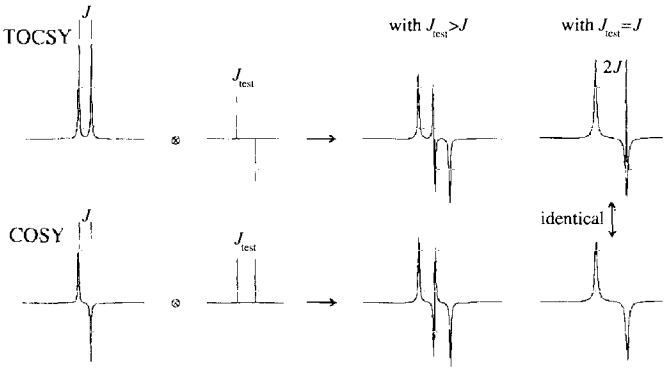

Fig. 8. Determination of a homonuclear coupling constant from COSY (antiphase) and TOCSY (in-phase) signals by convolution with a complementary multiplet coupling of J_{test} (see Fig. 7). When $J_{test} = J$, both of the multiplets are identical (far right), which can be used for a convergence criterium for the determination of the coupling constant J.

and an antiphase splitting of the same size $J = J_{test}$ (Fig 8, right). Therefore another criterion for optimization can be the similarity of the modulated multiplets obtained from both methods which can be determined with the help of the standard deviation of the two signals[43] or with vectorial algorithms.[44]

Another possibility, which is especially suited for the determination of homonuclear in-phase coupling constants, is the convolution of selectively decoupled spectra[45] with a test coupling which is then optimized. Two spectra serve as the data set: the conventional 1D spectrum (or a series of cross-sections taken from a 2D experiment containing a cross peak) and a further spectrum, in which the desired coupling $J_{B,D}$ was removed by irradiation of the frequency of the nucleus H_D (Fig. 9). The decoupled spectrum is again deconvoluted (i.e. the FID is multiplied by the function $\cos(\pi J_{test}t)$) resulting in an artificial in-phase coupling of size J_{test}. While varying J_{test}, the signal is compared with the decoupled spectrum either in the time or frequency domain until the deviation for $J = J_{test}$ is minimized. It is important to note that false minima can occur for sums or differences of the coupling constants included in the multiplet.

Such a selective decoupling is especially easy to perform if the coupling involves a heteronucleus. For example $^3J_{H,P}$ and $^3J_{C,P}$

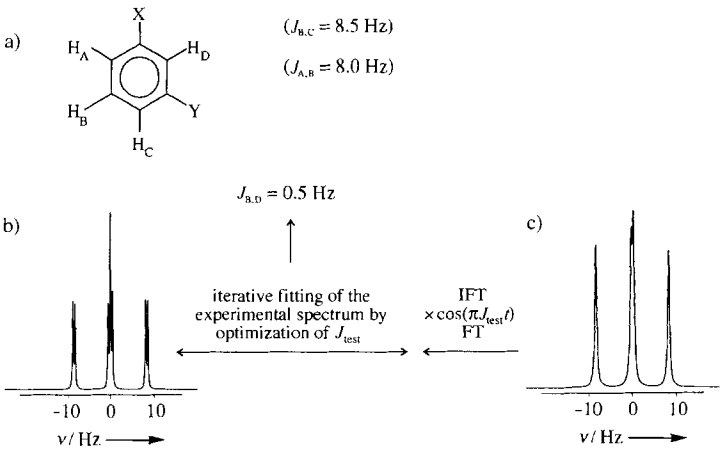

Fig. 9. Determination of the J(H,H) coupling constants for *meta*-disubstituted benzene (a). The values of the large ^3J coupling constants J(A,B) and J(B,C) can be read directly from the 1D spectrum (not shown). The multiplet of H_B coupled (b) and with selective decoupling of H_D (c). The selectively decoupled multiplet can be transformed into the coupled multiplet only when $J_{test} = J$.

in nucleic acids can be determined from two 2D-^{1}H,^{13}C-HSQC correlation spectra, one of which was recorded with ^{31}P decoupling (FIDS-HSQC).[76] The line widths in the ^{1}H (or ^{13}C) dimension in the two spectra differ from each other by the coupling of the proton (or carbon) atom to the phosphorus atom (Fig. 10).

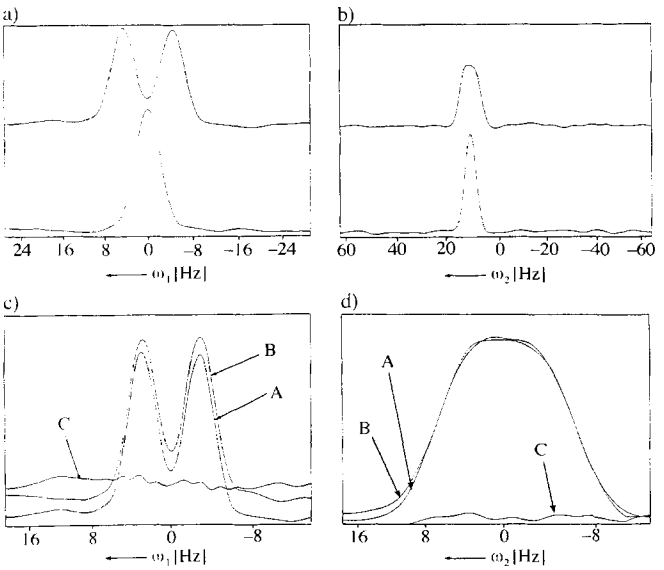

Fig. 10. FIDS-HSQC spectrum of a cyclic deoxyribose-methylphosphonate. a) Slices along the F_1 dimension (the ^{13}C dimension) through the (H5',C5') cross peak without (above) and with (below) ^{31}P-decoupling. b) Slices along the F_2 dimension (the ^{1}H dimension) through the (H3',C3') cross peak without (above) and with (below) ^{31}P-decoupling. c) Results from the simulation of the coupled multiplets (a) from the decoupled multiplet with the addition of the ^2J(C5',P) coupling; the optimal fit is obtained with ^2J(C5',P) = 8.9 Hz. d) Analogous to (c) from the multiplet shown in (b), producing ^3J(H3',P) = 4.5 Hz. A = experimental, B = simulated multiplet, C = difference (from ref. [76]).

These techniques have found widespread application in the determination of heteronuclear long-range coupling constants from HMBC (*h*eteronuclear *m*ulti-*b*ond *c*orrelation) cross peaks with samples with ^{13}C in natural abundance.[46] The major advantage is that the HMBC experiment is relatively sensitive because of inverse detection (e.g. compared to the COLOC experiment[47]) and that the identity of the heteronuclear long-range couplings directly ensues from the assignment of the 2D cross signals.[12, 48] The pulse sequence (including a low-pass J filter[49]) is shown in Figure 11.[12] The 180° ^{1}H pulse at the end of the sequence is not part of the standard HMBC experiment; it is only necessary in the determination of coupling constants with a homonuclear reference spectrum.

The HMBC experiment is a simple variation of the inverse heteronuclear correlation technique HMQC (*h*eteronuclear *m*ulti-*q*uantum *c*orrelation). During the time Δ_2 (in practice

Fig. 11. Pulse sequence for a HMBC experiment to determine heteronuclear coupling constants. The resulting spectrum correlates the protons through long-range coupling (i.e. ^2J and ^3J) with ^{13}C nuclei. The delay Δ_1, $1/(2^nJ(C,H))$, is for the low-pass J-filter and Δ_2 is set to approximately 60–80 ms.

60–80 ms), the long-range couplings $^nJ_{C,H}$ (n = 2,3) develop and the coherence is transferred to ^{13}C. The resulting 2D spectrum contains cross peaks between all protons and carbon nuclei which are not separated by more than three bonds.

In principle long-range coupling constants can be determined directly from the cross peaks which contain the active coupling, although modified sequences with better phase properties are recommended.[50] Long-range heteronuclear coupling constants are approximately of the same magnitude as homonuclear $^2J_{H,H}$ and $^3J_{H,H}$ coupling constants (1–10 Hz). Therefore, the rather small heteronuclear antiphase coupling constant $^nJ_{C,H}$ cannot be read directly because of overlapping and reciprocal cancellation of the numerous multiplet lines.

Keeler et al. have developed an eloquent procedure which allows one to determine the heteronuclear long-range coupling constants from the line shape even in such cases.[48] The multiplet of an HMBC cross peak is not purely absorptive in phase in F_2 because of the modulation through H-H couplings and through the development of the chemical shift evolution during the two delays Δ_1 and Δ_2. The multiplet includes all homonuclear couplings of the proton involved in the cross peak as well as the antiphase long-range coupling which causes the cross peak. In a homonuclear spectrum, (e.g. a 1D spectrum or a 2D RELAY or 2D TOCSY experiment) a cross peak of the same proton in the F_2 dimension has the same H–H couplings as the heteronuclear spectrum. The differences between this signal and the HMBC signal lie in the phase qualities of these couplings (here *in phase*) and the lack of the heteronuclear antiphase coupling.

To obtain the phase qualities of the heteronuclear spectrum in the ^{1}H spectrum, the 1D spectrum can be recorded with the sequence "90°(^{1}H)-(Δ_1 + Δ_2)-acquisition". However, this only applies to well-resolved signals. For overlapping signals, a TOCSY spectrum with pure phase (e.g. with the z-filter, cf. Section 2.1.1.) has to be recorded. The multiplet can then be read along the F_2 dimension, the remainder of the base line is set to zero and an IFT performed. The pseudo-FID represents the signal of this single multiplet in the time domain. The effect of the delays Δ_1 and Δ_2 can now be obtained by shifting the starting point of the FID by (Δ_1 + Δ_2) (i.e. discarding the first N data points, where $N = (\Delta_1 + \Delta_2)$/ "dwell-time"). At the end of the FID the missing points are substituted by zeros ("zero-filling"), which has been shown to produce negligible error.

The homonuclear reference multiplet which is contained in this modified FID now differs from the HMBC multiplet only by the absence of the heteronuclear antiphase coupling and the differing signal amplitude. As described in Section 2.1.3. this can be simulated by multiplication of the reference signal in the time domain with the term $\sin(\pi J_{test} t)$. The amplitude and J_{test} can now be varied by a nonlinear optimization until the deviation between the two spectra reaches a minimum, at which J_{test} should be equal to the desired coupling constant. An example of this method is shown in Figure 12.

This method has the advantage that a large number of coupling constants can be determined from one HMBC spectrum (which usually contains a large number of long-range correlations). However, the quality of the heteronuclear spectrum and especially the signal-to-noise ratio is of decisive importance for the convergence of the optimization (an elaborate analysis of errors associated with this method has appeared in the literature).[51]

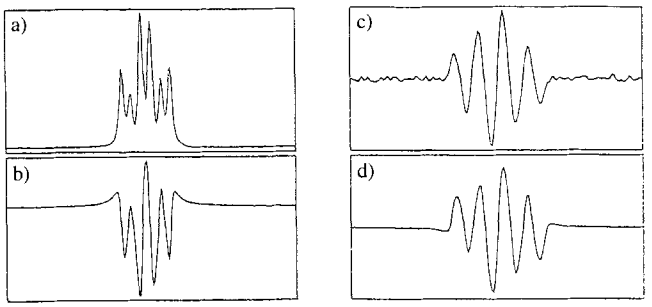

Fig. 12. Application of the Keeler-procedure for the determination of heteronuclear long-range coupling constants from an HMBC spectrum (see text). a) Reference multiplet from a z-filtered TOCSY spectrum; b) the multiplet of (a) after the phase correction of the HMBC spectrum; c) experimental multiplet from the HMBC cross peak, which differs from the multiplet in (b) by the antiphase, long-range heteronuclear coupling constant; d) the result of the simulation of the HMBC signal (c) using the reference signal (b).

2.1.5. *Inverse Fourier Transformation of In-Phase Multiplets*

Inverse FT of multiplets allows for the determination of the $^3J_{H^N,H^\alpha}$ coupling constant and is also suited for larger molecules. The method is preferably applied with NOESY spectra which have to be recorded anyway for structure determination and therefore does not increase the required measuring time.[115]

In a NOESY spectrum all cross signals of a certain proton in F_2 possess the same in-phase multiplet structure. The amide protons of amino acids in peptides (with the exception of glycine) are doublets because of the coupling to the α proton. The intraresidual (H^N,H^α) cross peak should not be used for the evaluation as it can be disturbed by scalar J coupling contributions.[52, 53] However, since the H^N signal is usually involved in a large number of NOEs to neighboring protons, another resolved signal can be selected. To determine the coupling constant $^3J_{H^N,H^\alpha}$ one uses a slice along the F_2 dimension through this signal (to increase the signal-to-noise ratio, several slices can be added, as in the DISCO procedure described above). From an IFT, a pseudo-FID corresponding to this signal is obtained (Fig. 13), which is already modulated by $\cos(\pi\ ^3J_{H^N,H^\alpha}t)$ because of the presence of the in-phase coupling.

As a first approximation the value $J^{(0)} = 1/2t_0$ for the $^3J_{H^N,H^\alpha}$ coupling constant can be estimated by using the time t_0 of the first zero crossing of the FID curve. The line width $\Gamma^{(0)}$ can be obtained from the width at half-height (naturally taking $J^{(0)}$ into consideration) (Fig. 13). Starting with these points it is possible to simulate an in-phase doublet [Eq. (2)], where t_{aq} corresponds to the experimental acquisition time; the line width is described by the decreasing exponential. The signal $S(t)$ is now submitted

$$S(t) = \cos(\pi\ ^3J_{H^N,H^\alpha}t)\,e^{-\pi\Gamma t} \quad 0 \le t \le t_{aq} \qquad (2)$$

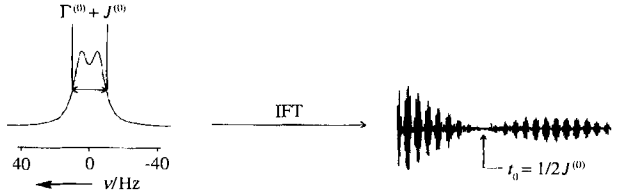

Fig. 13. The signal from a nonresolved doublet and the corresponding signal in the time domain (FID), obtained after IFT. Starting parameters for the coupling and line width, $J(0)$ and $\Gamma(0)$, can be obtained from the first null point of the FID. The exact method for the determination of the coupling constant is given in the text.

to the same procedure as the experimental signal (same filter function, zero-filling, etc.), and the deviation from the experimental FID is minimized in a nonlinear optimization with regard to $\Gamma^{(0)}$ and $J^{(0)}$.

Generally this procedure can be applied to in-phase multiplets, for example cross peaks from a (^{15}N, ^{1}H)-COSY, in which amide protons are detected. In Section 2.3.3 an alternative method, from which $^3J_{H^N,H^\alpha}$ coupling constants can be determined by signal intensities from a special (^{15}N,^{1}H)-COSY experiment, will be discussed. The advantage of the inverse Fourier transformation method is that only one spectrum is necessary, usually a NOESY spectrum. The experiment must be run in any case, for structure determination, and is relatively sensitive and needs no isotope enrichment.

2.2. The Determination of Coupling Constants with the E.COSY Principle

A large number of methods for the determination of coupling constants utilize the E.COSY principle. The name E.COSY stands for *e*xclusive *co*rrelation *s*pectroscop*y*.[10, 54, 55] It results in a simplification of the cross peak multiplet, as only the "connected transitions" are excited. The coupling can be read from the shifting of two in-phase multiplet components which are separated in the indirect dimension and therefore have no interfering influence on each other. Several procedures, which allow the measurement of homonuclear as well as heteronuclear coupling constants from signals of the E.COSY type, will be discussed in this chapter. But first the E.COSY principle, which forms the basis of all these techniques, will be described.

2.2.1. *The E.COSY Principle*

The advantage of the E.COSY experiment is a reduction of the multiplet lines in the cross peak. From this, the coupling constants can be read directly from the distance between the maximum intensity of the signal without error from line widths. This principle is illustrated in Figure 14 for a cross peak from a three-spin system, AMX, which would be observed in many common 2D experiments (e.g. COSY, TOCSY, NOESY).

In our three-spin system, the X atom is coupled to both A and M and therefore the cross peak for A,M is affected by the spin state of nucleus X. For the X nucleus in the α spin state (approximately 50% populated), we would expect the signal in Figure 14b, while for the X nucleus in the β spin state, the signal in Figure 14c would be observed. For the case of magnetization transfer from A to M, without excitation of the X nucleus, the cross peak shown in Figure 14d would be expected: the signal intensity can only be found at multiplet lines which correspond to the retention of the spin state of X ("connected transitions"), that is the left upper (α spin of X) and the lower right lines (β spin of X) in Figure 14d; the other two multiplet lines disappear. The resulting cross peak shows the typical oblique E.COSY pattern. In order to obtain such a E.COSY pattern, a mixture of spin states of X (e.g. by a 90° pulse) must be avoided.

The only requirement to reading coupling constants from an E.COSY cross peak is that the splitting in F_1 (the coupling between A and X) must be larger than the line width. The much smaller coupling constant J(M,X) can then be read from the dis-

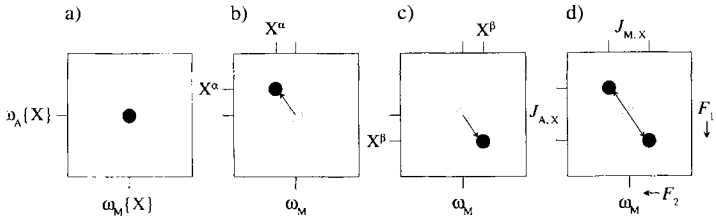

Fig. 14. The principle of the E.COSY technique. a) Schematic 2D cross peak correlating spins A and M from a system of three coupled nuclei (A, M, and X) with decoupling of spin X. b) and c) Without decoupling of X, the AM signal is shifted in both dimensions, an effect from the two different spin states (α and β) of spin X: b) X spin in the α-spin state, c) X spin in the β spin state. d) Under experimental conditions one expects a combination of spectra (b) and (c). The diagonal displacement of the signals in F_1 and F_2 contain both of the passive coupling constants J(A,X) and J(M,X).

placement in F_2 (in 2D) or F_3 (in 3D experiments), the dimension of detection which usually contains more data points and therefore higher digital resolution. The measurement can be made with the signal maxima or better yet from the mutual displacement of the coupling patterns. In addition, the direction of the displacement of the signal leads to the sign of the coupling constant.

2.2.2. *Homonuclear E.COSY Techniques*

In the homonuclear E.COSY experiment the effect outlined in the previous section is not obtained by the retention of the spin states of the passive spin, but by a suitable combination of several multiple quantum correlations. As reference [56] explains this in detail, it will not be fully developed here. The result is the same multiplet pattern as shown in Figure 14d, but all lines are additionally split in both dimensions by the active coupling, as decoupling cannot be performed in homonuclear experiments (Fig. 15). However, we would like to mention that in the case of linear combination of multiple components different transversal relaxation rates of the active in-phase and antiphase terms can influence the determination of the coupling constant.[57] In addition, longitudinal relaxation effects have been neglected in this analysis which can lead to a mixture of α and β components, which in turn leads to.[58]

A simple alternative to the E.COSY experiment is the P.E.COSY experiment (*p*rimitive E.COSY).[59] It is well known that the cross peaks in a COSY spectrum with a small flip angle of the mix pulse, $\beta' < 90°$ (β-COSY), contain strong signal components of connected transitions and that nonconnected transitions (i.e. transitions with a spin-flip of the passive nuclei) are partially suppressed. This is founded on the fact that the spin states of the passive nuclei can only be completely mixed by a 90° pulse; the influence of a very small flip angle β' on the passive spins is negligibly small [Eq. (3)].

$$\boldsymbol{I}^\alpha \xrightarrow{\beta'} \boldsymbol{I}^\alpha \cos^2\frac{\beta'}{2} + \boldsymbol{I}^\beta \sin^2\frac{\beta'}{2} \qquad (3)$$

The relation of the excitation of connected ($\boldsymbol{I}^\alpha \rightarrow \boldsymbol{I}^\alpha$) to nonconnected transitions ($\boldsymbol{I}^\alpha \rightarrow \boldsymbol{I}^\beta$) is therefore proportional to $\tan^2(\beta'/2)$. The same is true for the intensity of the corresponding multiplet lines. A problem with the β-COSY experiment is the phase difference between cross peaks and diagonal signals, which—analogous to the normal COSY spectrum—makes a simultaneous correction of both signals to absorptive signals impossible. However, the dispersive signal portions of the diagonal can easily be removed by subtracting a 2D reference spectrum with a mix pulse β' of 0° (i.e. $90° - t_1 - t_2$). This 2D reference spectrum can be obtained arithmetically from a single FID by shifting the data points in the time domain to the left by the single t_1 increments, so that the additional measurement time required corresponds to a good 1D spectrum. The P.E.COSY experiment is also more sensitive than the E.COSY experiment, since higher multiple quantum spectra (triple quantum, quadruple quantum) are not required.[10, 54, 55]

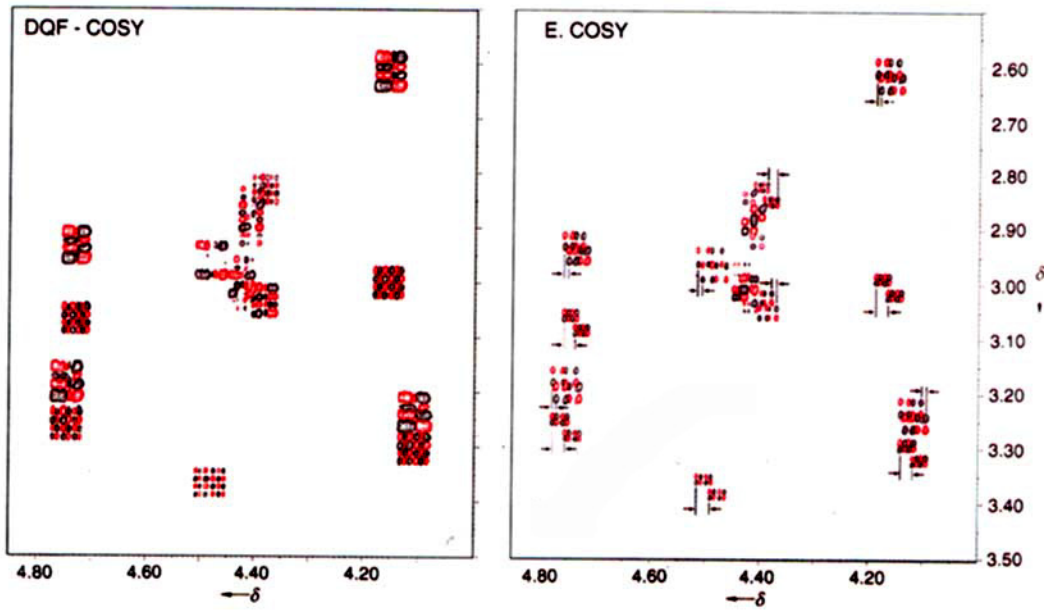

Fig. 15. A comparison of double quantum filtered COSY (left) and E.COSY (right) spectra from a cyclic hexapeptide, illustrating the H^α,H^β region. It is much easier to identifiy the multiplets in the cross peaks from the E.COSY spectrum; from the displacement of the multiplet patterns (arrows) the passive coupling constants (see Fig. 14) can be read with high accuracy.

2.2.3. *Heteronuclear E.COSY Techniques*

In heteronuclear spectroscopy multiplet cross peaks which contain only connected transitions (E.COSY pattern) can be obtained very easily. If no pulse is performed on the heteroatom (i.e. the states α and β are not mixed) each coupling of a proton with the heteroatom shows the typical

E.COSY structure. The easiest way to obtain this is by recording any homonuclear 2D experiment (e.g. H,H-TOCSY or NOESY) without any pulses on the heteronucleus; that is without heteronuclear decoupling in F_1 and F_2, and no heteronuclear pulses between F_1 and F_2. Thus an additional separation for every cross peak in two-dimensions is obtained through the coupling of the respective proton to the heteronucleus, yielding an E.COSY pattern for this coupling. Of course, this is only true for molecules with an NMR-active heteronucleus; for those nuclei in low abundance (e.g. ^{13}C and ^{15}N) the rest can be eliminated by heterofilters. For heteronuclei like ^{31}P and ^{19}F (or for samples which are enriched in NMR-active isotopes) this phenomenon can be observed effortlessly in every homonuclear 2D correlation spectra (Fig. 16).[75]

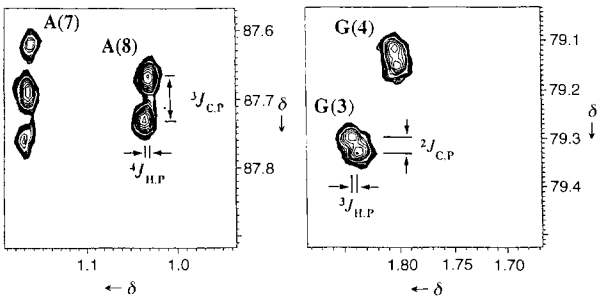

Fig. 16. $^1H,^{13}C$-HSQC spectrum from an oligonucleotide. Since the experiment was run without ^{31}P decoupling in F_1 and F_2, the coupling to the phosphorus nuclei results in the typical diagonal E.COSY cross peak pattern (see text).

Especially useful is the fact that the $^1J_{H,X}$ couplings are usually very large (^{13}C: ca. 140 Hz, ^{15}N: ca. 90 Hz), so that small coupling constants in molecules with very large line widths can easily be determined from E.COSY signals; the large ^1J couplings in the other dimension are used to separate the lines. If the NMR-active heteronucleus is in low natural abundance, the E.COSY pattern is weak and often overlapping within a normal COSY signal population. At natural abundance, the signal of E.COSY patterns is naturally very small and it is necessary to discriminate experiments which can be performed without isotopic enrichment.

Recently a large number of experiments, which in principle are all very similar, have been developed in this field. Here only a few basic experiments will be discussed. For further information we refer to Table 2, in which many experiments are summarized with respect to their field of application, measurement technique as well as advantages and disadvantages.

In principle, coupling constants with large line widths can also be determined accurately with the help of the E.COSY principle (see Sections 2.2.3.3 and 2.2.3.4). However, for heteronuclear E.COSY techniques a splitting of signals takes place, which naturally increases the probability of the overlapping of resonances. In addition, the signal intensity for E.COSY spectra is spread over two components (a doublet), which naturally leads to a loss of sensitivity by 50% in comparison to decoupled experiments (i.e. HMQC and HSQC). Again an error can arise from ignoring longitudinal relaxation which leads to a small mixture of the α and β states during the pulse sequence.

2.2.3.1. Heteronuclear ^{15}N-^1H Long-Range Coupling Constants

It was illustrated very early that in ^{15}N-enriched proteins heteronuclear $^3J_{N,H^\beta}$ and $^3J_{H^\alpha(i),N(i+1)}$ as well as $^3J_{N,H}$ coupling constants of ^{15}N spins of the side chains can be extracted from simple homonuclear scalar (RELAY or TOCSY) and dipole–dipole (NOESY or ROESY) correlated spectra.[60, 61] The coupling constant is determined from the cross peak of two protons, one of which is directly coupled to the ^{15}N spin and which is scalar coupled to the other proton. The cross peaks between the amide proton and other protons show E.COSY-like multiplet structures with the passive heteronuclear coupling constant in F_2, as no pulses are applied to the ^{15}N spins and therefore only connected transitions contribute to the signal (an analog of the HETLOC cross peak, see Fig. 17). Along the indirect dimension (F_1 in 2D spectra), the signals are split by the $^1J_{N,H}$ coupling (ca. 90 Hz) and along the direct dimension (F_2 in 2D spectra) by the smaller heteronuclear long-range coupling which is of interest. From the cross peak between the amide proton and the β-proton of the same amino acid the χ_1-dihedral angle, important for peptide and protein structures can be read (see Fig. 1). The $^3J_{H^\alpha(i)N(i+1)}$ coupling constant which depends on the ψ-dihedral angle of the peptide backbone can be determined from NOESY or ROESY spectra from the sequential (H^α_i,H^N_{i+1}) cross peak.

2.2.3.2. ω_1-Hetero-Filtered Experiments for Determination of Long-Range Coupling Constants

These methods are suited for the determination of long-range coupling constants of protons to a ^{13}C or ^{15}N nucleus in natural abundance, which carry a directly connected proton.[62–65] The pulse sequence for the HETLOC experiment is given in Figure 17.[62, 63, 180]

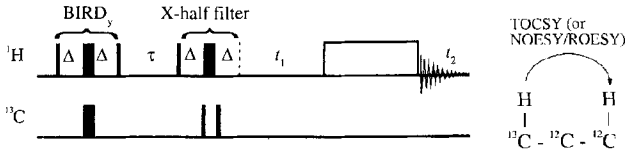

Fig. 17. Pulse sequence for a ω_1-filtered TOCSY without heteronuclear decoupling (HETLOC). The delay Δ is set to $1/(2^1J(C,H))$. In the resulting spectrum, protons directly bound to ^{13}C (frequency labeled during t_1) are correlated to other protons (frequency labeled during t_2) by scalar coupling (through chemical bonds, TOCSY) or dipole–dipole coupling (through-space, NOESY/ROESY). Since the spin states of the ^{13}C nuclei are not disturbed, the desired E.COSY cross peak pattern is produced (see text). The parameters for the BIRD pulse (i.e. relaxation delay τ and the aquisition time t_2) must be adjusted to obtain the optimal suppression of the signals of protons directly bound to ^{12}C [66]. The experiment can be easily modified to create a 3D experiment; one must simply add a ^{13}C evolution time in between the two ^{13}C-90° pulses [63].

Before the actual experiment starts, a BIRD-pulse sequence[56, 66] is used to suppress the signals of ^{12}C- or ^{14}N-coupled protons. The BIRD-pulse sequence allows one to greatly increase the pulse repetition rate, the relaxation time between two scans is reduced to approximately 1.3 T_1 from the commonly used $3T_1$, which cuts the measuring time by about one half. By using a heteronuclear ω_1-half-filter (X-half filter)[67] at the beginning of the experiment (before the t_1 delay) only protons which are directly coupled to the magnetically active heteroatom (^{13}C or ^{15}N) are selected and ^{12}CH or ^{14}NH protons are suppressed. Of course no heteronuclear decoupling can be

performed during the acquisition. The delay Δ is adjusted to the value of the heteronuclear coupling constant for the ω_1-half filter ($\Delta = 1/2(^1J_{H,C})$) resulting in in-phase magnetization at the end of these two delays, although with small phase distortions from the ^1H coupling. The following TOCSY sequence is only effective for the ^{13}C-coupled protons and transfers the magnetization through the complete spin system. In ω_1 the signals are split by the value of the $^1J_{C,H}$ coupling and in ω_2 by the value of the long-range heteronuclear coupling constant. When the proton peaks are severely overlapped the experiment can easily be expanded into a 3D-HMQC-TOCSY experiment[68] (again without decoupling). This can be accomplished simply by the addition of an evolution period during the heteronuclear half-filter. For example the approximately 200 heteronuclear, long-range coupling constants of the immunosuppressant FK506 were determined with *one* experiment.[69]

However, there are limitations of the HETLOC experiment; heteronuclear $^nJ_{H,X}$ coupling constants can only be determined for heteroatoms which have a directly bound proton. A great advantage is that many heteronuclear coupling constants can be determined for the molecule in natural abundance and with the sensitivity of an inverse detection experiment with one spectrum. In practice, a HETLOC spectrum for a sample with a concentration of about 20 mM can be obtained in approximately one day of measuring time with a high-field instrument. As an example, a HETLOC spectrum from a cyclic hexapeptide is given in Figure 18.

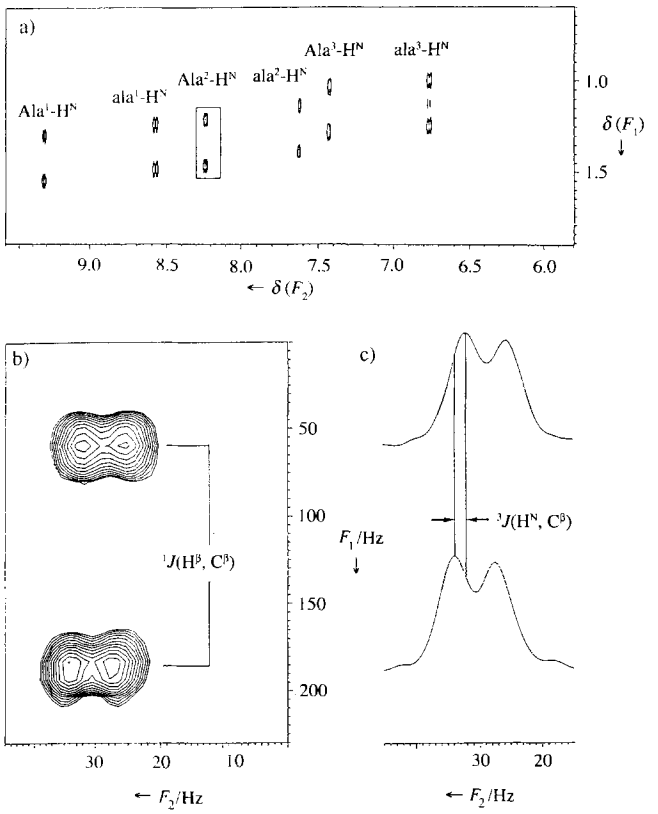

Fig. 18. HETLOC spectrum of a cyclic hexapeptide. a) The H^N,H^β region is shown. The signals are separated in F_1 by the large heteronuclear coupling constant. b) Expansion of the cross peak of Ala^2-H^N illustrating the displacement of the signal in F_2. c) From slices of the F_2 dimension through the signal the long-range heteronuclear coupling constant can be read.

2.2.3.3. Triple Resonance Experiments

Triple resonance experiments[9, 70–74] are pulse sequences which involve three different kinds of nuclei. In proteins and peptides, these are ^{13}C, ^{15}N, and ^1H. For nucleic acids ^{31}P is also of interest; for example $^3J_{C,P}$ or $^3J_{H,P}$ coupling constants can be measured.[75] As a rule, these experiments presuppose isotope enrichment of ^{13}C and often ^{15}N. For larger proteins the classification of signals is performed by triple resonance experiments, such as HNCA,[77] HN(CO)CA,[78] HCACO,[79] HNCO,[80] H(N)COCA,[81] HN(CA)H[82] to name only a few (Fig. 19). There are a large number of correlation experiments which can be modified to allow for passive couplings, producing the E.COSY-type cross peak.

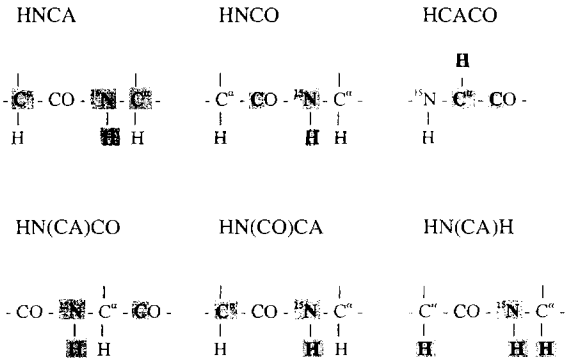

Fig. 19. Schematic representation of the more important 3D triple-resonance experiments for the assignment of the resonances of the protein backbone. The three atoms correlated in each of the three dimensions are highlighted (the HNCA and HN(CA)H produce correlations in the ^{13}C- and H^α dimension between both their own and the previous amino acid).

In the HNCA experiment amide protons, amide nitrogen nuclei, and the C^α nuclei of one residue and the preceding residue (i-1) are correlated. The H^α proton passively couples with the C^α_i, so that the option to determine the $^3J_{H^NH^\alpha}$ coupling constant presents itself.[83] An example of this will be discussed further below. But as there are a great number of other possibilities of correlation in completely enriched samples, a multitude of homo- and heteronuclear coupling constants can be determined by E.COSY techniques. Only a few of the existing experiments can be examined here, so as not to overemphasize the field of protein NMR; we refer to the references given in Table 2. Here, techniques for the determination of $^3J_{H^N,H^\alpha}$ and in the next section $^3J_{H^\alpha,H^\beta}$ will be discussed in detail for illustrative purposes.

Before the establishment of the HNCA experiment, Montelione and Wagner presented the so-called H^α-C^α-(ω_1)-N-selective-H^N-(ω_2) homonuclear RELAY experiment for the determination of the $^3J_{H^N,H^\alpha}$ coupling. The 2D experiment was first illustrated with a peptide enriched with ^{15}N. The pulse sequence is given in Figure 20.[113]

The experiment starts with a refocused INEPT pulse sequence[84] for the transfer of proton-magnetization to $^{13}C^\alpha$ nuclei. During the time of evolution a $^{13}C^\alpha$ chemical shift is developed which is decoupled from the ^{15}N nucleus, but coupled with the protons. In this way a splitting of the cross signals in the ω_1 dimension by the $^1J_{C,H}$ coupling of approximately 140 Hz is produced. The C^α magnetization is transferred to the amide nitrogen of the peptide bond by the $^1J_{C^\alpha N}$ coupling of approxi-

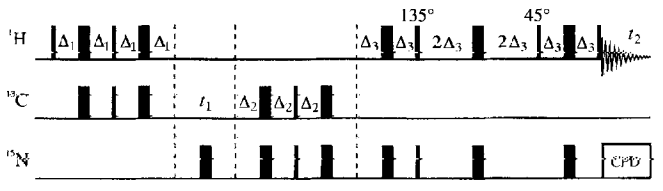

Fig. 20. Pulse sequence for a H^{α}-C^{α}-(ω_1)-N-selective-H^N-(ω_2)-heteronuclear RELAY experiment for the determination of the $^3J(H^N,H^{\alpha})$ coupling constant in peptides (see text). The delays are adjusted for the following coupling constants: $\Delta_1 = 1/(4^1J(C^{\alpha},H^{\alpha}))$, $\Delta_2 = 1/(4^1J(N,C^{\alpha}))$ and $\Delta_3 = 1/(4^1J(N,H))$.

mately 11 Hz during Δ_2. The amide nitrogen magnetization is then defocused with regard to the coupling with the amide proton and is transferred to the H^N nuclei with the help of a TANGO pulse.[85] The TANGO pulse is selective for protons which are directly coupled to ^{15}N and does not excite (change the spin state) of the α-protons. Antiphase proton-coherence is refocused and detected during t_2. The coupling constant can be read from the cross peak in the normal manner. The signal components are separated by the $^1J_{C,H}$ coupling to such an extent that the coupling constant can be determined independent of line width. The pulse sequence of Montelione and Wagner is the basis for a multitude of further experiments which are also founded on the magnetization transfer by ^1J scalar couplings.

However, for proteins with an especially high molecular weight, the pulse sequence must be modified to take into account the relaxation qualities of the molecule. An example of these methods for the HNCA-J experiment is given in Figure 21.[114, 177]

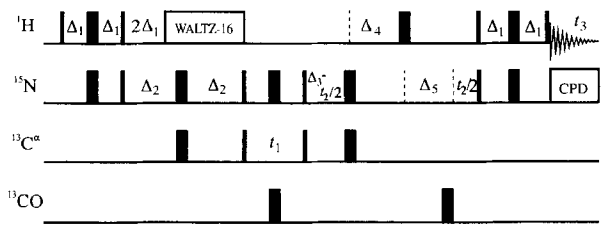

Fig. 21. Pulse sequence for the determination of the $^3J(H^N,H^{\alpha})$ coupling constant in large proteins. The delays are set to the following values: $\Delta_1 = 1/(4^1J(N,H))$, $\Delta_2 = 13$ ms, $\Delta_3 = 10$ ms, $\Delta_4 = 7.75$ ms and $\Delta_5 = 2.25$ ms.

Basically, the experiment corresponds to a constant-time 3D-HNCA experiment without proton decoupling in t_1. C^{α} spins are excited by H^N and ^{15}N and develop as antiphase magnetization with regard to ^{15}N without decoupling of the protons during t_1. After the constant-time evolution of ^{15}N in t_2 the magnetization is transferred back to the protons for detection in t_3. The ^{15}N nuclei are decoupled from the amide protons, through a switching (not mixing!) of populations of the α- and β-states with a 180° ^{1}H pulse. The E.COSY pattern is produced by the selective excitation of the protons which are coupled with ^{15}N. The spin states of the H^{α} protons must remain unperturbed by this. In this instance the effect of the last INEPT step is of importance. The ^{15}N does not strongly couple to the H^{α} nuclei during $2\Delta_1$ and therefore the last three ^{1}H pulses [$90^{\circ}_{(x)}$ - $180^{\circ}_{(x)}$ - $90^{\circ}_{(-x)}$] act as a normal 180° pulse to the α-protons along the z axis which along with the other 180° ^{1}H pulse, produces a 360° pulse, the same result after the t_1 evolution. The last portion of the sequence works similar to a 90°-BIRD pulse, selective for the amide protons, without disturbing the C^{α} protons.

2.2.3.4. HCCH-TOCSY Experiments

In a HCCH-TOCSY experiment the TOCSY transfer is applied to the ^{13}C framework. Because of this such techniques require a high enrichment in ^{13}C, which to date has been mainly limited to proteins. For very large line widths or overlapping of the H^{β} signals, the 2D E.COSY experiment cannot be used to determine the $^3J_{H^{\alpha},H^{\beta}}$ coupling and alternatives must be developed which separate the multiplet components by the large heteronuclear $^1J_{C,H}$ coupling constant along the indirect dimension. As many experiments which deal with this problem have appeared in the literature,[86-89] only one pulse sequence, for illustrative purposes, will be discussed here (Fig. 22).

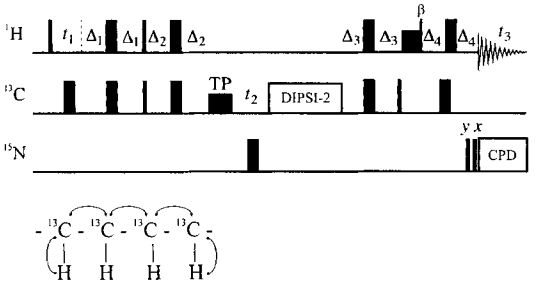

Fig. 22. Pulse sequence for a HCCH-TOCSY experiment [88] for the determination of homonuclear J(H,H) coupling constants in ^{13}C-enriched molecules. With this procedure, protons directly bound to carbon are correlated to each other by a TOCSY transfer through the ^{13}C framework. The delays are set to the following values: $\Delta_1 = 1/(4^1J(C,H))$, $\Delta_2 = 1.3$ ms, $\Delta_3 = 0.55$ ms, and $\Delta_4 = 1/(2^1J(C,H))$, $\beta \approx 35°$.

The refocused INEPT-transfer to begin the pulse sequence also contains the evolution time for the protons. During t_2 in-phase ^{13}C magnetization is developed. The TOCSY sequence is then used to transfer the magnetization to the neighboring ^{13}C nuclei. The magnetization is then transferred back to the protons for detection by reverse INEPT transfer. In comparison to analogous experiments, an advantage of this pulse sequence is that no selective pulses are necessary, and the E.COSY-pattern is obtained by a pulse with a small flip angle. A problem with the employment of selective pulses is that H^{α} nuclei must not be excited while H^{β} nuclei must be completely and uniformly excited. In practice, this cannot always be performed as the resonances of α and β protons may overlap (often the case for the amino acids threonine and serine). In addition, the signal intensities will vary with regard to the excitation profile of the selective pulse which depends on frequency. These problems can be avoided by using a pulse with a small flip angle in the reverse INEPT, especially for overlapping H^{α} and H^{β} resonances. In an (H^{α},H^{β}) cross signal the multiplet components are separated by the $^1J_{C,H}$ coupling along ω_1 and by the $^3J_{H^{\alpha},H^{\beta}}$ coupling along ω_2. An acceptable compromise between the excitation of connected and nonconnected transitions can be obtained with a flip angle β of 30°, suppressing nonconnected transitions by approximately a factor of 10 (see P.E.COSY, Section 2.2.2).

2.3. The Determination of Coupling Constants from Signal Intensities

The determination of coupling constants from signal intensities is founded on the quantification of the magnetization transfer. The precondition for this method is that the signal intensity

depends strongly on the coupling constant. The advantage is that a coupling constant in the range of only a few Hertz need not be read from the multiplet splitting, but is obtained from the signal intensity which can easily be measured.

Generally the signal intensities in most spectra are modulated in some manner by the scalar coupling, which are only in a few cases easy to interpret (e.g. COLOC, HMBC, see below). As a rule, special procedures in which the intensity is modulated by only *one* coupling and therefore easy to evaluate are necessary for the accurate measurement of couplings from signal intensities. In the following several principles will be presented with examples, in order to illustrate how intensity modulations can be evaluated: 1) simply looking at the cross signal intensities, 2) adjusting the analytical dependence of J to a series of measurements, and 3) comparison to a reference spectrum or comparing the intensities of cross peaks and diagonal signals in the same spectrum.

2.3.1. The COLOC Experiment

The COLOC experiment is an example of the determination of coupling constants directly from signal intensity. The pulse sequence is given in Figure 23.[47] The chemical shift evolution and polarization transfer is performed by shifting a pair of π pulses during the delay Δ_1 from 0 to $\Delta_1/2$. The careful optimization of both delays Δ_1 and Δ_2 is important for the suppression of direct couplings. Because of the direct detection of the heteronucleus the sensitivity of the COLOC experiment is relatively low.

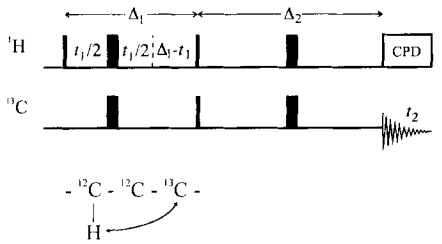

Fig. 23. Pulse sequence for the COLOC experiment for the correlation of ^1H to ^{13}C through long-range heteronuclear coupling constants. The delays Δ_1 and Δ_2 must be optimized. For peptides, values of $\Delta_1 = 25$ ms and $\Delta_2 = 30$ ms have been obtained.

The COLOC experiment was the first to use signal intensities for the determination of coupling constants.[90] For the *constant time* experiment the transfer amplitudes are easy to calculate. The general term of the transfer amplitude I_{ij} of a COLOC signal from proton i to carbon nucleus j is given in Equation 4. The letters k and l stand for passive proton nuclei, which couple with the active proton H_i and active C_j, respectively. For short delay times, $\Delta_1 \approx \Delta_2$ Equation 4 reduces to Equation 5.

As shown in Equation 4, the active coupling in question is developed with sine modulation in the constant delays Δ_1 and

$$I_{ij} = \sin(\pi J_{H_i,C_j}\Delta_1)\sin(\pi J_{H_i,C_j}\Delta_2)\prod_k \cos(\pi J_{H_i,H_k}\Delta_1)\prod_l \cdot \cos(\pi J_{H_i,C_j}\Delta_2) \quad (4)$$

$$I_{ij} \approx \sin^2(\pi J_{H_i,C_j}\Delta_2) \quad (5)$$

Δ_2, the other relevant couplings are cosine modulated. For short delays the difference in signal intensity is dominated by the sine term and therefore relative coupling constants are produced. Modulations due to homonuclear proton couplings in Δ_1 can be taken into account if the $J_{H,H}$ values are known.[90]

Often a qualitative analysis of the heteronuclear coupling constants is sufficient to obtain the stereospecific assignment of diastereotopic protons, for example, the C^β protons of amino acids in peptides. Along with the relatively easy to measure homonuclear coupling constants $^3J_{H^\alpha,H^{\beta pro-R}}$ and $^3J_{H^\alpha,H^{\beta pro-S}}$ (from an E.COSY or DISCO experiment, see Sections 2.1.2 and 2.2, respectively) the heteronuclear couplings provide an unambiguous analysis of the populations about the χ_1 side chain dihedral angle.

Of course, one can measure more than carbon heteronuclear coupling constants with the COLOC experiment. The size of ^1H-^{15}N long-range coupling constants in peptides in natural abundance can be determined, although the sensitivity is greatly reduced.[91, 92]

2.3.2. The HMBC Experiment

However, for most situations inverse detection techniques have many advantages over the methods with direct detection of the heteroatom. As already addressed in Section 2.1.4, the HMBC spectrum contains heteronuclear long-range couplings as antiphase splitting in the cross peak. If couplings for only a few selected carbon atoms are to be determined (e.g. carbonyl-carbons of a peptide) the selective HMBC is favorable to increase the resolution of the carbon dimension.[192, 193] Two illustrative pulse sequences are given in Figure 24.[93]

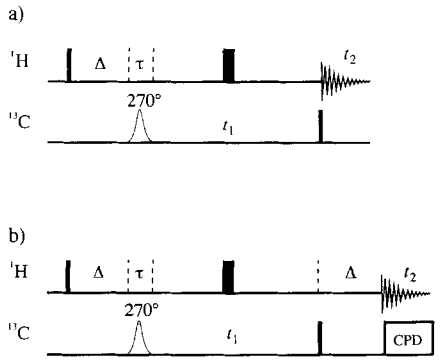

Fig. 24. Pulse sequence for heteronuclear long-range correlation with selective pulses (see the HMBC sequence, Fig. 11). a) Selective HMBC experiment for excitation of a specific region of the heteronuclei. b) Similar to (a) but with refocusing and decoupling during t_2. The delay Δ is set to 60–80 ms. τ is the length of the selective pulse. The utilization of the self-refocusing 270°-Gauss pulse has the advantage that data phase-sensitive in t_1 can be collected.

The signal intensities (transfer amplitude) for these experiments can be easily calculated with the help of the product operator formalism [Eqs. (6a) and (6b)], where H'_k stands for the

$$I = \prod_{H'_k}\cos(\pi J_{H,H'_k}(\Delta + \tau + t_1 + t_2)) \cdot \sin\left(\pi J_{C,H}\left(\Delta + \frac{\tau}{2}\right)\right)\sin(\pi J_{C,H}t_2) \quad (6a)$$

$$I = \prod_{H'_k}\cos(\pi J_{H,H'_k}(\Delta + \tau + t_1 + t_2 + \Delta))\sin\left(\pi J_{C,H}\left(\Delta + \frac{\tau}{2}\right)\right) \cdot \sin(\pi J_{C,H}\Delta)\sin(\pi J_{C,H}t_2) \quad (6b)$$

passive protons. In Equation (6a) (corresponding to the sequence in Fig. 24a) the amplitude varies very little with the coupling, constant, whereas in Equation (6b) (corresponding to the sequence in Fig. 24b) a much stronger influence of the coupling constant on the intensity is observed, as the factor $\sin(\pi J_{C,H}\Delta)$ increases the dependence of the signal amplitude on the coupling constant. Large coupling constants produce an intensive signal in both spectra, whereas small couplings with the second sequence produce a much smaller one.

2.3.3. The J-Modulated (^{15}N,^{1}H)-COSY Experiment

This experiment is used to determine the homonuclear $^{3}J_{H^N,H^\alpha}$ coupling constant. A precondition is an ^{15}N-enriched sample.[94] The desired information about the coupling constant is obtained by the temporary evolution of the proton coherence at the end of a heteronuclear correlation experiment. This procedure allows for an accurate determination of the coupling constant over a large range of J values. The coupling constant can be read from the cross peak intensities with the help of a nonlinear fitting procedure.

Recently an improved version of this method has been presented,[95] which will be discussed in the following. The pulse sequence, shown in Figure 25, is also suitable for proteins with high molecular weight.

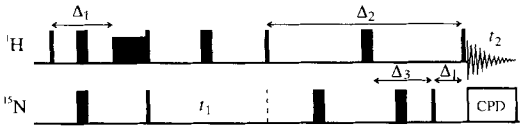

Fig. 25. Pulse sequence for a J-modulated [^{15}N,^{1}H]-COSY experiment for the determination of the $^{3}J(H^N,H^\alpha)$ coupling constants in peptides. The pulse sequence correlates ^{15}N nuclei with the directly bound amide proton. The delay Δ_1 is set to $1/(2^1J(N,H))$; Δ_2 is a variable delay, during which the $^{3}J(H^N,H^\alpha)$ coupling constant is developed; $\Delta_3 = \Delta_2 - \Delta_1 - 180°(^{15}N)$. To determine the coupling constant, a series of spectra with different Δ_2 are collected and the volume of the cross peak is fitted using Equation (7) (see Fig. 26) [93].

The experiment begins as with the related [^{15}N,^{1}H]-HSQC experiment with a spin-lock pulse for water suppression. At the beginning of the delay Δ_2 transversal heteronuclear two-spin coherence $2H_yN_y^H$ is selected, in which the coupling to H^α is developed with $\cos(\pi J\Delta_2)$. The volume of the cross peak is a function of the delay Δ_2 and is given by Equation (7), where A

$$V(\Delta_2) = A\left(\cos(\pi J\Delta_1)\cos(\pi J\Delta_2) - \frac{1}{2}\sin(\pi J\Delta_1)\sin(\pi J\Delta_2)\right) \cdot \exp\left(-\frac{\Delta_2}{T_2'}\right) \quad (7)$$

is the volume of the cross peak for $\Delta_2 = 0$, J is the $^{3}J_{H^N,H^\alpha}$ coupling constant and T_2' is the approximate transversal relaxation time. The coupling constant $^{3}J_{H^N,H^\alpha}$ is obtained by adjusting Equation (7) to the experimental dependence of the volume of the cross peaks with respect to Δ_2. An example for some amino acids from the PTS protein IIB^{Glc}[96] is shown in Figure 26.

For this method several spectra with good signal-to-noise ratio are required and therefore considerable measuring time must be invested.

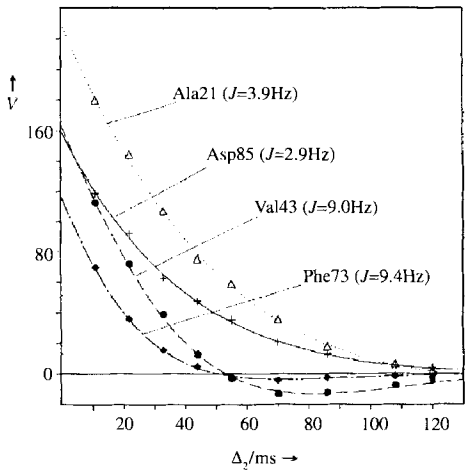

Fig. 26. Results from the fitting using Equation (7) for four amino acids (Ala21, Val43, Phe73, and Asp85) from the IIB^{Glc}-domain of the phosphotransferase transport system from *E.coli*. The volume of the cross peaks V is plotted against the length of the Δ_2 delay. The lines represent the optimal fitting from Equation (7), leading to the values of $^{3}J(H^N,H^\alpha)$ given in the Figure.

2.3.4. The HNHA Experiment

The $^{3}J_{H^N,H^\alpha}$ coupling constant in ^{15}N-enriched proteins can be determined by the HNHA experiment (Fig. 27). An advantage with regard to E.COSY techniques, which are also often used in

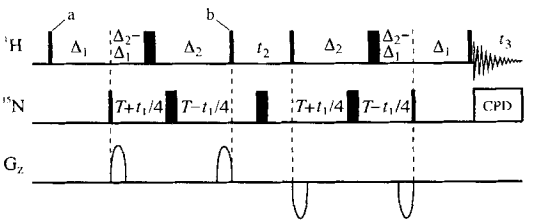

Fig. 27. Pulse sequence for the HNHA experiment. The delays Δ_1 and Δ_2 are set to values 4.5 ms and 13.05 ms, respectively. The pulse sequence is described in detail in the text.

3D NMR spectra, is that signal intensities are easier to determine than precise signal positions in multidimensional spectra with bad digital resolution. The determination of the $^{3}J_{H^N,H^\alpha}$ coupling constant is founded on the quantitative analysis of the intensity of the diagonal signal relative to the cross peak.[16] Basically, the experiment corresponds to several procedures which have already been discussed in the literature with regard to the determination of coupling constants in isotopically enriched proteins.[97-99] In addition, the intraresidual (H^N,H^α) correlation is obtained in the HNHA experiment, so that—besides the measurement of the $^{3}J_{H^N,H^\alpha}$ coupling constant—the assignment of the H^α resonances can also be obtained. The experiment is similar to the ^{15}N-edited [H^N,H^α] COSY spectrum. This sequence is therefore not very useful for large proteins, since the signal intensity is greatly reduced because of the short T_2 relaxation times.

The pulse sequence for the HNHA experiment shown in Figure 27 utilizes pulse field gradients. The gradient pulses are not essential, but they do reduce artifacts from pulse inaccuracies

and allow for a shorter phase cycle.[100] The first 90°-^{1}H pulse produces proton magnetization, which dephases during the delay Δ with respect to the $^1J_{H,N}$ coupling. The first 90°-^{15}N pulse produces zero and double quantum magnetization similar to the HMQC sequence. A ^{15}N chemical shift is developed during the simultaneous shift of the first and the third 180°-^{15}N pulse during the delays $4T$ as in constant-time experiments. Between a and b (marked in Fig. 27) in the pulse sequence the magnetization is dephased as a result of the $^3J_{H^N,H^\alpha}$ coupling. This produces the development of amide proton antiphase magnetization with regard to the H^α nucleus which is proportional to $\sin(2\pi J_{H,H}\Delta_2)$. The amide proton antiphase term is transformed to antiphase H^α magnetization by the second 90°-^{1}H pulse. After a short t_2-period it is converted back to the amide proton antiphase term with regard to the H^α magnetization. In the following period $2\Delta_2$, during which the $^3J_{H^N,H^\alpha}$ coupling is active again, the magnetization is re-phased with regard to the H^α nuclei. The last 90°-^{15}N pulse produces H^N-magnetization from the multiple quantum term which is antiphase with regard to ^{15}N and then rephases, leading to in-phase amide proton magnetization during the delay Δ_1. The detected signal is described by Equation (8), where Ω_{H^N}, Ω_N, and Ω_{H^α} are the chemical shifts

$$I = A(\cos^2(2\pi J_{H,H}\Delta_2)\cos(\Omega_N t_1)\cos(\Omega_{H^N} t_2) - \sin^2(2\pi J_{H,H}\Delta_2)\cos(\Omega_N t_1)\cos(\Omega_{H^\alpha} t_2))\exp(i\Omega_{H^N} t_3) \quad (8)$$

of amide proton, amide nitrogen, and H^α proton, respectively, and A is a constant.[*] The first term corresponds to the diagonal signal ($\Omega_{H^N}t_2$, $\Omega_{H^N}t_3$) and the second to the cross peak ($\Omega_{H^\alpha}t_2$, $\Omega_{H^N}t_3$). The value of the $^3J_{H^N,H^\alpha}$ coupling constant can now easily be determined from the intensity relation of I_{cross}/II_{diag} [Eq. (9)].

$$\frac{I_{cross}}{I_{diag}} = -\tan^2(2\pi J_{H,H}\Delta_2) \quad (9)$$

Equation 9 implies implicitly that the magnetization components which lead to the intensity of the diagonal and cross peaks relax identically during the re- and dephasing delays Δ_2. The HNHA cross peaks are the result of the antiphase, whereas diagonal signals develop from in-phase terms. Antiphase terms are known to relax faster [101–103] so that the cross peaks are less intense and the value of the measured coupling constant is too small. However, it has been shown that for proteins a simple correction of 11% (this is the estimate of the error in the measurement which arises from relaxation effects) can be used to account for this.[16]

2.3.5. {^{15}N} *Spin Echo Differences CT-HSQC*

The experiments for the determination of coupling constants from J-correlated spectra which were discussed so far dealt with either coupling constants between two protons or a proton and a heteronucleus. Here, an experiment will be discussed which is suited for the determination of ^{15}N-^{13}C coupling constants;[104] other couplings between heteronuclei can be measured analogously, for example, ^{13}C-^{13}C and ^{13}C-^{31}P. Of course, the determination of the ^{15}N-^{13}C coupling constant requires a doubly enriched sample. So far there has been little discussion of $^3J_{N,C}$ couplings in the literature[105] and therefore further study in this area is of great interest.

This method[104] allows for the determination of a multitude of ^{15}N-^{13}C couplings with doubly enriched proteins. In combination with $^3J_{C,C}$ couplings, which can measured by using similar methods,[97] the $^3J_{N,C}$ coupling constants of amide nitrogen to γ-methyl-carbon atoms can be used for the characterization of the χ_1 angle of valine, isoleucine, and threonine. As a rule, coupling constants between two heteroatoms are smaller than coupling constants involving protons and therefore cannot be resolved. Procedures which utilize the quantification of the coherence transfer are especially suited and are to be preferred to other techniques.

The pulse sequence in Figure 28 is basically a 2D difference experiment.[104] If the 180°-^{15}N pulse is performed in position A, the experiment corresponds to a normal constant-time

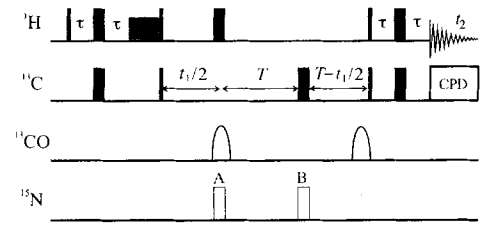

Fig. 28. Pulse sequence for the constant-time-HSQC experiment, which correlates the protons with the directly bound ^{13}C nuclei. The 180° nitrogen pulse is switched between position A and B for the two experiments. The delays τ and T are set to 1.7 ms and 28.6 ms, respectively. The second selective ^{13}CO pulse is to compensate for the Bloch–Siegert effect of the non-carbonyl carbon atoms and the resulting phase error.

HSQC experiment decoupled from ^{13}CO and ^{15}N in t_1 (signal intensity S_a). The delay 2T which corresponds to the constant-time evolution should be adjusted to $1/(^1J_{C,C})$ in order to exclude effects of ^{13}C-^{13}C couplings. In a second experiment the 180°-^{15}N pulse is performed in position B. Due to this the ^{15}N-^{13}C coupling is active during the whole period 2T. The signal intensity is decreased by the factor $\cos(2\pi J_{N,C}T)$ (signal intensity S_b). The ^{15}N-^{13}C coupling constant is the direct result of the relative signal intensities [Eq. (10)].

$$\frac{S_a - S_b}{S_a} = 1 - \cos(2\pi J_{C,N}T) = 2\sin^2(\pi J_{C,N}T) \quad (10)$$

As in other experiments of this kind sources of error derive mainly from relaxation effects. In addition, the percentage of ^{15}N-enrichment and the efficiency of the 180°-^{15}N inversion pulse are decisive for the signal intensity. The authors state that these sources of error are taken into account by scaling the measured coupling constants with the factor 1.075.

[*] In the Equations the same letters are sometimes used for constants and variables in an attempt to be consistent with the literature, they do not necessarily refer to the same quantities.

3. Coupling Constants and Computer Simulations for the Determination of Molecular Structure

The utilization of NMR data for the calculation of the three-dimensional structure of molecules is carried out by computer simulations. For these calculations, distances from NOESY and ROESY spectra are certainly important.[106, 107] Recently, it has become possible to use coupling constants in computer structural refinement,[17, 18] which has increased the quality of the structures as well as allowed for study of the dynamics and flexibility of these biomolecular systems. In this Section we detail the utilization of coupling constants in the computational refinement of protein/peptide structures. Before we can address this point, a few basic aspects about the computational methods themselves are discussed.

3.1. Computational Methods

The computational methods used in the refinement of structures from NMR data, can be broken down into two general categories: molecular mechanics/dynamics (MM or MD) [108–112] and distance geometry (DG) calculations.[113–116] Of course, there is a great variety of different computational approaches, many which utilize a combination of the two listed here, but for our purposes this general division will suffice. A discussion of the precise differences and technical details of the separate procedures could constitute a review alone.

By MM and MD we refer to the utilization of a force field to describe the molecule and produce an estimate of the potential energy of the current conformation. Many different approaches are then used in an attempt to try to minimize the potential energy of this function. The standard force field contains a term for distortion of bond lengths, bond angles, and dihedral angles plus nonbonded terms for Coulombic interactions and Lennard-Jones description of the attraction/repulsion of atoms. There are many different functional forms of the force field,[117–122] varying greatly in the detail in which the molecule is described (i.e. polarization). The greater the detail, the more intense the calculation and longer computational time required. Different recipes to increase the conformational searching to find the global minimum have been described. Many involve varying the weights of the various terms in the force field or scaling of the temperature during molecular dynamics simulations during different stages of the simulation.

The application of experimental restraints in the molecular mechanics type of calculations is achieved by simply adding an additional term, a so-called penalty function. As was mentioned above, NOEs and distance restraints are the most often used constraints; coupling constants were considered to be too difficult to interpret to be used as restraints. The penalty function minimizes the differences between the calculated value and that measured experimentally. This can be illustrated for distance restraints from NOEs simply by Equation (11), where K_{NOE} is

$$\text{energy violation} = \frac{1}{2} \cdot K_{NOE}(R_{exp} - R_{calc})^2 \qquad (11)$$

the force constant, R_{exp} the experimentally measured distance, and R_{calc} the current distance in the computer refinement. The force constant can be adjusted to vary the relative weights of the experimental restraints with respect to the remainder of the force field.

The other general approach, distance geometry calculations, utilizes a description of the molecule based solely on distances.[113] Bond lengths, bond angles, and torsions are converted into ranges of allowed distances. Distances, which satisfy these ranges, are chosen randomly to create a distance matrix. The diagonalization of this matrix, or often a metric matrix, then produces Cartesian coordinates. The procedure of choosing distances can be repeated many times, to better sample conformational space, producing many structures fulfilling the distance matrix.

The application of distance restraints into distance geometry is quite straightforward: the experimental distances are compared with the distances generated from the covalent structure; if the experimental distances are tighter, they are used in place of those from the consideration of the covalent geometry. It is important to note that chirality is not maintained with the description of the molecule solely with distances. Both enantiomers are equally probable. Chirality is maintained by inclusion of an additional penalty term applied after the generation of the Cartesian coordinates.[115]

3.2. Conformation and Coupling Constants

Similar to the NOE which provides information of the distance between the two nuclei, the coupling constant is dependent on structure. The coupling constant provides information about the dihedral angle subtended by the coupled atoms. The equation most often used is that proposed by Karplus [Eq. (12)].[5, 6]

$$^3J = A\cos^2\theta + B\cos\theta + C \qquad (12)$$

The equation was developed from simple valance bond electron calculations, and the coefficients were adjusted with structure parameters, for example from X-ray structure analyses.[123–125] The equation holds for almost all coupling constants, only the coefficients, A, B, and C are adjusted. Even if the coefficients have been determined, the multiple answers possible from Equation (12) (up to four answers can be obtained, see Fig. 29) remains a problem.

The problems with Equation 12 have limited the use of coupling constants as conformational restraints. The standard use of coupling constants was as a secondary check; after the development of a conformation from NOE data, temperature coefficients, or chemical shifts, the dihedral angles would be used to calculate the coupling constants and the agreement with the experimental values examined. The agreement was almost always found to be good, because of the range of values, up to four dihedral angles, that are produced by Equation (12). One method to address the wide range of allowed values is the measurement of additional coupling constants.[126, 127] Using this approach, only the dihedral angles that are in agreement with all of the couplings are retained. This usually allows for some of the solutions (from Equation 12) to be removed from further con-

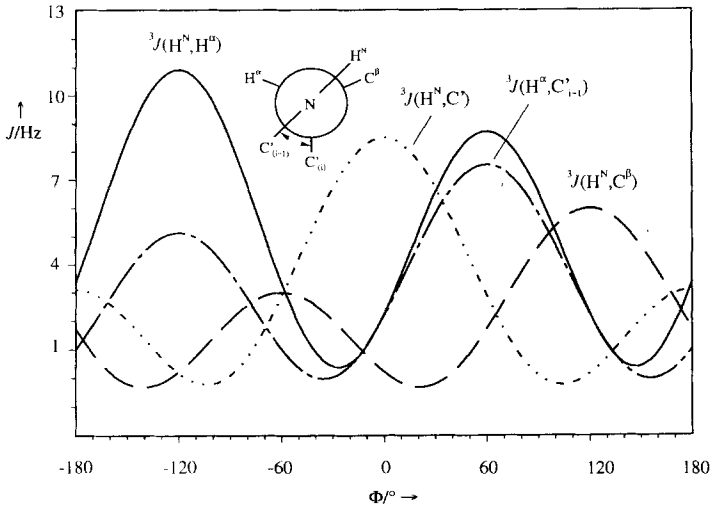

Fig. 29. The Karplus curve for four coupling constants about the ϕ dihedral angle of an L-amino acid. Because of the form of the curve, there are four dihedral angles per coupling constant. Utilizing a combination of all four coupling constants, it is usually possible to eliminate three of the possible dihedral angles.

sideration. However, the coupling constants are frequently only used to confirm an existing structure, and not to determine a conformation.

3.3. Restraints on Dihedral Angles

The first use of coupling constants in refinement calculations was to assume a range of acceptable dihedral angles from Equation (12) and then restrain the torsion to these values. This method is often referred to as dihedral angle restraining. The information from the couplings is used in the refinement, not after the fact. Of course, the problem is how to employ conformational restraints that are consistent with the multiple answers from Equation (12).

One approach to this problem is to utilize only extreme coupling constants.[128-130] For the $^3J_{H^N,H^\alpha}$ coupling constant, values greater than 8.0 Hz or smaller than 6.5 Hz are considered extreme. Couplings between these arbitrary values are considered consistent with conformational averaging and therefore not utilized. For a coupling of 8.0 Hz, the $^3J_{H^N,H^\alpha}$ curve shown in Figure 29 yields four possible dihedral angles. The two answers with positive ϕ dihedral angles are often ignored, which can be very problematic indeed. Ignoring the positive ϕ dihedral angles, a $^3J_{H^N,H^\alpha}$ coupling constant of 8.0 Hz would indicate two minima centered around $-120°$. Typical ranges of acceptable values would be $-140°$ to $-100°$ for $^3J_{H^N,H^\alpha} > 9.0$ Hz, $-160°$ to $-80°$ for 9.0 Hz $> {}^3J_{H^N,H^\alpha} > 8.0$ Hz, and $-160°$ to $-40°$ for $^3J_{H^N,H^\alpha} < 6.0$ Hz.

For each of these couplings a penalty function is applied and added to the energy function or force field that is utilized to refine the conformation. The penalty function can take many different forms. One robust approach uses the calculation of a chiral volume, calculated from the triple product of the three vectors from any of the four atoms defining the dihedral angle.[131] A target chiral volume, CH_{target}, consistent for the dihedral angle, is then calculated and used in a simple penalty function similar to that for NOEs [Eq. (13)],

$$V_{chiral} = \frac{1}{2} K_{CH} (CH_{target} - CH_{theo})^2 \quad (13)$$

where K_{CH} is an adjustable force constant and CH_{theo} is the theoretical chiral volume calculated from the present dihedral angle. Equation (13) is then minimized, along with the remainder of the penalty function, to ensure that the selected dihedral angle adopts a conformation consistent with the experimental value. This method has found widespread use in distance geometry calculations in which chiral volumes are used to maintain the stereochemistry at chirality centers, which is not possible with distances alone.

Another approach utilizes a penalty function identical to that used for dihedral angles in standard molecular dynamics or mechanics programs. For values larger than 8.0 Hz a minimum at $-120°$ is assumed, while for small coupling constants a minimum centered about -80 or $-60°$ is used. The penalty function defined in Equation (14), where K_{DH} is a scaling constant,

$$V = K_{DH} (1 + \cos(\theta - \delta)) \quad (14)$$

θ the dihedral angle, and δ a phase shift, has been shown to be useful for the refinement of conformation using molecular dynamics.[128] Depending on the coupling constant the energy minimum can be adjusted by variation of the phase shift. The K_{DH} can be adjusted to allow for a small range of values centered about the minimum (e.g. for a K_{DH} of 6.8 kJ mol^{-1}, the allowed range of the dihedral angle at 300 K would be $\pm 11°$).

The use of dihedral angle restraints assumes that some of the solutions to Equation (12) are not likely. It is often assumed that positive ϕ values are not possible, and therefore these solutions are ignored. This was done since, up till recently, there have been very few amino acids in protein structures with positive ϕ torsion angles. Recently, as more high-resolution protein structures have been determined, there have been numerous reports of amino acids, not only glycines, with positive ϕ dihedral angles.[132-134] For cyclic or otherwise constrained peptides, it is not safe to assume that the general Ramachandran energy profile will be applicable and one must consider the possibility of positive ϕ values.[135]

3.4. Direct Use of Coupling Constants

A more direct application of coupling constants in the structural refinement calculations was introduced by Kim and Prestegard.[17] The penalty function proposed [Eq. (15)] is similar to that utilized for NOE distance restraints [see Eq. (11)], where K_J is a force constant to weigh each coupling individually, J_{exp} is the experimental coupling constant, and J_{theo} is the theoretical coupling calculated using Equation (12). The difference between the experimental value and that calculated from Equation (12) is minimized during the refinement calculation. This

$$V_J = \frac{1}{2} K_J (J_{exp} - J_{theo})^2 \quad (15)$$

approach allows for all of the coupling constants to be utilized in the refinement calculations without any approximations of which ranges of dihedral angles are appropriate. In addition, multiple couplings about the same dihedral angle can be easily utilized.[137]

Equation (15) has been applied in the conformational analysis of many different peptides and proteins in molecular mechanics and dynamics calculations.[118, 119, 136] In simulations of small cyclic peptides the sole use of coupling constants has produced structures almost identical to those developed from NOE data. However, for a larger cyclic undecapeptide peptide, cyclosporin A, the sole use of coupling constants failed to produce the structure derived from NOE data.[137] There were significant differences in the backbone conformations from the application of the two different experimental restraints. The penalty-energy function for three different coupling constants for the ϕ dihedral angle of D-Ala^8 in cyclosporin A is given in Figure 30. The global minimum of the sum of the coupling constants is given at $+80°$.[138] A similar dihedral angle was obtained for the structure calculated by using only NOE restraints.

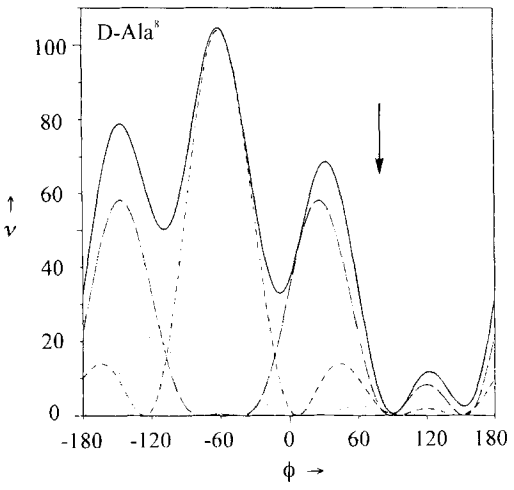

Fig. 30. The potential energy V [kJ mol^{-1}] penalty function for the coupling constants as a function of the ϕ dihedral angle of the amino acid D-Ala^8 in cyclosporin A. The "energy" is calculated from Equations (12) and (15) with a force constant, K_J, of 1.0 kJ mol^{-1} Hz^{-2}. The coefficients for Equation (12) must be known for each individual coupling. The penalty for the $^3J(H^N,H^\alpha)$ (- · -), $^3J(H^N,H^\beta)$ (···), $^3J(C'(i-1),H^\alpha(i))$ (– – –), and the sum of all of the couplings (——) are shown. The arrow indicates the ϕ dihedral angle observed from the structure calculated by using only NOEs.

The populations of the side chain conformations were identical from both calculations. The reason why no structure can be determined for cyclosporin A solely on the basis of coupling constants is because, firstly, seven of the eleven residues are N-methylated and thus only four ϕ angles can be determined from the $^3J_{H^N,H^\alpha}$ coupling constants, and secondly, the ψ dihedral angle is generally difficult to define with J values. Because of the limited number of coupling constants available, many conformations fulfilled the coupling constant restraints (multiple minima) and there was no convergence. It is important to note that the NOE structure satisfied the coupling constant restraints.

One question with the utilization of different coupling constants as conformational restraints, is the appropriate weighting of the various couplings. The experimental error in J varies greatly for the different types of coupling constants. As a general rule, homonuclear coupling constants can be measured with far greater accuracy than heteronuclear couplings. In addition, a great deal of effort must be invested in the development of the A, B, and C coefficients of Equation (12), which to date has only been carried out for the $^3J_{H^N,H^\alpha}$ coupling constant. In general the vicinial heteronuclear coupling constants are greatly influenced by substitution effects and therefore studies to develop standard coefficients for Equation 12 as has been achieved for $^3J_{H,H}$ are much more difficult.[139] The studies that have appeared to date in this area are based on purely quantum mechanical calculations or very few experimental data.

3.5. Identification of Dynamics

One of the most interesting aspects of the use of Equation (12), is the identification of conformational dynamics taking place fast on the NMR time scale.[140, 141] In situations where conformational averaging is taking place, the NOEs are averaged as a function of the sixth power of the distance R between the two participating protons (e.g. R^{-6}). On the other hand, coupling constants are averaged as a function of the cosine series of the dihedral angle subtended by the coupled atoms (i.e. $\cos^2\theta$ and $\cos\theta$). Therefore the NOE restraints will produce a different conformation from that consistent with the coupling constants. This is a clear indication that the molecule is undergoing averaging fast on the NMR time scale. The differences between the "NOE structure" and the structure from coupling constants comes from the different averaging; (R^{-6}) for NOEs and $\cos^2\theta$ and $\cos\theta$ for the coupling constants. It is important to differentiate this finding, with that discussed in the previous Section for cyclosporin A, which can be simply defined as a multiple minima problem (i.e. with the sole application of the coupling constants there exists numerous energy minima, so that the NOE conformation is not found, even though it is one of the minima).

The consideration of dynamic aspects is extremely important in the development of conformations using NMR data, particularly for smaller systems such as peptides or many natural products. Under conformational averaging, the distances calculated from the NOEs are consistent with the average structure, a structure that may not exist in solution or be even physically possible.[142] Only with the use of these two restraints which average differently is it possible to unambiguously identify such averaging. The results of the simultaneous application of coupling constant and NOE restraints to analyze a situation like this was reported recently.[22] Fast conformational averaging can also be identified when one has more than one coupling constant about the same dihedral angle, which cannot be fulfilled by one value. Here it is important to recall that the associated error in the heteronuclear coupling constants is larger, and thus one may wish to give the homonuclear couplings more weight (e.g. four $J_{H,H}$ values describe the angle YCH_2-CH_2X).

3.6. Time-Dependent Restraints

As stated in the previous section, the presence of conformational mobility would have a great influence on the NMR observables (NOEs, coupling constants, chemical shifts) and therefore on the restraints developed from these experimental parameters measurements (distances, dihedral angles), which are used for the simulation calculations. One approach to handle this situation is to apply the restraints as time averages.[143, 144] This method was first utilized for NOE restraints and recently in the use of Equation (11).[145, 146] Rather than comparing the instantaneous value of the coupling constant (or distance) to the experimentally measured coupling constant (or NOE), the time-averaged value, averaged over a short time span, is utilized. The theoretical coupling constant can be calculated by using Equation (16), where the brackets denote an

$$J_{\text{theo}} = A\langle\cos^2\theta\rangle + B\langle\cos\theta\rangle + C \qquad (16)$$

average over a specific period of time, which is usually kept rather small (10–40 ps) so that sufficient periods can be run to allow for a better statistical evaluation of the data. The method has been shown to correctly reproduce molecular dynamics that were not observed with application of more traditional constant-time restraints. As an example for the application of time-dependent restraints, results from two simulations of a cyclic tripeptide, *cyclo*(L-Pro^1-L-Pro^2-D-Pro^3-), are given in Figure 31.

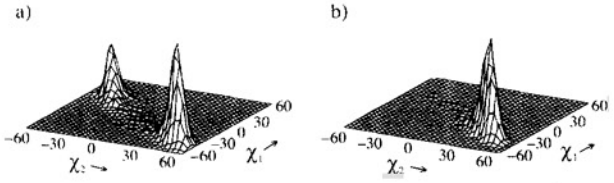

Fig. 31. Relative populations of the dihedral angles χ_1 and χ_2 of L-Pro^2 in *cyclo*(-L-Pro^1-L-Pro^2-D-Pro^3). a) Results from a 1 ns simulation, calculated with time-dependent restraints. After 400 ps both of the conformations are clearly observed with significant populations. b) Results from a 500 ps simulation with constant restraints, which produces only one of the conformations, and therefore fails to reproduce the experimental data.

We can conclude from the discrepancy of the vicinial coupling constants[147, 148] that Pro^1 and to some extent Pro^2 are undergoing fast dynamics which is in agreement with relaxation time measurements[149] and the results of an X-ray structure.[150] If the measured coupling constants are used as constant restraints then, for example, the ring of Pro^2 is drawn into one, single conformation which does not reproduce the experimentally obtained coupling constant. If the calculation is carried out with time-dependent restraints one finds two minima and excellent agreement with the measured J values. The results from these simulations are shown in Figure 31.

3.7. The Ensemble Method

Whenever an experimental measurement is carried out, the observable is an average, this can be considered a time-average over the length of the measurement or as an ensemble average, over a large (infinitely large) number of molecules. For example, the average distance from the ensemble of molecules must fulfill the experimental distance derived from NOEs.[151] Of course if the system is ergodic, the results—time-averaged and ensemble-averaged—must be the same. Recently, ensemble averaging of coupling constants has been incorporated into a refinement procedure to be used after distance geometry calculations.[22, 152] It is standard to repeat distance geometry calculations a large number of times, producing a larger number of structures. The ensemble approach then utilizes these structures to calculate an ensemble average. This ensemble average is then used to compare with the experimental values [Eq. (17)], where the sum is

$$J_{\text{theo}} = \frac{1}{N}\Sigma J_{\text{N}} \qquad (17)$$

run over the number of structures in the ensemble N. This theoretical coupling constant from Equation (17) is then utilized in the calculation of the error by using Equation (15). There can be a great variety of coupling constants, but if the average over the complete ensemble is fulfilled, the penalty function is zero and no forces are applied.

The consideration of dynamics or molecular motion is no more obvious than with the rotation about side chains. It is clear that for coupling constants involving side chains, that the observable is an average. Because of this the use of the side chain homonuclear coupling constants $^3J_{\text{H}^\alpha,\text{H}^\beta}$ for conformational information has often been limited to "extreme" couplings (i.e. $^3J_{\text{H}^\alpha,\text{H}^\beta}$ smaller than 4.0 Hz or larger than 10 Hz). However, with the measurement of numerous coupling constants about the side chain torsion and with the application of the restraint as an average, such information can be safely used in structure refinement calculations.

3.8. Assignments of the Signals of Diastereotopic Protons

The correct assignment of the signals of diastereotopic protons greatly increases the quality of structures simulated from distance restraint calculations, since the use of pseudoatoms or large modifications of the NOE-derived distances (to allow for both *pro-R* and *pro-S* protons) are not required.[153] The assignment of β-methylene protons of amino acids such as phenylalanine can be obtained from the homonuclear $^3J_{\text{H}^\alpha,\text{H}^\beta}$ along with the heteronuclear $^3J_{\text{C}',\text{H}^\beta}$ or $^3J_{\text{N},\text{H}^\beta}$. In the case of a large number of local NOEs, it is sometimes possible to make the assignments of the diastereotopic protons without the heteronuclear coupling constants, using only the homonuclear coupling constants.

One calculation procedure to facilitate the diastereotopic assignment is floating chiralities.[154–156] Floating chirality requires the removal of the energy term that is present in the force field which maintains the stereoposition of the two β-methylene protons. With this term removed, the protons can switch relative stereopositions (*pro-R* and *pro-S*) during the calculation. The adoption of the chirality is driven solely by the NOE restraints. This method originally illustrated in distance geometry calculations,[154] has been shown to work very well for proteins where the number of NOEs are often sufficient to obtain an unambiguous assignment. With peptides, there are usually not

enough NOEs to develop the diastereotopic assignment. We have recently examined the possibility of using both experimental parameters—NOEs and coupling constants—and allowing the chiralities to float. Application of this approach was successful for five out of six β-methylene groups of a substance P analog recently studied.[157] One cautionary note with the use of floating chiralities should be given. The method will produce an answer, no matter what the extent of the experimental restraints. For underdetermined systems there is a high probability of finding a local minimum. The number of restraints gives no insight into the confidence of the assignment. Also important is the nature of the restraints, a few restraints from different angles or orientations will be of more use than more NOEs from one direction. The method that we employ is a graphical representation of the NOEs to examine the confidence in the diastereotopic assignment.

3.9. Conformational Restraints from Other Coupling Constants

Above we have concentrated on the application of vicinal coupling constants, which have been traditionally the most informative, and therefore, there is more data within the literature to develop conformational parameters. However, with the large number of proteins that have been isotopically enriched, the number of interesting couplings besides the three-bond couplings has greatly increased. It is therefore foreseeable that conformational information could be obtained from two-bond or even one-bond coupling constants. One example is the $^1J_{C,H}$ coupling constant in glycosides which varies by up to 10 Hz for the axial and equatorial protons, allowing for the determination of the anomeric configuration.[158, 159] For peptides and proteins, Egli and von Philipsborn reported many years ago that the one-bond coupling between the α-carbon and the α-proton, $^1J_{C^\alpha,H^\alpha}$, is dependent on both the ϕ and ψ backbone dihedral angles.[160] The relationship for an L-amino acid is given in Equation (18). The $^1J_{C^\alpha,H^\alpha}$ coupling constant is a function of

$$^1J = A + B\cos^2(\phi - 30^\circ) + C\cos^2(\psi - 30^\circ) \quad (18)$$

both of the backbone dihedral angles, ϕ and ψ, and can be used to develop a penalty-energy profile similar to that shown in Figure 30; however, now the dependence on two dihedral angles is illustrated (Fig. 32).

The coefficients A, B, and C for Equation 18 have been recently determined (136.4, 13.7, and -5.2, respectively), from a series of cyclic alanine-containing peptides. This expression was recently introduced into molecular dynamics program to add a conformational restraint to the ψ dihedral angle, and then use of the ^1J coupling to reduce the allowed ranges of the ψ dihedral has been shown to be useful in the examination of peptide conformation. From examination of a few proteins, a modified version of Equation (18) for the ^1J coupling has been proposed;[162] however, the conformational minima are very similar.

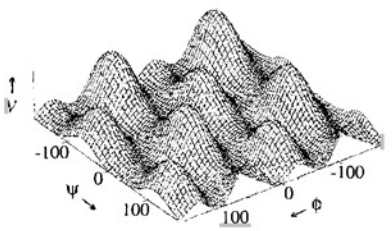

dral angles of a peptide backbone for a $^1J(C^\alpha,H^\alpha)$ coupling constant of 143.2 Hz. The penalty energy is calculated from Equations (15) and (18) with a force constant, K_J, of 1.0 kJ mol^{-1} Hz^{-2}.

Recent studies have illustrated some interesting correlations between conformation and coupling constants greater than ^3J. For example, the $^4J_{H^N(i),H^\alpha(i-1)}$ coupling constant is usually between -0.5 and 0.5 Hz and therefore would seem of little use. However, with a ψ dihedral angle of $+120^\circ$ and the ϕ of the next residue of $+60^\circ$, this coupling adopts values between -0.8 and -2.6 Hz.[163]

4. Conclusions

We have summarized the most important methods for the measurement of homo- and heteronuclear coupling constants for biomolecules in natural abundance, as well as for those systems isotopically enriched in ^{15}N and ^{13}C. In such a review article, all of the techniques which have appeared in the literature cannot be discussed, although we have attempted to give a more comprehensive listing in Tables 1–3. This should serve as a useful guide for the methods that have been developed and give the spectroscopist a place to begin in the literature. In addition, the use of coupling constants in computer simulations, many of which have recently been developed, has been highlighted. It is a matter of concern of this article to stress the necessity of the combined usage of distances *and* dihedral angles which is especially important when dealing with the structure of small molecules since dynamic phenomena have to be recognized and interpreted carefully.

Small molecules confront the scientist with the additional difficulty that the number of available NOEs is not sufficient for a reliable structure analysis. This is due to the fact that the ratio of surface to the inner core is much larger than in globular structures (e.g. proteins). Therefore, the structure calculations require the additional conformational information of coupling constants. The same situation, a small number of NOEs, is often observed for surface-exposed regions and active sites of many proteins. For the analysis of nucleic acids where the NOEs are often difficult to interpret, coupling constants can be very informative.

In closing, we would like to say a few words about the structure of molecules and their representation in the literature. Most methods employed today for structure analysis use MD calculations (at least to refine the results). The structure coordinates are averaged over the time profile of the simulation and presented in *one* figure. The averaging causes distorted distances and angles and therefore the structure is usually partially energy minimized. As all molecules are flexible and undergoing dynamics such a representation is not 100% accurate (i.e. it does not represent the "real" conformation). This fact must always be kept in mind when dealing with structures derived from NMR data (or any experimental data).

It is usual to begin with the simple assumption that the molecule adopts a single conformation. When all of the experimental data is reproduced by the results from the structure calculations,

this presents one and only one possible model of the conformation. The number and quality of the experimental data and the force field determine if further solutions exist (keywords: local minimum and under-determined structure). If the experimental parameters do not confirm the experiment—even if the trivial case of falsely classified or quantitatively wrong values (which in practice requires very careful scrutiny) is excluded internal dynamics must be taken into consideration. For this, extensive MD calculations, in addition to time-dependent or ensemble methods for application of experimental restraints, are suitable.

We would like to thank the Deutsche Forschungsgemeinschaft and the Fonds des Chemischen Industrie for the many years of support. Over the years, a large number of coworkers have produced significant contributions for the determination of coupling constants and their evaluation, of which only a few can be mentioned: U. Anders, J. Balbach, W. Bermel, S. Golic Grdadolnik, C. Griesinger, T. Huber, H. Oschkinat, P. Schmieder, and S. Seip. Numerous insights came from cooperation and discussion with colleagues of which three deserve special mention: R. R. Ernst (ETH, Zurich), R. Freeman (Oxford), and W. F. van Gunsteren (ETH, Zurich). We want to thank: S. Golic Grdadolnik (Figs. 29, 32), P. Schmieder (Figs. 16, 18), and T. Huber (Fig. 31) for supplying figures. Finally we want to thank M. Bachelin for his careful proof reading as well as helpful remarks.

Received: June 25, 1994
Revised version: January 23, 1995 [A 701E]
German version: *Angew. Chem.* **1995**, *107*, 1813–1838

[1] H. S. Gutowsky, D. W. McCall, *Phys. Rev.* **1951**, *82*, 748–749.
[2] H. S. Gutowsky, D. W. McCall, P. Slichter, *Phys. Rev.* **1951**, *84*, 589–590.
[3] E. L. Hahn, D. E. Maxwell, *Phys. Rev.* **1951**, *84*, 1246–1247.
[4] E. L. Hahn, D. E. Maxwell, *Phys. Rev.* **1952**, *88*, 1070–1084.
[5] M. Karplus, *J. Chem. Phys.* **1959**, *30*, 11–13.
[6] M. Karplus, *J. Am. Chem. Soc.* **1963**, *85*, 2870–2871.
[7] K. Wüthrich, *NMR of Proteins and Nucleic Acids*, Wiley, New York, **1986**.
[8] R. Kaptein, R. Boelens, R. M. Scheek, W. F. van Gunsteren, *Biochemistry* **1988**, *27*, 5389–5395.
[9] G. Wagner, *Prog. Nucl. Magn. Reson. Spectrosc.* **1990**, *22*, 101–139.
[10] H. Kessler, A. Müller, H. Oschkinat, *Magn. Reson. Chem.* **1985**, *23*, 844–852.
[11] C. Griesinger, O. W. Sørensen, R. R. Ernst, *J. Magn. Reson.* **1987**, *75*, 474–492.
[12] J. J. Titman, D. Neuhaus, J. Keeler, *J. Magn. Reson.* **1989**, *85*, 111–131.
[13] G. T. Montelione, G. Wagner, *J. Am. Chem. Soc.* **1989**, *111*, 5474–5475.
[14] S. Seip, J. Balbach, H. Kessler, *Angew. Chem.* **1992**, *104*, 1656–1658; *Angew. Chem. Int. Ed. Engl.* **1992**, *31*, 1609–1611.
[15] T. Szyperski, P. Güntert, G. Otting, K. Wüthrich, *J. Magn. Reson.* **1992**, *99*, 552–560.
[16] G. W. Vuister, A. Bax, *J. Am. Chem. Soc.* **1993**, *115*, 7772–7777.
[17] Y. Kim, J. H. Prestegard, *Proteins: Struct. Funct. Genet.* **1990**, *8*, 377–382.
[18] D. F. Mierke, H. Kessler, *Biopolymers* **1992**, *32*, 1277–1282.
[19] M. Eberstadt, D. F. Mierke, M. Köck, H. Kessler, *Helv. Chim. Acta* **1992**, *75*, 2583–2592.
[20] D. F. Mierke, S. Golic Grdadolnik, H. Kessler, *J. Am. Chem. Soc.* **1992**, *114*, 8283–8284.
[21] D. F. Mierke, H. Kessler, *Biopolymers* **1993**, *33*, 1003–1017.
[22] D. F. Mierke, M. Kurz, H. Kessler, *J. Am. Chem. Soc.* **1994**, *116*, 1042–1049.
[23] IUPAC-IUB Commission on Biochemical Nomenclature (CBN), *Eur. J. Biochem.* **1970**, *17*, 193–201.
[24] J. D. Roberts, *An Introduction to the Analysis of Spin-Spin Splitting in High-Resolution Nuclear Magnetic Resonance Spectra*, Benjamin, New York, **1962**.
[25] R. R. Ernst, G. Bodenhausen, A. Wokaun, *Principles of Nuclear Magnetic Resonance in One and Two Dimensions*, Clarendon, Oxford, **1987**.
[26] H. Günther, *NMR-Spektroskopie*, Thieme, Stuttgart, **1992**.
[27] J. W. Emsley, J. Feeney, L. H. Sutcliffe, *High Resolution NMR Spectroscopy*, Macmillan (Pergamon), New York, **1965**, Chapter 8.
[28] J. A. Pople, W. G. Schneider, H. J. Bernstein, *High Resolution NMR Spectroscopy*, McGraw Hill, New York, **1959**, Chapter 6.
[29] G. Hägele, M. Engelhardt, W. Boenigk, *Simulation und automatisierte Analyse von Kernresonanzspektren*, VCH, Weinheim, **1987**.
[30] O. W. Sørensen, M. Rance, R. R. Ernst, *J. Magn. Reson.* **1984**, *56*, 527–534.
[31] M. Rance, *J. Magn. Reson.* **1987**, *74*, 557–564.
[32] S. J. F. Vincent, C. Zwahlen, G. Bodenhausen, *J. Am. Chem. Soc.* **1992**, *114*, 10989–10990.
[33] H. Kessler, H. Oschkinat, C. Griesinger, W. Bermel, *J. Magn. Reson.* **1986**, *70*, 106–133.
[34] H. Kessler, S. Mronga, G. Gemmecker, *Magn. Reson. Chem.* **1991**, *29*, 527–557.
[35] a) L. D. Hall, T. J. Norwood, *J. Magn. Reson.* **1988**, *76*, 325–330; b) *ibid.* **1988**, *78*, 582–587.
[36] K. E. Köver, D. Jiao, D. Uhrin, P. Forgo, V. J. Hruby, *J. Magn. Reson. Ser. A* **1994**, *106*, 119–122.
[37] D. Neuhaus, G. Wagner, M. Vasak, J. H. R. Kägi, K. Wüthrich, *Eur. J. Biochem.* **1985**, *151*, 257–273.
[38] Y. Kim, J. H. Prestegard, *J. Magn. Reson.* **1989**, *84*, 9–13.
[39] H. Oschkinat, R. Freeman, *J. Magn. Reson.* **1984**, *60*, 164–169.
[40] H. Kessler, H. Oschkinat, *Angew. Chem.* **1985**, *97*, 689–690; *Angew. Chem. Int. Ed. Engl.* **1985**, *24*, 690–692.
[41] R. Freeman, L. McIntyre, *Isr. J. Chem.* **1992**, *32*, 231–244.
[42] L. McIntyre, R. Freeman, *J. Magn. Reson.* **1992**, *96*, 425–431.
[43] J. J. Titman, J. Keeler, *J. Magn. Reson.* **1990**, *89*, 640–646.
[44] P. Huber, C. Zwahlen, S. J. F. Vincent, G. Bodenhausen, *J. Magn. Reson. Ser. A* **1993**, *103*, 118–121.
[45] F. del R. Portilla, R. Freeman, *J. Magn. Reson. Ser. A* **1993**, *104*, 358–362.
[46] A. Bax, M. F. Summers, *J. Am. Chem. Soc.* **1986**, *108*, 2093–2095.
[47] H. Kessler, C. Griesinger, J. Zarbock, H. R. Loosli, *J. Magn. Reson.* **1984**, *57*, 331–336.
[48] J. Keeler, D. Neuhaus, J. J. Titman, *Chem. Phys. Lett.* **1988**, *146*, 545–548.
[49] H. Kogler, O. W. Sørensen, G. Bodenhausen, R. R. Ernst, *J. Magn. Reson.* **1983**, *55*, 157–163.
[50] L. Poppe, H. van Halbeck, *J. Magn. Reson.* **1991**, *92*, 636–641.
[51] J. M. Richardson, J. J. Titman, J. Keeler, *J. Magn. Reson.* **1991**, *93*, 533–553.
[52] S. Macura, Y. Huang, D. Suter, R. R. Ernst, *J. Magn. Reson.* **1981**, *43*, 259–281.
[53] M. Rance, G. Bodenhausen, G. Wagner, K. Wüthrich, R. R. Ernst, *J. Magn. Reson.* **1985**, *62*, 497–510.
[54] C. Griesinger, O. W. Sørensen, R. R. Ernst, *J. Chem. Phys.* **1986**, *64*, 6837–6852.
[55] C. Griesinger, O. S. Sørensen, R. R. Ernst, *J. Am. Chem. Soc.* **1985**, *107*, 6394–6396.
[56] H. Kessler, M. Gehrke, C. Griesinger, *Angew. Chem.* **1988**, *100*, 507–554; *Angew. Chem. Int. Ed. Engl.* **1988**, *27*, 490–536.
[57] T. J. Norwood, K. Jones, *J. Magn. Reson. Ser. A* **1993**, *104*, 106–110.
[58] S. Wimperis, G. Bodenhausen, *Mol. Phys.* **1989**, *66*, 897–919.
[59] L. Müller, *J. Magn. Reson.* **1987**, *72*, 191–196.
[60] G. T. Montelione, M. E. Winkler, P. Rauhenbuehler, G. Wagner, *J. Magn. Reson.* **1989**, *82*, 198–204.
[61] G. Wider, D. Neri, G. Otting, K. Wüthrich, *J. Magn. Reson.* **1989**, *85*, 426–431.
[62] M. Kurz, P. Schmieder, H. Kessler, *Angew. Chem.* **1991**, *103*, 1341–1342; *Angew. Chem. Int. Ed. Engl.* **1991**, *30*, 1330–1331.
[63] P. Schmieder, M. Kurz, H. Kessler, *J. Biomol. NMR* **1991**, *1*, 403–420.
[64] A. S. Edison, W. M. Westler, J. L. Markley, *J. Magn. Reson.* **1991**, *92*, 434–438.
[65] U. Wollborn, D. Leibfritz, *J. Magn. Reson.* **1992**, *98*, 142–146.
[66] A. Bax, S. Subramanian, *J. Magn. Reson.* **1986**, *67*, 565–569.
[67] G. Otting, H. Senn, G. Wagner, K. Wüthrich, *J. Magn. Reson.* **1986**, *70*, 500–505.
[68] S. Fesik, E. R. P. Zuiderweg, *J. Am. Chem. Soc.* **1989**, *111*, 770–772.
[69] D. F. Mierke, P. Schmieder, P. Karuso, H. Kessler, *Helv. Chim. Acta* **1991**, *74*, 1027–1047.
[70] G. M. Clore, A. M. Groneborn, *Prog. Nucl. Magn. Reson. Spectrosc.* **1991**, *23*, 43–92.
[71] M. Ikura, L. E. Kay, R. Tschudin, A. Bax, *J. Magn. Reson.* **1990**, *86*, 204–209.
[72] E. R. P. Zuiderweg, L. P. McIntosh, F. W. Dahlquist, S. W. Fesik, *J. Magn. Reson.* **1991**, *86*, 210–216.
[73] L. E. Kay, M. Ikura, R. Tshudin, A. Bax, *J. Magn. Reson.* **1990**, *89*, 496–514.
[74] H. Oschkinat, T. Müller, T. Dieckmann, *Angew. Chem.* **1994**, *106*, 284–300; *Angew. Chem. Int. Ed. Engl.* **1994**, *33*, 277–293.
[75] P. Schmieder, J. H. Ippel, H. van Elst, G. A. van der Marel, J. H. van Boom, C. Altona, H. Kessler, *Nucleic Acids Res.* **1992**, *20*, 4747–4751.
[76] H. Schwalbe, W. Samstag, J. W. Engels, W. Bermel, C. Griesinger, *J. Biomol. NMR* **1993**, *3*, 479–486.
[77] B. T. Farmer, R. A. Venters, L. D. Spicer, M. G. Wittekind, L. Müller, *J. Biomol. NMR* **1992**, *2*, 195–202.
[78] R. T. Clubb, V. Thanabal, G. Wagner, *J. Magn. Reson.* **1992**, *97*, 213–217.
[79] R. Powers, A. M. Groneborn, M. G. Clore, A. Bax, *J. Magn. Reson.* **1991**, *94*, 209–213.

[80] S. Grzesiek, A. Bax, *J. Magn. Reson.* **1992**, *96*, 432–440.
[81] S. Seip, J. Balbach, H. Kessler, *J. Biomol. NMR* **1993**, *3*, 233–237.
[82] S. Seip, J. Balbach, H. Kessler, *J. Magn. Reson.* **1992**, *100*, 406–410.
[83] O. W. Sørensen, *J. Magn. Reson.* **1990**, *90*, 433–438.
[84] G. A. Morris, R. Freeman, *J. Am. Chem. Soc.* **1979**, *101*, 760–762.
[85] S. Wimperis, R. Freeman, *J. Magn. Reson.* **1984**, *58*, 348–353.
[86] G. Gemmecker, S. W. Fesik, *J. Magn. Reson.* **1991**, *95*, 208–213.
[87] C. Griesinger, U. Eggenberger, *J. Magn. Reson.* **1992**, *97*, 426–434.
[88] S. D. Emerson, G. T. Montelione, *J. Magn. Reson.* **1992**, *99*, 413–420.
[89] Y. Karimi-Nejad, J. M. Schmidt, H. Rüterjans, H. Schwalbe, C. Griesinger, *Biochemistry* **1994**, *33*, 5481–5492.
[90] U. Anders, G. Gemmecker, H. Kessler, C. Griesinger, *Fresenius' Z. Anal. Chem.* **1987**, *327*, 72–73.
[91] H. Kessler, C. Griesinger, K. Wagner, *J. Am. Chem. Soc.* **1987**, *109*, 6927–6933.
[92] L. Emsley, G. Bodenhausen, *J. Magn. Reson.* **1989**, *82*, 211–221.
[93] W. Bermel, K. Wagner, C. Griesinger, *J. Magn. Reson.* **1989**, *83*, 223–232.
[94] D. Neri, G. Otting, K. Wüthrich, *J. Am. Chem. Soc.* **1990**, *112*, 3663–3665.
[95] M. Billeter, D. Neri, G. Otting, Y. Q. Quian, K. Wüthrich, *J. Biomol. NMR* **1992**, *2*, 257–274.
[96] S. Golic Grdadolnik, M. Eberstadt, G. Gemmecker, H. Kessler, A. Buhr, B. Erni, *Eur. J. Biochem.* **1994**, *219*, 945–952.
[97] A. Bax, D. Max, D. Zax, *J. Am. Chem. Soc.* **1992**, *114*, 6923–6925.
[98] S. Grzesiek, G. W. Vuister, A. Bax, *J. Biomol. NMR* **1993**, *3*, 487–493.
[99] G. W. Vuister, T. Yamazaki, D. Torchia, A. Bax, *J. Biomol. NMR* **1993**, *3*, 297–306.
[100] G. Bodenhausen, H. Kogler, R. R. Ernst, *J. Magn. Reson.* **1984**, *56*, 370–388.
[101] A. Bax, M. Ikura, L. E. Kay, D. A. Torchia, R. Tshudin, *J. Magn. Reson.* **1990**, *86*, 304–318.
[102] R. E. London, *J. Magn. Reson.* **1990**, *86*, 410–415.
[103] L. E. Kay, L. K. Nicholson, F. Delaglio, A. Box, D. A. Torchia, *J. Magn. Reson.* **1992**, *97*, 359–375.
[104] G. W. Vuister, A. Bax, *J. Am. Chem. Soc.* **1993**, *115*, 5334–5335.
[105] S. Berger, J. D. Roberts, *J. Am. Chem. Soc.* **1974**, *96*, 6757–6759.
[106] R. Kaptein, E. R. P. Zuiderweg, R. Scheek, R. Boelens, W. F. van Gunsteren, *J. Mol. Biol.* **1985**, *182*, 179–182.
[107] G. M. Clore, A. M. Gronenborn, A. T. Brünger, M. Karplus, *J. Mol. Biol.* **1985**, *186*, 435–455.
[108] M. P. Allen, D. J. Tildesly, *Computer Simulations of Liquids*, Wiley, New York, **1987**.
[109] J. A. McCammon, S. Harvey, *Dynamics of Proteins and Nucleic Acids*, Cambridge University Press, Cambridge, **1987**.
[110] C. L. Brooks III, M. Karplus, B. M. Pettitt, *Proteins: A Theoretical Perspective of Dynamics, Structure and Thermodynamics*, Wiley, New York, **1988**.
[111] J. M. Haile, *Molecular Dynamics Stimulation*, Wiley, New York, **1992**.
[112] W. F. van Gunsteren, H. J. C. Berendsen, *Angew. Chem.* **1990**, *102*, 1020–1055; *Angew. Chem. Int. Ed. Engl.* **1990**, *29*, 992–1023.
[113] W. Braun, N. Go, *J. Mol. Biol.* **1985**, *186*, 611–626.
[114] W. Braun, *Q. Rev. Biophys.* **1987**, *19*, 115–157.
[115] G. M. Crippen, T. F. Havel, *Distance Geometry and Molecular Conformation*, Wiley, New York, **1988**.
[116] T. F. Havel, *Prog. Biophys. Mol. Biol.* **1991**, *56*, 33–56.
[117] A. T. Hagler, E. Huler, S. Lifson, *J. Am. Chem. Soc.* **1974**, *96*, 5319–5327.
[118] F. A. Momany, R. F. McGuire, A. W. Burgess, H. A. Scheraga, *J. Phys. Chem.* **1975**, *79*, 2361–2383.
[119] S. J. Weiner, P. A. Kollman, D. T. Nguygen, D. A. Case, *J. Comput. Chem.* **1986**, *7*, 230–249.
[120] B. R. Brooks, R. E. Bruccoleri, B. D. Olafson, D. J. States, S. Swaminathan, M. Karplus, *J. Comput. Chem.* **1986**, *7*, 591–608.
[121] W. F. van Gunsteren, H. J. C. Berendsen, *Groningen Molecular Simulation (GROMOS) Library Manual*, Biomos, Groningen, The Netherlands, **1987**.
[122] N. L. Allinger, Y. H. Huh, J.-H. Lii, *J. Am. Chem. Soc.* **1989**, *111*, 8551–8566; J.-H. Lii, N. L. Allinger, *ibid.* **1989**, *111*, 8566–8575, 8776–8582.
[123] V. F. Bystrov, Y. D. Gavrilov, V. T. Ivanov, Y. A. Ovchinnikov, *Eur. J. Biochem.* **1977**, *78*, 63–82.
[124] A. DeMarco, M. Llinas, K. Wüthrich, *Biopolymers* **1978**, *17*, 2727–2742.
[125] A. Pardi, M. Billeter, K. Wüthrich, *J. Mol. Biol.* **1984**, *180*, 741–751.
[126] D. Cowburn, D. H. Live, A. J. Fischman, W. C. Agosta, *J. Am. Chem. Soc.* **1983**, *105*, 7435–7442.
[127] P. Schmieder, H. Kessler, *Biopolymers* **1992**, *32*, 435–440.
[128] D. de Vlieg, R. Boelens, R. M. Scheek, R. Kaptein, W. F. van Gunsteren, *Isr. J. Chem.* **1986**, *27*, 181–186.
[129] A. D. Kline, W. Braun, K. Wüthrich, *J. Mol. Biol.* **1988**, *204*, 675–694.
[130] M. J. Moore, D. A. Case, W. J. Chazin, G. P. Gippert, T. F. Havel, R. Powls, P. E. Wright, *Science* **1988**, *240*, 314–317.
[131] T. F. Havel, K. Wüthrich, *J. Mol. Biol.* **1985**, *182*, 281–294.
[132] S. Ludvigsen, F. M. Poulsen, *J. Biomol. NMR* **1992**, *2*, 227–233.
[133] H. Nicholson, E. Söderlind, D. E. Tronrud, B. W. Matthews, *J. Mol. Biol.* **1989**, *210*, 181–193.
[134] J. Overington, M. S. Johnson, A. Sali, T. L. Blundell, *Proc. R. Soc. London B* **1990**, *241*, 132–145.
[135] G. N. Ramachandran, C. Ramakrishnan, V. Sasisekharan, *J. Mol. Biol.* **1963**, *7*, 95–99.
[136] R. K. Konat, D. F. Mierke, H. Kessler, B. Kutscher, M. Bernd, R. Voegeli, *Helv. Chim. Acta* **1993**, *76*, 1649–1666.
[137] D. F. Mierke, T. Huber, H. Kessler, *J. Comput. Aided Mol. Des.* **1994**, *8*, 29–40.
[138] H.-R. Loosli, H. Kessler, H. Oschkinat, H.-P. Weber, T. J. Petcher, A. Widmer, *Helv. Chim. Acta* **1985**, *68*, 682–704.
[139] P. E. Hansen, *Prog. Nucl. Magn. Reson. Spectrosc.* **1983**, *14*, 175–296.
[140] F. A. A. M. de Leeuw, C. Altona, H. Kessler, W. Bermel, A. Friedrich, G. Krack, W. E. Hull, *J. Am. Chem. Soc.* **1983**, *105*, 2237–2246.
[141] H. Kessler, C. Griesinger, J. Lautz, A. Müller, W. F. van Gunsteren, H. J. C. Berendsen, *J. Am. Chem. Soc.* **1988**, *110*, 3393–3396.
[142] O. Jardetzki, *Biochim. Biophys. Acta* **1980**, *621*, 227–232.
[143] A. E. Torda, R. M. Scheek, W. F. van Gunsteren, *Chem. Phys. Lett.* **1989**, *157*, 289.
[144] A. E. Torda, R. M. Scheeck, W. F. van Gunsteren, *J. Mol. Biol.* **1990**, *214*, 223–235.
[145] A. E. Torda, R. M. Brunner, T. Huber, H. Kessler, W. F. van Gunsteren, *J. Biomol. NMR* **1993**, *3*, 55–66.
[146] D. A. Pearlman, *J. Biomol. NMR* **1994**, *4*, 279–299.
[147] F. A. A. M. de Leeuw, C. Altona, H. Kessler, *J. Am. Chem. Soc.* **1983**, *105*, 2237–2246.
[148] Z. L. Mädi, C. Griesinger, R. R. Ernst, *J. Am. Chem. Soc.* **1990**, *112*, 2908–2914.
[149] R. Deslaurier, I. C. P. Smith, *Top. Carbon-13C NMR Spectrosc.* **1976**, *2*, 1–80.
[150] H. Kessler, A. Friedrich, G. Krack, W. E. Hull, *Proc. Am. Pept. Symp. 7th* **1981**, 335–338.
[151] J. Kenmik, C. P. M. van Mierlo, R. M. Scheek, T. E. Creighton, *J. Mol. Biol.* **1993**, *230*, 312–322.
[152] D. F. Mierke, R. M. Scheek, H. Kessler, *Biopolymers* **1994**, *34*, 559–563.
[153] K. Wüthrich, M. Billeter, W. Braun, *J. Mol. Biol.* **1983**, *169*, 949–961.
[154] P. L. Weber, R. Morrison, D. Hare, *J. Mol. Biol.* **1988**, *204*, 483–487.
[155] T. A. Holak, D. Gondol, J. Otlewski, T. Wilusz, *J. Mol. Biol.* **1989**, *210*, 635–648.
[156] N. A. J. van Nuland, J. Grutzinger, K. Dijkstra, R. M. Scheek, G. T. Robillard, *Eur. J. Biochem.* **1992**, *210*, 881–891.
[157] S. Golic Grdadolnik, D. F. Mierke, G. Byk, I. Zeltser, C. Gilon, H. Kessler, *J. Med. Chem.* **1994**, *37*, 2145–2152.
[158] K. Bock, C. Pedersen, *J. Chem. Soc. Perkin Trans. 2* **1974**, 293–297.
[159] S. Wolfe, B. M. Pinto, V. Varma, R. Y. N. Leung, *Can. J. Chem.* **1990**, *68*, 1051–1062.
[160] H. Egli, W. von Philipsborn, *Helv. Chim. Acta* **1981**, *64*, 976–988.
[161] D. F. Mierke, S. Golic Grdadolnik, H. Kessler, *J. Am. Chem. Soc.* **1992**, *114*, 8283–8284.
[162] G. W. Vuister, F. Delaglio, A. Bax, *J. Am. Chem. Soc.* **1992**, *114*, 9674–9675.
[163] G. W. Vuister, A. Bax, *J. Biomol. NMR* **1994**, *4*, 193–200.
[164] L. E. Kay, B. Brooks, S. W. Sparks, D. A. Torchia, A. Bax, *J. Am. Chem. Soc.* **1989**, *111*, 5488–5490.
[165] L. E. Kay, A. Bax, *J. Magn. Reson.* **1990**, *86*, 110–126.
[166] T. Jippo, O. Kamo, K. Nagayama, *J. Magn. Reson.* **1986**, *66*, 344–348.
[167] D. Uhrin, T. Liptaj, M. Hricovini, P. Capek, *J. Magn. Reson.* **1989**, *85*, 137–140.
[168] G. Bodenhausen, R. Freeman, G. A. Morris, D. L. Turner, *J. Magn. Reson.* **1978**, *21*, 75–95.
[169] A. Bax, R. Freeman, *J. Am. Chem. Soc.* **1982**, *104*, 1099–1100.
[170] B. Coxon, *J. Magn. Reson.* **1986**, *66*, 230–239.
[171] T. Parella, F. Sánchez-Ferrando, A. Virgili, *Magn. Reson. Chem.* **1994**, *32*, 343–347.
[172] H. Oschkinat, A. Pastore, P. Pfändler, G. Bodenhausen, *J. Magn. Reson.* **1986**, *69*, 559–566.
[173] R. Brüschweiler, J. C. Madsen, C. Griesinger, O. W. Soørensen, R. R. Ernst, *J. Magn. Reson.* **1987**, *73*, 380.
[174] J. Cavanagh, J. P. Waltho, J. Kecler, *J. Magn. Reson.* **1987**, *74*, 386–393.
[175] W. Willker, D. Leibfritz, *J. Magn. Reson.* **1992**, *99*, 421–425.
[176] M. D. Sørensen, S. M. Kristensen, J. J. Led, O. W. Sørensen, *J. Magn. Reson. Ser. A* **1993**, *103*, 364–368.
[177] R. Weisemann, H. Rüterjans, H. Schwalbe, J. Schleucher, W. Bermel, C. Griesinger, *J. Biomol. NMR* **1994**, *4*, 231–240.
[178] S. D. Emerson, G. T. Montelione, *J. Am. Chem. Soc.* **1992**, *114*, 354–356.
[179] H. Kessler, U. Anders, G. Gemmecker, *J. Magn. Reson.* **1988**, *78*, 382–388.
[180] M. Sattler, H. Schwalbe, C. Griesinger, *J. Am. Chem. Soc.* **1992**, *114*, 1126–1127.
[181] E. R. P. Zuiderweg, S. W. Fesik, *J. Magn. Reson.* **1991**, *93*, 653–658.
[182] U. Eggenberger, Y. Karimi-Nejad, H. Thüring, H. Rüterjans, C. Griesinger, *J. Biomol. NMR* **1992**, *2*, 583–590.

[183] G. Wagner, N. R. Nirmala, G. T. Montelione, S. Hyberts, *Frontiers of NMR in Molecular Biology*, Liss, New York, **1990**, pp. 129–143.
[184] P. Schmieder, V. Thanabal, L. P. McIntosh, F. W. Dahlquist, G. Wagner, *J. Am. Chem. Soc.* **1991**, *113*, 6323–6324.
[185] G. Wagner, P. Schmieder, V. Thanabal, *J. Magn. Reson.* **1991**, *93*, 436–440.
[186] G. T. Montelione, S. D. Emerson, B. A. Lyons, *Biopolymers* **1992**, *32*, 327–334.
[187] J. C. Madsen, O. W. Sørensen, P. Sørensen, F. M. Poulsen, *J. Biomol. NMR* **1993**, *3*, 239–244.
[188] M. Görlach, M. Wittekind, B. T. Farmer, L. E. Kay, L. Mueller, *J. Magn. Reson. Ser. B* **1993**, *101*, 194–197.
[189] W. Willker, U. Wollborn, D. Leibfritz, *J. Magn. Reson. Ser. B* **1993**, *101*, 83–86.
[190] S. Seip, J. Balbach, H. Kessler, *J. Magn. Reson. Ser. B* **1994**, *104*, 172–179.
[191] K. V. R. Chary, G. Otting, K. Wüthrich, *J. Magn. Reson.* **1991**, *93*, 218–224.
[192] P. Schmieder, S. Zimmer, H. Kessler, *Magn. Reson. Chem.* **1991**, *29*, 375–380.
[193] H. Kessler, P. Schmieder, M. Köck, M. Kurz, *J. Magn. Reson.* **1990**, *88*, 615–618.
[194] F. Löhr, H. Rütherjans, *J. Biomol. NMR* **1995**, *5*, 25–36.

Thermotropic Liquid Crystals Formed by Intermolecular Hydrogen Bonding Interactions

Constantinos M. Paleos* and Dimitris Tsiourvas

The role of hydrogen bonding in the formation or stabilization of liquid crystalline phases has only recently been appreciated. Following the first, well-established examples of liquid crystal formation from the dimerization of aromatic carboxylic acids, through hydrogen bonding, several classes of compounds have recently been synthesized, the liquid crystalline behavior of which is also dependent on intermolecular hydrogen bonds between similar or dissimilar molecules. In this review the main classes of compounds exhibiting liquid crystallinity due to hydrogen bonding are presented to show the diversity of organic compounds that can be used as building elements in liquid crystals. The molecules are either of the rigid-rod anisotropic or amphiphilic types such as molecules appropriately functionalized with pyridyl and carboxyl groups, whose interaction leads to the formation of liquid crystals; amphiphilic carbohydrates and amphiphilic and bolaamphiphilic compounds with multiple hydroxyl groups whose dimerization or association is indispensable for the formation of liquid crystals; and certain amphiphilic carboxylic acids with monomeric or polymeric mesogens and amphiphilic-type compounds bearing different moieties, whose interaction may lead to the formation of mesomorphic compounds. Associated with the macroscopic display of liquid crystalline phases is the supramolecular structure, and therefore rather extended discussion of these structures are included in this review.

Keywords: hydrogen bonds · liquid crystals · supramolecular chemistry

1. Introduction

Intermolecular hydrogen bonds have been considered of crucial importance in inducing aggregation in nature. The most well-known example of hydrogen bonding in the biological world is the interaction of complementary nucleobases stabilizing the double helical structure of nucleic acids. However, in liquid crystals, whose formation is attributed to intermolecular interactions, the role of hydrogen bonding has not been greatly appreciated, in particular during the early years of research in this area, and only a limited number of publications and reviews[1–6] deal with the subject. This development is probably related to the fact that simple compounds such as phenols and amines, which form hydrogen bonds, are not generally mesomorphic. The investigation of the synthesis and characterization of hydrogen-bonded liquid crystals was thus somewhat delayed.

The first compounds found to exhibit liquid crystalline behavior due to hydrogen bond formation were carboxylic acids.[1–2] These compounds dimerize through intermolecular hydrogen bonds leading to a lengthening of the rigid-rod moiety, which in turn induces liquid crystallinity. Among the carboxylic acids that form liquid crystalline phases are *trans-p*-methoxy- and *trans-p*-ethoxycinnamic acids[1, 7] and their higher alkoxy derivatives,[8] as well as *p-n*-alkoxybenzoic acids.[1, 9] Aliphatic carboxylic acids do not generally exhibit mesomorphic character. However 2,4-nonadienoic acid is liquid crystalline[10] due to the presence of the double bonds, which because of their polarizabilities increase the intermolecular attraction between the molecules. Another interesting case of liquid crystallinity exhibited by an aliphatic carboxylic acid is that of 2-hydroxy-1,2,3-nonadecanetricarboxylic acid reported in 1919.[11] The segregation of the aliphatic lipophilic moiety from the hydrophilic carboxyl groups and the hydroxyl group, coupled with their ability to form multiple hydrogen bonds, explains the liquid crystalline behavior. This is in line with the now-accepted views on the formation of liquid crystals from analogous compounds, as will be discussed further below.

The two components of the acceptor–donor complex may or may not be mesomorphic. In both cases, however, and primarily for nonmesomorphic molecules, hydrogen bonding is responsible for the formation of liquid crystalline phases. As will be examined further below, this mode of liquid crystal formation can be extended to polymers with structures modified by hydrogen bonds.

Hydrogen bonding has also been employed for the formation of liquid crystals derived from amphiphilic mesogens[6] consisting of two distinct and segregated segments, one hydrophobic

[*] Dr. C. M. Paleos, Dr. D. Tsiourvas
NRC "Demokritos"
15310 Aghia Paraskevi, Attiki (Greece)
Telefax: Int. code + (1651)1766

and one hydrophilic. Here, the hydrophilic moiety is a group that can form one or more hydrogen bonds leading to the formation of thermotropic liquid crystals (in analogy to ionic or nonionic amphiphiles). As with typical amphiphiles, in hydrogen-bonded amphiphiles segregation occurs between the polar groups primarily hydroxyl or carboxyl groups—and the lipophilic segments. This is the driving force for the formation of lamellar or discotic structures. Among the classes of compounds that have been found to form thermotropic liquid crystals and molecular organizates in solution are certain carbohydrate amphiphiles, some polyhydroxy compounds, and long-chain alkyl derivatives of iminodiacetic acid. In addition, a novel class of amphiphilic liquid crystalline materials now under development is prepared by molecular recognition, through the formation of multiple hydrogen bonds between amphiphiles bearing complementary groups. From this introductory discussion it is apparent that hydrogen bonding either extends the rigid-rod structure of the mesogens resulting in stabilization of the liquid crystalline phases, or it positively affects the segregation of the polar and the lipophilic groups inducing the formation of liquid crystals.

2. Liquid Crystalline Behavior of Anisotropic, Hydrogen-Bonded, Rigid-Rod Molecules

2.1. Hydrogen-Bonded Liquid Crystals from Monomeric Mesogens

Hydrogen-bonded systems composed of different components, for example molecules bearing pyridyl or bipyridyl moieties and carboxylic acid molecules, have been used to prepare new liquid crystals or stabilize already existing liquid crystalline materials. This type of interaction is shown schematically in Figure 1 and can be described in the terminology of structural chemistry as a molecular self-complementary system.[12]

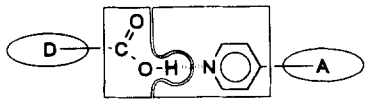

Fig. 1. Schematic representation of the interaction of pyridyl and carboxyl groups (from ref. [12]).

Liquid crystalline complex **1** was formed by the intermolecular interaction of 4-butoxybenzoic acid (nematic range 147–160 °C) with *trans*-4-[(4-ethoxybenzoyl)oxy]-4′-stilbazole (nematic range 165–213 °C).[13] Complex **1** exhibits a smectic phase as evidenced by its focal conic texture (range

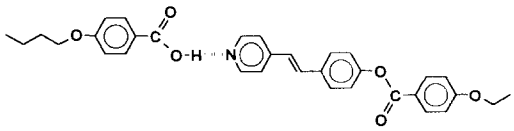

1

136–160 °C), which was not exhibited by either of the individual components. However, this transition was not apparent in DSC studies, and the observed smectic texture has not not been characterized. The subsequent nematic phase appeared in the region 160–238 °C. The stabilization of the mesophase of the 1:1 complex **1** was attributed to the formation of a new and elongated mesogen through intermolecular hydrogen bonding which allows **1** to behave as a one-component, liquid crystalline compound. The formation of the complex was supported by FTIR measurements, which show that the spectrum of the 4-butoxy benzoic acid dimer was replaced by that of complex **1**. The primarily adopted method for the preparation of complex **1** and analogous liquid crystalline compounds is the slow evapo-

Constantinos M. Paleos was born in 1941 in Chios, Greece, and studied chemistry from 1960 to 1964 at the Universities of Salonica and Athens, where he obtained his undergraduate degree in chemistry. He received his Ph.D. at Drexel University in Philadelphia, USA, under the supervision of Dr. M. M. Labes for studies on reactivity in liquid crystalline media. In 1973, after three years with Standard Oil (Illinois) and Motor Oil (Athens), he joined the Institute of Physical Chemistry at the National Center for Scientific Research "Demokritos" in Athens, where he has been Director since 1994. From 1991 to 1992 he was visiting professor at the University of Strasbourg. His main research interests include the formation and characterization of novel liquid crystals resulting from molecular recognition of complementary molecules, and the development of organized molecular assemblies such as micelles, vesicles, and liquid crystals.

Dimitris Tsiourvas was born in 1962 in Larisa, Greece, and completed his undergraduate studies in chemical engineering at the National Technical University of Athens. He obtained his Ph.D. at "Demokritos" in 1992 under the direction of Dr. C. M. Paleos for research on liquid crystals formed from polymeric mesogens. He is currently employed by the Research and Development Department of ARGO SA and collaborates with the Institute of Physical Chemistry at Demokritos. His research focuses on the synthetic and physicochemical aspects of supramolecular organization and molecular recognition.

ration of an equimolar solution of the components in pyridine. In this way the hydrogen bonds of 4-butoxybenzoic acid dimer were broken.

In similar fashion mesogens **2** were formed by hydrogen bond formation between a nonmesogenic dicarboxylic acid with $n = 5-9$ and mesogenic *trans*-4-[(ethoxybenzoyl)oxy]-4′-stilbazole.[14] These compounds form twin-type liquid crystalline complexes[14] and exhibit both smectic and nematic phases. These complexes display an effect dependent on the number of C atoms (odd–even effect) similar to that reported for twin-type liquid crystals formed through covalent bonding between a mesogen and a flexible spacer.[15]

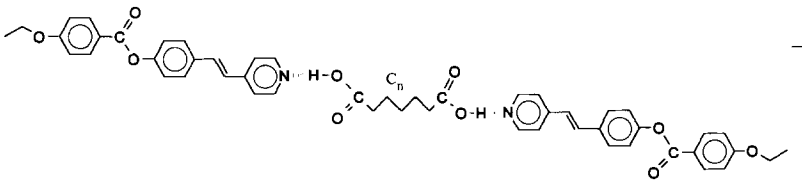

2

Liquid crystalline complexes were formed by treating 4-alkoxybenzoic acids ($n = 1-8$, 10) or alkylbenzoic acids ($n = 4$, 5, 8) with 4,4′-bipyridine[16] or *trans*-1,2-bis(4-pyridyl)ethylene.[16, 17] For instance, liquid crystals **3** and **4** formed by hydrogen bond formation between 4,4′-bipyridine and 4-butyl- or 4-butoxybenzoic acid in a molar ratio of 1:2. Sharp phase transitions and homogeneous mesophases were observed. Complex **3** exhibits only a smectic phase that it is not observed for either single component, while complex **4** shows both smectic and nematic phases.

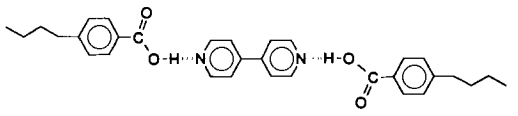

3

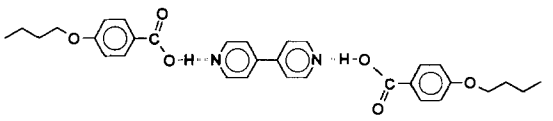

4

The interaction of phthalic or isophthalic acid with *trans*-4-alkoxy-4′-stilbazole ($n = 7$, 8, and 10) led to complexes **5** and **6** with bent structures.[12] The complexes exhibit liquid crystalline behavior even though they are not linear and the mesogenic groups form an angle. It is interesting to note that compounds consisting of covalently bonded, nonlinear structural units do not generally exhibit liquid crystallinity.[12]

In analogous fashion, the interaction of two stilbazole units linked by a triethyleneglycol spacer, in other words a nonmesogenic compound, with fatty and aromatic acids yielded liquid crystalline compounds **7** and **8**, respectively.[18] Monotropic smectic B phases were observed for complexes with carboxylic

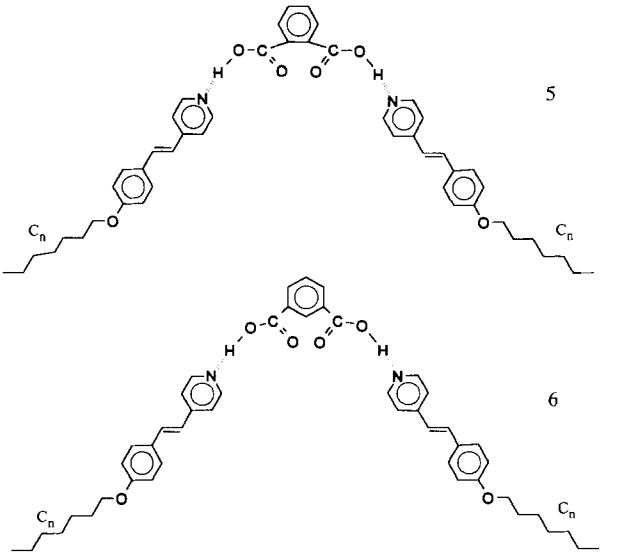

5

6

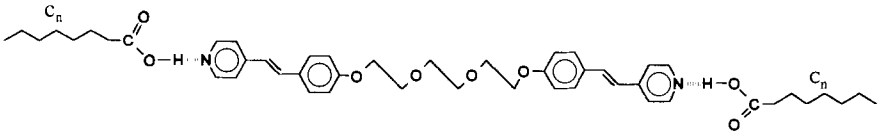

7

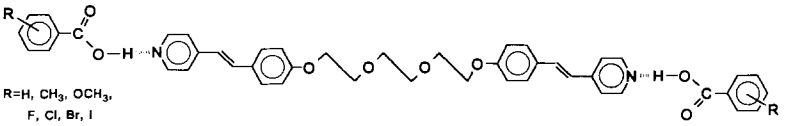

8

acids ranging from nonanoic up to tetradecanoic acids. Enantiomeric nematic and in some cases monotropic smectic A phases were obtained with 4-methyl-, 4-methoxy-, and 4-halobenzoic acids as donors. The stability of the induced mesophases decreased with 3- and 2-substituted benzoic acids, and with aliphatic dicarboxylic acid donors liquid crystalline phases were not observed.

Liquid crystals of the general formula **9** with a mesomorphic range near room temperature formed by complex formation between 4-alkoxybenzoic acids ($n = 6-8$, 10, 12) and 4-octyl pyridine. Thus, the simple hydrogen-bonded complex that results from two nonmesogenic aromatic compounds is sufficient to induce a nematic phase below 50 °C. Nematic phases are broadened by mixing several 1:1 complexes within this homologous series.

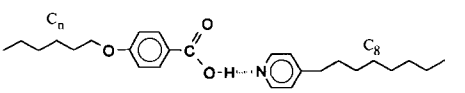

9

Ferroelectric liquid crystals like **10** have also been prepared by hydrogen bond formation between the mono-2(methylbutyl)

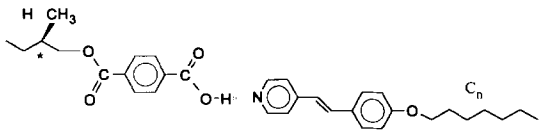

10

ester of terephthalic acid and 4-alkoxy-4'-stilbazoles with a smectic B phase ($n = 1-10$, 12, 14, 16).[20] Depending upon the chain length of the components in the complexes, blue phases, chiral nematic (N*) phases, and chiral smectic C (S_c^*) phases were obtained.

In analogous experiments Kresse et al.[21] investigated liquid crystalline materials obtained from selected monocarboxylic or dicarboxylic acids and alkylpyridine derivatives or bipyridine. One of the conclusions of this study is that the length of the pyridine component is important for inducing stability in the liquid crystalline phase of the complex, at least at the low temperatures at which the (pyridine)N $\cdots$ H–O bond is not broken.

It is therefore apparent that by simply mixing compounds functionalized by carboxyl and pyridyl groups in the bulk or in solution a wealth of liquid crystalline materials are formed with broad mesomorphic ranges. These complexes have been investigated mainly by thermal, optical, and FTIR spectroscopic studies.[22]

Early examples of complexes not bearing a central pyridyl–carboxyl unit that self-organize through multiple hydrogen bonds are the diacylhydrazines **11** ($n = 5-7$), **12** ($n = 5-9$), and **13** ($n = 6-9$), which were synthesized by Schubert et al.[23a] These compounds exhibit relatively broad smectic liquid crystalline phases. Models of their supramolecular structures were not presented by the authors. Another class of compounds, the chiral carbonylbis(amino acid esters),[23b] which bear a urea moiety, was investigated as early as 1973 and found to exhibit smectic mesophases. It was suggested that formation of hydrogen bonds between the urea moieties would yield supramolecular structures of parallel molecular layers, thus explaining the appearance of smectic liquid crystalline phases. These mesogens and analogous compounds resulting from the simple functionalization of urea warrant further investigation for the development of new hydrogen-bonded liquid crystals.

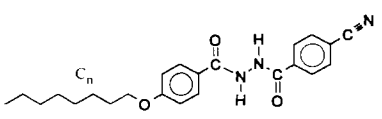

11

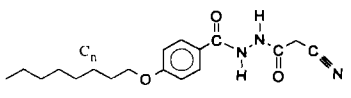

12

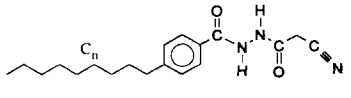

13

The previously mentioned mesogenic diacylhydrazines are not the only examples of compounds that self-assemble through hydrogen bond formation and exhibit liquid crystalline properties. It has been reported[24] that hydrogen bonding enhances the possibility of the exhibition of smectic C phase in troponoid-based liquid crystals **14** ($m = 6$, 8, 11, 12, 14, 18 and $n = 1$, 4, 12) and **15** ($m = 12$, 14, 18 and $n = 8$, 10, 12, 18). Considering intermolecular hydrogen bonding, two arrangements may be envisaged for these compounds in the liquid crystalline phase: the folded and extended structures shown in Figure 2. The extended structure explains the appearance of the smectic C phase, since the molecules are tilted with respect to the layer plane. It should be noted that only molecules with long alkyl chains exhibit the smectic C phase; those with short chains are nonmesomorphic, since hydrogen bonding raises the melting point above the mesophase–isotropic transition.

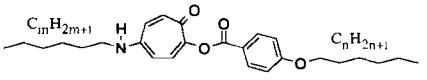

14

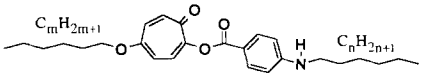

15

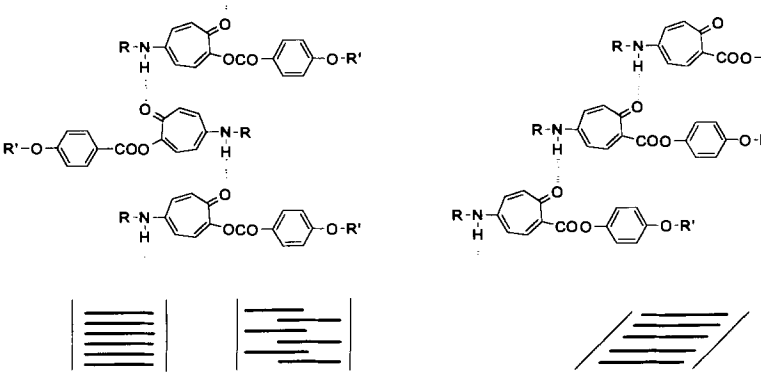

Fig. 2. Molecular arrangements for compound **14**: folded (left) and extended structure (right) (from ref. [24]).

2.2. Hydrogen-Bonded Liquid Crystals Formed from Polymeric Mesogens

Liquid crystalline phases in polymers can be stabilized or induced by interaction of carboxyl and pyridyl moieties. Liquid crystalline polymers bearing a carboxyl in the side chain were mixed with 4-*trans*-stilbazole derivatives bearing a pyridyl group, and the effect on their mesomorphic properties was investigated. In this way polymer **16** was formed by the interaction

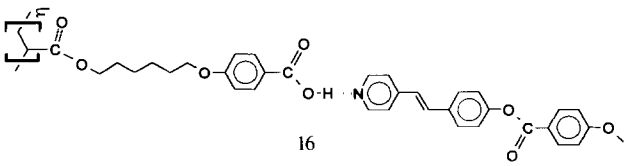

16

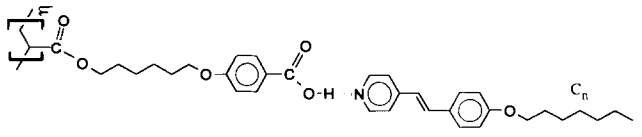

17

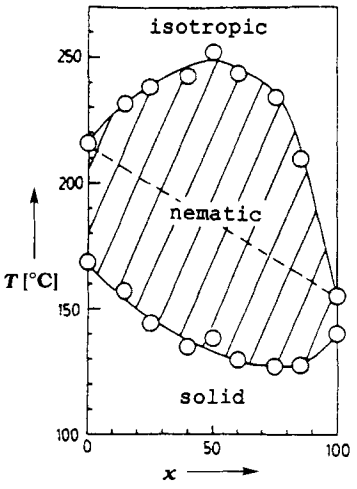

Fig. 3. Phase diagram of the binary mixture of the components forming polymer **16**, i.e. a poly(acrylic acid) and a *trans*-stilbazole ester derivative (from ref. [25]). x = mole ratio.

of a poly(acrylic acid) derivative with a *trans*-stilbazole ester.[25] Both components exhibit mesomorphic behavior: the polymer has a mesomorphic range between 140 and 155 °C and *trans*-stilbazole derivative between 168 and 216 °C. These two components are miscible over the whole range of composition, and the binary mixture exhibits a broad mesomorphic range (Fig. 3). This extension of the temperature range of liquid crystallinity again results from the formation of an extended mesogenic unit through hydrogen bond formation. Furthermore, a similar polymer was complexed with various *trans*-4-alkoxy-4′-stilbazoles having a linear alkyl chain spacer ($\eta = 1-8$ and 10) to afford compounds **17**.[26] Thermally stable smectic A phases were formed, and the isotropization and melting temperatures depend on the number of carbon atoms in the terminal alkoxy group (odd–even effect). Analogous monomeric 1:1 complexes were also prepared which, as expected, show lower transition temperatures than the polymeric complexes.

Combining the same poly(acrylic acid) derivative with the bifunctional hydrogen bond acceptor 4,4′-bipyridine and also with the monofunctional acceptor *trans*-4-hexyloxy-4′-stilbazole yielded the cross-linked polymer **18** in which two polymer

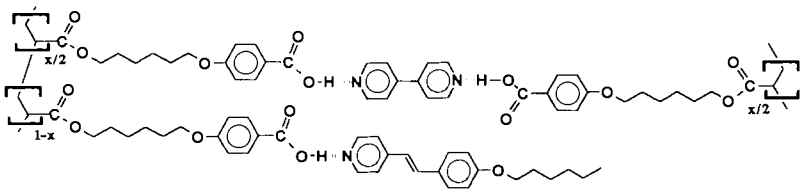

18

chains are bound.[27] As the proportion of the bifunctional acceptor increased, the glass transition also increases and the melting temperature decreases. The 1:1 complexes show mesomorphic character for the whole composition range of hydrogen bond acceptors. The isotropization temperature is roughly 200 °C for all these complexes. Reversible (noncovalent) cross-linking is assumed, since the smectic–isotropic transitions are reversible. On heating to the isotropic phase, some of the hydrogen bonds between the carboxyl group and the bipyridyl group are broken. On cooling from the isotropic melt, some of the hydrogen bonds are reformed, affording the smectic phase again. It should be noted that for covalently bonded and highly cross-linked polymers, molecular orientations are preserved in the solid phase and mesomorphic character is not observed.[26]

Similarly, polysiloxanes, specifically poly(methylsiloxanes) and poly(methyl-*co*-dimethylsiloxanes) with a benzoic acid moiety in their side chain, which themselves exhibit liquid crystalline properties due to dimerization, form hydrogen bonds with the mesogenic *trans*-4-[(4-methoxybenzoyl)oxy]-4′-stilbazole and the nonmesogenic *trans*-4-ethoxy-4′-stilbazole, affording polymers **19** and **20**, respectively, with $x = 5, 8, 10$.[28] Stilbazoles are

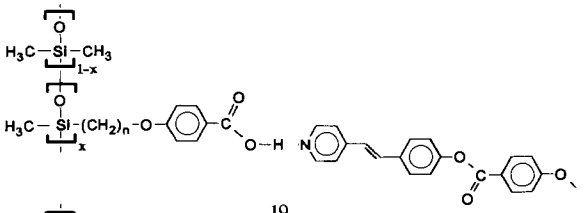

19

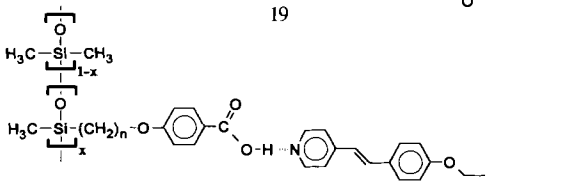

20

used so frequently as hydrogen bond acceptors because of the high enthalpy value for the formation of complexes between carboxyl and pyridine groups.[29] In this case it has also been established that formation of a liquid crystalline complex of a side-chain polymer does not require that either of the hydrogen bonding components exhibit liquid crystallinity. In addition, these polymers are completely miscible over the whole composition range and the liquid crystalline phase has excellent thermal stability. X-ray diffraction studies on nonoriented samples show smectic C or A phases for the various hydrogen-bonded complexes.

Polymers with potential practical applications were prepared by combining polymeric donors with acceptors bearing appropriate functionalities. Thus polysiloxane donors bearing a pendant propyloxybenzoic acid group were mixed with stilbazole-*N*-oxide as an acceptor leading to the formation of the polymers **21** (**21a**: $x = 1.00$, Y = H; **21b**: $x = 1.00$, Y = F; **21c**: $x = 0.43$, Y = H; **21d**: $x = 0.43$, Y = F).[30] These polymers exhibit

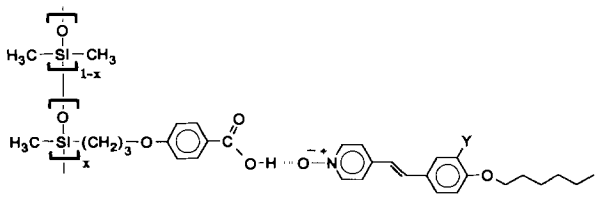

21

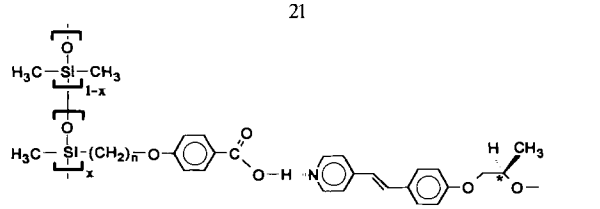

22

smectic A or smectic C phases above their glass-transition temperature, and since none of the components of the complexes exhibit liquid crystalline behavior, the observed phases reflect the formation of mesogenic moieties by hydrogen bonding. The strong dipole along the molecular axis is expected to result in liquid crystalline materials with strong positive dielectric anisotropy, which is a prerequisite for certain electrooptic applications.

In studies of analogous polysiloxanes ferroelectricity was induced when polysiloxanes bearing a pendant *p*-alkoxybenzoic acid group were complexed with the optically active (*S*)-(−)-*trans*-4-(2-methoxypropyloxy)-4′-stilbazole forming polymers **22** ($n = 5$, $x = 0.29$; $n = 5$, $x = 0.43$; $n = 8$, $x = 0.29$; $n = 8$, $x = 0.43$).[31] X-ray diffraction data of annealed unoriented samples showed an intense ring, sometimes accompanied by its second-order reflection which, together with the spontaneous polarization of the polymers, point to the formation of a smectic C phase composed of two overlapping hydrogen-bonded moieties. In **22** the $S_A \rightarrow S_C$ phase transition was proved by optical microscopy but not by DSC measurements.

In a recent study the interaction of 4-polyvinylpyridine with a mesogenic biphenyl derivative bearing a carboxyl group at one end gave polymer **23**. The monotropic liquid crystalline phase

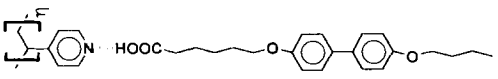

23

observed for the mesogenic compound alone disappears on mixing, and the mesophases of the resulting complexes are dependent on the ratio of interacting components and exhibited thermal stability.[32]

A reaction analogous to polycondensation may occur when dicarboxylic acid **24a** is mixed with bipyridines **24b–d**, which contain two pyridyl groups. All three complexes form enantiotropic nematic mesophases, while their starting components do not have liquid crystalline properties.[33] In complexes **24a**/**24b** and **24a**/**24d** the nematic–isotropic transition exhibits only a small hysteresis, while this is quite large, about 25 °C, for complex **24a**/**24c**. In addition polymer **24a**/**24b** exhibits smectic A phase, as evidenced by the focal conic fan-type texture in polarized light microscopy.

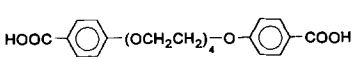

24a

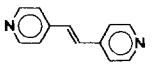

24b

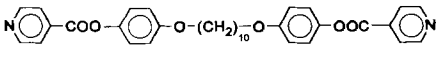

24c

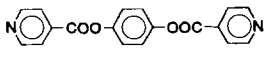

24d

To conclude the discussion on monomeric and polymeric liquid crystals resulting from the interaction of pyridyl and carboxyl groups, we will briefly describe a model of these systems.[34] The mesogen complexes are termed "living systems", since their bonding properties are determined by subtle interactions. Because of the weak hydrogen bonding interactions the complexes form, separate, and recombine at the melt temperature. In the models presented for a "living" low molecular weight nematic and a "living" liquid crystalline polymer, nematic effects induce hydrogen bonding between the components, resulting in discontinuous jumps in concentration variables at the nematic–isotropic transition.

3. Hydrogen-Bonded Liquid Crystalline Compounds Derived from Amphiphilic Mesogens

3.1. Liquid Crystalline Behavior of Amphiphilic Carbohydrates

The structural versatility of carbohydrate moieties provides the basis for the synthesis of a great variety of amphiphilic carbohydrates. The first example of an amphiphilic liquid crystalline carbohydrate was a β-hexadecyl-D-glucoside prepared by E. Fischer et al.[35] more than eighty years ago. This compound showed an "anomalous" melting behavior which could not be explained at the time. Two years later Salway[36] synthesized ceryl-β-D-glucopyranosides which had similar melting behavior. No mention was made of liquid crystallinity at that time; it was thought that two modifications had been obtained. The subject of carbohydrate liquid crystals was neglected for many years. In one paper, which appeared in 1938, Noller et al.[37] interpreted the "double melting" of the amphiphilic glucoside prepared by Fischer as resulting from liquid crystalline behavior. Extensive synthetic work on alkyl carbohydrates, including amphiphilic derivatives, was performed by Hori[38] in the late 1950s. Research on liquid crystalline carbohydrates intensified in the 1980s, and interest in this area continues to increase. The subject has been reviewed by Jeffrey et al.[39, 40] and van Doren et al.[41]

Carbohydrate liquid crystals are formed by the functionalization of carbohydrate moieties with one or more long aliphatic chains. Considering the wealth of carbohydrate moieties and the nature and number of aliphatic chains, it is not surprising that numerous, diverse liquid crystals have already been synthesized.[42–61] We do not intend to describe the mesomorphic properties of the known carbohydrate liquid crystals in detail; rather we will focus on supramolecular models that rationalize the macroscopic appearance of liquid crystalline phases.

From a survey of the literature it can be seen that carbohydrate amphiphiles with one lipophilic chain form smectic phases, while carbohydrates with more than one lipophilic chain typically form columnar mesophases based on the formation of hydrogen-bonded multimers.

3.1.1. Smectic Phases Resulting from Amphiphilic Carbohydrates

The *n*-alkyl-β-D-glucopyranosides reported by Goodby[42] exhibit smectic A liquid crystalline phases. A bilayer structure was postulated in which the carbohydrate moieties overlap each

other and are held together in the middle through extensive hydrogen bonding, while the alkyl chains are located in the exterior of the supramolecular structure. At about the same time Marcus and Finn[43] performed miscibility experiments for identifying the phases of *n*-decyl-β-glucopyranoside. They found that its smectic phase is thermodynamically identical to the lyotropic lamellar phase exhibited by a 20% solution of sodium bis-2-ethylhexylsulfosuccinate (Aerosol OT). In analogous manner it was found[44] that liquid crystalline phases of *n*-alkylgluconamides are miscible with those of *n*-alkyl-β-D-glucopyranosides, forming phases classified as smectic A (S_A) and tentatively as smectic A_d (S_{Ad}), in which an interdigitated bilayer structure is formed. The *d*-spacing in these phases should be equal to twice the length of the aliphatic chain plus the length of the carbohydrate moiety. It should be pointed out that in the smectic phase the molecules are in a dynamic state; the lipophilic chains are relatively flexible and the hydrogen bonds in the polar cores often break and reform as the molecules undergo reorientational motion. In the same period, however, Baeyens-Volant et al.[45] proposed a monolayer smectic phase based on the determination of the length of the *d*-spacing.

Smectic phases were also reported for the amphiphilic derivatives of 1-*O*-alkyl derivatives of 2,5-anhydrohexitols,[46] some of which are liquid crystals even at room temperature. Also, for a variety of acyclic carbohydrates, for example 1-deoxy-1-(*N*-methylalkanamido)-D-glucitols **25** ($n = 5-11$) and the closely related series of *N*-(2-(alkanamido)ethyl)-D-gluconamides **26** ($n = 5, 7, 9$) and *N*-(2-(*N*-methylalkanamido)ethyl)-D-gluconamides **27** ($n = 5, 7, 9$), it was shown[47] that they exhibit smectic A_d phases due to the interdigitated bilayer ordering of the supramolecular structures. It should also be mentioned that smectic A mesophases were observed for 1-*O*-alkyl-D-glucitols[48] originating from alkyl D-glucopyranosides and for carbohydrates incorporating calamitic mesogens.[49] For the latter compounds the introduction of the calamitic mesogenic units greatly increases the potential number of carbohydrate liquid crystalline phases and allows greater control of the thermal properties. In addition, several α- and β-glucosides were prepared,[50] and the liquid crystalline properties of mono-, di-, and trisaccharides were compared. Smectic A phases were obtained in all cases.

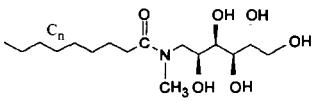

25

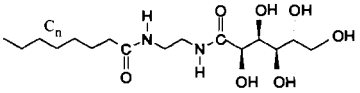

26

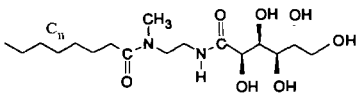

27

In a comparative paper[41] the liquid crystalline behavior of six homologous series of D-glucose and 2-deoxy-D-glucose derivatives with an amino-linked alkyl chain was investigated. All these compounds with diverse structures, **28**–**33** ($n = 7-16$), exhibit smectic A_d phases (i.e. partially overlapping structures). In all cases the *d*-spacing corresponds to $l < d < 2l$, where l is the length of the fully extended molecule and d is the calculated layer thickness.

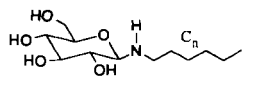

28

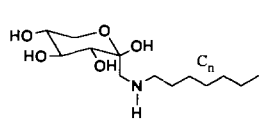

29

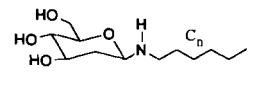

30

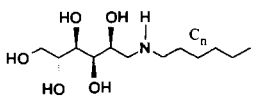

31

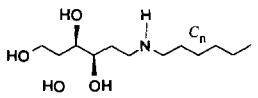

32

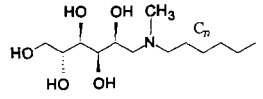

33

A_d phases are well-established for amphiphilic carbohydrates with one aliphatic chain. However, the originally proposed model for the arrangement of molecules within the layers (Model I in Fig. 4)[40, 51] has been questioned. In this model the car-

Model I

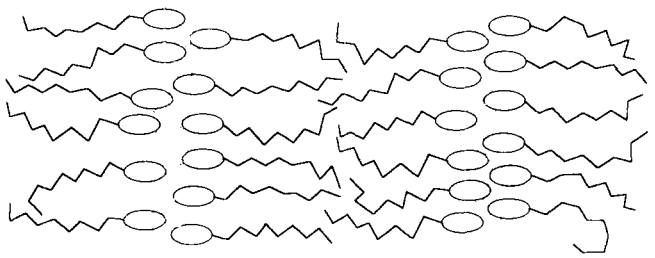

Model II

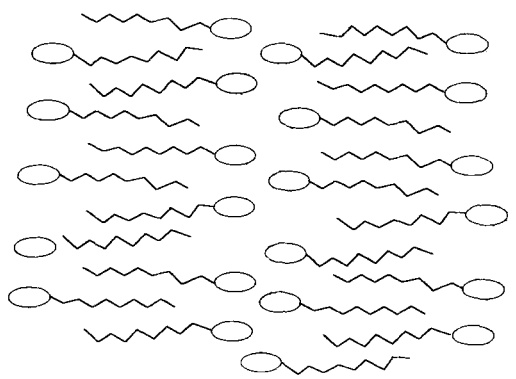

Fig. 4. Models I and II for carbohydrate mesogens.

bohydrate moieties constitute the core held together in a dynamic hydrogen bonding network, and the aliphatic chains are in the exterior of the supramolecular structure. A new model, Model II (Fig. 4), was proposed by Jeffrey[52] and further supported by van Doren and Wingert.[51] Contrary to Model I, the alkyl chains constitute the core of the smectic bilayer and the carbohydrate moieties are located on the outside. This latter model is identical, with the exception of the exclusion of water, with the lamellar lyotropic phase (L_α) and consistent with experimental data. It also explains the thermal behavior and the influence of minor structural changes in the carbohydrate moiety.[40,41] Model II corresponds to the view that carbohydrate moieties are more sensitive to the increase of thermal energy than are van der Waals forces between interdigitating alkyl chains.[40]

3.1.2. Discotic Columnar Phases from Amphiphilic Carbohydrates

Dithioacetals having two aliphatic chains were investigated[53–55] almost simultaneously by three research groups. In these studies a smectic A_d[53] and a smectic B[54] phase were identified initially. Shortly thereafter a hexagonal columnar structure[56] was assigned to these Y-shaped molecules based on X-ray diffraction data showing three sharp peaks.[56] Dithioacetals with two chains R **34**–**37** (R = C_8 unit for **34**, **35**, **37** and R = C_7–C_9 unit for **36**), although different in stereochemistry,

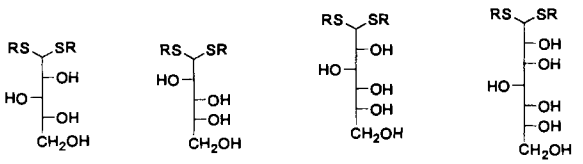

34 35 36 37

form only one type of hydrogen-bonded disk-shaped structure through multimer formation. The supramolecular structure in Figure 5, which may rationalize these findings, was proposed by Jeffrey and Wingert.[40] The terminal hydroxyl group is essential for the formation of the columnar hexagonal mesophase, since the 6-deoxy carbohydrate dithioacetals were shown not to be mesomorphic.[56]

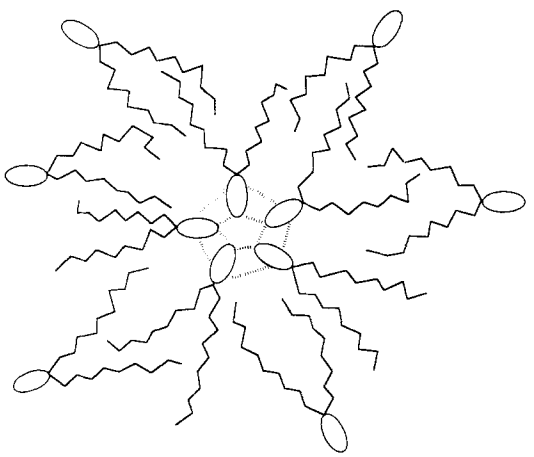

Fig. 5. Schematic representation of the molecular arrangement for the formation of a hexagonal columnar mesophase.

Similarly, 6,6-dialkyl-D-galactopyranoses with two alkyl chains also form columnar supramolecular structures due to the formation of multimers held together by hydrogen bonds. The miscibility of 6,6-di-*C*-*n*-octyl-α/β-D-galactopyranose with *S*,*S*-dioctyl-D-*arabino*-dithioacetal, which has a hexagonal-columnar structure,[57] verifies the formation of columnar phases.

Inositol(1,2,3,4,5,6-hexahydroxycyclohexane) mono-, di-, tri-, tetra-, and pentaethers allow detailed studies to be performed on the relationship between the type of substitution in the cyclohexane ring and the liquid crystalline character. The type of mesomorphism formed depends on the number and stereochemical arrangement of the hydroxyl groups, the length of alkyloxy chains, and also on their positions on the six-membered ring. Among the most important findings on the liquid crystalline behavior of inositol ethers[58] are that axial groups in these compounds weaken the mesophase since molecular symmetry does not favor the formation of mesophases, and that the transformation from hexagonal columnar to the smectic phase shown for compounds **38** and **39** is due to the stereochemical effect of two vicinal hydroxyl groups.

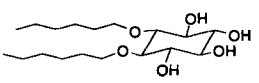

38

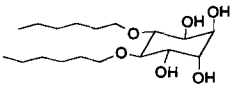

39

Further detailed studies were performed on a homologous series of cellobiose octaalkanoates[59] with alkyl chain lengths C_n ranging from $n = 7$ to $n = 14$. All the compounds form enantiotropic discotic columnar phases in which the columns are formed by the regular stacking of the cellobiose moieties in a two-dimensional lattice. The types of phases formed depend on the homologue and on the temperature. Thus homologues with $n = 9$–14 form hexagonal ordered columnar (D_{ho}) phases, whereas the member with $n = 7$ forms a rectangular ordered columnar (D_{ro}) phase. The carbohydrate with $n = 8$ forms the D_{ho} phase at higher temperatures and the D_{ro} phase at lower temperatures.

Besides the intensively investigated substituted dithioacetal carbohydrates,[53–56] several new related compounds[60] were prepared (**40**: $n = 8$; **41**: $n = 12$; **42**, $n = 12$, $m = 15$). Carbohydrates **40** and **41** exhibit enantiomeric hexagonal columnar disordered phases, as identified by polarization microscopy and X-ray diffraction. Compound **42** forms monotropic phases, the first of which has been identified as a hexagonal columnar dis-

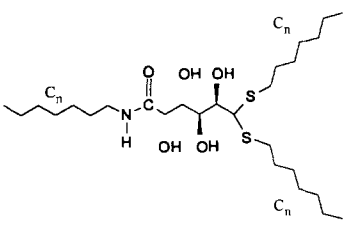

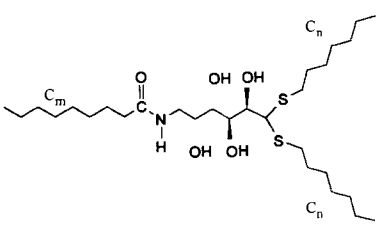

ordered (D_{hd}) phase at 91 °C, while the second as a rectangular columnar disordered (D_{rd}) phase at 70 °C. The columnar phases observed for these acyclic trialkylated compounds are surprising and in contrast to the previously mentioned dialkylated derivatives which form hexagonal columnar phases; in the former, multimers cannot form. It is suggested that the columns of **40** and **41** are constructed from single molecules stacked without preferred orientation. This arrangement is supported by strong hydrogen bording interactions and by the segregation of the hydrophilic and lipophilic moieties.

The synthesis of alkyl-6-*O*-acyl-glycopyranosides **43**–**46** by a chemoenzymatic procedure led to the development of new supramolecular model[61] for the observed liquid crystalline properties. The β-glycosides **43** and **44** form columnar discotic mesophases with clearing points above 80 °C, while the α-glycosides **45** and **46**, which presumably form discotic phases, show

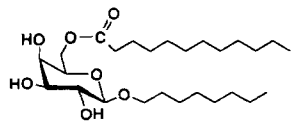

43

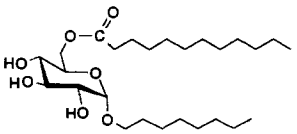

45

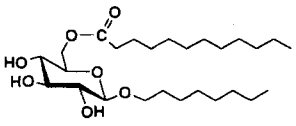

44

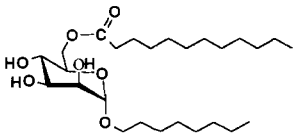

46

clearing points below 20 °C. Detailed textures have not been assigned for these two latter compounds. The proposed model shown in Figure 6 indicates that the driving force for the formation of these mesophases is the tendency of the hydrophilic and lipophilic moieties to segregate. In this way the surface between these stacked units constitutes a cylindrical jacket. Along this bent plane the amphiphilic carbohydrates can move in two dimensions and rotate along the longitudinal axis. Since carbohydrates **43** and **44** have equatorial-bound aglycons, the alkyl groups enclose a smaller angle than that in carbohydrates **45** and **46**, which bear an axial aglycon. It is concluded that **43** and **44** are favorably packed within the mesophase and have a higher freedom of movement and consequently higher entropy (an acute triangle rotates faster than an obtuse one). From these results and those previously mentioned, the postulated model of multimers for the formation of columnar phases, which was developed for dialkyl thiols,[56] cannot be generalized. But we can say with certainty that the supramolecular structures of amphiphilic carbohydrates remain a challenge and that further structural elaborations are expected.

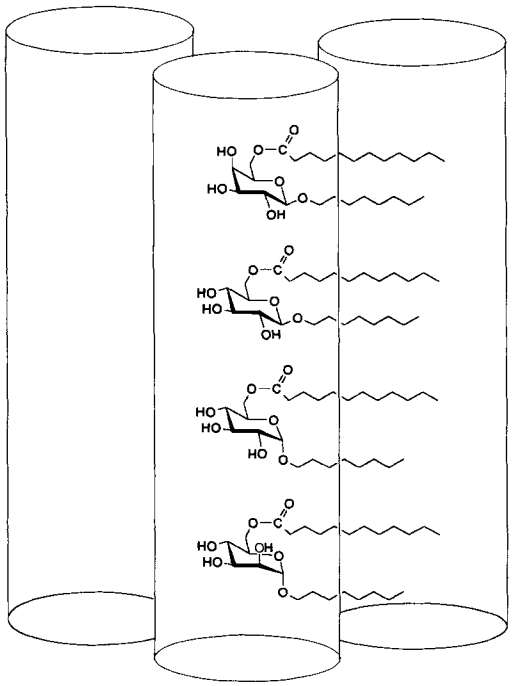

Fig. 6. A model for the formation of discotic mesophases for certain alkyl-6-*O*-acylglycopyranosides (from ref. [61]).

3.2. Liquid Crystalline Behavior of Amphiphilic and Bolaampiphilic Polyols

The crucial factors for the formation of liquid crystals from amphiphiles containing multiple hydroxyl groups are the tendency of the hydroxyl groups to form a dynamic network of cooperative hydrogen bonds and also their location at the ends of lipophilic chains. Diols and polyols with one polar head,[62] as well as bolaamphiphilic polyols,[63] exhibit thermotropic liquid crystalline behavior. Examples of such polyhydroxy amphiphiles with one polar head are compounds **47**–**50**. Compound **51** ($n = 5$) exhibits monotropic mesophase[64] that is stabilized by the addition of water. These polyols are structurally related to carbohydrate liquid crystals and can be regarded as the simplest members of this large class of amphiphilic mesogens.

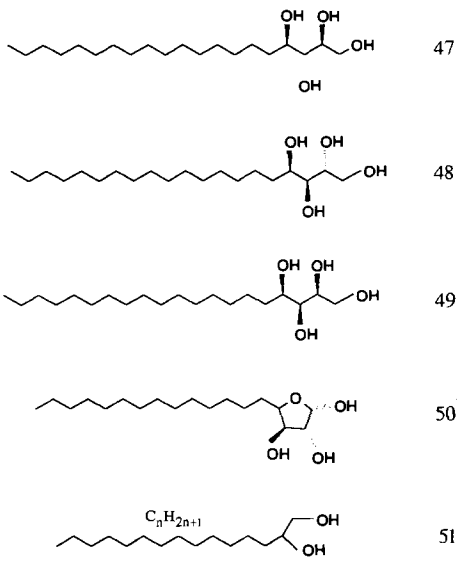

47

48

49

50

51

Recently, it has been found that the liquid crystalline phases of these compounds can be modified and stabilized by the introduction of rigid-rod moieties. For instance the introduction of

a 1,2-diol unit at the end of the *n*-alkoxy group of a nonamphiphilic phenyl benzoate affords compound **52**, which exhibits a smectic phase rather than the nematic phase exhibited by the starting material.[65] In addition, the introduction of a diol moiety to the known, liquid crystalline 4-alkoxy-4′-cyanobiphenyl results in compounds of the general formula **53** ($n = 1, 2, 4, 6, 8, 9$). The latter compounds have enhanced thermal stability but

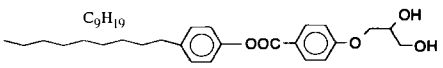

52

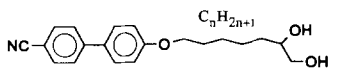

53

do not induce the formation of smectic phases. Since these compounds are amphiphilic, their mesogenic properties are affected by the addition of water, which stabilizes the mesophase and induces the formation of smectic phases. One explanation for this behavior is that water molecules penetrate the network of hydrogen bonds of the diol head groups, strengthening their interactions and therefore hindering the parallel movement of single molecules. It is therefore clear that by affecting hydrogen bonds it is possible to specifically control the molecular arrangement of amphiphilic molecules.

In connection with the above polyhydroxy compounds, 1,3-cyclohexanediols **54** ($n = 6, 8, 9, 10, 12, 14$) and **55** ($n = 4-14$), which are linked through an ester group to a benzene ring with two and three alkoxy chains, respectively, have been synthesized. Following detailed characterization studies,[66-71] including X-ray diffraction, it was concluded that the molecules aggregate even in the isotropic phase. In the mesophase they pack in a hexagonal array giving a phase with a structure similar to that of a columnar discotic phase. The mesogen is not a disklike unit, but six molecules assembled through hydrogen bonding to give the hexagonal structure.

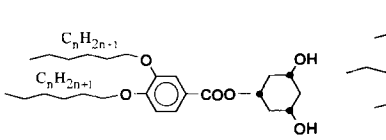

54

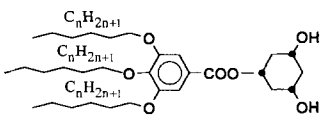

55

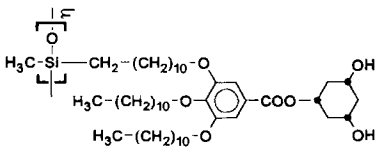

56

In addition to these monomeric diols a polymeric counterpart was synthesized by employing a hydrosilylation reaction analogous to that for polysiloxane preparation.[71] Polymer **56** was obtained bearing the 1,3-cyclohexanediol moiety. As was the case with analogous monomeric compounds, hydrogen bonding between the diols is responsible for the formation of a liquid crystalline phase, the texture of which needs further investigation.[71]

The liquid crystalline phases of these polyhydroxy derivatives can be stabilized by coupling two amphiphilic diols through their hydrophobic subunits ($n \geq 5$), affording the bolaamphiphilic compounds **57**–**62**.[63] Among these compounds the unsymmetrical tetraol **58** has the greatest mesophase diversity. Thus, when **58** is cooled from the isotropic melt, a fanlike texture

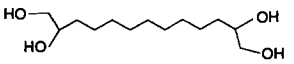

57

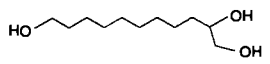

60

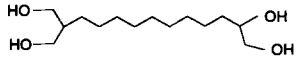

58

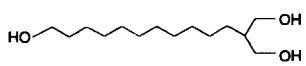

61

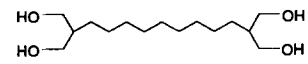

59

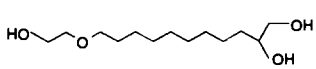

62

typical of lamella α-phases is obtained, which can be very easily oriented homoetropically by shearing. The hydroxyl groups, like those of amphiphilic diols, should be coupled through a dynamic network of cooperative hydrogen bonds, which are separated by the polymethylene chains, forming an L_α phase. On further cooling down to 75 °C, the texture changes and viscosity increases probably due to transition to a more highly ordered mesophase with rigid parallel polymethylene chains, that is, an L_β phase. At 43 °C another transformation occurs which cannot be studied in detail since crystallization starts. The liquid crystalline phases of polyols can again be modified by the addition of water. Specifically, the water-saturated mesophases of compounds with long aliphatic chains are stabilized, while those with shorter polymethylene chains are destabilized.

3.3. Liquid Crystalline Behavior of Monomeric and Polymeric Carboxylic Acid Amphiphiles

As previously established[11] and discussed in the introduction, liquid crystalline behavior is displayed not only by aromatic acids; certain amphiphilic-type acids also exhibit mesomorphic character. Thus polymers **63**–**65**, prepared by the reaction of poly(maleic anhydride)[72,73] or poly(acryloyl chloride)[74] with long-chain primary (**63**) and secondary amines (**64**) or ω-aminoundecanoic acid (**65**), exhibit liquid crystalline properties. In analogy with the dimers formed by aromatic acids, for example cinnamic

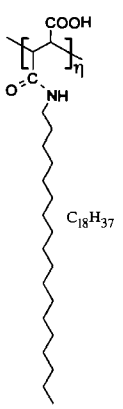

63

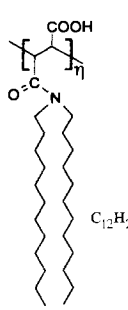

64

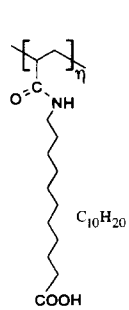

65

acid derivatives, the liquid crystalline character of **63**–**65** was attributed to the formation of supramolecular structures resulting from the association of the carboxylic groups of the polymers through hydrogen bonding.[72–74] The observed smectic phases were attributed to the lamellar structure formed by lipophilic and hydrophilic layers. These, in turn, arise owing to segregation of the aliphatic chains from the facing hydrogen-bonded carboxyl groups, which form eight-membered rings, as shown schematically for these polymers in Figure 7 (structures A and B). However, in addition to structures A and B one can envisage structures in which the adjacent carboxyl groups are linked through hydrogen bonds in a zig-zag fashion (Fig. 7, structures C and D). FTIR spectroscopy[74] and X-ray diffraction studies[75] reveal that these two supramolecular arrangements coexist in the solid and liquid crystalline phase and that the sample temperature determines which structure predominates.

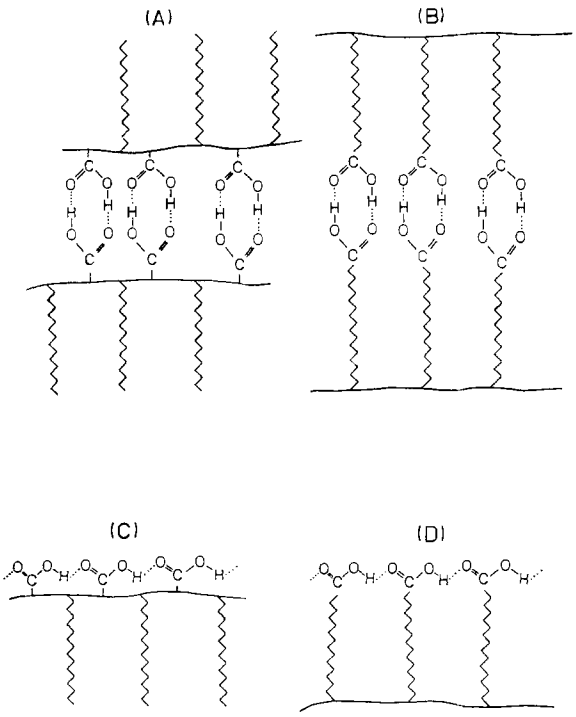

Fig. 7. Schematic representation of the dimerization of polymers **63**–**65**.

Derivatives of iminodiacetic acids with long aliphatic chains, **66** ($n = 12, 14, 16, 18$), exhibits a smectic phase in analogy with ionic amphiphilic compounds.[76, 77] Taking into consideration the zwitterionic character[78] of iminodiacetic acids, the presence of proton donors and acceptors that could lead to multiple hydrogen bonds between the two acid molecules, and the nonmiscibility of the alkyl chains, one can envisage for these acids a lamellar structure in the liquid crystalline phase. It should be noted that in the crystalline phase the hydroxyl group does not act as an acceptor, since carbonyl and carboxyl are better acceptors than hydroxyl groups.[78] Because the Bragg *d*-spacings[77] are shorter than the dimensions estimated by molecular modeling, we assume that either the aliphatic chains overlap or the molecules are tilted within the layers.

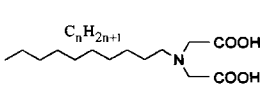

66

3.4. Liquid Crystalline Character of Amphiphiles Bearing Complementary Functional Groups

The formation of liquid crystalline phases through dimerization of certain carboxylic acids can be considered as the starting point for the formation of mesophases by hydrogen bonding between dissimilar molecules bearing complementary functional groups. A very well-known example is the interaction of nucleobases in nucleic acids.

The first reported examples of compounds that could, in principle, form liquid crystals were 2,6-diaminopyridines and uracil derivatives with long aliphatic chains.[79] In fact these compounds with complementary moieties for hydrogen bonding formed both crystalline and liquid crystalline phases. Three hydrogen bonds form between the interacting heterocyclic bases (Fig. 8, bottom). In this case the bases together with the hydrogen bonding system constitute the "polar segment" which is segregated from their lipophilic moiety. The supramolecular structure of the complex is shown in Figure 8 (top). In general, the complexes can be prepared either by allowing the interaction of the complementary bases in organic solvents, usually chloroform, by melt crystallization, or even by solid mixing. For the complex shown in Figure 8 the heterocyclic bases were dissolved in chloroform.

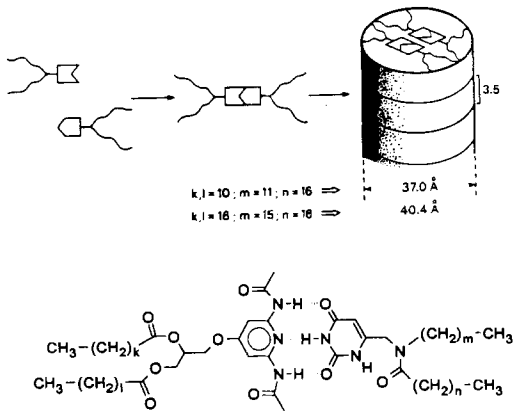

Fig. 8. Formation of a complex through hydrogen bonding (bottom) and a schematic representation of the columnar mesomorphic (top) structure (from ref. [4]).

A series of compounds was prepared by Lehn et al.[79] by modifying the length of the alkyl chain while maintaining the same basic core. The pure compounds show solid polymorphism but none of them exhibits a mesomorphic phase. All of the 1:1 mixtures of these bases that were investigated[79] showed crystalline polymorphism and five of them having long aliphatic chains exhibited a metastable mesomorphic phase. There is no direct evidence for the formation of the complex in the mesomorphic phase. The fact, however, that an analogous complex with three hydrogen bonds was found both in the solid state and in solution[79] is a convincing argument that the structure main-

tained in the melt may be the one responsible for the formation of the liquid crystalline phase. In X-ray diffraction studies of the mixtures with the chain lengths specified in Figure 8, mesophases of the columnar hexagonal type were identified. The columns have diameters of 37 and 40.4 Å and are formed by a stack of disks, each of which contains two supermolecules side by side, with a contact distance of 3.5 Å between successive disks (Fig. 8). Thus the molecular information coded by recognition between the two amphiphiles is amplified and expressed macroscopically in the formation of a liquid crystalline phase.

The interaction of a molecule having at least two functional groups with a molecule having corresponding complementary functional groups can lead, in principle, to the formation of polymeric structures. Such a bifunctional system is shown schematically in Figure 9.

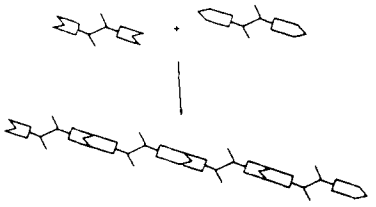

Fig. 9. Schematic representation of the interaction of two compounds each bearing two complementary recognition groups.

Compounds with two complementary groups were prepared[80] and their complexes characterized as far as their liquid crystalline character is concerned. Specifically, uracil (U) and 2,6-diacylaminopyridine (P) were introduced in tartaric acid (T), and the compounds were allowed to interact, forming complementary pairs with three hydrogen bonds (Scheme 1). Since tartaric acid has chiral centers, it is also possible to study their effect on the properties of the materials.

The components LP_2, LU_2, DP_2, MP_2, and MU_2 were prepared from uracil or pyridine components and L(+)-, D(−)-, and *meso*-(M) tartaric acid and can associate through their heterocyclic moieties.[80] In fact, 1:1 mixtures of the complementary pairs (LP_2 + LU_2) and (MP_2 + MU_2) gave complexes that differed from their components both in the bulk and in solution, as established by NMR and circular dichroism spectra of (LP_2 + LU_2).

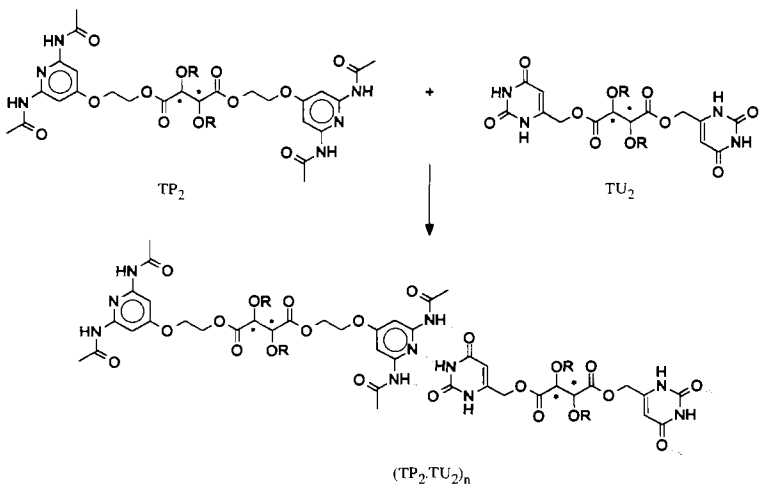

Scheme 1.

The thermal transitions of the individual components and of 1:1 mixtures were studied by DSC and polarizing microscopy. The pure compounds are polymorphic solids, whereas 1:1 mixtures exhibit liquid crystalline behavior from below room temperature to above 200 °C. The optical textures were different for LL and MM mixtures, as the mixtures (LU_2 + LP_2) and (MU_2 + MP_2) showed.[4]

The X-ray patterns of LL, DL, and MM mixtures reveal hexagonal columnar liquid crystalline phases. Details of the X-ray diffraction studies on the supramolecular structures affording these liquid crystals were reported by Lehn et al.[80] More recently, electron microscopy studies[4] were used to further explore the structure of these materials. It was shown that as the concentration of equimolar solutions of LP_2 and LU_2 increases, a progressive assembly of supramolecular entities occurs up to very large species. Initially small nuclei are formed, which grow into filaments, and finally associate laterally to give treelike species, strings, and fibers.[4] The materials formed are helical as a result of the chirality of the subunits.

Mesophases were also obtained by the interaction of a component containing two recognition sites and a second component containing one recognition site in a 1:2 molar ratio. This is the case when two uracil components combine with the complementary LP_2 component to form the supermolecule shown in Scheme 2, having a columnar structure of rectangular section.[4]

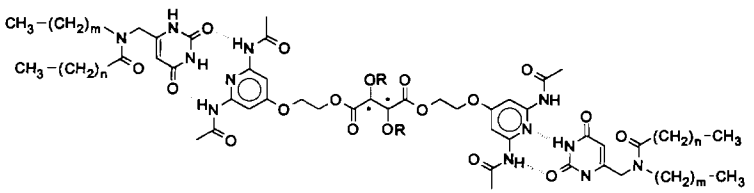

Scheme 2.

To mimic the interaction of complementary nucleobases in nucleic acids, adenine and thymine nucleobases were functionalized with long aliphatic chains, transforming these bases to amphiphilic-type compounds. Since it is known that recognition in nonbiological systems is significantly enhanced by solvents that do not form hydrogen bonds,[81–85] the amphiphilic nucleobases were mixed in chloroform or in the melt. It is of interest to note that in aqueous media vertical stacking predominates.[85] The alkylated derivatives of adenine and thymine **67**–**70** (n = 16) were prepared.[86, 87] The obvious question was whether the amphiphilic-type nucleobases exhibit liquid crystalline behavior alone or as complementary complexes. The aliphatic chains were introduced at 1- and 9-positions of thymine and adenine, respectively, in other words, at sites remote from the functionalities involved in the recognition process. This strategy must be followed in all cases when molecular recognition is required to occur.

Since the amino group in adenine has two hydrogens available for hydrogen bonding, it may in principle recognize two molecules of thymine. This is the

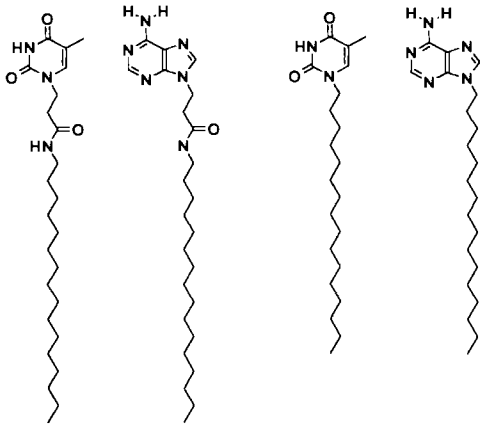

67 68 69 70

reason why adenine–thymine complexes with molar ratios of 1:1 and 1:2 could be prepared.[86, 87] The types of hydrogen bonds formed in these complexes, Watson–Crick and Hoogsteen interactions, are shown in Scheme 3. The amide group of the derivatives **67** and **68** may affect their organizational characteristics since it is capable of forming hydrogen bonds.

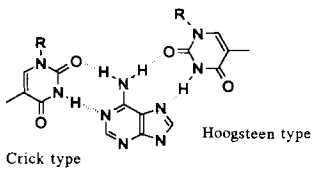

Scheme 3. Watson–Crick and Hoogsteen hydrogen bonds in adenine–thymine complexes.

The results of detailed optical and DSC studies as well as X-ray diffraction analyses of these novel nucleobases can be summarized as follows: Pure adenine and thymine derivatives and their binary mixtures have an organized arrangement in the solid state at low temperatures and form the lamellar structures typical for amphiphilic compounds. X-ray diffraction studies show that this ordering is maintained up to the isotropic phase. The optical textures indicate the formation of metastable mesomorphic phases which seems to contradict the X-ray results. Thus, these mesomorphic phases may be interpreted as transient monotropic phases, occurring on cooling from the isotropic melt and not stable enough to be detected by X-ray diffraction. We may attribute the absence of stable mesomorphic phases to the structure and shape of the molecules and their complexes, which cannot properly be accommodated in the type of supramolecular structure that affords liquid crystalline phases. Further investigations are needed to determine the order of the amphiphiles in stable liquid crystalline phases and also to assess the role of amphiphilicity and molecular recognition in the formation of novel liquid crystals.

The mesomorphic properties of diamides of alkyl-substituted 1,3-diaminobenzenes, initially prepared by Matsunaga et al.,[88] were reinvestigated in detail by Malthête et al.[89] together with some analogous compounds. The presence of methyl groups at appropriate positions on the benzene ring is crucial for the formation of the mesomorphic phases. In the example shown in Figure 10 it may be assumed that a methyl group close to an amide (4-position) or between two amide groups (2-position) turns at least one amide group out of the plane of the benzene ring. This should favor self-association and formation of supramolecular structures leading to mesomorphic phases.

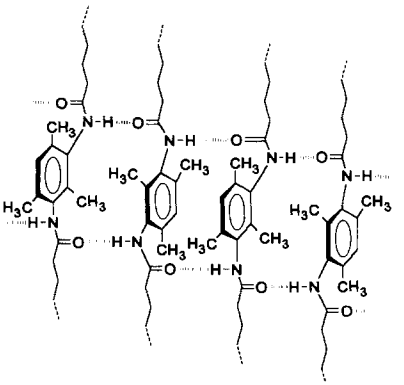

Fig. 10. Schematic representation of the potential supramolecular structure of a hydrogen-bonded associated diamide (from ref. [89]).

In an analogous manner, hydrogen bonding explains the "unconventional nematic phases" exhibited by the homologous series of benzdiamides—*N,N'*-dialkanoyl-2,5-dimethyl-4-alkanoyloxy-1,3-benzdiamines **71a** (R = CH_3; $n = m = 8-11, 13, 15$) and 2-methyl-5-isopropyl- **71b** (R = *i*Pr; $n = 8-11, 13, 15$ and $m = 4-15$) and 2-methyl-5-*tert*-butyl-4-alkanoyloxy-1,3-benzdiamines **71c** (R = *t*Bu; $n = m = 10, 11, 13, 15$). These results are included in the latest work[90] of Matsunaga et al.

The liquid crystalline character of 3,4,5-tris(alkoxybenzamides) can be interpreted by assuming a supramolecular structure analogous to that of the alkylated diamides previously discussed.[89] Based on optical textures only, Beginn and Lattermann[91] deduced a columnar or stacklike structure and proposed a dimeric structure (Fig. 11). It was also proposed that since the amide groups are tilted against the plane of the aromatic rings, not only intradimer but also interdimer hydrogen bonding is exercised, stabilizing the columnar structure. The existence of interdimer hydrogen bonds was supported by infrared spectroscopy and also by substitution of the benzene ring, which results in loss of mesomorphism. Apparently steric hindrance suppresses interdimeric hydrogen binding.

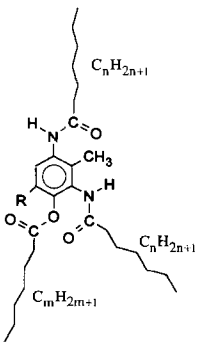

71

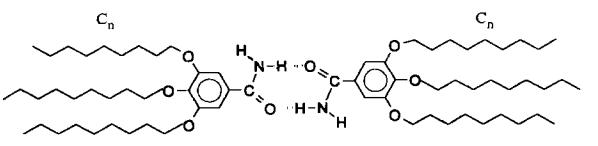

Fig. 11. Hydrogen-bonded dimers of trisalkylated primary benzamides.

In preliminary experiments[92] the mesomorphic character of some 2,4,6-trichloro-1,3,5-triazine derivatives with long alkyl chains was investigated. These molecules, which contain in their core a typical unit for molecular recognition, N=C–NH,[93] were mixed in the melt with molecules bearing a complementary

moiety. In a typical experiment, lauric acid was combined in the melt with a disubstituted triazine derivative, affording the structure shown in the Scheme 4. In DSC and optical studies of the complex a mesomorphic texture was found which was not characterized further.

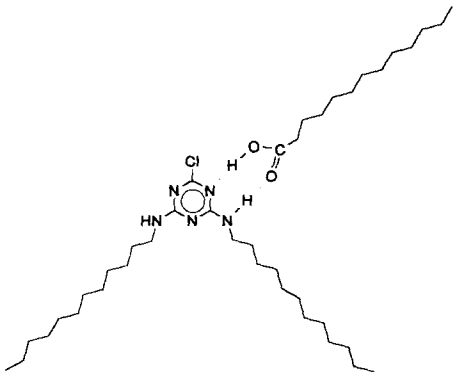

Scheme 4.

The examples described were the first attempts at preparing liquid crystalline phases through molecular recognition of dissimilar molecules. Further study is required on the structure of interacting components in order to lead to stable and diverse liquid crystalline phases. Thus, in addition to having the proper geometry and being complementary, the interacting components must also benefit from cooperativity[94] or secondary electrostatic interactions, as invoked by Jorgensen et al.[95, 96] According to a model proposed by Jorgensen, the most stable supramolecular structure is obtained when all or at least most of the donors are located in one of the interacting molecules, while the acceptors are on the other. The preparation of liquid crystals stabilized by secondary interactions is thus of current interest.

4. Summary and Outlook

The results presented in this review clearly demonstrate that hydrogen bonding is of significant importance in the formation of liquid crystalline phases and the stabilization of existing mesophases of both rigid-rod and amphiphilic molecules. In future work hydrogen bonding must be put on a more quantitative basis, taking into consideration not only the typical interaction of donor–acceptor pairs but also secondary electrostatic interactions. The development of the structural features of the recognition moieties for a more effective binding of supramolecular assemblies will be certainly the main objective of future work in the domain of hydrogen-bonded liquid crystals. These exploratory studies may very well trigger interest in identifying and synthesizing new building-block molecules with the prescribed hydrogen bonding properties, whose supramolecular assemblies may lead to novel liquid crystalline materials.

5. Addendum

A number of new studies on compounds displaying liquid crystalline phases induced by hydrogen bonding have appeared since this review was accepted for publication in September 1994. Most of this new work refers to amphiphilic polyhydroxy liquid crystalline compounds[97–100] including carbohydrates.[97–99] But there has also been research activity focusing on the formation of liquid crystalline complexes incorporating pyridyl or bipyridyl moieties.[101, 102] Some examples of these types of liquid crystals are discussed below.

Liquid crystalline amphiphilic carbohydrates[97] based on glucosamine and 6-amino-6-deoxyhexopyranoses have been prepared. In previously synthesized aminocarbohydrates[41] the secondary amino group was placed in the bridge between the hydrophilic and hydrophobic segment, while in the new glucosamines a primary amino group is located in the hydrophilic section of carbohydrates. In addition to the simple alkyl glucosamines **72** ($n = 8$, 10, 12, 14, and 18) and its hydrochloride salt **73** ($n = 12$), which exhibit smectic phases, the hydroxyl derivative **74** ($n = 16$) also shows smectic behavior. The amides of 6-amino-6-deoxygalactose **75** ($R = SO_2C_{16}H_{33}$, $COC_{17}H_{35}$)

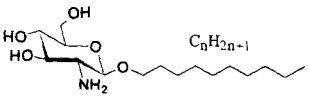

72

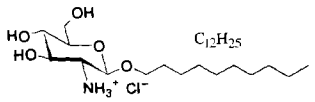

73

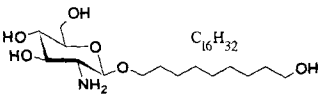

74

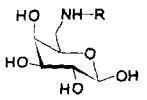

75

with only one alkyl group connected at the amino group form smectic S_A phases. The clearing temperatures are higher than those of the alkyl glucosides, and the sulfonamide derivative has a higher clearing temperature than the carbonamide because of differing polarities.[97] A particularly interesting feature of aminocarbohydrates is their ability to form intra- and intermolecular salts with organic acids, giving a multiplicity of liquid crystalline materials. Thus, depending on the organic acid used, smectic, discotic, or cubic phases can be prepared. The liquid crystalline properties of aminocarbohydrates are summarized as follows: *N*-Alkylglucosamines show S_A phases with lower clearing points than those of alkyl glucosides; high clearing points are induced when the amino group is located at the bridge position between the hydrophilic and the hydrophobic segments.

A quite recent paper extends the work on amphiphilic carbohydrates to the preparation and characterization of nonamphiphilic carbohydrate liquid crystals.[98] Thus, a coumarin moiety was incorporated in the carbohydrate and compounds **76** ($R = C_7H_{13}$, C_9H_{19}, and $C_{13}H_{27}$) were prepared. The rigid and relatively flat coumarin unit is flanked by the hydrophilic carbohydrate head group and a lipophilic tail. Although the structures of these carbohydrates are not typical for compounds exhibiting mesomorphic character, two of these compounds form liquid crystalline phases. Thus, the heptyl derivative is not liquid crystalline, while nonyl

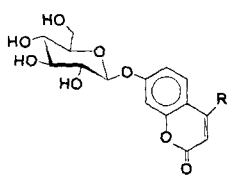

76

and tridecyl derivatives exhibit a smectic S_A liquid crystalline phase.

Studies on bolamphiphillic tetraols have been continued by a detailed investigation of the homologous series of 1,2,ψ,ω,*n*-alkanetetraols **77** (n = 5–18, 20).[99] The compounds that bear a rather long polymethylene chain exhibit a lamellar α phase and a mesophase at low temperatures, whereas the derivatives with short chains exhibit only a low-temperature mesophase. Characterization by X-ray diffraction showed the low-temperature phase to be an L_x phase. On the basis of the experimental d values and the estimated tilt angle of 28°, a model was proposed (Fig. 12). It is assumed that the primary hydroxyl groups interact through hydrogen bonding with the secondary hydroxyl groups of the neighboring molecule. In this way the tilt angle of about 30° can be rationalized. This low-temperature mesophase is highly ordered and viscous. Its layer thickness decreases at the transition to the high-temperature phase. This transition is accompanied by a high enthalpy change and gives rise to a mesophase in which the methylene chains are liquidlike, as is also the case with the L_α phase of lyotropic systems. The melting of the aliphatic chains should be accompanied by a reorganization of the hydrogen bonds, which would also contribute to the high transition enthalpy. With respect to the high transition enthalpy between the two mesophases and the high viscosity, the low-temperature phase may be considered to have a solidlike character although the X-ray patterns are very similar to those of the low-temperature mesophases of the amphiphilic diol compounds.[100]

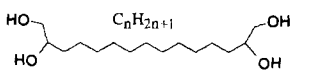

77

In studies of complexes bearing pyridyl or bipyridyl moieties as acceptors two classes of compounds were investigated. The nonmesomorphic *N*-(*p*-methoxy-*o*-hydroxybenzylidene)-*p*-aminopyridine[101] was combined with *p*-alkoxybenzoic acids affording complexes **78** (n = 1–5, 10, 12). The anil moiety is protected from hydrolysis by the *ortho*-hydroxyl group. Complexes originating from methoxy-, ethoxy-, propoxy-, butoxy-, and pentyloxybenzoic acids afforded complexes with nematic liquid crystalline phases, while the complexes of decyloxy- and dodecyloxybenzoic acid with the same anil exhibit smectic and nematic phases.

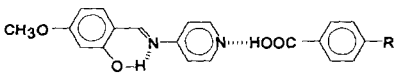

78

In this context 4,4′-bipyridine was combined for the first time with phenols rather than with acids to yield complexes **79** and **80**.[102] Neither of the interacting components exhibit liquid crystalline character; for the formation of their complexes a stoichiometric ratio of 2:1 (phenol:bipyridine) was employed.

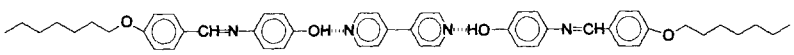

79

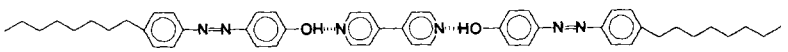

80

Long alkyl or alkoxy chains are needed to obtain liquid crystalline character. Thus, for complexes **79** smectic phases were observed only for the members having an alkoxy chain longer than C_9. In complexes **80** the members with an alkyl chain shorter than C_7 do not show liquid crystalline behavior. Thus derivatives with short alkyl and alkoxy chains do not form a nematic phase.

Received: February 1, 1994
Revised version: November 21, 1994
Addendum: April 18, 1995 [A 53 IE]
German version: *Angew. Chem.* **1995**, *107*, 1839–1855

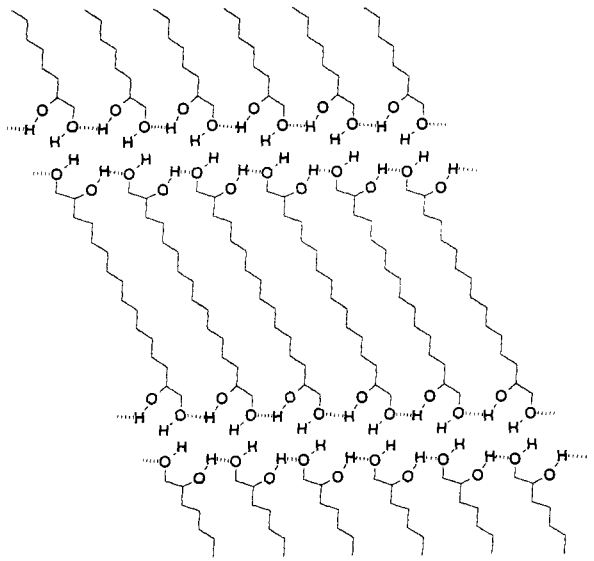

Fig. 12. Supramolecular structure of **77**; the components are linked through hydrogen bonds between the diol groups in the low-temperature mesophase.

[1] G. W. Gray, *Molecular Structure and Liquid Crystals*, Academic Press, London, **1967**, p. 161, and references therein.
[2] H. Kelker, R. Hatz, *Handbook of Liquid Crystals*, Verlag Chemie, Weinheim, **1980**, and references therein.
[3] J. M. Lehn, *Angew. Chem.* **1990**, *102*, 1347; *Angew. Chem. Int. Ed. Engl.* **1990**, *29*, 1304.
[4] J. M. Lehn, *Makromol. Chem. Macromol. Symp.* **1993**, *69*, 1.
[5] V. Percec, H. Jonsson, D. Tomazos in *Polymerization in Organized Media* (Ed.: C. M. Paleos), Gordon and Breach, Philadelphia, **1992**, p. 1.
[6] C. M. Paleos, *Mol. Cryst. Liq. Cryst.* **1994**, *243*, 159
[7] D. Vorländer, *Ber. Dtsch. Chem. Ges.* **1908**, *41*, 2033.
[8] G. W. Gray, B. Jones, *J. Chem. Soc.* **1954**, 1467.
[9] G. W. Gray, B. Jones, *J. Chem. Soc.* **1953**, 4179.
[10] C. Weygand, R. Gabler, J. Hoffmann, *Z. Phys. Chem. Abt. B* **1941**, *50*, 124.
[11] M. P. Gaubert, *C. R.* **1919**, *168*, 277.
[12] T. Kato, H. Adachi, A. Fujishima, J. M. J. Frechet, *Chem. Lett.* **1992**, 265.
[13] T. Kato, J. M. J. Frechet, *J. Am. Chem. Soc.* **1989**, *111*, 8533.
[14] T. Kato, A. Fujishima, J. M. J. Frechet, *Chem. Lett.* **1990**, 919.
[15] J. I. Jin, J. H. Park, *Mol. Cryst. Liq. Cryst.* **1984**, *110*, 221.
[16] T. Kato, P. G. Wilson, A. Fujishima, J. M. J. Frechet, *Chem. Lett.* **1990**, 2003.
[17] T. Kato, J. M. J. Frechet, P. G. Wilson, T. Saito, T. Uryu, A. Fujishima, C. Jin, F. Kaneuchi, *Chem. Mater.* **1993**, *5*, 1094.
[18] L. J. Yu, J. S. Pan, *Liq. Cryst.* **1993**, *14*, 829.
[19] M. Fukumasa, T. Kato, T. Uryu, J. M. J. Frechet, *Chem. Lett.* **1993**, 65.
[20] L. J. Yu, *Liq. Cryst.* **1993**, *14*, 1303.
[21] H. Kresse, I. Szulzewsky, S. Diele, R. Paschke, *Mol. Cryst. Liq. Cryst.* **1994**, *13*, 238.

[22] T. Kato, T. Uryu, F. Kaneuchi, C. Jin, J. M. J. Frechet, *Liq. Cryst.* **1993**, *14*, 1311.
[23] a) H. Schubert, S. Hoffmann, J. Hauschild, *Z. Chem.* **1977**, *17*, 414; b) C. H. Lochmueller, R. W. Souter, *J. Phys. Chem.* **1973**, *77*, 3016.
[24] A. Mori, H. Takeshita, R. Nimura, M. Isobe, *Liq. Cryst.* **1993**, *14*, 821.
[25] T. Kato, J. M. J. Frechet, *Macromolecules* **1989**, *22*, 3818.
[26] T. Kato, H. Kihara, T. Uryu, A. Fujishima, J. M. J. Frechet, *Macromolecules* **1992**, *25*, 6836.
[27] T. Kato, H. Kihara, U. Kumar, A. Fujishima, T. Uryu, J. M. J. Frechet, *Polym. Prepr.* **1993**, *34*(2), 722.
[28] U. Kumar, T. Kato, J. M. J. Frechet, *J. Am. Chem. Soc.* **1992**, *114*, 6630.
[29] S. E. Odinokov, A. A. Mashkovsky, V. P. Glazunov, A. V. Logangen, B. V. Rassadin, *Spectrochim. Acta Part A* **1976**, *32*, 1355.
[30] U. Kumar, J. M. J. Frechet, *Adv. Mater.* **1992**, *4*, 665.
[31] U. Kumar, J. M. J. Frechet, T. Kato, S. Ujiie, K. Timura, *Angew. Chem.* **1992**, *104*, 1545; *Angew. Chem. Int. Ed. Engl.* **1992**, *31*, 1531.
[32] F. A. Brandys, C. G. Bazuin, *Polym. Prepr.* **1993**, *34*(1), 186.
[33] C. Alexander, C. P. Jariwala, C. M. Lee, A. C. Griffin, *Polym. Prepr.* **1993**, *34*(1), 168.
[34] P. Bladon, A. C. Griffin, *Macromolecules* **1993**, *26*, 6604.
[35] E. Fischer, B. Helferich, *Justus Liebigs Ann. Chem.* **1911**, *383*, 68.
[36] A. H. Salway, *J. Chem. Soc.* **1913**, 1022.
[37] C. R. Noller, W. C. Rockwell, *J. Am. Chem. Soc.* **1938**, *60*, 2076.
[38] a) R. Hori, *Yakugaku Zasshi* **1958**, *78*, 523 [*Chem. Abstr.* **1958**, *52*, 17118i]; b) *Yakugaku Zasshi* **1958**, *78*, 999 [*Chem. Abstr.* **1959**, *53*, 3073d]; c) *Yakugaku Zasshi* **1958**, *78*, 1171 [*Chem. Abstr.* **1958**, *53*, 5140f]; d) *Yakugaku Zasshi* **1959**, *79*, 80 [*Chem. Abstr.* **1959**, *54*, 10049f].
[39] G. A. Jeffrey, *Acc. Chem. Res.* **1986**, *19*, 168.
[40] G. A. Jeffrey, L. M. Wingert, *Liq. Cryst.* **1992**, *12*, 179.
[41] H. A. Van Doren, R. Van der Geest, C. F. De Ruijter, R. M. Kellogg, H. Wynberg, *Liq. Cryst.* **1990**, *8*, 109.
[42] J. W. Goodby, *Mol. Cryst. Liq. Cryst.* **1984**, *110*, 205.
[43] M. A. Marcus, P. L. Finn, *Mol. Cryst. Liq. Cryst. Lett. Sect.* **1985**, *2*, 159.
[44] B. Pfannemüller, W. Welte, E. Chin, J. W. Goodby, *Liq. Cryst.* **1986**, *1*, 357.
[45] D. Baeyens-Volant, R. Fornasier, E. Szalai, C. David, *Mol. Cryst. Liq. Cryst.* **1986**, *135*, 93.
[46] P. Köll, M. Oelting, *Angew. Chem.* **1986**, *98*, 362; *Angew. Chem. Int. Ed. Engl.* **1986**, *25*, 368.
[47] J. W. Goodby, M. A. Marcus, E. Chin, P. L. Finn, B. Pfannemüller, *Liq. Cryst.* **1988**, *3*, 1569.
[48] W. V. Dahlhoff, *Liebigs Ann. Chem.* **1990**, 811.
[49] C. Tschierske, A. Lunow, H. Zaschke, *Liq. Cryst.* **1990**, *8*, 885.
[50] V. Vill, T. Bocker, I. Thiem, F. Fischer, *Liq. Cryst.* **1989**, *6*, 349.
[51] H. A. van Doren, L. M. Wingert, *Mol. Cryst. Liq. Cryst.* **1991**, *198*, 381.
[52] G. A. Jeffrey, *Mol. Cryst. Liq. Cryst.* **1990**, *185*, 209.
[53] H. van Doren, T. J. Buma, R. M. Kellogg, H. Wynberg, *J. Chem. Soc. Chem. Commun.* **1988**, 460.
[54] W. V. Dahlhoff, *Z. Naturforsch. B* **1987**, *42*, 661.
[55] A. Eckert, B. Kohne, K. Praefcke, *Z. Naturforsch. B* **1988**, *43*, 878.
[56] K. Praefcke, A. M. Levelut, B. Kohne, A. Eckert, *Liq. Cryst.* **1989**, *6*, 263.
[57] R. Miethchen, M. Schwarze, J. Holz, *Liq. Cryst.* **1993**, *15*, 185.
[58] K. Praefcke, D. Blunk, *Liq. Cryst.* **1993**, *14*, 1181.
[59] A. Takada, T. Fukuda, T. Miyamoto, Y. Yakoh, J. Watanabe, *Liq. Cryst.* **1992**, *12*, 337.
[60] H. Fischer, V. Vill, C. Vogel, U. Jeschke, *Liq. Cryst.* **1993**, *15*, 733.
[61] V. Vill, B. Sauerbrei, H. Fischer, J. Thiem, *Liq. Cryst.* **1992**, *11*, 949.
[62] K. Praefcke, B. Kohne, S. Diele, D. Pelzl, A. Kjaer, *Liq. Cryst.* **1992**, *11*, 1.
[63] F. Hentrich, C. Tschierske, H. Zaschke, *Angew. Chem.* **1991**, *103*, 429; *Angew. Chem. Int. Ed. Engl.* **1991**, *30*, 440.
[64] C. Tschierske, G. Brezesinski, F. Kuschel, H. Zaschke, *Mol. Cryst. Liq. Cryst. Lett. Sect.* **1989**, *6*, 139.
[65] D. Joachimi, C. Tschierske, H. Müller, J. H. Wendorff, L. Schneider, *Angew. Chem.* **1993**, *105*, 1205; *Angew. Chem. Int. Ed. Engl.* **1993**, *32*, 1165.
[66] G. Lattermann, G. Staufer, *Liq. Cryst.* **1989**, *4*, 347.
[67] G. Lattermann, G. Staufer, *Mol. Cryst. Liq. Cryst.* **1990**, *191*, 199.
[68] M. Ebert, R. Kleppinger, M. Soliman, M. Wolf, J. H. Wendorff, G. Lattermann, G. Staufer, *Liq. Cryst.* **1990**, *7*, 553.
[69] G. Lattermann, G. Staufer, G. Brezesinski, *Liq. Cryst.* **1991**, *10*, 169.
[70] R. Festag, R. Kleppinger, M. Soliman, J. H. Wendorff, G. Lattermann, G. Staufer, *Liq. Cryst.* **1992**, *11*, 699.
[71] G. Staufer, G. Lattermann, *Macromol. Chem.* **1991**, *192*, 2421.
[72] D. Tsiourvas, C. M. Paleos, P. Dais, *J. Appl. Polym. Sci.* **1989**, *38*, 257.
[73] D. Tsiourvas, C. M. Paleos, P. Dais, *J. Polym. Sci. Part A Polym. Chem.* **1990**, *28*, 1263.
[74] C. M. Paleos, D. Tsiourvas, J. Anastassopoulou, T. Theophanides, *Polymer* **1992**, *33*, 4047.
[75] D. Tsiourvas, Dissertation, National Technical University of Athens, **1992**.
[76] C. M. Paleos, J. Michas, A. Malliaris, *Mol. Cryst. Liq. Cryst.* **1990**, *186*, 251.
[77] J. Michas, C. M. Paleos, A. Skoulios, P. Weber, *Mol. Cryst. Liq. Cryst.* **1993**, *237*, 175.
[78] J. Bernstein, M. C. Etter, J. C. MacDonald, *J. Chem. Soc. Perkin Trans.* **1990**, *2*, 695.
[79] M. J. Brienne, J. Galard, J. M. Lehn, J. Stibor, *J. Chem. Soc. Chem. Commun.* **1989**, 1868.
[80] C. Fouquey, J. M. Lehn, A. M. Levelut, *Adv. Mater.* **1990**, *2*, 254.
[81] L. Katz, S. Penman, *J. Mol. Biol.* **1966**, *15*, 220.
[82] R. M. Hamlin, Jr., R. C. Lord, A. Rich, *Science* **1965**, *148*, 1734.
[83] J. Pitha, R. N. Jones, P. Pithova, *Can. J. Chem.* **1966**, *44*, 1045.
[84] Y. Kyogoku, R. C. Lord, A. Rich, *J. Am. Chem. Soc.* **1967**, *89*, 496.
[85] J. Rebek, Jr., *Angew. Chem.* **1990**, *102*, 261; *Angew. Chem. Int. Ed. Engl.* **1990**, *29*, 245.
[86] J. Michas, C. M. Paleos, *Liq. Cryst.* **1993**, *11*, 773.
[87] J. Michas, C. M. Paleos, A. Skoulios, P. Weber, *Mol. Cryst. Liq. Cryst.* **1994**, *239*, 245.
[88] Y. Matsunaga, M. Terada, *Mol. Cryst. Liq. Cryst.* **1986**, *141*, 321.
[89] J. Malthête, A. M. Levelut, L. Liébert, *Adv. Mater.* **1992**, *4*, 37.
[90] T. Akutagawa, Y. Matsunaga, S. Sakamoto, *Mol. Cryst. Liq. Cryst.* **1994**, *239*, 141.
[91] U. Beginn, G. Lattermann, *Mol. Cryst. Liq. Cryst.* **1994**, *241*, 215.
[92] C. M. Paleos, D. Tsiourvas, S. Fillipakis, L. Fillipaki, *Mol. Cryst. Liq. Cryst.* **1994**, *242*, 9.
[93] M. Etter, *Acc. Chem. Res.* **1990**, *23*, 120.
[94] S. C. Zimmerman, M. H. Baloga, B. F. Duerr, E. E. Fenlon, J. J. Murray, *Polym. Prepr.* **1993**, *34*(1), 94.
[95] W. L. Jorgensen, J. Pranata, *J. Am. Chem. Soc.* **1990**, *112*, 2008.
[96] J. Pranata, S. G. Wierschke, W. L. Jorgensen, *J. Am. Chem. Soc.* **1991**, *113*, 2810.
[97] P. Stangier, V. Vill, S. Rohde, U. Jeschke, J. Thiem, *Liq. Cryst.* **1994**, *17*, 589.
[98] D. Blunk, K. Praefcke, G. Legler, *Liq. Cryst.* **1995**, *18*, 149.
[99] L. F. Tietze, K. Boge, V. Vill, *Chem. Ber.* **1994**, *127*, 1065.
[100] F. Hentrich, S. Diele, C. Tschierske, *Liq. Cryst.* **1994**, *17*, 827.
[101] Z. Sideratou, C. M. Paleos, A. Skoulios, *Mol. Cryst. Liq. Cryst.* **1995**, *265*, 19.
[102] T. Koga, H. Ohba, H. Takase, S. Sakagami, *Chem. Lett.* **1994**, 2071.

Two at One Blow: The New Chemical Elements 110 and 111

Günter Herrmann*

Nothing significant has happened at the very end of the periodic table for about a decade, since a research group around Peter Armbruster, Sigurd Hofmann, and Gottfried Münzenberg produced and identified the three then heaviest chemical elements—element 107 in February 1981, 109 in August 1982, and 108 in March 1984—at the heavy-ion accelerator UNILAC of the Gesellschaft für Schwerionenforschung (GSI) in Darmstadt (Germany). Rather, scepticism about progress beyond this limit seemed to be appropriate. "Their synthesis [of the heaviest nuclei] is strongly hindered—much more than was initially anticipated. It is this hindrance rather than the decreasing nuclear stability which seems to presently limit the extent of the periodic table: even heavier elements should be able to exist, but no way has yet been found to produce them" is pointed out in 1988 in a report[2] in this journal. Nuclear properties are the key when the limit of the periodic table is approached. The electron shell does not play a role here, but it is decisive, of course, if we ask where the heaviest elements are located in the periodic table and whether its systematics continues consistently up to this point.

Now, the same research group has again created a great stir in a very eventful beam time late in 1994: On November 9 at 16:39 h, the group discovered element 110 in form of an atomic nucleus of mass number 269.[3] On November 23 at 20:07 h a second isotope of element 110 with mass number 271 was detected.[4, 5] Rapidly thereafter, on December 8 at 05:49, element 111 followed with mass number 272.[6] Four nuclei of $^{269}110$ were observed, nine of $^{271}110$, and three of $^{272}111$.[5] Each of these new nuclei fed a long decay chain of well known α-emitters with a total of 68 registered α-particles.[4] Lifetimes and decay energies of the chain links present a very characteristic fingerprint which cannot appear accidentally. Furthermore, the information on the formation and decay of the heaviest atomic nuclei fuels the hope for still heavier elements: The "superheavy" elements around element 114, in discussion for three decades, appear now to be within reach.

The group's strategy for synthesis and detection was basically the same as for the elements 107 to 109 (for more details see the review articles[1, 2]). The heaviest elements are created by fusion of two atomic nuclei. One of them, the target nucleus at rest, is lead-208 (proton number $Z = 82$) or bismuth-209 ($Z = 83$), the two heaviest stable nuclei in nature. The other, the projectile nucleus, adds exactly the number of protons required to make the sought element. To induce a nuclear reaction, projectile and target nucleus have to be brought into contact; the repulsive electrostatic force between the two nuclei has to be overcome. The projectile, therefore, is accelerated in the UNILAC to about ten per cent of the velocity of light. To build element 110 from lead and element 111 from bismuth, nickel ($Z = 28$) is needed as the projectile. Used are its rare neutron-rich isotopes 62 or 64 (not the most abundant ones 58 or 60) to provide, at least to some extent, the neutron excess typical for very heavy nuclei.

Written as nuclear chemical reactions, the fusion processes leading to the new elements are given by Equations (1)–(3). After fusion of the two reaction partners the resulting compound nucleus is more or less heated, because the kinetic energy of the projectile, necessary to get the nuclei in contact, is not completely consumed in the nuclear reaction but remains as residual excitation energy. The hot nucleus cools down by evaporation of neutrons leaving the element unchanged but reducing the mass number accordingly. In the three synthetic reactions (1)–(3) of the new elements a single neutron (n) is sufficient for cooling. This is a peculiarity of nuclear fusions starting with lead or bismuth nuclei; they proceed without excessive excitation of the compound system.

$$^{62}_{28}\mathrm{Ni} + ^{208}_{82}\mathrm{Pb} \longrightarrow ^{269}110 + 1\,^{1}_{0}\mathrm{n} \quad (1)$$

$$^{64}_{28}\mathrm{Ni} + ^{208}_{82}\mathrm{Pb} \longrightarrow ^{271}110 + 1\,^{1}_{0}\mathrm{n} \quad (2)$$

$$^{64}_{28}\mathrm{Ni} + ^{209}_{83}\mathrm{Bi} \longrightarrow ^{272}111 + 1\,^{1}_{0}\mathrm{n} \quad (3)$$

Because of that, such reactions—first proposed 1974 by Yuri Oganessian from the Joint Institute for Nuclear Research in Dubna (Russia)—are considered the most promising for the synthesis of new elements. That they are so mild has to do with the closure of nuclear shells in lead and bismuth; such nuclei are strongly bound—deep frozen, so to speak—as are the nickel projectiles. One could aptly call such reactions "cold fusion" if this term did not recall the recent notorious flop of cold fusion of deuterium nuclei. The shell structure of atomic nuclei is a quantum mechanical phenomenon, quite analogous to the shell structure of the electron cloud and has the same stabilizing effect.

The realization of such fusion reactions are as difficult as their formulations on paper appear easy, because quite different processes predominate by far. In such heavy nuclei the repulsive force between the protons becomes competitive with the attractive nuclear force between the nucleons. Hence, the two touching nuclei may separate again before a reaction has started at all,

[*] Prof. Dr. G. Herrmann
Institut für Kernchemie der Universität
Fritz-Strassmann-Weg 2, D-55099 Mainz (Germany)
Telefax: Int. code + (6131)39-4488

or when fusion is still incomplete. If the reaction proceeds to yield a (hot) compound nucleus, it most likely breaks into two fragments rather than surviving as the desired nuleus after neutron evaporation. Fusion could be promoted by increasing the projectile energy, but the compound nucleus would get even hotter and more susceptible to nuclear fission; thus, nothing would be gained.

Just how delicate the situation is can be illustrated by a few numbers. The probability for a collision between projectile and target nucleus is approximately given by their geometric cross section. This is about 10^{-24} cm^2 or 1 barn, to introduce a unit popular in nuclear research. According to the results of the Darmstadt SHIP group—called after their principal instrument *S*eparator for *H*eavy *I*on Reaction *P*roducts—the production cross sections decrease from 10^{-32} cm^2 for element 104 to 10^{-35} cm^2 for element 109, that is, to only 10 picobarn. In more illustrative terms: Only one single collision between projectile and target among 10^{11} yields element 109. Extrapolated to still heavier elements, this trend predicts figures around one picobarn for element 111, equivalent to a square millimeter in an area of a square kilometer. This level seemed to be inaccessible a decade ago even to the SHIP group. All technical resources seemed to be exhausted, and laws of nature are inviolable anyway.

But then the SHIP group succeeded in approaching the picobarn cross section level by many small improvements of their facilities.[3] At this level one would expect to observe, on average, one nucleus every six days at the UNILAC, provided the projectile energy is optimized, namely to one percent. Fusion reactions depend very sensitively on the bombarding energy. The SHIP group has studied this effect thoroughly in the synthesis of the elements 104 and 108 in order to chose the right energies in attacking the new elements.

However, the potential now available did not have to be fully exploited in the synthesis of elements 110 and 111. The two nuclei ^{269}110 and ^{272}111 are produced with cross sections of about 3 picobarn,[3, 6] and for ^{271}110 even 15 picobarn were measured[5] multiples of what had been anticipated.

But how can a few atoms of a new element be found and identified unambiguously in the profusion of uninteresting nuclei? The sorting process takes place within a few microseconds during the flight of positively charged ions through SHIP, an 11 m long recoil spectrometer. It consists of the rotating target, the actual separator—equipped with magnetic lenses and crossed electric and magnetic fields—and the detector. Fed in the instrument are all kinds of reaction products that recoil out of the target during collisions of the pulsed projectile beam with nuclei in the target foil. But the strong projectile beam also passes through the target in nearly unattenuated intensity, because most projectiles do not undergo nuclear reactions. To catch the very few, very heavy reaction products, the direction and velocity of the flying atoms are utilized: fusion products are collimated in forward direction whereas products of other reactions are more likely to escape sidewards, and fusion products move more slowly than projectiles. Only nuclei with the right direction and velocity pass through this extremly efficient filter to reach the detector.

The identification of the very rare nuclei is based on their emission of α-particles, helium nuclei with nuclear charge 2 and mass number 4. Auspicious are events with high α-particle energy, because towards the end of the periodic table this energy should increase from element to element. The presence of a new element is proven conclusively by its α-decay into a whole chain of known atomic nuclei. The α-decay of the new element yields a known nucleus, lighter by two protons and four nucleons, which is recognized by its lifetime and α-energy, and feeds a known decay chain linked together again by α-transitions.

This principle of genetic linking of new with known nuclei is ingeniously realized in SHIP in a semiconductor detector, 80 mm wide and 35 mm high, which is mechanically and electronically divided into 3700 tiny individual detectors of 0.8 mm^2 area. If an atom passing SHIP hits the detector, an electric signal is produced indicating the time and location of the event. All subsequent events at the same location are recorded: what kind of decay occurs at what time, and what energy is released. Thus, the fate of the original nucleus is followed, step by step, by the lifetimes and α-energies of its descendants.

Figure 1 shows three decay chains of the new elements. When element 110 was observed for the first time, this individual nucleus ^{269}110 decayed 393 μs after its implantation, by emitting an α-particle of 11.13 MeV energy, into a nucleus that proved to be the known ^{265}108 by its 10.57 MeV α-particle emission after

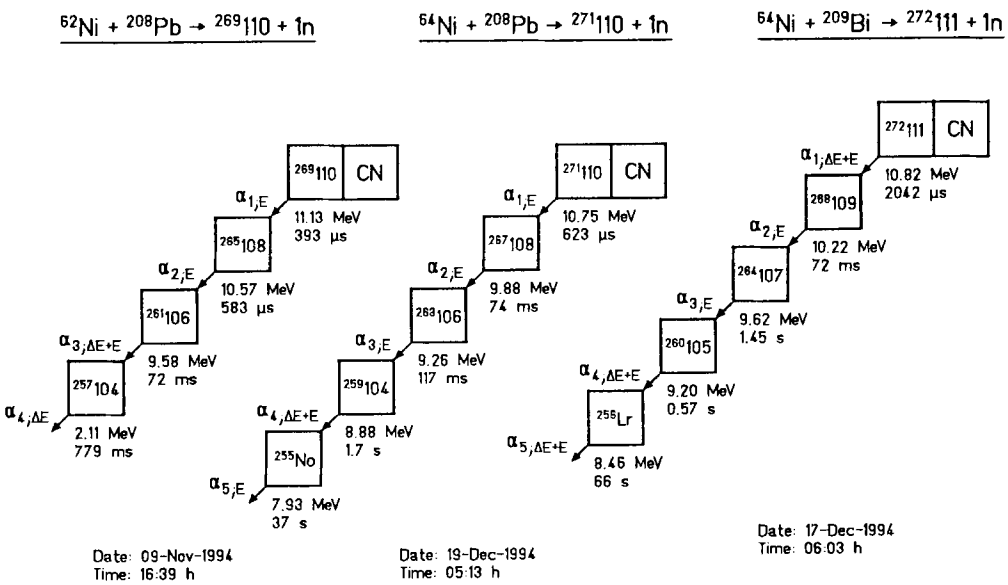

Fig. 1. Three decay chains characteristic of the elements 110 and 111 [5]. The top line gives the synthesis reactions. CN represents the compound nucleus produced by fusion of projectile and target nuclei; on its left is indicated the nucleus formed by evaporation of one neutron. This nucleus is the starting point for the decay chain. For each chain link i the measured α-particle energy α_i is given and, below, the observed individual lifetime (E and ΔE refer to details of the energy measurement). The bottom line indicates when that nucleus of the new element hit the detector.

 © VCH Verlagsgesellschaft mbH, D-69451 Weinheim, 1995 0570-0833/95/1616-1714 $ 10.00+.25/0

583 μs lifetime. Also for the following decay chain originating in ^{265}108, lifetimes—or, deduced from that, half-lives—and α-particle energies of all chain members agreed with known data. Therefore, the new α-emitter right at the beginning of the whole decay series had to be assigned to the nucleus ^{269}110. In the same way ^{271}110 was identified. In the case of element 111 the first two decay products, ^{268}109 and ^{264}107, were not yet known, but since three long decay chains were observed terminating at well-known isotopes of the elements 105 or 103, the initial nucleus had to be attributed to ^{272}111.

The decay data of the new elements are summarized in Table 1 as average values of all observed nuclei. The α-particle energies can be reproduced very precisely even with very few events; half-lives and production cross sections fluctuate more due to the statistical nature of radioactive processes. In the case of ^{271}110, one of the nine observed nuclei was identified to be a nuclear isomer of longer lifetime.[6]

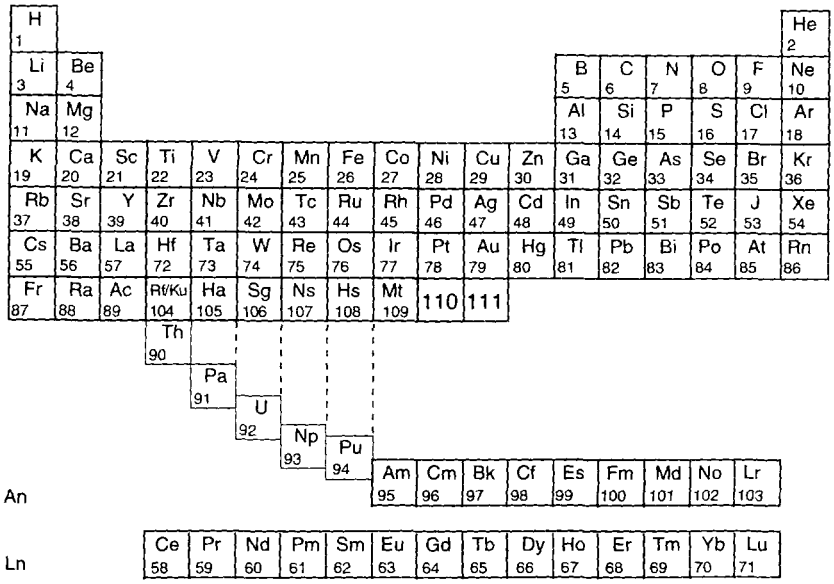

Fig. 2. The periodic table of the elements today. In this somewhat unusual presentation, the actinide elements (An) are arranged above the lanthanides (Ln) in a form that emphasizes similarities of the first actinides with subgroup elements. For the heaviest elements the names and symbols preferred by heavy-element researchers are used.

Table 1. Nuclear properties of the new elements and production cross sections x, from results of the SHIP group at the UNILAC heavy-ion accelerator [3–6].

Element	Mass number	Half-life [ms]	α-Particle energy [MeV]	x [picobarn]
110	269	0.17	11.112	3.5
	271	1.1	10.738 10.681	15
	271m [a]	56	10.709	
111	272	1.5	10.820	3.5

[a] Isomeric nucleus.

That the method of genetic linkage can be performed to such perfection with very few nuclei was demonstrated when the SHIP group repeated in this latest beam time the fusion of iron-58 ($Z = 26$) with lead-208 to form element 108 with mass number 265. Now, with 79 observed nuclei, what had been found before with only three nuclei when element 108 was discovered was confirmed.

Evidence for the synthesis of element 110 was also presented at recent conferences by two other research groups. Albert Ghiorso[7] reported in Juni 1994 on a single event observed at the Lawrence Berkeley Laboratory during fusion experiments of cobalt-59 ($Z = 27$) with bismuth-209, which may be assigned to mass number 267. However, the decay chain is rather incomplete and cannot be interpreted without making assumptions. The experiment cannot be repeated in Berkeley because the SuperHILAC heavy-ion accelerator is shut down, and the recoil separator has been dismantled. Also apparently incomplete is the single event described by Yuri Lazarev[8] in April 1995, found in Dubna in the "hot" fusion of sulfur-34 ($Z = 16$) with plutonium-244 ($Z = 94$), which may lead to mass number 273. In contrast to these events, the SHIP researchers present their assignments of element 110 as unambigous, and justifiably so.[3]

Figure 2 shows where the new elements should be located in the periodic table: 110 below platinum, 111 below gold, if after completion of the actinide series the table is continued with element 104 in the 4th subgroup and is simply carried on to the right. The chemical behavior[9] of the first two elements following the actinides, the elements 104 and 105, indeed characterizes them as part of the subgroups 4 and 5. Studies of the chemistry of heaviest elements have not yet progressed beyond element 105, hahnium, since short half-lives and extremely low production rates lead to a very unusual situation: When a new atom appears, the preceding one has already decayed, and chemical experiments have, thus, to be carried out with single atoms. Apart from the technical problems, the question arises whether studies with single atoms are representative for determining macroscopic properties. According to theoretical studies this is indeed the case for certain classes of experiments.

The chemistry of element 105, hahnium, is investigated on its isotope 262 (half-life 34 s) produced by fusion of oxygen-18 ($Z = 8$) with berkelium-249 ($Z = 97$). The production rate is so low that a hahnium decay is observed, statistically distributed, only in one out of ten experiments. What is needed under these circumstances are fully automated, miniaturized techniques; automation is required to perform thousands of experiments, miniaturization to minimize losses by radioactive decay. Nevertheless, several properties of the first two transactinide elements are already well characterized; consequently they can be compared with those of the homologous elements, for example, the species occurring in aqueous solutions or in gas phases.[9] In general, the elements 104 and 105 exhibit the expected oxidation states IV and V, respectively. In detail, they often follow more their "pseudohomologues" at the beginning of the actinide series. Element 105 behaves more like protactinium (Pa), than niobium (Nb), and scarcely like tantalum (Ta), its immediate neighbor. This could be due to rearrangements of the electron clouds caused by the relativistic mass increase of the very fast moving inner electrons. It is challenging to ask how this trend will continue at element 106 whose chemistry is not known at

all; it will soon be attacked by chemists studying the heaviest elements.

When reporting new elements one can hardly ignore the recent discussion of the names of the heaviest elements. Since controversies about the priority for some of the discoveries led to much confusion, the International Union of Pure and Applied Chemistry (IUPAC) and the corresponding Union of Physics (IUPAP) charged a working group to follow the history of all transfermium elements, that is, elements beyond 100. The group has summarized the evaluations[10] in form of discovery profiles which clearly show that several cases are quite complex and priorities should be shared. For the elements 107 to 109, however, the priority of the SHIP group is undisputed. Hence, in a celebration[11] at GSI on September 7, 1992, element 107 was named nielsbohrium (Ns), element 108 hassium (HS), and element 109 meitnerium (Mt), honoring the physicists Niels Bohr and Lise Meitner and after the state of Hessen where GSI is located. After the evaluation by the IUPAC–IUPAP working group, which did not propose names, the research groups involved apparently agreed to a large extent on names that had been established some time and are also used in this report; really in dispute remained only element 104.

Unfortunately the IUPAC Commission on Nomenclature of Inorganic Chemistry presented a rather different list of names[12] for ratification by the IUPAC Council. The proposals of the SHIP group are adopted for element 109, meitnerium; for 107 bohrium (Bh) is proposed, and for 108 hahnium, so far in use for element 105. No argument is given why element 108 should not be named after a geographic term linked to the discovery—as is the case for many natural and artificial elements—although in the same paper this tradition is followed with the name dubnium for element 104. A single sentence merely points out that naming the neighboring elements 108 and 109 after Otto Hahn and Lise Meitner is proposed as a recognition of their decisive role in the discovery of nuclear fission.[12] It might appear appealing to see these two scientists who cooperated over decades immortalized side by side in the periodic table, but the idea of moving the chemist Otto Hahn away from element 105 is nevertheless disappointing. We are already sure that the chemistry of hahnium can be studied; whether this will ever be possible for element 108 is a very open question. The other deviating proposals[12] are: dubnium instead of rutherfordium for element 104, joliotium instead of hahnium for 105, and rutherfordium instead of seaborgium for 106.

On behalf of the SHIP group, Peter Armbruster protested against this violation of the traditional right of the discoverers to choose the name for a new element.[13] Obviously the IUPAC has also violated its own rules[14] (Bylaw B2.11) that recommendations of such consequence should be considered provisional when first published, and the comments invited. Now the IUPAC seems to wish to revert to these rules.[15] Thus, the severe criticism would appear to have succeeded, and whoever already adopted the "new" names seem to have been a bit overzealous.

What about the future? How stable are nuclei beyond element 111 and how can they be made? First of all, this is a question of the shell structure of atomic nuclei; from element 108 onwards nuclei exist merely because they are held together by nuclear shells.

The strength of shell energies in kown nuclei is deduced from nuclear masses or α-decay energies, which amounts to the same thing. These experimental shell energies are input data for nuclear-model calculations used to extrapolate the shell energy of still unknown nuclei. Figure 3 shows the results of recent

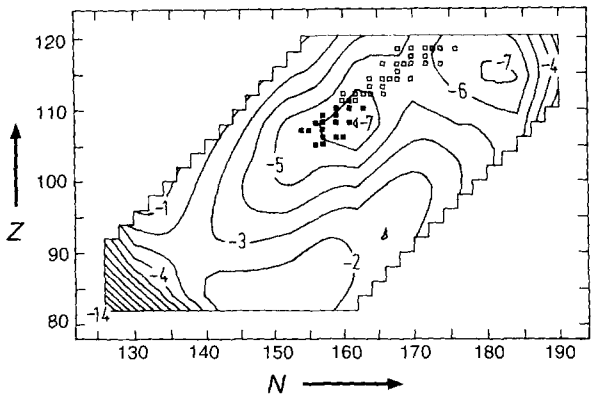

Fig. 3. Shell energies of heaviest nuclei calculated for nuclear models [16], plotted versus proton number Z and neutron number N. Contour lines connect nuclei of equal shell energy (in MeV). The more negative this energy, the more stabilized the nucleus. Three minima for nuclei with closed proton and neutron shells can be seen: in the left lower corner the steep minimum at lead-208 ($Z = 82$, $N = 126$), in the center a flat minimum at $Z = 108$ and $N = 162$, and at the upper right end a shallow minimum at $Z = 114$ and $N = 182$. Filled squares indicate the heaviest known nuclei; empty squares are compound nuclei that can be reached, in principle, by fusion of lead-208 with the appropriate projectile [5].

calculations,[16] which take into account complicated nuclear shapes. At the lower left corner this landscape of shell energy opens with a deep valley (−14.3 MeV) around lead-208. The belt of known nuclei (not indicated) then follows a steep ascent up to a saddle (− 3 MeV) at the uranium nuclei with $Z = 92$, $N \approx 146$. A gentle descent leads to a plateau oriented northeastwards with a rather flat valley (−7.2 MeV) around element 108 at neutron number 162. Here we find the heaviest known nuclei, as can be seen in Figure 3. Then the plateau continues towards the east, in the direction of more neutron-rich nuclei, and after crossing a rarely visible saddle enters another shallow valley (again −7.2 MeV) around element 114 with neutron number 182. According to another recent calculation[17] the deepest point in this valley is expected somewhat further to the west, at element 115 and 179 neutrons.

The prediction of spherical superheavy nuclei with 114 protons has kept nuclear theorists and experimentalists busy for three decades, but these nuclei were considered to form an island well separated from the mainland by the sea of instability. Now, after new nuclei have been found and nuclear models and extrapolations improved, the landscape has changed completely: The sea has gone, replaced by a broad ridge of shell-stabilized nuclei that are not spherical but look like elongated cylinders with rounded edges. Such more complicated shapes were not considered in those earlier days.

What implications do the shell energies have for the half-lives? This can be quite well estimated, but the picture is somewhat complicated by the fact that two decay modes—α-particle emission and spontaneous fission—play a role and follow different trends. In summary, α-decay with half-lives between a microsecond and a second is predicted for most of the nuclei that

can be produced with stable projectiles and accessible targets. Spontaneous fission does not yet predominate. Thus, seen in the light of nuclear stability, the limit of the periodic table is not yet in sight. This limit will finally be reached when nuclei do not hold together at all but immediately break into two fragments.

The process that produce heavy nuclei remain more difficult to judge. They are not yet well understood, and what is known about fusion reactions in lighter systems cannot be applied. Thus, one relies upon empirical extrapolations; the 15 picobarn production cross section of the nucleus ^{271}110 opens exciting perspectives, of course. The cross section extrapolated for element 112 is about three picobarn, that for element 113 and element 114 one picobarn,[5] if zinc-70 ($Z = 30$) or germanium-76 ($Z = 32$) are fused with lead or bismuth– all within reach of the SHIP group. However, the center of stability, the mountain lake around element 114, cannot be reached from lead-208. As shown in Figure 3, the channel of accessible nuclei goes past to the west. Other strategies would also not lead to success, because no combination of accessible projectile and target nuclei would provide enough neutrons. Nevertheless, it seems not to be utopian to step onto the broad western beach. If the landscape would appear there as predicted, one would also catch a glimpse of that glorious lake.

German version: *Angew. Chem.* **1995**, *107*, 1857–1861

Keywords: element 110 · element 111 · nuclear stability · transuranium elements

[1] G. Münzenberg, *Rep. Prog. Phys.* **1988**, *51*, 57–104.
[2] G. Herrmann, *Angew. Chem.* **1988**, *100*, 1471–1491; *Angew. Chem. Int. Ed. Engl.* **1988**, *27*, 1417–1436.
[3] S. Hofmann, V. Ninov, F. P. Heßberger, P. Armbruster, H. Folger, G. Münzenberg, H. J. Schött, A. G. Popeko, A. V. Yeremin, A. N. Andreyev, S. Saro, R. Janik, M. Leino, *Z. Phys. A* **1995**, *350*, 277–280.
[4] S. Hofmann, V. Ninov, F. P. Heßberger, P. Armbruster, H. Folger, G. Münzenberg, H. J. Schött, A. G. Popeko, A. V. Yeremin, A. N. Andreyev, S. Saro, R. Janik, M. Leino, *GSI Nachrichten* **1995** (2), 4–15.
[5] a) Conference: *Low Energy Nuclear Dynamics*, St. Petersburg, **1995**, April 18–22; Preprint *GSI-95-25* **1995**; Proceedings in press. b) S. Hofmann, paper in [5a].
[6] S. Hofmann, V. Ninov, F. P. Heßberger, P. Armbruster, H. Folger, G. Münzenberg, H. J. Schött, A. G. Popeko, A. V. Yeremin, A. N. Andreyev, S. Saro, R. Janik, M. Leino, *Z. Phys. A* **1995**, *350*, 281–282.
[7] A. Ghiorso, D. Lee, L. P. Somerville, W. Loveland, J. M. Nitschke, W. Ghiorso, G. T. Seaborg, P. Wilmarth, R. Leres, A. Wydler, M. Nurmia, K. Gregorich, R. Gaylord, T. Hamilton, N. J. Hannink, D. C. Hoffman, C. Jarzynski, C. Kacher, B. Kadkhodayan, S. Kreek, M. Lane, A. Lyon, M. A. McMahan, M. Neu, T. Sikkeland, W. J. Swiatecki, A. Türler, J. T. Walton, S. Yashita, *Nucleus-Nucleus Collisions V* (Eds.: M. Di Toro, E. Migneco, P. Piatelli) (*Nucl. Phys. A* **1995**, *583*, 861–866).
[8] Yu. A. Larazev, paper in [5a]. Quoted from S. Hofmann, personal communication.
[9] J. V. Kratz, *Actinides-93* (Eds.: D. L. Clark, D. E. Hobart, J. Fuger) (*J. Alloys Compd.* **1994**, *213/214*, 20–27); D. C. Hoffman, *Chem. Eng. News* **1994**, *72* (18), 24–34.
[10] Transfermium Working Group of IUPAC and IUPAP (D. H. Wilkinson, A. H. Wapstra, I. Ulehla, R. C. Barber, N. N. Greenwood, A. Hrynkiewicz, Y. P. Jeannin, M. Lefort, M. Sakai, *Pure Appl. Chem.* **1993**, *65*, 1757–1814).
[11] *Die Benennung der schwersten Elemente 107, 108 und 109* (Ed.: P. Armbruster), Gesellschaft für Schwerionenforschung, Darmstadt, **1993**.
[12] IUPAC Commission on Nomenclature of Inorganic Chemistry (A. M. Sargeson, Chair, *Pure Appl. Chem.* **1994**, *66*, 2419–2421).
[13] P. Armbruster, *Nachr. Chem. Tech. Lab.* **1995**, *43*(1), 53.
[14] D. C. Hoffman, personal communication, **1995**.
[15] Quoted from M. Freemantle, *Chem. Eng. News* **1995**, *73*(19), 7.
[16] R. Smolańczuk, A. Sobiczewski, paper in [5a].
[17] P. Möller, J. R. Nix, W. D. Myers, W. J. Swiatecki, *At. Data Nucl. Data Tables* **1995**, *59*, 185–381.

Catalytic Asymmetric Carbonyl–Ene Reactions

David J. Berrisford* and Carsten Bolm*

As one of the fundamental bond-forming reactions, the carbonyl–ene reaction between an aldehyde and an alkene bearing an allylic hydrogen attracts considerable attention[1] from the synthetic community. Given the versatile chemistry of the resulting homoallylic alcohols, both the intra- and intermolecular versions of asymmetric carbonyl–ene reactions are valuable processes.[2] Within the field of catalysis[3] the continuing improvements in the efficiency of chiral Lewis acids and the development of novel ene chemistry occur in concert. We wish to highlight a number of these developments.

A recent publication by Carreira et al.[4] documents further advances in this already topical area. The authors describe a titanium-catalyzed asymmetric carbonyl–ene reaction of the commodity chemical 2-methoxypropene ($ 49.30 L^{-1}/Janssen) with aldehydes (Scheme 1). When a catalyst prepared in situ

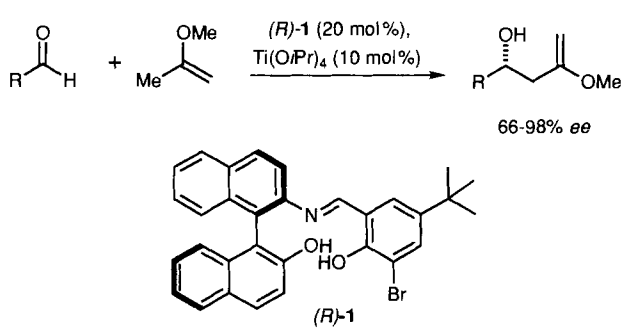

Scheme 1.

[*] Dr. D. J. Berrisford
Department of Chemistry
University of Manchester Institute of Science and Technology
PO Box 88, GB-Manchester M60 1QD (UK)
Telefax: Int. code +(161) 236-7677
Prof. Dr. C. Bolm
Fachbereich Chemie der Universität Marburg
D-35032 Marburg (Germany)
Telefax: Int. code +(6421) 28-8917

from the tridentate ligand (*R*)-**1** and $Ti(OiPr)_4$ in a 2:1 ratio is used, the yields and enantioselectivities of the new process are generally high (Table 1). The most encouraging results, up to 98% *ee*, are obtained with α,β-ynals. Thus, this reaction offers an alternative catalytic method for the synthesis of propargylic alcohols. The reaction with benzaldehyde proceeds with only modest selectivity, 66% *ee*, which is unusual for asymmetric addition processes. The only α-branched aldehyde reported to undergo addition, cyclohexanecarboxaldehyde, affords a product with 75% *ee*.

Table 1. Yields and enantiomeric excesses of the Ti-catalyzed asymmetric carbonyl–ene reaction [5] (see Scheme 1).

Aldehyde	Yield [%] [a]	*ee* [%] [a]
$Ph(CH_2)_3-C\equiv C-CHO$	99	98
$TBSOCH_2-C\equiv C-CHO$	85	93
$Ph-C\equiv C-CHO$	99	91
$Ph(CH_2)_2CHO$	98	90
PhCHO	83	66
$C_6H_{11}CHO$	79	75

[a] The corresponding β-hydroxy ketones, which were obtained by treatment of the reaction mixture with Et_2O/2N HCl, were isolated and analyzed.

The vinyl ethers obtained from asymmetric ene reactions are valuable precursors for synthetically important optically active compounds (Scheme 2). Acid hydrolysis affords the corresponding methyl ketones, thus providing an alternative to asymmetric methyl ketone aldol additions.[5, 6] Oxidative cleavage of the enol ethers with ozone affords the corresponding β-hydroxy esters, and osmium-catalyzed dihydroxylation with *N*-morpholine-*N*-oxide (NMO) gives ketodiols.

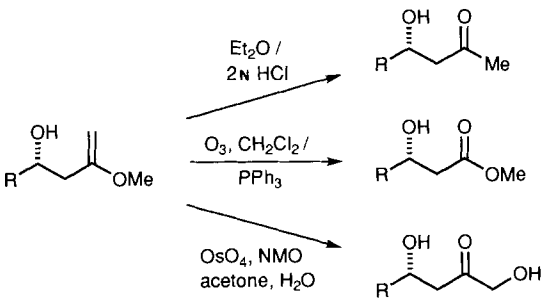

Scheme 2.

The recent work by Carreira et al. is an extension of earlier studies[5] in which a titanium(IV) catalyst prepared in situ from the tridentate ligand (*R*)-**1** and $Ti(OiPr)_4$ was used to achieve Mukaiyama aldol additions with high enantioselectivities. The chiral ligand used in both the ene and aldol chemistry is prepared from 3-bromo-5-*tert*-butylsalicylaldehyde and 2-amino-2′-hydroxy-1,1′-binaphthol. This enantiomerically pure amino alcohol is obtained from the convenient oxidative coupling procedure[7] of Smrčina et al. We expect further applications of this valuable chiral biaryl ligand.

Usually intermolecular ene reactions of simple aldehydes with otherwise inactivated 1,1-disubstituted alkenes require stoichiometric amounts of powerful Lewis acids.[1] Therefore, asymmetric variants using milder Lewis acids as catalysts have been restricted to especially reactive aldehydes in intermolecular processes or to intramolecular reactions. For example, Yamamoto et al. used the aluminum-based chiral Lewis acid (*R*)-**2** in catalyzed asymmetric carbonyl–ene reactions (Scheme 3).[8] However, the choice of enophile is limited to highly electron-deficient aromatic aldehydes such as pentafluorobenzaldehyde and chloral. Both simple 2,2-disubstituted alkenes and vinyl sulfides undergo enantioselective reaction with a maximum *ee* of 88% even with catalytic quantities (20 mol%) of the Lewis acid.

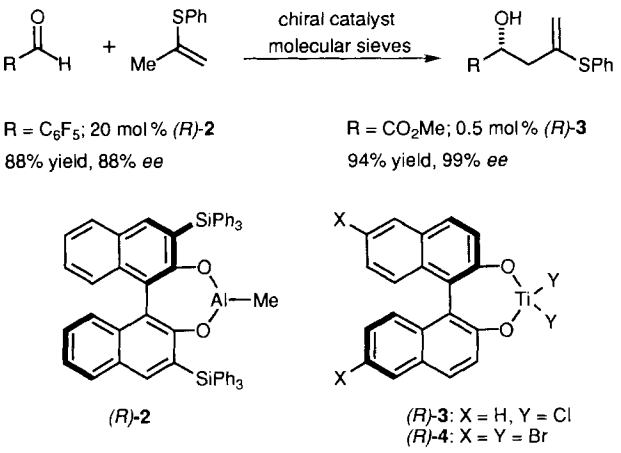

Scheme 3.

The asymmetric carbonyl–ene reaction has also been developed further by Mikami et al.[1b, c] The reaction of glyoxylate enophiles with the readily available Lewis acids $[TiX_2BINOL]$[9] (X = Cl, Br), for example (*R*)-**3** (Scheme 3), gives outstanding enantioselectivities. Many of the earlier developments have been thoroughly reviewed.[1] However, a number of important recent advances are worth highlighting.[10–15] Extremely low catalyst loadings (0.5 mol%) can be used with vinyl sulfides and selenides in the glyoxylate–ene reaction.[10] Changing the Lewis acid to (*R*)-**4** enables certain trisubstituted alkenes to be used with excellent enantio- and diastereocontrol.[11] Vinyl ethers, which are more reactive than their thioether counterparts, undergo ene reactions with high enantioselectivities when (*R*)-**3** is employed as catalyst.[12] Thus, addition of 2-phenoxybutene to chloroacetaldehyde in the presence of 10 mol% of (*R*)-**3** gives the corresponding ene product in 53% yield with 97% *ee* (Scheme 4).[12] Under these Lewis acidic conditions phenoxy

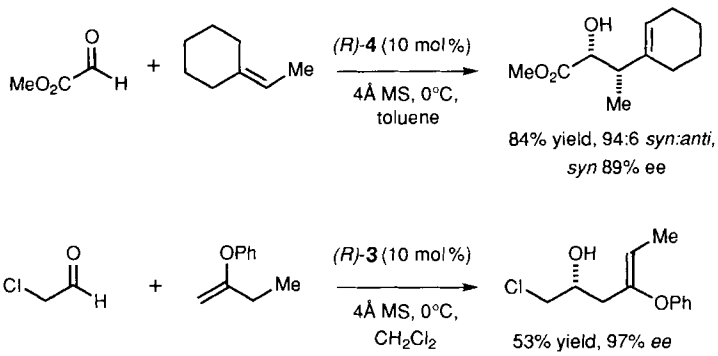

Scheme 4. MS = molecular sieves.

ethers are more stable than the corresponding hexyl and methyl ethers.

Owing to the impressive levels of stereocontrol achieved with this method, a number of concise syntheses[1] of important bioactive targets can be devised. Recent studies by the Mikami group focus on two fragments of the immunosuppressant rapamycin[13] and the prostacyclin analogue isocarbacylin; the latter application is notable for using a formaldehyde–ene reaction.[14]

An ene mechanism is also implicated in the asymmetric "aldol" additions of ketene silyl acetals of thioesters to aldehydes[15] and of silyl enol ethers to glyoxylate esters (Scheme 5).[16] The lack of accompanying silyl transfer is in contrast to other asymmetric Mukaiyama-type aldol reactions.[17]

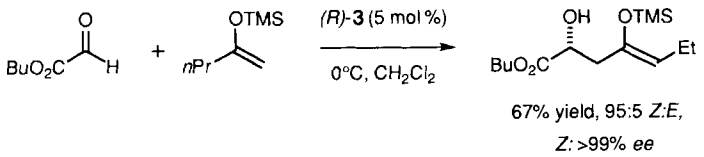

Scheme 5.

The new methods developed by Carreira, Mikami, and others widen the scope of asymmetric catalytic ene reactions. Studies on new catalysts[18] often provide the necessary mechanistic insights from which further developments in reaction protocol ensue. With a high degree of confidence we can predict that discoveries of even more practical chiral Lewis acid catalysts, displaying wider substrate tolerance and requiring lower catalyst loadings, will continue apace.

German version: *Angew. Chem.* **1995**, *107*, 1862–1864

Keywords: asymmetric syntheses · carbonyl–ene reactions · catalysis · chiral auxiliaries · titanium compounds

[1] a) B. B. Snider in *Comprehensive Organic Synthesis, Vol. 2* (Eds.: B. M. Trost, I. Fleming), Pergamon, Oxford, **1991**, p. 527; *ibid Vol. 5*, p. 1; b) K. Mikami, M. Shimizu, *Chem. Rev.* **1992**, *92*, 1021; c) K. Mikami, M. Terada, S. Narisawa, T. Nakai, *Synlett* **1992**, 255; d) R. M. Borzilleri, S. M. Weinreb, *Synthesis* **1995**, 347.

[2] a) S. Sakane, K. Maruoka, H. Yamamoto, *Tetrahedron Lett.* **1985**, *26*, 5535; b) *Tetrahedron* **1986**, *40*, 2203; c) K. Narasaka, Y. Hayashi, S. Shimada, *Chem. Lett.* **1988**, 1609.

[3] a) K. Maruoka, H. Yamamoto in *Catalytic Asymmetric Synthesis* (Ed.: I. Ojima), VCH, Weinheim, **1993**, p. 413; b) R. Noyori, *Asymmetric Catalysis in Organic Synthesis*, Wiley, New York, **1994**; c) K. Narasaki, *Synthesis* **1991**, 1.

[4] E. Carreira, W. Lee, R. A. Singer, *J. Am. Chem. Soc.* **1995**, *117*, 3649.

[5] E. Carreira, R. A. Singer, W. Lee, *J. Am. Chem. Soc.* **1994**, *116*, 8837.

[6] Catalyzed Mukaiyama-type aldol reactions of silyl enol ethers or silyl ketene acetals with aldehydes lead to the same products. For recent advances see: G. E. Keck, D. Krishnamurthy, *J. Am. Chem. Soc.* **1995**, *117*, 2363, and references therein.

[7] a) M. Smrčina, M. Lorenc, V. Hanus, P. Sedmera, P. Kočovský, *J. Org. Chem.* **1992**, *57*, 1917; b) M. Smrčina, J. Poláková, S. Vyskočil, P. Kočovský, *ibid.* **1993**, *58*, 4534.

[8] K. Maruoka, Y. Hoshino, T. Shirasaka, H. Yamamoto, *Tetrahedron Lett.* **1988**, *29*, 3967.

[9] The formulae in this article merely imply the stoichiometric composition rather than the solution structure. For recent investigations of the structures of chiral Ti complexes see: a) T. J. Boyle, N. W. Eilerts, J. A. Heppert, F. Takusagawa, *Organometallics* **1994**, *13*, 2218; b) E. J. Corey, M. A. Letavic, M. C. Noe, S. Sarshar, *Tetrahedron Lett.* **1994**, *35*, 7553; c) K. V. Gothelf, R. G. Hazell, K. A. Jørgensen, *J. Am. Chem. Soc.* **1995**, *117*, 4435.

[10] M. Terada, S. Matsukawa, K. Mikami, *J. Chem. Soc. Chem. Commun.* **1993**, 327.

[11] a) M. Terada, Y. Motoyama, K. Mikami, *Tetrahedron Lett.* **1994**, *35*, 6693; b) K. Mikami, Y. Motoyama, M. Terada, *Inorg. Chim. Acta* **1994**, *222*, 71.

[12] We thank Professor Mikami, Tokyo Institute of Technology, for helpful discussions and disclosure of unpublished material. a) K. Mikami, E. Sawa, M. Terada, unpublished results; b) E. Sawa, *Master's Thesis*, Tokyo Institute of Technology, **1992**.

[13] a) K. Mikami, A. Yoshida, *Tetrahedron Lett.* **1994**, *35*, 7793; b) K. Mikami, S. Narisawa, M. Shimizu, M. Terada, *J. Am. Chem. Soc.* **1992**, *114*, 6566, 9242.

[14] K. Mikami, A. Yoshida, *Synlett* **1995**, 29.

[15] K. Mikami, S. Matsukawa, *J. Am. Chem. Soc.* **1994**, *116*, 4077.

[16] a) K. Mikami, S. Matsukawa, *J. Am. Chem. Soc.* **1993**, *115*, 7039; b) *Tetrahedron Lett.* **1994**, *35*, 3133.

[17] T. K. Hollis, B. Bosnich, *J. Am. Chem. Soc.* **1995**, *117*, 4570.

[18] For a new type of highly active titanium catalysts for asymmetric glyoxylate–ene reactions: a) M. Terada, K. Mikami, *J. Chem. Soc. Chem. Commun.* **1994**, 833; b) D. Kitamoto, H. Imma, T. Nakai, *Tetrahedron Lett.* **1995**, *36*, 1861.

 © VCH Verlagsgesellschaft mbH, D-69451 Weinheim, 1995 0570-0833/95/1616-1719 $ 10.00+.25/0

Total Synthesis of (±)-Dynemicin A**

Matthew D. Shair,* Tae-young Yoon, and Samuel J. Danishefsky

Dynemicin A (**1**) (Scheme 1), a metabolite isolated from *Micromonospora chersina*, which has DNA cleaving capacity and demonstrated in vitro antitumor properties, has elicited a great deal of excitement among chemists.[1] While it is not likely to be developed as a drug (owing to issues of abundance, formulatability, and biological specificity), the interest in dynemicin is sustained by its fascinating structure. Questions as to the mechanism of its bioactivation,[2] the search for simpler analogues that retain the central motif of dynemicin,[3] and the need to catalog modalities of recognition of the drug by DNA targets, continue to engender research.[4]

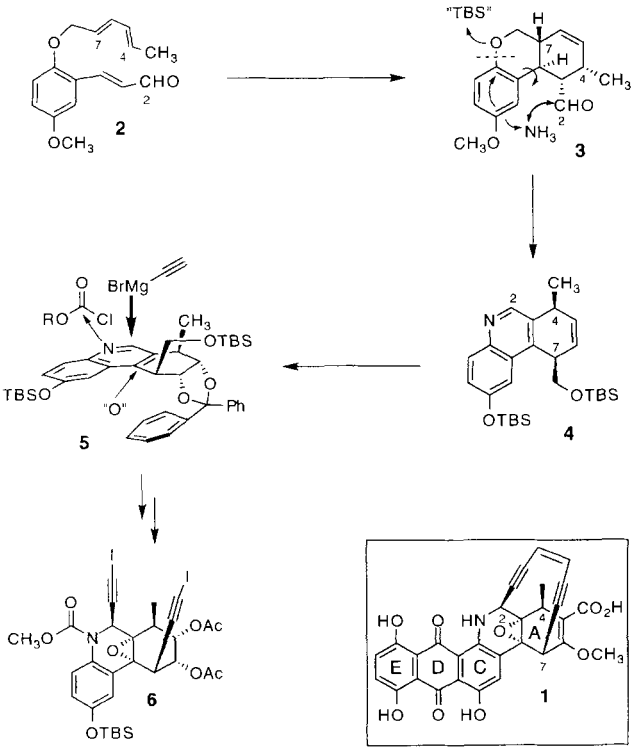

Scheme 1. Synthesis of diiodoalkyne **6**. TBS = *tert*-butyldimethylsilyl.

[*] M. D. Shair, T. Yoon, Prof. S. J. Danishefsky[+]
Department of Chemistry, Havemeyer Hall
Columbia University, New York, NY 10027 (USA)
Telefax: Int. code + (212)854-7142

[+] Alternative address:
Sloan-Kettering Institute for Cancer Research
Laboratory for Bioorganic Chemistry
1275 York Avenue, Box 106, New York, NY 10021 (USA)
Telefax: Int. code + (212)772-8691

[**] This work was supported by the National Institutes of Health (grant CA 28824) and by the Memorial Sloan-Kettering Cancer Center (predoctoral fellowship to M. D. S.). We thank Dr. I. J. Kim for the preparation of bromoarene **17**, and Dr. Dolatrai M. Vyas of Bristol-Myers Squibb Pharmaceutical Research Institute for supplying an authetic sample of dynemicin A.

No less challenging is the issue of total synthesis. Major progress in this domain was registered by Schreiber et al., who first demonstrated methods for constructing truncated versions of dynemicin, lacking the anthraquinone sector.[5a] Eventually, these studies culminated in a striking synthesis of protected versions of dynemicin.[5b] Even in the face of these large accomplishments, the novelty of the dynemicin molecule continued to elicit new conjectures at the level of synthesis. The goal of preparing dynemicin in its full and exquisite structural detail continued to be worthy of attention.

Our own efforts were initially directed toward exploring some fresh departures which might eventually accomplish such a total synthesis. We demonstrated that an intramolecular Diels–Alder reaction could be used to dictate the *cis* stereochemical relationship of C-4 and C-7 (dynemicin numbering) (see **2** → **3** → **4**, Scheme 1) in pre-dynemicin structures.[6] We learned how to functionalize the C5–C6 double bond, not only for developmental purposes regarding the synthesis, but also for implementing the required stereochemical disposition of C-2 and C-7 (see **4** → **5** → **6**, Scheme 1).[6, 7] A rather new reaction type, the palladium-mediated cross-coupling reaction of a diiodoalkyne with a (*Z*)-distannylethene (see **6** + **7** → **8**, Scheme 2) was implemented to assemble the enediyne linkage.[7] In due course, we learned how to fashion the β-ketoacid enol ether moiety at C-5 and C-6 (see **8** → **9** → **10**).[7]

The time was at hand to deal with installation of the CDE trihydroxyanthraquinone ensemble. Toward this end, we reported a method for synthesizing a quinone imine of the type **11** (Scheme 2).[3a] This quinone imine linkage readily undergoes

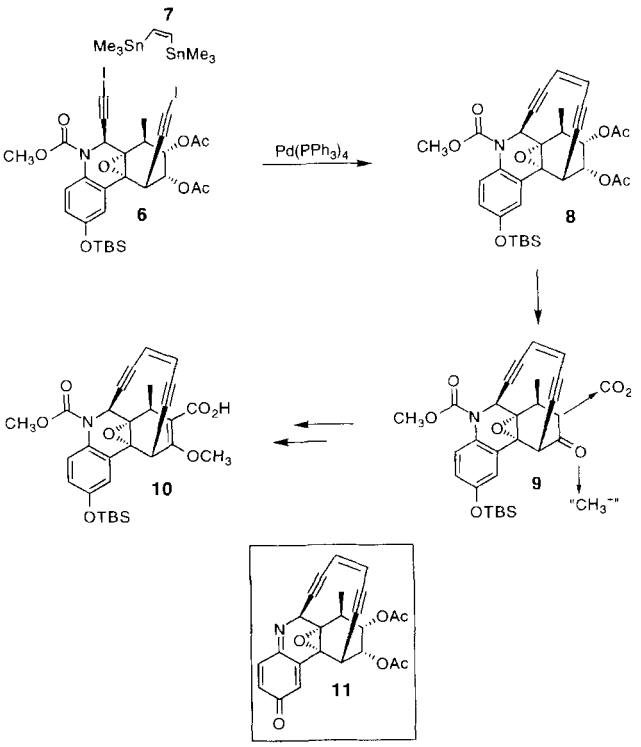

Scheme 2. Synthesis of enediyne **10**.

cycloaddition reactions of pertinence to the construction of the anthraquinone segment.

Concurrently with our own work, although through totally different premises, Myers and associates disclosed the synthesis of a closely related quinone imine[8] and also demonstrated its amenability to cycloaddition with dienes of relevance to the "DE problem."[9] Indeed, in a striking accomplishment, the Caltech workers announced the first total synthesis of dynemicin A by Diels–Alder reaction of a quinone imine with a suitable isobenzofuran. This cycloaddition was followed by eventual oxidative development of the DE system and unveiling of the C5–C6 functionality.[9]

We describe here the culmination of our own efforts leading to a total synthesis of dynemicin A (**1**). We report the application of a rather different annulation strategy for the conversion of quinone imine **16** (Scheme 3) to dynemicin A. The construction of the anthraquinone follows a concise route and should be applicable to the synthesis of congeners of dynemicin or other classes of anthracycline-based antitumor agents.

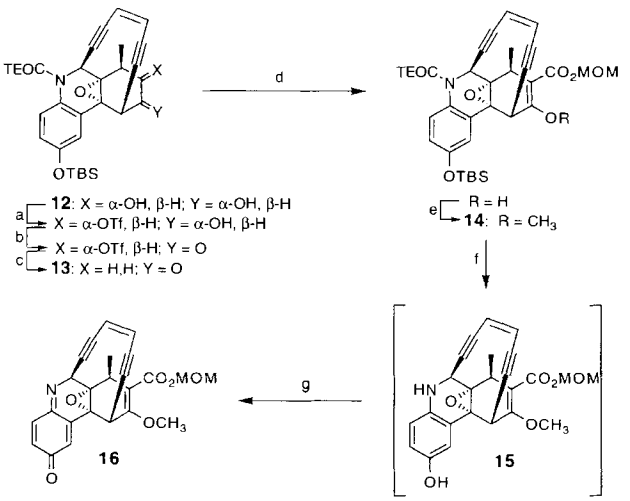

Scheme 3. Synthesis of quinone imine **16**. a) 1.8 equiv Tf_2O, 40 equiv C_5H_5N, CH_2Cl_2, −20 °C, 1 h (95%); b) 3.0 equiv Dess–Martin periodinane, CH_2Cl_2, 25 °C, 2 h (91%); c) 7.0 equiv $CrCl_2$, THF, 25 °C, 2 h (75%); d) 5.5 equiv $MgBr_2$, 30.0 equiv Et_3N, CO_2, CH_3CN, 25 °C, 2.5 h, then 7.0 equiv MOMCl, 50.0 equiv iPr_2NEt, THF, 25 °C, 5 min (60%); e) excess CH_2N_2, MeOH, 0 °C, 1 h (70%); f) 5.0 equiv TBAF, THF, 0 °C, 3.5 h; g) 5.0 equiv $PhI(OAc)_2$, 0 °C, 0.5 h (60%). TEOC = trimethylsilylethoxycarbonyl, TBAF = tetra-*n*-butylammonium fluoride.

The synthesis started with compound **12**[3a] (Scheme 3) which was converted to ketone **13** and thence to **14**, in which C-5 and C-6 have been suitably functionalized.[7] Simultaneous removal of the two blocking groups TEOC and TBS generated the highly labile, uncharacterized tetrahydroquinolinol derivative **15**, which was immediately oxidized to provide **16**.[10]

The synthesis of the protected homophthalic anhydride **20**, which would deliver the DE segment of dynemicin A, is denoted in Scheme 4.[11] Doubly MOM-protected bromoarene **17** was

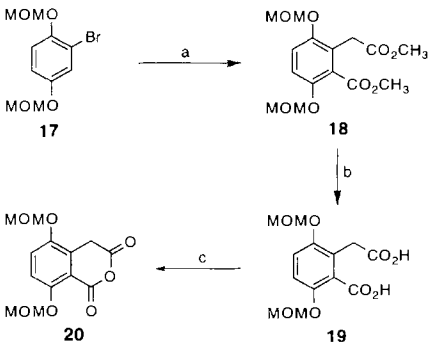

Scheme 4. Synthesis of homophthalic anhydride **20**. a) 1.2 equiv $CH_2(CO_2CH_3)_2$, 2.4 equiv LiTMP, THF, −78 °C, 30 min (71%); b) 20 equiv KOH, H_2O, MeOH, reflux, 3 h (91%); c) TMSC≡COEt, CH_2Cl_2, 25 °C, 2 h (100%). LiTMP = lithium tetramethylpiperidide.

condensed with the lithium salt of dimethylmalonate and lithium tetramethylpiperidide (LiTMP) at low temperature. The homophthalic ester **18** formed immediately, presumably arising from the addition of lithium dimethylmalonate to the benzyne followed by intramolecular carboxylation of the resulting aryl anion.[12] Saponification of the diester **18** led to the formation of dicarboxylic acid **19**, which was dehydrated with ethyl trimethylsilylethynyl ether to provide the desired anhydride **20** in high yield.[13]

After much experimentation, we developed a workable annulation sequence (Scheme 5).[11] Treatment of **16** with the anion

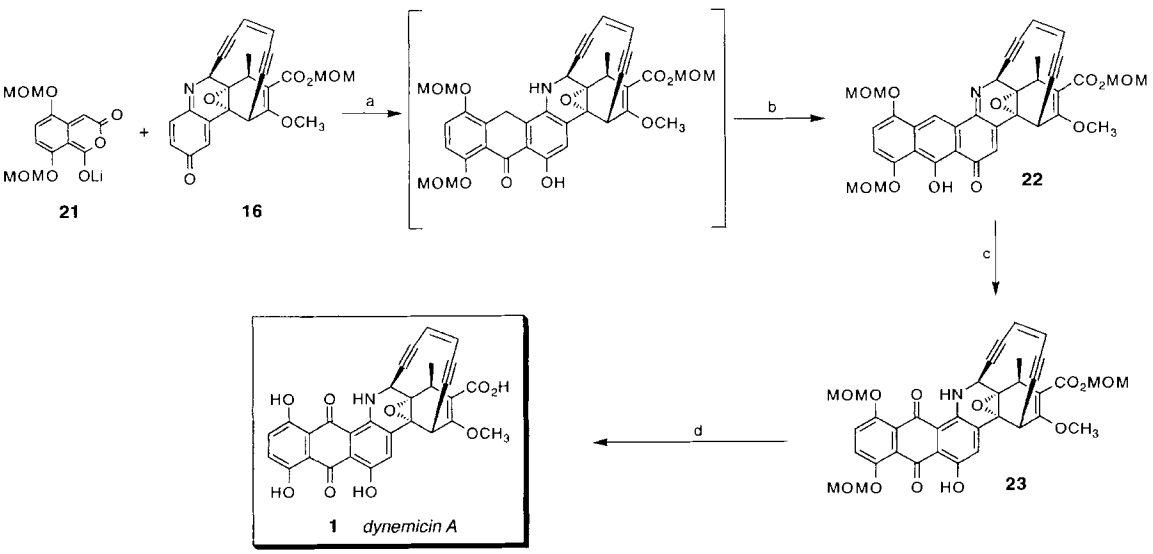

Scheme 5. Anthraquinone annulation sequence and deprotection of **23** to provide dynemicin A (**1**). a) 5.0 equiv 2,5-bis(methoxymethyl)-homophthalic anhydride, 4.8 equiv LHMDS, 0 °C, 1 h; b) 7.0 equiv $PhI(OCOCF_3)_2$, THF, 0 °C, 5 min; c) air, high concentration, 25 °C, daylight, THF, 24 h; d) 15 equiv $MgBr_2$, Et_2O, 0–25 °C, 36 h (15% yield over 4 steps). LHMDS = lithium 1,1,1,3,3,3-hexamethyldisilazane.

21, derived from doubly MOM-protected homophthalic anhydride **20**, followed by oxidation with phenyliodondium bis(trifluoroacetate) resulted in a substance which we provisionally formulate as **22**.[14] The proposal advanced in Scheme 5 for the progression from **16** to **22** should be implemented in a formal rather than a chronological context. When a highly concentrated solution of **22** in THF was exposed to the action of oxygen and daylight, a violet-red product presumed to be the protected goal structure **23** was obtained.[15] Deprotection of **23** afforded dynemicin A (**1**). The ^{1}H NMR spectrum and TLC properties of the synthetic material matched those of an authentic sample. The relative configuration at C-4 had been independently verified by crystallography at an earlier stage.[6] The comparisons with the severely limited authentic material available, the nature of the steps, and the inherent properties of our final product, fully establish that (±)-dynemicin A (**1**) had been synthesized. Studies directed to higher yielding anthraquinone annulation protocols are underway. Also, with increased quantities of dynemicin now available to us by synthesis, investigations of some of the bioorganic issues identified above have already been initiated.

Received: April 20, 1995 [Z79131E]
German version: *Angew. Chem.* **1995**, *107*, 1883–1885

Keywords: anthraquinones · dynemicin A · enediynes · total syntheses

[1] a) M. Konishi, H. Ohkuma, T. Tsuno, T. Oki, G. D. VanDuyne, J. Clardy, *J. Am. Chem. Soc.* **1990**, *112*, 3715 and references therein; b) For a review of the chemistry and biology of the enediyne antibiotics, see: K. C. Nicolaou, W.-M. Dai, *Angew. Chem.* **1991**, *103*, 1453; *Angew. Chem. Int. Ed. Engl.* **1991**, *30*, 1387.

[2] M. F. Semmelhack, J. Gallagher, D. Cohen, *Tetrahedron Lett.* **1990**, *31*, 1521.

[3] a) M. D. Shair, T. Yoon, T.-C. Chou, S. J. Danishefsky, *Angew. Chem.* **1994**, *106*, 2578; *Angew. Chem. Int. Ed. Engl.* **1994**, *33*, 2477; b) K. C. Nicolaou, W.-M. Dai, S.-C. Tsay, V. A. Estevez, W. Wrasildo, *Science* **1992**, *256*, 1387; c) P. A. Wender, C. K. Zercher, S. Beckham, E.-M. Haubold, *J. Org. Chem.* **1993**, *58*, 5867.

[4] a) Y. Sugiura, T. Shiraki, M. Konishi, T. Oki, *Proc. Nat. Acad. Sci. USA* **1990**, *87*, 3831; b) D. R. Langley, T. W. Doyle, D. L. Beveridge, *J. Am. Chem. Soc.* **1991**, *113*, 4395; c) P. A. Wender, R. C. Kelly, S. Beckham, B. L. Miller, *Proc. Natl. Acad. Sci. USA* **1991**, *88*, 8835.

[5] a) J. L. Wood, J. A. Porco, Jr., J. Taunton, A. Y. Lee, J. Clardy, S. L. Schreiber, *J. Am. Chem. Soc.* **1992**, *114*, 5898; b) J. Taunton, J. L. Wood, S. L. Schreiber, *ibid.* **1993**, *115*, 10378.

[6] T. Yoon, M. D. Shair, S. J. Danishefsky, G. K. Schulte, *J. Org. Chem.* **1994**, *59*, 3752.

[7] M. D. Shair, T. Yoon, S. J. Danishefsky, *J. Org. Chem.* **1994**, *59*, 3755.

[8] A. G. Myers, M. E. Fraley, N. J. Tom, *J. Am. Chem. Soc.* **1994**, *116*, 11556.

[9] A. G. Myers, M. E. Fraley, N. J. Tom, S. B. Cohen, D. J. Madar, *Chem. Biol.* **1995**, *2*, 33.

[10] For the use of the trimethylsilylethoxycarbonyl (TEOC) group to protect amino functions in sensitive molecules, see: a) S. A. Hitchcock, S. H. Boyer, M. Y. Chu-Moyer, S. H. Olson, S. J. Danishefsky, *Angew. Chem.* **1994**, *106*, 928; *Angew. Chem. Int. Ed. Engl.* **1994**, *33*, 858; b) G. Kim, M. Y. Chu-Moyer, S. J. Danishefsky, *J. Am. Chem. Soc.* **1990**, *112*, 2003.

[11] For the use of a base-induced cycloaddition between homophthalic anhydrides and quinones to form polycyclic compounds, see: Y. Tamura, M. Sasho, K. Nakagawa, T. Tsugoshi, Y. Kita, *J. Org. Chem.* **1984**, *49*, 473.

[12] M. Guyot, D. Molho, *Tetrahedron Lett.* **1973**, 3433.

[13] Y. Kita, S. Akai, N. Ajimura, M. Yoshigi, T. Tsugoshi, H. Yasuda, Y. Tamura, *J. Org. Chem.* **1986**, *51*, 4150.

[14] The direct product of the cycloaddition between **16** and **21** prior to oxidation may also exist as the anthracenol rather than the anthrone as depicted. In addition, the C ring may have not undergone aromatization. However, the spectroscopic properties observed for the product following in situ oxidation would fit **22**.

[15] For the conversion of anthracenols to anthraquinones in the presence of ground-state oxygen and light, see: D. W. Cameron, P. E. Schultz, *J. Chem. Soc. C.* **1967**, 2121; P. L. Julian, W. Cole, G. Diemer, *J. Am. Chem. Soc.* **1945**, *67*, 1721.

A Total Synthesis of Taxol**

John J. Masters,* J. T. Link, Lawrence B. Snyder, Wendy B. Young, and Samuel J. Danishefsky

Taxol (**1**) is a clinically useful antitumor agent. First approved for the treatment of ovarian cancer, it is currently being evaluated for efficacy against a broader range of tumors.[1] The combination of the beneficial chemotherapeutic effects of taxol, its limited availability from phytochemical sources, and its novel, multifunctional structure has stimulated a great deal of interest among organic chemists.[2] The accessibility of taxol (**1**) was improved by the development of several efficient acylation sequences commencing with baccatin III (**2**, Scheme 1).[3] Since this compound is reasonably available from renewable plant sources, it is improbable that total synthesis will ever impact the availability of **2**. Thus, questions pertaining to strategy, reaction development, and access to certain classes of analogs rather than a solution of the taxol "supply problem" fuel interest in these targets.

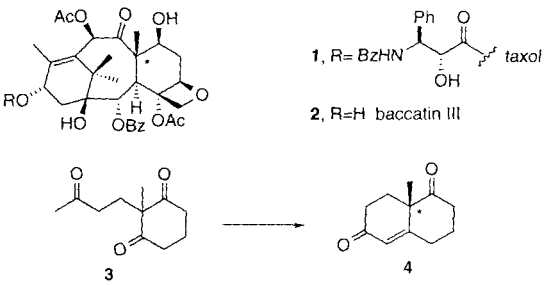

Scheme 1.

Indeed, the challenge associated with assembling baccatin III (**2**) in the laboratory has brought forth a myriad of fascinating ideas. Most of the published works have centered on issues relating to the elaboration of the ABC ring system. Fewer have provided sound prospects for appropriate functional group development. In early 1994, Nicolaou et al. and Holton et al. reported the first and only total syntheses of baccatin III and taxol in virtually concurrent disclosures.[4, 5] The steep barrier that separates a comprehensive solution (total synthesis) from advances of a more local nature had been surmounted. Here, we report our total synthesis of baccatin III (**2**) and thence, by well-known steps, of taxol (**1**) itself.[3]

Since our synthesis also requires a multistep sequence, it does not constitute a plausible alternative to phytochemical routes to **2**. However, the synthesis described herein has the merit of not relying upon resolutions, synthetic relays, or on difficultly accessible starting materials for entering the "chiral pool". In fact, in our program, all asymmetric induction ultimately accrues from

[*] J. J. Masters, J. T. Link,[+] L. B. Snyder, W. B. Young, Prof. S. J. Danishefsky[+]
Sloan-Kettering Institute for Cancer Research
1275 York Avenue, New York, NY 10021 (USA)
Telefax: Int. code + (212)772-8691

[+] Alternative address:
Department of Chemistry, Havemeyer Hall
Columbia University, New York, NY 10027 (USA)
Telefax: Int. code + (212)854-7142

[**] This research was supported by National Institutes of Health (NIH, grant no. AI 16949). A Damon Runyon-Walter Winchell Cancer Fund Postdoctoral Fellowship to J. J. M. and an American Cancer Society Postdoctoral Fellowship to W. B. Y. are gratefully acknowledged. We thank Susan de Gala, Yale University, for crystallographic analysis and Dr. G. Sukenick, Memorial Sloan-Kettering Cancer Center, for mass spectrometric analyses.

(*S*)-Wieland Miescher ketone **4**, which, in turn, arises from the catalytically induced enantioselective aldol condensation of the prochiral trione **3** (Scheme 1).[6] Another distinguishing element of our synthesis is an early introduction of the oxetane moiety by displacement of a leaving group at C-5 with a hydroxymethyl nucleophile stationed at C-4 (Scheme 2).[7] This protocol, which we first demonstrated on a fully functionalized C ring,[8] found application at late stages in each of the first two total syntheses. Early emplacement of the oxetane seemed to offer the advantage of enhancing the convergency of the total synthesis.

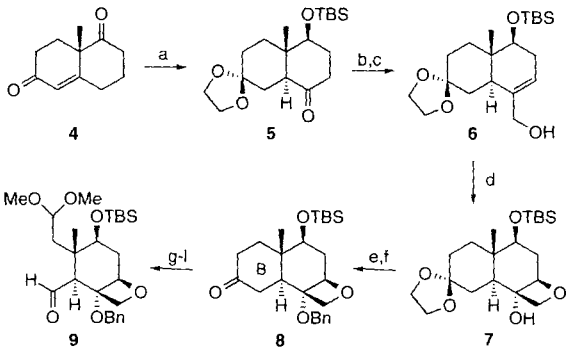

Scheme 2. a) See ref. [7]; b) $Me_3S^+I^-$, potassium hexamethyldisilazide (KHMDS), THF, 0 °C, 99%; c) $Al(OiPr)_3$, PhMe, reflux, 99%; d) see ref. [7]; e) BnBr, NaH, tetrabutylammonium iodide (TBAI), THF, 0 °C → room temperature (RT), 98%; f) TsOH, acetone, H_2O, 70 °C, 84%; g) TMSOTf, Et_3N, CH_2Cl_2, −78 °C; h) 3,3-dimethyldioxirane, CH_2Cl_2, 0 °C; i) camphorsulfonic acid (CSA), acetone, RT, 89%; j) $Pb(OAc)_4$, MeOH, PhH, 0 °C, 97%; k) MeOH, 2,4,6-collidine *p*-toluenesulfonate, 70 °C, 97%; l) $LiAlH_4$, THF, 0 °C, 100%; j) *o*-$NO_2C_6H_4SeCN$, PBu_3, THF, RT, 88%; k) 30% H_2O_2, THF, RT, 90%; l) O_3, CH_2Cl_2, −78 °C, PPh_3, 79%.

As described earlier with racemic material, **4** was converted to ketone **5** by classical, high-yielding steps.[9] A significant improvement in the conversion of **5** to the previously described **6** was achieved as shown in Scheme 2.[10] Compound **6** was then converted to the oxetane **7** and thence to the ketone **8** by known methods.[7] The B ring of the latter was cleaved in an easily conducted, high-yielding sequence to produce aldehyde acetal **9**.[11]

In related efforts to assemble a baccatin–cholesterol hybrid, the dienyl iodide **10** was prepared and lithiated to provide **11** (Scheme 3).[11a] In that simpler setting, the equivalence of **11** and the hypothetical **12** had been demonstrated. However, it was unclear that joining **10** (via **11**) and **9** would be feasible in the presence of the labile oxetane. After much effort, an efficient coupling leading to **13** was accomplished under the conditions shown.

The strategy of connecting suitably functionalized A and C fragments (in this case A and CD) to build 1,2-constrained

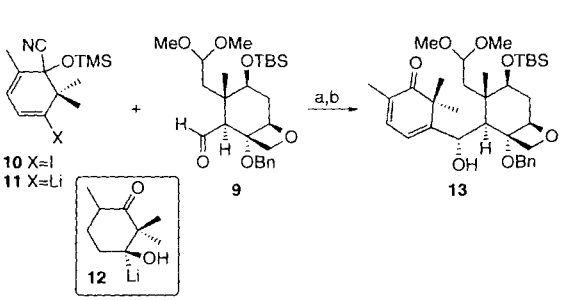

Scheme 3. a) **10**, *t*BuLi, THF, −78 °C, then **9**, 93%; b) TBAF, THF, −78 °C, 80%.

seco-B structures en route to closure of the B ring, had been implicit in our earliest publications in the taxol area.[12] Clearly the idea was central to the Nicolaou total synthesis (see Scheme 4, **14** → **15**), in which the C9–C10 bond was closed through a pinacol construction.[5] In our work, we studied possible C10–C11 closures of highly functionalized substrates. This

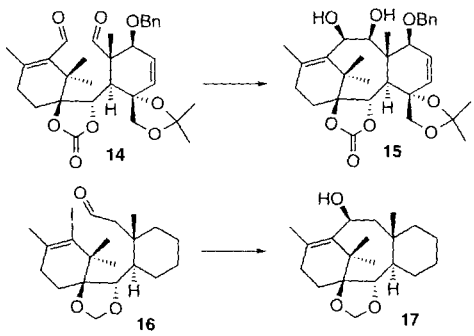

Scheme 4.

possibility was being investigated concurrently by Kishi and associates who pursued, broadly speaking, a Barbier-type bond formation (specifically focusing on Ni^{II}/Cr^{II}-induced closures of a C-10 aldehyde and a C-11 vinyl nucleophile; see **16** → **17**).[13] While we could reach intermediates that were substrates for this and analogous Barbier reactions, we were never able to achieve such a closure in syntheses of either the baccatin–cholesterol hybrid or baccatin itself.

We had also investigated the possibility of closing the C10–C11 bond through an intramolecular Heck reaction.[14] The first indications of feasibility were recorded in the construction of an aryl taxane (see Scheme 5, **18** → **19**).[11c] A more convinc-

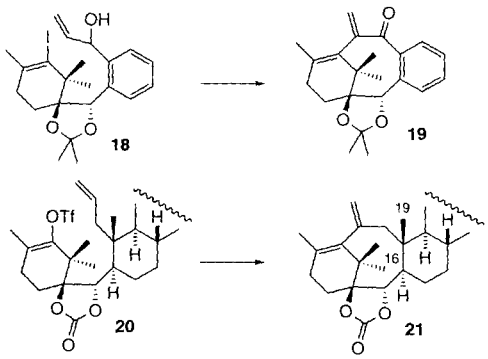

Scheme 5.

ing demonstration was achieved in the conversion of **20** to **21**. Here, ring formation succeeded despite the emerging abutment of the methyl groups at C-16 and C-19.[11a] The question remaining was whether this chemistry could be conducted with highly functionalized baccatin III precursors containing the oxetane ring.

After considerable experimentation, advances toward our goal were achieved (Scheme 6). Directed epoxidation of **13** was accomplished,[15] as was subsequent reduction to **22**. Particularly challenging, in the highly hindered and marginally stable setting of **22**, was the efficient protection of the C-1 and C-2 hydroxyl groups. This too was realized (see compound **23** and

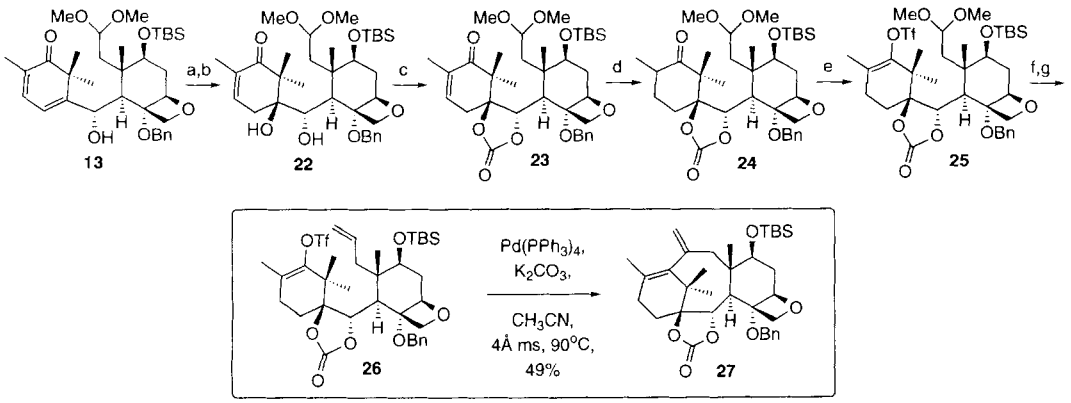

Scheme 6. a) *meta*-chloroperbenzoic acid (mCPBA), CH_2Cl_2, RT, 80%; b) H_2, Pd/C, −5 °C, EtOH, 65%; c) carbonyl diimidazole (CDI), NaH, DMF, 81%; d) L-Selectride, THF, −78 °C, 93%; e) $PhNTf_2$, KHMDS, THF, −78 °C, 98%; f) pyridinium *para*-toluenesulfonate (PPTS), acetone, H_2O, 96%; g) $Ph_3P{=}CH_2$, THF, −78 °C → 0 °C, 77%. ms = molecular sieves.

its subsequent conversion to ketone **24**). Given the dense array of functional groups in **24**, its conversion to vinyl triflate **25** was gratifying. Cleavage of the dimethylacetal linkage was conducted and elongation afforded **26**. The critical reaction was now at hand. The Heck ring closure was achieved on a highly functionalized substrate (**26** → **27**).

In reaching **27** we had deliberately relied on a robust *tert*-butyldimethylsilyl (TBS) protecting group at C-7. Preliminary studies revealed that the silyl ether could not be readily removed when the functionality in the core tetracyclic structure became more complex.[16] Accordingly, **27** was converted to the triethylsilyl (TES) ether **28** (Scheme 7). In related work on the

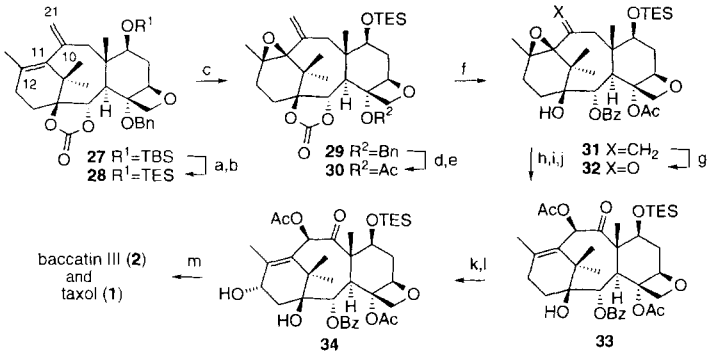

Scheme 7. a) TBAF, THF, RT, 92%; b) TESOTf (TES = triethylsilyl), Et_3N, CH_2Cl_2, −78 °C, 92%; c) mCPBA, $NaHCO_3$, CH_2Cl_2, RT, 45%; d) H_2, Pd/C, EtOH, RT, 82%; e) Ac_2O, *para*-dimethylaminopyridine (DMAP), Pyr, RT, 66%; f) PhLi, THF, −78 °C, 93%; g) OsO_4, Pyr, 105 °C; $Pb(OAc)_4$, PhH, MeOH, 0 °C, 61%; h) SmI_2, Ac_2O, THF, −78 °C, 92%; i) KO*t*Bu, $(PhSeO)_2O$, THF, −78 °C; KO*t*Bu, THF, −78 °C, 81%; j) Ac_2O, DMAP, Pyr, 76%; k) pyridinium chlorochromate (PCC), NaOAc, PhH, reflux, 64%; l) $NaBH_4$, MeOH, 79%; m) HF·Pyr, THF, 85% yield of **2**; for the conversion of **34** to **1** see ref. [3c].

construction of a baccatin III–steroid hybrid we showed how to accomplish the unexpectedly difficult conversion of the diene unit to the required functionality.[17] In the present case, the reaction sequence was initiated with epoxidation leading to **29**. The status of the oxygen substituent at C-4 was changed from benzyl ether to acetate (**29** → **30**). Phenylation of **30**, following valuable precedent, afforded benzoate **31**.[4, 5, 18] The *exo*-methylene group was cleaved to provide **32** as indicated. Deoxygenation of the oxirane was accomplished with samarium diiodide in the presence of acetic anhydride.[19] Oxidation at C-9, followed by an α-ketol interchange and acetylation provided **33**.[4] From here, allylic oxidation followed by reduction afforded 7-triethylsilyl baccatin III (**34**)[5] and thence, following deprotection, to baccatin III (**2**) itself.[20] Also, for the sake of the record, we repeated the Ojima protocol for the introduction of the side chain, thus completing the total synthesis of taxol (**1**).[3c]

These studies, featuring a remarkable intramolecular Heck reaction (**26** → **27**) to establish the core tetracyclic system, have demonstrated new and, perhaps, unsuspected capacity to carry the oxetane through complex maneuvers. As such, this chemistry is likely to be influential in accomplishing totally synthetic ventures to simpler taxol analogs.

Received: May 17, 1995 [Z.8001IE]
German version: *Angew. Chem.* **1995**, *107*, 1886–1888

Keywords: baccatin III · Heck reactions · taxol · total syntheses

[1] For reviews see: a) G. I. Georg, T. T. Chen, I. Ojima, D. M. Vyas, *Taxane Anticancer Agents*, American Cancer Society, San Diego, **1995**; b) D. G. I. Kingston, A. A. Molinero, J. M. Rimoldo, *Prog. Chem. Org. Nat. Prod.* **1993**, *61*, 1.

[2] For reviews see: a) K. C. Nicolaou, W. M. Dai, R. K. Guy, *Angew. Chem.* **1994**, *106*, 38; *Angew. Chem. Int. Ed. Engl.* **1994**, *33*, 15; b) C. S. Swindell, *Stud. Nat. Prod. Chem.* **1993**, *12*, 179.

[3] a) I. Ojima, C. M. Sun, M. Zucco, Y. M. Park, O. Duclos, S. Kuduk, *Tetrahedron Lett.* **1993**, *34*, 4149; b) I. Ojima, I. Habus, M. Zhao, M. Zucco, Y. H. Park, C. M. Sun, T. Brigaud, *Tetrahedron* **1992**, *48*, 6985; c) I. Ojima, I. Habus, M. Zhao, G. I. Georg, L. R. Jayasinghe, *J. Org. Chem.* **1991**, *56*, 1681; d) R. A. Holton, Workshop on Taxol and Taxus, **1991**; R. A. Holton, Eur. Pat. Appl. EP400,971 **1990**; *Chem. Abstr.* **1990**, *114*, 164568q; e) J. N. Denis, A. E. Greene, D. Guenard, F. Gueritte-Voegelein, L. Mangatal, P. Potier, *J. Am. Chem. Soc.* **1988**, *110*, 5917; f) J. N. Denis, A. Correa, A. E. Greene, *J. Org. Chem.* **1990**, *55*, 1957; g) L. Deng, E. N. Jacobsen, *ibid.* **1992**, *57*, 4320.

[4] a) K. C. Nicolaou, Z. Zang, J. J. Liu, H. Ueno, P. G. Nantermet, R. K. Guy, C. F. Claiborne, J. Renaud, E. A. Couladouros, K. Paulvannan, E. J. Sorensen, *Nature* **1994**, *367*, 630; b) K. C. Nicolaou, P. G. Nantermet, H. Ueno, R. K. Guy, E. A. Coulandouros, E. J. Sorensen, *J. Am. Chem. Soc.* **1995**, *117*, 624; c) K. C. Nicolaou, J. J. Liu, H. Yang, H. Ueno, E. J. Sorensen, C. F. Claiborne, R. K. Guy, C. K. Hwang, M. Nakada, P. G. Nantermet, *ibid.* **1995**, *117*, 634; d) K. C. Nicolaou, Z. Yang, J. J. Liu, P. G. Nantermet, C. F. Claiborne, J. Renaud, R. K. Guy, K. Shibayama, *ibid.* **1995**, *117*, 645; e) K. C. Nicolaou, H. Ueno, J. J. Liu, P. G. Nantermet, Z. Yang, J. Renaud, K. Paulvannan, R. Chadha, *ibid.* **1995**, *117*, 653.

[5] a) R. A. Holton, C. Somoza, H. B. Kim, F. Liang, R. J. Biediger, D. Boatman, M. Shindo, C. C. Smith, S. Kim, H. Nadizadeh, Y. Suzuki, C. Tao, P. Vu, S. Tang, P. Zhang, K. K. Murthi, L. S. Gentile, J. H. Liu, *J. Am. Chem. Soc.* **1994**, *116*, 1597; b) R. A. Holton, H. B. Kim, C. Somoza, F. Liang, R. J. Biediger, D. Boatman, M. Shindo, C. C. Smith, S. Kim, H. Nadizadeh, Y. Suzuki, C. Tao, P. Vu, S. Tang, P. Zhang, K. K. Murthi, L. S. Gentile, J. H. Liu, *ibid.* **1994**, *116*, 1599.

[6] P. Wieland, K. Miescher, *Helv. Chim. Acta* **1950**, *33*, 2215.

[7] a) T. V. Magee, W. G. Bornmann, R. C. A. Isaacs, S. J. Danishefsky, *J. Org. Chem.* **1992**, *57*, 3274. b) For alternative, but related, synthesis of the CD fragment and the oxetane see: R. C. A. Isaacs, M. J. Di Grandi, S. J. Danishefsky, *ibid.* **1993**, *58*, 3938.

[8] L. Ettouate, A. Ahond, C. Poupat, P. Potier, *Tetrahedron* **1991**, *47*, 9823.

[9] C. H. Heathcock, R. Ratcliffe, *J. Am. Chem. Soc.* **1971**, *93*, 1746.

 © VCH Verlagsgesellschaft mbH, D-69451 Weinheim, 1995 0570-0833/95/1616-1725 $ 10.00+.25/0

[10] a) E. J. Corey, M. Chaykovsky, *J. Am. Chem. Soc.* **1965**, *87*, 1353; b) T. G. Waddell, P. A. Ross, *J. Org. Chem.* **1987**, *52*, 4802. – We thank Dr. Craig A. Coburn and Dr. William G. Bornmann for developing and optimizing these steps.

[11] a) J. J. Masters, D. Jung, S. J. Danishefsky, L. B. Snyder, T. K. Park, R. C. A. Isaacs, C. A. Alaimo, W. B. Young, *Angew. Chem.* **1995**, *107*, 495; *Angew. Chem. Int. Ed. Engl.* **1995**, *34*, 452; b) For a related degradation of a CD fragment see: M. J. Di Grandi, C. A. Coburn, R. C. A. Isaacs, S. J. Danishefsky, *J. Org. Chem.* **1993**, *58*, 7728; c) J. J. Masters, D. K. Jung, W. G. Bornmann, S. J. Danishefsky, *Tetrahedron Lett.* **1993**, *34*, 7253.

[12] a) Y. Queneau, W. J. Krol, W. G. Bornmann, S. J. Danishefsky, *J. Org. Chem.* **1992**, *57*, 4043; b) M. J. Di Grandi, D. K. Jung, W. J. Krol, S. J. Danishefsky, *ibid.* **1993**, *58*, 4989. c) For an earlier example of this strategy see: A. S. Kende, S. Johnson, P. Sanfilippo, J. C. Hodges, L. N. Jungheim, *J. Am. Chem. Soc.* **1986**, *108*, 3513.

[13] a) M. H. Kress, R. Ruel, W. H. Miller, Y. Kishi, *Tetrahedron Lett.* **1993**, *34*, 5999; b) *ibid.* **1993**, *34*, 6003.

[14] For a review on the Heck reaction see: A. de Meijere, F. E. Meyer, *Angew. Chem.* **1994**, *106*, 2473; *Angew. Chem. Int. Ed. Engl.* **1994**, *33*, 2379.

[15] G. Berti, *Top. Stereochem.* **1973**, *7*, 93, and references therein.

[16] Deprotection of **31a** proved to be problematic and revealed that protecting group manipulations must be performed on compounds containing the carbonate group. The crystal structure of **31a** secured all of the stereochemical assignments made in the course of the synthesis before the target system was reached.

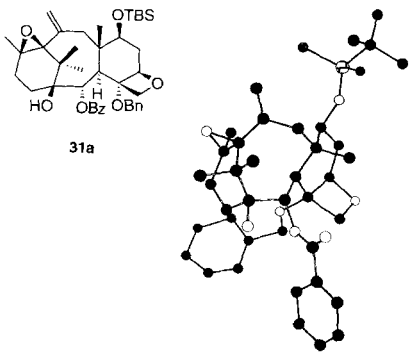

31a

[17] W. B. Young, J. T. Link, J. J. Masters, L. B. Snyder, S. J. Danishefsky, *Tetrahedron Lett.*, **1995**, *36*, 4963.

[18] K. C. Nicolaou, J. Renaud, P. G. Nantermet, E. A. Couladouros, R. K. Guy, W. Wrasidlo, *J. Am. Chem. Soc.* **1995**, *117*, 2409.

[19] For a review on the applications of samarium diiodide in organic synthesis see: G. A. Molander, *Chem. Rev.* **1992**, *92*, 29.

[20] Synthetic baccatin III (**2**) was identical to a natural sample by TLC, ^{1}H NMR, ^{13}C NMR, and IR spectroscopy, high-resolution mass spectrometry, and optical rotation.

Asymmetric Reaction of Arylalkenes with Diselenides**

Thomas Wirth*

Reactions for the functionalization of non-activated C=C double bonds are an integral part in the repertoire of the synthetic chemist; however there are not many stereoselective variants of these reactions.[1, 2] Stoichiometric addition reactions of chiral reagents can be used advantageously for asymmetric synthesis, especially since some of these adducts can also be further functionalized. Functionalizations of non-activated alkenes with selenium compounds, in particular, offer attractive possibilities. However, so far only a few asymmetric variants of these reactions are known since the chiral precursors can only be prepared by multistep syntheses with low overall yields.[3, 4]

In the following new and readily accessible chiral diselenides will be described, which show interesting stereoselectivities on addition to alkenes. After activating the diselenides by conversion into selenium cations, the alkenes are added in the presence of a nucleophile, and subsequently the addition products can be isolated in good yields. The selenium compounds obtained in this way are suitable for further reactions.[5] Since they are potential radical precursors, the whole palette of radical reactions is available. Deprotonation of the selenides in the α-position to the selenium and oxidative elimination offer possibilities for further functionalizations.

The diselenides (*S*,*S*)-**2** are synthesized from the chiral alcohols (*S*)-**1**,[6] which are obtained by reduction of the ketones with (−)-*B*-chlorodiisopinocampheylborane [(Ipc)$_2$BCl] in enantiomeric excesses of 93–96%.[7] The ketones are accessible by Grignard reaction from 2-bromobenzaldehyde and the subsequent oxidation with chromium(VI) oxide.[8] After alkylation of **1** (only if the desired product is **2**, R ≠ H) the resulting product is lithiated and worked up oxidatively after the addition of elemental selenium. The chiral diselenides **2** are isolated in overall yields of 50–60%.

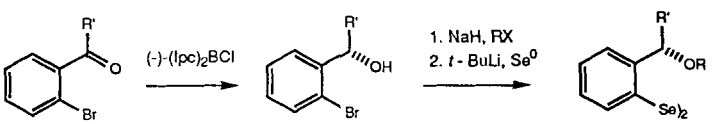

A (*S*)-**1** (*S*,*S*)-**2**

The diselenides **2** were initially treated with bromine to yield the bromides, which were subsequently allow to react with silver triflate to give the more reactive triflates. Coordination of the oxygen of the OR group to the selenium cation leads to the formation of a heterocycle in a fixed conformation; on addition of the alkene the chirality is transferred to the newly formed asymmetric centers. This is confirmed by analysis of the addition products **3**. For the diselenides **2a**–**2d** (R′ = Me, Table 1) the ability of the oxygen to coordinate to selenium is influenced by the size of the substituents R: the larger the substituent R the weaker the coordination of oxygen to selenium and therefore the weaker the inducing effect on the newly formed stereocenter. Thus, compound **2a** with R = H shows the highest diastereoselectivity on addition to styrene. A further indication of the coordinative effect is revealed by the ^{77}Se NMR shifts of the diselenides: the signal of the diselenide **2a** at δ = 446 is shifted

Table 1. Reaction of (*S*,*S*)-diselenides with styrene to give the addition products **3**.

Diselenide	R	R′	^{77}Se NMR [a]	*T* [°C]	Yield **3** [%]	*de* [b] **3** [%]
2a	H	Me	446	−78	70	77
2a	H	Me	446	−100	67	83
2b	Me	Me	428	−78	63	74
2c	Et	Me	425	−78	58	74
2d	*t*Bu	Me	414	−78	68	36
2e	CH_2CH_2OMe	Et	429	−78	54	70
5			447	−78	63	60

[a] δ values. [b] The *ee* values of **4** determined by GC [7] differ only slightly (±3% from the *de* values of the addition products **3**.

[*] Dr. T. Wirth
Institut für Organische Chemie der Universität
St. Johanns-Ring 19, CH-4056 Basel (Switzerland)
Telefax: Int. code + (61)322-6017
e-mail: wirth@ubaclu.unibas.ch

[**] This work was supported by the Fonds der Chemischen Industrie with a Liebig-Stipendium. I would like to thank Professor B. Giese for his generous support.

by approximately 30 ppm to lower field in contrast to that of **2d** ($\delta = 414$). The diastereomeric ratios of the addition products **3** were determined by ^1H and ^{13}C NMR spectroscopy as well as by GC analysis[7] of the cleavage products **4**.[9] In a separate synthesis of (*S*)-**4**[10] it could be shown that the *S*-configurated center in **2** induces an *S*-configuration of a new asymmetric center in **3**, thus the main diastereomer of the addition products **3** is (*S*,*S*)-configurated. The diastereoselectivity of the addition reaction is improved if the reaction temperature of $-78\,^\circ C$ is lowered to $-100\,^\circ C$.

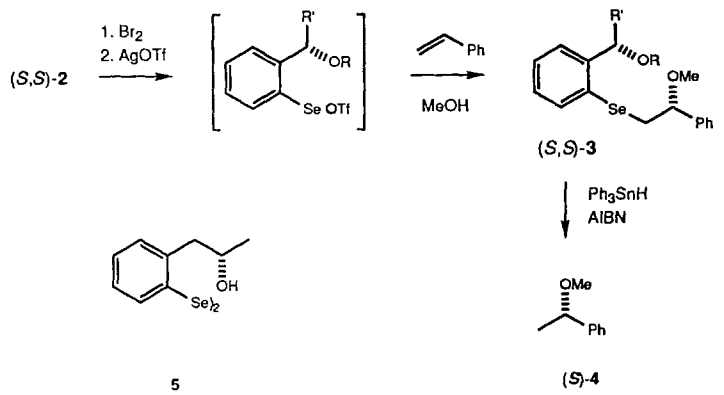

Unprotected hydroxy groups (R = H) thus appear to coordinate the intermediate selenium cations well. An ethoxymethoxy substituent in **2e** which, in principle, contains two oxygen atoms capable of coordinating to selenium causes no increase in the diastereoselectivity in the addition reaction. The position of the hydroxy group in the side chain in the diselenide **5** is varied, and the coordination no longer leads to the formation of a five-membered ring but a six-membered ring. Because of the evidently greater flexibility of the conformation, the diastereomeric excess decreases on the addition to styrene to approximately 4:1 (60% *de*).

In contrast, if the steric demand of R' in the diselenides **2** with R = H is altered, a better side selectivity than in **2a** is achieved for **2f** with R' = Et and **2g** with R = *n*Pr for the addition to styrene; the diastereomeric ratio increases up to 16:1 (88% *de*, Table 2). For **2h** with R = *t*Bu this ratio decreases to about 2:1 (35% *de*). This effect is presumably based on the steric strain of the five-membered ring, which is formed by coordination of the oxygen atom to selenium.

Table 2. Reaction of (*S*,*S*)-diselenides with styrene to give the addition products **3**. $T = -100\,^\circ C$.

Di-selenide	R	R'	^{77}Se NMR [a]	Yield **3** [%]	*de* [b] **3** [%]
2a	H	Me	446	67	83
2f	H	Et	456	53	88
2g	H	*n*Pr	456	54	87
2h [c]	H	*t*Bu	[d]	33	35

[a] and [b] See Table 1. [c] Compound **2h** was employed as a racemate [11]. [d] Not determined.

Other arylalkenes were also treated successfully with **2f**: **2f** reacts with (*E*)-1-phenyl-prop-1-ene **6** to give the addition product **7** in 61% yield and 72% *de*; with 2-phenyl-but-1-ene **10** the compound **11** was formed in 60% yield and 82% *de*.

An intramolecular trapping of the selenonium compounds formed by addition of the electrophilic selenium species is also possible. Thus, the carboxylic acids **8a**[12] and **12a**[13] react to give the lactones **9a** and **13a**, respectively; the alcohols[14] **8b** and **12b** yield the substituted tetrahydrofurans **9b** and **13b**, respectively. The intramolecular addition of the nucleophile is preferred; even on addition of six equivalents of methanol, the alkenes **8** and **12** do not form selenium-containing products with methoxy groups. As the products **11** and **13** show, quaternary carbon centers with good asymmetric induction can be formed by the title reaction. Alkenes without aryl groups sometimes yield mixtures of regioisomers with lower diastereoselectivities.

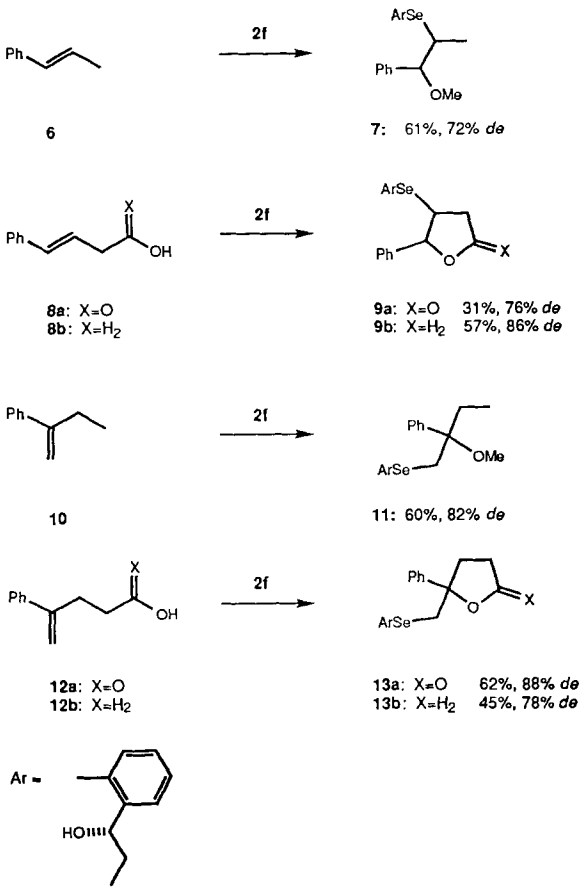

New chiral diselenides have been presented that are readily accessible in a few steps. In the addition to arylalkenes, diastereoselectivities up to 88% were achieved. The chiral diselenides open up new routes to asymmetric syntheses through further functionalization of the addition products. The use of other nucleophiles in the addition reactions as well as the synthesis of diselenides with different coordinating heteroatoms are currently under investigation.

Experimental Procedure

Synthesis of the diselenides **2**: 1-(2-bromophenyl)alcohol **1** [or 1-(2-bromophenyl) ether **1**, OR instead of OH] (10 mmol) was placed in dry THF (100 mL) under argon at $-78\,^\circ C$ and treated slowly with *t*BuLi (30 mmol). After the mixture had been stirred for 30 min at $0\,^\circ C$, selenium (1.18 g, 15 mmol; gray) was added. The mixture was stirred for an additional 3 h at $20\,^\circ C$, then 1 N HCl (100 mL) was added. The resulting mixture was extracted three times with *tert*-butylmethyl ether, and the combined organic phases were dried with $MgSO_4$. After subsequent addition of KOH (100 mg), the solvent was removed under vacuum. Purification by column chromatography on silica (pentane: *tert*-butylmethyl ether 2:1) afforded the dise-

 © VCH Verlagsgesellschaft mbH, D-69451 Weinheim, 1995 0570-0833/95/1616-1727 $ 10.00+.25/0

lenides **2** in 50–80% yields as yellow oils. Selected spectroscopic data for **2f**: ^{1}H NMR (300 MHz, $CDCl_3$): $\delta = 0.82$ (t, $J = 7.0$ Hz, 6H), 1.65 (dq, $J = 7.0$, 7.0 Hz, 4H), 2.28 (s, 2H), 4.76 (t, $J = 7.0$ Hz, 2 H), 7.19 (dd, $J = 7.5$, 7.5 Hz, 2H), 7.33 (dd, $J = 7.5$, 7.5 Hz, 2H), 7.45 (d, $J = 7.5$ Hz, 2H), 7.75 (d, $J = 7.5$ Hz, 2H); ^{13}C NMR (75 MHz, $CDCl_3$): $\delta = 10.3$, 31.3, 74.7, 126.4, 128.3, 129.1, 130.0, 135.3, 146.5; ^{77}Se NMR (76 MHz, $CDCl_3$): $\delta = 456.1$; $[\alpha]_D^{20} = +262.0$ ($c = 1$, $CHCl_3$); correct elemental analysis for $C_{18}H_{22}O_2Se_2$.

Addition of the diselenides **2** to styrene: **2** (0.1 mmol) was placed in dry diethyl ether (4 mL) under argon at -78 °C and bromine (0.11 mmol, 0.11 mL of a 1 M solution in CCl_4) was added. After 10 min silver triflate (72 mg, 0.28 mmol) in methanol (0.1 mL) was added and the mixture was stirred for 20 min at -78 °C. The reaction solution was cooled to -100 °C and treated with styrene (0.4 mmol, 0.046 mL). After the mixture had been stirred for 2 h, *sym.*-collidine (0.3 mmol, 0.04 mL) was added, and the resultant mixture was heated to 20 °C and washed with 7% aqueous citric acid solution (5 mL). The organic phase was dried with $MgSO_4$, and after removal of the solvent under vacuum, the addition product **3** was purified by column chromatography on silica (pentane: *tert*-butylmethyl ether 3:1). Selected spectroscopic data for **3f**: ^{1}H NMR (300 MHz, $CDCl_3$): $\delta = 0.98$ (t, $J = 7.4$ Hz, 3H), 1.79 (quin, $J = 7.4$ Hz, 2H), 2.41 (s, 1H), 3.10–3.30 (m, 2H), 3.24 (s, 3H), 4.36 (dd, $J = 8.5$, 5 Hz, 1H), 5.04 (m, 1H), 7.13–7.51 (m, 9H); ^{13}C NMR (75 MHz, $CDCl_3$): $\delta = 10.4$, 31.2, 36.2, 57.0, 74.7, 83.0, 126.4, 126.7, 127.6, 128.0, 128.2, 128.6, 129.7, 133.7, 140.8, 146.0; correct elemental analysis for $C_{18}H_{22}O_2Se$.

Received: March 30, 1995
Revised version: April 28, 1995 [Z 7848 IE]
German version: *Angew. Chem.* **1995**, *107*, 1872–1873

Keywords: asymmetric syntheses · chiral diselenides · selenium compounds

[1] H. C. Kolb, M. S. VanNieuwenhze, K. B. Sharpless, *Chem. Rev.* **1994**, *94*, 2483–2547.
[2] a) E. N. Jacobsen in *Catalytic Asymmetric Synthesis* (Ed.: I. Ojima), VCH, Weinheim, **1993**, pp. 159–202; b) B. D. Brandes, E. N. Jacobsen, *J. Org. Chem.* **1994**, *59*, 4378–4380.
[3] a) S. Tomoda, K. Fujita, M. Iwaoka, *J. Chem. Soc. Chem. Commun.* **1990**, 129–131; b) K. Fujita, M. Iwaoka, S. Tomoda, *Chem. Lett.* **1994**, 923–926.
[4] R. Déziel, S. Goulet, L. Grenier, J. Bordeleau, J. Bernier, *J. Org. Chem.* **1993**, *58*, 3619–3621.
[5] C. Paulmier, *Selenium Reagents and Intermediates in Organic Synthesis*, Pergamon, Oxford, **1986**.
[6] M. Srebnik, P. V. Ramachandran, H. C. Brown, *J. Org. Chem.* **1988**, *53*, 2916–2920.
[7] Determination by GC, chiral column: Chrompack, β-CD permethylated, 25 m.
[8] F. Bickelhaupt, C. Jongsma, P. de Koe, R. Lourens, N. R. Mast, G. L. van Mourik, H. Vermeer, R. J. M. Weustink, *Tetrahedron* **1976**, *32*, 1921–1930.
[9] An enrichment of a diastereomer in the workup by column chromatography was ruled out since the NMR spectra of the crude products show identical diastereomeric ratios.
[10] H. C. Brown, J. Chandrasekharan, P. V. Ramachandran, *J. Am. Chem. Soc.* **1988**, *110*, 1539–1546.
[11] In the synthesis of the diselenide **2h**, the ketone could not be reduced with (−)-(Ipc)$_2$BCl. Compound **2h** was thus employed as a racemate; the additional determination of the diastereoselectivity by the *ee* values of the ether **4** was not carried out.
[12] T. R. Hoye, W. S. Richardson, *J. Org. Chem.* **1989**, *54*, 688–693.
[13] S. Handa, K. Jones, C. G. Newton, *Tetrahedron Lett.* **1988**, *29*, 3841–3844.
[14] Synthesis of the alcohols by reduction of the carboxylic acids with $LiAlH_4$.

New Fluorescent Model Compounds for the Study of Photoinduced Electron Transfer: The Influence of a Molecular Electric Field in the Excited State**

A. Prasanna de Silva,* H. Q. Nimal Gunaratne, Jean-Louis Habib-Jiwan, Colin P. McCoy, Terence E. Rice, and Jean-Philippe Soumillion

The elucidation of the structure and some functions of the bacterial photosynthetic reaction center (PRC)[1] has inspired chemists to develop synthetic supramolecular systems[2] and models[3] to mimic and understand some of these natural features. One of the most intriguing features of the photosynthetic reaction center is that photoinduced electron transfer (PET) occurs preferentially along one of two nearly identical paths. Here we describe two simple systems, **1** and **2**, which display remarkably different PET behavior because of the presence of different PET paths. We infer that PET in **1** and **2** is directed by the electrical properties of the excited state itself: in other words, PET is self-regulated.[4]

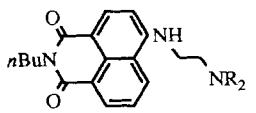

1a-c

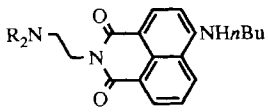

2a-c

a; R = Et
b; R = Me
c; R,R = $(CH_2)_2O(CH_2)_2$

We and others have shown how PET can be exploited for the design of fluorescent sensors for many analytes according to the fluorophore–spacer–receptor format.[5] While some of the factors that control PET have been uncovered in recent years,[6] the influence of regiochemistry is unknown. Regioisomers **1** and **2**[7] were designed as fluorescent PET pH sensors[8] with very different electron transfer paths; all other factors were kept as constant as possible. We report here that the influence of regiochemistry on PET is very large.

The fluorescence of compound **1a** is strongly enhanced upon protonation (Fig. 1), as required of a fluorescent PET pH sensor based on an aliphatic amine receptor.[5] PET occurs from the unprotonated amine[9] to the fluorophore and causes fluorescence quenching. The PET process stops when the amine is protonated, resulting in recovery of fluorescence. In complete contrast, regioisomer **2a**, in which the spacer–receptor unit is linked to the fluorophore through the imide, shows only a small reduction in fluorescence upon protonation (Fig. 1). This can be attributed to fluorescence quenching in the protonated, in-

[*] Dr. A. P. de Silva, Dr. H. Q. N. Gunaratne, Dr. C. P. McCoy, T. E. Rice
School of Chemistry, Queen's University
Belfast BT9 5AG (Northern Ireland)
Telefax: Int. code + (1232) 382117
Dr. J.-L. Habib-Jiwan, Prof. J.-P. Soumillion
Laboratoire de Chimie Organique Physique et de Photochimie
Université Catholique de Louvain
B-1348 Louvain-la-Neuve (Belgium)
Telefax: Int. code + (10) 472989

[**] This work was supported by the following organizations: NATO (grant no. 921408), SERC/EPSRC (UK), FNRS (Belgium), Department of Education in Northern Ireland, and The Nuffield Foundation (UK). We thank Dr. P. L. M. Lynch for support and help.

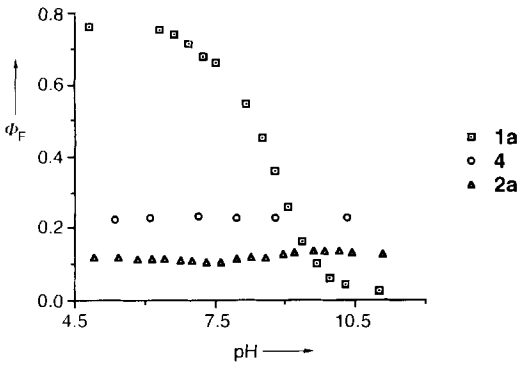

Fig. 1. Fluorescence quantum yield Φ_F versus pH for **1a**, **2a**, and **4**. Strong fluorescent sensor behavior is displayed by **1a** only.

tramolecularly hydrogen-bonded structure **3**.[10] The fluorescence of the fluorophore unit is intrinsically pH-independent, as evidenced by the behavior of **4** (Fig. 1). Other parameters that

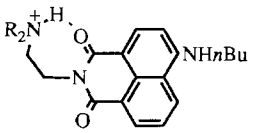

3

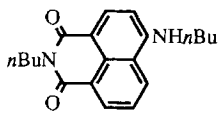

4

reflect the contrasting regiochemistry of compounds **1** and **2** are listed in Table 1.

The remarkably different fluorescence behavior can be easily rationalized according to Figure 2. The 4-aminonaphthalimide fluorophore in compounds **1** and **2** is a "push–pull" π electron system with the 4-amino group as donor and the naphthalimide as acceptor. This leads to strong internal charge transfer (ICT) in the lowest excited singlet state and considerable dipole character (positive pole at the 4-amino terminus).[11] The dipole moment of the excited state of the model fluorophore **4** is 11 D according to our measurements of solvent effects on its fluorescence and absorption spectra.[12] A large dipole moment in an excited state gives rise to a strong photogenerated electric field. Such a molecular electric field can, depending on its sign and magnitude, inhibit or accelerate a transiting electron in **2** or **1**, respectively.[13, 14] Thus the fluorescence quenching PET process is observed only if the electron leaving the unprotonated amine donor can enter the space of the 4-aminonaphthalimide fluorophore across the 4-position in **1** with its attractive electric field (Fig. 2). The corresponding PET path in **2** is just as feasible thermodynamically but requires the electron to enter the fluorophore across the imide moiety with its repulsive electric field and is not observed. We note that the PET process, which proceeds in opposite directions in **1** and **2** with respect to the orientation of the fluorophore, is strongly controlled by the excited state itself without the intervention of any outside agent. This self-regulation of PET is unprecedented and an important addition

Table 1. Parameters of the absorption and fluorescence spectra of **1a–c**, **2a–c**, and **4** [a].

Parameter	**1a**	**2a**	**4**	**1b**	**2b**	**1c**	**2c**
λ_{Abs}(acid)[nm]	431	455	454	432	455	431	456
lgε(acid)	4.22	4.13	4.19	4.15	4.20	4.18	4.07
λ_{Abs}(base)[nm]	449	455	454	447	455	447	455
lgε(base)	4.22	4.11	4.18	4.18	4.20	4.19	4.07
λ_{Isos}[nm]	440	–[i]	–[i]	439	–[i]	437	[i]
pK_a[b]	8.4	–[j]	–[j]	7.8	–[j]	6.1	[j]
λ_{Flu}(acid)[nm][c]	538	559	555	538	558	538	558
Φ_F(acid)[d]	0.76	0.12	0.23	0.70	0.12	0.73	0.14
λ_{Flu}(base)[nm][c]	549	557	555	548	557	551	556
Φ_F(base)[d]	0.030	0.15	0.23	0.050	0.16	0.070	0.17
FE[e]	25	0.8	1.0	14	0.8	11	0.8
pK'_a[f]	8.7	8.6	–[k]	8.2	8.3	6.0	6.3
τ_F(acid)[ns][g]	7.1	3.0	4.2	7.0	3.3	6.9	3.2
k_F[10^9 s^{-1}][h]	0.11	0.040	0.055	0.10	0.036	0.11	0.044
k_{PET}[10^9 s^{-1}][h]	3.3	–[l,m]	–[l]	1.7	–[l,m]	1.3	–[l,m]
k_D[10^9 s^{-1}][h]	0.034[n]	0.23	0.18	0.043[n]	0.19	0.039[n]	0.21
k_{IHB}[10^9 s^{-1}][h]	–[i]	0.07	–[l]	–[l]	0.07	–[l]	0.06
Φ_F(cyclohexane)[d]	0.95	0.41	0.94				
Φ_F(ethanol)[d]	0.020	0.50	0.83				
τ_F(cyclohexane)[ns]	7.4	6.0[o]	7.6				
τ_F(ethanol)[ns]	0.2	4.7	8.3				

[a] All the compounds (**1a–c**, **2a–c**, and **4**) were characterized by the full set of molecular spectroscopic techniques. **4** is a known compound and has been photophysically characterized [7a]. Electronic spectra (absorption and emission) were measured with 10^{-5} M solutions in aerated methanol:water (1:4, v/v), except in the studies of solvent effects; the same conditions were also used for phase modulation fluorometry. The possibility of naphthalimide ring hydrolysis was considered, but this did not occur under our conditions (pH range 4–12). pH-Dependent fluorescence measurements were carried out with excitation at isosbestic wavelengths λ_{Isos}. [b] These values were obtained by analyzing the pH dependence of the absorbance A at appropriate wavelengths with the equation $\lg[(A_{max}-A)/(A-A_{min})] = \mp$ pH $\pm$ pK_a [18]. Either set of signs on the right hand side of this equation can be valid, depending on the analytical wavelength chosen. Isosbestic points λ_{Isos} were observed for **1a–c**. [c] Obtained from fluorescence spectra which were corrected for wavelength dependence of response of the photon detection system by using quinine bisulfate [19]. [d] Rhodamine B ($\Phi_F = 0.65$ in EtOH [20]) was employed as a secondary standard. Comparison of corrected spectra was necessary since the spectrum of the secondary standard has a different shape than those of **1a–c**, **2a–c**, and **4**. [e] Factor for fluorescence enhancement induced by protons: FE = Φ_F(acid)/Φ_F(base). [f] These values are obtained by analyzing the pH dependence of fluorescence quantum yield Φ_F with the equation $\lg[(\Phi_{F,max}-\Phi_F)/(\Phi_F-\Phi_{F,min})]$ = pH – pK'_a [5a]. [g] The τ_F values in basic solution (pH 12) are 0.2 and 4.2 ns for **1a** and **4**, respectively. [h] Obtained from the following relations (J. B. Birks, *Photophysics of Aromatic Molecules*, Wiley, New York, **1970**) in acidic and basic solution: for **4**: $\Phi_F = k_F/(k_F + k_D)$ and $\tau_F = (k_F + k_D)^{-1}$; for **1a–c** with the extra PET deactivation channel, $\Phi_F = k_F/(k_F + k_D + k_{PET})$ and $\tau_F = (k_F + k_D + k_{PET})^{-1}$; for **2a–c** with the extra internal hydrogen bonding (IHB) deactivation channel, $\Phi_F = k_F/(k_F + k_D + k_{IHB})$ and $\tau_F = (k_F + k_D + k_{IHB})^{-1}$. k_F is the fluorescence rate constant; k_D is the rate constant for all the other deexcitations except PET and IHB. PET processes occur only in basic solution and IHB processes only in acidic. [i] No clear isosbestic point due to the negligible spectral shift upon protonation. [j] Cannot be determined by this method due to the small spectral shift upon protonation. [k] Cannnot be determined with this method. [l] There is no evidence for the presence of this term, and it was therefore ignored during the kinetic analysis. [m] An upper limit can be calculated as the difference of the k_D values of **2** and **4**, e.g. 0.05×10^9 s^{-1} for **2a**. Even this estimate is too high, since this can include contributions from other deexcitation processes such as those arising from solvation and/or aggregation. [n] These values refer to acidic solution. In basic solution, a value of 0.18×10^9 s^{-1} (the corresponding k_D value for model **4**) is assumed. [o] There is an additional shorter-lived component (1.0 ns) in this instance.

 © VCH Verlagsgesellschaft mbH, D-69451 Weinheim, 1995 0570-0833/95/1616-1729 $ 10.00+.25/0

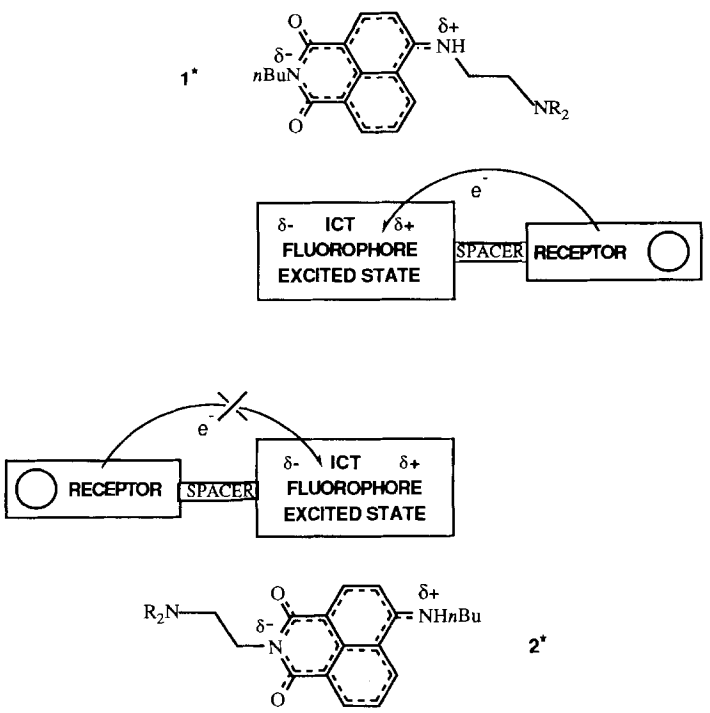

Fig. 2. Schematic representation of electron transfer to an ICT excited state of a fluorophore from an intramolecular but "external" electron donor (which is also a proton receptor) in two regioisomers. Structures of the excited states **1*** and **2*** are also shown alongside. The scheme does not distinguish between through-space or through-bond electron transfer.

to the growing number of molecular processes regulated by self-organization.[15]

Large solvent effects on fluorescence quantum yields (Φ_F) and lifetimes (τ_F) (obtained from phase modulation fluorometry[16]) are found for **1a** (Table 1) because its PET process is accelerated in polar solvents.[17] The corresponding effects are very small for the regioisomer **2a**, since PET processes are suppressed as discussed above. Model fluorophore **4**, which lacks an external aliphatic amine as electron donor, does not undergo PET processes, and solvent effects are minor.

Table 1 also gives detailed rate constants which are calculated from Φ_F and τ_F data as described in the footnotes. We estimate the PET rate in **2** to be less than $0.05 \times 10^9\ s^{-1}$, which is the difference in the k_D values (see in footnote h of Table 1) of **2** and the model fluorophore **4**, which lacks an "external" aliphatic amino group. Since k_{PET} values ranging from $1.3 \times 10^9\ s^{-1}$ to $3.3 \times 10^9\ s^{-1}$ are found for **1a–c**, we can deduce that the self-regulation of electron transfer by the ICT excited state of the 4-aminonaphthalimide fluorophore allows the discrimination between the two directions by a factor of at least 26–66.

In conclusion, the examination of the effects of pH and solvent on absorption and fluorescence behavior of **1** and **2** shows that the excited state dipole of the 4-aminonaphthalimide fluorophore can lower the kinetic barrier to electron transfer in **1** but not in **2**, since the two compounds have opposite configurations in terms of the placement of the "external" aliphatic amino group with respect to the fluorophore.

Received: March 3, 1995 [Z 7758 IE]
German version: *Angewandte Chemie* **1995**, *107*, 1889–1891

[1] a) J. Deisenhofer, H. Michel, *Angew. Chem.* **1989**, *101*, 872; *Angew. Chem. Int. Ed. Engl.* **1989**, *28*, 829; b) R. Huber, *ibid.* **1989**, *101*, 849 and **1989**, *28*, 848; c) *The Photosynthetic Reaction Center, Vol. I, II* (Eds.: J. Deisenhofer, J. R. Norris), Academic, San Diego, CA, USA, **1993**.

[2] Sensitized electron transfer: J.-P. Sauvage, J.-P. Collin, J.-C. Chambron, S. Guillerrez, C. Coudret, V. Balzani, F. Barigelletti, L. de Cola, L. Flamigni, *Chem. Rev.* **1994**, *94*, 993; D. Gust, T. A. Moore, A. L. Moore, *Acc. Chem. Res.* **1993**, *26*, 198; M. R. Wasielewski, *Chem. Rev.* **1992**, *92*, 435; Energy transfer from antenna groups: L. Jullien, J. Canceill, B. Valeur, E. Bardez, J.-M. Lehn, *Angew. Chem.* **1994**, *106*, 2582; *Angew. Chem. Int. Ed. Engl.* **1994**, *33*, 2438; Modulation of quinone redox properties: P. A. Brooksby, C. A. Hunter, A. J. McQuillan, D. H. Purvis, A. E. Rowan, R. J. Shannon, R. Walsh, *Angew. Chem.* **1994**, *106*, 2584; *Angew. Chem. Int. Ed. Engl.* **1994**, *33*, 2489.

[3] W. Rettig, *Top. Curr. Chem.* **1994**, *169*, 253.

[4] With sensors **1** and **2** we were interested in demonstrating some degree of analogy with the PRC from a functional, rather than structural, viewpoint. We used two regioisomeric sensors, each of which has only one PET pathway, such that the arguments for self-regulation could be developed with maximum clarity. Two PET pathways are possible for one sensor molecule when two distinguishable dialkylaminoethyl groups are attached to the imide nitrogen and the 4-amino group of the 1,8-naphthalimide nucleus. Then the analogy with the PRC becomes apparent even in structural terms. While sensors **1** and **2** do not display symmetry breaking during PET, we note that symmetry breaking within the PRC assumes that the effects of the protein matrix and the carotenoid can be neglected. See refs. [1c,3]. We thank the referees for initiating these comments.

[5] a) R. A. Bissell, A. P. de Silva, H. Q. N. Gunaratne, P. L. M. Lynch, G. E. M. Maguire, K. R. A. S. Sandanayake, *Chem. Soc. Rev.* **1992**, *21*, 187; b) R. A. Bissell, A. P. de Silva, H. Q. N. Gunaratne, P. L. M. Lynch, G. E. M. Maguire, C. P. McCoy, K. R. A. S. Sandanayake, *Top. Curr. Chem.* **1993**, *168*, 223; c) A. W. Czarnik, *Acc. Chem. Res.* **1994**, *27*, 302.

[6] Influence of thermodynamic driving force: R. A. Marcus, *Angew. Chem.* **1993**, *105*, 1161; *Angew. Chem. Int. Ed. Engl.* **1993**, *32*, 111; Influence of distance and stereochemistry: G. L. Closs, J. R. Miller, *Science* **1988**, *240*, 440; M. M. Paddon-Row, *Acc. Chem. Res.* **1994**, *27*, 18; Influence of conformation: F. D. Lewis, E. L. Burch, *J. Am. Chem. Soc.* **1994**, *116*, 1159.

[7] The sensors were prepared in two stages. The derivatization of 4-chloronaphthalic anhydride with an amine to yield the corresponding 4-chloronaphthalimide is much faster than the subsequent nucleophilic aromatic substitution of the 4-chloro group by an amino moiety. Proper choice of *N,N*-dialkyl-*N*-(2-aminoethyl)amine or 1-butylamine as the reactant in the second step allows the synthesis of **1** and **2**. Synthetic procedures were adapted from a) M. S. Alexiou, V. Tychopoulos, S. Ghorbanian, J. H. P. Tyman, R. G. Brown, P. I. Brittain, *J. Chem. Soc. Perkin Trans. 2* **1990**, 837; b) Q. Xuhong, Z. Zhenghua, C. Kongchang, *Dyes Pigm.* **1989**, *11*, 13.

[8] Protons were studied in the first instance. Other guests can be studied by changing the receptor since the fluorescent PET sensor principle is quite general [5].

[9] For the unprotonated forms of both **1a** and **2a** the PET process from the aliphatic amine to the 4-aminonaphthalimide fluorophore across the dimethylene spacer has near-zero ΔG_{PET} according to the equation $\Delta G_{PET} = -E_{ox,\,fluorophore} + E_{ox,\,receptor} + \Delta G_{ion\ pair}$ [5a,b]. The oxidation potential E_{ox} of the fluorophore is 1.09 and that of the receptor 1.19 or 1.00 V (versus SCE, acetonitrile solvent; with **4** and triethylamine as models). The data for triethylamine are from H. Siegerman in *Techniques of Electroorganic Synthesis, Part II* (Ed.: N. L. Weinberg), Wiley, New York, **1975**, p. 667; C. K. Mann, K. K. Barnes, *Electrochemical Reactions in Nonaqueous Solvents*, Dekker, New York, **1970**. The attractive energy $\Delta G_{ion\ pair}$ between the radical ion pair (which is the product of the PET process) is assumed to be −0.1 V (Z. R. Grabowski, J. Dobkowski, *Pure Appl. Chem.* **1983**, *55*, 245).

[10] A. Pardo, E. Martin, J. M. L. Poyato, J. J. Camacho, M. F. Brana, J. M. Castellano, *J. Photochem. Photobiol. A Chem.* **1987**, *41*, 69, propose **3** as an explanation of the shift in fluorescence wavelength but not with regard to quenching. The presence of hydrogen bond donors near the negative pole of ICT excited states is known to result in fluorescence quenching (M. D. P. de Costa, A. P. de Silva, S. T. Pathirana, *Can. J. Chem.* **1987**, *69*, 1416). A recent report on a system closely related to **2** shows pH-independent fluorescence (D. Yuan, R. G. Brown, *J. Chem. Res. (M)* **1994**, 2346).

[11] For a theoretical study, see A. Pardo, J. Campanario, J. M. L. Poyato, J. J. Camacho, D. Reyman, E. Martin, *J. Mol. Struct. (Theochem.)* **1988**, *166*, 463.

[12] Our measurements of solvent effects on fluorescence and absorption spectra of **4** can be analyzed with the equations $1/\lambda_{abs} = [-2\mu_0(\mu_1-\mu_0)/hca^3]\{[(\varepsilon-1)/(2\varepsilon+1)]-[(n^2-1)/(2n^2+1)]\}$ + const. and $1/\lambda_{flu} = [-2\mu_1(\mu_1-\mu_0)/hca^3]\{[(\varepsilon-1)/(2\varepsilon+1)]-[(n^2-1)/(2n^2+1)]\}$ + const.' (J. B. Birks, *Photophysics of Aromatic Molecules*, Wiley, New York, **1970**). In these equations μ_0 and μ_1 are the dipole moments of the ground and excited states, respectively, ε the solvent dielectric constant, n the refractive index, h Planck's constant, c the velocity of light, and a the Onsager cavity radius (taken to be 3.3 Å for **4**). Ref. [7a] and A. Pardo, J. M. L. Poyato, E. Martin, J. J. Camacho, D. Reyman, J. M. Castellano, *J. Photochem. Photobiol. A* **1989**, *46*, 323 report on solvatochromism and corresponding fluorescence effects of **4** and related compounds but do not determine dipole moments.

[13] For other effects caused by molecular electric fields due to ICT excited states, see J. F. Ireland, P. A. H. Wyatt, *Adv. Phys. Org. Chem.* **1976**, *12*, 131; M. M. Martin, P. Plaza, N. DaiHung, Y. H. Meyer, J. Bourson, B. Valeur, *Chem.*

Phys. Lett. **1993**, *202*, 425; J. F. Letard, R. Lapouyade, W. Rettig, *Pure Appl. Chem.* **1993**, *65*, 1705; E. M. Kosower, D. Huppert, *Annu. Rev. Phys. Chem.* **1986**, *37*, 127; H. Shizuka, *Acc. Chem. Res.* **1985**, *18*, 141; A. P. de Silva, H. Q. N. Gunaratne, P. L. M. Lynch, A. J. Patty, G. L. Spence, *J. Chem. Soc. Perkin Trans. 2* **1993**, 1611.

[14] When the thermodynamic driving force for PET is calculated by the usual Weller-type thermodynamic cycle with redox potentials, ion pairing energy, and singlet energy [9], there is no opportunity to allow for the effect of the photogenerated internal electric field. This appears to be due to the fact that the internal field is only generated after photon absorption. Thus the effect of the internal field can be viewed as being largely kinetic. We are grateful to a referee for catalyzing this discussion.

[15] See, for example D. Amabilino, J. F. Stoddart, *New Scientist* **1994**, *141(1913)*, 25; P. Baxter, J.-M. Lehn, A. DeCian, J. Fischer, *Angew. Chem.* **1993**, *105*, 92; *Angew. Chem. Int. Ed. Engl.* **1993**, *32*, 69; C. O. Dietrich-Buchecker, J. F. Nierengarten, J.-P. Sauvage, *Tetrahedron Lett.* **1992**, *33*, 3625.

[16] E. Gratton, D. M. Jameson, R. D. Hall, *Annu. Rev. Biophys. Bioeng.* **1984**, *13*, 105.

[17] R. A. Bissell, A. P. de Silva, W. T. M. L. Fernando, S. T. Patuwathavithana, T. K. S. D. Samarasinghe, *Tetrahedron Lett.* **1991**, *32*, 425.

[18] K. Connors, *Binding Constants: The Measurement of Molecular Complex Stability*, Wiley, New York, **1987**.

[19] R. A. Velapoldi, K. D. Mielenz, *NBS Spec. Publ.* **1980**, 260–264.

[20] I. Lopez-Arbeloa, K. K. Rohatgi-Mukerjee, *Chem. Phys. Lett.* **1986**, *128*, 474.

Intramolecular Allylsilane Addition to Chiral Alkylidene-1,3-dicarbonyl Compounds for the Synthesis of Enantiomerically Pure *trans*-1,2-Disubstituted Cyclopentanes and Cyclohexanes**

Lutz F. Tietze* and Christian Schünke

Dedicated to Professor Herbert W. Roesky on the occasion of his 60th birthday

The cyclization of compounds containing an allylsilane and a carbonyl group provides a simple and elegant synthesis of five- and six-membered ring compounds.[1] In an analogous way, α,β-unsaturated ketones and aldehydes can also be converted in a type of intramolecular Sakurai reaction.[2] The simple and induced diastereoselectivities of these transformations are, however, often unsatisfactory.[3] For instance, in particular the stereoselective construction of enantiomerically pure 1,2-*trans*-disubstituted cyclopentanes has not yet been achieved successfully with this method. Such compounds are, however, of great interest for natural product synthesis.[4]

Recently we showed that racemic 1,2-*trans*-disubstituted cyclopentanes and cyclohexanes can be obtained in very good simple diastereoselectivity through intramolecular allylsilane addition from alkylidene malonates (for example, **2** from **1**); the best results were obtained with trimethylsilyl trifluoromethanesulfonate (TMSOTf) as promoter.[5]

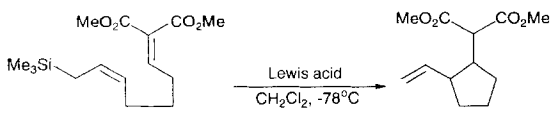

1 **2**

TMSOTf : *trans* : *cis* = 99.6 : 0.4 ; 97 % yield

Here we describe the synthesis of enantiomerically pure *trans*-1,2-disubstituted cyclopentanes and cyclohexanes with three stereogenic centers on using the chiral malonic acid derivatives **5b–d**, which were transformed by Knoevenagel condensation with aldehydes **6** and **7** into the alkylidene-1,3-dicarbonyl compounds **8b–d** and **9d** required for the cyclization. The chiral malonic acid derivatives **5b–d** were synthesized by acylation of the oxazolidinones **4b–d**[6] with malonic acid methyl ester chloride (**3**) in the presence of 4-dimethylaminopyridine (DMAP) and triethylamine in 60–64% yield. The achiral oxazolidinone **4a** was also converted into **5a** in 90% yield. With the acid chloride **3** the conventional procedure of acylation with deprotonated oxazolidinones[7] did not lead to the products **5**, probably because in this case the primary step is a deprotonation of the malonyl chloride **3**.

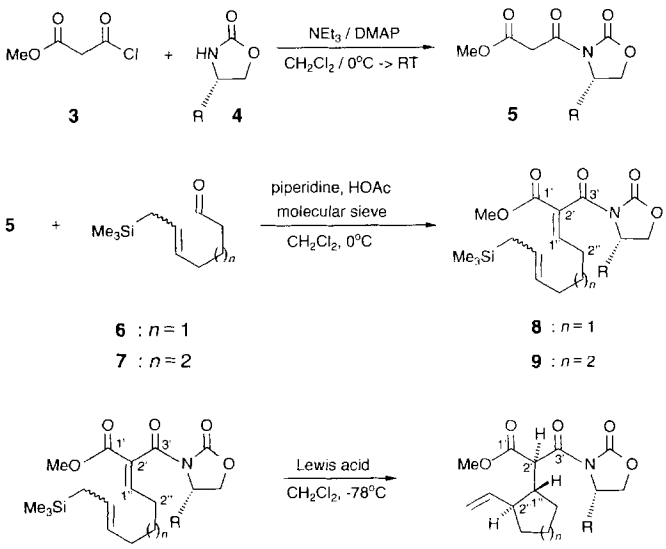

3 **4** **5**

6 : $n = 1$
7 : $n = 2$

8 : $n = 1$
9 : $n = 2$

10 : $n = 1$
11 : $n = 2$

4, 5, 8 - 11 : **a**, R = H; **b**, R = *i*Pr; **c**, R = *t*Bu; **d**, R = Bn

The Knoevenagel condensation of **5a–d** with the aldehyde **6**, which is easily accessible from 2-trimethylsilylmethylcyclohexanone by a photochemical Norrish type I cleavage,[8] gave, in the presence of piperidine and acetic acid virtually exclusively the (*E*) isomers **8a–d** ($E:Z > 95:5$) in yields of 54–75%. The configuration of the newly formed double bond in **8a–d** was determined by NOESY measurements on **8d** as well as by comparison with **14**, which was obtained as the major product ($E:Z > 95:5$) on condensation of **5d** and benzaldehyde and characterized by X-ray crystal structure analysis.[9]

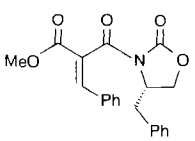

14

For the conversion of **8a–d** the Lewis acids Me_2AlCl, $EtAlCl_2$, $ZrCl_4$, $AlCl_3$, $TiCl_4$, and $SnCl_4$, as well as TMSOTf (1.0 equiv in each case) were used as promoters. During the cyclization of **8a–d** three new stereogenic centers apart from those in the auxiliary were constructed. Eight enantiomerically pure diastereomers can therefore be formed. On conversion of the achiral compound **8a**, four diastereomers are expected as

[*] Prof. Dr. L. F. Tietze, Dipl.-Chem. C. Schünke
Institut für Organische Chemie der Universität
Tammannstrasse 2, D-37077 Göttingen (Germany)
Telefax: Int. code + (551)39-9476

[**] This work was supported by the Deutsche Forschungsgemeinschaft and the Fonds der Chemischen Industrie.

racemic mixtures. In contrast to the reaction of **1**, the use of TMSOTf in the conversion of **8d** led exclusively to the protodesilylated product. On the other hand, with the Lewis acids the cyclization was successful (Table 1).

Table 1. Lewis acid initiated allylsilane cyclization of **8a–d** to form **10a–d** and **9d** to form **11d**.

Substrate No.	R	Lewis-acid	Yield [%]	Major product	Product ratio [a]
8a	H	$SnCl_4$	80	**10a**	86/14
8b	*i*Pr	$SnCl_4$	57	**10b**	3/10/82/3/2
8c	*t*Bu	$SnCl_4$	65	**10c**	4/79/14/1/1/1
8d	Bn	$SnCl_4$	80	**10d**	95/5 [a, b]
9d	Bn	$SnCl_4$	80	**11d**	>96/4
8a	H	Me_2AlCl	92	**10a**	24/71/1/4
8b	*i*Pr	Me_2AlCl	61	**10b**	12/15/54/2/12/5
8c	*t*Bu	Me_2AlCl	81	**10c**	9/44/13/3/6/13/6/6
8d	Bn	Me_2AlCl	77	**10d**	8/13/63/1/11/4
8d	Bn	TMSOTf	68	–	[c]
8d	Bn	$EtAlCl_2$	74	**10d**	14/49/3/28/6
8d	Bn	$ZrCl_4$	78	**10d**	18/77/2/3
8d	Bn	$AlCl_3$	75	**10d**	86/1/11/2
8d	Bn	$TiCl_4$	61	**10d**	15/65/5/15

[a] Analytical capillary gas chromatography of the crude product. [b] ^{13}C NMR spectroscopy of the crude product. [c] Protodesilylation.

The high induced diastereoselectivity in the cyclization of **8d** and **9d** is surprising, because this is a 1,5-induction. Recently, however, we detected even a 1,6-induction with a very good simple and induced diastereoselectivity in hetero-Diels–Alder reactions.[13] Interestingly, in the hetero-Diels–Alder reaction the only auxiliary that gave good selectivities was the oxazolidinone derived from *tert*-leucine, whereas in the allylsilane cyclization of **8c** the oxazolidinone containing a *tert*-butyl group gave the worst results. At the moment it is not clear whether the particularly good results of the cyclization of **8d** with a benzyl group at the oxazolidinone can be attributed to π-stacking.[14]

We assume in the reaction of **8d** and **9d** that a reactive metal chelate complex like **15d** is first formed and that subsequently a *Si* side attack of the allylsilane moiety on the alkylidene-1,3-dicarbonyl unit forming the enolate **16d** takes place. Surprisingly,

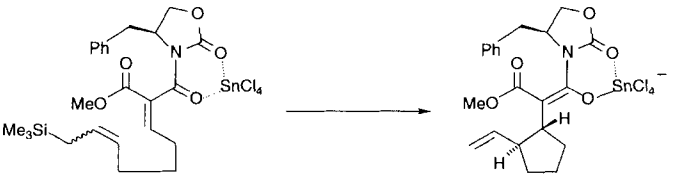

15d **16d**

The best results were obtained with $SnCl_4$ and the substrate **8d** containing the auxiliary which was derived from (*S*)-phenylalanine. Two products in a 95:5 ratio were formed in an 80% yield. The major product was **10d**, which could be obtained pure by recrystallization from ether/petroleum ether; the by-product is thought to be 2′-*epi*-**10d**. This was confirmed by the results of the conversion of the achiral substrate **8a** with $SnCl_4$, which also yielded two products, however, in an 86:14 ratio. Since the results of the cyclization of **1**[5] suggest a *trans* arrangement of the substituents on the pentane ring, the products must be the two C-2′-epimers **10a** and 2′-*epi*-**10a**.

To construct a cyclohexane derivative, **5d** was transformed selectively with (*Z*)-**7** into (2′*E*,5″*Z*)-**9d**,[10] which on reaction with $SnCl_4$ gave almost exclusively the 1,2-*trans*-disubstituted cyclohexane **11d** beside a very small amount of 2′-*epi*-**11d** (>96:4) in 80% yield. Recrystallization from ether/petroleum ether furnished pure **11d**. The configuration of the two major products **10d** and **11d** of the cyclization of **8d** and **9d**, respectively, was proved by X-ray crystal structure analyses.[11]

The chiral auxiliaries in **10d** and **11d** were removed simply by the usual methods.[12] Thus, the reduction of **10d** with $LiAlH_4$ in THF at −78 °C, for example, gave the enantiomerically pure cyclopentane derivative **12** with retention of configuration at all stereogenic centers in 77% yield; in addition **4d** could be recovered by chromatography. Similarly, **11d** was transformed into the cyclohexane derivative **13**.

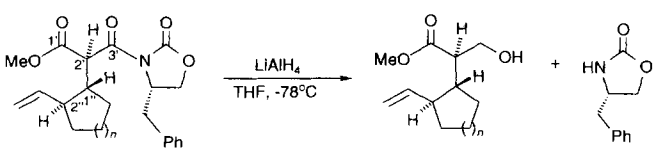

10d : *n* = 1 **12** : *n* = 1 **4d**

11d : *n* = 2 **13** : *n* = 2

even the protonation to form the stereogenic center C-2′ is highly stereoselective. To test whether thermodynamic or kinetic control is operative here, we stirred **10d** and 2′-*epi*-**10d** under the reaction conditions for several days; in neither case did we observe isomerization. It must therefore be assumed that the stereogenic center C-2′ is formed under kinetic control. The possibilities suggested by this work for stereoselective protonation of enolates that are derived from **5b–d** are under investigation.[16]

Experimental Procedure

To a solution of **8a–d** or **9d** in dichloromethane (20 mL) under argon at −78 °C was added the Lewis acid (1 equiv). After two days of stirring under argon at −78 °C, the reaction was terminated by addition of a saturated aqueous solution of $NaHCO_3$ or of 2N HCl.

10d: ^1H NMR (300 MHz, $CDCl_3$): δ = 1.37 (m_c, 2H, 3″-H_2), 1.58 (m_c, 2H, 4″-H_2), 1.81 (m_c, 2H, 5″-H_2), 2.39 (m_c, 2H, 1″-H, 2″-H), 2.63 (dd, *J* = 13.5, 10.0 Hz, 1H, benzyl-CH), 3.26 (dd, *J* = 13.5, 3.0 Hz, 1H, benzyl-CH), 3.58 (s, 3H, OMe), 4.06 (dd, *J* = 9.0, 3.0 Hz, 1H, 5-H), 4.12 (dd, *J* = 9.0, 7.5 Hz, 1H, 5-H), 4.59 (d, *J* = 7.5 Hz, 1H, 2′-H), 4.65 (m_c, 1H, 4-H), 4.86 (dd, *J* = 10.0, 2.0 Hz, 1H, 2‴-H_{cis}), 4.88 (dd, *J* = 17.5, 2.0 Hz, 1H, 2‴-H_{trans}), 5.62 (ddd, *J* = 17.5, 10.0, 8.0 Hz, 1H, 1‴-H), 7.10–7.28 (m, 5H, phenyl-H). M.p. 119 °C (ether/petroleum ether), $[\alpha]_D^{20} = +48°$ (*c* = 0.6, $CHCl_3$). In the ^1H NMR spectrum of 2′-*epi*-**10d** the signal for the 2′-H appears as a doublet at δ = 4.71 with *J* = 6.0 Hz and for the methoxy group as a singlet at δ = 3.77.

11d: ^1H NMR (500 MHz, $CDCl_3$): δ = 1.18–1.29 (m, 2H, 3″-H_2), 1.32–1.42 (m, 1H, 4″-H*), 1.54 (m_c, 1H, 5″-H*), 1.69–1.82 (m, 3H, 4″-H*, 5″-H*, 6″-H*), 1.91 (m_c, 1H, 6″-H*), 2.02 (m_c, 1H, 1″-H), 2.30 (m_c, 1H, 2″), 2.60 (dd, *J* = 13.0, 10.0 Hz, 1H, benzyl-CH), 3.42 (dd, *J* = 13.0, 3.0 Hz, 1H, benzyl-CH), 3.70 (s, 3H, OMe), 4.12 (dd, *J* = 8.5, 3.0 Hz, 1H, 5-H), 4.18 (dd, *J* = 10.0, 8.5 Hz, 1H, 5-H), 4.70–4.77 (m_c, 1H, 4-H), 4.76 (d, *J* = 5.0 Hz, 1H, 2′-H), 4.95 (dd, *J* = 15.5, 2.0 Hz, 1H, 2‴-H_{trans}), 4.96 (dd, *J* = 10.0, 2.0 Hz, 1H, 2‴-H_{cis}), 5.65 (ddd, *J* = 15.5, 11.0, 10.0 Hz, 1H, 1‴-H), 7.22–7.36 (m, 5H, phenyl-H). M.p. 139 °C (ether/petroleum ether), $[\alpha]_D^{20} = +48°$ (*c* = 0.4, $CHCl_3$).

Received: March 4, 1995 [Z7762IE]
German version: *Angew. Chem.* **1995**, *107*, 1901–1903

Keywords: allylsilanes · asymmetric syntheses · cyclizations cyclohexanes · cyclopentanes

[1] Reviews on syntheses and reactions of allylsilanes, in particular the intramolecular addition to carbonyl compounds: a) Y. Yamamoto, N. Asao, *Chem. Rev.* **1993**, *93*, 2207; b) G. Majetich, K. Hull, A. M. Casares, V. Khetani, *J. Org. Chem.* **1991**, *56*, 3958; c) T. K. Sarkar, *Synthesis* **1990**, *969*, 1101; d) G. Majetich in *Organic Synthesis, Theory and Applications, Vol. 1* (Ed.: T. Hudlicky), JAI Press, London, **1989**, pp. 173–240; e) I. Fleming, J. Dunogues, R. Smithers, *Org. React.* **1989**, *37*, 57; f) G. L. Larson, *J. Organomet. Chem.* **1989**, *360*, 39; g) G. Majetich, J. Defauw, C. Ringold, *J. Org. Chem.* **1988**, *53*, 50; h) G. Majetich, R. W. Desmond, S. J. Soria, *ibid.* **1986**, *51*, 1753; i) T. A. Blumenkopf, L. E. Overman, *Chem. Rev.* **1986**, *86*, 857.

[2] a) A. Hosomi, *Acc. Chem. Res.* **1988**, *21*, 200; b) D. Schinzer, *Synthesis* **1988**, 263; c) H. Sakurai, *Pure Appl. Chem.* **1985**, *57*, 1759.

[3] However, see: a) M.-J. Wu, J.-Y. Yeh, *Tetrahedron* **1994**, *50*, 1073; b) M.-J. Wu, C.-C. Wu, P.-C. Lee, *Tetrahedron Lett.* **1992**, *33*, 2547; c) L.-R. Pan, T. Tokoroyama, *ibid.* **1992**, *33*, 1469; d) K. Nishitani, K. Yamakawa, *ibid.* **1991**, *32*, 387.

[4] a) T. Hudlicky, J. D. Pridce, *Chem. Rev.* **1989**, *89*, 1467; b) B. M. Trost, *Angew. Chem.* **1986**, *98*, 1; *Angew. Chem. Int. Ed. Engl.* **1986**, *25*, 1; c) L. A. Paquette, *Top. Curr. Chem.* **1984**, *119*, 1; d) B. M. Trost, *Chem. Soc. Rev.* **1982**, *11*, 141.

[5] L. F. Tietze, M. Ruther, *Chem. Ber.* **1990**, *123*, 1387; see also: L. F. Tietze, U. Beifuss, M. Ruther, *J. Org. Chem.* **1989**, *54*, 3120.

[6] a) D. A. Evans, J. R. Gage, *Org. Synth.* **1989**, *68*, 77; b) D. A. Evans, K. T. Chapman, J. Bisaha, *J. Am. Chem. Soc.* **1988**, *110*, 1238; c) D. A. Evans, D. J. Mathre, W. L. Scott, *J. Org. Chem.* **1985**, *50*, 1830; d) D. A. Evans, *Aldrichim. Acta* **1982**, *15*, 23.

[7] a) L. F. Tietze, C. Schneider, *Synlett* **1992**, 755; b) D. A. Evans, M. D. Ennis, J. D. Mathre, *J. Am. Chem. Soc.* **1982**, *104*, 1737. Another possible acylation has been described: P. Kocienski, C. Thom, *Synthesis* **1992**, 582.

[8] L. F. Tietze, J. R. Wünsch, *Synthesis* **1990**, 985. For the conversion an (*E*/*Z*) mixture of about 6:1 was used. Studies with pure (*E*)- and (*Z*)-allylsilanes **1** have shown that the simple diastereoselectivity of the cyclization to give the cyclopentane derivative is virtually independent of the configuration of the allylsilane group: L. F. Tietze, C. Schünke, unpublished.

[9] E. Pohl, C. Schünke, L. F. Tietze, *Acta Crystallogr. Sect. C*, in press.

[10] For the conversion the pure (*Z*)-allylsilane was used, because (*E*)-allylsilanes gave a lower simple diastereoselectivity. For the synthesis of the corresponding allylsilanecarbaldehydes, see ref. [5].

[11] M. Schäfer, R. Herbst-Irmer, E. Pohl, C. Schünke, L. F. Tietze, *Acta Crystallogr. Sect. C*, submitted.

[12] a) L. F. Tietze, A. Montenbruck, C. Schneider, *Synlett* **1994**, 509; b) D. A. Evans, D. A. Evrard, S. D. Rychnovsky, T. Früh, W. G. Whittingham, K. M. DeVries, *Tetrahedron Lett.* **1992**, *33*, 1189; c) R. E. Damon, G. M. Coppola, *ibid.* **1990**, *31*, 2849; d) T. D. Penning, S. W. Djuric', R. A. Haack, V. J. Kalish, J. M. Miyashiro, B. W. Rowell, S. S. Yu, *Snyth. Commun.* **1988**, *20*, 307; e) D. A. Evans, M. D. Ennis, J. D. Mathre, *J. Am. Chem. Soc.* **1982**, *104*, 1737; f) J. I. Levin, E. Turos, S. M. Weinreb, *Synth. Commun.* **1982**, *12*, 989.

[13] L. F. Tietze, C. Schneider, A. Montenbruck, *Angew. Chem.* **1994**, *106*, 1031; *Angew. Chem. Int. Ed. Engl.* **1994**, *33*, 980.

[14] D. A. Evans, K. T. Chapman, D. T. Hung, A. T. Kawaguchi, *Angew. Chem.* **1987**, *99*, 1197; *Angew. Chem. Int. Ed. Engl.* **1987**, *26*, 1184.

[15] Studies on the structure of adducts of Lewis acids and carbonyl compounds: a) S. Castellino, W. J. Dwight, *J. Am. Chem. Soc.* **1993**, *115*, 2986; b) S. E. Denmark, N. G. Almstead, *ibid.* **1993**, *115*, 3133; c) M. A. McCorrick, Y.-D. Wu, K. N. Houk, *J. Org. Chem.* **1993**, *58*, 3330; d) S. Shambayati, W. E. Crowe, S. L. Schreiber, *Angew. Chem.* **1990**, *102*, 273; *Angew. Chem. Int. Ed. Engl.* **1990**, *29*, 256.

[16] Studies on the stereoselective protonation of enolates: a) C. Fehr, J. Galindo, *Angew. Chem.* **1994**, *106*, 1967; *Angew. Chem. Int. Ed. Engl.* **1994**, *33*, 1888; b) N. Krause, *ibid.* **1994**, *106*, 1845 bzw. **1994**, *33*, 1764; c) A. Yanagisawa, T. Kuribayashi, T. Kikuchi, H. Yamamoto, *ibid.* **1994**, *106*, 129 bzw. **1994**, *33*, 107; d) E. Vedejs, N. Lee, S. T. Sakata, *J. Am. Chem. Soc.* **1994**, *116*, 2175; e) T. Haubenreich, S. Hünig, H.-J. Schulz, *Angew Chem.* **1993**, *105*, 443; *Angew. Chem. Int. Ed. Engl.* **1993**, *32*, 398; f) F. Rehders, D. Hoppe, *Synthesis* **1992**, 859.

A Phycocyanobilin Seryliminoester as a New Model for the Chromophore–Protein Interaction in Phytochrome**

Ronald Micura and Karl Grubmayr*

Dedicated to Professor Albert Eschenmoser on the occasion of his 70th birthday

Phytochrome is the photoreceptor of photomorphogenesis in higher plants.[1] It exists in two forms (Pr = phytochrome red, Pfr = phytochrome far red) which differ in their absorption spectra (660 and 730 nm, respectively) and can be interconverted photochemically. Structurally, phytochrome Pr **1** is a biliprotein. It can be transformed into the physiologically active Pfr form by photoisomerization[2] and a sequence of dark reactions.[3] These dark reactions are well characterized by spectroscopy, but the structures of the intermediates involved, and that of the Pfr form itself, are largely unknown.[4]

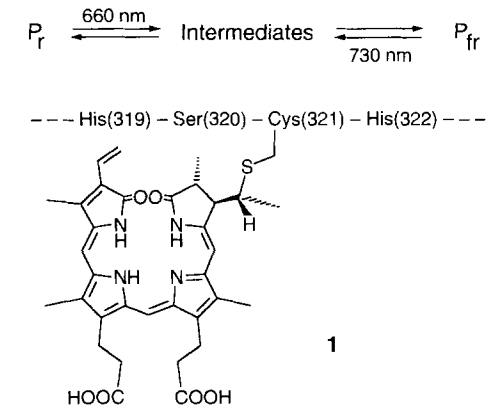

1

Here we report on a new phytochrome model based on model compound **2**,[5, 6] whose chromophore is derived from that of the structurally related phycocyanobilin, and whose dipeptide component corresponds to the Ser(320)-Cys(321) structural component of the Pr form. The most important aspect of this model is the covalent linkage of the chromophore and the hydroxyl group of the serine to give iminoester **3**. This reaction represents a possible form of chromophore–protein interaction that has not yet been considered, and which has characteristic effects on reactivity and light absorption.

The synthesis of **3** from **2** (Scheme 1; Table 1) was carried out in a one-pot reaction and was designed on the basis of the synthesis and reactivity of oxoniaporphinato-[7] and oxoniachlorinatometal complexes.[8] The crucial change in the chromophore structure, tautomerization of the ring-A lactam into its lactim form, occurs in the first step with formation of the zinc chelate **I**. The subsequent O-acetylation serves merely to activate this chelate chemically, leading to the kinetically favored cyclization to the oxoniachlorinatozinc acetate **II** and allowing regioselective attack of the serine hydroxyl group on ring A. Decomplexation takes place during workup with aqueous sodium hydrogen carbonate.

[*] Univ.-Doz. Dr. K. Grubmayr, Dipl.-Ing. R. Micura
Institut für Chemie der Universität
Altenbergerstrasse 69, A-4040 Linz (Austria)
Telefax: Int. code + (732)2468-10
e-mail: karl.grubmayr@jk.uni-linz.ac.at

[**] This work was supported by the Fonds zur Förderung der wissenschaftlichen Forschung (project no. P-9166).

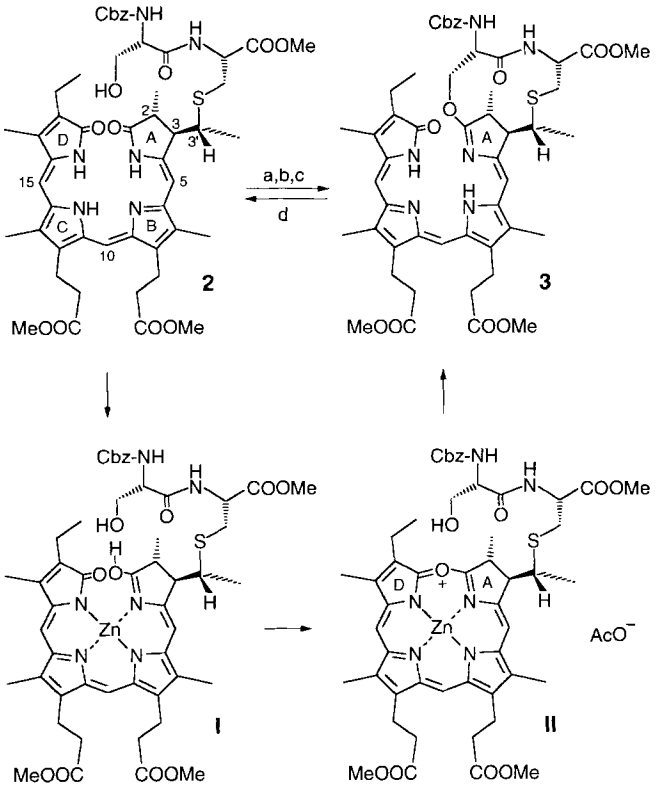

Scheme 1. a) $CHCl_3$, $Zn(OAc)_2$/*t*BuOH, Et_3N, 25 °C, 10 min; b) Ac_2O, 55 °C, 50 min; c) $NaHCO_3/H_2O$ (22%); d) $H_2O/CHCl_3$, CF_3COOH, 25 °C, 10 min (100%). Cbz = benzyloxycarbonyl.

Table 1. Selected NMR spectroscopic data for compounds **2** and **3**.

2: ^{1}H NMR (360 MHz, $CDCl_3$, 25 °C, TMS): δ = 6.65 (s, 1H; H-(C10)), 5.97 (s, 1H; H-(C15)), 5.56 (s br., 1H; H-(C5)), 4.30 (ddd, ^3J(H,H) = 8.1 Hz, ^3J(H,H) = 3.9 Hz, ^3J(H,H) = 3.0 Hz, 1H; H$^\alpha$-Ser), 3.82 (dd, ^2J(H,H) = 11.0 Hz, ^3J(H,H) = 3.0 Hz, 1H; H(1)$^\beta$-Ser), 3.49 (dd, ^2J(H,H) = 11.0 Hz, ^3J(H,H) = 3.9 Hz, 1H; H(2)$^\beta$-Ser); ^{13}C NMR (90 MHz, $CDCl_3$, 25 °C, TMS): δ = 178.50 (C1), 112.38 (C10), 96.80 (C15), 92.55 (C5), 62.89 (C$^\beta$-Ser)

3: ^{1}H NMR (360 MHz, $CDCl_3$, 25 °C, TMS): δ = 11.85 (br., 1H; NH ring B), 9.98 (s, 1H; NH ring D), 6.81 (s, 1H; H-(C10)), 6.06 (d, ^2J(H,H) = 11.5 Hz, ^3J(H,H) = 0 Hz, 1H; H(1)$^\beta$-Ser), 5.90 (s, 1H; H-(C15)), 5.76 (d, ^4J(H,H) = 0.5 Hz, 1H; H-(C5)), 4.15 (dd, ^3J(H,H) = 6.9 Hz, ^3J(H,H) = 3.5 Hz, ^3J(H,H) = 0 Hz, 1H; H$^\alpha$-Ser), 3.69–3.65 (m, 1H; H(2)$^\beta$-Ser); ^{13}C NMR (90 MHz, $CDCl_3$, 25 °C, TMS): δ = 182.23 (C1), 116.65 (C10), 101.63 (C5), 97.66 (C15), 68.17 (C$^\beta$Ser)

The conversion of **2** to **3** is associated with a conspicuous color change from reddish blue to turquoise. The bathochromic shift is about 75 nm (Fig. 1, bottom) and may be explained by a donor–acceptor reversal on transformation of the ring-A lactam (N → C=O) into a lactim ether (N=C←O). In contrast to **2**, in **3** the conjugative donor–acceptor stabilization covers the entire chromophore and extends from the ring-A lactim oxygen to the ring-D lactam oxygen atom. The partial structures **A** and **B** therefore suffice for a qualitative description of electronic excitation. The porphyrin-like geometry of the chromophore leads in **A** to a short distance between the lactim ether and the

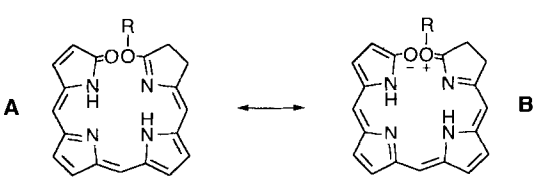

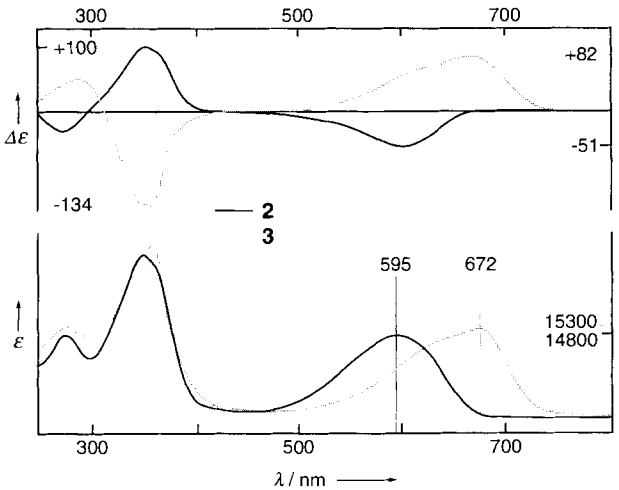

Fig. 1. CD spectra (top) and UV/Vis spectra (bottom) of **2** and **3** in $CHCl_3$ (ca. 3×10^{-5} M).

lactam and in **B** to a small (O^+/O^-) separation; the development of the electric dipole transition is therefore favored. Other experimental data also agree with this geometry: the (4*Z*,10*Z*,15*Z*,5*syn*,9*syn*,14*syn*) configuration of the chromophore can be deduced from the presence of characteristic cross peaks in the H,H-NOESY spectra;[9] the corresponding *P*-helix can be deduced from the sign alternation of the Cotton effects at 354 and 667 nm (Fig. 1, top).[10]

In view of the photochromism of phytochrome, the assumption of a seryl–ring-A iminoester allows a first experimentally supported approach to understanding the analogous chromophore–protein interaction. The model not only correctly reflects the changes in the absorption spectrum but also the possibility of the reverse reaction, which is compulsory for biological regulatory systems: hydrolysis of iminoester **3** to lactam **2** proceeds under acid catalysis within a few minutes.

A Ser(320) iminoester would be assigned a role in the reaction scheme of phytochrome as an intermediate close to the Pfr form, on the basis of its absorption properties and its chemical potential. In principle nothing speaks against the assumption that the iminoester structural element is retained even in the Pfr form itself, because **3**, like **2**, is photoisomerizable at the double bond exocyclic to ring D. This would therefore afford the photoreversibility required of a useful phytochrome model.

Received: April 7, 1995 [Z7876IE]
German version: *Angew. Chem.* **1995**, *107*, 1896–1898

Keywords: enzyme models · phycocyanobilin · phytochrome

[1] a) L. C. Sage, *Pigment of the Imagination. A History of Phytochrome Research*, Academic Press, San Diego, **1992**; b) W. Rüdiger, F. Thümmler, *Angew. Chem.* **1991**, *103*, 1242–1254; *Angew. Chem. Int. Ed. Engl.* **1991**, *30*, 1216–1228; c) K. Schaffner, S. E. Braslavsky, A. R. Holzwarth, *Adv. Photochem.* **1990**, *15*, 229–277.

[2] W. Rüdiger, F. Thümmler, E. Cmiel, S. Schneider, *Proc. Natl. Acad. Sci. USA* **1983**, *80*, 6244–6248.

[3] a) Y. Inoue, W. Rüdiger, R. Grimm, M. Furuya, *Photochem. Photobiol.* **1990**, *52*, 1077–1083; b) C.-F. Zhang, D. L. Farrens, S. C. Björling, P.-S. Song, D. S. Kliger, *J. Am. Chem. Soc.* **1992**, *114*, 4569–4580; c) R. D. Scurlock, S. E. Braslavsky, K. Schaffner, *Photochem. Photobiol.* **1993**, *57*, 690–695.

[4] a) W. Rüdiger, *Photochem. Photobiol.* **1992**, *56*, 803–809; b) H. Kandori, K. Yoshihara, S. Tokutomi, *J. Am. Chem. Soc.* **1992**, *114*, 10958–10959.

[5] Compound **2** was synthesized by addition of Cbz-Ser-Cys-OMe to racemic phycocyanobilin dimethyl ester, followed by chromatographic separation of the mixture of four diastereomers with 2,3-*trans* configuration: H. Stumpe, N. Müller, K. Grubmayr, *Tetrahedron Lett.* **1993**, *34*, 4165–4168.

 © VCH Verlagsgesellschaft mbH, D-69451 Weinheim, 1995 0570-0833/95/1616-1734 $ 10.00+.25/0

[6] The assignment of the configuration of **2** is based on the (*l,l*) relative configuration of the 2, 3, and 3′ centers determined by H,H-NOESY (see ref. [9]), and on chemical correlation with enantiomerically pure (*2R*)-phycocyanobilin dimethyl ester. This latter compound was obtained by chromatographic separation of the enantiomers of the ring-D methyliminoester (see ref. [8b]) on triacetylcellulose, and subsequent hydrolysis. The (*2R*) configuration was determined by comparison of the CD spectra: J. E. Bishop, J. O. Nagy, J. F. O'Connell, H. Rapoport, *J. Am. Chem. Soc.* **1991**, *113*, 8024–8035.

[7] a) J.-H. Fuhrhop, P. Krüger, W. S. Sheldrick, *Justus Liebigs Ann. Chem.* **1977**, 339–359; b) J.-H. Fuhrhop, P. Krüger, *ibid.* **1977**, 360–370.

[8] a) J. Iturraspe, A. Gossauer, *Photochem. Photobiol.* **1991**, *54*, 43–49; b) R. Micura, K. Grubmayr, *Bioorg. Med. Chem. Lett.* **1994**, *21*, 2517–2522.

[9] Cross peaks in the H,H-NOESY spectra of **2** and **3** that are relevant to the configuration: 3↔5↔3′; 2↔3↔3″; 5↔7′; 8′↔10↔12′; 13′↔15↔17′.

[10] a) G. Wagnière, G. Blauer, *J. Am. Chem. Soc.* **1975**, *97*, 1949–1954; b) *ibid.* **1976**, *98*, 7806–7810; c) H. Falk, *The Chemistry of Linear Oligopyrroles and Bile Pigments*, Springer, Vienna – New York, **1989**, p. 426.

[11] The (15*Z* →15*E*) photoisomerization requires thiol catalysis: a) F. Thümmler, W. Rüdiger, *Tetrahedron* **1983**, *39*, 1943–1951; b) H. Falk, N. Müller, T. Schlederer, *Monatsh. Chem.* **1980**, *111*, 159–175. The (15*E* →15*Z*) photoisomerization does not require addition of thiol.

Calculation of the Thermodynamic Properties of Polycyclic Aromatic Hydrocarbons by an Incremental Procedure**

Karen Nass, Dieter Lenoir,* and Antonius Kettrup

Dedicated to Professor Paul von Ragué Schleyer on the occasion of his 65th birthday

Uniform substances are characterized by both their thermodynamic and their molecular properties.[1] After the triumphs of quantum chemistry,[2] it has been possible in the past decade to calculate the inherent molecular properties of compounds in the gas phase.[3] Certain thermodynamic properties of substances, like the melting and boiling point, the vapor pressure, and the corresponding energy values of the phase transitions, are ensemble properties of molecules and thus not accessible with these methods.[4] Apart from group theoretical procedures, several empirical methods are used for the prediction of these properties.[5] The vapor pressure and the enthalpy of sublimation of synthetic compounds (xenobiotics) are important properties relevant for the environment,[6] and a relationship between structure and these thermodynamic quantities can be used in model calculations for otherwise unknown values.

We studied the group of polycyclic aromatic hydrocarbons and found a general relationship between structure and vapor pressure, and between structure and enthalpy of sublimation. The results are based on the data from thirty polycyclic aromatic hydrocarbons containing five- and six-membered rings that are found in the environment.

The vapor pressure of several substances are known, but the quoted values vary mostly by an order of magnitude. We further developed the gas saturation method of vapor pressure determination and measured the vapor pressures and enthalpies of sublimation of the selected compounds.[9] This method can be used to measure vapor pressue over a wide range as well as in mixtures. The results of the experiments are collated in Table 1. In all cases the temperature range of between 40 and 180 °C lay well below the critical temperature for each substance. The logarithm of the value of the measured vapor pressure was plotted against the reciprocal temperature. For a linear relation this corresponds to the intergration of the Clausius–Clapeyron equation in which the temperature dependence of the enthalpy can be neglected if the measurements are made well below the critical temperature. The enthalpy of the relevant phase transition was determined from the slope of the lines.

Table 1. Vapor pressure and enthalpy of sublimation for 30 polycyclic aromatic hydrocarbons measured in the temperature range 40–180 °C in 5 °C steps; the average of three experimental values were determined at each temperature step.

	Substance	$p\,(25\,^{\circ}C)_{extrapolated}$ [Pa]	$\Delta_{sub}H_m$ [kJ mol^{-1}]
1	naphthalene	10.86	71.7
2	biphenyl	1.56	81.8
3	biphenylene	3.75×10^{-1}	82.7
4	acenaphthene	3.97×10^{-1}	83.2
5	acenaphthylene	1.26×10^{-1}	77.2
6	fluorene	1.10×10^{-1}	84.9
7	anthracene	1.21×10^{-3}	99.7
8	dihydroanthracene	3.28×10^{-2}	93.9
9	phenanthrene	2.57×10^{-2}	88.9
10	1-phenylnaphthalene	3.20×10^{-3}	88.6
11	fluoranthene	1.60×10^{-3}	98.3
12	4,5-dimethylphenanthrene	1.23×10^{-2}	85.9
13	benzo[a]fluorene	1.11×10^{-4}	105.4
14	benzo[b]fluorene	3.12×10^{-4}	111.2
15	triphenylene	2.80×10^{-6}	114.5
16	tetracene	2.20×10^{-7}	126.5
17	pyrene	7.60×10^{-4}	97.9
18	chrysene	1.36×10^{-6}	118.8
19	benzanthracene	2.12×10^{-6}	115.5
20	9-phenylanthracene	4.50×10^{-6}	118.7
21	binaphthalene	2.17×10^{-8}	138.3
22	benzo[b]fluoranthene	1.00×10^{-6}	119.2
23	dibenz[a,c]anthracene	5.65×10^{-9}	135.0
24	dibenz[a,h]anthracene	4.93×10^{-9}	134.1
25	benzo[a]pyrene	5.30×10^{-8}	122.5
26	benzo[e]pyrene	7.89×10^{-7}	117.9
27	perylene	5.54×10^{-7}	123.2
28	benzo[g,h,i]perylene	1.01×10^{-8}	129.9
29	9,10-diphenylanthracene	1.88×10^{-8}	137.5
30	coronene	3.56×10^{-10}	143.2

The magnitude of the vapor pressure and the enthalpy of sublimation of these compounds can be derived from the structure. If naphthalene or fluorene is the reference compound, each higher homologue can be developed through the following structural features:[10]

Structural feature 1: linear *ortho* annelation
Structural feature 2: angular *ortho* annelation
Structural feature 3: angular *peri* annelation
Structural feature 4: phenyl group substitution

Each annelation step contributes a fixed increment to the magnitude of the vapor pressure and enthalpy of sublimation. The vapor pressure p at 25 °C and the enthalpy of sublimation $\Delta_{sub}H_m$ of the homologous series of polycyclic aromatic hydrocarbons can be described by Equations (a) and (b).

$$p(25\,^{\circ}C) = A\,X_1^{n_1}\,X_2^{n_2}\,X_3^{n_3}\,X_4^{n_4} \quad (a)$$

$$\Delta_{sub}H_m = B + n_1Y_1 + n_2Y_2 + n_3Y_3 + n_4Y_4 \quad (b)$$

[*] Prof. Dr. D. Lenoir, Dr. K. Nass, Prof. Dr. A. Kettrup
Institut für Ökologische Chemie, GSF-Forschungszentrum für Umwelt und Gesundheit GmbH
Ingolstädter Landstrasse 1, D-85758 Oberschleissheim (Germany)
Telefax: Int. code + (89)3187-3371
e-mail: lenoir@gsf.de

[**] We thank Prof. Cammenga, Braunschweig, and Dr. Utschick, GSF, for valuable suggestions.

 © VCH Verlagsgesellschaft mbH, D-69451 Weinheim, 1995 0570-0833/95/1616-1735 $ 10.00+.25/0

In the Equations (a) and (b), n_1, n_2, n_3, and n_4 are the number of structural features 1, 2, 3, and 4; $A = 10.86$ Pa, $B = 71.7$ kJ mol^{-1} for the reference substance naphthalene; $A = 1.1 \times 10^{-1}$ Pa, $B = 84.9$ kJ mol^{-1} for the reference substance fluorene; and X_m and Y_m are constants having the values shown in Table 2.

Table 2. Values of the constants from Equations (a) and (b).

m	X_m	Y_m [kJ mol^{-1}]
1	1.29×10^{-4}	27.7
2	1.81×10^{-3}	17.7
3	2.22×10^{-2}	10.2
4	3.50×10^{-3}	18.3

The method of calculation will be demonstrated for the example of coronene (Fig. 1). The vapor pressure p at 25 °C for coronene is given as 3.58×10^{-8} and 2.01×10^{-10} Pa;[7] the published enthalpy of sublimation is 112.05 and 138.02 kJ mol^{-1}. The calculation according to Equations (a) and (b) yield a vapor pressure value of 3.4×10^{-10} Pa and an enthalpy of sublimation of 140.2 kJ mol^{-1}.

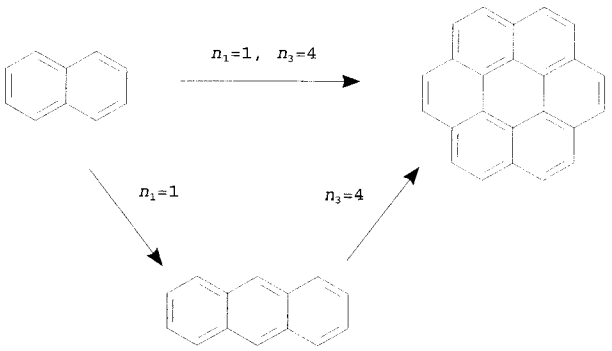

Fig. 1. Representation of the method of calculation of the vapor pressure and the enthalpy of sublimation of coronene with naphthalene as reference on the basis of Equations (a) and (b).

The results show that within a class of substances a relationship between structure and vapor pressure, and structure and enthalpy of sublimation exists.[11] To our knowledge no relationship could previously be derived for these thermodynamic parameters. The relations (a) and (b) have the mathematical form of a linear free energy relationship (LFER) somewhat like the Hammett or Hammett–Taft equation.[12] Additive relations have been derived by Benson for certain molecular properties.[13]

Thus we have shown that a relationship exists between the ensemble property of molecules and the structural elements. Through the relation between vapor pressure or enthalpy of sublimation and other thermodynamic parameters like melting and boiling points, a general derivation of thermodynamic parameters is possible.

Experimental Procedure

The measurements were performed with the VPA 434 instrument of the company Netzsch-Gerätebau, based on the gas saturation method [9a], in which a stream of inert gas flows over the sample. The saturated stream of gas is passed over an adsorption segment and after a predetermined time diverted into a gas chromatograph while heating the segment to release adsorbed substances. In this way a quantitative determination is possible. All the substances under investigation were commercially available compounds with a purity of 99.9% or greater.

The overall error of the method includes the error in calibration and the in the temperature measurement. If this error is taken into account for the linear regression of the vapor pressure curve according to $y = a + bx$, an error of $\pm 0.5\%$ is inherent in the constant a and $\pm 1\%$ in the constant b. The error in the extrapolation of the vapor pressure to 25 °C and in the calculation of the enthalpy of sublimation thus depend on the values a and b and are therefore different for each substance. Use of this error calculation with the reference substance anthracene gives a maximum error of about 36% for the extrapolated vapor pressure and about 1% for the enthalpy of sublimation. In contrast, the studies on the reproducibility for 15 measurements of anthracene yielded a standard deviation of 2.5%. The vapor pressure of anthracene therefore is 1.21×10^{-3} Pa $\pm 7.4\%$ with a statistical reliability of 99%, while the enthalpy of sublimation is 99.8 kJ mol^{-1} $\pm 1.2\%$.

Received: October 4, 1994
Revised: March 17, 1995 [Z 7373 IE]
German version: *Angew. Chem.* **1995**, *107*, 1865–1866

Keywords: polycyclic arenes · vapor pressure

[1] a) See textbooks of physical chemistry such as G. M. Barrow, *Physikalische Chemie*, 8th ed., Vieweg, Braunschweig, **1990**; b) Landoldt-Börnstein, *Zahlenwerte und Funktionen aus Physik, Chemie, Astronomie, Geophysik und Technik*, 6th ed., Springer, Berlin, **1980**; c) *Handbuch of Chemistry and Physics, 75th Ed.* (Ed.: D. L. Lide), CRC Press, Boca Raton, FL, USA, **1994**.

[2] a) H. Primas, *Chemistry, Quantum mechanics and Reductionism*, Springer, Berlin, **1981**; b) H. Primas in *Der Pauli-Jung-Dialog und seine Bedeutung für die moderne Wissenschaft* (Ed.: H. Atmanspacher), Springer, Berlin, **1995**.

[3] a) T. Clark, *A Handbook of Computational Chemistry*, Wiley, New York, **1985**; b) W. J. Hehre, L. Radom, P. von R. Schleyer, J. A. Pople, *Ab initio Molecular Orbital Theory*, Wiley, New York, **1986**; c) see papers on calculated moleculs in Chemical Abstracts.

[4] H. Primas, *Chem. Unserer Zeit* **1985**, *19*, 109–119; *ibid. 19*, 160–167.

[5] W. J. Lymann, W. F. Reehl, D. H. Rosenblatt, *Handbook of Chemical Property Estimation Methods*, American Chemical Society, Mc Graw Hill, **1990**.

[6] a) R. P. Schwarzenbach, P. M. Gschwend, D. M. Imboden, *Environmental Organic Chemistry*, Wiley, New York, **1993**, S. 56 75; b) K. Ballschmiter, *Angew. Chem.* **1992**, *104*, 501–528; *Angew. Chem. Int. Ed. Engl.* **1992**, *31*, 487–515.

[7] G. Grimmer in *Handbook of Polycyclic Aromatic Hydrocarbons* (Ed.: A. Bjorseth), Dekker, New York, **1983**, S. 149–182.

[8] M. Stephenson, S. Malanowski, *Handbook of the Thermodynamics of Organic Compounds*, Elsevier, Amsterdam, **1987**.

[9] a) K. Naß, Dissertation, TU München, **1994**; b)review on vapor pressure measurements: W. Hessler, *Wissenschaftliche Zeitschrift der Wilhelm-Pieck-Universität Rostock, Mathematisch-Naturwissenschaftliche Reihe* **1976**, *10* 1047–1066; *ibid.* **1977**, *7*, 759–784; c) F. Wania, W. Y. Shiu, D. Mackay, *J. Chem. Eng. Data* **1994**, *39* (3), 572–577.

[10] In principle, the relation can be derived from the parent compound benzene. The vapor pressure data for this compound is, however, inaccurate for technical reasons connected with the gas saturation method.

[11] a) A relation has been defined for the vapor pressure of *n*-alkanes; every CH_2 group contributes an increment to the vapor pressure: K. Ružička, V. Majer, *J. Phys. Chem. Ref. Data* **1994**, *23*, 1–39; b) a relation has been described for the enthalpy of sublimation of aliphatic hydrocarbons: J. S. Chikos, R. Annuziata, L. H. Hadon, A. S. Hyman, J. F. Liebman, *J. Org. Chem.* **1986**, *51*, 4311–4314; c) a relation between vapor pressure and the number of chlorine atoms in the compound can be derived for certain chloroarenes: B. F. Rordorf, *Thermochim. Acta* **1985**, *85*, 435–438; K. Liu, R. M. Dickhut, *Chemosphere* **1994**, *29*, 581–589.

[12] a) N. B. Chapman, J. Shorter, *Advances in Linear Free Energy Relationships*, Plenum Press, London, **1972**; b) C. Hansch, *Acc. Chem. Res.* **1993**, *26*, 147–153.

[13] S. W. Benson, *Thermochemical Kinetics*, Wiley, New York, **1976**.

The First Olefin-Substituted Peroxomolybdenum Complex: Insight into a New Mechanism for the Molybdenum-Catalyzed Epoxidation of Olefins**

Werner R. Thiel,* and Thomas Priermeier

Dedicated to Professor Henri Brunner on the occcasion of his 60th birthday

Molybdenum complexes of type $(L-L)MoO(O_2)_2$ (L–L) = chelate ligand), with seven-fold coordination, are employed as catalysts for the epoxidation of olefins.[2] Whether these complexes function as the actual catalytic species in this commercially important reaction or as catalyst precursors is one of the central problems of the still controversial reaction mechanism.[3] Associated with this are questions as to the origin of the transferred oxygen atom, the regeneration of the catalyst, and the influence of the solvent and oxidizing agent on the rate of the reaction.

For some time our studies have focused on the design of ligands for the adaptation of known catalysts for new solvent systems. For the peroxomolybdenum complexes $(L-L)MoO(O_2)_2$, which are only sparingly soluble in most common solvents, we have succeeded, through substitution of 2-(pyrazol-3-yl)pyridine (**1**) with long-chain alkyl groups, in raising their solubility dramatically such that we may epoxidize olefins in hydrocarbon solvents.[1,4] Moreover, spectroscopic investigations into the reaction mechanism are now made possible with these soluble complexes. Indications that seven-coordinate peroxomolybdenum complexes should not epoxidize olefins in stoichiometric reactions[5] led us to the synthesis of olefin-substituted derivatives of **1**.

The synthesis of the ligands **3** was accomplished through nucleophilic substitution of bromoolefins **2** with **1**. The conversions of allyl bromide (**2a**) and 4-bromo-but-1-ene (**2b**) afforded 2-(1-allyl-pyrazol-3-yl)pyridine (**3a**) and 2-(1-but-3-enyl-pyrazol-3-yl)pyridine (**3b**), respectively, in virtually quantitative yield. Reaction of a methanolic solution of the ligand with a solution of molybdic acid in 30% H_2O_2 gave rise to the chelate complexes **4a** and **4b** (Scheme 1).

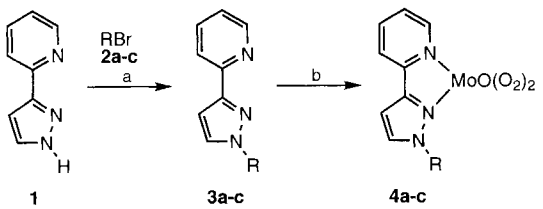

Scheme 1. a) THF, NaH, **2a–c**, 12 h, RT (**3a**: 87%, **3b**: 85%, **3c**: 55%); b) **3a–c** in MeOH, H_2MoO_4 in H_2O_2 /**4a**: 95%, **4b**: 95%, **4c**: 87%); **a**: R = $CH_2CH{=}CH_2$, **b**: R = $CH_2CH_2CH{=}CH_2$, **c**: R = cyclooct-1-enylmethyl.

Owing to their short-chain substituents, **4a** and **4b** are, however, only poorly soluble in organic solvents and are thus unsuitable for detailed spectroscopic investigations. We nevertheless succeeded in obtaining single crystals of **4a** (see Fig. 1). To increase the solubility of the molybdenum complexes **4**, we chose a methylcyclooctenyl moiety instead of a long-chain substituent, since cyclooctene is a standard substrate for investigations on olefin epoxidation (high reactivity, low tendency towards epoxide opening). The allylic precursor 1-(bromomethyl)cyclooct-1-ene (**2c**) is obtained by a five-step synthesis starting from cyclooctene.[6] The synthesis of the chelate ligand 2-[1-(cyclooct-1-ylmethyl)-pyrazol-3-yl)pyridine (**3c**) and complex **4c** proceeds analogously to that of **3a,b**/**4a,b** (Scheme 1).

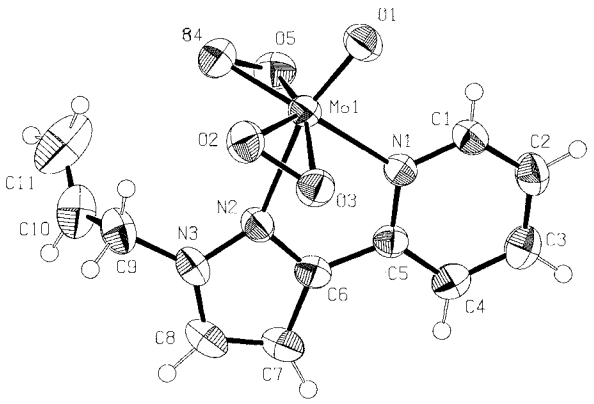

Fig. 1. Crystal structure of **4a** [7]. Selected distances [pm] and bond angles [°]: Mo-O1 167.2(1), Mo-O2 192.4(1), Mo-O3 196.3(1), Mo-O4 191.8(2), Mo-O5 194.5(1), Mo-N1 222.1(2), Mo-N2 239.1(2), O2-O3 146.8(2), O4-O5 146.9(2); N1-Mo-O1 92.37(7), N2-Mo-O1 162.72(7), N2-Mo-N1 70.49(6).

Complexes **4** exist as a mixture of two isomers. Whereas the oxo ligand adopts one of the two axial positions in the pentagonal-bipyramidal ligand sphere of the seven-coordinate Mo atom, the remaining axial position may be occupied by either the pyridine or the pyrazole ring of the ligand.[4] The single-crystal structure determination[7] of an arbitrarily selected crystal of **4a** shows the isomer with the pyrazole ring in the axial position (Fig. 1). As with all other previously known molecular structures of this type,[4,8] the Mo–N2 distance ($Mo-N_{ax}$: 239.1(2) pm) is distinctly longer than the Mo–N1 distance ($Mo-N_{eq}$: 222.1(2) pm), which may be attributed to the *trans* influence of O1. The angle N2-Mo-O1 (162.72(7)°) likewise corresponds to values found for other structures. An intra- or intermolecular interaction of the olefinic side chain at N3 with one of the oxygen ligands at molybdenum or with the central atom is not observed, even in the solid state.

The complexes **4a–c** are stable in solution as well as in the solid state. This indicates that transfer (intra- or intermolecular) of an oxygen atom from a peroxo ligand to the CC double bond does not occur for this type of complex or is otherwise very slow. This step is, however, the central element of the reaction mechanism for the olefin epoxidation discussed in the literature (Scheme 2).[3] As is shown by NMR investigations with the highly soluble compound **4c**, the cyclooctenyl ring is epoxidized only in the presence of *tert*-butyl hydroperoxide (Fig. 2).

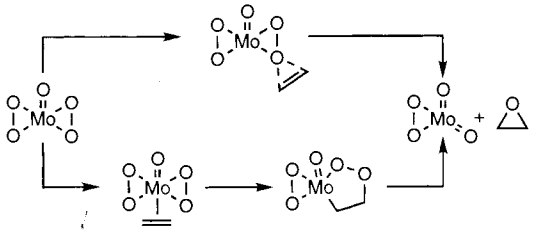

Scheme 2. Previously accepted mechanisms for the Mo-catalyzed epoxidation of olefins [3].

[*] Dr. W. R. Thiel, Dipl.-Chem. T. Priermeier
Anorganisch-chemisches Institut der Technischen Universität München
Lichtenbergstrasse 4, D-85747-Garching (Germany)
Telefax: Int. code + (89)3209-3473
e-mail: thiel@zaphod.anorg.chemie.tu-muenchen.de

[**] Metal-Catalyzed Oxidations, Part 3. We thank Professor W. A. Herrmann and the Deutsche Forschungsgemeinschaft (Schwerpunktprogramm "Peroxidchemie") for support of our work. Part 2: ref. [1].

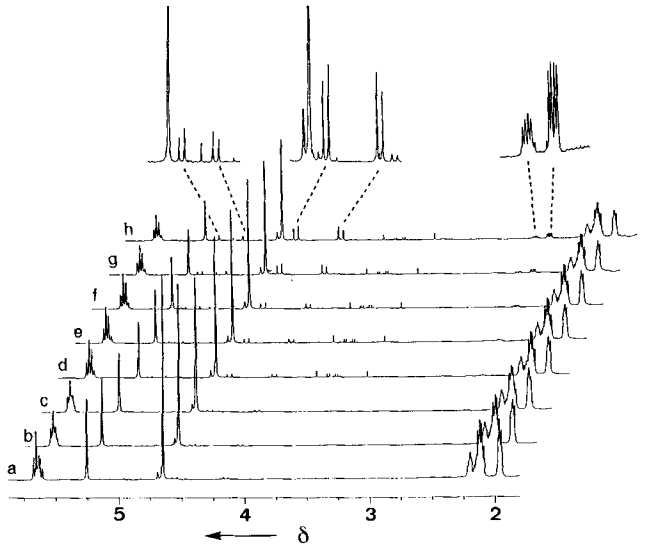

Fig. 2. Reaction of **4c** with *t*BuOOH (NMR experiment): a) **4c** in $CDCl_3$, b) after 15 min, c) after 1 h, d) after addition of 4.3 equiv of *t*BuOOH, e) 30 min after addition, f) 1 h after addition, g) 2 h after addition, h) 3 h after addition; the signals of the aromatic protons and a part of the cyclooctenyl protons are omitted.

The progress of the reaction is evident by the emergence of six new signals in the ^{1}H NMR spectrum. Whereas the spectrum of the starting compound (two isomers) displays two signals for both the $N-CH_2$ group ($\delta = 5.24$ and 4.63, $2 \times s$) and the olefinic proton of the cyclooctenyl ring ($\delta = 5.64$ and 5.63, $2 \times t$, $^3J_{HH} = 8.0$ Hz), the epoxidized product (likewise two isomers) shows a more complex spectrum for these protons. Two new chiral centers are introduced into the molecule through the epoxidation. As a consequence, the protons of the $N-CH_2$ groups are no longer equivalent, and two doublets are observed for each isomer ($\delta = 5.15$, 4.92, $^2J_{HH} = 15.3$ Hz; $\delta = 4.52$, 4.16, $^2J_{HH} = 14.9$ Hz). Similarly, the signals for the protons at the epoxide C atom are split into doublets of doublets, because the protons of the neighboring CH_2 group are no longer equivalent ($\delta = 2.61$, $^3J_{HH} = 10.1$ Hz, $^3J_{HH} = 4.6$ Hz; $\delta = 2.50$, $^3J_{HH} = 10.1$ Hz, $^3J_{HH} = 4.4$ Hz).

These observations are consistent with catalytic epoxidations with alkyl-substituted peroxomolybdenum complexes and *tert*-butyl hydroperoxide as oxidant:[4] In the absence of the oxidant no reaction takes place; the olefin reacts rapidly only upon addition of TBHP. No decomposition of the catalyst is found within the limits of the accuracy of our monitoring. From these studies it may be inferred that for the complexes investigated here, the oxygen atom transferred to the olefin in the epoxidation derives not from a peroxo ligand, but from the *tert*-butyl hydroperoxide. The molybdenum complex thus activates the oxidizing agent. This activation may proceed in analogous fashion to the mechanism postulated for the epoxidation of allylic alcohols with titanium alkoxides (Sharpless epoxidation) (Scheme 3),[9a] which at the same time provides a simple explanation for the regeneration of the catalyst.

This step was also suggested by Sharpless et al. for the molybdenum-catalyzed epoxidations,[9b] but was not, however, verified further. The η^2-coordination of hydroperoxides to Lewis acidic centers has been established structurally for vanadium complexes.[10] The resulting oxenoid character of the hydroperoxide has been calculated for model systems.[11] The activation of hydroperoxide with regard to reaction with nucleophiles is demonstrated preparatively by the reaction of Li(η^2-OOR) with organolithium, -magnesium, and -copper compounds.[11a]

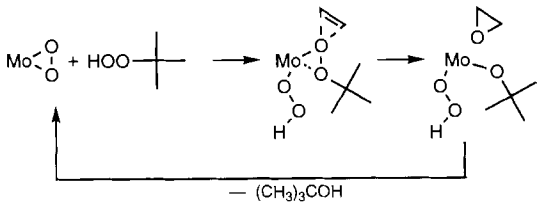

Scheme 3. Mechanism for the Mo-catalyzed epoxidation of olefins (formulated analogously to the postulated mechanism for the Ti-catalyzed epoxidation of allylic alcohols; cf. ref. [9]).

Through the synthesis of olefin-substituted peroxomolybdenum complexes we have succeeded in obtaining the first indications of a new reaction mechanism for olefin epoxidation with peroxo complexes. Further investigations are planned, specifically on the influence of the ligand on the activity and selectivity of the catalyst. In addition to this, the ligands introduced here should prove suitable for the synthesis of polymer-supported catalyst systems.

Received: March 1, 1995
Revised version: May 3, 1995 [Z 7752 IE]
German version: *Angew. Chem.*, **1995**, *107*, 1870–1871

Keywords: catalysis · epoxidations · molybdenum compounds

[1] W. R. Thiel, M. Angstl, N. Hansen, *J. Mol. Catal.* **1995**, in press.
[2] a) *Catalytic Oxidations with Hydrogen Peroxide as Oxidant* (Ed.: G. Strukul), Kluwer, Rotterdam, **1992**; b) K. A. Jørgensen, *Chem. Rev.* **1989**, *89*, 431; c) *Organic Synthesis by Oxidation with Metal Compounds* (Eds.: W. J. Mijs, C. H. R. I. de Jonge), Plenum, New York, **1986**; d) S. Campestrini, F. Di Furia, P. Rossi, A. Torboli, G. Valle, *J. Mol. Catal.* **1993**, *83*, 95.
[3] a) K. B. Sharpless, J. M. Townsend, D. R. Williams, *J. Am. Chem. Soc.* **1972**, *94*, 295; b) H. Mimoun, I. Seree de Roch, L. Sajus, *Tetrahedron* **1970**, *26*, 37; c) H. Arakawa, Y. Moro-Oka, A. Ozaki, *Bull. Chem. Soc. Jpn.* **1974**, *47*, 2958; d) P. Chaumette, H. Mimoun, L. Saussine, J. Fischer, A. Mitschler, *J. Organomet. Chem.* **1983**, *250*, 291; e) K. Purcell, *ibid.* **1983**, *252*, 181; f) K. A. Jørgensen, R. Hoffmann, *Acta Chem. Scand. Ser. B* **1986**, *40*, 411; g) V. Schurig, K. Hintzer, U. Leyrer, C. Mark, P. Pitchen, H. B. Kagan, *J. Organomet. Chem.* **1989**, *370*, 81.
[4] W. R. Thiel, M. Angstl, T. Priermeier, *Chem. Ber.* **1994**, *127*, 2373.
[5] M. J. Filatov, K. V. Shalyaev, E. P. Talsi, *J. Mol. Catal.* **1994**, *87*, L5.
[6] L. Pagès, A. Llebaria, F. Camps, E. Molins, C. Miravitlles, J. Motetó, *J. Am. Chem. Soc.* **1992**, *114*, 10449.
[7] Crystal structure analysis of **4a** (crystallized from CH_2Cl_2): $Mo_{K\alpha}$, $\lambda = 0.71703$ Å, ω-scan, solution: Patterson methods (SHELXS-86), refinement with CRYSTALS, all hydrogen atoms located and refined without restrictions, $C_{11}H_{11}MoN_3O_5$, $M = 361.2$ g mol^{-1}, space group $P2_1/c$, $a = 1310.5(2)$, $b = 1202.4(1)$, $c = 846.7(2)$ pm, $\beta = 103.79(1)°$, $V = 1296 \cdot 10^6$ pm^3, $Z = 4$, $\rho_{calc.} = 1.851$ g cm^{-3}, $\mu = 10.1$ cm^{-1}, measurement temperature + 23 °C, 5231 measured reflections, 2112 independent reflections used for the refinement ($I > 0$), 225 refined parameters, $R = 0.021$, $R_w = 0.020$, residual electron density 0.57 and -0.28 e Å^{-3}. Further details of the crystal structure investigation may be obtained from the Fachinformationszentrum Karlsruhe, D-76344 Eggenstein-Leopoldshafen (Germany), on quoting the depository number CSD-58989.
[8] a) E. O. Schlemper, G. N. Schrauzer, L. A. Hughes, *Polyhedron* **1984**, *3*, 377; b) W. A. Herrmann, W. R. Thiel, J. G. Kuchler, J. Behm, E. Herdtweck, *Chem. Ber.* **1990**, *123*, 1963.
[9] a) T. Katsuki, K. B. Sharpless, *J. Am. Chem. Soc.* **1980**, *102*, 5976; b) A. O. Chong, K. B. Sharpless, *J. Org. Chem.* **1977**, *42*, 1587.
[10] a) H. Mimoun, P. Chaumette, M. Mignard, L. Saussine, J. Fischer, R. Weiss, *New J. Chem.* **1983**, *7*, 467; b) H. Szentivanyi, R. Stomberg, *Acta Chem. Scand. Ser. A* **1984**, *38*, 101.
[11] a) G. Boche, F. Bosold, J. C. W. Lohrenz, *Angew. Chem.* **1994**, *106*, 1228; *Angew. Chem. Int. Ed. Engl.* **1994**, *33*, 1161; b) R. D. Bach, M.-D. Su, J. L. Andrés, H. B. Schlegel, *J. Am. Chem. Soc.* **1993**, *115*, 8763.

Design of Novel, Nonpeptidic Thrombin Inhibitors and Structure of a Thrombin–Inhibitor Complex**

Ulrike Obst, Volker Gramlich, François Diederich,* Lutz Weber,* and David W. Banner

Dedicated to Professor Albert Eschenmoser on the occasion of his 70th birthday

In the context of our work on host–guest interactions, we have developed receptors for various substrates.[1] The availability of high resolution X-ray structures of enzymes now allows the reverse process of rational design of inhibitors with the aid of molecular modeling. To this end, instead of using the enzyme's substrate as model, a small molecule, complementary to the active site with respect to hydrogen bonding as well as ionic and dispersive interactions, should be designed *de novo*.

Enzymes that are best suited for the rational design approach are those with rigid, well-defined binding pockets in the active site. Thrombin, a trypsin-like serine protease[2] with a central role in the blood coagulation process,[3] meets these requirements. The natural substrate for thrombin is fibrinogen, which is dissolved in the blood plasma. The enzyme selectively cleaves the peptide bond next to an arginine residue to form fibrin, which can polymerize. Thrombin is also the main activator of platelet aggregation. A selective inhibition of thrombin has potential therapeutic application in thrombotic diseases.

A number of X-ray structures of thrombin–inhibitor complexes were available,[4] which allowed the study of the important interactions crucial for inhibition. The active site of thrombin features three binding pockets (see Fig. 1). The bottom of the recognition pocket S1 contains Asp189 for interactions with guanidinium or ammonium groups of arginine or lysine residues. The large hydrophobic pocket (D-pocket, signifying a pocket "distal" to the catalytic site[4b]) is preferentially occupied by arene rings, which can undergo CH···π arene–arene interactions with the indole unit of Trp215. Fibrinogen, the natural substrate for thrombin, places the benzyl group of a phenylalanine residue in this pocket. An additional smaller hydrophobic pocket is positioned close to the catalytic site ("proximal": P-pocket[4b]). In the thrombin–fibrinogen complex this pocket is occupied by a valine residue. It was our goal to develop a nonpeptidic cyclic template to which three side chains could be attached in order to reach each of the three binding pockets (hydrophobic side chains for the P and D pockets, and an aromatic unit with a basic group for the recognition pocket S1 of the enzyme). The template should be rigid to avoid hydrophobic collapse of the side chains[6] and to avoid the loss of conformational degrees of freedom on complexation to the enzyme. In addition, the template should contain a hydrogen-bond acceptor (for example, a carbonyl group) to form a hydrogen bond to the amide NH of Gly216, a feature present in all known thrombin–inhibitor complexes. The synthesis should be simple and short and allow variation of the side chains. With such a synthesis, affinity and selectivity can be subsequently optimized through combinatorial solid-phase synthesis. The design of the target molecule was undertaken with the programs Insight II and Discover;[7] the force field used was the CVFF. A result of the modeling was molecule **1** (see Fig. 1). It has no structural similarity to either the natural thrombin substrate, fibrinogen, or other known synthetic thrombin inhibitors. This molecule has a series of potential interactions with the enzyme (Fig. 1): 1) a salt bridge between the amidinium group of the inhibitor and the carboxylate of Asp189 in the recognition pocket S1 of the enzyme, 2) two hydrogen bonds of the NH of Gly216 and the OH of Tyr60A to the carbonyl groups of the succinimide residue, 3) edge-to-face interactions between the indole ring of Trp215 and the benzyl group of the inhibitor in the D-pocket of the enzyme, where the benzyl group experiences additional benefits from the neighboring hydrophobic residues Ile174 and Leu99 (not shown in Fig. 1), and 4) contacts between two methyl groups of the inhibitor and the hydrophobic P-pocket of thrombin.

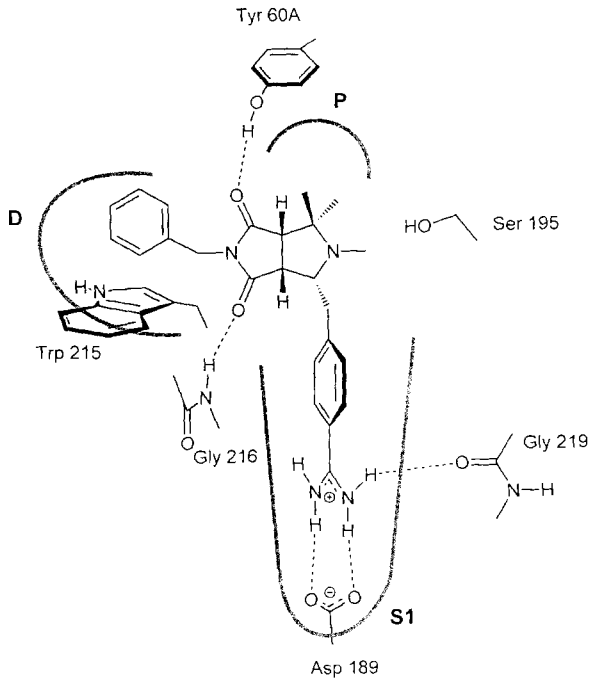

Fig. 1. Schematic representation of inhibitor **1** energy-minimized in the active site of thrombin.

The synthesis of **1** (Scheme 1) began with a 1,3-dipolar cycloaddition in a three component reaction. An azomethine ylide was generated in situ from 4-bromophenylalanine (**2**) and acetone (**3**) with decarboxylation and treated with *N*-benzylmaleimide (**4**). The pyrrolidine nitrogen atom of the cycloadduct (**5**) was methylated (→ **6**), and the bromo substituent converted into a cyano group. The conversion of the nitrile **7** into amidine **1** was achieved with a Pinner reaction.[10]

In the preparation of the bicyclic templates, it is also possible to make shorter basic benzamidinium "needles"[4c] lacking the methylene group, by using 4-cyanobenzaldehyde in the 1,3-dipolar cycloaddition (Scheme 2). Compounds **11a–m** are more easily prepared than the analogous cycloadduct **5**. In addition, their synthesis allows a larger structural variation of the "upper" side chains, a significant feature with respect to the planned

[*] Prof. F. Diederich, Dipl.-Chem. U. Obst
Laboratorium für Organische Chemie, ETH Zentrum
Universitätstrasse 16, CH-8092 Zürich (Switzerland)
Telefax: Int. code + (1)632-1109
e-mail: Diederich @ org.chem.ethz.ch
Dr. L. Weber, Dr. D. W. Banner
Pharma Division, Präklinische Forschung
F. Hoffmann–La Roche AG
CH-4002 Basel (Switzerland)
Dr. V. Gramlich
Institut für Kristallographie und Petrographie
ETH-Zentrum
Sonneggstrasse 5, CH-8092 Zürich (Switzerland)

[**] This work was supported by F. Hoffmann-La Roche AG, Basel. U. O. thanks the Fonds der Chemischen Industrie, Germany, for a Kekulé stipend.

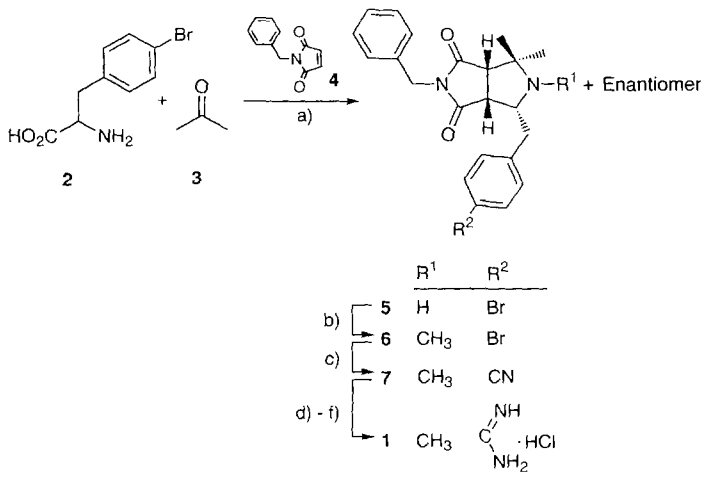

Scheme 1. Synthesis of the designed thrombin inhibitor **1**, as racemate: a) toluene, reflux, 68 h, 25%; b) HCHO, HCO_2H, 100 °C, 10 h, 81%; c) CuCN, *DMF*, reflux, 56 h, 63%; d) HCl, MeOH, 4 °C, 48 h; e) $NaHCO_3$; f) NH_4Cl, MeOH/H_2O, 65 °C, 3 h, 57%.

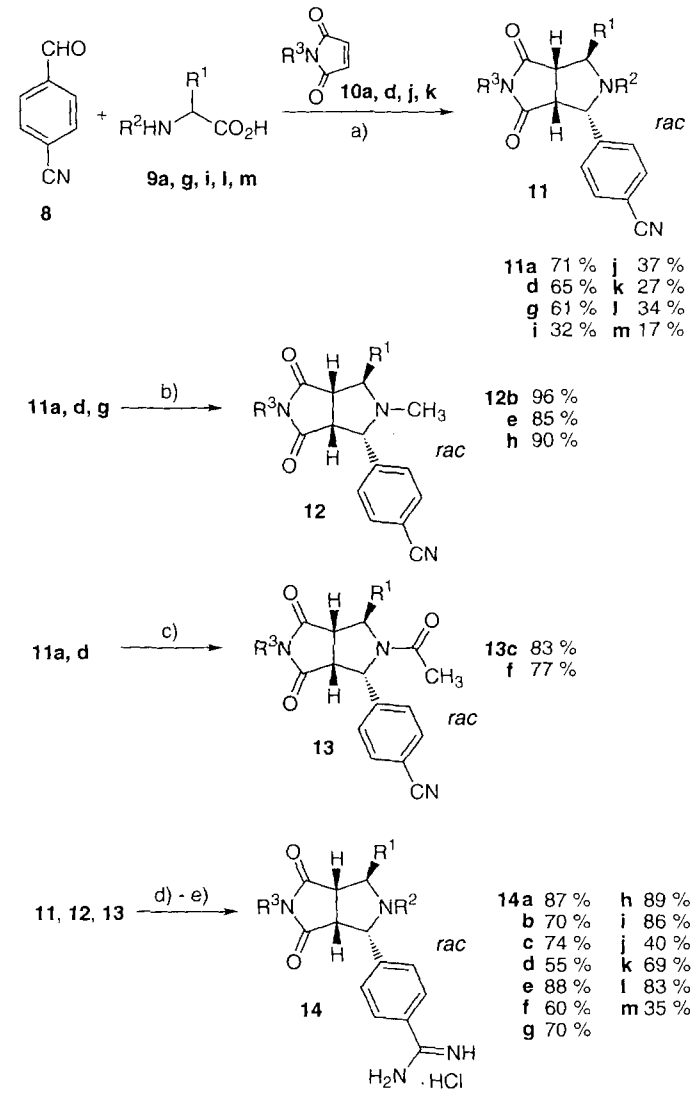

Scheme 2. Synthesis of the benzamidinium chlorides **14a–m** as analogs of **1**: a) DMF, 80 °C, 5 h; b) HCHO, HCO_2H, 100 °C, 10 h; c) Ac_2O, pyridine, 0 °C to room temperature, 2 h; d) HCl, MeOH, 4 °C, 48 h; e) NH_3, MeOH, 65 °C, 3 h. For the residues R^1–R^2 see Table 1. Racemic mixtures are formed at all stages.

combinatorial synthesis. The structure of the major diastereomer formed in the cycloaddition was determined by X-ray crystallography of nitrile **12b**. The product was formed from an *anti*-ylide through an *endo* transition state[11] and was shown to have a different conformation in the crystal[12] (Fig. 2) than is required for the binding of the final product **14b** to thrombin. In the structure of **12b** an intramolecular CH···π arene–arene interaction and a different conformation of the pyrrolidine ring can be observed. At any rate, the structure of **12b** in the crystal does not provide information about the conformation of amidine **14b** either in solution or in the active site of thrombin.

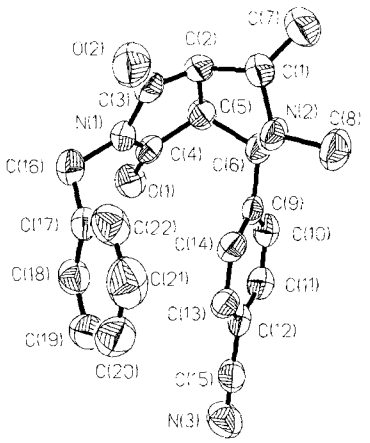

Fig. 2. Crystal structure of **12b**.

The originally proposed compound **1** was found to have a K_i value for thrombin of 18 μM as a racemic mixture[14] (for comparison: benzamidine has a K_i value of 300 μM[4c]). Compounds **14a–m**, lacking the CH_2 group in the benzamidinium needle, were significantly more active (Table 1). These compounds are conformationally more restricted than **1** because of the rigid framework and the attachment of the needle, and are therefore excellent candidates on which to study structure–activity relationships. These compounds can all be expected to follow the same binding mode.

Table 1. Activities of the thrombin inhibitors **14a–m** and selectivities with respect to complexation to trypsin.

Compd.	R^1	R^2	R^3	K_i [μM]	Selectivity [a]
14a	Me	H	Bn	1.1	4.6
14b	Me	Me	Bn	0.67	7.3
14c	Me	Ac	Bn	170	2.5
14d	Me	H	Bu	11	1.3
14e	Me	Me	Bu	2.9	7.6
14f	Me	Ac	Bu	160	2.3
14g	*i*Bu	H	Bn	1.5	3.4
14h	*i*Bu	Me	Bn	1.0	2.8
14i	$-(CH_2)_3-$		Bn	0.22	12
14j	$-(CH_2)_3-$		piperonyl [b]	0.09	7.8
14k	$-(CH_2)_3-$		cyclohexyl-methyl	0.35	15
14l	$-(CH_2)_4-$		Bn	10	0.6
14m	$-CH_2SCH_2-$		piperonyl [b]	0.44	20

[a] K_i (trypsin)/K_i (thrombin). [b] Piperonyl =

On the pyrrolidine nitrogen on the right in the depicted structural formula, three structural modifications were evaluated. The compounds with a methylated nitrogen atom (**14b,e,h**) showed increased activity relative to the unmethylated ones (**14a,d,g**), whereas a dramatic reduction of activity was observed with acetylated compounds (**14c,f**). A possible explanation is that acetylation leads to a conformational change in the bicyclic template. Another possibility is that the pyrrolidine is preferentially bound in the protonated state: with acetylation

 © VCH Verlagsgesellschaft mbH, D-69451 Weinheim, 1995 0570-0833/95/1616-1740 $ 10.00+.25/0

protonation is no longer possible. The highest thrombin affinities (lowest K_i values) were achieved with the addition of a five-membered ring on the right side of the molecule (**14i–k**). A six membered ring led to a reduction in affinity (**14l**), probably because this large hydrophobic moiety displaces a water molecule close to the catalytic group Ser195. A thiazolidine ring (**14m**) is probably also too big. The activity is less influenced by the substituents on the succinimide nitrogen atom for the "aryl binding pocket" (D-pocket). Butyl, benzyl, and cyclohexylmethyl substituents give rise to no large variations. The highest activity was achieved with a benzodioxol-5-ylmethyl (= piperonyl) substituent (**14j**, $K_i = 90$ nM).

The binding mode of the currently most active compound **14j** was revealed by X-ray crystallography[15] of its complex with thrombin. The inhibitor was bound in the active site of thrombin in the predicted fashion (Figs. 3 and 4). As expected, based on the rigidity of the molecule and the molecular modeling, only the (3a*S*,4*R*,8a*S*,8b*R*) enantiomer of the racemic mixture was found in the crystal structure. The benzamidinium side chain binds well in the recognition pocket S1 of the enzyme. Hydrogen bonds are formed to the carboxylate group of Asp189, to the carbonyl group of Gly219, and to a water molecule present at the bottom of the pocket. One carbonyl group of the inhibitor acts as a hydrogen bond acceptor for the NH of Gly216, whereas the other is located in the enzyme's P-pocket. The move of this carbonyl group from aqueous solution to the small hydrophobic P-pocket of thrombin must cost desolvation energy. This energy is not required for the binding of the inhibitor to trypsin, because it lacks the loop which in thrombin forms the P-pocket. This could explain why this class of inhibitors is only slightly more selective (up to 20-fold) for thrombin than for trypsin. Another hydrogen bond is formed between Tyr60A and an oxygen of the piperonyl group. The aromatic portion of the piperonyl group is located in the D-pocket of the enzyme and is involved in the expected CH $\cdots\pi$ interaction with Trp215.

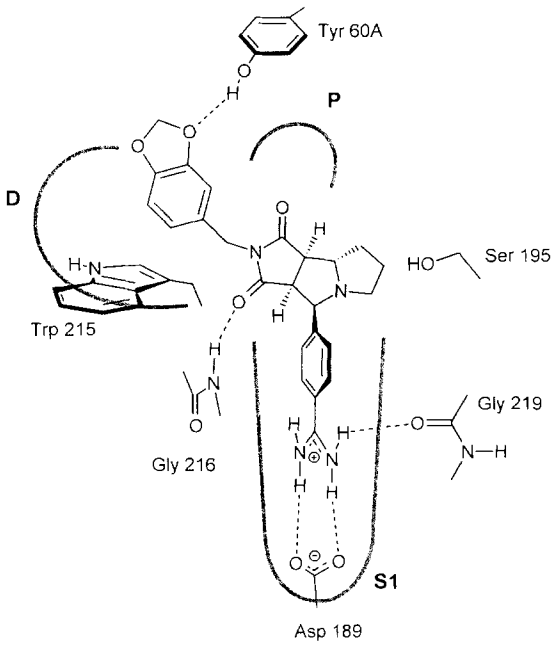

Fig. 3. Schematic representation of the interactions of **14j** with thrombin according to the crystal structure.

This inhibitor is still not optimal, especially with respect to its selectivity. Nevertheless, our results show that with a rational approach it is possible to develop new lead structures for enzyme inhibition in a relatively short time.

The synthetic strategy with 1,3-dipolar cycloaddition provides a large potential for structural variation. Most α-amino acids and several carbonyl compounds are feasible reagents to generate the azomethine ylides.[11] Most electron-poor olefins or acetylenes are conceivable dipolarophiles. Investigations involving the 1,3-dipolar cycloaddition with azomethine ylides on a solid phase are in progress. We hope that these combinatorial methods on a resin will lead to thrombin inhibitors with improved activity, selectivity, and good pharmacological properties.

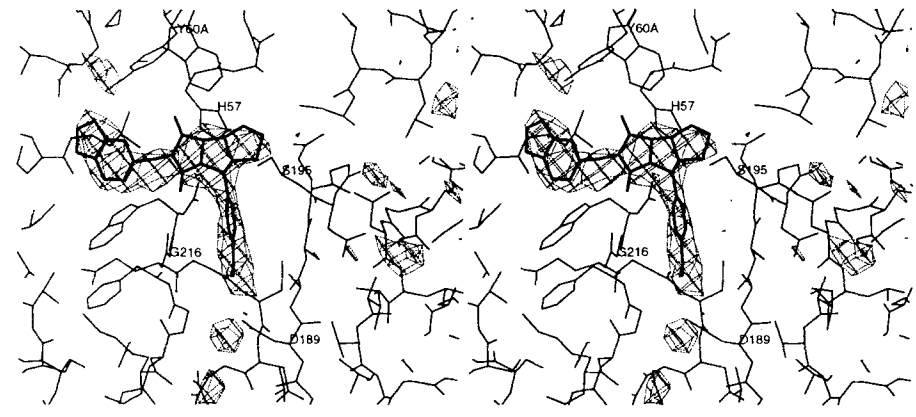

Fig. 4. Stereorepresentation of the difference electron densities of **14j** (dashed lines), thrombin (thin lines), and a model of the inhibitor (thick lines) [15]. The very small peaks represent water molecules or small changes of the protein compared to the (unrefined) model. Comparative calculations showed that the electron densities of the carbonyl groups must be weak at this resolution due to truncation of the Fourier series.

Experimental Procedure

11j: A mixture of proline (1.15 g, 10 mmol), 4-cyanobenzaldehyde (1.31 g, 10 mmol), and *N*-piperonylmaleimide (2.31 g, 10 mmol) was heated in DMF (10 mL) for 5 h at 80 °C. The solvent was removed under high vacuum, and the residue purified chromatographically on silica gel (hexane/AcOEt/NEt_3 49.5:49.5:1). Yield 37%; colorless needles (recrystallized from methanol), m.p. 176–179 °C.

14j: Dry HCl was passed through a solution of **11j** (831 mg, 2 mmol) in dry $CHCl_3$/CH_3OH 5:1 (6 mL) at 0 °C for 10 min. The reaction mixture was kept for two days at 4 °C. After addition of Et_2O a precipitate was formed, which was dried and mixed with a $NaHCO_3$ solution (5%, 8 mL) and $CHCl_3$ (20 mL). After a quick extraction the aqueous layer was again extracted twice with $CHCl_3$. The organic phase was dried over Na_2SO_4, and the solvent was distilled off. The residue was dissolved in MeOH (7 mL) and NH_4Cl (150 mg) in H_2O (1.5 mL) was added. The mixture was stirred at 65 °C for 3.5 h. After cooling, the solvent was distilled off, and the residue was separated chromatographically (RP18 silica gel, gradient from H_2O to MeOH). Yield 40%; colorless powder, m.p. 177–181 °C; IR (KBr): $\tilde{\nu} = 1701$ (C=O), 1678 (C=N) cm^{-1}; ^1H NMR (250 MHz, $(CD_3)_2SO$): $\delta = 1.68$ (m, 2H), 1.98 (m, 2H), 2.45 (m, 1H), 2.77 (m, 1H), 3.47 (d, $J = 7.8$ Hz, 1H), 3.56 (m, 1H), 3.76 (t, $J = 8.3$ Hz, 1H), 4.22 (d, $J = 8.5$ Hz, 1H), 4.33 (s, 2H), 6.02 (s, 2H), 6.67, 6.88 (AB, $J = 7.8$ Hz, 2H), 6.70 (s, 1H), 7.44, 7.71 (AB, $J = 8.2$ Hz, 4H), 9.08 (s, 2H), 9.38 (s, 2H); ^{13}C NMR (62.5 MHz, $(CD_3)_2SO$): $\delta = 23.0$, 29.0, 41.2, 48.6, 50.3, 67.4, 67.5, 101.0, 108.1, 108.2, 121.2, 126.5, 127.5, 128.7, 129.7, 145.6, 146.6, 147.2, 165.4, 175.4, 178.1; ESI(electrospray)-MS: *m/z* 433.4 ($[M + H]^+$, 100); satisfactory anal. for C, H, N, Cl.

Received: April 12, 1995 [Z 7884 IE]
German version: *Angew. Chem.* **1995**, *107*, 1874–1877

Keywords: azomethine ylides · cycloadditions · de novo design · enzyme inhibitors · thrombin

[1] a) B. R. Peterson, F. Diederich, *Angew. Chem.* **1994**, *106*, 1688–1690; *Angew. Chem. Int. Ed. Engl.* **1994**, *33*, 1625–1628; b) V. Alcazar, F. Diederich, *ibid.* **1992**, *104*, 1503–1505 and **1992**, *31*, 1521-1523; c) F. Diederich, *Cyclophanes*, The Royal Society of Chemistry, Cambridge, **1991**.

[2] I. V. Kurinov, R. W. Harrison, *Struct. Biol.* **1994**, *1*, 735–743.

[3] M. C. E. van Dam-Mieras, A. D. Muller in *Blood Coagulation* (Eds.: R. F. A. Zwaal, H. C. Hemker), Elsevier, Amsterdam, **1986**, pp. 1–11.

[4] a) W. Bode, I. Mayr, U. Baumann, R. Huber, S. R. Stone, J. Hofsteenge, *EMBO J.* **1989**, *8*, 3467–3475; b) D. W. Banner, P. Hadváry, *J. Biol. Chem.* **1991**, *266*, 20085–20093; c) K. Hilpert, J. Ackermann, D. W. Banner, A. Gast, K. Gubernator, P. Hadváry, L. Labler, K. Müller, G. Schmid, T. B. Tschopp, H. van de Waterbeemd, *J. Med. Chem.* **1994**, *37*, 3889–3901.

[5] Chymotrypsinogen numbering [4a].

[6] a) D. H. Rich in *Perspectives in Medicinal Chemistry* (Eds.: B. Testa, W. Fuhrer, E. Kyburz, R. Giger), Verlag Helvetica Chimica Acta, Basel/VCH, Weinheim 1993, pp. 15–25; b) R. Hirschmann, K. C. Nicolaou, S. Pietranico, E. M. Leahy, J. Salvino, B. Arison, M. A. Cichy, P. G. Spoors, W. C. Shakespeare, P. A. Sprengeler, P. Hamley, A. B. Smith III, T. Reisine, K. Raynor, L. Maechler, C. Donaldson, W. Vale, R. M. Freidinger, M. R. Cascieri, C. D. Strader, *J. Am. Chem. Soc.* **1993**, *115*, 12550–12568; c) P. Y. S. Lam, P. K. Jadhav, C. J. Eyermann, C. N. Hodge, Y. Ru, L. T. Bacheler, J. L. Meek, M. J. Otto, M. M. Rayner, Y. N. Wong, C.-H. Chang, P. C. Weber, D. A. Jackson, T. R. Sharpe, S. Erickson-Viitanen, *Science* **1994**, *263*, 380–384.

[7] Insight II, Version 2.3.0: San Diego, Biosym Technologies, **1993**; Discover, Version 2.9.5: San Diego, Biosym Technologies, **1994**. Modeling procedure: The proposed inhibitor was separately geometry optimized and docked into its expected binding site. The coordinates of the enzyme were fixed, and the energy of the inhibitor inside the enzyme was minimized.

[8] a) O. Tsuge, S. Kanemasa, M. Ohe, S. Takenaka, *Bull. Chem. Soc. Jpn.* **1987**, *60*, 4079–4089; b) R. Grigg, S. Thianpatanagul, *J. Chem. Soc. Chem. Commun.* **1984**, 180–181; c) R. Grigg, S. Surendrakumar, S. Thianpatanagul, D. Vipond, *ibid.* **1987**, 47–49.

[9] All new compounds gave satisfactory analytical results.

[10] G. Wagner, I. Wunderlich, *Pharmazie* **1977**, *32*, 76–79.

[11] Review on azomethine ylides: O. Tsuge, S. Kanemasa, *Adv. Heterocycl. Chem.* **1989**, *45*, 231–347.

[12] **12b**: $C_{22}H_{21}N_3O_2$; colorless plates, crystal dimensions $0.4 \times 0.4 \times 0.3$ mm; $M_r = 359.43$; triclinic, space group $P\bar{1}$, $a = 9.352(8)$, $b = 10.004(7)$, $c = 10.882(9)$ Å, $\alpha = 95.55(6)$, $\beta = 94.39(7)$, $\gamma = 110.73(7)°$, $V = 941.0(13)$ Å^3, $Z = 2$, $\rho_{calcd} = 1.269$ g cm^{-3}, Syntex P3/V diffractometer ($Mo_{K\alpha}$ radiation, $\lambda = 0.71073$ Å, graphite monochromator, $T = 293$ K), 1885 reflections measured, 1763 independent reflections, 1365 reflections with $F > 4.0\sigma(F)$. The structure was solved by direct methods [13] and refined by full-matrix, least-squares analysis (heavy atoms anisotropic, H atoms fixed isotropically; H positions are based on stereochemical considerations), $R = 0.0471$, $wR = 0.0422$. Further details of the crystal structure investigations may be obtained from the Director of the Cambridge Crystallographic Data Centre, 12 Union Road, GB-Cambridge CB2 1EZ (UK), on quoting the full journal citation.

[13] Siemens SHELXTL PLUS (VMS), Siemens Analytical Instruments, Madison, USA, **1986**.

[14] The activity of the thrombin inhibitors was determined according to R. Lottenberg, J. A. Hall, J. W. Fenton, G. M. Jackson, *Thromb. Res.* **1982**, *28*, 313 (chromogenic substrate S-2238).

[15] The data (75% complete to a resolution of 3.16 Å) were measured and worked up as described in [4b,c]. For calculation of the difference electron densities (Fig. 4) the coordinates for protein and water molecules of human thrombin were used (refined to a resolution of 2.6 Å, see Fig. 4 in ref. [4c]). Despite the modest quality of the data the binding mode of the inhibitor could be clearly identified. After refinement of protein and inhibitor the crystallographic R value was 12.9% for 7043 reflections with $F > \sigma$ with acceptable geometry (standard deviation for the bond lengths 0.012 Å and for the bond angles 2.0°). The atoms of the inhibitor have an average B value of 50 Å^2, significantly higher then the atoms of the protein. Either not all inhibitor sites are occupied or the inhibitor is present in several similar conformations. We have recently confirmed this result at higher resolution (1.9 Å) in a different crystal type (C2); details of this better defined structure will be published elsewhere.

σ Metathesis as a Critical Step for the Transition Metal Catalyzed Formation of Formic Acid from CO_2 and H_2? An Ab Initio Investigation**

François Hutschka, Alain Dedieu,* and Walter Leitner

The homogeneous catalytic hydrogenation of carbon dioxide into formic acid has been the subject of recent experimental studies,[1-3] and hydridorhodium(I) complexes have been shown to be very efficient catalysts.[1, 2] It is generally believed that the catalytic cycle starts with the CO_2 insertion into the metal–hydrogen bond, a process that is well understood, experimentally and theoretically.[4, 5] The subsequent steps are more speculative. A sequence involving Rh^I and Rh^{III} intermediates was put forward in the two most recent examples. In these either $[Rh(nbd)(PMe_2Ph)_3]BF_4$ (nbd = norbornadiene)[2] or $[\{Rh(cod)(\mu\text{-}H)\}_4]$ and $[\{Rh(cod)(\mu\text{-}Cl)\}_2]$ (cod = 1,5-cyclooctadiene) in the presence of the bidendate phosphane ligand $Ph_2P(CH_2)_4PPh_2$ were used as the hydrogenation catalyst.[1a, 1d] In the former case the catalytically active species is believed to be the cationic dihydridorhodium(III) complex $[Rh(PMe_2Ph)_3(H)_2(solvent)]^+$, and insertion of CO_2 has been shown to yield a hydridoformatorhodium(III) complex. Reductive elimination of formic acid and subsequent oxidative addition of H_2 are assumed to regenerate the dihydridorhodium(III) cation. In the second, much more efficient system, the neutral species $[\{Ph_2P(CH_2)_4PPh_2\}Rh(H)]$ is believed to carry the catalytic cycle by insertion of CO_2. H_2 would then oxidatively add to the formatorhodium(I) intermediate and reductive elimination of formic acid from a dihydridorhodium(III) intermediate would lead back to the rhodium(I) compound (path A in Scheme 1). In the course of our theoretical studies of CO_2 coordination and reactivity,[6] we have started to investigate these catalytic processes.[7] The purpose of this preliminary communcation is to propose on the basis of our calculations an alternative mechanism (summarized in path B in Scheme 1) in which the rhodium center retains the formal oxidation state I throughout the reaction. Change of oxidation state is avoided by a σ metathesis reaction between the H_2 molecule and the formate complex.

Ab initio MO/MP2 calculations were carried out on the *cis*-$[HRh(PH_3)_2] + H_2 + CO_2$ model system using the Gaussian 92 program system.[8] Geometries were optimized by the gradient technique at the MP2 level, with the LANL1DZ basis set.[8, 9] Single-point MP2 energy values, to be discussed here, were obtained with an all electron basis set and with polarization functions on the active hydrogen atoms and on the carbon and oxygen atoms of CO_2.[13] We have checked that the use of the LANL1DZ basis set was appropriate for the geometry opti-

[*] Dr. A. Dedieu, F. Hutschka
Laboratoire de Chimie Quantique, UPR 139 du CNRS
Université Louis Pasteur
4 rue Blaise Pascal, F-67000 Strasbourg (France)
Telefax: Int. code +88 61 20 85
e-mail: dedieu@quantix.u-strasbg.fr

Dr. W. Leitner[+]
Max Planck Gesellschaft, Arbeitsgruppe CO_2-Chemie
an der Universität Jena (Germany)

[+] New address:
Max-Planck-Institut für Kohlenforschung, Mülheim/Ruhr (Germany)

[**] This work was partly supported by a French–German PROCOPE contract (no. 94132). Calculations were carried out on the IBM RS 6000 workstations of our laboratory and of the Institut du Developpement et de Ressources en Informatique Scientifique (IDRIS, Orsay), and on the DEC 3000/600S workstations of the Centre Universitaire Régional de Ressources Informatiques (CURRI, Strasbourg). We thank the staff of these two centers for their cooperation. We are also grateful to Dr. L. Padel and Mrs. Fersing for their help and technical assistance.

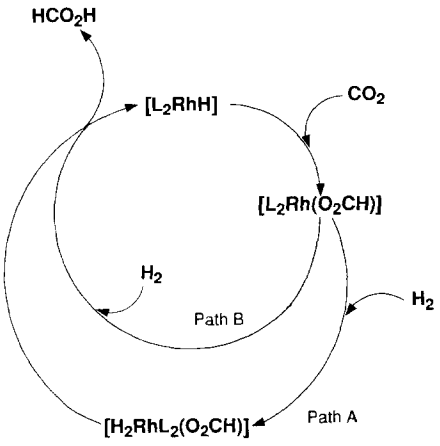

Scheme 1. L = phosphane.

mization by performing, for some key structures, additional geometry determinations with the all electron basis set (with and without polarization functions). Similarly the validity of the conclusions reached at the MP2 level was assessed by carrying out a few calculations at the QCISD(T) level.[7a]

The optimized geometries of the various intermediates and transition states of path B (Scheme 1) are sketched in Figure 1 together with the corresponding relative energies.[16] The first

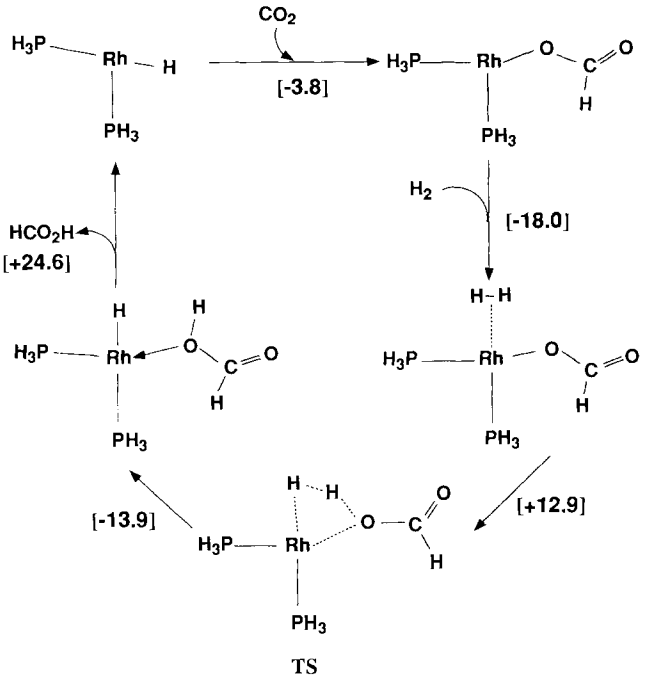

Fig. 1. Structures of various intermediates and transition states (TS) of path B in Scheme 1 (relative energies in kcal mol^{-1}).

step, which is common to paths A and B (Scheme 1), is the insertion of CO_2 into the Rh–H bond of $[HRh(PH_3)_2]$. The corresponding transition state is shown in Figure 2a with the most important geometrical parameters. This CO_2 insertion is a relatively easy process: an initially formed association complex between CO_2 and $[HRh(PH_3)_2]$[7] rearranges with a calculated energy barrier of only 4.2 kcal mol^{-1}. The overall reaction leading to the η^1-formate complex in Figure 1 is exothermic

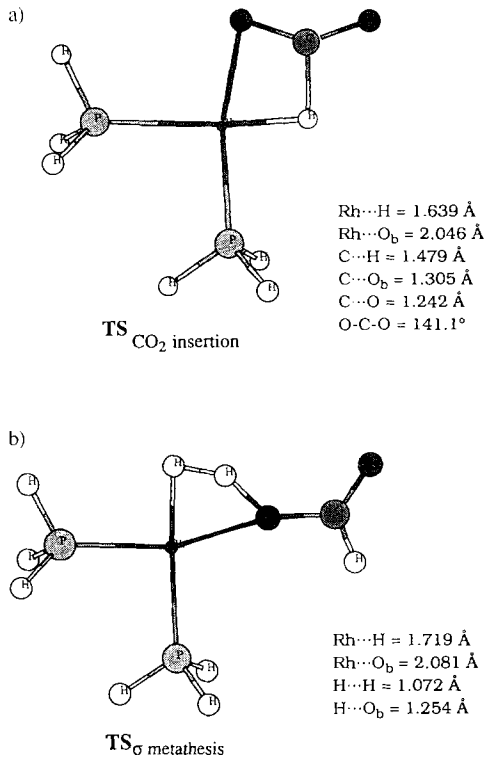

Fig. 2. a) Optimized structure of the transition state (TS) for the CO_2 insertion into the Rh–H bond of $[HRh(PH_3)_2]$. b) Optimized structure of the transition state for the $2\sigma + 2\sigma$ metathesis reaction between H_2 and $[Rh(PH_3)_2(\eta^1\text{-}O_2CH)]$.

(3.8 kcal mol^{-1}).[17, 19] The geometry of the transition state (Fig. 2a) is rather similar to the one found by Sakaki and Musahi[5e] for the insertion of CO_2 into the Rh–H bond of $[HRh(PH_3)_3]$. Only the Rh–O distance is much shorter in our case owing to the propensity of the oxygen atom to fill the vacant fourth coordination site of rhodium.

The path B is characterized by a transition state corresponding to a $2\sigma + 2\sigma$ metathesis reaction (Fig. 2b).[20] This transition state is bracketed by two intermediates. The first one is an association complex between H_2 and $[Rh(PH_3)_2(O_2CH)]$ that may be characterized as a dihydrogen complex: The Rh–H distances are 1.940 and 1.932 Å and the H–H bond length is 0.764 Å (i.e. only slightly elongated from that in H_2 (computed value 0.738 Å)). This complex is more stable than $H_2 + [Rh(PH_3)_2(O_2CH)]$ by 18.0 kcal mol^{-1}. An energy barrier of 12.9 kcal mol^{-1} must be overcome to go through the transition state of the σ metathesis reaction from this intermediate. After the transition state the formic acid remains bound to the rhodium atom, its hydroxy oxygen atom occupying the fourth coordination site. The calculated Rh–O bond length is 2.140 Å, in contrast to 1.889 Å in the three-coordinate formate complex. The dative-type interaction between rhodium and oxygen accounts for the relatively high energy requirement (+ 24.6 kcal mol^{-1}) for the complete dissociation into HCO_2H and $[HRh(PH_3)_2]$.

The most salient feature of the pathway B, however, is that none of the steps lead to large energy changes. In particular the energy barrier for the $2\sigma + 2\sigma$ metathesis reaction is rather low, and the corresponding step is not the most energy demanding in the complete cycle. We interpret this as an additional indication of the possibility of such reactions. The low energy barrier is due, as shown by previous theoretical studies,[22] to the involvement of the $d_{x^2-y^2}$ orbital of rhodium in the σ bond which is broken and in the σ bond which is formed.

According to our calculations, the dissociation of the HCO_2H molecule from the $[HRh(PH_3)_2]$ complex requires the largest energy change; but the energy requirement may be less important in solution. Moreover since CO_2 forms a preassociation complex with $[HRh(PH_3)_2]$, the substitution of HCO_2H by CO_2 in the catalytic cycle could follow an associative mechanism that might be less energy demanding than the dissociative one.

In comparison with path B, greater variations are observed for the individual steps of path A. The oxidative addition of H_2, which leads to an isomer with a geometrical arrangement favorable for the subsequent reductive elimination of HCO_2H, is computed to be exothermic by 32.6 kcal mol^{-1}. It is therefore not surprising that the reductive elimination to yield the separated HCO_2H and $[HRh(PH_3)_2]$ systems is in turn endothermic by 38.3 kcal mol^{-1}.[23] The energy barrier for the elimination of formic acid is also rather large, 23.8 kcal mol^{-1}. (The transition state lies at lower energy than the separated products of the reaction. However, as we have already mentioned the HCO_2H and $[HRh(PH_3)_2]$ can form an association complex; the association complex obtained in this case lies 4.4 kcal mol^{-1} lower in energy than the transition state.[24])

It is therefore clear from these calculations that the path B represents an alternative to the more traditional path A.[25] There are some precedents for invoking pathways that do not use reduction/reoxidation sequences.[26] For example, a σ bond metathesis pathway has also been considered, both experimentally[27] and theoretically[28] as an alternative in metal-catalyzed hydroboration reactions. We have already mentioned the importance of the involvement of a d orbital in allowing the [2 + 2] process[22] which otherwise would be forbidden according to the Woodward–Hoffmann rules. Another important factor for driving the σ metathesis reaction is the strength of the O–H bond formed during the process. One might object that our finding will apply only to the neutral hydridobis(phosphane)rhodium complex and not to the $[H_2Rh(PMe_2Ph)_3(solvent)]^+$ cation, which has been proposed as the active species for the formation of formic acid from H_2 and CO_2 catalyzed by $[Rh(nbd)(PMe_2Ph)_3]BF_4$.[2] But we can make use of the isolobal analogy between the T-shaped d^8-$[ML_3]$ and the square-pyramidal d^6-$[ML_5]$ complexes,[29] and consider now a σ metathesis reaction that would take place between H_2 and the five-coordinate d^6 complex cation $[HRh(PMe_2Ph)_3(O_2CH)]^+$ (after dissociation of the solvent). There would be no need to invoke reductive elimination of formic acid and subsequent oxidative addition of H_2— the rhodium atom would remain in the oxidation state III throughout the whole catalytic cycle. We are currently investigating this possibility.

Received: March 17, 1995
Revised version: May 13, 1995 [Z 7804IE]
German version: *Angew. Chem.* **1995**, *107*, 1905–1908

Keywords: ab initio calculations · carbon dioxide · catalysis · hydrogenations · rhodium compounds

[1] a) E. Graf, W. Leitner, *J. Chem. Soc. Chem. Commun.* **1992**, 623; b) F. Gassner, W. Leitner, *ibid.* **1993**, 1465; c) T. Burgemeister, F. Kastner, W. Leitner, *Angew. Chem.* **1993**, *105*, 781; *Angew. Chem. Int. Ed. Engl.* **1993**, *32*, 739; d) W. Leitner, E. Dinjus, F. Gassner, *J. Organomet. Chem.* **1994**, *475*, 257.

[2] J.-C. Tsai, K. M. Nicholas, *J. Am. Chem. Soc.* **1992**, *114*, 5117.

[3] P. G. Jessop, T. Ikariya, R. Noyori, *Nature* **1994**, *368*, 231.

[4] Recent examples: a) D. J. Darensbourg, M. Y. Darensbourg, L. Y. Goh, M. Ludvig, P. Wiegreffe, *J. Am. Chem. Soc.* **1987**, *109*, 7539; b) D. J. Darensbourg, H. P. Wiegreffe, P. W. Wiegreffe, *ibid.* **1990**, *112*, 9252.

[5] a) S. Sakaki, K. Ohkubo, *Inorg. Chem.* **1988**, *27*, 2020; b) C. Bo, A. Dedieu, *ibid.* **1989**, *28*, 304; c) S. Sakaki, K. Ohkubo, *Organomet.* **1989**, *8*, 2973; d) S. Sakaki, K. Ohkubo, *Inorg. Chem.* **1989**, *28*, 2583; e) S. Sakaki, Y. Musahi, *J. Chem. Soc. Dalton Trans.* **1994**, 3047.

[6] a) S. Sakaki, A. Dedieu *Inorg. Chem.* **1987**, *26*, 3278; b) A. Dedieu, F. Ingold, *Angew. Chem.* **1989**, *101*, 1711; *Angew. Chem. Int. Ed. Engl.* **1989**, *28*, 1694; c) A. Dedieu, C. Bo, F. Ingold, *Enzymatic and Model Carboxylation and Reduction Reactions for Carbon Dioxide Utilization* (Eds.: M. Aresta, J. V. Schloss), (*NATO ASI Ser. Ser. C* **1990**, *176*, 23); d) A. Dedieu, C. Bo, F. Ingold, *Metal-Ligand Interactions; from Atoms to Clusters, to Surfaces*, (Ed.: D. Salahub), (*NATO ASI Ser. Ser. C* **1992**, *378*, 175); e) C. Jegat, M. Fouassier, M. Tranquille, J. Mascetti, I. Tommasi, M. Aresta, F. Ingold, A. Dedieu, *Inorg. Chem.* **1993**, *32*, 1279.

[7] a) F. Hutschka, A. Dedieu, F. Gassner, W. Leitner, unpublished. b) In the preassociation complex, the CO_2 is η^2-coordinated to the rhodium center.

[8] a) Gaussian 92, Revision E.2., M. J. Frisch, G. W. Trucks, M. Head-Gordon, P. M. W. Gill, M. W. Wong, J. B. Foresman, B. G. Johnson, H. B. Schlegel, M. A. Robb, E. S. Replogle, R. Gomperts, J. L. Andres, K. Raghavachari, J. S. Binkley, C. Gonzales, R. L. Martin, D. J. Fox, D. J. Defrees, J. Baker, J. J. P. Stewart, J. A. Pople, Gaussian, Inc., Pittsburgh, PA, **1992**. b) The MP2 calculations were carried out with a frozen core.

[9] This basis set, of valence double zeta quality, is derived from the Dunning and Hay basis [10] for the first row atoms and from the Huzinaga basis [11a] for the hydrogen atom. For rhodium and phosphorus an effective core potential (up to the 4p electrons of Rh) [12] was used and the valence electrons were described by double zeta basis sets [12].

[10] T. H. Dunning, P. J. Hay in *Modern Theoretical Chemistry* (Ed.: H. F. Schäfer III), Plenum, New York, **1977**, p. 1.

[11] a) S. Huzinaga, *J. Chem. Phys.* **1965**, *42*, 1293; b) *Technical Report*, University of Alberta, Edmonton **1971**.

[12] P. J. Hay, W. R. Wadt, *J. Chem. Phys.* **1985**, *82*, 270.

[13] For Rh a (15,10,8) ⟨6,4,4⟩ basis [14] was used. The phosphorus, carbon, and oxygen atoms were described by the standard (11,7) and (9,5) basis sets of Huzinaga [11b] contracted into ⟨4,3⟩ and ⟨3,2⟩. The hydrogen atoms were described by a (4)⟨2⟩ basis set [11a]. These basis sets were supplemented by polarization functions for the C (exponent 0.63), O (exponent 1.33), and the H atoms (exponent 0.8) actively participating in the catalytic process (i.e. the hydrogen atoms originating from H_2 and the hydride of the $[HRh(PH_3)_2]$ system).

[14] The original (15,9,8) basis set [15] was modified by the addition of a p function of exponent 0.15.

[15] A. Veillard, A. Dedieu, *Theor. Chim Acta* **1984**, *65*, 215.

[16] Zero-point energies are not taken into account. The corresponding total energies (in Hartree) are: H_2 −1.1553, CO_2 −188.0083, $[HRh(PH_3)_2]$ −5360.8454, $[Rh(PH_3)_2(\eta^1\text{-}O_2CH)]$ −5548.8597, $[H_2\cdots Rh(PH_3)_2(\eta^1\text{-}O_2CH)]$ −5550.0437, TS(σ metathesis), −5550.0231, $[HRh(PH_3)_2(HCO_2H)]$, −5550.0452, HCO_2H, −189.1606.

[17] These values have been computed on the singlet potential energy surface. One might argue that the ground state of the *cis*-$[HRh(PH_3)_2]$ system is a triplet, by analogy with what has been found for *trans*-$[RhCl(PH_3)_2]$ [18]. In our case however the singlet state is found to be, after a MP2 optimization of both the singlet state and triplet state structures, lower than the triplet state by 16.6 kcal mol^{-1} [7]. For the three-coordinate formate complex the energy difference is less important but still in favor of the singlet state by 2.2 kcal mol^{-1}.

[18] N. Koga, K. Morokuma, *J. Phys. Chem.* **1990**, *94*, 5454.

[19] Of course, the η^2 isomer is more stable (by 27.2 kcal mol^{-1}) than the η^1 isomer. But in accordance with Tsai and Nicholas [2], one can reasonably expect that because of this high stability the η^2 species is an unproductive shunt in the catalytic cycle.

[20] The transition state was characterized by an imaginary frequency of 1511*i* cm^{-1} with an eigenvector corresponding to the σ metathesis reaction. A second imaginary frequency was obtained in the frequency analysis, but with a very low value of 43*i* cm^{-1}. This residual frequency corresponds to the departure from C_s symmetry. However the very low value indicates that the C_s restriction is not a severe one and that upon a very slight move from the C_s symmetry this frequency would disappear, thus leaving only one imaginary frequency. A similar situation has been reported in the determination of the four-center transition state corresponding to the addition of the methane C–H bond across the metal nitrogen double bond of $[H_2Zr{=}NH]$ [21].

[21] T. R. Cundari, *J. Am. Chem. Soc.* **1992**, *114*, 10557.

[22] a) M. L. Steigerwald, W. A. Goddard III, *J. Am. Chem. Soc.* **1984**, *106*, 308; b) T. H. Upton, A. K. Rappé, *ibid.* **1985**, *107*, 1206; c) C. A. Jolly, D. S. Marynick, *ibid.* **1989**, *111*, 7968.

[23] The endothermicity is of course much greater if one starts from a η^2-formate $[H_2Rh^{III}(PH_3)_2(\eta^2\text{-}O_2CH)]$ complex which is again found more stable than the η^1 complex by 12.6 kcal mol^{-1}. This six-coordinate η^2 complex might in turn result from the oxidative addition of H_2 to the four-coordinate $[Rh^I(PH_3)_2(\eta^2\text{-}O_2CH)]$ complex [19]. Thus, taken together, these features probably rule out the η^2 formate complex of either Rh^I or Rh^{III} as *productive* intermediates in the catalytic cycle.

[24] After the transition state of the reductive elimination initially an association complex forms between HCO_2H and $[HRh(PH_3)_2]$ with the hydrogen atom bound to the rhodium atom, and with the formate plane perpendicular to the $[HRh(PH_3)_2]$ plane. This intermediate is more stable than the transition state by 4.4 kcal mol^{-1}. It can then easily rearrange to yield the square-planar

[HRh(PH$_3$)$_2$(HCO$_2$H)] intermediate which has been characterized in path B and which lies a further 5.7 kcal mol^{-1} lower in energy [7a].
[25] A similar conclusion has been obtained for the formation of the *cis* isomer of the formic acid [7a].
[26] a) T. Hosokawa, S. I. Murahashi, *Acc. Chem. Res.* **1990**, *23*, 49; b) A. M. Joshi, B. R. James, *Organometallics* **1990**, *9*, 199; c) L. Versluis, T. Ziegler, *ibid.* **1990**, *9*, 2985; d) R. H. Morris, *Inorg. Chem.* **1992**, *31*, 1471.
[27] J. F. Hartwig, S. Bhandari, P. R. Rablen, *J. Am. Chem. Soc.* **1994**, *116*, 1839.
[28] D. G. Musaev, A. M. Mebel, K. Morokuma, *J. Am. Chem. Soc.* **1994**, *116*, 10693.
[29] a) R. Hoffmann, *Angew. Chem.* **1982**, *94*, 781; *Angew. Chem. Int. Ed. Engl.* **1982**, *21*, 711; b) T. A. Albright, J. K. Burdett, M. H. Whangbo, *Orbital Interactions in Chemistry*, Wiley, New York, **1985**, pp. 352–356.

Designed Assemblies in Open Framework Materials Synthesis: An Interrupted Sodalite and An Expanded Sodalite**

Pingyun Feng, Xianhui Bu, and Galen D. Stucky*

A number of new framework materials based on zinc–oxygen and phosphorus–oxygen tetrahedra have recently been characterized,[1, 2] some of which are structural analogs of natural zeolites.[2] These include zeolite X and hydro-sodalite[3] whose structures were established by Rietveld refinement of X-ray powder data. The synthesis of solids with zinc phosphate open frameworks can be carried out from $-20\,^{\circ}C$ (zeolite X) to 200 °C.[2] This composition also pushes the limits with respect to the ionic radii of the tetrahedrally surrounded atoms (T atoms) of materials with open frameworks; Zn^{2+} (0.60 Å) is the largest for a pure (TO_2^{n+}, $T'O_2^{m-}$) phase zeolite and P^{5+} (0.17 Å) is one of the smallest ions.[4]

One important aspect in the synthesis of framework materials is the mechanism by which the inorganic framework is assembled by the templating molecule. The piperazine molecule has a number of features which can be used for such a study. The recent studies on the trioxane-templated silica sodalite[5] suggest that the molecular dimension of the similarly sized piperazine molecule is ideal for organization of four-ring units into a cage configuration. The directed hydrogen bonding should also impose at least one symmetry operation of the molecule on the framework, that is, the crystallographic site symmetry should be a subgroup of the molecular point group symmetry. This is distinct from dynamic templating in which the inorganic condensation is around a spatially averaged distribution of the organic molecules.

In this study, we were interested in those cases in which the symmetry of host frameworks is determined by nonframework template ordering.[6] A complication occurs for sodalite structures when the templating molecules are not only ordered but also have a charge less than +3, as required to balance the charge of a sodalite cage with (T^{3+}/T^{4+}) or (T^{2+}/T^{5+}) composition. We describe here two mechanisms by which the negative charge of the framework is lowered to match that of guest molecules while preserving the sodalite type cage linking: cage interruption and expansion as discovered in two newly synthesized zincophosphates. The cage interruption mechanism involves the removal of a tetrahedrally coordinated atom from the sodalite cage which reduces the negative charge from -3 to -1 per cage. The cage expansion mechanism involves the insertion of tetrahedral atom groups into the sodalite cage, which reduces the cage charge from -3 to -2 per cage. In both cases, the symmetry of template molecules (inversion center and twofold axis of piperazine molecule, respectively) plays a structure-directing role in the formation of the new cage assemblies.

Crystals of ZnPO/PPZ$^+$ (zincophosphate with a monoprotonated piperazine) were grown by "nonaqueous" synthesis from a mixture of $Zn(NO_3)_2 \cdot 6\,H_2O$, H_3PO_4, ethylene glycol, and piperazine. The molar ratio of the corresponding precursor oxides (ZnO and P_2O_5), piperazine, and ethylene glycol was 1.0:0.96:0.91:25. The gel was stirred at room temperature for about 30 minutes. The mixture was heated at 170 °C for four days in a teflon-coated steel autoclave. The product was recovered by filtration and washed with deionized water. Clear needlelike crystals of typical dimensions $0.3 \times 0.1 \times 0.1$ mm^3 were obtained, which were suitable for an X-ray structure analysis (Fig. 1a).

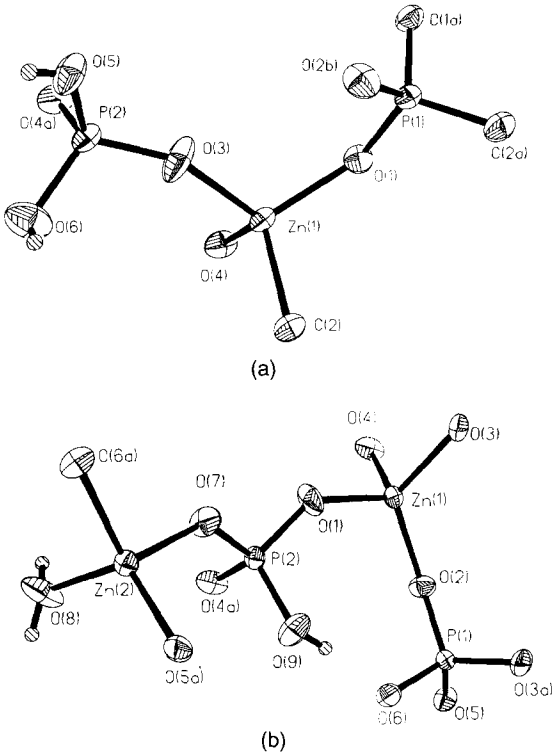

Fig. 1. Crystal structures of a) ZnPO/PPZ$^+$ and b) ZnPO/PPZ^{2+}: ORTEP views of zinc and phosphorus tetrahedra. Atom labels having "a" and "b" refer to symmetry generated atoms.

Crystals of ZnPO/PPZ^{2+} (zincophosphate with a diprotonated piperazine) were grown from a mixture of $Zn(NO_3)_2 \cdot 6\,H_2O$, H_3PO_4, H_2O, and piperazine. The molar ratio of the corresponding precursor oxides (ZnO and P_2O_5), piperazine, and water was 1.0:0.95:0.89:85. A white gel was formed at an approximate pH of 3 after stirring the mixture for about 15 minutes. The mixture was heated at 170 °C for four days in a teflon-coated steel autoclave. The product was recovered by filtration and washed with deionized water. Clear platelike crystals of typical dimensions $0.20 \times 0.17 \times 0.03$ mm^3 were obtained, which were suitable for an X-ray structure analysis (Fig. 1b).

[*] Prof. Dr. G. D. Stucky, P. Feng, Dr. X. Bu
Chemistry Department, University of California at Santa Barbara
Santa Barbara, CA 93106 (USA)
Telefax: Int. code + (805)893-4120
e-mail: stucky@sbxray.ucsb.edu

[**] This research was supported in part by the National Science Foundation under Grant DMR 92-08511.

$ZnPO/PPZ^+$ has an interrupted sodalite-type structure which is obtained by removal of a T atom (Zn^{2+} in this case) from sites related by one of the three twofold axes through opposing four-rings of the normal sodalite cage structure (Fig. 2a and 3a). One piperazine molecule per cage, whether mono- or diprotonated, is unable to provide the three positive charges which are needed to balance the negatively charged framework of an uninterrupted zincophosphate sodalite structure. The charge compensation is achieved instead by removal of one lower charged T atom (Zn^{2+}) for every six T atoms, and the addition of four protons, which form hydroxyl groups with oxygen atoms for a net charge gain of +2 per cage. The remaining −1 charge on the cage is balanced by one monoprotonated piperazine molecule located at the center of the cage.

$ZnPO/PPZ^{2+}$ has an expanded sodalite structure with eight eight-rings instead of six-rings (Figs. 2c and 3b). The structural relationship between the expanded sodalite and the normal sodalite is described below. Starting with a normal zincophosphate sodalite[3] cage ($[Zn_{12}P_{12}O_{48}]^{12-}$), oriented such that there are four four-rings on the equatorial plane, one four-ring above and one four-ring below (Fig. 2b), a hypothetical expanded structure can be derived by rotation of the top and bottom four-rings by 90° followed by insertion of four $ZnO(H_2O)_2$ units and four $PO(OH)_2^+$ units into eight T-O-T connections between the four equatorial four-rings and two four-rings above and below. This gives a stoichiometry of $[Zn_{12}P_{12}O_{48}]^{12-}$ $[Zn_4P_4O_8(H_2O)_8(OH)_8]^{4+}$ which is identical to the observed one, but with two water molecules coordinated to each of the four inserted zinc atoms and two OH groups coordinated to each of the inserted four P atoms. In the actual structure (Fig. 2c) one of the two water molecules on each zinc and one of the two OH groups on each phosphorus in the above hypothetical structure are distributed onto zinc and phosphorus atoms across the eight-rings. This gives rise to the sodalite-type cage linkage with elongated cages sharing single four-rings or single eight-rings (Fig. 3b). The reduction of the negative charge from −3 for a normal sodalite cage to −2 for an expanded cage is achieved with the introduction of one $PO(OH)_2^+$ unit per cage.

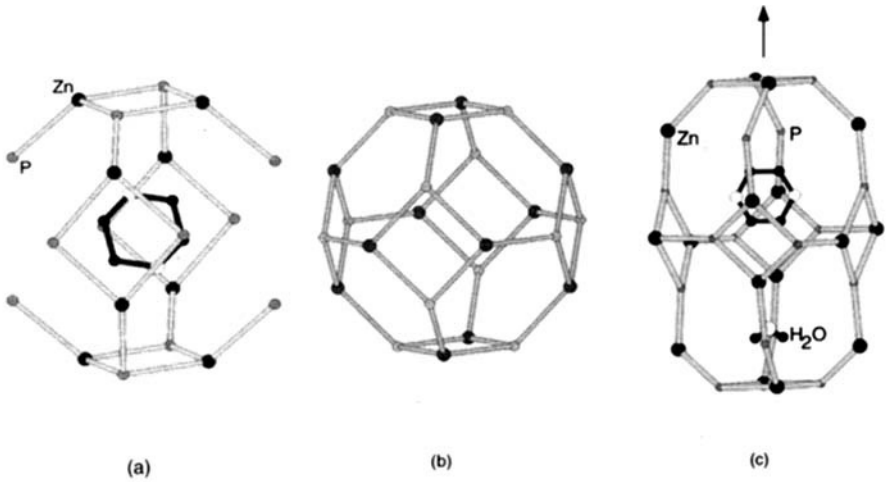

Fig. 2. a) The interrupted sodalite cage with the template molecule located on the inversion center at the cage center; b) the normal aluminosilicate sodalite cage; c) the expanded sodalite cage with the piperazinium dication and water molecule on the twofold axis.

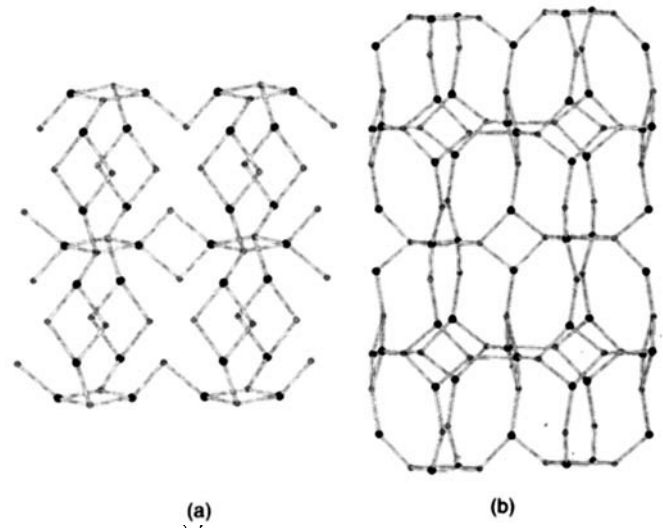

Fig. 3. Illustration of the framework structure and sodalite-type cage linkage. a) Four interrupted sodalite cages sharing single four-rings; there are no six-rings due to the T atom removal; b) four expanded sodalite cages sharing single four-rings.

The unit cell volume of $ZnPO/PPZ^+$ is 1403.8(7) Å^3 which is slightly more than twice the cell volume of 688.01(3) Å^3 for the normal zincophosphate sodalite.[3] This is consistent with four interrupted cages per unit cell. The volume increase per cage over the normal sodalite is only 2.0% which suggests that the dimension of the template molecule is ideally suited for such a four-ring assembly. In contrast, the volume increase per cage is as large as 53.7% for $ZnPO/PPZ^{2+}$ due to the cage elongation. This extra space inside the cage is occupied by ordered nonframework water molecules.

Both the interrupted and expanded sodalite cages have a point group symmetry lower than that of a regular sodalite cage. The interrupted cage is built around the inversion center on which the template molecule is located, while a twofold axis runs through the expanded cage on which both the piperazinium dications and water molecules are located. Since the carbon and nitrogen atoms in the chair conformation of the piperazine molecule have a point symmetry of $2/m$ with three individual symmetry elements (i, 2, m), the template molecule therefore imposes its individual symmetry constraint onto both types of framework structures. In the expanded cage, the symmetry match is achieved between the framework and two different template molecules, piperazine and water.

In both structures, the symmetry information of the template molecule is passed onto the framework mainly through guest–framework hydrogen bonding as illustrated in Figure 4. In $ZnPO/PPZ^+$, the extra proton in the piperazinium monocation is statistically distributed on two nitrogen sites. Each template nitrogen atom forms at least one N–H···O bond to one of four four-rings and may have another N–H···O bond depending on whether the extra proton is located on it (Fig. 4a). This observation is in contrast with the results with trioxane silica sodalite in which the guest–framework hydrogen bonding may only involve the weak C–H···O interactions due to the lack of OH groups and the trioxane molecule is orientationally disordered to preserve the cubic symmetry of the sodalite cage.[5]

 © VCH Verlagsgesellschaft mbH, D-69451 Weinheim, 1995 0570-0833/95/1616-1746 $ 10.00+.25/0

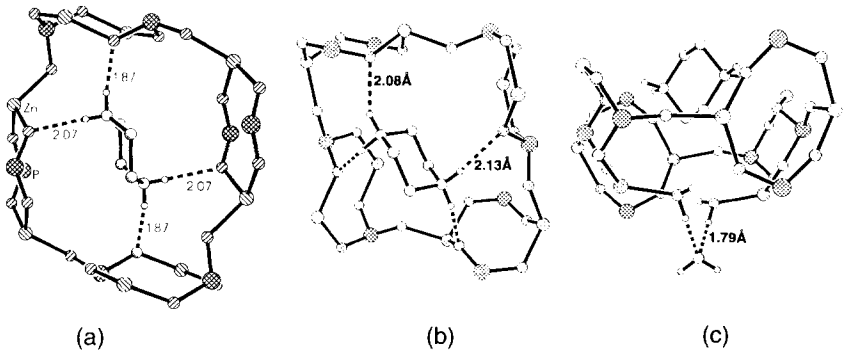

Fig. 4. Guest-framework hydrogen bonding. a) $ZnPO/PPZ^{+}$, monoprotonated piperazinium shown as di-protonated due to its statistical distribution on the two sites; b) $ZnPO/PPZ^{2+}$, top view of the four equatorial four-rings showing host-guest hydrogen bonds between piperazine NH_2 groups and framework oxygen atoms; c) $ZnPO/PPZ^{2+}$, side view of the four equatorial four-rings showing host guest hydrogen bonds between extra-framework H_2O and H_2O on Zn tetrahedra in the lower portion of the cage.

In $ZnPO/PPZ^{2+}$, one bridging oxygen atom from each of the four equatorial four-rings forms the N–H···O type bonding to each of the hydrogen atoms on NH_2 groups of piperazine molecules (Fig. 4b and 4c). All four participating oxygen atoms are on the same side of the four four-ring cluster due to the symmetry constraint imposed by a twofold axis. This is different from $ZnPO/PPZ^{+}$ where four participating oxygen atoms are divided on the two sides of the cluster formed from four four-rings, an arrangement consistent with the center of inversion. The hydrogen bonding between $Zn(H_2O)$ groups and extra-framework H_2O molecules gives OH_4 tetrahedra (Fig. 4c).

As shown in Figure 4, the molecular dimension of the piperazine molecule and the 90°/180° distribution of hydrogen atoms on the two nitrogen atoms make piperazine a perfect molecule for the organization of four four-ring units. In $ZnPO/PPZ^{+}$, these four four-rings units share single four-rings to form layers that are interconnected into the three-dimensional sodalite type framework by bridging bidentate -O-P(OH)$_2$-O- groups (Fig. 3a). Similar layers are also found in $ZnPO/PPZ^{2+}$ (Fig. 3b).

Both structures contain interruptions between tetrahedrally surrounded atoms. Due to the charge difference of the piperazine molecules in the two structures as well as the inclusion of a water molecule in the expanded structure, the style of interruption is different, leading to two unique novel cages assemblies. However, they are similar to each other in that the cages are interlinked in a manner analogous to that of sodalite. The interruption of the framework structure is one of the key structural features for several zincophosphates[7] as well as aluminophosphates.[8] In the cases discussed herein it helps to reduce the negative charge on the framework.

The symmetry matching between the inorganic host and template molecules are not limited to purely tetrahedral zincophosphate systems as described above. Recently, we discovered a new piperazine-templated vanadium(IV) phosphate (space group: *Cm*) in which the symmetry of the tetrahedral–octahedral framework is determined by the mirror symmetry of the template molecule.[9] In this structure both two-centered and three-centered hydrogen bonds are used to direct the assembly of the vanadium(IV) phosphate into an extended array.

In conclusion, we have demonstrated that all three individual symmetry elements of a piperazine molecule can direct framework formation and that partial zeolite-like cage structures can be synthesized by using a template design strategy. The results are important for the elucidation of the synthesis mechanism of sodalite-based zeolite materials in general and indicate that in future it may be possible to derive a strategy for the design of new framework structures as well as modification of existing types utilizing template symmetry, charge matching, and directed hydrogen bonding between guest and host. This strategy should apply to both interrupted and noninterrupted zeolitic systems since the directed hydrogen bonds described above are between the bridging framework oxygen atoms and piperazine molecules.

Received: November 3, 1994
Revised version: March 27, 1995 [Z 7451 IE]
German version: *Angew. Chem.* **1995**, *107*, 1911–1913

Keywords: hydrogen bonding · sodalites · solid-state structures · template syntheses · zeolites

[1] R. H. Jones, J. Chen, G. Sankar, J. M. Thomas in *Zeolites and Related Microporous Materials* (Eds.: J. Weitkamp, H. G. Karge, H. Pfeifer, W. Holderich), Elsevier, Amsterdam, **1994**, p. 2229.
[2] T. E. Gier, G. D. Stucky, *Nature (London)* **1991**, *349*, 508.
[3] T. M. Nenoff, W. T. A. Harrison, T. E. Gier, G. D. Stucky, *J. Am. Chem. Soc.* **1991**, *113*, 378.
[4] T. M. Nenoff, W. T. A. Harrison, T. E. Gier, N. L. Keder, C. M. Zaremba, V. I. Srdanov, J. M. Nicol, G. D. Stucky, *Inorg. Chem.* **1994**, *33*, 2472.
[5] K. Futterer, W. Depmeier, F. Altorfer, P. Behrens, J. Felsche, *Z. Kristallogr.* **1994**, *209*, 517.
[6] W. Depmeier, *Z. Kristallogr.* **1992**, *199*, 75.
[7] W. T. A. Harrison, T. E. Martin, T. E. Gier, G. D. Stucky, *J. Mater. Chem.* **1992**, *2*, 175.
[8] Q. Huo, R. Xu, S. Li, Z. Ma, J. M. Thomas, R. H. Jones, A. M. Chippindale, *J. Chem. Soc. Chem. Commun.* **1992**, 875.
[9] X. Bu, P. Feng, G. D. Stucky, *J. Chem. Soc. Chem. Commun.*, in press.
[10] a) Crystal data for $ZnPO/PPZ^{+}$: $[Zn_2(PO_4)(H_2PO_4)_2](C_4H_8N_2H_3)$, $M = 506.9$, space group $C2/c$, $a = 13.370(4)$, $b = 12.829(4)$, $c = 8.207(3)$ Å, $\beta = 94.79(1)°$, $V = 1402.8(7)$ Å^3, $Z = 4$, $\rho_{calcd} = 2.40$ g cm^{-3}, colorless needle, crystal size $0.28 \times 0.10 \times 0.07$ mm^3, $Mo_{K\alpha}$, $\lambda = 0.71073$ Å, $\mu = 3.91$ mm^{-1}, empirical absorption correction, $T_{min} = 0.56$, $T_{max} = 0.86$, $\theta_{max} = 60°$, $R = 0.048$, $wR = 0.061$ for 138 parameters and 1587 unique reflections with $I > 3\sigma(I)$. b) Crystal data for $ZnPO/PPZ^{2+}$: $[Zn(H_2O)Zn(PO_4)(HPO_4)]_2 \cdot (H_2O)(C_4H_8N_2H_4)$, $M = 785.61$, space group $C2/c$, $a = 12.093(7)$, $b = 14.897(8)$, $c = 11.849(6)$ Å, $\beta = 97.821(3)°$, $V = 2115(2)$ Å^3, $Z = 4$, $\rho_{calcd} = 2.468$ g cm^{-3}, colorless plate, crystal size $0.20 \times 0.17 \times 0.03$ mm^3, $Mo_{K\alpha}$, $\lambda = 0.71073$ Å, $\mu = 4.99$ mm^{-1}, empirical absorption correction, $T_{min} = 0.53$, $T_{max} = 0.86$, $\theta_{max} = 60°$, $R = 0.049$, $wR = 0.06$ for 191 parameters and 2452 unique reflections with $I > 3\sigma(I)$. c) Further details of the crystal structure investigation are available on request from the Director of the Cambridge Crystallographic Data Center, 12 Union Road, GB-Cambridge CB2 1EZ (UK), on quoting the full journal citation.

Synthesis of dTDP-6-Deoxy-4-ketoglucose and Analogues with Native and Recombinant dTDP-Glucose-4,6-dehydratase**

Andreas Stein, Maria-Regina Kula, Lothar Elling,* Stefan Verseck, and Werner Klaffke*

Activated ketoglucose derivatives play a key role in the biosynthesis of deoxygenated oligo- and polysaccharides, because they represent the branching points in many biosynthetic pathways leading to 2,6- and 3,6-dideoxy- and -aminodeoxysugars, and branched deoxysugars. Although the gene clusters for the biosynthesis of deoxysugars in bacteria have been localized and the corresponding enzymes should now be available, the insufficient availability of the intermediates and the lack of effective analytical methods still hampers detailed investigations.[1-3] Solving these problems is necessary before the chemoenzymatic synthesis of deoxyoligosaccharides is as successful as that of N-glycosidically bound glycans.

In one of the activating pathways in bacteria leading to deoxyoligosaccharides, dTDP-D-glucose **1** (dTDP = thymidine-5′-diphosphate) is converted into dTDP-L-rhamnose via the corresponding 6-deoxy-4-keto intermediate **2**, which in turn is synthesized by dTDP-D-glucose-4,6-dehydratase [EC 4.2.1.46] (Scheme 1). This enzyme from different sources has been used for the synthesis of labeled substrates.[4, 5] The recent enzymatic synthesis of dTDP-6-deoxy-4-ketoglucose **2** marks progress in this area.[6] During the preparation of this manuscript, a paper by Lindqvist et al.[7] appeared which describes the biosynthesis of CDP-D-abequose (CDP-3,6-dideoxy-D-galactose; CDP = cytidine-5′-diphosphate) and the analytical separation of the activated sugars involved.

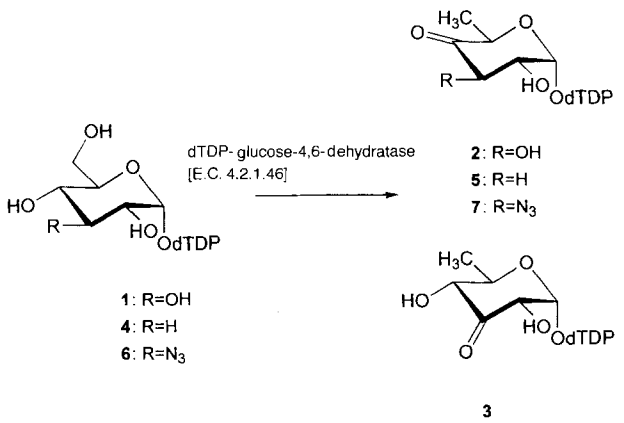

Scheme 1.

We describe here the synthesis and the first NMR spectroscopic characterization of dTDP-6-deoxy-α-D-*xylo*-hexopyran-4-ulose (**2**) in pure form as well as the enzymatic conversion of structurally related, nonnatural dTDP-glucose analogues into the corresponding 6-deoxysugars. We also present an ion-pair HPLC method for the analytical and preparative separation of dTDP-activated hexoses.

We first used the native enzyme in the crude extract of *Escherichia coli* B for deoxygenation.[8] In addition to dTDP-D-glucose (**1**), its 3-deoxy- and 3-azido-3-deoxy derivatives **4** and **6**, respectively, were incubated to demonstrate the range of application of the preparative method. The synthesis of the 4-ulose **2** was monitored by TLC. Surprisingly, the ^{1}H NMR spectrum recorded after the reaction mixture had been worked up by passage through a basic ion exchange column and subsequent desalting showed two products not identical to **1**. Detailed analysis revealed the products to be a 3:2 mixture of **2** and **3**. The analogues **4** (K_m = 200 μM, v_{max} = 130 μmol h^{-1} mg^{-1}) and **6** (K_m = 350 μM, v_{max} = 90 μmol h^{-1} mg^{-1}) were identified as substrates in the enzyme assay;[9] however, they show only 1/5 and 1/10, respectively, of the natural selectivity (v_{max}/K_m) of **1** (K_m = 80 μM, v_{max} = 260 μmol h^{-1} mg^{-1}). In the reactions of **4** and **6** the formation of a more unpolar product after roughly 1 d at 37 °C was detected by TLC; after 3 d the reaction was complete. Since compounds **5** and **7** are much more prone to hydrolysis than **2**, the workup had to be conducted quickly at + 4 °C and with lower concentrations of LiCl. The dideoxyhexo-4-ulose **5** was obtained as white foam (20 mg) in 41% yield and was characterized by NMR spectroscopy. As expected, dTDP-3-azido-3,6-dideoxyhexo-4-ulose (**7**) was also obtained in the form of a colorless foam (23 mg, 24% yield from a 166 μmol-scale reaction).

In the course of our work we developed an HPLC method based on the reversed-phase ion-pair chromatography described by Aw et al.,[10] which allows the highly selective separation of dTDP-activated hexoses and can be scaled up for preparative-scale batches. (In preparative HPLC ca. 5 mg of the crude product is loaded on the column, whereas loads of roughly 0.01 mg are typically applied in analytical separations.) Furthermore for the synthesis of **2** the wild-type enzyme was exchanged for recombinant dTDP-glucose-4,6-dehydratase from *Salmonella typhimurium* LT2 which was overexpressed in *E. coli* BL21. With the higher specific enzyme activity the effect of contaminating activities can be nearly excluded. Figure 1 shows the chro-

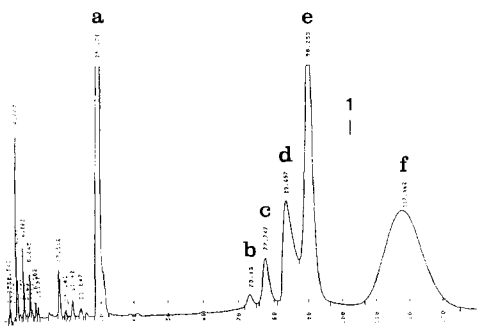

Fig. 1. Chromatogram of an analytical HPLC separation of a) dTMP, b, c) contaminants from commercial dTDPG, d) dTDP, e) dTDPG, and f) dTDP-6-deoxy-D-xylo-4-hexulose. The retention time of dTDP-L-rhamnose, which was added in other separations to demonstrate selectivity, is marked with a 1.

[*] Dr. L. Elling, Dipl.-Chem. A. Stein, Prof. Dr. M.-R. Kula
Institut für Enzymtechnologie der Universität Düsseldorf
im Forschungszentrum Jülich
Postfach 2050, D-52404 Jülich (Germany)
Telefax: Int. code + (2461) 61-2490
e-mail: L. Elling@kfa-juelich.de
Dipl.-Biol. S. Verseck
Institut für Chemische Mikrobiologie der Universität Wuppertal (Germany)
Dr. W. Klaffke
Universität Hamburg
Martin-Luther-King-Platz 6, D-20146 Hamburg (Germany)
and
Unilever Research, Bio-Organic Chemistry
Olivier van Noortlaan 120, NL-3133 AT Vlaardingen (The Netherlands)
Telefax: Int. code + (10) 460-5384
e-mail: werner.klaffke@a.2488bns.urlnl.sprint.com

[**] This work was supported by the Deutsche Forschungsgemeinschaft (W. K.), the Fonds der Chemischen Industrie (W. K.), and the Studienstiftung des Deutschen Volkes (A. S.). We thank Dr. V. Sinnwell and Dr. C. Schulze (Universität Hamburg) for recording the NMR and ESI spectra, respectively. dTDP = thymidine-5′-diphosphate.

matogram of the analytical separation of a mixture consisting of dTDP-glucose, the resulting 6-deoxy-4-ulose **2**, two contaminants present in the commercial starting material, and dTMP and dTDP.

In general the instability of product **2** leads to problems.[6, 11] We found that **2** partially decomposed with formation of dTMP and dTDP during storage in salt and buffer solutions at + 4 °C and −20 °C, respectively, and on lyophilization from volatile buffers and uncompletely desalted solutions, as well as on precipitation with organic solvents. Ulose **2** was isolated after preparative HPLC with an overall yield of 70%. The product can be stored at −20 °C for at least four months. Spectroscopic characterization of compound **2** as a 1:5 mixture of the keto and hydrate forms proved it to be a pure compound.

Table 1. Selected physical data of compounds **2**, **5**, and **7**.

2: ^{1}H NMR (400 MHz, D_2O): δ = 1.13 (d, 3H, 6″-H), 1.84 (d, 3H, CH_3), 2.24–1.32 (m, 2H, 2a′-H, 2b′-H), 3.53 (ddd, 2″-H), 3.69 (d, 3″-H), 4.01 (q, 5″-H), 4.07–4.11 (m, 3H, 4′-H, 5a′-H, 5b′-H), 4.53 (m, 3′-H), 5.46 (dd, 1″-H), 6.25 (dd, 1′-H), 7.65 (d, 6-H); $J_{1',2'}$ = 3.6, $^3J_{1',P}$ = 7.0, $^4J_{2',P}$ = 3.1, $J_{2',3'}$ = 10.2, $J_{5'',6''}$ = 6.5 Hz; ^{13}C NMR (100.7 MHz, D_2O): δ = 11.7 (C-6″), 12.1 (CH_3), 39.0 (C-2′), 65.9 (C-5′), 70.0 (C-5″), 71.1 (C-2″), 71.4 (C-3′), 73.6 (C-3″), 85.4 (C-1′), 85.8 (C-4′), 94.1 (C-4″, hydrated), 95.8 (C-1″), 112.2 (C-5), 137.7 (C-6), 152.2 (C-2), 167.0 (C-4); $^2J_{C-1',P}$ = 8.6, $^3J_{C-5',P}$ = 5.7 Hz; ESI-MS (negative mode, + 3 kV): *m/z*: 562.7 [M^- − Na]; keto form: ^{13}C NMR (100.7 MHz, [D$_6$]DMSO): δ = 206.4 (C″-4); ESI-MS (negative mode, + 3 kV): *m/z*: 545 [M^- − Na].

5: ^{1}H NMR (400 MHz, D_2O): δ = 1.09 (d, 3H, 6″-H), 1.84 (s, 3H, CH_3), 2.25–2.47 (≈dd and dd, 2H, 3a″-H and 3b″-H), 3.74 (m, 2″-H), 4.02 (q, 5″-H), 5.38 (dd, 1″-H); $J_{1'',2''}$ = 3.1, $^3J_{1'',P}$ = 6.5, $J_{2'',3a''}$ = 5.5, $J_{2'',3b''}$ = 11.6, $^2J_{3a'',3b''}$ = 12.6, $J_{5'',6''}$ = 6.6 Hz; ^{13}C NMR (100.7 MHz, D_2O): δ = 11.6 (CH_3), 12.2 (C″-6), 32.4 (C″-3), 69.1 (d, C″-2), 69.8 (C″-5), 93.2 (C″-4, hydrated), 95.7 (d, C″-1); $^2J_{C-1',P}$ = 6.4, $^3J_{C-2',P}$ = 8.5 Hz; ^{13}C NMR (100.7 MHz, [D$_6$]DMSO): δ = 203.1 (C″-4, not hydrated).

7: ^{1}H NMR (400 MHz, D_2O): δ = 1.21 (d, 3H, H″-6), 1.84 (s, 3H, CH_3), 3.40 (m, 2H, H″-2, H″-3), 4.21 (q, H″-5), 5.43 (dd, H″-1); $J_{1'',2''}$ = 3.8, $^3J_{1'',P}$ = 7.0, $J_{5'',6''}$ = 6.4 Hz; ^{13}C NMR (100.7 MHz, D_2O): δ = 13.3 (CH_3), 13.6 (C″-6), 60.2 (C″-3), 82.3 (d, C″-2), 94.1 (C″-4, hydrated), 95.7 (d, C″-1); $^2J_{1'',2''}$ = 6.4, $^3J_{C-2',P}$ = 8.1 Hz; ^{13}C NMR (100.7 MHz, [D$_6$]DMSO): δ = 201.4 (C″-4, not hydrated).

To the best of our knowledge, these experiments describe the first NMR spectroscopic characterization of the dehydratase-catalyzed synthesis of the deoxy intermediate **2**. The successful conversion of nonnatural dTDP-3-deoxy-α-D-*ribo*- and -3-azido-α-D-*xylo*-hexopyranoses **4** and **6**, respectively, open a new enzymatic route to artificial nucleoside diphosphate activated glycosyl donors in which easily available crude extracts are used. The HPLC method described should enable the first complete characterization of the dTDP-L-rhamnose biosynthesis in one step. In addition, preparative amounts of **2** and related compounds can now be isolated.

Experimental Procedure

2, **5**, and **7**: The disodium salt of dTDP-glucose **1** (50 mg, 82 μmol) or its 3-deoxy derivatives **4** and **6** (available by ion exchange from the chemically synthesized dilithium salts [12,13]) was dissolved in 5 mL of Tris/HCl buffer pH 7.5 (50 mM, 0.5 mM DTT). The dehydratase was added (0.083 U; 1 U = 1 μmol min^{-1}; 1.45 mL crude extract from *E. coli* B [8]), the reaction flask filled with 10 mL of distilled water, and the solution incubated at 37 °C with constant shaking. After 2 d the reaction was complete according to TLC (2-propanol/ethanol/water = 5:3:2, 5% HOAc, 2% triethylamine; product R_F = 0.4, starting material **1** R_F = 0.3, dTMP R_F = 0.5, dTDP R_f = 0.2). The enzyme reaction was stopped by heating for 30 s in boiling water; the reaction mixture was lyophilized to a volume of 3 mL and separated on a Sephadex G-10 column (2 × 160 cm; 1 mL min^{-1}). The fractions containing the nucleotide sugars were collected, purified by ion exchange chromatography (Dowex 1 × 2, Cl$^-$ form, 5 × 18 cm, 800 mL linear gradient 0–0.8 M LiCl), and concentrated. Desalting on Sephadex G-10 and subsequent lyophilization gave the dilithium salts of the products as white foams. Yield of **2** and **3** (ca. 3:2 according to ^{1}H NMR): 26 mg (54%); yield of **5**: 20 mg (41%); yield of **7**: 23 mg (24%).

2: The disodium salt of dTDP-glucose (41 mg, 60 μmol; Sigma) was dissolved in 2 mL of Tris/HCl buffer pH 7.5 (50 mM) in a 2 mL Eppendorf flask. 1 U of recombinant dTDP-D-glucose-4,6-dehydratase (65 μL crude extract, 9.5 mg mL^{-1} protein) was added, and the reaction mixture was incubated at 37 °C. After complete conversion (ca. 2 h) the reaction mixture was incubated for 2 min at 95 °C, centrifuged for 2 min at 12400 × *g*, and filtered through a 0.45 μm membrane. The separation was performed by preparative HPLC (Hypersil ODS-10 μ, 2 × 25 cm, Macherey Nagel, Düren (Germany), 0.04 M NH_4CO_3 solution (pH 3), 0.0038% (v/v) octylamine, 1% (v/v) methanol, isocratic elution, flow rate 20 mL min^{-1}, detection at 260 nm). The fractions containing the product were collected, diluted with doubly distilled water, and pumped with 250 mL min^{-1} onto a membrane anion-exchange module (KN107Q, Sartorius, Göttingen (Germany)). The salts of the HPLC solvent were removed with a 5 mM NaCl solution, and **2** was eluted with 150 mM NaCl solution. The product solution was concentrated to 10 mL under vacuum at 30 °C and subsequently desalted on a Sephadex G-10 column (2.6 × 93 cm, flow rate 1 mL min^{-1}). After lyophilization the disodium salt of the product was obtained as fluffy white solid. Yield: 24 mg (70%). Even traces of **3** were not detectable in this batch.

Received: March 17, 1995 [Z7806IE]
German version: *Angew. Chem.* **1995**, *107*, 1881–1883

Keywords: biotechnology · chromatography · dehydratases · deoxycarbohydrates · enzymes

[1] S. F. Lo, V. P. Miller, Y. Lei, J. S. Thorson, H.-W. Liu, J. L. Schottel, *J. Bacteriol.* **1994**, *176*(2), 460–468.
[2] S. Chang, B. Duerr, G. Serif, *J. Biol. Chem.* **1988**, *263*(4), 1693–1697.
[3] B. W. Jarvis, C. R. Hutchinson, *Arch. Biochem. Biophys.* **1994**, *308*(1), 175–181.
[4] C. E. Snipes, C. J. Chang, H. G. Floss, *J. Am. Chem. Soc.* **1979**, *101*, 701–706.
[5] C. E. Snipes, G. U. Brillinger, L. Sellers, L. Mascaro, H. G. Floss, *J. Biol. Chem.* **1977**, *252*, 8113–8117.
[6] K. Marumo, L. Lindqvist, N. Verma, A. Weintraub, P. R. Reeves, A. A. Lindberg, *Eur. J. Biochem.* **1992**, *204*, 539–545.
[7] L. Lindqvist, K. H. Schweda, P. R. Reeves, A. A. Lindberg, *Eur. J. Biochem.* **1994**, *225*, 863–872.
[8] R. D. Bevill in *Methoden der enzymatischen Analyse* (Ed.: H. U. Bergemeyer), Verlag Chemie, Weinheim, **1974**, pp. 2268–2269.
[9] R. Okazaki, T. Okazaki, J. L. Strominger, A. M. Michelson, *J. Biol. Chem.* **1962**, *237*, 3014–3026.
[10] T. Y. Aw, D. P. Jones, *Anal. Biochem.* **1982**, *127*, 32–36.
[11] H. P. Wahl, H. Grisebach, *Biochim. Biophys. Acta* **1979**, *568*, 243–252.
[12] J. G. Moffatt, *Methods Enzymol.* **1966**, 136–142.
[13] B. Leon, S. Liemann, W. Klaffke, *J. Carbohydr. Chem.* **1993**, *12*, 597–610; A. Naundorf, S. Liemann, W. Klaffke, *Synthesis of Deoxy Sugar Phosphates*, Eurocarb VII, Krakow, **1993**, Abstr. C004.

Estramycins: A New Diyl Precursor Family Derived from Estradiol**

Jing Wang and Pierre J. De Clercq*

The recent discovery of a new class of anticancer antibiotics from a bacterial source, presently consisting of neocarzinostatin, the esperamycin and calicheamycin families, dynemicin, kedarcidin, and C-1027, which exert their biological activity through DNA cleavage, opens new perspectives in cancer chemotherapy.[1] DNA cleavage is effected by diradicals that are generated from cyclic polyunsaturated core structures upon suitable activation. Quite recently diyl-based DNA cleaving agents have been reported in which the core of the diradical precursor is tethered to known minor groove DNA binding agents or DNA intercalators.[2] Also, a new family of artificial enediynes (taxamycins) has been described in which the unsatu-

[*] Prof. Dr. P. J. De Clercq, Dr. J. Wang
University of Gent, Department of Organic Chemistry
Krijgslaan, 281 (S.4), B-9000 Gent (Belgium)
Telefax: Int. code + (9)264-4998

[**] This work was supported by the National Fund for Scientific Research.

rated core is intimately embedded within a structure with known antitumor activity, like taxol.[3] In the same context we aimed to study the chemotherapeutic potential of estramycins, derivatives in which the diradical precursor core is incorporated into estradiol. It is indeed known that the chemotherapeutic activity of cytostatics against hormone-responsive tumors can be enhanced by linking them to hormones.[4] Since human mammary cancers are usually rich in estrogen receptor, estrogens, and estradiol in particular, are potential vectors to transfer cytotoxic agents into the nuclei of receptor rich cells.[5] As shown in Scheme 1 potential candidates include cyclic enediynes and enyne–allenes that would generate the diradical intermediates through Bergman and Myers cyclization processes, respectively.[6, 7]

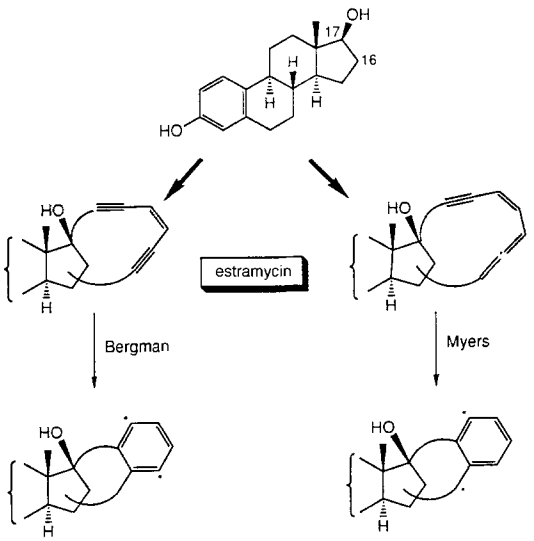

Scheme 1. Possible routes from estramycins to diradicals.

Obviously, in designing such hybrid molecules both the binding affinity of the modified estradiol for the estrogen receptor and the reactivity of the unsaturated system should be taken into account. The knowledge of the various structural features that are necessary for the activity of estradiol is crucial to the design of a successful candidate. The structure **1** (see Scheme 2) was proposed based on the following:[8] 1) Both the phenolic C3-hydroxy and β-oriented C17-hydroxy groups are intimately involved in the recognition process. 2) An α-oriented ethynyl group at C17 enhances the binding affinity. 3) Estradiol derivatives α-substituted at C16 bind well to the estrogen receptor.[9]

For the design of an appropriate enediyne core one can apply, at least in the first instance, the critical distance (*cd*) criterium introduced by Nicolaou.[10] The distance between the terminal alkyne atoms of the enediyne is taken as a measure of its ease of cyclization; the crucial turning point from stability to spontaneous cyclization lies between 331 and 320 pm. Depending on ring size candidates **1** possess varying *cd*s (Scheme 2);[11] only the ten-membered ring derivative (**1**, $n = 2$) is of potential use. From the low distance of 305 pm that is found in the lowest energy conformation of this compound one may expect the derivative to be rather unstable. Consequently, in the design of a synthesis, the enediyne core should be realized at a very late stage.[12] We now further describe the synthesis of a few derivatives of **1** and their cyclization behavior.

After protection of estrone as the *tert*-butyldimethylsilyl (TBDMS) ether,[13] the required stereoselective introduction of

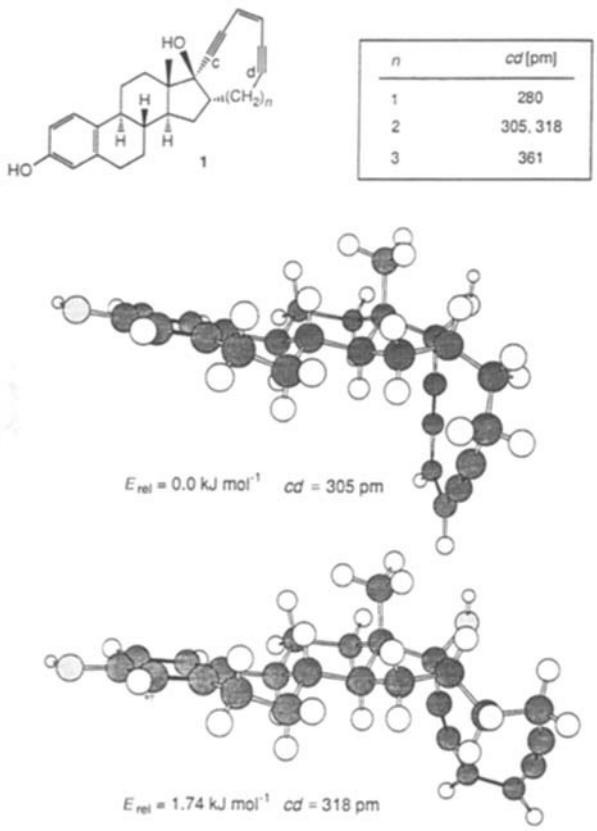

n	cd [pm]
1	280
2	305, 318
3	361

Scheme 2. Calculated *cd* values in estramycin **1**.

a 2,2-dimethoxyethyl side chain in α position at C16, as in **4**, was accomplished as follows (Scheme 3): 1) Ketone **2** was enolized (0.95 equiv. of lithium diisopropylamide (LDA), THF), and subsequently treated with 3-bromo-1-propene to form the corresponding 16α-(2-propenyl) derivative (83% yield).[13, 14] 2) Oxidative cleavage of the double bond with osmium tetroxide/sodium periodate gave the aldehyde **3** (71% yield). 3) Selective protection of the aldehyde with trimethyl orthoformate in tetrachloromethane, catalyzed by Montmorillonite K-10 clay, resulted in a mixture of desired **4** (57% yield) besides the cyclic mixed double acetal **5** as a mixture of two isomers (30% yield).[15] The stereochemistry at C16 predicted on steric grounds was further corroborated by ^{1}H NMR NOE difference spectroscopy: irradiation of the angular methyl group led to an increase of the signal of the H atom on C16.

Quite recently the intramolecular version of Nozaki's chromium(II)/nickel(II) salt mediated coupling of haloalkynes with aldehydes has been applied successfully in the synthesis of enediyne ring systems.[16, 17] The method is especially useful when dealing with enolizable aldehydes as in our case. The required cyclization precursor **8** was obtained by reaction of **4** with the alkynyl anion obtained from **6**,[18] which led to **7** as an approximate 1:1 mixture of diastereomers at C22 in 67% yield, and subsequent protection of the hydroxy group at C17 with trimethylsilyl trifluoromethanesulfonate (TMSOTf) and 2,6-lutidine in dichloromethane. Simultaneously the aldehyde function was deprotected (86% yield of **8a**, but contaminated with about 30% of deiodinated **8b**, which could not be separated at this stage).[19] The β-hydroxy configuration at C17 (shown in Scheme 3) was assigned on the basis of literature precedents and of the magnitude of the ^{1}H NMR shift of the resonance for the angular methyl group that is observed for **7** in pyridine relative to that in chloroform ($\Delta(\delta_{CDCl_3} - \delta_{C_5D_5N}) = -0.22$).[20, 21] The

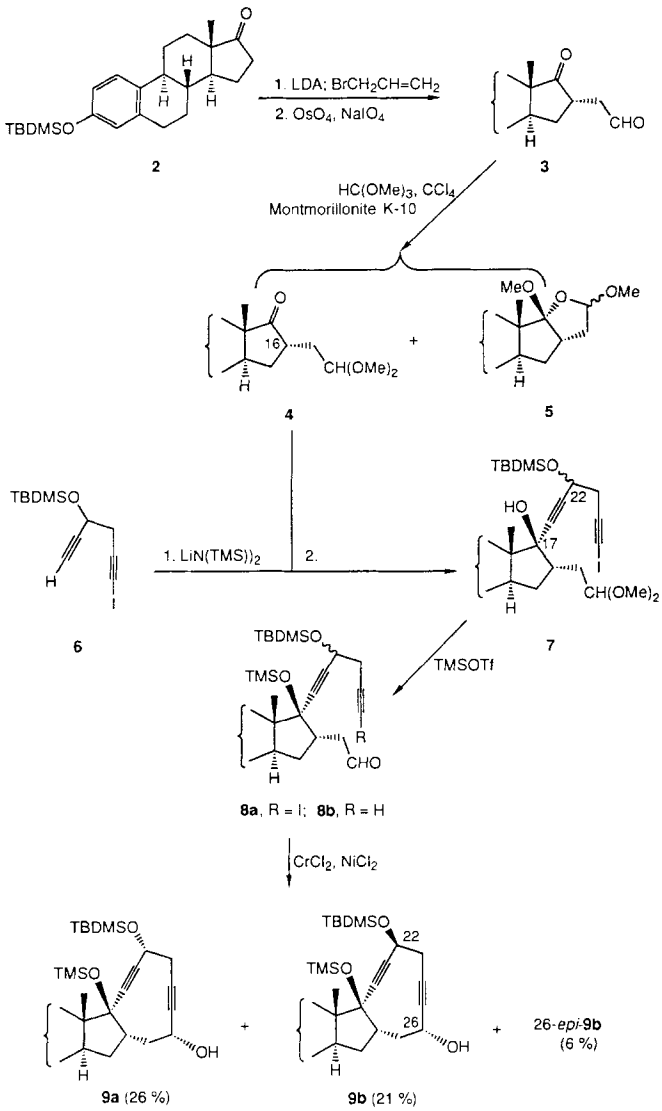

Scheme 3. The synthesis of the ten-membered ring estradiol derivative **9**. TMSOTf = trimethylsilyl trifluormethanesulfonate.

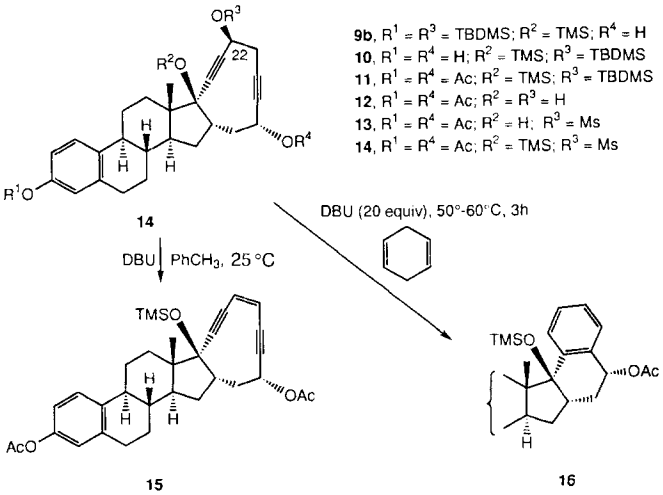

Scheme 4. Synthesis and cycloaromatization of estramycins **15**. Ms = methanesulfonyl.

crucial intramolecular cyclization of the iodoalkyne–aldehyde **8a** succeeded in the presence of seven equivalents of chromium(II) chloride and 10 mol% of nickel(II) chloride in THF at room temperature. The ring-closed alcohol was obtained in 54% yield (based on the 80% iodide content of the starting material) and consisted of a mixture of three out of the four possible diastereomers, which could be separated by careful chromatography: **9a** (26%), **9b** (21%), and 26-*epi*-**9b** as a minor component (6%). The relative stereochemistry at positions 22 and 26 was assigned on the following basis: the stereochemistry at C26 in **9b** follows from the elucidation by ^{1}H NMR spectroscopy of a later intermediate (**16**); comparison of the calculated vicinal coupling constants for H22[11] with the experimental values, (for **9a**: calcd. 5.3/2.7 Hz, exp. 5.4/5.4 Hz; for **9b**: calcd 9.0/6.9 Hz, exp. 8.4/6.7 Hz)[22] and for 26-*epi*-**9b** (8.2/6.7 Hz); oxidation of 26-*epi*-**9b** with Dess–Martin periodinane leads to an alkynone that is identical with the one obtained from **9b**, but different from that obtained from **9a**.

The conversion of **9** into a precursor for cycloaromatization further requires the elimination of the C22-oxy function in a selective manner.[12] Scheme 4 depicts the laborious sequence by which this was accomplished for **9b**. Selective deprotection of the phenolsilyl ether (81% yield) followed by acetylation of **10** afforded diacetate **11** (95% yield). After further desilylation with hydrofluoric acid in acetonitrile to **12** (95% yield), the free C22-hydroxy group was converted into the corresponding methanesulfonate **13** (86% yield). The elimination of the methanesulfonate was first attempted on the unprotected 17-oxy derivative **13**.[23] Treatment with ten equivalents of 1,8-diazabicyclo[5.4.0]undec-5-ene (DBU) at room temperature proved difficult. Even after six hours most of the starting methanesulfonate was still present. When the reaction was followed by ^{1}H NMR spectroscopy (25 °C, [D_2]dichloromethane), an isolated AB system (δ = 6.01, 5.93, J = 9.4 Hz; integration indicated less than 10% of the starting material) as expected for the two hydrogen atoms of a (*Z*)-enediyne system was observed but gradually disappeared, presumably through Bergman cyclization.

At several stages during the synthesis we found that C17-alkynylated derivatives were rather unstable when they possessed a free C17-hydroxy group. The same procedure was therefore also studied on derivative **14**, in which the C17-hydroxy group is protected as the trimethylsilyl ether (90% yield with TMSOTf and 2,6-lutidine, CH_2Cl_2, −78 °C, 45 min). Upon treatment of **14** with DBU in toluene at room temperature for 1 h the expected enediyne **15** could be isolated in about 50% yield after fast workup and chromatography as well as 31% of starting methanesulfonate. The rate of its disappearance, presumably through Bergman cyclization, was estimated by means of ^{1}H NMR spectroscopy ([D]chloroform, 25 °C) at $t_{1/2}$ = 108 min (25 °C). When methanesulfonate **14** was treated with 20 equivalents of DBU in the presence of 1,4-cyclohexadiene (50 °–60 °C, 3 h), the expected cycloaromatized acetate **16** was isolated in 33% yield. The assignment of the configuration at C26 was based on comparison with calculated vicinal coupling constant values for H26,[11] (3.2/3.0 Hz for **16**; 11.1/4.3 Hz for 26-*epi*-**16**);[24] the experimental values are 3.0/3.0 Hz.

Although the estramycin derivative that has been synthesized and shown to cycloaromatize still possesses a protected C17-hydroxy group, we have shown that a 10-membered ring derivative of this type, in particular with a *cis*-ring fusion, does cycloaromatize at a rate useful for possible chemothera-

peutic use. We are convinced that this knowledge will be crucial in the development of more sophisticated estramycin derivatives.

Received: March 11, 1995
Revised version: May 3, 1995 [Z 7790 IE]
German version: *Angew. Chem.* **1995**, *107*, 1898–1901

Keywords: antibiotics · antitumor agents · diradicals · enediynes · estrogens

[1] Review: K. C. Nicolaou, W.-M. Dai, *Angew. Chem.* **1991**, *103*, 1453–1481; *Angew. Chem. Int. Ed. Engl.* **1991**, *30*, 1387–1416; recent progress in the chemistry of enediyne antibiotics: *Tetrahedron* **1994**, *50* (Tetrahedron Symposia-in-print no. 53).

[2] a) K. C. Nicolaou, Y. Ogawa, G. Zuccarello, H. Kataoka, *J. Am. Chem. Soc.* **1988**, *110*, 7247–7248; b) M. Tokuda, K. Fujiwara, T. Gomibuchi, M. Hirama, M. Uesugi, Y. Sugiura, *Tetrahedron Lett.* **1993**, *34*, 669–672; c) D. Boger, J. Zhou, *J. Org. Chem.* **1993**, *58*, 3018–3024; d) M. F. Semmelhack, J. J. Callaghes, W.-D. Ding, G. Krishnamurthy, R. Babine, G. A. Ellestad, *J. Org. Chem.* **1994**, *59*, 4357–4359; e) K. Toshima, K. Onta, A. Ohashi, T. Nakamura, M. Nakata, S. Matsumura, *J. Chem. Soc. Chem. Commun.* **1993**, 1525–1527; Review: K. Nicolaou, A. Smith, E. Yue, *Proc. Natl. Acad. Sci. USA* **1993**, *90*, 5881–5888.

[3] Y.-F. Lu, C. W. Harwig, A. G. Fallis, *J. Org. Chem.* **1993**, *58*, 4202–4204.

[4] *Cytotoxic Estrogens in Hormone Receptive Tumors* (Eds.: J. Raus, H. Martens, G. Leclercq), Academic Press, London, **1980**.

[5] For example, estramustine (estradiol to which nitrogen mustard [bis(2-chloroethyl)sulfide] is bound): H. Hamacher, *Arzneim. Forsch.* **1979**, *29*, 463; see also: S. Top, A. Vessières, G. Jaouen, *J. Chem. Soc. Chem. Commun.* **1994**, 453–454, and references therein.

[6] R. G. Bergman, *Acc. Chem. Res.* **1973**, *6*, 25–31.

[7] A. G. Myers, F. Y. Kuo, N. S. Finney, *J. Am. Chem. Soc.* **1989**, *111*, 8057–8059.

[8] T. Ojasoo, J.-P. Raynaud, J.-P. Mornon in *Comprehensive Medicial Chemistry, Vol. 3* (Eds.: C. Hansch, P. G. Sammes, G. B. Taylor), Pergamon, New York, **1990**, pp. 1175–1226.

[9] a) D. F. Heiman, S. G. Senderoff, J. A. Katzenellenbogen, R. L. Neeley, *J. Med. Chem.* **1980**, *23*, 994–999; b) D. O. Kiesewetter, J. A. Katzenellenbogen, M. R. Kilbourn, M. J. Welch, *J. Org. Chem.* **1984**, *49*, 4900–4905.

[10] K. C. Nicolaou, G. Zuccarello, Y. Ogawa, E. J. Schweiger, T. Kumazawa, *J. Am. Chem. Soc.* **1988**, *110*, 4866–4868; but see also: J. P. Snyder, *ibid.* **1990**, *112*, 5367–5369; P. Magnus, P. Carter, J. Elliot, R. Lewis, J. Harling, T. Pitterna, W. E. Bauta, S. Fortt, *ibid.* **1992**, *114*, 2544–2559.

[11] Calculations were performed with MacroModel (MM2): W. C. Still, F. Mohamadi, N. G. J. Richards, W. C. Guida, M. Lipton, R. Liskamp, G. Chang, T. Hendrickson, F. De Gunst, W. Hasel, *MacroModel V3.0*, Department of Chemistry, Columbia University, New York.

[12] An excellent, recent account of the strategies for the generation of reactive enediynes from stable precursors: M. E. Maier, *Kontakte* **1994** (2), 3–17.

[13] T. L. Fevig, J. A. Katzenellenbogen, *J. Org. Chem.* **1987**, *52*, 247–251.

[14] K. M. Sam, R. P. Boivin, S. Auger, D. Poirier, *Bioorg. Med. Chem. Lett.* **1994**, *4*, 2129–2131.

[15] E. C. Taylor, C.-S. Chiang, *Synthesis* **1977**, 467.

[16] K. Takai, T. Kuroda, S. Nakatsukasa, K. Oshima, H. Nozaki, *Tetrahedron Lett.* **1985**, *26*, 5585–5588.

[17] a) C. Crevisy, J.-M. Beau, *Tetrahedron Lett.* **1991**, *32*, 3171–3174; b) M. E. Maier, T. Brandstetter, *ibid.* **1992**, *33*, 7511–7514; c) see also: P. A. Wender, J. A. McKinney, C. Mukai, *J. Am. Chem. Soc.* **1990**, *112*, 5369–5370.

[18] Complete details (synthesis, experimental procedures, spectral data) will be published in a full paper.

[19] H. Emde, D. Domsch, H. Feger, U. Frick, A. Götz, H. H. Hergott, K. Hofmann, W. Kober, K. Krägeloh, T. Oesterle, W. Steppan, W. West, G. Simchen, *Synthesis* **1982**, 1.

[20] G. Neef, U. Eder, R. Wiechert, *J. Org. Chem.* **1978**, *43*, 4679–4680.

[21] P. V. Demarco, E. Farkas, D. Doddrell, B. Mylari, E. Wenkert, *J. Am. Chem. Soc.* **1968**, *90*, 5480–5486.

[22] Calculations were performed on an unprotected model lacking the C26-substituent.

[23] An example in which the enediyne system is generated by the elimination of a methanesulfonate (4 equiv of DBU in THF: 1,4-cyclohexadiene, 3:1): a) H. Audrain, T. Skrydstrup, G. Ulibarri, D. S. Grierson, *Synlett* **1993**, 20–22; b) H. Audrain, T. Skrydstrup, G. Ulibarri, C. Riche, A. Chiaroni, D. S. Grierson, *Tetrahedron* **1994**, *50*, 1469–1502.

[24] Calculations were performed on the unprotected triol derivative.

Substituent-Controlled Reactions of Iminophosphoranes with Methyllithium**

Alexander Steiner and Dietmar Stalke*

Dedicated to Professor Paul von Ragué Schleyer on the occasion of his 65th birthday

Phosphorus ylides $R_3P{=}CR_2$ and phosphine oxides $R_3P{=}O$ can react with nucleophiles via hypervalent intermediates. These intermediates might be regarded as electronically similar to the valence-expanded $[PX_4]^-$ ions.[1, 2] The Wittig reaction, in which an intermediately formed oxaphosphetane resulting from the reaction of a phosphorus ylide and a carbonyl compound decomposes to give phosphine oxide and the related olefin, has been well studied.[3] Another example of the above-mentioned reactions is that of a pyridyl-substituted phosphine oxide with organometallic bases.[4] Aryl- and heteroaryl-substituted tertiary phosphanes can react to give either substituent-exchange[5] (Scheme 1, top) or substituent-coupling[6] products (Scheme 1, bottom).

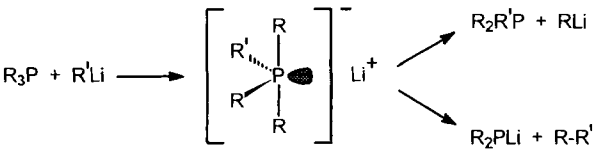

Scheme 1.

In our ongoing studies of the influence of pyridyl substituents at phosphorus,[7] we were interested in the reaction of organolithium compounds with iminophosphoranes $R_3P{=}NR'$, which can be regarded as unsaturated $P^V{-}N$ compounds and hence as N analogues of phosphorus ylides and phosphine oxides.[8]

Both $Py_3P{=}NSiMe_3$ (**1**) (Py = 2-pyridyl) and the isoelectronic phenyl derivative $Ph_3P{=}NSiMe_3$ (**2**) were treated with methyllithium, and the structures of the resulting lithium compounds were determined. Compound **1** can readily be made by the Staudinger reaction of tri(2-pyridyl)phosphane and trimethylsilylazide [Eq. (a)].

$$Py_3P + Me_3SiN_3 \xrightarrow[-N_2]{160\,^\circ C/12\,h} \underset{\mathbf{1}}{Py_3P{=}NSiMe_3} \qquad \text{(a)}$$

Compound **1** reacts spontaneously with methyllithium in diethyl ether even at $-78\,^\circ C$, during which the solution changes from colorless to dark green. Golden brown needles can be grown from the reaction mixture on storing the flask at $0\,^\circ C$ for two days.

The results of the single-crystal X-ray structure analysis[9] are shown in Figure 1. The iminophosphorane **1** is converted into the lithium phosphine amide **3** during which the oxidation state of the central phosphorus atom decreases from V to III. The coordination sphere of the lithium ion is saturated by the substituent-coupling product 2,2′-bipyridyl obtained in this reaction. Scheme 2 shows one plausible reaction mechanism.

[*] Priv.-Doz. Dr. D. Stalke, Dr. A. Steiner
Institut für Anorganische Chemie der Universität
Tammannstrasse 4, D-37077 Göttingen (Germany)
Telefax: Int. code + (551)392582

[**] This work was supported by the Deutsche Forschungsgemeinschaft and the Fonds der Chemischen Industrie.

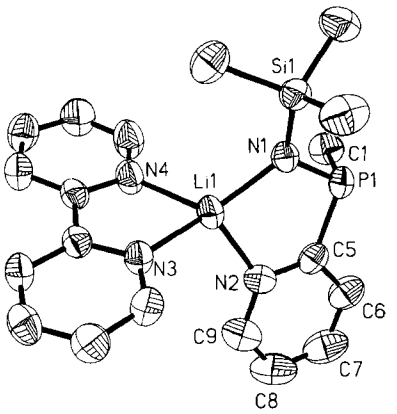

Fig. 1. Molecular structure of **3** in the crystal. Selected bond lengths [pm] and angles [°]: P1–N1 163.4(3), N1–Si1 167.5(3), P1–C1 183.8(4), P1–C5 184.9(4), C5–N2 134.7(4), Li1–N1 195.1(6), Li1–N2 203.3(6), Li1–N3 209.5(6), Li1–N4 207.0(7); N1–P1–C5 102.8(2), P1–N1–Si1 123.1(2), N1–Li1–N2 91.7(2), N3–Li1–N4 78.6(2).

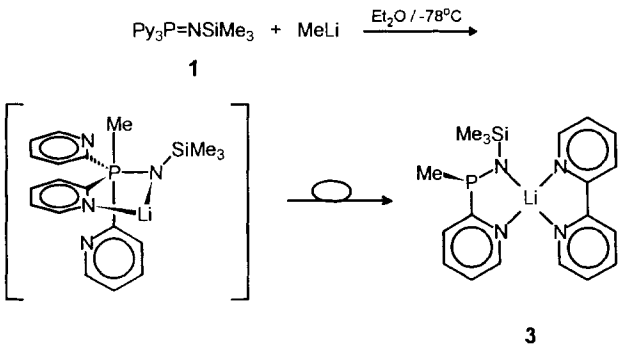

Scheme 2.

Methyllithium initially adds to the P=N bond in such a way that the methanide anion binds to the phosphorus atom and the lithium ion is coordinated by the peripheral nitrogen atoms. The hypervalent species subsequently rearranges through substituent coupling of two pyridyl groups to form the 2,2′-bipyridyl adduct **3**. Alternatively, a reaction mechanism analogous to that suggested by Wittig et al. for their phosphorane syntheses[10] is also plausible [Eq. (b)].

$$Py_3P{=}NSiMe_3 + MeLi \longrightarrow [Py_2(Me)P{=}NSiMe_3 + PyLi] \longrightarrow MeP(Py)(Me_3SiN)LiPy_2 \quad (b)$$

The P–N distance of 163.4(3) pm in **3** is remarkably short for a P–N single bond; the standard value is 170 pm.[11] In comparison the P=N bond length in iminophosphanes varies from 147 to 162 pm.[12] The P–N bond (167.2 pm) in the lithium phosphine amide $[Li(PhNPPh_2)(OEt)_2]_2$, which exhibits Li–N as well as Li–P contacts, was also considered to be relatively short.[13] A conceivable delocalization of the negative charge in the P–N unit of phosphine amide and iminophosphoranide resonance structures, which would explain the short P–N distance, however, could not be confirmed on the basis of the results of theoretical calculations on the $[H_2PNH]^-$ ion.[14] According to these calculations the negative charge is almost entirely localized at the nitrogen atom.

Li1 resides in a distorted tetrahedral environment, coordinated to its four neighboring atoms. The Li–N distance to the negatively charged N1 atom of 195.1(6) pm is 5 pm shorter than that in the $[Li(PhNPPh_2)(OEt)_2]_2$ dimer. The Li–N contacts to the neutral 2,2′-bipyridyl donor molecule (Li1–N3 209.5(6), Li1–N4 207.0(7) pm) are slightly longer than those to the pyridyl substituent of the anion (Li1–N2 203.3(6) pm).

When the phenyl-substituted iminophosphorane **2** is treated with methyllithium in diethyl ether in an analogous way to **1**, the reaction mixture only turned pale yellow at −78 °C. After the reaction mixture had been allowed to warm to room temperature, no spontaneous reaction was observed. Only after constant stirring for three days is the formation of a colorless precipitate apparent. Colorless single crystals were grown from the filtrate in two days at 3 °C. According to NMR spectroscopic studies the composition of the colorless precipitate and the single crystals growing from the solution is identical.

The single-crystal X-ray structure analysis[9] (Fig. 2) shows that, in contrast to the reaction of **1** with methyllithium, this

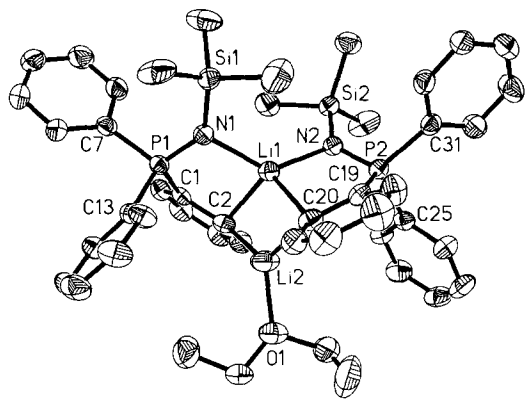

Fig. 2. Molecular structure of **4** in the crystal. Selected bond lengths [pm] and angles [°]: P1–N1 156.2(2), P1–N2 156.2(3), P1–C1 180.2(2), P1–C7 181.9(3), P1–C13 181.6(2), P1–C19 180.4(3), P1–C25 181.3(3), P1–C31 181.6(3), N1–Si1 170.1(2), N2–Si2 170.8(2), Li1–N1 203.7(5), Li1–N2 202.7(4), Li1–C2 213.8(6), Li1–C20 226.3(5), Li2–C2 213.8(6), Li2–C20 212.0(6), Li2–O1 189.7(5); P1–N1–Si1 135.2(1), P2–N2–Si2 133.5(1), C1–C2–C3 113.0(2), C19–C20–C21 113.0(2), N1–Li1–N2 132.2(2), C2–Li1–C20 107.7(2), C2–Li2–C20 121.2(2).

reaction does not involve nucleophilic attack at the phosphorus atom but deprotonation at the *ortho* position of one phenyl substituent leading to the dimeric organolithium complex **4** [Eq. (c)].

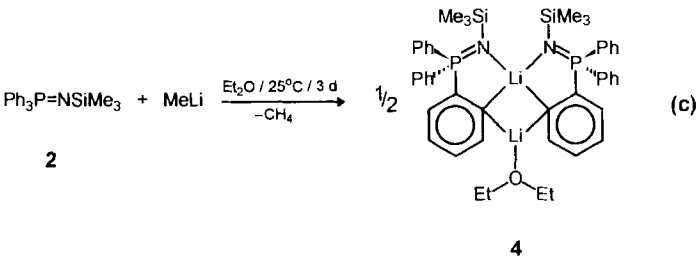

(c)

In the solid state **4** consists of two $Ph_3P{=}NSiMe_3$ units each deprotonated at the *ortho* position of one phenyl ring. The iminophosphorane units chelate through these *ortho*-carbon atoms and the N donor centers with a single central lithium ion (Li1; Fig. 2). A second lithium ion (Li2; Fig. 2) is coordinated to the two *ortho* ring carbon atoms and the oxygen atom of a diethyl ether molecule. Compound **4** adopts almost local C_2 symmetry.

Li1 resides in a tetrahedrally distorted environment, Li2 in an almost trigonally planar one. The Li1–C distances (C2–Li1 226.3, C20–Li1 233.1 pm) are on average 20 pm longer than the Li2–C distances (C2–Li2 213.8, C20–Li2 212.0 pm). The latter are comparable to the Li–C distances in the monomeric phenyllithium complex [PhLi·PMDETA] (PMDETA = *N*,*N*,*N*′,*N*″,*N*″-pentamethyldiethylenetriamine).[15] In the oligomeric aggregates $[PhLi \cdot TMEDA]_2$ (TMEDA = *N*,*N*,*N*′,*N*′-tetramethylethylenediamine) and $[PhLi \cdot OEt_2]_4$, the related distances[16] are almost identical to the Li1–C distances in **4**. The lithium–nitrogen distances (N1–Li1 203.7(5), N2–Li1 202.7(4) pm) are comparable to the related distances in monomeric $(THF)_2Li(NSiMe_3)_2PPh_2$.[17] The Li2–O1 distance of 189.7(5) pm is within the range found for lithium ether adducts.[18] The coordination behavior of the phosphazene-substituted aryl anion in **4** is closely related to that of other bidentate monoanionic C,N-chelate ligands.[19] The phosphazene unit acts as an N-donating side arm. Preliminary results show that both lithium atoms can be replaced in a transmetalation reaction by E^{II} (E = Sn,Pb). In the solid-state structures of these compounds, the heavy p-block metal cations are coordinated in a bidentate way to both the *ortho*-carbon atoms and the two nitrogen atoms of the chelating phosphazene units.[20] Furthermore, **4** can be oxidatively coupled in the *ortho*-C positions to give the iminodiphosphorane **5**.[20] This appears to be particularly interesting in light of oligomeric phosphazenes as potential polymeric materials.

$Ph_2P(NSiMe_3)-(C_6H_4)-(C_6H_4)(NSiMe_3)PPh_2$ **5**

The ^{7}Li NMR spectrum of **4** at room temperature shows only one signal at $\delta = 3.0$ (standard: LiCl ext.). However, upon cooling the signal broadens, and beyond the coalescence point two signals can be resolved at $\delta = 3.4$ and 2.2.

The P=N bond (156.2(2) pm) in **4** is only 2 pm longer than that in the structure of the starting material **2**.[21] The P=N stretching vibration in the IR spectrum of **4** appears at $\tilde{\nu} = 1184\ cm^{-1}$. In comparison to the corresponding vibration for **2**, this is red-shifted by $120\ cm^{-1}$ as a result of the N–Li coordination.[22] The P–C bond lengths do not differ significantly (180.2(2)–181.9(3) pm).

The different reaction behavior of **1** and **2** can be attributed to the inductive effects of the substituents at the phosphorus atom. The pyridyl substituents in **1** are electron-withdrawing and facilitate the nucleophilic attack at the phosphorus atom, while the triphenyl-substituted phosphorus atom in **2** remains inert under the same conditions. Furthermore, the N donor functions of the pyridyl substituents can coordinate the lithium ion in the periphery of the molecule. This enables the attack of the methanide ion at the electrophilic P center of the molecule. Under the same conditions no nucleophilic attack at the phosphorus atom of **2** occurs, not even at 25 °C. The phenyl substituents lower the nucleophilicity of the central phosphorus atom and they themselves react as CH-acidic components with methyllithium.

The reaction of iminophosphoranes with organolithium bases controlled by pyridyl substituents opens new synthetic routes in phosphorus–nitrogen chemistry, and further interesting reactions can be expected in the near future. Because the phosphorus atom in **3** is a chiral center, diastereomeric products can be assumed when the related chiral organometallic compounds are used in syntheses. Currently we are investigating such reactions with phosphorus ylides.

Experimental Procedure

All manipulations were performed under an inert atmosphere of dry nitrogen with Schlenk techniques or in an argon glove box. Diethyl ether was dried over Na/K alloy and distilled prior to use.

1: Tri(2-pyridyl)phosphane (7.5 g, 28.0 mmol) was added to trimethylsilylazide (3.6 g, 31.0 mmol 1.1 eq), and the reaction mixture was heated to 160 °C for 12 h. At an oil bath temperature of 230 °C the dirty brown crude product was distilled off at reduced pressure (10^{-2} Torr). The resulting colorless oil solidified after addition of *n*-pentane (30 mL). This solid was washed twice with *n*-pentane (30 mL) and dried under high vacuum. Yield: 9.2 g (93%). M.p. 77 °C. IR (Nujol, KBr): $\tilde{\nu}\ [cm^{-1}] = 1574, 1424, 1295, 1234, 989, 863, 831, 746, 731, 538$. ^{1}H NMR ($CDCl_3$, 25 °C, TMS): $\delta = -0.76$ (d, $^4J(H,P) = 0.4$ Hz, 9H, $SiMe_3$), 7.26 (dddd, $^3J(H,[4]H) = 7.7$ Hz, $^3J(H,[6]H) = 4.8$ Hz, $^5J(H,P) = 2.5$ Hz, $^4J(H,[3]H) = 1.3$ Hz, 3H, [5]H), 7.72 (dddd, $^3J(H,[3]H) = 7.8$ Hz, $^3J(H,[5]H) = 7.7$ Hz, $^4J(H,P) = 3.9$ Hz, $^4J(H,[6]H) = 1.8$ Hz, 3H, [4]H), 8.05 (dddd, $^3J(H,[4]H) = 7.8$ Hz, $^3J(H,P) = 6.0$ Hz, $^4J(H,[5]H) = 1.3$ Hz, $^5J(H,[6]H) = 1.0$ Hz, 3H, [3]H), 8.68 (dddd, $^3J(H,[5]H) = 4.8$ Hz, $^4J(H,[4]H) = 1.8$ Hz, $^5J(H,[3]H) = 1.0$ Hz, $^4J(H,P) = 0.5$ Hz, 3H, [6]H). ^{13}C NMR ($CDCl_3$, 25 °C, TMS): $\delta = 3.4$ (d, $^3J(C,P) = 3.5$ Hz, $SiMe_3$), 124.5 (d, $^3J(C,P) = 3.2$ Hz, C[5]), 128.3 (d, $^2J(C,P) = 21.4$ Hz, C[3]), 135.6 (d, $^4J(C,P) = 9.4$ Hz, C[4]), 149.8 (d, $^3J(C,P) = 19.2$ Hz, C[6]), 158.0 (d, $^1J(C,P) = 131.1$ Hz, C[2]). ^{29}Si NMR ($CDCl_3$, 25 °C, TMS): $\delta = -8.0$ (d, $^2J(Si,P) = 15.8$ Hz). ^{31}P NMR ($CDCl_3$, 25 °C, H_3PO_4 / 85%): $\delta = -6.9$. MS(EI) $m/z = 337$ ($M^+ - Me$, 100%).

3: To a solution of **1** (1.0 g, 3.0 mmol) in diethyl ether (20 mL) methyllithium (3.0 mmol, 1.9 mL of a 1.6 M solution in diethyl ether) was added dropwise over 30 min at −78 °C. Subsequently the dark green reaction mixture was stirred for 3 d at 25 °C. After storage for 2 d at 0 °C golden brown needles were obtained. Yield: 0.7 g (64%). M.p. 134 °C. IR (Nujol, KBr): $\tilde{\nu}\ [cm^{-1}] = 1584, 1458, 1415, 1229, 1060, 823, 755, 498$. ^{1}H NMR ($C_6D_6$, 25 °C, TMS): $\delta = 0.45$ (s, 9H, $SiMe_3$), 1.88 (d, $^2J(H,P) = 4.3$ Hz, 3H, PMe, 6.3–8.5 (m, 12H, Py). ^{7}Li NMR (C_6D_6, 25 °C, LiCl): $\delta = 4.2$. ^{13}C NMR (C_6D_6, 25 °C, TMS): $\delta = 5.06$ (s, $SiMe_3$), 29.1 (d, $^1J(C,P) = 39.1$ Hz, PMe), 117–187 (m, Py). ^{29}Si NMR (C_6D_6, 25 °C, TMS): $\delta = -10.1$ (d, $^2J(Si,P) = 36.3$ Hz). ^{31}P NMR (C_6D_6, 25 °C, H_3PO_4/85%): $\delta = 52.5$. MS(EI) $m/z = 375$ (M^+, 32%), 79 ($[PyH]^+$, 100%).

4: To a solution of **2** (7.0 g, 20 mmol) in diethyl ether (100 mL) methyllithium (20 mmol, 12.5 mL of a 1.6 M solution) in diethyl ether was added dropwise at 25 °C. Within 3 d of stirring the formation of a colorless precipitate was observed. This was filtered and after storage of the filtrate at room temperature for 2 d colorless crystals were obtained. Spectroscopic data for the crystals and the precipitate were identical. Yield: 4.4 g (56%). M.p. 131 °C (decomp.). IR (Nujol, KBr): $\tilde{\nu}\ [cm^{-1}] = 1435, 1184, 1107, 859, 830, 725, 714, 659, 534$. ^{1}H NMR ($C_6D_6$, 25 °C, TMS): $\delta = -0.01$ (s, 18H, $SiMe_3$), 0.38 (t, $^3J(H,H) = 7.0$ Hz, 6H, Et_2O), 2.66 (q, $^3J(H,H) = 7.0$ Hz, 4H, Et_2O), 7.1–8.3 (m, 28H, Ph). ^{7}Li NMR (C_6D_6, 25 °C, LiCl): $\delta = 3.1$. ^{13}C NMR (C_6D_6, 25 °C, TMS: $\delta = 4.1$ (d, $^3J(C,P) = 3.8$ Hz, $SiMe_3$), 14.6 (s, Et_2O), 65.3 (s, Et_2O), 120–195 (m, Ph). ^{29}Si NMR (C_6D_6, 25 °C, TMS): $\delta = -5.2$ (d, $^2J(Si,P) = 4.7$ Hz). ^{31}P NMR (C_6D_6, 25 °C, H_3PO_4 / 85%): $\delta = 19.8$. MS(EI) $m/z = 334$ ($[Ph_3P{=}NSiMe_2]^+$, 100%).

Received: February 27, 1995
Revised: May 3, 1995 [Z 7736 IE]
German version: *Angew. Chem.* **1995**, *107*, 1908–1910

Keywords: iminophosphoranes · lithium compounds · NMR spectroscopy · phosphanes · solid-state structures

[1] S. Oae, Y. Uchida, *Acc. Chem. Res.* **1991**, *24*, 202.
[2] K. B. Dillon, *Chem. Rev.* **1994**, *94*, 1441.
[3] G. Wittig, *Pure Appl. Chem.* **1964**, *9*, 245.
[4] Y. Uchida, K. Onoue, N. Tada, F. Nagao, S. Oae, *Tetrahedron Lett.* **1989**, *30*, 567.
[5] a) G. Wittig, A. Maercker, *J. Organomet. Chem.* **1967**, *8*, 491; b) E. P. Kyba, *J. Am. Chem. Soc.* **1976**, *98*, 4805.
[6] a) Y. Uchida, M. Kawai, H. Masauji, S. Oae, *Heteroatom Chem.* **1993**, *4*, 421; b) Y. Uchida, Y. Takaya, S. Oae, *Heterocycles* **1990**, *30*, 347.
[7] a) A. Steiner, D. Stalke, *J. Chem. Soc. Chem. Commun.* **1993**, 444; b) A. Steiner, D. Stalke, *Organometallics*, **1995**, *14*, 2422.
[8] A. W. Johnson, *Ylides and Imines of Phosphorus*, Wiley, New York, **1993**.
[9] Crystallographic data for **3**: $C_{19}H_{24}LiN_4PSi$, $M = 374.4$, triclinic, space group $P\bar{1}$, $a = 906.3(4)$, $b = 958.1(4)$, $c = 1378.7(6)$ pm, $\alpha = 73.43(2)$, $\beta = 72.48(2)$, $\gamma = 74.81(2)°$, $V = 1.0737\ nm^3$, $Z = 2$, $\rho_{calcd} = 1.158\ Mg\,m^{-3}$, $\lambda = 71.073$ pm, $T = 153(2)$ K, $\mu(Mo_{K\alpha}) = 0.193\ mm^{-1}$. All data were collected by using an oil-coated shock-cooled crystal [23] with dimensions of $0.6 \times 0.4 \times 0.3$ mm in the range $8° \geq 2\theta \geq 50°$ on a Stoe-Siemens AED diffractometer. Of the 4461 collected reflections, 3371 were unique. The structure was solved by direct methods [24] and refined by full-matrix least-squares on F^2 [25]. $R1 = (I > 2\sigma(I)) = 0.061$ and $wR2 = 0.180$ (all data) with $R1 = \Sigma||F_o| - |F_c||/\Sigma|F_o|$ and $wR2 = \Sigma w(F_o^2 - F_c^2)^2/\Sigma w(F_o^2)^2)^{0.5}$; highest residual electron density peak: $948\ e\,nm^{-3}$. Crystallographic data for **4**: $C_{46}H_{56}Li_2N_2OP_2Si_2$,

$M = 784.9$, monoclinic, space group $P2_1/c$, $a = 1482.81(1)$, $b = 1691.9(2)$, $c = 1806.0(2)$ pm, $\beta = 4.42(1)$°, $V = 4.517$ nm^3, $Z = 4$, $\rho_{calcd} = 1.154$ Mg m^{-3}, $\lambda = 71.073$ pm, $T = 173(2)$ K, $\mu(Mo_{K\alpha}) = 0.184$ mm^{-1}. All data were collected by using an oil-coated shock-cooled crystal [23] with dimensions of $0.8 \times 0.7 \times 0.4$ mm in the range of $8° \geq 2\theta \geq 45°$ on a Stoe-Siemens AED diffractometer. Of the 6980 collected reflections, 5899 were unique. The structure was solved by direct methods [24] and refined by full-matrix least-squares on F^2 [25]. $R1 = (I > 2\sigma(I)) = 0.042$ and $wR2 = 0.110$ (all data) with $R1 = \Sigma||F_o| - |F_c||/\Sigma|F_o|$ and $wR2 = (\Sigma w(F_o^2 - F_c^2)^2/\Sigma w(F_o^2)^2)^{0.5}$; highest residual electron density peak: 349 e nm^{-3}. Further details of the crystal structure investigations are available on request from the Director of the Cambridge Crystallographic Data Centre, 12 Union Road, GB-Cambridge CB2 1EZ (UK), on quoting the full journal citation.

[10] a) G. Wittig, E. Kochendörfer *Angew. Chem.* **1958**, *70*, 506; b) G. Wittig, D. Hellwinkel *Angew. Chem.* **1962**, *74*, 76.
[11] P. Rademacher *Strukturen organischer Moleküle*, VCH, Weinheim, **1987**, p. 56.
[12] E. Niecke, D. Gudat, *Angew. Chem.* **1991**, *103*, 251; *Angew. Chem. Int. Ed. Engl.* **1991**, *30*, 217.
[13] M. T. Ashby, Z. Li, *Inorg. Chem.* **1992**, *31*, 1321.
[14] G. Trinquier, M. T. Ashby, *Inorg. Chem.* **1994**, *33*, 1306.
[15] U. Schümann, J. Kopf, E. Weiss, *Angew. Chem.* **1985**, *97*, 222; *Angew. Chem. Int. Ed. Engl.* **1985**, *24*, 215.
[16] a) D. Thoennes, E. Weiss, *Chem. Ber.* **1978**, *111*, 3157; b) H. Hope, P. P. Power, *J. Am. Chem. Soc.* **1983**, *105*, 5320.
[17] A. Steiner, D. Stalke, *Inorg. Chem.* **1993**, *32*, 1977.
[18] W. Setzer, P. von R. Schleyer, *Adv. Organomet. Chem.* **1985**, *24*, 353.
[19] G. van Koten, *Pure Appl. Chem.* **1989**, *61*, 1681.
[20] S. Wingerter, D. Stalke, unpublished results.
[21] R. Fleischer, A. Steiner, D. Stalke, unpublished results.
[22] H. Schmidbaur, W. Wolfsberger, *Chem. Ber.* **1967**, *100*, 1000.
[23] T. Kottke, D. Stalke, *J. Appl. Crystallogr.* **1993**, *26*, 615.
[24] G. M. Sheldrick, *Acta Crystallogr. Sect. A* **1990**, *46*, 467.
[25] G. M. Sheldrick, SHELXL-93, program for crystal structure refinement, University of Göttingen, **1993**.

Reaction of (Butadiene)zirconocene with Tris(pentafluorophenyl)borane—A Novel Way of Generating Methylalumoxane-Free Homogeneous Ziegler-Type Catalysts**

Bodo Temme, Gerhard Erker,* Jörn Karl, Heinrich Luftmann, Roland Fröhlich, and Sirpa Kotila

Homogeneous Ziegler-type catalysts based of bent metallocenes of the Group 4 metals have become enormously important in recent years.[1] They will probably develop into the next generation of Ziegler catalyst systems for industrial α-olefin polymer production.[2] Activation of the metallocene is mostly achieved by treatment with a very large excess of methylalumoxane.[3] New ways of activation for such CC-coupling catalysts employing only stoichiometric amounts of reagents are being developed to extend their use to other synthetic fields besides α-olefin polymerization. These methods are particularly attractive when they lead to well-characterized active catalysts or their direct precursors. Some progress has been achieved in this respect by using $[\{Cp_2ZrR^+\}\{BR_4^-\}]$-type ion pairs and related systems that are converted into active homogeneous Ziegler catalysts upon exposure to reactive α-olefins.[4] We have now found a very simple way to prepare metallocene–borate–betaine systems[5] in which the cationic and anionic parts are combined into a neutral molecule in such a way that the catalytic reactivity of the essential alkylmetallocene cation is retained. These novel organometallic compounds constitute neutral, covalently bonded molecules that rapidly polymerize α-olefins without further activation.

We have recently shown that (butadiene)zirconocene (**1a**) adds aluminum compounds $XAlR_2$ to form the heterodimetallacyclic complexes **2a**. These exhibit dynamic properties that

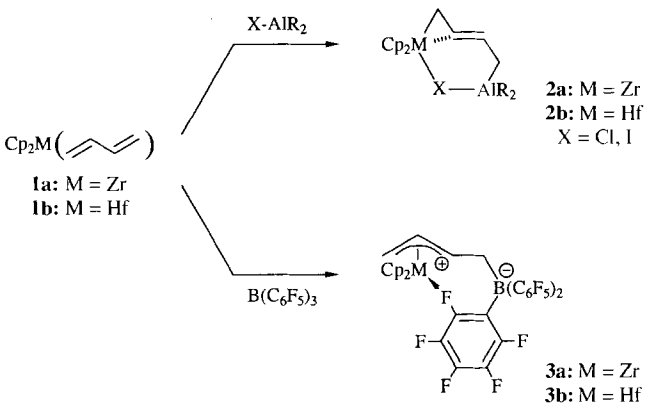

have been shown to originate from a reversible opening (with low activation barrier) of the Al–X bond.[6] To activate such complexes as metallocene–betaine catalysts for olefin polymerization, cleavage of the Zr–X linkage has to be facilitated by suitable molecular design. We have achieved this by introducing a more weakly coordinating bridging ligand between the main group metal and the zirconium center, and by increasing the electronic stabilization of the negative end of the potential betaine dipole.

Treatment of (butadiene)zirconocene (**1a**)[7] with tris(pentafluorophenyl)borane in toluene (−78 °C to room temperature) gives the 1:1 addition product (**3a**). It was isolated in 85% yield. The isolated material can be dissolved in tetrahydrofuran and characterized by spectroscopy and subsequent reactions in this solvent. Although complex **3a** can also be handled conveniently in toluene or benzene, it must be freshly prepared in these aromatic solvents since, once precipitated, the zirconium–boron complex **3a** is only slightly soluble in noncoordinating solvents. Single crystals of **3a** for the X-ray crystal structure analysis were obtained from toluene. A distorted π-allyl moiety is coordinated to the bent metallocene unit (Zr–C1 2.339(5), Zr–C2 2.494(6), Zr–C3 2.710(5), C1–C2 1.414(9), C2–C3 1.342(8) Å, angle C1-C2-C3 123.5(6)°; Fig. 1). The $B(C_6F_5)_3$ group is bonded to C4 (C3–C4 1.521(8), C4–B 1.633(9) Å). A characteristic feature of the structure of **3a** is the weak coordination of an *ortho*-fluoro substituent (F42) to the zirconium atom (Zr–F42 2.423(3), C42–F42 1.402(6) Å, angle C42-F42-Zr 140.0(3)°). The free coordination site of the zirconium–boron-betaine **3a** is occupied by this zirconium–fluorine interaction[4a, 5c] to give a stable metallacyclic complex.

From a comparison with the complexes **2a**, we assign complex **3a** a dimetallacyclic structure containing a distorted (π-allyl)metallocene unit in solution [^{13}C NMR spectrum in [D_8]toluene: δ = 52.7, 123.8, 131.1, 28.5 (C1–C4)]. Complex **3a** is chiral and thus exhibits two resonances for the diastereotopic Cp ligands (^{1}H NMR spectrum: δ = 5.32 and 5.28 in [D_6]benzene), as well as fast exchange on the NMR time scale

[*] Prof. Dr. G. Erker, Dr. B. Temme, Dipl.-Chem. J. Karl, Dr. H. Luftmann, Dr. R. Fröhlich, Dr. S. Kotila
Organisch-chemisches Institut der Universität
Corrensstrasse 40, D-48149 Münster (Germany)
Telefax: Int. code + (251)83-9772
e-mail: erker@uni-muenster.de

[**] This work was supported by the Fonds der Chemischen Industrie, the Alfried-Krupp-von-Bohlen-und-Halbach-Stiftung, the Ministerium für Wissenschaft und Forschung des Landes Nordrhein-Westfalen, and the Hoechst AG.

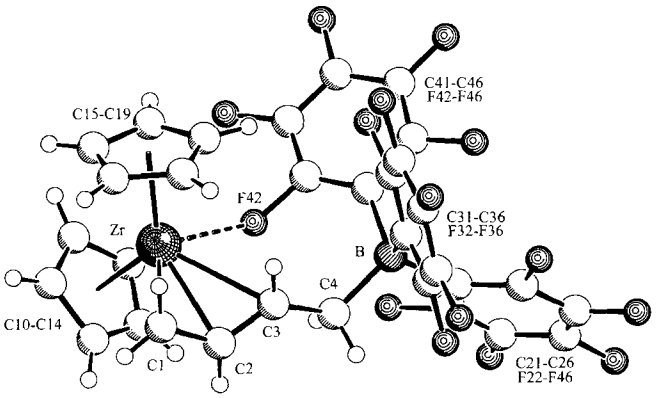

Fig. 1. Molecular structure of **3a** in the crystal.

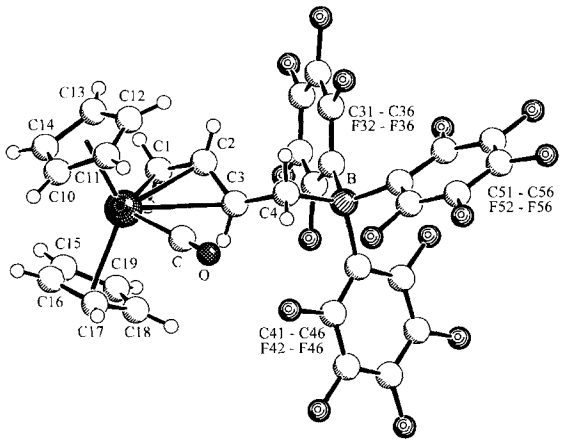

Fig. 2. Molecular structure of **5**; selected bond lengths [Å] and angles [°]: 2.246(7) (Hf–C), 1.109(8) (C–O), 2.396(5) (Hf–C1), 2.514(5) (Hf–C2), 2.742(5) (Hf–C3), 1.399(8) (C1–C2), 1.369(8) (C2–C3), 1.497(7) (C3–C4), 1.675(8) (C4–B), 176.2(6) (Hf-C-O).

of the 1-H_{syn}/H_{anti} and 4-H/H′ protons at high temperature ($\Delta G^{\ddagger}_{enant.} \approx 17.2 \pm 0.5$ kcal mol^{-1} at 350 K).[8] Also the ^{19}F NMR spectrum of **3a** indicates dynamic behavior. Only in an oversaturated [D_8]toluene solution at 187 K are the signals of the ^{19}F NMR spectrum of **3a** resolved (external reference $CFCl_3$): three *para*-fluorine ($\delta = -158.5$, -159.2 and -160.9) and six *meta*-fluorine resonances ($\delta = -163.6$, -164.7 (three overlapping signals), -165.1, -165.3) in addition to six clearly separated *ortho*-fluorine signals, five of which appear in the usual range ($\delta = -126.4$, -130.6, -131.8, -134.0 and -137.5) are observed, whereas one signal is found at much more negative δ values (-213.2). This indicates that a single *ortho*-fluorine substituent of the $B(C_6F_5)_3$ unit coordinates to zirconium in solution, too.[5e] In [D_8]tetrahydrofuran the dynamics of **3** are still rapid on the NMR time scale at even much lower temperatures. The activation barrier of the formal allyl inversion process was estimated from the dynamic ^{1}H NMR spectra at 600 MHz in this solvent to be $\Delta G^{\ddagger}_{enant.}$(207 K) $\approx 10.0 \pm 0.5$ kcal mol^{-1}. In this solvent the ^{13}C NMR chemical shifts of the μ-C_4H_6 ligand [$\delta = 46.8$, 114.2, 147.1, 35.0 (C1–C4)] are so different from those in [D_8]toluene (see above) that we assume the presence of a THF-coordinated species.

Upon standing at room temperature for two days in [D_8]toluene solution the corresponding hafnium/boron complex **3b** quantitatively rearranges to the isomeric betaine complex **4**.[9] In the coordinating solvent THF this hydrogen migration reaction was not observed.[10] Treatment of **3b** with carbon monoxide yields the d^0-configurated (π-allyl)carbonylhafnium complex **5**, which was characterized by X-ray diffraction (Fig. 2).[11]

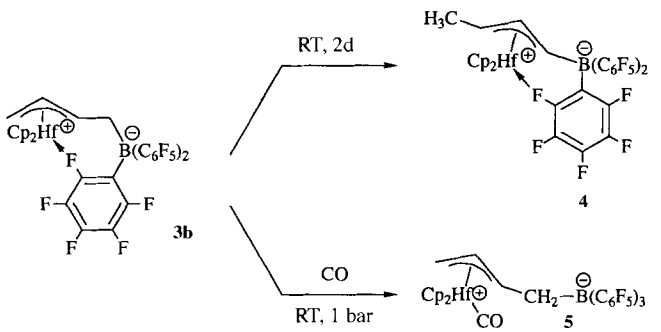

All these features of the zirconium complex **3a** (and its hafnium analogue **3b**) indicate that the C_6F_5 bridge is easily opened to generate a very reactive (μ-C_4H_6)M/B–betaine system. Consequently, introduction of ethylene to the Zr/B system **3a** resulted in rapid formation of polyethylene (the activity *a* is about 135 g polyethylene per mmol [Zr] per hour at 20 °C in dilute toluene solution). Complex **3a** also catalyzes the polymerization of propene. In toluene solution at 50 °C polypropylene formed with an activity of about 28 g polymer per mmol [Zr] per hour. As expected, the polymerization reaction catalyzed by **3a** is more efficient in liquid propene. A polymerization experiment employing 100 mg (0.36 mmol) of (butadiene)zirconocene and 186 mg (0.36 mmol) $B(C_6F_5)_3$ (to generate **3a** in situ) in 10 L of liquid propene at 70 °C (30 bar, 1 h) yielded about 800 g of polypropylene (*a* about 2.2 kg of polymer per mmol [Zr] per hour).[12] Both polymers have characteristics typical of polyethylene (m.p. 126 °C) and polypropylene (atactic, rather low molecular weight) formed at homogeneous Ziegler-type catalysts containing the parent bis(cyclopentadienyl)zirconium unit.[1–3]

In view of the typical chemical properties of **3a** (and **3b**, see above) one must assume that the fluoride bridge is very easily opened under the polymerization conditions. This may result in the generation of a betaine species (**6** or **7**) containing a very electrophilic zirconium center that can readily coordinate and insert α-olefins.[13] Experimental evidence for such a reaction path for betaines derived from **3a** was obtained from a laser desorption ionization MS experiment (LDI) [14] that could monitor even small quantities of anionic polymers originating

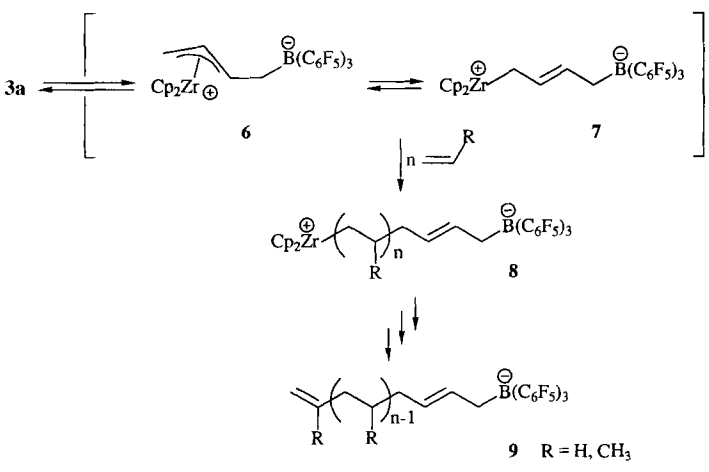

from some initial phases of the polymerization process in the presence of the "MS-silent" neutral polypropylene.

In a typical series of experiments propene was polymerized at ambient pressure in toluene at + 40 °C with **3a**. The reactions were stopped after short polymerization times (about 10 min). The solvent was removed, and an aliquot of the residue dissolved in tetrahydrofuran and treated with tetrabutylammonium bromide. The sample was introduced into the mass spectrometer, where the solvent evaporated. Laser desorption from targets treated in this manner gave time of flight mass spectra of the anions; a typical example is depicted in Figure 3. Aside from

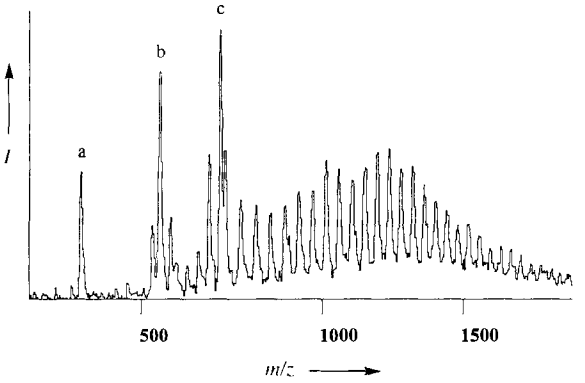

Fig. 3. LDI-TOF mass spectrum of the anions **9** (the features a–c originate from $B(C_6F_5)_3$-derived secondary products).

a few discrete features (for example, $[(C_6F_5)_3BOH]^-$ at $m/z = 529$), a broad molecular weight distribution of the anions of the general composition of $[H_2C=C(CH_3)-(propene)_{n-1}(butadiene)B(C_6F_5)_3]^-$ (**9**) are registered (for example, $m/z = 1280$ for $n = 17$). The example shown in Figure 3 contains a distribution of oligomeric anions ranging from about $n = 5$ to 27 with a broad maximum around propene insertion values of $n \approx 16-18$. This analysis shows that upon propene polymerization at the catalyst **3a**, anionic polymers containing borate groups are obtained with the typical molecular weight distribution of such a consecutive insertion process. The borate groups are probably incorporated in the initial phases of the catalytic process from **6** and **7**. Our experiment has indicated that in the reaction starting from **3a** and α-olefins, polymer modified catalyst systems are formed. This is very interesting since a covalently bound α-olefin polymer is, by the nature of its favored secondary structure, probably able to increasingly protect the active section of the catalyst system during the course of the polymerization process. The catalytic process starting from **3a** could, therefore, open new ways toward a dynamic stabilization of active catalysts that is achieved by the catalysis itself and is even enhanced as it proceeds.

Received: April 1, 1995 [Z 7857 IE]
German version: *Angew. Chem.* **1995**, *107*, 1867–1869

Keywords: alkenes · polymerization · sandwich complexes · Ziegler catalysts · zirconium compounds

[1] W. Kaminsky, K. Külper, H. H. Brintzinger, F. R. W. P. Wild, *Angew. Chem.* **1985**, *97*, 507; *Angew. Chem. Int. Ed. Engl.* **1985**, *24*, 507.

[2] Review: M. Aulbach, F. Küber, *Chemie Unserer Zeit* **1994**, *28*, 197; H.-H. Brintzinger, D. Fischer, R. Mülhaupt, B. Rieger, R. Waymouth, *Angew. Chem.* **1995**, *107*, 1255; *Angew. Chem. Int. Ed. Engl.* **1995**, *34*, 1143.

[3] H. Sinn, W. Kaminsky, *Adv. Organomet. Chem.* **1980**, *18*, 99, and references therein.

[4] $[\{Cp_2ZrR\}^+\{RB\}^-]$ ion pairs and related systems: a) M. Bochmann, G. Karger, A. J. Jaggar, *J. Chem. Soc. Chem. Commun.* **1990**, 1038; A. D. Horton, J. H. G. Frijns, *Angew. Chem.* **1991**, *103*, 1181; *Angew. Chem. Int. Ed. Engl.* **1991**, *30*, 1152; X. Yang, C. L. Stern, T. J. Marks, *J. Am. Chem. Soc.* **1991**, *113*, 3623; *Angew. Chem.* **1992**, *104*, 1406; *Angew. Chem. Int. Ed. Engl.* **1992**, *31*, 1375; C. Sishta, R. M. Hathorn, T. J. Marks, *J. Am. Chem. Soc.* **1992**, *114*, 1112; G. G. Hlatky, R. R. Eckman, H. W. Turner, *Organometallics* **1992**, *11*, 1413; C. J. Schaverien, *Organometallics* **1992**, *11*, 3476; C. Pellecchia, A. Immirzi, A. Grassi, A. Zambelli, *Organometallics* **1993**, *12*, 4473; C. Pellecchia, A. Grassi, A. Immirzi, *J. Am. Chem. Soc.* **1993**, *115*, 1160; J. J. Eisch, S. I. Pombrik, G.-X. Zheng, *Organometallics* **1993**, *12*, 3856; D. J. Gillis, M. J. Tudoret, M. C. Baird, *J. Am. Chem. Soc.* **1993**, *115*, 2543; F. Calderazzo, G. Pampaloni, L. Rocchi, U. Englert, *Organometallics* **1994**, *13*, 2592; reviews: M. Bochmann, *Angew. Chem.* **1992**, *104*, 1206; *Angew. Chem. Int. Ed. Engl.* **1992**, *31*, 1181; J. L. Kiplinger, T. G. Richmond, C. E. Osterberg, *Chem. Rev.* **1994**, *94*, 373; b) X. Yang, C. L. Stern, T. J. Marks, *J. Am. Chem. Soc.* **1994**, *116*, 10015.

[5] a) For a different Zr/B betaine type see G. G. Hlatky, H. Turner, R. R. Eckman, *J. Am. Chem. Soc.* **1989**, *111*, 2728; D. M. Amorose, R. A. Lee, J. L. Petersen, *Organometallics* **1991**, *10*, 2191; b) it was recently reported that treatment of $[Cp^*TaMe_2(butadiene)]$ with $B(C_6F_5)_3$ in $[D_6]$benzene gives a solution that shows a very low polymerization activity at high ethylene pressure: K. Mashima, S. Fujikawa, A. Nakamura, *J. Am. Chem. Soc.* **1993**, *115*, 10990; c) A. R. Siedle, R. A. Newmark, W. M. Lamanna, J. C. Huffman, *Organometallics* **1993**, *12*, 1491.

[6] G. Erker, R. Noe, C. Krüger, S. Werner, *Organometallics* **1992**, *11*, 4174; G. Erker, R. Noe, D. Wingbermühle, *Chem. Ber.* **1994**, *127*, 805.

[7] G. Erker, J. Wicher, K. Engel, F. Rosenfeldt, W. Dietrich, C. Krüger, *J. Am. Chem. Soc.* **1980**, *102*, 6344; H. Yasuda, Y. Kajihara, K. Mashima, K. Nagasuna, K. Lee, A. Nakamura, *Organometallics* **1982**, *1*, 388; Review: G. Erker, C. Krüger, G. Müller, *Adv. Organomet. Chem.* **1985**, *24*, 1.

[8] M. L. H. Green, L.-L. Wong, A. Sella, *Organometallics* **1992**, *11*, 2660, and references therein.

[9] **3a**: 820 mg (85%) isolated from toluene, m.p. 121 °C. ^{1}H NMR ([D$_8$]THF, 229 K): $\delta = 6.20$ (s, 10H, Cp), 6.05 (m, 1H, 2-H), 4.78 (m, 1H, 3-H), 2.83 (m, 2H, 4-H), 2.06 (m, 2H, 1-H). ^{1}H NMR ([D$_6$]benzene, 300 K): $\delta = 5.88$ (m, 1H, 2-H), 5.32, 5.28 (br. s, each 5H, Cp), 5.23 (m, 1H, 3-H), 2.56 ($\delta =$, $^2J = 18$ Hz, 1H, 4-H'), 2.25 (dd, $^2J = 18$ Hz, $^3J = 6$ Hz, 1H, 4-H), 1.85 (dd, $^2J = 12$ Hz, $^3J = 5$ Hz, 1-H'), 1.47 (dd, $^2J = 8$ Hz, $^3J = 5$ Hz, 1H, 1-H). ^{11}B NMR ([D$_6$]benzene): $\delta = -14.7$. X-ray crystal structure analysis of **3a**: Formula $C_{32}H_{16}BF_{15}Zr$, M 787.48, $0.35 \times 0.20 \times 0.10$ mm, $a = 14.930(1)$, $b = 11.213(2)$, $c = 17.248(1)$ Å, $\beta = 97.23(1)°$, $V = 2864.5(6)$ Å^3, $\rho_{calcd} = 1.826$ g cm^{-3}, $\mu = 5.1$ cm^{-1}, $Z = 4$, monoclinic, space group $P2_1/n$ (No. 14), Enraf-Nonius-CAD4 diffractometer, $\lambda = 0.71073$ Å, 6001 reflections measured ($\pm h$, + k, + l), $[\sin\theta/\lambda]_{max} = 0.62$ Å^{-1}, 5806 independent and 3095 observed reflections, 442 refined parameters, $R = 0.055$, $wR^2 = 0.145$. **3b**: 850 mg (80%) isolated. ^{1}H NMR ([D$_8$]THF, 205 K): $\delta = 6.21$ (s, 10H, Cp), 5.78 (m, 1H, CH), 4.81 (m, 1H, CH), 2.61 (m, 2H, 4-H), 1.80 (m, 2H, 1-H). ^{13}C NMR ([D$_8$]THF): $\delta = 149.0$, 138.6, 137.3, 126.5 (BAr_3), 148.0 ($^1J_{CH} = 147$ Hz, CH), 114.7 ($^1J_{CH} = 148$ Hz, CH), 110.4 (Cp), 46.8 ($^1J_{CH} = 140$ Hz, allyl-CH_2), 35.0 (broad, B-CH_2-). ^{11}B NMR ([D$_8$]THF): $\delta = -13.0$. **4**: ^{1}H NMR ([D$_8$]toluene): $\delta = 5.88$ (m, 1H, CH), 5.43, 5.09 (s, each 5H, Cp), 5.33 (m, 1H, CH), 2.98 (m, 1H, CH), 1.23 (d, 3H, CH_3). ^{13}C NMR ([D$_8$]toluene): $\delta = 148.9$, 139.0, 137.5 (BAr_3, one signal beneath solvent signal), 150.6 ($^1J_{CH} = 145$ Hz, CH), 110.3 (Cp), 102.0 (br., B-CH), 68.5 ($^1J_{CH} = 149$ Hz, CH), 18.2 ($^1J_{CH} = 128$ Hz, CH_3).

[10] G. Erker, R. Noe, D. Wingbermühle, J. L. Petersen, *Angew. Chem.* **1993**, *105*, 1216; *Angew. Chem. Int. Ed. Engl.* **1993**, *32*, 1213.

[11] X-ray crystal structure analysis of **5**: Formula $C_{33}H_{16}BF_{15}OH \cdot C_6H_6$, $M = 980.87$, $0.30 \times 0.20 \times 0.15$ mm, $a = 11.684(1)$, $b = 12.071(1)$, $c = 14.357(1)$ Å, $\alpha = 99.16(1)°$, $\beta = 105.20(1)°$, $\gamma = 110.84(1)°$, $V = 1753.2(2)$ Å^3, $\rho_{calcd} = 1.858$ g cm^{-3}, $\mu = 30.89$ cm^{-1}, empirical absorption correction, $Z = 2$, triclinic, space group $P\bar{1}$ (No. 2), Enraf-Nonius-CAD4 diffractometer, $\lambda = 0.71073$ Å, ω-2θ scan, 7444 reflections measured ($\pm h, -k, \pm l$), $[\sin\theta/\lambda]_{max} = 0.62$ Å^{-1}, 7091 independent and 5441 observed reflections, [$F > 4\sigma(F)$] 514 refined parameters, $R = 0.037$, $wR^2 = 0.088$, max. residual electron density 1.15(−1.00) e Å^{-3}, direct methods, hydrogen atoms calculated. Programs used SHELX 86, SHELX 93, SCHAKAL. Further information about the X-ray structure analyses can be obtained from the Fachinformationszentrum Karlsruhe, D-76344 Eggenstein-Leopoldshafen, on quoting the depository numbers CSD-401927 and 401928; other examples of d^0-configurated (carbonyl)metallocene complexes: D. M. Antonelli, E. B. Tjaden, J. M. Stryker, *Organometallics* **1994**, *13*, 763; Z. Guo, D. C. Swenson, A. S. Guram, R. F. Jordan, *ibid.* **1994**, *13*, 766; A. S. Guram, D. C. Swenson, R. F. Jordan, *J. Am. Chem. Soc.* **1992**, *114*, 8991.

[12] We thank the metallocene group of the Hoechst AG for carrying out this experiment.

[13] R. F. Jordan, *Adv. Organomet. Chem.* **1991**, *32*, 325, and references therein.

[14] a) Time-of-flight mass spectrometer (home-built by H. Luftmann): N_2 laser, $\lambda = 340$ nm, 3 ns pulse width, single stage acceleration 16 kV, flight path 1 m, resolution $m/\Delta m$ 100–250 (50% valley), MS accuracy ±0.1%. It was not necessary to use a matrix (MALDI) for ionizing the compounds **9**; b) F. Hillenkamp, *Laser Induced Ion Formation from Organic Solids* in *Springer Ser. in Chem. Phys.* **1983**, *25*, 190; M. A. Posthumus, P. G. Kristemaker, H. L. C. Meuselaar, M. C. T. N. De Brauw, *Anal. Chem.* **1978**, *50*, 985; H. S. Creel, *TRIP* **1993**, *1*, 336; D. Price, G. J. Milne, *Int. J. Mass Spectrom. Ion Proc.* **1990**, *99*, 1.

The Preparation of Salts of $[Pd_2(\mu\text{-}Se_2N_2)Cl_6]^{2-}$, the First Adducts of Diselenium Dinitride**

Paul F. Kelly* and Alexandra M. Z. Slawin

The continued interest in sulfur–nitrogen chemistry is prompted by the diverse range of species involved and the remarkable, and often unique, properties they exhibit.[1] Recent years have witnessed the gradual development of an important extention to this area, in the form of the synthesis of selenium analogues of many sulfur–nitrogen compounds.[2] Although this may appear to be a relatively trivial chemical alteration, in practice the preparation of such species is fraught with difficulties, not least of which is the severely explosive nature of the most obvious starting material, Se_4N_4. Despite these hurdles, there have now been reports of the preparation of a number of noncoordinated compounds, including $(Se_3N_2)^{2+}$ and Se_4N_2, as well as complexes of a variety of Se–N ligands.[3–5]

The reactions leading to these compounds serve to highlight the likelihood that the chemistry of Se–N compounds in fact mirrors that of S–N compounds to a far greater extent than was previously thought. One area in which the latter conclusion has so far proved untrue, however, is in the preparation of Se_2N_2 and $(SeN)_x$; here we present the first conclusive evidence of the existence of the former species, in the form of a palladium adduct.

Reaction of a suspension of Se_4N_4 in CH_2Cl_2 with the salt **1**, which has a Pd^{II} dimer as the anion, in a sealed tube at 100 °C

$[PPh_4]_2[Pd_2Cl_6]$ **1**

yields a dark solution from which orange crystals may be grown by slow diffusion of ether. X-ray crystallography reveals this product to be the salt **2a** (Fig. 1).[6] The planar anion in **2a**

$[PPh_4]_2[Pd_2(Se_2N_2)Cl_6]$ **2a**

(maximum deviation from mean plane is shown by Cl2, 0.02 Å) contains the first known example of a bidentate, neutral Se_2N_2 ligand. The latter exhibits an average Se–N bond length of 1.79 Å, which is essentially identical to that in Se_4N_4.[7] In contrast, the average bond length in the sulfur analogue of **2a** (1.65 Å) is markedly longer than that in S_4N_4 (1.62 Å) although equal to that in free S_2N_2.[8]

These bond lengths in **2a** are not equivalent, reflecting a slight degree of asymmetry exhibited by the molecule as a whole. This asymmetry may be traced back to the different N1-Pd-Cl angles at each palladium atom; for Cl1 this angle is 85.6° compared to the tighter 83.6° for Cl3. (The fact that both chlorines show a substantial deformation in towards the Se_2N_2 unit mirrors an effect noted many times for S_2N_2 adducts.[9]) Thus it appears that the slightly different degree of interaction between Cl1–Se1* and Cl3–Se1 produces a concomitant difference in the N1–Se1* and N1–Se1 distances. A view of the packing arrangements in the structure of **2a** reveals a Cl3–Cl3* interaction of about 3.5 Å between neighboring anions (Fig. 2), which is probably the ultimate source of the asymmetry in the anion; Cl3

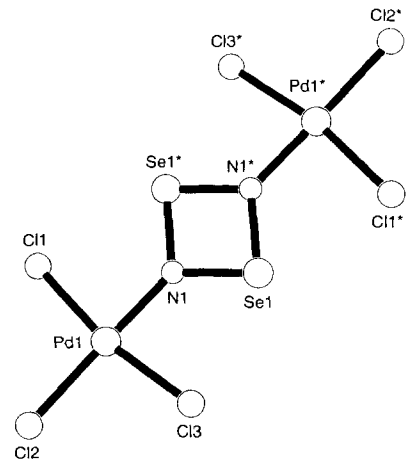

Fig. 1. X-ray structure of the $[Pd_2(Se_2N_2)Cl_6]^{2-}$ anion in **2a**. Selected distances [Å] and angles [°]: Pd1-Cl2 2.286(1), Pd1-Cl3 2.289(2), Pd1-Cl1 2.310(2), Pd1-N1 1.946(4), N1-Se1 1.779(4), N1-Se1* 1.804(5), N1-Pd1-Cl3 83.6(1), N1-Pd1-Cl1 85.6(1), Pd1-N1-Se1 130.6(3), Pd1-N1-Se1* 130.8(2), Se1*-N1-Se1 98.6(2), N1-Se1-N1* 81.4(2).

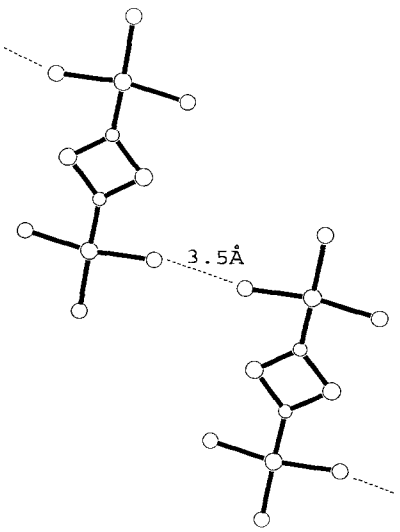

Fig. 2. The close approach of anions in the crystal packing of **2a**.

is presumably "repelled" by Cl3* into a closer approach to the nearest selenium atom. These effects at Pd1 are mirrored at Pd1*, reflecting the center of symmetry of the molecule as a whole.

The reaction gives **2a** in reasonable yield (ca. 20%) and, interestingly, this appears to be the only crystallizable product. In contrast, the analogous reaction of S_4N_4 with **1** generates a variety of species, including the S_2N_2 adduct **3** (which is

$[Pd_2(S_2N_2)Cl_6]^{2-}$ **3**

isostructural with the anion in **2a**) as well as $[Pd_2(S_3N_2)Cl_4]^{2-}$ and $[Pd(S_2N_2H)Cl_2]^-$, both of which crystallize readily.[8, 10] This implies that a different reaction mechanism applies in the two cases. We have previously suggested that for S_4N_4 this involves the initial formation of a Pd^{II}–S_4N_4 adduct, $[Pd(S_4N_4)Cl_3]^-$, which can then either react with more **1** to give **3**, or undergo a redox process leading to an unstable Pd^{IV} complex of tridentate $[S_4N_4]^{2-}$. The latter in turn decomposes to the two other isolated compounds. In the case of Se_4N_4 it may be that the latter redox process is not favorable and hence only the

[*] Dr. P. F. Kelly, A. M. Z. Slawin
Department of Chemistry
Loughborough University of Technology
GB-Loughborough LE11 3TU (UK)
Telefax: Int. code + (509) 233-163
e-mail: P. F. KELLY@LUT. AC. UK

[**] We are grateful to Johnson Matthey for loans of precious metals.

Se_2N_2 adduct is ever formed (Scheme 1). On this point, it is noteworthy that reactions that are known to generate complexes of $[S_4N_4]^{2-}$ give entirely different products with Se_4N_4.[5]

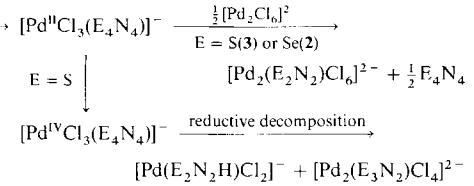

Scheme 1. Possible mechanisms for the reaction of E_4N_4 (E = S or Se) with $[Pd_2Cl_6]^{2-}$.

The reaction can be extended to $[Pd_2Cl_6]$ salts with different cations than that in **1**. Thus $[n\mathrm{Bu}_4\mathrm{N}]_2[Pd_2Cl_6]$ reacts in similar conditions to give **2b**. In this case the product may be isolated

$[n\mathrm{Bu}_4\mathrm{N}]_2[Pd_2(Se_2N_2)Cl_6]$ **2b**

as well-formed needles by cooling a CH_2Cl_2 solution for roughly 12 h. (A common feature of both salts is their surprisingly low solubility, which has caused problems in the measurement of their ^{77}Se NMR spectra.) As in the preparation of **2a**, IR spectroscopy shows the insoluble residue from the reaction to be mostly Se_4N_4.

The yield of **2b** prepared in this way (33%) is significantly higher than that of **2a**. Interestingly, when a 1:1 molar ratio of Se_4N_4 and the palladium salt are used, the yield (based upon Pd) actually increases to 53%. This is clearly a more efficient reaction; the observation fits with the mechanism in Scheme 1 insofar as the existence of only one reaction route for Se_4N_4 would allow a reaction with an overall stoichiometry of 1:1 to proceed efficiently. (For S_4N_4 the presence of the two competing routes, one of which does not result in S_4N_4 being liberated, would require a higher ratio, and we have previously shown that even at a 2:1 ratio very little S_4N_4 is left at the end of the reaction.) It is not clear, however, why the presence of an excess of Se_4N_4 should result in lower yields of **2b**.

The IR spectrum (KBr disc, Perkin-Elmer 2000R spectrometer) of **2b** is more informative than that of **2a** due to the presence of fewer strong cation vibrations. In addition to a metal–halogen stretch at 334 cm^{-1} a band at 777 cm^{-1} is observed. This is a ν(Se–N) stretch analogous to the ν(S–N) stretch seen at 877 cm^{-1} in **3**; a comparable frequency difference is observed between the bands of S_4N_4 (927, 700, 548 cm^{-1}) and Se_4N_4 (788, 570, 425 cm^{-1}).[7] In contrast to the spectrum of **3**, in which both the S–N and Pd–Cl stretches are of similar intensity, in **2b** the Se–N band is the markedly weaker of the two. A further band is seen in **3**, at 436 cm^{-1}; no analogous vibration appears in the spectrum of **2b**, although it may well be obscured by the Pd–Cl stretch.

Despite the obvious dangers associated with their preparation, it does appear that once formed, **2a** and **2b** are quite stable. This clearly bodes well for the chances of preparing free Se_2N_2, possibly by means of elimination from the adduct (as has been noted for S_2N_2 from adducts with $AlCl_3$ for example),[11] and hence $(SeN)_x$. This route may actually prove to be the best hope of making the aforementioned polymer, which has so far eluded preparation (mainly because of the involatility of Se_4N_4 and its consequent inability to mirror the vapor-phase cleavage of S_4N_4 to S_2N_2)[12].

Experimental Procedure

The salts containing the $[Pd_2Cl_6]$ anions and Se_4N_4 were prepared as reported previously. **Extreme caution** was taken with the latter since it is **severely explosive** [10,13].

2a: Solid Se_4N_4 (150 mg, 0.4 mmol) was added to a solution of **1** (222 mg, 0.2 mmol) in CH_2Cl_2 (50 mL) in a thick-walled reaction tube fitted with a Youngs greaseless joint. The mixture was stirred at room temperature under a nitrogen atmosphere. More CH_2Cl_2 was added to just below the seal of the joint, which was then closed. The tube was immersed in a preheated oil bath at 100 °C. After ca. 1 h with continuous stirring the mixture consisted of a dark solution with dark colored suspension. After cooling, the solution was filtered through celite in air and reduced in volume to 2 mL. Layering with ether followed by slow diffusion yielded a large crop of well-formed dark orange crystals of **2a**. Yield 48 mg (20%).

2b: This salt was prepared in similar manner to **2a** by the reaction of Se_4N_4 (100 mg, 0.27 mmol) with $[n\mathrm{Bu}_4\mathrm{N}]_2[Pd_2Cl_6]$ (122 mg, 0.14 mmol) in CH_2Cl_2 at 100 °C for 1.5 h. The resulting mixture was filtered and the volume reduced to ca. 10 mL in vacuo. At this point the solution was heated to redissolve any solid and then cooled at −20 °C overnight. The mass of orange needles that formed were separated from the mother liquor and redissolved in CH_2Cl_2 (50 mL). This solution was filtered through celite and the solvent then removed leaving an orange solid. Yield 44 mg; a further small amount of impure crystals was obtained by evaporation of the mother liquor; recrystallization gave a further 4 mg of pure product. Total yield 48 mg, 33% based upon Pd.

The reaction between $[n\mathrm{Bu}_4\mathrm{N}]_2[Pd_2Cl_6]$ and Se_4N_4 in a molar ratio of 1:1 was performed exactly as above, using half the amount of Se_4N_4 (50 mg, 0.135 mmol). Final yield of **2b** 78 mg (53% based upon Pd).

Received: January 9, 1995
Revised version: April 27, 1995 [Z7609IE]
German version: *Angew. Chem.* **1995**, *107*, 1903–1905

Keywords: heterocycles · nitrides · selenium compounds

[1] a) H. G. Heal, *The Inorganic Heterocyclic Chemistry of Sulphur, Nitrogen and Phosphorus*, Academic Press, **1980**; b) *Gmelin Handbook of Inorganic Chemistry; Sulfur-Nitrogen Compounds (Part 2)*, Springer, Berlin, **1985**.
[2] "The Chemistry of Inorganic Ring Systems": T. M. Klapötke, *Stud. Inorg. Chem.* **1992**, *14*, 409.
[3] E. G. Awere, J. Passmore, P. S. White, T. Klapötke, *J. Chem. Soc. Chem. Commun.* **1989**, 1415.
[4] K. Dehnicke, F. Schmock, K. F. Köhler, G. Frenking, *Angew. Chem.* **1991**, *103*, 564; *Angew. Chem. Int. Ed. Engl.* **1991**, *30*, 577.
[5] P. F. Kelly, J. D. Woollins, *Chem. Soc. Rev.*, **1992**, 245.
[6] Crystal data of **2a**: $C_{48}H_{40}Cl_6P_2N_2Se_2Pd_2$, $M_r = 1290.24$; triclinic, $a = 9.786(2)$, $b = 14.456(3)$, $c = 9.582(2)$ Å; $\alpha = 107.89(2)$, $\beta = 95.79(2)$, $\gamma = 81.72(2)$°; $V = 1274.2(5)$ Å^3, space group $P\bar{1}$ (No. 2), $Z = 1$, $\rho_{calcd} = 1.68$ g cm^{-3}, $\mu(Cu_{K\alpha}) = 110.8$ cm^{-1}. All measurements were made on a Rigaku AFC7S diffractometer with graphite-monochromated $Cu_{K\alpha}$ radiation, $\omega - 2\theta$ scan technique to a maximum 2θ value of 120.4°. An empirical absorption correction was applied, which resulted in transmission factors ranging from 0.67 to 1.00. The structure was solved by heavy-atom Patterson methods and expanded using Fourier techniques. All non-hydrogen atoms were refined anisotropically to give an R value of 0.034 for 2894 observed reflections ($I > 3\sigma(I)$). Further details of the crystal structure investigation may be obtained from the Director of the Cambridge Crystallographic Data Centre, 12 Union Road, GB-Cambridge CB2 1EZ (UK), on quoting the full journal citation.
[7] H. Folkerts, B. Neumüller, K. Dehnicke, *Z. Anorg. Allg. Chem.* **1994**, *620*, 1011.
[8] P. F. Kelly, A. M. Z. Slawin, D. J. Williams, J. D. Woollins, *Polyhedron*, **1991**, *10*, 2337.
[9] See, for example U. Thewalt, M. Burger, *Angew. Chem.* **1982**, *94*, 646; *Angew. Chem. Int. Ed. Engl.* **1982**, *21*, 634.
[10] V. C. Ginn, P. F. Kelly, A. M. Z. Slawin, D. J. Williams, J. D. Woollins, *J. Chem. Soc. Dalton Trans.* **1992**, 963.
[11] H. W. Roesky, J. Anhaus, *Chem. Ber.* **1982**, *115*, 3682.
[12] G. Wolmershäuser, G. R. Brulet, G. B. Street, *Inorg. Chem.* **1978**, *17*, 3586.
[13] J. Adel, C. Ergezinger, R. Figge, K. Dehnicke, *Z. Naturforsch. B* **1988**, *43*, 639.

Rhodium-Catalyzed Hydroformylation of Internal Alkynes to α,β-Unsaturated Aldehydes**

John R. Johnson, Gregory D. Cuny, and Stephen L. Buchwald*

The hydroformylation of alkenes has been widely studied and is an important industrial process.[1] The hydroformylation of alkynes has received relatively scant attention. The first reported alkyne hydroformylations with cobalt and rhodium catalysts resulted in the formation of saturated aldehydes.[2, 3] These can arise by hydrogenation of an initially formed unsaturated aldehyde intermediate, as observed with internal alkynes.[3, 4] Alternatively they may be produced by the hydroformylation of an alkene formed by alkyne hydrogenation, as observed with terminal alkynes.[3, 5]

Few examples of the selective hydroformylation of alkynes to yield unsaturated aldehydes have been reported. Conjugated enynes undergo hydroformylation with a rhodium catalyst to give formylbutadienes in low yields.[6] In addition, diphenylacetylene can be converted into 2,3-diphenylpropenal under hydroformylation conditions (approximately 30 atm CO/H_2, 80 °C) in low to moderate yield.[6a, e] However, attempts to generalize the reaction to include other alkynes have had minimal success.[6c] β-Alkynylamines were found to undergo rhodium-catalyzed hydroformylation to give substituted pyrroles.[7] These reactions are believed to proceed through α,β-unsaturated aldehyde intermediates.

Related carbonylation reactions of alkynes have also been reported. Hydrocarboxylation and hydrocarboalkoxylation of alkynes to give (*E*)-alkenoic acids[8] or (*E*)-alkenoate esters,[9] respectively, have been achieved with palladium catalysts. In addition, rhodium catalysts silylformylate alkynes in the presence of a trialkylsilane and CO to yield β-silyl-2-enals.[10] A high degree of regiocontrol has been obtained with terminal alkynes; disubstituted alkynes are silylformylated with moderate selectivity.[10]

A catalyst capable of the stereoselective hydroformylation of alkynes to provide the conjugated aldehyde, without producing significant amounts of either the corresponding saturated aldehyde or noncarbonylated alkene, would be useful as a method for the stereoselective synthesis of trisubstituted olefins.[11] Herein, we report our initial results utilizing the catalyst system formed from $[Rh(CO)_2(acac)]$ (acac = acetylacetonate) and **1** to effect the selective hydroformylation of alkynes to α,β-unsaturated aldehydes under mild reaction conditions.

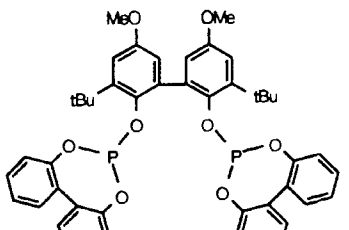

1

We recently reported that the catalyst system **1**/$[Rh(CO)_2(acac)]$ regioselectively hydroformylates α-olefin substrates that contain a variety of functional groups.[12] The reaction conditions that we employed for the hydroformylation of alkenes led to extensive hydrogenation of the enal product before conversion of the alkyne was complete. Further studies revealed that overreduction of the conjugated olefin could be suppressed if the reaction pressure was decreased to approximately 1 atm. In the presence of 2 mol% of $[Rh(CO)_2(acac)]$, 2.1 mol% of **1**, and synthesis gas (1:1 CO/H_2 mixture, 1 atm) in CH_2Cl_2 as solvent, symmetric alkynes were converted at room temperature into α,β-unsaturated aldehydes without significant formation of the saturated aldehydes (Scheme 1, Table 1). The stereochemistry

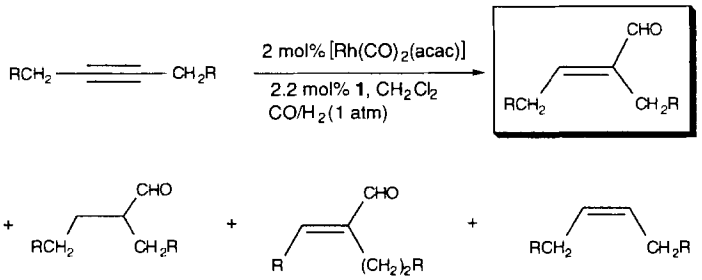

Scheme 1.

of the hydroformylation products was determined by NOE experiments to arise from the net *cis* addition of the formyl group and hydrogen.[13] The aldehyde products were obtained in good yield after Kugelrohr distillation or chromatography on silica gel.

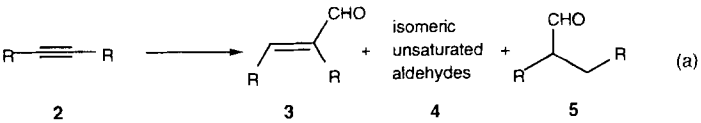

Table 1. Hydroformylation of the symmetric alkynes **2** according to Equation (a).

No.	R	Product distribution [a]		
		3	**4**	**5**
1	C_2H_5	63 (92)	(4)	(1)
2	C_3H_7	85 (96)	–	(2)
3	C_4H_9	90 (97)	(2)	(1)
4 [b]	C_5H_{11}	83 (92)	(1)	(4)
5 [c]	Ph	56 (67)	–	3 (3)
6 [d]	$CH_3OC_6H_4$	84 (86)	–	–

[a] Yield of isolated product, followed by relative percent of crude products in parentheses (uncorrected for GC response factors; numbers do not always total 100%, because small quantities of unidentified products are present). [b] 4 mol% catalyst and 4.4 mol% **1**. [c] 29% (*Z*)-stilbene formed (GC). [d] 14% (*Z*)-olefin formed (GC).

Careful monitoring of the hydroformylation of 4-octyne indicates that the saturated aldehyde can arise from the hydrogenation of the desired unsaturated aldehyde. If the reactions are allowed to continue under the standard reaction conditions for an extended period of time after complete consumption of the substrate, the saturated aldehyde increases in quantity as the amount of enal decreases and can be obtained as the major product. Diaryl-substituted alkynes, however, exhibit different behavior. In the most clear-cut case, diphenylacetylene (Table 1, Entry 5) is hydrogenated to *cis*-stilbene at a rate competitive with hydroformylation to 2,3-diphenyl-2-propenal. Upon complete consumption of the starting material, the ratio of enal to alkene was typically 3:1.[14] Allowing the reaction to continue

[*] Prof. Dr. S. L. Buchwald, Dr. J. R. Johnson, Dr. G. D. Cuny
Department of Chemistry, Massachusetts Institute of Technology
Cambridge, MA 02139 (USA)
Telefax: Int. code + (617)253-3297
e-mail: sbuchwal@mit.edu

[**] We thank Union Carbide for financial support. G.D.C. thanks the National Science Foundation for a graduate fellowship. S.L.B. acknowledges additional support as a Fellow of the Alfred P. Sloan Foundation and a Camille and Henry Dreyfus Teacher-Scholar.

results in conversion of *cis*-stilbene into 2,3-diphenylpropanal by hydroformylation and to *trans*-stilbene by isomerization. Other diaryl-substituted alkynes such as di(*p*-methoxyphenyl)-acetylene (Table 1, Entry 6) are hydrogenated to a lesser extent and correspondingly higher yields of the enal are realized.

After the development of suitable reaction conditions for the hydroformylation of symmetrical alkynes, a study of the regioselectivity of the hydroformylation of unsymmetrical alkyne substrates was undertaken (Table 2). Both steric and electronic factors appear to play a role. For example, hydroformylation of 4,4-dimethyl-2-pentyne (Table 2, Entry 5) gave approximately a 5:1 ratio of enal products, in which the major regioisomer arose from the intermediacy of the less hindered vinylrhodium isomer. In contrast, hydroformylation of 1-phenyl-1-propyne (Table 2, Entry 1) gave a 2.5:1 mixture of 2-phenyl-2-butenal and 2-methyl-3-phenyl-2-propenal; the major product stems from the

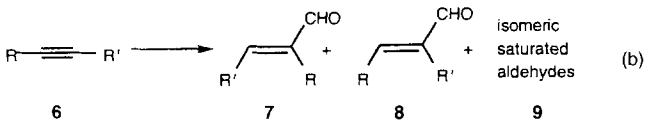

6 7 8 9

Table 2. Hydroformylation of the unsymmetric alkynes **6** according to Equation (b).

No.	R	R'	Product distribution [a] 7	8	9
1	Ph	Me	51 (65)	(26)	(4)
2 [b]	Ph	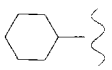	64 (69)	(18)	(5)
3	Ph	*t*Bu	46 (74)	(14)	
4 [b]	Me	nC_5H_{11}	83 [c]		(2)
5 [d]	Me	*t*Bu	56 (67)	(13)	(11)

[a] See footnote [a] of Table 1. [b] 3 mol% $[Rh(CO)_2(acac)]$ and 3.3 mol% **1**. [c] Yield of isolated products from the purified mixture containing the α,β-unsaturated aldehyde regioisomers in a 1.3:1 ratio. [d] 4 mol% $[Rh(CO)_2(acac)]$ and 4.4 mol% **1**.

more hindered alkylrhodium isomer.[15] This example also demonstrates that competitive hydrogenation does not occur to a significant extent when at least one alkyne substituent is an alkyl group. Hydroformylation of 2-octyne led to approximately a 1:1 mixture of 2-methyl-2-octenal and 2-pentyl-2-butenal, which points to little differentiation between the methyl and the *n*-pentyl group.

In conclusion, we have shown that the catalyst system generated from $[Rh(CO)_2(acac)]$ and **1** is the first selective, reasonably general catalyst for the hydroformylation of internal alkynes to α,β-unsaturated aldehydes. With further research to optimize the regioselectivity with unsymmetrical alkyne substrates, this method should prove useful for the stereoselective synthesis of trisubstituted olefins.

Received: February 27, 1995 [Z 7743 IE]
German version: *Angew. Chem.* **1995**, *107*, 1877–1879

Keywords: alkenes · alkynes · catalysis · hydroformylation · rhodium compounds

[1] a) J. K. Stille in *Comprehensive Organic Synthesis, Vol. 4* (Eds.: B. M. Trost, E. I. Fleming), Pergamon, Oxford, **1991**, p. 913; b) G. W. Parshall, S. D. Ittel, *Homogeneous Catalysis*, 2nd ed., Wiley-Interscience, New York, **1992**, pp. 106–111.

[2] a) I. Tkatchenko in *Comprehensive Organometallic Chemistry, Vol. 8* (Eds.: G. Wilkinson, F. G. A. Stone, E. W. Abel), Pergamon, Oxford, **1982**, p. 115–157; b) B. Cornils in *New Syntheses with Carbon Monoxide* (Ed.: J. Falbe), Springer, New York, **1980**, pp. 1–181.

[3] B. Fell, M. Beutler, *Erdöl, Kohle, Erdgas, Petrochem.* **1976**, *29*, 149–153.

[4] a) B. Fell, M. Beutler, *Tetrahedron Lett.* **1972**, 3455–3456; b) C. Botteghi, C. Salomon, *ibid.* **1974**, 4285.

[5] a) H. Greenfield, J. H. Wotiz, I. Wender, *J. Org. Chem.* **1957**, *22*, 542; b) P. G. M. Wuts, A. R. Ritter, *ibid.* **1989**, *54*, 5180–5182.

[6] a) K. Doyama, J. Takashi, S. Takahashi, *Tetrahedron Lett.* **1986**, *27*, 4497–4500; b) K. Doyama, J. Takashi, T. Shiohara, S. Takahashi, *Bull. Chem. Soc. Jpn.* **1988**, *61*, 4353–4360; c) E. M. Campi, W. R. Jackson, *Aust. J. Chem.* **1989**, *42*, 471–478.

[7] E. M. Campi, W. R. O. Jackson, Y. Nilsson, *Tetrahedron Lett.* **1991**, *32*, 1093–1094.

[8] D. Zargarian, H. Alper, *Organometallics* **1993**, *12*, 712–724, and references therein.

[9] a) J. F. Knifton, *J. Mol. Catal.* **1977**, *2*, 293–299; b) H. Alper, B. Despeyroux, J. B. Woell, *Tetrahedron Lett.* **1983**, *24*, 5691–5694.

[10] a) I. Matsuda, A. Ogiso, S. Sato, Y. Izumi, *J. Am. Chem. Soc.* **1989**, *111*, 2333–2334; b) I. Ojima, P. Ingallina, R. J. Donovan, N. Clos, *Organometallics* **1991**, *10*, 38–41; c) M. P. Doyle, M. S. Shanklin, *ibid.* **1993**, *12*, 11–12, and references therein.

[11] Leading references: S. F. Martin, D. Daniel, R. J. Cherney, S. Liras, *J. Org. Chem.* **1992**, *57*, 2523–2525.

[12] G. D. Cuny, S. L. Buchwald, *J. Am. Chem. Soc.* **1993**, *115*, 2066–2068.

[13] a) A difference NOE experiment was performed on the hydroformylation product of 3-hexyne (Table 1, Entry 1). b) Little or none of the *Z* isomers was detected in the crude reaction mixtures by ^1H NMR spectroscopy. c) A. Stefani, G. Consiglio, C. Botteghi, P. Pino, *J. Am. Chem. Soc.* **1977**, *99*, 1058–1063.

[14] 2,3-Diphenyl-2-propenal, the initial product, was not hydrogenated under the reaction conditions.

[15] The regiochemistry is similar to that observed in the hydroformylation of styrene: R. Lazzaroni, A. Raffaelli, R. Settambolo, S. Bertozzi, G. Vitulli, *J. Mol. Catal.* **1989**, *50*, 1, and references therein.

$(Sr_6N)[Ga_5]$ and $(Ba_6N)[Ga_5]$: Compounds with Discrete (M_6N) Octahedra and $[Ga_5]$ Clusters**

Gerhard Cordier, Matthias Ludwig, Dagmar Stahl, Peter C. Schmidt, and Rüdiger Kniep*

The majority of intermetallic ternary compounds comprising an alkaline earth metal, an earth metal, and an element of Group 15 are electrovalent and contain complex anions (e.g. $Ca_3[AlSb_3]$[1]). Also nitrogen, as the lightest element of the Group 15 elements, participates as a ligand in the formation of covalent anionic structures (e.g. $Sr_3[Al_2N_4]$[2]). At the same time, however, the nitrido nitrogen tends to occupy—as isolated (ionic) species—the centers of coordination polyhedra formed exclusively by alkaline earth metal cations. Such structural elements with an overall positive charge form (M_6N) octahedra (M = alkaline earth metal cations) as found recently in a series of nitride compounds: Isolated (M_6N) octahedra exist in the crystal structure of $Na_{16}Ba_6N$;[3] the crystal structure of $NaBa_3N$[4] contains one-dimensional columns (Ba_3N) of face-sharing (Ba_6N) octahedra. Layer structures result by edge-sharing $((Ca_3N)_2[GaN_3]$[5]) or corner-sharing $((Ca_4N)[In_2]$[6]) of (Ca_6N) octahedra. Three-dimensional frameworks are generated by condensation of (Ca_6N) octahedra through common corners $((Ca_3N)[Au]$[7]) or common corners and edges $(Ca_{18.5}Ga_8N_7$[8]).

[*] Prof. Dr. R. Kniep, Dr. G. Cordier, Dipl.-Ing. M. Ludwig, Dr. D. Stahl
Eduard-Zintl-Institut der Technischen Hochschule
Hochschulstrasse 10, D-64289 Darmstadt (Germany)
Telefax: Int. code + (6151)166029
Prof. Dr. P. C. Schmidt
Institut für Physikalische Chemie, TH-Darmstadt (Germany)

[**] This work was supported by the Deutsche Forschungsgemeinschaft, the Fonds der Chemischen Industrie, and the Vereinigung von Freunden der TH Darmstadt.

Cationic partial structures in nitrido compounds with alkaline earth metals can thus be varied in terms of size and volume over a wide range. This is surely one of the reasons why rather uncommon anions such as trigonal-planar $[GaN_3]^{6-}$ units ($(Ca_3N)_2[GaN_3]$[5]), helical $^1_\infty[NiN_{2/2}]$ polyanions ($Ba_2\{(Ba_6N)[NiN]_6\}$[9]), and auride ions ($(Ca_3N)[Au]$[7]) can be stabilized in the solid state.

With a view to gaining further insight into this situation, we decided to investigate the formation of compounds in the ternary systems alkaline earth metal – gallium – nitrogen. These systems are particularly attractive because of the well-known tendency of gallium to form homonuclear bonds, for example, tetrahedral Ga_4 clusters ($Ca_{18.5}Ga_8N_7$[8]), planar zigzag chains ($Ca_5[Ga_2N_4]$[10]), or even layers of tetragonal pyramids (Ca[GaN][11]). We report here the first ternary phases with the higher homologues of calcium. The isotypic compounds $(Sr_6N)[Ga_5]$ and $(Ba_6N)[Ga_5]$ contain isolated octahedral cations $(M_6N)^{9+}$ and trigonal-bipyramidal anions $[Ga_5]^{7-}$. The ionic isles $(M_6N)^{9+}$ together with the homonuclear clusters $[Ga_5]^{7-}$ form the motif of a rock-salt structure.

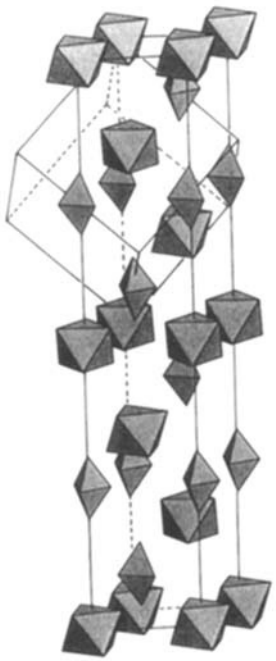

Fig. 1. Crystal structure of $(Sr_6N)[Ga_5]$ and $(Ba_6N)[Ga_5]$: Hexagonal and pseudocubic unit cell. Octahedra: $(Sr_6N)^{9+}$, trigonal bipyramids: $[Ga_5]^{7-}$.

For the preparation of $(Sr_6N)[Ga_5]$ and $(Ba_6N)[Ga_5]$, the metals were initially added together and heated to about 1000 °C and then subsequently treated with nitrogen.[12] The crystal structure of the isotypic phases[13] is shown in Figure 1. The Sr–N (Ba–N) distances in the isolated octahedra (M_6N) are 260.3(1) (273.4(1) pm). Comparable Ba–N distances were observed in the subnitrides $NaBa_3N$ (273 pm; strings of face-sharing (NBa_6) octahedra[4]) and $Na_{16}Ba_6N$ (283 pm; isolated (NBa_6) octahedra[3]). The (M_6N) octahedra in the crystal structures of $(Sr_6N)[Ga_5]$ and $(Ba_6N)[Ga_5]$ are arranged in the form of a cubic closest packing, with Ga_5 clusters (trigonal bipyramids) occupying the octahedral holes. The Ga–Ga distances of 272.5(3) and 273.6(3) pm for the strontium compound and 272.5(3) and 272.5(3) pm for the barium compound correspond to the bond lengths in elemental gallium (271 pm[14]). The trigonal axes of the Ga_5 bipyramids are aligned parallel to the c axis. A pseudo-cubic cell is outlined in Figure 1.

The Sr–Ga distances (328.7(2)–349.4(1) pm) and the Ba–Ga distances (346.4(2)–367.1(3) pm) are comparable to those found in the intermetallic phases Sr_8Ga_7[15] (325–359 pm), Ba_8Ga_7[15] (340–368 pm), and Ba_5Ga_6[16] (332–359 pm). The shortest Sr–Sr and Ba–Ba distances (octahedral edges) (362.8(2) pm and 378.6(2) pm, respectively) are clearly shorter than the bond lengths in the elements (425 pm and 434 pm, respectively[17]).

According to the results of the crystal structure determination, the bonding in $(Sr_6N)[Ga_5]$ and $(Ba_6N)[Ga_5]$ can be described by the following simple picture: the nitride ions (N^{3-}) octahedrally surrounded by six alkaline earth metal ions (M^{2+}) form positively charged units $(M_6N)^{9+}$, whose charge is compensated at least partly by the negatively charged Ga_5 clusters. If the Ga_5 cluster is considered as a Zintl anion, there are two three-coordinate (axial) Ga atoms ($\triangleq Ga^{2-}$) and three four-coordinate (equatorial) Ga atoms ($\triangleq Ga^{-}$), resulting in a total charge of $[Ga_5]^{7-}$. According to Wade, the homonuclear 22-electron system can be described as a *closo* cluster $[Ga_5]^{7-}$ with $2n + 2 = 12$ electrons in the skeleton. This situation is similar to that already known for the isoelectronic species $[Sn_5]^{2-}$[18], $[Bi_5]^{3+}$,[18] and $[Tl_5]^{7-}$.[19] For the title compounds this results in the formula $\{(M_6N)^{9+}[Ga_5]^{7-} \cdot 2e^-\}$, as a simple model of the chemical bonding; the charge is balanced by two electrons in metallic states.

For a more detailed characterization of the chemical bonding, band structure calculations for the strontium compound were carried out according to the standard ASW[20] technique (ASW = augmented spherical wave). From the total density of states ($N(E)$), metallic character ($N(E_F) \neq 0$) can be derived, as shown in Figure 2. The partial density of states of Sr (Fig. 2)

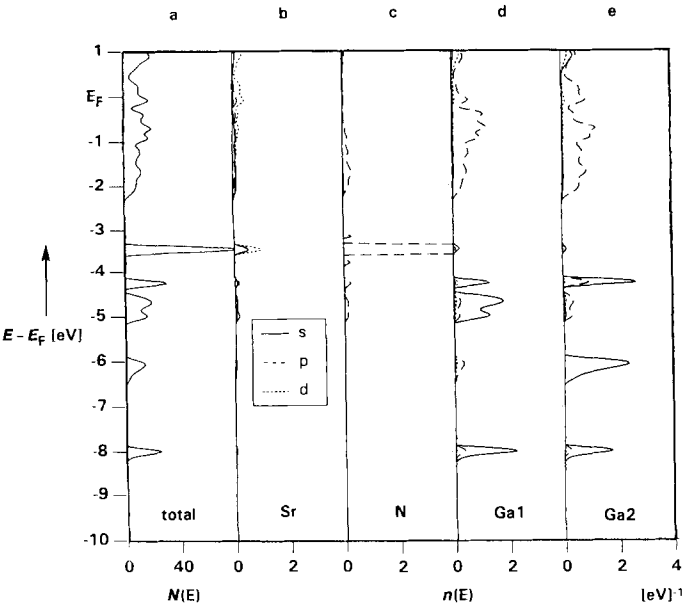

Fig. 2. Density of states (total (a) and partial (b–e)) of $(Sr_6N)[Ga_5]$ vs. energy [eV] of the valence states (calculation by ASW technique).

shows only scattering contributions below the Fermi energy corresponding to an Sr^{2+} ion.[21] The partial density of states of the nitrogen atoms exhibits a large 2p-like contribution at -3 eV. The integral of these states yields six electrons per N atom, therefore indicating that a N^{3-} species results (the 2s states of nitrogen are not shown in Fig. 2). The 2p states of the nitride ions overlap at approximately -3 eV with the scattering contributions of strontium (Sr^{2+}) and thus reflect the cationic $(Sr_6N)^{9+}$ units derived from the crystal structure determination. All further states below the minimum at -0.35 eV can be assigned to the partial density of states of the Ga atoms (Fig. 2, d and e). The integral of these states below -0.35 eV results in 22 electrons per formula unit and thus corresponds to the anionic cluster $[Ga_5]^{7-}$ already discussed. The states of two conduction electrons remain from the minimum at -0.35 eV up to the Fermi energy. The band structure of the p-like states of gallium in the range -2 eV up to E_F shows a dispersion, which is possibly consistent with a delocalization of these states over the $[Ga_5]^{7-}$ clusters and slightly over the Sr atoms. Crystal orbital

overlap population (COOP) analyses[22] of these states indicate delocalized bonds within the homonuclear clusters and only weak overlap between gallium and strontium. A direct bond between the $[Ga_5]^{7-}$ clusters can be ruled out because of the large distances ($d(Ga\cdots Ga \geq 493$ pm).

In recent work Hoffmann and Liu[23] discussed the question of whether the intermetallic phase Ba_5Ga_6[16] might not actually be a hydride "$Ba_5Ga_6H_2$". Therefore with respect to the compounds presented here, the formula "$(M_6N)[Ga_5][H_2]$" comes into contention. However, experimental indications of a hydride are certainly not evident. Suitable regions for the uptake of hydrogen would be available in the appropriate number with the relatively large trigonal-prismatic holes formed along [001] from the corners of the isolated (Sr_6N) octahedra. ($Sr\cdots Sr > 372$ pm; tetrahedral holes of the closest (Sr_6N) packing). To evaluate the possibility whether these tetrahedral holes are occupied by hydrogen atoms, we have estimated the enthalpy of formation $\Delta H(\Delta H = E((Sr_6N)[Ga_5][H_2]) - E((Sr_6N)[Ga_5]) - E[H_2])$ by calculating the total ASW energy E of the compounds $(Sr_6N)[Ga_5][H_2]$ and $(Sr_6N)[Ga_5]$ and taking the energy $E(H_2)$ of the H_2 molecule from the literature.[24, 25] These calculations gave a value of ΔH of -0.03 eV per unit cell. Since, in general an ASW calculation[26] overestimates the bonding energy, we conclude that ΔH_{exp} lies above -0.03 eV and that a reaction with hydrogen should be endothermic.

Received: March 24, 1995 [Z 7828 IE]
German version: *Angew. Chem.* **1995**, *107*, 1879–1881

Keywords: clusters · gallium compounds · nitrogen compounds · solid-state structures

[1] G. Cordier, H. Schäfer, M. Stelter, *Z. Naturforsch. B* **1984**, *39*, 727.
[2] W. Blase, G. Cordier, M. Ludwig, R. Kniep, *Z. Naturforsch. B* **1994**, *49*, 501.
[3] G. J. Snyder, A. Simon, *Angew. Chem.* **1994**, *106*, 713; *Angew. Chem. Int. Ed. Engl.* **1994**, *33*, 689.
[4] P. E. Rauch, A. Simon, *Angew. Chem.* **1992**, *104*, 1505; *Angew. Chem. Int. Ed. Engl.* **1992**, *31*, 1519.
[5] G. Cordier, P. Höhn, R. Kniep, A. Rabenau, *Z. Anorg. Allg. Chem.* **1990**, *591*, 58.
[6] G. Cordier, S. Rönninger, *Z. Naturforsch. B* **1987**, *42*, 825.
[7] J. Jäger, D. Stahl, P. C. Schmidt, R. Kniep, *Angew. Chem.* **1993**, *105*, 738; *Angew. Chem. Int. Ed. Engl.* **1993**, 709.
[8] G. Cordier, S. Rönninger, *Z. Kristallogr.* **1988**, *Suppl. 27. AGKr/DMG-Tagg.* 60.
[9] A. Gudat, W. Milius, S. Haag, R. Kniep, A. Rabenau, *J. Less-Common Met.* **1991**, *168*, 305.
[10] G. Cordier, *Z. Naturforsch. B* **1988**, *43*, 1253.
[11] P. Verdier, P. L'Haridon, M. Maunaye, R. Marchand, *Acta Crystallogr. Sect. B* **1974**, *30*, 226.
[12] Preparation of $(Sr_6N)[Ga_5]$ and $(Ba_6N)[Ga_5]$: Sr and Ga (molar ratio 8:1; total weight 5 g) were heated in a sintered corundum crucible under an argon atmosphere to 1100 °C, cooled to room temperature, ground in inert gas atmosphere, and finally allowed to react with nitrogen at 1050 °C in a corundum crucible (stationary nitrogen atmosphere, 1 atm) and cooled to room temperature within 10 h. The barium compound was obtained by heating Ba and Ga (molar ratio 5:1) to 1000 °C in a corundum crucible, followed by reaction of the powdered product with nitrogen at 1100 °C. After a reaction period of 30 min, the melt was quickly cooled by removing the reaction tube from the oven. According to X-ray powder investigations, both compounds, are the main crystalline products, other phases obtained in addition have not been identified. Single crystals have a dark metallic luster and are brittle.
[13] Crystallographic data of $(Sr_6N)[Ga_5]$ and $((Ba_6N)[Ga_5])$: $R\bar{3}c$; $Z = 6$; $a = 758.0(3)$ pm (790.5(3) pm), $c = 4041.3(1)$ pm (4196.5(7)) pm; $\rho_{calcd} = 4.40$ (5.21) g cm^{-3}. PW-1100 four-circle diffractometer, graphite monochromator, scintillation counter, $Mo_{K\alpha}$, $5° \leq 2\theta \leq 50°$, $\theta/2\theta$ scan. Solution/refinement: SHELXS-86/SHELX-93; direct methods; full-matrix least-squares refinement; 20 variables. $R_1 = 0.0674$ (0.0570); wR_2(aniso) = 0.157 (0.133) for $N_{hkl} = 660$ (680). Further details of the crystal structure investigation may be obtained from the Fachinformationszentrum Karlsruhe, D-76344 Eggenstein-Leopoldshafen (Germany), on quoting the depository number CSD-59104.
[14] J. Donohue, *The Structures of the Elements*, Wiley, London, **1972**.
[15] M. L. Fornasini, *Acta Crystallogr. Sect. C* **1983**, *39*, 943.
[16] M. L. Fornasini, M. J. Pani, *J. Alloys Compds.* **1994**, *205*, 179.
[17] W. B. Pearson, *Handbook of Lattice Spacings and Structures of Metals and Alloys*, Vol. 2, Pergamon Press, London **1967**.
[18] H. G. von Schnering, *Angew. Chem.* **1981**, *93*, 44; *Angew. Chem. Int. Ed. Engl.* **1981**, *20*, 681.
[19] Z. Dong, J. D. Corbett, *J. Am. Chem. Soc.* **1994**, *116*, 3429.
[20] A. R. Williams, J. Kübler, C. D. Gelatt, jr., *Phys. Rev. B* **1978**, *19*, 604. The atomic radii employed in this work are: $r_{Sr} = 187$ pm, $r_N = 155$ pm, $r_{Ga} = 177$ pm, $r_{empty\ sphere} = 317$ pm (on 12 c, $z = 0.4168$).
[21] P. C. Schmidt, D. Stahl, B. Eisenmann, R. Kniep, V. Eyert, J. Kübler, *J. Solid State Chem.* **1992**, *97*, 93.
[22] R. Hoffmann, *Angew. Chem.* **1987**, *99*, 871; *Angew. Chem. Int. Ed. Engl.* **1987**, *26*, 846.
[23] Q. Liu, R. Hoffmann, *J. Phys. Chem.* **1994**, *98*, 9360.
[24] $E(H_2)$ is equal to the sum of the total energy of two spin polarized H atoms, the bond energy of one H_2, and the zero-point oscillation energy (O. Gunnarson, B. I. Lundqvist, *Phys. Rev. B* **1976**, *13*, 4274).
[25] J. F. Janak, *Phys. Rev.* **1974**, *9*, 3985.
[26] V. L. Moruzzi, J. F. Janak, A. R. Williams, *Calculated Electronic Properties of Metals*, Pergamon Press, New York, **1978**.

Solid-Phase Synthesis of Vinylogous Sulfonyl Peptides**

Cesare Gennari,* H. Peter Nestler, Barbara Salom, and W. Clark Still

The construction of synthetic combinatorial libraries with a focus on the incorporation of pharmacophore units is currently of great interest.[1] Combinatorial libraries on solid supports have helped elucidate subtle biasing of intermolecular interactions and have opened the way to new lead structures for drugs. Among the most interesting structures for clinical and biological purposes are peptides along with their analogues and isosteres.[2] Phosphoryl peptides (phosphonamidates and phosphonates) are intensively studied analogues and have been recognized as transition state mimics of peptide hydrolysis.[1b, 3] Although sulfonamides feature the same tetrahedral structure of the amide group as their phosphorus counterparts, their potential has not yet been investigated as thoroughly. Nevertheless, sulfonamides might also be interesting pharmacophores for protease inhibition.[4] Furthermore the stronger polarization of the sulfonamide bond compared to the regular peptide bond favors the formation of hydrogen bonds and leads to a more distinct preorganization of the sulfonyl peptides, which makes them interesting objects for studies of noncovalent molecular interactions.[5, 6]

Because the problem of determining the structures of the compounds in combinatorial libraries has been solved by encoding procedures,[7] the greatest current challenge is the development of techniques for organic synthesis on solid supports. In

[*] Prof. Dr. C. Gennari, B. Salom
Dipartimento di Chimica Organica e Industriale
Università di Milano
Centro CNR per lo Studio delle Sostanze Organiche Naturali
via G. Venezian 21, I-20133 Milano (Italy)
Telefax: Int. code + (2)236-4369
e-mail: Cesare@iumchx.chimorg.unimi.it
Dr. H. P. Nestler
Cold Spring Harbor Laboratory (USA)
Prof. Dr. W. C. Still
Department of Chemistry, Columbia University (USA)

[**] We thank NATO for a Collaborative Research Grant (NATO 921422) to C. G. and W. C. S. We acknowledge the support of the U. S. National Institutes of Health (grant HL25634 to W. C. S.) and the Fonds der Chemischen Industrie (Liebig fellowship to H. P. N.).

this communication we report a method for the solid-phase synthesis of vinylogous sulfonyl peptides that is compatible with peptide synthesis using Boc chemistry (Boc = *tert*-butoxycarbonyl). This method enables the construction of combinatorial libraries containing vinylogous sulfonyl peptides and thus represents an important advance in the development of synthetic combinatorial libraries—the incorporation of pharmacophore units within natural and unnatural oligomers.[1] The first solution synthesis of vinylogous sulfonyl peptides, which is based on the same strategy, was described recently.[5] Five glycine-derived sulfonyl peptides **3a–e** were prepared starting from Boc-glycine PEG-resin **1**[8] (PEG = poly(ethylene glycol)) and the sulfonyl chlorides **2a–e** (Boc-vsAA-Cl).[9] We cleaved the coupling products from the resin by methanolysis and obtained the sulfonyl peptide methyl esters **4a–e** in good yields (Scheme 1).

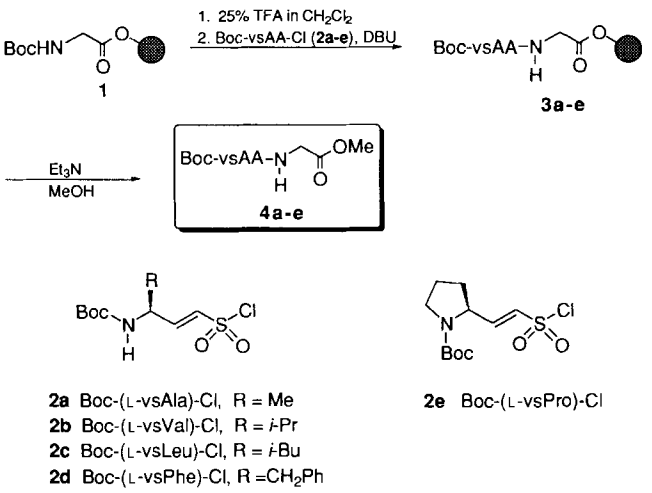

Scheme 1. Sulfonyl monopeptides synthesized on a solid support. See text for abbreviations.

Our synthesis of the sulfonyl peptides follows an adapted Boc-protection strategy. The Boc group was removed by treating the resin with 25% TFA (TFA = trifluoroacetic acid) in CH_2Cl_2 for 30 min, and the resulting ammonium salts were neutralized by washing with 2.5% DBU (DBU = 1,8-diazabicyclo[5.4.0]undec-7-ene) in CH_2Cl_2 three times. After one equivalent of the sulfonyl chloride **2** was added, DBU was added in small portions at a rate of about 1.5 equivalents per hour until no more sulfonyl chloride was present in solution. The resin was washed five times with CH_2Cl_2, and the coupling was repeated three times to achieve complete conversion of the amines on the support. Finally, any unreacted amino groups were capped by treatment with acetic anhydride.

The sulfonyl peptides were cleaved by treatment of the resin with 10% Et_3N in MeOH to yield the corresponding methyl esters **4a–e** in 60–70% yield after purification by preparative TLC. The degree of conversion was determined from the ratio of the intensities of the ^1H NMR signals of the Boc group of the sulfonyl peptide ($\delta \approx 1.45$) and the acetyl group of acetyl glycine methyl ester ($\delta \approx 2.06$) in the crude cleavage mixture. After the four coupling cycles described above the conversion was greater than 95%. The acetyl glycine methyl ester used in these studies was prepared in 67% yield by deprotection of resin **1**, acetylation with acetic anhydride, methanolysis, and TLC purification.

In our studies of the synthesis of the vinylogous sulfonyl peptides in solution we found that excess DBU leads to decomposition of the sulfonyl chlorides, but also that DBU crucial to the coupling.[5] Nevertheless, we tried several methods for catalysis of the the solid-phase coupling. The addition of one or more equivalents of DBU at the beginning of the coupling favored the decomposition of the sulfonyl chloride over the coupling to the resin. When, in analogy to the protocol for the solution synthesis, we added several equivalents of sulfonyl chloride stepwise in one coupling cycle without removing the soluble byproducts and with stepwise neutralization with DBU, only partial conversion of the amino groups was achieved; the products of the sulfonyl chloride decomposition apparently prevented completion of the coupling reaction. This phenomenon was also observed when we used slightly impure sulfonyl chlorides: although all of the sulfonyl chloride was consumed, the amino group had not reacted. The replacement of DBU by 2,6-lutidine, *N*-methylimidazole, or triethylamine was not successful either. Although 2,6-lutidine gave good coupling yields for the reaction of Boc-vsAla-Cl **2a** with glycyl-polystyrene resin, the attempt to synthesize the sulfonyl dipeptide Boc-(L-vsAla)-(L-vsAla)-Gly-OMe **5** resulted in a complex mixture of products. Our studies also revealed that the PEG-resin is much more suitable for the synthesis of the sulfonyl peptides than the regular polystyrene support often used in solid-phase peptide synthesis.[8]

During our studies we encountered an unexpected problem in monitoring the coupling reaction. Neither the traditional Kaiser ninhydrin test[10] nor the use of bromophenol blue as a simple acid–base indicator[11] were suitable to test for the presence of free amines on the support. The coupling reaction apparently yields small amounts of amino compounds that evoke positive amine assays even after virtually complete conversion of the amines. Nevertheless we found bromophenol blue very helpful for the in situ monitoring of the consumption of the sulfonyl chlorides during the addition of DBU. As long as DBU is not in excess, the solution is yellow, and on neutralization the solution turns green. After a while a further color change to blue indicates the complete consumption of sulfonyl chloride, thus offering a convenient way for monitoring the coupling of vinylogous sulfonyl peptides during the synthesis of a combinatorial library.

After having established the conditions for the synthesis of the monopeptides, we prepared two sulfonyl dipeptides to show the applicability of the method described here for the synthesis of oligomers (Scheme 2).

Both products were obtained in satisfactory yield (57% for **5**, 52% for **6**). The synthesis of **5** proved that the coupling on the solid support occurs, like its solution counterpart, without loss of stereochemical integrity; only one diastereomer of **5** could be detected in the crude cleavage product. In the synthesis of **6** we were especially interested in the special properties of the secondary amine of proline. We could show that this amino group

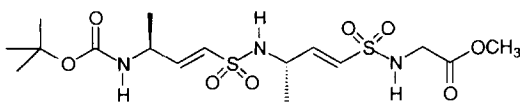

Boc-(L-vsAla)-(L-vsAla)-Gly-OMe **5**

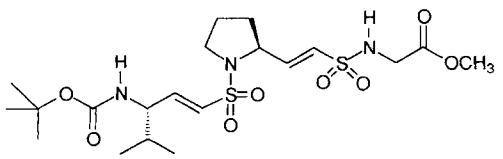

Boc-(L-vsVal)-(L-vsPro)-Gly-OMe **6**

Scheme 2. Sulfonyl dipeptides synthesized on a solid support.

does not affect the coupling with sulfonyl chlorides. Neither the reactivity on solid support nor in solution was distinctively altered compared to those of primary amino functionalities of other amino acids.

This method for coupling vinylogous sulfonyl peptides on solid supports should allow the incorporation of these peptide analogues into combinatorial libraries. Currently we are exploring the scope and limitations of this method as well as expanding the monomer basis set to include functionalized side chains (e.g. vs-Ser, vs-Gln, vs-Lys). In addition we are engaged in constructing receptors composed of vinylogous sulfonyl peptides and screening them for their affinity towards combinatorial libraries of peptides.[6]

Experimental Procedure

6: 600 mg of Boc-Gly-OPEG-resin **1** was deprotected by treatment with 10 mL of 25% TFA in CH_2Cl_2 for 30 min. After the resin was washed with CH_2Cl_2 (5 × 10 mL), the TFA salt was neutralized by washing the resin with 2.5% DBU in CH_2Cl_2 (3 × 10 mL). Excess DBU was removed by washing with CH_2Cl_2 (3 × 10 mL). Three drops of a solution of 1% bromophenol blue in dimethylacetamide (DMA) were added to monitor the reaction. The resin was then subjected to four coupling cycles. Each coupling cycle consisted of the addition of 2 mg of 4-dimethylaminopyridine (DMAP) and 40 mg of **2e** in 5 mL of CH_2Cl_2 followed by the addition of 0.4 mL of 2.5% DBU in CH_2Cl_2 every 10 min, until the reaction mixture was basic (intense blue color of bromophenol blue). (For the first cycle a total of 2 equiv DBU was necessary, but the amount of DBU had to be increased in every cycle (up to 4 equiv).) The reaction mixture was agitated for another 30 min and then washed with CH_2Cl_2 (5 × 10 mL). After the last coupling cycle the resin was treated for 1 h with 0.5 mL of Ac_2O in 10 mL of CH_2Cl_2 and washed with CH_2Cl_2 (5 × 10 mL), DMF (3 × 10 mL), and CH_2Cl_2 (3 × 10 mL) to yield **3e**. 300 mg of the resin was washed with MeOH (5 × 10 mL) and transferred into a 10 mL round-bottom flask equipped with a magnetic stirrer and treated overnight with 5 mL of 10% Et_3N in anhydrous MeOH. The suspension was filtered, and the filtrate concentrated under reduced pressure. According to the ^1H NMR spectrum, the crude residue contained less than 5% acetyl glycine methyl ester. Purification by preparative TLC (silica gel, hexanes/ethyl acetate 1:1) yielded 18 mg (75%) of **4e**. ^1H NMR (400 MHz, $CDCl_3$, 25 °C, TMS): δ = 1.44 (9H, s), 1.78 (1H, m), 1.88 (2H, m), 2.10 (1H, m), 3.35–3.47 (2H, m), 3.78 (3H, s), 3.82 (2H, s), 4.45 (1H, br. s), 4.96 (1H, br. s), 6.21 (1H, d, ^3J(H,H) = 15.0 Hz), 6.65 (1H, dd, ^3J(H,H) = 15.0, ^3J(H,H) = 5.7 Hz); ^{13}C NMR (75.4 MHz, $CDCl_3$): δ = 23.546 (CH_2), 28.354 (CH_3), 30.912 (CH_2), 43.844 (NCH_2), 46.513 (CH_2N), 52.550 (OCH_3), 57.012 (CHN), 127.443 (=CH), 145.714 (=CH), 158.848 (C=O), 169.638 (C=O). High-resolution MS calcd. for $C_{14}H_{25}N_2O_6S$ (M + H): m/z: 349.1433; found: 349.1441. The remaining resin **3e** was deprotected and reacted with **2b** (21 mg in each cycle) as described above. Acetylation and release from the resin according to the aforementioned protocol yielded **6** in ca. 90% purity (^1H NMR). Purification by preparative TLC (silica gel, hexanes/ethyl acetate 2:1) yielded 18 mg (52%) of **6**. ^1H NMR (400 MHz, $CDCl_3$, 25 °C, TMS): δ = 0.95 (3H, d, ^3J(H,H) = 6.7 Hz), 0.96 (3H, d, ^3J(H,H) = 6.7 Hz), 1.44 (9H, s), 1.75–2.00 (4H, m), 2.00–2.20 (1H, m), 3.25–3.50 (2H, m), 3.76 (3H, s), 3.87 (2H, d, ^3J(H,H) = 5.5 Hz), 4.13 (1H, m), 4.28 (1H, m), 4.75 (1H, d, ^3J(H,H) = 8.2 Hz), 5.44 (1H, t, ^3J(H,H) = 5.5 Hz), 6.27 (1H, d, ^3J(H,H) = 15.1 Hz), 6.46 (1H, d, ^3J(H,H) = 15.0 Hz), 6.65 (2H, dd, ^3J(H,H) = 15.0, ^3J(H,H) = 5.5 Hz); ^{13}C NMR (75.4 MHz, $CDCl_3$): δ = 18.178 (CH_3), 18.769 (CH_3), 23.927 (CH_3), 28.173 (CH_3), 31.549 (CH), 31.858 (CH_2), 43.835 (NCH_2), 48.712 (NCH_2), 52.579 (OCH_3), 56.695 (CHN), 59.157 (CHN), 124.999 (=CH), 128.911 (=CH), 144.349 (=CH), 145.616 (=CH). High-resolution MS calcd. for $C_{20}H_{36}N_3O_8S$ (M + H): m/z 510.1944; found: 510.1956. The data are in agreement with the data obtained from material that was synthesized in solution.

Received: March 24, 1995 [Z 7826 IE]
German version: *Angew. Chem.* **1995**, *107*, 1892–1893

Keywords: combinatorial chemistry · peptides · solid-phase synthesis · sulfonamides

[1] a) For recent reviews see M. A. Gallop, R. W. Barrett, W. J. Dower, S. P. A. Fodor, E. M. Gordon, *J. Med. Chem.* **1994**, *37*, 1233–1251, *ibid.* **1994**, *37*, 1385–1401; b) D. A. Campbell, J. C. Bermak, *J. Am. Chem. Soc.* **1994**, *116*, 6039–6040.

[2] A. Giannis, T. Kolter, *Angew. Chem.* **1993**, *105*, 1303–1326; *Angew. Chem. Int. Ed. Engl.* **1993**, *32*, 1244–1267; J. Gante, *ibid.* **1994**, *106*, 1780–1802 and **1994**, *33*, 1699–1720.

[3] K. Teraishi, M. Saito, I. Fujii, H. Nakamura, *Tetrahedron Lett.* **1992**, *33*, 7153–7156; D. Maffre-Lafon, R. Escale, P. Dumy, J.-P. Vidal, J.-P. Girard, *ibid.* **1994**, *35*, 4097–4098; J.-M. Campagne, J. Coste, P. Jouin, *ibid.* **1995**, *36*, 2079–2082; A. Mucha, P. Kafarski, F. Plenat, H.-J. Christau, *Tetrahedron* **1994**, *50*, 12743–12754; W. P. Malachowski, J. K. Coward, *J. Org. Chem.* **1994**, *59*, 7616–7624; *ibid.* **1994**, *59*, 7625–7634; H.-J. Musiol, F. Grams, S. Rudolph-Bohner, L. Moroder, *ibid.* **1994**, *59*, 6144–6146, and references therein.

[4] R. M. J. Liskamp, *Angew. Chem.* **1994**, *106*, 661–664; *Angew. Chem. Int. Ed. Engl.* **1994**, *33*, 633–636; W. J. Moree, L. C. van Gent, G. A. van der Marel, R. M. J. Liskamp, *Tetrahedron* **1993**, *49*, 1133–1150; W. J. Moree, G. A. van der Marel, R. M. J. Liskamp, *Tetrahedron Lett.* **1992**, *33*, 6389–6392.

[5] C. Gennari, B. Salom, D. Potenza, A. Williams, *Angew. Chem.* **1994**, *106*, 2181–2183; *Angew. Chem. Int. Ed. Engl.* **1994**, *33*, 2067–2069.

[6] C. Gennari, H. P. Nestler, B. Salom, W. C. Still, *Angew. Chem.* **1995**, *107*, 1894–1896; *Angew. Chem. Int. Ed.* **1995**, *34*, 1765–1768.

[7] a) M. H. J. Ohlmeyer, R. N. Swanson, L. W. Dillard, J. C. Reader, G. Asouline, R. Kobayashi, M. Wigler, W. C. Still, *Proc. Natl. Acad. Sci. USA* **1993**, *90*, 10922–10926; b) H. P. Nestler, P. A. Bartlett, W. C. Still, *J. Org. Chem.* **1994**, *59*, 4723–4724.

[8] E. Bayer, *Angew. Chem.* **1991**, *103*, 117–133; *Angew. Chem. Int. Ed. Engl.* **1991**, *30*, 113–124. PEG-resin (TentaGel S-OH resin) was obtained from Rapp Polymere, Ernst-Simon-Strasse 9, D-72072 Tübingen, Germany (order number S 30900); hydroxymethyl polystyrene resin was obtained from Bachem California, 3132 Kashiwa Street, Torrance, CA 90505 (order number RM1S35).

[9] vsAA-OH = vinylogous sulfonyl amino acid. Defined vinylogous sulfonyl amino acid residues are described by the vs prefix to the three-letter code of the corresponding amino acid, e.g. vsAla = vinylogous sulfonyl alanyl. The sulfonyl chlorides Boc-vsAA-Cl **2a–e** were prepared according to ref. [5]. Before use in the solid phase coupling, they were purified by additional flash chromatography on silica gel (hexanes/ethyl acetate 1:1).

[10] E. Kaiser, R. L. Colescott, C. D. Bossinger, P. I. Cook, *Anal. Biochem.* **1970**, *34*, 595–598; V. K. Sarin, S. B. H. Kent, J. P. Tam, R. B. Merrifield, *ibid.* **1981**, *117*, 147–157.

[11] V. Krchňák, J. Vágner, P. Safár, M. Lebl, *Collect. Czech. Chem. Comm.* **1988**, *53*, 2542–2548.

Synthetic Receptors Based on Vinylogous Sulfonyl Peptides**

Cesare Gennari, H. Peter Nestler,* Barbara Salom, and W. Clark Still

For a long time noncovalent intermolecular interactions have been a prime topic of interest in drug research and design. Understanding the nature of these interactions and using this knowledge for the rational prediction of receptor agonists or antagonists is one of the most intriguing tasks in supramolecular chemistry. The interaction of oligopeptides and proteins with peptides is the basis for most biochemical functions, and encoded combinatorial chemistry libraries offer an efficient means of gathering empirical information about these interactions.[1] We describe here the binding of tweezerlike molecular receptors based on vinylogous sulfonyl peptides[2] to an encoded combinatorial tripeptide library. We show that these receptors bind oligopeptides with low binding strength but high selectivity, and that the binding strength and selectivity are just as good as that of analogous receptors built with natural α-amino acids. We also

[*] Dr. H. P. Nestler
Cold Spring Harbor Laboratory
P. O. Box 100, Cold Spring Harbor, NY 11724 (USA)
Telefax: Int. code + (516) 367-8873
e-mail: nestler@phage.cshl.org
Prof. Dr. C. Gennari, B. Salom
Dipartimento di Chimica Organica e Industriale, Università di Milano (Italy)
Prof. Dr. W. C. Still
Department of Chemistry, Columbia University (USA)

[**] We thank NATO for a Collaborative Research Grant (NATO 921422) to C. G. and W. C. S. We acknowledge the support of the U. S. National Institutes of Health (grant HL25634 to W. C. S.) and the Fonds der Chemischen Industrie (Liebig fellowship to H. P. N.).

show that the binding selectivity of sulfonyl peptide based receptors differs from their peptide counterparts.

Among the peptide bond analogues, sulfonyl peptides have not received as much attention as the phosphoryl peptides (phosphonamidates and phosphonates).[3] Since the amide group in sulfonamides has a tetrahedral structure, which is recognized as a mimic of the amide hydrolysis transition state, these compounds may be potential pharmacophores for the inhibition of proteases.[4] The sulfonamide group is also more polar and more acidic than the regular peptide bond, which may lead to stronger intra- and intermolecular hydrogen bonds. Indeed, the group from Milan reported earlier that vinylogous sulfonyl peptides tend to adopt well-defined conformations.[2a] This conformational bias could aid in the preorganization of selective receptors.

First, we wanted to know if simple vinylogous sulfonyl peptides show significant binding to peptides. Several arbitrarily chosen sulfonyl peptides (**1a–c**) were derivatized with a red dye (Disperse Red 1 = DR = **4**) using glutaric acid as a linker (Fig. 1). The red-dyed sulfonyl peptides **2a–c** thus obtained

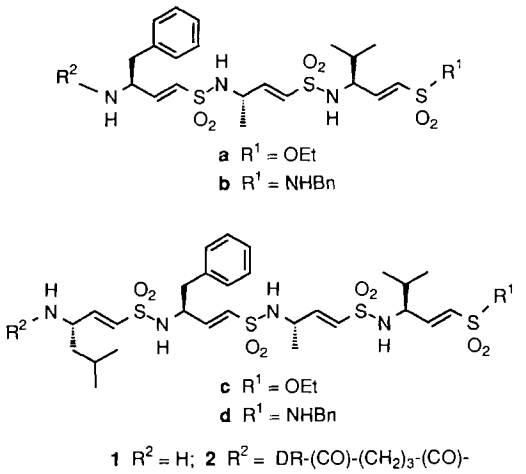

Fig. 1. Vinylogous sulfonyl peptides used in these studies. Bn = benzyl.

were screened for binding against an encoded combinatorial library of 50625 acylated tripeptides R-(C=O)-AA_3-AA_2-AA_1-NH-$(CH_2)_5$-(C=O)NHCH_2-polystyrene that was described earlier (R and AA_n are specified in Fig. 2).[5] Interestingly none of the three dyed sulfonyl peptides **2a–c** showed detectable binding to any of the tripeptide library members at sulfonyl peptide concentrations as high as 500 μM. As with regular peptides, higher molecular mass and a more preformed spatial structure seem to be required for significant binding.

Tweezerlike, two-armed molecules have been used previously to create receptors for simple biopolymers.[6] We therefore looked for a convenient linker that would allow the facile attachment of two sulfonyl peptide arms and also provide an anchor point for the dye molecule.

We chose 1,3,5-benzenetricarboxylic acid (trimesic acid, **3**) as the linker and used it in the three-step synthesis of the two-armed receptors **6a–d**. Tricarboxylic acid 3 was converted into the monoester by treatment with Disperse Red 1 (DR = **4**), and the two remaining carboxyls were esterified using pentafluorophenol (Scheme 1). The resulting bispentafluorophenyl ester **5** was then coupled with two equivalents of the corresponding sulfonyl peptides **1a–d** to afford the colored receptors **6a–d** in good yields (75–85%) (e.g. **6b** in Scheme 1).

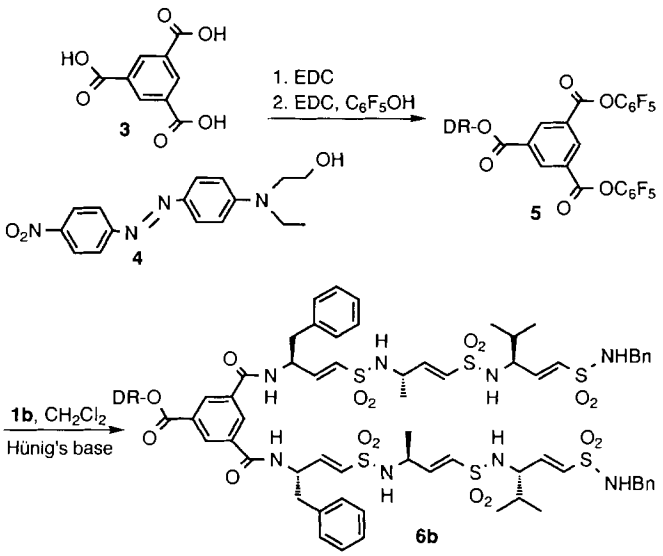

Scheme 1. Synthesis of vinylogous sulfonyl peptide based receptor **6b**. EDC = 1-(3-Dimethylaminopropyl)-3-ethylcarbodiimide hydrochloride, DR = Disperse Red 1 (= **4**), Hünig's base = diisopropylethylamine.

Receptors **6a–d** were screened against the aforementioned tripeptide library following the standard protocol.[7] The procedure included the following steps: 24 h equilibration of the receptor solution in chloroform with the bead-supported tripeptide library, separation of the red-stained beads, and decoding of the information on the beads by photolytic release of the molecular tags followed by EC-GC (electron capture gas chromatographic) analysis.[7]

While receptor **6d** did not significantly bind to any of the tripeptides in the library at receptor concentrations as high as 500 μM,[8] receptors **6a–c** showed sequence-selective peptide binding at concentrations of about 200 μM. Such concentrations suggest binding constants for **6a–c** and the library tripeptides in chloroform on the order of 10^2–10^3. Of the three receptors, **6b** showed the highest selectivity, and its properties are discussed below.

At a receptor concentration of 160 μM, **6b** bound approximately 250 peptide sequences out of a total of 50625 in the library.[9] **6b** shows a distinct single residue selectivity for D-Pro at position AA_3 (41% of the decoded beads), for D-Asn/D-Gln at position AA_2 (47% of the decoded beads), and for L-Gln at position AA_1 (76% of the decoded beads). Thus the highest residue selectivity was found at AA_1, while the nature of the N-terminal acyl group was almost completely ignored (Fig. 2). Statistical analysis of the sequence data[10] revealed an even more interesting feature: **6b** has strong sequence selectivity for the tripeptide (D-Pro)-(D-Gln)-(L-Gln) (found in 18% of the decoded beads, statistically expected in 0.03%[11a]) and for (L-Pro)-(D-Val)-(D-Pro) (found in 5% of the decoded beads, statistically expected in 0.03%[11a]). The high occurrence of the former sequence is not surprising, given the high frequency of the single residues (41% D-Pro at position AA_3, 47% D-Gln at position AA_2, and 76% L-Gln at position AA_1, see above). On the other hand, the high occurrence of the second sequence is quite remarkable, given the low frequency of the single residues (16% L-Pro at position AA_3, 10% D-Val at position AA_2, and 10% D-Pro at position AA_1). This implies that recognition of this second sequence must result from synergistic multiresidue interactions within the tripeptide.

We next asked what the binding properties of the corresponding peptidic receptor would be. Would it bind tripeptides under

 © VCH Verlagsgesellschaft mbH, D-69451 Weinheim, 1995 0570-0833/95/1616-1766 $ 10.00+.25/0

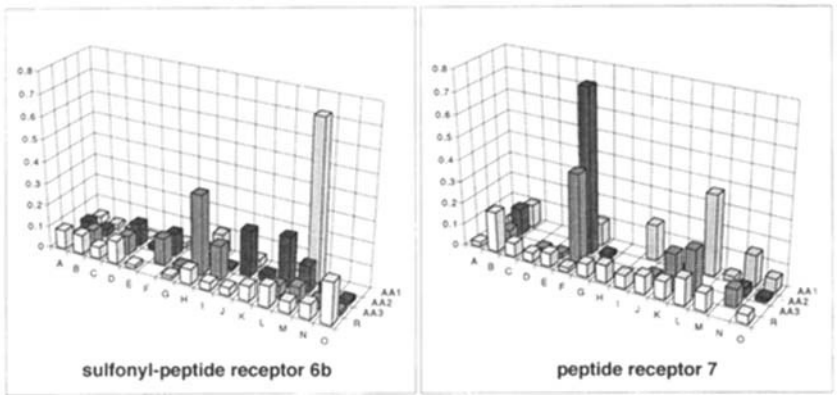

Fig. 2. Frequencies of different residues in the tripeptide library R-(C=O)-AA_3-AA_2-AA_1-NH-$(CH_2)_5CONHCH_2$-polystyrene binding **6b** and **7**. Codes for R: A = methyl, B = ethyl, C = isopropyl, D = *tert*-butyl, E = neopentyl, F = CF_3, G = isobutyl, H = methoxymethyl, I = cyclopropyl, J = cyclobutyl, K = cyclopentyl, L = acetoxymethyl, M = phenyl, N = $N(CH_3)_2$, O = morpholino; codes for AA_n: A = Gly, B = D-Ala, C = L-Ala, D = D-Ser(O*t*Bu), E = L-Ser(O*t*Bu), F = D-Val, G = L-Val, H = D-Pro, I = L-Pro, J = D-Asn(β-trityl), K = L-Asn(β-trityl), L = D-Gln(γ-trityl), M = L-Gln(γ-trityl), N = D-Lys(ε-Boc), O = L-Lys(ε-Boc).

similar conditions? If so, would a different selectivity profile be obtained than that of **6b**?

The synthesis of peptide receptor **7** followed the outline shown in Scheme 1. Interestingly, while sulfonyl peptide receptor **6b** is readily soluble in chloroform, the peptide receptor dissolves only sparingly, which already pointed to strong intermolecular peptide interactions.

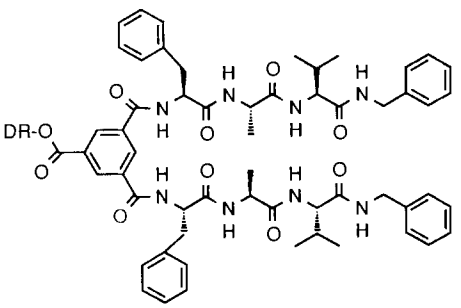

7

The binding properties of **7** in chloroform were determined as described for **6b**. At a concentration of 130 μM, **7** bound approximately 270 sequences out of a total of 50625 in the library.[9] The recognition ability of **7** for specific tripeptides was as distinct as that of **6b**. Like its sulfonyl counterpart, **7** neglects the terminal acylating group but is selective for the amino acid residues. In particular, **7** recognizes D-Val at positions AA_3 (37% of the decoded beads) and AA_2 (78% of the decoded beads), and D-Gln at position AA_1 (33% of the decoded beads) (Fig. 2). Thus not only does receptor **7** bind different amino acids than **6b** does, but its selectivity is greatest at a different site, namely AA_2. The tripeptide sequence derived from the most selectively bound residues, (D-Val)-(D-Val)-(D-Gln), occurs with high frequency as expected (found in 11% of the decoded beads, statistically expected in 0.03%[11a]). The most striking finding was the extraordinary sequence selectivity of **7** for a different tripeptide: (D-Gln)-(D-Val)-(L-Pro) (found in 24% of the decoded beads, statistically expected in 0.03%[11a]). Interestingly, L-Pro in position AA_1 occurred exclusively in this sequence. Furthermore the receptor recognizes the (D-Ala)-(D-Ala) dipeptide sequence (found in 5% of the decoded beads, statistically expected in 0.4%[11b]) in the position AA_3/AA_2.

We describe here nonmacrocyclic, tweezerlike molecules having significant binding selectivities for certain oligopeptides. Although the receptors studied here do not provide the large binding strengths reported recently for more rigid receptors,[5, 12] they have significant specificity in the recognition of tripeptides. Furthermore, these results and others recently described[6b–d] show that molecules having a simple motif consisting of a central linker and two oligomeric arms can act as remarkably selective receptors. The results support the idea that extensive rigidity of receptors is not necessary for selective binding.

In summary, we have shown that two-armed receptors based on sulfonyl peptides and regular peptides bind oligopeptides in chloroform with comparable binding constants (low) and selectivity (high). Not surprisingly, the particular binding properties are different for the two families. As the receptors described here are readily preparable linear molecules, they may serve as prototypes for combinatorial libraries of tweezerlike, vinylogous sulfonyl peptide based receptors, which can be screened to find specific binders of given substrates.

Experimental Procedure

6b: Sulfonyl tripeptide **1b** (7 mg) was dissolved in 2 mL of CH_2Cl_2. 0.5 mL of trifluoroacetic acid was added, and the resulting mixture was stirred for 30 min. The volatiles were removed at reduced pressure, and the residue was dried in vacuo for 2 h and then dissolved in 1 mL of CH_2Cl_2. After 20 μL of diisopropylethylamine and 3.5 mg of bispentafluorophenyl ester **5** were added, the mixture was stirred for 2 d at room temperature. The reaction mixture was purified by flash chromatography on 20 g of silica gel ($CHCl_3$/MeOH 95/5) and size exclusion chromatography on 30 g of LH20 ($CHCl_3$) to yield 5 mg (70%) of **6b**. ^{1}H NMR (400 MHz, [D_8]DMF, 25 C, TMS): δ = 0.94 (12H, d, J(H,H) = 6.8 Hz), 1.26 (3H, t, J(H,H) = 7.0 Hz), 1.32 (6H, d, J(H,H) = 7.0 Hz), 1.92 (2H, m), 3.19 (4H, m), 3.71 (2H, q, J(H,H) = 6.9 Hz), 3.85 (2H, m), 4.00 (2H, t, J(H,H) = 6.6 Hz), 4.06 (2H, m), 4.18 (4H, d, J(H,H) = 6.3 Hz), 4.63 (2H, m), 5.17 (2H, m), 6.58 6.70 (10H, m), 6.87 (2H, dd, J(H,H) = 15.1, J(H,H) = 5.6 Hz), 7.11 (2H, d, J(H,H) = 9.2 Hz), 7.18–7.41 (20H, m), 7.54 (2H, d, J(H,H) = 7.6 Hz), 7.59 (2H, d, J(H,H) = 8.4 Hz), 7.65 (2H, t, J(H,H) = 6.4 Hz), 7.94 (2H, d, J(H,H) = 9.3 Hz), 8.01 (2H, d, J(H,H) = 9.1 Hz), 8.42 (2H, m, J(H,H) = 9.1 Hz), 8.67 (2H, d, J(H,H) = 1.8 Hz), 8.71 (1H, s), 9.20 (2H, d, J(H,H) = 8.2 Hz). High-resolution MS calcd. for $C_{90}H_{95}N_{12}O_{18}S_6$ (M + H): m/z 1691.5210; found: 1691.5240.

Peptide binding assay of receptor **6b**: The general screening procedure is described in ref. [5a]. The red-dyed receptor **6b** (initial concentration ca. 250 μM) in $CHCl_3$ solution was equilibrated with the acylated tripeptide library for 24 h on a wrist-action shaker; the final concentration of the receptor in solution was found to be 160 μM. Assuming that at least 10% of the peptides on the deep red-stained beads are bound by the receptor (i.e. ≥ 10% saturated), the minimum binding constant (K_a) for the assay is estimated to be 694 ($\Delta G = -15.9$ kJ mol^{-1}). 66 of the most intensely colored beads were selected and decoded, and 58 unique four-residue sequences were found. Statistical analysis of the number of duplicate sequences found indicated that ca. 250 unique four-residue sequences are tightly bound out of the total pool of 50625 acylated tripeptides under the conditions of our assay [10].

7: Boc-(L-Phe)-(L-Ala)-(L-Val)-NHBn (120 mg) was dissolved in 7.5 mL of CH_2Cl_2, 2.5 mL of trifluoroacetic acid was added, and the mixture was stirred for 1 h. The volatiles were removed at reduced pressure, and the residue was washed with diethyl ether (2 × 10 mL) and then dried in vacuo for 4 h. The residue was dissolved in 10 mL of CH_2Cl_2, and 100 μL of diisopropylethylamine was added. After the addition of 84 mg of bispentafluorophenyl ester **5**, the mixture was stirred for 3 d at room temperature. During this time a red precipitate formed. The reaction mixture was filtered through 50 g of silica gel ($CHCl_3$/MeOH 95/5), and fractions containing only **7** (TLC analysis) were further purified by size exclusion chromatography on 30 g of LH20 ($CHCl_3$) to yield 12 mg (9%) of **7**. ^{1}H NMR (400 MHz, [D_8]DMF, 25 C, TMS): δ = 0.90 (12H, m), 1.25 (3H, t, J(H,H) = 6.9 Hz), 1.34 (6H, d, J(H,H) = 7.2 Hz), 2.13 (2H, m), 3.16 (2H, m), 3.32 (2H, dd, J(H,H) = 13.6, J(H,H) = 3.6 Hz), 3.61 (2H, q, J(H,H) = 6.9 Hz), 3.99 (2H, t, J(H,H) = 5.7 Hz),

4.31 (2H, t, J(H,H) = 6.6 Hz), 4.34 (4H, d, J(H,H) = 6.0 Hz), 4.51 (2H, t, J(H,H) = 7.2 Hz), 4.63 (2H, m), 4.94 (2H, m), 7.08 (2H, d, J(H,H) = 9.1 Hz), 7.14 (2H, d, J(H,H) = 7.4 Hz), 7.17–7.30 (14H, m), 7.41 (4H, m), 7.86 (2H, d, J(H,H) = 8.8 Hz), 7.92 (2H, d, J(H,H) = 9.1 Hz), 8.01 (2H, d, J(H,H) = 7.6 Hz), 8.43 (4H, m), 8.62 (2H, s), 8.68 (2H, d, J(H,H) = 7.2 Hz), 8.75 (1H, d, J(H,H) = 6.2 Hz), 9.27 (2H, d, J(H,H) = 8.3 Hz). High-resolution MS calcd. for $C_{73}H_{82}N_{12}O_{12}Na$ (M + Na): m/z 1341.6070, found: 1341.6050.

Peptide binding assay of receptor **7**: Receptor **7** was assayed as described above for **6b**. The final concentration of the receptor was 130 μM, and the minimum binding constant (K_a) is estimated to be 855 ($\Delta G = -16.5$ kJ mol^{-1}). 54 beads were decoded, yielding 49 unique sequences. Replicate analysis [10] indicated that under these conditions, 269 unique sequences are bound.

Received: March 24, 1995 [Z 7827 IE]
German version: *Angew. Chem.* **1995**, *107*, 1894–1896

Keywords: combinatorial chemistry · peptide analogues · receptors · supramolecular chemistry

[1] For recent reviews, see: M. A. Gallop, R. W. Barrett, W. J. Dower, S. P. A. Fodor, E. M. Gordon, *J. Med. Chem.* **1994**, *37*, 1233–1251; *ibid.* **1994**, *37*, 1385–1401.

[2] a) C. Gennari, B. Salom, D. Potenza, A. Williams, *Angew. Chem.* **1994**, *106*, 2181–2183; *Angew. Chem. Int. Ed. Engl.* **1994**, *33*, 2067–2069; b) C. Gennari, H. P. Nestler, B. Salom, W. C. Still, *ibid.* **1995**, *107*, 1892–1893 and **1995**, *34*, 1763–1765.

[3] a) K. Teraishi, M. Saito, I. Fujii, H. Nakamura, *Tetrahedron Lett.* **1992**, *33*, 7153–7156; b) D. Maffre-Lafon, R. Escale, P. Dumy, J.-P. Vidal, J.-P. Girard, *ibid.* **1994**, *35*, 4097–4098; c) A. Mucha, P. Kafarski, F. Plenat, H.-J. Christau, *Tetrahedron* **1994**, *50*, 12743–12754; d) H.-J. Musiol, F. Grams, S. Rudolph-Bohner, L. Moroder, *J. Org. Chem.* **1994**, *59*, 6144–6146; e) D. A. Campbell, J. C. Bermak, *J. Am. Chem. Soc.* **1994**, *116*, 6039–6040; f) W. P. Malachowski, J. K. Coward, *J. Org. Chem.* **1994**, *59*, 7616–7624; g) *ibid.* **1994**, *59*, 7625–7634; h) J.-M. Campagne, J. Coste, P. Jouin, *Tetrahedron Lett.* **1995**, *36*, 2079–2082.

[4] a) R. M. J. Liskamp, *Angew. Chem.* **1994**, *106*, 661–664; *Angew. Chem. Int. Ed. Engl.* **1994**, *33*, 633–636; b) W. J. Moree, L. C. van Gent, G. A. van der Marel, R. M. J. Liskamp, *Tetrahedron* **1993**, *49*, 1133–1150; c) W. J. Moree, G. A. van der Marel, R. M. J. Liskamp, *Tetrahedron Lett.* **1992**, *33*, 6389–6392.

[5] a) S. S. Yoon, W. C. Still, *Tetrahedron* **1995**, *51*, 567–578; b) A. Borchardt, W. C. Still, *J. Am. Chem. Soc.* **1994**, *116*, 373–374.

[6] a) S. C. Zimmerman, W. Wu, Z. Zeng, *J. Am. Chem. Soc.* **1991**, *113*, 196–201; b) R. Boyce, G. Li, H. P. Nestler, T. Suenaga, W. C. Still, *ibid.* **1994**, *116*, 7955–7956; c) S. R. LaBrenz, J. W. Kelly, *ibid.* **1995**, *117*, 1655–1656; d) H. Wennemers, S. S. Yoon, W. C. Still, *J. Org. Chem.* **1995**, *60*, 1108–1109.

[7] M. H. J. Ohlmeyer, R. N. Swanson, L. W. Dillard, J. C. Reader, G. Asouline, R. Kobayashi, M. Wigler, W. C. Still, *Proc. Natl. Acad. Sci. USA* **1993**, *90*, 10922–10926.

[8] The affinity of **6d** for the library peptides could be as much as one-tenth of the binding affinities of **6a–c** and not be detected by our assays.

[9] Since there are 15 different possibilities for R and for each of the three amino acids AA_1, AA_2, AA_3, there are $15^4 = 50625$ total possibilities. R and AA_n are listed in Fig. 2.

[10] The statistical analysis of the binding sequence data was performed using the SACCS program by Dr. Peter Shenkin (Columbia University). The total number of unique sequences bound from the pool is estimated by binomial analysis of the multiple occurrences of identical sequences and gives an approximation of the selectivity of the receptor.

[11] a) One out of 15^3 possibilities = 0.03%; b) one out of 15^2 possibilities = 0.4%.

[12] a) A. Borchardt, W. C. Still, *J. Am. Chem. Soc.* **1994**, *116*, 7467–7468; b) S. S. Yoon, W. C. Still, *Angew. Chem.* **1994**, *106*, 2517–2519; *Angew. Chem. Int. Ed. Engl.* **1994**, *33*, 2458–2460.

Miller, R.J.D. (ed.)

Surface Electron Transfer Processes

1995. XII, 368 pages
with 137 figures and 3 tables.
Hardcover. DM 128.00.
ISBN 1-56081-036-X
(VCH, New York)

This book gives an extensive theoretical treatment of its theme. The emphasis is on electronic coupling of molecular potentials to conducting band states. The essential role of surface electron transfer in catalysis, electrochemistry, photo imaging, and virtually all charge transfer solid state devices make this process one of the most important single chemical events.

Sandifer, J. R.

Ion-Transfer Kinetics

1995. X, 142 pages with
38 figures and 16 tables.
Hardcover. DM 165.00.
ISBN 1-56081-508-6
(VCH, New York)

In six concise, well-referenced chapters, this book covers the essentials of ion-transfer principles and applications, including computer simulation techniques for ion-transfer kinetics models.

It is addressed to chemists in academia and industry, to physical chemists and to chemical engineers.

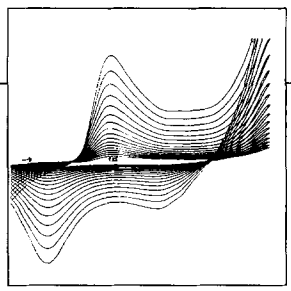

ELECTRO CHEMISTRY

To order please contact your bookseller or:

VCH, P.O. Box 10 11 61,
D-69451 Weinheim,
Telefax (0) 62 01 - 60 61 84

VCH, Hardstrasse 10, P.O. Box,
CH-4020 Basel

VCH, 8 Wellington Court,
Cambridge CB1 1HZ, UK

VCH, 220 East 23rd Street,
New York, NY 10010-4606, USA
(toll free: 1-800-367-8249)

VCH, Eikow Building,
10-9 Hongo 1-chome,
Bunkyo-ku, Tokyo 113
Japan

VCH

A Whole New Ball Game

The Most Beautiful Molecule. An Adventure in Chemistry. By *H. Aldersey-Williams*. Aurum Press, London, 1994. 340 pp., hardcover £ 18.95.—ISBN 1-85410-302-2

Fullerene—die Bucky-Balls erobern die Chemie. By *J. Dettmann*. Birkhäuser, Basel, 1994. 248 pp., hardcover DM 59.80.—ISBN 3-7643-2947-5

In *The Most Beautiful Molecule—An Adventure in Chemistry* H. Aldersey-Williams has set out to convey the fascination and elegance of modern chemistry to a wide readership, using the history of the fullerenes for illustration. He has therefore been careful to avoid too much scientific jargon. The account contains a wealth of historical detail which the author has meticulously researched by personal interviews, and only a few examples are mentioned here.

The author describes in great detail and in chronological order all the events that led up to the discovery of the fullerenes. The experiments and the participants are described so vividly as to give the reader the feeling of having been present at the time. Where there is a possibility that difficulties of understanding might arise, these are avoided very effectively by including explanatory sections (e.g. on spectroscopic methods).

Readers will certainly also be interested in the analysis of the article by Kroto, Heath, O'Brien, Curl, and Smalley (*Nature* **1985**, *318*, 162). That publication, which reported the first "proof" of the existence of C_{60}, is examined in detail sentence by sentence. This chapter will undoubtedly provide new food for thought, not only for the authors of the paper but for everyone who publishes research results.

Equally good is the detailed description of the events at a conference. Here again the reader is held engrossed by the author's lucid and yet gripping style.

The author succeeds in the ambitious aims mentioned above, and at the same time shows through the fullerenes story how science works. Furthermore, he has managed to reveal the apparently unromantic world of chemistry in a more favorable light than recently. Thus, it is one of those rare books which hold the attention of the reader who is interested in science to the extent that he or she cannot put it down until it is finished. It is a fantastic book which occupies a high position in the literature of chemistry. The only complaint is that up to now there is only an English version.

In *Fullerene—die Bucky-Balls erobern die Chemie* Joachim Dettmann states at the outset that his aim is to show, through the example of the fullerenes, the fundamental importance of chemical research for developing future applications and new technologies, and at the same time to convey the beauty of nature at the molecular level. He brings to this task a clear and readily understandable style of writing, so that non-scientists as well as scientists will benefit from reading the book.

A preface by Wolfgang Krätschmer is followed by an eight-page introduction giving a short and succinct history of the fullerenes. In the following two chapters (100 pages altogether) the author gives an excellent and comprehensive overview of the element carbon, including the different forms in which it occurs, their structures, and methods of preparing them, and of clusters (definition, properties, preparation, magic numbers, applications). Armed with this considerable body of sound knowledge, the reader is then led into the fascinating world of the fullerenes. First the complete "fullerene story" is recounted in a chapter of 28 pages. This is followed by a 48-page chapter which takes the reader aside for a thorough discussion of symmetry. The historical origins of the concept of symmetry, the different symmetry elements, topology, and point groups are all explained clearly and in great detail. These principles, including especially Euler's theory of polyhedrons, are then applied to the case of the fullerenes.

The book is completed by a brief discussion of microarchitectures resembling the fullerenes, a chapter on the chemistry of the fullerenes (a mere 18 pages), and a summing-up which also considers the future of fullerenes. In this the author has sensibly resisted the temptation to overstate the future potential for applications of fullerenes. He takes the view that, as the field is still very new, it is too early to make firm predictions about future applications of fullerenes. The only thing that seems certain, according to Dettmann, is that the future micro-robots of nanotechnology should find that the bucky-ball is the ultimate "pill" to be kicked.

The book offers a good introduction to the chemistry of carbon. However, the title does not clearly reflect the contents, as the chemistry of the fullerenes is treated only very superficially and incompletely. In view of this a more appropriate title would be something like "Carbon Modifications—Carbon and Bucky-Balls".

Andreas Gügel
Max-Planck-Institut für
Polymerforschung
Mainz (Germany)

Chemische Kabinettstücke. By *H. W. Roesky* and *K. Möckel*. VCH Verlagsgesellschaft, Weinheim, 1994. 314 pp., hardcover DM 68.00.—ISBN 3-527-29220-9

Even at the end of the 20th century, experiments still form the cornerstone of chemistry, and particular credit is due to H. W. Roesky and K. Möckel for taking appropriate account of this by writing "Chemische Kabinettstücke", a book that is hard to put down once one has started to enjoy

This section contains book reviews and a list of new books received by the editor. Book reviews are written by invitation from the editor. Suggestions for books to be reviewed and for book reviewers are welcome. Publishers should send brochures or (better) books to Dr. Ralf Baumann, Redaktion Angewandte Chemie, Postfach 101161, D-69451 Weinheim, Federal Republic of Germany. The editor reserves the right of selecting which books will be reviewed. Uninvited books not chosen for review will not be returned.

the excellent experimental "firework display" which the authors present in just over 300 pages. This volume, which can only be described as a success in both presentation and content, carries the reader back to the pre-video era of the great experimental lectures, and its descriptions convey the strange, almost magical fascination that the present reviewers experienced as students in Münster when those great masters of the experiment Wilhelm Klemm, Fritz Micheel, Harald Schäfer, and Claus Brendel were "on-stage".

One hundred and twenty-four experiments are described and presented with great care and in great detail. Apart from clear instructions on the experimental setup and procedure, each section includes a list of chemicals and apparatus, a short explanation of the principles, and tips on safety and waste disposal as well as literature references; these are complemented by historical, anecdotal, and even lyrical comments. This fresh approach, the strength of the book, prevents an austere "cookbook" atmosphere from developing. The descriptions of the experiments are extremely precise and complete, and are prepared with great didactic skill; they deal with subject matter which reflects the past, present, and future of chemistry and which in part represents a distillate of the authors' long experience in teaching and research. The many color plates that illustrate, and at the same time elucidate, the experiments do much to reinforce the positive impression made by the book. The majority of the experiments (almost 90%) deal with optical and color effects, while about 7% appeal to the ear, and the remainder to the senses of taste or smell.

This brilliantly structured experimental concept is unique on the German book market. The authors are not afraid to grapple with the manifold modern developments in chemistry (experiments dealing with fractals, superconductors, and crown ethers will not be looked for in vain!), and their book is not just a compendium of spectacular experimental descriptions. A perusal of the literature references does, however, make it difficult for the reviewers to stifle a little sigh of regret: was the transfer of experimental chemistry to the New World really so successful that new experiments today come almost entirely from there? (poor didacticians!). If one fault can be found with the book, then perhaps it is the "literary quotations" that accompany the experiments and sometimes appear too artificial, and of course the criticism that these do not stem from the authors' own pen.

This book sets standards and will become a "must" for all those whose job it is to organize experimental lectures, to be responsible for a "magic show" or a Christmas demonstration, or who as secondary school teachers are looking for suggestions for experiments to extend their own repertoire. The highly readable "Kabinettstücke" presented by the all-rounders Roesky and Möckel achieve flagship status in the field of experimental literature and do a great honor to the chemists' guild. The book will provide pleasure and delight for nonscientists and scientists alike and could make history by serving as the screenplay for the first video published by VCH.

Hans Georg von Schnering, Dietmar Raschke
Max-Planck-Institut für Festkörperforschung, Stuttgart (Germany)

Photochemical Key Steps in Organic Synthesis—An Experimental Coursebook. Edited by *J. Mattay* and *A. Griesbeck*. VCH Verlagsgesellschaft, Weinheim, 1994. 350 pp., paperback DM 68.00/$ 40.00.—ISBN 3-527-29214-4

The field of photochemistry has grown dramatically over the past 20 years, unveiling many exciting applications to organic synthesis, physical organic chemistry, and organometallic chemistry. However, most advanced texts of organic chemistry do not sufficiently cover the breadth of photochemical reactions, nor do they introduce important industrial applications in fields such as polymer chemistry. Furthermore, photochemical reactions have infrequently been introduced into experimental courses for students. Professors Mattey and Griesbeck have developed an experimental coursebook consisting of several multistep syntheses, each highlighting one or more photochemical key reactions. In all, this book is a compilation of nearly 100 synthetic sequences contributed by 50 or so experts in the field of organic photochemistry. Most of the experimental procedures involve multiple steps leading up to the photochemical reaction, and so this book contains a total of about 300 actual synthetic reactions. Opening each chapter, a brief (approximately 3-page) introduction provides a commentary for the reactions presented and some discussion of the mechanisms involved. In addition, a general introduction discusses the experimental considerations that are particularly important to carrying out photochemical reactions.

One of the most valuable characteristics of this book is the breadth of coverage, which includes nearly all important types of photochemical reactions. Many of the specific reactions chosen for this series are especially interesting and display the power of photochemistry for the construction of complex and strained molecules which would be available by no other means. This makes the book an especially valuable resource for graduate students and researchers in organic synthesis. The organization is excellent and contains many examples of each specific class of photochemical reactions. Furthermore, many of the most current and exciting areas of research in organometallic chemistry, asymmetric synthesis, and photolithography have representative experiments. For the reaction types covered, optimum experimental conditions (including light filters, solvents, and possible sensitizers) are detailed quite thoroughly, representing the valuable experience of the contributors.

For supervisors of laboratory courses, this experimental coursebook would provide the opportunity to introduce photochemistry early in the training of young chemists. However, there are several nontrivial reasons why photochemical experiments present difficulties in laboratory courses—most notably, the expense of the equipment and the specific hazards unique to using photochemical equipment. From the standpoint of safety, the most appropriate photochemical reactions in this coursebook for use in a laboratory course involve: a) 5 g scale or less; b) relatively non-flammable solvents; c) convenient photolysis times (preferably not unattended for long periods). In addition, reactions employing a Rayonet® photochemical reactor are perhaps more convenient for a laboratory course than reactions involving the medium-pressure mercury lamps. There are many excellent experiments in this coursebook that could be performed conveniently and within these considerations. These include the syntheses of dehydrovaline, Ibuprofen, and *trans*-bicyclo[5.3.1]undecanone, the single crystal photolysis of an ethenylanthracene compound, and the synthesis and photolithography of poly(4-ethenyl-5-methylthiadiazole).

In contrast, however, many of the others are truly research-level experiments requiring highly specialized equipment or the handling of sensitive intermediates. Some experiments employ photochemical conditions involving such forcing or potentially dangerous conditions as to make them highly inappropriate for an under-

 © VCH Verlagsgesellschaft mbH, D-69451 Weinheim, 1995 0570-0833/95/1616-1770 $ 10.00+.25/0

graduate laboratory course. For example, one reaction involves photolysis of 2.5 L of an *ether* solution with a 450 W Hanovia immersion lamp for 20 h. Another reaction involves the photolysis of 125 g of vinyl acetylene with a 500 W immersion lamp for 9 days. Not all experiments in this text provide the expected photolysis time, and almost none of the experiments has any specific notes pertaining to safety. It appears in some cases that the experimental procedures are identical to those appearing in the original literature, and neither the contributor nor the editors have investigated modifications in scale or procedure which would make them appropriate for a laboratory course.

The introduction to this book (10 pages) describes several important considerations for photochemical reactions and how these conditions are studied for optimization of a specific reaction. In addition, a brief section describes the hazards of using photochemical equipment. Although this section is very helpful and interesting, the beginner would benefit from a much expanded section including pictures of photochemical set-ups, operating instructions, and safety concerns. In addition, if each chapter were introduced with a more comprehensive presentation of the mechanisms and applications of the reactions in question, the result would be a much more powerful learning tool.

In conclusion, Mattay and Griesbeck have accumulated a collection of procedures from many of the leaders in the field of synthetic organic photochemistry which will be a valuable resource for researchers in the field of organic chemistry. The wealth of reaction sequences covers nearly all aspects of this field and is excellently organized. However, the use of this resource as an experimental course book would demand a good deal of responsibility and planning on the parts of the instructor and student, to assure that the experiments can be reproduced accurately and safely in a laboratory course setting.

Scott Virgil
Massachusetts Institute of Technology
Cambridge, MA (USA)

Radical Chemistry. (Ellis Horwood Series in Organic Chemistry.) By *M. J. Perkins*. Ellis Horwood, New York, 1994. 182 pp., paperback $ 18.00.– ISBN 0-13-320920-2

Although M. J. Perkins' *Radical Chemistry* is a book of less than 200 pages, it covers in a very thorough way the most important aspects of the subject. A short introduction, mainly concerned with the history of radical chemistry, is followed by Chapter 2 dealing with the kinetics of free radical reactions and introducing the most important concepts: chain initiation, unimolecular and bimolecular radical reactions, radical-induced fragmentations, radical rearrangements, and radical–radical and radical–molecule reactions. Chapter 3 contains a more detailed treatment of chain initiation, methods for generating radicals, and radical–radical reactions, with particular emphasis on free radicals and radical pairs in solvent cages. In Chapter 4 the author discusses reactivity and selectivity in radical reactions, beginning with the bromination or chlorination of alkanes, then with regard to radical additions to double bonds. Next the three main factors influencing selectivity, namely stereoelectronic effects (e.g. in cyclizations forming five-membered rings), polar effects, and steric effects (in stable radicals), are discussed in separate sections. This chapter ends with a discussion of intra- and intermolecular competing reactions and the competition between addition and abstraction, illustrated by the bromination of cyclohexene using *N*-bromosuccinimide.

It is not until Chapter 5 that methods for detecting radicals and determining their structures are discussed (ESR spectroscopy, hyperfine splittings, σ- and π-radicals, spin trapping, etc.). The chapter ends with an introduction to ENDOR and CIDNP spectroscopies.

Chapter 6 is devoted to the role of radicals in organic synthesis. Under the heading of chain reactions the author first describes transformations of functional groups: NBS bromination reactions, the Toray process, the Hoffmann–Löffler–Freytag reaction, and reactions using Barton esters. Under carbon–carbon bond-forming reactions the tin hydride method, used especially for cyclizations forming five-membered rings, is given prominence. The chapter ends with radical reactions not involving the chain mechanism, such as the free radical oxidation of phenols to quinones. Chapter 7 is concerned with stereochemical aspects, including a discussion of intramolecular asymmetric induction for various reactions of prochiral radical centers. Chapter 8, which deals briefly with radical ions and electron transfer reactions, deserves special praise. Chapter 9 is entitled "Some Special Topics", and discusses some other important aspects of radical reactions, including FMO theory, an introduction to the SOMO concept, nucleophilic and electrophilic radicals, radical kinetics and thermodynamics, capto-dative substituent effects, autoxidation (e.g. of unsaturated lipids), and antioxidants. Lastly Chapter 10, "Radicals in Biology", is an introduction to this most topical area of radical chemistry. The author begins by discussing the role of the hydroxy radical and the mode of action of Vitamin E, followed by enzymatic reactions. The chapter ends with the Bergman cyclization of ene-diynes.

An appendix contains a list of some absolute rate constants for elementary free radical reactions. The book ends with a selected bibliography for further reading and a set of exercises, in which references to the original papers are provided to help the reader.

Altogether this book gives an excellent overview of radical chemistry, and very few aspects are neglected (although I found nothing on radical clocks nor on the stabilities of radicals). The organization of the contents is not always ideal—for example, NBS bromination is mentioned in three different places. Also in Chapter 5 on the structure of radicals and their detection, the relationship between reactivity and selectivity on the one hand (Ch. 4) and synthetic aspects on the other hand (Ch. 6) is not treated as well as it might be. However, the book is a good introduction to and general survey of free radical chemistry and is reasonably priced.

Ulrich Lüning
Institut für Organische Chemie
der Universität Kiel (Germany)

Chaos and Order. The Complex Structure of Living Systems. By *F. Cramer*. VCH Verlagsgesellschaft, Weinheim, 1993. 250 pp., hardcover DM 48.00.—ISBN 3-527-29067-2/1-56081-812-3

This book is a work of art. Like all truly inspiring scientific books it has the virtue of brevity and is also a piece of literature, on a par with classics such as G. H. Hardy's *A Mathematician's Apology* or Peter Medawar's *The Limits of Science*. In his foreword Professor Prigogine writes that *Chaos and Order* is "first and foremost an excellent introduction to the main problems of molecular biology [seen in the] context of the progress that has recently been achieved in the theory of non-linear

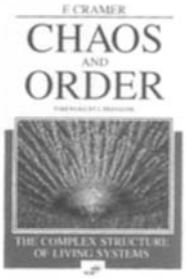

systems far from equilibrium". But it is much more than this, for Professor Cramer easily straddles the gap between the two cultures, in a virtuoso display of cross-references and interconnections. Taking his own research as a starting point he aims at the general picture, deftly crossing the boundaries between scientific disciplines and artistic fields. Poems by Hölderlin and paintings by Kandinsky are used to make a point about the delicate transition between order and chaos. He is right to use this approach, for it is at the fuzzy borders where different disciplines meet that innovation thrives. The book is also a very personal work (Professor Cramer even confesses his reluctance to part with it), and thus more universal in its appeal.

In *Chaos and Order* some fundamental questions are asked—what is life? how do ideas arise in our brain? what does evolution mean?—but the author is careful to separate the methods of science and philosophy. As he puts it, "scientific research cannot yield moral values and cannot teach us the meaning of life". Only children ask "why?" and only the selfish start their enquiries with "what for?"; the scientist's business is to answer the "how?" According to Goethe, what cannot be investigated is better left to contemplation. But Professor Cramer does not eschew ethical matters, stating very forcefully that "gene therapy is a violation of the personal rights of future human beings". He also does not shy away from denouncing the dangers of a capitalistic exploitation of publicly funded research with its potential for the prostitution of science. These matters are all the more important because, as he persuasively argues in the last chapter, intellectual evolution has now overtaken biological evolution. We do not develop any more organs; we invent domestic appliances instead. Information is passed from generation to generation not only through genes but also through libraries, data banks, social traditions, etc.

It is only fitting that a book about structure should itself be highly structured. Each chapter starts with a partly fictitious dialogue and ends with a poem (authors ranging from Yeats to Chemistry Nobel Prize winner Roald Hoffmann). The dialogues are constructed around an assortment of scientists (Einstein, Pauli, Darwin, the 18th century Göttingen physicist Lichtenberg, etc.), writers (Kleist, Goethe), philosophers (Socrates and Wittgenstein) and various fictional characters (Shakespeare's Hamlet or Bottom and Carroll's Alice, the latter because scientific nonsense can be very meaningful). *Chaos and Order* can thus be read on several levels—as a collection of dialogues intended to show that difficult problems are neither new nor difficult to discuss, as an anthology of poetry (in the author's words "poetic language is often capable of describing truths in a more valid, concise and enduring form", which is not unlike mathematics) or as a masterly essay on the complex structure of living systems.

Nonlinear systems with feedback coupling and a strong dependence on the initial conditions have the potential for chaotic behavior. Inevitably Professor Cramer invokes Wallace Stevens's poem *Connoisseur of Chaos*, which proclaims that a violent order and a great disorder are one and the same thing. One of the book's most impressive sections shows that esthetic harmony can be found at the irrational boundary separating order from disorder. The evidence that the famed golden section is somehow related to this transition strikes us as a true coup de théatre. The whole book, even the more difficult sections, is a pleasure to read, and is admirably illustrated with examples and illuminating parallels. Thus a tree can be looked upon as an upside-down bolt of lightning which propagates very slowly, and the phenomenon of the sudden boiling of superheated water is not all that different from a stock market crash (both are cusp catastrophes).

I was expecting the book to start—like some modern-day Genesis—with chaos, but Professor Cramer devotes the first chapter to life, seen as a dynamic system between order and decay. It is a process governed by entropy, the "arrow of time" (Eddington). This is the "leitmotiv" of the book. Once taken apart, living systems die and cannot be reassembled; in other words, the whole of life is always greater than the sum of its parts. As far as life is concerned, the Cartesian method should thus be applied with caution. All living matter is made from the same building blocks: for instance, there are more than 10000 different proteins in the human organism, but they are made from only twenty aminoacids! A sort of atomistic model seems to prevail, and the various ways of combining the structural units make for a tremendous information capability. It is clear why life is too complex to have been left to chance. The molecules of life and cells have developed recognition mechanisms of the lock and key type; these can be rather selective and sophisticated, given the complex geometry of molecular surfaces. No wonder some of the fundamental problems in biology are topological (and fractal)!

Much of the book is involved with self-organization and evolution. Along with heaviness (mass), self-organization is a basic property of matter. Eigen's theory of hypercycles (a mathematical formulation of all possible evolution systems) is imaginatively presented. Professor Cramer insists that, like quantum mechanics, Eigen's formulation is not an explanation but a description, but surely with the loss of visualization ("anschaulichkeit") that was brought about by modern physics, mathematical description became the equivalent of meaning. Then there is the question of complexity of highly-organized systems which can be quantified (a reincarnation of Boltzmann's equation for the entropy). The occurrence of bifurcation or fulguration points in the evolutionary schemes confers a kind of history on the process, and the systems become adaptable, even intelligent. In the old order of Newtonian systems, forever following their predictable paths, aging was inconceivable. If equilibrium is abandoned and bifurcations are possible, the future of the systems cannot be predicted, and Leibnitz's famous assertion "Natura non facit saltus" no longer holds. Instead of following determinism, the player has to learn the rules of the game. Predictability has ceased to be a criterion for scientific truth. But, as Professor Cramer explains in another context, growing old brings wisdom and freedom; ambitions are no longer necessary. There is a moral to this book, too.

Jorge C. G. Calado
Department of Chemistry
and Chemical Engineering
Instituto Superior Tecnico
Lisbon (Portugal)

Group Theory in Chemistry and Spectroscopy. A Simple Guide to Advanced Usage. By *B. S. Tsukerblat*. Academic Press, London, 1994, 430 pp., hardcover £ 40.00.—ISBN 0-12-702285-6

The fundamentals of symmetry methods and their applications to chemistry and spectroscopy are already well covered by many excellent textbooks and monographs. In the book reviewed here B. S. Tsukerblat aims to give an account of the principles and applications of the theory of finite groups, illustrated by detailed discussion of simple examples, and to enable the reader to solve practical problems using these methods. The main fields of application covered are the symmetry aspects of the ligand field theory, including spin–orbit interaction, and of molecular

 © VCH Verlagsgesellschaft mbH, D-69451 Weinheim, 1995 0570-0833/95/1616-1772 $ 10.00+.25/0

orbital theory, selection rules, vibrational spectroscopy, electron spin resonance spectroscopy (an area that has hitherto seldom been treated from this standpoint), and exchange interaction in coordination compounds.

The choice of topics and the methods used are well suited to serve the author's aims. If more care had been taken in writing the book it might have successfully filled a large gap that exists in the present range of student textbooks on chemistry and spectroscopy. There is an unusually high incidence of printing errors, mistakes, and incorrect statements, and the fact that about 15% of the literature citations refer to publications in Russian must be a serious obstacle to readers of a book in English. It should at least have been possible to refer the reader to translations, or to English-language books covering similar ground.

The book begins with three introductory chapters dealing with symmetry operations, point groups, and their representations, which according to the preface "might well be assimilated at a pre-university level". Here we already find numerous printing errors, such as those in Table 2.3 listing the 32 crystal point groups, and in the scheme showing their sub-groups (Table 2.5), examples of poor choice of words or ambiguous phrases, such as "reflection within a plane" (p. 7), and ill-chosen examples; thus, the chair form of cyclohexane is used to illustrate a body with S_6 symmetry (Fig. 2.12), whereas there is no mention of it as an example of a body with the higher symmetry D_{3d}. Many of the statements are simply wrong; some examples are: "C_{2v} has three classes" (p. 33) this should be four; on page 29 it is stated that for odd values of n the operation S_n is "not a new symmetry operation", despite the fact that the groups C_{nh} are not introduced until later; on page 42 we read "all planar molecules possessing a C_n axis belong to D_{nh}" the last symbol should be C_{nh}. Errors such as these are confusing to the novice. Equally annoying are the occasional inconsistencies; for example, in Equation (3.88) a symmetry operation is applied to the variables of a function rather than, as previously defined in Equation (3.57), to the function itself. Also the setting up of character tables is not quite so simple as is implied in Section 3.6; the quadratic equations used here have some redundant solutions.

Some important topics of representation theory, such as the classification of energy eigenfunctions, the direct product of representations, Clebsch–Gordan coefficients, the Wigner–Eckart theorem, projection operators, and the basis functions of irreducible representations are treated in connection with the ligand field theory (Chapters 4–6). The solution to the problem of classifying energy eigenfunctions in terms of irreducible representations is "proved" on page 99, despite the fact that the concept of irreducibility must be introduced as a postulate or via the definition of "accidental degeneracy". Even some statements that are given special prominence by being enclosed in a "box" are badly formulated. For example, in restricting a group to a subgroup, an irreducible representation does not necessarily give a reducible one (p. 101). Clebsch–Gordan coefficients are introduced by means of tables (pp. 135, 232), but the discussion does not include a brief explanation of how they are calculated, which would make the tables understandable. These important topics, the results of which are needed frequently in later parts of the book, deserved to be treated in a separate chapter. The description of the ligand field theory is not very satisfactory. On many aspects, such as the calculation of energy level splittings, the relationships are not properly explained, and the reader must be content with mere literature references. Even some minor aspects are not discussed thoroughly enough, for example the effect of configuration mixing on the energy terms of a d^2 ion (p. 148).

In Chapter 7 on directed valences, the orbitals given for a trigonal-bipyramidal structure such as that of PF_5 include not only the correct hybrid orbitals of the sp^3d and spd^3 types but also some incorrect ones, including sp^3 (p. 186). In Chapter 8 it is explained how molecular orbitals are classified according to group theory; here the author even manages to make mistakes in calculating the π-MOs of benzene (p. 207).

Selection rules can be expressed in the form of conditions applied to the integrands of the corresponding transition matrix elements. However, in Chapter 9 on optical transitions, it is disturbing to find that the descriptions of "necessary" and "sufficient" conditions ("only if" and "if", respectively) are often used incorrectly (pp. 225, 238). Furthermore, through the uncritical use of the formalism of representational theory, the Laporte rule forbidding pure d–d dipole transitions is wrongly described as a "supplementary restriction" in the case of systems without an inversion center (p. 235). On the other hand, the discussion of two-photon transitions in terms of symmetry in Section 9.5 is very useful, especially as this is unlikely to be found in other books on the subject.

Chapter 10 is devoted to double groups. Chapter 11 then builds on that discussion by treating the spin–orbit interaction. Chapters 12 and 13, dealing respectively with the symmetry aspects of ESR spectroscopy and with exchange interaction in coordination compounds, are the best ones in the book, after one has corrected a few errors in the signs and terms of some of the formulas. In particular, the author constructs effective Hamiltonian operators for a paramagnetic ion in ligand fields of different symmetries, and those for describing electric field effects in ESR spectroscopy, which is especially interesting. The use of group theory for the classification of exchange multiplets in polynuclear complexes and of systems with ions in different valence states is also explained, with many examples. The main text ends with Chapter 14, dealing with normal vibrations and the Jahn–Teller effect, and with vibrational coupling in mixed-valence systems.

The appendix contains the matrices of the irreducible representations for various important point groups, the associated basis functions in the form of symmetry-adapted linear combinations of harmonic functions, the decomposition of product representations into their components, and symmetry-adapted Hamiltonian operators for special ESR problems. It would also have been useful here to include answers to the exercise problems.

The work is not, as claimed in the preface, a handbook on the subject. Unfortunately it contains too many errors, far more than have been mentioned here, and too often the author fails to explain the relationships correctly. It cannot be recommended for beginners, except for gaining a general impression of the extent to which group theory and representation theory can be successfully applied to problems of chemistry and spectroscopy. On the other hand, the more advanced reader who is prepared to tolerate the errors in the book will find in it many interesting examples and problems that are not treated in other books on the subject.

Dietrich Haase
Institut für Physikalische
und Theoretische Chemie
der Freien Universität Berlin (Germany)

 © VCH Verlagsgesellschaft mbH, D-69451 Weinheim, 1995 0570-0833/95/1616-1773 $ 10.00+.25/0

Novel Porphyrinoids for Chemistry and Medicine by Biomimetic Syntheses

Burchard Franck* and Ansgar Nonn

In 1926 Hans Fischer and Bruno Walach synthesized the first porphyrins.[1] Currently more than 1400 new articles concerning the synthesis and uses of porphyrins are published every year.[2] However, the strong interest in these compounds indicated by this is in sharp contrast to their restricted availability. This is reflected in the current price of up to 500 DM for 5 mg of the most important porphyrins used in research and other applications (see Scheme 3).

Biomimetic syntheses offer possibilities for an improved approach to porphyrins. By following the example set by nature it is also possible to obtain novel porphyrinoids which are different from naturally occurring porphyrins. This is exemplified by *N*,*N'*-bridged porphyrinogens, which have cage structures, inverted porphyrinoids (N atoms in the outer periphery) and, in particular, porphyrins with expanded systems. Among the family of expanded porphyrins are superarenes with up to 34 π electrons. Their pronounced aromaticity is indicated by ^{1}H NMR spectra, bond length equivalence, planar structures, and electrophilic substitution. With their strong absorption bands, the strongest of which have ε values of > 1 000 000, a value which exceeds the absorption intensity of all other organic pigments observed until now, and their ability to act as efficient photosensitizers, the expanded porphyrins open interesting perspectives in the fields of photochemistry and photomedicine.

Keywords: aromaticity · biomimetic syntheses · dyes · porphyrins · tumor therapy

1. Introduction

Porphyrins are important for all organisms.[3, 4] They are indispensible because of their function as complexing ligands for catalytically active metals. This relates not only to metabolism, but also to the provision of energy in living creatures and photosynthesis in the plant kingdom. The deep red porphyrin **1** contains an annulene-type cyclic conjugated 18 π-electron system. Addition of six hydrogen atoms leads to the colorless and highly reactive porphyrinogen **2**. The porphyrinogens are air sensitive and are readily reoxidized to the porphyrins.

Due to the large number of natural products and synthetic products derived from the porphyrin system, it has proved appropriate to group these products under the heading *porphyrinoids* (cf. steroids, alkaloids). This approach can today be further justified for the naturally occuring porphyrins, porphyrinogens, chlorins, and corrins not only formally but also biogenetically, since, according to current knowledge, all four groups of compounds are derived from a common precursor, uroporphyrinogen III (**3**) (Scheme 1).[5–7]

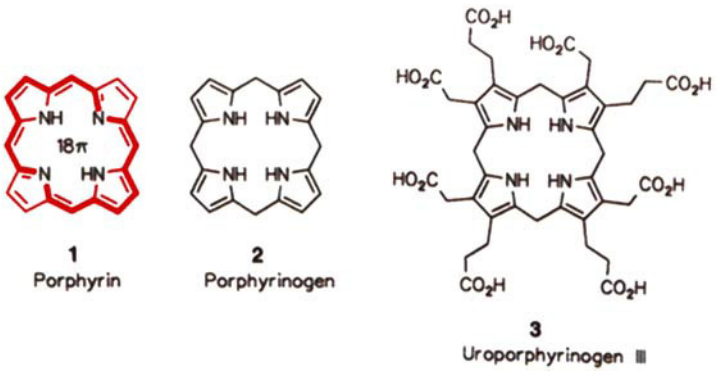

1 Porphyrin **2** Porphyrinogen **3** Uroporphyrinogen III

Scheme 1.

In order to satisfy the requirements of living organisms, nature has developed the bioproduction of porphyrinoids, the extent of which can be estimated. Let us begin with the porphyrinoid vitamin B_{12}, deficiency of which causes pernicious anemia. Humans have a daily requirement of only 0.001 mg vitamin B_{12}, an extremely tiny amount, corresponding to a total annual requirement for the earth's population of approximately 2000 kg. Heme, the red blood pigment necessary for respiration, is produced to the extent of 500 000 tonnes per year by the world's population, an amount corresponding to 25 000 full railway wagons.[8, 9] Thus, one can estimate that the total production of heme by all breathing organisms is of the order of 10 million tonnes. Even more extensive is the estimated annual production of 10^9 tonnes[10, 11] of chlorophyll by plants.

[*] Prof. Dr. B. Franck
Organisch-chemisches Institut der Universität
Corrensstrasse 40, D-48149 Münster (Germany)
Telefax: Int. code + (251)83-9772
e-mail: franck@uni-muenster.de
Dr. A. Nonn
Bayer AG
Rheinuferstrasse 7–9, D-47829 Krefeld (Germany)
Telefax: Int. code + (2151)88-7703

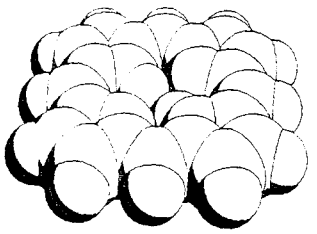

Fig. 1. MOPLO representation [12] of the unsubstituted porphyrin framework.

Aside from the bioproduction of porphyrinoids, their chemical synthesis is of growing importance. Increasingly, the porphyrin system is characterized by a multitude of reactions, properties, and transformations, which, given their compact structure (Fig. 1), at first sight appears to be surprising. In the last 27 years *Chemical Abstracts* has registered more than 20000 publications relating to porphyrins of various structures.[2] In this time the annual number of publications has risen from 234 (1967) to 1414 (1994). In addition, numerous structurally related porphyrinoids containing ring systems different from that in **1** must also be taken into consideration. A selection of applications of porphyrinoids in chemistry and medicine is given in Scheme 2.

Chemistry	Medicine
complexes	diagnosis of porphyria
light conversion	cytochrome oxidase models
autoxidation catalysis	phototoxicity
aromaticity	tumor therapy
UV/Vis/NIR sensors	virus eradication

Scheme 2. Applications and research uses of porphyrins.

With regard to the areas mentioned in Scheme 2, the following goals can be set: 1) The development of more efficient processes for the synthesis of porphyrinoids. 2) Research into access to and structural limitations of novel porphyrinoids. 3) The synthesis of tailor-made porphyrinoids for investigations into aromaticity, electron spectroscopy, and photomedicinal applications. The results of research into these three areas form the content of the following discussion.

2. Do Synthetic Porphyrinoids Have To Be More Expensive Than Gold?

Despite the promising developments made with porphyrinoids in chemistry and medicine, this area of research suffers from a severe handicap: Access to the majority of the required porphyrinoids demands cumbersome, multistep syntheses with very low overall yields.

In order to illustrate the availability of porphyrins, the current commercial prices of four important examples (**1**,**4**–**6**) are shown (Scheme 3).[13] Although the simple porphyrin **1** is one of

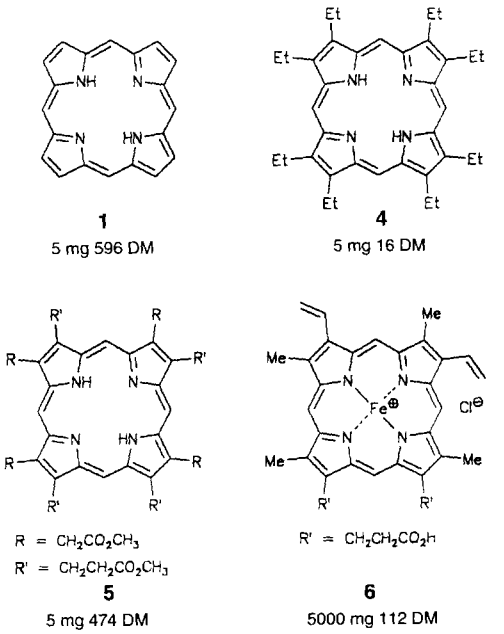

Scheme 3. Commercial prices for porphyrin (**1**), octaethylporphyrin (**4**), uroporphyrin-III octamethyl ester (**5**) and hemin **6** [13] (5 g of gold cost ca. 90 DM [19]).

Burchard Franck, born in 1926 in Hamburg, studied chemistry at the Universities of Hamburg and Göttingen. After his Diplomarbeit on digitalis glycosides with R. Tschesche in Hamburg he received his doctorate under the supervision of H. Brockmann in Göttingen in 1952 for work on antibiotics from streptomycetes. In 1959 he was awarded his habilitation for organic chemistry at the University of Göttingen. In 1963 he accepted a call to the University of Kiel and since 1968 he has been Professor of Organic Chemistry at the University of Münster. He has been a Guest-Professor in the USA, Norway, Switzerland, China, and India. Among the awards he has received for his research are the Richard-Kuhn-Medaille der Gesellschaft Deutscher Chemiker and the Adolf-Windaus-Medaille der Universität Göttingen. His recent research work has focussed on mycotoxins, biosynthesis and biomimetic syntheses, isotopic labeling, novel porphyrins, superaromaticity, and phototherapy.

B. Franck

A. Nonn

Ansgar Nonn, born in 1962 in Bad Honnef, studied chemistry from 1984 to 1989 at the Universities of Cologne and Münster. He received his doctorate in 1991 under the supervision of B. Franck for work on selective porphyrin syntheses by conformational control of the cyclization. From 1991 to 1992 he carried out post-doctoral reseach with K. P. C. Vollhardt in Berkeley, USA, on the cyclization of N-heterocycles with cobalt complexes. In 1992 he joined the Bayer AG and carried out fundamental research. Since 1993 he has been a project leader in diagnostics development at Bayer AG in Uerdingen.

the most important naturally occuring aromatic systems, it cannot be easily synthesized. Accordingly, it is very expensive (Scheme 3). Octaethylporphyrin (**4**)[14, 15] is an intensively used synthetic porphyrin due to its similarity to the natural porphyrins and its much lower price. Uroporphyrin-III octamethyl ester (**5**) is a derivative of uroporphyrinogen III (**3**), which is the common biosynthetic precursor to all porphyrins and cyclic tetrapyrroles in the biosphere.[5–7] Thus, according to what has previously been stated, the annual natural production of **3** is more than 1 billion tonnes. Its price is nevertheless very high (Scheme 3), because, for practical purposes, it cannot be isolated from natural sources and its chemical synthesis requires numerous steps.[16, 17] In contrast, hemin **6** is available in abundance[18] as a porphyrin raw material from slaughterhouse blood.

A chemist who considers embarking on the synthesis of porphyrins is well advised to learn from nature and concentrate on porphyrins bearing substituents in all eight pyrrole β positions. Cyclizations leading to porphyrins lacking these substituents, of which porphyrin **1** is an extreme example, suffer from the drawbacks of low cyclization yield, as well as instability and poor solubility of the product unless the C–H bridges between the pyrrole nuclei carry stabilizing groups.

The three most commonly used synthetic routes to β-substituted porphyrinoids are summarized in Scheme 4. These are the optimized dipyrrylmethane method **A** of Hans Fischer,[21] as modified by McDonald et al.,[20] the biladiene process **B**,[22] and the ring-forming cyclization of four monopyrroles (**C**) which resembles the biosynthesis of porphyrins.[23] All three methods are based on the tendency of open-chain tetrapyrrole intermediates to cyclize in an astonishingly selective manner.[24, 25] The biomimetic route has proved to be the most powerful of the three methods, not only from the point of view of the yields attained but also because of the lower number of steps required and the variety of products which can be synthesized using this method.[23, 26–29]

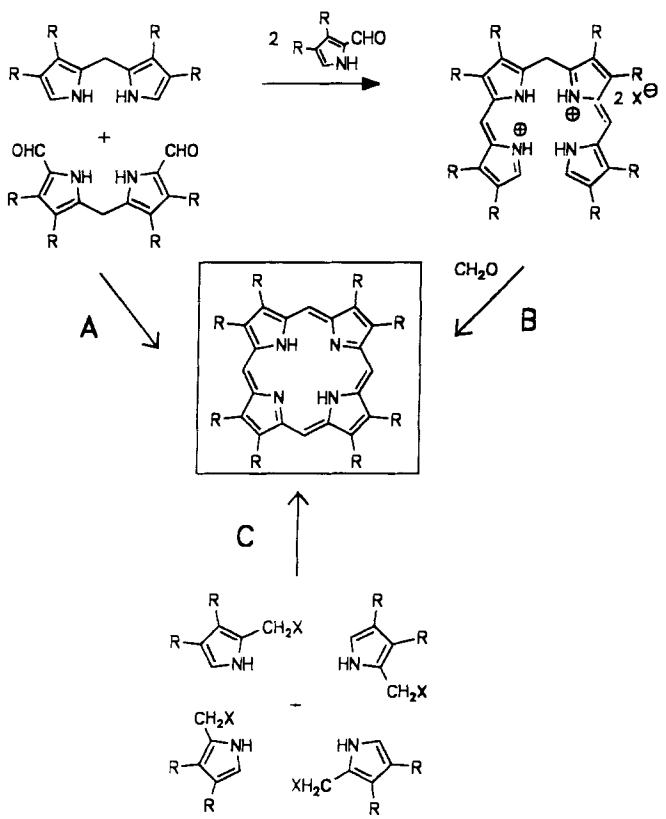

Scheme 4. Three synthetic routes to porphyrins.

Nature provides a model of biomimetic synthesis of porphyrins with the biosynthesis of the essential cyclic tetrapyrroles from the monopyrrole porphobilinogen **9** (Scheme 5).[5, 6] As

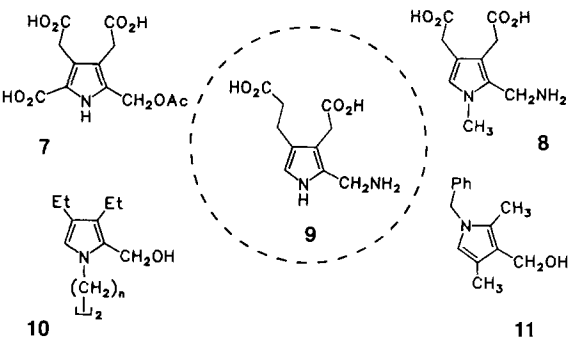

Scheme 5. Pyrroles for biomimetic synthesis.

first demonstrated by Cookson and Rimington,[23] **9** can be converted under conditions of acid catalysis to uroporphyrinogens and further to uroporphyrins, as represented by path **C** in Scheme 4. In order to explore the potential and the limitations of biomimetic syntheses of porphyrins from pyrrole precursors, we synthesized a series of derivatives of **9** (Scheme 5) and investigated their reactivity towards condensation under acid catalysis. The results obtained exceeded all expectations. Despite considerable structural variations in the monopyrroles **7**, **8**, **10**, and **11** (Scheme 5), in comparison with the biosynthetic starting material **9**, the condensations proceeded in high yields.

3. A Variety of Porphyrins through Biomimetic Synthesis: Reasonably Priced, *N*-substituted, *N,N'*-Bridged, and Inverted Porphyrinoids

Due to the presence of different side chains in the β-positions of porphobilinogen **9**, its acid-catalyzed cyclocondensation yields a mixture of isomeric uroporphyrins. Thus, the porphobilinogen derivative **7**, which contains two identical acetic acid side chains, is better suited as a reactant for biomimetic synthesis.[27] Additionally, the amino group of **9** is replaced in **7** by the better leaving group *O*-acetyl and the other α-position is reversibly protected by a carboxyl group. The cyclocondensation of **7** proceeds to give the porphyrinogen octaacetic acid **12** in high yield (Scheme 6). This can undergo autoxidation and is isolated after oxidative workup as the octamethyl ester **14**. Compound **14** differs from the expensive uroporphyrin-III derivative **5** (see Scheme 3) only by the replacement of propionic acid side chains by acetic acid units and has thus proved itself to be an

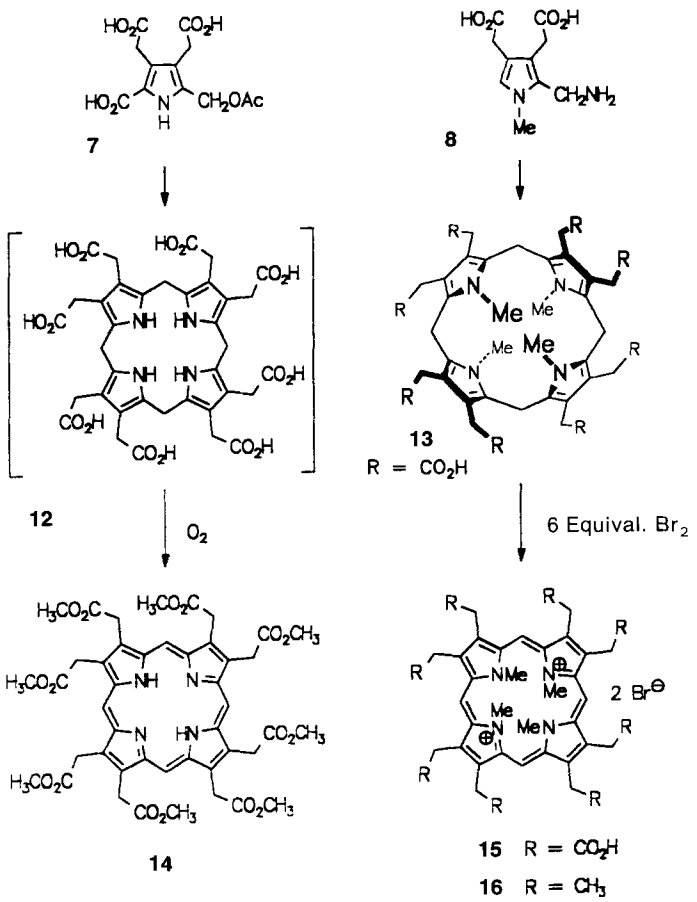

Scheme 6. Biomimetic syntheses of [18]porphyrins.

easily accessible, useful model compound for biological investigations.

The fact that exhaustive *N*-methylation of porphyrins had been shown not to be possible[30, 31] led to the assumption that *N*,*N*′,*N*″,*N*‴-tetramethylporphyrins are not capable of existence. Thus, the possibility of biomimetic condensation of the *N*-methylnorporphobilinogen **8** to the *N*,*N*′,*N*″,*N*‴-tetramethylporphyrinogen **13** seemed rather remote. We could, nevertheless, show that the acid-catalyzed condensation of **8** delivered the crystalline *N*,*N*′,*N*″,*N*‴-tetramethyporphyrinogen **13** in a yield of 17%.[26] This represents a particularly convincing example of the capability of the biomimetic principle in the synthesis of porphyrins. According to its crystal structure,[32] **13** has a structure unusual for porphyrinogens, in which the neighboring pyrrole rings are highly twisted relative to each other. This does not, however, lead to instability, but rather to high resistance towards oxidation.

In order to convert **13**, the first autoxidation-resistant porphyrinogen, to the corresponding bis-quaternary *N*,*N*′,*N*″,*N*‴-tetramethylporphyrin **15**, one requires very powerful oxidants such as elemental bromine or cerium(IV) ammonium nitrate.[6, 33] Although **15** cannot have a completely planar structure, the ^{1}H NMR spectrum of the octamethyl ester displays a significant diamagnetic ring current effect which resembles that of Sondheimers [18]annulene **33** (see Scheme 12).[34] Thus, the resonance signals of the methine protons are strongly shifted to low field, appearing at $\delta = 10.40$, while the NCH_3 protons resonate at $\delta = -4.31$.[6] These values were confirmed by the synthesis of a similar octaethyl-*N*,*N*′,*N*″,*N*‴-tetramethylporphyrinogen (**13**, R = CH_3 instead of CO_2H)[35, 36] and also the synthesis and crystal structure of the corresponding porphyrin **16** by Vogel et al.[36]

Encouraged by these findings we took in hand the synthesis and biomimetic condensation of *N*,*N*′-bridged dipyrrole precursors.[28] Since in the *N*,*N*′,*N*″,*N*‴-tetramethylporphyrinogen **13**, the diametrically opposing *N*-methyl groups project out of the same side of the molecular plane, it could be possible to bridge the two nitrogens with an alkylene chain of the appropriate length. To this end the two principle possibilities **A** (parallel *N*,*N*′-bridges) and **B** (crossed *N*,*N*′-bridges) shown in Scheme 7 can be considered. In both cases cyclization would lead to novel polycyclic tetraaza systems.

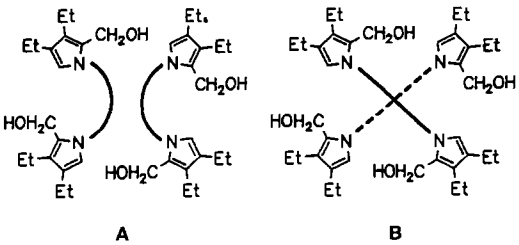

Scheme 7. Two product types potentially accessible by the acid-catalyzed condensation of *N*,*N*′-α,ω-alkylenedipyrroles.

The synthesis of the required *N*,*N*′-α,ω-alkylenedipyrroles **19a–e** was successfully carried out by condensation of the potassium salt of the diethylpyrrolecarbaldehyde **17** with the α,ω-alkylene dibromides **18a–e** (Scheme 8).[28] The di(pyrrole-

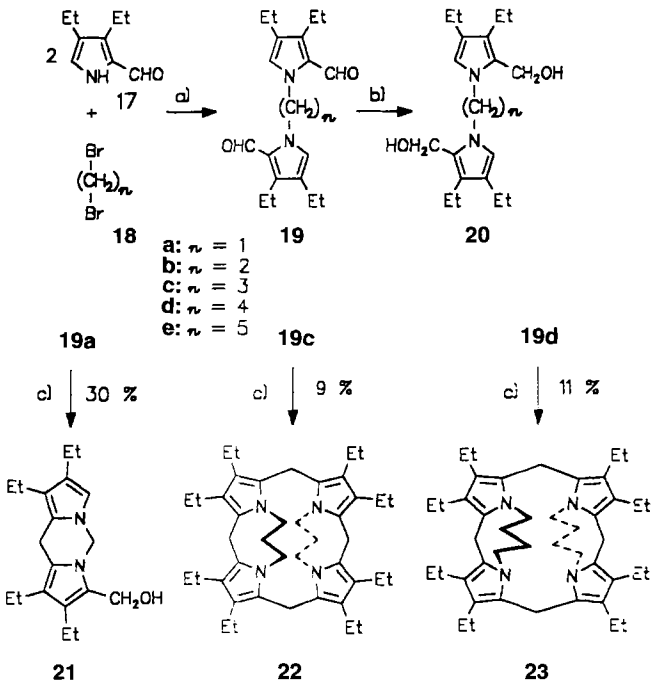

Scheme 8. Synthesis of *N*,*N*′-α,ω-alkylenedipyrroles **19a–e** and the conversion of **19a**, **19c**, and **19d** into the bridged polycycles **21–23** by reduction and biomimetic cyclization [28,37]. a) KOH/DMSO, 20 °C; b) $NaBH_4$/MeOH, 20 °C; c) TosOH/MeOH/AcOH, −60 °C.

carbaldehydes) **19a–e** thus obtained are vinylogous amides and are thus stable compounds capable of being stored. Before further reaction they were activated by reduction with $NaBH_4$ to the diols **20a–e** and used in situ. The yields of **21–23** obtained by the acid-catalyzed condensation over one or four steps display a marked dependency not only on the chain length of the alkylene moiety but also on the transannular interactions within the heteropolycycles formed during the reaction (Scheme 8).

While the *N*,*N*′-methylenedipyrrole **19a** undergoes exclusively intramolecular condensation to give the novel dipyrrolo-1,3-piperazine **21**, the ethylenedipyrrole **19b** reacts to give undefined intermolecular polycondensates. The desired intra-/intermolecular condensation leading to *N*,*N*′-bridged [18]porphyrinogens only succeeds with the higher *N*,*N*′-α,ω-alkylenedipyrroles, starting from the 1,3-propanediylpyrrole **19c**. This is to be expected from inspection of molecular models.

Compounds **19c** and **19d** condense intra-/intermolecularly to the [18]porphyrinogens **22** and **23**, respectively. Both of these structures contain two novel heterotricyclic ring systems which can be classified as dipyrrolo-1,5-diazocane and dipyrrolo-1,5-diazonane, respectively. According to the following evidence, it can be concluded that both pairs of neighboring N atoms are connected by parallel bridges (cf. **A** in Scheme 7) rather than the alternative arrangement with crossed *N*,*N*′-bridges (**B** in Scheme 7): 1) In the conversion of **19c**, it was possible to isolate a dipyrrolo-1,5-diazocane (half molecule) which is an intermediate in the synthesis of the parallel-bridged **22**.[28] 2) The ^1H NMR spectrum of **22** displays two triplets for the ethyl-CH_3 groups, which shows that the molecule is not C_4 symmetrical, and thus is not a [18]porphyrinogen with crossed *N*,*N*′-bridges (cf. **B** in Scheme 7).

The yields of porphyrinogens **22** and **23** (Scheme 8), based on the pyrrolecarbaldehydes, are remarkably high, taking into account the multistep nature of the reaction sequence. Due to Prelog strain in medium ring systems lower yields are expected for **25**, unless the transannular interactions are reduced by substitution of CH_2 with oxygen atoms. This effect is clearly seen in the acid-catalyzed condensation of the bipyrroles **19e** and **24** (Scheme 9). While the yield of **25** is only 7%, due to Prelog strain in the dipyrrolo-1,5-diazecane ring system, the exchange of CH_2 for O in the *N*,*N*′-bridge, which leads to the dipyrrole **24**, causes the yield of **26** to jump significantly to 49%.

Similarly to the *N*,*N*′,*N*″,*N*‴-tetramethyl[18]porphyrinogen **13**, the N,N′-bridged porphyrinogens **22**, **23** and **25**, **26** are stable towards oxidation. As would be expected from their three-dimensional cage structure, **22** and **26** are incapable of dehydrogenation to [18]porphyrins even under energetic conditions, this behavior being in contrast to that of **13**. The octaethyl *N*,*N*′,*N*″,*N*‴-di(3-oxapentylene)-porphyrinogen **26** deserves consideration as a potential ligand for metal complexes because of its spherical center which contains six donor atoms.[37]

The question of whether porphyrinogens with inverted pyrrole units could be obtained by biomimetic condensation (Scheme 10) was of interest for a variety of reasons. Such invertoporphyrinogens like **30**,[38] whose nitrogen atoms are located on the periphery rather than in the center of the molecule, should provide much revealing information regarding, for example, the electronic structure, the complex formation, and the conformational control of the cyclocondensation.

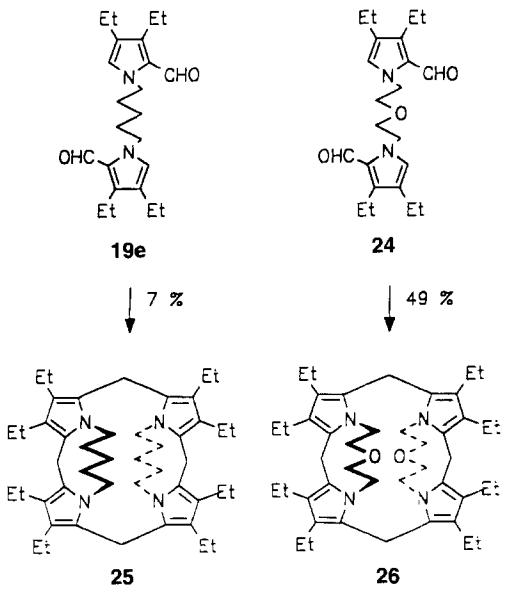

Scheme 9. Biomimetic condensation of α,ω-pentanediyldipyrrole **19e** and 3-oxa-α,ω-pentanediyldipyrrole **24** to the doubly *N*,*N*′-bridged [18]porphyrinogens **25** and **26**, respectively. (For reaction conditions see Scheme 8) [28].

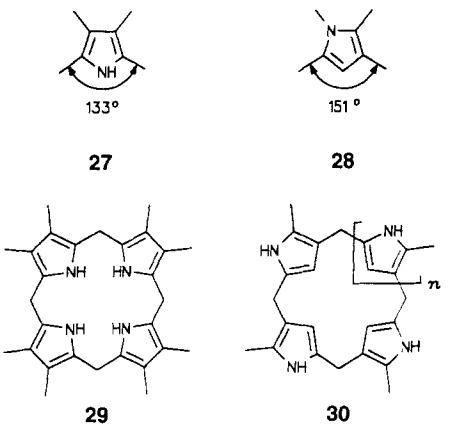

Scheme 10. Comparative bond angles for the formation of porphyrinogens **29** and invertoporphyrinogens **30**.

It had to be considered for such a cyclocondensation, that the inverted pyrrole units take up a larger proportion of the sum of the internal angles of the porphyrinogen product than the non-inverted units (Scheme 10). Thus, for the normal porphyrinogen **29**, the relevant angle, that between the α-substituents of the pyrrole unit **27**, is 133°,[39] whereas the angle between the macrocycle-forming substituents for the invertoporphyrinogen **30** is 151°. Thus, each inverted pyrrole nucleus should either cause an increase in size of the macrocycle formed or lead to increased ring strain. Accordingly, one would expect that acid-catalyzed condensation would lead to a cyclic pentapyrrole.

The initially considered isomer of porphobilinogen **9** (Scheme 5), as well as a range of similar monopyrroles, proved to be unsuitable for the biomimetic synthesis of invertoporphyrinogens. Success in the acid-catalyzed condensation was achieved by using the *N*-benzylpyrrole **11**, in which the large, space-filling benzyl groups favor the ring closure[29] along the lines of the conformational helix effect (Scheme 11).[24]

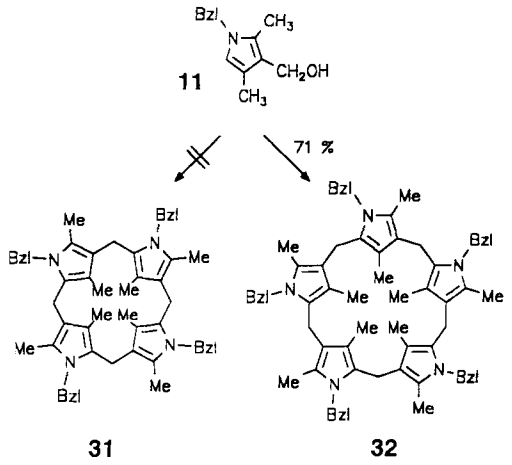

Scheme 11. Biomimetic synthesis of the invertopentaphyrinogen **32** [29].

Compound **11** gave the colorless cyclic pentapyrrole **32** in 71 % yield. The pyrrole homolog of porphyrin was named pentaphyrin by Gossauer et al.[40] Following this system we have named **32** invertopentaphyrinogen.[29]

The cyclic tetrapyrrole **31** (invertoporphyrinogen) corresponding to **32**, which, due to bond angle considerations (see Scheme 10), should display substantial ring strain, could not be detected in the condensation. The pentapyrrole **32** is characterized by its high resistance to oxidation. While normal porphyrinogens are very sensitive towards oxidation and the *N*,*N*′,*N*″,*N*‴-tetramethylporphyrinogen **13** can be dehydrogenated to the corresponding deep red porphyrin **15**, albeit under more forcing conditions, such a reaction does not take place with the invertopentaphyrinogen **32**. A possible explanation for this resistance to oxidation[29] is the fact that aromatization of **32** would require a destabilizing accumulation of charge on quaternary centers.

Recently, Furuta et al.[41a] and Chmilewski et al.[41b] succeeded in demonstrating that, in the non-biomimetic synthesis of porphyrins from pyrrole and arylaldehydes (Rothemund synthesis[41c]), the major products (tetraphenylporphyrins) are accompanied by smaller amounts of isomeric monoinvertoporphyrins. This interesting observation indicates that the formation of normal porphyrins is preferred to monoinvertoporphyrins in the equilibrium-controlled acid-catalyzed condensation of simple pyrroles. This is in agreement with the conclusions which can be drawn from bond angle considerations.

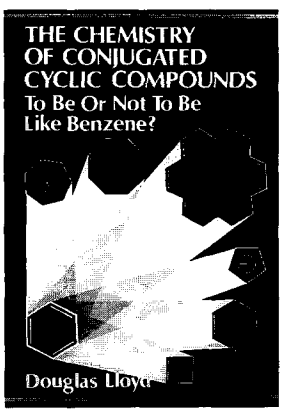

Fig. 2. Front cover of a monograph by Lloyd [42] (Copyright 1989 reprinted with kind permission from John Wiley & Sons Ltd. New York).

4. Routes to Novel Superarenes

The subtitle of a monograph by Lloyd[42] (cover design, Fig. 2) poses the question which has perplexed chemists since Kekulé, almost as much as Shakespeare's Hamlet was troubled by his famous existential contemplation.[43] Thanks to the pioneering work of Sondheimer[34] we know that the [18]annulene displayed in the upper right part of the cover, with its cyclic conjugated 18-π-electron system, can be considered to be a hexavinylogous benzene.

The aromaticity of **33** (Scheme 12) is indicated by the following experimental evidence: The π-electron count of the [18]annulene obeys E. Hückel's $(4n + 2)$ rule,[44] the crystal structure analysis[45] yields a planar structure with bond length equivalence, and finally, the ^{1}H NMR spectrum of **33** indicates a pronounced diatropic ring current. As with **33**, the porphyrin **1** contains a cyclic conjugated 18-π electron system, which can be designated a diazaannulene. Three further azaannulene systems related to the porphyrins are the corrole **34**,[46] the homoporphyrin **35**,[47] and the porphycene **36**.[48]

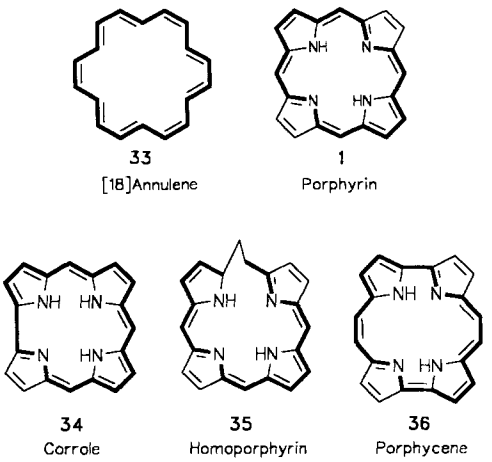

Scheme 12. 18π-electron systems.

4.1. Biomimetic Synthesis of [26]- and [34]Porphyrins

We had hoped that it might be possible to prepare vinylogous porphyrins using the biomimetic approach and related processes. Indeed it was possible to synthesize the four vinylogous porphyrin systems with 22π- (**39**), 26π-(**37**,**40**), and 34π-electron perimeters (**38**) shown in Scheme 13. We have proposed a system of nomenclature for such compounds[49, 50] in analogy to that used for the annulenes. Thus, vinylogous porphyrins are represented by a prefix in square brackets corresponding to the number of π electrons in their conjugated perimeter. Accordingly, the systems **37**–**40** in Scheme 13 would be designated [22]-, [26]-, and [34]porphyrins. Furthermore, it is sensible to extend this system to the precursors of these porphyrins. In this way one can use the names [22]-, [26]-, and [34]porphyrinogens.

The experimental[34] and theoretical[51] results from annulene chemistry represent the first hurdles standing in the way of a synthesis of vinylogous porphyrins. It has been shown that for annulenes, the resonance energies of annulenes up to [22]annulene allow the stabilization of a planar, aromatic conformation, whereas higher annulenes behave more like conjugated olefins. The experimental and theoretical studies of this subject are in good agreement. The situation regarding porphyrinoids appears to be more favorable. From the finding that simple [18]porphyrins are more chemically stable than

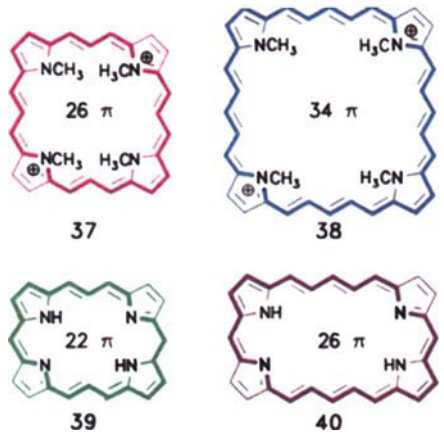

Scheme 13. Four vinylogous porphyrins with 22π-, 26π-, and 34π-electron systems.

[18]annulenes, one can presume that the rigid pyrrole units of the system can provide conformational stability, without adverse affect on the annulenoid conjugation.

All four porphyrinoids shown in Scheme 13 are characterized by previously unknown extremes in properties related to aromaticity and light absorption. Very high diatropic ring current effects in their ^{1}H NMR spectra justify the name superarenes. Their Soret band molar extinction coefficients of $\varepsilon > 10^6$ exceed the highest previously known, found in pigments.

Following the ring closure principle of porphyrin biosynthesis, pyrrolylpropenals of type **42** (Scheme 14) were considered as starting materials for the synthesis of vinylogous porphyrinogens.[24c, 49] They differ from the biosynthetic precursor of porphyrin, porphobilinogen **9** (see Scheme 5), by the replacement of the β-position side chains by alkyl groups and the replacement of the aminomethylene group by a propenal unit. Additionally, it was found to be necessary, for reasons of stability, to replace the NH hydrogen atom with a methyl group. In order to obtain information about conformational influences on the ring closure reaction, pyrrole units with increasing steric congestion at their β-positions were chosen.

The pyrrolylpropenals **42a–e** were obtained in high yields by vinylogous Vilsmeier formylation[52, 53] in two steps from the monopyrroles **41a–e**.[24c, 49] Finally, reduction of the aldehyde group and acid-catalyzed condensation of the so-formed reactive pyrrolylpropenols in situ yielded the [26]porphyrinogens **44a–e** (Scheme 14). A significant correlation between the yields of the ring closure and the spatial requirements of the β-substituents can be detected. As in the biomimetic synthesis of normal [18]porphyrins,[24] this effect can be explained by a preferred helical conformation in the transition state of the cyclization of the intermediate tetrapyrrole **43** being favored by interactions between the β-substituents of neighboring pyrrole units. When one considers the structures of **44a** and **44e** (Scheme 15) it appears at first sight astonishing that the isobutyl groups which project far out from **44e** do not hamper the ring closure, but rather, in comparison to **44a**, significantly favor it.

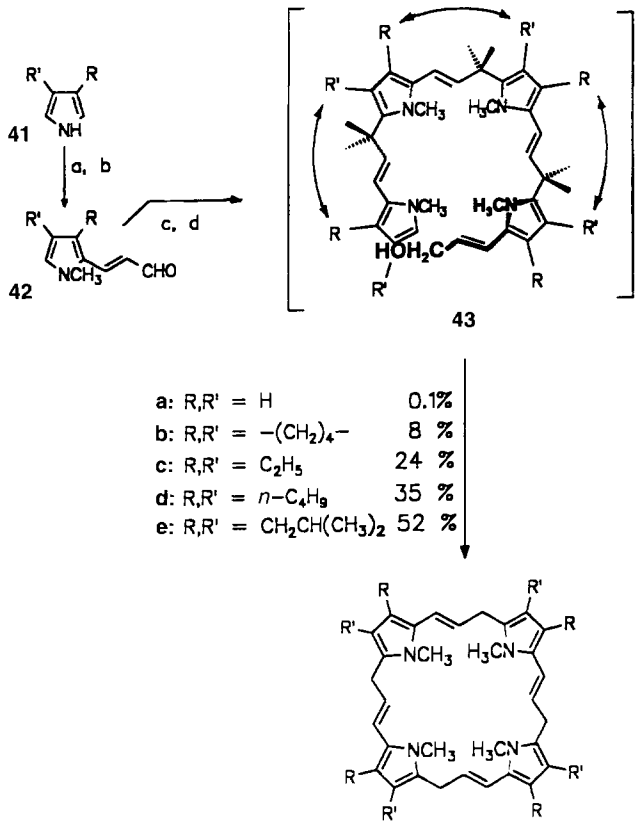

Scheme 14. Biomimetic synthesis of the [26]porphyrinogens **44a–e** [24c,49]. Reaction conditions: a) dimethylaminoacrolein ($Me_2NCH{=}CH{-}CHO$)/$POCl_3$; b) KOH/DMSO, CH_3I; c) $NaBH_4$/MeOH; d) TosOH/AcOH.

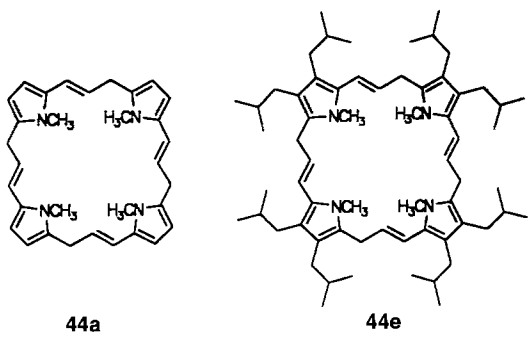

Scheme 15. Structures of **44a** and **44b**.

The question that arises next is whether the helical effect[24c] can also play an effective part in the biomimetic cyclotetramerization of monopyrroles carrying pentadienyl side chains. Such condensations should lead to octavinylogous porphyrinogens and [34]porphyrins. The starting materials **45a,b** were obtained in a similar manner to the aldehydes **42a–e** by the bis-vinylogous Vilsmeier formylation of the dialkylpyrroles **41c,e** (Scheme 14) with dimethylaminopentadienal (Scheme 16). Subsequently, the NH was methylated, the aldehyde function reduced, and the resulting, highly reactive pyrrolylpentadienol then underwent the acid-catalyzed cyclization in situ. An especially mild workup delivered the [34]porphyrinogens **46a** and **46b**.[53, 54] The yield of porphyrinogen **46b** with its sterically demanding isobutyl groups is almost twice as high as that of the octaethylporphyrinogen **46a** and indicates that, in this case too, the helical effect[24] is active in providing effective conformational control.

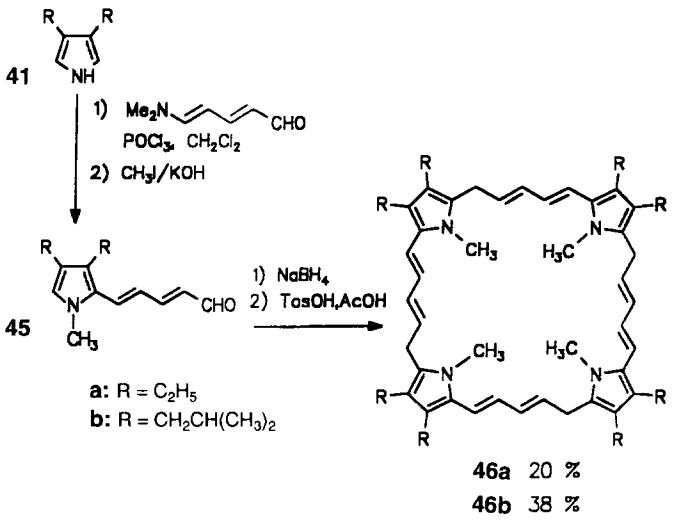

Scheme 16. Biomimetic synthesis of the [34]porphyrinogens **46a** and **46b** [53, 54].

The four [26]porphyrinogens **44b–e** and also the two [34]porphyrinogens **46a** and **46b** can be dehydrogenated with exactly six equivalents of bromine in the presence of polymeric base to give the deeply colored and aromatic porphyrins **47a–d**, **48a**, and **48b**, respectively (Scheme 17).[24c, 53, 54] The smooth

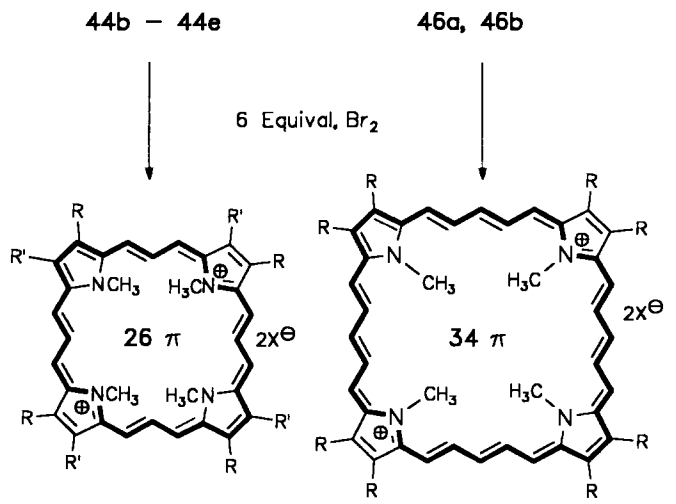

47a R,R' = $-(CH_2)_4-$ 24 %
47b R,R' = C_2H_5 41 %
47c R,R' = n-C_4H_9 39 %
47d R,R' = $CH_2CH(CH_3)_2$ 34 %
48a R = C_2H_5 12.6 %
48b R = $CH_2CH(CH_3)_2$ 13.0 %

Scheme 17. Dehydrogenation of the tetra- and octavinylogous porphyrinogens to the [26]porphyrins **47** and the [34]porphyrins **48**.

progress of this dehydrogenation of cyclic polyenes each with four reactive allyl groups would be almost inexplicable were it not for the aromatic stabilization of the reaction products. The good yields obtained in the dehydrogenation reactions proved to be essentially independent of the steric demands of the β-substituents (Scheme 17).

4.2. Synthesis of [22]- and [26]Porphyrins with the Biladiene Process

Because of the already mentioned extensive applications of Hans Fischer's octaethyl[18]porphyrin (**4**),[14] particular interest is being shown in its di- and tetravinylogues, the [22]porphyrin **49a** and the [26]porphyrin **49b**, respectively (Scheme 18). While the synthesis developed for **4** is based on the condensation of monopyrroles, a vinylogous version of the biladiene process could be applied to the synthesis of the "rectangular" C_2-symmetric porphyrins **49a,b**.[22] This would require that the vinylogous biladiene, formed as an intermediate, is capable of adopting the necessary hairpin conformations **50a** or **50b**, respectively (Scheme 18). As previously discussed for the biomimetic synthesis of "square" C_4-symmetric porphyrins, helical effects[24] of the β-substituents should favor the required conformation **50** over the linear form **51**. A further prerequisite is that the biladiene, with its vinylogous amidine structure, must possess sufficient stability.

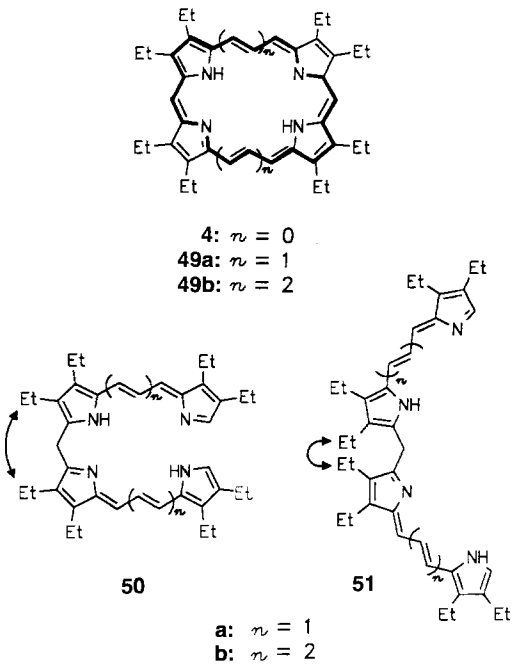

Scheme 18. The octaethyl[18]porphyrin **4** of Hans Fischer [14] together with its di- and tetravinylogues **49a** and **49b**, respectively, and the possible conformations **50** and **51** of the biladiene precursor.

The pyrrolylacroleins **53a** and **53b** are key building blocks in the synthesis of the bisvinylogous biladiene **54a** and the tetravinylogous biladiene **54b**, respectively.[24c, 53] Their condensation with the dipyrrolylmethane **52**, a porphyrin building block described by Paine and Woodward,[55] provided the highly colored vinylogous biladienes **54a** and **54b** in surprisingly high yields (Scheme 19).[50, 56]

The highly crystalline, aromatic porphyrinoids **49a** and **49b** can be obtained by the acid-catalyzed condensation of **54a** and **54b** with formaldehyde, followed by the dehydrogenation of the initially formed hydroporphyrinoids with 2,3-dichloro-5,6-dicyano-1,4-benzoquinone (DDQ) (Scheme 20).[56] Similarly, the

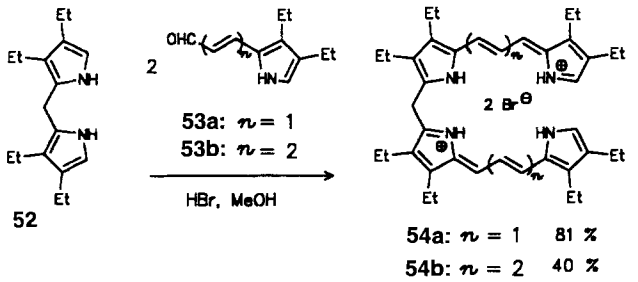

Scheme 19. Synthesis of the di- and tetravinylogous biladienes **54a** and **54b**, respectively [50, 56].

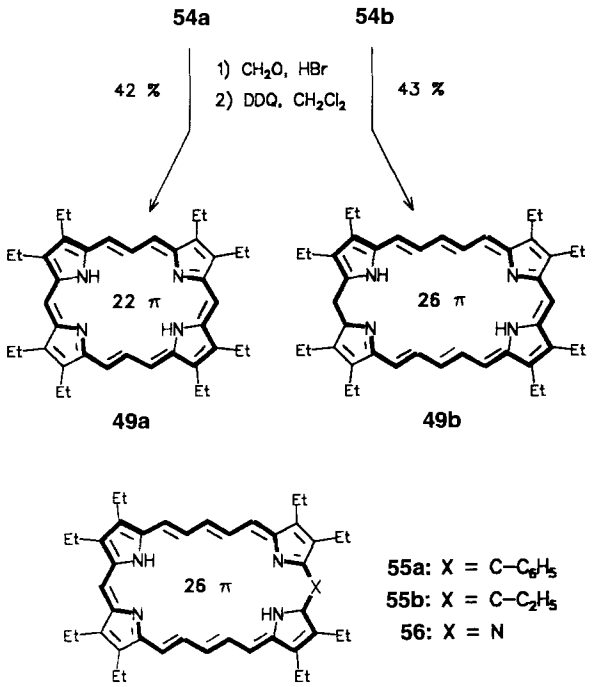

Scheme 20. Acid-catalyzed condensation of the vinylogous biladienes **54a** and **54b** to give [22]- and [26]porphyrins [50, 56].

phenyl- and ethyl-substituted [26]porphyrins **55a** and **55b** were prepared by condensation of the tetravinylogous biladiene **54b** with benzaldehyde and propionaldehyde, respectively. Condensation of **54b** with ammonia gave the aza[26]porphyrin **56**.[50]

5. The Fascination of Superaromaticity

Sondheimers synthesis of the [18]annulene **33a**[34] (Scheme 21) has had far-reaching implications for organic chemistry. For example, 40 years after the Hückel rule for benzenoid arenes[44] was postulated, this synthesis provided confirmation of the validity of this rule for systems up to and including the hexavinylogue of benzene **33a**. Furthermore, as previously mentioned, the annulenes proved the power and capabilities of HMO calculations as a method for predicting the stability of unknown molecules.[51]

These findings have stimulated intensive efforts to obtain access to higher aromatics by constraining the conformational

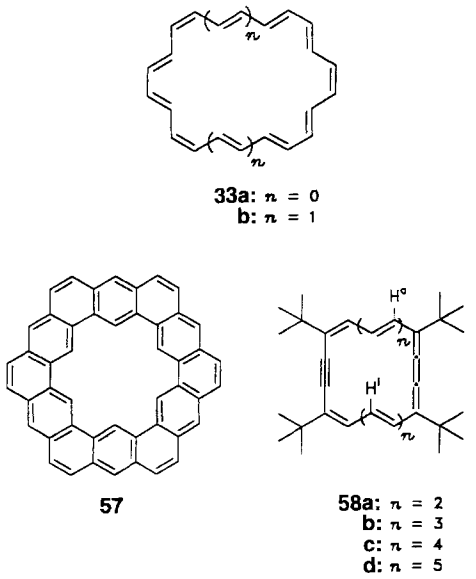

Scheme 21. [18]- and [22]annulenes **33a** and **33b**, respectively [34], as well as kekuléne **57** [57] and dehydroannulene **58** [58].

flexibility of annulenes. Two studies proved to be particularly informative: The synthesis of the kekuléne **57** by Staab et al.[57] and of the didehydroannulene **58** by Nagakawa et al.[58] (Scheme 21). In the case of kekuléne **57** the [18]annulene is embedded in a wreath of twelve benzene rings. This allows a direct comparison of the resonance stabilization of the benzene sextet with that of the conjugated 18π- and 30π-perimeters (inner and outer rings in **57**). As can be seen from the ^{1}H NMR spectra, **57** is a system composed of annelated benzenoid π-sextets, in which annulenoid conjugation plays no part.[57]

In the cases of the dehydroannulenes **58a–d** the alkyne and allene units provide the conjugated perimeter with steric rigidity and resonance stabilization. The ^{1}H NMR signals of the inner (H^i) and outer (H^a) protons at the conjugated perimeter indicate a correspondingly larger ring current effect than that displayed by annulenes of the same π-electron count (Table 1). The $\Delta\delta$ values ($\delta(H^a) - \delta(H^i)$), which serve as a measure of the size of the ring current effect, become smaller, starting from [18]didehydroannulene **58a**, as the molecule becomes less rigid.[58]

Table 1. ^{1}H NMR data for the didehydroannulenes **58a–d** [58] (see Scheme 21). δ values of the inner (H^i) and outer (H^a) protons at the conjugated perimeter, and the differences $\Delta\delta = \delta(H^a) - \delta(H^i)$.

Didehydroannulene	$\delta(H^i)$	$\delta(H^a)$	$\Delta\delta$
58a (18π)	−3.42	9.87	13.29
58b (22π)	−0.83	9.16	9.99
58c (26π)	1.95	8.23	6.28
58d (30π)	3.5	7.5	4.0

An unequivocal indication of the aromaticity of higher annulene derivatives should include, in addition to the ring current effects in the ^{1}H NMR spectrum, the proof of a planar structure with bond length equivalence in the conjugated perimeter, and the ability of the perimeter to undergo electrophilic substitution. Therefore, with regard to theoretical utility, it is desirable that

the measures taken to ensure a stable planar structure allow the molecule to remain structurally as close as possible to the annulenes. These requirements are essentially fulfilled in the case of the [22]- and [26]porphyrins **49a** and **49b**, respectively (see Scheme 20).[50, 56]

The ^{1}H NMR data for Hans Fischer's octaethyl[18]porphyrin (**4**) are summarized in Table 2 along with those of the octaethyl[22]porphyrin **49a** and the octaethyl[26]porphyrin **49b**. As is already known, the diatropic ring current effect of the normal [18]porphyrin **4**, with a $\Delta\delta$ value of 13.92, is comparable

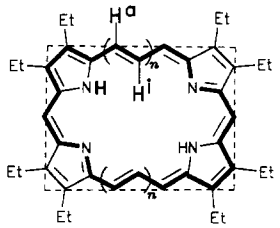

4: $n = 0$
49a: $n = 1$
49b: $n = 2$

Table 2. ^{1}H NMR data for the vinylogous porphyrinoids. δ values of the inner protons (H^i, NH) and outer protons (H^a, NH) at the conjugated perimeter, the difference $\Delta\delta = \delta(H^a) - \delta(H^i)$, and the areas S of the rings in Å^2.

Porphyrinoid	$\delta(H^i)$	$\delta(H^a)$	δ(NH)	$\Delta\delta$	S
4 [18]	–	10.18	−3.74	13.92	50
49a [22]	−9.54	12.78	−6.61	20.2	68
49b [26]	−9.79	14.35	−5.77	24.1	84

to that of the [18]didehydroannulene **58a** (Table 1). It must be kept in mind, however, that, in the case of **4**, the δ values of the NH protons were used, replacing those of the absent inner CH protons. For the [22]porpyhrin **49a** and the [26]porphyrin **49b** the $\Delta\delta$ values increase steadily from 20.2 to 24.1. In contrast to the situation in the corresponding didehydroannulene series (Table 1), the criterion of ring current indicates no reduction in aromaticity due in some way to conformational flexibility.

The rigidity of the three porphyrinoids **4**, **49a**, and **49b** leads to an almost linear correlation between the magnitude of the ring current effect, expressed by the $\Delta\delta$ values, and the area of the ring, defined as the area within the dotted line in the formulas of the compounds above Table 2. Thus the ring areas S of **4**, **49a**, and **49b** expressed in Table 2 are approximately proportional to the $\Delta\delta$ values of the ring current effect. This relationship corresponds to that developed by Haddon[60] between the resonance stabilization (RE), the ring current (RC), and the area (S) of carbocyclic aromatic ring systems [Eq.(a)].

$$RE = \pi^2 RC/3S \qquad (a)$$

As already discovered in 1973 with the determination of the crystal structure of the octaethyl[18]porphyrin **4**,[59a] porphyrins with ethyl groups in the β-positions of the pyrrole units tend to crystallize readily as single crystals. This was confirmed in the cases of the vinylogous porphyrins **49**. Crystal structures of the bistrifluoroacetates of the [22]porphyrin **49a** and the [26]porphyrin **49b** indicated molecules with bonds of equivalent length of 136.6–138.8 pm and 137.1–139.6 pm in their respective perimeters (Figs. 3 and 4). The ring systems are almost

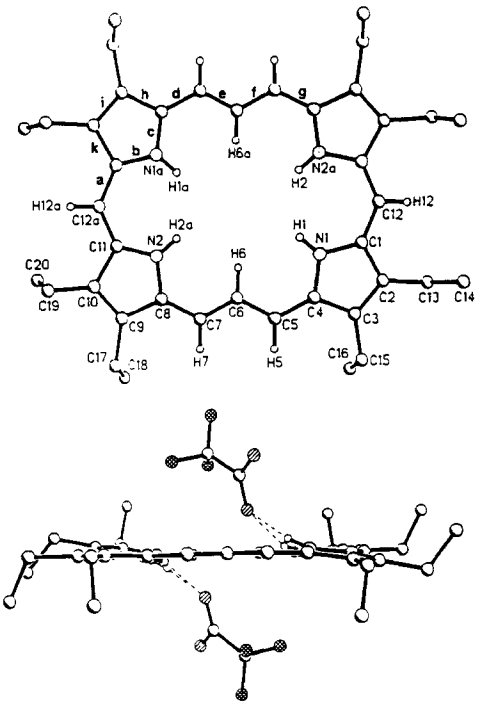

Fig. 3. Crystal structure of the bistrifluoroacetate of octaethyl[22]porphyrin **49a**; top: viewed perpendicular to the crystal plane, bottom: side view [56].

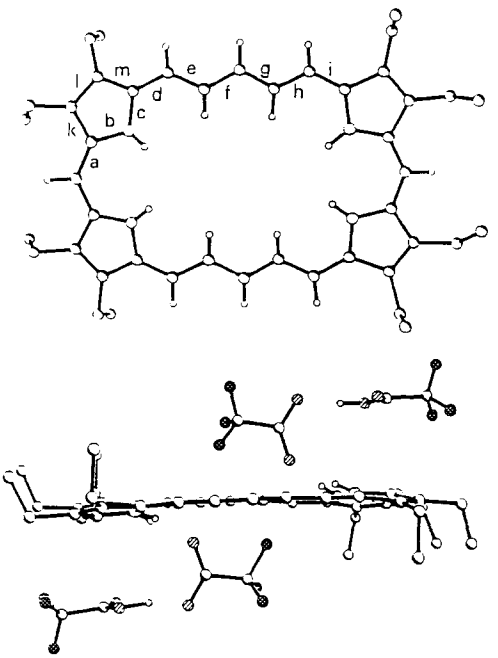

Fig. 4. Crystal structure of the bistrifluoroacetate of octaethyl[26]porphyrin **49b**; top: viewed perpendicular to the crystal plane, bottom: side view [50].

planar with maximum deviation from the central plane of 19 pm.[50, 56] The crystal structure data thus obtained for bond length equivalence and planarity for the [22]porphyrin **49a** and the [26]porphyrin **49b** agree completely with those measured by Lauher et al.[59a] and by Cetinkaya et al.[59b] for the [18]porphyrin **4**.

The vinylogous [22]- and [26]porphyrins **49a** and **49b**, respectively, offered the first opportunity to extend the investigation of

aromaticity in cyclic conjugated superarenes to the study of electrophilic substitution. The most suitable candidate for this purpose appeared to be electrophilic deuteration, for which steric considerations are minimal, and the results can be conveniently interpreted by NMR spectroscopy. Both porphyrins were treated with D_2SO_4/D_2O under identical conditions,[61] and the extent of deuteration was subsequently measured by mass spectrometry and the position and level of deuterium substitution determined by NMR spectroscopy. Significant differences in the behavior of the two porphyrins were seen (Scheme 22).

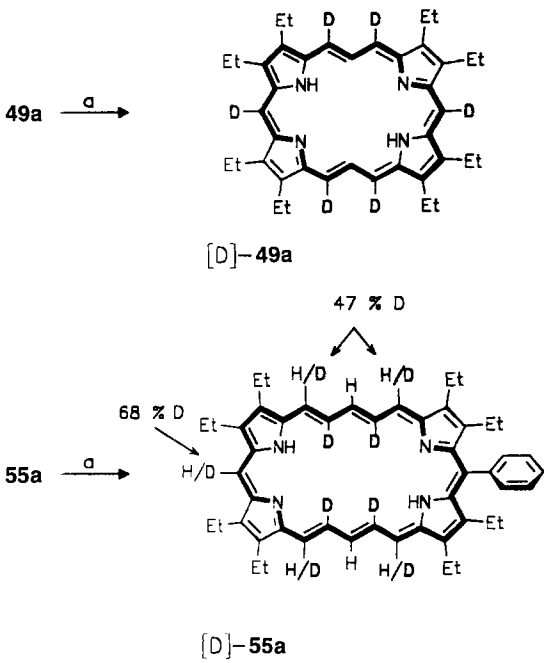

Scheme 22. Deuteration of octaethyl[22]porphyrin **49a** and 14-phenyl octaethyl-[26]porphyrin **55a**. Reaction conditions: a) $D_2SO_4/D_2O = 10:1$, 120 h, 20 °C.

In the case of the [22]porphyrin **49a**, the outer perimeter protons were almost quantitatively substituted with deuterium, with the formation of the hexadeuterio[22]porphyrin [D]-**49a**. Both inner protons proved to be inert towards electrophilic deuteration. One must assume that the NH groups undergo a D/H exchange on aqueous workup. The [26]porphyrin **49b** which is more acid sensitive than **49a**, was replaced by its phenyl derivative **55a**. Analysis of its deuteration product [D]-**55a** indicated that complete electrophilic substitution of the four inner CH protons by deuterium had taken place.

The preferred exchange of the inner protons in **55a** (→ [D]-**55a**) should be attributed to the activating effect of the phenyl substituent, rather than to the larger space inside the ring. The phenyl group proved to be an effective donor under the conditions of deuteration, compared to the more electronegative, protonated 22π-electron system. Correspondingly, the 12-phenyl[22]porphyrin underwent complete deuteration of its inner protons under the same conditions.[56b] The deuteration experiments with the [22]- and [26]porphyrins provide convincing chemical evidence for the aromaticity of these compounds. They also stimulate further interesting questions about the reactivity and regioreactivity of these novel, easily accessible[62,63] superarenes.

Conformationally stabilized diazaannulenes can similarly be represented by the [22]platyrin **59** and the [26]platyrin **60** of LeGoff et al.[64,65] (Scheme 23). These 22-π- and 26π-electron systems, prepared by a conceptually different synthetic route, can be considered to be aromatic according to the ^{1}H NMR ring current effect. Thus, **59** has a $\Delta\delta$ value of 20.6 and the less stable **60** a value of 26.0, similar to the $\Delta\delta$ values found for the [22]- and [26]porphyrins **49** (Table 2).

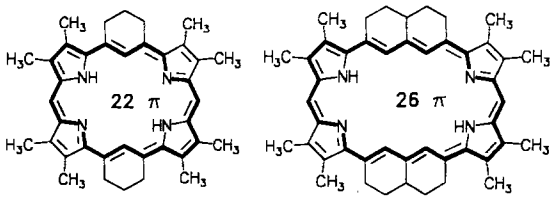

Scheme 23. Platyrins with aromatic 22π- and 26π-electron systems [64,65].

An interesting class of expanded porphyrins are the pyrrole-homologous systems, two groups of which are represented in Scheme 24. Penta- and hexaphyrins **61a** and **61b**, respectively, were described by Gossauer et al.[40] Pyrrologous macrocycles

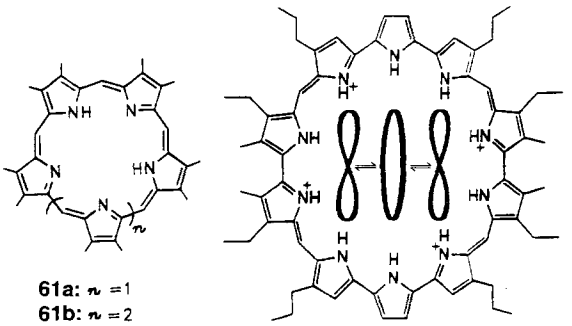

Scheme 24. Pyrrole-homologous porphyrins: penta- and hexaphyrin **61a** and **61b**, respectively [65]; and turcasarin **62** [66].

with up to ten pyrrole units, such as the turcasarin **62** which is turquoise in solution, were achieved by Sessler et al.[66] by the insertion of di- and tripyrrole units. As was anticipated from the consideration of the angles in the perimeters (see Scheme 10), the additional pyrrole units give rise to increasing deviation from the planar structure. This leads finally, as with the cyclic decapyrrole **62**, to the formation of twisted conformations with exciting stereochemistry (Scheme 24).

The octaethyl[26]porphyrin salts **47a–d** also display pronounced aromaticity according to the ^{1}H NMR ring current effect (Table 3).[24c,49] The resonance signals of their perimeter protons are almost completely independent of the nature of the peripheral alkyl groups and lie at $\delta = -11.45$ to -11.68 for the inner protons (H^i) and at $\delta = 8.98-9.10$ for the outer protons (H^a). This gives a $\Delta\delta$ value of 25.0–25.3, which agrees very well with the values for the [26]porphyrin **49b** (Table 2) and for the [26]platyrin **60**.[64,65]

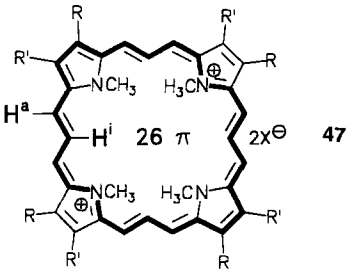

47

Table 3. ^{1}H NMR data for the salts of octaalkyl[26]porphyrins. δ values of the inner protons (H^i, CH_3N) and outer protons (H^a) at the conjugated perimeter, and the difference $\Delta\delta = \delta(H^a) - \delta(H^i)$ in $CDCl_3$.

[26]Porphyrin	$\delta(H^i)$	$\delta(H^a)$	$\delta(H_3CN)$	$\Delta\delta$
47a: R, R' = $-(CH_2)_4-$ [a]	−11.68	13.52	−9.10	25.2
47b: R, R' = C_2H_5 [a]	−11.64	13.67	−9.09	25.3
47c: R, R' = *n*-C_4H_9 [b]	−11.54	13.61	−8.98	25.2
47d: R, R' = $CH_2CH(CH_3)_2$ [b]	−11.45	13.58	−9.01	25.0

[a] Measured as the bistrifluoroacetate. [b] Measured as the dibromide.

Initial attempts to measure the diatropic ring current effect of the octaethyl[34]porphyrin salts **48a,b** from their ^{1}H NMR spectra were frustrated by the occurrence of an unexpected problem. The signals at very high field and at very low field displayed no spin splitting. It was initially presumed that this could be attributed to interconversion of conformers, as is the case with the annulenes. Therefore measurements were performed at −60 °C and at 50 °C. However, no improvements were seen. It was found that the inner (H^i) and outer protons (H^a) gave the expected splitting patterns (Fig. 5) only at extremely high dilution (0.1 mg mL^{-1}) in [D_6]DMSO.

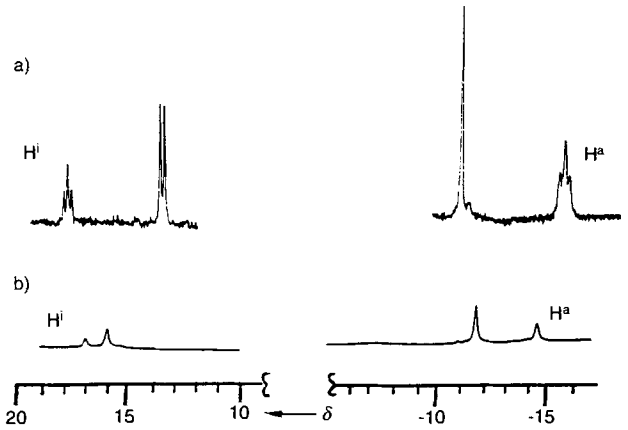

Fig. 5. ^{1}H NMR spectrum of the octaethyl[34]porphyrin **48a** in [D_6]DMSO [53]. Concentrations: a) 0.1 g L^{-1}; b) 3.0 g L^{-1}.

The eight H^i protons of the octaethyl[34]porphyrins **48a** and **48b**, which lie in identical positions on the inside of the C_5 bridges, display triplets at $\delta = -14.13$ and -14.23 in their ^{1}H NMR spectra (Table 4). The singlets of the CH_3N protons resonate at slightly lower field, namely $\delta = -11.30$ and -11.16, because of their somewhat larger distance from the perimeter. The twelve outer protons (H^a) on the C_5 bridges of the perimeter display two signals at $\delta = 17.18$ and at 17.04, of which the signal at lower field is derived from the protons in the center of the

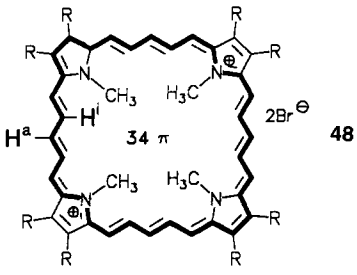

48

Table 4. ^{1}H NMR data for the octaalkyl[34]porphyrin dibromides **48a, b**. δ values of the inner protons (H^i, CH_3N) and outer protons (H^a) at the conjugated perimeter, and the difference $\Delta\delta = \delta(H^a) - \delta(H^i)$ in [D_6]DMSO.

[34]Porphyrin	$\delta(H^i)$	$\delta(H^a)$	$\delta(H_3CN)$	$\Delta\delta$
48a: R = C_2H_5	−14.23	17.18	−11.30	31.4
48b: R = $CH_2CH(CH_3)_2$	−14.13	17.04	−11.16	31.2

bridges. The resulting $\Delta\delta$ value is thus greater than $\Delta\delta = 31$. Thus, the ring current effects of the [34]porphyrins **48a,b** are higher than those measured for all of the previously described arenes. Such a large span between high and low field signals in a ^{1}H NMR spectrum has only previously been observed for organometallic compounds. It is remarkable that the pyrrole units at the corners of the molecule can stabilize a planar conformation over bridges as long as C_5 and thus allow the [34]porphyrins to display aromaticity.

The fact that the spin splittings in the ^{1}H NMR spectra of the [34]porphyrins are only resolved at extremely high dilution can be considered as being due to strong associative behavior in solution. This behavior, which is also recognizable in the crystal structures of the porphyrins, might not only be due to the ring size of the octavinylogous [34]porphyrins, but may also be strengthened by the possible intercalation of anions. In contrast to the [18]porphyrins, the inner space of the octavinylogues would be well suited for this purpose, as is shown by the space-filling models in Figure 6.

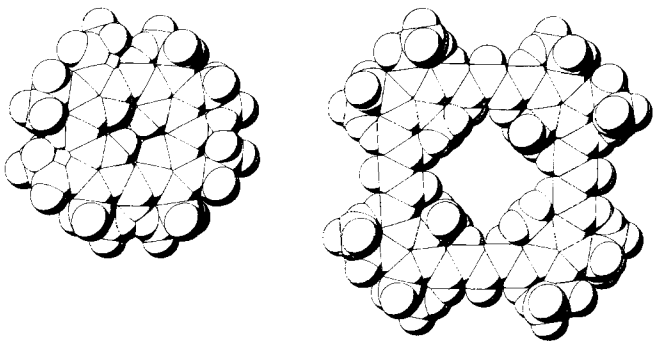

Fig. 6. Space-filling representations of the octaethyl[18]porphyrin **4** (left) and the *N,N',N'',N'''*-tetramethyl octaethyl[34]porphyrin dibromide **48a** (right) [12].

6. High Intensity Pigments with Future Perspectives

Chlorophylls cause the formation of huge amounts of biomass using energy absorbed from sunlight. In comparison with this, the light absorption of the other porphyrinoids plays a relatively minor role. Some porphyrins do have, however,

pathological or medicinally useful effects. Examples include their role as photosensitizers in porphyria[67, 68] or in photodynamic tumor therapy (PDT).[69, 70]

The new vinylogous porphyrinoids are of current interest as pigments because they display the following properties: 1) Extremely high intensity of absorption with values of the molar extinction coefficient ε as high as 1 100 000; 2) a linear relationship between the number of π-electrons and the wavelength of the most intense absorption band (Soret band); 3) high light stability, and 4) activity as photosensitizers.

The pigments, which are characterized by high extinction coefficients, could allow dyeing techniques with small amounts of substance. Up until now, the most industrially important pigments have molar extinction coefficients ε ranging from 20 000 (indigo) up to 220 000 (copper phthalocyanin).[71] The ε values of the vinylogous porphyrinoids are fifty times higher than those of indigo and three to four times higher than those of the phthalocyanins (Table 5). This fact, if supported by other useful pigment properties, may lead to interesting opportunities.

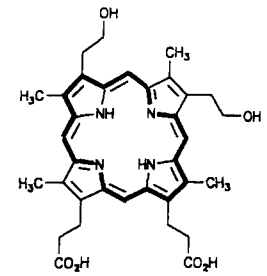

64

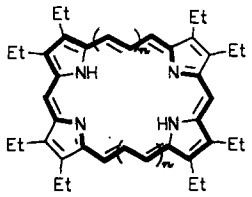

49a: $n = 1$
49b: $n = 2$

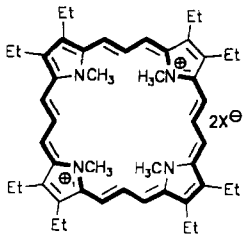

47b

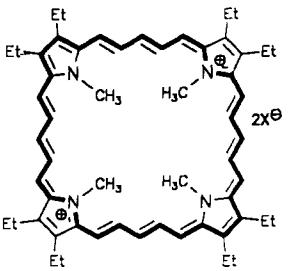

48a

Table 5. Absorption bands of vinylogous porphyrins.

Porphyrinoid	Soret band		Longest wavelength band	
	λ_{max}	ε	λ_{max}	ε
[18]isohematoporphyrin **64**[a]	399	130 000	621	2 570
[22]porphyrin(1.3.1.3) **49a**[b]	460	1 120 000	691	7 960
[26]porphyrin(1.5.1.5) **49b**[b]	512	694 000	694	40 600
[26]porphyrin(3.3.3.3) **47b**[a]	547	909 600	783	28 000
[34]porphyrin(5.5.5.5) **48a**[c]	663	370 000	997	24 000

[a] $CHCl_3$. [b] CH_2Cl_2 + 1% TFA. [c] MeOH.

One of the prerequisites for narrow, intense absorption bands with high ε values and small half widths is a substantially symmetrical structure. Thus, the unprotonated [22]porphyrin **49a** displays a less intense Soret band ($\lambda_{max} = 463$, $\varepsilon = 419\,000$), when measured without the addition of trifluoroacetic acid (TFA) (Table 5).

The crystal structures of the bistrifluoroacetate salts of the [22]porphyrin **49a** and the [26]porphyrin **49b** (Figs. 3 and 4, respectively) indicate an almost complete bond length equivalence in the aromatic perimeter. An independent confirmation of this finding is provided for the vinylogous porphyrins from their absorption spectra. It can be seen that, as for the cyanin pigments—for the vinylogous C_4 symmetric 18π-, 26π-, and 34π-porphyrinoids—there exists a linear relationship between λ_{max} and the number of π-electrons in the aromatic perimeter (Fig. 7). According to this, the vinylogous porphyrins have fully delocalized π-electron systems comparable to those of the cyanins.[72] Because of the formal similarity, the term "Babuschka porphyrins" (in analogy with the Russian dolls in which a small doll fits inside a larger doll which fits inside an even larger doll, known as Babuschka dolls in German) is proposed for the C_4-symmetric vinylogous porphyrinoids.

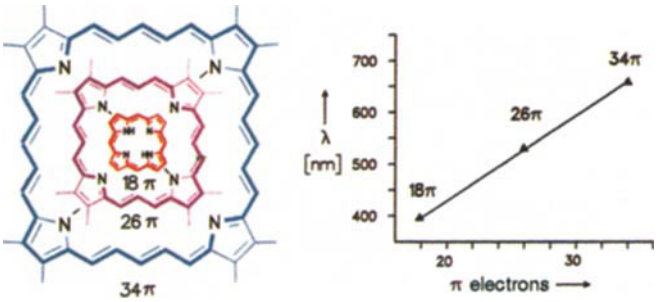

Fig. 7. Left: [18]-, [26]-, and [34]porphyrins in the colors of their solutions in CH_2Cl_2 (simplified formulas). Right: Relationship between λ_{max} (Soret band) and the number of π-electrons in the aromatic perimeter for the porphyrinoids **64**, **47b**, and **48a** with 18π-, 26-, and 34π-electron systems, respectively.

7. Tailor-Made Porphyrinoids for Photomedicine

As physiologically acceptable, effective photosensitizers, which differ only slightly from the body's own blood pigment heme, the porphyrinoids find two important applications in the field of photomedicine. These are photodynamic tumor therapy (PDT)[69, 70] and photodynamic destruction of viruses (PDV)[73] in transfusion blood. In connection with the necessity of reliably preventing viral or parasitic infections arising from blood transfusions, the second technique is of topical significance.

Thus, at the Baylor Research Institute in Dallas, it was found that viruses and other parasites in transfusion blood can be destroyed by adding a trace of a suitable photosensitizer to the blood and then irradiating it with visible light.[73] This technique is based on the fact that the photosensitizer causes the formation of singlet oxygen, which kills the virus, without causing any significant damage to the essential blood cells. Figure 8[74] shows AIDS viruses which, after multiplication within a cell, penetrate the membrane and enter into the blood stream and are, at this point, particularly exposed to attack by singlet oxygen. At present, thanks to various other techniques, particularly heat treatment of transfusion blood, the risk of infection can be substantially reduced, but not completely excluded.

In photodynamic therapy (PDT), after uptake of the photosensitizer, the tumor is irradiated with visible laser light of a suitable wavelength. This leads to inhibition and destruction of

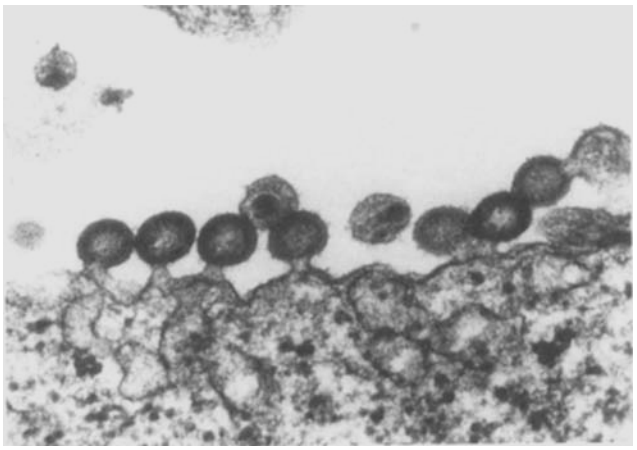

Fig. 8. Electron microscopic picture of budding AIDS viruses [74] (reprinted with kind permission of the Dana-Farber Cancer Institute, Division of Human Retrovirology, Boston, MA, USA).

the tumor, an effect which has already been demonstrated in several thousand clinical applications.[69] Because of the success achieved up to now, and the much milder nature of the treatment in comparison to the treatment of cancer by X-ray irradiation, this area is the subject of intensive development in a worldwide collaboration between medicine and chemistry.[69, 70, 73, 75]

To explain the mechanism of action of photosensitisers in tumor therapy and in the destruction of viruses in transfusion blood, it has been assumed that the singlet oxygen which is formed on irradiation in the presence of light and oxygen, reacts with nucleosides. From this, the rapidly proliferating tumor cells are more strongly affected than the healthy tissue. Cadet et al.[76] have described oxidative transformation of deoxyguanosine acetate by singlet oxygen in a relevant model study (Scheme 25).

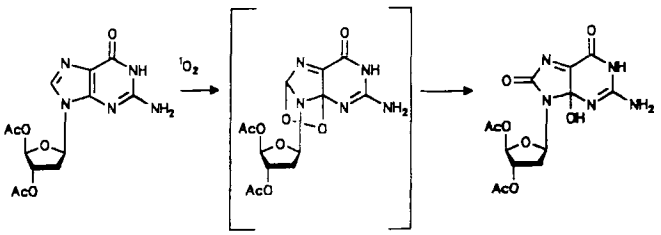

Scheme 25. Reaction of deoxyguanosine acetate with singlet oxygen [76].

In order to compare the photosensitizer activity of the vinylogous porphyrins, their ability to form singlet oxygen under the conditions encountered in photodynamic therapy was chemically determined (Scheme 26). The trapping reaction with 2,5-dimethylfuran and the subsequent iodometric titration of the hydroperoxide formed after the methanolysis, was chosen for this purpose.[79–81] This indicated that the divinylogous [22]porphyrin **49a** performs almost as efficiently as Rose Bengal, and exceeds the [18]porphyrin system, for example **4**, which has been predominantly used in photomedicine until now. In the case of the [34]porphyrin **48a**, the relatively low energy of the

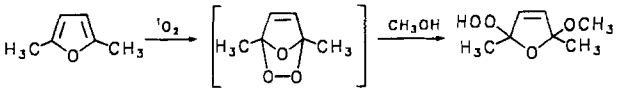

Scheme 26. Formation of $^1O_2$ by various photosensitizers under standard conditions [79–81]. Photosensitizers used (yield %): octaethyl[18]porphyrin **4** (22); octaethyl[22]porphyrin **49a** (40); octaethyl[26]porphyrin **49b** (12); octaethyl[34]porphyrin **48a** (0); Bengal Rose (44); blank (0).

higher wavelength fluorescence emission ($\lambda_{max} = 1310$ nm)[82] is not sufficient for $^1O_2$ formation.

An ideal photosensitizer for photomedicinal applications should fulfill the following criteria:[70] 1) be readily available and chemically stable; 2) be a good photosensitizer; 3) its absorption of light should differ from that of the blood pigment heme; 4) have minimal dark toxicity; 5) be pharmacokinetically innocuous; 6) be rapidly eliminated from the organism after phototherapy.

The most widely used photosensitizers have been hitherto derivatives of the hematoporphyrin **63** (Scheme 27), which have

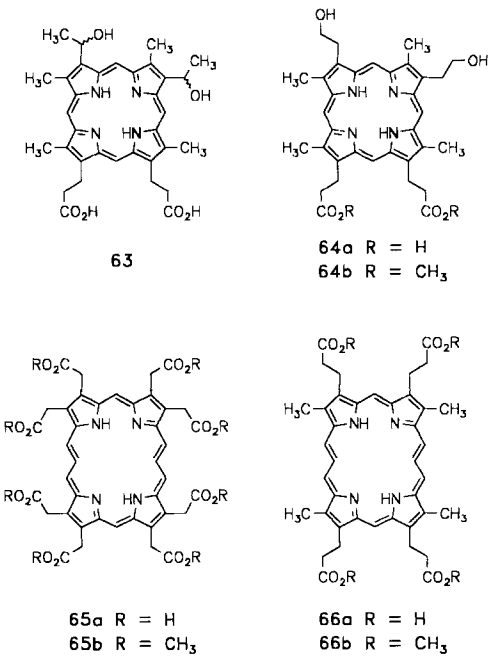

Scheme 27. Hematoporphyrin (**63**), isohematoporphyrin (**64a**) [77], [22]porphyrin-octaacetic acid (**65a**) [78a]and [22]coproporphyrin II (**66a**) [78b] and esters.

been named Photofrin.[69] They fulfill the majority of the above-mentioned criteria. The hematoporphyrin **63** is somewhat chemically unstable due to its allylic secondary hydroxy group, which leads to mixtures of derivatives. This problem can be overcome by the use of the more stable isohematoporphyrin **64**.[77] Of greater significance is the improvement in the penetration depth of the laser light used for the photosensitization. Due to the similarity of the chromophore of hematoporphyrin **63** to that of the natural blood pigment heme, present in large excess, part of the laser light is lost during phototherapy. A remedy to this problem is offered by photosensitizers which, as in the case of the vinylogous porphyrins **65a** and **66a**, are structurally similar to the hematoporphyrin **63**, but absorb light at longer wavelengths (Scheme 27). Compound **66a**[78b] is a divinylogue of the

naturally occuring coproporphyrin II. It has a more intense UV/Vis absorption which is shifted to longer wavelengths than the blood pigments, and thus appears to be a candidate for selective photoactivation (Fig. 9).

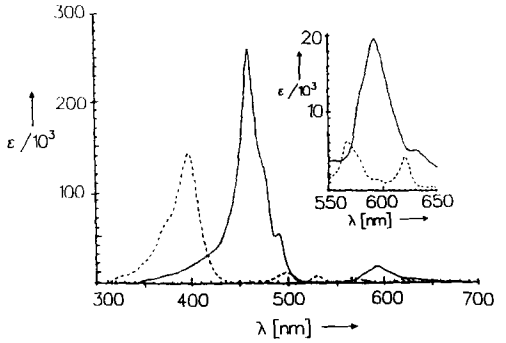

Fig. 9. UV/Vis spectra of [22]coproporphyrin II ester (**66b**) (– – –) [78b] and isohematoporphyrin (**64b**) (——) [77] in CH_2Cl_2. Because of the instability of hematoporphyrin (**63**), the spectrum of **64b**, which has the same chromophore, is shown for comparison.

Due to the short half life and therefore limited range of action of $^1O_2$,[82] the photosensitizer can only display its effect inside the viral or tumor cells. Therefore, a decisive factor for the photomedicinal application of porphyrinoids is, apart from their photosensitizing ability, their polarity. In order to investigate this, the ability to inhibit tumors in a leukemia cell line was studied for two derivatives of the isohematoporphyrin **64b** and **67**[77b] as well as for a [22]porphyrin **65b**[78a] and a [26]porphyrin **47b**[24c] (Table 6).[83] This showed that the tumor inhibitory activity of the nonpolar isohematoporphyrin dimethyl ester **64b** significantly exceeded that of the isohematoporphyrin digalactoside **67**. The nonpolar [22]porphyrin octaacetic acid octamethyl ester **65b** has similar activity to **64**, while the polar, bisquaternary [26]porphyrin **47b** has a lower activity which corresponds roughly to that of **67**.

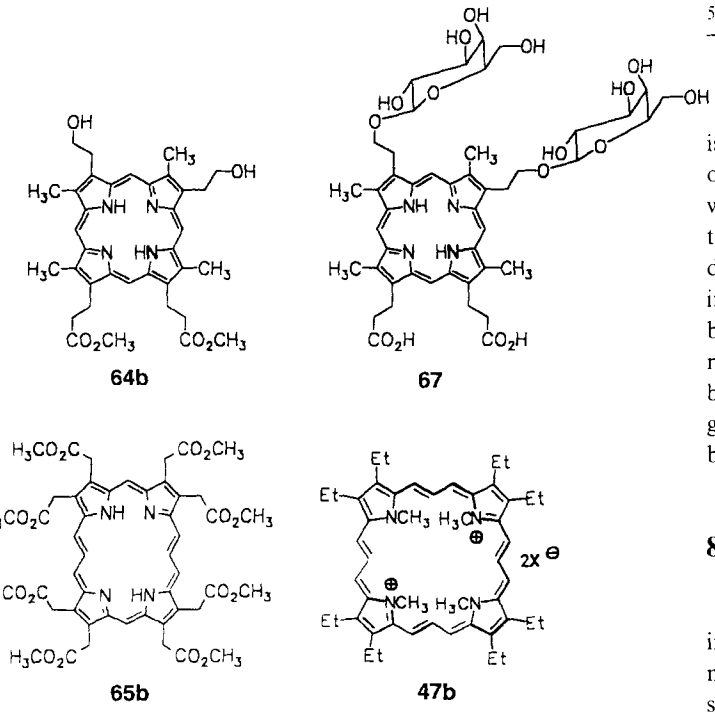

Table 6. Inhibition of tumors by the four porphyrinoids **64b**, **65b**, **67**, and **47b** of different polarity against leukemia cell lines [83]. Colony building after laser irradiation (93.6 J cm^{-2}) as a percentage of the initial value.

Concentration [%] [μg mL^{-1}]	Colony formation **64b** [77b]	**67** [77b]	**65b** [78a]	**47b** [24c]
2.5	32	78	48	62
5	12	49	29	48
7.5	8	39	1	30
10	0	10	0	15

The isohematoporphyrin dimethyl ester **64b** proved itself to be just as well suited for the photodynamic destruction of viruses in blood. Table 7 shows the destruction of Herpes simplex virus (HSV) using **64b** and 458 nm laser light. A concentration of 1 μg mL^{-1} (corresponding to 0.5 mg in a transfusion blood unit of 500 mL) is sufficient to kill 99.996% of the virus. Under the same conditions the blood leukocytes are hardly affected.

Table 7. Phototoxicity of the isohematoporphyrin dimethyl ester **64b** against Herpes simplex virus (HSV) and against blood leukocytes with laser light of 458 nm [83].

Concentration [μg mL^{-1}]	Destruction of HSV dark	laser	Surviving leukocytes dark	laser
0	–	18000000		
1	1500000	750	58	43
2.5	1500000	500	42	28
5	1400000	250	36	22

In the flow cells of a test apparatus (Fig. 10) the film thickness is so low that the absorption of laser light by blood pigments is of no importance.[73b, 83] By using the vinylogous porphyrins which absorb light at longer wavelengths, it would be possible to photodynamically sterilize blood in thicker films, potentially directly in the transfusion units. This would not only be of use in the reduction of infection from AIDS and hepatitis viruses, but also from malaria parasites. Taking into consideration the risk of infection which is always present in the use of transfusion blood and other infusion liquids, the development of safer, more generally applicable, and cheaper processes of sterilization is becoming more and more important.

8. Summary and Outlook

The results gained with the porphyrins have reinforced the importance of understanding the biosynthesis of a group of natural products, the knowledge of which opens the door to a series of novel methods and insights. In particular this holds true for the development of biomimetic syntheses, as was shown first of all in the pioneering work by Robinson and Schöpf for the alkaloids,[84, 85] then Johnson[86] for the steroids, and Rimington et al.[23] for the porphyrins. Through this approach possibilities for efficient syntheses have been realized, which allow an alternative route to active substances, generally preferable to their isolation from biological material. In the case of the porphyrins, the biomimetic principle has provided a remarkable versatility and flexibility, which has allowed access to viny-

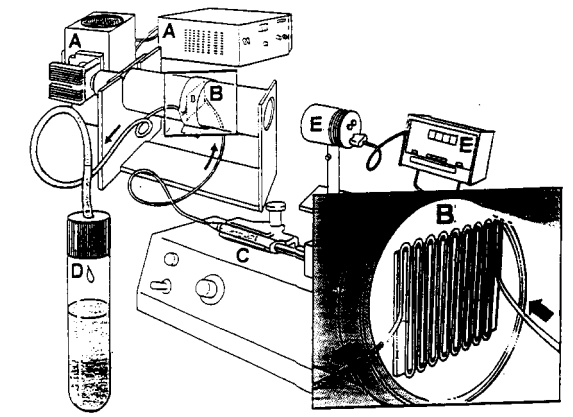

Fig. 10. Flow apparatus for the sterilization of blood (Baylor Research Foundation) [73b,83] (reproduced with kind permission of the Baylor Research Institute, Dallas, Tx, USA). Top: Schematic diagram: A)laser light assembly, B) flow cell, C) syringe pump, D) sterile collecting vial, E) light meter. Bottom: Apparatus in operation.

logously expanded, *N*,*N*′,*N*″,*N*‴-tetrasubstituted, *N*,*N*′-bridged, and inverted (*N* atoms in the periphery) porphyrins.

While we are still in the early stages, the new porphyrinoids have already displayed properties which are of great promise in the fields of chemistry and medicine. If one looks for a reason for the unusually broad variability encountered in biomimetic porphyrin synthesis, one is forced to suppose that this has to do with the very early prebiotic formation of porphyrins.[87] The evolution of organisms required a versatile system with strong formation tendency, which could satisfy the demand for ligands for the essential elements Mg, Fe, Co, Ni, and V.

Our work was generously supported by the Deutsche Forschungsgemeinschaft, the Fonds der Chemischen Industrie, and BASF AG (Ludwigshafen). B. F. would, in particular, like to thank all the co-authors of the cited work, carried out in Münster. The readiness of numerous colleagues (refs. [15, 18, 25, 32, 36, 40, 46, 60, 68, 69, 72, 73, 75, 79, 82, 83]) to contribute much valuable advice or to collaborate was decisive for the success of the interdisciplinary research.

Received February 24, 1995 [A 107 IE]
German version: *Angew. Chem.* **1995**, *107*, 1941–1957
Translated by Dr. D. Marquarrie, Naters (Switzerland)

[1] H. Fischer, B. Walach, *Justus Liebigs Ann. Chem.* **1926**, *450*, 164–181.
[2] CAS Online search for **1994**.
[3] a) *Biochemistry: The Porphyrins, Vol. VI, Part A and Vol. VII, Part B* (Ed.: D. Dolphin), Academic Press, New York, **1978**; b) A. L. Lehninger, D. L. Nelson, M. M. Cox, *Prinzipien der Biochemie*, Spektrum Akademischer Verlag, Berlin, **1994**.
[4] *Heme and Hemoproteins* (Ed.: F. de Matteis, W. N. Aldrige), Springer, Berlin, **1978**.
[5] a) F. J. Leeper, *Nat. Prod. Rep.* **1989**, *6*, 171–203; b) L. R. Milgrom, *Chem. Br.* **1994**, *31*, 923–927.
[6] B. Franck, *Angew. Chem.* **1982**, *94*, 327–337; *Angew. Chem. Int. Ed. Engl.* **1982**, *21*, 323–353.
[7] A. I. Scott, *Angew. Chem.* **1993**, *105*, 1281–1302; *Angew. Chem. Int. Ed. Engl.* **1993**, *32*, 1223–1243.
[8] The blood of an adult human (ca. 5 L) contains approximately 30 g heme. Biosynthesis replaces this completely every 120 days [9].
[9] G. H. Tait, *The Biosynthesis and Degradation of Heme*, in ref.[4], pp. 1–48.
[10] B. Kräutler, B. Jaun, K. Bortlik, M. Schellenberg, P. Matile, *Angew. Chem.* **1991**, *103*, 1354–1357; *Angew. Chem. Int. Ed. Engl.* **1991**, *30*, 1315–1318.
[11] G. A. Hendry, J. D. Houghton, S. B. Brown, *New Phytol.* **1987**, *107*, 255.
[12] G. Thiele, Moplo. Ein elektronischer Molekülbaukasten auf dem PC, VCH, Weinheim, **1992**.
[13] Catalogue of Sigma-Aldrich Chemie GmbH, D-82041 Deisenhofen, **1995**.
[14] H. Fischer, R. Bäumler, *Justus Liebigs Ann. Chem.* **1929**, *468*, 58–98.
[15] H. H. Inhoffen, J.-H. Fuhrhop, H. Voigt, H. Brockmann, *Justus Liebigs Ann. Chem.* **1966**, *695*, 133–143.
[16] E. J. Tarlton, S. F. McDonald, E. Baltazzi, *J. Am. Chem. Soc.* **1960**, *82*, 4389–4395.
[17] B. Franck, D. Gantz, F. Hüper, *Angew. Chem.* **1972**, *84*, 432–433; *Angew. Chem. Int. Ed. Engl.* **1972**, *11*, 420–421.
[18] The company Harimax, Loenen, Holland recovers annually 10–12 t hemin from 40 million liters of blood from slaughterhouses. The hemin is used in chemical and medicinal applications. This amount represents ca. 80% of the world requirement. Currently, the industrial price of hemin is approximately 600 DM per kg (Personal communication from Harimax, and also Prof. Mueller von der Haegen, Seehof-Laboratorium, D-25764 Wesselburenerkoog Seehof.
[19] Price from February 15, 1995.
[20] G. P. Arsenault, E. Bullock, S. F. MacDonald, *J. Am. Chem. Soc.* **1960**, *82*, 4384–4389.
[21] H. Fischer, J. Klarer, *Justus Liebigs Ann. Chem.* **1926**, *448*, 178.
[22] A. W. Johnson, I. T. Kay, *J. Chem. Soc.* **1961**, 2418–2423.
[23] G. H. Cookson, C. Rimington, *Biochem. J.* **1954**, *57*, 476–484.
[24] a) B. Franck, A. Rowold, C. Wegner, H. G. Eckert, *Philos. Trans. R. Soc. London B* **1976**, *273*, 181–189; b) G. Bringmann, B. Franck, *Liebigs Ann. Chem.* **1982**, 1272–1279; c) B. Franck, A. Nonn, K. Fuchs, M. Gosmann, *ibid.* **1994**, 503–510.
[25] L. F. Tietze, H. Geisler, *Angew. Chem.* **1993**, *105*, 1087–1089; *Angew. Chem. Int. Ed. Engl.* **1993**, *32*, 1038–1040.
[26] B. Franck, C. Wegner, *Angew. Chem.* **1975**, *87*, 419–420; *Angew. Chem. Int. Ed. Engl.* **1975**, *14*, 424.
[27] B. Franck, G. Bringmann, C. Wegner, U. Spiegel, *Liebigs Ann. Chem.* **1980**, 263–274.
[28] a) R. Timmermann, R. Mattes, B. Franck, *Angew. Chem.* **1987**, *99*, 74–76; *Angew. Chem. Int. Ed. Engl.* **1987**, *26*, 64–65; b) B. Franck, R. Timmermann, W. Sirges, *Liebigs Ann. Chem.* **1993**, 1075–1080.
[29] K.-H. Schumacher, B. Franck, *Angew. Chem.* **1989**, *101*, 1292–1293; *Angew. Chem. Int. Ed. Engl.* **1989**, *28*, 1243–1245.
[30] R. Grigg, A. Sweeney, G. R. Dearden, A. H. Jackson, A. W. Johnson, *J. Chem. Soc. D.* **1970**, 1273–1274.
[31] H. M. G. Al-Hazimi, A. J. Jackson, A. W. Johnson, M. Winter, *J. Chem. Soc. Perkin Trans. 1* **1977**, 98–103.
[32] G. Sawitzki, H. G. von Schnering, *Angew. Chem.* **1976**, *88*, 616–617; *Angew. Chem. Int. Ed. Engl.* **1976**, *15*, 552.
[33] B. Franck, W. Bock, G. Bringmann, G. Fels, F. Grubenbecher, M. Marsmann, R. Pietschmann, K. Schäpers, U. Spiegel, R. Steinkamp, G. Ufer, C. Wegner, *Int. J. Biochem.* **1980**, *12*, 671–679.
[34] F. Sondheimer, *Acc. Chem. Res.* **1972**, *5*, 81–91.
[35] M. Gosmann, Dissertation, Universität Münster, **1986**.
[36] E. Vogel, *Pure Appl. Chem.* **1990**, *62*, 557–564.
[37] We would like to thank Prof. G. Wilke and Dr. K. R. Pörschke of the Max-Planck-Institut für Kohlenforschung, Mülheim a. d. Ruhr, for valuable discussions and for the possibility of carrying out direction-finding investigations.
[38] According to our proposed nomenclature [29] porphyrins and porphyrinogens with inverted pyrrole units are designated mono-, di-, tri- and tetra-invertoporphyrins, or invertoporphyrinogens respectively.
[39] a) L. Nygard, J. T. Nielsen, J. Kirchheiner, G. Maltesen, J. Rastrup-Andersen, G. O. Sorensen, *J. Mol. Struct.* **1969**, *3*, 491–506; b) A. Gossauer, *Die Chemie der Pyrrole*, Springer, Berlin, **1974**, p. 7.
[40] H. Rexhausen, A. Gossauer, *J. Chem. Soc. Chem. Commun.* **1983**, 275; R. Carriere, T. Jenny, H. Rexhausen, A. Grossauer, *Heterocycles*, **1993**, *36*, 1561–1575.

[41] a) H. Furuta, T. Asano, T. Ogawa, *J. Am. Chem. Soc.* **1994**, *116*, 767–768; b) P. J. Chmielewski, L. Latos-Grazynski, K. Rachlewicz, T. Glowiak, *Angew. Chem.* **1994**, *106*, 805–808; *Angew. Chem. Int. Ed. Engl.* **1994**, *33*, 779–781; c) P. Rothemund, *J. Am. Chem. Soc.* **1936**, *58*, 625–627.

[42] D. Lloyd, *The Chemistry of Conjugated Cyclic Compounds*, Wiley, New York, **1989**.

[43] W. Shakespeare, *The Tragedy of Hamlet, Prince of Denmark*, monologue in III–I, **1601**.

[44] E. Hückel, *Z. Phys.* **1931**, *72*, 310.

[45] H. Baumann, J. F. M. Oth, *Helv. Chim. Acta* **1982**, *65*, 1885–1893.

[46] A. W. Johnson, I. T. Kay, *J. Chem. Soc.* **1965**, 1620–1629.

[47] H. J. Callot, E. Schaeffer, *J. Org. Chem.* **1977**, 1567–1570.

[48] E. Vogel, M. Köcher, H. Schmickler, J. Lex, *Angew. Chem.* **1986**, *98*, 262–264; *Angew. Chem. Int. Ed. Engl.* **1986**, *25*, 257–259.

[49] M. Gosmann, B. Franck, *Angew. Chem.* **1986**, *98*, 1107–1108; *Angew. Chem. Int. Ed. Engl.* **1986**, *25*, 1100–1101.

[50] T. Wessel, B. Franck, M. Möller, U. Rodewald, M. Läge, *Angew. Chem.* **1993**, *105*, 1201–1203; *Angew. Chem. Int. Ed. Engl.* **1993**, *32*, 1148–1151.

[51] M. J. S. Dewar, G. J. Gleicher, *J. Am. Chem. Soc.* **1965**, *87*, 685–692.

[52] F. W. Ulrich, E. Breitmeier, *Synthesis* **1983**, 641–645.

[53] G. Knübel, B. Franck, *Angew. Chem.* **1988**, *100*, 1203–1211; *Angew. Chem. Int. Ed. Engl.* **1988**, *27*, 1170–1172.

[54] A. Nonn, Dissertation, Universität Münster, **1991**.

[55] J. B. Paine, R. B. Woodward, *J. Org. Chem.* **1976**, *41*, 2826–2835.

[56] a) H. König, C. Eickmeier, M. Möller, U. Rodewald, B. Franck, *Angew. Chem.* **1990**, *102*, 1437–1439; *Angew. Chem. Int. Ed. Engl.* **1990**, *29*, 1393–1394; b) C. Eickmeier, Dissertation, Universität Münster, **1993**.

[57] a) H. A. Staab, F. Diederich, *Chem. Ber.* **1983**, *116*, 3487–3503; b) H. A. Staab, F. Diederich, C. Krieger, D. Schweitzer, *ibid.* **1983**, *116*, 3504–3512.

[58] M. Nakagawa, *Pure Appl. Chem.* **1975**, *44*, 885–924.

[59] a) J. W. Lauher, J. A. Ibers, *J. Am. Chem. Soc.* **1973**, *95*, 5148–5152; b) E. Cetinkaya, A. W. Johnson, M. F. Lappert, G. M. MacLaughlin, K. W. Muir, *J. Chem. Soc. Dalton Trans.* **1974**, 1236–1243.

[60] R. C. Haddon, *J. Am. Chem. Soc.* **1979**, *101*, 1722–1728.

[61] B. Franck, G. Krautstrunk, *Liebigs Ann. Chem.* **1993**, 1069–1073.

[62] a) *Preparation of azaporphyrins from biladienes*: B. Franck, H. König, C. Eickmeier, M. Völker, T. Wessel (BASF AG), *Eur. Pat. Appl.* 477611, **1992**; [*Chem. Abstr.* **1992**, *117*, 7740j]; b) *Preparation of biladiene derivatives as intermediates for vinylogous porphyrins*: B. Franck, H. König, C. Eickmeier (BASF AG), DE-A 4029768, **1992**; [*Chem. Abstr.* **1992**, *117*, 26197d].

[63] B. Franck, *Chimia* **1994**, *48*, 490.

[64] a) R. A. Berger, E. LeGoff, *Tetrahedron Lett.* **1978**, 4225–4228; b) E. LeGoff, O. G. Weaver, *J. Org. Chem.* **1987**, *52*, 710–711.

[65] LeGoff and co-workers name their compounds "platyrins" (from the Greek πλατυσ = wide). Here they will be differentiated from each other by using the nomenclature of annulenes and vinylogous porphyrins as [22]- and [26]platyrins.

[66] a) J. L. Sessler, S. J. Weghorn, V. Lynch, M. R. Johnson, *Angew. Chem.* **1994**, *106*, 1572–1575; *Angew. Chem. Int. Ed. Engl.* **1994**, *33*, 1509–1512; b) J. L. Sessler, T. Morishima, V. Lynch, *ibid.* **1991**, *103*, 1018–1021 and **1991**, *30*, 977–980.

[67] U. A. Meyer, R. Schmid in *The Metabolic Basis of Inherited Diseases* (Eds.: J. B. Stanbury, J. B. Wyngarden, D. S. Frederickson), 4th ed., McGraw-Hill, New York, **1978**, p. 1166–1220.

[68] H. Ippen in *The Science of Photomedicine* (Eds.: J. D. Regan, J. A. Parrish), Plenum, New York, **1982**, S. 349–394.

[69] T. J. Dougherty, *Adv. Photochem.* **1992**, *17*, 275–311.

[70] B. Franck, U. Schneider, D. Schröder, K. S. Gulliya, J. L. Matthews in *Biologic Effects of Light 1993* (Eds.: E. G. Jung, M. F. Holick), de Gruyter, Berlin, **1994**, p. 289–302.

[71] H. Zollinger, *Color Chemistry*, VCH, Weinheim, **1987**, p. 78.

[72] M. Klessinger, *Chem. Unserer Zeit* **1978**, *12*, 1–11.

[73] a) J. L. Matthews, J. T. Newman, F. Sogandares-Bernal, M. M. Judy, H. Skiles, J. E. Leveson, A. J. Marengo-Rowe, T. C. Chan, *Transfusion (Philadelphia)* **1988**, *28*, 81–83; b) J. L. Matthews, S. Sogandares-Bernal, M. M. Judy, A. J. Marengo-Rowe, J. E. Leveson, H. Skiles, J. T. Newman, T. C. Chan, *ibid.* **1991**, *31*, 636–641.

[74] H. Göttlinger, J. G. Sodroski, W. A. Haseltine, *Proc. Natl. Acad. Sci. USA*, **1989**, *86*, 5781–5785.

[75] K. S. Gulliya, B. Franck, U. Schneider, R. Sharma, L. Arnold, J. L. Matthews, *Anti-Cancer Drugs* **1994**, *5*, 557–566.

[76] J. Cadet, M. Berger, C. Decarroz, J. R. Wagner, J. E. van Lier, Y. M. Ginot, P. Viny, *Biochimie* **1986**, *68*, 813–834.

[77] a) G. W. Kenner, S. W. McCombie, K. M. Smith, *Justus Liebigs Ann. Chem.* **1973**, 1329–1338; b) G. Fülling, D. Schröder, B. Franck, *Angew. Chem.* **1989**, *101*, 1550–1552; *Angew. Chem. Int. Ed. Engl.* **1990**, *28*, 1519–1521.

[78] a) M. Gosmann, A. Vogt, B. Franck, *Liebigs Ann. Chem.* **1990**, 163–168; b) S. Beckmann, T. Wessel, B. Franck, W. Hönle, H. Borrmann, H. G. von Schnering, *Angew. Chem.* **1990**, *102*, 1439–1441; *Angew. Chem. Int. Ed. Engl.* **1990**, *29*, 1395–1397; c) S. Beckmann, Dissertation, Universität Münster, **1990**.

[79] C. S. Foote, M. T. Wuesthoff, S. Wexler, I. G. Burstein, R. Denny, G. O. Schenck, K.-H. Schulte-Elte, *Tetrahedron* **1967**, *23*, 2583–2599.

[80] B. Franck, M. Dust, A. Stange, P. P. Hoppe, *Naturwissenschaften* **1982**, *69*, 401–402.

[81] W. Wiegrebe, K. Müller, K. K. Mayer, *Arch. Pharm. (Weinheim, Ger.)* **1986**, *319*, 1009–1018.

[82] a) G. Schermann, R. Schmidt, A. Völcker, D.-D. Brauer, H. Mertes, B. Franck, *Photochem. Photobiol.* **1990**, *52*, 741–744; b) D.-D. Brauer, unpublished.

[83] We are thankful to Dr. J. L. Matthews, Baylor Research Institute, Dallas, TX, USA for valuable discussions and investigations as well as for the pictures on blood sterilization (Fig. 10).

[84] R. Robinson, *J. Chem. Soc.* **1917**, *111*, 762–768.

[85] C. Schöpf, *Justus Liebigs Ann. Chem.* **1935**, *518*, 1–37.

[86] W. S. Johnson, *Angew. Chem.* **1976**, *88*, 33–41; *Angew. Chem. Int. Ed. Engl.* **1976**, *15*, 9–17.

[87] R. M. Lemmon, *Chem. Rev.* **1970**, *70*, 95–109.

Molecular Imprinting in Cross-Linked Materials with the Aid of Molecular Templates—A Way towards Artificial Antibodies

Günter Wulff*

Can binding sites be produced in organic or inorganic polymers—similar to those in antibodies—which are able to recognize molecules and which may have catalytic action? In this article we review a method, analogous to a mechanism of antibody formation proposed earlier, by which in the presence of interacting monomers a cross-linked polymer is formed around a molecule that acts as a template. After removal of the template, an imprint containing functional groups capable of chemical interaction remains in the polymer. The shape of the imprint and the arrangement of the functional groups are complementary to the structure of the template. If chiral templates are used, the success of the imprinting process can be assessed by the ability of the polymer to resolve the racemate of the template molecule. Thorough optimization of the process has led to chromatographic separation factors of $\alpha = 4-8$, and to base line separations. There is also great interest in the surface imprinting of solid materials and monolayers. In all cases, the structure of the polymeric matrix in the imprinted materials and the function of the binding groups are of crucial importance. The mechanisms of imprinting and molecular recognition of substrates are by now well understood. A large number of potential applications for this class materials are being intensively developed, for example in the chromatographic resolution of racemates, and as artificial antibodies, chemosensors, and selective catalysts. The use of similarly produced materials as enzyme models is also of great interest.

Keywords: catalysis · enantiomeric resolution · imprinting · molecular recognition · polymers

1. Introduction

In nature, molecular recognition plays a decisive role in biological activity, for example, in receptors, enzymes, and antibodies. The chemist, too, has discovered how to develop more and more selective recognition systems. Extremely high selectivity is obtained if, as in nature, a cavity exists that has a shape to match that of the substance to be embedded in it and binding sites in a definite spatial arrangement. To form the cavity, low molecular weight ring or cage systems[1] such as crown ethers,[2] cryptates,[3] cyclodextrins,[4] cyclophanes,[5] or concave molecules[6] are usually used. The additional incorporation of catalytically active groups that can lead to enzymelike catalysts is of particular interest. Using a conceptually simpler process, similar cavities can now be created in synthetic polymers. In a technique analogous to what was formerly thought to be the mechanism of formation of antibodies,[7] cross-linked polymers are formed around a molecule that acts as a template, and this template is then removed. An imprint containing reactive groups with binding capability remains behind in the polymer.[8] This process differs from the usual template effect[9] in which a template is used to bring low molecular weight reactants into an arrangement that favors the formation of a particular low molecular weight (usually cyclic) product. It also differs from true template polymerization,[10] in which monomers are bound to a polymer that acts as a template to give defined linear polymers. In contrast to this, during the imprinting process the newly formed polymer is cross-linked, so that the three-dimensional structure formed remains unchanged after removal of the template.

The imprinting of organic polymers was first reported by our research group in 1972.[8, 11, 12] The early part of the work necessitated tedious optimization experiments. However, the process is now established and is used in many research groups. The promising areas of development include chromatography, catalysis research, biosensor technology, and the production of artificial antibodies that offer a broad range of potential practical uses. Numerous patents in the field testify to this claim.

Many papers review the subject of molecular imprinting. In addition to comprehensive review articles,[13] there are many shorter articles[14–21] and articles dealing with specific aspects such as chromatography[22–24] and binding groups.[25–27]

[*] Prof. Dr. G. Wulff
Institut für Organische Chemie und Makromolekulare Chemie der Universität Universitätsstrasse 1, D-40225 Düsseldorf (Germany)
Telefax: Int. code + (211)311-4788

 © VCH Verlagsgesellschaft mbH, D-69451 Weinheim, 1995 0570-0833/95/3417-1812 $ 10.00+.25/0

2. The Concept of Imprinting

To obtain highly specific binding sites of a definite shape containing functional groups in a predetermined orientation,[8, 11, 12] we bound the functional groups in a polymerizable form to a suitable template molecule (see Fig. 1a). This monomer (Fig. 1b) was then copolymerized under conditions

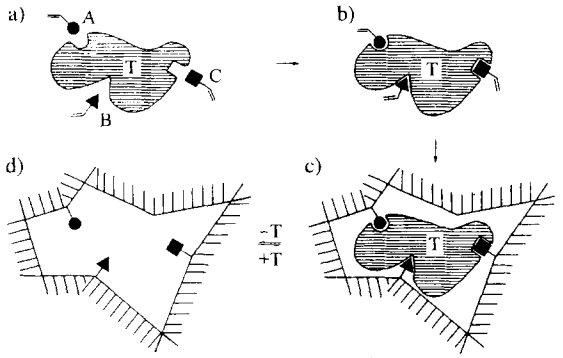

Fig. 1. Schematic representation of the imprinting of specific cavities in a cross-linked polymer by a template (T) with three different binding groups.

that led to the formation of highly cross-linked polymers with chains in a fixed arrangement (c). After removal of the template, polymers with well-defined cavities (d) were obtained, whose structure and arrangement of functional groups were predetermined by the chemical nature of the template. The functional groups in these cavities are located at various points in the polymer chain, and are held in a definite mutual orientation simply by the cross-linking. In this case, the stereochemical information is not carried by a low molecular weight part of the molecule. Instead, the entire arrangement of the polymer chains (topochemistry) is responsible for the stereochemical structure. This is reminiscent of the structure of the active centers of enzymes; we have therefore termed these polymers enzyme-analogous. The relationship of the template to the imprinted cavity corresponds to the key/lock principle proposed by Emil Fischer for enzyme catalysis around 100 years ago.[28] The imprinting process has a certain analogy to the attempts of F. H. Dickey to imprint silica gel by precipitation in the presence of template molecules (see Section 3.2.2).[29, 30]

The polymerization of the template monomer **1a** is an example of the imprinting method. Extensive optimization work was carried out on the methodology with this system.[31–42] The template is phenyl-α-D-mannopyranoside (**1b**) to which two molecules of 4-vinylphenylboronic acid are bound by esterification with two OH groups of the sugar. Boronic acid was chosen

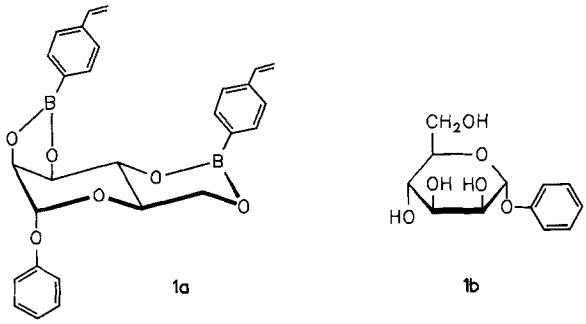

as the binding group (binding site) as this undergoes a rapid and reversible reaction with diols. The monomer **1a** is subjected to radical copolymerization with large amounts of a cross-linking agent such as ethylene dimethacrylate in the presence of an inert solvent (which acts as a porogen to give a porous structure). This yields macroporous polymers with a large inner surface area and a permanent pore structure. Up to 95% of the templates can be split off again from polymers of this type by treatment with water or methanol (Fig. 2).

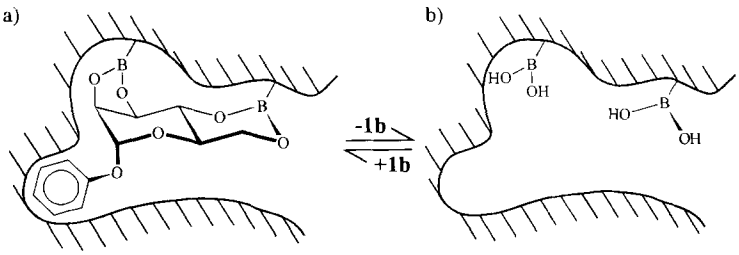

Fig. 2. Schematic representation of a cavity a) obtained by polymerization of **1a**. The template **1b** can be removed with water or methanol to give b). Addition of **1b** causes the cavity to be reoccupied, giving a) again. In this case, the binding of the template is by covalent bonds [13, 34].

Günter Wulff was born in 1935 in Hamburg where he began his chemistry studies. He was awarded his Ph.D. in Bonn in 1963 for a dissertation on the isolation and characterization of glycosidic natural products from plants under the supervision of R. Tschesche. His habilitation, dealing with glycoside synthesis, was completed in 1969 in Bonn. Since 1979 he has held the chair of Organic and Macromolecular Chemistry at the University of Düsseldorf. His present research interests include the synthesis of polymers with enzyme-analogous properties through imprinting with template molecules, the synthesis and investigation of optically active (main-chain chiral) vinyl polymers, and the application of renewable resources (monosacchaides and starch) for the synthesis of specialty polymers.

Since the template **1b** is optically active, the correct structure of the cavity can be verified by racemate resolution experiments. After the template has been removed, the polymer is equilibrated in a batch process with the racemate of **1b**, whereupon the enantiomer used as the template is preferentially taken up. The selectivity is expressed by the separation factor α, which is well known from chromatography (ratio between the distribution coefficients in solution and in the polymer for the D and L forms, K_D/K_L). Depending on the polymer structure and the equilibration conditions, values of α between 1.20 and 6.0 are obtained. With the highest values of α, the D-**1b** can be enriched to 60–70 % *ee* on the polymer in a batch process. With these polymers as stationary phases in HPLC, base line separations of the racemates can be achieved (see Section 6.1).

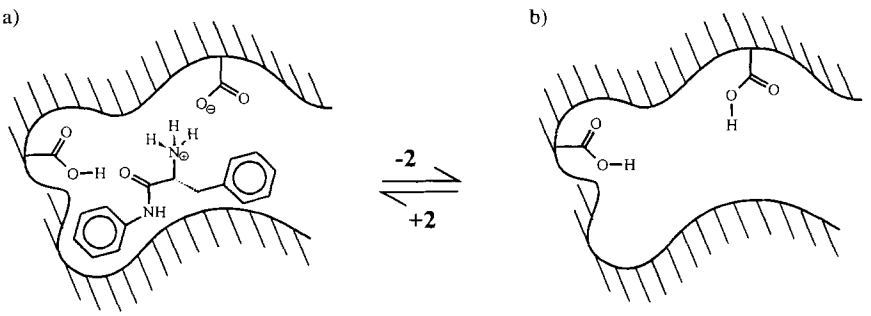

Fig. 3. Schematic representation of a cavity produced in the presence of **2**. The polymerization takes place in the presence of acrylic acid. Noncovalent electrostatic interactions and hydrogen bond formation occur [16, 43].

The extremely high selectivities for the resolution of the racemate clearly show that it is indeed possible to produce cavities with a definite structure and a precise arrangement of functional groups. Although optimization of the polymers extended their properties very considerably, only when K. Mosbach et al.[43] achieved an effective imprinting effect by using exclusively noncovalent interactions could the usefulness of the process be considerably widened. Many investigations in this direction were carried out with L-phenylalanine anilide (**2**) as template. This was polymerized with methacrylic acid as the comonomer under the polymerization conditions established for **1a**. One methacrylic acid unit forms an electrostatic bond with the template **2**, and another forms a hydrogen bond (Fig. 3).[43] The research groups of K. Mosbach and K. J. Shea extensively optimized the process, and achieved high selectivities for resolution similar to those obtained with **1b**.[43–54]

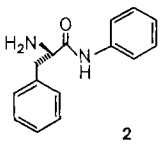

2

Figures 4 and 5 show schematic representations produced by computer graphics of the imprints produced by templates **1b**

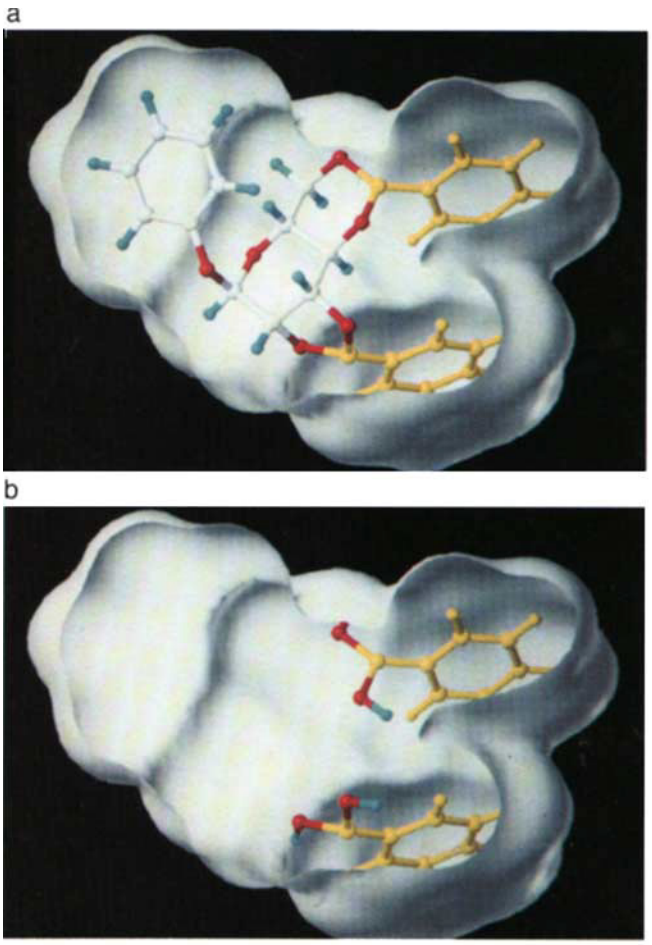

Fig. 4. Computer graphical representation of an occupied cavity a) and an unoccupied cavity b) analogous to Fig. 2. The cavities correspond to the electrostatic potential surfaces of **1a** and were computed by the program MOLCAD 1.0.

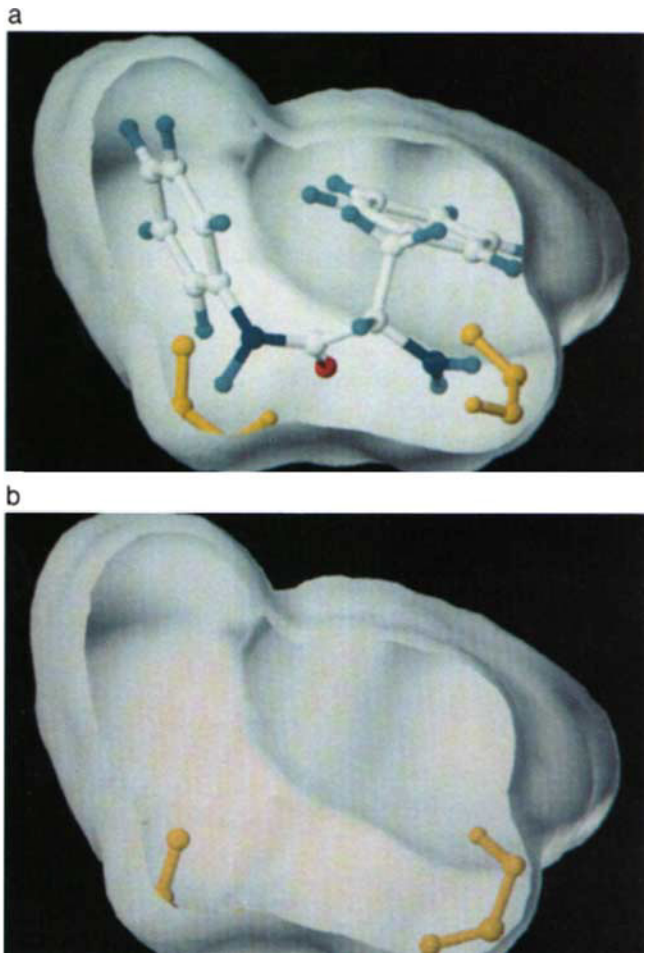

Fig. 5. Computer graphical representation of an occupied cavity a) and an unoccupied cavity b) analogous to Fig. 3. Computation by the same method as for Fig. 4.

and **2**. The shape of the cavity is highly schematic, because the boundaries of the cavities are formed by polymer chains whose dimensions are actually of the same order as those of the templates; consequently, smooth surfaces are not formed.

Since then many other substances have been used as templates to produce imprinted polymers. A list of classes of substances so far used for imprinting polymers is given in Table 1.

Table 1. Classes of substances used as template molecules for imprinting polymers.

Class of substance	Reference
sugars and sugar derivatives	[18, 23, 31, 32, 34, 35, 37, 39–42, 55, 56]
diols, polyols	[8, 57]
hydroxycarboxylic acids	[8, 58–63]
amino acid derivatives	[16, 21, 43, 44, 54, 64–75]
peptides	[76]
proteins	[26, 77]
nucleosides and nucleotides	[78–80]
purine derivatives	[78, 81]
steroids	[72, 73, 82]
basic drugs	[47, 83, 84]
acidic drugs	[85]
dialdehydes	[86]
diketones	[87–90]
dicarboxylic acids	[71–91]
disulfides	[92]
dyes	[93, 94]
coenzyme analogs	[95–97]
basic condensed aromatics	[74, 98]
bisimidazoles	[26, 99, 100]
phosphonate esters	[101, 104a]
pesticides	[104b]

3. The Structure of the Polymeric Matrix

3.1. Imprinted Cavities in Synthetic Polymers

The structure of the matrix is crucial in the imprinting process. As the specific structure of the cavity is not determined by low molecular weight molecules, but by the fixed arrangement of the polymer chains, the optimization of the polymer structure is extremely important. The polymer should have the following properties:[13a]

a) *Stiffness of the polymer structure* enables the cavities to retain their shape even after removal of the template, thus giving high selectivity.
b) *High flexibility* of the polymer structure works against the above, but is essential for the kinetics, to give rapid equilibration with the substrate to be embedded.
c) *Good accessibility* of as many cavities as possible in the highly cross-linked polymer can be achieved by forming a particular polymer morphology.
d) *Mechanical stability* of the polymer particles is of great importance for many applications, for example, for use in an HPLC column at high pressure or as a catalyst in a stirred reactor.
(e) *Thermal stability* of the polymers enables them to be used at higher temperatures, at which the kinetics are considerably more favorable.

From the beginning, macroporous structures have been used almost exclusively for imprinted polymers. Macroporous polymers are obtained if polymerization of the monomers is carried out with a relatively high content of cross-linking agent (5–90%) in the presence of inert solvents (also known as porogens). During the polymerization, phase separation takes place, and, after removal of the porogen and drying, a permanent pore structure remains. The pores can change size on subsequent swelling, but usually remain present.[105] The relatively large inner surface area (50–600 $m^2 g^{-1}$) and large pores (about 10–60 nm) ensure that the specific microcavities formed by the imprinting process (about 0.5–1.5 nm in diameter) are readily accessible, and smaller molecules can diffuse freely inside the pores. If high levels of cross-linking agent are used, the cavities retain their shape quite well after removal of the templates.

The polymers first produced, however, showed relatively low selectivities ($\alpha = 1.03–1.80$) for racemate resolution,[8, 31–33, 57, 61] and their thermal and mechanical stability properties were also below par. Detailed investigations into polymer optimization in our laboratory then brought great improvements. The ratio of porogen to monomer should be approximately 1:1 (mL:g). The type of porogen (solvent or precipitating agent for the polymer being formed) has a strong influence on the morphology of the polymer, but the effect on the selectivity of the cavities formed is small.[13, 39, 54] The decisive factor for high selectivity is the type and quantity of the cross-linking agent used in the production of the macroporous polymers.[34]

Figure 6 shows the selectivity of the polymers (expressed as separation factor α) for the resolution of phenyl-D,L-mannopyranoside in a batch process as a function of the type and amount of cross-linking agent. Ethylene dimethacrylate will be used as a typical example of cross-linking agent (Fig. 6a). The cross-linking agent shows no specificity below a certain concentration (about 10%). The shape of the cavities cannot be stabilized unless the matrix is adequately cross-linked. Increase in the content of cross-linking agent from 10% to 50% increases the α value from 1.0 to approximately 1.5. Increase from 50% to 70% then leads to an unexpected increase from $\alpha = 1.5$ to $\alpha = 3.0$, corre-

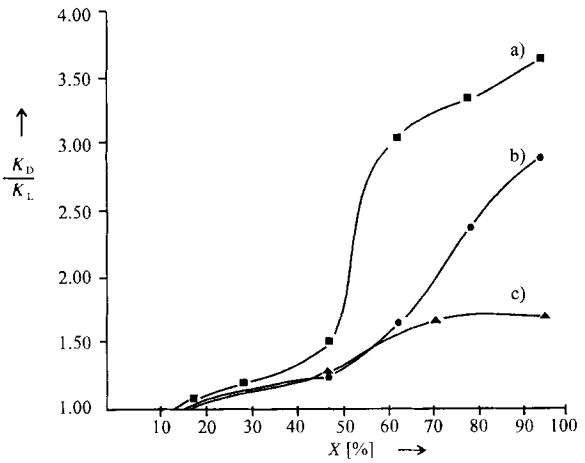

Fig. 6. Selectivity of polymers as a function of the type and amount (X) of cross-linking agent [34]. The polymers were prepared in the presence of **1a** with various proportions of the cross-linking agents ethylene dimethacrylate a), tetramethylene dimethacrylate b), and divinylbenzene c). After removal of the template **1b**, the separation factor $\alpha = K_D/K_L$ was determined for the resolution of D,L-**1b** in a batch process.

sponding to a fourfold increase in selectivity in this range. At present we cannot correlate this sudden increase with a structural change in the polymer matrix. Further increase in the content of cross-linking agent to 95% causes a further increase in selectivity to $\alpha = 3.7$ under these conditions. An even higher selectivity (up to $\alpha = 6.0$) is obtained by reducing the ratio of racemate to polymer and by equilibration at a higher temperature.

If divinylbenzene is used as the cross-linking agent (Fig. 6c), the increase in selectivity at higher content of cross-linking agent is considerably smaller. This cross-linking agent might be increasing the stiffness of the polymer network severely, thereby decreasing the accessibility of the cavities significantly, as shown by the smaller percentage of templates that can be removed. Pure *ortho*-, *meta*-, or *para*-divinylbenzene cross-linking agents behave similarly in this respect.[39] Tetramethylene dimethylacrylate is apparently too flexible as cross-linking agent to give sufficient stabilization of the cavities (Fig. 6b). Thus, a compromise must be found between an inflexible arrangement of the polymer chains to give high selectivity and an appropriate degree of flexibility, which is necessary for good accessibility of the cavities and rapid attainment of binding equilibrium.

Many other cross-linking agents, some synthesized for the first time, have been investigated in the same way.[39] However, it became apparent that ethylene dimethacrylate is not only the cheapest cross-linking agent and easy to purify, but also the most suitable for the imprinting process. Even new, optically active cross-linking agents[39, 106] did not give better selectivity for resolution. The thermal and mechanical stability of materials incorporating higher proportions of ethylene dimethacrylate is very good. Chromatographic columns based on this material did not lose their selectivity even at 80 °C and 6–10 MPa during periods of constant use over many months.[23, 37] For information on good thermal stability, see also Ref. [54]. Polymers cross-linked with divinylbenzene are subject to significant loss of selectivity on prolonged use at 70 °C.[33] Because of the superior properties of imprinted polymers produced with ethylene dimethacrylate, most research groups today use these for work on imprinting.[43, 46, 51, 53, 54, 81, 83, 84, 100, 107–109]

The cavities in polymers of this kind are quite well accessible. If the template is fixed with readily hydrolyzable or noncovalent bonds, over 90% of the templates incorporated in the polymer can be removed again. The remaining templates are located in the interior of the highly cross-linked parts of the macroporous polymer and are not accessible for reactions. Of the empty cavities, about 80–90% can be reoccupied on subsequent equilibration with an excess of template molecules. If the templates are bound by noncovalent interactions, this figure is only 10–15%.[48, 52, 54] (For a thorough discussion refer to Ref. [54].) Almost 90% of the cavities from which the noncovalently bound templates were removed cannot therefore be reoccupied; this leads to a significantly lower capacity. Evidently, after removal of the templates, relaxation of strain and swelling of the matrix cause some of the cavities to change their shape to such an extent that it is no longer possible for substances to be taken up. If the templates are bound covalently, the polar binding groups are located only in the cavity, which swells preferentially and therefore can absorb substances well. In the case of noncovalent binding, three quarters of the binding groups are situated outside the cavity.

The accessibility of the cavities depends not only on the type of cross-linking, but also essentially on the porosity and the inner surface area. The porosity in the dry state has been determined by Hg-porosimetry,[57] BET measurements (determination of the adsorption isotherms of N_2 at low temperatures), and electron microscopy.[33, 54] The porosity in the swollen state is even more important during separations. This was determined by inverse gel permeation chromatography,[33] which shows that in optimized polymers the average pore diameter is 10–30 nm, and the fraction of small pores that hinder diffusion is relatively small. The inner surface area of the polymers is about 300–600 $m^2 g^{-1}$ (determined by BET).

Interpenetrating networks should be especially favorable for imprinting. Here, the stabilizing effect of a very stiff cross-linked polymer combined with a more flexible polymer is utilized. For example, a very rigid, wide-pore polymer of styrene and divinylbenzene is first prepared. This polymer, swollen in an inert solvent containing dissolved template monomer and ethylene dimethacrylate, is then polymerized a second time. The resulting polymers are very stable and show good selectivity, although the percentage of templates that can be removed is somewhat lower.[13a, 39] In another useful technique, monodisperse microparticles are produced by a two-stage swelling/polymerization process[110] in the presence of templates.[111]

If the template is attached to the polymer matrix by bonds that are difficult to break (ester, amide, acetal), these must be cleaved by hydrolysis under vigorous conditions. As this can also cleave ethylene dimethacrylate units, the less effective divinylbenzene must be used as the cross-linking agent.[8, 63, 66, 82a] Shea et al. found that in such a case diisopropenylbenzene was a significantly better cross-linking agent.[88–90]

Extensive polymer optimization and characterization work on macroporous imprinted polymers has been carried out recently in the research group of K. J. Shea.[54, 89, 90] The properties of diffusion and reactivity in the cavities were investigated by fluorescence measurements on dansyl derivatives.[89] Also, ^{13}C CP/MAS NMR and FTIR spectroscopic investigations gave important results.[90] During the polymerization, not all the double bonds of the template monomers react; consequently, some templates are bound through only one binding group instead of two.[32, 54] On removal of the template, the unpolymerized binding group is then also split off.[32] In the cross-linking agent 6–9% of the double bonds also remain unchanged.[54] This proportion can be reduced by subsequent heating, and the polymer structure is thereby considerably improved[54] (see also Refs. [32, 55, 59]). This effect is especially marked if a photopolymerization is initially carried out at low temperature.[54]

3.2. Imprinted Cavities on and in Inorganic Carriers

3.2.1. Organic Polymer Layers on Inorganic Carriers

Thin layers (5–10 nm) of macroporous polymers that have a structure very similar to that described in the previous Section can be produced on the surface of wide-pore silica gels. For this, methacrylate groups are bound covalently to the surface of the silica gel, for example by reaction with 3-(trimethoxysilyl)propyl methacrylate. The surface is then coated with a monomer mix-

ture typical for the imprinting process and polymerized by radical initiation. In this way, highly selective adsorbents consisting of nonswellable particles with the desired particle size are obtained. These products are especially suitable for the chromatographic resolution of racemates.[35, 36, 112, 113]

3.2.2. Imprinted Silica Gels

As already mentioned in the introduction, F. H. Dickey prepared imprinted adsorbents for the first time. Developing the key/lock principle of Emil Fischer,[28] Linus Pauling recognized the great importance of shape selectivity for the action of enzymes and antibodies.[114] He recommended to his doctoral candidate Dickey that he prepare substrate-selective adsorbents.[29, 30] Dickey precipitated silica gel in the presence of dyes (methyl orange and homologues). After drying, the dyes were washed out, and the silica gels obtained showed an increased affinity for the template dye. During the formation of the rigid silica gel matrix around the template molecule, silanol groups are apparently so arranged that interactions with the template can occur.

After these initial investigations, silica gels of this type were also imprinted with optically active templates and used for racemate resolution.[115] The separation of pesticides and other substances was investigated with these silica gels as well.[116] However, as the separations were not particularly good and the selectivity disappeared readily,[117] the direction was not pursued further.

An interesting application in another direction has been reported recently.[118] The compound $CH_3-Si(OCH_3)_3$ was hydrolyzed in the presence of various amphiphiles that form double layers in the form of vesicles, lamellae, tubes, helixes, etc. After removal of the amphiphiles acting as templates, special microstructures were obtained in the silica gel.

3.2.3. Imprinted Inorganic Layers on Solid Materials

In a further development of the Dickey process, layers of cross-linked polysiloxanes were produced in the presence of template molecules on previously prepared silica gel particles in order to utilize their particle structure. Polycondensation was carried out in the presence of functional silanes containing binding groups in order to obtain additional and well-defined interactions between the template molecule and the monomer mixture to give increased affinity and selectivity in the final adsorbent.[23, 119–121] This process employs similar interactions to those used to produce imprinted polymers, except that instead of polymerizable double bonds there are polycondensable silane groups attached to the binding groups. Noncovalent interactions were used during imprinting with dyes,[119] and covalent boronate interactions with glycoproteins,[113a, 119] NAD-dimers,[121] and sugars.[23, 120] Overall, however, this methodology seems to have no advantage over imprinting in polymers.

With a view to subsequent applications as catalysts, Morihara et al.[122, 123] used a somewhat different method of modifying the surface of silica gel (described by him as the "footprint" method, see Section 6.5.).

3.2.4. Surface Modification of Solid Materials

In the typical imprinting of polymers or silica gels, the selectivity of the products so obtained depends on the shape of the cavity and the arrangement of the functional groups within it. We asked ourselves whether the distance between two binding groups on a surface could also lead to substrate selectivity.[86] To test this, bisazomethines were condensed on the surface of wide-pore silica gels. The most promising substances for the condensation were of the type $RSi(CH_3)(OCH_3)_2$.[124] The free silanol groups on the surface were then blocked by hexamethyldisilazane to prevent nonspecific adsorption. After removing the template, two amino groups were left behind at a definite distance apart (Fig. 7). To obtain good selectivity, the number of

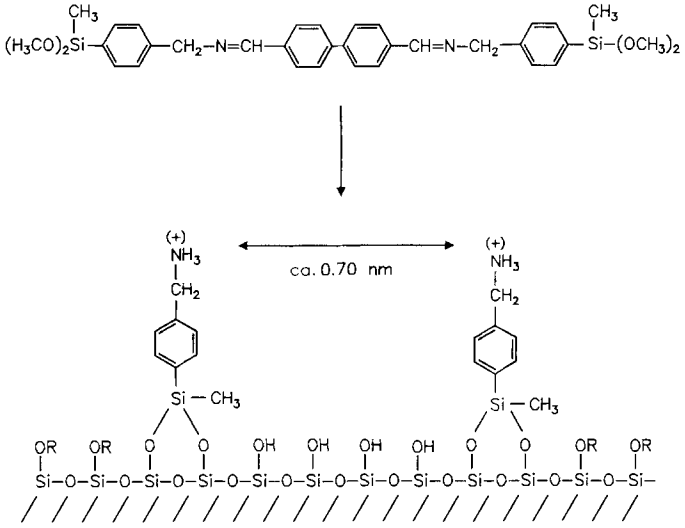

Fig. 7. Preparation of a silica gel with two amino groups on the surface a definite distance apart. The distance between the groups (about 0.70 nm) is fixed by using a biphenyl-4,4'-dialdehyde as the template [86, 124].

condensed templates must not be too high, as otherwise, after removal of the templates and subsequent equilibration with dialdehydes, bonding through adjacent amino groups that did not originally form a pair takes place. If dialdehydes in which the aldehyde groups are at various distances apart are exposed to silica gels so modified, the dialdehyde that was used to carry out the imprinting is bound preferentially.[86] Dicarboxylic acids with different distances between the carboxyl groups can also be very effectively separated on these silica gels by HPLC (Table 2),[124] because the terephthalic acid with the correct distance between the carboxyl groups (0.70 nm) is retarded the most, and those acids in which the distance is greater or smaller are less strongly retarded. Remarkably high α values can be obtained in this way. If an aldehyde is used as the binding group and a diamine as the template, diamines should also be separable after removal of the diamine and oxidation of the aldehyde to carboxyl groups.[125] In a similar way, trios of amino groups in a definite arrangement can be placed on the surface of SiO_2.[126] If the remaining silanol groups are blocked with space-filling silanes (for example, phenyldimethylmethoxysilane) after condensation of the template, contours of the size of the templates are obtained after removal of the template on the surface where the

Table 2. HPLC separations with the silica gel described in Fig. 7. Capacity factors (k') of some dicarboxylic acids with various distances (d) between the carboxyl groups (loading: 4.23×10^{-2} mmol NH_2 groups per g) and the separation factors α for certain pairs of substances are given [124]. Eluent: 2-propanol/acetonitrile/formic acid 67.9/32.0/0.1.

No.	Chromatographed substance	d [nm]	k'	α
1	HOOC–C$_6$H$_4$–COOH	1.14	0.015	
2	HOOC–C$_6$H$_4$–COOH	0.70	0.314	$\alpha_{2,1} = 20.9$
3	HOOC–CH$_2$–C$_6$H$_4$–CH$_2$–COOH	0.85	0.226	$\alpha_{3,1} = 15.1$
4	HOOC–CH$_2$–CH$_2$–C$_6$H$_4$–CH$_2$–CH$_2$–COOH	1.11	0.037	$\alpha_{3,4} = 6.1$

functional groups are located (Fig. 8).[86] Long-chain aliphatic silanes can also be used for blocking for this purpose.[127]

An interesting method of modifying surfaces by self-assembling systems was used by J. Sagiv.[128] Mixed monolayers of trichloro-*n*-octadecylsilane and a dye modified with a detergent as the template were adsorbed on glass and chemically bound as siloxanes. The modified dye molecule that was not covalently bound could then be dissolved out. This left holes within the stable network of chemisorbed and polycondensed silane molecules. Such layers showed preferential adsorption of the template used (Fig. 9). However, the kinetics of the sorption–desorption process are unfavorable, as the mass transfer must take place through a channel formed by the dense arrangement

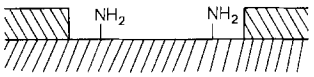

Fig. 8. Schematic representation of the surface of a silica gel with two amino groups at a definite distance apart and the contour of the original template [86].

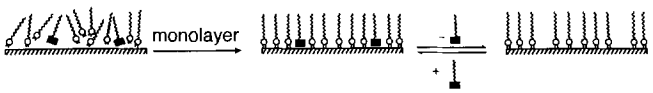

Fig. 9. Schematic representation of the production of mixed monolayers with template molecules on glass. Components that are only physisorbed can be removed [128].

of long alkyl chains in the monolayer. Molecules similar to the template can also be adsorbed in the cavities. Here, it is important that amphiphilic groups should be present in the molecule.[129] This readsorption was investigated mainly electrochemically,[130] by surface-enhanced resonance Raman spectroscopy,[129] and by ellipsometry.[131] Solid carriers included glass, tin dioxide, and gold. Tin dioxide and gold, in particular, could be used as substrates in sensors.[132]

For use in sensors, templates with different properties from those of the rest of the monolayer (for example, insulator–semiconductors) were cocondensed onto the solid carrier. If the alkyl chains are very much longer than the templates, they again form specific channels through which only certain substances penetrate to emit a signal (Fig. 10).[133, 134] Surface imprints on monolayers and vesicles are described in Section 4.4, and on microparticles in Section 4.5.

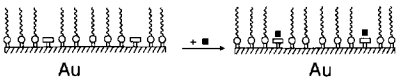

Fig. 10. Schematic representation of the production of mixed monolayers with a chemically bound template molecule. Certain substances (■) can penetrate to the template and cause a signal to be emitted [133, 134].

3.3. Imprinting in Biopolymers (Bioimprinting)

3.3.1. In Proteins

M. H. Keyes et al.[135] have thoroughly investigated the problem of converting proteins by an imprinting process into semisynthetic enzymes. These can sometimes have similar efficiency to that of natural enzymes, but have other defined properties. First the protein is partially denatured, and then brought into contact with a modifying agent, which may, for example, be an inhibitor for the enzyme to be modeled. The protein is subsequently cross-linked, and the substance acting as a template removed. In this way products with new types of enzymatic activity were obtained, although the starting proteins had either no activity (for example, albumin, concanavalin A) or a completely different type of activity (ribonuclease, trypsin, glucose oxidase, α-amylase). The partially denatured protein is assumed to bind the template, which leads to the formation of a new active center similar to that of the enzyme to be modeled.

Another method of bioimprinting was independently investigated by the research groups of A. M. Klibanov[136] and K. Mosbach.[137a] Klibanov freeze-dried proteins dissolved in water in the presence of a large excess of added multifunctional substances, and then removed the template with organic solvents. These artificial receptors had considerable selectivity for binding the template molecules. The reason for the selectivity is the increased rigidity of the protein conformation in organic solvents. In water the selectivity is completely lost, as, in contrast to the experiments of Keyes, no covalent cross-linking was carried out. Even more interesting are the results of Mosbach et al. They precipitated, for example, α-chymotrypsin in the presence of *N*-acetyl-D-phenylalanine with 1-propanol, and then dried it. In nonaqueous solution, after removal of the templates, this modified α-chymotrypsin had good selectivity for the formation of D-phenylalanine ethyl ester, whereas an enzyme analogously treated in the absence of a template showed virtually no selectivity for this reaction. A similar bioimprinting was used for the investigation of the photochemistry of labeled chymotrypsin.[137b]

3.3.2. In Carbohydrates

S. Shinkai et al.[138] cross-linked water-soluble starch with cyanuric chloride in the presence of methylene blue. The insoluble products, after removal of the methylene blue, adsorbed methylene blue considerably better than a starch cross-linked in the absence of methylene blue. The reason was that a much greater number of accessible binding sites were present in the imprinted starch.

Recently our research group has carried out detailed investigations into the stabilization of certain helical conformations in amylose. Inclusion compounds of the amylose with selected organic complexing agents were prepared and thoroughly charac-

terized.[139, 140] Depending on the bulk of the complexing agents, six, seven, or eight glucose units are obtained per turn in the amylose helix. If this complex is intramolecularly cross-linked with epichlorohydrin, or intra- and intermolecularly with cyanuric chloride, soluble or insoluble (respectively) cross-linked amylose complexes are obtained. After removal of the complexing agents (the templates), these amyloses show very different selectivity for the adsorption of substances, depending on the complexing agent used as template.[140]

The cross-linking of chitosans in the presence of metal ions is described in Section 4.5.

4. The Function of the Binding Groups

4.1. General

In the imprinting procedure, the binding groups have several functions.[13a, 22, 25, 27, 36, 54] On the one hand, the bond between the template and the binding group should be as strong as possible during the polymerization to enable the binding groups to be fixed by the template in a definite orientation on the polymer chains during cross-linking. Then the templates should be able to be removed as completely as possible. The next very important function is the interaction of the binding groups with the substrates to be bound, for example, with the compound that acted as the template. This process should be as fast and reversible as possible to enable application in chromatographic separations or catalysis. Thus, although a high activation energy is desirable for the first function, it should be as low as possible for the two other functions.

Interactions can be covalent or noncovalent. Covalent interactions have the advantage that the binding groups are precisely fixed in space during the polymerization. Covalent interactions are very suitable if a high percentage of the templates can be removed and the interactions with substrates can be strongly accelerated by catalysis. The same is true for templates fixed by bonding through metal complexes. With noncovalent interactions, a considerable excess (usually at least fourfold) of binding groups is required in the polymerization mixture so that the binding sites in the template are completely saturated at equilibrium. In this way, a considerable proportion of the binding groups are incorporated randomly. On the other hand, the template is usually very easily removed, and reversible interactions with substrates are, in principle, rapid. The structure of the template molecule determines which interactions are the most favorable in the specific case. When producing chromatographic materials for analytical purposes, noncovalent interactions are usually preferred, as the materials are more readily obtainable and an excess of binding groups apparently does not have a detrimental effect on the separations. For the construction of catalysts, the orientation of the binding groups and catalytically active groups in the cavity are of greater significance, so that covalent interactions should be more advantageous here.

4.2. Covalent Interactions

The boronic acid group is very suitable for covalent binding. Poly(vinylphenylboronic acid)s are commercially available and are used in chemoselective affinity chromatography in alkaline aqueous solution for diol-containing compounds.[141] They can also be used in a similar way for imprinting. The advantage is that relatively stable trigonal boronic acid esters are formed [Eq. (a)]. However, in aqueous alkaline solution or in the presence of certain nitrogen bases (for example, NH_3, piperidine), tetragonal boronic acid esters are formed [Eq. (b)], which equilibrate extremely rapidly with tetragonal boronic acid and diol.[22, 142] In these cases, the rate of equilibration is comparable to that for noncovalent interaction.

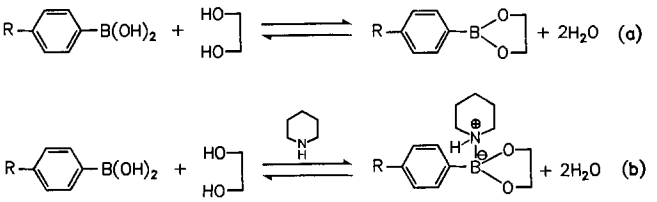

These exchange equilibria with diols are extremely rapid when the intramolecular interaction is with nitrogen bases.[22, 36, 143] A further advantage of the boronic acid group is that the B–C bond can be cleaved afterwards, and the boron acts as leaving group. In this way, other functional groups can also be introduced into the polymer.[55, 144] A large number of diols have been used as templates and polymerized as esters with 4-vinylphenylboronic acid (see, for example, **1a** and Fig. 2). Polymers have also been prepared with only one binding group present, such as those formed from glyceric acid esters[14, 58, 59, 61, 145] and propanediol.[57] These had significant ability to resolve racemates. The mandelic acid polymers prepared by A. Sarhan had remarkably good resolving power.[62, 63, 146, 147] Templates that were bound to the polymer by two boronic acid groups gave polymers with very much higher selectivity for resolution of racemates.[31–33, 35–40, 55, 56a] The optimization of the polymer structure for imprinted polymers was mainly carried out on the example of phenyl-α-D-mannopyranoside. Recently, the resolution of the racemates of free sugars (fructose, mannose, and galactose) was also possible on polymers prepared for the purpose. Thus, for the first time, sugar racemates could be resolved without first having to prepare derivatives.[41, 55, 56a]

One would think that three covalent interactions should be especially favorable for imprinting and for the subsequent molecular recognition. However, it has been shown that three boronic acid interactions,[8, 12, 57] three different covalent interactions,[35] or three or more noncovalent interactions[44, 49, 51, 148] all lead to poorer resolving powers (small number of theoretical plates N_{th}) of the polymers. Here the main factor must be the low rate of formation of polymer–substrate complexes of this type.

In the example of the boronic acids, the effect of the flexibility of the binding group on the resolving power of the polymers was also investigated.[40, 41, 145] For example, nine different polymerizable boronic acids with different degrees of mobility between the boron and the polymerizable double bond were used, with phenyl-α-D-mannopyranoside as the template.[40] As the mobility of the groups in the cavity increased, the selectivity in racemate resolution decreased.

The suitability of Schiff bases for covalent binding was also extensively investigated.[25, 64, 65, 86, 150] Schiff bases are, in principle, suitable for imprinting and subsequent binding, since the position of the equilibrium is favorable. The rate of equilibration is, however, too low for rapid chromatography.[64] By using suitable intramolecular neighboring groups, the rate of equilibration can be considerably increased.[25] With amino acids, racemic resolution in the form of anilides is especially suitable,[64] an experience which was later also confirmed with noncovalent interactions.[43] In this case, the template monomer was *N*-(4-vinylbenzylidene)-L-phenylalanine anilide (**3**) or the 5-vinylsalicylidene derivative.[64]

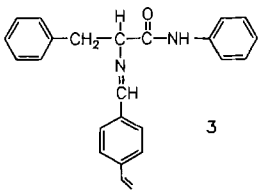

3

Binding with Schiff bases was successfully used either with double fixation as Schiff bases[86, 149] or in combination with other interactions.[35, 65, 150] For binding monoalcohols, both intramolecular monoesters of boronic acids (1-hydroxy-1-bora-2-oxaindene derivatives)[22, 25] and certain cyclic hemiacetals are suitable,[151] and in both cases relatively rapid equilibration takes place.

Ester groups[66, 82a, 91] and amide groups[8] are not very suitable for introducing binding groups into imprinted polymers, as only a small proportion (20%) of these can be removed. In the case of amide, the covalent bond present during polymerization can be used later in the binding of substrates as an electrostatic interaction between carboxylic acids and amino groups.[8, 11, 12, 14, 58, 59, 64]

An interesting way to combine the advantages of covalent bonding during imprinting with noncovalent interaction during equilibration was used by M. J. Whitcombe et al.[82b] They employed 4-vinylphenyl carbonate esters during imprinting. The ester is afterwards efficiently cleaved hydrolytically with loss of CO_2. The resulting binding site phenol is capable of interacting with an alcohol through hydrogen bonding.

K. J. Shea et al.[87–90] used ketals for introducing binding groups. Diketones with various distances between the keto groups were treated with polymerizable diols and after removal of the template showed considerable selectivity for the template originally used when they were reloaded with a mixture of diketones. Unlike the reloading experiments mentioned earlier, this bond formation takes place slowly, and therefore seems to be kinetically controlled, unlike the bonding reactions described so far, which are thermodynamically controlled.

An overview of covalent interactions used to date (including the interaction through metal complexes discussed in Section 4.4.) is given in Table 3.

Table 3. Covalent interactions during the imprinting process.

Polymerizable binding group	Binding site to the template	Type of bond	Reference
4-vinylphenylboronic acid	diol	boronic acid ester	[22, 142]
amines	aldehyde	Schiff base	[86, 149]
aldehydes	amine	Schiff base	[25, 35, 64, 65, 150]
diols	ketone	ketal	[87–90]
hemiacetals	alcohols	full acetal	[151]
boronaphthalide	alcohol	boronic acid ester	[22, 25]
acrylic acid	amine	amide	[8, 11, 12, 14, 58]
acrylic acid	alcohol	ester	[66, 82a, 91]
4-vinylphenyl carbonate	alcohol	ester	[82b]
cobalt chelate	amino acid	chelate complex	[68, 69]
copper chelate	imidazole	chelate complex	[26, 77, 99, 100]
alcohols	carboxylic acid	ester	[71, 91]
vinylimidazole + Co^{2+}	amino acids	chelate complex	[152]

4.3. Noncovalent Interactions

The simplest method of producing selective polymers by imprinting uses noncovalent interactions. Here, monomers that can undergo noncovalent interactions are brought together with the template molecule and the cross-linking agent to form more or less well-defined aggregates of template and monomer. These monomers ligated to the template are in rapid equilibrium with monomers in solution. To ensure that, on average, as many interactions as possible occur during the polymerization, the ratio of ligand monomer to template in the solution must be at least 4:1.[43] As in imprinting silica gels, the first templates used when imprinting polymers with noncovalent interactions were dyes, and these were cross-linked in the presence of monomers that undergo less definite interactions.[93, 94] Selectivity properties were similar to those of silica gels, namely, rather poor. Only after careful optimization by K. Mosbach et al.[43] of imprinting using noncovalent interactions could extremely good separations be performed, and in many cases these were just as good as those obtained with covalent interactions. Noncovalent interactions are considerably easier to use, and many new interacting pairs for the imprinting were found (Table 4).

The most important type of noncovalent interaction is the electrostatic one. For example, when imprinting with L-phenylalanine anilide (**2**) in the presence of methacrylic acid, the influence of this interaction on the selectivity was thoroughly inves-

Table 4. Noncovalent interactions used in the imprinting process.

Polymerizable binding groups	Binding sites to the matrix	References
Electrostatic interaction		
acrylic acid, methacrylic acid	amine	[53, 74]
acrylic acid	amidine	[153]
itaconic acid	amine	[83]
sulfonic acid	amine	[98]
2-vinypyridine, 4-vinylpyridine	acid	[154]
	in combination with covalent interactions	[14, 59, 64, 155]
	in combination with carboxylic acid binding groups	[67]
amine	phosphate (ATP)	[79]
Hydrogen bond formation		
acrylic acid, methacrylic acid	amide	[107]
	amide in combination with electrostatic interaction	[43–54]
acrylic acid	purine base	[78]
ethylene dimethacrylate	nucleoside	[156]
Other interactions		
charge transfer interactions	in combination with covalent interactions	[14, 61]
hydrophobic interactions	in combination with covalent interactions	[60, 61]
interactions of dyes through intercalation	in DNA	[80]

tigated.[21, 43, 48, 53] The strength of the interaction depends on the pK_a values of the methacrylic acid and the amine group in the anilide **2**, on the pH of the solution, and in some circumstances on competing ions present. The interaction during imprinting takes place in a comparatively nonpolar solution (45% ethylene dimethacrylate, 50% acetonitrile, 5% **2** and methacrylic acid), whereas subsequent equilibration (chromatography) of the polymer (from which the templates have been removed) with the racemate of the template is carried out in an aqueous solution with variable pH and foreign ion concentration or a solution containing acetic acid.

However, an electrostatic interaction alone leads to relatively low selectivity,[157] so that another interaction must be present. Remarkably, a polymerizable acid and base can simultaneously interact with a template by electrostatic bonding. For this to occur, the template carboxyl group must be more acidic than methacrylic acid to enable it to react preferentially with the added base.[67]

A useful second interaction is hydrogen-bond formation, for example, as it occurs between the methacrylic acid OH group and an amide oxygen atom. Under these conditions, very selective cavities with α values for racemate resolution of 3–8 are obtained. However, if hydrogen bonds are the only interaction during imprinting and in subsequent interaction, the α values for the racemate resolution are only 1.1–2.5.[107] Examples of the influence of the binding sites are provided by templates **2**,[54] **4**,[157] **5**,[47] and **6**,[44] which were polymerized under comparable conditions in the presence of methacrylic acid or acrylic acid (Fig. 11). The capacity for resolving the racemate of the template becomes considerably less if only one interaction is possible (**4** and **5**).

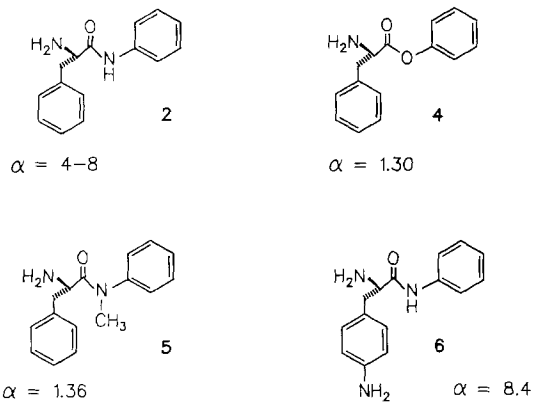

Fig. 11. Separation factors α for the resolution of the racemates of **2**, **4**, **5**, and **6**. The separation factors α were determined for polymers produced under comparable conditions with the appropriate templates.

With noncovalent interactions, it is beneficial to carry out the polymerizations at a low temperature, as these conditions favor the association equilibrium.[46, 49, 50, 54]

Interesting separations with noncovalent interactions have also been carried out on nucleotides and nucleosides. S. A. Piletski et al. used 2′-deoxyadenosine[156] and adenosine triphosphate (ATP)[79] for imprinting based on hydrogen bond formation and electrostatic interactions. The selectivity for the molecule of the template was considerably increased: ADP and ATP, for instance, could be separated considerably better than by chromatography on nonimprinted polymers. High selectivities of imprinted polymers with binding constants of $K_a = 76000\,M^{-1}$ were recently obtained by K. J. Shea et al.[78] They used 9-ethyladenine as the template and methacrylic acid as the binding group. The selectivity of the binding is considerably higher or similar to that of low molecular weight receptors that were prepared in multistep syntheses.[158]

New binding groups for noncovalent binding must also be developed. Ideally, they must undergo a stoichiometric reaction with the template (for example, in the ratio 1:1 or 2:1) during polymerization. This way, no excess of binding groups will be distributed unspecifically within the polymer after polymerization and after removing the template. This is especially important for the formation of catalysts. The percentage of reoccupation for noncovalent binding might then also be significantly improved, which will at the same time increase the capacity for preparative separations. In subsequent equilibrations, adaptation of the medium (nature of solvent, pH, addition of adventitious compounds) will allow the position of the equilibrium to be varied in the desired way.

Noncovalent interactions have also been used in combination with covalent interactions. Thus, electrostatic,[14, 59, 86] charge-transfer,[14, 61] and hydrophobic interactions[60, 61] could be combined with covalent interactions. The resulting polymers sometimes had considerably higher selectivities than those of polymers with a simple covalent bond to the template.

4.4. Binding by Interaction through Metal Complexes

A very promising type of binding during polymerization and later in the final polymer can be achieved by coordinative bonds to metals. This type of bond is analogous to that used in ligand exchange chromatography.[159] The advantage of this kind of bond is that its strength can be controlled by experimental conditions. Definite interactions occur during the polymerization, and an excess of binding groups is not necessary. The subsequent binding of the substrate to the polymer is so rapid that in many cases even rapid chromatography is possible. This method was first used for imprinting by Y. Fujii et al.[68, 69] They obtained a remarkably high selectivity in the optical resolution of *N*-benzyl-D,L-valine using a chiral Schiff base ligand of (*1R*,*2R*)-1,2-diaminocyclohexane and 4-(4-vinylbenzyloxy)salicylaldehyde to which amino acids could be bound through a Co^{2+} cation (see **7**). The exceptionally high separation factor for the race-

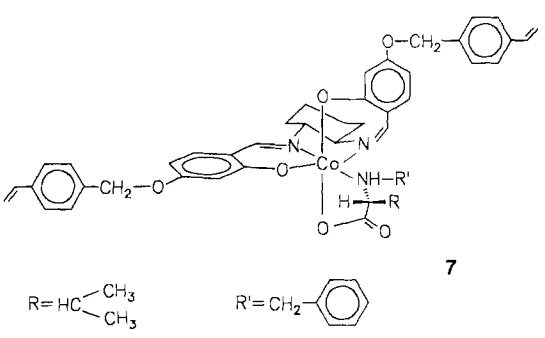

mate resolution of the template molecule was found to be $\alpha = 682$. The enantiomeric excess *ee* was 95.5% in the batch process.

More detailed investigations showed that most of the separating ability was due to the cavity effect.[69] The observed selectivity is greater than that of many enzymes. Unfortunately, the mass transfer rate in the case of the Co^{2+} complex is very slow in the chromatographic separation, so that practical separations are very difficult.[160]

Recently, F. H. Arnold, P. K. Dhal et al. investigated the bonding of imidazole-containing compounds with Cu^{2+} complexes like **8** in great detail [Eq. (c)].[26, 77, 99, 100] Model experi-

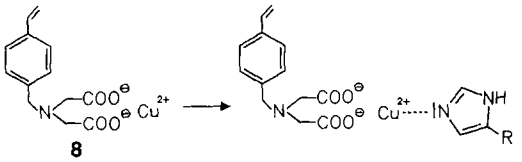

8 (c)

ments were first carried out in which bisimidazoles with various distances between the imidazole groups were used as templates to position polymerizable iminodiacetate groups in the polymer.[99, 100] These experiments were aimed at developing an effective recognition for proteins that depends on the correct spatial arrangement of a few binding sites on a polymer. Polymerizable monolayers or vesicles were used. Surface imprinting with a protein then oriented the Cu^{2+} binding sites in a definite arrangement (corresponding to the imidazole units in the protein), and these were in turn fixed by polymerization (Fig. 12).[26, 77] No more detailed results are yet available on the potential of surface imprinting by proteins.

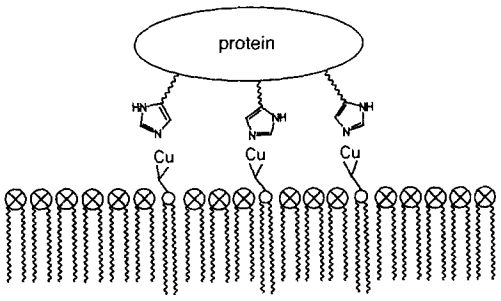

Fig. 12. Schematic representation of a monolayer with copper iminodiacetate groups that are brought into a definite arrangement by interaction with imidazole groups of a protein. The arrangement in the monolayer is then fixed by polymerization (see text) [26, 77].

4.5. Ion-Selective Imprinted Polymers

Metal cations can also serve as templates for imprinting cross-linked polymers. Suitable ligand groups are brought into contact with the cations to form a complex. This is then converted into a cross-linked polymer. After removal of the template (the cation), the adsorption of the cation used as template by such polymers is strongly enhanced and in many cases is also considerably more selective. The selectivity depends on various factors:

1. the specificity of the interaction of the ligand with the cation
2. the coordination geometry and coordination number of the cations
3. the charge on the cation and
4. to some extent, the size of the cation.

Table 5. Examples of ion-selective imprinted polymers.

Imprinting method [a]	Functional polymer/monomer	Imprinting cations	Cross-linking agent	Ref.
a	poly(4-vinylpyridine)	Cu^{2+}, Fe^{3+}, Co^{2+}, Zn^{2+}, Ni^{2+}, Hg^{2+}	1,4-dibromobutane	[161]
	poly(4-vinylpyridine)	Cu^{2+}	1,4-dibromobutane	[162]
	poly(4-vinylpyridine) on silica	Cu^{2+}	1,4-dibromobutane	[163]
a	poly(vinylphosphonic acid-diethylester-co-acrylic acid)	Cu^{2+}	methylenebis(acrylamide)	[164]
		Cu^{2+}, Co^{2+}, Ni^{2+}	methylenebis(acrylamide)	[165]
a	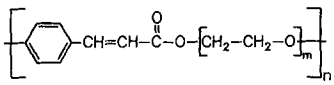	K^+	photochemical cross-linking	[166]
a	poly(ethylenepolyamine)	Cu^{2+}, Ni^{2+}	epichlorohydrin	[167]
a	chitosan	Cu^{2+}	epichlorohydrin	[168]
	chitosan	Cu^{2+}, Cd^{2+}, Zn^{2+}, Ni^{2+}, Fe^{3+}	epichlorohydrin	[169]
b	vinylimidazole	Ni^{2+}, Co^{2+}, Zn^{2+}	1-vinyl-2-pyrrolidone and γ-rays	[170]
b	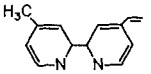	Ni^{2+}, Co^{2+}, Cu^{2+}	divinylbenzene	[171]
b	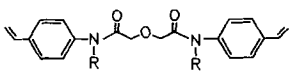	Mg^{2+}, Ca^{2+}	divinylbenzene	[172]
c	Cu_2(methacrylate)$_4$(H_2O)$_2$	Cu^{2+}	EDMA [b]	[108]
c	Cu_2(methacrylate)$_4$(4-vinylpyridine)$_2$	Cu^{2+}	EDMA [b]	[108]
c	Cu_2(acrylate)$_4$(4-vinylpyridine)$_2$	Cu^{2+}	divinylbenzene	[173]
c	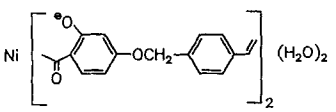	Ni^{2+}	methylenebis(acrylamide)	[174]
d	carboxylated microparticles	Cu^{2+}, Ni^{2+}, Co^{2+}	divinylbenzene	[175]

[a] For the description of the methods see text. [b] EDMA = ethylene dimethacrylate

The polymers can be prepared in various ways (see Table 5):

a) From linear polymers. Linear polymers with groups that can bind to a metal (for example, poly(4-vinylpyridine)) are treated with certain metal cations in solution and allowed to equilibrate for some time. Metal–polymer complexes are formed in which the conformation of the polymer chains is optimized, and many coordinations are possible. These complexes are then cross-linked to stabilize the optimum polymer conformation, and the metal is leached out. This method was used, independently of each other, by V. A. Kabanov, A. A. Efendiev et al.[164, 165] and H. Nishide, E. Tsuchida et al.[161, 176] The Russian research group found considerably increased adsorption, while the Japanese group also established for the first time an increased selectivity for the imprinting cation. The method was subsequently developed very extensively (see Table 5).

b) Polymerization of a mixture of monomers containing complexing groups. In the presence of certain metal cations, intermediate complexes are formed and polymerized with cross-linking. The method is very simple, but the selectivities are relatively poor.

c) Preparation of definite polymerizable complexes of metal cations as pure substances. Using this somewhat more laborious method, the type of complex can be precisely determined, and the polymerization proceeds under strictly controlled conditions. It is also important that the complex should not dissociate during the polymerization. This can be influenced by, for example, the choice of polymerization medium.

W. Kuchen et al.[108, 177] were the first to show that very selective ion exchangers could be prepared with the aid of certain metallic complexes of methacrylic acid and 4-vinylpyridine (Table 6). Unusually high selectivities with the imprinting technique were observed when mixtures of cations were equilibrated. Relative to a reference polymer with the same binding groups but without imprinting, Cu^{2+} was taken up 10–60 times as selectively. With a smaller degree of cross-linking, the selectivity decreases but the capacity remains high.[173]

Table 6. Selectivity of a Cu^{2+}-imprinted resin for the separation of cationic pairs on loading with mixtures of two cations [108], together with that of a blank resin (not imprinted) for comparison.

Metal ions	α [a]	α_{blank} [b]	α' [c]
Cu^{2+}/Zn^{2+}	58	4.2	14
Cu^{2+}/Cd^{2+}	136	3.3	41
Cu^{2+}/Pb^{2+}	28	0.46	62

[a] $\alpha = K_1/K_2$ = selectivity coefficient. [b] α_{blank} = selectivity coefficient for blank resin. [c] $\alpha' = \alpha/\alpha_{blank}$

d) M. Takagi et al.'s method.[175, 178] Selective chelate resins can also be prepared by a new method of surface imprinting. Emulsion polymerization with methacrylic acid as one of the comonomers is used to produce microparticles ($d = 0.4$–$0.7\ \mu m$). The particles are afterwards swollen by a cross-linking agent, and the carboxyl groups become concentrated at the surface by the action of NaOH. They are then oriented specifically by complexation with Cu^{2+}, Co^{2+}, or Ni^{2+} ions, and this arrangement is fixed by a further cross-linking step (Fig. 13). Considerable selectivity for the imprinted cation is observed. Thus, at low Cu^{2+} concentrations, the polymer imprinted with Cu^{2+} takes up 10^3 times as much Cu^{2+} as the nonimprinted polymer.

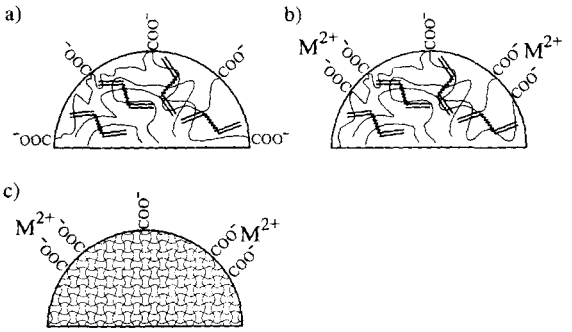

Fig. 13. Surface imprinting in the preparation of ion-selective polymers [178]. Micro-particles containing carboxyl groups are treated with NaOH and swollen with divinylbenzene (a). The carboxyl groups are positioned in a definite manner with the aid of cations (b), and are then cross-linked, for example, by using radiation from ^{60}Co (c).

5. The Imprinting Mechanism

The substance used as the template is, in general, embedded preferentially in the imprinted cavities. By using a pure enantiomer as the template, very effective racemate resolutions could be achieved with these imprinted polymers. In these cases the cavity must thus have an asymmetric structure. The question arises as to the origin of the asymmetry. It was established quite early that the asymmetry is not caused by optically active templates remaining in the polymer.[13a, 32, 43, 58] The possibility that the linear parts of the polyvinyl chains were responsible for the asymmetry was considered after monomer residues bound to a chiral template molecule were found to give optically active vinyl polymers in an asymmetric cyclocopolymerization.[179] However, monomers with a structure like **1a** do not tend to undergo such asymmetric cyclocopolymerization.[180] One must therefore conclude that it is not the configuration, but a fixed asymmetric conformation of the polymer chains that is responsible for the asymmetry.

Surprisingly, the asymmetry of the cavities can also be determined by direct measurement of their optical rotation as well as by their ability to resolve racemates.[18, 42] To measure the optical rotation, the insoluble polymer is suspended in a solvent that has exactly the same refractive index as that of the polymer. This technique has already been used with other insoluble substances.[181a] Whereas monomer **1a** has a molar optical rotation of $[M]_D^{20} = -448.9°$, after incorporation into a polymer the molar optical rotation is $[M]_D^{20} = -61.7°$. After removal of the template, the polymer has a molar optical rotation of $[M]_D^{20} = +110.0°$. This figure is not due to low molecular weight chiral compounds, but is caused by the asymmetric conformations of the polymer chains that form the chiral cavities. Thus, direct measurements on the highly cross-linked polymer are possible. If templates are again in contact with the polymer from which the templates have been removed, it first shows a

high positive molar rotation of $[M]_D^{20} \approx +200°$, which slowly (or rapidly at higher temperatures) changes to the original molar rotation of the polymer ($[M]_D^{20} = -61.7°$). As shown by parallel calorimetric measurements, the template is first bound through one boronic acid only (one-point binding), and this then changes to the stable two-point binding (Fig. 14).

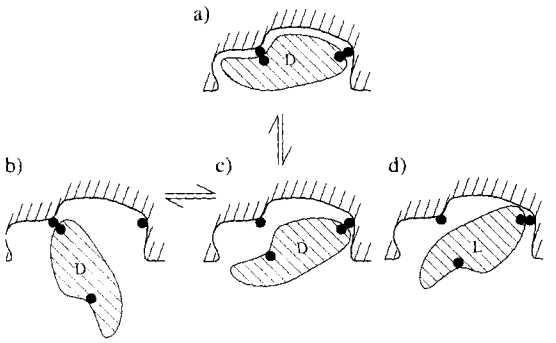

Fig. 14. Schematic representation of two-point binding (a), unproductive one-point binding (b), a productive one-point binding (c), and a one-point binding of the "wrong" enantiomer (d).

An important question is: to what extent can imprinted polymers also bind substances other than the template. For example, are racemates of other substances resolvable? In the first experiments on glyceric acid esters with a certain ester as template, imprinted polymers were shown to resolve a whole series of racemates even when the alcohol group in the racemate is varied (methyl, ethyl, benzyl, or 4-nitrophenyl).[61] Aromatic amino acids were shown to behave similarly. Here, the aromatic group in the racemates can vary. A racemate resolution is possible provided that the rest of the structure remains the same.[45] However, if the arrangement of functional groups is the same, the size and shape of the rest of the molecule are important factors for the separability, as shown, for example, in various bisketals.[88]

To determine to what extent the arrangement of the binding groups in the cavity, rather than its shape, affects the resolving power, we polymerized a series of similar monomers with various arrangements of the functional groups or with different spatial properties.[18, 23, 55, 56a] For example, imprinted polymers were prepared in the usual way with template monomers **1a**, **9a–c**, and **10**. After removal of the template, the resolving power was determined for various sugar racemates (Table 7). All polymers were able, as expected, to resolve racemates of

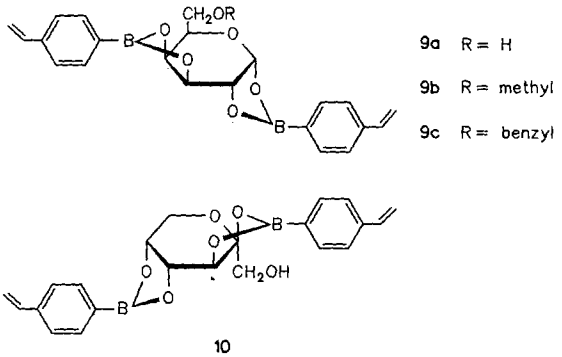

9a R = H
9b R = methyl
9c R = benzyl

10

Table 7. Selectivity of various polymers for racemate resolution [55, 56a].

Template monomer	Racemate	α
1a	phenyl-α-D,L-mannoside	5.0
1a	D,L-mannose	1.60
1a	D,L-fructose	1.34
9a	D,L-galactose	1.38
9c	D,L-galactose	1.58
10	D,L-fructose	1.63
10	D,L-galactose	0.85 (1.17) [a]
9a	D,L-fructose	0.80 (1.25) [a]
9b	D,L-fructose	0.71 (1.41) [a]

[a] To give a better comparison of the selectivities, reciprocal values are given in parentheses (K_L/K_D).

their own template; consequently sugars can now be directly resolved chromatographically even without the need for derivatization.[41]

D,L-Mannose can be resolved on a polymer that has been imprinted with phenyl-α-D-mannopyranoside (entry 2, Table 7). This shows that even racemates with significantly smaller spatial requirements than the template can be resolved. The same is true for the resolution of D,L-galactose on a polymer imprinted with 6-*O*-benzyl-D-galactose (entry 5, Table 7). In these cases, the template and racemate have the same arrangement of functional groups. However, with the exception of D,L-fructose, it was not possible to resolve other sugar racemates on a polymer imprinted with **1b**. The cross-equilibration of polymers that had been imprinted with D-galactose (P-**9a**) or D-fructose (P-**10**) is interesting. Whereas on equilibration with its own racemate, the template is bound preferentially, the polymer imprinted with D-fructose preferentially binds L-galactose, and the polymer imprinted with D-galactose preferentially binds L-fructose out of the racemic mixture. This inverse selectivity on cross-equilibration can be explained if one considers models of the preferred conformations of the molecules.[55] As an example, Figure 15 shows the structures of β-L-fructopyranose and α-D-galactopyranose, which are both preferentially bound by polymer P-**9a**. Both compounds have the same arrangement of hydroxyl groups that react with the boronic acids (in black). Only the hydroxymethyl groups (crosshatched) are at different positions in the molecule, which causes significantly different shapes for the molecules.

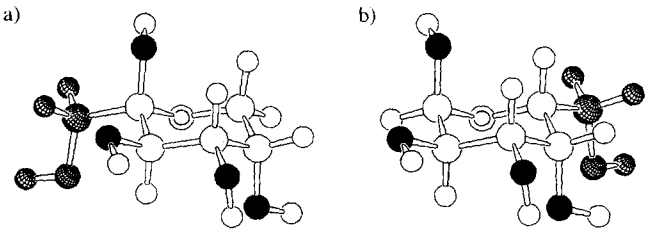

Fig. 15. Ball-and-stick model of the preferred conformations of β-L-fructopyranose (a) and α-D-galactopyranose (b). The OH groups that react with the boronic acid are represented in black. The hydroxymethylene groups which influence the shape are hatched.

Similar considerations apply to β-L-galactopyranose and α-D-fructopyranose and are also valid for phenyl-α-D-mannopyranoside and β-D-fructopyranose.[55] From these results it follows

that the arrangement of the functional groups in the cavity is the decisive factor for the selectivity, while the shape of the cavity is somewhat less important. Classes of substances with the same arrangement of interacting groups therefore have a group selectivity.

In the synthesis of catalytically active polymers, the possibility of introducing functional groups in a definite arrangement is of great importance. However, this is only possible with interactions through covalent or metal-complex bonds, or stoichiometric noncovalent interaction.

A substrate must be embedded in a specific cavity in the correct orientation so that the interactions correspond with the binding groups and the substrate fits with its shape into the cavity. With most template monomers there are two binding groups which, although often chemically identical, produce in the imprinted cavity nonidentical binding sites to the template or substrate (see Fig. 14).[36] Initial one-point binding can be productive (as in Fig. 14c) and lead to the correct two-point binding (a) on further reaction. If a "wrong" one-point bond is formed (unproductively as shown in (b)), a second bond is no longer possible. One of the two productive one-point bonds can only be made after breaking this unproductive bond. Also it can be seen that although the "wrong" (L) enantiomer (or other isomer, diastereomer, etc.) can easily form one bond (for example, (d)), this is unproductive, because a second bond cannot be formed because of the nonfitting geometry of the molecule. The correct two-point bond (as in (a)) has a significantly higher binding constant than the one-point bond. However, as shown by chromatographic investigations, it is formed much more slowly.[23, 35-37]

As already mentioned in connection with optical rotation measurements in the solid state, the formation of the two-point bond can be much accelerated at higher temperatures. Also, in the experiments of K. J. Shea et al., a considerable proportion of one-point bonds were found.[88, 90] No systematic investigations into one- and two-point noncovalent binding have been made, but similar relationships to those observed with covalent binding would be expected.

If the template is removed from the cavity, an interaction of the solvent with the binding groups occurs. The considerable volume increase of the polymer (up to 100%) that results, and especially of the cavities, facilitates embedding of the templates into the expanded cavities. Surprisingly, on binding of the original template, the volume of the cavity decreases again, approximately to the former volume.[14, 59] As the selectivity is fully maintained, the cavity must have kept its shape (memory effect). This phenomenon resembles to some degree the "induced fit" effect known from enzymology.[181b] On equilibration of the polymer with the substrate, and also during chromatography, a rapid equilibrium is established between the free and occupied cavities; consequently a rapid pulsation in the volumes of the cavities must take place. It is not known how the solvent leaves the cavity during embedding of the substrate, or whether it can penetrate the polymer matrix as it does in the case of enzymes. It is to be expected that this type of "induced fit" plays no role in noncovalent bonding.[54]

At increased temperatures the selectivity of the imprinted polymers increases considerably. This is partly because the more selective two-point binding takes place considerably more rapidly at higher temperatures. Also, swelling makes accessible more cavities (binding sites) that have particularly high selectivity and that cannot be occupied at room temperature. This leads to the unusual effect that at higher temperatures even more substance is adsorbed and the retention increases.[37] This fact makes a detailed investigation of the thermodynamics and kinetics of the binding process difficult.

In this connection it must be mentioned that, as with polyclonal antibodies, the individual cavities have varying degrees of selectivity. The selectivity distribution was determined in a multisite model where association constants for each newly occupied binding site were calculated.[31] This showed that a certain proportion of the cavities have relatively low selectivity (changes due to shrinkage or swelling, position on the surface), while the others have a distribution of selectivities around an average figure that can give very high selectivities.[31] When comparing the selectivity of different polymers, the degree of embedding during equilibration or during chromatography is of crucial importance. Figure 17b illustrates this in the case of chromatography.[54]

6. Applications of Imprinted Materials

6.1. Chromatography

Imprinted materials can be used as stationary phases in chromatography, especially for the resolution of racemates. Although the selectivity was good, strong peak broadening in the chromatographic process at first made it impossible to get complete separation, for example, of the racemate of the template **1b**.[22, 32, 33] When significantly more selective adsorbents and improved chromatographic processes coupled with higher temperatures became available, we were able for the first time in 1986 to perform a complete racemate resolution with $R_s = 2.1$.[38] Later, we achieved resolutions of $R_s = 4.3$ by using gradient elution (see Fig. 16a).[41] (The quality of a chromatographic separation is expressed by the resolution R_s, which is mainly governed by the separation factor α of the substance pair and the number of theoretical plates of the column. Satisfactory separations are obtained with $R_s \geq 1$.)

With noncovalent interactions, for example using polymers imprinted with **2**, it was thought that a separation would have been much easier to achieve. However, these systems were found to be very complicated in chromatographic practice. Strong interactions with the medium occurred, and the mass transfer was also very slow. In 1988 K. Mosbach et al. obtained a complete resolution of D,L-**2**, with $R_s = 1.2$,[43] and B. Sellergren and K. J. Shea achieved considerable improvement five years later after very careful optimization work.[53] Protonation of the substrate could be achieved in an aqueous buffer system of pH = 4, in which the carboxyl groups inside the cavities were partially deprotonated, and those outside the cavities were not deprotonated at all. This gave selective binding by an ion exchange mechanism only inside the cavities. Kinetics were good, and could be further improved by use of a heat-treated polymer[54] to give a resolution of $R_s = 2.2$ (see Fig. 16b).

Remarkably, in these separations the more strongly retarded enantiomer (corresponding to the template molecule) gives

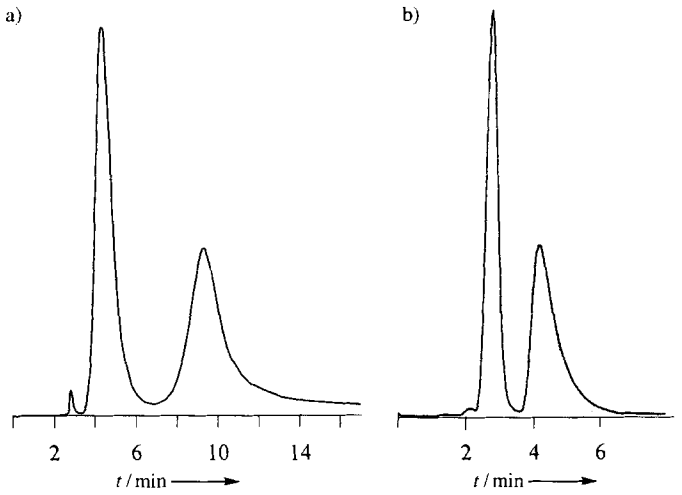

Fig. 16. Chromatographic resolutions of D,L-**1b** on a polymer imprinted with **1a** (a, elution with a solent gradient at 90 °C [41]) and D,L-**2** on a polymer imprinted with L-**2** (b, separation by isocratic elution at 80 °C [53]).

much more pronounced peak broadening if a solvent gradient is not used during chromatography. The number of theoretical plates for this compound is at most half that of the less strongly retarded compound. The reason must be essentially the two-point binding of the template molecule and the one-point binding of the other enantiomer. The difference also shows itself in the temperature dependence of the number of theoretical plates for the two enantiomers. Whereas the template molecule shows hardly any temperature dependence because of the increased two-point bonding with slow binding rates at higher temperatures, the number of theoretical plates for the second enantiomer increases rapidly, as expected (see Fig. 17a).[38] The effect of concentration on retention is also very different for the two enantiomers (see Fig. 17b).[54] The "wrong" enantiomer does not show much effect, whereas the retention in the case of the template molecule is greatly increased at lower concentrations at which only the most selective cavities are occupied by the template molecule. The selectivity therefore increases sharply.[31] Preparative separations are also possible. For example, 30 mg of the racemate of **1b** were effectively resolved by 20 g of polymer.[23]

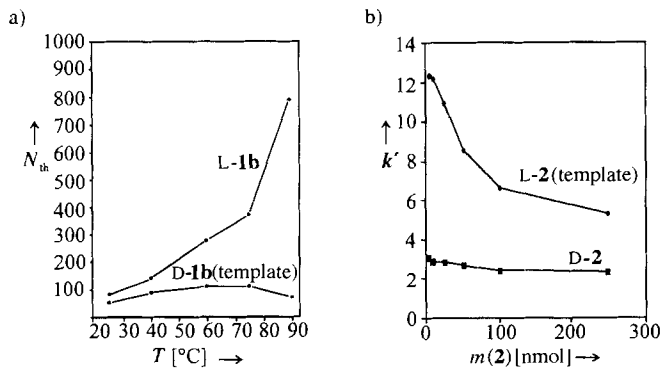

Fig. 17. Differences in the effect of temperature on number of theoretical plates and of the amount chromatographed on the retention for template molecules and their enantiomers. a) Temperature dependence of the number of theoretical plate (N_{th}) in the resolution of D-**1b** and L-**1b** on a polymer imprinted with D-**1b**. b) Dependence of the capacity factors k' on amount treated in the resolution of L-**2** and D-**2** on a polymer imprinted with L-**2**.

Many of the imprinted polymers listed in Table 1 are also used for chromatographic separations. The resolution of drugs is especially interesting, as here it is worthwhile synthesizing a suitable polymer especially for racemic resolution when such a substance is produced. Racemate resolutions of β-blockers,[83] anti-inflammatory agents,[85] and group separations of pentamidines[153a] have been described.

A method originally developed by Svec and Fréchet[182] should also be very suitable for such purposes. Here, a microparticulate polymer is produced directly inside a column. With this process, imprinted polymers can be prepared which have cavities suitable for separations.[153b, 183a] In another approach the direct preparation of imprinted microparticles for chromatography has recently been described.[110] Electrophoretic separations in capillaries filled with imprinted polymers are also of interest.[153c] Extremely high theoretical plate numbers can be obtained in this way, although selectivity in this process still leaves something to be desired. Another possibility is utilizing imprinted polymers as the basis of TLC stationary phases.[183b]

6.2. Imprinted Polymers for Radioimmunoassay

Mosbach et al. used imprinted polymers in place of antibodies for the determination of drugs in a radioimmunoassay.[81, 84] They imprinted polymers with theophylline, diazepam,[81] and morphine,[84] and for theophylline, for example, good linearity was achieved in the range between 14 and 224 μM. The cross-reactions that occur with drugs of similar structure were the same as those of antibodies. In contrast to the determinations with antibodies that are monoclonal, problems arose due to the different binding powers of the individual cavities ("polyclonal"). On further optimization of the process, an effective alternative both to the very laborious isolation of antibodies from animals and to producing them in bacteria was obtained.

6.3. Membranes and Sensors

Imprinted polymer membranes or polymer surfaces could be used as the basis of chemosensors. These are considerably more stable than biosensors and therefore have a longer lifetime. In principle, layers selective for many substances can be prepared by molecular imprinting. In practice, the preparation of effective and selective sensors is still beset with considerable difficulties. One problem is the development of a suitable detection system.

I. Tabushi et al. were the first to prepare sensors purely by surface imprinting.[132] They used Sagiv's method[128] and bound octadecylsilyl monolayers, together with inert template hosts (*n*-hexadecane, 2-cholesteryl-3,6-dioxadecylcarbonate, or decyladamantane-1-carboxylate) covalently to tin dioxide or silicon dioxide layers. After extraction of the hosts, vitamin K_1, K_2, and E, as well as cholesterol and adamantane have been detected by strong electrochemical signals.

Silicon wafers with SiO_2 coatings function similarly.[184a] The templates (nucleotides, nucleosides, and amino acids) were applied to the coatings, and the free silanol groups were then

treated with trimethylchlorosilane or octadecyltrichlorosilane. The same method was used on the surface of glass electrodes.

As already mentioned, the template molecules can also remain in the inert monolayer, thus forming molecular defect sites of definite size and binding power. Only certain molecules can then cause an electrochemical signal, which can lead to considerably increased ion selectivity.[133]

S. A. Piletsky et al.[71-73, 104b, 184b] have also investigated the development of sensors based on imprinted polymers. They prepared imprinted polymers in the form of free-standing[71] membranes or membranes supported on glass frits.[72, 73, 104b] The polymers were prepared from monomeric (2-diethylaminoethyl)methacrylate and ethylene dimethacrylate, and were imprinted with adenosine monophosphate, amino acids, cholesterol, or artrazine by noncovalent interactions. Electrodialysis showed that these membranes were selectively permeable. Also, considerable selectivity for racemates was obtained.[72, 73] The mechanism of these remarkable separations does not yet seem to be fully explained.

In a recent paper on sensors for sialic acid, fluorescence was used for the first time for detection.[184b] In another experiment a membrane was imprinted with tryptophan, and this compound could be selectively transported through it, but the capacity for selective transport was destroyed by photoisomerization of the polymer.[75] Sensors were also prepared by polymerization of an imprinted polymer layer on a silicon wafer with a thin coating of SiO_2.[185a] This very refined design gives a product with selectivity for various amino acids. Differences in embedding of the substances on the polymer coating are measured by the capacitive resistance.

An interesting new route for the construction of sensors was found by D. C. Sherrington et al.[185b] They succeeded in synthesizing imprinted macroporous polymers as completely transparent monoliths. The template molecules bound to the polymer (for example, Michler's ketone) are irradiated with polarized light, and the molecules lying in the direction of excitation react with the polymer matrix. After removal of the unchanged template molecules the anisotropic polymer contains empty cavities that not only preferentially bind the templates, but orient them in a particular direction. The polymers therefore show a pronounced dichroism in UV light, which enables nonselective binding to be distinguished.

6.4. Selective Reactions in Imprinted Cavities

An important reason for producing cavities with a definite shape and a predetermined arrangement of functional groups is the desire to produce highly selective catalysts and enzyme models. Stereoselective and regioselective reactions in these cavities, which are then termed microreactors, constitute a step in this direction. The cavity is first imprinted with the end product of the reaction, and a precursor is then embedded into the cavity so that a reaction can convert it into the product. The first experiments were carried out by the research groups of K. J. Shea[71] and D. C. Neckers[91], who performed cycloadditions to obtain cyclopropanedicarboxylic and cyclobutanedicarboxylic acids. The latter compounds were obtained with remarkable regio- and diastereoselectivity.[91] Y. N. Belokon et al.[70, 96, 186] established that on removal of a proton from a template still located in a cavity, the carbanion formed maintains its original configuration (unlike its behavior in solution), and therefore reacts under retention.

The first asymmetric syntheses in the chiral cavity were achieved in our research group.[13, 65, 150] A cavity was made with an L-DOPA methyl ester. After removal of the template, glycine was embedded in the cavity, deprotonated, and alkylated. So far, the highest enantiomeric excesses (36% *ee*) on using imprinted polymers have been with the amino acids formed in this way. This excess is purely a result of the shape of the asymmetric cavity.

In some very remarkable experiments, S. E. Byström et al.[82a] were recently able to demonstrate high regio- and stereoselectivity in reactions inside the imprinted cavity. The steroid **11** was copolymerized as the template monomer, and removed by reduction. The hydroxyl group in the polymer newly formed from the carboxyl group was converted into an active hydride by $LiAlH_4$. On this polymer, androstan-3,17-dione was reduced exclusively in position 17 to the alcohol, whereas in solution or with a polymer with statistically distributed hydride groups it is reduced exclusively in position 3. Figure 18 shows that the reduction in the cavity is only favored at position 17. A considerable stereochemical preference (ratio of α- to β-OH groups formed) was observed, as well.

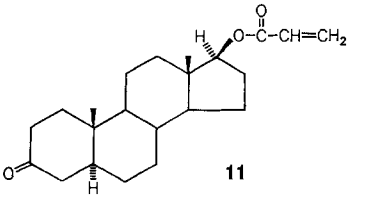

11

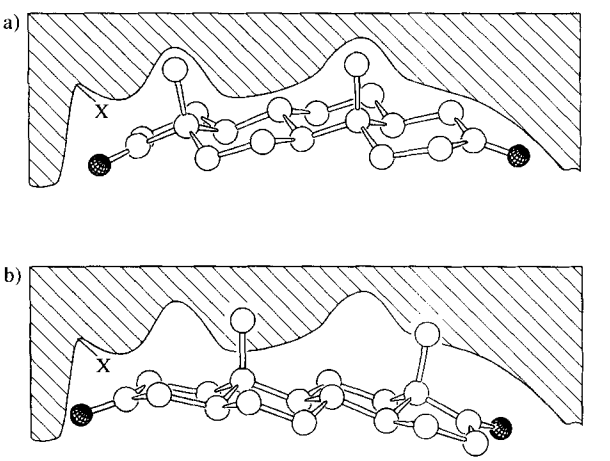

Fig. 18. Schematic representation of the embedding of androstan-3,17-dione in a cavity produced by imprinting with **11** (X = CH_2OH or $CH_2OAlH_3^-$ [82a]: Embedding when the 17-keto group (a) and the 3-keto group (b) is in close proximity to the X group. Poor fitting is obtained in (b).

6.5. Catalysis with Imprinted Polymers and Silica Gels

The imprinting of polymers is immediately recognized as a method for producing catalysts, especially those which function similarly to enzymes.[8, 14] It is possible to produce a cavity with a shape similar to that of the active center of enzymes. In addition, it is necessary to incorporate binding sites for substrates as

well as catalytically active groups in an optimal mutual spatial orientation. This should be possible with suitable template monomers. In these cases, as with enzymes, Michaelis–Menten kinetics are probable, and the catalytic activity should depend on k_{cat}/K_m, where k_{cat} is the rate constant of the catalyzed reaction, and K_m is a binding constant which describes the affinity of the substrate to the catalyst (enzyme). It is important that the binding to the catalyst takes place in a definite (productive) orientation, as otherwise no reaction would occur (unproductive orientation).

In addition it should be possible to use transition state analogs as templates, so producing effective catalysts similar to the catalytically active antibodies.[187] The advantage of these synthetic catalysts lies in their ease of production and stability. However, in contrast to monoclonal antibodies, the active centers are variously structured, more closely resembling polyclonal antibodies.

The first investigations into catalysis were carried out by A. A. Efendiev, V. A. Kabanov et al.[188] Cobalt complexes of linear polymers were equilibrated with, for example, ethylbenzene, the starting material of the reaction to be catalyzed, and the polymer was then cross-linked. Such polymers had two to three times the catalytic activity for the oxidation than catalysts that were not imprinted. The activity was somewhat better if imprinting was carried out with the reaction's product, α-phenylethyl hydroperoxide.

A retroracemization with an imprinted polymer containing 4-vinylpyridine units was carried out by A. Sarhan.[63] Pyridoxal-containing imprinted polymers gave some acceleration of the proton exchange in amino acid derivatives,[97] and imprinted polymers produced with vinylimidazole resulted in an increased esterolytic activity towards the template molecules.[152] However, in all cases, the template effect was very limited. This is also true of attempts to imprint polymers with phosphonic esters that function as transition state analogs for ester hydrolysis.[101–104a] Very similar phosphonic esters have been used as antigens in the preparation of antibodies, and antibodies of this type in some cases showed much increased catalytic activity for the ester hydrolysis.[187] In the imprinted polymers, acceleration by only a factor of 2 was observed,[101–103] but with a large excess of vinylimidazole the acceleration factor was 6.8.[104a] More significant catalytic acceleration was obtained by Shea et al.[109] They used benzylmalonic acid as the template to position polymerizable amines in a definite arrangement in the cavity. After removal of the template, this polymer catalyzed the dehydrofluorination of 4-fluoro-4-(*para*-nitrophenyl)butanone by a factor of 8.6 compared with the corresponding reaction in solution [Eq. (d)]. Although the

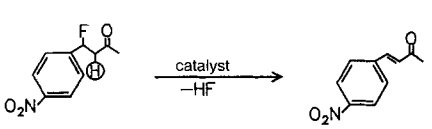

(d)

corresponding catalysis with antibodies was more effective,[189a] turnover, Michaelis–Menten kinetics, and competitive inhibition are observed. Even stronger accelerations (25-fold) were obtained during decarboxylations of 3-carboxybenzisoxazoles. In this case two amino groups were introduced a suitable distance apart in the cavity by means of a polymerizable di-Schiff base.[189b] Apparently, a cavity analogous to a transition state is not sufficient for the catalysis, and the additional cooperative effects of catalytically active groups are necessary.

Prior to some of the investigations described above, the research group of K. Morihara was working very intensively on the preparation of catalysts on the surface of silica gel. In a process described as "footprint catalysis", commercial silica gel is treated with Al^{3+} ions. Incorporation of Al^{3+} in the silicate matrix by isomorphous substitution of silicate by aluminate causes the formation of surface Lewis acid groups. The surface is then loaded with template molecules that contain Lewis base groups (the method is described in detail in Refs. [192, 196]). After aging and drying, surface cavities with Lewis acids (Al^{3+}) in a definite arrangement are formed by regrouping (Fig. 19).

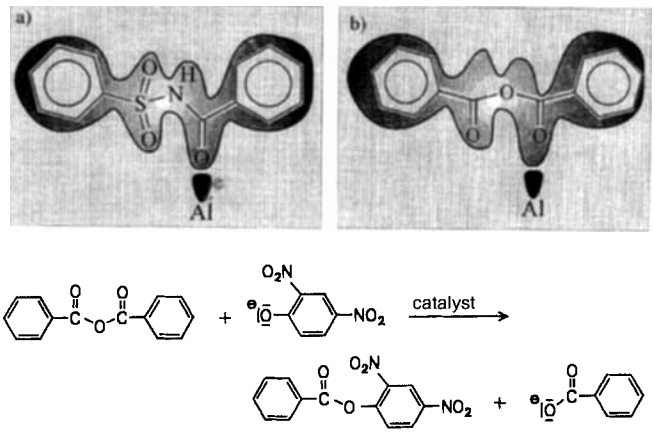

Fig. 19. Schematic representation of footprint catalysis [192, 194]. a) Imprinting with **12** on the surface and orientation of an Al^{3+} Lewis acid in the vicinity of a Lewis base. b) Embedding of the substrate benzoic acid anhydride for the reaction with 2,4-dinitrophenolate.

After removal of the templates, the suitability of the compounds as catalysts was investigated, for example, for the esterification of 2,4-dinitrophenolate with anhydrides. An example is given in Table 8,[192, 194] which shows that on imprinting with a template molecule analogous to the substrate, the binding ability of the substrate corresponding to Michaelis–Menten kinetics is much increased, but k_{cat} becomes smaller. Overall, k_{cat}/K_m increases by a factor of 2–8 over that of control catalysts without imprinting.[191, 193–105] However, if an imprinting molecule analogous to the transition state and containing tetrahedral phosphorus is used (**13**),[192] the binding power is increased, along with a large increase in k_{cat}. Increases of k_{cat}/K_m by a factor of 22 are possible

Table 8. Kinetic parameters for the catalyzed esterification of 2,4-dinitrophenolate with benzoic anhydride [192, 194].

Catalyst imprinted with	$10^4 \times K_m$ [a] [L mol^{-1}]	$10^{-2} \times k_{cat}$ [b] [L^{-1} mol s^{-1}]	$10^{-5} \times k_{cat}/K_m$ [L^{-2} mol^2 s^{-1}]
12	3.36	4.04	12.02 (3.19) [c]
13	4.06	33.36	82.23 (21.81) [c]
Control (no imprinting)	18.0	6.79	3.77

[a] K_m = Michaelis constant. [b] k_{cat} = Rate constant of the catalyzed reaction. [c] Factor for a corresponding catalyst not imprinted in parentheses.

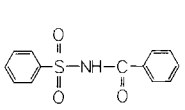

12

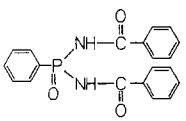

13

in this way. In many cases, high substrate specificity is found.[122, 190, 194] If an optically active template is used for imprinting,[123, 193, 195, 198, 200] these catalysts cause enantiomers to react at different rates (kinetic racemic resolution). The enantiomer used for imprinting reacts two to four times more rapidly than the other.[123, 193, 195, 198] Extensive investigations into competitive inhibition and into productive and nonproductive binding[194, 195, 198] in catalysis have contributed greatly to the understanding of the process. Important applications are to be expected in the future. It is even speculated that "prebiotic enzymes" may have been produced in similar ways and may have played a part in the origin of life.[197]

Maier et al. produced a transesterification catalyst by imprinting with a phosphonate ester in silica gel.[201] The catalyst contains cavities with phosphoric acid centers acting as Lewis acid, and showed high substrate selectivity. On transesterification of ethyl phenylacetate, the octyl ester was formed eight to ten times more rapidly than the phenylethyl ester.

7. Future Prospects

The generation of imprints in polymers and other materials including surfaces has now reached a high degree of sophistication. The applications of these materials are becoming more and more interesting. As described in Section 6, such materials could find application in the near future as artificial antibodies, chemosensors, and catalysts. Application in the chromatographic resolution of racemates is especially likely. The following problems are in the forefront of investigation today:

1. When high molecular weight biopolymers such as proteins, glycoproteins etc. have to be used as templates, special methods must be used. Surface imprinting is likely to be a useful solution here.[19, 26, 77, 119, 202, 203] The further development of monolayers and vesicles[77] seems to be especially promising.
2. To enable a wider range of substrates to be used for imprinting, a broader array of binding groups must be developed, which are specific for interaction with particular functional groups.
3. In spite of considerable improvement of the mass transfer in imprinted polymers, the attainment of equilibrium in the embedding of the substrate in cavities with two-point bonding needs to be accelerated.
4. It would be very useful if the selectivity differences between individual cavities ("polyclonality") could be further minimized.
5. For preparative chromatography, the capacity of the columns must be further increased. In this context, if noncovalent interactions are used for the imprinting, it is important to increase significantly the proportion of cavities that can be refilled.
6. An important simplification of the chromatographic process would be achieved if compounds could be directly separated without first forming derivatives.
7. When imprinted polymers are used as chemosensors, extremely sensitive methods are required for the detection of substances bound to the imprinted membrane.

Special thanks are due to my co-workers who have been involved with me in research on this topic and who, through their commitment and their ideas, have contributed a significant share of these results. We have received financial support over a long period, and especially in the difficult initial phase, from the Deutsche Forschungsgemeinschaft, whom we thank in particular. Also, support from the Fonds der Chemischen Industrie has helped us considerably. I thank the following colleagues for providing me with unpublished results: S. E. Byström, Stockholm; P. K. Dhal, Cambridge; A. A. Efendiev, Baku; Y. Fujii, Ibaraki; W. Kuchen, Düsseldorf; K. Morihara, Nara; S. A. Piletsky, Kiev; B. Sellergren, Mainz; K. J. Shea, Irvine; D. C. Sherrington, Glasgow; M. J. Whitecombe, Reading. I also thank Dr. M. Aust, Düsseldorf, for drawing some of the diagrams and for the computer graphics in Figures 4 and 5, and Dr. A. Kraft, Düsseldorf, for assistance in the preparation of the English manuscript.

Received: August 22, 1994
Revised version: November 30, 1994 [A781E]
German version: *Angew. Chem.* **1995**, *107*, 1958–1979
Translated by R. G. Leach, Basingstoke (UK)

[1] F. Vögtle, *Supramolekulare Chemie*, 2nd ed., Teubner, Stuttgart, **1992**; *Supramolecular Chemistry*, Wiley, New York, **1991**.
[2] D. J. Cram, *Angew. Chem.* **1988**, *100*, 1041–1052; *Angew. Chem. Int. Ed. Engl.* **1988**, *27*, 1009–1020.
[3] J. M. Lehn, *Angew. Chem.* **1988**, *100*, 91–106; *Angew. Chem. Int. Ed. Engl.* **1988**, *27*, 89–104.
[4] G. Wenz, *Angew. Chem.* **1994**, *106*, 851–870; *Angew. Chem. Int. Ed. Engl.* **1994**, *33*, 803–822.
[5] H.-J. Schneider, *Angew. Chem.* **1991**, *103*, 1419–1548; *Angew. Chem. Int. Ed. Engl.* **1991**, *30*, 1417–1546.
[6] J. Rebek, *Angew. Chem.* **1990**, *102*, 261–272; *Angew. Chem. Int. Ed. Engl.* **1990**, *29*, 245–256.
[7] L. Pauling, *J. Am. Chem. Soc.* **1940**, *62*, 2643–2657.
[8] G. Wulff, A. Sarhan, K. Zabrocki, *Tetrahedron Lett.* **1973**, 4329–4332.
[9] R. Hoss, F. Vögtle, *Angew. Chem.* **1994**, *106*, 389–398; *Angew. Chem. Int. Ed. Engl.* **1994**, *33*, 375–386.
[10] C. H. Bamford in *Developments in Polymerisation–2* (Ed.: R. N. Haward), Applied Science Publ., London, **1979**; Y. Y. Tan, G. Challa, *Encycl. Polym. Sci. Eng.1985*- **1989**, *16*, 554–569.
[11] G. Wulff, A. Sarhan, *Angew. Chem.* **1972**, *84*, 364; *Angew. Chem. Int. Ed. Engl.* **1972**, *11*, 341.
[12] G. Wulff, A. Sarhan, DOS 2242796, **1974** [*Chem. Abstr.* **1975**, *83*, P60300w]; G. Wulff, A. Sarhan, US-A 4127730, **1978** (greatly extended version of the previous patent).
[13] a) G. Wulff in *Polymeric Reagents and Catalysts* (Ed.: W. T. Ford) (*ACS Symp. Ser.* **1986**, *308*), pp. 186; b) I. R. Dunkin, J. H. G. Steinke, D. C. Sherrington, *Adv. Polym. Sci.* **1995**, in press.
[14] G. Wulff, A. Sarhan in *Chemical Approaches to Understanding Enzyme Catalysis: Biomimetic Chemistry and Transition-State Analogs* (Eds.: B. S. Green, Y. Ashani, D. Chipman), Elsevier, Amsterdam, **1982**, pp. 106–118.
[15] T. Kunieda, *Yuki Gosei Kagaku Kyokaishi* **1982**, *40*, 686–693; G. Wulff, *Ann. NY Acad. Sci.***1984**, *434*, 327–333; K. Ichimura, *Kobunshi* **1986**, *35*, 934–937 [*Chem. Abstr.* **1987**, *106*, 33682j]; U. H. Cho, K. C. Kim, K. D. Anh, *Hwahak Kwa Kongop Ui Chinbo* **1987**, *27*, 821–827 [*Chem. Abstr.* **1988**, *109*, 210218x]; W. Huang, P. Ho, *Lizi Jiaohuan Yu Xifu* **1988**, *4*, 225–234 [*Chem. Abstr.* **1989**, *111*, 126106t]; K. Tsukagoshi, M. Takagi, *Kagaku (Kyoto)* **1992**, *47*, 500–501 [*Chem. Abstr.* **1992**, *117*, 92771]; M. M. Green, *Chemtracts: Macromol. Chem.* **1991**, *2*, 338–370.
[16] B. Ekberg, K. Mosbach, *Trends Biotechnol.* **1989**, *7*, 92–96.
[17] G. Wulff in *Biomimetic Polymers* (Ed.: C. G. Gebelein), Plenum, New York, **1990**, pp. 1–14.
[18] G. Wulff in *Bioorganic Chemistry in Healthcare and Technology* (Eds.: U. K. Pandit, F. C. Alderweireldt), Plenum, New York, **1991**, pp. 55–68.
[19] F. Flam, *Science* **1994**, *263*, 1221–1222.
[20] K. J. Shea, *Trends Polym. Sci. (Cambrigde, UK)* **1994**, *2*, 166–173.
[21] K. Mosbach, *Trends Biochem. Sci.* **1994**, *19*, 9–14.
[22] G. Wulff, W. Dederichs, R. Grotstollen, C. Jupe in *Affinity Chromatography and Related Techniques* (Eds.: T. C. J. Gribnau, J. Visser, R. J. F. Nivard), Elsevier, Amsterdam, **1982**, pp. 207–216.

[23] G. Wulff, M. Minarik in *Chromatographic Chiral Separations* (Eds.: M. Zief, L. J. Crane), Dekker, New York, **1988**, pp. 15–52; G. Wulff in *Molecular Interactions in Bioseparations* (Ed.: T. T. Ngo), Plenum, New York, **1993**, pp. 363–381.

[24] L. I. Andersson, B. Ekberg, K. Mosbach in *Molecular Interactions in Bioseparations* (Ed.: T. T. Ngo), Plenum, New York, **1993**, pp. 383–394; B. Sellergren in *Chiral Separations by Liquid Chromatography* (Ed.: G. Subramanian), VCH, Weinheim, in press; L. I. Andersson, I. A. Nicholls, K. Mosbach in *Highly Selective Separations in Biotechnology* (Ed.: G. Street), Blackie, New York, **1994**, pp. 206–224; M. Kempe, K. Mosbach, *J. Chromatogr. A* **1995**, *694*, 3–13.

[25] G. Wulff, *Pure Appl. Chem.* **1982**, *54*, 2093–2102.

[26] S. Mallik, S. D. Plunkett, P. K. Dhal, R. D. Johnson, D. Pack, D. Shnek, F. H. Arnold, *New J. Chem.* **1994**, *18*, 299–304.

[27] G. Wulff, *Trends Biotechnol.* **1993**, *11*, 85–87.

[28] E. Fischer, *Ber. Dtsch. Chem. Ges.* **1894**, *27*, 2985–2993; F. W. Lichtenthaler, *Angew. Chem.* **1994**, *106*, 2456–2467; *Angew. Chem. Int. Ed. Engl.* **1994**, *33*, 2364–2374.

[29] F. H. Dickey, *Proc. Natl. Acad. Sci. USA* **1949**, *35*, 227–229.

[30] F. H. Dickey, *J. Phys. Chem.* **1955**, *59*, 695–707.

[31] G. Wulff, R. Grobe-Einsler, W. Vesper, A. Sarhan, *Makromol. Chem.* **1977**, *178*, 2817–2825.

[32] G. Wulff, W. Vesper, R. Grobe-Einsler, A. Sarhan, *Makromol. Chem.* **1977**, *178*, 2799–2816.

[33] G. Wulff, W. Vesper, *J. Chromatogr.* **1978**, *167*, 171–186.

[34] G. Wulff, R. Kemmerer, J. Vietmeier, H.-G. Poll, *Nouv. J. Chim.* **1982**, *6*, 681–687.

[35] G. Wulff, D. Oberkobusch, M. Minarik, *React. Polym. Ion Exch. Sorbents* **1985**, *3*, 261–275.

[36] G. Wulff, D. Oberkobusch, M. Minarik in *Proceedings of the XVIIIth Solvay Conference on Chemistry, Brussels 1983* (Ed.: G. von Binst), Springer, Berlin, **1986**, pp. 229–233.

[37] G. Wulff, H.-G. Poll, M. Minarik, *J. Liq. Chromatogr.* **1986**, *9*, 385–405.

[38] G. Wulff, M. Minarik, *HRC & CC, J. High Resolut. Chromatogr. Chromatogr. Commun.* **1986**, *9*, 607–608.

[39] G. Wulff, J. Vietmeier, H.-G. Poll, *Makromol. Chem.* **1987**, *188*, 731–740.

[40] G. Wulff, H.-G. Poll, *Makromol. Chem.* **1987**, *188*, 741–748.

[41] G. Wulff, M. Minarik, *J. Liquid Chromatogr.* **1990**, *13* (15), 2987–3000.

[42] G. Wulff, G. Kirstein, *Angew. Chem.* **1990**, *102*, 706–708; *Angew. Chem. Int. Ed. Engl.* **1990**, *29*, 684–686.

[43] B. Sellergren, M. Lepistö, K. Mosbach, *J. Am. Chem. Soc.* **1988**, *110*, 5853–5860.

[44] A. Moradian, K. Mosbach, *J. Mol. Recognit.* **1989**, *2*, 167–169.

[45] D. J. O'Shannessy, L. I. Andersson, K. Mosbach, *J. Mol. Recognit.* **1989**, *2*, 1–5.

[46] D. J. O'Shannessy, B. Ekberg, L. I. Andersson, K. Mosbach, *J. Chromatogr.* **1989**, *470*, 391–399.

[47] M. Lepistö, B. Sellergren, *J. Org. Chem.* **1989**, *54*, 6010–6012.

[48] B. Sellergren, *Makromol. Chem.* **1989**, *190*, 2703–2711.

[49] B. Sellergren, *Chirality* **1989**, *1*, 63–68.

[50] D. J. O'Shannessy, B. Ekberg, K. Mosbach, *Anal. Biochem.* **1989**, *177*, 144–149.

[51] L. I. Andersson, D. J. O'Shannessy, K. Mosbach, *J. Chromatogr.* **1990**, *513*, 167–179.

[52] M. Kempe, K. Mosbach, *Anal. Lett.* **1991**, *24*, 1137–1145.

[53] B. Sellergren, K. J. Shea, *J. Chromatogr.* **1993**, *654*, 17–28.

[54] B. Sellergren, K. J. Shea, *J. Chromatogr.* **1993**, *635*, 31–49.

[55] G. Wulff, S. Schauhoff, *J. Org. Chem.* **1991**, *56*, 395–400.

[56] a) G. Wulff, J. Haarer, *Makromol. Chem.* **1991**, *192*, 1329–1338; b) A. G. Mayes, L. Andersson, K. Mosbach, *Anal. Biochem.* **1994**, *222*, 483–488.

[57] G. Wulff, I. Schulze, K. Zabrocki, W. Vesper, *Makromol. Chem.* **1980**, *181*, 531–544.

[58] A. Sarhan, G. Wulff, *Makromol. Chem.* **1982**, *183*, 85–92.

[59] A. Sarhan, G. Wulff, *Makromol. Chem.* **1982**, *183*, 1603–1614.

[60] G. Wulff, A. Sarhan, J. Gimpel, E. Lohmar, *Chem. Ber.* **1974**, *107*, 3364–3376.

[61] G. Wulff, E. Lohmar, *Isr. J. Chem.* **1979**, *18*, 279

[62] A. Sarhan, *Makromol. Chem. Rapid Commun.* **1982**, *3*, 489–493.

[63] A. Sarhan, M. A. El-Zahab, *Makromol. Chem. Rapid Commun.* **1987**, *8*, 555–561.

[64] G. Wulff, W. Best, A. Akelah, *React. Polym. Ion Exch. Sorbents* **1984**, *2*, 167–174; G. Wulff, A. Akelah, *Macromol. Chem.* **1978**, *179*, 2647–2651; H Naarmann, G. Wulff, A. Akelah (BASF A.G.) DOS 2849112, **1978** [*Chem. Abstr.* **1980**, *93*, 133081 n].

[65] G. Wulff, J. Vietmeier, *Makromol. Chem.* **1989**, *190*, 1727–1735.

[66] B. Sellergren, L. Andersson, *J. Org. Chem.* **1990**, *55*, 3381–3383.

[67] O. Ramström, L. I. Andersson, K. Mosbach, *J. Org. Chem.* **1993**, *58*, 7562–7564.

[68] Y. Fujii, K. Kikuchi, K. Matsutani, K. Ota, M. Adachi, M. Syoji, I. Haneishi, Y. Kuwana, *Chem. Lett.* **1984**, 1487–1490.

[69] Y. Fujii, K. Matsutani, K. Kikuchi, *J. Chem. Soc., Chem. Commun.* **1985**, 415–417.

[70] Y. N. Belokon, V. I. Tararov, T. F. Savel'eva, S. V. Vitt, V. I. Bakhmutov, V. M. Belikov, *Makromol. Chem.* **1980**, *181*, 89–104.

[71] K. J. Shea, E. A. Thompson, *J. Org. Chem.* **1978**, *43*, 4253–4255; S. A. Piletsky, I. J. Dubey, D. M. Fedoryak, V. P. Kukhar, *Biopolim. Kletka* **1990**, *6*, 55–58; K. J. Shea, E. A. Thompson, S. D. Pandey, P. S. Beauchamp, *J. Am. Chem. Soc.* **1980**, *102*, 3149–3151.

[72] S. A. Piletsky, I. A. Butovich, V. P. Kukhar, *Zh. Anal. Khim.* **1992**, *47*, 1681–1684.

[73] S. A. Piletsky, Y. P. Parhometz, N. V. Lavryk, T. L. Panasyuk, A. V. El'skaya, *Sens. Actuators B* **1994**, *18–19*, 629–631.

[74] J. Matsui, T. Kato, T. Takeuchi, M. Suzuki, K. Yokoyama, E. Tamiya, I. Karube, *Anal. Chem.* **1993**, *65*, 2223.

[75] S. Marx-Tibbon, I. Willner, *J. Chem. Soc. Chem. Commun.* **1994**, 1261–1262.

[76] a) O. Ramström, I. A. Nicholls, K. Mosbach, *Tetrahedron: Asymmetry* **1994**, *5*, 649–656; b) M. Kempe, K. Mosbach, *J. Chromatogr. A* **1995**, *691*, 317–323.

[77] F. H. Arnold, P. K. Dhal, D. Shnek, S. Plunkett, *PCT Int. Appl.*, WO-9213447, **1992** [*Chem. Abstr.* **1993**, *118*, 164712q]; D. R. Shnek, D. W. Pack, D. Y. Sasaki, F. H. Arnold, *Langmuir* **1994**, *10*, 2382–2388.

[78] K. J. Shea, D. A. Spivak, B. Sellergren, *J. Am. Chem. Soc.* **1993**, *115*, 3368–3369.

[79] S. A. Piletsky, D. M. Fedoryak, V. P. Kukhar, *Dokl. Akad. Nauk Ukr. SSR Ser. B* **1990** (4), 53–54 [*Chem. Abstr.* **1991**, *114*, 165457q].

[80] H. Bünemann, N. Dattagupta, H. J. Schuetz, W. Müller, *Biochemistry* **1981**, *20*, 2864–2874.

[81] G. Vlatakis, L. I. Andersson, R. Müller, K. Mosbach, *Nature (London)* **1993**, *361*, 645–647; K. Mosbach, G. Vlatakis, L. I. Andersson, R. Müller, *PCT Int. Appl.* WO 94/11403, **1994** [*Chem. Abstr.* **1994**, *121*, 132213 y].

[82] a) S. E. Byström, A. Boerje, B. Akermark, *J. Am. Chem. Soc.* **1993**, *115*, 2081–2083; b) M. J. Whitcombe, M. E. Rodriguez, E. N. Vulfson, *Separations for Biotechnology 3* (Ed.: D. L. Pyle) (*Spec. Publ. R. Soc. Chem.* **1994** (158), 565); M. J. Whitcombe, M. E. Rodriguez, P. Villar, E. N. Vulfson, *J. Am. Chem. Soc.* **1995**, *117*, 7105–7111.

[83] L. Fischer, R. Müller, B. Ekberg, K. Mosbach, *J. Am. Chem. Soc.* **1991**, *113*, 9358–9360; L. Fischer, R. Müller, K. Mosbach, B. Ekberg, *PCT Int. Appl.* WO 93 09075, **1993** [*Chem. Abstr.* **1993**, *119*, 108196 h].

[84] G. Vlatakis, L. I. Andersson, K. Mosbach, *Proc. Natl. Acad. Sci. USA*, in press.

[85] M. Kempe, K. Mosbach, *J. Chromatogr. A* **1994**, *664*, 276–279.

[86] G. Wulff, B. Heide, G. Helfmeier, *J. Am. Chem. Soc.* **1986**, *108*, 1089–1091; *React. Polym. Ion Exch. Sorbents* **1987**, *6*, 299–310.

[87] K. J. Shea, T. K. Dougherty, *J. Am. Chem. Soc.* **1986**, *108*, 1091–1093.

[88] K. J. Shea, D. Y. Sasaki, *J. Am. Chem. Soc.* **1989**, *111*, 3442–3444.

[89] K. J. Shea, D. Y. Sasaki, G. J. Stoddard, *Macromolecules* **1989**, *22*, 1722–1730.

[90] K. J. Shea, D. Y. Sasaki, *J. Am. Chem. Soc.* **1991**, *113*, 4109–4120.

[91] J. Damen, D. C. Neckers, *Tetrahedron Lett.* **1980**, *21*, 1913–1916; *J. Am. Chem. Soc.* **1980** 102, 3265–3267.

[92] G. Wulff, I. Schulze, *Angew. Chem.* **1978**, *90*, 568–570; *Angew. Chem. Int. Ed. Engl.* **1978**, *17*, 537–538; G. Wulff, I. Schulze, *Isr. J. Chem.* **1978**, *17*, 291–297.

[93] T. Takagishi, I. M. Klotz, *Biopolymers* **1972**, *11*, 483–491; T. Takagishi, A. Hayashi, N. Kuroki, *J. Polym. Sci. Polym. Chem. Ed.* **1982**, *20*, 1533–1547; T. Takagishi, T. Sugimoto, H. Hamano, Y.-J. Lim, N. Kuroki, H. Kozuka, *J. Polym. Sci. Polym. Lett. Ed.* **1984**, *22*, 283–289.

[94] R. Arshady, K. Mosbach, *Makromol. Chem.* **1981**, *182*, 687–692.

[95] Y. N. Belokon, V. I. Tararov, T. F. Saveleva, V. M. Belikov, *Makromol. Chem. Macromol. Chem. Phys.* **1980**, *181*, 2183–2197.

[96] Y. N. Belokon, V. I. Tararov, T. F. Savel'eva, O. I. Lependina, G. I. Timofeyeva, V. M. Belikov, *Makromol. Chem.* **1982**, *183*, 1921–1934.

[97] L. I. Andersson, K. Mosbach, *Makromol. Chem. Rapid Commun.* **1989**, *10*, 491–495.

[98] I. R. Dunkin, J. Lenfeld, D. C. Sherrington, *Polymer* **1993**, *34*, 77.

[99] P. K. Dhal, F. H. Arnold, *J. Am. Chem. Soc.* **1991**, *113*, 7417–7418.

[100] P. K. Dhal, F. H. Arnold, *Macromolecules* **1992**, *25*, 7051–7059.

[101] K. Mosbach, US-A 5110833, **1992** [*Chem. Abstr.* **1992**, *117*, 107313r].

[102] D. K. Robinson, K. Mosbach, *J. Chem. Soc. Chem. Commun.* **1989**, 969–970.

[103] B. Sellergren, K. J. Shea, *Tetrahedron Asymmetry* **1994**, *5*, 1403–1406.

[104] a) K. Ohkubo, Y. Urata, S. Hirota, Y. Honda, T. Sagawa, *J. Mol. Catal.* **1994**, *87*, L21–L24; K. Ohkubo, Y. Urata, S. Hirota, Y. Honda, Y. Fujishita, T. Sagawa, *ibid.* **1994**, *93*, 189–193; K. Ohkubo, Y. Urata, Y. Honda, Y. Nakashima, K. Yoshinga, *Polymer* **1994**, *35*, 5372–5374; b) S. A. Piletsky, E. V. Piletskaya, A. V. Elgersma, K. Yano, I. Karube, Yu. P. Parhometz, A. V. Elskaya, *Biosens. Bioelectron.*, submitted.

[105] J. R. Millar, D. G. Smith, T. R. E. Kressman, *J. Chem. Soc.* **1965**, 304–310; A. Guyot in *Synthesis and Separation Using Functional Polymers* (Eds.: D. C. Sherrington, P. Hodge), Wiley, Chichester, **1989**, pp. 1–42.

[106] L. Andersson, B. Ekberg, K. Mosbach, *Tetrahedron Lett.* **1985**, *26*, 3623–3624.

[107] L. I. Andersson, K. Mosbach, *J. Chromatogr.* **1990**, *516*, 313–322.

[108] W. Kuchen, J. Schram, *Angew. Chem.* **1988**, *100*, 1757–1763; *Angew. Chem. Int. Ed. Engl.* **1988**, *27*, 1695–1701.

[109] J. V. Beach, K. J. Shea, *J. Am. Chem. Soc.* **1994**, *116*, 379–380; see also R. Müller, L. J. Andersson, K. Mosbach, *Makromol. Chem. Rapid Commun.* **1993**, *14*, 637–641.

[110] K. Hosoya, J. M. J. Fréchet, *J. Polym. Sci. Part A Polym. Chem.* **1993**, *31*, 2129.

[111] K. Hosoya, K. Yoshizako, N. Tanaka, K. Kimata, T. Araki, J. Haginaka, *Chem. Lett.* **1994**, 1437–1438.

[112] O. Norrlöw, M. Glad, K. Mosbach, *J. Chromatogr.* **1984**, *299*, 29–41.

[113] a) M. Glad, M. Kempe, K. Mosbach, *PCT Int. Appl.* WO9305068, **1993** [*Chem. Abstr.* **1993**, *119*, 4425r]; b) F. H. Arnold, S. Plunkett, P. K. Dhal, S. Vidyasankar, *Polym. Prepr.* **1995**, *36*, 97–98.

[114] L. Pauling, *Chem. Eng. News* **1949**, *27*, 913–916.

[115] R. Curti, U. Colombo, *J. Am. Chem. Soc.* **1952**, *74*, 3961; A. H. Beckett, P. Anderson, *Nature (London)* **1957**, *179*, 1074–1075; *J. Pharm. Pharmacol.* **1960**, *12*, 228T–236T; H. Erlenmeyer, H. Bartels, *Helv. Chim. Acta* **1964**, *47*, 46–51, 1285–1288.

[116] V. V. Patrikeev, A. F. Sholin, *Mol. Khromatogr. 1964* **1964**, 66–72 [*Chem. Abstr.* **1965**, *62*, 11127d]; E. S. Kosmatyi, K. A. Chebot'ko, V. I. Galinskaya, V. V. Strelko, *Zh. Anal. Khim.* **1974**, *29*, 168–170 [*Chem. Abstr.* **1974**, *81*, 59097n].

[117] S. B. Bernhard, *J. Am. Chem. Soc.* **1952**, *74*, 4946–4947.

[118] K. Sakata, T. Kunitake, *Chem. Lett.* **1989**, 2159–2162.

[119] M. Glad, O. Norrlöw, B. Sellergren, N. Siegbahn, K. Mosbach, *J. Chromatogr.* **1985**, *347*, 11–23.

[120] T. Huver, *Dissertation, Düsseldorf*, **1987**, see also Review [23].

[121] O. Norrlöw, M.-O. Mansson, K. Mosbach, *J. Chromatogr.* **1987**, *396*, 374–377.

[122] K. Morihara, S. Kurihara, J. Suzuki, *Bull. Chem. Soc. Jpn.* **1988**, *61*, 3991–3998.

[123] K. Morihara, M. Kurokawa, Y. Kamata, T. Shimada, *J. Chem. Soc. Chem. Commun.* **1992**, 358–360.

[124] G. Wulff, T. Görlich, unpublished; T. Görlich, *Dissertation, Düsseldorf*, **1991**.

[125] G. Wulff, R. Poensgen, unpublished.

[126] D. C. Tahmassebi, T. Sasaki, *J. Org. Chem.* **1994**, *59*, 679–681.

[127] Y.-T. Tao, Y.-H. Ho, *J. Chem. Soc. Chem. Commun.* **1988**, 417–418.

[128] J. Sagiv, *Isr. J. Chem.* **1979**, *18*, 346–353; *J. Am. Chem. Soc.* **1980**, *102*, 92–98; S. R. Cohen, R. Naaman, J. Sagiv, *J. Phys. Chem.* **1986**, *90*, 3054–3056.

[129] J.-H. Kim, T. M. Cotton, R. A. Uphaus, *Thin Solid Films* **1988**, *160*, 389–397.

[130] J.-H. Kim, T. M. Cotton, R. A. Uphaus, *J. Phys. Chem.* **1988**, *92*, 5575–5578.

[131] L. I. Andersson, C. F. Mandenius, K. Mosbach, *Tetrahedron Lett.* **1988**, *29*, 5437–5440.

[132] K. Yamamura, H. Hatakeyama, K. Naka, I. Tabushi, K. Kurihara, *J. Chem. Soc. Chem. Commun.* **1988**, 79–81; I. Tabushi, K. Kurihara, K. Naka, K. Yamamura, H. Hatakeyama, *Tetrahedron Lett.* **1987**, *28*, 4299–4302.

[133] I. Rubinstein, S. Steinberg, Y. Tor, A. Shanzer, J. Sagiv, *Nature (London)* **1988**, *332*, 426–429; O. Chailapakul, R. M. Crooks, *Langmuir* **1993**, *9*, 884–888; R. Bilewicz, M. Majda, *J. Am. Chem. Soc.* **1991**, *113*, 5464–5466.

[134] S. Steinberg, Y. Tor, E. Sabatani, I. Rubinstein, *J. Am. Chem. Soc.* **1991**, *113*, 5176–5182; S. H. Chen, C. W. Frank, *Langmuir* **1991**, *7*, 1719–1726.

[135] M. H. Keyes, DOS 3147947 A1, **1982**; UK-B 2088880, **1984** [*Chem. Abstr.* **1982**, *97*, 211561z]; S. Saraswathi, M. H. Keyes, *Enzyme. Microb. Technol.* **1985**, *6*, 98–100; M. H. Keyes, D. E. Albert, S. Saraswathi, *Ann. N. Y. Acad. Sci.* **1987**, *501*, 201–204.

[136] L. Braco, K. Dabulis, A. M. Klibanov, *Proc. Natl. Acad. Sci. USA* **1990**, *87*, 274–277; K. Dabulis, A. M. Klibanov, *Biotechnol. Bioeng.* **1992**, *39*, 176–185.

[137] a) M. Stahl, M.-O. Mansson, K. Mosbach, SE-B 84040215-4, **1989**; M. Stahl, M.-O. Mansson, K. Mosbach, *Biotechnol. Lett.* **1990**, *12*, 161–166; M. Stahl, U. Jeppsson-Wistrand, M.-O. Mansson, K. Mosbach, *J. Am. Chem. Soc.* **1991**, *113*, 9366–9368; b) I. Willner, M. Lion-Dagan, S. Rubin, J. Wonner, F. Effenberger, P. Bäuerle, *Photochem. Photobiol.* **1994**, *59*, 491–496.

[138] S. Shinkai, M. Yamada, T. Sone, O. Manabe, *Tetrahedron Lett.* **1983**, *24*, 3501–3504.

[139] G. Wulff, S. Kubik, *Makromol. Chem.* **1992**, *193*, 1071–1080; *Carbohydr. Res.* **1992**, *237*, 1–10.

[140] G. Wulff, S. Kubik, H.-G. Breitinger in *Nachwachsende Rohstoffe – Perspektiven für die Chemie* (Eds.: M. Eggersdorfer, S. Warwel, G. Wulff), VCH, Weinheim, **1993**, pp. 311–322; S. Kubik, G. Wulff, *Starch / Staerke* **1993**, *45*, 220–225.

[141] A. Bergold, W. H. Scouten in *Solid Phase Biochemistry* (Ed.: W. H. Scouten), Wiley, New York, **1983**, pp. 149–187; M. J. Benes, A. Stambergova, W. H. Scouten in *Molecular Interactions in Bioseparations* (Ed.: T. T. Ngo), Plenum, New York, **1993**, S. 313–322.

[142] M. Lauer, G. Wulff, *J. Chem. Soc. Perkin Trans. 2* **1987**, 745–749.

[143] G. Wulff, M. Lauer, H. Böhnke, *Angew. Chem.* **1984**, *96*, 714–715; *Angew. Chem. Int. Ed. Engl.* **1984**, *23*, 741–742; M. Lauer, H. Böhnke, R. Grotstollen, M. Salehnia, G. Wulff, *Chem. Ber.* **1985**, *118*, 246–260; G. Wulff, H. Stellbrink, *Recl. Trav. Chim. Pays-Bas* **1990**, *109*, 216–221.

[144] G. Wulff, H. Schmidt, H. Witt, R. Zentel, *Angew. Chem.* **1994**, *106*, 240–243; *Angew. Chem. Int. Ed. Engl.* **1994**, *33*, 188–191.

[145] G. Wulff, J. Gimpel, *Makromol. Chem.* **1982**, *183*, 2469–2477.

[146] A. Sarhan, M. M. Ali, M. Y. Abdelaal, *React. Polym.* **1989**, *11*, 57–70.

[147] A. Sarhan, *Makromol. Chem.* **1989**, *190*, 2031–2039.

[148] B. Sellergren, K. G. I. Nilsson, *Methods Mol. Cell. Biol.* **1989**, *1*, 59–62.

[149] K. J. Shea, G. J. Stoddard, D. M. Shavelle, F. Wakui, R. M. Choate, *Macromolecules* **1990**, *23*, 4497–4507.

[150] G. Wulff, J. Vietmeier, *Makromol. Chem.* **1989**, *190*, 1717–1726.

[151] G. Wulff, G. Wolf, *Chem. Ber.* **1986**, *119*, 1876–1889.

[152] A. Leonhardt, K. Mosbach, *React. Polym. Ion Exch. Sorbents* **1987**, *6*, 285.

[153] a) B. Sellergren, *Anal. Chem.* **1994**, *66*, 1578–1582; b) B. Sellergren, *J. Chromatogr. A* **1994**, *673*, 133–141; c) K. Nilsson, J. Lindell, O. Norrlöw, B. Sellergren, *ibid.* **1994**, *680*, 57–61.

[154] M. Kempe, L. Fischer, K. Mosbach, *J. Mol. Recognit.* **1993**, *6*, 25–29.

[155] G. Wulff, M. Minarik, S. Schauhoff, *GIT Fachz. Lab.* **1991**, *35*, 10–17.

[156] S. A. Piletsky, V. P. Kukhar, D. M. Fedoryak, *Ukr. Khim. Zh. (Russ. Ed.)* **1989**, *55*, 872–875 [*Chem. Abstr.* **1990**, *112*, 159517b].

[157] B. Sellergren, B. Ekberg, K. Mosbach, *J. Chromatogr.* **1985**, *347*, 1–10.

[158] K. Williams, B. Askew, P. Ballester, C. Buhr, K. S. Jeong, S. Jones, J. Rebek, *J. Am. Chem. Soc.* **1989**, *111*, 1090–1094; S. C. Zimmerman, Z. Zeng, *J. Org. Chem.* **1990**, *55*, 4789–4791; J. C. Adrian, C. S. Wilcox, *J. Am. Chem. Soc.* **1989**, *111*, 8055–8057.

[159] V. A. Davankov, A. V. Semechkin, *J. Chromatogr.* **1977**, *141*, 313–353; V. A. Davankov, A. A. Kurganov, S. A. Bochkov, *Adv. Chromatogr.* **1983**, *22*, 71–116.

[160] Y. Fujii, personal communicaton, Ibaraki, Japan.

[161] H. Nishide, J. Deguchi, E. Tsuchida, *Chem. Lett.* **1976**, 169–174; *J. Polym. Sci. Polym. Chem. Ed.* **1977**, *15*, 3023–3029.

[162] L. S. Molochnikov, L. V. Demidova, Y. M. Sultanov, R. A. Gaibli, D. D. Orudzhev, E. B. Amanov, A. A. Efendiev, *Vysokomol. Soedin. Ser. B* **1990**, *32*, 945–947 [*Chem. Abstr.* **1991**, *114*, 83404f]; A. A. Efendiev, E. B. Amanov, D. D. Orudzhev, V. A. Kabanov, *Dokl. Akad. Nauk SSSR* **1988**, *300*, 1393–1395.

[163] M. Chanda, G. L. Rempel, *React. Polym.* **1992**, *16*, 149–158.

[164] V. A. Kabanov, A. A. Efendiev, D. D. Orudzhev, Russ.-Pat. 502907, **1976** [*Chem. Abstr.* **1976**, *85*, 6685d]; A. A. Efendiev, D. D. Orudzhev, V. A. Kabanov, *Vysokomol. Soedin. Ser. B* **1977**, *19*, 91 [*Chem. Abstr.* **1977**, *86*, 140873n]; V. A. Kabanov, A. A. Efendiev, D. D. Orudzhev, N. M. Samedova, *Dokl. Akad. Nauk. SSSR* **1978**, *238*, 356–358 [*Chem. Abstr.* **1978**, *88*, 90425m].

[165] A. A. Efendiev, V. A. Kabanov, *Pure Appl. Chem.* **1982**, *54*, 2077–2092.

[166] M. Shirai, T. Orikata, M. Tanaka, *Makromol. Chem. Rapid Commun.* **1983**, *4*, 65; M. Shirai, A. Ueda, M. Tanaka, *Makromol. Chem.* **1985**, *186*, 493–496; M. Shirai, M. Tanaka, *Eur. Polym. J.* **1985**, *21*, 999–1003.

[167] A. A. Efendiev, Y. M. Sultanov, B. K. Abbasova, S. I. Bagbanly, V. A. Kabanov, *Vysokomol. Soedin. Ser. B* **1985**, *27*, 264–266.

[168] K. Inoue, Y. Baba, K. Yoshizuka, H. Noguchi, M. Yoshizaki, *Chem. Lett.* **1988**, 1281–1284.

[169] K. Ohga, Y. Kurauchi, H. Yanase, *Bull. Chem. Soc. Jpn.* **1987**, *60*, 444–446.

[170] M. Kato, H. Nishide, E. Tsuchida, T. Sasaki, *J. Polym. Sci. Polym. Chem. Ed.* **1981**, *19*, 1803–1809.

[171] S. N. Gupta, D. C. Neckers, *J. Polym. Sci. Polym. Chem. Ed.* **1982**, *20*, 1609–1622.

[172] T. Rosatzin, L. I. Andersson, W. Simon, K. Mosbach, *J. Chem. Soc. Perkin Trans. 2* **1991**, 1261–1265.

[173] D. A. Harkins, G. K. Schweitzer, *Sep. Sci. Technol.* **1991**, *26*, 345–354.

[174] Y. Fujii, H. Maie, S. Kumagai, T. Sugai, *Chem. Lett.* **1992**, 995–998.

[175] K. Yu, K. Tsukagoshi, M. Maeda, M. Takagi, *Anal. Sci.* **1992**, *8*, 701–703; K. Tsukagoshi, K. Y. Yu, M. Maeda, M. Takagi, *Bull. Chem. Soc. Jpn.* **1993**, *66*, 114–120.

[176] H. Nishide, E. Tsuchida, *Makromol. Chem.* **1976**, *177*, 2295.

[177] U. Braun, W. Kuchen, *Chem.-Ztg.* **1984**, *108*, 255; W. Kuchen, J. Schram, DOS DE 3804646, **1989** [*Chem. Abstr.* **1990**, *112*, 140473n]; unpublished results in dissertations at the Heinrich-Heine-Universität Düsseldorf: H. Zoch, 1991, S. Kümmel, 1992, S. Pausch, 1994.

[178] H. Kido, T. Miyajima, K. Tsukagoshi, M. Maeda, M. Makoto, *Anal. Sci.* **1992**, *8*, 749–753; K. Tsukagoshi, K. Yu, M. Maeda, M. Takagi, *Kobunshi Ronbunshu* **1993**, *50*, 455–458 [*Chem. Abstr.* **1993**, *119*, 73583c]; H. Kido, H. Sonoda, K. Tsukagoshi, M. Maeda, M. Takagi, H. Maki, T. Miyajima, *ibid* **1993**, *50*, 403–410 [*Chem. Abstr.* **1993**, *119*, 73662c].

[179] G. Wulff, K. Zabrocki, J. Hohn, *Angew. Chem.* **1978**, *90*, 567–568; *Angew. Chem. Int. Ed. Engl.* **1978**, *17*, 535–537; G. Wulff, R. Kemmerer, B. Vogt, *J. Am. Chem. Soc.* **1987**, *109*, 7449–7457; G. Wulff, *Angew. Chem.* **1989**, *101*, 22–38; *Angew. Chem. Int. Ed. Engl.* **1989**, *28*, 21–37; *Chemtech* **1991**, 364–370; *Polym. News* **1991**, *16*, 167–173.

[180] G. Wulff, J. Hohn, *Macromolecules* **1982**, *15*, 1255–1261.

[181] a) P. Pino, I. Bartus, O. Vogl, *Polym. Prepr. (Am. Chem. Soc. Div. Polym. Chem.)* **1988**, *29*, 254–255; O. Vogl, J. Bartus, J. R. Murdoch, *Monatshefte Chem.* **1990**, *121*, 311–316; J. Bartus, O. Vogl, *Polymer Int.* **1994**, *33*, 25–36; b) D. E. Koshland, Jr., *Angew. Chem.* **1994**, *106*, 2468-2472; *Angew. Chem. Int. Ed. Engl.* **1994** *33*, 2408-2412; M. Gerstein, A. M. Lesk, C. Chotia, *Biochemistry* **1994**, *33*, 6739-6749.

[182] F. Svec, J. M. J. Fréchet, *Anal. Chem.* **1992**, *64*, 820–822.
[183] a) J. Matsui, T. Kato, T. Takeuchi, M. Suzuki, K. Yokoyama, E. Tamiya, I. Karube, *Anal. Chem.* **1993**, *65*, 2223–2224; B. Sellergren, SE-B 9303164-9, **1993**; b) D. Kriz, C. B. Kriz, L. I. Andersson, K. Mosbach, *Anal. Chem.* **1994**, *66*, 2636–2640.
[184] a) S. A. Piletsky, N. F. Starodub, *Zh. Anal. Khim.* **1992**, *47*, 623–628; N. F. Starodub, S. A. Piletsky, N. V. Lavryk, A. V. Elskaya, *Sens. Actuators B* **1994**, *18–19*, 629–632; b) S. A. Piletsky, E. V. Piletskaya, K. Yano, A. Kugimiya, A. V. Elgersma, R. Levi, U. Kahlow, T. Takeuchi, I. Karube, T. J. Panasyuk, A. V. Elskaya, *Anal. Lett.*, submitted. See also D. Kriz, O. Ramström, A. Svensson, K. Mosbach, *Anal. Chem.* **1995**, *67*, 2142–2144.
[185] a) E. Hedborg, F. Winquist, I. Lundström, L. I. Andersson, K. Mosbach, *Sens. Actuators A* **1993**, *37–38*, 796–799; b) J. H. G. Steinke, J. R. Dunkin, D. C. Sherrington, *Macromolecules*, submitted.
[186] Y. N. Belokon, V. I. Tararov, T. F. Savel'eva, M. M. Vorob'ev, S. V. Vitt, V. F. Sizoy, N. A. Sukhacheva, G. V. Vasil'ev, V. M. Belikov, *Makromol. Chem.* **1983**, *184*, 2213–2223.
[187] R. A. Lerner, S. J. Benkovic, P. G. Schultz, *Science* **1991**, *252*, 659–667; P. G. Schultz, *Angew. Chem.* **1989**, *101*, 1336–1348; *Angew. Chem. Int. Ed. Engl.* **1989**, *28*, 1283–1295; B. S. Green, D. S. Tawfik, *Trends Biotechnol.* **1989**, *7*, 304–309.
[188] A. A. Efendiev, D. D. Orujew, T. N. Shakhtakhinsky, V. A. Kabanov in *Homogeneous and heterogeneous catalysis* (Eds.: Y. Yermakov, V. Likholobov), VNU Science, Utrecht, **1986**, pp. 717–725; A. A. Efendiev, *Makromol. Chem. Makromol. Symp.* **1994**, *80*, 289–313; A. A. Efendiev, J. J. Orujew, E. B. Amanov, Y. M. Sultanov in *Metal-Containing Polymer Materials* (Ed.: C. Pittman, Jr.), Plenum, New York, in press.
[189] a) K. M. Shokat, C. J. Leumann, R. Sugasawara, P. G. Schultz, *Nature (London)* **1989**, *338*, 269–271; b) S. Kato, K. J. Shea, *J. Am. Chem. Soc.*, in press.
[190] K. Morihara, E. Nishihata, M. Kojima, S. Miyake, *Bull. Chem. Soc. Jpn.* **1988**, *61*, 3999–4003.
[191] K. Morihara, E. Tanaka, Y. Takeuchi, K. Miyazaki, N. Yamamoto, Y. Sagawa, E. Kawamoto, T. Shimada, *Bull. Chem. Soc. Jpn.* **1989**, *62*, 499–505.
[192] T. Shimada, K. Nakanishi, K. Morihara, *Bull. Chem. Soc. Jpn.* **1992**, *65*, 954–958.
[193] T. Matsuishi, T. Shimada, K. Morihara, *Chem. Lett.* **1992**, 1921–1924.
[194] T. Shimada, R. Kurazona, K. Morihara, *Bull. Chem. Soc. Jpn.* **1993**, *66*, 836–840.
[195] K. Morihara, S. Kawasaki, M. Kofuji, T. Shimada, *Bull. Chem. Soc. Jpn.* **1993**, *66*, 906–913.
[196] K. Morihara, S. Doi, M. Takiguchi, T. Shimada, *Bull. Chem. Soc. Jpn.* **1993**, *66*, 2977–2982.
[197] K. Morihara, T. Iijima, H. Usui, T. Shimada, *Bull. Chem. Soc. Jpn.* **1993**, *66*, 3047–3052.
[198] T. Matsuishi, T. Shimada, K. Morihara, *Bull. Chem. Soc. Jpn.* **1994**, *67*, 748–756.
[199] T. Shimada, R. Hirose, K. Morihara, *Bull. Chem. Soc. Jpn.* **1994**, *67*, 227–235.
[200] K. Morihara, M. Takiguchi, T. Shimada, *Bull. Chem. Soc. Jpn.* **1994**, *67*, 1078–1084.
[201] J. Heilmann, W. F. Maier, *Angew. Chem.* **1994**, *106*, 491–493; *Angew. Chem. Int. Ed. Engl.* **1994**, *33*, 471–473.
[202] M. Glad, M. Kempe, K. Mosbach, *PCT Int. Appl.* Se9200610, **1992**.
[203] N. B. Afeyan, L. Varady, F. E. Regnier, (Perspective Biosystems) *PCT Int. Appl.* WO9319844, **1993** [*Chem. Abstr.* **1994**, *120*, 265352u].

CHIRALITY '95 JERUSALEM

7th International Symposium on Chiral Discrimination (ISCD 7)

Jerusalem, Israel, November 12-16, 1995

Plenary Speakers

David Avnir, *Hebrew University of Jerusalem, Jerusalem, Israel*
Samuel J. Danishefsky, *Columbia University, New York, USA*
Ben L. Feringa, *University of Groningen, Groningen, The Netherlands*
Joseph Gal, *University of Colorado, Denver, Colorado, USA*
Ryoji Noyori, *University of Nagoya, Nagoya, Japan*
Frank Volker Schurig, *University of Tubingen, Tubingen, Germany*
J. Fraser Stoddart, *University of Birmingham, Birmingham, UK*
Sidney Topiol, *Sandoz Research Institute, New Jersey, USA*
David M. Walba, *University of Colorado at Boulder, Colorado, USA*
Chi-Huey Wong, *Scripps Research Institute, La Jolla, California, USA*

The Scientific Program will Highlight Advances in the Following Topics:

- Stereospecific analytical methodology
- Stereocontrol in organic synthesis
- Chiral recognition
- Chirality in pharmacodynamics, drug-action, and therapeutics
- Stereochemical aspects of drug metabolism, and pharmacokinetics
- Chirality and the future of drug design
- Regulatory aspects and intellectual property issues
- Molecular chirality
- Quantitative evaluation of chirality
- Electronic materials and chirality
- Chirality in Archeology

For further information please contact the Symposium Secretariat:
ORTRA Ltd., 2 Kaufman Street, P.O. Box 50432, Tel Aviv 61500, Israel FAX: 972-3-5174433

Catalytic Ring-Closing Metathesis: A New, Powerful Technique for Carbon–Carbon Coupling in Organic Synthesis

Hans-Günther Schmalz*

Introduction

Owing to the rapidly growing human population and the consequent increasing demand for the products of organic synthesis, the development of highly efficient and selective synthetic methods is one of the most urgent tasks for chemical science. In this connection, transition metal mediated reactions and, in particular, catalytic C–C bond forming processes have a great and still relatively unexplored potential.[1]

From the point of view of organic synthesis, olefin metathesis, that is, the metal-catalyzed exchange of the alkylidene groups of two olefins, is a highly interesting process.[2] This general reaction, which was previously used almost exclusively in polymer chemistry and above all for ring-opening metathesis polymerization (ROMP),[3] was recently proven to be of value in many cases for the preparation of low molecular weight compounds, in particular for cyclization reactions like that in Scheme 1.[4]

The alkylidene complexes $[M]=CH_2$ are proposed to be the catalytically active species, and the reactions are thought to proceed according to the mechanism outlined in Scheme 1 (via metallacyclobutane intermediates). If terminal 1,(ω – 1)-dienes

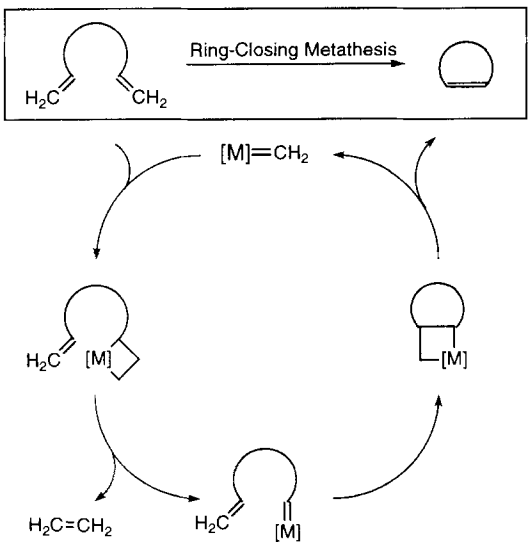

Scheme 1. The mechanism of cyclizations by olefin metathesis.

[*] Prof. Dr. H.-G. Schmalz
Institut für Organische Chemie der Technischen Universität
Strasse des 17. Juni 135, D-10623 Berlin (Germany)
Telefax: Int. code + (30) 314-22429

are employed as substrates, ethylene is formed as the only stoichiometric by-product. Therefore, these reactions may certainly be classified as being "atom economic".[5]

Cyclization Reactions by Olefin Metathesis

Early reports[6] including a paper by D. Villemin[6a] from 1980 on the preparation of an Exaltolid precursor by WCl_6/Me_4Sn-catalyzed metathesis cyclization went mostly unnoticed. Only when well-defined and highly active catalysts that also tolerate functional groups were discovered at the beginning of the 1990s, did research on ring-closing metathesis chemistry take off. In 1992 two key papers from the research group of R. H. Grubbs[7] appeared, which marked the beginning of intensive and still continuing research activity in this field. Initially, the molybdenum complex **1** developed by R. R. Schrock[8] was employed in most cases, but in the meantime, the easily accessible and much less air-sensitive ruthenium complex **2**

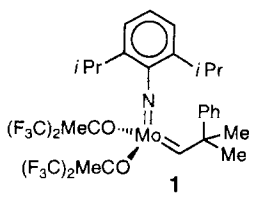

1

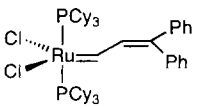

2

(Cy = cyclohexyl)[9] enjoys at least the same popularity. With these catalysts the construction of cyclopentene and cyclohexene derivatives[10–12] as well as five-, six-, and seven-membered (even highly functionalized) heterocycles can be achieved usually in excellent yield (Scheme 2).[7,13–15]

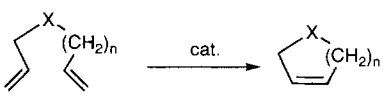

Scheme 2. Synthesis of heterocycles by olefin metathesis. cat = **1** or **2**.

In many cases, ring-closing methathesis reactions proceed with remarkable high efficiency, as exemplified by the examples shown in Scheme 3. Thus, (optically active) methylcyclopentene **4**, which is of interest as a monomer for the production of main chain chiral polymers using ROMP and very difficult to obtain by other techniques, can be prepared easily from β-citronellene

 © VCH Verlagsgesellschaft mbH, D-69451 Weinheim, 1995 0570-0833/95/3417-1833 $ 10.00+.25/0

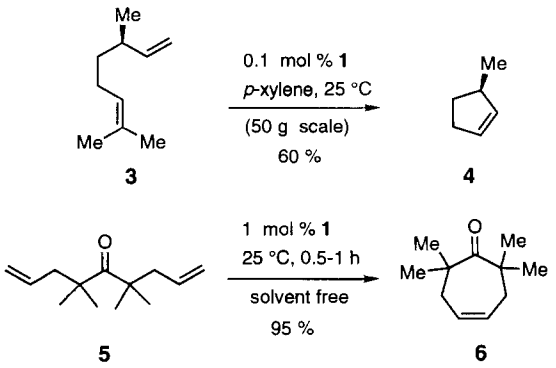

Scheme 3.

(**3**) by the action of minute amounts of catalyst **1**.[12] Another striking example is the solvent-free cyclization of diene **5** to give cycloheptenone **6**.[16] In this case, the conformational preorganization of the substrate is crucial, since the methyl-free analogue of **5** polymerizes under the same conditions—a good example of the Thorpe–Ingold effect.

Metathesis can also be used for the construction of condensed ring systems as demonstrated by the transformations shown in Scheme 4. For the synthesis of partially hydrogenated azulenes (e.g. **7** → **8**),[17] methyltrioxorhenium (MTO)[18] was employed.

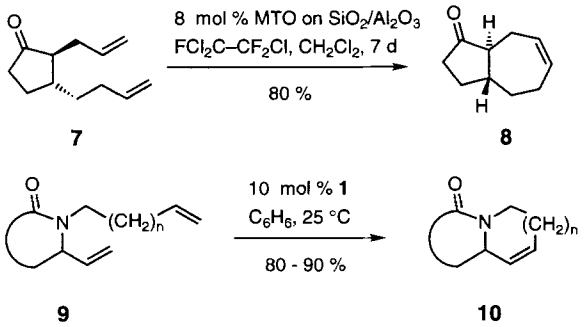

Scheme 4. Synthesis of condensed ring systems by olefin metathesis.

However, this catalyst seems to be less active than **1** or **2** and also exhibits a somewhat lower tolerance towards functional groups. The synthesis of condensed nitrogen heterocycles (**9** → **10**) was achieved using **1**.[19] This opens up a new entry to the frameworks of a number of biological active alkaloids.

Even eight-membered rings may be closed by metathesis, but only when they are not too strained and when the substrate is structurally preorganized to a certain degree.[20] S. J. Miller and R. H. Grubbs recently reported the synthesis of cyclic peptides, demonstrating the high tolerance of the Ru catalyst **2** towards NH groups.[20b] Especially remarkable is the transformation displayed in Scheme 5, in which the conformationally preformed substrate **11** smoothly metathesizes to give the 14-membered macrocycle **12** (with β-turn-type structure).

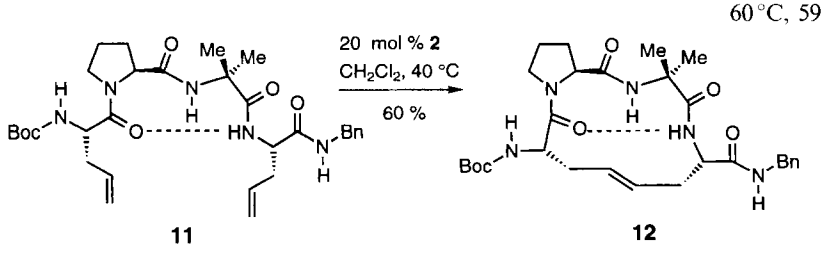

Scheme 5.

Metathesis of Enynes and Dienynes

At this point it is mentioned only briefly that metathesis chemistry can be extended with great success to conversions of enynes and dienynes.[21, 22] Thus, for example, substrate **13** reacts in excellent yield (and in a mechanistically straightforward manner) to afford the bicyclic product **14**,[21] while the enyne **15** gives the conjugated diene **16**.[22a]

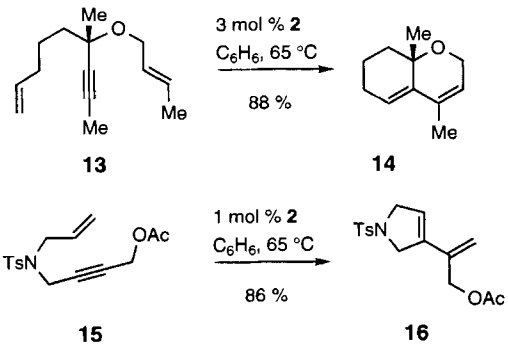

Synthetic Applications

Considering the great success of the methodological studies, it is not surprising that ring-closing metathesis was promptly applied to the synthesis of specific target molecules. For instance, C. M. Huwe and S. Blechert[23] used catalyst **2** for the cyclization of diene **17** to give the dehydroprolinol derivative **18**, which is an ideal precursor for pharmacologically interesting azasugars of type **19**.

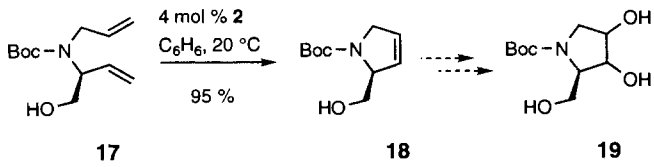

In the course of model studies directed towards the synthesis of the antitumor antibiotic FR-900482, the cyclization of dienes of type **20** to give azabenzocyclooctadienes **21** was accomplished independently by two research groups. S. F. Martin et al.[24] employed the Mo catalyst **1** (15 mol % **1**, benzene, 50 °C, 77 %), whereas R. H. Grubbs and co-workers accomplished the desired reaction with the aid of the Ru catalyst **2** (10 mol % **2**, benzene, 60 °C, 59 %).

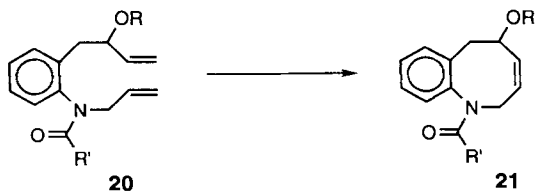

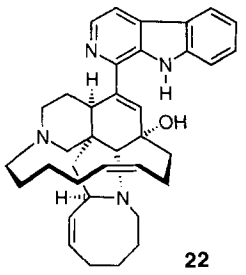

22

The metathesis cyclization reaction has also proven itself in connection with the planned total syntheses of manzamine A (**22**), a highly interesting antitumor alkaloid with an unusual structure, which presents a particular challenge for synthetic chemists. S. F. Martin et al.[25] used a metathesis reaction for the construction of the eight-membered ring (**23** → **24**), and U. K. Pandit and co-workers[26] demonstrated that even the macrocyclic ring can be closed by this method (Ru catalysis) (**25** → **26**, TBDPS = tBuPr$_2$Si). At this point, the power of metathesis chemistry for solving difficult synthetic problems becomes evident.

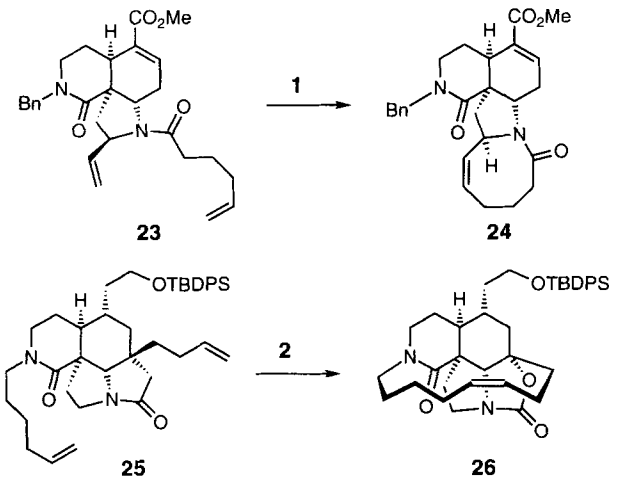

23 **24** **25** **26**

Total Synthesis of the Fluvirucin B_1 Aglycon

Recently A. H. Hoveyda and co-workers[27] described a remarkable total synthesis of the fluvirucin B_1 aglycon (**27**) in which a metathesis cyclization is employed for the formation of a 12-membered ring. Fluvirucin B_1 (also known as Sch 38516) is a naturally occurring macrolactam glycoside with interesting antifungal and antiviral properties. Retrosynthetically, Hoveyda et al. traced the target molecule back to an open-chain amide of type **29** (Scheme 6), which is cyclized in the key metathesis

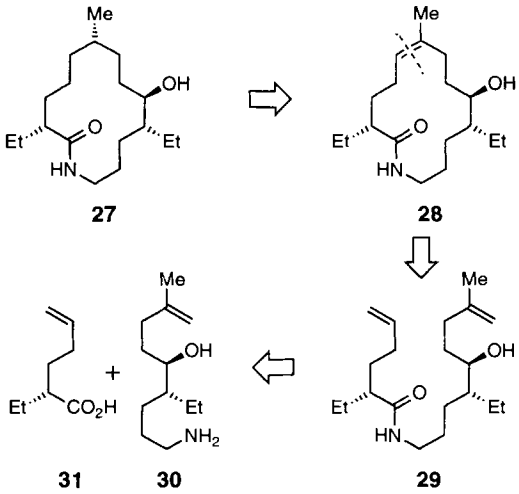

27 **28** **31** **30** **29**

Scheme 6. Strategy of the fluvirucin synthesis by A. H. Hoveyda et al. in a retrosynthetic representation.

step to give **28**. Compared to alternative synthetic strategies, in which the macrolactam ring is closed by formation of the amide bond, the cyclization precursor **29** is accessible here in a simple and convergent manner by coupling the amide **30** with the carboxylic acid **31**.

The fascinating feature of the Hoveyda synthesis is not only its clear strategic conception but the extended sequences of transition metal catalyzed reactions involved (Scheme 7). A Sharpless-type Ti-catalyzed kinetic resolution provides the optically active starting material **32**, which is regio- and diastereoselectively further converted by Zr-catalyzed carbomagnesation.[28] The resulting Grignard intermediate **33** is then

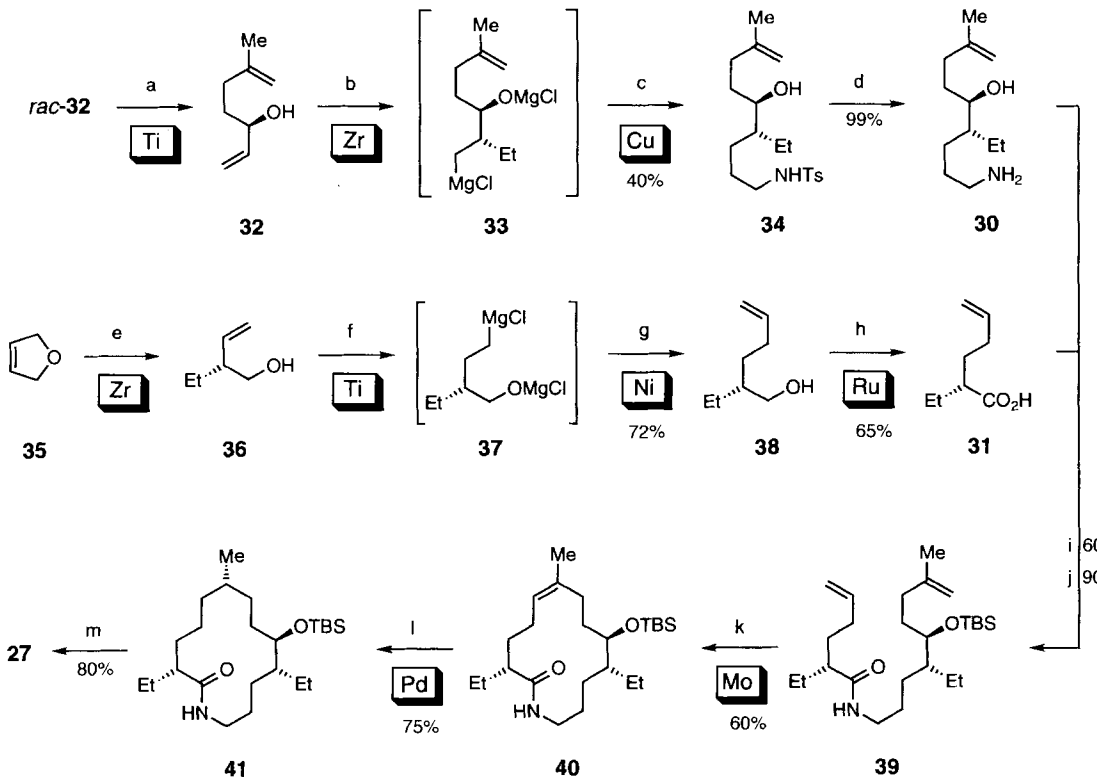

32 **33** **34** **30** **35** **36** **37** **38** **31** **41** **40** **39**

Scheme 7. Synthesis of the fluvirucin by A. H. Hoveyda et al. The element symbols in boxes indicate transition metal catalyzed transformations. For the reaction conditions for steps a–m see ref. [27].

coupled with *N*-tosyl aziridine under Cu catalysis (→ **34**). The preparation of the second fragment, the carboxylic acid **31**, starts with an enantioselective carbomagnesation[28] of **35**. The homoallylic alcohol **36** thus obtained is then homologized to **38** by Ti-catalyzed hydromagnesation (→ **37**) and Ni-catalyzed cross-coupling. Finally, **38** is oxidized to **31** in a Ru-catalyzed reaction.

After the two components **30** and **31** are coupled (→ **39**) the crucial metathesis cyclization using the Mo catalyst **1** furnishes alkene **40** with almost complete *Z*-selectivity. Considering the general problem of constructing 12-membered rings, the obtained yield of 60% is remarkably high. The synthesis is completed by (completely diastereoselective) catalytic hydrogenation of **40** (→ **41**) and desilylation.

All in all, Hoveyda et al. needed little more than ten synthetic steps, including five transition metal catalyzed C–C couplings and four other metal-catalyzed transformations. The synthesis is short, highly selective, and should be flexible enough to allow the preparation of a wide variety of fluvirucin analogues. Only a few protecting groups are needed because simple (nonactivated) double bonds, which are stable under all sorts of reaction conditions, serve as functional anchor groups for the crucial C–C bond forming reactions.

Conclusion

There is no question that transition metal mediated processes in general and catalytic C–C bond forming reactions in particular will be of increasing importance in organic synthesis. The catalytic ring-closing metathesis discussed here is only one of several new interesting methods. In some respect, the Hoveyda synthesis of the fluvirucin B_1 aglycon (see Scheme 7) can be regarded as a prototype of a new generation of total syntheses in which the multifariousness of metal-catalyzed reactions is consequently and successfully utilized. Though some of the yields achieved leave much to be desired, this synthesis emphasizes the potential of transition metal catalysis for the synthesis of challenging target molecules in a wealth of selective transformations. Yet, this masterpiece in catalytic synthetic organometallic chemistry would not have been possible without work from the laboratories of R. H. Grubbs and R. R. Schrock, who paved the way for almost all of the ring-closing metathesis reactions mentioned above.[29]

German version: *Angew. Chem.* **1995**, *107*, 1981 – 1984

Keywords: alkylidene complexes · catalysis · cyclizations · fluvirucin · metathesis reactions

[1] L. S. Hegedus, *Transition Metals in the Synthesis of Complex Organic Molecules*, University Science Books, Mill Valley, CA, **1994**.
[2] a) R. H. Grubbs, S. H. Pine in *Comprehensive Organic Synthesis, Vol. 5* (Eds.: B. M. Trost, I. Fleming, L. A. Paquette), Pergamon, New York, **1991**, Chapter 9.3; b) R. R. Schrock, *The Strem Chemiker, Vol. XIV*, Strem Chemicals, Newburgport, MA, **1992**. No. 1, pp. 1 – 6.
[3] a) R. H. Grubbs, W. Tumas, *Science* **1989**, *243*, 907 – 915; b) D. J. Brunelle, *Ring-Opening Polymerization, Mechanisms, Catalysis, Structure, Utility*, Hanser, Munich, **1993**.
[4] For recent work on the preparation of low molecular weight metathesis products see, for instance: W. E. Crowe, D. R. Goldberg, *J. Am. Chem. Soc.* **1995**, *117*, 5162 – 5163.
[5] B. M. Trost, *Angew. Chem.* **1995**, *107*, 285 – 307; *Angew. Chem. Int. Ed. Engl.* **1995**, *34*, 259 – 281.
[6] a) D. Villemin, *Tetrahedron Lett.* **1980**, *21*, 1715 – 1718; b) S. Warwel, H. Kätker, *Synthesis* **1987**, 935 – 937; c) M. F. C. Plugge, J. C. Mol, *Synlett* **1991**, 507 – 508.
[7] G. C. Fu, R. H. Grubbs, *J. Am. Chem. Soc.* **1992**, *114*, 5426 – 5427, 7324 – 7325.
[8] R. R. Schrock, J. S. Murdzek, G. C. Bazan, J. Robbins, M. DiMare, M. O'Regan, *J. Am. Chem. Soc.* **1990**, *112*, 3875 – 3886.
[9] a) S. T. Nguyen, L. K. Johnson, R. H. Grubbs, J. W. Ziller, *J. Am. Chem. Soc.* **1992**, *114*, 3974 – 3975; b) S. T. Nguyen, R. H. Grubbs, J. W. Ziller, *ibid.* **1993**, *115*, 9858 – 9859.
[10] G. C. Fu, R. H. Grubbs, *J. Am. Chem. Soc.* **1993**, *115*, 3800 – 3801.
[11] N. B. Bespalova, M. A. Bovina, M. B. Sergeeva, V. G. Zaikin, *Russ. Chem. Bull.* **1994**, *43*, 1425 – 1426.
[12] L. R. Sita, *Macromolecules* **1995**, *28*, 656 – 657.
[13] G. C. Fu, S. T. Nguyen, R. H. Grubbs, *J. Am. Chem. Soc.* **1993**, *115*, 9856 – 9857.
[14] J. P. Morken, M. T. Didiuk, M. S. Visser, A. H. Hoveyda, *J. Am. Chem. Soc.* **1994**, *116*, 3123 – 3124.
[15] O. Fujimura, G. C. Fu, R. H. Grubbs, *J. Org. Chem.* **1994**, *59*, 4029 – 4031.
[16] M. D. E. Forbes, J. T. Patton, T. L. Myers, H. D. Maynard, D. W. Smith, Jr., G. R. Schulz, K. B. Wagener, *J. Am. Chem. Soc.* **1992**, *114*, 10978 – 10980.
[17] H. Junga, S. Blechert, *Tetrahedron Lett.* **1993**, *34*, 3731 – 3732.
[18] a) W. A. Herrmann, W. Wagner, U. N. Flessner, H. Komber, *Angew. Chem.* **1991**, *103*, 1704; *Angew. Chem. Int. Ed. Engl.* **1991**, *30*, 1636; b) W. A. Herrmann, F. E. Kühn, R. W. Fischer, W. R. Thiel, C. C. Romao, *Inorg. Chem.* **1992**, *31*, 4431 – 4432.
[19] S. F. Martin, Y. Liao, H.-J. Chen, M. Pätzel, M. N. Ramser, *Tetrahedron Lett.* **1994**, *35*, 6005 – 6008.
[20] a) S. J. Miller, S. H. Kim, Z. R. Chen, R. H. Grubbs, *J. Am. Chem. Soc.* **1995**, *117*, 2108 – 2109; b) S. J. Miller, R. H. Grubbs, *ibid.* **1995**, *117*, 5855 – 5856.
[21] S. H. Kim, N. Bowden, R. H. Grubbs, *J. Am. Chem. Soc.* **1994**, *116*, 10801 – 10802.
[22] a) A. Kinoshita, M. Mori, *Synlett* **1994**, 1020 – 1022; b) S. Watanuki, N. Ochifuji, M. Mori, *Organometallics* **1994**, *13*, 4129 – 4130.
[23] C. M. Huwe, S. Blechert, *Tetrahedron Lett.* **1995**, *36*, 1621 – 1624.
[24] S. F. Martin, A. S. Wagman, *Tetrahedron Lett.* **1995**, *36*, 1169 – 1170.
[25] S. F. Martin, Y. Liao, Y. Wong, T. Rein, *Tetrahedron Lett.* **1994**, *35*, 691 – 694.
[26] a) B. C. Borer, S. Deerenberg, H. Bieräugel, U. K. Pandit, *Tetrahedron Lett.* **1994**, *35*, 3191 – 3194; b) *Pure Appl. Chem.* **1994**, *66*, 2131 – 2134.
[27] A. F. Houri, Z. M. Xu, D. A. Cogan, A. H. Hoveyda, *J. Am. Chem. Soc.* **1995**, *117*, 2943 – 2944.
[28] a) A. F. Houri, M. T. Didiuk, Z. M. Xu, N. R. Horan, A. H. Hoveyda, *J. Am. Chem. Soc.* **1993**, *115*, 6614 – 6624; b) for a review see: H.-G. Schmalz, *Nachr. Chem. Tech. Lab.* **1994**, *42*, 724 – 729.
[29] For another recent short review of ring-closing olefin metathesis see: U. Koert, *Nachr. Chem. Tech. Lab.* **1995**, *43*, 809.

 © VCH Verlagsgesellschaft mbH, D-69451 Weinheim, 1995 0570-0833/95/3417-1836 $ 10.00+.25/0

Distorted Sandwich Compounds: [1]Ferrocenophanes and [2]Ruthenocenophanes**

Max Herberhold*

Strained cyclic compounds are potential monomers for ring-opening polymerization, and strained metallocenophanes have consequently attracted interest as precursors for polymers containing transition metals such as Fe or Ru in the cage of sandwich units that are incorporated into the macromolecule.[1] The propensity towards polymerization depends on the ring strain, as may be seen for the sila[*n*]ferrocenophanes[2] fc[$(SiMe_2)_n$] with $n = 1$ (**1**) and $n = 2$ (**2**). Whereas **1** polymerizes in the melt above 130 °C to give silaferrocenylene polymers,[3] **2** requires temperatures above 350 °C to undergo ring-opening polymerization.[2, 3] Nevertheless, it is easy to oxidize fc[$(SiMe_2)_2$] **2** to 1,3-bis(dimethylsila)-2-oxa-[3]ferrocenophane fc[$(SiMe_2)_2O$] which, like fc[$(SiMe_2)_3$] **3**, is strain-free and therefore not prone to polymerization.[4]

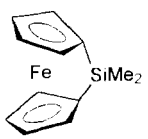

fc[$SiMe_2$]
1

α = 20.8(5)° [3]
δ = 164.74(8)°

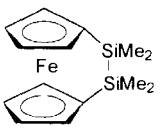

fc[Si_2Me_4]
2

α = 4.19(2)° [3]
(4.3° [2])
δ = 176.48(3)° [3]

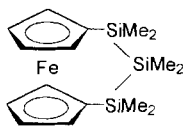

fc[Si_3Me_6]
3

The ring strain in [1]ferrocenophanes, which contain just a single bridging atom as a link between the two cyclopentadienyl ligands, is conveniently described by the tilt angle α of the rings and the deformation angle δ at the metal between the midpoints of the rings. (Fig. 1, cf. ref. [3]). The tilt angle α increases as the size (i.e. the covalent radius) of the bridging element E decreases, for example in the series **4**–**6**. To date [1]ferrocenophanes containing elements of the second row of the periodic table (E = B, C, N, O) as bridges have not been synthesized. The smallest bridging element possible appears to be sulfur, and the new thia[1]ferrocenophane fc[S] **6**, prepared by Ian Manners and co-workers,[5] holds the present world record for the largest tilt angle in [1]ferrocenophanes with $\alpha = 31.05(10)°$. The conformation of the two cyclopentadienyl rings in **1** and **4**–**6** is almost exactly eclipsed.

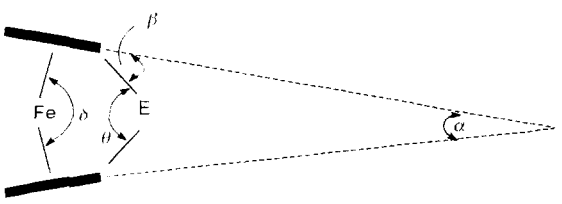

Fig. 1. Parameters describing the deformations in [1]ferrocenophanes.

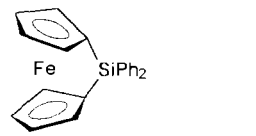

fc[$SiPh_2$] (red)
4 [6a]

α = 19.2°
δ = 167.3°
β = 40°
θ = 99.1(3)°

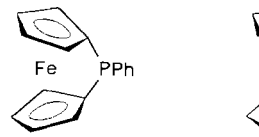

fc[PPh] (red-purple)
5 [7]

α = 26.9°
δ = 159.8°
β = 32.3°
θ = 90.7(2)°

(Very similar angles are given in ref. [6b])

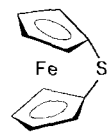

fc[S] (violet)
6 [5]

α = 31.05(10)°
δ = 156.9(1)°
β = 28.8; 29.1°
θ = 89.03(9)°

As expected, the ring strain is reduced when the bridging atom is a heavier homologue, as for example in diphenylgerma-[1]ferrocenophane fc[$GePh_2$] ($\alpha = 16.6$, $\delta = 170$, $\beta = 32.5$, and $\theta = 90.6°$)[6b] and in the substituted phenylarsa[1]ferrocenophane fc'[AsPh] (fc' = $(C_5H_4)Fe(C_5H_3R)$, R = $CHMeNMe_2$; α = 22.9, $\delta = 162.5$, $\beta = 32.8$, and $\theta = 87.90(7)$).[7] Apparently only a single metalla[1]ferrocenophane has been structurally characterized: fc[$Zr(C_5H_4tBu)_2$] **7** ($\alpha = 6.0$, $\delta = 177.27(8)°$);[8] the metal–metal separation, d(Fe–Zr) = 296.21(5) pm, might indicate a weak bonding interaction.

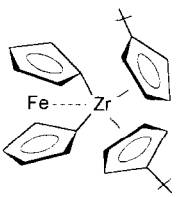

fc[$Zr(C_5H_4tBu)_2$]
7 [8]

α = 6.0°
δ = 177.28(8)°

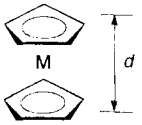

MCp_2

8a : M = Fe (d = 332 pm)
8b : M = Ru (d = 368 pm)
8c : M = Os (d = 371 pm)

Whereas a fair number of [1]ferrocenophanes are now available, the isolation of the first [1]ruthenocenophane, rc[$SiMe_2$], was mentioned only in 1994,[9] and the first [2]ruthenocenophanes have been described by Ian Manners and his group only recent-

[*] Prof. Dr. M. Herberhold
Laboratorium für Anorganische Chemie der Universität
Postfach 10 12 51, D-95440 Bayreuth (Germany)
Telefax: Int. code + (921) 55 21 57
e-mail: max.herberhold@uni-bayreuth.de

[**] Abbreviations: Cp = η^5-cyclopentadienyl, η^5-C_5H_5; Fc = 1-ferrocenyl, CpFe(C_5H_4)-; fc = 1,1'-ferrocenediyl, Fe(C_5H_4)$_2$; rc = 1,1'-ruthenocenediyl, Ru(C_5H_4)$_2$; thf = tetrahydrofuran ligand, dmso = dimethylsulfoxide ligand.

ly.[10,11] As the intramolecular ring–ring distance in the parent metallocenes MCp_2 **8a–c** expands on going from ferrocene to ruthenocene and osmocene, the distortion in the corresponding [1]- and [2]metallocenophanes must similarly increase. This might explain why dimethyldichlorosilane Me_2SiCl_2 reacts with 1,1′-dilithioferrocene $fcLi_2$ to give fc[$SiMe_2$] **1**,[12] while the corresponding reaction with 1,1′-dilithioruthenocene $rcLi_2$ leads preferentially to oligomers and polymers. The binuclear bis(dimethylsila)[1.1]metallocenophanes **9a,b** were prepared by a different route [Eq. (a)];[13] it is conceivable that small amounts of the strained mononuclear monomers fc[$SiMe_2$] **1** and rc[$SiMe_2$][9] are formed under these conditions as well.

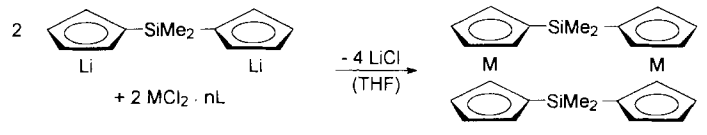

(M = Fe ; nL = 2thf ;
M = Ru ; nL = 4dmso)

9a : fc($SiMe_2$)$_2$fc[13]
9b : rc($SiMe_2$)$_2$rc[13]

(a)

In all cases (**2**, **10**–**12**) where analogous [2]ferrocenophanes and [2]ruthenocenophanes have been structurally characterized, the ruthenium complex is always the more strained.[13] As expected, an almost linear correlation exists between the distortion angles α and δ in [1]- and [2]metallocenophanes.

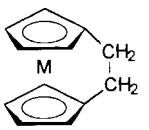

10a : M = Fe[14]
α = 21.6(5)°

10b : M = Ru[10]
α = 29.6(5)°
δ = 159.3(2)°

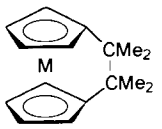

11a : M = Fe[15]
α = 23°
δ = 163.4(6)°

11b : M = Ru[16]
α = 30.6/31.5°
δ = 159.2/158.3°

(two independent molecules in the cell)

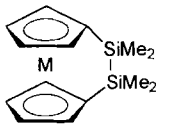

12a : M = Fe[3]
α = 4.19(2)°
δ = 176.48(3)°

12b : M = Ru[11]
α = 7.8(5)°
δ = 174.2(2)°

The ring-opening polymerization of the highly strained monomer fc[S] **6** is expected to lead to poly(ferrocenylene sulfide) $[fcS]_n$. A yellow product of this composition was obtained earlier from the reaction of 1,1′-diiodoferrocene fcI_2 with the copper salt of 1,1′-dimercaptoferrocene $fc(SCu)_2$ in boiling pyridine;[17] it is insoluble in all common solvents. The presence of substituents on the rings is apparently necessary to obtain tractable sulfur-bridged ferrocene polymers, which might be new materials with special properties due to the regularly arranged Fe centers.

A modified ring-opening polymerization leading to poly(ferrocenylene disulfide) $[fcS_2]_n$ **14** (R = H) was discovered by T. B. Rauchfuss and co-workers [Eq. (b)].[19–22] Starting from the unstrained 1,2,3-trithia[3]ferrocenophanes **13**, abstraction of the central sulfur atom using $PnBu_3$ generates one-dimensional

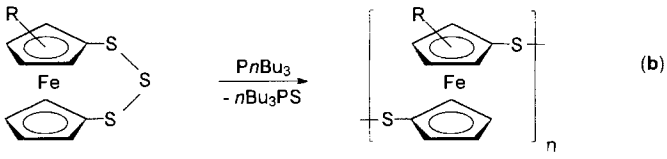

(b)

13 **14**

R = H : fc[S_3][18]
α = 2.85°
δ = 177.7°

(R = H, *n*Bu, *t*Bu)

macromolecules **14**; again substituents on the rings are required to obtain soluble products. When 4-*t*ert-butyl-1,1′,2,2′-bis(1,2,3-trithia[3])ferrocenophane (**15**) is used as the monomer, giant three-dimensional networks containing disulfide bridges can be obtained.[21]

In spite of the synthetic achievements in the chemistry of distorted sandwich compounds, some questions still remain open. Thus, points of discussion are the disturbed intramolecular interactions between

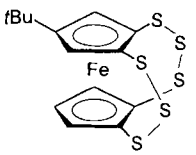

15

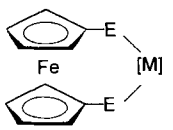

16

E = S, Se, Te
[M] = metal complex fragment

iron and the cyclopentadienyl rings or the possible contacts of iron to the bridge elements. An attractive synthetic target for the near future will be the preparation of polymeric materials with different metals, either from metalla[1]ferrocenophanes[8,23] or from [3]ferrocenophanes **16**, which contain transition metal complex fragments in the bridge system (cf. ref. [24]).

German version: *Angew. Chem.* **1995**, *107*, 1985–1987

Keywords: iron compounds · metallocenophanes · polymerization · ruthenium compounds · sandwich complexes

[1] I. Manners, *Ring-Opening Polymerization of Metallocenophanes: A New Route to Transition Metal-Based Polymers* (*Adv. Organomet. Chem.* **1995**, *37*, 131–168); I. Manners, *Phosphorus Sulfur Silicon* **1994**, *93/94*, 143–151.
[2] V. V. Dement'ev, F. Cervantes-Lee, L. Parkanyi, H. Sharma, K. H. Pannell, M. T. Nguyen, A. Diaz, *Organometallics* **1993**, *12*, 1983–1987.
[3] W. Finckh, B.-Z. Tang, D. A. Foucher, D. B. Zamble, R. Ziembinski, A. Lough, I. Manners, *Organometallics* **1993**, *12*, 823–829.
[4] C. Angelakos, D. B. Zamble, D. A. Foucher, A. J. Lough, I. Manners, *Inorg. Chem.* **1974**, *33*, 1709–1718.
[5] J. K. Pudelski, D. P. Gates, R. Rulkens, A. J. Lough, I. Manners, *Angew. Chem.* **1995**, *107*, 1633–1635; *Angew. Chem. Int. Ed. Engl.* **1995**, *34*, 1506–1508.
[6] a) H. Stoeckli-Evans, A. G. Osborne, R. H. Whiteley, *Helv. Chim. Acta* **1976**, *59*, 2402–2406; b) *J. Organomet. Chem.* **1980**, *194*, 91–101.
[7] I. R. Butler, W. R. Cullen, F. W. B. Einstein, S. J. Rettig, A. J. Willis, *Organometallics* **1983**, *2*, 128–135.
[8] R. Broussier, A. Da Rold, B. Gautheron, Y. Dromzee, Y. Jeannin, *Inorg. Chem.* **1990**, *29*, 1817–1822.
[9] J. M. Nelson, A. J. Lough, I. Manners, *Phosphorus Sulfur Silicon* **1994**, *93/94*, 361–362.

[10] J. M. Nelson, A. J. Lough, I. Manners, *Angew. Chem.* **1994**, *106*, 1019–1021; *Angew. Chem. Int. Ed. Engl.* **1994**, *33*, 989–991.
[11] J. M. Nelson, A. J. Lough, I. Manners, *Organometallics* **1994**, *13*, 3703–3710.
[12] A. B. Fischer, J. B. Kinney, R. H. Staley, M. S. Wrighton, *J. Am. Chem. Soc.* **1979**, *101*, 6501–6506.
[13] M. Herberhold, Th. Bärtl, *Z. Naturforsch.* **1995**, *50b*, in press.
[14] J. M. Nelson, H. Rengel, I. Manners, *J. Am. Chem. Soc.* **1993**, *115*, 7035–7036.
[15] M. Burke Laing, K. N. Trueblood, *Acta Crystallogr.* **1965**, *19*, 373–381.
[16] W. Milius, Universität Bayreuth, unpublished results.
[17] J. C. W. Chien, R. O. Gooding, C. P. Lillya, *Polym. Mater. Sci. Eng.* **1983**, *49*, 107–111.
[18] B. R. Davis, I. Bernal, *J. Cryst. Mol. Struct.* **1972**, *2*, 107–114.
[19] P. F. Brandt, T. B. Rauchfuss, *J. Am. Chem. Soc.* **1992**, *114*, 1926–1927.
[20] D. L. Compton, T. B. Rauchfuss, *Polym. Prepr. (Am. Chem. Soc. Div. Polym. Chem.)* **1993**, *34*, 351–543.
[21] C. P. Galloway, T. B. Rauchfuss, *Angew. Chem.* **1993**, *105*, 1407–1409; *Angew. Chem. Int. Ed. Engl.*, **1993**, *32*, 1319–1321.
[22] T. B. Rauchfuss, C. P. Galloway, *Phosphorus Sulfur Silicon*, **1994**, *93/94*, 117–128.
[23] R. Broussier, A. Da Rold, M. Kubicki, B. Gautheron, *Bull. Soc. Chim. France* **1994**, *131*, 951–958.
[24] M. Herberhold, *Ferrocenophane Compounds Containing Heteroelements* in *Ferrocenes, Homogeneous Catalysis – Organic Synthesis – Materials Science* (Eds.: A. Togni, T. Hayashi), VCH, Weinheim, **1995**, pp. 219–278.

Woollins, J. D. (ed.)

Inorganic Experiments

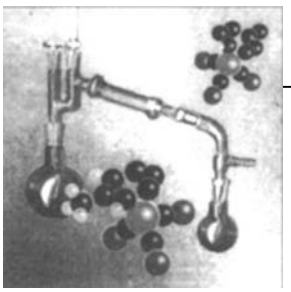

1994. XV, 286 pages
with 86 figures and
8 tables.
Hardcover. DM 148.00.
ISBN 3-527-29235-7

Renew your inorganic chemistry lab course!
This book offers detailed descriptions of more than 60 experiments ranging from undergraduate to graduate level, covering organometallic, main group, solid state and coordination chemistry. Almost all reaction types, laboratory techniques and classes of compounds which constitute current curricula are exemplarily represented.

Experiments have been contributed from university teachers all over Europe. Each experiment has been thoroughly tested. Special safety instructions are always provided, hazardous substances have been substituted by less harmful ones wherever possible. Products are characterized by modern spectroscopic techniques. Also included are excercises, questions and hints to further reading. The experiments illustrate modern research directions: many compounds have only very recently been described in key journals – here you learn how to prepare them in your lab course.

To order please contact your bookseller or:
VCH, P.O. Box 10 11 61,
D-69451 Weinheim,
Telefax (0) 62 01 - 60 61 84
VCH, Hardstrasse 10, P.O. Box,
CH-4020 Basel
VCH, 8 Wellington Court,
Cambridge CB1 1HZ, UK
VCH, 303 N.W. 12th Avenue,
Deerfield Beach, FL 33442-1788,
USA, toll-free: 1-800-367-8249 or
fax: 1-800-367-8247
VCH, Eikow Building, 10-9 Hongo
1-chome, Bunkyo-ku, Tokyo 113

VCH

Determination of the Bioactive Conformation of the Carbohydrate Ligand in the E-Selectin/ Sialyl Lewis^x Complex**

Karoline Scheffler, Beat Ernst, Andreas Katopodis, John L. Magnani, Wey Tong Wang, Rüdiger Weisemann, and Thomas Peters*

The expression of E-selectin receptors on the surface of endothelial cells stimulated by cytokines is one of the first steps in inflammatory processes.[1, 2] E-selectin is a membrane-resident glycoprotein belonging to the selectin family (E-selectin, L-selectin, P-selectin) which specifically binds the sialyl Lewis^x antigen present on neutrophilic granulocytes. To understand the recognition and binding processes at the molecular level, the three-dimensional (3D) structure of the complex formed between E-selectin and sialyl Lewis^x must be analyzed. In this connection a considerable advance was marked by the elucidation of the crystal structure of E-selectin.[3] Unequivocal experimental data for the determination of the conformation of the ligand sialyl Lewis^x in the E-selectin complex have been lacking until now. Although two recent publications[4, 5] described transfer NOE experiments[6] for the conformational analysis of complexed sialyl Lewis^x, different conformations for the bound ligand were given and the orientation of the fucose residue in the complex was not even mentioned.

We now describe transfer NOE experiments on the E-selectin/ sialyl Lewis^x complex. The tetrasaccharide sialyl Lewis^x was prepared synthetically;[7] the E-selectin used is a recombinant chimera of E-selectin and human IgG, in which the lectin, the EGF, and six CR domains of the E-selectin replace the antigen binding sites in IgG.[8] NOESY spectra were recorded with different mixing times to determine the transfer NOEs.[9] In order to suppress the interfering proton resonance signals of the E-selectin and thus enable the quantitative evaluation of the spectra, a spinlock filter[10] was used. For comparison purposes NOESY experiments were performed on pure E-selectin and free sialyl Lewis^x.[11] The assignments of the proton resonance signals were carried out using available data.[12]

Comparison of the NOESY spectra of E-selectin and free sialyl Lewis^x shows that no interfering superposition of proton signals from the glycan portion of E-selectin occurs with those of the tetrasaccharide. As reported in previous publications,[12] small negative NOEs are observed for free sialyl Lewis^x (Fig. 1a). Interglycosidic NOEs occur which correspond with known NOEs; however, no interglycosidic NOE is observed

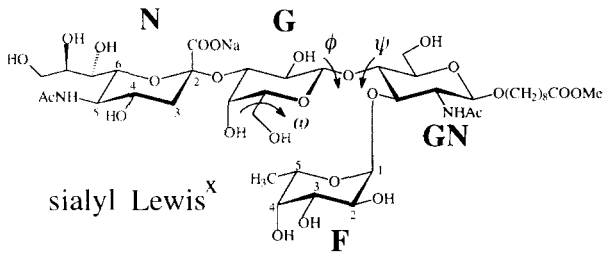

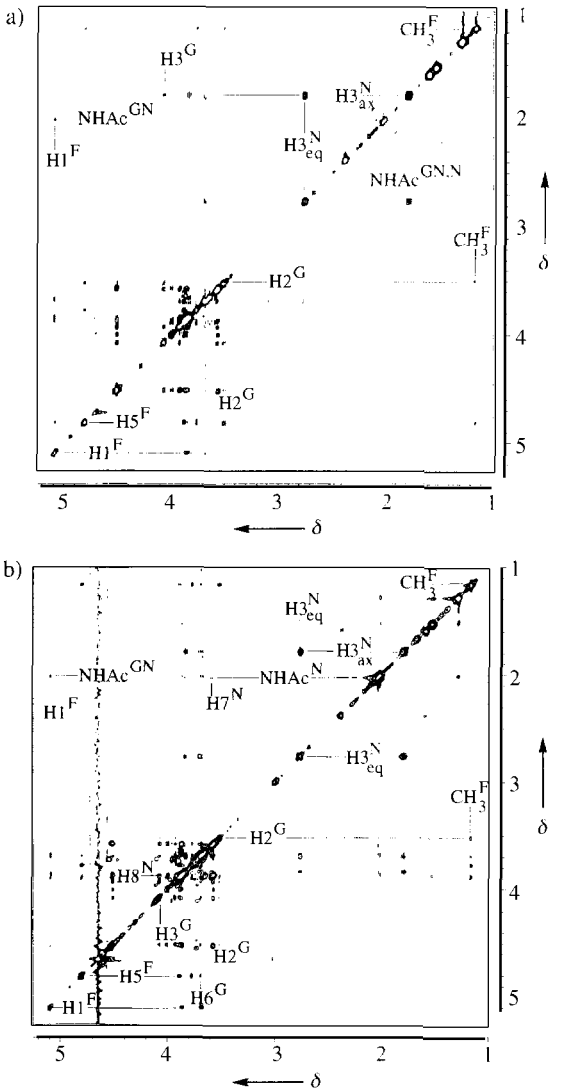

Fig. 1. 2D NOESY spectra [9, 11] of free sialyl Lewis^x (a) and sialyl Lewis^x complexed with E-selectin (b). Spectrum a was recorded with a mixing time of 900 ms without a spinlock filter, spectrum b with a mixing time of 150 ms and a spinlock filter.

[*] Prof. Dr. T. Peters, Dipl.-Chem. K. Scheffler
Institut für Chemie der Medizinischen Universität
Ratzeburger Allee 160, D-23538 Lübeck (Germany)
Telefax: Int. code (451) 500-4241
e-mail: tp@chemie.mu-luebeck.de
Dr. B. Ernst, Dr. A. Katopodis
Zentrale Forschungslaboratorien, Rosental, CIBA-GEIGY AG
CH-4002 Basel (Switzerland)
Dr. J. L. Magnani, W. T. Wang
Glyco Tech Corporation
14915 Broschart Road, Rockville, MD 20850 (USA)

[**] This work was supported by the Deutsche Forschungsgemeinschaft (Sonderforschungsbereich 169). T. P. wishes to thank NATO for a research grant (CRG.890356).

between $H8^N$ and $H3^G$ as was found in ROESY experiments.[13] The corresponding effect was also observed with sialyl-$\alpha(2 \rightarrow 3)$-*N*-acetyllactosamine.[12a] The reason for these differing results is that the correlation time τ_c of the tetrasaccharide leads to a value $\omega\tau_c$ (ω = spectrometer frequency, 600 MHz) of approximately 1. In this region the intensities of the NOEs are extremely sensitive to even small changes in the local mobility of individual parts of the molecule. This is clearly shown in the C9 chain at the reducing end of sialyl Lewis^x for which no, or even very weak positive, NOEs are observed. Similarly the glycerol side chain of the *N*-acetylneuraminic acid residue may show a local correlation time τ that deviates from the global correlation time τ_c, such that NOEs in this side chain, for example NOE $H8^N/H3^G$, are no longer detectable. Taking into consideration the experiments carried out by other research groups[12a, 13] it appears that, in general, the sialyl Lewis^x tetrasaccharide exists in solution as an equilibrium of several conformations,[13] which to a large extent are characterized by the orientation of the *N*-acetylneuraminic acid residue. The ^{1}H NMR data for the tetrasaccharide are summarized in Table 1.

Table 1. ^{1}H NMR chemical shifts (δ values) for the tetrasaccharide sialyl Lewis^x in D_2O at 303 K and 600 MHz. Reference signal: δ(HDO) = 4.722.

	NeuNAc (N)	Gal (G)	GlcNAc (GN)	Fuc (F)	Spacer $O(CH_2)_8COOMe$	
H1		4.51	4.51	5.09		
H2		3.52	3.89	3.68	$4\times CH_2$	1.28
H3	1.79	4.08	3.82	3.91	$1\times CH_2$	1.52
	2.76				CH_2	1.59
H4	3.68	3.92	3.77		CH_2	2.38
H5	3.86	3.58	3.58	4.81	CH_2	3.82–3.92
H6	3.66	3.68	4.0	1.16	OCH_3	3.68
			3.88			
H7	3.59					
H8	3.89					
H9	3.64					
	3.87					
N-CH_3	2.01		2.01			

Even with a mixing time of 25 ms, transfer NOEs occur for the complex. Since complete transfer NOE curves were obtained by recording NOESY spectra at different mixing times,[9] spin diffusion effects can be excluded from the following discussion of the NOEs. The intensities of the transfer NOEs and the position of the maxima in the transfer NOE curves clearly indicate that the observed effects are indeed transfer NOEs. Transfer NOEs between E-selectin and sialyl Lewis^x protons could not be observed at the selected protein:ligand ratio.[9] The following discussion concerns only the NOESY spectrum recorded with a mixing time of 150 ms (Fig. 1b). A precise analysis of the transfer NOE data and other NMR experiments in particular with consideration of exchange equilibria and the involvement of the amino acid protons[14] in the binding pocket of E-selectin will be published elsewhere. For comparison the corresponding section from the 2D NOESY spectrum of free sialyl Lewis^x is shown in Figure 1a. Sections of the corresponding 1D NOESY spectra relevant to the discussion of the most important effects are collected in Figure 2.

The interglycosidic transfer NOEs between the *N*-acetylneuraminic acid and galactose protons differ considerably from the corresponding NOEs in free sialyl Lewis^x (Figs. 1 and 2). The most obvious difference is the absence of a transfer NOE between $H3^N_{ax}$ and $H3^G$. However, a clear transfer NOE between $H8^N$ and $H3^G$ is observed (Figs. 2b and 2c). A weak transfer NOE is observed between the methyl group of the *N*-acetyl function attached to $C5^N$ and $H7^N$ within the *N*-acetyl-

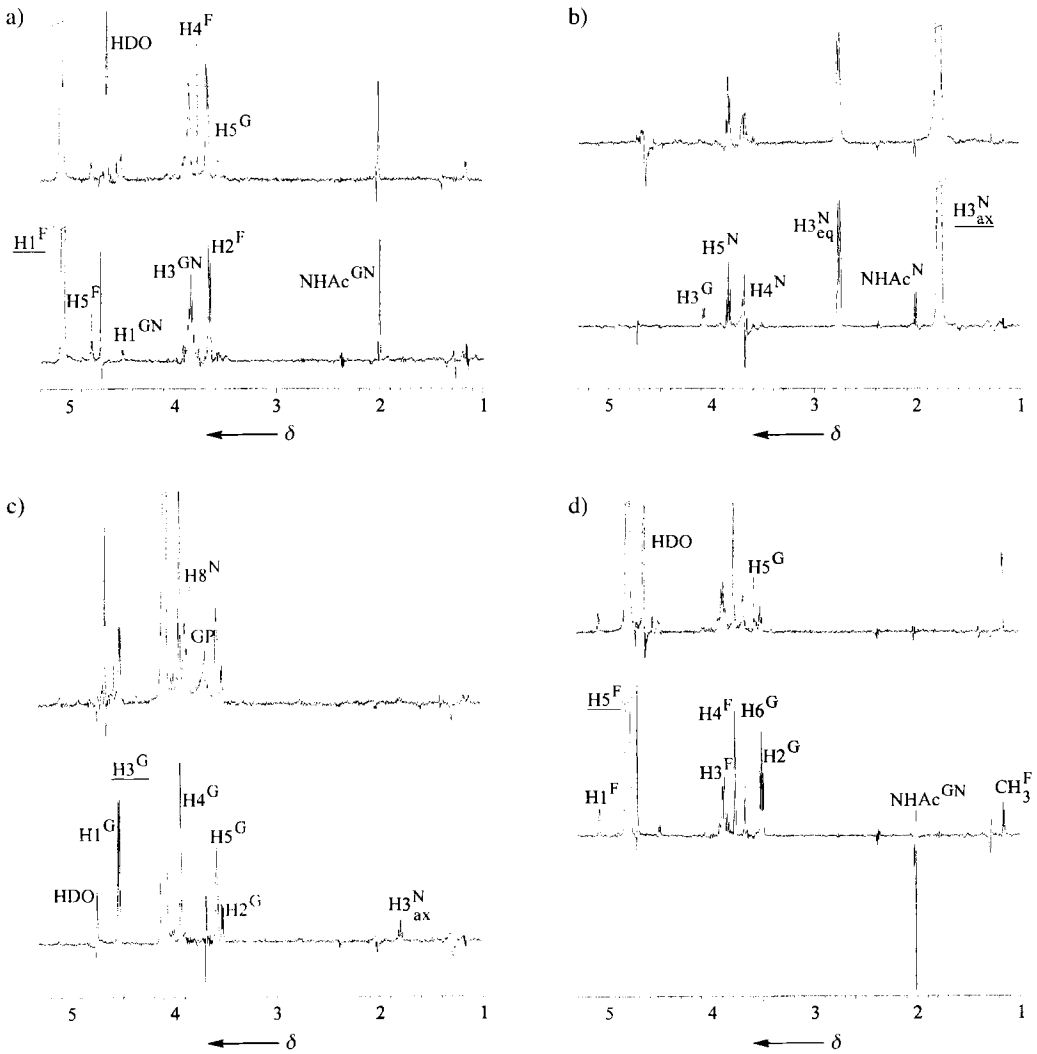

Fig. 2. 1D representations of the NOESY spectra from Figure 1, obtained by the addition of traces of F1. The lower traces are taken from the NOESY spectrum of free sialyl Lewis^x (cf. Fig. 1a); the upper traces correspond to complexed sialyl Lewis^x (cf. Fig. 1b). a) $\delta = H1^F$; b) $\delta = H3^N_{ax}$; c) $\delta = H3^G$; d) $\delta = H5^F$. The signal labeled GP arises from E-selectin. This can be shown by comparison with NOESY spectra of free E-selectin (not shown).

 © VCH Verlagsgesellschaft mbH, D-69451 Weinheim, 1995 0570-0833/95/3417-1842 $ 10.00+.25/0

neuraminic acid residue. This supports the preferred *gg* (*gg* = *gauche,gauche*) orientation at the $C6^N$–$C7^N$ bond. With regard to the orientation at the $C7^N$–$C8^N$ bond, analysis of the vicinal homo- and heteronuclear coupling constants and the determination of the ^{13}C spin-lattice relaxation times have shown that in aqueous solution the hydroxyl groups attached to the $C7^N$–$C8^N$ bond[12a, 15] are oriented exclusively *trans* and that a conformational equilibrium is observed only for the hydroxymethyl group on C9. Hence, the glycerol side chain of the *N*-acetylneuraminic acid is thought to assume an orientation like that described in ref. [12a].

The transfer NOEs observed between galactose and *N*-acetylglucosamine correspond to the NOEs in the free tetrasaccharide (Fig. 1). The interglycosidic transfer NOEs originating from fucose, on the other hand, differ considerably from the corresponding NOEs in the free tetrasaccharide. Only an extremely weak transfer NOE is observed between $H5^F$ and $H2^G$ (Fig. 2d). Similarly there is a slightly weaker transfer NOE between the methyl group of the *N*-acetyl function on $C2^{GN}$ and $H1^F$ (Fig. 2a). A very weak transfer NOE between $H1^F$ and $H5^G$ or $H5^{GN}$, which is marked in Figure 2a, most likely arises by spin diffusion (based on consideration of the NOE buildup curves). The intensity of the transfer NOE between CH_3-6^F and $H2^G$, on the other hand, resembles that of the corresponding NOE in the free tetrasaccharide (Fig. 1). A transfer NOE is also detected between $H5^F$ and $H6^G$, which in sialyl Lewis^x lies at the detection limit (Fig. 2d).

For further evaluation the transfer NOEs were integrated;[16] the intensities of the intraglycosidic transfer NOEs between $H3^N_{ax}$ and $H3^N_{eq}$ were used as calibration values. The relative NOEs were converted into distance restrictions (Table 2) by

Table 2. Experimentally determined interglycosidic transfer NOEs from the NOESY spectrum (Fig. 1b) used for distance restrictions. (The NOEs for the NOESY spectrum (Fig. 1a) of the free tetrasaccharide are also given for comparison.) For the determination of the distance restrictions, r_a (lower limit) and r_b (upper limit), calibration was carried out with a known intraglycosidic distance, $H1^F$–$H2^F$ = 2.3 Å according to the "Isolated Spin Pair Approximation" (ISPA) [16]. For the determination of the NOEs a relatively large error of ±40% was used. The values of the distance restrictions r_a and r_b were then obtained from the distances calculated from the NOEs by means of ISPA and the estimated errors.

	NOE [%] complex (free)	r_a [Å]	r_b [Å]
$H1^F$-$H3^{GN}$	−37 (−8)	2.3	2.6
$H1^F$-NAc^{GN}	−9 (−1)	2.8	3.3
$H5^F$-$H2^G$	−8 (−15)	2.9	3.4
$H5^F$-$H6^G$	−12 (−1)	2.7	3.1
CH_3^F-$H2^G$	−20 (−4)	2.5	2.9
$H1^G$-$H4^{GN}$	−45 (−20)	2.2	2.5
$H3^G$-$H8^N$	−37 (0)	2.3	2.6
$H3^N_{ax}$-$H3^G$	0 (−4)	4.0	
$H3^N_{eq}$-$H3^G$	0 (0)	4.0	

application of the ISPA approximation,[17] and these in turn were used to find the conformation of bound sialyl Lewis^x. For this a 10^6-step Metropolis Monte Carlo (MMC) simulation[18] with a temperature parameter of 2000 K was performed which completely encompassed the conformational space available to sialyl Lewis^x.[19] From the 457309 conformations obtained, 29 structures were selected which fulfilled all the distance restrictions. The conformations thus found populate only a very restricted region of the conformational space and thus yield the conformation of bound sialyl Lewis^x (Fig. 3).

From their experiments Cooke et al. derived a conformation in which the *N*-acetylneuraminic acid has an orientation similar

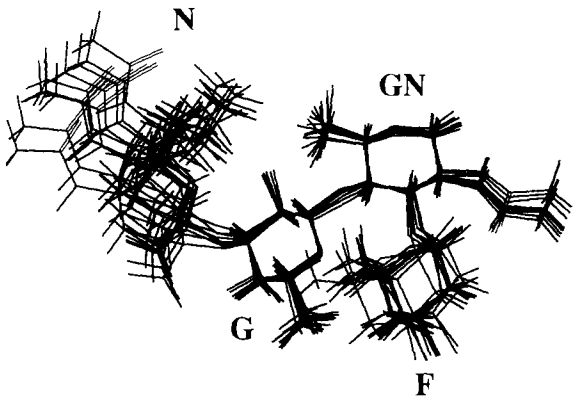

Fig. 3. Representation of the conformation of sialyl Lewis^x in the bound state. Ten of the 29 conformations obtained are shown. The following average values were obtained for the dihedral angles at the glycosidic bond (cf. Table 2): $\phi_{N\ G} = -76° +/- 10°$, $\psi_{N-G} = 6° +/- 10°$, $\phi_{G\ GN} = 39° +/- 10°$, $\psi_{G\ GN} = 12° +/- 6°$, $\phi_{F\ GN} = 38° +/- 7°$, $\psi_{F\ GN} = 26° +/- 6°$.

to that described here. However, they neither observed nor discussed a transfer NOE between $H8^N$ and $H3^G$, which is an essential distance restriction for deriving the bound conformation. The authors therefore used already published force field calculations[11b] and molecular dynamics (MD) simulations[13] to be able to suggest a possible conformation for the bound ligand. The use of the exclusion principle—only the missing NOE $H3^G$/$H3^N_{ax}$ is enlisted for an upper distance restriction—favors the conformation C suggested by Ichikawa et al.[11b] Transfer NOEs between the fucose and the *N*-acetylglucosamine unit were not discussed, and as a result the fucose residue in sialyl Lewis^x is assigned the orientation present in aqueous solution. In the recent publication of Hensley et al.[5] a "transfer NOE" between $H3^N_{ax}$ and $H3^G$ was found which, it is claimed, shows that the conformation in the bound state is identical with the conformation of sialyl Lewis^x in solution. It is not clear, however, which solution conformation is meant. Probably conformations A or B suggested by Ichikawa are implied.[11b] This cannot be reconciled with the results of Cooke et al.[4] nor can it be correlated with our results. Possibly the "transfer NOE" observed by these authors[5] may be explained by the use of a large excess of ligand and the presence of unbound sialyl Lewis^x.

Our experiments enable the determination of the conformation of bound sialyl Lewis^x on the basis of MMC simulations at 2000 K. The high temperature parameter was chosen in order to encompass, as fully as possible, the sterically available conformational space. It should be emphasized that the orientations of both the *N*-acetylneuraminic acid and the fucose residue in bound ligands lead to transfer NOEs that differ considerably from those for free sialyl Lewis^x (Figs. 1 and 2).

The most important conclusions are that E-selectin complexes exclusively a conformation of sialyl Lewis^x from the conformational mixture in aqueous solution in which the neuraminic acid shows an orientation corresponding approximately to conformation A of Rutherford et al.[13] or conformation C of Ichikawa et al.[11b] and in which fucose differs in its orientation from that preferred in aqueous solution (cf. Fig. 3). From more precise evaluation of the transfer NOE data it is possible to derive possible conclusions as to the flexibility of the $\alpha(1 \rightarrow 3)$-glycosidic bond between the fucose and the *N*-acetylglucosamine residue. These results are used at present as a basis for the modeling of potent inhibitors for E-selectin receptors.

Received: February 25, 1995 [Z 7735 IE]
German version: *Angew. Chem.* **1995**, *107*, 2034–2037

Keywords: carbohydrates · glycoproteins · NMR spectroscopy · selectins · sialyl Lewis^x

[1] M. P. Bevilacqua, S. Stengelin, M. A. Gimbrone, Jr., B. Seed, *Science* **1989**, *243*, 1160–1165.
[2] L. A. Lasky, *Science* **1992**, *258*, 964–969.
[3] B. J. Graves, R. L. Crowther, C. Chandran, J. M. Rumberger, S. Li, K.-S. Huang, D. H. Presky, P. C. Familletti, B. A. Wolitzky, D. K. Burns, *Nature* **1994**, *367*, 532–538.
[4] R. M. Cooke, R. S. Hale, S. G. Lister, G. Shah, M. P. Weir, *Biochemistry* **1994**, *33*, 10591–10596.
[5] P. Hensley, P. J. McDevitt, I. Brooks, J. J. Trill, J. A. Feild, D. E. McNulty, J. R. Connor, D. E. Griswold, N. V. Kumar, K. D. Kopple, S. A. Carr, B. J. Dalton, K. Johanson, *J. Biol. Chem.* **1994**, *269*, 23949–23958.
[6] a) G. M. Clore, A. M. Gronenborn, *J. Magn. Reson.* **1982**, *48*, 402–417; b) G. M. Clore, A. M. Gronenborn, *ibid.* **1983**, *53*, 423–442; c) F. Ni, *J. Magn. Resonan.* **1992**, *96*, 651–656.
[7] B. Ernst, N. Cooke, P. M. Åberg, unpublished. The synthetic tetrasaccharide corresponds to the formula shown in the text.
[8] The ectodomains of human E-selectin were combined by means of the polymerase chain reaction (PCR) with the Fc region of human IgG1, and subcloned in the expression vector pcDNAI/neo (Invitrogen). Following transfection of CHO-K1 cells (ATCC CCL-61) and selection with G418 (Gibco), a stable cell line was obtained which secreted ca. 25 $\mu g\,mL^{-1}$ recombinant E-selectin/hIgG. For the production of larger amounts this cell line was cultivated in a hollow fiber bioreactor (1.1 m^2, 50 mL, Cellco) in Opti. MEM culture medium (Gibco) supplemented with 2% fetal calf serum and 200 mL^{-1} gentamycin. The supernatant of conditioned cells was first purified by affinity chromatography on protein A/agarose (Sigma). The protein fraction obtained by elution with 20 mM glycine–HCl, pH 3.0, was neutralized and chromatographed directly on an anti-human-E-selectin affinity column (2 mg monoclonal antibody 7A9 per mL affigel). Specifically bound E-selectin/IgG was eluted with 5 M urea in buffered salt solution and finally dialyzed against Dubeccos PBS solution (PBS = phosphate buffered saline). The protein thus obtained showed, in SDS (sodium decyl sulfate) polyacrylamide gel electrophoresis under reducing conditions, a single band at ca. 140 kD. For NMR analysis ca. 6 mg E-selectin/hIgG was dialyzed against 50 mM perdeuterated imidazol (Sigma), 1 mM $CaCl_2$, pH 7.4, in D_2O and concentrated by means of Centricon YM-50 (Amicon) to a final volume of 0.5 mL.
[9] a) All NMR experiments were performed in the Institut für Biophysikalische Chemie der Universität Frankfurt on a Bruker DMX600 spectrometer. We wish to thank Prof. Dr. H. Rüterjans for the the opportunity to make the measurements. b) For the NMR experiments on the complex an E-selectin(IgG chimera)/tetrasaccharide ratio of 1:15 was chosen. The concentration of sialyl Lewis^x was 0.81 mM, that of E-selectin(IgG chimera) 54 μM. [D_4]Imidazole (30 mM) was used as buffer. In addition the solution contained NaCl (50 mM) and $CaCl_2$ (1 mM). The pH was 7.4. Spinlock filtered NOESY spectra [10] with mixing times τ_m of 25, 50, 75, 100, 125, 150, 175, and 200 ms were recorded at 600 MHz and 310 K. The relaxation time was 1.85 s. The spectral width was 3000 Hz (5 ppm) in all cases. 512 Increments in τ_1 were recorded. For each increment 32 transients were acquired each with 2K data points. After zero-filling and multiplication with squared cos functions in τ_1 and τ_2, a 2K × 1K data matrix was obtained by 2D Fourier transformation.
[10] T. Scherf, J. Anglister, *Biophys. J.* **1993**, *64*, 754–761.
[11] NOESY spectra of free E-selectin(IgG chimera) and sialyl Lewis^x tetrasaccharide were recorded as described in ref. [9] with the following changes. For free E-selectin mixing times τ_m of 50, 100, 150, 200, and 400 ms (with spinlock filter) were used; for free sialyl Lewis^x mixing times of 200, 300, 500, 600, 800, and 900 ms (without spinlock filter) were used. For free sialyl Lewis^x a measurement temperature of 303 K was chosen.
[12] a) J. Breg, L. M. J. Kroon-Batenburg, G. Strecker, J. Montreuil, J. F. G. Vliegenthart, *Eur. J. Biochem.* **1989**, *178*, 727–739; b) Y. Ichikawa, Y.-C. Lin, D. P. Dumas, G.-J. Shen, E. Garcia-Junceda, M. A. Williams, R. Bayer, C. Ketcham, L. E. Walker, J. C. Paulson, C.-H. Wong, *J. Am. Chem. Soc.* **1992**, *114*, 9283–9298; c) C. Mukhopadhyay, K. E. Miller, C. A. Bush, *Biopolymers* **1994**, *34*, 21–29.
[13] T. J. Rutherford, D. G. Spackman, P. J. Simpson, S. W. Homans, *Glycobiology* **1994**, *4*, 59–68.
[14] a) N. Murali, G. K. Jarori, S. B. Landy, B. D. N. Rao, *Biochemistry* **1993**, *32*, 12941–12948; b) F. Ni, H. A. Scheraga, *Acc. Chem. Res.* **1994**, *27*, 257–264; c) F. Ni, Y. Zhu, *J. Magn. Reson. Ser. B* **1994**, *102*, 180–184.
[15] a) L. Poppe, R. Stuike-Prill, B. Meyer, H. van Halbeek, *J. Biomol. NMR* **1992**, *2*, 109–136; b) G. Zhu, A. Renwick, A. Bax, *J. Magn. Reson. Ser A* **1994**, *110*, 257–261; c) L. W. Jaques, S. Glant, W. Weltner, Jr., *Carbohydr. Res.* **1980**, *80*, 207–211; d) M. F. Czarniecki, E. R. Thornton, *J. Am. Chem. Soc.* **1977**, *99*, 8273–8279.
[16] Integrations of the NOE cross signals were carried out with UXNMR software (Bruker, Karlsruhe). The spectra shown in Figure 1 were selected for integration. The NOE cross signal between $H3^N_{ax}$ and $H3^N_{eq}$ was used as a reference (100%). Transfer NOEs are roughly an order of magnitude more intensive than NOEs for free sialyl Lewis^x.
[17] A. M. Gronenborn, G. M. Clore, *Prog. Nucl. Magn. Reson. Spectrosc.* **1985**, *17*, 1–32.
[18] a) T. Peters, B. Meyer, R. Stuike-Prill, R. Somorjai, J.-R. Brisson, *Carbohydr. Res.* **1993**, *238*, 49–73; b) R. Stuike-Prill, B. Meyer, *Eur. J. Biochem.* **1990**, *194*, 903–919.
[19] The MMC simulations for sialyl Lewis^x were carried out with a temperature parameter of 2000 K and 1×10^6 macrosteps. The maximum step size was 20° (ϕ, ψ) and 25° (ω). The dihedral angles were defined as follows: ϕ = H1-C1-O1-Cx (for NeuNAc: C1-C2-O2-Cx), ψ = C1-O1-Cx-Hx (for NeuNAc: C2-O2-Cx-Hx), and ω = O5-C5-C6-O6 (for NeuNAc corresponding designations are used to indicate the orientation of the side chain). The acceptance ratio was 46%. The choice of a high temperature parameter ensured that all sterically possible conformations were considered. The evaluation of the MMC data and the extraction of the conformations that satisfied the experimentally determined distance restrictions (see Table 2) were performed with Fortran and MATLAB programs. All calculations were performed on a Silicon Graphics Indy II workstation.

Palladacycles as Structurally Defined Catalysts for the Heck Olefination of Chloro- and Bromoarenes**

Wolfgang A. Herrmann,* Christoph Brossmer, Karl Öfele, Claus-Peter Reisinger, Thomas Priermeier, Matthias Beller, and Hartmut Fischer

Dedicated to Professor Henri Brunner on the occasion of his 60th birthday

The Heck reaction has developed into a standard method of organic synthesis since its discovery in 1971.[1, 2] With it, styrene derivatives, amongst others, can be prepared as vinylic C–C coupling products in one step from iodo- and bromoarenes. Because the reaction is both regio- and stereoselective, it is often used in heterocycle and natural product chemistry.[3] The Heck reaction is also beginning to make headway in polymer chemistry.[4] However, attempts to submit the cheap chloroarenes to the Heck olefination were not an unqualified success.[5] We have found new, structurally defined, easy-to-handle palladium complexes, that surpass all previously known catalysts of the Heck reaction as regards stability and lifetime. They also enable the activation of chloroarenes.

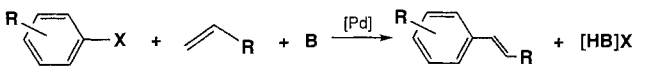

X = Br, I
[Pd] = $Pd(CH_3CO_2)_2/P(C_6H_5)_3$
B = Base, e.g. $N(C_2H_5)_3$, K_2CO_3, $Na(CH_3CO_2)$

[*] Prof. Dr. W. A. Herrmann, Dr. C. Brossmer, Dr. K. Öfele, C.-P. Reisinger, T. Priermeier
Anorganisch-chemisches Institut der Technischen Universität München
Lichtenbergstrasse 4, D-85747 Garching (Germany)
Telefax: Int. code + (89) 3209-3473
e-mail: herrmann@zaphod.anorgchemie.tu-muenchen.de
Dr. M. Beller, Dr. H. Fischer
Hoechst AG, Zentralforschung, D-65926 Frankfurt am Main (Germany)

[**] Coordination Chemistry and Mechanisms of Metal-Catalyzed C–C Coupling Reactions, Part 5. This work was supported by the Fonds der Chemischen Industrie and the Deutsche Forschungsgemeinschaft. Part 4: Ref. [7a].

In kinetic studies we discovered that the standard catalysts used virtually exclusively till now—comprising 1 mol% $Pd(OAc)_2$ and 2–6 mol% of a triaryl phosphane—are rapidly deactivated (Fig. 1) as a result of cleavage of the PC bond at the stage of the arylpalladium(II) halide at temperatures above 120 °C.[6, 7] This also causes the Pd deposits reported in the literature, because the constant PC cleavage depletes the system of (catalyst-stabilizing) phosphane. As is thoroughly confirmed, this degradation thwarted the application of these catalysts with technically particularly interesting chloroarenes, as well as deactivated bromoarenes.[6, 7]

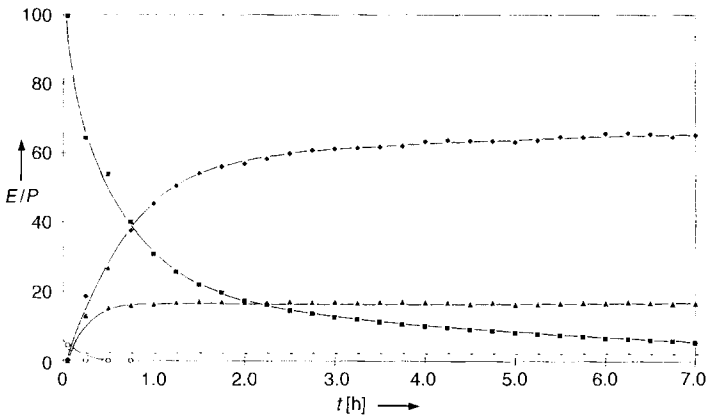

Fig. 1. Diagram of the concentration (C in mol%) vs. reaction time (t) of the Heck olefination of 4-bromoanisole (■) with n-butyl acrylate at 140 °C to form n-butyl 4-methoxycinnamate (●); catalyst $Pd(OAc)_2 + 4P(C_6H_5)_3$ (Pd/P = 1/4); for details see [7b]. The rapid cleavage of the PC bond is evident in the formation of n-butyl E-cinnamate (▲), which correlates with the degradation of the ligand $P(C_6H_5)$ (○). For this reason by-products containing the aryl groups of the particular phosphane are formed. In addition triphenylphosphane oxide forms (---).

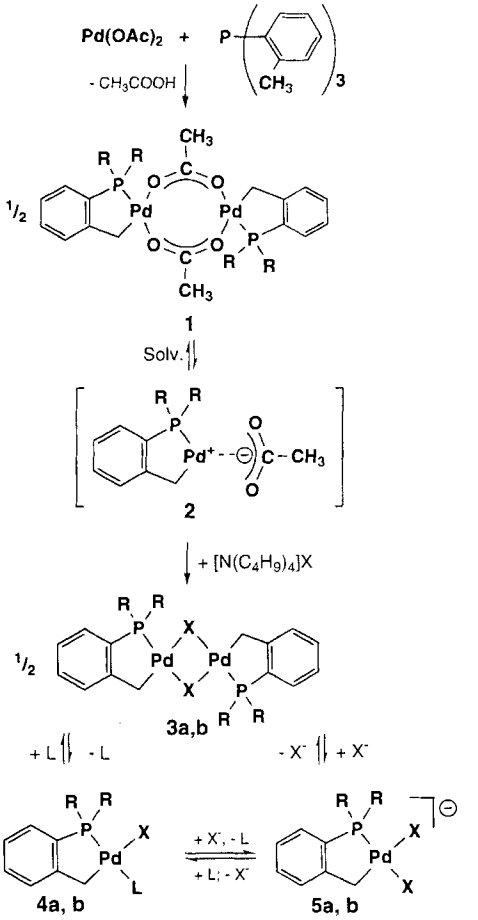

Scheme 1. Ac = CH_3CO_2; R = o-tolyl; L = DMSO, DMF, CH_3CN, $P(C_6H_5)_3$, pyridine; **a**, X = Cl; **b**, X = Br. **3b′**: as **3b**, but R = mesityl; **4b′**: L = DMF.

Treatment of palladium(II) acetate with tris(o-tolyl)phosphane in toluene affords the cyclometalation product **1** (R = o-tolyl) in 93% yield according to Scheme 1. The crystal packing and molecular structure of **1** are shown in Figure 2.[8] The approximately C_2-symmetric, dinuclear molecule has two acetate bridges which brings the two metal centers to within 311.5 pm, a nonbonding distance. In solution the cyclopalladated five-membered moieties are preserved, but the more weakly bound acetate ligands enter into monomer/dimer equilibria in which the solvent molecules are involved (^{31}P and ^1H NMR studies). The substituents R are variable (for example, o-xylyl, C_6H_5, iC_4H_9, cC_6H_{11}); tris(mesityl)phosphane also yields a palladacycle analogous to **1**.

The palladacycles **1** and **3a,b** are thermally about 100 °C more stable than conventional adducts like **6** and **7**. According to

$[Pd\{P(C_6H_5)_3\}_2(OAc)_2]$ **6**

$[Pd_2\{P(C_6H_5)_3\}_2(\mu\text{-}OAc)_2(OAc)_2]$ **7**

TG/MS studies, **1** and **3a,b** decompose only above 250 °C. Cyclometalated Pd^{II}–phosphane complexes like **1** have proven to be the most active catalysts for the Heck reaction of arenes. Figure 3 shows that for the system 4-bromoanisole/n-butyl acrylate the isolated catalyst **1**, is more active and productive than a conventional "in situ catalyst", produced from equimolar amounts of $Pd(OAc)_2$ and $P(o\text{-tol})_3$ and thus having the identical Pd/P ratio (Table 1).

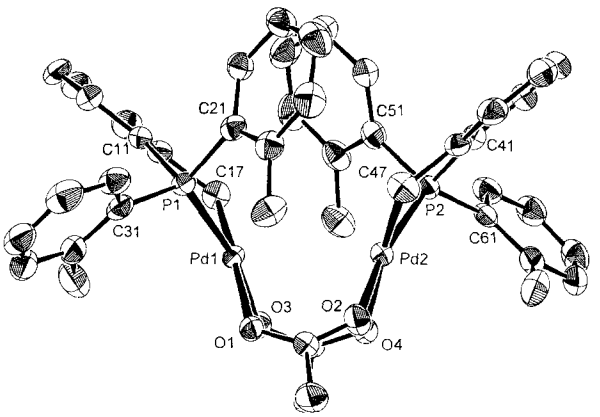

Fig. 2. PLATON representation of the crystal structure of the cyclometalation product **1** (single-crystal X-ray analysis) [8]. The thermal ellipsoids correspond to 50% probability; only one of the two independent molecules in the asymmetric unit is depicted. CH_2Cl_2 found in the unit cell is not shown. Selected distances [pm] and angles [°]: Pd1-C17 202.1(5), Pd1-O1 214.7(3), Pd1-O3 211.1(3), Pd1-P1 221.6(1), Pd2-C47 203.5(5), Pd2-P2 221.3(1), C16-C17 150.6(7); P1-Pd1-C17 82.3(2), O3-Pd1-O1 87.9(1), O1-Pd1-C17 175.8(2).

The new catalysts have the following advantages:

1) Palladium deposits, notorious in Heck reactions and formed because of the higher temperatures (usually 100–140 °C), are observed either not at all, or only in trace amounts (after longer reaction times of more than 25 h). This alone explains

Table 1. Heck olefinations of haloarenes with palladacycles as catalysts. Compound **3b′** is the same as **3b**, but with R = mesityl instead of *o*-tolyl. Reaction conditions: 50(100) mmol haloarene, 70(140) mmol *n*-butyl acrylate, 55(110) mmol sodium acetate (dry), 50(100) mL dimethylacetamide, 1 g(2 g) diethyleneglycol di-*n*-butyl ether (GC standard).

No.	[mmol]	Haloarene	Catalyst [mmol]	Stabilizer [mmol]	*T* [°C]	*t* [h]	Conversion [%] [a]	Yield [%] [a]	TON [b]
1	100	4-bromobenzaldehyde	0.5 **1**	-	100	2	100	>99	200
2	100		0.005 **1**	-	130	3	100	>99	20000
3	100		0.0005 **1**	-	135	12	100	>99	200000
4	100		0.005 **3b′**	-	130	2	100	>99	20000
5	100		0.0005 **3b′**	-	135	10	100	>99	200000
6	50	4-bromobenzonitrile	0.005 **1**	-	135	1	100	>99	10000
7	100	bromobenzene	1 **1**	-	140	48	100	96	96
8	100	2-bromotoluene	1 **1**	-	140	48	100	92	92
9	100	4-bromoanisole	1 **1**	-	140	48	100	94	94
10	100		1 $Pd(OAc)_2$	1 P(*o*-Tol)$_3$	140	93	84	75	75
11	100		0.5 **1**	-	140	48	93	87	174
12	50		0.5 **3b′**	-	138	44	85	74	74
13	50	4-chlorobenzaldehyde	0.5 **1**	-	140	24	22	12	12
14	50		0.05 **1**	10 NaI	130	24	14	10	100
15	50		0.05 **1**	50 LiBr	135	6	71	61	610
16	50		0.05 **1**	10 LiBr	130	22	70	63	630
17	50		0.05 **1**	10 $[NBu_4]Br$	130	24	90	81	810
18	50		0.5 **3b′**	-	140	24	8	8	8
19	50		0.05 **3b′**	50 LiBr	130	24	48	40	400
20	50		0.05 **3b′**	50 LiBr	140	4	45	40	400

[a] Determined by GC, based on haloarene. [b] TON = turnover number [mol product per mol catalyst].

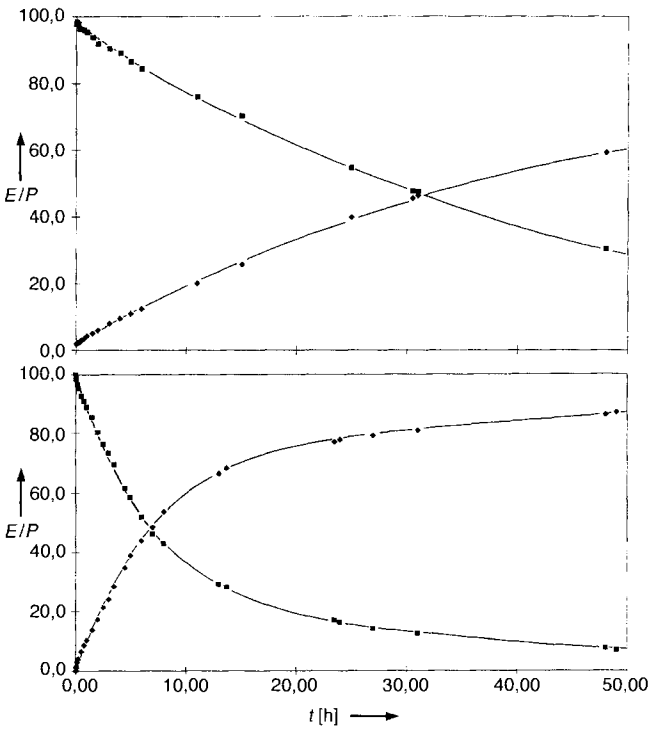

Fig. 3. Diagram of concentration (*C* in mol%) vs. reaction time (*t*) for the Heck olefination of 4-bromoanisole (deactivated bromoarene) with *n*-butyl acrylate at 140 °C; for reaction conditions see Table 1. The decrease in the concentration of the starting material 4-bromoanisole (■) and the increase in the concentration of the product *n*-butyl (*E*)-4-methoxycinnamate (◆) are shown. Top: In situ catalyst $Pd(OAc)_2$/P(*o*-Tol)$_3$ with Pd/P = 1/1 (1 mol% Pd); bottom: palladacycle **1** as catalyst (1 mol% Pd).

the increased lifetimes (long-term stability), because in no form is elemental palladium a reasonably active Heck catalyst.[9]

2) Relative to the catalyst systems $Pd(OAc)_2$ + *n* phosphane (*n* = 2–6) in common practice, they offer a saving of several phosphane equivalents.
3) The turnover numbers (TON) with bromoarenes (for example, 4-bromobenzaldehyde) reach values of 200000 [mol product per mol **1**], and the catalytic turnover frequencies (TOF) lie in the range 5000–50000 [mol product per mol **1** per hour] (Table 1).
4) Palladacycles like **1** can be used as catalysts *without* addition of phosphane: Whereas a major proportion of palladium precipitates from the $Pd(OAc)_2$/P(*o*-tolyl)$_3$ (Pd/P = 1:1) system as the element at 140 °C, **1** is stable at this temperature for days without added phosphane. Unusually small concentrations of catalyst (about 5×10^{-3} mol%) are sufficient for Heck coupling of activated bromoarenes, while up to now 0.5–5 mol% were required.
5) PC bond cleavage is insignificant at the commonest reaction temperatures around 130 °C, with the result that no yield-reducing by-products are formed.
6) Many variants of the effective structural principle of metallacyclic stabilization are possible. Compounds of this type catalyze, for instance, the Suzuki coupling of aryl boronic acids.[10]

The acetate-bridged palladacycle **1** becomes catalytically active at about 80 °C. Significant mechanistic aspects are that in Heck olefinations the bromoarenes undergo an acetate/bromide exchange at the beginning of the reaction. With increasing conversion *x*, the anionic complex **5b** is formed towards the end as a result of increasing Br^- concentration (Fig. 4). After the reaction the bromine-bridged derivative **3b**, which crystallizes well, can be isolated from the cold reaction mixture. Instead of **1**, **3b** can also be used as catalyst (cf. Scheme 1).

Interestingly, in reactions with **1** as catalyst, chloroarenes give rise to palladium deposits above 120 °C. However, the addition of special salts, in particular alkali metal salts and tetrabutylammonium bromide, leads to a substantial stabilization of the catalyst. As a result of the higher temperatures thus achievable (130–140 °C), the conversion increases. In the Heck coupling with 4-chlorobenzaldehyde, 80% butyl (*E*)-4-formylcinnamate was obtained at a TON of 600–800. By-products were not detected (no cleavage of the P–C bond). The salt effect is due to

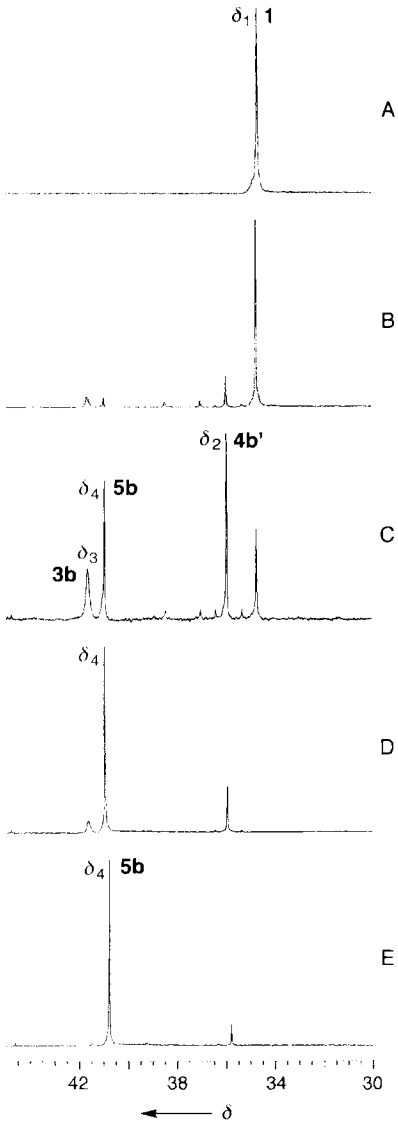

Fig. 4. $^{31}P\{^1H\}$ NMR investigation (−40 °C, [D$_7$]DMF, 161.85 MHz) on the Heck olefination of 4-bromobenzaldehyde with *n*-butyl acrylate in [D$_7$]DMF; T = 80 °C, **1** as catalyst. A: At the start (conversion x = 0), B: after 10 min (x = 2%), C: after 1 h (x = 5%), D: after 1.5 h (x = 8%), E: after 5 h (x = 10–12%). For formulas see Scheme 1.

the action of bromide ions and appears to be a concept that can be extended to optimize the new catalyst generation further.

The accelerating effect of *o*-tolyl groups in the Heck coupling has till now been explained by the steric effect of *ortho* substitution,[11a] and palladacycles were excluded as active species.[11b] This interpretation has now finally been refuted. In fact, the PC chelate structures, described here for the first time, actually compete sucessfully with the conventional electron-rich P ligands.[5a, b]

Our results suggest that, contrary to the existing textbook opinion,[12] no uniform mechanism forms the basis of the Heck reaction. Whereas the earlier assumption was that the phosphane ligands reduce the Pd^{II} salts to Pd^0 complexes at which the actual activation of the bromoarenes begins with oxidative addition,[2, 5e, 11, 12] no evidence points to a reduction of **1** and the active species derived from it under the conditions of the Heck reaction. A $Pd^{II} \rightarrow Pd^{IV}$ step also seems possible.[13] It is conspicuous that the new catalysts react with bromoarenes only when the olefin is present.

The extension of the new catalyst principle to other metallacycles (for example, rhodium) and to other carbon–carbon and carbon–heteratom coupling reactions is in progress.[14]

Experimental Procedure

1) *trans*-Di(μ-acetato)-bis[*o*-(di-*o*-tolylphosphino)benzyl]dipalladium(II) (**1**): $Pd(OAc)_2$ (4.50 g, 20.0 mmol) was dissolved in toluene (500 mL). The red-brown solution was treated with tris(*o*-tolyl)phosphane (8.00 g, 26.3 mmol). The solution, which rapidly bleached to light orange, was heated to 50 °C for 3 min and then cooled to 25 °C. The solution was reduced under vacuum to a quarter of its volume. After addition of *n*-hexane (500 mL), the precipitate was filtered off and dried under vacuum. Yield 8.80 g (93%), yellow solid. Crystallization from toluene/*n*-hexane or dichloromethane/*n*-hexane and filtration of the solution over Celite affords analytically pure, crystalline **1**.

2) Catalyst solution: **1** (5×10^{-4}–0.5 mmol) was dissolved in *N*,*N*-dimethylacetamide (DMA). The catalyst solution was degassed and purged with argon several times before use.

3) Catalytic procedure: The haloarene (50 mmol), dry sodium acetate (4.51 g, 55 mmol), and diethyleneglycol di-*n*-butyl ether (1.00 g) were placed in a 100 mL three-necked flask fitted with a septum, interior thermometer, and a condensor (with mercury check valve). After repeated degassing under oil-pump vacuum and purging with argon, *n*-butyl acrylate (10 mL, 70 mmol) was injected through the septum. The batch was heated to 100 °C. When the temperature was reached, a freshly prepared solution of **1** (see above) was injected, and the reaction mixture heated to the final reaction temperature. The course of the reaction was monitored by removing 500 μL samples after 1, 3, 6, and 24 hours, washing them with 5% HCl solution, and extracting them with 3.5 mL dichloromethane. The organic phases were transferred to GC sample bottles and analysed by gas chromatography (GC/FID, GC–MS, GC–IR–MS). The reaction is worked up by addition of water and extraction of the organic phases with CH_2Cl_2 or ether. After drying ($MgSO_4$) and removal of the solvent (CH_2Cl_2, Et_2O, DMA), the products are purified by distillation or recrystallization.

Received: October 4, 1994 [Z 7376 IE]
publication delayed at authors' request
German version: *Angew. Chem.* **1995**, *107*, 1989–1992

Keywords: catalysis · Heck olefination · palladacycles

[1] a) T. Mizoroki, K. Mori, A. Ozaki, *Bull. Chem. Soc. Jpn.* **1971**, *44*, 581; b) R. F. Heck, J. P. Nolly, *J. Org. Chem.* **1972**, *37*, 2320.

[2] Summaries: a) R. F. Heck, *Palladium Reagents in Organic Synthesis*, Academic Press, London, **1985**; b) J. Mulzer, H.-J. Altenbach, M. Braun, K. Krohn, H.-U. Reissig, *Organic Synthesis Highlights*, VCH, Weinheim, **1991**, p. 174; c) *Vinyl Substitutions with Organopalladium Intermediates*: R. F. Heck in *Comprehensive Organic Synthesis, Bd. 4* (Eds.: B. M. Trost, I. Fleming), Pergamon, Oxford, **1991**, Chap. 4.3, p. 833; d) A. de Meijere, F. Meyer, *Angew. Chem.* **1994**, *106*, 2473; *Angew. Chem. Int. Ed. Engl.* **1994**, *33*, 2379; e) W. Cabri, I. Caudiani, *Acc. Chem. Res.* **1995**, *28*, 2.

[3] a) H.-G. Schmalz, *Nachr. Chem. Tech. Lab.* **1994**, *42*, 270; b) J.-M. Gaudin, *Tetrahedron Lett.* **1991**, *32*, 6113; c) L. F. Tietze, W. Buhr, *Angew. Chem.* **1995**, *107*, 1485–1487; *Angew. Chem. Int. Ed. Engl.* **1995**, *34*, 1366–1368.

[4] a) W. Heitz, W. Brügging, L. Freund, M. Gailberger, A. Greiner, H. Jung, K. Kampschulte, N. Nießner, F. Osan, H.-W. Schmidt, M. Wicher, *Makromol. Chem.* **1988**, *189*, 119; b) M. Brenda, A. Greiner, W. Heitz, *ibid.* **1990**, *191*, 1083.

[5] a) Y. Ben-David, M. Portnoy, M. Gozin, D. Milstein, *Organometallics* **1992**, *11*, 1995; b) M. Portnoy, Y. Ben-David, D. Milstein, *ibid.* **1993**, *12*, 4734; c) J. J. Bozell, C. E. Vogt, *J. Am. Chem. Soc.* **1988**, *110*, 2655; d) A. Spencer, *J. Organomet. Chem.* **1984**, *270*, 115; e) Summary: H. Alper, V. V. Grushin, *Chem. Rev.* **1994**, *94*, 1047–1062.

[6] Chloroarenes and deactivated bromoarenes can also not be induced to react with the phosphane-free catalysts of T. Jeffery et al. ($Pd(OAc)_2$/[NBu_4]X/K_2CO_3/DMF; (deposition of palladium), cf. T. Jeffery, *Tetrahedron Lett.* **1984**, *26*, 2667.

[7] a) W. A. Herrmann, C. Brossmer, K. Öfele, M. Beller, H. Fischer, *J. Organomet. Chem.* **1995**, *491*, C1; b) C. Brossmer, Dissertation, Technische Universität München, **1994**.

[8] Compound **1** crystallized from dichloromethane/*n*-hexane at room temperature in the monoclinic space group $P2_1/c$ (no. 14) with a = 1877.2(2), b = 2417.8(1), c = 2082.9(2) pm, β = 115.70(1)°, Z = 8, V = 8519(1) × 10^6 pm^3, ρ_{calcd} = 1.496 g cm^{-3}, μ = 9.9 cm^{-1}, $F(000)$ = 3892; $Mo_{K\alpha}$ radiation, T = −50 °C, Enraf-Nonius CAD4, ω scan, 15772 measured reflections, of which 12276 for which $I > 1.0\sigma(I)$ were used in the refinement. Solution with Patterson methods, empirical absorption correction, not decomposition correction. $R = \sum(||F_o| - |F_c||)/\sum|F_o| = 0.0406$, $R_w = [\sum w||F_o| - |F_c||^2/\sum w|F_o|^2]^{1/2} = 0.0435$, residual electron density +1.99/−0.57 e Å^{-3}. Further details of the crystal structure investigation may be ob-

tained from the Fachinformationszentrum Karlsruhe, D-76344 Eggenstein-Leopoldshafen (Germany), on quoting the depository number CSD-59103.
[9] Colloidal palladium and Pd/activated carbon were catalytically active, but not very stable as catalysts in Heck reactions. In this case they can give rise, at best, to short-term effects.
[10] M. Beller, H. Fischer, W. A. Herrmann, K. Öfele, C. Brossmer, *Angew. Chem.* **1995**, *107*, 1992–1993; *Angew. Chem. Int. Ed. Engl.* **1995**, *34*, 1848–1849.
[11] a) C. B. Ziegler, R. F. Heck, *J. Org. Chem.* **1978**, *43*, 2941; b) T. Mitsudo, W. Fischetti, R. F. Heck, *ibid.* **1984**, *49*, 1640.
[12] J. P. Collman, L. S. Hegedus, J. R. Norton, R. G. Finke, *Principles and Applications of Organotransition Metal Chemistry*, University Science Books, Mill Valley, CA, USA, **1987**.
[13] Preparative examples: a) A. J. Canty, *Acc. Chem. Res.* **1992**, *25*, 83; b) G. Bocelli, M. Catellani, S. Ghelli, *J. Organomet. Chem.* **1993**, *458*, C12.
[14] Alkyne coupling: W. A. Herrmann, C.-P. Reisinger, C. Broßmer, K. Öfele, M. Beller, H. Fischer, *J. Mol. Catal.*, in press.

Palladacycles as Efficient Catalysts for Aryl Coupling Reactions**

Matthias Beller,* Hartmut Fischer, Wolfgang A. Herrmann, Karl Öfele, and Christoph Brossmer

In recent years a large number of palladium-mediated syntheses for complex synthetic building blocks and also for structurally simple industrially important intermediate products have been found and further developed.[1] Commercially available palladium compounds in the presence of different ligands were often used as catalysts. However, the quality of the used catalysts[2] is generally not sufficient for industrial demands. "Real" catalytic reactions of palladium complexes in the field of C–C couplings with turnover numbers (TON) larger than 10000 were described only in exceptional cases. Just recently, with the palladacycles **1** a new structure principle was discovered for Heck reactions, which allows TON > 100000.[3]

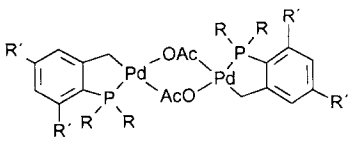

1a, b

a, R = o-tolyl, R' = T H
b, R = mesityl, R' = CH_3

As a result of the increasing importance of unsymmetrically substituted biaryl derivatives, for example as drug intermediates,[4] we were interested in the transferability of the catalytic properties of the complexes **1a, b** to the cross coupling between aryl halides and arylboronic acids.[5] We show here that palladacycles **1** catalyze this type of reaction known as Suzuki coupling with an unusual efficiency.

[*] Dr. M. Beller, Dr. H. Fischer
Hoechst AG, Zentralforschung
D-65926 Frankfurt am Main (Germany)
Telefax: Int. code + (69)305-313320
Prof. Dr. W. A. Herrmann, Dr. K. Öfele, Dr. C. Brossmer
Anorganisch-chemisches Institut der Technischen Universität München (Germany)

[**] Coordination Chemistry and Mechanisms of Metal-Catalyzed C–C Coupling Reactions, Part 6. The authors thank Mrs. Susanne Klein for her support with the experimental work. - Part 5: Ref. [3]

When 4-bromoacetophenone **2a** is treated with phenylboronic acid **3** under conditions analogous to the Heck olefination (solvent: dimethylacetamide; 1.1 molar equivalents sodium acetate as base),[3] only low turnovers (< 40%) were observed to give the desired 4-acetylbiphenyl **4a**, even after 24 h at temperatures > 130 °C and in the presence of 0.1 mol% **1a**. However, under different reaction conditions (see Table 1)[6] this product forms in over 90% yield. Turnover numbers up to 75000 with good yields (75%) were achieved with only 0.001 mol% **1a** as catalyst. Thus, the palladacycles are the most active catalysts which are known for aryl couplings catalyzed by organometallic compounds. In contrast to traditional Suzuki reactions, which were carried out with triphenylphosphanepalladium complexes $[Pd(PR_3)_n]$,[7] we did not observe any aryl scrambling at the catalyst or the associated unselective aryl transfer of the phosphane to side products.[7a, 8] Only biphenyl was detected as a minor side product in the crude solutions (< 5%, GC). A comparison of the reaction of several bromoarenes with phenylboronic acid makes it clear that the reactions occur in a similar way regardless of the substitution pattern of the arene. Thus under standard conditions (Table 1) TON of 65000–74000 were obtained both for 4-bromoacetophenone **2a** and for 4-bromoanisole **2d** (yields > 65%).

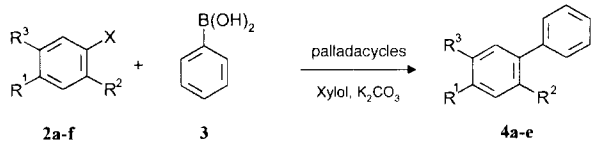

2a-f **3** **4a-e**

Table 1. Palladacycle-catalyzed couplings of aryl halides **2** with phenylboronic acid **3** to give biphenyl derivatives **4**. Standard reaction conditions: aryl halides **2** (10 mmol), phenylboronic acid **3** (15 mmol), K_2CO_3 (20 mmol), catalyst (0.1–0.001 mmol), *o*-xylene (30 mL), $T = 130$ °C.

Nr.	R^1	R^2	R^3	X	Starting material	Product	catalyst [Mol-%][a]	Yield [%]	TON
1	CH_3CO	H	H	Br	**2a**	**4a**	**1a** 0.05	92	1840
2	CH_3CO	H	H	Br	**2a**	**4a**	**1a** 0.001	74	74000
3	CH_3CO	H	H	Br	**2a**	**4a**	**1b** 0.001	71	71000
4	F	H	H	Br	**2b**	**4b**	**1a** 0.02	90	4500
5	Cl	Cl	F	Br	**2c**	**4c**	**1a** 0.02	70	3500
6	CH_3O	H	H	Br	**2d**	**4d**	**1a** 0.01	76	7600
7	CN	H	H	Br	**2e**	**4e**	**1a** 0.02	83	4150
8	CH_3CO	H	H	Cl	**2f**	**4a**	**1a** 0.1	82	820
9	CH_3CO	H	H	Cl	**2f**	**4a**	**1a** 0.01	21	2100

[a] mol% catalyst related to used haloarenes.

From this it follows that the oxidative insertion of the catalyst species into the aryl–halogen bond is not the rate-determining step in contrast to the situation in the Heck reaction.[3] With regard to the reaction mechanism we did not find any indication of an intermediate reduction to an active palladium(0) intermediate. Associated coupling products between the benzylic carbon atom of the ligand and the phenyl or aryl group could not be isolated. Thus Pd^{II}/Pd^{IV} intermediates have to be considered as essential intermediates in the catalysis.[9]

For the conversion of **2e** to **4e**, a catalyst system prepared in situ from 0.01 mol% palladium acetate and 0.01 mol% tri-*o*-tolylphosphane was used. In this case the yield (38%) was significantly lower than that from the direct use of **1a** (83%). Fur-

thermore, after only a short time at 130 °C palladium deposition was observed. Since under standard conditions a 50% excess of phenylboronic acid **3** was used, the reaction of **2a** to **4a** was carried out with a 1 molar equivalent (with respect to the aryl halide) of phenylboronic acid. It was shown that the yield (69%) was only marginally less than that obtained from reaction 2 in Table 1 (74%).

Since the application of the less reactive chloroarenes was particularly desirably from an industrial point of view, we investigated the reaction of 4-chloroacetophenone **2f** with phenylboronic acid **3** (reaction 8 and 9). Surprisingly, this reaction which was carried out in *o*-xylene with 2 molar equivalents of potassium carbonate as base is likewise directly catalyzed with 0.1 mol% **1a**. The desired product 4-acetylbiphenyl **4a** is isolated in 82% yield! Even when the amount of catalyst used is reduced by a power of ten, 21% of **4a** is still isolated, the corresponding turnover number is 2100. Such excellent activations of chloroarenes to aryl coupling are possible for the first time with palladacycles: as expected the comparable reaction with 0.1 mol% palladium acetate and 0.1 mol% triphenylphosphane under otherwise analogous conditions does not yield[5a, e] the desired product (< 1% **4a**).

Our investigations show that the use of palladacycles of type **1** is by no means limited to the Heck reaction.[3] On the contrary, this is a new general type of catalyst, which with regard to its efficiency exceeds all previously described catalyst systems for aryl couplings[5, 10] and which because of its single site character should allow for a rational further development. The evaluation of additional catalysis potential as well as the extension of the chloroarene activation with these new catalyst systems are in progress.[11]

Experimental Procedure

Aryl halide **2** (100 mmol), phenylboronic acid **3** (150 mmol), and potassium carbonate (200 mmol) were heated for 16 h at 130 °C with 0.01 mmol **1a** in *o*-xylene (200 mL). Subsequently the cooled reaction mixture was extracted twice with H_2O (100 mL) and the organic phase was separated. The solvent was removed under vacuum and the crude product was purified by chromatography on silica gel or by recrystallization.

Received: October 19, 1994 [Z74121E].
publication delayed at authors' request
German version: *Angew. Chem.* **1995**, *107*, 1992–1993

Keywords: catalysis · palladacycles · Suzuki coupling

[1] Reviews: a) R. F. Heck, *Palladium Reagents in Organic Synthesis*, Academic Press, London, **1985**; b) A. de Meijere, F. Meyer, *Angew. Chem.* **1994**, *106*, 2473; *Angew. Chem. Int. Ed. Engl.* **1994**, *33*, 2379; c) R. F. Heck, *Org. React.* **1982**, *27*, 345; d) *Comprehensive Organic Synthesis*, *Vol. 4* Eds.: B. M. Trost, I. Fleming), Pergamon, Oxford, **1991**; e) R. F. Heck in [1d], p. 833; f) S. A. Godleski in [1d], p. 585; g) J.-E. Bäckvall, *New J. Chem.* **1990**, *14*, 447; h) C. G. Frost, J. Howarth, J. M. J. Williams, *Tetrahedron Asymmetry* **1992**, *3*, 1089; i) J. Tsuji, *Organic Synthesis with Palladium Compounds*, Springer, Berlin, **1980**; j) J. Tsuji, *Synthesis* **1990**, 739; k) L. S. Hegedus, *Tetrahedron* **1984**, *40*, 2415.

[2] The quality of a catalyst is mainly characterized by turnover number (TON) and catalytic turnover frequency (TOF). Definitions: TON = mol product × mol^{-1} catalyst; TOF = mol product × mol^{-1} catalyst × h^{-1}.

[3] W. A. Herrmann, C. Brossmer, K. Öfele, C.-P. Reisinger, T. Priermeier, M. Beller, H. Fischer, *Angew. Chem.* **1995**, *107*, 1989–1992; *Angew. Chem. Int. Ed. Engl.* **1995**, *34*, 1844–1848.

[4] a) W. V. Murray, *Chemtracts-Org. Chem.* **1993**, *6*, 263; b) K.-H. Hsieh, T. LaHann, R. Speth, *J. Med. Chem.* **1989**, *32*, 898; c) D. Williams, R. Kannan, *J. Org. Chem.* **1987**, *52*, 5435.

[5] a) N. Miyaura, T. Yanagi, A. Suzuki, *Synth. Commun.* **1981**, *11*, 513; b) W. J. Thompson, J. Gaudino, *J. Org. Chem.* **1984**, *49*, 5237; c) M. A. Siddqui, V. Snieckus, *Tetrahedron Lett.* **1988**, *29*, 5463; d) M. J. Sharp, W. Cheng, V. Snieckus, *ibid.* **1987**, *28*, 5093; e) N. M. Ali, A. McKillop, M. B. Mitchell, R. A. Rebelo, P. J. Wallbank, *ibid.* **1992**, *33*, 8117; f) V. Kalinin, *Synthesis* **1992**, 413; g) A. R. Martin, Y. Yang, *Acta Chem. Scand.* **1993**, *47*, 221; h) G. Marck, A. Villiger, R. Buchecker, *Tetrahedron Lett.* **1994**, *35*, 3277; i) Y. Satoh, C. Shi, *Synthesis* **1994**, 1146; j) G. B. Smith, G. Dezeny, D. L. Hughes, A. O. King, T. R. Verhoeven, *J. Org. Chem.* **1994**, *59*, 8151.

[6] W.-C. Sieh, J. A. Carlson, *J. Org. Chem.* **1992**, *57*, 379.

[7] a) D. F. O'Keefe, M. C. Dannock, S. M. Marcuccio, *Tetrahedron Lett.* **1992**, *33*, 6679; b) A. Suzuki, *Pure Appl. Chem.* **1991**, *63*, 419.

[8] a) W. A. Herrmann, C. Brossmer, K. Öfele, M. Beller, H. Fischer, *J. Organomet. Chem.* **1995**, *491*, C1–C4; b) A. R. Hunt, S. K. Stewart, A. Whiting, *Tetrahedron Lett.* **1993**, *34*, 3599.

[9] Palladium(IV) complexes in the catalysis: a) G. Bocelli, M. Catellani, S. Ghelli, *J. Organomet. Chem.* **1993**, *458*, C12; b) O. Reiser, M. Weber, A. de Meijere, *Angew. Chem.* **1989**, *101*, 1037; *Angew. Chem. Int. Ed Engl.* **1989**, *28*, 1037; c) A. J. Canty, *Acc. Chem. Res.* **1992**, *25*, 83; d) D. Milstein, J. K. Stille, *J. Am. Chem. Soc.* **1979**, *101*, 4981; e) A. Gillie, J. K. Stille, *ibid.* **1980**, *102*, 4933; f) B. M. Trost, C. Chan, G. Ruther, *ibid.* **1987**, *109*, 3486; g) K. Albrecht, O. Reiser, M. Weber, B. Kieriem, A. de Meijere, *Tetrahedron* **1994**, *50*, 383; h) G. Dyker, *Angew. Chem.* **1994**, *106*, 117; *Angew. Chem. Int. Ed. Engl.* **1994**, *33*, 103.

[10] a) T. I. Wallow, B. M. Novak, *J. Org. Chem.* **1994**, *59*, 5034; b) G. M. Carrera, G. S. Sheppard, *Synlett* **1994**, 93.

[11] Initial investigations of the palladium-catalyzed aminations of aryl halides – discovered by Buchwald et al. and Hartwig et al. – showed that palladacycles of $Pd(OAc)_2$ and P(*o*-tolyl)$_3$ are catalysts for this type of reaction. a) A. S. Guram, R. A. Rennels, S. L. Buchwald, *Angew. Chem.* **1995**, *107*, 1456; *Angew. Chem. Int. Ed. Engl.* **1995**, *34*, 1348; b) J. Louie, J. F. Hartwig, *Tetrahedron Lett.* **1995**, *36*, 3609.

Carbenoid or Lithium Complex of a Carbanion? Synthesis and Structure of $(Me_3Si)_2C{=}P(aryl){=}C(Cl)Li(thf)_3$ and LiCl Elimination To Give the Phosphirene**

Edgar Niecke,* Petra Becker, Martin Nieger, Dietmar Stalke, and Wolfgang W. Schoeller

Dedicated to Professor Manfred Regitz on the occasion of his 60th birthday

The unusual reactivity of carbenoids towards both electrophiles and nucleophiles has made them important for organic synthesis up to the present day.[1] Their unusual bonding, which was substantiated experimentally by the elucidation of a structure of an alkylidenecarbenoid,[2] has been the subject of numerous theoretical studies.[3] Of particular interest is the integration of the carbenoid center in a pπ-electron system[4] and thus the possibility of an intramolecular rearrangement (Fritsch–Buttenberg–Wiechell rearrangement[5]). Phosphanylcarbenoids also undergo a rearrangement of this kind;[6] these compounds are of increasing interest as synthetic building blocks in organophosphorus chemistry.[7]

In the context of our work on anions containing a P–C pπ-bond,[8] we have been interested in ylene(phosphoranylidene)carbenoids, in which the "carbenoid" center as a component of a delocalized four-electron–three-center pπ-system appears to be capable of reacting in numerous ways.[9] We report here on the synthesis and X-ray structure analysis of a methylene(phosphoranylidene)carbenoid, which forms a phosphirene with the elimination of LiCl and ring closure.

The bis(methylene)phosphorane **2**, prepared by the treatment of aryl[bis(trimethylsilyl)methylene]phosphane (**1**)[10] with trichloromethyllithium,[11] reacts with n-butyllithium in THF at −80 °C to give the two carbenoids **3a**,**b** (**3a**:**3b** = 1:6), which

[*] Prof. Dr. E. Niecke, Dipl.-Chem. P. Becker, Dr. M. Nieger
Anorganisch-chemisches Institut der Universität
Gerhard-Domagk-Strasse 1, D-53121 Bonn (Germany)
Telefax: Int. code + (228)735327
Priv.-Doz. Dr. D. Stalke
Institut für Anorganische Chemie der Universität Göttingen (Germany)
Prof. Dr. W. W. Schoeller
Fakultät für Chemie der Universität Bielefeld (Germany)

[**] This work was supported by the Deutsche Forschungsgemeinschaft and the Fonds der Chemischen Industrie.

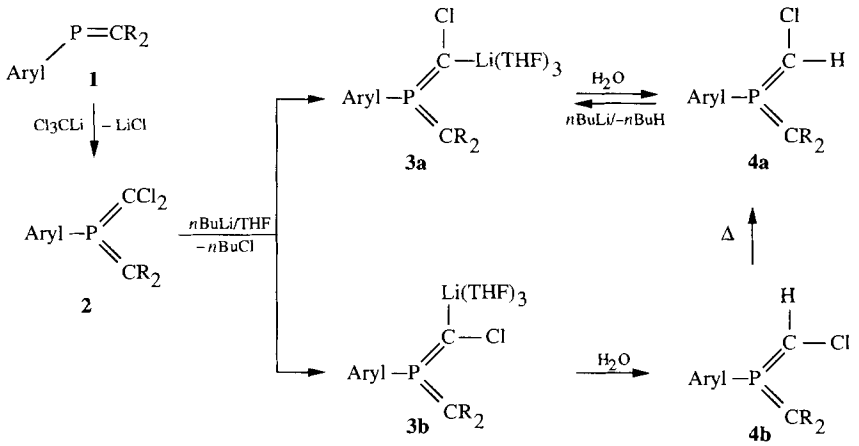

Scheme 1. Aryl = 2,4,6-tBu$_3$C$_6$H$_2$; R = SiMe$_3$.

were characterized by their low-temperature NMR spectra (Scheme 1). Quenching the reaction solution with water at $-50\,^{\circ}C$ affords the two bis(methylene)phosphoranes **4a,b** (in the ratio 1:6); above $0\,^{\circ}C$ **4b** rearranges into the thermodynamically more stable form **4a**. This product can be isolated in the form of pale yellow single crystals. The H/Li exchange in **4a** (n-butyllithium/THF, $-80\,^{\circ}C$) leads selectively to the carbenoid **3a** only, single crystals of which suitable for X-ray structure analysis can be obtained at $-60\,^{\circ}C$.

Figure 1 shows the molecular structure[12] of bis(methylene)-phosphorane **4a**. Like in all known bis(methylene)phosphoranes the phosphorus atom is trigonal-planar coordinated.

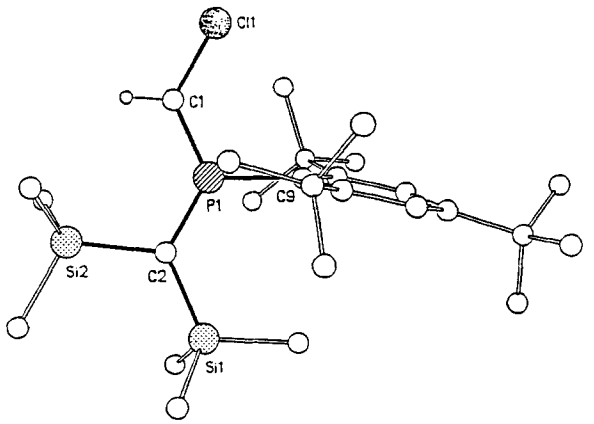

Fig. 1. Molecular structure of **4a** in the crystal. Selected bond lengths [pm] and angles [°]: P1-C1 164.5(7), P1-C2 165.6(6), P1-C9 181.6(5), C1-Cl1 171.2(8), C2-Si1 185.7(6), C2-Si2 188.6(5); C1-P1-C2 125.2(4), C1-P1-C9 115.1(3), C2-P1-C9 119.6(3), P1-C1-Cl1 123.4(5), P1-C2-Si1 126.5(3), P1-C2-Si2 113.3(3), Si1-C2-Si2 119.8(3).

The hydrogen atom is in *endo* position, which, in agreement with the isomerization **4b** → **4a**, shows **4a** to be the energetically more favored form. In this conformation the twisting of the two methylene carbon units, as observed for bis(methylene)phosphoranes with sterically demanding substituents,[13] is avoided. Steric conditions are also responsible for the almost ideal orthogonal alignment of the aryl group with regard to the PC_2 unit. The bond angle at the phosphorus center (C1-P1-C2 125.2(4)°) and the lengths of the bonds to the sp^2 hybridized carbon centers (P1–C9 181.6(5), P1–C1 164.5(7), P1–C2 165.6(6) pm) correspond to those of comparably substituted compounds.[13]

The structural changes during the metal substitution of **4a** to give **3a** are shown in Figure 2.[12] As in **4a** the geometry of the central PC_3 framework in **3a** is determined by the formation of a delocalized π-electron system extending over three centers; the atoms $Si_2CP(C)CCl(Li)$ lie in the same plane ($\sigma = 0.054$ Å). The large P1-C1-Li1 angle (155.7(5)°) is unusual; this angle is mainly compensated by a compression of the Cl1-C1-Li1 angle to 94.8(4)° (and from P1-C1-Cl1 to 109.4(3)°). This is accompanied with a significantly longer C1–Cl1 distance (181.6(6) pm) than that in **4a** (171.2(8) pm). However, the approach of the Li atom to the Cl atom (296(1) pm) caused by this structure is not sufficient for a binding interaction between these atoms.[14] The angle deformations at the "carbenoid" center here exceed that in the alkylidenecarbenoid **5** (C-C-Li 137, Cl-C-Li 109°). The comparatively longer C–Li (219.3 pm) and shorter C–Cl distances (**3a**: 181.6; **5**: C–Li 214.4, C–Cl 185.5 pm[2]) indicate a stronger nucleophilic character of **3a**.[15] In contrast, the effects of the structural changes in the bis(ylene) unit in comparison to **4a** are small. For a similar central bond angle (C-P-C 124.7(3)°) only a small increase of the two P–C bond lengths (167.1(6), 167.5(5) pm) is observed. Noteworthy is the relatively short C–Si(*exo*) distance (182.0(6) vs. 185.7(6) pm in **4a**), which indicates a hyperconjugative charge stabilization in **3a**.[16] The lithium atom attains the coordination number four by solvatation with three THF molecules. The observed distortion of the pyramidal LiO_3 geometry (O-Li-O: 97, 99, 111°) and the different C-Li-O bond angles (106, 108, 135°) should be attributed to steric effects. The Li–O distances (196–202 pm) are not unusual. An inter-

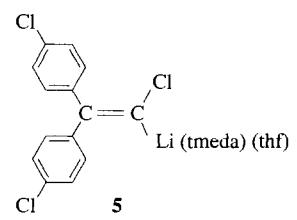

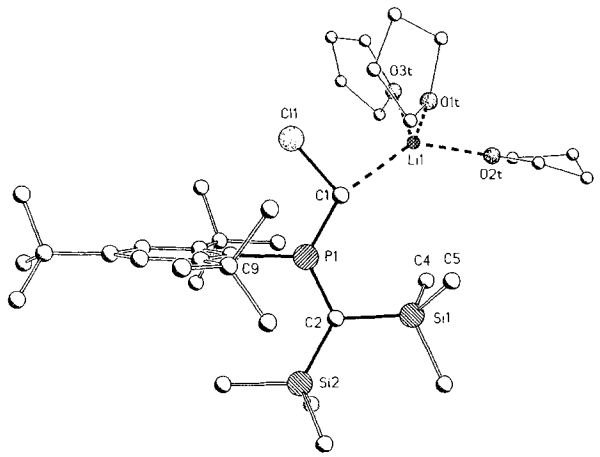

Fig. 2. Molecular structure of **3a** in the crystal. Selected bond lengths [pm] and angles [°]: P1-C1 167.1(6), P1-C2 167.5(5), P1-C9 181.7(5), C1-Cl1 181.6(6), C1-Li1 219.3(12), C2-Si1 186.8(6), C2-Si2 182.0(6), Li1-O1t 196.3(13), Li1-O2t 200.9(12), Li-O3t 201.6(12); C1-P1-C2 124.7(3), C1-P1-C9 118.1(3), C2-P1-C9 117.1(3), P1-C1-Li1 155.7(5), P1-C1-Cl1 109.4(3), Cl1-C1-Li1 94.8(4), P1-C2-Si1 113.6(3), P1-C2-Si2 126.9(3), Si1-C2-Si2 119.0(3), O1t-Li1-O2t 96.8(5), O1t-Li1-O3t 111.0(6), O2t-Li1-O3t 99.3(5), C1-Li1-O1t 105.9(6), C1-Li1-O2t 134.7(6), C1-Li1-O3t 107.9(5).

 © VCH Verlagsgesellschaft mbH, D-69451 Weinheim, 1995 0570-0833/95/3417-1850 $ 10.00+.25/0

molecular Li···Cl interaction cannot be deduced from the observed packing of the molecules in the crystal lattice.

From the structures of **3a** and **4a** as well as the results of multinuclear NMR measurements (Table 1) it follows that **3b** and **4b** are the corresponding stereoisomers with an *endo*-chlorine atom; additional solvent molecules (THF) should be coordinated to the lithium atom also in **3b**. The ^{31}P and ^{13}C NMR data of the protonated compounds **4** are typical for this class of compounds.[13, 17] The different chemical environment of the

Table 1. Relevant chemical shifts δ and coupling constants J of **3** and **4**.

	$\delta^{31}P$ ($^2J_{PH/PLi}$)	$\delta^{13}C$ ($^1J_{CP}$)	
		P=C(Li/H)Cl	P=C(SiMe$_3$)$_2$
3a	164 (br., <5 Hz)	147.3 (93 Hz)	40.0 (18.3 Hz)
4a	147 (33.8 Hz)	79.5 (137 Hz)	50.3 (48.5 Hz)
3b	146 (19 Hz)	139.7 (96 Hz)	49.7 (10 Hz)
4b	134 (35.3 Hz)	77.7 (139.5 Hz)	50.0 (42 Hz)

carbon atoms in the "allyl anion system"[18] leads to an asymmetric charge distribution; the silyl groups are more capable of stabilizing the negative charge. The high field position of the corresponding ^{13}C NMR signal correlates with a significantly smaller value for the coupling constant J_{CP}. As expected, changes in the ^{13}C chemical shifts in the metal substitution to **3** are evident with a strong deshielding of the neighboring ^{13}C nucleus ($\Delta\delta$ = 67.8 **3a/4a** and 62.0 **3b/4b**, respectively). A comparable change in chemical shift on metalation is documented for halogen lithium vinylidenecarbenoids (e.g. H(Cl)C=C(H)Cl/H(Cl)C=C(Li)Cl: $\Delta\delta$ = 68[19]). There is an apparent decrease of the coupling constants J_{PC} in the conversion of **4** to **3**, which indicates a weakening of the P=C bond in the allyl system. Surprisingly, the different stereochemistry of the hydrogen atoms in **4** is not apparent from the value of $^2J_{HP}$, whereas the well-resolved ^{31}P-^7Li coupling constant (19 Hz) in **3b**, in contrast to that of **3a**, (for comparable line width, $\nu_{1/2}$ = 5 Hz) is possibly attributed to differences in the bonding at the carbenoid center.[20]

Quantum chemical ab initio calculations[21] on the model compounds **I**, **II**, **IV**, and **III** (for the modeling of solvation effect[24]) gave the following trends (Scheme 2). The formal

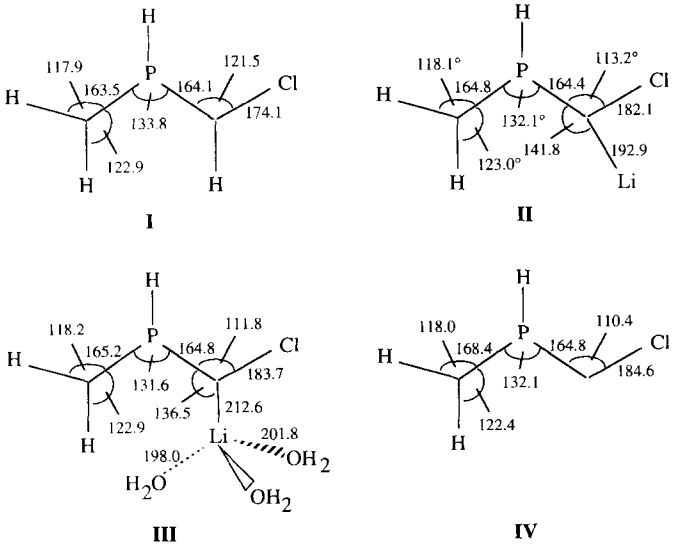

Scheme 2. Optimized geometries of the model compounds **I**–**IV**.

replacement of H by Li (**I** → **II**) leads to a significant reduction of the P-C-Cl angle (Δ 8.3°) which is accompanied by a considerable increase in the length of the P–Cl bond (Δ 8.0 pm). The C–Li distance in **II** (192.9 pm) indicates a relatively "strong" bond between these two atoms. The influence of solvation (**II** → **III**) as expected is apparent in a considerable extension of the C–Li bond (Δ 19.8 pm). The associated structural changes in the P-C-Cl angle and the r(P–Cl) bond are comparatively small, and in the series **II** → **III** → **IV** a slight compression of the angle is accompanied by a small bond extension. Population analysis implies the formal "kinship" of the solvate **III** with the free carbanion **IV**; some of the excess charge is stabilized by the allyl system.[25]

However, the carbenoid character of the remarkably stable "carbenoid" **3a** is apparent in the LiCl elimination, which in solution occurs above −10 °C and leads to the λ^3-phosphirene **6**, whose constitution is confirmed by the NMR data typical for this type of compound[26] ($\delta(^{31}P) = -184$; $\delta(^{13}C) = 159.4$, $^1J_{C,P} = 71.4$ Hz).

Model calculations[27] on the postulated neutral intermediates **V** ($H_2C{=}P(H){=}C$, $^1A'$ state)[28] and **VI** ($HP\dot{C}H_2\dot{C}$, ^1A state) deriving from an LiCl elimination however gave very high energy structures for them (**V**: 111; **VI**: 48 kcal mol^{-1}; relative to the

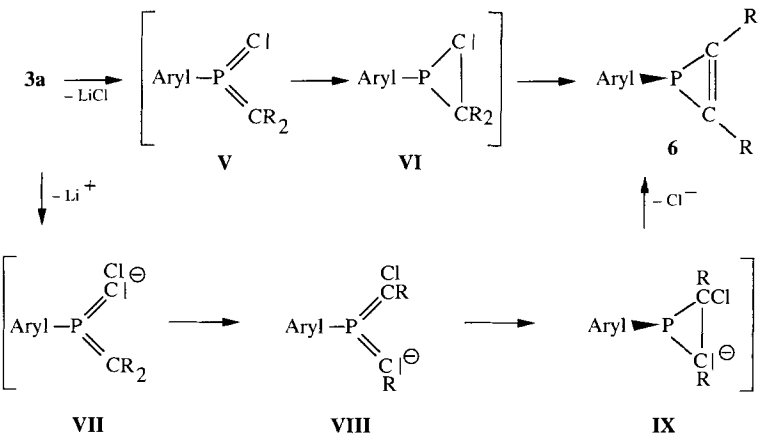

λ^3-phosphirene $HP(CH)_2$). This finding therefore makes a two-step elimination with the integration of a carbanionic intermediate **VII** as primary step of the reaction seem more likely. In a subsequent 1,3-silyl group shift the "carbanion" **VII** should rearrange to give the more stable isomer **VIII**, which by ring closure forms the phosphirane anion **IX**. The subsequent chloride elimination affords the phosphirene **6**.[29]

Experimental Procedure

2: A solution of CH_3Cl (0.47 g, 4 mmol) in THF (40 mL) and ether (10 mL) was treated with *n*BuLi (4.4 mmol, in *n*-hexane (c = 1.6 mol L^{-1})) at −100 °C. This was stirred for 1 h and then added dropwise to a solution of **1** (1.51 g, 3.5 mmol) in ether (10 mL). After the solution was allowed to warm to 25 °C, the volatiles were removed under vacuum, the residue was taken up in pentane, and the insoluble material (LiCl) was separated by filtration. Compound **2** crystallized from the concentrated filtrate at 25 °C. Yield: 78%; m.p. 140–142 °C. NMR (without aryl group): $^{31}P\{^1H\}$ NMR (ext.): δ = 127 (s); ^1H NMR (C_6D_6): δ = 0.6 (s, $SiMe_3$), 0.11 (s, $SiMe_3$); ^{13}C NMR (C_6D_6): δ = 90.0 (d, ^1J(C,P) = 156 Hz, $PCCl_2$), 54.5 (d, ^1J(C,P) = 48.5 Hz, $PC(SiMe_3)_2$), 4.8 (d, ^4J(C,P) = 4.7 Hz, $PCSiC_3$), 4.3 (d, ^4J(C,P) = 4.8 Hz, $PC(SiC_3)$); MS (70 eV) m/z (%): 516 (11) [M^+], 73 (100) [$SiMe_3$].

4a [**3b**, **4b**]: **2** (0.15 mg, 0.3 mmol) was dissolved in THF (3 mL), and then metalated with *n*BuLi (0.2 mL, 0.33 mmol, in hexane (c = 1.6 mol L^{-1})) at −78 °C in 10 min under constant stirring. The deep red reaction solution was subsequently quenched with H_2O (0.005 mL, 0.3 mmol) at −78 °C. After the solution was allowed to warm to 25 °C the solvent was removed under vacuum, the residue was taken up in a little pentane, and the solution was filtered through Celite. Compound

4a crystallized as yellow crystals from the yellow solution after 2 d at + 2 °C. Yield: 97%; m.p. 129–131 °C. NMR (25 °C; without aryl group): ^{31}P NMR (ext.): $\delta = 147$ (d, ^2J(P,H) = 33.8 Hz, PCHCl); ^{1}H NMR (C_6D_6): $\delta = 4.9$ (d, ^2J(H,P) = 34 Hz, PCHCl), 0.47 (s, $SiMe_3$), 0.07 (s, $SiMe_3$); ^{13}C NMR (C_6D_6): $\delta = 79.5$ (d, ^1J(C,P) = 137.1 Hz, PCHCl), 50.3 (d, ^1J(C,P) = 48.5 Hz, $PC(SiMe_3)_2$), 3.8 (d, ^4J(C,P) = 4.6 Hz, $PCSiC_3$), 1.9 (d, ^4J(C,P) = 5.7 Hz, $PC(SiC_3)$); MS (70 eV) *m/z* (%): 482 (6) [M^+], 73 (100) [$SiMe_3$].

The NMR spectroscopic characterization of the deep red reaction solution at −60 °C shows the preferred formation (> 85%) of the carbenoid **3b** (by product **3a**, < 15%). NMR (THF, −60 °C; without aryl group): ^{31}P{^{1}H} NMR (ext.): $\delta = 146$ (q, ^2J(P,Li) = 19 Hz; ^{13}C NMR ([D_8]THF): $\delta = 139.7$ (d, ^1J(C,P) = 96.1 Hz, PCLiCl), 49.7 (d, ^1J(C,P) = 10 Hz, $PC(SiMe_3)_2$), 6.1 (s, $PCSiC_3$), 4.6 (s, $PC(SiC_3)$).

The NMR spectroscopic characterization of **4b** was undertaken from the reaction solution of **3a** (**3b**) quenched with water at −20 °C. As a result of the isomerization **4b** → **4a** only occuring above 0 °C, there was a high excess of **4b** (< 85%). NMR data, without aryl group: ^{31}P NMR (ext.): $\delta = 134$ (d, ^2J(P,H) = 35.3 Hz, PCHCl); ^{1}H ([D_8]THF): $\delta = 4.2$ (d, ^2J(H,P) = 35 Hz, PCHCl), 0.35 (s, $SiMe_3$), 0.26 (s, $SiMe_3$); ^{13}C NMR ([D_8]THF): $\delta = 77.7$ (d, J(C,P) = 139.6 Hz, PCClH), 50.0 (d, J(C,P) = 42 Hz, $PC(SiMe_3)_2$), 4.8 (br, $PC(SiC_3)$), 3.6 (br, $PC(SiC_3)$).

3a and **5**: **4a** (0.14 mg, 0.3 mmol) was dissolved in THF (3 mL). The reaction solution was deprotonated at −78 °C with *n*BuLi (0.2 mL, 0.33 mmol in hexane (c = 1.6 mol L^{-1})) under constant stirring. Yellow crystals suitable for X-ray structure analysis were obtained from the deep red reaction solution after 4 months at −78 °C. **3a**: NMR (THF; −60 °C; without aryl group): ^{31}P{^{1}H} NMR (ext.): $\delta = 164$ (br); ^{13}C NMR ([D_8]THF): $\delta = 147.3$ (d, ^1J(C,P) = 93 Hz, PCClLi), 40.0 (d, ^1J(C,P) = 18.3 Hz, $PC(SiMe_3)_2$), 4.6 (s, $PCSiC_3$), 4.0 (s, $PC(SiC_3)$).

If, after the reaction mixture was allowed to warm to room temperature, the solvent was removed under vacuum, the residue was taken up in pentane, and the insoluble material (LiCl) was separated by filtration over Celite, **5** was obtained as a yellow-brown oil. **5**: Yield: 91%, b.p. 90–92 °C/10^{-2} Torr. NMR (25 °C; without aryl group): ^{31}P{^{1}H} NMR (ext.) $\delta = -184$(s); ^{1}H NMR (C_6D_6): $\delta = 0.23$ (s, $SiMe_3$), 0.20 (s, $SiMe_3$); ^{13}C NMR (C_6D_6): $\delta = 159.4$ (d, 71.4 Hz, $PCSiMe_3$), 0.07 (s, $PC(SiC_3)$); MS (70 eV) *m/z* (%): 446 (6) [M^+], 73 (100) [$SiMe_3$].

Received: March 8, 1995 [Z 7774 IE]
German version: *Angew. Chem.* **1995**, *107*, 2012–2015

Keywords: carbenoids · lithium compounds · phosphorus compounds · structure elucidation

[1] Reviews: a) G. Köbrich, *Angew. Chem.* **1967**, *79*, 15–27; *Angew. Chem. Int. Ed. Engl.* **1967**, *6*, 41; b) W. Kirmse, *Angew. Chem.* **1965**, *77*, 1–10; *Angew. Chem. Int. Ed. Engl.* **1965**, *4*, 1.

[2] G. Boche, M. Marsch, A. Müller, K. Harms, *Angew. Chem.* **1993**, *105*, 1081–1082; *Angew. Chem. Int. Ed. Engl.* **1993**, *32*, 1033; A. Maercker, *ibid.* **1993**, *105*, 1072–1074 and **1993**, *32*, 1023.

[3] a) T. Clark, P. von R. Schleyer, *J. Chem. Soc. Chem. Commun.* **1979**, 883–884; b) *J. Am. Chem. Soc.* **1979**, *101*, 7747–7748; c) P. von R. Schleyer, T. Clark, A. J. Kos, G. W. Spitznagel, C. Rohde, D. Arad, K. N. Houk, N. G. Rondan, *ibid.* **1984**, *106*, 6467–6475.

[4] Reviews: a) P. J. Stang, *Methoden Org. Chem. (Houben-Weyl) 4th Ed. 1952–*, Bd. E 19b, **1989**, p. 84–165; b) H. Yamamoto in *Comprehensive Organic Synthesis, Bd. 2* (Eds.: I. Fleming, B. M. Trost, C. H. Heathcock), Pergamon, Oxford, **1992**, p. 81; c) J. P. Stang, *Acc. Chem. Res.* **1982**, *15*, 348–354.

[5] a) A. A. Bothner-By, *J. Am. Chem. Soc.* **1955**, *77*, 3293–3296; b) G. Köbrich, H. Trapp, *Chem. Ber.* **1966**, *99*, 680–688.

[6] a) R. Appel, C. Casser, M. Immenkeppel, *Tetrahedron Lett.* **1985**, *30*, 3551–3554, b) M. Yoshifuji, T. Niitsu, N. Inamoto, *Chem. Lett.* **1988**, *10*, 1733–1734.

[7] a) R. Appel, M. Immenkeppel, *Z. Anorg. Allg. Chem.* **1987**, *553*, 7–14; b) S. J. Goede, F. Bickelhaupt, *Chem. Ber.* **1991**, *124*, 2677–2684; c) E. Niecke, A. Fuchs, F. Baumeister, M. Nieger, W. W. Schoeller, *Angew. Chem.* **1995**, *107*, 640–642; *Angew. Chem. Int. Ed. Engl.* **1995**, *34*, 555–557.

[8] E. Niecke, M. Nieger, P. Wenderoth, *J. Am. Chem. Soc.* **1993**, *115*, 6989–6990; b) *Angew. Chem.* **1994**, *106*, 362–363; *Angew. Chem. Int. Ed. Engl.* **1994**, *33*, 353–354; c) *ibid.* **1994**, *106*, 2045–2046 and **1994**, *33*, 1953; d) K. Paasch, M. Nieger, P. Wenderoth, E. Niecke, unpublished.

[9] W. Schilbach, V. von der Gönna, D. Gudat, M. Nieger, E. Niecke, *Angew. Chem.* **1994**, *106*, 1037–1039; *Angew. Chem. Int. Ed. Engl.* **1994**, *33*, 982–983.

[10] R. Appel, C. Casser, M. Immenkeppel, *Tetrahedron Lett.* **1985**, *26*, 3551–3554.

[11] G. Köbrich, K. Flory, R. H. Fischer, *Chem. Ber.* **1966**, *99*, 1793–1804.

[12] X-ray structure analysis of **3a** and {**4a**}: $[C_{26}H_{47}ClPSi_2]^-[(C_4H_8O)_3Li]^+ \cdot 0.5C_6H_{12}$ {$C_{26}H_{48}ClPSi_2$}, yellow {yellow} crystals, crystal dimensions $0.2 \times 0.2 \times 0.4$ mm {$0.13 \times 0.20 \times 0.48$ mm}; $M = 747.6$ {483.2}; monoclinic {orthorhombic}, space group $C2/c$ (no. 15) {$Pca2_1$ (no. 29)}, $a = 39.483(7)$ {13.033(1)}, $b = 11.416(4)$ {12.173(1)}, $c = 25.636(6)$ {18.596(1)} Å, $\beta = 127.55(1)$ {90}°, $V = 9161(4)$ {2950.3(6)} Å^3, $Z = 8$ {4}, $\mu(Cu_{K\alpha}) = 1.81$ {2.50} mm^{-1}, $T = 193$ {208} K, $F(000) = 3280$ {1056}. 6936 {3848} reflections up to $2\theta = 120$ {120}° were collected on an Enraf-Nonius CAD4 diffractometer with $Cu_{K\alpha}$ radiation, of these 6797 {3720} were independent and used for the calculations. The structure was solved with direct methods and refined on F^2 anisotropic, the H atoms were refined with a "riding" model (program SHELXL-93 (G. M. Sheldrick, SHELXL-93, Universität Göttingen, **1993**)). The final quality factor *wR2* (F^2) was 0.256 {0.164}, with a conventional $R(F) = 0.079$ {0.054} for 445 {281} parameters and 203 {67} restraints. An absorption correction (DIFABS [N. Walker, D. Stuart, *Acta Crystallogr. Sect. A*, **1983**, *39*, 158–166] {ψ scans}) and an extinction correction were carried out. One molecule of THF and one *t*Bu group are disordered {one tBu group is disordered}. The absolute structure was determined for **4a** (Flack parameter $x = 0.03(4)$). Further details of the crystal structure investigations may be obtained from the Fachinformationszentrum Karlsruhe, D-76344 Eggenstein-Leopoldshafen (Germany) on quoting the depository number CSD-59028.

[13] R. Appel in *Multiple Bonding and Low Coordination in Phosphorus Chemistry* (Eds.: M. Regitz, O. J. Scherer), Thieme, **1990**, pp. 367–374.

[14] W. N. Setzer, P. von R. Schleyer, *Adv. Organomet. Chem.* **1985**, *24*, 353–451.

[15] M. Topolski, M. Duraisamy, J. Richon, J. Gawronski, K. Gawronska, V. Goedken, H. W. Walborsky, *J. Org. Chem.* **1993**, *58*, 546–555.

[16] G. Boche, G. Decker, H. Etzrodt, H. Dietrich, W. Mahdi, A. J. Kos, P. von R. Schleyer, *J. Chem. Soc. Chem. Commun.* **1984**, 1493–1494.

[17] P. Becker, H. Brombach, G. David, M. Leuer, H.-J. Metternich, E. Niecke, *Chem. Ber.* **1992**, *125*, 771–782.

[18] W. W. Schoeller, J. Niemann, *J. Am. Chem. Soc.* **1986**, *108*, 22–26.

[19] a) D. Seebach, H. Siegel, J. Gabriel, R. Hässig, *Helv. Chim. Acta* **1980**, *63*, 2046–2053; b) D. Seebach, R. Hässig, J. Gabriel, *ibid.* **1983**, *66*, 308–337.

[20] The investigations on the corresponding ^{6}Li-labeled derivatives will be discussed elsewhere.

[21] The calculations at the RHF/6-31 + G* level [22] were carried out with the Gaussian 92/DTF program (Revision G.3) [23].

[22] 6-31 + G* basis set with diffuse functions: T. Clark, J. Chandrasekhar, G. W. Spitznagel, P. von R. Schleyer, *J. Comput. Chem.* **1983**, *4*, 294; M. J. Frisch, J. A. Pople, J. S. Binkley, *J. Chem. Phys.* **1984**, *80*, 3265.

[23] M. J. Frisch, G. W. Trucks, H. B. Schlegel, P. M. W. Gill, B. G. Johnson, M. W. Wong, J. B. Foresman, M. A. Robb, M. Head-Gordon, E. S. Replogle, R. Gomperts, J. L. Andres, K. Raghavachari, J. S. Binkley, C. Gonzalez, R. L. Martin, D. J. Fox, D. J. Defrees, J. Baker, J. J. P. Stewart, J. A. Pople, Gaussian, Inc., Pittsburgh, PA, **1993**.

[24] For the problem of the solvation and electron correlation effects in vinylidenecarbenoids see: W. W. Schoeller, *Chem. Phys. Lett.* in press.

[25] W. W. Schoeller, unpublished results.

[26] F. Mathey, *Chem. Rev.* **1990**, *90*, 997–1025.

[27] Relative energies for **V** and **VI** at the RHF/6 + 31G* level plus MP4SDTQ(cf) plus zero-point vibrational energy correction.

[28] The methylenephosphorane carbene, $H_2C{=}P(H){=}C$, has a triplet ground state (^{3}A″), which is energetically more favorable by 25.7 kcal mol^{-1} than the singlet ground state (^{1}A′). ^{3}A″ (^{1}A′) : C–P = 1.710 (1.702), $C(H_2)P = 1.714$ Å, ∢ C-P-C = 129.0 (141.9), ∢ H_{endo}-C-P = 120.2 (122.0), ∢ H_{exo}-C-P = 121.0 (118.6). The energy separation between the singlet and triplet state ($\langle S^2 \rangle$ = 2009) was determined from the energy difference between a MP4SDTQ(fc)/6-31 + G*//(U)RHF/ 6-31 + G* (^{1}A′) and a (P)UMP4SDTQ(fc)/6-31 + G*//(U)RHF/6-31 + G* (^{3}A″) calculation. For the triplet state, this corresponds to a spin projection according to the formalism of Schlegel (H. B. Schlegel, *J. Chem. Phys.* **1986**, *84*, 4530). According to vibrational analysis (harmonic approximation, R(U)HF/6-31 + G* level) both the singlet and the triplet state have C_s symmetry.

[29] The conversion of a phosphirane into a phosphirene via an elimination is known: H. J. Metternich, E. Niecke, *Tetrahedron Lett.* **1991**, *32*, 6537–6538.

Ylidediyl Halophosphane Oligomers, $(Ph_3PCPX)_n$—A Structurally Diverse Class of Compounds**

Hans-Peter Schrödel, Georg Jochem, Alfred Schmidpeter,* and Heinrich Nöth

Dedicated to Professor Rolf Huisgen on the occasion of his 75th birthday

Triphenylphosphonium ylidyl substituents $Ph_3P{=}CR-$,[1-4] exert a stronger +M effect than the corresponding isolobal amino groups and, for example, lead to spontaneous dissociation of halophosphanes.[1, 2] In the same way, the ylidediyl unit $Ph_3P{=}C{=}$, which is isolobal to an imino group, is expected to form halophosphaalkenes **1** (X = Cl, Br); upon dissociation, **1** would yield the triphenylphosphoniophosphaethyne ion **2**.[5]

$$\underset{\mathbf{1}}{Ph_3\bar{P}-C{=}PX} \cdot \rightarrow Ph_3P{=}C{=}PX \rightleftharpoons \underset{\mathbf{2}}{Ph_3\overset{+}{P}-C{\equiv}P\,X^-}$$

The attempted synthesis of **1** actually affords its oligomers $(Ph_3PCPX)_n$, (n = 2, 3, 4). They are related to cyclophosphazanes,[6] $(RNPX)_n$, by a formal RN/Ph_3PC exchange,[7] and consequently, similar symmetrical ring structures are predicted. However, such an analogous structure is only encountered for n = 2, whereas partial dissociation leads to structures of lower symmetry for n = 3, 4.

Treatment of bis(trimethylsilyl)ylide **3** with phosphorus trichloride or phosphorus tribromide affords the dihalophosphanyl ylides **4** and **5** (Scheme 1).[2] The mixed trimethylsilyl- and dihalophosphanyl-substituted ylides **4** (route 1) are isolable; in solution, however, self-condensation (route 3) takes place to afford the oligomers **6**–**8**. Similarly, the condensation of bis(dihalophosphanyl)ylide **5** with bis(trimethylsilyl)ylide **3** (route 4) yields oligomers **6** and **7**.

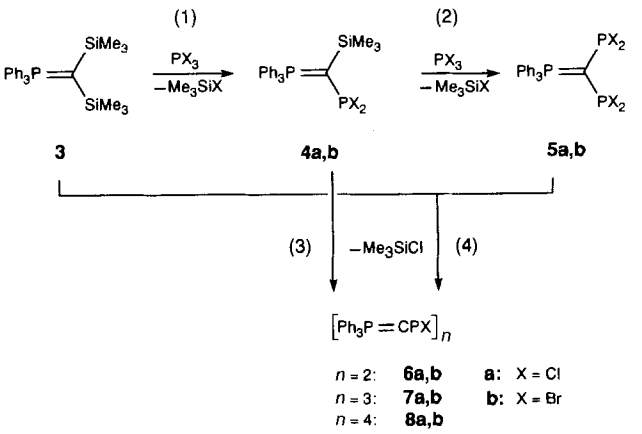

Scheme 1.

Which of these oligomers forms predominantly is frequently determined by only small changes in the reaction conditions. The choice of starting materials, solvent (benzene or pyridine), concentration, and temperature are all factors that influence the product distribution. Most often, the synthesis can be directed in such a way that *one* oligomer becomes the main product. If a mixture of oligomers is obtained, the components can be separated by their different solubilities. All oligomers have been characterized in detail by NMR spectroscopy, which yields unambiguous structure assignments. Furthermore, the dimers **6** and tetramers **8** crystallize well enough for their molecular structures to be determined by X-ray diffraction analyses of single-crystals of **6a**, **8a**, and **8b**. Unfortunately, trimers **7** could so far only be isolated as microcrystalline powders precluding their structure determination in the solid state. As expected for a structure containing a four-membered ring, the $^{31}P\{^1H\}$ NMR spectra of dimers **6** reveal an A_2B_2 spin system (Table 1). The

Table 1. $^{31}P\{^1H\}$ NMR spectra of the dimers **6** and the cations **9** and **10** derived from them (in CD_2Cl_2); coupling constants J in Hz; ν_0 = 109.379 MHz.

	6a	**6b**	**9** [a]	**9** [b]	**10**
$\delta_A(\sigma^3P)$	194.6	214.6	76.0	76.0	21.1
$\delta_B(C\text{-}PPh_3)$	16.5	15.6	19.4	17.1	19.7
$\delta_C(\sigma^2P)$			407.8	413.5	441.7
$\delta_D(P\text{-}PPh_3)$					1.7
$J_{AB}(^2J_{PP})$	51.9	48.1	32.6	34.9	22.4
$J_{AC}(^2J_{PP})$			122.1	119.1	91.6
$J_{AD}(^1J_{PP})$					444.6
$J_{BC}(^2J_{PP})$			50.7	45.0	54.9
$J_{CD}(^3J_{PP})$					39.7

[a] Y = $AlCl_4$. [b] Y = CF_3SO_3.

chemical shift of the ring phosphorus is in a region typical of diazadiphosphetidines halogen-substituted at the P atom; only *one* conformer is observed. An X-ray structure analysis[8] of **6a** shows that the chlorine atoms are *cis* to each other (Fig. 1).[9] The diphosphetane ring is almost planar (angle sum 358°). The carbon atoms C1 and C2 are surrounded in an almost planar

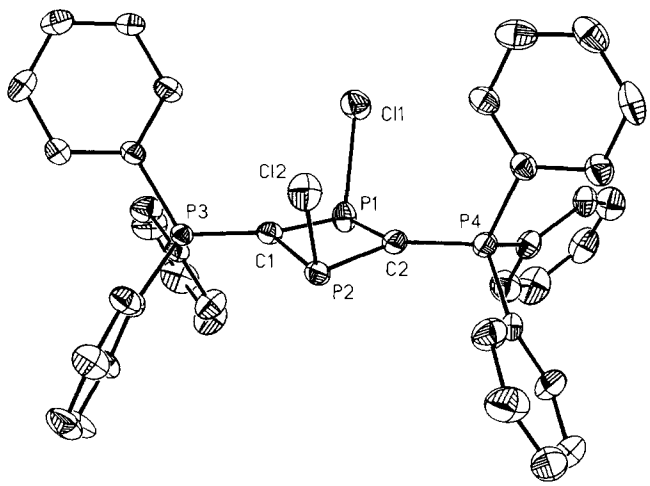

Fig. 1. Crystal structure of **6a** (thermal ellipsoids with 25% probability). Significant bond lengths [pm] and angles [°]: P1-Cl1 220.4(4), P2-Cl2 225.1(3), P1-C1 175.9(8), P1-C2 176.1(7), P2-C1 176.2(7), P2-C2 178.1(8), C1-P3 170.9(8), C2-P4 168.3(8); C1-P1-C2 84.3(4), Cl1-P1-C1 107.3(3), Cl1-P1-C2 105.8(3), C1-P2-C2 83.7(4), Cl2-P2-C1 106.1(3), Cl2-P2-C2 105.4(3), P1-C1-P2 95.7(4), P1-C1-P3 131.3(4), P2-C1-P3 130.7(5), P1-C2-P2 95.0(4), P1-C2-P4 133.9(5), P2-C2-P4 131.0(4).

[*] Prof. Dr. A. Schmidpeter, Dipl.-Chem. H.-P. Schrödel, Dr. G. Jochem, Prof. Dr. H. Nöth[+]
Institut für Anorganische Chemie der Universität
Meiserstrasse 1, D-80333 München (Germany)

[+] X-ray structure analysis.

[**] This work was supported by the Deutsche Forschungsgemeinschaft and the Fonds der Chemischen Industrie. We thank Dipl.-Chem. M. Schmidt for the structural determination of **8a**.

manner (angle sum 357.7° and 359.9°, respectively) despite the small interior angle of 95° and the resulting distortion of their trigonal symmetry.[10] The filled p_z orbitals of the carbon atoms and the P–Cl bonds are virtually eclipsed. This arrangement favors charge transfer to the antibonding orbitals of the P–Cl bond[11] and therefore leads to the unusual elongation of this bond to more than 220 pm (PCl_3: 204 pm). The P–Cl bond in **6a** is thus not only longer than that in another *cis* structured compound, the cyclodiphosphazane $(-t\mathrm{BuN}-\mathrm{PCl}-)_2$ (211 pm[12]), which at the time it was determined was the longest known, but also surpasses any other previously reported P^{III}–Cl distance.[2, 13]

Treatment of **6a** with aluminum trichloride or trimethylsilyl trifluoromethanesulfonate causes one P–Cl bond to dissociate; in the presence of triphenylphosphane a dication is formed (Table 1, Scheme 2).

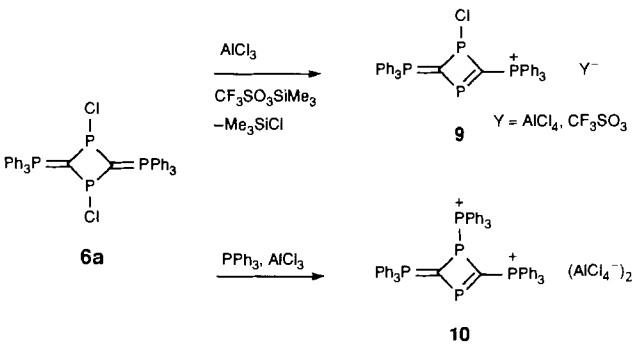

Scheme 2.

^{31}P NMR spectra of trimers **7a, b** recorded at room-temperature show an $[AB]_3$ spin system and are thus indicative of a structure with a symmetrical six-membered ring. The signal for the trivalent phosphorus in **7a** is broad, and the coalescence temperature is approximately −10 °C; in **7b** the same signal broadens upon cooling and splits into two at approximately −60 °C. Below these temperatures the signal in **7a** splits into a low-field resonance and a high-field resonance that is twice as intense, while the signal in **7b** gives rise to one low-field and two high-field resonances of equal intensity (Table 2). The signal at $\delta = 311$ is without doubt attributable to a two-coordinate phosphenium-type phosphorus atom, providing evidence for an ionic structure. The signals at $\delta = 61$ to 68 are assigned to a halogen-substituted phosphorus in a pyramidal coordination environment. In addition, a broad, averaged signal (**7a**: $\delta \approx 180$, **7b**: $\delta \approx 190$) close to the original position and with approximately one-third of the initial intensity is discernible in the low-temperature spectra. Upon further cooling the sample these signals become even broader; however, complete coalescence is not achieved at the lowest temperature of −95 °C. The nonequivalency of the two pyramidally coordinated ring phosphorus atoms in **7b** can tentatively be explained by their different conformations: While all other ring atoms are coplanar,[14] the carbon atom opposite the two-coordinate phosphorus atom is expected to be bent out-of-plane,[15] and hence substituents on its two neighboring ring phosphorus atoms can assume either axial or equatorial positions (Scheme 3).[16]

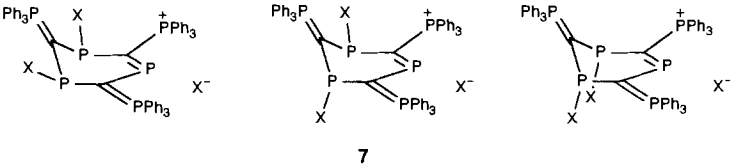

Scheme 3.

In solution the three nonequivalent Ph_3PCPX moieties in **7** rapidly alter their identity by exchange of ionic and covalently bound halogen. At any given temperature this exchange process occurs more rapidly for bromide-containing **7b** than for chloride-containing **7a**. Replacing the bromide in **7b** with tosylate (by reaction of **7b** with silver tosylate) slows the exchange process to allow the observation, even at room temperature, of separate signals for each of the three phosphorus ring atoms (Fig. 2).

Table 2. $^{31}P\{^1H\}$ NMR data of the trimers **7** (in CD_2Cl_2); coupling constants J in Hz; $\nu_0 = 109.379$ MHz. P-5 indicates the site of the dissociating phosphorus–halogen bond in the 1,3,5-trihalo-2,4,6-triphosphoranediyl-1,3,5-triphosphinanes **7a,b**.

	7a [a] 20 °C	**7a** [b] −85 °C	**7b** [a] 20 °C	**7b** −95 °C	**7b** [c] 20 °C
δ(P-1)	168.5 [d]	61.6 [d]	194.2	61.0 [d]	58.9 [d]
δ(P-3)				68.2 [d]	66.8 [d]
δ(P-5)		311.8 [d]		311.4 [d]	330.6 [d]
δ(2-PPh_3)	28.3	32.1	27.8	28.6 [e]	29.4 [e]
δ(4,6-PPh_3)		29.6			
^2J(P-1, 2-PPh_3)	152.6 [f]	170.9	151.1 [f]		
^2J(P-1/P-5, 6-PPh_3)		143.4 [g]			

[a] Both P-1,3,5 and 2,4,6-PPh_3 are dynamically equivalent, with the result that an $[AB]_3$ spin system is observed; its A and B signals approximate a 1:2:1 triplet. [b] The part of the spectrum showing splitting on cooling. Both P-1,3 and 4,6-PPh_3 atoms are equivalent and give an $[AB]_2CD$ spin system. [c] With $TosO^-$ instead of Br^- as counterion. [d] Broad signal because of exchange processes; coupling cannot be deduced. [e] Overlapping signals of 2- ,4-, and 6-PPh_3; couplings cannot be deduced. [f] Actually $N/2$ [23]; the value can be considered as $^2J_{PP}$ with sufficient approximation, since $^4J_{PP}$ is very small in comparison. [g] Average of the two similar $^2J_{PP}$ couplings; the two $^4J_{PP}$ couplings are very small in comparison.

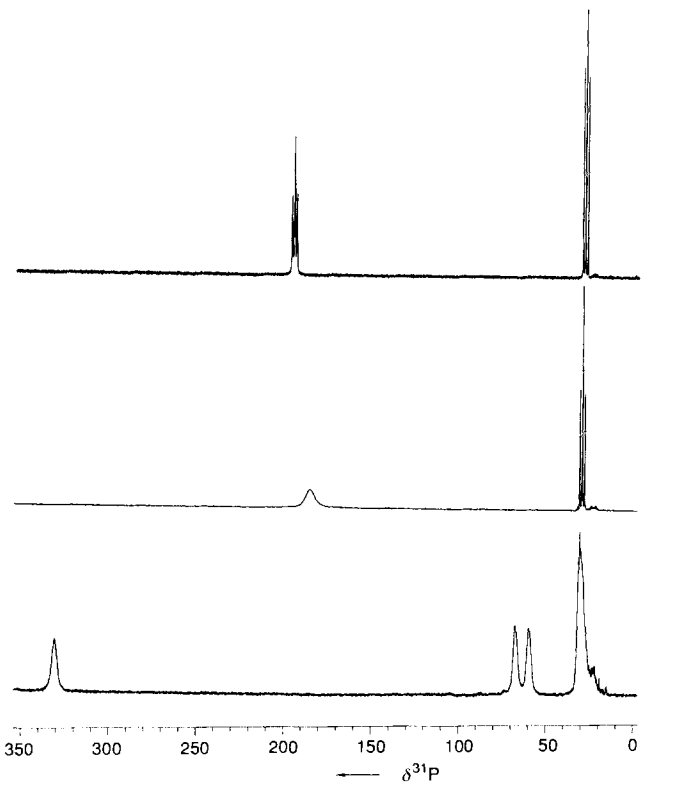

Fig. 2. ^{31}P NMR spectra of **7b** in CD_2Cl_2 at room temperature before (top) and after addition of 1 (center) and 2.5 (bottom) equivalents of silver tosylate.

An eight-membered ring structure is commonly assumed for cyclotetraphosphazanes[6] The presence of this structural element in the permethyl derivative[17] and in several other related compounds[18] has been confirmed by X-ray structure analysis. However, the tetramers **8** do not follow the same building principle. Like the trimers **7**, tetramers **8** are ionic compounds that, however, do not undergo rapid halogen exchange. Their $^{31}P\{^{1}H\}$ spectra reveal an $[AC]_3BD$ spin system (Table 3), and no resonances attributable to a phosphenium-type phosphorus

Table 3. $^{31}P\{^{1}H\}$ NMR data of the tetramers **8** (in CD_2Cl_2); coupling constants J in Hz; $\nu_0 = 109.379$ MHz.

	8a	**8b**
δ_A(PX)	215.4	248.5
δ_B(4-PPh_3)	37.3	35.8
δ_C(2,6,8-PPh_3)	25.3	23.3
δ_D(P-1)	−88.2	−85.0
$J_{AB}(^2J_{PP})$	94.0	90.0
$J_{BC}(^4J_{PP})$	7.6	7.7
$J_{CD}(^2J_{PP})$	138.1	128.2

are present. Instead, the phosphorus affected by dissociation gives rise to a ^{31}P NMR resonance (δ_D) at strikingly high field, whereas the NMR resonance (δ_A) for the three undissociated PX units is observed at unusually low field. The symmetry of the spin system of **8** is in accord with a barrelane structure. This conclusion was confirmed for the solid state as well by an X-ray structure analysis for **8a**·4.5 pyridine and the preliminary results for **8b**. The observation of the crystallographic space group $R\bar{3}$ for **8a** requires the presence of a threefold rotational axis (Fig. 3). As observed for **6a**, the P–Cl bonds and the p_z orbital of the ylidic carbon atoms (dihedral angle Cl1-P1-C2-P3 = 90.5°) are virtually eclipsed, and the bond length of 235 pm makes these P–Cl bonds even longer than those of **6a** and by far the longest known to date. The small P1–C2 distance of 171 pm, which is of the same magnitude as the P–C distance reported for a phosphaalkene (161–171 pm[19]), is in accord with the strong negative hyperconjugation, and the consequently relatively large bond length of 174 pm for P3–C2, which corresponds to the P–C distance in acylylides.[10] The pyridine molecules and chloride ions assume vacant positions in the cation lattice (Fig. 4).

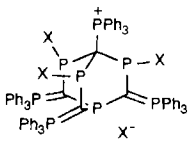

8

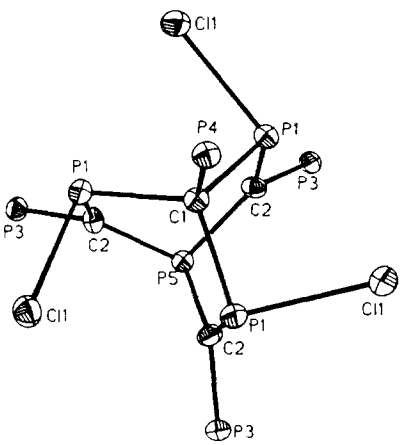

Fig. 3. Crystal structure of **8a** (thermal ellipsoids with 25% probability). For each of the four Ph_3P groups, only the phosphorus atom P3,4 is shown. Significant bond lengths [pm] and angles [°]: P1-Cl1 235.3(2), P1-C1 190.8(3), P1-C2 171.1(5), P4-C1 189.5(8), P3-C2 174.0(5), P5-C2 181.6(5); C1-P1-C2 101.3(3), Cl1-P1-C1 93.97(8), Cl1-P1-C2 109.7(2), C2-P5-C2 100.1(2), P1-C1-P4 108.4(2), P1-C1-P1 110.5(2), P1-C2-P3 117.8(3), P1-C2-P5 124.0(3), P3-C2-P5 118.1(3).

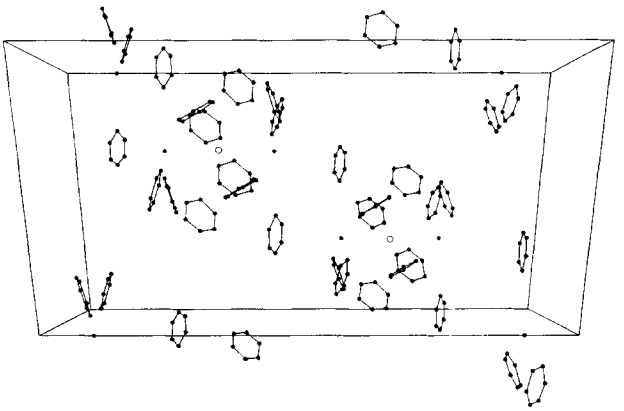

Fig. 4. Unit cell of **8a**·4.5 pyridine. View along the a axis. The packing of the six cations (not shown) leaves three vacancies about the inversion center (indicated by o). Each is filled by two chloride anions and pyridine molecules in twelve orientations with an occupancy factor of 0.75; that is, nine molecules.

The structures reported here for the oligomers of **1** forms a parrallel to the structures of the compounds obtained by cyclooligomerization of *tert*-butylphosphaethyne within the coordination sphere of transition metals. This leads, for example, to complexes of 1,3-diphosphets,[20] 1,3,5-triphosphinine,[21, 22] and 1,3,5,7-tetraphosphabarrelene.[20] An extension of this analogy seems feasible.

Experimental Procedure

6a: At room temperature, PCl_3 (1.44 mL, 11.1 mmol) was added dropwise to a well-stirred solution of **3** (4.66 g, 11.1 mmol) in benzene (150 mL). The initially yellow solution turned colorless and, upon standing, honey-yellow. Light-yellow crystals of **6a** formed after approximately 10 d. Yield: 2.51 g (67%), m.p. (decomp.) 200 °C.

6b: At room temperature, a solution of **3** (2.96 g, 7.05 mmol) in benzene (15 mL) was added dropwise to a stirred mixture of **5b** (4.62 g, 7.05 mmol) in benzene (150 mL). The suspension turned orange. After 10 d the reaction mixture was concentrated to one-half its original volume, and the yellow precipitate of **6b** was collected on a glass frit. Yield: 4.89 g (90%).

7a: A solution of **4a** (3.21 g, 7.14 mmol) in pyridine (10 mL) was stirred for 10 h at 50 °C. The resulting deep-red solution was concentrated and filtered; upon addition of benzene/pentane (30 mL, 1:1 by volume), **7a** precipitated as an orange-red crystalline powder. Yield: 1.78 g (75%). Compound **7a** crystallized from benzene with one mol of solvent.

7b and **8b**: PBr_3 (1.71 g, 6.33 mmol) was added by syringe to a warm (55 °C) solution of **3** (2.66 g, 6.33 mmol) in a mixture of benzene (7 mL) and pyridine (3 mL). The solution color changed from orange to red, and after 10 h a yellow precipitate had formed which ^{31}P NMR spectroscopy showed to be a 10:1 mixture of **7b** and **8b**. This mixture was dissolved in benzene/dichloromethane (1:1 by volume), and pentane was added until the solution began to turn cloudy. Within 12 h, **8b** precipitated in the form of yellow crystals, which were collected by filtration. On evaporating the filtrate to dryness, **7b**·1.5 pyridine was left as a yellow powder, which was recrystallized from pyridine.

8a: A stirred suspension of **3** (846 mg, 2.01 mmol) in pyridine (6 mL) was heated to 60 °C and PCl_3 (276 mg, 2.01 mmol) was added with a syringe. Within 15 min the solution turned red, and stirring was discontinued. The solution was then allowed to stand for 5–10 h at 60 °C during which time large, yellow crystals of **8a**·4.5 pyridine formed. Yield: 481 mg (43%); m.p.(decomp.) 124 °C.

Received: February 10, 1995 [Z 7708 IE]
German version: *Angew. Chem.* **1995**, *107*, 2006–2010

Keywords: heterocycles · NMR spectroscopy · phosphorus compounds · ylides

[1] A. Schmidpeter, G. Jochem, *Tetrahedron Lett.* **1992**, *33*, 471–474.

[2] A. Schmidpeter, H. Nöth, G. Jochem, H.-P. Schrödel, K. Karaghiosoff, *Chem. Ber.* **1995**, *128*, 379–393, and references therein.

[3] A. Schmidpeter, G. Jochem, K. Karaghiosoff, C. Robl, *Angew. Chem.* **1992**, *104*, 1420–1421; *Angew. Chem. Int. Ed. Engl.* **1992**, *31*, 1350–1352.

[4] G. Jochem, H. Nöth, A. Schmidpeter, *Angew. Chem.* **1993**, *105*, 1117–1119; *Angew. Chem. Int. Ed. Engl.* **1993**, *32*, 1084–1091.

[5] A phosphonio-phosphaethyne $(Me_2N)_3P^+-C\equiv P\ BPh_4^-$ had been reported: U. Fleischer, H. Grützmacher, U. Krüger, *J. Chem. Soc. Chem. Commun.* **1991**, 302–303. However, the compound has only been identified by its ^{31}P NMR spectrum and trapping reactions. This data does not allow for unique identification and could also be in accord with its precursor $(Me_2N)_3P{=}CH{-}PCl_2$.

[6] R. Keat in *The Chemistry of Inorganic Homo- and Heterocycles, Vol. 2* (Ed.: I. Haiduc, D. B. Sowerby), Academic Press, London, **1987**, p. 467–499.

[7] In general, coordination of a phosphane to a carbon atom renders the latter isolobal to an imino group or a chalcogen atom. As such the carbon atom becomes a suitable building block for the formation of saturated rings. The first such heterocycles, that is, four-membered rings consisting of two R_3PC and two $SiMe_2$ moieties have been reported by H. Schmidbaur, W. Malisch, *Chem. Ber.* **1970**, *103*, 9–103, and isosteric four-membered rings consisting of Ph_3PC and PPh_2^+ moieties by R. Appel, F. Knoll, H.-D. Wihler, *Angew. Chem.* **1977**, *89*, 415–416; *Angew. Chem. Int. Ed. Engl.* **1977**, *16*, 402–403. For compounds in which Ph_3PC and CO are combined to rings, see H. J. Bestmann, T. G. Fürst, A. Schier, *ibid.* **1993**, *105*, 1783–1784, 1784–1788 and **1993**, *32*, 1746–1747, 1747–1751. For cyclic compounds of the isoelectronic cationic unit $(Me_2N)_3PP^+$ with $PNMe_2$ and CH_2, see A. Schmidpeter, S. Lochschmidt, *ibid.* **1986**, *98*, 271–273, and **1986**, *25*, 253–254.

[8] X-ray structure analyses: data collection at 293 K, Siemens-P4-diffractometer, $Mo_{K\alpha}$ radiation ($\lambda = 0.71073$ Å), graphite monochromator. The structure was solved by direct methods (SHELXTL PLUS, PC version). Non-hydrogen atoms anisotropic, H atoms in calculated positions and included in the refinement with constant U. **6a** Pale yellow prisms, $C_{38}H_{30}Cl_2P_4$, $M = 681.5$, orthorhombic, space group *Pbca*; $a = 18.340(8)$, $b = 16.939(7)$, $c = 22.47(1)$ Å, $V = 6980(6)$ Å^3, $Z = 8$, $\rho_{calcd} = 1.297$ g cm^{-3}, $F(000) = 2816$, $\mu = 3.96$ cm^{-1}; ω scans, $3.0° \le 2\theta \le 48.0°$, 5703 measured reflections, of which 5400 are independent ($R_{int} = 0.0172$), 2824 with $|I| > 3\sigma(I)$. Refinement in block mode gave $R = 0.074$ and $R_w = 0.069$. – **8a** · 4.5 pyridine: yellow crystals, $C_{98.5}H_{82.5}Cl_4N_{4.5}P_8$, $M = 1718.9$, rhombohedral, space group $r\bar{3}$ with hexagonal axes (no. 148); $a = 21.403(5)$, $c = 36.154(9)$ Å, $V = 14343(6)$ Å^3, $Z = 6$, $\rho_{ber.} = 1.194$ g cm^{-3}, $F(000) = 5358$, $\mu = 0.304$ cm^{-1}; ω scans, $2.4° \le 2\theta \le 46°$, 5300 measured reflections, of which 4400 ($4\sigma|F|$) are independent and observed ($R_{int} = 0.0932$). Refinement with complete matrix according to the method of least squares gave $R = 0.064$ and $wR2 = 0.167$ (referred to F^2). The positions of the pyridine molecules have an occupation factor of 0.75. Further details of the crystal structure investigation are available from the Fachinformationszentrum Karlsruhe, D-76344 Eggenstein-Leopoldshafen (Germany) on quoting the depository number CSD-401551 (**8a**) or 401552 (**6a**).

[9] Quantum chemical calculation on diazadiphosphetidines (I. Silaghi-Dumitrescu, I. Haiduc, *Phosphorus, Sulfur Silicon Relat. Chem.* **1994**, *91*, 21–36) suggest that the *cis* arrangement is also the more favorable for **6**.

[10] The ylide carbon atom in triphenylphosphonium perfluorocyclobutylide $Ph_3P{=}C(CF_2)_3$ is also still in a planar environment with an interior ring angle of 93.4°: M. A. Howells, R. D. Howells, N. C. Baenziger, D. J. Burton, *J. Am. Chem. Soc.* **1993**, *95*, 5366–5370; in contrast in triphenylphosphonium cyclopropylide $Ph_3P{=}C(CH_2)_2$ it is pyramidal with an interior ring angle of 58.8° (angle sum 293.7°): H. Schmidbaur, A. Schier, B. Milewski-Mahrla, U. Schubert, *Chem. Ber.* **1982**, *115*, 722–731; M. A. Vincent, H. F. Schaefer III, A. Schier, H. Schmidbaur, *J. Am. Chem. Soc.* **1983**, *105*, 3806–3811.

[11] Similar situations and consequences [2] are discussed as anomeric effects, negative hyperconjugation, or no-bond resonance. A. J. Kirby, *The Anomeric Effect and Related Stereoelectronic Effects at Oxygen*, Springer, Berlin, **1983**, p. 37, 52; *Pure Appl. Chem.* **1987**, *59*, 1605–1612; P. von Ragué Schleyer, A. J. Kos, *Tetrahedron* **1983**, *39*, 1141–1150.

[12] K. W. Muir, *J. Chem. Soc. Dalton Trans.* **1975**, 259–262.

[13] N. M. Zapirov, V. A. Naumov, L. L. Tuzova, *Phosphorus* **1974**, *4*, 179–182.

[14] This planarity is confirmed by the molecular structure of the corresponding acyclic structural unit [1].

[15] The isoelectronic S_4N_2 ring has the identical half-chair structure: R. W. H. Small, A. J. Banister, Z. V. Hauptman, *J. Chem. Soc. Dalton Trans.* **1981**, 2188–2191; T. Chivers, P. W. Codding, R. T. Oakley, *J. Chem. Soc. Chem. Commun.* **1981**, 584–585.

[16] The chemical shifts of phosphorus ring atoms with axial or equatorial substituents are significantly different: M. J. Gallagher in *^{31}P NMR Spectroscopy in Stereochemical Analysis* (Ed.: J. G. Verkade, L. D. Quin), VCH, Deerfield Beach, **1987**, p. 296–329; L. D. Quin, A. N. Hughes in *The Chemistry of Organophosphorus Compounds, Vol. 1* (Ed.: F. R. Hartley), Wiley, Chichester, **1990**, p. 295–384.

[17] W. Zeiss, W. Schwarz, H. Hess, *Angew. Chem.* **1977**, *89*, 423–424; *Angew. Chem. Int. Ed. Engl.* **1977**, *16*, 407–408.

[18] A. Schmidpeter, H. Tautz, J. von Seyerl, G. Huttner, *Angew. Chem.* **1981**, *93*, 420–421; *Angew. Chem. Int. Ed. Engl.* **1981**, *20*, 408–409; A. N. Chernega, M. Yu. Antipin, Yu. T. Struchkov, Yu. V. Balitskii, Yu. G. Gololobov, I. E. Boldeskul, *Zh. Obshch. Khim.* **1984**, *54*, 271; *J. Gen. Chem. USSR* **1984**, *54*, 238; C. Malavaud, T. N'Gando M'Pondo, L. Lopez, J. Barrans, J.-P. Legros, *Can. J. Chem.* **1984**, *62*, 43–50; M. Haddad, F. Dahan, J.-P. Legros, L. Lopez, M.-T. Boisdon, J. Barrans, *J. Chem. Soc. Perkin Trans. 2* **1992**, 671–678; J. M. Barendt, E. G. Bent, R. C. Haltiwanger, A. D. Norman, *J. Am. Chem. Soc.* **1989**, *111*, 6883–6884.

[19] R. Appel in *Multiple Bonds and Low Coordination in Phosphorus Chemistry* (Ed.: M. Regitz, O. J. Scherer), Thieme, Stuttgart **1993**, p. 157–219.

[20] P. Binger, G. Glaser, B. Gabor, R. Mynott, *Angew. Chem.* **1995**, *107*, 114–116; *Angew. Chem. Int. Ed. Engl.* **1995**, *34*, 81–83, and references therein.

[21] A. R. Barron, A. H. Cowley, *Angew. Chem.* **1987**, *99*, 956; *Angew. Chem. Int. Ed. Engl.* **1987**, *26*, 907; meanwhile the result has been queried: J. Nixon, *Chem. Ind. (London)* **1993**, 403–407.

[22] P. Binger, S. Leininger, J. Stannek, B. Gabor, R. Mynott, J. Bruckmann, C. Krüger, *Angew. Chem.*, in press.

[23] R. G. Jones, R. C. Hirst, H. J. Bernstein, *Can. J. Chem.* **1965**, *43*, 683–699.

Carbene Complex Functionalized Sugars**

Karl Heinz Dötz,* Wolfgang Straub, Richard Ehlenz, Klaus Peseke, and Roland Meisel

Electrophilic Fischer-type carbene complexes are of interest in stereoselective organic synthesis as building blocks for metal- and ligand-centered cycloadditions,[1a–c] as ketene equivalents,[1c] and as enolate analogues for aldol and Michael reactions.[1d] In C–C bond forming reactions the transition metal may serve as a template,[2] and, moreover, the analogy between the carbonyl metal fragment and the oxygen atom in carbonyl compounds,[3a] as described by the isolobal relationship,[3b] is exploited. The stereochemical information available in carbohydrates with their wealth of chiral centers[4] has been employed in organometallic coordination chemistry only in rare cases. Whereas the capacity of sugars to serve as O-coordinated, optically active ligands for chiral induction is convincingly documented for titanium-mediated C–C bond forming reactions,[5] examples of C-metalated carbohydrates are limited for the most part to lithium and tin derivatives. Transition metals have been used in isolated cases for C-glycosidation;[6a–d] however, glycosyl complexes are known only for manganese,[6c,d] cobalt,[6e] and iron.[6f] We set out to transfer the synthetic potential of carbene complexes to carbohydrates[7] and report here on the conversion of the exposed C-1 atom of a sugar into a metal-coordinated carbene center.

We used a synthetic approach complementary to the Fischer route and constructed the metal–carbene function by addition of a metal nucleophile to an acid chloride followed by O-alkylation.[8a] Suitable metal nucleophiles are available by reduction of binary carbonyl metal compounds with graphite–potassium[8b] or sodium. We chose 2,3,4,5,6-penta-*O*-acetyl-D-galactonic acid chloride (**1**) to serve as the electrophilic sugar component; it can be prepared from D-galactose by electrochemical oxidation[9] followed by acidic acetylation and chlorination,[10]

[*] Prof. Dr. K. H. Dötz, Dipl.-Chem. W. Straub, Dipl.-Chem. R. Ehlenz
Institut für Organische Chemie und Biochemie der Universität
Gerhard-Domagk-Strasse 1, D-53121 Bonn (Germany)
Telefax: Int. code + (228) 73-5609
Prof. Dr. K. Peseke, Dipl.-Chem. R. Meisel
Fachbereich Chemie der Universität Rostock (Germany)

[**] Organotransition Metal Modified Sugars, Part 1. This work was supported by the Volkswagen-Stiftung and the Fonds der Chemischen Industrie.

and its protecting groups are stable to carbonyl metalates **2**–**5**. Under mild conditions these reagents rather attack the acid chloride function to give the acylmetalates **6**–**9**, which react with strong alkylating agents to afford the C-1-metalated sugar derivatives **10**–**13** (Scheme 1). In the alkylation of ferrate **9** the acylmetalate function competes with the iron center for the electrophile. Collman-type ketone formation can be suppressed by the presence of HMPA and the use of ethyl trifluoromethanesulfonate,[11] but the yields of carbene complex **13** are lower than those of the pentacarbonyl analogues **10**–**12**. The carbene complexes are thermally stable in the solid state and easy to handle; nevertheless, chromatographic purification should be conducted at lower temperatures to preclude decomposition.

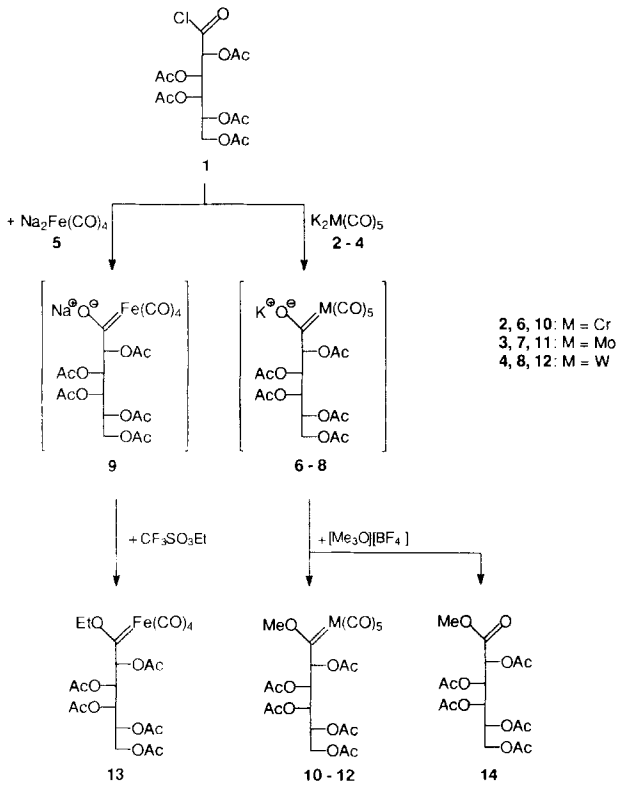

Scheme 1. Synthesis of sugar-carbene complexes **10**–**13**.

The NMR spectra (Table 1) show compounds **10**–**13** to be typical Fischer carbene complexes with a pronounced electrophilic C-1 atom; its ^{13}C NMR signal, for example for the chromium complex **10** ($\delta = 355.0$), is shifted distinctly downfield in comparison to that of the analogous D-galactose ester **14** ($\delta = 167.3$). The acceptor character of the metal–carbene function is also evident at the adjacent C–H fragment (**10**: ^{13}C NMR: $\delta = 84.5$; ^1H NMR: $\delta = 5.41$; **14**: ^{13}C NMR: $\delta = 69.0$; ^1H NMR: $\delta = 5.00$). The chemical shifts of the hydrogen atoms on the C3–C6 chain and their vicinial H,H coupling constants are very similar in the carbene complexes **10**–**13** and in ester **14**. This indicates that the incorporation of the metal–carbene function into the sugar framework does not impose any significant changes in the configuration and conformation.

Table 1. Characteristic ^{13}C NMR data for compounds **10**–**14** (100 MHz, $CDCl_3$, δ values). See Experimental Procedure for full charactization of **10**.

Compound	C-1	C-2	Yield [a]
10	355.0	84.5	64%
11	346.2	84.4	44%
12	328.2	86.0	42%
13	327.6	84.9	28%
14	167.3	69.0	–

[a] Yields of **10**–**13** based on **1**.

Based on the spectroscopic properties of complexes **10**–**13**, it can be expected that the electrophilicity of the carbene carbon atom and the acidity of the neighboring C–H function can be used for further controlled modification of the sugar framework.

Experimental Procedure

All experiments were conducted under argon with strict exclusion of air and moisture.

10: A suspension of **2** was prepared from potassium (0.45 g, 11.51 mmol), graphite (1.10 g, 92 mmol) and hexacarbonylchromium (1.18 g, 5.4 mmol) in 100 mL of THF. This suspension was cooled to −60 °C and a solution of **1** (2.16 mmol, 5.10 mmol) in 20 mL of THF was added dropwise. The reaction mixture was stirred a further 30 min, the solvent removed under vacuum, and the residue taken up in 120 mL of dichloromethane. This solution was cooled to −30 °C, trimethyloxonium tetrafluoroborate (0.73 g, 5.00 mmol) added, and the resulting solution stirred 5 h at 0–5 °C. To ensure complete alkylation another portion of trimethyloxonium tetrafluoroborate (0.44 g, 3.00 mmol) was added. After a further 5 h the crude product was absorbed onto silica gel (−60 °C), the solvent removed under vacuum, and the residue chromatographed (SiO_2, −15 °C, ether/petroleum ether/dichloromethane (1/1/1)) to give a fraction from which 1.93 g (64%) of **10** was isolated as an orange solid. A subsequent fraction yielded 0.21 g (10%) of methyl ester **14**. **10**: R_f (SiO_2, ether/petroleum ether, dichloromethane(1/1/1)): 0.70. M.p. 113–115 °C. FT-IR (KBr): ν(CO) [cm^{-1}] = 2071 (m), 1994 (m), 1959 (s), 1943 (vs), 1755 (s). ^1H NMR (400 MHz, $CDCl_3$): $\delta = 5.46$ (d, $J_{3,4} = 10.2$ Hz, H-3), 5.41 (bs, H-2), 5.26–5.34 (m, 2H, H-4, H-5), 4.82 (s, 3H, OCH_3), 4.30 (dd, $J_{6,6'} = 11.6$ Hz, $J_{5,6} = 4.5$ Hz, H-6), 3.72 (dd, $J_{6,6'} = 11.6$ Hz, $J_{5,6'} = 8.3$ Hz, H-6'), 2.31, 2.11, 2.04, 2.01, 1.99 (jeweils s, 3H, $OCOCH_3$). ^{13}C-NMR (100 MHz, $CDCl_3$): $\delta = 355.0$ (C=Cr), 223.0 (*trans*-CO), 215.5 (*cis*-CO), 170.5, 170.3, 170.1, 169.8, 169.3 ($OCOCH_3$), 84.5 (C-2), 68.9 (C-3), 68.0 (C-4), 67.7 (OCH_3), 67.5 (C-5), 62.4 (C-6), 20.9, 20.6, 20.6, 20.6, 20.5 ($OCOCH_3$). MS (FAB, mNBA (*m*-nitrobenzyl alcohol): m/z = 596 (12%, M^+), 456 (4%, $M^+ - 5\,CO$), 405 (12%, $M^+ - Cr(CO)_5$), 230 (100%, $M^+ - Cr(CO)_5 - Ac_2O - CH_2OAc$).

Compounds **11** and **12** were synthesized in an analogous fashion. **11**: yellow solid. M.p. 115–117 °C. MS (FAB, mNBA): m/z = 642 (14%, M^+). **12**: red solid. M.p. 130–132 °C. MS (FAB, mNBA): m/z = 728 (10%, M^+).

13: A suspension of anhydrous **5**·1.5 dioxane [12] was prepared from pentacarbonyliron (0.72, 5.4 mmol) dissolved in 5 mL of 1,4-dioxane, sodium (0.24 g, 10.7 mmol), and benzophenone (0.22 g, 1.2 mmol). This suspension was cooled to −60 °C and a solution of **1** (2.29 g, 5.4 mmol) in 15 mL of THF was added dropwise over 30 min. After 3 h the resulting red solution was concentrated to dryness under vacuum (oil pump) and the resulting reddish brown residue was taken up in 15 mL of diethyl ether and 2.5 mL of HMPA. This solution was cooled to −70 °C, a solution of ethyl trifluoromethanesulfonate (1.05 mL, 8.1 mmol) was added over 5 min, and the resulting solution was stirred for 16 h. The reaction mixture was absorbed onto silica gel and chromatographed (SiO_2, 0 °C, diethyl ether/petroleum ether/dichloromethane (1/1/1)) to provide 0.90 g (1.5 mmol, 28%) of **13** as a red solid (m.p. 91–93 °C).

Received: April 6, 1995 [Z 7873 IE]
German version: *Angew. Chem.* **1995**, *107*, 2023–2025

Keywords: carbene complexes · carbohydrates · metal-modified sugars · optically active carbene complexes

[1] Reviews: a) K. H. Dötz, *Angew. Chem.* **1984**, *96*, 573; *Angew. Chem. Int. Ed. Engl.* **1984**, *23*, 587; b) R. Aumann, *ibid.* **1988**, *100*, 1512 and **1988**, *27*, 1456; c) L. S. Hegedus, *Pure Appl. Chem.* **1990**, *62*, 691; d) W. D. Wulff in *Comprehensive Organic Synthesis, Vol. 5* (Eds.: B. M. Trost, I. Fleming), Pergamon, New York, **1991**, p. 1065.

[2] K. H. Dötz, *Angew. Chem.* **1975**, *87*, 672; *Angew. Chem. Int. Ed. Engl.* **1975**, *14*, 644.

[3] a) R. Hoffmann, *Angew. Chem.* **1982**, *94*, 725; *Angew. Chem. Int. Ed. Engl.* **1982**, *21*, 711; b) F. G. A. Stone, *ibid.* **1984**, *96*, 85 and **1984**, *23*, 89.

[4] Reviews: a) F. W. Lichtenthaler in *Modern Synthetic Methods* (Ed.: R. Scheffold), Helvetica Chimica Acta, Basel, **1992**; b) H. Kunz, K. Rück, *Angew. Chem.* **1993**, *105*, 355; *Angew. Chem. Int. Ed. Engl.* **1993**, *32*, 336.

[5] Reviews: a) R. O. Duthaler, A. Hafner, M. Riediker, *Pure Appl. Chem.* **1990**, *62*, 631; b) R. O. Duthaler, A. Hafner, M. Riediker in *Organic Synthesis via Organometallics* (Eds.: R. W. Hoffmann, K. H. Dötz), Vieweg, Wiesbaden, **1991**, p. 285; c) R. O. Duthaler, A. Hafner, *Chem. Rev.* **1992**, *92*, 807.

 © VCH Verlagsgesellschaft mbH, D-69451 Weinheim, 1995 0570-0833/95/3417-1857 $ 10.00+.25/0

[6] a) T. Kametani, K. Kawamura, T. Honda, *J. Am. Chem. Soc.* **1987**, *109*, 3010; b) J. C.-Y. Cheng, G. D. Daves, *J. Org. Chem.* **1987**, *52*, 3083; c) P. DeShong, G. A. Slough, V. Elango, G. L. Trainor, *J. Am. Chem. Soc.* **1985**, *107*, 7788; d) P. DeShong, G. A. Slough, V. Elango, *Carbohydr. Res.* **1987**, *171*, 342; e) A. Rosenthal, H. J. Koch, *Tetrahedron Lett.* **1967**, 871; f) G. L. Trainor, B. E. Smart, *J. Org. Chem.* **1983**, *48*, 2447.
[7] Only a few sugar-functionalized carbene complexes have been reported: a) products of the Michael addition of sugars to alkynyl carbene complexes: R. Aumann, *Chem. Ber.* **1992**, *125*, 2773; *ibid.* **1994**, *127*, 725; b) manganese, rhenium, gold, and platinum complexes: H. Fischer, J. Schleu, G. Roth, *ibid.* **1995**, *128*, 373; T. Pill, K. Polborn, W. Beck, *ibid.* **1990**, *123*, 11.
[8] a) M. F. Semmelhack, G. R. Lee, *Organometallics* **1987**, *6*, 1839; b) M. A. Schwindt, T. Lejon, L. S. Hegedus, *ibid.* **1990**, *9*, 2814.
[9] H. S. Isabell, H. L. Frush, *Bur. Stand. J. Res.* **1931**, *6*, 1145.
[10] M. L. Wolfrom, M. J. Berkebile, A. Thompson, *J. Am. Chem. Soc.* **1949**, *71*, 2360.
[11] M. F. Semmelhack, R. Tamura, *J. Am. Chem. Soc.* **1983**, *105*, 4099.
[12] R. G. Finke, T. N. Sorrell, *Org. Synth.* **1979**, *59*, 102.

Fluorocarbonate, $[FCO_2]^-$: Preparation and Structure**

Xiongzhi Zhang, Udo Gross, and Konrad Seppelt*

Fluorocarbonate (fluoroformate), $[FCO_2]^-$, should be a stable anion, because it is isoelectronic with nitrate. The only reports about it are of matrix reactions of CO_2 or COF_2 with vaporized and matrix-deposited CsF and Tl_2O in argon to form $[FCO_2]^-$,[1, 2] as well as an ion-cyclotron resonance experiment of the reaction of F^- with CO_2 in the gas phase.[3] The postulated reaction under pressure of CO_2 with CsF in CH_3CN could not be confirmed.[4, 5] According to calculations, the conjugate acid to the base $[FCO_2]^-$, fluoroformic acid, should be metastable with respect to decomposition into CO_2 and HF;[6] this, however, says nothing about intermolecular decomposition. Very recently a photoelectron spectrum of $[FCO_2]^-$, generated by reaction of F^- with CO_2 in a molecular beam, was recorded.[7]

Supplementary to earlier data,[5] we showed that neither crystalline CsF nor AgF underwent a significant increase in mass, even after long contact times with liquid CO_2 under pressure at room temperature. NOF also does not react. In contrast, CO_2 reacts spontaneously with anhydrous quaternary ammonium fluorides like tetramethylammonium fluoride,[8] neopentyl(trimethyl)ammonium fluoride, and 1,1,3,3,5,5-hexamethylpiperidinium fluoride (pip^+F^-)[9] both without solvent or dissolved in CH_2F_2 and CF_3CHFCF_3, which are particularly suitable solvents for piperidinium fluoride. $[FCO_2]^-$ salts are obtained as colorless, almost insoluble solids [Eq. (a) gives the reaction equation for the synthesis of the anion]. Because of the extremely poor solubility in nearly all conceivable solvents, the growth of single crystals has not yet been achieved, and structural analysis has had to be done by other methods.

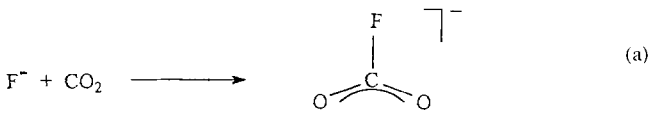

(a)

Besides the complete elemental analysis of $pip^+CO_2F^-$, the ^{13}C MAS NMR signal of $[(CH_3)_4N][FCO_2]$ is an almost unambiguous indication of the presence of the $[FCO_2]^-$ ion (Fig. 1), because it shows a $J_{C,F}$ coupling of 292 Hz. The splitting is independent of the NMR frequency (100.55 or 75.41 Hz), but disappears in a $\{^{19}F\}^{13}C$ decoupling experiment.

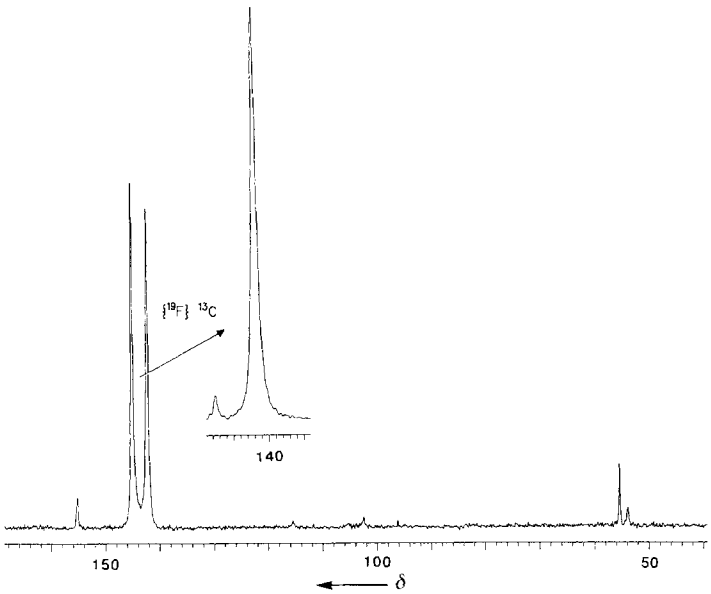

Fig. 1. $\{^1H\}^{13}C$ solid-state MAS NMR spectrum of $[(CH_3)_4][F^{13}CO_2]$, prepared from $[(CH_3)_4]F$ and $^{13}CO_2$. $B_0 = 100.557$ MHz, 5000 Hz angular velocity. $^1J(^{19}F,^{13}C) = 280.8$ Hz. The signal at $\delta = 55.39$ is attributable to the CH_3 groups with natural abundance of ^{13}C, that at $\delta = 155.21$ to a CO_3H^- impurity. Inset: $\{^{19}F\}^{13}C$ MAS NMR spectrum.

In freshly prepared solutions of $[FCO_2]^-$ in purest CH_3CN[10] a singlet is observed in the ^{19}F NMR spectrum. Depending on the fluoride content of the sample, this signal appears between $\delta = -65$ and $+18$, which suggests an exchange between F^- ions and $[FCO_2]^-$; the chemical shift of the fluoride ion in CH_3CN is $\delta = -71$. In the ^{13}C NMR spectrum of $[F^{13}CO_2]^-$ in CH_3CN a singlet appears at $\delta = 134.4$; the anticipated doublet splitting is not observed because of the exchange processes mentioned above.

The presence of moisture leads spontaneously to the formation of hydrogen carbonate,[11] hydrogen fluoride, and gaseous CO_2. Protic solvents, for example alcohols, cleave the CF bond immediately with evolution of CO_2 and the solvation of fluoride.

Indications about the structure of $[FCO_2]^-$ can be found in the IR (Fig. 2) and Raman spectra. Four of the six bands anticipated for a C_{2v} spectrum are definitely present; two further bands are weak as expected and are partly hidden by the intense bands of νCF and $\delta_s CO_2$ (Table 1). The Raman spectrum is dominated by cation bands, which have been well described;[8] the Raman emissions of the anion with its strongly polar bonds are very weak. Striking features among the stretching bands are the large difference between $\nu_{as}CO_2$ (1798 cm^{-1}) and $\nu_s CO_2$ (1275 cm^{-1}) and the low value for νCF (570 cm^{-1}). Qualitatively these observations can be explained by a very large O-C-O angle and a very weak C–F bond. To elucidate this problem we

[*] Prof. Dr. K. Seppelt, Dipl.-Chem. X. Zhang, Dr. U. Gross
Institut für Anorganische und Analytische Chemie der
Freien Universität Berlin
Fabeckstrasse 34–36, D-14195 Berlin (Germany)
Telefax: Int. code + (30)838-2424

[**] This work was supported by the Deutsche Forschungsgemeinschaft and the Fonds der Chemischen Industrie. Our thanks are also due to Hoechst AG for the gifts of fluorocarbons, Dr. Simon, Varian, Darmstadt, and Prof. Limbach and his research group, FU Berlin, for the measurement of the solid-state MAS NMR spectrum.

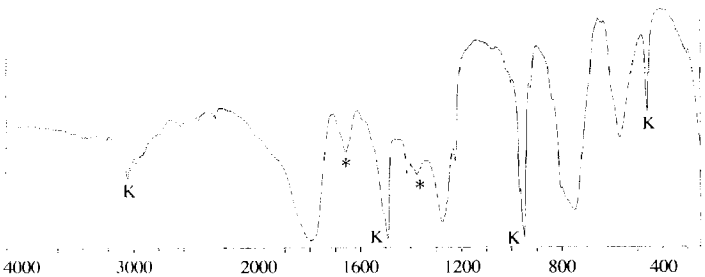

Fig. 2. IR spectrum of $[(CH_3)_4][FCO_2]$ (KBr [cm^{-1}]). K = cation bands; the two asterisks indicate the bands of the HCO_3^- impurity.

Table 1. Anion bands in the IR and Raman spectra of $[(CH_3)_4][FCO_2]$.

	$\nu_{as}CO_2(B_2)$	$\nu_sCO_2(A_1)$	$\gamma(B_1)$	$\delta_sCO_2(A_1)$	$\nu_{CF}(A_1)$	$\delta_{as}CO_2(B_2)$
IR ($[F^{12}CO_2]^-$)	1798vs	1275s	795sh	752s	570s	610?
IR ($[F^{13}CO_2]^-$)	1748vs	1261s		734s	567s	
Raman ($[F^{12}CO_2]^-$)	1795sh	1277m			570w	
Raman ($[F^{13}CO_2]^-$)	1750sh	1259m			569w	
MP2 ($[F^{12}CO_2]^-$)	1804(100)	1362(25)	760(2.5)	701(28)	483(20)	523(1.3)
MP3 ($[F^{12}CO_2]^-$)	1771	1262	788	763	574	551

calculated the structure with ab initio methods (Table 2). Even with small basis sets our calculations establish that $[FCO_2]^-$ is a stable anion, and the C_{2v} structure is apparently the global minimum on the potential hypersurface. The calculations indeed indicate (see Table 2) a large O-C-O angle of 136–138° and a strikingly long C–F bond (144–150 pm).[12] These results agree with those that were recently published.[7]

Table 2. Bond lengths and angles of the C_{2v} structure of $[FCO_2]^-$ (calculated) and NO_2F (calculated and experimental).

$[FCO_2]^-$	MP2	MP3	NO_2F	MP2	MP3	exp. [13]
C-F [pm]	150.5	144.6	N-F	153.6	141.2	146.7(15)
C-O [pm]	122.5	122.0	N-O	117.9	117.4	118.0(5)
O-C-O [°]	137.9	136.2	O-N-O	137.9	134.5	136.0(15)

The vibrational bands determined by ab initio calculations are in accord with experimental results after scaling. The intensities of the IR bands are correctly predicted as well. The weakness of the C–F bond in $[FCO_2]^-$ is also reflected in the strikingly small affinity of CO_2 for the F^- ion. This was determined to be $-132.6\ kJ\ mol^{-1}$ in the gas state[3] by ion-cyclotron resonance spectroscopy and calculated by us to be $-110.7\ kJ\ mol^{-1}$. For comparison, NO_2F, whose structure in the gas state has been reliably analyzed by microwave spectroscopy, was also calculated.[13] The results show that in particular the N–F bond length (like the C–F bond length) depends markedly on the basis set and on the approximations for electron correlation. Nevertheless, very long C–F or N–F bonds and a large O-C-O or O-N-O angle are always predicted. These are indeed found experimentally[13] in the case of NO_2F.

In one limit $[FCO_2]^-$ can be considered as a F^- ion solvated by CO_2, and it also behaves as such. After prolonged periods in CH_3CN a basic attack on the solvent takes place with formation of $[NC\ C(CO_2)_2H]^-$[14] and HF_2^-. $[FCO_2]^-$ therefore belongs to the fluoride oxides like NO_2F, NOF, NOF_3, and $[COF_3]^-$,[15, 16] which show pronounced negative hyperconjugation. The radical FCO_2, however, which has one electron less and which plays a role in the atmospheric chemistry of F–Cl compounds, apparently has a more normal structure: C–F 130–140 pm, C–O 121–127 pm, O-C-O ≈ 120°.[7, 17] The special features of the $[FCO_2]^-$ ion also become evident when it is compared with $[HCO_2]^-$, which has an O-C-O angle of 125.5° and C–O bond lengths of 125.6 pm.[18]

We have no evidence yet for the $[CO_2F_2]^{2-}$ ion, whose existence has already been postulated[2, 4] but questioned.[6] Products with the correct analytical composition have vibrational spectra that indicate a mixture of $[FCO_2]^-$ and F^-. Ab initio calculations for $[CO_2F_2]^{2-}$ with several basis sets yield no minimum on the potential hypersurface.

Molecules related to CO_2 like N_2O and $H_2C{=}C{=}CH_2$, and also CO, do not react with pip^+F^-. Apparently the fluoride affinities of these molecules are already so small that they no longer exceed that of the solvent or the cation. Our calculations gave the values depicted in Scheme 1 for the equilibrium structures and fluoride affinities. The small fluoride affinities compete with those of the solvent or the cation, for example, CH_2F_2 (see Scheme 2). Since the fluoride affinity of a CH_2F_2 molecule is the same size as that of CO, N_2O, and $H_2C{=}C{=}CH_2$, it is not surprising that in condensed phase no reaction takes place, especially as in this case a crystal structure study showed that a F^- ion is solvated by up to five CH_2F_2 molecules.[9] To force the reaction of CO, N_2O, and $CH_2C{=}C{=}CH_2$ with F^- a still less acidic solvent *and* cation is needed, because according to the crystal structure analysis, cation and CH_2F_2 associate almost as

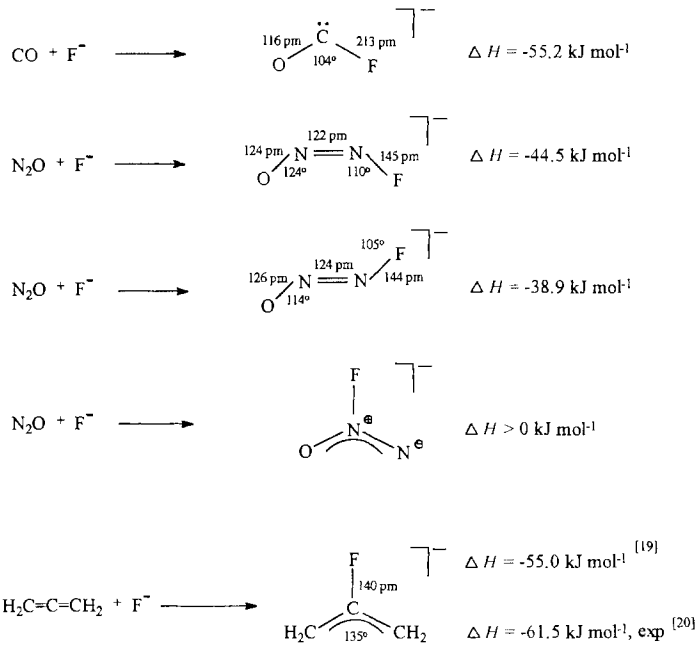

Scheme 1.

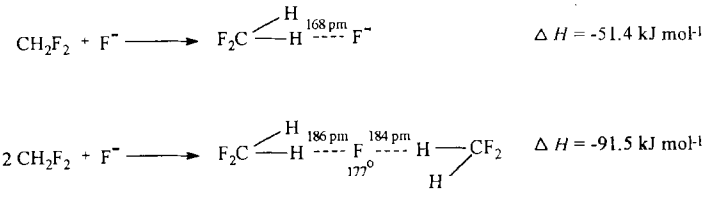

Scheme 2.

strongly with F^-.[7] The fluoride affinity of CO_2 in the presently known systems with "naked" fluoride ions appears to be the approximate lower limit for a reaction.

Received: March 15, 1995
Revised version: May 24, 1995 [Z 7797 IE]
German version: *Angew. Chem.* **1995**, *107*, 2019–2021

Keywords: ab initio calculations · carbon dioxide · fluoride ions fluorocarbonate · nonmetal chemistry

[1] B. S. Ault, *Inorg. Chem.* **1982**, *21*, 756–759.
[2] S. J. David, B. S. Ault, *Inorg. Chem.* **1985**, *24*, 1238–1241.
[3] T. B. McMahon, C. J. Northcott, *Can. J. Chem.* **1978**, *56*, 1069–1074.
[4] E. Martineau, J. B. Milne, *J. Chem. Soc. Chem. Commun.* **1971**, 1327.
[5] L. Lawlor, J. Passmore, *Inorg. Chem.* **1979**, *18*, 2923–2930.
[6] Z. Havlas, T. Kovar, R. Zahradnik, *J. Am. Chem. Soc.* **1985**, *107*, 7243–7246.
[7] D. W. Arnold, S. E. Bradforth, E. H. Kim, D. M. Newmark, *J. Chem. Phys.* **1995**, *102*, 3439–3509.
[8] K. O. Christe, W. W. Wilson, R. D. Wilson, R. Bau, J. Feng, *J. Am. Chem. Soc.* **1990**, *112*, 7619–7625.
[9] A.-R. Mahjoub, X. Zhang, K. Seppelt, *Chem. Eur. J.* **1995**, *1*, 261–265.
[10] J. M. Winfield, *J. Fluorine Chem.* **1984**, *25*, 91–98.
[11] 1,1,3,3,5,5,-Hexamethylpiperidinium hydrogen carbonate · CH_3CN: $a = 1210.6(2)$, $b = 830.7(2)$, $c = 1715.8(2)$, $\beta = 109.98(1)^\circ$, $P2_1/c$, $Z = 4$. Well-formed crystals of $pip^+CO_3H^-$ are easy to confuse with $pip^+[FCO_2]^-$ in a crystal structure analysis.
[12] Gaussian 92, basis set 6-311 + G(d,p), Møller–Plesset approximation MP2 and MP3 for the electron correlation.
[13] A. C. Legon, D. J. Millen, *J. Chem. Soc. A* **1968**, 1736–1740.
[14] To our knowledge cyanomalonic acid has not been described. Only the monoester of the acid is known: E. Lehman, B. Züge, *Chem. Ber.* **1954**, *87*, 443.
[15] J. Arlt, M. Jansen, *Chem. Ber.* **1991**, *124*, 321–327.
[16] W. B. Farnham, B. E. Smart, W. J. Middleton, J. C. Calabrese, D. A. Dixon, *J. Am. Chem. Soc.* **1985**, *107*, 4565–4567.
[17] G. A. Argüello, H. Grothe, M. Kronenberg, H. Willner, *J. Phys. Chem.*, in press.
[18] H. Fuess, J. W. Bats, H. Damöhl, H. Meyer, A. Schweig, *Acta Crystallogr. Sect. B* **1982**, *38*, 736–743.
[19] See also: S. M. Khalil, H. M. Jarjis, *Z. Naturforsch. A* **1987**, *42*, 761–766; on the relative stability of $[CH_2C{=}CF{-}CH_2]^-$ versus $CH_2C{=}C{=}CH{-}H\cdots F^-$, see also M. Roy, T. B. McMahon, *Can. J. Chem.* **1985**, *63*, 708–715.
[20] The fluoride ion affinity of $[H_2C{=}C{=}CH_2]^-$ was calculated to be 15 kcal mol^{-1} by using the acidity of $CH_3CF{=}CH_2$ measured by ion-cyclotron resonance spectroscopy [3].

$[Ni_3(alkyne)_4]$—The First Homoleptic Alkyne–Metal Oligomer (Alkyne: 2,5,5-Trimethylhex-3-yn-2-ol)**

Dirk Walther,* Thomas Klettke, and Helmar Görls

Compounds that consist solely of a combination of a d^{10} metal(0) center and an alkyne should be able to form a "homologous series" of composition $[M_n(alkyne)_{n+1}]$, in which each alkyne connects two metal centers and the ends of the chain of metal atoms are coordinated to terminally bound alkynes.

[*] Prof. Dr. D. Walther, Dipl.-Chem. T. Klettke
Institut für Anorganische und Analytische Chemie der Universität
August-Bebel-Strasse 2, D-07743-Jena (Germany)
Telefax: Int. code + (3641) 6-35538
e-mail: cdw@fsuj50.rz.uni-jena.de
Dr. H. Görls
Max-Planck-Gruppe CO_2-Chemie an der Universität Jena (Germany)

[**] This work was supported by the Deutsche Forschungsgemeinschaft (SFB 247, Heidelberg), the Max-Planck-Gesellschaft (Arbeitsgruppe CO_2-Chemie), and the Fonds der Chemischen Industrie.

Oligomeric examples of these homoleptic compounds are of interest on account of their bonding relationships,[1] and also because of the possibility of simulating interactions of alkynes on metal surfaces. Catalytic properties and reactions of the chain ends might be of some practical significance, and may also be exploited for the construction of multimetal systems with different metals.

Until now, there has been no proof of the existence of such series. Apart from monomers,[2, 3] only $[Pt_2L_3]$ has been isolated and investigated by NMR spectroscopy,[4] but the solid-state structure is not known. The complex $[Fe_2L_4]$ (L: bis(trimethylsilyl)acetylene) is more electron-rich, as the d^8 system contains iron(0) centers.[5] The concept of utilizing peripheral hydrogen-bonding as a means of stabilizing homoleptic alkyne–Ni compounds[3] also proved successful in the synthesis of the first homoleptic alkyne–metal trimer.

Upon reaction of 2,5,5-trimethylhex-3-yn-2-ol with [Ni(cdt)] (cdt: cyclododeca-1,5,9-triene) in pentane, the red, crystalline air-sensitive compound $[Ni_3(alkyne)_4]$ **1** may be isolated, even when the reactants are introduced in a molar ratio of 2:1. Complex **1** dissolves well in THF, is reasonably soluble in ether and pentane, and is stable in the solid state at room temperature.

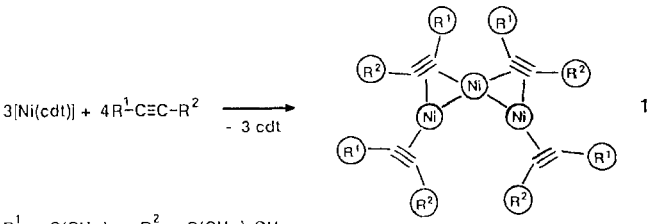

1

$R^1 = C(CH_3)_3$; $R^2 = C(CH_3)_2OH$

According to the crystal structure analysis,[6] the nickel(0) centers form a bent three-membered chain with a Ni-Ni-Ni angle of approximately 118° and an average Ni–Ni distance of 2.56 Å (Fig. 1). The terminal Ni centers each bind one bridging and one terminal alkyne ligand, whereas the central Ni atom is surrounded by two bridging alkynes.

Thus, **1** is held together by metal–metal bonds as well as twelve Ni–C bonds. The Ni–C bonds display normal bond lengths (1.88–1.97 Å). The groups R^1 and R^2 exert an influence only on the Ni–C bond lengths of the bridging alkynes: shorter bonds are formed between the terminal Ni centers and the C atoms bearing R^2 substituents, whereas this is reversed for Ni2. As expected, the C≡C bond lengths of the terminally bound alkynes are shorter than those of the bridging alkynes (average lengths 1.25 and 1.32 Å, respectively). Agostic interactions between the

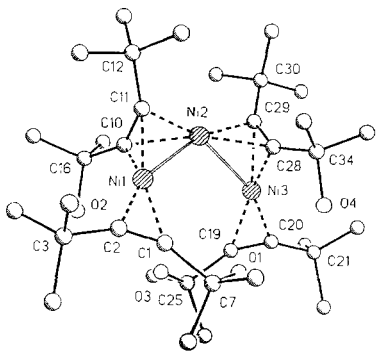

Fig. 1. Crystal structure of **1**. Selected distances [Å] and angles [°]: Ni1-Ni2 2.5468(6), Ni2-Ni3 2.5682(6), Ni1-C1 1.889(3), Ni1-C2 1.879(3), Ni1-C10 1.887(3), Ni1-C11 1.958(3), Ni2-C10 1.975(3), Ni2-C11 1.917(3), Ni2-C28 1.965(3), Ni2-C29 1.927(3), Ni3-C19 1.883(4), Ni3-C20 1.892(4), Ni3-C28 1.889(3), Ni3-C29 1.941(3), C1-C2 1.250(5), C10-C11 1.320(4), C19-C20 1.259(5), C28-C29 1.323(5); Ni1-Ni2-Ni3 118.03(2), C1-C2-C3 153.4(4), C2-C1-C7 152.7(3), C10-C11-C12 146.0(3), C11-C10-C16 146.3(3), C19-C20-C21 155.1(4), C20-C19-C25 153.1(4), C28-C29-C30 147.1(3), C29-C28-C34 146.8(3).

H atoms of the methyl groups and the metal atoms are not observed. Finally, the tolerance of the Ni_3 chain towards the peripheral OH groups is noteworthy.

The OH groups form three intramolecular and two intermolecular hydrogen bonds, such that the trimeric units are joined into a polymeric "rope" (Fig. 2). Since only a slight difference in energy is anticipated for the individual members of the hypothetical series $[M_n(alkyne)_{n+1}]$, these additional possibilities for stabilization might be crucial for the synthesis.

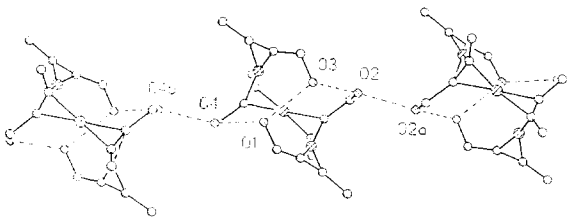

Fig. 2. Hydrogen bonding system in **1**. For clarity the methyl groups are omitted. Selected distances [Å]: O1-O3 2.842(4), O1-O4 2.751(4), O2-O3 2.780(4), O2-O2a 2.862(4), O4-O4b 2.817(4); symmetry transformation for a: $-x, 1-y, -z$; and for b: $1-x, 2-y, 1-z$.

As expected, in the IR spectrum of **1**, only two bands for C≡C stretching vibrations occur in the region for coordinated triple bonds, at 1638 and 1887 cm^{-1} (bridging and terminal alkynes, respectively).

In the 400 MHz ^{13}C NMR spectrum of **1** ([D$_8$]THF, −15 °C), the four signals of the coordinated bridging and terminal C≡C groups may be identified between $\delta = 147.1$ and 130.5. The signals for $C(CH_3)_2OH$ occur at $\delta = 69.0$ and 69.9. The highest field signals are those of $C(CH_3)_3$ at $\delta = 31.4$ and 31.5. A further eight signals in the region $\delta = 32.0-34.8$ are assigned to the methyl groups. The ^1H NMR spectrum ([D$_8$]THF, −15 °C) shows, as expected, only signals in the methyl group region and for the two OH groups. A more extensive evaluation of the spectrum is made difficult by the considerable overlap of the signals, such that it is not possible to identify which methyl signals are doubled.

Complex **1** reacts in the presence of *N*,*N*,*N*′,*N*′-tetramethylethylenediamine (tmeda) to form the dinuclear complex **2**, which may be isolated as red crystals. The two nickel

$[(tmeda)Ni_2(alkyne)_2]$ **2**

centers in **2** are connected by a bridging alkyne and a Ni–Ni bond, as demonstrated by a crystal structure analysis.[7] The second alkyne is terminally bound to one of the nickel centers, whereas at the other nickel center the tmeda functions as a chelate ligand. Thus, **2** has a structure analogous to that of the dinuclear complex $[(tmeda)Ni_2L_2]$ [L = 2,5-dimethylhex-3-yn-2,5-diol (tetramethylbutynediol)], which we reported previously.[3]

Complex **1** catalyzes the cyclooligomerization of prop-2-yn-1-ol; the selectivity is very solvent- and temperature-dependent. At 114 °C and without additional solvent, 95% cyclooctatetraene and 5% benzene derivatives are formed, according to NMR spectroscopic evidence.[8] Of the cyclotetramers, the symmetrical cycloocta-1,3,5,7-tetraene-1,3,5,7-tetramethanol predominates (70%); in addition, roughly 30% of the isomeric 1,3,5,8-tetramethanol is formed.

At −25 °C in THF, the oligoselectivity is far lower: a molar ratio of cyclooctatetraene:benzene derivatives of 63:37 was determined by NMR spectroscopy. We attribute this difference to a partial blocking of the coordination sites at the central Ni atom by alkyne ligands at −25 °C, which favors the cyclotrimerization. At 114 °C, on the other hand, the cyclotetramerization proceeds at "naked" nickel center and is reflected in the higher selectivity.[8]

Experimental Procedure

All transformations were carried out under argon.

1: Ni(cdt) (1.8 mmol) and 2,5,5-trimethylhex-3-yn-2-ol (3.6 mmol) were allowed to react together in *n*-pentane (10 mL) at −40 °C. After the reaction mixture was warmed to room temperature and filtered, dimethoxyethane (2 mL) was added. After 5 h the mixture was cooled to −78 °C and the precipitate recrystallized from *n*-pentane. Burgundy microcrystals, yield ca. 30%. Ni 23.72 (calc. 23.67)%. Single crystals from ether (with 0.5 mol ether). IR(Nujol): $\tilde{\nu} = 1887$ (C≡C), 1638 (C≡C), 3246 cm^{-1} (OH). ^1H-NMR ([D$_8$]THF, −15 °C, 400 MHz): $\delta = 1.21$, 1.26, 1.33, 1.38, 1.46, 1.50, 1.66 (CH_3), 5.65, 6.62 (OH). ^{13}C-NMR ([D$_8$]THF, −15 °C, 400 MHz): $\delta = 31.4$, 31.5 ($C(CH_3)_3$), 32.0, 32.2, 32.4, 32.6, 33.6, 33.9, 34.4, 34.8 (CH_3), 69.0, 69.9 ($C(CH_3)_2OH$), 130.5, 136.6, 142.5, 147.1 (C≡).

2: Ni(cdt) (1.4 mmol) and 2,5,5-trimethylhex-3-yn-2-ol (1.7 mmol) were allowed to react together in *n*-pentane (10 mL) at −60 °C. After warming to room temperature and filtration, the mixture was cooled to −40 °C and tmeda (23 mmol) added. Warming to 20 °C during 2 h and concentration of the solution to 4 mL led, at 0 °C, to **2**. Black-red crystals, yield 47%. Ni 22.78 (calc. 22.83)%. IR (Nujol): $\tilde{\nu} = 1839$ (C≡C), 1587 (C≡C), 3429 cm^{-1} (OH); crystal structure determination: ref. [7].

Received: March 31, 1995 [Z 7852 IE]
German version: *Angew. Chem.* **1995**, *107*, 2022–2023

Keywords: alkyne complexes · nickel compounds · oligomers

[1] D. M. Hoffman, R. Hoffmann, *J. Chem. Soc. Dalton Trans.* **1982**, 1471–1482.
[2] a) F. D. Rochon, T. Theophanides, *Can. J. Chem.* **1972**, *50*, 1325–1327; b) R. J. Dubey, *Acta Crystallogr. Sect. B* **1975**, *31*, 1860–1864; c) N. M. Boag, M. Green, D. M. Grove, J. A. K. Howard, J. L. Spencer, F. G. A. Stone, *J. Chem. Soc. Dalton Trans.* **1980**, 2170–2190.
[3] D. Walther, A. Schmidt, T. Klettke, H. Görls, W. Imhof, *Angew. Chem.* **1994**, *106*, 1421–1424; *Angew. Chem. Int. Ed. Engl.* **1994**, *33*, 1373–1376.
[4] N. M. Boag, M. Green, J. A. K. Howard, F. G. A. Stone, H. Wadepohl, *J. Chem. Soc. Dalton Trans.* **1981**, 862–872.
[5] H. Schäufele, H. Pritzkow, U. Zenneck, *Angew. Chem.* **1988**, *100*, 1577–1578; *Angew. Chem. Int. Ed. Engl.* **1988**, *27*, 1519.
[6] Crystal data for **1**: Four-circle diffractometer CAD4 (Enraf-Nonius), $Mo_{K\alpha}$ radiation, $\lambda = 0.71069$ Å, $\omega - 2\theta$ scan, empirical absorption correction (psi scan, max.–min. transmission: 0.99–0.89), structure solution: direct methods (SHELXS-86), refinement with SHELXL-93 versus F_o^2; $C_{36}H_{64}O_4Ni_3 \cdot 0.5\,C_4H_{10}O$, dark red parallelepiped, $0.40 \times 0.38 \times 38$ mm^3, $M = 777.1$ $g\,mol^{-1}$, triclinic, $a = 12.051(1)$, $b = 14.111(1)$, $c = 14.379(2)$ Å, $\alpha = 99.43(1)$, $\beta = 101.74(1)$, $\gamma = 93.84(1)°$, $V = 2219.9(4)$ $Å^3$, space group $P\bar{1}$ (No. 2), $Z = 2$, $\rho = 1.16$ $g\,cm^{-3}$, $\mu = 12.9$ cm^{-1}, $T = 183(2)$ K, 10539 measured reflections, 10128 symmetry-independent reflections, of which 7874 were observed ($I > 2\sigma(I)$), hydrogen atoms of the OH groups located by difference-Fourier syntheses, the remaining hydrogen atoms calculated for ideal positions and incorporated in the refinement as rigid groups with a common isotropic temperature factor, 443 refined parameters, $R1 = 0.043$, $wR2 = 0.125$, residual electron density 1.01 $eÅ^{-3}$. Further details of the crystal structure investigation may be obtained from the Director of the Cambridge Crystallographic Data Center, 12 Union Road, GB-Cambridge CB2 1EZ (UK), on quoting the full literature citation.
[7] T. Klettke, Diplomarbeit, Universität Jena, **1994**.
[8] D. Walther, D. Braun, W. Schulz, W. Rosenthal, *Z. Anorg. Allg. Chem.* **1989**, *577*, 270–282.

 © VCH Verlagsgesellschaft mbH, D-69451 Weinheim, 1995 0570-0833/95/3417-1861 $ 10.00+.25/0

Molecular Mosaics Formed by a Square Cyclophane and Its Inclusion Complex with Ferrocene**

Peter R. Ashton, Christian G. Claessens, Wayne Hayes, Stephan Menzer, J. Fraser Stoddart,* Andrew J. P. White, and David J. Williams

Self-assembly processes have been employed[1] successfully to create with precision molecular assemblies and supramolecular arrays previously unattainable by conventional chemistry. One-, two-, and three-dimensional solid-state arrays and networks incorporating hydrogen bonds,[2] metal–ligand interactions,[3] and π–π stacks as recognition motifs[4] have all been designed rationally and to some extent, realized.[5] There is a feeling growing in the scientific community that the range of novel molecular and supramolecular architectures being developed at present will lead ultimately to the emergence of a new generation of materials.[6] In order to exploit the novel properties already being exhibited[7] by some of these architectures, a more fundamental understanding of the molecular recognition phenomena that give rise to these properties is required. With all these features and criteria in mind, we have designed a self-complementary cyclophane **4**·4PF_6, which can express itself simultaneously as both an *exo* and an *endo* receptor (Scheme 1). The incorporation of two hydroquinone rings and two bipyridinium units in diametrically opposite positions creating a boxlike shape gives 4^{4+} the potential to form a highly structured two-dimensional array of stacked π-donor/π-acceptor systems after a mosaiclike fashion, while retaining the ability to bind either π-electron rich or π-electron deficient substrates. Here, we report (i) the synthesis of the cyclophane **4**·4PF_6, (ii) its ability to form a 1:1 adduct with the organometallic sandwich compound ferrocene (Fc) in solution, as evidenced by UV and ^{1}H NMR spectroscopic studies, and (iii) the X-ray crystallographic characterization of both the molecular and supramolecular structures of the free (**4**·4PF_6) and complexed (**4**/Fc·4PF_6) cyclophane, respectively.

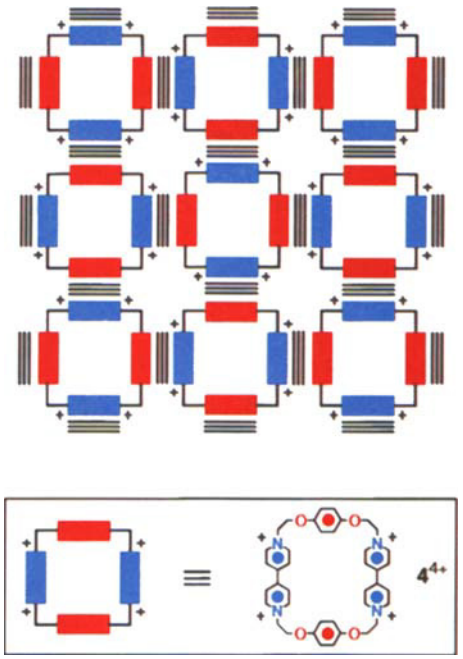

Scheme 1. Schematic representation of the expected solid-state structure of cation 4^{4+} in a crystalline salt.

The tetracationic cyclophane 4^{4+} was prepared as a PF_6 salt by the route shown in Scheme 2. The dibromide **2** was obtained by bromination[8] of the diol **1** with PPh_3Br_2 in MeCN. Portionwise addition of **2** over seven days to a tenfold excess of bipyridine in MeCN afforded, after counterion exchange, **3**·2PF_6.[9, 10] Reaction of **3**·2PF_6 with the dibromide **2** in DMF using 1,5-bis[(2-hydroxyethoxy)ethoxy]naphthalene (BHEEN) as a template afforded, after counterion exchange, the desired salt **4**·4PF_6 in 12% yield.

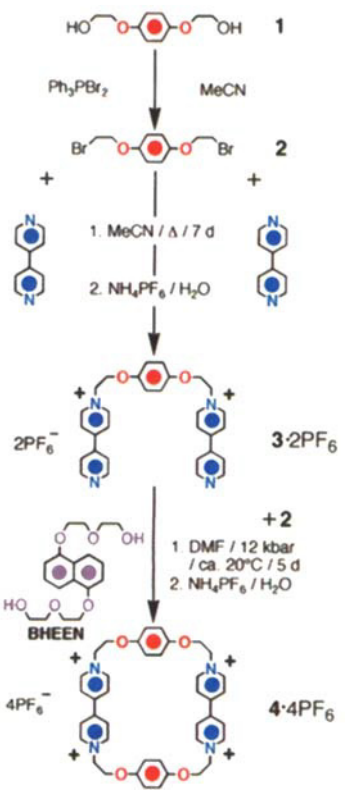

Scheme 2. Template-directed synthesis of the square tetracationic cyclophane 4^{4+}.

The X-ray structural analysis[10, 11] of **4**·4PF_6 reveals that the cyclophane has an open geometry with C_2 symmetry and with the two $CH_2OC_6H_4OCH_2$ units having a *syn* relationship of their OCH_2 groups (Fig. 1). The profile of the molecule is almost square with distances between the corner NCH_2 carbon atoms of 9.88 Å and 9.94 Å for the sides incorporating the bipyridinium units and the hydroquinone rings, respectively.[12] The vectors joining these four carbon atoms form a parallelogram[13] with angles of 88 and 92°. There is a retention of near coplanarity of the oxybismethylene units with the hydroquinone ring. There are marked twists (20°) about the central C–C bonds of the two bipyridinium units and a small amount of bowing, with the two NCH_2 bonds in both instances subtending angles of 11°. Whereas the planes of the bipyridinium units are essentially orthogonal to the mean plane of the cyclophane, the planes of the hydroquinone rings are appreciably inclined (by 59°). A study of the packing of the tetracation 4^{4+} shows that the expected two-dimensional π-donor/π-acceptor mosaic is present in the solid state (Fig. 1). Adjacent cyclophanes within any two-dimensional sheet are slightly stepped (Fig. 1b), whilst still retaining a proximal relationship between one of the pyridinium rings in one tetracation and a hydroquinone ring in the next and vice versa. The centroid–centroid separation between these rings in adjacent cyclophanes is 4.0 Å and the planes

[*] Prof. J. F. Stoddart, P. R. Ashton, C. G. Claessens,[+] W. Hayes
School of Chemistry, University of Birmingham
Edgbaston, Birmingham B15 2TT (UK)
Telefax: Int. code + (121) 414-3531
Dr. S. Menzer, Dr. A. J. P. White, Dr. D. J. Williams
Chemical Crystallography Laboratory
Imperial College, London (UK)
[+] Permanent address: Ecole Normal Supérieure de Lyon (France)

[**] This research was supported by the Engineering and Physical Sciences Research Council and the Wolfson Foundation in the UK and by the Minstère de la Recherche et de l'Enseignement Supérieur in France. We are grateful to Prof. A. Collet (Lyon) for helpful discussions.

 © VCH Verlagsgesellschaft mbH, D-69451 Weinheim, 1995 0570-0833/95/3417-1862 $ 10.00+.25/0

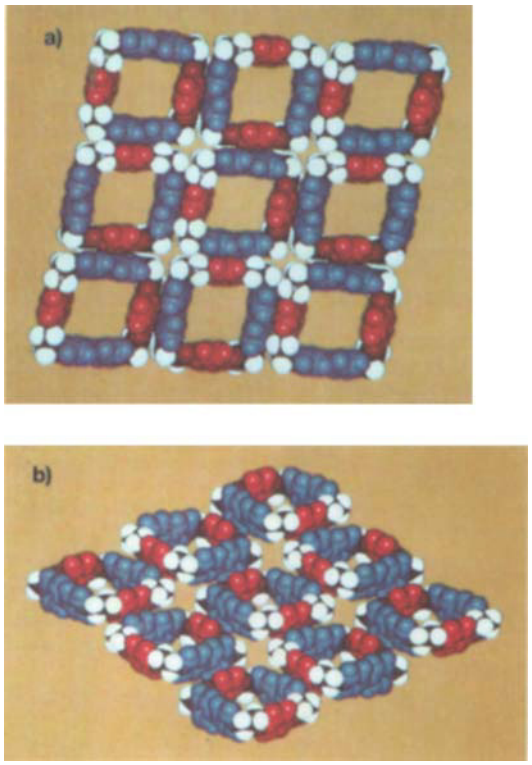

Fig. 1. a) Front view and b) side view in perspective of the packing of $\mathbf{4}^{4+}$ in the solid state (space-filling representations).

of the rings are inclined by 22°. Although adjacent sheets are separated by layers of disordered PF_6^- ions and MeCN molecules, the tetracations are in register and form channels that extend through the crystal (Fig. 2).[14]

Mixing equimolar amounts of $\mathbf{4}\cdot 4PF_6$ and ferrocene (Fc) in MeCN produces a bright green solution, which we associate with the formation of a 1:1 adduct $\mathbf{4}/Fc\cdot 4PF_6$ in the form of an inclusion complex that also displays a charge transfer (CT) interaction.[15] A UV spectrophotometric titration, using the CT band centered on 602 nm, yields an association constant K_a of $44 \pm 3\ dm^3\,mol^{-1}$ for the 1:1 adduct $\mathbf{4}/Fc\cdot 4PF_6$ in MeCN at 25°C. This K_a value corresponds to a free energy of adduct formation of $-2.2\ kcal\,mol^{-1}$. In the ^1H NMR spectrum of $\mathbf{4}/Fc\cdot 4PF_6$ (5.5×10^{-3} M in CD_3CN) significant upfield shifts are observed for the resonances of the cyclopentadienyl ring protons of Fc ($\Delta\delta = -0.29$) and also for the bipyridinium β-protons of $\mathbf{4}^{4+}$ ($\Delta\delta = -0.08$), indicating that the ferrocene molecule resides within the tetracationic cyclophane with its cyclopentadienyl rings oriented parallel to the plane of the two bipyridinium units in the tetracation. Consequently, it was anticipated that inclusion of ferrocene in this manner should permit the retention (Scheme 3) of the mosaiclike array proposed (Scheme 1) and observed (Fig. 1) in the solid state for $\mathbf{4}\cdot 4PF_6$.

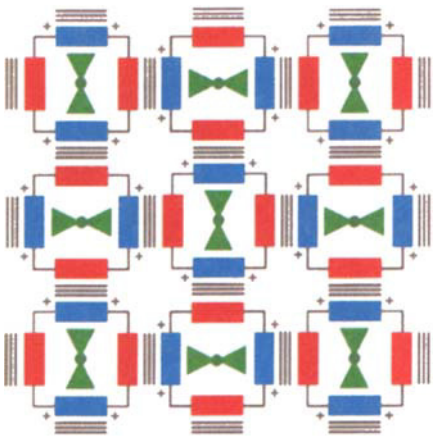

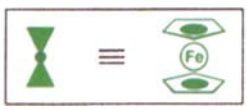

Scheme 3. Schematic representation of the anticipated structure of the 1:1 adduct $\mathbf{4}/Fc^{4+}$ in a crystalline salt.

The X-ray crystallographic analysis[10, 16] of $\mathbf{4}/Fc\cdot 4PF_6$ reveals a C_i-symmetric adduct in which the iron atom of the ferrocene molecule is located on a crystallographic symmetry center and the cyclopentadienyl rings are sandwiched between the faces of the two bipyridinium units (Fig. 3). The structure of the cyclophane is very similar to that of $\mathbf{4}\cdot 4PF_6$; the *syn* arrangement of the $CH_2OC_6H_4OCH_2$ groups is retained and the distances between the corner NCH_2 carbon atoms are 9.83 and 9.95 Å with associated angles of 88 and 92° (as before!).[17] The

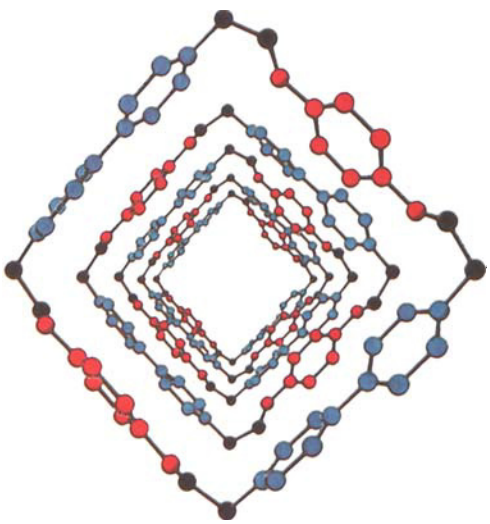

Fig. 2. View down a channel of $\mathbf{4}^{4+}$ ions in the solid state (ball-and-stick representation).

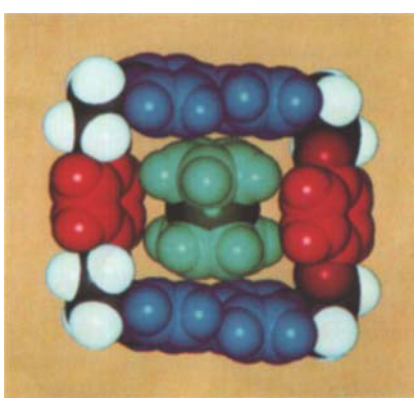

Fig. 3. Space-filling representation of $\mathbf{4}/Fc^{4+}$ in the X-ray structure of $\mathbf{4}/Fc\cdot 4PF_6$.

torsional twists within the bipyridinium units are 19° and these units are bowed by 7°. The planes of the bipyridinium units are again essentially orthogonal with respect to the mean plane of the cyclophane, but the inclination of the hydroquinone rings is increased by 5° to 54°. The bipyridinium/bipyridinium and hydroquinone/hydroquinone centroid–centroid separations are 10.1 and 10.2 Å, respectively. The distance from the center of the C–C bond of the bipyridinium unit and the centroid of the adjacent cyclopentadienyl ring of the ferrocene is 3.4 Å, and the vector linking these two centroids is inclined by 88° to the cyclopentadienyl ring plane. The packing of the 1:1 adducts (Fig. 4) is virtually identical to that of the free cyclophane

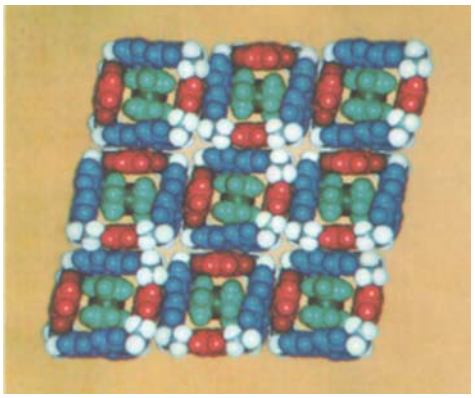

Fig. 4. View of the packing of the 1:1 adduct $\mathbf{4}/Fc^{4+}$ in the solid state (space-filling representation).

(Fig. 1a). A slightly stepped two-dimensional mosaic is observed with improved π–π stacking between the hydroquinone ring of one molecule and one of the pyridinium rings of the bipyridinium unit in an adjacent molecule. The pyridinium/hydroquinone ring centroid separations are reduced to 3.8 Å and their planes are much closer to parallel, with an inclination of only 6° (cf. 22° in $\mathbf{4}\cdot 4PF_6$). The packing of the sheets is again virtually identical to that observed for the free cyclophane; adjacent sheets are approximately in register and form partially filled channels that extend in the crystallographic *a* direction. The distance between the sheets is 9.8 Å and the interstices are occupied by MeCN and H_2O molecules and by the PF_6^- ions.

The self-assembly of $\mathbf{4}\cdot 4PF_6$ is possible as a result of sufficient information in the form of molecular recognition elements being programmed into its constituent molecular components. The information present in the symmmetrical cyclophane facilitates the efficient self-organization of a regular repeating two-dimensional supramolecular array in the solid state. The symmetrically oriented molecular recognition elements of the cyclophane $\mathbf{4}\cdot 4PF_6$ have also allowed the directionally specific inclusion of ferrocene within its cavity to form the 1:1 adduct $\mathbf{4}/Fc\cdot 4PF_6$. The ability of both $\mathbf{4}\cdot 4PF_6$ and $\mathbf{4}/Fc\cdot 4PF_6$ to generate supramolecular order on the nanometer scale in the crystalline state marks a significant development in the fields of both crystal engineering[5] and supramolecular chemistry.[6] Furthermore, it is believed that, in the solution state, the inclusion of organometallic species[18] within cyclophanes of this type, featuring π–π stacking molecular recognition motifs, will open up novel routes to new mechanically interlocked molecular systems.[19] Also, as further fascinating examples of second-sphere coordination,[20] they could find application in the design of artificial enzymes[21]—or indeed they might ultimately play a significant role in the construction[22] of functioning nanoscale devices.[23]

Experimental Procedure

$\mathbf{3}\cdot 2PF_6$: During seven days, **2** (1.05 g, 3.2 mmol) was added portionwise three times a day (50 mg per portion) to a refluxing solution of 4,4′-bipyridine (5.05 g, 32.4 mmol) in dry MeCN (100 mL) under nitrogen. The reaction mixture was maintained under reflux for a further 48 h before it was allowed to cool down to room temperature. The greenish brown precipitate was filtered, dissolved in a mixture of acetone and water, and purified by column chromatography [SiO_2; MeOH/2N aqueous $NH_4Cl/MeNO_2$ (7:2:1)] to yield, after counterion exchange, $\mathbf{3}\cdot 2PF_6$ as a yellow solid (1.3 g, 50%, m.p. >250 °C); FABMS: *m/z*: 621 ($[M - PF_6]^+$); ^1H NMR (300 MHz, CD_3COCD_3): $\delta = 4.65$ (t, 4H), 5.32 (t, 4H), 6.92 (s, 4H), 7.99 (d, 4H), 8.72 (d, 4H), 8.87 (d, 4H), 9.42 (d, 4H); ^{13}C NMR (75.5 MHz, CD_3CN): $\delta = 61.7, 67.5, 116.8, 123.2, 127.0, 142.1, 146.6, 152.2, 153.6, 155.7$. Single crystals suitable for X-ray crystallography were grown from aqueous acetone.

$\mathbf{4}\cdot 4PF_6$: A solution of **2** (32.4 mg, 0.1 mmol), $\mathbf{3}\cdot 2PF_6$ (76.6 mg, 0.1 mmol), and BHEEN (100.9 mg, 0.3 mmol) in dry DMF (10 mL) was transferred to a high-pressure reaction Teflon tube and compressed (12 kbar) at room temperature for 5 d. The precipitate that resulted on addition of Et_2O (150 mL) was filtered off and purified by column chromatography [SiO_2; MeOH/2N aqueous $NH_4Cl/MeNO_2$ (7:2:1)] to yield, after counterion exchange, $\mathbf{4}\cdot 4PF_6$ as a deep yellow solid (15 mg, 12%, m.p. >260 °C, FABMS: *m/z*: 1075 ($[M - PF_6]^+$); ^1H NMR (300 MHz, CD_3CN): δ: = 4.31 (t, 8H), 4.98 (t, 8H), 6.71 (s, 8H), 8.36 (d, 8H), 8.94 (d, 8H); ^{13}C NMR (75.5 MHz, CD_3CN): δ: = 62.3, 67.5, 116.3, 127.6, 147.3, 150.8, 153.5. Single crystals suitable for X-ray crystallography were grown by vapor diffusion of iPr_2O into a solution of $\mathbf{4}\cdot 4PF_6$ in MeCN.

$\mathbf{4}/Fc\cdot 4PF_6$ (5.5×10^{-3} M): ^1H NMR (300 MHz, CD_3CN): $\delta = 3.87$ (s, 10H), 4.31 (t, 8H), 4.96 (t, 8H), 6.74 (s, 8H), 8.28 (d, 8H), 8.89 (d, 8H). Single crystals suitable for X-ray crystallography were grown by vapor diffusion of iPr_2O into a 1:1 solution of $\mathbf{4}\cdot 4PF_6$ and ferrocene in MeCN.

Received: April 6, 1995 [Z 7872 IE]
German version: *Angew. Chem.* **1995**, *107*, 1994–1997

Keywords: host–guest chemistry · nanotubes · sandwich complexes · self-assembly

[1] J. S. Lindsey, *New J. Chem.* **1991**, *15*, 153–180; G. M. Whitesides, J. P. Mathias, C. T. Seto, *Science* **1991**, *254*, 1312–1319; D. Philp, J. F. Stoddart, *Synlett* **1991**, 445–461.

[2] H. M. Colquhoun, J. F. Stoddart, D. J. Williams, *J. Chem. Soc. Chem. Commun.* **1981**, 847–849; H. M. Colquhoun, D. F. Lewis, J. F. Stoddart, D. J. Williams, *J. Chem. Soc. Dalton Trans.* **1983**, 607–613; Y.-L. Chang, M.-A. West, F. W. Fowler, J. W. Lauher, *J. Am. Chem. Soc.* **1993**, *115*, 5991–6000; J. C. MacDonald, G. M. Whitesides, *Chem. Rev.* **1994**, *94*, 2383–2420; M. Kotera, J.-M. Lehn, J.-P. Vigneron, *J. Chem. Soc. Chem. Commun.* **1994**, 197–199; J. Yang, J.-L. Marendaz, S. J. Geib, A. D. Hamilton, *Tetrahedron Lett.* **1994**, *35*, 3665–3668; J. C. Besson, L. J. Fitzgerald, J. C. Gallucci, R. E. Gerkin, J. T. Rademacher, A. W. Czarnik, *J. Am. Chem. Soc.* **1994**, *116*, 4621–4622; A. Houlton, D. Michael, P. Mingos, D. J. Williams, *J. Chem. Soc. Chem. Commun.* **1994**, 503–504.

[3] Y. S. Obeng, M. E. Laing, A. C. Friedli, H. C. Yang, D. Wang, E. W. Thulstrup, A. J. Bard, J. Michl, *J. Am. Chem. Soc.* **1992**, *114*, 9943–9952; H. O. Stumpf, L. Ouahab, Y. Pei, D. Grandjean, O. Kahn, *Science* **1993**, *260*, 1762–1763; M. Munakata, T. Kuroda-Sowa, M. Maekawa, M. Nakamura, S. Akiyama, S. Kitagawa, *Inorg. Chem.* **1994**, *33*, 1284–1291; S. Kawata, S. Kitagawa, M. Kondo, I. Furuchi, M. Munakata, *Angew. Chem.* **1994**, *106*, 1861–1863; *Angew. Chem. Int. Ed. Engl.* **1994**, *33*, 1759–1761; C. M. Drain, J.-M. Lehn, *J. Chem. Soc. Chem. Commun.* **1994**, 2313–2315; D. M. L. Goodgame, S. Menzer, A. M. Smith, D. J. Williams, *ibid.* **1994**, 1825–1826; L. R. MacGillivray, S. Subramanian, M. J. Zaworotko *ibid.* **1994**, 1325–1326; M. Fujita, Y. J. Kwon, M. Miyazawa, K. Ogura, *ibid.* **1994**, 1977–1978; P. J. Stang, K. Chen, *J. Am. Chem. Soc.* **1995**, *117*, 1667–1668; D. M. L. Goodgame, S. Menzer, A. M. Smith, D. J. Williams, *Angew. Chem.* **1995**, *107*, 605–607; *Angew. Chem. Int. Ed. Engl.* **1995**, *34*, 574–575.

[4] P. R. Ashton, T. T. Goodnow, A. E. Kaifer, M. V. Reddington, A. M. Z. Slawin, N. Spencer, J. F. Stoddart, C. Vicent, D. J. Williams, *Angew. Chem.* **1989**, *101*, 1404–1408; *Angew. Chem. Int. Ed. Engl.* **1989**, *28*, 1396–1399; C. A. Hunter, J. K. M. Sanders, *J. Am. Chem. Soc.* **1990**, *112*, 5525–5534; P. R. Ashton, D. Philp, N. Spencer, J. F. Stoddart, D. J. Williams, *J. Chem. Soc. Chem. Commun.* **1994**, 181–184; D. B. Amabilino, P. R. Ashton, J. F. Stoddart, S. Menzer, D. J. Williams, *ibid.* **1994**, 2475–2478; C. A. Hunter, *Chem. Soc. Rev.* **1994**, 101–109.

[5] G. R. Desiraju, *Crystal Engineering. The Design of Organic Solids*, Elsevier, Amsterdam, **1989**; M. C. Etter, *Acc. Chem. Res.* **1990**, *23*, 120–126;

 © VCH Verlagsgesellschaft mbH, D-69451 Weinheim, 1995 0570-0833/95/3417-1864 $ 10.00+.25/0

C. B. Aakeröy, K. R. Seddon, *Chem. Soc. Rev.* **1993**, 397–407; M. J. Zaworotko, *ibid.* **1994**, 283–288.

[6] J.-M. Lehn, *Science*, **1993**, *260*, 1762–1763; F. N. Diederich, *Nature* **1994**, *369*, 199–207; D. B. Amabilino, J. F. Stoddart, D. J. Williams, *Chem. Mater.* **1994**, *6*, 1159–1167; V. A. Russel, M. C. Etter, M. D. Ward, *ibid.* **1994**, *6*, 1206–1217; N. J. Long, *Angew. Chem.* **1995**, *107*, 37–56; *Angew. Chem. Int. Ed. Engl.* **1995**, *34*, 21–38.

[7] J. Y. Sze, H. W. Gibson, *Polym. Prepr. (Am. Chem. Soc. Div. Polym. Chem.)* **1992**, *33*(2), 331–332; R. Ballardini, V. Balzani, M. T. Gandolfi, L. Prodi, M. Venturi, D. Philp, H. G. Ricketts, J. F. Stoddart, *Angew. Chem.* **1993**, *105*, 1362–1364; *Angew. Chem. Int. Ed. Engl.* **1993**, *32*, 1301–1303.

[8] R. Machinek, W. Lüttke, *Synthesis* **1975**, 255–256.

[9] Crystal data for $\mathbf{3}\cdot 2PF_6$: triclinic, space group $P\bar{1}$, $a = 10.459(7)$, $b = 11.811(8)$, $c = 14.522(12)$ Å, $\alpha = 92.56(2)$, $\beta = 110.81(2)$, $\gamma = 90.67(2)^\circ$, $V = 1675$ Å^3, $Z = 2$, $\rho_{calcd} = 1.54$ g cm^{-3}, $\mu(Cu_{K\alpha}) = 21.4$ cm^{-1}, 4216 independent reflections measured, 2411 observed reflections with $[|F_o| > 4\sigma(|F_o|)$, $2\theta \leq 110^\circ]$ refined to $R = 0.138$, $R_w = 0.157$.

[10] Siemens P4/RA diffractometer for $\mathbf{3}\cdot 2PF_6$ and $\mathbf{4}\cdot 4PF_6$ and Siemens P4/PC diffractometer for $\mathbf{4}\cdot Fc\cdot 4PF_6$, ω scans, $Cu_{K\alpha}$ radiation, (graphite monochromator). The structures were solved by direct methods and refined anisotropically. Further details of the crystal structures can be obtained from the Cambridge Crystallographic Data Centre, 12 Union Road, GB-Cambridge CB2 1EZ (UK), on quoting the full journal citation.

[11] Crystal data for $\mathbf{4}\cdot 4PF_6\cdot 2.3MeCN$: monoclinic, space group $C2/c$, $a = 22.990(7)$, $b = 20.372(6)$, $c = 17.476(5)$ Å, $\beta = 124.00(2)^\circ$, $V = 6785$ Å^3, $Z = 4$, $\rho_{calcd} = 1.29$ g cm^{-3}, $\mu(Cu_{K\alpha}) = 19.9$ cm^{-1}, 4268 independent reflections measured, 2512 observed reflections with $[|F_o| > 4\sigma(|F_o|)$, $2\theta \leq 110^\circ]$ refined to $R = 0.118$, $R_w = 0.127$.

[12] The separation between the centers of the C–C bonds within diametric bipyridinium units is 10.3 Å and the centroid-centroid separation between the two hydroquinone rings is 10.2 Å.

[13] The overall array in $\mathbf{4}^{4+}$ is perfectly symmetric; the centroids of immediately adjacent cyclophanes form a rhombus with an edge length of 13.4 Å and angles of 81 and 99°.

[14] This arrangement is reminiscent of the stacking exhibited by cyclobis(paraquat-*p*-cyclophane) tetrakis(hexafluorophosphate)·3MeCN in the solid state. See B. Odell, M. V. Reddington, A. M. Z. Slawin, N. Spencer, J. F. Stoddart, D. J. Williams, *Angew. Chem.* **1988**, *100*, 1605–1608; *Angew. Chem. Int. Ed.* **1988**, *27*, 1547–1550.

[15] R. E. Lehmann, J. K. Kochi, *J. Am. Chem. Soc.* **1991**, *113*, 501–512.

[16] Crystal data for $\mathbf{4}\cdot Fc\cdot 4PF_6\cdot 2MeCN\cdot 2H_2O$: monoclinic, space group $P2_1/c$, $a = 9.834(2)$, $b = 20.450(4)$, $c = 16.767(3)$ Å, $\beta = 103.09(2)^\circ$, $V = 3284(1)$ Å^3, $Z = 2$ (the complex has C_i symmetry), $\rho_{calcd} = 1.54$ g cm^{-3}, $\mu(Cu_{K\alpha}) = 38.5$ cm^{-1}, 4860 independent reflections measured, 2348 observed reflections with $[|F_o| > 4\sigma(|F_o|)$, $2\theta \leq 120^\circ]$ refined to $R = 0.118$, $R_w = 0.116$.

[17] In $\mathbf{4}\cdot Fc\cdot 4PF_6$, adjacent iron atoms within the mosaic also define a rhombus with sides of 13.2 Å and angles of 79 and 101°.

[18] B. Siegel, R. Breslow, *J. Am. Chem. Soc.* **1975**, *97*, 6869–6870; A. Harada, S. Takahashi, *J. Chem. Soc. Chem. Commun.* **1984**, 645–646; Y. Odagaki, K. Hirotsu, T. Higuchi, A. Harada, S. Takahashi, *J. Chem. Soc. Perkin Trans. 1* **1990**, 1230–1231; M. Shimada, A. Harada, S. Takahashi, *J. Organomet. Chem.* **1992**, *428*, 199–205; T. Tomohiro, H. Okuno, *Inorg. Chim. Acta* **1993**, *204*, 147–152; L. Zhang, A. Macias, T. Lu, J. I. Gordon, G. W. Gokel, A. E. Kaifer, *J. Chem. Soc. Chem. Commun.* **1994**, 1017–1019; D. J. Cram, J. M. Cram, *Container Molecules and their Guests (Monographs in Supramolecular Chemistry)* (Ed.: J. F. Stoddart), The Royal Society of Chemistry, **1994**; P. D. Beer in *Transition Metals in Supramolecular Chemistry* (Eds.: L. Fabbrizzi, A. Poggi), Kluwer, Dordrecht, **1994**, pp. 33–54; G. van de Goor, C. C. Freyhardt, P. Behrens, *Z. Anorg. Allg. Chem.* **1995**, *621*, 311–322.

[19] A. M. De Blas, G. De Santis, L. Fabbrizzi, M. Licchelli, P. Pallavicini, A. Poggi in *Supramolecular Chemistry* (Eds.: V. Balzani and L. De Cola), Kluwer, Dordrecht, **1992**, pp. 87–103; R. Isnin, A. E. Kaifer, *Pure Appl. Chem.* **1993**, *65*, 495–498.

[20] M. F. Czarniecki, R. Breslow, *J. Am. Chem. Soc.* **1978**, *100*, 7771–7772; W. J. le Noble, S. Srivastava, R. Breslow, G. Trainor, *ibid.* **1983**, *105*, 2745–2748; R. Breslow, *Recl. Trav. Chim. Pays-Bas* **1994**, *113*, 493–498; R. Breslow, *Pure Appl. Chem.* **1994**, *66*, 1573–1582.

[21] H. M. Colquhoun, J. F. Stoddart, D. J. Williams, *Angew. Chem.* **1986**, *98*, 483–503; *Angew. Chem. Int. Ed. Engl.* **1986**, *25*, 487–507; J. F. Stoddart, R. Zarzycki, *Recl. Trav. Chim. Pays-Bas* **1988**, *107*, 515–528; J. E. Kickham, S. J. Loeb, *Inorg. Chem.* **1994**, *33*, 4351–4359.

[22] The solid-state structures in this communication display the same gridlike patterns as the 3×3 molecular array described by Lehn et al. See P. N. W. Baxter, J.-M. Lehn, J. Fischer, M.-T. Youinou, *Angew. Chem.* **1994**, *106*, 2432–2434; *Angew. Chem. Int. Ed. Engl.* **1994**, *33*, 2284–2287.

[23] K. E. Drexler, *Nanosystems, Molecular Machinery, Manufacturing and Computation*, Wiley, New York, **1992**.

Dialkylammonium Ion/Crown Ether Complexes: The Forerunners of a New Family of Interlocked Molecules**

Peter R. Ashton, Paul J. Campbell, Ewan J. T. Chrystal, Peter T. Glink, Stephan Menzer, Douglas Philp, Neil Spencer, J. Fraser Stoddart,* Peter A. Tasker, and David J. Williams

Since Pedersen's discovery[1] that crown ethers form complexes with organic as well as metal cations, numerous investigations[2] of the binding of NH_4^+ and RNH_3^+ ammonium ions to macrocyclic polyethers have been reported. Almost without exception, the mode of binding (Fig. 1a) is face-to-face in character and usually 1:1 in its stoichiometry,[3] though occasionally, in closely related situations, 2:1 complexes occur.[4] By contrast, reports describing[5] the complexation of dialkylammonium ions ($R_2NH_2^+$) by crown ethers are relatively sparse. These investigations were limited almost entirely to complexes formed with medium-ring macrocycles, for example 1,7-dimethyl-1,7-diaza[12]crown-4, in which a face-to-face arrangement is inevitable and the ammonium center forms hydrogen bonds with the heteroatoms of the macrocycle.[6] In principle, increasing the size of the ring should enable the complete insertion (Fig. 1b) of an $R_2NH_2^+$ ion into and through the macro-ring center. The formation of such pseudorotaxanes[7] would be the prelude to the construction of a whole new family of interlocked molecules,[8] such as rotaxanes (Fig. 1c) and catenanes (Fig. 1d). Here, we report our first two examples of pseudorotaxanes formed between $R_2NH_2^+$ ions and dibenzo[24]crown-8 (**DB24C8**)[9] fully characterized by computational, crystallographic, and spectroscopic methods.

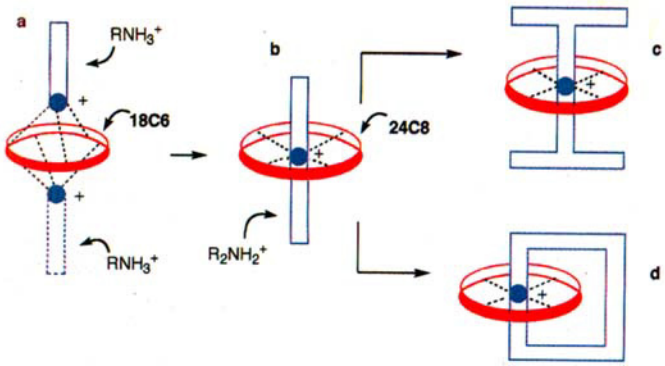

Fig. 1. Schematic representation of a) the face-to-face mode of binding RNH_3^+ to derivatives of [18]crown-6 (**18C6**) and how, in the case of $R_2NH_2^+$ and even larger macrocyclic polyethers such as **24C8**, one might expect a 1:1 complex of pseudorotaxane type (b) to form. Such a 1:1 complex can be envisioned to lead to a [2]rotaxane (c) and a [2]catenane (d).

[*] Prof. J. F. Stoddart, P. R. Ashton, Dr. P. J. Campbell, Dr. P. T. Glink, Dr. D. Philp, Dr. N. Spencer
School of Chemistry, University of Birmingham
Edgbaston, Birmingham B15 2TT (UK)
Telefax: Int. code + (121) 414-3531

Dr. E. J. T. Chrystal
ZENECA Agrochemicals, Bracknell (UK)

Dr. S. Menzer, Dr. D. J. Williams
Chemical Crystallography Laboratory
Imperial College, London (UK)

Dr. P. A. Tasker
ZENECA Specialities, Manchester (UK)

[**] This work was sponsored by the ZENECA Strategic Research Fund and supported additionally by the Engineering and Physical Sciences Research Council.

 © VCH Verlagsgesellschaft mbH, D-69451 Weinheim, 1995 0570-0833/95/3417-1865 $ 10.00+.25/0

Computer modeling of the 1:1 complex in which the di-*n*-butylammonium ion is threaded through the center of the **DB24C8** ring in both vacuum[10] and solution[11] produced several low-energy assemblies with pseudorotaxane-like geometries. Encouraged by these calculations, we proceeded to

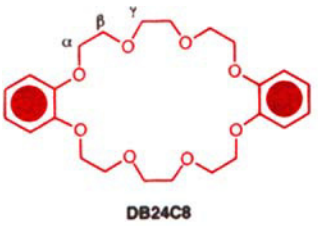

DB24C8

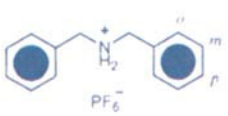

1-H·PF$_6$

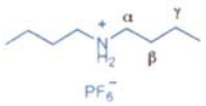

2-H·PF$_6$

investigate the ability of **DB24C8** to form complexes in solution with dibenzylammonium (**1**-H·PF$_6$) and di-*n*-butylammonium (**2**-H·PF$_6$) hexafluorophosphates. Although these salts are quite soluble in MeOH, Me_2CO, MeCN, and Me_2SO, they are virtually insoluble in $CHCl_3$ and CH_2Cl_2. The first indication that **1**-H·PF$_6$ and **2**-H·PF$_6$ form 1:1 complexes with **DB24C8** was the observation of the ready solubilization of both these salts in $CHCl_3$ and CH_2Cl_2 solutions on addition of the crown ether. The ^{1}H NMR spectrum (Fig. 2) of a 1:1 mixture of **DB24C8**

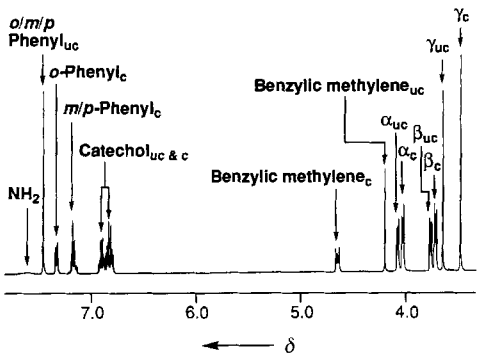

Fig. 2. The ^{1}H NMR spectrum recorded at 400 MHz in CD_3CN of an equimolar mixture of **DB24C8** and **1**-H·PF$_6$ at 20 °C. The concentrations of both the crown ether and the salt are 1.0×10^{-2} M. Three sets of resonances are evident in this spectrum: for the uncomplexed crown ether (**uc**), and uncomplexed salt (**uc**), and for the 1:1 complex between **DB24C8** and **1**-H·PF$_6$ (**c**).

and **1**-H·PF$_6$ in CD_3CN shows three sets of resonances for 1) free **DB24C8**, 2) free **1**-H·PF$_6$, and 3) the 1:1 complex[12] between the crown ether and the dibenzylammonium ion. The presence of both free and complexed species in equilibrium implies that the rates of complexation and decomplexation are both slow on the ^{1}H NMR time scale at room temperature—an observation that is not too surprising since space-filling models indicate that a phenyl ring has some difficulty threading its way through the cavity of **DB24C8**. By contrast, the ^{1}H NMR spectrum[13] of a 1:1 mixure of **DB24C8** and **2**-H·PF$_6$ shows a time-averaged set of signals consistent with the much decreased bulk of the *n*-butyl groups in **2**-H$^+$ relative to the benzyl groups in **1**-H$^+$. The much more rapid rates of complexation and decomplexation, implied by the time-averaging for association and dissociation of [**DB24C8**·**2**-H]PF$_6$, are also consistent with a pseudorotaxane-like structure for the 1:1 complex[12] in solution, given the substantial shifts observed[13] in the resonances of the butyl protons.

Crystals[14] of both 1:1 complexes were analyzed by mass spectrometry (FABMS).[15] Both [**DB24C8**·**1**-H]PF$_6$ and [**DB24C8**·**2**-H]PF$_6$ displayed very strong peaks, at *m*/*z* 646 for the [**DB24C8**·**1**-H]$^+$ ion and at *m*/*z* 578 for the [**DB24C8**·**2**-H]$^+$ ion. Indeed, the peak for the [**DB24C8**·**1**-H]$^+$ ion is by far the most abundant in the mass spectrum, an observation commensurate with a very strong 1:1 complex. Elemental microanalyses of the crystalline complexes confirmed their 1:1 stoichiometries. The solid-state structures of these 1:1 complexes were established by X-ray crystallography on suitable single crystals.[14]

[**DB24C8**·**1**-H]PF$_6$ crystallizes[16] with two crystallographically independent 1:1 complexes, **A** and **B** (Fig. 3), in the asymmetric unit. In both complexes, the **1**-H$^+$ ion is threaded

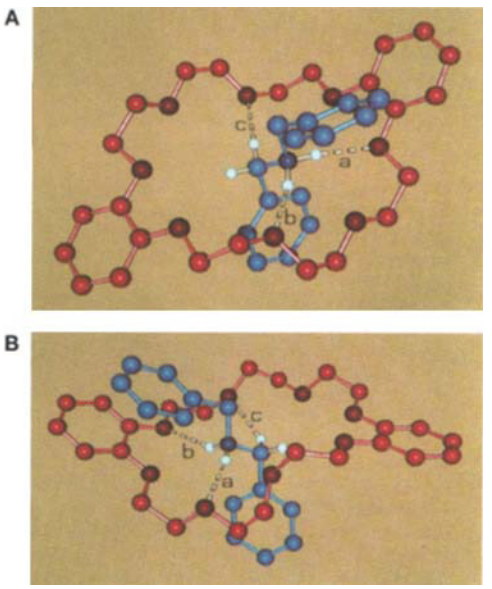

Fig. 3. The superstructures of the 1:1 complexes **A** and **B** of [**DB24C8**·**1**-H]$^+$ in the solid state. In **A**, the hydrogen bonds have the following distances and angles a) [N···O] 3.12 Å, [H···O] 2.24 Å, [N–H···O] 167°; b) [N···O] 2.85 Å, [H···O] 1.99 Å, [N–H···O] 159°; c) [C···O] 3.16 Å, [H···O] 2.21 Å, [C–H···O] 174°. In **B**, the hydrogen bonds have the following distances and angles a) [N···O] 2.99 Å, [H···O] 2.14 Å, [N–H···O] 157°; b) [N···O] 3.12 Å, [H···O] 2.28 Å, [N–H···O] 155°; c) [C···O] 3.27 Å, [H···O] 2.45 Å, [C–H···O] 143°.

through the center of the **DB24C8** macrocycle, which adopts an extended all-*gauche* (O-C-C-O) conformation. The structures of the two independent cations differ, as does the nature of the threading through the macrocyclic polyethers. The cation in **A** has a "gull-wing" conformation in which the planes of the aromatic rings are approximately orthogonal to the C–CH_2–NH_2^+–CH_2–C backbone. In **B**, one of the phenyl rings is inclined by roughly 52° to the backbone while the other one is essentially orthogonal. In both complexes, the NH_2^+ center and one of the adjacent CH_2 groups lie more or less within the plane of their polyether macrocycles. Also, in **A** and **B**, *both* NH_2^+ hydrogen atoms and *one* CH_2 hydrogen atom are directed toward polyether oxygen atoms which lie within *H*-bonding distances. However, the oxygen atoms involved in these hydrogen bonds are different in **A** and **B**, demonstrating that alterna-

 © VCH Verlagsgesellschaft mbH, D-69451 Weinheim, 1995 0570-0833/95/3417-1866 $ 10.00+.25/0

tive three-point binding geometries can be accommodated within these 1:1 complexes. In **B**, there is an additional $\pi-\pi$ stacking interaction between one of the phenyl groups in the cation and one of the catechol rings in the crown ether (mean plane separation, 3.48 Å, centroid–centroid separation, 3.79 Å, angle formed by the ring planes, 11°). The macrocyclic components of **A** and **B** pack (Fig. 4) to form channels that extend in the crystallographic c direction with the cations threaded in such a manner as to suggest the potential for the formation of polyrotaxanes. The centrally located phenyl groups are aligned parallel to each other, with a mean interplanar separation of 3.50 Å and a centroid–centroid distance of 3.73 Å. The distance between adjacent NH_2^+ centers in the stack are 9.3 and 9.7 Å.

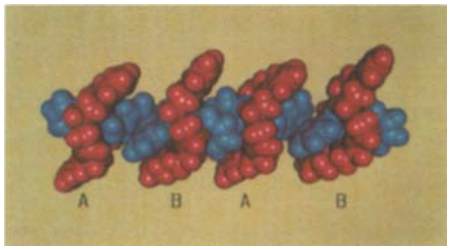

Fig. 4. Part of one of the continuous cation-threaded channels present in the crystals of [**DB24C8**·**1**-H]PF_6. The sequence of complexes from left to right is **ABAB**.

The X-ray crystal structure[16] of [**DB24C8**·**2**-H]PF_6 reveals (Fig. 5) that the macrocyclic polyether adopts an extended all-*gauche* (O-C-C-O) conformation very similar to that in [**DB24C8**·**1**-H]PF_6. The **2**-H^+ ion is threaded through the center of the **DB24C8** and bound by means of one [C–H···O] and two [N–H···O] hydrogen bonds. Although there are no dominant intercomplex interactions, the packing of the complexes suggests the possibility for polyrotaxane formation.

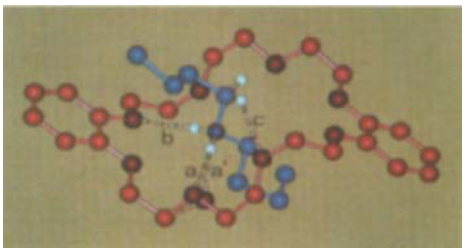

Fig. 5. The superstructure of the 1:1 complex [**DB24C8**·**2**-H]$^+$ in the solid state. The hydrogen bonds have the following distances and angles a) [N···O] 3.09 Å, [H···O] 2.20 Å, [N–H···O] 175°; a') [N···O'] 2.90 Å, [H···O'] 2.04 Å, [N–H···O'] 161°; b) [N···O] 3.25 Å, [H···O] 2.35 Å, [N–H···O] 172°; c) [C···O] 3.23 Å, [H···O] 2.48 Å, [C–H···O] 134°.

In the ^{1}H NMR spectra of an equimolar mixture of **1**-H^+ and **DB24C8** in a number of different solvents, signals for the complexed and uncomplexed species are observed (see Fig. 2). Since absolute concentrations can be determined readily from the relative abundances of the three species at equilibrium when the initial concentrations of both **1**-H^+ and **DB24C8** are known, single point determination[17] of the association constants (K_a) and derived free energies of complexation (ΔG°) are possible. The values of K_a at 25 °C are given in Table 1 for a range of common NMR solvents. A clear trend is observed: an increase in K_a values corresponds to the decrease in the Gutmann donor numbers[18] of the solvents. For instance, $CDCl_3$, a very weak hydrogen bond acceptor, gives the highest K_a value (Table 1, Entry 5), whereas, in CD_3SOCD_3, no complex formation could be observed (Entry 1).

Table 1. Effect of solvent on the association constants K_a for the 1:1 complex formed between of **DB24C8** and **1**-H·PF_6 at 25 °C.

Entry	Solvent	ε [a]	n_G [a]	K_a [M^{-1}] [b]	ΔG° [kcal mol^{-1}]
1	CD_3SOCD_3	46.5	29.8	0	-
2	CD_3COCD_3	20.6	17.0	360	−3.5
3	CD_3CN	35.9	14.1	420	−3.6
4	$CDCl_3$/CD_3CN (1:1)	–	–	1700	−4.4
5	$CDCl_3$	4.81	4.0	27000	−6.0

[a] Values of the solvent dielectric constants ε and the Gutmann donor numbers n_G were obtained from ref. [18]. [b] Association constants K_a were obtained from single-point measurements of the concentrations of the complexed and uncomplexed species in the relevant ^{1}H NMR spectra at 25 °C and using the expression $K_a = \frac{[\mathbf{DB24C8}\cdot\mathbf{1}\text{-}H]^+}{[\mathbf{DB24C8}][\mathbf{1}\text{-}H^+]}$. [c] The free energies of complexation ΔG° were calculated from the K_a values by applying the equation $\Delta G^\circ = -RT\ln K_a$.

By contrast, the time-averaged ^{1}H NMR signals associated with complexation between **DB24C8** and **2**-H^+ ions in various solvents requires the calculation of the K_a values by dilution or titration methods.[19] In $CDCl_3$, dilution from 5×10^{-2} to 5×10^{-4} M resulted in only negligible shifts for all of the resonances of the host and guest species.[20] This result reflects the low solubility of the salt **2**-H·PF_6 in $CDCl_3$ in the absence of **DB24C8** and the resulting very high K_a value of $>10^4\,M^{-1}$. In CD_3CN, in which **2**-H·PF_6 is readily soluble, dilution over the same range of concentrations resulted in significant shifts ($\Delta\delta$) of the four butyl proton resonances of between 25 and 55 Hz. Plots of $\Delta\delta$ against $(\Delta\delta/c)^{1/2}$ for different probe protons gave straight lines,[21] the slopes of which yielded K_a values of consistently around $70\,M^{-1}$. Use of the titration method,[19] in which the ratio of **DB24C8** was varied with respect to **2**-H·PF_6 in CD_3CN, gave a value of approximately $50\,M^{-1}$ for K_a. These K_a values for [**DB24C8**·**2**-H]PF_6 complexation are somewhat lower than the value (Table 1, Entry 3) of K_a for the [**DB24C8**·**1**-H]PF_6 complex in CD_3CN. This observation reflects the greater flexibility—and hence lower preorganization—of the **2**-H^+ ion compared with the more rigid **1**-H^+ ion. A mixture of **DB24C8** and **2**-H·PF_6 in a 2:1 molar ratio was dissolved in CD_2Cl_2 and investigated by variable-temperature ^{1}H NMR spectroscopy. At + 30 °C, the spectrum obtained displays a time-averaged set of resonances for both the host and guest species (Fig. 6a). At −27 °C, the signals associated with the α- and γ-OCH_2 protons in the crown ether exist as two sets of equally intense resonances arising from complexed and uncomplexed **DB24C8** molecules (Fig. 6b). The coalescence temperatures were found to be −3 °C for the α-OCH_2 protons ($\Delta\delta$ = 24 Hz at −27 °C) and −7 °C for the γ-OCH_2 protons ($\Delta\delta$ = 20 Hz at −27 °C). From these parameters, the activation barrier ($\Delta G_c^{\ddagger}$) for the exchange of the di-*n*-butylammonium ion from one crown ether molecule to another was calculated to be roughly 13.5 kcal mol^{-1}.

We have demonstrated that an extremely simple recognition motif—the binding of dialkylammonium salts with suitably sized crown ethers—can result in the self-assembly of pseudorotaxanes. The roots of this supramolecular phenomenon lie in 1) *hydrogen bonding interactions* involving charged and/or activated donors and neutral acceptors, 2) *electrostatic pole–dipole interactions* between onium centers and precisely positioned ligating atoms, as well as, in some instances, 3) *dispersive interactions*, including stabilizing $\pi-\pi$ and/or CH–π interactions. The extension of this exciting and potentially rewarding line of in-

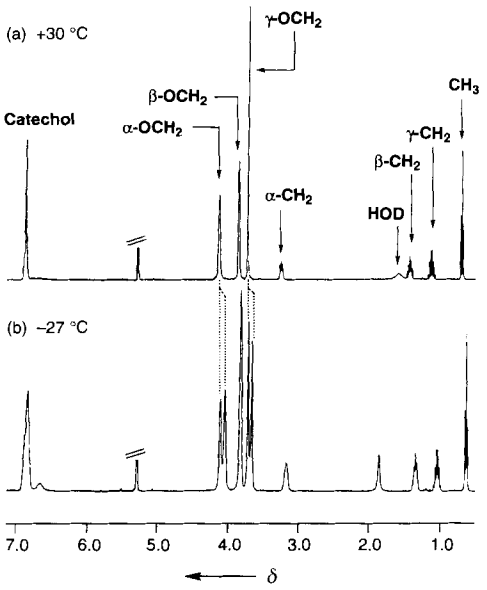

Fig. 6. The ^{1}H NMR spectrum recorded at 400 MHz in CD_2Cl_2 of a solution of **DB24C8** and **2**-H·PF_6 in a 2:1 molar ratio at a) + 30 °C and b) −27 °C. The spectrum recorded at higher temperature (a) shows a time-averaged set of signals for both **DB24C8** and **2**-H$^+$. In the spectrum recorded at lower temperature (b), signals associated with one equivalent of complexed and one equivalent of uncomplexed **DB24C8** are evident for the α-OCH_2 and γ-OCH_2 protons. The concentrations of the crown ether and the salt are 2.4×10^{-2} M and 1.2×10^{-2} M, respectively.

quiry into the elaboration of a new range of interlocked molecular compounds, specifically catenanes and rotaxanes as indicated conceptually in Figure 1, is now the subject of detailed study in our research laboratories.[2,3] It is remarkable to reflect on the fact that in the intervening three decades since Pedersen[1] first reported the complexation of (substituted) ammonium salts by crown ethers, no publications have appeared to our knowledge in which dialkylammonium ions have been shown to thread through macrocyclic polyethers.

Experimental Procedure

General procedure for the synthesis of $[R_2NH_2]PF_6$ salts: 2 M HCl (250 mL) was added to R_2NH (ca. 25 mmol) and the solution stirred for 4 h. Water was removed under vacuum and the residue dissolved in H_2O (100 mL). Saturated aqueous NH_4PF_6 was added until no further precipitation occurred. The white solid was filtered off and dried.

1-H·PF_6: Yield 91%; m.p. 205–208 °C; Analysis: found: C 48.72, H 4.53, N 4.28%; calcd for $C_{14}H_{16}NPF_6$: C 48.98, H 4.66, N 4.08%; MS (FAB): *m/z*: 198 [*M* − PF_6]$^+$; ^{1}H NMR (300 MHz, CD_3SOCD_3): δ = 4.20 (s, 4H, CH_2), 7.39–7.53 (m, 10H, aromatic protons), 9.19 (br s, 2H, NH_2); ^{13}C NMR (75 MHz, CD_3SOCD_3): δ = 50.3 (CH_2), 128.8, 129.1, 130.0, 131.9 (*ipso*-C).

2-H·PF_6: Yield 92%; m.p. 187–188 °C; Analysis: found: C 35.03, H 7.39, N 5.11%; calcd for $C_8H_{20}NPF_6$: C 34.91, H 7.27, N 5.09%; MS (CI): *m/z* 130 [*M* − PF_6]$^+$; ^{1}H NMR (300 MHz, $CDCl_3$): δ = 0.97 (t, *J* = 7.5 Hz, 6H, CH_3), 1.36–1.48 (m, 4H, γ-CH_2), 1.74–1.85 (m, 4H, β-CH_2), 2.96–3.05 (m, 4H, α-CH_2), 7.65 (br s, 2H, NH_2); ^{13}C NMR (75 MHz, $CDCl_3$): δ = 13.5 (CH_3), 19.9 (γ-CH_2), 27.6 (β-CH_2), 47.6 (α-CH_2).

Received: May 15, 1995 [Z 7989 IE]
German version: *Angew. Chem.* **1995**, *107*, 1997–2001

Keywords: crown ethers · hydrogen bonds · inclusion compounds · rotaxanes · self-assembly

[1] C. Pedersen, *J. Am. Chem. Soc.* **1967**, *89*, 7017–7036.

[2] a) I. O. Sutherland, *Chem. Soc. Rev.* **1986**, *15*, 63–91; b) J. F. Stoddart, *Top. Stereochem.* **1988**, *17*, 205–288; c) G. W. Gokel, *Crown Ethers and Cryptands*, The Royal Society of Chemistry, Cambridge, **1991**.

[3] I. Goldberg in *Inclusion Compounds, Vol. 2* (Eds.: J. L. Atwood, J. E. D. Davies, D. D. MacNicol), Academic Press, London, **1984**, pp. 261–335.

[4] a) M. J. Bovill, D. J. Chadwick, M. R. Johnson, N. F. Jones, I. O. Sutherland, R. F. Newton, *J. Chem. Soc. Chem. Commun.* **1979**, 1065–1066; b) M. R. Johnson, N. F. Jones, I. O. Sutherland, R. F. Newton, *J. Chem. Soc. Perkin Trans. 1* **1985**, 1637–1643.

[5] a) J. C. Metcalfe, J. F. Stoddart, G. Jones, *J. Am. Chem. Soc.* **1977**, *99*, 8317–8319; b) J. Krane, O. Aune, *Acta Chem. Scand. Ser. B* **1980**, *34*, 397–401; c) H. Tsukube, *Bull. Chem. Soc. Jpn.* **1984**, *57*, 2685–2686; d) S. S. Abed-Ali, B. J. Brisdon, R. England, *J. Chem. Soc. Chem. Commun.* **1987**, 1565–1566; e) S. Misumi, *Top. Curr. Chem.* **1993**, *165*, 163–192.

[6] J. C. Metcalfe, J. F. Stoddart, G. Jones, W. E. Hull, A. Atkinson, I. S. Kerr, D. J. Williams, *J. Chem. Soc. Chem. Commun.* **1980**, 540–543.

[7] The name "rotaxane" is derived from the Latin words *rota* meaning wheel and *axis* meaning axle (G. Schill, *Catenanes, Rotaxanes, and Knots*, Academic Press, New York, **1971**). In the chemical sense, this type of molecule contains a linear component (the axle) encircled by a macrocyclic component (the wheel). In order to prevent the wheel from slipping off the axle, the linear component must be terminated at both ends by large blocking groups or stoppers. The addition of the prefix pseudo to the term rotaxane indicates that in a "pseudorotaxane" the wheels are free to dissociate from the axle in the same way as ligands may in a more conventional type of complex. The molecular components of a pseudorotaxane are held together only by their mutual noncovalent bonding interactions. See P. R. Ashton, D. Philp, N. Spencer, J. F. Stoddart, *J. Chem. Soc. Chem. Commun.* **1991**, 1677–1679.

[8] a) J.-C. Chambron, C. O. Dietrich-Buchecker, J.-P. Sauvage, *Top. Curr. Chem.* **1993**, *165*, 131–162; b) G. Wenz, *Angew. Chem.* **1994**, *106*, 851–870; *Angew. Chem. Int. Ed. Engl.* **1994**, *33*, 803–822; c) H. W. Gibson, M. C. Bheda, P. T. Engen, *Prog. Polym. Sci.* **1994**, *19*, 843–945; d) D. B. Amabilino, J. F. Stoddart, *Chem. Rev.*, submitted.

[9] I. R. Hanson, D. L. Hughes, M. R. Truter, *J. Chem. Soc. Perkin Trans. 2* **1976**, 972–976.

[10] Calculations were performed on a Silicon Graphics 4B/35 workstation using the CVFF forcefield as implemented in the Insight II/Discover package (Version 2·3.0, Biosym Technologies, San Diego, 1993).

[11] Calculations were performed on a Silicon Graphics Crimson Elan Workstation using the MM3* forcefield, a modified version of the original MM3 forcefield (N. L. Allinger, M. Rahman, J.-H. Lii, *J. Am. Chem. Soc.* **1990**, *112*, 8293–8307) and the GB/SA solvent model (W. C. Still, A. Tempczyk, R. C. Hawley, T. Hendrickson, *J. Am. Chem. Soc.* **1990**, *112*, 6127–6129) for $CHCl_3$ as implemented by Macromodel V3.5X (F. Mohamadi, N. G. J. Richards, W. C. Guida, R. Liskamp, C. Canfield, G. Chang, T. Hendrickson, W. C. Still, *J. Comput. Chem.* **1990**, *11*, 440–467; Version 3.5X, Columbia University, 1992). Initial input structures were minimized using the Polak–Ribiere Conjugate Gradient method to a gradient of < 0.1 kJ mol^{-1} Å^{-1}. Conformational searching was performed using the Monte Carlo (MC) method. Global minima were located by 1000-step MC simulations, and the structures generated by the conformational search were minimized to a gradient of < 0.01 kJ mol^{-1} Å^{-1} using the Full-Matrix Newton–Raphson (FMNR) method. Two starting geometries were used. The same set of minimum-energy structures emerged in both cases.

[12] An NOE experiment was also undertaken in which each of the resonances associated with the protons in the 1:1 complex formed between **DB24C8** and **1**-H·PF_6 in $CDCl_3$ was irradiated in turn. The signals of the *o*-phenyl and benzylic methylene protons of the **1**-H$^+$ ion in the complex were enhanced upon irradiation of the β- and γ-OCH_2 protons of the complexed **DB24C8**, but only the signal for the *o*-phenyl protons was enhanced upon irradiation of the α-OCH_2 resonance. Conversely, irradiation of the *o*- and *m*/*p*-phenyl resonances of the complexed **1**-H$^+$ ion resulted in enhancement of all three OCH_2 signals, but irradiation of the benzylic methylene resonance of the complexed **1**-H$^+$ ion enhanced only the β- and γ-signals of the complexed **DB24C8**. Irradiation of the NH_2 signal produced small enhancements in all three **DB24C8** OCH_2 resonances. Irradiation of the signals for the aromatic protons in **DB24C8** had a negligible effect on the resonances of the bound **1**-H$^+$ ion. These NOE experiments are consistent with a 1:1 complex having a pseudorotaxane structure in solution.

[13] The Δδ values for the α-CH_2, β-CH_2, γ-CH_2, and Me protons from ^{1}H NMR spectra recorded on **2**-H·PF_6 and [**DB24C8** · **2**-H]PF_6 at 300 MHz in $CDCl_3$ are + 0.19, − 0.30, − 0.25, and − 0.23, respectively.

[14] Both 1:1 complexes were crystallized by liquid diffusion of *n*-hexane into a $CHCl_3$ solution of an equimolar mixture of the dialkylammonium salt (**1**-H·PF_6 or **2**-H·PF_6) and **DB24C8**.

[15] FAB mass spectra were recorded with a Kratos MS80RF mass spectrometer (accelerating voltage 4 kV; resolution 1000) coupled to a DS90 data system with an off-line Sun Workstation for data processing. The atom gun was an adapted saddle field source (Ion Tech Limited) operating at 7 keV with a tube current of roughly 2 mA. Krypton was used to provide a primary beam of atoms, and samples of the complexes were dissolved in a small volume (ca. 1–2 μL) of *m*-nitrobenzyl alcohol and loaded on to a stainless steel probe tip. Spectra were recorded in the positive-ion mode at a scan speed of 10 s per decade.

[16] X-ray data for [**DB24C8**·**1**-H]PF_6·0.5H_2O: triclinic, space group $P\bar{1}$, $a = 14.430(3)$, $b = 15.788(4)$, $c = 18.536(5)$ Å, $\alpha = 73.30(2)$, $\beta = 75.79(2)$, $\gamma = 84.10(2)°$, $V = 3939(2)$ Å^3, $Z = 4$, $\mu(Cu_{K\alpha}) = 1.32$ mm^{-1}, $\rho_{calc} = 1.35$ g cm^{-3}, Siemens P4/PC diffractometer, graphite-monochromated $Cu_{K\alpha}$ radiation. The structure was solved using direct methods, and anisotropic refinement gave

$R = 0.063$, $R_w = 0.068$ for 6629 independent observed reflections for $[|F_o| > 4\sigma(F_o|)$, $2\theta < 110^\circ]$. X-ray data for **[DB24C8·2-H]PF$_6$**: monoclinic, space group Ia (body-centered cell chosen because C-face-centered cell has $\beta = 124^\circ$), $a = 18.597(4)$, $b = 10.362(3)$, $c = 20.265(3)$ Å, $\beta = 105.48(2)^\circ$, $V = 3763(2)$ Å^3, $Z = 4$, $\mu(Cu_{K\alpha}) = 1.30$ mm^{-1}, $\rho_{calc} = 1.28$ g cm^{-3}. Siemens P4/PC diffractometer, graphite-monochromated $Cu_{K\alpha}$ radiation. The structure was solved using direct methods, and anisotropic refinement gave $R_1 = 0.063$, $\omega R_2 = 0.169$ for 2747 independent observed reflections with $[|F_o| > 4\sigma(|F_o|)$, $2\theta < 125^\circ]$. Further details of the X-ray crystal structure investigations may be obtained from the Director of the Cambridge Crystallographic Data Centre, 12 Union Road, GB-Cambridge CB2 1EW (UK).

[17] For an alternative type of single-point analysis for the determination of K_a values, see J. C. Adrian, Jr., C. S. Wilcox, *J. Am. Chem. Soc.* **1991**, *113*, 678–680.

[18] The Gutmann donor number provides a semiquantitative measurement of the ability of the solvent to donate its electrons into noncovalent bonds. See a) V. Gutmann, E. Wychera, *Inorg. Nucl. Chem. Lett.* **1966**, *2*, 257–260; b) C. Reichardt, *Solvents and Solvent Effects in Organic Chemistry*, 2nd ed., VCH, Weinheim, **1988**.

[19] C. S. Wilcox in *Frontiers of Supramolecular Organic Chemistry and Photochemistry* (Eds.: H.-J. Schneider, H. Durr), VCH, Weinheim, **1991**, pp. 123–143.

[20] The determination of K_a values by either titration or by Job's method of continuous variation cannot be undertaken in $CDCl_3$ because these techniques both require at some stage that the concentration of the ammonium salt be in excess relative to that of the crown ether. This situation cannot be achieved in practice on account of the low solubility of **1**-H·PF$_6$ in the absence of a molar equivalent of **DB24C8**.

[21] In the case of the dilution experiment, the values of K_a and $\Delta\delta_{max}$ were obtained after linearization of the binding data according to Equation (a), where $\Delta\delta_{max}$ corresponds to the value of the complexation-induced chemical shift, $\Delta\delta_o$ is the observed difference in chemical shift between the complex and free species for a probe proton of either host or guest, and c is the concentration of an equimolar solution of host and guest.

$$\Delta\delta_o = \Delta\delta_{max} - (\Delta\delta_o \Delta\delta_{max}/cK_a)^{1/2} \quad (a)$$

[22] The Eyring equation was employed to calculate $\Delta G_c^{\ddagger}$ values at the coalescence temperatures T_c, at which the rate constants k_c can be calculated (I. O Sutherland, *Annu. Rep. NMR Spectrosc.* **1971**, *4*, 71–235) from the approximate expression, $k_c = \pi(\Delta\nu)/(2)^{1/2}$, where $\Delta\nu$ is the chemical shift difference (in Hertz) between the coalescing signals in the absence of exchange.

[23] **Note added in proof** (August 18, 1995): After this paper had been submitted, Busch et al. (A. G. Kolchinski, D. H. Busch, N. W. Alcock, *J. Chem. Soc. Chem. Commun.* **1995**, 1289–1291) reported the synthesis of a [2]rotaxane composed of a dumbell, which incorporates a secondary dialkylammonium center, and a **DB24C8** bead. The [2]rotaxane was self-assembled by acylation of a primary amine—in a molecule also containing a secondary amino center—in the presence of the macrocycle.

Doubly Encircled and Double-Stranded Pseudorotaxanes**

Peter R. Ashton, Ewan J. T. Chrystal, Peter T. Glink, Stephan Menzer, Cesare Schiavo, J. Fraser Stoddart,* Peter A. Tasker, and David J. Williams

In the preceeding communication,[1] we described the formation of pseudorotaxanes from $R_2NH_2^+$ ions (R = $PhCH_2$ in **1**-H·PF$_6$ and R = *n*Bu in **2**-H·PF$_6$) and dibenzo[24]crown-8 (**DB24C8**) both in the solution and solid states. Subsequently, in our evaluation of the propensities of other crown ethers to bind with $R_2NH_2^+$ ions, we discovered that **1**-H·PF$_6$ forms a complex with bis-*para*-phenylene[34]crown-10 (**BPP34C10**)[2] in which two dibenzylammonium ions are threaded simultaneously through the macrocyclic polyether. Here, we describe (i) the X-ray crystal structure of this 1:2 complex, [**BPP34C10**·(**1**-H)$_2$][PF$_6$]$_2$, a "double-stranded pseudorotaxane", and also those of the solid-state superstructures that self-assemble spontaneously from solutions of α,α′-bis(benzylammonium)-*para*-xylene bis(hexafluorophosphate) (**3**-H$_2$·2PF$_6$) and (ii) **BPP34C10** and also (iii) **DB24C8**; these latter structures are intriguing examples of a double-stranded and a doubly encircled 2:2 complex and a doubly encircled 2:1 complex, respectively. Evidence that the 1:2 and 2:1 complexes ("a double-stranded pseudorotaxane" and "a doubly encircled pseudorotaxane", respectively) also exist with the same stoichiometries in solution is provided by ^{1}H NMR spectroscopy.

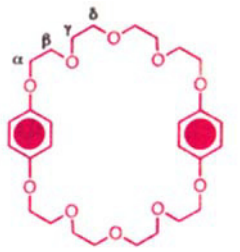

BPP34C10

3-H$_2$·2PF$_6$

The complex formed between **BPP34C10** and **1**-H·PF$_6$ crystallized with a 1:2 stoichiometry when an equimolar mixture of the two components was dissolved in acetone and the solution layered with *n*-pentane. The resulting single crystals were analyzed[3] by X-ray crystallography (Fig. 1). The **BPP34C10** component has the expected[2] open centrosymmetric structure; its hydroquinone rings are aligned parallel to each other with a centroid–centroid separation of 6.99 Å. Pairs of **1**-H$^+$ ions are threaded symmetrically through the macrocyclic ring. The conformation of the C-CH_2-NH_2^+-CH_2-C backbone departs from the all-*anti* geometry adopted by the **1**-H$^+$ ion in [**DB24C8**·**1**-H][PF$_6$] in its solid-state superstructure.[1] The NH_2^+ hydrogen atoms of each cationic center are directed toward polyether oxygen atoms at either end of the macrocycle. However, the 1:2 complex does not have additional stabilization through any significant [C–H···O] hydrogen bonds. Secondary stabilization is achieved by edge-to-face interactions[4] between one of the phenyl rings in each cation and the hydroquinone rings of the crown ether. The centroid–centroid distances for these pairs of symmetrically related interactions are 5.06 Å, and in each case the approach of one of the

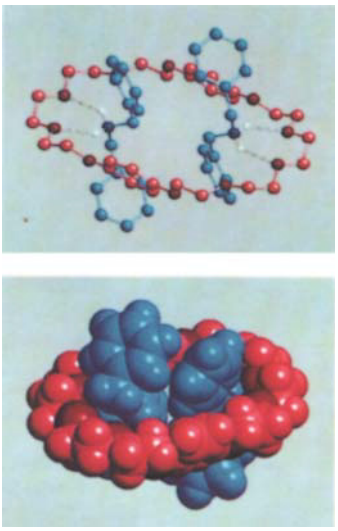

Fig. 1. Top: Ball-and-stick representation of [**BPP34C10**·(**1**-H)$_2$]$^{2+}$ in the solid state. The **BPP34C10** component is depicted in red and the $(PhCH_2)_2NH_2^+$ cations in blue. The [N–H···O] hydrogen bonds have the following distances and angles [N···O] 2.83, 2.82 Å; [H···O] 2.10, 2.06; [N–H···O] 137, 141°. Bottom: Space-filling representation of the complex.

[*] Prof. J. F. Stoddart, P. R. Ashton, Dr. P. T. Glink, C. Schiavo
School of Chemistry, University of Birmingham
Edgbaston, Birmingham B15 2TT (UK)
Telefax: Int. code + (121)414-3531

Dr. E. J. T. Chrystal
ZENECA Agrochemicals, Bracknell (UK)

Dr. S. Menzer, Dr. D. J. Williams
Chemical Crystallography Laboratory
Imperial College, London (UK)

Dr. P. A. Tasker
ZENECA Specialities, Manchester (UK)

[**] This work was sponsored by the ZENECA Strategic Research Fund and supported additionally by the Engineering and Physical Sciences Research Council.

ortho hydrogen atoms of the hydroquinone ring to the phenyl ring center is almost linear (171°; H···ring centroid distance, 2.73 Å). The distance between the two NH_2^+ centers in the complex is 8.4 Å. The **BPP34C10** rings are arranged to form channels (Fig. 2) that extend in the crystallographic *c* direction, again conjuring up the prospect of the formation of polyrotaxanes.[5] The distance between the closer NH_2^+ centers within the stack is 6.9 Å.

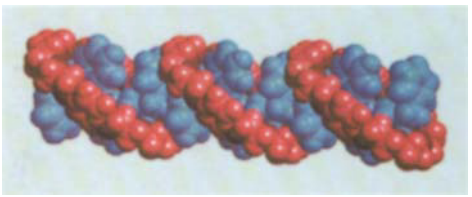

Fig. 2. Space-filling representation showing the pseudopolyrotaxane stacking motif in the crystals of $[\mathbf{BPP34C10}\cdot(\mathbf{1}\text{-}H)_2]^{2+}$.

Single crystals suitable for X-ray analysis were also obtained when an equimolar mixture of **BPP34C10** and $\mathbf{3}\text{-}H_2\cdot 2PF_6$ was dissolved in acetone and the solution layered with *n*-pentane. The X-ray crystal structure showed the complex to have 2:2 stoichiometry (Fig. 3).[3] In this superstructure, both dications

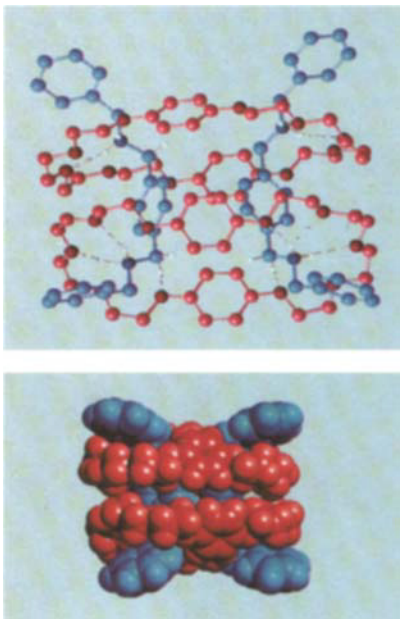

Fig. 3. Top: Ball-and-stick representation of $[(\mathbf{BPP34C10})_2\cdot(\mathbf{3}\text{-}H_2)_2]^{4+}$ in the solid state. The **BPP34C10** components are depicted in red and the $[(PhCH_2NH_2^+CH_2)_2C_6H_4]$ dications in blue. The [N–H···O] hydrogen bonds have the following distances and angles [N···O] 2.85–3.10, [H···O] 2.02–2.27 Å, and [N–H···O] 127–168°. The [C–H···O] hydrogen bonds have the following distances and angles [C···O] 3.25–3.43, [H···O] 2.32–2.48 Å, and [C–H···O] 158–167°. Bottom: Space-filling representation of the complex.

are threaded through two **BPP34C10** macrocycles positioned immediately adjacent to each other, producing an extended torus (Fig. 4). This double-stranded, doubly encircled superstructure is stabilized by a series of nine [N–H···O] and three [C–H···O] hydrogen bonds between the NH_2^+ centers and benzylic CH_2 groups of the dicationic threads and oxygen atoms of the encircled macrocyclic polyethers, respectively. The con-

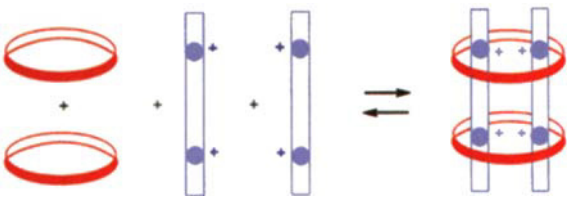

Fig. 4. Schematic representation of the formation of the 2:2 complex between two **BPP34C10** macrocycles (red) and two $[\mathbf{3}\text{-}H_2]^{2+}$ ions (blue).

formations of the two **BPP34C10** macrocycles are similar, with centroid–centroid distances between the hydroquinone rings in the upper and lower macrocycles of 7.18 and 7.00 Å, respectively. However, unlike the parallel alignments of these matching rings in $[\mathbf{BPP34C10}\cdot(\mathbf{1}\text{-}H)_2][PF_6]_2$, here they are inclined by 30° and 26°, respectively. In common with the 1:2 complex, the 2:2 complex packs with pairs of tori oriented in tubelike arrays; the enthreaded dications in each complex are aligned with respect to each other along the crystallographic *b* direction. When the crown ether is changed from **BPP34C10** to **DB24C8**, a 2:1 complex[3, 6] results in which the $[\mathbf{3}\text{-}H_2]^{2+}$ dication is threaded through the centers of two **DB24C8** macrocycles (Fig. 5). The

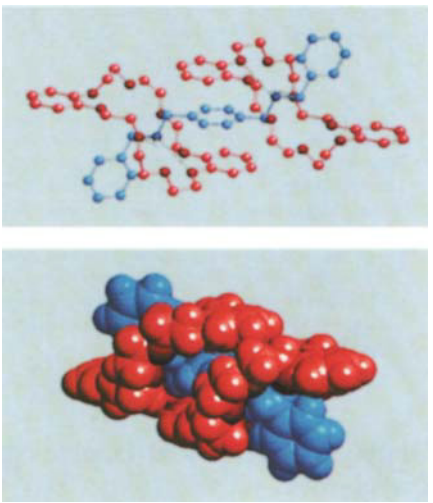

Fig. 5. Top: Ball-and-stick representation of $[(\mathbf{DB24C8})_2\cdot\mathbf{3}\text{-}H_2]^{2+}$ in the solid state. The **DB24C8** macrocycles are depicted in red and the $[(PhCH_2NH_2^+CH_2)_2C_6H_4]$ dication in blue. The [N–H···O] hydrogen bonds have the following distances and angles [N···O] 3.10, 3.05, 3.00 Å; [H···O] 2.25, 2.39, 2.33 Å; [N–H···O] 155, 133, 131°. The [C–H···O] hydrogen bonds have the following distances and angles [C···O] 3.24 Å; [H···O] 2.30 Å; [C–H···O] 163°. Bottom: Space-filling representation of the complex.

complex is centrosymmetric with respect to the central *para*-xylyl unit of the dication. Once again, the complex is stabilized by a combination of [N–H···O] and [C–H···O] hydrogen bonds. In addition, there are π–π stacking interactions between the almost parallel, aligned catechol and *para*-xylyl units within the superstructure (these rings are inclined by ca. 5° and have centroid–centroid separations of 3.65 Å). In this complex, there is an absence of any pronounced channel formation within the crystals.

Both $\mathbf{1}\text{-}H\cdot PF_6$ and $\mathbf{3}\text{-}H_2\cdot 2PF_6$ have very low solubilities[7] in CD_2Cl_2. On the addition of **BPP34C10**, the solubility of $\mathbf{1}\text{-}H\cdot PF_6$ increases significantly (ca. tenfold). The ^1H NMR spectrum of a saturated solution of $\mathbf{1}\text{-}H\cdot PF_6$ in CD_2Cl_2 in the presence of **BPP34C10** exhibits signals[8] that integrate for the

 © VCH Verlagsgesellschaft mbH, D-69451 Weinheim, 1995 0570-0833/95/3417-1870 $ 10.00+.25/0

expected stoichiometry associated with the 1:2 complex [**BPP34C10**·(**1**-H)$_2$][PF$_6$]$_2$. By contrast, in the case of **3**-H$_2$·2PF$_6$, when **BPP34C10** is added to a saturated solution of the salt in CD_2Cl_2/CD_3CN (4:1, v/v), an approximately 1:1 ratio[9] of salt to crown ether is observed by integration. It was also noted that **3**-H$_2$·2PF$_6$ does not dissolve in $CDCl_3$, even in the presence of a large excess of **DB24C8**. However, when the spectrum of a 10:1 mixture of **DB24C8** and **3**-H$_2$·2PF$_6$ in $CDCl_3/CD_3CN$ (1:1, v/v) was recorded, only signals for the expected 2:1 complex[10] and the excess of **DB24C8** were observed under conditions of slow exchange on the ^{1}H NMR time scale. The stoichiometry of the complex was established by direct integration of the signals associated with its **DB24C8** and [**3**-H$_2$]$^{2+}$ components.

When positive-ion FAB mass spectrometry[11] was used to characterize these complexes, peaks for $[M - PF_6]^+$ ions were observed at *m/z* 1077 and 1360 for [**BPP34C10**·(**1**-H)$_2$][PF$_6$]$_2$ and [(**DB24C8**)$_2$·**3**-H$_2$][PF$_6$]$_2$, confirming the respective 1:2 and 2:1 stoichiometries of these species. The 2:2 complex formed between **3**-H$_2$·2PF$_6$ and **BPP34C10** in the solid state (Fig. 3) was not observed by positive-ion FABMS. However, a peak with *m/z* 999, corresponding to a species with 1:1 stoichiometry that has lost one counterion, is observed.

The ease with which both the monocationic (**1**-H$^+$) and dicationic ([**3**-H$_2$]$^{2+}$) species containing NH_2^+ recognition sites self-assemble with crown ether receptors such as **DB24C8** and **BPP34C10** to give highly ordered superstructures in solution, as well as in the solid state, could herald some new and fascinating developments in macromolecular science as a result of a productive marriage[12] between macrocyclic and supramolecular chemistry.

Experimental Procedure

3-H$_2$·2PF$_6$: A solution of benzylamine (5.14 g, 0.048 mol) and terephthaldehyde (3.26 g, 0.024 mol) was heated under reflux with stirring in a Dean–Stark apparatus for 10 h. After the reaction mixture was cooled down to room temperature, the solvent was evaporated off under vacuum to give the 1,4-bis(benzyliminomethyl)benzene as a brown solid [^{1}H NMR ($CDCl_3$): δ = 4.84 (s, 4H), 7.18–7.47 (m, 10H), 7.82 (s, 4H), 8.41 (s, 2H)] which was dissolved in MeOH (50 mL). $NaBH_4$ (3.80 g, 0.10 mol) was added in small portions to the reaction mixture which was heated under reflux with stirring for 8 h. It was then allowed to cool down to room temperature and concentrated HCl was added (pH < 2). After evaporation of the solvent, the residue was suspended in H_2O (30 mL) and extracted with CH_2Cl_2 (4 × 30 mL). The combined extracts were washed with 5% aqueous $NaHCO_3$ (2 × 60 mL), H_2O (50 mL), and then dried ($MgSO_4$). Removal of the solvent under vacuum afforded 1,4-bis(benzylaminomethyl)benzene (4.00 g) as a colorless solid [^{1}H NMR ($CDCl_3$): δ = 3.80 (s, 4H), 3.81 (s, 4H), 7.15–7.45 (m, 14H)] of which 2.00 g (0.006 mol) was dissolved in MeOH (30 mL). Concentrated HCl was added (pH < 2) and the reaction mixture was stirred for a further hour. Evaporation of the solvent afforded a colorless solid which was suspended in acetone (30 mL). An aqueous solution of NH_4PF_6 was added until dissolution occurred. Evaporation of acetone afforded colorless crystals of **3**-H$_2$·2PF$_6$, which were isolated, washed with H_2O, and air-dried (3.50 g, 90%, m.p. 238 °C with decomp.). Positive-ion FABMS: *m/z* 463 $[M - PF_6]^+$; ^{1}H NMR (CD_3CN): δ = 4.24 (s, 4H), 4.25 (s, 4H), 7.45–7.51 (m, 10H), 7.52 (s, 4H); ^{13}C NMR (CD_3CN): δ = 51.6, 52.4, 129.9, 130.6, 131.0, 131.2, 131.6, 132.9.

Received May 15, 1995 [Z 7990 IE]
German version: *Angew. Chem.* **1995**, *107*, 2001–2004

Keywords: crown ethers · molecular recognition · rotaxanes · self-assembly

[1] P. R. Ashton, P. J. Campbell, E. J. T. Chrystal, P. T. Glink, S. Menzer, D. Philp, N. Spencer, J. F. Stoddart, P. A. Tasker, D. J. Williams, *Angew. Chem.* **1995**, *107*, 1997–2001; *Angew. Chem. Int. Ed. Engl.* **1995**, *34*, 1869–1871.

[2] P. L. Anelli, P. R. Ashton, R. Ballardini, V. Balzani, M. Delgado, M. T. Gandolfi, T. T. Goodnow, A. E. Kaifer, D. Philp, M. Pietraszkiewicz, L. Prodi, M. V. Reddington, A. M. Z. Slawin, N. Spencer, J. F. Stoddart, C. Vicent, D. J. Williams, *J. Am. Chem. Soc.* **1992**, *114*, 193–218 and references therein.

[3] Crystal data for [**BPP34C10**·(**1**-H)$_2$][PF$_6$]$_2$: monoclinic, space group $P2_1/a$, a = 12.132(9), b = 18.378(7), c = 13.824(5) Å, β = 105.03(2)°, V = 2977(2) Å^3, Z = 2 (the complex has C_i symmetry), ρ_{calc} = 1.36 g cm^{-3}, $\mu(Cu_{K\alpha})$ = 15 cm^{-1}, Siemens P4/PC diffractometer, graphite-monochromated $Cu_{K\alpha}$ radiation. The structure was solved by direct methods and the anisotropic refinement gave R = 0.084, Rw = 0.093 for 3237 independent observed reflections with [$|F_o| > 4\sigma(|F_o|)$, $2\theta < 125°$]. Crystal data for [(**BPP34C10**)$_2$·(**3**-H$_2$)$_2$][PF$_6$]$_4$: monoclinic, space group $P2_1/n$, a = 18.101(4), b = 28.232(6), c = 27.525(6) Å, β = 99.71(3)°, V = 13865(5) Å^3, Z = 4, ρ_{calc} = 1.17 g cm^{-3}, $\mu(Cu_{K\alpha})$ = 12 cm^{-1}, Siemens P4/RA diffractometer, graphite-monochromated $Cu_{K\alpha}$ radiation. The structure was solved by direct methods and anisotropic refinement gave R_1 = 0.154, wR_2 = 0.398 for 6773 independent observed reflections with [$|F_o| > 4\sigma(|F_o|)$, $2\theta < 110°$]. Crystal data for [(**DB24C8**)$_2$·**3**-H$_2$][PF$_6$]$_2$: monoclinic, space group $P2_1/c$, a = 11.538(3), b = 29.293(7), c = 10.820(3) Å, β = 91.39(2)°; V = 3656(2) Å^3, Z = 2, ρ_{calc} = 1.37 g cm^{-3}, $\mu(Cu_{K\alpha})$ = 14 cm^{-1}, Siemens P4/PC diffractometer, graphite-monochromated $Cu_{K\alpha}$ radiation. The structure was solved by direct methods and refined anisotropically (based on F^2) to give R_1 = 0.087, wR_2 = 0.202 for 2516 independent observed reflections with [$|F_o| < 4\sigma(|F_o|)$, $2\theta < 114°$]. Further details of the crystal structure investigations may be obtained from the Director of the Cambridge Crystallographic Data Centre, 12 Union Road, GB-Cambridge CB2 1EW (UK).

[4] a) W. L. Jorgensen, D. L. Severance, *J. Am. Chem. Soc.* **1990**, *112*, 4768–4774; b) M. C. Grossel, A. K. Cheetham, D. A. Hope, S. C. Weston, *J. Org. Chem.* **1993**, *58*, 6651–6661; c) S. Paliwal, G. Geib, C. S. Wilcox, *J. Am. Chem. Soc.* **1994**, *116*, 4497–4498.

[5] a) D. B. Amabilino, I. W. Parsons, J. F. Stoddart, *Trends in Polym. Sci. (Cambridge, UK)* **1994**, *2*, 146–152; b) H. W. Gibson, M. C. Bheda, P. T. Engen *Prog. Polym. Sci.* **1994**, *19*, 843–945; c) H. W. Gibson, S. Lui, P. Lecavalier, C. Wu, Y. X. Shen, *J. Am. Chem. Soc.* **1995**, *117*, 852–874.

[6] The 2:1 complex was crystallized by vapor diffusion of diisopropyl ether into an acetonitrile solution of the bisammonium salt **3**-H$_2$·2PF$_6$ and **DB24C8** (1:2 stoichiometry).

[7] The solubility of **1**-H·PF$_6$ is roughly 8 mg in 10 mL of CD_2Cl_2, while **3**-H$_2$·2PF$_6$ is virtually insoluble in this solvent.

[8] The $\Delta\delta$ values (with reference to the uncomplexed crown ether) for the C_6H_4, α-CH_2, β-CH_2, γ-CH_2, and δ-CH_2 protons in **BPP34C10** deduced from the ^{1}H NMR spectrum of [**BPP34C10**·(**1**-H)$_2$][PF$_6$]$_2$ recorded in CD_2Cl_2 are +0.18, −0.03, −0.12, −0.31, and −0.43, respectively.

[9] For an equimolar mixture of **BPP34C10** and **3**-H$_2$·2PF$_6$ in CD_2Cl_2/CD_3CN (3:1, v/v), $\Delta\delta$ values (with reference to the free salt) of −0.34 and −0.11, respectively, are observed in the ^{1}H NMR spectrum for the aromatic and benzylic methylene protons associated with the bridging *para*-xylyl group in the [**3**-H$_2$]$^{2+}$ dication.

[10] The $\Delta\delta$ values (with reference to the uncomplexed crown ether and the free salt) for different protons obtained from the ^{1}H NMR spectrum of this sample recorded in $CDCl_3/CD_3CN$ (1:1, v/v) range a) from −0.05 to −0.19 for protons in **DB24C8** and b) from −0.67 to +0.35 for protons in **3**-H$_2$·2PF$_6$.

[11] FABMS were recorded on a Kratos MS80RF mass spectrometer (accelerating voltage 3 kV, resolution 1000) coupled to a DS data system and off-line Sun Workstation for processing the raw data. The atom gun was an adapted saddle field source (Ion Tech Limited) that operated at ca. 8 keV and with a tube current of ca. 2 mA. Krypton was used to provide a primary beam of atoms and the samples were dissolved in a small volume of 3-nitrobenzyl alcohol which had previously been coated on to a stainless steel probe tip. Spectra were recorded in the positive-ion mode at a scan speed of 30 s per decade.

[12] The double-stranded inclusion complexes that are formed when γ-cyclodextrin threads simultaneously on to two poly(ethylene glycol) chains is one of the very few examples in the literature of this particular form of supermolecule involving a macrocycle. See A. Harada, J. Li, M. Kamachi, *Nature*, **1994**, *370*, 126–128. The formation of molecular nanotube aggregates of β- and γ-cyclodextrins has been reported. See G. Li, L. B. McGown, *Science* **1994**, *264*, 249–251.

 © VCH Verlagsgesellschaft mbH, D-69451 Weinheim, 1995 0570-0833/95/3417-1871 $ 10.00+.25/0

$(C_5Me_5)TiF_2$—A Versatile Building Block for Generating Large Soluble Dimetallic Aggregates**

Feng-Quan Liu, Dietmar Stalke, and Herbert W. Roesky*

Dedicated to Professor Herbert Schumann on the occasion of his 60th birthday

In 1826 Berzelius observed the formation of heteropolyanions in the reaction of molybdate with phosphate and arsenate; however, it is only in the last two decades that this field of research has received tremendous attention in theory and practice.[1] Organometallic complexes of polyoxoanions were investigated for example by Day, Klemperer, and Finke.[2]

Neutral metal clusters containing up to 146 metal atoms have been structurally investigated.[3] However, the only characterized examples of systems of this size have contained one kind of metal atom. We are not aware that any organometallic fluorides have been used for dimetallic cluster formation up to now. Recently, we described the preparation and structure of $[Cp^*_6Ti_6Na_7F_{19}]$ ($Cp^* = C_5Me_5$).[4] Here we report on the preparation and structural characterization of the two large dimetallic clusters **1** and **2**, which were formed in the reaction

$[Cp^*_{12}Ti_{14}Na_{18}F_{48}(thf)_6]$ **1** $[(Cp^*TiF_2)_6CaF_2(thf)_2]$ **2**

of $[Cp^*TiF_3]$[5, 6] with the corresponding alkali and alkaline earth metal as a reducing agent in THF (THF = tetrahydrofuran) in the presence of mercury.

From the filtered reaction mixture of **1**, green, oxygen- and moisture-sensitive single crystals were obtained by recrystallization from THF/hexane. Surprisingly, no NaF precipitated during the reaction. DMPE (DMPE = 1,2-bis(dimethylphosphino)ethane) was added during the reduction to stabilize the low oxidation state of the titanium center. As expected, no DMPE is present in the final product because of the better donor properties of the fluoro ligands in this system.

The structure of this cluster was determined by single-crystal X-ray analysis[7] at low temperature. Twelve Cp^*TiF_2 groups almost completely enclose two TiF_3 and eighteen NaF molecules (Fig. 1).

The central inorganic $[(TiF_3)_2(NaF)_{18}]$ unit is covered with a hydrocarbon layer consisting of twelve Cp^*TiF_2 units and six sodium-coordinated thf molecules. This provides—although poor—solubility of the aggregate in hydrocarbon solvents. The average $Ti-Cp^*_{(centroid)}$ distance (202 pm; range from 199 to 204 pm) is in accordance with literature values;[11] the same is true for the average Na–O(thf) distance of 235 pm (range from 226 to 242 pm).[12]

The kidney-shaped inorganic core consists of 14 Ti^{III}, 18 Na, and 48 F atoms. Twelve of the 14 Ti atoms are approximately square-based pyramidal coordinated; four F atoms form the base of the pyramid and the Cp* ligand centroid adopts the apical position. The Ti–F bonds can be divided into a set of long and short distances. The two shorter Ti–F bonds (198 pm; range from 195 to 202 pm) are in accordance with the distances

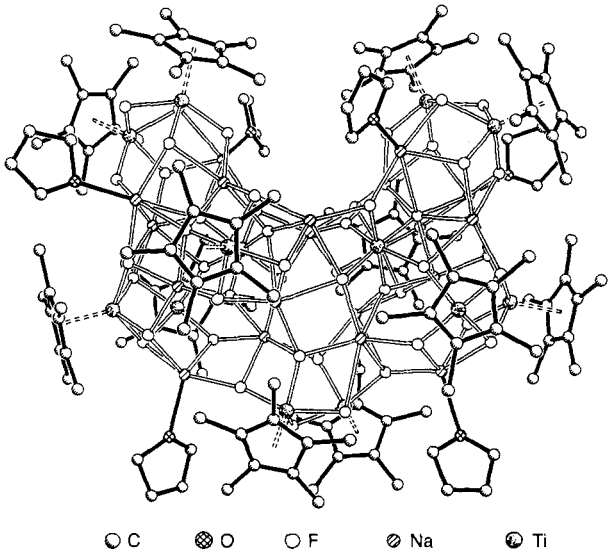

Fig. 1. The solid state structure of **1**. For clarity the nine uncoordinated THF solvent molecules are not depicted. Average bond lengths [pm] and (range): $Cp^*_{(centroid)}-Ti$ 202 (199–204), short Ti–F 198 (195(1)–202(1)), long Ti–F 205 (202(1)–210(1)), Na–F 232 (215(1)–291(2)).

in TiF_3.[13] The longer distances (205 pm; range from 202 to 210 pm) are found in the coordination to adjacent F atoms which are shared by two Ti atoms. Two of the fourteen Ti atoms are distorted octahedral coordinated by six F atoms at an average distance of 197 pm (range from 194 to 206 pm).

The eighteen Na atoms of the molecule are coordinated in four different ways: two are five-coordinate, surrounded by four F atoms and one thf molecule, four are six-coordinate surrounded by five F atoms and one thf molecule, four are five-coordinate and eight are six-coordinate surrounded exclusively by F atoms. The average Na–F distances of the four different coordination polyhedra are 226, 242, 226, and 232 pm, respectively. The average of the 96 independent distances of 232 pm is consistent with the corresponding distances in NaF.[14] The remaining nine THF molecules are not coordinated to any metal; they occupy vacant lattice sites. As a result of the paramagnetic properties and relatively poor solubility of compound **1** at low temperature, we were unable to confirm the structure in solution by NMR spectroscopy or by cryoscopic molecular weight determination. However, the presence of even larger aggregates (100–1000 Å) in solution is assumed because of the Tyndall effect of the solution (Fig. 2).

Fig. 2. The Tyndall effect of a sodium-reduced solution of $[Cp^*TiF_3]$ in THF.

[*] Prof. Dr. H. W. Roesky, Dr. F.-Q. Liu, Priv.-Doz. Dr. D. Stalke
Institut für Anorganische Chemie der Universität
Tammannstrasse 4, D-37077 Göttingen (Germany)
Telefax: Int. code + (551)393373

[**] We gratefully acknowledge support by the Deutsche Forschungsgemeinschaft, the Fonds der Chemischen Industrie, the Volkswagen-Stiftung, the BMBF, and the Hoechst AG.

 © VCH Verlagsgesellschaft mbH, D-69451 Weinheim, 1995 0570-0833/95/3417-1872 $ 10.00+.25/0

The second example of the formation of a large aggregate with Cp^*TiF_2 units is the first soluble CaF_2 complex $[(Cp^*TiF_2)_6CaF_2(thf)_2]$ (**2**). Calcium difluoride is prepared in situ by adding a solution of Cp^*TiF_3 to a suspension of calcium metal in the presence of mercury at 0 °C. The reaction mixture was filtered and pale green crystals were obtained at 0 °C. Also, under these conditions the Ti^{IV} centers were reduced to Ti^{III} centers. The result of the crystal structure determination[7] of **2** is shown in Figure 3. The center between two $[Cp^*_3Ti_3F_7(thf)]$ moieties is a single Ca atom. Like in the solid-state structure of CaF_2,[15] the Ca atom is coordinated to eight F atoms but in a rather distorted way. Four Ca–F bonds are long (average 253 pm), while the other four are much shorter (average 226 pm). Hence the central unit can be described as two penetrating distorted tetrahedrons.

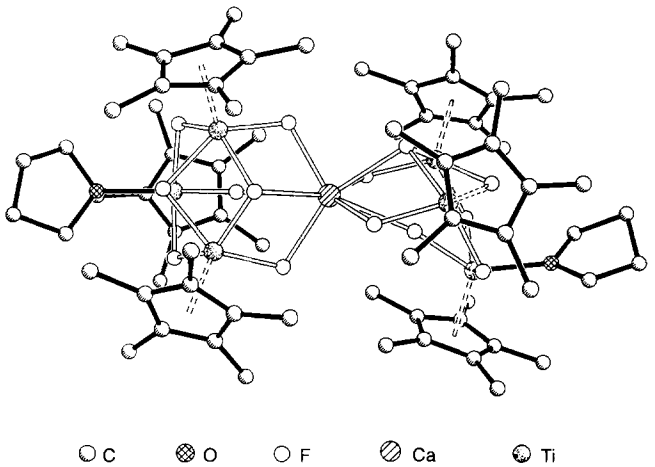

Fig. 3. The solid state structure of **2**. For clarity, the four uncoordinated THF solvent molecules are not depicted. Average bond lengths [pm] and (range): $Cp^*_{(centroid)}$ Ti 204 (201–206), Ti–F 206 (198.4(2)–213.3(2)), long Ca–F 253 (266.3(2) 244.6(2)), short Ca–F 226 (225.2(2)–227.2(2)).

Although the structural features from CaF_2 are not maintained in the structure of **2**, the average value of the Ca–F bond is in accordance with that in fluorite.[15a] To our knowledge there is only one other highly aggregated complex akin to **2**, however, it contains Ti^{IV} centers. In $[M\{Ti_2(OR)_9\}_2]$ (M = Ca, Ba), eight Ti^{IV}-bound oxygen atoms are coordinated in a similar way to the central calcium or barium atom.[16]

Unlike in **1** there are no different sets of Ti–F distances in **2**; on average (206 pm), they are even longer than the long Ti–F distances in **1**. Also the average $Ti-Cp^*_{(centroid)}$ distance (204 pm) is 2 pm longer than that in **1**. In **2** the titanium ligand distances are not influenced by the different coordination of the Ti atoms. While four Ti atoms are coordinated by four F atoms and one Cp* ligand, two are only coordinated by three F atoms and one Cp* ligand. The remaining four THF molecules are not coordinated to any metal center but occupy vacant lattice sites.

Although CaF_2 has broad applications in chemistry, up to now it was not available to organometallic chemistry because of its poor solubility in common organic solvents.[17] With the Cp^*TiF_2 building block, it now seems possible to establish a new field of chemistry at the borders of solid state and organometallic chemistry. While the dimetallic inorganic core of compounds **1** and **2** resembles that in many solid phases with respect to its structural parameters, solubility of the cluster in common organic solvents is provided by wrapping that core with the Cp^*TiF_2 unit. The generation of solids in solution and their encapsulation by organometallic moieties might have a broad application. CaF_2, which was already known from work by Agricola[18] in 1529, now seems to be accessible to well-established organometallic techniques.

Experimental Procedure

All reactions must be carried out under careful exclusion of water and oxygen.

1: A solution of $[Cp^*TiF_3]$ (0.72 g, 3.0 mmol) and DMPE (0.9 mL) in THF (40 mL) was added dropwise to a suspension of sodium metal (0.07 g, 3.0 mmol, 12 g Hg) in THF (20 mL) at 0 °C. The mixture was stirred for 12 h at room temperature during which time the solution changed from orange to green. The solution was filtered and the solvent was concentrated to 30 mL and cooled to 0 °C. Under these conditions X-ray suitable green crystals were obtained after 4 d and more crystalline material was obtained by concentrating the solution to 15 mL. The solvent-free green product was obtained at 25 °C/10^{-2} Torr after 12 h. It decomposed at 221 °C. Correct elemental analyses. IR (Nujol): 1494w, 1290m, 1054s, 934m, 719s, 492s, 403s cm^{-1}.

2: A solution of $[Cp^*TiF_3]$ (0.72 g, 3.0 mmol) in THF (40 mL) was added dropwise to Ca/Hg alloy (0.06 g, 1.5 mmol Ca in 30 g mercury) in THF (25 mL) at room temperature. The mixture was stirred for 12 h at this temperature during which time the solution changed from orange to green. The reaction mixture was subsequently filtered and the solvent was removed in vacuum. The residue was recrystallized from THF/hexane (30 mL/30 mL) which yielded 0.47 g of **2** (62%). M.p. 268 °C (decomp.). Correct elemental analyses from the solvent-free compound (10^{-2} Torr, 25 °C, 12 h). IR (Nujol) : 1496w, 1342m, 1260m, 1165m, 1074s, 874s, 477s, 394s cm^{-1}.

Received: April 1, 1995 [Z 7856 IE]
German version: *Angew. Chem.* **1995**, *107*, 2004–2006

Keywords: aggregates · fluorine compounds · structure elucidation · titanium compounds

[1] M. T. Pope, A. Müller, *Polyoxometalates: From Platonic Solids to Anti-Retroviral Activity*, Kluwer, Dordrecht, **1994**.
[2] V. W. Day, W. G. Klemperer, *Science* **1985**, *228*, 533; M. Pohl, Y. Lin, T. J. R. Weakley, K. Nomiya, M. Kaneko, H. Weiner, R. G. Finke, *Inorg. Chem.* **1995**, *34*, 767, and references therein.
[3] H. Krautscheid, D. Fenske, G. Baum, M. Semmelmann, *Angew. Chem.* **1993**, *105*, 1364; *Angew. Chem. Int. Ed. Engl.* **1993**, *32*, 1303.
[4] F.-Q. Liu, A. Kuhn, R. Herbst-Irmer, D. Stalke, H. W. Roesky, *Angew. Chem.* **1994**, *106*, 577; *Angew. Chem. Int. Ed. Engl.* **1994**, *33*, 555.
[5] H. W. Roesky, M. Sotoodeh, M. Noltemeyer, *Angew. Chem.* **1992**, *104*, 896; *Angew. Chem. Int. Ed. Engl.* **1992**, *31*, 864.
[6] A. Herzog, F.-Q. Liu, H. W. Roesky, A. Demsar, K. Keller, M. Noltemeyer, F. Pauer, *Organometallics* **1994**, *13*, 1251.
[7] Crystal data of **1**·9THF, $M = 4620.45$, monoclinic, space group $P2_1/c$, $a = 1643.9(2)$, $b = 4213.5(8)$, $c = 3158.1(4)$ pm, $\beta = 92.25(1)°$, $V = 21.857(6)$ nm^3, $Z = 4$, $\rho_{calcd} = 1.404$ $Mg\,m^{-3}$, $F(000) = 9560$, $\lambda = 0.71073$ Å, $T = 153$ K, $\mu(Mo_{K\alpha}) = 0.609$ mm^{-1}, data were collected on a Stoe-Siemens-AED diffractometer. Intensities of a $0.6 \times 0.55 \times 0.45$ mm rapidly cooled crystal in an oil drop [8] were collected by the $2\theta/\omega$ method in the range of $4° \le 2\theta \le 42°$. Of a total of 26618 reflections, 23345 ($R_{int} = 0.145$) were independent and 22550 used to refine 2530 parameters (3915 restraints), largest difference peak and hole: 598 and -656 $e\,nm^{-3}$, $R1(F > 4\sigma(F)) = 0.116$ and $wR2 = 0.405$ (all data) with $R1 = \Sigma||F_o| - |F_c||/\Sigma|F_o|$ and $wR2 = (\Sigma w(F_o^2 - F_c^2)^2/\Sigma w(F_o^2)^2)^{0.5}$. The relativly high R value is due to a severe decay of intensities (about 60%) during the data collection which lasted 15 days with an conventional scintillation detector. Crystal data of **2**·4THF, $M = 1833.48$, triclinic, space group $P\bar{1}$, $a = 1147.93(8)$, $b = 1624.0(1)$, $c = 2489.7(2)$ pm, $\alpha = 87.431(7)$, $\beta = 82.210(5)$, $\gamma = 72.401(5)°$, $V = 4.4069(6)$ nm^3, $Z = 2$, $\rho_{calcd} = 1.382$ $Mg\,m^{-3}$, $F(000) = 1936$, $\lambda = 0.71073$ Å, $T = 153$ K, $\mu(Mo_{K\alpha}) = 0.653$ mm^{-1}, data were collected on a Stoe-Siemens-AED diffractometer. Intensities of a $0.8 \times 0.8 \times 0.6$ mm rapidly cooled crystal in an oil drop [8] were collected by the $2\theta/\omega$ method in the range of $4° \le 2\theta \le 45°$. Of a total of 15866 reflections 11629 ($R_{int} = 0.030$) were independent and 11626 used to refine 1138 parameters, largest difference peak and hole: 507 and -518 $e\,nm^{-3}$, $R1(F > 4\sigma(F)) = 0.040$ and $wR2 = 0.103$ (all data) with $R1 = \Sigma||F_o| - |F_c||/\Sigma|F_o|$ and $wR2 = (\Sigma w(F_o^2 - F_c^2)^2/\Sigma w(F_o^2)^2)^{0.5}$. Both structures were solved with direct methods (SHELXS-92) [9]. Compound **1** was refined by full-matrix-block least-squares and **2** by full-matrix least-squares on F^2 (SHELXL-93) [10]. A riding model was applied to refine the hydrogen atom positions. Further details of the crystal structure investigations are available on request from the Director of the Cambridge Crystallographic Data Centre, 12 Union Road, GB-Cambridge CB2 1EZ (UK), on quoting the full journal citation.
[8] T. Kottke, D. Stalke, *J. Appl. Crystallogr.* **1993**, *26*, 615.
[9] G. M. Sheldrick, *Acta Crystallogr. Sect. A* **1990**, *46*, 467.

 © VCH Verlagsgesellschaft mbH, D-69451 Weinheim, 1995 0570-0833/95/3417-1873 $ 10.00+.25/0

[10] G. M. Sheldrick, SHELXL-93, program for crystal structure refinement, Göttingen, **1993**.
[11] F.-Q. Liu, H. Gornitzka, D. Stalke, H. W. Roesky, *Angew. Chem.* **1993**, *105*, 447; *Angew. Chem. Int. Ed. Engl.* **1993**, *32*, 441.
[12] C. Schade, P. von R. Schleyer, *Adv. Organomet. Chem.* **1987**, *27*, 169.
[13] a) P. Ehrlich, G. Pietzka, *Z. Anorg. Allg. Chem.* **1954**, *275*, 121; b) S. Siegel, *Acta Crystallogr.* **1956**, 684; c) R. Hoppe, S. Becker, *Z. Anorg. Allg. Chem.* **1989**, *568*, 126.
[14] a) W. L. Bragg, *Nature* **1920**, 648; b) T. Barth, *Z. Phys.* **1926**, *40*, 804.
[15] For typical studies: a) D. N. Batchelder, R. O. Simmons, *J. Chem. Phys.* **1964**, *41*, 2324; b) A. K. Cheetham, B. E. F. Fender, M. J. Cooper, *J. Phys.* **1952**, *4*, 3107; c) B. T. M. Willis, *Acta Crystallogr.* **1965**, *18*, 75; d) A. Weiss, H. Witte, E. Wölfel, *Z. Phys. Chem.* **1957**, *10*, 98.
[16] E. P. Turevskaya, V. G. Kessler, N. Y. Turova, A. P. Pisarevsky, A. I. Yanovsky, Y. T. Struchkov, *J. Chem. Soc. Chem. Commun.* **1994**, 2303.
[17] H. J. Emeléus, *The Chemistry of Fluorine and its Compounds*, Academic Press, New York, **1969**.
[18] *Gmelin Handbuch der Anorganische Chemie, Fluor* 8th ed. **1926** p. 1.

Platination Pathways for Reactions of Cisplatin with GG Single-Stranded and Double-Stranded Decanucleotides**

Kevin J. Barnham, Susan J. Berners-Price, Tom A. Frenkiel, Urban Frey, and Peter J. Sadler*

The anticancer drug cisplatin, *cis*-$[PtCl_2(NH_3)_2]$, disrupts cellular replication and transcription by the formation of Pt-DNA adducts, largely guanine–guanine (GG) and adenine–guanine (AG) intrastrand cross-links.[1, 2] Therefore it is important to understand the mechanisms of DNA platination and the perturbations of DNA structure which these adducts cause. The rate-determining step in GG platination is believed to be hydrolysis of cisplatin, followed by monofunctional binding to N7 of either the 3′- or 5′-G, and finally macrocyclic ring closure to give the bifunctional GG adduct. However, direct detection of aquated cisplatin during the course of DNA reactions has proved to be difficult. None was seen by Bancroft et al.[3] by ^{195}Pt NMR spectroscopy, even with enriched ^{195}Pt and high concentrations of DNA oligomers (ca. 14–32 mM). These workers were able to detect monofunctional adducts and determine the rate of ring closure by independent studies of reactions of the aqua-chloro complex with DNA. In an alternative approach, Chottard et al.[4, 5] have recently determined the rates of attack of "diaqua cisplatin" (Cl replaced by H_2O) on GG oligonucleotides and rates of ring closure using an HPLC trapping method. We report here that the major species in the pathways of platination of both single- and double-stranded GG oligonucleotides by ^{15}N-cisplatin can all be detected simultaneously by $[^1H,^{15}N]$ NMR spectroscopy. We have determined directly, for the first time, the lifetime of the aqua-chloro intermediate present at only micromolar concentrations, and investigated differences in the platination pathways for single- and double-stranded DNA. Both ^1H and ^{15}N NMR resonance signals are sensitive to cisplatin-induced helix melting. The method will be generally applicable to a wide range of DNA substrates and platinum ammine and amine complexes, and promises to provide new insights into the factors which influence Pt-DNA recognition.

We have studied platination of the deoxydecanucleotide **I** and its duplex with **II** (**I** + **II** = **III**) using ^{15}N-labeled cisplatin, *cis*-$[PtCl_2(^{15}NH_3)_2]$ (**1**) to allow the selective detection of ^1H and ^{15}N NMR resonances of Pt-NH_3 groups by the use of $^1H\{^{15}N\}$ inverse detection methods.[6] This, combined with the use of sequences incorporating pulsed-field gradients,[7] enabled detection of intermediates present at only micromolar concentrations, and also peaks whose chemical shifts lie very close to the resonance signal of the H_2O protons.

	1	2	3	4	5	6	7	8	9	10	
5′-d(	A	C	A	T	**G**	**G**	T	A	C	A)	**I**
3′-d(	T	G	T	A	C	C	A	T	G	T)	**II**
	20	19	18	17	16	15	14	13	12	11	

Duplex from **I** + **II** = **III**

The reaction between **1** and single-stranded DNA **I** (ca. 1:1 mol ratio, 1.3 mM, 10 mM sodium phosphate pH 7.1, 90% H_2O/10% D_2O, 310 K), was followed by recording a series of ^{15}N-edited ^1H NMR spectra. Assignments of peaks for products and intermediates were aided by ^{15}N chemical shifts from 2D $[^1H,^{15}N]$ spectra. These are diagnostic of the ligand (X) *trans* to the ammine group of the platinum complex: For X = O $\delta = -95$ to -75; for X = N or Cl $\delta = -70$ to -50.[8]

Within the first few minutes, resonances 2a (^{15}N *trans* to Cl) and 2b (^{15}N *trans* to O) assignable to the hydrolysis product *cis*-$[PtCl(H_2O/OH)(NH_3)_2]^+$ (**2**) were detected (Fig. 1).[9] These attained their maximum intensities after about 40 min and then gradually decreased in intensity. They were no longer visible (i.e. accounted for <1% of total Pt-NH_3) after 5 h. The hydrolysis product **2** was clearly detectable by this method even at concentrations of about 10 μM.

The pair of peaks for compound **3** (3a: $\delta = 4.45/-65.8$ and 3b: $\delta = 4.11/-68.7$) also became visible within the first 30 min (Fig. 1). They reached a maximum intensity after about 4.5 h, and then gradually decreased in intensity. Their $^1H/^{15}N$ shifts are similar to those of the monosubstituted 5′-guanosine monophosphate (GMP) complex[10] *cis*-$[PtCl(GMP\text{-}N7)(NH_3)_2]^+$,[6, 11] and therefore a reasonable assignment is to a monofunctional N7-G adduct in which Pt is bound to either the 3′- or 5′-G of the oligonucleotide **I** (G(5) or G(6), respectively).

Shortly after this, peaks for another intermediate species **4** (4a: $\delta = 4.40/-65.9$, 4b: overlapped with the signal 3b and with a ^{195}Pt satellite of the signal 1) became visible (Fig. 1). In view of their similar ^1H and ^{15}N NMR shifts and their similar time dependences, intermediates **3** and **4** can be assigned to be the monofunctional N7-G(5) and N7-G(6) adducts *cis*-$[PtCl(\mathbf{I}\text{-}N7\text{-}G)(NH_3)_2]$. Both **3** and **4** can undergo ring closure to form the bifunctional GG chelate complex *cis*-$[Pt(\mathbf{I}\text{-}N7\text{-}G(5),N7\text{-}G(6))(NH_3)_2]$ (**5**). Peaks assignable to **5** (5a: $\delta = 4.55/-68.4$, 5b: $\delta = 4.62/-66.6$) were first observed after 90 min and continued

[*] Prof. Dr. P. J. Sadler, Dr. K. J. Barnham
Department of Chemistry, Birkbeck College, University of London
Gordon House and Christopher Ingold Laboratories
29 Gordon Square, GB-London WC1H 0PP (UK)
Telefax: Int. code +(171) 380-7464
e-mail: ubca424@ccs.bbk.ac.uk
Dr. S. J. Berners-Price
Faculty of Science and Technology
Griffith University, Nathan, Brisbane 4111 (Australia)
Dr. T. A. Frenkiel
Biomedical NMR Centre, National Institute for Medical Research
The Ridgeway, Mill Hill, GB-London NW7 1AA (UK)
Dr. U. Frey
Institut de Chimie Minerale et Analytique
University of Lausanne
BCH, CH-1015 Lausanne (Switzerland)

[**] This work was supported by the Medical Research Council, Australian NH&MRC (R. Douglas Wright Award to S. J. B.-P.), The British Council, Association for International Cancer Research, and EC HCM (CHRX-CT92-0016) and COST (D1-0002-92) programs, the members of which we also thank for stimulating discussions.

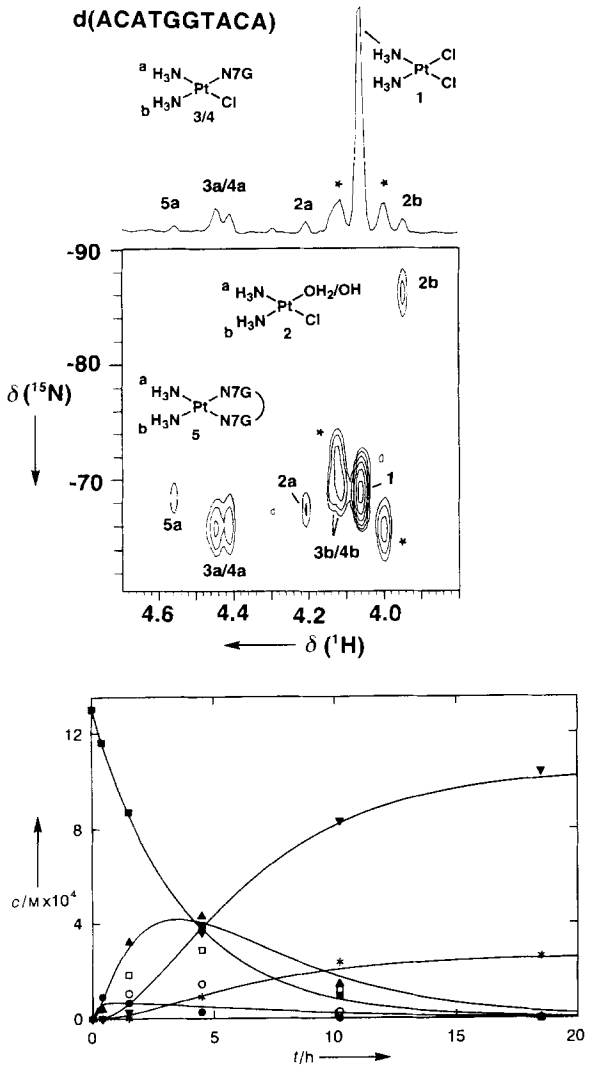

Fig. 1. Platination of single-stranded d(ACATGGTACA) (**I**) with *cis*-$[PtCl_2(^{15}NH_3)_2]$ **1** at 310 K. Top: Typical 500 MHz 2D [^{1}H,^{15}N] HSQC spectrum after 1.5 h reaction time, 310 K, acquired in 21 min, showing peaks assigned to NH_3 in the structures **1**–**5**. Peak 5b (NH_3 *trans* to N7-G6/5) is obscured by suppression of the H_2O peak (low frequency filter, Varian software), but is revealed in a ^{15}N-coupled spectrum at $\delta = 4.62/-66.6$. A broad peak for other adducts (**6**) appears after 4 h (see text). Bottom: Plot of relative concentrations of species **1**–**6** (based on Pt-NH_3 peak integrals) versus time. Cisplatin [**1**] (■), aqua-chloro intermediate [**2**] (●), monofunctional Pt-G intermediates [**3**] or [**4**] (□ and ○), sum of **3** + **4** (▲), GG chelate [**5**] (▼), and [**6**] (unassigned) (*). The curves are the computer best fits for the rate constants given in Scheme 1 (where errors represent one standard deviation).

to increase in intensity until the reaction was complete (ca. 20 h). It is notable that peak 5b is very close to the H_2O peak, and previously we have observed such large low-field shifts only for Pt-NH groups strongly H-bonded to terminal 5′-phosphates in nucleotide complexes of Pt^{II} ammines and amines.[11, 12]

At reaction times less than 4 h, no other Pt-NH_3 resonances were detected. However, after this time, a new broad Pt-NH_3 resonance signal became visible with a ^{1}H/^{15}N cross-peak at about $\delta = 4.52/-65.1$. The time-dependent increase in concentration of the species (**6**) associated with this peak is shown in Figure 1 bottom. By comparison of peak integrals, **6** accounts for about 20% of the total Pt-NH_3 species present at equilibrium, the bifunctional adduct **5** accounting for the remaining 80%. Since the signal for **6** was not seen during reactions of **1** with duplex DNA (vide infra), it can be assigned to interstrand cross-linked complexes involving for example N1-G (not accessible in duplexes).

Kinetic analysis of the data as a series of consecutive first- and second-order processes gave rise to the rate constants in Scheme 1.[13] The half-life for the first aquation step of **1** (2.51 h) is close to the values reported previously for cisplatin

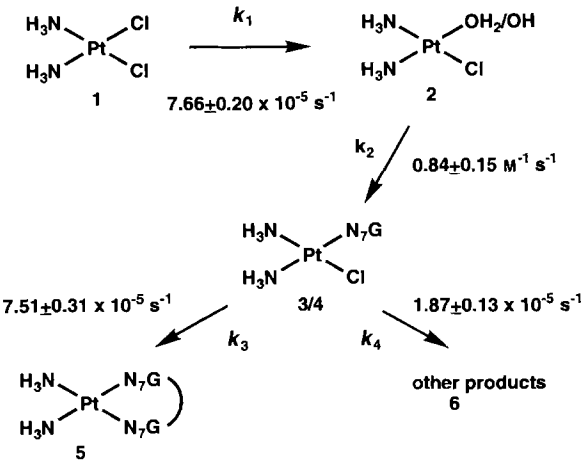

Scheme 1.

hydrolysis,[14] and to that determined by Bancroft et al.[3] for the disappearance of cisplatin during reactions with double-stranded chicken erythrocyte DNA by ^{195}Pt NMR spectroscopy (1.9 h) under similar conditions, and the half-life for the aqua intermediate of only 0.14 h is close to their estimated value of 0.1 h.[3] One of the N7-G monofunctional intermediates is present during the reaction in a greater proportion than the other (ratio ca. 2:1). This may be the 5′-G (G(5)) adduct **3** since Gonnet et al.[4] have shown that 3′-G monofunctional adducts formed from *cis*-$[Pt(NH_3)_2(H_2O)_2]^{2+}$ undergo ring closure reactions about ten times faster than 5′-G monofunctional adducts. In our experiments the half-life for the conversion of monofunctional into bifunctional adducts was 2.6 h, similar to that reported for single-stranded chicken erythrocyte DNA[3] (2.1 h), and consistent with aquation controlling this step too.

The platinated duplex *cis*-[Pt(**III**-N7-G(5),N7-G(6))$(NH_3)_2$] **7** was formed by the addition of 1 mol equivalent of the complementary strand **II** to the equilibrium solution containing platinated **I**. The ^{15}N-edited ^{1}H NMR spectrum contained two sharp peaks at $\delta = 4.48$ and 4.26 (283 K), assignable to the Pt-NH_3 protons of the bifunctional adduct **7**, together with a very broad unresolved resonance at about $\delta = 4.6$ from other Pt-NH_3 species. Platinated duplex was formed also by direct reaction of cisplatin **1** with the preformed duplex **III**[15] (at 293 K to ensure that the DNA was double-stranded). The reaction was slow (in agreement with hydrolysis being the rate-limiting step) with only about 60% of the cisplatin reacting in the first 24 h, during which time peaks assignable to **2**, N7-G(5) and N7-G(6) monofunctional adducts, and at least one other intermediate were observed, as well as peaks for the products **7** and **8** described below. A kinetic analysis has not yet been attempted.

Figure 2 shows the ^{15}N-edited ^{1}H NMR spectrum after complete reaction of the duplex **III** with 1 mol equivalent cisplatin **1**. The chemical shifts and temperature dependences of the pair of peaks for the bifunctional adduct **7** are identical to those observed for the product formed on addition of **II** to the platinated single strand **I** (data not shown). Between 298 and 303 K, peaks

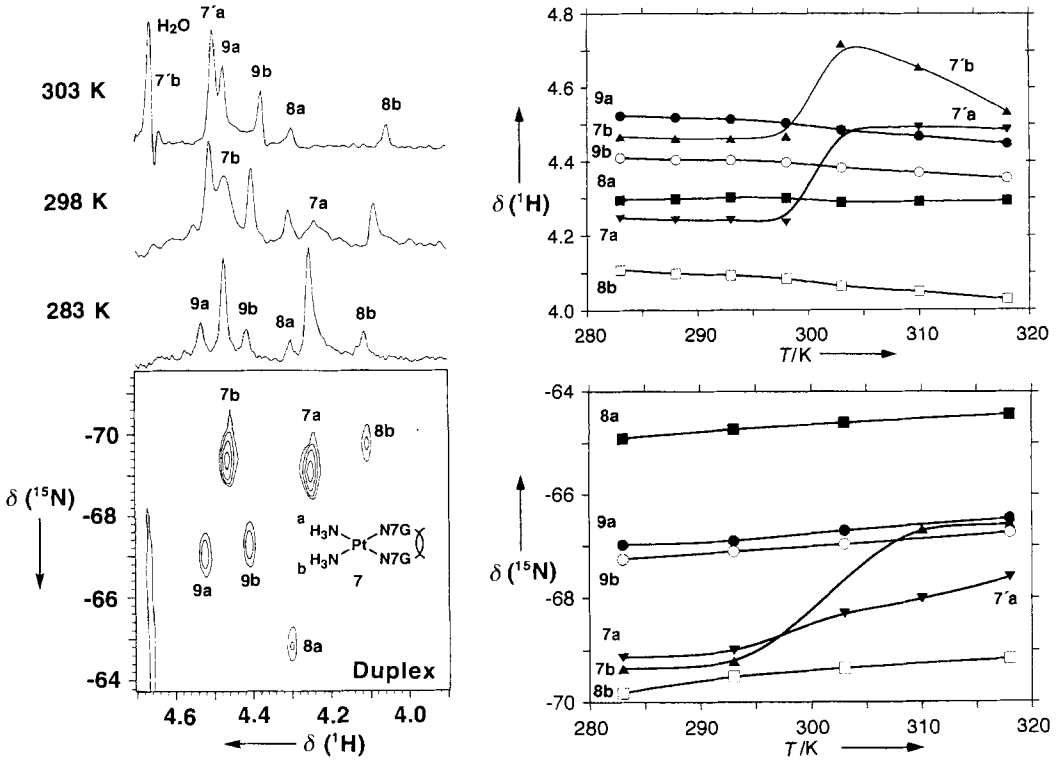

Fig. 2. Effect of temperature on the ^1H and ^{15}N NMR shifts of the platinated duplex formed by complete reaction (5 d, ca. 297 K) of 1 mol equivalent *cis*-$[PtCl_2(^{15}NH_3)_2]$ with d(ACATGGTACA)-d(TGTACCATGT) (**III**). Left: 600 MHz 2D $[^1H,^{15}N]$ HSQC spectrum at 283 K, showing peaks for *cis*-[Pt(**III**-N7-G(5),N7-G(6))$(NH_3)_2$] (**7**), and species **8** and **9** (unassigned, see text). 1D $^1H\{^{15}N\}$-edited NMR spectra for Pt-NH_3 resonances at various temperatures are also shown. Right: Temperature dependence of the ^1H and ^{15}N NMR shifts of platinated duplex. Between 298 and 303 K the peaks for **7** gradually disappear, and at >303 K two new peaks (7′a and 7′b) appear with shifts similar to those of the single-stranded GG chelate (species **5**). As for the platinated single strand, peak 7′b is obscured by the H_2O peak (but revealed in ^{15}N-coupled spectrum). Note the behavior of this peak at high temperature.

for **7** disappear, and at >303 K two new peaks (7′a and 7′b) appear with shifts similar to those assigned to the GG-platinated single strand (species **5**). This (reversible) temperature-dependent behavior can be attributed to melting of the platinated duplex with a T_m value of about 300 K,[16] an approximate 10 K lowering from the value for the unplatinated duplex, as expected.[17]

Two other stable adducts (**8** and **9**, Fig. 2) were produced by reaction of cisplatin **1** with duplex **III**. As these were not observed in spectra of the duplex formed by addition of **II** to the platinated single strand **I**, and were not sensitive to duplex melting (Fig. 2 right), they are likely to arise from Pt binding to the two G residues (G(12) and G(19)) near the terminii of the complementary strand **II**. For **9**, the ^{15}N chemical shifts of the two Pt-NH_3 groups are similar, whereas for **8** they are significantly different (Fig. 2). Their shifts, although very different, lie in the range expected for Pt-NH_3 *trans* to either N or Cl but it is not possible to distinguish between monofunctional and bifunctional adducts on this basis alone, and interstrand cross-links cannot be ruled out.

The large low-field shift of one of the Pt-NH_3 resonances (5 b) of the platinated single-strand GG adduct **5** is intriguing. Such a shift was not observed for the GG platinated duplex **7** until it melted (signal 7′b). The loss of this low-field shift at high temperature (Fig. 2 right), suggests that a GG platinated single-strand lesion has secondary structure which is destroyed on heating. This could have important functional consequences for platinated DNA. Whether this secondary structure involves a looped-back structure similar to that proposed[18] for *cis*-$[Pt(NH_3)_2\{$d-TCTCGGTCTC)-N7(5),N7(6)$\}]$, or a close interaction with the terminal bases giving rise to a ring-current shift, or hydrogen bonding to Pt-NH_3,[11] requires further investigation.

In summary, $[^1H,^{15}N]$-NMR spectroscopy can be used to study the mechanisms of DNA platination reactions at low concentration, and the major intermediates can all be detected. Aquated cisplatin had a half-life of only 8 min at 310 K in reactions of cisplatin with a single-stranded GG deoxydecanucleotide. One monofunctional Pt-N7-G intermediate dominated (by ca. 2:1) over the other, consistent with either preferential 3′- or 5′-G attack on GG and/or preferential chelate ring closure. Further experiments with the aqua-chloro complex should address this problem in a complementary manner to the reported HPLC experiments.[4] As expected, both the initial attack by cisplatin and the rate of ring closure appear to be determined by the Pt–Cl hydrolysis rate. The NH_3 resonances are very sensitive to melting of the platinated duplex and suggest that platinated lesions on single strands possess secondary structure. The method should be applicable to a wide range of oligonucleotides and lead to an improved understanding of the preferential attack by Pt on selected DNA sequences, which, in turn, will be invaluable in the drug design process.

Experimental Procedure

cis-$[PtCl_2(^{15}NH_3)_2]$ (**1**) was synthesized as described previously [19] and recrystallized from aqueous KCl. $^1H\{^{15}N\}$ NMR spectra were recorded on either a Varian UNITYplus-500 or a UNITY-600 spectrometer fitted with pulsed field gradient modules. ^1H spectra were referenced to TSP (TSP = $(Me_3Si(CD_2)_2CO_2Na)$, and ^{15}N spectra to 1.5 M NH_4Cl in 1 M HCl (external). Both 1D ^{15}N-edited ^1H NMR spectra and 2D $[^1H,^{15}N]$ HSQC spectra (optimized for $^1J(N,H) = 72$ Hz) were recorded by using the sequence of Stonehouse et al. [7]. In this sequence coherence selection and suppression of the ^1H_2O signal is achieved by the use of gradient pulses and the water magnetization is returned to its equilibrium position (z axis) before the start of data acquisition. The ^{15}N-spins were decoupled by irradiating with the GARP-1 sequence at field strength of 1 KHz during the acquisition time.

Received: March 24, 1995 [Z 7832 IE]
German version: *Angew. Chem.* **1995**, *107*, 2040–2043

Keywords: antitumor agents · DNA · NMR spectroscopy · nucleotides · platinum compounds

[1] S. E. Sherman, S. J. Lippard, *Chem. Rev.* **1987**, *87*, 1153–1181.
[2] J. Reedijk, *Inorg. Chim. Acta* **1992**, *198–200*, 873–881.
[3] D. P. Bancroft, C. A. Lepre, S. J. Lippard, *J. Am. Chem. Soc.* **1990**, *112*, 6860–6871.
[4] F. Gonnet, J. Kozelka, J.-C. Chottard, *Angew. Chem.* **1992**, *104*, 1494; *Angew. Chem. Int. Ed. Engl.* **1992**, *31*, 1483–1485.
[5] J. C. Chottard, *Proc. EUROBIC II*, Florence, Italy, Aug 30–Sept 3, **1994**, Abs. p 84.

 © VCH Verlagsgesellschaft mbH, D-69451 Weinheim, 1995 0570-0833/95/3417-1876 $ 10.00+.25/0

[6] S. J. Berners-Price, T. A. Frenkiel, J. D. Ranford, P. J. Sadler, *J. Chem. Soc. Dalton Trans.* **1992**, 2137–2139.
[7] J. Stonehouse, G. L. Shaw, J. Keeler, E. D. Laue, *J. Magn. Reson. Ser. A* **1994**, *107*, 174–184.
[8] T. G. Appleton, J. R. Hall, S. F. Ralph, *Inorg. Chem.* **1985**, *24*, 4685–4693.
[9] S. J. Berners-Price, T. A. Frenkiel, U. Frey, J. D. Ranford, P. J. Sadler, *J. Chem. Soc. Chem. Commun.* **1992**, 789–791. Some phosphate coordination may also be present.
[10] The charges on the nucleotides are ignored in the formulae.
[11] S. J. Berners-Price, U. Frey, J. D. Ranford, P. J. Sadler, *J. Am. Chem. Soc.* **1993**, *115*, 8649–8659; $\delta = 4.38/-66.4$ N *trans* to Cl; $\delta = 4.09/-69.1$ N *trans* to NH_3.
[12] S. J. Berners-Price, J. D. Ranford, P. J. Sadler, *Inorg. Chem.* **1994**, *33*, 5842–5846.
[13] The appropriate differential equations were integrated numerically and rate constants determined by a non-linear optimization procedure. The errors quoted represent one standard deviation. To simplify the kinetic treatment, it was assumed that each monofunctional intermediate (**3** or **4**) gives rise to the same products (**5** and **6**). To achieve a good fit for complex **2**, it was necessary to assume that a small excess (20%) of strand **I** over **1** was present in the reaction solution; about 20% of **I** appeared to be unreacted at equilibrium. We were able to exclude a model in which each intermediate gives rise to only one product (e.g., **3** gives **5**, and **4** gives **6**) since this did not fit the data. A more elaborate kinetic analysis will require a more detailed assessment of the errors in measurement of concentrations from peak intensities (problems of overlap and nearness to the solvent peak) and identification of unknown products.
[14] S. E. Miller, D. A. House, *Inorg. Chim. Acta* **1989**, *161*, 131–137.
[15] By mixing **I** and **II** in an equimolar ratio (1.5 mM; 10 mM phosphate buffer, pH 6.82). Seven of the ten imino proton resonances were observed at 278 K: four in the downfield region ($\delta = 13.4$ to 13.6, A–T base pairs) and three in the G–C region ($\delta = 12.5$ to 12.7), consistent with end-fraying so that the imino resonances of the terminal A–T base-pairs and either the C(9)–G(12) or C(2)–G(19) base pairs are in rapid exchange with solvent. One G–C resonance and one A–T resonance began to undergo exchange-broadening at 293 K and were in rapid exchange with solvent by 303 K, slightly below the exchange temperature of the remaining G–C and A–T resonances (303–310 K).
[16] The ^{1}H NMR spectrum of **III**-Pt (formed either from direct platination of **III**, or addition of **II** to **I**-Pt) supports the assignment of **7** as *cis*-[Pt(**III**-N7-G(5), N7-G(6))$(NH_3)_2$] and also melting of the platinated duplex at ca. 300 K. A sharp peak at $\delta = 8.62$ at 283 K began to broaden at 293 K, and by 303 K had disappeared. Above ca. 313 K a new broad signal appeared at $\delta = 8.96$ which sharpened at 328 K. This chemical shift is similar to a broad resonance at $\delta = 8.98$ for **I**-Pt at 310 K assignable to one of the G H8 protons of the bifunctional adduct **5**, and similar to the reported behavior of single- and double-stranded GG chelates of d-TCTGGTCTC: J. H. J. den Hartog, C. Altona, J. H. van Boom, G. A. van der Marel, C. A. G. Hasnoot, J. Reedijk, *J. Biomol. Struct. Dyn.* **1985**, *2*, 1137.
[17] C. J. van Garderen, H. van den Elst, J. H. van Boom, J. Reedijk, *J. Am. Chem. Soc.* **1989**, *111*, 4123–4125. Lowerings of 9–27° are typical.
[18] T. P. Kline, L. G. Marzilli, D. Live, G. Zon, *J. Am. Chem. Soc.* **1989**, *111*, 7057–7068.
[19] S. J. S. Kerrison, P. J. Sadler, *J. Chem. Soc. Chem. Commun.* **1977**, 861–864.

The $[Zr_6X_{18}H_5]^{3-}$ Ions with X = Cl, Br, and Related Species**

Linfeng Chen, F. Albert Cotton,* and William A. Wojtczak

Our work with low-valent zirconium cluster compounds began in 1988 with the accidental preparation and characterization of the compound $[Zr_6Cl_{12}(PMe_2Ph)_6]$.[1] It was clear that this molecule contained no atom or atoms within the Zr_6 octahedron with the possible exception of hydrogen, thus differentiating it from the many $Zr_6X_{12}Z$ type compounds, where Z is an atom such as B, C, N, or even larger atoms, at the center of the Zr_6 octahedron.[2] The first result of an effort to find an efficient and reproducible synthetic method for the $[Zr_6Cl_{12}(PR_3)_6]$ species was the preparation of a class of slightly less reduced compounds, $[Zr_6Cl_{14}(PR_3)_4]$,[3] in which, again, it was clear that no other atoms except possibly hydrogen could be present in or on the cluster. In none of these structures was there any X-ray evidence for the presence of hydrogen atoms and until recently NMR results were inconclusive. It has also been shown[4] that further reduction of $[Zr_6Cl_{14}(PMe_2Ph)_4]$ by Na/Hg in presence of PMe_2Ph affords the long-sought improved route to $[Zr_6Cl_{12}(PMe_2Ph)_6]$.

We wish to report here additional synthetic results in this area. As shown in Scheme 1, we now have routes to products containing the $[Zr_6Cl_{18}H_n]^{x-}$ ions ($x = 3,4$). Moreover, we have

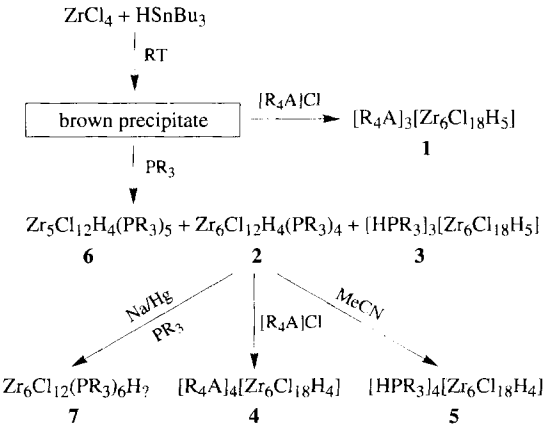

Scheme 1. For **1**–**5** the number of hydrogen atoms shown is that obtained by ^{1}H NMR spectroscopic measurements. For **6** the number (4) is that previously found by X-ray crystallography. For **7** even the presence of H atoms remains uncertain.

been able to establish conclusively by ^{1}H NMR spectroscopy that there are hydrogen atoms present in these anions such that their actual formulas are $[Zr_6Cl_{18}H_5]^{3-}$ and $[Zr_6Cl_{18}H_4]^{4-}$. Again, by ^{1}H NMR spectroscopy, we find that the previously reported $[Zr_6Cl_{14}(PMe_3)_4]$ is actually $[Zr_6Cl_{14}H_4(PMe_3)_4]$. These results have been obtained by employing scrupulously pure, crystalline samples and integrating the cluster hydrogen atom signals against the ^{1}H signals from the cations or the PMe_3 ligands, as appropriate. Results for three representative compounds are shown in Figure 1 and tabulated in Table 1.

The structural characterization of the compounds containing the new $[Zr_6X_{18}H_n]^{x-}$ ions ($x = 3,4$) was first carried out without attempting to obtain evidence concerning the presence or location of hydrogen atoms. A list of the compounds so charac-

Table 1. ^{1}H NMR Data (in CD_3CN).

Compound	δ[a]	n[b]
$[Ph_4P]_3[Zr_6Cl_{18}H_5]$	−3.07	5
$[Ph_4P]_4[Zr_6Cl_{18}H_4]$	−5.19	4
$Zr_6Cl_{14}H_4(PMe_3)_4$	−5.17	4

[a] Signals of the hydrogen atoms in the cluster relative to TMS ($\delta = 0$). [b] The number n of hydrogen atoms in the cluster was calculated from the ratio of integrated intensities of cluster H signal to that of the selected cation or ligand signals.

[*] Prof. F. A. Cotton, Dr. L. Chen, Dr. W. A. Wojtczak
Department of Chemistry and Laboratory
for Molecular Structure and Bonding
Texas A & M University
College Station, TX 77843-3255 (USA)
Telefax: Int code + (409)845-9351

[**] This work was supported by the Robert A. Welch Foundation (Grant No. A494). We thank Dr. Gong Chen for contributions to the preparative work and Dr. Lee M. Daniels for advice concerning the crystallography.

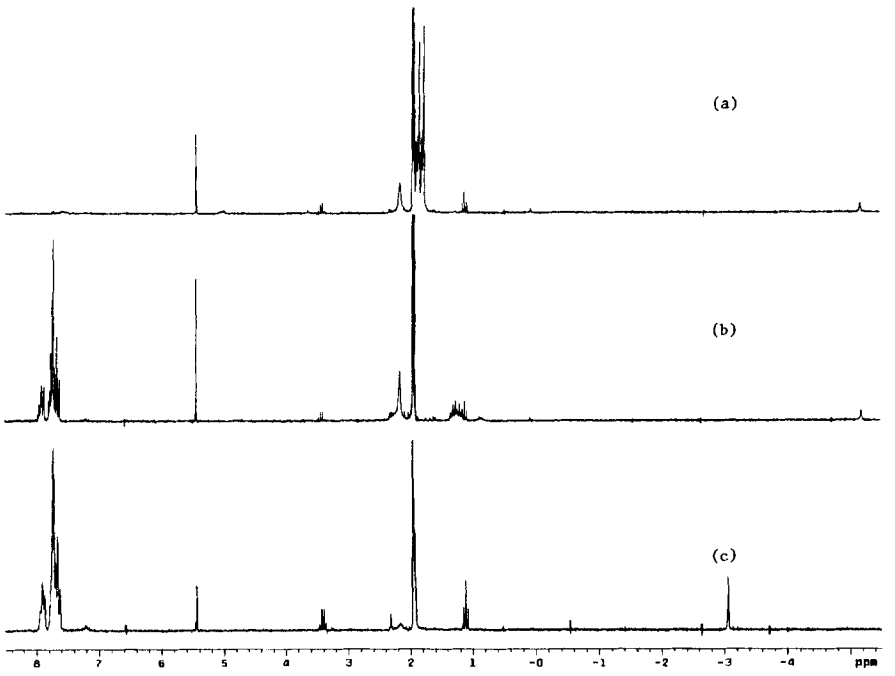

Fig. 1. ^{1}H NMR spectra of a) $[Zr_6Cl_{14}H_4(PMe_3)_4]$, b) $(Ph_4P)_4[Zr_6Cl_{18}H_4]$, and c) $(Ph_4P)_3[Zr_6Cl_{18}H_5]$.

terized and the mean values of the principal internuclear distances, Zr–Zr, Zr–X_b, and Zr–X_t (b and t indicating bridging and terminal, respectively) is given in Table 2.

Table 2. Summary of structural parameters for $[Zr_6Cl_{18}H_4]^{4-}$ and $[Zr_6X_{18}H_5]^{3-}$ ions (X = Cl,Br).

Compound	mean distance [Å]			
	Zr–Zr	Zr–X_t	Zr–X_b	Zr–H
1a: $[Ph_4P]_3[Zr_6Cl_{18}H_5]\cdot 3CH_2Cl_2$ [a]	3.404	2.565	2.479	1.971
1b: $[Ph_4P]_3[Zr_6Cl_{18}H_5]$ [a]	3.414	2.569	2.483	1.978
1c: $[Pr_4N]_3[Zr_6Cl_{18}H_5]$ [b]	3.393	2.559	2.484	1.970
1d: $[Pr_4N]_3[Zr_6Br_{18}H_5]$ [b]	3.438	2.687	2.661	1.985
1e: $[Et_4N]_3[Zr_6Cl_{18}H_5]\cdot 4.5$ MeCN [c]	3.416	2.574	2.481	
3: $[HP(tBu)_2Ph]_3[Zr_6Cl_{18}H_5]\cdot 2CH_2Cl_2\cdot 2C_6H_6$ [b]	3.416	2.573	2.486	
4: $[HPMe_2Ph]_4[Zr_6Cl_{18}H_4]\cdot 2$ MeCN [b]	3.356	2.573	2.549	
5a: $[Ph_4P]_4[Zr_6Cl_{18}H_4]\cdot 4$ MeCN [b]	3.370	2.566	2.544	
5b: $[Et_4N]_4[Zr_6Cl_{18}H_4]\cdot 2$ MeCN [b]	3.366	2.565	2.540	
5c: $[Et_3NCH_2Ph]_6[ZrCl_6]\cdot[Zr_6Cl_{18}H_4]\cdot 4$ MeCN [b]	3.371	2.568	2.538	

[a] At 20 °C. [b] At −60 °C. [c] At −100 °C.

The dimensions of the $[Zr_6Cl_{18}H_5]^{3-}$ and $[Zr_6Cl_{18}H_4]^{4-}$ ions are practically identical. The mean Zr–Zr distances (followed by the ranges) are 3.411 (3.393–3.438) Å and 3.366 (3.356–3.371) Å for the 3– and 4– ions, respectively. There appears to be a small but real contraction; not only do the mean values differ by 0.045 Å, but the ranges do not overlap. As for Zr–Cl_b distances, there is also a significant difference, but now the mean value for the 4– species (2.542 Å) is greater than that for the 3– species (2.484 Å), and again the ranges do not overlap. As for Zr–Cl_t distances, they are indistinguishable for the two classes of anion.

It has previously been reported[5] that in the compound $[Zr_5Cl_{12}H_4(PMe_3)_5]$ the hydrogen atoms could be found and refined by using X-ray diffraction data. Here, of course, there was no reason to expect that the hydrogen atoms would be distributed fractionally over more than one equivalent site and thus the chance of seeing and refining them at full occupancy was optimal. In view of the NMR results suggesting the presence of four or five hydrogen atoms in the $[Zr_6Cl_{18}H_n]^{x-}$ species ($x = 3,4$) and four hydrogen atoms in the $[Zr_6Cl_{15}H_4(PMe_3)_4]$ compound, we were guardedly hopeful that by employing the powerful new computational tools available in the SHELXL-93 program package,[6] we might be able to locate hydrogen atoms in at least some of these cases, despite the fact that individual sites might have only about 50% occupancy. We can now report four instances in which this has been successfully done.

As shown in Table 2, for the $[Zr_6Cl_{18}H_5]^{3-}$ ions in compounds **1a**–**c** and also in the $[Zr_6Br_{18}H_5]^{3-}$ ion in compound **1d**, hydrogen atoms have been found and refined, at partial occupancy, in or very near the centers of all triangular faces of the Zr_6 octahedra. The structure of one such anion is shown in Figure 2. The average occupancy number for all the faces is 5/8, but since the faces are, in general, not crystallographically equivalent, the occupation numbers need not be equal and do, in fact, vary about this mean value, in the range 0.50–0.80.

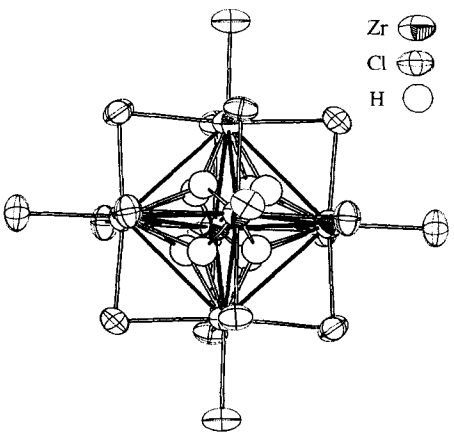

Fig. 2. ORTEP drawing of one of the two independent molecules in the unit cell for compound **1a**.

There is, as expected, a high degree of correlation between the occupancy numbers and the thermal displacement parameters. When the mean occupancy number was changed in any of the four cases from that corresponding to a total of five, to four or six hydrogen atoms, the thermal displacement parameters became *very* unrealistic.

The results presented are highly reminiscent of the classic $Th_6Br_{15}D_7$ structure of Simon et al.,[7, 8] where seven D atoms are disordered on the eight faces of the Th_6 octahedron, lying just slightly (0.22 Å) outside. They are also consistent with the results previously reported for $[Zr_5Cl_{12}H_4(PMe_3)_5]$, wherein it may be imagined that if the octahedron were completed by adding a zirconium atom, there would be four H atoms just over the centers of four alternating faces.

 © VCH Verlagsgesellschaft mbH, D-69451 Weinheim, 1995 0570-0833/95/3417-1878 $ 10.00+.25/0

Experimental Procedure

All manipulations were carried out under an argon atmosphere using standard vacuum-line and Schlenk techniques. The solvents were freshly distilled under nitrogen from the appropriate drying reagents. Phosphonium and ammonium salts were dried in vacuum at 180 °C. Other reactants were used as received from the suppliers. **1**–**7**: ZrX_4 (X = Cl: 0.466 g, 2.0 mmol; X = Br: 0.822 g, 2.0 mmol) was reduced with Bu_3SnH (1.05 mL, 4.0 mmol) in benzene or toluene (20 mL) for 36 h. The resulting red-brown precipitate (dark blue for X = Br) was washed with two portions of freshly distilled toluene or benzene (each 10 mL) to remove excess Bu_3SnH. Addition of $R_4A^+X^-$ in CH_3CN or CH_2Cl_2 afforded **1** in about 30% yield. Approximately 50% of starting material was unreacted and isolated as $[R_4A]_2[ZrX_6]$. Addition of PR_3 to the red-brown precipitate yielded a purple solution of compound **6** and a purple precipitate. Compounds **2** were isolated in about 15% yield by dissolving the purple precipitate in CH_2Cl_2 and layering with hexane. When phosphanes with a higher number of carbon atoms (i.e., PBu_3, $P(tBu)_2Ph$) were used, the only isolable products from crystallization were compounds **3** in about 15% yield. Compounds **2** were converted into compounds **4** by treating with $[R_4A]^+Cl^-$ in over 90% yield. Compounds **2** were also converted gradually into compounds **5** in MeCN solution at room temperature over a period of 30 days in about 50% yield. When compounds **2** were further reduced with Na/Hg in the presence of PR_3 compounds **7** were formed in yields of about 20%.

^1H NMR measurements were made at 200 MHz on a Varian XL-200 spectrometer. Hydride signals were detected at $\delta = -3.07$ for $[Zr_6Cl_{18}H_5]^{3-}$ and at $\delta = -5.19$ for $[Zr_6Cl_{18}H_4]^{4-}$ in CH_3CN. X-ray data were collected on an Enraf-Nonius CAD-4 diffractometer or Enraf-Nonius FR590 area detector. Full reports on the structures will be published elsewhere at a later time.

Received: April 18, 1995 [Z 7891 IE]
German version: *Angew. Chem.* **1995**, *107*, 2050–2052

Keywords: clusters · hydrides · structure elucidation · zirconium compounds

[1] F. A. Cotton, P. A. Kibala, W. J. Roth, *J. Am. Chem. Soc.* **1988**, *110*, 298.
[2] See, for example, F. Rogel, J. D. Corbett, *J. Am. Chem. Soc.* **1990**, *112*, 8198.
[3] F. A. Cotton, X. Feng, M. Shang, W. A. Wojtczak, *Angew. Chem.* **1992**, *104*, 1117; *Angew. Chem., Int. Ed. Engl.* **1992**, *31*, 1050.
[4] F. A. Cotton, W. A. Wojtczak, *Inorg. Chim. Acta* **1994**, *223*, 93.
[5] F. A. Cotton, J. Lu, M. Shang, W. A. Wojtczak, *J. Am. Chem. Soc.* **1994**, *116*, 4364.
[6] G. M. Sheldrick, A Fortran-77 program for the refinement of crystal structures from diffraction data; University of Göttingen, Göttingen, Germany, **1993**.
[7] A. Simon, F. Böttcher, J. K. Cockcroft, *Angew. Chem.* **1991**, *103*, 79; *Angew. Chem., Int. Ed. Eng.* **1991**, *30*, 101.
[8] The senior author would like to acknowledge that Dr. Arndt Simon made him a friendly wager at the time ref. [3] was submitted that hydrogen atoms would eventually be found in our Zr_6 clusters.

New Tellurometalates of Gallium and Indium: $K[K([18]crown\text{-}6)]_2[GaTe_3] \cdot 2CH_3CN$ and $[(NEt_4)_5][In_3Te_7] \cdot 0.5Et_2O$**

Chang-Woo Park, Robert J. Salm, and James A. Ibers*

The number of known tellurometalates has increased rapidly in the past few years through the use of the traditional techniques of nonaqueous solution chemistry as well as the nontraditional techniques of cathodic dissolution of electrodes composed of metal telluride alloys,[1–6] solvent extraction of metal telluride phases,[7, 8] and solventothermal sealed-tube reactions.[9–18] Among these nontraditional techniques, the first two have been especially effective for the synthesis of main group tellurometalates. The cathodic dissolution technique is based on the constant discharge of tellurometalate anions into the cathodic cell from the metal telluride electrode by application of a steadily increasing potential at room temperature; once sufficient concentration has been achieved, crystallization may occur in that chamber. The solvent extraction technique involves the high-temperature fusion of an alkali metal with the desired elements for the tellurometalate, followed by extraction with polar solvents such as ethylenediamine.

We have developed another synthetic route for the preparation of tellurometalates, namely a chemical reduction method in which binary metal tellurides are reduced in liquid NH_3 by K in the presence of an encapsulating ligand.[19] Through the use of a chemical reducing agent, such as K, the potential remains constant and is lower than is usual for cathodic dissolution experiments. Through the use of liquid NH_3 as the solvent, the reductions occur at much lower temperatures than are commonly used in the solvent extraction method or in redox reactions in organic solvents, for example in the preparation of $[Ba(en)_4]_2[As_4Te_6]$ in refluxing ethylenediamine (en).[20] For this chemical reduction method to work an alkali-metal sequestering agent is necessary, since encapsulation of the cation helps to prevent tight-ion pairing that otherwise would cause reversion of the compounds formed to insoluble materials.[8, 21] The features of lower reduction potential and lower temperature in this chemical reduction method may enable the preparation of tellurometalates that are not accessible by other techniques. We illustrate that here with the synthesis and structural characterization of two new tellurometalates **1** and **2**.

$K[K([18]crown\text{-}6)]_2[GaTe_3] \cdot 2CH_3CN$ **1**

$[(NEt_4)_5][In_3Te_7] \cdot 0.5Et_2O$ **2**

Compound **1** was obtained as yellow plates from the chemical reduction of Ga_2Te_3. Its crystal structure includes two $[K([18]crown\text{-}6)]^+$ ions, one K^+ ion, and two CH_3CN solvent molecules per $[GaTe_3]^{3-}$ ion. The $[GaTe_3]^{3-}$ ion, which has a crystallographically imposed mirror plane through atoms Ga and Te(1), consists of a trigonal planar arrangement of Te atoms about a central Ga atom (Fig. 1). The Ga–Te distances are 2.495(3) and 2.513(2) Å, the Te-Ga-Te angles are 114.76(11) and 122.38(6)°, and the Ga atom lies 0.10 Å above the plane of the three Te atoms. These small distortions from strict trigonal planar geometry may be a result of the differing environments of the Te atoms. For example, the K^+ ion, K(4), is 3.429(1) Å from Te(1) and 3.797(1) Å from Te(2). The Ga–Te distances in $[GaTe_3]^{3-}$ are similar to those reported for $[PPh_4][GaTe_2(en)_2]$ (2.509(1) Å),[6] but are signifi-cantly shorter than those in the intermetallic compounds GaTe (average, 2.665(2) Å),[22] Ga_2Te_5 (2.641(1) Å),[22] and $K_6Ga_2Te_6$ (2.591 and 2.680 Å).[23] Among the combinations of Group 13 (M) and Group 16 (Q) elements there are number of isolated $[MQ_3]^{3-}$ ions found in compounds prepared by high-temperature solid-state methods (for example, the $[BSe_3]^{3-}$ ion in

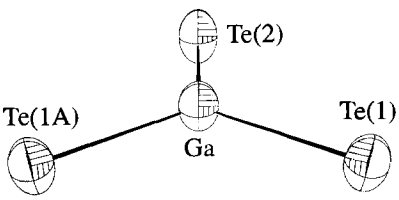

Fig. 1. Structure of the $[GaTe_3]^{3-}$ ion in **1**. Thermal ellipsoids are shown at 50% probability. Relevant distances [Å] and angles [°]: Ga–Te(1) 2.513(2), Ga–Te(2) 2.495(3); Te(1)-Ga-Te(2) 122.38(6); Te(1)-Ga-Te(1A) 114.76(11). The anion has a crystallographically imposed mirror plane through atoms Ga and Te(1).

[*] Prof. J. A. Ibers, C.-W. Park, R. J. Salm
Department of Chemistry, Northwestern University
Evanston, IL 60208-3113 (USA)
Telefax: Int. code + (708)491-7713
e-mail: ibers@chem.nwu.edu

[**] This work was supported by the U. S. National Science Foundation, Grant CHE92-24469.

Tl_3BSe_3[24]), but the $[GaTe_3]^{3-}$ ion appears to be the first to be prepared at low temperatures by a solution method.

Compound **2** was obtained as orange needles from the chemical reduction of In_2Te_3. The $[In_3Te_7]^{5-}$ ion, which has no known analogues, consists of an $[In_3Te_4]^{+}$ cuboidal framework (where one corner is missing) with one Te^{2-} ligand on each of the three In^{3+} centers (Fig. 2). This structure may be described as three edge-sharing "$InTe_4$" tetrahedra; each tetrahedron shares an edge with each of the other two tetrahedra. The In–$Te_{terminal}$ distances range from 2.685(2) to 2.692(2) Å; the In–(μ_2-Te) distances range from 2.802(2) to 2.824(2) Å; the In–(μ_3-Te) distances range from 2.881(2) to 2.907(2) Å. All of the "$InTe_4$" tetrahedra are distorted and have Te-In-Te angles between 94.16(5) and 120.56(7)°. This lengthening of the In–Te bonds with increasing coordination number of the Te atom is also seen in related systems. For example, the "$InTe_4$" tetrahedral moiety is contained in Na_5InTe_4,[25] in which the In–$Te_{terminal}$ distances range from 2.758(2) to 2.811(2) Å and the Te-In-Te angles are all nearly tetrahedral. The In–(μ_2-Te) bond lengths in $[NBu_4]_2[In_2Te_4]$[26] and in $Na_5In_2Te_6$[25] range from 2.786(2) to 2.814(2) Å and from 2.818(5) to 2.836(5) Å, respectively. The "In_4Te_4" cubane core is found in $[Cp(CO)_3Mo]_4In_4Te_4$;[27] in this compound the In-(μ_3-Te) distances range from 2.839(1) to 2.989(1) Å.

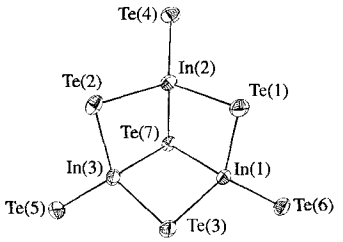

Fig. 2. Structure of the $[In_3Te_7]^{5-}$ ion in **2**. Thermal ellipsoids are shown at 50% probability. Relevant distances [Å] and angles [°]: In(1)–Te(1) 2.802(2), In(1)–Te(3) 2.820(2), In(1)–Te(6) 2.691(2), In(1)–Te(7) 2.881(2), In(2)–Te(1) 2.812(2), In(2)–Te(2) 2.824(2), In(2)–Te(4) 2.692(2), In(2)–Te(7) 2.907(2), In(3)–Te(2) 2.809(2), In(3)–Te(3) 2.816(2), In(3)–Te(5) 2.685(2), In(3)–Te(7) 2.897(2); Te(6)-In(1)-Te(1) 117.98(6), Te(6)-In(1)-Te(3) 120.56(7), Te(1)-In(1)-Te(3) 107.72(6), Te(6)-In(1)-Te(7) 114.09(6), Te(1)-In(1)-Te(7) 96.30(6), Te(3)-In(1)-Te(7) 95.36(5), Te(4)-In(2)-Te(1) 118.30(7), Te(4)-In(2)-Te(2) 116.65(6), Te(1)-In(2)-Te(2) 112.73(6), Te(4)-In(2)-Te(7) 114.83(6), Te(1)-In(2)-Te(7) 95.51(6), Te(2)-In(2)-Te(7) 94.16(5), Te(5)-In(3)-Te(2) 116.88(7), Te(5)-In(3)-Te(3) 117.15(7), Te(2)-In(3)-Te(3) 113.00(6), Te(5)-In(3)-Te(7) 115.73(7), Te(2)-In(3)-Te(7) 94.70(5), Te(3)-In(3)-Te(7) 95.09(5).

Experimental Procedure

Ga_2Te_3 and In_2Te_3 were prepared by the fusion of stoichiometric amounts of the constituent elements under an inert atmosphere and were finely ground before use.

1: NH_3 (ca. 60 mL) was condensed into a flask that contained [18]crown-6 (528 mg, 2.0 mmol) and K (80 mg, 2.0 mmol) at liquid N_2 temperature and the resultant blue solution was stirred for 30 min at −78 °C. Ga_2Te_3 (522 mg, 1 mmol) was then added to the flask and the resultant mixture was stirred for 2 days to provide a light brown solution. The NH_3 was allowed to evaporate at room temperature and CH_3CN (30 mL) was added to the residual material. The resultant solution was then filtered. Et_2O (80 mL) was layered on top of the filtrate to afford yellow plates of **1** (110 mg, yield 10% based on Te) after 5 days.

X-ray structural analysis: $C_{28}H_{54}GaK_3N_2O_{12}Te_3$; crystal dimensions, 0.04 × 0.16 × 0.23 mm; monoclinic, $C2/m$; a = 24.469(5), b = 14.073(3), c = 12.875(3) Å, β = 97.47(3)°, V = 4369(2) Å^3; T = 113 K; Z = 4; ρ_{calc} = 1.784 g cm^{-3}; Enraf-Nonius CAD4 diffractometer; $2\theta_{max}$ = 120.6°; $Cu_{K\alpha}$; $\lambda(K\alpha_1)$ = 1.540562 Å; ω–2θ scan mode; 11538 reflections measured, 3342 independent reflections all of which were included in the refinement; data corrected for Lorentz-polarization effects and for absorption (analytical method), μ = 192 cm^{-1}, min./max. trans. = 0.065/0.446; solution by direct methods [28], refinement on F^2 by full-matrix least-squares [29], 228 parameters, anisotropic refinement of non-hydrogen atoms, H atoms placed in calculated positions before final cycle of refinement; one CH_3CN solvent molecule is disordered; use was made of the SQUEEZE subroutine [30] of the PLATON software package [31] to account for its electron density; R_1 = 0.080; wR_2 = 0.177; residual electron density = 1.03 e Å^{-3}.

2: NH_3 (ca. 60 mL) was condensed into a flask that contained [2.2.2]cryptand (753 mg, 2 mmol) and K (80 mg, 2.0 mmol) at liquid N_2 temperature and the resultant blue solution was stirred for 30 min at −78 °C. In_2Te_3 powder (613 mg, 1.0 mmol) was then added to the flask and the resultant mixture was stirred for 2 days to provide a red-brown solution. The NH_3 was allowed to evaporate at room temperature and CH_3CN (15 mL) was added to the residual material. The resultant solution was then filtered and NEt_4Br (473 mg, 2.5 mmol) in CH_3CN (15 mL) was added to the filtrate. Et_2O (90 mL) was layered on top of the solution to yield orange needles of **2** (180 mg, yield 22% based on Te).

X-ray structural analysis: $C_{42}H_{105}In_3N_5O_{0.5}Te_7$, 0.58 × 0.12 × 0.049 mm; monoclinic, $P2_1/n$, a = 12.419(6), b = 23.005(9), c = 24.171(10) Å, β = 104.210(14)°, V = 6694(5) Å^3; T = 113 K; Z = 4, ρ_{calc} = 1.911 g cm^{-3}; Picker diffractometer; $2\theta_{max}$ = 49.5°; $Mo_{K\alpha}$; $\lambda(K\alpha_1)$ = 0.7093 Å; θ-2θ mode; 13584 reflections measured, 11544 independent reflections of which 11540 were included in the refinement; data corrected for Lorentz-polarization effects and for absorption (analytical method), μ = 40.4 cm^{-1}, min./max. trans. = 0.604/0.779; solution by direct methods [28], refinement on F^2 by full-matrix least-squares [29], 244 parameters, 21 restraints, anisotropic refinement of In and Te atoms, isotropic refinement of other non-hydrogen atoms; R_1 = 0.083, wR_2 = 0.180, residual electron density = 2.27 e Å^{-3}. Of the five independent NEt_4^+ ions only N(1)Et_4^+ is well defined; for this cation hydrogen atoms were included at calculated positions. The N atoms and the four α-C atoms of the other four cations were modeled as rigid tetrahedra with N–C bond lengths of 1.50 Å and C-N-C angles of 109.45°; β-C atoms, when located, were restrained so that αC–βC bond lengths were 1.50(3) Å. The number of β-C atoms found for the N(n)Et_4^+ ions are: n = 2, four, but two disordered over two sites; n = 3, four; n = 4, none; n = 5, three. Some of the resultant displacement parameters are unreasonably large, probably because the model of isotropically vibrating rigid groups is inadequate. An Et_2O solvent of crystallization is disordered about the origin. Further details of the crystal structure investigations may be obtained from the Director of the Cambridge Crystallographic Data Center, 12 Union Road, GB-Cambridge CB21EZ (UK), on quoting the full journal citation.

Received: March 29, 1995 [Z 7839 IE]
German version: *Angew. Chem.* **1995**, *107*, 2044–2045

Keywords: gallium compounds · indium compounds · metalates · tellurium compounds · Zintl phases

[1] C. J. Warren, D. M. Ho, R. C. Haushalter, A. B. Bocarsly, *Angew. Chem.* **1993**, *105*, 1684; *Angew. Chem. Int. Ed. Engl.* **1993**, *32*, 1646.
[2] B. Eisenmann, *Angew. Chem.* **1993**, *105*, 1764; *Angew. Chem., Int. Ed. Engl.* **1993**, *32*, 1693.
[3] C. J. Warren, D. M. Ho, A. B. Bocarsly, R. C. Haushalter, *J. Am. Chem. Soc.* **1993**, *115*, 6416.
[4] C. J. Warren, S. S. Dhingra, D. M. Ho, R. C. Haushalter, A. B. Bocarsly, *Inorg. Chem.* **1994**, *33*, 2709.
[5] C. J. Warren, R. C. Haushalter, A. B. Bocarsly, *Chem. Mater.* **1994**, *6*, 780.
[6] C. J. Warren, D. M. Ho, R. C. Haushalter, A. B. Bocarsly, *J. Chem. Soc. Chem. Commun.* **1994**, 361.
[7] R. C. Burns, J. D. Corbett, *Inorg. Chem.* **1981**, *20*, 4433.
[8] S. S. Dhingra, R. C. Haushalter, *Inorg. Chem.* **1994**, *33*, 2735.
[9] W. S. Sheldrick, H.-J. Häusler, *Z. Anorg. Allg. Chem.* **1988**, *557*, 105.
[10] W. S. Sheldrick, H.-J. Häusler, *Z. Anorg. Allg. Chem.* **1988**, *557*, 98.
[11] W. S. Sheldrick, *Z. Anorg. Allg. Chem.* **1988**, *562*, 23.
[12] W. S. Sheldrick, J. Kaub, *Z. Anorg. Allg. Chem.* **1986**, *535*, 179.
[13] J.-H. Liao, M. G. Kanatzidis, *Inorg. Chem.* **1992**, *31*, 431.
[14] H. M. Haendler, D. Mootz, A. Rabenau, G. Rosenstein, *J. Solid State Chem.* **1974**, *10*, 175.
[15] W. Milius, *Z. Naturforsch. B* **1989**, *44*, 990.
[16] C. Stergiou, P. J. Rentzeperis, *Z. Kristallogr.* **1985**, *172*, 111.
[17] J.-H. Chou, M. G. Kanatzidis, *Inorg. Chem.* **1994**, *33*, 1001.
[18] W. Milius, A. Rabenau, *Z. Naturforsch. B* **1988**, *43*, 243.
[19] C.-W. Park, R. J. Salm, J. A. Ibers, *Can. J. Chem.* **1995**, in press.
[20] B. Eisenmann, R. Zagler, *Z. Naturforsch. B* **1987**, *42*, 1079.
[21] J. D. Corbett, *Chem. Rev.* **1985**, *85*, 383.
[22] F. Alapini, J. Flahaut, M. Guittard, S. Jaulmes, M. Julien-Pouzol, *J. Solid State Chem.* **1979**, *28*, 309.
[23] B. Eisenmann, A. Hofmann, *Z. Kristallogr.* **1991**, *197*, 145.
[24] B. Krebs, W. Hamann, *J. Less-Common Metals* **1988**, *137*, 143.
[25] B. Eisenmann, A. Hofmann, R. Zagler, *Z. Naturforsch. B* **1990**, *45*, 8.
[26] C. J. Warren, S. S. Dhingra, R. C. Haushalter, A. B. Bocarsly, *J. Solid State Chem.* **1994**, *112*, 340.
[27] K. Merzweiler, F. Rudolph, L. Brands, *Z. Naturforsch. B* **1992**, *47*, 470.
[28] G. M. Sheldrick, in *Crystallographic Computing 3*, (Eds.: G. M. Sheldrick, C. Krüger, R. Goddard), Oxford University, London, **1985**, pp. 175–189.
[29] G. M. Sheldrick, *J. Appl. Crystallogr.* **1995**, in press.
[30] P. van der Sluis, A. L. Spek, *Acta Crystallogr. Sect. A* **1990**, *46*, 194.
[31] A. L. Spek, *Acta Crystallogr. Sect. A* **1990**, *46*, C34.

A New Quantitative Description of the Distance Dependence of Through-Space $^{19}F,^{19}F$ Spin–Spin Coupling**

Ludger Ernst* and Kerstin Ibrom

When NMR-active atomic nuclei approach each other at distances equal to or less than the sum of their van der Waals radii, their scalar spin–spin coupling can be transmitted through space.[1–3] This has been well proved experimentally for interactions between ^{19}F nuclei.[4] The efficiency of through-space spin–spin coupling is strongly dependent upon the distance between the interacting nuclei, and several attempts have been made to formulate a quantitative relationship between the magnitude of the $^{19}F,^{19}F$ through-space coupling, J_{FF}, and the nonbonding distance, d_{FF}, between the fluorine nuclei.[5–7] In this communication we demonstrate that the correlations derived previously do not reproduce the experimental facts very well. From a series of tailored difluorocyclophanes, in which we varied the F–F distance systematically, we have derived a d_{FF}/J_{FF} correlation that describes the distance dependence very much better. This correlation will be useful for structural investigations of multiply fluorinated molecules in solution.

We observed the first through-space F,F coupling (J_{FF} = 42.1 Hz) in a difluorocyclophane in **1**,[4j] a *syn*-dithia[3.3]metacyclophane, in which the aromatic rings are tilted such

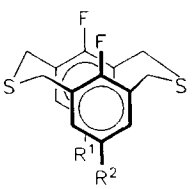

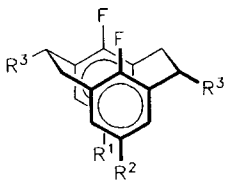

	R^1	R^2
1	H	H
2	*t*Bu	*t*Bu
6	*t*Bu	H

	R^1	R^2	R^3
3	H	H	SMe
4	H	H	H
5	*t*Bu	*t*Bu	H
7	*t*Bu	H	H

that the F–C bonds point towards each other and the F–F distance amounts to 278.1 pm according to molecular mechanics computations.[8] A decrease of the distance had been achieved, on the one hand, by introducing two *tert*-butyl groups *para* to the fluorine atoms (**2**: d_{FF} = 259.7 pm). By their mutual repulsion these *tert*-butyl groups force the fluorine substituents into closer contact. Shortening the cyclophane bridges, on the other hand, diminished the F–F distance even more efficiently (**3**, **4**: d_{FF} = 251.7 and 248.1 pm, respectively). By means of these structural changes, J_{FF} had been increased to 99.3 Hz (Table 1). In order to increase the attainable range of F–F distances towards smaller values, we have now prepared the *syn*-di-*tert*-butyl[2.2]metacyclophane **5**, in which substituents are introduced and the bridges are shortened as well. The synthesis of **5** was analogous to that of **4**:[9] Stevens rearrangement of the *S*,*S*′-dimethylbissulfonium salt of **2** and subsequent removal of the methylthio groups with Raney nickel/H_2. We omitted, however, the complexation of the starting material with $Cr(CO)_3$, which proceeds with very low yield and, in the synthesis of **4**, had been meant to prevent *syn*–*anti* isomerization.[9] The *anti* isomer of **5**, which amounted to only one-third in spite of the bulky substituents, could be separated by chromatography (see Experimental Procedure). Expectedly, the desired *syn* isomer **5** displayed the largest F,F coupling constant, 110.1 Hz, because the related F–F distance, computed with MM2, is the shortest in the series (241.9 pm). The data of **6**[10] and **7**[11] show that J_{FF} is not increased by a single *tert*-butyl substituent.

Table 1. Nonbonding F–F distances d_{FF} as computed by MM2 and experimental coupling constants J_{FF} in **1**–**10**.

Cmpd.	d_{FF} [pm]	J_{FF} [Hz]	Cmpd.	d_{FF} [pm]	J_{FF} [Hz]
1	278.1	42.1	**6**	273.3	40.6
2	259.7	60.5	**7**	248.5	97.6
3	251.7	89.3	**8**	299.8	13.7
4	248.1	99.3	**9**	318.0	7.2
5	241.9	110.1	**10**	301.7	1.9

In paracyclophanes **8** and **9**[12] the best planes through the aromatic rings lie parallel to each other. Therefore, the F–F distances are larger than in the corresponding metacyclophanes and the J_{FF} values are smaller. The overall range of F–F distances in **1**–**9** extends from 318 to 242 pm and the respective F,F coupling constants lie between 7 and 110 Hz (Table 1). The relatively large number of data points permits the derivation of a function that describes the correlation between d_{FF} and J_{FF} within the range of distances covered [Eq. (a)]. Figure 1 gives a comparison of this function (curve c) with the previous d_{FF}/J_{FF} relationships.

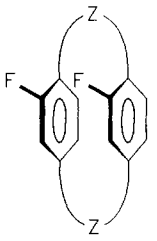

Z	
8	CH_2CH_2
9	CH_2SCH_2

$$J_{FF} = 275000\ e^{-0.03211 d_{FF}} \qquad (a)$$

Clearly, through-space coupling does not come into effect only at $d_{FF} = 2r_{vdW}(F) = 270$ pm, but already amounts to more than 40 Hz at this distance. Thus, as pointed out before,[4j, 6] not only are the values obtained from semiempirical calculations by Buckingham et al.[5] (curve a) distinctly too small (by a factor ≥ 10), but the empirical correlation suggested instead by Hilton and Sutcliffe[6] (curve b) also yields coupling constants that, in the range of smaller distances, are only half as large as the values we observed; this can be traced back to these authors' unrealis-

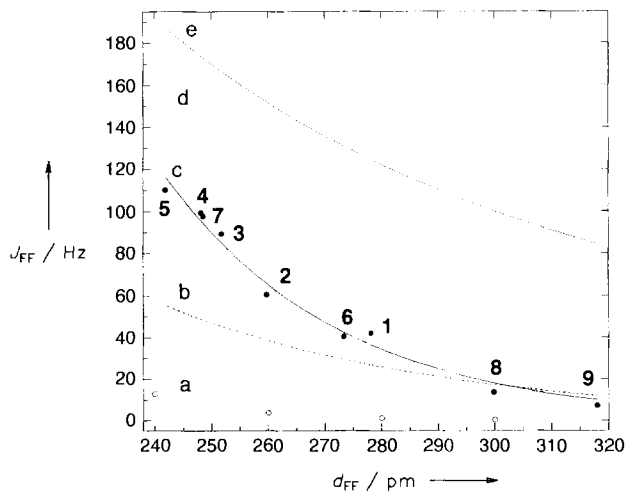

Fig. 1. Postulated dependencies of the through-space F,F coupling constant J_{FF} [Hz] upon the nonbonding distance d_{FF} [pm]. a) Values according to ref. [5]; b) $J_{FF} = 6800\ \exp(-0.0199 d_{FF})$ [6]; c) J_{FF} according to Equation (a) and appropriate experimental data (data points are labeled with the compound numbers); d) $J_{FF} = |-431\ \exp(-1.6\times10^{-5}\ d_{FF}^2) + 1.2|$ [7b]; e) $J_{FF} = 2.6\times10^9\ d_{FF}^{-3} + 3.6$ [7a].

[*] Prof. L. Ernst, Dr. K. Ibrom
NMR-Labor der Chemischen Institute
und Institut für Organische Chemie der Technischen Universität
Hagenring 30, D-38106 Braunschweig (Germany)
Telefax: Int. code (531) 391-5387
e-mail: L. Ernst@tu-bs.de

[**] This work was supported by the Fonds der Chemischen Industrie.

tic assumptions of the molecular geometries.[6] In contrast, both functions suggested by Russian authors[7] (curves d and e) for a given distance substantially overestimate the magnitude of J_{FF}. The main reason for this should lie in the debatable method by which the authors tried to extract the through-space component from $^4J_{FF}$ in fluorinated allyl cations. Their prediction of nonbonding F–F distances by semiempirical MO calculations is not unproblematic either.[13]

For some of our compounds the F–F distances in the solid state are known from X-ray structural analyses.[4j, 14, 15] These distances can be used to derive a function similar to Equation (a), yet it is not as good because it is based on fewer data points and d_{FF} is restricted to the range of 245 to 275 pm. Moreover, in some cases, several molecules with different F–F distances are present in the asymmetric unit, which indicates that d_{FF} is influenced by packing forces in the solid state. We therefore suppose that the structures calculated with MM2 are better suited to describe the geometries in solution.

We tested the usefulness of the new d_{FF}/J_{FF} correlation with 1,8-difluoro-4-methylnaphthalene, which has a calculated d_{FF} of 258.7 pm and a J_{FF} of 65.6 Hz. Equation (a) predicts J_{FF} to be 67.9 Hz, whereas the correlations from the literature give J_{FF} values of 39.5,[6] 153.8,[7a] and 146.5 Hz,[7b] respectively. Thus, our equation gives by far the best prediction.

Finally, we have observed a very small J_{FF} value of 1.9 Hz in the [2.2]metaparacyclophane **10**,[16] although d_{FF} in this compound is calculated to be 301.7 pm, only slightly larger than in **8** (299.8 pm) where J_{FF} is 13.7 Hz. Since the F–C bonds in **10** form a substantially larger angle than those in the other molecules studied, the small coupling constant could be a first indication that the magnitude of the through-space coupling is influenced not only by the distance d_{FF} but also by the relative spatial orientation of the interacting parts of the molecules. This has hardly been considered in the previous discussions.[20]

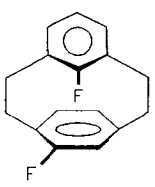

10

Experimental Procedure

5: Cyclophane **2** was methylated with $(MeO)_2CH^+ BF_4^-$ according to ref. [17], but the carbenium salt was added at the boiling temperature of dichloromethane instead of at −78 °C. Of the resulting dimethylbissulfonium salt (m.p. 186–188 °C, quantitative yield), 1.73 g (2.77 mmol) was subjected to an S-analogous Stevens rearrangement according to ref. [18], with a reaction time of 2 h. From the mixture of isomeric 1,9-/1,10-bis(methylthio)[2.2]metacyclophane derivatives obtained (brown oil, 1.03 g, 83%), 346 mg of the *anti*-(1*RS*,9*SR*) isomer could be precipitated by adding petroleum ether to a CH_2Cl_2 solution. Roughly 7 g of Raney nickel W7 was added to 688 mg (1.53 mmol) of the remaining isomers in 250 mL of ethanol and the mixture was hydrogenated for 5 h at 60–65 °C with 1 bar of H_2. The catalyst was filtered off and the solvent removed. After filtration over silica gel with CH_2Cl_2, 223 mg (41%) of **5** and 131 mg (24%) of its *anti* isomer were obtained by thin layer chromatography (silica gel, CH_2Cl_2/petroleum ether 1:3). **5**: m.p. 146–148 °C; *anti* isomer of **5** [19]: m.p. 214–215 °C. NMR data: see Table 2. All new compounds gave correct C,H,S analyses or high-resolution mass spectra. The NMR spectra were assigned by H,H- and C,H-COSY, C,H-COLOC, and NOE measurements.

Received May 8, 1995 [Z 7966 IE]
German version: *Angew. Chem.* **1995**, *107*, 2010–2012

Keywords: cyclophanes · fluoroarenes · NMR spectroscopy

Table 2. NMR spectroscopic data of **5**–**7** [a].

5: ^{1}H NMR: δ = 6.38 ("t", $A_2A'_2XX'$, N = 6.6 Hz, H_{ar}), 3.49 (m_c, bridge-H *syn* to F), 2.57 (m_c, bridge-H *anti* to F), 1.08 (s, *t*Bu); $^{13}C\{^1H\}$ NMR [b]: δ = 159.5 (ABX, 6 lines, J_{FC} = −251.0, +0.5 Hz, CF), 145.3 (ABX, "t", $\sum J_{FC}$ = 4.1 Hz, C*t*Bu), 125.8 (ABX, "dd", $\sum J_{FC}$ = 18.3 Hz, CCH_2), 125.1 (ABX, "t", $\sum J_{FC}$ = 5.4 Hz, CH), 33.8 [s, $C(CH_3)_3$], 31.3 [ABX, "t", $\sum J_{FC}$ = 0.7 Hz, $C(CH_3)_3$], 29.5 [ABX, "t", $\sum J_{FC}$ = 4.2 Hz, CH_2]; $^{19}F\{^1H\}$ NMR: δ = −109.7 (s)

anti Isomer of **5**: ^{1}H NMR: δ = 7.07 (d, J_{FC} = 5.9 Hz, H_{ar}), 2.76 (m_c, bridge-H *anti* to F), 2.65 (m_c, bridge-H *syn* to F), 1.31 (s, *t*Bu); $^{13}C\{^1H\}$ NMR [b]: δ = 158.6 (ABX, 4 lines, J_{FC} = −245.7, +2.9 Hz, CF), 147.5 (ABX, "t", $\sum J_{FC}$ = 4.0 Hz, C*t*Bu), 126.7 (ABX, "dd", $\sum J_{FC}$ = 18.6 Hz, CCH_2), 125.5 (ABX, "t", $\sum J_{FC}$ = 6.9 Hz, CH), 34.3 [ABX, "t", $\sum J_{FC}$ = 0.5 Hz, CH_2], 34.2 [s, $C(CH_3)_3$], 31.7 [ABX, "t", $\sum J_{FC} \geq$ 0.3 Hz, $C(CH_3)_3$]; $^{19}F\{^1H\}$ NMR: δ = −129.1, J_{FF} = 3.1 Hz (from ^{13}C satellites)

6: ^{1}H NMR: δ = 6.97 (m_c, J_{FH} = 6.8 Hz, H-5,7), 6.94 (m_c, J_{FH} = 8.5, $^3J_{HH}$ = 7.9 Hz, H-14,16), 6.67 (td, $J_{FH} \approx$ 0.5 Hz, H-15), 4.33 (d, $^2J_{HH}$ = 15.0 Hz, H-3,10, *syn* to F), 4.33 (d, $^2J_{HH}$ = 15.0 Hz, H-1,12, *syn* to F), 3.40 (m_c, H-3,10, *anti* to F), 3.39 (m_c, H-1,12, *anti* to F), 1.16 (s, *t*Bu); $^{13}C\{^1H\}$ NMR: δ = 158.2 (d, J_{FC} = 244.6 Hz, C-18), 156.9 (d, J_{FC} = 242.9 Hz, C-9), 146.6 (d, J_{FC} = 2.1 Hz, C-6), 129.5 (d, J_{FC} = 3.8 Hz, C-14,16), 126.6 (d, J_{FC} = 3.5 Hz, C-5,7), 125.2 (d, J_{FC} = 15.7 Hz, C-13,17), 124.2 (d, J_{FC} = 4.4 Hz, C-15), 124.0 (d, J_{FC} = 15.4 Hz, C-4,8), 35.1 [s, $C(CH_3)_3$], 33.6 [d, J_{FC} = 0.3 Hz, $C(CH_3)_3$], 32.7 (d, J_{FC} = 2.1 Hz, C-3), 32.5 (d, J_{FC} = 2.4 Hz, C-1); $^{19}F\{^1H\}$ NMR: δ = −125.5 (d, J_{FF} = 40.6 Hz, F-18), −130.6 (d, F-9), assignment based on ^{13}C satellites

7: ^{1}H NMR: δ = 6.37 (m_c, H-12,13,14), 6.32 (d, J_{HH} = 6.6 Hz, H-4,6), 1.08 (s, *t*Bu), CH_2 signals hidden; $^{19}F\{^1H\}$ NMR: δ = −105.8 (d, J_{FF} = 97.6 Hz, F-16), −112.5 (d, F-8)

[a] Solvent: $CDCl_3$; measuring frequencies: 400 MHz (^{1}H), 101 MHz (^{13}C), 188 MHz (^{19}F); internal standards: TMS (^{1}H), $CDCl_3$ (^{13}C, δ = 77.05), $CFCl_3$ (^{19}F); atom numbering according to the nomenclature employed. [b] In the ABX spin systems the A and B nuclei are F.

[1] J. Hilton, L. H. Sutcliffe, *Prog. Nucl. Magn. Reson. Spectrosc.* **1975**, *10*, 27–39.
[2] R. H. Contreras, M. A. Natiello, G. E. Scuseria, *Magn. Reson. Rev.* **1985**, *9*, 239–321.
[3] R. H. Contreras, J. C. Facelli, *Annu. Rep. NMR Spectrosc.* **1993**, *27*, 255–356.
[4] Selected references: a) J. Jonas, L. Borowski, H. S. Gutowsky, *J. Chem. Phys.* **1967**, *47*, 2441–2448; b) K. L. Servis, K.-N. Fang, *J. Am. Chem. Soc.* **1968**, *90*, 6712–6717; c) R. A. Fletton, R. D. Lapper, L. T. Thomas, *Chem. Commun.* **1969**, 1049; d) R. D. Chambers, L. H. Sutcliffe, G. J. T. Tiddy, *Trans. Faraday Soc.* **1970**, *66*, 1025–1038; e) F. B. Mallory, C. W. Mallory, M.-C. Fedarko, *J. Am. Chem. Soc.* **1974**, *96*, 3536–3542; f) F. B. Mallory, C. W. Mallory, W. M. Ricker, *ibid.* **1975**, *97*, 4770–4771; g) T. Schaefer, W. Niemczura, K. Marat, *J. Chem. Soc. Faraday Trans. 2* **1975**, *71*, 1526–1528; h) R. S. Matthews, *J. Fluorine Chem.* **1990**, *48*, 7–15; i) P. Szczeciński, J. Zachara, *J. Organomet. Chem.* **1993**, *447*, 241–249; j) L. Ernst, K. Ibrom, K. Marat, R. H. Mitchell, G. J. Bodwell, G. W. Bushnell, *Chem. Ber.* **1994**, *127*, 1119–1124.
[5] A. D. Buckingham, J. E. Cordle, *J. Chem. Soc. Faraday Trans. 2* **1974**, *70*, 994–1004.
[6] J. Hilton, L. H. Sutcliffe, *Spectrochim. Acta Part A* **1976**, *32*, 201–213.
[7] a) V. I. Bakhmutov, M. V. Galakhov, E. I. Fedin, *Magn. Reson. Chem.* **1985**, *23*, 971–972; b) V. I. Bakhmutov, M. V. Galakhov, N. I. Raevskii, V. A. Petrov, Y. A. Borisov, E. I. Fedin, *Bull. Acad. Sci. USSR Div. Chem. Sci. (Engl. Transl.)* **1987**, *36*, 1747–1749.
[8] N. L. Allinger, *MM2(91)*, Quantum Chemistry Program Exchange, Indiana University, Bloomington, IN 47405, USA.
[9] R. H. Mitchell, G. J. Bodwell, T. K. Vinod, K. S. Weereawarna, *Tetrahedron Lett.* **1988**, *29*, 3287–3290.
[10] **6**: M.p. 83–84.5 °C. NMR data: see Table 2. In a previous description of compound **6** with m.p. 82.5–83.5 °C the conformation was not specified: T. Yamato, A. Miyazawa, M. Tashiro, *J. Org. Chem.* **1992**, *57*, 266–270.
[11] Cyclophane **7** was obtained as a side product (3%) together with the *anti* isomer and the 11,12,13,14-tetrahydro derivative, which had formed in the energetic desulfurization (Raney nickel/H_2, 1.5 bar, 60–65 °C, 6 h) of the bis(methylthio) precursor. NMR data of **7**: see Table 2.
[12] Compounds **8** and **9** were prepared and analyzed as mixtures of the four stereoisomers (pseudogeminal, pseudo-*ortho*, pseudo-*meta*, pseudo-*para*): L. Ernst, K. Ibrom, unpublished.
[13] T. Clark, *A Handbook of Computational Chemistry*, Wiley, New York, **1985**, Chapter 4.
[14] a) P. G. Jones, L. Ernst, K. Ibrom, *Z. Kristallogr.* **1995**, *210*, in press; b) P. G. Jones, L. Ernst, A. Reisner, K. Ibrom, *ibid.* **1995**, *210*, in press.
[15] In the complex $[(\eta^6$-**4**$)Cr(CO)_3]$ J_{FF} amounts to 102.2 Hz. X-ray structural data: P. G. Jones, L. Ernst, K. Ibrom, A. Chrapkowski, R. H. Mitchell, G. J. Bodwell, *Z. Kristallogr.* **1994**, *209*, 464–465.
[16] Compound **10** is obtained as two *syn*/*anti* rotamers: L. Ernst, K. Ibrom, unpublished. We discuss only the *syn* rotamer here.
[17] V. Boekelheide, P. H. Anderson, *J. Org. Chem.* **1973**, *38*, 3928–3931.
[18] R. H. Mitchell, V. Boekelheide, *J. Am. Chem. Soc.* **1974**, *96*, 1547–1557.
[19] M. Tashiro, T. Yamato, *J. Org. Chem.* **1985**, *50*, 2939–2942.
[20] **Note added in proof** (August 2, 1995): Recently we learned about two additional papers that treat the distance dependence of through-space F,F couplings: a) C. Schumann, F. Cavagna, *J. Magn. Reson.* **1975**, *18*, 172–184; b) F. Cavagna, C. Schumann, *ibid.* **1976**, *22*, 333–344. The F–F distances assumed there are based upon model considerations and are presumably too small because the data points (e.g. J_{FF} = 35.4 Hz at d_{FF} = 247 pm and 45.5 Hz at 220 pm) lie even distinctly below curve b in Figure 1. Due to the unusual nomenclature employed ("non-bond couplings") these papers had not been found in a CAS Online search.

Double Helical Dinuclear Copper(I) Complexes of Macrocyclic Bis(dithiadiimine) Ligands**

Peter Comba,* Andreas Fath, Trevor W. Hambley, and David T. Richens*

A [2 + 2] condensation reaction[1] was used to prepare 32- and 34-membered macrocyclic Schiff base type ligands with $(N_2S_2)_2$ donor sets (Scheme 1). Both imines and thiaethers favor soft metal centers and thus stabilize the +1 oxidation state of copper, which has a preference for tetrahedral coordination geometry. Because of our interest in the comparison of solid-state and solution structures of transition metal compounds,[2] the structural and spectroscopic properties of compounds **6** and **7** were of particular interest. In this communication we describe the syntheses of the ligands **4** and **5** and of their dicopper(I) complexes **6** and **7**, as well as their structural, spectroscopic, and electrochemical properties.

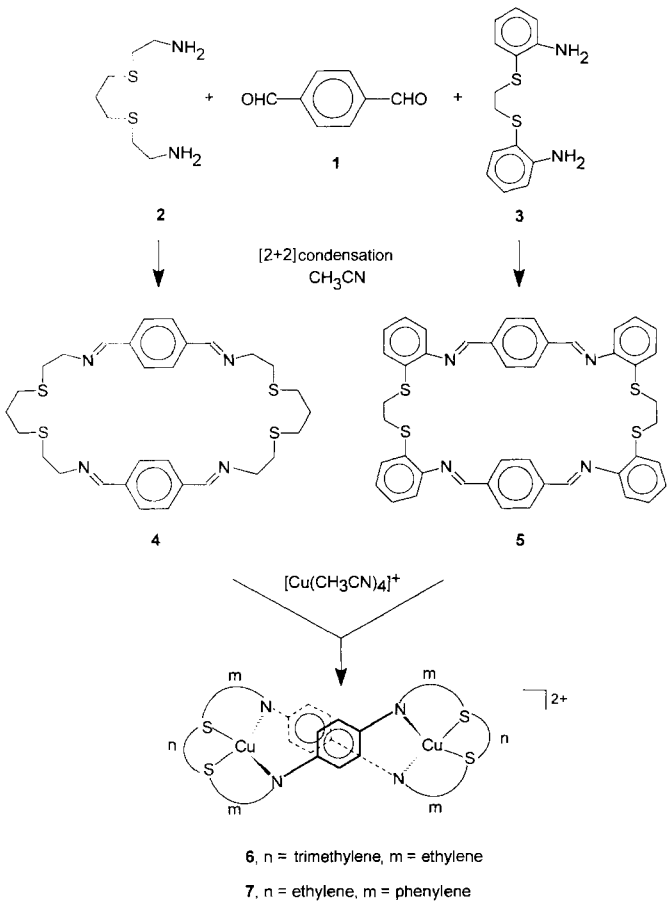

6, n = trimethylene, m = ethylene

7, n = ethylene, m = phenylene

Scheme 1. Counterion: ClO_4^-

[*] Prof. Dr. P. Comba, Dipl.-Chem. A. Fath
Anorganisch-chemisches Institut der Universität
Im Neuenheimer Feld 270, D-69120 Heidelberg (Germany)
Telefax: Int. code + (6221) 56-3617
e-mail: comba @akcomba.oci.uni-heidelberg.de
Dr. T. W. Hambley
School of Chemistry, University of Sydney (Australia)
Dr. D. T. Richens
School of Chemistry, University of St. Andrews
The Purdie Building,
GB-St. Andrews KY16 9 ST (Scotland)

[**] This project was supported by the DFG, the DAAD, the Australian Research Council and the British Council (ARC Project 484).

The addition of stoichiometric amounts of terephthalaldehyde (**1**) to solutions (CH_3CN) of 3,7-dithia-1,9-diaminononane (**2**) and 1,2-bis(1-aminothiophenyl)ethane (**3**) affords the ligands **4** and **5**, respectively, as white (yellow) solids in good yields (60–70%). The analytical data (elemental analyses, FAB^+-MS, IR, ^1H and ^{13}C NMR spectra) are compatible with symmetrical macrocycles containing four Schiff base units each. The ^1H and ^{13}C NMR spectra, in particular, demonstrate that the ligands **4** and **5** are highly symmetrical. Addition of $[Cu(CH_3CN)_4]ClO_4$ to **4** and **5** in CH_3CN/CH_2Cl_2 (1:1) produces yellow-orange or red solutions, respectively, from which orange or red-brown air-stable crystals, suitable for X-ray diffraction, were isolated after slow evaporation of the solvents.

The structural analyses of **6** and **7** (Figs. 1 and 2)[4, 5] reveal that the basic structural properties of the two dicopper(I) com-

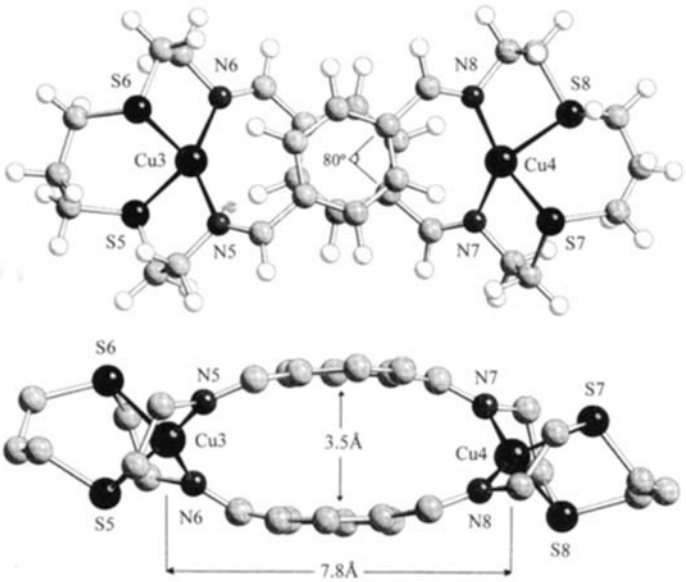

Fig. 1. Crystal structure of **6**-$(ClO_4)_2 \cdot H_2O$ (molecule A) (SCHAKAL plots [3]). Selected bond lengths [Å] and angles [°]: Cu3–S5 2.333(3), Cu3–S6 2.347(3), Cu3–N5 2.024(8), Cu3–N6 2.023(9), Cu4–S7 2.347(3), Cu4–S8 2.388(4), Cu4–N7 2.007(9), Cu4–N8 2.011(9), S5-Cu3-S6 106.0(1), S5-Cu3-N5 90.6(3), S5-Cu3-N6 113.0(2), S6-Cu3-N5 116.4(3), S6-Cu3-N6 90.4(3), N5-Cu3-N6 138.4(4), S7-Cu4-S8 99.1(1), S7-Cu4-N7 90.3(3), S7-Cu4-N8 115.3(3), S8-Cu4-N7 120.8(3), S8-Cu4-N8 89.3(3), N7-Cu4-N8 137.7(4).

pounds are rather similar. The main features are the following: a) The two N_2S_2 donor sets are each tetrahedrally coordinated to the Cu^I centers; b) the two bridging *para*-substituted phenyl rings are parallel, about 3.5 Å apart, indicative of a stabilization by π-stacking; c) the dihedral angles between the bridging phenyl rings are about 80°, resulting in a double helical arrangement (figure-of-eight loop) of the ligand backbone. The molecules **6** and **7** shown in Figures 1 and 2 have Λ configurations (both compounds crystallize as racemates; there are two crystallographically independent molecules in the asymmetric unit of **6**). The distance between the two copper(I) centers is about 7.8 Å in both compounds.

Helical metal complexes have recently attracted much attention, and aspects related to the topology and intrinsic chirality of helicates, and their relevance to biological systems and supramolecular chemistry, as well as to material sciences, have been extensively reviewed.[8] Many of the reported systems are based on open-chain ligands with polypyridine or phenanthroline donors[8, 9] but macrocyclic systems and ligands with other donor sets have also been studied.[10] The helicates reported so

 © VCH Verlagsgesellschaft mbH, D-69451 Weinheim, 1995 0570-0833/95/3417-1883 $ 10.00+.25/0

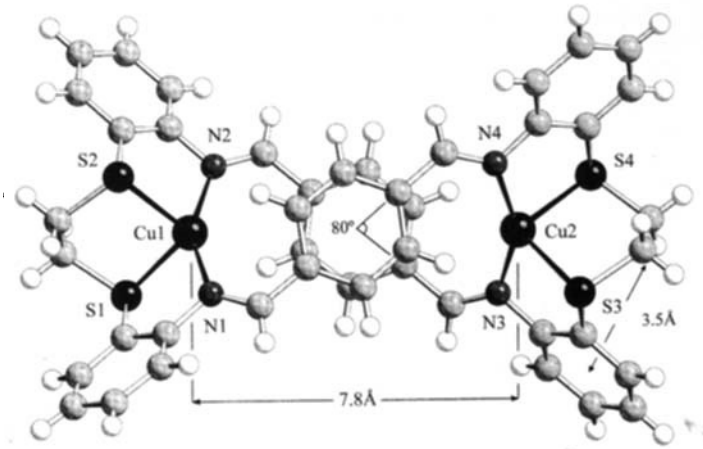

Fig. 2. Crystal structure of 7-$(ClO_4^-)_2 \cdot 0.5\,H_2O \cdot 0.5\,CH_3CN$ (SCHAKAL plots [3]). Selected bond lengths [Å] and angles [°]: Cu1–S1 2.330(3), Cu1–S2 2.341(3), Cu1–N1 2.022(8), Cu1–N2 1.985(9), Cu2–S3 2.315(4), Cu2–S4 2.356(4), Cu2–N3 2.009(9), Cu2–N4 1.995(9), S1-Cu1-S2 92.9(1), S1-Cu1-N1 87.8(3), S1-Cu1-N2 111.5(3), S2-Cu1-N1 115.4(3), S2-Cu1-N2 88.1(3), N1-Cu1-N2 149.4(4), S3-Cu2-S4 93.2(1), S3-Cu2-N3 88.1(3), S3-Cu2-N4 111.9(3), S4-Cu2-N3 114.1(3), S4-Cu2-N4 87.8(3), N3-Cu2-N4 150.1(4).

far include double and triple helical systems. Preorganization of the ligands, self-assembly, and chiral self-organization have also been observed and studied.[8–10] The simplicity of the figure-of-eight loop resulting from the copper(I)-induced folding of **4** and **5** is an interesting new motif in this area.

The following questions arise: a) are the helical structures of the dicopper(I) species preserved in solution and b) are the metal-free ligands preorganized, that is, do they have helical structures or the open macrocyclic structures shown in Scheme 1. As in other systems[9, 10] these questions were addressed by ^{1}H NMR spectroscopy. The methylene protons of the metal-free ligand **5** are chemically equivalent (singlet at $\delta = 2.68$). In the dicopper(I) complex **7** these protons are diastereotopic and appear as a single AX system with a geminal coupling of 10.5 Hz and a chemical shift difference of $\Delta\delta = 1.5$. These observations imply that the dicopper(I) complex **7** is chiral in solution and kinetically inert on the NMR time scale, while the corresponding metal-free ligand **5** has an open macrocyclic structure (see Scheme 1). Preliminary model calculations[11] of the dicopper(I) complex **7** with δ conformations of the chelate rings (as in the crystal structure, see Figure 2; Λ helix of the complex) lead to a structure that is in good agreement with that observed in the solid state. The axial methylene protons are about 3.5 Å from the phenyl rings of the five-membered chelate rings separated by a methylene group (see arrow in Figure 2). In addition, complex **7** with λ conformations of the five-membered chelate rings (Λ configuration of the complex) has been refined by molecular mechanics.[11] In this configuration the complex is at least 6 kJ mol^{-1} more stable, and the axial methylene protons are separated from the phenyl rings of the neighboring chelate rings by about 3.4 Å. We interpret the chemical shift difference of the AX system of the methylene protons of $\Delta\delta = 1.5$ to be due to the ring current. The symmetry of the dicopper(I) complex and the small difference in proton to phenyl ring distance of the two conformers resulting from our preliminary calculations does not allow the assignment of the spectrum to one of the two possible conformers.

There are two possible effects contributing to the stabilization of the helical arrangement of the macrocyclic rings, namely, the preference of copper(I) for tetrahedral coordination geometry and π stacking of the phenyl rings. The solution structures of the free ligand **5** and the dicopper(I) complex **7**, deduced from ^{1}H NMR spectroscopy, indicate that stabilization by π stacking alone is not sufficient to induce helicity. Future structural studies, supported by molecular modeling studies, of metal complexes with a series of ligands with the basic structure of **4** and **5** coordinated to copper(I) and other metal centers might help to quantify the stabilization by π stacking. An important fact emerging from the arrangement of the bridging *para*-substituted phenyl rings, induced by the tetrahedral coordination geometry, is that an enforced helical arrangement of a metal-free ligand of the type discussed here would lead to tetrahedral preorganization of the ligating atoms and thus selectively stabilize metal centers with a preference for tetrahedral coordination.

Electrochemical properties of **6** have been studied by cyclic voltammetry in CH_3CN.[14] The voltammogram indicates that, due to the Cu–Cu separation of about 7.8 Å, both Cu^I centers behave largely independently. The oxidation from Cu^I to Cu^{II} at a potential of $E_{1/2} = 1.34$ V (vs NHE) is independent of the scan rate (0.1–2 Vs^{-1}). The E_p value of 55 mV indicates the presence of a reversible electron process. The stabilization of Cu^I by a tetrahedral arrangement of thioether and imine donors is demonstrated by the highly positive redox potential.

Experimental Procedure

The diaminodithiaalkanes **2** and **3** were prepared as described in [15]. The dialdehyde **1** is commercially available.

For the syntheses of the macrocyclic ligands **4** [5], the dialdehyde **1** (4.2 g, 31.5 mmol, dissolved in 500 mL CH_3CN) was added slowly (24 h) to a stirred solution of **2** (6.2 g, 31.5 mmol) [**3** (7.7 g, 31.5 mmol)] dissolved in 800 mL CH_3CN. The isolated white [yellowish] solids were recrystallized twice from CH_3CN/CH_2Cl_2 (1:1). **4**: Yield: 5.6 g (9.7 mmol, 62%); correct C,H,N,S analysis; MS (FAB$^+$, NOBA): *m/z* 585 (M^+, 30%); ^{1}H NMR (200.1 MHz, $CDCl_3$): $\delta = 8.27$ (s, 4H, NCH), 7.74 (s, 8H, Ar-H), 3.79 (t, 8H, $^3J = 6.5$ Hz, NCH_2) 2.82 (t, 8H, $^3J = 6.9$ Hz, NCH_2CH_2) 2.62 (t, 8H, $^3J = 7.1$ Hz, $CH_2CH_2CH_2$), 1.85 (p, 4H, $^3J = 7.2$ Hz, $CH_2CH_2CH_2$); ^{13}C NMR (50.3 MHz, $CDCl_3$): $\delta = 161.56$ (NCH), 137.95 (Ar-*C*-CHN), 128.42 (*o*-Ar-C), 61.87 (NCH_2), 32.82 (NCH_2CH_2), 31.22 ($CH_2CH_2CH_2$), 29.37 ($CH_2CH_2CH_2$); IR (KBr): $\tilde{\nu}$ [cm^{-1}] = 1639(s), (C=N)s. [**5**: Yield: 7.9 g (10 mmol, 68%); correct C,H,N,S analysis; ^{1}H NMR (200.1 MHz, C_6D_6): $\delta = 7.82$ (s, 4H, NCH), 7.30 (s, 8H, *p*-Ar-H), 2.68(s, 8H, SCH_2), 6.25–7.90 (m, 16H, *m*-Ar-H); ^{13}C NMR (50.3 MHz, C_6D_6): $\delta = 159.52$ (NCH), 149.82 (Ar-*C*-NC), 137.87 (Ar-C-S), 135.77 (Ar-*C*-CN), 129.95, 129.84 (S-*m*-Ar-C, N-*m*-Ar-C), 129.24 (C-*o*-Ar-C), 116.43 (S-*o*-Ar-C), 114.37 (N-*o*-Ar-C), 33.50 (CH_2); IR (KBr): $\tilde{\nu}$ [cm^{-1}] = 1616(s), (C=N)s.

Complex **6** [7] was synthesized under an Ar atmosphere in dry and degassed solvents. An excess of freshly prepared $[Cu(CH_3CN)_4]ClO_4$ in CH_3CN [16] was added slowly to a stirred solution of **4** (200 mg, 0.34 mmol) [**5** (200 mg, 0.27 mmol)] in 200 mL CH_3CN/CH_2Cl_2 (1:1). The yellow-orange [red] solution was filtered after 1 h and reduced to 50 mL by evaporation of the solvent under reduced pressure to afford yellow-orange [red-brown] solids. Excess $[Cu(CH_3CN)_4]ClO_4$ that precipitated with the dinuclear species was oxidized with air and removed with CH_3CN. **6**: Yield: 134 mg (0.15 mmol, 43%); correct C,H,N,S analysis. ^{1}H NMR (200.1 MHz, CD_3CN): $\delta = 8.67$ (s, 4H, NCH), 7.48 (s, 8H, Ar-H), 4.04–4.22 (m, 8H, NCH_2), 2.92–3.38 (m, 16H, $NCH_2CH_2 + CH_2CH_2CH_2$) 2.18–2.25 (m, 4H, $CH_2CH_2CH_2$); ^{13}C NMR (50.3 MHz, CD_3CN): $\delta = 166.64$ (NCH), 138.10 (Ar-*C*-NC), 129.07 (*o*-Ar-C), 61.01 (NCH_2), 36.17 (NCH_2CH_2), 32.91 ($CH_2CH_2CH_2$), 26.14 ($CH_2CH_2CH_2$); IR (KBr): $\tilde{\nu}$ [cm^{-1}] = 1619(s), (C=N)s, 1093 (br. s), (Cl–O)s. [**7**: Yield: 140 mg (0.13 mmol, 47%); correct C,H,N,S analysis. ^{1}H NMR (200.1 MHz, CD_3CN): $\delta = 9.05$ (s, 4H, NCH), 8.23 (s, 8H, *m*-Ar-H), 7.95 (d, 4H, $^3J = 6.0$ Hz, N-*o*-Ar-H) 7.54–7.65 (m, 12H, Ar-H + S-*o*-Ar-H), 3.96 (d, 4H, $^2J_{AX} = 10.5$ Hz, SCH_2) 2.47 (d, 4H, $^2J_{AX} = 10.5$ Hz, SCH_2), $\Delta\nu = 298.9$ Hz; ^{13}C NMR (50.3 MHz, CD_3CN): $\delta = 165.60$ (NCH), 152.36 (Ar-*C*-NC), 140.98 (Ar-C-S), 135.42 (Ar-*C*-CN), 132.51 (S-*o*-Ar-C), 131.54 (*m*-Ar-H), 128.08 (C-*o*-Ar-C), 122.34 (N-*o*-Ar-C), 38.25 (CH_2); IR (KBr): $\tilde{\nu}$ [cm^{-1}] = 1593(s), (C=N)s, 1088 (br. s), (Cl–O)s.

Received: February 22, 1995 [Z 7730 IE]
German version: *Angew. Chem.* **1995**, *107*, 2047–2050

Keywords: complexes with macrocyclic ligands · copper compounds · helical structures · molecular modeling · supramolecular chemistry

[1] a) S. R. Cooper in *Crown Compounds Toward Future Applications* (Ed.: S. R. Cooper). VCH. Weinheim, **1992**, p. 112; b) R. Menif, A. E. Martell, *J. Chem. Soc. Chem. Commun.* **1989**, 1521.

[2] a) P. V. Bernhardt, P. Comba, T. W. Hambley, S. S. Massoud, S. Stebler, *Inorg. Chem.* **1992**, *31*, 2644; b) P. Comba, *Inorg. Chem.* **1994**, *33*, 4577; c) *Comments Inorg. Chem.* **1994**, *16*, 133; d) P. Comba, H. Jakob, B. K. Keppler, B. Nuber, *Inorg. Chem.* **1994**, *33*, 3396; e) P. Comba, T. W. Hambley, M. A. Hitchman, H. Stratemeier, *Inorg. Chem.* **1995**, *34*, in press.

[3] E. Keller, SCHAKAL 92, Universität Freiburg, Germany, **1992**.

[4] Crystal structure determination of **6**-$(ClO_4)_2 \cdot 0.5H_2O$ ($C_{30}H_{38}Cl_2Cu_2N_4O_{8.5}S_4$), $M = 916.74$; yellow prisms (crystal dimensions 0.45·0.25·0.20 mm^3); triclinic space group $P\bar{1}$, $a = 13.364(4)$, $b = 24.126(11)$, $c = 12.266(6)$ Å, $\alpha = 102.62(3)$, $\beta = 100.02(3)$, $\gamma = 90.64(3)$°; $V = 3795(3)$ Å^3; $Z = 4$; $\rho_{calcd} = 1.604$ g cm^{-3}; $F(000) = 1880$; $\mu = 46.34$ cm^{-1}; min./max. transmission 0.693–1.000; 10155 reflections were measured at 21 °C on a Rigaku AFC7R four-circle diffractometer employing graphite monochromated $Cu_{K\alpha}$ radiation ($\lambda = 1.5418$ Å); ω 2θ scan ($1° < \theta < 110°$); data reduction and application of Lorenz, polarization absorption, and decomposition corrections were carried out with teXsan Systems [6]; the structure was solved by direct methods with SHELXS-86 [7]; hydrogen atoms were included at calculated sites with fixed isotropic thermal parameters; full-matrix least-squares methods were used to refine 909 variables out of 6037 reflections with $I > 2.5\sigma(I)$ converged at $R = 0.070$ and $R_w = 0.075$; residual electron density 0.5, 0.6 e Å^{-3}; the unit cell consists of two independent molecular cations; a carbon atom in cation A (C6) is disordered [6].

[5] Crystal structure analysis of **7**-$(ClO_4)_2 \cdot 0.5H_2O \cdot 0.5CH_3CN$ ($C_{43}H_{41.5}Cl_2Cu_2N_{4.5}O_{8.5}S_4$), $M = 1100.43$; brown prisms (crystal dimensions 0.45·0.25·0.20 mm^3); monoclinic space group $P2_1/n$ (No. 2); $a = 16.085(5)$; $b = 17.999(6)$, $c = 16.919(4)$ Å; $\beta = 101.61(4)$°; $V = 4798(3)$ Å^3; $Z = 4$; $\rho_{calcd} = 1.523$ g cm^{-3}, $F(000) = 2254$, $\mu = 41.72$ cm^{-1}; min./max. transmission 0.903–0.993; 6597 reflections were measured under the same conditions as for **6**, and the structure was solved analogously; full-matrix least-squares methods were used to refine 585 variables out of 3402 reflections with $I > 2.5\sigma(I)$ converged at $R = 0.069$ and $R_w = 0.072$; residual electron density 0.54, −0.54 e Å^{-3}; further details of the crystal structure analysis are available on request from the Director of the Cambridge Crystallographic Data Centre, 12 Union Road, GB-Cambridge CB21EZ, on quoting the full journal citation.

[6] teXsan, Crystal Structure Analysis Package, Molecular Structure Corporation, **1985**, **1992**.

[7] G. M. Sheldrick, SHELXS-86, in *Crystallographic Computing 3*, (Eds.: G. M. Sheldrick, C. Krüger, R. Goddard), Oxford University Press, Oxford pp. 175–189).

[8] a) E. C. Constable, *Nature (London)* **1990**, *346*, 314; b) J.-P. Sauvage, *Acc. Chem. Res.* **1990**, *23*, 319; c) J.-M. Lehn, *Angew. Chem.* **1990**, *102*, 1347; *Angew. Chem. Int. Ed. Engl.* **1990**, *29*, 1304; d) E. C. Constable, *Chem. Ind. (London)* **1994**, 56.

[9] a) U. Koert, M. M. Harding, J.-M. Lehn, *Nature(London)* **1990**, *346*, 339; b) W. Zarges, J. Hall, J.-M. Lehn, *Helv. Chim. Acta* **1991**, *74*, 1843; c) J. K. Judice, S. J. Keipert, D. J. Cram, *J. Chem. Soc. Chem. Commun.* **1993**, 1323; d) K. T. Potts, M. Keshavarz-K, F. S. Tham, H. D. Abruña, C. Arana, *Inorg. Chem.* **1993**, *32*, 4436; e) R. Krämer, J.-M. Lehn, A. De Cian, J. Fischer, *Angew. Chem.* **1993**, *105*, 764; *Angew. Chem. Int. Ed. Engl.* **1993**, *32*, 703; f) E. C. Constable, A. J. Edwards, P. R. Raithby, J. V. Walker, *ibid.* **1993**, *105*, 1486 and **1993**, *32*, 1465; g) A. Bilyk, M. M. Harding, *J. Chem. Soc. Dalton Trans.* **1994**, 77.

[10] a) C. Piguet, G. Bernardinelli, B. Bocquet, A. Quattropani, A. F. Williams, *J. Am. Chem. Soc.* **1992**, *114*, 7440; b) R. Ziessel, M.-T. Youinou, *Angew. Chem.* **1993**, *105*, 929; *Angew. Chem. Int. Ed. Engl.* **1993**, *32*, 877; c) D. E. Fenton, R. W. Matthews, M. McPartlin, B. P. Murphy, I. J. Scowen, P. A. Tasker, *J. Chem. Soc. Chem. Commun.* **1994**, 1391; d) T. Adatia, N. Beynek, B. P. Murphy, *Polyhedron* **1995**, *14*, 335.

[11] Molecular mechanics calculations were performed with the program MOMEC [12] which uses HyperChem (HyperCube Inc., Waterloo, Ontario, Canada) as graphics surface, and a published forcefield [13] (the metal–ligand distances were constrained at the experimentally observed distance).

[12] P. Comba, T. W. Hambley, N. Okon, MOMEC, *a molecular mechanics program for coordination compounds*, Attenhof & Schmitz, Dortmund, **1995**.

[13] P. V. Bernhardt, P. Comba *Inorg. Chem.* **1992**, *31*, 2638.

[14] The cyclic voltammogram of **6** (1.0 mM in dry CH_3CN with 0.1 M tetrabutylammonium perchlorate as electrolyte and ferrocene as internal standard) was measured on a BAS 100B instrument with a glassy carbon working electrode, a Pt auxiliary electrode, and a $AgCl/Ag^0$ reference electrode. The potential of ferrocene (+ 0.44 V) was reference (reversability of the proceess was only observed upon addition of at least one equivalent of ferrocene). The potentials are converted into potentials vs. the NHE.

[15] R. W. Hay, P. M. Gidney, *J. Chem. Soc. Dalton Trans.* **1975**, 779.

[16] J. van Rijn, J. Reedijk, *J. Chem. Soc. Dalton Trans.* **1987**, 2579.

Pseudo-Spherical Host Molecules: Synthesis, Dimerization, and Nucleation Effects**

Carlos Valdés, Urs P. Spitz, Stefan W. Kubik, and Julius Rebek, Jr.*

We recently synthesized structure **1** and gave evidence for its self-assembly into **1**–**1**, a pseudo-spherical dimer.[1] The internal cavity of the dimerization acts as a host for small guests of complementary shape and volume.[2]

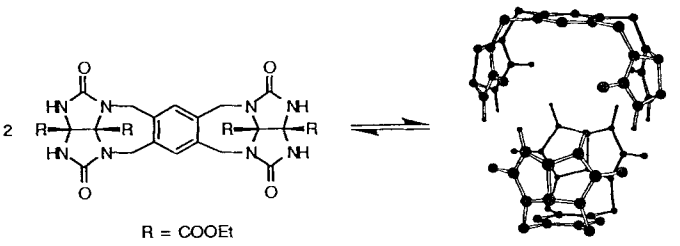

By replacing the benzene spacer in **1** with a bridged anthracene unit, an extended structure **2** is generated that maintains the self-complementarity required for dimerization (Scheme 1). The synthesis and characterization of **2** is outlined here, along with the unexpected formation of a recombinant (or hybrid) structure in solutions of **1** and **2**. The effects of guest nucleation on the assembly processes, as determined through NMR measurements, are also described.

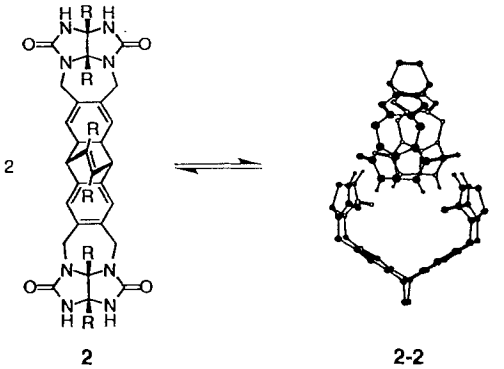

Scheme 1. MM2-minimized structure of the homodimer **2**–**2**. Hydrogen atoms and the glycouril ester groups have been omitted for clarity.

The core of monomer **2** (Scheme 2) was made through tandem benzyne additions to furan as described earlier by Hart.[3] The reaction of tetrabromobenzene (**3**) with BuLi in the presence of excess disubstituted furan **4** gave mixtures of two isomeric endoxides *syn*- and *anti*-**5** in 30% (R = Bn) or 65% (R = TBDMS) combined yield. Tetrasubstituted anthracene **6**

[*] Prof. J. Rebek Jr., Dr. C. Valdés, Dr. U. P. Spitz, Dr. S. W. Kubik
Department of Chemistry
Massachusetts Institute of Technology
Cambridge, MA 02139 (USA)
Telefax: Int. + (617)253-7929

[**] We thank the National Institutes of Health for support of this work. C. V. is grateful to the Ministerio de Educación y Ciencia (Spain) for a MEC-Fulbright postdoctoral fellowship, U. P. S. to the Swiss National Science Foundation for a postdoctoral fellowship, and S. W. K. to the Deutscher Akademischer Austauschdienst for a NATO postdoctoral fellowship.

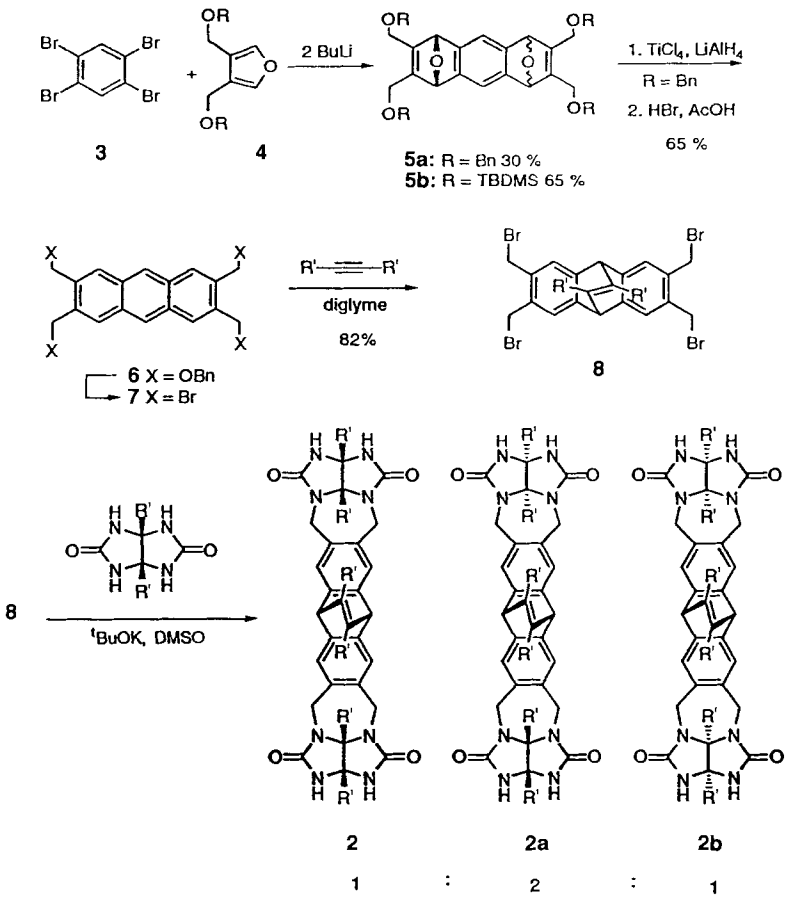

Scheme 2. Synthesis of **2**. TBDMS = $tBuMe_2Si$, R' = CO_2Et.

was obtained from **5a** by reduction[4] of the *syn/anti* mixture with Ti^0. Treatment of the tetrabenzyl ether **6** with HBr/AcOH solution in $CHCl_3$ yielded the tetrabromide **7** in 65% yield. The Diels–Alder reaction of anthracene **7** with diethyl acetylenedicarboxylate proceeded well in hot diglyme to give the desired ethenoanthracene tetrabromide **8**. Reaction of **8** with an excess of the soluble glycoluril **9**[2b] in DMSO produced a mixture of the three possible isomers of **2**[5] in the expected statistical ratio (1:2:1). Target compound **2** (12% yield), the only isomer soluble in nonpolar organic solvents, was separated from the mixture by extraction with $CHCl_3$ and was further purified by flash chromatography.

Spectroscopic studies in $CDCl_3$ indicate a fully dimerized structure (**2**–**2**) in solution. The chemical shift of the NH protons in the ^1H NMR spectrum of **2** appear downfield at $\delta = 8.45$; the IR spectrum in $CHCl_3$ shows a broad absorption band at 3229 cm^{-1}. These values are very similar to those for **1**,[6] and do not change as a function of concentration. In contrast, reference compound **10**[7] shows concentration-dependent NMR signals for the NH protons (between $\delta = 6.17$ at 35 mM and $\delta = 5.45$ at 1.5 mM) and a sharp absorption band at 3442 cm^{-1} in its FTIR spectra of **2**. The dimeric arrangement proposed allows formation of the maximum number of hydrogen bonds and accounts for the spectroscopic features.

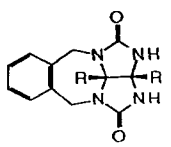

10, R = CO_2Et

Encapsulation behavior was also observed by NMR spectroscopy. When a solution of **1**–**1** in $CDCl_3$ (a guest too large to fit comfortably in **1**–**1**) was titrated with CD_2Cl_2, the appearance and growth of a new, broad NH signal at $\delta = 8.5$ was observed. This new signal represents the dimer **1**–**1** containing CD_2Cl_2 in its cavity. The shift upfield relative to "empty"[8] **1**–**1** ($\delta_{1-1} = 9.13$) is attributed to the elongation and weakening of the hydrogen bonds upon encapsulation of the guest. The signal for the empty dimer disappears completely as the concentration of CD_2Cl_2 in $CDCl_3$ reaches 20%. *Direct observation of the guest inside the cavity* of **1**–**1** is possible with ^{13}C NMR and ^{13}C-labeled samples. Addition of 10% $^{13}CH_2Cl_2$ to a solution of **1** in $CDCl_3$ results in a new signal in the ^{13}C NMR spectrum at 0 °C (Fig. 1), shifted by $\Delta\delta = 2$ upfield from free $^{13}CH_2Cl_2$.[9] Its intensity, relative to that of the ^{13}C NMR signals of the host **1**–**1** (marked with Δ), suggested that the majority of hosts contained labeled guests, and confirmed the earlier ^1H NMR assignments of signals for "full" and "empty" **1**–**1**.

In encapsulation experiments with the dimer **1**–**1**, the spectra invariably showed two sets of ^1H NMR signals, which correspond to slow exchange between the empty host and the filled host.[1, 2] However, this is not the case with **2**. Presumably, a dynamic solvent exchange, fast on the NMR time scale, takes place even at low temperatures. The openings on both sides of the dimer (Scheme 1) appear large enough for guest molecules to enter and escape the cavity without affecting many of the host's hydrogen bonds. Nonetheless, tiration experiments support encapsulation phenomena. For example, a solution of **2** in $CDCl_2CDCl_2$ (a poor guest for **2**–**2**, as its size appears too big) was titrated with $CDCl_3$ (an ideally sized guest for **2**–**2**). The resonance for the NH signal gradually shifted downfield from $\delta = 7.75$ and stabilized at $\delta = 8.25$ after 20% $CDCl_3$ had been added. As $CDCl_3$ replaces $CDCl_2CDCl_2$ inside the cavity, the host's hydrogen bonds shorten, which causes the downfield shift of its NH signals.

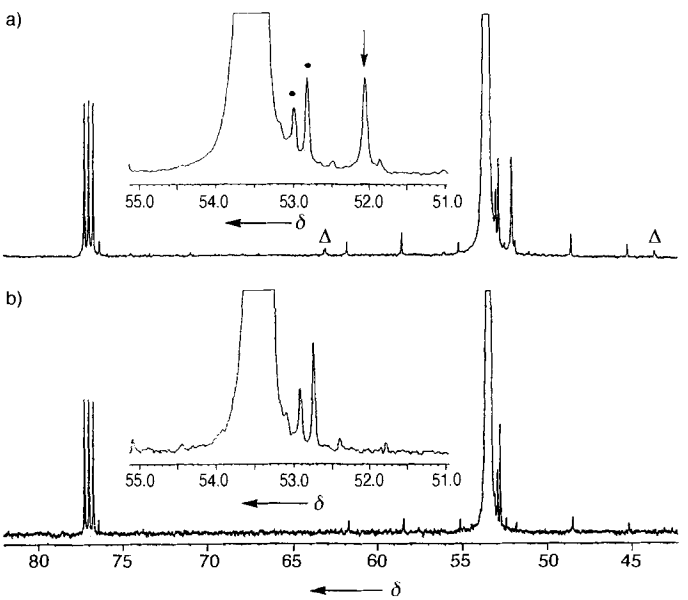

Fig. 1. a) ^{13}C NMR spectrum of **1**–**1** in a solution that contains 10% $^{13}CH_2Cl_2$. The arrow indicates the signal of encapsulated $^{13}CH_2Cl_2$, and the dots those of impurities. b) ^{13}C NMR spectrum of solvent reference.

Structures **1** and **2** are self-complementary but they are also mutually well suited. The hybrid aggregate (**1**–**2**) of **1** and **2** is shown in Scheme 3. The calculated structure of the pear shaped **1**–**2** adducts suggests the formation of only six "strong" hydrogen bonds. The two additional bonds are significantly longer.

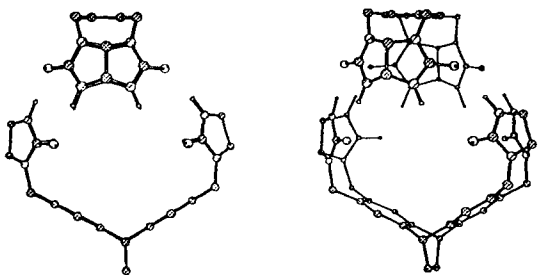

Scheme 3. Two views of MM2-minimized hybrid dimer **1**–**2**. Some hydrogen atoms and the ester groups have been omitted for clarity.

In the experiment **1**–**1** and **2**–**2** were shown to be capable of recombination to form hybrid species. Specifically, the ^{1}H NMR spectrum of an equimolar mixture of **1** and **2** in $CDCl_3$ showed signals corresponding to three different species. Besides the signals of the two homodimers **1**–**1** and **2**–**2**, a third set of signals, which we assigned to the "heterodimer" **1**–**2**, was present. This assignment was supported by NOE experiments: at $-40\,^{\circ}C$ a strong NOE was observed in the heterodimer's spectrum on irradiation of the NH protons of either of its half shells, **1** and **2**. The disproportionation constants K and the thermodynamic values for the hybrid formation were determined by ^{1}H NMR spectroscopy. In $CDCl_3$ K is 11.6 at 298 K (titrations of **1** with **2** and vice versa gave the same value). The enthalpy for heterodimerization in $CDCl_3$ was measured to be -3 kcal mol^{-1} and the entropy -5 cal K^{-1} mol^{-1}.

What is the driving force for the recombination, particularly if hydrogen bonding is better in **1**–**1** than in **1**–**2**? Nucleation by guest species is the likely answer. The distribution of the hydrogen-bonded pairs at equilibrium is influenced by the presence of suitable guests. Though all three pairs are capable of accommodating guest molecules, the cavity size of each varies. For instance, the dimer **1**–**1** readily encapsulates CH_2Cl_2 but not $CHCl_3$. Only the bridged anthracene dimer **2**–**2** appears large enough to encapsulate $CHCl_2CHCl_2$, but both **2**–**2** and the heterodimer **1**–**2** are large enough to accommodate $CHCl_3$ or even $CHBr_3$.

These surmises are borne out by the data of Table 1: in $CHCl_3$ (or even more so in $CHBr_3$) the formation of the hybrid ball **1**–**2** is favored, but very little heterodimer **1**–**2** is formed in CD_2Cl_2 or $CDCl_2CDCl_2$. These results suggest that a species is favored if its cavity can be well-filled.

Table 1. Equilibrium constants for the disproportionation (recombination) of **1**–**1** and **2**–**2** in solvents of increasing size.

Solvent	CD_2Cl_2	$CDCl_3$	$CDBr_3$	$CDCl_2CDCl_2$
$K^{298} = \frac{[1\text{–}2]^2}{[1\text{–}1][2\text{–}2]}$	no **1**–**2**	11.6	42	traces of **1**–**2**

Further evidence for these nucleation effects was provided by titration experiments and will be reported elsewhere. In the meantime, the surprisingly stable heterodimer found here augurs well for the formation of new hybrids from other self-assembly processes.[10]

Received: March 27, 1995 [Z 78401E]
German version: *Angew. Chem.* **1995**, *107*, 2031–2033

Keywords: host–guest chemistry · pseudodimers · self-assembly

[1] R. Wyler, J. de Mendoza, J. Rebek, Jr., *Angew. Chem.* **1993**, *105*, 1820–1821; *Angew. Chem. Int. Ed. Engl.* **1993**, *32*, 1699–1701.
[2] a) N. Branda, R. Wyler, J. Rebek, Jr., *Science* **1994**, *263*, 1267–1268; b) N. Branda, R. M. Grotzfeld, C. Valdés, J. Rebek, Jr., *J. Am. Chem. Soc.* **1995**, *117*, 85–88.
[3] H. Hart, C. Lay, G. C. Nwokogu, S. Shamouilian, *Tetrahedron* **1987**, *43*, 5203.
[4] N. Z. Huang, Y. D. Xing, D. Y. Ye, *Synthesis* **1982**, 1041–1044.
[5] The unambiguous distinction between C-shaped structure **2** and W-shaped **2b** is difficult. However, **2b** is expected to form polymeric, ribbon-type hydrogen-bonded structures of low solubility in nonpolar solvents.
[6] The NH protons of **2** are $\delta = 0.68$ upfield from the corresponding protons in **1**; modeling suggests that the upfield shift is a consequence of a somewhat less ideal arrangement of the hydrogen bond array in **2**–**2**.
[7] Compound **10** was prepared from bis(chloromethyl)benzene by a previously described procedure [2].
[8] The empty **1**–**1** probably contains dissolved atmospheric gases.
[9] This ^{13}C NMR technique has the advantage of eliminating overlapping signals as only enriched materials become visible.
[10] For two component assemblies based on calixarenes see K. Koh, K. Araki, S. Shinkai, *Tetrahedron Lett.* **1994**, *35*, 8255.

Synthesis and Structure of a Free Germacyclopentadienide Ion: $[Li([12]crown\text{-}4)_2][C_4Me_4GeSi(SiMe_3)_3]$**

William P. Freeman, T. Don Tilley,* Frederick P. Arnold, Arnold L. Rheingold, and Peter K. Gantzel

Numerous investigations have focused on characterization of the electronic structures for sila- and germacyclopentadienides.[1–6] Theoretical studies generally have concluded that the silacyclopentadienide ion $(HSiC_4H_4)^-$ would have some delocalization,[2] and recent high-level ab initio calculations suggest that it would have about half the aromatic stabilization energy of $C_5H_5^-$, despite possessing pyramidal silicon.[3] NMR parameters for the lithium and sodium derivatives of $(Ph_4C_4SiBu)^-$ in THF suggest some delocalization of negative charge in the ring.[4] Germacyclopentadienide ions have also been generated in solution,[5] and an analysis of NMR parameters for $(C_4Me_4GePh)^-$ was consistent with substantial localization of negative charge on germanium.[6] Given the level of interest in possible aromatic character for these anions, we have

[*] Prof. Dr. T. D. Tilley, W. P. Freeman
Department of Chemistry
University of California
Berkeley, CA 94720-1460 (USA)
Telefax: Int. code + (510) 642-8940
email: tdtilley@violet.berkeley.edu
F. P. Arnold, Prof. Dr. A. L. Rheingold
Department of Chemistry, University of Delaware
Newark, DE 19716 (USA)
Dr. P. K. Gantzel
Department of Chemistry, 0314
University of California, San Diego
9500 Gilman Drive
La Jolla, CA 92093-0314 (USA)

[**] This research was supported by the National Science Foundation.

sought to establish the structures for uncomplexed sila- and germacyclopentadienide ions. Here we report the synthesis of an isolated germacyclopentadienide ion, $[C_4Me_4GeSi(SiMe_3)_3]^-$ as the alkali metal salt, and its crystal structure.

For comparative purposes, the molecular structure of $C_4Me_4Ge(H)Si(SiMe_3)_3$ (**1**) was determined (Fig. 1).[7] The planar C_4Ge ring contains inequivalent C–C distances that reflect isolated single (1.504(4) Å) and double (1.342(3), 1.343(3) Å) bonds. The Ge–Si distance of 2.387(1) Å is only slightly longer than the comparable distance in $[(\eta^5\text{-}C_5Me_5)Ru\{\eta^5\text{-}C_4Me_4GeSi(SiMe_3)_3\}]$ (2.357(2) Å),[8] and the angle between the C_4Ge plane and the Ge–Si bond is 131.0°.

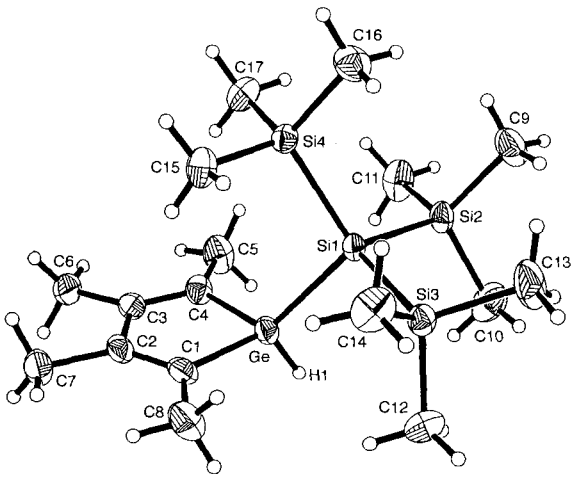

Fig. 1. Molecular structure of **1**. Selected interatomic distances [Å] and angles [°]: Ge–Si1 2.387(1), Ge–C1 1.944(3), Ge–C4 1.948(3), Ge–H1 1.43(2), C1–C2 1.342(3), C2–C3 1.504(4), C3–C4 1.343(3), C4–C5 1.502(4), C1–C8 1.510(4), C2–C7 1.510(4), C3–C6 1.513(3); Si1-Ge-C1 116.3(1), Si1-Ge-C4 119.6(1), Si1-Ge-H1 110(1), C1-Ge-C4 89.7(1), Ge-C1-C2 107.6(2), Ge-C1-C8 125.9(2), Ge-C4-C3 107.6(2), Ge-C4-C5 126.3(2).

Deprotonation of **1** in the presence of a crown ether produces the alkali metal germacyclopentadienides **2** and **3**, which were isolated as crystalline solids. The NMR parameters for these compounds suggest that the anions have identical structures. The ^{13}C NMR shifts for the ring carbons ($\delta(C_\alpha) = 137$, $\delta(C_\beta) = 157$) are somewhat downfield-shifted relative to analogous resonances for **1** ($\delta(C_\alpha) = 132.89$, $\delta(C_\beta) = 146.45$)[8] and $Li(Me_4C_4GePh)$ ($\delta(C_\alpha) = 138.7$, $\delta(C_\beta) = 151.5$).[6]

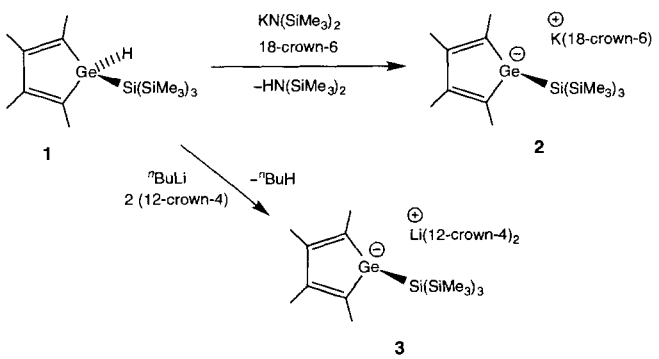

The germacyclopentadienide **5** was obtained by a different route (Scheme 1) involving silylation of the $[Me_4C_4Ge]^{2-}$ dianion, followed by heterolytic cleavage of the Ge–Si bond of **4** with benzylpotassium. Compound **5** appears to possess a structure analogous to that for **2** and **3** ($\delta(^{13}C)$ of the ring carbons: $C_\alpha = 136.72$, $C_\beta = 158.56$), involving free germacyclopentadienide ions which do not interact strongly with the cations.

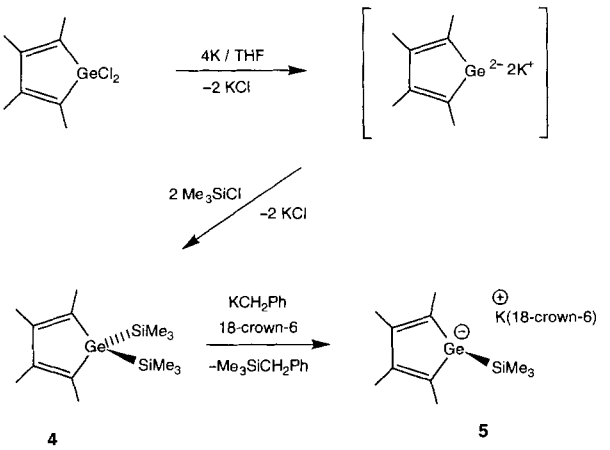

Scheme 1.

X-ray quality crystals of **3** were obtained by slow, vapor diffusion of pentane into a solution of the compound in diethyl ether. The structure contains well-separated cations and anions, and Figure 2 provides a view of the free anion.[9] A pyramidalization

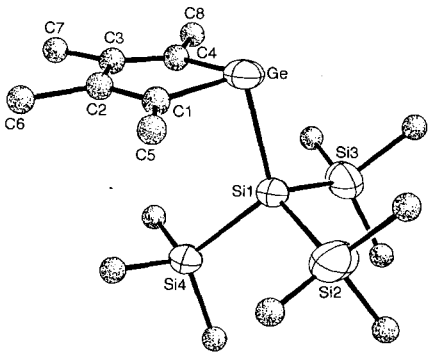

Fig. 2. Molecular structure of the anion in **3**. Selected interatomic distances [Å] and angles [°]: Ge–Si1 2.446(9), Ge–C1 2.01(3), Ge–C4 1.96(3), C1–C2 1.36(6), C2–C3 1.46(6), C3–C4 1.35(5), C4–C8 1.49(4), C1–C5 1.33(5), C2–C6 1.51(4), C3–C7 1.52(6); Si1-Ge-C1 98.0(9), Si1-Ge-C4 96.7(8), C1-Ge-C4 86(2), Ge-C1-C2 107(3), Ge-C1-C5 132(3), Ge-C4-C3 111(2), Ge-C4-C8 125(2).

at the germanium center is clear, as evidenced by the angle between the C_4Ge plane and the Ge–Si bond of only 100.1°. Furthermore, the carbon portion of the ring has considerable diene character, as indicated by the C1–C2, C2–C3, and C3–C4 bond lengths of 1.36(6), 1.46(6), and 1.35(5) Å, respectively. The Ge–Si(1) distance of 2.446(9) Å is about 0.06 Å longer than the Ge–Si distance in **1**. These data therefore suggest that $[Me_4C_4GeSi(SiMe_3)_3]^-$ gains very little stabilization by π-delocalization of the negative charge.

We have performed calculations on $(C_4H_4ESiH_3)^-$ ions at the RHF level of theory,[10] with an interest in examining the structural trends to be expected for Group 14 derivatives. The results for three structural parameters are given in Table 1: the (C-E-C plane)–(E–Si bond) angle at E (α), and the two independent C–C bond lengths (C_s symmetry) in the ring. As expected, the cyclopentadienide ion (E = C) is flat ($\alpha = 177.3°$), and the angle bends sharply as this group is descended and the bonding orbitals for E develop more p-character. This is accompanied by

 © VCH Verlagsgesellschaft mbH, D-69451 Weinheim, 1995 0570-0833/95/3417-1888 $ 10.00+.25/0

Table 1. Selected calculated geometric parameters for $(H_4C_4ESiH_3)^-$ ions.

E	C	Si	Ge [a]	Sn
α [ ]	177.3	104.5	99.7 (100.1)	94.7
$d(EC_1\text{-}C_2) = d(C_3\text{-}C_4E)$ [Å]	1.408	1.367	1.361 (1.36)	1.358
$d(C_2\text{-}C_3)$ [Å]	1.428	1.477	1.484 (1.46)	1.493

[a] Experimental values in parentheses.

increased localization of the π system in the ring. The agreement between the calculated and experimental values for E = Ge is excellent. Note that the silacyclopentadienide ion is also expected to have a pyramidal, non-aromatic structure. Löwdin charges for the ring atoms are given in Table 2. The trend in the charge at E clearly parallels the Pauling electronegativities, and expected polarities for the E–C bonds. Charge differences as a function of E diminish rapidly at C1 and all but vanish at C2. For $(C_4H_4GeSiH_3)^-$, the homodesmotic aromatic stabilization energy (ASE, 5.3 kcal mol^{-1}) and the Julg parameter[13] (A, 0.532) indicate less aromaticity than is expected for $(C_4H_4SiH)^-$ (ASE = 13.8 kcal mol^{-1}; A = 0.926, based on the ab initio calculations of Schleyer et al.[3, 14]).

Table 2. Löwdin charges for ring atoms in $(H_4C_4ESiH_3)^-$ ions.

Atom	E = C	Si	Ge	Sn
E	−0.50	0.06	−0.03	0.14
C1 = C4	−0.36	−0.51	−0.48	−0.52
C2 = C3	−0.37	−0.33	−0.33	−0.33
electronegativity [a]	2.55	1.90	2.01	1.96

[a] Electronegativities are modified Pauling values from W. L. Jolly, *Modern Inorganic Chemistry*, McGraw-Hill, New York, **1984**.

The results reported here clearly characterize the title germacyclopentadienide ion as a non-aromatic ring with a pyramidal germanium center. It is interesting to compare this structure with that of $[(\eta^5\text{-}C_5Me_5)Ru\{\eta^5\text{-}C_4Me_4GeSi(SiMe_3)_3\}]$,[8] which contains the same germacyclopentadienide ring bonded to ruthenium. In the latter case, the ring appears to be highly delocalized, as indicated by (for example) the summation of bond angles at Ge (358.1°) and the equivalent C–C distances of 1.42 Å. Interestingly, then, coordination of a transition metal fragment induces considerable π-delocalization and apparent aromatic character for the germacyclopentadienide ring. Coordination of the analogous silacyclopentadienide ring $[Me_4C_4Si\text{–}Si(SiMe_3)_3]^-$ to $[(\eta^5\text{-}C_5Me_5)Ru]$ also leads to a delocalized ring,[15] and interestingly, Goldfuss and Schleyer have recently predicted that coordination of Li^+ would induce considerable π-delocalization in $(C_4H_4SiH)^-$.[3b]

Experimental Procedure

2: Toluene (50 mL) was added to a Schlenk flask containing **1** [8] (0.20 g, 0.47 mmol), [18]crown-6 (0.12 g, 0.47 mmol), and $KN(SiMe_3)_2$ (0.094 g, 0.47 mmol). After stirring the reaction mixture for 30 min at room temperature, the solution was reduced in volume to about 10 mL and then cooled to −40 °C to produce yellow crystals of **2** in 45% yield. Anal. calcd for $C_{29}H_{63}GeKO_6Si_4$: C 47.59, H 8.68; found: C 47.44, H 8.57. ^{1}H NMR (300 MHz): δ = 0.59 (s, 27 H, $SiMe_3$), 2.22, 2.62 (s, 6 H, CMe), 3.09 (s, 24 H, [18]crown-6). $^{13}C\{^1H\}$ NMR (75.5 MHz): δ = 3.98 ($SiMe_3$), 15.96, 20.46 (*CMe*), 69.91 ([18]crown-6), 137.13, 157.06 (*C*Me); $^{29}Si\{^1H\}$ NMR (59.63 MHz, DEPT): δ = −125.03 (s, *Si*$SiMe_3$), −8.22 (s, $SiMe_3$).

3: To a mixture of **1** (0.26 g, 0.60 mmol) and [12]crown-4 (0.22 g, 1.20 mmol) in diethyl ether (25 mL) was added *n*BuLi (0.395 mL, 0.632 mmol of a 1.6 M solution in hexanes) dropwise over 1 min, and the resulting yellow solution was stirred for 30 min. Slow diffusion of pentane into this solution via vapor transport provided X-ray quality crystals in 42% yield. Anal. calcd for $C_{33}H_{71}GeLiO_8Si_4$: C 50.30, H 9.10; found: C 50.22, H 9.10. ^{1}H NMR (300 MHz): δ = 0.62 (s, 27 H, $SiMe_3$), 2.26, 2.69 (s, 6 H, CMe), 3.18 (s, 32 H, [12]crown-4); $^{13}C\{^1H\}$ NMR (100.6 MHz, THF/[D$_6$]benzene): δ = 3.77 ($SiMe_3$), 15.59, 20.30 (*CMe*), 69.19 ([12]crown-4), 136.95, 157.03 (*C*Me); $^{29}Si\{^1H\}$ NMR (59.63 MHz, INEPT): δ = −125.57 (s, *Si*$SiMe_3$), −8.43 (s, $SiMe_3$).

4: THF (250 mL) was added to a flask containing $C_4Me_4GeCl_2$ [16] (2.28 g, 9.06 mmol) and finely divided potassium chunks (1.45 g, 37.14 mmol) at room temperature, and the reaction mixture was stirred for 4 days. To the resulting deep red solution was added Me_3SiCl (4.71 mL, 37.14 mmol) dropwise. After stirring for 5 min, the volatiles were removed by vacuum transfer and the resulting residue was extracted with pentane (3 × 40 mL). The pentane extracts were concentrated and cooled (−40 °C) to give the product as an oil at room temperature in 60% yield. Anal. calcd for $C_{14}H_{30}GeSi_2$: C 51.39, H 9.26; found: C 50.40, H 8.98. ^{1}H NMR (300 MHz): δ = 0.22 (s, 18 H, $SiMe_3$), 1.86, 2.11 (s, 6 H, CMe); $^{13}C\{^1H\}$ NMR (100.6 MHz): δ = 0.51 ($SiMe_3$), 14.71, 17.53 (*CMe*), 134.86, 145.67 (*C*Me); $^{29}Si\{^1H\}$ NMR (59.63 MHz, INEPT): δ = −7.55 (s, $SiMe_3$).

5: To KCH_2Ph (0.138 g, 1.01 mmol) and [18]crown-6 (0.247 g, 0.935 mmol) was added **4** (0.329 g, 1.01 mmol) in toluene (100 mL), and the resulting solution was stirred for 30 min. Removal of volatiles and addition of diethyl ether (25 mL) produced a red solution. Slow vapor diffusion of pentane into this solution over 3 days gave the product in 45% yield. Anal. calcd for $C_{23}H_{45}GeKO_6Si$: C 49.55, H 8.15; found: C 49.55, H 8.01. ^{1}H NMR (400 MHz): δ = 0.54 (s, 9 H, $SiMe_3$), 2.26, 2.67 (s, 6 H, CMe), 3.19 (s, 24 H, [18]crown-6); $^{13}C\{^1H\}$ NMR (100.6 MHz): δ = 2.49 ($SiMe_3$), 15.86, 20.06 (*CMe*), 70.07 ([18]crown-6), 136.72, 158.56 (*C*Me); $^{29}Si\{^1H\}$ NMR (59.63 MHz, INEPT): δ = −3.86 (s, $SiMe_3$).

Received: April 18, 1995 [Z 7897 IE]
German version: *Angew. Chem.* **1995**, *107*, 2029–2031

Keywords: aromaticity · germacyclopentadienide · heterocycles · silacyclopentadienide

[1] J. Dubac, A. Laporterie, G. Manuel, *Chem. Rev.* **1990**, *90*, 215; E. Colomer, R. J. P. Corriu, M. Lheureux, *ibid.* **1990**, *90*, 265; H. Grützmacher, *Angew. Chem.* **1995**, *107*, 323; *Angew. Chem. Int. Ed. Engl.* **1995**, *34*, 295.

[2] M. S. Gordon, P. Boudjouk, F. Anwari, *J. Am. Chem. Soc.* **1983**, *105*, 4972; J. R. Damewood, Jr., *J. Org. Chem.* **1986**, *51*, 5028.

[3] a) P. von R. Schleyer, P. K. Freeman, H. Jiao, B. Goldfuss, *Angew. Chem.* **1995**, *107*, 332; *Angew. Chem. Int. Ed. Engl.* **1995**, *34*, 337; b) B. Goldfuss, P. von R. Schleyer, *Organometallics* **1995**, *14*, 1553.

[4] J.-H. Hong, P. Boudjouk, *J. Am. Chem. Soc.* **1993**, *115*, 5883.

[5] M. D. Curtis, *J. Am. Chem. Soc.* **1967**, *89*, 4241; *ibid.* **1969**, *91*, 6011; P. Jutzi, A. Karl, *J. Organomet. Chem.* **1981**, *215*, 19.

[6] P. Dufour, J. Dubac, M. Dartiguenave, Y. Dartiguenave, *Organometallics* **1990**, *9*, 3001.

[7] a) X-ray structure analysis of **1**: $C_{17}H_{40}GeSi_4$, M_r = 429.4, triclinic, $P\bar{1}$, a = 9.065(3), b = 9.585(4), c = 15.925(7) Å, α = 92.49(4), β = 98.27(3)°, γ = 113.74(3)°, V = 1245.6(9) Å^3, Z = 2; ρ_{calcd} = 1.145 g cm^{-3}, $\mu(Mo_{K\alpha})$ = 13.99 cm^{-1}, T = 173 K; 4381 independent reflections with 3° ≤ 2θ ≤ 50° were collected, of which 3812 reflections with F_0 greater than 4$\sigma(F_0)$ were used in refinement. $R(F)$ = 0.0253, $R_w(F)$ = 0.0370, GOF = 0.96. A semiempirical absorption correction was applied, T(max)/T(min) = 1.47. All the non-hydrogen atoms were refined anisotropically with the hydrogen atoms treated as idealized isotropic contributions, except H(1) which was located and refined. b) Further details of the crystal structure investigation are available on request from the Director of the Cambridge Crystallographic Data Centre, 12 Union Road, GB-Cambridge CB2 1EZ (UK), on quoting the full journal citation.

[8] W. P. Freeman, T. D. Tilley, A. L. Rheingold, R. L. Ostrander, *Angew. Chem.* **1993**, *105*, 1841; *Angew. Chem. Int. Ed. Engl.* **1993**, *32*, 1744.

[9] X-ray structure analysis of **3**: $C_{33}H_{71}GeLiO_8Si_4$, M_r = 787.8, monoclinic, $P2_1/n$, a = 17.73(3), b = 14.871(10), c = 18.83(2) Å, β = 111.60(3)°, V = 4617(9) Å^3, Z = 4; ρ_{calcd} = 1.133 g cm^{-3}, $\mu(Mo_{K\alpha})$ = 8.06 cm^{-1}, T = 296 K; 4916 independent reflections with 4° ≤ 2θ ≤ 35° were collected (Siemens P4), of which 2327 with F_0 greater than 5$\sigma(F_0)$ were used in refinement. $R(F)$ = 0.1263, $R_w(F)$ = 0.1684, GOF = 2.68. All specimens that were screened showed extremely broad diffraction that did not sharpen or intensify significantly at 220 K. The diffuseness of diffraction likely arises from the considerable disorder seen in the cationic complex, $[Li([12]crown\text{-}4)_2]^+$, the high thermal activity of the tris(trimethylsilyl)silyl group, and the low lattice energy resulting from the extreme isolation of cationic charge. Observed diffraction data was found only to 2θ = 35°. Full profile data collection was performed at 2° min^{-1} and a learned profile routine was applied to improve the accuracy of the measurement of weak reflections. The C–Si bond distances were constrained to a distance of 1.82 Å [7b].

[10] Calculations were performed with the GAMESS [11] package on an SGI Indigo-2 computer, at the RHF level of theory, and employed the SBKJ CEP-31 basis set, supplemented by d-polarization and shared exponent (s = p) diffuse functions on all heavy atoms. C_s symmetry was employed. Geometries were confirmed to be minima by vibrational analyses. It may be noted that Mopac-6

calculations with either the AM1 or PM3 parameters of Stewart [12] failed to predict a folding of the dihedral angle at Ge, also the calculations for E = Si, Ge, and Sn indicate slight non-planarity for the C_4E rings, such that the E atom is displaced in the direction away from the SiH_3 group by folding along the C_1–C_4 vector (fold angles: Si, 6.3°; Ge, 6.0°; Sn, 4.5°). Thus, α is defined as the angle between the C_1-E-C_4 plane and the E–Si bond.

[11] M. W. Schmidt, K. K. Baldridge, J. A. Boatz, S. T. Elbert, M. S. Gordon, J. J. Jensen, S. Koseki, N. Matsunaga, K. A. Nguyen, S. Su, T. L. Windus, M. Dupuis, J. A. Montgomery, *J. Comput. Chem.* **1993**, *14*, 1347.

[12] J. J. P. Stewart, *J. Comput. Aided Mol. Des.* **1990**, *4*, 1, and references therein.

[13] A. Julg, P. Francois, *Theor. Chim. Acta* **1967**, *7*, 249.

[14] Our methods produced an ASE value for $C_5H_5^-$ that is 3.7 kcal mol^{-1} (13%) lower than the value calculated by Schleyer et al. [3a]. Our calculations did not include zero-point energy corrections, but were performed with a more complete basis set at the RHF level of theory.

[15] W. P. Freeman, T. D. Tilley, A. L. Rheingold, *J. Am. Chem. Soc.* **1994**, *116*, 8428.

[16] P. J. Fagan, W. A. Nugent, *J. Am. Chem. Soc.* **1988**, *110*, 2310.

$C_4S_6^{2-}$: A Bridging Bis(dithiolato) Ligand for the Preparation of Semiconducting Inorganic Polymers**

Lisa F. Szczepura, Collin P. Galloway, Yifan Zheng, Pengdi Han, Arnold L. Rheingold, Scott R. Wilson, and Thomas B. Rauchfuss*

Difunctional ligands are key to the preparation of coordination polymers.[1, 2] Especially relevant to the design of new electronic materials are those ligands that promote strong electronic coupling between pairs of metal atoms, as is optimally effected by ligands with delocalized π-electron systems. To confer stability to the intermetallic linkage, it is further desirable that the ligands engage the metals through binding sites that are both anionic and chelating. We report a new inorganic ligand that incorporates these design features and forms inorganic polymers with a delocalized π-electron system.

We have recently reported[3] the preparation of the dithiocarbonate C_3S_7O in two steps from the Steimecke anion $[Zn(C_3S_5)_2]^{2-}$.[4] Since dithiocarbonates are susceptible to alkaline hydrolysis, this C-S-O heterocycle represents a potential precursor to novel dithio chelates. With this in mind we treated a methanolic suspension of C_3S_7O with two equivalents of NaOMe, causing the yellow solid to dissolve to give a brown-purple solution. Treatment of the reaction solution with NEt_4Br and fractional crystallization from $MeCN/Et_2O$ gave $(NEt_4)_2C_4S_6$ in 59% yield as dark blue, air-sensitive crystals [Eq. (a)]. The mechanism of this transformation has not been

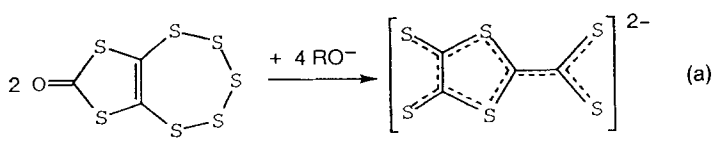

(a)

[*] Prof. T. B. Rauchfuss, Dr. L. F. Szczepura, C. P. Galloway, Dr. Y. Zheng, Dr. P. Han, Dr. S. R. Wilson
School of Chemical Sciences
and the Materials Research Laboratory
University of Illinois, Urbana, IL 61801 (USA)
Telefax: Int. code + (217)333-2685

Prof. A. L. Rheingold
Department of Chemistry
University of Delaware, Newark, DE 19716 (USA)

[**] This research was supported by the Department of Energy (DE-FG02-91ER45439). L. F. S. thanks the National Science Foundation for a postdoctoral fellowship.

investigated; however, it is obvious that it involves condensation of a pair of C_2S_x units. We observed the formation of elemental sulfur as a by-product.

The ^{13}C NMR spectrum of $(NEt_4)_2C_4S_6$ shows resonances at $\delta = 217, 189$, and 143 in an approximate ratio of 1:2:1. Solutions of $(NEt_4)_2C_4S_6$ display a rich optical spectrum including low-energy bands at $\tilde{\nu} \approx 10000\ cm^{-1}$ and a band at higher energy showing a distinct solvatochromic effect ($\tilde{\nu}$(MeCN) = 29400 cm^{-1}, $\tilde{\nu}$(MeOH) = 31100 cm^{-1})[5] (Fig. 1). These data indicate that $C_4S_6^{2-}$ is highly polarizable with a small HOMO–LUMO gap. Single-crystal X-ray diffraction[6] showed that

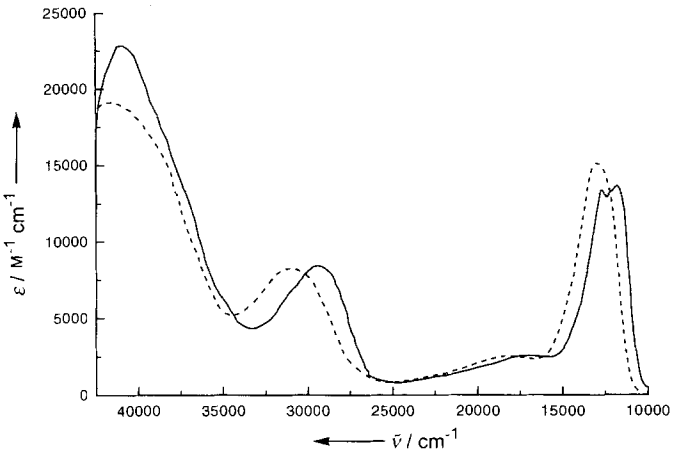

Fig. 1. Optical spectra of $(NEt_4)_2C_4S_6$ in MeCN (solid line) and MeOH (dashed line).

$C_4S_6^{2-}$ is planar with crystallographically imposed C_{2v} symmetry (Fig. 2). This is the largest anionic carbon sulfide structurally characterized.[7] The anion is disordered over two orientations within a rectangular framework defined by the four terminal sulfur atoms. The planarity and short C–S distances indicate extensive delocalization of the π system. The differing C1–S1 and C3–S3 distances suggest that the anion could be described as a 1,1-alkenedithiolate fused to a 1,2-dithione.[8]

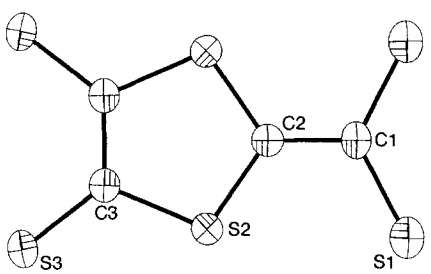

Fig. 2. Molecular structure of the dianion in $(NEt_4)_2C_4S_6$. Important bond lengths [Å] and angles [°]: S1-C1 1.745(2), S2-C2 1.700(2), S2-C3 1.742(3), S3-C3 1.638(3), C1-C2 1.402(6), C3-C3e' 1.424(5); S1-C1-S1' 126.0(2), S3-C3-C3' 127.95(10).

Vast numbers of complexes are known for 1,2- and 1,1-dithiolates[9] but the combination of the two ligand types as in $C_4S_6^{2-}$ is unique to this work. It was therefore of interest to test the ability of this bis(dithiolate) to serve as a bridging ligand. Qualitative tests showed that solutions of $C_4S_6^{2-}$ react in acetonitrile with many simple metal salts to give black insoluble solids. Starting with $[Ni(H_2O)_6]Cl_2$ we were able to prepare solids that undergo ion exchange with additional $[Ni(H_2O)_6]^{2+}$

to give a product of approximate composition $[NiC_4S_6]$. The microanalytical data fit well for $(NBu_4)_2[Ni_{45}(C_4S_6)_{46}]$, an inorganic polymer terminated by $C_4S_6^{2-}$ units. Based on the composition, diamagnetism, and semiconducting properties of this material (see below), we propose that it is a one-dimensional polymer consisting of a ribbonlike strand of edge-shared square-planar complexes [Eq. (b)].

$$Ni^{2+} + C_4S_6^{2-} \longrightarrow \left[\text{S}_2\text{C}_2\text{S}_2\text{Ni}\right]_n \qquad \text{(b)}$$

In related experiments, solutions of $C_4S_6^{2-}$ in acetonitrile were found to react with $[Cu(MeCN)_4]BF_4$ to afford black diamagnetic solids analyzing as $(NEt_4)_2[Cu_{60}(C_4S_6)_{31}]$. The IR spectra of these inorganic polymers are very simple and dominated by a single intense absorption assigned to ν_{CS} (1196 cm^{-1} for the Ni polymer, 1172 cm^{-1} for the Cu polymer). Compressed pellets of $[Cu_2C_4S_6]$ and $[NiC_4S_6]$ exhibit four-point conductivities (294 K) of 0.1 and 0.9 $S\,cm^{-1}$, respectively. In both cases the temperature dependence of the conductivities indicate that these are semiconductors. It is unusual for simple coordination polymers to exhibit such conductivities.[10]

To elucidate the structures of these semiconducting polymers we investigated bimetallic complexes of $C_4S_6^{2-}$. This proved to be quite challenging, as again most experiments produced insoluble products. The reaction with $[(p\text{-cymene})RuCl_2]_2$ (*p*-cymene = 4-isopropyltoluene) proved successful and afforded the purple compound $[(p\text{-cymene})_2Ru_2Cl_2(C_4S_6)]$ [Eq. (c)].

$$[(p\text{-cymene})_2Ru_2Cl_4] + C_4S_6^{2-} \longrightarrow [(p\text{-cymene})_2Ru_2Cl_2(C_4S_6)] + 2\ Cl^- \qquad \text{(c)}$$

A crystallographic study of the Ru_2 complex[11] established the structure shown in Figure 3. This unsymmetrical structure is maintained in solution, since both ^1H and ^{13}C NMR analyses indicate that the cymene groups are nonequivalent but that both

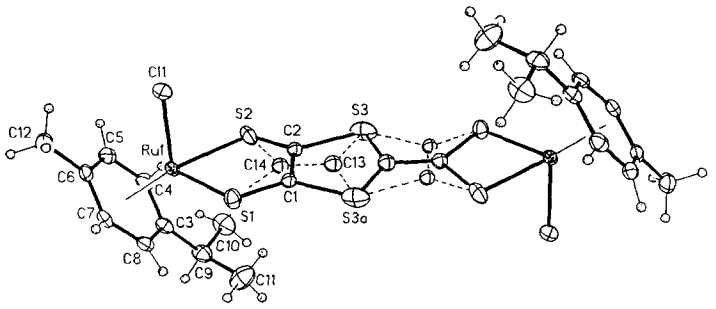

Fig. 3. Molecular structure of $[(p\text{-cymene})_2Ru_2Cl_2(C_4S_6)]$ showing the end-to-end disorder about a crystallographic inversion center. Carbon atoms C1, C2, C3, and C4 were refined isotropically at half occupancy; the remaining non-hydrogen atoms are shown with 40% probability ellipsoids.

are bisected by a symmetry plane. This diruthenium complex provides a well-defined model for a subunit of $[NiC_4S_6]$. The means by which the C_4S_6 unit bridges more than two metals, as is assumed to occur in $[Cu_2C_4S_6]$, must await further study.

Since $C_4S_6^{2-}$ is itself electroactive (it can be reduced), it should be possible to dope the new inorganic polymers reported in this paper to enhance their electrical conductivity.

Experimental Procedure

All preparative operations were conducted under purified nitrogen. C_3S_7O was prepared from "C_3S_7" [3] synthesized from the reaction of $(NBu_4)_2[Zn(C_3S_5)_2]$ [4] with purified S_2Cl_2. Electrical conductivity measurements (AC technique) were performed on pellets (ca. 0.08 g) pressed at roughly 2250 $kg\,cm^{-2}$, and the contacts were made with silver paint.

$(NEt_4)_2C_4S_6$: A fresh solution of NaOMe in 13 mL of MeOH, prepared from 0.083 g of Na, was added to 0.5 g of C_3S_7O. After stirring for 2 d, the solution was combined with NEt_4Br and concentrated to dryness. This material was extracted into MeCN, filtered to remove NaBr, and crystallized by addition of Et_2O to give 0.27 g (59% yield) of the dark blue, air-sensitive crystals. Anal. calcd for $C_{20}H_{40}N_2S_6$ (found): C 47.95 (47.65), H 8.05 (8.09), N 5.59 (5.66). IR (KBr): $\tilde{\nu} = 1173\ cm^{-1}$. UV-Vis (MeCN): λ [nm] (ε [$M^{-1}cm^{-1}$]) 240 (25000), 340 (8500), 800 (14000), 856 (13000).

The NBu_4^+ salt was obtained similarly and used in all subsequent reactions.

$[NiC_4S_6]$: Equimolar methanol solutions of $(NBu_4)_2C_4S_6$ (0.328 g) and $[Ni(H_2O)_6]Cl_2$ (0.132 g) in MeOH were added simultaneously to a flask containing 40 mL MeOH. A black solid precipitated immediately. This solid was collected, washed with MeOH, ground, and resuspended in a solution of $[Ni(H_2O)_6]Cl_2$ (1.42 g) in MeOH for 8 h. The solid was collected and dried under vacuum at 94 °C. Yield 86%. Anal. calcd for $(NBu_4)_2[Ni_{45}(C_4S_6)_{46}]$ (found): C 18.29 (18.48), H 0.51 (0.47), N 0.20 (0.23), Ni 18.62 (17.32). IR (KBr): $\tilde{\nu} = 1196\ cm^{-1}$ (vs).

$[Cu_2C_4S_6]$: Solutions of $[Cu(MeCN)_4]BF_4$ (0.254 g) and $(NBu_4)_2C_4S_6$ (0.290 g) in acetonitrile were combined to give a black precipitate, which was washed with solvent and dried under vacuum at 85 °C. Yield 87%. Anal. calcd for $(NBu_4)_2[Cu_{60}(C_4S_6)_{31}]$ (found): C 15.94 (15.84), H 0.62 (0.37), N 0.24 (0.30), Cu 32.45 (31.80). IR (KBr): $\tilde{\nu} = 1172\ cm^{-1}$ (vs).

$[(p\text{-Cymene})_2Ru_2Cl_2C_4S_6]$: Equimolar solutions of $(NBu_4)_2C_4S_6$ (0.20 g) and $[(p\text{-cymene})RuCl_2]_2$ (0.18 g) in CH_2Cl_2 were combined. After 4 h, the reaction solution was concentrated and diluted with MeCN to precipitate the purple product. Yield: 46%. Single crystals were obtained from CH_2Cl_2/MeCN. Anal. calcd for $C_{24}H_{28}Cl_2Ru_2S_6$ (found): C 36.88 (36.63), H 3.59 (3.69), Cl 9.09 (10.90), Ru 25.85 (24.43), S 24.58 (23.73). IR (KBr): $\tilde{\nu} = 1308, 1252\ cm^{-1}$ (vs). ^1H NMR ($CDCl_3$): $\delta = 1.22$ (d, 6H), 1.27 (d, 6H), 2.24 (s, 3H), 2.28 (s, 3H), 2.80 (m, 2H), 5.37 (d, 2H), 5.41 (d, 2H), 5.52 (d, 2H), 5.61 (d, 2H). ^{13}C NMR ($CDCl_3$): $\delta = 17.5$, 18.4, 21.4, 21.8, 30.2, 31.1, 84.1, 84.4, 84.8, 85.3, 101.8, 102.7, 104.9, 105.4, 154.0, 186.0, 210.6.

Received: April 11, 1995 [Z7881IE]
German version: *Angew. Chem.* **1996**, *107*, 2027–2029

Keywords: polymers · semiconductors · sulfur compounds · thiones

[1] Recent developments on coordination polymers include advances in one-dimensional polymers: J. Kröber, E. Codjovi, O. Kahn, F. Groliere, C. Jay, *J. Am. Chem. Soc.* **1993**, *115*, 9810; two-dimensional polymers: G. De Munno, M. Julve, F. Nicolo, F. Lloret, J. Faus, R. Ruiz, E. Sinn, *Angew. Chem.* **1993**, *105*, 588; *Angew. Chem. Int. Ed. Engl.* **1993**, *32*, 613; and three-dimensional polymers: S. R. Batten, B. H. Hoskins, R. Robson, *ibid.* **1995**, *107*, 884 and **1995**, *34*, 820; B. F. Abrahams, B. F. Hoskins, R. Robson, *J. Am. Chem. Soc.* **1991**, *113*, 3606; L. R. Macgillivray, S. Subramian, M. J. Zaworotko, *J. Chem. Soc. Chem. Commun.* **1994**, 1325; O. M. Yaghi, Z. Sun, D. A. Richardson, T. L. Groy, *J. Am. Chem. Soc.* **1994**, *116*, 807.

[2] G. Cao, H.-G. Hong, T. E. Mallouk, *Acc. Chem. Res.* **1992**, *25*, 420; A. Stein, S. W. Keller, T. E. Mallouk, *Science* **1993**, *259*, 1558.

[3] C. P. Galloway, D. D. Doxsee, D. Fenske, T. B. Rauchfuss, S. R. Wilson, X. Yang, *Inorg. Chem.* **1994**, *33*, 4537. An overview of binary carbon sulfides: C. P. Galloway, T. B. Rauchfuss, X. Yang in *The Chemistry of Inorganic Ring Systems* (Ed.: R. Steudel), Elsevier, Amsterdam, **1992**.

[4] G. Steimecke, H.-J. Sieler, R. Kirmse, E. Hoyer, *Phosphorus Sulfur* **1979**, *7*, 49; R.-M. Olk, B. Olk, W. Dietzsch, R. Kirmse, E. Hoyer, *Coord. Chem. Rev.* **1992**, *117*, 99.

[5] C. Reichardt, *Chem Rev.* **1994**, *94*, 2319.

[6] Crystal data for $C_{20}H_{40}N_2S_6$: black prisms, orthorhombic, *Immm*, $a = 8.793(3)$, $b = 12.052(4)$, $c = 13.047(4)$ Å; $Z = 2$; $V = 1382.6(8)$ Å^3, $T = 292$ K, $\mu(Mo_{K\alpha}) = 17.33\ cm^{-1}$, $R(F) = 0.0371$, $wR_2 = 0.0742$. In the refinement the anion was constrained to *m2m* symmetry [11b].

[7] G. Seitz, *Phosphorus, Sulfur, Silicon* **1989**, *43*, 311.

[8] R. Mattes, D. Altmeppen, G. Johann, M. Schulte-Coerne, H. Weber, *Monatsh. Chem.* **1982**, *113*, 191; R. Grenz, F. Götzfried, U. Nagel, W. Beck, *Chem. Ber.* **1986**, *119*, 1217; C. Wolf, H.-U. Hummel, *J. Chem. Soc. Dalton Trans.* **1986**, 43; H.-U. Hummel, C. Wolf, *Z. Naturforsch. B* **1986**, *41*, 1206.

[9] P. Cassoux, L. Valade, H. Kobayashi, A. Kobayashi, R. A. Clark, A. E. Underhill, *Coord. Chem. Rev.* **1991**, *110*, 115; M. R. Bryce, *Chem. Soc. Rev.* **1991**, *20*, 355; J. R. Ferraro, J. M. Williams, *Introduction to Synthetic Electrical Conductors*, Academic Press, New York, **1987**; U. T. Mueller-Westerhoff, B. Vance in *Comprehensive Coordination Chemistry, Vol. 2* (Eds.: G. Wilkinson, R. D. Gillard, J. A. McCleverty) Pergamon, Oxford, **1987**.

[10] Coordination polymers with significant conductivities ($>1\ S\,cm^{-1}$) have been prepared from tetrathiafulvalene-tetrathiolate and -tetrathiaoxalate: N. M. Rivera, E. M. Engler, R. R. Schumaker, *J. Chem. Soc. Chem. Commun.* **1979**, 184; J. Ribas, P. Cassoux, *C. R. Acad. Sc. Paris* **1981**, *293*, 665; J. R. Reynolds, C. A. Jolly, S. Krichene, P. Cassoux, C. Faulmann, *Synth. Met.* **1986**, *13*, 265; J. R. Reynolds, C. P. Lillya, J. C. W. Chien, *Macromolecules* **1987**, *20*, 1184.

[11] a) Crystal data for $C_{24}H_{28}Cl_2Ru_2S_6$: red plates, monoclinic, $P2_1/c$, $a = 14.089(6)$, $b = 8.219(3)$, $c = 12.090(4)$ Å, $\beta = 92.27(3)°$, $V = 1398.9(9)$ Å^3, $Z = 2$, $T = 292$ K, $\mu(Mo_{K\alpha}) = 17.33\ cm^{-1}$, $R(F) = 0.0406$, $R(wF) = 0.0441$. The molecule sits on a crystallographic inversion center producing end-for-end disorder. The thermal ellipsoids for the S atoms reveal the presence of unresolved dual positions. The position of C(14) was obtained after refinement with the C(1)–C(2) distance fixed at the value found in the $C_4S_6^{2-}$. b) Further details of the crystal structure investigations may be obtained from the Director of the Cambridge Crystallographic Data Centre, 12 Union Road, GB-Cambridge CB21EZ (UK), on quoting the full journal citation.

Synthesis of New Sworski-Type Dehydroannulenes: 3,4-Benz-1,2,5,6,8,9,12,13-octadehydro[14]-annulenes**

Yoshiyuki Kuwatani* and Ikuo Ueda

Recently, highly unsaturated conjugated compounds have attracted considerable attention as possible precursors of two- and three-dimensional carbon networks.[1] Two-dimensional carbon networks should have a rigid and planar cyclic conjugated system as a unit structure. Some compounds for these systems can be designed by insertion of two sp-hybridized carbons into appropriate C–C bonds in benzene, as shown by T. J. Sworski.[2] We had been interested in these dehydroannulenes[3] and reported the the synthesis of the dodecadehydro[18]-annulene derivative (**1**).[4]

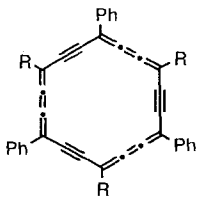

1

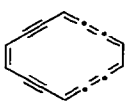

2

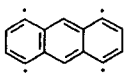

3

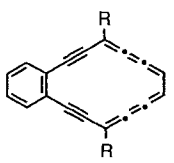

4

[*] Dr. Y. Kuwatani
Institute for Fundamental Research of Organic Chemistry
Kyushu University
Hakozaki, Higashiku, Fukuoka, 812 (Japan)
Telefax: Int. code +(92) 651-8285
Prof. Dr. I. Ueda
The Institute of Scientific and Industrial Research
Osaka University
Mihogaoka, Ibaraki, Osaka, 567 (Japan)

[**] This work was supported by a Grant-in-Aid (No. 05740394) for Scientific Research from the Ministry of Education, Science and Culture (Japan).

Octadehydro[14]annulene (**2**), which is classified as a Sworskii-type dehydroannulene, is represented by two equivalent canonical structures and should show properties of an aromatic $(4n + 2)$ π-electron system. Therefore it is an interesting candidate for a unit structure of two-dimensional carbon networks. Furthermore, the dehydroannulene **2** can give rise to an anthracene tetraradical **3** through the Bergman reaction, which plays important role in some antitumor antibiotics.[5] In this paper, we describe the synthesis of the benzannelated dehydroannulenes **4** and their physical properties.

Since the selective synthesis of (*Z*)-[3]cumulenes is very difficult, we decided to construct the 14-membered ring prior to introduction of cumulative double bonds. The annulenedione **5** was chosen as a synthetic intermediate and prepared from **6** as shown in Scheme 1. Trimethylsilylethynyl-1,3-dioxane (**6**) was

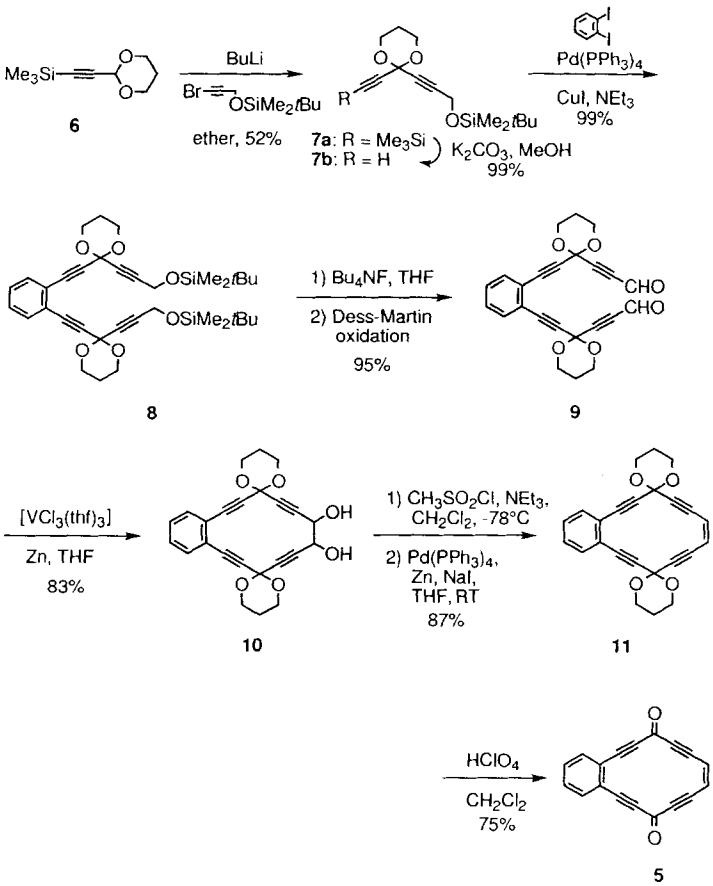

Scheme 1. Preparation of annulenedione **5** from **6**.

lithiated by *n*-butyllithium in ether[6] and then reacted with 1-bromo-3-(*tert*-butyldimethyl)silyloxy-1-propyne[7] to give the diyne **7a** in 52% yield. After removal of the trimethylsilyl group of **7a** by treatment with K_2CO_3 in methanol, the terminal alkyne **7b** was coupled with *ortho*-diiodobenzene in the presence of a palladium(0) complex and CuI to afford tetrayne **8** in quantitative yield.[8] The bis(silyloxy)tetrayne **8** was deprotected with tetrabutylammonium fluoride, and the resulting diol was oxidized to the dialdehyde **9** with Dess–Martin periodinane[9] in 95% yield. Cyclization of **9** was achieved in 83% yield by the modified Pedersen method—a pinacol coupling reaction using a low-valent vanadium complex generated from $[VCl_3(thf)_3]$ and zinc dust.[10] The pinacol **10** obtained as a mixture of two diastereoisomers was reduced to the cyclic enediyne derivative

11 via the corresponding dimesylate in 87% yield. This procedure provides a new and effective method for the construction of cyclic enediyne systems.[11, 12] The diacetal **11** was hydrolyzed by perchloric acid in dichloromethane to give the annulenedione **5** in 75% yield (see Table 1).

The transformation of **5** to the dehydroannulenes **4** was achieved by three different methods depending on the substituents (Scheme 2). The aryl-substituted derivatives **4a** and **4b** were synthesized via diols **12a** and **12b** prepared from **5** and the

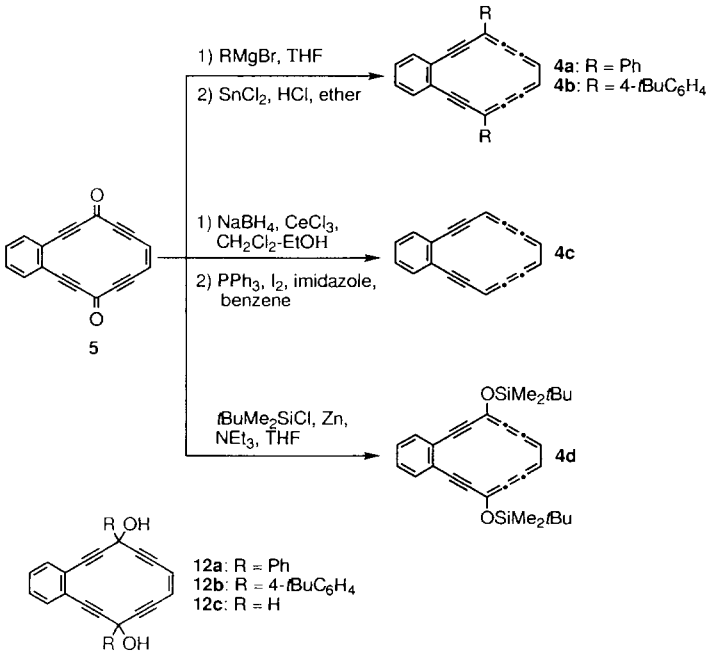

Scheme 2. Synthesis of dehydroannulenes **4** from **5**.

appropriate Grignard reagent. The Grignard reaction of **5** with PhMgBr gave the diol **12a** as a mixture of diastereomers, which was reduced by $SnCl_2$ and gaseous HCl in ether[13] to afford the diphenyl-substituted dehydroannulene **4a** in 21% yield. The bis(4-*tert*-butylphenyl)-substituted derivative **4b** was also obtained by the same method in 27% yield.[14] The unsubstituted dehydroannulene **4c** was synthesized by reduction of **5** with a hydride under Luche's conditions[15] and dehydroxylation of the resultant diol (**12c**) by treatment with PPh_3, I_2, and imidazole in benzene. The direct reduction of **5** to the bis(silyloxy) derivative **4d** was achieved under electron-transfer conditions.[16] The reaction of **5** with zinc powder in the presence of *tert*-butyldimethylchlorosilane and triethylamine gave **4d**.[17]

The two diaryl-substituted derivatives **4a** and **4b** were obtained as moderately stable violet needles, but the other derivatives, **4c** and **4d**, could be obtained only in dilute, red solution. These two compounds polymerized readily in concentrated solution. Dehydroannulenes **4** show characteristic properties of arenes (Table 1). In their ^1H NMR spectra, all the signals are observed at very low field indicating the existence of a diatropic ring current, the most common criterion for aromaticity. For example, the signals of H-10 and H-11 on the 14-membered ring in **4a**, **4b**, **4c**, and **4d** are observed at $\delta = 8.18$, 8.13, 8.23, and 7.80, respectively. These signals are about 2 ppm downfield from the corresponding signal of **11**, which is observed at $\delta = 6.04$. The number of signals in the ^{13}C NMR spectra of **4** corresponds to half the number of carbon atoms, which reflects the symmetry of the compounds (C_{2v}) and is in good agreement

Table 1. Selected physical data of compounds **4**, **5**, and **11**. *J* in Hz.

4a: Deep violet needles (CH_2Cl_2/hexane), m.p. >120 °C (decomp.); MS (FAB): *m/z* 376 (M^+); ^1H NMR (270 MHz, $CDCl_3$): $\delta = 9.03-8.96$ (2H, AA'm), 8.78 (4H, d, $J = 7.3$), 8.18 (2H, s), 8.13–8.06 (2H, BB'm), 7.67 (4H, t, $J = 7.3$), 7.49 (2H, t, $J = 7.3$); ^{13}C NMR (67.5 MHz, $CDCl_3$): $\delta = 138.4$ (s), 132.2 (s), 131.9 (d), 130.5 (s), 129.2 (d), 129.1 (d), 128.4 (d), 127.1 (d), 121.6 (s), 111.7 (d), 104.8 (s), 103.9 (s), 100.6 (s); UV/Vis ($CHCl_3$): λ_{max} [nm] (log ε) = 295 sh (4.45), 306 (4.56), 340 sh (4.67), 353 (4.97), 393 (3.55), 535 sh (4.40), 572 (4.80); IR (KBr): $\tilde{\nu}$[cm^{-1}] = 1908 (cumulene).

4b: Deep violet needles (CH_2Cl_2/ethanol), m.p. >120 °C (decomp.); MS (FAB): *m/z* 488 (M^+); ^1H NMR (270 MHz, $CDCl_3$): $\delta = 8.98-8.94$ (2H, AA'm), 8.64 (4H, d, $J = 8.3$), 8.13 (2H, s), 8.09–8.05 (2H, BB'm), 7.70 (4H, d, $J = 7.3$), 1.46 (18H, s); ^{13}C NMR (67.5 MHz, $CDCl_3$): $\delta = 152.6$ (s), 135.9 (s), 131.8 (d), 131.6 (s), 129.9 (s), 128.2 (d), 126.9 (d), 126.2 (d), 121.5 (s), 111.2 (d), 104.5 (s), 103.5 (s), 100.6 (s), 35.0 (s), 31.3 (q); UV/Vis ($CHCl_3$): λ_{max} [nm] (log ε) = 295 sh (4.45), 306 (4.52), 340 sh (4.58), 356 (4.89), 397 (3.69), 542 sh (4.38), 581 (4.78); IR (KBr): $\tilde{\nu}$[cm^{-1}] = 1914 (cumulene).

4c: ^1H NMR (270 MHz, $CDCl_3$): $\delta = 8.95-8.92$ (2H, AA'm), 8.23 (2H, dd, $J = 4.0, 1.5$), 8.15–8.11 (2H, BB'm), 8.03 (2H, dd, $J = 4.0, 1.5$); UV/Vis ($CHCl_3$): λ_{max} [nm] = 275 sh, 296 sh, 312 sh, 328, 440, 452, 481, 530, 554.

4d: ^1H NMR (270 MHz, $CDCl_3$): $\delta = 8.87-8.82$ (2H, AA'm), 8.03–7.99 (2H, BB'm), 7.80 (2H, s), 1.18 (18H, s), 0.62 (12H, s); ^{13}C NMR (67.5 MHz, $CDCl_3$): $\delta = 131.2$ (s), 130.7 (d), 126.9 (s), 126.4 (d), 119.0 (s), 116.6 (s), 102.2 (d), 100.6 (s), 98.2 (s), 25.9 (q), 18.7 (s), 3.8 (q); UV/Vis ($CHCl_3$): λ_{max} [nm] = 296, 321 sh, 340, 480 sh, 504, 556.

5: Pale yellow needles (CH_2Cl_2/acetone), m.p. >130 °C (decomp.); MS (EI): *m/z* (rel. int. [%]) 254 (M^+, 45), 226 ($M^+ - CO$, 45), 198 ($M^+ - 2CO$, 100); ^1H NMR (270 MHz, $CDCl_3$): $\delta = 7.68-7.65$ (2H, AA'm), 7.52–7.49 (2H, BB'm), 6.32 (2H, s); ^{13}C NMR (67.5 MHz, $CDCl_3$): $\delta = 159.6$ (s), 135.3 (d), 131.7 (d), 126.6 (d), 96.7 (s), 93.0 (s), 88.7 (s), 85.6 (s); IR (KBr): $\tilde{\nu}$[cm^{-1}] = 2210 (C≡C), 1605, 1580 (C=O).

11: Colorless needles (CH_2Cl_2/hexane), m.p. >180 °C (decomp.); MS (EI): *m/z* 370 (M^+); ^1H NMR (270 MHz, $CDCl_3$): $\delta = 7.56-7.52$ (2H, AA'm), 7.35–7.30 (2H, BB'm), 6.04 (2H, s), 4.19 (t, 8H), 1.95–1.71 (m, 4H); ^{13}C NMR (67.5 MHz, $CDCl_3$): $\delta = 133.0$ (d), 128.9 (d), 124.0 (s), 120.9 (d), 91.8 (s), 87.84 (s), 87.78 (s), 82.3 (s), 81.2 (s), 60.6 (t), 24.7 (t); IR (KBr): $\tilde{\nu}$[cm^{-1}] = 2255, 2230 (C≡C).

with the ^1H NMR spectra. Nine signals corresponding to the benzannulene skeleton are observed in the ^{13}C NMR spectra of **4a**, **4b**, and **4d** between $\delta = 132$ and $\delta = 98$. No signals were observed in the typical area for acetylenic carbons (e.g., $\delta = 88$ to 81 in **11**) or cumulenic sp-hybridized carbons (e.g., $\delta = 156$ in 1,4-diphenylbutatriene). This observation suggests that **4** is represented well by the hybrid resonance structures although they are nonequivalent (Scheme 3).

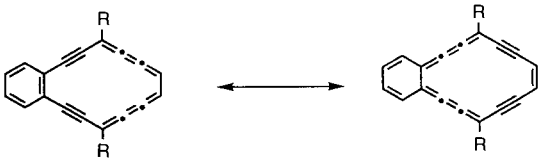

Scheme 3. Resonance structures of **4**.

In conclusion, the novel dehydroannulenes **4** were synthesized by means of the new strategy for the construction of cyclic enediynes. These compounds showed considerable aromaticity in spite of only nominal stability.

Received: March 29, 1995 [Z 7845 IE]
German version: *Angew. Chem.* **1995**, *107*, 2017–2019

Keywords: dehydroannulenes · enediynes · pinacol coupling

[1] For a review see: F. Diederich, Y. Rubin, *Angew. Chem.* **1992**, *104*, 1123; *Angew. Chem. Int. Ed. Engl.* **1992**, *31*, 1101; R. Gleiter, D. Kratz, *ibid.* **1993**, *105*, 884 and **1993**, *32*, 842; U. H. F. Buntz, *ibid.* **1994**, *106*, 1127 and **1994**, *33*, 1073; F. Diederich, *Nature (London)* **1994**, *369*, 199; R. H. Baughman, H. Eckhardt, M. Kertesz, *J. Chem. Phys.* **1987**, *87*, 6687.

[2] T. J. Sworski, *J. Chem. Phys.* **1948**, *16*, 550.
[3] Several types of dehydroannulenes have been studied extensively. For a review see: M. Nakagawa, *Cyclic Acetylenes* in *The Chemistry of Carbon Carbon Triple Bond, Part II.* (Ed.: S. Patai), Wiley, Chichester, **1978**, Chapter 15.
[4] Y. Kuwatani, N. Watanabe, I. Ueda, *Tetrahedron Lett.* **1995**, *36*, 119.
[5] For a review see: K. C. Nicolaou, W.-M. Dai, *Angew. Chem.* **1991**, *103*, 1453; *Angew. Chem. Int. Ed. Engl.* **1991**, *30*, 1387.
[6] K. J. H. Kruithof, R. F. Schmitz, G. W. Klumpp, *Tetrahedron* **1983**, *39*, 3073.
[7] This compound was prepared from 3-bromo-2-propyne-1-ol under standard conditions (treatment with tBuMe$_2$SiCl and NEt$_3$ in the presence of 4-dimethylaminopyridine in CH_2Cl_2).
[8] K. Sonogashira, Y. Tohda, N. Hagihara, *Tetrahedron Lett.* **1975**, 4467; S. Takahashi, Y. Kuroyama, K. Sonogashira, N. Hagihara, *Synthesis* **1980**, 627.
[9] D. B. Dess, J. C. Martin, *J. Am. Chem. Soc.* **1991**, *113*, 7277; *J. Org. Chem.* **1983**, *48*, 4155.
[10] A. S. Raw, S. F. Pederson, *J. Org. Chem.* **1991**, *56*, 830; A. G. Myers, P. S. Dragovich, *J. Am. Chem. Soc.* **1992**, *114*, 5859. In this procedure, it is important to use THF as the solvent.
[11] The direct coupling of **9** to give **11** by the McMurry reaction failed.
[12] A related strategy, the use of cyclic diynediols as precursors of cyclic enediyne systems, was reported: M. F. Semmelhack, J. Gallagher, *Tetrahedron Lett.* **1993**, *34*, 4121.
[13] M. Iyoda, Y. Kuwatani, M. Oda, *J. Am. Chem. Soc.* **1989**, *111*, 3761.
[14] The low yield of this transformation came from the first step in which an electron transfer occurred. Like quinone, dione **5** is susceptible toward reduction.
[15] J.-L. Luche, *J. Am. Chem. Soc.* **1978**, *100*, 2226; A. L. Gemel, J.-L. Luche, *ibid.* **1981**, *103*, 5454; J.-L. Luche, L. Rodriquez-Hahn, P. Crabbe, *J. Chem. Soc. Chem. Commun.* **1978**, 601.
[16] Related transformations have been reported: M. Iyoda, Y. Onishi, M. Nakagawa, *Tetrahedron Lett.* **1981**, *22*, 3645.
[17] The yields of **4c** and **4d** were not determined because of their instability.

A Gold(I) [2]Catenane**

D. Michael P. Mingos,* John Yau, Stephan Menzer, and David J. Williams

Recently we have described the charcterization of some linear gold(I) complexes with nitrogen donor ligands,[1-3] which are very labile and therefore provide excellent precursors for the development of the coordination and organometallic chemistry of gold. When $[Au(NH_3)_2]^+$ [2] is treated with PhC≡CH the colorless crystalline compound **1** is obtained in excellent yield

$[(H_3N)Au(C{\equiv}CPh)]$ **1**

and has been characterized by elemental analyses and IR spectroscopy. When the reaction is repeated with tBuC≡CH the resultant compound is yellow and the elemental analysis suggests that the ammonia is no longer coordinated to the gold and that it is best formulated as $[Au(C{\equiv}Ct\text{Bu})]_n$. Coates and Parkin[4] have reported an identical compound and proposed that it is probably polymeric and have tentatively suggested the tetrameric structure shown in Scheme 1.

Single crystals of $[Au(C{\equiv}Ct\text{Bu})]_n$ can be obtained from EtOH from the above-mentioned synthesis, starting from $[Au(NH_3)_2]^+$. The yellow color of the crystals is unusual for linear gold(I) ethynyl compounds, the compound also has ν(C=C) stretching modes at 2002, 1983, and 1964 cm^{-1} suggesting three inequivalent triple bond environments.

[*] Prof D. M. P. Mingos, Dr. S. Menzer, J. Yau, Dr. D. J. Williams
Chemistry Department, Imperial College of Science, Technology and Medicine
GB-London SW7 2AY (UK)
Telefax: Int. code + (171) 594-5804

[**] This work was supported by British Petroleum and the Engineering and Physical Science Research Council.

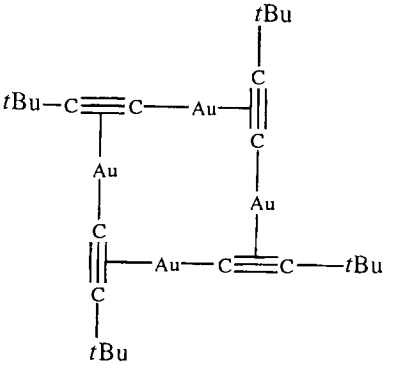

Scheme 1. Possible structure of a [Au(C≡CtBu)] oligomer.

The single-crystal X-ray crystallographic analysis of the oligomer[5] has demonstrated that it actually has a novel catenane structure based on two interlocked rings each containing six gold atoms and thus has the formula $[\{Au(C{\equiv}Ct\text{Bu})\}_6]_2$ (**2**) (Fig. 1). A crystallographically imposed C_2 axis passes through

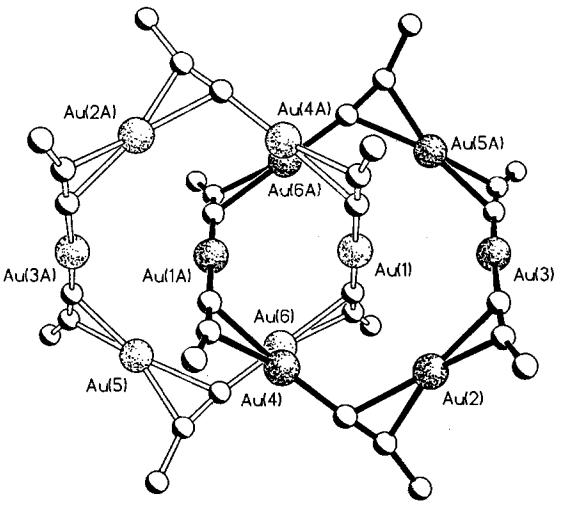

Fig. 1. Molecular structure of [2]catenane-$[\{Au(C{\equiv}Ct\text{Bu})\}_6]_2$. For reasons of clarity the methyl groups have been excluded. The crystallograhic C_2 axis is perpendicular to the page and passes through the mid-point of Au(1)–Au(1A).

the midpoint of the Au(1)–Au(1A) vector. The ethynyl ligands in **2** adopt both η^1 and η^2 coordination modes, a feature which has been noted previously in Group 11 ethynyl complexes.[6] Each ring of (**2**) contains pairs of gold(I) atoms with the different ligand arrangements and formal charges (Scheme 2) because

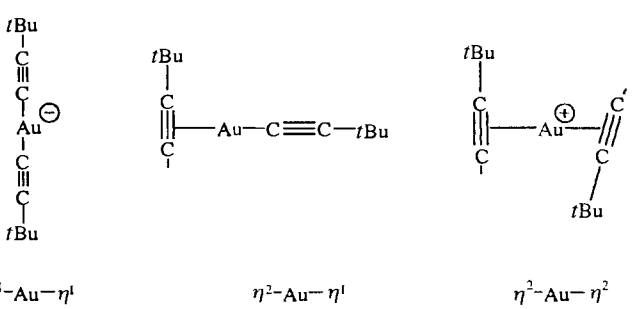

Scheme 2.

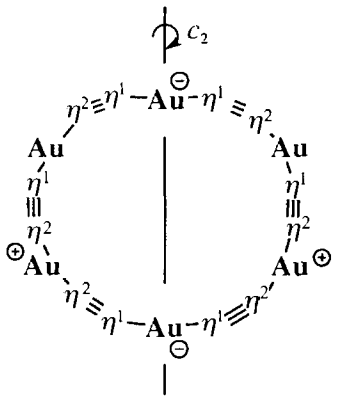

Scheme 3.

some of the ethynyl ligands in [Au(C≡C*t*Bu)] have migrated in the oligomerization process. The arrangement of these coordination modes around the ring is shown in Scheme 3.

Within each ring the gold atoms form an almost regular hexagon (Au–Au contacts between 3.304(2)–3.361(2) Å) and define a plane (maximum deviation 0.1 Å). The two interlocking rings make a dihedral angle of 64.5° and inter-ring gold–gold contacts lie in the range between 3.215(2)–3.351(2) Å, leading to a symmetrical [2]catenane structure. The individual rings have approximately C_2 symmetry as a result of the ethynyl ligand bonding modes described above, and if one ignores the ligands the central Au_{12} core has approximately D_2 symmetry.

The η^2-η^2 coordination mode, not previously observed in gold(I) chemistry, results in the ethynyl ligands being mutually perpendicular in a manner similar to that reported previously for $[Pt^0(ethyne)_2]$ complexes.[7] The utilization of orthogonal C≡C π orbitals is also evident in the η^1-η^1 and η^2-η^1 coordination centers, (see Fig. 1).

The gold–gold distances within the rings and between the rings are significantly longer than those in the bulk metal (2.88 Å) but are nonetheless in the range where weak "aurophilic"[8] interactions may occur. The narrow range of the Au–Au contacts and the symmetrical nature of the structure suggests that the "aurophilic" interactions may contribute significantly to the self-assembly of the catenane.

The manner in which the basic [Au(C≡C*t*Bu)] fragments rearrange their coordination environments in solution and self-assemble in order to realize the observed solid-state structure remains a mystery. IR studies on the [2]catenane in solution have indicated that the three ν(C≡C) bands observed in the solid are also observed in solution (IR (CCl_4): ν(C≡C) 2003, 1985, 1965 cm^{-1}) suggesting that the ring structure is maintained in solution. Two ^1H resonances for the *t*Bu groups in the ratio of 2:1 in the ^1H NMR spectrum at room temperature (see experimental) are also consistant with the C_2 symmetry of the individual rings.

The observation of such an interesting catenane structure based on such simple homoleptic organometallic complex is really most unexpected and novel. Previous examples of [2]catenane complexes have the metal atoms involved in much more complex polyaromatic nitrogen ligand systems[9] and in some cases two different metal ions.[10] We are currently investigating similar compounds in order to establish the extent to which the "aurophilicity" of the gold atoms is contributing to the spontaneous formation of the [2]catenane.

Experimental Procedure

1: PhC≡CH (0.025 mL, 0.228 mmol) was added dropwise to $[Au(NH_3)_2]BF_4$ (0.065 g, 0.204 mmol) dissolved in pre-dried, degassed acetonitrile (10 mL). The colorless solution was allowed to stir for 1 h, after about 10 minutes a white microcrystalline solid separated, which was eventually collected by filtration, washed with acetonitrile (3 × 5 mL), and dried under reduced pressure. Yield 94%; elemental analysis for C_8H_8AuN; found: C 30.0, H 2.4, N 4.4; calcd: C 30.5, H 2.6, N 4.5; IR(KBr): ν(NH) bands at 3318 and 3239 cm^{-1}, ν(CH) at 3078, 3050, and 3030 cm^{-1} and ν(C≡C) at 2112 cm^{-1}.

2: *t*BuC≡CH (0.06 mL, 0.487 mmol) was added dropwise to $[Au(NH_3)_2]BF_4$ (0.10 g, 0.487 mmol) dissolved in pre-dried, degassed acetonitrile (10 mL). After about 30 min a pale yellow solution was observed, the solution was then allowed to stir for a further 30 min, after which time the volume was concentrated under reduced pressure to give a dark yellow precipitate. This was filtered, dissolved in a minimum volume of hot EtOH and left in a refrigerator at about 4°C, to give pale yellow cubes after about 2 days. Yield 65%; elemental analysis for $[(C_6H_9Au)_6]_2$; found: C 25.6, H 2.4; calcd: C 25.9, H 3.2; IR(KBr): ν(CH) bands at 2966, 2945, 2922, 2895, and 2864 cm^{-1} and ν(C≡C) at 2002, 1983 and 1964 cm^{-1}; ^1H NMR (270 MHz, C_6D_6, 25 °C, TMS): δ = 1.2 (S, 36H; 4*t*Bu), 0.5 (s, 18H; 2*t*Bu).

Received: April 18, 1995 [Z 7892 IE]
German version: *Angew. Chem.* **1995**, *107*, 2045–2047

Keywords: aurophilicity · catenanes · gold compounds · self-assembly

[1] D. M. P. Mingos, J. Yau, *J. Organomet. Chem.* **1994**, *479*, C16–C17.
[2] D. M. P. Mingos, J. Yau, S. Menzer, D. J. Williams, *J. Chem. Soc. Dalton Trans.* **1995**, 319–320.
[3] J. Yau, D. M. P. Mingos, H. Powell, *Polyhedron* **1995**, in press.
[4] G. E. Coates, C. Parkin, *J. Chem. Soc.* **1962**, 3220–3226.
[5] Crystal data for **2**: monoclinic, $a = 29.378(4)$, $b = 13.112(2)$, $c = 25.805(3)$ Å, $\beta = 117.14(1)°$; $V = 8846(2)$ Å^3; space group $C2/c$; $Z = 4$; $\rho = 2.506$ g cm^{-3}; $\mu(Mo_{K\alpha}) = 19.847$ mm^{-1}; Siemens P4/PC diffractometer, ω scans, graphite monochromated $Mo_{K\alpha}$ radiation; data corrected for absorption. The structure was solved by the heavy-atom method. All six *tert*-butyl groups are severely disordered, however, only three of these could be split into pairs with alternative partial occupancy orientations. All the *tert*-butyl groups were refined subject to C–C distance constraints. Least-squares refinement based on F^2 with the gold atoms anisotropic, and the remaining non-hydrogen atoms isotropic, gave $R_1 = 0.0722$ and $wR_2 = 0.1879$ for 3350 independent observed data [$|F_0| > 4\sigma |F_0|$, $2\theta < = 45°$]. Further details of the crystal study can be obtained from the Director of the Cambridge Crystallographic Data Centre, 12 Union Road, GB-Cambridge, CB12 1EZ, (UK), on quoting the full literature citation.
[6] G. E. Coates, M. L. H. Green, K. Wade, *Organometallic Compounds - Transition Elements Vol 2*, 3rd ed., Methuen, London, **1968**, pp. 271–287.
[7] N. M. Boag, M. Green, D. M. Grove, J. A. K. Howard, J. L. Spencer, F. G. A. Stone, *J. Chem. Soc. Dalton Trans.* **1980**, 2170–2181.
[8] H. Schmidbaur, *Gold Bull.* **1990**, *32*, 11–21.
[9] C. Dietrich-Buchecker, J.-P. Sauvage, *Bull. Soc. Chim. Fr.* **1992**, *129*, 113–120; J.-C. Chambron, C. Dietrich-Buchecker, J.-P. Sauvage, *Top. Curr. Chem.* **1993**, *165*, 131–162.
[10] C. Piquet, G. Bernardinelli, A. F. Williams, B. Bocquet, *Angew. Chem.* **1995**, *107*, 618–621; *Angew. Chem. Int. Ed. Engl.* **1995**, *34*, 582–584.

Novel Networks of Unusually Coordinated Silver(I) Cations: The Wafer-Like Structure of $[Ag(pyz)_2][Ag_2(pyz)_5](PF_6)_3 \cdot 2G$ and the Simple Cubic Frame of $[Ag(pyz)_3](SbF_6)$**

Lucia Carlucci, Gianfranco Ciani,* Davide M. Proserpio, and Angelo Sironi

The crystal engineering of two- (2D) and three-dimensional (3D) coordination polymers is of great current interest,[1–3] both for the theoretical aspects related to the topologies of novel networks, and for their potential physicochemical properties, such as electrical conductivity,[4] magnetism,[5] and applications in host–guest chemistry,[1, 6] and catalysis.[7] In the supramolecular chemistry of hydrogen-bonded organic molecules,[8] coordination polymers offer a higher potential because of the variety of coordination modes and the peculiarities of the metallic cen-

[*] Dr. L. Carlucci, Prof. G. Ciani, Dr. D. M. Proserpio, Prof. A. Sironi
Dipartimento di Chimica Strutturale e Stereochimica Inorganica
and
Centro CNR
Via G. Venezian 21, 20133 Milano (Italy)
Telefax: Int. code + (2)-70635288

[**] pyz = pyrazine, G = CH_2Cl_2, $CHCl_3$, CCl_4.

 © VCH Verlagsgesellschaft mbH, D-69451 Weinheim, 1995 0570-0833/95/3417-1895 $ 10.00+.25/0

ters. We are currently investigating the self-assembly of silver(I) cations and bidentate N–N′-donor ligands and have already reported interesting 2D and 3D networks including the fourfold interpenetrating super-diamond structures of the complexes $[Ag(N-N')_2]X$ (N–N′ = 4,4′-bipyridyl, $X^- = CF_3SO_3^-$; N–N′ = 4-cyanopyridine, $X^- = BF_4^-$),[9] and the threefold interpenetrating 3D 3-connected frame of $[Ag_2(pyz)_3](BF_4)_2$ (pyz = pyrazine),[10] topologically related to the prototypal structure of α-$ThSi_2$.

In this paper we describe two novel Ag^I polymeric species, which contain only the linear bidentate pyz ligand as bridge: a 2D wafer-like polymer **1a**, consisting of alternating layers of different nature and composition, and containing guest solvent molecules (G) between the sheets, and a 3D polymer **2** with cubic symmetry, related to the structure of α-polonium.

$[Ag(pyz)_2][Ag_2(pyz)_5](PF_6)_3 \cdot 2G$ $[Ag(pyz)_3](SbF_6)$

1a, G = CH_2Cl_2 **2**

1b, G = $CHCl_3$

1c, G = CCl_4

These types of frameworks are unprecedented in the chemistry of coordination polymers based on molecular rods (cationic polymers), and are particularly exceptional because of the unusual coordination modes adopted by the silver ions (see below).

Compound **1** is obtained on layering a solution of $AgPF_6$ in ethanol on a solution of pyz (between 2:1 to 3:1 molar ratio of pyrazine to Ag^I salt) in the appropriate chlorinated solvent. Platelike crystals, rather unstable when removed from the mother liquor, are recovered in the three cases, the most suitable ones for a single-crystal X-ray analysis being those from CH_2Cl_2 (**1a**).[11] Variable amounts of needle-shaped crystals of the linear polymer $[Ag(pyz)](PF_6)$ (**3**) are also obtained; their nature was also established by a single-crystal X-ray analysis.[12]

The structure of **1a** (Fig. 1) consists of stacks of two different 2D layers alternating along the direction of the tetragonal *c* axis. The first one (layer I) comprises cubes of silver ions, the edges of which are formed by the pyz ligands; four faces are shared to give an infinite 2D tessellation (see Fig. 2). Each cubic unit [equatorial and axial Ag···Ag edges 7.548(2) and 7.645(3) Å, respectively] is centered by a PF_6^- anion. The metal ions, lying

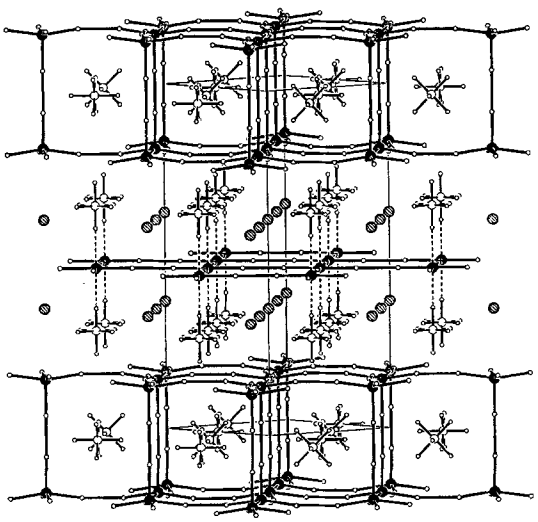

Fig. 1. The crystal packing of **1a** (SCHAKAL representation), viewed approximately down [110]. The pyz ligands are represented as rods connecting the nitrogen atoms. Solid, open, and cross-hatched spheres indicate Ag, P, and the guest molecules G, respectively.

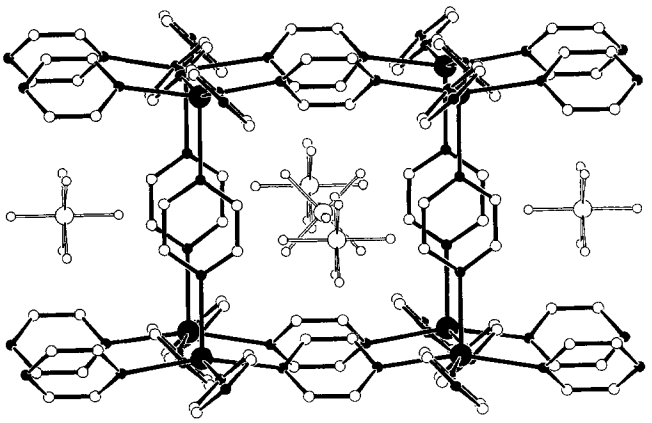

Fig. 2. The structure of layer I of **1a**. Only one model for the axially disordered pyz ligand is shown.

on fourfold axes, are five-coordinate in a square-pyramidal environment [out-of-plane displacement of Ag equal to 0.367(9) Å, N_{ax}-Ag-N_{eq} 98.6(2)° and N_{eq}-Ag-N_{eq} 162.8(4)°], with four Ag–N_{eq} bonds of 2.454(9) Å and one Ag–N_{ax} bond of 2.44(2) Å. The four equatorial pyz ligand display a propeller-like disposition and are not in line with the metal ions [Ag–N···N 166.9(2)°].

The second type of layer (layer II) is an infinite flat grid of square meshes of Ag^I ions linked by pyz ligands [Ag···Ag contact of 7.548(2) Å]. The silver ions, lying on *mmm* special positions, are in a square-planar environment, with two Ag–N bonds of 2.32(2) Å and two of 2.45(2) Å. However, they also present two long contacts [2.685(11) Å] with the fluorine atoms of two axially disposed anions (Fig. 3); taking into account

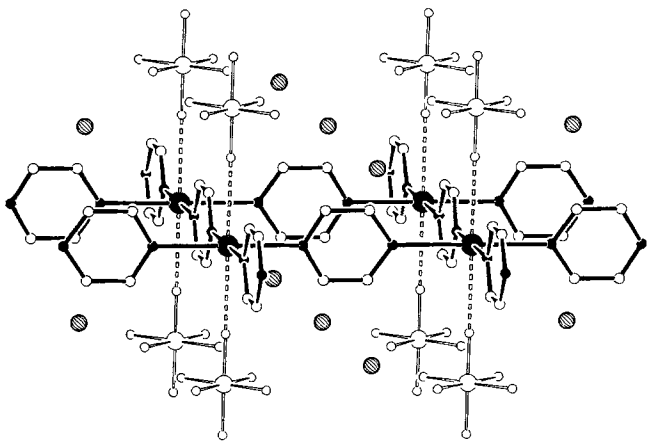

Fig. 3. The structure of layer II of **1a** (SCHAKAL representation). The axially disposed, disordered PF_6^- anions are shown in the positions with the highest occupancy factor.

these weak interactions the Ag^+ coordination can be described as a tetragonally distorted octahedron (4 + 2). The layers of this type, of composition $[Ag(pyz)_2](PF_6)_2$, are therefore negatively charged, whereas the others of composition $[Ag_2(pyz)_5](PF_6)$, are positively charged. The wafer-like structure of **1a** derives from the assembly of these layers with an *ABAB* sequence. Stacking occurs in such a manner that the metal ions of one layer are in the centers of the squares of the adjacent layers. Between each pair of layers there are cavities (approximately 100 $Å^3$) that can contain CH_2Cl_2 as guest solvent molecules.

 © VCH Verlagsgesellschaft mbH, D-69451 Weinheim, 1995 0570-0833/95/3417-1896 $ 10.00+.25/0

The analogous products containing the other solvent molecules (**1b** and **1c**) are isomorphous with **1a** and exhibit cell parameters[13] that increase with an increasing number of chlorine atoms in the guest (about 1.7% of the cell volume in each step).

The simultaneous presence of different extended structural motifs in the same compound is quite rare in coordination polymers; another example is the polyselenide K_2PdSe_{10},[14] which consists of two interpenetrating diamondoid sublattices of different nature.

On performing the same reactions above described with $AgSbF_6$, compound **2** is obtained as beautiful multifaced crystals, irrespective of the chlorinated solvent used.

The unit cell of **2** is shown in Figure 4. It consists of a simple cubic framework of silver ions, lying on special positions having 222 symmetry, octahedrally bound to six pyz ligands, with Ag–N bond lengths between 2.481(7) and 2.519(8) Å. All the

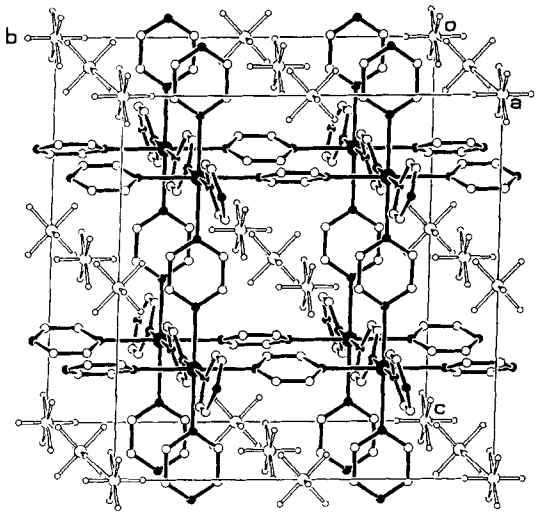

Fig. 4. The unit cell of **2** (SCHAKAL representation). The disordered SbF_6^- anions are represented in the positions with the highest occupancy factor, and a little reduced for clarity.

cubes (average Ag···Ag edge of 7.761 Å) are similar to the cubic cells of layer I of **1a** (Fig. 2) and are similarly centered by the anions. Along the linear pyz-Ag-pyz-Ag chains developing in the directions of the three crystal axes the pyz ligands are alternately rotated in opposite directions, with different rotation angles [16.5(5)°, 18.3(4)° and 2.9(7)° along *a*, *b*, and *c*, respectively].

The 6-connected framework of **2** is topologically related to the structure of α-polonium or, better, to that of ReO_3; other well-known examples are compounds like Prussian blue. It is of interest as fundamental structural types, since it represents the first cationic frame linked by molecular rods only and consisting of a single network, different from some other known interpenetrating α-polonium type frames, like the two recently reported cyano-bridged polymers $Rb[Cd(Ag(CN)_2)_3]$[16] and $[Cd(pyz)(Ag_2(CN)_3)(Ag(CN)_2)]$.[17]

The networks of **1a** and **2** are particularly surprising and unpredictable in the presence of metal centers like Ag^I, which usually adopt linear, trigonal, or tetrahedral coordination geometries.[18] It is worth mentioning that, in contrast, the known polymeric complexes of some M^{2+} octahedral cations with pyz exhibit a maximum of four M–pyz (equatorial) bonds, resulting in 2D flat sheets of squares, the other two (axial) coordination sites being involved in interactions with the counterions.[5, 19] The very existence of **2** suggests the possibility of obtaining similar 3D frames with divalent metal cations and suitable dianions, and work is in progress. However, the self-assembly of these polymers is highly influenced by factors such as the solvent system and the steric requirements of the counterion. $AgPF_6$ in H_2O/EtOH gives $[Ag(pyz)_2](PF_6)$, composed of 2D, markedly undulated sheets of squares,[20] and $AgBF_4$ in EtOH affords, inter alia, $[Ag(pyz)_3](BF_4)$, with a composition analogous to that of **2** but forming a 1D zigzag polymer of tetrahedral silver ions bearing two monodentate pyz molecules.[10] Indeed, this high structural versatility of Ag^I can be a problem for the design of new solids, but it also offers the opportunity to discover unprecedented polymeric motifs potentially extendible to other transition metal systems.

Experimental Procedure

Compound **1a**: A solution of $AgPF_6$ (0.104 g, 0.410 mmol) in EtOH (3 mL) was layered on a solution of pyz (0.103 g, 1.290 mmol) in CH_2Cl_2 (3 mL). After a few days a crystalline precipitate was recovered, which was filtered and washed with EtOH. The product slowly decomposes in air. After some needle-shaped crystals of $[Ag(pyz)](PF_6)$ (**3**) had been hand-picked, it was submitted to elemental analysis. Yield 57%. Anal. calcd. for $C_{30}H_{32}Ag_3Cl_4F_{18}N_{14}P_3$: C 25.66, H 2.28, N 13.97; found C 25.02, H 2.02, N 13.57. IR (Nujol): ν(pyz) = 1417(s), 1047(m), $\nu(PF_6^-)$ = 843(s) cm^{-1}.

Compound **2**: A solution of $AgSbF_6$ (0.230 g, 0.670 mmol) in EtOH (4 mL) was layered on a solution of pyz (0.161 g, 2.010 mmol) in CH_2Cl_2 (3 mL). After two days a crystalline precipitate was obtained, which was filtered and washed with EtOH. The product is stable in air. Yield 88%. Anal. calcd. for $C_{12}H_{12}AgF_6N_6Sb$: C 24.68, H 2.07, N 14.39; found C 24.47, H 1.98, N 14.20. IR in Nujol: ν(pyz) = 1411(s), 1031(s), $\nu(SbF_6^-)$ = 650(s) cm^{-1}.

Received: April 18, 1995 [Z 7896 IE]
German version: *Angew. Chem.* **1995**, *107*, 2037–2040

Keywords: coordination polymers · complexes with nitrogen ligands · solids · silver compounds

[1] a) B. F. Hoskins, R. Robson, *J. Am. Chem. Soc.* **1990**, *112*, 1546; b) R. Robson, B. F. Abrahams, S. R. Batten, R. W. Gable, B. F. Hoskins, J. Liu, *Supramolecular Architecture* (*ACS Symp. Ser.* **1992**, *449*, **1992**, chap. 19).
[2] M. J. Zaworotko, *Chem. Soc. Rev.* **1994**, 283.
[3] J. S. Moore, S. Lee, *Chem. Ind.* **1994**, 556.
[4] a) A. Aumuller, P. Erk, G. Klebe, S. Hünig, J. U. von Schütz, H.-P. Werner, *Angew. Chem.* **1986**, *98*, 759, *Angew. Chem. Int. Ed. Engl.* **1986**, *25*, 740; b) O. Ermer, *Adv. Mater.* **1991**, *3*, 608, and references therein.
[5] See for example, G. De Munno, M. C. Munoz, M. Julve, *Inorg. Chem.* **1991**, *30*, 2701, and references therein.
[6] See for example, a) T. Kitazawa, S. Nishikiori, R. Kuroda, T. Iwamoto, *J. Chem. Soc. Dalton Trans.* **1994**, 1029 and references therein; b) H. Yuge, T. Iwamoto, *ibid.* **1994**, 1237.
[7] M. Fujita, Y. J. Kwon, S. Washizu, K. Ogura, *J. Am. Chem. Soc.* **1994**, *116*, 1151.
[8] a) G. R. Desiraju, *Crystal Engineering: Design of Organic Solids*, Elsevier, Amsterdam, **1989**; b) O. Ermer, *J. Am. Chem. Soc.* **1988**, *110*, 3747; c) O. Ermer, A. Eling, *J. Chem. Soc. Perkin Trans.* **1994**, 925, and references therein; d) D. Venkataraman, S. Lee, J. Zhang,, J. S. Moore, *Nature*, **1994**, *371*, 591.
[9] L. Carlucci, G. Ciani, D. M. Proserpio, A. Sironi, *J. Chem. Soc. Chem. Commun.* **1994**, 2755.
[10] L. Carlucci, G. Ciani, D. M. Proserpio, A. Sironi, *J. Am. Chem. Soc.* **1995**, *117*, 4562.
[11] A single crystal of **1a** was mounted under a coating of cyanoacrylic glue, to prevent decomposition, on an Enraf–Nonius CAD-4 diffractometer. Crystal data: tetragonal, *P4/mbm* (no. 127), $a = b = 10.675(3)$, $c = 23.290(2)$ Å, $V = 2654.0(11)$ Å^3, $Z = 2$, $\rho_{calcd} = 1.863$ Mg m^{-3}, $Mo_{K\alpha}$ radiation ($\lambda = 0.71069$ Å). The data collection was performed at 293 K, by the ω-scan method, within the limits $3 < \theta < 26°$. The structure was solved by direct methods (SIR92) and refined by full-matrix least-squares methods (SHELX93). The pyz ligands linking the double layers to give cubes lie on fourfold axes and therefore exhibit a statistical disorder of the carbon atoms, which form two half-rings rotated by 90° about the *c* axis (only one model is shown in Fig. 2). The equatorial fluorine atoms of the PF_6^- anions axially bound to the layers of squares are disordered (two models with population 0.58 and 0.42; only the dominant model is depicted). The solvated CH_2Cl_2 molecules are also disordered: the two chlorine atoms lie on a fourfold axis, and the CH_2 groups are statistically distributed. $R = 0.0751$ for 799 independent significant [$F_0 > 3\sigma(F_0)$] absorption corrected data. Anisotropic thermal factors were assigned to all the non-hydrogen atoms [21].

[12] Crystal data for **3**: tetragonal, *I4/mcm* (no. 140), $a = b = 8.026(2)$, $c = 14.203(6)$ Å, $V = 914.9(5)$ Å^3, $Z = 4$, $\rho_{calcd} = 2.417$ Mgm^{-3}. Final $R = 0.0621$ for 190 significant $[F_0 > 2\sigma(F_0)]$ absorption corrected data. The structure consists of strictly linear polymers propagating in the direction of the tetragonal axis and exhibiting pyz ligands alternately rotated by 90°, with Ag–N bonds of 2.168(14) Å [21].

[13] Compound **1b**: $a = b = 10.725(6)$, $c = 23.481(6)$ Å, $V = 2700.9$ Å^3. Compound **1c**: $a = b = 10.794(3)$, $c = 23.566(15)$ Å, $V = 2745.7$ Å^3.

[14] K. W. Kim, M. G. Kanatzidis, *J. Am. Chem. Soc.* **1992**, *114*, 4878.

[15] The crystals of **2** are orthorhombic, *Fmmm* (no. 69), with $a = 15.442(2)$, $b = 15.495(3)$, $c = 15.630(3)$ Å, $V = 3739.8(11)$ Å^3, $Z = 8$, $\rho_{calcd} = 2.074$ Mgm^{-3}. The data collection was performed within the limits $3 < \theta < 25°$. The SbF_6^- anions were both disordered and occupied two different special positions (only the dominant model is shown in Fig. 4). $R = 0.0432$ for 565 independent significant $[F_0 > \sigma(F_0)]$ absorption corrected data. Other experimental features are as in **1a** [21]. The crystals are pseudo-cubic, but their orthorhombic nature has been confirmed by the splitting of selected peaks in the X-ray powder diffraction spectrum, which also shows the homogeneous nature of the bulk powders.

[16] a) B. F. Hoskins, R. Robson, N. V. Y. Scarlett, *J. Chem. Soc. Chem. Commun.* **1994**, 2025; b) a referee has pointed out that $Rb[Cd(Ag(CN)_2)_3]$ is isomorphous with $K[Co(Au(CN)_2)_3]$: S. C. Abrahams, J. L. Bernstein, R. Liminga, E. T. Eisenmann, *J. Chem. Phys.* **1980**, *73*, 4585.

[17] T. Soma, H. Yuge, T. Iwamoto, *Angew. Chem.* **1994**, *106*, 1746; *Angew. Chem. Int. Ed. Engl.* **1994**, *33*, 1665.

[18] Only two examples of Ag^IN_6 chromophores, both with macrocyclic ligands, have previously been reported: a) J. de Mendoza, E. Mesa, J.-C. Rodríguez-Ubis, P. Vazquez, F. Vogtle, P.-M. Windscheif, K. Rissanen, J.-M. Lehn, D. Lilienbaum, R. Ziessel, *Angew. Chem.* **1991**, *103*, 1365; *Angew. Chem. Int. Ed. Engl.* **1991**, *30*, 1331; b) C. Stockheim, K. Wieghardt, B. Nuber, J. Weiss, U. Florke, H.-J. Haupt, *J. Chem. Soc. Dalton Trans.* **1991**, 1487.

[19] a) P. W. Carreck, M. Goldstein, E. M. McPartlin, W. D. Unsworth, *J. Chem. Soc. Chem. Commun.* **1971**, 1634; b) J. Darriet, M. S. Haddad, E. N. Duesler, D. N. Hendrickson, *Inorg. Chem.* **1979**, *18*, 2679; c) J. S. Haynes, S. J. Rettig, J. R. Sams, R. C. Thompson, J. Trotter, *Can. J. Chem.* **1987**, *65*, 420.

[20] L. Carlucci, G. Ciani, D. M. Proserpio, A. Sironi, unpublished.

[21] Further details of the crystal structure investigations can be obtained from the Director of the Cambridge Crystallographic Data Center, 12 Union Road, GB-Cambridge CB2 1EZ (UK), on quoting the full journal citation.

A One-Step Synthesis of Squalene from Farnesol under Prebiotic Conditions**

Martin Keller, Doris Hafenbradl, Karl O. Stetter, Gérard Teller, Yoichi Nakatani, and Guy Ourisson*

We have recently recognized that a large number of terpenoids play the same role in all living organisms: forming or stabilizing membranes.[1] Among these terpenoids, squalene (**1**) is apparently present in the cells of all living organisms. It serves in particular as the precursor of membrane reinforcers: cholesterol in eucaryotes through its epoxide[2] and hopanoids in many bacteria by direct cyclization.[3] But squalene is also present in archea species in uncyclized form which apparently serves as a spacer between the lipid chains.[4] We describe now its formation under hypothetical, but plausible prebiotic conditions, namely those postulated by Wächtershäuser to have been operative in a "pyrite-driven" chemoautotrophic world.[5]

[*] Prof. Dr. G. Ourisson, Dr. G. Teller, Prof. Dr. Y. Nakatani
Centre de Neurochimie, Laboratoire de Chimie des Substances Naturelles, associé au CNRS
Université Louis Pasteur
5, rue Blaise Pascal, F-67084 Strasbourg (France)
Telefax: Int. code +88 60 76 20

Dr. M. Keller, Dipl.-Biol. D. Hafenbradl, Prof. Dr. K. O. Stetter
Lehrstuhl für Mikrobiologie, Universität Regensburg (Germany)

[**] This work was supported by the Deutsche Forschungsgemeinschaft, the Fonds der Chemischen Industrie, the Centre National de la Recherche Scientifique, and the Université Louis Pasteur as part of the "Supermolecules" Program (ULP/Research Development Corporation of Japan).

The complex biosynthesis of squalene has been studied in remarkable detail.[6] It starts with the formation of the sesquiterpene alcohol farnesol (**2**), the pyrophosphate of which forms the presqualene alcohol pyrophosphate, which in turn is

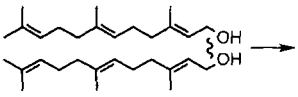

2

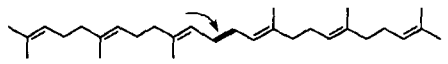

1

finally reduced to squalene by an NADPH reductase after a series of steps. We have noted that farnesol, along with its lower and higher homologues, could be derived by very simple nonenzymatic reactions of type (a) from simple C_4 and C_1 or C_5

$$-C^+ + C{=}C \longrightarrow -C-C-C^+ \qquad \text{(a)}$$

precursors.[7] We have also shown that aqueous solutions of the sodium salts of the phosphate esters of farnesol and its higher and lower homologues (di-[8] and even monopolyterpenyl phosphates[9]) spontaneously form vesicles that can be considered as models of the most primitive cell membranes. However, no reaction is known, nor have any been postulated, by which farnesol or its pyrophosphate can be transformed into squalene under potentially prebiotic conditions, and the complexity of the present biosynthetic pathway can hardly be compatible with its early operation.

Stoichiometrically, the doubling of farnesol or of its pyrophosphate is a reductive coupling,[10] which is analogous to several standard chemical reactions, for example the classical Wurtz coupling of alkyl halides, in which the reducing agent is a metal like sodium, or the van Tamelen–McMurry couplings of allylic alcohols, which rely on low-valent titanium (obtained from a mixture of a dichlorotitanium(IV) dialkoxide and molten potassium[11] or from titanium trichloride and lithium aluminum hydride[12]). While both methods give squalene from farnesol in appreciable yields (30–40%), these reducing conditions can of course in no way be considered as prebiotic.

We now show that this doubling can be achieved, albeit in low yield, by the direct reduction of farnesol to squalene with the system (b), which was advocated by Wächtershäuser as a prim-

$$H_2S + FeS \longrightarrow FeS_2 + 2[H^+] \qquad \text{(b)}$$

itive reducing system and provided a basis for his unified theory of the chemoautotrophic origin of the constituents of life.[5]

We used conditions described earlier to reduce various organic substrates.[13] All experiments were carried out under fastidiously anaerobic conditions. Farnesol was heated at 100 °C for six days in the presence or absence of FeS and H_2S. The reaction mixture then showed the glistening appearance characteristic of anaerobic pyrite formation. Analysis of a chloroform extract by thin-layer chromatography and gas chromatography showed that farnesol had disappeared and new products had been formed in significant amounts when both FeS and H_2S were present. In the absence of FeS, none of these new products were observed; however, in the presence of FeS alone, which was partially hydrolyzed to H_2S under these conditions, the new products were observed but in smaller amounts. The products were analyzed by GCMS. All the experiments yielded a series of

peaks with retention times very similar to that of squalene and all with a mass peak at m/z 410. The peak having exactly the same retention time as squalene gave a mass spectrum entirely identical to that of an authentic sample.

The eight major fragmentations can be interpreted as indicated in Scheme 1, with incidental H transfers. Squalene was isolated in about 0.2% yield. The other GC peaks with m/z 410 gave

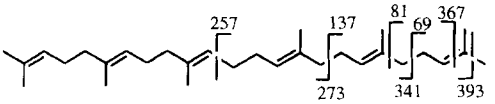

Scheme 1. Main fragments in the mass spectrum of squalene.

similar mass spectra and may be double-bond isomers, in which one or more of the double bonds in squalene are *cis*-configurated; these products were not studied further.

Squalene was accompanied by four products with longer retention times, all characterized by a molecular peak at m/z 442, corresponding to $C_{30}H_{50}$ (410) + S (32). (The expected isotopic satellite corresponding to the ^{34}S analogue was observed at m/z 444.) The very remarkable similarity of the mass spectra of these products and the presence of most of the fragments observed in the mass spectrum of squalene itself suggest that they are probably close derivatives of squalene, probably squalenethiols. The high intensity of the new fragment at m/z 305 (with an isotopic satellite at m/z 307), which is absent in the mass spectrum of squalene, completely excludes structures based on difarnesyl sulfide and suggests that this cleavage corresponds to the formation of the highly stabilized allylic sulfanylcarbenium ion **3** (Scheme 2). Major peaks at m/z 237 (+239), and at 373 (+375) are attributed to isomeric squalenethiols. The

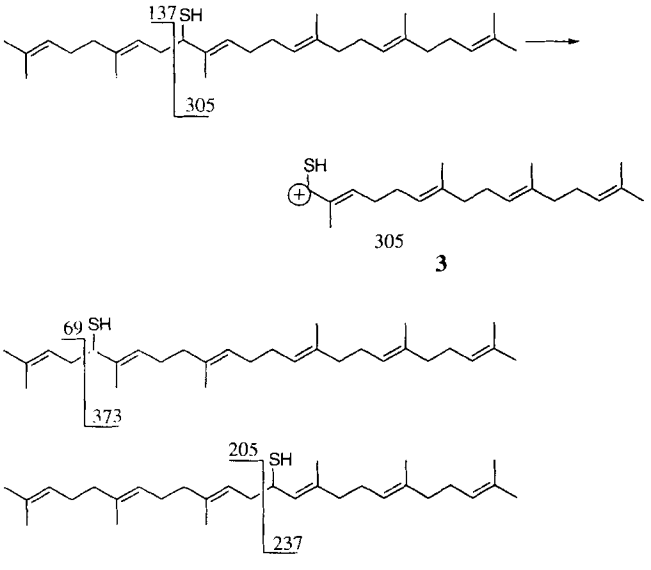

Scheme 2. Fragmentation of squalenethiols yielding allylic sulfanylcarbenium ions.

various isomers may again be double-bond isomers. These monothio derivatives are accompanied by smaller amounts of doubly sulfur-substituted squalenes (M_r (476) = squalene + S + H_2S, isotopic satellites at m/z 478 and 480).

To better evaluate the yield of the reductive coupling, we attempted to simplify the reaction mixture by desulfurizing the various thio derivatives with Raney nickel. This was not successful, because it was difficult to recover products from the nickel reagent, and some partial hydrogenation was observed. We have therefore treated the crude reaction mixture first with Raney nickel at 80 °C, which led to desulfurization and partial hydrogenation, and then completed the hydrogenation by treatment under an atmosphere of hydrogen with platinum (from platinum oxide). Only about one-fourth of the product could be recovered from this sequence. This was chromatographed and analyzed by GCMS. No farnesol remained; the mixture was mostly (90%) C_{15} products of its cyclization or isomerization. A family of C_{30} peaks were observed, the most intense of which had a retention time and a mass spectrum entirely identical with those of squalene. It was isolated in about 2% yield from farnesol.

The formation of squalene in such a low yield can of course not be construed as evidence in support of Wächterhäuser's conditions in the prebiotic formation of this hydrocarbon. We must, however, note that farnesol itself could be produced under general acidic conditions in the homogeneous or heterogeneous phase by three successive condensations of isopentenyl units, which in turn could possibly originate from isobutene and formaldehyde.[1, 5] The intermediates might be, like in the biosynthetic processes, polyprenyl phosphates. If squalene was ever produced, even in a low yield, in a system containing vesicles of polyterpenoid phosphates like those we have described, these would necessarily extract it specifically within their lipidic layer, as a most lipophilic component.[4] This would be one example of stepwise build-up of complexity in simple vesicles.[1]

Experimental Procedure

All reactions were carried out under argon. The solutions were prepared from doubly distilled water through which argon had been bubbled for 2 h. Amorphous FeS was prepared in an anaerobic chamber by adding a solution of $Na_2S \cdot 9H_2S$ to 0.6 M Fe_2SO_4, filtering the precipitate, washing it with water, and drying it under N_2:H_2 (95:5). Hydrogen sulfide was prepared by adding 50% H_2SO_4 to $Na_2S \cdot 9H_2S$ in an evacuated serum bottle. Serum bottles (120 mL) were charged with 10 mL of water, 100 mmol of farnesol, and then with 2 mmol of FeS in the anaerobic chamber. They were closed with a "Viton" diaphragm (Ochs), filled to 200 KPa with argon, and subsequently charged with H_2S (2 mmol). The pH was adjusted to 7.5. All incubations were carried out at 100 °C in a rotatory shaker (100 rpm) for 6 d. The reaction mixture was centrifuged and the supernatant extracted with chloroform. GCMS spectra were recorded with a Fisons MD800 quadrupole instrument from 50 to 500 Da. The gas chromatograph had a direct injector and a JW DB5 column (30 m, internal diameter 0.32 mm, 0.1 mm film). The samples were injected as a solution in acetone or dichloromethane.

The yields are based on farnesol. In the absence of FeS, no squalene and no squalenethiols were detected. In the presence of only FeS, we obtained 0.2 mmol of squalene, 1.7 mmol of squalenemonothiols, and 0.02 mmol of squalenedithiols. When both FeS and H_2S were used, we obtained 0.2 mmol of squalene, 3.0 mmol of squalenemonothiols, and 0.5 mmol of squalenedithiols.

Received: January 26, 1995
Revised version: March 17, 1995 [Z 7664 IE]
German version: *Angew. Chem.* **1995**, *107*, 2015–2017

Keywords: iron sulfide · prebiotic syntheses · squalene · terpenoids

[1] G. Ourisson, Y. Nakatani, *Chem. Biol.* **1994**, *1*, 10–23.
[2] K. Bloch, *Steroids* **1992**, *57*, 378–383.
[3] M. Rohmer, C. Anding, G. Ourisson, *Eur. J. Biochem.* **1980**, *112*, 541–547.
[4] T. G. Tornabene, M. Kates, E. Gelpi, J. Oro, *J. Lipid. Res.* **1969**, *10*, 294–303.
[5] G. Wächtershäuser, *Microbiol. Rev.* **1988**, *52*, 452–484; *Proc. Natl. Acad. Sci. USA* **1990**, *87*, 200–204, and references therein.
[6] C. D. Poulter, H. C. Rilling in *Biosynthesis of Isoprenoid Compounds, Vol. 1* (Eds.: J. W. Porter, S. L. Spurgeon), Wiley, New York, **1981**, p. 413.
[7] G. Ourisson, *Pure Appl. Chem.* **1990**, *62*, 1401–1404.
[8] N. Plobeck, S. Eifler, A. Brisson, Y. Nakatani, G. Ourisson, *Tetrahedron Lett.* **1992**, *33*, 5249–5252.
[9] G. Pozzi, V. Bizault, B. Werner, O. Dannenmuller, Y. Nakatani, G. Ourisson, S. Tenakawa, unpublished.

[10] The nonreductive version of this coupling, leading to a double bond between the two polyprenyl chains, is an analogous reaction; it converts geraniol pyrophosphate into the unsaturated homologue of squalene prephytoene, the precursor of carotenoids [6].
[11] E. E. van Tamelen, M. A. Schwartz, *J. Am. Chem. Soc.* **1965**, *87*, 3277–3278.
[12] J. E. McMurry, M. Silvestri, *J. Org. Chem.* **1975**, *40*, 2687–2688; J. E. McMurry, M. G. Silvestri, M. P. Fleming, T. Hoz, M. W. Grayston, *ibid.* **1978**, *43*, 3249–3255.
[13] E. Drobner, H. Huber, G. Wächtershäuser, D. Rose, K. O. Stetter, *Nature* **1990**, *346*, 742–744; E. Blöchl, M. Keller, G. Wächtershäuser, K. O. Stetter, *Proc. Natl. Acad. Sci. USA* **1992**, *89*, 8117–8120.

Radical Cation [4 + 2] Cycloadditions with 2-Vinylindoles**

Christoph F. Gürtler, Siegfried Blechert,* and Eberhard Steckhan

Numerous organic reactions can be traced back to electron transfer (ET) processes, which are among the most important elementary reactions in chemistry.[1] In addition to intensified mechanistic/theoretical investigations[2, 4] of ET reactions in all areas of chemistry, there is increasing interest in the preparative potential of these reactions.[3, 4]

Neutral Diels–Alder reactions that proceed slowly or not at all can in certain cases be accelerated by transforming either the diene or the dienophile into its radical cation by single electron transfer (SET). The electron-deficient radical cation reacts with the electron-rich component to form a cycloadduct radical cation, which in the catalytic case can undergo back electron transfer with the starting material. Cycloadducts of a higher oxidation state can be formed by one-electron oxidation of the product radical cation and subsequent deprotonation.

The versatility of 2-vinylindoles especially in natural product synthesis has been demonstrated[5] several times. A wide range of 2-vinylindoles are accessible[6] by a process developed by our group. Until now these Diels–Alder reactions could only be performed with electron-poor dienophiles.[7]

2-Vinylindoles react with electron-rich dienophiles in high-yielding, electron transfer induced Diels–Alder reactions under mild reaction conditions by photoelectron transfer catalysis or electrochemical initiation. We reported earlier on the reaction of 2-vinylindoles **1** with cyclohexadienes and styrene.[8] Similar reactions with enamidoesters[9] lead directly to heteroaromatic compounds by an elimination process.

Here we report the application of this type of reaction to relatively electron-rich heterosubstituted dienophiles. In contrast to known reactions of vinylindoles with carbocyclic dienes and styrenes, neither formation of carbazole derivatives nor aromatization is observed in reactions with either the 1,4,5,6-tetrahydroyridines **2** (Scheme 1) or with β-aminomethacrylates like **7** or -nitriles like **5**. Instead the preparatively interesting tetracycles **3** (indolo[1,2-*a*]-1,8-naphthyridine) result which have

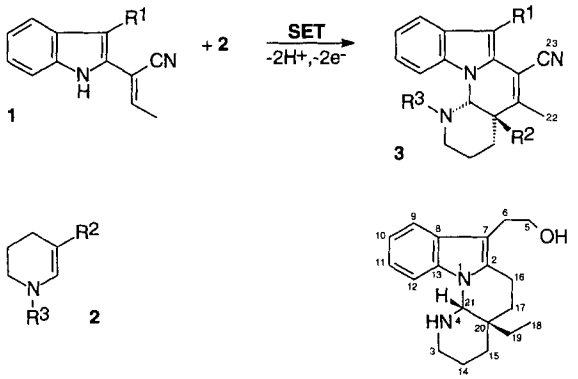

Scheme 1. SET = single electron transfer.

the pyrrocoline skeleton of alkaloids (e.g. goniomitine (**4**)) (Table 1). Ring closure is effected by the indole nitrogen, which allows the electron transfer induced [*a*]annelation of the dienophiles to the indole nucleus. It is, thus, an electron transfer induced hetero [4 + 2] cycloaddition proceeding via an electrochemically generated vinylindole radical cation.

Table 1. Results of the ET-induced [4 + 2] cyclization of 2-vinylindoles **1** (diene) with 1,4,5,6-tetrahydropyridines **2** and with acceptor-substituted enamines having different steric demands (**5** and **7**) (dienophiles).

Diene	R^1	Dienophile	R^2	R^3	Product	Yield [%] [a]
1a	Me	**2a**	CN	H	**3a**	68
1b	$EtOCH_2CH_2$	**2a**	CN	H	**3b**	53
1a	Me	**2b**	COOMe	H	**3c**	90
1a	Me	**2c**	COOMe	Me	**3d**	62
1a	Me	**5**			**6**	50
1a	Me	**7**			**8**	53

[a] Based on 80% conversion; see Experimental Procedure.

By potentiostatically controlled electrolysis[10] at a potential allowing only for one-electron oxidation of the vinylindole, it was acertained that only the radical cation of the diene component is formed initially.

β-Substituted enamines that do not have radical-stabilizing substituents such as cyano or methoxycarbonyl groups do not react even if they have an appropriate oxidation potential. We, therefore, assume that the stabilization of a radical intermediate is of prime importance (Scheme 2). The oxidation potentials of

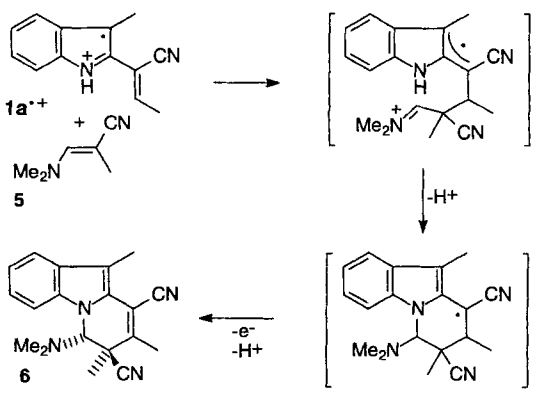

Scheme 2. Proposed mechanism for the ET-induced [4 + 2] cyclization illustrated by the reaction $\mathbf{1a}^{\bullet+} + \mathbf{5} \rightarrow \mathbf{6}$.

[*] Prof. Dr. S. Blechert, Dipl.-Chem. C. F. Gürtler
Institut für Organische Chemie der Technischen Universität
Strasse des 17. Juni 124, D-10623 Berlin (Germany)
Telefax: Int. code + (30) 31423619
e-mail: gurt0531@mailszrz.zrz.tu-berlin.de
Prof. Dr. E. Steckhan
Institut für Organische Chemie und Biochemie der Universität Bonn (Germany)

[**] This work was supported by the Volkswagen-Stiftung (I/69415) and the Fonds der Chemischen Industrie. We would like to thank Mr. P. Pritschow for recording the NMR spectra.

the dienophiles employed in this reaction are about 100 to 200 mV higher than those of the dienes. The requirement that the oxidation potentials of the two components should not differ by more than 500 mV is thus fulfilled.[11] A rather small difference of the oxidation potentials usually has a positive effect on the reaction rates.

Based on our experience with 2-vinylindoles, we propose the mechanism outlined in Scheme 2. We assume that the first step is an addition of the enamine to the electrochemically formed vinylogous iminium radical cation, followed by cyclization via the electrophilic iminium cation. Deprotonation and subsequent electron transfer terminate the reaction. Thus **6** is formed as the exclusive product in good yield.

A nonconcerted mechanism is consistent with earlier mechanistic investigations on radical cation Diels–Alder reactions.[12] At the stage of the initially formed radical cation addition product, rotation about the C–C single bond and formation of *cis*/*trans* diastereomers should generally be possible, in particular when the dienophile is bulky. If ring closure is much faster than rotation, a uniform product is to be expected. In case of acrylonitrile **5** and the sterically demanding enaminolactone **7**, (*E*)-configurated olefins lead most remarkably to *trans* products **6** and **8** exclusively (Table 1).

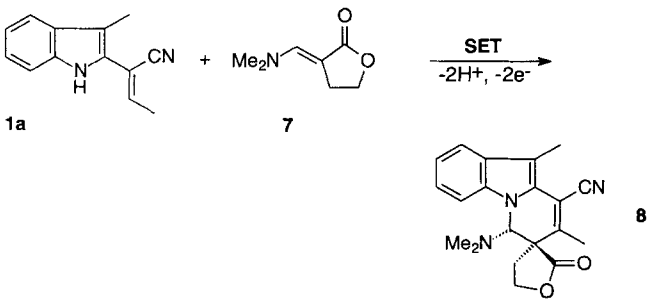

1a **7** **8**

The reaction described here extends the application of ET-induced Diels–Alder reaction with 2-vinylindoles as the diene component in a preparatively interesting way. It enables the rapid construction of alkaloid skeletons in high to very high yield. The mechanism and further application, especially towards the synthesis of indole alkaloids, are topics of current investigations.

Experimental Procedure

General procedure for ET-induced reactions: 1 mmol diene **1** and 0.7 mmol dienophile were dissolved in 50 mL of acetonitrile (+ 0.1 M $LiClO_4$). The solution was degassed in an electrolysis cell (undivided) and subsequently subjected to a potentiostatically controlled electrolysis at a working potential of 490 mV vs a $Ag/AgNO_3$ reference electrode. Electrolysis was performed until about 80% conversion was reached (working electrode: graphite, auxiliary electrode: graphite). For workup the solvent was removed and the residue was treated with water and extracted several times with dichloromethane. The product was purified by column chromatography (*tert*-butyl methyl ether/petroleum ether 1:3) or by HPLC (Nucleosil RP-18, water/methanol 7:3). All new compounds were characterized unequivocally by spectroscopy. 2D-NMR techniques (COLOC) and NOE experiments were used for structure determination. Selected spectroscopic data e.g. for **3c**: ^{1}H NMR (200 MHz, $CDCl_3$): δ = 7.56 (d, 1H, J = 7.5 Hz, H-9), 7.36 (d, 1H, J = 7.5 Hz, H-12), 7.24 (dd, 1H, J = 7.5, 7.5 Hz, H-11), 7.12 (dd, 1H, J = 7.5, 7.5 Hz, H-10), 5.52 (s, 1H, H-21), 3.58 (s, 3H, $COOCH_3$), 3.08 (ddd, 1H, J = 3.5, 4.5, 13.0 Hz, H-3eq) 2.88 (ddd, 1H, J = 4.0, 8.0, 13.0 Hz, H-3ax), 2.52 (m, 1H, H-15eq), 2.48 (s, 3H, H-6), 2.42 (s, 3H, H-22), 2.02 (ddd, 1H, J = 4.0, 8.0, 13.0 Hz, H-15ax), 1.72 (dddd, 1H, J = 3.5, 4.0, 4.0, 14.0 Hz, H-14eq), 1.32 (m, 1H, H-14ax). ^{13}C NMR (100.6 MHz, $CDCl_3$): δ = 172.4 (C-19), 146.2 (C-17), 135.6 (C-13), 130.0 (C-8), 124.2 (C-7), 124.1 (C-11), 120.4 (C-10), 119.7 (C-9), 116.1 (C-23), 111.9 (C-2), 108.7 (C-12), 106.1 (C-16), 67.6 (C-21), 53.0 (C-24), 52.5 (C-20), 44.6 (C-3), 31.3 (C-15), 22.9 (C-14), 19.3 (C-22), 8.7 (C-6). C calc.: 71.62%, found: 71.40%; H calc.: 6.31%, found: 6.40%.

Received: April 21, 1995 [Z 7915 IE]
German version: *Angew. Chem.* **1995**, *107*, 2025–2026

Keywords: cyclizations · electrochemistry · electron transfer · radical cations

[1] For reviews see for example a) L. Eberson, *Electron Transfer Reactions in Organic Chemistry*, Springer, Berlin, **1987**; b) J. Mattay, *Angew. Chem.* **1987**, *99*, 849; *Angew. Chem. Int. Ed. Engl.* **1987**, *26*, 825.
[2] a) N. L. Bauld, *Tetrahedron* **1989**, *45*, 5307; b) B. Harirchian, N. L. Bauld, *J. Am. Chem. Soc.* **1989**, *111*, 1826.
[3] a) F. Müller, J. Mattay, *Chem. Rev.* **1993**, *93*, 99; b) J. Mattay, *Synthesis* **1989**, 233; c) M. Schmittel, H. V. Seggern, *Angew. Chem.* **1991**, *103*, 981; *Angew. Chem. Int. Ed. Engl.* **1991**, *30*, 999; d) F. Müller, J. Mattay, *ibid.* **1992**, **104**, 207 and **1992**, *31*, 209.
[4] a) A. Gieseler, E. Steckhan, O. Wiest, *Synlett* **1990**, 275; b) A. Gieseler, E. Steckhan, O. Wiest, F. Knoch, *J. Org. Chem.* **1991**, *56*, 1405; O. Wiest, E. Steckhan, F. Grein, *ibid.* **1992**, *57*, 4034.
[5] a) S. Blechert, R. Knier, H. Schroers, T. Wirth, *Synthesis* **1995**, 592; b) S. Blechert, *Liebigs Ann. Chem.* **1985**, 673; c) J. Wilkens, A. Kühling, S. Blechert, *Tetrahedron* **1987**, *43*, 3237.
[6] T. Wirth, S. Blechert, *Synlett* **1994**, 717.
[7] a) H. Schroers, Dissertation, Universität Bonn, **1989**; b) J. Levy, J. Sapi, J.-Y. Laronze, D. Royer, L. Toupet, *Synlett* **1992**, 601.
[8] O. Wiest, E. Steckhan, *Angew. Chem.* **1993**, *105*, 932; *Angew. Int. Ed. Engl.* **1993**, *32*, 901.
[9] C. F. Gürtler, S. Blechert, E. Steckhan, *Synlett* **1994**, 141.
[10] J. Mlcoch, E. Steckhan, *Angew. Chem.* **1985**, *97*, 429; *Angew. Chem. Int. Ed. Engl.* **1985**, *24*, 412.
[11] J. Mlcoch, E. Steckhan, *Tetrahedron Lett.* **1987**, *28*, 1081.
[12] O. Wiest, E. Steckhan, *Tetrahedron Lett.* **1993**, *34*, 6391.
[13] Semiempirical calculations (AM-1,RHF) show that thermodynamical stability of the *cis* and *trans* adducts should be comparable.

 © VCH Verlagsgesellschaft mbH, D-69451 Weinheim, 1995 0570-0833/95/3417-1901 $ 10.00+.25/0

New Dimensions to Familiar Themes

Two Dimensional NMR Spectroscopy. Applications for Chemists and Biochemists. 2nd Edition. Edited by *W. R. Croasmun* and *R. M. K. Carlson*. VCH Publishers, New York, 1994. 958 pp., hardcover DM 199.00.—ISBN 1-56081-664-3

Compared with the first edition of this work (published in 1987), this new edition has not only been extended and updated to take account of the latest state of development in NMR methods, it must actually be regarded for the most part as a newly written book. I therefore commend it even to readers who already have the first edition. Most of the authors have recognized that two-dimensional and multidimensional NMR techniques have undergone further radical changes during the 1990s, and that new examples were needed, especially of reverse heteronuclear experiments, to emphasize the enormous advances that these new methods have brought to the already available strategies for structure determination.

In Chapter 1 the already well-proven introduction by G. A. Gray to multidimensional NMR spectroscopy of solutions has been extended to include reverse heteronuclear correlation experiments, spin-locking pulses, and pulsed field gradients. Gray's introduction is intended for chemists who are already familiar with traditional NMR methods. Nevertheless, these readers are likely to have difficulties with Chapters 2–4, which constitute the heart of the book. W. E. Hull's chapter on experimental aspects of two-dimensional NMR spectroscopy has been completely reorganized and enlarged to 357 pages. This and the new chapters by C. Griesinger and coauthors on proton-detected heteronuclear and multidimensional NMR spectroscopy, and by H. R. Kalbitzer on computer-aided analysis of multidimensional NMR spectra, together make up over half the book. However, these chapters are definitely for practising NMR spectroscopists! Even they will be impressed by the wealth of information, and will perhaps be surprised that they have missed so much that has occurred in the last few years.

W. E. Hull describes all the technical aspects: shim systems, locks, mechanical vibration effects, probe-heads, amplitude and phase modulation of r.f. pulses for selective excitation, suppression of solvent peaks, gradient echo spectroscopy. This is followed by an explanation of the fundamental principles of 2D NMR spectroscopy and of all the important homonuclear and directly-detected heteronuclear experiments. The description and comparison of the different acquisition methods for phase-sensitive experiments deserves a special mention. The author also makes an effort to avoid using software nomenclature that is specific to individual instrument manufacturers, and altogether this Chapter 2 is a very welcome contribution. I doubt if there exists any other treatment that is so detailed and comprehensive.

In Chapter 3 Griesinger and his coauthors round off their account by describing the latest highlights: proton-detected heteronuclear spectroscopy and the 3D NMR techniques. Their introduction to the product operator formalism seems rather too condensed, and this can be better understood by reading the original publications. In contrast the reverse methods (HMQC, HMBC, HSQC, double-INEPT) and their modifications for correlation experiments with improved sensitivity, constant time experiments, and spectral editing are described in great detail; product operators are used to describe the state of the spin system at critical points in the pulse sequences. The authors compare the effectiveness of phase cycles and pulsed field gradients for suppressing the signals of solvents and of protons attached to ^{12}C atoms. 3D NMR methods help to overcome problems of assignment and enable one to measure "J-values for homonuclear and heteronuclear couplings with improved accuracy.

Chapters 5–11 describe applications of many of the NMR techniques introduced earlier to special structural problems, with particular emphasis on the considerable increase in sensitivity obtained with the reverse procedures. Regrettably, however, there are no examples of the use of pulsed field gradients that would have illustrated the saving in time or the reduction of noise in the t_1 channel. These seven chapters will probably be sufficiently understood by chemists and biochemists working in the relevant areas, and should provide these readers with an excellent introduction to the capabilities and limitations of NMR spectroscopy. In a completely rewritten Chapter 5 H. Kessler and S. Seip describe the conformational analysis of peptides, now in a more general context and no longer concentrating solely on cyclosporin A. Some very nice examples of the use of DEPT-HMQC sequences are included. However, there is some lack of coordination between this chapter and the following one by H. J. Dyson and P. E. Wright on protein structure calculations based on NMR constraints; for example, the two chapters use completely different nomenclature systems to describe the NOE effect. There is an interesting discussion about the maximum size of a protein molecule whose structure can be determined by NMR spectroscopy (stated here as 30000 u); it is concluded that the limitation is due to the increased correlation time for molecular reorientation rather than to the severe overlapping of the resonances. Next there are chapters on the structural analysis of nucleic acids (I. Goljer and P. H. Bolton), oligo- and polysaccharides (J. Dabrowski), and steroids (W. R. Croasmun and R. M. K. Carlson), all well worth reading. In Chapter 10 P. L. Rinaldi discusses applications to structural problems in organic syntheses, giving as examples an organometallic compound, a Diels–Alder product, and a polymer, and considers the merits of different NMR strategies. He also describes triple resonance experiments whereby one can selectively detect the signals of ^1H or ^{13}C nuclei adjacent to a suitable isotopically labeled site (containing ^2H, for ex-

This section contains book reviews and a list of new books received by the editor. Book reviews are written by invitation from the editor. Suggestions for books to be reviewed and for book reviewers are welcome. Publishers should send brochures or (better) books to Dr. Ralf Baumann, Redaktion Angewandte Chemie, Postfach 101161, D-69451 Weinheim, Federal Republic of Germany. The editor reserves the right of selecting which books will be reviewed. Uninvited books not chosen for review will not be returned.

ample) or to a third NMR-active nucleus (e.g. ^{19}F, ^{31}P, or a suitable metal nuclide). In Chapter 11 G. E. Martin and R. C. Crouch describe examples in which the structures of natural products and compounds of pharmaceutical importance have been determined. These authors indicate that by using a microprobe head it may be possible to further reduce the amount of sample needed for an NMR analysis. They show examples of reverse 2D NMR spectra obtained with 10 μg samples in reasonable measurement times.

Lastly there is a glossary explaining nearly 300 of the acronyms that are so beloved by NMR spectroscopists. This book can be thoroughly recommended.

Jürgen Lauterwein
Organisch-chemisches Institut
der Universität Münster (Germany)

Ferrocenes. Homogeneous Catalysis. Organic Synthesis. Materials Science. Edited by *A. Togni* and *T. Hayashi*. VCH Verlagsgesellschaft, Weinheim, 1995. 540 pp., hardcover DM 248.00, $ 145.00.—ISBN 3-527-29048-6

M. Rosenblum's book *Chemistry of Iron Group Metallocenes* was published in 1965. Now, just 30 years later, we again have a new book on the same subject area, *Ferrocenes*, edited by A. Togni and T. Hayashi. In this monograph the editors have set out to cover the most important areas of research in which ferrocenes play a major role, and to extend and update the material in the ten volumes of the Gmelin Handbook devoted to ferrocenes, and in the annual reviews of ferrocenes research in the *Journal of Organometallic Chemistry*.

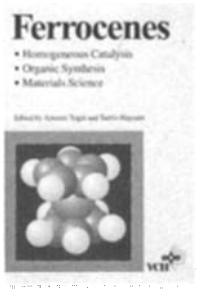

The book is divided into three parts: I. Homogeneous Catalysis, II. Organic Synthesis—Selected Aspects, and III. Materials Science. Chapter 1 of Part I (K.-S. Gan and T. S. A. Hor) describes the coordination chemistry and catalytic properties of 1,1′-bis(diphenylphosphano)ferrocene, and in the second chapter T. Hayashi continues this theme by describing the use of chiral ferrocenylphosphanes for asymmetric catalysis. Hayashi sets out clearly and concisely the reasons why chiral ferrocenylphosphanes are so important as catalysts and inductors in organic synthesis: the ferrocenylmethyl group of the side-chain contains suitable functional groups, the planar chirality of the 1,2-substituted ferrocene cannot racemize, both mono- and diphosphines can be prepared from the same chiral source, and lastly the characteristic orange-red color of the ferrocene derivative facilitates chromatographic work-up. Part I ends with a chapter on "Enantioselective Addition of Dialkylzinc to Aldehydes Catalyzed by Chiral Ferrocenyl Aminoalcohols" (Y. Butsugan, S. Araki, and M. Watanabe). Part II again begins with a report on chiral ferrocenes (Ch. 4, G. Wagner and R. Herrmann). However, it was not clear to me why this excellent contribution was not included in Part I, where synthetic aspects had already become an important part of the discussions.

In Chapter 5, "Ferrocene Compounds Containing Heteroelements" (M. Herberhold), the inorganic chemist's heart will certainly beat a little faster on discovering with pleasure that it contains all those compounds that would otherwise require laborious searching through the Gmelin volumes or recent original papers. It is especially commendable that this and several other chapters include some "Notes added in proof", bringing the book as up-to-date as possible by including references to publications appearing up to about August 1994. The resulting total number of references is around 2000, greatly easing the task of finding one's way into the primary literature.

However, in Chapter 6, "Macrocycles and Cryptands Containing the Ferrocene Unit" (C. D. Hall), the reader will suffer some disappointment, as this chapter compares poorly with the rest of the book. First one notices that the layout of the formula schemes is inconsistent, varying from page to page in size, quality, and line thickness. On two successive pages a σ-donor bond between sulfur and a metal ion is represented variously by a dashed line, a full line, and an arrowed line. Elsewhere ferrocene is shown as an iron atom between two cyclopentadienyl rings (represented by cpd) with no connection at all. On closer inspection one notices that about 50% of the structural formulas in this chapter are identical with the diagrams in a recent review article by P. D. Beer (*Adv. Inorg. Chem.* **1992**, *39*, 79–157). This becomes painfully obvious when small errors in symbols or in reproduction in Beer's review reappear at exactly the same positions in this chapter. But worse still, a detailed reading reveals that this copying is not confined to the formula diagrams, as some passages of text seem to have been reproduced from the above-mentioned article with only minor changes, and without acknowledging the source. For example, this is clearly seen in Section 6.4.2, which has only been very slightly altered and contains the same literature references in exactly the same sequence.

But these serious criticisms of Chapter 6 must not be allowed to give the impression that the style is typical of the book as a whole. On the contrary, the other authors' contributions are flawless and are convincingly presented. Chapter 7 (P. Zanello) gives a thorough account of the electrochemistry and structural characteristics of ferrocenes, and includes an extensive tabulation of redox potentials. Part III of the book, with the highly topical title "Materials Science", describes the many different aspects of ferrocenes as materials, ranging from charge-transfer complexes and magnetic materials (Ch. 8, A. Togni) through liquid crystalline compounds (Ch. 9, R. Deschenaux and J. W. Goodby) to organometallic polymers (Ch. 10, K. E. Gonsalves and X. Chen). These three chapters are especially enjoyable to read, as they afford a glimpse beyond the world of synthetic chemistry. After reading *Ferrocenes* it seems well justified to regard ferrocene as the organometallic counterpart of benzene in organic chemistry; this viewpoint helps one to understand why the range of topics treated in this book is so broad. On the other hand, this wide-ranging character might be seen by some readers as a disadvantage, because the ferrocene chemist, for whom this book with its wide coverage would be of greatest interest, does not really exist as such, and the individual chapters are more orientated towards the specialist. Nevertheless, this is a good book, and for that reason especially it is unfortunate that the high price is likely to restrict its effective market mainly to libraries and the above mentioned specialist.

Herbert Plenio
Institut für Anorganische
und Analytische Chemie
der Universität Freiburg (Germany)

The Chemistry of the Fullerenes. By *A. Hirsch*. Thieme, Stuttgart, 1994. 203 pp., paperback DM 80.00.—ISBN 3-13-136801-2

About ten years after the discovery of the fullerenes, and five years after they became available on a preparative scale, this book by A. Hirsch now gives us for the first time a well-written survey of the rapidly evolving chemistry of this new

 © VCH Verlagsgesellschaft mbH, W-6940 Weinheim, 1995 0570-0833/95/3417-1904 $ 10.00+.25/0

allotropic (and molecular) form of carbon. The book covers the most important published work up to about the beginning of 1994, lucidly summarizing the results in nine chapters.

The first chapter gives a brief outline of the discovery of the fullerenes. The author describes the methods for preparing and isolating some important fullerenes and a few of their endohedral derivatives, and briefly discusses their structure and spectroscopic properties. Chapter 2 is concerned with reduced forms of fullerene-C_{60}, which are of special interest because of the extraordinary solid-state (superconducting) properties of alkali metal fullerides. Chapter 3 deals with nucleophilic addition of carbanions, amines, and hydroxide ions to fullerenes-C_{60} and -C_{70}. Special attention is given here to the important problems of regioselectivity, the initial step in additions to C_{70}, and multiple additions to the highly symmetrical C_{60}. Chapter 4 is devoted to the important organic cycloaddition chemistry of C_{60}, with a lucid treatment of [4 + 2]-, [3 + 2]-, [2 + 2]-, and [2 + 1]-cycloaddition reactions and the resulting products, as well as the possibilities for further functionalization of these fullerene derivatives. Chapter 5 is concerned with the hydrogenation of C_{60} and C_{70}. The available data on the many structural variations of constitutionally isomeric hydrogenation products and on their relative stabilities are systematically reviewed and are discussed from a theoretical standpoint. Chapter 6 discusses single and multiple additions of organic and organometallic free radicals to C_{60}, and the free radical-initiated formation of dimers and polymers. Chapter 7 deals with complexes formed by fullerenes with transition metals. Single and multiple additions of this kind can show considerable selectivity, and structural factors influencing this are briefly discussed. Chapter 8 discusses the complex oxygenation and oxidation chemistry of C_{60} and C_{70}, as well as reactions with halogens and other electrophiles. A separate section in this chapter is devoted to the pioneering work on the functionalization of fullerenes using osmium tetroxide. In the final chapter the author summarizes the general features of the reactive properties of C_{60} and C_{70}, and considers likely future developments in the chemistry of fullerenes (e.g. multiple addition products with controlled constitution, heterofullerenes, endohedral fullerenes).

This easily readable book gives an excellent insight into the still very rapidly developing chemistry of the fullerenes. It is mainly intended for chemists and materials scientists in academic and industrial laboratories, and provides a good coverage of the original literature, including much that is still novel and speculative. It is a highly valuable source of information both for those already working in the fullerenes area and for newcomers. I recommend everyone who wishes to learn about the current state of knowledge in fullerenes chemistry to buy this book.

Bernhard Kräutler
Institut für Organische Chemie
der Universität Innsbruck (Austria)

Brian Kaye
Chaos & Complexity
Discovering the Surprising Patterns of Science and Technology

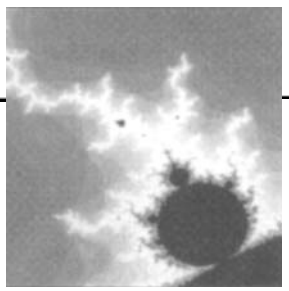

1993. XXII, 593 pages with 257 figures, 2 in color
Hardcover. DM 148.-/öS 1154.-/sFr 140.-.
ISBN 3-527-29039-7 (VCH, Weinheim)
Softcover. DM 78.-/öS 608.-/sFr 75.-.
ISBN 3-527-29007-9 (VCH, Weinheim)

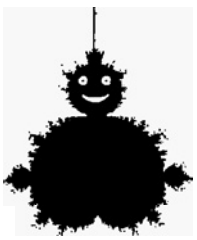

The surprising patterns of chaos and complexity are to be found in many areas of nature and science, examples ranging from cabbages to coastlines.

Quite often, those who could benefit most from an understanding of the principles behind chaos and complexity are denied access to the power and wonders of the field by the mathematical and unnecessarily convoluted way the topic is usually presented.

This book makes these sometimes complicated wonders accessible to students and professionals alike. Amusing tales and cartoons are used to explain the concepts and demonstrate the fascinating applications of this powerful technique.

To order please contact your bookseller or:

VCH, P.O. Box 10 11 61,
D-69451 Weinheim,
Telefax (0) 62 01 - 60 61 84

VCH, Hardstrasse 10, P.O. Box,
CH-4020 Basel

VCH, 8 Wellington Court,
Cambridge CB1 1HZ, UK

VCH, 220 East 23rd Street,
New York, NY 10010-4606, USA
(toll free: 1-800-367-8249)

VCH, Eikow Building,
10-9 Hongo 1-chome,
Bunkyo-ku, Tokyo 113
Japan

VCH

Chemistry of Inositol Lipid Mediated Cellular Signaling**

Barry V. L. Potter* and Dethard Lampe

It is now slightly more than a decade since Michael Berridge and his collaborators reported in *Nature* "... micromolar concentrations of Ins(1,4,5)P_3 (1D-*myo*-inositol 1,4,5-trisphosphate) release Ca^{2+} from a non-mitochondrial intracellular Ca^{2+} store in pancreatic acinar cells. Our results strongly suggest that this is the same Ca^{2+} store that is released by acetylcholine". This observation ushered in a new era in the field of signal transduction with the discovery of a small-molecule second messenger linking the spatially separated events of cell surface receptor activation and intracellular Ca^{2+} mobilization. This event, which has spawned what is now one of the most active fields of current biology, also stimulated a renaissance in inositol and inositol phosphate chemistry. The synthesis of inositol polyphosphates presents a number of problems: the regiospecific protection of inositol and the optical resolution of the resulting precursors, the phosphorylation of the polyol, removal of all phosphate protecting groups without phosphate migration, and finally the purification of the water-soluble target polyanion. With the solution of these problems over the last few years it is now possible to look beyond the synthesis of naturally occurring inositol polyphosphates, whose number has been steadily increasing, to the design of chemically modified inositol phosphate analogues with the prospect of developing enzyme inhibitors, rationally modified receptor ligands and antagonists, and perhaps, through pharmacological intervention in signal transduction pathways, even the therapeutical agents of the future.

Keywords: inositol phosphates · second messengers · signal transduction

1. Transmembrane Signaling

The cells in multicellular organisms must communicate with each other in order to work together. They convey signals by using substances such as hormones and neurotransmitters (Fig. 1). Lipophilic hormones such as steroids, for example, can pass through the lipid bilayer of cell membranes and bind to their target receptors within the cell. Many chemical messengers, however, are too hydrophilic to cross membranes. In order to deliver their message they have to bind to specific receptors on the outside of the cell membrane and activate mechanisms that transmit the signal into the cell, a process known as transmembrane signaling or signal transduction. Several different classes of receptors are involved in signal transduction. If the receptor is linked to an ion channel, the opening of this channel can trigger the influx or efflux of ions into or out of the cell. A change of ion concentration in the cytosol will then activate cellular enzymes, evoking an ultimate response to the stimulatory cell surface ligand. Another class of receptor is the receptor tyrosine kinase, which is intrinsically an enzyme. It is embedded in the cell membrane and has binding sites able to recognize

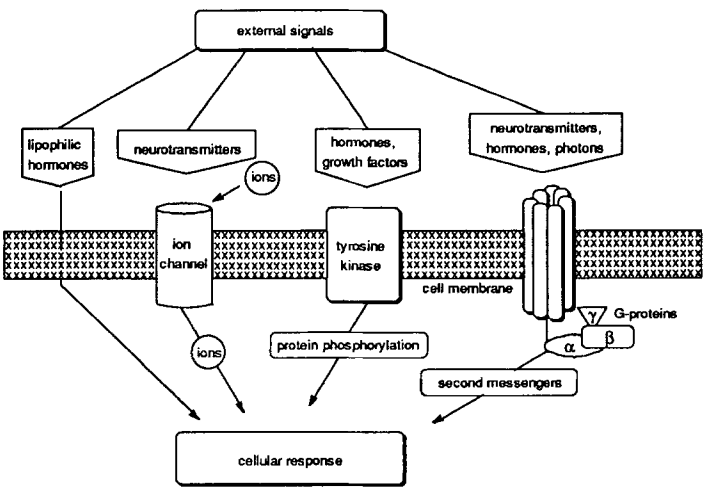

Fig. 1. Getting the message across: signal transduction mechanisms.

[*] Prof. Dr. B. V. L. Potter, Dr. D. Lampe
School of Pharmacy and Pharmacology, University of Bath
Bath BA2 7AY (UK)
Telefax: Int. code + (1225) 826-114
e-mail: B. V. L. Potter@bath.ac.uk

[**] Abbreviations used in this review: All = allyl, Bn = benzyl, Bz = benzoyl, Cb = (*R*)-1-phenylethylcarbamoyl, Cbz = benzyloxycarbonyl, Gro = glycero, MEM = methoxyethoxymethyl, MOM = methoxymethyl, Ms = methylsulfonyl, Piv = pivaloyl, PMB = *p*-methoxybenzyl, Prop = prop-1-enyl, Ptd = phosphatidyl, Tf = trifluoromethanesulfonyl, TBDMS = *tert*-butyldimethylsilyl. All references to inositol refer to the *myo* isomer unless otherwise specified. Inositol phosphates are abbreviated Ins, Ins$P$, InsP_2, InsP_3, InsP_4, InsP_5, and InsP_6 (inositol, inositol mono-, bis-, tris-, tetrakis-, pentakis-, and hexakisphosphate, respectively), with positioning of phosphate groups, as indicated in parentheses. Deoxyfluoro analogues are identified by a prefix consisting of a number indicating the position at which the fluorine substitution has taken place and the letter F, e.g. 2-F-Ins(1,4,5)P_3 = 2-deoxy-2-fluoro-inositol 1,4,5-trisphosphate. Phosphorothioate analogues are similarly identified by a suffix including the letter S, e.g. Ins(1,4,5)P_3-5S = inositol 1,4-bisphosphate 5-phosphorothioate.

 © VCH Verlagsgesellschaft mbH, D-69451 Weinheim, 1995 0570-0833/95/3418-1933 $ 10.00+.25/0

agonists on the outer surface, and an active site on the inner surface of the membrane. Binding of agonists activates the enzyme and leads to the phosphorylation of tyrosine residues on target proteins within the cell. This signal transduction mechanism is used by many growth factors and hormones including insulin.[1] Recently, the role of specific protein–protein interactions in mediating the flow of information from receptor tyrosine kinases to *ras* proteins was elucidated.[2]

Many water-soluble hormones make use of a signal transduction system whereby the receptor is coupled to the production of an internal signaling molecule via an intracellular effector. After the hormone binds to its receptor protein on the cell surface, a membrane-bound GTP-binding protein (G-protein),[3–5] which is associated with the receptor, is activated. The family of G-proteins includes several members which regulate different intracellular pathways. G-proteins are composed of three subunits designated α, β, and γ in order of decreasing mass. On activation, guanosine diphosphate (GDP) bound to the α subunit is replaced by guanosine triphosphate (GTP), causing the $\beta\gamma$ subunit to dissociate from the activated α-GTP subunit. The free subunits can now stimulate or inhibit other membrane-bound enzymes acting as amplifiers (e.g. K^+ channels, Ca^{2+} channels, adenylate cyclase (AC), guanylate cyclase (GC), PtdIns(4,5)P_2-specific phospholipase C (PtdIns-PLC)), which in turn generate so-called second messengers on the cytosolic side of the cellular membrane. The intrinsic GTPase activity of the α subunit then hydrolyzes GTP to GDP, the α-GDP subunit recombines with the $\beta\gamma$ subunit, and the G-protein returns to its basal state.

1.1. Second Messengers

Second messengers identified so far include adenosine 3′,5′-cyclic monophosphate (cAMP), guanosine 3′,5′-cyclic monophosphate (cGMP), diacylglycerol (DAG), Ins(1,4,5)P_3, and of course Ca^{2+} ions. Considerable current interest is also focused upon phosphatidylinositol 3,4,5-trisphosphate as a potential second messenger (see Section 2). Recent studies suggest that cyclic adenosine diphosphate ribose (cADP-ribose), a metabolite of NAD^+, may also have Ca^{2+}-mobilizing second messenger properties,[6–8] and the sphingolipid metabolite sphingosine 1-phosphate has been implicated as a potential second messenger in signal transduction pathways activated by certain mitogens.[9]

1.2. The Role of Ca^{2+} in Signal Transduction

The first indication that calcium ions play a role in the regulation of cellular events was an observation by Ringer in 1883.[10] On examining muscle tissue, he found that he could not induce contraction when he replaced the tap water in his medium with distilled water. The missing component was found to be Ca^{2+}.

Today, it is known that a large number of different cellular processes are controlled by protein phosphorylation induced by changes in intracellular Ca^{2+} concentration, and the mobilization of Ca^{2+} has been found to be the primary function of many

B. V. L. Potter

D. Lampe

Barry Potter was born in Brighton (UK) in 1953. He studied chemistry at the University of Oxford as an Exhibitioner of Worcester College, graduating with first-class honors and winning the Part II Thesis Prize in Organic Chemistry. He completed his doctorate in bioorganic chemistry in 1981 in Oxford under Professor Gordon Lowe with research on enzyme-catalyzed phosphoryl transfer reactions using chiral [^{16}O,^{17}O,^{18}O]phosphate esters. During that time he was a Graduate Scholar and subsequently Junior Research Fellow of Wolfson College. After postdoctoral research in nucleic acid chemistry and molecular biology as a European Exchange Fellow of the Royal Society with Professor Fritz Eckstein at the Max-Planck-Institut für Experimentelle Medizin in Göttingen, he accepted the post of Lecturer in Biological Chemistry at the University of Leicester in 1984 and was awarded a Lister Institute Research Fellowship in 1987. In 1990 he moved to the Chair of Medicinal Chemistry in the School of Pharmacy and Pharmacology, University of Bath, where he is Lister Institute Research Professor. He received his DSc from Oxford University in 1993. His fields of research activity lie in biological and medicinal chemistry, in particular enzyme mechanisms and nucleic acid and phosphorus chemistry. Special interests are the chemistry of second messengers and the synthesis of receptor ligands and enzyme inhibitors.

Dethard Lampe was born in Delmenhorst (Germany) in 1963. He studied chemistry at the Universities of Hamburg and Göttingen, where he obtained his diploma in clinical biochemistry in 1989 under Professor H.-D. Söling. In the same year he joined the research group of Dr. B. V. L. Potter in Leicester on a Wellcome Trust Prize Studentship. He moved to the School of Pharmacy and Pharmacology at the University of Bath in 1990 and completed his PhD on the synthesis of novel inositol phosphate analogues in 1993. He continued research in Bath in the area of inositol polyphosphates as a Wellcome Trust Prize Fellow. At the beginning of 1995 he moved to the Instituto de Química Orgánica General, CSIC (Prof. M. Martín-Lomas) in Madrid, where he is involved in the synthesis of biologically active oligosaccharides.

agonists. The cytosolic Ca^{2+} concentration can be regulated by two different mechanisms:

1. Many agonists operate by inducing a change in the potential difference across the membrane. This causes voltage-sensitive Ca^{2+} channels in the cell membrane to open. As most Ca^{2+} within the cell is bound to membranes or proteins, the intracellular level of free Ca^{2+} is low. Therefore there is a large gradient in favor of influx of ions into the cell and the cytosolic Ca^{2+} concentration is increased.

2. Other agonists mobilize sequestered Ca^{2+} from intracellular stores so that the Ca^{2+} concentration in the cytosol is increased and Ca^{2+}-dependent enzymes are activated. The cellular response effected depends on the type of cell targeted as well as the nature of the agonist.

2. Inositol 1,4,5-Trisphosphate: A Second Messenger

In 1850 Scherer isolated an optically inactive isomer of cyclohexanehexol from muscle, which he designated "Inosit".[11] Just over a century after this discovery and a few years prior to the discovery of the now well-established second messenger 3',5'-cyclic AMP by Rall and Sutherland,[12, 13] Lowell and Mabel Hokin demonstrated that acetylcholine stimulates the turnover of inositol-containing phospholipids in pancreas and brain cortex slices.[14] Folch had discovered the inositol-containing phospholipids in brain some ten years earlier.[15] Later work showed that the phospholipid effect described by the Hokins was observable in a number of other systems exposed to agonist stimulation, and this suggested a role for these lipids in stimulus–response coupling. In the late 1950s new analytical techniques facilitated the separation of the inositol-containing phospholipids into phosphatidylinositol (PtdIns), phosphatidylinositol-4-phosphate [PtdIns(4)*P*], and phosphatidylinositol-4,5-bisphosphate [PtdIns(4,5)P_2][16] (Fig. 2), and the chemical structures of these species were soon established by Ballou et al.[17] Despite this progress, little headway was made in understanding the physiological significance of the stimulated turnover of inositol-containing phospholipids in subsequent years, primarily since too much attention was given to the major phospholipid, PtdIns.

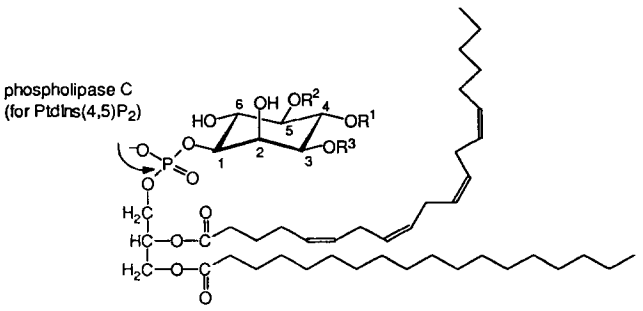

PtdIns: $R^1 = R^2 = R^3 = H$;
PtdIns(4)*P*: $R^1 = PO_3^{2-}$, $R^2 = R^3 = H$;
PtdIns(4,5)P_2: $R^1 = R^2 = PO_3^{2-}$, $R^3 = H$;
PtdIns(3)*P*: $R^1 = R^2 = H$, $R^3 = PO_3^{2-}$
PtdIns(3,4)P_2: $R^1 = R^3 = PO_3^{2-}$, $R^2 = H$;
PtdIns(3,4,5)P_3: $R^1 = R^2 = R^3 = PO_3^{2-}$

Fig. 2. Location of phospholipase C attack on inositol phospholipids.

A key breakthrough, however, came in 1975 when Michell[18] realized the connection between agonist-stimulated phospholipid turnover and the increased intracellular Ca^{2+} levels, which had already been in focus with regard to regulation of a variety of cellular functions. Despite this, there was no obvious contender for a chemical link between these events. Finally, at the end of 1983, Berridge and his co-workers in Cambridge, UK, and Frankfurt am Main, Germany,[19] identified the missing second messenger in the form of a *myo*-inositol polyphosphate generated from the minor phospholipid PtdIns(4,5)P_2 with the statement: "micromolar concentrations of Ins(1,4,5)P_3 (1D-*myo*-inositol 1,4,5-trisphosphate) release Ca^{2+} from a non-mitochondrial intracellular Ca^{2+} store in pancreatic acinar cells. Our results strongly suggest that this is the same Ca^{2+} store that is released by acetylcholine".

These discoveries opened up a whole new chapter in signal transduction and since then, progress in this field has been dramatic, as evidenced by the comment of Hokin:[20] "the phosphoinositide field is currently the number one field in biochemistry in the number of citations (excluding molecular biology)". Activity was still further stimulated by the mapping out of a highly complex metabolic pathway for inositol phosphates,[21, 22] including the involvement of higher inositol phosphates such as InsP_6 and even the pyrophosphate-containing InsP_7 and InsP_8.[23] Still more intriguing is the characterization of the new inositol-containing phospholipids PtdIns(3)*P*, PtdIns(3,4)P_2, and PtdIns(3,4,5)P_3 (Fig. 2) formed after the stimulation of a 3'-kinase in cells by growth factors.[24] The latter phospholipid, in particular, may be a second messenger in its own right. This whole area is under considerable scrutiny and appears to be a completely new branch of polyphosphoinositide-mediated signal transduction. Additionally, it was discovered that the cell nucleus appears to have its own autonomous phosphoinositide signaling machinery.[25, 26] Some of these newer aspects of the polyphosphoinositide signaling pathway have been reviewed.[27] Although a discrete molecule has yet to be structurally identified, much excitement has been generated recently by the discovery of a Ca^{2+} influx factor (CIF).[28, 29] CIF appears to be a diffusable messenger that is released from activated intracellular compartments in stimulated cells and stimulates Ca^{2+} influx across the plasma membrane.[30, 31] Also, attention is drawn to recent reports showing that the affinity of the *Penicillium brevicompactum* metabolites adenophostin A and B for the Ins(1,4,5)P_3 receptor is higher than that of Ins(1,4,5)P_3 itself[32–34] (Fig. 3).

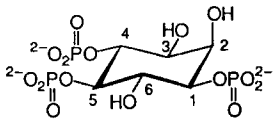

Fig. 3. The second messenger D-*myo*-inositol 1,4,5-trisphosphate.

While most of the rapid progress of the last ten years has been focused on biological aspects, it is clear that current and future efforts are, and will be directed towards pharmacological intervention in the phosphoinositide signaling system. First syntheses of Ins(1,4,5)P_3 were reported in 1986–1987, and these have been followed by significant synthetic progress to the extent that essentially all of the problems inherent to inositol phosphate

synthesis have now been overcome. The complex nature of inositol phosphate metabolism, however, which is still being uncovered, is providing new targets for synthesis with regularity. Moreover, receptors that bind second messengers, enzymes that metabolize them, and the generative pathways responsible for their formation are naturally seen as potential targets for rational drug design.[35-37] Thus, the focus of synthetic activity is now moving towards structurally modified inositol phosphates with novel biological properties.

This review focuses primarily on recent chemical progress in this area. Although attempts will be made to place the essential biological background in context, a completely comprehensive coverage of the biology of the past ten years is well beyond the scope of this article and the reader is referred to the many existing reviews[22, 38-47] and books[48-52] currently available on this topic. Several reviews and books on more recent aspects of the synthesis of inositol phosphates have also appeared.[53-56] For information on synthetic approaches prior to this, the reader is referred to two other major works.[57, 58]

3. Stereochemistry and Nomenclature of Inositol Derivatives

3.1. Stereochemistry and Nomenclature

After Scherer's discovery of "Inosit",[11] the suffix -ol was added, and when other isomers were discovered or synthesized they were also named "inositols". There are nine possible isomeric inositols, including one enantiomeric pair,[59] with the prefixes *scyllo*-, *myo*-, *neo*-, *epi*-, *cis*-, *muco*-, *allo*-, D-*chiro*-(+)-, and L-*chiro*-(−)- (Fig. 4). The large number of inositols and their derivatives has caused difficult problems of nomenclature, not all of which have been fully resolved. The publication of the "1967 IUPAC Tentative Rules for Cyclitols"[60] has gone a considerable way towards standardization, but difficulties still exist. Some aspects of these rules are outlined in the treatment of *myo*-inositol in the following section. Proposals were made that the system of stereospecific numbering should be adopted for inositol derivatives,[61] but these have not yet found widespread acceptance. A note on recent attempts to simplify nomenclature and abbreviations has appeared.[62] For a simplified discussion of this topic, the reader is referred to an excellent review.[63]

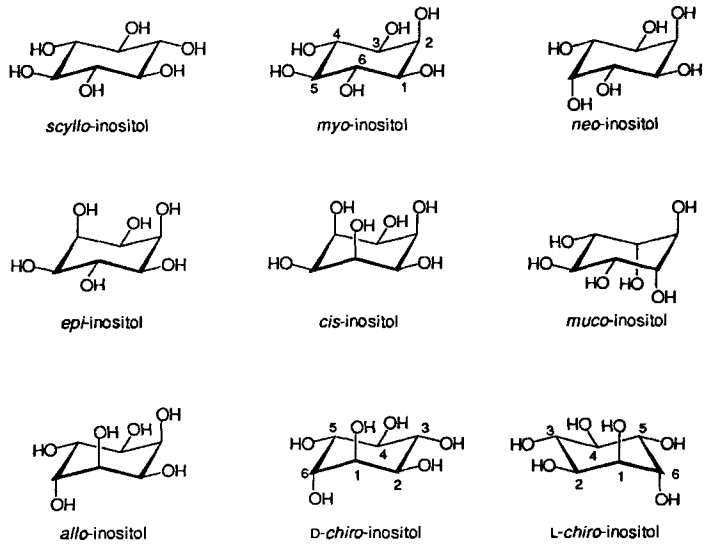

Fig. 4. The nine inositol isomers.

3.2. *myo*-Inositol

myo-Inositol is a *meso*-cyclohexane hexol, or cyclitol, and consequently possesses a plane of symmetry with five equatorial hydroxyl groups and one axial hydroxyl group. The carbon bearing the axial hydroxyl is designated C-2 and the other ring carbons can be numbered from C-1 to C-6 starting from a C-1 atom on either side of C-2 and proceeding around the ring in a clockwise or anticlockwise fashion. According to convention, an anticlockwise numbering in an asymmetrically substituted inositol leads to a configurational D prefix, and a clockwise numbering gives a substituted inositol with an L prefix. The choice of prefix is normally determined by giving preference to that which results in the lowest numbering of substituents. Thus, in *myo*-inositol the symmetry plane is through C-2 and C-5.

The substitution of one of the symmetry-related pairs of carbon atoms C-1, C-3 and C-4, C-6 gives rise to D and L enantiomers. Substitution of C-2 and/or C-5 clearly gives a *meso* product and a prefix is inappropriate. In Figure 5 the enantiomers of Ins(1,4)P_2 are shown. D-Ins(1,4)P_2 is an Ins(1,4,5)P_3 metabolite formed by phosphatase action, and L-Ins(1,4)P_2 is its synthetic enantiomer. The numberings shown were chosen since the alternatives, namely L-Ins(3,6)P_2 and D-Ins(3,6)P_2, have higher position numbers for the substituents. However, problems can arise when the IUPAC rules are adhered to strictly; in particular, when a metabolic pathway is traversed, confusing changes in nomenclature can occur. For example, D-*myo*-inositol-3,4-bisphosphate (name according to the IUPAC convention: L-*myo*-inositol-1,6-bisphosphate) is metabolized by phosphatases to the monophosphate L-*myo*-inositol-1-phosphate although the nonconventional name D-*myo*-inositol-3-phosphate allows more immediate appreciation of this fact. An IUPAC recommendation allowing all biologically relevant compounds to be denoted as D derivatives has now been proposed.[64] This convention, where possible, is adopted in this review.

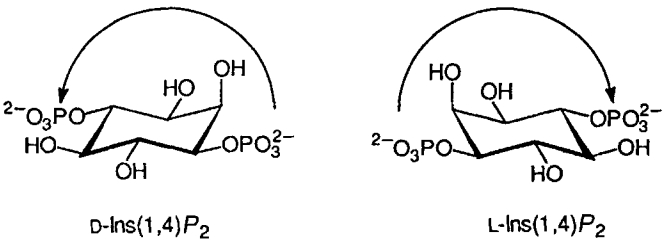

Fig. 5. The enantiomers of *myo*-inositol 1,4-bisphosphate.

4. Biosynthesis and Metabolism of *myo*-Inositol Phosphates

4.1. Biosynthesis of *myo*-Inositol

In humans the greater part of *myo*-inositol intake is from plants and only a small fraction is biosynthesized. De novo synthesis is, however, possible in both plants and animals by the isomerization of D-glucose 6-phosphate catalyzed by L-*myo*-inositol 1-phosphate synthase (D-*myo*-inositol 3-phosphate synthase). This enzyme was purified to homogeneity from yeast,[65] mammalian testis,[66,67] and brain.[68] The biosynthetic pathway has been reviewed[69,70] and stereochemical aspects have been discussed.[63] Surprisingly, the D-glucose-6-phosphate analogue D-glucose-6-phosphorothioate is not a substrate for L-*myo*-inositol-1-phosphate synthetase.[71]

myo-Inositol is then generated by the action of inositol monophosphatase on L-*myo*-inositol-1-phosphate. The monophosphatase is a key enzyme in the phosphatidylinositol cycle since it hydrolyzes both isomers of Ins(1)*P*; the L isomer arises by the above pathway and the D isomer by the hydrolysis of phosphatidylinositol phospholipids. It was shown that this single enzyme also dephosphorylates D- and L-Ins(4)*P* and in vitro Ins(5)*P*.[72] *myo*-Inositol monophosphatase was purified from brain[73-75] and an X-ray crystal structure of this enzyme has now been published.[76]

This enzyme is also of great current interest on account of its sensitivity to inhibition by lithium ions. It was observed in 1971 that levels of free *myo*-inositol decreased significantly in the brains of Li^+-treated rats.[77] Currently, links between the known therapeutic effects of lithium in the treatment of manic depression and its inhibition of *myo*-inositol 1-phosphatase are being actively sought. Since the brain does not have access to dietary *myo*-inositol, which cannot cross the blood–brain barrier, the de novo biosynthetic pathway via D-glucose 6-phosphate must be in effect. If the final stage in this pathway, the dephosphorylation of L-Ins(1)*P*, is blocked by lithium ions, the brain is unable to replenish its stores of phosphatidylinositol lipids, and the messenger system based on these lipids (see Section 4.2), which is used by neurotransmitters in cell signaling to alter electrical activity, is unable to operate. This is thought to be particularly important in hyperactive cells, as may also be the case in some forms of mania.[78,79] These important aspects have been reviewed.[80-82]

The inhibition of inositol-1-phosphatase by Li^+ ions[83] is unusual in that it is uncompetitive. Li^+ is thought to inhibit the second step of the dephosphorylation reaction, namely the breakdown of a phosphorylenzyme intermediate, possibly by coordination to an attacking water molecule at the active site, thus reducing its nucleophilicity.[83,84] It is clear that a better understanding of the molecular mechanism of Li^+ inhibition together with the crystal structure of the enzyme and the extensive medicinal chemistry which has now been carried out will go a long way towards assisting the rational design of mimics with potential antimanic properties. Several potent, albeit competitive, enzyme inhibitors have now been synthesized (see Section 9).

4.2. The Phosphatidylinositol Cycle

Inositol-containing phosphatides (Fig. 2) comprise less than 10% of the total phospholipid in animal cells. PtdIns is the most abundant (over 90%) and is primarily located in the endoplasmic reticulum (ER). The polyphosphoinositides PtdIns(4)*P* and PtdIns(4,5)P_2 are, together with a small proportion of PtdIns, located in the inner leaflet of the plasma membrane.

PtdIns isolated from plants has a different structure than that from animal sources. (The development of plant phosphoinositide signaling is beyond the scope of this article, but has been reviewed recently.[85]) In plants the *sn*-2 glycerol carbon is linked to the C_{18} fatty acid linoleic acid (18:2) and the *sn*-1 position is linked to fatty acids of the (16:0), (18:0), or (18:2) form. In contrast, in animals arachidonic acid (20:4) at C-2 and stearic acid (18:0) at C-1 predominate. PtdIns is phosphorylated by a specific kinase (PtdIns 4-kinase) to give the 4-phosphate PtdIns(4)*P*, which in turn is phosphorylated by another kinase (PtdIns*P* 5-kinase) to generate the key lipid PtdIns(4,5)P_2. On the other hand, specific phosphomonoesterases can dephosphorylate PtdIns(4)*P* and PtdIns(4,5)P_2.[86] Upon receptor activation the associated G-protein activates a membrane-bound phosphodiesterase (or phosphoinositidase), phospholipase C,[87] which cleaves PtdIns(4,5)P_2 into two second messengers, D-*myo*-inositol 1,4,5 trisphosphate (Fig. 3) and 1,2-di-*O*-acylglycerol (DAG), which together form a bifurcating signaling pathway. The hydrophilic Ins(1,4,5)P_3 diffuses into the cytosol and activates the receptor of a Ca^{2+} channel on the ER, resulting in the release of Ca^{2+} from an internal store (see Section 5).

The other product of this signaling pathway, DAG, was demonstrated to activate protein kinase C (PKC) by Nishizuka et al.[88,89] PKC was identified as the long-sought "receptor" for the tumor-promoting phorbol esters.[90] PKC was originally thought to be a single entity, but it is now clear that a large family of such protein kinase C isozymes exists.[91-93] DAG is hydrophobic, remains in the plane of the membrane, and can be metabolized by two major pathways involving a kinase or a lipase. In the first case the fatty acid moieties are conserved and DAG is phosphorylated to phosphatidic acid, which then combines with cytidine 5′-monophosphate (CMP) to form CMP-phosphatidate, which in turn can be coupled to a molecule of inositol to reform PtdIns. This reaction is catalyzed by the enzyme PtdIns synthetase. In the second case the DAG is hydrolyzed by a lipase to give a monoacylglycerol with the release of the eicosanoid precursor arachidonic acid,[94] used in prostaglandin synthesis. Structural aspects of the DAG limb of the signaling pathway have been studied by using DAG analogues,[95,96] and the structural requirements for PKC activation by lipids have been reviewed.[97]

Aside from the well-established phosphatidylinositol lipids discussed above, whose signaling involvement is now clear, a major new area has emerged recently due to the discovery of three phospholipids bearing a phosphate group at the D-3 position of the inositol ring. These lipids are PtdIns(3)*P*, PtdIns(3,4)P_2, and PtdIns(3,4,5)P_3 (Fig. 2). While their source has been the subject of some debate,[98] it is now accepted that direct phosphorylation of PtdIns(4,5)P_2 by a 3-kinase (PtdIns-3K)[99] is the main route of formation of PtdIns(3,4,5)P_3 in stimulated

cells. PtdIns(3)P and PtdIns(3,4)P_2 are derived from the parent PtdIns(3,4,5)P_3 by phosphatase action.[24, 100] The 3-phosphorylated lipids, unlike PtdIns(4,5)P_2, are not substrates for phospholipase C and thus cannot give rise to inositol phosphates as signaling molecules.[101] PtdIns-3K activation is intrinsic to mitogenic signaling by growth factor receptor tyrosine kinases[102] and has been implicated in signaling by many receptor and non-receptor protein tyrosine kinases.[103, 104] A distinctive second messenger role for PtdIns(3,4,5)P_3 is not yet apparent and the hunt is on for an intracellular effector. It may be possible that, like PtdIns(4,5)P_2,[105] PtdIns(3,4,5)P_3 interacts with the cytoskeleton.

4.3. Metabolism of *myo*-Inositol 1,4,5-Trisphosphate

Once released inside the cell, a second messenger must be efficiently deactivated in order to terminate its action and return the cell to a basal state in preparation for a new stimulus. Additionally, metabolites of the second messenger may well have physiological activities within the cell. These aspects have come under close scrutiny for Ins(1,4,5)P_3 in the past few years, and it has become clear that its metabolism to free inositol, which is then recycled into lipid synthesis, is quite complex, generating many inositol phosphates which are often difficult to separate. Only very basic features of this aspect of the PtdIns cycle will be discussed here. For more details the reader should consult the extensive reviews available.[21, 22, 106] The important features of Ins(1,4,5)P_3 metabolism are detailed in Figure 6.

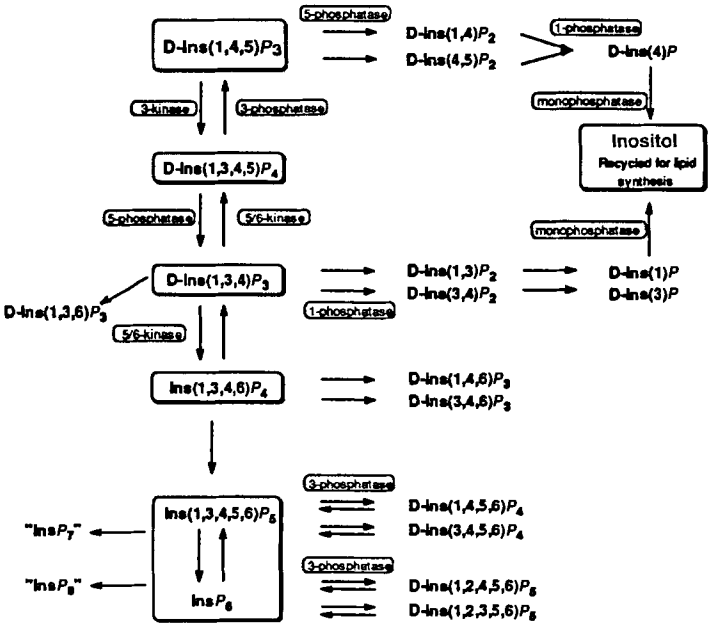

Fig. 6. Metabolism of inositol phosphates.

The PLC-mediated cleavage of PtdIns(4,5)P_2 is complicated by the fact that Ins(1,4,5)P_3 is not the sole hydrophilic product. Attack by H_2O on the phosphodiester linkage of PtdIns(4,5)P_2 gives Ins(1,4,5)P_3 and DAG, but cleavage may also be accomplished by attack of the 2-hydroxyl group at phosphorus, to yield inositol 1,2-cyclic-4,5-trisphosphate [Ins(1:2-cyclic 4,5)P_3], for example in thrombin-stimulated platelets.[107] Initial reports led to the suggestion that Ins(1:2-cyclic 4,5)P_3 is a second messenger in its own right,[108] but it proved impossible to confirm some of the earlier results.[109] The long half-life of Ins(1:2-cyclic,4,5)P_3 in parotid cells is also not compatible with a physiological function in Ca^{2+} release,[110] and its low concentration in some stimulated cells argues against an important messenger role for this compound.[111] There is no reason at present to assume that the production of Ins(1:2-cyclic 4,5)P_3 is anything other than an unavoidable and nonfunctional consequence of the mechanism of action of phospholipase C.[112]

The role of Ins(1,4,5)P_3 as a second messenger is now well established. Two major routes of metabolism have been discovered. It was known for some time that Ins(1,4,5)P_3 is metabolized by the action of a 5-phosphatase; this was first demonstrated in erythrocytes[113] and subsequently in many other cells.[21] There appear to be multiple types of this enzyme and both soluble, cytosolic forms and particulate, membrane-bound forms exist. Human platelet cytosol, for example, contains two 5-phosphatases, designated type I and type II, and the particulate type I 5-phosphatase from human placental membranes has recently been purified and characterized.[114] Since the product of the action of 5-phosphatase, Ins(1,4)P_2, has no known physiological role in this signaling pathway (there have, however, been reports that Ins(1,4)P_2 acts as an activator of DNA polymerase α[115] and 6-phosphofructo-1-kinase[116]), it seems clear that this enzyme acts merely to terminate the Ca^{2+} mobilization signal. Ins(1,4)P_2 is metabolized to Ins(4)P and subsequently converted to inositol, which reenters the cycle.

In 1985 the higher polyphosphate Ins(1,3,4,5)P_4 was discovered[117] closely followed by the 3-kinase enzyme,[118] which has been purified,[119, 120] sequenced, and cloned,[121, 122] adding a further complication to the metabolic pathway and initiating speculations about the possible function of this molecule. Despite fierce debate, no unambiguous role for this molecule has yet been elucidated. Readers are referred to recent reports on the topic.[123–126] Considerable controversy has been raised by the suggestion that Ins(1,3,4,5)P_4 acts as a second messenger in its own right and may be responsible for mediating the entry of extracellular Ca^{2+} through plasma membrane ion channels.[127] No end to this debate is yet in sight.

Whatever the function of Ins(1,3,4,5)P_4, it appears to be metabolized by the same 5-phosphatase as Ins(1,4,5)P_3. However, the situation is complicated by the existence of both soluble and particulate forms of the enzyme and more than one subtype of the former.[128] The particulate and type I soluble enzymes cleave both substrates and Ins(1,3,4,5)P_4 is a better substrate, but the type II enzyme has a very poor affinity for the tetrakisphosphate.[21, 128, 129] The product, Ins(1,3,4)P_3, has also been proposed to have a physiological function on the basis of a report that it is a moderately potent mobilizer of intracellular Ca^{2+}.[130] However, this was not confirmed[131] and there is no further evidence for a physiological role for this compound. The metabolism of Ins(1,3,4)P_3 is tissue-dependent. The products, Ins(1,3)P_2 and/or Ins(3,4)P_2, are subsequently converted into the monophosphates Ins(1)P and Ins(3)P, respectively, and these are ultimately dephosphorylated to inositol by inositol monophosphatase.

Studies on the action of Ins(1,3,4,5)P_4 have been complicated by the observation that in many tissues it can be converted to Ins(1,4,5)P_3 by a 3-phosphatase.[132, 133] It is now thought that InsP_5 and InsP_6 are the physiological substrates of this enzyme since these compounds are attacked with much higher affinity than Ins(1,3,4,5)P_4.[134] Ins(1,3,4,5)P_4 3-phosphatase was purified from hepatocytes[134] where it is compartmentalized inside the ER.[135]

Other metabolic pathways have also emerged. It is now apparent that Ins(1,3,4)P_3 can be phosphorylated by a 5/6-kinase to Ins(1,3,4,6)P_4,[136, 137] which has a weak, but distinct, Ca^{2+}-mobilizing activity.[138, 139] The 5/6-kinase will also convert Ins(1,3,4)P_3 to Ins(1,3,4,5)P_4. In animal cells Ins(1,3,4,5)P_4 is phosphorylated by 5/6-kinase to Ins(1,3,4,5,6)P_5, which is metabolized to three compounds, InsP_6 (phytic acid) and the normally inseparable enantiomeric pair Ins(3,4,5,6)P_4 and Ins(1,4,5,6)P_4. Ins(1,4,5)P_3 5/6-kinase was purified from liver with an InsP_6-linked affinity column.[140]

Such higher inositol polyphosphates have long been known to be present in plants and in avian erythrocytes[57, 70] where they function to provide phosphate storage and to modulate the oxygen affinity of hemoglobin. Their presence in mammalian cells, however, together with observations indicating that these compounds may provide intracellular and extracellular signals in brain[141, 142] indicate an interesting future for this area,[143] although it seems unlikely that these higher polyphosphates are directly involved in signal transduction. A physiological role for InsP_6 as an inhibitor of iron-catalyzed hydroxyl radical formation was suggested.[144] InsP_6 is, surprisingly, not the limit for phosphorylation, and evidence has been put forward for the existence of the pyrophosphate-containing higher polyphosphates InsP_7 and InsP_8,[23] which as yet have not been securely structurally characterized. These compounds apparently occur naturally in the slime mould *Dictyostelium*, but inositol polyphosphate pyrophosphates can also be generated by lyophilization of an inositol polyphosphate in the presence of a phosphoryl donor.[23] It seems certain that more surprises are in store.

To aid in the investigation of inositol polyphosphate metabolism in various tissues two major instrumental analytical methods were developed: one involves anion exchange HPLC[145] with on-line enzymatic hydrolysis of the phosphates, using a post-column reactor containing immobilized alkaline phosphatase, and molybdate detection of inorganic phosphate.[146] The other method relies on a metal-dye detection system not requiring dephosphorylation, in which trivalent transition metal ions are bound with high affinity to the dye 4-(2-pyridylazo)resorcinol and inositol phosphate polyanions.[147] This method permits picomolar-range detection of inositol phosphates.

Several NMR studies on inositol phosphates were also reported. Multinuclear NMR spectra were measured to confirm the structures and conformations of Ins(1,4,5)P_3,[148, 149] Ins(1,3,4,5)P_4,[149, 150] Ins(1,4,5,6)P_4,[151] InsP_6,[152] and a variety of lower inositol phosphates.[149] The data on phytic acid indicate that the conformation of this molecule varies with its degree of protonation. At high pH the molecule assumes a conformation having one axial and five equatorial phosphate groups, whereas between pH 2 and 5 it adopts a conformation with one equatorial and five axial phosphate groups, which is stabilized by intramolecular hydrogen bonding.

5. The Inositol 1,4,5-Trisphosphate Receptor

The inositol 1,4,5-trisphosphate receptor (InsP_3R) is now recognized to be a ligand-gated ion channel, activated by the binding of Ins(1,4,5)P_3 and gating Ca^{2+} (Fig. 7). In the last five years much information has accrued concerning the molecular structure of the InsP_3R, its distribution in tissues and in the cell, and its regulation.[153–158] In brain, Ins(1,4,5)P_3 receptors are highly expressed in cerebellar Purkinje cells, the hippocampus, striatum, and cerebral cortex. Peripherally, they were identified

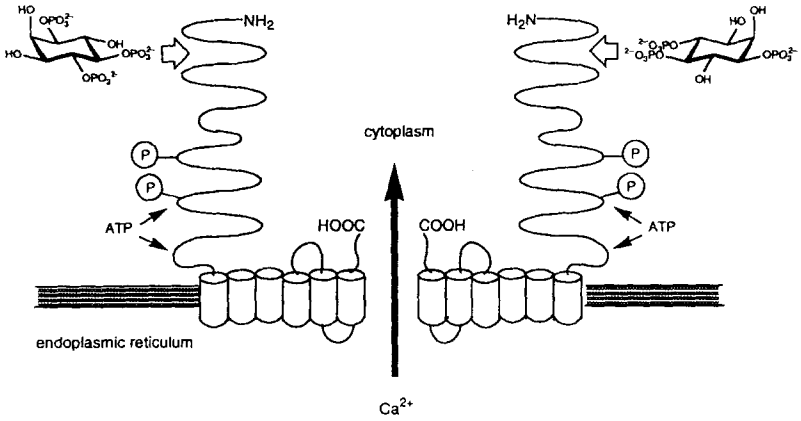

Fig. 7. Schematic representation of the Ins(1,4,5)P_3 receptor (cross section).

in the smooth muscle of arteries, uterus, and oviducts, as well as in the contractile smooth muscle of the intestine and esophagus. In Purkinje cells electron microscopy showed that the receptor is mainly associated with the smooth ER, but it is also present in the rough ER and outer nuclear membrane.

InsP_3R was purified in 1988 as two immunologically identical polypeptides: an Ins(1,4,5)P_3-binding protein[159] and the Purkinje cell enriched protein P_{400}.[160] Since then, cloning of the receptor cDNA from mouse,[161, 162] rat,[163, 164] *Drosophila*,[165] and human[164] has shown that the general structure of the receptor, first deduced from mouse cDNA, appears to be highly conserved. The receptor protein binds Ins(1,4,5)P_3 and activates Ca^{2+} channels, and reconstitution into lipid vesicles allowed the demonstration of Ins(1,4,5)P_3-gated Ca^{2+} transport.[166] The receptor is a homotetramer, as demonstrated by electron microscopy[167, 168] and cross-linking experiments.[168] Each subunit binds one molecule of Ins(1,4,5)P_3, as revealed by examination of deletion mutants,[169, 170] and InsP_3R apparently binds four molecules of Ins(1,4,5)P_3 in a noncooperative fashion;[159] however, contradictory finding have also been reported.[171]

There is no homology between the primary sequence of InsP_3R and Ca^{2+} channels on the plasma membrane,[161, 172]

but a significant partial homology does exist with the ryanodine receptor of skeletal and cardiac muscle sarcoplasmic reticulum.[161, 173, 174] InsP_3R has a transmembrane domain close to the C-terminus with long N-terminal and short C-terminal portions projecting into the cytoplasm. Examination of the hydropathy profile of the highly conserved amino acid sequence suggests that the transmembrane domain has six[165] or eight[169] membrane-spanning regions. The large N-terminal region incorporates some 650 amino acid residues, which are highly conserved between species[161, 169, 170] and thought to contain the critical sequence that forms the three-dimensional Ins(1,4,5)P_3 binding site,[169, 170] since deletion of sequences within this region abolished Ins(1,4,5)P_3 binding activity. This region is enriched in positively charged arginine and lysine residues, which may have a role in binding the phosphate groups of Ins(1,4,5)P_3. A peptide labeled by an Ins(1,4,5)P_3 photoaffinity ligand has been isolated whose sequence matches that of the N-terminal 20% of InsP_3R.[175] Binding of Ins(1,4,5)P_3 must stimulate a large conformational change in the receptor, which spans almost 1400 amino acid residues from the extreme N-terminal Ins(1,4,5)P_3 binding site to the extreme C-terminal putative Ca^{2+} channel site.[153] The coupling region between the Ins(1,4,5)P_3 binding site and the Ca^{2+} channel contains sites that modulate the effect of Ins(1,4,5)P_3 on channel opening. Two serine residues present in this region can be phosphorylated by cAMP-dependent protein kinase,[153, 161, 176] which results in uncoupling Ins(1,4,5)P_3 binding from the opening of the Ca^{2+} channel in the cerebellar receptor. The receptor also binds equimolar amounts of ATP,[168] and ATP at low concentrations has a potentiating effect upon Ins(1,4,5)P_3-stimulated Ca^{2+} release. Ca^{2+} itself can also modulate channel opening, but by an unknown mechanism.[177]

InsP_3R is known to exhibit significant heterogeneity as a result of alternative mRNA splicing, giving receptors that differ in the coupling region and perhaps in the ligand binding domain. The original cerebellar receptor is now termed Type 1. New types of receptors encoded by separate genes were also reported.[164, 178] While Type 2 InsP_3R shares a significant homology with the Type 1 receptor, it has a higher affinity for Ins(1,4,5)P_3 and is 48 amino acids shorter.[164] A Type 3 InsP_3R was characterized from rats[179] and recently from humans[180] which has 63 and 64% identity with the Type 1 and 2 receptors, respectively. It is expressed in kidney, in the gastrointestinal tract, and in brain and binds Ins(1,3,4,5)P_4 and InsP_6 as well as Ins(1,4,5)P_3. A partial sequence for the C-terminal domain of a Type 4 receptor was reported.[156, 164] It is possible that the InsP_3Rs identified so far may only be the first examples of a larger family of receptors. If such receptors differ in their ligand binding affinities and specificity, they may offer an exciting prospect for the selective targeting of drugs.

6. Synthesis and Activity of Inositol Analogues

Inositol is taken up by many cells[181–183] and is incorporated into PtdIns by the enzyme PtdIns synthetase. The incorporation of synthetic analogues into phosphatidylinositol lipids offers an attractive route for pharmacological intervention in the signaling pathway. Since a large number of growth stimuli are now known to stimulate inositol lipid hydrolysis,[184] the presentation of fraudulent phospholipid species to the cell, especially those which cannot be further phosphorylated, could inhibit phospholipase C or reduce the availablity of PtdIns(4,5)P_2, thus affecting cell proliferation inter alia. A particular advantage of this route is that problems intrinsic to the introduction of highly charged phosphate-containing compounds into the cell are avoided. Fluorinated inositol analogues have proved to be particularly attractive in this respect.

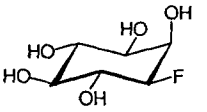

1

Fig. 8. 1-Deoxy-1-fluoro-*myo*-inositol (**1**).

Kozikowski et al. prepared 1D-1-deoxy-1-fluoro-*myo*-inositol (**1**) (Fig. 8) from 1D-3-*O*-methyl-*chiro*-inositol in five steps, including fluorination with diethylaminosulfur trifluoride (DAST), via the 1,2:5,6-di-*O*-isopropylidene derivative. Direct regioselective fluorination of 1D-3-*O*-methyl-*chiro*-inositol with DAST followed by demethylation gave 1D-1,5-dideoxy-1,5-difluoro-*neo*-inositol.[185] The same group had earlier reported a ten-step synthesis of both enantiomers of 1-deoxy-1-fluoro-*myo*-inositol[186] by DAST fluorination at the 2-position of a suitably protected *myo*-inositol derivative and the optical resolution of the resulting fluoro-*scyllo*-inositol intermediate. Recovery of the *myo*-inositol configuration by Swern oxidation of the 1-hydroxyl group followed by stereospecific reduction of the keto function with L-selectride, gave, after deprotection of the respective enantiomeric intermediates, 1D- and 1L-1-deoxy-1-fluoro-*myo*-inositol.

The synthesis of 1D- and 1L-1-deoxy-1-fluoro-*myo*-inositol was also reported by Offer et al.[187, 188] Here, the problems of recovering the *myo*-inositol configuration and optical resolution were efficiently addressed in a single step by displacing a tosylate group of a fluorinated *scyllo*-inositol intermediate with (*S*)-(−)-cesium camphanate. The resulting diastereoisomers were separated and deprotected to produce the D- and L-1-fluoro analogues of *myo*-inositol. The respective 2-^{3}H-labeled analogues were prepared by an exchange of the tritium radiolabel from [2-^{3}H]-*myo*-inositol catalyzed by inositol dehydrogenase.[189]

1-Deoxy-1-fluoro-*scyllo*-inositol (**2**) (Fig. 9), the first fluorinated analogue of inositol,[190] was obtained from 1-*O*-benzoyl-3,4,5,6-tetra-*O*-benzyl-*myo*-inositol by treatment with DAST at elevated temperature and deblocking of the protected fluorinated *scyllo*-inositol intermediate. The preparation of **2** was subsequently described by another group.[191] Lowe and McPhee[192] reported the synthesis of **2** and 2-deoxy-2-fluoro-*myo*-inositol (**3**) together with their 2-^{3}H-labeled derivatives **4** and **5**. Fluorination of 1,3,4,5,6-penta-*O*-benzyl-*myo*-inositol with DAST proceeded with inversion at the 2-position to give the fluorinated *scyllo*-inositol, which was debenzylated with dry HBr to af-

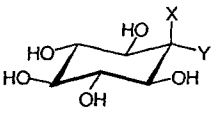

2: X = H, Y = F:
3: X = F, Y = H:
4: X = ^{3}H, Y = F:
5: X = F, Y = ^{3}H:
6: X = Y = F:
7: X = F, Y = CH_2OH
8: X = OH, Y = CH_2F
9: X = SH, Y = H:

Fig. 9. C-2-modified inositol analogues.

ford **2**. In order to prepare **3**, the configuration at C-2 was inverted by triflation followed by displacement of the triflate moiety with sodium trifluoroacetate. Ester hydrolysis, reaction of the product with DAST, and deprotection produced **3**. Oxidation of 1,3,4,5,6-penta-*O*-benzyl-*myo*-inositol with Jones' reagent and reduction of the resulting inosose with $[^3H]NaBH_4$ gave predominantly the tritiated *scyllo*-inositol and some 1,3,4,5,6-penta-*O*-benzyl-2-[^{3}H]-*myo*-inositol. Treatment with DAST and deprotection as before gave **4** and **5**.[192] A synthesis of **3** and **5** reported by another group[189] followed a route similar to the one outlined above.

2-Deoxy-2,2-difluoro-*myo*-inositol (**6**) was prepared by oxidizing 1-*O*-allyl-3,6-di-*O*-benzyl-4,5-*O*-isopropylidene-*myo*-inositol to the corresponding 2-inosose, which was fluorinated with DAST to give the *gem*-difluoro derivative. Deprotection was carried out first by removal of the allyl and isopropylidene groups and subsequent hydrogenolysis.[191] Yang et al. used 1-*O*-benzoyl-3,4,5,6-tetra-*O*-benzyl-2-oxiranyl-*myo*-inositol to prepare 2-deoxy-2_{ax}-fluoro-2_{eq}-hydroxymethyl-*myo*-inositol (**7**)[193] and 2-deoxy-2-*C*-fluoromethyl-*myo*-inositol (**8**).[194]

The synthesis of the 2-mercapto [sulfanyl (IUPAC)] analogue **9** of *myo*-inositol was described:[195] Selective iodination of the 2-position of racemic 1,4,5,6-tetra-*O*-benzyl-*myo*-inositol using triphenylphosphine/imidazole/iodine proceeded with inversion of configuration. The free 3-hydroxyl group was silylated and the equatorial iodine displaced with sodium benzylsulfide, thus reestablishing the *myo*-inositol configuration. Fluoride-induced desilylation, debenzylation, acetylation of the crude product, purification, and methanolysis gave the thio analogue **9**.

Kozikowski et al. reported the synthesis of a number of enantiomerically pure inositol analogues modified at the 3-position (**18**–**25**, Fig. 10).[196–200] A two-step synthesis of 1D-3-deoxy-3-fluoro-*myo*-inositol (**18**) was possible by direct fluorination of L-quebrachitol (1L-2-*O*-methyl-*chiro*-inositol, **10**) with DAST,

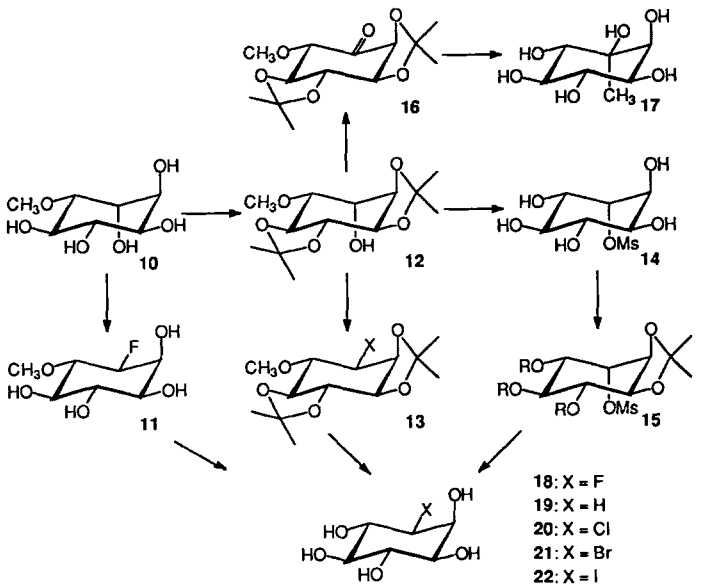

Fig. 10. C-3-modified D-*myo*-inositols from L-quebrachitol (**10**) (Kozikowski et al.).

resulting in selective reaction at the 1-position with inversion to give the *myo*-inositol configuration in **11**. Demethylation gave **18**.[196] D-3-Deoxy-*myo*-inositol (**19**) was prepared from L-3,4:5,6-di-*O*-isopropylidene-2-*O*-methyl-*chiro*-inositol (**12**) by treatment with 1,1′-thiocarbonyldiimidazole, tributyltin hydride, and finally boron tribromide.[198] Intermediate **12** was also employed in the preparation of the D-3-halogeno analogues **20**–**22**. The free hydroxyl group of this intermediate was displaced with inversion of configuration by activation with triphenylphosphine and employing CCl_4, Br_2, or I_2 as electrophilic sources of halogen. Deprotection of **13** (X = Cl, Br, or I) with boron tribromide furnished the corresponding D-3-halogenoinositols.[197] Compounds **23**–**25** were prepared by employing mesylate **15**, obtained from **12** via **14**.[198] Introduction of the azido group with inversion of configuration was achieved by displacing the mesylate in **15** (R = ethoxyethyl) with sodium azide/hexamethylphosphoramide (HMPA). Acid hydrolysis furnished D-3-azido-3-deoxy-*myo*-inositol (**23**), which could be converted into D-3-amino-3-deoxy-*myo*-inositol hydrochloride (**24**) by catalytic reduction in dilute HCl. The 3-mercaptoinositol **25** was obtained by reaction of **15** (R = Ac) with $(CH_3)_2NC(S)SNa$/HMPA, followed by reduction with $LiAlH_4$, and removal of the protecting groups. Oxidation of the hydroxyl group in **12** and treatment of the resulting ketone **16** with MeMgBr resulted in an axial attack to give the protected 3-*C*-methyl derivative, which was deblocked as described previously to yield **17**.[197]

The growth inhibitory properties of these inositol analogues on wild-type NIH 3T3 cells and v-*sis*-transformed cells were examined. v-*sis*-Transformed cells exhibit an increased PtdIns 3′-kinase activity and can therefore be expected to be more sensitive towards inhibitors of the PtdIns 3′-kinase signaling pathway than the nontransformed cells. Initial experiments[185] showed that D-3-deoxy-3-fluoro-*myo*-inositol (**18**) is a potent and selective inhibitor of cell growth, although the potency was decreased by about an order of magnitude in the presence of *myo*-inositol in the growth medium. The fluoro analogue was also found to act as a potent competitive inhibitor of [^{3}H]-*myo*-inositol uptake, suggesting that the compound is incorporated into inositol phospholipids. In further studies[197,198] on a number of C-3-modified D-*myo*-inositol analogues, D-3-azido-*myo*-inositol (**23**) was found to be highly potent (IC_{50} = 0.04 mM) and selective for v-*sis*-transformed cells (more than 1200-fold over the wild-type) in inositol-free medium. Addition of *myo*-inositol, however, caused a considerable decrease in the inhibitory properties of this compound, whereas the inhibition of growth by D-3-amino-3-deoxy-*myo*-inositol (**24**) was only moderately affected. Also investigated were D-3-deoxy-3-methylene-, -3-(hydroxymethyl)-, -3-(iodomethyl)-, and -3-phosphonomethyl-*myo*-inositol as well as the dimethyl ester of the latter compound; none of these analogues displayed any significant inhibitory activity.[199]

Both D- and L-4-deoxy-4-fluoro-*myo*-inositol were obtained from DL-1,3,4,5-tetra-*O*-benzyl-*myo*-inositol by selective tosylation of the 6-OH group, fluorination at C-2 with DAST (giving the *scyllo* derivative), and treatment with (*S*)-(−)-cesium camphanate (reestablishing the *myo*-inositol configuration by inversion at C-6 which becomes the new 2-position). The resulting mixture of two diastereoisomers could be separated by HPLC or

partial crystallization. Deprotection afforded D- and L-4-deoxy-4-fluoro-*myo*-inositol.[189] Whereas a ^{3}H-radiolabel could be introduced into the 2-position of the L isomer by employing inositol dehydrogenase and [^{3}H]-*myo*-inositol, the D isomer was not a substrate for this enzyme. The radiolabeled D analogue was prepared by oxidizing D-1,3,5,6-tetra-*O*-benzyl-4-deoxy-4-fluoro-*myo*-inositol, reducing the resulting 2-inosose with [^{3}H]$NaBH_4$, and removing the protecting groups. Syntheses of racemic 4-deoxy-, 4-deoxy-4-fluoro-, and 4-deoxy-4-methyl-*myo*-inositol employing a precursor obtained from benzene by microbial oxidation were also reported.[201]

6-*O*-Benzyl-1,2:3,4-di-*O*-cyclohexylidene-*myo*-inositol was employed in the preparation of 5-deoxy-5-fluoro-*myo*-inositol (**26**) (Fig. 11) by two different groups. DAST fluorination gave

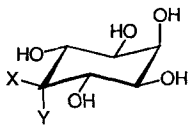

26: X = F, Y = H:
27: X = Y = F:
28: X = Cl, Y = H
29: X = Br, Y = H
30: X = H, Y = Cl
31: X = H, Y = Br
32: X = H, Y = I
33: X = Y = H
34: X = OCH_3, Y = H:

Fig. 11. C-5-modified inositol analogues.

the product resulting from inversion of configuration and as well as minor amounts of that resulting from retention; the latter was deprotected to **26**.[202] This low-yield method was subsequently improved upon by inversion of configuration at the 5-position prior to DAST fluorination.[187, 188, 203] Thus, tosylation[187, 188] or triflation[203] of the 5-hydroxyl group followed by nucleophilic displacement with cesium propionate afforded the *neo*-inositol derivative. After saponification, fluorination with DAST reestablished the *myo*-inositol configuration and deprotection furnished **26**.

Deuteriation studies revealed that the equatorial H-2 proton of **26** is the one most rapidly exchanged.[203] Incubation of **26** with inositol dehydrogenase and [2-^{3}H]-*myo*-inositol led to an exchange of the radiolabel, which was again incorporated at the 2-position of the fluorinated analogue.[189] The 5-deoxy-5,5-difluoro analogue **27**[203] was prepared from the oxo derivative of 1,4,6-tri-*O*-benzyl-2,3-*O*-cyclohexylidene-*neo*-inositol, an intermediate in the synthesis of **26**.

Apart from the synthesis of **26** and **27** and *myo*-inositol analogues deoxygenated at positions 1, 4, and 5, Baker et al. also reported the preparation of further 5-deoxyhalogeno-*myo*- (**28**, **29**) and epimeric *neo*-inositols (**30**–**32**),[202] as well as racemic 4-deoxy-4-fluoro-*myo*-inositol. DAST fluorinations generally proceed with inversion of configuration,[204] but surprisingly, fluorination of the intermediate 3-*O*-benzyl-1,2:5,6-di-*O*-cyclohexylidene-*myo*-inositol gave predominantly the product of retention of configuration. This was rationalized as being due to steric hindrance to the backside attack of fluoride ion on the intermediate adduct with DAST.[202]

These inositol analogues were then evaluated as substrates and inhibitors of PtdIns synthetase,[205] as were a number of C-3-modified D-*myo*-inositols.[206] The enzyme showed very stringent requirements for the cyclitol substrate. All compounds examined were less effective substrates than *myo*-inositol. 5-Deoxy-5-fluoro-*myo*-inositol (**26**), the best analogue found in these studies, was incorporated into the cellular phospholipid at a rate equal to 26% of that of *myo*-inositol. Analogue **26** was further phosphorylated to give the corresponding 5-fluoro-PtdIns(4)*P* derivative but, not surprisingly, no lipid bisphosphate was detected. Other 5-deoxy-5-halogeno derivatives were very poor or inactive substrates. The 5-deoxy analogue **33**, however, was found to be well recognized. In the series of C-3-modified derivatives tested, D-3-amino- (**24**), D-3-fluoro- (**18**), and D-3-deoxy-*myo*-inositol (**19**) as well as the 3-oxo analogue were substrates for PtdIns synthetase,[206] albeit $\geq 90\%$ less well tolerated than the natural substrate. The general conclusion derived from these observations appears to be that substrate activity diminishes with increased steric bulk of the substituent. In the inhibition assay, the rank order of analogues was similar to their effectiveness as substrates, with the exception of 5-deoxy-5,5-difluoro-*myo*-inositol (**27**) which was not a substrate for PtdIns synthase but an effective inhibitor of the enzyme.

In another study[207] the inhibition of incorporation of [^{3}H]Ins into PtdIns by inositol analogues modified at the 1-, 2-, 3-, 4-, or 5-position was investigated. 1-Deoxy-1-fluoro-*scyllo*-inositol (**2**) and 5-*O*-methyl-*myo*-inositol (**34**) were found to be the most effective competitive inhibitors of both PtdIns synthase and a nucleotide-independent PtdIns/Ins exchange enzyme, whilst a number of other analogues also displayed significant inhibitory effects mainly on the exchange activity. Both [1-^{3}H]-1-deoxy-1-fluoro-*scyllo*-inositol (**4**) and [2-^{3}H]-2-deoxy-2-fluoro-*myo*-inositol (**5**) are very poor substrates for the two enzymes. However, once **5** was incorporated into the phospholipid, the corresponding analogues of PtdIns(4)*P* and PtdIns(4,5)P_2 could be detected.

Offer et al. investigated the uptake of ^{3}H-labeled monodeoxyfluoro-*myo*-inositols[189] into thymocytes and their incorporation into the phospholipid.[208] Only D-3-F-Ins **18**, 5-F-Ins **26** and to a lesser extent D-6-F-Ins showed activity as substrates for PtdIns synthase, and only **18** was both taken up actively into the cells and incorporated into the phospholipid. However, it was concluded that because of the overall selectivity for *myo*-inositol both by the uptake mechanism and by PtdIns synthase, monodeoxyfluoro analogues, unless made cell permeable, were unlikely to be of any use as inhibitors of PtdIns(4,5)P_2 formation or breakdown in intact cells.

Deoxy inositols were the subject of a report demonstrating chemoenzymatic methods for the synthesis of selectively protected derivatives of 3-deoxy-*epi*-inositol and 1-deoxy-*scyllo*-inositol, taking advantage of the preference of *Candida cylindracea* lipase for (*R*)-configurated esters.[209]

7. Synthesis of Specific *myo*-Inositol Phosphates

Recognition of Ins(1,4,5)P_3 as a second messenger has stimulated renewed interest in the chemistry of inositol phosphates. Many inositol phosphates had already been synthesized before this recent revival, and this earlier work has been discussed.[57, 58] In spite of this, some of the older procedures used were not entirely satisfactory. This was especially true for the phosphorylation of polyols, where the presence of vicinal diols

makes simultaneous polyphosphorylation difficult and encourages the formation of cyclic five-membered phosphates (for exceptions see ref.[210]). Nevertheless, Ins(4,5)P_2 was originally synthesized in 1961.[211] More recent work is covered in a new book.[56]

7.1. General Synthetic Considerations

Five distinct problems are intrinsic to inositol polyphosphate synthesis (Fig. 12): 1. Suitably protected derivatives must be prepared to facilitate later incorporation of phosphate groups at selected positions. 2. Since the D enantiomer of Ins(1,4,5)P_3 is

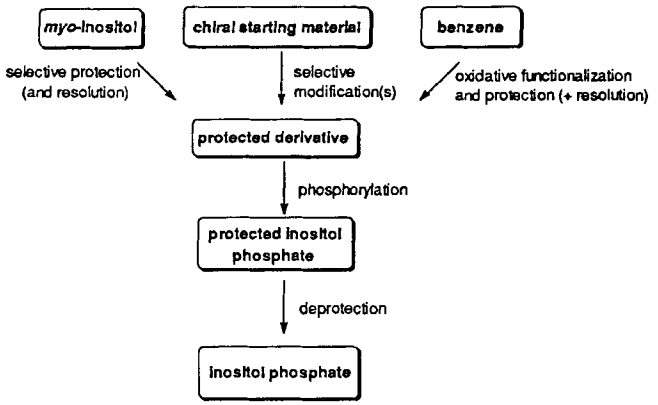

Fig. 12. Steps in the synthesis of inositol phosphates.

the natural messenger, such derivatives must be optically resolved. 3. An efficient phosphorylation strategy is required, which overcomes the difficulties associated with cyclic phosphate formation. 4. The phosphorylated intermediate must be deprotected under conditions that preclude any migration of phosphate groups onto neighboring hydroxyls. 5. The anionic polyphosphate must be efficiently purified and separated from minor potentially regioisomeric impurities, which might possess activity.

7.1.1. *Protecting Group Chemistry*

Protection strategies for the synthesis of inositol polyphosphates already have a long historical development,[57, 58] but several new approaches have been described.[212–218] The subject has been discussed in two review articles.[53, 54] The most popular temporary and permanent hydroxyl protecting groups are acetyl, benzoyl, benzyl, *p*-methoxybenzyl, allyl, isopropylidene, cyclohexylidene, and orthoformate. This will become apparent from examination of individual syntheses.

7.1.2. *Synthesis of Optically Active Compounds*

If benzene or the *meso* compound *myo*-inositol are used as starting material in the synthesis of inositol phosphates, optical resolution is required to separate D and L isomers of the inositol phosphate precursors. Most optical resolutions in the synthesis of inositol phosphates rely on the conversion of racemic inositol derivatives into a pair of diastereoisomers, which is then separated by crystallization or chromatography. Until recently, the procedures of Shvets,[219, 220] employing orthoesters of D-mannose **35** (Fig. 13), were the only methods available. Recent work, however, has highlighted the advantages of several other resolving agents such as (*S*)-(+)-*O*-acetylmandelic acid (**36**), (*R*)-(+)-camphor dimethyl acetal (**37**) and its (*S*) isomer, L-menthyl chloroformate (**38**), L-menthyloxyacetylchloride (**39**), and (*R*)-(+)-1-phenylethyl isocyanate (**40**). Optical resolution by formation of camphanates seems to be the most generally useful method available at the present time, and both (*S*)-(−)-camphanic acid chloride (**41**) and its (*R*)-(+) isomer have been employed to obtain optically active inositol derivatives. Chiral HPLC columns were used to resolve intermediates in syntheses of Ins(1,3,4)P_3[221] and Ins(1,3,4,5)P_4.[222]

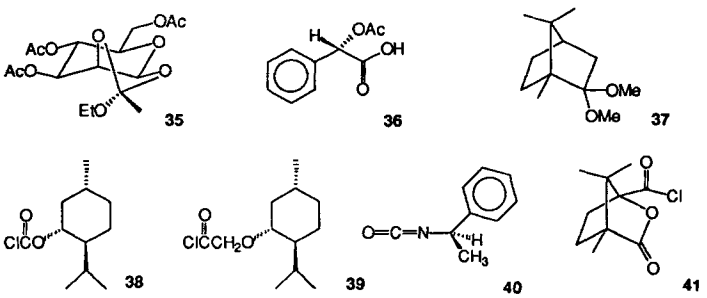

Fig. 13. Agents employed in inositol phosphate synthesis for optical resolution.

In a number of studies, enzymes such as esterases, lipases, and proteases were examined for their ability to hydrolyze enantio- and regioselectively racemic or *meso* carboxylic esters of *myo*-inositol,[223–226] 3-deoxy-*epi*-inositol and 1-deoxy-*scyllo*-inositol.[209] A new method is enzyme-catalyzed selective esterification, which was applied to resolve racemic 1,2:5,6- and 1,2:3,4-di-*O*-cyclohexylidene-*myo*-inositol,[227, 228] and to obtain enantiomerically pure D-1-*O*-butyryl-4,6-di-*O*-benzoyl-*myo*-inositol.[229]

The problem of optical resolution can be avoided altogether by employing chiral starting materials, for example naturally occurring compounds such as L-quebrachitol (**10**), D-3-*O*-methyl-*chiro*-inositol (**42**), (−)-quinic acid (**43**), D-glucurono-6,3-lactone (**44**), and galactinol (**45**) (Fig. 14). The Ferrier reac-

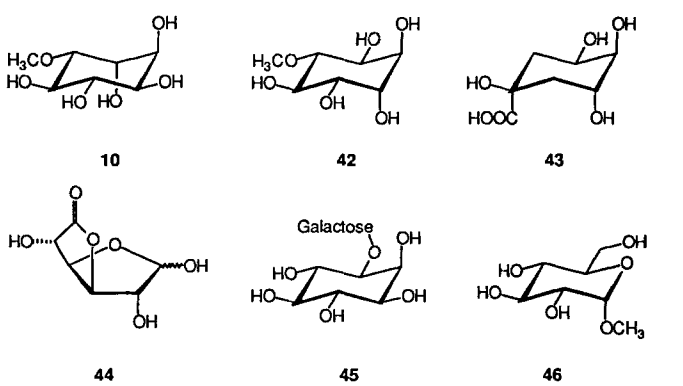

Fig. 14. Chiral starting materials for the synthesis of inositol phosphates.

tion[230] has been used to generate *myo*-inositol derivatives from D-galactose,[231] D-glucose,[232–234] and in a biomimetic approach from methyl α-D-glucopyranoside (**46**).[235, 236] A samarium diiodide promoted reductive carbocyclization of an intermediate derived from D-mannitol was employed to gain access to enantiomerically pure *myo*-inositol derivatives.[237]

7.1.3. Phosphorylating Agents

Phosphorylation of free hydroxyl groups in suitably protected inositol is performed primarily by two methods: a) employing a P^V reagent in which the phosphorus atom is already at the correct oxidation level, and b) phosphitylating the hydroxyl group with a P^{III} reagent and then oxidizing the resulting phosphite ester to give the protected phosphate ester (Fig. 15).

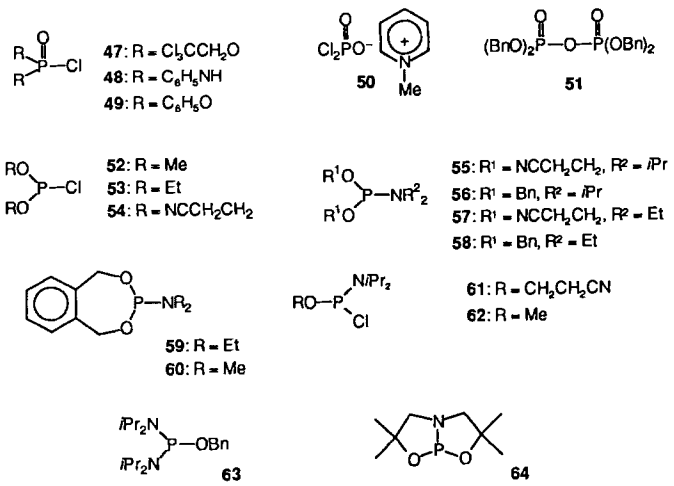

Fig. 15. Phosphorylating and phosphitylating reagents.

The advantages of P^V reagents for phosphorylation are the relative stability of reagent and products. However, problems have been encountered because of the low reactivity of the secondary hydroxyl groups of inositols; the phosphorylation of vicinal diols has proved to be especially difficult. The intermediate phosphate triesters formed upon phosphorylation of the first free hydroxyl group are prone to attack by the neighboring second hydroxyl group. The bulkiness of most P^V reagents may prevent a second reagent molecule from gaining access to the phosphorylation site after monosubstitution of the diol has taken place. Cyclization reactions are therefore able to compete successfully with substitution at the second hydroxyl group, affording five-membered cyclic phosphates rather than the desired bisphosphates.

Phosphorus(v) oxychloride was first used as a phosphorylating reagent in 1857[238] and more recently in a stepwise phosphorylation of the vicinal 4,5-diol in *myo*-inositol derivatives with two P^V reagents.[239] Phosphorylation with bis(2,2,2-trichloroethyl)phosphorochloridate (**47**) only gave a mixture of the 4- and 5-monophosphorylated inositols but not the bisphosphate presumably due to steric hindrance. When $POCl_3$ was used, however, this mixture could be converted into the mixed 4,5-bisphosphate triesters. Phosphorochloridate **47** was also applied in the preparation of Ins(1,4,5)P_3 and its 5-phosphorothioate analogue.[240–242] Dianilidophosphorochloridate (**48**) was used in the first reported synthesis of D-Ins(1,4,5)P_3;[243] however, this phosphorylation method and the removal of the protecting groups with isoamyl nitrite in pyridine/acetic acid/acetic anhydride was unsatisfactory. Diphenyl phosphorochloridate (**49**) was employed in many phosphate ester preparations, including an early synthesis of Ins(2)P[244] and the synthesis of L-Ins(1)P.[245]

Phosphorodichloridates can react with two different partners, thus forming a phosphate bridge between these moieties. As phosphodiester links are common features of many natural compounds (e.g. oligonucleotides and phospholipids), a number of phosphorodichloridates were developed for the synthesis of these substances. *N*-Methylpyridinium phosphorodichloridate (**50**) was employed in the synthesis of Ins(1:2-cyclic)P.[246]

Polyphosphates and mixed anhydrides are widely used although they react nonspecifically and often lead to the formation of cyclic phosphates or other side products. Phosphoric acid, potassium hydrogen phosphate, and pyrophosphoric acid were all employed in syntheses of carbohydrate phosphates; the latter was also used to phosphorylate *epi*- and *muco*-inositols.[247]

Tetrabenzyl pyrophosphate (TBPP, **51**)[248] is a commercially available crystalline solid formed by condensation of two equivalents of dibenzyl phosphate with dicyclohexylcarbodiimide (DCC). It is the only P^V reagent that has been employed successfully in inositol phosphate chemistry for the phosphorylation of vicinal diols.[249–251] For efficient phosphorylation with TBPP, it is necessary to convert the free hydroxyl groups into alkoxides. The strongly basic conditions can cause problems with some compounds and lead to decomposition.

P^{III} reagents are more reactive than most P^V reagents. Good results were obtained by phosphitylation with P^{III} reagents and subsequent oxidation in cases where P^V reagents failed to give the desired products, for example phosphorylation of vicinal diol precursors to Ins(1,4,5)P_3. The formation of undesired cyclic phosphodiesters is avoided. One further advantage of the P^{III} approach is that the phosphite triesters can be sulfoxidized by elemental sulfur in pyridine[252] or by phenacetyl disulfide,[253] thereby also making available phosphorothioates, which were shown to be useful nonhydrolyzable analogues of nucleotides[254] and inositol phosphates (see Section 8.4).

Although phosphorochloridites are unstable towards moisture, they have found widespread use in inositol phosphate synthesis. Dimethoxychlorophosphine (**52**) was employed in preparations of Ins(1,4,5)P_3, Ins(1,3,4,5)P_4, and Ins(1,4,5,6)P_4,[255] diethoxychlorophosphine (**53**) for Ins(1,2,4,5)P_4,[256] and di(2-cyanoethoxy)chlorophosphine (**54**) for Ins(1,3,4)P_3.[257]

The more stable phosphoramidites are used under catalytic activation by a weak acid (1*H*-tetrazole). Compounds **55**–**57** are examples of these reagents. The use of di(benzyloxy)-(diethylamino)phosphine (**58**) was considered to be less advantageous than **56**, since the latter can be easily purified by column chromatography.[258]

3-Diethylamino-2,4,3-benzodioxaphosphepane (**59**),[259] prepared by the reaction of hexaethylphosphorus triamide with 1,2-bis(hydroxymethyl)benzene, and the related dimethylamino

compound **60** are increasingly applied in preparations of inositol phosphates. 2-Cyanoethoxy(diisopropylamino)chlorophosphane (**61**) and the corresponding methoxy derivative **62** have also been extensively used, the former inter alia in syntheses of Ins(1,4,5)P_3 and Ins(4,5)P_2.[260-262] The phosphoramidites initially obtained are usually converted into phosphite triesters prior to oxidation. As bifunctional P^{III} reagents, **61** and **62** are also suitable for the preparation of phosphorothioate analogues of inositol phospholipids.[263-265] The same is true of **63**, which was employed by van Boom et al. in syntheses of a PtdIns(4,5)P_2 analogue[266] and an inositol-containing mycobacterial phospholipid.[267] Finally, the less conventional aminobicyclophosphane **64** was employed in the synthesis of inositol monophosphates.[268]

The efficiency of different methods for the oxidation of phosphite triesters was studied;[269] in inositol phosphate chemistry this transformation is usually effected with *tert*-butyl hydroperoxide (*t*BuOOH) or *m*-chloroperoxybenzoic acid (*m*-CPBA).

7.1.4. Deprotection and Purification

In order to avoid migration of protected phosphate esters to adjacent free hydroxyl groups it is essential to deblock the phosphate groups prior to the alcohols. When benzyl groups are used for protection of both hydroxyls and phosphates, deprotection in one step is possible, since the benzylphosphate esters are cleaved much more rapidly.[270] Purification after the protecting groups are removed with sodium/liquid ammonia usually involves anion-exchange chromatography. It may be possible, however, to obtain the final compound without further purification by catalytic hydrogenolysis.

7.2. Inositol Monophosphates

Four possible *myo*-inositol monophosphates exist: the symmetrical 2- and 5-phosphates and the two enantiomeric pairs inositol 4(6)-phosphate and 1(3)-phosphate. Many syntheses of racemic and optically active *myo*- and other inositol monophosphates have been published prior to and after the demonstration that the hydrolysis of brain phosphoinositides gives D-Ins(1)*P*.[271, 272] Such earlier synthetic work has been reviewed.[53, 57]

The D[273, 274] and L enantiomers[273] of Ins(1)*P* were prepared from 1L-quebrachitol (**10**) via 1L-3,4:5,6-di-*O*-cyclohexylidene-2-*O*-methyl-*chiro*-inositol. For the synthesis of D-Ins(1)*P*, this compound was oxidized to the inosose which was stereoselectively reduced to give D-1,2:5,6-di-*O*-cyclohexylidene-4-*O*-methyl-*myo*-inositol. In a six-step sequence, this intermediate was converted into the 1-silyl pentabenzoate. Desilylation, phosphorylation, and successive deblocking gave D-Ins(1)*P*. In addition, L-Ins(1)*P* [= D-Ins(3)*P*] was obtained from **12** via the 1-tosylate. An elegant route to D-Ins(1)*P*[275, 276] involved resolution of inositol by formation of the *myo*-inositol-D-camphor 2,3-acetal and selective phosphorylation of the 1-OH group with dibenzyl phosphorochloridate. L-Ins(1)*P* was accessible by using the L-camphor dimethyl acetal.[276] Optically active Ins(1)*P* was also synthesized from 1,2,4,5,6-penta-*O*-benzyl-*myo*-inositol [resolved as the (*R*)(−)-camphanate][270] and the corresponding pentaacetate (resolved as the acid oxalate),[277] which was also used in the synthesis of racemic Ins(1)*P*.[278] DL-Ins(1)*P* could be resolved on a chiral GC column after persilylation.[279]

Ins(2)*P* was first synthesized by taking advantage of the highly selective oxidation of *myo*-inositol to *scyllo*-inosose by *Acetobacter suboxydans*.[244] A more recent approach relied upon selective dibenzylation of the 4- and 6-OH groups of *myo*-inositol orthoformate and phosphorylation of the free 2-OH groups with TBPP.[280]

Synthesis of Ins(4)*P* was possible by selective benzoylation of the 3-OH group of 1,2:4,5-di-*O*-cyclohexylidene-*myo*-inositol, phosphorylation of the remaining free hydroxyl group, and deprotection.[211, 220] The corresponding 3-*O*-benzyl derivative was also used to produce racemic and, after resolution via its camphanate, optically active Ins(4)*P*.[270] A short synthesis of DL-Ins(4)*P* by chelation-controlled selective phosphorylation of the monoanion of *myo*-inositol orthoformate[281] with TBPP was reported.[280, 282] Reaction of 1,2-*O*-cyclohexylidene-*myo*-inositol with 1,3-dichloro-1,1,3,3-tetraisopropyldisiloxane gave selectively the 3,4-disiloxanylidene-inositol, which was benzoylated at the 6-position. Whereas reaction with TBPP resulted in phosphorylation at the 6-position due to benzoate migration and gave racemic Ins(4)*P* after deblocking, phosphitylation with PCl_3 and benzyl alcohol, followed by oxidation and deprotection furnished Ins(5)*P*.[283] The latter was first prepared from 2-amino-2-deoxy-*neo*-inositol,[211] which was obtained by hydrolysis of hygromycin A.

D-Ins(1,2-cyclic)*P* was synthesized from D-3,4,5,6-tetra-*O*-benzyl-*myo*-inositol by reaction with **50**.[246] Direct phosphorylation of inositol with bicycloaminophosphane **64** followed by oxidation of the resulting bicyclophosphorane, which has a five-coordinate P atom, and acid hydrolysis gave mixtures of Ins(1)*P*, Ins(2)*P*, and Ins(1,2-cyclic)*P* separable by HPLC.[268]

7.3. Inositol Bisphosphates

The synthesis of racemic inositol 1,4-, 1,6-, and 4,5-bisphosphates by phosphorylation of di-*O*-cyclohexylidene-inositols biscyclohexylidene acetals with phosphorochloridate was described as early as 1961.[211] Enantiomerically pure bisphosphates were prepared by employing the optically active diacetals obtained by resolution with orthoesters of D-mannose.[284]

Ins(1,3)P_2 was synthesized by regioselective phosphorylation of 2,4,6-tri-*O*-benzyl-*myo*-inositol using chlorophosphate **49**.[270, 280] The 1,3-bisphosphorylated product was crystallized from the mixture of 1,3- and 1,5-bisphosphorylated products. Deprotection with lithium in liquid ammonia gave Ins(1,3)P_2. Racemic Ins(1,4)P_2 was prepared by phosphitylation of 1,2:4,5-di-*O*-isopropylidene-*myo*-inositol with chlorophosphine **61**, conversion of the product into a bisphosphite ester, oxidation, and deprotection.[285] As an alternative to the resolution of 1,2:4,5-di-*O*-cyclohexylidene-*myo*-inositol via orthoacetates,[286] formation of chromatographically separable dicamphanates gives access to the enantiomers of Ins(1,4)P_2.[251] A short route to D-Ins(1,4)P_2 from *myo*-inositol D-camphor 2,3-acetal was reported.[276, 287] D-Ins(1,4)P_2 was also obtained semisynthetically by periodate treatment of deacylated phos-

phoinositides.[288] The two enantiomers of Ins(1,5)P_2[289] were synthesized from D- and L-1,2,4,6-tetra-*O*-benzyl-*myo*-inositol and **57**. Resolution of the tetrabenzyl compounds obtained by selective benzylation of 2,4,6-tri-*O*-benzyl-*myo*-inositol was possible via the mono-(−)-camphanates. DL-Ins(4,5)P_2 was prepared from 1,2,3,4-tetra-*O*-benzyl-*myo*-inositol by a P^{III} approach.[262, 290] Conduritol B derivatives obtained from benzene have also been used.[291]

7.4. Inositol Trisphosphates

7.4.1. *Inositol 1,4,5-Trisphosphate*

Not surprisingly, most attention has been focused upon the synthesis of Ins(1,4,5)P_3, which is still by far the most important inositol phosphate biologically. The first synthesis of D-Ins(1,4,5)P_3 was reported by Ozaki et al. in 1986 (Fig. 16).[243]

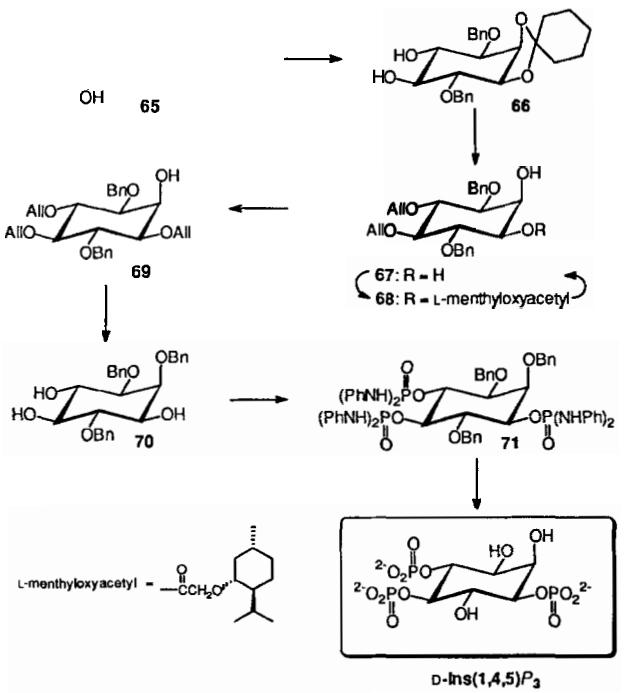

Fig. 16. The first synthesis of D-Ins(1,4,5)P_3 (Ozaki et al.)

DL-1,2:4,5-Di-*O*-cyclohexylidene-*myo*-inositol (**65**) was benzylated and the *trans*-4,5-acetal selectively removed to afford **66**. Allylation and acid hydrolysis of the remaining *cis*-acetal gave the 1,2-diol **67**, which was resolved by conversion into the diastereomeric esters **68**. Regioselective allylation of D-**67** gave **69**, which was benzylated and deallylated to yield **70**. Phosphorylation with **48** provided **71**, and deblocking of phosphate and hydroxyl groups with isoamyl nitrite and H_2/5% Pd–C, respectively, gave D-Ins(1,4,5)P_3. The use of TBPP **51** or phosphoramidite **59** allowed significant improvements to this synthesis.[292]

Racemic Ins(1,4,5)P_3 was subsequently synthesized[260, 261] by modified routes to triol **70**[213, 214] and by employing a P^{III} approach (Fig. 17). Thus, **72** was dibenzylated and the acetals

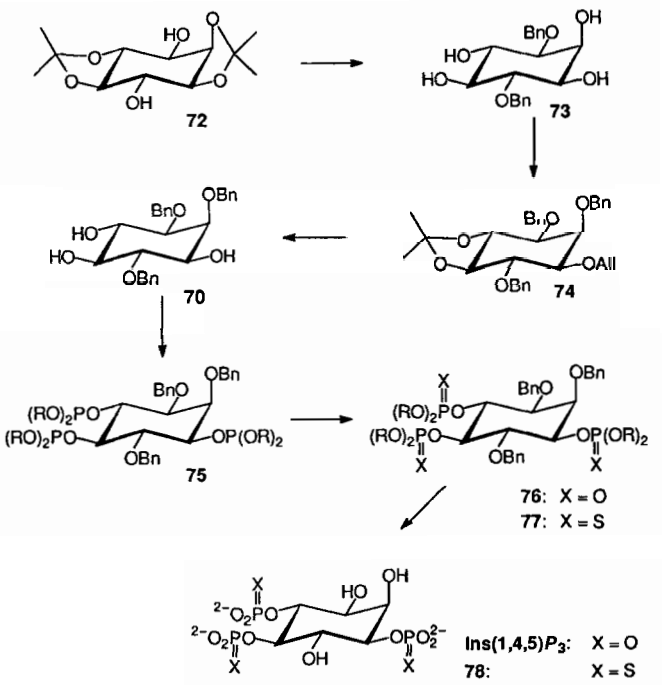

Fig. 17. Syntheses of Ins(1,4,5)P_3 and Ins(1,4,5)PS_3 by a P^{III} approach (Cooke et al.) R = CH_2CH_2CN.

removed to give **73**. Conversion to the fully protected derivative **74** required tin-mediated allylation of the 1-OH group, formation of the 4,5-acetal, and benzylation of the 2-OH group. Isomerization of the allyl group in **74** and hydrolysis of acid-labile protecting groups furnished triol **70**, which was phosphitylated with **61**, converted into **75**, and oxidized to **76**. All protecting groups were removed in one step by reaction with sodium in liquid ammonia to give DL-Ins(1,4,5)P_3. When resolved D-[214] and L-1,2,4-tri-*O*-benzyl-*myo*-inositol were employed, L-Ins(1,4,5)P_3[261] and D-Ins(1,4,5)P_3[293] were obtained, respectively.

D- and L-Ins(1,4,5)P_3 were also prepared from **79** (Fig. 18) by phosphorylation with **48** to give **80**, removal of the ketal, and resolution of the resulting intermediate via **81**. The 1-hydroxyl

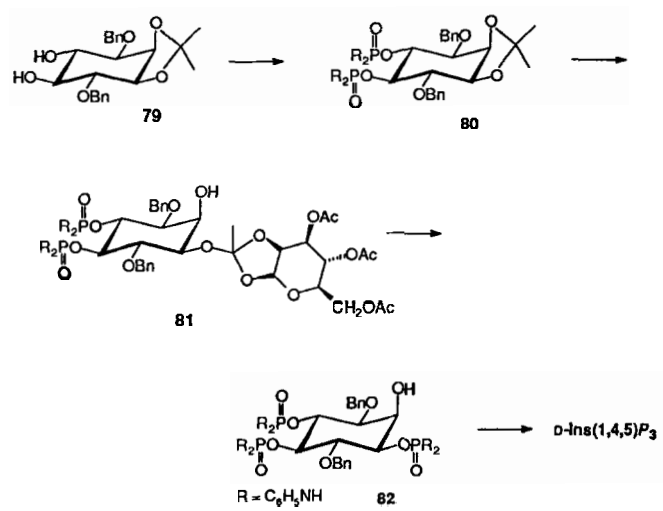

Fig. 18. Synthesis of D-Ins(1,4,5)P_3 utilizing mannose-orthoester resolution (Shvets et al.)

groups of the enantiomeric 1,2-diols obtained were then selectively phosphorylated with **48** to give **82**. Successive removal of *N*-phenyl- and benzyl protecting groups yielded the respective enantiomers of Ins(1,4,5)P_3.[294] Other phosphorylating methods are now preferred.[295]

Cyclopentylidene acetal **84** (from **83**, Fig. 19) was employed in a different approach in which silylation of the 1- and 4-hydroxyl groups afforded **85** and reaction with 2,7-dibromo-9-phenyl-9-xanthenyl chloride gave triol **86** after desilylation.

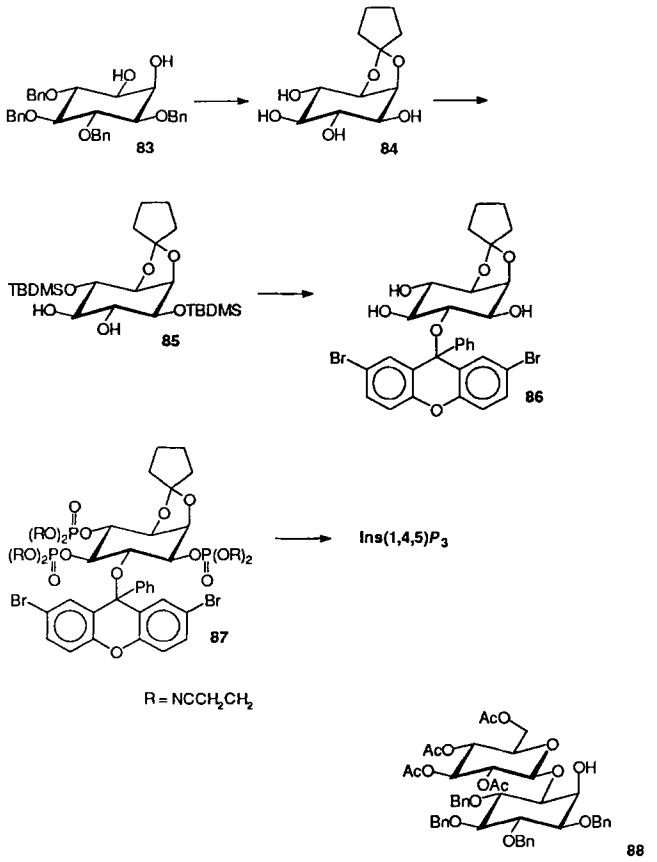

Fig. 19. Synthesis of D-Ins(1,4,5)P_3 employing the xanthenyl protecting group (Reese and Ward).

Phosphitylation with phosphine **57**, oxidation, and deblocking gave DL-Ins(1,4,5)P_3.[296] This route was also used to prepare D-Ins(1,4,5)P_3[296] by resolving diol **83** as its glucopyranosyl derivative **88**.[286]

Diastereoisomeric camphanate derivatives of 2,3:4,5-di-*O*-cyclohexylidene-6-*O*-benzyl-*myo*-inositol, synthesized by selective benzylation of the corresponding racemic 1,6-diol,[216] were used to prepare D- and L-6-*O*-benzyl-2,3-*O*-cyclohexylidene-*myo*-inositol. Phosphorylation of the tripotassium salts of these intermediates using TBPP **51**[249, 270, 280] followed by deprotection gave the enantiomers of Ins(1,4,5)P_3.[251, 297]

A short synthesis of racemic Ins(1,4,5)P_3 from 3,6-di-*O*-benzoyl-*myo*-inositol was reported.[255] Partial phosphitylation with chlorophosphite **52**, acetylation of the 2-OH group, and oxidation gave predominantly the 1,4,5-tris(dimethyl phosphate). Demethylation and saponification afforded Ins(1,4,5)P_3.

Phosphine **56** was proposed for the synthesis of inositol phosphates[258] and used to prepare DL-Ins(1,4,5)P_3 from triol **70**. The intermediate phosphite esters were oxidized with *m*-CPBA.

D-Ins(1,4,5)P_3 was synthesized from 3,6-di-*O*-allyl-1,2-*O*-cyclohexylidene-*myo*-inositol. The 4-OH group was benzylated and the 5-OH group allylated to give 3,5,6-tri-*O*-allyl-4-*O*-benzyl-1,2-*O*-cyclohexylidene-*myo*-inositol. Hydrolysis of the 1,2-ketal, optical resolution via monomenthyloxyacetyl derivatives, removal of the chiral auxiliary, dibenzylation, and deallylation produced enantiomerically pure **70**. Treatment with phosphine **58** and *t*BuOOH followed by hydrogenolysis gave D-Ins(1,4,5)P_3.[298]

Ins(1,4,5)P_3 was also synthesized by using a mixed P^{III}/P^{V} approach.[240, 242] Phosphorylation of 2,3,6-tri-*O*-benzyl-4,5-*O*-isopropylidene-*myo*-inositol[213] with **47**, removal of the ketal, and phosphorylation of the exposed vicinal diol gave a mixture of the 1,4- and 1,5-bisphosphates. The former crystallized from the reaction mixture and was phosphitylated with chlorophosphine **61**, and the resulting phosphoramidite was converted into the phosphate triester.[260] Deprotection afforded Ins(1,4,5)P_3.

3,6-Di-*O*-benzyl-4,5-bis(dibenzylphosphoryl)-*myo*-inositol was employed in an approach to D-Ins(1,4,5)P_3.[246] The enantiomers were resolved either as the 1-*O*-monomenthyloxyacetyl derivatives or with a chiral HPLC column. Regioselective silylation of the equatorial hydroxyl group, benzoylation of the 2-hydroxyl group, and desilylation exposed the 1-hydroxyl group which was phosphitylated with PCl_3/benzyl alcohol. Oxidation, hydrogenolysis, and alkaline treatment gave D-Ins(1,4,5)P_3.

D-Ins(1,4,5)P_3 was also synthesized by using enantiomerically pure 1,2:5,6-di-*O*-cyclohexylidene-*myo*-inositol,[224, 226] obtained either via the diastereomeric di(L-menthyloxyacetate) esters or by conversion into the diacetate or dibutyrate followed by regio- and enantiospecific enzymatic deacylation.

The use of 2-(*tert*-butyldimethylsilyloxy)phenylacetyl chloride for the selective protection of the 1-OH group of 2,3-*O*-cyclohexylidene-*myo*-inositol was the key step in another synthesis of enantiomerically pure Ins(1,4,5)P_3.[299] Treatment of the resulting mixture of diastereomeric esters with 1,3-dichloro-1,1,3,3-tetraisopropyldisiloxane gave the 4,5-*O*-silyl derivatives. Methoxymethylation of the free 6-OH group, chromatographic separation of the fully protected diastereoisomers, and removal of acyl and silyl groups of the individual isomers followed by phosphorylation with **56**/*m*-CPBA, and hydrogenolysis gave D- and L-Ins(1,4,5)P_3, respectively.

Regioselective 1-*O*-acylation of inositol was effected by perborylation, transmetalation with bis(acetylacetonato)-di-*n*-butyltin, and treatment of the dibutyltin intermediate with (−)-menthyl chloroformate.[300] Separation of the diastereoisomers by crystallization and treatment of the D isomer with 2,2-dimethoxypropane gave D-1-*O*-menthyloxycarbonyl-2,3:4,5-di-*O*-isopropylidene-*myo*-inositol. Benzylation of the 6-OH group, cleavage of the ester, and selective removal of the 4,5-acetal afforded, after phosphorylation and hydrogenolysis, D-Ins(1,4,5)P_3.

An elegant short route to D-Ins(1,4,5)P_3 was devised,[287] employing 2,3-*O*-(D-1,7,7-trimethyl[2.2.1]bicyclohept-2-ylidene)-*myo*-inositol (**89**) (Fig. 20),[301] prepared from inositol and D-camphor dimethyl acetal by way of a precipitation-driven

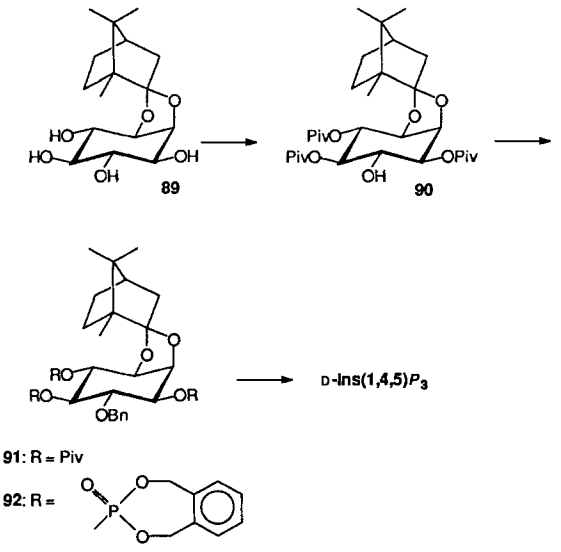

Fig. 20. Short route to D-Ins(1,4,5)P_3 via camphor acetal **90** (Salamonczyk and Pietrusiewicz).

equilibrium reaction.[275] Reaction of **89** with five equivalents of pivaloyl chloride afforded **90**, which was benzylated to provide **91**. After removal of the pivaloyl esters, phosphorylation with phosphepane **60**, and oxidation, **92** was obtained, which was deblocked to give D-Ins(1,4,5)P_3.

A conceptually different approach was developed by Ley et al.,[201, 302] who took advantage of the observation that microbiological oxidation of benzene by *Pseudomonas putida* affords *cis*-1,2-dihydroxycyclohexa-3,5-diene (**93**) (Fig. 21a).[303] The

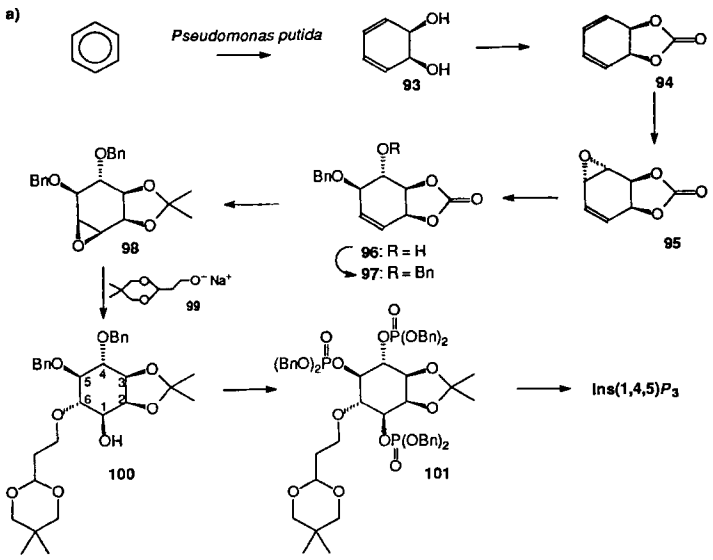

Fig. 21. Approach to D-Ins(1,4,5)P_3 employing microbial oxidation of benzene (Ley et al.): a) synthesis of Ins(1,4,5)P_3, b) reaction of intermediate **95** giving diastereomers separable by HPLC.

cyclic carbonate **94** derived from this diol was stereoselectively oxidized to the α-epoxide **95**. Regioselective ring opening of **95** with benzyl alcohol gave **96** and benzylation of the free hydroxyl group afforded **97**. Hydrolysis of the 1,2-carbonate, epoxidation of the double bond, and reprotection of the *cis*-1,2-diol as an isopropylidene acetal gave **98**. The β-epoxide was opened with **99** to give the protected inositol **100**. Debenzylation and phosphorylation with TBPP afforded **101**, which was deprotected to give racemic Ins(1,4,5)P_3, D- and L-Ins(1,4,5)P_3[201] were obtained by opening epoxide **95** with (*R*)-(+)-*sec*-phenethyl alcohol, giving diastereoisomers **102a** and **102b**, which were separable by HPLC (Fig. 21b).

Benzene was also used as starting material in a synthesis of racemic Ins(1,4,5)P_3 (Fig. 22).[291] *trans*-1,2-Dihydroxycyclo-

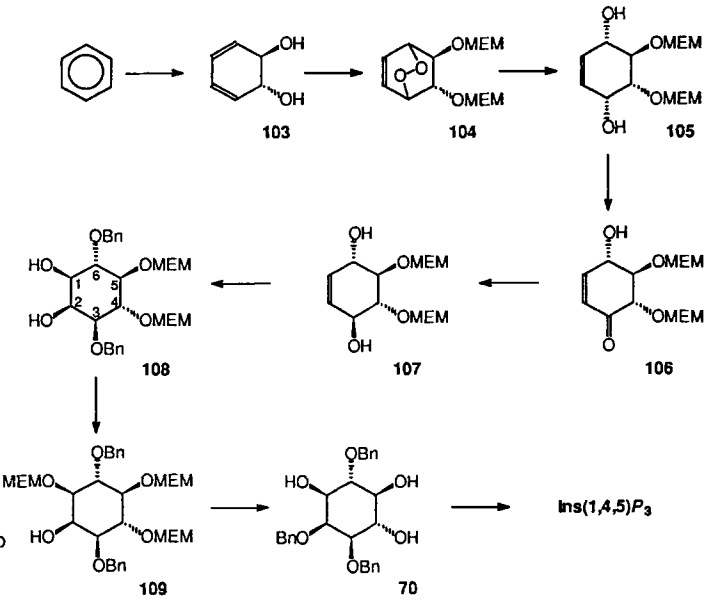

Fig. 22. Access to Ins(1,4,5)P_3 from benzene via conduritol B derivative **107** and with photooxidation of **103** as a key reaction (Carless and Busia).

hexa-3,5-diene (**103**) was prepared in 40% overall yield by Birch reduction, bromination, *trans*-hydroxylation, acetylation, and dehydrobromination. Protection of the hydroxyl groups as methoxyethoxymethyl (MEM) ethers and [4 + 2] addition of singlet oxygen furnished endoperoxide **104**, which was reduced stereospecifically to **105**.[304] Inversion at C-1 by an oxidation–reduction sequence gave the conduritol B derivative **107**. Benzylation of **107** and *cis*-hydroxylation of the double bond afforded **108**, which was regioselectively methoxyethoxymethylated to give **109**. Benzylation and removal of the MEM groups furnished **70**, and, after phosphorylation with TBPP and hydrogenolysis, Ins(1,4,5)P_3.

Falck and Yadagiri used (−)-quinic acid (**43**) to prepare D-Ins(1,4,5)P_3 (Fig. 23).[305] A four-step conversion gave ester **10**. Sequential protection of the 1-hydroxyl group as a β-(trimethylsilyl)ethoxymethyl (SEM) ether, reduction of the ester, and selenylation of the resulting primary alcohol furnished **111**. Stereoselective [2,3] sigmatropic rearrangement of the allylic selenoxide derived from **111** and benzylation generated **112** as a single stereoisomer. Transformation to silyl enol ether

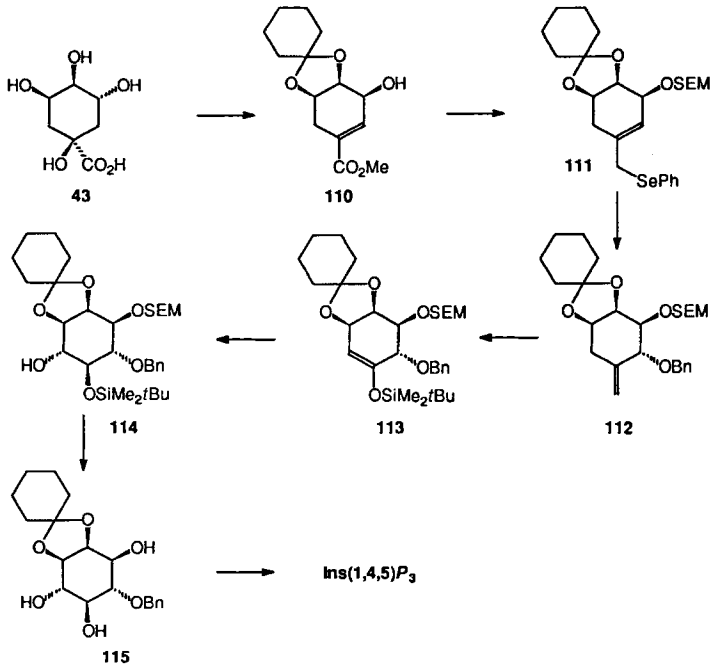

Fig. 23. Enantiospecific synthesis of D-Ins(1,4,5)P_3 from (−)-quinic acid (**43**) (Falck and Yadagiri).

113 by ozonolysis and treatment with TBDMS triflate proceeded with nearly complete regiospecificity. Hydroboration of the enol ether followed by oxidation furnished alcohol **114**, which on desilylation gave **115**. TBPP phosphorylation and hydrogenolysis afforded D-Ins(1,4,5)P_3.

Tegge and Ballou employed D- and L-*chiro*-inositol, derived by demethylation of 1D-3-*O*-methyl-*chiro*-inositol (**42**) and L-quebrachitol (**10**), respectively, to obtain both enantiomers of Ins(1,4,5)P_3 (Fig. 24).[306] Formation of the *cis,cis*-dicyclohexylidene acetal **116** (from D-*chiro*-inositol), benzylation, hydrolysis, and benzoylation gave mainly **117**. Inversion of the configuration at C-1 via the triflate afforded **118**, which was debenzylated to give **119** and then converted into D-Ins(1,4,5)P_3 by employing phosphine **56**. The L isomer was synthesized similarly from L-*chiro*-inositol.

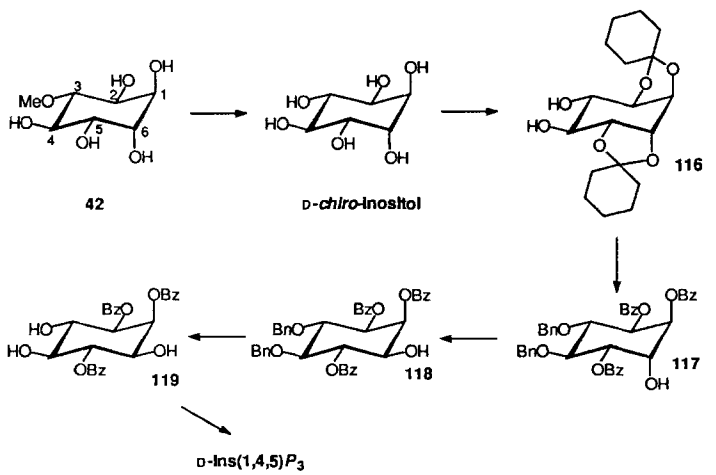

Fig. 24. Synthesis of D-Ins(1,4,5)P_3 from 1D-3-*O*-methyl-*chiro*-inositol (**42**) (Tegge and Ballou).

Other preparations of optically active[307, 308] Ins(1,4,5)P_3 were also published, including the synthesis of ^{3}H-labeled D- and L-Ins(1,4,5)P_3 by reduction of a protected inosose with [^{3}H]NaBH$_4$.[309]

7.4.2. Other Inositol Trisphosphates

D-Ins(1:2-cyclic 4,5)P_3 was synthesized by treatment of D-3,6-di-*O*-benzyl-4,5-bis(dibenzylphospho)-*myo*-inositol with **50**,[246] and (in low yield) from D-Ins(1,4,5)P_3 by using 1-ethyl-3-(3-dimethylaminopropyl)carbodiimide.[310] In the latter reaction the product was isolated by HPLC and was shown to be converted to Ins(1,4,5)P_3 by treatment with acid.

Racemic Ins(2,4,5)P_3 was prepared from 4,5-di-*O*-allyl-3,6-di-*O*-benzyl-*myo*-inositol, which was selectively benzylated at the 1-position, deallylated, and phosphorylated with TBPP.[250, 251] DL- Ins(2,4,5)P_3 was also obtained from benzene via conduritol B derivatives.[291] The synthesis of a fully protected, phosphorylated, and enantiomerically pure precursor of D-Ins(2,4,5)P_3 was reported, but the final deprotection step was not achieved.[311] The same authors did, however, prepare D-Ins(2,4,5)P_3 by phosphorylation of 3,6-di-*O*-benzyl-1,2-*O*-cyclohexylidene-*myo*-inositol with TBPP, removal of the acetals, and resolution via the diastereomeric 1-menthyloxyacetates. The equatorial hydroxyl group was regiospecifically silylated and the 2-hydroxyl group was phosphorylated by treatment with PCl_3/benzyl alcohol followed by *t*BuOOH oxidation.[246] Both D- and L-Ins(2,4,5)P_3 were prepared from L- and D-1,3,4-tri-*O*-benzoyl-*myo*-inositol, respectively,[312] which were generated in turn from D- and L-*chiro*-inositol.[306]

Ins(1,3,4)P_3 was synthesized from 2,4,5-tri-*O*-benzyl-*myo*-inositol, prepared from the corresponding 1,2:4,5-di-*O*-cyclohexylidene acetal. Phosphitylation with chlorophosphine **54**, followed by oxidation and deprotection gave racemic Ins(1,3,4)P_3,[257] which was also prepared from the same precursor by using TBPP **51**[250, 251] and phosphine **56**.[258] D-Ins(1,3,4)P_3 was prepared by resolution of 5,6-di-*O*-benzyl-3,4-di-*O*-*p*-methoxybenzyl-*myo*-inositol using a chiral HPLC column or via the diastereomeric 1-menthyloxyacetates.[221] Optically active 1,2:5,6-di-*O*-cyclohexylidene-*myo*-inositol, obtained either by an enzymatic process or by conversion into the di(L-menthylcarbonates),[224] was used in another synthesis of D-Ins(1,3,4)P_3 via D-2,5,6-tri-*O*-benzyl-*myo*-inositol.[225, 226] Finally, Boehm and Prestwich synthesized both enantiomers of Ins(1,3,4)P_3 as well as radiolabeled [1-^{3}H]-Ins(1,3,4)P_3.[313] 2,4,5-Tri-*O*-benzyl-inositol was converted to the isopropylidene ketal and resolved by means of diastereoisomeric (−)-camphanates. Saponification and oxidation of the alcohol gave the 1-inosose, which was reduced with [^{3}H]NaBH$_4$ to give the alcohol with the equatorial OH group as the major product. Phosphorylation using TBPP followed by deprotection furnished D-[1-^{3}H]-Ins(1,3,4)P_3. Despite the availability of Ins(1,3,4)P_3, there has been some doubt about its Ca^{2+}-mobilizing activity. An unambiguous synthesis of the enantiomers of this compound has now been published.[314]

A synthesis of Ins(1,4,6)P_3[315] relied upon diallylation of 1,2:4,5-di-*O*-isopropylidene-*myo*-inositol, removal of the *trans*-ketal, and tin-mediated *p*-methoxybenzylation of the 4,5-diol, which gave mainly the desired 6-alkylated derivative. Benzyla-

tion of the 5-OH group, acid hydrolysis of the *cis*-ketal, benzylation of the 1- and 2-OH groups, isomerization of the allyl ethers, and removal of the resulting prop-1-enyl as well as the *p*-methoxybenzyl groups gave the 1,4,6-triol, which was phosphorylated with **56**/*t*BuOOH. Ins(1,4,6)P_3 was also prepared by another research group both as a racemate and in optically active form.[316]

7.5. Inositol Tetrakisphosphates

7.5.1. Inositol 1,3,4,5-Tetrakisphosphate

Ins(1,3,4,5)P_4 was first synthesized in racemic form from the symmetrical inositol orthoformate **120** (Fig. 25). Chelation-controlled monoallylation of **120** gave **121**, which was benzylated to give **122**. The allyl and orthoformate groups were removed to furnish tetrol **123**, which was phosphorylated with TBPP to give **124** and Ins(1,3,4,5)P_4 after catalytic hydrogenation.[282] A similar route was adopted by another group[250] except that the benzyloxymethyl group was used instead of the allyl group for initial hydroxyl protection and a combined report has appeared.[280] 2,6-Di-*O*-benzyl-*myo*-inositol (**123**) was also used for two P^{III} approaches to Ins(1,3,4,5)P_4, employing either **60**[317] or **56**[258] as phosphitylating agents.

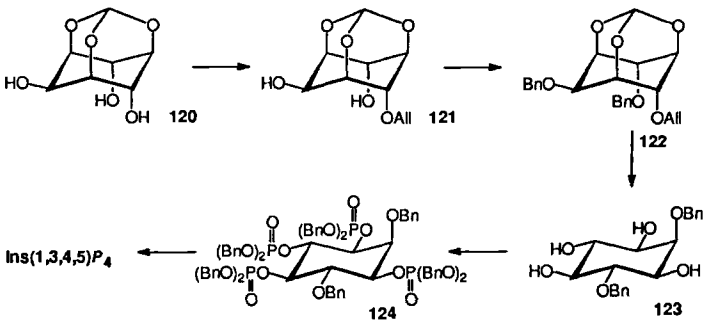

Fig. 25. Synthesis of Ins(1,3,4,5)P_4 by chelation-controlled monoallylation of *myo*-inositol orthoformate (Billington et al.).

Orthoformate ester protection of *myo*-inositol was also a key step in a synthesis by Vasella et al., which led to both enantiomers of Ins(1,3,4,5)P_4 (Fig. 26).[223] Benzylation of the silylated orthoester **125**[281] gave the racemic monobenzyl compound **126**, which was reacted with (*R*)-(+)-1-phenylethyl isocyanate to give diastereoisomeric carbamate derivatives, which could be separated as **127a** and **b** after removal of the silyl group. Subsequent benzylation of each diastereoisomer followed by removal of the carbamate and orthoformate groups gave the enantiomers of **123**, which were phosphorylated with **56**/*m*-CPBA and hydrogenolyzed to give D- and L-Ins(1,3,4,5)P_4. The enantiomeric dibenzylinositols **123** could also be derived by enantioselective monodeacylation of the symmetrical dibutyrate **128** formed by acylation and desilylation of **125**. Thus, treatment of **128** with porcine liver esterase (PLE) gave monobutyrate **129** in >95% enantiomeric excess. Dibenzylation, deacylation, and removal of the orthoester gave the precursor (L-**123**) for L-Ins(1,3,4,5)P_4. The D isomer was eventually obtained from **129** by a protection–deprotection sequence

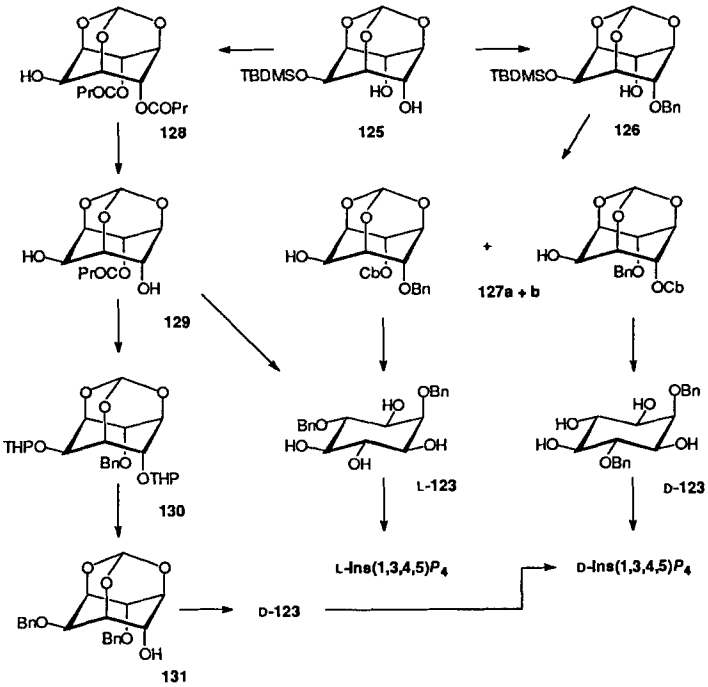

Fig. 26. Chemoenzymatic route to the enantiomers of Ins(1,3,4,5)P_4 (Vasella et al.).

via **130** and **131**. Surprisingly, L-Ins(1,3,4,5)P_4 is a higher affinity ligand than D-Ins(1,3,4,5)P_4 at Ins(1,3,4,5)P_4 binding sites in pig cerebellum, and this difference in affinity is greater than that between L-Ins(1,4,5)P_3 and D-Ins(1,4,5)P_3 at the Ins(1,4,5)P_3 receptor.[318]

Meek et al.[255] employed a base-catalyzed isomerization of the 1-benzoyl group in the readily available *myo*-inositol 1,4-dibenzoate to give inter alia the 2,4-dibenzoate. Phosphitylation with chlorophosphane **52**, oxidation, demethylation, and alkaline hydrolysis gave racemic Ins(1,3,4,5)P_4.

D-Ins(1,3,4,5)P_4 was synthesized by resolution of 3,4,5-tri-*O*-benzoyl-6-*O*-benzyl-*myo*-inositol, prepared from the 1,2:4,5-di-*O*-cyclohexylidene ketal by selective benzoylation of the 3-OH group, benzylation of the 6-OH group, removal of the *trans*-ketal, benzoylation of the 4- and 5-OH groups, and finally hydrolysis of the *cis*-1,2-ketal. Resolution by means of the monomenthyloxyacetyl derivatives and benzylation of the desired diastereoisomer followed by deacylation afforded D-**123**, which was phosphorylated with TBPP and deblocked to give D-Ins(1,3,4,5)P_4.[319] D-Ins(1,3,4,5)P_4 was also prepared from 1,4,5-tri-*O*-allyl-6-*O*-benzyl-*myo*-inositol, which was resolved via its monomenthyloxyacetyl derivative. Chemoselective tin-mediated allylation of the equatorial hydroxyl group, followed by benzylation of the 2-hydroxyl group and deallylation gave tetrol **123**, which was phosphitylated with phosphine **58**.[298] D-1,2:5,6-Di-*O*-cyclohexylidene-*myo*-inositol, obtained by chemoenzymatic means, served a starting material for another synthesis of D-Ins(1,3,4,5)P_4 via D-**123**.[225, 226]

A short route devised by Ozaki et al.[222] involved selective benzoylation of inositol. The 1,3,4,5-tetrabenzoate was isolated as major product in 34% yield. Benzylation with benzyl trichloroacetimidate and debenzoylation afforded the 2,6-protected inositol, which was phosphitylated with phosphoramidite **59**. Resolution of the tetrabenzoate by means of chiral column

chromatography gave access to enantiomerically pure Ins(1,3,4,5)P_4. The same group described the enantioselective acylation of inositol derivatives using tartaric acid monoester.[320] Thus, 1,3,5-tri-*O*-benzoyl-*myo*-inositol, obtained from direct benzoylation of inositol, was transformed enantioselectively into the 4-tartrate and the 2- and 6-OH groups were protected as silyl ethers. Separation of the fully protected diastereoisomers followed by deacylation with ethylmagnesium bromide, phosphorylation, and hydrogenolysis afforded D-Ins(1,3,4,5)P_4.[308]

7.5.2. *Other Inositol Tetrakisphosphates*

Racemic Ins(1,4,5,6)P_4 was synthesized from the 1,2-*O*-isopropylidene ketal of *myo*-inositol by phosphitylation with **52** followed by hydrogen peroxide oxidation. Demethylation was accomplished with bromotrimethylsilane, since HBr in acetic acid led to premature hydrolysis of the ketal and phosphate migration.[255] DL-Ins(1,4,5,6)P_4 was also prepared by phosphitylation of the corresponding 1,2-ketal with chlorophosphine **61**.[321] D-Ins(1,4,5,6)P_4 was obtained by resolution via the *O*-camphanylidene-*myo*-inositol *cis*-monoacetals.[276]

Ins(1,3,4,6)P_4 was prepared by treating inositol with 1,3-dichloro-1,1,3,3-tetraisopropyldisiloxane, which gave the symmetrical 1,6:3,4-*O*-bis(disiloxanylidene) regioselectively. Benzoylation and removal of the siloxanes with HF produced the 2,5-dibenzoate, which was phosphitylated with phosphoramidite **59**.[283]

DL-Ins(1,2,4,5)P_4 was previously synthesized by benzoylation of 1,2:4,5-di-*O*-cyclohexylidene-*myo*-inositol, hydrolysis of the ketal, phosphorylation with **52**/hydrogen peroxide, and stepwise deblocking.[255] A similar strategy in a more recent synthesis employed the isopropylidene ketal and **53** as phosphitylating agent.[256] Conduritol B derivatives obtained from benzene were also used to prepare Ins(1,2,4,5)P_4,[291] and L-quebrachitol served as starting material in a synthesis of L-*chiro*-Ins(1,2,3,5)P_4.[322]

8. Inositol Phosphate Analogues

Now that the second messenger properties of Ins(1,4,5)P_3 are well established, attention has turned to the synthesis of inositol phosphate analogues, which are hoped to have novel biological properties. There is currently considerable interest in the concept of pharmacological intervention in cellular signaling pathways. If suitable cell-permeable receptor antagonists and enzyme inhibitors can be synthesized, some of these compounds may have potential therapeutic value.

8.1. Deoxy Analogues

The racemic 2- and 6-deoxy analogues of Ins(1)*P* were synthesized in the search for inhibitors of inositol monophosphatase[323] (see Section 9). D-2-Deoxy-Ins(1)*P* was prepared by employing D-3,4,5,6-tetra-*O*-benzyl-*myo*-inositol, which was transformed into the 1-tetrahydropyranyl (THP) ether and deoxygenated at C-2 by the Barton–McCombie method. Cleavage of the THP ether, phosphorylation, and hydrogenolysis furnished D-2-deoxy-Ins(1)*P*.[276]

By using 4,5-di-*O*-benzoyl-3,6-di-*O*-benzyl-1,2-*O*-cyclohexylidene-*myo*-inositol, DL-2-deoxy-Ins(1,4,5)P_3 was prepared.[324] Hydrolysis of the ketal was followed by tin-mediated monomethoxymethylation of the 1-hydroxyl group. Deoxygenation at C-2 was accomplished by first oxidizing the hydroxyl group to give the inosose, which was then converted into the tosyl hydrazone and reduced. The resulting hydrazine was removed with sodium acetate. Cleavage of MOM and benzoyl protecting groups gave the 1,4,5-triol, which was phosphorylated with TBPP and deblocked.

Both D-3-deoxy-Ins(1,4,5)P_3 and D-3-deoxy-Ins(1,5,6)P_3[325, 326] were prepared from D-3-deoxy-*myo*-inositol (viburnitol), which was obtained from *O*-diisopropylidene-L-quebrachitol, by Barton deoxygenation of the free hydroxyl group, and removal of all protecting groups with boron tribromide. On treatment with 2-methoxypropene/acid, viburnitol gave a mixture of the 1,2:4,5- and the 1,2:5,6-di-*O*-isopropylidene derivatives. After benzylation, removal of the *trans*-ketals, and benzoylation, the two regioisomers could be separated by chromatography. Cleavage of the ketal of 4,5-di-*O*-benzoyl-6-*O*-benzyl-3-deoxy-1,2-*O*-isopropylidene-*myo*-inositol followed by benzoylation of the 1-hydroxyl group, protection of the axial hydroxyl group as its ethoxyethyl ether, and removal of the benzoate esters furnished the 1,4,5-triol, which was treated with TBPP and deblocked to give D-3-deoxy-Ins(1,4,5)P_3. D-3-Deoxy-Ins(1,5,6)P_3 was prepared analogously from the other regioisomer.

DL-6-Deoxy-Ins(1,4,5)P_3 **133** (Fig. 27) was synthesized by utilizing precursors derived from benzene by microbial oxidation.[201, 327] The key step was the selective ring opening of the

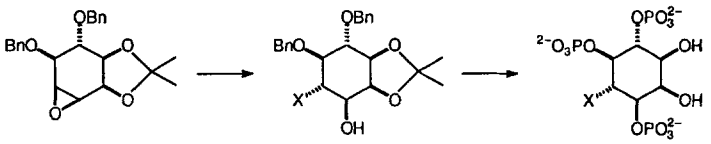

98

132: X = H
134: X = F
136: X = Me
138: X = OMe

133: X = H
135: X = F
137: X = Me
139: X = OMe

Fig. 27. Synthesis of C-6-modified Ins(1,4,5)P_3 analogues via epoxide **99** (Ley et al.).

intermediate epoxide **98** with $LiAlH_4$, giving predominantly the 6-deoxy-*myo*-inositol derivative **132**. D-6-Deoxy-Ins(1,4,5)P_3 was prepared from D-galactose by the Ferrier reaction. Interactions of this inositol phosphate with the Ins(1,4,5)P_3 receptor and metabolic enzymes were studied,[231] although details of the synthesis remain to be published.

Syntheses of 1D-2,3-dideoxy- and 1D-2,3,6-trideoxy-Ins(1,4,5)P_3 from 1D-1,4,5-tri-*O*-benzoyl-6-*O*-benzyl-3-deoxy-*myo*-inositol, an intermediate in the preparation of D-3-deoxy-Ins(1,4,5)P_3, were described.[326] Earlier, racemic 2,3,6-trideoxy-Ins(1,4,5)P_3 (= DL-cyclohexane 1,2,4-trisphosphate) had been synthesed by another group.[328]

8.2. Fluorinated Analogues of Inositol Phosphates

2-F-*scyllo*-Ins(1,4,5)P_3 and 2,2-F_2-Ins(1,4,5)P_3 were both synthesized from 1-*O*-allyl-3,6-di-*O*-benzyl-4,5-*O*-isopropylidene-*myo*-inositol. Treatment with DAST resulted in monofluorination at the 2-position with inversion of configuration, and the *gem*-difluoro derivative was obtained after oxidation to the 2-inososse. Deblocking of the 1-, 4-, and 5-OH groups, phosphorylation with TBPP, and hydrogenolysis gave 2-F-*scyllo*-Ins(1,4,5)P_3 and 2,2-F_2-Ins(1,4,5)P_3, respectively.[329] Syntheses of these compounds by a similar approach have also been published.[191, 330] The enantiomers of 3,6-di-*O*-benzyl-2-deoxy-2,2-difluoro-4,5-isopropylidene-*myo*-inositol were resolved by separation of the camphanates, thus giving access to D- and L-2,2-F_2-Ins(1,4,5)P_3.[191, 331, 332]

The protected *scyllo*-inositol **140** was used to prepare 2-F-Ins(1,4,5)P_3 **146** (Fig. 28).[333] Isomerization of the allyl group

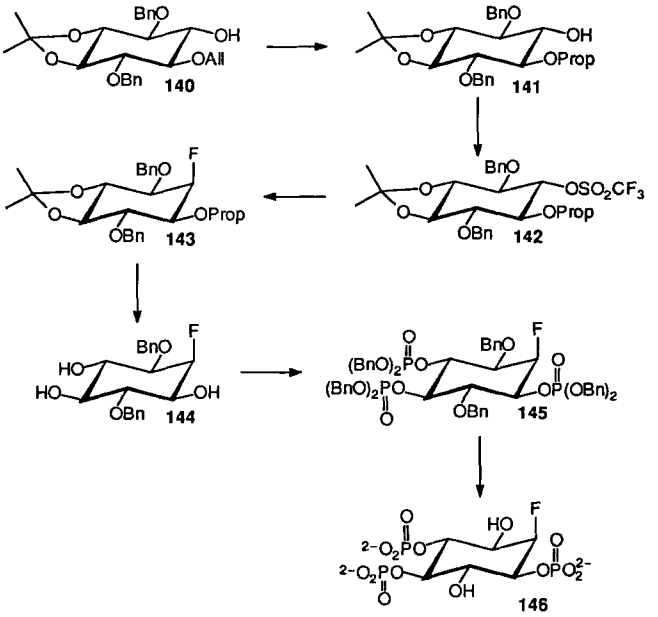

Fig. 28. Synthesis of 2-F-Ins(1,4,5)P_3 **146** (Lampe and Potter).

of **140** gave the prop-1-enyl derivative **141**, whose free 2-hydroxyl group was triflated giving **142**. Displacement of the sulfonate with tetrabutylammonium fluoride furnished the fluoroinositol **143**. Removal of acid-labile protecting groups followed by treatment of the resulting triol **144** with **56**/*t*BuOOH gave **145** and, after deprotection, **146**. An earlier attempt to synthesize 2-F-Ins(1,4,5)P_3 from **140** using DAST failed because the reaction unexpectedly proceeded with retention of configuration.[329]

Treatment of D-3-deoxy-3-fluoro-*myo*-inositol (**18**) (obtained from L-quebrachitol as above) with 2-methoxypropene/camphorsulfonic acid (cat.) produced a mixture of the 1,2:5,6- and the desired 1,2:4,5-di-*O*-isopropylidene acetal **147** (Fig. 29). The latter was benzylated to **148**, and cleavage of the *trans*-acetal followed by benzoylation gave **149**. Hydrolysis of the remaining acetal, selective benzoylation of the equatorial hydroxyl group, and protection of the free axial hydroxyl group as its

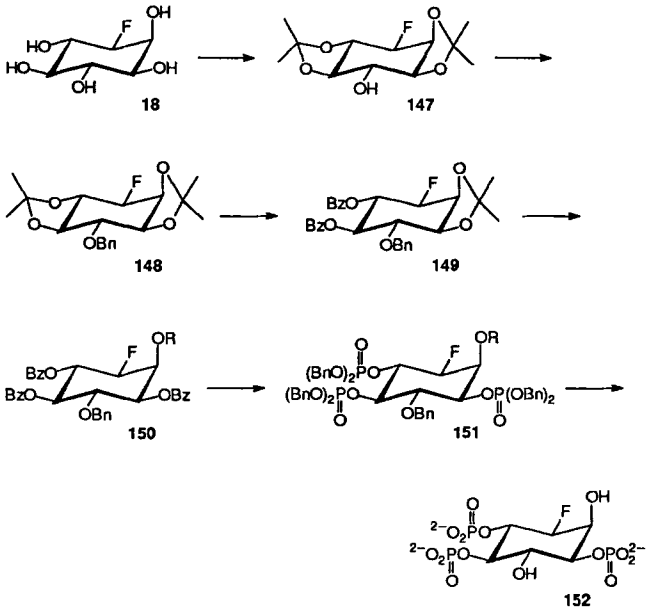

Fig. 29. Synthesis of optically active 3-F-Ins(1,4,5)P_3 **152** (Kozikowski et al.).

ethoxyethyl derivative afforded **150**. Removal of the benzoate groups and phosphorylation with TBPP gave **151**, which was deblocked stepwise to yield D-3-F-Ins(1,4,5)P_3 **152**.[334] The synthesis of D-3-*C*-(trifluoromethyl)-Ins(1,4,5)P_3 was recently described by the same group.[322]

Racemic 6-F-Ins(1,4,5)P_3 **135** was accessible from benzene by microbial oxidation via epoxide **98** (Fig. 27).[201, 327] Ring opening with $LiAlH_4$ gave mainly **134**. Debenzylation, phosphorylation with TBPP, and deprotection with trimethylsilyl bromide gave **135**.

1,3,4-Tri-*O*-allyl-5,6-di-*O*-benzyl-*myo*-inositol was employed in syntheses of 2-F-*scyllo*-Ins(1,3,4)P_3 and 2,2-F_2-Ins-(1,3,4)P_3.[313] Reaction with DAST proceeded with inversion of configuration introducing an equatorial fluoro substituent. Deallylation, TBPP phosphorylation, and hydrogenolysis afforded 2-F-*scyllo*-Ins(1,3,4)P_3. The difluoro derivative was obtained similarly by fluorination of the 2-inosose. Synthesis of the *myo*-inositol derivative was also attempted by inverting the configuration at C-2 prior to fluorination; however, the fluorinated *myo*-inositol intermediate could not be selectively deallylated.[313]

8.3. Ring-Modified Inositol Phosphate Analogues

The versatile benzene-derived epoxide **98** (Fig. 27) was employed in syntheses of racemic 6-deoxy-6-methyl-Ins(1,4,5)P_3 **137** and 6-*O*-methyl-Ins(1,4,5)P_3 **139**.[201, 302, 327] Whereas ring opening with methanolic sodium methoxide afforded mainly **136**, the precursor for **137**, reaction of **98** with lithium dimethyl(cyano)copper(I) gave **138**, which can be used to prepare **139**. DL-6-*O*-Methyl-Ins(1,4,5)P_3 was also prepared and evaluated by another group.[328]

An Ins(1,4,5)P_3 analogue with an equatorial 2-hydroxyl group, DL-*scyllo*-Ins(1,2,4)P_3, was prepared from 1-*O*-allyl-3,6-di-*O*-benzyl-4,5-*O*-isopropylidene-*myo*-inositol[333] by trifla-

tion of the 2-hydroxyl group followed by displacement of the triflate moiety with cesium acetate.

Syntheses of *chiro*-Ins(2,3,5)P_3 **159**, an Ins(1,4,5)P_3 analogue with inverted configuration at C-3, were reported by two groups. Racemic **159** (Fig. 30) was prepared from the conduri-

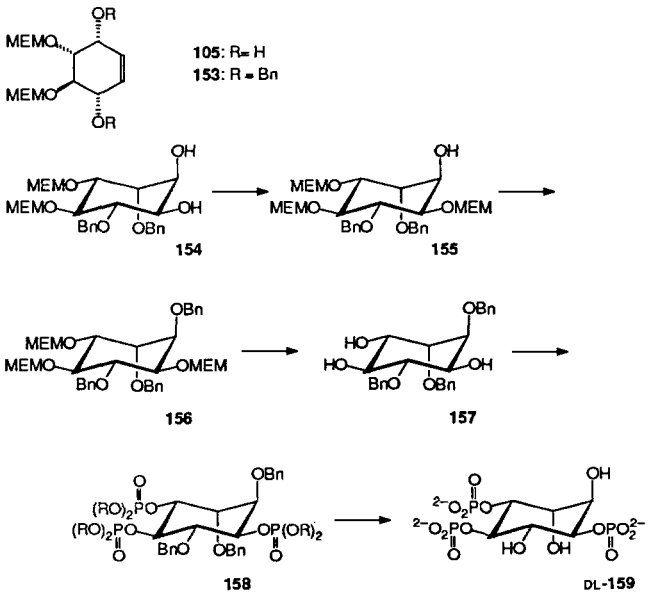

Fig. 30. Photooxidation approach to DL-*chiro*-inositol-2,3,5-trisphosphate (**159**) (Carless and Busia).

tol F derivative **105** (obtained from benzene, see Fig. 22), which was benzylated to **153** and *cis*-hydroxylated to give the *chiro*-inositol derivative **154**. Selective protection of the equatorial hydroxyl group as its methoxymethyl ether (**155**) followed by benzylation gave the fully protected **156**. Acidic hydrolysis furnished **157**, which was phosphorylated with TBPP to give **158**, and hydrogenolysis gave DL-**159**.[304] L-*chiro*-Ins(2,3,5)P_3[335, 336] was synthesized from L-*chiro*-inositol (Fig. 31). A selective tin-mediated benzylation yielded the key intermediate **160** as the major product. Perbenzoylation and cleavage of the benzyl ethers furnished **161**, which was phosphitylated with either chlorophosphine **53** or phosphine **55**. Oxidation gave **162**, which was deblocked to yield **159**. The corresponding thiophosphate **164** was prepared by sulfoxidation of the trisphosphite ester of **161** to give **163** followed by deprotection. Phosphitylation of intermediate **160** and (sulf)oxidation of the resulting trisphosphite ester gave **165** and **166**, respectively, which were deblocked to afford L-*chiro*-Ins(1,4,6)P_3 **167** and its trisphosphorothioate analogue L-*chiro*-Ins(1,4,6)PS_3 **168**.[337]

Carless and Busia[271] reported the synthesis of DL-6-F-*chiro*-Ins(2,3,5)P_3 employing the *cis*-1,4-diol **105** (see Fig. 21). Benzylation and *cis*-hydroxylation gave 1,4-di-*O*-benzyl-2,3-di-*O*-methoxymethyl-*chiro*-inositol. Selective methoxymethylation of the equatorial hydroxyl group and DAST fluorination (which proceeded with retention of configuration) furnished the fully protected fluorinated *chiro*-inositol. Hydrolysis of MOM ethers, TBPP phosphorylation, and hydrogenolysis gave DL-6-F-*chiro*-Ins(2,3,5)P_3.

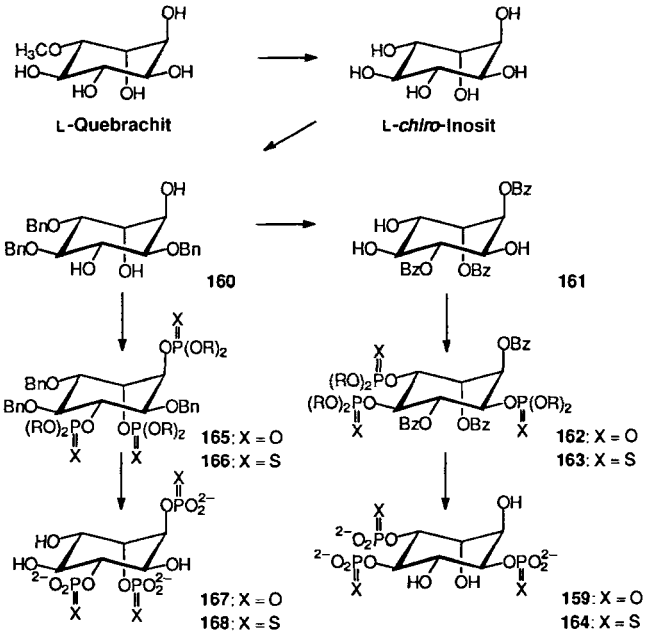

Fig. 31. Synthesis of L-*chiro*-Ins(1,4,6)P_3 **167**, L-*chiro*-Ins(2,3,5)P_3 **159**, and their trisphosphorothioate analogues from L-quebrachitol (Liu and Potter).

Other C-3-modified analogues reported include D-3-chloro-, D-3-bromo-, and D-3-O-methyl-Ins(1,4,5)P_3.[338] Recently, the first synthesis of an amino analogue of Ins(1,4,5)P_3, D-3-amino-3-deoxy-Ins(1,4,5)P_3, was published.[339]

8.4. Phosphorothioates

Phosphorothioate analogues of nucleotides have proved to be invaluable in studies in mechanistic enzymology and molecular biology[340] and in examining the stereochemistry of enzymatic phosphoryl transfer reactions,[254, 341] and phosphorothioate analogues of the established second messengers cAMP and cGMP have been available for some time. Indeed, it should be noted that phosphorothioate substitution has generated the only known competitive cAMP antagonists from the manhundreds of cAMP analogues, (R_P)-adenosine cyclic-3',5'-monophosphorothioate and the corresponding phosphorodithioate. The applicability of these analogues to the inositol phosphate field stems from their resistance to phosphatase-catalyzed degradation.[285] Already inositol phosphorothioates are emerging as the first partial agonists at the Ins(1,4,5)P_3 receptor (see Section 11.1). Synthesis of phosphorothioate analogues also provides an excellent method to introduce ^{35}S radiolabels. Since sulfoxidation is usually the final synthetic step before deprotection and can be effected with elementary sulfur, the handling of radioactive material can be kept to a minimum. Thus, D-[^{35}S]Ins(1,4,5)PS_3 was synthesized and used for enzyme[342] and receptor binding studies,[343] in which it was found to label two different sites, the Ins(1,4,5)P_3 receptor and possibly a different conformation of the receptor. Furthermore, since sulfur is a better nucleophile than oxygen, the selective attachment of reporter groups such as fluorescent labels to phosphorothioates in the presence of phosphates is possible.[344]

8.4.1. Phosphorothioate Analogues of Inositol Mono- and Bisphosphates

DL-*myo*-Inositol 1-phosphorothioate [Ins(1)*P*S] was initially obtained by treatment of inositol 1,2,4,5,6-pentaacetate with thiophosphoryl chloride followed by ester hydrolysis.[278] A synthesis of racemic as well as enantiomerically pure Ins(1)*P*S[71, 345] relied upon phosphitylation of the corresponding penta-*O*-benzylinositol (which could be resolved via camphanates) with phosphoramidite **61** and sulfoxidation. L-Ins(1)*P*S was also prepared by another group.[346]

Direct thiophosphorylation of, for example, DL-1,4,5,6-tetra-*O*-acetyl-*myo*-inositol with thiophosphoryl chloride afforded a 1:1 mixture of the *endo* and *exo* diastereoisomers of the protected 1,2-cyclic-phosphorothioates, which was separated by reverse-phase flash chromatography. Deacylation and precipitation with potassium chloride produced *endo*- and *exo*-DL-*myo*-inositol 1:2-cyclic-phosphorothioate.[347] A different approach relied upon the monophosphitylation of 1,4,5,6-tetra-*O*-benzyl-*myo*-inositol at either the 1- or 2-position using **61**, followed by cyclization of the phosphoramidites to the *exo*- and *endo*-methoxyphosphites using tetrazole. Sulfoxidation gave a mixture of the respective protected diastereoisomeric phosphorothioates which were separated by chromatography and deblocked.[263] Ins(1,4)PS_2[285] and Ins(4,5)PS_2[262] were obtained from DL-1,2:4,5-di-*O*-isopropylidene- and 1,2,3,4-tetra-*O*-benzyl-*myo*-inositol, respectively.

8.4.2. Phosphorothioate Analogues of Inositol Trisphosphates

myo-Inositol 1,4,5-trisphosphorothioate [Ins(1,4,5)PS_3, **78**] (Fig. 17)[348] was the first Ins(1,4,5)P_3 analogue reported and has proved to be a valuable tool in the elucidation of the biochemical role of Ins(1,4,5)P_3 (see Section 12). Ins(1,4,5)PS_3 was prepared from triol **70**, which was converted into the trisphosphoramidite by reaction with chlorophosphine **55** and then into trisphosphite **75** on reaction with tetrazole and 2-cyanoethanol. Sulfoxidation to **77** and deprotection produced the trisphosphorothioate **78**. A second synthesis[253] also employing triol **70** involved phosphitylation with **56** to give the intermediate trisphosphite triester. Sulfurization with phenacetyl disulfide produced the phosphorothioate which was deblocked to provide Ins(1,4,5)PS_3.

2,3,6-Tri-*O*-benzyl-4,5-*O*-isopropylidene-*myo*-inositol was used in syntheses of both the 5-phosphorothioate and the 4,5-bisphosphorothioate analogues of Ins(1,4,5)P_3, Ins(1,4,5)P_3-5S,[240, 242] and Ins(1,4,5)P_3-4,5S_2. Treatment of this intermediate with phosphorochloridate **47** resulted in phosphorylation of the 1-OH group. After removal of the ketal, phosphorylation with **47** afforded a mixture of the 1,4- and 1,5-bisphosphate triesters, from which the 1,4-bisphosphate triester crystallized. Phosphitylation of the free 5-hydroxyl group using chlorophosphine **61**, sulfoxidation, and deblocking gave Ins(1,4,5)P_3-5S. Alternatively, the 4,5-diol obtained after acetal hydrolysis could be phosphitylated with **55** or **56**, sulfoxidized, and deblocked to give Ins(1,4,5)P_3-4,5S_2. The 4,5-bisphosphorothioate was used in the synthesis of the 4,5-cyclic pyrophosphate, obtained by desulfurization with *N*-bromosuccinimide (NBS).[349] Phosphitylation of a fully benzyl-protected inositol 1,4-bisphosphate with a free 5-hydroxyl group with phosphine **56** followed by reaction with phenacetyl disulfide featured in another synthesis of Ins(1,4,5)P_3-5S.[253]

Ins(1,4,5)P_3-1S was synthesized from 1-*O*-allyl-2,3,6-tri-*O*-benzyl-*myo*-inositol by isomerization of the allyl group to give the corresponding prop-1-enyl derivative, which was then 4,5-bisphosphorylated by using P^{III} chemistry. Removal of the prop-1-enyl ether and phosphitylation of the 1-hydroxyl group followed by sulfoxidation and deprotections gave Ins(1,4,5)P_3-1S.[350] Ins(1,4,5)P_3-1S, which was used in the preparation of an Ins(1,4,5)P_3 analogue carrying a fluorescent reporter group, was obtained in optically active form by employing 1D-1-*O*-allyl-2,3,6-tri-*O*-benzyl-*myo*-inositol.[344] DL-Ins(1,4,5)P_3-1S was also prepared by using **56** as the phosphitylating reagent and phenacetyl disulfide to effect sulfoxidation.[253]

Other reported trisphosphorothioates include D-6-deoxy-Ins(1,4,5)PS_3 and L-*chiro*-Ins(2,3,5)PS_3[351, 352] as well as Ins(1,3,5)PS_3, L-Ins(1,4,5)PS_3, and L-*chiro*-Ins(1,4,6)PS_3.[353]

A different approach to the preparation of phosphorothioate analogues of Ins(1,4,5)P_3 was adopted by thiophosphorylating PtdIns and PtdIns(4)*P* using kinases in human erythrocyte ghosts and ATPγS.[354] This method can naturally be adapted to prepare the highly desirable ^{35}S radiolabeled compounds. Thus, incubation of [^{35}S]γATP with erythrocyte ghosts produced ^{35}S-labeled PtdIns(4,5)P_2 analogues, with the ^{35}S label in both the 4- and 5-positions or only in the 5-position. Activation of phospholipase C with Ca^{2+} cleaved this modified lipid to give a mixture of inositol 1,4-bisphosphate-5-[^{35}S]phosphorothioate and inositol 1-phosphate 4,5-[^{35}S]bisphosphorothioate, which was shown to be resistant to 5-phosphatase.

8.4.3. Phosphorothioate Analogues of Inositol Tetrakisphosphates

Ins(1,3,4,5)P_4-5S was obtained by phosphitylation of 2,6-di-*O*-benzyl-1,3,4-tris[(dibenzoxy)phospho]-*myo*-inositol with **56** and in situ sulfurization to produce the fully protected Ins(1,3,4,5)P_4-5S analogue. Debenzylation yielded the 5-phosphorothioate derivative.[253]

Ins(1,3,4,5)P_4-3S **176** was prepared from **169** (Fig. 32). Hydrolysis of the ketals and tin-mediated *para*-methoxybenzylation of the 1-OH group gave **170**, which was converted into **171** by simultaneous protection of the 4- and 5-OH groups as the isopropylidene ketal and benzylation of the 2-OH groups. Removal of acid-labile protecting groups and isomerization of the allyl ether gave **172**, and phosphorylation gave the 1,4,5-trisphosphate triester **173**. Hydrolysis of the prop-1-enyl ether furnished **174**. Thiophosphorylation of the free 3-hydroxyl group gave **175** and deblocking in sodium/liquid ammonia afforded Ins(1,3,4,5)P_4-3S **176**,[355] a potent inhibitor of Ins(1,3,4,5)P_4 3-phosphatase.[356] The synthesis of enantiomerically pure D-Ins(1,3,4,5)P_4-3S from L-quebrachitol was also reported.[357]

8.5. Phosphonate Analogues

The monoammonium salt of benzylphosphonic acid was employed in the synthesis of inositol 1,4,5-tris(hydrogenphosphonate). Thus, phosphonylation of **70** with the salt of the activated acid, followed by debenzylation of the product with

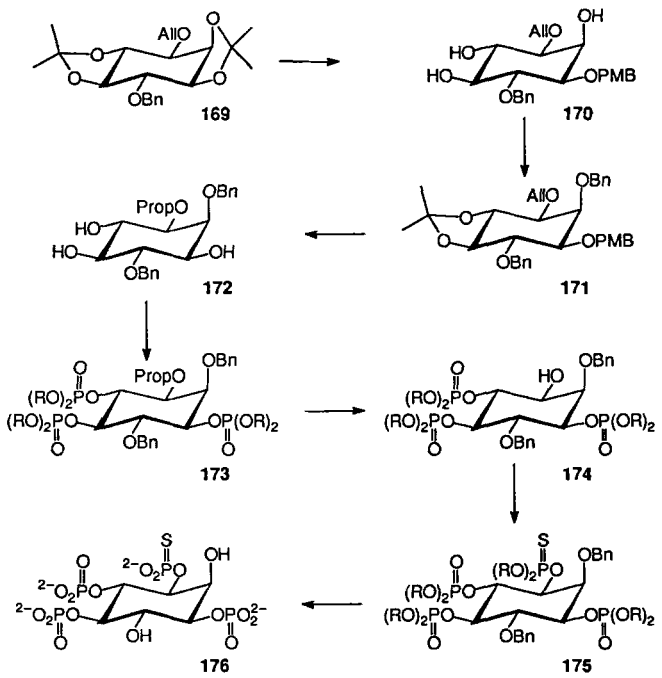

Fig. 32. Synthesis of Ins(1,3,4,5)P_4-3S **176** (Liu and Potter).

base provided the racemic 1,4,5-tris(hydrogenphosphonate).[358]

The 5-methylenephosphonate analogue of Ins(1,4,5)P_3, **180**, was also prepared (Fig. 33).[359] Compound **112**, an intermediate in the synthesis of Ins(1,4,5)P_3 from (−)-quinic acid (see Fig. 23), was desilylated, and kinetically controlled addition of

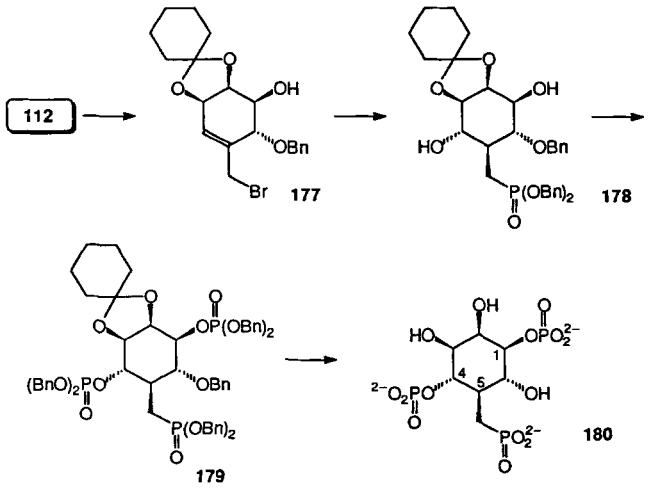

Fig. 33. Synthesis of the 5-methylenephosphonate analogue of Ins(1,4,5)P_3 from quinic acid (Falck et al.).

phenylselenyl bromide to the exocyclic alkene gave predominantly the anti-Markovnikov adduct. Oxidative elimination furnished the allylic bromide **177**, which was converted into **178** by Michaelis–Becker phosphorylation, hydroboration, and oxidative workup. Phosphorylation of the 1- and 4-hydroxyl groups gave **179**, which was deprotected to **180**.

Also synthesized were the 5-methylphosphonate analogues and the 5-(difluoromethyl)phosphonate analogues of Ins(1,4,5)P_3

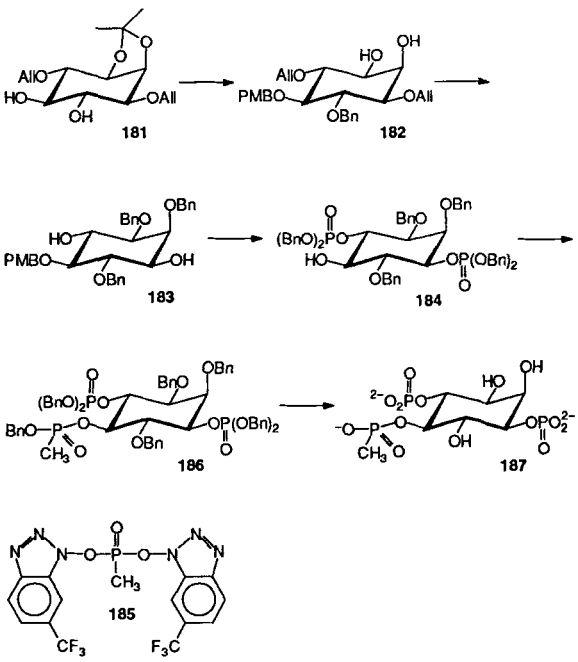

Fig. 34. Preparation of the 5-methylphosphonate analogue of Ins(1,4,5)P_3 employing phosphonylating agent **185** (van Boom et al.).

(Fig. 34) and Ins(1,3,4,5)P_4, by employing the new bifunctional phosphonylating agents bis[6-(trifluoromethyl)benzotriazol-1-yl]methylphosphonate (**185**) and (difluoromethyl)phosphonic di(1,2,4-triazolide), respectively.[360, 361] Thus, regioselective benzylation of **181** gave the 6-benzyl ether as the main product. Protection of the free 5-hydroxyl group by *p*-methoxybenzylation and removal of the *cis*-ketal furnished **182**, which was benzylated and deallylated to give **183**. Phosphorylation of the 1- and 4-OH groups with **56** and acidic removal of the *p*-methoxybenzyl group gave **184**, which was phosphonylated with **185**/benzyl alcohol. Hydrogenolysis of **186** gave the 5-methylphosphonate analogue **187**. Syntheses of racemic 3-methylphosphonate analogues of Ins(3,4)P_2 and Ins(1,3,4)P_3 were also described.[362] Additionally, phosphonylating agent **185** was used in syntheses of the methylphosphonate analogue of D-Ins(1)P[363] and DL-*myo*-inositol 1-*O*-methylphosphonate 4,5-bisphosphate.[364]

Syntheses of racemic *myo*-inositol 5-methylphosphonate, -4,5-bis(methylphosphonate), and -1,4,5-tris(methylphosphonate) were accomplished via the corresponding phosphinates.[365, 366]

8.6. "Caged" Analogues

The photochemically induced release of an active molecule of physiological interest such as ATP, GTP, second messengers, or even ions from an inactive precursor has considerable potential for studies in cellular physiology, especially kinetic aspects, since diffusional delay of agents into tissues is often a limitation. Inactive precursors which on irradiation yield, for example, a free second messenger are known as "caged" compounds[367, 368] and can be used for time-resolved measurements. Esterification of the three phosphate monoester groups

of Ins(1,4,5)P_3 with 1(2-nitrophenyl)diazoethane[369] yielded caged inositol 1,4,5-trisphosphate[370] as a mixture of singly and multiply caged compounds. The singly caged material was resolved into P-1, P-4, and P-5 isomers **188**, **189**, and **190**, respectively, by HPLC (Fig. 35). All three compounds released

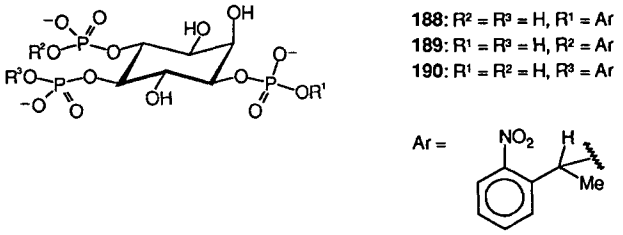

Fig. 35. Regioisomers of caged Ins(1,4,5)P_3 (Trentham et al.).

Ins(1,4,5)P_3 on irradiation. **188** is a potent releaser of Ca^{2+} and a substrate for 5-phosphatase. By contrast, **189** and **190** are inactive in Ca^{2+} release and resistant to 5-phosphatase, and **190** is a 3-kinase inhibitor. Analogues **189** and **190** were used to investigate the role of Ins(1,4,5)P_3 in excitation–contraction coupling in muscle.[371, 372] The results indicate an essential role for this compound in pharmacomechanical coupling in smooth but not striated muscle. Studies in stomatal guard cells have shown that the reversible inactivation of K^+ channels follows the photolysis of caged Ins(1,4,5)P_3 **190**.[373]

8.7. Photoaffinity Analogues and Affinity Matrices

To aid studies on localization and purification of Ins(1,4,5)P_3 receptors, it is desirable to synthesize photoaffinity analogues of Ins(1,4,5)P_3. Initially, the preparation of an arylazide derivative of Ins(1,4,5)P_3 was reported.[374] Thus, Ins(1,4,5)P_3 was coupled to *p*-azidobenzoic acid by using *N,N'*-carbonyldiimidazole. Unfortunately, the site of location of the *p*-azidobenzoic acid moiety was not determined, although hydroxyl group substitution was presumed, and a mixture was used. However, an irreversible inhibition of Ins(1,4,5)P_3-induced Ca^{2+} release in saponin-permeabilized photoirradiated macrophages was observed, which could be prevented by the presence of a large excess of Ins(1,4,5)P_3. This photoaffinity label was shown to label three proteins in macrophages.[375]

Acylation of the 2-OH group of Ins(1,4,5)P_3 yielded analogues[376] that were immobilized on Sepharose for the preparation of affinity matrices.[377] 2-*O*-*p*-Aminobenzoyl-Ins(1,4,5)P_3 was utilized in the synthesis of the photoaffinity probe **191** (Fig. 36) carrying a biotin moiety as a nonradioactive marker. This compound was successfully used to label the Ins(1,4,5)P_3 5-phosphatase of erythrocyte ghosts.[378] The same research group recently reported the preparation of affinity columns employing 2-substituted Ins(1,3,4,5)P_4 and Ins(1,3,4,5,6)P_5 analogues and their application in the isolation of Ins(1,3,4,5)P_4-binding proteins.[379]

(±)-(1*R*,3*R*,4R)-*trans*-*N*-(2-Aminoethyl)-3,4-bis(phosphonyloxy)cyclohexane-1-carboxamide was used for the preparation of an affinity matrix and a photolabel,[380] but the utility of these derivatives remains to be established. However, 6-*O*-substituted

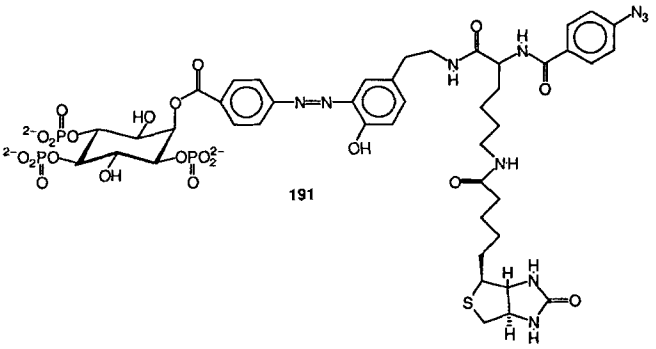

Fig. 36. Biotinylated C-2-modified Ins(1,4,5)P_3 (Ozaki et al.).

D-Ins(1,4,5)P_3 analogues were successfully applied in the production and purification of antibodies against Ins(1,4,5)P_3, by allowing the preparation of Ins(1,4,5)P_3-based immunogens and an affinity matrix.[381]

"Tetherable" derivatives of Ins(1,4,5)P_3,[382] Ins(1,3,4,5)P_4,[383] and InsP_6[384] with an ω-aminoalkyl group at P-1 were employed in the preparation of affinity matrices for the purification of binding proteins[382, 385] and [^{125}I]-labeled photoaffinity analogues.[175, 386, 387] Thus, [^{125}I](azidosalicyl)aminopropyl-Ins(1,4,5)P_3 **194** (Fig. 37) was used to identify the major

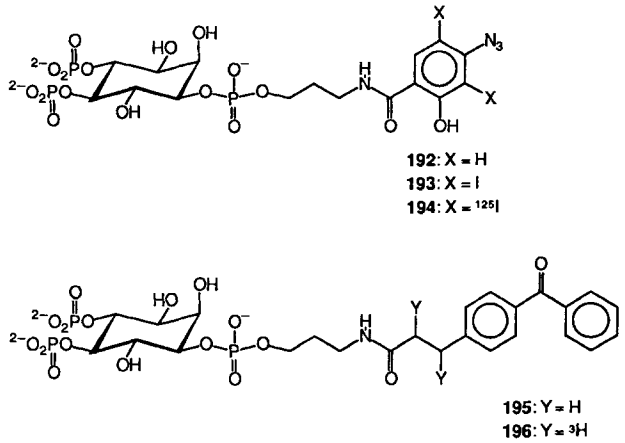

Fig. 37. Photoaffinity labeling by modification of the 1-position of Ins(1,4,5)P_3 (Prestwich et al.).

Ins(1,4,5)P_3-binding protein in olfactory cilia.[387] With the help of the new photoaffinity label [^{3}H](benzoyldihydrocinnamyl)-aminopropyl-Ins(1,4,5)P_3 **196**, which was incorporated into the rat cerebellar receptor at a substantially higher level than **194**, it was possible to purifiy and sequence a peptide matching specific sequences in the N-terminal portion of the Ins(1,4,5)P_3 receptor,[175] an area suggested to contain the Ins(1,4,5)P_3 recognition site. An InsP_6 receptor isolated by these means was subsequently identified as the clathrin assembly protein AP-2.[388] Syntheses of tetherable Ins(1,3,4)P_3 and Ins(2,4,5)P_3 derivatives and their application in the preparation of bioaffinity matrices were also described.[389]

Tethered D-Ins(1,3,4,5)P_4[235, 236] was prepared in a biomimetic synthesis involving Ferrier rearrangement of a suitably protected D-glucose derivative (Fig. 38). Thus, the primary hydroxyl group in **46** was tritylated, the secondary alcohols were

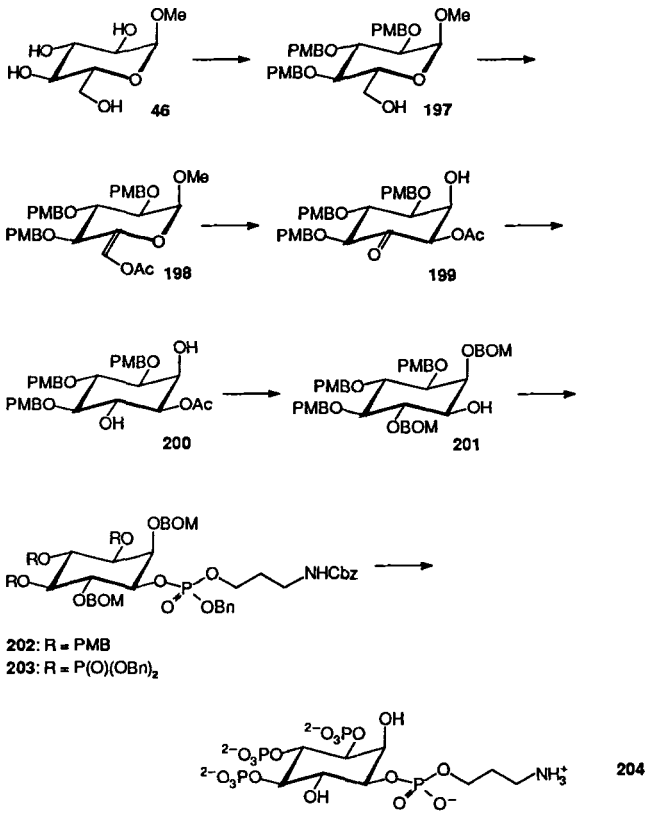

Fig. 38. Biomimetic synthesis of a precursor to an Ins(1,3,4,5)P_4 affinity label (Estevez and Prestwich).

p-methoxybenzylated, and the trityl group removed to produce **197**. Swern oxidation and treatment of the resulting aldehyde with acetic anhydride and base gave the (*Z*)-enol acetate **198**, which after Ferrier rearrangement furnished inosose **199**. Stereoselective reduction of the keto function with sodium triacetoxyborohydride gave the inositol derivative **200**. The 6- and 2-hydroxyl groups were then protected stepwise as their benzyloxymethyl ethers to minimize acetyl migration. Basic methanolysis gave **201**, and condensation with benzyloxy-{[3-(*N*-carbobenzyloxyamino)propyl]oxy}(diisopropylamino)-phosphane/tetrazole followed by oxidation provided **202**. Cleavage of the PMB ethers and phosphorylation gave **203**, hydrogenolysis of which afforded the P-1-tethered D-Ins(1,3,4,5)P_4 **204**, used to synthesize an ^{125}I-labeled affinity probe analogous to **192**.

8.8. Lipophilic Analogues

Cell-permeable inositol phosphate analogues would obviously find considerable applications. To this end the synthesis of racemic 2,3,6-tributyryl-Ins(1,4,5)P_3 was addressed[390] by phosphorylation of 1,2,4-tri-*O*-butyryl-*myo*-inositol with dianilidophosphorochloridate followed by removal of the phosphate protecting groups. The utility of this molecule, however, remains to be established.

Masking the negative charges of anionic biomolecules is another strategy that has already been successfully employed in the synthesis of a lipophilic cAMP analogue.[391] Here, the phosphate groups were esterified with acetoxymethyl bromide. Acetoxymethyl esters are rapidly cleaved intracellularly, releasing the second messenger. A preliminary report on the synthesis of membrane-permeable Ins(1,4,5)P_3 and Ins(1,3,4,5)P_4 analogues has been published.[392]

8.9. Miscellaneous

A number of C-1-modified Ins(1,4,5)P_3 analogues were prepared by chemical modification of the deacylated lipid 1-(*sn*-glycero-3-phospho)-D-*myo*-inositol-4,5-bisphosphate.[393] Syntheses of racemic sulfonamide, sulfate, and carboxymethyl analogues,[366, 394] an enantiomerically pure hexadeoxy-1,4,5-tris(methylenesulfonic acid) analogue of Ins(1,4,5)P_3,[395] and the 3-methylenecarboxylate analogue of Ins(1,3,4,5)P_4[396] were also described.

9. Inhibitors of Inositol Monophosphatase

Efforts towards the synthesis of inositol monophosphatase inhibitors by the Merck, Sharpe and Dohme group[323, 397–404] have shown encouraging results. A number of active compounds have been prepared (Fig. 39), although they are not

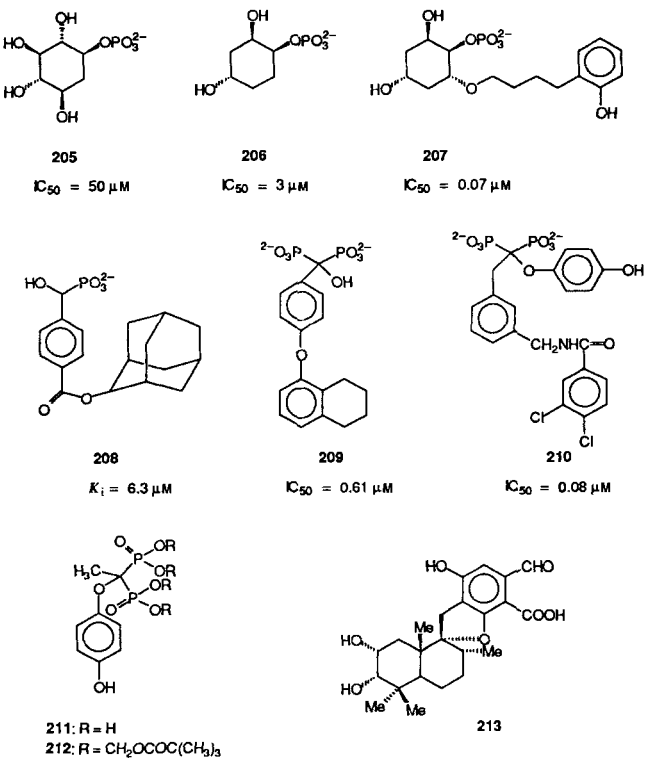

Fig. 39. Inositol monophosphatase inhibitors.

uncompetitive inhibitors like lithium. It was found that the hydroxyl groups in the 2- and 6-positions play very different roles in the hydrolysis of Ins(1)*P* by inositol monophosphatase. The 2-hydroxyl group is important for substrate recognition by the enzyme (2-deoxy-Ins(1)*P* is only a weak substrate), whereas the 6-hydroxyl group is involved in the mechanism of phosphate hydrolysis (6-deoxy derivatives like **205** have inhibitory proper-

ties). The first approach to inhibitors was based on this observation, and by a "hydroxyl group deletion" strategy, D-3,5,6-trideoxy-Ins(1)*P* **206** was synthesized and found to be a potent inhibitor,[397] indicating that the 3- and 5-hydroxyl groups are not necessary for enzyme recognition.

Inositol monophosphatase is known to be very unspecific, and the enzyme is capable of hydrolyzing 2′-nucleotides including adenosine-2′-monophosphate (2′-AMP)[74] as well as inositol monophosphates. When the molecular structures of 2′-AMP and D-3,5,6-tri-deoxy-Ins(1)*P* **206** were superimposed, it was concluded that substituents in the 6-position (the purine heterocycle in 2′-AMP) would be tolerated by the enzyme. This led to the synthesis of 6-substituted 3,5-dideoxy-Ins(1)*P* derivatives, amongst them **207**, the most potent monophosphatase inhibitor reported to date.[398]

However, phosphate esters are biologically labile and tend to have short half-lives due to hydrolysis by nonspecific phosphatases. Therefore, attempts to improve the stability of the inhibitor by replacement of the phosphate ester with an isosteric, but stable, monophosphonate group have been made. Since *myo*-inositol 1-methylenephosphonate did not show any inhibitory properties, the search for inhibitors was based on hydroxymethylene phosphonate, which had been identified as a weak inhibitor. In a series of analogues, the adamantyl ester **208** was the most potent inhibitor with a K_i value of 6.3 μM. Further studies on hydroxymethylene bisphosphonic acid derivatives[400, 403, 404] showed that compounds unrelated to the enzyme substrate like the tetralin derivative **209** can also be very potent monophosphatase inhibitors. The 3-(3,4-dichlorobenzamido)benzyl derivative **210** is the most potent, nonhydrolyzable inhibitor of inositol monophosphatase reported to date.[402] The observation that the potent bisphosphonate **211**[403] was only poorly taken up into cells led to the development of prodrug **212** with reduced polarity.[404] Synthetic efforts of the research group at Merck, Sharpe and Dohme have now been extended towards derivatives and analogues of adenosine-2′-monophosphate,[405] and molecular modeling, kinetic, and mutagenesis studies[406] are being employed to further elucidate the enzyme mechanism. Attention should be drawn to a report on the noncompetitive inhibition of inositol monophosphatase by the fungal metabolite K-76 monocarboxylic acid **213**.[407]

10. Structure–Activity Studies on Ins(1,4,5)P_3 Analogues

This section will address the consequences of structural modifications to Ins(1,4,5)P_3 on its interactions with the three binding proteins—the Ins(1,4,5)P_3 receptor and the two metabolic enzymes 5-phosphatase and 3-kinase.

10.1. Structural Requirements for Ca^{2+} Release

The Ins(1,4,5)P_3 receptor shows considerable stereo- and regiospecifity in its structural requirements for Ins(1,4,5)P_3 analogues in order to effect Ca^{2+} release. However, of the three key binding proteins Ins(1,4,5)P_3 3-kinase appears to be the most specific in its recognition of Ins(1,4,5)P_3; Ins(1,4,5)P_3 5-phosphatase is much less specific. The specificity of the Ins(1,4,5)P_3 receptor lies apparently between these two extremes.

The stereospecifity of the receptor is apparent since L-Ins(1,4,5)P_3, [= D-Ins(3,5,6)P_3] is unable to mobilize Ca^{2+}.[131, 408] The binding of this synthetic enantiomer to the receptor is roughly 2000 times weaker than that of natural D-Ins(1,4,5)P_3.[328, 409] Likewise, the enantiomers of 2-deoxy-2,2-difluoro-Ins(1,4,5)P_3 display very different agonist properties.[331, 332] D-2,2-F_2-Ins(1,4,5)P_3 was found to be a full agonist, slightly less potent than Ins(1,4,5)P_3, whereas the L isomer is only a very poor agonist.

Ins(1:2,4,5)P_3, Ins(4,5)P_2, and GroPtdIns(4,5)P_2 were shown to be 13–15 times,[109, 410] 650 times,[411] and 3–10 times[109, 393] more weakly bound than Ins(1,4,5)P_3, respectively; however, most other natural inositol phosphates including Ins(1)*P*, Ins(1:2)*P*, Ins(1,4)P_2,[19] Ins(1,3,4)P_3,[131, 328] Ins(1,3,4,5,6)P_5,[138, 412] and InsP_6 (phytic acid)[131] are ineffective as agonists at the Ins(1,4,5)P_3 receptor. Although the precise role of Ins(1,3,4,5)P_4 is still controversial, it was shown to mobilize Ca^{2+},[138] probably however via the Ins(1,4,5)P_3 receptor.[413] Ins(1,4,6)P_3 was surprisingly found to be a full agonist at the Ins(1,4,5)P_3 receptor.[315, 414] D-Ins(1,3,6)P_3 [= L-Ins(1,3,4)P_3], obtained by an unambiguous route, was shown to have Ca^{2+}-mobilizing activity in *Limulus* photoreceptors,[314] and this finding along with other data[414] helped to resolve a long-standing confusion.

The Ca^{2+}-releasing ability of a number of semisynthetic 1-substituted Ins(1,4,5)P_3 analogues[393] showed that large groups can be introduced at this position without major loss of activity. Similar results were obtained when these compounds were tested as inhibitors of aldolase A, an enzyme found to be a potent isomer-selective binder of inositol polyphosphates.[415] Similarly, the 1-*O*-(3-aminopropyl) ester of Ins(1,4,5)P_3 and a derived photoaffinity analogue[382] were able to effect Ca^{2+} release; the binding of both compounds was roughly eight times weaker than that of Ins(1,4,5)P_3. The binding of these derivatives by the receptor was equally good, and the photoaffinity derivatives were successfully used to label Ins(1,4,5)P_3 binding sites.[175] The 1-phosphorothioate analogue of Ins(1,4,5)P_3 as well as fluorescently labeled Ins(1,4,5)P_3-1S were also found to be potent Ca^{2+}-mobilizing agonists.[344]

The introduction of large groups is also tolerated at the axial 2-position and does not affect the ability of the analogue to act as a full agonist at the Ins(1,4,5)P_3 receptor.[410] Deoxygenation resulted in only a slight loss of activity,[410] and inversion of the configuration of the hydroxyl-bearing carbon [*scyllo*-Ins(1,2,4)P_3[333]] gave a highly potent full agonist.[416] DL-2-F-Ins(1,4,5)P_3[333] had the same potency as Ins(1,4,5)P_3 in mobilizing sequestered Ca^{2+} ions. Comparison with 2-F-*scyllo*-Ins(1,4,5)P_3 and 2,2-F_2-Ins(1,4,5)P_3 (which are also full agonists at the Ins(1,4,5)P_3 receptor)[330, 417] shows that the greater structural similarity of 2-F-Ins(1,4,5)P_3 to Ins(1,4,5)P_3 is reflected in its biological activity. The assumption that the 2-hydroxyl group of Ins(1,4,5)P_3 may interact with the receptor by acting as a hydrogen bond acceptor rather than a donor[330, 417] thus appears to be strengthened: the fluoro substituent of 2-F-Ins(1,4,5)P_3 can no longer donate a hydrogen bond, but the ana-

logue is still as potent as Ins(1,4,5)P_3. DL-Ins(1,2,4,5)P_4 was pharmacologically evaluated and found to be the most potent inositol tetrakisphosphate described to date.[256]

D-3-Deoxy-Ins(1,4,5)P_3,[325] D-3-F-Ins(1,4,5)P_3,[334] and D-3-*C*-(trifluoromethyl)-Ins(1,4,5)P_3[322] all mobilized Ca^{2+} as full agonists. The potency of these compounds is similar to that of Ins(1,4,5)P_3. Analogues with substituents at C-3 of increasing steric bulk (3-chloro, 3-bromo, and 3-*O*-methyl) were found to display decreasing activity with respect to receptor binding and Ca^{2+} release.[200, 338] L-*chiro*-Ins(2,3,5)P_3,[335, 336] an Ins(1,4,5)P_3 analogue with an axial rather than equatorial 3-hydroxyl group, is a potent agonist for the mobilization of sequestered Ca^{2+} with an EC_{50} only 5 to 10 times higher than that of Ins(1,4,5)P_3.[335, 417] The pharmacological properties of DL-6-F-*chiro*-Ins(2,3,5)P_3[271] are not yet available. Ins(1,3,4,5)P_4, the product of 3-kinase action on Ins(1,4,5)P_3, was shown to inhibit the binding of [^{3}H]Ins(1,4,5)P_3 to cerebellar membranes. The receptor affinity of this tetrakisphosphate is, however, about 60-fold lower than that of Ins(1,4,5)P_3,[418] and a similar decrease in potency was observed in Ca^{2+} release.[328] By analogy, an axial phosphate group at the 3-position is likewise not well tolerated.[322] These results show that the 3-hydroxyl group surprisingly plays a relatively insignificant role in receptor binding and Ca^{2+} release. Substituents at this position with increased steric demand (like an additional phosphate group), however, reduce receptor binding properties considerably. It has therefore been proposed that phosphorylation to Ins(1,3,4,5)P_4 may be the major regulatory mechanism for Ins(1,4,5)P_3 receptor binding.[417] Interestingly, a recently published study on D-3-amino-3-deoxy-Ins(1,4,5)P_3 appears to indicate that this compound is a pH-dependent partial agonist.[339]

Since the early work of Berridge and Irvine[419] the 4,5-bisphosphate motif has been thought to be crucial for Ca^{2+}-mobilizing activity. The phosphate group at C-4 appears to be essential for recognition by the Ins(1,4,5)P_3 receptor: all inositol phosphates lacking this moiety are inactive (for exceptions see ref. [420]). Ins(1,4,5)P_3-4,5S_2 is a potent Ca^{2+}-mobilizing agonist, suggesting that at least phosphorothioate substitution at C-4 is well tolerated.[349] However, no Ins(1,4,5)P_3 analogues selectively modified at the 4-position have yet been studied, and this is a clear area for future synthetic activity.

Ins(1,4,5)P_3-5S[241, 242] was found to bind with high affinity to the Ins(1,4,5)P_3 receptor and as a full agonist for mobilization of sequestered Ca^{2+} is only about seven times less potent than Ins(1,4,5)P_3. Similar to the trisphosphorothioate Ins(1,4,5)PS_3, Ins(1,4,5)P_3-5S is not dephosphorylated by the 5-phosphatase and is therefore able to produce a sustained release of Ca^{2+}. Only preliminary evaluations were carried out on the 5-methylenephosphonate analogue **180**, but these initial studies showed that this compound releases Ca^{2+} from bovine adrenal gland microsomes in a sustained fashion similar to other nonhydrolyzable analogues of Ins(1,4,5)P_3.[359] 5-Methylphosphonate **187** was reported to antagonize Ins(1,4,5)P_3-stimulated Ca^{2+} release in a pH-dependent manner, and to act as a competitive inhibitor of [^{3}H]Ins(1,4,5)P_3 binding to bovine adrenocortical microsomes.[360, 361] Full biological data for this compound and the 5-difluoromethylphosphonate analogue, which is also supposed to act as a weak antagonist,[360, 361] are awaited with interest, as these would be the first small-molecule antagonists of Ins(1,4,5)P_3 action. If these results can be confirmed, then clearly the phosphate group at C-5 is crucial for the activity of Ins(1,4,5)P_3.

D-6-Deoxy-Ins(1,4,5)P_3 was found to be a full agonist for Ca^{2+} release in permeabilized SH-SY5Y human neuroblastoma cells and is roughly 70 times less potent than Ins(1,4,5)P_3.[231] Other C-6-modified Ins(1,4,5)P_3 analogues were synthesized, including the fluoro, methyl, and methoxy derivatives.[201, 302, 327, 421] The biological properties of these compounds have not been reported to date except those of DL-6-*O*-methyl-Ins(1,4,5)P_3. This derivative was found to mobilize Ca^{2+} with an EC_{50} value over 200 times higher than that of Ins(1,4,5)P_3,[328] a result similar to those obtained for other 6-*O*-substituted analogues.[381] DL-Ins(1,4,5,6)P_4 exhibited no Ca^{2+}-releasing activity and did not appear to influence the Ins(1,4,5)P_3-mediated Ca^{2+} release at concentrations of up to 10 μM.[138] Clearly, the 6-OH group plays a significant role in receptor binding or fixing the conformation of the 5-phosphate group by hydrogen bonding. Substitution of this hydroxyl group by both uncharged and charged groups effectively abolishes activity. There is a clear need to examine the potency of 6-F-Ins(1,4,5)P_3, which remains as yet unevaluated.

The unnatural inositol phosphates Ins(2)P,[422] Ins(2,4)P_2, Ins(1,2,6)P_3,[423] Ins(1,3,5)P_3,[328] and 3-deoxy-Ins(1,5,6)-P_3[325] are all, like inositol, unable to release Ca^{2+}. Ins(1:2-cyclic 4,5)P_3 was initially reported as being equipotent to Ins(1,4,5)P_3,[130, 424] and there were speculations that this cyclic inositol phosphate may be a second messenger in its own right.[424] Further studies,[109] however, showed that Ins(1:2-cyclic 4,5)P_3 is only a weak agonist more than an order of magnitude less potent than Ins(1,4,5)P_3. Ins(2,4,5)P_3 was found to effect Ca^{2+} release and is 12–68 times less potent than Ins(1,4,5)P_3.[109, 328, 410, 411, 425] Tegge et al.[312, 425] obtained the same EC_{50} value [roughly 30 times higher than that of Ins(1,4,5)P_3] for D-Ins(2,4,5)P_3 and for D-*chiro*-Ins(1,3,4)P_3, an analogue of Ins(2,4,5)P_3 with an axial 1-hydroxyl group. It thus appears that the difference between the two compounds, an equatorial rather than an axial hydroxyl group at C-1, is insignificant with respect to Ca^{2+}-mobilizing activity. The L enantiomers of both compounds were much less active than the D isomers and roughly 800 to 960 times less active than Ins(1,4,5)P_3.[312, 425] D-3-Azido-3-deoxy-Ins(2,4,5)P_3 was considerably less potent than Ins(1,4,5)P_3 in Ca^{2+} release studies;[426] its affinity for binding to the receptor is reduced by a factor of 2000. The compound was found to mobilize 21% of sequestered Ca^{2+} at a concentration of 100 μM, whereas Ins(1,4,5)P_3 released 53% at 10 μM. The binding affinity of D-2,3-dideoxy-Ins(1,4,5)P_3 to bovine adrenal cortices was only six times lower than that of Ins(1,4,5)P_3, and its potency in effecting Ca^{2+} release was reduced by a factor of 3.5. In sharp contrast, additional deletion of the 6-hydroxyl group resulted in a further 100-fold reduction in binding affinity, and D-2,3,6-trideoxy-Ins(1,4,5)P_3 was also a very poor receptor agonist with an EC_{50} value more than 200 times higher than Ins(1,4,5)P_3.[326] This confirmed results of an earlier study in which the trideoxy analogue, albeit in racemic form, had been shown to effect Ca^{2+} release from permeabilized smooth muscle cells

with an EC_{50} value some 130 times higher than that of Ins(1,4,5)P_3.[328]

Benzene 1,2,4-trisphosphate was found to block the binding of Ins(1,4,5)P_3 to adrenal cortex microsomes competitively with an IC_{50} value of 34 μM. The affinity for the receptor is about 10000 less than that of Ins(1,4,5)P_3, and no Ca^{2+} release could be induced.[427] Benzene 1,2,4-tris(methylenephosphonate) was likewise inactive in binding and Ca^{2+} release assays, as were (1*R*,2*R*,4*R*)-cyclohexane 1,2,4-trismethylenephosphate, -tris(methylenephosphonate), -tris(methylenesulfonate), and the (4*S*) isomer of the latter.[428] Racemic trissulfate, trissulfonamide, triscarboxymethyl, and trismethylphosphonate analogues of Ins(1,4,5)P_3 did not show any biological activity;[365,366] neither did the 4,5-dimethylenephosphonate analogue of DL-Ins(4,5)P_2.[429] Inositol-1-phosphate-4,5-pyrophosphate[349] and an enantiomerically pure hexadeoxy-1,4,5-tris(methylenesulfonic acid) analogue of Ins(1,4,5)P_3[395] were also found to be inactive.

A report by Schultz et al.[420] that *cis,cis*-cyclohexane 1,3,5-trisphosphate and related analogues with a 1,5-bisphosphate arrangement are able to effect Ca^{2+} release from isolated vacuoles of *Neurospora crassa* should be treated with caution, because Ins(1,3,5)P_3 was shown not to act as an agonist in bovine aortic smooth muscle cells.[328] If these results were to be confirmed, it would imply that the vacuolar receptor of *Neurospora crassa* is different from mammalian receptors, which seems remarkable since Ins(1,4,5)P_3 receptors in different species have to date been found to be highly similar. It seems possible that Ca^{2+} contamination of the synthetic compound may be responsible for this effect.

These results suggest that the vicinal 4,5-bisphosphate moiety is essential for receptor recognition and that the presence of an additional phosphate group at C-1 greatly enhances Ca^{2+}-mobilizing properties. The fact that Ins(2,4,5)P_3 is also a full and relatively potent agonist may possibly be explained by an interaction of the axial 2-phosphate with the receptor site normally occupied by the equatorial 1-phosphate of Ins(1,4,5)P_3. Clearly, however, analogues can be synthesized with bulky substituents at the 2-hydroxyl and the 1-phosphate groups, suggesting that this area is probably relatively open to solvent. It remains to be seen which substituents can be tolerated at the 3-position, but the low activity of Ins(1,3,4,5)P_4 makes it unlikely that this is an attractive site for chemical modification (Fig. 40).

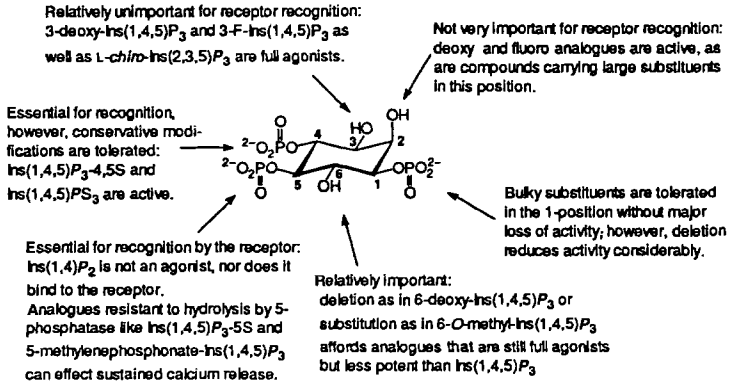

Fig. 40. Structure–activity relationships for the Ins(1,4,5)P_3 receptor.

10.2. Structure–Recognition Studies on Ins(1,4,5)*P*3 3-Kinase

The specifity of 3-kinase is in many respects greater than that of the Ins(1,4,5)P_3 receptor itself;[46] Ins(1,4,5)P_3 and Ins(1,3,4,5)P_4 are the only natural inositol polyphosphates known to be recognized with high affinity.[328]

Removal of the 1-phosphate group greatly decreases affinity for the 3-kinase: Ins(4,5)P_2 and Ins(2,4,5)P_3 are both very poor substrates for this enzyme,[328,430] and Ins(1:2 cyclic 4,5)P_3 is not phosphorylated.[431] The 1-phosphate group therefore appears to be essential for substrate recognition, which is in agreement with the observation that whilst both Ins(1,4,5)P_3-5S[241,432] and Ins(1,4,5)P_3-4,5S_2[433] are substrates for 3-kinase, an additional phosphorothioate substitution at C-1 is not tolerated: Ins(1,4,5)PS_3 is not a substrate.[434,435]

DL-2-Deoxy-Ins(1,4,5)P_3 effectively inhibits phosphorylation of [^{3}H]Ins(1,4,5)P_3 by 3-kinase;[410] the apparent K_i value is close to that of Ins(1,4,5)P_3. Other analogues carrying bulky substituents at C-2 were also recognized well by the enzyme. However, no data indicating whether these analogues act as substrates or inhibitors were given. Both DL-2-F-*scyllo*-Ins(1,4,5)P_3 and DL-2,2-F_2-Ins(1,4,5)P_3 appeared to be substrates for 3-kinase.[330] After resolution of the racemic *gem*-difluoride, however, the substrate properties of D- and L-2,2-F_2-Ins(1,4,5)P_3 were found to be quite different. Whereas the D isomer is a substrate for 3-kinase, the L isomer is a potent inhibitor of this enzyme.[332] The reason for this inhibitory activity is not yet known; however, L-2,2-F_2-Ins(1,4,5)P_3 represents a novel lead in the design of further effective inhibitors for the pharmacological intervention in the polyphosphoinositide pathway and has the advantage that it does not mobilize intracellular Ca^{2+}. 2-F-Ins(1,4,5)P_3 is also a good substrate for 3-kinase,[416] acting as a potent competitive inhibitor of the phosphorylation of [^{3}H]Ins(1,4,5)P_3 by this enzyme (apparent K_i = 3.0 μM; for comparison: 2-F-*scyllo*-Ins(1,4,5)P_3 and 2,2-F_2-Ins(1,4,5)P_3 have K_i values of 8.8 and 11.0 μM, respectively).

As can be expected with C-3-modified Ins(1,4,5)P_3 analogues, both D-3-F-Ins(1,4,5)P_3[325,334] and L-*chiro*-Ins(2,3,5)P_3,[335,336] a D-Ins(1,4,5)P_3 analogue with inverted configuration at C-3, are resistant to phosphorylation by the 3-kinase, and they are potent inhibitors of this enzyme.[436] Ins(1,3,4,5)P_4, the product of Ins(1,4,5)P_3 phosphorylation by 3-kinase, is a weak inhibitor (IC_{50} = 90 μM). However, based upon the IC_{50} data it seems unlikely that sufficient Ins(1,3,4,5)P_4 can accumulate to affect the rate of Ins(1,4,5)P_3 phosphorylation significantly, suggesting that it plays no role in any "feedback" mechanism.[328] Phosphorylation of the 3-OH group results in effective exclusion from the Ins(1,4,5)P_3 receptor, and this could be a regulatory mechanism to modulate Ins(1,4,5)P_3 binding.[417] Similarly, Ins(1,3,4,5)P_4-5S was reported to be a competitive inhibitor of 3-kinase.[253]

No compounds with selective modifications at the 4-position have been pharmacologically evaluated to date. However, the affinity of Ins(1,4,5)P_3-4,5S_2 for 3-kinase was ten times less than that of Ins(1,4,5)P_3-5S,[433] indicating that the 4-phosphate group is important for substrate recognition.

Unlike Ins(1,4,5)PS_3, DL-Ins(1,4,5)P_3-5S is a substrate for 3-kinase.[253, 432] but phosphorylation of this compound was much slower than that of the natural substrate. The 5-methylenephosphonate analogue of Ins(1,4,5)P_3, reported to elicit a sustained release of Ca^{2+},[360, 361] is presumably therefore not a substrate for 3-kinase, although full biological details on this compound remain to be published. It appears that only conservative modifications are tolerated in this position.

6-Deoxy-Ins(1,4,5)P_3 is one of the few compounds that is recognized by the highly selective 3-kinase.[231] The kinetics of its metabolism indicate that it is a substrate for this enzyme, and the phosphorylation of Ins(1,4,5)P_3 is inhibited competitively by 6-deoxy-Ins(1,4,5)P_3. It appears that hydroxyl group deletion remote from the site of action of the 3-kinase has no major effect on the binding properties of the substrate. In contrast to the 6-deoxy analogue, DL-6-methoxy-Ins(1,4,5)P_3 showed a marked drop in affinity (by roughly a factor of 120) for 3-kinase.[328] Since the hydrogen bonding potential at the 6-position is removed in both analogues, it seems possible that the increased steric bulk at the 6-position of DL-6-methoxy-Ins(1,4,5)P_3 is the cause for the low affinity of this analogue. Once again it would be useful to evaluate 6-fluoro-Ins(1,4,5)P_3 in this context.

DL-Cyclohexane 1,2,4-trisphosphate is only a weak inhibitor of [^{3}H]Ins(1,4,5)P_3 phosphorylation (IC_{50} = 327 μM).[328] Surprisingly, benzene 1,2,4-trisphosphate was relatively well recognized by 3-kinase (IC_{50} = 6.1 μM) with an affinity about ten times less than that of Ins(1,4,5)P_3.[427] D-2,3-Dideoxy- and D-2,3,6-trideoxy-Ins(1,4,5)P_3 displayed K_i values of 19 and 36 μM, respectively, whereas various other multiply deoxygenated analogs did not show any interaction[428] (Fig. 41). Interestingly, 3-kinase is also inhibited by adriamycin.[437]

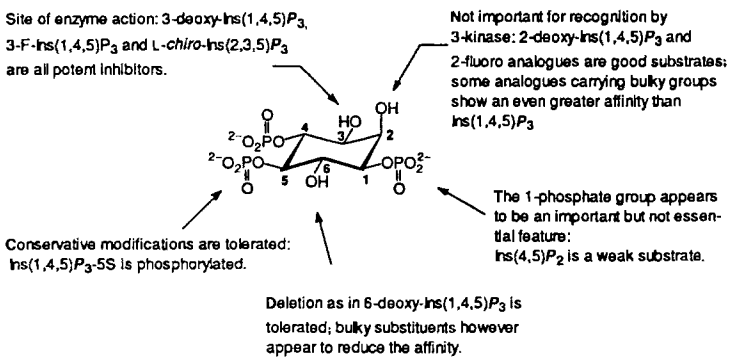

Fig. 41. Structure activity relationships for Ins(1,4,5)P_3 3-kinase.

10.3. Structure–Recognition Studies on Ins(1,4,5)P_3-5-Phosphatase

In contrast to the Ins(1,4,5)P_3 receptor and the 3-kinase, Ins(1,4,5)P_3 5-phosphatase seems to be relatively nonspecific. However, while many analogues bind to the phosphatase, only a few appear to be substrates.

The 1-phosphate group is an important feature in substrate recognition by 5-phosphatase, since Ins(4,5)P_2 is a very poor substrate.[433]

A number of racemic Ins(1,4,5)P_3 analogues modified at the 2-hydroxyl group were examined for their ability to interact with erythrocyte ghost and brain cytosol 5-phosphatase.[410] It was found that all compounds are competitive inhibitors of the enzyme and substrates for 5-phosphatase, although the extent of hydrolysis varied. Surprisingly, 2-deoxy-Ins(1,4,5)P_3 and most of the other C-2-modified analogues showed an even greater affinity for 5-phosphatase than Ins(1,4,5)P_3. 2-F-*scyllo*-Ins(1,4,5)P_3 was found to be recognized but is a weaker substrate than Ins(1,4,5)P_3.[330] The 5-phosphatase substrate properties of D- and L-2,2-F_2-Ins(1,4,5)P_3 are quite different. Whereas D-2,2-F_2-Ins(1,4,5)P_3 is a good substrate, the L enantiomer is a potent inhibitor of the enzyme.[332] Since 5-phosphatase is known to be specific for the D isomer of Ins(1,4,5)P_3, and analogues of the L enantiomer are usually not recognized very well by this enzyme [cf. L-Ins(1,4,5)P_3[438]], this result is surprising. However, there were reports of 2-substituted analogues that also display 5-phosphatase resistance,[439] and surprisingly, the L isomer of 2-aminobenzoyl-Ins(1,4,5)P_3 was found to be a potent inhibitor. Interactions of DL-2-F-Ins(1,4,5)P_3 with 5-phosphatase were also studied, and this derivative was found to be a moderately potent competitive inhibitor of this enzyme. It may be tentatively assumed that by analogy with the difluoro analogue 2,2-F_2-Ins(1,4,5)P_3, the inhibitory effect of DL-2-F-Ins(1,4,5)P_3 is due to the presence of L-2-F-Ins(1,4,5)P_3 in the racemic mixture, whereas the D isomer, like D-2,2-F_2-Ins(1,4,5)P_3, is probably a substrate for this enzyme. Thus, it may be concluded that the 2-hydroxyl group is involved in substrate recognition by Ins(1,4,5)P_3 5-phosphatase, although it does not appear to be an essential feature.

3-Deoxy-Ins(1,4,5)P_3 is a good substrate, binding with a slightly higher affinity than Ins(1,4,5)P_3 itself,[433] and 3-F-Ins(1,4,5)P_3 is also a substrate for erythrocyte 5-phosphatase.[436] In contrast, L-*chiro*-Ins(2,3,5)P_3, which can be visualized as Ins(1,4,5)P_3 with inverted configuration at C-3, was found to be a potent inhibitor.[335, 336, 436] This is surprising, since the hydroxyl group at C-3 in this molecule is remote from the site of attack of the enzyme. Two possible explanations for this phenomenon were given: The conformation of L-*chiro*-Ins(2,3,5)P_3 in solution and/or bound to 5-phosphatase may be sufficiently different from that of Ins(1,4,5)P_3 that although the analogue binds to the enzyme in a similar mode as Ins(1,4,5)P_3, the catalytic mechanism of the enzyme is interrupted. Alternatively, the inhibition may be the result of nonproductive binding of the inverted substrate L-*chiro*-Ins(2,3,5)P_3 in a rotated fashion. In this arrangement the analogue would mimic three elements of Ins(1,4,5)P_3 correctly, namely the ring pucker, the crucial vicinal 4,5-bisphosphate moiety (as the 2,3-bisphosphate pair), and the 3-hydroxyl group (as the 4-hydroxyl group). The 5-phosphate group of L-*chiro*-Ins(2,3,5)P_3 in this arrangement mimics an equatorial 2-phosphate group of an Ins(1,4,5)P_3 analogue, and such a phosphate could presumably still bind reasonably well to the hydrophilic pocket of the enzyme, which usually interacts with the equatorial 1-phosphate group of Ins(1,4,5)P_3. In this inverted binding mode the axial 1-hydroxyl group of L-*chiro*-Ins(2,3,5)P_3 now mimics the axial 6-hydroxyl group of an Ins(1,4,5)P_3 analogue. As discussed below, the equatorial 6-hydroxyl group of Ins(1,4,5)P_3 may play an important role in the mechanism of 5-phosphatase-catalyzed hydrolysis, and the inhibitory proper-

ties of L-*chiro*-Ins(2,3,5)P_3 may possibly be ascribed to the pseudo-axial 6-hydroxyl group in the inverted binding conformation.

Phosphorothioate substitution at the 5-position creates a potent inhibitor of Ins(1,4,5)P_3-5-phosphatase, Ins(1,4,5)P_3-5S.[241, 242] The 5-methylenephosphonate analogue of D-Ins(1,4,5)P_3 is another long-lived agonist of Ca^{2+} mobilization.[359] The sustained release of Ca^{2+} by this compound indicates that it is not dephosphorylated and thus deactivated by the 5-phosphatase. Full data have yet to be published, and details on interactions of the 5-methylphosphonate and 5-difluoromethylphosphonate analogues of Ins(1,4,5)P_3[360, 361] are also awaited with interest.

D-6-Deoxy-Ins(1,4,5)P_3[231] inhibited the dephosphorylation of [^{32}P]Ins(1,4,5)P_3 by erythrocyte 5-phosphatase and is a moderately potent inhibitor of this enzyme. The nonselectivity of this enzyme is underlined by the moderate reduction in affinity of D-6-deoxy-Ins(1,4,5)P_3 (ca. twofold) and DL-6-methoxy-Ins(1,4,5)P_3 (ca. fourfold) for the aortic smooth muscle 5-phosphatase[328] relative to the natural substrate. The resistance of these two analogues to dephosphorylation confirms that the minimal structural requirements for substrate hydrolysis by the 5-phosphatase include the vicinal 4,5-bisphosphate moiety and a free 6-hydroxyl group. It is possible that the function of the 6-hydroxyl group of Ins(1,4,5)P_3 is similar to the role that the 6-hydroxyl group of Ins(1)P plays in the dephosphorylation of this compound by inositol monophosphatase; in other words, the absence of this group has no significant effect on binding, but its presence is essential for the enzyme to act on the substrate.

Whereas Ins(2,4,5)P_3[410] and Ins(1:2-cyclic 4,5)P_3[310] are substrates for the 5-phosphatase, DL-Ins(1,4,5)PS_3 is resistant to degradation by this enzyme.[440] DL-Cyclohexane 1,2,4-trisphosphate is a weak competitive inhibitor (K_i = 124 mM), and no inorganic phosphate release due to hydrolysis by the enzyme was detected.[328] Benzene 1,2,4-trisphosphate[427] and (1*R*,2*R*,4*S*)-cyclohexane 1,2,4-tris(methylenesulfonate)[428] were found to inhibit the degradation of [^{3}H]Ins(1,4,5)P_3 by 5-phosphatase surprisingly well, indicating that even radical structural alterations can be tolerated by the enzyme. The trisphosphorothioates L-Ins(1,4,5)PS_3, Ins(1,3,5)PS_3, and L-*chiro*-Ins(1,4,6)PS_3 were found to be 5-phosphatase inhibitors of the highest potency with submicromolar K_i values of 0.50, 0.43, and 0.3 μM, respectively.[353] The latter two compounds do not interact with 3-kinase, nor do they mobilize Ca^{2+}.[441, 442] These analogues are therefore ideal tools for the selective inhibition of 5-phosphatase (Fig. 42).

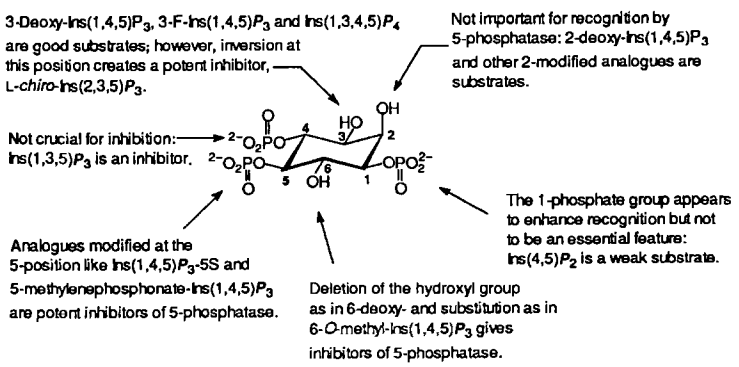

Fig. 42. Structure–activity relationships for Ins(1,4,5)P_3 5-phosphatase.

11. Ins(1,4,5)P_3 Partial Agonists and Antagonists

Only a small number of chemical agents are available for intervention in the phosphatidylinositol signaling pathway, which is underlined by the lack of a simple small-molecule Ins(1,4,5)P_3 antagonist. To aid the design of such an antagonist, extensive structure–activity studies are required. In the rational search for an agent having high affinity for the receptor yet not releasing Ca^{2+}, it is necessary to dissect the structural features of Ins(1,4,5)P_3 that determine binding affinity from those that trigger opening of the Ca^{2+} ion channel. Many naturally occurring and synthetic inositol phosphates display lower binding affinity than Ins(1,4,5)P_3 for the receptor, which can be correlated with correspondingly lower Ca^{2+}-releasing ability. However, no compound lacking a D-vicinal 4,5-bisphosphate grouping has yet been found to release Ca^{2+}. Modifications at this locus may be the way to design a small molecule that can directly affect channel opening, providing that high binding affinity can be maintained in such an analogue.

11.1. Partial Agonists at the Ins(1,4,5)P_3 Receptor

A number of partial agonists at the Ins(1,4,5)P_3 receptor have been identified: Ins(1,3,4,6)P_4 was found to have moderate affinity for the receptor and to give a maximal Ca^{2+} release only some 80% of that of mobilized by Ins(1,4,5)P_3. If the maximally effective Ca^{2+}-releasing concentration of Ins(1,3,4,6)P_4 is administered together with Ins(1,4,5)P_3, the EC_{50} value of the latter is increased.[138] This has led to the conclusion that the Ca^{2+} released is not only from the same intracellular store, but it also strongly indicates that Ins(1,3,4,6)P_4 and Ins(1,4,5)P_3 compete for the same receptor site.[138, 139] As Ins(1,3,4,6)P_4 does not nominally possess the vicinal 4,5-bisphosphate moiety normally required for agonist activity, it is not obvious why this tetrakisphosphate should release Ca^{2+}. However, two alternative binding conformations of Ins(1,3,4,6)P_4 to the Ins(1,4,5)P_3 receptor can be visualized, in which a number of important recognition features are mimicked, including the 4,5-bisphosphate unit and the 1-phosphate group. It may be that one or both of these binding conformations are the cause of the partial agonist behavior exhibited by Ins(1,3,4,6)P_4. Chemical modification of Ins(1,3,4,6)P_4 may provide a solution to this.

Weaker partial agonist behavior was found for 6-deoxy-Ins(1,4,5)PS_3 and L-*chiro*-Ins(2,3,5)PS_3.[351, 352] They were able to mobilize only 42 and 34% of the Ins(1,4,5)P_3-sensitive Ca^{2+} pool, respectively. As weak partial agonists they can be used to antagonize Ins(1,4,5)P_3-induced Ca^{2+} release, albeit at relatively high concentrations. It should be noted that both compounds are C-3- or C-6-modified analogues of Ins(1,4,5)P_3, respectively, in addition to carrying phosphorothioate groups rather than phosphates in the 1-, 4-, and 5-positions. As the weakest partial agonists, these compounds and L-*chiro*-Ins(2,3,5)PS_3 in particular represent key leads in the hunt for a small-molecule Ins(1,4,5)P_3 receptor antagonist. Partial agonist properties were also demonstrated for *scyllo*-Ins(1,2,4,5)PS_4.[416]

11.2. Ins(1,4,5)P_3 Receptor Antagonists

At present, none of the Ins(1,4,5)P_3 analogues synthesized has shown any antagonistic properties apart from the 5-methylphosphonate analogue of Ins(1,4,5)P_3[360,361] and L-*chiro*-Ins(2,3,5)PS_3.[433] The latter, however, has significant intrinsic activity. The only molecules that have been clearly demonstrated to potently inhibit Ins(1,4,5)P_3-receptor binding are heparin[443-449] and decavanadate;[19,450-452] neither of them, however, shows specifity for the Ins(1,4,5)P_3 receptor,[418,453] and they are therefore of only limited use as pharmacological tools.

11.2.1. Heparin

Heparin is a polysulfated polysaccharide with a molecular weight between 6000 and 20000, depending on origin and preparation. Initial indications that heparin could interact with Ins(1,4,5)P_3 binding sites came from the observation that the cerebellar site first described by Worley et al.[454] is sensitive to heparin.[443] Indeed, subsequently the protein representing this site was significantly purified using heparin-agarose affinity chromatography.[159] Heparin was also found to inhibit Ins(1,4,5)P_3-induced Ca^{2+} release in hepatocytes,[447] pancreatic β-cells,[448] and rat liver microsomes.[449] The potent antagonism of Ins(1,4,5)P_3-activated Ca^{2+} release by heparin was demonstrated to be both competitive and reversible, with an affinity of heparin for the binding site of roughly 3 nM.[444] It was also found that the heparin fragment TV84558-51 (average $M_r = 5100$) is as potent as heparin itself in inhibiting [^{3}H]Ins(1,4,5)P_3 binding, whereas smaller heparin fragments and less sulfated or unsulfated glycosaminoglycans (chondroitin sulfate and hyaluronic acid) did not affect binding.[443] This is also the case for O- and N-desulfated, N-reacetylated heparin; N-desulfated heparin showed a decreased inhibitory activity at the Ins(1,4,5)P_3 receptor but not at the Ins(1,3,4,5)P_4 binding site, whilst pentosan polyphosphate is another potent but nonelective inhibitor at both Ins(1,4,5)P_3 and Ins(1,3,4,5)P_4 binding sites.[418] In contrast to the inhibitory effects of heparin and related substances observed in many animal and plant tissues, Ins(1,4,5)P_3-induced Ca^{2+} mobilization in fungi is heparin-insensitive.[455] Heparin also inhibits Ins(1,4,5)P_3 3-kinase activity (but not that of Ins(1,4,5)P_3 5-phosphatase),[445] the specific binding of Ins(1,3,4,5)P_4 to cerebellar membranes,[418] and the ability of Ins(1,3,4,5)P_4 to release Ca^{2+} from cerebellar microsomes.[412]

It seems likely that the negatively charged sulfate groups of heparin interact with the hydrophilic pockets in the receptor binding site that usually accommodate the phosphate groups of Ins(1,4,5)P_3. However, it is interesting to note here that *myo*-inositol-1,4,5-trissulfate, in spite of carrying sulfate groups in the positions that are occupied by the phosphate groups in Ins(1,4,5)P_3, does not seem to have any antagonistic properties.[366] Although fragments of lower molecular weight have been investigated with some success,[456] their effectiveness is still an order of magnitude away from that of a true Ins(1,4,5)P_3 analogue. Clearly, a closer study of the heparin-receptor interaction is essential in the search for structural features that can be incorporated into a small-molecule antagonist.

11.2.2. Decavanadate

Different vanadates were examined for their ability to inhibit Ins(1,4,5)P_3-receptor binding and Ca^{2+} release. It was found that decavanadate ($V_{10}O_{28}^{6-}$ at pH 7)[457] inhibits Ins(1,4,5)P_3-induced Ca^{2+} mobilization in permeabilized rat insulinoma and PC12 cells (IC_{50} 5 μM)[310] and SH-SY5Y cells (K_i = 1.2 μM),[451] and inhibits the binding of [^{3}H]Ins(1,4,5)P_3 to its receptor in cerebellar and adrenal cortex membranes.[451] Orthovanadate and oligovanadate on the other hand do not inhibit Ins(1,4,5)P_3-receptor binding,[450] possibly because they are unable to bridge the multiple Ins(1,4,5)P_3 binding sites suggested by Meyer et al.[458] Decavanadate also suppresses Ins(1,3,4,5)P_4-induced Ca^{2+} release from permeabilized SH-SY5Y cells and inhibits Ins(1,4,5)P_3 5-phosphatase, 3-kinase, and Ins(1,3,4,5)P_4 5-phosphatase.[451]

Although decavanadate is a potent and competitive antagonist at the Ins(1,4,5)P_3 receptor, the fact that its specifity is low will most likely prevent it from becoming a useful tool to investigate the second messenger role of Ins(1,4,5)P_3. However, molecular modeling studies based upon decavanadate, and indeed heparin, may provide important leads.

12. Applications of Inositol Phosphate Analogues

Apart from caged and photoaffinity analogues of Ins(1,4,5)P_3 with obvious applications, Ins(1,4,5)PS_3 has proved to be the most versatile Ins(1,4,5)P_3 analogue synthesized to date. Ins(1,4,5)P_3 receptors recognize Ins(1,4,5)PS_3 with high affinity in brain[409,440] and liver.[459] The analogue, a full intracellular Ca^{2+}-releasing agonist, is only three to four times less potent than Ins(1,4,5)P_3 in a number of cells, including *Xenopus* oocytes,[408,460] permeabilized Swiss 3T3 cells,[131,408] GH_3 cells,[131] hepatocytes,[435] pancreatic[461-463] and parotid[464] acinar cells, skeletal muscle triads,[465] mouse lacrimal cells,[466] and SH-SY5Y neuroblastoma cells.[46] Ins(1,4,5)PS_3 is resistant to dephosphorylation by 5-phosphatase[435,440] and can produce a sustained cellular Ca^{2+} transient.[46,435] Ins(1,4,5)PS_3 was the first competitive inhibitor of 5-phosphatase reported,[432,438] but is not bound by 3-kinase and does not compete with Ins(1,4,5)P_3 for this enzyme.[432,435] Ins(1,4,5)PS_3, which is resistant to all known routes of Ins(1,4,5)P_3 metabolism, is now commercially available, and is finding an increasing number of biological applications, as illustrated here.

The possibility of synergistic interactions between Ins(1,4,5)P_3 and its metabolite, Ins(1,3,4,5)P_4, in promoting Ca^{2+} entry at the plasma membrane has been the subject of considerable recent debate.[123,124,126] When a Ca^{2+}-activated K^+ current in singly internally perfused mouse lacrimal acinar cells was monitored by using a patch-clamp technique for whole-cell current recording, addition of Ins(1,4,5)PS_3 alone gave rise to a single transient response, independent of external Ca^{2+} and typical of Ins(1,4,5)P_3. In the presence of Ins(1,3,4,5)P_4, however, this analogue gave a sustained response dependent upon external Ca^{2+}. The transient response of Ins(1,4,5)P_3 is therefore presumed not to be a consequence of rapid metabolism, and Ins(1,3,4,5)P_4 does not act by protecting Ins(1,4,5)P_3 against dephosphorylation by 5-phosphatase, for which it is also a substrate.[466]

Intracellular Ca^{2+} oscillations are often observed in cells stimulated by extracellular agonists coupled to polyphosphoinositide hydrolysis, and the role and generative mechanisms of such oscillations have been the subject of significant recent interest and controversy.[47,467] Models of the processes underlying these oscillations have been developed.[467,468] Singly perfused mouse pancreatic acinar cells treated with Ins(1,4,5)PS_3 [or Ins(1,4,5)P_3], applied through a patch pipette, were found to evoke repetitive pulses of Ca^{2+}-activated Cl^- current, similar in amplitude and frequency to the response to acetylcholine, acting through muscarinic receptors. Pulsatile Ca^{2+} release is possible, therefore, even at a constant level of the analogue, and presumably therefore also of Ins(1,4,5)P_3, which is an argument against a receptor-controlled oscillator in the generation of local maxima in Ca^{2+} concentration, and a role for the periodic phosphorylation or degradation of Ins(1,4,5)P_3.[462] Different types of cytosolic Ca^{2+} fluctuation patterns, mimicking those produced by the natural agonist, can be generated by Ins(1,4,5)PS_3 depending on its concentration.[463] Low Ins(1,4,5)PS_3 concentrations evoke repetitive local maxima in the Ca^{2+} concentration, whereas at relatively high concentrations repetitive Ca^{2+} waves are produced.

When invertebrate microvillar photoreceptors are exposed to light, Ca^{2+} release from the ER is effected by the intermediacy of Ins(1,4,5)P_3 acting through an Ins(1,4,5)P_3 receptor. In ventral photoreceptors of the horseshoe crab *Limulus* Ins(1,4,5)PS_3 was used to investigate mechanisms that terminate Ins(1,4,5)P_3-induced Ca^{2+} mobilization. The action of Ins(1,4,5)P_3 in these cells is stereospecific for the D enantiomer and the second messenger is normally rapidly deactivated by metabolism. In the *Limulus* photoreceptor, Ins(1,4,5)PS_3 generates sustained repetitive oscillation of Ca^{2+}-dependent membrane potential which persists for tens of minutes.[469] Oscillations of membrane potential[408] and Ca^{2+}-dependent Cl^- current[460] can be generated by microinjection of Ins(1,4,5)PS_3 into *Xenopus* oocytes. Such oscillations are not sustained here, however, indicating that factors other than metabolism are important in terminating the response. Ins(1,4,5)PS_3-evoked membrane potential oscillations differ from those generated by Ins(1,4,5)P_3, and resemble more those of Ins(2,4,5)P_3. The reason for this is not clear, but different mechanisms for setting up Ca^{2+} oscillations may be possible.[126] Oscillations in Ca^{2+}-dependent Cl^- current induced by Ins(1,4,5)PS_3 appear to resemble those induced by Ins(1,3,4,5)P_4 rather than Ins(1,4,5)P_3.[470]

The free intracellular Ca^{2+} concentration increased in a localized cellular area through the action of stimulus-induced elevation of Ins(1,4,5)P_3 can give rise to actively propagated Ca^{2+} waves, which extend this signal to other parts of this cell. Ins(1,4,5)PS_3 was employed to investigate the propagation of Ca^{2+} waves through the cytoplasm of *Xenopus* oocytes.[471] Ins(1,4,5)PS_3-stimulated Ca^{2+} waves were found to be very similar to those induced by stimulation of acetylcholine receptors and probably therefore result from the same intracellular mechanisms. However, since Ins(1,4,5)PS_3 cannot be hydrolyzed and is not readily metabolized by *Xenopus* oocytes,[460] it can be inferred that such Ca^{2+} waves do not require fluctuations in Ins(1,4,5)P_3 levels and may be derived by a mechanism dependent upon Ca^{2+} stimulation of Ins(1,4,5)P_3-induced Ca^{2+} release.

When receptor activation in *Xenopus* oocytes is followed, complex spatial and temporal patterns of Ca^{2+} release in the form of regenerative circular and spiral waves can be observed. Such spiral waves could be generated by injection of the nonmetabolizable Ins(1,4,5)PS_3 and were indistinguishable from receptor-induced Ca^{2+} patterns.[472] Stimulation of Ca^{2+} release by such a compound, however, did not result in gross alteration of the Ca^{2+} release pathway. This and other similar behavior suggested that the metabolism of Ins(1,4,5)P_3 is not responsible for the cessation of Ca^{2+} activity. Clearly the Ins(1,4,5)P_3 concentration remains relatively constant during the period of regenerative wave stimulation. Regenerative activity is probably due to the cyclical nature of stimulation and inhibition of the Ins(1,4,5)P_3 receptor channel as governed by cytoplasmic Ca^{2+} concentrations. Ins(1,4,5)PS_3 has also been employed to study the influence of Ca^{2+} influx on Ca^{2+} waves induced by microinjection of the analogue. Receptor-activated Ca^{2+} influx was found to modulate the frequency and velocity of Ins(1,4,5)P_3-dependent Ca^{2+} waves in *Xenopus* oocytes.[473]

Microinjection of cGMP into unfertilized sea urchin eggs elicits its activation by stimulating a rise in the intracellular free Ca^{2+} concentration by means of an unknown mechanism. This Ca^{2+} release and activation are prevented in eggs in which the Ins(1,4,5)P_3-sensitive Ca^{2+} stores were emptied by prior injection of Ins(1,4,5)P_3. Indeed, injection of Ins(1,4,5)PS_3 into sea urchin eggs caused a Ca^{2+} transient of similar magnitude and duration to that elicited by Ins(1,4,5)P_3. However, subsequent injections of Ins(1,4,5)PS_3 resulted in only small subsequent repetitive Ca^{2+} transients in contrast to the much larger ones elicited by Ins(1,4,5)P_3. This is because, as a result of the nonhydrolyzable nature of Ins(1,4,5)PS_3, the resting Ca^{2+} level is relatively greater in Ins(1,4,5)PS_3-injected eggs. Thus, the Ca^{2+} store can be progressively depleted by successive injections of Ins(1,4,5)PS_3.[474]

Ins(1,4,5)PS_3 was exploited to help distinguish functionally between Ins(1,4,5)P_3-sensitive and -insensitive nonmitochondrial MgATP-dependent Ca^{2+} pools in rat pancreatic acinar cells.[461] The Ins(1,4,5)P_3-sensitive Ca^{2+} pool was kept empty by Ins(1,4,5)PS_3 and Ca^{2+} reuptake occurred into the Ins-(1,4,5)P_3-insensitive pool.

Ins(1,4,5)PS_3 and the related monophosphorothioate analogue Ins(1,4,5)P_3-5S are potent 5-phosphatase inhibitors[432,438] and have been employed to inhibit Ins(1,4,5)P_3 breakdown in electrically permeabilized SH-SY5Y human neuroblastoma cells.[475] Inhibition of 5-phosphatase-mediated metabolism of exogenously added 5[^{32}P]Ins(1,4,5)P_3 was about ten times greater than that of cell-membrane-derived [^{3}H]Ins(1,4,5)P_3, indicating the possibility of Ins(1,4,5)P_3 compartmentation, in other words that homogenous mixing of exogenously added and endogenously generated Ins(1,4,5)P_3 does not occur. Ins(1,4,5)P_3-5S is a substrate for Ins(1,4,5)P_3 3-kinase and inhibits the phosphorylation of [^{3}H]Ins(1,4,5)P_3 by this enzyme.[432]

Intracellular Ca^{2+} release can be "quantized", where the size of the Ins(1,4,5)P_3-sensitive Ca^{2+} pool is apparently dependent upon the concentration of Ins(1,4,5)P_3.[124] Ins(1,4,5)PS_3 has been employed in the investigation of quantal Ca^{2+} release in permeabilized hepatocytes.[476] The failure of submaximal con-

centrations of Ins(1,4,5)P_3 or Ins(1,4,5)PS_3 to empty the Ca^{2+} store completely was not due to stimulus deactivation or to receptor desensitization. Use of the metabolically stable Ins(1,4,5)PS_3 allowed Ca^{2+} efflux experiments to be performed at a high cell density, at which metabolic degradation of Ins(1,4,5)P_3 would normally have posed significant problems.

Ins(1,4,5)P_3 activates a novel voltage-dependent K^+ conductance in rat CA1 hippocampal pyramidal cells.[477] When injected into these cells, Ins(1,4,5)PS_3 inhibited action potential firing. The metabolic stability of Ins(1,4,5)PS_3 was crucial for these observations. Ins(1,4,5)P_3 itself did not elicit this conductance, presumably because of its rapid enzymatic metabolism. Thus, importantly, the use of Ins(1,4,5)PS_3 may uncover activities of Ins(1,4,5)P_3 that may not be observable experimentally with the natural messenger because of rapid metabolism or the slow diffusion of exogenously added agonist.

In rabbit skeletal muscle triads, Ins(1,4,5)PS_3 released up to 20% of an actively loaded Ca^{2+} pool, although activation of ryanodine receptor Ca^{2+} channels was zero or minimal,[465] raising the possibility that the Ca^{2+}-mobilizing activity may be mediated by other channels or mechanisms. Evidence was provided for two types of intracellular Ca^{2+}-sensitive channels displaying fast activation kinetics, namely Ins(1,4,5)P_3-sensitive and Ca^{2+}-sensitive channels. The kinetics of Ca^{2+} release by Ins(1,4,5)PS_3 in rabbit skeletal muscle SR were surprisingly fast (20–150 ms, depending upon agonist concentration), indicating that Ins(1,4,5)P_3 receptors of skeletal muscle may be kinetically competent to signal the raid elevation of cytosolic Ca^{2+} that preceeds muscle contraction.[478]

A role for Ins(1,4,5)P_3 in red blood cells has yet to be established, although the turnover of polyphosphoinositides is well known. In permeabilized human red blood cells Ins(1,4,5)P_3 evokes transient release of Ca^{2+}, disorganization of the spectrin network, and reversible shape changes, as measured by immunofluorescence.[479] However, Ins(1,4,5)PS_3 evokes sustained release of Ca^{2+} and irreversible shape changes and disorganization of the spectrin network. The polyphosphoinositide signaling pathway evidently plays an important role in the shape maintenance of red blood cells.

13. Syntheses of Inositol Lipids and Analogues

Much of the earlier work on the synthesis of phosphatidylinositol lipids and their analogues has been covered in a review.[480] The synthesis of four stereoisomers of dipalmitoyl phosphatidylinositol to probe the substrate stereospecificity of PtdIns 4-kinase was reported.[481,482] The PtdIns(4,5)P_2 phospholipid analogue 1-*O*-(1,2-di-*O*-palmitoyl-*sn*-glycero-3-phospho)-D-Ins(4,5)P_2 was synthesized using a P^{III} approach.[266] (The preparation of the di-*O*-stearoyl phospholipid had been described previously by a Russian group,[219,483,484] and the work of this group in this area has been reviewed.[480,485]) A synthesis of optically active 1-*O*-(1,2-di-*O*-stearoyl-*sn*-glycero-3-phospho)-D-Ins(3,4,5)P_3 from (−)-quinic acid[486] has been complemented by a short synthesis of this PtdIns(3,4,5)P_3 analogue in racemic form.[487]

The first synthesis of a fluoro analogue of an inositol lipid was described as early as 1982.[190] 2-Deoxy-2-fluoro-1-phosphatidyl-*scyllo*-inositol was obtained by condensation of 2-fluoro-2-deoxy-3,4,5,6-tetra-*O*-benzyl-*scyllo*-inositol with the sodium salt of dipalmitoyl-L-α-phosphatidic acid, followed by hydrogenolysis. More recently, preparations of D-3-deoxy-3-fluoro-1-phosphatidyl-*myo*-inositol and the respective 3-chloro derivative were reported.[488–490] The former PtdIns analogue displayed cytostatic properties, inhibiting cell growth of NIH 3T3 cells at concentrations on the order of 100 μM.

The synthesis of 2-deoxy-PtdIns was described.[491] Racemic 3,4,5,6-tetra-*O*-benzyl-*myo*-inositol was selectively acetylated at the 1-hydroxyl group. Deoxygenation was effected employing the Robins' variation of the Barton–McCombie sequence: thionocarbonate formation and radical reduction. Saponification and optical resolution of the resulting alcohol via its camphanates afforded D-3,4,5,6-tetra-*O*-benzyl-2-deoxy-*myo*-inositol, which was phosphitylated with the novel coupling agent bis(diisopropylamino)(2-trimethylsilylethoxy)phosphine. Reaction with dipalmitoylglycerol and oxidation of the phosphite triester gave the protected deoxy-PtdIns analogue as a mixture of diastereoisomers at phosphorus. Stepwise deblocking then gave 2-deoxy-PtdIns, which was used to study the specificity of phospholipase C (PLC).

Syntheses of the PtdIns analogue 1,2-dipalmitoyl-*sn*-glycero-3-thiophospho-*myo*-inositol (DPPsI) were reported by two groups.[263–265] In the first synthesis,[263,264] 1D-2,3:5,6-di-*O*-cyclohexylidene-4-*O*-methoxymethyl-*myo*-inositol was phosphitylated with methoxy(diisopropylamino)chlorophosphine (**61**) and then converted directly to the protected 1,2-dipalmitoyl-*sn*-glycero-3-thiophospho-*myo*-inositol by reaction with 1,2-dipalmitoyl-*sn*-glycerol and sulfoxidation. Deprotection with acid and demethylation with trimethylamine afforded (R_P + S_P)-DPPsI as a mixture of diastereoisomers, which was used to examine the stereochemical mechanism by which PtdIns-specific PLCs cleave their substrates. In the second approach,[265] 1,2-dipalmitoyl-*sn*-glycerol was reacted with **61** to produce the phosphoramidite, which was then condensed with 1D-2,3,4,5,6-penta-*O*-benzyl-*myo*-inositol. Sulfoxidation afforded a mixture of the phosphorothioate diastereoisomers separable by chromatography. Deprotection produced the individual diastereoisomers of 1,2-dipalmitoyl-*sn*-glycero-3-thiophospho-1-*myo*-inositol. The synthesis of a number of PtdIns analogues with thiophosphoester bonds designed to inhibit PtdIns-PLC was also reported.[492]

Phosphonylating agent **185** was employed in syntheses of optically active phosphonate analogues of PtdIns and PtdIns(4)P[493] as well as in the preparation of the diastereomeric uncharged methylphosphonate analogues of PtdIns.[363] The phosphonate analogue of PtdIns has proved to be a potent antiinflammatory and analgesic agent.[494] Phosphonate derivatives of PtdIns with a single alkyl chain in place of the diacylglycerol moiety were also described,[495] as were isosteric methylenephosphonate and isopolar difluoromethylenephosphonate analogues of PtdIns containing short-chain ethers rather than lengthy acyl chains on the *sn*-1 and *sn*-2 oxygens of the glycerol unit to improve the water solubility of these compounds.[496]

14. Glycosyl-Phosphatidylinositol Anchors

Many proteins are bound to biological membranes. Whereas integral membrane proteins have one or more hydrophobic domains and are embedded to a great extent in the lipid bilayer, other proteins are covalently attached to lipids which serve as anchors to the cell membrane. It has been shown that many of these latter proteins are linked to the membrane by phosphatidylinositol anchors attached to the C-terminal amino acid of the protein through an intervening glycan structure [glycosylphosphatidylinositol (GPI) anchor].[497-500] More than 30 different cell surface proteins with a GPI anchor have been identified (for the biosynthesis of GPI anchors see ref. [501]), including hydrolytic enzymes (e.g. alkaline phosphatase and acetylcholinesterase[502]), mammalian antigens (e.g. Thy-1[503]), and cell adhesion proteins. The generic structure of GPI anchors is PtdIns-glucosamine-mannose$_3$-phosphoethanolamine-protein; however, modifications of the core mannosyl residues by additional side chains are common and other variations (e.g. in the fatty acid composition of PtdIns) have also been observed.

The discovery of GPI anchors has attracted the interest of bioorganic chemists, and efforts to synthesize the GPI anchor of the variant surface glycoprotein (VSG) of the parasitic protozoan *Trypanosoma brucei*[504] (Fig. 43) have been successful.[505, 506] The survival of African trypanosomes depends on the integrity of their cell-surface coat, which is formed by VSGs arranging into tightly packed monolayers and which protects the parasite from lytic factors of the host serum. By expressing different VSGs at different times the parasite is able to evade the host's immune response. This antigenic variation makes it difficult for the immune system to supply the appropriate antibodies at the right time, and it also renders drugs against specific VSGs ineffectual. Inhibition of the biosynthesis of the VSG GPI anchor, however, or drugs targeting specific features of this GPI anchor, could prove successful. This explains the interest this particular GPI anchor has attracted. Whereas the backbone structure of the VSG GPI anchor is similar to that of other GPI anchors, the α-galactose side chain of the VSG GPI anchor seems to be parasite-specific. Thus the design of drugs aiming at this side chain may prove successful.

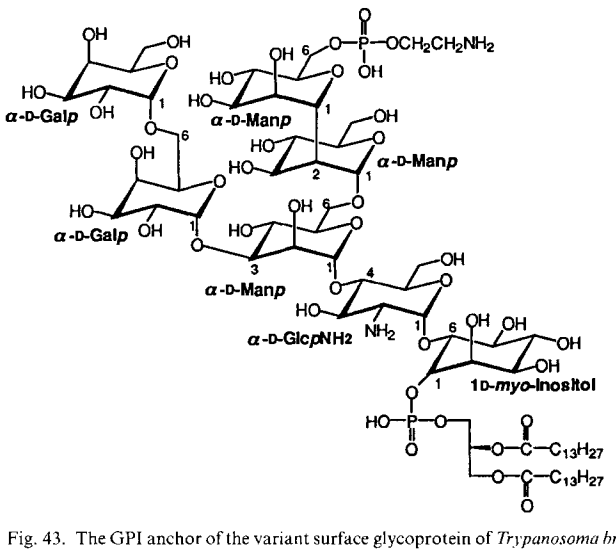

Fig. 43. The GPI anchor of the variant surface glycoprotein of *Trypanosoma brucei*.

Some metabolic fragments of the protein–GPI complex formed by the combined actions of specific endogeneous proteases and a glycosyl-phosphatidylinositol-specific phospholipase C (GPI-PLC) were found to display certain biochemical properties previously associated with crude preparations of putative insulin mediators (PIMs). (This GPI-PLC is distinct from the PtdIns-PLC, which hydrolyzes PtdIns, PtdIns(4)P and PtdIns(4,5)P_2 and is located on the inner membrane rather than the cell surface.) PIMs are phosphorylated inositol-glycans generated after insulin stimulation of the cell surface receptor and can mimic some biochemical properties of insulin in vitro.[500, 507, 508] However, it is as yet still premature to regard inositol phosphate glycans as second messengers of insulin action. Several groups directed their attention towards the preparation of PIMs[234, 509-512] and related GPIs. Syntheses of fragments of mycobacterial inositol phospholipids were also reported.[267, 513]

15. Summary and Outlook

The first evidence of a second messenger role for Ins(1,4,5)P_3[19, 419] catapulted the study of polyphosphoinositide metabolism and its effects from the position of a relatively modest backwater to one of the most active fields at the forefront of modern biology. The resulting upsurge in interest in cyclitol and inositol phosphate chemistry shows no current signs of subsiding. Indeed, it is likely that a significant proportion of future progress in inositol phosphate biology will be underpinned by the current interest in inositol phosphate chemistry. Continuing development of synthetic inositol phosphate analogues with novel biological properties can be envisaged, including receptor antagonists, caged compounds, cell-penetrating compounds, affinity, photoaffinity, and spin-labeled inositol phosphate analogues, fluorescent probes, and inositol phosphates linked to affinity columns for the purification of receptors and enzymes. The prospect of a whole new signaling pathway based upon PtdIns(3,4,5)P_3 opening up, the anticipation of the structural characterization of the as yet elusive "Ca^{2+}-influx factor", and the advent of novel potent Ins(1,4,5)P_3 receptor ligands unrelated to Ins(1,4,5)P_3 such as adenophostins (Fig. 44) together with the real possibility of devising drugs of the future by pharmacological intervention in signaling transduction pathways means that interdisciplinary collaborations by chemists with cell biologists, biochemists, and pharmacologists will be crucial to meet these new challenges and apply the results.

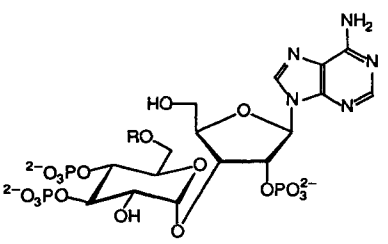

Fig. 44. Adenophostin A (R = H) and B (R = $COCH_3$).

We thank the Wellcome Trust for a Prize Fellowship (to D. L.) and S. J. Mills for a critical reading of the manuscript. B. V. L. P. is a Lister Institute Research Professor.

Received: June 10, 1994 [A 69 IE]
German version: *Angew. Chem.* **1995**, *107*, 2085–2125

[1] D. J. Takemoto, J. M. Cunnick, *Cell Signalling* **1990**, *2*, 99–104.
[2] F. McCormick, *Nature (London)* **1993**, *363*, 15–16, and references therein.
[3] E. J. Neer, D. Clapham, *Nature (London)* **1988**, *333*, 129–134.
[4] A. G. Gilman, *Annu. Rev. Biochem.* **1987**, *56*, 615–649.
[5] L. Stryer, H. R. Bourne, *Annu. Rev. Cell Biol.* **1986**, *2*, 391–419.
[6] A. Galione, *Trends Pharmacol. Sci.* **1992**, *13*, 304–306.
[7] A. Galione, A. White, N. Willmott, M. Turner, B. V. L. Potter, S. P. Watson, *Nature (London)* **1993**, *365*, 456–459.
[8] M. J. Berridge, *Nature (London)* **1993**, *365*, 388–389.
[9] A. Olivera, S. Spiegel, *Nature (London)* **1993**, *365*, 557–560.
[10] S. Ringer, *J. Physiol. (London)* **1883**, *4*, 29–42.
[11] J. Scherer, *Justus Liebigs Ann. Chem.* **1850**, *73*, 322–328.
[12] T. W. Rall, E. W. Sutherland, *J. Biol. Chem.* **1958**, *232*, 1065–1076.
[13] E. W. Sutherland, T. W. Rall, *J. Biol. Chem.* **1958**, *232*, 1077–1091.
[14] L. E. Hokin, M. Hokin-Neaverson, *Biochim. Biophys. Acta* **1989**, *1000*, 465–469.
[15] J. Folch, *J. Biol. Chem.* **1942**, *146*, 35–44.
[16] R. M. C. Dawson, *Biochim. Biophys. Acta* **1989**, *1000*, 459–461.
[17] H. Brockerhoff, C. E. Ballou, *J. Biol. Chem.* **1961**, *236*, 1907–1911.
[18] R. H. Michell, *Biochim. Biophys. Acta* **1975**, *415*, 81–147.
[19] H. Streb, R. F. Irvine, M. J. Berridge, I. Schulz, *Nature (London)* **1983**, *306*, 67–69.
[20] R. S. Rana, L. E. Hokin, *Physiol. Rev.* **1990**, *70*, 115–164.
[21] S. B. Shears, *Biochem. J.* **1989**, *260*, 313–324.
[22] S. B. Shears in *Advances in Second Messenger and Phosphoprotein Research* (Ed.: J. W. Putney, Jr.), Raven, New York, **1992**, pp. 63–92.
[23] G. W. Mayr, T. Radenberg, U. Thiel, G. Vogel, L. R. Stephens, *Carbohydr. Res.* **1992**, *234*, 247–262.
[24] L. R. Stephens, K. T. Hughes, R. F. Irvine, *Nature (London)* **1991**, *351*, 33–39.
[25] N. Divecha, H. Banfic, R. F. Irvine, *EMBO J.* **1991**, *10*, 3707–3714.
[26] R. H. Michell, *Curr. Biol.* **1992**, *2*, 200–202.
[27] P. J. Hughes, R. H. Michell, *Curr. Opin. Neurobiol.* **1993**, *3*, 383–400.
[28] C. Randriamampita, R. Y. Tsien, *Nature (London)* **1993**, *364*, 809–814.
[29] A. B. Parekh, H. Terlau, W. Stühmer, *Nature (London)* **1993**, *364*, 814–818.
[30] J. W. Putney, Jr., G. S. J. Bird, *Cell* **1993**, *75*, 199–201.
[31] J. W. Putney, Jr., *Science* **1993**, *262*, 676–678.
[32] M. Takahashi, T. Kagasaki, T. Hosoya, S. Takahashi, *J. Antibiot.* **1993**, *46*, 1643–1647.
[33] M. Takahashi, K. Tanzawa, S. Takahashi, *J. Biol. Chem.* **1994**, *269*, 369–372.
[34] S. Takahashi, T. Kinoshita, M. Takahashi, *J. Antibiot.* **1994**, *47*, 95–100.
[35] R. C. Young, C. P. Downes, *Drug Des. Delivery* **1990**, *6*, 1–13.
[36] P. Workman, *Annal. Oncol.* **1990**, *1*, 100–111.
[37] B. V. L. Potter, *Pharmacochem. Libr.* **1993**, *20*, 185–214.
[38] A. A. Abdel-Latif, *Pharmacol. Rev.* **1986**, *38*, 227–272.
[39] M. J. Berridge, *J. Exp. Biol.* **1986**, *124*, 323–335.
[40] K. Muraki, Y. Imaizumi, M. Watanabe, *Pflügers Arch.* **1992**, *420*, 461–469.
[41] J. Altman, *Nature (London)* **1988**, *331*, 119–120.
[42] P. W. Majerus, T. M. Connolly, V. S. Bansal, R. C. Inhorn, T. S. Ross, D. L. Lips, *J. Biol. Chem.* **1988**, *263*, 3051–3054.
[43] L. E. Hokin, *Annu. Rev. Biochem.* **1985**, *54*, 205–235.
[44] S. R. Nahorski, *Trends Neurosci.* **1988**, *11*, 444–448.
[45] G. W. Mayr, *Topics in Biochemistry – Boehringer Mannheim* **1987**, 1–18.
[46] S. R. Nahorski, B. V. L. Potter, *Trends Pharmacol. Sci.* **1989**, *10*, 139–144.
[47] M. J. Berridge, *Nature (London)* **1993**, *361*, 315–325.
[48] *Inositol and Phosphoinositides: Metabolism and Regulation* (Eds.: J. E. Bleasdale, J. Eichberg, G. Hauser), Humana, Clifton, NJ, **1985**.
[49] *Molecular Mechanisms of Transmembrane Signalling* (Eds.: P. Cohen, M. D. Houslay), Elsevier, Amsterdam, **1985**.
[50] J. W. Putney, Jr., *Phosphoinositides and Receptor Mechanisms*, Liss, New York, **1986**.
[51] *Inositol Lipids and Transmembrane Signalling* (Eds.: M. J. Berridge, R. H. Michell), The Royal Society, London, **1988**.
[52] *Inositol Lipids and Cell Signalling* (Eds.: R. H. Michell, A. H. Drummond, C. P. Downes), Academic Press, London, **1989**.
[53] D. C. Billington, *Chem. Soc. Rev.* **1989**, *18*, 83–122.
[54] B. V. L. Potter, *Nat. Prod. Rep.* **1990**, *7*, 1–24.
[55] *Inositol Phosphates and Derivatives – Synthesis, Biochemistry and Therapeutic Potential* (Ed.: A. B. Reitz), American Chemical Society, Washington, DC, **1991**.
[56] D. C. Billington, *The Inositol Phosphates: Chemical Synthesis and Biological Significance*, VCH, Weinheim, **1993**.
[57] D. J. Cosgrove, *Inositol Phosphates, their Chemistry, Biochemistry and Physiology*, Elsevier, Amsterdam, **1980**.
[58] T. Posternak, *The Cyclitols*, Holden-Day, San Francisco, **1965**.
[59] L. Bouveault, *Bull. Soc. Chim. Fr.* **1894**, *11*, 144.
[60] *Inf. Bull. IUPAC* **1968**, *32*, 51.
[61] B. A. Klyashchitskii, V. I. Shvets, N. A. Preobrazhenskii, *Chem. Phys. Lipids* **1969**, *3*, 393.
[62] R. H. Michell, M. J. Berridge, *Phil. Trans. R. Soc. London Ser. B* **1988**, *320*, 237–238.
[63] R. Parthasarathy, F. Eisenberg, Jr., *Biochem. J.* **1986**, *235*, 313–322.
[64] Nomenclature Committee-IUB, *Biochem. J.* **1989**, *258*, 1–2.
[65] T. F. Donahue, S. A. Henry, *J. Biol. Chem.* **1981**, *256*, 7077–7085.
[66] T. Maeda, F. Eisenberg, Jr., *J. Biol. Chem.* **1980**, *255*, 8458–8461.
[67] L. A. Mauck, Y.-H. Wong, W. R. Sherman, *Biochemistry* **1980**, *19*, 3623–3629.
[68] F. Eisenberg, Jr., T. Maeda in *Inositol and Phosphoinositides: Metabolism and Regulation* (Eds.: J. E. Bleasdale, J. Eichberg, G. Hauser), Humana, Clifton, NJ, **1985**, pp. 3–11.
[69] F. A. Loewus, *Recent Adv. Phytochem.* **1974**, *8*, 179.
[70] F. A. Loewus, M. W. Loewus, *Annu. Rev. Plant Physiol.* **1983**, *34*, 137–161.
[71] G. R. Baker, D. C. Billington, D. Gani, *Bioorg. Med. Chem. Lett.* **1991**, *1*, 17–20.
[72] N. S. Gee, C. I. Ragan, K. J. Watling, S. Aspley, R. G. Jackson, G. G. Reid, D. Gani, J. K. Shute, *Biochem. J.* **1988**, *249*, 883–889.
[73] K. Takimoto, M. Okada, Y. Matsuda, H. Nakagawa, *J. Biochem. (Tokyo)* **1985**, *98*, 363.
[74] P. V. Attwood, J.-B. Ducep, M.-C. Chanal, *Biochem. J.* **1988**, *253*, 387–394.
[75] J. L. Meek, T. J. Rice, E. Anton, *Biochem. Biophys. Res. Commun.* **1988**, *156*, 143–148.
[76] R. Bone, J. P. Springer, J. R. Atack, *Proc. Natl. Acad. Sci. USA* **1992**, *89*, 10031–10035.
[77] J. H. Allison, M. A. Stewart, *Nature (London), New Biol.* **1971**, *233*, 267–268.
[78] M. J. Berridge, C. P. Downes, M. R. Hanley, *Biochem. J.* **1982**, *206*, 587–595.
[79] W. R. Sherman, L. Y. Munsell, B. G. Gish, M. P. Honchar, *J. Neurochem.* **1985**, *44*, 798–807.
[80] W. R. Sherman in *Inositol Lipids in Cell Signalling* (Eds.: R. H. Michell, A. H. Drummond, C. P. Downes), Academic Press, London, **1989**, pp. 39–79.
[81] A. H. Drummond, *Trends Pharmacol. Sci.* **1987**, *8*, 129–133.
[82] S. R. Nahorski, C. I. Ragan, R. A. J. Challiss, *Trends Pharmacol. Sci.* **1991**, *12*, 297–303.
[83] J. K. Shute, R. Baker, D. C. Billington, D. Gani, *J. Chem. Soc. Chem. Commun.* **1988**, 626–628.
[84] G. R. Baker, D. Gani, *Bioorg. Med. Chem. Lett.* **1991**, *1*, 193–196.
[85] B. J. Drøbak, *Biochem. J.* **1992**, *288*, 697–712.
[86] Y. Uemura, M. Sakon, J. Kambayashi, T. Tsujinaka, T. Mori, *Biochem. Int.* **1988**, *16*, 639–646.
[87] S. Cockcroft, G. M. H. Thomas, *Biochem. J.* **1992**, *288*, 1–14.
[88] Y. Nishizuka, *Nature (London)* **1984**, *308*, 693–698.
[89] U. Kikkawa, Y. Nishizuka, *Annu. Rev. Cell Biol.* **1986**, *2*, 149–178.
[90] M. Castagna, Y. Takai, K. Kaibuchi, K. Sano, U. Kikkawa, Y. Nishizuka, *J. Biol. Chem.* **1982**, *257*, 7847–7851.
[91] Y. Nishizuka, *Science* **1986**, *233*, 305–312.
[92] Y. Nishizuka, *Nature (London)* **1988**, *334*, 661–665.
[93] H. Hug, T. F. Sarre, *Biochem. J.* **1993**, *291*, 329–343.
[94] W. L. Smith, *Biochem. J.* **1989**, *259*, 315–324.
[95] B. R. Ganong, C. R. Loomis, Y. A. Hannun, R. M. Bell, *Proc. Natl. Acad. Sci. USA* **1986**, *83*, 1184–1188.
[96] J. C. Briggs, A. H. Haines, R. J. K. Taylor, A. P. Dawson, I. Gibson, J. Hook, A. Lloyd, S. Meiners, *Carbohydr. Res.* **1992**, *234*, 23–35.
[97] R. R. Rando, *FASEB J.* **1988**, *2*, 2348–2355.
[98] R. F. Irvine, *Curr. Opin. Cell Biol.* **1992**, *4*, 212–219.
[99] P. J. Parker, M. D. Waterfield, *Cell Growth Differ.* **1993**, *3*, 747–752.
[100] T. R. Jackson, L. R. Stephens, P. T. Hawkins, *J. Biol. Chem.* **1992**, *267*, 16627–16636.
[101] D. L. Lips, P. W. Majerus, F. R. Gorga, A. T. Young, T. L. Benjamin, *J. Biol. Chem.* **1989**, *264*, 8759–8763.
[102] M. J. Pazin, L. T. Williams, *Trends Biochem. Sci.* **1992**, *17*, 374–378.
[103] L. C. Cantley, K. R. Auger, C. Carpenter, B. Duckworth, A. Graziani, R. Kapeller, S. Soltoff, *Cell* **1991**, *64*, 281–302.
[104] P. C. Downes, A. W. Carter, *Cell. Signalling* **1991**, *3*, 501–513.
[105] K. Fukami, K. Furuhashi, M. Inagaki, T. Endo, S. Hatano, T. Takenawa, *Nature (London)* **1992**, *359*, 150–152.
[106] P. W. Majerus, *Annu. Rev. Biochem.* **1992**, *61*, 225–250.
[107] H. Ishii, T. M. Connolly, T. E. Bross, P. W. Majerus, *Proc. Natl. Acad. Sci. USA* **1986**, *83*, 6397–6401.
[108] P. W. Majerus, T. M. Connolly, H. Deckmyn, T. S. Ross, T. E. Bross, H. Ishii, V. S. Bansal, D. B. Wilson, *Science* **1986**, *234*, 1519–1526.
[109] A. L. Willcocks, J. Strupish, R. F. Irvine, S. R. Nahorski, *Biochem. J.* **1989**, *257*, 297–300.

[110] A. R. Hughes, T. Takemura, J. W. Putney, Jr. , *J. Biol. Chem.* **1988**, *263*, 10314–10319.
[111] **N. S. Wong, C.** J. Barker, S. B. Shears, C. J. Kirk, R. H. Michell, *Biochem. J.* **1988**, *252*, 1–5.
[112] M. J. Berridge, R. F. Irvine, *Nature (London)* **1989**, *341*, 197–205.
[113] C. P. Downes, M. C. Mussat, R. H. Michell, *Biochem. J.* **1982**, *203*, 169–177.
[114] **K. M. Laxminarayan,** M. Matzaris, C. J. Speed, C. A. Mitchell, *J. Biol. Chem.* **1993**, *268*, 4968–4974.
[115] V. Sylvia, G. Curtin, J. Norman, J. Stec, D. Busbee, *Cell* **1988**, *54*, 651–658.
[116] G. W. Mayr, *Biochem. J.* **1989**, *259*, 463–470.
[117] I. H. Batty, S. R. Nahorski, R. F. Irvine, *Biochem. J.* **1985**, *232*, 211–215.
[118] R. F. Irvine, A. J. Letcher, J. P. Heslop, M. J. Berridge, *Nature (London)* **1986**, *320*, 631–634.
[119] **R. A. Johanson, C. A. Hansen, J. R. Williams**on, *J. Biol. Chem.* **1988**, *263*, 7465–7471.
[120] **S. Y. Lee, S. S. Sim, J. W. Kim, K. H. Moon,** J. H. Kim, S. G. Rhee, *J. Biol. Chem.* **1990**, *265*, 9434–9440.
[121] **K. Y. Choi, H. K. Kim, S. Y. Lee, K. H. Moon**, S. S. Sim, J. W. Kim, H. K. **Chung, S. G. Rhee,** *Science* **1990**, *248*, 64–66.
[122] **K. Takazawa, J. Vandekerck, J. E. Dumont, C.** Erneux, *Biochem. J.* **1990**, *272*, 107–112.
[123] R. F. Irvine, *Bioessays* **1991**, *13*, 419–427.
[124] R. F. Irvine, *FEBS Lett.* **1990**, *263*, 5–9.
[125] E. Neher, *Nature (London)* **1992**, *355*, 298–299.
[126] A. Lückhoff, D. E. Clapham, *Nature (London)* **1992**, *355*, 356–358.
[127] R. F. Irvine in *Advances in Second Messenger and Phosphoprotein Research* (Ed.: J. W. Putney, Jr.), Raven, New York, **1992**, pp. 161–186.
[128] C. Erneux, M. Lemos, B. Verjans, P. Vanderhaeghen, A. Delvaux, J. E. Dumont, *Eur. J. Biochem.* **1989**, *181*, 317–322.
[129] C. A. Hansen, R. A. Johanson, M. T. Williamson, J. R. Williamson, *J. Biol. Chem.* **1987**, *262*, 17319–17326.
[130] R. F. Irvine, A. J. Letcher, D. J. Lander, M. J. Berridge, *Biochem. J.* **1986**, *240*, 301–304.
[131] J. Strupish, A. M. Cooke, B. V. L. Potter, R. Gigg, S. R. Nahorski, *Biochem. J.* **1988**, *253*, 901–905.
[132] C. Doughney, M. A. McPherson, R. L. Dormer, *Biochem. J.* **1988**, *251*, 927–929.
[133] A. Höer, D. Höer, E. Oberdisse, *Biochem. J.* **1990**, *270*, 715–719.
[134] K. Nogimori, P. J. Hughes, M. C. Glennon, M. E. Hodgson, J. W. Putney, Jr., S. B. Shears, *J. Biol. Chem.* **1991**, *266*, 16499–16506
[135] N. Ali, A. Craxton, S. B. Shears, *J. Biol. Chem.* **1993**, *268*, 6161–6167.
[136] S. B. Shears, J. B. Parry, E. K. Y. Tang, R. F. Irvine, R. H. Michell, C. J. Kirk, *Biochem. J.* **1987**, *246*, 139–147.
[137] **T. Balla, G. Guillemette, A. J. B**aukal, K. J. Catt, *J. Biol. Chem.* **1987**, *262*, 9952–9955.
[138] **D. J. Gawler, B. V. L. Potter, R.** Gigg, S. R. Nahorski, *Biochem. J.* **1991**, *276*, 163–167.
[139] I. Ivorra, R. Gigg, R. F. Irvine, I. Parker, *Biochem. J.* **1991**, *273*, 317–321.
[140] M. Abdullah, P. J. Hughes, A. Craxton, R. Gigg, T. Desai, J. F. Marecek, G. D. Prestwich, S. B. Shears, *J. Biol. Chem.* **1992**, *267*, 22340–22345.
[141] M. Vallejo, T. Jackson, S. Lightman, M. R. Hanley, *Nature (London)* **1987**, *330*, 656.
[142] M. R. Hanley, T. R. Jackson, M. Vallejo, S. I. Patterson, O. Thastrup, S. Lightman, J. Rogers, G. Henderson, A. Pini, *Phil. Trans. R. Soc. London Ser. B* **1988**, *320*, 381–398.
[143] D. Carpenter, M. R. Hanley, P. T. Hawkins, T. R. Jackson, L. R. Stephens, M. Vallejo, *Biochem. Soc. Trans.* **1989**, *17*, 3–5.
[144] P. T. Hawkins, D. R. Poyner, T. R. Jackson, A. J. Letcher, D. J. Lander, R. F. Irvine, *Biochem. J.* **1993**, *294*, 929–934.
[145] J. L. Meek, F. Nicoletti, *J. Chromatogr.* **1986**, *351*, 303–311.
[146] J. L. Meek, *Proc. Natl. Acad. Sci. USA* **1986**, *83*, 4162–4166.
[147] G. W. Mayr, *Biochem. J.* **1988**, *254*, 585–591.
[148] J. C. Lindon, D. J. Baker, R. D. Farrant, J. M. Williams, *Biochem. J.* **1986**, *233*, 275–277.
[149] **S. Cerdan, C. A. Hansen, R. Johanson, T. Inubushi, J. R. Williamson, *J. Biol. Chem.* 1986, *261*, 14676–14680.**
[150] **J. C. Lindon, D. J. Baker, J. M.** Williams, R. F. Irvine, *Biochem. J.* **1987**, *244*, 591–595.
[151] G. W. Mayr, W. Dietrich, *FEBS Lett.* **1987**, *213*, 278–282.
[152] J. Emsley, S. Niazi, *Phosphorus Sulfur Relat. Elem.* **1981**, *10*, 401.
[153] C. D. Ferris, S. H. Snyder, *Annu. Rev. Physiol.* **1992**, *54*, 469–488.
[154] C. D. Ferris, S. H. Snyder, *J. Neurosci.* **1992**, *12*, 1567–1574.
[155] S. K. Joseph, *Annu. Rep. Med. Chem.* **1992**, *27*, 261–270.
[156] K. Mikoshiba, *Trends Pharmacol. Sci.* **1993**, *14*, 86–89.
[157] K. Mikoshiba, T. Furuichi, A. Miyawaki, S. Yoshikawa, T. Nakagawa, N. Yamada, Y. Hamanaka, I. Fujino, T. Michikawa, Y. Ryo, H. Okano, S. Fujii, S. Nakade, *Phil. Trans. R. Soc. London Ser. B* **1993**, *340*, 345–349.
[158] C. W. Taylor, A. Richardson, *Pharmacol. Ther.* **1991**, *51*, 97–137.
[159] S. Supattapone, P. F. Worley, J. M. Baraban, S. H. Snyder, *J. Biol. Chem.* **1988**, *263*, 1530–1534.
[160] N. Maeda, M. Niinobe, K. Nakahira, K. Mikoshiba, *J. Neurochem.* **1988**, *51*, 1724–1730.
[161] **T. Furuichi, S. Yoshikawa, A. Miyawaki,** K. Wada, N. Maeda, K. Mikoshiba, *Nature (London)* **1989**, *342*, 32–38.
[162] M. C. Glennon, S. B. Shears, *Biochem. J.* **1993**, *293*, 583–590.
[163] G. A. Mignery, C. L. Newton, B. T. Archer III, T. C. Südhof, *J. Biol. Chem.* **1990**, *265*, 12679–12685.
[164] **T. C. Südhof, C. L. Newton, B. T. Archer III, Y. A. Ushkaryov,** G. A. Mignery, *EMBO J.* **1991**, *10*, 3199–3206.
[165] **S. Yoshikawa, T. Tanimura, A. Miyawaki, M. Nakamura, M.** Yuzaki, T. **Furuichi, K. Mikoshiba,** *J. Biol. Chem.* **1992**, *267*, 16613–16619.
[166] **C. D. Ferris, R. L. Huganir, S. Supattapone, S. H. Snyder,** *Nature (London)* **1989**, *342*, 87–89.
[167] N. Maeda, M. Niinobe, K. Mikoshiba, *EMBO J.* **1990**, *9*, 61–67.
[168] N. Maeda, T. Kawasaki, S. Nakade, N. Yokota, T. Taguchi, M. Kasai, K. **Mikoshiba,** *J. Biol. Chem.* **1991**, *266*, 1109–1116.
[169] G. A. Mignery, T. C. Südhof, *EMBO J.* **1990**, *9*, 3893–3898.
[170] A. Miyawaki, T. Furuichi, Y. Ryou, S. Yoshikawa, T. Nakagawa, T. Saitoh, **K. Mikoshiba,** *Proc. Natl. Acad. Sci. USA* **1991**, *88*, 4911–4915.
[171] T. Meyer, T. Wenzel, L. Stryer, *Biochemistry* **1990**, *29*, 32.
[172] Y. Mori, T. Friedrich, M.-S. Kim, A. Mikami, J. Nakai, P. Ruth, E. Bosse, F. Hofmann, V. Flockerzi, T. Furuichi, K. Mikoshiba, K. Imoto, T. Tanabe, S. Numa, *Nature (London)* **1989**, *350*, 398–402.
[173] G. A. Mignery, T. C. Südhof, K. Takei, P. De Camilli, *Nature (London)* **1989**, *342*, 192–195.
[174] H. Takeshima, S. Nishimura, T. Matsumoto, H. Ishida, K. Kangawa, N. Minamino, H. Matsuo, M. Ueda, M. Hanaoka, T. Hirose, S. Numa, *Nature (London)* **1989**, *339*, 439–445.
[175] R. J. Mourey, V. A. Estevez, J. F. Marecek, R. K. Barrow, G. D. Prestwich, S. H. Snyder, *Biochemistry* **1993**, *32*, 1719–1726.
[176] S. K. Danoff, C. D. Ferris, C. Donath, G. A. Fischer, S. Munemitsu, A. Ullrich, S. H. Snyder, C. A. Ross, *Proc. Natl. Acad. Sci. USA* **1991**, *88*, 2951–2955.
[177] I. Bezprozvanny, J. Watras, B. E. Ehrlich, *Nature (London)* **1991**, *351*, 751–754.
[178] C. A. Ross, S. K. Danoff, M. J. Schell, S. H. Snyder, A. Ullrich, *Proc. Natl. Acad. Sci. USA* **1992**, *89*, 4265–4269.
[179] O. Blondel, J. Takeda, H. Janssen, S. Seino, G. I. Bell, *J. Biol. Chem.* **1993**, *268*, 11356–11363.
[180] A. R. Maranto, *J. Biol. Chem.* **1994**, *269*, 1222–1230.
[181] J. D. Moyer, N. Malinowski, E. A. Napier, J. Strong, *Biochem. J.* **1988**, *254*, 95–100.
[182] R. Spector, *Neurochem. Res.* **1988**, *13*, 785.
[183] M. D. Tuersley, L. Best, S. Tomlinson, *J. Neurochem.* **1988**, *51*, 1610.
[184] M. J. Berridge, *Biochim. Biophys. Acta* **1987**, *907*, 33–45.
[185] A. P. Kozikowski, A. H. Fauq, G. Powis, D. C. Melder, *J. Am. Chem. Soc.* **1990**, *112*, 4528–4531.
[186] **A. P. Kozikowski, Y. Xi**a, J. M. Rusnak, *J. Chem. Soc. Chem. Commun.* **1988**, 1301–1303.
[187] **J. L. Offer, G. A. Smith,** J. C. Metcalfe, *Biochem. Soc. Trans.* **1990**, *18*, 590–591.
[188] **J. L. Offer, J. C. Metcalfe,** G. A. Smith, *J. Chem. Soc. Chem. Commun.* **1990**, 1312–1313.
[189] **J. L. Offer, H. P. Voorhei**s, J. C. Metcalfe, G. A. Smith, *J. Chem. Soc. Perkin Trans. 1* **1992**, 953–960.
[190] S. S. Yang, T. R. Beattie, T. Y. Shen, *Tetrahedron Lett.* **1982**, *23*, 5517–5520.
[191] D. A. Sawyer, B. V. L. Potter, *J. Chem. Soc. Perkin Trans. 1* **1992**, 923–932.
[192] G. Lowe, F. McPhee, *J. Chem. Soc. Perkin Trans. 1* **1991**, 1249–1253.
[193] S. S. Yang, T. R. Beattie, T. Y. Shen, *Synth. Commun.* **1986**, *16*, 131–138.
[194] S. S. Yang, J. M. Min, T. R. Beattie, *Synth. Commun.* **1988**, *18*, 899–905.
[195] J. P. Guidot, T. Le Gall, *Tetrahedron Lett.* **1993**, *34*, 4647–4650.
[196] A. P. Kozikowski, A. H. Fauq, J. M. Rusnak, *Tetrahedron Lett.* **1989**, *30*, 3365–3368.
[197] A. P. Kozikowski, A. H. Fauq, G. Powis, D. C. Melder, *Med. Chem. Res.* **1991**, *1*, 277–282.
[198] G. Powis, I. A. Aksoy, D. C. Melder, S. Aksoy, H. Eichinger, A. H. Fauq, A. P. Kozikowski, *Cancer Chemother. Pharmacol.* **1991**, *29*, 95–104.
[199] A. P. Kozikowski, G. Powis, A. Gallegos, W. Tückmantel, *Bioorg. Med. Chem. Lett.* **1993**, *3*, 1323–1326.
[200] A. P. Kozikowski, A. H. Fauq, M. J. Malaska, W. Tückmantel, V. I. Ognyanov, G. Powis, *Curr. Med. Chem.* **1994**, *1*, 1–12.
[201] S. V. Ley, M. Parra, A. J. Redgrave, F. Sternfeld, *Tetrahedron* **1990**, *46*, 4995–5026.
[202] C. Jiang, J. D. Moyer, D. C. Baker, *J. Carbohydr. Chem.* **1987**, *6*, 319–355.
[203] C. Jiang, D. J. A. Schedler, P. E. Morris, Jr. , A. A. Zayed, D. C. Baker, *Carbohydr. Res.* **1990**, *207*, 277–285.
[204] G. Lowe, B. V. L. Potter, *J. Chem. Soc. Perkin Trans. 1* **1980**, 2029
[205] J. D. Moyer, O. Reizes, A. Surender, C. Jiang, N. Malinowski, D. C. Baker, *Mol. Pharmacol.* **1988**, *33*, 683–689.
[206] **S. C. Johnson, J. Dahl, T.-L. Shih, D. J. A. Schedler, L.** Anderson, T. L. Benjamin, D. C. Baker, *J. Med. Chem.* **1993**, *36*, 3628–3635.

[207] F. McPhee, C. P. Downes, G. Lowe, *Biochem. J.* **1991**, *277*, 407–412.
[208] J. L. Offer, J. C. Metcalfe, G. A. Smith, *Biochem. J.* **1993**, *291*, 553–560.
[209] H. Hönig, P. Seufer-Wasserthal, A. E. Stütz, E. Zenz, *Tetrahedron Lett.* **1989**, *30*, 811–812.
[210] K.-L. Yu, K.-Y. Ko, B. Fraser-Reid, *Synth. Commun.* **1988**, *18*, 465–468.
[211] S. J. Angyal, M. E. Tate, *J. Chem. Soc.* **1961**, 4122–4128.
[212] J. Gigg, R. Gigg, S. Payne, R. Conant, *Carbohydr. Res.* **1985**, *142*, 132–134.
[213] J. Gigg, R. Gigg, S. Payne, R. Conant, *J. Chem. Soc. Perkin Trans. 1* **1987**, 423–429.
[214] J. Gigg, R. Gigg, S. Payne, R. Conant, *J. Chem. Soc. Perkin Trans. 1* **1987**, 1757–1762.
[215] J. Gigg, R. Gigg, S. Payne, R. Conant, *J. Chem. Soc. Perkin Trans. 1* **1987**, 2411–2414.
[216] P. J. Garegg, T. Iversen, R. Johansson, B. Lindberg, *Carbohydr. Res.* **1984**, *130*, 322–326.
[217] P. J. Garegg, B. Lindberg, I. Kvarnström, S. C. T. Svensson, *Carbohydr. Res.* **1985**, *139*, 209–215.
[218] P. J. Garegg, B. Lindberg, I. Kvarnström, S. C. T. Svensson, *Carbohydr. Res.* **1988**, *173*, 205–216.
[219] V. I. Shvets, A. E. Stepanov, V. N. Krylova, P. V. Gulak, *myo-Inositol and Phosphoinositides*, Nauka, Moscow, **1987**.
[220] A. E. Stepanov, V. I. Shvets, *Chem. Phys. Lipids* **1979**, *25*, 247–263.
[221] S. Ozaki, M. Kohno, H. Nakahira, M. Bunya, Y. Watanabe, *Chem. Lett.* **1988**, 77–80.
[222] Y. Watanabe, T. Shinohara, T. Fujimoto, S. Ozaki, *Chem. Pharm. Bull.* **1990**, *38*, 562–563.
[223] G. Baudin, B. I. Glänzer, K. S. Swaminathan, A. Vasella, *Helv. Chim. Acta* **1988**, *71*, 1367–1378.
[224] Y.-C. Liu, C.-S. Chen, *Tetrahedron Lett.* **1989**, *30*, 1617–1620.
[225] D.-M. Gou, C.-S. Chen, *Tetrahedron Lett.* **1992**, *33*, 721–724.
[226] D.-M. Gou, Y.-C. Liu, C.-S. Chen, *Carbohydr. Res.* **1992**, *234*, 51–64.
[227] L. Ling, Y. Watanabe, T. Akiyama, S. Ozaki, *Tetrahedron Lett.* **1992**, *33*, 1911–1914.
[228] L. Ling, X. Li, Y. Watanabe, T. Akiyama, S. Ozaki, *Bioorg. Med. Chem.* **1993**, *1*, 155–159.
[229] P. Andersch, M. P. Schneider, *Tetrahedron: Asymmetry* **1993**, *4*, 2135–2138.
[230] R. J. Ferrier, *J. Chem. Soc. Perkin Trans. 1* **1979**, 1455–1458.
[231] S. T. Safrany, R. J. H. Wojcikiewicz, J. Strupish, S. R. Nahorski, D. Dubreuil, J. Cleophax, S. D. Gero, B. V. L. Potter, *FEBS Lett.* **1991**, *278*, 252–256.
[232] K. Sato, S. Sakuma, S. Muramatsu, M. Bokura, *Chem. Lett.* **1991**, *1991*, 1473–1474.
[233] K. Sato, M. Bokura, M. Taniguchi, *Bull. Chem. Soc. Jpn.* **1994**, *67*, 1633–1640.
[234] C. Jaramillo, J.-L. Chiara, M. Martin-Lomas, *J. Org. Chem.* **1994**, *59*, 3135–3141.
[235] S. L. Bender, R. J. Budhu, *J. Am. Chem. Soc.* **1991**, *113*, 9883–9885.
[236] V. A. Estevez, G. D. Prestwich, *J. Am. Chem. Soc.* **1991**, *113*, 9885–9887.
[237] J. L. Chiara, M. Martin-Lomas, *Tetrahedron Lett.* **1994**, *35*, 2969–2972.
[238] H. Schiff, *Justus Liebigs Ann. Chem.* **1857**, *102*, 334–339.
[239] T. Desai, A. Fernandez-Mayoralas, J. Gigg, R. Gigg, S. Payne, *Carbohydr. Res.* **1992**, *234*, 157–175.
[240] A. M. Cooke, N. J. Noble, S. Payne, R. Gigg, B. V. L. Potter, *J. Chem. Soc. Chem. Commun.* **1989**, 269–271.
[241] A. M. Cooke, N. J. Noble, R. Gigg, A. L. Willcocks, J. Strupish, S. R. Nahorski, B. V. L. Potter, *Biochem. Soc. Trans.* **1988**, *16*, 992–993.
[242] N. J. Noble, A. M. Cooke, B. V. L. Potter, *Carbohydr. Res.* **1992**, *234*, 177–187.
[243] S. Ozaki, Y. Watanabe, T. Ogasawara, Y. Kondo, N. Shiotani, H. Nishii, T. Matsuki, *Tetrahedron Lett.* **1986**, *27*, 3157–3160.
[244] B. M. Iselin, *J. Am. Chem. Soc.* **1949**, *71*, 3822–3825.
[245] D. Mercier, J. E. G. Barnett, S. D. Gero, *Tetrahedron* **1969**, *25*, 5681–5687.
[246] Y. Watanabe, T. Ogasawara, H. Nakahira, T. Matsuki, S. Ozaki, *Tetrahedron Lett.* **1988**, *29*, 5259–5262.
[247] D. J. Cosgrove, *Carbohydr. Res.* **1975**, *40*, 380–384.
[248] H. G. Khorana, A. R. Todd, *J. Chem. Soc.* **1953**, 2257–2260.
[249] Y. Watanabe, H. Nahahira, M. Bunya, S. Ozaki, *Tetrahedron Lett.* **1987**, *28*, 4179–4180.
[250] S. J. DeSolms, J. P. Vacca, J. R. Huff, *Tetrahedron Lett.* **1987**, *28*, 4503–4506.
[251] J. P. Vacca, S. J. DeSolms, J. R. Huff, D. C. Billington, R. Baker, J. J. Kulagowski, I. M. Mawer, *Tetrahedron* **1989**, *45*, 5679–5702.
[252] P. M. J. Burgers, F. Eckstein, *Tetrahedron Lett.* **1978**, *40*, 3835–3838.
[253] C. E. Dreef, G. W. Mayr, J.-P. Jansze, H. C. P. F. Roelen, G. A. van der Marel, J. H. van Boom, *Bioorg. Med. Chem. Lett.* **1991**, *1*, 239–242.
[254] F. Eckstein, *Angew. Chem.* **1983**, *95*, 431–514; *Angew. Chem. Int. Ed. Engl.* **1983**, *22*, 423–506.
[255] J. L. Meek, F. Davidson, F. W. Hobbs Jr, *J. Am. Chem. Soc.* **1988**, *110*, 2317–2318.
[256] S. J. Mills, S. T. Safrany, R. A. Wilcox, S. R. Nahorski, B. V. L. Potter, *Bioorg. Med. Chem. Lett.* **1993**, *3*, 1505–1510.
[257] C. E. Dreef, G. A. van der Marel, J. H. van Boom, *Recl. Trav. Chim. Pays-Bas* **1987**, *106*, 161–162.
[258] K. L. Yu, B. Fraser-Reid, *Tetrahedron Lett.* **1988**, *29*, 979–982.
[259] Y. Watanabe, Y. Komoda, K. Ebisuya, S. Ozaki, *Tetrahedron Lett.* **1990**, *31*, 255–256.
[260] A. M. Cooke, B. V. L. Potter, R. Gigg, *Tetrahedron Lett.* **1987**, *28*, 2305–2308.
[261] A. M. Cooke, R. Gigg, B. V. L. Potter, *Biochem. Soc. Trans.* **1987**, *15*, 904–906.
[262] M. R. Hamblin, B. V. L. Potter, R. Gigg, *Biochem. Soc. Trans.* **1987**, *15*, 415–416.
[263] G. Lin, M. D. Tsai, *J. Am. Chem. Soc.* **1989**, *111*, 3099–3101.
[264] G. Lin, F. Bennett, M. D. Tsai, *Biochemistry* **1990**, *29*, 2747–2757.
[265] G. M. Salamonczyk, K. S. Bruzik, *Tetrahedron Lett.* **1990**, *31*, 2015–2016.
[266] C. E. Dreef, C. J. J. Elie, P. Hoogerhout, G. A. van der Marel, J. H. van Boom, *Tetrahedron Lett.* **1988**, *29*, 6513–6516.
[267] C. J. J. Elie, C. E. Dreef, R. Verduyn, G. A. van der Marel, J. H. van Boom, *Tetrahedron* **1989**, *45*, 3477–3486.
[268] B. Duthu, D. Houalla, R. Wolf, *Can. J. Chem.* **1988**, *66*, 2965–2974.
[269] W. Bannwarth, A. Trzeciak, *Helv. Chim. Acta* **1987**, *70*, 175–186.
[270] D. C. Billington, R. Baker, J. J. Kulagowski, I. M. Mawer, *J. Chem. Soc. Chem. Commun.* **1987**, 314–316.
[271] H. A. J. Carless, K. Busia, *Carbohydr. Res.* **1992**, *234*, 207–215.
[272] C. E. Ballou, L. I. Pizer, *J. Am. Chem. Soc.* **1960**, *82*, 3333–3335.
[273] T. Akiyama, N. Takechi, S. Ozaki, *Tetrahedron Lett.* **1990**, *31*, 1433–1434.
[274] T. Akiyama, N. Takechi, S. Ozaki, K. Shiota, *Bull. Chem. Soc. Jpn.* **1992**, *65*, 366–372.
[275] G. M. Salamonczyk, K. M. Pietrusiewicz, *Tetrahedron Lett.* **1991**, *32*, 4031–4032.
[276] K. M. Pietrusiewicz, G. M. Salamonczyk, K. S. Bruzik, W. Wieczorek, *Tetrahedron* **1992**, *48*, 5523–5542; *ibid.* **1994**, *50*, 573.
[277] J. G. Molotkovsky, L. D. Bergelson, *Tetrahedron Lett.* **1971**, *50*, 4791–4794.
[278] T. Metschies, C. Schultz, B. Jastorff, *Tetrahedron Lett.* **1988**, *29*, 3921–3922.
[279] A. L. Leavitt, W. R. Sherman, *Carbohydr. Res.* **1982**, *103*, 203–212.
[280] D. C. Billington, R. Baker, J. J. Kulagowski, I. M. Mawer, J. P. Vacca, S. J. DeSolms, J. R. Huff, *J. Chem. Soc. Perkin Trans. 1* **1989**, 1423–1429.
[281] H. W Lee, Y. Kishi, *J. Org. Chem.* **1985**, *50*, 4402–4404.
[282] D. C. Billington, R. Baker, *J. Chem. Soc. Chem. Commun.* **1987**, 1011–1013.
[283] Y. Watanabe, M. Mitani, T. Morita, S. Ozaki, *J. Chem. Soc. Chem. Commun.* **1989**, 482–483.
[284] V. N. Krylova, N. I. Kobelkova, G. F. Oleinik, V. I. Shvets, *Zhur. Org. Khim.* **1980**, *16*, 62–68.
[285] M. R. Hamblin, J. S. Flora, B. V. L. Potter, *Biochem. J.* **1987**, *246*, 771–774.
[286] A. E. Stepanov, B. A. Klyashchitskii, V. I. Shvets, R. P. Evstigneeva, *Bioorg. Khim.* **1976**, *2*, 1627.
[287] G. M. Salamonczyk, K. M. Pietrusiewicz, *Tetrahedron Lett.* **1991**, *32*, 6167–6170.
[288] I. M. Bird, I. H. Sadler, B. C. Williams, S. W. Walker, *Mol. Cell. Endocrinol.* **1989**, *66*, 215–229.
[289] P. Westerduin, H. A. M. Willems, C. A. A. van Boeckel, *Tetrahedron Lett.* **1990**, *31*, 6915–6918.
[290] M. R. Hamblin, B. V. L. Potter, R. Gigg, *J. Chem. Soc. Chem. Commun.* **1987**, 626–627.
[291] H. A. J. Carless, K. Busia, *Tetrahedron Lett.* **1990**, *31*, 3449–3452.
[292] S. Ozaki, Y. Kondo, N. Shiotani, T. Ogasawara, Y. Watanabe, *J. Chem. Soc. Perkin Trans. 1* **1992**, 729–737.
[293] A. M. Cooke, Dissertation, University of Leicester, **1991**.
[294] A. E. Stepanov, O. B. Runova, V. N. Krylova, V. I. Shvets, V. N. Bochkov, G. Schlewer, B. Spiess, *Bioorg. Khim.* **1991**, *17*, 258–267.
[295] V. I. Shvets, A. E. Stepanov, L. Schmitt, B. Spiess, G. Schlewer in *Inositol Phosphates and Derivatives – Synthesis, Biochemistry, and Therapeutic Potential* (Eds.: A. B. Reitz), American Chemical Society, Washington, DC, **1991**, pp. 155–171.
[296] C. B. Reese, J. G. Ward, *Tetrahedron Lett.* **1987**, *28*, 2309–2312.
[297] J. P. Vacca, S. J. DeSolms, J. R. Huff, *J. Am. Chem. Soc.* **1987**, *109*, 3478–3479.
[298] C. E. Dreef, R. J. Tuinman, C. J. J. Elie, G. A. van der Marel, J. H. van Boom, *Recl. Trav. Chim. Pays-Bas* **1988**, *107*, 395–397.
[299] K. S. Bruzik, J. Myers, M. D. Tsai, *Tetrahedron Lett.* **1992**, *33*, 1009–1012.
[300] A. Aguilo, M. Martin-Lomas, S. Penades, *Tetrahedron Lett.* **1992**, *33*, 401–404.
[301] K. S. Bruzik, G. M. Salamonczyk, *Carbohydr. Res.* **1989**, *195*, 67–73.
[302] S. V. Ley, F. Sternfeld, *Tetrahedron Lett.* **1988**, *29*, 5305–5308.
[303] S. V. Ley, F. Sternfeld, S. Taylor, *Tetrahedron Lett.* **1987**, *28*, 225–226.
[304] H. A. J. Carless, K. Busia, *Tetrahedron Lett.* **1990**, *31*, 1617–1620.
[305] J. R. Falck, P. Yadagiri, *J. Org. Chem.* **1989**, *54*, 5851–5852.
[306] W. Tegge, C. E. Ballou, *Proc. Natl. Acad. Sci. USA* **1989**, *86*, 94–98.
[307] A. E. Stepanov, O. B. Runova, G. Schlewer, B. Spiess, V. I. Shvets, *Tetrahedron Lett.* **1989**, *30*, 5125–5128.
[308] Y. Watanabe, T. Fujimoto, T. Shinohara, S. Ozaki, *J. Chem. Soc. Chem. Commun.* **1991**, 428–429.
[309] J. F. Marecek, G. D. Prestwich, *J. Labelled Compd. Radiopharm.* **1989**, *27*, 917–925.

[310] R. J. Auchus, S. L. Kaiser, P. W. Majerus, *Proc. Natl. Acad. Sci. USA* **1987**, *84*, 1206–1209.
[311] Y. Watanabe, T. Ogasawara, N. Shiotani, S. Ozaki, *Tetrahedron Lett.* **1987**, *28*, 2607–2610.
[312] W. Tegge, G. V. Denis, C. E. Ballou, *Carbohydr. Res.* **1991**, *217*, 107–116.
[313] M. F. Boehm, G. D. Prestwich, *Tetrahedron Lett.* **1988**, *29*, 5217–5220.
[314] A. M. Riley, R. Payne, B. V. L. Potter, *J. Med. Chem.* **1994**, *37*, 3918–3927.
[315] S. J. Mills, J. Al-Hafidh, J. Westwick, B. V. L. Potter, *Bioorg. Med. Chem. Lett.* **1993**, *3*, 2599–2604.
[316] Y. Watanabe, T. Ogasawara, S. Ozaki, M. Hirata, *Carbohydr. Res.* **1994**, *258*, 87–92.
[317] A. M. Cooke, D. C. Billington, B. V. L. Potter, unpublished results.
[318] R. A. Wilcox, R. A. J. Challiss, G. Baudin, A. Vasella, B. V. L. Potter, S. R. Nahorski, *Biochem. J.* **1993**, *294*, 191–194.
[319] S. Ozaki, Y. Kondo, H. Nakahira, S. Yamaoka, Y. Watanabe, *Tetrahedron Lett.* **1987**, *28*, 4691–4694.
[320] Y. Watanabe, A. Oka, Y. Shimizu, S. Ozaki, *Tetrahedron Lett.* **1990**, *31*, 2613–2616.
[321] M. R. Hamblin, L. R. Stephens, B. V. L. Potter, unpublished results.
[322] A. P. Kozikowski, V. I. Ognyanov, A. H. Fauq, R. A. Wilcox, S. R. Nahorski, *J. Chem. Soc. Chem. Commun.* **1994**, 599–600.
[323] R. Baker, J. J. Kulagowski, D. C. Billington, P. D. Leeson, I. C. Lennon, N. J. Liverton, *J. Chem. Soc. Perkin Trans. 1* **1989**, 1383–1385.
[324] S. Ozaki, Y. Watanabe in *Inositol Phosphates and Derivatives – Synthesis, Biochemistry, and Therapeutic Potential* (Eds.: A. B. Reitz), American Chemical Society, Washington, DC, **1991**, pp. 43–65.
[325] M. J. Seewald, I. A. Aksoy, G. Powis, A. H. Fauq, A. P. Kozikowski, *J. Chem. Soc. Chem. Commun.* **1990**, 1638–1639.
[326] A. P. Kozikowski, V. I. Ognyanov, A. H. Fauq, S. R. Nahorski, R. A. Wilcox, *J. Am. Chem. Soc.* **1993**, *115*, 4429–4434.
[327] S. V. Ley, M. Parra, A. J. Redgrave, F. Sternfeld, A. Vidal, *Tetrahedron Lett.* **1989**, *30*, 3557–3560.
[328] M. A. Polokoff, G. H. Bencen, J. P. Vacca, S. J. DeSolms, S. D. Young, J. R. Huff, *J. Biol. Chem.* **1988**, *263*, 11922–11927.
[329] J. F. Marecek, G. D. Prestwich, *Tetrahedron Lett.* **1989**, *30*, 5401–5404.
[330] S. T. Safrany, D. Sawyer, R. J. H. Wojcikiewicz, S. R. Nahorski, B. V. L. Potter, *FEBS Lett.* **1990**, *276*, 91–94.
[331] D. A. Sawyer, B. V. L. Potter, *Bioorg. Med. Chem. Lett.* **1991**, *1*, 705–710.
[332] S. T. Safrany, D. A. Sawyer, S. R. Nahorski, B. V. L. Potter, *Chirality* **1992**, *4*, 415–422.
[333] D. Lampe, B. V. L. Potter, *Tetrahedron Lett.* **1993**, *34*, 2365–2368.
[334] A. P. Kozikowski, A. H. Fauq, I. A. Aksoy, M. J. Seewald, G. Powis, *J. Am. Chem. Soc.* **1990**, *112*, 7403–7404.
[335] C. Liu, S. R. Nahorski, B. V. L. Potter, *J. Chem. Soc. Chem. Commun.* **1991**, 1014–1016.
[336] C. Liu, S. R. Nahorski, B. V. L. Potter, *Carbohydr. Res.* **1992**, *234*, 107–115.
[337] C. Liu, S. T. Safrany, S. R. Nahorski, B. V. L. Potter, *Bioorg. Med. Chem. Lett.* **1992**, *2*, 1523–1528.
[338] A. H. Fauq, A. P. Kozikowski, V. I. Ognyanov, R. A. Wilcox, S. R. Nahorski, *J. Chem. Soc. Chem. Commun.* **1994**, 1301–1302.
[339] A. P. Kozikowski, A. H. Fauq, R. A. Wilcox, R. A. J. Challiss, S. R. Nahorski, *J. Med. Chem.* **1994**, *37*, 868–872.
[340] F. Eckstein, G. Gish, *Trends Biochem. Sci.* **1989**, *14*, 97–100.
[341] F. Eckstein, *Annu. Rev. Biochem.* **1985**, *54*, 367–402.
[342] R. A. J. Challiss, E. R. Chilvers, A. L. Willcocks, S. R. Nahorski, *Biochem. J.* **1990**, *265*, 421–427.
[343] R. A. J. Challiss, S. M. Smith, B. V. L. Potter, S. R. Nahorski, *FEBS Lett.* **1991**, *281*, 101–104.
[344] D. Lampe, S. J. Mills, B. V. L. Potter, *J. Chem. Soc. Perkin Trans. 1* **1992**, 2899–2906.
[345] G. R. Baker, D. C. Billington, D. Gani, *Tetrahedron* **1991**, *47*, 3895–3908.
[346] A. M. Cooke, L. James, S. R. Nahorski, B. V. L. Potter, *Phosphorus Sulfur Silicon Relat. Elem.* **1990**, *51/52*, 19–22.
[347] C. Schultz, T. Metschies, B. Jastorff, *Tetrahedron Lett.* **1988**, *29*, 3919–3920.
[348] A. M. Cooke, R. Gigg, B. V. L. Potter, *J. Chem. Soc. Chem. Commun.* **1987**, 1525–1526.
[349] N. J. Noble, D. Dubreuil, B. V. L. Potter, *Bioorg. Med. Chem. Lett.* **1992**, *2*, 471–476.
[350] D. Lampe, B. V. L. Potter, *J. Chem. Soc. Chem. Commun.* **1990**, 1500–1501.
[351] S. T. Safrany, R. A. Wilcox, C. Liu, D. Dubreuil, B. V. L. Potter, S. R. Nahorski, *Mol. Pharmacol.* **1993**, *43*, 499–503.
[352] C. Liu, J. Al-Hafidh, J. Westwick, B. V. L. Potter, *Bioorg. Med. Chem.* **1994**, *2*, 253–257.
[353] D. Lampe, C. Liu, B. V. L. Potter, *J. Med. Chem.* **1994**, *37*, 907–912.
[354] P. Folk, E. Kmonickova, L. Krpejsova, A. Strunecka, *J. Labelled Compd. Radiopharm.* **1988**, *25*, 793–803.
[355] C. Liu, B. V. L. Potter, *Tetrahedron Lett.* **1994**, *35*, 1605–1608.
[356] R. A. Wilcox, E. M. Whitham, C. Liu, B. V. L. Potter, S. R. Nahorski, *FEBS Lett.* **1993**, *336*, 267–271.
[357] A. P. Kozikowski, A. H. Fauq, R. A. Wilcox, S. R. Nahorski, *J. Org. Chem.* **1994**, *59*, 2279–2281.
[358] C. E. Dreef, G. A. van der Marel, J. H. van Boom, *Recl. Trav. Chim. Pays-Bas* **1987**, *106*, 512–513.
[359] J. R. Falck, A. Abdali, S. J. Wittenberger, *J. Chem. Soc. Chem. Commun.* **1990**, 953–955.
[360] C. E. Dreef, W. Schiebler, G. A. van der Marel, J. H. van Boom, *Tetrahedron Lett.* **1991**, *32*, 6021–6024.
[361] C. E. Dreef, J.-P. Jansze, C. J. J. Elie, G. A. van der Marel, J. H. van Boom, *Carbohydr. Res.* **1992**, *234*, 37–50.
[362] C. E. Dreef, R. J. Tuinman, A. W. M. Lefeber, C. J. J. Elie, G. A. van der Marel, J. H. van Boom, *Tetrahedron* **1991**, *47*, 4709–4722.
[363] C. E. Dreef, M. Douwes, C. J. J. Elie, G. A. van der Marel, J. H. van Boom, *Synthesis* **1991**, 443–447.
[364] L. Schmitt, B. Spiess, G. Schlewer, *Tetrahedron Lett.* **1993**, *34*, 7059–7060.
[365] H. A. M. Willems, G. H. Veeneman, P. Westerduin, *Tetrahedron Lett.* **1992**, *33*, 2075–2078.
[366] P. Westerduin, H. A. M. Willems, C. A. A. van Boeckel, *Carbohydr. Res.* **1992**, *234*, 131–140.
[367] J. H. Kaplan, A. P. Somlyo, *Trends Neurosci.* **1989**, *12*, 54–59.
[368] J. A. McCray, D. R. Trentham, *Annu. Rev. Biophys. Biophys. Chem.* **1989**, *18*, 239.
[369] J. W. Walker, G. P. Reid, J. A. McCray, D. R. Trentham, *J. Am. Chem. Soc.* **1988**, *110*, 7170–7177.
[370] J. W. Walker, J. Feeney, D. R. Trentham, *Biochemistry* **1989**, *28*, 3272–3280.
[371] J. W. Walker, A. V. Somlyo, Y. E. Goldman, A. P. Somlyo, D. R. Trentham, *Nature (London)* **1987**, *327*, 249–252.
[372] A. V. Somlyo, K. Horiuti, D. R. Trentham, T. Kitazawa, A. P. Somlyo, *J. Biol. Chem.* **1992**, *267*, 22316–22322.
[373] M. R. Blatt, G. Thiel, D. R. Trentham, *Nature (London)* **1990**, *346*, 766–769.
[374] M. Hirata, T. Sasaguri, T. Hamachi, T. Hashimoto, M. Kukita, T. Koga, *Nature (London)* **1985**, *317*, 723–725.
[375] T. Ishimatsu, Y. Kimura, T. Ikebe, K. Yamaguchi, T. Koga, M. Hirata, *Biochem. Biophys. Res. Commun.* **1988**, *155*, 1173–1180.
[376] S. Ozaki, Y. Watanabe, T. Ogasawara, M. Hirata, T. Kanematsu, *Carbohydr. Res.* **1992**, *234*, 189–206.
[377] M. Hirata, Y. Watanabe, T. Ishimatsu, F. Yanaga, T. Koga, S. Ozaki, *Biochem. Biophys. Res. Commun.* **1990**, *168*, 379–386.
[378] Y. Watanabe, M. Hirata, T. Ogasawara, T. Koga, S. Ozaki, *Bioorg. Med. Chem. Lett.* **1991**, *1*, 399–402.
[379] S. Ozaki, Y. Koga, L. Ling, Y. Watanabe, Y. Kimura, M. Hirata, *Bull. Chem. Soc. Jpn.* **1994**, *67*, 1058–1063.
[380] A. N. Jina, J. Ralph, C. E. Ballou, *Biochemistry* **1990**, *29*, 5203–5209.
[381] D.-M. Gou, W.-R. Shieh, P.-J. Lu, C.-S. Chen, *Bioorg. Med. Chem.* **1994**, *2*, 7–13.
[382] G. D. Prestwich, J. F. Marecek, R. J. Mourey, A. B. Theibert, C. D. Ferris, S. K. Danoff, S. H. Snyder, *J. Am. Chem. Soc.* **1991**, *113*, 1822–1825.
[383] G. D. Prestwich, V. A. Estevez, *Tetrahedron Lett.* **1991**, *32*, 1623–1626.
[384] J. F. Marecek, G. D. Prestwich, *Tetrahedron Lett.* **1991**, *32*, 1863–1866.
[385] A. B. Theibert, V. A. Estevez, C. D. Ferris, S. K. Danoff, R. K. Barrow, G. D. Prestwich, S. H. Snyder, *Proc. Natl. Acad. Sci. USA* **1991**, *88*, 3165–3169.
[386] A. B. Theibert, V. A. Estevez, R. J. Mourey, J. F. Marecek, R. K. Barrow, G. D. Prestwich, S. H. Snyder, *J. Biol. Chem.* **1992**, *267*, 9071–9079.
[387] D. L. Kalinoski, S. B. Aldinger, A. G. Boyle, T. Huque, J. F. Marecek, G. D. Prestwich, D. Restrepo, *Biochem. J.* **1992**, *281*, 449–456.
[388] S. M. Voglmaier, J. H. Keen, J.-E. Murphy, C. D. Ferris, G. D. Prestwich, S. H. Snyder, A. B. Theibert, *Biochem. Biophys. Res. Commun.* **1992**, *187*, 158–163.
[389] J. F. Marecek, V. A. Estevez, G. D. Prestwich, *Carbohydr. Res.* **1992**, *234*, 65–73.
[390] W. Tegge, Dissertation, Universität Bremen, **1986**.
[391] C. Schultz, M. Vajanaphanich, A. T. Harootunian, P. J. Sammak, K. E. Barrett, R. Y. Tsien, *J. Biol. Chem.* **1993**, *268*, 6316–6322.
[392] C. Schultz, R. Y. Tsien, *FASEB J.* **1992**, *6*, A1924.
[393] V. Henne, G. W. Mayr, B. Grabowski, B. Koppitz, H.-D. Söling, *Eur. J. Biochem.* **1988**, *174*, 95–101.
[394] P. Westerduin, H. A. M. Willems, C. A. A. van Boeckel, *Tetrahedron Lett.* **1990**, *31*, 6919–6922.
[395] A. P. Kozikowski, V. I. Ognyanov, C. Chen, P. Kurian, F. T. Crews, *Tetrahedron Lett.* **1993**, *34*, 219–222.
[396] C. Liu, N. F. Thomas, B. V. L. Potter, *J. Chem. Soc. Chem. Commun.* **1993**, 1687–1689.
[397] R. Baker, P. D. Leeson, N. J. Liverton, J. J. Kulagowski, *J. Chem. Soc. Chem. Commun.* **1990**, 462–464.
[398] R. Baker, C. Carrick, P. D. Leeson, I. C. Lennon, N. J. Liverton, *J. Chem. Soc. Chem. Commun.* **1991**, 298–300.
[399] A. M. MacLeod, R. Baker, M. Hudson, K. James, M. B. Roe, M. Knowles, G. MacAllister, *Med. Chem. Res.* **1992**, *2*, 96–101.
[400] S. R. Fletcher, R. Baker, P. D. Leeson, M. Teall, E. A. Harley, C. I. Ragan, *Bioorg. Med. Chem. Lett.* **1992**, *2*, 627–630.

[401] R. Baker, J. J. Kulagowski, P. D. Leeson, N. J. Liverton in *Trends in Medicinal Chemistry '90* (Eds.: S. Sarel, R. Mechoulam, I. Agranat), Blackwell, Oxford, **1992**, pp. 199–205.
[402] S. R. Fletcher, R. Baker, T. Ladduwahetty, A. Sharpe, M. Teall, J. R. Atack, *Bioorg. Med. Chem. Lett.* **1993**, *3*, 141–146.
[403] J. R. Atack, S. M. Cook, A. P. Watt, S. R. Fletcher, C. I. Ragan, *J. Neurochem.* **1993**, *60*, 652–658.
[404] J. R. Atack, A. M. Prior, S. R. Fletcher, K. Quirk, R. McKernan, C. I. Ragan, *J. Pharmacol. Exp. Ther.* **1994**, *270*, 70–76.
[405] P. D. Leeson, K. James, I. C. Lennon, N. J. Liverton, S. Aspley, R. G. Jackson, *Bioorg. Med. Chem. Lett.* **1993**, *3*, 1925–1930.
[406] S. J. Pollack, J. R. Atack, M. R. Knowles, G. McAllister, C. I. Ragan, R. Baker, S. R. Fletcher, L. L. Iversen, H. B. Broughton, *Proc. Natl. Acad. Sci. USA* **1994**, *91*, 5766–5770.
[407] J. A. Pachter, *Mol. Pharmacol.* **1991**, *40*, 107–111.
[408] C. W. Taylor, M. J. Berridge, K. D. Brown, A. M. Cooke, B. V. L. Potter, *Biochem. Biophys. Res. Commun.* **1988**, *150*, 626–632.
[409] A. L. Willcocks, A. M. Cooke, B. V. L. Potter, S. R. Nahorski, *Biochem. Biophys. Res. Commun.* **1987**, *146*, 1071–1078.
[410] M. Hirata, Y. Watanabe, T. Ishimatsu, T. Ikebe, Y. Kimura, K. Yamaguchi, S. Ozaki, T. Koga, *J. Biol. Chem.* **1989**, *264*, 20303–20308.
[411] D. L. Nunn, C. W. Taylor, *Biochem. J.* **1990**, *270*, 227–232.
[412] S. K. Joseph, C. A. Hansen, J. R. Williamson, *Mol. Pharmacol.* **1989**, *36*, 391–397.
[413] R. A. Wilcox, R. A. J. Challiss, C. Liu, B. V. L. Potter, S. R. Nahorski, *Mol. Pharmacol.* **1993**, *44*, 810–817.
[414] M. Hirata, Y. Watanabe, M. Yoshida, T. Koga, S. Ozaki, *J. Biol. Chem.* **1993**, *268*, 19260–19266.
[415] B. Koppitz, F. Vogel, G. W. Mayr, *Eur. J. Biochem.* **1986**, *161*, 421–433.
[416] R. A. Wilcox, S. T. Safrany, D. Lampe, S. J. Mills, S. R. Nahorski, B. V. L. Potter, *Eur. J. Biochem.* **1994**, *223*, 115–124.
[417] R. A. Wilcox, S. R. Nahorski, D. A. Sawyer, C. Liu, B. V. L. Potter, *Carbohydr. Res.* **1992**, *234*, 237–246.
[418] R. A. J. Challiss, A. L. Willcocks, B. Mulloy, B. V. L. Potter, S. R. Nahorski, *Biochem. J.* **1991**, *274*, 861–867.
[419] M. J. Berridge, R. F. Irvine, *Nature (London)* **1984**, *312*, 315–321.
[420] C. Schultz, G. Gebauer, T. Metschies, L. Rensing, B. Jastorff, *Biochem. Biophys. Res. Commun.* **1990**, *166*, 1319–1327.
[421] S. V. Ley, *Pure Appl. Chem.* **1990**, *62*, 2031–2034.
[422] G. M. Burgess, R. F. Irvine, M. J. Berridge, J. S. McKinney, J. W. Putney, Jr., *Biochem. J.* **1984**, *224*, 741–746.
[423] K. S. Authi, T. O. Gustafsson, N. Crawford, *Thromb. Haemostasis* **1989**, *62*, 250.
[424] D. B. Wilson, T. M. Connolly, T. E. Bross, P. W. Majerus, W. R. Sherman, A. N. Tyler, L. J. Rubin, J. E. Brown, *J. Biol. Chem.* **1985**, *260*, 13496–13501.
[425] G. V. Denis, C. E. Ballou, *Cell Calcium* **1991**, *12*, 395–401.
[426] A. P. Kozikowski, A. H. Fauq, G. Powis, P. Kurian, F. T. Crews, *J. Chem. Soc. Chem. Commun.* **1992**, 362–364.
[427] M. Poitras, S. Bernier, G. Boulay, A. Fournier, G. Guillemette, *Eur. J. Pharmacol.* **1993**, *244*, 203–210.
[428] A. P. Kozikowski, V. I. Ognyanov, C. Chen, A. H. Fauq, S. T. Safrany, R. A. Wilcox, S. R. Nahorski, *J. Med. Chem.* **1993**, *36*, 3035–3038.
[429] J. P. Lyssikatos, M. D. Bednarski, *Bioorg. Med. Chem. Lett.* **1993**, *3*, 685–688.
[430] A. J. Morris, K. J. Murray, P. J. England, C. P. Downes, R. H. Michell, *Biochem. J.* **1988**, *251*, 157–163.
[431] T. M. Connolly, V. S. Bansal, T. E. Bross, R. F. Irvine, P. W. Majerus, *J. Biol. Chem.* **1987**, *262*, 2146–2149.
[432] S. T. Safrany, R. J. H. Wojcikiewicz, J. Strupish, J. McBain, A. M. Cooke, B. V. L. Potter, S. R. Nahorski, *Mol. Pharmacol.* **1991**, *39*, 754–761.
[433] S. T. Safrany, Dissertation, University of Leicester, **1993**.
[434] C. W. Taylor, M. J. Berridge, A. M. Cooke, B. V. L. Potter, *Biochem. Soc. Trans.* **1988**, *16*, 995–996.
[435] C. W. Taylor, M. J. Berridge, A. M. Cooke, B. V. L. Potter, *Biochem. J.* **1989**, *259*, 645.
[436] S. T. Safrany, R. A. Wilcox, C. Liu, B. V. L. Potter, S. R. Nahorski, *Eur. J. Pharmacol.* **1992**, *226*, 265–272.
[437] C. P. da Silva, F. Emmrich, A. H. Guse, *J. Biol. Chem.* **1994**, *269*, 12521–12526.
[438] A. M. Cooke, S. R. Nahorski, B. V. L. Potter, *FEBS Lett.* **1989**, *242*, 373–377.
[439] M. Hirata, F. Yanaga, T. Koga, T. Ogasawara, Y. Watanabe, S. Ozaki, *J. Biol. Chem.* **1990**, *265*, 8404–8407.
[440] A. L. Willcocks, B. V. L. Potter, A. M. Cooke, S. R. Nahorski, *Eur. J. Pharmacol.* **1988**, *155*, 181–183.
[441] S. G. Ward, D. Lampe, C. Liu, B. V. L. Potter, J. Westwick, *Eur. J. Biochem.* **1994**, *222*, 515–523.
[442] S. T. Safrany, S. J. Mills, C. Liu, D. Lampe, N. J. Noble, S. R. Nahorski, B. V. L. Potter, *Biochemistry* **1994**, *33*, 10763–10769.
[443] P. F. Worley, J. M. Baraban, S. Supattapone, V. S. Wilson, S. H. Snyder, *J. Biol. Chem.* **1987**, *262*, 12132–12136.
[444] T. K. Ghosh, P. S. Eis, J. M. Mullaney, C. L. Ebert, D. L. Gill, *J. Biol. Chem.* **1988**, *263*, 11075–11079.
[445] G. Guillemette, S. LaMontagne, G. Boulay, B. Mouillac, *Mol. Pharmacol.* **1989**, *35*, 339–344.
[446] M. A. Tones, M. D. Bootman, B. F. Higgins, D. A. Lane, G. F. Pay, *FEBS Lett.* **1989**, *252*, 105–108.
[447] T. D. Hill, P.-O. Berggren, A. L. Boynton, *Biochem. Biophys. Res. Commun.* **1987**, *149*, 897–901.
[448] T. Nilsson, J. Zwiller, A. L. Boynton, P.-O. Berggren, *FEBS Lett.* **1988**, *229*, 211–214.
[449] P. J. Cullen, J. G. Comerford, A. P. Dawson, *FEBS Lett.* **1988**, *228*, 57–59.
[450] K. J. Föhr, J. Scott, G. Ahnert-Hilger, M. Gratzl, *Biochem. J.* **1989**, *262*, 83–89.
[451] J. Strupish, R. J. H. Wojcikiewicz, R. A. J. Challiss, S. T. Safrany, A. L. Willcocks, B. V. L. Potter, S. R. Nahorski, *Biochem. J.* **1991**, *227*, 294.
[452] M. Bencherif, R. J. Lukas, *Neurosci. Lett.* **1992**, *134*, 157–160.
[453] R. A. J. Challiss, S. T. Safrany, B. V. L. Potter, S. R. Nahorski, *Biochem. Soc. Trans.* **1991**, *19*, 888–893.
[454] P. F. Worley, J. M. Baraban, J. S. Colvin, S. H. Snyder, *Nature (London)* **1987**, *325*, 159–161.
[455] G. Cornelius, G. Gebauer, D. Techel, *Biochem. Biophys. Res. Commun.* **1989**, *162*, 852–856.
[456] M. J. Bamford, P. L. Coe, R. T. Walker, *J. Med. Chem.* **1990**, *33*, 2488–2494.
[457] L. Petterson, B. Hedman, I. Andersson, N. Ngri, *Chem. Scr.* **1983**, *22*, 254–264.
[458] T. Meyer, D. Holowka, L. Stryer, *Science* **1988**, *240*, 653–656.
[459] D. L. Nunn, B. V. L. Potter, C. W. Taylor, *Biochem. J.* **1990**, *265*, 393–398.
[460] S. DeLisle, K. H. Krause, G. Denning, B. V. L. Potter, M. J. Welsh, *J. Biol. Chem.* **1990**, *265*, 11726–11730.
[461] F. Thevenod, M. Dehlinger-Kremer, T. P. Kemmer, A. L. Christian, B. V. L. Potter, I. Schulz, *J. Membr. Biol.* **1989**, *109*, 173–186.
[462] M. Wakui, B. V. L. Potter, O. H. Petersen, *Nature (London)* **1989**, *339*, 317–320.
[463] C. C. H. Petersen, E. C. Toescu, B. V. L. Potter, O. H. Petersen, *FEBS Lett.* **1991**, *293*, 179–182.
[464] F. S. Menniti, G. S. J. Bird, H. Takemura, O. Thastrup, B. V. L. Potter, J. W. Putney, Jr., *J. Biol. Chem.* **1991**, *266*, 13646–13653.
[465] C. Valdivia, H. H. Valdivia, B. V. L. Potter, R. Coronado, *Biophys. J.* **1990**, *57*, 1233–1243.
[466] L. Changya, D. V. Gallacher, R. F. Irvine, B. V. L. Potter, O. H. Petersen, *J. Membr. Biol.* **1989**, *109*, 85–93.
[467] M. J. Berridge, P. H. Cobbold, K. S. R. Cuthbertson, *Phil. Trans. R. Soc. London Ser. B* **1988**, *320*, 325–343.
[468] O. H. Petersen, *J. Physiol. (London)* **1992**, *448*, 1–51.
[469] R. Payne, B. V. L. Potter, *J. Gen. Physiol.* **1991**, *97*, 1165–1186.
[470] J. E. Ferguson, B. V. L. Potter, R. Nuccitelli, *Biochem. Biophys. Res. Commun.* **1990**, *172*, 229–236.
[471] S. DeLisle, M. J. Welsh, *J. Biol. Chem.* **1992**, *267*, 7963–7966.
[472] J. D. Lechleiter, D. E. Clapham, *Cell* **1992**, *69*, 283–294.
[473] D. Clapham, S. Girard, *Science* **1993**, *260*, 229–232.
[474] T. Whalley, A. McDougall, I. Crossley, K. Swann, M. Whitaker, *Mol. Biol. Cell* **1992**, *3*, 373–383.
[475] R. J. H. Wojcikiewicz, A. M. Cooke, B. V. L. Potter, S. R. Nahorski, *Eur. J. Biochem.* **1990**, *192*, 459–467.
[476] C. W. Taylor, B. V. L. Potter, *Biochem. J.* **1990**, *266*, 189–194.
[477] M. McCarren, B. V. L. Potter, R. Miller, *Neuron* **1989**, *3*, 461–471.
[478] C. Valdivia, D. Vaughan, B. V. L. Potter, R. Coronado, *Biophys. J.* **1992**, *61*, 1184–1193.
[479] A. Strunecka, E. Kmonickova, N. El Desouki, L. Krpejsova, J. Palacek, B. V. L. Potter, *Receptor* **1991**, *1*, 141–153.
[480] R. Gigg, *Chem. Phys. Lipids* **1980**, *26*, 287–404.
[481] J. G. Ward, R. C. Young, *Tetrahedron Lett.* **1988**, *29*, 6013–6016.
[482] R. C. Young, C. P. Downes, D. S. Eggleston, M. Jones, C. H. Macphee, K. K. Rana, J. G. Ward, *J. Med. Chem.* **1990**, *33*, 641–646.
[483] V. N. Krylova, N. P. Gornaeva, V. I. Shvets, R. P. Evstigneeva, *Dokl. Akad. Nauk SSSR* **1979**, *246*, 339.
[484] V. N. Krylova, A. I. Lyutik, N. P. Gornaeva, V. I. Shvets, *Zh. Obshch. Khim.* **1981**, *51*, 210.
[485] A. E. Stepanov, V. I. Shvets, *Chem. Phys. Lipids* **1986**, *41*, 1–51.
[486] J. R. Falck, A. Abdali in *Inositol Phosphates and Derivatives – Synthesis, Biochemistry and Therapeutic Potential* (Ed.: A. B. Reitz), American Chemical Society, Washington,DC, **1991**, pp. 145–154.
[487] Y. Watanabe, H. Hirofuji, S. Ozaki, *Tetrahedron Lett.* **1994**, *35*, 123–124.
[488] A. P. Kozikowski, W. Tückmantel, G. Powis, *Angew. Chem.* **1992**, *104*, 1408–1410; *Angew. Chem. Int. Ed. Engl.* **1992**, *31*, 1381–1383.
[489] A. H. Fauq, A. P. Kozikowski, A. Gallegos, G. Powis, *Med. Chem. Res.* **1993**, *3*, 17–23.
[490] A. P. Kozikowski, G. Powis, A. H. Fauq, W. Tückmantel, A. Gallegos, *J. Org. Chem.* **1994**, *59*, 963–971.
[491] S. P. Seitz, R. F. Kaltenbach, R. H. Vreekamp, J. C. Calabrese, F. W. Perrella, *Bioorg. Med. Chem. Lett.* **1992**, *2*, 171–174.

[492] M. A. Alisi, M. Brufani, L. Filocamo, G. Gostoli, S. Maiorana, M. C. Cesta, E. Ferrari, S. Lappa, P. Pagella, *Tetrahedron Lett.* **1992**, *33*, 7793–7796.
[493] C. E. Dreef, C. J. J. Elie, G. A. van der Marel, J. H. van Boom, *Tetrahedron Lett.* **1991**, *32*, 955–958.
[494] S. S. Yang, T. R. Beattie, P. L. Durette, T. F. Gallagher, T. Y. Shen, US-A 4515722, **1985**.
[495] M. S. Shashidhar, J. F. W. Keana, J. J. Volwerk, O. H. Griffith, *Chem. Phys. Lipids* **1990**, *53*, 103–113.
[496] T. K. Vinod, O. H. Griffith, J. F. W. Keana, *Tetrahedron Lett.* **1994**, *35*, 7193–7196.
[497] M. A. J. Ferguson, A. F. Williams, *Annu. Rev. Biochem.* **1988**, *57*, 285–320.
[498] M. G. Low, M. A. J. Ferguson, A. H. Futerman, I. Silman, *Trends Biochem. Sci.* **1986**, *11*, 212–215.
[499] M. G. Low, *Biochem. J.* **1987**, *244*, 1–13.
[500] M. G. Low, A. R. Saltiel, *Science* **1988**, *239*, 268–275.
[501] T. L. Doering, W. J. Masterson, G. W. Hart, P. T. Englund, *J. Biol. Chem.* **1990**, *265*, 611–614.
[502] W. L. Roberts, S. Santikarn, V. N. Reinhold, T. L. Rosenberry, *J. Biol. Chem.* **1988**, *263*, 18776–18784.
[503] S. W. Homans, M. A. J. Ferguson, R. A. Dwek, T. W. Rademacher, R. Anand, A. F. Williams, *Nature (London)* **1988**, *333*, 269–272.
[504] M. A. J. Ferguson, S. W. Homans, R. A. Dwek, T. W. Rademacher, *Science* **1988**, *239*, 753–759.
[505] C. Murakata, T. Ogawa, *Carbohydr. Res.* **1992**, *234*, 75–91.
[506] C. Murakata, T. Ogawa, *Tetrahedron Lett.* **1991**, *32*, 671–674.
[507] A. R. Saltiel, D. G. Osterman, J. C. Darnell, L. R. Sorbara-Cazan, B. L. Chan, M. G. Low, P. Cuatrecasas, *Phil. Trans. R. Soc. London Ser. B* **1988**, *320*, 345–358.
[508] M. P. Czech, J. K. Klarlund, K. A. Yagaloff, A. P. Bradford, R. F. Lewis, *J. Biol. Chem.* **1988**, *263*, 11017–11020.
[509] W. K. Berlin, W. S. Zhang, T. Y. Shen, *Tetrahedron* **1991**, *47*, 1–20.
[510] A. Zapata, M. Martin-Lomas, *Carbohydr. Res.* **1992**, *234*, 93–106.
[511] R. Plourde, M. D'Alarcao, *Tetrahedron Lett.* **1990**, *31*, 2693–2696.
[512] R. Verduyn, C. J. J. Elie, C. E. Dreef, G. A. van der Marel, J. H. van Boom, *Recl. Trav. Chim. Pays-Bas* **1990**, *109*, 591–593.
[513] C. J. J. Elie, R. Verduyn, C. E. Dreef, D. M. Brounts, G. A. van der Marel, J. H. van Boom, *Tetrahedron* **1990**, *46*, 8243–8254.

C–H and C–C Bond Activation by Bare Transition-Metal Oxide Cations in the Gas Phase

Detlef Schröder and Helmut Schwarz*

Dedicated to Michael Henchman and Rudolf Zahradnik

Over the last decade the gas-phase chemistry of bare transition-metal oxide cations MO^+ has received considerable attention. This interest is primarily due to the particular role of metal oxides in the oxidation of organic compounds in a variety of chemical and biochemical transformations. At a molecular level the simplest model system for these processes deals with reactions of bare metal-oxide ions in the gas phase. Due to the high oxophilicities of the early transition metals, their monoxide cations MO^+ do not mediate O-atom transfer to any organic compounds at all. In contrast, monoxide cations of late transition metals can oxygenate a variety of hydrocarbons, and the most reactive ions, MnO^+, FeO^+, NiO^+, OsO^+, and PtO^+, even activate methane. Insight into the reaction mechanisms of these oxidation processes can be obtained by analysis of reaction kinetics, isotope effects, product distributions etc., and for the reactions of MO^+ with alkanes the initial C–H bond activation by MO^+ is often rate-determining. Interestingly, the high reactivity of some MO^+ ions is not always associated with a decrease in regioselectivity; for example, FeO^+ ions induce regiospecific γ-C–H bond activation of dialkylketones in the gas phase. The situation for the epoxidation of olefins in the gas phase turns out to be even more complex than for condensed-phase analogues. This is primarily because the metal ion that mediates O-atom transfer to the olefin also catalyzes the isomerization of the epoxides formed, to afford the energetically more stable aldehydes or ketones. Aromatic compounds can also be hydroxylated by MO^+ ions, and particularly the oxidation of benzene by bare FeO^+ ions in the gas phase reveals striking parallels to the metabolism of arenes. Furthermore, the storing capabilities of ion cyclotron resonance mass spectrometers even permit the design of catalytic processes in which a single metal ion converts more than one substrate molecule into an oxygenated product in a sequence of strictly bimolecular reactions. The most outstanding examples are the Pt^+-mediated oxidation of methane by molecular oxygen and the Co^+-mediated hydroxylation of benzene by N_2O as oxidant. Finally, the key features of the gas-phase reactions are compared with observations in condensed-phase systems in which metal oxides are anticipated as central intermediates. The result of this comparison is promising in the sense that, in general, the understanding of transition-metal-mediated oxidations in the gas phase may lead to a more uniform description of these processes at a molecular level. Ultimately, it is hoped that gas-phase studies will serve as one of the building blocks in the evolution of tailor-made catalysts.

Keywords: bond activation · gas-phase chemistry · kinetics · mass spectrometry · transition-metal oxides

The selective activation of carbon–hydrogen bonds of alkanes constitutes the search for the chemists' Holy Grail.
Sir Derek Barton, 1990

1. Introduction

Transition-metal-mediated oxidation of organic compounds is of fundamental importance in various branches of chemistry, biology, and chemical engineering. In general, three basic areas can be distinguished: 1) Heterogeneous catalysis for the conversion of hydrocarbons into more valuable products by use of economical oxidants such as peroxides, oxygen, or even air. Numerous methods are applied in large scale processes, for example, the conversion[1] and coupling[2] of methane, or the olefin epoxidation on silver contacts.[3] 2) Homogeneous catalysis for similar purposes as well as for small-scale synthetic applications, for example, the Wacker process,[4, 5] the oxidation of cyclohexane,[5] or many preparative procedures, as for example the enantioselective Katsuki–Sharpless epoxidation.[6] 3) Biochemical transformations that involve one or several transition metals in the enzymes' reaction centers. For example, metal-containing enzymes are essential for oxygen transportation, storage, and activation in living organisms.[7] In this context the iron-centered cytochromes, the methane monooxygenases and related systems are of particular relevance.[8]

[*] Prof. Dr. H. Schwarz, Dr. D. Schröder
Institut für Organische Chemie
Technische Universität Berlin
Strasse des 17. Juni 135, D-10623 Berlin (Germany)
Telefax: Int. code + 030/314-21102

Although in view of the tremendous variety of metals, ligands, and oxidants many mechanistic routes may exist, it has been repeatedly conjectured that a large number of these otherwise different systems involve transition-metal oxides [M]=O as the catalytically active species;[9] here, [M] refers to a ligated mono- or oligonuclear transition-metal compound or even a metal atom embedded in the surface of a solid catalyst. Therefore, considerable interest focused on the synthesis, characterization, and reactivity studies of these species and their appropriate model compounds in the condensed phase.[10] One of the most fundamental processes mediated by [M]=O deals with the hydroxylation of organic compounds, and a simplified mechanism for C–H bond activation of a hydrocarbon RH by a metal-oxide fragment is depicted in Scheme 1. The initial (and

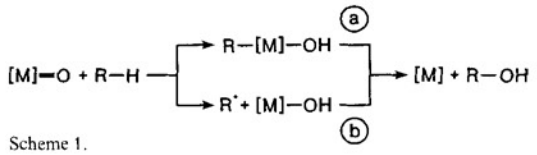

Scheme 1.

frequently rate-determining) step commences with the activation of an R–H bond resulting in the formation of an inserted species R–[M]–OH or a pair of cage-trapped radicals R˙ and [M]˙–OH. Subsequent product formation can proceed by reductive elimination (path ⓐ) or an OH-rebound process[11] (path ⓑ); the latter is sometimes described in terms of a radical recombination. Both pathways yield the oxygenated hydrocarbon ROH and reduced [M]. Alternatively, if R has a second α-H atom, water elimination can give rise to carbene intermediates $[M]=CR^1R^2$ which, subsequently, can be converted into the corresponding carbonyl compound by an appropriate O-atom donor.[12] For catalytic applications the oxidant should also be capable of reoxidizing [M] to the active species [M]=O. Frequently O_2, H_2O_2, and hydroperoxides are used for this purpose.

The ultimate goal is to unravel the mechanistic features of transition-metal-catalyzed oxidation at a molecular level. One of the simplest and most straightforward approaches to tackle this problem deals with reactivity studies of ionic transition-metal oxides in the gas phase by mass-spectrometric methods.[13] Here, any contribution of ligand effects, counterions, solvents etc. can be rigorously excluded. In addition, by studying ligated metal fragments, the sequential effects of ligands L on the reactivity may be evaluated. Consequently, this approach allows an evaluation of whether the catalytic activity of L[M]=O represents an intrinsic property of the corresponding molecule in a certain oxidation state, or if the reactivity is governed by the ligands, solvation phenomena, surface properties, cooperative effects etc. of the "real life" catalysts. As a prerequisite for the evaluation and the proper understanding of mass-spectrometric experiments, it is important to note that due to the net coulombic charge of the ions as well as the absence of counter ions and solvation, these coordinatively unsaturated ("naked") species will, in general, be much more reactive than their condensed-phase analogues.[14] Thus, the gas-phase studies to be described here will, in principal, *never* account for the precise mechanisms, energetics, and kinetics operating for applied catalysis. Yet, the gas-phase experiments are not meaningless, for they provide an efficient means to obtain insight into reactivity patterns, the role of ligands, the chemo- and regioselectivities, and the intermediates operative at molecular level. In fortunate cases predictions may be possible for those condensed-phase systems that are suggested to involve "free" metal-oxide species. In general, the studies of isolated molecules under well-defined conditions may be viewed as one of the key features stones in the evolution of paradigms aimed at a more comprehensive understanding of elementary steps, knowledge of which is mandatory for the design of tailor-made catalysts.

In this review we will describe the current status of knowledge of the reactivity of bare transition-metal-oxide ions towards various classes of organic compounds. We shall focus on the chemistry of mononuclear, cationic transition-metal monoxides, MO^+, since hitherto most of the reactivity studies deal with these species. However, where appropriate some representative

Helmut Schwarz, born in 1943, spent four years as a chemical technician before reading chemistry at the Technische Universität Berlin (TUB), where he obtained his Ph.D under the supervision of F. Bohlmann in 1972 and his habilitation in 1974. Since 1978 he has been associated with the TUB as a Professor of Chemistry and has resisted all temptation to leave Berlin for good. He held visiting appointments in Cambridge, Lausanne, Jerusalem and Haifa, and Canberra. Among his several awards are the Otto-Klung, Otto-Bayer, and Leibniz Prizes, and the Max-Planck Research Award, which he received jointly with C. Lifshitz. In 1992 the Hebrew University of Jerusalem conferred an honorary doctorate on him and in 1994 the J. J. Thomson Gold Medal. H. Schwarz is a fellow of the Lepoldina (Halle), the Academy of Sciences at Erfurt and at Berlin-Brandenburg, and an Overseas Fellow of the Churchill College Cambridge. His current interests, besides the topic of this review, focus on the generation and characterization of elusive molecules of interstellar and atmospheric importance.

Detlef Schröder, born in 1963, began to study chemistry at the TUB in 1983. In 1988 he joined the group H. Schwarz and completed his Ph. D. on the topic of ligand effects in organometallic gas-phase chemistry in 1992. He is author of more than sixty papers and recipient of the Klaus-Koch Award of the TUB and the Schering Prize (1993). His prime interests are in the field of gas-phase ion chemistry of organometallic compounds, with special emphasis on C–H and C–C activation, oxidation, and the reactive intermediates, as well as reaction mechanisms, isotope effects, and mass spectrometry.

examples of reactions of anionic, neutral, and high-valent transition-metal oxides will be included.

The review begins with a brief description of the experimental methods used for gas-phase reactivity studies. Then, the formation, thermochemistry, and bonding of MO^+ ions are discussed, followed by chapters that deal with reactions of metal-oxide ions with alkanes, olefins, arenes, and monofunctionalized hydrocarbons. A comparison of reactivity patterns, isotope effects, and regioselectivities of MO^+ ions with some representative condensed-phase analogues will be presented in terms of simplified mechanistic schemes. In an extra section, the design of catalytic processes in the gas phase is described, and the implications for the condensed phase are discussed. Finally, an outlook is given on the possible development of this field in the near future. To limit the size of the article, we will refrain from describing experimental and theoretical findings in detail, as these are available in the original references.

2. Experimental Procedure and Theoretical Methods

This section serves as a brief survey of the experimental methods that are used to examine the reactivity of metal-monoxide cations as well as high-valent transition-metal-oxide cations in the gas phase; to illustrate the techniques we refer to the oxidation of methane by FeO^+ as an example. Similar techniques have been applied for reactivity studies of the corresponding anionic[15] and neutral[16] transition-metal oxides.

Most of the experimental studies have been performed by ion cyclotron resonance (ICR) mass spectrometry or its modern variant, Fourier transform (FT)ICR.[17] Here, MO^+ ions are trapped in the magnetic field of an ion cyclotron setup and mass-selected by specifically modulated radio-frequency pulses. Reactivity studies are performed by leaking in neutral reactants and monitoring the time dependencies of the MO^+ and product-ion signal intensities (for example, $FeO^+ + CH_4 \rightarrow Fe^+ + CH_3OH$); neutral products cannot be detected by (FT)ICR. Provided the MO^+ species are properly thermalized,[18] the reactions can be considered to take place at thermal energies (300 K) at which only exothermic or almost thermoneutral processes can occur.[14, 19] consequently, the observation of a particular ion/molecule reaction can be used to bracket thermodynamic thresholds for reactant and product channels.[20] Furthermore, the time dependencies of the ion signals can be analyzed in terms of pseudo-first-order kinetics, and the corresponding rate constants k_R (in general determined with an experimental error of $\pm 25\%$)[21] can be compared to the capture rates k_C as derived from collision theory.[22] The efficiency, defined as $\phi = k_R/k_C$, is a measure of the reactivity of a given MO^+ ion towards a neutral molecule, and the magnitude of ϕ is a measure of the importance of thermodynamic or kinetic restrictions that are associated with the process of interest. Furthermore, isotopically labeled substrates permit the evaluation of kinetic isotope effects (KIEs)[23] on the rate constants k_R and product branching ratios.[24] These, in turn, provide insight into the reaction mechanism, reveal the rate-determining step (RDS), and may uncover structural and energetical features of reaction intermediates. In addition, other techniques such as ligand-exchange reactions[13, 25] and collision-induced dissociation experiments[26] permit the elucidation of the structures of the ionic reaction products. In spite of this richness, (FT)ICR mass spectrometry often does not provide a complete picture of the reaction mechanisms for the oxidation of organic compounds RH by MO^+ cations. This is mostly due to 1) the instability of the rovibrationally highly excited eneounter complexes $[RH \cdot MO^+]^*$ formed in the absence of stabilizing collision partners and 2) the high exothermicities of the oxidation reactions: Consequently, in (FT)ICR often only the final ionic products, but no reaction intermediates or neutral species, are detected.

Fortunately, tandem mass spectrometry[27] with multi-sector-field instruments constitutes a complementary approach and can be used to generate and characterize possible reaction intermediates of the process of interest. In these experiments structural isomers of the proposed intermediates are generated by chemical ionization (CI) of appropriate precursor molecules. For example,[28] intermediates of the elemental composition $[Fe,C,H_4,O]^+$, which are believed to be involved in the formation of methanol from FeO^+ and methane, can be generated by CI, starting from different precursor mixtures: 1) $Fe(CO)_5$, N_2O, and CH_4 yield the encounter complex of the reactants, $(CH_4)FeO^+$; 2) $Fe(CO)_5$ and CH_3SO_3H give rise to the inserted species H_3C-Fe^+-OH; 3) $Fe(CO)_5$, c-C_3H_6, and H_2O lead to the carbene complex $H_2C=Fe^+-OH_2$; and finally, 4) $Fe(CO)_5$ and CH_3OH form the product complex $(CH_3OH)Fe^+$. The structures of the so-formed isomeric ions as well as interconversion processes between various isomers can be probed by means of collisional activation (CA) of mass-selected ion beams and related techniques.[27] Most recently, neutralization–reionization mass spectrometry (NRMS)[29] was added to the repertoire and successfully applied to examine transition-metal-mediated oxidation reactions. For details of the slightly more complex NRMS setup, we refer to the original sources; however, it should be pointed out that this technique permits insight into the structures of not only the ionic, but also of *neutral* products being formed in the course of an oxidation process.

Most of the experiments that address the thermochemistry[20] of transition-metal oxides as well as a few reactivity studies have been performed with another sophisticated mass-spectrometric method, the guided ion beam (GIB)[30] technique. In this type of experiment mass-selected ions of interest are made to collide at well-defined collision energies with either an unreactive neutral, for example a rare gas, or a reactive substrate that has a potential-energy hypersurface related to that of the molecule of interest. For example, the experimental threshold for the formation of Fe^+ by colliding translationally excited FeO^+ with xenon can be converted into the bond dissociation energy (BDE) of the Fe^+–O bond; similarly, the appearance of an endothermic ion/molecule reaction can be related to thermodynamic and kinetic barriers, for example, $Fe^+ + CH_3OH \rightarrow FeO^+ + CH_4$. Because of its well-defined energy scale, this technique is an excellent tool for the evaluation of the thermodynamics of ionic and neutral molecules; furthermore, GIB has been applied for state-specific reactivity studies of transition-metal fragments.[31] Exothermic ion/molecule reactions can also be studied by means of GIB experiments; however, their quantification in terms of reaction energetics is not as straightforward as for endothermic processes. In addition, flow-tube measurements,[32] ion-trap mass spectrometry,[33] and flame-ionization methods[34] have been used to examine metal-oxide ions in the gas phase.

In a more general sense, these complementary experimental methods probe different parts of a potential-energy hypersurface of an MO^+/RH system, as depicted in Figure 1 for an exothermic hydroxylation process. The (FT)ICR method establishes whether an exothermic ion/molecule reaction of thermalized MO^+ ions with the substrate RH occurs, and sheds light on

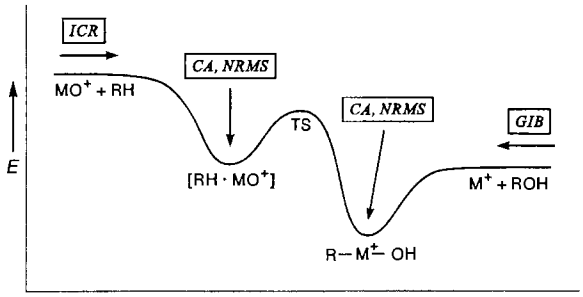

Fig. 1. Exothermic hydroxylation of RH with MO^+. The x axis represents the reaction coordinate. TS = transition structure.

the kinetics and isotope effects. Collisional activation of ions generated by chemical ionization in a sector instrument permit insight into connectivity, stability, and interconversion processes of the reaction intermediates. Furthermore, NRMS can be used to derive the structure(s) of the neutral oxidation products being formed. Finally, the GIB technique is particularly valuable for probing the endothermic (reverse) reactions to establish thermodynamic and kinetic thresholds for the reaction of interest as well as reaction dynamics.

In principle, the currently available experimental methods permit reactivity studies of almost all metal-oxide cations and anions with a large variety of substrates. However, in practice these experiments are sometimes limited by the problems associated with the generation of the corresponding metal-oxide ions in reasonable quantities. Furthermore, in many laboratories the lack of isotopic labeling facilities hampers the unambiguous interpretation of data with respect to intermediates and reaction mechanisms.

Finally, enormous progress in the last decade has been brought about by theoretical methods. Besides conventional high-level molecular orbital calculations,[35] the recent density functional theory (DFT)[36] approach gained particular relevance because of its economical use of computer time.[37] Although transition-metal complexes often have a vast number of energetically closely spaced electronic states, computational methods now permit relatively reliable predictions of the energetics and structures of many of these species, at least for small systems.[38] These computational results represent a versatile and complementary extension of the experimental methods and permit an interpretation with respect to minima on the potential-energy hypersurface, that is, possible reaction intermediates. More importantly, even the salient features of the corresponding transition structures (TS) connecting the minima can be probed. Thus, geometries, activation barriers, and harmonic vibrational frequencies are available and can be used to refine the analysis of experimental data. In fact, the successful interplay of theoretical and experimental studies gives hope that reaction pathways will be reliably mapped out and mechanisms for transition-metal-mediated oxidations will be understood.[39]

3. Formation, Energetics, and Bonding Features of Metal-Oxide Ions

Transition-metal oxides can be generated by a variety of mass spectrometric means starting from different precursors (Scheme 2). Of course, for reactivity studies, the method of choice is determined by both the particular experimental setup and the absolute yields associated with making the metal-oxide ion of interest.

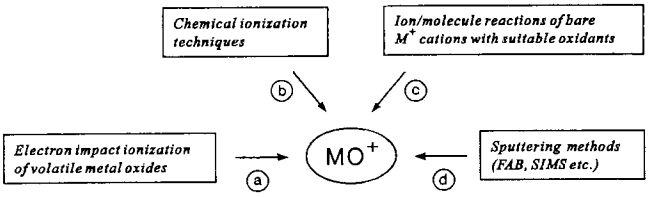

Scheme 2.

Electron impact ionization (method ⓐ) has been applied to generate metal-oxide ions from volatile precursors, for example, CuO_n^+ from anhydrous copper(II) nitrate ($n = 1, 2$),[40] OsO_n^+ from osmium(VIII) tetraoxide ($n = 1-4$),[41] and the high-valent organometal-oxide cation radical $CH_3ReO_3^+$ from the corresponding neutral compound.[42] Chemical ionization of mixtures of organometallic compounds with appropriate oxidants (method ⓑ) has been applied for various metals, for example, FeO^+ from $Fe(CO)_5$ and N_2O,[28] and FeO_n^- from $Fe(CO)_5$ and O_2 ($n = 1-4$).[43] For most of the reactivity studies metal-oxide ions have been generated by ion/molecule reactions of bare metal ions M^+ with O-atom donors such as molecular oxygen, oxirane, dinitrogen oxide, or ozone (method ⓒ).[44] These methods are of particular relevance, since they occur under well-defined conditions, and thus the formation of electronically excited ions can be more or less excluded. Almost all MO^+ ions can be generated from the corresponding metal salts by sputtering methods (ⓓ) such as secondary ion mass spectrometry (SIMS) or fast atom bombardment mass spectrometry (FAB-MS);[45] however, the absolute ion currents obtained for MO^+ by the latter methods as well as the experimental setups themselves often hamper further reactivity studies.

In addition, thermoionization in flames[34] has been used for the generation of MO^+; however, the experimental conditions do not always allow their reactivity with organic substrates to be probed. Unfortunately, only a few MO^+ ions have so far been examined by photoionization methods. Among these studies, those of Dyke et al. should be pointed out.[46] Photoionization experiments are highly desirable, because they may allow the assignment of electronic ground states, the investigation of state-specific reactivities, and also the spectroscopic characterization of reactants, intermediates, and products.

The evaluation of the thermodynamics of MO^+ began in the 1960s with the evolution of Knudsen cell mass spectrometry.[47] Nowadays, most of these early data have been refined by more sophisticated techniques; in particular, the accurate GIB studies by Armentrout et al. brought about significant progress.[48] Figure 2 displays the bond dissociation energies (BDEs) of the MO^+ cations of the first-row transition metals. In accordance

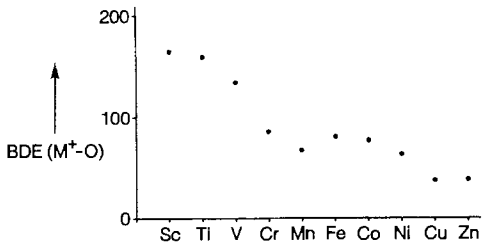

Fig. 2. Bond dissociation energies (BDE in kcal mol^{-1}) of the first-row transition-metal monoxide ions MO^+ (Data taken from Ref. [48]).

with the well-known high oxophilicities of the early transition metals (Sc, Ti, and V), the corresponding BDEs (M^+–O) are fairly high (Table 1) and exceed that of many other atoms and molecules. For example, bare Sc^+ is capable of abstracting an oxygen atom from carbonyl compounds to yield ScO^+ and the corresponding alkenes as neutral products.[49] For Group 6–10 transition metals (Cr–Ni) the values for BDE (M^+–O) are moderate and vary between 63 and 86 kcal mol^{-1}, whereas for Cu and Zn the BDEs amount to less than 40 kcal mol^{-1}. In general, these trends are in line with the bond dissociation energies of other transition-metal cations, for example, BDE(M^+–H) or BDE(M^+–CH_3).[50] Due to the higher oxidation state in MO^+, most of the BDEs of the corresponding neutral transition-metal oxides exceed that of the cations by 10–20 kcal mol^{-1},[51] as is apparent from the increase of the ionization energies (IEs) for the metal oxides relative to the bare metal atoms (Table 2). For second- and third-row transition-metal oxides a comprehensive set of data is not yet available, and the reported figures are less precise than those determined by GIB experiments, as demonstrated by the error bars in Table 1. Nevertheless, the general trend parallels the features observed for the first-row transition-metal series (high BDEs for the early and lower ones for the late transition metals). Within a group of the periodic table, the BDEs seem to increase for heavier elements; however, the precise orderings are determined by an interplay of electronic ground states, orbital-overlap factors, and relativistic effects.[52, 53]

Table 1. Experimental bond dissociation energies BDE [kcal mol^{-1}] with error limits F of diatomic transition-metal oxide cations.

MO^+	BDE	F	MO^+	BDE	F	MO^+	BDE	F
ScO^+	164 [a]	±2	YO^+	170 [c]	±5	LaO^+	206 [f]	±4
TiO^+	159 [a]	±2	ZrO^+	201 [c]	±8	HfO^+	173 [c]	±5
VO^+	134 [a]	±2	NbO^+	207 [d]	±53	TaO^+	188 [c]	±15
CrO^+	86 [b]	±3	MoO^+	113 [c]	±19	WO^+	126 [c]	±10
MnO^+	68	±3	TcO^+	–	–	ReO^+	–	–
FeO^+	81 [b]	±2	RuO^+	88 [i]	±2	OsO^+	100 [g]	±12
CoO^+	77 [b]	±2	RhO^+	70 [i]	±2	IrO^+	59 [c]	[e]
NiO^+	63 [b]	±2	PdO^+	34 [i]	±3	PtO^+	59 [c]	±7
CuO^+	37 [b]	±3	AgO^+	28 [i]	±2	AuO^+	[h]	–
ZnO^+	38 [b]	±3	CdO^+	–	–	HgO^+	–	–

[a] Ref. [48b]. [b] Ref. [48a]. [c] Ref. [20b, d]. [d] Ref. [44b]. [e] No errors have been reported. [f] D. E. Clemmer, N. F. Dalleska, P. B. Armentrout, *Chem. Phys. Lett.* **1992**, *190*, 259. [g] Ref. [41.] [h] For the observation of AuO^+, see A. Hecq, M. Vandy, M. Hecq, *J. Chem. Phys.* **1980**, *72*, 2876; C. R. Alten, *J. Appl. Phys.* **1987**, *61*, 5182. [i] Y.-M. Chen, P. B. Armentrout, *J. Chem. Phys.*, in press.

Table 2. Ionization energies IE [eV] of transition-metal atoms M and diatomic oxides MO [a].

M	IE (M)	IE (MO)	M	IE (M)	IE (MO)	M	IE (M)	IE (MO)
Sc	6.5	6.4	Y	6.4	5.9	La	5.6	4.9
Ti	6.1	6.6	Zr	6.8	6.1	Hf	7.0	7.6
V	6.7	7.5	Nb	5.5	6.1	Ta	7.9	7.9
Cr	6.7	7.9	Mo	7.1	8.0	W	8.0	9.1
Mn	7.4	8.7	Tc	7.3		Re	7.9	
Fe	7.9	8.9	Ru	7.4	8.9	Os	8.5	10.1
Co	7.9	8.9	Rh	7.5	8.6	Ir	9.0	10.1
Ni	7.6	9.5	Pd	8.3	9.8	Pt	9.0	10.1
Cu	7.7	9.0	Ag	7.6	8.6	Au	9.2	
Zn	9.4	> 10.1 [b]	Cd	9.0		Hg	10.4	

[a] Values derived form the references given in Table 1 and Ref. [51a]. [b] Lower limit according to Refs. [47c, 48a].

For the first-row transition-metal series Carter and Goddard III predicted the electronic ground states and analyzed the binding situations of the MO^+ cations on the basis of valence-bond (VB) theory.[54] While organic chemists are perhaps more familiar with describing bonding properties in terms of the equivalent molecular orbital (MO) picture, both theories cover the basic features of the bonding in metal-oxide cations, they account for most of the thermodynamics, and also allow a prediction of symmetries and multiplicities of the electronic ground states.[39, 55] Figure 3 shows the occupancy of the valence molecular orbitals for three representative examples, ScO^+, FeO^+, and ZnO^+. In the low-spin ground state of ScO^+ ($^1\Sigma^+$) all bonding valence orbitals, 1σ, 2σ, and 1π, are doubly occupied, while the remaining orbitals are empty, thus giving rise to a low-spin ground state ($^1\Sigma^-$) and a high BDE (164 kcal mol^{-1}). This description also accounts well for the high oxophilicities of the other early transition metals. In contrast, in the high-spin ground state of FeO^+ ($^6\Sigma^+$), besides the doubly occupied bonding orbitals, all five 1δ, 2π, and the 3σ orbitals are singly occupied, and consequently, BDE (Fe^+–O) is moderate (81 kcal mol^{-1}). Finally, in ZnO^+ ($^2\Pi$), with the exception of one antibonding orbital, all orbitals are doubly occupied, resulting in a fairly low BDE (38 kcal mol^{-1}). As a rule of thumb,[54] the bonding in the oxides from ScO^+ through

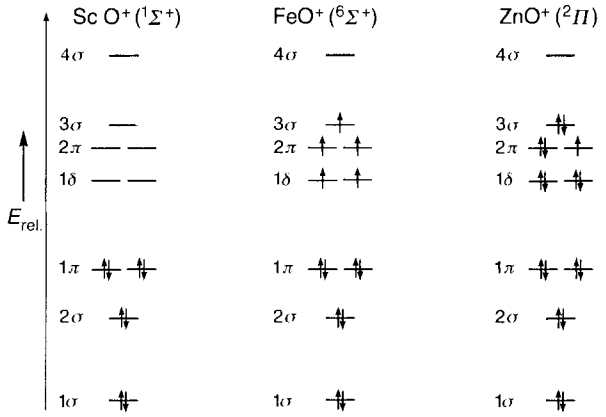

Fig. 3. Schematic molecular orbital diagram for the representative first-row transition-metal-monoxide cations ScO^+, FeO^+, and ZnO^+ (only the valence orbitals are depicted; for a discussion, see Ref. [39]).

CrO^+ can be viewed as analogous to carbon monoxide, whereas for those from FeO^+ through CuO^+ the bonding resembles that of triplet dioxygen.[39, 54] This simple analogy of the MO^+ ground states to CO and O_2 is of particular relevance for the interpretation of the observed reactivity patterns, as will be demonstrated later.

Recently the pictorial description of the bonding in MO^+ has been evaluated quantitatively by means of ab initio molecular orbital calculations (Table 3),[39, 55] which predict CO-like bonding for the low-spin ground states of the early transition-metal oxides from ScO^+ through CrO^+ and O_2-like bonding from FeO^+ to CuO^+. MnO^+ occupies an intermediate position.

Table 3. Promotion energies ΔE and bond lengths r_{MO} of the electronic ground and the first excited states of the first-row transition-metal-oxide cations MO^+ [a].

MO^+	State	Occupancy [b]	r_{MO} [Å]	ΔE [eV]
ScO^+	$^1\Sigma^+$	$1\sigma^2 2\sigma^2 1\pi^4$	1.60	0.0
TiO^+	$^2\Delta$	$1\sigma^2 2\sigma^2 1\pi^4 1\delta^1$	1.58	0.0
	$^2\Sigma^+$	$1\sigma^2 2\sigma^2 1\pi^4 3\sigma^1$	1.58	1.3
VO^+	$^3\Sigma^-$	$1\sigma^2 2\sigma^2 1\pi^4 1\delta^2$	1.54	0.0
	$^3\Delta$	$1\sigma^2 2\sigma^2 1\pi^4 1\delta^1 3\sigma^1$	1.55	1.4
CrO^+	$^4\Sigma^+$	$1\sigma^2 2\sigma^2 1\pi^4 1\delta^2 3\sigma^1$	1.55	0.0
	$^4\pi$	$1\sigma^2 2\sigma^2 1\pi^4 1\delta^2 2\pi^1$	1.57	0.1
	$^2\Delta$	$1\sigma^2 2\sigma^2 1\pi^4 1\delta^3$	1.50	1.2
MnO^+	$^5\pi$	$1\sigma^2 2\sigma^2 1\pi^4 1\delta^2 2\pi^1 3\sigma^1$	1.59	0.0
	$^5\Sigma^+$	$1\sigma^2 2\sigma^2 1\pi^4 1\delta^2 2\pi^2$	1.58	0.1
	$^7\pi$	$1\sigma^2 2\sigma^2 1\pi^3 1\delta^2 2\pi^2 3\sigma^1$	1.83	0.5
	$^3\Delta$	$1\sigma^2 2\sigma^2 1\pi^4 1\delta^3 3\sigma^1$	1.51	1.5
FeO^+	$^6\Sigma^+$	$1\sigma^2 2\sigma^2 1\pi^4 1\delta^2 2\pi^2 3\sigma^1$	1.62	0.0
	$^4\Delta$	$1\sigma^2 2\sigma^2 1\pi^4 1\delta^3 1\pi^2$	1.56	1.0
CoO^+	$^5\Delta$	$1\sigma^2 2\sigma^2 1\pi^4 1\delta^3 2\pi^2 3\sigma^1$	1.63	0.0
	$^3\Sigma$	$1\sigma^2 2\sigma^2 1\pi^4 1\delta^3 1\pi^2$	1.55	1.0
NiO^+	$^4\Sigma$	$1\sigma^2 2\sigma^2 1\pi^4 1\delta^4 2\pi^2 3\sigma^1$	1.63	0.0
	$^4\Delta$	$1\sigma^2 2\sigma^2 1\pi^4 1\delta^3 2\pi^2 1\sigma^2$	1.74	1.1
	$^2\Delta$	$1\sigma^2 2\sigma^2 1\pi^4 1\delta^4 2\pi^2 3\sigma^1$	1.62	1.3
CuO^+	$^3\Sigma$	$1\sigma^2 2\sigma^2 1\pi^4 1\delta^4 2\pi^2 3\sigma^2$	1.76	0.0
	$^3\pi$	$1\sigma^2 2\sigma^2 1\pi^4 1\delta^4 1\pi^3 3\sigma^1$	1.75	0.8
	$^1\Delta$	$1\sigma^2 2\sigma^2 1\pi^4 1\delta^4 2\pi^2 3\sigma^2$	1.73	1.4
ZnO^+	$^2\Pi$	$1\sigma^2 2\sigma^2 1\pi^4 1\delta^4 2\pi^3 3\sigma^2$	1.83	0.0
	$^4\Pi$	$1\sigma^2 2\sigma^2 1\pi^4 1\delta^4 2\pi^3 3\sigma^1 4\sigma^1$	1.74	1.6

[a] According to ab initio calculations using a density functional theory approach [39, 55]. [b] For nomenclature of the orbitals, see Fig. 2.

In accordance with this picture, FeO^+, CoO^+, NiO^+, and CuO^+ exhibit high-spin ground states rather than their perfect-pairing, low-spin electromers, analogous to the singlet/triplet splitting in dioxygen. These assignments of the electronic ground states agree well with the predictions by Carter and Goddard III,[54] although some differences in the occupancy of the 1δ and 3σ orbitals exist. These differences are because, in the electronic ground states of MO^+, the metal atom participates in its s^1d^n configuration. In addition, these results reveal that the description of a metal oxide in terms of a double bond between the metal and oxygen atoms, for example, [M]=O, is somewhat misleading; however, for the sake of simplicity we keep using this description.[56]

Unfortunately, not much effort has yet been expended to characterize metal-oxide ions spectroscopically. However, the electronic ground state assignments derived from these few experimental studies are in good agreement with the theoretical predictions: TiO^+ ($^2\Delta$) and TiO^+ ($^2\Sigma^+$) with an experimentally measured excitation energy ($\Delta E_{exp.}$) of 1.5 eV;[57] VO^+ ($^3\Sigma^-$) and VO^+ ($^3\Delta$) with $\Delta E_{exp.} = 1.2$ eV;[58] CrO^+ ($^4\Sigma^+$),[59] FeO^+ ($^4\Delta$),[60] ZrO^+ ($^2\Sigma^+$),[61] and HfO^+ ($^2\Sigma^+$).[61]

From a chemical point of view, we can expect catalytic activity for those metals for which on one hand BDE (M^+-O) is sufficiently low but BDE (M^+-H) and/or BDE (M^+-CH_3)[50] are high enough to render the initial activation reaction (step ⓐ in Scheme 3) exothermic. On the other hand, BDE (M^+-O) must be high enough to permit the reoxidation of the reduced metal to the corresponding oxide by a suitable O-atom donor by reaction ⓒ.

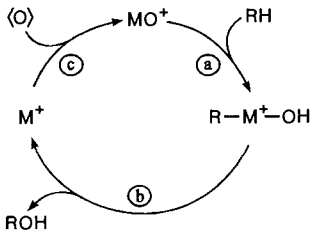

Scheme 3.

Furthermore, the ionization energy (IE) of the metal oxide (Table 2) should not exceed that of the organic substrate RH. A high IE of MO would give rise to an electron-transfer process from the substrate to the MO^+ ion, to yield the corresponding organic cation radicals, which are expected to lead to less specific product formation in subsequent reactions. Different reactivities have been predicted for different electronic states of the MO^+ cations. The high-spin metal-oxide ions, for example FeO^+ ($^6\Sigma^+$), should preferentially involve atom- or group-abstraction reactions as well as electron-transfer processes, whereas the low-spin states, for example, FeO^+ ($^4\Delta$), should also permit more complex reactions, such as multibond rearrangements or hydride transfers.[39] This enhanced reactivity of the low-spin states in synchronous C–H bond activation can be attributed to the fact that these states have both high-lying doubly occupied as well as low-lying unoccupied molecular orbitals that can interact with the σ^* and σ orbitals of the R–H bond to be broken.[62] In metal-oxide cations with high-spin ground states, such favorable HOMO/LUMO interactions are not possible. However, as outlined below, for transition-metal compounds this simple picture is complicated by the ease of curve crossing mediated by spin–orbit coupling between states of different multiplicities and symmetries. Indeed, the facile interconversion of various electronic states is quite probably the most crucial issue for the particular reactivity of transition-metal compounds.

4. Reactions of Metal-Oxide Cations with Hydrocarbons

Before we address reactions of MO^+ cations with organic substrates, it is worthwhile to discuss briefly the simplest system, the reaction of MO^+ with dihydrogen to yield M^+ and H_2O as products. The particular simplicity of this reaction renders it an attractive model system for experimentalists and theoreticians. First, most of the thermochemical data of reactants and products are well established, and for the few missing species one can derive reasonable estimates from literature, and thermochemical thresholds for reactions ⓐ and ⓑ can be evaluated (Scheme 4). Second, the reaction of MO^+ with H_2 (or HD

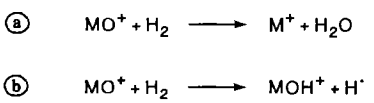

Scheme 4.

and D_2) can be measured in almost all experimental setups without serious difficulties. Finally, this four-atom system is small enough to allow high-level calculations with reasonable accuracy and reliability.

For the early transition-metal oxide cations from ScO^+ through VO^+ and also for ZrO^+ and NbO^+ neither reaction ⓐ nor ⓑ can proceed at room temperature on simple thermodynamic grounds (Table 4).[62, 63] However, both reactions occur

Table 4. Efficiencies ϕ [%], product branching ratios [%], and reaction exothermicities ΔH_r (kcal mol^{-1}) associated with the formation of M^+ and H_2O in the reactions of MO^+ with molecular hydrogen [a, b].

MO^+	ϕ	$MOH^+ + H^\cdot$	$M^+ + H_2O$	ΔH_r
ScO^+	<0.01			46
TiO^+	<0.01			43
VO^+	<0.01			21
CrO^+	<0.01			−31
MnO^+	15	75	25	−49
FeO^+	1 [c]		100	−36
CoO^+	0.1 [c]		100	−41
NiO^+	0.2		100	−54
OsO^+	0.5		100	−17

[a] H-atom abstraction reactions are observed for a number of other MO^+ ions when these are subjected to translational excitation [63]. [b] The data are extracted from Refs. [18, 41, 62, 64, 66, 70, 80]; for further details, see text and the original sources. [c] Note the somewhat lower efficiencies measured by Armentrout et al. [65].

at the thermochemical thresholds when the MO^+ cations (M = Sc, Ti, V) are subjected to translational excitation, which indicates the absence of significant kinetic barriers for reactions ⓐ and ⓑ for these systems.[62] In contrast, from CrO^+ through ZnO^+ the formation of water (reaction ⓐ) is quite exothermic, and for MnO^+, CuO^+, and ZnO^+ the H-atom abstraction ⓑ is also energetically feasible. Despite a favorable thermochemistry, CrO^+, CoO^+, and NiO^+ hardly react with molecular hydrogen (or even not at all), and for FeO^+ the reaction rate k_R is surprisingly slow and occurs only once in every hundred collisions.[18, 64] More recently, the value of the thermal rate constant for the reaction of FeO^+ with H_2 came under criticism;[65] however, the general features of the reaction were confirmed. Only the reaction of MnO^+ with H_2 is efficient, leading to both $MnOH^+$ (75%) and Mn^+ (25%) as ionic products.[66] Unfortunately, CuO^+ and ZnO^+ have not yet been studied experimentally, because they could not be generated in reasonable quantities. In addition, slow occurrence of reaction ⓐ was observed for OsO^+, the third-row homologue of FeO^+.[41]

The high efficiency observed for MnO^+ can be easily rationalized by a mechanism involving initial exergonic abstraction of a hydrogen atom to give a loosely bound complex $[H\cdots MnOH^+]$; this rovibrationally excited intermediate may either rearrange to form a second O–H bond followed by reductive elimination of water, reaction ⓐ, or the complex may lose an H atom, reaction ⓑ.[66] A more detailed analysis reveals[66] that the hallmark of the MnO^+/H_2 system (and also for other MnO^+/RH couples) is a nearly barrier-free[67] H-atom abstraction. The reaction is therefore primarily driven by the intrinsic thermodynamics of the system, instead of by the lowering of an activation barrier associated with H–H bond activation. As far as metal-catalyzed oxidation processes are concerned, the inefficiency of the exothermic reaction ⓐ for the other MO^+ cations is much more telling: the low rate constants for these processes imply the existence of considerable kinetic barriers associated with H–H bond activation. Recently, independent studies from Armentrout's[65] and our laboratories[18, 39] have shown that the barrier associated with water formation by reaction ⓐ originates not only from a tight, four-centered transition state en route to the products, but also from a curve crossing between the high-spin to the low-spin potential-energy hypersurfaces of FeO^+ and H_2.

Some of the salient features of the FeO^+/H_2 system are given in the simplified potential-energy hypersurface depicted in Figure 4. The reaction of FeO^+ ($^6\Sigma^+$) with H_2 to yield Fe^+ (^6D) and water has been examined by high-level ab initio calculations in

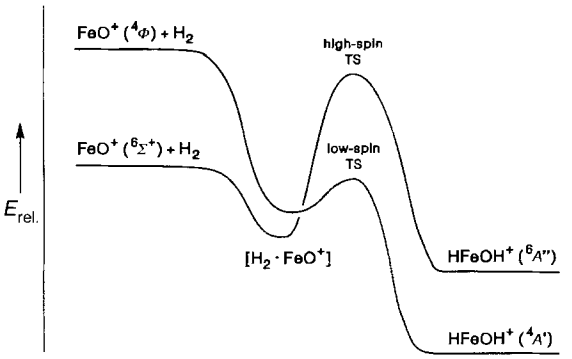

Fig. 4. Reaction of FeO^+ ions with H_2. TS = transition structure.

which DFT and MO approaches were combined.[39] According to these computations the corresponding transition structure (TS) on the high-spin entrance channel is too high in energy to account for the reactivity observed at thermal energies. In contrast, the TS on the low-spin surface, which is derived from an excited quartet state of FeO^+ ($^4\Phi$ or $^4\Delta$), is relatively low in energy. Consequently, at thermal energies reaction ⓐ has to involve a curve crossing mediated by spin–orbit coupling from the sextet to the quartet surface for M = Fe. These arguments agree well with the absence of a significant intermolecular kinetic isotope effect for the activation of H_2, HD, and D_2, respectively.[18] Furthermore, a qualitative analysis indicates that the lower activation barrier associated with the low-spin surface reveals a general phenomenon for H–H and C–H bond activation by late transition-metal-oxide ions, since only in the low-spin states can bond formation and breaking occur synchronously. Consequently, the very small efficiencies of the reactions of the late transition-metal oxide cations MO^+ (M = Cr, Fe, Co, and Ni) with H_2 do not reflect unfavorable thermochemistry; rather, they are controlled by reaction barriers and the ease of curve crossing from the high-spin ground state of MO^+ to the low-spin surface; it is the latter that leads to product formation.

4.1. Reactions of MO^+ Ions with Alkanes

Hydroxylation of nonactivated C–H bonds is a central issue in contemporary chemistry. Recently the efficient conversion of methane into methanol has been listed as one of the ten chal-

lenges for catalysis.[68] Furthermore, the activation of C–H bonds of higher saturated hydrocarbons is of economic interest—for example, the oxidation of cyclohexane to cyclohexanone.[5] In this section we will review the current status and the scope of reactions of alkanes in the gas phase with transition-metal oxide cations.

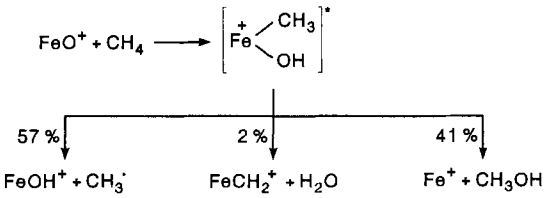

Scheme 5.

4.1.1. Methane

The efficiencies ϕ and the product branching ratios for the reactions of methane with the MO^+ cations studied so far are collated in Table 5. If one takes into account that the larger polarizability of methane (relative to that of H_2) increases the efficiency of an ion/molecule reaction, the trends for the first-row transition-metal oxides are similar to those already discussed for the activation of H_2. For example, MnO^+ reacts in a fast process by facile hydrogen-atom abstraction to yield exclusively $MnOH^+$.[66] In contrast, FeO^+ reacts somewhat less efficiently; however, most interestingly methanol is also formed as neutral product.[28, 39, 69] Not unexpectedly, the early transition-metal oxides ScO^+, and TiO^+ do not react at all, and the activation of methane by VO^+ and CoO^+ hardly occurs.[44, 62, 65, 70] The only exception deals with NiO^+ which reacts much faster with methane and other alkanes than with H_2.[71]

Table 5. Efficiencies ϕ [%] and product branching ratios [%] for the reactions of MO^+ with methane [a, b].

MO^+	ϕ	$MOH^+ + CH_3^\cdot$	$MCH_2^+ + H_2O$	$M^+ + CH_3OH$
MnO^+	40	100		<1
FeO^+	20 [c]	57	2	41
CoO^+	0.5 [c]			100
NiO^+	20			100
PtO^+	100		75	25

[a] The data are extracted from Refs. [66, 69–71, 75]; for further details, see text and the original sources. [b] OsO^+ also reacts efficiently with methane [41]; however, the only product corresponds to dehydrogenation rather than oxidation (see text). [c] Note the somewhat lower efficiencies measured by Armentrout et al. [65].

Again, it is the reaction of FeO^+ that has attracted particular interest.[28] Here, reductive elimination of methanol corresponds to a formal O-atom transfer from the metal oxide to methane, and this process can be viewed as a model for alkane hydroxylation. Experimental and theoretical analysis of this reaction revealed that it commences with activation of the C–H bond of methane to yield the iron(III) insertion compound H_3C-Fe^+-OH (Scheme 5).[28, 39] This rovibrationally excited species is the key intermediate which subsequently decomposes to the products, $FeOH^+ + CH_3^\cdot$, $FeCH_2^+ + H_2O$, and $Fe^+ + CH_3OH$. As mentioned in Section 2, chemical ionization of appropriate precursor molecules, isotopic labeling studies, and collisional activation (CA) mass spectrometry were applied to characterize structural isomers formed en route to the products.[28] The essential CA data and the respective precursors are collected in Table 6. The isomer (Table 6, line 1) corresponds to the encounter complex of the reactants, $(CH_4)FeO^+$, as evident from the signal indicative of the structure of FeO^+. The key intermediate of methane hydroxylation, H_3C-Fe^+-OH, is generated independently from methanesulfonic acid and $Fe(CO)_5$ and is characterized by competitive losses of $CH_3^\cdot$ and $HO^\cdot$, which in turn yield $FeOH^+$ and $FeCH_3^+$. The ratio of both fragment ions is in line with the larger BDE for Fe^+-OH (79 kcal mol^{-1}) than for Fe^+-CH_3 (59 kcal mol^{-1}).[20, 72] The carbene complex $H_2C=Fe^+(OH_2)$ undergoes a characteristic loss of water, which accounts for the $FeCH_2^+$ product ion observed in the reaction of FeO^+ with methane at thermal energies. Finally, the CA mass spectrum of the product complex $(CH_3OH)Fe^+$ is dominated by an intense loss of the intact methanol ligand to yield Fe^+. Like the reaction of FeO^+ with H_2, hydroxylation of methane also most likely involves curve crossing from the high-spin to the low-spin surface of the metal oxide as crucial step. As mentioned above, the larger efficiency of the methane oxidation ($\phi = 0.2$) than that of H_2 ($\phi = 0.01$) can be accounted for by the larger polarizability of methane, which increases the lifetime of the encounter complex and lowers the energy demand of the more polarized four-center transition structure in the case of methane.[39, 74]

Methane activation has also been reported for the third-row transition-metal oxides OsO^+ and PtO^+. Interestingly, these third-row transition metal oxides exhibit quite another reactivity than their first-row congeners. For example, PtO^+ reacts with methane at the collisional limit ($\phi = 1$) to yield the carbene complex $PtCH_2^+$ and water as predominant products,[75] whereas the isoelectronic NiO^+ reacts five times more slowly and gives rise to Ni^+ and methanol only.[71] Similarly, while FeO^+ oxygenates methane, its third-row congener OsO^+ ($\phi = 0.6$)[41] exclusively dehydrogenates methane to yield a complex of composition $[Os,C,H_2,O]^+$. Secondary reactions indicate that this product ion has the oxo–osmium carbene structure $O=Os^+=CH_2$ rather than that of a formaldehyde complex,

Table 6. Characteristic fragments (ion intensities in % relative to the base peak) in the CA mass spectra of $[Fe,C,H_4,O]^+$ isomers generated by chemical ionization of various organic precursors with $Fe(CO)_5$ [a, b].

Precursors	Ion Structure	$Fe(OH_2)^+$	$FeOH^+$	FeO^+	$FeCH_3^+$	$FeCH_2^+$	Fe^+
CH_4/N_2O	$(CH_4)FeO^+$	1	20	100	1	15	50
CH_3SO_3H	CH_3-Fe^+-OH		100	4	9	4	
c-C_3H_6/H_2O	$CH_2=Fe^+-OH_2$	25	6			100	15
CH_3OH	$(CH_3OH)Fe^+$		50	2			100

[a] For the sake of clarity intensities smaller than 1% are omitted. [b] Data from Ref. [28].

that is, $(CH_2O)Os^+$. This agrees with the observation that methane is also dehydrogenated by bare Os^+ itself to yield $H_2C{=}Os^+$.[41, 76] Apparently the oxygen atom is not actively involved in methane activation by OsO^+. The different reactivity of third-row MO^+ ions relative to their first-row analogues can partly be traced back to thermodynamic grounds, which originate from the significantly increased $M^+{=}CH_2$ bond strengths for third-row transition metals.[77]

4.1.2. Higher Alkanes

In general, higher alkanes react much more efficiently with MO^+ than methane does (Table 7). This is not primarily due to the increase in polarizability; rather, a new reaction channel

Table 7. Efficiencies ϕ [%] for the reactions of MO^+ with alkanes [a].

MO^+	CH_4	C_2H_6	C_3H_8	n-C_4H_{10}
ScO^+	<0.01	<0.01		
TiO^+	<0.01	<0.01		
VO^+	<0.01	<0.01	[b]	[b]
CrO^+	<0.01	100	100	100
MnO^+	40	100	100	100
FeO^+	20	50	100	100
CoO^+	0.5	50	50	100
NiO^+	20	100	100	100
OsO^+	60	[c]	[c]	[c]
PtO^+	100	[c]	[c]	[c]

[a] The data are extracted from Refs. [41, 62, 64, 66, 69–71, 75, 78]; for further details, see text and the original sources. [b] In Ref. [78] the occurrence of dehydrogenation was reported; however, kinetic data were not examined. [c] In Refs. [41] and [75] no efficiencies were given; however, these reactions are likely to occur with $\phi \approx 1$.

opens for these alkanes, namely, β-hydrogen transfer to the metal center after initial C–H bond activation (Scheme 6). Since β-hydrogen transfer is by far the most facile reaction of organometallic compounds and is often associated with low activation barriers, the major products of the reactions of MO^+ with higher homologues of methane reflect losses of molecular hydrogen, water, alkanes, alkenes, and alkanols. Because these processes are not limited to transition-metal-oxide species, and β-hydrogen transfer also follows initial hydroxylation, we restrict ourselves to the discussion of a few representative and some exceptional studies.

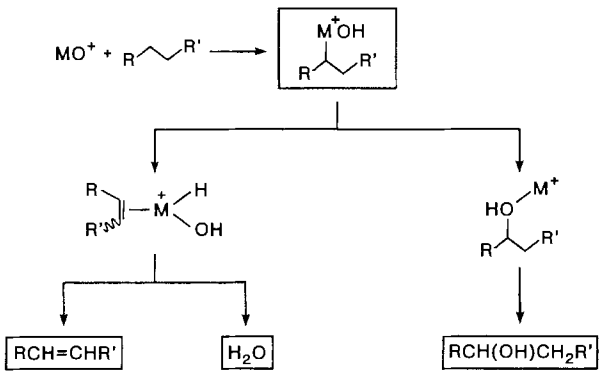

Scheme 6.

As expected, the oxides of the early transition metals are, in general, much less reactive towards alkanes than the bare metal cations. For example, V^+ dehydrogenates propane quite rapidly, whereas VO^+ is completely unreactive.[78] Similarly, the bare V^+ cation induces oligomerization of butanes, whereas VO^+ does not. Thus, for the highly oxophilic early transition metals the oxide ligand decreases the reactivity relative to that of bare M^+, and this effect can be ascribed to the high BDEs of these metal oxides. As a consequence, the early transition-metal oxides are not good catalyst for the oxidation of alkanes, since their high BDEs do not allow transfer of the oxide ligand to the substrate. Moreover, bare Sc^+ ion even deoxygenates methanol to yield ScO^+ and methane, precisely the reverse of the desired hydroxylation process (Scheme 7).[79]

$$Sc^+ + CH_3OH \rightleftharpoons ScO^+ + CH_4$$

Scheme 7.

In contrast, for many other transition metals the presence of an oxygen ligand dramatically enhances the reactivity towards hydrocarbons.[80] For example, at thermal energies none of the first-row M^+ ions reacts with methane, but MnO^+ through NiO^+ do. Similarly, none of the M^+ ions (M = Cr–Ni) activate ethane at thermal energies, but all the corresponding MO^+ ions lead to C–H bond activation and subsequent losses of ethanol, ethene, or water.[64, 66, 71, 80] The ease of these reactions can also be ascribed to the moderate strength of the M^+–O bonds, rendering initial C–H bond activation probable. Subsequent β-hydrogen transfer is expected to be associated with small activation barriers,[81] and the reaction rates approach the collision limit ($\phi = 1$). Once more, a typical example is the reaction of FeO^+ with alkanes (Scheme 6; M = Fe):[80] Ethane (R = R′ = H) is rapidly oxidized to ethene (20%), water (70%), and ethanol (10%) as neutral products. Similarly, propene (10%), water (50%), and propanol (20%) are formed when FeO^+ reacts with propane. In addition, a new product (20%) originates from the loss of a methyl radical in the FeO^+/C_3H_8 system to yield a species of composition $[Fe,C_2,H_5,O]^+$; this ion is most likely an ethene/$FeOH^+$ complex (**3**) rather than an iron(II) ethoxide cation ($Fe(OC_2H_5)^+$). Freiser et al.[80] explained the formation of **3** by a mechanism (Scheme 8, path ⓐ) which involves an initial insertion of the iron center into a C–C bond to form **1**; subsequent $CH_3^{\bullet}$ loss to give **2**, followed by two consecutive hydrogen rearrangements, will lead to the product structure (**1** → **2** → **3**). However, as outlined above, the initial step in the reactions of MO^+ with alkanes is most likely O–H bond formation, thus generating the key intermediate **4**, which

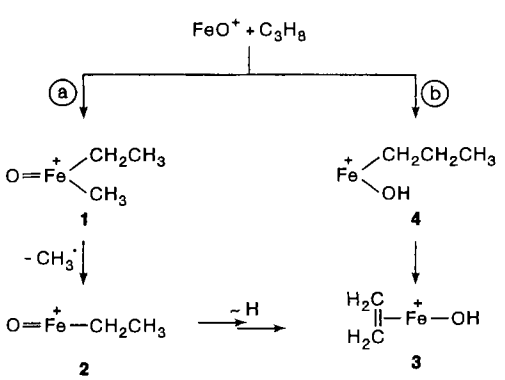

Scheme 8.

upon facile β-C–C bond cleavage dissociates to **3**. Path ⓑ of Scheme 8 is also expected to be energetically favored over the generation of the formally high-valent iron(v) compound **1**. This mechanism is further supported by the observation of a sizable $CH_3^{\bullet}$ loss from the 1-propanol/Fe^+ complex upon collisional activation.[82] Moreover, losses of alkyl radicals are also prominent in the reactions of MnO^+ with alkanes, and, as shown above, initial C–H bond activation is the hallmark in the gas-phase chemistry of MnO^+.[66] Because of the high exothermicity of the oxidation of RH by MO^+, alkanes larger than propane also give rise to consecutive, facile losses of H_2O and H_2, thus leading to alkadiene complexes: for example, $MO^+ + n\text{-}C_4H_{10} \rightarrow M(C_4H_6)^+ + H_2O + H_2$ (M = Mn, Fe, Co, Ni). In addition, if the IE of R$^{\bullet}$ is small enough, initial C–H bond activation of RH by CoO^+ is completed by single-electron transfer from R$^{\bullet}$ to the $CoOH^+$ unit, resulting in the production of a carbocation R^+ and neutral CoOH: for example, $CoO^+ + n\text{-}C_4H_{10} \rightarrow C_4H_9^+ + CoOH$.[70] Interestingly, for CrO^+ yet another mechanism is operative. In their comprehensive study Kang and Beauchamp[64] demonstrated by using labeled substrates that water loss from propane and CrO^+ includes the conventional 1,2-elimination and, in addition, a formal 1,3-dehydrogenation to yield cyclopropane was proposed (Scheme 9).

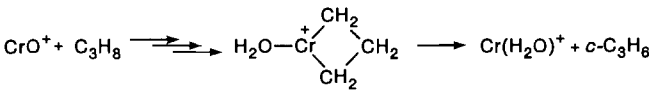

Scheme 9.

Similar mechanisms were reported for the reactions of MO^+ with branched alkanes. The product distribution can be explained if one takes into account the larger tendency for C–C bond activation in branched molecules concomitant with a decreased formation of alkadiene/M^+ complexes (Scheme 10).[13] For *iso*-butane, rather than C–C bond activation (path ⓐ), the initial step for these alkanes is more likely to be C–H bond activation, followed by either β-H or β-alkyl transfer or rearrangement of the carbon skeleton (path ⓑ). As for the larger linear alkanes, selectivity decreases with the size

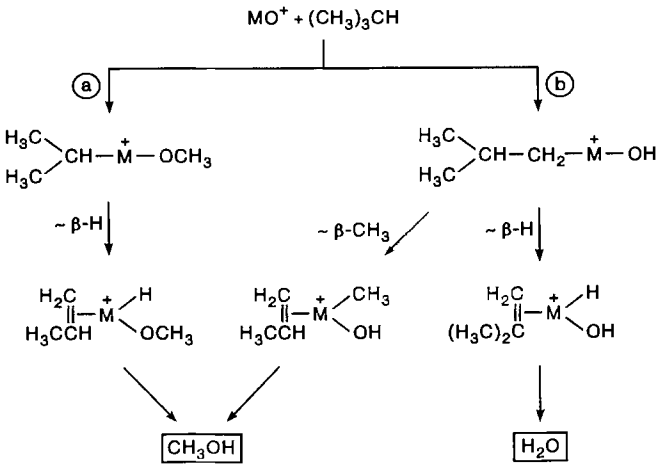

Scheme 10.

of branched alkanes. For example, FeO^+ reacts with *neo*-hexane to yield no less than ten products.[80]

In only two cases has clear evidence for initial C–C bond activation by MO^+ been reported, and both deal with small ring compounds (cyclopropane and cyclobutane).[64, 80] For example, in the reaction of FeO^+ with cyclopropane[83] the carbene complex $FeCH_2^+$ constitutes a major product ion, and its formation can easily be explained by C–C bond activation to yield a metallacyclic intermediate.[85] Here, C–C bond activation can be ascribed to the particular bonding in the three-membered ring, which results in stronger C–H bonds and weaker C–C bonds than in acyclic systems or less-strained rings.[86]

The diversity of competing C–H bond activation of primary and secondary positions, potential radical losses, carbocation formation, and consecutive processes gives rise to quite complex product mixtures for larger alkanes. Thus, the activation of alkanes by late transition-metal-oxide cations is facile, but it lacks chemo- and regioselectivity. Similar mechanisms to those for reactions of the corresponding atomic M^+ ions (M = Cr–Ni) with alkanes and alkanols are operative,[87] but the large exothermicities of the primary oxidation processes (for example, water formation) enforce subsequent fragmentations. For example, though $Fe(C_6H_6)^+$ is the sole product ion in the reaction of FeO^+ with cyclohexane, Fe^+ also transforms cyclohexane and cyclohexanol to the intermediate dehydrogenation products $Fe(c\text{-}C_6H_{10})^+$ and $Fe(c\text{-}C_6H_8)^+$ respectively.[80]

At the end of this section, two experiments in which gas-phase reactions of alkanes with high-valent transition-metal oxides were examined should be mentioned briefly. In their comprehensive study of the OsO_n^+ chemistry ($n = 0$–4), Irikura and Beauchamp[41] demonstrated that not only OsO^+ but also OsO_2^+ ions react efficiently with hydrogen, methane, and larger alkanes. In particular, the reaction of OsO_2^+ with methane (Scheme 11) is noteworthy in that it may be viewed as a model for the catalytic conversion of methane into formaldehyde. Interestingly, the higher valent OsO_3^+ was found to be much less reactive than OsO_n^+ ($n = 0$–2); for example, OsO_3^+ does not react at all with methane, whereas OsO^+ and OsO_2^+ are quite efficient ($\phi = 0.6$ and 0.5, respectively). OsO_4^+ also reacts with methane ($\phi = 0.7$), but the sole product corresponds to a hydrogen abstraction to yield the protonated species $Os(O)_3OH^+$ (actually a typical reaction for a cation radical such as OsO_4^+). Similar behavior was found for the higher alkanes, and OsO_3^+ turned out to be the least reactive species of all OsO_n^+ ($n = 0$–4) ions.

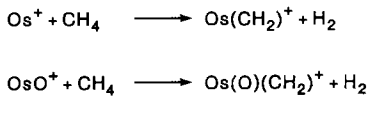

Scheme 11.

Another study addressed the reactions of the formal iron(IV) compound $OFeOH^+$ with small alkanes.[88] In this unusual oxidation state of iron, the metal oxide is somewhat less reactive than its formal iron(III) analogue FeO^+. For example, $OFeOH^+$ oxidizes methane ($\phi = 0.1$) half as fast as FeO^+ ions. Perhaps more important is the observation that the complex of $OFeOH^+$ with CH_4 does not yield any open-shell neutral species as products, whereas $CH_3^{\bullet}$ loss amounts to 57% in the reaction of FeO^+

These examples demonstrate that high-valent transition-metal oxides are indeed accessible in the gas phase and need not necessarily be stabilized by a highly coordinating ligand environment. In addition, high-valent species are expected to exhibit distinct reactivities and selectivities towards alkanes and similar substrates, which render these cationic oxides attractive candidates for further studies.[89, 90]

4.2. Reactions of MO^+ with Alkenes

From the point of view of applications, by far the most important oxidation reaction of alkenes is O-atom transfer from an oxidant to yield the epoxides.[91] Numerous preparative methods as well as large-scale industrial processes deal with this important topic. In fact, nowadays many sophisticated methods for the epoxidation of a large variety of alkenes are available, including regio- and stereospecific epoxidation (and also dihydroxylation) of alkenes.[91b–c, 92] Reaction mechanisms differ for classical methods (for example, employing peracids) and transition-metal-catalyzed epoxidations.[91a] In the latter reactions metal-oxide species are often involved; however, a huge number of mechanistic routes prevail in the condensed phase. At least five different pathways can be distinguished for the rate-determining step of epoxidation processes mediated by [M]=O (Scheme 12):[93] 1) In a more or less concerted [2+2] cycloaddition a metallaoxacyclobutane (**5**) is formed as central

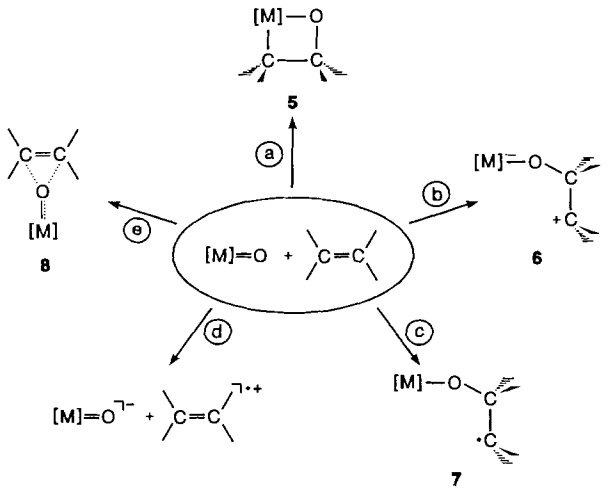

Scheme 12.

intermediate (path ⓐ); 2) stepwise bond breaking and formation, having either an ionic (**6**) or radical nature (**7**), take place (paths ⓑ and ⓒ); 3) initial single-electron transfer from the alkene to the metal oxide (path ⓓ) is followed by subsequent transformation of the alkene cation radical; 4) direct O-atom transfer from the metal to the alkene proceeds through a multicentered structure (**8**, path ⓔ). Obviously, depending on the mechanistic details not only the stereochemical outcome of the epoxidation may vary, but also characteristic side-products are likely to be formed in nonconcerted pathways. In the condensed phase, the elucidation of the mechanism(s) of epoxidations was studied in detail with H/D kinetic isotope effects and isotope exchange processes,[94] to probe regio- and stereochemical features,[95] and analysis of the side-products[95b, c] to identify the reaction intermediates.[96]

Previously, gas-phase studies focused on the characterization of the reaction intermediates and determination of the rate-determining step(s) of olefin epoxidation, and one may rightly raise the question whether the models developed are suitable to improve the understanding of the condensed-phase analogues.

4.2.1. Ethene

A number of gas-phase studies have addressed the epoxidation of ethene by MO^+ ions or the reverse reaction of M^+ with oxirane.[97–101] According to thermochemistry, oxidation of ethene to its epoxide can only occur if $BDE(M^+-O) \leqq 85\ kcal\,mol^{-1}$.[20] Consequently, the oxophilic early transition-metals need not be considered further. In fact, Sharpless epoxidation, which is one of the most powerful tools in contemporary organic oxidation chemistry, does not involve [Ti]=O species as intermediates.[6b, c] In the gas phase, TiO^+ only undergoes adduct formation with ethene to yield $(C_2H_4)_3TiO^+$ as final product, whereas naked Ti^+ is capable of inducing polymerization of ethene.[97]

For CrO^+ ($BDE = 86\ kcal\,mol^{-1}$), the formation of oxirane is almost thermoneutral, and may thus occur in a thermal ion/molecule reaction. Indeed, Kang and Beauchamp reported rapid O-atom transfer from CrO^+ to ethene to yield Cr^+ and a compound of composition $[C_2,H_4,O]$.[98] However, comparative studies of the reverse reaction of Cr^+ with oxirane and with acetaldehyde revealed that not oxirane, but rather, the energetically more stable acetaldehyde is formed as the neutral product in the reaction of CrO^+ with ethene. Although these authors did not suggest a reaction mechanism, they provided evidence for the formation of the metallacycle **9** as central intermediate (Scheme 13). This assignment was based on the occurrence of a

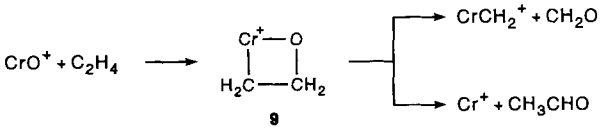

Scheme 13.

metathesis-like ring-opening of **9** to yield formaldehyde and $CrCH_2^+$ as products. In fact, the reaction of CrO^+ with C_2H_4 demonstrates the central problem in studying olefin oxidation in the gas phase: While the initial addition of MO^+ to the C–C double bond quite likely leads to the metallacycle **9**, this intermediate does not necessarily undergo a one-step reductive elimination to generate the epoxide. Unfortunately, the transition-metal ion that mediates O-atom transfer to the olefins preferably catalyzes the isomerization of the so-formed epoxides to the corresponding carbonyl compounds (Scheme 14). Thus, instead of providing a conceptually simple model system aimed at improving the understanding of the condensed phase analogues, in the gas phase the situation is even more complicated because of subsequent M^+-mediated intramolecular H-migration (**10** → **11**). In other words, the reactivity of naked MO^+ ions

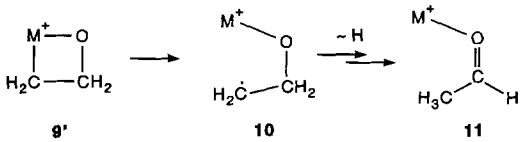

Scheme 14.

is simply too high to permit selective gas-phase epoxidation of olefins.

Similarly, the late transition-metal oxides MnO^+, FeO^+, CoO^+, and NiO^+ rapidly oxidize ethene, and most likely acetaldehyde rather than oxirane is formed as neutral product.[99-104] This interpretation was further supported by Armentrout et al. who studied the reverse reactions, that is, oxirane with M^+ (M = Fe, Co, Ni, Cu), by means of GIB mass spectrometry.[100, 101] On the basis of the experimental findings the formation of acetaldehyde was attributed to the bonding in **9'**, for which homolytic ring opening to **10** and subsequent H transfer to yield the aldehyde complex **11** are expected to be facile (Scheme 14). However, this picture needs further investigation; in particular, a detailed description of the rearrangement **10** → **11** and the overall mechanism is not yet available. Furthermore, the current experimental findings cannot exclude the formation of the enol form of acetaldehyde (that is, vinylalcohol) as a reaction product or at least a role as for it as an intermediate en route to the products.

A formal O-atom transfer to ethene has also been reported for OsO^+.[41] Here, the high BDE of the Os^+–O bond (100 kcal mol^{-1}) precludes oxirane formation, and again, acetaldehyde is most likely generated as the neutral product. As in the reaction of OsO^+ with alkanes (see above), dehydrogenation of ethene to yield $[Os,C_2,H_2,O]^+$ competes with its oxidation, indicating that for Os^+ the oxygen atom can also serve simply as a spectator ligand. Interestingly, the high-valent dioxide OsO_2^+ reacts much more slowly than OsO^+ with ethene to yield exclusively a compound of composition $[Os,H_2,O_2]^+$ and acetylene. Furthermore, the higher oxides OsO_3^+, OsO_4^+, and also the organometal oxide $(CH_3)_4OsO^+$ do not epoxidize ethene at all.[41, 105]

As far as other high-valent transition-metal oxides are concerned, CrO_2Cl^+, $CH_3ReO_3^+$, and CeO_2^+ have been shown to bring about stoichiometric O-atom transfer with ethene.[42, 107, 108] Whereas the formal Cr^{VI} compound CrO_2Cl^+ as well as the lanthanide dioxide CeO_2^+ presumably lead to acetaldehyde, collisional activation studies of the $[C_2H_4/CH_3ReO_3^+]$ system and related ions revealed that for this rhenium-based organometal oxide, formation of oxirane is indeed observed and competes with olefin metathesis (Scheme 15).[42] Interestingly, the competition of olefin epoxidation and metathesis parallels the chemistry of CH_3ReO_3 in the condensed phase, where it was demonstrated that this organometal oxide catalyzes both reactions.[109]

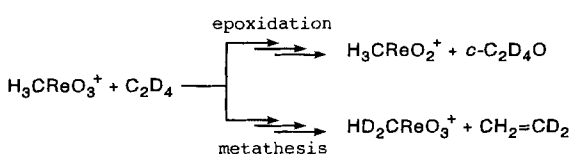

Scheme 15.

4.2.2. *Ligand Effects*

As outlined in the previous paragraph, the rapid isomerization of the desired product, that is, of the epoxides to the energetically more stable carbonyl compounds, constitutes a severe problem in the gas-phase olefin oxidation. Thus, instead of representing a conceptually simple model system for elucidating mechanistic aspects of epoxidation processes, the consecutive rearrangements render the gas-phase experiments even more complicated than their condensed-phase analogues. Since this isomerization usually does not affect epoxidation in condensed-phase chemistry, this pitfall might be overcome by sequential addition of appropriate ligands to the reactive MO^+ center.[110] The approach may moderate the reactivity of MO^+ and 1) permit a stabilization of reaction intermediates and 2) suppress the subsequent isomerization processes. Such a ligand effect is already illustrated in the epoxidation of ethene with $CH_3ReO_3^+$, as described above (Scheme 15).[42] Unfortunately, the high reactivity of MO^+ towards a variety of substrates that may serve as ligands renders this concept quite difficult to realize. For example, the attempt to mediate the reactivity of FeO^+ by adding a hexafluorobenzene ligand failed:[111] even hexafluorobenzene is rapidly oxidized by FeO^+ through C–F bond activation. The generation of $(C_6F_6)FeO^+$ and further reactivity studies with this system were thus precluded.[84] Yet another problem was encountered by Irikura and Beauchamp, who tried to add an oxide ligand to a metalloporphyrin ion in order to mimic cytochrome chemistry directly.[112] The porphyrin system seems to be too large to permit rapid reactions of the metal center with various O-atom donors to produce oxide species, and none of the (porphyrin)FeO_x^+ species ($x = 1, 2$) were observed. The intermediacy of (porphyrin)$FeO^{+/-}$ ions has been reported for NO_2 as an oxidant and (porphyrin)$Fe^{+/-}$; unfortunately, further reactivity studies were precluded on experimental grounds.[113] Furthermore, the reactivity of an metalloporphyrin–oxide species might be too low to be monitored in the time window of gas-phase experiments. Obviously, the direct translation of results of condensed-phase systems to gas-phase studies and vice versa is not a very promising prospect. In this context, a study which describes consecutive formal O-atom transfers from oxirane to $(c\text{-}C_5H_5)Fe^+$ to yield $(c\text{-}C_5H_5)FeO^+$ and $(c\text{-}C_5H_5)FeO_2^+$ is relevant.[114] These reactions demonstrate that the additional cyclopentadienyl ligand influences not only the reactivity, but also the thermochemistry of the formal metal-oxide species, since on thermochemical grounds the reverse reaction of ethene epoxidation is unlikely to occur. However, neither mechanistic insight nor energetic details were given in this study;[114] in particular, these experiments lack a thorough thermalization of precursor ions as well as a definitive characterization of the reaction products.

Most recently, the idea of mediating a gas-phase epoxidation by ligand effects has been realized:[115] The ligated metal oxide $(C_6H_6)FeO^+$, generated by treating $(C_6H_6)Fe^+$ with N_2O, serves as an excellent gas-phase oxidant for alkenes (Scheme 16). Although bare FeO^+ itself is capable of oxidizing benzene,[116] the integrity of the $(C_6H_6)FeO^+$ formed in this way was established by collisional activation studies and the occurrence of a clean, degenerate ligand exchange with C_6D_6 to yield $(C_6D_6)FeO^+$. As expected, the presence of the additional

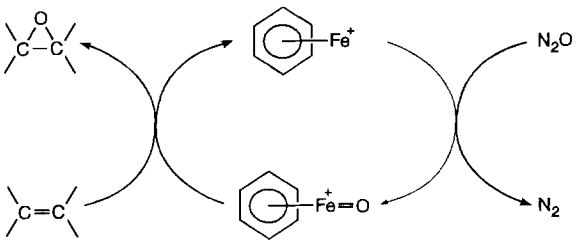

Scheme 16.

benzene ligand both decreases and modifies the reactivity of $(C_6H_6)FeO^+$ dramatically relative to that of bare FeO^+; for example, $(C_6H_6)FeO^+$ does not react at all with alkanes such as methane or even *iso*-butane. However, recent results of ion/molecule reactions of $(C_6H_6)FeO^+$ with various alkenes indicate that this ligated metal oxide brings about O-atom transfer to yield the neutral epoxides; rearrangement to the carbonyl compound is indeed prevented.[115] Thus, addition of suitable ligands to the reactive metal-oxide center can enhance the selectivity at the expense of reactivity, and systematic studies on tuning chemical reactivity by suitable ligands are under way in our laboratory.

4.2.3. Higher Alkenes

In the epoxidation of alkenes larger than ethene the competing activation of allylic C–H bonds is a serious problem. For example, while oxirane is produced in large amounts by oxidation of ethene with molecular oxygen on silver contacts,[3] the related oxidation of propene often leads to allyl alcohol or other products.[117]

As far as gas-phase experiments are concerned, allylic C–H bond activation and the problems associated with epoxidation of ethene by MO^+ are expected to bring about a vast complexity in the reactions of MO^+ with higher alkenes. Consequently, detailed mechanistic studies of gas-phase oxidation of alkenes larger than ethene have not yet been conducted. This is particularly regrettable, since only with alkenes larger than ethene can the intriguing aspects of the regio- and stereospecificity of gas-phase epoxidations in competition with C–H and C–C bond activation be explored. As discussed in the previous section, it will be mandatory to modify the reactivity of MO^+ by adding suitable ligands to the metal in order to tackle this important topic successfully.

Not surprisingly, all MO^+ ions which oxidize ethene also react rapidly with higher alkenes to yield a variety of products. The complexity of these processes leads us only to refer to the quite comprehensive study on gas-phase epoxidation by Kang and Beauchamp.[98] In their study of the reactions of CrO^+ with alkenes it was demonstrated that indeed allylic C–H bond activation competes with olefin epoxidation (Scheme 17). Furthermore, consecutive isomerization of the intermediates to carbonyl compounds was also observed. Despite this isomerization, CrO^+ was found to exhibit a significant selectivity in its reactions with olefins. For example, the product distributions for 1- and *cis*-2-butene were clearly distinguishable, demonstrating that allylic C–H bond activation does not lead to a complete loss of positional integrity of the carbon–carbon double bond

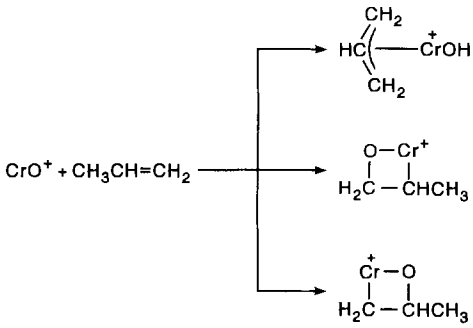

Scheme 17.

within the butene skeleton. We note in passing that this observation, which appears to be trivial, constitutes one of the rare examples in which the butene isomers have been differentiated by mass-spectrometric means. Unfortunately, these authors did not report the reactions of CrO^+ with the *cis*- and *trans*-stereoisomers of 2-butene.

Finally, other unsaturated hydrocarbons such as dienes[84] and acetylenes[44a] are also efficiently oxidized by cationic late transition-metal oxides in the gas phase; for example, FeO^+ reacts with C_2H_2 to yield an approximate 1:1 ratio of $FeCH_2^+$ and Fe^+ as ionic products, accompanied by CO and C_2H_2O formation; the latter neutral species is most probably a ketene.

4.3. Reactions of MO^+ with Arenes

Hydroxylation of arenes is a process of industrial relevance. It is also the most important pathway in the metabolization of aromatic compounds. In common with other oxidations, several mechanistic pathways for arene hydroxylation have been suggested.[8a] As far as processes in which metal oxides play a central role are concerned, the arene–oxide path has received considerable attention.[118] Here, O-atom transfer from an appropriate donor, depicted as [M]=O, leads to an arene oxide (**12**), which subsequently undergoes rearrangement ("NIH" shift)[119] to the corresponding phenol (Scheme 18). However, the arene-oxide path came under criticism, and alternative mechanisms involving σ-complexes (for example, **13**) or electron-transfer reactions were suggested.[120]

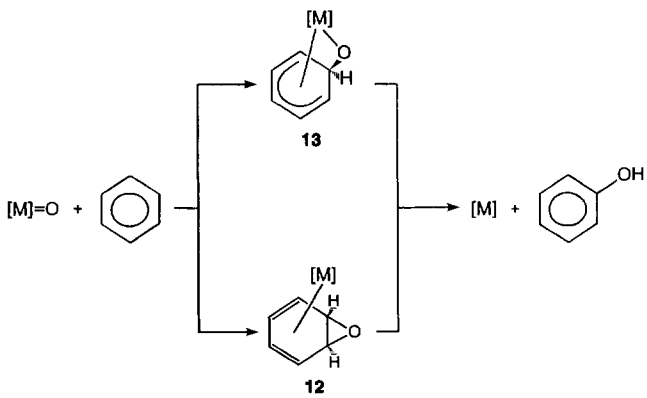

Scheme 18.

Although the conjectured reaction mechanisms are highly dependent on substrate and oxidant,[121] gas-phase studies may open up a new view on aromatic hydroxylation processes. Previously, detailed mechanistic gas-phase studies have only been reported for the reactions of FeO^+ with arenes. Therefore, in the following discussion we will primarily address iron oxide, which is also believed to play a central role in the cytochrome P-450 mediated metabolization of arenes.[8a]

4.3.1. Benzene

In a recent study the ion/molecule reactions of benzene with the first-row transition-metal oxides ScO^+–NiO^+ have been examined (Table 8).[122] Early and late transition-metal oxides can by and large be classified as for C–H bond activation of alkanes: The early transition-metal oxides ScO^+, TiO^+, and VO^+ do not hydroxylate benzene, but undergo adduct formation exclusively. As found for alkanes, MnO^+ is highly reactive ($\phi = 1$) and acts as a potent H-atom abstraction reagent, as evidenced by the formation of $MnOH^+$ with concomitant loss of a neutral phenyl radical among other products. CrO^+, CoO^+ and NiO^+ also react efficiently (all, $\phi = 1$) to yield the bare metal cations and neutral C_6H_6O as major products; for these reactions no mechanistic studies have yet been conducted.

Table 8. Efficiencies ϕ [%] and product ion branching ratios [%] in the reactions of MO^+ with benzene [a].

MO^+	ϕ	$(C_6H_6)MO^+$ [b]	$M(C_6H_4)^+$	$M(C_5H_6)^+$	$M(OH)^+$	M^+
ScO^+	15	100				
TiO^+	30	100				
VO^+	95	100				
CrO^+	100					100
MnO^+	100		18		15	67
FeO^+	100		5	37 [c]		56
CoO^+	100			30		70
NiO^+	100					100

[a] Data taken from Refs. [116] and [122]. [b] The entry corresponds to the formation of the adduct complexes. [c] In addition, the so-formed $Fe(C_5H_6)^+$ undergoes consecutive $H^\cdot$ loss (2%) to yield $Fe(C_5H_5)^+$.

Mechanistic aspects of the benzene hydroxylation by bare MO^+ ions have been studied in quite some detail for FeO^+.[116, 123] In particular, the combination of isotopic labeling studies with ion/molecule reactions under ICR conditions, and collisional activation experiments in a sector field instrument provided significant insight into the reaction intermediates and the potential-energy hypersurface of the species $[Fe,C_6,H_6,O]^+$. NRMS was used to the structure of neutral C_6H_6O and unequivocally established that a C–O bond was present in the FeO^+/C_6H_6 system.[116a] Further experiments strongly favored the phenol structure.[116b] The results indicate that besides the *arene–oxide path*, an alternative mechanistic route must exist, which most probably involves formation of the σ-complex **13** (M = Fe^+ in Scheme 18). This conclusion was derived from comparative CA studies in which the complex of benzene oxide with Fe^+ was found to behave similar to authentic phenol/Fe^+, whereas in the reaction of FeO^+ with benzene significant amounts of the keto form, cyclohexadienone/Fe^+, were formed. Consequently, the arene–oxide path has to be questioned in bimolecular gas-phase chemistry as well. Interestingly, these studies also revealed that bare Fe^+ does not significantly affect the barrier for the interconversion of the keto and enol forms of phenol; however, isomerization of cyclohexadienone/Fe^+ to phenol/Fe^+ was achieved in the presence of a single water molecule added to the ligand sphere of the metal.[116b]

3.2. Alkylbenzenes

In the previous section it has been demonstrated that FeO^+ ions are capable of hydroxylating benzene with a reaction rate near the collisional limit, while the reaction with methane is less efficient. Consequently, it is intriguing to probe the chemistry of FeO^+ ions with toluene; in addition to the kinetic aspect, the site of the activation (benzylic or aromatic C–H bond) or possible competition between the two are points of interest.[124]

In spite of the high reactivity of FeO^+, the reaction of FeO^+ with toluene is highly selective and favors C–H bond activation at the benzylic position. The predominant products of the reaction of FeO^+ with toluene are a benzyl cation and neutral FeOH (Scheme 19).[125] Three aspects of this ion/molecule reaction

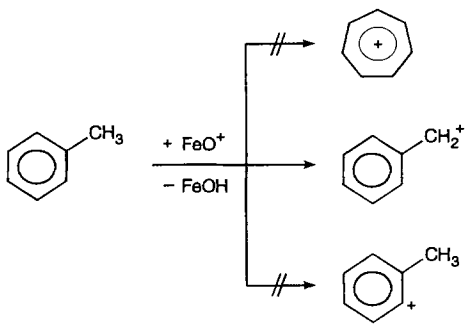

Scheme 19.

deserve mention: 1) Although the IEs of FeO and $C_6H_5CH_3$ are very similar,[20] electron transfer to yield the toluene cation radical hardly competes with oxidation. Since electron-transfer processes are assumed to take place very rapidly in such large molecules, its absence in the $C_6H_5CH_3/FeO^+$ system underlines the high intrinsic chemical reactivity of the iron oxide cation. 2) MS/MS studies establish that the $C_7H_7^+$ cation formed from FeO^+ and $C_6H_5CH_3$ exhibits exclusively the benzylium structure, rather than that of the energetically more stable tropylium ion.[126] Thus, the iron does not induce the interconversion of the two isomers. Further, the labeling studies reveal that activation of the aromatic C–H bonds does not take place. 3) As demonstrated by the preferential benzylic C–H bond activation, the high reactivity of FeO^+ is not necessarily accompanied by a decrease of selectivity.

We currently cannot decide whether the reaction mechanism for the formation of $C_6H_5CH_2^+$ involves a direct hydride anion transfer from the benzylic position to FeO^+ or whether it involves stepwise single-electron and H-atom transfers, or vice versa. Obviously, further studies with donor- and acceptor-substituted toluenes are indicated to probe this subtle question.

Not surprisingly, FeO^+ also reacts efficiently with the higher alkylbenzenes, for example, ethyl-, propyl-, *n*-butyl, and *n*-pentylbenzene.[127] Again, isotopic labeling studies demonstrate that activation of aromatic C–H bonds does not take place. With respect to site-selectivity, these reactions turn out to be more complicated in the sense that C–H as well as C–C bond activation of benzylic positions compete with activation of remote groups. For example, one pathway in the reaction of FeO^+ with ethylbenzene involves C–H bond activation in the β-position, thus, initiating C–C bond activation and subsequent loss of ethene (Scheme 20).[116b, 127]

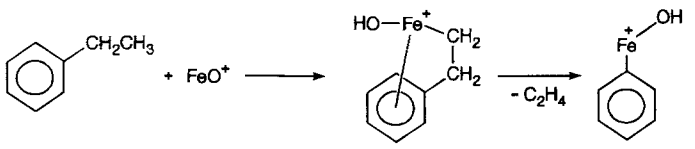

Scheme 20.

4.4. Comparison with the Condensed Phase

A major issue in the evaluation of gas-phase experiments concerns their relevance for condensed-phase analogues. Since iron–oxide species play a central role in metalloporphyrin chemistry[8, 9] as well as in artificial systems (for example, the *Gif* mixtures)[12] and in view of the fact that FeO^+ has been studied quite comprehensively in the gas phase, we restrict the comparison to the iron system. As mentioned in the introduction, gas-phase experiments refer to reactions of isolated, and often almost entirely unligated molecules, bearing a real coulombic charge (no counterions) in a highly diluted atmosphere under strictly bimolecular conditions. Therefore, the characteristic features of an ion/molecule reaction are a priori different from a formally related reaction in solution. Furthermore, the binding in an unligated transition-metal oxide like FeO^+ is completely different nature to that of an iron–oxide species embedded in a large ligand like a porphyrin skeleton.[128] Besides the electronic differences in structure, the steric requirements may have an influence as well. For example, for bare FeO^+ it is easy to form an additional covalent bond to another atom, whereas the planar ligand environment in a porphyrinatoiron oxide renders the formation of an additional covalent bond on the same site as the oxygen atom much more difficult, if not impossible. Consequently, products as well as their distributions can vary substantially between the gas and the condensed phase. And yet, a comparison of mechanistic features is both interesting and promising, as it may provide insight into the role of reaction intermediates, the rate-determining steps, and, in particular, H/D kinetic isotope effects, prevailing under otherwise quite different conditions.

In the gas phase, the H/D kinetic isotope effects associated with hydroxylation of alkanes by FeO^+ are quite large; for example, $k_H/k_D = 4.6$ has been observed for FeO^+ and methane.[69] Similarly, aliphatic C–H bond activation by iron porphyrins and related systems display effects within this range or even larger.[129] Also, initial C–H bond activation is the rate-determining step in both cases. Furthermore, in the gas phase the H/D kinetic isotope effects (both inter- and intramolecular) associated with hydroxylation of benzene by FeO^+ are close to unity, that is, $k_H/k_D = 1.00 \pm 0.03$ for C_6H_6, C_6D_6, and $C_6H_3D_3$.[116a] This finding parallels that in condensed-phase systems, in which negligible kinetic isotope effects were reported for the hydroxylation of arenes by a variety of [M]=O-based oxidants.[8a, 130] The absence of an H/D kinetic isotope effect for both the gas-phase and the solution chemistry in these systems was attributed to the formation of either an arene oxide or a σ-complex in the rate-determining step. Likewise, the studies reveal that in both cases the arene-oxide path cannot be the only reaction mechanism responsible for product formation (see Section 4.3.2). For toluene, yet another mechanism is operative. In the condensed phase the H/D kinetic isotope effects associated with benzylic C–H bond activation vary from moderate to quite large, depending on the nature of the oxidant.[131] In the gas phase the reaction of FeO^+ with toluene is also associated with a primary kinetic isotope effect ($k_H/k_D = 1.8$);[125] however, its magnitude is substantially smaller than in the condensed phase. This relatively low value can be attributed to the high exothermicity for the formation of a benzyl cation and neutral FeOH (-24 kcal mol^{-1}), which diminishes the role of differing C–H and C–D bond energies in the transition structures, and k_H/k_D decreases. Alternatively, the small KIE may point to a reaction mechanism in which in the rate-determining step, stretching of the benzylic C–H bond is negligible (for example, an electron-transfer process). Finally, in the reaction of FeO^+ with labeled ethylbenzenes,[127] a distinct influence of the isotopic labeling on the product distribution has been reported, which indicates the existence of isotopically sensitive branching ("metabolic switching"), which has been observed earlier in hydroxylation of α-labeled ethylbenzene by cytochrome P-450.[132]

In spite of these pleasing similarities, we emphasize once more that beause of the principal differences of gas- and condensed-phase systems, any overinterpretation of the findings should be avoided. In fact, in some cases such as the reactions of bare MO^+ ions with alkenes, the current knowledge of the gas-phase process is even much worse than that of the condensed-phase analogues. Thus, instead of providing solutions to mechanistic problems that are not addressable in large-scale epoxidations, the situation for even the simplest system, namely MO^+/C_2H_4, turns out to be quite complex at the molecular level.

However, as demonstrated above in the hydroxylation of hydrocarbons, some analogies between the two media are obvious, and the gas-phase data may complement if not guide further research. In particular, the size of the systems under study renders them promising candidates for more sophisticated theoretical approaches. Finally, we should like to address one of the most promising processes in contemporary oxidation research, the Gif Systems introduced by Barton et al.[12] These rather complex mixtures bring about the transformation of hydrocarbons to ketones without formation of alcohols as intermediates.[133] Unfortunately, none of the gas-phase systems studied so far provided any evidence for the occurrence of these or related processes. Most likely, this failure is because for the transformation of a methylene group into R_2CH_2 into the corresponding ketone R_2CO, formally two O-atom equivalents are mandatory to yield water as an energetically stable oxidation product. Thus, the cationic metal monoxides will, on fundamental grounds, not be capable of satisfying the stoichiometry of this oxidation.

5. Reactions of MO^+ with Other Substrates

This chapter deals primarily with the reactions of monofunctionalized alkanes RX[87] with MO^+ ions. Due to its polar character any functional group will preferentially bind the charged metal center ("docking"). Therefore, in an ion/molecule reaction of an MO^+ ion with a functionalized alkane, the ion will initially coordinate to the heteroatom moiety[134] rather than directly activate C–H or C–C bonds as for pure hydrocarbons. Consequently the regioselectivity of C–H bond activation of the alkane backbone by coordinated MO^+ ions will be subject to additional conformational constraints, which, in turn, may determine the product formation.

For bare transition-metal cations M^+, coordination of the metal cation definitely leads to highly selective C–H and C–C bond activation remote from the functional group, and regioselective derivatization of nonactivated bonds in flexible alkyl chains thus becomes feasible. In analogy to Breslow's terminology[135] this process has been referred to as remote functionalization of nonactivated C–H and C–H bonds in the gas phase; Scheme 21 illustrates this mechanism for a metal-induced dehydrogenation.[136]

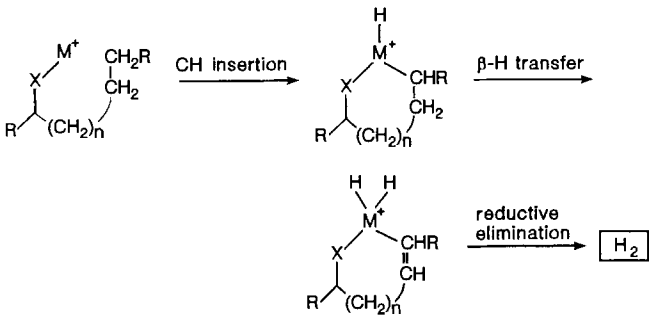

Scheme 21.

As shown in Section 4, late transition-metal oxide cations are very reactive towards alkanes, and for larger alkanes hardly any regiospecificity is observed, since all C–H bonds are more or less equivalent. Thus, it is an intriguing question, whether coordination of a reactive MO^+ species to a functional group will introduce any specificity or if the intrinsically high reactivity of the MO^+ ions will preclude selective processes. In fact, the former prospect is quite attractive, since nowadays only few procedures are known which allow regio- or even stereospecific hydroxylation of C–H bonds embedded in simple alkyl chains or rings.[137] Unfortunately, the gas-phase experiments performed so far are limited almost exclusively to reactions of FeO^+ with only a few substrates.

5.1. [C,H,O] Compounds

Oxygen-containing organic compounds are particularly suited for probing the regioselectivity in the gas-phase reactions of R–X with MO^+ on the following grounds: 1) Numerous gas-phase studies have shown that O-functionalities are among the weakest ligands for metal cations;[13, 87, 138] consequently, the intrinsic reactivity of MO^+ may override the stabilization from initial coordination to the functional group. On the other hand, remote functionalization of O-compounds by bare metal ions M^+ has been shown to exhibit high regio- and even stereoselectivity.[139] Therefore, O-compounds can be expected to serve as versatile probes for regioselectivity, when competition with nonselective processes within the hydrocarbon backbone is feasible. 2) Oxygen compounds, such as alcohols, ketones, or carbonic acids, are easily oxidized in the α-position. Thus, the competition between hydroxylation of activated and nonactivated C–H bonds can be examined. 3) Finally, oxygen compounds fulfill another requirement of mass spectrometric studies: Due to the high electronegativity of oxygen, hydride abstraction by MO^+ to yield neutral MOH and the corresponding organic cations is less favorable than for other heteroatom-containing substrates. Hence, the thermodynamic driving force for charge transfer from the metal to the functional group is small for [C,H,O] compounds and will not interfer reactivity studies.

5.1.1. *Alcohols*[84, 140]

A large variety of oxidants are capable of converting primary and secondary alcohols into the corresponding carbonyl compounds, for example, ketones, aldehydes, or even acids in the condensed phase. In these processes the activated C–H bond next to the hydroxyl moiety is involved.[141]

Indeed, if FeO^+ undergoes a reaction with methanol, formation of formaldehyde or its organometallic complexes by C–H bond activation is observed (Scheme 22). Similarly, FeO^+ oxidizes ethanol, 1-propanol, and 2-propanol to the corresponding

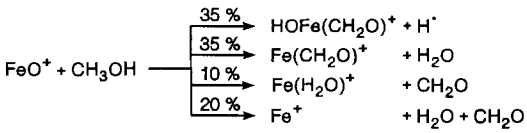

Scheme 22.

aldehydes, ketones, and their Fe^+ complexes. Interestingly, these substrates also exhibit formal transfer of a hydroxide anion to the metal center to yield the corresponding carbocations and neutral OFeOH.[84, 88] For larger alcohols, such as 1-pentanol, oxidation to the aldehyde and OH^- transfer become less important, and new reaction pathways open up with FeO^+. Among these, products arising from C–H and C–C bond activation remote from the functional group are observed.

5.1.2. *Ketones*

From a chemical point of view three different types of initial bond activations can be envisaged when a ketone is allowed to react with a reactive transition-metal-oxide cation such as FeO^+ (Scheme 23): 1) Hydroxylation of an activated C–H bond in the α-position leading to α-hydroxyketone/Fe^+ complexes and subsequent fragmentations (path ⓐ). 2) C–H bond activation of other positions in terms of remote functionalization (path ⓑ). 3) O-atom insertion into the C–C bond next to the keto group, giving rise to the corresponding ester/Fe^+ complexes (path ⓒ).

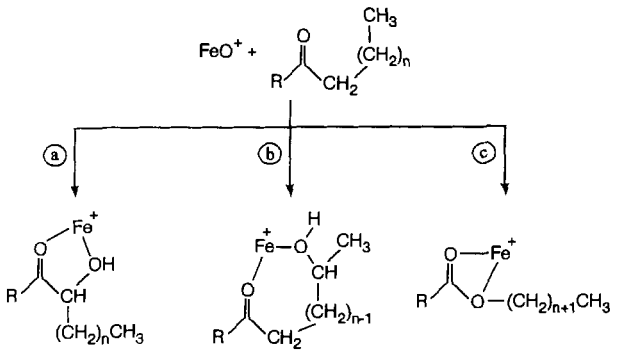

Scheme 23.

Surprisingly, in the reaction of the simplest ketone, namely acetone, α-C–C bond cleavage dominates and leads to subsequent loss of CH_3^+ and—most likely—formation of a cationic iron(II) acetate, $H_3CCOOFe^+$ (path ©).[142, 143] Since for almost all alkanes studied so far, C–H bond activation by FeO^+ was found to predominate, its apparent suppression in the acetone/FeO^+ system implies a substantial influence of the coordinating carbonyl group. Most probably, the complexation renders the C–H bonds of acetone less accessible for the metal oxide, and thus, for geometric reasons, C–C bond activation prevails.

Larger ketones exhibit a significantly different reactivity towards FeO^+ cations. The symmetrical ketones 4-heptanone and 5-nonanone have been shown to undergo regiospecific functionalization of nonactivated C–H bonds in the alkyl side chains when treated with FeO^+ (Scheme 24).[144] The supposition that geometric reasons influence the chemoselectivity of FeO^+ in the reaction with acetone (that is, C–C rather than C–H bond activation) is further supported by these findings. Moreover, the regioselective C–H bond activation of remote positions (namely the γ- and δ-C–H bonds) further emphasizes that the high reactivity of FeO^+ is not necessarily associated with a loss of specificity. We note in passing that the selectivity for the oxidative dehydrogenation of ketones by FeO^+ in the gas phase resembles the one observed in the derivatization of carbonyl compounds mediated by cytochrome P-450.[145]

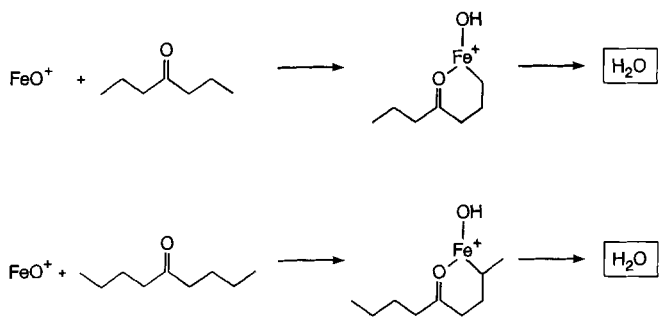

Scheme 24.

5.1.3. *Other [C,H,O] compounds*

Previously only a few other oxygen-containing organic substrates have been treated with MO^+ ions. Most of these studies did not explicitly address the reactions of MO^+ but rather reported them as secondary processes or side reactions, often in a quite different context.[41, 79a, 146] However, one example is of interest for fundamental reasons and should therefore be discussed here:[84] When acetaldehyde is treated with FeO^+, among other products, the pairs $FeOH^+/CH_3CO^\bullet$ (35%) and $CH_3CO^+/FeOH$ (15%) are formed. Since these product channels differ only in the location of the positive charge, it is somewhat surprising in view of the relative magnitudes of the ionization energies of $CH_3CO^\bullet$ (IE = 7.0 eV) and FeOH (IE = 7.9 eV) that less CH_3CO^+ is generated than $FeOH^+$. Either electron transfer from the initially charged iron center to the acetyl moiety must be hampered by a significant kinetic barrier, or that instead of $CH_3CO^\bullet$ the isomeric $^\bullet CH_2CHO$ radical must accompany $FeOH^+$ formation. Both possibilities are quite intriguing, and the results clearly indicate the need for further studies to probe the intrinsic reactivity of FeO^+ and other metal oxides towards aldehydes.

5.2. Miscellaneous Substrates

Experimental studies of the reactions of bare MO^+ with various substrates have been reported in the literature. However, these efforts did not always investigate the mechanistic features of MO^+ chemistry; rather, they dealt with side reactions.[147] Specific studies that deal with oxidation processes were performed for MO^+ when it was treated with hexafluorobenzene, pyridine and other nitrogen-containing heterocycles, aliphatic amines, and nitriles.[90, 111, 114, 148, 149] In general, the products observed correlate with the reactions of hydrocarbons and oxygen-containing compounds if one takes into account the additional effects of the heteroatom(s) present in the substrates. Furthermore, the differences in relative reactivities of the various metal-oxide cations are also noteworthy for these substrates. For example, the reactive metal oxides MnO^+ and FeO^+ are capable of oxygenating such a robust substrate as hexafluorobenzene,[66, 111] whereas in the reaction of pyridine with the early transition-metal-oxide cation NbO^+ only loss of HCN, rather than oxidation processes are observed. Moreover, loss of HCN from pyridine is also affected by the bare Nb^+ ion itself.[90]

The only two reactions of MO^+ (M = Fe) which should be discussed in this section involve the polycyclic hydrocarbons norbornane and adamantane.[140, 150] These alkanes serve as probes for regio- and stereoselectivity as well. The ion/molecule reactions of FeO^+ with norbornane and adamantane give rise to a variety of products, and the selectivities associated with the C–H and C–C bond activations were derived from extensive labeling experiments. Moreover, the carbon skeletons of both substrates are broken up in the reaction with FeO^+; for example, both precursors yield $Fe(C_6H_6)^+$ among other products.[151] Without going into detail, two points should be mentioned here: 1) C–H bond activation of norbornane by FeO^+ proceeds at the 2-position preferentially, with an *endo*-site selectivity (Scheme 25). This contrasts with the preferential *exo*-selectivity reported for hydroxylation of norbornane by cytochrome P-450.[152] 2) In the C–H bond activation of adamantane by FeO^+ to yield $C_{10}H_{15}^+$ and neutral FeOH, only a methyne group is involved, and this process is associated with an H/D kinetic isotope effect of $k_H/k_D = 2.7$. The reactivity of

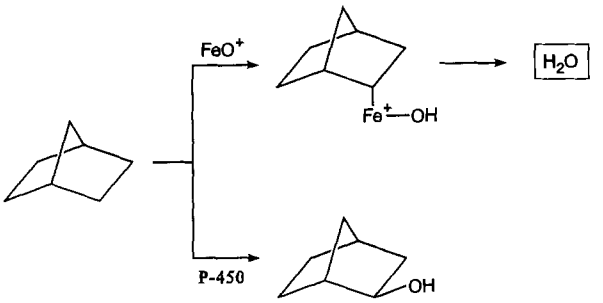

Scheme 25.

FeO^+ in the gas phase parallels the selectivities found for P-450-mediated oxidation of adamantane in the condensed phase,[129e] whereas in the *Gif* systems preferential attack at a methylene group takes place.[153]

6. Catalytic Oxidations in the Gas Phase

The storage capability of (FT)ICR mass spectrometry permits the examination of catalytic processes occurring in the gas phase.[154] In this context, catalysis is defined as a sequence of reactions in which *one* charged species converts more than one substrate molecule into a product. Since ion/molecule reactions in the low-pressure regime of (FT)ICR mass spectrometry can only proceed if they are exergonic (or more or less thermoneutral), the catalytic cycle must be designed so that each individual bimolecular step of the whole sequence must fulfill the condition of $\Delta G \leq 0$. Moreover, the bimolecular nature of the reactions permits modeling of the complete catalytic cycle in terms of a set of differential equations which, in turn, allows a determination of the reaction kinetics, the turnover number, and cooperative effects.

6.1. Earlier Studies and the "Perfect" Catalytic Cycle

The first gas-phase catalysis was described by Kappes and Staley, who reported that Fe^+ ions mediate the catalytic combustion of carbon monoxide to carbon dioxide with N_2O as oxidant.[44a] The reaction sequence is quite simple and commences with the oxidation of Fe^+ to FeO^+ by N_2O. Fe^+ is regenerated in the second step in which CO is converted into CO_2 (Scheme 26a). However, no further details concerning reaction kinetics and the turnover number were reported. Other authors proposed catalytic cycles for methane activation and olefin epoxidation in the gas phase, but did not examine them in great detail.[41, 102]

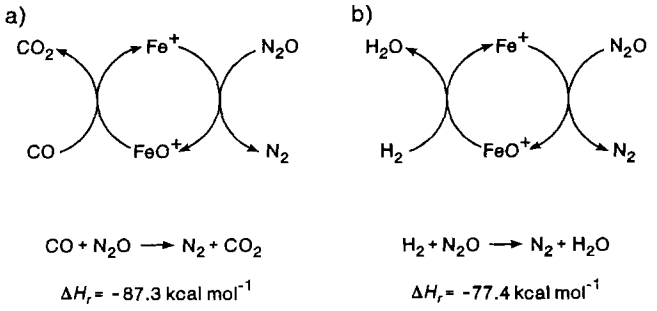

Scheme 26.

A example well-suited for a catalytic gas-phase reaction is, again, the simplest system, that is, the Fe^+-mediated oxidation of H_2 to H_2O with N_2O as an oxidant.[18] As outlined above, Fe^+ reacts with N_2O to yield FeO^+ and N_2, and in the second step Fe^+ is recovered in the reaction of FeO^+ with H_2; water is formed in the reaction. Thus, when N_2O and H_2 are leaked into an (FT)ICR mass spectrometer, the Fe^+ ions are capable of catalyzing the reaction $N_2O + H_2 \rightarrow N_2 + H_2O$, which itself does not occur at room temperature in the absence of a catalyst (Scheme 26b). Furthermore, the "catalyst" is inert towards reactants and products in that the oxidant N_2O does not react with the oxidized form FeO^+, nor does the substrate H_2 react with the reduced form Fe^+. If background contaminants as well as trapping losses from the cyclotron setup are neglected,[17] the catalytic cycle depicted in Scheme 26b proceeds with an infinite turnover number; in practice, however, side reactions with background hydrocarbons and water limit the turnover number to about 100. Of course, this process has no practical importance, since combustion of hydrogen does not need to be performed catalytically; rather, the strong exothermicity permits an efficient chain reaction to occur. In addition, it is obvious that catalysis in an (FT)ICR mass spectrometer cannot be used for real applications, since the ion concentrations are extremely low (about 10^{-15} mol L^{-1}). However, these studies are more than "l'art pour l'art" exercises, since intrinsic properties of the reactive center of a catalyst can be evaluated at a molecular level. In fact, the principles uncovered for the isolated system may hold true to some extent for applied catalysis, for example, an [M]=O species on the surface of a heterogeneous catalyst.

6.2. Catalytic Oxidation of Alkanes

The principles outlined above for the Fe^+-catalyzed oxidation of H_2 by N_2O can also be applied to mediate the oxidation of methane.[69] However, the formation of $FeOH^+$ is substantial, and this ion is unreactive towards methane on thermochemical grounds;[155] consequently, first-principle considerations limit the turnover number to 1.6. However, in a more general view, the release of a methyl radical in the course of $FeOH^+$ formation can also be seen as a model for methane oxidation or coupling processes[1, 2] by recombination of $CH_3^{\bullet}$ with other radicals, for example, $CH_3^{\bullet}$ or $HO^{\bullet}$. Of course, these bimolecular reactions of neutral species are precluded in the low-pressure regime of the (FT)ICR instrument, and the radicals are simply pumped away.

The same concept has also been applied to the ethane/N_2O/Fe^+ system.[156] The overall sequence of reactions can be described as an Fe^+-catalyzed oxidation of ethane to yield ethanol and acetaldehyde as major products with a turnover number of about 2.5 (Scheme 27). Here, the sink in the catalytic cycle is caused by the irreversible formation of $Fe(OH)_2^+$ as a side product. The nonreactivity of $Fe(OH)_2^+$ towards ethane emphasizes the essential function of the metal-oxide moiety in FeO^+, rather than the formal oxidation state iron(III). Moreover, as $Fe(OH)_2^+$ can be described as hydrated FeO^+, the reactive spe-

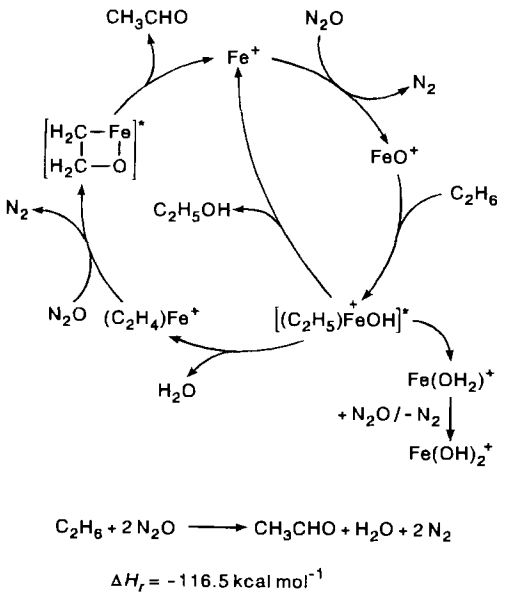

Scheme 27.

cies might be regenerated by loss of water. Actually, this finding illustrates, to some extent, an analogy to applied catalytic processes in which desorption of the product, in this case, loss of the water ligand, is often rate-limiting. In practice, dehydration is achieved by performing the oxidation at elevated temperatures. Irion et al.[154a–d] mimicked the effect of temperature in gas-phase catalytic processes by kinetically exciting the unreactive product complexes of a catalytic cycle in order to regenerate the active species.

Most recently, a turnover number of about 6.0 was found for the Pt^+-mediated oxidation of methane.[75] In this example it is particularly interesting that molecular oxygen can be used as the oxidant. The overall reaction sequence is somewhat more complicated (Scheme 28), since not only PtO^+, but also bare Pt^+ itself and the intermediate $PtCH_2^+$ activate methane. The sink in the catalytic cycle is a result of minor consecutive reactions of $PtCH_2^+$ with methane. Furthermore, the reactions reveal a general problem also encountered in the applied catalysis: On one hand increasing the excess of oxygen in its mixture with methane minimizes the side reactions, and thus increases the turnover, but on the other hand, this procedure will decrease the overall

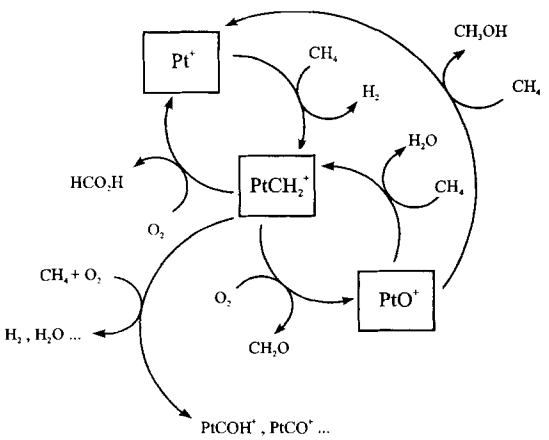

Scheme 28.

rate of methane oxidation. In addition, the product distribution reveals that in the gas phase, as in the condensed phase, oxidation of methane is associated with overoxidation to yield formic acid and eventually CO_2. Obviously, we are a long way from finding the ideal "methane → methanol" conversion catalyst.

6.3. Catalytic Oxidation of Other Hydrocarbons

Upon increasing the size of the substrate the reactions often become less selective than those of methane or ethane. A drop in the turnover numbers can therefore be expected. Not many examples of gas-phase catalysis have been examined yet. In all reactions reported so far for other substrates, Fe^+ catalyzes the oxidation of acetylene[44a] and ethene[102, 157] with N_2O as oxygen source. As described above for olefin epoxidation by MO^+ the highest selectivity and also the largest turnover number can be achieved for ligated metal oxides rather than the bare MO^+ species. For example, $Fe(L)^+$ ions (L = benzene, pyridine, naphthalene) catalyze the epoxidation of ethene, propene, *iso*-butene, and cyclohexene by N_2O as oxidant with turnover numbers up to 6 (Scheme 29).[158]

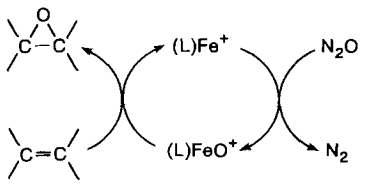

Scheme 29.

Recently Co^+-catalyzed oxidation of benzene, most probably to phenol, has been reported.[122] This process is particularly interesting in the sense that it mimics heterogeneous catalysis (Scheme 30): In the first step benzene coordinates to bare Co^+ to afford the corresponding $(C_6H_6)Co^+$ complex. Subsequently, the oxidant N_2O also coordinates to the complex, and the reaction yields neutral C_6H_6O and regenerates the catalytically active Co^+. Here, the cobalt–oxygen species just serves as an intermediate en route to product formation. Moreover, the reaction exothermicity leads to dissociation of the product complex $((C_6H_6O)Co^+)$; consequently product formation does not represent a sink for the overall cycle. The turnover number for the Co^+-catalyzed hydroxylation of benzene is therefore quite high for a gas-phase process (about 18).

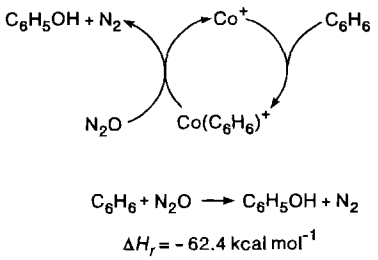

Scheme 30.

7. Conclusions

Gas-phase reactions of bare transition-metal-oxide ions represent the simplest model systems for oxidation processes that involve metal-oxide species [M]=O. In particular, these systems are ideally suited for a combination of state-of-the-art experimental and theoretical approaches. As demonstrated above, the oxides of the late transition-metal cations undergo O-atom

transfer to alkanes, alkenes, arenes, as well as functionalized alkanes. In fact, hardly any substrates exist that are not oxidized by highly reactive species such as MnO^+ and FeO^+. As far as the reaction mechanisms are concerned, C–H bond activation by MO^+ proceeds either by direct H-atom abstraction (provided this process is thermochemically feasible) or by a multicentered transition structure as well as curve crossing—mediated by spin–orbit coupling—between the high-spin and low-spin surfaces of the intermediates.[55a]

Despite the high reactivity of FeO^+, it is rather selective with respect to the site of C–H bond activation. Furthermore, gas-phase reactions of FeO^+ with various substrates reveal interesting parallels to related processes occurring in the condensed phase, which involve metal oxides as central intermediates. In particular, selectivities and kinetic isotope effects of the gas-phase reactions are often similar to those observed in solution chemistry, and to the reactions of cytochrome P-450 in particular. These results are promising in the sense that the elementary steps of C–H bond activation may be elucidated. Within this context, further experiments with specifically designed substrates are indicated, for example, ring-substituted toluenes or cyclopropyl derivatives which may serve as a probe for radicaloid intermediates.[159] Furthermore, additional significant information might be obtained by using other experimental approaches, as for example the powerful analysis of kinetic energy release distributions and related techniques.[160]

However, the example of epoxidation reactions demonstrates that the translation of gas-phase results to well-known condensed-phase analogues is not at all straightforward. Indeed, for olefin oxidation the situation in the gas phase turns out to be more complicated than in solution. Here, the neglect of ligand effects is critical, and these effects deserve to be studied much more carefully in the future. Actually, recent results of ligated FeO^+ cations that mediate selective epoxidation reactions already indicate a potential route towards higher selectivity and are likely to stimulate further research. Similarly, the design of catalytic variants for gas-phase processes might bring about a more detailed understanding of the principles of catalysis, as demonstrated for the few examples given in Section 6.

In addition, the activation of molecular oxygen for oxidation processes represents an attractive prospect that should be addressed in the future. Preliminary gas-phase experiments[161] demonstrate that olefin/Fe^+ complexes are efficiently oxidized by O_2, whereas other olefin/M^+ complexes (M = Na, Mg, Sc–Mn, Co–Zn, Ru–Pd, and Os–Pt)[84, 161, 162] do not promote olefin oxidation. Interestingly, the exceptional reactivity of the cationic iron complexes in the gas phase parallels the relevance of iron for transportation, storage, and activation of molecular oxygen in the condensed phase, and in biochemistry in particular.[7] Obviously, continuing experimental and theoretical studies on the reactions of dioxygen and transition-metal dioxygen complexes are indicated.[89, 163, 164] In addition, gas-phase reactions of organometallics with other O-atom donors, for example, peroxides, need to be considered.

Last but not least, the impetus of theoretical methods will improve significantly our understanding of oxidation reactions mediated by transition metals. In particular, theoretical approaches can shed light on reaction dynamics and the role of the various electronic states in these processes.

In conclusion, gas-phase studies of bare and ligated transition-metal-oxide ions provide valuable insight into the elementary steps of oxidation processes. However, when gas-phase data are compared to data from the condensed phase, the fundamental differences of both approaches must always be considered. Thus, despite the considerable progress witnessed in the chemistry of transition-metal-oxide species in the condensed as well as the gas phase, continuous efforts are needed to unify these fields and to bring about a more uniform understanding of oxidation catalysis at a molecular level to account for the experimentally observed effects.[165] Ultimately, it is hoped that the combination of theoretical and experimental gas-phase studies and its cautious comparison with results from applied processes may help to realize the design of tailor-made catalysts.

The generous and continuous financial support of our work by the Deutsche Forschungsgemeinschaft, the Fonds der Chemischen Industrie, the Volkswagen-Stiftung, and the Freunde der Technischen Universität Berlin is gratefully acknowledged. We are indebted to our co-workers for helpful discussions and additional information, in particular to Dr. Jan Hrušák, Matthew F. Ryan PhD, Dr. Detlef Stöckigt, Dr. Hansjürgen Becker, Dipl.-Chem. Andreas Fiedler, Dipl.-Chem. Christoph Heinemann, Dipl.-Chem. Josef Schwarz, and Dipl.-Chem. Ralf Wesendrup. Likewise, we thank Professors Peter B. Armentrout, Diethard K. Böhme, Wolfgang A. Herrmann, Nico M. M. Nibbering, Tom Ziegler, and Dr. K. K. Irikura for sending preprints and communicating unpublished results. We also appreciate enlightening discussions on theoretical aspects with Professors Wolfram Koch, Keiji Morokuma, Sason Shaik, and Per E. M. Siegbahn. H. S. is grateful to the Alexander-von-Humboldt Foundation for support (Max-Planck Research Award). In particular, he appreciates the hospitality of Professor Leo Radom and the Research School of Chemistry at the Australian National University for a Visiting Fellowship, which made possible his stay in Canberra where part of this review was completed.

Received: August 15, 1994 [A 79 IE]
German version: *Angew. Chem.* **1995**, *107*, 2126–2150

Keywords: catalysis · C–C activation · C–H activation · oxidations · transition-metal oxides

[1] a) S. T. Ceyer, *Science* **1990**, *249*, 133; b) J. C. Mackie, *Catal. Rev. Sci. Eng.* **1991**, *33*, 169; c) D. Eng, M. Stoukides, *ibid.* **1991**, *33*, 375; d) see also H. Schwarz, *Angew. Chem.* **1991**, *103*, 837; *Angew. Chem. Int. Ed. Engl.* **1991**, *30*, 820.

[2] a) J. S. Lee, S. T. Oyama, *Catal. Rev. Sci. Eng.* **1988**, *30*, 249; b) J. Kiwi, K. R. Thampi, M. Grätzel, P. Albers, K. Seibold, *J. Phys. Chem.* **1992**, *96*, 1344; c) J. M. Fox III, *Catal. Rev. Sci. Eng.* **1993**, *35*, 169; d) Z. Zhang, X. E. Verykios, M. Baerns, *ibid.* **1994**, *36*, 507.

[3] Discussions and leading references: a) K. A. Jørgensen, R. Hoffmann, *J. Phys. Chem.* **1990**, *94*, 3046; b) J. T. Gleaves, A. G. Sault, R. J. Madix, J. R. Ebner, *J. Catal.* **1990**, *121*, 202; c) K. A. Jørgensen, E. Larsen, *J. Chem. Soc. Dalton Trans.* **1990**, 1053.

[4] J. E. Baeckvall, B. Akermark, S. O. Ljunggren, *J. Am. Chem. Soc.* **1979**, *101*, 2411.

[5] a) K. Weissermel, H. J. Arpe, *Industrielle Organische Chemie*, VCH, Weinheim, **1988**; b) C. Elschenbroich, A. Salzer, *Organometallchemie*, Teubner, Stuttgart, **1989**; c) C. Elsenbroich, A. Salzer, *Organometallics: A Concise Introduction*, 2nd ed., VCH, Weinheim, **1992**.

[6] a) T. Katsuki, K. B. Sharpless, *J. Am. Chem. Soc.* **1980**, *102*, 5974; b) S. S. Woodard, M. G. Finn, K. B. Sharpless, *ibid.* **1991**, *113*, 106; c) M. G. Finn, K. B. Sharpless, *ibid.* **1991**, *113*, 113.

[7] a) E. F. Elstner, *Der Sauerstoff: Biochemie, Biologie und Medizin*, Wissenschaftsverlag, Mannheim, **1990**; b) L. I. Simándi, *Dioxygen Activation and Homogeneous Catalytic Oxidation*, Elsevier, Amsterdam, **1991**; c) *The Activation of Dioxygen and Homogeneous Catalytic Oxidation (Eds.: D. H. R. Bar-*

ton, A. E. Martell, D. T. Sawyer), Plenum, New York, **1993**; d) A. L. Fery, S. J. Lippard, *Chem. Rev.* **1994**, *94*, 759.

[8] a) *Cytochrome P-450: Structure, Mechanism and Biochemistry (Ed.: P. R. Ortiz de Montellano)*, Plenum, New York, **1986**; b) F. P. Guengerich, *FASEB J.* **1992**, *6*, 667; c) M. J. Coon, X. Ding, S. J. Pernecky, A. D. N. Vaz, *ibid.* **1992**, *6*, 699.

[9] a) P. R. Ortiz de Montellano in Ref. [8a], p. 217; b) J. T. Groves, Y. Watanabe, *J. Am. Chem. Soc.* **1986**, *108*, 507; c) F. P. Guengerich, T. L. McDonald, *FASEB J.* **1990**, *4*, 2453; d) R. A. Leising, B. A. Brennan, L. Que, Jr., B. G. Fox, E. Münck, *J. Am. Chem. Soc.* **1991**, *113*, 3988; e) A. Satsuma, Y. Tanaka, A. Hattori, T. Hattori, Y. Murakami, *J. Chem. Soc. Chem. Commun.* **1994**, 1073; see also f) W. A. Oertling, R. T. Kean, R. Wever, G. T. Babcock, *Inorg. Chem.* **1990**, *29*, 2633.

[10] a) T. J. McMurry, J. T. Groves in Ref. [8a], p. 1; b) P. Inchley, J. R. Lindsay Smith, R. J. Lower, *New J. Chem.* **1989**, *13*, 669; c) T. G. Taylor, *Pure Appl. Chem.* **1991**, *63*, 265.

[11] a) J. T. Groves, *J. Chem. Educat.* **1985**, *62*, 928; b) V. W. Bowry, K. U. Ingold, *J. Am. Chem. Soc.* **1991**, *113*, 5699.

[12] Survey: D. H. R. Barton, D. Doller, *Pure Appl. Chem.* **1991**, *63*, 1567.

[13] Recent reviews: a) S. W. Buckner, B. S. Freiser, *Polyhedron* **1988**, *7*, 1583; b) K. Eller, H. Schwarz, *Chem. Rev.* **1991**, *91*, 1121.

[14] a) *Gas Phase Ion Chemistry (Ed.: M. T. Bowers)*, Academic Press, New York, **1979**; b) *Gaseous Ion Chemistry and Mass Spectrometry (Ed.: J. H. Futrell)*, Wiley, New York, **1986**.

[15] R. R. Squires, *Chem. Rev.* **1987**, *87*, 623.

[16] Surveys, including main-group elements: a) J. R. Blackborow, D. Young, *Metal Vapour Synthesis in Organometallic Chemistry*, Springer, Berlin, **1979**; b) *Gas-Phase Metal Reactions* (Ed.: A. Fontijn), Elsevier, Amsterdam, **1992**.

[17] Recent review: A. G. Marshall, P. B. Grosshans, *Anal. Chem.* **1991**, *63*, 215A.

[18] D. Schröder, A. Fiedler, M. R. Ryan, H. Schwarz, *J. Phys. Chem.* **1994**, *98*, 68.

[19] a) M. Meot-Ner (Mautner) in Ref. [14a], p. 198; b) P. B. Armentrout, *Comments At. Mol. Phys.* **1988**, *22*, 133; see also: c) B. D. Nourse, H. I. Kenttämaa, *J. Phys. Chem.* **1990**, *94*, 5809; d) B. D. Wladkowski, J. L. Wilbur, J. I. Brauman, *J. Am. Chem. Soc.* **1992**, *114*, 9706.

[20] Reliable thermochemical data for a large variety of organic and inorganic compounds can be extracted from the following sources: a) S. G. Lias, J. F. Liebman, R. D. Levin, *J. Phys. Chem. Ref. Data* **1984**, *13*, 695; b) S. G. Lias, J. E. Bartmess, J. F. Liebman, J. L. Holmes, R. D. Levin, W. G. Mallard, *ibid.* **1988**, *17*, Suppl. 1; c) J. Berkowitz, G. B. Ellison, D. Gutman, *J. Phys. Chem.* **1994**, *98*, 2744; d) NIST Standard Reference Database 19A; S. G. Lias, J. F. Liebman, R. D. Levin, S. A. Kafafi; National Institute of Standards and Technology, Gaithersburg, MD 20899, USA, Version 2.01, **1994**.

[21] For a recent discussion of the reliability of experimental rate constants obtained in (FT)ICR mass spectrometry, see: Y. Lin, D. P. Ridge, B. Munson, *Org. Mass Spectrom.* **1991**, *26*, 550.

[22] a) T. Su, M. T. Bowers, *Int. J. Mass Spectrom. Ion Phys.* **1973**, *12*, 347; b) W. J. Chesnavich, T. Su, M. T. Bowers, *J. Chem. Phys.* **1980**, *72*, 2641; c) T. Su, W. J. Chesnavich, *ibid.* **1982**, *76*, 5183.

[23] E. K. Thornton, E. R. Thornton in *Isotope Effects in Chemical Reactions*, (ACS Monogr. Ser. **1970**, *167*, 274.

[24] A. Thibblin, P. Ahlberg, *Chem. Soc. Rev.* **1989**, *18*, 209.

[25] B. S. Freiser, *Chemtracts: Anal. Phys. Chem.* **1989**, *1*, 65.

[26] a) R. C. Burnier, R. B. Cody, B. S. Freiser, *J. Am. Chem. Soc.* **1982**, *104*, 7436; b) R. B. Cody, B. S. Freiser, *Int. J. Mass Spectrom. Ion Phys.* **1982**, *41*, 199.

[27] K. L. Busch, G. L. Glish, S. A. McLuckey, *Mass Spectrometry/Mass Spectrometry: Techniques and Applications of Tandem Mass Spectrometry*, VCH, Weinheim, **1988**.

[28] D. Schröder, A. Fiedler, J. Hrušák, H. Schwarz, *J. Am. Chem. Soc.* **1992**, *114*, 1215.

[29] Recent reviews: a) F. W. McLafferty, *Science* **1990**, *247*, 925; b) *Int. J. Mass Spectrom. Ion Processes* **1992**, *118/119*, 221; c) N. Goldberg, H. Schwarz, *Acc. Chem. Res.* **1994**, *27*, 347.

[30] a) K. M. Ervin, P. B. Armentrout, *J. Chem. Phys.* **1985**, *83*, 166; b) R. H. Schultz, P. B. Armentrout, *Int. J. Mass Spectrom. Ion Processes* **1991**, *107*, 29.

[31] a) P. B. Armentrout, *Annu. Rev. Phys. Chem.* **1990**, *41*, 313; b) *Science* **1991**, *251*, 175.

[32] a) J. M. van Doren, S. E. Barlow, C. H. DePuy, V. M. Bierbaum, *Int. J. Mass Spectrom. Ion Processes* **1987**, *81*, 85. Application examining neutral metal oxides: b) D. E. Clemmer, K. Honma, I. Koyano, *J. Chem. Phys.* **1993**, *97*, 11480.

[33] Reviews: a) R. G. Cooks, R. E. Kaiser, Jr., *Acc. Chem. Res.* **1990**, *23*, 213; b) R. G. Cooks, G. L. Glish, S. A. McLuckey, R. E. Kaiser, Jr., *Chem. Eng. News* **1991**, *69* (12), 26; c) application to transition-metal oxide chemistry: Y. Matsuo, H. Maeda, M. Takami, *Chem. Phys. Lett.* **1993**, *201*, 341.

[34] Examples: a) D. E. Jensen, G. A. Jones, *J. Chem. Soc. Faraday Trans. 1* **1973**, *69*, 1448; b) N. S. Ham, T. McAlister, *Aust. J. Chem.* **1983**, *36*, 1299; c) J. M. Goodings in Ref. [16b], p. 493; d) K. Schofield in Ref. [16b], p. 529; e) J. M. Goodings, C. S. Hassanali, P. M. Patterson, C. Chow, *Int. J. Mass Spectrom. Ion Processes* **1994**, *132*, 83.

[35] a) S. R. Langhoff, C. W. Bauschlicher, Jr., *Annu. Rev. Phys. Chem.* **1988**, *39*, 181; b) C. Tsipis, *Coord. Chem. Rev.* **1991**, 108, 163; c) A. Vaillard, *Chem. Rev.* **1991**, *91*, 743.

[36] T. Ziegler, *Chem. Rev.* **1991**, *91*, 651.

[37] See for example: a) H. Chen, M. Krasowski, G. Fitzgerald, *J. Chem. Phys.* **1993**, *98*, 8710; b) F. U. Axe, J. M. Coffin, *J. Phys. Chem.* **1994**, *98*, 2567; c) R. H. Hertwig, Diploma Thesis, Technische Universität Berlin, **1994**; d) R. H. Hertwig, W. Koch, *J. Comput. Chem.*, in press; see also: e) P. W. Gill, B. G. Johnson, J. A. Pople, M. J. Frisch, *Chem. Phys. Lett.* **1992**, *197*, 499.

[38] For outstanding examples, see: a) A. L. Sargent, M. B. Hall, M. F. Guest, *J. Am. Chem. Soc.* **1992**, *114*, 517; b) H. Kawamura-Kuribayashi, N. Koga, K. Morokuma, *ibid.* **1992**, *114*, 2359; c) D. G. Musaev, N. Koga, K. Morokuma, *J. Phys. Chem.* **1993**, *97*, 4064; d) M. C. Holthausen, C. Heinemann, M.-C. Cornehl, W. Koch, H. Schwarz, *J. Chem. Phys.* **1995**, *102*, 4931.

[39] A. Fiedler, D. Schröder, S. Shaik, H. Schwarz, *J. Am. Chem. Soc.* **1994**, *116*, 10734.

[40] D. Sülzle, H. Schwarz, K. H. Moock, J. K. Terlouw, *Int. J. Mass Spectrom. Ion Processes* **1991**, *108*, 269.

[41] K. K. Irikura, J. L. Beauchamp, *J. Am. Chem. Soc.* **1989**, *111*, 75.

[42] D. Schröder, W. A. Herrmann, R. W. Fischer, H. Schwarz, *Int. J. Mass Spectrom. Ion Processes* **1992**, *122*, 99.

[43] K. Lane, L. Sallans, R. R. Squires, *J. Am. Chem. Soc.* **1984**, *106*, 2719.

[44] a) M. M. Kappes, R. H. Staley, *J. Am. Chem. Soc.* **1981**, *103*, 1286; b) *J. Phys. Chem.* **1981**, *85*, 942.

[45] See, for example, a) J. C. Pivin, C. Roques-Carmes, G. Slodzian, *Int. J. Mass Spectrom. Ion Phys.* **1979**, *31*, 293; b) S. M. McCullough, A. D. Jones, C. B. Lebrilla, *Int. J. Mass Spectrom. Ion Processes* **1991**, *107*, 545; c) S. McCullough-Catalono, C. B. Lebrilla, *J. Am. Chem. Soc.* **1993**, *115*, 1441.

[46] a) J. M. Dyke, *J. Chem. Soc. Faraday Trans. 2*, **1987**, *83*, 69; b) J. M. Dyke, A. M. Shaw, T. G. Wright in Ref. [16b], p. 467. c) In contrast, *neutral* transition-metal oxides are spectroscopically well characterized; for many examples, see A. J. Merer, *Annu. Rev. Phys. Chem.* **1989**, *40*, 407; see also d) J. C. Green, *Acc. Chem. Res.* **1994**, *27*, 131.

[47] a) For examples, see J. H. Norman, H. G. Staley, W. E. Bell *Adv. Chem. Ser.* **1970**, *72*, 101. Recent Knudsen-cell studies of transition-metal oxides: b) D. L. Hildenbrand, K. H. Lau, *J. Phys. Chem.* **1992**, *96*, 2325; c) L. R. Watson, T. L. Thiem, A. Dressler, R. H. Salter, E. Murad, *ibid.* **1993**, *97*, 5577.

[48] a) E. R. Fisher, J. L. Elkind, D. E. Clemmer, R. Georgiadis, S. K. Loh, N. Aristov, L. S. Sunderlin, P. B. Armentrout, *J. Phys. Chem.* **1990**, *93*, 2676; b) D. E. Clemmer, J. L. Elkind, N. Aristov, P. B. Armentrout, *ibid.* **1991**, *95*, 3387; c) D. E. Clemmer, N. F. Dalleska, P. B. Armentrout, *J. Chem. Phys.* **1991**, *95*, 7263.

[49] M. A. Tolbert, J. L. Beauchamp, *J. Am. Chem. Soc.* **1984**, *106*, 8117.

[50] a) J. A. Martinho-Simões, J. L. Beauchamp, *Chem. Rev.* **1990**, *90*, 629; b) *Energetics of Organometallics Species, NATO ASI Ser. Ser. C*, **1992**, 367; c) P. B. Armentrout, B. L. Kickel, in *Organometallic Ion Chemistry*, (Ed.: B. S. Freiser), Kluwer, Dordrecht, in press.

[51] a) Thermochemistry of neutral transition-metal oxides: J. B. Pedley, E. M. Marshall, *J. Phys. Chem. Ref. Data* **1983**, *12*, 967; b) lanthanide oxides: M. C. R. Cockett, L. Nyulászi, T. Veszprémi, T. G. Wright, J. M. Dyke, *J. Electron Spectrosc. Relat. Phenom.* **1991**, *57*, 373.

[52] Computational studies of neutral second-row transition-metal oxides: a) P. E. M. Siegbahn, *Chem. Phys. Lett.* **1993**, *201*, 15; b) *J. Phys. Chem.* **1993**, *97*, 9096.

[53] P. Pyykkö, *Chem. Rev.* **1988**, *88*, 563.

[54] E. A. Carter, W. A Goddard III, *J. Phys. Chem.* **1988**, *92*, 2109.

[55] a) S. Shaik, D. Danovich, A. Fiedler, D. Schröder, H. Schwarz, *Helv. Chim. Acta*, in press; b) A. Fiedler, H. Schwarz, unpublished.

[56] Previous computations of transition-metal monoxides that are not mentioned explicitly: a) S. P. Walch, W. A. Goddard III, *J. Am. Chem. Soc.* **1978**, *100*, 1338; b) K. Yamaguchi, Y. Takahara, T. Fueno, in *Applied Quantum Chemistry* (Eds.: V. H. Smith, Jr., H. F. Schaefer III, K. Morokuma), Reidel, Boston, **1984**, p. 155; c) M. Krauss, W. J. Stevens, *J. Chem. Phys.* **1985**, *82*, 5584; d) C. W. Bauschlicher, Jr., S. R. Langhoff, A. Komornicki, *Theor. Chim. Acta* **1990**, *77*, 263; e) D. Hippe, S. D. Peyerimhoff, *Mol. Phys.* **1992**, *76*, 293; f) E. Broclawik, D. R. Salahub, *Int. J. Quant. Chem.* **1992**, *26*, 393; g) A. Fiedler, J. Hrušák, W. Koch, H. Schwarz, *Chem. Phys. Lett.* **1993**, *211*, 242; h) E. Broclawik, D. R. Salahub, *J. Mol. Catal.* **1993**, *82*, 117; i) J. Hrušák, W. Koch, H. Schwarz, *J. Chem. Phys.* **1994**, *101*, 3898; see also j) E. M. van Wezenbeek, E. J. Baerends, J. G. Snijders, *Theor. Chim. Acta* **1991**, *81*, 139.

[57] J. M. Dyke, B. W. J. Gravenor, G. D. Josland, R. A. Lewis, A. Morris, *Mol. Phys.* **1984**, *53*, 465.

[58] a) J. M. Dyke, B. W. J. Gravenor, M. P. Hastings, A. Morris, *J. Phys. Chem.* **1985**, *89*, 4613; b) J. Harrington, J. C. Weisshaar, *J. Chem. Phys.* **1992**, *97*, 2809.

[59] a) J. M. Dyke, B. W. J. Gravenor, R. A. Lewis, A. Morris, *J. Chem. Soc. Faraday Trans. 2* **1983**, *79*, 1083. However, the state assignment has been criticized; for details, see b) J. F. Harrison, *J. Phys. Chem.* **1986**, *90*, 3313; c) P. G. Jasien, W. J. Stevens, *Chem. Phys. Lett.* **1988**, *147*, 72.

[60] a) P. C. Engelking, W. C. Lineberger, *J. Chem. Phys.* **1977**, *66*, 5054; b) J. Fan, L.-S. Wang, *J. Phys. Chem.* **1995**, *102*, 8714.

[61] R. J. Van Zee, S. Li, W. Weltner, Jr., *Chem. Phys. Lett.* **1994**, *217*, 381.
[62] D. E. Clemmer, N. Aristov, P. B. Armentrout, *J. Phys. Chem.* **1993**, *97*, 544.
[63] Excited TiO^+ and VO^+ cations, formed directly from the corresponding bare metal cations and N_2O, were found to react with H_2, whereas ZrO^+ and NbO^+ are unreactive regardless of the oxidant used (Ref. [44b]).
[64] H. Kang, J. L. Beauchamp, *J. Am. Chem. Soc.* **1986**, *108*, 7502.
[65] a) D. E. Clemmer, Y.-M. Chen, F. A. Khan, P. B. Armentrout, *J. Phys. Chem.* **1994**, *98*, 6522; b) Y.-M. Chen, D. E. Clemmer, P. B. Armentrout, *J. Am. Chem. Soc.* **1994**, *116*, 7815.
[66] M. F. Ryan, A. Fiedler, D. Schröder, H. Schwarz, *J. Am. Chem. Soc.* **1995**, *117*, 2033.
[67] a) K. J. Børve, L. G. M. Pettersson, *J. Phys. Chem.* **1991**, *95*, 3214; b) D. P. Belyung, A. Fontijn, P. Marshall, *ibid.* **1993**, *97*, 3456; c) K. D. Dobbs, D. A. Dixon, A. Komornicki, *J. Chem. Phys.* **1993**, *98*, 8852; d) Y. Aray, J. Rodríguez, J. Murgich, F. Ruette, *J. Phys. Chem.* **1993**, *97*, 8393; see also: e) C. Shi, M. Xu, M. P. Rosynek, J. H. Lunsford, *ibid.* **1993**, *97*, 216; f) N. W. Cant, E. M. Kennedy, P. F. Nelson, *ibid.* **1993**, *97*, 1445.
[68] *Chem. Eng. News* **1993**, *71* (21), 27.
[69] D. Schröder, H. Schwarz, *Angew. Chem.* **1990**, *102*, 1468; *Angew. Chem. Int. Ed. Engl.* **1990**, *29*, 1433.
[70] M. F. Ryan, A. Fiedler, D. Schröder, H. Schwarz, *Organometallics* **1994**, *13*, 4072.
[71] M. F. Ryan, H. Schwarz, unpublished.
[72] Experimental values for BDE (Fe^+–OH) range from 73 to 87 kcal mol^{-1} [73]. Due to this uncertainty it is not clear whether its formation from FeO^+ and H_2 is endothermic or not; therefore, we refer to the "standard" value of 79 kcal mol^{-1} given in Ref. [20b]; for discussions, see Refs. [65a] and [73d] as well as P. B. Armentrout, D. E. Clemmer in Ref. [50b], p. 321.
[73] a) E. Murad, *J. Chem. Phys.* **1980**, *73*, 1381; b) C. J. Cassady, B. S. Freiser, *J. Am. Chem. Soc.* **1984**, *106*, 6176; c) T. F. Magnera, D. E. David, J. Michl, *ibid.* **1989**, *111*, 4100; d) Y.-M. Chen, D. E. Clemmer, P. B. Armentrout, University of Utah, personal communication.
[74] D. K. Böhme, personal communication of data obtained with a SIFT mass spectrometer; see also: V. I. Baranov, G. Javahevy, D. K. Bohme, *Chem. Phys. Lett.* **1995**, *239*, 339.
[75] R. Wesendrup, D. Schröder, H. Schwarz, *Angew. Chem.* **1994**, *106*, 1232; *Angew. Chem. Int. Ed. Engl.* **1994**, *33*, 1174.
[76] a) K. K. Irikura, J. L. Beauchamp, *J. Am. Chem. Soc.* **1989**, 111, 75; b) S. W. Buckner, T. J. McMahon, G. D. Byrd, B. S. Freiser, *Inorg. Chem.* **1989**, *28*, 3511; c) K. K. Irikura, J. L. Beauchamp, *J. Am. Chem. Soc.* **1991**, *113*, 2769; *J. Phys. Chem.* **1991**, *95*, 8344.
[77] a) K. K. Irikura, W. A. Goddard III, *J. Am. Chem. Soc.* **1994**, *116*, 8733; b) C. Heinemann, R. H. Hertwig, R. Wesendrup, W. Koch, H. Schwarz, *ibid.* **1995**, *117*, 495.
[78] T. C. Jackson, T. J. Carlin, B. S. Freiser, *J. Am. Chem. Soc.* **1986**, *108*, 1120.
[79] a) M. Azzaro, S. Breton, M. Decouzon, S. Geribaldi, *Int. J. Mass Spectrom. Ion Processes* **1993**, *128*, 1. b) Neutral Sc exhibits a similar reactivity for O-atom abstraction, see K. Liu, J. M. Parson, *J. Phys. Chem.* **1979**, *83*, 970; see also: c) T. J. Groshens, K. J. Klabunde, *Inorg. Chem.* **1990**, *29*, 2979; d) J. M. Parnis, R. D. Lafleur, D. M. Rayner, *Chem. Phys. Lett.* **1994**, *218*, 544.
[80] T. C. Jackson, D. B. Jacobson, B. S. Freiser, *J. Am. Chem. Soc.* **1984**, *106*, 1252.
[81] For a survey, see a) M. Brookhart, M. L. H. Green, L.-L. Wong, *Prog. Inorg. Chem.* **1988**, *36*, 1; recent examples of experiments addressing the activation barriers associated with β-H transfer reactions: b) M. Brookhart, A. F. Volpe, Jr., D. M. Lincoln, *J. Am. Chem. Soc.* **1990**, *112*, 5634; c) M. L. Burke, R. J. Madix, *ibid.* **1991**, *113*, 3675.
[82] S. Karrass, T. Prüsse, K. Eller, H. Schwarz, *J. Am. Chem. Soc.* **1989**, *111*, 9018.
[83] In contrast to Ref. [80], cyclopropane reacts efficiently with FeO^+ to yield a variety of products, among them $Fe(OCH_2)^+$, $Fe(C_2H_4)^+$, FeO^+, $FeCH_2^+$, and Fe^+ [84].
[84] D. Schröder, Ph.D. Thesis, Technische Universität Berlin, D83, **1993**.
[85] In the case of FeO^+/c-C_3H_6 the initial product corresponds to a metallaoxacyclopentane. For the formation of metallacycles in the gas phase, see a) D. B. Jacobson, B. S. Freiser, *Organometallics* **1984**, *3*, 513. For theoretical aspects, see b) P. Swanstrøm, K. A. Jørgensen, *J. Chem. Soc. Dalton Trans.* **1990**, 115.
[86] a) K. C. Ferguson, E. Whittle, *Trans. Faraday Soc.* **1971**, *67*, 2618; b) M. H. Baghal-Vayjooee, S. W. Benson, *J. Am. Chem. Soc.* **1979**, *101*, 2838.
[87] K. Eller, *Coord. Chem. Rev.* **1993**, *126*, 93.
[88] D. Schröder, H. Schwarz, *Angew. Chem.* **1991**, *103*, 987; *Angew. Chem. Int. Ed. Engl.* **1991**, *30*, 991.
[89] For example, the high-valent iron(v) dioxide cation could be generated by chemical ionization of a mixture of $Fe(CO)_5$ and O_2. For further details and preliminary reactivity studies, see D. Schröder, A. Fiedler, J. Schwarz, H. Schwarz, *Inorg. Chem.* **1994**, *33*, 5094.
[90] a) R. M. Pope, S. L. VanOrden, B. T. Cooper, S. W. Buckner, *Organometallics* **1992**, *11*, 2001; b) R. Marshall, S. W. Buckner, *Org. Mass Spectrom.* **1993**, *28*, 1616; see also: C. J. Cassady, S. W. McElvany, *Organometallics* **1992**, *11*, 2367.
[91] a) K. A. Jørgensen, *Chem. Rev.* **1989**, *89*, 431; b) J. P. Collman, X. Zhang, V. J. Lee, E. S. Uffelman, J. I. Brauman, *Science* **1993**, *261*, 1404; For a recent survey, see c) P. Besse, H. Veschambre, *Tetrahedron* **1994**, *50*, 8885.
[92] a) E. N. Jacobsen, I. Markó, W. S. Mungall, G. Schröder, K. B. Sharpless, *J. Am. Chem. Soc.* **1988**, *110*, 1968. For mechanistic discussions and further references, see b) A. Veldkamp, G. Frenking, *ibid.* **1994**, *116*, 4937; c) P.-O. Norrby, H. C. Kolb, K. B. Sharpless, *ibid.* **1994**, *116*, 8470.
[93] a) D. Ostovic, T. C. Bruice, *J. Am. Chem. Soc.* **1989**, *111*, 6511; b) D. Ostovic, T. C. Bruice, *Acc. Chem. Res.* **1992**, *25*, 314.
[94] a) Refs. [9a] and [10a]; b) J. T. Groves, G. E. Avaria-Neisser, K. M. Fish, M. Imachi, R. L. Kuczkowski, *J. Am. Chem. Soc.* **1986**, *108*, 3837.
[95] a) T. G. Traylor, A. R. Miksztal, *J. Am. Chem. Soc.* **1989**, *111*, 7443; b) J. P. Collman, P. D. Hampton, *ibid.* **1990**, *112*, 2977, 2986; c) P. R. Ortiz de Montellano, J. A. Fruetel, J. R. Collins, D. L. Camper, G. H. Loew, *ibid.* **1991**, *113*, 3195; d) G.-X. He, H.-Y. Mei, T. C. Bruice, *ibid.* **1991**, *113*, 5644; e) J. A. Fruetel, J. R. Collins, D. L. Camper, G. H. Loew, P. R. Ortiz de Montellano, *ibid.* **1992**, *114*, 6987.
[96] a) Y. Naruta, F. Tami, N. Ishihara, K. Maruyama, *J. Am. Chem. Soc.* **1991**, *113*, 6865; see also b) K. A. Jørgensen, B. Schiøtt, *Chem. Rev.* **1990**, *90*, 1483.
[97] B. C. Guo, A. W. Castleman, Jr., *J. Am. Chem. Soc.* **1992**, *114*, 6152.
[98] H. Kang, J. L. Beauchamp, *J. Am. Chem. Soc.* **1986**, *108*, 5663.
[99] A. E. Stevens, J. L. Beauchamp, *J. Am. Chem. Soc.* **1979**, *101*, 6449.
[100] a) P. B. Armentrout, J. L. Beauchamp, *J. Chem. Phys.* **1981**, *74*, 2819; b) R. Georgiadis, P. B. Armentrout, *Int. J. Mass Spectrom. Ion Processes* **1989**, *89*, 227; c) S. K. Loh, E. R. Fisher, L. Lian, R. H. Schultz, P. B. Armentrout, *J. Phys. Chem.* **1989**, *93*, 3159.
[101] E. R. Fisher, P. B. Armentrout, *J. Phys. Chem.* **1990**, *94*, 1674.
[102] S. W. Buckner, J. R. Gord, B. S. Freiser, *J. Am. Chem. Soc.* **1988**, *110*, 6606.
[103] A. Fiedler, Diploma Thesis, Technische Universität Berlin, 1992.
[104] Both CoO^+ and NiO^+ react with ethene essentially at the collision rate to yield exclusively the corresponding bare metal cations: M. F. Ryan, H. Schwarz, unpublished.
[105] However, $(CH_3)_4OsO^+$ undergoes metathesis with ethene to yield neutral propene [84]. Interestingly, in the condensed phase $(CH_3)_4OsO$ also mediates metathesis of olefins, but does not catalyze epoxidation [106].
[106] W. A. Herrmann, S. J. Eder, P. Kiprof, K. Rypdal, *Angew. Chem.* **1990**, *102*, 1460; *Angew. Chem. Int. Ed. Engl.* **1990**, *29*, 1445.
[107] D. M. Walba, C. H. DePuy, J. J. Grabowski, V. M. Bierbaum, *Organometallics* **1984**, *3*, 498.
[108] C. Heinemann, H. H. Cornehl, H. Schwarz, unpublished.
[109] a) W. A. Herrmann, W. Wagner, U. N. Flessner, U. Volkhardt, H. Komber, *Angew. Chem.* **1991**, *103*, 1704; *Angew. Chem. Int. Ed. Engl.* **1991**, *30*, 1636; b) W. A. Herrmann, R. W. Fischer, D. W. Marz, *ibid.* **1991**, *103*, 1706 and **1991**, *30*, 1638.
[110] Examples on mediating the reactivity of bare transition-metal ions by additional ligands: a) D. B. Jacobson, B. S. Freiser, *J. Am. Chem. Soc.* **1983**, *105*, 7484; b) A. Tsarbopoulos, J. Allison, *Organometallics* **1984**, *3*, 86; c) J. Allison, A. Mavridis, J. F. Harrison, *Polyhedron* **1988**, *7*, 1559; d) R. Stepnowski, J. Allison, *J. Am. Chem. Soc.* **1989**, *111*, 449; e) R. L. Hettich, B. S. Freiser, *Organometallics* **1989**, *8*, 2447; f) D. Schröder, K. Eller, T. Prüsse, H. Schwarz, *ibid.* **1991**, *10*, 2052; g) D. Stöckigt, S. Sen, H. Schwarz, *Chem. Ber.* **1993**, *126*, 2553.
[111] a) D. Schröder, J. Hrušák, H. Schwarz, *Helv. Chim. Acta* **1992**, *75*, 2215. Review of transition-metal-mediated C–F bond activation: b) J. L. Kiplinger, T. G. Richmond, C. E. Osterberg, *Chem. Rev.* **1994**, *94*, 373.
[112] K. K. Irikura, J. L. Beauchamp, *J. Am. Chem. Soc.* **1991**, *113*, 2767.
[113] H. L. Chen, T. E. Hagan, S. E. Groh, D. P. Ridge, *J. Am. Chem. Soc.* **1991**, *113*, 9669.
[114] W. J. Gwathney, L. Lin, C. Kutal, I. J. Amster, *Org. Mass Spectrom.* **1992**, *27*, 840.
[115] D. Stöckigt, H. Schwarz, *Chem. Ber.* **1994**, *127*, 2499.
[116] a) D. Schröder, H. Schwarz, *Helv. Chim. Acta* **1992**, *75*, 1281; b) H. Becker, D. Schröder, W. Zummack, H. Schwarz, *J. Am. Chem. Soc.* **1994**, *116*, 1096.
[117] a) R. Graselli, J. D. Burrington, *Adv. Catal.*, **1981**, *30*, 133; b) B. Blumenberg, *Nachr. Chem. Techn. Lab.* **1994**, *42*, 480.
[118] D. M. Jerina, J. W. Daly, *Science* **1974**, *185*, 573.
[119] G. Guroff, J. W. Daly, D. M. Jerina, B. Witkop, S. Udenfriend, *Science* **1967**, *157*, 1254.
[120] a) J. E. Tomaszewki, D. M. Jerina, *Biochemistry* **1975**, *14*, 2024; b) B. D. Preston, J. A. Miller, E. C. Miller, *J. Biol. Chem.* **1983**, *258*, 8304; c) F. P. Guengerich, T. L. McDonald, *FASEB J.* **1990**, *4*, 2453.
[121] a) H. L. Holland, F. M. Brown, M. Conn, *J. Chem. Soc. Perkin Trans. 2* **1990**, 1651; see also: b) J. Green, H. Dalton, *J. Biol. Chem.* **1989**, *264*, 17698.
[122] M. F. Ryan, D. Stöckigt, H. Schwarz, *J. Am. Chem. Soc.* **1994**, *116*, 9565.
[123] D. Schröder, W. Zummack, H. Schwarz, *Organometallics* **1993**, *12*, 1079.
[124] a) W. D. Jones, F. J. Feher, *Acc. Chem. Res.* **1989**, *22*, 91; b) A. D. Ryabov, *Chem. Rev.* **1990**, *90*, 403.
[125] D. Schröder, H. Florencio, W. Zummack, H. Schwarz, *Helv. Chim. Acta* **1992**, *75*, 1792.
[126] Recent survey on the benzylium/tropylium ion controversy: C. Lifshitz, *Acc. Chem. Res.* **1994**, *27*, 138.
[127] H. Becker, Diploma Thesis, Technische Universität Berlin, **1993**.

[128] For a recent review of computational approaches to describe the bonding of [M]=O and dioxygen complexes in metalloporphyrins as well as leading references, see I. Bytheway, M. B. Hall, *Chem. Rev.* **1994**, *94*, 639.
[129] a) A. B. Sorokin, A. M. Khenkin, *J. Chem. Soc. Chem. Commun.* **1990**, 45; b) M. J. Rataj, J. E. Kauth, M. I. Donnelly, *J. Biol. Chem.* **1991**, *266*, 18684; c) Ref. [121a]; d) R. A. Leising, T. Kojima, L. Que, Jr. in Ref. [7c], p. 321; e) A. Sorokin, A. Robert, B. Meunier, *J. Am. Chem. Soc.* **1993**, *115*, 7293; f) see also K. R. Korzekwa, J. P. Jones, J. R. Gilette, *ibid.* **1990**, *112*, 7042.
[130] a) J. E. Tomaszewski, D. M. Jerina, J. W. Daly, *Biochemistry* **1975**, *14*, 2024; b) F. P. Guengerich, *Chem. Res. Toxicol.* **1990**, *3*, 21. Detailed discussion of intra- versus intermolecular kinetic isotope effects: c) R. P. Hanzlik, K. Hogberg, C. M. Judson, *Biochemistry* **1984**, *23*, 3048.
[131] a) Ref. [121]; b) K. H. J. Ling, R. P. Hanzlik, *Biochem. Biophys. Res. Commun.* **1989**, *160*, 844; c) R. P. Hanzlik, K.-H. J. Ling, *J. Am. Chem. Soc.* **1993**, *115*, 9363.
[132] R. E. White, J. P. Miller, L. V. Favreau, A. Bhattacharyya, *J. Am. Chem. Soc.* **1986**, *108*, 6024.
[133] a) D. H. R. Barton, J. Boivin, M. Gastiger, J. Morzycki, R. S. Hay-Motherwell, W. B. Motherwell, N. Ozbalik, K. M. Schwartzentruber, *J. Chem. Soc. Perkin Trans. 1.* **1986**, 947; b) D. H. R. Barton, S. D. Bévière, W. Chavasiri, E. Csuhai, D. Doller, W.-G. Liu, *J. Am. Chem. Soc.* **1992**, *114*, 2147; see also: c) C. Sheu, S. A. Richert, P. Cofré, B. Ross, Jr., A. Sobkowiak, D. T. Sawyer, J. R. Kanofsky, *ibid.* **1990**, *112*, 1936; d) C. Knight, M. J. Perkins, *J. Chem. Soc. Chem. Commun.* **1991**, 925.
[134] For this concept, see D. J. Hankinson, C. B. Miller, J. Allison, *J. Phys. Chem.* **1989**, *93*, 3624.
[135] a) R. Breslow, *Chem. Soc. Rev.* **1972**, *1*, 533; b) *Acc. Chem. Res.* **1980**, *13*, 170; an industrial application: c) U. Kerb, M. Stahnke, P.-E. Schulze, R. Wiechert, *Angew. Chem.* **1981**, *93*, 89; *Angew. Chem. Int. Ed. Engl.* **1981**, *20*, 88.
[136] H. Schwarz, *Acc. Chem. Res.* **1989**, *22*, 283.
[137] a) A. E. Shilov, *Activation of Saturated Hydrocarbons by Transition Metal Complexes*, Reidel, Dordrecht, **1984**; b) *Activation and Functionalization of Alkanes* (Ed.: C. L. Hill), Wiley, New York, **1989**. c) *Selective Hydrocarbon Activation* (Eds.: J. A. Davies, P. L. Watson, J. F. Liebman, A. Greenberg), VCH, Weinheim, **1990**.
[138] For example, the ligand binding energies of methanol/Fe^+ and acetone/Fe^+ are of the order of 40 kcal mol^{-1} [84], whereas the known BDEs for most of the other heteroatom ligands are significantly larger [13a, 25]; see also: D. Schröder, H. Schwarz, *J. Organomet. Chem.*, in press.
[139] Surveys: a) Ref. [87]; b) D. Schröder, H. Schwarz, *J. Am. Chem. Soc.* **1990**, *112*, 5947; c) D. Schröder, W. Zummack, H. Schwarz, *ibid.* **1994**, *116*, 5857.
[140] D. Schröder, W. Zummack, H. Schwarz, unpublished.
[141] a) G. Cainelli, G. Cardillo, *Chromium Oxidations in Organic Synthesis*, Springer, Berlin, **1984**; b) J. Muzart, *Chem. Rev.* **1992**, *92*, 113.
[142] D. Schröder, H. Schwarz, unpublished.
[143] D. Schröder, H. Schwarz, *Organometallics* **1992**, *11*, 2296.
[144] D. Schröder, K. Eller, H. Schwarz, *Helv. Chim. Acta* **1990**, *73*, 380.
[145] J. R. Collins, D. L. Camper, G. H. Loew, *J. Am. Chem. Soc.* **1991**, *113*, 2736.
[146] O. Blum, D. Stöckigt, D. Schröder, H. Schwarz, *Angew. Chem.* **1992**, *104*, 637; *Angew. Chem. Int. Ed. Engl.* **1992**, *31*, 603.
[147] a) C. J. Cassady, B. S. Freiser, S. W. McElvany, J. Allison, *J. Am. Chem. Soc.* **1984**, *106*, 6125; b) K. Eller, H. Schwarz, *Inorg. Chem.* **1990**, *29*, 3250; c) C. Heinemann, D. Schröder, H. Schwarz, *Chem. Ber.* **1994**, *127*, 1807; d) H. H. Cornehl, C. Heinemann, D. Schröder, H. Schwarz, *Organometallics* **1995**, *14*, 992.
[148] C. J. Cassady, B. S. Freiser, *J. Am. Chem. Soc.* **1984**, *106*, 6176.
[149] D. Stöckigt, Ph.D. Thesis, Technische Universität Berlin D83, **1994**.
[150] J. Schwarz, H. Schwarz, *Helv. Chim. Acta* **1995**, *78*, 1013.
[151] In addition, also $Fe(C_7H_8)^+$, $Fe(C_5H_6)^+$, and neutral FeOH with concomitant organic cations are formed as reaction products.
[152] a) T. J. Groves, G. A. McGlusky, R. E. White, M. J. Coon, *J. Biochem. Biophys. Res. Commun.* **1978**, *81*, 154; b) T. G. Traylor, K. W. Hill, W.-P. Fann, S. Tsuchiyn, B. E. Dunlap, *J. Am. Chem. Soc.* **1992**, *114*, 1308.
[153] a) D. H. R. Barton, F. Halley, N. Ozbalik, M. Schmitt, E. Young, G. Balavoine, *J. Am. Chem. Soc.* **1989**, *11*, 7144; for a review see b) D. H. R. Barton, *Aldrichimica Acta* **1990**, *23*, 3.
[154] Other examples of catalytic gas-phase processes that do not involve O-atom transfer: a) P. Schnabel, M. P. Irion, K. G. Weil, *J. Phys. Chem.* **1991**, *95*, 9688; b) P. Schnabel, M. P. Irion, K. G. Weil, *Chem. Phys. Lett.* **1992**, *190*, 255; c) M. P. Irion, P. Schnabel, *Chem. Ber.* **1992**, *96*, 1091; d) P. Schnabel, K. G. Weil, M. P. Irion, *Angew. Chem.* **1992**, *104*, 633; *Angew. Chem. Int. Ed. Engl.* **1992**, *104*, 633; e) S. Karraß, D. Schröder, H. Schwarz, *Chem. Ber.* **1992**, *125*, 751.
[155] Rather, at thermal energies the reverse reaction, $CH_3Fe^+ + H_2O \rightarrow HOFe^+ + CH_4$, takes place [146].
[156] D. Schröder, H. Schwarz, *Angew. Chem.* **1990**, *102*, 1466; *Angew. Chem. Int. Ed. Engl.* **1990**, *29*, 1431.
[157] D. Stöckigt, Diploma Thesis, Technische Universität Berlin, **1991**.
[158] D. Stöckigt, H. Schwarz, *Chem. Ber., Liebigs Ann.* **1995**, 429.
[159] a) K. U. Ingold, *Acc. Chem. Res.* **1980**, *13*, 317. Recent applications of "radical clocks" in oxidation chemistry: b) V. W. Bowry, K. U. Ingold, *J. Am. Chem. Soc.* **1991**, *113*, 5699; c) K. E. Liu, C. C. Johnson, M. Newcomb, S. J. Lippard, *ibid.* **1993**, *115*, 939.
[160] Examples: a) P. A. M. van Koppen, D. B. Jacobson, A. Illies, M. T. Bowers, M. Hanratty, J. L. Beauchamp, *J. Am. Chem. Soc.* **1989**, *111*, 1991; b) P. A. M. van Koppen, M. T. Bowers, E. R. Fisher, P. B. Armentrout, *ibid.* **1994**, *116*, 3780.
[161] D. Schröder, H. Schwarz, *Angew. Chem.* **1993**, *105*, 1493; *Angew. Chem. Int. Ed. Engl.* **1993**, *32*, 1420.
[162] R. Wesendrup, Diploma Thesis, Technische Universität Berlin, **1994**.
[163] D. Stöckigt, H. Schwarz, *Chem. Ber.* **1994**, *127*, 791.
[164] a) J. S. Valentine, *Chem. Rev. 1973*, *73*, 235; b) E. C. Niederhoffer, J. H. Timmons, A. E. Martell, *ibid.* **1984**, *84*, 137; c) R. S. Drago, *Coord. Chem. Rev.* **1992**, *117*, 185. d) The whole June issue of *Chem. Rev.* **1994** deals with dioxygen complexes and related topics; for a discussion, see I. M. Klotz, D. M. Kurtz, *ibid.* **1994**, *94*, 567.
[165] a) V. R. Choudhury, A. M. Raiput, B. Prabhahm, *Angew. Chem.* **1994**, *106*, 2179; *Angew. Chem. Int. Ed. Engl.* **1994**, *33*, 2104; b) R. Zahradnik, *Acc. Chem. Res.* **1995**, *28*, 306; c) *J. Mol. Catal.* **1993**, *82*, 265.

Terminal E_1 Ligands from Elements of Group 15**

Manfred Scheer*

In recent years interest in complexes containing multiple bonds between transition metal and main group elements has risen sharply.[1] This field is dominated by compounds with terminal ligands from elements of the first row of the periodic table with M=E units (e.g. E = CR_2, NR, O) or M≡E (E = CR, N). The synthesis of complexes with ligands of higher homologues of the main group elements was first achieved at the beginning of the nineties. Thus, Parkin et al. succeeded in synthesizing the first complexes with terminal tellurido ligands.[2]

For complexes containing ligands from elements of group 15 the situation is as follows: Coordination compounds with terminal nitrogen ligands have been known for some time.[3, 4] Examples include the square-pyramidal complexes of type $[MNCl_4]^-$ (M = Mo, W, Re, Ru, Os),[5] which have a very short metal–nitrogen bond. The Lewis base properties of the nitrido ligands are expressed above all in the addition to Lewis acids such as BF_3, and in their tendency towards intermolecular association.[3, 6] For the heavier elements of group 15 there have been, up to now, no examples of this type of coordination, whilst numerous other coordination polyhedra with E_1 ligands are known.[7] Only recently has there been a breakthrough in the successful synthesis of isolable phosphido complexes,[***] and the following discussion traces their development from objects of speculation to manipulable compounds.

Ziegler et al., who were working on the reactivity of trinuclear clusters capped by As, postulated $[Cp(CO)_2M{\equiv}As]$ (M = Mo, W) as intermediates during the co-photolysis of $[\{CpM(CO)_2\}_3(\mu_3\text{-As})]$ with $[CpM'(CO)_2]$ (M' = Co, Rh)[8a, b] or with $[Fe_2(CO)_9]$ and $[Fe(CO)_5]$.[8c] The transformation of the trinuclear cluster into species of the types $[Cp(CO)_2M{\equiv}As]$ and $[\{CpM(CO)_2\}_2]$ ($M{\equiv}M$) can be deduced from the nature of the reaction products.

Rheingold et al. recently reported a gas-phase reaction of Sb_2^- species, generated by laser evaporation of antimony metal, with carbonyl complexes in an ion-cyclotron spectrometer (FT-ICR).[9] Under these conditions the formation of the anionic complexes $[(CO)_nM{\equiv}Sb]^-$ (n = 4, M = Cr, Mo, W; n = 3, M = Fe) could be observed. Ab-initio-MP2 calculations on the Mo complex indicated a square-pyramidal structure (C_{4v} symmetry) with a Mo≡Sb bond length of 2.55 Å.

In 1987 Chisholm et al. found that during the reaction of $[W_2(ONp)_6(HNMe_2)_2]$ (Np = neopentyl) with P_4 a complex with a P_1 and a complex with a P_3 ligand are formed (Scheme 1).[10] Here it was proposed that a phosphido complex

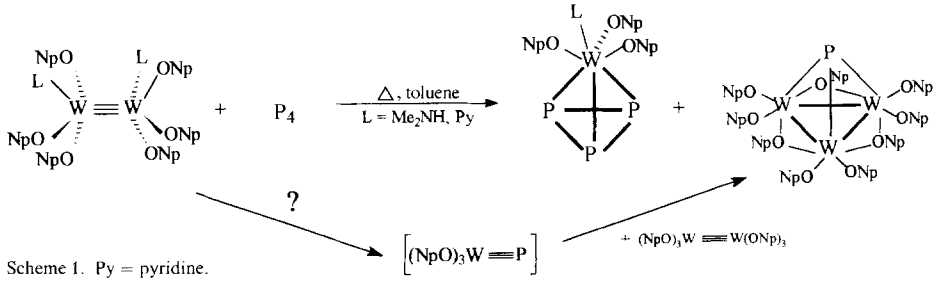

Scheme 1. Py = pyridine.

of type $[(NpO)_3W{\equiv}P]$ could be an intermediate in this reaction. This reacts further with the dimeric W^{III} alkoxide to give a trinuclear cluster with a capping phosphorus ligand. This assumption is supported by the fact that the reaction of $[W_2(O\mathit{t}Bu)_6]$ with alkynes generates alkylidynetungsten complexes[11] and that $[(RO)_3W{\equiv}CR']$ adds to $[(RO)_3W{\equiv}W(OR)_3]$ to form $[W_3(\mu_3\text{-}CR')(OR)_9]$.[12]

A phosphido complex intermediate is also suggested by Becker et al.,[13] for the reaction of $[W_2(O\mathit{t}Bu)_6]$ with the phosphaalkyne $\mathit{t}BuC{\equiv}P$. A reaction pathway as shown in Scheme 2 is proposed.[14] This is based on the identification of **3** with a WC_2P four-membered ring and on data from ^{31}P NMR spectroscopy which indicates the existence of a possible product **4**. Accordingly, there should be a metathesis reaction between the phosphaalkyne $\mathit{t}BuC{\equiv}P$ and the tungsten complex $[W_2(O\mathit{t}Bu)_6]$ to afford alkylidyne compound **1** and the phosphido complex **2**. Subsequent rapid reactions produce intermediates with four-membered rings which stabilize themselves by a 1,3-migration of an alkoxy group to the give the final products **3** and **4**.

[*] Priv.-Doz. Dr. M. Scheer
Institut für Anorganische Chemie der Universität
Engesserstrasse, D-76128 Karlsruhe (Germany)
Telefax: Int. code + (721) 661921

[**] My thanks go to Dr. M. Häser (University of Karlsruhe) for the very valuable discussions which contributed to the development of this work.

[***] The term phosphido ligand for the P^{3-} ligand complies with the IUPAC guidelines (and analogously: arsenido-, antimonido- and bismutido ligand). Hitherto this name has been used incorrectly for the R_2P ligand. This name should be given to $[L_nM{\equiv}P]$, in analogy to the nitrido complex, in preference to terms such as metallaphosphaalkyne or phosphinidyne complex. The latter is derived from the isolobal relationship of the P ligand with the CR fragment.

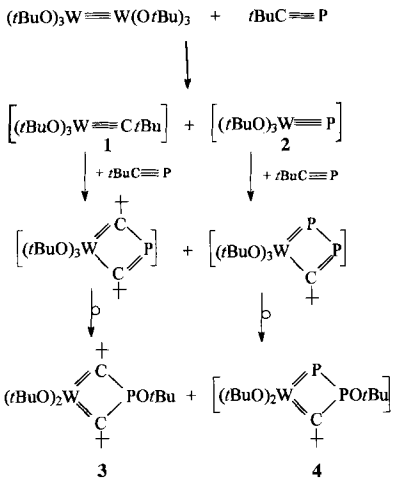

Scheme 2. Postulated course of the reaction between $[W_2(OtBu)_6]$ and $tBu{\equiv}P$.

In recent years we have developed a concept for the elucidation of the transformation pathway of the P_4 tetrahedron in the coordination sphere of transition metal complexes.[15] By addition of simple carbonyl complexes such as $[Cr(CO)_5(thf)]$ to the appropriate reaction solutions containing P_4 it is possible to stabilize intermediates through the coordination of the lone pairs on the phosphorus atoms to the carbonyl complex. If the reaction given in Scheme 2 is carried out in the presence of pentacarbonyl complexes, the alkylidyne complex **1** and the product **5** are obtained.[16] However, a subsequent reaction with $tBuC{\equiv}P$ followed by 1,3-migration of the alkoxy ligand to form the compounds **3** and **6**, with four-membered rings, cannot be completely prevented. Since the reaction mixture could not be separated by column chromatography, only the enrichment of **5a,b** by fractional crystallization was achieved. The ^{31}P NMR chemical shifts at $\delta = 595.4$ (**5a**) and 544.6 (**5b**), the large $^1J(^{183}W,^{31}P)$ coupling constants of 535.8 Hz (**5a**) and 554 Hz (**5b**), and the appearance of a second coupling in the case of the $[W(CO)_5]$-substituted product **5b** of $J = 163$ Hz together with the ratio of signal integrals proves the existence of the compounds.

$[(tBuO)_3W{\equiv}P \rightarrow M(CO)_5]$ (M = Cr, W) **5a,b**

$[(tBuO)_2W\{(CtBu)P(M(CO)_5)P(OtBu)\}]$ (M = Cr or W) **6a,b**

The first isolated and structurally characterized complexes containing metal–phosphorus triple bonds were obtained by the groups of Cummins[17] and Schrock,[18] and marked a breakthrough in this field.

The phosphido complex **8** can be obtained from the reaction of the molybdenum(III) complex **7** with P_4 (Scheme 3).[17] The molybdenum starting material **7** is planar, probably without any $N \rightarrow Mo$ $p\pi$-$d\pi$ bonds. The three unpaired electrons are localized on the Mo atom.[19] This complex is extremely reactive and can cleave N–N bonds in N_2O[19] and even in N_2[20] under very mild conditions (Scheme 3). In the former case the nitrido complex **9** and the nitrosyl complex **10** are obtained. In the latter reaction, with N_2, a η^1-N_2 coordinated intermediate is proposed, onto which a second molecule of the starting material can coordinate to form a $(\mu,\eta^1$-$N_2)$ complex. Subsequent cleavage of

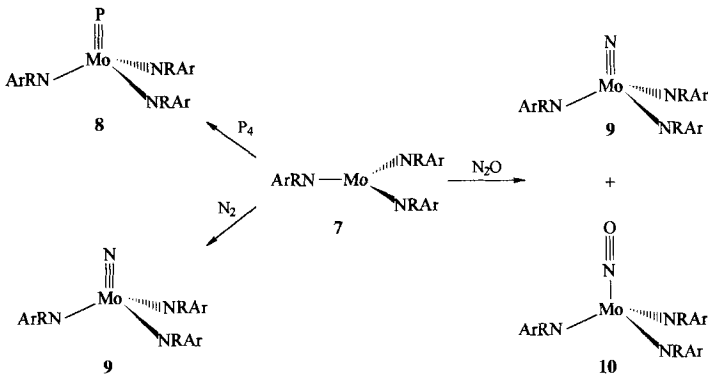

Scheme 3. $R = C(CD_3)_2CH_3$; $Ar = 3,5\text{-}C_6H_3Me_2$.

the N–N bond generates the nitrido complex **9**. Investigations on the reactivity of the molybdenum starting complex are in their infancy, so that further very interesting results can be expected.

Schrock et al. used the N_3N ligand ($N_3N = (Me_3SiNCH_2CH_2)_3N$) for the synthesis of the phosphido complexes **11a,b**. This figand promotes the formation of a multiple bond (between the transition metal and the ligand) *trans* to the intramolecular N donor. Thus, the phosphinidene complex **12** is obtained from the reaction of $[(N_3N)TaCl_2]$ with LiPHR.[21] Treatment of $[(N_3N)SnBu]$ with $[(tBuO)_3Mo{\equiv}N]$ leads to the nitrido complex **13**.[22] Therefore, the chloro complexes $[(N_3N)MCl]$ (M = Mo, W) are predestined as starting materials for a M–E triple bond system. They react with MeLi to give the corresponding methyl derivatives; under mild thermal conditions (80 °C), $[(N_3N)WCH_3]$ loses H_2 to form the alkylidyne complex **14**.[23] Using the same principle of synthesis (halogeno complex and LiPHPh) the phosphido complexes **11a,b** are now accessible. The reaction pathway is not completely understood; however, the phenylphosphanido complexes **15a,b** should be precursors of **11a,b**.

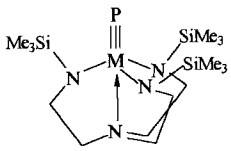

11a: M = Mo
11b: M = W

$[(N_3N)Ta{=}PR]$, $N_3N = (Me_3SiNCH_2CH_2)_3N$; R = Ph, Cy, *t*Bu **12**

$[(N_3N)Mo{\equiv}N]$, $N_3N = (MeNCH_2CH_2)_3N$ **13**

$[(N_3N)W{\equiv}CH]$, $N_3N = (Me_3SiNCH_2CH_2)_3N$ **14**

$[(N_3N)M{-}PPhH]$, $N_3N = (Me_3SiNCH_2CH_2)_3N$; M = Mo, W **15a,b**

Formal metal–phosphorus triple bonds are also present in phosphinidene complexes with an almost linear MPR arrangement (Scheme 4, type **A**). The p orbitals of phosphorus can form π bonds with the d orbitals of the metal. A comparison of the metal–phosphorus bond lengths in **12** (2.145(7) Å),[21] **16** (2.169(1) Å), and **11b** (2.162(4) Å) justifies this view. The bond lenghts are almost

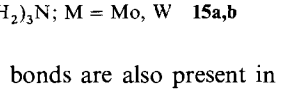

A **B**

Scheme 4. Coordination modes of phosphinidene complexes.

identical in two tungsten compounds (**11b** and **16**). On the other hand, the observed coupling constants $^1J(^{183}W,^{31}P)$ of **11b** (138 Hz) and **16** (649 Hz) seem to contradict themselves, and even for **5a,b** values of 535 and 554 Hz are found.[16] In the bent phosphinidene complex **17b**,[25] in which there is only a

$[CO(Me_3P)_2Cl_2W{\equiv}PAr']$, Ar' = 2,4,6-$tBu_3C_6H_2$ **16**

$[Cp_2M{=}PAr']$, Ar' = 2,4,6-tBu$_3$C$_6$H$_2$; M = Mo, W **17a,b**

double bond present (Scheme 4, type **B**; cf. structure of **17a**) the value of $^1J(^{183}W,^{31}P)$ amounts to 153.5 Hz.[26] It seems sensible to attribute the small coupling constants of **11b** to the high oxidation state of the metal center (tungsten(VI)). However, the W^{II} complex $[CpW(CO)_2(SnMe_3)PR_3]$ (R = OMe) shows, for example, a coupling of 493.6 Hz, whilst smaller values have been found for W^0 complexes.[27a] There is also the consideration that the Fermi-contact term, which is essentially determined by the s-character of the bonding orbital, is not the sole controlling factor for the resulting coupling constants, but coupling contributions which are transmitted through the π-electron system (spin dipole contribution or the paramagnetic orbital contribution) must be taken more effectively into account.[27b] It is noteworthy that there is always a relatively large coupling constant $^1J(^{183}W,^{31}P)$ when the phosphido ligand is coordinated in a linear fashion to a second bonding partner, for example an aryl group as in **16** or a pentacarbonyl-metal complex fragment as in **5**. Indeed, the comparative analysis of the electronic structures of uncoordinated and coordinated phosphido ligand complexes shows that with approximately constant π-bonding contributions, the phosphorus-3s orbital contribution to a W–P bond increases by about 30% whilst at the same time the phosphorus-3p σ-contribution decreases.[28] There must certainly be a connection between the enormous increase of $^1J(^{183}W,^{31}P)$ in linear coordination of phosphorus in the experimentally investigated complexes **5** and **15**.

Summary: The synthesis of the first stable complexes with terminal phosphido ligands is of fundamental importance and will lend the field of coordination chemistry considerable impetus. The synthesis of analogous complexes with ligands of the heavier homologues have now moved within reach. Both synthetic pathways should give access to, for example, the corresponding arsenido complexes. Moreover, we can now set about answering fundamental questions on the properties of P_1 ligands both experimentally and theoretically.

German version: *Angew. Chem.* **1995**, *107*, 2151–2153

Keywords: complexes with elements of group 15 · molybdenum compounds · multiple bonds · phosphorus compounds · tungsten compounds

[1] W. A. Nugent, J. M. Mayer, *Metal-Ligand Multiple Bonds*, Wiley, New York, **1988**.

[2] D. Rabinovich, G. Parkin, *J. Am. Chem. Soc.* **1991**, *113*, 9421.

[3] K. Dehnicke, J. Strähle, *Angew. Chem.* **1981**, *93*, 451; *Angew. Chem. Int. Ed. Engl.* **1981**, *20*, 413; K. Dehnicke, J. Strähle, *ibid.* **1992**, *104*, 978 and **1992**, *31*, 955.

[4] W. A. Herrmann, *Angew. Chem.* **1986**, *98*, 57; *Angew. Chem. Int. Ed. Engl.* **1986**, *25*, 56.

[5] a) B. Knopp, K.-P. Lörcher, J. Strähle, *Z. Naturforsch. B* **1977**, *32*, 1361; b) W. Liese, K. Dehnicke, R. D. Rogers, R. Shakir, J. L. Atwood, *J. Chem. Soc. Dalton Trans.* **1988**, 1061; c) F. L. Phillips, A. C. Skapski, *Acta Crystallogr. Sect. B* **1975**, *31*, 2667; d) W. Liese, K. Dehnicke, I. Walker, J. Strähle, *Z. Naturforsch. B* **1979**, *35*, 693.

[6] See also recent work on cyclotrimerization: a) W. A. Herrmann, S. Bogdanovic, T. Priermeier, R. Poli, J. C. Fettinger, *Angew. Chem.* **1995**, *107*, 63; *Angew. Chem. Int. Ed. Engl.* **1995**, *34*, 112; b) M. H. Chisholm, K. Folting-Streib, D. B. Tiedtke, F. Lemoigno, O. Eisenstein, *ibid.* **1995**, *107*, 61 or **1995**, *34*, 110.

[7] Reviews: a) M. Scheer, E. Herrmann, *Z. Chem.* **1990**, *30*, 41; b) O. J. Scherer, *Angew. Chem.* **1990**, *102*, 1137; *Angew. Chem. Int. Ed. Engl.* **1990**, *29*, 1104.

[8] a) M. L. Ziegler, H.-P. Neumann, *Chem. Ber.* **1989**, *122*, 25; b) C. Caballero, D. Lehne, B. Nuber, M. L. Ziegler, *ibid.* **1991**, *124*, 1327; c) H. P. Neumann, M. L. Ziegler, *J. Organomet. Chem.* **1989**, *377*, 255.

[9] F. P. Arnold, D. P. Ridge, A. L. Rheingold, *J. Am. Chem. Soc.* **1995**, *117*, 4427.

[10] a) M. H. Chisholm, K. Folting, J. W. Pasterczyk, *Inorg. Chem.* **1988**, *27*, 3057; b) M. H. Chisholm, J. C. Huffman, J. W. Pasterczyk, *Inorg. Chim. Acta* **1987**, *133*, 17.

[11] R. R. Schrock, M. L. Listemann, L. G. Sturgeoff, *J. Am. Chem. Soc.* **1982**, *104*, 4291; M. L. Listemann, R. R. Schrock, *Organometallics* **1985**, *4*, 74.

[12] M. H. Chisholm, K. Folting, J. A. Heppert, D. M. Hoffman, J. C. Huffman, *J. Am. Chem. Soc.* **1985**, *107*, 1234.

[13] G. Becker, W. Becker, R. Knebl, H. Schmidt, U. Hildenbrand, M. Westerhausen, *Phosphorus Sulphur* **1987**, *30*, 349.

[14] P. Binger in *Multiple Bonds and Low Coordination in Phosphorus Chemistry* (Eds.: M. Regitz, O. J. Scherer), Thieme, Stuttgart, **1990**, p. 100.

[15] a) M. Scheer, C. Troitzsch, P. G. Jones, *Angew. Chem.* **1992**, *104*, 1395; *Angew. Chem. Int. Ed. Engl.* **1992**, *31*, 1377; b) M. Scheer, C. Troitzsch, L. Hilfert, M. Dargatz, E. Kleinpeter, P. G. Jones, J. Sieler, *Chem. Ber.* **1995**, *128*, 251; c) M. Scheer, U. Becker, M. H. Chisholm, J. C. Huffman, J. Organomet. Chem. **1993**, *461*, C1.

[16] M. Scheer, K. Schuster, T. A. Budzichowski, M. H. Chisholm, W. E. Streib, *J. Chem. Soc. Chem. Commun.* **1995**, 1671.

[17] C. E. Laplaza, W. M. Davis, C. C. Cummins, *Angew. Chem.* **1995**, *107*, 2181; *Angew. Chem. Int. Ed. Engl.* **1995**, *34*, 2042.

[18] N. C. Zanett, R. R. Schrock, W. M. Davis, *Angew. Chem.* **1995**, *107*, 2184; *Angew. Chem. Int. Ed. Engl.* **1995**, *34*, 2044.

[19] C. E. Laplaza, A. L. Odom, W. M. Davis, C. C. Cummins, *J. Am. Chem. Soc.* **1995**, *117*, 4999.

[20] C. E. Laplaza, C. C. Cummins, *Science* **1995**, *268*, 861.

[21] C. C. Cummins, R. R. Schrock, W. D. Davis, *Angew. Chem.* **1993**, *105*, 758; *Angew. Chem. Int. Ed. Engl.* **1993**, *32*, 756.

[22] W. Plass, J. G. Verkade, *J. Am. Chem. Soc.* **1992**, *114*, 2275.

[23] K.-Y. Shin, K. Totland, S. W. Weidel, R. R. Schrock, *J. Am. Chem. Soc.* **1994**, *116*, 12103.

[24] A. H. Cowley, B. Pellerin, *J. Am. Chem. Soc.* **1990**, *112*, 6734.

[25] P. B. Hitchcock, M. F. Lappert, W. P. Leung, *J. Chem. Soc. Chem. Commun.* **1987**, 1282.

[26] Die ^{31}P NMR chemical shifts behave inversely **8**: δ = 1216 [17]; **11b**: δ = 1080 ($^1J(^{183}W,^{31}P)$ = 138 Hz) [18]; **12**: δ = 209.8 [21]; **16**: δ = 193 (649 Hz) [24]; **17a**: δ = 799.4; **17b**: δ = 661.1 (153.5 Hz) [25]).

[27] a) P. S. Pregosin, R. W. Kunz in *^{31}P- and ^{13}C NMR of Transition Metal Phosphine Complexes*, Springer, Berlin, **1979**, p. 101; b) *ibid.*, pp. 75ff.

[28] M. Häser (Universität Karlsruhe), personal communication.

 © *VCH Verlagsgesellschaft mbH, D-69451 Weinheim, 1995* *0570-0833/95/3418-1999 $ 10.00+.25/0*

Endotoxin Antagonists: Possible Candidates for the Treatment of Gram-Negative Sepsis**

Otto Holst*

The endotoxins [lipopolysaccharides (LPS)] of Gram-negative bacteria are amphiphilic macromolecules located in the outer membrane of the cell wall.[1, 2] LPS are essential for bacterial survival; they augment the rigidity of the cell wall and protect bacteria from bile acids, gut enzymes, and defense mechanisms of the host, and from antibiotics. In higher animals and humans, however, endotoxins exhibit a variety of pathophysiological effects. Even in minor amounts they may invoke a sepsis which, accompanied by hypotension and multiple organ failure, leads to septic shock that is the major cause of death in intensive care units worldwide. Moreover, LPS are antigens and thus involved in the process of recognition of bacteria and the host's defense. The biological activities of LPS and their clinical relevance are main impulses for tremendous international research on the structure and function of LPS and possible approaches to sepsis therapy.

LPS of all Gram-negative bacteria share a common architecture (Scheme 1).[2] They consist of a lipidic portion, the lipid A,[3] which anchors the molecule in the outer membrane

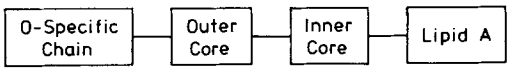

Scheme 1. General structure of bacterial LPS.

and which is linked to a more or less complex carbohydrate chain. In various bacterial families (e.g. *Enterobacteriaceae, Vibrionaceae*) this is an oligosaccharide unit with up to 15 monosaccharides (the core region), which is substituted with a polysaccharide of repeating units (the O-antigen, S-form LPS).[4] A second type of LPS, which was first identified in mutants carrying a defect in the gene cluster responsible for O-antigen biosynthesis (*rfb*), consists only of lipid A and the core region (R-form LPS). Later, this type of LPS was also found in bacteria without known genetic defects, for example, in *Bordetella pertussis* (whooping cough) and *Neisseria gonorrhoeae* (gonorrhea).

During infection, LPS are liberated from bacteria, for example after cell death. These LPS react with various serum components, a prominent member of which is the "lipopolysaccharide binding protein" (LBP). LPS complex with LBP and may then be bound to a receptor (CD14) of macrophages, which through a not yet elucidated signal transduction pathway are stimulated to synthesize and release distinct mediator substances such as tumor necrosis factor-α (TNF-α) and the interleukins (Il) 1, 6, and 8.[5] Overproduction of mediators results in the pathophysiological effects of endotoxins. The initialization of this cascade does not require a complete LPS molecule. As postulated in the 1950s and verified in the 1980s[6, 7] in various biological experiments using natural isolates and synthetic *Escherichia coli* lipid A (Scheme 2), lipid A represents the toxic principle of LPS.

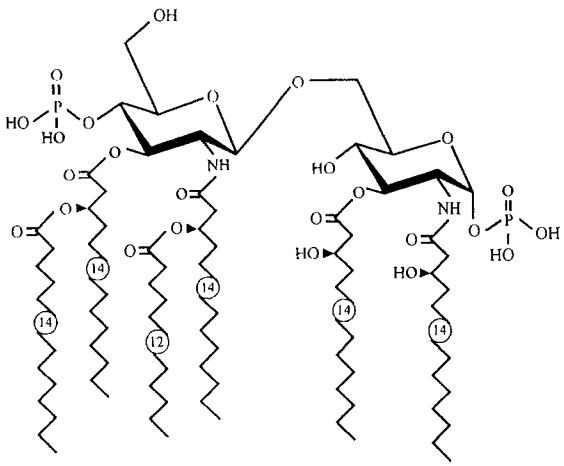

Scheme 2. Structure of lipid A from *E. coli*. The circled numbers refer to the length of the carbon chain.

Today, the mortality rate of Gram-negative sepsis is still as high as 60%, owing to an increasing distribution of antibiotic-resistent bacteria in hospitals. Additionally, LPS are liberated from bacteria by antibiotics. New strategies to avoid or treat Gram-negative sepsis could affect different stages of the endotoxin cascade: the LPS, the interaction of LPS with serum components/cell receptors, or the production and secretion of mediators. Besides efforts to obtain cross-reactive and -protective antibodies in particular against lipid A, an inhibitor of the TNF-α synthesis was identified which protects mice against the lethal effects of endotoxin. One monoclonal antibody (HA-1A) was applied clinically; however, its distribution has been stopped in the meantime, since it proved to be a failure.

In my opinion recent investigations concerning the effects of nontoxic endotoxin antagonists are also very important. These are structural analogues of lipid A, some of which are shown in Scheme 3. One example is tetraacyl lipid A (**A**) (precursor Ia), a precursor in lipid A biosynthesis which has also been synthesized chemically (Compound 406).[8, 9] As shown by different research groups, precursor Ia inhibits the LPS-induced specific mRNA production for monokines in human macrophages. Comparison of investigations using different structural analogues revealed that the effectiveness of these disaccharide an-

[*] Priv.-Doz. Dr. O. Holst
Forschungsinstitut Borstel
Institut für Experimentelle Biologie und Medizin
Parkallee 22, D-23845 Borstel (Germany)
Telefax: Int. code +(4537) 10419

[**] I thank Dr. U. Zähringer for help in preparing the schemes and Professor H. Brade for critical reading of the manuscript.

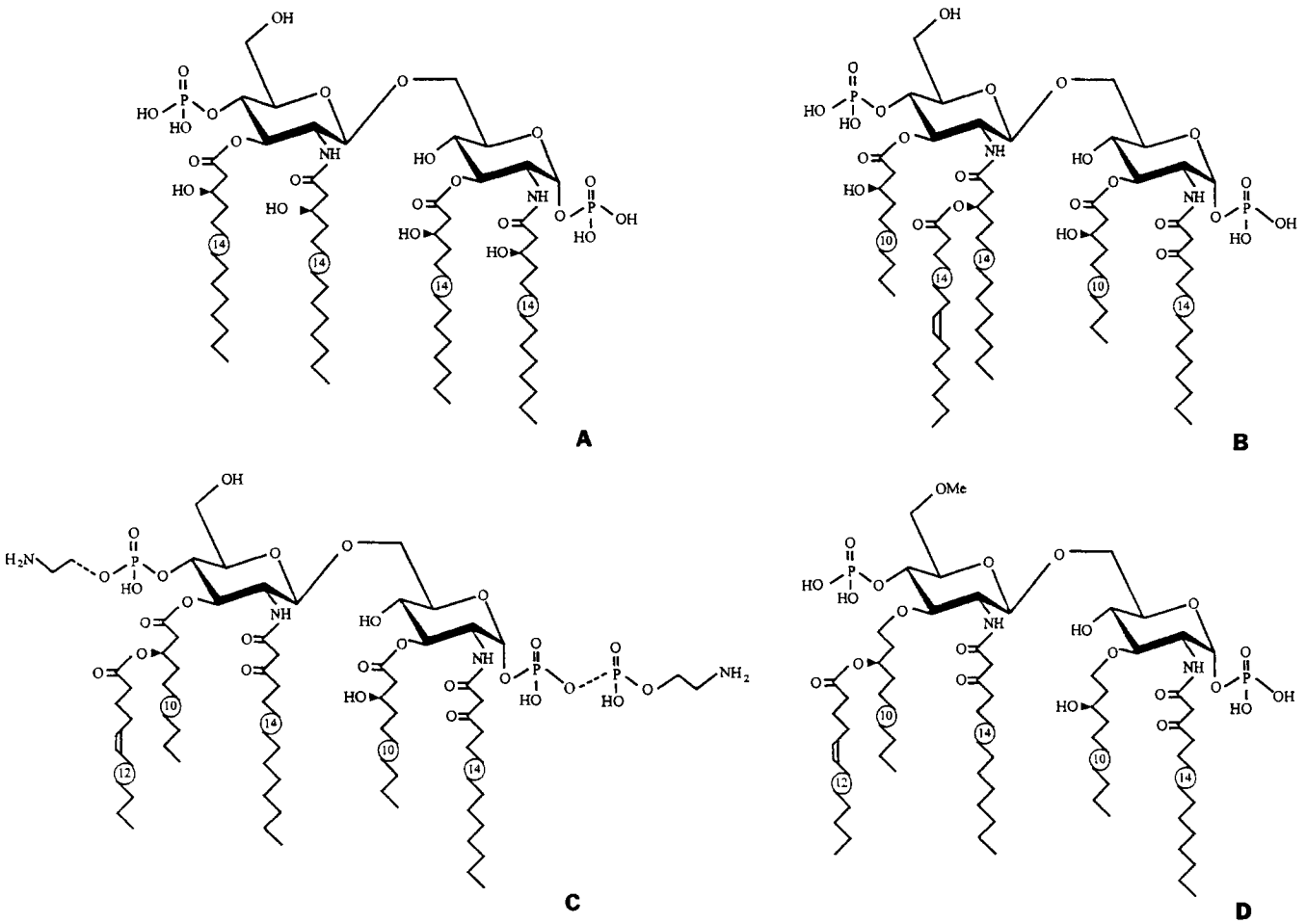

Scheme 3. Structures of precursor Ia (**A**), lipid A from *R. sphaeroides* (**B**), lipid A from *R. capsulatus* (**C**), and E5531 (**D**).

tagonists depends on their acylation and phosphorylation pattern. Tetraacylated and bisphosphorylated precursor Ia is one of the most effective inhibitors known to date. In macrophages and monocytes, the mechanism of the inhibition is based on competitive binding of the antagonist to CD14. However, since precursor Ia exhibits agonistic activities in vitro and in vivo in mice (but not in humans), it is not possible to test this substance in a murine sepsis model.

Other antagonists are the nontoxic lipid A of *Rhodobacter sphaeroides* (**B**) and *R. capsulatus* (**C**) (Scheme 3).[10–15] The lipid A of *R. sphaeroides* (**B**) was also chemically synthesized.[16] A spectroscopic analysis identified differences with the structure of the natural isolate, most likely in the fatty acids. The authors thus suggested that the published structure of the isolated lipid A is not correct. However, the discrepancy has not yet been finally clarified. Recently, the synthesis of a structural analogue (E5531, **D** in Scheme 3) of the lipid A from *R. capsulatus* was described along with a broad characterization of its toxic and antagonistic properties.[17] Since the chemically synthesized *R. capsulatus* lipid A (**C**) appeared to be unstable during storage (hydrolytic cleavage of the acyl groups at C-3 and C-3′ of the glucosamine disaccharide) and, thus, did not fulfill an important prerequisite of a drug, it was necessary to synthesize a stable derivative thereof. This was possible by introducing ether substituents at positions C-3 and C-3′. Just as fascinating as the chemical synthesis are the results of the biological in vitro and in vivo experiments using E5531 (**D**). First of all, the LPS-induced monokine production in human monocytes and whole blood was inhibited by E5531. Notably, and in contrast to precursor Ia (**A**), E5531 (**D**) did not show any agonistic activity in either human or murine cells. Therefore, murine in vivo models could be established. It was shown that the LPS-induced increase in the TNF-α concentration in plasma and the 100% mortality rate of the animals could be negated by coinjection of E5531 (**D**). Even more important is the establishment of a murine infection model, in which the animals can be protected from experimental *E. coli* peritonitis by combined injection of E5531 and a β-lactam antibiotic. This was not possible by injection of either E5531 or the antibiotic alone, and in the latter case it was found that the antibiotic killed the bacteria but also liberated higher amounts of LPS. This infection model seems to represent important processes of human sepsis and may thus be an essential instrument in future in vivo investigations. Owing to its favorable biological properties, E5531 (**D**) has already been tested in a clinical phase I study; it did not show agonistic activity and decreased dose-dependant endotoxic LPS-effects, for example the amount of released cytokines.

The results obtained to date indicate that nontoxic structural analogues of lipid A such as precursor Ia and E5531 are potent endotoxin antagonists in vitro and, partially, also in vivo. Most

promising is E5531, a compound that may lead to an important progress in the treatment of Gram-negative sepsis.

German version: *Angew. Chem.* **1995**, *107*, 2154 - 2156

Keywords: drugs · endotoxins · lipopolysaccharides · medicinal chemistry

[1] B. Lugtenberg, L. van Alphen, *Biochim. Biophys. Acta* **1983**, *737*, 51 - 115.
[2] E. T. Rietschel, H. Brade, *Sci. Am.* **1992**, *267*, 54 - 61.
[3] U. Zähringer, B. Lindner, E. T. Rietschel, *Adv. Carbohydr. Chem. Biochem.* **1994**, *50*, 211 - 276.
[4] a) *Bacterial Endotoxic Lipopolysaccharides, Vol. 1* (Eds.: D. C. Morrison, J. L. Ryan), CRC, Boca Raton, FL, **1992**; b) O. Holst, H. Brade in ref. [4a], p. 135.
[5] E. T. Rietschel, H. Brade, O. Holst, L. Brade, S. Müller-Loennies, U. Mamat, U. Zähringer, F. Beckmann, U. Seydel, K. Brandenburg, A. J. Ulmer, T. Mattern, H. Heine, J. Schletter, S. Hauschildt, H. Loppnow, H.-D. Flad, U. F. Schade, F. Di Padova, R. R. Schumann, *Curr. Top. Microbiol. Immunol.*, unpublished.
[6] O. Westphal, O. Lüderitz, *Angew. Chem.* **1954**, *66*, 407 - 417.
[7] H. Brade, L. Brade, E. T. Rietschel, *Zbl. Bakt. Hyg. A* **1988**, *268*, 151 - 179.
[8] C. R. H. Raetz in ref. [4a], p. 67.
[9] S. Kusumoto in ref. [4a], p. 81.
[10] N. Qureshi, K. Takayama, R. Kurtz, *Infect. Immun.* **1991**, *59*, 441 - 444.
[11] H. Loppnow, E. T. Rietschel, H. Brade, U. Schönbeck, P. Libby, M.-H. Wang, H. Heine, W. Feist, I. Dürrbaum-Landmann, M. Ernst, E. Brandt, E. Grage-Griebenow, A. J. Ulmer, S. Campos-Portuguez, U. Schade, T. Kirikae, S. Kusumoto, J. Krauss, H. Mayer, H.-D. Flat in *Bacterial Endotoxin: Recognition and Effector Mechanisms* (Eds.: J. Levin, C. R. Alving, R. S. Munford, P. L. Stütz), Elsevier, Amsterdam, **1993**, p. 337.
[12] P. V. Salimath, J. Weckesser, W. Strittmatter, H. Mayer, *Eur. J. Biochem.* **1983**, *136*, 195 - 200.
[13] N. Qureshi, J. P. Honovich, H. Hara, R. J. Cotter, K. Takayama, *J. Biol. Chem.* **1988**, *263*, 5502 - 5504.
[14] T. Merkofer, A. Neszmelyi, H. Mayer, *Workshop Endotoxine und Exotoxine als bakterielle Pathogenitätsfaktoren*, **1995**, Forschungsinstitut Borstel, P 1.3.
[15] J. H. Krauss, U. Seydel, J. Weckesser, H. Mayer, *Eur. J. Biochem.* **1989**, *180*, 519 - 526.
[16] W. J. Christ, P. D. McGuinness, O. Asano, Y. Wang, M. A. Mullarkey, M. Perez, L. D. Hawkins, T. A. Blythe, G. R. Dubuc, A. L. Robidoux, *J. Am. Chem. Soc.* **1994**, *116*, 3637 - 3638.
[17] W. J. Christ, O. Asano, A. L. Robidoux, M. Perez, Y. Wang, G. R. Dubuc, W. E. Gavin, L. D. Hawkins, P. D. McGuinness, M. A. Mullarkey, M. D. Lewis, Y. Kishi, T. Kawata, J. R. Bristol, J. R. Rose, D. P. Rossignol, S. Kobayashi, I. Hishinuma, A. Kimura, N. Asakawa, K. Katayama, I. Yamatsu, *Science* **1995**, *268*, 80 - 83.

Third, Revised and Enlarged Edition

E. V. Dehmlow / S. S. Dehmlow

Phase Transfer Catalysis

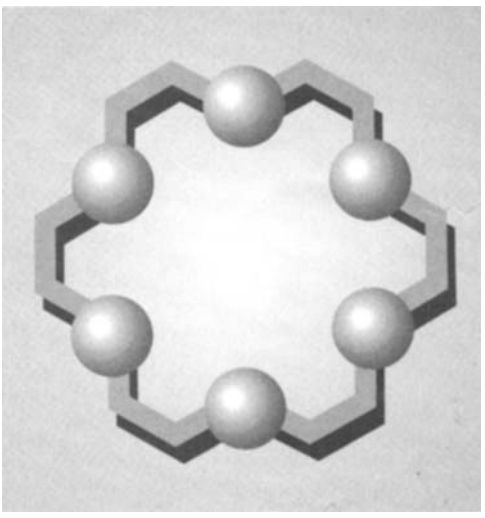

1993. XIII, 499 pages with 49 tables.
Hardcover. DM 198,00.
ISBN 3-527-28408-7

Phase Transfer Catalysis has matured and so has this book. Certain PTC-variants have become standard techniques in the lab, and PTC may be on the brink of large-scale use.
This new edition describes important new developments in PTC.
Furthermore, it has been extensively updated and offers a comprehensive list of very recent references.

New material has been added on

- solid/liquid PTC
- enantioselective reactions
- metal-organic reactions
- reduction and oxidation reactions
- elimination and substitution reactions.

To order please contact your bookseller or:

VCH, P.O. Box 10 11 61,
D-69451 Weinheim,
Fax (0) 62 01 - 60 61 84

VCH, Hardstrasse 10,
P.O. Box, CH-4020 Basel

VCH

 © VCH Verlagsgesellschaft mbH, D-69451 Weinheim, 1995 0570-0833/95/3418-2002 $ 10.00+.25/0

The Metallic Bond—Dead or Alive? A Comment and a Reply

Comment by Leland C. Allen* and Jeremy K. Burdett*

In a recent 'Highlight' J. C. Schön discussed[1] a point of view put forward by ourselves[2, 3] that the term 'Metallic Bond' should be dropped from the chemical vernacular. Although Dr. Schön gives a useful summary of the thrust of our work, his conclusions are the opposite to ours—the metallic bond is alive and well, he believes, as a distinct entity on a par with the ionic, van der Waals, and covalent bonds which chemists use to categorize compounds. There are some other points that support our view, which are worth stating here. We will show once again that 'metallic bonds' are a subset of that large group of bonds we loosely call 'covalent'.

1) To estimate the strength of ionic interactions, one would use an interatomic potential of the form $-e^2/r + A/r^6$, where the electrostatic interaction is balanced by a repulsive term. This approach has been used for years to estimate the cohesive energies of ionic materials. To estimate the strength of van der Waals interactions we would use a potential of the form of $-B/r^6 + C/r^{12}$, the age-old Lennard–Jones 6–12 potential. To estimate the strength of covalent bonding we would try to evaluate the integral $\int \phi_1 H^{\text{eff}} \phi_2 d\tau$, or use empirical expressions to access these overlap terms. But what do we use to estimate the strength of 'metallic bonding'? What is the special electronic characteristic that distinguishes it from the other three types? In fact, we use the same considerations as for covalent bonding. Tight-binding theory used in the solid state, for metals as well as insulators, is just like the Hückel theory of the organic chemist.[4] The use of the terms 'ionic', 'covalent', and van der Waals, are of course frequently imprecise, but in a perfectly accurate electronic structure calculation, all of these considerations are included. Importantly no special theory is included for the 'metallic' bond.

2) Energy differences between the bcc, fcc, and hcp crystal structures of the transition elements[5, 6] as a function of electron count may readily be calculated, and thus the most stable structure identified. Excellent agreement with the observed structures is found. These particular calculations[5, 6] used tight-binding theory—as we pointed out in (1), the solid state analog of molecular orbital theory. No special 'metallic bonding' was used to get these results—just orbital overlap considerations. Thus the crystal structures, and indeed their cohesive energies, are determined by d-band covalency. The Hume–Rothery electron compounds, often very complex crystal structures that are found for metallic alloys with between 11 and 12 valence electrons per atom are also completely accessible[7] using this solid-state equivalent of Hückel theory. Again no special 'metallic bonding' needs to be implied.

3) Pauling[8] regarded metals as really no different from large molecules where there are not enough electrons to form electron pair bonds between all close atomic contacts. He used the concept of resonance to get over this problem, just as he used resonance to view the electronic structure of the π manifold of benzene. His Resonating Valence Bond model certainly has an appeal, and has recently found new uses in the physics community. Thus, as pointed out in our paper,[2] and hardly a new observation, there are strong similarities between the electronic descriptions of metallic solids and molecules with delocalized electrons such as benzene.

4) Important in this regard too are aspects of the van Arkel–Ketelaar diagram.[3] The electronic underpinnings of the scheme come from 'covalent' arguments. Particularly interesting, is the reduction of a three variable scheme (the original triangle itself, with 'ionic', 'covalent' and 'metallic' bonding variables) to a two variable scheme,[3] essentially 'ionic' and 'covalent' indices.

In view of these comments, which surely put the electronic structures of metals within the same electronic framework as the 'covalent' bond, our argument stands, that the 'metallic bond' as a separate term with equal weight to the other three traditional schemes should be abandoned. Certainly it does not have a mathematical framework distinct from the other three categories as shown in (1) above. However, if one wishes to use the term to describe that subset of 'covalent' systems, which are metals then one should be aware of the discussion above.

[*] Prof. J. K. Burdett
Department of Chemistry and James Franck Institute
The University of Chicago
Chicago, IL 60637 (USA)
Telefax: Int. code +(312) 702-0805
Prof. L. C. Allen
Department of Chemistry
Princeton University
Princeton, NJ 08544 (USA)

[1] J. C. Schön, *Angew. Chem.* **1995**, *107*, 1183; *Angew. Chem. Int. Ed. Engl.* **1995**, *34*, 1081.
[2] W. P. Anderson, J. K. Burdett, P. T. Czech, *J. Am. Chem. Soc.* **1994**, *116*, 8808.
[3] L. C. Allen, J. F. Capitani, *J. Am. Chem. Soc.* **1994**, *116*, 8810.
[4] J. K. Burdett, *Prog. Solid State Chem.* **1984**, *15*, 173.
[5] J. K. Burdett, S. Lee, *J. Am. Chem. Soc.* **1985**, *107*, 3050.
[6] D. G. Pettifor, *CALPHAD* **1977**, *1*, 305.
[7] S. Lee, *J. Am. Chem. Soc.* **1991**, *113*, 101.
[8] L. Pauling, *The Nature of The Chemical Bond*, Third Edition, Cornell University Press, Ithaca, NY, **1960**.

 © *VCH Verlagsgesellschaft mbH, D-69451 Weinheim, 1995* *0570-0833/95/3418-2003 $ 10.00+.25/0*

Reply by J. Christian Schön*

It appears to me that L. C. Allen and J. K. Burdett are not really far away from the point of view I have presented in the Highlight.[1] It seems that we would agree that the proper way to deal with solids from the theoretical point of view is the use of quantum mechanics, preferably on the level of ab initio calculations. Clearly, on this level one would not make a distinction between different types of bonding; only after having done the calculation, one could try to classify the electronic structure according to some criteria, by which one would *define* what should constitute a covalent, metallic, or ionic bond.

If one leaves the level of ab initio calculations, one becomes concerned with the calculation of band structures for some effective potential seen by the electrons. As I have pointed out in the Highlight, there are a number of techniques to perform such a calculation. The most popular ones derive from expansions of the wave function in Bloch functions of either the plane-wave or the atomic/molecular orbital type (nearly-free-electron theory or tight-binding approach). Both sets are complete systems of eigenfunctions (at least, if one includes ionized states with the atomic arbitals), and a proper diagonalization of the Hamiltonian matrix within either set should lead to the same spectrum of energies, that is, to the same band structure. Note that, in principle, all pairs of eigenfunctions must be used in evaluating the matrix elements of the Hamiltonian (unless they vanish by some symmetry considerations); it is, in general, not sufficient to restrict oneself, for example, to atomic/molecular orbitals belonging to neighboring sites.

The authors now point out in (1) and (2) that in many systems good results are found with the tight-binding theory. I agree; the only surprise is the great success of the band approximation. From this they conclude that tight-binding theory should be the language of choice for discussing the electronic structure of solids. So far, this is a matter of personal choice, and I do not object. However, I disagree if tight-binding theory is now to be set equivalent with the theory of covalent bonding—a much more local concept than the full tight-binding theory necessary to correctly describe the solid within the band approximation—and all the historic associations and visualizations of, for example, directed bonds that go along with this term.

Results as good as those obtained with the tight-binding method can be achieved with sufficiently large plane-wave expansions. I think Allen and Burdett would agree that one should not use the latter fact to claim that, since all substances can basically be viewed as more or less perturbed free-electron systems, they should be considered as "metals". Such a claim would lead us to describe covalent or ionic insulators as "metals" with an energy gap. To conclude, once we treat the solid on a high enough quantum mechanical level, the distinction among the different chemical concepts of bonding is no longer very meaningful. As an example, consider the Group 4 elements C (diamond) through Pb. Their electronic structure can be calculated with either plane-waves or atomic orbitals, and exhibit the closing of the energy gap in the band structure for Pb. But if one tried a classification with regard to the bonding situation, one would clearly ascribe "directed" covalent bonds to carbon in the diamond structure and "undirected" metallic bonds to lead in the fcc-structure.

Finally, judging by the feel of the arguments presented in (1), it appears that the authors would always like to associate with the term "bond" some two-body interaction, either in the form of an effective potential or an overlap integral. But already for the π-manifold mentioned in (3) or the "three-center, one-electron-pair bonds" such a view is rather problematic. One might perhaps argue that the "bonds" in the benzene molecule are still between (nearest) neighbors, and that the π-electrons just "strengthen" these bonds. But if that were allowed, then one could also treat the metallic bond as, for example, a van der Waals bond cleverly strengthened by the energetic advantage gained by letting the valence electrons become delocalized over the whole crystal. Of course, it is difficult to write down a simple heuristic variant of, for example, the Lennard-Jones potential suitable for a two-body description of the cohesive energy of a metal, but the same problem applies to the covalent picture, where because of the directionality of the bonds at least three-body terms are necessary for a proper effective potential.

German version: *Angew. Chem.* **1995**, *107*, 2157–2158

Keywords: bond theory · metallic bond · solid-state chemistry

[*] Dr. J. C. Schön
Institut für Anorganische Chemie der Universität
Gerhard-Domagk-Strasse 1, D-53121 Bonn (Germany)
Telefax: Int. code +(228) 73-5660
e-mail: unc419@ibm.rhrz.uni-bonn.de

[1] J. C. Schön, *Angew. Chem.* **1995**, *107*, 1183; *Angew. Chem. Int. Ed. Engl.* **1995**, *107*, 1081.

Chiral Titanium Alkoxides as Catalysts for the Enantioselective Reduction of Ketones with Boranes

Guido Giffels, Claus Dreisbach, Udo Kragl, Michael Weigerding, Herbert Waldmann, and Christian Wandrey*

Asymmetric catalysis has gained much significance during the last 15 years.[1] In this area, chiral titanium alkoxides have proven to be very versatile tools and have been employed successfully in enantioselective epoxidations of allyl alcohols,[2] asymmetric Diels–Alder and ene reactions, syntheses of cyanohydrins, aldol reactions,[3] and addition reactions of diethylzinc to aldehydes.[4] We recently introduced the use of the bicyclic diols **1** and **3** as ligands in the latter reaction type.[5] Currently we are interested in to what extent the enantioselective titanate-catalyzed hydride transfer can be applied to keto-carbonyl substrates.

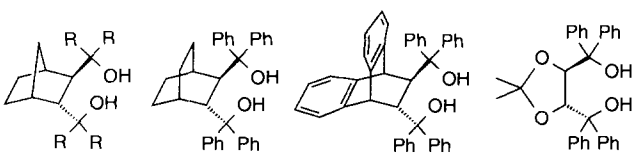

1: R = Ph **2**: R = 2-Naphthyl **3** **4** **5**

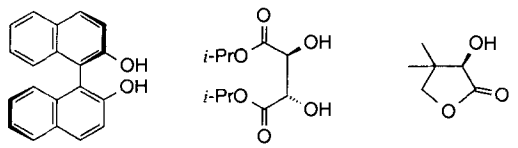

6 **7** **8**

Catalytic reductions with boron-containing Lewis acids have been thoroughly investigated,[6, 7] titanium(IV) alkoxide-catalyzed reductions, on the other hand, are unknown.[8] We have now been able to show that reductions of this kind are feasible and result in good enantiomeric excesses when boranes are used as the reducing agents. Several chiral diols, including **1**–**7** and (D)-pantolactone (**8**), were employed as the Ti ligands. The best results were accomplished with the TADDOL-analogous ligands **1**–**4**, in particular with **1** and **3**, as well as with TADDOL **5**.[9] The corresponding titanium alkoxides **1a**–**8a** were prepared in situ from 1.15 equivalents of the ligand and 1.0 equivalents of titanium tetraisopropoxide in *n*-hexane by azeotropic removal of isopropyl alcohol [Eq. (a)]. The reducing agents used

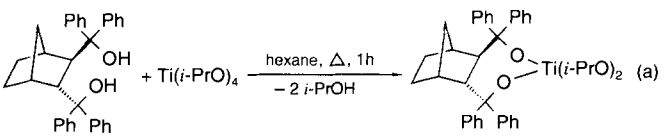

1 **1a** (a)

include the adducts borane-tetrahydrofuran (1 M in THF), borane-dimethylsulfide, and 1,3,2-benzodioxaborole (catecholborane).

Initially, we investigated the reduction of acetophenone to 1-phenylethanol [Eq. (b)]. The results are summarized in Table 1. The best results were obtained with **1** or **3** as the ligand,

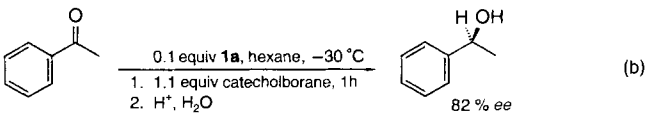

82 % *ee* (b)

Table 1. Enantioselective reduction of acetophenone with catecholborane in the presence of titanium alkoxide catalysts (10 mol%), unless noted otherwise.

Catalyst	Solvent	(*S*)/(*R*)	Conversion [%] (reaction time)
1a [a]	*n*-hexane	59:41	100 (1 h)
1a [b]	*n*-hexane	39:61	100 (1 h)
1a	*n*-hexane	91: 9	100 (1 h)
1a [c]	*n*-hexane	90:10	77 (1 h) >95 (15 h)
1a [d]	*n*-hexane	50:50	5 (15 h)
1a	THF	86:14	95 (1 h)
1a	*n*-hexane/THF 9/1	55:45	90 (1 h)
1a	CCl_4	84:16	85 (15 h)
2a	*n*-hexane	85:15	85 (0.5 h)
3a	*n*-hexane	92: 8	90 (1 h)
4a	*n*-hexane	88:12	83 (1 h)
5a	*n*-hexane	79:21	100 (1 h)
6a	toluene	60:40	77 (15 h)
7a	*n*-hexane	55:45	86 (15 h)
8a	*n*-hexane	36:64	10 (15 h)

[a] BH_3-THF (1 M). [b] Reducing agent BH_3-SMe_2. [c] 2.5 mol%. [d] Control experiment without titanium tetraisopropoxide.

catecholborane as the reducing agent, and *n*-hexane as the solvent. The enantioselectivities obtained in these transformations did not decrease even with catalyst concentrations as low as 2.5 mol%.

An excess of titanium tetraisopropoxide with respect to the ligand decreases the observed enantiomeric excess. This can be explained by the fact that the achiral alkoxide catalyzes the reduction in the same way as the chelate complex. We assume that the borate ester of phenylethanol is formed as the reduction

[*] Prof. Dr. C. Wandrey, Dipl.-Chem. G. Giffels, Dr. C. Dreisbach, Dr. U. Kragl
Institut für Biotechnologie, Forschungszentrum Jülich GmbH
D-52425 Jülich (Germany)
Telefax: Int. code + (2461)61-3870
e-mail: u.kragl@kfa-juelich.de
Dipl.-Chem. M. Weigerding, Prof. Dr. H. Waldmann
Institut für Organische Chemie der Universität
D-76128 Karlsruhe (Germany)

[**] This work was supported by the Deutsche Forschungsgemeinschaft.

product. Therefore, it is not necessary to use an excess of titanium tetraisopropoxide to regenerate the chiral alkoxide in the catalytic cycle as in the addition of diethylzinc to aldehydes.[10] Without a catalyst, hardly any reduction takes place; however, when using 0.1 equivalents of **1a** (with respect to the ketone) and 1.1 equivalents of catecholborane, numerous ketones can be reduced quantitatively with moderate to good enantioselectivities within 1 h as shown in Table 2.

Table 2. Results of the reduction of various ketones with 0.1 equiv of **1a** as the catalyst and 1.1 equiv of catecholborane after a reaction time of 1 h.

Ketone	(*S*)/(*R*)	Conversion [%]
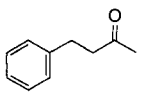	65:35	100
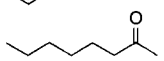	67:33	100
	79:21	100
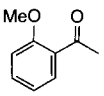	80:20	100
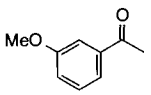	85:15	100
	74:26	100
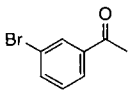	88:12	95
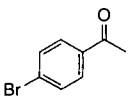	91: 9	95
	91: 9	100

A reduction of the titanate in the presence of catecholborane does not occur. Furthermore, there is no evidence that low-valent titanium species are involved in the transformation. Upon the addition of BH_3-THF to a solution of **1a** in *n*-hexane, the colorless reaction solution turns pale violet after a reaction time of more than half an hour, which indicates the presence of titanium(III). However, in the presence of a ketone, this color change does not take place. On the other hand, adding an excess of BH_3-SMe_2 results in the formation of a titanium precipitate.

To rule out the possibility that the asymmetric induction is based on an interaction between the borane and any excess ligand, we performed control experiments in which we used the ligand in the absence of titanium tetraisopropoxide. In these experiments, the reduction was significantly slower and produced only racemic product (see Table 1).

At present, we can only speculate about the mechanism of the reaction. The steric model introduced by Seebach et al.[11] for the titanate-catalyzed addition of diethylzinc to benzaldehyde cannot be applied to the system titanium-acetophenone-catecholborane, since it does not adequately explain the observed product configurations. When employing catecholborane and BH_3-THF, an attack of the nucleophile to the *re*-face of the carbonyl group can be observed, as is the case for example in the reduction of ketones with AlH_x-TADDOLates[10] or in the addition of primary Grignard reagents to ketones in the presence of Mg-TADDOLate.[12] Surprisingly, the enantioselectivity is reversed when using BH_3-SMe_2 (see Table 1). Similar to Grignard additions, the reaction exhibits a strong solvent dependence.[12]

The reaction introduced herein constitutes the first example of the asymmetric reduction of ketones with readily available achiral boranes in which chiral titanates are used as catalysts. The variety of available ligands offers the possibility for further optimization of the enantiomeric excesses obtained in these reactions.

Experimental Procedure

Preparation of the titanium alkoxides: **1** (320 mg, 0.69 mmol) or a corresponding amount of one of the other chiral ligands **2**–**8** in *n*-hexane (250 mL) in an inert gas atmosphere was treated with titanium tetraisopropoxide (175 μL, 0.6 mmol), and the reaction mixture was heated to reflux for 1–2 h. Thereafter, about 25 mL of the solvent was removed by distillation. To this catalyst solution were added consecutively at −30 °C acetophenone (700 μL, 6 mmol) and catecholborane (700 μL, 6.6 mmol). After 1 h (conversion >95% according to GC), 1 M HCl (50 mL) was added and the mixture was extracted with ethyl acetate (3 × 50 mL). The combined organic layers were washed with 1 M NaOH (3 × 50 mL), dried over sodium sulfate, and the solvent was removed by distillation. Chromatography on silica gel (eluent: dichloromethane) afforded (*S*)-1-phenylethanol (560 mg, 78%) in a purity of >99% and with 82% *ee* according to GC on a permethylated β-cyclodextrin phase. $[\alpha]_D^{25} = -38.5$ (*c* = 1 in toluene).

Received: April 24, 1995
Revised version: June 3, 1995 [Z 7914 IE]
German version: *Angew. Chem.* **1995**, *107*, 2165–2166

Keywords: asymmetric syntheses · catalysis · chiral auxiliaries · reductions

[1] I. Ojima, *Catalytic Asymmetric Synthesis*, VCH, New York, **1993**.
[2] T. Katsuki, K. B. Sharpless, *J. Am. Chem. Soc.* **1980**, *102*, 5974–5976.
[3] K. Narasaka, *Synthesis* **1991**, 1–11 (review).
[4] B. Schmidt, D. Seebach, *Angew. Chem.* **1991**, *103*, 100–101; *Angew. Chem. Int. Ed. Engl.* **1991**, *30*, 99–101.
[5] C. Dreisbach, U. Kragl, C. Wandrey, *Synthesis*, **1994**, 911–912; H. Waldmann, M. Weigerding, C. Dreisbach, C. Wandrey, *Helv. Chim. Acta* **1994**, *77*, 2111–2116.
[6] E. J. Corey, R. K. Bakshi, S. Shibata, *J. Am. Chem. Soc.* **1987**, *109*, 5551–5553.
[7] C. Bolm, M. Felder, *Tetrahedron Lett.* **1993**, *34*, 6041–6044.
[8] The hydrosilylation of ketones introduced by Buchwald et al. that employs a titanocene catalyst proceeds via a low-valent titanium species (M. B. Carter, B. Schiøtt, A. Gutiérrez, S. L. Buchwald, *J. Am. Chem. Soc.* **1994**, *116*, 11667–11670).
[9] TADDOLs: *Tetraaryldioxolandimethanols*; see for example A. K. Beck, B. Bastani, D. A. Plattner, W. Petter, D. Seebach, H. Braunschweiger, P. Gysi, L. La Vecchia, *Chimia* **1991**, *45*, 238–244.
[10] D. Seebach, D. A. Plattner, A. K. Beck, Y. M. Wang, D. Hunziker, W. Petter, *Helv. Chim. Acta* **1992**, *75*, 2171–2209.
[11] Y. N. Ito, X. Ariza, A. K. Beck, A. Boháč, C. Ganter, R. E. Gawley, F. M. N. Kühnle, J. Tuleja, Y. M. Wang, D. Seebach, *Helv. Chim. Acta* **1994**, *77*, 2071–2110.
[12] B. Weber, D. Seebach, *Tetrahedron* **1994**, *50*, 6117–6128.

Diastereoselective Cathodic Cyclization of 1-(4- and 1-(3-Oxoalkyl)pyridinium Salts to Quinolizidine and Indolizidine Derivatives**

Rüdiger Gorny, Hans J. Schäfer,* and Roland Fröhlich

Dedicated to Professor Hans Jürgen Bestmann on the occasion of his 70th birthday

The umpolung of reactivity by electron transfer has developed into a powerful synthetic principle for cyclizations. In this process, in acyclic molecules with two functional groups of the same reactivity, one of these groups has its reactivity reversed by oxidation or reduction, thereby initiating intramolecular C–C bond formation. The electrode has proven to be a useful reagent for this, as documented by numerous cyclizations at both the anode[1] and the cathode.[2]

Acetone and pyridine can be coupled cathodically in acidic electrolytes to form tetrahydropyridyl alkyl alcohols.[3–5] We report here on an intramolecular version of this C–C bond formation, which opens up a facile route to heterobicyclic systems. We chose oxoalkylpyridinium halides as starting materials, which are readily available by nucleophilic substitution of halogen ketones with pyridine and in which the arene is additionally activated for the reduction by the quaternization of nitrogen.

Compound **1** was obtained in 68% yield from pyridine and 5-chloropentan-2-one.[6] The potential-controlled electrolysis of **1** in a divided cell at −1.37 V (relative to the saturated calomel electrode) in 10% aqueous H_2SO_4 gave, after current consumption of 18 F mol^{-1}, 12% **2a,b** in a 1.3:1.0 ratio and 28% **3**;[7] at the same time a strong evolution of hydrogen was observed. An electrolysis with a current consumption of 4 F mol^{-1} gave 9% yield of **2a,b** (**a**:**b** = 1.3:1.0).

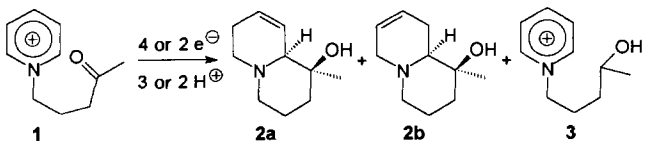

The yield of **2** can be increased by reducing the competing reduction of protons. A decrease of the H^+ concentration to 5% did not improve the yield; at pH 7 **2** was not formed at all. However, if the electrolysis was carried out at a constant current the yield of **2** was improved to 30% by reducing the current density ($\bar{i}$ = 4.2 mA cm^{-2}). A further increase in yield of **2** to 58% was possible by doubling the amount of charge. Under these conditions the best yield was obtained with a 0.2 M solution of **1**; higher (0.4 M **1**: 44% **2**) or lower concentrations of **1** (0.1 M **1**: 50% **2**) led to decreases in the yield. The most favorable sulfuric acid concentration is 10%; in 5% H_2SO_4 the yield drops slightly, in 20% H_2SO_4 more strongly. The temperature only slightly influenced the yield in the range of 3 to 40 °C. In every case the ratio of **2a**:**2b** remained 1.3:1.0. A more or less pronounced passivation takes place when the mercury cathode is replaced with a graphite, glassy carbon, or lead cathode. On the lead cathode, if the electrolysis is repeatedly interrupted and the cathode surface is polished a 38% yield of **2** was obtained. The more pronounced passivation on graphite or glassy carbon cannot be alleviated in this way: **1** was not transformed on these cathodes.

The structure of **2a,b** was determined by NMR spectroscopy and in the case of **2a** confirmed by X-ray analysis (Fig. 1a). The ^{1}H NMR signals of the olefinic protons at δ = 5.7 and 5.8 are only consistent with **2a** and **2b** among the conceivable double-bond isomers. The quinolizidines **2a** and **2b** were converted by catalytic hydrogenation (H_2/Pd/C) to the known (1*S**, 9a*S**)-1-methylquinolizidin-1-ol (**4**)[9] in 92% yield (not shown).

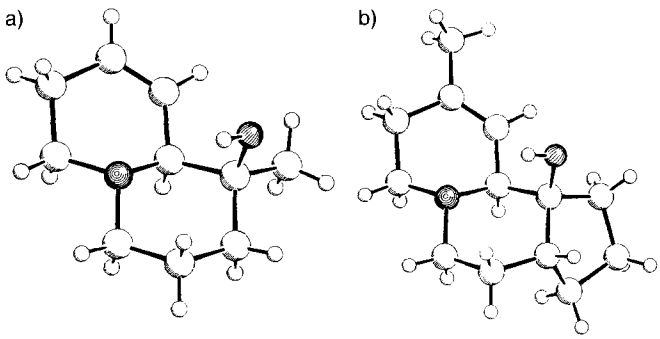

Fig. 1. a) Structure of **2a** and b) of **29a** in the crystal [8].

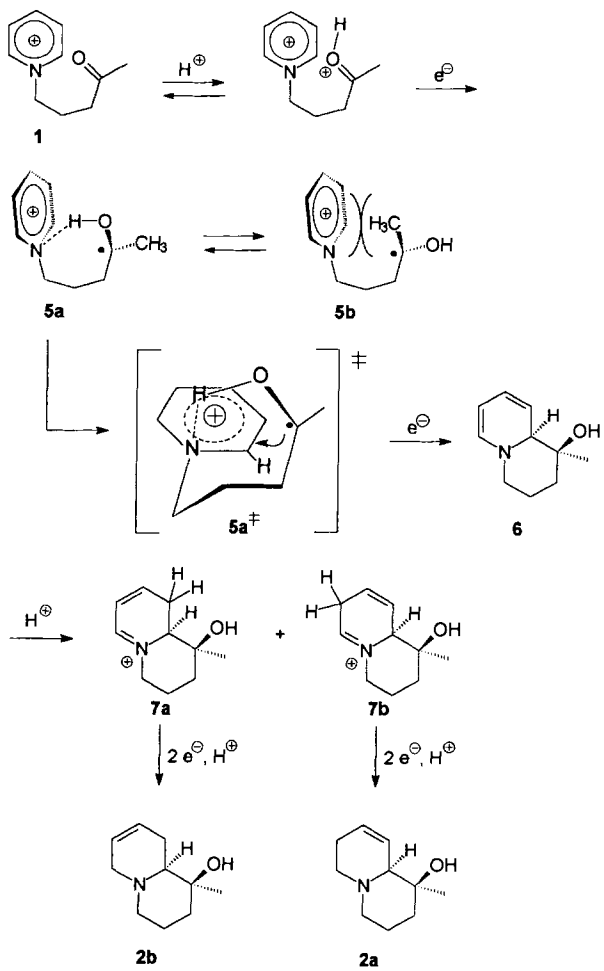

Scheme 1. Postulated course of the reaction **1** → **2**.

[*] Prof. H. J. Schäfer, Dr. R. Gorny, Dr. R. Fröhlich[+]
Organisch-chemisches Institut der Universität
Corrensstrasse 40, D-48149 Münster (Germany)
Telefax: Int. code + (251)83 9772
e-mail: schafeh@uni-muenster.de

[+] X-ray structure analyses.

[**] Electroorganic Syntheses, Part 61. This work was supported by the Fonds der Chemischen Industrie with a doctoral grant to R. G. and from the Graduiertenkolleg "Hochreaktive Mehrfachbindungssysteme". Part 60, B. Klotz-Berendes, H. J. Schäfer, M. Grehl, R. Fröhlich, *Angew. Chem.* **1995**, *107*, 218–220; *Angew. Chem. Int. Ed. Engl.* **1995**, *34*, 189–191.

Measurements with differential pulse polarography at pH values from 1–4 and extrapolation of the values to 10% sulfuric acid indicate that the pyridinium group and the carbonyl group are reduced at −1.43 V and −1.37 V, respectively. The relative positions of these potentials, the structures of the products, and postulated course[10] of the cathodic coupling of acetone with pyridine support the mechanism outlined in Scheme 1.

The protonated carbonyl group is reduced to the radical, which adds to the pyridinium ring. According to AM1-calculations the nitrogen in the radical cation **5** has a negative partial charge, thus the cyclization from conformation **5a** is favored possibly through a hydrogen bond, whereas cyclization from conformation **5b** is sterically hindered because of the interaction between the methyl group and the pyridinium ring. Compound **6** is formed from **5a** and has the (1*S**, 9a*S**) configuration; **6** is then protonated to form the immonium ions **7a** and **7b**, whose 2e reduction leads to **2b** and **2a**, respectively.

In order to demonstrate the utility of this reductive cyclization, substituents were placed on the pyridinium ring and the size of the annulated ring was varied. Thus, the pyridinium salts **8**–**12** were prepared from the corresponding pyridines and 5-chloropentan-2-one in 33–63% yield and subsequently cyclized under the optimal conditions for **2** to give the quinolizidines **13**–**17** (Table 1).

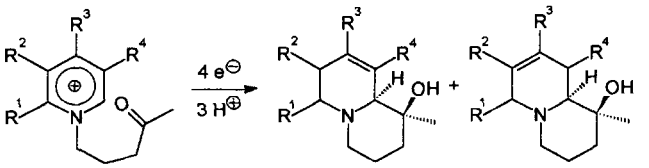

Table 1. Reductive cyclization of the 1-(4-oxopentyl)pyridinium chloride **1** and **8**–**12** to the quinolizidines **2** and **13**–**17**, respectively [a].

Entry	Pyridinium salt	R^1	R^2	R^3	R^4	Product	Yield [%]
1	**1**	H	H	H	H	**2**	58
2	**8**	CH_3	H	H	H	**13**	40
3	**9**	H	CH_3	H	H	**14**	45
4	**10**	H	H	CH_3	H	**15**	59
5	**11**	H	H	*t*Bu	H	**16**	62
6	**12**	CH_3	H	H	*n*Bu	**17**	41

[a] Conditions: Charge used: 8 F mol^{-1}, current density: 4.2 mA cm^{-2}, 10% sulfuric acid, 0.2 M pyridinium salt solution, 20 °C.

The structures of **13**–**17** were determined by ^{1}H and ^{13}C NMR spectroscopy and mass spectrometry and in the case of **16a** confirmed by X-ray structure analysis.[8] Owing to the alkyl substituents, several diastereomers were formed in the reduction of **8**, **9**, and **12**. Six diastereomers were obtained from **9** in the ratio 2.4:1.5:1.2:1.0:3.6:3.6 (according to gas chromatography); however, these could not be separated by liquid chromatography. The unsubstituted carbon C-6 of the pyridinium ring in **8** couples preferentially; products of the coupling at the substituted C-2 were only identified in trace amounts. Double-bond isomers and C-2 epimers from the coupling at C-6 were obtained from **12**. The yields for the cyclizations of the 4-substituted pyridinium chlorides **10** and **11** are comparable with those for the unsubstituted **1**. The yields of the cyclizations of **8**, **9**, and **12** are slightly lower, possibly because of steric interaction with the substituents on the pyridinium ring.

The reductive cyclization of **18** and **19** should lead to the indolizidine skeleton. Compounds **18** and **19** were prepared in 80 and 88% yield, respectively, by the alkylation of pyridine and 4-*tert*-butylpyridine, respectively, with 2-(2-bromoethyl)-2-methyl-1,3-dioxolane. Their cathodic reduction under the optimized conditions for **2** gave in each case only one double-bond isomer of the indolizidines **20** and **21**, respectively (Table 2).

The structures of **20** and **21** were determined by comparison of their spectroscopic data with those of **2a** and **16a** and in the case of **20** additionally confirmed by an X-ray structure analysis.[8]

While the yield of the cyclization to the five-membered ring is hardly reduced in comparison to that of **2**, as expected this is not the case for the annulation of the seven-membered ring. Compounds **24a,b** (14%) and **25a,b** (16%) were obtained together with the acyclic alcohols **26** (16%) and **27** (16%) from **22** and **23** (prepared from the reaction of 6-bromohexan-2-one with pyridine and 4-*tert*-butylpyridine, respectively, in 83% and 87% yield), respectively, using the optimized conditions for **2** (Table 2).

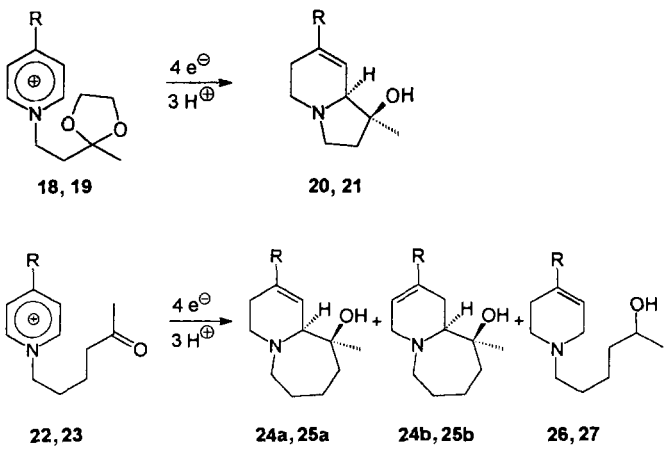

Table 2. Reductive cyclization of the 1-[2-(2-methyl-1,3-dioxolan-2-yl)ethyl]pyridinium bromides **18** and **19** to the indolizidines **20** and **21**, respectively, and 1-(5-oxohexyl)pyridinium bromides **22** and **23** to the pyridoazepines **24** and **25**, respectively, as well as the alcohols **26** and **27**, respectively. For conditions see Table 1.

Entry	Pyridinium salt	R	Products	yield [%]		yield [%]
1	**18**	H	**20**	55		
2	**19**	*t*Bu	**21**	58		
3	**22**	H	**24a, b**	14	**26**	16
4	**23**	*t*Bu	**25a, b**	16	**27**	16

A tricyclic quinolizidine is also readily available in only three steps from **28**. The pyridinium bromide **28** was prepared by alkylation of γ-picoline with 2-(2-bromoethyl)cyclopentanone in 83% yield. The cathodic cyclization of this compound gave **29a,b** in 46% yield in the ratio >20:1. The structure of **29a** was determined spectroscopically and confirmed by an X-ray structure analysis (Fig. 1b).[8]

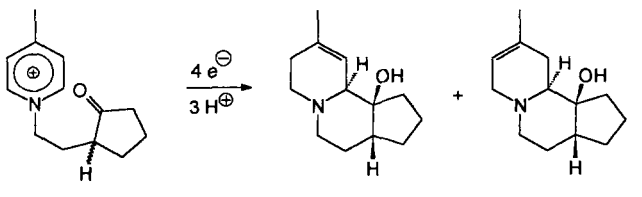

 © VCH Verlagsgesellschaft mbH, D-69451 Weinheim, 1995 0570-0833/95/3418-2008 $ 10.00+.25/0

In this case a double-bond isomer was formed regioselectively, and at the same time three stereogenic centers were formed diastereoselectively. The preferential formation of the (3a*R**,9a*S**,9b*S**) diastereoisomer in this case can be explained by the smaller steric interaction between the 2-H of the pyridinium ring and the *exo*-orientated angular H atom of the side chain.

Quinolizidine and indolizidine derivatives are diastereoselectively accessible in only two or three steps in a simple reaction in which the key step is the new cathodic cyclization described here.

Experimental Procedure

28: 4-Methylpyridine (2.79 g, 30 mmol) and 2-(2-bromoethyl)cyclopentanone [11] (3.82 g, 20 mmol) were heated to 120 °C for 20 min. After cooling to room temperature the reaction mixture was treated with ether (80 mL), stirred for 10 min and then the ether was decanted off. This procedure was repeated twice with ether (with 50 mL). The residue was then dissolved in methanol (5 mL) with gentle warming, treated with ether (80 mL) and stirred for 5 min before the supernatant was decanted off. After the final wash with ether (50 mL) and subsequent decanting, the residue was filtered through a short column filled with silica using methanol as eluant. After removal of the methanol under vacuum, 4.82 g (17 mmol, 83%) **28** remained. ^{1}H NMR (CD_3OD): δ = 1.61–2.00 (m, 2H, NCH_2CH_2), 2.03–2.45 (m, 7H, cyclopentanone-H), 2.73 (s, 3H, CH_3), 4.65–4.86 ((partially covered by CH_3OH) NCH_2), 7.99 (d, ^3J = 6.5 Hz, 2H, NCHC*H*), 8.91 (d, ^3J = 6.5 Hz, 2H, NCH). ^{13}C NMR (CD_3OD): δ = 21.9 (t, NCH_2CH_2), 22.3 (q, CH_3), 30.9 (t, $OCCH_2CH_2$), 32.8 (t, $OCCHCH_2$), 38.8 (t, $OCCH_2$), 47.3 (d, OCCH), 60.7 (t, NCH_2), 130.3 (d, NCHCH), 145.3 (d, NCH), 161.7 (s, CCH_3), 222.0 (s, CO).

29: **28** (2.84 g, 10.0 mmol) was dissolved in 10% sulfuric acid (50 mL) and electrolyzed in a divided beaker type cell with a mercury pool cathode (19 cm^2) and a platinum anode (1 cm^2), a current density of 4.2 mA cm^{-2} (related to the cathode), at a temperature of 20 °C, until the consumption of 8.2 F mol^{-1}. The catholyte was made basic by addition of solid sodium carbonate and shaken with dichloromethane. After drying the organic phase with magnesium sulfate, it was concentrated and the solution filtered through silica with diethyl ether as eluant to give 0.95 g (4.6 mmol, 46%) **29a,b**. ^{1}H NMR ($CDCl_3$): δ = 1.44–2.03 (m, 10H), 1.68 (s, CH_3), 2.23–2.36 (m, 3H, 7-H_{ax}, 8-H_{ax}, 5-H_{ax}), 2.51–2.58 (m, 2H, 5-H_{eq} and 10a-H), 2.61 (s, 1H, OH), 2.71–2.81 (m, 1H, 7-H_{eq}), 5.35 (s, 1H, 10-H). ^{13}C NMR ($CDCl_3$): δ = 19.4 (t, C-2), 23.3 (q, CH_3), 23.5 (t, C-4), 26.1 (t, C-3), 30.4 (t, C-1), 33.5 (t, C-8), 43.8 (d, C-3a), 51.3 (t, C-5), 52.5 (t, C-7), 63.2 (d, C-10a), 78.5 (s, C-10b), 118.5 (d, C-10), 135.8 (s, C-9).

Received: April 18, 1995 [Z 7894 IE]
German version: *Angew. Chem.* **1995**, *107*, 2188–2191

Keywords: cyclizations · electrochemistry · heterocycles · indolizidines · quinolizines

[1] H. J. Schäfer in *Organic Electrochemistry* (Eds.: H. Lund, M. M. Baizer), Dekker, New York, **1991**, p. 949, there p. 985; H. J. Schäfer, W. Eilenberg, *Heterocycles* **1989**, *28*, 979–985; L. V. Tinao-Wooldridge, K. D. Moeller, C. M. Hudson, *J. Org. Chem.* **1994**, *59*, 2381–2389; S. Maki, K. Toyoda, S. Kosemura, S. Yamamura, *Chem. Lett.* **1993**, 1059–1062; S. Yamamura, Y. Shizuri, H. Shigemori, Y. Okuno, M. Ohkubo, *Tetrahedron* **1991**, *47*, 635–644; E. G. Corley, N. L. Abramson, J. S. Amato, L. M. Weinstock, *ibid.* **1991**, *47*, 757–766.

[2] M. M. Baizer in *Organic Electrochemistry* (Eds.: H. Lund, M. M. Baizer), Dekker, New York, **1991**, p. 879; R. D. Little, C. G. Sowell in *Electroorganic Synthesis* (Eds.: R. D. Little, N. L. Weinberg), Dekker, New York, **1991**, p. 323; T. Shono, N. Kise, T. Suzumoto, T. Morimoto, *J. Am. Chem. Soc.* **1986**, *108*, 4676–4677; C. G. Sowell, R. L. Wolin, R. D. Little, *Tetrahedron Lett.* **1990**, *31*, 485–488; N. Kise, T. Suzumoto, T. Shono, *J. Org. Chem.* **1994**, *59*, 1407–1413; R. D. Little, R. Wolin, G. Sowell, *Denki Kagaku oyobi Kogyo Butsuri Kagaku* **1994**, *62*, 1105–1108; [*Chem. Abstr.* **1995**, *122*, 117416u]; S. Donnelly, J. Grimshaw, J. Trocha-Grimshaw, *J. Chem. Soc. Chem. Commun.* **1994**, 2171–2172.

[3] T. Nonaka, K. Sugino, *J. Electrochem. Soc.* **1969**, *116*, 615–616.

[4] M. Ferles, M. Vanka, A. Šilhánková, *Collect. Czech. Chem. Commun.* **1969**, *34*, 2108–2113.

[5] T. Nonaka, T. Sekine, K. Odo, K. Sugino, *Electrochim. Acta* **1977**, *22*, 271–277.

[6] D. A. Jaeger, M. R. Frey, *J. Org. Chem.* **1982**, *47*, 311–315.

[7] The salts **1**, **3**, **8**–**12** are present as chlorides and the salts **18**, **19**, **22**, **23**, and **28** as bromides. For reasons of clarity the anions are not shown in the diagrams.

[8] Data for the four X-ray structure determinations: The structures were solved on an Enraf-Nonius CAD4 diffractometer, (λ = 1.54178 Å, T = 223 K, ω-2θ scan) by direct methods with the hydrogen atoms in calculated positions. **2a** $C_{10}H_{17}NO$, M = 167.25, crystal dimensions 1.0 × 1.1 × 1.2 mm^3, a = 7.513(1), b = 8.557(1), c = 8.769(1) Å, α = 66.70(1), β = 73.41(2), γ = 66.91(1)°, V = 470.6(1) Å^3, ρ_{calcd} = 1.180 g cm^{-3}, μ = 5.9 cm^{-1}, Z = 2, triclinic, space group $P\bar{1}$ (no. 2), 2179 measured reflections ($\pm h$, $\pm k$, $\pm l$), 1965 independent and 1949 observed [$I \geq 2\sigma(I)$] reflections, 112 refined parameters, R = 0.043, wR^2 = 0.118, max. residual electron density 0.19 (−0.28) e Å^{-3}. **16a** $C_{14}H_{25}NO$, M = 207.31, crystal dimensions 1.2 × 1.0 × 1.0 mm^3, a = 7.871(1), b = 9.231(1), c = 9.991(1) Å, α = 76.22(1), β = 81.79(1), γ = 73.65(1)°, V = 674.3(1) Å^3, ρ_{calcd} = 1.110 g cm^{-3}, μ = 5.2 cm^{-1}, Z = 2, triclinic, space group $P\bar{1}$ (no. 2), 3027 measured reflections ($\pm h$, $\pm k$, $\pm l$), 2812 independent and 2749 observed [$I \geq 2\sigma(I)$] reflections, 151 refined parameters, R = 0.032, wR^2 = 0.075, max. residual electron density 0.25 (−0.17) e Å^{-3}. **20** $C_9H_{15}NO$, M = 153.22, crystal dimensions 1.0 × 0.7 × 0.6 mm^3, a = 7.153(1), b = 8.375(1), c = 8.733(1) Å, α = 99.47(1), β = 109.60(1), γ = 110.89(1)°, V = 435.80(9) Å^3, ρ_{calcd} = 1.168 g cm^{-3}, μ = 6.0 cm^{-1}, Z = 2, triclinic, space group $P\bar{1}$, 1896 measured reflections ($\pm h$, $\pm k$, $\pm l$), 1773 independent and 1750 observed [$I \geq 2\sigma(I)$] reflections, 103 refined parameters, R = 0.043, wR^2 = 0.117, max. residual electron density 0.30 (−0.17) e Å^{-3}. **29a** $C_{13}H_{21}NO$, M = 207.31, crystal dimensions 0.4 × 0.3 × 0.3 mm^3, a = 7.134(1), b = 9.402(3), c = 9.326(3) Å, α = 101.39(3), β = 98.03(2), γ = 105.46(3)°, V = 578.6(3) Å^3, ρ_{calcd} = 1.190 g cm^{-3}, μ = 5.7 cm^{-1}, Z = 2, triclinic, space group $P\bar{1}$, 2514 measured reflections ($\pm h$, $\pm k$, $\pm l$), 2363 independent and 2118 observed [$I \geq 2\sigma(I)$] reflections, 139 refined parameters, R = 0.066, wR^2 = 0.239, max. residual electron density 0.36 (−0.37) e Å^{-3}. Programs used: SHELX-86, SHELX-93, SCHAKAL-92. Further details of the crystal structure investigations may be obtained from the Fachinformationszentrum Karlsruhe, D-76344 Eggenstein-Leopoldshafen (Germany) on quoting the depository numbers CSD-401870 for **2a**, CSD-401868 for **16a**, CSD-401869 for **20**, and CSD-401867 for **29a**.

[9] A. Šilhánková, J. Lávicka, S. Kafka, M. Ferles, *Collect. Czech. Commun.* **1983**, *48*, 1435–1439.

[10] T. Nonaka, S. Miyaji, K. Odo, *Denki Kagaku* **1973**, *41*, 142–149, [*Chem. Abstr.* **1973**, *79*, 4677e].

[11] K. Jarowicki, T. Jaworski, *Monatsh. Chem.* **1984**, *115*, 605–612; J. K. Crandall, R. J. Seidewand, *J. Org. Chem.* **1970**, *35*, 697–701.

Automerizations and Isomerizations in Propynylidene (HCCCH), Propadienylidene (H_2CCC), and Cyclopropenylidene (c-C_3H_2)**

Randal A. Seburg and Robert J. McMahon*

The structure and rearrangements of triplet propynylidene (**1**, propargylene) and its derivatives remain topics of current interest.[1–8] Despite considerable experimental and theoretical effort spanning 35 years, a detailed understanding of the structure of **1** emerged only recently. Experimental[1] and theoretical[2] investigations implicate a C_2-symmetric, 1,3-diradical-like structure for **1**, rather than the linear structure concluded from early experiments[3] or the bent C_s structure predicted by other theoretical studies[4, 5] (Scheme 1). Our ^{13}C-labeling studies not

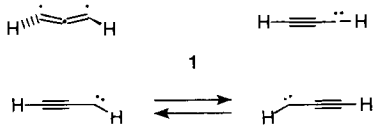

Scheme 1. Currently accepted and previously proposed structures for triplet propynylidene (**1**).

[*] Prof. Dr. R. J. McMahon, R. A. Seburg
Department of Chemistry
University of Wisconsin-Madison
Madison, WI 53706-1396 (USA)
Telefax: Int. code +(608) 265-4534

[**] This work was supported by the National Science Foundation. We acknowledge Eric V. Patterson for providing the QCISD/6-31G* calculations on triplet propynylidene.

only establish the structure of propynylidene (**1**),[1] but also provide a probe of the photochemical rearrangements on the C_3H_2 energy surface.[4a] The presence of the ^{13}C label breaks the symmetry of the system, thereby revealing a manifold of rearrangement pathways that was not evident in previous investigations. We describe here the rearrangements leading to scrambling of the ^{13}C label in isomeric C_3H_2 carbenes. The automerization of propadienylidene (**2**) can be rationalized by a mechanism involving cyclopropyne as an intermediate or transition state. Although Maier et al. recently reported evidence for a silacyclopropyne intermediate on the C_2SiH_2 energy surface,[6] our studies provide no direct spectroscopic evidence for the corresponding cyclopropyne intermediate on the C_3H_2 energy surface.

Photolysis ($\lambda > 472$ nm) of either [1-^{13}C]diazopropyne (**4a**) or [3-^{13}C]diazopropyne (**4b**), isolated in an argon matrix at 8 K, yields exclusively [1-^{13}C]propynylidene (**1a**).[1] Subsequent irradiation of **1a** at $\lambda > 237$ nm for 15.4 h results in the decrease of **1a** and the appearance of IR signals due to [2-^{13}C]propynylidene (**1b**), three ^{13}C-isotopomers of propadienylidene (**2a–c**), and two ^{13}C-isotopomers of cyclopropenylidene (**3a, b**) (Scheme 2). The photoproducts show complete scrambling of the ^{13}C label.[9] Table 1 contains both experimental and computed vibrational frequencies and intensities of the seven ^{13}C-labeled species. Assignment of the bands was made by comparison with the experimental IR spectra of unlabeled **1**, **2**, and **3**,[4a]

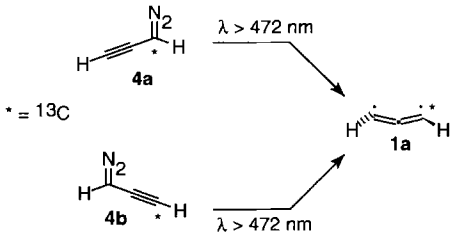

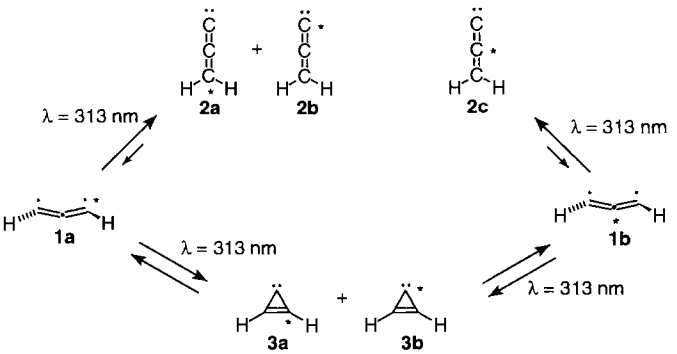

Scheme 2. Proposed mechanism for automerization of **1a** upon irradiation with $\lambda = 313$ nm.

by comparison with the calculated IR spectra of the ^{13}C-isotopomers of **1**, **2**, and **3**,[10] and by comparison with the known photochemical behavior of the unlabeled C_3H_2 isomers.[4a] Ab initio calculations at the QCISD/6-31G* level of theory yield an IR spectrum that agrees best with the spectrum of unlabeled **1** obtained experimentally;[2a] we therefore used this method to compute the IR spectra of **1a** and **1b**. The RHF/6-31G* level of theory, which reliably reproduces the IR spectra of the unlabeled singlets **2** and **3**, was used to calculate the IR spectra of **2a–c** and **3a, b**. When a matrix containing only **1a** is warmed to 37 K neither thermal automerization to **1b** nor rearrangement to any of the ^{13}C-propadienylidenes or ^{13}C-cyclopropenylidenes is observed.

Irradiation ($\lambda = 313$ nm) of a matrix containing only propynylidene **1a** leads to scrambling of the ^{13}C label in the various photoproducts. The scrambling process was monitored by IR spectroscopy. Automerization of **1a** to **1b** is evident after only 0.4 h; the absorption of **1b** grows quickly to a maximum at 3.0 h, after which its intensity decreases (Fig. 1). Propynylidenes **1a** and **1b** reach a 2:1 ratio (statistical distribution) after about 10 h. Cyclopropenylidenes **3a** and **3b** appear immediately in a 2:1 ratio (statistical distribution) and maintain the same relative

Table 1. Experimental [a] and calculated [b] IR absorptions of propynylidenes **1a, b**, cyclopropenylidenes **3a, b**, and propadienylidenes **2a–c**.

1a		**1b**		**3a**		**3b**	
exp.	calcd. [c]	exp.	calcd. [c]	exp.	calcd. [d]	exp.	calcd. [d]
3273 (10)	3424 (18)	3273 (6) [e]	3426 (6)		3108 (0)		3115 (0)
3257 (57)	3410 (29)	3265 (35)	3420 (40)		3074 (0)		3080 (0)
1612 (7)	1618 (29)	1581 (3)	1583 (28)		1563 (0)		1584 (0)
	1244 (0)		1266 (0)	1268 (100)	1267 (56)	1252 (52)	1251 (56)
547 (36)	502 (33)	549 (17) [e]	502 (35)		1054 (22)		1063 (21)
	425 (7)		418 (7)		973 (0)		979 (0)
402 (23)	413 (24)	394 (13)	407 (24)		894 (3)		889 (13)
	361 (20)		361 (6)	888 (114) [f]	892 (13)	881 (114) [f]	888 (3)
247 (100)	297 (103)	247 (38) [e]	298 (103)	781 (77) [f]	774 (25)	781 (77) [f]	776 (25)

2a		**2b**		**2c**	
exp.	calcd. [d]	exp.	calcd. [d]	exp.	calcd. [d]
	3031 (2)		3043 (2)		3043 (2)
	2962 (11)		2968 (12)		2967 (12)
1944 (81)	1944 (390)	1937 (74)	1939 (380)	1903 (100)	1903 (368)
1438 (4)	1444 (9)	1445 (15) [g]	1450 (12)	1445 (15) [g]	1452 (12)
	1100 (0)		1096 (1)		1115 (0)
993 (3)	1032 (18)	1002 (7) [g]	1042 (18)	1002 (7) [g]	1041 (18)
	1017 (3)		1025 (4)		1020 (4)
	301 (3)		299 (3)		295 (3)
	269 (0)		267 (0)		262 (0)

[a] In cm^{-1}; relative experimental intensities in parentheses; argon matrix, 8 K. [b] In cm^{-1}; absolute calculated intensities [km mol^{-1}] in parentheses; absolute intensities less than 0.5 are reported as 0. [c] QCISD/6-31G*, uncorrected. [d] RHF/6-31G*, corrected by a factor of 0.893. [e] Obtained by subtraction of the intensity due to **1a** from the total intensity of the peak. [f] Intensity is the sum of both **3a** and **3b**. [g] Intensity is the sum of both **2b** and **2c**.

 © VCH Verlagsgesellschaft mbH, D-69451 Weinheim, 1995 0570-0833/95/3418-2010 $ 10.00+.25/0

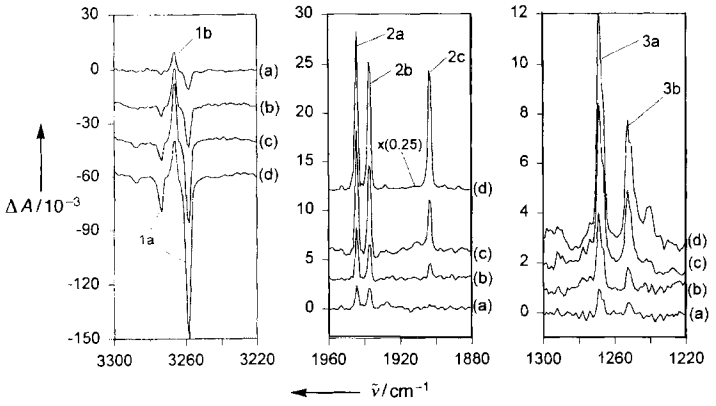

Fig. 1. IR difference spectra obtained upon photolysis (λ = 313 nm) of **1a** in an argon matrix at 8 K, showing generation of **1b**, **2a–c**, and **3a**, **b**. Irradiation time: a) 0.4, b) 1.2, c) 3.0, and d) 24.5 h. The spectra (b) through (d) are offset to facilitate viewing.

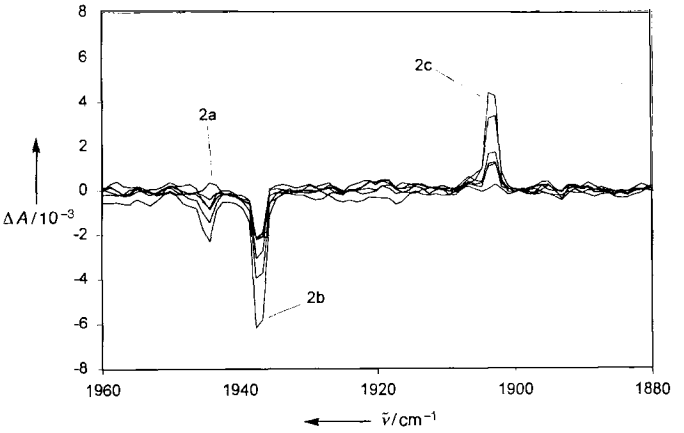

Fig. 2. IR difference spectra obtained upon irradiation (λ > 444 nm) of an argon matrix containing **1a**, **b**, **2a–c**, and **3a**, **b** (see text), illustrating automerization of **2b** and **2c**. Irradiation time: 20, 40, 50, 80, 180, and 240 min.

intensity ratio as their intensities grow during the photolysis. Their growth slows as the photolysis continues. Propadienylidenes **2a** and **2b** are also produced immediately in a 1:1 ratio and grow at the same rate. Appearance of center-labeled **2c** lags well behind **2a** and **2b**. Even after 24.5 h of irradiation, the intensity of the **2c** band at 1903 cm^{-1} has reached only about 70% of its photoequilibrium magnitude (see Table 1). Thus, photolysis of triplet propynylidene **1a** affords statistical label distribution in **3** at the earliest detection times and statistical label distribution in **1** within 10 h, yet incomplete label distribution in **2** after 76 h.

The time evolution of the photolysis (λ = 313 nm) provides information regarding the mechanism of the label scrambling, for which we suggest the mechanism shown in Scheme 2. Photolysis of triplet propynylidene **1a** affords cyclopropenylidenes **3a** and **3b** in a ratio of roughly 2:1. A hydrogen shift must accompany the formation of **3b**, although we do not know whether migration precedes or follows cyclization. Simple ring closure of **1a** followed by rapid 1,2-hydrogen shifts in the nascent **3a** accounts for statistical distribution of the ^{13}C label in **3**.[11] Once **3b** is formed, a sequence of two reversible photoequilibria serve to scramble the label rapidly into propynylidene **1b** and then slowly from **1b** into propadienylidene **2c**.[4a, b] Conversion of **1** to **2** must occur by a photochemical 1,3-hydrogen shift, since only **2a** and **2b** are formed initially from photolysis of **1a**. The third isotopomer **2c** appears only after a significant amount of **1b** is present, consistent with the proposed mechanistic scheme. Conversion of **1** to **2** is slow relative to interconversion of **1** and **3**, for **1b** appears quickly relative to **2c**, and **1a** and **1b** reach their equilibrium intensity ratio after roughly 10 h whereas the proportion of **2c** is still increasing relative to **2a** and **2b** after 76 h. In order to account for the continued growth of **2c** at long irradiation times, we postulate that **2** must return to **1** during irradiation at λ = 313 nm. This process must be very slow, since statistical distribution of the label in **2** is not reached even after 76 h.

Using different irradiation conditions, we obtain evidence for a distinct label-scrambling mechanism in ^{13}C labeled propadienylidenes **2**. At short irradiation times (8.3 h), photolysis (λ = 313 nm) of a matrix containing only **1a** produces **1**, **2**, and **3** with incomplete scrambling of the ^{13}C label in **2** (vide infra). The concentration of **2c** is only 60% of that of **2b**. Broadband irradiation (λ > 444 nm, up to 4 h) results in rapid conversion of **2b** to **2c** with virtually no change in the concentration of **2a** (Fig. 2). Control experiments impose important constraints on possible mechanisms for this automerization process. First, triplet propynylidenes **1a** and **1b** are stable to these irradiation conditions and are therefore not possible intermediates in the transformation of **2b** to **2c**. Second, the conversion of cyclopropenylidenes **3a**, **b** to propadienylidenes **2a–c** is extremely slow under these irradiation conditions. Reversible photoequilibration of **2** and **3** cannot account for the rapid changes observed for **2b** and **2c**, nor can it account for the substantial difference in disappearance rates between **2a** and **2b**. Thus, we conclude that the automerization of **2b** to **2c** does not proceed via **1** or **3** and suggest that **2b** and **2c** interconvert through a cyclopropyne (**5**) intermediate or transition state (Scheme 3). In

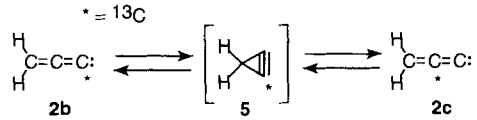

Scheme 3. Proposed mechanism for automerization of **2b** and **2c** upon irradiation with λ > 444 nm.

our experiments, no IR bands were observed that could be attributed to **5**. Theory indicates that singlet cyclopropyne is not a discrete energy minimum but a transition state approximately 40 kcal mol^{-1} higher in energy than propadienylidene (**2**).[5c, 7] The atomic motion in the vibrational mode of cyclopropyne characterized by an imaginary frequency corresponds to ring opening to **2**.[7] A second mechanism that accounts for automerization of **2b** to **2c** involves photochemical cleavage of **2b** to yield methylene and C_2 followed by rapid recombination at either end of the C_2 fragment. This process is analogous to the known fragmentation/recombination reactions that occur upon photolysis of diazomethane or ketene in low-temperature matrices.[12] It seems unlikely to us that fragmentation of **2b** would occur upon irradiation with visible light (photon energy $\leq$64 kcal mol^{-1}).

In summary, our experiments reveal two distinct photochemical processes leading to scrambling of a ^{13}C label in C_3H_2 isomers. UV photolysis (λ = 313 nm) scrambles the label during the photoisomerization of **1** to **3** (Scheme 2). Broadband visible irradiation (λ > 444 nm) scrambles the label in **2** by means of an automerization reaction (Scheme 3). Both mechanisms proceed under the conditions of broadband UV photolysis (λ > 237 nm) to produce rapid, statistical distribution of the ^{13}C label.

Experimental Procedure

[1-^{13}C]- and [3-^{13}C]diazopropyne (**4a** and **4b**, respectively) were prepared by pyrolysis of the corresponding tosylhydrazone salts. Experimental details of the syntheses of the tosylhydrazones are described in ref. [1]. The apparatus and techniques for matrix-isolation spectroscopy have been described elsewhere [13].

Received: March 10, 1995
Revised version: May 22, 1995 [Z 7784 IE]
German version: *Angew. Chem.* **1995**, *107*, 2198–2201

Keywords: automerizations · carbenes · cycloalkynes · photochemistry

[1] R. A. Seburg, J. T. DePinto, E. V. Patterson, R. J. McMahon, *J. Am. Chem. Soc.* **1995**, *117*, 835–836.
[2] a) R. Herges, A. Mebel, *J. Am. Chem. Soc.* **1994**, *116*, 8229–8237; b) the results of early STO-3G calculations also suggested a 1,3-diradical structure: W. J. Hehre, J. A. Pople, W. A. Lathan, L. Radom, E. Wasserman, Z. R. Wasserman, *ibid.* **1976**, *98*, 4378–4383.
[3] ESR experiments: R. A. Bernheim, R. J. Kempf, J. V. Gramas, P. S. Skell, *J. Chem. Phys.* **1965**, *43*, 196–200; R. A. Bernheim, R. J. Kempf, E. F. Reichenbecher, *J. Magn. Reson.* **1970**, *3*, 5–9; IR experiment: F. K. Chi, Ph.D. Dissertation, Michigan State University, **1972**.
[4] a) G. Maier, H. P. Reisenauer, W. Schwab, P. Čársky, B. A. Hess, Jr., L. J. Schaad, *J. Am. Chem. Soc.* **1987**, *109*, 5183–5188; b) G. Maier, H. P. Reisenauer, W. Schwab, P. Čársky, V. Špirko, B. A. Hess, Jr., L. J. Schaad, *J. Chem. Phys.* **1989**, *91*, 4763–4773; c) G. Maier, T. Preiss, H. P. Reisenauer, B. A. Hess, Jr., L. J. Schaad, *J. Am. Chem. Soc.* **1994**, *116*, 2014–2020; d) G. Maier, T. Preiss, H. P. Reisenauer, *Chem. Ber.* **1994**, *127*, 779–782.
[5] a) D. J. DeFrees, A. D. McLean, *Astrophys. J.* **1986**, *308*, L31–L35; b) P. Čársky, V. Špirko, B. A. Hess, Jr., L. J. Schaad, *J. Phys. Chem.* **1990**, *94*, 5493–5496; c) V. Jonas, M. Böhme, G. Frenking, *ibid.* **1992**, *96*, 1640–1648.
[6] G. Maier, H. P. Reisenauer, H. Pacl, *Angew. Chem.* **1994**, *106*, 1347–1349; *Angew. Chem. Int. Ed. Engl.* **1994**, *33*, 1248–1250.
[7] a) P. Saxe, H. F. Schaefer III, *J. Am. Chem. Soc.* **1980**, *102*, 3239–3240; b) G. Fitzgerald, H. F. Schaefer III, *Isr. J. Chem.* **1983**, *23*, 93–96.
[8] For a review of carbenes in interstellar space see: P. Thaddeus, C. A. Gottlieb, R. Mollaaghababa, J. M. Vrtilek, *J. Chem. Soc. Faraday Trans.* **1993**, *89*, 2125–2129.
[9] ESR spectroscopy provides further evidence for automerization of **1a** to **1b**. A matrix containing **1a** (Ar, 15 K, $|D/hc| = 0.641\ cm^{-1}$, $|E/hc| = 0.00130\ cm^{-1}$, hyperfine coupling constant $A_X = A_Y = 38$ G) [1] was irradiated ($\lambda > 237$ nm, 19 h; then $\lambda > 200$ nm, 7 h) to effect complete scrambling of the ^{13}C label. The signal of a second ^{13}C-propynylidene (**1b**) with the ^{13}C-hyperfine coupling constant $A_X = A_Y = 24$ G appears. Simulation [1] of the hyperfine splitting in the X_2Y_2 region of the ESR spectrum satisfactorily reproduces the experimental spectrum only when a 2:1 mixture of **1a** and **1b** is assumed.
[10] Gaussian 92, Revision A: M. J. Frisch, G. W. Trucks, M. Head-Gordon, P. M. W. Gill, M. W. Wong, J. B. Foresman, B. G. Johnson, H. B. Schlegel, M. A. Robb, E. S. Replogle, R. Gomperts, J. L. Andres, K. Raghavachari, J. S. Binkley, C. Gonzales, R. L. Martin, D. J. Fox, D. J. DeFrees, J. Baker, J. J. P. Stewart, J. A. Pople, Gaussian Inc., Pittsburgh, PA, USA, **1992**.
[11] An alternative mechanism, involving ring closure in concert with 1,2-hydrogen shift, is apparently inconsistent with the experimental observations. This mechanism predicts that **1a** should produce **3a** and **3b** in an approximate ratio of 1:1.
[12] C. B. Moore, G. C. Pimentel, *J. Chem. Phys.* **1964**, *41*, 3504–3509.
[13] R. A. Seburg, R. J. McMahon, *J. Am. Chem. Soc.* **1992**, *114*, 7183–7189, and references therein.

Synthesis of Chiral γ,δ-Unsaturated Amino Acids by Asymmetric Ester Enolate Claisen Rearrangement**

Uli Kazmaier* and Achim Krebs

The synthesis of γ,δ-unsaturated amino acids has received more attention in recent years, since some of these amino acids,[1] which also occur in nature, showed distinct antibiotic activity and could be applied as enzyme inhibitors.[2] From a point of view of the synthesis, these unsaturated amino acids are likewise of great interest, since more complex compounds may be generated readily by functionalization of the double bond.[3] Besides electrophilic and nucleophilic allylations,[4] sigmatropic rearrangements are extremely well suited for the stereoselective introduction of unsaturated side chains.[5]

As early as 1975, Steglich et al. reported the thermal Claisen rearrangement of the allylic esters of *N*-(benzoyl)-α-amino acids under dehydrating conditions via an intermediate 5-allyloxazole.[6] Owing to the highly diastereoselective course of the [3,3] sigmatropic rearrangement, brought about by a highly ordered transition state, this elegant method has found plenty of applications, especially in the synthesis of α-alkylated amino acids.[7] Bartlett et al. published their investigations on the Ireland–Claisen rearrangement[8] of allylic esters of amino acids in 1982.[9] By employing esters of chiral allylic alcohols in this rearrangement, optically active amino acids were generated under transfer of chirality. The rearrangement of chiral allylic amides gave similarly good results.[10]

Although great advances have been made in the field of asymmetric catalysis in recent years, no catalytic asymmetric version of the [3,3] sigmatropic rearrangement has been found to date. Yamamoto et al. reported for the first time a Lewis acid catalyzed asymmetric Claisen rearrangement of allylvinyl ethers by employing chiral aluminum complexes.[11] Shortly thereafter Corey et al. described an interesting asymmetric boron enolate version of the Claisen rearrangement.[12]

We recently published a new version of the ester enolate Claisen rearrangement which occurs via chelate-bridged ester enolates (Scheme 1).[13] As a result of the enolate geometry

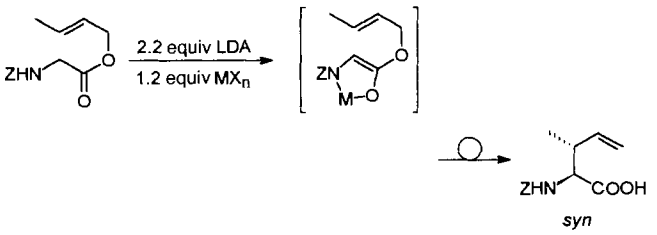

Scheme 1. Chelate-bridged ester enolate Claisen rearrangement. Z = benzyloxycarbonyl, LDA = lithium diisopropylamide.

fixed by chelation, the rearrangement proceeds with high diastereoselectivity; the chairlike transition state is clearly preferred. This rearrangement can be applied to acyclic and cyclic allylic esters[14] and even to peptides.[15] Thus unsaturated side

[*] Dr. U. Kazmaier, Dipl.-Chem. A. Krebs
Organisch-chemisches Institut der Universität
Im Neuenheimer Feld 270, D-69120 Heidelberg (Germany)
Telefax: Int. code + (6221)564205

[**] This work was supported by the Deutsche Forschungsgemeinschaft and the Fonds der Chemischen Industrie. We would like to express our gratitude to the Bayer AG as well as to Prof. G. Helmchen, Heidelberg.

chains can be introduced into peptides at a later stage. In addition to the greater reactivity of the chelate enolates in comparison with the corresponding silylketene acetals, and the fixed enolate geometry, the chelate enolate Claisen rearrangement we investigated has the advantage that it enables the possibility of coordination of chiral ligands to the chelating metal.

We report herein the first asymmetric ester enolate Claisen rearrangement of chelate-bridged enolates in the presence of chiral bidentate ligands. As a standard reaction to investigate the influence of the metal salts and ligands used, we chose the rearrangement of *N*-(trifluoroacetyl) glycine crotyl ester (Scheme 2).[1,6] Some of the results are listed in Table 1.

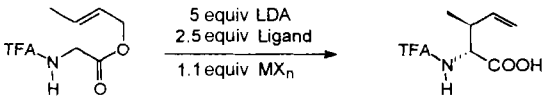

Scheme 2. Rearrangement of *N*-(trifluoroacetyl) glycine crotyl ester.

Table 1. Rearrangement of *N*-(trifluoroacetyl) glycine crotyl ester in the presence of different ligands and metal salts MX_n (see Scheme 2).

Ligand	MX_n	Yield [%]	*ds* [a] [%]	*ee* [a] [%]	Conf. [b]
(*S*)-valinol	$Al(OiPr)_3$	73	97	4	(2*R*,3*S*)
(−)-ephedrine	$Al(OiPr)_3$	70	96	27	(2*S*,3*R*)
(+)-ephedrine	$Al(OiPr)_3$	72	96	27	(2*R*,3*S*)
(−)-norephedrine	$Al(OiPr)_3$	56	96	24	(2*R*,3*S*)
quinine	$ZnCl_2$	95	90	10	(2*R*,3*S*)
quinine	$MgCl_2$	98	91	69	(2*R*,3*S*)
quinine	$CaCl_2$	73	96	65	(2*R*,3*S*)
quinine	$Al(OiPr)_3$	70	98	86	(2*R*,3*S*)

[a] Ratio determined by GLC (Chira-Si-(L)-Val). [b] Configuration determined after catalytic hydrogenation by correlation with the naturally occurring stereoisomers of isoleucine.

Thus a multitude of metal salts could be employed for the asymmetric version of the chelate enolate Claisen rearrangement; the best results were achieved by using $Al(OiPr)_3$. The selectivity and yield were significantly lower with $ClTi(OiPr)_3$ and $Ti(OiPr)_4$; the lower yield is attributed to partial transesterification reactions. Among the bidentate ligands, amino alcohols have proven to be particularly suitable, whereas diols and diamines gave no significant induction. By far the best results with regard to diastereoselectivity and enantioselectivity were achieved by using the cinchona alkaloids. Rearrangements in the presence of quinine gave the corresponding γ,δ-unsaturated amino acids in very high yields and large enantiomeric excesses. The highest enantioselectivity was found when two to three equivalents of quinine were employed. Therefore the rearrangement of a range of allylic esters under these conditions was investigated (Scheme 3, Table 2). Application of lithium hexamethyldisilazide (LHMDS) as base again led to a considerable increase in the yields.

In all cases, the observed diastereoselectivity (98% *ds*) was clearly higher than in rearrangements without addition of ligand.[1,3] The same is true with regard to the the yields. Quinine

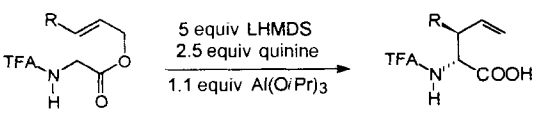

Scheme 3.

Table 2. Rearrangement of different *N*-(trifluoroacetyl)glycine allylic esters (see Scheme 3).

Ligand	R	Yield [%]	*ds* [a] [%]	*ee* [a] [%]	Conf.
quinine	H	92	–	80	(2*R*)
quinine	CH_3	98	98	86	(2*R*,3*S*)
quinine	C_2H_5	88	98	88	(2*R*,3*S*)
quinine	C_3H_7	87	98	80	(2*R*,3*S*)
quinine	$CH(CH_3)_2$	72	98	88	(2*R*,3*S*)
quinine	$C(CH_3)_3$	66	98	90	(2*R*,3*R*)
quinine	Ph	97	98	79	(2*R*,3*R*)
quinidine	CH_3	96	98	86	(2*S*,3*R*)
quinidine	Ph	95	98	82	(2*S*,3*S*)

[a] Ratio determined by GLC (Chira-Si-(L)-Val).

presumably coordinates as a bidentate ligand to the aluminum, thus leading to the liberation of 2-propanol. No induction could be observed after blocking the alcoholic moiety of quinine by acylation or alkylation. In the presence of *O*-methylquinine, the same yield and diastereoselectivity were found as in the case without ligand addition, therefore strongly indicating an absence of coordination.

The enantiomeric excess was found to lie in the range 80–90% *ee* in all cases. The introduction of sterically demanding moieties onto the allylic esters evidently raises the enantiomeric excess (see Table 2). The rearrangement in the presence of quinine gave the unnaturally configured (2*R*) amino acids. The corresponding (2*S*) derivatives were generated analogously, by using quininidine as inducing ligand. The yields and the selectivities were comparable to those achieved with quinine. Simple recrystallization with 1-phenylethyl amine afforded the optically pure amino acids.

The major advantages of this method over the classsical procedure are that the reaction is extremely simple to carry out and that the possibility exists to regenerate the chiral auxiliary. Thus, for example, the quinine employed could be recovered to more than 90% by simple extraction, especially when used on a larger scale.

Experimental Procedure

General procedure for rearrangements: LHMDS solution was prepared by adding *n*-butyllithium (1.6 mL of a 1.55 M solution in hexane, 2.5 mmol) at −20 °C under argon to hexamethyldisilazane (470 mg, 2.9 mmol) in dry THF (1.5 mL) and stirring for 20 min. The glycine ester (0.5 mmol), $Al(OiPr)_3$ (0.55 mmol), and the ligand (1.25 mmol) were dissolved under argon in dry THF, cooled to −78 °C, and the freshly prepared LHMDS solution was added slowly. The reaction mixture was allowed to warm to room temperature over 12 h. After dilution with ether (50 mL), the reaction mixture was hydrolyzed by addition of aqueous $KHSO_4$ solution (25 mL, 1 M). The organic layer was washed again with $KHSO_4$ solution (1 M), before the reaction product was extracted with saturated aqueous $NaHCO_3$ solution (3 × 25 mL). The basic solution was subsequently acidified by careful addition of solid $KHSO_4$ to pH 1 and extracted with ether (3 × 25 mL). The combined ethereal extracts were dried with Na_2SO_4 and the solvent was evaporated under reduced pressure. For the determination of the enantiomeric and diastereomeric ratios of the product, the residue was treated with diazomethane in ethereal solution. Subsequent chromatography on silica gel gave the corresponding methyl esters.

Received: May 30, 1995 [Z8041IE]
German version: *Angew. Chem.* **1995**, *107*, 2213–2214

Keywords: amino acids · asymmetric syntheses · chiral auxiliaries · enolates · rearrangements

[1] a) K. Katagiri, K. Tori, Y. Kimura, T. Yoshida, T. Nagasaki, H. Minato, *J. Med. Chem.* **1967**, *10*, 1149; b) U. Cramer, A. G. Rehfeldt, F. Spener, *Biochemistry* **1980**, *19*, 3074; c) S. Tsubotani, Y. Funabashi, M. Takamoto, S. Hakoda, S. Harada, *Tetrahedron* **1991**, *47*, 8079.

[2] a) R. L. Dennis, W. J. Plant, C. G. Skinner, G. L. Sutherland, *J. Am. Chem. Soc.* **1955**, *77*, 2362; b) J. Edelson, J. D. Fissekis, C. G. Skinner, W. Shive, *ibid.*

 © VCH Verlagsgesellschaft mbH, D-69451 Weinheim, 1995 0570-0833/95/3418-2013 $ 10.00+.25/0

1958, *80*, 2698; c) P. Shannon, P. Marcotte, S. Coppersmith, C. Walsh, *Biochemistry* **1979**, *18*, 3917; d) S. Santoso, T. Kemmer, W. Trowitzsch, *Liebigs Ann. Chem.* **1981**, 658.

[3] a) P. A. Bartlett, D. J. Tanzella, J. F. Barstow, *Tetrahedron Lett.* **1982**, *23*, 619; b) Y. Ohfune, N. Kurokawa, *ibid.* **1985**, *26*, 5307; c) N. Kurokawa, Y. Ohfune, *J. Am. Chem. Soc.* **1986**, *108*, 6041; d) Q. B. Broxterman, B. Kaptein, J. Kamphuis, H. E. Schoemaker, *J. Org. Chem.* **1992**, *57*, 6286.

[4] R. M. Williams *Synthesis of Optically Active α-Amino Acids, Organic Chemistry Series, Vol. 7*), (Eds.: J. E. Baldwin, P. D. Magnus), Pergamon, Oxford **1989**.

[5] Reviews about sigmatropic rearrangements: a) P. A. Bartlett, *Tetrahedron* **1980**, *36*, 3; b) F. E. Ziegler, *Chem. Rev.* **1988**, *88*, 1423; c) S. Blechert, *Synthesis* **1989**, 71; d) P. Wipf in *Comprehensive Organic Synthesis, Vol. 5* (Eds.: B. M. Trost, I. Fleming, L. A. Paquette) Pergamon, New York, **1991**, p. 827; e) H.-J. Altenbach in *Organic Synthesis Highlights* (Eds.: J. Mulzer, H.-J. Altenbach, M. Braun, K. Krohn, H.-U. Reissig), VCH, Weinheim, **1991**, p. 111, 116; f) S. Pereira, M. Srebnik, *Aldrichimica Acta* **1993**, *26*, 17.

[6] a) B. Kübel, G. Höfle, W. Steglich, *Angew. Chem.* **1975**, *87*, 64; *Angew. Chem. Int. Ed. Engl.* **1975**, *14*, 58; b) N. Engel, B. Kübel, W. Steglich, *ibid.* **1977**, *89*, 408 and **1977**, *16*, 394.

[7] a) J. Fischer, C. Kilpert, U. Klein, W. Steglich, *Tetrahedron* **1986**, *42*, 2063; b) K. Burger, K. Geith, K. Gaa, *Angew. Chem.* **1988**, *100*, 860; *Angew. Chem. Int. Ed. Engl.* **1988**, *27*, 848; c) A. L. Castelhano, S. Horne, G. J. Taylor, R. Billedeau, A. Krantz, *Tetrahedron* **1988**, *44*, 5451; d) L. Colombo, G. Casiraghi, A. Pittalis, *J. Org. Chem.* **1991**, *56*, 3897; e) M. W. Holladay, A. M. Nadzan, *ibid.* **1991**, *56*, 3900.

[8] R. E. Ireland, R. H. Mueller, A. K. Willard, *J. Am. Chem. Soc.* **1976**, *98*, 2868.

[9] P. A. Bartlett, J. F. Barstow, *J. Org. Chem.* **1982**, *47*, 3933.

[10] T. Tsunoda, S. Tatsuki, Y. Shiraishi, M. Akasaka, I. Sho, *Tetrahedron Lett.* **1993**, *34*, 3297.

[11] a) K. Maruoka, H. Banno, H. Yamamoto, *J. Am. Chem. Soc.* **1990**, *112*, 7791; b) K. Maruoka, H. Yamamoto, *Synlett* **1991**, 793; c) K. Maruoka, S. Saito, H. Yamamoto, *J. Am. Chem. Soc.* **1995**, *117*, 1165.

[12] E. J. Corey, D. Lee, *J. Am. Chem. Soc.* **1991**, *113*, 4026.

[13] U. Kazmaier, *Angew. Chem.* **1994**, *106*, 1096; *Angew. Chem. Int. Ed. Engl.* **1994**, *33*, 998.

[14] U. Kazmaier, *Tetrahedron* **1994**, *50*, 12895.

[15] U. Kazmaier, *J. Org. Chem.* **1994**, *59*, 6667.

[16] The trifluoracetyl group allows a simple determination of the diastereomeric and enantiomeric excess of the rearrangement products (after esterification with diazomethane) by GLC on the chiral phase Chira-Si-(L)-Val.

Synthesis of Hexagonally Packed Mesoporous TiO_2 by a Modified Sol–Gel Method**

David M. Antonelli and Jackie Y. Ying*

In 1992 researchers at Mobil first demonstrated[1, 2] that hexagonally packed, mesoporous silicate and aluminosilicate materials (MCM-41) with uniformly sized pores and surface areas approaching 1400 $m^2 g^{-1}$ could be synthesized by an micelle-assisted crystallization of the inorganic phase[3, 4] Since then there have been many unsuccessful attempts to extend this methodology to the synthesis of related transition metal oxide structures.[5, 6] Such materials would be very attractive as adsorbents and in a wide variety of catalytic processes, because the large and uniform pore sizes should lead to fast diffusion to the active sites during catalysis, even for large molecules. Most attempts aimed at synthesizing these structures have led to lamellar phases in which the surfactant and metal oxide phases are layered. Few purely transition metal based hexagonal phases have been reported.[5] However, these tungsten and antimony systems are thermally unstable and their structures collapse readily upon surfactant removal during calcination such that mesoporous hexagonal oxide phases cannot be attained. Until recently,[7, 8] the only reported example of a hexagonally packed, mesoporous material containing a transition metal is one in which a small percentage of TiO_2 has been incorporated into a silica structure.[9] Herein we report the first synthesis of a thermally stable titanium-based hexagonally packed, transition metal oxide molecular sieve (Ti-TMS1), which has been accomplished through a novel modified sol–gel process involving titanium isopropoxide bis-acetylacetonate and alkylphosphate surfactants.

Previous work demonstrated that basic hydrolysis of $Si(OEt)_4$ in the presence of 0.3–0.6 mol equivalents of alkyl(trimethyl)-ammonium bromide surfactants led to MCM-41 structures.[10] Other work showed that 1 mol% Ti could be incorporated into these structures by addition of titanium isopropoxide.[9, 11] We postulated that it would also be possible to use metal alkoxides in the presence of the appropriate surfactant to synthesize hexagonal mesoporous phases comprising purely transition metal oxides. Initial attempts at hydrolysis of titanium isopropoxide in the presence of alkyl(trimethyl)ammonium bromide surfactants at pH 8–10 produced only the TiO_2 anatase phase after calcination. Similarly, hydrolysis at lower pH with alkyl(trimethyl)ammonium bromide surfactants, or anionic sulfate, carboxylate, and phosphate surfactants gave either anatase or amorphous titania. It is known that 1 mol equivalent of acetylacetone is required in the hydrolysis of zirconium alkoxides in order to obtain stable gels.[12] In the absence of acetylacetone, gel formation was disfavored due to the rapid precipitation of oxide–alkoxide aggregates. When we employed titanium acetylacetonate tris-isopropoxide as a precursor, the desired hexagonally packed titanium oxide mesostructures (Ti-TMS1) were obtained with phosphate surfactants (10 wt%) at pH 3–6 after two days of aging at 80 °C. This strategy was successful with surfactants with phosphate head groups, but not with cationic surfactant or other anionic surfactants we tried, such as those with carboxylate or sulfate head groups.

The powder X-ray diffraction (XRD) pattern (Fig. 1a) for isolated as-synthesized Ti-TMS1 made with 0.5–1 mol equivalents of potassium tetradecylphosphate gives the expected (100)

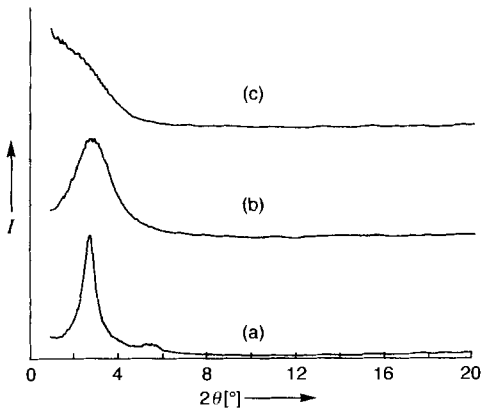

Fig. 1. XRD patterns of three samples of Ti-TMS1 prepared with tetradecylphosphate-to-titanium ratios of a) 1:1, b) 1:3, and c) 1:9. All samples were synthesized at pH = 4 with an acetylacetone-to-metal ratio of 1:1 after five days aging at 80 °C. The most distinct hexagonal crystalline pattern was associated with the sample prepared with 1:1 surfactant-to-metal ratio and had a *d* spacing for the (100) reflection at 36 Å. The (110) and (200) peaks are not clearly resolved. *I* = intensity in arbitrary units.

[*] Prof. J. Y. Ying, D. M. Antonelli
Department of Chemical Engineering, Massachusetts
Institute of Technology
Cambridge, MA 02139 (USA)
Telefax: Int. code +(617) 258-8224

[**] This work was supported by the National Science Foundation (CTS-9257223, CTS-9411901 and DMR-9400334). The authors acknowledge M. Frongillo for his assistance with the transmission electron microscopy and Dr. T. Sun for helpful discussions.

peak at a d spacing of 36 Å. No amorphous or layered phases were observed in this material. The low-intensity (110), (200), and (210) peaks became more distinct when the sample was aged for longer periods. The material isolated after only one day aging at room temperature gives a diffraction pattern in which the (100) peak is broad and the smaller peaks are not clearly distinguished. This phenomenon has been observed before in MCM-41 materials and has been attributed to either disordered packing of the individual tubes in the mesostructure[9] or very small crystallite size.

Samples of Ti-TMS1 calcined to 350 °C in air for 4 h (heating rate 1 K min^{-1}) have narrow pore size distributions as determined by N_2 adsorption (Fig. 2) and BET (BET = Brunauer-Emmett-Teller) surface areas of approximately 200 m^2 g^{-1}. This is the first example of a non-alumina or non-silica based hexagonally packed mesoporous material retaining its pore structure after surfactant removal by calcination. Although the surface area is only one-third that expected on the basis of MCM-41, taking into account the difference in molecular mass between silica and titania, we feel this process can be optimized to yield greater surface areas. When calcination is conducted in pure O_2 a light-off occurs at about 180 °C resulting in a greater degree of pore collapse as evidenced by a reduction of the BET surface area to about 100 m^2 g^{-1}. IR spectroscopic studies of the calcined material revealed a strong band at 1087 cm^{-1} indicative of the phosphate ion. This result suggests that phosphate is still present in the calcined structure. The XRD pattern of this material (Fig. 3) indicated that the diffraction intensity has diminished and the (110) and (200) reflections are no longer distinctive due to reduced crystalline domain sizes in the calcined mesostructure. Transmission electron microscopy (TEM) illustrated that there was still considerable retention of the hexagonal pore structure (Fig. 4) for the Ti-TMS1 sample calcined under O_2 at 500 °C, demonstrating the thermal stability of this material even after calcination. The domain size for hexagonally packed structures is about 100 nm. We are currently investigating the optimization of the surfactant removal step to yield materials with higher surface areas.

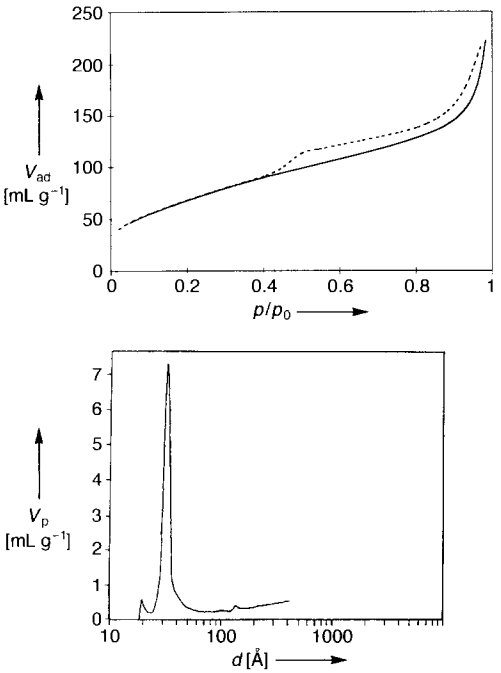

Fig. 2. Top: Nitrogen adsorption (—) desorption (- - -) isotherm for Ti-TMS1 synthesized from tetradecylphosphate after surfactant removal at 350 °C in air for four hours. The sharp decline in the desorption curve is indicative of mesoporosity, while the hysteresis between the two curves demonstrates that there is a diffusion bottleneck, possibly caused by pore damage. V_{ad} = volume adsorbed. p/p_0 = relative pressure. Bottom: BJH (BJH = Barrett-Joyner-Halenda method) desorption pore size distribution of the same sample with sharp peak at 32 Å illustrating the narrow pore size distribution and mesoporous nature of Ti-TMS1. V_p = pore volume. d = pore diameter.

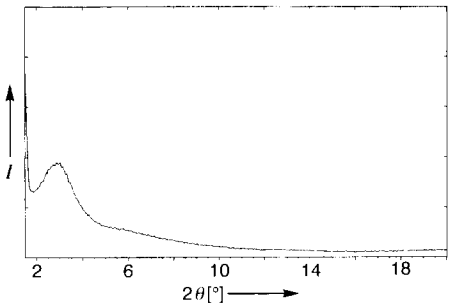

Fig. 3. XRD pattern for a sample of Ti-TMS1 synthesized from tetradecylphosphate at a surfactant:Ti ratio of 1:2 with one equivalent of acetylacetone at pH = 5 after surfactant removal at 350 °C in air for four hours. There is a considerable reduction in the intensity and sharpness of this pattern as compared to the as-synthesized sample. This is consistent with the results of nitrogen adsorption and TEM studies which reveal that there is partial loss of structure and reduction in crystalline domain size on calcination. The d spacing of the (100) reflection is centered at 34 Å as compared to 35 Å in the as-synthesized material, indicative of a small degree of pore shrinkage on thermal treatment. I = intensity in arbitrary units.

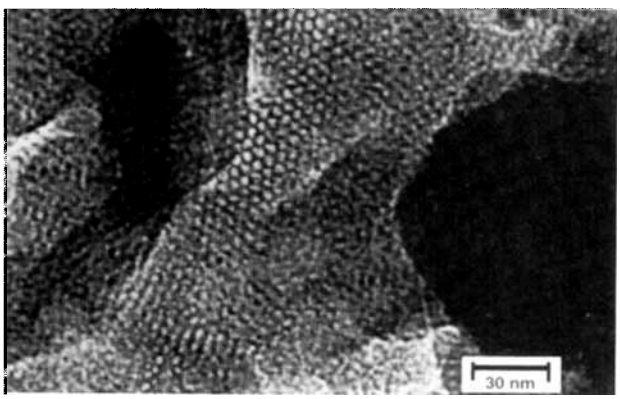

Fig. 4. TEM image of Ti-TMS1 prepared from tetradecylphosphate and calcined at 500 °C under O_2 for ten hours showing the retained 32 Å pores ordered in a hexagonal array.

A series of 120 experiments were conducted to determine the optimal pH, molar ratio of surfactant, and molar ratio of acetylacetone in the synthesis of Ti-TMS1. The pH was varied in integer steps from 2–6, the acetylacetone-to-Ti ratio was varied from 0–3 in integer steps, and the surfactant-to-Ti ratio was studied at levels of 1:9, 1:6, 1:4, 1:3, 1:2, and 1:1. In all cases, one parameter was changed while the other two were held constant. The aging temperature and time were always held at 80 °C and five days, respectively. The weight percent of surfactant used was 7–10% depending on the pH. This slight variation was necessary because the surfactant is less soluble at lower pH and higher ionic strength. In the appropriate weight percent and pH ranges, liquid crystal micelle formation for phosphates of chain length greater than 10 carbon atoms is favored.[13, 14] The quality of the materials was assessed by XRD which elucidates the presence and crystallinity of the hexagonal phase in the

as-synthesized material. The parameters that seemed most critical were the acetylacetone concentration and the surfactant-to-Ti ratio. The effect of the pH was not dramatic in the precursor compositions which favor the formation of mesostructures. The optimum surfactant-to-Ti ratio under all conditions examined was 1:1. Figure 1 shows the XRD patterns obtained for as-prepared samples synthesized with tetradecylphosphate-to-Ti ratios of 1:1, 1:3, 1:9 at pH = 4 after five days aging at 80 °C. Hexagonal structures with poorly defined XRD patterns were obtained for surfactant-to-Ti ratios of 1:2–1:4, while the materials were largely amorphous at a ratio of 1:6. At 1:9 the surfactant effect was so small that only anatase was observed at all pH and acetylacetone concentrations.

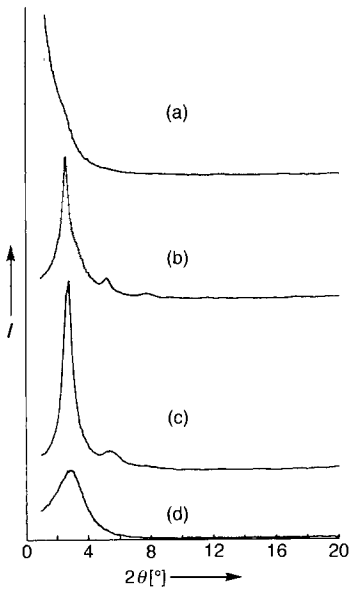

Fig. 5. XRD patterns of samples of Ti-TMS1 prepared from tetradecylphosphate at pH = 4 with a surfactant-to-Ti ratio of 1:1 at acetylacetone-to-Ti ratios of a) 0:1, b) 1:1, c) 2:1, and d) 3:1 illustrating that the optimal amount of acetylacetone is 1–2 equivalents. The (100) reflection for samples b) and c) appear at 36 Å as expected. I = intensity in arbitrary units.

The optimal molar ratio of acetylacetone to Ti was established at 1:1 as shown in Figure 5. In the absence of acetylacetone only amorphous materials or anatase were formed in all surfactant-to-Ti ratios and pH ranges. With one equivalent of acetylacetone, the results were the best at a pH of 4–6, while at two equivalents the results were best at a pH of 2–3, with precipitation time required increasing from less than five minutes to over one day. This is not unexpected since the effect of the acetylacetone is to slow down the hydrolysis. The chelating six-membered metallo-acetylacetonate ring is kinetically quite stable to hydrolysis in the absence of acid.[8] Thus, lower pH was required to promote the hydrolysis when two equivalents of acetylacetone per mol Ti were used. Since the phosphate surfactant becomes less soluble at a pH of less than 3, it is better to use a higher pH with only one equivalent of acetylacetone. In excess of three equivalents of acetylacetone, no precipitation occurred at all. This may be due to the formation of a hydrolytically inert cationic octahedral tris(acetylacetonate) complex.

The alteration of pH had little effect on the system in acetylacetone and surfactant concentration domains where Ti-TMS1 formation was favored. The main effect seemed to be one of acceleration or deceleration of the hydrolysis process. At very low pH however, there was a tapering off of the product crystallinity which may be due to protonation of the phosphate head group, reducing the strength of the interaction between the organic micellar phase and the inorganic phase. At pH values lower than 1, alkylphosphates exist almost exclusively as the dihydrogen phosphates.[13, 14] This would be expected to disfavor Ti-TMS1 formation, and in fact it does. Also, at higher basic pH where the Ti layer was expected to develop a negative charge and interact more strongly with OH^- ions than with the surfactant, no mesoporous structures were obtained. In summary, these experiments revealed that the best conditions for Ti-TMS1 synthesis were a molar ratio of surfactant-to-Ti of 1:1, a molar ratio of acetylacetone-to-Ti of 1:1, and a pH of 4–6.

In order to determine the ideal surfactant head group for the synthesis of Ti-TMS1, a series of studies were conducted with C_{14} hydrocarbons functionalized at the 1-position with trimethylammonium, sulfate, carboxylate, phosphate, amine, and acetylacetone. Two general approaches were used. The first was to dissolve the monopotassium salt of the anionic surfactant or the bromide salt of the tetradecyl(trimethyl)ammonium cation in water at a concentration above the critical micelle concentration (cmc) for that particular system followed by adjustment of the pH and addition of the Ti precursor. This room-temperature route was not applicable to the amine and acetylacetone surfactants because of the very low pK_b of the deprotonated form. The second approach involved first mixing the protic form of the anionic or neutral surfactant in ethanol with the titanium alkoxide precursor followed by hydrolysis with water of a preadjusted pH at −78 °C. This low-temperature approach was not used for tetradecylammonium bromide since it has no conjugate acid. Metal alkoxides react quickly with a wide variety of donor ligands. Thus, we would expect the precursor molecules formed in this step to have a structure in which the head group is chemically bonded to the titanium alkoxide fragment. In general, the strength of the resulting metal–ligand interaction decreases as follows: acetylacetonate > carboxylate > phosphate > sulfate. Amine ligands are difficult to place on this scale since they can form amino, amido, and imido complexes, the stability of which is largely dependent on the metal center and ancillary ligands. In all cases the surfactant-to-Ti ratio was held at 1:1. After aging at room or higher temperatures, the crystallinity of the materials was characterized by XRD (Fig. 6).

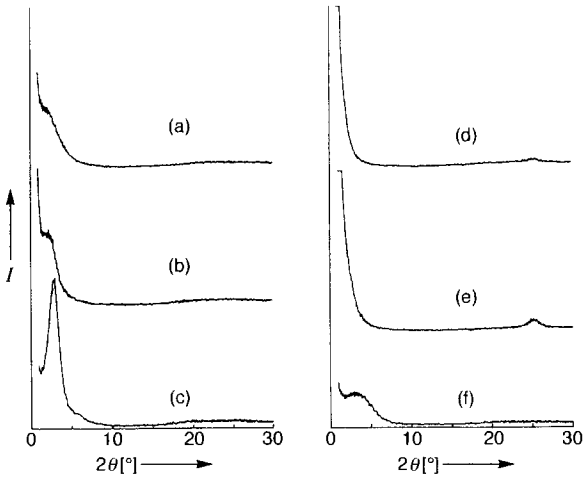

Fig. 6. XRD patterns of samples of Ti-TMS1 prepared with a surfactant chain length of 14 carbon atoms at pH = 4, 1:1 surfactant-to-Ti ratio, 1:1 acetylacetone-to-Ti ratio, and aged at room temperature for 24 h: a) Amino, b) carboxylate, c) acetylacetonate, d) sulfate, e) trimethylammonium bromide, and f) phosphate are employed as the surfactant head groups. I = intensity in arbitrary units.

Systems involving trimethyl(tetradecyl)ammonium bromide and sodium sulfate gave no mesoporous materials at pH values ranging from 2–9 under both the room-temperature and low-temperature routes. By the room-temperature route, the carboxylate system gave anatase at basic pH, but could not be extended to acidic pH because the surfactant was not very soluble under those conditions. However, by using the low-temperature route, low-crystallinity hexagonal materials were isolated after aging at room temperature for pH 4–7. Further aging at

80 °C led to phase separation and isolation of amorphous materials. The acetylacetonate-functionalized surfactant (3-tetradecyl-2,5-pentanedione) worked the best in the series studied with the low-temperature route, producing materials with broadened hexagonal patterns after one day aging at room temperature. Further heating led to the leaching away of the insoluble surfactant as a separate phase on top of the water layer. Potassium hydrogen tetradecylphosphate works almost as well as tetradecyl acetylacetone in the low-temperature preparation, but vastly surpasses the latter during the aging process. While acetylacetone is a much better ligand to the Ti ion than phosphate, the fact that the phosphate surfactant is soluble at pH 2–12 makes it possible to age these materials without phase separation induced surfactant loss from the liquid crystal phase. The materials produced by the low-temperature route are identical to those obtained by using the room-temperature route as long as KCl is added to the mixture after warming the former to room temperature. The quality of the materials obtained by the low-temperature route without any further aging follows the trend of the head group's donor abilities listed above: acetylacetonate > carboxylate > phosphate. Further aging, however, favors the phosphate system, presumably because of the solubility of the free surfactant in the supernatant. Under the conditions described the amine surfactants gave materials with weak hexagonal patterns which collapsed on aging at 80 °C.

The effects of aging temperatures and ionic strength of the medium were also investigated. In general, temperatures higher than 120 °C led to degradation of the as-synthesized material, possibly indicating low hydrothermal stability. The absence of KCl in the aging medium was found to yield poorly crystalline materials, while the presence of more than three equivalents of KCl led to formation of layered phases. For example, treatment of a 10 wt% solution of dodecyl phosphoric acid with titanium bis(acetylacetonate)isopropoxide gave only poorly crystalline materials after three days of aging at 80 °C without KCl.

In summary, the best synthesis conditions for Ti-TMS1 involve either: a) the prior addition of tetradecylphosphate to titanium acetylacetonate tris-isopropoxide, followed by hydrolysis at −78 °C and subsequent aging to 80 °C at pH 4–6 at a 1:1 surfactant-to-Ti ratio in the presence of 1 equivalent of KCl, or b) the addition of titanium acetylacetonate tris-isopropoxide to a 10 wt% solution of the monopotassium salt of the surfactant at pH 4–6 followed by aging at 80 °C for several days.

In this study we have prepared the first hexagonally packed mesoporous materials based on early transition metal oxides. The synthesis of this novel system proceeds by a modified sol–gel method. This approach should be extendable to a wide range of mesoporous and microporous materials well beyond the typical aluminosilicate based compositions. We have also reported the first examples of hexagonal mesoporous materials based on transition metal oxides which retain their pore structure on removal of surfactant by calcination. These new materials should have applications in a variety of areas, including catalysis, molecular adsorption, nonlinear optics, and thermal or acoustic insulation.

Experimental Procedure

X-ray powder diffraction data were recorded on either a Siemens D-5000 θ-θ diffractometer using Cu_{K_α} radiation and a scintillation detector at 2.2 kW or a Rigaku RU-300 θ-2θ with a rotating anode using Cu_{K_α} radiation at 10 kW. High-resolution transmission electron microscopy (TEM) images and electron diffraction patterns were obtained on a JEOL 2010 transmission electron microscope operated at 200 kV. Samples were prepared by sonication in isopropyl alcohol and suspension on carbon-coated copper grids. Nitrogen adsorption data were collected on a Micromeritics ASAP 2000 Sorption Analyzer.

In a typical preparation, tetradecylphosphate (3.75 g, 8.8 mmol) was dissolved in water (25 mL) with KOH (0.49 g, 8.8 mmol) and the pH adjusted to 5.0 with 12.5 M HCl. In a separate beaker, titanium isopropoxide (5.0 g, 8.8 mmol) was treated with acetylacetone (0.9 mL, 8.8 mmol). The solution immediately turned yellow and heat was liberated. This solution was cooled and then added to the surfactant solution with vigorous stirring. The thick yellow meringue was then aged at ambient temperature for two hours and then at 80 °C for five days. The resulting fawn powder was then collected by filtration, washed with water (3 × 100 mL) and subsequently dried in an oven at 120 °C overnight. Calcination at 350 °C in air yielded a mesoporous sample of Ti-TMS1 with 196 $m^2 g^{-1}$ surface area and a pore size of 32 Å as determined by nitrogen adsorption.

Received: May 3, 1995 [Z 7957 IE]
German version: *Angew. Chem.* **1995**, *107*, 2202–2206

Keywords: mesoporous materials · molecular sieves · sol–gel process · titanium dioxide

[1] C. T. Kresge, M. E. Leonowicz, W. J. Roth, J. C. Vartulli, J. S. Beck, *Nature* **1992**, *359*, 710.
[2] J. S. Beck, J. C. Vartuli, W. J. Roth, M. E. Leonowicz, C. T. Kresge, K. D. Schmitt, C. T-W. Chu, D. H. Olson, E. W. Shepard, S. B. McCullen, J. B. Higgins, J. L. Schlenker, *J. Am. Chem. Soc.* **1992**, *114*, 10834.
[3] C.-Y. Chen, H.-X Li, M. E. Davis, *Microporous Mater.* **1993**, *2*, 17.
[4] M. E. Davis, *Nature* **1993**, *364*, 391.
[5] a) Q. Huo, D. I. Margolese, U. Ciesla, P. Feng, T. E. Gier, P. Sieger, R. Leon, P. M. Petroff, F. Schüth, G. Stucky, *Nature* **1994**, *368*, 317; b) U. Ciesla, D. Demuth, R. Leon, P. Petroff, G. Stucky, K. Unger, F. Schüth, *J. Chem. Soc. Chem. Commun.* **1994**, 1387.
[6] Q. Huo, D. I. Margolese, U. Ciesla, D. G. Demuth, P. Feng, T. E. Gier, P. Sieger, A. Firouzi, B. F. Chmelka, F. Schüth, G. Stucky, *Chem. Mater.* **1994**, *6*, 1176.
[7] D. M. Antonelli, J. Y. Ying, *Nature*, submitted.
[8] J. Y. Ying, D. M. Antonelli, submitted patent, USA.
[9] a) A. Corma, M. T. Navarro, J. Pérez-Pariente, *J. Chem. Soc. Chem. Commun.* **1994**, 147; b) P. T. Tanev, M. Chibwe, T. J. Pinnavaia, *Nature* **1994**, *368*, 321.
[10] J. C. Vartuli, K. D. Schmitt, C. T. Kresge, M. J. Roth, M. E. Leonowicz, S. B. McCullen, S. D. Hellring, J. S. Beck, J. L. Schlenker, D. H. Olson, E. W. Sheppard, *Chem. Mater.* **1994**, *6*, 2317.
[11] P. T. Tanev, T. J. Pinnavaia, *Science* **1995**, *267*, 865.
[12] J. C. Debsikdar, *J. Non-Cryst. Solids* **1986**, 231.
[13] R. S. Cooper, *J. Am. Oil Chem. Soc.* **1963**, *40*, 642.
[14] R. S. Cooper, A. D. Urber, *J. Am. Oil Chem. Soc.* **1964**, *41*, 337.

A Facile Access to $1\lambda^5,3\lambda^5$-Benzodiphospholes

Hans Jürgen Bestmann,* Helmut Paul Oechsner, Lothar Kisielowski, Claudia Egerer-Sieber, and Frank Hampel

Dedicated to Professor Manfred Regitz on the occasion of his 60th birthday

Diphosphaheterocycles that contain a pentacoordinate and a tetracoordinate phosphorus atom as part of their PCP unit have not previously been reported. We have discovered a facile route to the first compound of this type, namely the 1,1,1,3,3-pentaphenyl-$1\lambda^5,3\lambda^5$-benzodiphospholes (**10**).

When hexaphenylcarbodiphosphorane **1**[1] is treated with halides **2**, the cationic 1,3-diphosphaallyl salts **3**[2] form. The same type of compound can be obtained if alkynyl phosphonium salts **4** are treated with phosphonium ylides **5** (except for $R^2 = R^3 = H$). The reactions probably take place via a cycloaddition intermediate, which opens to **7**.[3]

[*] Prof. Dr. H. J. Bestmann, Dr. H. P. Oechsner, Dr. L. Kisielowski, Dipl.-Chem. C. Egerer-Sieber, Dr. F. Hampel
Institut für Organische Chemie der Universität Erlangen-Nürnberg
Henkestrasse 42, D-91054 Erlangen (Germany)
Telefax: Int. code + (9131)85-6864
e-mail: bestmann@organik.uni-erlangen.de

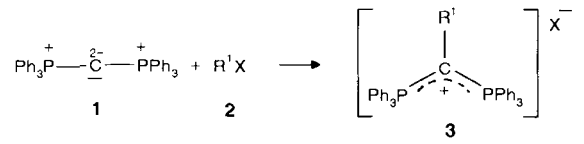

1 2 3

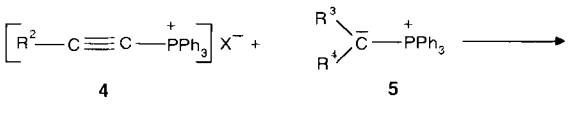

4 5

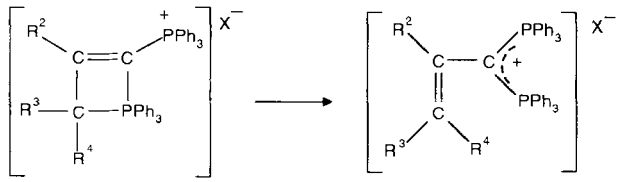

6 7

Reaction of **3** or **7** with sodium hexamethyldisilazanide (**8**) in benzene or pyridine gives 1,1,1,3,3-pentaphenyl-1λ^5,3λ^5-benzodiphospholes (**10**). The heterocyclic ring system consists of a pentacoordinated and a tetracoordinated phosphorus atom in 1, 3 juxtaposition. The carbon atom of the ligand between the two phosphorus atoms, has ylidic character.

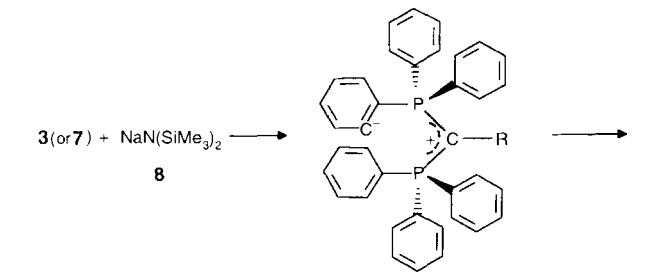

8 9

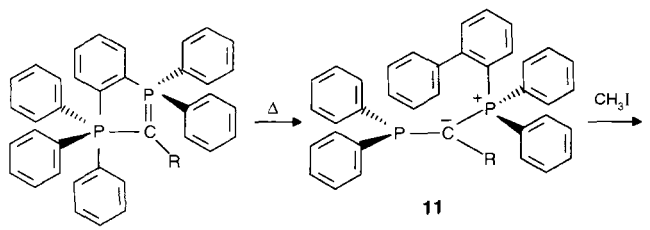

10 11

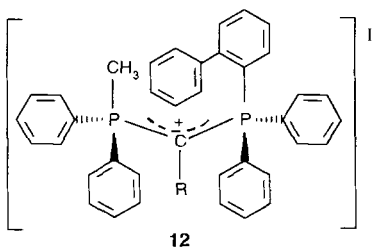

12

Apparently an ortho proton is removed from one of the six phenyl rings of **3** or **7**.[4] The resulting zwitterion **9** undergoes ring closure to create a new C–P bond (→ 10). Thus, a trigonal bipyramid is formed with a pentacoordinate phosphorus atom at its center. The rules governing attack and departure of ligands in reactions involving the mutual interconversion of tetra- and pentacoordinate phosphorus[5] predict that the incoming ligand should be located in the apical site. Pseudo rotation of the five-membered ring in a,e position should be strongly hindered, since the ylidic ligand, which serves as an electron donor, prefers an equatorial position.[6] A crystal structure analysis of **10a** (R = CH_3) was performed[7] (Fig. 1).

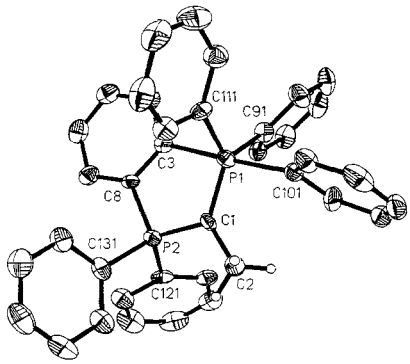

Fig. 1. Crystal structure of **10a** (R = CH_3) with selected bond lengths [pm] and bond angles [°]: C1-C2 150.9(9), C1-P1 176.2(6), C1-P2 171.7(6), P1-C3 198.8(7), P1-C111 185.1(6), P1-C91 188.6(7), P1-C101 197.7(7), C3-C8 138.5(9), P2-C8 180.0(6), P2-C131 182.1(7), P2-C121 182.5(7); P1-C1-P2 116.9(4), C1-P1-C101 90.9(3), C1-P1-C91 124.6(3), C1-P1-C111 120.3(3), C1-P1-C3 90.8(3), C91-P1-C101 88.6(3), C91-P1-C111 115.0(3), C3-P1-C111 87.2(3), C2-C1-P1 128.4(5), C2-C1-P2 89.6(3), C1-P2-C8 103.4(3), C1-P2-C131 114.6(3), C1-P2-C121 114.6(3), C8-P2-C131 110.7(3), C121-P2-C131 104.6(3), P1-C3-C8 119.9(5), P2-C8-C3 109.0(5), C3-P1-C101 178.0(3) [7].

A nearly ideal trigonal bipyramid can be detected in the molecule. As expected, the newly formed C–P bond is located in an apical position and forms part of the five-membered ring. The ylidic C atom is situated in an equatorial position.

The P1–C1 bond (1.76 Å) is considerably shorter than the two equatorial C–P bonds (1.85 and 1.88 Å). However, it is longer than the C1–P2 bond (1.72 Å). The five-membered ring is perpendicular to the equatorial plane and is distorted, as expected, but nearly flat. C2 lies in the plane of the five-membered ring (angle sum about C1 357.8°). It can be assumed that the ylidic electron pair is as π-donor perpendicular to this plane and therefore lies in the equatorial plane. This is in accord with molecular orbital calculations for the pentavalent phosphorus by R. Hoffmann et al.[6] The ^{31}P NMR spectrum shows a doublet at $\delta = -80$ to -81 for the pentacoordinate P atom of compound **10** derived from **3** and another doublet at $\delta = 10.0$ to 11.5 for the tetracoordinate P atom. The coupling constant ^2J(P,P) is 93 Hz. For **10** obtained from **7** the analogous values are $\delta = -81 - -83$ and $\delta = 3.5 - 5.5$. In these cases the coupling constants ^2J(P,P) are 94–102 Hz. Between −60 °C and +40 °C the ^{31}P NMR spectra are not temperature-dependent. In the ^{1}H NMR spectrum of **10a** the CH_3 moiety gives rise to a doublet at $\delta = 1.1$ (^2J(P,H) = 12 and 16 Hz). The signal of the C atom of the same CH_3 group is again a doublet in the ^{13}C NMR spectrum at $\delta = 12.4$ (determined from ^{31}P–^{13}C satellites). The resonance of the quaternary C atom could not be observed. Table 1 gives an overview of some of the 1λ^5,3λ^5-benzodiphospholes **10** synthesized in our group.

If **10** is heated in refluxing benzene (5 days) or toluene (8 hours), compound **11** is obtained by migration of a phenyl ring and formation of a biphenyl moiety at the ylidic P atom. The new substrate now contains a tricoordinate and tetracoordinate phosphorus atom. The latter is part of an ylide moiety.[8] Structure **11a** (R = CH_3) was confirmed by X-ray analysis.[9]

We assume that the phosphorane–phosphane rearrangement[10] follows an a,a cheletropic reaction mechanism. At the

 © VCH Verlagsgesellschaft mbH, D-69451 Weinheim, 1995 0570-0833/95/3418-2018 $ 10.00+.25/0

Table 1. Formation of $1\lambda^5,3\lambda^5$-benzodiphospholes **10a–e** from **3a–c** or **7d,e** with sodium hexamethyldisilazanide (**8**). **a**, R = CH_3; **b**, R = $CH_2C_6H_5$; **c**, R = $CH_2CH{=}CH_2$; **d**, R = (*z*)-PhC=CHPh; **e**, R = (*z*)-H_3CSC=CHPh.

Starting material	Product	Yield [%]	M.p. [°C] [a]	^{31}P NMR in $CDCl_3$ [b] $P\sigma^5$	$P\sigma^4$	J(P,P) [Hz]
3a	**10a**	75	145–147	−80.3	+11.1	94.6
3b	**10b**	80	120–122	−80.5	+11.3	94.6
3c	**10c**	95	123–126	−80.2	+10.0	93.1
7d	**10d**	81	114–116	−82.5	+4.0	102.2
7e	**10e**	67	133–135	−81.8	+5.5	102.2

[a] Decomposition. [b] δ values. σ indicates the number of bonds.

trigonal bipyramid of **10** a diaxial bond is broken, while simultaneously the *o*-biphenyl system is formed. According to R. Hoffmann[16] thermal cheletropic reactions at the pentavalent phosphorous atom that involve e,e and a,a bond breakage are allowed, while those with a,e bond cleavage are forbidden. Since we were unable to detect any biphenyl by a thermal treatment of **10**, ring strain and steric congestion at the five-membered ring in **10** might be the determining factor that steers the rearrangement exclusively into the a,a path. However, alternative mechanisms cannot be excluded. Investigations of the rearrangement by ESR spectroscopy gave no evidence for radicals.

The ^{31}P NMR spectra of the compounds **11** show two doublets with chemical shifts between $\delta = +2$ and -6 for P^{III} and $\delta = +20$ and $+27$ for P^{IV}. The geminal coupling constants ^2J(P,P) lie between 175 and 200 Hz (Table 2).

Table 2. Biphenyl-2-yl-[1-(diphenylphosphenyl)alkylidene]diphenylphosphoranes **11a–d** obtained from thermal rearrangement of **10a–d**.

Product	Yield [%]	M.p. [°C]	^{31}P NMR in $CDCl_3$ [a] $P\sigma^3$	$P\sigma^4$	J(P,P) [Hz]
11a	75	142	+2.5	+26.5	200
11b	75	155	+2.2	+26.4	179
11c	70	157	−0.2	+27.1	185
11d	82	163	−5.9	20.5	197

[a] δ values. σ indicates the number of bonds.

If a suspension of compound **10** is stirred in benzene with excess of phenol or cresol for approximately 6 days, an oil is obtained. On addition of iodomethane the cationic 1,3-diphosphaallyl salts of **3** (X = I) are recovered. Furthermore, anisol **17** is obtained; the oil is therefore assigned the structure **16**. On carrying out the reaction with hexadeuterophenol, deuterium is introduced in the *ortho* position of a phenol ring, as can be proven by FD-MS and NMR experiments (^{1}H,^{13}C coupling).

Treatment of **10** with HCl leads to a number of products that have not yet been identified. However, **3** could not be detected among them (^{31}P NMR). If **10** is treated with iodomethane, a small amount of the cationic diphosphaallyl iodide **12a** (R = CH_3) can be isolated after stirring for several days. Compound **12** also can be obtained by treatment of **11a** with iodomethane.[11] We cannot therefore conclude that formation of **16** from **10** and **13** occurs by primary elimination of a phenylic anion from the apical position. We rather tend to the view that a hexacoordinated species **14**[12] is formed, which then ring-opens with formation of a phenylic anion. This anion accepts the phenolic proton to afford **15**, which transforms into **16**.[13] On treatment of **16** with iodomethane, **3** (X = I) and anisole **17** are obtained.

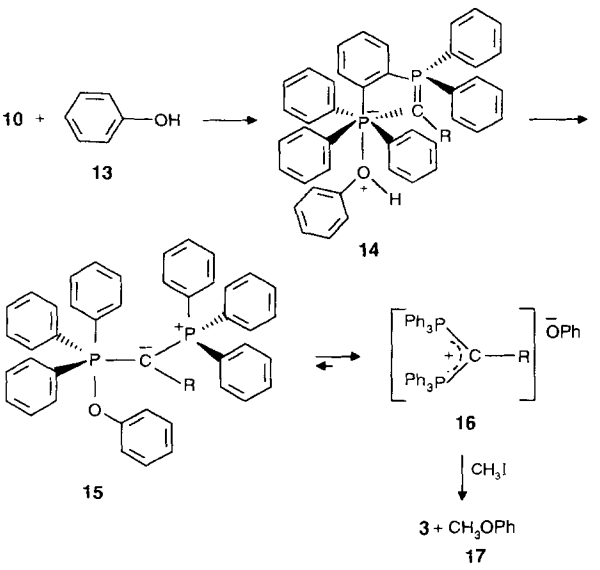

Experimental Procedure

Synthesis of **10**: **8** (510 mg, 2.8 mmol) and **3** or **7** (2.0 mmol) were dissolved in dry pyridine (8 mL). After stirring for six days with exclusion of light the product was filtered off, rinsed with 2 portions each of dry pyridine (5 mL) and dry petroleum ether (5 mL), and dried under high vacuum for 24 h at room temperature.

Received: April 12, 1995 [Z 7888 IE]
German version: *Angew. Chem.* **1995**, *107*, 2186–2188

Keywords: benzodiphospholes · diphosphaallylic cations · phosphorus compounds · rearrangements

[1] F. Ramirez, N. B. Desai, B. Hansen, N. McKelvie, *J. Am. Chem. Soc.* **1961**, *83*, 3539–3540; see also H. Schmidbaur, *Nachr. Chem. Tech.* **1979**, *27*, 620.
[2] H. J. Bestmann, H. P. Oechsner, *Z. Naturforsch. B* **1983**, *38*, 861–865.
[3] H. J. Bestmann, L. Kisielowski, *Tetrahedron Lett.* **1990**, *23*, 3301–3304.
[4] For *o*-metalation of phosphonium salts phosphinimines and phosphonium ylides, see D. Seyferth, M. A. Eisert, J. K. Heeren, *J. Organomet. Chem.* **1964**, *2*, 101–108; G. Wittig, G. Geissler, *Justus Liebigs Ann. Chem.* **1953**, *580*, 44–57; H. Hoffmann, *Chem. Ber.* **1962**, *95*, 2563–2566; J. C. Baldwin, W. C. Kaska, *Inorg. Chem.* **1979**, *18*, 686–691; C. G. Stuckwisch, *J. Org. Chem.* **1976**, *41*, 1173–1178; B. Schaub, T. Jenny, M. Schlosser, *Tetrahedron Lett.* **1984**, *25*, 4097–4100; B. Schaub, M. Schlosser, *ibid.* **1985**, *26*, 1623–1626.
[5] D. Marquarding, F. Ramirez, I. Ugi, P. Gillespie, *Angew. Chem.* **1973**, *85*, 99–127; *Angew. Chem. Int. Ed. Engl.* **1973**, *12*, 91–119.
[6] R. Hoffmann, J. M. Howell, E. L. Muetterties, *J. Am. Chem. Soc.* **1972**, *94*, 3047–3058.
[7] X-ray structure analysis of **10a** (R = CH_3): $C_{38}H_{32}P_2$; M = 550.58; triclinic; space group P1; a = 9.007(5), b = 11.51(7), c = 16.234(9) Å, α = 71.40(5), β = 109.68(3), γ = 85.01(5)°; V = 1581(2) Å^3; Z = 2, ρ_{calcd} = 1.131 Mgm^{-3}, F(000) = 556, T = 200(2) K. Collection of data was obtained on an automatic Nicolet R3mV diffractometer, with graphite monochromated $Mo_{K\alpha}$ radiation (λ = 0.71073 Å) in the range $4.0° \le 2\theta \le 52.0°$; ω scan method (6552 reflections were measured; of these 6210 were independent and 2902 with $I > 2\sigma(I)$). The structure was solved by direct methods with SHELXTL Plus V4.11. The parameters were refined with full-matrix least squares on F^2 using SHELXL 93, G. M. Sheldrick, Göttingen 1993. All non-hydrogen atoms were refined anisotropically. The hydrogen atoms were fixed in idealized positions with the riding model; 389 refined parameters; R-values $R1$ = 0.0931 ($I > \sigma(I)$), $wR2$ = 0.4148 (all data) with $R1 = \sum|F_o - F_c|/\sum F_o$ and $wR2 = \sum w\sigma|(F_o^2 - F_2^2)^2|/\sum w^{0.5}$; maximum/minimum final difference map: 0.893/−0.671 e Å^{-3}. Further details of the crystal structure analysis are available on request from the Director of the Cambridge Crystallographic Data Centre, 12 Union Road, GB-Cambridge CB2 1EZ, by quoting the full journal citation.
[8] [1-(diphenylphosphenyl)alkylidene]triphenylphosphoranes have been synthesized from [alkylidene]triphenylphosphoranes and diphenylchlorophosphane by transylidation: K. Issleib, R. Lindner, *Liebigs Ann. Chem.* **1966**, *699*, 40–52.

[9] Since the X-ray structural analysis doesn't show any exceptional features, it hasn't been depicted; see F. Hampel, H. J. Bestmann, H. P. Oechsner, C. Egerer-Sieber, *Zeitschr. für Kristallographie*, in press.
[10] D. Hellwinkel, W. Lindner, *Chem. Ber.* **1976**, *109*, 1497–1505.
[11] m.p. 143 °C; ^{1}H NMR (400 MHz, [D$_1$] $CHCl_3$, 31 °C, TMS): $\delta = 1.6$ (dd, appears as t, $^3J(P,H) = 15$ Hz, 3H, (CH_3)), 1.65 (dd, $^2J(P,H) = 12$ Hz, $^4J(P,H) = 1.5$ Hz, 3H, PCH_3); ^{13}C NMR (125 MHz, [D$_1$] $CHCl_3$, 31 °C, TMS): $\delta = 0.5$ (dd, appears as t, $^1J(P,C) = 119$ Hz, 1C, PCP), 14.5 (dd, $^1J(P,C) = 60$ Hz, $^3J(P,C) = 5$ Hz, 1C, Ph_2P-CH_3), 16.5 (dd, $^2J(P,C) = 4.6$ and 1.5 Hz, 1C, CCH_3); ^{31}P NMR (162 MHz, [D$_1$] $CHCl_3$, 31 °C, H_3PO_4): $\delta = 24.3$ (dd, $^2J(P,P) = 55$ and 101 Hz, 2P, PCP).
[12] See F. Ramirez, K. Tasaka, N. B. Desai, C. P. Smith, *J. Am. Chem. Soc.* **1968**, *90*, 751–755; D. Hellwinkel, *Top. Curr. Chem.* **1983**, *109*, 1–64.
[13] See H. Schmidbaur, H. Stühler, W. Buchner, *Chem. Ber.* **1973**, *106*, 1238–1250.

Octathioporphyrazine Crown Ethers: An Octanuclear Ag^I Complex with Coordination in the *meso* Pocket**

John W. Sibert, Steven J. Lange, Charlotte L. Stern, A. G. M. Barrett,* and Brian M. Hoffman*

Porphyrazines (tetraazaporphyrins) and porphyrins are related by the isoelectronic replacement of the *meso* CH unit in the latter with the *meso* N atom in the former (Scheme 1).[1] This

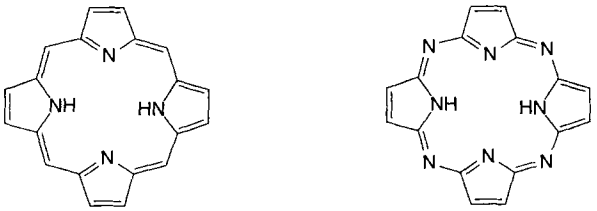

Scheme 1.

replacement influences the binding of a metal ion in the central cavity.[2] However, it has not been widely recognized that the *meso* N atoms' lone-pair electrons, which are in the plane of the macrocycle and directed away from it, potentially can coordinate to additional metal ions at the macrocycle's periphery. We recently reported the first structurally characterized example displaying this behavior, a peripherally metalated porphyrazine where each *meso* N atom of porphyrazineoctathiolate acts together with its two nearby peripheral S atoms to function as a tridentate "*meso*-pocket" ligand that binds a dialkyltin molecule.[3] Because the metal-binding capabilities of the thiolato sulfur atoms are strong, it was by no means clear that coordination by the *meso* N atom made a major contribution to the binding. This is now shown to be the case for the remarkable peripheral ligation of eight silver(I) ions by an octakis(alkylthio)-tetraazaporphyrin containing four crown ether units, in which both crown ether and *meso*-pocket coordination is exhibited.[4]

We[5] and others[6] have reported on the synthesis and coordination chemistry of crown ether derivatives ("oxa-crowned" derivatives) of dithiomaleonitrile (for example, **1** and **2** in Scheme 2). The mix of soft sulfur and hard oxygen donor atoms

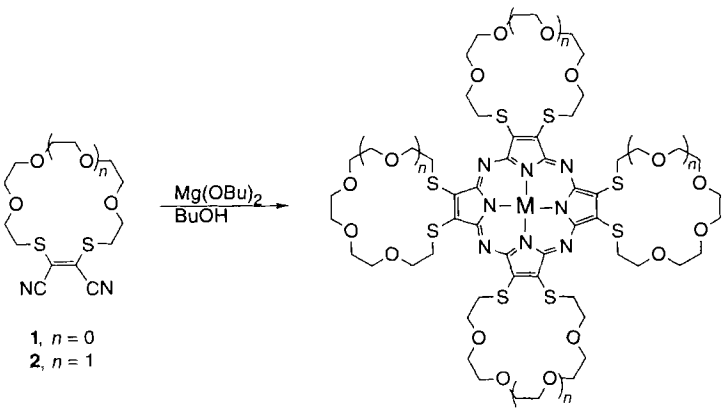

Scheme 2. Synthesis of the porphyrazine crown ethers **3**–**10**.

renders these crown ethers particularly well suited for the ligation of heavy metal ions; endocyclic complexes of $HgCl_2$,[5a] and Ag^I,[5b] and exocyclic complexes of PdX_2 (X = Cl, Br),[6a] are known. In addition to being ligands themselves, **1** and **2** are the direct precursors to oxa-crowned octakis(alkylthio)tetraazaporphyrins.[4, 7]

The oxa-crowned porphyrazines were synthesized by the Mg^{II} template cyclization of the appropriate crowned derivative of dithiomaleonitrile as described (Scheme 2).[8] Consistent with the work of Linstead and co-workers for the synthesis of octamethyltetraazaporphyrin,[9] we obtain the highest yields for the preparation of the Mg^{II} porphyrazines **3** and **7** (about 35%) using butanol as the reaction medium. van Nostrum et al. reported yields of 20–22% for a similar synthesis of **3** and **7** in propanol.[7] Treatment of the Mg-porphyrazines with trifluoroacetic acid provided the metal-free porphyrazines **4** and **8**. Subsequent reaction with $Ni(OAc)_2$ or $Cu(OAc)_2$ in chlorobenzene/DMF (5/1) quantitatively produced the corresponding centrally metalated porphyrazines (**5**, **9** and **6**, **10**; see Table 1 for the characterization).

Preliminary studies of the binding of Ag^I, $HgCl_2$, $CdCl_2$, and Pb^{II} to the periphery of **5** dissolved in chloroform/methanol (3/1) solutions employed UV/Vis spectroscopy. Reactions with $HgCl_2$ and $CdCl_2$ caused the precipitation of compounds that could not be sufficiently purified. No evidence for complexation with Pb^{II} was observed. However, the addition of a large excess of $AgBF_4$ led to significant color changes, from blue to greenish-blue, that could be monitored.[10] The spectrum of the parent compound **5** has strong π–π^* absorptions at 326 and 672 nm and an n–π^* transition at 485 nm that involves the peripheral S atoms.[11] The color change upon addition of Ag^I ions corre-

[*] Prof. Dr. A. G. M. Barrett
Department of Chemistry
Imperial College of Science, Technology and Medicine
South Kensington, GB-London SW72AY (UK)
Telefax: Int. code + (171) 59-45805
e-mail: barrett@ic.ac.uk
Prof. Dr. B. M. Hoffman, Dr. J. W. Sibert, S. J. Lange, C. L. Stern
Department of Chemistry, Northwestern University
Evanston, IL 60208 (USA)
Telefax: Int. code + (708) 491-7713
e-mail: bmh@mercury.chem.nwu.edu

[**] This work was supported by the National Science Foundation (CHE-9408561).

Table 1. Analytical (elemental analysis), spectroscopic (UV/Vis, ^{1}H NMR), and mass spectrometric data (HR-FAB-MS) for compounds **4**–**6**, **8**–**10**, and [**11**·8 BF_4].

Compound	Elemental analysis [%] [a]			λ_{max} [nm] [b]	δ [c]		*m/z* [a]
	C	H	N		CH_2O	CH_2S	
4	48.14 (47.91)	5.69 (5.53)	8.90 (9.32)	346, 502, 644, 716	3.54 (32H, m) 3.93 (16H, t)	4.21 (16H, t)	1203.280 (1203.264)
5	44.89 (45.13) [d]	5.13 (5.21)	8.90 (8.78)	326, 485, 672	3.58 (32H, m) 3.94 (16H, t)	4.20 (16H, t)	1259.186 (1259.184)
6	43.94 (44.96) [d]	4.62 (5.19)	7.88 (8.74)	348, 498, 676			1264.182 (1264.178)
8	48.20 (48.75)	6.05 (6.00)	7.86 (8.13)	356, 504, 643, 716	3.62 (48H, m) 4.01 (16H, t)	4.31 (16H, t)	1379.367 (1379.369)
9	46.38 (46.85)	5.57 (5.62)	7.69 (7.81)	324, 342 (sh), 486, 671	3.61 (48H, m) 3.94 (16H, t)	4.19 (16H, t)	1435.294 (1435.289)
10	46.21 (46.69)	5.84 (5.60)	7.57 (7.78)	356, 495, 614 (sh), 672			1440.275 (1440.283)
11	19.36 (19.50) [e]	2.48 (2.57)	3.69 (3.25)	333, 605 (sh), 664			

[a] Theoretical values are given in parentheses. [b] Compounds **4**–**6**, **8**–**10** in chloroform, [**11**·8 BF_4] in methanol. [c] The chemical shifts of the internal NH protons for **4** and **8** are $\delta = -2.31$ and -2.18, respectively. [d] Analysis of the monohydrate. [e] The analytical and crystallographic data for the two crystalline forms of [**11**·8 BF_4] are consistent with ten Ag^I ions, of which eight are directly coordinated to the porphyrazine, and four water molecules per molecule.

sponded to the disappearance of the transition at 485 nm and sharpening (but not shifts) in the $\pi-\pi^*$ transitions.

The absence of the $n-\pi^*$ transition indicates that the Ag^I ions coordinate to the peripheral S donor atoms. The small changes in the $\pi-\pi^*$ transitions are unlike those observed for the *meso*-coordinated tin adduct of porphyrazineoctathiolate. In the latter case the Soret band is shifted out of the visible region of the spectrum, presumably as a result of the stabilization of the a_{1u} molecular orbital through coordination to the *meso* N atoms. *Thus, in solution* **5** *appears to coordinate* Ag^I *ions through the crown moieties alone without participation of the meso* N atoms.

Slow evaporation in the dark of a chloroform/methanol solution containing **5** and an excess of $AgBF_4$ produced complex **11**

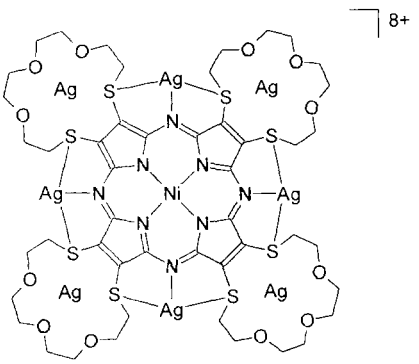

11

as blue crystals with a red reflex in two distinct morphologies (needles and cubes). The analysis of both types of crystals indicates more than eight Ag^I ions per porphyrazine. Importantly, when only eight or fewer equivalents of $AgBF_4$ were added to **5**, no crystalline product was obtained.

X-ray diffraction studies on [**11**·8 BF_4][12, 13] yield the first structural characterization of a crowned porphyrinic macrocycle incorporating metal ions in the crowns. They disclose a far more interesting situation than inferred from the behavior in solution: a crystal having the needle morphology[12] has not four, but eight Ag^I ions coordinated to the periphery of the porphyrazine (Fig. 1).[14] Four Ag^I ions are coordinated in an endocyclic fashion by the crown moieties, consistent with the

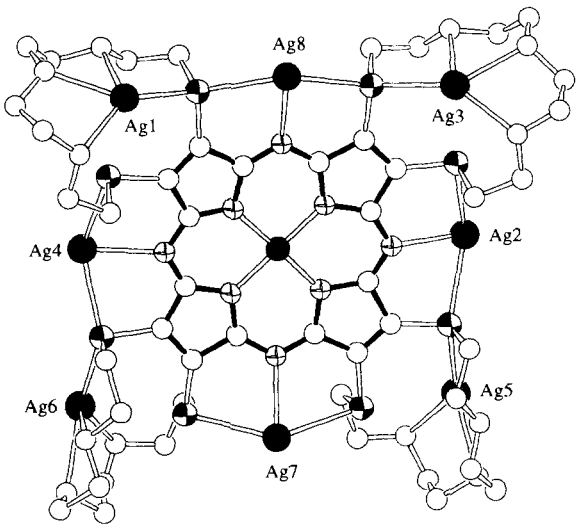

Fig. 1. X-ray structure of the porphyrazine cation **11** with all other atoms of the complex [**11**·8 BF_4] removed for clarity.

inferences based on optical spectra of solutions. However, four additional Ag^I ions occupy the *meso* pockets and undergo tridentate, S-N-S coordination by the peripheral thioether S and the *meso* N atoms (the coordination sphere of these Ag^I ions is completed by O atoms from solvent). The lack of evidence for *meso* coordination in solution suggests a preference for the ligation of Ag^I by the crown moieties of **5**.

As shown in Figure 2a, each of the four Ag^I ions in the crown subunit is coordinated by one S atom (average distance 2.55(1) Å; range 2.50(1)–2.60(1) Å), and all three macrocyclic O atoms (average distance 2.52(3) Å; range 2.39(3)–2.69(3) Å). In addition there is a weaker interaction with the remaining S donor atom (average 2.98(1) Å; range 2.95(1)–3.04(1) Å). The Ag–S and Ag–O bond lengths are typical and similar to those in the related Ag^I complexes of macrocycles **1**, **2**,[15b] and 1,4-dithia-7,10,13-trioxacyclopentadecane.[15] Each of the four Ag^I ions in the *meso* pockets is coordinated unsymmetrically by the two S donor atoms (Fig. 2b). The short Ag_{meso}–S bond lengths average 2.69(1) Å (range 2.65(1)–2.74(1) Å), whereas the long Ag_{meso}–S bond lengths average 2.81(1) Å (range 2.71(1)–

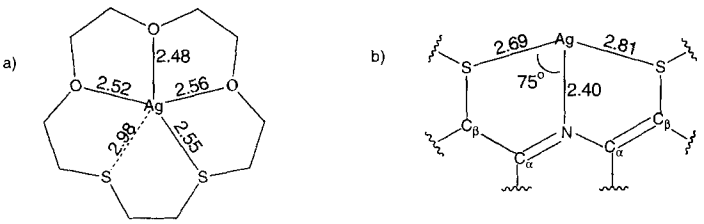

Fig. 2. Coordination geometry about Ag^{I} ions in the crown ether units (a) and in the *meso* pockets (b) of the porphyrazine cation **11**. The average bond lengths are given in angstroms.

2.88(1) Å). The Ag–N_{meso} bonds are slightly longer (average 2.40(3) Å; range 2.37(3)–2.43(3) Å), though similar to those reported for Ag–N(pyridine) bonds.[16]

The ability of S-appended porphyrazines to coordinate metal ions in two distinct binding sites is due to the flexibility of the C_{β}–S bond. This flexibility can be gauged by examining the "bite" distance between the two S atoms on each pyrrole unit. In the tin-capped porphyrazine octathiolate, a purely *meso*-coordinated complex, the S···S distance is 3.74 Å. This distance decreases to 3.25 Å in the nickel-capped porphyrazine octathiolate, a complex exhibiting the classic bidentate "dithiolene" coordination of a Ni^{II} ion by both S atoms on each pyrrole ring.[17] An intermediate value for the S···S separation might be expected for **11**, because it contains both types of bonding in the same molecule, and such is the case. The average S···S distance in **11** is 3.58 Å (range 3.57–3.60 Å), comparable to that in an octathiomethylporphyrazine (S···S = 3.53 Å) with no peripherally coordinated metal ions.[3b]

As first seen with the tin-capped porphyrazine octathiolate, heteroatoms at the β positions of the pyrrole ring can function together with the *meso* N atom to form a tridentate binding pocket that readily accepts metal ions. This is now found to be true in both thiolate- and thioether-appended porphyrazines, thus establishing that porphyrazines should not be viewed simply as modified porphyrins, but as a discrete class of molecules with its own unique properties. We anticipate that a rich chemistry with *meso*-pocket coordination will grow from the study of functionalized porphyrazines.

Experimental Procedure

4: A suspension of magnesium turnings (30 mg; 1.23 mmol) in butanol (8–10 mL) was heated at reflux for 24 hours with iodine as an initiator. To the resulting magnesium butoxide suspension was added solid **1** (1.0 g; 3.3 mmol). The solution rapidly turned yellow, then green and, after several minutes, settled at a deep blue color. The reaction was kept at reflux under a nitrogen atmosphere for 18 h. The butanol was then removed under reduced pressure, and the residue taken up in chloroform and filtered. The filtrate was passed through a silica column (5% CH_3OH in $CHCl_3$ as eluent) to afford the Mg-porphyrazine **3**, which was used without further purification. Compound **3** was dissolved in neat trifluoroacetic acid (10 mL) and stirred at room temperature for 1 h. The solution was poured over ice and neutralized with ammonium hydroxide. The resulting precipitate was filtered and washed with water and methanol. Column chromatography on silica (3% CH_3OH in $CHCl_3$) produced pure **4** as a blue solid: yield 35–40% (based on **1**). Porphyrazine **8** was prepared from crown ether **2** by an identical procedure.

5 (M = Ni) and **6** (M = Cu): The 21*H*,23*H*-porphyrazine **4** (150 mg) and a large excess of $M(OAc)_2$ (M = Ni or Cu) were added to a mixture of chlorobenzene/DMF (5/1; 10 mL). The reaction was heated to 100 °C under a nitrogen atmosphere and stirred for 18 h. The solvent was then removed under reduced pressure, and the solid residue washed with methanol and filtered. The product was isolated in nearly quantitative yield following column chromatography on silica (3% CH_3OH in $CHCl_3$). Porphyrazines **9** and **10** were prepared from **8** by an identical procedure.

11: To a solution (chloroform/methanol 3/1, 50 mL) of **5** (40 mg) was added $AgBF_4$ (> 10 equiv). The color of the solution immediately changed from blue to greenish-blue. Slow evaporation of the solvent in the dark produced **11** as blue crystals with a red sheen.

Received: May 2, 1995 [Z 7952 IE]
German version: *Angew. Chem.* **1995**, *107*, 2173–2176

Keywords: coordination · crown ethers · porphyrazines · silver compounds

[1] *Phthalocyanines: Properties and Applications* (Eds.: C. C. Leznoff, A. B. P. Lever), VCH, New York, **1989**.
[2] See, for example, J. P. Fitzgerald, B. S. Haggerty, A. L. Rheingold, L. May, G. A. Brewer, *Inorg. Chem.* **1992**, *31*, 2006.
[3] a) C. S. Velazquez, W. E. Broderick, M. Sabat, A. G. M. Barrett, B. M. Hoffman, *J. Am. Chem. Soc.* **1990**, *112*, 7408; b) C. S. Velazquez, G. A. Fox, W. E. Broderick, K. A. Andersen, O. P. Anderson, A. G. M. Barrett, B. M. Hoffman, *ibid.* **1992**, *114*, 7416.
[4] Preliminary accounts of this work: a) J. W. Sibert, S. J. Lange, C. Stern, B. M. Hoffman, A. G. M. Barrett, *Abstr. Pap. Am. Chem. Soc. 206th National Meeting* (Chicago, IL) **1993**, INOR 60; b) A. G. M. Barrett, presented at the Macrocycles Group Meeting of the Royal Society of Chemistry (UK), University of Warwick, UK, **1994**.
[5] a) J. W. Sibert, S. J. Lange, C. Stern, B. M. Hoffman, A. G. M. Barrett, *J. Chem. Soc. Chem. Commun.* **1994**, 1751; b) J. W. Sibert, S. J. Lange, B. M. Hoffman, D. J. Williams, A. G. M. Barrett, *Inorg. Chem.* **1995**, *34*, 2300.
[6] a) H.-J. Holdt, *Pure Appl. Chem.* **1993**, *65*, 477; b) H.-J. Holdt, J. Teller, *Z. Chem.* **1988**, *28*, 249.
[7] C. F. van Nostrum, F. B. G. Benneker, N. Veldman, A. L. Spek, A.-J. Schouten, R. J. M. Nolte, *Recl. Trav. Chim. Pays-Bas* **1994**, *113*, 109.
[8] C. J. Schramm, B. M. Hoffman, *Inorg. Chem.* **1980**, *19*, 383.
[9] M. E. Baguley, H. France, R. P. Linstead, M. Whalley, *J. Chem. Soc.* **1955**, 3521.
[10] van Nostrum et al. noted changes in the visible spectrum of **7** upon addition of up to six equivalents of Ag^{I} ions per porphyrazine. They ascribe the uptake of more than four equivalents of Ag^{I} to dimerization caused when the metal ions are sandwiched between neighboring porphyrazines [7].
[11] P. Doppelt, S. Huille, *New J. Chem.* **1990**, *14*, 607.
[12] Crystal data: triclinic, space group $P\bar{1}$ (no. 2), $a = 15.377(8)$, $b = 17.685(6)$, $c = 19.002(7)$ Å, $\alpha = 104.94(3)$, $\beta = 95.57(4)$, $\gamma = 99.71(4)°$, $V = 4867(8)$ Å^3, $Z = 2$, $\rho_{calcd} = 2.161$ g cm^{-3}, $\mu(Mo_{K\alpha}) = 4.20$ cm^{-1}. A blue, platelike crystal ($0.48 \times 0.14 \times 0.02$ mm) was mounted on an Enraf-Nonius CAD-4 diffractometer with graphite monochromated $Mo_{K\alpha}$ radiation ($\lambda = 0.71069$ Å). Data collection at $T = -120$ °C, ω–θ scan, $2\theta_{max} = 45.9°$, 14110 measured reflections, 13512 unique ($R_{int} = 0.065$), of which 6424 with $I > 3\sigma(I)$ were used in all calculations. An analytical absorption correction was applied which resulted in transmission factors ranging from 0.74 to 0.96. The data were corrected for Lorentz and polarization effects. The structure was solved by direct methods (SHELXS-86) and refined by the full-matrix least-squares technique (Texsan 5.0). The Ag, Ni, S, and O atoms were refined anisotropically; the remaining atoms were refined isotropically. The residual electron density was not completely modeled. The positions of the porphyrazine atoms and the peripheral coordination of eight silver ions are unambiguous. The highest peak in the final difference Fourier map was 2.90 e Å^{-3}. At final convergence, $R = \sum||F_o| - |F_c||/\sum|F_o| = 0.109$, $R_w = [(\sum w(|F_o| - |F_c|)^2/\sum wF_o^2)]^{1/2} = 0.136$ for 632 parameters. Further details of the crystal structure investigation are available on request from the Director of the Cambridge Crystallographic Data Centre, 12 Union Road, GB-Cambridge CB21EZ (UK) on quoting the full journal citation.
[13] Crystals having cubic morphology have also been isolated. Crystal data: cubic, $a = b = c = 30.200(5)$ Å.
[14] Additional Ag^{I} ions, not bonded to the porphyrazine, are cocrystallized in the lattice.
[15] A. J. Blake, G. Reid, M. Schröder, *J. Chem. Soc. Chem. Commun.* **1992**, 1074.
[16] Recent examples a) G. Smith, A. N. Reddy, K. A. Byriel, C. H. L. Kennard, *Polyhedron* **1994**, *13*, 2425; b) S. O. Sommerer, B. L. Westcott, K. A. Abboud, *Acta Crystallogr. Sect. C* **1994**, *50*, 48; c) H. Adams, N. A. Bailey, D. E. Fenton, Y.-S. Ho, *Inorg. Chim. Acta* **1993**, *212*, 65.
[17] C. S. Velazquez, T. F. Baumann, M. M. Olmstead, H. Hope, A. G. M. Barrett, B. M. Hoffman, *J. Am. Chem. Soc.* **1993**, *115*, 9997.

Routes to Dendritic Networks: Bis-Dendrimers by Coupling of Cascade Macromolecules through Metal Centers**

George R. Newkome,* Ralf Güther, Charles N. Moorefield, Francesca Cardullo, Luis Echegoyen, Eduardo Pérez-Cordero, and Heinrich Luftmann

The chemistry of cascade molecules (or dendrimers)[1] has allowed the construction of macromolecular assemblies possessing vast numbers of precisely juxtaposed nuclei by the iterative connection of multifunctional building blocks. A notable feature of the dendritic method is the ability to control spatial or topological relationships between similar and dissimilar macromolecular subunits incorporated into a branched polymeric framework. Consequently, this controlled synthesis of branched (or linear) macroassemblies has potential in such areas of supramolecular chemistry as molecular devices[2] and molecular information processing.[3] Thus, the potential creation of precisely ordered dendritic "superclusters" or "networks"[4] has provided the impetus for the investigation of definite dendritic conjointment. Reports of contructing cascade molecules by connecting preconstructed dendrimers as macroassembly subunits include the random, nonspecific linking of "starburst dendrimers" to yield "starburst polymers"[5] and the highly branched poly(arylamide) polymers.[6] Specific connectivity is noted in the connection of dendritic wedges with both ends of polyethylene glycol or polyethylene oxide producing polyethereal copolymers,[7] in the trapping of living polystyrene to afford linear - globular ABA copolymers,[8] and in the attachment of dendrimers to a polyfunctional core.[9, 10, 11]

We now report the ruthenium-mediated assembly of a novel series of well-defined cascade macroassemblies[12] possessing maximal $1 \rightarrow 3$ branching multiplicity at a carbon atom. The use of a ruthenium(II) metal center (**<Ru>**)[13] allowed the formation of stable complexes between the discrete terpyridine receptor units attached to different cascade macromolecules. Since the proof of the structure of specific organic networks is often difficult, the use of metal spacers will help to establish the network patterns. The electrochemical results presented here for the complexes, when compared to those of several model systems, clearly establish the presence of the **<Ru>** center bound to two O-substituted terpyridine ligands. These results, coupled with the other spectroscopic evidence and the synthetic strategy utilized, confirm the presence of the bis-dendrimers. Used in this fashion, electrochemical results become useful tools for rapid assessment of the structure of nanoscopic complex formation.

[*] Prof. G. R. Newkome, Dr. R. Güther, Dr. C. N. Moorefield, F. Cardullo
Center for Molecular Design and Recognition
Department of Chemistry
University of South Florida, Tampa, FL 33620-5250 (USA)
Telefax: Int. code + (813)974-1733

Prof. L. Echegoyen, E. Perez-Cordero
University of Miami (USA)

Dr. H. Luftmann
Westfälische Wilhelms-Universität, Münster (Germany)

[**] Chemistry of Micelles, Part 49. These results were first presented, in part, at the Royal Society of Chemistry International Symposium on "Recognition Processes" held in Birmingham, England, July 24–29, 1994. This work was supported by the National Science Foundation (G.R.N.: DMR-92-17331, 92-08925; L.E.: DMR-91-19986, CHE-93-13018), the U.S. Army Office of Research (G.R.N.: DAAH04-93-0048), and the Petroleum Research Fund administered by the American Chemical Society, (G.R.N.: PRF 26365-AC7,3; L.E.: PRF 27827-AC1), as well as by Engelhard Industries (gift of metals). R. G. thanks the Alexander-von-Humboldt-Stiftung for the Feodor Lynen fellowship. We also thank Prof. E. Constable (Basel) for his invaluable discussions and Dr. G. R. Baker and G. H. Escamilla for their time preparing the computer graphics.

The second-tier, metal-cascade molecule **9 < Ru** (Scheme 1) was prepared in the following manner: 4'-chloro-2,2':6'2''-terpyridine[14] (**3**) and 1-hydroxydodecanoic acid (**1**) were converted with KOH in DMSO into the terpyridinecarboxylic acid **4**. Peptide-type coupling of **4** with amine **6** under standard conditions[15] led to triester **7a**, which was readily hydrolyzed to the corresponding polyacid **7b**. Repetition of the amide coupling gave the well-defined nonaester **9**. Treatment of **7a** and **9** with $RuCl_3 \cdot 3H_2O$ generated the desired Ru-containing cascades (**7a<Ru** and **9<Ru**), as microcrystalline, paramagnetic, orange-brown complexes. Because of their paramagnetic nature, definitive NMR spectra could not be obtained, but elemental analysis and MALDI-TOF mass spectra support the desired structures. The series of receptor cascades was similarly synthesized by utilizing a shorter connecting moiety, for example 1-hydroxybutyric acid monosodium salt (**2**), and treating it with **3** to afford the terpyridinecarboxylic acid **5** as the core precursor. Subsequent repetitive amidation and hydrolysis procedures, as described above, gave the first, second, third, and fourth generation receptor cascades **8**, **10**, **11**, and **12**, respectively (Schemes 1 and 2). ^1H and ^{13}C NMR spectra and correct ele-

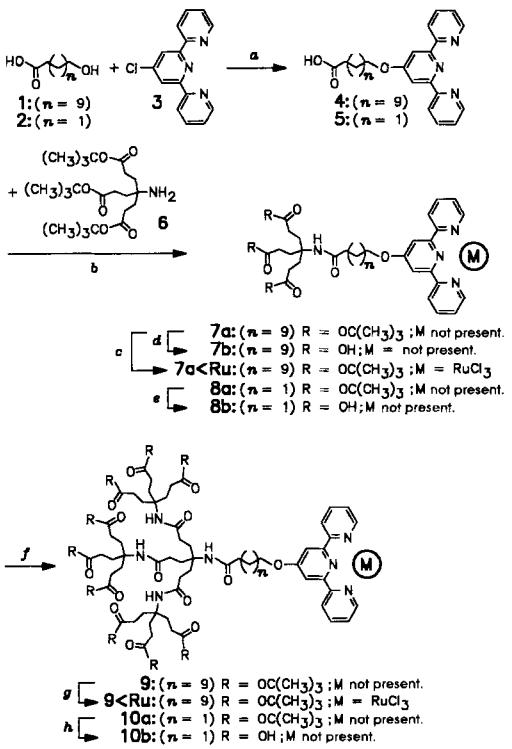

Scheme 1. Synthesis of the donor and receptor cascades. a) KOH/DMSO, 24 h, 65 °C, **4**: 82%; **5**: 58%; b) *N,N*-dicyclohexylcarbodiimide (DCC)/1-hydroxybenzotriazol (1-HBT), 24 h, room temperature (RT), **7a**: 58%; **8a**: 60%; c) $RuCl_3 \cdot H_2O$, EtOH, 24 h, reflux, **7a<Ru**: 78%; **9<Ru**: 80%; d,e) HCO_2H, 24 h, RT, **7b**,**8b**: 98%; f) DCC/1-HBT, 24 h, RT, **9**: 58%; **10a**: 52%; g) $RuCl_3 \cdot H_2O$, EtOH, 24 h, reflux, 78%; h) HCO_2H, 24 h, RT, **10b**: 98%.

mental analysis of the higher generations **11** and **12** support the structure of the cascade molecules. MALDI-TOF mass spectra[16] of the second generation **10a** gave the correct molecular peak ($[M + H^+]$ *m/z* 1758; $[M + Na^+]$ *m/z* 1780). In the mass spectra of the third and the fourth generation **11a** and **12**, fragmentation was observed. The spectrum of **11a** showed several fragmentation peaks in addition to a broad peak near the expected molecular peak. Only fragmentation peaks (from 6500 to

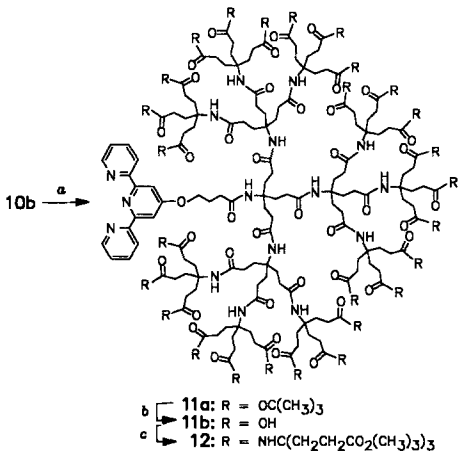

Scheme 2. Synthesis of the higher generations of the receptor cascade. a) DCC/1-HBT, 24 h, RT, **11a**: 58%; b) HCO_2H, 24 h, RT, **11b**: 98%; c) DCC/1-HBT, 24 h, RT, **12**: 58%.

11200 amu) were observed in the spectra of **12**; however, the observed chemical and spectral properties as well as other analytical data confirm the desired structure.

The complementary metallo-donor and receptor cascade macromolecules were readily connected by a single Ru^{II} center. This coupling was performed in MeOH with 4-ethylmorpholine[17] as the reducing agent, and, in each case, afforded the resultant red, crystalline bis-dendrimer complex with the general formula (***X*<Ru>*Y***;[18] Scheme 3). Five different Ru complexes were synthesized with either **7a<Ru>** or **9<Ru>** and receptors **8a**, **10a**, **11a**, and **12**. Evidence for complexation was provided by NMR and UV spectroscopy, elemental analysis, and electrochemistry data. The ^{13}C NMR spectra proved the most useful for structure verification; for example, the NMR spectrum of complex **9<Ru>10a** combines the characteristic signals of both cascade parts at $\delta = 27.91$ ($C(CH_3)_3$), 57.47, 57.65 (C-quat.), 69.11, 70.37 (CH_2Otpy), 80.46 ($C(CH_3)_3$) 172.83 ($CO_2C(CH_3)_3$), as well as the significant doubling of all the terpyridine signals, due the dissymmetry of the two terpyridine moieties. The characterization of complex **9<Ru>12** was, however, difficult with NMR techniques because of the presence of the 90 *tert*-butyl groups, which masked the signals of the internal terpyridine unit. The UV spectra were consistent with complex formation: the electronic spectra of all ***X*<Ru>*Y*** complexes in MeCN showed exactly the same characteristic MLCT transitions in the visible region at 486 nm. The absorption maximum at 394 nm for **9<Ru>** is also distinctive. The MALDI-TOF mass spectrum of **9<Ru>10a** gave the correct mass with the highest intensity for the $[M + Na^+]$ peak. In the mass spectra of **9<Ru>11a**, a small parent peak at the correct mass can be observed, as well as several fragmentation peaks (around 2200 for the metal-donor cascade part and from 3400 to 5100 for the receptor cascade part). The Ru complexes appear to be unstable under the conditions used for MALDI-TOF spectrometry.

The Ru–terpyridine redox-active centers of these bis-dendritic complexes are readily probed with electrochemical techniques.[19] Both terpyridine-based cathodic cyclic voltammetry (CV) as well as Ru-based anodic CV are presented in Figure 1. These results were obtained with a glassy carbon working electrode for 1 mM solutions of the complex in acetonitrile containing 0.1 M tetrabutylammonium hexafluorophosphate ($TBAPF_6$) as supporting electrolyte.

Figure 1a depicts the cyclic voltammogram of the simplest member (**7a<Ru>8a**) of this bis-dendrimer family. Both the cationic and anionic scans yield electrochemically and chemically reversible processes. The two electron transfer steps in the cathodic scan correspond to the two terpyridine ligands. The Ru^{2+}/Ru^{3+} couple seen on the anodic scan is also chemically reversible, as evidenced by the i_C/i_A ratio, and electrochemically quasi-reversible with $\Delta E_{pp} =$ 76 mV (Table 1). The complex **7a<Ru>8a** thus displays the expected electrochemistry. There is a slight splitting of the anodic wave corresponding to the second cathodic process, which is not currently well understood but ascribed to an electrode surface effect.

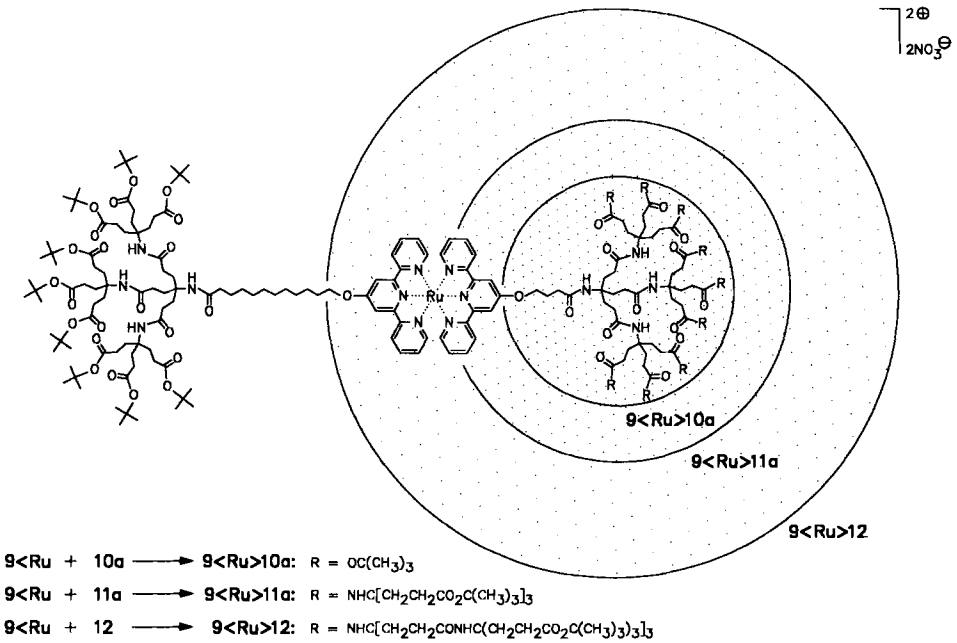

Scheme 3. Synthesis of the bis-dendritic metal complexes. 4-Ethylmorpholine, EtOH, 1.5 h at reflux. Yields: **9<Ru>10a**: 65%; **9<Ru>11a**: 61%; **9<Ru>12**: 63%.

Although the steric hindrance around the redox active centers increases in going from **7a<Ru>8a** to **9<Ru>10a** (Fig. 1b), hardly any difference is observed in the corresponding cathodic electrochemistry (Table 1). However, the Ru^{2+}/Ru^{3+} couple exhibits a larger ΔE_{pp}, indicative of slower electron transfer than for **7a<Ru>8a**. Nevertheless, the overall difference in electrochemical behavior between these 1:1- and 2:2-tier complexes is negligible.

In going from the **9<Ru>10a** (2:2 tier) to **9<Ru>11a** (2:3 tier) the redox couples remain electrochemically and chemically reversible except for the first cathodic couple (Fig. 1c). Thus,

Table 1. Peak potentials, E_c and E_a, ΔE_{pp} and $E_{1/2}$ values [mV] for the complexes studied in 0.1 M nBu$_4$PF$_6$/CH$_3$CN [a].

Complex [b]	Oxidation				Reduction							
	$E_a(1)$	$E_c(1)$	ΔE_{pp}	$E_{1/2}$ [c]	E_a [c]	$E_c(1)$	ΔE_{pp}	$E_{1/2}(1)$	$E_a(2)$	$E_c(2)$	ΔE_{pp}	$E_{1/2}(2)$
a) **7a⟨Ru⟩8a** (1:1)	+747	+672	76	+709	−1701	−1772	71	−1736	−1885	−1969	84	−1927
b) **9⟨Ru⟩10a** (2:2)	+791	+650	140	+721	−1699	−1774	75	−1737	−1892	−1972	80	−1932
c) **9⟨Ru⟩11a** (2:3)	+757	+675	82	+716	−1693	−1810	117	−1751	−1893	−1971	78	−1932
d) **7a⟨Ru⟩12** (1:4)	+880	+520	360	+700	−1659	−1863 [d]	204	−1761	−1859 [c]	−2026	167	−1942
e) **9⟨Ru⟩12** (2:4)	+1089 [c]	+532	557	+810	-	−1712 [d]	-	-	-	−1977	-	-

[a] F_c/F_c^+ as internal standard. [b] a)–e): see Fig. 1. Numbers in parentheses refer to the number of generations in the components of the cascade molecule. [c] Inflection point. [d] Very poorly defined.

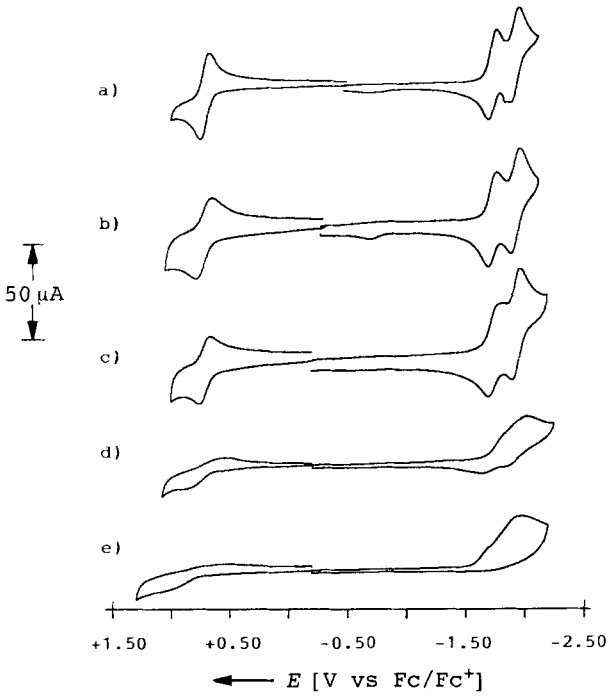

Fig. 1. Cyclic voltammograms of a) **7a<Ru>8a**; b) **9<Ru>10a**; c) **9<Ru>11a**; d) **7a<Ru>12**; and e) **9<Ru>12**. Numbers in parentheses indicate the ratio of the number of tiers in the two dendrimer components. All voltammograms were obtained from MeCN/100 mM TBAPF$_6$ at a scan rate of 100 mV s^{-1}, with a glassy-carbon working electrode, a Pt counter electrode, and a Ag wire pseudo-reference electrode. The potential is referred to the internally added ferrocene/ferrocenium (Fc/Fc^+) couple.

even though the steric hindrance has increased considerably at this stage, there is still a high degree of permeability for electron transfer to and from the redox centers. However, for the first time electrochemical irreversibility is detected for this first cathodic couple, with a $\Delta E_{pp} = 117$ mV. The second cathodic process remains electrochemically quasi-reversible and chemically reversible.

Drastic irreversible behavior first becomes evident for the more sterically congested 1:4-tiered complex **7a<Ru>12** (Fig. 1d). All redox couples exhibit electrochemically irreversible behavior and, more importantly, for the first time in the series there is evidence of chemical irreversibility. This is clear from the small currents upon scan reversal, both for cathodic as well as anodic waves. The wave exhibiting the largest ΔE_{pp} is the Ru^{2+}/Ru^{3+} couple, at 360 mV. Interestingly, the $E_{1/2}$ values for the three couples remain essentially constant relative to those of the 1:1-, 2:2-, and 2:3-tiered complexes (Table 1). This is in contrast to the recent report by Diederich et al.[20] on potential shifts for zinc porphyrin dendrimers upon successive generation buildup. These authors also observed increased chemical irreversibility as the steric hindrance increased, although they did not mention this explicitly in their work. Since the intervening chemical groups in their systems are nearly the same as those reported here, it is interesting to note this difference in the electrochemical behavior as the dendrimer generation increases; potential shifts could also possibly reflect the difference in counterion penetration in the various dendrimer generations.

Completely irreversible behavior is clearly seen (Fig. 1e) for **9<Ru>12** (2:4). Since it was difficult to measure peak potentials for any of the processes upon scan reversal, no ΔE_{pp} values are reported in Table 1. Note that the peak potential of the

Table 2. Selected physical data of the compounds **9**, **11a**, **12**, **9<Ru>10a**, **9<Ru>11a**.

9: $C_{103}H_{165}N_7O_{23}$; ^{1}H NMR (250 MHz, $CDCl_3$): δ = 1.24 (brs, CH_2; 12H), 1.37 (s, $C(CH_3)_3$; 81H), 1.40 (m, CH_2; 2H), 1.53 (m, CH_2; 2H), 1.78 (m, CH_2; 2H), 1.90 (m, CCH_2; 24H), 2.12 (m, CH_2CO; CCH_2CH_2, m; 26H), 4.15 (t, CH_2Otpy; 2H), 6.07 (brs, NH; 3H), 7.25 (td, J = 6 Hz, 1.2 Hz, C^5H; 2H), 7.46 (brs, NH; 1H), 7.77 (td, J = 8 Hz, 1.8 Hz, C^4H; 2H), 7.94 (s, C^3H; 2H), 8.55 (dm, J = 8 Hz, C^3H; 2H), 8.62 (d, J = 5 Hz, C^6H; 2H); ^{13}C NMR (62.9 MHz, $CDCl_3$): δ = 25.68 (CH_2), 25.83 (CH_2), 27.94 (27$C(CH_3)_3$), 28.92 (CH_2), 29.24 (2CH_2), 29.27 (2CH_2), 29.45 (2CH_2), 29.68 (12CH_2), 29.75 (6CH_2), 31.68 (3CH_3), 31.98 (3CH_2), 37.36 (CH_2CO), 57.29 (3C-quat.), 57.33 (C-quat.), 68.08 (CH_2Otpy), 80.39 (9$OC(CH_3)_3$), 107.26 ($C^{3'}$), 121.17 (C^3), 123.59 (C^5), 136.59 (C^4), 148.85 (C^6), 156.06 (C^2), 156.88 ($C^{2'}$), 167.20 ($C^{4'}$), 172.53 (9$CO_2C(CH_3)_3$), 172.77 (3CON), 173.54 (CON).

11a: $C_{257}H_{428}N_{16}O_{78}$; ^{1}H NMR (250 MHz, $CDCl_3$): δ = 1.40 (s, $C(CH_3)_3$; 243H), 1.88, 2.10 (br, CH_2; 160H), 4.20 (CH_2Otpy; 2H), 6.0–6.8 (br, NH; 13NH), 7.23 (t, C^5H; 2H), 7.76 (t, C^4H; 2H), 7.98 (s, $C^{3'}$H; 2H), 8.54 (d, C^3H; 2H), 8.61 (d, C^6H; 2H); ^{13}C NMR (62.9 MHz, $CDCl_3$): δ = 24.84 (CH_2), 27.94 (81$C(CH_3)_3$), 29.83 (CH_2), 31.30 (CH_2), 34.56 (CH_2CO), 57.20, 57.92 (13C-quat.), 67.41 (CH_2Otpy), 80.18 (9$OC(CH_3)_3$), 107.34 ($C^{3'}$), 121.07 (C^3), 123.59 (C^5), 136.49 (C^4), 148.49 (C^6), 155.92 (C^2), 156.94 ($C^{2'}$), 166.92 ($C^{4'}$), 172.24 (3CON), 172.53 (27$CO_2C(CH_3)_3$), 172.88 (9CON); correct C,H,N analysis.

12: $C_{743}H_{1205}N_{43}O_{213}$; (250 MHz, $CDCl_3$): δ = 1.38 (s, $C(CH_3)_3$; 729H), 1.88, 2.10 (br, CH_2; 484H), 4.20 (CH_2Otpy; 2H), 6.0–7.0 (br, NH; 40NH), 7.2 (br, C^5H; 2H), 7.75 (br, C^4H; 2H), 7.90 (br, C^3H; 2H), 8.50 (br, C^3H; 2H), 8.58 (br, C^6H; 2H); ^{13}C NMR (62.9 MHz, $CDCl_3$): δ = 25.34 (CH_2), 27.99 (243$C(CH_3)_3$), 29.62 (CH_2), 30.94 (CH_2), 31.30 (CH_2), 33.49 (CH_2CO), 57.19, 57.94 (40C-quat.), 67.57 (CH_2Otpy), 80.09 (81$OC(CH_3)_3$), 107.46 ($C^{3'}$), 121.20 (C^3), 123.72 (C^5), 136.61 (C^4), 148.98 (C^6), 155.88 (C^2), 156.98 ($C^{2'}$), 166.90 ($C^{4'}$), 172.56 (40CON; 81$CO_2C(CH_3)_3$); correct C,H,N anylysis.

9⟨Ru⟩10a: red microcrystalline powder, $C_{198}H_{314}N_{16}O_{52}Ru$; ^{1}H NMR (250 MHz, $CDCl_3$): δ = 1.35 (s, $C(CH_3)_3$; 81H), 1.38 (s, $C(CH_3)_3$; 81H), 1.1–1.6 (brm, CH_2; 20H), 1.90 (br, CCH_2; 48H), 2.18 (br, CH_2CO; CCH_2CH_2, m; 52H), 4.5 (brm, CH_2Otpy; 4H), 6.2–6.8 (br, NH; 8H), 7.0–8.8 (m, tpy-H; 20H); ^{13}C NMR (62.9 MHz, $CDCl_3$): δ = 25.67 (CH_2), 27.91 ($C(CH_3)_3$), 28.60 (CH_2), 29.16 (CH_2), 29.68 (CH_2), 31.58 (CH_2), 32.19 (CH_2), 37.15 (CH_2CO), 57.47, 57.65 (C-quat.), 69.11, 70.37 (CH_2Otpy), 80.46 ($OC(CH_3)_3$), 110.84, 111.42 ($C^{3'}$), 124.49, 124.94 (C^3), 127.26, 127.61 (C^5), 137.62, 137.98 (C^4), 151.58, 152.07 (C^6), 155.88, 155.99 (C^2), 157.92, 158.38 ($C^{2'}$), 165.90, 166.10 ($C^{4'}$), 172.83 ($CO_2C(CH_3)_3$), 173.09, 173.46 (CON); MALDI-TOF-MS: m/z 3878.4 (M + Na)

9⟨Ru⟩11a: red microcrystalline powder, $C_{360}H_{593}N_{25}O_{107}Ru$; ^{1}H NMR (250 MHz, $CDCl_3$): δ = 1.35 (s, $C(CH_3)_3$; 243H), 1.38 (s, $C(CH_3)_3$; 81H), 1.9 (br, CCH_2), 2.2 (br, CCH_2), 4.5 (br m, CH_2Otpy), 6.2–6.8 (br, NH), 7.0–8.8 (brm, tpy-H; 20H); ^{13}C NMR (62.9 MHz, CD_3CN): δ = 28.42 ($C(CH_3)_3$), 30.2 (br, CH_2), 32.0 (br, CH_2), 58.0 (C-quat.), 80.78 ($OC(CH_3)_3$), 112–167 (C-tpy), 173.56 ($CO_2C(CH_3)_3$); correct C,H,N analysis; MALDI-TOF-MS: m/z 6966 (M − 2HNO_3)

oxidation of the Ru^{2+} center is much more positive than that of the other complexes, but the peak reduction potentials remain remarkably constant. However, what is clear is that the electrochemical processes are chemically irreversible, showing almost no perceptible return upon scan reversals. There is only a hint of a return cathodic wave for Ru^{3+}/Ru^{2+} at + 0.532 V, but none could be detected upon anodic reversal after reduction of the terpyridines.

The reason for the observed chemically irreversible voltammetric responses is currently not well understood. It is possible to speculate that, due to the increased steric hindrance for **9**<**Ru**>**12**, either reduction or oxidation leads to sufficient destabilization. These redox processes occur in the vicinity of the metal center and could result in decomposition of the complex. Such a redox-driven "unlocking" of a complex could form the basis for a reversible formation–decomposition mechanism. This possibility, as well as the full characterization of the redox products, are currently under intense investigation.

In summary, this construction concept allows the synthesis of specific polymacrocascade networks, as well as the incorporation of metal receptor units on or at a precise depth inside the macromolecule, to be controlled. We confirmed earlier that it is possible to encapsulate relevant molecules[21] randomly within a lipophilic region or to bind them covalently at a specific locus in the interior of cascades.[22] We now demonstrate the application of directed complex formation to generate the first stages in the construction of dendritic networks through metal-centered connectivity.

Received: April 19, 1995 [Z 7905 IE]
German version: *Angew. Chem.* **1995**, *107*, 2159–2162

Keywords: dendrimers · electrochemistry · macromolecules · ruthenium compounds

[1] Recent reviews: C. N. Moorefield, G. R. Newkome in *Advances in Dendritic Macromolecules, Vol. 1* (Ed.: G. R. Newkome), JAI Press, Greenwich, CT, **1994**, p. 1; D. A. Tomalia, A. M. Naylor, W. A. Goddard III, *Angew. Chem.* **1990**, *102*, 119; *Angew. Chem. Int. Ed. Engl.* **1990**, *29*, 138; J. Issberner, R. Moors, F. Vögtle, *ibid.* **1994**, *106*, 2507 or **1994**, *33*, 2413; H. B. Mekelburger, W. Jaworek, F. Vögtle, *ibid.* **1992**, *104*, 1606 or **1992**, *31*, 1571; J. M. J. Fréchet, C. J. Hawker, K. L. Wooley, *J. Macromol. Sci. A* **1994**, *31*(11), 1627.

[2] J. M. Lehn, *Angew. Chem.* **1988**, *100*, 91; *Angew. Chem. Int. Ed. Engl.* **1988**, *27*, 89; J. S. Lindsey, *New J. Chem.* **1991**, *15*, 153; D. Philp, J. F. Stoddart, *Synlett* **1991**, 445.

[3] J. M. Lehn, *Angew. Chem.* **1990**, *102*, 1347; *Angew. Chem. Int. Ed. Engl.* **1990**, *29*, 1304.

[4] The term "network" as used in this communication refers to the specific connection of multiple dendritic macroassemblies and not a single branched structure commonly known as a dendrimer.

[5] D. A. Tomalia, H. Baker, J. Dewald, M. Hall, G. Kallos, S. Martin, J. Roeck, J. Ryder, P. Smith, *Polymer J.* **1985**, *17*, 117.

[6] "Rigid Polymer Networks": S. M. Aharoni, S. F. Edwards, *Adv. Polym. Sci.* **1994**, *118*, 117; S. M. Aharoni, US-A 249992, **1992**.

[7] I. Gitsov, K. L. Wooley, J. M. J. Fréchet, *Angew. Chem.* **1992**, *104*, 1282; *Angew. Chem. Int. Ed. Engl.* **1992**, *31*, 1200; I. Gitsov, K. L. Wooley, C. J. Hawker, P. T. Ivanovo, J. M. J. Fréchet, *Macromolecules* **1993**, *26*, 5621.

[8] I. Gitsow, J. M. J. Fréchet, *Macromolecules* **1994**, *27*, 7309.

[9] K. L. Wooley, C. J. Hawker, J. M. J. Fréchet, F. Wudl, G. Srdanov, S. Shi, C. Li, M. Kao, *J. Am. Chem. Soc.* **1993**, *115*, 9836.

[10] K. L. Wooley, C. J. Hawker, J. M. J. Fréchet, *J. Am. Chem. Soc.* **1993**, *115*, 11496.

[11] T. Kawaguchi, J. S. Moore, *Polym. Prep. Am. Chem. Soc. Div. Polym. Chem.* **1994**, *35*(2), 872; K. L. Wooley, C. J. Hawker, J. M. J. Fréchet, *J. Chem. Soc. Perkin Trans. 1* **1991**, 1059.

[12] J. K. Young, G. R. Baker, G. R. Newkome, K. F. Morris, C. S. Johnson, Jr., *Macromolecules* **1994**, *27*, 3464.

[13] G. R. Newkome, F. Cardullo, E. C. Constable, C. N. Moorefield, A. M. Cargill Thompson, *J. Chem. Soc. Chem. Commun.* **1993**, 925.

[14] 4′-Chloro-2,2′:6′2″-terpyridine was prepared to the following procedure: E. C. Constable, M. D. Ward, *J. Chem. Soc. Dalton Trans.* **1990**, 1405; K. T. Potts, D. Konwar, *J. Org. Chem.* **1991**, *56*, 4815.

[15] Y. S. Klausner, M. Bodansky, *Synthesis*, **1972**, 453.

[16] MALDI-TOF experiments were conducted with a 340 nm N2 laser (1-stage acceleration, 1 m pathlength, 100–250 FWHM resolution, and accuracy of mass determination ±0.15 %).

[17] K. T. Potts, D. A. Usifer, A. Guadalupe, H. D. Abruna, *J. Am. Chem. Soc.* **1987**, *109*, 3961; E. C. Constable, A. M. W. Cargill Thompson, D. A. Tocher, M. A. M. Daniels, *New J. Chem.* **1992**, *16*, 855.

[18] In ***X*** < **Ru** > ***Y***, ***X*** and ***Y*** refers to the connected dendritic components.

[19] Cyclic voltammograms at 20 °C were recorded on a BAS-100-W electrochemical apparatus from Bioanalytical Systems, Inc. A conventional three-electrode configuration was used with a 3 mm diameter glassy-carbon disk as the working electrode, a platinium counter electrode, and a silver wire pseudo-reference electrode. Electrochemical grade $TBAPF_6$ was recrystallized twice from pure EtOH and pulverized. HPLC grade MeCN was dried over P_4O_{10}, and the vapor transferred directly into the electrochemical cell after three freeze-pump-thaw degassing cycles at 10^{-5}–10^{-6} mm Hg. In general, a 0.5 mL sample solution containing 1 mM metal complex and 100 mM $TBAPF_6$ was prepared by drying the solid reagents directly in the electrochemical cell at 10^{-5}–10^{-6} mm Hg and then transferring the solvent directly into it through the vacuum line.

[20] P. J. Dandliker, F. Diederich, M. Gross, C. B. Knobler, A. Lovati, E. M. Sanford, *Angew. Chem.* **1994**, *106*, 1821; *Angew. Chem. Int. Ed. Engl.* **1994**, *33*, 1739.

[21] G. R. Newkome, C. N. Moorefield, G. R. Baker, M. J. Saunders, S. H. Grossman, *Angew. Chem.* **1991**, *103*, 1207; *Angew. Chem. Int. Ed. Engl.* **1991**, *30*, 1178; G. R. Newkome, C. N. Moorefield, US-A 5154853, **1992**; see also: M. F. Ottaviani, S. Bossmann, M. J. Turro, D. A. Tomalia, *J. Am. Chem. Soc.* **1994**, *116*, 661.

[22] G. R. Newkome, C. N. Moorefield, J. M. Keith, G. R. Baker, G. H. Escamilla, *Angew. Chem.* **1994**, *106*, 701; *Angew. Chem. Int. Ed. Engl.* **1994**, *33*, 666; G. R. Newkome, C. N. Moorefield, *Polym. Prep. Am. Chem. Soc. Div. Polym. Chem.* **1993**, *34*(1), 75; G. R. Newkome, R. Güther, F. Cardullo, *Macromol. Symp.* **1994**, in press; G. R. Newkome, C. N. Moorefield, *Macromol. Symp.* **1993**, *77*, 66; G. R. Newkome, C. N. Moorefield, U.S. Pat. Application.

Stereoselective Syntheses of Retro-Isomers of *N*-Glucoasparagine**

Oliver Frey, Matthias Hoffmann, and Horst Kessler*

Dedicated to Professor Dr. Richard R. Schmidt on the occasion of his 65th birthday

The extension of the structural diversity of peptides is important for the discovery of new lead structures in drug design. For this purpose carbohydrate moieties can be linked to peptides, because they can modulate the biological activity, increase the bioavailability, and improve the solubility of the compounds.[1]

If the sugars are bound, by the natural O-glycosidic linkage, to a serine residue (**1**), or by a N-glycosidic bond to the amide nitrogen of asparagine (**2**), one obtains glycopeptides having a glycosidic bond that is unstable towards base,[2] acid,[3] or enzymes.[4] A more stable linkage between the carbohydrate moiety and the peptide backbone results from a carbon–carbon bond (C-glycoside **3**). Up to now there have been only a few examples of C-glycosylated amino acids in which either the O or N atom is replaced by an isosteric methylene group[5] or the oxygen atom is omitted.[6]

[*] Prof. Dr. H. Kessler, Dipl.-Chem. O. Frey, Dipl.-Chem. M. Hoffmann
Institut für Organische Chemie und Biochemie
der Technischen Universität München
Lichtenbergstrasse 4, D-85747 Garching (Germany)
Telefax: Int. code + (89)3209-3210
e-mail: kessler@joshua.org.chemie.tu-muenchen.de

[**] This work was supported by the Fonds der Chemischen Industrie and Deutsche Forschungsgemeinschaft.

We report now a simple and stereoselective access to the glucoheptonamides **4** and **5**, in which the amide group between the sugar and amino acid is inverted relative to that of the natural N-glycosides (retroamide) to give a pyranose linked by a C-glycosidic bond to the amino acid. Though there are some examples of glucoheptonamides in the literature,[7] none has a retroamide bond between a carbohydrate moiety and an amino acid.

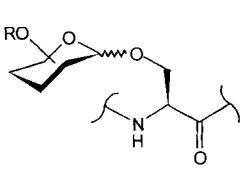

1

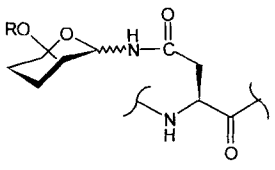

2

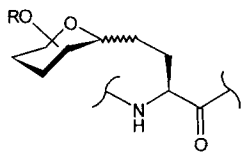

3

To synthesize the desired compounds **4** and **5**, it was necessary to prepare the corresponding sugar acids derived from D-glucose and an amino acid derivative containing an amino function in the β position. The α-configurated acid is particularly interesting, because there is only a single report of an α-heptonic acid,[7b] whereas the β-configurated acids are well known.[8]

The required acid **6** was prepared according to a procedure already described by us:[9] The chlorohydrin **7** was deprotonated with *n*-butyllithium and treated with lithium naphthalenide to give the dianion **8**, which was then trapped by carbon dioxide. The acid was purified by flash chromatography, and then acetylated to give **6** to avoid side reactions during the coupling step to the amide. With this procedure the α-heptonic acid **6** could be isolated in 57% overall yield, starting from **7**.

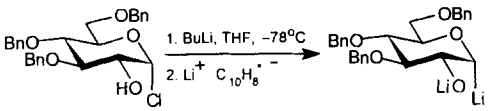

7 **8**

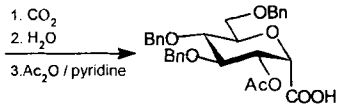

6

The β-heptonic acid **9** was also synthesized according to a procedure that we developed for the stereoselective synthesis of β-C-glycosides:[9b, 10] The readily accessible triphenyltin compound **10**[9] was deprotonated with an excess of *n*-butyllithium and transmetalated to **11**. This dianion was trapped by carbon dioxide, and purified and acetylated in analogy to **6**. The β-heptonic acid **9** could be isolated in 82% overall yield starting from **10**.

The β-aminoalanine derivative **12**, required for the coupling with the sugar acids **6** and **9**, was synthesized according to a procedure of Ranganathan et al., starting from the methyl ester

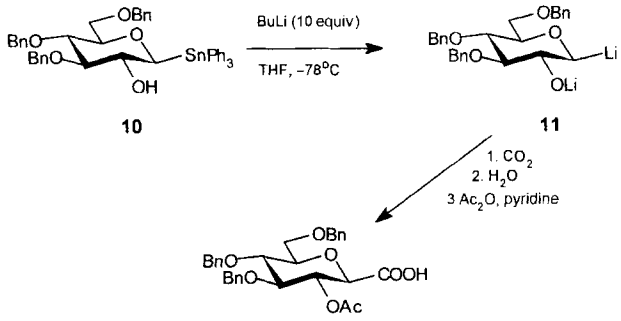

10 **11** **9**

of Cbz-protected asparagine, and using iodobis(trifluoroacetoxy)benzene.[11] Compound **12** was isolated as trifluoroacetate salt and used in subsequent reactions without purification.

The acid and amino components was first coupled by synthesizing a mixed anhydride of the sugar acid, which was then treated with the amine **12** in analogy to a procedure of Bemiller et al.[12] In the case of the α-heptonic acid **6**, the coupling product **4** was isolated after purification by chromatography in 82% yield. The β-heptonic acid **9** was coupled only in 55% yield by this method to give compound **5**.

An improved procedure was then developed in which the coupling was performed with the classical peptide coupling reagents *O*-(1*H*-benzotriazol-1-yl)-*N*,*N*,*N*′,*N*′-tetramethyluronium tetrafluoroborate (TBTU)[13] and 1-hydroxybenzotriazol (HOBt) in the presence of 2 equivalents of diisopropylethylamine (DIEA) in *N*-methylpyrrolidone (NMP) as solvent. Compound **4** was isolated in 88% by this method, and **5** was now prepared in 70% yield.

The α and β configuration at the anomeric centers of the pyranoses were deduced from the coupling constants between H^1 and H^2 in the ^{1}H NMR spectra, which were found to be 3.2 Hz for compound **4** and 9.2 Hz for compound **5** (Table 1).

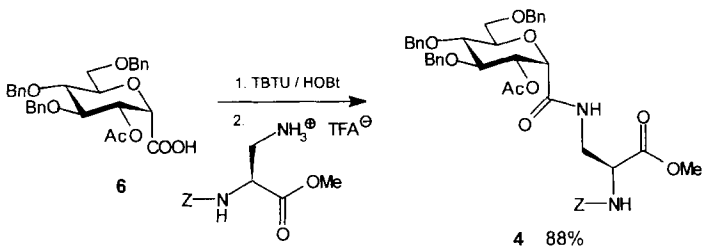

6 **12** **4** 88%

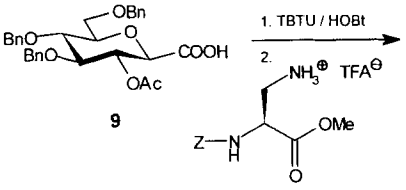

9 **12**

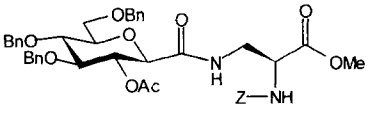

5 70%

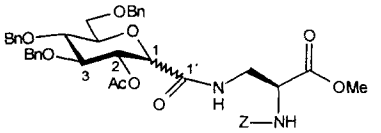

4, 5

Scheme 1. Atom numbering for compounds **4** and **5**, which is analogous to that for compound **7** (cf. Table 1).

Table 1. Some ^1H and ^{13}C NMR chemical shifts (δ values) and coupling constants ([Hz]) as well as R_f values and results from mass spectrometry for **4** and **5** [a, b].

Cmpd.	H-1	H-2	C-1	C-2	^3J(H-1,H-2) [Hz]	R_f [c]	*m/z* [d]
4	4.49	5.36	70.9	68.5	3.2	0.22	777
5	3.72	4.98	76.7	72.2	9.2	0.12	777

[a] NMR spectra in $CDCl_3$ at 300 K, internal standard TMS. ^1H: 500 MHz, ^{13}C: 125 MHz. [b] For better comparability the atoms were numbered as in sugar **7** (see Scheme 1). [c] Eluent: *n*-hexane/ethyl acetate = 1/1. [d] FAB-MS in nitrobenzylic alcohol matrix, $(M + Na)^+$.

Two new, unnatural, glycosylated amino acid compounds are now readily available, in good yield, from **7** and **10**. In addition, the Cbz protecting group of **4** and **5** could be selectively cleaved with H_2/Pd, without removing the benzyl ether protecting groups of the sugar.

Received: May 5, 1995
Revised version: June 16, 1995 [Z 7960IE]
German version: *Angew. Chem.* **1995**, *107*, 2194–2195

Keywords: C-glycosides · glycosylated amino acids · heptonamides

[1] a) J. F. Fisher, A. W. Harrison, G. L. Bundy, K. F. Wilkinson, B. D. Rush, M. J. Ruwart, *J. Med. Chem.* **1991**, *34*, 3140–3143; b) J. Kihlberg, J. Ahman, B. Walse, T. Drakenberg, A. Nilsson, C. Söderberg-Ahlm, B. Bengtsson, H. Olsson, *ibid.* **1995**, *38*, 161–169.
[2] K. Wakabayashi, W. Pigman, *Carbohydr. Res.* **1974**, *35*, 3–14.
[3] a) F. K. Hartley, F. R. Jerons, *Biochem. J.* **1962**, *84*, 134–139; b) A. Gottschalk, W. H. Murphy, *Biochim. Biophys. Acta* **1961**, *46*, 81–90.
[4] A. Gottschalk, *Glycoproteins: Their Composition, Structure and Function*, Elsevier, New York, **1972**, p. 361–364.
[5] a) M. K. Gurjar, A. S. Mainkar, M. Syamala, *Tetrahedron Asymmetry* **1993**, *4*, 2343–2346; b) C. R. Bertozzi, P. D. Hoeprich, M. D. Bednarski, *J. Org. Chem.* **1992**, *57*, 6092–6094; c) L. Petrus, J. N. Bemiller, *Carbohydr. Res.* **1992**, *230*, 197–200.
[6] H. Kessler, V. Wittmann, M. Köck, M. Kottenhahn, *Angew. Chem.* **1992**, *104*, 874–877; *Angew. Chem. Int. Ed. Engl.* **1992**, *31*, 902–904.
[7] a) G. Cruciani, K. A. Watson, *J. Med. Chem.* **1994**, *37*, 2589–2601; b) K. A. Watson, E. P. Mitchell, L. N. Johnson, C. J. Bichard, M. G. Orchart, G. W. J. Fleet, N. G. Oikonomakos, D. P. Leonidas, J. Son, *Biochemistry* **1994**, *33*, 5745–5758; c) J. N. Bemiller, R. J. Gilson, R. W. Myers, M. M. Santoro, M. P. Yadav, *Carbohydr. Res.* **1993**, *250*, 93–100.
[8] a) E. F. Fuchs, J. Lehmann, *Chem. Ber.* **1975**, *108*, 2254–2260; b) H. Fritz, J. Lehmann, P. Schlesselmann, *Carbohydr. Res.* **1983**, *113*, 71–92.
[9] a) V. Wittmann, H. Kessler, *Angew. Chem.* **1993**, *105*, 1138–1140; *Angew. Chem. Int. Ed. Engl.* **1993**, *32*, 1091–1093; b) M. Hoffmann, H. Kessler, *Tetrahedron Lett.* **1994**, *35*, 6067–6070.
[10] O. Frey, M. Hoffmann, V. Wittmann, H. Kessler, P. Uhlmann, A. Vasella, *Helv. Chim. Acta* **1994**, *77*, 2060–2069.
[11] S. Ranganathan, D. Ranganathan, W. P. Singh, *Tetrahedron Lett.* **1988**, *29*, 3111–3114.
[12] J. N. Bemiller, M. P. Yadav, V. N. Kalabokis, R. W. Myers, *Carbohydr. Res.* **1990**, *200*, 111–126.
[13] R. Knorr, A. Trzeciak, W. Bannwarth, D. Gillessen, *Tetrahedron Lett.* **1989**, *30*, 1927–1930.

Unexpected Course of the Darzens Reaction of Phenyl Esters of α-Chlorocarboxylic Acids with Carbonyl Compounds—A Novel One-Step Synthesis of α-Chloro-β-lactones**

Christine Wedler, Annamarie Kunath, and Hans Schick*

The Darzens reaction, the classical procedure for the preparation of glycidic esters by condensation of aldehydes or ketones with α-halocarboxylic esters in the presence of a base, has been known for more than 100 years[1, 2] and thoroughly exploited for the synthesis of a large variety of α-halo-β-hydroxy esters and α,β-epoxy esters. By hydrolysis and decarboxylation of the epoxy esters, aldehydes[3] and ketones[4] have been prepared. In most cases methyl, ethyl, isopropyl, and *tert*-butyl esters of α-chlorocarboxylic acids have been used as starting material.[2] To our knowledge the phenyl esters have never been employed in a Darzens reaction. A simple and broadly applicable one-step synthesis of α-chloro-β-lactones, which we report here, has therefore been overlooked until now.

Recently our group found that indium[5] as well as lithium[6] enolates derived from phenyl esters of α-branched or straight-chain carboxylic acids react with ketones to form α,α,β,β-tetrasubstituted or α,β,β-trisubstituted β-lactones in good yields. The question arose whether, instead of the phenyl ester of α-branched carboxylic acids, the phenyl esters of α-halocarboxylic acids could be used for the synthesis of β-lactones with two substituents in α-position, one of them an alkyl group, the other a halogen atom. The success of this idea should depend on whether lithium phenoxide is eliminated more easily than lithium halide from the anticipated intermediate **4**.

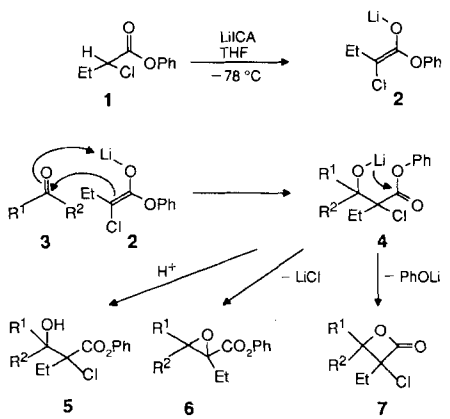

Scheme 1. Formation of α-chloro-β-lactones **7** by reaction of the carbonyl compounds **3** with the lithium phenyl ester enolate **2**. (The meaning of R^1 and R^2 is given in Table 1).

In order to decide this question, phenyl 2-chlorobutanoate (**1**) was deprotonated with lithium *N*-cyclohexyl-*N*-isopropylamide (LiICA) in THF at −78 °C to give the ester enolate **2**, which was treated with cyclohexanone **3a**. After workup the α-chloro-β-lactone **7a** was isolated in 80% yield (Table 1, entry 1). This

[*] Prof. Dr. H. Schick, Dr. C. Wedler, Dr. A. Kunath
Institut für Angewandte Chemie Berlin-Adlershof
Rudower Chaussee 5, D-12489 Berlin (Germany)
Telefax: Int. code + (30) 6392-4103
e-mail: schick@aca.fta-berlin.de in INTERNET

[**] This work was supported by the Deutsche Forschungsgemeinschaft and the Fonds der Chemischen Industrie

Table 1. Yields and positions of the carbonyl bands of the α-chloro-β-lactones **7**, synthesized from phenyl 2-chlorobutanoate (**1**) and carbonyl compounds **3**.

No.	7 [a]	R^1	R^2	Yield [%]	ν(CO) [cm^{-1}]
1	**7a**	$(CH_2)_5$		83	1835
2	**7b**	$-(CH_2)_4-$		80	1835
3	**7c**	Et	Et	68	1834
4	**7d**	Et	Me	73 [b, c]	1835
5	**7e**	Me	Me	72	1837
6	**7f**	Ph	Me	78 [d, e]	1840
7	**7g**	*t*Bu	H	62 [d, f]	1840
8	**7h**	$Ph(CH_2)_2$	H	40 [b, e]	1842

[a] All compounds were characterized by ^1H and ^{13}C NMR spectra. Correct elemental analysis for C, H, and Cl. [b] The mixture of *syn* and *anti* compound could not be separated by flash chromatography on silica gel. [c] *syn*/*anti*: 2/3. [d] The mixture of *syn* and *anti* compound was separated by flash chromatography on silica gel. [e] *syn*/*anti*: 1/1. [f] *syn*/*anti*: 2/1.

experiment revealed that the elimination of lithium phenoxide is the only observed reaction of the O-lithiated phenyl α-chloro-β-hydroxyalkanoate **4a**. Neither the anticipated α,β-epoxy ester **6a** nor the α-chloro-β-hydroxy ester **5a** seemed to be formed by elimination of lithium chloride from, or protonation of, the intermediate **4a**. The same course of reaction was observed when ketones **3b–f** were treated with the lithium phenyl ester enolate **2**. Again the α-chloro-β-lactones **7b–f** were obtained in acceptable yields (entries 2–6).

It was of interest for the synthesis of less substituted α-chloro-β-lactones to determine whether aldehydes could be included in this reaction. Indeed, the enolizable 3-phenylpropanal **3h** afforded the β-lactone **7h** in 40% yield (entry 8). The nonenolizable pivalaldehyde (**3g**) even gave the β-lactone **7g** in 62% yield (entry 7). However, the reaction was unsatisfactory with butanal. In this case a complicated reaction mixture was formed, from which the corresponding β-lactone could be isolated in contaminated form in only about 10% yield.

Unsymmetrically substituted carbonyl compounds such as butan-2-one (**3d**), acetophenone (**3f**), pivalaldehyde (**3g**), and 3-phenylpropanal (**3h**) yielded diastereomeric products. In all these cases mixtures of *syn* and *anti* β-lactones were obtained in a ratio between 1:1 and 1:2. The β-lactones **7f** and **7g** could be separated into the *syn* and *anti* diastereoisomers by flash chromatography. The configuration of these isomers was assigned on the basis of NOE difference spectroscopy (NOE = *n*uclear *O*verhauser *e*nhancement).

The low diastereoselectivity of the reaction of unsymmetrically substituted carbonyl compounds with the lithium ester enolate **2** (derived from phenyl α-chlorobutanoate **1**) parallels that of the normal Darzens reaction. For instance, the reaction of acetophenone[7] or benzaldehyde[8] with ethyl α-bromopropanoate provides the *syn* and *anti* diastereoisomers in a ratio of about 1:1.

Notwithstanding the outlined stereochemical problems, the described process opens a new one-step approach to many α,β,β-trisubstituted and α,β-disubstituted α-chloro-β-lactones. This class of compounds was previously available from α-chloro-β-hydroxyalkanoic acids by reaction with benzenesulfonyl chloride,[9] but only a few examples have been found in the literature. Except for **7b**[9] all α-chloro-β-lactones **7** described in this paper seem to be new compounds.

In conclusion it can be emphasized that the simple substitution of an alkyl α-chlorocarboxylate by a phenyl α-chlorocarboxylate in the Darzens reaction causes the elimination of lithium phenoxide instead of lithium chloride from the O-lithiated phenyl α-chloro-β-hydroxyalkanoate intermediate **4** and turns the classical Darzens reaction for glycidic ester synthesis into a useful α-chloro-β-lactone synthesis. To our knowledge only one observation in the literature is related to this possibility. Wemple et al. described the formation of **7a** (Me instead of Et) as a side product in the Darzens reaction of cyclohexanone with *S*-*t*-butyl 2-chloropropanethioate.[10] In this case, a competition between lithium chloride and lithium *t*-butyl sulfide elimination from the intermediate **4a** (*t*BuS instead of PhO) led to an α-chloro-β-lactone, but in a yield of only 10%.

Experimental Procedure

A solution of *n*-butyllithium in hexane (1.35 N, 4.4 mL, 6.0 mmol) was added by syringe at −10 °C within 1 min to *N*-cyclohexyl-*N*-isopropylamine (1.10 mL, 6.6 mmol) in THF (20 mL). The mixture was allowed to warm to ambient temperature over 15 min and thereafter cooled again to −78 °C. Then the phenyl α-chlorocarboxylate **1** (1.19 g, 6 mmol), dissolved in THF (5 mL), was precooled with acetone and dry ice to −70 °C in a dropping funnel equipped with a cooling jacket. This solution was slowly added over 30 min to the solution of lithium amide. During the addition the temperature was kept below −70 °C. After the mixture was stirred for additional 20 min at this temperature, a precooled solution of the carbonyl compound **3** (5 mmol) in THF (5 mL) was added over 20 min from the dropping funnel, while the temperature was again kept below −70 °C. Then the mixture was allowed to warm to 0 °C within 2 h. After addition of diethyl ether (50 mL), aqueous NaOH (1 N, 15 mL, 15 mmol), and water (50 mL), the organic phase was separated, washed with 1 N NaOH (2 × 7.5 mL) and brine (2 × 20 mL), dried over Na_2SO_4, and filtered. Removal of the solvent under reduced pressure afforded a pale yellow oil, from which the corresponding α-chloro-β-lactone **7** was isolated by flash chromatography on silica gel with hexane/ethyl acetate (10/1) as eluent.

Received: May 6, 1995 [Z 7964 IE]
German version: *Angew. Chem.* **1995**, *107*, 2201–2202

Keywords: 2-chlorocarboxylic acids · α-chloro-β-lactones · Darzens reaction · heterocycles · β-lactones

[1] a) E. Erlenmeyer, Jr., *Justus Liebigs Ann. Chem.* **1892**, *271*, 137; b) G. Darzens, *C. R. Acad. Sci.* **1904**, *139*, 1214; c) W. S. Johnson, J. S. Belew, L. J. Chinn, R. H. Hunt, *J. Am. Chem. Soc.* **1953**, *75*, 4995–5001.
[2] Reviews: a) M. S. Newman, B. J. Magerlein, *Org. React.* **1949**, *5*, 413–429; b) M. Ballester, *Chem. Rev.* **1955**, *55*, 283–300; c) T. Rosen in *Comprehensive Organic Synthesis, Vol. 2* (Eds.: B. M. Trost, I. Fleming), Pergamon, Oxford, **1991**, p. 409–439.
[3] a) M. E. Dullaghan, F. F. Nord, *J. Org. Chem.* **1953**, *18*, 878–881; b) O. Bayer, *Methoden Org. Chem.* (Houben-Weyl) **1954**, Vol. VII/1, p. 326–329.
[4] a) R. A. Kuroyan, A. I. Markosyan, A. P. Engoyan, S. A. Vartanyan, *Zh. Org. Khim.* **1983**, *19*, 1947–1953; b) H. Hennecka, *Methoden Org. Chem.* (Houben-Weyl) **1976**, Vol. VII/2b, p. 1371–1374.
[5] H. Schick, R. Ludwig, K. Kleiner, A. Kunath, *Tetrahedron* **1995**, *51*, 2939–2946.
[6] C. Wedler, A. Kunath, H. Schick, *J. Org. Chem.* **1995**, *60*, 758–760.
[7] L. M. Alekseeva, A. I. Bokanov, V. I. Shvedov, Yu. N. Sheinker, *Zh. Org. Khim.* **1986**, *22*, 1854–1857.
[8] J. Kagan, B. E. Firth, *J. Org. Chem.* **1974**, *39*, 3145–3147.
[9] T. H. Black, T. S. McDermott, G. A. Brown, *Tetrahedron Lett.* **1991**, *32*, 6501–6502.
[10] D. J. Dagli, P.-S. Yu, J. Wemple, *J. Org. Chem.* **1975**, *40*, 3173–3178.

Fluxionality Induced by High Pressure: [9-D]9-Homocubyl Triflate, a Pressure-Sensing Molecule**

Urs P. Spitz and Philip E. Eaton*

1

2

The solvolysis of 9-homocubyl triflate (**1**) and similar derivatives occurs by ionization to a tight ion pair containing the σ-bridged homocubyl cation (**2**).[1, 2] Recently, and in accord with this interpretation, we reported that [9-D]9-homocubyl triflate ([9-D]-**1**) on exposure to heat or to polar solids like silica gel undergoes multiple automerizations that result in scrambling of the deuterium label over five positions of the homocubyl skeleton [Equation (a)].[1] Starting material recovered from incomplete solvolyses of [9-D]-**1** has the label scrambled in the same way. It follows from these

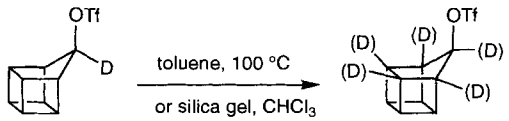

[9-D]-**1** [D]-**1** (a)

observations that only C–C bonds anti to the ionizing group undergo Wagner–Meerwein shifts. Continual automerization results in a formal rotation of a cyclopentyl cation against a cyclobutane ring. Herein we report that these automerizations occur simply upon pressurizing solutions of [9-D]9-homocubyl triflate.

Samples of labeled triflate [9-D]-**1**[1] in dichloromethane were subjected to hydrostatic pressures of about 10000 atm.[3] After various periods of time the triflate was recovered, and the label distribution was determined by proton and deuterium NMR spectroscopy. Under the conditions of high pressure, as is apparent from the data in Table 1, a nonsolvolytic, highly stereoselective scrambling process took place.[4] Exposure for several days (entry 5) led to essentially statistical distribution of the deuterium label [20% C(9), 40% C(1,8) 40% C(2,3)] over the syn face. At normal pressure under otherwise the same conditions no significant scrambling of the label occurred. Although the solution of the triflate darkened during the pressure-induced scrambling process, no significant decomposition could be detected by NMR spectroscopy. This is remarkable because at least ten automerizations, each involving the formation of the ion pair and internal return of the triflate, are necessary to spread the label evenly (±3%) over the five positions. In contrast, thermally induced scrambling of the label of [9-D]-**1**, for example in hot toluene, was accompanied by complete decomposition of the triflate well before the statistical distribution of the label could be reached.[1]

Table 1. Pressure-induced scrambling in labeled triflate [9-D]-**1** as a function of time.

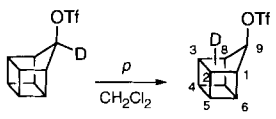

[9-D]-**1** [D]-**1**

Entry	Pressure [atm]	Time [h]	D at position [a] C(9)	C(1,8)	C(2,3)
1	10000	0.25	70	30	≈0
2	10700	1.75	52	41	7
3	9400	6	46	41	13
4	10000	12	23	40	37
5	10000	72	20	40	40

[a] In % (±3%); determined by integration of ^{1}H NMR signals. The comparison with data from the ^{2}H NMR spectra was satisfactory.

Pressure has two very particular effects on chemical reactions.[5] The first, intuitively obvious, follows the ancient principle of Le Chatelier: Increasing pressure is countered by a decrease in volume. Thus, reaction rates are strongly enhanced by pressure if in the transition state molecules associate (negative volume of activation). The second important effect, electrostriction, is less obvious: The polarization induced by a charge (an ion) in a dielectric (a solvent) increases intermolecular forces. This causes the dielectric medium to pack more densely and decrease its volume. Consequently, processes involving charge separation can be promoted by pressure. We suppose that the electrostriction effect is the operating principle in the present examples. In this case, quite extraordinarily, pressure controls the relative rate with which a cyclobutane rotates relative to a cyclopentane ring. This pressure-regulated "molecular gear" is certainly unique.

Received: May 8, 1995 [Z 7967 IE]
German version: *Angew. Chem.* **1995**, *107*, 2206–2207

Keywords: automerization · carbocations · electrostriction · fluxionality · high-pressure chemistry

[*] Prof. P. E. Eaton, Dr. U. P. Spitz
Department of Chemistry
The University of Chicago
5735 S. Ellis Avenue, Chicago, IL 60637 (USA)
Telefax: Int. code + (312)702-0805
e-mail: pde2@midway.uchicago.edu

[**] This work was supported by the National Science Foundation.

[1] U. P. Spitz, *J. Am. Chem. Soc.* **1993**, *115*, 10174.
[2] a) P. von R. Schleyer, J. J. Harper, G. L. Dunn, V. J. DiPasquo, J. R. E. Hoover, *J. Am. Chem. Soc.* **1967**, *89*, 698; b) R. E. Leone, P. von R. Schleyer, *Angew. Chem.* **1970**, *82*, 889; *Angew. Chem. Int. Ed. Engl.* **1970**, *9*, 860; c) R. E. Leone, J. C. Barborak, P. von R. Schleyer, *Carbonium Ions*, Wiley Interscience, New York, **1973**, pp. 1863–1869; d) A. P. Marchand, *Chem. Rev.* **1989**, *89*, 1011; e) J. C. Barborak, R. Pettit, *J. Am. Chem. Soc.* **1967**, *89*, 3080; f) P. Ahlberg, G. Jonsäll, C. Engdahl, *Adv. Phys. Org. Chem.* **1983**, 223.
[3] The apparatus (LECCO model PG-200 HPC) consisted of a steel chamber containing a pressure transmission fluid (castor oil) in which a sample holder was immersed. The system was pressurized by a hydraulically driven differential area piston. The sample was contained in Teflon tubing sealed with glass stoppers.
[4] Significant adiabatic heat is produced during pressurization and might affect the experimental results. To reduce the problem, the experiments were run with samples pre-cooled in ice water, and the pressure was raised relatively slowly.
[5] For an excellent and detailed overview of the effects of pressure on organic reactions, see W. J. le Noble in *High Pressure Organic Chemistry, Vol 37*, (Ed.: W. J. le Noble), Elsevier, New York, **1988**, 1.

Catalytic Photoinduced Charge-Transfer Osmylation: A Novel Pathway from Arenes to Cyclitol Derivatives**

William B. Motherwell* and Alvin S. Williams

The ability of the enzymatic system present in strains of *Pseudomonas putida* to achieve stereospecific vicinal *cis* dihydroxylation[1] of benzene has spawned recent intense interest among synthetic organic chemists. The resultant *cis* diene diol and functionalized chiral derivatives have been widely used as starting materials for the syntheses of a diverse array of biologically important molecules including conduritols, inositols, prostaglandins, and carbohydrates.[2-4] It was therefore of interest to devise a simple *chemical* method for the production of these useful building blocks, particularly since the commonly encountered reagents for in vitro oxidation of arenes, such as ozone and ruthenium tetraoxide, also lead to the concomitant cleavage of the carbocyclic ring. We now present the results of a preliminary study in which we have achieved the first direct metal-catalyzed, one-pot conversion of benzene and some simple arenes to conduritol and inositol derivatives.

The basis for our work rests on an elegant study by Kochi and Wallis,[5] who demonstrated that actinic (UV) irradiation of the Electron Donor–Acceptor (EDA) complex[6] (**1**) formed on mixing benzene and osmium tetraoxide led, in the presence of an excess of the OsO_4 and at a frequency equal or greater than that of the absorption maxima, to a polymeric 2:1 adduct (**4** Scheme 1), which could be isolated as a monomer (**5**) by the addition of pyridine. The proposed mechanism involves photochemically induced charge transfer from the complex (**1**) to form an ion pair (**2**), which can collapse to the osmate ester of benzene diol (**3**) followed by a second thermal *anti* osmylation.

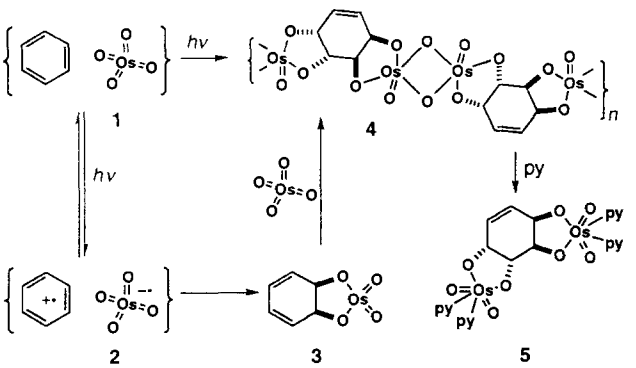

Scheme 1.

Although yields of the isolated adducts such as **5** were low even in the stoichiometric reaction, we envisaged that such a process could be made catalytic in osmium through careful selection of a suitable solvent system and oxygen atom transfer reagent. In this respect, since the heat of formation of the EDA complex between benzene and osmium tetraoxide has been estimated to be of the order of 0.5 kcal mol^{-1},[6] it was of paramount importance to avoid the use or generation of any molecule whose donor ability would give more stable OsO_4 complexes. Thus a series of simple control experiments served to indicate that *N*-methylmorpholine, pyridine, acetone, and *tert*-butanol were all fatal competitive inhibitors of the EDA complex. The use of aqueous solutions of barium chlorate[7] in a biphasic system with the arene were shown to provide suitable conditions for a catalytic photoosmylation.

In a typical early experiment, irradiation of benzene (0.65 mL) in the presence of aqueous barium chlorate (0.22 M, 75 mL) and osmium tetraoxide (25 mg; 1.3 mol%) led, after reductive workup with sodium disulfite and acetylation, to the *meso* derivative *allo*-inositol hexaacetate (**6**) in 31% yield[8] (Scheme 2). Conduritol E tetraacetate (**7**),[9] which is derived from the major but less reactive *anti*-isomer at the tetrol stage,[10] was also formed in 5% yield. This corresponds to a catalytic turnover for osmium tetraoxide of 76.

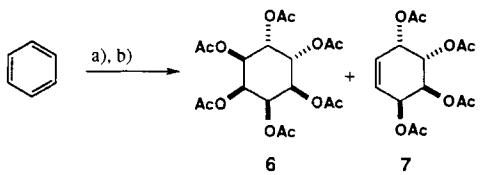

Scheme 2. a) OsO_4 (cat.), *hv*, $Ba(ClO_3)_2$ (0.22 M); b) Ac_2O, Et_3N, DMAP; **6**:**7** (6.2:1) 36%.

At a later stage, during studies using a higher chlorate concentration (1.10 M) and a reduced water:arene ratio (1:1.5) (see Experimental Procedure), we were intrigued to note that the formation of deoxychloroinositols is possible (Scheme 3). In this manner, photoosmylation of benzene (15 mL) followed by acetylation provided not only the anticipated *allo*-inositol hexaacetate on a gram scale (1.120 g) but also the deoxychloro-*chiro*- (**8**), *-neo*- (**9**) and *-epi*-inositols (**10**) (0.616 g, 2:2:1 respectively) corresponding to a catalytic turnover of 108 for osmium tetraoxide.

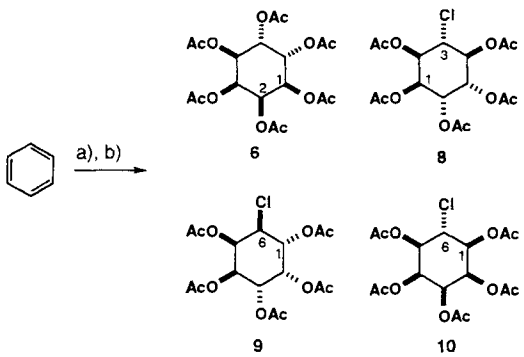

Scheme 3. a) OsO_4 (cat.), *hv*, $Ba(ClO_3)_2$ (1.10 M); b) Ac_2O, Et_3N, DMAP; **8**:**9**:**10** (2:2:1).

Since the formation of derivatives **8**, **9**, and **10** was indicative of competitive *trans* addition of hypochlorous acid at an early intermediate stage, it was of interest to examine the behavior of the inherently even more reactive bromate anion as the oxygen transfer reagent. Even under the original "standard" conditions that led only to vicinal dihydroxylation products with the chlorate anion, brominated derivatives were formed (Scheme 4), and even predominated over *allo*-inositol hexaacetate (**6**; 7.7%). The structure of the major diastereoisomer, isolated in 15.7% yield, was based on its ^1H and ^{13}C NMR

[*] Prof. W. B. Motherwell, A. S. Williams
Department of Chemistry, Christopher Ingold Laboratories
University College London, GB-London, WC1H 0AJ (UK)
Telefax: Int. code + (171)380-7524

[**] We thank B. P. Research for a studentship to A. S. W.

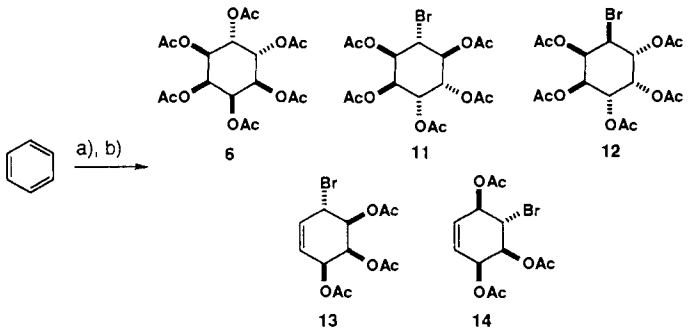

Scheme 4. a) OsO_4 (cat.), *hv*, $NaBrO_3$ (0.22 M); b) Ac_2O, AcOH; **6** 7.7%, **11**:**12** (5.1:1) 18.8%, **13**:**14** (1:5) 2.3%.

spectra and confirmed by X-ray analysis[11] to be the deoxybromo-*chiro*-inositol (**11**). Minor amounts of the deoxybromo-*neo*-inositol (**12**) (3.1%) and the bromoconduritols C (**13**) and F (**14**) (2.3% yield; **13**:**14** = 1:5) were also isolated.

A preliminary screening of some simple monosubstituted arenes gave the following results: Oxidation of the stereochemically more complex toluene (Scheme 5) was achieved in 13% overall yield (catalytic turnover 29) to the single C-methyl conduritol isomer E (**15**) and an isomeric mixture (ratio 2:1:1) of C-methyl-*allo*-inositols **16**, **17**, and **18** in a conduritol:inositol ratio of 1:5. Inspection of the relative configuration of **15** (X-ray analysis)[11] reveals it to be the precursor of the major portion of the inositol derivatives **16** and **17**, and also suggests that the initial photoosmylation step occurs at either the 1,2 or 3,4 positions. Interestingly, in contrast with the Etard oxidation,[12] which also involves metal-mediated electron transfer, only trace amounts of benzaldehyde were formed.

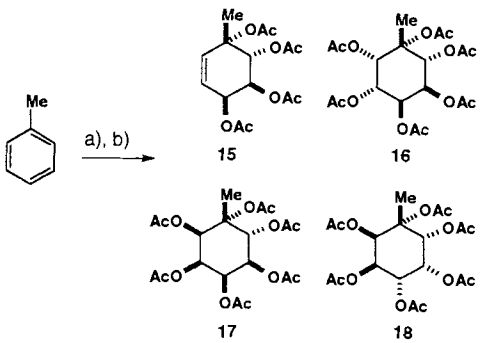

Scheme 5. a) OsO_4 (cat.), *hv*, $Ba(ClO_3)_2$ (0.22 M); b) Ac_2O, Et_3N, DMAP; **15** 2.2%, **16**:**17**:**18** (2:1:1) 10.8%.

As expected on the basis of their higher ionization potentials, the "catalytic" turnover of the oxidation of halogenated arenes under our initial conditions is very slow indeed (Scheme 6; combined yields: **19** 0.6%, **20** 3.4%, **21** 2.6%). Nevertheless, it is significant to note that no inositol derivatives were detected, presumably since the remaining double bond—a vinylic halide—is resistant to further osmylation on electronic grounds. In these experiments the preference for the formation of the *anti*-tetrols is much higher[13] than in the OsO_4-catalyzed vicinal dihydroxylation of the 2,3-diol produced by oxidation of bromobenzene with *Pseudomonas putida*, where the ratio of **21a**:**21b** is 1.1:1.0.[3c]

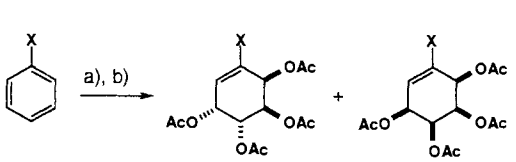

19: X=F	**19a**	4.4:1	**19b**
20: X=Cl	**20a**	5.0:1	**20b**
21: X=Br	**21a**	5.5:1	**21b**

Scheme 6. a) OsO_4 (cat.), *hv*, $Ba(ClO_3)_2$ (0.22 M); b) Ac_2O, Et_3N, DMAP; **19** 0.6%, **20** 3.4%, **21** 2.6%.

In view of the many kinetically discrete photochemical and thermal steps involving formation and oxidative hydrolysis of different regio- and stereoisomeric osmate esters during a single reaction sequence, it is not surprising that the nature and relative ratios of the products isolated are influenced by temperature, relative concentrations of reactants and reagents, and the duration of the radiation and its intensity. Although we have not yet carried out systematic optimization studies for each system, the present work indicates for the first time that the controlled catalytic vicinal dihydroxylation of benzene and simple arenes can lead to a variety of usefully functionalized inositol and conduritol derivatives without cleavage of the carbocyclic ring.

Experimental Procedure

6, **8**, **9**, **10**: To deionized water (10 mL) in a 25 mL Pyrex florentine flask fitted with a Teflon tap was added $Ba(ClO_3)_2$ (3.53 g), benzene (15 mL), and OsO_4 (25 mg, 0.1 mmol) in CCl_4 (0.25 mL). The biphasic system was stirred vigorously and irradiated with a 400 W medium-pressure Hg bulb for 43 h. The solution was then cooled to 0 °C and reduced with $Na_2S_2O_5$ (15 g), stirred for a further 2 h, and evaporated to dryness under reduced pressure. The dried salts were then powdered, treated with Et_3N (70 mL), Ac_2O (20 mL), and 4-dimethylaminopyridine (DMAP, catalytic amount), and heated (70 °C) for 3 h. The reaction mixture was cooled (0 °C), water was added (100 mL), and the mixture was filtered through a pad of Celite and extracted with ether (3 × 100 mL). The extract was washed with brine (100 mL), dried over $MgSO_4$, and concentrated at reduced pressure to give a yellow oil, which crystallized on standing. Column chromatography (SiO_2, 70% ether in petroleum spirits) gave, in order of elution, **8** and **9** as a 1:1 mixture (0.495 g, 1.21 mmol), **10** (0.121 g, 0.30 mmol), and **6** (1.120 g, 2.59 mmol). Compound **8** was separated from **9** by HPLC (SiO_2, 25% EtOAc in hexane).

6: ^1H NMR (400 MHz, $CDCl_3$, 55 °C, $CHCl_3$): δ = 2.05 (bs, 18H; 6 × CH_3), 5.30 (m, 2H; H-3, 6), 5.44 (m, 4H, H-1, 2, 4, 5); ^{13}C NMR (100 MHz): δ = 20.5–20.6 (6 × CH_3), 67.4–67.7 (6 × CH), 169.2, 169.3, 169.5 (6 × OCOMe); MS (70 eV, NH_3): *m/z*(%): 450 $[M + NH_4]^+$. Correct elemental analysis; m. p. 140–141 °C (methanol; ref. [10]: 138–139 °C).

8: ^1H NMR (400 MHz, $CDCl_3$, RT, $CHCl_3$): δ = 2.00, 2.07, 2.11, 2.17, 2.20 (5 × s, 15H, 5 × CH_3), 4.15 (t, $^3J(H,H)$ = 10.9, 10.9 Hz, 1H, H-3), 5.21 (dd, $^3J(H,H)$ = 10.3, 2.8 Hz, 1H, H-5), 5.31 (dd, $^3J(H,H)$ = 11.0, 2.7 Hz, 1H, H-2), 5.36 (m, $^3J(H,H)$ = 2.9, 5.6 Hz, 2H, H-1, 6), 5.49 (dd, $^3J(H,H)$ = 10.3, 10.3 Hz, 1H, H-4); ^{13}C NMR (100 MHz): δ = 20.4, 20.5, 20.5, 20.6, 20.7 (5 × CH_3), 57.4 (CH, C-3), 67.1, 67.5, 69.3, 70.5, 70.8 (5 × CH), 168.7, 169.0, 169.3, 169.3, 169.7 (5 × OCOMe); MS (70 eV, NH_3): *m/z*(%): 428 (34.8), 426 (100) $[M + NH_4]^+$. Correct elemental analysis; m. p. 146–147 °C (ethanol; ref. [14]: 144 °C).

9: ^1H NMR (400 MHz, $CDCl_3$, RT, $CHCl_3$): δ = 2.00 (s, 6H, 2 × CH_3), 2.07, 2.16, 2.20 (3 × s, 9H, 3 × CH_3), 4.34 (dd, $^3J(H,H)$ = 11.1, 3.0 Hz, 1H, H-6), 5.23 (dd, $^3J(H,H)$ = 11.0, 3.0 Hz, 1H, H-4), 5.32 (dd, $^3J(H,H)$ = 11.2, 2.8 Hz, 1H, H-1), 5.34 (dd, $^3J(H,H)$ = 11.2, 3.0 Hz, 1H, H-3), 5.65 (dd, $^3J(H,H)$ = 3.0, 3.0 Hz, 1H, H-2), 5.72 ((dd, $^3J(H,H)$ = 3.0, 2.9 Hz, 1H, H-5); ^{13}C NMR (100 MHz): δ = 20.4, 20.5, 20.6 (5 × CH_3), 54.7 (CH, C-6), 67.0, 68.4, 68.6, 69.4, 69.5 (5 × CH), 169.3, 169.4, 169.6, 169.7, 169.9 (5 × OCOMe); MS (70 eV, NH_3): *m/z*(%): 428 (34.7), 426 (100) $[M + NH_4]^+$. Correct elemental analysis; m. p. 137–139 °C (ethanol).

10: ^1H NMR (400 MHz, $CDCl_3$, RT, $CHCl_3$): δ = 2.08 (s, 6H, 2 × CH_3), 2.10 (s, 6H, 2 × CH_3), 2.12 (s, 3H, CH_3), 4.36 (dd, $^3J(H,H)$ = 11.1, 3.0 Hz, 1H, H-6), 5.37 (m, 5H, H-1, 2, 3, 4, 5). ^{13}C NMR (100 MHz, 55 °C): δ = 20.4 (4 × CH_3), 20.6 (CH_3), 54.0 (CH, C-6), 67.7 (CH, C-3), 68.3 (2 × CH, C-1, 5), 71.1 (2 × CH, C-2, 4), 169.0–169.2 (5 × OCOMe); MS (70 eV, NH_3): *m/z*(%): 428 (33.1), 426 (92.4) $[M + NH_4]^+$. Correct elemental analysis; m. p. 170–171 °C (ethanol; ref. [15]: 185 °C from 2-propanol).

Received: May 16, 1995 [Z 7991 IE]
German version: *Angew. Chem.* **1995**, *107*, 2207–2209

Keywords: arene oxidation · charge transfer · conduritols · inositols · osmylation

[1] D. T. Gibson, J. R. Koch, R. E. Kallio, *Biochemistry* **1968**, *7*, 2653.
[2] a) S. V. Ley, F. Sternfeld, S. Taylor, *Tetrahedron Lett.* **1987**, *28*, 225; b) S. V. Ley, F. Sternfeld, *ibid.* **1988**, *29*, 5305; c) S. V. Ley, A. J. Redgrave, *Synlett* **1990**, 393.
[3] a) H. A. J. Carless, O. Z. Oak, *Tetrahedron Lett.* **1989**, *30*, 1719; b) H. A. J. Carless, K. Busia, *ibid.* **1990**, *31*, 1617; c) H. A. J. Carless, K. Busia, Y. Dove, S. S. Malik, *J. Chem. Soc. Perkin Trans. 1* **1993**, 2505.
[4] a) T. Hudlicky, M. Mandel, J. Rouden, R. S. Lee, B. Bachmann, T. Dudding, K. J. Yost, J. S. Merola, *J. Chem. Soc. Perkin Trans. 1* **1994**, 1553; b) T. Hudlicky, J. Rouden, H. Luna, S. Allen, *J. Am. Chem. Soc.* **1994**, *110*, 5099; c) T. Hudlicky, H. F. Olivo, B. McKibben, *ibid.* **1994**, *110*, 5108.
[5] J. M. Wallis, J. K. Kochi, *J. Org. Chem.* **1988**, *53*, 1679; *J. Am. Chem. Soc.* **1988**, *110*, 8207.
[6] P. R. Hammond, R. R. Lake, *J. Chem. Soc. (A)* **1971**, 3819.
[7] K. A. Hoffman, *Chem. Ber. Dtsh. Chem. Ges.* **1912**, *45*, 3329.
[8] Yields are based on amount of starting material used originally.
[9] Synthesis of (+)- and (−)-conduritol E: S. Takano, T. Yoshimitsu, K. Ogasawara, *J. Org. Chem.* **1994**, *59*, 54; Z.-M. Wang, K. Kakiuchi, K. B. Sharpless, *ibid.* **1994**, *59*, 6895.
[10] T. Tschamber, F. Backenstrass, H. Fritz, J. Streith, *Helv. Chim. Acta* **1992**, *75*, 1052–1060.
[11] X-ray crystal structure: W. B. Motherwell et al., unpublished.
[12] W. H. Hartford, M. Darin, *Chem. Rev.* **1958**, *58*, 1.
[13] For an analysis of this selectivity see H. C. Kolb, M. S. VanNieuwenhze, K. B. Sharpless, *Chem. Rev.* **1994**, *94*, 2483.
[14] G. E. McCasland, *Adv. Carbohydr. Chem.* **1965**, *20*, 24.
[15] G. E. McCasland, S. Furuta, V. Bartuska, *J. Org. Chem.* **1963**, *28*, 2096.

Tantalum-Mediated Coupling of Methane and Carbon Dioxide in the Gas Phase**

Ralf Wesendrup and Helmut Schwarz*

Dedicated to Professor Rolf Huisgen on the occasion of his 75th birthday

Activation of carbon dioxide and its use as a C_1 building block in chemical reactions has been a challenge for chemists for decades.[1] Nature has solved the problem impressively, for example in photosynthesis. Driven by both the advances in organometallic chemistry and in the insights into the mechanisms of biochemical processes that involve reactions of CO_2, substantial progress in CO_2 activation has been made in the past years.[2] For example, quite efficient catalytic systems for the hydrogenation of CO_2 to formic acid have become available, at least on a laboratory scale.[3] However, inherent thermochemical and kinetic problems result in a partial solution at best for the ultimate goal of CO_2 chemistry, the simultaneous coupling of CO_2 with alkanes RH to yield the corresponding carboxylic acids RCO_2H. Formation of acetic acid from CH_4 and CO_2, for example, is endergonic under standard conditions and even 9 kcal mol^{-1} endothermic in the gas phase.[4] Thus, it can only be accomplished by taking advantage of solvation enthalpies in polar solutions or by complexation of the reactants and/or products to a metal center.[1] While ion–molecule reactions in the gas phase are a valuable tool for investigating the elementary steps of organometallic reactions,[5] gas-phase studies on the reactivity of CO_2 are relatively scarce, and a few examples are summarized in Scheme 1.

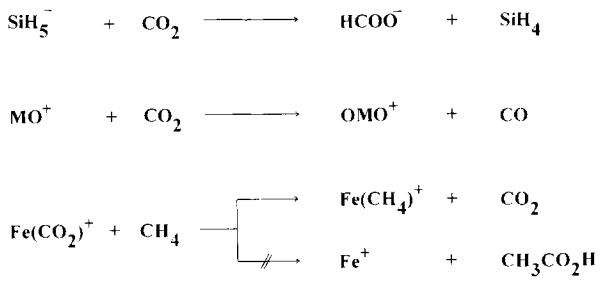

Scheme 1.

Anions like SiH_5^- can reduce carbon dioxide by hydride transfer to yield the formate anion HCO_2^- [Scheme 1, reaction (a)];[6] analogous results have not yet been reported for cationic systems and are not likely ever to emerge. Of course, CO_2 can be deoxygenated to carbon monoxide by "naked" metal cations or by oxo cations MO^+ [reaction (b)], provided the bond energy of the newly formed (O)M–O bond exceeds 127 kcal mol^{-1}.[7] Recently, Schwarz and Schwarz successfully isolated an $Fe(CO_2)^+$ complex and probed its reactivity towards dihydrogen and methane [reaction (c)].[8a] Unfortunately, hydrogen does not react at all, and only the slow ligand exchange of the intact CO_2 molecule for a methane molecule [reaction (c)] has been observed, but no evidence for the activation of CO_2/CH_4 to generate CH_3CO_2H has been found. Since methane itself is not activated by "bare" Fe^+ [5a, b] cations in the ground state, and the weakly bound CO_2 ligand does not significantly alter the electronic situation of the metal center,[8b, c] this negative finding is not really surprising. However, a transition metal cation that can react with both methane and carbon dioxide might also activate them simultaneously and lead to coupling. Previous experiments demonstrate that the third-row metal ions Ta^+, W^+, Os^+, Ir^+, and Pt^+ dehydrogenate methane in an exothermic reaction to form the corresponding carbene complexes MCH_2^+ as primary ionic product.[9] Only Ta^+ and W^+ form a strong enough M^+–O bond to enable an exothermic reduction of CO_2.[4] For example, when W^+ is treated with CO_2 under single-collision conditions the oxo cation WO^+ is the primary and WO_2^+ the secondary product.[9d] Although Ta^+ cations are highly reactive species that activate even inert molecules like O_2,[10a] NH_3,[10b] benzene,[10c] and SF_6,[10d] to the best of our knowledge its reactivity towards CO_2 has not yet been reported.

In this article we describe the gas-phase reactions of "bare" Ta^+ and its carbene complex $TaCH_2^+$ with CO_2, and we will demonstrate that this system can indeed couple CH_4 and CO_2. All experiments were performed with a Spectrospin CMS 47X FT-ICR mass spectrometer equipped with an external ion source.[11] Ta^+ cations were generated by laser desorption/laser ionization of pure tantalum,[12] and the ions were transferred to the analyzer cell through a system of electric potentials and lenses. Isolation of $^{181}Ta^+$ and all other isolation steps were performed with FERETS.[13] The ions were thermalized by collisions with pulsed-in nitrogen and subsequently reisolated. Background argon pressures of $2-5\times10^{-7}$ mbar was used as a collision gas for additional thermalization and collision induced dissociation (CID) experiments. The oxo cations TaO^+ and TaO_2^+ were generated by the reaction of bare Ta^+ with pulsed-in CO_2, the carbene $TaCH_2^+$ with pulsed-in CH_4, and $[TaCH_2O]^+$ by consecutive pulses of CH_4 and CO_2. Reactant gases were bled into the FT-ICR cell at constant pressure through a leak valve. The pseudo-first-order rate constants were determined from the logarithmic decay of the precursor-ion intensity with

[*] Prof. Dr. H. Schwarz, Dipl.-Chem. R. Wesendrup
Institut für Organische Chemie der Technischen Universität
Strasse des 17. Juni 135, D-10623 Berlin (Germany)
Telefax: Int. code + (30)314-21102

[**] This work was supported by the Deutsche Forschungsgemeinschaft and the Fonds der Chemischen Industrie. Abbreviations: ICR = ion cyclotron resonance spectroscopy, FERETS = front-end resolution enhancement using tailored sweeps, CID = collision-induced dissociation, ADO = averaged dipole orientation.

time and corrected for reactions with background impurities. The error in the rate constants determined in this way is ±50%.

The temporal evolution and disappearance of the ions in the reaction of Ta^+ with CO_2 are plotted in Figure 1. As expected, TaO^+ is the primary ionic product and reacts further to form the dioxocation TaO_2^+. Both reactions are highly exothermic (−57 and −29 kcal mol^{-1}, respectively) and proceed at collision

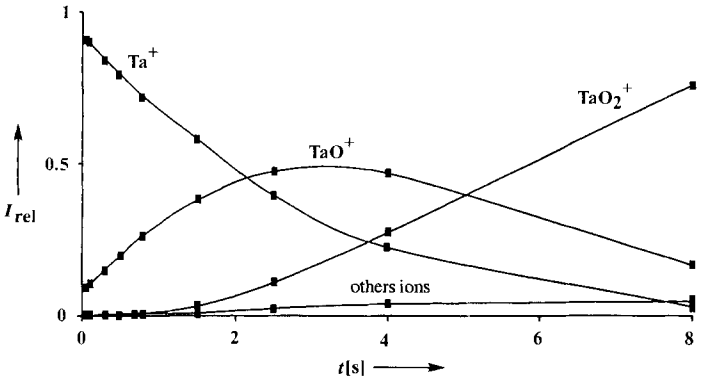

Fig. 1. Intensity vs time curves for the ions in the reaction of Ta^+ and CO_2.

rate.[14] In contrast to many late transition metal oxides,[15] neither TaO^+ nor TaO_2^+ activate methane; this corresponds to an experimental rate constant k_r smaller than 10^{-14} cm^3 molecule^{-1} s^{-1}. We decided therefore to treat CH_4 with Ta^+ first and then to investigate the reactivity of the resulting carbene complex $TaCH_2^+$ towards CO_2.

In fact, $TaCH_2^+$, like the bare Ta^+ cation, is able to deoxygenate CO_2 rapidly ($k_r = 6.9 \times 10^{-10}$ cm^3 molecule^{-1} s^{-1}; $k_{ADO} = 6.4 \times 10^{-10}$ cm^3 molecule^{-1} s^{-1}) to yield CO and a complex of the elemental composition $[TaCH_2O]^+$ (Fig. 2). The formulas **1**–**5** depict possible connectivities for this species. The

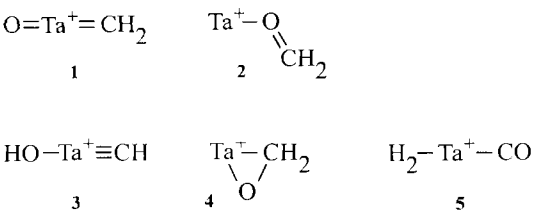

formation of a Ta^+–formaldehyde complex (**2**) can be excluded on thermochemical grounds, since this would require a Ta^+–(CH_2O) bond dissociation energy of more than 70 kcal mol^{-1}. The generation of a mixed dihydrogen carbonyl complex (**5**) can also be ruled out on energetic considerations. More likely, the complex contains a covalent Ta^+–carbon and a Ta^+–oxygen bond. This supposition is reinforced by CID experiments, which generate TaO^+ (44%) and Ta^+ (40%) as major products. As by-products $TaCO^+$ (10%) and TaH_2^+ (6%) are presumably generated by a collision-induced isomerization/dissociation path via intermediate **5**. Since no loss of an OH radical is observed, the hydroxo(carbyne) HO–Ta^+–CH **3** is also not likely to be formed in the reaction of $TaCH_2^+$ with CO_2. However, both the oxo(carbene) **1** and the cyclic structure **4** are in accord with the experimental data, and an unequivocal distinction cannot be made.

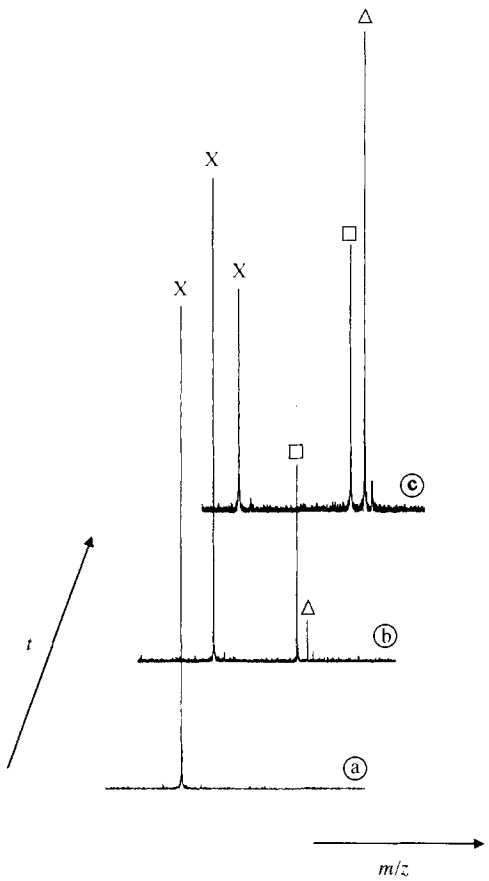

Fig. 2. Section of the mass spectra of $TaCH_2^+$ in the presence of CO_2, recorded after a) 0.3 s, b) 6 s, and c) 16 s reaction time (X: $TaCH_2^+$; □: $Ta[CH_2O]^+$; Δ: TaO_2^+).

Most interestingly, regardless of its actual connectivity, the tantalum complex $[TaCH_2O]^+$ reacts slowly ($k_r = 1.3 \times 10^{-10}$ cm^3 molecule^{-1} s^{-1}; $k_{ADO} = 6.3 \times 10^{-10}$ cm^3 molecule^{-1} s^{-1}) with a further equivalent of CO_2 to yield the dioxo cation TaO_2^+ as the only ionic product (Fig. 2). The more important aspect of this reaction concerns the nature of the neutral product. Although the FT-ICR mass spectrometer does not provide direct structural information on the neutral "C_2H_2O", thermochemical data can be used to narrow down the number of possibilities. Table 1 summarizes the heats of formation for different isomers of "C_2H_2O" or dissociation products thereof. According to this data, the overall reaction $Ta^+ + CH_4 + 2CO_2 \rightarrow TaO_2^+ + H_2 + CO + C_2H_2O$ is exothermic only if genuine ketene ($\Delta H_r = -53$ kcal mol^{-1}) or hydroxyacetylene ($\Delta H_r = -16$ kcal mol^{-1}) (Scheme 2)[16] are formed. On mechanistic grounds, the formation of HC≡COH from either **1** or **4** is quite difficult. The tantalum-mediated coupling of the C_1 units

Table 1. Heats of formation for isomers of C_2H_2O and fragmentation products [a].

Species	ΔH_R [kcal mol^{-1}]
$CH_2=C=O$	−11.4
HC≡COH	25.6 [b]
oxirene	66 [c]
$CH_2 + CO$	67
$C_2HO^{\cdot} + H^{\cdot}$	94
$H_2O + C_2$	141
$CH_2O + C$	145
$HCO^{\cdot} + CH^{\cdot}$	153

[a] See ref. [4]. [b] Calculated value from ref. [16]. [c] Calculated value from ref. [17].

$$Ta^+ + CH_4 \longrightarrow TaCH_2^+ + H_2$$

$$TaCH_2^+ + CO_2 \longrightarrow Ta(O)CH_2^+ + CO$$

$$Ta(O)CH_2^+ + CO_2 \longrightarrow TaO_2^+ + C_2H_2O$$

$$Ta^+ + CH_4 + 2\,CO_2 \longrightarrow TaO_2^+ + H_2 + CO + C_2H_2O$$

Scheme 2.

CO_2 and CH_4 and their conversion to ketene by a metathesis reaction involving **1** and **6** (Scheme 3) is more plausible. Interestingly, a related reaction has recently been discovered by Proulx and Bergman in the condensed phase.[18] They investigated the reactivity of a tantalum–carbene complex towards a CO donor and obtained a product containing a vinylidene ($C{=}CH_2$) and a TaO unit. Common to both processes is the fact that new C–C and Ta–O multiple bonds are formed at the cost of C–O and Ta–C bonds. Although the exact mechanism of the metathesis reaction is not yet known, it is quite attractive to suggest a Wittig-like process. This may involve the formation of an oxametallacyclobutanone **6**, followed by ring opening and cleavage to yield the observed products (Scheme 3). While Proulx and Bergman favor a ring fragmentation by a zwitterionic intermediate for their system, a concerted process is more appropriate for the cationic system reported here.

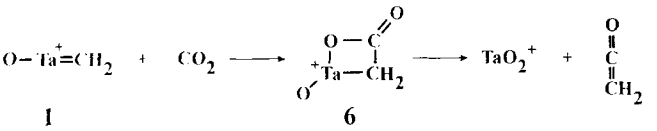

1 **6**

Scheme 3.

The reported sequence of reactions (Scheme 2) demonstrates for the first time that, at a molecular level, activation and coupling of CO_2 and CH_4 to form an acetic acid equivalent, most likely $CH_2{=}C{=}O$, can be achieved by a relatively simple system. Nevertheless, the reaction suffers from the drawback that Ta^+ is used in stoichiometric amounts and consumed as TaO_2^+. While the formation of strong tantalum–oxygen bonds is, on one hand, the driving force for ketene formation, on the other hand the fact that TaO_2^+ cannot be reduced to Ta^+ by any of the common reagents such as dihydrogen or alkanes limits the scope of the reaction. Obviously, the task of developing a genuine catalytic system for acetic acid synthesis, based on methane and carbon dioxide coupling, remains a challenge.

Received: May 18, 1995 [Z 8003 1E]
German version: *Angew. Chem.* **1995**, *107*, 2176–2179

Keywords: carbon dioxide activation · mass spectrometry · methane activation · tantalum

[1] Recent monographs: a) A. Behr, *Carbon Dioxide Activation by Metal Complexes*, VCH, Weinheim, **1988**; b) W. M. Ayers, *Catalytic Activation of Carbon Dioxide*, *ACS Symp. Ser. 363*, **1988**; c) M. Aresta, J. V. Schloss, *Enzymatic and Model Carboxylation and Reduction Reactions for Carbon Dioxide Utilization*, *NATO ASI Ser. Ser. C*, *314*, **1990**.

[2] See, for example, a) D. Walther, *Nachr. Chem. Tech. Lab.* **1992**, *40*, 1214; b) N. Kitajima, S. Hikichi, M. Tanaka, Y. Moro-oka, *J. Am. Chem. Soc.* **1993**, *115*, 5496; c) W. Leitner, *Angew. Chem.* **1994**, *106*, 183; *Angew. Chem. Int. Ed. Engl.* **1994**, *33*, 173; d) I. Willner, B. Willner, *Top. Curr. Chem.* **1991**, *159*, 153.

[3] a) J.-C. Tsai, K. M. Nicholas, *J. Am. Chem. Soc.* **1992**, *114*, 5117; b) T. Burgemeister, F. Kastner, W. Leitner, *Angew. Chem.* **1993**, *105*, 781; *Angew. Chem. Int. Ed. Engl.* **1993**, *32*, 739; c) F. Gassner, W. Leitner, *J. Chem. Soc. Chem. Commun.* **1993**, 1465; d) W. Leitner, E. Dinjus, F. Gaßner, *J. Organomet. Chem.* **1994**, *475*, 257; e) P. G. Jessop, T. Ikariya, R. Noyori, *Nature (London)* **1994**, *368*, 231; f) W. Leitner, *Angew. Chem.* **1995**, *107*, Nr. 20; *Angew. Chem. Int. Ed. Engl.* **1995**, *34*, Nr. 20.

[4] If not stated otherwise, all thermochemical data are taken from: a) S. G. Lias, J. E. Bartmess, J. F. Liebman, J. L. Holmes, R. D. Levin, W. G. Mallard, *Gas-Phase Ion and Neutral Thermochemistry*, *J. Phys. Chem. Ref. Data, Suppl. 1* **1988**; b) S. G. Lias, J. F. Liebman, R. D. Levin, S. A. Kafafi, *NIST Standard Reference Database, Positive Ion Energetics*, Version 2.01, Gaithersburg, MD, USA, **1994**.

[5] Recent reviews: a) P. B. Armentrout, *Annu. Rev. Phys. Chem.* **1990**, *41*, 313; b) K. Eller, H. Schwarz, *Chem. Rev.* **1991**, *91*, 1121; c) K. Eller, *Coord. Chem. Rev.* **1993**, *123*, 93; d) B. S. Freiser, *Acc. Chem. Res.* **1994**, *27*, 353.

[6] D. J. Hajdasz, Y. Ho, R. R. Squires, *J. Am. Chem. Soc.* **1994**, *116*, 10751, and references therein.

[7] a) See, for example, M. M. Kappes, R. H. Staley, *J. Phys. Chem.* **1981**, *85*, 942. See also: b) D. E. Lersen, R. L. Asher, P. J. Brucat, *J. Chem. Phys.* **1991**, *95*, 1414; c) M. R. Sievers, P. B. Armentrout, *ibid.* **1995**, *102*, 754.

[8] a) J. Schwarz, H. Schwarz, *Organometallics* **1994**, *13*, 1518; b) J. Schwarz, C. Heinemann, H. Schwarz, *J. Phys. Chem.*, **1995**, *99*, 11405. c) Inefficient activation of CO_2 by Fe_n^+ clusters ($n = 2$–4) has been recently observed: O. Gehret, M. P. Irion, *Chem. Eur. J.*, submitted. We thank Prof. Irion for this information.

[9] a) K. K. Irikura, J. L. Beauchamp, *J. Am. Chem. Soc.* **1989**, *111*, 75; b) S. W. Buckner, T. J. MacMahon, G. L. Byrd, B. S. Freiser, *Inorg. Chem.* **1989**, *28*, 3511; c) K. K. Irikura, J. L. Beauchamp, *J. Am. Chem. Soc.* **1991**, *113*, 2769; d) *J. Phys. Chem.* **1991**, *95*, 8344; e) R. Wesendrup, D. Schröder, H. Schwarz, *Angew. Chem.* **1994**, *106*, 1232; *Angew. Chem. Int. Ed. Engl.* **1994**, *33*, 1174; f) C. Heinemann, R. Wesendrup, H. Schwarz, *Chem. Phys. Lett.*, **1995**, *239*, 75.

[10] a) Y. Matsuo, H. Maeda, M. Takami, *Chem. Phys. Lett.* **1993**, *201*, 341; b) S. W. Buckner, J. R. Gord, B. S. Freiser, *J. Am. Chem. Soc.* **1988**, *110*, 6606; c) R. M. Pope, S. L. VanOrden, B. T. Cooper, S. W. Buckner, *Organometallics* **1992**, *11*, 2001; d) C. Q. Jiao, B. S. Freiser, *J. Am. Chem. Soc.* **1993**, *115*, 6268.

[11] a) K. Eller, H. Schwarz, *Int. J. Mass Spectrom. Ion Processes* **1989**, *93*, 243; b) K. Eller, W. Zummack, H. Schwarz, *J. Am. Chem. Soc.* **1990**, *112*, 621.

[12] a) B. S. Freiser, *Talanta* **1982**, *32*, 697; b) B. S. Freiser, *Anal. Chim. Acta* **1985**, *178*, 137.

[13] R. A. Forbes, F. H. Laukien, J. Wronka, *J. Int. Mass Spectrom. Ion Processes* **1988**, *83*, 23.

[14] $k_r(Ta^+ + CO_2) = 6.0 \times 10^{-10}\ cm^3\,molecule^{-1}\,s^{-1}$; $k_r(TaO^+ + CO_2) = 5.8 \times 10^{-10}\ cm^3\,molecule^{-1}\,s^{-1}$; k_{ADO} (for both reactions) $= 6.4 \times 10^{-10}\ cm^3\,molecule^{-1}\,s^{-1}$. See: T. Su, M. T. Bowers, *Int. J. Mass Spectrom. Ion Phys.* **1973**, *12*, 347.

[15] Recent review: D. Schröder, H. Schwarz, *Angew. Chem.* **1995**, *107*, 2126–2150; *Angew. Chem. Int. Ed. Engl.* **1995**, *34*, 1973–1995.

[16] B. van Baar, T. Weiske, J. K. Terlouw, H. Schwarz, *Angew. Chem.* **1986**, *98*, 275; *Angew. Chem. Int. Ed. Engl.* **1986**, *25*, 282.

[17] A. P. Scott, R. H. Nobes, H. F. Schaefer III, L. Radom, *J. Am. Chem. Soc.* **1994**, *116*, 10159.

[18] G. Proulx, R. G. Bergman, *J. Am. Chem. Soc.* **1993**, *115*, 9802.

$[Pb_{18}I_{44}]^{8-}$—An Iodoplumbate with an Unusual Structure**

Harald Krautscheid* and Frieder Vielsack

The synthesis and characterization of polynuclear complexes of various compositions have been the subject of increasing interest in the past several years. These types of compounds can be regarded as a link between mononuclear complexes and the corresponding binary solids and may possibly provide insight into the molecular steps in the precipitation of the corresponding insoluble binary phase from solution. The heavier elements of Group 15 form anionic halogeno complexes with either discrete or polymeric anions with a surprising diversity of structures.[1]

[*] Dr. H. Krautscheid, F. Vielsack
Institut für Anorganische Chemie der Universität
Engesserstrasse, Geb.-Nr. 30.45, D-76128 Karlsruhe (Germany)
Telefax: Int. code + (721)661 921

[**] This work was supported by the Fonds der Chemischen Industrie. We thank Prof. Dr. D. Fenske for his support.

In the synthesis of iodobismutate complexes, the solvent, the stoichiometric ratio $Bi^{3+}:I^-$, and the nature and size of the counterion used for crystallization control the structure of the resulting complexes. For example, salts such as $[Li(thf)_4]_4[Bi_5I_{19}]$, with isolated anions, and compounds with infinite one-dimensional anions like $(Bu_4N)[Bi_2I_7]$ or $(Et_3PhN)_2[Bi_3I_{11}]$ can be isolated and characterized by X-ray structure analysis.[2] PbI_2 is also known to form complexes with halide ions; for example $Cs_4[PbI_6]$ contains octahedral $[PbI_6]^{4-}$ ions.[3] Although the compositions of a large number of halogeno complexes of Pb^{II} are known, their structures are mainly undetermined.[4]

PbI_2 has a low solubility in polar organic solvents such as dimethylformamide, acetonitrile, and acetone, which increases upon the addition of an alkali metal iodide. Treatment of the resulting yellow solution with quaternary ammonium salts leads to the formation of ionic lead(II) complexes. According to their elemental analyses, some of these salts have the composition $(R_4N)[PbI_3]$. A single-crystal X-ray structure analysis for the $(Me_4N)[PbI_3]$ complex confirmed the composition and showed that the polymeric anion $[PbI_3]^-$ consists of an infinite chain of *trans*-face-sharing PbI_6 octahedra.[5]

We are currently investigating the possibility of synthesizing iodoplumbate complexes of different structure types and report here the structure of $(Bu_4N)_8[Pb_{18}I_{44}]$ (**1**), which is formed according to Equation (a).

$$18\,PbI_2 + 8\,NaI + 8\,Bu_4NPF_6 \xrightarrow[-8\,NaPF_6]{\text{acetone/ether}} \underset{\mathbf{1}}{(Bu_4N)_8[Pb_{18}I_{44}]} \qquad \text{(a)}$$

Compound **1** crystallizes in space group $I4/m$[6] with two formula units and 32 molecules of acetone in the unit cell.[7] According to the results of the X-ray structure analysis the anion of **1** has crystallographic $4/m$ symmetry (D_{4h}) approaching even O_h symmetry. Figure 1 shows that the outer 38 (I1, I2, I4, I5, I6, I7, I9) of a total of 44 I atoms are arranged as a v_3-octahedron (an octahedron with a threefold edge length; thus with four I atoms on each edge and ten I atoms on each face of the octahedron). Inside the v_3-I-octahedron there is a v_2-octahedron (three Pb atoms on each edge of the octahedron) consisting of 18 Pb atoms. Inside this lies a simple octahedron formed by six I atoms (I3, I8). The I structure is reminiscent of the metal framework in the cluster $[Ni_{38}Pt_6(CO)_{48}H_2]$.[8] The Pb atoms in **1** occupy the octahedral sites of the I_{44} framework. In contrast to the above-mentioned iodoplumbate $(Me_4N)[PbI_3]$,[5] the anion in **1** consists of edge-sharing PbI_6 octahedra. If the $[Pb_{18}I_{44}]^{8-}$ ion is schematically divided into shells of atoms around the unoccupied center, one finds, with increasing distance from the center, an I_6 octahedron (I3, I8), a Pb_{12} cuboctahedron (Pb2, Pb3), an I_8 cube (I4), a Pb_6 octahedron (Pb1, Pb4), a truncated octahedron formed by 24 I atoms (I2, I5, I6, I7) and, on the outside again, an I_6 octahedron (I1, I9).

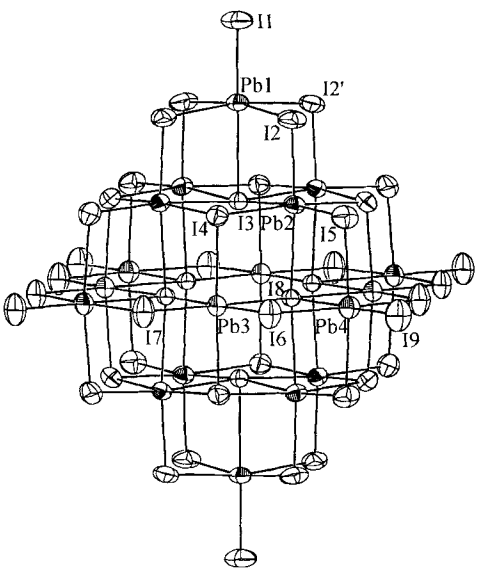

Fig. 1. ORTEP representation of the structure of the anion in **1** (ellipsoids drawn at the 50% probability level). I1, Pb1, I3 and equivalent atoms lie on the fourfold axis. The Pb atoms are marked by hatching of the ellipsoids. Important distances [pm] and angles [°]: Pb1–I1 296.8(2), Pb1–I2 324.57(9), Pb1–I3 352.50(13), Pb2–I2 303.65(9), Pb2–I3 339.19(5), Pb2–I4 323.35(8), Pb2–I5 304.53(9), Pb2–I8 339.34(5), Pb3–I4 322.64(8), Pb3–I6 304.59(11), Pb3–I7 304.46(12), Pb3–I8 337.94(10), Pb4–I5 323.46(9), Pb4–I6 324.69(13), Pb4–I8 352.21(10), Pb4–I9 295.85(12), Pb1–Pb2 474.55(7), Pb3–Pb4 471.43(8), I1–Pb1–I2 95.17(2); I1-Pb1-I3 180, I2-Pb1-I2' 89.536(3), I2-Pb1-I3 84.83(2), I2-Pb2-I3 90.48(3), I2-Pb2-I4 93.14(2), I2-Pb2-I5 95.95(2), I2-Pb2-I8 173.36(2), I3-Pb2-I5 173.56(3), I5-Pb2-I8 90.69(2).

Neglecting the vacant site in the center, $[Pb_{18}I_{44}]^{8-}$ can be described—with idealized symmetry—as an octahedral fraction of the solid-state structure of NaCl. This relationship to the structure of NaCl is reflected in the layered structure of the anion (see Fig. 1). The stacking of the Pb and I layers alternates and can be described as "A γ B α C β A" (where A, B, and C are layers of I atoms, and α, β, γ are layers of Pb atoms). The mean distance between layers formed from I atoms is 373 pm. In contrast, PbI_2 crystallizes in the CdI_2 structure type with "A γ B □, A ..." stacking; other polytype forms are observed as a consequence of variants of stacking. For the most common 2H-form, the distance between I layers for an occupied (Pb) intermediate layer γ is 373 pm, that between I layers for an unoccupied intermediate layer[9] 324 pm. The distances between the Pb atoms in **1** range from 471 to 480 pm, indicating the absence of Pb–Pb bonds. As expected, the Pb–I bond lengths (295.85(12)–352.50(13) pm) depend on the bridging mode of the I ligands: I_{term}–Pb 295.85(12), 256.8(2) pm (I1, I9); μ_2-I-Pb 303.65(9)–324.69(13) pm (I2, I5, I6, I7); μ_3-I-Pb 322.64(8)–323.35(8) pm (I4); μ_5-I-Pb 337.94(10)–352.50(13) pm (I3, I8).

The distances between the Pb atoms in PbI_2 are 456 pm. All I atoms bridge three Pb atoms each; the Pb–I bonds (323 pm) are as long as the μ_3-I-Pb distances in **1**. The μ_2-I ligands in $(Me_4N)[PbI_3]$ bridge the Pb atoms symmetrically with Pb–I distances of 322.3(1) pm; the distance between the Pb atoms is 395.8(1) pm.

The octahedral anions of **1** with edge lengths of 1364 and 1366 pm occupy the vertices and the center of the tetragonal unit cell. The equatorial plane of the octahedra formed by I9 and symmetry equivalent atoms is twisted by 13.4° around the crystallographic *c* axis with respect to the unit cell; thus the shortest distance between two anions is 715 pm (I6 to I9 of the neighboring anions).

Experimental Procedure

Synthesis of **1**: PbI_2 (0.50 g, 1.1 mmol) and NaI (0.09 g, 0.6 mmol) were dissolved in acetone (100 mL). After addition of $(Bu_4N)(PF_6)$ (0.42 g, 1.1 mmol) the solution was filtered, concentrated to 30 mL and over one week ether (20 mL) was condensed into the acetone solution. Highly refractive, yellow, octahedral crystals of **1** are formed in 45% (0.30 g) yield. Reaction of PbI_2 (0.50 g, 1.1 mmol) with NaI (0.16 g, 1.1 mmol) followed by the addtion of $(Bu_4N)(PF_6)$ (0.42 g, 1.1 mmol) led to the formation of $(Bu_4N)[PbI_3]$ [10].

Received: May 19, 1995 [Z 8007 IE]
German version: *Angew. Chem.* **1995**, *107*, 2166–2168

Keywords: crystal structure elucidation · iodine compounds · lead compounds

[1] G. A. Fisher, N. C. Norman, *Adv. Inorg. Chem.* **1994**, *41*, 233; S. Pohl, M. Peters, D. Haase, W. Saak, *Z. Naturforsch. B* **1994**, *49*, 741; W. D. Sheldrick, J. Kiefer, *ibid.* **1992**, *47*, 1079.
[2] H. Krautscheid, *Z. Anorg. Allg. Chem.* **1994**, *620*, 1559; *ibid.* in press.
[3] B. D. Stepin, G. M. Serebrennikova, G. P. Chicherina, V. K. Trunov, Yu. V. Oboznenko, *Zh. Neorg. Khim.* **1976**, *21*, 3148.
[4] N. N. Greenwood, A. Earnshaw, *Chemistry of the Elements*, 1st ed., Pergamon Press, Oxford, **1984**, p. 444; E. W. Abel in *Comprehensive Inorganic Chemistry*, *Vol. 2*, Pergamon, Oxford, **1973**, Chapter 18 (lead), p. 105.
[5] J. G. Contreras, G. V. Seguel, B. Ungerer, W. F. Maier, F. J. Hollander, *J. Mol. Struct.* **1983**, *102*, 295.
[6] X-ray structure analysis of **1**·16 Me_2CO: STOE IPDS diffractometer (imaging plate), $Mo_{K\alpha}$ radiation, $T = 200$ K, data collection, structure solution (SHELXS-86) and refinement (SHELXL-93): crystal dimensions $0.10 \times 0.10 \times 0.10$ mm^3, 329 images with rotation increments $\Delta\varphi = 0.4^\circ$, cell parameters $a = 2137.5(2)$, $c = 2850.6(3)$ pm, $V = 13024(2) \times 10^6$ pm^3, tetragonal, space group $I4/m$ (No. 87), $Z = 2$, $\mu(Mo_{K\alpha}) = 168.5$ cm^{-1}; $2\theta_{max} = 48^\circ$, 27556 reflections, 5175 independent reflections ($R_{int} = 0.089$), 4500 [$I > 2\sigma(I)$] reflections observed; 188 parameters (Pb, I refined anisotropically, C, N refined isotropically); $R1 = 0.044$ (observed reflections), $wR2 = 0.115$ (all data). **1** crystallizes with acetone which is given off under decomposition of the crystals outside the mother liquor at room temperature [7]. The Bu_4N^+ ions and the solvent molecules are disordered; most of the C atoms of the butyl groups could be localized. Further details of the crystal structure investigation may be obtained from the Fachinformationszentrum Karlsruhe, 76344 Eggenstein-Leopoldshafen (Germany), on quoting the depository number CSD-404031.
[7] ^1H and ^{13}C NMR spectra (250 and 62.9 MHz, respectively, 25 °C) of crystals of **1**, washed with pentane and dissolved in [D_6]DMSO, show signals of the Bu_4N^+ ions and of acetone in a molar ratio of 1:1.3. In a N_2 stream the crystals loose acetone very quickly.
[8] A. Ceriotti, F. Demartin, G. Longoni, M. Manassero, M. Marchionna, G. Piva, M. Sansoni, *Angew. Chem.* **1985**, *97*, 708; *Angew. Chem. Int. Ed. Engl.* **1985**, *24*, 697.
[9] T. Minagawa, *Acta Crystallogr. Sect. A* **1975**, *31*, 823; M. Chand, G. C. Trigunayat, *Acta Crystallogr. Sect. B* **1975**, *31*, 1222; *ibid.* **1976**, *32*, 1619; R. S. Mitchell, *Z. Kristallogr.* **1959**, *111*, 372.
[10] $(Bu_4N)[PbI_3]$: cell parameters ($T = 300$ K): $a = 2446(2)$, $c = 835.5(5)$, $V = 4999 \times 10^6$ pm^3, $Z = 8$, space group $I\bar{4}2d$ (No. 122). The polymeric $[PbI_3]^-$ ion consists, like in $(Me_4N)[PbI_3]$, of infinite chains of *trans*-face-sharing PbI_6 octahedra.

Low-Temperature Tandem Enyne Allene Radical Cyclizations: Efficient Synthesis of 2,3-Dihydroindenes from Simple Enediynes**

Janet W. Grissom* and Dahai Huang

In recent years, the enediyne antitumor antibiotics[1] have received widespread attention due to their unique mechanism of DNA cleavage and unusual structures, which represent a challenging synthetic problem. Synthesis and cyclization of less complex models of enediyne,[2, 3] enyne allene,[4, 5] and enyne ketene[6] systems have also been studied. While considerable effort has been devoted to the synthetic and DNA cleaving studies of these enediynes and enyne allenes,[1-5] limited attention has been focused on trapping the intermediate diyl in further radical cyclizations.[7-10]

[*] Prof. Dr. J. W. Grissom, D. Huang
Department of Chemistry, University of Utah
Salt Lake City, UT 84112 (USA)
Telefax: Int. code + (801) 581-8433
e-mail: GrissomJ@Chemistry.Chem.Utah.Edu

[**] This research was supported by the University of Utah, University of Utah Biomedical Research Grant (Nos. SO7RR07092 and 2807RR0792-26), University of Utah Research Committee Grant, American Cancer Society (IRG-178A), Petroleum Research Fund (PRF24681 61), and the National Institutes of Health (GM 49991-01).

Previously, we have reported that benzindene derivatives can be synthesized in excellent yields by a tandem enediyne radical cyclization of aromatic enediynes.[8a-f] The corresponding non-aromatic enediynes also undergo a similar cyclization to provide indene derivatives;[8g] however, the yields are only moderate. Both reactions require high temperatures (ca. 170–230 °C). More recently, we have developed the tandem enyne allene radical cyclization for the preparation of 2,3-dihydrobenz[*e*]-indenes.[9] Although the reaction proceeds at low temperature (ca. 75 °C) and in excellent yield, the synthesis of the cyclization precursors requires eight to nine steps. In line with our effort to lower the reaction temperature, improve the cyclization of non-aromatic systems, and simplify the synthesis of the reaction precursors, we herein report the synthesis of 2,3-dihydroindenes by a tandem enyne allene radical cyclization that proceeds at 37 °C.

Enediynes **10**–**13** were readily synthesized in four steps from chloroenyne **1**, which can be prepared from commercially available *cis*-dichloroethylene (Scheme 1).[8g] Two consecutive Pd^0-

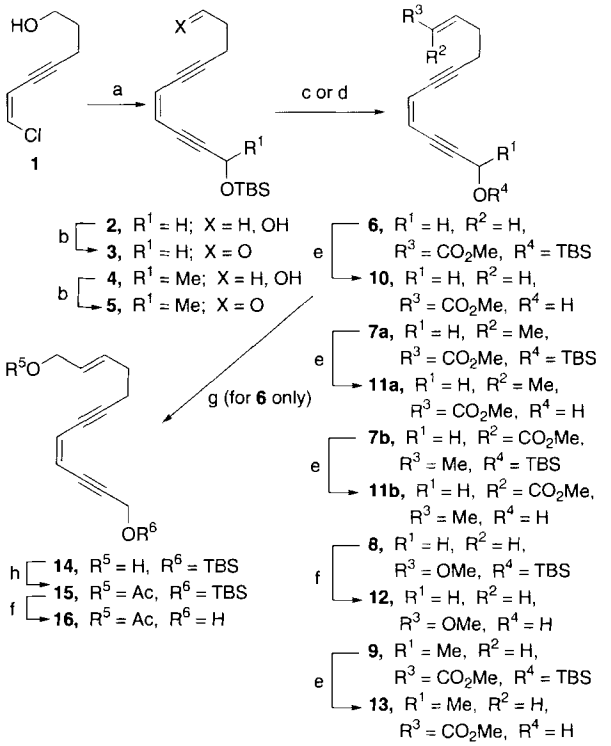

Scheme 1. a) 3-(*tert*-Butyldimethylsilyloxy)propyne or 3-(*tert*-butyldimethylsilyloxy)butyne (1.2 equiv), $[Pd(PPh_3)_4]$ (0.017 equiv), CuI (0.04 equiv), $nBuNH_2$ (1.7 equiv), benzene, 50 °C (85% for **2**, 79% for **4**); b) PCC, CH_2Cl_2 (75% for **3**, 77% for **5**); c) trimethyl phosphonoacetate or trimethyl (2-methyl)phosphonoacetate (1.5 equiv), LiCl (2.0 equiv), 1,8-diazabicyclo[5.4.0]undec-7-ene (DBU) (1.5 equiv), CH_3CN, room temperature (RT) (86% for **6**, 82% for **7a** and **7b**, $E/Z = 8:1$, 92% for **9**); d) (methoxymethyl)triphenylphosphonium chloride (2.5 equiv), *t*BuOK (2.5 equiv), THF, −78 °C (62% for **8**, $E/Z = 6:1$); e) $Et_2O \cdot BF_3$, CH_2Cl_2, RT (86% for **10**, 80% for **11a**, 82% for **11b**, 84% for **13**); f) tetrabutylammonium fluoride, THF, RT (88% for **12**, $E/Z = 6:1$, 83% for **16**); g) DIBAL, CH_2Cl_2, 0 °C (78%); h) Ac_2O, NEt_3, CH_2Cl_2 (95%). TBS = *tert*-butyldimethylsilyl.

catalyzed coupling reactions under modified Castro–Stephens conditions[11] followed by oxidation with pyridinium chlorochromate (PCC) provided aldehydes **3** and **5**.[8g] A subsequent Horner–Emmons reaction or Wittig reaction followed by desilylation afforded **10**–**13** in excellent yields. Enediyne **16** was

obtained by reduction of **6** with diisobutylaluminum hydride (DIBAL) followed by acetylation and desilylation.[8g]

Given the reliability of the α,β-unsaturated ester as a radical acceptor in tandem enediyne and enyne allene radical cyclizations,[8, 9] we initially decided to investigate the enyne allene **17** (Table 1). When enediyne **10** was treated with PPh_2Cl and NEt_3 in CH_2Cl_2 at −78 °C and the mixture allowed to stir at 0 °C, enyne allene **17** was formed by a [2,3] sigmatropic rearrangement.[5a, b, j] Unfortunately, **17** was isolated in poor yield (ca. 10%) since it decomposes on silica gel and alumina. Therefore the subsequent cyclization was performed without the purification of **17**. Upon mild thermolysis of the crude enyne allene **17** in anhydrous benzene at 37 °C in the presence of 1,4-cyclohexadiene (1,4-CHD, 3.5 M) for 12 h, 2,3-dihydroindene **22** was isolated in 68% overall yield from **10**. It is noteworthy that 2,3-dihydroindene **22** was produced at 37 °C in excellent yield from the tandem enyne allene radical cyclization, whereas synthesis of similar compounds via a tandem enediyne radical cyclization proceeded both at much higher temperatures (ca. 170–230 °C) and in lower yields.[8g]

Table 1. Tandem enyne allene radical cyclization.

Enediyne	Enyne allene	R^1	R^2	R^3	Product	Yield [%] [a]
10	**17**	H	H	CO_2Me	**22**	68
11a	**18a**	H	Me	CO_2Me	**23a, b** [b]	70
11b	**18b**	H	CO_2Me	Me	**23a, b** [b]	67
12 [c]	**19**	H	H	OMe	**24**	55
16	**20**	H	H	CH_2OAc	**25**	62
13	**21**	Me	H	CO_2Me	**26**	52

[a] Overall yield for two steps. [b] Isolated as a 3.5:1 mixture of diastereomers. [c] $E/Z = 6:1$.

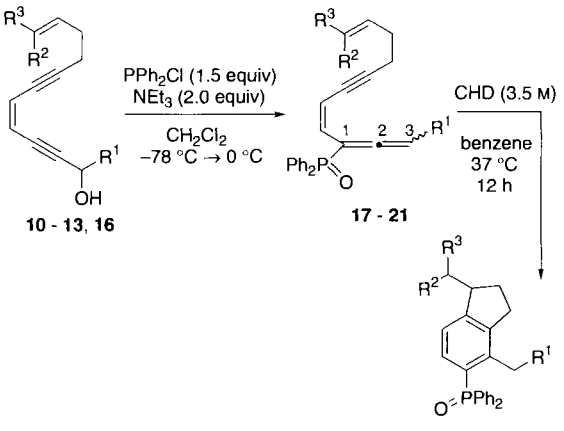

22 - 26

Encouraged by the successful tandem enyne allene radical cyclization of **17**, we thermolyzed enyne allene **18a**, which was generated from **11a** by a [2,3] sigmatropic rearrangement, at 37 °C in the presence of 1,4-CHD (3.5 M) to provide 2,3-dihydroindenes **23a** and **23b** as a 3.5:1 diastereomeric mixture in 70% overall yield from **11a**. When the same reaction sequence was applied to **11b**, 2,3-dihydroindenes **23a** and **23b** were obtained as an identical 3.5:1 diastereomeric mixture in 67% overall yield from **11b**. The fact that the diastereoselectivities observed in both reactions are identical with previous results observed in the tandem enediyne radical cyclizations and the comparable tributyltin hydride mediated radical cyclizations[8b] indicates that the current reaction likely proceeds through a radical intermediate and that the configuration of the double bond within the α,β-unsaturated ester affects neither the diastereoselectivity nor the yield of the radical cyclization.

To test our method with other radical acceptors and to determine the scope of the reaction, both vinyl ether **12** and allylic acetate **16** were subjected to the standard reaction conditions. Treatment of **12** and **16** with PPh_2Cl followed by thermolysis of the corresponding enyne allenes **19** and **20** at 37 °C in the presence of 1,4-CHD (3.5 M) produced 2,3-dihydroindenes **24** and **25** in 55% and 62% overall yields, respectively. It should be pointed out that the tandem enyne allene radical cyclization of **19** bearing a methyl vinyl ether in the side chain occurred smoothly at 37 °C, while the vinyl ether functionality in a nonaromatic enediyne similar to **12** did not survive the tandem enediyne radical cyclization at high temperatures.[8f, g]

Finally, enediyne **13** was chosen to determine how a simple alkyl substituent at the C-3 position of the resulting allene would affect the enyne allene cyclization.[4] When **13** was treated with PPh_2Cl and NEt_3 at −78 °C and the mixture allowed to stir at 0 °C, enyne allene **21** was formed as the major product along with an impurity (ca. 15% based on ^1H NMR). Subsequent thermolysis of the crude **21** at 37 °C in the presence of 1,4-CHD (3.5 M) afforded 2,3-dihydroindene **26** in 52% overall yield from **13** and 12% of a minor product, which is identical with the impurity formed in the [2,3] sigmatropic rearrangement. NMR data suggest that the minor product may be phosphonate **28**, which could arise from oxidation of the corresponding phosphinite **27**.

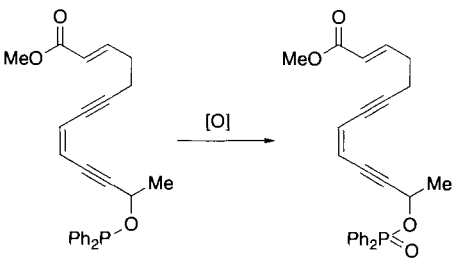

The mechanism of the overall transformation is outlined in Scheme 2. Enyne allene **17**, generated from a [2,3] sigmatropic rearrangement of the corresponding enediyne **10**, undergoes an enyne allene cyclization to form the biradical **29**. Subsequent 5-*exo* radical cyclization of the aryl radical within **29** followed by H· abstraction from 1,4-CHD furnish the 2,3-dihydroindene derivative **22**.

In conclusion, we have extended the tandem enyne allene radical cyclization to the preparation of 2,3-dihydroindene derivatives. The cyclization precursors can be readily synthesized from commercially available starting materials. In contrast to the tandem enediyne radical cyclization that proceeds at high temperatures (ca. 170–230 °C) and in moderate yields,[8g] the tandem enyne allene radical cyclization of nonaromatic enyne allenes occurs at physiological temperature (ca. 37 °C), and the 2,3-dihydroindenes are formed in good to excellent overall yields. Furthermore, the present method should tolerate a variety of functional groups due to the mild reaction condi-

 © VCH Verlagsgesellschaft mbH, D-69451 Weinheim, 1995 0570-0833/95/3418-2038 $ 10.00+.25/0

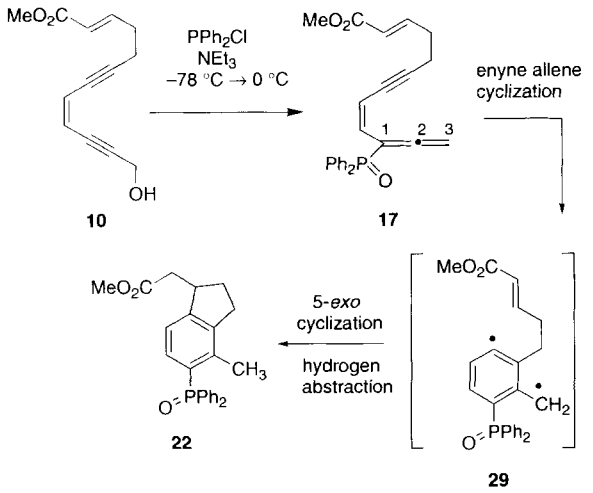

Scheme 2. Mechanism of the tandem enyne allene radical cyclization.

tions. Employment of other radical acceptors and the applications of this protocol towards the synthesis of natural products are currently underway and will be reported in due course.

Received: April 1, 1995 [Z 7860IE]
German version: *Angew. Chem.* **1995**, *107*, 2196–2198

Keywords: cyclizations · dihydroindenes · enyne allenes · radicals

[1] For reviews of enediyne chemistry, see: a) K. C. Nicolaou, W.-M. Dai, *Angew. Chem.* **1991**, *103*, 1453; *Angew. Chem. Int. Ed. Engl.* **1991**, *30*, 1387; b) K. C. Nicolaou, A. L. Smith, *Acc. Chem. Res.* **1992**, *25*, 497; c) K. C. Nicolaou, W.-M. Dai, S.-C. Tsay, V. A. Estevez, W. Wrasidlo, *Science* **1992**, *256*, 1172; d) K. C. Nicolaou, A. L. Smith, E. W. Yue, *Proc. Natl. Acad. Sci. USA* **1993**, *90*, 5881; e) M. E. Maier, *Synlett* **1995**, 13.

[2] a) R. G. Bergman, R. R. Jones, *J. Am. Chem. Soc.* **1972**, *94*, 660; b) T. P. Lockhart, C. B. Mallon, R. G. Bergman, *ibid.* **1980**, *102*, 5976; c) R. G. Bergman, T. P. Lockhart, P. B. Comita, *ibid.* **1981**, *103*, 4082; d) T. P. Lockhart, R. G. Bergman, *ibid.* **1981**, *103*, 4091; e) K. N. Bharucha, R. M. Marsh, R. E. Minto, R. G. Bergman, *ibid.* **1992**, *114*, 3120; f) R. G. Bergman, *Acc. Chem. Res.* **1973**, *6*, 25; g) G. C. Johnson, J. J. Stofko, T. P. Lockhart, D. W. Brown, R. G. Bergman, *J. Org. Chem.* **1979**, *44*, 4215.

[3] For other preparative enediyne cyclizations, see: a) K. C. Nicolaou, P. Maligres, T. Z. Suzuki, S. V. Wendeborn, W.-M. Dai, R. K. Chadhi, *J. Am. Chem. Soc.* **1992**, *114*, 8890; b) K. C. Nicolaou, W.-M. Dai, *ibid.* **1992**, *114*, 8908; c) K. C. Nicolaou, A. Liu, Z. Zeng, S. McComb, *ibid.* **1992**, *114*, 9279; d) P. A. Magriotis, K. D. Kim, *ibid.* **1993**, *115*, 2972; e) M. F. Semmelhack, T. Neu, F. Foubelo, *Tetrahedron Lett.* **1992**, *33*, 3277; f) D. L. Boger, J. Zhou, *J. Org. Chem.* **1993**, *58*, 3018; g) M. F. Semmelhack, J. J. Gallagher, *ibid.* **1994**, *59*, 4357; h) W. R. Roth, H. Hopf, C. Horn, *Chem. Ber.* **1994**, *127*, 1765.

[4] a) A. G. Myers, E. Y. Kuo, N. S. Finney, *J. Am. Chem. Soc.* **1989**, *111*, 8057; b) A. G. Myers, P. S. Dragovich, *ibid.* **1989**, *111*, 9130; c) A. G. Myers, P. S. Dragovich, E. Y. Kuo, *ibid.* **1992**, *114*, 9369.

[5] For other enyne allene cyclizations, see: a) I. Saito, R. Nagata, H. Yamanaka, E. Okazaki, *Tetrahedron Lett.* **1989**, *30*, 4995; b) I. Saito, R. Nagata, H. Yamanaka, E. Murahashi, *ibid.* **1990**, *31*, 2907; c) M. Hirama, K. Fujiwara, A. Kurisaki, *ibid.* **1990**, *31*, 4329; d) K. Toshima, K. Ohta, T. Ohtake, K. Tatsuka, *ibid.* **1991**, *32*, 391; e) P. A. Wender, M. Tebbe, *ibid.* **1991**, *32*, 4863; f) M. Shibuya, Y. Sakai, Y. Bando, K. Shishido, *ibid.* **1992**, *33*, 957; g) M. Hirama, M. Tokuda, K. Fujiwara, T. Gomibuchi, M. Uesugi, Y. Sugiura, *ibid.* **1993**, *34*, 669; h) M.-J. Wu, C.-F. Lin, J.-S. Wu, H.-T. Chen, *ibid.* **1994**, *35*, 1879; i) M. Hirama, K. Fujiwara, K. Shigematu, Y. Fukazawa, *J. Am. Chem. Soc.* **1989**, *111*, 4120; j) K. C. Nicolaou, P. Maligres, J. Shin, E. de Leon, D. Rideout, *ibid.* **1990**, *112*, 7825; k) K. Morokuma, N. Koga, *ibid.* **1991**, *113*, 1907; l) M. Hirama, T. Gomibuchi, K. Fujiwara, *ibid.* **1991**, *113*, 9851; m) R. R. Squires, P. G. Wenthold, S. G. Wierschke, J. J. Nash, *ibid.* **1993**, *115*, 12611; n) K. Fujiwara, H. Sakai, M. Hirama, *J. Org. Chem.* **1991**, *56*, 1688; o) K. K. Wang, Z. Wang, *ibid.* **1994**, *59*, 4738; p) K. Toshima, K. Ohta, A. Ohashi, A. Ohtsuka, M. Nakata, K. Tatsuta, *J. Chem. Soc. Chem. Commun.* **1992**, 1306; q) K. Toshima, K. Ohta, T. Kano, T. Nakamura, M. Nakata, S. Matsumura, *ibid.* **1994**, 2295; r) M. Hirama, M. Tokuda, K. Fujiwara, *Synlett* **1991**, 651; s) P. A. Wender, M. J. Tebbe, *Tetrahedron* **1994**, *50*, 1419; t) M. Hirama, K. Fujiwara, H. Sakai, T. Tanaka, *Chem. Lett.* **1994**, 457.

[6] For enyne ketene cyclizations, see: a) I. Saito, K. Nakatani, S. Isoe, S. Maekawa, *Tetrahedron Lett.* **1994**, *35*, 605; b) H. W. Moore, R. W. Sullivan, V. M. Coghlan, S. A. Munk, M. W. Reed, *J. Org. Chem.* **1994**, *59*, 2276.

[7] a) A. Padwa, D. J. Austin, U. Chiacchio, J. M. Kassir, A. Rescifina, S. L. Xu, *Tetrahedron Lett.* **1991**, *32*, 5923; b) S. L. Xu, M. Taing, H. W. Moore, *J. Org. Chem.* **1991**, *56*, 6104; c) H. W. Moore, S. L. Xu, *ibid.* **1992**, *57*, 326; d) H. W. Moore, H. Xia, *ibid.* **1992**, *57*, 3765; e) H. W. Moore, J. E. Ezcurra, C. Pham, *ibid.* **1992**, *57*, 4787; f) K. K. Wang, Y. W. Andemichael, Y. G. Gu, *ibid.* **1992**, *57*, 794; g) K. K. Wang, Y. W. Andemichael, Y. Huang, *ibid.* **1993**, *58*, 1651.

[8] a) J. W. Grissom, T. L. Calkins, *Tetrahedron Lett.* **1992**, *33*, 2315; b) J. W. Grissom, T. L. Calkins, M. L. Egan, *J. Am. Chem. Soc.* **1993**, *115*, 11744; c) J. W. Grissom, T. L. Calkins, *J. Org. Chem.* **1993**, *58*, 5422; d) J. W. Grissom, D. Klingberg, *ibid.* **1993**, *58*, 6559; e) J. W. Grissom, T. L. Calkins, H. A. McMillen, Y. Jiang, *ibid.* **1994**, *59*, 5833; f) J. W. Grissom, T. L. Calkins, D. Huang, H. A. McMillen, *Tetrahedron* **1994**, *50*, 4635; g) J. W. Grissom, T. L. Calkins, H. A. McMillen, *J. Org. Chem.* **1993**, *58*, 6556.

[9] a) J. W. Grissom, D. Huang, *J. Org. Chem.* **1994**, *59*, 5114; b) J. W. Grissom, B. J. Slattery, *Tetrahedron Lett.* **1994**, *35*, 5137.

[10] J. W. Grissom, D. Klingberg, S. Meyenburg, B. L. Stallman, *J. Org. Chem.* **1994**, *59*, 7876.

[11] a) D. Guillerm, G. Linstrumelle, *Tetrahedron Lett.* **1985**, *26*, 3811; b) C. Crévisy, J.-M. Beau, *ibid.* **1991**, *32*, 3171.

A Series of Well-Defined Metathesis Catalysts—Synthesis of $[RuCl_2(=CHR')(PR_3)_2]$ and Its Reactions**

Peter Schwab, Marcia B. France, Joseph W. Ziller, and Robert H. Grubbs*

Over the past three years there has been considerable effort in our group to explore the metathesis activity of vinylcarbene ruthenium complexes **1** and **2** which are available from

$RuCl_2(=CH-CH=CPh_2)(PR_3)_2]$, R = Ph (**1**),[1] R = Cy (**2**)[2]

$[RuCl_2(PPh_3)_3]$ and diphenyl cyclopropene. Although these complexes exhibit both high metathesis activity and remarkable stability towards functional groups, the multistep synthesis of the carbene precursors and the low initiation rates of **1** and **2** at present limit their use. The latter phenomenon leads to relatively broad molecular weight distributions in Ring Opening Metathesis Polymerization (ROMP)[3–5] and prolonged reaction times in Ring Closing Metathesis (RCM).[6] We now report that the use of diazoalkanes[7] as an alternative carbene source provides a series of novel alkylidene ruthenium complexes $[RuCl_2(=CHR')(PR_3)_2]$ (R' = alkyl, aryl; R = Ph, Cy) in high yields and that these complexes have high initiation rates.

$[RuCl_2(PPh_3)_3]$ reacts at −78 °C in CH_2Cl_2 with alkyl and aryl diazoalkanes to form **3**–**6**, which are isolated as air-stable green solids in 80–89% yield (Scheme 1). In contrast to **1**, **3**–**6**

[*] Prof. Dr. R. H. Grubbs, Dr. P. Schwab
The Arnold and Mabel Beckman Laboratory of Chemical Synthesis
Division of Chemistry and Chemical Engineering
California Institute of Technology
Pasadena, CA 91125 (USA)
Telefax: Int. + 818/564-9297
Prof. Dr. M. B. France
Washington and Lee
Lexington, VA 24450 (USA)
Telefax: Int. +703/463-8479
Dr. J. W. Ziller
Department of Chemistry
University of California
Irvine, CA 92717-2025 (USA)
Telefax: Int. +714/824-8571

[**] This work was supported by the Alexander von Humboldt Foundation, the National Science Foundation, and the National Institutes of Health.

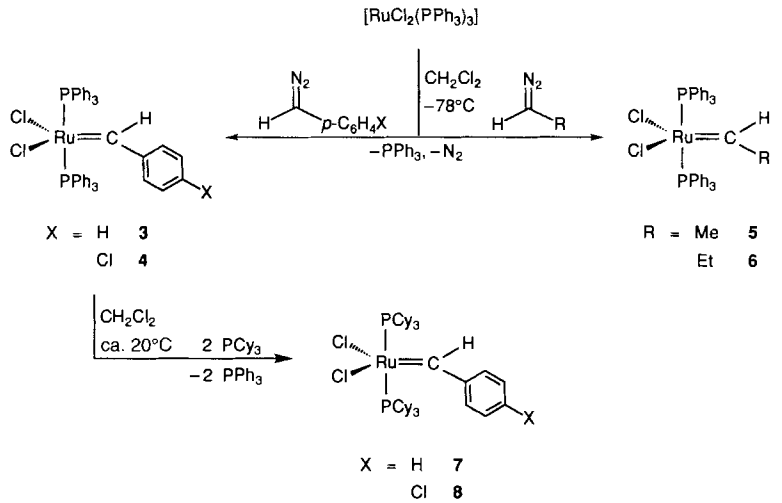

Scheme 1. Synthesis of alkylidene complexes from diazoalkanes and subsequent phosphane exchange. Cy = cyclohexyl.

Table 1. Selected spectroscopic data for compounds **3**–**13** (omitting the ^1H and ^{13}C NMR data for the phosphane ligands).

3: ^1H NMR (300 MHz, C_6D_6): $\delta = 19.56$ (t, $J(P,H) = 10.2$ Hz, Ru=CH), 7.80–7.64 and 6.99–6.66 (both m, C_6H_5); ^{13}C NMR (125.8 MHz, CD_2Cl_2): $\delta = 310.12$ (t, $J(P,C) = 11.4$ Hz, Ru=CH), 155.36 (s, *ipso*-C of C_6H_5), 130.03, 128.71 and 127.09 (all s, C_6H_5); ^{31}P NMR (161.9 MHz, CD_2Cl_2): $\delta = 30.63$ (s, PPh_3).

4: ^1H NMR (500 MHz, CD_2Cl_2): $\delta = 19.27$ (t, $J(P,H) = 9.2$ Hz, Ru=CH), 7.51–7.44 and 6.88–6.84 (both m, C_6H_4Cl); ^{13}C NMR (125.8 MHz, CD_2Cl_2): $\delta = 307.34$ (t, $J(P,C) = 10.6$ Hz, Ru=CH), 153.82 (s, *ipso*-C of C_6H_4Cl), 128.87, 128.81 and 128.07 (all s, C_6H_4Cl); ^{31}P NMR (161.9 MHz, CD_2Cl_2): $\delta = 30.47$ (s, PPh_3).

5: ^1H NMR (300 MHz, CD_2Cl_2): $\delta = 18.47$ (tq, $J(P,H) = 10.2$, $^3J(H,H) = 5.1$ Hz, Ru=CH), 2.59 (d, $^3J(H,H) = 5.1$ Hz, CH_3); ^{13}C NMR (75.5 MHz, CD_2Cl_2): $\delta = 320.65$ (t, $J(P,C) = 9.9$ Hz, Ru=CH), 49.17 (s, CH_3); ^{31}P NMR (161.9 MHz, CD_2Cl_2): $\delta = 29.99$ (s, PPh_3).

6: ^1H NMR (300 MHz, CD_2Cl_2): $\delta = 18.21$ (tt, $J(P,H) = 10.8$, $^3J(H,H) = 6.6$ Hz, Ru=CH), 3.11 (dq, $^3J(H,H) = {}^3J(H,H') = 6.6$ Hz, CH_2CH_3), 0.79 (t, $^3J(H,H) = 6.6$ Hz, CH_2CH_3); ^{13}C NMR (125.8 MHz, CD_2Cl_2): $\delta = 320.88$ (t, $J(P,C) = 10.0$ Hz, Ru=CH), 53.20 (s, CH_2CH_3), 29.74 (s, CH_2CH_3); ^{31}P NMR (161.9 MHz, CD_2Cl_2): $\delta = 30.02$ (s, PPh_3).

7: ^1H NMR (500 MHz, CD_2Cl_2): $\delta = 20.02$ (s, Ru=CH), 8.44 (d, $^3J(H,H) = 7.6$ Hz, *o*-H of C_6H_5), 7.56 (t, $^3J(H,H) = 7.6$ Hz, *p*-H of C_6H_5), 7.33 (dd, $^3J(H,H) = {}^3J(H,H') = 7.6$ Hz, *m*-H of C_6H_5); ^{13}C NMR (125.8 MHz, CD_2Cl_2): $\delta = 294.72$ (s(br.), Ru=CH), 153.17 (s, *ipso*-C of C_6H_5), 131.21, 129.49 and 129.27 (all s, C_6H_5); ^{31}P NMR (202.5 MHz, CD_2Cl_2): $\delta = 36.61$ (s, PCy_3).

8: ^1H NMR (500 MHz, CD_2Cl_2): $\delta = 19.98$ (s, Ru=CH), 8.43 (d, $^3J(H,H) = 8.7$ Hz, *o*-H of C_6H_4Cl), 7.29 (d, $^3J(H,H) = 8.7$ Hz, *m*-H of C_6H_4Cl); ^{13}C NMR (125.8 MHz, CD_2Cl_2): $\delta = 291.46$ (t, $J(P,C) = 8.0$ Hz, Ru=CH), 151.81 (s, *ipso*-C of C_6H_4Cl), 134.64, 132.56, and 129.51 (all s, C_6H_4Cl); ^{31}P NMR (202.5 MHz, CD_2Cl_2): $\delta = 36.81$ (s, PCy_3).

9: ^1H NMR (500 MHz, CD_2Cl_2): $\delta = 18.94$ (s, Ru=CH_2); ^{13}C NMR (125.8 MHz, CD_2Cl_2): $\delta = 294.71$ (t, $J(P,C) = 7.6$, $J(C,H) = 164.0$ Hz, Ru=CH_2); ^{31}P NMR (161.9 MHz, CD_2Cl_2): $\delta = 43.74$ (s, PCy_3).

10: ^1H NMR (500 MHz, CD_2Cl_2): $\delta = 19.26$ (q, $^3J(H,H) = 5.1$ Hz, Ru=CH), 2.57 (d, $^3J(H,H) = 5.1$ Hz, CH_3); ^{13}C NMR (125.8 MHz, CD_2Cl_2): $\delta = 316.32$ (t, $J(P,C) = 7.6$ Hz, Ru=CH), 49.15 (s, CH_3); ^{31}P NMR (161.9 MHz, CD_2Cl_2): $\delta = 35.54$ (s, PCy_3).

11: ^1H NMR (500 MHz, CD_2Cl_2): $\delta = 19.12$ (t, $^3J(H,H) = 5.0$ Hz, Ru=CH), 2.79 (dq, $^3J(H,H) = 5.0$, $^3J(H,H') = 7.1$ Hz, CH_2CH_3), 1.35 (t, $^3J(H,H) = 7.1$ Hz, CH_2CH_3); ^{13}C NMR (125.8 MHz, CD_2Cl_2): $\delta = 322.59$ (t, $J(P,C) = 9.3$ Hz, Ru=CH), 53.48 (s, CH_2CH_3), 29.57 (s, CH_2CH_3); ^{31}P NMR (161.9 MHz, CD_2Cl_2): $\delta = 36.39$ (s, PCy_3).

12: ^1H NMR (300 MHz, CD_2Cl_2): $\delta = 19.06$ (d, $^3J(H,H) = 10.5$ Hz, Ru=CH), 8.11 (ddd, $^3J(H,H) = 10.5$, $^3J(H,H^{cis}) = 9.3$, $^3J(H,H^{trans}) = 16.8$ Hz, CH=CH_2), 6.25 (d, $^3J(H,H) = 9.3$ Hz, H^{cis} of CH=CH_2), 6.01 (d, $^3J(H,H) = 16.8$ Hz, H^{trans} of CH=CH_2); ^{13}C NMR (125.8 MHz, CD_2Cl_2): $\delta = 296.00$ (t, $J(P,C) = 7.6$ Hz, Ru=CH), 153.61 (s, CH=CH_2), 115.93 (s, CH=CH_2); ^{31}P NMR (161.9 MHz, CD_2Cl_2): $\delta = 36.17$ (s, PCy_3).

13: ^1H NMR (300 MHz, CD_2Cl_2): $\delta = 3.63$ (s, Ru=C=CH_2); ^{13}C NMR (125.8 MHz, CD_2Cl_2): $\delta = 327.41$ (t, $J(P,C) = 17.2$ Hz, Ru=C=CH_2), 99.34 (s, Ru=C=CH_2); ^{31}P NMR (161.9 MHz, CD_2Cl_2): $\delta = 35.36$ (s, PCy_3).

decompose in solution (**3** and **4** faster than **5** and **6**) within several hours through bimolecular pathways, as shown by the formation of the corresponding disubstituted olefins R'HC=CHR' (R' = Ph, *p*-C_6H_4Cl, Me, Et). This instability is attributed to a lack of conjugation, which can be inferred from the significant downfield shift of the carbene resonances in the ^1H and ^{13}C NMR spectra [$\delta(^1H) = 17.94$ (**1**), 19.56 (**3**); $\delta(^{13}C) = 288.9$ (**1**), 310.1 (**3**)].

Complexes **3**–**6** are efficient catalysts for the living ROMP of norbornene and substituted cyclobutenes. For example, monodisperse polynorbornene (PDI = $\bar{M}_W/\bar{M}_N = 1.04$) may be prepared from reaction of **3** with 100 equivalents of norbornene in CH_2Cl_2 or C_6H_6 at room temperature (PDI = 1.25 with **1**[11]). Kinetic studies have shown that the initiation rate for **3** is about 1000 times greater than for **1** (for comparison, the ratio of initiation rate to propagation rate $k_i/k_p = 9$ for **3** compared to 6×10^{-3} for **1**[8].)

Treatment of **3** or **4** with two equivalents of tricyclohexyl phosphane results in facile phosphane exchange to give **7** or **8**, respectively, as air-stable solids in 85–90% yield (Scheme 1). In contrast to **3** and **4**, **7** and **8** are stable at 60 °C in C_6D_6 for more than 48 h. Single-crystal X-ray analysis of **8** (Fig. 1)[9] reveals

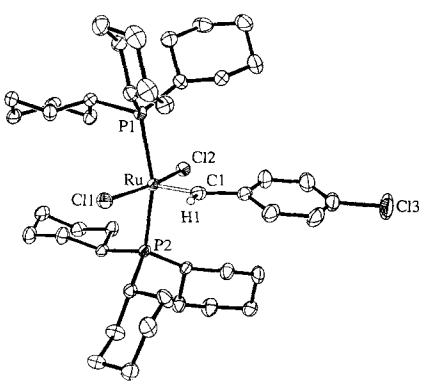

Fig. 1. Crystal structure of **8**. Selected bond distances [Å] and angles [°]: Ru–C1 1.839(3), Ru–Cl1 2.401(1), Ru–Cl2 2.395(1), Ru–P1 2.397(1), Ru–P2 2.435(1), Cl1-Ru-P1 87.2(1), P1-Ru-C1 97.5(1), P1-Ru-Cl2 91.5(1), Cl1-Ru-P2 90.8(1), C1-Ru-P2 101.2(1), Cl1-Ru-C1 88.7(1), Cl1-Ru-Cl2 167.6(1), C1-Ru-Cl2 103.7(1), P1-Ru-P2 161.1(1), Cl2-Ru-P2 86.5(1).

distorted square-pyramidal coordination with a nearly linear Cl1-Ru-Cl2 angle (167.61°). The carbene unit is perpendicular to the P1-Ru-P2-plane, and the aryl ligand is only slightly twisted out of the Cl1-Ru-Cl2-C1-plane. The Ru–C1 bond distance is shorter [1.838(3) Å] than that in **2** [1.851(21)] or in [RuCl(=C(OMe)–CH=CPh_2)(CO)($PiPr_3$)$_2$](BF_4) [1.874(3)].[10]

Besides its remarkable activity in ROMP and RCM reactions, **7** has great potential as a catalyst for metathesis of acyclic olefins (Scheme 2) and is significantly more reactive than the vinylcarbene derivative **2**.[11] Complex **7** is quantitatively converted into [$RuCl_2$(=CH_2)(PCy_3)$_2$] (**9**) by reaction with excess ethylene. To our knowledge, **9** is the *first isolable methylidene complex which is an active metathesis catalyst*. Alkylidene complexes with alkyl substituents on the carbene carbon, such as **10** and **11**, are quantitatively available on reaction of **7** with a small excess of the corresponding terminal olefin and rapid workup.

 © VCH Verlagsgesellschaft mbH, D-69451 Weinheim, 1995 0570-0833/95/3418-2040 $ 10.00+.25/0

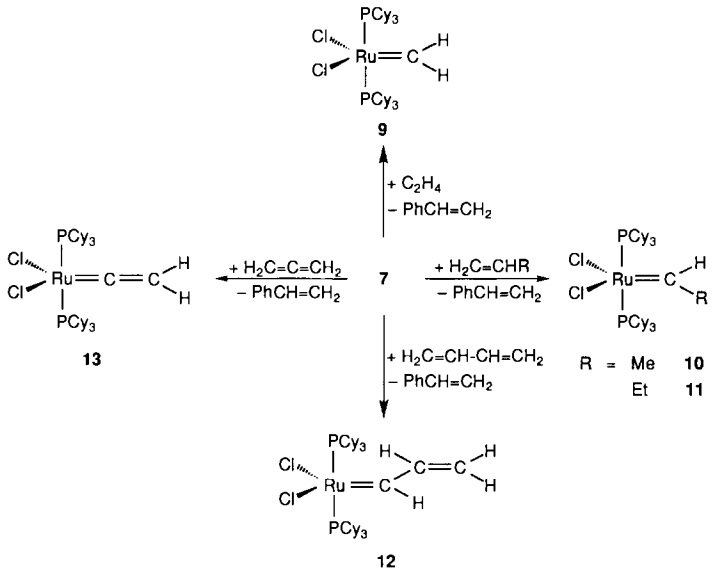

Scheme 2. Methathesis of acyclic alkenes with **7** as catalyst.

However, longer reaction times favor the formation of **9**, which is the sole product after 20 h. This suggests that alkylidene complexes (**10**, **11**) are kinetic products, and the methylidene complex **9** is the thermodynamic product. Complex **7** may be used to prepare substituted carbenes by reaction with excess conjugated and cumulated olefins: The reaction of **7** with 1,3-butadiene leads to the formation of complex **12** with an unsubstituted vinylalkylidene ligand, which cannot be synthesized by ring opening of cyclopropene.[11] In addition, reaction of **7** with excess 1,2-propadiene (allene) leads to the formation of vinylidene complex **13** in essentially quantitative yield.

These results demonstrate that diazoalkanes are excellent carbene sources for the facile synthesis of a wide range of well-defined ruthenium metathesis catalysts of the type $[RuCl_2(=CHR')(PR_3)_2]$. These complexes display greater metathesis activity than **1** and **2** because of facile initiation. The complex with R' = Ph, R = Cy (**7**) not only yields the first metathesis-active methylidene complex (**9**) in quantitative yield, but also serves as an efficient precursor to a variety of alkylidene complexes by cross metathesis. The use of functionalized alkylidenes in the preparation of telechelic polymers, as well as detailed investigations into the kinetics and mechanisms of olefin metathesis processes, are under investigation.

Experimental Procedure

3: A solution of $[RuCl_2(PPh_3)_3]$ (2.37 g, 2.47 mmol) in CH_2Cl_2 (20 mL) was treated at −78 °C with a solution (−50 °C) of phenyldiazomethane (584 mg, 4.94 mmol, 2.0 equiv) in CH_2Cl_2 (3 mL). After the cool-bath had been removed, the solution was stirred for 5 min, and the brown-green solution concentrated to about 3 mL. Upon addition of pentane (20 mL) a green solid precipitated, which was separated from the brown mother liquor, redissolved in CH_2Cl_2 (3 mL), and reprecipitated with pentane. This procedure was repeated until the mother liquor was almost colorless. After drying in vacuo, a grey-green, air-stable microcrystalline solid was recovered; yield 1.67 g (89%). C,H analysis: found: C 65.83, H 4.59%; calcd: C65.65, H 4.61%. Compounds **4**, **5**, and **6** were prepared in a similar way; yield 80–85%.

7: A solution of **3** (242 mg, 0.31 mmol) in CH_2Cl_2 (10 mL) was treated with a solution of tricyclohexylphosphane (190 mg, 0.68 mmol, 2.2 equiv) in CH_2Cl_2 (3 mL) and stirred at room temparature for 30 min. The solvent was removed in vacuo, and the residue repeatedly washed with acetone (5 mL) and dried in vacuo. A purple, air-stable microcrystalline solid was obtained; yield 209 mg (89%). C,H analysis: found: C 62.84, H 8.71%; calcd: C62.76, H 8.82%. Compound **8** was prepared analogously; yield 87%.

9: A solution of **7** (821 mg, 1.00 mmol) in CH_2Cl_2 (15 mL) was stirred under an atmosphere of ethylene for 20 min at room temperature. The solvent was removed in vacuo, and the residue repeatedly washed with acetone or pentane (5 mL) and dried thoroughly in vacuo. A red-purple, air-stable microcrystalline solid was obtained; yield 745 mg (quant.). C,H analysis: found: C 59.42, H 9.29%; calcd: C 59.50, H 9.18%. Compounds **10**–**13** were prepared similarly; yield about 95%.

Polynorbornene from **3**: A solution of norbornene (59 mg, 0.63 mmol) in CH_2Cl_2 (0.7 mL) was treated with a solution of **3** (4.9 mg, 6.25 μmol) in CH_2Cl_2 (0.3 mL). The viscous solution was stirred at room temperature for 1 h, then exposed to air, and treated with CH_2Cl_2 (2 mL) containing traces of 2,6-di-*tert*-butyl-4-methylphenol and ethyl vinyl ether. The solution was stirred for 20 min and, after filtration through a short column of silica gel, precipitated by pouring into vigorously stirred methanol. The white, tacky polymer was washed several times with methanol and dried in vacuo; yield 56 mg (95%), 90% *trans*, M_n = 34.5 kg mol^{-1}, PDI (toluene): 1.04.

Received: May 2, 1995 [Z7950IE]
German version: *Angew. Chem.* **1995**, *107*, 2179–2181

Keywords: carbene complexes · diazo compounds · metathesis · ruthenium compounds

[1] S. T. Nguyen, L. K. Johnson, R. H. Grubbs, *J. Am. Chem. Soc.* **1992**, *114*, 3974–3975.
[2] S. T. Nguyen, R. H. Grubbs, J. W. Ziller, *J. Am. Chem. Soc.* **1993**, *115*, 9858–9859.
[3] Reviews on ROMP: a) R. H. Grubbs in *Comprehensive Organometallic Chemistry, Vol. 8* (Ed.: G. Wilkinson), Pergamon, New York, **1982**, pp. 499–551; b) K. J. Ivin, *Olefin Metathesis*, Academic Press, London, **1983**; c) M. Leconte, J. M. Basset, F. Quignard, C. Larroche in *Reactions of Coordinated Ligands, Vol. 1* (Ed.: P. S. Braterman), Plenum, New York, **1986**, pp. 371–420; d) R. H. Grubbs, W. Tumas, *Science* **1989**, *243*, 907–915; e) R. R. Schrock, *Acc. Chem. Res.* **1990**, *23*, 158–165; f) J. Feldman, R. R. Schrock, *Prog. Inorg. Chem.* **1991**, *39*, 1–74; g) D. S. Breslow, *Prog. Polym. Sci.* **1993**, *18*, 1141–1195.
[4] Z. Wu, A. D. Benedicto, R. H. Grubbs, *Macromolecules* **1993**, *26*, 4975–4977.
[5] M. Hillmyer, Ph. D. thesis, California Institute of Technology, **1994**.
[6] a) G. C. Fu, S. T. Nguyen, R. H. Grubbs, *J. Am. Chem. Soc.* **1993**, *115*, 9856–9857; b) S.-H. Kim, N. Bowden, R. H. Grubbs, *ibid.* **1994**, *116*, 10801–10802; c) S. J. Miller, S.-H. Kim, Z.-R. Chen, R. H. Grubbs, *ibid.* **1995**, *117*, 2108–2109.
[7] For the use of diazoalkanes in organometallic synthesis, see a) W. A. Herrmann, *Angew. Chem.* **1978**, *90*, 855–868; *Angew. Chem. Int. Ed. Engl.* **1978**, *17*, 800–813; b) *Chem. Ber.* **1975**, *108*, 486–499; c) W. A. Herrmann, I. Schweizer, M. Creswick, I. Bernal, *J. Organomet. Chem.* **1979**, *65*, C17–C20; c) W. A. Herrmann, C. Bauer, G. Kriechbaum, H. Kunkely, M. L. Ziegler, D. Speth, E. Guggolz, *Chem. Ber.* **1982**, *115*, 878–900; d) W. A. Herrmann, C. Bauer, M. L. Ziegler, H. Pfisterer, *J. Organomet. Chem.* **1983**, *243*, C54–C58; e) W. A. Herrmann, G. W. Kriechbaum, C. Bauer, B. Kombouris, H. Pfisterer, E. Guggolz, M. L. Ziegler, *ibid.* **1984**, *262*, 89–122; f) P. Schwab, N. Mahr, J. Wolf, H. Werner, *Angew. Chem.* **1993**, *105*, 1498–1500; *Angew. Chem. Int. Ed. Engl.* **1993**, *32*, 1480–1482; A. Stumpf, E. Saive, A. Demoncean, A. F. Noels, *Chem. Commun.* **1995**, 1127–1128.
[8] P. Schwab, R. H. Grubbs, unpublished results.
[9] Crystals from CH_2Cl_2/pentane; crystal size 0.2·0.3·0.5 mm; triclinic, space group $P\bar{1}$, $Z = 2$; $a = 10.6413(14)$, $b = 12.392(2)$, $c = 17.730(2)$ Å; $\alpha = 107.088(8)$, $\beta = 93.811(7)$, $\gamma = 105.750(9)°$; $V = 2123.5(5)$ Å^3, $\rho_{calcd} = 1.341$ g cm^{-3}; $2\theta = 4.0–50.0°$ ($Mo_{K\alpha}$, $\lambda = 0.71073$ Å, graphite monochromator, $2\theta–\theta$ scan, $T = 158$ K); 7782 reflections measured, 7347 independent, 6411 observed, $[F > 3.0\sigma(F)]$ semiempirical absorption corrections (min./max. transmission 0.7742/0.8871); direct methods (SHELXTL PLUS), refinement with Full-Matrix Least-Squares, hydrogen atoms refined isotropically, all other atoms refined anisotropically; $R = 0.035$, $R_w = 0.036$; reflection/parameter ratio 8.8; residual electron density +0.63/−0.52 e Å^{-3}. Further details of the X-ray structure analysis are available on request from the Fachinformationszentrum Karsruhe, Gesellschaft für wissenschaftlich-technische Information mbH, D-76344 Eggenstein-Leopoldshafen (Germany), on quoting the depository number CSD-59036.
[10] M. A. Esteruelas, F. J. Lahoz, E. Onate, L. A. Oro, B. Zeier, *Organometallics* **1994**, *13*, 4258–4265.
[11] S. T. Nguyen, Ph. D. thesis, California Institute of Technology, **1995**.

 © VCH Verlagsgesellschaft mbH, D-69451 Weinheim, 1995 0570-0833/95/3418-2041 $ 10.00+.25/0

A Molybdenum–Phosphorus Triple Bond: Synthesis, Structure, and Reactivity of the Terminal Phosphido (P^{3-}) Complex $[Mo(P)(NRAr)_3]$**

Catalina E. Laplaza, William M. Davis, and Christopher C. Cummins*

In two recent reports we showed that the three-coordinate molybdenum(III) complex $[Mo(NRAr)_3]$ (**1**, R = $C(CD_3)_2CH_3$, Ar = 3,5-$C_6H_3Me_2$) is an avid nitrogen-atom acceptor; the reactions of **1** with nitrous oxide[1] and dinitrogen[2] both occur with N–N bond cleavage to give the molybdenum(VI) complex $[Mo(N)(NRAr)_3]$ having a terminal nitrido ligand. To determine whether the tendency of **1** to abstract a trivalent atom would extend to a heavier homologue, we investigated the reaction of $[Mo(NRAr)_3]$ (**1**) with white phosphorus (P_4). Accordingly, we present herein the synthesis and structure of the monomeric phosphido (P^{3-}) complex $[Mo(P)(NRAr)_3]$ (**2**), which contains a molybdenum–phosphorus triple bond. Doubly and triply bridging bonding modes for P_1 ligands in bimetallic or trimetallic systems, respectively, are well-documented,[3] but terminal P_1 ligation has not been established previously.[4]

Orange-red $[Mo(NRAr)_3]$ (**1**) is a trigonal-planar, high-spin complex isolobal[5] with a nitrogen or a phosphorus atom. Its stability as a monomeric entity derives at least in part from the considerable steric demands imposed by an array of three NRAr ligands. The monomeric nature of **1** stands in stark contrast with the stability of triply bonded dimers (M≡M) of formula $[M_2X_6]$ (M = Mo, W; X = alkyl, amide, alkoxide).[6] Addition of 0.35 equiv of solid P_4 (a 40% excess) directly to an agitated solution of **1** (0.05 M in ether) resulted in a color change to brown-green over about 45 min (Scheme 1). The deep color of the reaction mixture does not reflect the color of the isolated product, $[Mo(P)(NRAr)_3]$ (**2**), which is yellow-gold both in solution and in the crystalline state. ^1H and ^2H NMR spectra[7] of aliquots taken from the reaction mixture at times varying from 5 to 60 min did not reflect the presence of any intermediate complexes. Analytically pure **2** was obtained in good yield (ca. 79%) by recrystallization from ether at −35 °C. The phosphido (P^{3-}) ligand in **2** is substantially deshielded, exhibiting a ^{31}P NMR signal at $\delta = 1216$. ^1H, ^2H, and ^{13}C NMR spectra of diamagnetic **2** (see Experimental Procedure) are reminiscent of those for the related nitrido complex, $[Mo(N)(NRAr)_3]$.[1] Complex **2** is soluble in standard organic solvents, and is perfectly stable in an inert atmosphere at 28 °C for days in the solid state and in solution.

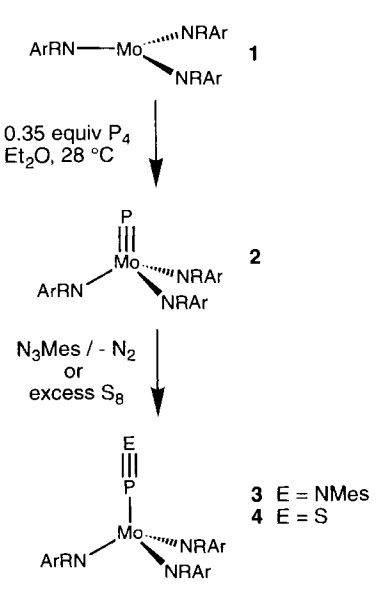

Scheme 1. Synthesis of **2**–**4**.

The structure of $[Mo(P)(NRAr)_3]$ (**2**, Fig. 1) was determined by single-crystal X-ray diffraction in order to verify its monomeric nature, and to corroberate the proposed terminal bonding mode of the P_1 ligand.[8] The molecule crystallizes as a discrete neutral species with its Mo–P vector on a crystallographic threefold axis. The Mo–P interatomic distance is 2.119(4) Å and is consistent with the presence of a molybdenum–phosphorus triple bond.[9] Complex **2** possesses a pseudotetrahedral $MoPN_3$ core geometry as observed previously for $[Ti(Cl)(NRAr)_3]$[10] and $[Sn(I)(NRAr)_3]$.[11] The latter molecules likewise exhibit the familiar propellor arrangement of the three NRAr ligands, with the unique axial substituent shielded by *tert*-butyl groups. In the crystal structure of **2** this feature is evidenced by an *inter*molecular Mo–P distance of 9.553(3) Å.

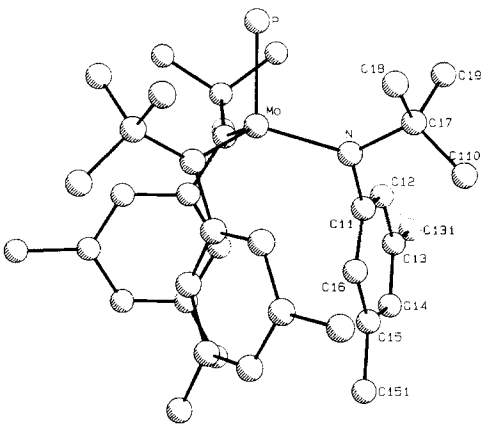

Fig. 1. PLUTO drawing of the molecular structure of **2**. Selected bond lengths [Å] and angles [°]: Mo1–P1 2.119(4), Mo1–N1 1.966(7), N1–C11 1.46(1), N1–C17 1.52(1); P1-Mo1-N1 104.8(2), N1-Mo1-N1 113.7(1), Mo1-N1-C11 111.1(5), Mo1-N1-C17 133.7(5), C11-N1-C17 114.1(6).

Derivatization of $[Mo(P)(NRAr)_3]$ was achieved by treatment with mesityl azide[12] (see Experimental Procedure for details). A process reminiscent of the Staudinger reaction,[13] the reaction proceeded (Scheme 1) with slow (ca. 22 h at 28 °C) conversion to $[Mo(PNMes)(NRAr)_3]$ (**3**). Conversion of **2** to diamagnetic, dark blue-green **3** transpired with no significant accumulation of any observable intermediates (the reaction was monitored by ^1H NMR). We attribute a ^{31}P NMR signal at $\delta = 159$ to the single phosphorus atom in **3**, a reasonable value for two-coordinate phosphorus.[3] It was anticipated for **3** that the angle at phosphorus would be nearly linear, because the molecule is isolobal with the linear nitrosyl derivatives $[Mo(NO)(NRAr)_3]$[14] and $[Cr(NO)\{N(SiMe_3)_2\}_3]$.[15] This expectation was borne out by a single-crystal X-ray diffraction study of $[Mo(PNMes)(NRAr)_3]$ (**3**, Fig. 2).[16] The $PMo(NRAr)_3$ portion of molecule **3** is largely unperturbed relative to **2**. As far as we are aware, **3** provides a unique example of a terminally complexed iminophosphenium ("monophosphadiazonium") (PNR^+) residue.[17]

A unique deep-red phosphorus monosulfide complex $[Mo(PS)(NRAr)_3]$ (**4**) was also readily obtained (Scheme 1)

[*] Prof. Dr. C. C. Cummins, C. E. Laplaza, Dr. W. M. Davis
Department of Chemistry 2-227
Massachusetts Institute of Technology
Cambridge, MA 02139 (USA)
Telefax: Int. code + (617) 253-7030
e-mail: ccummins@mit.edu

[**] This work was supported by a National Science Foundation CAREER award to C. C. C. (CHE-9501992) and by the MITDepartment of Chemistry. Michael G. Fickes is hereby acknowledged for a generous gift of mesityl azide, and we thank Aaron L. Odom for assistance with the X-ray crystallography.

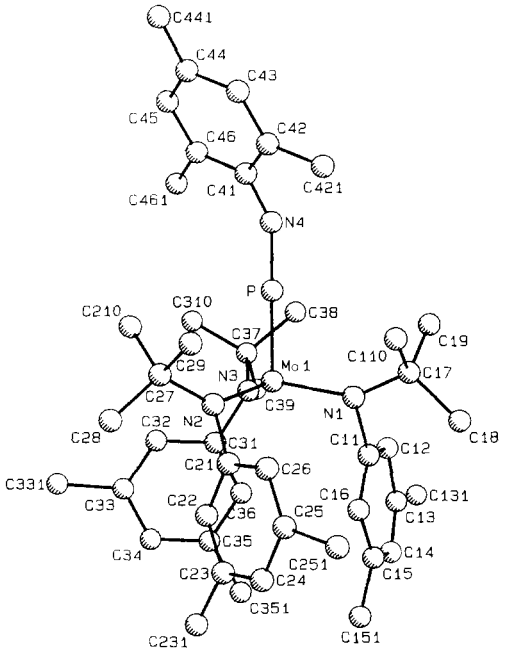

Fig. 2. PLUTO drawing of the molecular structure of **3** [15].

upon treatment of **2** with either an episulfide or excess S_8 (see Experimental Procedure for details).[18] ^{1}H, ^{2}H and ^{13}C NMR spectral data for **4** are consistent with its formulation as a monomeric entity; a ^{31}P NMR signal attributable to **4** was located at $\delta = 383$. Further characterization of **4** is in progress.

Interest in multiple bonding between transition metals and phosphorus has climaxed in recent studies of terminal phosphinidene (PR) complexes[19] (such as those summarized in Scheme 2) following the seminal preparation of $[M(PAr^*)Cp_2]$

$[W(PAr^*)(CO)(PMePh_2)_2(Cl)_2]$ [20] $[Ta(PCy)\{(Me_3SiNCH_2CH_2)_3N\}]$ [21]

$[ZrCp_2(PAr^*)(PMe_3)]$ [22] $[Ta(PPh)(OSi^tBu_3)_3]$ [23]

Scheme 2. Complexes with terminal phosphinidene (PR) ligands. Cy = cyclohexyl, $Ar^* = 2,4,6\text{-}^t Bu_3\text{-}C_6H_2$.

(M = Mo, W; $Ar^* = 2,4,6\text{-}^t Bu_3C_6H_2$) by Lappert and coworkers.[24] Prior reports of naked phosphido ligands engaged in triple bonding to a metal center have been confined to the speculation, by Chisholm and coworkers, that $[W(P)(OCH_2{}^tBu)_3]$ (not observed) was generated upon addition of P_4 to $[W_2(OCH_2{}^tBu)_6(HNMe_2)_2]$.[25] (The *cyclo*-$P_3$ complex $[W(\eta^3\text{-}P_3)(OCH_2{}^tBu)_3(HNMe_2)]$[26] and the tritungsten cluster $[W_3(\mu_3\text{-}P)(OCH_2{}^tBu)_9]$ were ultimately isolated from that reaction.) The work we report here is unique in that a robust complex containing a metal–phosphorus triple bond has been prepared by simple addition of elemental phosphorus (P_4) to a complex of known structure. In a report submitted concurrently with this one, Zanetti, Schrock, and Davis describe an alternative means for installing a terminal P_1 ligand. They report the synthesis of $[M(P)\{(Me_3SiNCH_2CH_2)_3N\}]$ (M = Mo, W) complexes in which the phosphorus atom derives from breakdown of a bound phenylphosphido (PHPh) unit.[4] Many interesting questions concerning the chemical reactivity of the terminal P_1 ligand are now open for study. $[Mo(P)(NRAr)_3]$ (**2**), as a terminal phosphido (P^{3-}) complex, joins phosphaalkynes[3] as a representative of the growing class of one-coordinate phosphorus compounds.

Experimental Procedure

All manipulations were carried out in an atmosphere of dry, oxygen-free nitrogen inside a Vacuum Atmospheres glovebox using appropriately dried and deaerated solvents. $[Mo(NRAr)_3]$ (**1**) was prepared as described previously [1].

2: White phosphorus (136 mg, 1.10 mmol, 0.35 equiv) was added in small pieces to a stirred orange-red solution of $[Mo(NRAr)_3]$ (**1**, 2.015 g, 3.13 mmol) in ether (60 mL) at 28 °C. Over 90 min the color of the reaction mixture became brown-green. The ^{2}H NMR spectrum of an aliquot taken at this time showed that **1** had been completely consumed. The reaction mixture was filtered and the filtrate was concentrated to a volume of about 30 mL. Storing the concentrated filtrate at −35 °C for several hours provided $Mo(P)(NRAr)_3$ (**2**, 1.661 g, 2.46 mmol, 78.7% yield) as a yellow crystalline solid (m.p. 221–224 °C). ^{1}H NMR (C_6D_6): δ = 6.59 (s, 3H, *para* $C_6H_3Me_3$), 5.50 (s, 6H, *ortho* $C_6H_3Me_3$), 1.97 (s, 18H, *meta* $C_6H_3Me_2$), 1.35 (s, 9H, $C(CD_3)_2CH_3$); ^{13}C NMR ($CDCl_3$): δ = 150.03 (s, *ipso* $C_6H_3Me_2$), 136.35 (q, *meta* $C_6H_3Me_2$), 129.84 (d, *ortho* $C_6H_3Me_2$), 127.15 (d, *para* $C_6H_3Me_2$), 59.93 (s, $C(CD_3)_2CH_3$), 33.40 (s, $C(CD_3)_2CH_3$), 32.80 (m, $C(CD_3)_2CH_3$), 21.23 (q, *meta* $C_6H_3Me_2$); ^{31}P NMR (C_6D_6): δ = 1216 (s). Anal. calcd for $C_{36}H_{36}D_{18}MoN_3P$: C 64.17, H 8.08, N 6.24; found: C 64.40, H 8.13, N 6.09.

3: A solution of mesityl azide (253 mg, 1.57 mmol) in ether (2 mL) was added to a stirred solution of **2** (0.400 g, 0.594 mmol) in ether (10 mL). The reaction mixture acquired a blue-green color over several (3 to 4) hours. After a total of 22 h, the reaction mixture was concentrated and cooled to −35 °C to provide [Mo(PNMes)$(NRAr)_3$] (**3**, 0.35 g, 0.43 mmol, 73%) as a dark blue-green crystalline solid (m.p. 181–183 °C). ^{1}H NMR (C_6D_6): δ = 6.95 (s, 2H, *meta* $C_6H_2Me_3$), 6.67 (s, 3H, *para* $C_6H_3Me_2$), 6.00 (br, 6H, *ortho* $C_6H_3Me_2$), 2.80 (s, 6H, *ortho* $C_6H_2Me_3$), 2.28 (s, 3H, *para* $C_6H_2Me_3$), 2.08 (s, 18H, *meta* $C_6H_3Me_2$), 1.45 (s, 9H, $C(CD_3)_2CH_3$); ^{13}C NMR ($CDCl_3$): δ = 149.79 (s, *ipso* $C_6H_3Me_2$), 136.65 (q, *meta* $C_6H_3Me_2$), 131.66 (s), 131.03 (d, *ortho* $C_6H_3Me_2$), 130.00 (s), 129.47 (s), 127.90 (d), 127.82 (d), 61.58 (s, $C(CD_3)_2CH_3$), 34.33 (q, $C(CD_3)_2CH_3$), 34.00 (m, $C(CD_3)_2CH_3$), 21.38 (q, *meta* $C_6H_3Me_2$), 20.68 (q, *para* $C_6H_2Me_3$), 20.21 (q, *ortho* $C_6H_2Me_3$)]; ^{31}P NMR (C_6D_6): δ = 159 (s). Anal. calcd for $C_{45}H_{47}D_{18}MoN_4P$: C 66.97, H 8.12, N 6.94; found: C 67.31, H 8.09, N 6.89.

4: Method a: Elemental sulfur (S_8, 575 mg, 2.24 mmol) was added to a solution of **2** (301 mg, 0.447 mmol) in ether (10 mL). The agitated reaction mixture changed color slowly, over 1.5 d, to purple-red. Consumption of **2** was complete after 43 h according to the ^{1}H NMR spectrum of an aliquot. The excess sulfur was removed by filtration, and the filtrate was cooled and concentrated to give $[Mo(PS)(NRAr)_3]$ (**4**, 197 mg, 0.279 mmol, 62%) as a dark red crystalline solid. Method b: Cyclohexene sulfide (7-thiabicyclo[4.1.0]heptane) (ca. 70 mg, 0.6 mmol, 1.1 equiv) was added dropwise to a magnetically-stirred solution of **2** (353 mg, 0.524 mmol) in ether (10 mL). A color change to purple-red was observed. After 1.5 h, the reaction mixture was filtered, and all volatile material was removed from the filtrate in vacuo. Recrystallization (ether, −35 °C) provided $[Mo(PS)(NRAr)_3]$ (**4**, 186 mg, 0.26 mmol, 50%) as a dark red crystalline solid (m.p. 175–180 °C (decomp)). ^{1}H NMR (C_6D_6): δ = 6.62 (s, 3H, *para* $C_6H_3Me_2$), 5.89 (s, 6H, *ortho* $C_6H_3Me_2$), 2.01 (s, 18H, *meta* $C_6H_3Me_2$), 1.45 (s, 9H, $C(CD_3)_2CH_3$); ^{13}C NMR ($CDCl_3$): δ = 148.37 (s, *ipso* $C_6H_3Me_2$), 136.90 (q, *meta* $C_6H_3Me_2$), 130.76 (d, *ortho* $C_6H_3Me_2$), 128.32 (d, *para* $C_6H_3Me_2$), 63.01 (s, $C(CD_3)_2CH_3$), 33.86 (q, $C(CD_3)_2CH_3$), 33.36 (m, $C(CD_3)_2CH_3$), 21.30 (q, *meta* $C_6H_3Me_2$); ^{31}P NMR (C_6D_6): δ = 383 (s). Anal. calcd for $C_{36}H_{36}D_{18}MoN_3PS$: C 61.25, H 7.71, N 5.95; found: C 61.58, H 7.61, N 5.95.

Received: April 28, 1995 [Z 7940IE]
German version: *Angew. Chem.* **1995**, *107*, 2181–2183

Keywords: complexes with phosphido ligands · molybdenum compounds · multiple bonds · phosphorus compounds

[1] C. E. Laplaza, A. L. Odom, W. M. Davis, C. C. Cummins, J. D. Protasiewicz, *J. Am. Chem. Soc.* **1995**, *117*, 4999.

[2] C. E. Laplaza, C. C. Cummins, *Science* **1995**, *268*, 861.

[3] The following fine treatises should be consulted for information on low-coordinate phosphorus: *Multiple Bonds and Low Coordination in Phosphorus Chemistry* (Eds.: M. Regitz, O. J. Scherer), Thieme, New York, **1990**; O. J. Scherer, *Angew. Chem.* **1990**, *102*, 1137; *Angew. Chem. Int. Ed. Engl.* **1990**, *29*, 1104; W. A. Herrmann, *ibid.* **1986**, *98*, 57 and **1986**, *25*, 56; for a phosphido ligand bridging two early metal centers see: M. C. Fermin, J. W. Ho, D. W. Stephan, *J. Am. Chem. Soc.* **1994**, *116*, 6033.

[4] Schrock et al. have also been able to synthesize a complex with a terminal P_1 ligand: N. Zanetti, R. R. Schrock, W. M. Davis, *Angew. Chem.* **1995**, *107*, 2184; *Angew. Chem. Int. Ed. Engl.* **1995**, *34*, 2044; following paper in this issue.

[5] R. Hoffmann, *Angew. Chem.* **1982**, *94*, 725; *Angew. Chem. Int. Ed. Engl.* **1982**, *21*, 711.

[6] F. A. Cotton, R. A. Walton, *Multiple Bonds Between Metal Atoms*, 2 ed., Oxford University, New York, **1993**; M. H. Chisholm, *Acc. Chem. Res.* **1990**, *23*, 419–425.

[7] We use ^{2}H NMR routinely to monitor reactions involving ^{2}H-labeled paramagnetic complexes such as [Mo(NRAr)$_3$] (**1**); see: *NMR of Paramagnetic Molecules* (Eds.: G. N. La Mar, W. D. Horrocks Jr., R. H. Holm), Academic Press, New York, **1973**.

[8] a) A suitable crystal of **2**·THF, of approximate dimensions $0.28 \times 0.24 \times 0.12$ mm, was obtained by cooling a THF solution of **2** to -35 °C. The crystal was mounted on a glass fiber in a stream of cold N_2. Data were collected at -86 °C on an Enraf-Nonius CAD-4 diffractometer with graphite monochromated $Mo_{K\alpha}$ radiation. A total of 2109 reflections were collected to a 2θ value of 45.0°. The structure was solved by direct methods. Non-hydrogen atoms were refined anisotropically except for the THF atoms; the THF molecule is disordered about a symmetry element. The final cycle of least-squares refinement was based on 1585 observed reflections ($I > 3.00\sigma(I)$) and 263 variable parameters and converged with $R = 0.058$ and $R_w = 0.062$. A final difference Fourier map showed no chemically significant features. Crystal data are $a = 11.434(1)$, $c = 18.051(3)$ Å, $V = 2043.7(5)$ Å^3, space group $P6_3$, $Z = 2$, $M_r = 719.80$, and $\rho_{calcd} = 1.169$ g cm^{-3}. b) Further details of the crystal structure investigation may be obtained from the Director of the Cambridge Crystallographic Data Centre, 12 Union Road, GB-Cambridge CB21EZ (UK), on quoting the full journal citation.

[9] The P≡P distance in gaseous P_2 is 1.895 Å: N. N. Greenwood, A. Earnshaw, *Chemistry of the Elements*, Pergamon, Oxford, **1984**. The Mo≡Mo distance in [Mo$_2$(NMe$_2$)$_6$] is 2.214 Å: M. H. Chisholm, F. A. Cotton, B. A. Frenz, W. W. Reichert, L. W. Shive, B. R. Stults, *J. Am. Chem. Soc.* **1976**, *98*, 4469. The sum of Mo and P triple bond covalent radii may therefore be taken as 2.055 Å.

[10] A. R. Johnson, P. W. Wanandi, C. C. Cummins, W. M. Davis, *Organometallics* **1994**, *13*, 2907.

[11] C. E. Laplaza, W. M. Davis, C. C. Cummins, *Organometallics* **1995**, *14*, 577.

[12] We prepared mesityl azide (caution! organic azides are potentially explosive) according to the procedure given in the following paper: I. Ugi, H. Perlinger, L. Behringer, *Chem. Ber.* **1958**, *91*, 2330.

[13] Y. G. Gololobov, L. F. Kasukhin, *Tetrahedron* **1992**, *48*, 1353.

[14] C. E. Laplaza, W. M. Davis, C. C. Cummins, unpublished results. See reference [1] above for the synthesis of [Mo(NO)(NRAr)$_3$].

[15] D. C. Bradley, C. W. Newing, *J. Chem. Soc., Chem. Commun.* **1970**, 219.

[16] A crystal of **3** having approximate dimensions $0.38 \times 0.29 \times 0.12$ mm was mounted on a glass fiber in a stream of cold N_2. Data were collected at -86 °C on an Enraf-Nonius CAD-4 diffractometer with graphite monochromated $Mo_{K\alpha}$ radiation. A total of 5628 reflections were collected to a 2θ value of 54.9°. The structure was solved by direct methods. Non-hydrogen atoms were refined either anisotropically or isotropically. Aromatic rings were refined as rigid groups. Because of poor crystal quality we regard this structure as a confirmation of atom connectivity only, and offer no detailed discussion of bond lengths and angles at this time. The final cycle of least-squares refinement was based on 2943 observed reflections ($I > 3.00\sigma(I)$) and 160 variable parameters and converged with $R = 0.095$ and $R_w = 0.084$. A final difference Fourier map showed no chemically significant features. Crystal data are $a = 22.626(2)$, $b = 18.380(2)$, $c = 10.619(1)$ Å, $V = 4416(2)$ Å^3, space group $Pna2_1$, $Z = 4$, $M_r = 788.95$, and $\rho_{calcd} = 1.186$ g cm^{-3} [8b].

[17] The free "monophosphadiazonium" cation [PNAr*]$^+$ (Ar* = 2,4,6-tBu$_3$C$_6$H$_2$) has been isolated and structurally characterized as its tetrachloroaluminate salt: E. Niecke, M. Nieger, F. Reichert, *Angew. Chem.* **1988**, *100*, 1781; *Angew. Chem. Int. Ed. Engl.* **1988**, *27*, 1715

[18] We believe this to be the first example of a terminal PS ligand. For discussions of complexed phosphorus monoxide see: O. J. Scherer, J. Braun, P. Walther, G. Heckmann, G. Wolmershäuser, *Angew. Chem.* **1991**, *103*, 861; *Angew. Chem. Int. Ed. Engl.* **1991**, *30*, 852; W. A. Herrmann, *ibid.*, **1991**, *30*, 818; **1991**, *103*, 835; J. F. Corrigan, S. Doherty, N. J. Taylor, A. J. Carty, *J. Am. Chem. Soc.* **1994**, *116*, 9799.

[19] A. H. Cowley, A. R. Barron, *Acc. Chem. Res.* **1988**, *21*, 81.

[20] A. H. Cowley, B. Pellerin, J. L. Atwood, S. G. Bott, *J. Am. Chem. Soc.* **1990**, *112*, 6734.

[21] C. C. Cummins, R. R. Schrock, W. M. Davis, *Angew. Chem.* **1993**, *105*, 758; *Angew. Chem. Int. Ed. Engl.* **1993**, *32*, 756.

[22] Z. Hou, T. L. Breen, D. W. Stephan, *Organometallics* **1993**, *12*, 3158.

[23] J. B. Bonanno, P. T. Wolczanski, E. B. Lobkovsky, *J. Am. Chem. Soc.* **1994**, *116*, 11159.

[24] P. B. Hitchcock, M. F. Lappert, W.-P. Leung, *J. Chem. Soc. Chem. Commun.* **1987**, 1282; P. Bohra, P. B. Hitchcock, M. F. Lappert, W.-P. Leung, *Polyhedron* **1989**, *8*, 1884.

[25] M. H. Chisholm, K. Folting, J. W. Pasterczyk, *Inorg. Chem.* **1988**, *27*, 3057.

[26] M. H. Chisholm, J. C. Huffman, J. W. Pasterczyk, *Inorg. Chim. Acta* **1987**, *133*, 17.

Monomeric Molybdenum and Tungsten Complexes That Contain a Metal–Phosphorus Triple Bond**

Nadia C. Zanetti, Richard R. Schrock,* and William M. Davis

Monomeric complexes of the type [(N$_3$N)Ta=PR] (N$_3$N = [(Me$_3$SiNCH$_2$CH$_2$)$_3$N]$^{3-}$; R = Ph, cyclohexyl, tBu) can be prepared by treating [(N$_3$N)TaCl$_2$] with two equivalents of LiPHR.[1] A crystal structure of [(N$_3$N)Ta=P(cyclohexyl)] showed that the Ta=P bond length is 2.145(7) Å and the Ta-P-C angle is 170(1)°, consistent with strong donation of the phosphorus lone pair to give a Ta–P pseudo triple bond. More recently we have shown that tungsten–carbon triple bonds form remarkably readily by ejection of dihydrogen from d^2 alkyl complexes of the type [(N$_3$N)W(CH$_2$R)],[2] even when β protons are present in the alkyl ligands, which suggests that the W≡C bond in this type of d^0 alkylidyne complex[3] is highly favored thermodynamically. Therefore we speculated that for both steric and electronic reasons, and because of the diagonal relationship between some C and P chemistry,[4] [(N$_3$N)W≡P], a monomeric compound containing the heretofore unknown transition metal to phosphorus triple bond,[4–7] would be a worthwhile and achievable goal. We describe here the synthesis of [(N$_3$N)W≡P] and [(N$_3$N)Mo≡P] by an unconventional route. These results should be compared with the synthesis and structure of [{3,5-Me$_2$C$_6$H$_3$)(tBu)N}$_3$Mo≡P] reported by Cummins et al. in the preceding article in this issue.[8]

The slow reaction between [(N$_3$N)WCl][2] and two equivalents of LiPPhH (toluene/tetrahydrofuran, 4/1, two days) yields yellow, crystalline, pentane-soluble, diamagnetic [(N$_3$N)W≡P] in approximately 50% yield [Eq. (a)]. An X-ray study revealed

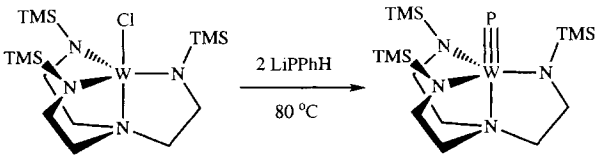

(a)

a structure (Fig. 1) that is unremarkable for heavy metal monomeric complexes of this general type[1, 9] except for the presence of a terminal phosphorus ligand 2.162(4) Å from tungsten, a metal–P distance that is essentially the same as that in [(N$_3$N)Ta=P(cyclohexyl)].[1] The ^{31}P NMR signal of [(N$_3$N)W≡P] is found at $\delta = 1080$, but J(P,W) is only 138 Hz (Table 1). This value for J(P,W) should be compared with that of 410 Hz for the planar phosphido phosphorus in [W(CtBu)(PPhH)(PEt$_3$)$_2$Cl$_2$],[10] in which the metal also can be said to be d^0, and J(P,W) = 719 Hz in [(N$_3$N)W(PPhH)] (see below). Such a low value for J(P,W) in the W≡P bond could be indicative of a low % s character in the σ portion of the bond, if the relationship that is so well-known for C–H bonds were to hold also for W–P bonds. The IR spectrum of [(N$_3$N)W≡P]

[*] Prof. Dr. R. R. Schrock, Dr. N. C. Zanetti, Dr. W. M. Davis[+]
Department of Chemistry 6-331
Massachusetts Institute of Technology
Cambridge, MA 02139 (USA)
Telefax: Int. code + (617)253-7670
e-mail: rrs@mit.edu

[+] X-ray structure analysis.

[**] This work is an extension of a program supported by the National Institutes of Health (GM 31978) designed to elucidate chemistry of N$_3$N complexes relevant to the reduction of dinitrogen.

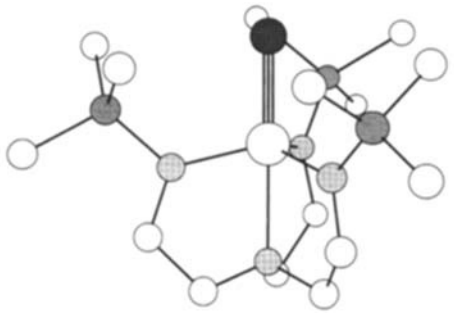

Fig. 1. A Chem 3D drawing of the structure of $[(N_3N)W{\equiv}P]$. Selected bond lengths [Å]: W–P 2.162(4), W–N_{eq} 1.975(6), W–N_{ax} 2.34(1).

Table 1. Selected NMR data for compounds with M(PPhH) and M≡P units.

Complex	δP(J(P,W))	δH(J(H,P)·J(H,W))	δ^1H value [a]
$[(N_3N)W(PPhH)]$	91 (719)	18.68 (300,36)	3.37 (t, CH_2) 2.21 (t, CH_2) 0.33 (s, TMS)
$[(N_3N)Mo(PPhH)]$	142	12.16 (283)	3.38 (t, CH_2) 2.35 (t, CH_2) 0.28 (s, TMS)
$[(N_3N)W{\equiv}P]$	1080 (138)	–	3.52 (t, CH_2) 1.69 (t, CH_2) 0.72 (s, TMS)
$[(N_3N)Mo{\equiv}P]$	1346	–	3.36 (t, CH_2) 1.77 (t, CH_2) 0.73 (s, TMS)

[a] N_3N ligand. TMS = trimethylsilyl.

above 550 cm^{-1} is similar to that of $[(N_3N)WCl]$ except for a medium strength peak at 935 cm^{-1}, but we are cautious about ascribing this to the W≡P stretch until further studies are carried out. Since examples of M≡E (M = Mo or W) stretching frequencies include ν(Mo≡N) at 991 cm^{-1} in $[\{(MeNCH_2CH_2)_3N\}Mo{\equiv}N]$[11] and ν(W≡C) at 911 cm^{-1} in $[Cl(Me_3P)_4W{\equiv}CH]$,[12] we would expect the value for ν(W≡P) to be lower than 935 cm^{-1}.

Before the reaction shown in Equation (a) is complete a diamagnetic threefold symmetric species can be observed by NMR spectroscopy along with $[(N_3N)W{\equiv}P]$ and paramagnetic $[(N_3N)WCl]$. We propose that this intermediate is $[(N_3N)W(PPhH)]$ (Table 1) by analogy with the NMR data for the crystallographically characterized $[(N_3N)Mo(PPhH)]$ (see below). $[(N_3N)W(PPhH)]$ is diamagnetic because the lone pair on phosphorus is donated to the metal and the d_{xz}/d_{yz} orbital degeneracy thereby is split, but it still has C_3 symmetry on the NMR time scale. The NMR data for the PPhH ligand in $[(N_3N)W(PPhH)]$ should be compared with those for the PPhH ligand in $[W(CtBu)(PPhH)(PEt_3)_2Cl_2]$[10] ($\delta$P = 233, δH = 10.0, J(P,W) = 410 Hz, J(P,H) = 362 Hz, and J(H,W) = 65 Hz). Reactions between $[(N_3N)WCl]$ and *one* equivalent of LiPPhH also give mixtures that contain $[(N_3N)W{\equiv}P]$, $[(N_3N)WCl]$, and $[(N_3N)W(PPhH)]$.

The reaction between $[(N_3N)MoCl]$ and one equivalent of LiPPhH [Eq. (b)] yields an orange, crystalline diamagnetic

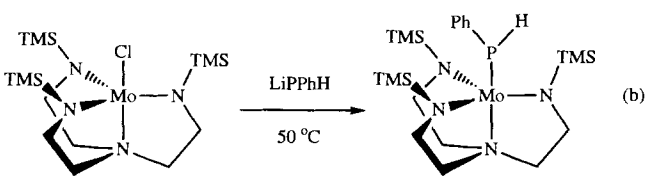

(b)

threefold symmetric species in more than 60% yield that has NMR parameters similar to those for $[(N_3N)W(PPhH)]$ (Table 1) and which was shown in an X-ray study (Fig. 2) to contain a planar phenylphosphido ligand in which Mo–P distance is 2.227(3) Å and the Mo-P-C and Mo-P-H angles are 129.7(2)° and 134(1)°, respectively. The distance between Mo

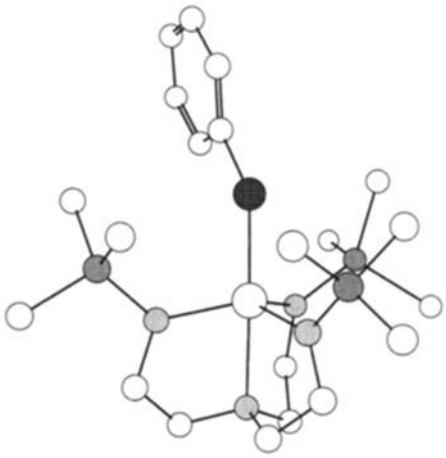

Fig. 2. A Chem 3D drawing of the structure of $[(N_3N)Mo(PPhH)]$. Selected bond lengths [Å] and angles [°]: Mo–P 2.227(3), Mo–N_{eq} 1.992(5), 2.014(5), 2.010(5), Mo–N_{ax} 2.251(5); Mo-P-C 129.7(2), Mo-P-H 134(1).

and H (3.23(1) Å) is too great to invoke any bonding interaction. These data are consistent with a Mo–P pseudo double bond being formed by using one of the two available π-type orbitals pointing toward P along the N-Mo-P (z) axis. An electron pair must be present on Mo in the remaining π-type orbital that lies approximately in the C-P-H-Mo plane. It is interesting to note that a hydrido(phosphinidene) analog of the recently characterized cyclopentylidene hydrido complex, $[(N_3N)W(C_5H_8)(H)]$,[13] is disfavored. Note also that the Mo–N_{axial} distance in $[(N_3N)Mo(PPhH)]$ is shorter (2.26 Å) than the W–N_{axial} distance in $[(N_3N)W{\equiv}P]$ (2.34 Å), consistent with a larger *trans* effect for the W–P triple bond than for the Mo–P pseudo double bond.

Addition of *two* equivalents of LiPPhH to $[(N_3N)MoCl]$ (toluene/THF, 80 °C, 12 h) or one equivalent of LiPPhH to $[(N_3N)Mo(PPhH)]$ (toluene/THF, 25 °C, 2 days) yields yellow crystalline $[(N_3N)Mo{\equiv}P]$ in about 75% yield in which the ^{31}P NMR signal is found at δ = 1346, $\Delta\delta$ = 266 further downfield than the corresponding signal in $[(N_3N)W{\equiv}P]$.

The mechanism of formation of $[(N_3N)M{\equiv}P]$ complexes is not clear at this stage. So far we know that $[(N_3N)Mo{\equiv}P]$ is not observed when a $[D_8]$toluene solution of pure $[(N_3N)Mo(PPhH)]$ is heated at temperatures up to 120 °C for up to three days, even though a solution of pure $[(N_3N)Mo{\equiv}P]$ remains unchanged after being heated to 120 °C for three days. We also have found that $[(N_3N)Mo(PPhH)]$ does not react with butyllithium in $[D_8]$toluene at 25 °C over a period of one day. Preliminary experiments suggest that the reaction between $[(N_3N)WCl]$ and two equivalents LiP(cyclohexyl)H also yields $[(N_3N)W{\equiv}P]$ in more than 50% yield.

The results reported here demonstrate that d^0 terminal phosphido complexes can be formed readily in the sterically protected C_3 environments found in $[\{(Me_3SiNCH_2CH_2)_3N\}M]$ complexes. In future studies we will attempt to elucidate the mechanism of forming terminal phosphido complexes and explore their reactivity patterns, and attempt to prepare analogous terminal arsenido complexes by similar techniques.

Experimental Procedure

All operations were performed under dinitrogen using appropriately dried and degassed solvents. NMR data are reported in [D_6]benzene at 20°C unless otherwise noted. See Table 1 for selected NMR data.

[$(N_3N)W{\equiv}P$]: A mixture of [$(N_3N)WCl$] (164 mg, 0.28 mmol) and LiPPhH (66 mg, 0.57 mmol) in a mixture of toluene (20 mL) and tetrahydrofuran (5 mL) was heated for 2 days at 80°C. The color changed from orange to deep red. The solvent was removed in vacuo and the residue was dissolved in pentane (100 mL). The mixture was filtered and the solvent was removed from the filtrate in vacuo. The resulting orange residue was recrystallized from ether at −40°C; yield 87 mg (53%). Anal. calcd (found) for $WC_{15}H_{39}N_4P$: C 31.36 (31.54), H 6.84 (6.55), N 9.75 (9.48).

[$(N_3N)Mo(PPhH)$]: A solution of [$(N_3N)MoCl$] (135 mg, 0.27 mmol) and LiPPhH (38 mg, 0.33 mmol) in a mixture of toluene (15 mL) and tetrahydrofuran (5 mL) was heated for 12 h at 50°C. The solvent was removed in vacuo and the residue was taken up in pentane (50 mL). The mixture was filtered and the solvent was removed from the filtrate in vacuo. The orange residue was recrystallized from ether at −40°C; yield 109 mg (70%).

[$(N_3N)Mo{\equiv}P$]: A solution of [$(N_3N)MoPPhH$] (60 mg) and LiPPhH (16 mg) in a mixture of toluene (20 mL) and tetrahydrofuran (5 mL) was heated to 70°C for 12 h. The color changed from orange to yellow. The solvent was removed in vacuo and the residue was dissolved in pentane (50 mL). Concentration of the pentane solution in vacuo produced a yellow crystalline solid; yield 42 mg (81%). [$(N_3N)Mo{\equiv}P$] also can be prepared directly from [$(N_3N)MoCl$] in a manner analogous to that used to prepare [$(N_3N)W{\equiv}P$]. Anal. calcd (found) for $MoC_{15}H_{39}N_4P$: C 37.02 (36.80), H 8.08 (7.85), N 11.51 (11.53).

X-ray diffraction study of [$(N_3N)W{\equiv}P$], $WC_{15}H_{39}N_4Si_3P$, $M = 574.58$. A yellow, cubic crystal ($0.280 \times 0.280 \times 0.280$ mm) was determined to possess cubic metric symmetry (25 reflections, 14.0–22.0° in 2θ): $a = 17.166(4)$ Å, $V = 5058(1)$ Å^3, $\rho_{calcd} = 1.509$ g cm^{-3}, space group $Pa\bar{3}$ (no. 205), $Z = 8$, $F(000) = 2304$, $\mu(Mo_{K\alpha}) = 48.72$ cm^{-1}. Data were collected on an Enraf-Nonius CAD4 diffractometer, $Mo_{K\alpha}$ ($\lambda = 0.71069$ Å) radiation, at 187 K. Reflections were measured with widths of $(0.80 + 0.35 \tan\theta)°$ in ω in the ω-2θ mode at a rate of between 1.9 and 16.0° min^{-1} in ω to a $2\theta_{max}$ of 44.9°. A total of 3693 reflections were collected, of which 1239 were unique ($R_{int} = 0.08$). Lorentz-polarization, absorption (trans. factors: 0.91–1.06), and secondary extinction (0.30939×10^{-7}) corrections were applied. The structure was solved by standard Patterson and difference Fourier techniques. Full-matrix least squares converged at $R(R_w) = 0.028(0.025)$ and GOF = 1.05 using neutral atom scattering factors and anomalous dispersion terms for all non-hydrogen atoms. Hydrogen atoms were placed in calculated positions. Final cycles based upon |F| with 683 observations ($I > 3\sigma(I)$) and 74 variables gave rise to residual electron density of 0.69 e Å^{-3}. All calculations were performed with TEXSAN crystallographic package.

X-ray diffraction study of [$(N_3N)Mo(PPhH)$], $MoC_{21}H_{45}N_4Si_3P$, $M = 564.78$. An orange, prismatic crystal ($0.280 \times 0.140 \times 0.280$ mm) was determined to possess monoclinic metric symmetry (25 reflections, 20.0–30.0° in 2θ): $a = 16.32(2)$, $b = 9.82(2)$, $c = 19.55(2)$ Å, $\beta = 110.7(1)°$, $V = 2932(7)$ Å^3, $\rho_{calcd} = 1.279$ g cm^{-3}, space group $P2_1/n$ (no. 14), $Z = 4$, $F(000) = 1192$, $\mu(Mo_{K\alpha}) = 6.25$ cm^{-1}. Data were collected on a Rigaku AFC6S diffractometer, $Mo_{K\alpha}$ ($\lambda = 0.71069$ Å) radiation, at 173 K. Reflections were measured with widths of $(1.31 + 0.30 \tan\theta)°$ in ω in the ω-2θ mode at a rate of 16.0° min^{-1} in ω (8 rescans) to a $2\theta_{max}$ of 45.2°. A total of 4193 reflections were collected of which 4025 were unique ($R_{int} = 0.125$). Lorentz-polarization, absorption (trans. factors: 0.91–1.06), and secondary extinction (0.16781×10^{-7}) corrections were applied. The structure was solved by standard Patterson and difference Fourier techniques. Full-matrix least squares converged at $R(R_w) = 0.040(0.037)$ and GOF = 1.75 using neutral atom scattering factors and anomalous dispersion terms for all non-hydrogen atoms. Hydrogen atoms were placed in calculated positions. Final cycles based upon |F| with 2889 observations ($I > 3\sigma(I)$) and 272 variables gave rise to residual electron density of 0.35 e Å^{-3}. All calculations were performed with TEXSAN crystallographic package. Further details of the crystal structure investigations may be obtained from the Director of the Cambridge crystallographic Data Centre, 12 Union Road, GB-Cambridge CB2 1EZ (UK), on quoting the full journal citation.

Received: April 28, 1995 [Z 7941 IE]
German version: *Angew. Chem.* **1995**, *107*, 2184–2186

Keywords: complexes with phosphido ligands · molybdenum compounds · multiple bonds · phosphorus compounds · tungsten compounds

[1] C. C. Cummins, R. R. Schrock, W. M. Davis, *Angew. Chem.* **1993**, *105*, 758; *Angew. Chem. Int. Ed. Engl.* **1993**, *32*, 756.
[2] K.-Y. Shih, K. Totland, S. W. Seidel, R. R. Schrock, *J. Am. Chem. Soc.* **1994**, *116*, 12103.
[3] J. S. Murdzek, R. R. Schrock in *High Oxidation State Alkylidyne Complexes*, VCH, New York, **1988**.
[4] O. J. Scherer, *Angew. Chem.* **1990**, *102*, 1137; *Angew. Chem. Int. Ed. Engl.* **1990**, *29*, 1104.
[5] M. H. Chisholm, J. C. Huffman, J. W. Pasterczyk, *Inorg. Chim. Acta* **1987**, *133*, 17.
[6] *Multiple Bonds and Low Coordination in Phosphorus Chemistry* (Eds.: M. Regitz, O. J. Scherer) Thieme, New York, **1990**.
[7] M. H. Chisholm, K. Folting, J. W. Pasterczyk, *Inorg. Chem.* **1988**, *27*, 3057.
[8] C. E. Laplaza, W. M. Davis, C. C. Cummins, *Angew. Chem.* **1995**, *107*, 2181; *Angew. Chem. Int. Ed. Engl.* **1995**, *34*, 2042.
[9] Z. Duan, J. G. Verkade, *Inorg. Chem.* **1995**, *34*, 1576.
[10] S. M. Rocklage, R. R. Schrock, M. R. Churchill, H. J. Wasserman, *Organometallics* **1982**, *1*, 1332.
[11] W. Plass, J. G. Verkade, *J. Am. Chem. Soc.* **1992**, *114*, 2275.
[12] J. Manna, R. J. Kuk, R. F. Dallinger, M. D. Hopkins, *J. Am. Chem. Soc.* **1994**, *116*, 9793.
[13] R. R. Schrock, K.-Y. Shih, D. A. Dobbs, W. M. Davis, *J. Am. Chem. Soc.* **1995**, *117*, 6609.

Cerium(III) Chloride Promoted Nucleophilic Addition of Organolithium Reagents to α-Alkyl-β-Ketophosphine Oxides: A New Protocol for the Synthesis of Stereochemically Defined Trisubstituted Olefins

Giuseppe Bartoli,* Enrico Marcantoni, Letizia Sambri, and Monica Tamburini

Given the importance of stereochemically defined carbon–carbon double bonds, extensive effort has been devoted over the years to their stereoselective construction.[1] Nevertheless, while efficient procedures are available for the synthesis of stereochemically defined disubstituted alkenes,[2] a general method for trisubstituted compounds is still needed. The classical Horner method offers poor stereocontrol in the formation of the key phosphine oxide intermediates with a tertiary hydroxyl group in the β-position.[2–4] An efficient access to trisubstituted olefins has been recently proposed by Denmark et al.,[4] who succeeded in adapting the Warren variant of the Horner–Wittig method[5] for the highly stereoselective construction of α-dialkyl-β-hydroxyphosphine oxide intermediates by using the chiral reagent **1** as starting material (Scheme 1). The method is

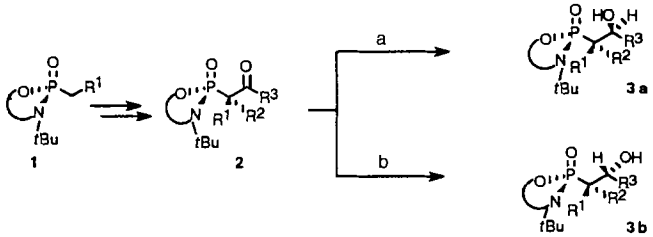

Scheme 1. Denmark synthesis of α-dialkyl-β-hydroxyphosphamidates. a) Diisobutylaluminum hydride (DIBAL), b) $CeCl_3$, $NaBH_4$, or $LiBHEt_3$ or $LiBH_sBu_3$.

[*] Prof. Dr. G. Bartoli, Dr. L. Sambri, Dr. M. Tamburini
Dipartimento di Chimica Organica
"A. Mangini", v. le Risiorgimento, 4, I-40136 Bologna (Italy)
Telefax: Int. code (51)6443654
Dr. E. Marcantoni
Università di Camerino (MC) (Italy)

useful for the synthesis of trisubstituted alkenes in both isomeric forms with high diastereoselectivity. However, there are some problems in the key step of the Denmark sequence, the stereoselective reduction of β-ketophosphine oxides **2** to hydroxyl derivatives **3**, the precursors of the alkenes. To ensure high selectivity in all cases, it was necessary to adopt a specific reduction method (with even opposite selectivity) for each pair of diastereomers depending on the nature of R^3 group. In addition, the stereoselective conversion of β-hydroxyphosphonoamidates into the corresponding alkenes requires very drastic conditions (thermal decomposition at 105 °C in THF).

The most straightforward method for constructing Wittig intermediates with high diastereoselectivity is the stereocontrolled addition of a carbon nucleophile to the carbonyl function of a β-ketophosphine oxide with a chiral carbon center in α position.

We report now that this goal can be achieved by using $RLi \cdot CeCl_3$ complexes. As shown in Scheme 2, when racemic

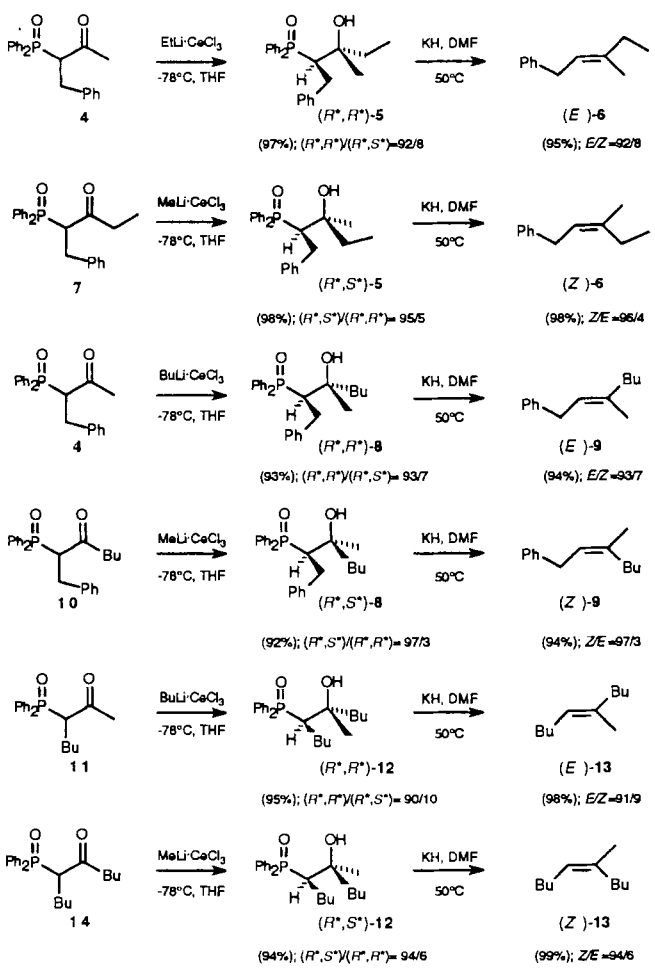

Scheme 2. Synthesis of trisubstituted olefins in both isomeric forms.

β-ketophosphine oxide **4** is allowed to react with the preformed $EtLi \cdot CeCl_3$ complex,[6] (*R**,*R**)-**5**[7] (see Table 1) is obtained in high yields (97%) and with excellent diastereoselectivity[8] (92/8). β-Hydroxyphosphine oxide (*R**,*R**)-**5** is transformed directly into alkene (*E*)-**6**[9] (see Scheme 2 and Table 2) without any purification from the small amount of the corresponding diastereomer. This conversion occurs in high yield (95%) and with excellent stereoselectivity ($E/Z = 92/8$). In an analogous manner, the isomer (*Z*)-**6** can be obtained in high yield (95%) and with excellent diastereoselectivity ($Z/E = 96/4$) from **7**. The same procedure can be used to synthesize olefins (*E*)- and (*Z*)-**9** from **4** and **10**, respectively.

Equally satisfactory results were obtained when the α-alkyl substituent was not a benzyl group. In fact, we were able to convert α-butyl-β-ketophosphine oxides **11** and **14** into (*E*)- and (*Z*)-6-methyl-5-decene ((*E*)- and (*Z*)-**13**), respectively, in comparable high yields and diastereoselectivities.

The present method is characterized by the following features:

a) The procedure is useful for preparing trisubstituted alkenes with excellent diastereoselectivity and in both isomeric forms. In particular the latter goal can be achieved easily by simply exchanging the aliphatic groups on the β-ketophosphine oxide with those of the lithium-cerium complex.

Table 1. Selected ^1H NMR data of α-alkyl-β-hydroxyphosphine oxides.

(*R**,*R**)-**5**: ^1H NMR (200 MHz, $CDCl_3$, 20 °C): $\delta = 0.77$ (t, 3H, $J = 7.4$ Hz, CH_2CH_3), 1.35 (s, 3H, CH_3), 1.6 (q, 2H, $J = 7.4$ Hz, CH_2CH_3), 2.9–3.2 (m, 3H, CH_2Ph and CH), 4.7 (br.s, 1H, OH), 4.8 (br.s, 1H, (*R**,*S**)-**5**-OH), 6.7–7.9 (m, 15H, 3Ph)

(*R**,*S*)-**5**: ^1H NMR (200 MHz, $CDCl_3$, 20 °C): $\delta = 0.83$ (t, 3H, $J = 7.4$ Hz, CH_2CH_3), 1.2 (s, 3H, CH_3), 1.7 (q, 2H, $J = 7.5$ Hz, CH_2CH_3), 2.8–3.3 (m, 3H, CH_2Ph and CH), 4.7 (br.s, 1H, (*R**,*R**)-**5**-OH), 4.8 (br.s, 1H, OH), 6.7–7.9 (m, 15H, 3Ph)

(*R**,*R**)-**8**: ^1H NMR (200 MHz, $CDCl_3$, 20 °C): $\delta = 0.57$ (t, 3H, $J = 6.9$ Hz, $(CH_2)_3CH_3$), 0.6–1.5 (m, 6H, $(CH_2)_3CH_3$), 1.3 (s, 3H, CH_3), 2.7–3.1 (m, 3H, CH_2Ph and CH), 4.79 (br.s, 1H, (*R**,*S**)-**8**-OH), 4.82 (br.s, 1H, OH), 6.6–7.8 (m, 15H, 3Ph)

(*R**,*S**)-**8**: ^1H NMR (200 MHz, $CDCl_3$, 20 °C: $\delta = 0.7$ (t, 3H, $J = 6.8$ Hz, $(CH_2)_3CH_3$), 0.9–1.7 (m, 6H, $(CH_2)_3CH_3$), 1.1 (s, 3H, CH_3), 2.7–3.3 (m, 3H, CH_2Ph and CH), 4.80 (br.s, 1H, OH), 4.83 (br.s, 1H, (*R**,*R**)-**8**-OH), 6.7–7.8 (m, 15H, 3Ph)

(*R**,*R**)-**12**: ^1H NMR (200 MHz, $CDCl_3$, 20 °C): $\delta = 0.57$ (t, 3H, $J = 6.8$ Hz, $CH_3(CH_2)_3$), 0.6–1.8 (m, 15H, $CH_3(CH_2)_3$ and $2CH_3(CH_2)_3$), 1.2 (s, 3H, CH_3), 2.3–2.45 (m, 1H, CH), 4.85 (br.s, 1H, (*R**,*S**)-**12**-OH), 4.92 (br.s, 1H, OH), 7.3–7.9 (m, 15H, 3Ph)

(*R**,*S**)-**12**: ^1H NMR (200 MHz, $CDCl_3$, 20 °C): $\delta = 0.60$ (t, 3H, $J = 6.6$ Hz, $CH_3(CH_2)_3$), 0.7–1.9 (m, 12H, $2CH_3(CH_2)_3$), 0.88 (t, 3H, $J = 6.9$ Hz, $CH_3(CH_2)_3$), 1.18 (s, 3H, CH_3), 2.35–2.45 (m, 1H, CH), 4.88 (br.s, 1H, OH), 5.0 (br.s, 1H, (*R**,*R**)-**12**-OH), 7.4–7.9 (m, 15H, 3Ph)

Table 2. Selected ^1H and ^{13}C NMR data of trisubstituted olefins.

(*E*)-**6**: ^1H NMR (200 MHz, $CDCl_3$, 20 °C: $\delta = 1.0$ (t, 3H, $J = 7.4$ Hz, CH_2CH_3), 1.7 (s, 3H, CH_3), 2.1 (q, 2H, $J = 7$ Hz, CH_2CH_3), 3.4 (d, 2H, $J = 7.3$ Hz, CH_2Ph), 5.3 (t, 1H, $J = 7.3$ Hz, CH), 7.1–7.3 (m, 5H, Ph); ^{13}C NMR (200 MHz, $CDCl_3$, 20 °C): $\delta = 12.9$, 16.3, 32.6, 34.3, 121.8, 125.8, 128.5, 138.6, 142.1

(*Z*)-**6**: ^1H NMR (200 MHz, $CDCl_3$, 20 °C: $\delta = 1.0$ (t, 3H, $J = 7.6$ Hz, CH_2CH_3), 1.7 (d, 3H, $J = 1.3$ Hz, CH_3), 2.1 (q, 2H, $J = 15$ Hz, CH_2CH_3), 3.3 (d, 2H, $J = 7.3$ Hz, CH_2Ph), 5.3 (t, 1H, $J = 7.3$ Hz, CH), 7.1–7.3 (m, 5H, Ph); ^{13}C NMR (200 MHz, $CDCl_3$, 20 °C): $\delta = 12.9$, 22.9, 24.9, 34.0, 122.8, 125.7, 128.4, 138.2, 141.9

(*E*)-**9**: ^1H NMR (200 MHz, $CDCl_3$, 20 °C): $\delta = 0.8$ (t, 3H, $J = 7.0$ Hz, $(CH_2)_3CH_3$), 1.2–1.4 (m, 4H, $CH_2(CH_2)_2CH_3$), 1.6 (s, 3H, CH_3), 2.0 (t, 2H, $J = 7.3$ Hz, $CH_2(CH_2)_2CH_3$), 3.3 (d, 2H, $J = 7.3$ Hz, CH_2Ph), 5.3 (t, 1H, $J = 7.3$ Hz, CH), 7.1–7.3 (m, 5H, Ph); ^{13}C NMR (200 MHz, $CDCl_3$, 20 °C): $\delta = 13.0$, 15.0, 21.4, 29.2, 33.2, 38.4, 121.7, 124.6, 127.3, 135.6, 140.9

(*Z*)-**9**: ^1H NMR (200 MHz, $CDCl_3$, 20 °C): $\delta = 0.8$ (t, 3H, $J = 7.1$ Hz, $(CH_2)_3CH_3$), 1.2–1.4 (m, 4H, $CH_2(CH_2)_2CH_3$), 1.7 (s, 3H, CH_3), 2.1 (d, 2H, $J = 7.3$ Hz, $CH_2(CH_2)_2CH_3$), 3.3 (d, 2H, $J = 7.0$ Hz, CH_2Ph), 5.2 (t, 1H, $J = 7.7$ Hz, CH), 7.1–7.3 (m, 5H, Ph); ^{13}C NMR (200 MHz, $CDCl_3$, 20 °C): $\delta = 14.3$, 23.0, 23.7, 30.5, 31.8, 34.3, 123.6, 125.9, 128.5, 136.9, 142.1

(*E*)-**13**: ^1H NMR (200 MHz, $CDCl_3$, 20 °C): $\delta = 0.8$–0.9 (m, 6H, $2CH_3(CH_2)_3$), 1.2–1.3 (m, 8H, $2CH_3(CH_2)_2CH_2$), 1.6 (s, 3H, CH_3), 1.9–2.1 (m, 4H, $2CH_3(CH_2)_2CH_2$), 5.1 (t, 3H, $J = 7.2$ Hz, CH); ^{13}C NMR (200 MHz, $CDCl_3$, 20 °C): $\delta = 14.2$, 16.0, 22.5, 27.8, 29.9, 30.4, 32.3, 39.6, 124.7, 135.3

(*Z*)-**13**: ^1H NMR (200 MHz, $CDCl_3$, 20 °C): $\delta = 0.8$–1.0 (m, 6H, $2CH_3(CH_2)_3$), 1.2–1.4 (m, 8H, $2CH_3(CH_2)_2CH_2$), 1.7 (s, 3H, CH_3), 1.9–2.1 (m, 4H, $2CH_3(CH_2)_2CH_2$), 5.1 (t, 3H, $J = 7.1$ Hz, CH); ^{13}C NMR (200 MHz, $CDCl_3$, 20 °C): $\delta = 14.2$, 22.6, 22.9, 23.6, 27.7, 30.5, 31.7, 32.6, 125.4, 135.5

 © VCH Verlagsgesellschaft mbH, D-69451 Weinheim, 1995 0570-0833/95/3418-2047 $ 10.00+.25/0

b) The method works well when the substituents are small and similar in size (CH_3, C_2H_5), in contrast to the classical Horner approach.[2]

c) Unlike the Denmark method, the stereochemical outcome is uniform: in all cases examined, the attack of the carbon nucleophile on the β-ketophosphine oxide occurs at the side opposite to the α-alkyl substituent.[10]

d) Stereospecific decomposition of β-hydroxyphosphine oxides to give alkenes requires very mild conditions.[5b, 11]

The method described here is a new protocol for the synthesis of trisubstituted alkenes with excellent diastereoselectivity and in both isomeric forms. It relies on easily available β-ketophosphine oxides as starting materials.[12] Studies are in progress in our laboratory to rationalize the unexpected selective alkylation and to explore the potential of this reaction especially in comparison with other strategies such as that recently published[13] based on addition of organocuprates to phenylthioacetylenes.

Experimental Procedure

α-Alkyl-β-hydroxyphosphine oxides: β-Ketophosphine oxide **6** (2 mmol), prepared according to Warren's method [12c], was added dropwise to a suspension [6] of $RLi \cdot CeCl_3$ (7 mmol) in THF (15 mL) at $-78\,^{\circ}C$. The mixture was stirred at this temperature for 2 h, then quenched with 5 mL of aqueous AcOH (5%) and extracted with Et_2O. The organic layer was washed with saturated $NaHCO_3$ (20 mL) and dried (Na_2SO_4). The product was purified by flash chromatography (SiO_2, ethyl acetate/Et_2O = 1/4) [14].

Trisubstituted alkenes: Compound **8** (1.5 mmol) was dissolved in anhydrous DMF (3 mL), treated with an excess of KH, and heated at 50 °C for 30 min. The mixture was cooled, 5 mL of pentane added, and the resulting solid removed by filtration and washed with pentane. The organic mother liquor was washed with water, dried, and concentrated to dryness. The olefins obtained had purities higher than 99%.

Received: March 29, 1995 [Z7847IE]
German version: *Angew. Chem.* **1995**, *107*, 2163–2164

Keywords: alkenes · alkylations · asymmetric syntheses · cerium compounds · Horner–Wittig reactions

[1] For reviews, see: a) S. E. Kelly in *Comprehensive Organic Synthesis, Addition to C-X π Bonds, Part 1*, Vol. 4, (Ed.: S. L. Schreiber), Pergamon, Oxford, **1991**, Chapter 3; b) J. Reucroft, P. G. Sammes, *Q. Rev. Chem. Soc.* **1971**, *25*, 135; c) M. Julia, *Pure Appl. Chem.* **1985**, *57*, 763; d) A. S. Arora, I. K. Ugi in *Methoden der Organischen Chemie (Houben-Weyl) 4th ed., 1952*, Vol. 5/1b, **1972**, p. 278.

[2] B. E. Maryanoff, A. B. Reitz, *Chem. Rev.* **1989**, *89*, 863.

[3] G. Etemad-Moghadam, J. Seyden-Penne, *Tetrahedron* **1984**, *40*, 5153.

[4] S. E. Denmark, J. Amburgey, *J. Am. Chem. Soc.* **1993**, *115*, 10386.

[5] a) A. D. Buss, S. Warren, *Tetrahedron Lett.* **1983**, *24*, 111; b) *J. Chem. Soc. Perkin Trans. 1* **1985**, 2307; c) D. Cavalla, W. B. Cruse, S. Warren, *ibid.* **1987**, 1883.

[6] G. Bartoli, E. Marcantoni, M. Petrini, L. Sambri, *Tetrahedron Lett.* **1994**, *35*, 8453.

[7] The descriptors *R**, *S** are used throughout the text and in Scheme 2 to indicate that the diastereomeric compounds are obtained as racemates.

[8] Diastereomeric ratios were determined on the basis of the relative intensity of OH signals in ^1H NMR spectrum of the reaction mixture. The configuration was assigned on the basis of the configuration of the final alkene.

[9] Ratios between (*Z*) and (*E*) alkenes were determined by GLC-GM analysis. Configuration of olefins was assigned by NOE experiments.

[10] A possible explanation of this stereochemical outcome is the formation of a six-membered intermediate, in which the Ce atom chelates the P=O and C=O groups. The nucleophile adds to the diastereotopic face of the C=O group opposite the alkyl group on the carbon atom between P=O and C=O. For an analogous situation see: J. Elliott, S. Warren, *Tetrahedron Lett.* **1986**, *27*, 649.

[11] A. D. Buss, W. B. Cruse, O. Kennard, S. Warren, *J. Chem. Soc. Perkin Trans. 1* **1984**, 243.

[12] For synthesis methods, see: a) E. E. Aboujaode, N. Collignon, P. Savignac, *J. Organomet. Chem.* **1984**, 264, 9; b) F. Mathey, P. Savignac, *Tetrahedron* **1978**, *34*, 649; c) R. S. Torr, S. Warren, *J. Chem. Soc. Pak.* **1979**, *1*, 15; d) P. D. Theisen, C. H. Heathcock, *J. Org. Chem.* **1988**, *53*, 2374.

[13] I. Creton, I. Marek, D. Brasseur, J. L. Jestin, J. F. Normant, *Tetrahedron Lett.* **1994**, *35*, 6837.

[14] All these compounds were unknown, except (*Z*)-6-methyl-5-decene ((*Z*)-**13**), see: E. Negishi, D. E. Van Horn, T. Yoshida, *J. Am. Chem. Soc.* **1985**, *107*, 6639.

An Alkylperoxoiron(III) Intermediate and Its Role in the Oxidation of Aliphatic C–H Bonds**

Jinheung Kim, Edmund Larka, Elizabeth C. Wilkinson, and Lawrence Que, Jr.*

Alkylperoxoiron(III) species have been invoked in mechanisms of alkane functionalization catalyzed by nonheme iron complexes in concert with alkyl hydroperoxides.[1] These catalytic systems have attracted interest as models for methane monooxygenase[2] and other nonheme iron oxygenases.[3] Ménage et al. have recently observed the transient formation of an intermediate when **1**[4] is treated with ROOH in the presence

$[Fe_2O(bpy)_4(H_2O)_2](ClO_4)_4$ **1**

of alcohols (R'OH).[5] This species has been formulated as a mononuclear Fe(III)-OOR complex, **2**, on the basis of a) its

$[Fe(bpy)_2(OOR)(R'OH)]^{2+}$ **2**

low-spin Fe(III) EPR signal which accounts for as much as 0.8 spin per Fe, b) resonance Raman features associated with the alkylperoxo moiety, and c) the perturbation of spectral features when different alcohols are used. In this paper, we demonstrate that an analogous intermediate can also be formed from a different (μ-oxo)diiron(III) catalyst, **3**, and establish its nature

$[Fe_2O(tpa)_2(H_2O)_2](CF_3SO_3)_4$ **3**

by resonance Raman spectroscopy and electrospray ionization mass spectrometry. We further show that this intermediate is directly responsible for the cleavage of aliphatic C–H bonds required for the oxidation of alcohols by this catalytic system.

Complex **3** has been synthesized and characterized as a (μ-oxo)diiron(III) complex with terminal aqua ligands.[6] In concert with *t*BuOOH (TBHP[4]), **3** catalyzes the oxidation of cyclohexane to cyclohexanol (7 turnovers) and the oxidation of cyclohexanol to cyclohexanone (18 turnovers).[7] In the case of alcohol substrates, treatment of **3** with excess TBHP in CH_3CN at $-40\,^{\circ}C$ affords a transient blue species **4** (λ_{max} 598 nm, Fig. 1)

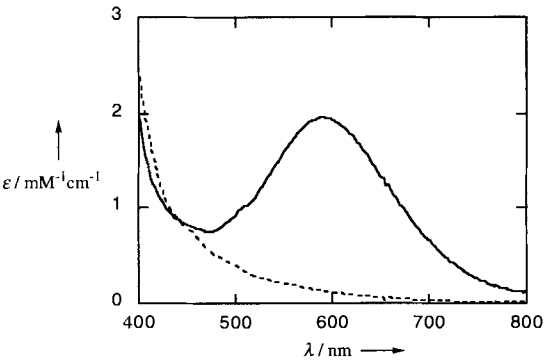

Fig. 1. Electronic spectra of **5** (----) and **4** (——) in CH_3CN for the case R'OH = cyclohexanol. Species **5** was prepared by mixing **3** (0.7 mM) and cyclohexanol (0.14 M). Species **4** was generated by adding TBHP (21 mM) to **5** at $-40\,^{\circ}C$ under argon.

[*] Prof. L. Que, Jr., J. Kim, Dr. E. Larka, E. C. Wilkinson
Department of Chemistry, University of Minnesota
Minneapolis, MN 55455 (USA)
Telefax: Int. code + (612)624-7029

[**] We thank Ms. Maren Bunge for her assistance with electrospray ionization mass spectrometry. This work was supported by the National Institutes of Health grant GM-38767.

with EPR and Raman properties similar to those of **2**.[5] Complex **4** exhibits an $S = 1/2$ EPR spectrum with $g = 2.19$, 2.14, and 1.98, typical of low-spin Fe(III) complexes and with a signal intensity that accounts for as much as 0.8 spin/Fe (Fig. 2). When excited at 597.8 nm, **4** exhibits resonance-enhanced Raman features at 490, 696, and 796 cm^{-1} (Fig. 3a) which are all

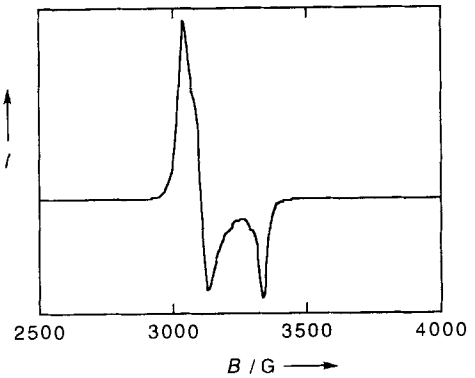

Fig. 2. EPR spectrum of **4** in CH_3CN generated by adding TBHP (21 mM) to **5** (1.4 mM, R'OH = cyclohexanol) at $-40\,^{\circ}C$ under argon. Spectrometer: 9.23 GHz, 15 μW power, modulation amplitude 10 G, temperature 20 K.

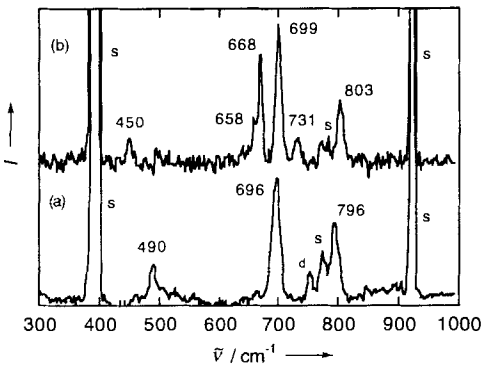

Fig. 3. Resonance Raman spectra (597.8 nm excitation, 77 K) of **4** derived from a) TBHP and b) $[D_9]$TBHP in CH_3CN. Peaks labeled s and d derive from solvent and decomposed product, respectively.

sensitive to the use of $[D_9]$TBHP[8] (Fig. 3b) but insensitive to the presence of $H_2{}^{18}O$; these observations suggest that the blue chromophore arises from an alkylperoxo-to-iron(III) charge transition and not from an iron-oxo species. Thus **4** is a mononuclear iron species with a coordinated alkylperoxo group.

Further spectroscopic studies provide new insight into the formation of the intermediate. NMR and EPR titrations show that the addition of alcohol to dinuclear **3** affords a mononuclear species **5** which is in equilibrium with its precursor. The NMR signals of **3** in the region $\delta = 5$–35 associated with the tpa pyridyl β- and γ-H's of a (μ-oxo)diiron(III) complex[9] are replaced by broader signals at $\delta = 120$, 114 (py β-H), and -18 (py γ-H), typical of a mononuclear high-spin iron(III) species; when dissolved in CD_3OD, **3** is quantitatively converted to **5**. Similarly, increasing amounts of alcohol elicit the appearance of an EPR signal at $g = 4.3$ which is characteristic of a mononuclear high-spin iron(III) center in a rhombic environment. Electrospray ionization mass spectrometry of a solution of **3** treated with 200 equiv $PhCH_2OH$ shows prominent positive and negative ion clusters at m/z 552 and 750, respectively, the observed masses and isotope patterns of which correspond to the ions $[\{Fe(tpa)(OCH_2C_6H_5)\}(ClO_4)]^+$ and $[\{Fe(tpa)(OCH_2C_6H_5)\}(ClO_4)_3]^-$ (Fig. 4a). These features respectively shift to m/z 544 and 742 when CF_3CH_2OH is used in place of $C_6H_5CH_2OH$, consistent with the decreased mass of CF_3 relative to C_6H_5. Species **5** is thus formulated as $[Fe(tpa)(OR')]^{2+}$.

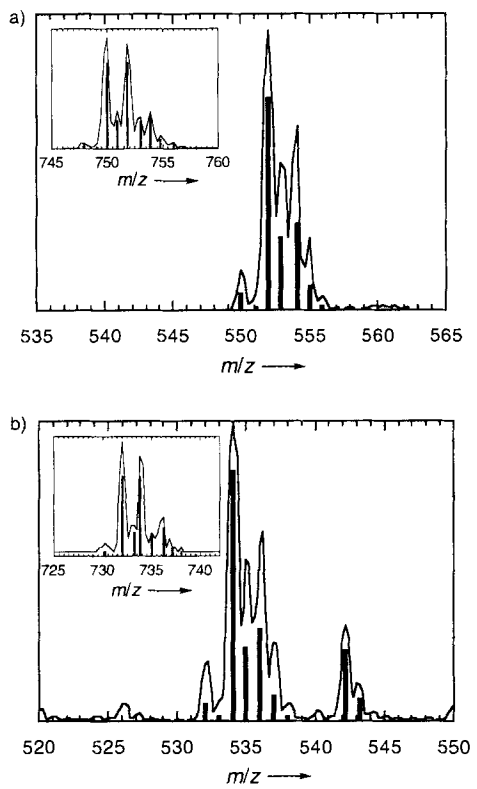

Fig. 4. Positive ion and (as insert) negative ion electrospray ionization mass spectral data. a) **3** + $PhCH_2OH$, b) **4**. Calculated isotope patterns are represented by bars under each peak cluster.

Electrospray ionization mass spectra of **4**, obtained by co-injecting solutions of **3** + alcohol and TBHP into a pre-cooled mixing chamber and channeling the output directly into the mass spectrometer, show prominent ion clusters at m/z 534 and 732, the masses and isotope patterns of which are consistent with the ions, $[\{Fe(tpa)(OO\mathit{t}Bu)\}(ClO_4)]^+$ and $[\{Fe(tpa)(OO\mathit{t}Bu)\}(ClO_4)_3]^-$, respectively (Fig. 4b). Furthermore these ion clusters shift by 62 mass units when CHP[4] is used in place of TBHP. Although these observations may suggest that **4** can be formulated as $[Fe(tpa)OOR]^{2+}$, its low-spin nature would require a six-coordinate species. The sixth ligand may be water or alcohol. The observed ions at m/z 534 and 732 would then derive from the loss of either water or benzyl alcohol from $[Fe(tpa)(OO\mathit{t}Bu)(HOR')]^{2+}$ (R' = H, benzyl) moiety. Evidence for the latter can be found in the positive ion mass spectrum of **4** which also shows a peak at m/z 542 (Fig. 4b). Its mass and isotope pattern correspond to $[Fe(tpa)(OO\mathit{t}Bu)(OCH_2Ph)]^+$ which would derive from the loss of $HClO_4$ from the parent ion $[\{Fe(tpa)(OO\mathit{t}Bu)(HOCH_2Ph)\}(ClO_4)]^+$. The coordination of the alcohol is also supported by kinetic evidence (see below).

Species **4** decomposes in a pseudo-first-order process as monitored by the disappearance of the 598 nm band, but further addition of TBHP re-generates **4**. Its rate of decomposition de-

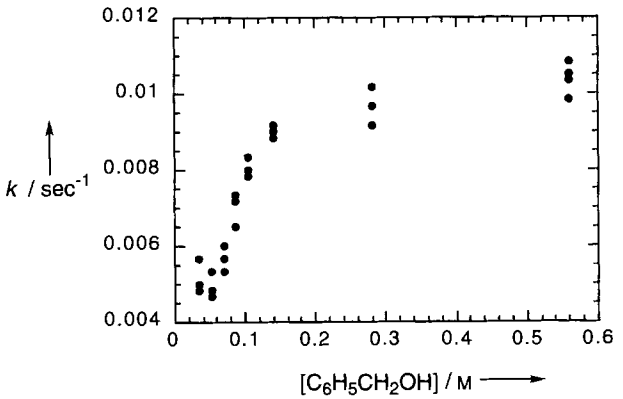

Fig. 5. Dependence of pseudo-first-order decomposition rate constants of **4** on benzyl alcohol concentration. The rates of decomposition were measured with 0.7 mM **3**, 21 mM TBHP, and 0.035–0.56 M benzyl alcohol in acetonitrile at −20 °C under argon. Each point represents one kinetic run.

pends on the amount of alcohol present. As shown in Figure 5, the pseudo-first-order rate constant for the decomposition of **4** increases as benzyl alcohol concentration is increased but reaches a plateau at high alcohol concentrations. The observed saturation kinetics implies the binding of alcohol to the complex prior to its decomposition. Furthermore, the decomposition rate decreases significantly in the presence of 200 equiv $C_6D_5CD_2OH$ ($k_H/k_D = 4.8$), indicating that the decomposition of the peroxide intermediate is accompanied by the breaking of the benzylic C–H bond.

Scheme 1 shows two mechanisms that are consistent with the observed substrate dependence for the decomposition of **4**.

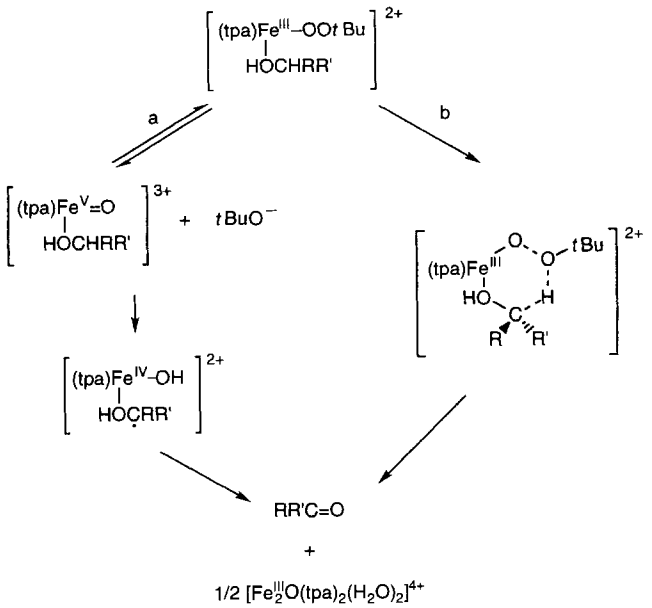

Scheme 1. Two possible mechanisms for the oxidation of alcohols by peroxides in the presence of **3**.

Pathway *a* is based on the heme precedent[10] but requires that the high-valent iron-oxo species responsible for the C–H bond attack be *reversibly* formed from **4**. That an O–O bond can be formed from a high-valent oxo species and OH^- is suggested by observations of Mascharak and Busch who have independently reported the formation of hydroperoxoiron(III) species by the reaction of iron(III) complexes with PhIO in basic media.[11] However, intermediate **4** is not formed when **5** is treated with PhIO and *t*BuO$^-$ ion. Furthermore, the addition of 100 equiv cumyl alcohol to a 1 mM solution of **4** does not result in the appearance of Raman features that can be attributed to a bound -OO-cumyl group.[12] Thus **4** is not in equilibrium with a high-valent iron-oxo species, and we consider pathway *a* unlikely.

Pathway *b*, on the other hand, involves contemporaneous O–O and C–H bond cleavage via an attractive six-membered ring transition state (Scheme 1). The direct participation of a metal-peroxo species in oxidation mechanisms has been considered in a number of studies involving nonheme systems,[2b, 3b, 13] because of the perceived difficulty of stabilizing a high-valent metal-oxo species in the absence of porphyrins. The data reported here however represents the first kinetic evidence that an alkylperoxoiron(III) species may directly cleave aliphatic C–H bonds. We cannot as yet establish whether an analogous alkylperoxoiron(III) species participates in the alkane oxidations catalyzed by **3**. Since alkanes lack the functionality to coordinate to the metal center, such a species would differ from **4** and may not have a sufficient lifewtime to be observed. Work is in progress to address this problem.

Experimental Procedure

3: A 1:1:4 ratio of $Fe(CF_3SO_3)_3 \cdot 6H_2O$, tpa·3$HClO_4$, and Et_3N was combined in CH_3OH to produce a red solution. A solid was obtained in 78% yield upon treatment with Et_2O. Recrystallization was accomplished by vapor diffusion of Et_2O into a CH_3CN solution of **3** to yield diffraction quality crystals. Anal. calcd for $C_{42}H_{40}F_{12}Fe_2N_8O_{15}S_4$: C 36.96, H 3.33, N 8.21, F 16.30; found: C 36.72, H 3.48, N 8.33, F 16.12.

Electrospray ionization mass spectra were acquired using a PE Sciex API III triple quadrupole mass spectrometer (Norwalk, CT). Samples in CH_3CN were infused into an Upchurch Scientific metal-free static mixing tee (Oak Harbor, WA) using a pair of Harvard Apparatus Model 22 syringe pumps (South Natick, MA), each delivering 20 μL min^{-1} of solution to the mixing tee. The syringes and the mixing tee were cooled with dry ice.

Kinetics: The decrease of the 598 nm band of **4** was monitored on a Hewlett-Packard 8452A diode array spectrometer fitted for low-temperature measurements with a dewar with quartz windows cooled by a Neslab Cryocool CC-100II immersion cooler.

Received: February 4, 1995
Revised version: June 19, 1995 [Z7691IE]
German version: *Angew. Chem.* **1995**, *107*, 2191–2194

Keywords: C–H activation · iron compounds · mass spectrometry · peroxo complexes

[1] a) R. A. Leising, J. Kim, M. A. Perez, L. Que, Jr., *J. Am. Chem. Soc.* **1993**, *115*, 9524–9530; b) T. Kojima, R. A. Leising, S. Yan, L. Que, Jr., *ibid.* **1993**, *115*, 11328–11335; c) S. Ménage, J.-M. Vincent, C. Lambeaux, G. Chottard, A. Grand, M. Fontecave, *Inorg. Chem.* **1993**, *32*, 4766–4773; d) D. H. R. Barton, S. D. Bèvière, W. Chavasiri, D. Doller, B. Hu, *Tetrahedron Lett.* **1992**, *33*, 5473–5476.

[2] a) A. C. Rosenzweig, C. A. Frederick, S. J. Lippard, P. Nordlund, *Nature (London)* **1993**, *366*, 537–543; b) J. D. Lipscomb, *Annu. Rev. Microbiol.* **1994**, *48*, 371–399.

[3] a) L. Que, Jr. in *Bioinorganic Catalysis* (Ed.: J. Reedijk), Marcel Dekker, New York, **1993**, pp. 347–393; b) A. L. Feig, S. J. Lippard, *Chem. Rev.* **1994**, *94*, 759–805.

[4] Abbreviations used: bpy = 2,2′-bipyridine;tpa = tris(2-pyridylmethyl)amine; TBHP = *tert*-butylhydroperoxide; CHP = cumene hydroperoxide.

[5] S. Ménage, M. Fontecave, E. C. Wilkinson, L. Que, Jr., *Angew. Chem.* **1995**, *107*, 198–199; *Angew. Chem. Int. Ed. Engl.* **1995**, *34*, 203–205.

[6] Diffraction quality crystals of **3** were obtained from acetonitrile/diethyl ether. The complex crystallizes in the monoclinic system, space group $P2_1/c$, with $a = 12.562(4)$, $b = 19.349(9)$, $c = 22.14$ Å, $\beta = 103.76(3)°$, $V = 5226(7)$, $Z = 4$. With the use of 5311 unique observed reflections, for which $I_{(obsd)} > 2.0\sigma(I)$, collected at 172 K with $Mo_{K\alpha}$ ($\lambda = 0.71069$ Å) radiation out to $2\theta_{max} = 56.0°$ on an Enraf-Nonius CAD4 X-ray diffractometer, the structure was solved by direct methods and refined to $R = 0.077$ and $R_w = 0.070$. Full structural details will be published elsewhere.

 © VCH Verlagsgesellschaft mbH, D-69451 Weinheim, 1995 0570-0833/95/3418-2050 $ 10.00+.25/0

[7] Turnover numbers were determined for a catalyst: TBHP:substrate ratio of 1:50:200 in CH_3CN under Ar at room temperature for a reaction time of 5 min.
[8] Prepared from [D$_9$]*t*BuMgCl using the synthetic method outlined in: C. Walling, S. A. Buckler, *J. Am. Chem. Soc.* **1955**, *77*, 6032–6038.
[9] Assignment of proton resonances in **3**: δ = 32 (py α-H), 19 (py β-H), and 6 (py γ-H).
[10] J. T. Groves, *J. Chem. Educ.* **1985**, *62*, 928–931.
[11] a) R. J. Guajardo, S. E. Hudson, S. J. Brown, P. K. Mascharak, *J. Am. Chem. Soc.* **1993**, *115*, 7971–7977; b) A. Sauer-Masarwa, N. Herron, C. M. Fendrick, D. H. Busch, *Inorg. Chem.* **1993**, *32*, 1086–1089.
[12] For comparison, the Raman spectrum of the Fe-OO-cumyl intermediate shows features at 454, 554, 574, 696, 728, and 792 cm^{-1}.
[13] a) G. Tian, J. A. Berry, J. P. Klinman, *Biochemistry* **1994**, *33*, 226–234; b) J. S. Valentine, W. Nam, R. Y. Ho in *The Activation of Dioxygen and Homogeneous Catalytic Oxidation* (Eds.: D. H. R. Barton, A. E. Martell, D. T. Sawyer), Plenum, New York, **1993**, pp. 183–198; c) W. Nam, R. Y. Ho, J. S. Valentine, *J. Am. Chem. Soc.* **1991**, *113*, 7052–7054; d) J. W. Sam, X.-J. Tang, J. Peisach, *ibid.* **1994**, *116*, 5250–5256; e) O. M. Reinaud, K. H. Theopold, *J. Am. Chem. Soc.* **1994**, *116*, 6979–6980; f) S. Mahapatra, J. A. Halfen, E. C. Wilkinson, L. Que, Jr., W. B. Tolman, *ibid.* **1994**, *116*, 9785–9786.

Novel Binuclear Cobalt Dioxygen Complex—A Step on the Path to Dioxygen Activation**

Olivia M. Reinaud, Glenn P. A. Yap, Arnold L. Rheingold, and Klaus H. Theopold*

The "activation" of dioxygen by complexation to transition metals is an important theme of contemporary chemical research.[1] The synthesis and characterization of novel dioxygen complexes (with O_2, O_2^-, or O_2^{2-} ligands) is thus part of the search for catalytic oxidation reactions that use air as an environmentally benign oxidant.[2] Such complexes may also serve as models for the active sites of biomolecules that facilitate transport and utilization of dioxygen in living organisms. Herein we describe the formation of a cobalt dioxygen complex containing an unprecedented structural motif. The cobalt is coordinated by sterically congested tris(pyrazolyl)borate moieties,[3] a class of ligands that have shown a propensity for stabilizing unusual binding modes in dioxygen complexes.[4]

As previously described, exposure of solid [Tp″Co(CO)] (Tp″ = hydrotris(3-isopropyl-5-methylpyrazolyl)borate) to an excess of O_2 gas yielded the dioxygen complex [Tp″Co(O_2)].[5] The spectroscopic characterization of this paramagnetic compound left little doubt that it is a close analogue of the structurally characterized complex [Tp′Co(O_2)] (Tp′ = hydrotris(3-*tert*-butyl-5-methylpyrazolyl)borate),[4b] which was the first example of a dioxygen complex with a symmetrically side-on bound superoxido ligand. However, in marked contrast to the very stable Tp′ complex, the sterically less encumbered [Tp″Co(O_2)] decomposed in solution at room temperature, producing [Tp″Co(μ-O_2)CoTp″] as a transient intermediate, and ultimately leading to hydrogen atom abstraction from the ligand. Below $-10\,^\circ$C [Tp″Co(O_2)] was stable for hours, but its variable-temperature NMR spectra revealed yet another difference between the Tp″ and the Tp′ complexes. Upon progressive cooling of a solution of the paramagnetic [Tp″Co(O_2)] complex in CD_2Cl_2, the five isotropically shifted ^{1}H NMR resonances were gradually replaced by a set of peaks in the range δ = 0–10, indicating the formation of a diamagnetic compound. These spectroscopic changes were reversible, and they were accompanied by changes in the color of the solution. At 270 K the solution appeared brown, similar to the color of [Tp′Co(O_2)]; cooling to 220 K produced a dark green solution. Similar color changes were observed in toluene, THF, and acetonitrile. Higher concentrations of [Tp″Co(O_2)] increased the fraction of the diamagnetic complex. Based on these observations we propose that a monomer–dimer equilibrium (Scheme 1) causes the spectroscopic changes.

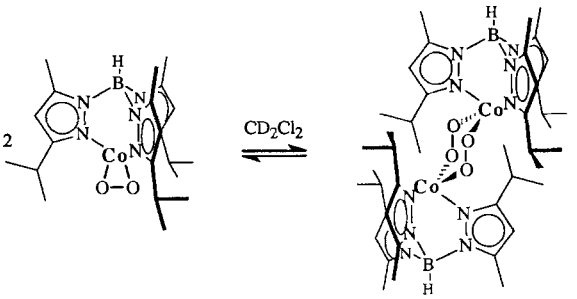

$$K_{eq} = \frac{[[Tp''Co(O_2)]_2]}{[Tp''Co(O_2)]^2}$$

Scheme 1. Equilibrium between monomeric and dimeric forms of [Tp″Co(O_2)].

Cooling a concentrated solution of [Tp″Co(O_2)] in acetonitrile to $-30\,^\circ$C yielded green crystals of [{Tp″Co(O_2)}$_2$·2CH_3CN] suitable for a low-temperature X-ray structure determination; apparently the dimer is much less soluble in this solvent and crystallizes out selectively. The molecular structure featuring crystallographic inversion symmetry is depicted in Figure 1.[6] Each cobalt atom is bound to three nitrogen atoms of its Tp″ ligand and to two oxygen atoms; the coordination environment about the metal closely approximates an idealized square pyramid. There are two dioxygen molecules, both linking

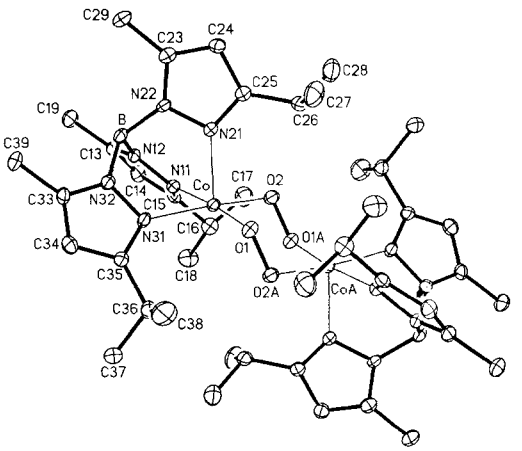

Fig. 1. The molecular structure of [{Tp″Co(O_2)}$_2$·2CH_3CN]; the solvent molecules are omitted for clarity. Selected interatomic distances [Å] and angles [°]: Co-O(1) 1.836(3), Co-O(2) 1.839(4), Co-N(11) 2.056(4), Co-N(21) 2.107(4), Co-N(31) 2.070(4), O(1)-O(2A) 1.354(5), Co-CoA 3.50; O(1)-Co-O(2) 88.8(2), Co-O(1)-O(2A) 110.4(3), Co-O(2)-O(1A) 110.9(3), O(1)-Co-N(11) 174.3(2), O(1)-Co-N(21) 95.5(2), O(1)-Co-N(31) 91.6(2), N(11)-Co-N(21) 89.8(2), N(11)-Co-N(31) 86.3(2), N(21)-Co-O(31) 90.9(2).

[*] Prof. Dr. K. H. Theopold, Dr. G. P. A. Yap, Prof. Dr. A. L. Rheingold
Department of Chemistry and Biochemistry
Center for Catalytic Science and Technology
University of Delaware
Newark, DE 19716 (USA)
Telefax: Int. code + (302)831-6335
e-mail: theopold@strauss.udel.edu
Dr. O. M. Reinaud
Laboratoire de Recherches Organiques del'ESPCI associé au CNRS
10 rue Vauquelin, F-75231 Paris Cedex 05 (France)

[**] This research was supported by the U. S. Department of Energy (ER14273) and by the CNRS and NATO.

the cobalt atoms in a *trans* μ-η^1:η^1 fashion; the resulting six-membered Co_2O_4 ring adopts a chair conformation. To our knowledge, this structural motif is unprecedented in the coordination chemistry of O_2. The O–O distance of 1.354(5) Å is intermediate between the ranges usually associated with μ-superoxido (1.24–1.32 Å) and μ-peroxido ligands (1.38–1.53 Å).[7] However, the Co–N bond lengths (average Co–N = 2.08 Å) are characteristic of a tris(pyrazolyl)borate moiety bound to Co^{II} centers. Besides, five-coordinate Co^{III} complexes are rather rare in general,[8] and we have yet to find an example of a stable Co^{III} complex containing one of these sterically demanding Tp ligands. Thus we suggest that the structural evidence is most consistent with the designation of $[\{Tp''Co(O_2)\}_2]$ as a Co^{II} superoxido complex.

Since thermochemical parameters for the interaction of O_2 with transition metals are important, we measured the temperature dependence of the monomer–dimer equilibrium described above. The relative concentrations of $[Tp''Co(O_2)]$ and $[\{Tp''Co(O_2)\}_2]$ were measured by ^1H NMR spectroscopy over the temperature range 220–260 K. The temperature dependence of the equilibrium constant in the form of a van't Hoff plot is depicted in Figure 2. The thermochemical parameters

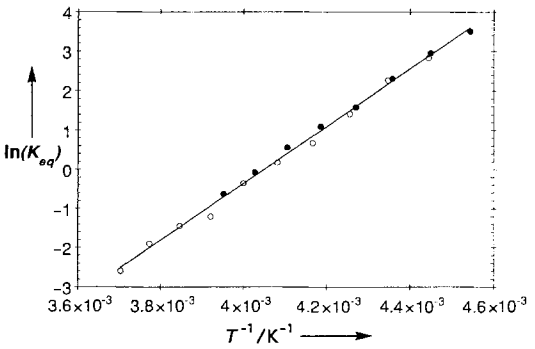

Fig. 2. Temperature dependence of the equilibrium constant K_{eq} (see Scheme 1). ○: [Co] = 0.033 M; ●: [Co] = 0.40 M in CD_2Cl_2 at 25 °C. Results of the van't Hoff analysis: $\Delta H = -14.5(5)$ kcal mol^{-1}, $\Delta S = -60(3)$ cal mol^{-1} K^{-1}.

derived therefrom are $\Delta H = -14.5(5)$ kcal mol^{-1} and $\Delta S = -60(3)$ cal mol^{-1} K^{-1}. As the conversion of the monomer into the dimer involves the opening of two strained CoO_2 rings and the formation of one six-membered ring, the reaction enthalpy provides a measure of the strain energy of roughly 7 kcal mol^{-1} per three-membered ring.

We also monitored the magnetic susceptibility of $[Tp''Co(O_2)]/[\{Tp''Co(O_2)\}_2]$ solutions at various temperatures by the Evans method.[9] At 270 K, where monomeric $[Tp''Co(O_2)]$ is the only species detectable by NMR, the effective magnetic moment μ_{eff} was 3.3(1) μ_B. This value is the same as that measured for solid $[Tp''Co(O_2)]$ at room temperature,[5] and it is consistent with two unpaired electrons ($S = 1$) resulting from strong antiferromagnetic coupling of a Co^{II} ion ($S = 3/2$) to the superoxido ligand ($S = 1/2$). When the solution was cooled, the magnetic moment decreased rapidly, concomitant with the appearance of the NMR signals of the dimer. Although we have not been able to extend these measurements to low enough temperatures to actually convert all of the cobalt complex into the dimeric form, extrapolation of the magnetic data indicates diamagnetic character for $[\{Tp''Co(O_2)\}_2]$. The narrow line widths, absence of isotropic shifts, and lack of significant temperature-dependence in the ^1H NMR spectrum of the dimer are also consistent with this notion.[10] The Co–Co distance of 3.50 Å rules out any direct interaction; instead we suggest that the diamagnetism of $[\{Tp''Co(O_2)\}_2]$ may result from strong antiferromagnetic coupling between low-spin Co^{II} ions ($S = 1/2$) and the adjacent superoxido ligands ($S = 1/2$).

Interestingly, dimeric $[\{Tp''Co(O_2)\}_2]$ is thermally less stable than monomeric $[Tp''Co(O_2)]$. Whereas the monomer is perfectly stable in the solid state at ambient temperature, green crystals of the dimer decomposed rapidly at room temperature, yielding a gas (O_2?) and a pink solid, very similar in nature to the decomposition products of $[Tp''Co(\mu\text{-}O_2)CoTp'']$. These observations suggest that $[\{Tp''Co(O_2)\}_2]$ may also be an intermediate in the solution reaction of $[Tp''Co(O_2)]$. Its formation, followed by loss of one of its two dioxygen moieties, constitutes a reasonable mechanistic pathway for the formation of $[Tp''Co(\mu\text{-}O_2)CoTp'']$, (much preferable to preequilibrium dissociation of O_2 from monomeric $[Tp''Co(O_2)]$) followed by trapping of the coordinatively unsaturated [Tp"Co] by $[Tp''Co(O_2)]$. The first proposal would also explain the surprising difference in reactivity between $[Tp''Co(O_2)]$ and its more hindered analogue $[Tp'Co(O_2)]$; a dimeric form of the latter is obviously much less accessible. Indeed, this reaction pathway may be crucial to our success in constructing a catalyst for the activation of O_2, which depends on simultaneous binding of one O_2 molecule to two metals atoms in the presence of excess O_2.

Experimental Procedure

$[Tp''Co(O_2)]$: An analytically pure sample of $[Tp''Co(CO)]$ (500 mg, 1.07 mmol) was ground into a fine powder in a dry box. The powder was transferred into a glass ampoule, which was then evacuated for 2 h to remove any trace of solvent. Upon exposure to 0.8 atm of dry O_2, the color of the solid changed rapidly from green to brown (within 1 min); the exposure was continued for 2 h. To ensure quantitative reaction, two more cycles of evacuation and exposure to O_2 were carried out. The solid thus obtained in quantitative yield was pure $[Tp''Co(O_2)]$.

$[\{Tp''Co(O_2)\}_2]$: Single crystals of $[\{Tp''Co(O_2)\}_2 \cdot 2CH_3CN]$ were obtained by cooling a solution of $[Tp''Co(O_2)]$ (50 mg) in MeCN (1 mL) to −30 °C for 2 d. The mother liquor was then pipetted out of the vial and cold oil introduced in order to coat the green crystals, and to protect them from contact with air during collection of the X-ray diffraction data. A crystal of dimensions $0.36 \times 0.38 \times 0.38$ mm was mounted on a Siemens P4 diffractometer at 222 K, and 4917 reflections were collected, of which 3033 were judged observed ($F < 4.0\sigma(F)$). The structure was solved by direct methods, using Siemens SHELXTL PLUS software.

Received: April 27, 1995 [Z 7935 IE]
German version: *Angew. Chem.* **1995**, *107*, 2171–2173

Keywords: cobalt compounds · dioxygen complexes · tris(pyrazolyl)borates

[1] a) R. A. Sheldon, J. K. Kochi, *Metal-Catalyzed Oxidations of Organic Compounds*, Academic, New York, **1981**; b) *Oxygen Complexes and Oxygen Activation by Transition Metals* (Eds.: A. E. Martell, D. T. Sawyer), Plenum, New York, **1988**; c) *Dioxygen Activation and Homogeneous Catalytic Oxidation*, *Stud. Surf. Sci. Catal.* **1991**, *66*.
[2] *Metal Dioxygen Complexes: A Perspective* (*Chem. Rev.* **1994**, *94*, 597).
[3] S. Trofimenko, *Chem. Rev.* **1993**, *93*, 943.
[4] a) M. J. Baldwin, D. E. Root, J. E. Pate, K. Fujisawa, N. Kitajima, E. I. Solomon, *J. Am. Chem. Soc.* **1992**, *114*, 10421; b) J. W. Egan, Jr., B. S. Haggerty, A. L. Rheingold, S. C. Sendlinger, K. H. Theopold, *ibid.* **1990**, *112*, 2445; c) K. Fujisawa, M. Tanaka, Y. Moro-oka, N. Kitajima, *ibid.* **1994**, *116*, 12079.
[5] O. M. Reinaud, K. H. Theopold, *J. Am. Chem. Soc.* **1994**, *116*, 6979.
[6] $[Tp''Co(O_2)]_2 \cdot 2CH_3CN$: monoclinic $P2_1/n$, $a = 13.256(6)$, $b = 13.868(4)$, $c = 16.463(6)$ Å, $\beta = 96.35(3)$°, $V = 3005(2)$ Å^3, $Z = 2$, $R = 0.0563$, $R_w = 0.0680$. Further details of the crystal structure investigation may be obtained from the Fachinformationszentrum Karlsruhe, D-76344 Eggenstein-Leopoldshafen (Germany), on quoting the depository number CSD-59113.
[7] R. R. Conry, K. D. Karlin in *Encyclopedia of Inorganic Chemistry*, *Vol. 3* (Ed.: R. B. King), Wiley, New York, 1994, p. 1036.
[8] a) L. G. Marzilli, M. F. Summers, N. Bresciani-Pahor, E. Zangrando, J.-P. Charland, L. Randaccio, *J. Am. Chem. Soc.* **1985**, *107*, 6880; b) S. Bruckner, M. Calligaris, G. Nardin, L. Randaccio, *Inorg. Chim. Acta* **1969**, *3*, 308.
[9] a) D. F. Evans, *J. Chem. Soc.* **1959**, 2003; b) D. Ostfeld, I. A. Cohen, *J. Chem. Ed.* **1972**, *49*, 829; c) S. K. Sur, *J. Magnet. Res.* **1989**, *82*, 169.
[10] I. Bertini, C. Luchinat, *NMR of Paramagnetic Molecules in Biological Systems*, Benjamin/Cummings, Menlo Park, CA, **1986**, p. 19ff.

Gas-Phase Micelles

Gary Siuzdak* and Brian Bothner

Surfactant micelles represent primitive vesicles associated with the origin of life. Their formation preceded the development of biochemical interactions, membrane assembly, and the beginning of cellular evolution. Micelles are used extensively in biochemistry to facilitate the transport of hydrophobic material and as a site for chemical reactions, thus mimicking their utility in the primordial pools. They are studied through a variety of methods, including gel permeation chromatography,[1] light scattering,[2] and interfacial tensiometry.[3,4] In this study, pneumatically assisted electrospray (ionspray) ionization (ESI) was used to transfer micelles from the condensed phase into the gas phase. Previous electrospray studies[5] on glycolipids resulted in the observation of Ca^{2+}-dependent glycolipid dimers. Evidence suggests that the origin of these dimers was, in part, due to the noncovalent disruption of glycolipid micelles. We now focus on the detection of the intact micelle.

The electrospray ionization technique (ESI) enables charged molecules to be transferred from a liquid solution to the gas phase by creating a fine spray of highly charged droplets. The sample solution is sprayed from the tip of a metal syringe maintained at approximately 5000 V. Dry gas is fed to the stream of droplets before they enter the vacuum of the mass spectrometer, which facilitates solvent evaporation. As each droplet decreases in size, the electric field density on its surface increases. The mutual repulsion between like charges on this surface becomes so great that it exceeds the forces of surface tension and results in the ion's ejection from the droplet. The ions are then directed into the mass analyzer by electrostatic lenses. This type of ionization is conducive to the formation of highly charged molecules and noncovalently bound molecular complexes.[6-9]

This study focused on CHAPS (3-[(3-cholamidopropyl)-dimethylammonio]-1-propanesulfonate) and SDS (sodium dodecylsulfate). The surfactants sodium octylsulfate, octylamine,

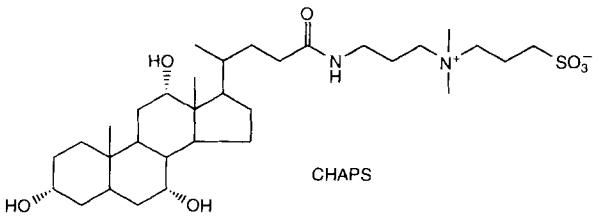

CHAPS

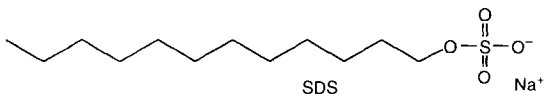

SDS

dodecylamine, sodium taurocholate, sodium taurodeoxycholate, and cholic acid were also analyzed. Experiments were performed with an API III Perkin Elmer Sciex triple-quadrupole mass spectrometer having an upper m/z range of 2400 and capable of analyzing for positive and negative ions. An electrospray interface potential of 5.0 kV was used for sample introduction. The declustering potential was varied between 30–250 V to control the orifice collisional energy. Samples with concentrations from 0.01 to 1.00 mM were dissolved either in water or 50:50 methanol:chloroform and introduced at a rate of 3.0 $\mu L\,min^{-1}$. Both positive and negative ions were monitored in these experiments and gave analogous results, although the positive ions generally gave a greater signal intensity.

Since ESI is an evaporation process, it is important to minimize the sample concentration and thus maximize evaporization efficiency to maintain a strong ion signal. To facilitate ionization in these experiments, the concentration of surfactants (1.0 mM) was kept below the critical micelle concentration (cmc; 6–10 mM for CHAPS and 7–10 mM for SDS).[10] However, since desolvation occurs more slowly[11] than micelle formation,[12] it can readily be assumed that the critical micelle concentration is been reached prior to ion ejection, and micelles are formed. Micelle formation in the droplet is likely, since the concentration of the solute in the droplet increases by a factor of 100[11] before ion ejection.

Micelle observation by mass spectrometry may be affected by a number of factors: 1) the size of the micelle, 2) the stability of the charged micelle in the gas phase, and 3) the conditions during evaporation of the droplets (temperature and pressure fluctuations). The first factor was addressed by using a variety of large and small micelle systems. An important feature of mass spectrometers is that they measure the mass-to-charge ratio, m/z, making it possible to observe very large molecules or molecular complexes with an instrument having a relatively small m/z range if the molecules are multiply charged. Micelles typically have counterions at the head group to minimize head group repulsion, and while removal or addition of these counterions (for example, H^+, Na^+, or Cl^-) is necessary in mass analysis in order to create a charged species, this may result in the destabilization and fragmentation of the micelle. Larger micelles would require many charges in order to be observed and could be destabilized by the numerous charges. The second factor was addressed with the choice of surfactants, some of which would potentially undergo intramicellar hydrogen bonding. Micelle formation in solution is driven by an entropy gain of the solvent; therefore, it is important that the molecules forming the micelle have strong intramicellar binding to preserve structure in the gas phase. Lastly, the inability to control droplet conditions precisely (third factor) could be detrimental to micelle formation; however, performing these experiments under identical conditions minimized these fluctuations.

The surfactants CHAPS, sodium taurocholate, sodium taurodeoxycholate, and cholic acid were selected because they have relatively low aggregation numbers and contain intermolecular binding sites[13] that could potentially stabilize association into the gas phase. The electrospray ionization source allows an ion's kinetic energy to be adjusted by means of the declustering potential; declustering potentials on the order of 70 V or lower are conducive to the observation of noncovalent complexes, while greater potentials usually promote the dissociation of noncovalent complexes and even covalent bonds. All of the experiments in which micelles were observed were performed at low declustering potentials, typically at or below 50 V. Figure 1 shows the mass spectra of CHAPS at declustering potentials of 50 V and 150 V. The spectrum acquired at 50 V contains oligomers that correlate with the expected micelle aggregation number (4–14).[10] Experiments performed at a declustering potential of 150 V gave no evidence of micelle formation. Similar results were obtained for sodium taurocholate and sodium taurodeoxy-

[*] Dr. G. Siuzdak, B. Bothner
Department of Chemistry
The Scripps Research Institute
La Jolla, CA 92037, (USA)

[**] The authors thank to Drs. Klaus Huber, Robert S. Cantor, and Joseph F. Krebs for helpful suggestions in the preparation of this manuscript and gratefully acknowledge funding from The Lucille P. Markey Charitable Trust and the National Institutes of Health (grant no 1 S10 RR07273-01).

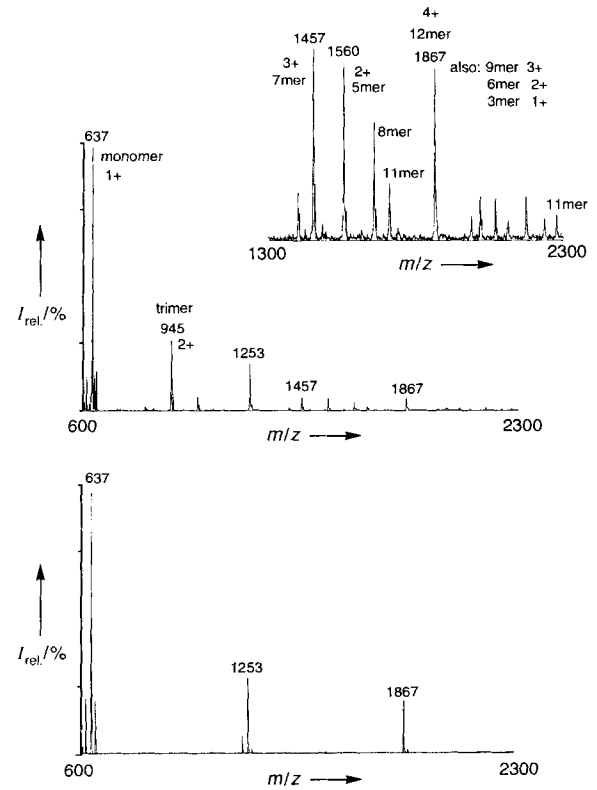

Fig. 1. Positive ion electrospray mass spectra of CHAPS micelles obtained from water at declustering potentials of 50 (a) and 150 V (b). At 50 V the micelles (as Na^+ adducts) vary in size and charge; for example, the ion m/z 1457 represents the $[(CHAPS)_7 + 3Na]^{3+}$. At 150 V only the singly charged monomer, dimer, and trimer were observed. Charge states were based on isotope distribution, cation addition, and MS/MS data.

cholate; however, cholic acid produced no evidence of micelle formation. From these results it is concluded that the zwitterionic nature of CHAPS, sodium taurodeoxycholate, and sodium taurocholate, and the hydrogen bonding interactions between their monomers may have facilitated the observation of gas phase micelles by stabilizing the charged (micelle) structure. Typically, CHAPS, sodium taurodeoxycholate, and sodium taurocholate produced micelles containing at least three charges.

The measured charge states were based on isotope patterns, cation addition, and MS/MS data. The spacing between isotope lines provides a means of determining charge state (Fig. 2); the

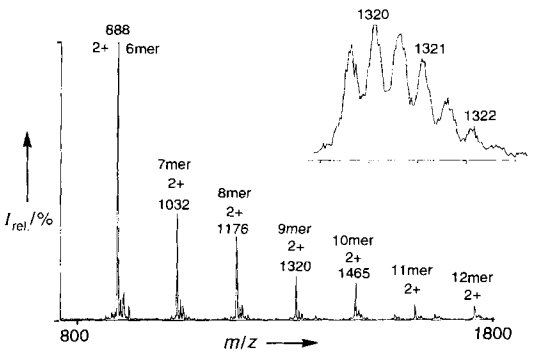

Fig. 2. Aggregates $[(SDS)_n + 2Na]^{2+}$ ($n = 6-12$) observed by positive ion electrospray mass analysis. Charge states determination can be based on spacing of the isotopes; for example, ^{13}C isotopes spaced 1.0 mass unit apart correspond to the 1 + charge state, those 0.5 mass units apart to the 2 + charge state, etc. This spectrum demonstrates the uniform stepwise addition typical of salt aggregates and nonspecific molecular aggregations.

resolving power of the quadrupole instrumentation allowed the determination of up to the 3 + charge state. Cation addition also served to identify the charge states (Fig. 3). The spacing between the cation adducts provided the same information as the isotope pattern without the need for high resolving power.

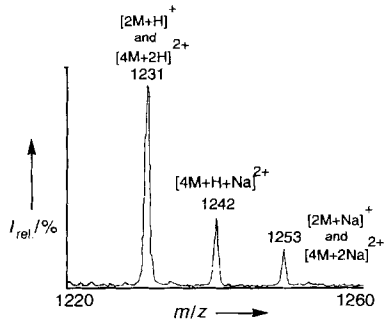

Fig. 3. Mass spectrum of CHAPS obtained at a declustering potential of 75 V. Cation addition is another way of determining an ion's charge state, analogous to examining the isotope distribution. The formation of cation adducts at half the mass of the ion is indicative of a 2 + charge state, at one third the mass of the ion of a 3 + charge state, and so on.

Cation addition was also used to test the effect different cation adducts may have on observing micelle formation. Here, Na was replaced with other alkali metals, Li, K, and Cs; however, no other significant changes were observed in the charge states or ion intensitites with the different cations. MS/MS data provided information about the charge states, since fragment ions were indicative of the minimum aggregation number.

SDS and other alkyl surfactants were also analyzed. In order to observe SDS micelles (aggregation number of 62)[10] with this instrumentation, they would require a positive or negative charge of at least 7. However, the mass spectrum of SDS shows no association that could correlate with micelle formation (Fig. 2), but is more consistent with spectra obtained from salt aggregates.[14] The same experiments were performed on structurally related surfactants, including sodium octyl sulfate, octylamine, and dodecylamine and gave results similar to those observed for SDS. No micelles were observed with these systems regardless of their size. The inability to observe micelles may be associated with significant head group repulsion on the highly charged micelles, as only charges of less than or equal to 2 + were observed for the aggregates. It was theorized that attempts to observe micelles with relatively high aggregation numbers may be difficult due to their instability when highly charged. Furthermore, the relatively weak van der Waal interactions of these molecules may be insufficient to stabilize micelles for transfer to the gas phase.

Tandem mass analysis was used along with the declustering potential to identify the micelle ions further. Tandem mass analysis through collision-induced dissociation (CID or MS/MS) is used to effect fragmentation. An ion of interest is selected with the mass analyzer and introduced into a collision cell, where, typically, argon is used as collision gas. The selected ion will collide with an inert gas molecule to give fragment ions, which are recorded with a second analyzer. Tandem mass spectrometry experiments were performed on the cholic acid derivatives at two different declustering potentials (50 V and 150 V) again to establish micelle formation at the low declustering potentials and a minimal aggregation number for the observed ions. The fragmentation data of the cholic acid derivatives under low declustering potentials (50 V) produced fragment ions (hep-

tamer, decamer, and undecamer) consistent with a dodecamer precursor ion. Figure 4 also illustrates the fragmentation of CHAPS at a declustering potential of 150 V to form only the monomer and dimer, fragments that are more consistent with the trimer precursor ion.

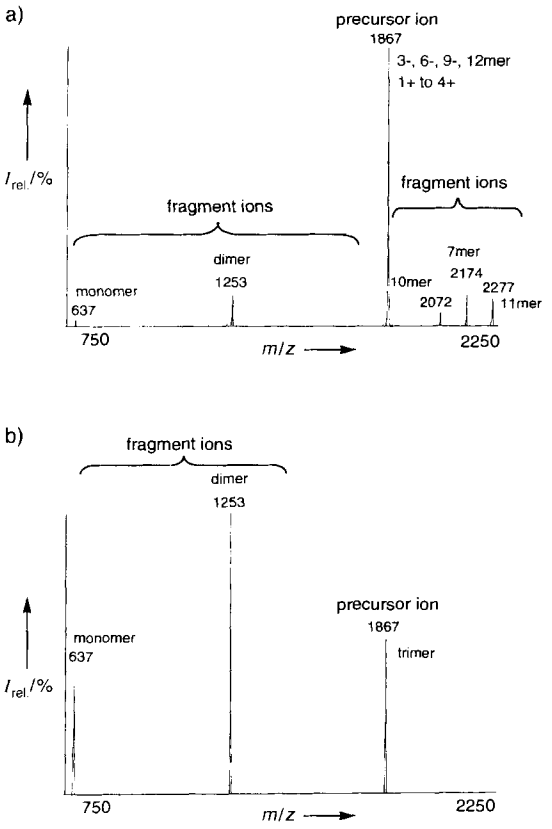

Fig. 4. Positive ion electrospray MS/MS analysis of the ion, m/z 1867, at declustering potentials of 50 V (a) and 150 V (b). The data at 50 V are consistent with the following structures: $[(CHAPS)_{12} + 4Na]^{4+}$, $[(CHAPS)_9 + 3Na]^{3+}$, $[(CHAPS)_6 + 2Na]^{2+}$, and $[(CHAPS)_3 + Na]^{1+}$. The data at 150 V are consistent with $[(CHAPS)_3 + Na]^{1+}$.

SDS and CHAPS were also evaluated in methanol:chloroform (50:50), a solvent system that is conducive to reverse micelle formation. Under these conditions the ion distribution for SDS closely resembled that under aqueous conditions, which further suggested that the clusters observed for these compounds were the result of nonspecific aggregation. However, CHAPS in methanol:chloroform (50:50) produced significantly different results in terms of ion distribution and relative ion intensity than those obtained in aqueous solution. This change could be attributed to the structural difference between reverse micelle and micelle formation.

Additional evidence of micelle formation in the gas phase was obtained from experiments monitoring the critical micelle concentration (cmc). The cmc is defined as the surfactant concentration above which micelles are formed.[10] The cmc's of CHAPS, taurocholate, and taurodeoxycholate are 6–10 mM, 3–11 mM, and 1–4 mM, respectively. The cholesterol-like surfactants were especially ideal for this study, because their similar structures are likely to produce similar evaporation conditions. In these experiments, the concentration of each surfactant was increased from a concentration of 0.01 mM in 0.01 mM increments, and the onset of micelle formation determined by the observation of the heptamer in the 2+ and 3+ charge states. The heptamer was chosen because it is consistent with the aggregation number of all three surfactants, and its signal does not overlap with that of any other oligomer ions in the 1+, 2+, or 3+ charge states.

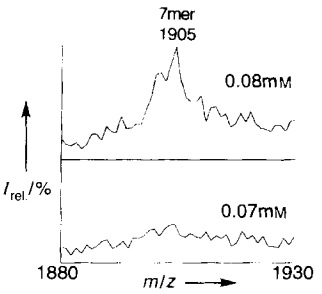

Fig. 5. Onset of micelle formation for taurocholate, monitored with the signal of the heptamer $[(TC)_7 + 2Na]^{2+}$ at 0.08 mM (top) and 0.07 mM (bottom).

The cmc for CHAPS, taurocholate (TC), and taurodeoxycholate (TDC) was found to be 0.06 mM, 0.08 mM, and 0.02 mM, respectively (Fig. 5, Table 1). Assuming evaporation increased the droplet surfactant concentration by a factor of approximately 100,[11] the results correlate with the absolute cmc values and are also consistent with respect to the relative cmc's of the surfactants. These experiments were also performed on SDS, cmc 7–10 mM, where SDS produced significant aggregation only at concentrations greater than 0.20 mM. The aggregation was deemed to be significant if the signal-to-noise ratio of the heptamer was greater than 2. The relatively high concentrations needed to observe aggregation of SDS is further evidence of the nonspecific nature of its aggregation, while the absolute and relative cmc correlations between the steroid surfactants further suggest that micelles were formed.

Table 1. A comparison of critical micelle concentrations (cmc) determined in solution and obtained with ESI for the surfactants CHAPS, TC, TDC, and SDS.

Surfactant	CHAPS	TC	TDC	SDS
cmc (solution) [mM]	6–10	3–11	1–4	7–10
cmc (ESI) [mM]	0.06	0.08	0.02	0.20
c [mM] [a]	6	8	2	20

[a] Estimated concentration of surfactant upon ion ejection.

The "soft" ionization/vaporization process of electrospray has allowed the transfer of micelles into the gas phase and thus the ability to analyze micelles by mass spectrometry. CHAPS, sodium taurodeoxycholate, and sodium taurocholate have provided useful models, probably because they form relatively small micelles and stable, multiply charged complexes.[15]

Received: January 10, 1995 [Z 7620 IE]
German version: *Angew. Chem.* **1995**, *107*, 2209–2212

Keywords: electrospray mass spectrometry · micelles

[1] N. Funasaki, *Adv. Colloid Interface Sci.* **1993**, *43*, 87.
[2] K. J. Mysels, L. H. Princen, *J. Phys. Chem.* **1959**, *63*, 1699.
[3] J. B. Chung, P. C. Shanks, R. E. Hanneman, E. I. Franses, *Colloids Surf.* **1990**, *43*, 223.
[4] M. J. Rosen, *Surfactants and Interfacial Phenomena*, Wiley, New York, **1978**.
[5] G. Siuzdak, Y. Ichikawa, T. J. Caulfield, B. Munoz, C.-H. Wong, K. C. Nicolaou, *J. Am. Chem. Soc.* **1993**, *115*, 2877.
[6] J. D. Henion, Y. T. Li, B. Ganem, *J. Am. Chem. Soc.* **1991**, *113*, 6294.
[7] V. Katta, B. T. Chait, *J. Am. Chem. Soc.* **1991**, *113*, 8534.
[8] R. D. Smith, K. J. Light-Wahl, B. E. Winger, J. A. Loo, *Org. Mass Spectrom.* **1992**, *27*, 811.
[9] G. Siuzdak, *Proc. Natl. Acad. Sci. USA* **1994**, *91*, 11290.
[10] L. M. Hjelmeland, *Proc. Natl. Acad. Sci. USA* **1980**, *77*, 6368; J. Neugebauer, *A Guide to the Properties and Uses of Detergents in Biology and Biochemistry*, CALBIOCHEM, CA, **1988**.
[11] P. Kebarle, L. Tang, *Anal. Chem.* **1993**, *65*, 972A.
[12] S. G. Oh, D. O. Shah, *J. Am. Oil Chem. Soc.* **1993**, *70*, 673.
[13] J. S. Nowick, T. Cao, G. Noronha, *J. Am. Chem. Soc.* **1994**, *116*, 3285.
[14] J. F. Anacleto, S. Pleasance, R. K. Boyd, *Org. Mass Spectrom.* **1992**, *27*, 660.
[15] G. Siuzdak, *Proc. 42nd Am. Soc. Mass Spectrom. Conf.* **1994**, 909.

 © VCH Verlagsgesellschaft mbH, D-69451 Weinheim, 1995 0570-0833/95/3418-2055 $ 10.00+.25/0

Incorporation of Membrane Proteins in Solid-Supported Lipid Layers

Renate Naumann,* Alfred Jonczyk, Ralf Kopp, Jan van Esch, Helmut Ringsdorf, Wolfgang Knoll, and Peter Gräber

Solid-supported lipid layers[1] are able to incorporate membrane proteins only if an aqueous layer separates the lipid layer from the substrate. This can be achieved by transferring lipids to hydrophilic surfaces either by Langmuir–Blodgett techniques[2] or by the fusion of liposomes.[3] Alternatively such layers can be formed by self-assembly if the lipid is attached to the substrate by a hydrophilic spacer group. For example, disulfide-functionalized amphiphilic copolymers (hydroxymethacrylates) form lipid layers on gold substrates separated by a swellable aqueous layer.[4, 5] The same holds for thiolipids having hydrophilic oxyethylene spacers of defined length, which were reported to form lipid mono- and bilayers[6] capable of incorporating intrinsic membrane proteins such as the $5HT_3$ receptor from calf brain.[7] Lipid layers having peptide spacers were first prepared on polymer beads. Bacteriorhodopsin incorporated in these layers was shown to operate as a proton pump.[8] Lipid layers on gold with peptide spacers will be described in the present paper.

In analogy to previous work[8] the relatively hydrophobic pentamer of alanine **1** (Fig. 1) was first functionalized with terminal sulfur groups followed by the more hydrophilic peptide **2**. These peptides have a tendency to form helical structures,[9] particularly when they are attached to gold substrates through sulfur groups and organize themselves by self-assembly.[10] Once the peptide **2** was covalently linked to the substrate, the free terminal COOH group was activated in situ and coupled to a lipid, for example DMPE (dimyristoylphosphatidyl ethanolamine), through the NH_2 group. A thiolipid monolayer with peptide spacer **3** is thus formed by further self-assembly. The formation of this layer was followed by electrochemical techniques such as cyclic voltammetry (CV) und impedance spectroscopy (IS) as well as by surface plasmon resonance spectroscopy (SPR). Table 1 shows the decrease in capacitance and the increase in layer thickness indicated by CV and SPR due to the formation of the lipid mono- and bilayers. The capacitance of perfect lipid monolayers determined by CV was reported to be as low as 0.5 $\mu F\ cm^{-2}$.[6, 7] The comparatively high capacitance found in our case indicates a lower degree of perfection. This conclusion is also supported by the fact that the layer thickness is much less than the calculated length of the molecule (Fig. 1), which can be explained by the incomplete coupling of the peptide in situ.

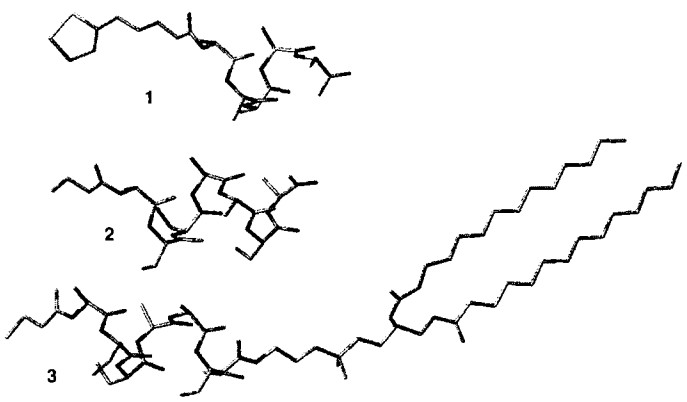

Fig. 1. Structures of peptides **1** and **2** as well as the thiolipid **3** with peptide spacer. Maximum lengths: **1**: 18.2 Å, **2**: 15.9 Å, **3**: 42.1 Å.

Table 1. Capacitance (measured by CV [6]) and layer thickness (measured by SPR and calculated using an effective refractive index of 1.5) of the films.

	Capacitance/$\mu F\ cm^{-2}$	layerthickness/nm
bare gold	18	–
lipid monolayer	2–3	2
lipid bilayer, no protein	1–2	4
lipid bilayer with ATPase	1–2	8.5

The thickness of these imperfect monolayers increases when they are exposed to a suspension of liposomes (Fig. 2). This increase does not occur below the transition temperature of the lipid and also when the peptide layer alone comes into contact with the liposomes (not shown). The shift in the resonance angle in SPR due to the formation of the mono- and bilayer with and without incorporated ATPase is shown in Figure 3. The layer thickness given in Table 1 is calculated from these shifts based on an effective refractive index of 1.5. In view of the theoretical thickness of 5 nm for a perfect lipid bilayer, the thickness of 4 nm is compatible with the formation of an imperfect bilayer. The thickness increases to 8.5 nm when the monolayer is exposed to liposomes with incorporated ATPase. Compared to the lateral extension of ATPase, which is also 8.5 nm,[11] and since a single orientation of the protein is possible only owing to the large F_0 part, this is a strong indication for the formation of a bilayer with incorporated ATPase. Figure 4 reflects the relative proportions.

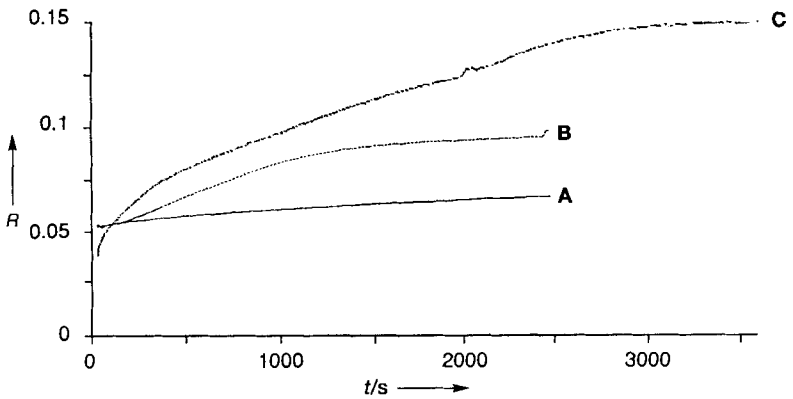

Fig. 2. Reflectivity R (arbitrary units) of the lipid monolayer as a function of time exposed to a suspension of liposomes without ATPase, at 20 °C (curve A) and 30 °C (curve B), and with incorporated ATPase at 30 °C (curve C).

[*] Dr. R. Naumann, Dr. A. Jonczyk, R. Kopp
E. Merck
D-64271 Darmstadt (Germany)
Telefax: Int. code + (6151) 71-0773
Dr. J. van Esch, Prof. H. Ringsdorf
Institut für Organische Chemie der Universität Mainz
Prof. W. Knoll
Max-Planck-Institut für Polymerforschung, Mainz (Germany)
Prof. P. Gräber
Institut für Biologie der Universität Stuttgart (Germany)

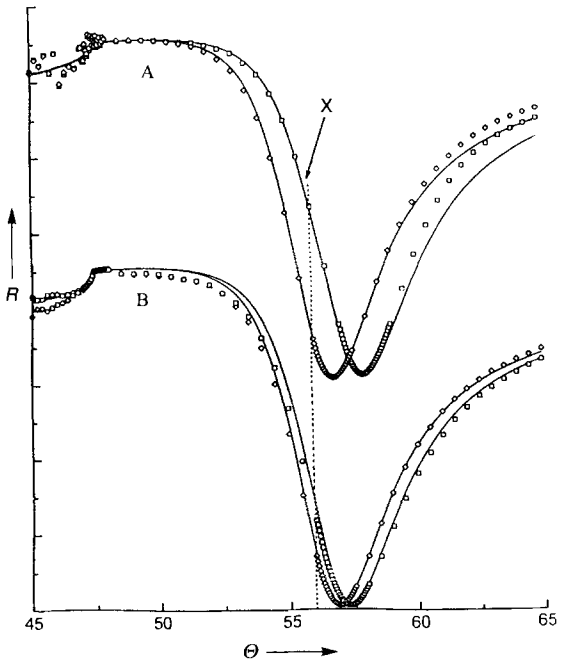

Fig. 3. Surface plasmon resonance spectrum of the lipid monolayer before and after fusion with liposomes with (curve A) and without incorporated ATPase CF_0F_1 (curve B). X is the angle for the kinetic measurements.

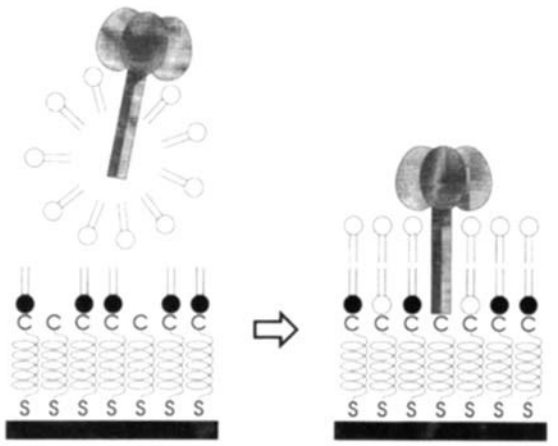

Fig. 4. Schematic representation of the fusion of liposomes with the lipid monolayer and formation of the lipid double layer with incorporation of ATPase.

Further indications of the incorporation of ATPase into the lipid layers are obtained by electrochemical techniques. ATPases CF_0F_1 from chloroplasts and EF_0F_1 from *E. coli*[13] catalyze the translocation of protons across the lipid membrane by hydrolysis of adenosine triphosphate (ATP). This process is possible only with an intact lipid layer and results in a pH gradient of pH 7–8 on the outside and pH 4 on the inside of the lipid.[12] Protons transported to the inside can be detected by the current when they are discharged at the gold surface. This discharge occurs only at relatively high negative potentials. To avoid damage to the lipid layers, fast pulse techniques such as square wave voltammetry (SWV) and chronoamperometry (CA) were employed. The SWV of a lipid layer with incorporated ATPase EF_0F_1 shows a peak at -0.7 V (Fig. 5), which increases in height as a function of the concentration of ATP. This indicates an increase in proton activity on the inside of the lipid layer to pH 4, while the pH of the solution remains the same, pH 7.4. A similar result was obtained for ATPase CF_0F_1 from chloroplasts (not shown). Figure 6 shows the decline of the

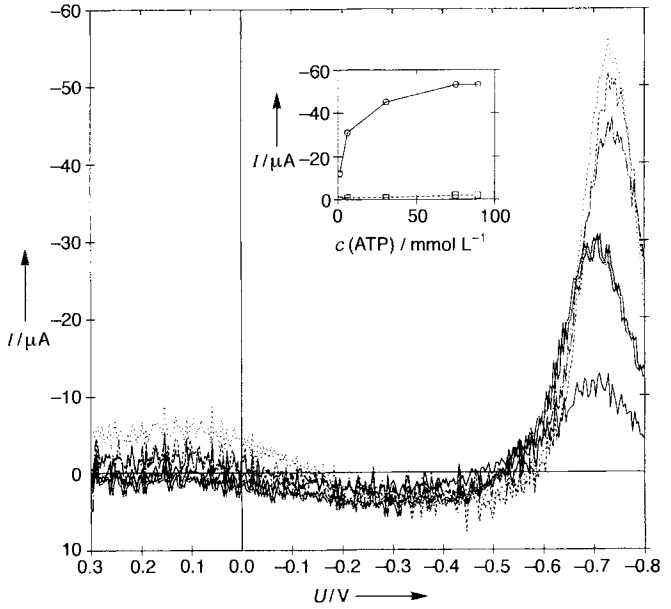

Fig. 5. Square wave voltammogram (corrected for the blank curve) of a lipid double layer with incorporated EF_0F_1 in the presence of 1 (—), 6 (═), 30 (—·—), 75 (- - - -), and 89 mmol L^{-1} ATP (····). Insert: Peak height as function of the concentration of ATP without (- - - -) and with EF_0F_1 (—).

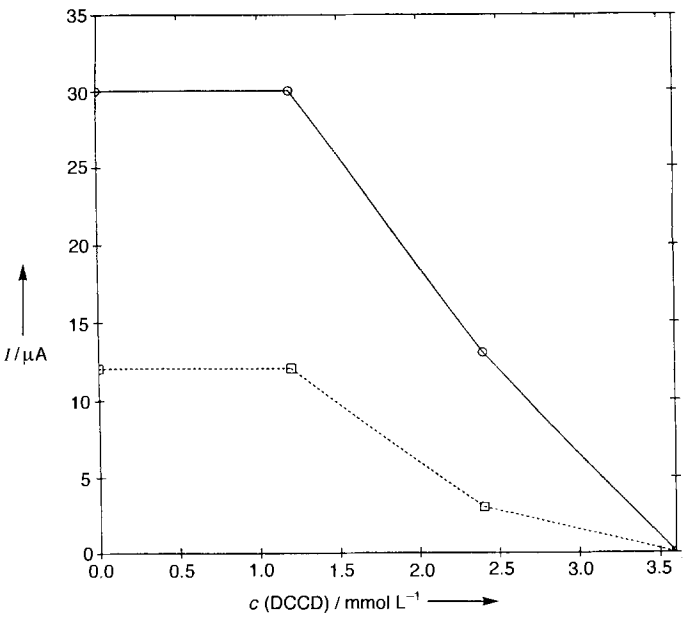

Fig. 6. Peak height in SWV of a lipid double layer with incorporated EF_0F_1 in the presence of constant concentrations of 1 (- - - -) and 6 mmol L^{-1} ATP (—), as a function of the concentration of DCCD.

SWV peak at -0.7 V caused by a specific inhibitor of ATPase, dicyclohexylcarbodiimide (DCCD).[14]

SWV measurements are designed to show only a static picture of proton translocation. Chronoamperometry, on the other hand, can be expected to yield information on the kinetics of the enzyme. In these measurements a current is recorded as a function of time while a potential pulse is applied to the electrode. The result is shown in Figure 7 for a lipid bilayer incorporating EF_0F_1 in the presence of increasing concentrations of ATP. In chronoamperometric measurements a double potential pulse technique is applied; that means the first pulse is applied at $+0.2$ V followed by a second at -0.7 V. The positive pulse is

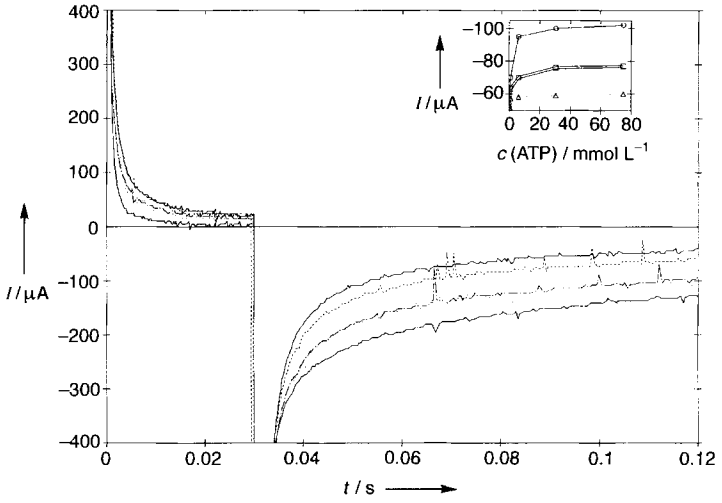

Fig. 7. Chronoamperometric measurements of the lipid double layer with incorporated EF_0F_1 as a function of the concentration of ATP (1–90 mmol L^{-1}). Insert: Stationary current as function of ATP concentration without ATPase (- - - -), with CF_0F_1 (═), and with EF_0F_1 (—).

conducive to the activation of the enzyme,[15] whereas the negative pulse causes discharge of protons. During this latter process, a decrease in the capacitive current is first observed. This is followed by a stationary cathodic current, indicating the activity of protons, which shows saturation behavior with respect to the concentration of ATP (insert, Fig 7). This stationary current is about two orders of magnitude higher than the current calculated from the kinetics of ATPases EF_0F_1 from *E. coli*[13] and CF_0F_1 from chloroplasts[12] (Table 2). Relative enzyme kinetics, however, are reasonably well reflected. Hence the activity of the enzymes appears to be preserved. This is possible only if the enzymes are properly arranged in space and above all if a lipid layer separates the inner aqueous layer from the outer solution. Only under these conditions is a pH gradient conceivable as long as the pH of the solution remains unchanged. Nonspecific adsorption of the enzyme is, therefore, highly unlikely. The relatively high current in the CA experiment could be due to an acceleration of proton translocation in the electric field. This will be investigated in further studies. The results so far are taken as a first indication that the enzymes in the lipid layer have comparable similar activities to those in liposomes, and that protein denaturation is apparently prevented by the peptide spacer.

Table 2. Stationary current I due to the discharge of protons at the gold electrode, compared to the current calculated from the amount of protons translocated by the enzymes.

Enzyme	$I/\mu A\,cm^{-2}$ calculated[a]	experimental
EF_0F_1	0.7	90
CF_0F_1	0.07–0.14	10

[a] From $G = 1.1 \times 10^{10}$ (enzymes per surface area, calculated from the concentration of enzymes in the liposomes and assuming a perfect lipid layer); activity: 100 ATP s^{-1} (EF0F1) und 10–20 ATP s^{-1} (CF0F1), at $4H^+$/ATP.

Experimental Procedure

Preparation of peptides: **1** and **2** were obtained by solid-phase peptide synthesis in a continuous flow synthesizer [16] using Fmoc (9-fluorenyl-methoxycarbonyl) strategy [17] with acid-labile protection of the side chain on an acid-labile Wang resin. The synthesis was monitored continuously by UV spectroscopy at 310 nm. After removal of the Fmoc groups the peptide was coupled with tritylmercaptopropionic acid. The peptide and side chain protecting groups were cleaved with TFA (trifluoroacetic acid). Purification was achieved by gel filtration and HPLC. The purity and identity of the peptide was determined by FAB-MS (fast atom bombardment mass spectroscopy), HPLC and capillary electrophoresis.

Gold (0.94 cm^2) was deposited onto clean glass slides by electrothermal evaporation over a sublayer of 30 nm of chromium at 300 °C and a pressure of 10^{-5} to 10^{-6} mbar using a Leybold-Heraeus L 650 vapor deposition apparatus. The thickness of the gold layer was 400 nm.

Preparation of the lipid monolayers: After the glass substrates were cleaned in a solution of 1 g of potassium bichromate in 100 mL of sulfuric acid (98%), they were incubated in a solution of the peptide in TFA (1 mg mL^{-1}) for 96 h. The substrates were then rinsed with TFA, dimethyl formamide (DMF), and dichloromethane (CH_2Cl_2). The terminal COOH groups of the peptide were activated with 20 μL mL^{-1} diisopropyl carbodiimide (DICD) and coupled in a solution of 1 mg mL^{-1} dimyristoyl phosphatidyl ethanolamine (DMPE) in a mixture of DMF, CH_2Cl_2, and LiCl (20:40:0.4). After addition of 10 μL mL^{-1} *N*-ethyl diisopropylamine, the substrates were incubated for a further 96 h. Activation and coupling were repeated using a fresh coupling mixture. The substrates were then rinsed with DMF and CH_2Cl_2 and dried in a stream of nitrogen.

Preparation of the lipid double layer: Liposomes were prepared from phophatidylcholine and phosphatidic acid (1:20). The ATPases CF_0F_1 and EF_0F_1 were incorporated into these liposomes by using biobeads [18]. Substrates with the lipid monolayers were incubated in suspensions of these liposomes at 30 °C; concentrations of the lipid and the protein were 1.4 mg mL^{-1} and 30 μg mL^{-1} of CF_0CF_1 and EF_0F_1, respectively.

CV, SWV, and CA measurements were carried out at 30 °C in a buffer solution of K_2SO_4 (0.1 mol L^{-1}), tricine (0.0005 mol L^{-1}), Na_2HPO_4 (0.0005 mol L^{-1}), and $MgSO_4$ (0.0002 mol L^{-1}) at pH 7.4, in a cell equipped with a silver rod as counter electrode and an Ag/AgCl (sat. KCl) reference electrode, and with an Autolab instrument (ECO Chemie) using GPES3 software. ATP was added from a stock solution of adenosine-5′-triphosphoric acid disodium salt (0.25 mol L^{-1} adjusted with NaOH to pH 7.4). Potential scan rate and range of potentials used in CV were 0.1 Vs^{-1} and 0.3 to −0.2 V, respectively. Frequency and range of potentials in SWV were 80 Hz and 0.3 to −0.8 V. Potential pulses applied in CA were 0.2 and −0.7 V. Duration of potential pulses was 0.07 s and duration of current sampling was 0.00011 s.

SPRS study was carried out in Kretschmann configuration [19] with a HeNe Laser (λ = 633 nm).

Received: March 18, 1995
Revised version: May 23, 1995 [Z78101E]
German version: *Angew. Chem.* **1995**, *107*, 2168–2171

Keywords: ATPase · electrochemistry · enzymes · lipid layers · membrane proteins

[1] A. Ulman, *An Introduction to Ultrathin Organic Films: From Langmuir Blodgett to Self-Assembly*, Academic Press, Boston, **1991**.
[2] G. Puu, I. Gustafson, P.-A. Ohlsson, G. Olofsson, A. Sellström in *Progress in Membrane Technology* (Eds.: J. C. Gomez-Fernandez, D. Chapman, L. Racker), Birkhäuser, Basel, **1991**, p. 279.
[3] M. Kühner, R. Tampe, E. Sackmann, *Biophys. J.* **1994**, *67*, 217.
[4] J. Spinke, J. Yang, H. Wolf, M. Liley, H. Ringsdorf, W. Knoll, *Biophys. J.* **1992**, *63*, 1667.
[5] C. Erdelen, L. Häussling, R. Naumann, H. Ringsdorf, H. Wolf, J. Yang, M. Liley, J. Spinke, W. Knoll, *Langmuir* **1994**, *10*, 1246.
[6] H. Lang, C. Duschl, H. Vogel, *Langmuir* **1994**, *10*, 197.
[7] H. Lang, B. Koenig, H. Vogel, WO-B93/21528, **1992**.
[8] U. Rothe, H. Aurich, *Biotech. Appl. Biochem.* **1988**, *11*, 18–25.
[9] J. D. Lear, Z. R. Wassermann, W. D. DeGrado, *Science* **1988**, *240*, 1179.
[10] E. P. Enriquez, E. T. Samuelski, *Mater. Res. Soc. Symp. Proc.* **1992**, *255*, 423.
[11] E. J. Boekema, P. Fromme, P. Gräber, *Ber. Bunsen-Ges. Phys. Chem.* **1988**, *92*, 1031.
[12] G. Schmidt, P. Gräber, *Z. Naturforsch. C* **1987**, *42*, 231.
[13] Y. Moriyama, A. Iwamoto, H. Hanada, M. Maeda, M. Futai, *J. Biol. Chem.* **1991**, *266*, 22141.
[14] R. McCarthy, E. C. Racker, *J. Biol. Chem.* **1967**, *242*, 3435.
[15] U. Junesch, P. Gräber, *Biochim. Biophys. Acta* **1987**, *893*, 275.
[16] A. Jonczyk, J. Meienhofer in *Peptides Proc. 8th Am. Pept. Symp.*, **1983**, pp. 73–77.
[17] C. D. Chang, A. M. Felix, M. H. Timinez, J. Meienhofer, *Int. J. Pept. Prot. Res.* **1980**, *15*, 485.
[18] P. Richard, J.-L. Rigaud, P. Gräber, *Eur. J. Biochem.* **1990**, *193*, 921.
[19] E. Kretschmann, *Z. Phys.* **1971**, *241*, 313.

Ammunition against Chemical Scaremongers

The Consumer's Good Chemical Guide. A Jargon-free Guide to the Chemicals of Everyday Life. By *J. Emsley*. W. H. Freeman, New York, 1994. XI, 347 pp., hardcover $ 24.95.—ISBN 0-7167-4505-4

For those concerned with the current epidemic of chemophobia and anti-science attitudes rampant in today's society—and that should include all of us—this book, which received the 1995 Rhône-Poulenc Science Book Prize, brings good news. Its author, John Emsley, recipient of the 1993 Glaxo Award for Science Writing, spent a quarter-century lecturing at the University of London and is now Science Writer in Residence at London's Imperial College of Science, Technology and Medicine. In this successful attempt to counter the "bad press" created for chemistry by scare-of-the-week stories, he deals with timely issues frequently in the news by systematically exposing misinformation disseminated by irresponsible media about chemicals with which we daily come in contact. In accessible, nontechnical language he presents up-to-date information on natural and artificial sweeteners, cholesterol, fats, fiber, painkillers, PVC, plastics, dioxins, nitrates, and carbon dioxide and the greenhouse effect. In separate chapters he shows how perfume chemists are trying to make the world a better place and simultaneously saving wildlife and how alcohol can not only improve the quality of life but may also prolong it. Some chemicals about which the public is worried, such as CFCs, lead, or radon are not included for the simple reason that they actually *are* dangerous (the book's title refers to good chemicals that are only generally *assumed* to be bad).

In contrast to the prevalent practice of accusing a given chemical of causing a disease or illness on the basis of alarming but unsound statistics, Emsley lucidly explains the chemistry involved and then shows that it is inconsistent with the accusations being made against the chemical. Intending his guide primarily for nonscientists, he eschews chemical formulas in the text but provides structural formulas and additional technical data on 193 substances (designated in the text by boldface type) from acesulfam to yohimbine in a 54-page cross-referenced alphabetical appendix. The information is not limited to the present-day controversial aspects of chemicals, such as their effects on life on earth and on the environment, but much fascinating and valuable background material, historical as well as anecdotal, is provided. For example, Emsley traces the evolution of perfumery from biblical times, discloses the fragrances in Chanel No. 5, discusses what makes a molecule taste sweet, reveals how to avoid a hangover, and shares with the reader the classical basis for successful dieting as well as "the boring diet that's guaranteed to work" according to the laws of chemistry. At the end of each chapter he summarizes his conclusions, and he is not afraid to take a stand, as, for example, when he declares, "As far as our animal friends are concerned we should continue to research the dioxins, but as far as humans are concerned the dioxin scare is over" (p. 203). A 10-page bibliography lists books and articles, divided according to each of the book's ten chapters and subdivided into general and specialist reading, as well as the sources that Emsley consulted in writing the book. A 17-page (2 columns per page) index facilitates location of topics.

This handy volume provides readers (with or without a scientific background) with unexpected, surprising, and reassuring answers that expose the misinformation and disinformation that surround many of the controversial chemicals that we all encounter today and that impinge on our lives. As such, it will be of interest not only to the public at large but also to instructors of chemistry, biology, environmental science, and risk assessment courses. Emsley promises a second volume in which he will deal with additional chemicals that have given rise to alarm such as phosphates, MSG, preservatives, chlorine, nicotine, methanol, and the HFCs and others that have led to unrealistic hopes of improved health, such as vitamin C and calcium.

George B. Kauffman, Laurie M. Kauffman
California State University
Fresno, CA (USA)

Practical Surface Analysis. A2, Vol. 1. Auger and X-Ray Photoelectron Spectroscopy. 2nd Edition. Edited by *D. Briggs* and *M. P. Seah*. Wiley, Chichester/Salle & Sauerländer, Aarau, 1994. 649 pp., paperback £ 49.95.—ISBN 0-471-9540-7

The first edition of this work, published in 1983 with a distinctive cover that gave it its common name "the blue book", soon became established as an indispensable handbook for the practitioner in the field of applied Auger spectroscopy (AES) and X-ray photoelectron spectroscopy (XPS). In 1990 it was followed by a second edition ("the red book"), enlarged and improved in many respects, and this has now also become available in a paperback version.

The declared aim of the editors is to provide a practical aid, within a single book, for users of AES and XPS, the two most important methods of electron spectroscopy, especially with beginners in mind. The ground covered ranges from introducing the theoretical basis of the methods to describing the most important areas of application. The contributions make up a well coordinated whole, which is undoubtedly an important reason why this has become *the* standard book, not just for beginners but for many surface analysts.

The book consists of ten chapters, of which the first five are devoted to the basic principles of AES and XPS, whereas Chapters 6 to 10 concentrate on the most important areas of application. Chapter 1 introduces general aspects of the analysis of surfaces and thin films by irradiation with electrons, ions, or photons. Chap-

This section contains book reviews and a list of new books received by the editor. Book reviews are written by invitation from the editor. Suggestions for books to be reviewed and for book reviewers are welcome. Publishers should send brochures or (better) books to Dr. Ralf Baumann, Redaktion Angewandte Chemie, Postfach 101161, D-69451 Weinheim, Federal Republic of Germany. The editor reserves the right of selecting which books will be reviewed. Uninvited books not chosen for review will not be returned.

ter 2, "Instrumentation", is of particular interest for newcomers to surface analysis, familiarizing them with the most important components of ultra-high vacuum systems and of electron spectrometers. Chapter 3 describes the characteristic features of Auger and photoelectron spectra, and explains in a clearly understandable way how such spectra are interpreted and what information they contain. Chapters 4 and 5 are concerned with depth profile analysis and with the methods used to establish quantitative scales of concentration and depth. All the most important theoretical relationships are given here, as well as practical methods for obtaining quantitative data, and the problems of depth profiling by ion sputtering are also treated. These two chapters are among the best in the book.

The following chapters describe important areas of application of AES and XPS, and this naturally involves reviewing the current state of progress in research and techniques. Some representative examples of applications in specialized fields are described. In the course of this the authors devote particular attention to experimental problems that must be overcome, such as surface charging, effects of radiation damage, and limitations on lateral and depth resolution, as well as some important complementary methods of analysis. Thus the editors' aim of providing an introduction to the various areas of application and also giving a broad survey is achieved in nearly every case. Chapter 6 deals with "Applications of AES in Microelectronics" and Chapter 7 with "AES in Metallurgy". The latter chapter begins with an interesting introduction and a discussion of ways of studying segregation, then deals in detail with theoretical aspects, thermodynamic processes, and the kinetics of segregation. In contrast to these two rather weak chapters, Chapter 8 contains an excellent account of the applications of electron spectroscopy in heterogeneous catalysis research, including a very good discussion of the experimental problems and possible sources of error. XPS studies of catalyst support materials, platinum metal catalysts, zeolites, and desulfuration methods are discussed in detail. Electron energy loss spectroscopy (EELS) is also included as an important complementary technique. Chapter 9 is devoted to "XPS in Polymer Technology"; in particular it contains very useful sections on bond energies and functional groups. Lastly, Chapter 10 describes the use of electrochemical measurements as an important complementary method in corrosion research, with detailed discussions of surface roughness and radiation effects. The book ends with nine appendices which cover physical aspects and experimental results of importance in electron spectroscopy. Appendices 5–9 contain useful and up-to-date tables of energies, sensitivity factors, and line positions.

To summarize, this book is a must for all analysts working in the field of Auger and photoelectron spectroscopy, and the availability of a paperback version now makes buying one's own copy easier from the standpoint of cost.

Henning Bubert
Institut für Spektrochemie
und Angewandte Spektroskopie
Dortmund (Germany)

Crystal Structure Analysis for Chemists and Biologists. By *J. P. Glusker, M. Lewis,* and *M. Rossi.* VCH Publishers, New York, 1994. 854 pp., hardcover $ 69.95, DM 120.00.—ISBN 0-89573-273-4

After many years during which chemical crystallography experienced a dearth of good or outstanding new monographs or textbooks, there has recently been a marked increase in the choice of material. Notwithstanding this welcome improvement, it is an exciting development when a further addition appears under the authorship of such a doyen of the discipline as Jenny Glusker, in collaboration with M. Lewis and M. Rossi. After a long wait since the first announcement, we at last have before us a work of 854 pages. As stated in the title, the book aims to make crystal structure analysis more easily accessible to chemists and biologists. In fact, the first sentence of the introduction narrows down the anticipated readership still further to those chemists and biochemists who, although not actually using the method themselves, need to be able to understand the results. On first picking up this bulky and comprehensive work, which does not merely deal with the applications but includes a careful and thorough treatment of the basic principles, one is almost inclined to say that it is not ideally suitable for the readership indicated, although that in no way detracts from the excellence of this book in covering nearly every facet of the subject that the title implies.

However, to discuss matters in their proper order: the book consists of 18 chapters covering the subject of chemical crystallography. About half the chapters are concerned mainly with the method itself, including the physical and mathematical fundamentals. The rest of the book concentrates on the results that it can give, and on their interpretation in terms of structure and the related chemistry and biochemistry. However, the boundary between theory and applications is a very fluid one, which is one reason why one can never become bored while reading the book. Another pleasing feature is that the authors avoid imposing too rigid a distinction between "small" and "large" molecules. In the examples discussed there is a strong emphasis on molecules and macromolecules related to biological systems, which comes as no surprise in view of the authors' backgrounds.

Each chapter ends with a brief résumé in which the main points covered are summarized with a paragraph for each, followed by a glossary of the most important terms and a comprehensive bibliography. For each of the publications cited the title is given in the original language, together with a translation of any title that is not in English. Altogether the book contains 102 (!) summary paragraphs, 435 (!!) glossary terms, and 1834 (!!!) literature references. The introduction alone contains 14 references. Even these rather dry statistics provide impressive evidence that the authors have not shirked their task, and the quality of the final result fully justifies the book's claims in every respect.

The manner in which the method and its applications are explained and discussed is very far from dry. Even the chapters devoted to the method itself impress one by the way in which applications are described for illustration, while ensuring that this does not detract from the thoroughness of the treatment. Historical aspects (some of which are little known) are also interwoven with the discussion, so that one often becomes really absorbed in the story. For example, where else would one discover that the first correct proposal for the structure of diborane appeared in an article by W. Dilthey in 1921 with the title "Über die Konstitution des Wassers" (*Z. Angew. Chem.* **1921**, *34*, 596)? Incidentally, this example also illustrates the point that by no means all the structures discussed relate to biological systems. In addition to boron and boranes, inorganic chemists will be pleased to find such ancient topics as the various tin modifications and blue (copper) vitriol, or may enjoy a glimpse at fullerenes.

The treatment of fundamentals begins with the structure and symmetry of crystals, then goes on to their physical properties, diffraction by crystals, superposition of waves, Fourier syntheses, measurement of structural amplitudes, the solution of the phase problem, electron density syntheses, and structure refinement. Al-

 © VCH Verlagsgesellschaft mbH, D-69451 Weinheim, 1995 0570-0833/95/3418-2060 $ 10.00+.25/0

though this arrangement of the subject matter largely follows the conventional pattern, the style of treatment is different in many respects from that in other books, with resulting benefits. The exceptionally clear way in which the subject is developed is no less than one expects from these authors. Although lengthy mathematical derivations are not completely absent, they are often avoided in favor of a more effective pictorial presentation. Where mathematical derivations do occur, they are enclosed in boxes separated from the main text, a device which again greatly improves the readability of the book. Despite this, the discussion is never simplified where that would be inappropriate, nor is the required depth of treatment ever sacrificed. The discussion is illustrated throughout by many examples (both old and new), and together with the carefully prepared figures, many of which are in stereoscopic form, these further serve to bring out the essentials in great clarity. The many tables and summaries also make the book a valuable reference source. The clear definitions and explanations of terms, which are provided in the text and in the glossary, are especially commendable.

In the part of the book devoted to applications the treatment is very different from that in other related texts (and is much better). The strong emphasis on biological aspects in the many examples of crystal structures has already been mentioned. Some of the topics to which considerable space is given are: molecular conformation (including its importance in biological macromolecules), chirality and absolute structure, structure comparisons including the use of data banks, receptors and molecular recognition, and stereochemical aspects of chemical reactions in crystals (although the latter topic appears under the rather misleading heading "Structure–Activity Results"). The authors have not neglected such highly topical (and difficult) areas as atomic and molecular scattering phenomena, molecular dynamics of polypeptides, and packing in molecular crystals. Atomic coordinates and their interpretation also receive careful treatment.

Although the book contains some practical advice and discusses the experimental aspects of crystal structure analysis, it is definitely not intended as a handbook for the practitioner. It does not even go into the details of crystallographic computer programs. In fact that would not be very desirable, as it would not fit in well with the character of the book in its present form. Moreover, a wide choice of other textbooks of a more practical kind is already available. On the other hand, one regrets that there is no discussion of the many different kinds of errors that can arise in crystal structure analysis and interpretation (and which regrettably occur increasingly often). In omitting this aspect the authors have missed a good opportunity to review the now extensive literature on "incorrect crystal structure analyses", to point out the most important kinds of errors that are likely to occur, and to persuade the reader to give some thought to this very important subject.

However, that is a very minor shortcoming in this thoroughly excellent book, and in no way detracts from the wide recognition that it deserves. The style of presentation, the construction of the book, and the treatment of the examples mark this out as a typical "Glusker". At almost every point one is aware that a lifetime's experience in both research and teaching have been distilled into the text. It can be confidently predicted that this book will remain one of the standard works in chemical crystallography for some years to come.

Gerhard Müller
Fakultät für Chemie
der Universität Konstanz (Germany)

The Conquest of Taxol

Kyriacos C. Nicolaou* and Rodney K. Guy

Much has been written about taxol, one of the newest weapons against cancer, and its producer, the Pacific Yew tree (*Taxus brevifolia*).[1] In this article, the authors give a frank and behind-the-scenes account of their encounter with this well-known molecule, which they and their collaborators faced as a synthetic target.[2–6] Once again total synthesis is found to offer excellent opportunities for developing new synthetic strategies and novel reactions. The team of chemists who took up this challenge emerged with valuable experience and confidence in their skills.

Keywords: natural products · taxol · total syntheses

1. Introduction

Rarely has a molecule received as much media attention as taxol (**1**, Fig. 1) has in recent years. Taxol and its producer, the Pacific Yew, earned their positions of public prominence after a long association between the yew and humans. By 1991 taxol was a "celebrity molecule", hailed as a miracle drug against cancer but in desperately short supply.[7, 8a] The media frenzy surrounding taxol focused daily attention on issues of life and death for cancer patients who desperately needed the drug, on the yew tree whose exclusive taxol-producing ability meant sure death for the tree, and on a rare owl species whose natural habitat was being destroyed systematically by the logging of the same forests that harbor the yew. The ethical and pragmatical dilemma that accompanied the discovery of taxol was fiercely argued by doctors, environmentalists, and politicians. The solution, they all agreed, was to find an alternative source of taxol. Chemists and biologists were challenged to find a solution. Today taxol is obtained semisynthetically from baccatin III, which is isolated from the needles of the European Yew, *Taxus baccata*.[8b]

Some chemists had been interested in the compound much earlier. Never before, however, had the urgency been so great. Anticipation of approval by the Food and Drug Administration (FDA) spurred on the 30 or so research groups around the world working on the total synthesis of taxol. It was at this juncture that we began to consider taking up the challenge of taxol's synthesis. Although we were attracted by the molecule's intricate structure, our initial feelings were mixed because we knew that we would be one of the last groups to enter the already heated race towards synthetic taxol, a race that had begun for some research groups shortly after the molecule's discovery in 1971.

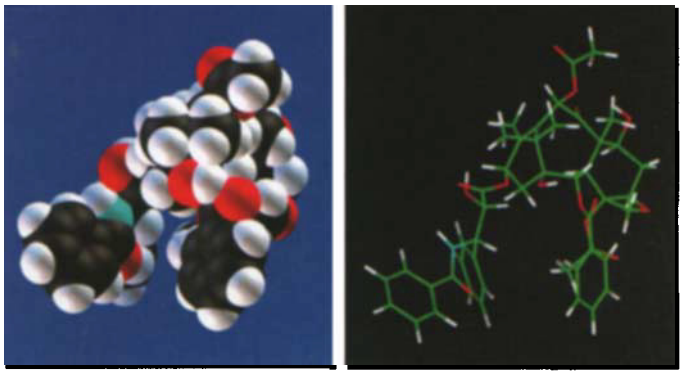

Fig. 1. Structure of taxol (**1**); top left: space-filling model, top right: stick model. The two models were generated by computer.

1

Before we describe our exciting journey, we should go back and trace the path of the yew tree and taxol through human history. The story of the yew is as old as the history of Western civilization itself.[9] Almost three millennia ago, Homer related the earliest tale of its use for bow-making in the Iliad. Alexander Pope translates:

Atrides, watchful of th' unwary foe,
Pierc'd with his Lance the Hand that grasp'd the Bow,
And nail'd it to the Eugh.

The yew has maintained its preeminence as the wood of choice for making bows to the present time. The Greeks, the Romans, and the English all appreciated its superiority and used the wood in their eras. Yew bows have figured prominently and decisively in wars over the years. For example, it was an arrow from a yew bow that killed King Harold the Saxon at the Battle

[*] Prof. Dr. K. C. Nicolaou,[+] R. K. Guy
Department of Chemistry
The Scripps Research Institute
10666 N. Torrey Pines Road, La Jolla, CA 92037 (USA)
[+] Alternative address: Department of Chemistry and Biochemistry
University of California, San Diego
9500 Gilman Drive, La Jolla, CA 92093 (USA)

 © VCH Verlagsgesellschaft mbH, D-69451 Weinheim, 1995 0570-0833/95/3419-2079 $ 10.00+.25/0

of Hastings in 1066 A. D., helping to turn the tide in favor of William the Conqueror.

A clue of the yew's cytotoxic properties comes from its long history as a producer of poison. In one of his books Julius Caesar recorded the death of Cativolcus, a chieftain of a Gaelic tribe, who committed suicide after his defeat at the hands of the Roman legions by drinking tea made from the bark of the yew. In fact, the Latin name for the Yew's genus, *Taxus*, probably has its origin in one or both of the Greek words *toxo*, for bow, and *toxikon*, for poison. It seems quite appropriate that a tree that has long represented death to man would provide one of the most potent weapons in our battle against cancer.

One of the seven major species of yews, *Taxus brevifolia*, commonly known as the Pacific Yew, grows in the oldest forests of the Pacific Northwest of North America.[9, 10] Long ago, Native Americans such as the Quinalt, the Tualitan, and the Nez Percé tribes recognized its unique qualities and used its bark as a disinfectant, an abortifacient, and even as a medicine for healing skin cancer. They also valued its wood, like the Europeans and the Asians did the wood of related yews, for bow-making and carving. It was in these forests, in 1962, that botanist Arthur Barclay encountered the Pacific Yew and collected its bark for chemical and biological studies. Little did he know that this particular sample would prove different from the others and would eventually catch the worldwide attention of scientists, doctors, politicians, environmentalists, and journalists.

The yew samples found their way, through the National Institutes of Health (NIH), to chemical, biological, and crystallographic laboratories, where eventually the structure of a compound active against leukemia cells was determined. Named taxol by its discoverers (Wani, Taylor, Wall, Coggen, and McPhail), this novel molecule was first described in the *Journal of the American Chemical Society* in 1971.[11] Despite its early promise and novel molecular architecture, taxol was not pursued further for several reasons. Scarcity, insolubility, and lack of knowledge regarding its mechanism of action were all responsible for this unfortunate delay. However, in 1979 this situation changed dramatically when S. Horwitz and her colleagues discovered that taxol acts by catalyzing tubulin polymerization and by stabilizing microtubules, essential fibers of the cytoskeleton.[12] The initial lethargy turned quickly into a campaign to rapidly develop the drug. By the time we started addressing a total synthesis, taxol was close to receiving approval by the FDA for clinical use against ovarian cancer.[13]

2. Embarking on the Taxol Project: The First Proposal to NIH

2.1. The Synthetic Efforts[*]

In 1991, Erik Sorensen, Chris Claiborne, and Kip Guy, three graduate students in my laboratories at the University of California at San Diego (E. S.) and Scripps (C. C., K. G.), were in search of Ph.D. projects. Intrigued by taxol's beautiful structure and therapeutic potential, they came to me with an interest in pursuing its total synthesis. Impressed by their courage and vision, and also attracted by the challenge, I immediately told them of my intentions of assembling a team to tackle the problem: they were the first to join. In the fall of 1991, we started to give serious thought as to how taxol could be put together in the laboratory. One of our most difficult problems was finding a route that did not merely duplicate the large body of chemistry already in the literature.

By February 1, 1992, we dispatched our first proposal requesting funding from the NIH for the total synthesis of taxol. Central to this proposal were: a) a convergent strategy (Fig. 2), b) the utilization of two metal-assisted C–C bond forming reactions to construct the eight-membered ring of taxol (Fig. 3, ring

[*] Abbreviations used in the schemes: Ac = acetyl, acac = acetylacetonate, AIBN = azobisisobutyronitrile, Bn = benzyl, Bz = benzoyl, CDI = carbonyldiimidazole, CSA = camphorsulfonic acid, DMAP = 4-dimethylaminopyridine, HMPA = hexamethylphosphoric triamide, LDA = lithium diisopropylamide, MEM = methoxyethoxymethyl, Ms = methanesulfonyl, NMO = *N*-methylmorpholine-*N*-oxide monohydrate, P = undefined protecting group, PCC = pyridinium chlorochromate, Piv = pivaloyl, pMB = *p*-methoxybenzyl, TBAF = tetra-*n*-butylammonium fluoride, TBS = *tert*-butyldimethylsilyl, TES = triethylsilyl, Tf = trifluoromethanesulfonyl, TMS = trimethylsilyl, TPAP = tetra-*n*-propylammonium perruthenate, TPS = 2,4,6-triisopropylsilyl, Ts = *p*-toluenesulfonyl, X = undefined leaving group.

K. C. Nicolaou was born in Cyprus and received his Ph.D. degree from the University of London under F. Sondheimer and P. Garratt. After postdoctoral work at Columbia University with T. Katz and at Harvard University with E. J. Corey, in 1976 he joined the faculty at the University of Pennsylvania, where he was promoted to Rhodes-Thompson Professor of Chemistry. In 1989 he accepted joint appointments as Professor of Chemistry at the University of California San Diego and as Darlene Shiley Professor of Chemistry and Chairman of the Department of Chemistry at The Scripps Research Institute. His awards include a Guggenheim Fellowship, a Humboldt Senior American Scientist Award, the American Chemical Society Award for Creative Work in Synthetic Organic Chemistry, and the Dr. Paul Janssen Prize for Creativity in Organic Synthesis. He has received honorary degrees from the Universities of Pennsylvania, London, and Athens. Nicolaou's research interests focus on chemical synthesis, molecular design and recognition, and the biological function of molecules. He is the author of 330 publications, 45 patents, and two books. A new textbook by Nicolaou, "Classics in Total Synthesis" (coauthor: E. J. Sorensen), will be published this year by VCH.

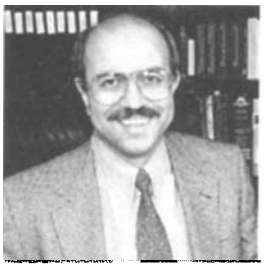

K. C. Nicolaou

R. K. Guy

Rodney "Kip" Guy was born in 1968 in Fort Rucker, Alabama (USA), and obtained his bachelor's degree from Reed College. He worked until the fall of 1991 at the Synthetic Development Laboratory of IBM's Almaden Research Center in San Jose, California. He then joined the Nicolaou group at the Scripps Research Institute as a doctoral student and has been working on the taxol project. He has received graduate fellowships from both the Office of Naval Research and the American Chemical Society Division of Organic Chemistry. His scientific interests include the synthesis of natural products and their use to probe cellular processes.

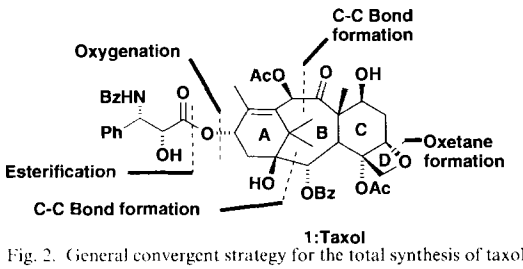

Fig. 2. General convergent strategy for the total synthesis of taxol (October 1991).

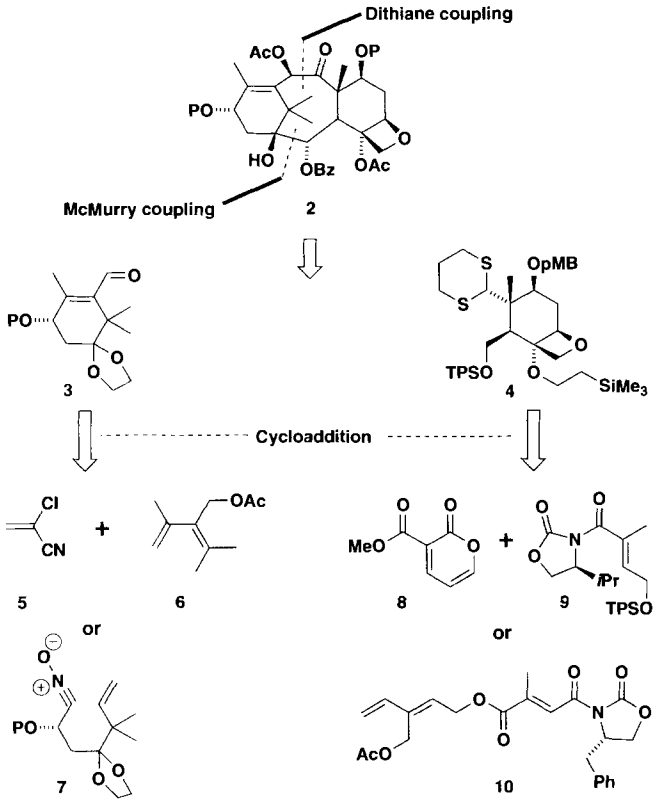

Fig. 3. The first plan for the convergent synthesis of taxol (January 1992).

B), c) the exploitation of Diels–Alder reactions to construct both rings A and C, and d) an alternative model study involving an oxy-Cope-based strategy to gain entry into the ABC tricyclic framework of taxol (Fig. 4). Despite our expectations, however, the study section found our first proposal unconvincing and sent us a depressing message, a score of 1.65 (39th percentile) [best possible evaluation: 1 (lowest percentile); worst possible evaluation: 5 (highest percentile)]. The squad was not deterred, and with stronger determination we wasted no time in preparing and submitting a new proprosal to NIH.

2.2. The Diels–Alder Approach to Ring A

In the meantime we had started our first assault on taxol. Our first goal was to explore the Diels–Alder chemistry outlined in Figure 3 for the construction of rings A and C. Erik, Chris, and C.-H. (Jack) Hwang, a research associate, concentrated on ring A, while research associates Jin-Jun Liu, Wei-Min Dai, and Jack, and graduate student Kip Guy focused on ring C. The designed route to ring A worked smoothly (Fig. 5), delivering a variety of related compounds of potential use in the total synthesis of taxol (e.g. **19**–**21**). Due to the success of this Diels–

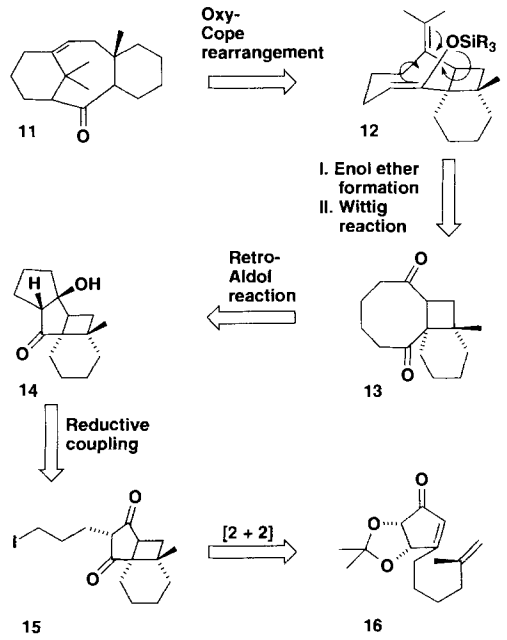

Fig. 4. An oxy-Cope strategy proposed as a model study (January 1992).

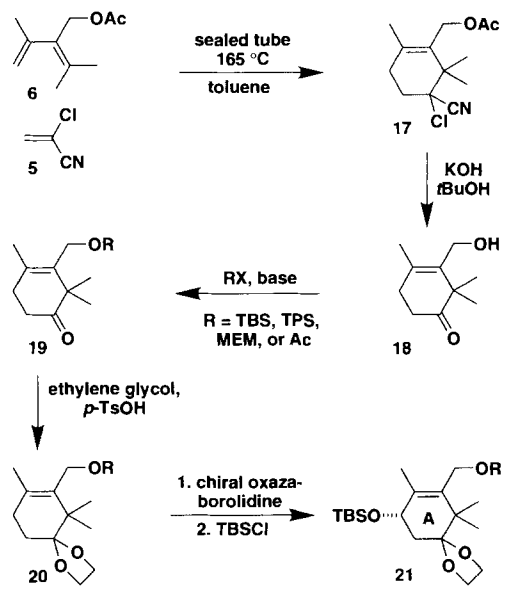

Fig. 5. The synthesis of the A ring unit proceeds as planned (Spring 1992).

Alder route, the alternative, intramolecular nitrile oxide/olefin cycloaddition approach (see Fig. 3) was never attempted. Because of the importance of this work to our taxol project and the fierce competition, we immediately dispatched a communication the synthesis of the A ring.[14] Parenthetically, this early report was rejected by *Angewandte Chemie*.

2.3. The Diels–Alder Approach to Ring C

In contrast to our experience with ring A, the initial attempts toward ring C met with frustrating failures (Fig. 6). While 2-methoxycarbonylpyrone **8** failed to react with chiral dienophile **9**, fusion of **8** with **22** proceeded in excellent yield in refluxing benzene. On examination of the product, however, we realized,

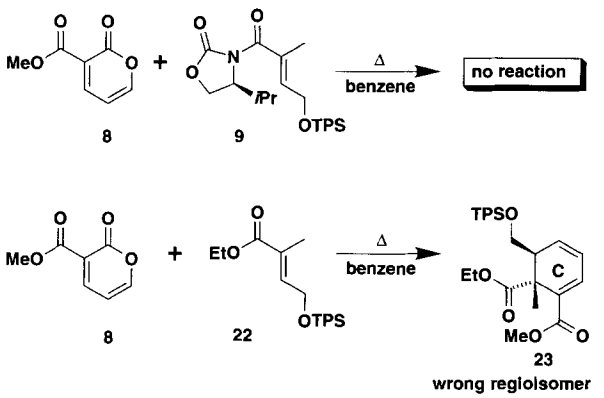

Fig. 6. Failed initial attempts to form taxol's C ring through Diels–Alder reactions (December 1991).

much to our disappointment, that the reaction furnished exclusively the undesired regioisomer **23**. In light of these discouraging results, we continued to search for new ideas.

One morning soon thereafter in my office I opened the latest issue of *Synthesis* and immediately noticed a paper by Koichi Narasaka et al. from the University of Tokyo.[15] I first turned to the paper because of my long-standing friendship with Koichi going back to the 1970s, when we were together at Harvard in the laboratories of E. J. Corey. The relevance of their work to our problem was unmistakable! As seen in Figure 7, the

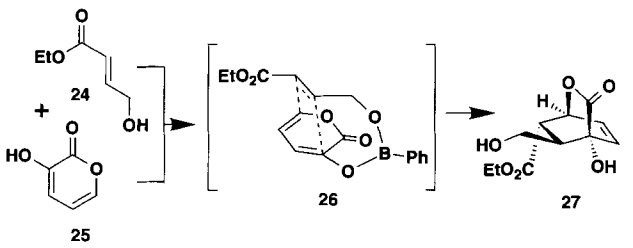

Fig. 7. A particularly propitious precendent from the group of Narasaka.

Narasaka reaction cleverly utilizes a boronate as a template for the assembly of a diene and a dienophile in a specific orientation, thus leading to the specific Diels–Alder regioisomer required for our taxol strategy! Only a methyl group was missing; a simple rearrangement would then provide ring C for our purposes.

Within days, the resistance of ring C to the Diels–Alder approach was broken and a beachhead was established by the application of Narasaka's brilliant boron-tethering device (Fig. 8). This facile process allowed the construction of the highly functionalized ring C in compound **31** in short order. Not only did the Diels–Alder reaction proceed in excellent yield with the requisite regioselectivity, but the desired skeletal rearrangement took place spontaneously under the reaction conditions (**30** → **31**), presumably because of the strain introduced by the extra methyl group. Intermediate **31** was quickly converted into a number of more advanced compounds, some of which are shown in Figure 9. Included among these compounds was the CD ring system **36**, in which taxol's oxetane ring is already installed. Due to the competitive nature of the taxol field, we sent a preliminary communication on this work along with the manuscript on our approach to ring A (vide supra)[16] to the

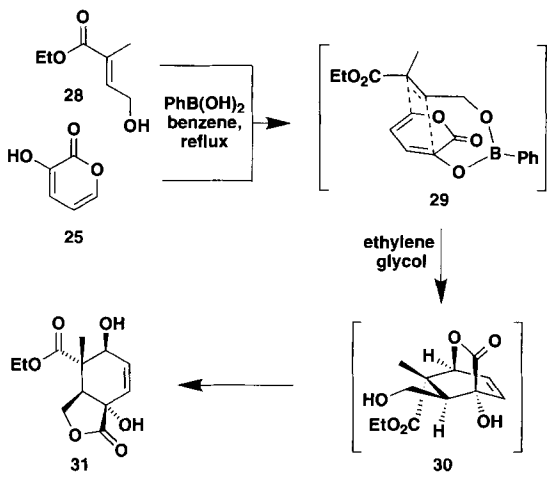

Fig. 8. Application of Narasaka's chemistry leads to an unexpected but advantageous rearrangement (December 1991).

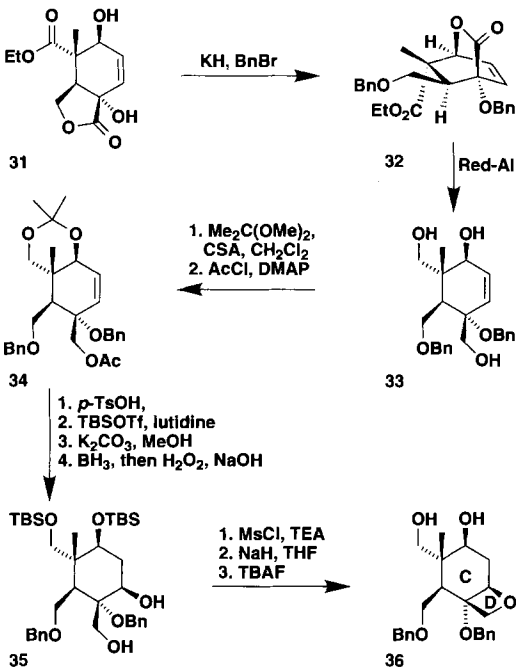

Fig. 9. The original synthesis of the CD ring system in taxol from the paper in *J. Chem. Soc. Chem. Commun.* (Spring 1992).

Journal of the Chemical Society, Chemical Communications. The anxiety one always feels on completion of a piece of work is amazing: it seems that the whole world is working on the same idea and that a "scoop" is imminent! More often than not, of course, one is mistaken, but the feeling cannot be avoided.

2.4. Initial Attempts to Couple "Top First, Bottom Second" Fail

With the two requisite fragments for taxol readily available, our attention turned next to their coupling. Given such functionalized intermediates as **37** and **38** (Fig. 10), one might surmise that final success would be just around the corner. Much to the surprise of the inexperienced (and there were some on the team at the time!), this would not be the case. Our first approach

was to attempt coupling of the two fragments at the "top" and then cyclize at the "bottom" to construct the eight-membered ring. As indicated in Figure 10, aldehyde **38** did not react either

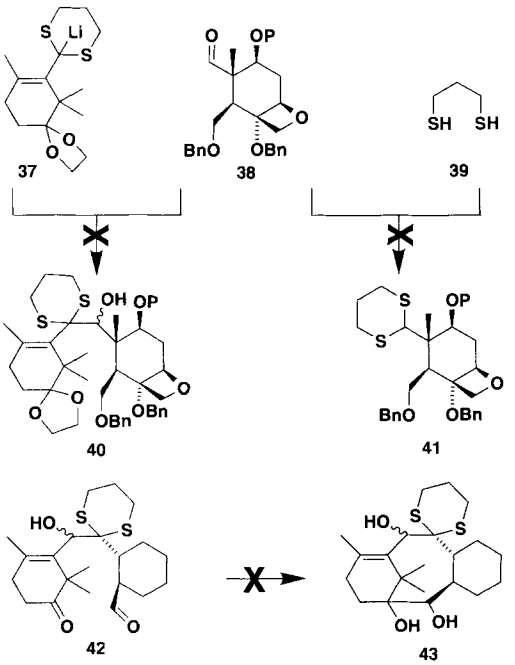

Fig. 10. Attempts to couple "top first, bottom second" fail (Spring 1992).

with lithiodithiane **37** to afford coupling product **40**, or with 1,3-propanedithiol (**39**) to give the expected dithiane **41**. At the same time a model study allowed the preparation of compound **42**, but its intramolecular McMurry coupling to yield compound **43** failed. Attributing these failures to severe steric hindrance within the systems, we decided to reverse the strategy and attempt coupling on the "bottom" first and then cyclizing on the "top" to construct ring B. The previous work by Pattenden[17] and Kende[18] gave us confidence in the McMurry reaction for closing the B ring. Therefore, we concentrated on the ways and means for coupling of the two fragments at the bottom.

2.5. A Crucial Observation and an Important Insight Point the Way

It was at this time that Erik Sorensen made a crucial observation. While attempting to benzylate hydroxy ketone **18** (Fig. 11) under standard basic conditions, he found that double C-alkylation adjacent to the carbonyl group occurred to afford compound **44**. This observation revealed how readily a second double bond is introduced in compound **18** in order to relieve transannular strain. Although useless for the benzylation of the hydroxyl group in **18**, this reaction pointed the way to intermediates such as **45** for our next generation of attempts at coupling fragments A and C. We first tested an enol triflate in a Stille-type coupling with an acid chloride (Fig. 12). Although this sequence worked quite well to give model compound **49**, more realistic intermediates were poor substrates. A new alternative was sought in haste.

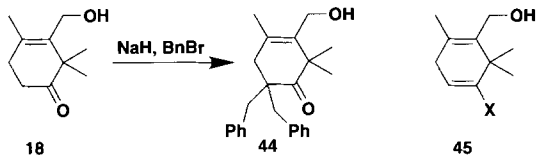

Fig. 11. Unusual preference for C-alkylation indicates that an additional double bond is advantageous for the A ring (June 1992).

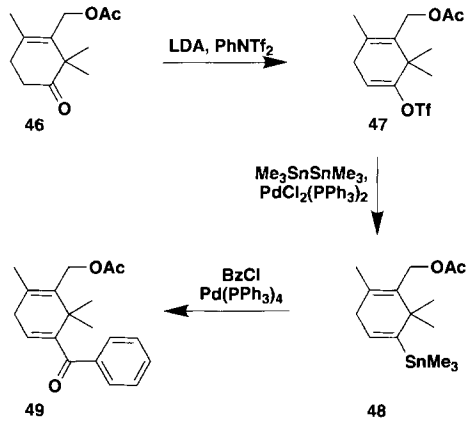

Fig. 12. Utilizing Stille chemistry to take advantage of the propensity for enolization works well in simple models but proves impractical with complex substrates (Summer 1992).

2.6. A Model Study for Exploring the Territory Ahead

The next insight came from Zhen Yang, who insisted on the Shapiro reaction as a means to connect rings A and C, despite the misgivings of several of his teammates and the lack of much precedent for such chemistry in complicated systems. The Shapiro approach was tried first with the model systems shown in Figure 13. The results were spectacular: coupling

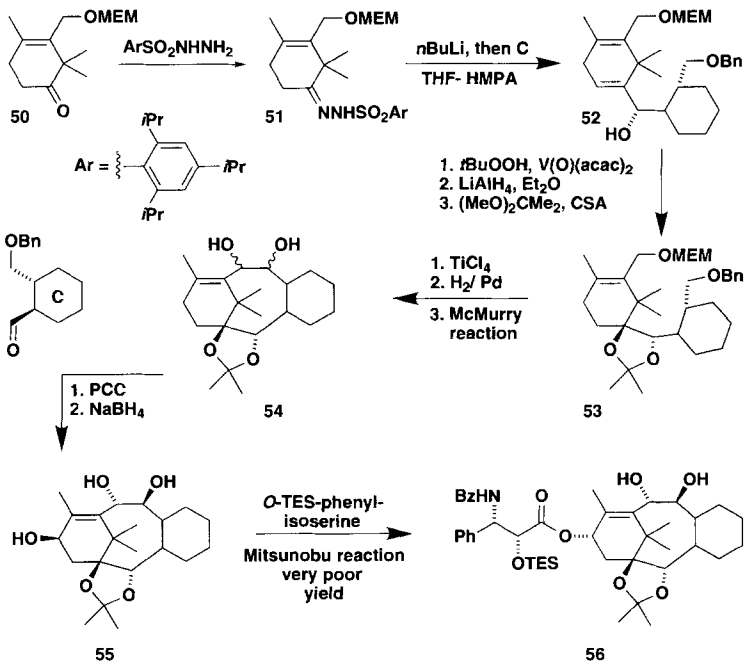

Fig. 13. The first successful closure of the B ring: validation of the Shapiro–McMurry approach (Summer–Fall 1992).

product **52** could be obtained in yields of over 80%. Furthermore, the prospects of stereochemical control in the actual synthesis of taxol added to the excitement of this discovery. This first model study carried out by Zhen, Erik, and Masahisa Nakada (visiting professor from the University of Tokyo) led to the successful synthesis of taxoid **56** (Fig. 13), thus exploring the territory ahead. The main findings of this exercise were that the Shapiro ("bottom first") and McMurry ("top second") reactions were viable options for constructing the desired ABC taxoid skeleton, and that unfortunately the acetonide functionality could not be removed at the final stages of the synthesis without destroying the molecule.[19] To find solutions for the remaining problems, yet another model study was designed and pursued.

2.7. A Second Model Study to Gather More Information of What Lies Ahead

The new model study, spearheaded by Chris, involved substituting a benzenoid framework for the CD ring system of taxol and utilized a cyclic carbonate to fix the 1,2-diol moiety in a highly preorganized conformation for the McMurry reaction (Fig. 14). The ready availability of the benzenoid CD equivalent, the stereoselectivity of the Shapiro coupling, and the high-yielding McMurry coupling observed in this study all contributed to the rapid and efficient synthesis of the benzenoid taxoid system **63**.[20] An important step in this synthesis was the efficient and regiospecific opening of the carbonate ring in **61**, which furnished the desired benzoate **62**. This reaction was originally developed in the ongoing retrosynthetic studies involving natural taxoids (see Section 2.9).

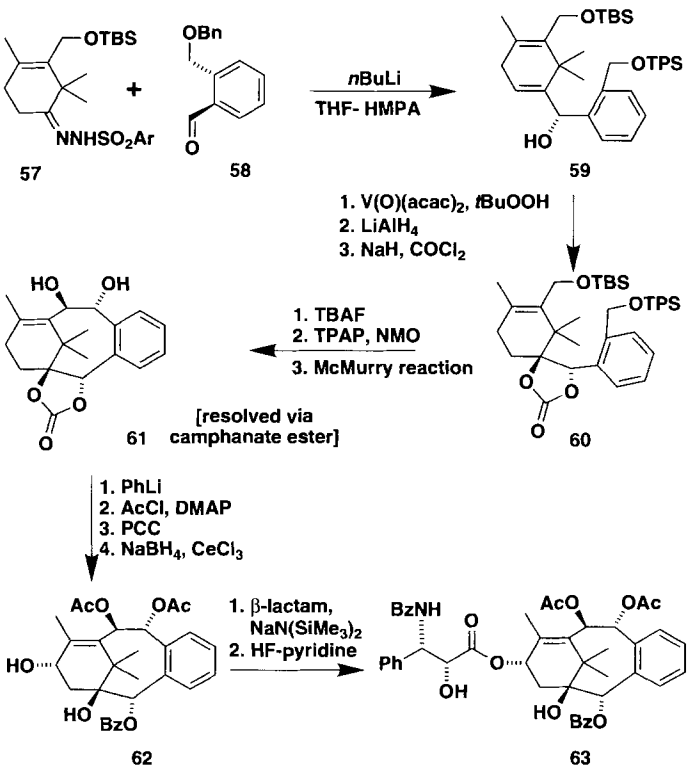

Fig. 14. A second model system helps establish the anticipated conclusion of the total synthesis (Summer - Fall 1992).

2.8. The Second Proposal to NIH

In the meantime a second research proposal had been assembled and submitted to NIH by October 1, 1992. This version described both model studies (Figs. 13 and 14), with considerable progress along the way, and a complete plan to finish the total synthesis of taxol. Additionally, the preparation of a series of designed taxoids was proposed. It was not long, however, before we learned that our revised proposal had the same fate as the first one: A score in the 37th percentile sent us back to the drawing board, and we scrambled for funding from other sources in order to maintain our momentum. A third proposal was prepared over the ensuing few months and sent back to NIH as our drive towards the target continued unabated.

As we entered 1993, the race for taxol was becoming quite heated. Rumors of imminent announcements of taxol's synthesis came and went without confirmation. Progress in our laboratory seemed rather slow; each problem that was solved gave way to another.

2.9. The Retrosynthetic Studies

It was decided at a relatively early stage that degradation studies with taxol would play a crucial role in answering questions about the final stages of the synthesis. There was a problem, however: the supply of taxol. No company would give us any taxol for our studies, despite repeated requests. We bought a small amount at an outrageous price, but that was not enough and unless we were prepared to risk bankruptcy something had to be done! It was finally through the generosity of Dr. Ezio Bombardelli of the Indena company, that we were given several grams of 10-deacetyl baccatin III (**64**, Fig. 15). Research associate Philippe Nantermet and Kip Guy, who were later joined by visiting scientist Hiroaki Ueno, probed taxol's chemistry systematically. Since a 13-deoxy-1,2-carbonate intermediate such as **68** (Fig. 15) was a projected key intermediate in our total synthesis of taxol, this compound became a target in our retrosynthetic studies. Thus, 10-deacetyl baccatin III (**64**) was converted into compound **65** by silylation and acetylation and then subjected to a variety of transformations (Fig. 15). After considerable experimentation, a sequence leading from **65** to **68** was established, and most importantly, the reverse path taking **68** back to **65** was worked out via compounds **67**, **66**, and **70**. Such exercises of securing a projected synthetic intermediate in advance from a natural product and converting it back into target compound are of considerable value in total synthesis. In this instance, these studies, along with the previously known conversion of **65** to taxol, allowed us to define, with complete confidence, compound **68** as an advanced intermediate for our total synthesis. At this stage, we knew that only six completely secured steps separated intermediate **68** and taxol.[21] Armed with this information, we pushed ahead in the synthetic direction to reach **68** from our ring A and ring C intermediates.

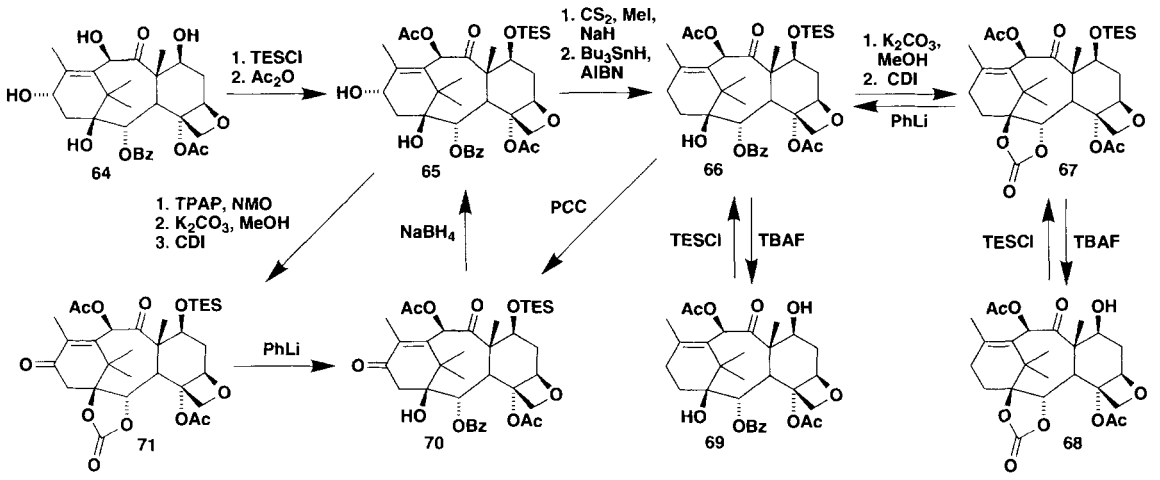

Fig. 15. Degradation studies facilitate planning of the final stages of the total synthesis (Summer 1992 to Summer 1993).

Achieving this goal still required walking a tightrope. A particularly important development was the application of a regioselective opening of the carbonate moiety to introduce the C2 benzoate system of taxol.

2.10. The Initial Attempts to Construct the Eight-Membered Ring of Taxol

Our initial efforts to construct an ABC taxoid system are summarized in Figure 16. The Shapiro coupling of fragments **72** and **57** proceeded in high yield, furnishing product **73** as a single diastereoisomer. Early attempts to generate the aldehyde function in **73**, however, gave mixed acetal **74**, which resisted further useful manipulation. We then turned our attention to the seven-membered ring carbonate **75** as a potential candidate for further advance. This compound proved elusive, however, as attempts to construct it by reaction of the diol with phosgene led to the tetrahydrofuran system **76** instead. Apparently, compound **77**, a presumed intermediate in this reaction, undergoes an internal attack by the C2 hydroxyl group at the primary carbon causing expulsion of CO_2 and HCl to afford **76**. The next attempt was directed towards the γ-lactone dialdehyde **79**, a potential McMurry substrate for the desired ring closure. The preparation of **79** proceeded according to plan, but unfortunately, all efforts to obtain **80** by the McMurry reaction failed, producing only diol **81**. At this point it became clear that this particular synthetic design did not favor the required ring closure and that a new tactic had to be adopted.

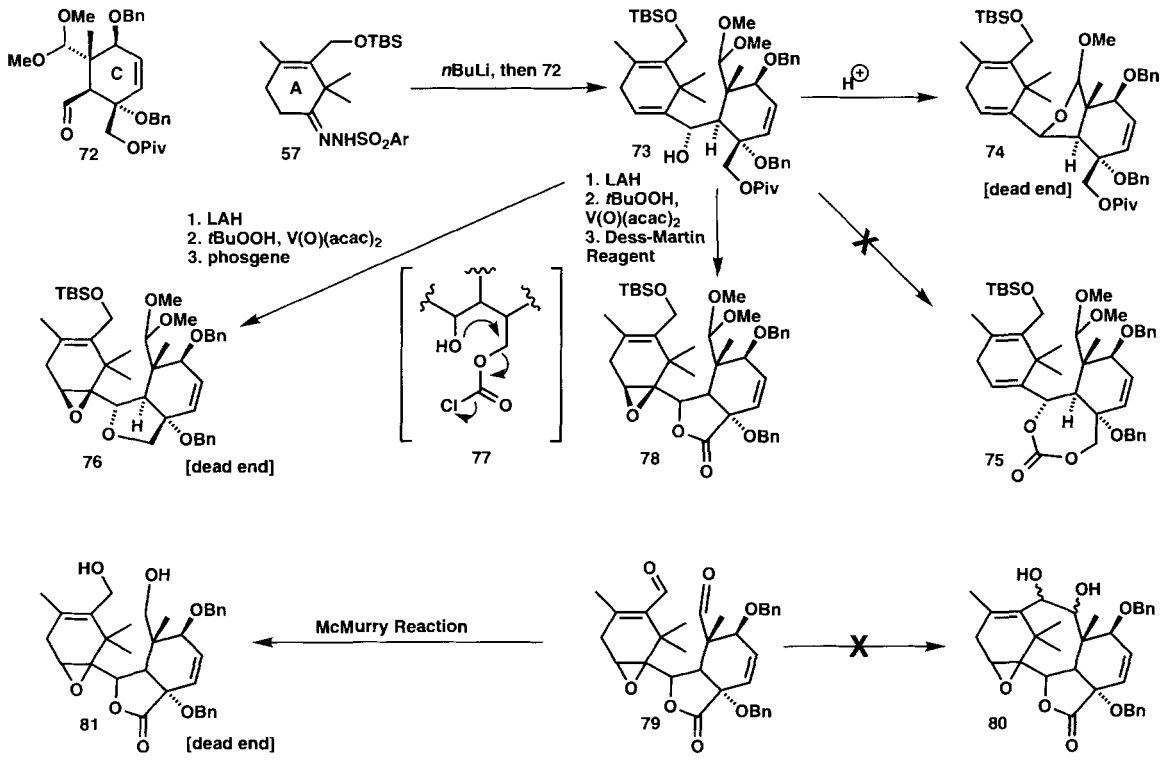

Fig. 16. Initial attempts to construct the eight-membered B ring of taxol fail (Fall 1992).

2.11. The Final Shapiro Elaboration and Preorganization of the Cyclization Precursor

The important results of the carbonate opening from the retrosynthetic studies (see Section 2.9) could not have come in a more timely fashion. We used that information to define a more specific strategy. According to this new plan, hydrazone **57** (ring A) and aldehyde **86** (ring C, Fig. 17) were paired as the Shapiro-coupling partners. The double bond in the resulting intermediate (**87**, Fig. 18) would serve in construction of the oxetane ring. Due to the sensitivity of the oxetane system, its construction was postponed until after the fabrication of the ABC skeleton.

The Shapiro coupling of **86** with **57** proceeded remarkably well (Fig. 18) both in terms of efficiency (80% yield) and stereoselectivity (a single isomer formed, whose configuration was later confirmed by X-ray crystallography). Figure 19 provides graphically a mechanistic rational for the observed stereoselectivity in this reaction. After many missteps along the way dialdehyde **92** was finally reached.

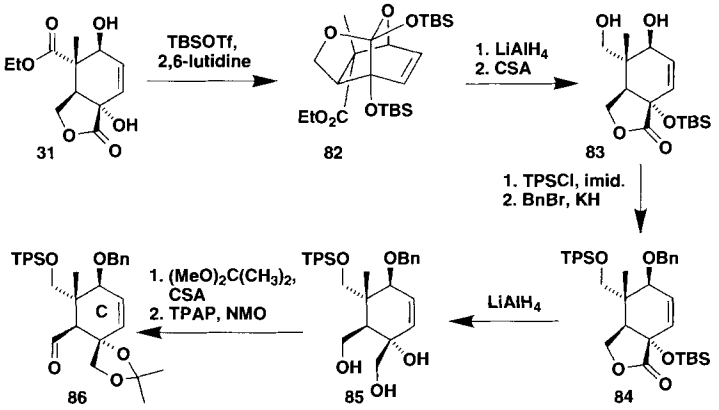

Fig. 17. Construction of the fully functionalized and protected C ring fragment aldehyde **86** (Spring 1993).

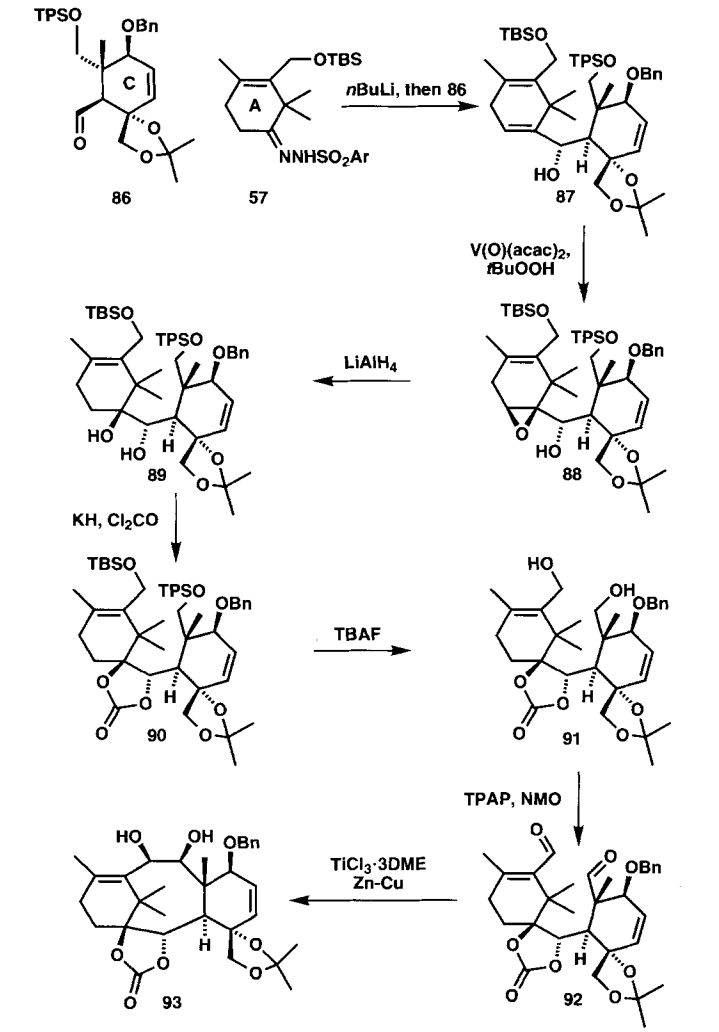

Fig. 18. Construction of compound **92** for the decisive McMurry reaction and formation of taxol's eight-membered ring (Spring–Summer 1993).

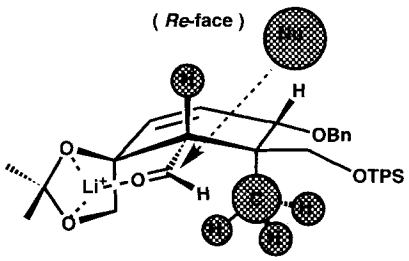

Fig. 19. A mechanistic rationale for the observed stereoselectivity of the Shapiro reaction. The Li^+ ion complexes the acetonide and aldehyde oxygen atoms, fixing the carbonyl group. The nucleophile attacks from the more accessible face, opposite the methyl group.

2.12. The McMurry Cyclization to Form the ABC Taxoid Skeleton

We then faced one of the most daunting problems of the entire campaign: the closure of taxol's B ring. With optimum preorganization, dialdehyde **92** seemed to be the best precursor we had synthesized thus far. Zhen Yang was chosen as the pointman to attempt the crucial McMurry cyclization—and it worked! The cyclized diol **93** (structure secured by spectroscopic and X-ray crystallographic analysis) was obtained, albeit in modest yield. The desired product **93** was accompanied by compounds **94**–**96** (Fig. 20). Despite many attempts by Chris and Zhen to improve the yield of **93** from this reaction, we could not prevail in the

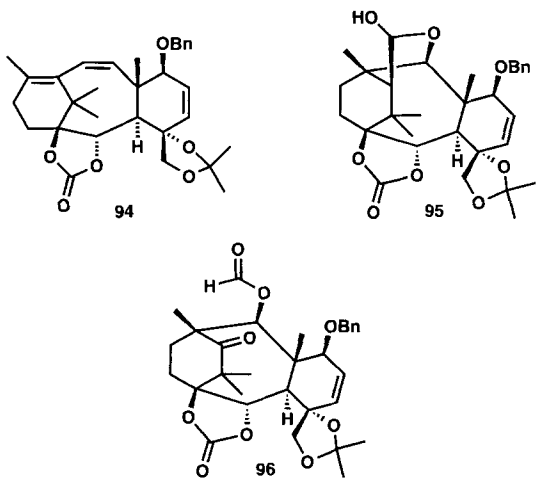

Fig. 20. The undesired side products of the McMurry reaction of **92** (see Fig. 18).

short time that we suspected we had. A major dilemma arose at this juncture. Should we continue to search for improvements of this cyclization method or should we abandon it to search for a new, more efficient procedure? Finally, Zhen Yang volunteered to become the "McMurry machine." But even this idea had its drawbacks, since the McMurry cyclization could not be scaled up to more than a few tens of milligrams without loss in efficiency. Nevertheless, Dr. Yang was able to provide a constant supply of diol **93** for the rest of the team, whose task was now to advance it further along the projected pathway to taxol.

At this stage, we chose a classical resolution to separate the two enantiomers of **93** for the production of natural taxol. Figure 21 illustrates this resolution, which relied on chromatographic separation of the diastereomeric camphanate esters **97a** and **97b**. Luckily, one of the diastereoisomers, the wrong one as it turned out, crystallized nicely, and X-ray crystallographic analysis revealed its absolute stereochemistry (**97b**, see ORTEP drawing, Fig. 21). This development enabled us to push forward to the next stage with the desired isomer, **93a**.

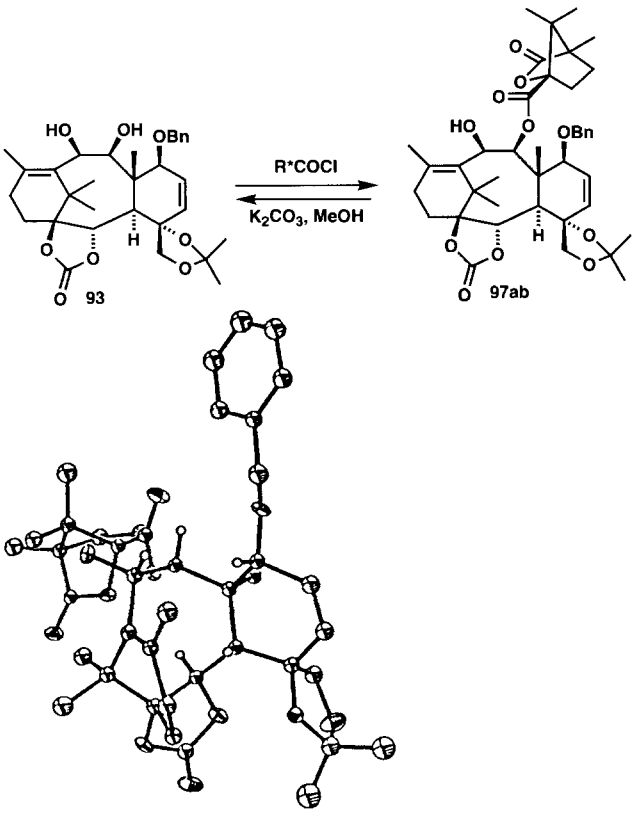

Fig. 21. Top: Resolution of the diol (±)-**93** via its camphanic esters provides (+)-**93** (Fall 1993). R*COCl = (1*S*)-camphanic anhydride. Bottom: X-ray structure of **97b**.

2.13. The Third NIH Proposal

In June 1993, while in the "heat of the battle" during final stages of the synthesis, we submitted the third version of our proposal to NIH. This latest revision included over ten alternative approaches to the eight-membered ring of taxol and a series of designed taxol mimics. Ironically, the announcement of the proposal's acceptance and eventual funding would come after we had completed the total synthesis of taxol. The positive response from NIH came hastily by fax on Saturday morning, February 19, 1994, providing us with a deep sense of the meaning of the expression "better late than never!"

2.14. The Fortunate Configurational Adjustments at C9 and C10

Since we had the enantiomerically pure diol **93**, the next objective was to settle the issue of the regio- and stereochemical arrangements in the C9–C10 region of the molecule. To our pleasant surprise, monoacetylation of **93** (Fig. 22) proceeded well, as did the ensuing NMO–TPAP oxidation of the remain-

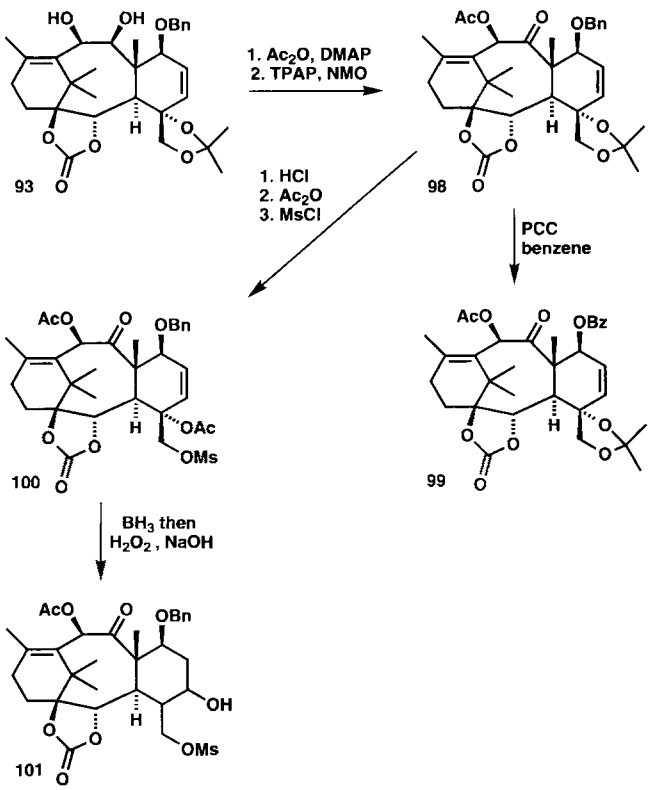

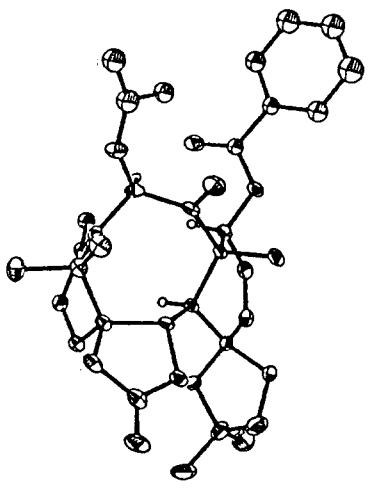

Fig. 22. Top: Attempts at hydroboration and allylic oxidation fail (Fall 1993). Bottom: X-ray structure of **99**.

ing free hydroxyl group. The regio- and stereochemical outcome of this sequence was the subject of much debate. NMR data pointed to the desired structure **98** but did not provide overwhelming evidence. Considering the X-ray crystallographic analysis of the camphanate ester **97b** mentioned above, we thought the regiochemistry of **98** odd, since it required acetylation at the other hydroxyl group, and this was not fully accepted at first by everyone on the team. Why should camphenyl chloride and acetic anhydride lead to opposite regiochemical outcomes in these esterifications? Soon thereafter, an unequivocal confirmation of the structure of **98** was obtained, largely through serendipity. Oxidation of **98** with PCC, aiming at oxidation at C13, gave unexpectedly the crystalline benzoate ester **99**, whose X-ray crystallographic analysis (Fig. 22 bottom) proved beyond doubt both the regio- and stereochemistry of the C9 acetate. This news was received with relief with regards to the C9–C10 region of the molecule, but also with chagrin since it implied that the protecting group at C7 must be replaced with one that would withstand an allylic oxidation. Could it be that the allylic alcohol at C10 is considerably more reactive than that at C9, but much less accommodating of a sterically demanding group such as the camphanate ester? Molecular models reveal only slight steric differences between the two positions.

2.15. Preparing for the Oxetane Ring: Introduction of the C5 Oxygen Atom

At this juncture we began to address the introduction of the hydroxyl group at C5. We placed hydroboration at the top of our list as a potential means of bringing in the required oxygen atom. The prospect of the two hydroxyls at C4 and C20 acting as directing groups was considered to be an advantage of such a substrate. Therefore, the acetonide group was removed from the substrate **98** to furnish the corresponding diol (Fig. 22). However, all our attempts to hydroborate this diol and a number of its derivatives met with a serious side reaction: cleavage of the allylic C–O bond leading to C4-deoxy systems as illustrated by the transformation of **100** to **101** (Fig. 22).

Faced with this new and serious problem, and putting aside for the moment the issue of the configuration of the carbon atom bearing the hydroxyl group, we decided to attempt the hydroboration reaction on acetonide **98**, hoping to avoid the undesired C–O bond cleavage. Much to our surprise, the reaction worked quite well, giving rise to a major isomer whose configuration became the subject of a major argument (Fig. 23). The orientation of the newly installed hydroxyl group at C5 in compound **102** was not easily deduced by NMR spectroscopy, but chemical correlation with authentic material, derived from natural compound by a degradation sequence (Fig. 24), showed this compound to be the α isomer.[3]

2.16. Installation of the Oxetane Ring

The next task in the drive towards taxol was the installation of the oxetane ring. Considering the work of P. Potier with naturally derived materials in which he and his collaborators at Gif-sur-Yvette formed an oxetane from a triol similar to **102**

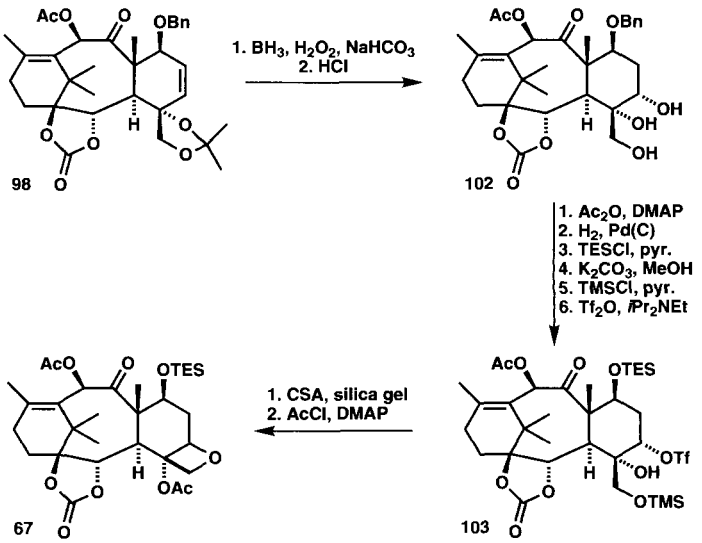

Fig. 23. Construction of the oxetane system and arrival at the desired tetracyclic intermediate **67** (Fall–Winter 1993).

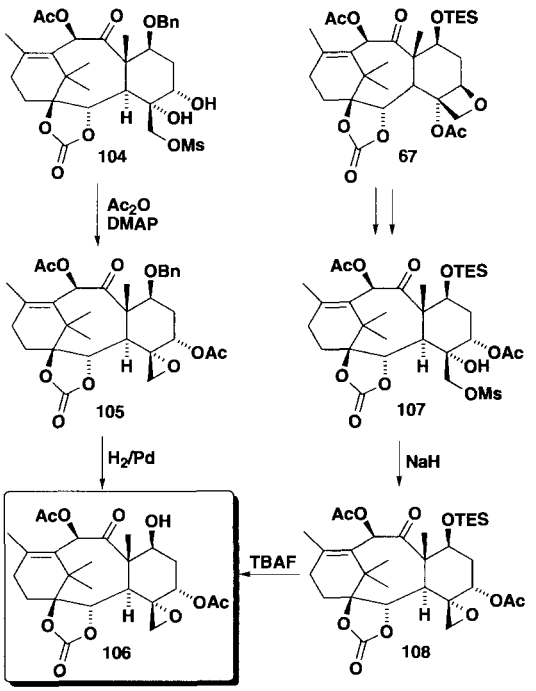

Fig. 24. Proof of the configuration at C5 by comparison of the degradation product **106** obtained from **67** with the derivative of **104** (Winter 1993).

(Fig. 23), we expected to solve this problem within a matter of days. But it took the team more than two months! First, and unforgivably so, we had missed Potier's important paper in *Tetrahedron*;[22] as a result this reference is missing from our review on the chemistry and biology of taxol, which was published in January 1994 in *Angewandte Chemie*.[1] Second, protection of the tetraol system in ring C presented a serious challenge. The problem was finally solved by utilizing the triflate group at C5 and displacing it intramolecularly with the hydroxyl nucleophile group at C20 by an S_N2-type reaction, a tactic used by Danishefsky et al. in a model system[*] (Fig. 23).[23] Application

[*] See footnote on p. 2089.

of Potier's mesylate protocol, which eventually came to our attention, worked even better. The final bulwark of taxol's fortress fell on January 19, 1994. Compound **67** matched an authentic sample by all the usual criteria, and as outlined in Figure 25, was carried through to taxol. The total synthesis of

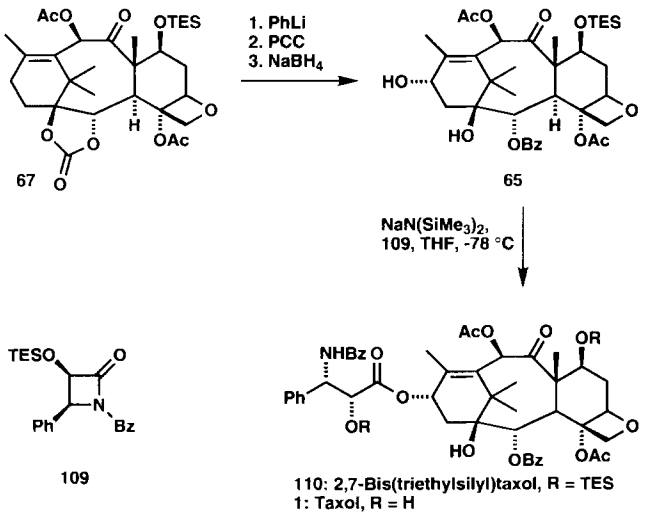

Fig. 25. Final stages of the total synthesis of taxol (January, February 1994).

taxol was reported in *Nature*, on February 17, 1994, shortly after the *Science* had designated taxol as a runner-up "Molecule of 1993".[24] Our publication appeared almost at the same time as another taxol total synthesis by the research group headed by Holton.[25, 26] Both syntheses met with highest acclaim.[27–29] Those early days of 1994 were quite dramatic and worth sharing here.

3. The Conquest

3.1. The Exhilarating Triumphant Moments

It was 11:00 pm on Wednesday, January 19, 1994, when the phone rang. Georgette, my wife, woke me up saying, "There's a man with an accent on the phone for you." Reluctant and very sleepy, I picked up the phone and said, "Hello?" It was Hiroaki Ueno asking me to come to the lab immediately because he wanted to talk to me. "What is it?" I said, "Can we talk tomorrow?" My thoughts started to turn to some bad accident in the lab. "No," he said, "You have to come now. It is very important, we have some news." To press me to come, Hiroaki put Jin-Jun on the line, who also insisted that I come to the lab, by saying, "We have the compound—we made taxol!" "I'll be there in five minutes," I said slamming the phone down and jumping out of bed. I put on my jogging suit and ran out the door to the car, saying to Georgette, "I have to go. They say they have some good news they finished taxol. I'll be back soon." In five minutes I was in my office looking at the spectra. The NMR spectra of synthetic and authentic intermediate **67** were identical. The synthetic and retrosynthetic sequences had been bridged! Only five already secured steps remained; our goal was only a matter of days if not hours from completion! Satisfied with what I saw, I left saying, "I'll see you tomorrow morning to discuss whatever we have to do to polish the work and write up the paper."

The next morning, I was in my office early pacing back and forth until everyone on the project arrived. Hiroaki was still in the lab when I arrived, having spent all night and morning bringing up material for a repeat of the final stages. Jin-Jun and Philippe were both away interviewing for jobs. The rest of the team, consisting of visiting professor Elias Couladouros from the University of Athens, research associates Johanne Renaud, K. Paulvannan, anad Zhen Yang, and graduate students Kip Guy, Chris Claiborne, and Erik Sorensen arrived shortly, and we decided that they would press around-the-clock until all intermediates leading to taxol were finally characterized and the final sequence was repeated; I was to immediately start working on preparing the manuscript. By the afternoon of Friday, January 21, 1994, the manuscript on the total synthesis of taxol was dispatched to *Nature*. Our paper was accepted, after peer review, on Monday, January 31, 1994, and scheduled to be published on Thursday, February 17, 1994.

3.2. The Competition

This story would not be complete without paying tribute to those researchers whose work in the area of taxol chemistry made the field so rich, exciting, and fruitful. In Europe, the groups of Potier, Greene, Pattenden, Commerçon, Blechert, Fetizon, and Jenkins contributed admirably to this area. In Japan, the work of Kuwajima, Kitagawa, Yamada, Ohtsuka, Takahashi, and Mukaiyama is nothing less than brilliant. In the USA, Wender, Trost, Danishefsky, Kende, Paquette, Swindell, Shea, Ojima, and Holton enriched considerably the field and provided much excitement and drama over the last two decades or so. A number of other groups have also touched upon various aspects of taxol's chemistry and biology.[1]

Particularly striking were the two papers from Holton's group at Florida State University. They not only describe the total synthesis of taxol itself, but also that of its enantiomer. One has to admire the courage of this group, who apparently risked all the glory of publishing first, by waiting to complete both syntheses before submitting their papers.[*]

4. Conclusion

The conquest of taxol as a synthetic target was both intense and exciting. Driven by the desire to succeed, the team of ten in the Nicolaou group (Fig. 26) proved themselves second to none and rose to the challenge. This was a magnificent opportunity for all of us to develop some new strategies in total synthesis and to discover chemistry leading to the synthesis of taxol and a series of designed analogues. This team came out of this project very proud of their success but also very tough, experienced, and ready to attack any challenge in synthesis placed in front of

[*] Comment from the editor: A third, equally instructive total synthesis of taxol appeared recently: J. J. Masters, J. T. Link, L. B. Snyder, W. B. Young, S. J. Danishefsky, *Angew. Chem.* **1995**, *107*, 1883; *Angew. Chem. Int. Ed. Engl.* **1995**, *34*, 1723.

Fig. 26. The triumphant taxol team. Front row (from left to right): Dr. Johanne Renaud (postdoc), R. Kip Guy (graduate student), Prof. K. C. Nicolaou, Chris Claiborne (graduate student. Back row: Dr. Elias Couladouros (visiting scientist), Dr. Jin-Jin Liu (postdoc), Dr. K. Paulvannan (postdoc), Dr. Zhen Yang (postdoc), Erik Sorensen (graduate student), Dr. Philippe Nanterment (postdoc), Dr. Hioaki Ueno (visiting scientist).

them. Such is the training that one receives in the total synthesis of challenging molecules.[30]

We are indebted to our talented collaborators all of whom worked on the taxol project with the outmost enthusiasm, dedication, and persistence (listed alphabetically): C. F. Claiborne, E. A. Couladouros, W.-M. Dai, C.-K. Hwang, J.-J. Liu, M. Nakada, P. G. Nantermet, K. Paulvannan, J. Renaud, K. Shibayama, E. J. Sorensen, H. Ueno, and Z. Yang. We are also grateful to Raj Chadha, Gary Siuzdak, and Dee-Hua Huang for their invaluable assistance with X-ray crystallography, mass spectrometry, and NMR spectroscopy, respectively. This work was carried out at The Scripps Research Institute and was supported financially by The National Institutes of Health, Merck Sharp & Dohme, Schering Plough, Pfizer, Hoffman-La Roche, Glaxo, and Rhône-Poulenc Rorer, and through fellowships by The Agricultural University of Athens (E. A. C.), Glaxo (C. F. C.), Mitsubishi Kasei Corporation (H. U.), NSERC (J. R.), The Office of Naval Research (R. K. G.), Rhône-Poulenc Rorer (P. G. N.), R. W. Johnson – ACS Division of Organic Chemistry (E. J. S.), and Mr. Richard Staley (C. F. C.).

Received: February 10, 1995 [A 105 IE]
German version: *Angew. Chem.* **1995**, *107*, 2047 - 2059

[1] K. C. Nicolaou, W.-M. Dai, R. K. Guy, *Angew. Chem.* **1994**, *106*, 38–69; *Angew. Chem. Int. Ed. Engl.* **1994**, *33*, 15 - 44.
[2] K. C. Nicolaou, Z. Yang, J.-J. Liu, H. Ueno, P. G. Nantermet, R. K. Guy, C. F. Claiborne, J. Renaud, E. A. Couladouros, K. Paulvannan, E. J. Sorensen, *Nature (London)* **1994**, *367*, 630 - 634.
[3] K. C. Nicolaou, J.-J. Liu, Z. Yang, H. Ueno, R. K. Guy, E. A. Couladouros, E. J. Sorensen, *J. Am. Chem. Soc.* **1995**, *117*, 624–633.
[4] K. C. Nicolaou, J.-J. Liu, Z. Yang, H. Ueno, E. J. Sorensen, C. F. Claiborne, R. K. Guy, C.-K. Hwang, M. Nakada, P. G. Nantermet, *J. Am. Chem. Soc.* **1995**, *117*, 634 - 644.
[5] K. C. Nicolaou, Z. Yang, J.-J. Liu, P. G. Nantermet, C. F. Claiborne, J. Renaud, R. K. Guy, K. Shibayama, *J. Am. Chem. Soc.* **1995**, *117*, 645–652.
[6] K. C. Nicolaou, H. Ueno, J.-J. Liu, P. G. Nantermet, Z. Yang, J. Renaud, K. Paulvannan, R. Chadha, *J. Am. Chem. Soc.* **1995**, *117*, 653–659.
[7] T. Junad, *Life* **1992** (5), 71.
[8] a) S. Borman, *Chem. Eng. News* **1991**, *69*(35), 11 - 18; b) D. G. I. Kingston *TIBTECH* **1994**, *12*, 221 - 227.
[9] H. Hartzell, Jr., *The Yew Tree. A Thousand Whispers*, Hugolosi, Eugene, OR, USA, **1991**.
[10] C. L. Bolsinger, A. E. Jaramillo in *Silvics of North American: Vol. 1, Conifers* (Eds.: R. M. Burns, B. H. Honkala), USDA Forest Service, Washington, DC, USA, **1990**, p. 573 - 579.
[11] M. C. Wani, H. L. Taylor, M. E. Wall, P. Coggen, A. T. McPhail, *J. Am. Chem. Soc.* **1971**, *93*, 2325–2327.
[12] S. B. Horwitz, J. Fant, P. B. Schiff, *Nature (London)* **1979**, *277*, 665 - 667.
[13] For a review see the special issue *Ann. Pharmacol.* **1994**, *28*(5) (Eds.: J. M. Koeller, R. T. Dorr).
[14] K. C. Nicolaou, C.-K. Hwang, E. Sorensen, C. Claiborne, *J. Chem. Soc. Chem. Commun.* **1992**, 1117–1118.
[15] K. Narasaka, S. Shimada, K. Osada, N. Iwasawa, *Synthesis* **1991**, 1171–1173.
[16] K. C. Nicolaou, J.-J. Liu, C.-K. Hwang, W.-M. Dai, R. K. Guy, *J. Chem. Soc. Chem. Commun.* **1992**, 1118–1120.
[17] M. J. Begley, C. B. Jackson, G. Pattenden, *Tetrahedron* **1990**, *46*, 4907–4924; see also: C. B. Jackson, G. Pattenden, *Tetrahedron Lett.* **1985**, *26*, 3393–3396.
[18] A. S. Kende, S. Johnson, P. Sanfilippo, J. C. Hodges, L. N. Jungheim, *J. Am. Chem. Soc.* **1986**, *108*, 3513 - 3515.
[19] K. C. Nicolaou, Z. Yang, E. J. Sorensen, M. Nakada, *J. Chem. Soc. Chem. Commun.* **1993**, 1024 - 1026.
[20] K. C. Nicolaou, C. F. Claiborne, P. G. Nantermet, E. A. Couladouros, E. J. Sorensen, *J. Am. Chem. Soc.* **1994**, *116*, 1591 - 1592.
[21] K. C. Nicolaou, P. G. Nantermet, H. Ueno, R. K. Guy, *J. Chem. Soc. Chem. Commun.* **1994**, 295–296.
[22] L. Ettovati, A. Ahond, C. Poupar, P. Potier, *Tetrahedron* **1991**, *47*, 9823 - 9831.
[23] T. V. Magee, W. G. Bornman, R. C. Isaacs, S. J. Danishfesky, *J. Org. Chem.* **1992**, *57*, 3274 - 3276.
[24] E. Culotta, D. E. Koshland, Jr., *Science* **1993**, *262*, 1958 - 1961.
[25] R. A. Holton, C. Somoza, H.-B. Kim, F. F. Liang, R. J. Biediger, P. D. Boatman, M. Shindo, C. C. Smith, S. Kim, H. Nadizadeh, Y. Suzuki, C. Tao, P. Vu, S. Tang, P. Zhang, K. K. Murchi, L. N. Gentile, J. H. Liu, *J. Am. Chem. Soc.* **1994**, *116*, 1597 - 1598.
[26] R. A. Holton, H.-B. Kim, C. Somoza, F. F. Liang, R. J. Biediger, P. D. Boatman, M. Shindo, C. C. Smith, S. Kim, H. Nadizadeh, Y. Suzuki, C. Tao, P. Vu, S. Tang, P. Zhang, K. K. Murchi, L. N. Gentile, J. H. Liu, *J. Am. Chem. Soc.* **1994**, *116*, 1599–1600.
[27] S. Borman, *Chem. Eng. News* **1994**, *72*(8), 32 - 34.
[28] S. B. Horwitz, J. Mann, *Nature (London)* **1994**, *367*, 593–594.
[29] L. Wessjohann, *Angew. Chem.* **1994**, *106*, 1011; *Angew. Chem. Int. Ed. Engl.* **1994**, *33*, 959.
[30] K. C. Nicolaou, E. J. Sorensen, *Classics in Total Synthesis*, VCH, Weinheim, **1995**.

Cytomimetic Organic Chemistry: Early Developments

Fredric M. Menger* and Kurt D. Gabrielson

This article describes how chemical and physical stimuli cause a simple system, the giant vesicle, to undergo a variety of "cytomimetic" transformations such as fusion, fission, endocytosis, budding, aggregation, birthing, and foraging. For example, when a giant vesicle, which happens to have a smaller vesicle inside it, is exposed to octyl glucoside, the smaller vesicle can pass through the outer membrane into the external medium ("birthing"). The resulting injury to the membrane of the host vesicle heals immediately. Addition of cholic acid, on the other hand, induces a feeding frenzy in which a vesicle grows rapidly as it consumes its smaller neighbors. After the food is gone, the giant vesicle then self-destructs (a case of "birth, growth, and death"). Such lifelike morphological changes were obtained by using commercially available chemicals; thus these processes should be assigned to organic chemistry, and not to biology or even biochemistry. Experimental details (e.g. the preparation and observation of the vesicles) are included in this review in hopes of helping others enter this undeveloped field.

Keywords: cytomimetic organic chemistry · microscopy · supramolecular chemistry vesicles

1. Introduction

The ancient Greeks believed that conversion of an unorganized universe ("chaos") into an organized one (the "cosmos") was the work of their dieties. Today, organization (especially in complex biological systems such as the cell) seems almost as puzzling as it did centuries ago. In mysterious ways, molecules organize themselves into elaborate assemblies to produce a phenomenon called "life". Since living systems presumably obey the fundamental laws of chemistry, biological behavior must, by default, originate from its collective and holistic nature. Biology is, in effect, organized organic chemistry. The question then becomes: Are the properties of organized organic molecules predictable from the familiar properties of individual molecules? Or in other words: Are organic "systems" simple extrapolations of single-molecule chemistry? We have already argued negatively to these questions.[1] To learn about organized assemblies, and ultimately about biology, one must forsake single-molecule organic chemistry and confront the assemblies themselves despite the difficulties, complications, and uncertainties that will undoubtedly ensue.

Consider the role of the π-meson in chemistry. Since π-mesons are components of all nuclei including that of carbon, organic chemistry necessarily embodies them. A decarboxylation, for example, entails a loss of π-mesons. Why then are chemists completely indifferent to these elementary particles? The answer is that chemists operate at a level of complexity and organization where particle physics is of absolutely no consequence. Three related quotes reinforce this general point. W. H. Thorpe: "The behavior of large and complex aggregates of elementary particles is not to be understood as a simple extrapolation of the properties of a few particles. Rather, at each level of complexity entirely new properties appear". P. W. Anderson: "At each level of organization, types of behavior open up which are entirely new and basically unpredictable from a...detailed analysis of the entities which make up the...higher level systems." And A. R. Peacocke: "Higher levels of complexity are distinguished by some genuinely new features and activities, and these require distinctive theories, language, and concepts to describe them". It is the philosophy embraced in these quotes that motivated the work that will be described in the following pages.

Vesicles, also called liposomes, are spherical structures composed of a closed lipid shell surrounding an aqueous interior (Fig. 1). Under certain conditions, lipids can self-assemble into giant vesicles the size of living cells.[2] As will be detailed later, giant vesicles engage in many cell-like activities such as aggregation, budding, fusion, and fission.[3] We refer to this behavior as "cytomimetic" chemistry.[4] Although we are hesitant to introduce such new jargon, the descriptor cytomimetic for the striking morphological changes (visible under a light microscope) seems appropriate enough. And, to paraphrase J. S. Mill, "Hardly any thoughts

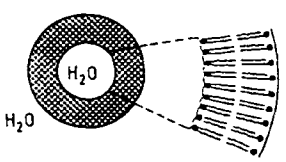

Fig. 1. Schematic representation of a unilamellar vesicle composed of a single bilayer of lipid molecules.

[*] Prof. F. M. Menger, Dr. K. D. Gabrielson
Department of Chemistry, Emory University
Atlanta, GA 30322 (USA)
Telefax: Int. code + (404)727-6586

ever make their way among mankind, even in the minds of their inventors, until aptly selected words nail them down and hold them fast".

We are hardly the first to become fascinated by cytomimetic chemistry. Over sixty years ago, in a brilliant piece of work, Crile et al.[5] combined the ether-soluble fraction of brain tissue (i.e. the lipids) with the water-soluble fraction (i.e. the proteins and nucleic acids).[6] Within minutes remarkable structures, called "autosynthetic cells", formed in the water. Each contained a microscopically visible central organelle resembling a nucleus. The structures grew slowly, multiplied by budding or direct division, and occasionally moved like an amoeba. They even exhibited a high rate of oxygen consumption. Although the findings have been confirmed independently,[7, 8] they have been largely ignored. We are currently resurrecting this work (the desire to do so being irresistible!), but the present article will deal only with much simpler systems composed of material that is not of direct biological origin.

It is necessary to stress the preliminary nature of what is about to unfold. Work began just two years ago in a small office made over to house a microscope. The plan was to watch the response of giant vesicles as they were exposed to chemicals, heat, touch, and various other irritations. At this early stage of research, we hoped more for a slow accumulation of information than for instant illuminative insights. J. F. Wilford described the situation succinctly: "Science proceeds first by open exploration, the time of initial discoveries. Then follows reconnaissance, gathering evidence on a broad front, pursuing leads to the far corners of the problem, and generating preliminary hypotheses. Finally, if warranted by the results of the exploration and reconnaissance, there comes the time for detailed studies and the testing of more informed hypotheses". By all counts, we are in the "open exploration" phase. Yet even so, the results to date have been sufficiently intriguing that their publication, in hopes that others join the enterprise, appears justified.

Since this article is intended for a broad range of nonexperts, an attempt has been made to avoid a technical, dehydrated style of writing. This was easy to do because "when we begin the study of any science, we are in a situation, respecting that science, similar to that of children" (A. Lavoisier). Indeed, many were the times when we gazed with a child's wonder at the dynamics of our giant vesicles.

2. A Brief History of Giant Vesicles

A. Einstein said "A hundred times every day, I remind myself that my inner and outer life are based on the labors of other men, living and dead, and that I must exert myself to give in the same measure as I have received." We too owe a debt to others who, before us, investigated giant vesicles and related systems. In 1911 Otto Lehmann wrote a book entitled "Die Flüssigen Kristalle" ("Fluid Crystals") in which he published optical micrographs of long tubules projecting from the edges of hydrated phospholipid films.[12] He also observed vesicle structures that he called "kunstliche Zellen" ("artificial cells"). As we shall see, Lehmann's tubules were important to our own research carried out eight decades later. D. Hammarskjold once asked, "Why this desire in all of us that, after we have disappeared, the thoughts of the living shall now and again dwell upon our name?" Otto Lehmann certainly had, at least in our laboratory, his wish fulfilled.

For all practical purposes, Lehmann's system lay dormant until the mid-1960s when it was revitalized by Alec Bangham. (Vesicles, in fact, were once referred to as "bangosomes"). Bangham was among the first to appreciate fully what now seems to be a rather obvious fact: Vesicles separate an interior volume from the external solvent by means of a semipermeable barrier (i.e. the lipid bilayer).[9] Substances placed within vesicles can, therefore, be protected (at least temporarily) from the surrounding bulk medium. This, plus the ability to target vesicles to specific biological sites, has stimulated considerable commercial interest. Since prospective uses of vesicles in pharmacology, medicine, cosmetics, diagnostics etc. are discussed elsewhere,[10] little more will be written about them here. Suffice it to state that the mundane lipid is a particularly interesting and useful substance not because of its molecular structure per se but because of its aggregated form. Organized lipid assemblies are, accordingly, ubiguitous in Nature. Even "our souls may reside in fat" (E. Chargaff).

The bulk of vesicle research has employed so-called small unilamellar vesicles (SUVs) or large unilamellar vesicles (LUVs).[11] Both are submicroscopic structures (about 30–50 nm and 100–200 nm in diameter, respectively). A typical SUV preparation is carried out as follows:[12] Lecithin or some other phospholipid (20 mg in 200 μL $CHCl_3$) is placed in a 4-dram vial

Fredric M. Menger was born, raised, and educated in the Northern temperate zone. His fondness for quotes, evident in the text, prompts one from the late rock star Frank Zappa: "I write because I am personally amused at what I do". Realizing that his professorial desk is a dangerous place from which to view the world, he travels extensively to far-flung places, often carrying his blues harmonica with him.

Kurt D. Gabrielson carried out most of the experiments described in this article. He has a BS from Rhode Island College, and he recently received his Ph.D. from Emory. He is now working for the Georgia Pacific Corporation.

F. M. Menger

K. D. Gabrielson

and the solvent evaporated with a stream of nitrogen. The resulting lipid film is then dried under reduced pressure, mixed with 2.0 mL buffer, and sonicated (probe or bath) for up to 15 min at a temperature exceeding the phase-transition temperature of the lipid (70 °C being sufficient for most lipids). Dynamic light scattering can be used to determine the size distribution of the resulting SUVs. LUVs are commonly prepared by rapidly injecting an alcoholic solution of the lipid into buffer.[13] Alternatively, an ether solution of the lipid is slowly injected into a warm aqueous phase where the ether evaporates, and the lipid assembles into large vesicles.[14]

Three disadvantages of SUV and LUV systems are worthy of note. a) Generally, SUVs and LUVs display a rather broad size distribution. This can present a problem if the various sizes within a population do not have identical properties (permeability, spectra etc.). b) SUVs and LUVs, being of small diameter, possess a high curvature compared to the much flatter cellular membranes. Curvature perturbs lipid packing and affects, therefore, the membrane behavior. c) Since one cannot visualize SUVs and LUVs under a light microscope, much information about them is necessarily difficult to obtain. It is not easy, for example, to differentiate SUV fusion from SUV aggregation. Undulation of membrane bilayers is almost impossible to monitor. And SUV/LUV systems do not lend themselves to the studies of injury and healing processes within the membrane. For all these reasons, we decided to switch to so-called giant vesicles that can be directly visualized under the light microscope.

At one time, when we were deeply immersed in SUV/LUV research,[15] we invoked the three famous questions of Kant: What can I know? What ought I do? What may I hope? With regard to the first question, we felt that there were important processes (e.g. membrane injury and healing as mentioned above) that could *not* be properly defined by using SUV/LUV systems. Therefore, in response to the question of what ought to be done, we thought it advisable to shift to giant vesicles. What may be hoped by doing this? That, of course, is a main theme of this paper.

Before proceeding, it might be useful to discuss an important parameter: vesicle size. Table 1 gives, in various units, the diameters of different types of vesicles and biological objects.

Table 1. Diameters of various chemical and biological entities.

	Å	nm	μm	mm
micelle	50	5		
SUV	300-500	30-50		
LUV	1000-2000	100-200	0.1-0.2	
rabies virus	1300	130	0.13	
typhoid bacillus	7000	700	0.70	
red blood cell	7×10^4	7×10^3	7	0.007
amoeba	10×10^5	10×10^4	100	0.10
giant vesicle	0.5 20×10^5	$0.5-20\times10^4$	5-200	0.01 0.20

Since giant vesicles equal or exceed cellular dimensions, they are microscopically visible. Although giant vesicle preparations are usually polydisperse (multisized), this takes on far less significance compared to SUV/LUV systems because, as will be shown, we select and operate on only one giant vesicle at a time. And the size of this vesicle is always known. Since this article is intended to be, in part, a primer on giant vesicles, it is worthwhile to summarize the methods that have been reported for their preparation.

2.1. Drying-Rehydration Method[16]

Phospholipid (1-3 mg) is dissolved in 1 mL $CHCl_3$/MeOH (10:1) in a 5 mL-round-bottom flask. The solvent is then removed by rotary evaporation (keeping the flask as horizontal as possible to maximize the film area). About 5 mL deionized water (or aqueous solution with less than 1 mM salt) is added carefully so as not to disturb the lipid film, and the flask is placed in warm water (70 °C) for 1 hour during which the hydrated film separates from the walls of the flask (Fig. 2). On continued

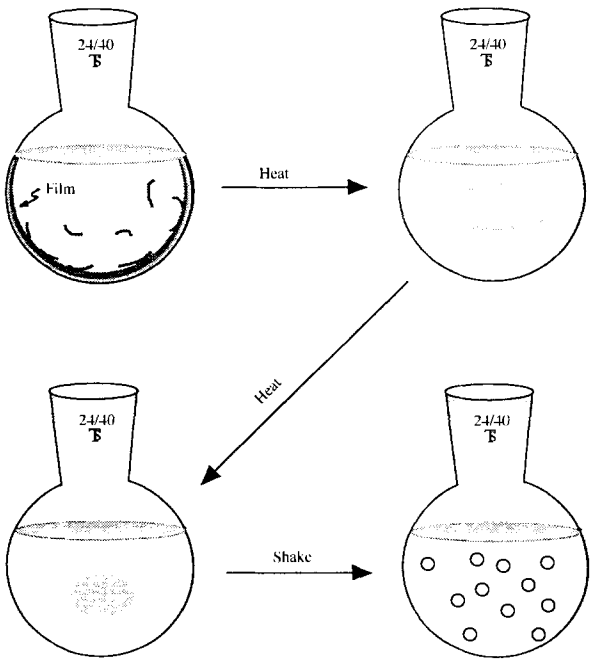

Fig. 2. The drying-rehydration method for making giant vesicles. Phospholipids are often hydrated at 70 °C, whereas 50 °C is sufficient for didodecyldimethylammonium bromide (DDAB).

heating (4 hours to 2 days), the lipid forms a single globule, perhaps 1 cm in diameter, that resembles a translucent sea-creature suspended in water. The flask is removed from the bath and shaken for only a few seconds (no more!) while it is still warm. This causes the globule to disintegrate into a polydisperse collection of giant vesicles suspended in a nearly clear solution. The vesicle size distribution depends upon the incubation time as well as the duration and vigor of the shaking step. Modifications of this procedure are described in the literature.[17]

2.2. Dialysis Method[18]

In this approach, 1-*O*-methylglucoside (200 mg) plus lipid (10 mg) in 400 μL methanol are dialyzed against pH = 7.4 buffer for two days. Giant vesicles are formed under conditions

where their internal contents are continuously hyperosmotic. Diameters range from 10–100 μm. It is claimed that the vesicles are mainly unilamellar (a single bilayer) as opposed to multilamellar (several bilayers in an onionlike configuration). Sodium trichloroacetate can also be used to achieve an osmotic gradient across the bilayer.[19] The dialysis method has an advantage over drying-rehydration in that it can be used with high salt concentrations. On the other hand, possible contamination by the "indifferent solute" is an ever-present concern.

2.3. Freeze-Thaw Method[20]

Giant vesicles are produced from SUV systems, generated in water by sonication, when the latter are repeatedly frozen in liquid nitrogen and then thawed. This method is advertized as being particularly suitable for lipid systems containing proteins because drying-rehydration and dialysis could conceivably denature the proteins.

2.4. Solid Hydration

From our point of view, it was especially important to minimize formation of multilamellar (onionlike) vesicles owing to their complexity. Vesicle fusion, for example, becomes difficult to interpret when multiple layers of varying curvature collectively get into the act. In our hands, all three of the above methods (especially dialysis and freeze-thaw) gave significant populations of multilamellar vesicles with both phospholipids and synthetic surfactants. We discovered, however, a fourth method that gives >90% unilamellar vesicles with a synthetic lipid, didodecyldimethylammonium bromide (DDAB).[4]

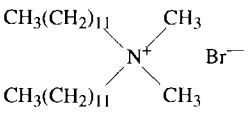

DDAB

In this method, DDAB (0.1–0.2 mg) was placed within a rubber washer (14 mm i.d.) cemented onto a glass slide. The powder was then immersed in 450 μL water and allowed to hydrate. (The amounts of DDAB and water are important; too much DDAB gives multilamellar vesicles; too little DDAB results in only a few vesicles by light microscopy). Hydration begins instantly as seen by wormlike tubules (myelin figures) forming at the surface of the solid particles (Fig. 3). After about five minutes, one observes many grapelike clusters some of which transform into 5–10 μm vesicles. Remaining clusters develop (via a poorly understood fusion process requiring about two hours) into giant unilamellar vesicles. These were easily distinguishable, by phase-contrast microscopy, from the small population of the more opaque multilamellar vesicles. Giant unilamellar vesicles will henceforth be symbolized by GUVs.

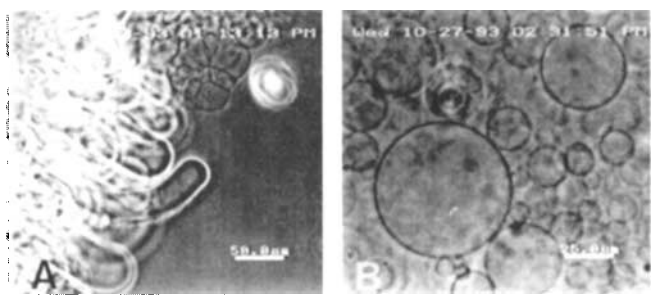

Fig. 3. Hydration of powdered DDAB as observed by phase-contrast microscopy. A: Initial formation of tubules. B: Subsequent formation of giant unilamellar vesicles (GUVs).

The preceding recipe works well for DDAB but not so well for phospholipids. In our experience, the conditions for making GUVs must be worked out individually for each particular lipid and temperature. Since DDAB gave such excellent preparations (even in the presence of additives such as cholesterol), and since the preparations displayed such a variety of cell-like morphological changes, we used DDAB exclusively for our initial studies. There is no reason in principle, however, why our experimental approach cannot be extended to all sorts of lipids, natural and synthetic alike.

Giant unilamellar vesicles, prepared by hydrating solid-state DDAB, are stable for two–three days after which they tend to aggregate. Note that GUVs do not lie in a global energy minimum despite their seemingly spontaneous formation.[21] The global energy minimum is in fact occupied by flat bilayer sheets; energy input is required to impose curvature upon such sheets. Convection currents and vibrations (usually unnoticed) suffice to achieve the mild curvature in GUVs (while, as mentioned, sonication generates high-curvature SUVs). Since GUVs, tubules, and many of their structural variations are all relatively flat, and thus of similar energy, a rich array of interconvertible morphology is possible.

Before continuing, the reader can rightly expect answers to some basic questions, the most important of which is: How do we know that our GUVs are indeed unilamellar (i.e. endowed with only a single lipid bilayer)? This is far from a trivial question as evidenced by the fact that we initially mistook multilamellar vesicles for unilamellar structures. The confusion arose from three sources: a) Literature reports on giant vesicles assume, often without sufficient supporting data, a unilamellar assembly. Initially, we did likewise. b) As mentioned above, unilamellar vesicles are far more desirable than multilamellar vesicles. We should have kept in mind the quote of H. J. Van Till: "The purpose of empirical research is to discover what the physical world is really like, not to verify its conformity to our preferences". c) Finally, as chemists we were novices with the light microscope. The unilamellar issue could not be resolved until we had become experienced in its use.

Vesicles turned out to be invisible by ordinary bright field microscopy because the refractive indices of the vesicle and aqueous medium are too similar. We thus called upon phase-contrast microscopy which is particularly useful in such cases. In phase-contrast microscopy, a hollow cone of light passes through the sample, and in this manner one achieves a variation in brightness across boundaries even when the difference between refractive indices is small. Phase-contrast illumination is easily produced with an inexpensive metal ring that is slipped into the microscope's condenser. Further details of phase-contrast optics can be found elsewhere.[22]

Figure 4 shows phase-contrast photomicrographs of giant DDAB vesicles (ca. 90 μm in diameter at 400× magnification). Although the vesicles are spherical, they appear flat because the microscope's depth of field (1.5 μm with a 40× objective lens)

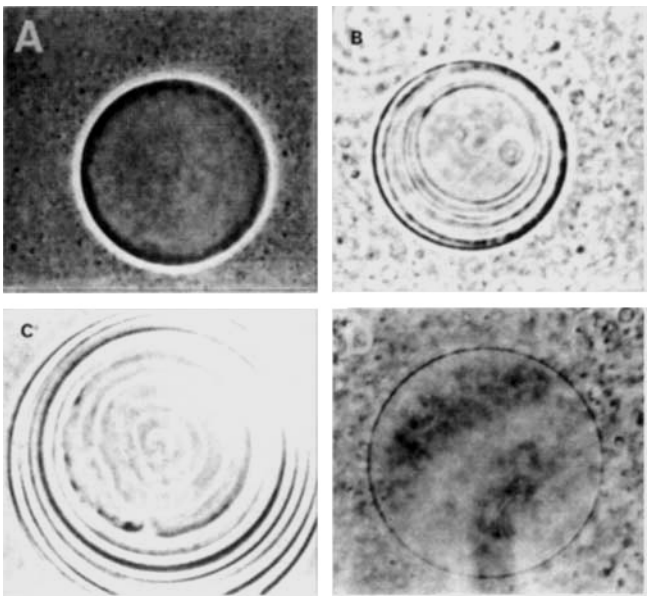

Fig. 4. Phase-contrast photomicrographs of a multilamellar giant vesicle (A), an oligolamellar giant vesicle (B and C), and a unilamellar giant vesicle (D).

is much less than the vesicle diameter. Phase-contrast microscopy can "see" only a narrow slice of lipid at the equator; attempts to focus above or below the equator produce only a blur. A typical multilamellar vesicle is given in Figure 4A. It is readily identified as such by an opacity and texture that differ from the medium surrounding the vesicle. The vesicles in Figures 4B and 4C are also multilamellar, but the layers can actually be resolved because they are, in this case, less densely packed. Finally, Figure 4D shows a giant unilamellar vesicle, the type that is most desirable for membrane research.

A lipid bilayer, being only about 40 Å thick, is obviously impossible to see by light microscopy. Thus, the dark ring in Figure 4D is an optical effect; in no way does it portray the actual membrane thickness. Similarly, light microscopy cannot differentiate between a membrane composed of a single bilayer (a true GUV) and a membrane composed of a few bilayers. Although the distinction makes little difference from the point of view of our experiments, we believe that true unilamellar vesicles are indeed formed for the following reasons: a) When GUVs are chemically or physically destroyed, the ring disappears as a unit, leaving no visible inner ring. (In contrast, multilamellar vesicles are often seen to "peel off" their layers one by one). b) Published cryoelectron micrographs on vesicles similar to those in Figure 4D suggest the presence of a single-layered configuration.[23] c) So-called bilayer lipid membranes (BLMs), in which a 60–100 Å film spans a 1 mm hole in a Teflon plate,[24] prove that one or two bilayers are capable of maintaining structural integrity over macroscopic distances.

3. The Literature

When the plan of studying giant vesicles was first initiated, we knew little about how to prepare, observe, and manipulate them. "Between the idea and reality stands the shadow" (T. S. Elliot). Past work of others helped illuminate the "shadow". Among the rather limited literature on giant vesicles, a few articles stand out as having been particularly relevant to our work. These will now be reviewed briefly.

Mueller et al.[25] published early experiments on giant vesicles prepared (by the dehydration-rehydration method) from brain lipids, egg lechithin, and synthetic phospholipids. A number of points are of interest: a) The vesicles can be made in distilled water and in solutions of non-electrolytes but not in salt solutions where the lipids precipitate. b) After growing in size for several days, the vesicles are stable for weeks. c) Vesicles can be fractionated according to size by centrifugation in specially designed tubes. Apparently, the giant vesicles can survive 40000 g for 30 min (our DDAB vesicles being too fragile to tolerate such abuse). d) Vesicles made in distilled water seem to be under osmotic stress (of unknown origin) because physically rupturing them causes interior contents to be rapidly expelled. e) Finally, and this is important, the micrographs of Mueller et al. were obtained by dark-field microscopy. This technique (which, like phase-contrast, uses a special attachment in the condenser) portrays the vesicles as a ring of light in an otherwise dark field (Fig. 5). In our experience, such a ring of light is seen primarily with multilamellar vesicles. One should resist the temptation to assume that a single shell in dark-field microscopy necessarily signifies a unilamellar structure.

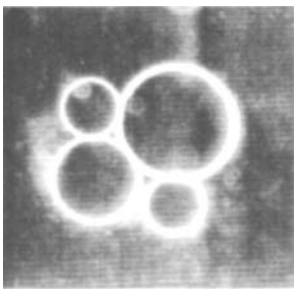

Fig. 5. Dark-field photomicrograph of giant multilamellar vesicles.

Zimmerman et al.[26] observed by light microscopy an electric-field-induced fusion of giant vesicles prepared from a 1:1 mixture of a cationic lipid and cholesterol. Application of an alternating electric field (200 Vcm^{-1}, 100 kHz) first caused the vesicles to move into direct contact with each other (Fig. 6). The fusion process, requiring about one second, was initiated by turning off the AC field and subjecting the sample to a 3–9 $kVcm^{-1}$ field pulse of 20–50 μs duration. The electric breakdown of the membrane creates, it is postulated, large numbers of aligned pores in the contact zone (Fig. 6). Reorganization of lipid then bridges the

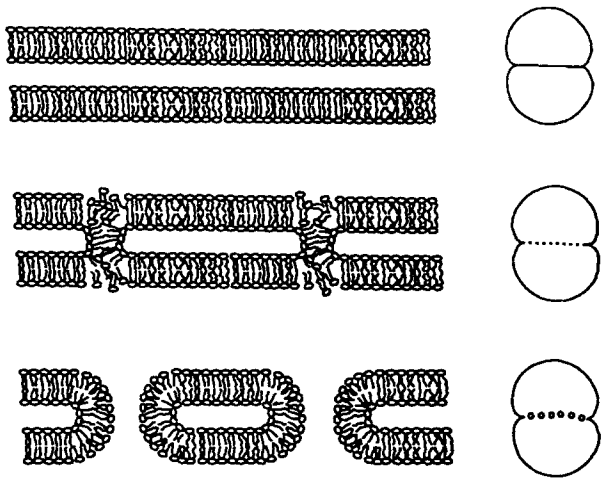

Fig. 6. Fusion induced by an electric field as adapted from ref. [26].

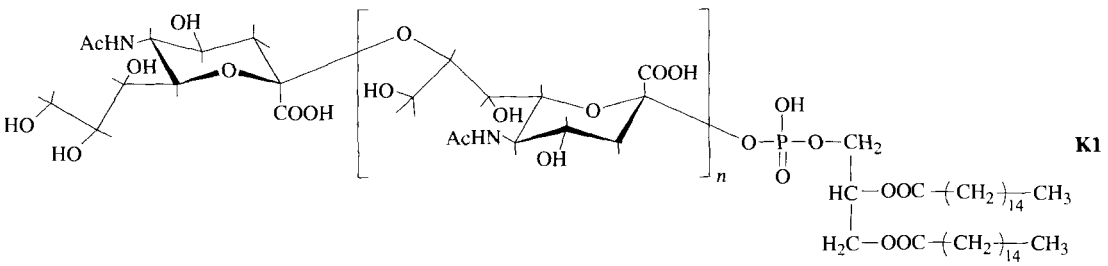

K1

two giant vesicles while simultaneously creating microscopically invisible SUVs that become trapped within the new vesicle.

The research group of H. Ringsdorf[27] injected a polysaccharide, isolated from *E. coli* and called K1, into a giant vesicle preparation. It was found that K1 inserts itself into the vesicle bilayer (presumably by means of K1's lipid moiety). Proof for binding of K1 to the vesicle was obtained by adding a fluorescent-labeled anti-K1 antibody to the preparation. Fluorescent microscopy showed giant vesicles with brightly fluorescent peripheries, clearly indicating that the antibody had concentrated itself at the external membrane surface. In the absence of K1, the antibody fluorescence remained distributed uniformly throughout the aqueous medium.

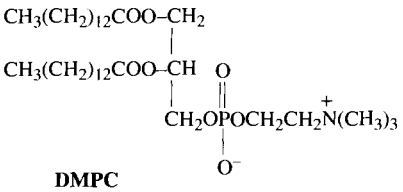

DMPC

It should be mentioned that the above work is only one of several beautiful experiments described in reference [27]. The 1988 review (which also discusses endocytosis, hole formation, vesicle domains, and polymerization processes) is "must" reading for anyone entering the field of giant vesicles. We ourselves owe it a special debt.

Among the diverse membrane papers of E. Sackmann, one finds a few devoted to the giant vesicle. Four experiments in particular will be mentioned here:

Experiment 1:[28] Giant vesicles were prepared from the quaternary ammonium lipid **1**, which has a phase-transition temperature of 42 °C. (A phase-transition temperature is the point at

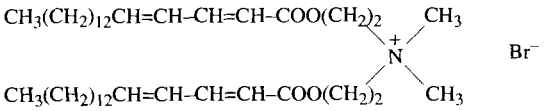

1

which a lipid transforms from a highly ordered gel state to a more disorganized liquid crystalline state). The normally spherical vesicle took on a discoid shape at 42 °C (Fig. 7). When the temperature was raised to 42.5 °C, the form of the vesicle changed to a "bowling pin", while at 41.5 °C the vesicle invaginated to a crescent. This extreme sensitivity of morphology to temperature was not observed in our experiments with the related DDAB vesicles. Membrane morphology obviously depends upon lipid structure in ways that are not yet understood.

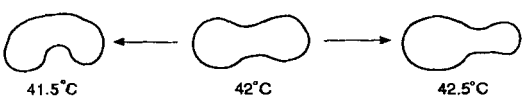

Fig. 7. Shape transformations in a giant vesicle composed of a synthetic lipid as the temperature is raised and lowered 0.5 °C above and below the phase-transition temperature of 42 °C [28].

Experiment 2:[29] Giant vesicles were prepared from a 4:1 mixture of dimyristoylphosphatidylcholine (DMPC) and a polymerizable phospholipid **2**. When polymerization was induced by UV irradiation, the vesicles were seen to invaginate

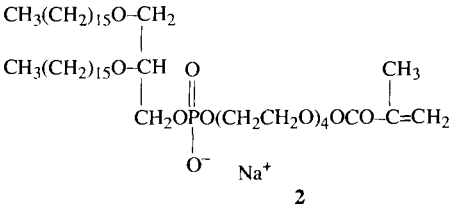

2

(a photochemically-induced endocytosis, Fig. 8). The explanation given for the phenomenon rests on two assumptions: a) Polymerizable lipid is of slightly higher concentration in the outer leaflet of the membrane bilayer than in the inner leaflet

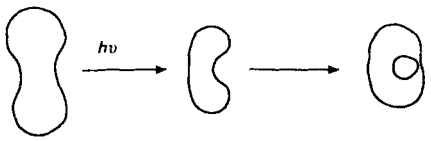

Fig. 8. A photochemically induced "endocytosis" with a giant vesicle composed of a 4:1 mixture of dimyristoyphosphatidylcholine (DMPC) and a polymerizable phospholipid [29].

(the former possessing slightly more room for the bulky headgroup). b) Polymerization decreases the area per molecule. If both factors are operative, polymerization will shrink the outer leaflet more than the inner one, and the composite bilayer will, therefore, distort inwardly. Svetina and Zeks,[30] in a classic article, were the first to propose that alterations in bilayer curvature arise because the two-component leaflets of a bilayer expand and contract independently from one another. We will have occasion to call upon this concept later on.

Experiment 3:[29] A vesicle composed of pure DMPC was shown to go from a spherical shape to an invaginated state and then to a two-vesicle form (Fig. 9) when the coverglass, resting

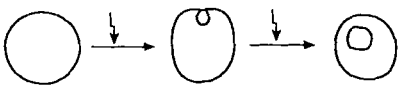

Fig. 9. Effect on a DMPC giant vesicle when the coverglass is lightly tapped [29].

on the sample, was lightly tapped. It was correctly argued that this experiment demonstrates the metastability of vesicle morphologies. One important question was not addressed however: Is the shape transformation (in this case triggered by mechanical agitation) seen frequently or is it a rare occurrence? We pose this question because in our experience many bizarre morphological events occur only infrequently, so that publishing their pictures without some statement as to their "probability" can be misleading.

The study of the physically induced vesicle transition is instructive for another reason. Vesicle preparations in experiment 3 were examined as thin films placed between a slide and a coverglass. We have avoided handling samples in this manner for two reasons: a) It is desirable to minimize vesicle/glass interactions especially those that might crush vesicles between two glass surfaces (recall that GUVs can have diameters of 0.2 mm or larger; see Table 1). b) We planned to manipulate our vesicles (i.e. move them about, inject into them etc.) much the way cytologists handle living cells. This precludes the use of a coverglass. Since uncovered thin films evaporate quickly, we invariably used a thick aqueous sample placed within the confines of a circular "wall" (details to be given later). A more sophisticated setup that accomplishes the same thing is given elsewhere.[31]

Experiment 4:[31] Shape transformations of DMCP GUVs in ion-free water were studied as a function of temperature (Fig. 10). The morphologies portrayed in Figure 10 occurred in

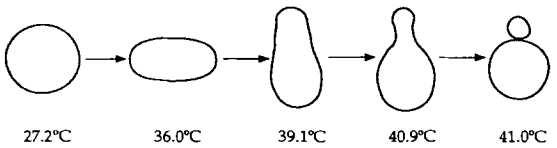

Fig. 10. Shape transformations of a DMPC GUV in ion-free water as a function of temperature [31].

35 out of 98 vesicles when "lateral stress" (of uncertain definition) was exerted upon the vesicles prior to heating. The GUVs changed from spherical (27.2 °C) to an ellipsoid (36.0 °C) to various pear-shapes (37.5–40.9 °C). All these morphologies were stable and reversible. A further temperature increase of 0.1 °C to 41.0 °C destabilized the pear-shape and created what appears to be an attached "bud" on the verge of becoming a separate daughter vesicle. Even more exotic transformations were observed but will not be detailed here. Suffice it to say that the shape transitions are qualitatively explainable in terms of the Svetina–Zeks model[30] in which the two component leaflets of the bilayers have slightly different thermal expansivities.

A degree of caution is necessary whenever vesicle morphologies are studied. It must never be forgotten that phase-contrast microscopy detects only a thin band around the equator of the vesicle. Consequently, it is possible to confuse a "sphere-to-pear" transition with a 90° rotation of a pear-shaped vesicle (Fig. 11). Similarly, a 90° rotation could be mistaken for a transition from an invaginated vesicle to a "vesicle inside a vesicle" (Fig. 11). Such ambiguity can be resolved by demonstrating the reversibility of the transition; it is unlikely that 90° rotations coordinate themselves with medium conditions as the latter switch back and forth between two states.

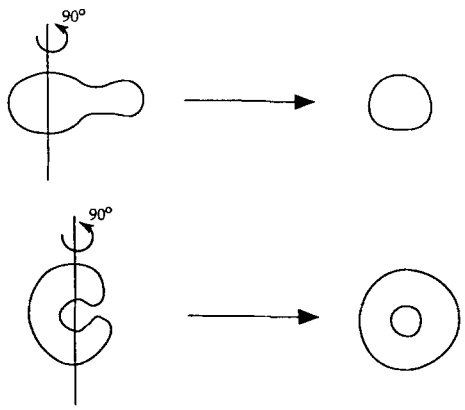

Fig. 11. Apparent shape changes in phase-contrast microscopy that arise from rotations rather than from true morphological changes.

The ingenious studies of giant vesicles by Evans and Needham[17, 32] can serve as a fitting conclusion to this historical section (which is by no means intended to be an all-inclusive review). Evans and Needham aspirated a 20 μm GUV with a 5 μm micropipet under a suction pressure of 0.03 atm or less. This caused the vesicle to be partially drawn into the pipet (Fig. 12) with a concomitant increase in the membrane area (as measured indirectly from the membrane projection length inside the pipet). Two types of experiments were performed: a) The suction pressure was increased at constant temperature. b) The temperature was increased at a fixed suction pressure. These experiments provided two thermoelastic coefficients: the compressibility modulus K and the thermal expansivity α. A few specific results, cited below, illustrate the power of the method.

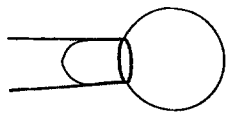

Fig. 12. Aspiration of a 20 μm GUV into a 5 μm pipet under a suction pressure of 0.03 atm or less [32].

When a GUV is cooled at constant pressure from above to below the phase-transition temperature, the membrane contracts abruptly by about 20%. In addition, the compressibility modulus increases dramatically. For example, the K value for DMPC (with a transition temperature of 24 °C) increases from 150 dyn cm^{-1} at 29 °C to 855 dyn cm^{-1} at 8 °C. Adding equimolar amounts of cholesterol to the DMPC at 29 °C increases the K value from 150 dyn cm^{-1} to 685 dyn cm^{-1} even though the membrane remains fluidlike (i.e. in its liquid-crystalline phase). Cholesterol apparently forms a tight complex with DMPC that greatly reduces the bilayer compressibility relative to a bilayer of pure DMPC above its transition temperature. Evans and Needham were also able to detect the presence of a "rippled membrane phase" from an unusually short projection length in the mircopipet at low tensions. A ripple phase has a corrugated structure with the lipid chains lying perpendicular to the overall membrane plane.

As is evident from the references cited thus far, the great majority of the giant vesicle work has appeared in the biochemical and biophysical literature. Chemists, especially organic chemists such as ourselves, have paid comparatively little attention to giant vesicles. In attempting now to publicize the topic to the chemical community, we face a severe communications problem, a problem stemming in part from the fact that giant

vesicle research is a composite of chemistry and biology. Whereas chemistry contributes its simple and defineable experimental conditions (composition, concentration, etc.), biology contributes a particular brand of data reporting (photography). As a result of the latter, chemists are (at least for the moment) denied the graphs, tables, equations, and spectra they love so well. Nonetheless, we ask that chemists resist exclaiming "This is not chemistry!" What else but chemistry could it be when, for example, a giant vesicle, prepared from a compound purchased from a chemical supplier, divides in two after being exposed to a synthetic surfactant? Eventually, of course, we will yield to reductionism and discuss our "chemical systems"[1] on more molecular terms. But before this can be accomplished, the fundamental behavioral modes of our membrane models must first be observed and recorded. Occasionally, explanations will be set forth here at the molecular level, but the reader will likely find them rather primitive. Remember, however, that we are at an early stage of understanding and that, at the moment, many problems in vesicle chemistry are, as J. Wiesner would say, "just too complicated for rational, logical solutions. They admit of insights, not solutions".

4. The Light Microscope

"The ladder of natural systems consists of elementary particles, atoms, molecules, macromolecules, cell parts, cells, organs, organisms, populations, and ecosystems" (R. Wesson). In the main, elemental particles have been the province of physicists; molecules the province of chemists; macromolecules the province of biochemists; and cells the province of cytologists. This division of labor is becoming increasingly obscure. Inevitably, as a particular level of science matures, the adventurous seek out the next higher level of complexity. Those who do so are of the same temperament as Thomas Lincoln who once remarked to his son (Abe) that people should move their homes as soon as they can see the smoke from their neighbor's chimney. Chemistry provides as good an example as any of this relentless move up the complexity scale. Thus, one hears more and more at chemistry conferences about DNA, antibodies, and receptor sites. The present paper recommends that chemists take a two-step jump from molecules to cell parts. A recommendation is hardly necessary because chemists have already applied their familiar methods (NMR, ESR, kinetics etc.) to membrane systems. What is unusual, however, is the suggestion that chemists befriend that old workhorse of the cytologist, the light microscope.

Those who have a mere passing interest in the subject of cytomimetic chemistry will wish to skip this section on light microscopy and move directly to the subsequent results section. But those who might be tempted to actually enter the field should read the following brief remarks on the light microscope. The light microscope has, in recent times, been upstaged by other techniques, but "it is not widely known outside the biological community that a renaissance and a revolution in light microscopy are now underway".[33]

Our laboratory is equipped with two instruments: A Leitz Laborlux S standard light microscope and a Nikon Diaphot-TMD inverted light microscope. The latter style, possessing the lens assembly below the stage and illumination above it, allows for easier micromanipulation of the vesicles (discussed later) and for less interference problems when water condenses on the coverslips at reduced temperatures.

Both microscopes are fitted with 10× ocular lenses. The objective lenses have four recommended features: a) They are specifically manufactured and sold for phase-contrast work. b) They are flat-field or PLANO to reduce the curvature of the field and thus bring into focus both the central portion and periphery of the image. c) They are achromatic which means they are corrected for one wavelength (yellow-green) with respect to spherical aberrations. Owing to this feature, a green filter is always placed in the path of illuminating light source. d) They are long working-distance lenses as required for our thick vesicle samples. The four features, specified when purchasing the lenses, are not recommended for high-quality bright-field, cross-polarizing, or fluorescence microscopy.

The microscope condensers, which focus the light onto the sample, are universal in the sense that they can handle many forms of light microscopy. Since their iris is always wide open in phase-contrast microscopy, the condensers are never touched once they are initially centered and focused.

Each objective lens is associated with a numerical aperture (NA) at the time of its manufacture. Our NAs vary from 0.25 to 0.55. Two important parameters, the resolution and depth-of-field, depend upon the NA value. Resolution can be defined as the smallest distance between two points that can be distinguished. According to the Rayleigh equation,[34] the greater the NA, the better the resolution. Note that objects smaller than the resolution can be detected but not in any detail. Resolutions of our various objective lenses vary from 0.52 μm to 0.87 μm.

Depth-of-field can be regarded as the distance from the nearest image plane to the farthest image plane that remains in acceptable focus. Depth-of-field can play a role, for example, in the study of a small vesicle departing from the inside of a larger one. As the depth-of-field diminishes, it becomes increasingly unlikely that the small and large vesicle will reside in the same image plane and thus both be in focus. Although a large NA enhances resolution, it decreases the depth-of-field, thereby making focusing more troublesome. For example, NA = 0.25 and DF = 8.5 μm; NA = 0.55 and DF = 1.5 μm. Working with light microscopes teaches the principle of compromise.

The light microscope can be used with an array of optional peripheral equipment (Fig. 13). Special mention should be made of a solid-state camera that is inserted into a microscope port made for that purpose. The camera's signal is sent to an Argus 10 image processor that digitally enhances images to give greater contrast. It also provides a "zooming" capability so that a 400× magnification becomes an 800× or 1600× magnification. The block diagram in Figure 13 also includes a VCR for making video tapes in real time, a monitor for viewing images on a screen, and a printer for making "stills". One should not be intimidated by the apparent complexity of Figure 13. All components are commercially available, attached quickly to the system, and easy to use.[35] Simple refocusing and stage repositioning are the main skills necessary to track "unidentified swimming objects".[36]

One of the major advantages of GUVs over their submicroscopic cousins is that they can be micromanipulated just like

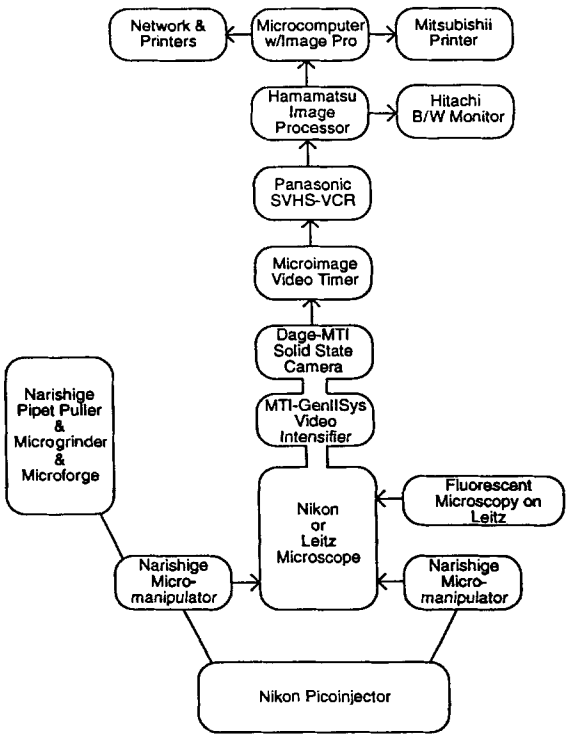

Fig. 13. Block diagram of video microscope setup and peripheral equipment used in our work. Many GUV experiments can, however, be carried out with a simple microscope equipped with a phase-contrast attachment and a Polaroid camera.

cells. Micropipets as small as 1000 Å in diameter can be made with a commercially available "pipet puller". A vertical glass capillary, weighted at the bottom end with suspended metal blocks, is threaded through an electric coil at the top end. When the switch is turned on, the hot coil melts the capillary section within it, the weights come crashing down, and the capillary is pulled into a narrow-diameter pipet. The pipet can be further fashioned with a microgrinding wheel or with a so-called microforge. The latter allows one to polish the end of the pipet or to bend it into any desired shape.

Micropipets were useful to us primarily for holding vesicles in place and for injecting into them. Holding pipets have large smooth ends that can latch onto a GUV when a slight suction is applied. Injection pipets are much smaller in diameter than the vesicles and are ground to a sharp point. Administration of both suction through an empty pipet and pressure on a filled pipet was carried out with a "picoinjector" hooked to a tank of nitrogen. A picoinjector can supply orders of magnitude less liquid than the nanoliter volume of a typical GUV.

Micropipets were directed toward a desired point in the microscope's image with the aid of a micromanipulator. This device, fixed to the microscope's stage, has a "joy-stick" that provides extremely small movements to the end of an attached pipet. All the micromanipulation techniques described here are commonplace in cytology.

Mention has already been made of sample preparation by the DDAB hydration method (see Section 2.4). The hydration took place within a rubber washer (14 mm i.d.) cemented onto a glass slide. Sufficient sample (0.45 mL) was used to fill the washer and to minimize the amount of air between the sample and the coverglass resting upon the washer. Coverglasses reduced evaporation and surface vibrations of the sample. Of course, when micromanipulation was desired, a coverglass was not possible. A simple homemade thermostated stage was installed when temperature control was necessary.

This concludes the background information pertinent to the subject of cytomimetic chemistry. Individual tastes and needs will dictate whether too much or too little detail has been provided. Either way, the time has arrived to inspect actual photomicrographs and view first-hand the intricacies of membrane behavior. Most of the photomicrographs in the next section have not been published previously.

5. Experimental Results

Our experimental results have been categorized below into various cytomimetic processes (aggregation, fusion, fission, etc.). Each process is portrayed by a series of still photographs selected from video films produced by the microscope setup. Admitedly, viewing the still photographs is like looking at a Mickey Mouse film one frame at a time. Fortunately, however, vesicle behavior can in fact be reasonably well described with still photographs as long as they span a suitable time period. This is not to say that nothing has been sacrificed by the unavoidable shift from a dynamic to a semistatic representation. No still photograph can, for example, elicit the delight of seeing, in real time, an entire vesicle fusion or fission. And no still photograph is likely to instill a sense of wonder of the type that once caused a visiting scientist to exclaim: "How do you make those cells do that?" Those "cells", we then revealed to the visitor, had been made from a compound purchased from Eastman Chemicals; and they do what they do because of simple chemical and physical stimuli.

5.1. Hydration

We have already described how hydration of lipid films leads to the production of giant vesicles (see Fig. 2). In our hands, this method led mainly to multilamellar vesicles (which is one reason why the solid-state hydration, pictured in Figure 3, was developed). It turns out that giant multilamellar vesicles, prepared by the drying-rehydration method, also tend to form unilamellar vesicles if allowed to sit around and hydrate for several days. This hydration process was examined under the microscope (Fig. 14).

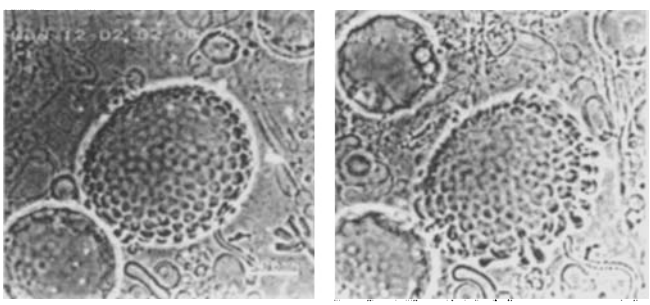

Fig. 14. Phase-contrast photomicrographs of a giant multilamellar vesicle hydrating to give, eventually, small unilamellar vesicles. Left: after 2.5 h. Right: after 4.5 h. Scale-bar in the bottom-right of photographs = 100 μm.

Multilamellar vesicles are seen first to "blister" at their outer shells. These blisters then grow into tubules that project radially from the vesicles' outer surface. Ultimately, the tubules break off to become unilamellar vesicles. Thus, one-by-one the layers of the multilamellar vesicles are eroded into GUVs. The apparent instability of multilamellar vesicles relative to their unilamellar counterparts may stem, in part, from electrostatic repulsion between the concentric DDAB layers within the onionlike configuration.

5.2. Aggregation

A. Einstein once wrote, "The only apparatus necessary for observing Brownian motion is the microscope, and it need not even be a particularly good one". Similarly, a simple microscope is all that is required to visualize vesicle aggregation. One merely adds low levels of Na_2SO_4 (1.0mM) to a sample containing widely spaced giant vesicles. Over the course of several minutes, the vesicles will assemble into clumps (Fig. 15). Note that this experiment, carried out early on in our research, used dark-field microscopy rather than the phase-contrast microscopy that we now prefer.

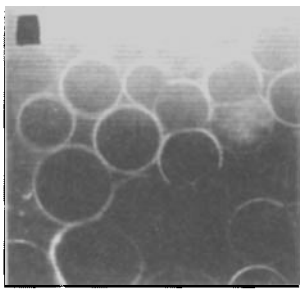

Fig. 15. Dark-field photomicrographs of sulfate-induced aggregation of giant vesicles. Prior to addition of sulfate, there were only three vesicles in the microscopic field.

The aggregation process is viewed as an electrostatic neutralization of the long-range double layer repulsion among the vesicles.[37] Dianionic sulfate can, apparently, serve as a far more effective "adhesive" than can the bromide counterion of DDAB (Scheme 1).

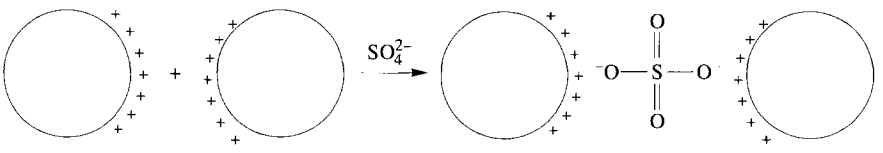

Scheme 1.

No sulfate-induced fusion was seen with the GUVs although this has been reported with vesicles only 80 nm in diameter.[38] Small vesicles have a high curvature and might be expected to show a greater propensity to fuse than the GUVs. One is reminded of the so-called "Ostwald ripening" in which large colloidal droplets grow at the expense of small ones.[39] Interfacial tension within the small droplets drives the coalescence. The absence of fusion with the sulfate-treated GUVs suggests that sulfate is unable to bring the vesicles sufficiently close together to overcome the "hydration repulsion" as would be necessary for fusion. Hydration repulsion reflects the need to desolvate headgroups prior to phase instability in the membrane.[40]

5.3. Fusion

If it were not for barriers to membrane fusion, humans would, like slime mold, exist as multinucleated masses of protoplasm. And if it were not for mechanisms that trigger fusion, many important biological events (infection, fertilization, conjugation etc.) would not be possible. Little wonder that fusion is a recurrent theme in treatises on membrane behavior. Unfortunately, a footnote number is the only homage we can give to the immensely fertile literature on membrane fusion.[41] Space restrictions force this embarassingly rapid trek through the subject of fusion in which the focus lies entirely on our own cursory experiments.

5.3.1. Physical Constraint

Two giant vesicles can be forced into intimate contact with the aid of holding pipets under slight suction (Fig. 16). Note that in the left photograph, the lefthand vesicle becomes distorted by the pressure from its neighbor. Moreover, when the vesicles are separated, the lefthand vesicle in the right photograph is pulled, however slightly, into an oval shape. The shape then restores itself instantly into a sphere. Despite the obvious close proximity of the vesicles, no fusion occurs for periods up to an hour. Fusion can be induced chemically (as we shall see next) but not physically.

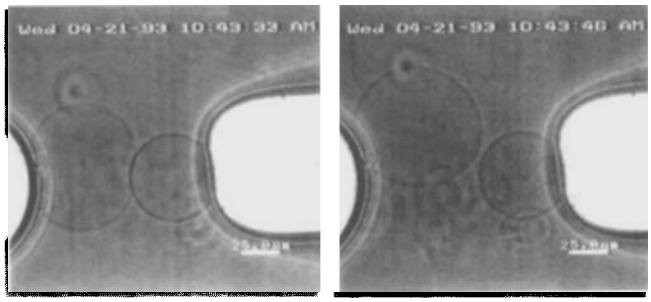

Fig.16. A failed attempt at physically inducing fusion in two DDAB giant vesicles. The vesicles were manipulated by means of holding pipets under slight suction. In the left photograph, the vesicles have just been pulled apart, an action that caused slight distortion in the lefthand vesicle.

5.3.2. Acetate-Induced Fusion

A remarkable sequence of events was observed when 100 μL of 0.25 M NaOAc was added, in tiny portions without stirring, to a sample of giant multilamellar vesicles (0.45 mL of 9×10^{-4} M DDAB; drying-rehydration method). First, the vesicles began immediately to disintegrate. In the course of 20 minutes, the vesicles deteriorated into structureless masses that eroded into submicroscopic material to give, finally, an absolutely clear microscopic field. (This vesicle disappearance was anticipated because didodecyldimethylammonium acetate is a highly water-soluble compound that does not form giant vesicles). But a peculiar thing happened when the samples were kept at or below

the DDAB phase-transition temperature of 17 °C. Small "globules" reappeared and began to speckle the microscopic field. The term globule is used because the structures were too opaque to be multilamellar vesicles. Whatever their exact morphology, the DDAB globules fused at a prodigious rate. Figure 17 shows

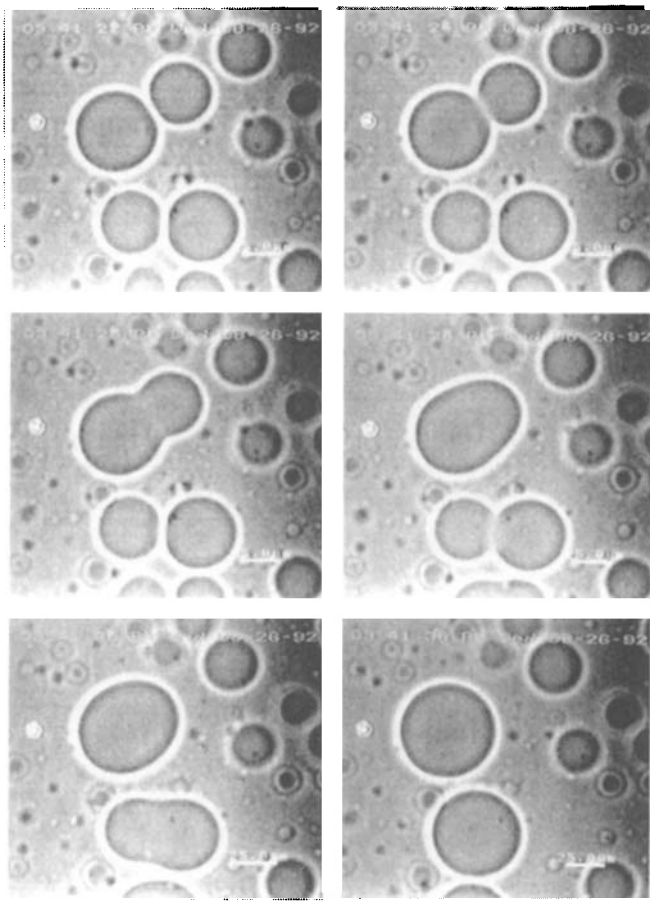

Fig. 17. Phase-contrast micrographs of an acetate-induced fusion taking place over a few seconds. Scale-bar = 25 μm.

a sequence in which two globules, after having resided side-by-side for many minutes, suddenly fused over the course of a few seconds. The fusion was reproducible in several experiments.

One cannot attribute the vesicle disappearance solely to osmotic stress since the effect was salt-dependent (being caused by acetate, fluoride, and hydroxide but not chloride). Two notions, however satisfactorily explain our observations: a) Strongly hydrated anions, such as acetate, bind relatively loosely to cationic surfaces.[42] b) According to the Svetina–Zeks model,[30] the coupled leaflets in a bilayer can act independently. Thus, when excess acetate is added externally to the DDAB vesicles, acetate exchanges with bromide to produce an outer leaflet that is more highly dissociated from its counterions. Owing to the resulting headgroup headgroup repulsion, the outer leaflet expands relative to the inner one. Such asymmetry would be expected to increase curvature[43] and, therefore, promote the expulsion of small vesicles and the eventual disappearance of microscopically visible structures (Scheme 2).

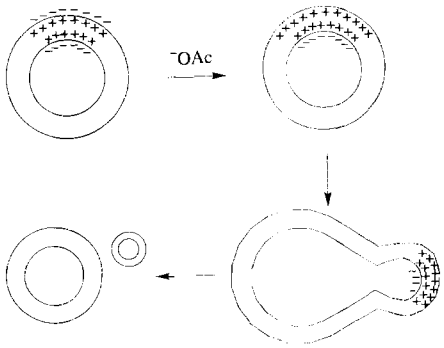

Scheme 2.

5.3.3. DPA-Induced Fusion

Engberts et al.[44] have reported that the dianion of dipicolinic acid (DPA) causes 3000 Å DDAB vesicles to fuse into vesicles 2–3 μm in diameter. The behavior of DPA is reminiscent of the well-known fusogenic effect of the Ca^{2+} ion on negatively charged vesicles.[45] Owing to the affinity of Ca^{2+} ions for anionic lipid, the Ca^{2+} ion enforces a vesicle/Ca^{2+}/vesicle association. The resulting surface dehydration and vesicle proximity trigger a fusion.

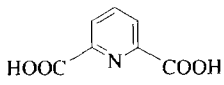

DPA

DPA (25 μL of 5 mM; pH adjusted to 7.0 with NaOH) was added to a vesicle preparation obtained by solid-state hydration. Scattered among the resulting GUVs were globules of undefined morphology that underwent rapid DPA-induced fusion (Fig. 18). The GUVs, on the other hand, converted from rigid spheres into floppy irregular enclosures (Fig. 19). Picolinic acid, with only one carboxylate, had no such effect.

We can only conjecture on the molecular basis for the loss of structural rigidity in the GUV membranes. One possibility is

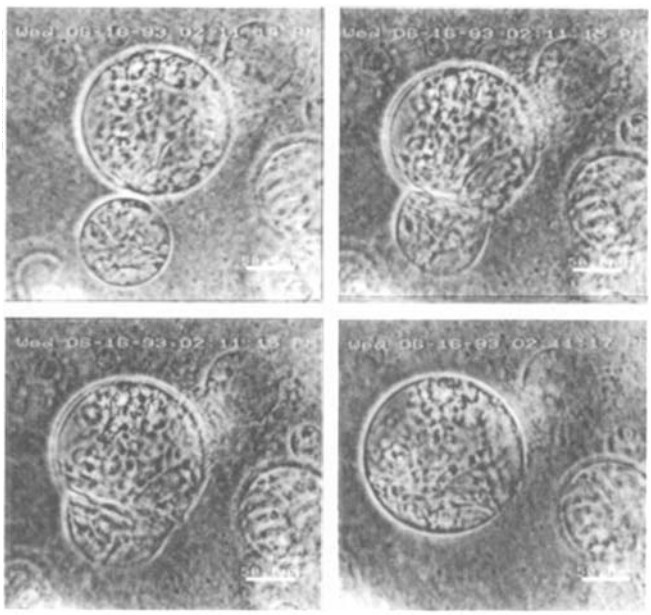

Fig. 18. Phase-contrast micrographs of a DPA-induced fusion of DDAB vesicles of unknown structure. Scale-bar = 50.0 μm. Process took place in less than four seconds.

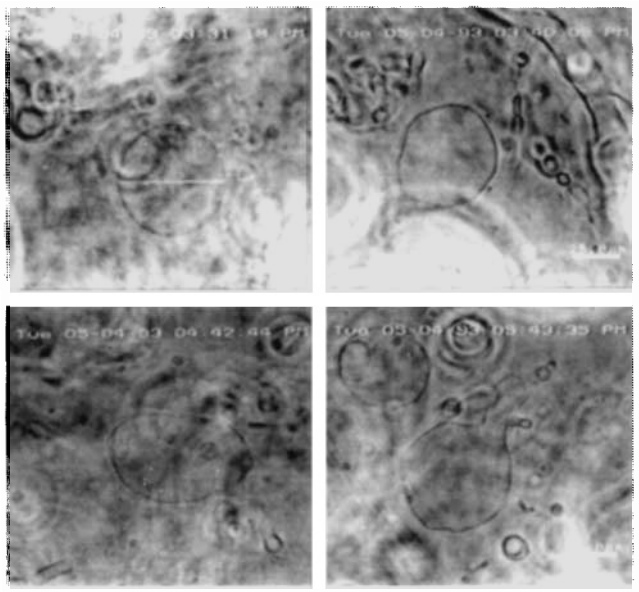

Fig. 19. Effect of DPA on DDAB GUVs. Top left to top right: 10 min. Top right to bottom left: 1 h. Bottom left to bottom right: 1 h.

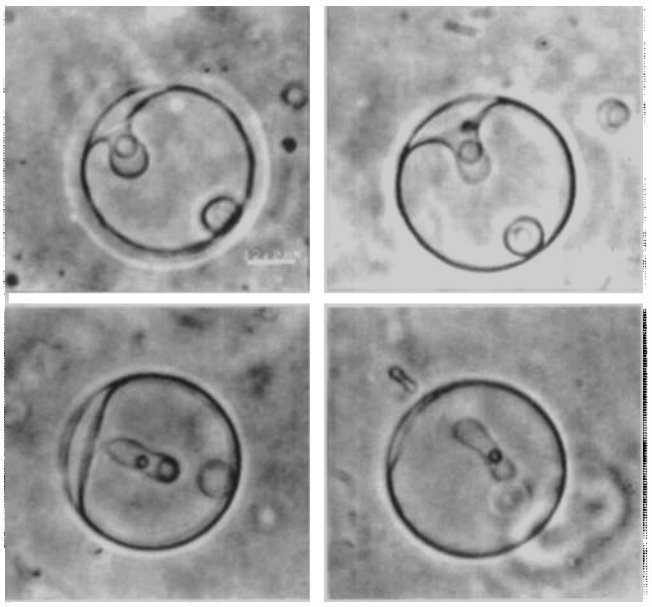

Fig. 20. Giant unilamellar vesicle undergoing a DPA-induced endocytosis over the course of about 30 min. Process was seen repeatedly but with only the occasional vesicle.

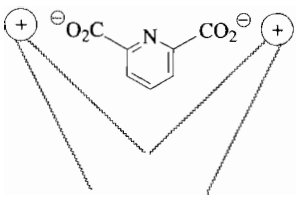

Scheme 3.

that the DPA incorporates itself into the headgroup region and spreads the lipid molecules apart (Scheme 3). Since the lipid packing is thereby loosened, distortions from the usual spherical shape become feasible. A second possibility relates to the fact, often observed in our work, that the GUVs seem to be under osmotic tension (i.e. internal pressure that inflates the vesicles). The source of the tension in the absence of any added salt is not yet understood. In any event, the DPA may render the vesicles permeable to water and small molecules, thus allowing pressures to equilibriate and vesicles to deflate.

5.4. Endocytosis

In many experiments with DPA, we saw an occasional GUV undergoing a process remarkably similar to cellular endocytosis (Fig. 20). A giant vesicle begins to engulf a smaller vesicle, and after about 30 minutes the smaller vesicle is completely "eaten". No doubt the DPA promotes the endocytosis by enhancing the membrane flexibility. One wonders what sort of endocytosis-stimulating substances are produced by an amoeba when it senses an edible morsel in its vicinity. Or how a virus manages to persuade a host cell to allow it to enter.

By now it should be obvious that a pattern is developing. We are enumerating wonderful morphological changes in a simple nonbiological membrane. But the readers are not being supplied with the molecular basis of these changes except at the most rudimentary level. There should never be an apology for the lack of detail when an area of science opens up and the investigation has only touched the surface. The pleasure of discovery in science derives not only from an incisive analysis but from the formulation of a problem which, according to A. Einstein, is "often more important than the solution". New observations leading to unanswered questions, unsolved puzzles, fresh possibilities, and untried experiments – that is what this paper is all about. In essence, we have taken the advice of R. Hoffmann: "Row a boat into that tall mysterious grass just because you have heard a strange bird call there". In our case, the "mysterious grass into which we rowed" is the world of chemical microscopy, and the "strange bird calling us" is the giant vesicle with all its amazing transformations.

5.5. Fission

Fission was of particular interest to us because the combination of fission, growth, and fission again is equivalent to self-replication, a long-range goal of ours (Scheme 4). As will be shown, fission has indeed been achieved but not the "one-vesicle-into-two-equal-vesicles" as would be ideal for a self-replicating process.

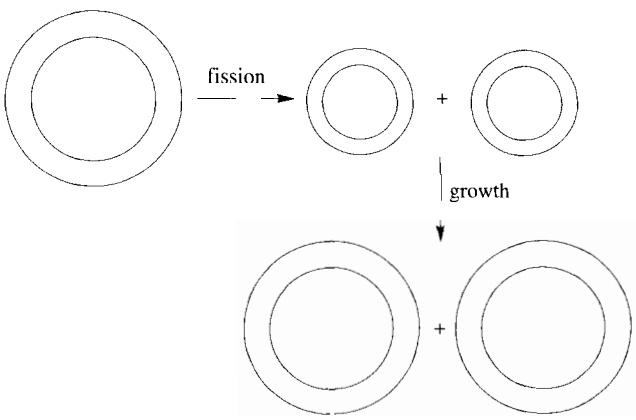

Scheme 4

5.5.1. Mechanical Agitation

Figure 21 represents an attempt to inject a sharp micropipet into a vesicle being held by a holding pipet under slight suction. This was an early experiment, and at the time we did not realize that the giant vesicle was multilamellar. In any event, the injecting pipet (being controlled by a micromanipulator fixed to the

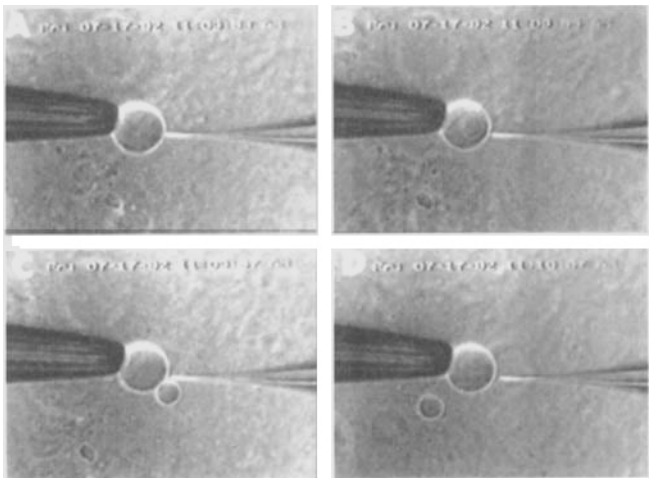

Fig. 21. Thigmatropic fission in which prodding of a multilamellar vesicle causes the formation and release of a smaller vesicle. The parent vesicle is held in place by a holding pipet, while a sharp pipet, controlled by a micromanipulator, prods the vesicle surface.

microscope stage) experienced great difficulty in penetrating the vesicle. Eventually, the prodding caused a new smaller vesicle to form. We surmise that the outermost bilayer of the multilamellar vesicle had been physically damaged by the pipet. Lipid molecules in the injured bilayer then had an opportunity to reorganize themselves into an independent unilamellar vesicle where bilayer–bilayer repulsion was not a factor.

Occasionally, one encounters an oligolamellar vesicle in which the concentric bilayers are sufficiently well-spaced that they are visible individually. Figure 22 shows the layer-by-layer

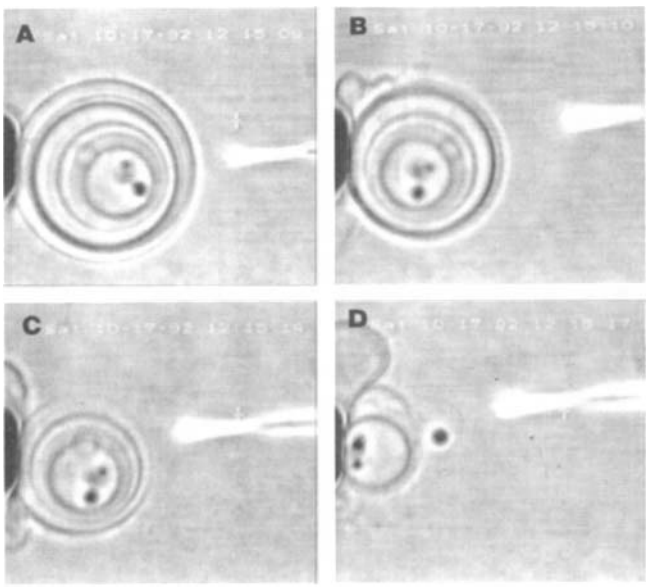

Fig. 22. Individual layers of an oligolamellar giant vesicle being ruptured by a sharp pipet, causing the vesicle to become smaller and smaller.

destruction of an oligolamellar vesicle when agitated by a sharp pipet. The vesicle becomes smaller and smaller as the layers are shed.

5.5.2. Dilution

When giant multilamellar vesicles are prepared by hydration of a lipid film (a method that, as mentioned, was supplanted by our solid-state hydration), the vesicles remain unchanged for at least a day unless the sample is diluted four- to twentyfold with water. Dilution stimulates the ejection of 5–30 μm GUVs from the multilamellar vesicles until the latter have entirely disappeared (Fig. 23). As small GUVs depart, their inner contents are

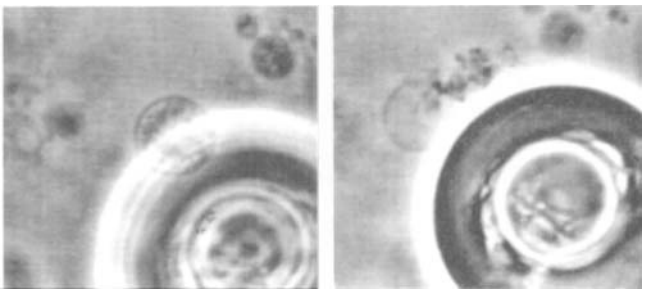

Fig. 23. Ejection of a small unilamellar vesicle from a multilamellar vesicle induced by dilution. Note how the particulate matter inside the unilamellar vesicle is expelled through a defect created at the contact point of the two vesicles. The two photographs are spaced three seconds apart. Less than five seconds later, the daughter vesicles had moved away from the parent and healed the defect.

rapidly expelled from the hole where the GUV and multilamellar vesicle had been momentarily attached. (The hole then heals immediately to give an intact GUV). Expulsion of the internal contents of the GUV is a further indication of the internal stress that seems to characterize GUV systems.[46]

Why does dilution with water induce fission? Osmotic stress does not seem to supply an answer because the vesicles, prepared in ion-free water, were also diluted with ion-free water. It seems, instead, that there is a delicate balance between vesicle–vesicle repulsion and bilayer–bilayer repulsion. When a sample is diluted, the vesicle–vesicle repulsion is diminished, but the bilayer–bilayer repulsion within the multilamellar vesicles remains unaffected. Consequently, GUV formation becomes thermodynamically favored. Small energy differences between different morphologies are key to giant vesicle behavior.

5.6. Birthing[4]

The interactions between surfactants and GUVs attracted our attention owing to the widespread use of surfactants in solubilizing biomembrane components.[47] M. N. Jones[48] proposed that surfactants bind to phosopholipid membranes by means of hydrophobic forces. When saturation levels are reached, the bilayer begins to expel mixed micelles composed of lipid plus surfactant. Ueno and Akechi,[49] who observed 200-nm vesicles by freeze fracture electron microscopy, found that octyl glucoside transforms a vesicle into a cluster of 20–30-nm spheres (resembling a raspberry). These tiny particles depart one-by-one

from the surface to become, soon thereafter, solubilized in the water as mixed micelles. We know of no example in which vesicle destruction by a surfactant has been observed by light microscopy.

Adding 25 μL of 5 mM octyl glucoside to a standard GUV preparation (20–21 °C), giving a surfactant concentration well below its critical micelle concentration of 25 mM, caused minimal vesicle destruction in the first hour. The most striking observation was a "birthing process" involving the occasional GUV that possessed a smaller vesicle within it. Under the influence of octyl glucoside, the entrapped vesicle can force its way through the bilayer wall of the parent vesicle (Fig. 24). A gap is created

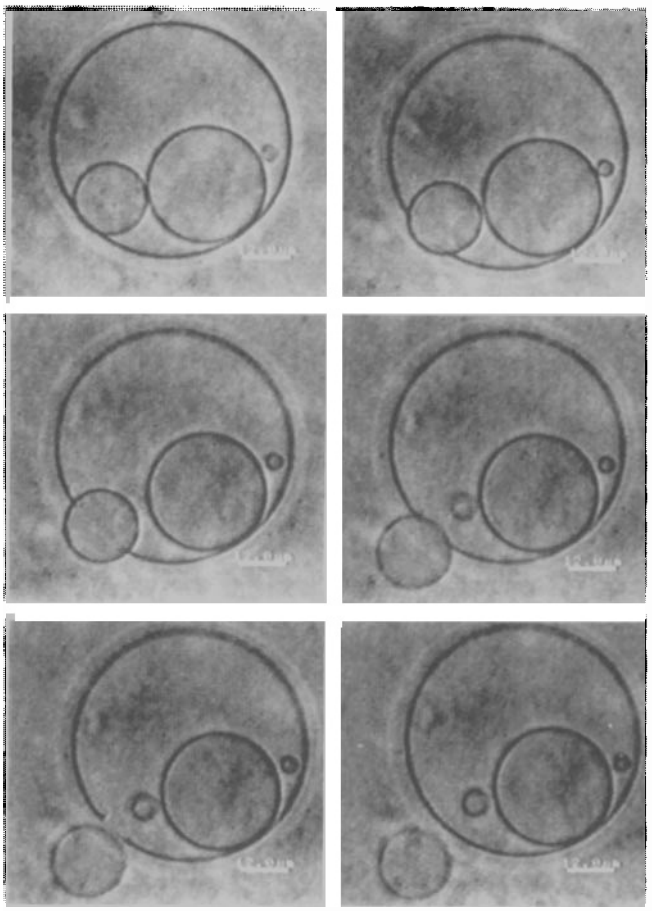

Fig. 24. "Birthing" of a vesicle induced by octyl glucoside (phase-contrast microscopy on giant unilamellar vesicles; scale-bar = 12.0 μm). Note how the hole in the parent vesicle (bottom left) heals itself instantly. The process takes about twelve seconds from start to finish.

in the parent vesicle that heals instantly (bottom photographs). The sequence of events was observed repeatedly with every preparation. Light microscopy can obviously capture dynamic events that are difficult to detect by the more commonly used electron microscope. Moreover, artifacts from drying, metal coating, etc., a problem in electron microscopy, are avoided.

Combining the results from both light microscopy and electron microscopy,[49] we surmise that octyl glucoside weakens the cohesion among the organized DDAB molecules, perhaps by the formation of weakly associated spherical particles. The membrane subunits are able to temporarily separate from one another and, thereby, allow the passage of an entrapped vesicle. Evidence for this model came from experiments using higher octyl glucoside concentrations (10–25 mM) that rapidly destroy the GUVs. During the process, 0.1–1.0-μm particles are seen to speckle the vesicle surface (not shown). These particles (which appear from bright-field microscopy to be either solid or multilamellar lipid) break away while, simultaneously, the diameter of the GUV diminishes at a rate dependent on the octyl glucoside concentration.

5.7. Foraging[4]

The dramatic effect of octyl glucoside on the giant vesicles led us to investigate a natural surfactant, sodium cholate **3**. The cholate **3** is a member of the bile salt family of steroids used to solubilize fatty material in the gut. Addition of cholate (50 μL of 5 mM) to GUV preparations induced a rapid fusion process among the vesicles. As seen in Figure 25, the GUV in the upper right hand corner consumes the smaller vesicles in the grapelike cluster beside it.

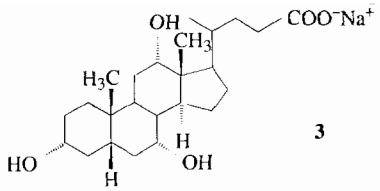

3

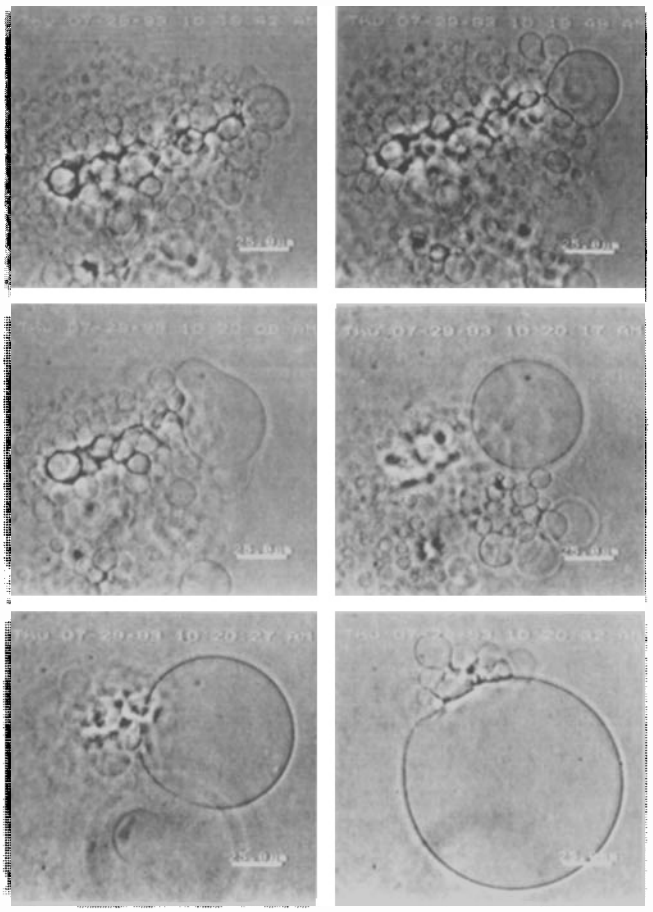

Fig. 25. Sodium cholate-induced foraging of a DDAB giant unilamellar vesicle. The vesicle in the upper right corner grows as it consumes its smaller nighbors. The entire process takes less than a minute.

The foraging vesicle grows in diameter with each small vesicle that is consumed. When small vesicles no longer exist in proximity of the foraging vesicle, an unexpected and previously unreported event occurs: The large vesicle disintegrates by a sequential ejection of lipid molecules (Fig. 26), a process that takes

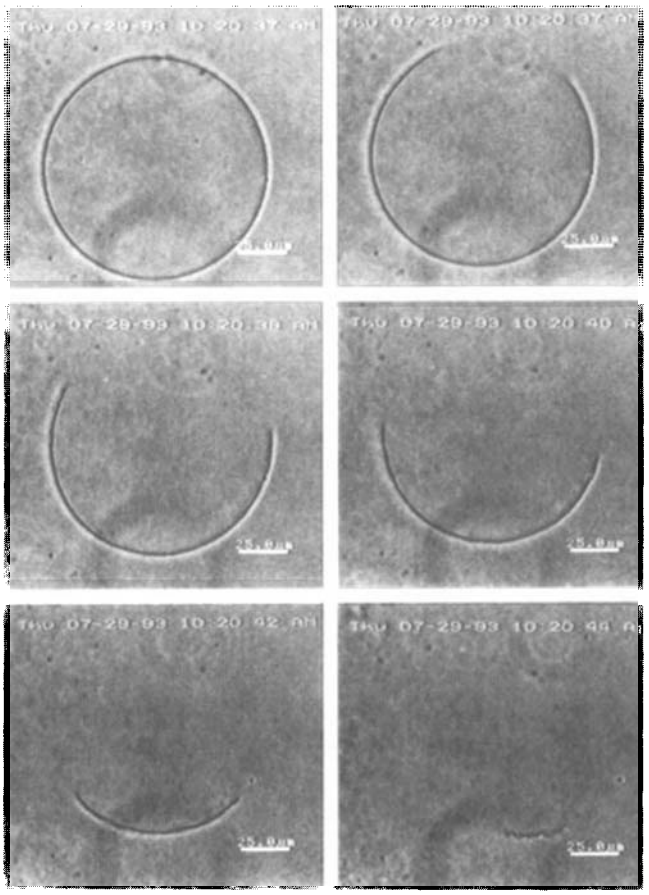

Fig. 26. Decay of giant unilamellar vesicle immediately following the foraging seen in Fig. 25. Entire dissolution of the membrane takes six seconds.

only a few seconds. It is as if a defect in the GUV created an edge of exposed lipid molecules. Lipid molecules are then continuously solubilized from this defect by the cholic acid until the vesicle bilayer disappears. Remarkably, the original spherical shape is retained throughout the process. The products of the membrane dissolution are submicroscopic and may well be the mixed micelles postulated by others.[48, 49] At higher concentrations, crystals of DDAB/cholate eventually fall out of solution. It should be noted that another steroid, cholesterol, has no such effect on the GUVs. In fact, 30% cholesterol incorporated into the DDAB bilayer actually stabilizes the vesicles.

5.8. Injection

Injection into giant vesicles has been a high-priority objective of ours since the very beginning. If a pipet could be inserted into a vesicle (the way cytologists routinely do with living cells), a host of experiments fall into place. For example, biological macromolecules, such as enzymes and DNA, could be examined within the confines of a giant vesicle. Or various volumes of water might be injected into a vesicle to test the bilayer's resilience to internal pressure. Or a perturbing solute might be introduced to determine how its effects on the interior and exterior leaflets of the bilayer compare.

Injection was not an easy thing to achieve. In the case of multilamellar vesicles, attempts to inject led to shedding of the bilayers (see Figs. 21 and 22). Most unilamellar vesicles, on the other hand, burst when prodded with a micropipet. We finally succeeded, however, with GUVs that are ≥ 200 μm in diameter containing 5% cholesterol. Such vesicles are pliable, and they resist bursting. A good example is shown in Figure 27. It is

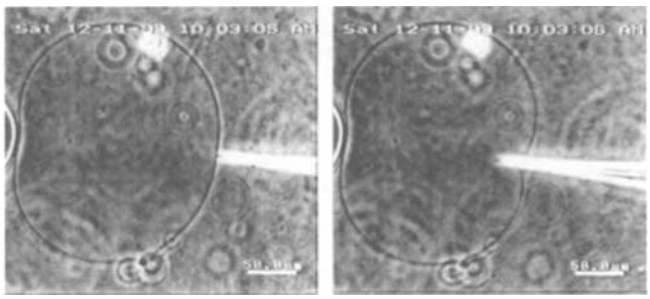

Fig. 27. Insertion of a micropipet into a giant unilamellar vesicle. The vesicle is composed of DDAB and cholesterol (95:5). Scale-bar = 50 μm.

believed that the pipet has actually penetrated the bilayer because the vesicle becomes distorted in the experiment and because both the tip of the pipet and the vesicle are in focus. A further indication of pipet entry into the vesicle interior is given in Figure 28. A bright particle within the vesicle is removed by the suction applied through the pipet. Note also the easy deformability of the vesicle as well as its ability to heal the wound created by the pipet.

5.9. Final Remarks

We finish, appropriately enough, with a quote from Albert Szent-Gyorgi in his "Personal Reminiscences":

"In my hunt for the secret of life, I started research in histology. Unsatisfied by the information that cellular morphology could give me about life, I turned to physiology. Finding physiology too complex, I took up pharmacology. Still finding the situation too complicated, I turned to bacteriology. But bacteria were even too complex, so I descended to the molecular level, studying chemistry and physical chemistry . After twenty years' work, I was led to conclude that to understand life we have to descend to the electronic level, and to the world of wave mechanics. But electrons are just electrons, and have no life at all. Evidently on the way I lost life; it had run out between my fingers."

The above words should not be regarded as a call for biologically oriented chemists to abandon their craft. Quite the contrary, their efforts should be intensified. But this should be done while bearing in mind that the living cell has an organizational complexity totally absent in the reaction flask. Future emphasis must, therefore, be away from "single-molecule chemistry" and

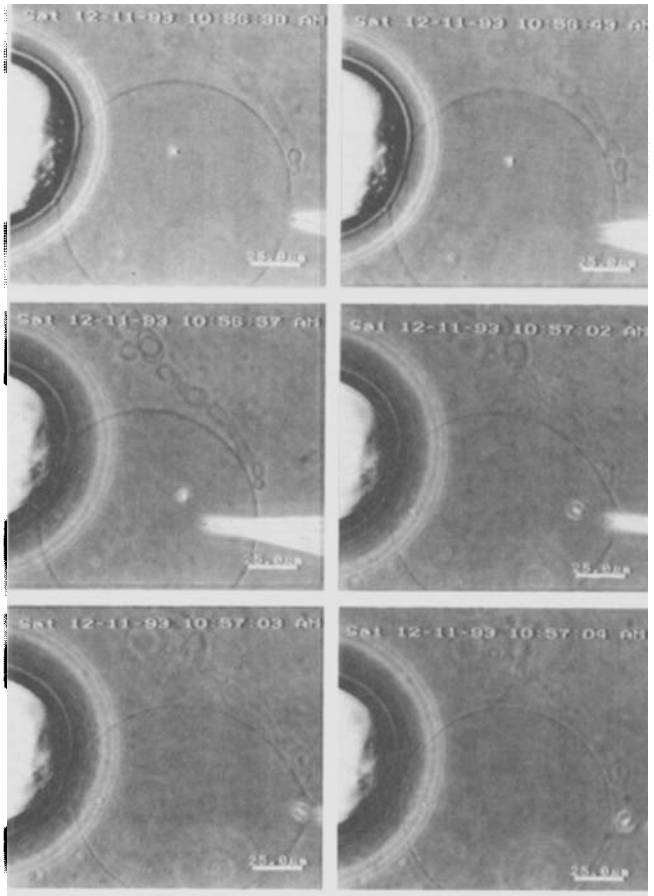

Fig. 28. Withdrawal of a particle (bright spot) from the interior of a giant unilamellar vesicle (DDAB + cholesterol 95:5) using an inserted micropipet under slight suction.

towards molecular assemblies. Because an organized group of molecules behaves differently from a molecule operating as a single entity, there is a need to define the differences. It is with this philosophy that our research group has worked over the past two decades;[1] and it is with this philosophy that "cytomimetic organic chemistry" was conceived.

It was a novelist, Tim O'Brien, who wrote the following words: "The thing about a story is that you dream it as you tell it, hoping that others might dream along with you, and in this way memory and imagination and language combine to make spirits in the head". Perhaps this is also the best that scientists can hope for: to create spirits in the mind.[50, 51]

Work was supported by the National Institutes of Health. The article is dedicated to— and, to some extent, written for—those special students whose days are controlled, measured, and defined by the pursuit of science.

Received: July 15, 1994 [A741E]
German version: *Angew. Chem.* **1995**, *107*, 2260–2278

[1] F. M. Menger, *Angew. Chem.* **1991**, *101*, 1104; *Angew. Chem. Int. Ed. Engl.* **1991**, *30*, 1086.
[2] D. D. Lasic, *Liposomes: From Physics to Applications*, Elsevier, Amsterdam, **1993**, p. 94, 118, 122, 189.
[3] F. M. Menger, N. Balachander, *J. Am. Chem. Soc.* **1992**, *114*, 5862.
[4] F. M. Menger, K. Gabrielson, *J. Am. Chem. Soc.* **1994**, *116*, 1567.
[5] G. Crile, M. Telkes, A. Rowland, *Protoplasma* **1932**, *15*, 337.
[6] We thank Dr. Adolph E. Smith for pointing out to us the Crile work.
[7] R. Beutner, *Physical Chemistry of Living Tissues and Life Processes*, Williams and Wilkens, Baltimore, **1933**.
[8] A. E. Smith, D. H. Kenyon, *Perspectives in Biol. and Med.* **1972**, 529.
[9] A. D. Bangham, M. W. Hill, N. G. A. Miller, *Meth. Memb. Biol.* **1973**, *1*, 1.
[10] *Liposomes as Drug Carriers* (Ed.: G. Gregoriadis), Wiley, Winchester, **1988**. *Liposomes*, (Ed.: M. J. Ostro), Dekker, New York, **1987**. G. Storm, H. P. Wilms, D. J. A. Crommelin, *Biotherapy* **1991**, 3, 25. G. L. Scherphof, T. Daemen, H. J. H. Spanjer, F. H. Roerdink, *Lipids* **1987**, *22*, 891. S. Wright, L. Huang, *Adv. Drug. Del. Rev.* **1989**, *3*, 343.
[11] R. R. C. New, *Liposomes, A Practical Approach*, IRL Press, Oxford, **1990**.
[12] F. M. Menger, J-J. Lee, P. Aikens, S. Davis *J. Colloid Interface Sci.* **1989**, *129*, 185.
[13] J. M. H. Kremer, M. W. J. Esker, C. Pathmamanoharan, P. H. Wiersema, *Biochemistry* **1977**, *16*, 3932.
[14] D. W. Deamer, A. D. Bangham, *Biochim. Biophys. Acta* **1976**, *443*, 629. M. J. Blandamer, B. Briggs, P. M. Cullis, J. B. F. N. Engberts, D. Hoekstra, *J. Chem. Soc. Faraday Trans.* **1994**, *90*, 1905.
[15] F. M. Menger, D. S. Davis, R. A. Persichetti, J-J. Lee, *J. Am. Chem. Soc. 1990*, **112**, 2451.
[16] J. P. Reeves, R. M. Dowben, *J. Cell. Physiol.* **1969**, *73*, 49; H. H. Hub, U. Zimmerman, H. Ringsdorf, *FEBS Lett.* **1982**, *140*, 254.
[17] D. Needham, E. Evans, *Biochemistry* **1988**, *27*, 8261.
[18] N. Oker, J. F. Scheerer, R. C. MacDonald, *Biochim. Biophys. Acta* **1982**, *692*, 384.
[19] N. Oker, R. C. MacDonald, *Biochim. Biophys. Acta* **1983**, *734*, 54.
[20] K. Higashi, S. Suzuki, H. Fujii, Y. Kirino, *J. Biochem.* **1987**, *101*, 433.
[21] D. D. Lasic, *J. Colloid Interface Sci.* **1990**, *140*, 302.
[22] J. H. Richardson, *Handbook for the Light Microscope. A User's Guide*, Noyes, Park Ridge, NJ, **1991**.
[23] A. Walter, P. K. Vinson, A. Kaplun, Y. Talmon, *Biophys. J.* **1991**, *60*, 1315.
[24] H. T. Tien, *Bilayer Lipid Membranes (BLM). Theory and Practice*, Dekker, New York, **1974**; X. K. Zhao, P. J. Herve, J. H. Fendler, *J. Phys. Chem.* **1989**, *93*, 908.
[25] P. Mueller, T. F. Chien, B. Rudy, *Biophys. J.* **1983**, *44*, 375. For another example of dark-field microscopy, see H. Hotani, *J. Mol. Biol.* **1984**, *178*, 113.
[26] R. Büschl, H. Ringsdorf, W. Zimmermann, *FEBS Lett.* **1982**, *150*, 38.
[27] H. Ringsdorf, B. Schlarb, J. Venzmer, *Angew. Chem.* **1988**, *100*, 117; *Angew. Chem. Int. Ed. Engl.* **1988**, *27*, 113.
[28] E. Sackmann, H-P. Duwe, K. Zeman, A. Zilker in *Structure and Dynamics of Nucleic Acids, Proteins, and Membranes*, (Eds.: E. Clementi, S. Chin), Plenum, New York, **1986**, p. 251.
[29] E. Sackmann, H-P. Duwe, H. Engelhardt, *Faraday Discuss. Chem. Soc.* **1986**, *81*, 281.
[30] S. Svetina, B. Zeks, *Biomed. Biochem. Acta* **1983**, *42*, 86.
[31] J. Käs, E. Sackmann, *Biophys. J.* **1991**, *60*, 825.
[32] E. Evans, D. Needham, *Faraday Discuss. Chem. Soc.* **1986**, *81*, 267.
[33] D. L. Taylor, M. Nederlof, F. Lanni, A. S. Waggoner, *Amer. Scientist* **1992**, *80*, 322.
[34] A. J. Lacey, *Light Microscopy in Biology. A Practical Approach*, IRL Press, Oxford, **1989**, p. 18.
[35] A fully equipped light microscope laboratory, including micromanipulation accessories, can be purchased for under $100000. A microscope with a Polaroid camera, which works well for many GUV experiments, can be obtained at only a fraction of this cost.
[36] We thank Professor J. B. F. N. Engberts for this moniker (name).
[37] D. Hoekstra, *Biochemistry* **1982**, *21*, 2833.
[38] D. Yogev, B. C. R. Guillaume, J. H. Fendler *Langmuir* **1991**, *7*, 623.
[39] J. H. Clint, *Surfactant Aggregation*, Chapman and Hall, New York, **1992**, p. 271.
[40] A. C. Cowley, N. L. Fuller, R. P. Rand, V. A. Parsegian, *Biochemistry* **1978**, 17, 3163.
[41] *Molecular Mechanisms of Membrane Fusion*, (Eds.: S. Ohki, D. Doyle, T. D. Flanagan, S. W. Hui, E. Mayhew), Plenum, New York, **1988**.
[42] E. W. Anacker, A. L. Underwood, *J. Phys. Chem. 1981*, *85*, 2463; D. F. Evans, *Langmuir*, *1988*, *4*, 3.
[43] D. J. Mitchell, B. W. Ninham, *J. Chem. Soc. Faraday Trans. 2*, **1981**, *77*, 601. Attention is also drawn to an important video-enhanced differential interference contrast microscopy study of the effect ofanions on vesicles: J. E. Brady, D. F. Evans, B. Kachar, B. W. Ninham, *J. Am. Chem. Soc.* **1984**, *106*, 4279.
[44] L. A. M. Rupert, J. B. F. N. Engberts, D. Hoekstra, *J. Am. Chem. Soc.* **1986**, *108*, 3920.
[45] D. Papahadjopoulos, *Cell. Surf. Rev.* **1978**, *5*, 765.
[46] P. Mueller, T. F. Chien, B. Rudy *Biophys. J.* **1983**, *44*, 375.
[47] J. Ruiz, F. M. Goni, A. Alonso, *Biochem. Biophys. Acta* **1988**, *937*, 127.
[48] M. N. Jones, *Chem. Soc. Rev.* **1992**, *21*, 127.
[49] M. Ueno, Y. Akechi *Chem. Lett.* **1991**, 1801.
[50] Two short pieces on vesicle behavior, one a review and the other an editorial, are well worth reading: R. Lipowsky, *Nature* **1991**, *349*, 475. J. Maddox, *ibid.* **1993**, *363*, 205.
[51] Additional examples of growth, fusion, undulation excretion, wounding and healing will be published shortly (F. M. Menger, S. J. Lee, *Langmuir*, in press).

Gold in Chains: Self-Assembly of a Gold(I) Catenane

Andreas Grohmann*

Catenane is the generic name for molecular assemblies consisting of interlocking rings that are arranged like the links of a chain (catena is Latin for chain).[1] Such compounds are characterized by the absence of any covalent bonds holding the rings together; instead, catenanes are systems with a "mechanical bond" between molecular subunits, and for this reason they have long intrigued chemists. The possibility of preparing linked-ring molecules was probably suggested as early as the beginning of this century by Willstätter, but it was not until the 1960s that catenanes and related species such as rotaxanes (that is, "threaded" macrocycles) and molecular knots became the subject of scientific inquiry.[2, 3]

In the beginning,[4] catenane chemistry involved herculean synthetic effort and was considered to be a highly specialized and somewhat esoteric area of science. It came to be seen in a different light, however, when DNA, the archetype of biomolecules, was shown to adopt catenated and knotted topologies in certain cases.[5] At the same time, the increasing appreciation of the importance of noncovalent bonding interactions (for example, van der Waals, charge–transfer interactions, and hydrogen bonding) in chemistry at large led to the conceptualization of a "chemistry beyond the molecule", namely supramolecular chemistry, which has been defined as the chemistry of molecular assemblies and of the intermolecular bond.[6] From these developments, the study of catenanes and related compounds gained new impetus, in particular with a view to creating materials with novel properties,[7] for example new types of polymer[2] and molecular-scale devices.[8]

Over the last fifteen years, template synthesis and the application of self-assembly have enabled chemists to synthesize a variety of catenated structures:[9] "Metal ion templating" allows the positioning of building blocks before ring closure in the synthesis of catenands (that is, catenanes with ligand properties, such as **1**),[10] while "organic templating" through hydrogen bonds and π–π interactions is instrumental in the preparation of **2**, the newest addition to the family of lactam catenanes.[11] The similarly facile synthesis of linked-ring molecules such as **3** relies on the preformation by self-assembly of a threaded crown ether macrocycle. While π-donor–acceptor interactions keep the two components locked in place, the open-chain bis(bipyridinium) ion may be formed into the second ring.[12]

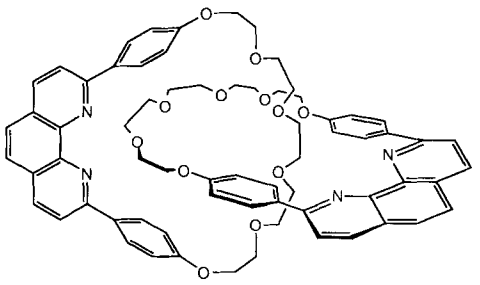

1

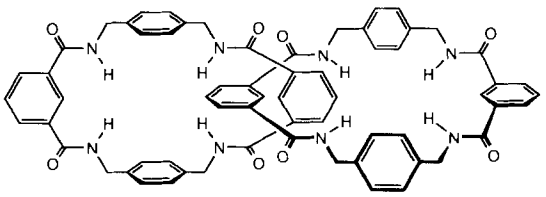

2

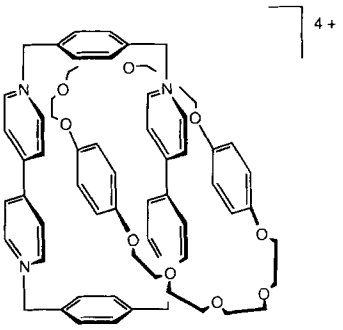

3

Whereas various types of wholly "organic" molecular chains are thus accessible, catenanes in which metal ions are incorporated into the macrocycles have remained a rarity.[13] The first such example was described in 1993 by Bickelhaupt and coworkers, who observed the formation of **4** from two preformed rings in an equilibrium that involves Mg–C bond dissociation, threading of the crown ether ring by an open-chain magnesium–organic intermediate, and reformation of the metal–carbon bond.[14] A variation on this theme was reported in 1994 by the group of Ogura and Fujita, who draw a parallel between their synthesis and the trick of interlinking "magic

[*] Dr. A. Grohmann
Institut für Anorganische Chemie der Universität Erlangen-Nürnberg
Egerlandstrasse 1, D-91058 Erlangen (Germany)
Telefax: Int. code +(91 31) 85 73 67

 © VCH Verlagsgesellschaft mbH, D-69451 Weinheim, 1995 0570-0833/95/3419-2107 $ 10.00+.25/0

rings".[15] Again, two preformed molecular rings are in equilibrium with a [2]catenane (**5**), and while the mechanism by which the two rings interlock has not yet been established, it is likely that two metal centers on different rings exchange ligands twice, with concomitant twisting of the rings around each other.[7]

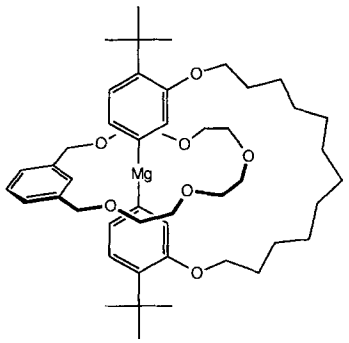

4

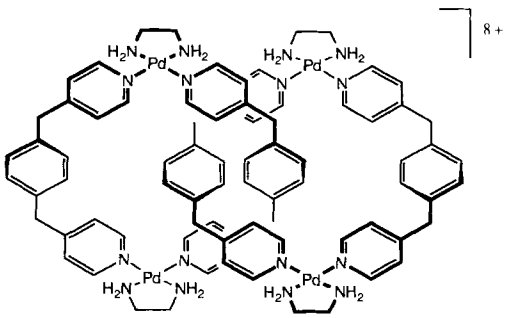

5

The most recent addition to the class of metal-containing catenanes comes from the laboratory of D. M. P. Mingos and coworkers, who describe the synthesis by self-assembly of a [2]catenane of monovalent gold (**6**).[16] It may be obtained from the reaction of $[Au(NH_3)_2]BF_4$ with *t*BuC≡CH in acetonitrile in a yield of 65%, and its solid-state structure is characterized by two interlocking cyclic [Au(C≡C*t*Bu)] hexamers. This compound, which is only the second example of an organometallic catenane, is highly unusual also against the backdrop of organogold chemistry.[17] With regard to other homoleptic alkynyl gold(I) species,[18] it is noteworthy that all the possible coordination modes of two alkynyl ligands about a gold(I) center (η^1-Au-η^1, η^1-Au-η^2, η^2-Au-η^2) are realized in **6**; the η^2-Au-η^2 arrangement of ligands is without precedent. While compounds of general formula $[Au(C{\equiv}CR)]_n$ (R = Ph, *t*Bu) were first obtained by a different route some 30 years ago, their polymeric nature has hampered structural characterization ever since. On the basis of a series of molecular weight determinations, Coates and Parkin[19] suggested a cyclic tetrameric structure for the *tert*-butyl derivative in which each gold atom is coordinated by two alkynyl residues in η^1-Au-η^2 fashion, but conclusive structural evidence has so far been lacking. It thus seems that the degree of association of monomers in $[Au(C{\equiv}Ct\text{Bu})]_n$ (n = 4, 6) depends on the reaction conditions, the influence of which requires further study.

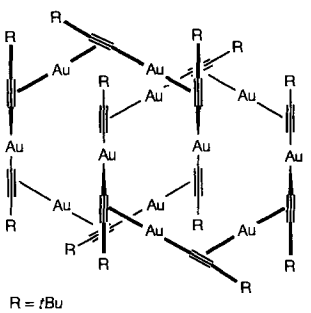

6

The most striking aspect about the formation of **6** is the apparent ease with which the [Au(C≡C*t*Bu)] units rearrange in solution and self-assemble in order to realize the observed catenane topology in the solid state. While there is evidence for the presence of $[Au(C{\equiv}Ct\text{Bu})]_6$ rings in solution, it is not yet clear whether separate rings and catenated species are in equilibrium. In this regard, it is interesting to note that the rearrangement necessary for the construction of **6** involves processes of ligand dissociation and association that are similar to the transmetalation reactions postulated in the formation of **5**.

In the solid state, the structure of **6** is characterized by close intra- and interring Au···Au contacts in a range between 3.2–3.5 Å, indicating a significant degree of attraction between the metal centers.[20] It is well known that aurophilic interactions of this kind, which are due to relativistic effects,[21] often have a decisive influence on the solid-state structures of gold compounds as well as on the course of reactions, the stability of main group element centered gold cluster cations being an example in point.[22] In the case of gold(I), the energy of the Au···Au interaction has been estimated to be of the order of 29–33 kJ mol^{-1} and thus of a magnitude comparable to the energy involved in hydrogen bonding.[23] Given the pivotal role that other types of noncovalent bonding interactions play in the self-assembly of supramolecular entities, it is reasonable to assume that the formation of **6** is due to secondary Au···Au bonding, which induces the rearrangement of the [Au(C≡C*t*Bu)] fragments and their subsequent formation into interlocking rings.

With a first synthesized gold catenane, the tantalizing vision of a gold rotaxane now appears on the horizon, and it will be interesting to see whether aurophilic interactions can be harnessed eventually to realize even more intricate ("knotted") molecular superstructures.

German version: *Angew. Chem.* **1995**, *107*, 2279–2281

Keywords: aurophilicity · catenanes · gold compounds · self-assembly · supramolecular chemistry

[1] In current nomenclature, the number of interlocking rings in a catenane is prefixed in square brackets, the simplest such compound being a [2]catenane.

[2] For a comprehensive review of catenanes and rotaxanes, see H. W. Gibson, M. C. Bheda, P. T. Eugen, *Prog. Polym. Sci.* **1994**, *19*, 843–945.

[3] Treatises on topology in molecular chemistry: a) *New J. Chem.* **1993**, *17*, No. 10, 11; b) J.-C. Chambron, C. Dietrich-Buchecker, J.-P. Sauvage, *Top. Curr. Chem.* **1993**, *165*, 131–162.

[4] G. Schill, *Catenanes, Rotaxanes, and Knots*, Academic Press, New York, **1971**.

[5] Three recent articles: a) W. M. Stark, C. N. Parker, S. E. Halford, M. R. Boocock, *Nature* **1994**, *368*, 76–78; b) N. R. Cozzarelli in *The Harvey Lectures, Series 87*, Wiley-Liss, New York, **1993**, pp. 35–55; c) J. E. Mueller, S. M. Du, N. C. Seeman, *J. Am. Chem. Soc.* **1991**, *113*, 6306–6308.

[6] J.-M. Lehn, *Supramolecular Chemistry*, VCH, Weinheim, **1995**, and references therein.

[7] R. Dagani, *Chem. Eng. News* **1994**, *72*(35), 28–34.

[8] Two recent articles: a) R. A. Bissell, E. Córdova, A. E. Kaifer, J. F. Stoddart, *Nature* **1994**, *369*, 133–137; b) A. Livoreil, C. O. Dietrich-Buchecker, J.-P. Sauvage, *J. Am. Chem. Soc.* **1994**, *116*, 9399–9400.
[9] R. Hoss, F. Vögtle, *Angew. Chem.* **1994**, *106*, 389–398; *Angew. Chem. Int. Ed. Engl.* **1994**, *33*, 375–384. For a collection of early thoughts on the possibilities of constructing a catenane about a "central core" see H. L. Frisch, E. Wasserman, *J. Am. Chem. Soc.* **1961**, *83*, 3789–3795.
[10] J.-C. Chambron, C. O. Dietrich-Buchecker, V. Heitz, J.-F. Nierengarten, J.-P. Sauvage, C. Pascard, J. Guilhem, *Pure Appl. Chem.* **1995**, *67*, 233–240, and references therein.
[11] a) A. G. Johnston, D. A. Leigh, R. J. Pritchard, M. D. Deegan, *Angew. Chem.* **1995**, *107*, 1324–1327; *Angew. Chem. Int. Ed. Engl.* **1995**, *34*, 1209–1212; b) A. G. Johnston, D. A. Leigh, L. Nezhat, J. P. Smart, M. D. Deegan, *ibid.* **1995**, *107*, 1327–1331 and **1995**, *34*, 1212–1216; c) S. Ottens-Hildebrandt, S. Meier, W. Schmidt, F. Vögtle, *ibid.* **1994**, *106*, 1818–1821 and **1994**, *33*, 1767–1770; d) C. A. Hunter, *J. Am. Chem. Soc.* **1992**, *114*, 5303–5311.
[12] D. B. Amabilino, P. R. Ashton, C. L. Brown, E. Córdova, L. A. Godínez, T. T. Goodnow, A. E. Kaifer, S. P. Newton, M. Pietraszkiewicz, D. Philp, F. M. Raymo, A. S. Reder, M. T. Rutland, A. M. Z. Slawin, N. Spencer, J. F. Stoddart, D. J. Williams, *J. Am. Chem. Soc.* **1995**, *117*, 1271–1293, and references therein.
[13] For a catenane containing a non-bridgehead metal atom in one of the rings see M. J. Gunter, D. C. R. Hockless, M. R. Johnston, B. W. Skelton, A. H. White, *J. Am. Chem. Soc.* **1994**, *116*, 4810–4823.
[14] a) G.-J. M. Gruter, F. J. J. de Kanter, P. R. Markies, T. Nomoto, O. S. Akkerman, F. Bickelhaupt, *J. Am. Chem. Soc.* **1993**, *115*, 12179–12180; b) P. R. Markies, O. S. Akkerman, F. Bickelhaupt, W. J. J. Smeets, A. L. Spek, *Organometallics* **1994**, *13*, 2616–2627; c) F. Bickelhaupt, *J. Organomet. Chem.* **1994**, *475*, 1–14.
[15] M. Fujita, F. Ibukuro, H. Hagihara, K. Ogura, *Nature* **1994**, *367*, 720–723; see also C. A. Hunter, *Angew. Chem.* **1995**, *107*, 1181–1183; *Angew. Chem. Int. Ed. Engl.* **1995**, *34*, 1079–1081.
[16] D. M. P. Mingos, J. Yau, S. Menzer, D. J. Williams, *Angew. Chem.* **1995**, *107*, 2045–2047; *Angew. Chem. Int. Ed. Engl.* **1995**, *34*, 1894–1895.
[17] A. Grohmann, H. Schmidbaur in *Comprehensive Organometallic Chemistry II Gold* (Eds.: E. W. Abel, F. G. A. Stone, G. Wilkinson), Pergamon, Oxford, **1995**.
[18] J. Vicente, M.-T. Chicote, M.-D. Abrisqueta, *J. Chem. Soc. Dalton Trans.* **1995**, 497–498, and references therein.
[19] G. E. Coates, C. Parkin, *J. Chem. Soc.* **1962**, 3220–3226.
[20] For distantly related polynuclear alkynyl- and arylgold(I) compounds see a) O. M. Abu-Salah, A. R. A. Al-Ohaly, *J. Chem. Soc. Dalton Trans.* **1988**, 2297–2300; b) E. M. Meyer, S. Gambarotta, C. Floriani, A. Chiesi-Villa, C. Guastini, *Organometallics* **1989**, *8*, 1067–1079.
[21] P. Schwerdtfeger, G. A. Bowmaker, *J. Chem. Phys.* **1994**, *100*, 4487–4497, and references therein.
[22] a) K. Angermaier, H. Schmidbaur, *J. Chem. Soc. Dalton Trans.* **1995**, 559–564, and references therein; b) O. D. Häberlen, H. Schmidbaur, N. Rösch, *J. Am. Chem. Soc.* **1994**, *116*, 8241–8248; c) J. K. Burdett, O. Eisenstein, W. B. Schweizer, *Inorg. Chem.* **1994**, *33*, 3261–3268; see also A. L. Balch, E. Y. Fung, M. M. Olmstead, *J. Am. Chem. Soc.* **1990**, *112*, 5181–5186.
[23] H. Schmidbaur, W. Graf, G. Müller, *Angew. Chem.* **1988**, *100*, 439–441; *Angew. Chem. Int. Ed. Engl.* **1988**, *27*, 417–419.

From *cyclo*-Te_8 to Te_x^{n-} Sheets: Are Nonclassical Polytellurides More Classical than We Thought?

Mercouri G. Kanatzidis*

The structural diversity of the allotropic forms of the chalcogenide elements diminishes when we move from sulfur to selenium and tellurium, and polymeric tellurium is the only stable form of this element known to date. The recent discovery of the *cyclo*-octatellurium ring Te_8 in the solid-state structure of Cs_3Te_{22} by Sheldrick and Wachhold[1] is an important landmark in polychalcogenide chemistry. Te_8, the stability of which has been debated by chemists for a long time, completes the chalcogen series S_8, Se_8, and Te_8; although, it must be noted that Te_8 is not a true allotrope, since it coexists with other components in Cs_3Te_{22}. The Te_8 molecule has the expected puckered ring structure (Fig. 1). It acts as a crown ether to a Cs^+ ion, which is presumably a major contributory factor to its stability in this compound. The ring seems to have been templated by the alkali metal ion, and this has broader implications for the role of the counterion effect in polychalcogenide and monochalcogenide chemistry in general. This role has not been properly appreciated in the past, but the accumulation of structural data seems to reveal a powerful influence of the counterion on the formation and structures of products, which in most cases shadows electronic factors. Given the great allotropy of sulfur and the abundance of rings such as S_6, S_7 etc., is it possible to template other Te_x rings ($x \neq 8$) by using, for example, Rb or K ions? Such expectations may no longer seem unrealistic. Another equally interesting component in the structure of Cs_3Te_{22} is the unusual $[Te_6]_n^{3n-}$ unit, which forms perfectly flat layers that sandwich the Te_8 molecules.

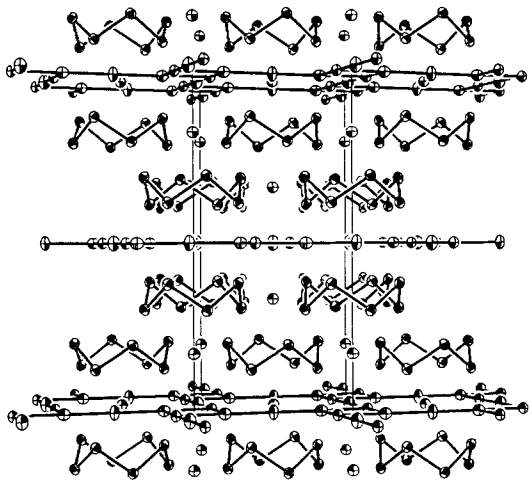

Fig. 1. Solid-state structure of Cs_3Te_{22}.

[*] Prof. Dr. M. G. Kanatzidis
Department of Chemistry, Michigan State University
East Lansing, MI 48824 (USA)
Telefax: Int. code +517-353-1793
e-mail: kanatzidis@cemvax.cem.msu.edu

[**] Financial support from the National Science Foundation DMR-9202428 and the Office of Naval Research (contract no. N00014-94-1-0935) for the authors research program are gratefully acknowledged.

The timing of the discovery of new Te structural features is not accidental, since it comes in a period in which polychalcogenide chemistry, especially that of the heavier members, is experiencing unprecedented development in laboratories around the world. The fascination of chemists with the chalcogen group arises for many reasons, not the least of which is the ability of the elements in this series to catenate and form intriguing polyanions and polycations.

The most unusual behavior ("nonclassical") among the chalcogens is undoubtedly displayed by tellurium, the most "classical" by sulfur. By "nonclassical" is meant the violation of the octet rule. Although violation of the octet rule is not at all unusual in main group compounds, most polysulfides, polyselenides and a few polytellurides do follow this rule. That tellurium chains associate even if they carry negative charge, and the ability of Te to form T-shaped three-coordinate centers or linear two-coordinate centers, set the behavior of tellurium distinctly apart from that of sulfur and selenium. This behavior can be considered as "nonclassical" (see Fig. 2). The structures of

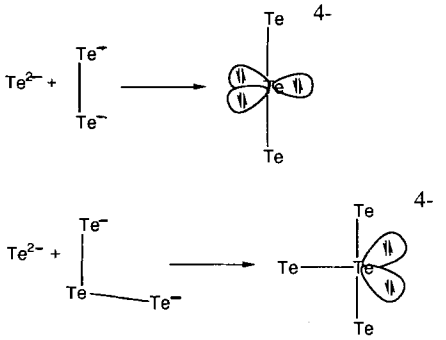

Fig. 2. The structures of Te_3^{4-} and Te_4^{4-} species formed by the association of two different Te_x^{2-} units. The stereochemically active lone pairs of electrons around the central Te atoms are shown. For the lighter polychalcogenides, such $\{Q_x^{2-} \cdot Q_y^{2-}\}$ (Q = chalcogen) interactions would normally be repulsive.

$\{Te_x^{2-} \cdot Te_y^{2-}\}$ adducts are consistent with VSEPR theory. The compounds $NaTe_3$,[2] $CsTe_4$,[3] Li_2Te_6,[2] Rb_2Te_5,[4] and Cs_2Te_5,[5] and $RbTe_6$[6] gave some of the early indications of the extraordinary structural behavior of tellurium. The $\{Te_x^{2-} \cdot Te_y^{2-}\}$ interactions are also found in coordination compounds such as $[NbTe_{10}]^{3-}$,[7] $[MTe_7]^{2-}$ (M = Zn, Hg),[8] and $[AuTe_7]^{3-}$,[9] $[Cu_3Te_{12}]^{9-}$,[10] and $(Et_4N)_2Te_{12}$.[11]

The normal polychalcogenide chains (Q_x or Q_x^{2-}) are characterized by Q-Q-Q angles and Q-Q-Q-Q dihedral angles of $105 \pm 5°$ and $100 \pm 5°$, respectively, which are responsible for the observed helical and cyclic structures of these species, including the structures of Te_8 and polymeric Te_x. These structures would now have to be considered classical. The special structural features of the polytellurides, that is Te-Te-Te angles of 90° or 180° and Te-Te-Te-Te dihedral angles of 0° or 180°, permit additional molecular structures. Thus not only helical chains and puckered rings, but also novel kinked chains, linear chains, branched, and spirocyclic chains (both finite and infinite), as well as puckered layers and strictly planar networks can be formed. For example, the polytellurides shown in Figure 3 have no analogues in sulfur or selenium chemistry. Occasionally, polyselenides have shown some of the same structural features but not nearly to the same extent as the polytellurides.

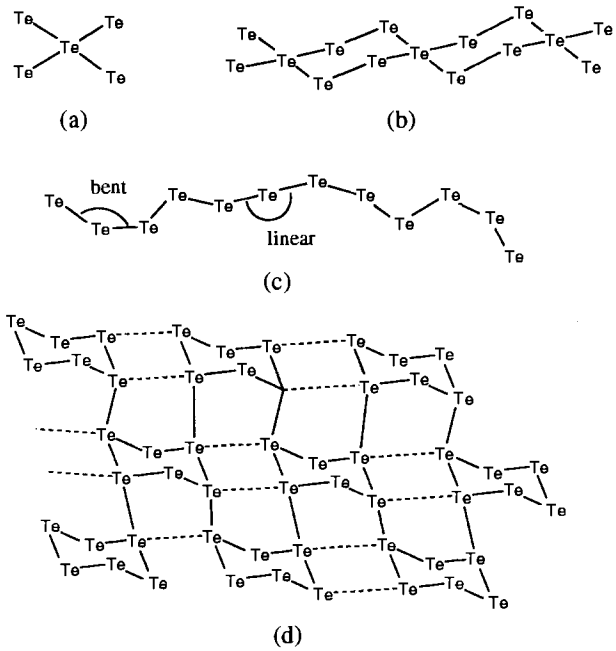

Fig. 3. Some examples of polytelluride anions with unique molecular structures: a) the Te_3^{2-} ion in Ga_2Te_3, b) the Te_5^{2-} spirocyclic chain in Rb_2Te_5, c) the Te_6^{2-} infinite chain in Li_2Te_6, and d) the puckered layer of $[Te_6]^-$ in $RbTe_6$. Undoubtedly, the counterion is paramount in controlling the form of the $\{Te_x^{2-} \cdot Te_y^{2-}\}$ interactions.

In Cs_3Te_{22} beautiful tetragonally symmetric, perfectly planar, $[Te_6]_n^{3n-}$ layers act as hosts for the Te_8 molecules. Such discoveries underscore the potential of polytellurides to teach us a great deal about the fundamental chemistry of chalcogenide elements. Although the properties of the $[Te_6]_n^{3n-}$ layers are not known yet, it would appear that they might be metallic. Topologically, these layers derive from planar 4^4 nets, in which 2/5 of the nodes (Te atoms) are removed. Such a 4^4 net has recently been discovered in $KBa_2[Ag_3Te_3][Te_3]$,[12] in which a strictly planar $[Te_3]_n^{2n-}$ square-net is sandwiched between two K/Ba layers. The relationship between these two structures is shown in Figure 4. The perfect square net of $[Te_3]_n^{2n-}$ is subject to electronically driven distortions which give rise to an incommensurate charge density wave (CDW). This leads to a metal-to-insulator transition. It would be very interesting to see if such phenomena are observed in the $[Te_6]_n^{3n-}$ layer as well. For example, the systems may be prone to distortion towards discrete Te_4^{2-} units. The puckered layer found in $RbTe_6$ (see Fig. 2d) is characterized by short and long bonds which suggest a strong localization of the bonding electrons and the presence of a band gap. The absence of any distortions in the $[Te_6]_n^{3n-}$ layer would make it the first one with completely delocalized electrons. The fact that the anionic polytelluride layers are electron-rich suggests that they may allow for a limited variation (fractional removal or addition of electrons) in the number of electrons, by redox chemistry, and therefore, modification if not control of their electronic properties. A more extensive change in the number of electrons would violate the Zintl–Klemm rules according to which another structure should be obtained. Undoubtedly, either way novel materials should result with semiconducting, metallic, and even magnetic

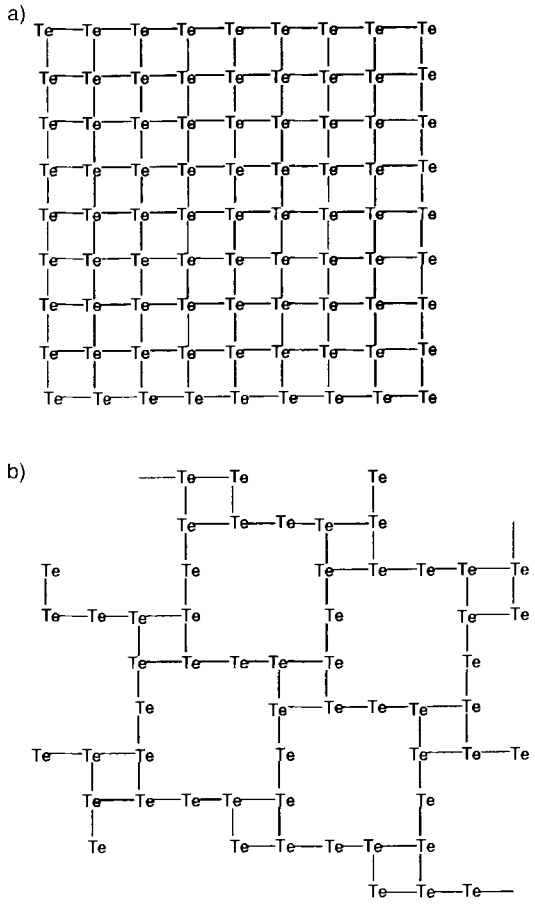

Fig. 4. The structural relationship between the $[Te_3]_n^{2n-}$ (a) and $[Te_6]_n^{3n-}$ (b) planar nets. The network in Fig. 4b can be derived from the network in Fig. 4a if 2/5 of the nodes (Te atoms) are removed.

properties that may exhibit interesting transitions to CDW and superconducting behavior.

The presence of well-separated polytelluride layers in the compounds mentioned above implies that it might be possible to obtain related compounds with more than one type of layer as part of a homologous family or other sheet-structure types. The pursuit of compounds of the type $A_xB_yTe_n$ (A = alkali metal; B = alkaline earth metal) is now justified because they may also contain nonclassical $[Te_x]^{n-}$ layers with varying electron count.

As every researcher active in this area knows, the synthetic and structural chemistry of polychalcogenides is characterized by a lack of predictability of both product composition and structure. While the results obtained can be rationalized, predictability depends on whether we understand the thermodynamics of crystallization and anion–cation packing in the solid state. However, little theoretical work has been carried out in this area. Thus, most of the exciting results have relied on a certain degree of serendipity, and the discovery of Te_8 seems to be no exception. All these highlight the paramount importance of *exploratory synthesis* in advancing inorganic chemistry, particularly in areas in which a deeper understanding of the mechanisms and thermodynamics is needed. This is also true for many areas of solid-state chemistry, and is in stark contrast to the procedure in organic chemistry in which the planned synthesis of compounds has been possible for a long time. In the coordination chemistry of main group elements and solid-state chemistry, imagination, creativity, and a lot of luck are still the prime tools of the trade. Zintl and Klemm would be proud to see how far the field of polychalcogenides has come since the 1920s and 1930s. The future of polychalcogenide chemistry seems indeed bright!

German version: *Angew. Chem.* **1995**, *107*, 2281–2283

Keywords: chalcogen compounds · polychalcogenides · tellurium compounds

[1] W. S. Sheldrick, M. Wachhold, *Angew. Chem.* **1995**, *107*, 490; *Angew. Chem. Int. Ed. Engl.* **1995**, *34*, 450.
[2] P. Böttcher, R. Keller, *J. Less Common Met.* **1985**, *109*, 311, and references therein.
[3] P. Böttcher, U. Kretschmann, *Z. Anorg. Allg. Chem.* **1985**, *523*, 145, and references therein.
[4] P. Böttcher, U. Kretschmann, *J. Less Common Met.* **1983**, *95*, 81.
[5] P. Böttcher, U. Kretschmann, *Z. Anorg. Allg. Chem.* **1982**, *491*, 39.
[6] W. S. Sheldrick, B. Schaaf, *Z. Naturforsch. B* **1994**, 49, 993.
[7] W. A. Flomer, J. W. Kolis, *J. Am. Chem. Soc.* **1988**, *110*, 3682.
[8] U. Müller, C. Grebe, B. Neumüller, B. Schreiner, K. Dehnicke, *Z. Anorg. Allg. Chem.* **1993**, *619*, 500.
[9] M. A. Ansari, J. C. Bollinger, J. A. Ibers, *J. Am. Chem. Soc.* **1993**, *115*, 3838.
[10] X. Zhang, J. L. Schindler, T. Hogan, J. Albritton-Thomas, C. R. Kannewurf, M. G. Kanatzidis, *Angew. Chem.* **1995**, *107*, 117; *Angew. Chem. Int. Ed. Engl.* **1995**, *34*, 68.
[11] C. J. Warren, R. C. Haushalter, *J. Alloys Compd.* **1995**, in press.
[12] X. Zhang, J. Li, B. Foran, S. Lee, H.-Y. Guo, T. Hogan, C. R. Kannewurf, M. G. Kanatzidis, *J. Am. Chem. Soc.* **1995**, *117*, in press.

 © VCH Verlagsgesellschaft mbH, D-69451 Weinheim, 1995 0570-0833/95/3419-2111 $ 10.00+.25/0

Condensed $RuSn_6$ Octahedra in $Ru_3Sn_{15}O_{14}$**

Werner Reichelt,* Tilo Söhnel, Otto Rademacher, Heinrich Oppermann, Arndt Simon,* Jürgen Köhler, and Hansjürgen Mattausch

The SnO_2/RuO_2 system is of interest with regard to the electronic properties of dimension stable anodes (DSA).[1] Detailed studies of the ternary system Ru/Sn/O[2] led to the discovery of new oxygen-poor phases. From the compound described as "$RuSn_5O_4$" by phase analysis, red translucent crystals can be obtained in a tin melt.[3] The X-ray structure analysis[4] of these crystals gave the composition $Ru_3Sn_{15}O_{14} \triangleq RuSn_5O_{4.67}$, in good agreement with the composition $RuSn_{4.95}O_{4.2}$ determined previously by systematic investigations of the phase equilibria and electron beam microanalysis of single crystals.[5] Due to the M:O ratio of greater than 1 for the compound, an unusual structure was expected. Indeed, the $Ru_3Sn_{15}O_{14}$ structure is remarkable for several reasons.

The projection of the monoclinic unit cell parallel to [010] (Fig. 1) shows characteristic triple chains of corner-sharing $RuSn_6$ octahedra. They run in the direction of the projection [010] and are surrounded from all sides by O atoms, which link the strands partially together. Each strand has the composition $Ru_3Sn_{14}O_{14}$. A polyhedral representation of the arrangement of the Sn atoms in the strand is given in Figure 2. In addition the

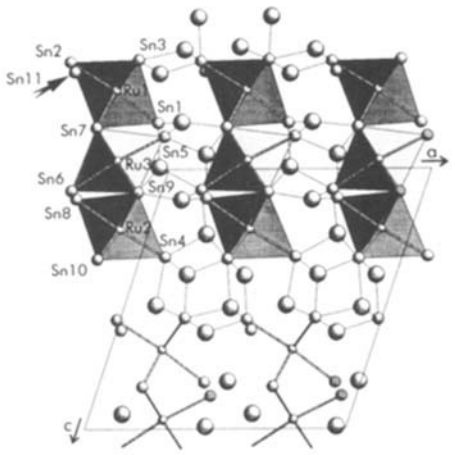

Fig. 1. Projection of the unit cell of $Ru_3Sn_{15}O_{14}$ parallel to [010]. The Ru, Sn, and O atoms are drawn with spheres of increasing size, and the $RuSn_6$ octahedra are highlighted in the top part of the figure. The Sn atom (Sn11) which does not belong to a $RuSn_6$ octahedron is marked with an arrow. Heterododecane units of Sn and O atoms can be seen between the cluster strands.

[*] Doz. Dr. W. Reichelt, Dipl.-Chem. T. Söhnel, Dr. O. Rademacher, Prof. Dr. H. Oppermann
Institut für Anorganische Chemie der Technischen Universität
Mommsenstrasse 13 D-01062 Dresden (Germany)
Telefax: Int. code + (351)643-7287
Prof. Dr. A. Simon, Dr. J. Köhler, Dr. H. Mattausch
Max-Planck-Institut für Festkörperforschung
Heisenbergstrasse 1, D-70569 Stuttgart (Germany)

[**] We thank Professor P. Böttcher and Professor H. G. von Schnering for helpful discussions, and the Deutsche Forschungsgemeinschaft and the Volkswagen-Stiftung for financial support.

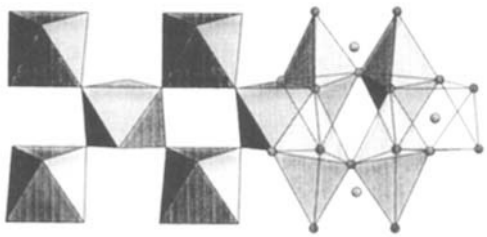

Fig. 2. Strand of corner-linked $RuSn_6$ octahedra (left) and the representation of the Sn_4 tetrahedra resulting from tilting the octahedra (right).

structure contains a further Sn atom (Sn 11) marked with an arrow in Figure 1, which does not belong to the assembly of the strand. This Sn atom leads to the loss of the symmetry centers (*Cm* instead of *C2/m*), whereas the variation of all other atom positions from the higher symmetry is small. Thus, there are two equivalent positions for the specially positioned Sn atom which are linked through a pseudo inversion center in the center of the strand. According to X-ray crystallographic findings[4] only one position is occupied (Fig. 1). Bond length–bond strength considerations[6, 7] show that the bonding around the occupied and the empty position are completely equivalent, which is manifested in the uniform bond order sums near 2 for the participating O atoms. The discrete Sn atom is also divalent. The corresponding analysis of the Sn–O bonds for the Sn atoms in the strand showed that all the terminal atoms likewise are divalent (type 1: Sn 1,2,3,4,5,6,8,10), whereas the atoms that function as linking elements in the strand (type 2: Sn 7,9) have bond order sums of almost 1.[8] The difference results directly from the coordination of the Sn atoms: eight atoms of the type 1 form the apices of SnO_4 pyramids such as in SnO, two atoms form the apices of trigonal SnO_3 pyramids. The apices of the pyramids each point towards the Ru atoms. The (four) atoms of type 2 are coordinated in a distorted tetrahedral fashion by two O and two Ru atoms. The most striking structural feature in $Ru_3Sn_{15}O_{14}$ are the corner-linked $RuSn_6$ octahedra. The Ru–Sn distances lie in the range between 251 and 262 pm and the Sn–Sn distances between 333 and 380 pm. $RuSn_6$ octahedra are also found in the intermetallic phase Ru_2Sn_3.[11] Here the Ru–Sn distances are (2×) 282 and (4×) 259 pm. The $RuSn_6$ octahedron is also known from the "inorganometallic complex" $[Ru(SnCl_3)_6]^{4-}$.[12]

The linkage scheme given in Figure 2 is closely related to the topology of the perovskite structure. In the latter, corner-sharing TiO_6 octahedra are arranged parallel. In the $GdFeO_3$ variant[13] the octahedra are tilted towards one another. Those in the strand found in $Ru_3Sn_{15}O_{14}$ correspond to a one-dimensional section of this structure. However, the tilting of the octahedra in the strand is so extreme that faces and edges of neighboring octahedra span almost regular tetrahedra, which in turn are linked together through a face, edge, and two corners. Thus, the sequence of the Sn atoms parallel to (001) corresponds to the section from a hexagonal close packing arrangement.

The above comparison with the perovskite structure is a rough simplification, in that in $Ru_3Sn_{15}O_{14}$ metal-centered metal octahedra are linked to one another. Systems of con-

densed clusters with such units, among others those with Ru as interstitial atom, are known for the electropositive rare earth metals, however only in terms of the motif of the edge linkage.[14, 15] A diverse range of corner-sharing systems of metal octahedra occur in metal-rich oxoniobates.[16] In contrast to $Ru_3Sn_{15}O_{14}$, here strong homonuclear metal–metal bonds are present, and the octahedra are empty. Indeed, the strand found in the latter compound corresponds to a one-dimensional section from the layers of octrahedra in $Ba_2Nb_5O_9$ with a tilting of the octahedra by about 30°. Interestingly, the special direction of this section in the metal-rich oxoniobates could so far not be detected despite a directed search.

The band structure calculation on the basis of the extended Hückel method[17, 18] shows $Ru_3Sn_{15}O_{14}$ to be a semiconductor (Fig. 3a), in agreement with the transparency of the compound. The COOP analysis reveals that, as expected, no Sn–Sn bonds but exclusively strong Sn–O and Ru–Sn bonds are present.

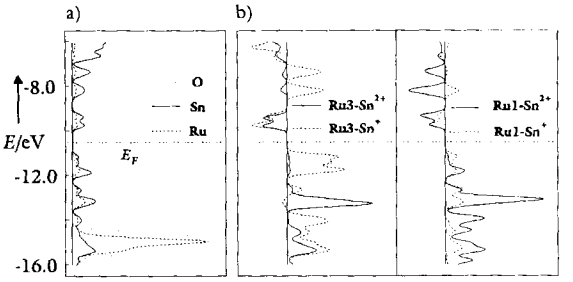

Fig. 3. a) Projected density of states for $Ru_3Sn_{15}O_{14}$. b) COOP curves for Ru3 Sn and Ru1–Sn interactions in the $RuSn_6$ octahedra (to the right bonding). Ru1 and Ru2 atoms center the peripheral octahedra. Ru3 atoms the central $RuSn_6$ octahedra. The COOP curves for Sn atoms of the same oxidation state are very similar within a $RuSn_6$ octahedron and therefore are each represented as a sum in the figure.

The corresponding analysis of the Ru–Sn interactions shows very similar bonding for the peripheral Ru1 and Ru2 atoms, however, considerably different bonding for the central Ru3 atom (Fig. 3b). The difference may at first be surprising due to the geometrically very similar coordination of the Ru atoms by Sn atoms; however, it is simply the result of the already stressed chemical dissimilarity of the Sn atoms. Up to the Fermi edge E_F only bonding Ru–Sn states are occupied. The upper edge of the valence band is dominated by Ru–Sn^{1+} interactions, and, since the central Ru3 atom is surrounded by four Sn atoms of this type, the electronic structure directly below the Fermi edge is particularly dominated by the states of this atom.

By using a simple approach, a picture of the distribution of valence electrons can be developed, which explains the electronic localization. Starting from the oxidation state II for all Sn atoms of the type 1 and the discrete Sn atom, an ionic limit $(Ru_3Sn_{8/2})^{6+}(Sn^{2+})_{10}Sn^{2+}(O^{2-})_{14}$ is reached. With the oxidation state I for the Sn atoms of the type 2 a possible charge distribution follows according to $(RuSn_{4/2})^{2+}(RuSn_{2/2})_2^{2+}$ with a formally zero valent central Ru atom and monovalent peripheral Ru atoms. The distribution is plausible since the Sn atoms of the type 2 (3-electron donors) together with four and two atoms, respectively, of the type 1 (2-electron donors) lead to the 18-electron configuration for all Ru atoms: $\overset{0}{Ru}\overset{1+}{Sn_4}\overset{2+}{Sn_2}$ with $8e + 4\times 1/2\times 3e + 2\times 1\times 2e = 18e$ (central octahedron), $\overset{1+}{Ru}\overset{1+}{Sn_2}\overset{2+}{Sn_4}$ with $7e + 2\times 1/2\times 3e + 4\times 1\times 2e = 18e$ (peripheral octahedra); the linking $\overset{1+}{Sn}$ (3e) counts half and the terminal $\overset{2+}{Sn}$ (2e) is fully included in the count. Thus $Ru_3Sn_{15}O_{14}$ forms a solid-state analogue of a hypothetical (polymeric) carbonyl–nitrosyl complex $[Ru_3(NO)_4(CO)_{10}]^{2-}$.

Received: June 9, 1995 [Z 8074 IE]
German version: *Angew. Chem.* **1995**, *107*, 2307–2309

Keywords: clusters · ruthenium compounds · solid-state structures · tin compounds

[1] C. Iwakura, K. Sakamoto, *J. Electrochem. Soc.* **1985**, *132*, 2420.
[2] G. Nichterwitz, H. Oppermann, W. Reichelt, *Z. Anorg. Allg. Chem.* **1992**, *615*, 61.
[3] Synthesis from $SnO_2/Ru_3Sn_{15}O_{14}/Sn_{liquid}$ or $Ru_3Sn_7/Ru_3Sn_{15}O_{14}/Sn_{liquid}$ mixtures. These were heated to 1000 °C in 1 h, then cooled to 700 °C at 1K h^{-1} and subsequently cooled to room temperature without controlling the rate of cooling. The single crystals are found in the Sn regulus and were extracted with HCl.
[4] Crystallographic data of $Ru_3Sn_{15}O_{14}$: $M = 2307.55\ g\,mol^{-1}$, monoclinic, *Cm* (no. 8), $a = 1239.0(2)$, $b = 707.4(2)$, $c = 1290.8(3)$ pm, $\beta = 108.60(2)°$, $Z = 2$, $\rho_{calcd} = 7.147\ g\,cm^{-3}$, $\rho_{pyc} = 7.2(2)\ g\,cm^{-3}$, 2603 measured reflections (CAD4, Enraf-Nonius), of which 2583 with $I > 2\sigma(I)$. The structure was solved by direct methods, FMLS refinement against F^2 (SHELX 93). Atomic positions: Ru 1: 0.69763(9), 0.0000, 0.69367(9); Ru 2: 0.38424(9), 0.5000, 0.23182(9); Ru 3: 0.78852(10), 0.5000, 0.96509(10); Sn 1: 0.90146(8), 0.0000, 0.82168(8); Sn 2: 0.48714(8), 0.0000, 0.58026(9); Sn 3: 0.74593(6), 0.74369(10), 0.57386(6); Sn 4: 0.59472(8), 0.5000, 0.33965(10); Sn 5: 0.94243(9), 0.5000, 0.87329(10); Sn 6: 0.65110(9), 0.5000, 0.08000(9); Sn 7: 0.66898(6), 0.75967(10), 0.83762(6) Sn 8: 0.17984(9), 0.5000, 0.11191(9) Sn 9: 0.40866(6), 0.26267(10), 0.08877(6); Sn 10: 0.83666(6), 0.74117(11), 0.34677(6); Sn 11: 0.51563(8), 0.5000, 0.61972(9); O 1: 0.9103(7), 0.2122(11), 0.5356(6); O 2: 0.9606(12), 0.0000, 0.9917(9); O 3: 0.6204(10), 0.5000, 0.5257(9); O 4: 0.1250(9), 0.5000, 0.9423(10); O 5: 0.4237(11), 0.0000, 0.4109(9); O 6: 0.3449(12), 0.0000, 0.6293(12); O 7: 0.7014(6), 0.7259(10), 0.4068(6); O 8: 0.5866(7), 0.7687(11), 0.1182(8); O 9: 0.9901(7), 0.7536(10), 0.8177(6); O 10: 0.7258(9), 0.5000, 0.2516(9); $R = 0.044$, $wR2 = 0.109$. The rhombohedral arrangement ($a = 1290.8$ pm, $\alpha = 31.74°$) which suggests itself is not applicable according to the splitting of the reflections in the powder diagram. The occurrence of *Cm* (instead of *C2/m*) is clearly evident from the refinement. The calculation in *C2/m* without Sn11 gives $R1 = 0.20$ ($wR2 = 0.47$), with half-filled Sn11 position $R1 = 0.20$ ($wR2 = 0.28$). Further details of the crystal structure investigation may be obtained from the Fachinformationszentrum Karlsruhe, D-76344 Eggenstein-Leopoldshafen (Germany) on quoting the depository number CSD-401827.
[5] Ru = 9.88 mol%, Sn = 48.89 mol%, O = 41.23 mol%: T. Söhnel, W. Reichelt, G. Nichterwitz, 7. Vortragstagung der Arbeitsgruppe Festkörperchemie der GDCh, Bonn, **1994**, Poster PO II 66.
[6] With $s_i(Sn–O) = [d(Sn–O)/1.86]^{-4.5}$ according to I. D. Brown [7] the following bond order sums $\Sigma s_i(Sn–O)$ were obtained for Sn1 = 1.86, Sn2 = 2.08, Sn3 = 2.03, Sn4 = 2.01, Sn5 = 1.85, Sn6 = 1.98, Sn7 = 0.88, Sn8 = 1.95, Sn9 = 0.93, Sn10 = 2.04, Sn11 = 2.09.
[7] I. D. Brown in *Structure and Bonding in Crystals, Vol. II* (Eds.: M. O'Keeffe, A. Navrotsky), Academic Press, New York, **1981**, S. 1 ff.
[8] Tin also exists in the unusual oxidation state + I in SrSnP [9,10].
[9] B. Eisenmann, H. Jordan, H. Schäfer, *J. Less-Common Met.* **1986**, *116*, 251.
[10] F. R. Wagner, Dissertation, Universität Saarbrücken, **1993**.
[11] O. Schwomma, H. Nowotny, A. Wittemann, *Monatsh. Chem.* **1964**, *95*, 1538.
[12] T. Yamakawa, H. Moriyama, S. Shinoda, Y. Saito, *Inorg. Chem.* **1987**, *26*, 3347.
[13] P. Coppens, M. Eibschütz, *Acta Crystallogr.* **1965**, *19*, 524.
[14] T. Hughbanks, J. D. Corbett, *Inorg. Chem.* **1989**, *28*, 631.
[15] M. W. Payne, P. K. Dorhout, S.-J. Kim, T. R. Hughbanks, J. D. Corbett, *Inorg. Chem.* **1992**, *31*, 1389.
[16] J. Köhler, G. Svensson, A. Simon, *Angew. Chem.* **1992**, *104*, 1463; *Angew. Chem. Int. Ed. Engl.* **1992**, *31*, 1437.
[17] R. Hoffmann, *J. Chem. Phys.* **1963**, *39*, 1397. H_{ij} matrix elements: J. H. Ammeter, H.-B. Bürgi, J. C. Thibeault, R. Hoffmann, *J. Am. Chem. Soc.* **1978**, *100*, 3686. Tight-binding-approach: M.-H. Whangbo, R. Hoffmann, *J. Am. Chem. Soc.* **1978**, *100*, 6093. Special k points: R. Ramirez, M. C. Böhm, *Int. J. Quantum Chem.* **1986**, *30*, 391; R. H. Summerville, R. Hoffmann, *J. Am. Chem. Soc.* **1976**, *98*, 7240.
[18] J. Köhler, P. Wunsch, PC-Version of the program EHMACC (extended-Hückel program by M.-H. Whangbo, R. Hoffmann, modified by M. Evain, J. Mitchell), Stuttgart, **1991**. Parameters for the EH calculations: atomic orbital energies H_{ij} [eV] (coefficients ζ_1) for O: 2s −32.36 (2.275), 2p −14.8 (2.275); Sn: 4s −16.16 (2.12), 4p −8.32 (1.82); Ru: 5s −10.4 (2.08), 5p −6.87 (2.04), 4d −14.90 (5.38). Double ζ functions were used for Ru: C_1 0.5340, ζ_2 2.30, and C_2 0.6365.

The "Submetalate" $Ba_{17}Al_3O_7$: The First Member of a New Class of Compounds**

Caroline Röhr* and Rita George

Recent investigations on metal-rich ternary oxides and nitrides have shown that these can have structural features, like those which occur in Rb/Cs suboxides, also with barium as an electropositive bonding partner. These structural features are namely units comprising face-linked oxygen-centered octahedra in a metallic matrix.[1] In the ternary sodium–barium subnitrides $NaBa_3N$[2] and Na_5Ba_3N,[3] octahedral chains ($^1_\infty[NBa_{6/2}]$) are present like those that occur in Cs_3O;[4] in the crystal structures of the isotypic series $Ba_{21}M_2O_5$ (M = In, Tl, Si, Ge),[5,6] $[O_5Ba_{18}]$ clusters consisting of five $[OBa_6]$ octahedra linked through four common faces were observed. The clusters in the above-mentioned compounds are separated by further metal atoms (Na, M, and Ba, respectively), comparable for example with the $[O_3Cs_{11}]$ units in Cs_7O.[7]

The synthesis of metallic, shining, brittle, extremely air-sensitive crystals of $Ba_{17}Al_3O_7$ (**1**) is achieved by the reduction of Al_2O_3 in barium-rich melts. Two crystallographically different Al and three crystallographically different O positions are found in the crystal structure (tetragonal, space group $P4_2/ncm$).[8] The Al1 atoms are tetrahedrally surrounded by oxide ions. Two tetrahedra each are linked through a common corner (O3) to give dialuminate ions $[Al_2O_7]^{8-}$ (Fig. 1a). The terminal oxygen

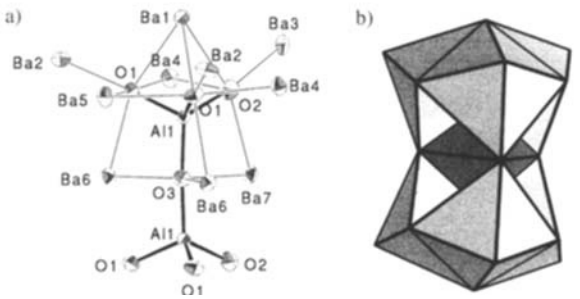

Fig. 1. The $[O_3(Al_2Ba_{17})]$ cluster with an internal dialuminate ion $[Al_2O_7]^{8-}$. a) ORTEP representation, b) polyhedral representation.

atoms of this anion (O1 and O2) are each centers of distorted octahedra comprising the Al1 atom and five Ba atoms. Three of these $[O(AlBa_5)]$ octahedra are linked through three common faces in such a way that the Al1–Ba1 edge is common to all three octahedra resulting in a $[O_3(AlBa_{10})]$ assembly. Thus, topologically, the linkage of the octahedra corresponds to those of the $[OCs_6]$ octahedra in the Cs suboxides (e.g. $Cs_{11}O_3$[9]). The bridging oxygen atom of the dialuminate ion is trigonal bipyramidally coordinated by three barium (Ba6 and Ba7) and two Al1 atoms. Two $[O_3(AlBa_{10})]$ clusters (light shading in Fig. 1b) are linked through common edges of the $[O(Al_2Ba_3)]$ trigonal bipyramids around O3 (dark) in such a way that clusters with the formula $[O_7(Al_2Ba_{17})]$ are formed. These subaluminate clusters are completely separated in the unit cell. The Al2 atoms are positioned in the region between the clusters, and these atoms achieve a distorted tetragonal antiprismatic coordination, surrounded by Ba atoms (Fig. 2). Clusters and coordination polyhedra about Al2 are corner-linked and form vertical [001] layers (Fig. 3).

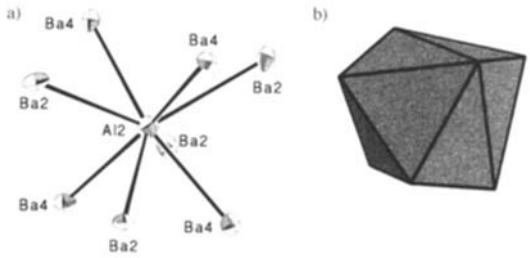

Fig. 2. The coordination polyhedron of the Al2 atom in the crystal structure of $Ba_{17}Al_3O_7$. a) ORTEP representation, b) polyhedral representation.

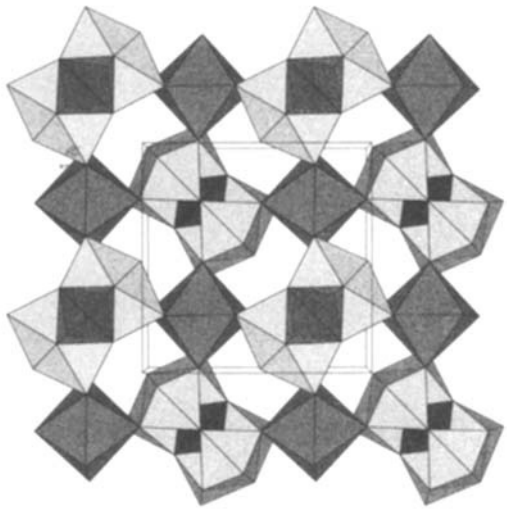

Fig. 3. View along [001] onto the layer of corner-linked $[O_7(Al_2Ba_{17})]$ clusters and distorted square antiprisms $[Al2Ba_8]$ ($z = 0$ to 1/2) in $Ba_{17}Al_3O_7$.

The Al–O distances (190.1–195.8 pm) in the dialuminate ion are significantly longer than the mean value of 176 pm found for aluminates. This result is not surprising considering the face linkage of the $[O(AlBa_5)]$ octahedra: like in the Rb/Cs suboxides with the same topology, the oxygen atoms in $Ba_{17}Al_3O_7$ (**1**) are shifted away from the centers of octahedra and the common octahedra faces; in good agreement with the findings in binary suboxides in this case are the longer Al–O bonds and the O–Ba distances which vary considerably (see below). Accordingly, the Al–O distance in the bridge—in contrast to the situation in the Si–O bonds of the disilicates—is shorter than the terminal Al–O bonds. The O-Al1-O angles deviate by up to 5° from the ideal tetrahedral angle; the angles to the bridging oxygen atom (111.9° and 114.5°, respectively) are larger and those between the terminal oxygen atoms are smaller (105.4° and 107.2°, respectively) than the ideal tetrahedral angle. The linear coordination of O^{2-} by Al^{3+} (for O3) is also found in the crystal structure of $BaAl_2O_4$.[10]

The O–Ba distances of the terminal oxygen atoms of the $[Al_2O_7]$ group vary from 252.2 (to "external" atoms Ba2/Ba3) to 299.1 pm and thus fluctuate—corresponding to the shift of O^{2-} from the octahedra centers—about the value in real salts (e.g. BaO: 275 pm). Similarly short O–Ba distances are known in the suboxides $Ba_{21}M_2O_5$.[6] The O–Ba distances of the bridging O3 atoms, which form the centers of trigonal bipyramids

[*] Dr. C. Röhr, R. George
Eduard-Zintl-Institut der Technischen Hochschule, Anorganische Chemie II
Hochschulstrasse 10, D-64289 Darmstadt (Germany)
Telefax: Int. code + (6151)166029

[**] We thank Prof. Dr. R. Kniep and Dr. habil. B. Eisenmann for their generous support and many stimulating discussions. This work was supported by the Dr.-Otto-Röhm-Gedächtnis-Stiftung.

$[O(Al_2Ba_3)]$, are of the same order of magnitude (265.3 and 273.9 pm). The Ba–Ba distances in the clusters are 372.1–444.7 pm and thus lie in the range of distances in salts (e.g. BaO: 389 pm). In contrast, the distances between the clusters (apart from Ba1–Ba4 with 406.6 pm) are greater than 443.7 pm and thus lie in the range typical for metals (Ba–Ba in the metal: 436 pm; metallic radius: 224 pm[11]). The same is true for the Ba–Al2 distances, which with values of 347.7–381.5 pm (for CN 8 for Al to Ba) are comparable to the atomic distances in the intermetallic phases Ba_4Al_5[12] and Ba_3Al_5[13] (352–370 pm).

The first dialuminate ion described to date occurs in $Ba_{17}Al_3O_7$ (**1**). However, the Al–O distances, as a result of the face linkage of the $[O(AlBa_5)]$ octahedra, are significantly longer than in comparable electrovalent[*] aluminates; thus, a description as $[Al_2O_7]^{8-}$ can be considered as a resonance formula.

Like the oxide ions in the suboxides, these dialuminate ions in **1** form the centers of clusters ($[[O_7(Al_2Ba_{17})]]$); thus the compound can be described as a "subaluminate" in analogy to the suboxides. The comparability is evident from the bond lengths and coordination numbers: *within* the clusters the conditions are typically ionic and *between* the clusters they are typically metallic. The direct structural analogy to the clusters comprising oxygen-centered face-sharing octahedra, characteristic for the suboxides, however, requires the inclusion of the Al centers of the complex anion in the octahedra, thus one may refer to heteroclusters. The relationship of $Ba_{17}Al_3O_7$ (**1**) to the suboxides is particularly apparent, since elements of the $[O_7(Al_2Ba_{17})]$ cluster are topologically identical with the $[O_3Cs_{11}]$ cluster in the Cs suboxides.

The possibility of including "metallic" M (M = element of group 13 and 14) into the regions between the subclusters in metal-rich oxides is already known for the series of isotypic compounds $Ba_{21}M_2O_5$ (M = In, Tl, Si, Ge).[6] As in this series, the metallic state of M in **1** is also revealed by the distances and coordination numbers characteristic for metals.

Thus, $Ba_{17}Al_3O_7$ (**1**) is the first compound that contains both cationic (within the clusters) and metallic aluminum (between the clusters). In analogy to the suboxides, this compound can be regarded as the first member of a new class of compounds, namely the submetalates.

Experimental Procedure

$Ba_{17}Al_3O_7$ (**1**) was formed by the reduction of dried powders of Al_2O_3 (Merck, analytical grade) and ZnO (Merck, analytical grade) with elemental barium (Degussa, 99.5%) with Ba:ZnO:Al_2O_3 ratios of 15:1:1. The samples were heated to 1020 K in dried corundum crucibles under argon, tempered for 5 h, and then cooled down again at a rate of 150 K h^{-1}. Compound **1** crystallized in a barium matrix together with $Ba_{21}Zn_2O_5$ ($Ba_{21}Si_2O_5$ type [6]) and BaZn in the form of brittle, xenomorphic crystals with a metallic shine, which decomposed in moist air within a few seconds. It is still unclear whether the ZnO acts as a mineralizer in the synthesis, however, it can be replaced by other transition metal oxides such as NiO. The synthesis of phase-pure **1** has so far not been achieved. The EDX analysis of the measured crystal confirms within the limits of error of the method the composition determined from X-ray investigations (results for the measured crystal (in wt%, theoretical values in parentheses): Ba 84.7(85.0), Al 15.3(15.0)). For the crystal structure analysis selected crystals were sealed in X-ray capillaries under Na-dried paraffin oil.

Received: April 20, 1995
Revised version: June 26, 1995 [Z 7910IE]
German version: *Angew. Chem.* **1995**, *107*, 2311–2313

Keywords: aluminates · barium compounds · subnitrides · suboxides

[*] Compounds are referred to as electrovalent when the valence electrons, in accord with common assumptions, can be attributed unequivocally to specific atoms.

[1] A. Simon, *Struct. Bonding* **1979**, *36*, 81.
[2] P. E. Rauch, A. Simon, *Angew. Chem.* **1992**, *104*, 1505; *Angew. Chem. Int. Ed. Engl.* **1992**, *31*, 1519.
[3] G. J. Snyder, A. Simon, *J. Am. Chem. Soc.* **1995**, *117*, 1996–1999.
[4] K. R. Tsai, P. M. Harris, E. N. Lassettre, *J. Phys. Chem.* **1956**, *60*, 345–347.
[5] C. Röhr in *3. Jahrestagung der Deutschen Gesellschaft für Kristallographie, Darmstadt Suppl. Issue Nr. 9, Z. Krist.*, p. 24, März **1995**.
[6] C. Röhr, *Z. Anorg. Allg. Chem.*, in press.
[7] A. Simon, *Z. Anorg. Allg. Chem.* **1976**, *422*, 208–218.
[8] a) Crystal structure data for $Ba_{17}Al_3O_7$ **1** at $T = 275$ K: tetragonal, space group $P4_2/ncm$ (no. 138), $a = 1480.8(9)$, $c = 1886.2(14)$ pm, $V = 4136(6)$ Å^3, $Z = 4$, $\rho_{X\ ray} = 4.06$ g cm^{-3}, diffractometer: Siemens P4 ($Mo_{K\alpha}$ radiation, graphite monchomator); $\mu(Mo_{K\alpha}) = 15.95$ mm^{-1}, $2\theta_{max} = 55^\circ$, 4520 measured reflections; 2467 independent reflections; Lorentz, polarization, and empirical absorption correction [8b]; structure solution by direct methods [8c]; least squares refinement (all atoms anisotropic) with SHELXL-93 [8d]; 76 free parameters, GoF = 1.16, R values ($I \geq 2\sigma(I)$): $R1 = 0.044$, $wR2 = 0.098$; residual electron density: 1.5/−1.6 e × 10^{-6} pm^{-3}. Further details of the crystal structure investigation may be obtained from the Fachinformationszentrum Karlsruhe, D-76344 Eggenstein-Leopoldshafen (Germany) on quoting the depository number CSD-401792. b) N. Walker, D. Stuart, program DIFABS, *Acta Crystallogr. Sect. A* **1983**, *39*, 158–166; c) G. Sheldrick, program SHELXS-86, *Acta Crystallogr. Sect. A*, **1990**, *46*, 467; d) G. Sheldrick, program SHELXL-93, *J. Appl. Crystallogr.* **1993**.
[9] A. Simon, E. Westerbeck, *Z. Anorg. Allg. Chem.* **1977**, *428*, 187–198.
[10] W. Hörkner, H. K. Müller-Buschbaum, *Z. Anorg. Allg. Chem.* **1979**, *451*, 40–44.
[11] W. B. Pearson, *The Crystal Chemistry and Physics of Metals and Alloys*, Wiley Interscience, New York, **1972**.
[12] M. L. Fornasini, *Acta Crystallogr. Sect. B* **1975**, *31*, 2551–2553.
[13] M. L. Fornasini, *Acta Crystallogr. Sect. C* **1975**, *44*, 1355–1357.

Synthesis and Properties of First to Third Generation Dendrimers with Doubly and Triply Branched Chiral Building Blocks**

Peter Murer and Dieter Seebach*

Dedicated to Professor Manfred Regitz on the occasion of his 60th birthday

In our work on the synthesis of chiral dendrimers[1] we have thus far used –with one exception[2]—only chiral central units and achiral branches[2–5] (cf. ref. [6]). We report here on the synthesis and properties of dendrimers of the zero to third generation[7] containing, without exception, chiral building blocks in both the central unit and the branches.

The method was outlined in our earlier work,[2, 5] and follows the convergent route first adopted by Fréchet et al.[8] For both, double and triple branching, (*R*)-3-hydroxybutanoic acid was used as the starting material. It was benzylated[9] for the double branching (see **1**) and hydroxybenzylated[10] for the triple branching, where two epimers **2** and **3** became available. For the peripheral building blocks, the OH groups of the branched diols and triols were etherified with MeI. The *tert*-butyldiphenylsilyl (TBDPS) protective groups in **1**–**3** (R = Me) were removed to construct the branches and a benzylic bromide was prepared, which was then used for the etherification of the OH groups of the corresponding diol or triol. Reaction of this branch bromide with the triols **4a** and **4b**[4] yielded dendrimers **5**–**7** with unextended and **8**–**11** with elongated central units, respectively (Scheme 1).

[*] Prof. Dr. D. Seebach, Dipl.-Chem. P. Murer
Laboratorium für Organische Chemie der
Eidgenössischen Technischen Hochschule
ETH-Zentrum, Universitätstrasse 16, CH-8092 Zürich (Switzerland)
Telefax: Int. code + (1)632-1144
e-mail: seebach@org.chem.ethz.ch

[**] Part of the proposed dissertation by P. Murer.

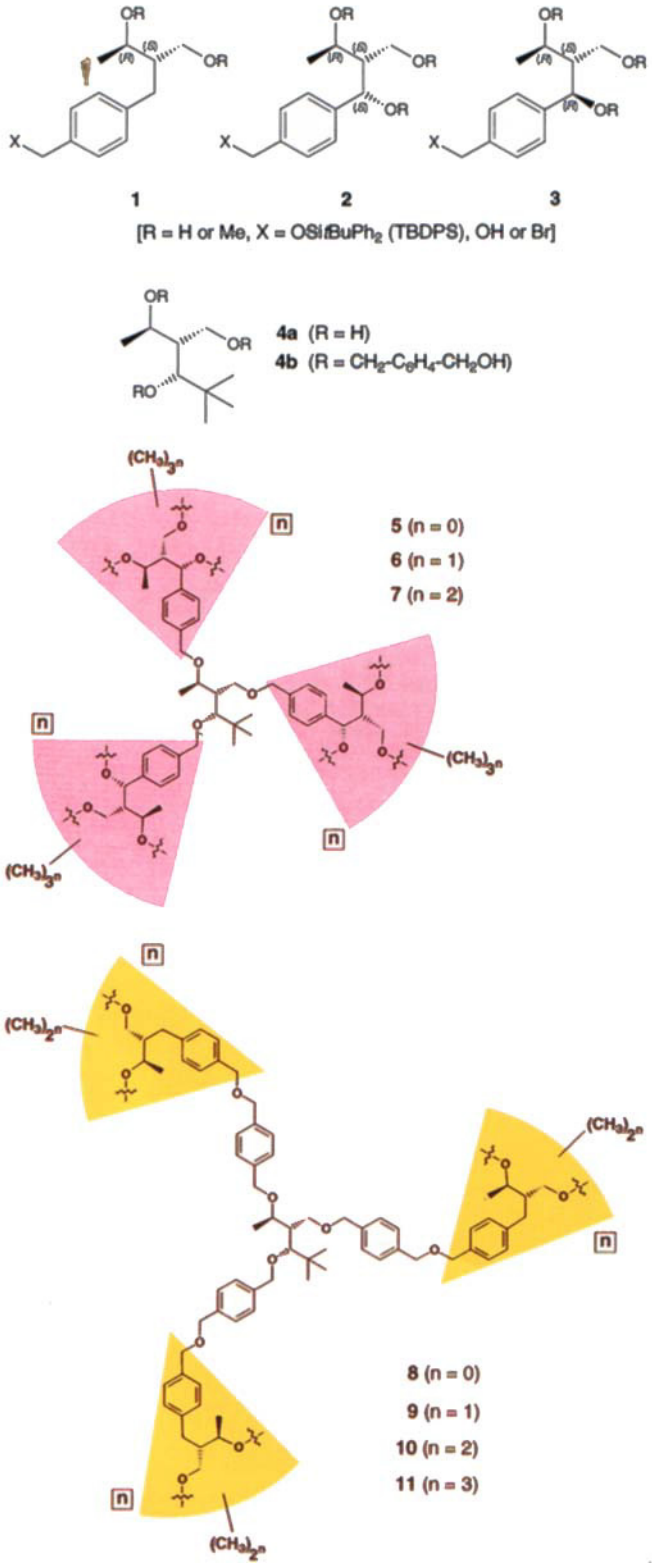

Scheme 1. Building blocks **1**–**4** for the construction of the dendrimers **5**–**11**; general formulae of the triply branched dendrimers **5**–**7** with unextended central units and the doubly branched dendrimers **8**–**11** with elongated central units.

As expected with an increasing number of generations, a higher degree of branching and the absence of an extension at the central unit, the coupling of three branches with triols of type **4** became increasingly more difficult.[11] Scheme 2 shows the largest molecules with triple or double branching which we have been able to prepare up to now; they are **7** (2nd generation, unextended central unit, 39 stereogenic centers) and **11** (3rd generation, extended central unit, 45 centers, 3.5×10^{13} possible stereoisomers, molecular weight 4911 Da). All branch building blocks and final dendrimers were fully characterized (IR, ^{1}H NMR, ^{13}C NMR, UV, CD, mass spectrometry, osmometry, and elemental analysis).

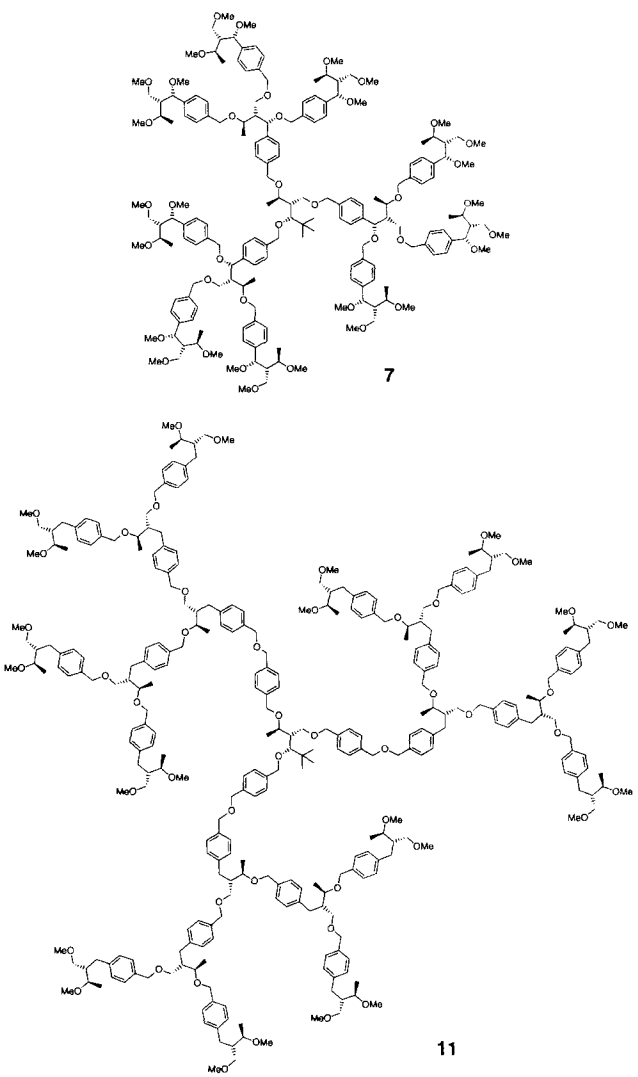

Scheme 2. The triply branched second generation dendrimer **7** with an unextended central unit and the doubly branched third generation dendrimer **11** with an elongated central unit.

In the synthesis of the most compact dendrimer **7**, we stumbled upon a spectacular case of diastereoselectivity (Scheme 3): when a branch bromide **12a** with (*S*)-configuration at the four benzylic stereogenic centers was used, the reaction proceeds smoothly to give the desired dendrimer **7** (51 % yield); if, on the other hand, the corresponding (*R*)-configured bromide **12b** was used, the reaction stopped at the doubly coupled product **13b** (88 % yield).[12]

At room temperature the dendrimers are very viscous, honey-like (**6**, **9**–**11**) or glassy (**7**, **13b**) substances, some of which retain solvent tenaciously (to obtain an analytically pure sample of **11**, it had to be kept at 80 °C/0.02 Torr for several days). These dendrimers are very soluble in moderately polar solvents such as CH_2Cl_2, $CHCl_3$, and Et_2O.[13]

The signal for the central hydrogen appears at $\delta = 2.46$ in the ^{1}H NMR spectrum of **7**. On the other hand, for **5** and **6**, for the analogues with elongated central units and for all doubly

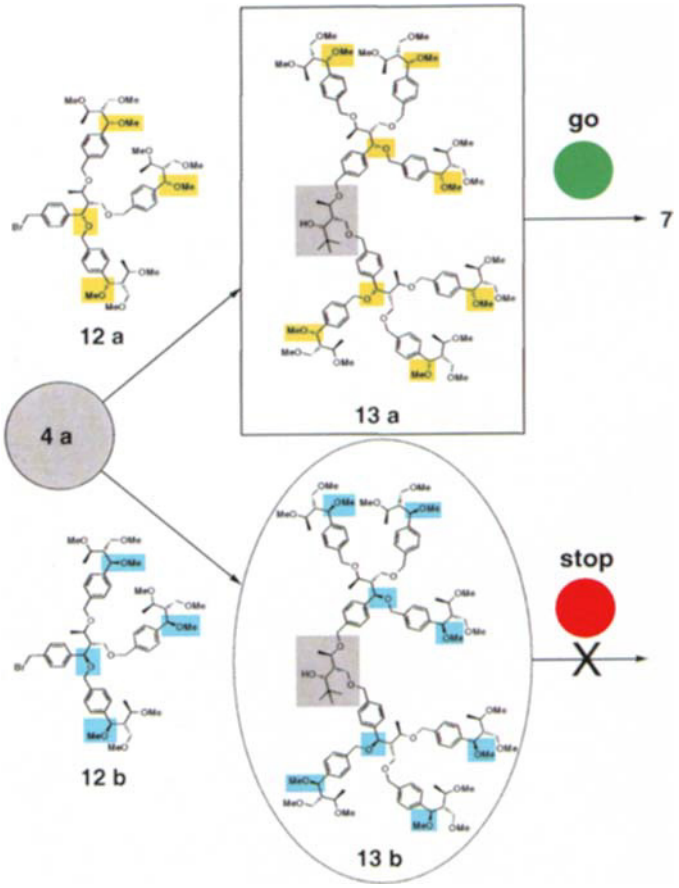

Scheme 3. Preparation of dendrimer **7** from the central unit **4a** and the branch bromide **12a** via **13a**. The attempted formation of a diastereoisomer of **7** by coupling with the branch bromide **12b** led to **13b** which carried only two branches and which did not react further.

branched dendrimers it appears at $\delta = 2.30$. The MALDI-TOF mass spectrum of **11** recorded in the linear mode is shown in Figure 1.

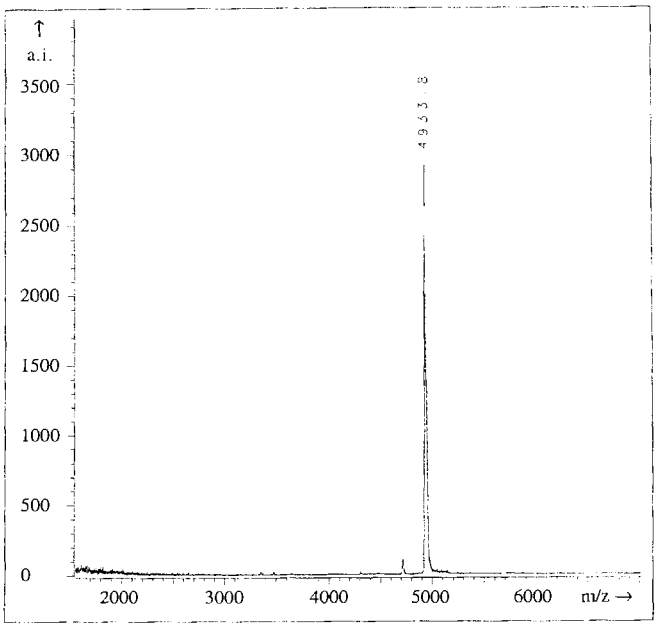

Fig. 1. MALDI-TOF mass spectrum of **11**. Recording conditions: linear mode, acceleration energy: 20.0 kV, N_2 laser (337 nm), α-cyano-4-hydroxycinnamic acid matrix, Bruker REFLEX. The peak at 4934 corresponds to $[M^+ + Na]$.

The chiroptical properties of the dendrimers presented here are informative. In the triply branched dendrimers, a reversal of the sense of rotation is observed on going from the first to the second generation (**6**: $[\alpha]_D = -38$; **7**: $[\alpha]_D = +12$). In the doubly branched dendrimers, this occurs on going from the second to the third generation (**10**: $[\alpha]_D = +4$; **11**: $[\alpha]_D = -5$). The CD spectra of the doubly branched compounds **8**–**11** in the region 220 to 270 nm are shown in Figure 2. As can be seen, the nature

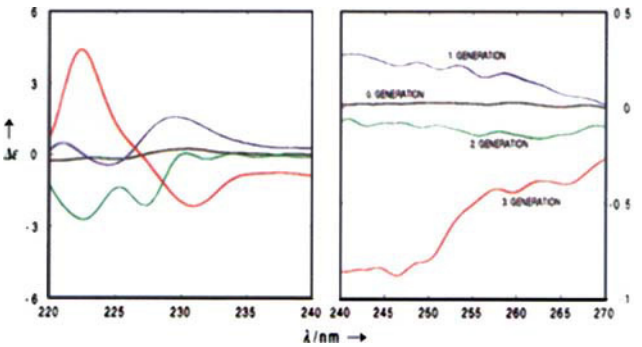

Fig. 2. CD spectra of the dendrimers **8**–**11** (10^{-3} to 10^{-4} M in CH_3CN, JASCO-J-710 spectrometer). Black: **8**, blue: **9**, green: **10**, red: **11**. The region of the spectrum usually used for the application of the benzene-sector and chirality rules [14] is shown on the right. The λ_{max} values for the long wavelength benzene absorption in the UV spectra of **8**–**11** alternate and lie at 261, 255, 263, and 254 nm, respectively.

of the curves changes from generation to generation; particularly large differences appear in moving from the second (**10**) to the third (**11**) generation. This may be an indication of conformationally chiral substructures in the dendrimer branches.

We are currently preparing larger quantities of chiral dendrimers to enable us to test their chemical behavior, for example, as additives to solvents for enantioselective reactions.

Received: March 10, 1995
Revised version: June 26, 1995 [Z 7795 IE]
German version: *Angew. Chem.* **1995**, *107*, 2297–2300

Keywords: asymmetric syntheses · chiral dendrimers · circular dichroism · dendrimers · mass spectrometry

[1] Recent reviews of all kinds of dendrimers: a) J. Issberner, R. Moors, F. Vögtle, *Angew. Chem.* **1994**, *106*, 2507; *Angew. Chem. Int. Ed. Engl.* **1994**, *33*, 2413; b) G. R. Newkome, *Advances in Dendritic Macromolecules, Vol. 1*, Jai, Greenwich, **1994**.

[2] The triply branched first generation dendrimer **2**: D. Seebach, J.-M. Lapierre, K. Skobridis, G. Greiveldinger, *Angew. Chem.* **1994**, *106*, 457; *Angew. Chem. Int. Ed. Engl.* **1994**, *33*, 440.

[3] D. Seebach, J.-M. Lapierre, W. Jaworek, P. Seiler, *Helv. Chim. Acta* **1993**, *76*, 459.

[4] J.-M. Lapierre, K. Skobridis, D. Seebach, *Helv. Chim. Acta* **1993**, *76*, 2419.

[5] D. Seebach, J.-M. Lapierre, G. Greiveldinger, K. Skobridis, *Helv. Chim. Acta* **1994**, *77*, 1673.

[6] Recent work on first generation dendrimers with chiral extension units [6a] or chiral peripheral building blocks [6b] and on dendrimers from amino acid building blocks [6c] see: a) H.-F. Chow, L. F. Fok, C. C. Mak, *Tetrahedron Lett.* **1994**, *35*, 3547; b) H. Brunner, J. Fürst, *Tetrahedron* **1994**, *50*, 4303; J. F. G. A. Jansen, H. W. I. Peerlings, E. M. M. de Brabander-Van den Berg, E. W. Meijer, *Angew. Chem.* **1995**, *107*, 1321; *Angew. Chem. Int. Ed. Engl.* **1995**, *34*, 1206; c) K. Rose, *J. Am. Chem. Soc.* **1994**, *116*, 30; C. Rao, J. P. Tam, *ibid.* **1994**, *116*, 6975.

[7] For nomenclature see: G. R. Newkome, G. R. Baker, J. K. Young, J. G. Traynham, *J. Polym. Sci. Part A: Polym. Chem.* **1993**, *31*, 641; [1b], pp. 169–186.

[8] C. J. Hawker, J. M. J. Fréchet, *J. Am. Chem. Soc.* **1990**, *112*, 7638; K. L. Wooley, C. J. Hawker, J. M. J. Fréchet, *J. Chem. Soc. Perkin Trans. 1* **1991**, 1059.

 © VCH Verlagsgesellschaft mbH, D-69451 Weinheim, 1995 0570-0833/95/3419-2118 $ 10.00+.25/0

[9] J. Zimmermann, D. Seebach, T.-K. Ha, *Helv. Chim. Acta* **1988**, *71*, 1143.
[10] W. Amberg, D. Seebach, *Chem. Ber.* **1990**, *123*, 2413.
[11] Conditions: 1 equiv triol, 9 equiv NaH in THF, 3.5 equiv branch bromide, 0 °C to reflux temperature.
[12] It was not confirmed that in **13b** the OH group adjacent to the *t*Bu group was actually present in the unetherified form.
[13] As already observed with other larger dendrimers, **11** showed an unusual elution behavior on chromatography; cf. Z. Xu, M. Kahr, K. L. Walker, C. L. Wilkins, J. S. Moore, *J. Am. Chem. Soc.* **1994**, *116*, 4537.
[14] K. Nakanishi, N. Berova, R. W. Woody, *Circular Dichroism*, VCH, New York, **1994**.

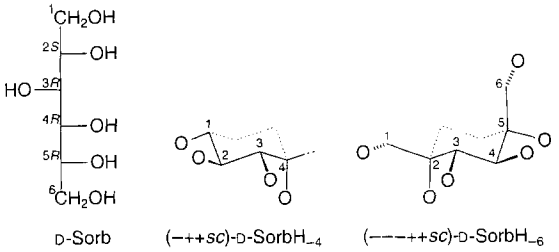

Scheme 1. D-Sorbitol (D-Sorb) in the Fischer projection (left), as a fourfold (center), and as a sixfold deprotonated ligand (right) in **1**; the additional dotted lines completing C_4 fragments leading to six-membered rings helps to provide a three-dimensional impression; charges have been omitted.

A Hexadecanuclear Polyolatometalate of Copper(II) Ions and Multideprotonated D-Sorbitol**

Peter Klüfers* and Jörg Schuhmacher

Polyols can be multideprotonated in aqueous alkali solutions of copper(II) salts to furnish polyolatocuprates; ligands with three or more functional groups, such as anions of glycerol or sugar alcohols, can be used as building blocks for the formation of oligo- or polymeric metalates.[1] For the synthesis of multinuclear alkoxo clusters, which for instance, could be interesting as low-dimensional magnetic materials, chiral hexitols seem to be the best ligands to choose: They are readily available, and the numerous potential sites for bonding to the metal atom are fixed in a pattern of low symmetry, and thus a complex molecular architecture can be deliberately imposed upon the end products.

Metal complexes of chiral hexitols have probably been known for a long time. Much attention has been paid to the compound arising from iron(III) ions and D-sorbitol in aqueous alkali solutions; the structure is not known, although a multinuclear framework is conceivable.[2] We report here on the crystallization and structural elucidation[3] of the D-sorbitol–copper(II) compound **1**, which is obtained on concentrating aqueous solutions of the composition LiOH:$Cu(OH)_2$:D-sorbitol in the molar ratio of 1:2:1 in the form of monoclinic, blue crystals of the same stoichiometry. In **1** (D-Sorb = D-sorbitol) half of the

$Li_8[Cu_{16}(D\text{-}SorbH_{-6})_4(D\text{-}Sorb1,2,3,4H_{-4})_4]\cdot ca.\ 46H_2O$ **1**

D-sorbitol ligands are completely deprotonated η^6,μ_5-hexaanions (Scheme 1), which form regardless of the protolytic equilibria and the competing aqua, hydroxo, and oxo ligands of the aqueous system. The other half of the D-sorbitol ligands are present as μ_3-tetraanions, in which four neighboring hydroxy groups have been deprotonated (H at O-1 to O-4 using the same numbering as for glucose, cf. Scheme 1). The eight polyolate ions are the sole ligands in this, therefore homoleptic, hexadecanuclear cuprate. To our knowledge there are no examples known of nonpolymeric copper(II) complexes with a greater number of metal atoms. It appears that such a multinuclear structure is necessary in order to achieve the largest possible number of metal–ligand contacts for a hexadentate, but C_1 symmetric ligand (cf. the simple structure of the coordination polymer from copper(II) ions and the anion of dulcitol, an isomeric hexitol of C_i symmetry[1b]).

The hexadecacuprate ion is toroidal with an oval cross-section and has approximate D_2 symmetry (Fig. 1).[3] It resembles the multinuclear polyolato metal structures obtained with cyclodextrin ligands. In contrast to compound **1**, the shape of the torus in $Pb_{16}(\gamma\text{-}CDH_{-16})_2$[4] is predetermined by the ligands. Common to both compounds is the fact that they do not need to be synthesized in metal-rich solutions; they can also be ob-

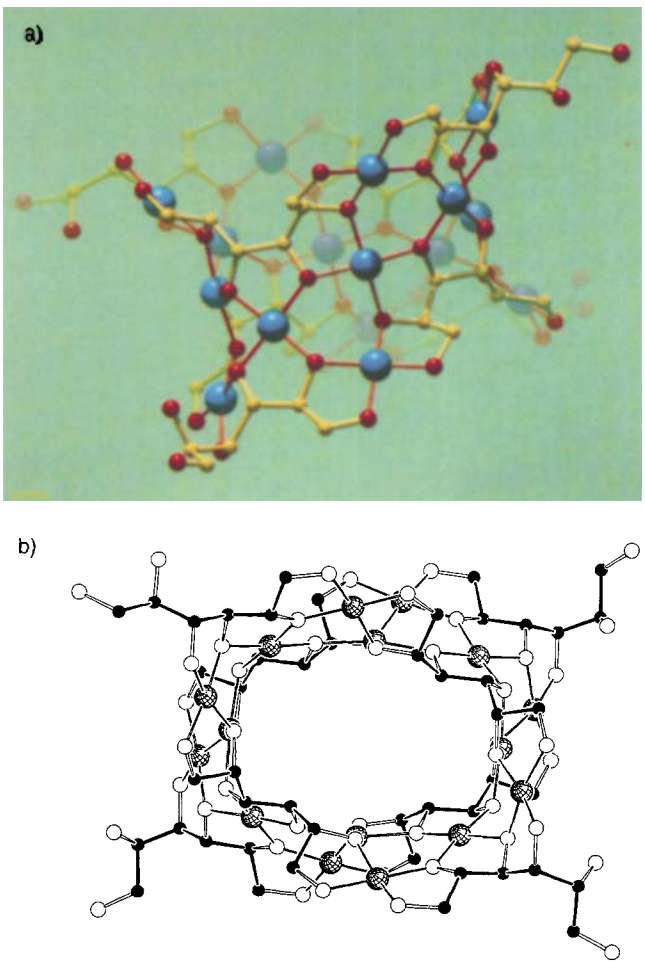

Fig. 1. Two views of the toroidal hexadecacuprate ion in **1**. a) Side view of the area of least curvature (blue: Cu, red: O, yellow: C). b) Oval cross-section (large circles: Cu, small circles: C (shaded), O (unshaded).

[*] Prof. Dr. P. Klüfers, Dipl.-Chem. J. Schuhmacher
Institut für Anorganische Chemie der Universität
Engesserstrasse, Gebäude 30.45, D-76128 Karlsruhe (Germany)
Telefax: Int. code + (721) 608-4290
e-mail: kluefers@achibm2.chemie.uni-karlsruhe.de

[**] Polyol · Metal Complexes, Part 15. This work was supported by the Bundesministerium für Forschung und Technologie (grant no. 0319368A) and by Akzo AG, Wuppertal (Germany). We would like to thank A. Geisselmann for his assistance during a practical. Part 14: J. Burger, G. Kettenbach, P. Klüfers, *Macromol. Symp.* in press.

tained from ligand-rich solutions, indicating a cooperative mode of formation. For example, the addition of a twofold amount of sorbitol ($LiOH:Cu(OH)_2$:D-Sorb = 2:1:1) still leads to crystals of compound **1**.

Vertex-sharing, six-membered rings of Cu_3O_3, which are found in an isolated form in the glycerol complex **2**[1a] consti-

$Li_3[Cu_3(GlycH_{-3})_3]\cdot 6H_2O$ **2**

tute the construction motif in compound **1**. The conformations of the four completely deprotonated sorbitol molecules are more or less the same. On account of the formation of five condensed five-membered chelate rings, all the diol fragments are found in a synclinal (sc) conformation to their neighboring fragments and the sign of their torsion angles gives the sequence $---++$ (Scheme 1, right). This is the conformation with the largest possible flattening of the C_6 chain under the limiting condition that all the ligating atom positions are synclinal. Likewise, the deprotonated fragments of the tetraanionic sorbitol ligands all have the same conformation, here there is a $(-++)$ synclinal arrangement (Scheme 1, center).

It is immediately apparent from the structure that the magnetic properties will be determined by the superexchange mechanism for which there are the optimal geometric conditions. In **1**, as in all known polyolatocuprates, the central atoms have a square-planar coordination geometry. In this mode of coordination the magnetic orbital of the d^9-Cu^{II} ions is directed towards the four ligating atoms which can, in addition, effectively pass on spin polarization through Cu-O-Cu angles which are to some extent unusually obtuse.[7] The magnetic properties are therefore determined by copper units which are still spin-coupled at room temperature, but whose net spins show further interactions at low temperatures.

The magnetic moment of **1** has been measured between 2 K and room temperature in a magnetic field with a flux density of 2 T.[5] The susceptibility follows an extended Curie–Weiss relationship (Fig. 2). The value of the Curie constant C is not the

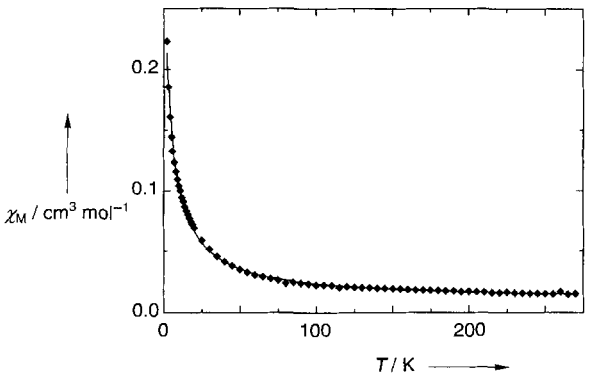

Fig. 2. Magnetic susceptibility of **1** (data points) and fitting by the Curie–Weiss law with an additive constant χ_0: $\chi = \chi_0 + C/T-\theta$ with $\chi_0 = 9.9\times10^{-3}$ cm³ mol⁻¹, $C = 1.4$ cm³ K mol⁻¹, and $\theta = -4.8$ K (solid line).

expected 16×0.374 cm³ K mol⁻¹ for 16 uncoupled $S=1/2$ spins, but a smaller value which corresponds to about 4 $S=1/2$ spins. The value of θ indicates a weak antiferromagnetic coupling of these four spins.

This behavior can be explained by the distribution of the Cu-O-Cu angles which determine the spin polarization. These angles are not all equal, as in the Cu_3-building unit in **2** with C_3 symmetry, but vary by about 25° (legends to Scheme 2 and

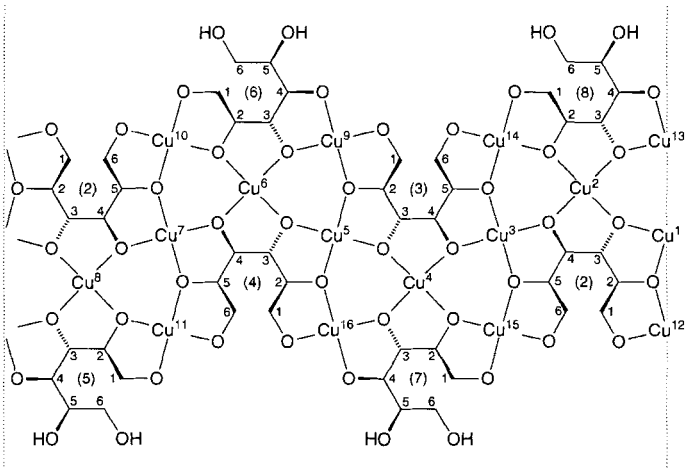

Scheme 2. Linkage within the anion of **1**, represented by a torus which has been cut open and flattened. C and O atoms are designated as C*mn* and O*mn*, respectively, *m* is the number for the sorbitol ligand given in parentheses, *n* follows the numbering in glucose (see Scheme 1); selected distances [pm] and angles [°]: average value Cu–O 191.9 (average standard deviation 1.2, standard deviation of the average value 2.5, smallest and largest value 187.6 and 198.8, respectively); Cu4-O33-Cu5 114.8(6), Cu8-O23-Cu1 115.2(6), Cu8-O53-Cu12 115.6(5), Cu6-O43-Cu5 116.6(6), Cu1-O13-Cu2 116.7(6), Cu16-O73-Cu4 116.9(6), Cu3-O15-Cu15 116.9(6), Cu9-O63-Cu6 117.3(5), Cu13-O83-Cu2 117.6(6), Cu11-O45-Cu7 119.2(5), Cu7-O25-Cu10 122.9(6), Cu5-O42-Cu16 128.3(6), Cu5-O32-Cu9 131.0(7), Cu3-O35-Cu14 131.2(7), Cu1-O22-Cu13 131.7(7), Cu2-O14-Cu3 136.7(7), Cu8-O52-Cu11 136.7(6), Cu4-O34-Cu3 137.2(7), Cu2-O82-Cu14 137.9(7), Cu8-O24-Cu7 138.3(6), Cu6-O62-Cu10 138.7(6), Cu4-O72-Cu15 139.2(7), Cu6-O44-Cu7 139.3(6).

Scheme 3, bottom). The smallest angles, which are approximately 115°, lie in the range expected for antiferromagnetic coupling, if they are compared to dihydroxo-bridged Cu_2 species.[7] However, it must be taken into account that each Cu_2 unit in **1** is bridged by only one O atom, so that the exchange constant J for the smaller angles could lie at around 0.[6] If it is assumed that there is a steep increase in $-J$ with the Cu-O-Cu angle, as found for the μ-hydroxocopper complexes,[7] the angle distribution as shown in Scheme 3 (bottom) also represents the hierarchy of the antiferromagnetic coupling. According to this

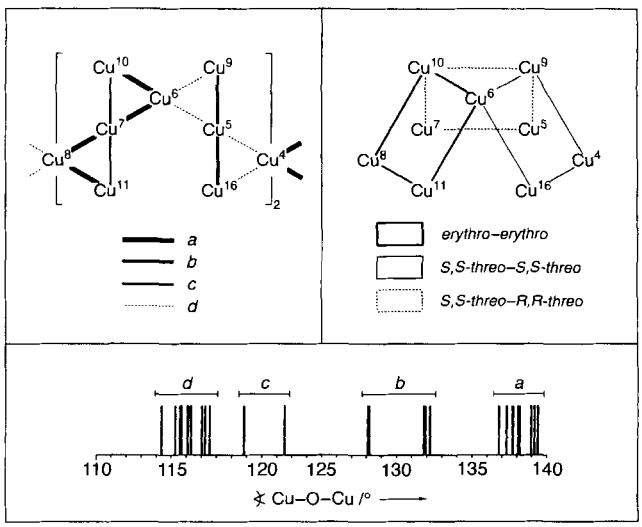

Scheme 3. Top left: Pathways of antiferromagnetic coupling, arranged according to Cu-O-Cu angles (*a*, *b*, *c*, *d* are defined in the bottom part of the Scheme); top right: stereochemistry of the diolato pairs (cf. Scheme 1 and the numbering of the C atoms in D-sorbitol), which bridge the long sides of the Cu_5 building blocks (highlighted by the three rectangles); bottom: frequency distribution of the Cu-O-Cu angles in **1**.

 © VCH Verlagsgesellschaft mbH, D-69451 Weinheim, 1995 0570-0833/95/3419-2120 $ 10.00+.25/0

the hexadecanuclear cluster can be divided into two groups of five copper atoms and two groups of three copper atoms, and within each group there is a strong antiferromagnetic coupling between the paramagnetic centers. Each group contributes with $S = 1/2$ towards the Curie constant as a consequence of the uneven number of copper atoms. Between the individual Cu_3 and Cu_5 groups there is only a weak antiferromagnetic coupling, this determines the observed value of θ: All the Cu-O-Cu angles between these groups are approximately equal and belong to the category with the smallest values (*d* in Scheme 3, bottom). The positive value of χ_0 indicates that the spin-coupled paramagnetic centers within the Cu_3 and/or Cu_5 groups are excited as the temperature increases, so that the susceptibility decreases more slowly as would be expected from a Curie–Weiss relationship.

The distribution of the Cu-O-Cu angles, along with the flattening of the torus shape, could also result from secondary interactions such as packing forces in the crystal. However, this is not the case here, rather the geometry of the hexadecacuprate ion reflects the linkage requirements arising from the stereochemistry of D-sorbitol. This is particularly apparent for the Cu_5 fragment. The O atoms participating in all of the Cu-O-Cu angles of category *a* (Scheme 3) are O-4 atoms from the $SorbH_{-6}$ ligands and O-2 atoms from the $SorbH_{-4}$ ligands (Scheme 2). Both sites are distinguished by the fact that they are the only ones with a (−+)-synclinal environment (Scheme 1). These correspond to the sequences eee or eae (e = equatorial, a = axial) in the chair conformation of a six-membered ring, and they give rise to an obtuse Cu-O-Cu angle. All the remaining triolato fragments bridge the copper atom pairs in a (−−) or (++) conformation (eea in the six-membered ring with *C* conformation; cf. Scheme 1), this results in a smaller angle at the bridging O atom. The Cu-O-Cu angles of category *b*, which determine the coupling in the Cu_3 fragment—here the bridging O atom is O-2 of the $SorbH_{-6}$ ligand—also belong qualitatively in this second class of the stereochemical classification, so that only the numerical values of the torsion angle along the C_6 chain reflect the further differentiation (average values for the size of the torsion angle O-C-C-O for the $SorbH_{-6}$ ligands: C1–C2 52.0(11), C2–C3 38.1(21), all the others 45.4(23)°, the standard deviation of the average value is given in parentheses).

The possibilities for a multifunctional polyol to adopt a favorable conformation for complexation are governed by the configuration. In order to explain this there are three possibilities depicted in Scheme 3 (right) of highlighting Cu_5 fragments as centered rectangles (in a D_2 torus only these three types are symmetry independent). A comparison with the left-hand side of the Scheme demonstrates the geometric relationship of the magnetically coupling Cu_3 and Cu_5 fragments. The different coupling behavior correlates with the different ligand configurations along the sides of the rectangles. A comparison with Scheme 2 shows that each of the four coordinating O atoms along the long sides of the rectangles differ with respect to the stereochemistry of the diolate function in the center. There is strong coupling within the Cu_5 rectangle which has *erythro*-configured μ-diolato fragments on both of its long sides; this is also the site of the least curvature in the torus. Spin-coupled Cu_3 units are found on both of the short sides of the flattened torus in a twofold *S,S-threo* environment, whilst there is no coupling between the Cu_3 and Cu_5 groups which have *S,S-threo-R,R-threo* configured diolate pairs.

Polyfunctional polyols should, according to these results, be suitable building blocks for self-assembling multinuclear alkoxo clusters. These complexes are thermodynamically very stable,[8] so that well-defined structures can be expected; in the case of Cu^{II} they are also kinetically labile, so that the complex frameworks also have the opportunity of undergoing self-organization. The construction of the complicated molecular architecture does not, in the case of the polyols, need a complicated synthesis of the ligand, which has an unsymmetrical shape and numerous linkage sites, because nature itself provides a wide range of such building blocks with differing stereochemistry. We are currently investigating whether the strong antiferromagnetic coupling along copper chains with uneven numbers of members can be used to construct ferrimagnets by the addition of further paramagnetic cations.[9]

Received: May 12, 1995 [Z 7978 IE]
German version: *Angew. Chem.* **1995**, *107*, 2290–2292

Keywords: alkoxo clusters · copper compounds · polyolato complexes · D-sorbitol · superexchange

[1] a) M. Klaassen, P. Klüfers, *Z. Anorg. Allg. Chem.* **1993**, *619*, 661–668; b) P. Klüfers, J. Schuhmacher, *Angew. Chem.* **1994**, *106*, 1839–1841; *Angew. Chem. Int. Ed. Engl.* **1994**, *33*, 1742–1744.

[2] A. Caneschi, A. Cornia, S. J. Lippard, *Angew. Chem.* **1995**, *107*, 511–513; *Angew. Chem. Int. Ed. Engl.* **1995**, *34*, 467–469, and references therein; H. W. Rich, K. Hegetschweiler, H. M. Streit, I. Erni, W. Schneider, *Inorg. Chim. Acta* **1991**, *187*, 9–15, and references therein.

[3] $C_{48}H_{72}Cu_{16}Li_8O_{48}\cdot 46H_2O$, $M_r = 3318.031$, crystal dimensions $0.25\times0.10\times0.05\ mm^3$, monoclinic, space group $P2_1$, $a = 1748.9(9)$, $b = 1639.3(7)$, $c = 2125.5(17)$ pm, $\beta = 100.75(5)°$, $V = 5987(6)\times10^6\ pm^3$, $Z = 2$, $\rho_{calcd} = 1.8407(18)\ g cm^{-3}$; $T = 190$ K, $2\theta_{max} = 42°$, 20239 reflections measured of which 12607 independent and included, 10948 with $|F_0| \geq 4\sigma(F_0)$. Lp correction, no correction for absorption, $\mu = 2.891\ mm^{-1}$, Cu anisotropic, 783 parameters, H atoms on C in calculated sites with common *U*, four of the eight Li atom sites are poorly defined, $wR(F^2) = 0.174$, $R(F)_{4\sigma} = 0.073$. $S = 1.090$, $\Delta\rho_{max} = 0.99\ eÅ^{-3}$; Stoe-IPDS area detector, $Mo_{K\alpha}$ (graphite monochromator, $\lambda = 0.71069$ Å), direct methods (SHELXS), refinement with full-matrix against F^2 (SHELXL), evaluation and depiction with PLATON and SCHAKAL. The water content given from the structural analysis is approximate; there were 55 oxygen sites, some of which were not fully occupied, which were refined as water; water content based on the mass loss on heating for five hours at 80 °C at 0.01 Torr: $45H_2O$. Further details of the crystal structure investigation may be obtained from the Fachinformationszentrum Karlsruhe, D-76344 Eggenstein-Leopoldshafen (Germany) on quoting the depository number CSD-401795.

[4] P. Klüfers, J. Schuhmacher, *Angew. Chem.* **1994**, *106*, 1925–1927; *Angew. Chem. Int. Ed. Engl.* **1994**, *33*, 1863–1865, and references therein.

[5] B. Pilawa, J. Schuhmacher, unpublished investigation by SQUID magnetometer (Quantum Design MPMS), sample size: 15 mg.

[6] The first magnetic measurements [B. Pilawa, J. Schuhmacher, unpublished] of a trinuclear complex of C_{2v} symmetry with propane triolato ligands [P. Klüfers, J. Schuhmacher, unpublished] gave magnetic exchange constants *J* of ca. −40 and −400 cm^{-1} from Cu-O-Cu angles of ca. 125 and 145°, respectively.

[7] O. Kahn, *Molecular Magnetism*, VCH, Weinheim, **1993**, p. 159 ff.

[8] W. Burchard, N. Habermann, P. Klüfers, B. Seger, U. Wilhelm, *Angew. Chem.* **1994**, *106*, 936–939; *Angew. Chem. Int. Ed. Engl.* **1994**, *33*, 884–887.

[9] O. Kahn, Y. Pei, Y. Journaux in *Inorganic Materials* (Eds.: D. W. Bruce, D. O'Hare), Wiley, New York, **1992**, p. 59–114.

 © VCH Verlagsgesellschaft mbH, D-69451 Weinheim, 1995 0570-0833/95/3419-2121 $ 10.00+.25/0

$[Mo_{154}(NO)_{14}O_{420}(OH)_{28}(H_2O)_{70}]^{(25\pm5)-}$: A Water-Soluble Big Wheel with More than 700 Atoms and a Relative Molecular Mass of About 24000

Achim Müller,* Erich Krickemeyer, Jochen Meyer, Hartmut Bögge, Frank Peters, Winfried Plass, Ekkehard Diemann, Stephan Dillinger, Fritz Nonnenbruch, Markus Randerath, and Carsten Menke

Dedicated to Professor Herbert W. Roesky on the occasion of his 60th birthday

In a previous paper we showed how, in the field of polyoxometalate chemistry, ever larger clusters with open shells can be constructed from small fragments.[1] Using the reaction system with which the giant cluster anions **1**, as well as **2** and **3**[1] (for which the conditions were adapted slightly) were synthesized, we have now succeeded in isolating the substantially larger, mixed-valent (type III; Mo^{V}/Mo^{VI}), diamagnetic compound **4** with a molar mass of about 30000 g mol^{-1}, and to grow

$[Mo_{57}V_6(NO)_6O_{180}(OH)_3(H_2O)_{18}]^{21-}$ **1**

$[Mo_{57}Fe_6(NO)_6O_{174}(OH)_3(H_2O)_{24}]^{15-}$ **2**

$[Mo_{36}(NO)_4O_{108}(H_2O)_{16}]^{12-}$ **3**

$(NH_4)_{25\pm5}[Mo_{154}(NO)_{14}O_{420}(OH)_{28}(H_2O)_{70}]\cdot$ ca. $350H_2O$ **4**

blue-black crystals suitable for X-ray structure analysis.[2] Spectroscopic methods (Vis/NIR, IR, Raman spectroscopy)[3] as well as elemental analyses and manganometric redox titrations served to confirm the information obtained from the X-ray structure analysis and to characterize the compound.

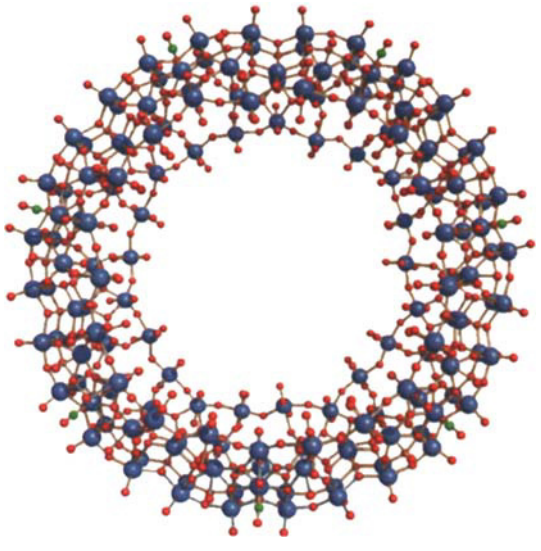

Fig. 1. Ball-and-stick model of the cluster anion of **4** (view parallel to the approximate C_7 axis; color code: Mo blue, O red, and N green).

[*] Prof. A. Müller, E. Krickemeyer, Dipl.-Chem. J. Meyer, Dr. H. Bögge, F. Peters, Dr. W. Plass, Dr. E. Diemann, Dr. S. Dillinger, F. Nonnenbruch, Dipl.-Chem. M. Randerath, Dipl.-Chem. C. Menke
Fakultät für Chemie der Universität
Lehrstuhl für Anorganische Chemie I
Postfach 100131, D-33501 Bielefeld (Germany)
Telefax: Int. code + (521) 106-6003
e-mail: amueller@cheops.chemie.uni-bielefeld.de

The approximately ring-shaped anion of **4** (Fig. 1) consists of 140 MoO_6 octahedra and 14 pentagonal bipyramids of the type $\{Mo(NO)O_6\}$. It can be described as a tetradecamer with approximate D_{7d} symmetry[4] (Fig. 2, top). Each of the fourteen subunits has a pentagonal-bipyramidal $\{Mo(NO)O_6\}$ center about which seven other MoO_6 octahedra are grouped by corner- and edge-sharing to form an $\{Mo_8\}$ fragment. The fragments arranged above and below the equatorial plane of the cluster anion are linked to each other by the oxygen atoms in this plane and the total of 14 equatorial Mo centers (Fig. 3, top), in accordance with the details given below.

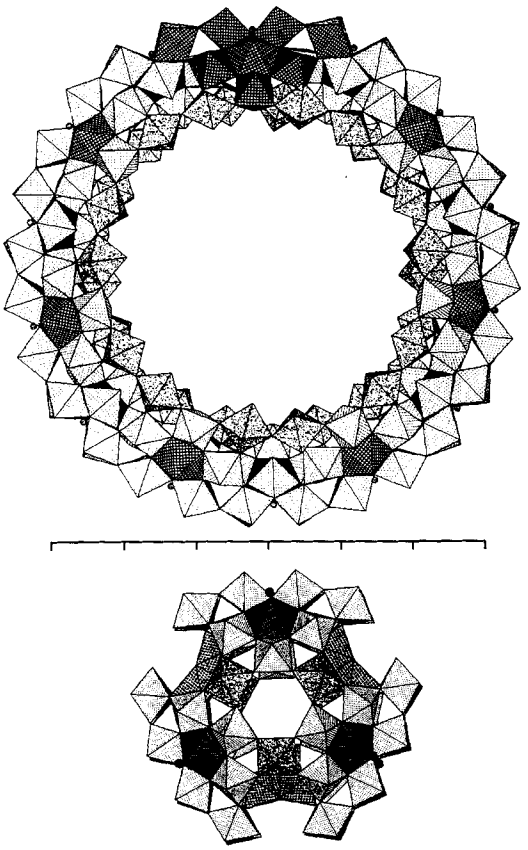

Fig. 2. Polyhedral representation of the cluster anion of **4** (top: view parallel to the approximate C_7 axis) and of **1** (or **2**) (bottom: view roughly parallel to the C_3 axis). In the top section, one example of the $\{Mo_8\}$ subunits constructed from seven MoO_6 octahedra and the central, pentagonal-bipyramidal $\{Mo(NO)O_6\}$ group has been highlighted by checkered shading. The other polyhedra, with the exception of the pentagonal bipyramids, which are also checkered, and the linking $\{MoO_2(H_2O)(\mu_2\text{-}O)MoO_2(H_2O)\}$ units, which are irregularly dotted, are shaded with regular dots. In the bottom section the polyhedra of $\{MoO_8\}$ units (or $\{MoO_7\}$ units)—that is, those with the central Mo(NO) groups—are represented as in the top section, but no $\{Mo_8\}$ unit is highlighted by special shading. In addition the $\{Mo^{V}(\mu\text{-}H_2O)_2(\mu\text{-}OH)Mo^{V}\}^{9+}$ fragments are indicated by crosses and the $\{V^{IV}O(H_2O)\}^{2+}$ (or $\{Fe^{III}(H_2O)_2\}^{3+}$) units by irregularly dotted shading (cf. ref. [1]). The distance between two graduations of the scale is 5 Å.

Corresponding, equivalent $\{Mo_8\}$ building blocks also occur in the anions **1** and **2**, which, however, have D_{3h} symmetry. The fundamental difference between the two structural types is that in **1** and **2** the $\{Mo_8\}$ fragments lie directly on top of each other and are transformed into each other by reflection across the equatorial mirror plane (Fig. 3, bottom), whereas in **4** they are twisted relative to each other about the approximate C_7 (S_{14}) axis by an angle of 360/14° (Fig. 3, top).

 © VCH Verlagsgesellschaft mbH, D-69451 Weinheim, 1995 0570-0833/95/3419-2122 $ 10.00+.25/0 Angew. Chem. Int. Ed. Engl. 1995, 34, No. 19

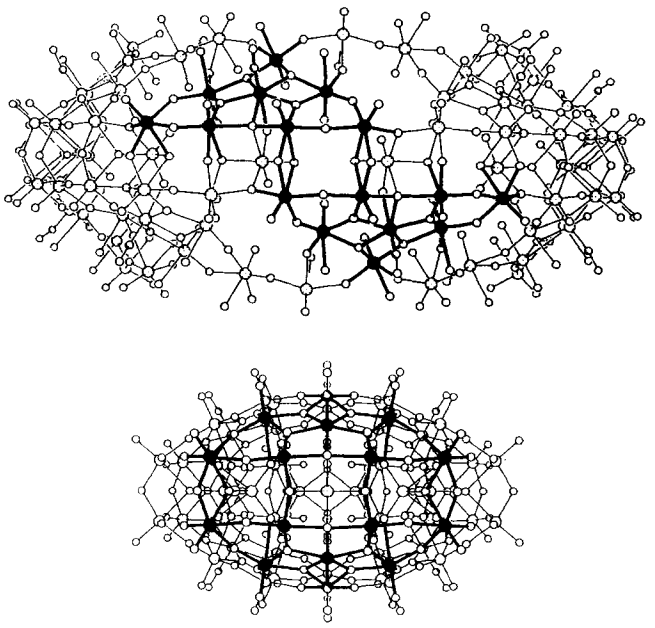

Fig. 3. Ball-and-stick model of the cluster anion of **4** (top: view parallel to an approximate C_2 axis and perpendicular to the view shown in Fig. 2, top; for reasons of clarity only the "half anion" has been drawn) and of **1** (or **2**) (bottom: view parallel to a C_2 axis and perpendicular to the view shown in Fig. 2, bottom). The $\{Mo_8\}$ units are in boldface in each case.

In **1** and **2** the pentagonal bipyramids of each unit are linked to each other through *one* additional Mo atom lying in the equatorial plane (Fig. 3, bottom), and therefore "discrete" $\{Mo_{17}\}$ fragments ($2 \times 8 + 1$) are formed. These are present as *transferrable ligands*, "isolated" from each other and linked solely through the cationic $\{V^{IV}O(H_2O)\}^{2+}$ or $\{Fe^{III}(H_2O)_2\}^{3+}$ and $\{Mo^{V}(\mu\text{-}H_2O)_2(\mu\text{-}OH)Mo^{V}\}^{9+}$ groups, respectively (Fig. 2, bottom).

In contrast, in **4** the shift of the $\{Mo_8\}$ units relative to each other (described above) means that in each case *two* equatorial Mo atoms are required to link two $\{Mo_8\}$ fragments (Fig. 3, top). Neighboring $\{Mo_8\}$ fragments above and below the equatorial plane are directly linked together through a μ_3-O atom, too (Fig. 2, top). The smaller curvature of the cluster ion relative to **1** and **2** correlates with the finding that in the region of the cavity there is enough space for a further linkage of the $\{Mo_8\}$ units through *two* Mo centers (or one $\{MoO_2(H_2O)(\mu_2\text{-}O)MoO_2(H_2O)\}$ unit) instead of only *one* V^{IV} or *one* Fe^{III} center as in **1** and **2**, respectively (Fig. 2, top). In this context the presence of two 42-membered rings containing alternating molybdenum and oxygen atoms, which give access to the cavity, is remarkable (Fig. 1).

The cavity itself, which, like a car tire, is broader at the equator, measures about 20 Å in diameter at its narrowest point, and thus corresponds fairly closely to the outer diameter of the cluster anions **1** and **2** (Fig. 2). A plausible hypothesis is therefore that the fragments in the solution that are also involved in the construction of **1**, **2**, and **3** induce the formation of the spherical cluster shell of **4**.

A further characteristic of the structure of the anion **4** is the exceptionally large number of protons resulting from the high degree of reduction. A careful analysis of the bond valence sums reveals 28 singly and 70 doubly protonated oxygen atoms. Singly protonated are the 28 equivalent μ_3-O atoms situated in the equatorial plane (Fig. 3, top) and linking two $\{Mo_8\}$ units as well as another Mo atom that also lies in this plane. Of the doubly protonated O atoms (the terminal H_2O ligands), 42 are coordinated to the Mo atoms that participate in the construction of the two 42-membered rings (one H_2O ligand per Mo atom). In these rings the H_2O ligands are arranged both above and below the ring's plane, and an alternating (*trans*) orientation between two adjacent centers is favored. The remaining 28 H_2O ligands are coordinated to the 28 equivalent metal centers in octahedral environments, which are in the immediate vicinity of the ring polyhedra. On considering all available data (degree of reduction and number of cations), further protonation is very unlikely.

Whereas the structure of the cluster ion could now be determined unequivocally, it will probably never be possible to ascertain the exact number of NH_4^+ ions because of disorder in the cationic lattice and the problematic nature of the analysis (about 2% nitrogen and an extremely high content of water of crystallization, which, moreover, decreases even at room temperature as a result of facile weathering).

A remarkable feature is that despite its large molar mass, **4** dissolves extremely well in water and on exclusion of air can be recovered from the solution without decomposition. The relatively high solubility can be attributed to the large surface area resulting from the tirelike form and the large number of H_2O and OH^- ligands (causing a large enthalpy of hydration). This also is manifest in the exceptionally large number of H_2O molecules in the crystal structure, with the result that even in the crystal the anions appear to be "swimming in water".

Interesting perspectives for further research are offered by the unusual potential and properties of the anion: the inclusion of substrates and their transformation within a host system that has mesoscopic dimensions, an extremely large surface area, and the electron-storage capability. Furthermore, the anion of **4** has a magnitude and surface area that places it on the border of the colloidal state, and yet it can still be included in a crystal lattice.

Experimental Procedure

A mixture of $Na_2MoO_4 \cdot 2H_2O$ (7.46 g, 30.8 mmol), NH_4VO_3 (1.19 g, 10.2 mmol), $NH_2OH \cdot HCl$ (12.83 g, 184.6 mmol), HCl (3.5%, 9.5 mL), and water (200 mL) was stirred for 1–2 min and then heated at 65–70 °C without stirring in a 300 mL, narrow-necked Erlenmeyer flask (covered with a watch glass) for 20 h. The resulting precipitate contained blue-black, rhombic crystals of **4**, suitable for X-ray structure analysis, but also water-insoluble, greenish crystals of a not yet more closely identified compound [5]. After separation from the hot reaction solution by filtration, the dark green filtrate was diluted with 100 mL hot water (70 °C), cooled to 20 °C, and allowed to stand to crystallize in a 300 mL, narrow-necked Erlenmeyer flask covered with a watch glass. Compound **4**, which precipitated within 2–3 days, was filtered off under exclusion of air and dried under inert atmosphere over $CaCl_2$. Yield: 0.3 g (5% based on Mo). (As a consequence of the differing solubility in H_2O, **4** can be separated from the greenish compound.)

Received: May 22, 1995 [Z8017IE]
German version: *Angew. Chem.* **1995**, *107*, 2293–2295

Keywords: clusters · complexes with oxygen ligands · molybdenum compounds · polyoxometalates

[1] a) A. Müller, W. Plass, E. Krickemeyer, S. Dillinger, H. Bögge, A. Armatage, A. Proust, C. Beugholt, U. Bergmann, *Angew. Chem.* **1994**, *106*, 897; *Angew. Chem. Int. Ed. Engl.* **1994**, *33*, 849; b) A. Müller, E. Krickemeyer, S. Dillinger, H. Bögge, W. Plass, A. Proust, L. Dloczik, C. Menke, J. Meyer, R. Rohlfing, *Z. Anorg. Allg. Chem.* **1994**, *620*, 599. The underlying principle is to generate highly negatively charged fragments in the reaction mixture (for example, by substitution of $\{MoO\}^{4+}$ by $\{MoNO\}^{3+}$ or Mo^{VI} by V^{IV}, as well as by reduction), which are stabilized by a high energy of hydration . This hampers the formation and crystallization of compounds with typical solid-state structures by further condensation—that is, by the operation of translation symmetry—and molecular growth processes can take place in the solution.

[2] **4**: space group $C2/m$; $a = 4790.2(8)$, $b = 4760.2(8)$, $c = 2100.2(3)$ pm, $\beta = 110.26(1)°$, $V = 44926(12) \times 10^6$ pm^3, ($\mu = 21.9$ cm^{-1}); $Z = 2$, Solution with direct methods, $R = 0.098$ for 16431 independent reflections ($F_0 > 4\sigma(F_0)$);

Siemens R3m/V diffractometer Mo_{K_α} radiation, graphite monochromator. Because of their air sensitivity, the blue-black, rhombic crystals were mounted in silicon oil when removed from the mother liquor, and the measurement was performed at −85 °C. Since the cationic lattice is partly disordered, it is not possible to distinguish between H_2O and NH_4^+ centers. The overall number of both of these groups found in lattice positions is about 320 per formula unit; however, it must be assumed that some of those units are so disordered that they are not detectable by difference Fourier syntheses. Thus, for instance, no relevant lattice positions could be localized in the vicinity of the center of the cavity of the cluster. Results of model calculations revealed that a further 50–70 positions that should be occupied by H_2O units are present. Elemental analyses, redox titrations, and the determination of the NH_4^+ content by the Kjeldahl method yielded the quoted formula. As a result of the quite characteristic bond valence sums, the positions of protonation could be unequivocally located. The calculated values lie between 0.15 and 0.45 for the 70 doubly protonated and between 1.1 and 1.3 for the 28 singly protonated oxygen atoms. This corresponds to what we expected from our experience with numerous other relevant cluster anions. Furthermore, significantly lowered bond valence sums (average 5.66) for 70 Mo atoms without H_2O ligands, which lie in the equatorial plane or above and below it on the periphery of the tire-shaped anion, show that the 4d electrons (and likewise the "Mo^V" centers without consideration of the $\{Mo(NO)\}^{3+}$ units) are predominantly localized here. This correlates with the degree of reduction corresponding to the molecular formula, which was also determined by manganometric redox titration (see ref. [1]). (Calculation of bond valence sums according to I. D. Brown in *Structure and Bonding in Crystals, Vol. II* (Eds.: M. O'Keefe, A. Navrotsky), Academic Press, New York, **1981**, p. 1.) Part of the $\{Mo(O_{br})_3(O_{term})_2(H_2O)\}$ and the $\{Mo(O_{br})_4(O_{term})(H_2O)\}$ octahedra (br = bridging, term = terminal) is disordered in such a way that the *trans* O_{term} and H_2O ligands exchange their positions (in each case unequivocally recognized in the individual octahedra through two Mo positions with apparent "distances" between 0.7 and 0.8 Å). Further details of the crystal structure investigation may be obtained from the Fachinformationszentrum Karlsruhe, D-76344 Eggenstein-Leopoldshafen (FRG) on quoting the depository number CSD-59058.

[3] Characterization of **4**: some characteristic IR bands (KBr disc prepared under argon): $\tilde{\nu}$ [cm^{-1}] = 1610 (m, br, $\delta(H_2O)$ and $\nu(NO)$), 1407 (m, $\delta_{as}(NH_4^+)$), 967 (m), 905 (m, $\nu(Mo{=}O)$), 812 (sh), 740 (s), 636 (s), 551 (s). Characteristic resonance Raman bands (solid/λ_e = 1064 nm): $\tilde{\nu}$ [cm^{-1}] = 806 (s, A_1), 536 (s), 462 (s), 326 (s), 221 (s). Vis/NIR (in H_2O): λ [nm] (ε_M [10^5 $L\,mol^{-1}\,cm^{-1}$]) = 750 (1.7, IVCT), 1080 (1.3, IVCT).

[4] The conditions required for the occurrence of D_{7d} symmetry were approximately fulfilled only for the Mo atoms. Deviations are observed mainly for the O_{term} and H_2O ligands of the $\{MoO_2(H_2O)(\mu_2\text{-}O)MoO_2(H_2O)\}$ units that are not transformed into each other by reflection across the dihedral planes.

[5] The exciting process of nucleus formation in the case of ionic crystals with "giant ions" will, after thorough examination, be reported elsewhere. The relevant stochastic process in the present case leads not only to (large) crystals but also to a noncrystalline part or to material with a different degree of crystallization, the powder diagram of which corresponds to the envelope of that calculated from single crystal data. The Raman, IR, and UV/Vis/NIR spectra, and the analyses, are identical for the crystalline and noncrystalline parts.

A Self-Assembled Bifunctional Receptor

Dmitry M. Rudkevich,* Alexander N. Shivanyuk, Zbigniew Brzozka, Willem Verboom, and David N. Reinhoudt*

Molecular self-assembly is an important part of life processes and biological systems.[1] It results in a wide variety of complex structures such as double-stranded DNA, viral protein coatings, lipid membranes, and globular proteins. Self-assembling processes have also found applications in the design of nanostructures such as inorganic clusters, tubes and channels, monolayers, and hydrogen-bonded networks. The functions of such assemblies can be extrapolated from molecular properties.[2, 3] Recently, Sessler et al. reported photoinduced energy transfer in noncovalently linked photosynthetic systems.[4] Molecular recognition by encapsulation of small guest molecules in cavities assembled through noncovalent interactions has been achieved.[5] Self-assembled nanotubes constructed from cyclic peptide subunits can transport glucose across lipid bilayers.[6]

Previously we have described bifunctional receptors having in the same molecule covalently connected cation and anion binding sites.[7] In this communication we describe the molecular recognition of ionic species by a bifunctional receptor system, in which a cation and an anion binding site are positioned in close proximity by means of self-assembly. Such a system is able to bind simultaneously both cationic and anionic guest species. The strategy applied is based on the assembly of known receptors through hydrogen bonding. The cation receptor calix[4]arene **1**, which contains one amide and three ester groups,

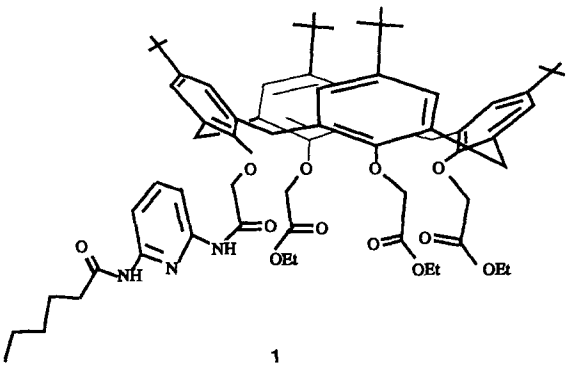

1

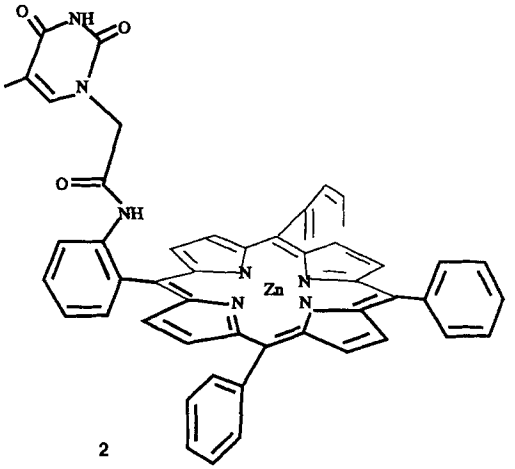

2

complexes alkali metal cations with a high selectivity for Na^+.[8] This calixarene was prepared in 78% yield from the corresponding triester monocarboxylic acid chloride[9] and 2-amino-6-(hexanamido)pyridine. The anion receptor porphyrin **2** was obtained in 49% overall yield by reaction of thymine with the appropriate bromoacetamidoporphyrin[10] in DMSO in the presence of K_2CO_3 as a base, followed by metalation with $Zn(OAc)_2 \cdot 2H_2O$. The Zn center in porphyrin **2** is expected[11] to bind anions in aprotic solution. For the assembly through hydrogen bonding, compounds **1** and **2** are functionalized with complementary diamidopyridine and thymine units, respectively.[12, 13]

[*] Dr. D. M. Rudkevich, Prof. Dr. Ir. D. N. Reinhoudt, Dr. A. N. Shivanyuk, Dr. habil. Z. Brzozka,[+] Dr. W. Verboom
Laboratory of Organic Chemistry, University of Twente
P. O. Box 217, NL-7500 AE Enschede (The Netherlands)
Telefax: Int. code + (53)312738

[+] Permanent address:
Department of Analytical Chemistry, Technical University of Warsaw (Poland)

 © VCH Verlagsgesellschaft mbH, D-69451 Weinheim, 1995 0570-0833/95/3419-2124 $ 10.00+.25/0

Calix[4]arene **1** strongly complexes Na^+ in $CDCl_3$, $[D_3]$MeCN, and $[D_8]$toluene solutions; from dilution experiments in $[D_3]$MeCN with $NaNO_3$ an association constant (K_{ass}) of $5.0 \times 10^4\ mol^{-1}$ was found. Calixarene **1** could be converted easily to the corresponding lipophilic complexes $(\mathbf{1}\cdot Na^+)ClO_4^-$, $(\mathbf{1}\cdot Na^+)I^-$, and $(\mathbf{1}\cdot Na^+)SCN^-$ by stirring a CH_2Cl_2 solution of **1** with saturated aqueous solutions of the appropriate sodium salts for three to five hours. With the more hydrophilic salts NaF and NaH_2PO_4 no complexes could be obtained.

Surprisingly, the diamidopyridine fragment in free **1** does not form hydrogen-bonded aggregates with complementary molecules such as *N*-butylthymine. In the ^1H NMR spectra no characteristic shifts[12] of C(O)NH signals were observed upon addition of *N*-butylthymine to $CDCl_3$, $[D_3]$MeCN, or $[D_8]$toluene solutions of **1**. The diamidopyridine moiety in **1** is apparently involved in intramolecular hydrogen bonding with the ethyl carboxylate groups, because the C(O)NH signals of **1** are shifted roughly $\Delta\delta = 0.3$ and 0.8 downfield in comparison with those of the $(\mathbf{1}\cdot Na^+)ClO_4^-$ complex in $CDCl_3$ and $[D_3]$MeCN, respectively. The Na^+ complexes of **1**, in which the carbonyls from the ester groups and the amide group are coordinated to the cation, do form hydrogen bonds with complementary molecules as indicated by the downfield shifts for the diamidopyridine C(O)NH protons of approximately $\Delta\delta = 0.5$–0.6 in $CDCl_3$, $[D_3]$MeCN, and $[D_8]$toluene upon addition of *N*-butylthymine to a solution of the $(\mathbf{1}\cdot Na^+)ClO_4^-$ complex. From dilution experiments in $[D_8]$toluene K_{ass} values of $1.5 \times 10^3\ mol^{-1}$ ($-\Delta G = 17.8\ kJ\,mol^{-1}$) and $1.7 \times 10^3\ mol^{-1}$ ($-\Delta G = 18.1\ kJ\,mol^{-1}$) were calculated for $(\mathbf{1}\cdot Na^+)ClO_4^-$ and $(\mathbf{1}\cdot Na^+)SCN^-$, respectively.[14, 15] This provides an interesting possibility of "switching on" the hydrogen bonding ability of **1** by complexation with Na^+ ions.[16] It means that anion receptor **2** can in principle be assembled with $(\mathbf{1}\cdot Na^+)ClO_4^-$ or $(\mathbf{1}\cdot Na^+)SCN^-$ complexes through a diamidopyridine–thymine interaction. UV/Vis experiments with porphyrin **2** show that it complexes I^- and SCN^- ions (introduced as tetrabutylammonium salts) in apolar solvents (CH_2Cl_2 and toluene). A bathochromic shift of the Soret band of 8–10 nm was found upon addition of $Bu_4N^+I^-$ and $Bu_4N^+SCN^-$ to a toluene solution of **2**, which is in agreement with the data published for simple tetraphenylporphyrins.[11] This binding is not strong; from dilution experiments a K_{ass} value of roughly $10\ mol^{-1}$ ($-\Delta G = 5.6\ kJ\,mol^{-1}$) was calculated for both I^- and SCN^- ions in toluene. No indication for complexation of the ClO_4^- ion was observed. Addition of *free* calix[4]arene **1** to a toluene solution of porphyrin **2** did not change the anion binding properties of **2**; K_{ass} values of roughly $10\ mol^{-1}$ for the complexation of I^- and SCN^- ions were found. Interactions between the hydrogen bonding sites of **1** and **2** were not observed in the ^1H NMR spectra upon mixing.

The final assembly experiment was carried out between $(\mathbf{1}\cdot Na^+)SCN^-$ and **2**.[17] Addition of porphyrin **2** to a $[D_8]$toluene solution of $(\mathbf{1}\cdot Na^+)SCN^-$ resulted in a pronounced thymine–diamidopyridine interaction. From the ^1H NMR chemical shifts of the C(O)NH signals a K_{ass} value of $2.8 \times 10^4\ mol^{-1}$ ($-\Delta G = 24.9\ kJ\,mol^{-1}$) for $(\mathbf{1}\cdot Na^+)(\mathbf{2}\cdot SCN^-)$ was calculated. This is significantly higher than those of the interactions in $(\mathbf{1}\cdot Na^+)\cdot$*N*-butylthymine$\cdot SCN^-$ and $Bu_4N^+(\mathbf{2}\cdot SCN^-)$ separately. A Job plot confirmed the 1:1 stoichiometry of the complex (Fig. 1).[18, 19] The $(\mathbf{1}\cdot Na^+)(\mathbf{2}\cdot SCN^-)$ assembly in toluene was also confirmed by UV/Vis spectroscopy; the Soret band displayed a bathochromic shift of 8 nm thus reflecting the Zn–SCN^- interaction (Fig. 2). From these experiments a K_{ass} value of $2.5 \times 10^4\ mol^{-1}$ was calculated, indicating strong anion binding.

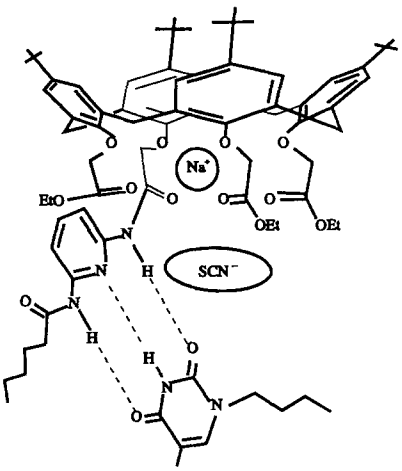

$(\mathbf{1}\cdot Na^+)\cdot$Thymine$\cdot SCN^-$

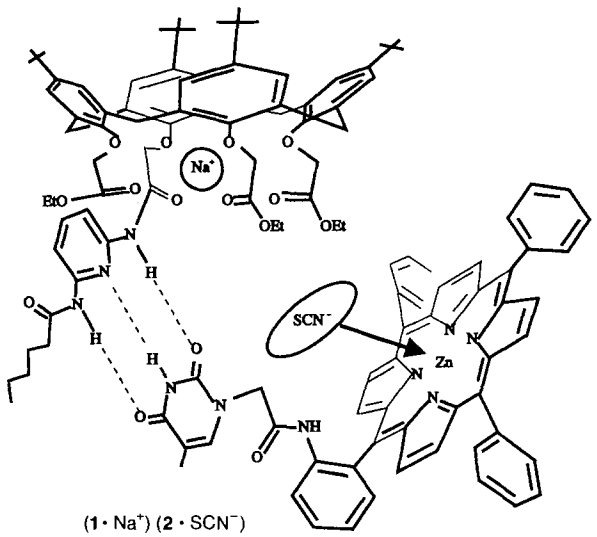

$(\mathbf{1}\cdot Na^+)\,(\mathbf{2}\cdot SCN^-)$

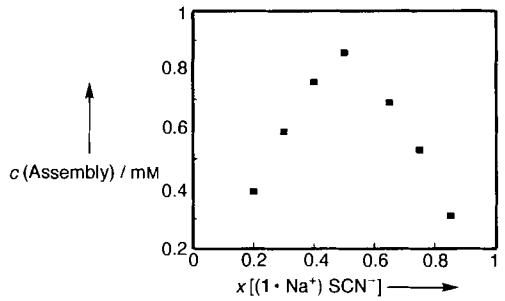

Fig. 1. Titration of 1 mmol of $(\mathbf{1}\cdot Na^+)SCN^-$ with 1 mmol of **2** in $[D_8]$toluene with formation of the assembly $(\mathbf{1}\cdot Na^+)(\mathbf{2}\cdot SCN^-)$ (Job plot).

These results prove the formation of the *noncovalently* organized bifunctional receptor system $(\mathbf{1}\cdot Na^+)(\mathbf{2}\cdot SCN^-)$ (Fig. 3).[20] The Na^+ ion is complexed by calixarene **1**, the SCN^- ion coordinates to the Zn-porphyrin **2**, and these cation and anion receptors are connected through hydrogen-bonded aggregation. The (significant) enhancement of the hydrogen bonding as well as the anion complexation points to a *coopera-*

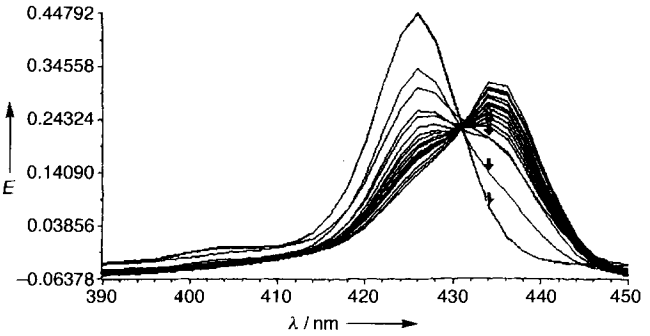

Fig. 2. Complexation of $(1\cdot Na^+)SCN^-$ with **2** in toluene. The assembly was monitored by UV/Vis spectroscopy between 390 and 450 nm (E = extinction). [**2**] = 1×10^{-3} mM; the concentration of $(1\cdot Na^+)SCN^-$ ranges from 5×10^{-4} to 1×10^{-1} mM.

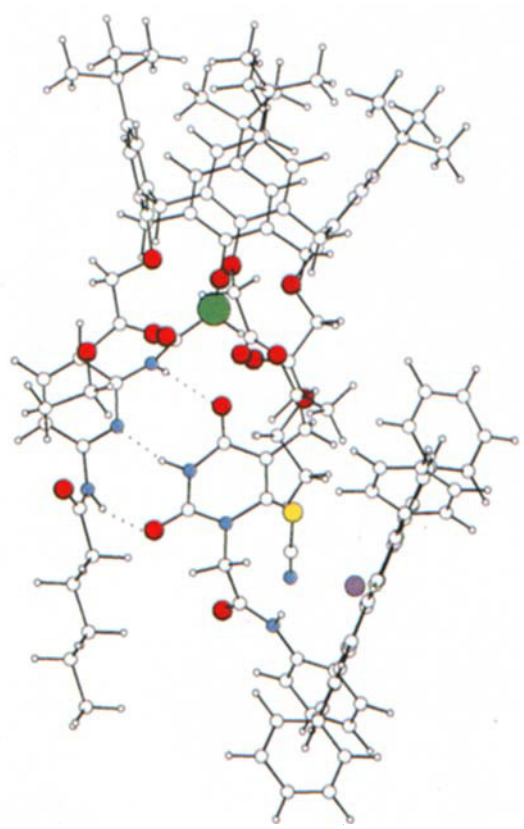

Fig. 3. Energy-minimized structure of the assembly $(1\cdot Na^+)(2\cdot SCN^-)$. Na = green, Zn = violet, S = yellow, O = red, N = blue, C,H = white.

tion of the individual interactions between calix[4]arene **1**, Zn-porphyrin **2**, and the Na^+ and SCN^- ions. The positions of all four components in the complex are fixed in solution by specific ion–dipole interactions and hydrogen bonding. The assembly can be "switched on" by complexation of the Na^+ ion with receptor **1**, and "switched off" by addition of MeOH, which is able to destroy hydrogen bonds.

Received: May 6, 1995 [Z 7965 IE]
German version: *Angew. Chem.* **1995**, *107*, 2300–2302

Keywords: hydrogen bonding · molecular recognition · self-assembly

[1] a) J.-M. Lehn, *Angew. Chem.* **1990**, *102*, 1347–1362; *Angew. Chem. Int. Ed. Engl.* **1990**, *29*, 1304–1319; b) G. M. Whitesides, J. P. Mathias, C. T. Seto, *Science* **1991**, *254*, 1312–1319; c) J. S. Lindsey, *New J. Chem.* **1991**, *15*, 153–180.

[2] a) G. A. Ozin, *Adv. Mater.* **1992**, *4*, 612–649; b) S. L. Suib, *Chem. Rev.* **1993**, *93*, 803–826.

[3] a) M. C. Etter, *Acc. Chem. Res.* **1990**, *23*, 120–126; b) E. Fan, C. Vicent, S. J. Geib, A. D. Hamilton, *Chem. Mater.* **1994**, *6*, 1113–1117; c) J. C. MacDonald, G. M. Whitesides, *Chem. Rev.* **1994**, *94*, 2383–2420.

[4] a) J. L. Sessler, B. Wang, A. Harriman, *J. Am. Chem. Soc.* **1993**, *115*, 10418–10419; b) *ibid.* **1995**, *117*, 704–714.

[5] a) N. Branda, R. Wyler, J. Rebek, Jr., *Science* **1994**, *263*, 1267–1268; b) C. A. Hunter, L. D. Sarson, *Angew. Chem.* **1994**, *106*, 2424–2426; *Angew. Chem. Int. Ed. Engl.* **1994**, *33*, 2313–2316; c) N. Branda, R. M. Grotzfeld, C. Valdés, J. Rebek, Jr., *J. Am. Chem. Soc.* **1995**, *117*, 85–88.

[6] J. R. Granja, M. R. Ghadiri, *J. Am. Chem. Soc.* **1994**, *116*, 10785–10786. For a few other examples see: a) O. F. Schall, K. Robinson, J. L. Atwood, G. W. Gokel, *J. Am. Chem. Soc.* **1993**, *115*, 5962–5969; b) O. F. Schall, G. W. Gokel, *J. Am. Chem. Soc.* **1994**, *116*, 6089–6100.

[7] a) D. M. Rudkevich, Z. Brzozka, M. Palys, H. C. Visser, W. Verboom, D. N. Reinhoudt, *Angew. Chem.* **1994**, *106*, 480–482; *Angew. Chem. Int. Ed. Engl.* **1994**, *33*, 467–468; b) D. M. Rudkevich, W. Verboom, D. N. Reinhoudt, *J. Org. Chem.* **1994**, *59*, 3683–3686;. c) D. M. Rudkevich, J. D. Mercer-Chalmers, W. Verboom, R. Ungaro, F. de Jong, D. N. Reinhoudt, *J. Am. Chem. Soc.* **1995**, *117*, 6124–6125.

[8] F. Arnaud-Neu, E. M. Collins, M. Deasy, G. Ferguson, S. J. Harris, B. Kaitner, A. J. Lough, M. A. McKervey, E. Marques, B. L. Ruhl, M. J. Schwing-Weill, E. Seward, *J. Am. Chem. Soc.* **1989**, *111*, 8681–8689.

[9] M. A. McKervey, M. Owens, H.-R. Schulten, W. Vogt, V. Böhmer, *Angew. Chem.* **1990**, *102*, 326–327; *Angew. Chem. Int. Ed. Engl.* **1990**, *29*, 280–282.

[10] S. Koeller, P. Cocolios, R. Guilard, *New J. Chem.* **1994**, *18*, 849–859.

[11] M. Nappa, J. S. Valentine, *J. Am. Chem. Soc.* **1978**, *100*, 5075–5080.

[12] a) B. Feibusch, M. Sahha, K. Onan, B. Karger, R. Giese, *J. Am. Chem. Soc.* **1987**, *109*, 7531–7533; b) A. D. Hamilton, D. Van Engen, *ibid.* **1987**, *109*, 5035–5036; c) A. V. Muehldorf, D. Van Engen, J. C. Warner, A. D. Hamilton, *ibid.* **1988**, *110*, 6561–6562.

[13] Selected data for **1**: M.p. 88–89 °C (MeCN); ^{1}H NMR ([D$_8$]toluene): δ = 9.61, 8.61 (2 br s, 2H, NH), 8.25, 8.12 (2 d, ^3J(H,H) = 8.0 Hz, 2H, diamidopyridine), 7.19 (t, ^3J(H,H) = 8.0 Hz, 1H, diamidopyridine), 6.92, 6.82, 6.69 (3 s, 8H, arom.), 5.12, 4.78 (2 d, ^3J(H,H) = 14.0 Hz, 4H, $CH_2C(O)$), 4.98, 4.72, 3.17, 3.10 (4 d, ^3J(H,H) = 13.0 Hz, 8H, CH_2-calix), 4.78, 4.53 (2 s, 4H, $CH_2C(O)$), 4.9–4.5 (m, 6H, OCH_2), 2.45 (t, ^3J(H,H) = 7.5 Hz, 2H, $CH_2C(O)N$), 1.85–1.75, 1.4–1.3 (2 m, 6H, CH_2), 1.15 (s, 18H, *t*Bu), 1.09, 1.03 (2 s, 18H, *t*Bu), 0.91 (t, ^3J(H,H) = 7.2 Hz, 9H, CH_3), 0.80 (t, ^3J(H,H) = 7.5 Hz, 3H, CH_3); FAB-MS (NBA matrix): *m/z*: 1154.4 (M^+, calcd 1154.5). Selected data for **2**: M.p. 253–255 °C; UV/Vis (toluene): λ_{max} = 426 nm; ^{1}H NMR ([D$_8$]toluene): δ = 9.06 (d, ^3J(H,H) = 8.0 Hz, 1H, arom.), 8.98 (s, 4H, porphyrin), 8.88, 8.67 (2 d, ^3J(H,H) = 4.8 Hz, 4H, porphyrin), 8.3–8.0 (m, 8H, arom.), 7.80 (d, ^3J(H,H) = 8.0 Hz, 1H, arom.), 7.6–7.4 (m, 10H, arom. + NH), 7.09 (t, ^3J(H,H) = 7.2 Hz, 1H, arom.), 5.30 (s, 1H, thymine), 2.70 (s, 2H, $NCH_2C(O)$), 2.01 (s, 3H, CH_3); FAB-MS (NBA matrix): *m/z*: 859.1 (M^+, calcd 859.3). NBA = nitrobenzyl alcohol.

[14] All K_{ass} values were obtained at 293 K using a constant concentration of the $(1\cdot Na^+)$ complex of 1.00 mM and a varying concentration of a guest of 0.25–5.00 mM. The values were calculated by nonlinear regression according to the procedure described in: J. A. A. de Boer, D. N. Reinhoudt, S. Harkema, G. J. van Hummel, F. de Jong, *J. Am. Chem. Soc.* **1982**, *104*, 4073–4076. The estimated error is 5%.

[15] The complex $(1\cdot Na^+)I^-$ appeared to be very light-sensitive and decomposed upon titration.

[16] A similar phenomenon has recently been reported, see: H. Murakami, S. Shinkai, *J. Chem. Soc. Chem. Commun.* **1993**, 1533–1535.

[17] Porphyrin **2** complexes F^- ions (as the tetrabutylammonium salt) very strongly; a K_{ass} value of 2.3×10^4 mol^{-1} in toluene was calculated. Since the complex $(1\cdot Na^+)F^-$ could not be obtained, a toluene solution of the complex $(1\cdot Na^+)(2\cdot ClO_4^-)$ was titrated (UV/Vis, ^{1}H NMR) with $Bu_4N^+F^-$. Despite the very strong interaction ($K_{ass} \approx 3.0\times10^4$ mol^{-1}) initially detected, fast precipitation of NaF from the toluene solution followed, which prevented further assembly.

[18] K. A. Connors, *Binding Constants*, Wiley, New York, **1987**, p. 24.

[19] ^{1}H NMR spectrum of $(1\cdot Na^+)/(2\cdot SCN^-)\cdot$([D$_8$]toluene): δ = 10.29, 10.18 (2 br s, 2H, NH), 8.99 (s, 4H, porphyrin), 8.95, 8.26 (2 d, ^3J(H,H) = 8.0 Hz, 2H, arom.), 8.83 (q, ^3J(H,H) = 4.8 Hz, 4H, porphyrin), 8.50 (d, ^3J(H,H) = 8.0 Hz, 2H, arom.), 8.2–8.0, 7.8–7.5 (2 m, 18H, arom. + NH), 7.38 (t, ^3J(H,H) = 8.0 Hz, 1H, arom.), 7.25, 7.17 (2 s, 8H, arom.), 5.60 (s, 1H, thymine), 4.60, 4.22 (2 s, 4H, $CH_2C(O)$), 4.55, 4.49, 3.30, 3.25 (4 d, ^3J(H,H) = 13.0 Hz, 8H, CH_2-calix), 4.38, 4.11 (2 d, ^3J(H,H) = 14.0 Hz, 4H, $CH_2C(O)$), 4.0–3.8 (m, 6H, OCH_2), 3.28 (s, 2H, $NCH_2C(O)$), 2.53 (t, ^3J(H,H) = 7.5 Hz, 2H, $CH_2C(O)N$), 2.01 (s, 3H, CH_3), 1.85–1.75, 1.4–1.1 (2 m, 6H, CH_2), 1.21 (s, 36H, *t*Bu), 1.03, 1.00 (2 t, ^3J(H,H) = 7.2 Hz, ^3J(H,H) = 7.5 Hz, 6H, CH_3), 0.80 (t, ^3J(H,H) = 7.2 Hz, 6H, CH_3).

[20] The proposed structures were additionally confirmed by molecular mechanics calculations performed with Quanta/CHARMm Version 3.3. Energy minimizations (conjugate gradient) were carried out (Steepest Descents followed by Adopted Based Newton Raphson) until the root mean square of the gradient was less than 0.01 kcal mol^{-1} Å^{-1}.

 © VCH Verlagsgesellschaft mbH, D-69451 Weinheim, 1995 0570-0833/95/3419-2126 $ 10.00+.25/0

Porous Solids by Design: $[Zn(4,4'\text{-bpy})_2(SiF_6)]_n \cdot x\,DMF$, a Single Framework Octahedral Coordination Polymer with Large Square Channels**

S. Subramanian* and Michael J. Zaworotko*

The concept of crystal engineering[1] has in recent years provided numerous examples of rationally designed one- (1D), two- (2D), and three-dimensional (3D) polymeric structures. Of particular potential interest to inclusion chemistry are 2D and 3D coordination polymers which, in principle at least, can be designed to have very specific pore size and type. In such a context, there already exist examples of 2D square[2] and hexagonal/honeycomb[3] grids generated from metal ions in square-planar or trigonal environments, respectively, coordinated to linear bifunctional ligands such as 4,4'-bipyridine or pyrazines. Furthermore, 3D diamondoid coordination polymers based upon tetrahedral or S_4 coordination environments have been generated by either coordinate covalent bonds or hydrogen bonding.[4] However, given the ubiquity of octahedral metal environments, it is somewhat surprising that simple 3D octahedral polymers[5] remain largely unexplored. Indeed, to our knowledge μ-cyano polymers such as $Fe^{III}_4[Fe^{II}(CN)_6]_3$, Prussian Blue,[6] the poorly characterized $[Cd(CN)_2(quinoxaline)]_n$,[7] and triply interpenetrated $[Cd(pyrazine)\{Ag_2(CN)_3\}\{Ag(CN)_2\}]$[8] represent the only examples of such structures.[9a] Recently a coordination polymer from silver ions and pyrazine was synthesized and structurally characterized.[9b] In this contribution we detail a potentially general strategy for generation of such polymers.

Scheme 1 illustrates how cross-linking of cationic square grids with suitable linear bifunctional anionic ligands could in principle afford neutral octahedral polymers with porosity controlled by the length, volume, and chemical type of the spacer ligands. Compound **1** polymerizes to afford square grids with sides of length 11.43 Å.[2] Unfortunately, unlike $[Cd(4,4'\text{-bpy})_2](NO_3)_2$, which eschews interpenetration,[2] the large cavity in **1** is self-included with hexafluorosilicate ions, which are bound through hydrogen bonds to water molecules, and a second independent $[Zn(4,4'\text{-bpy})_2]$ square grid. It occurred to us that the anhydrous form of **1** could be expected to fit the hypothetical network proposed in Scheme 1 since SiF_6^{2-} ions are capable of acting as a linear bridge between transition metal moieties such as $[Co(N\text{-vinylimidazole})_4]^{2+}$[10] and $[Cu(5\text{-phenylpyrazole})_4]^{2+}$.[11] We therefore synthesized the anhydrous form of **1**, namely **2**, and herein report its remarkable crystal structure.

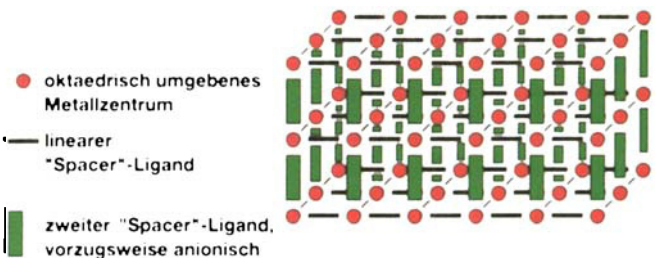

Scheme 1. Schematic illustration of how a three-dimensional coordination polymer might be generated by cross-linking of square grids.

$[Zn(4,4'\text{-bpy})_2(H_2O)_2]SiF_6$ **1**

$[Zn(4,4'\text{-bpy})_2]SiF_6$ **2**

The compound $\mathbf{2} \cdot x\,DMF$ crystallizes in the tetragonal space group $P4/mmm$ with $Z = 1$ and therefore sits around a crystallographic $4/mmm$ position.[12] This alone is quite a remarkable feature since the space group symmetry manifests the maximum D_{4h} point group symmetry that can be sustained by an MX_4Y_2 species. The space group symmetry and cell dimensions are therefore entirely rational or indeed predictable based upon the chemical composition of **2**. However, an even more remarkable feature of **2** is that it eschews interpenetration[13] and therefore, as Figure 1 reveals, large square channels are generated parallel

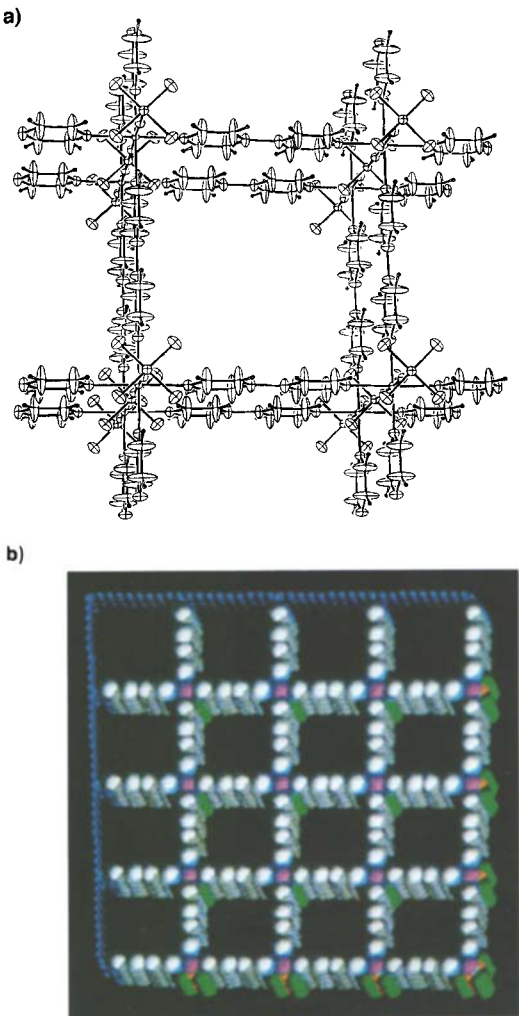

Fig. 1. ORTEP (a) and space-filling (b) views of the *ab* plane in **2**. The square channels have the same dimensions as the unit cell (11.396 × 11.396 Å) and therefore measure about 16 Å diagonally. The effective cross-sectional area is given by subtracting the van der Waals radius of an aromatic ring (ca. 1.7 Å) from each face of the channel, thereby affording a void that should hold molecules with a cross-sectional area of about 8 × 8 Å.

[*] Prof. Dr. M. J. Zaworotko
Department of Chemistry, Saint Mary's University
Halifax, Nova Scotia, B3H 3C3 (Canada)
Telefax: Int. code + (902)420 5261
e-mail: mzaworot@science.stmarys.ca
Dr. S. Subramanian
Department of Chemistry, Sir Wilfred Grenfell College
Memorial University of Newfoundland
Corner Brook, Newfoundland, A2H 6P9 (Canada)

[**] This work was supported by the N. S. E. R. C. (Canada) and the Environmental Science and Technology Alliance Canada. bpy = bipyridyl, DMF = dimethylformamide.

to the crystallographic c axis. As would be anticipated, these channels have essentially the same dimensions as those seen in the interpenetrated dihydrate, 11.3959(11) × 11.3959(11) Å, and the effective size of their pores (8 × 8 Å) compares well with the pore sizes of large zeolites.[14] The volume of the channels is about 50% of the total volume.[15] The μ-SiF_6^{2-} ions form perfectly linear bridges, and the Zn–F distances of 2.082(10) Å, are shorter than the M–F distances encountered in previous studies concerning μ-SiF_6^{2-} units.[10, 11] The Zn–N distances (2.157(8) Å) are also within the expected range. That there is no interpenetration in **2** can possibly be attributed to the orientation of the 4,4′-bipyridine ligands (Fig. 2). These ligands are

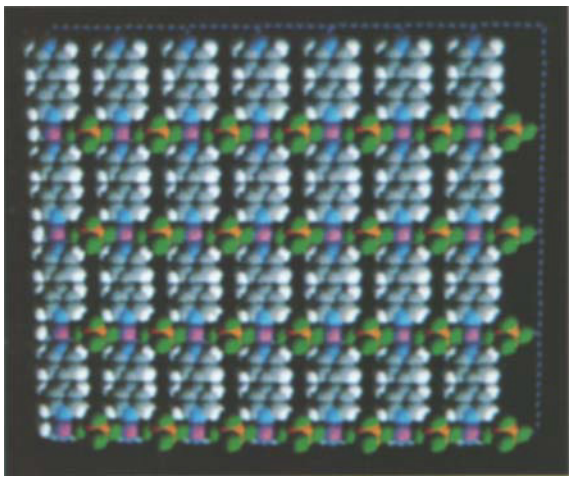

Fig. 2. A view of the *ac* plane in **2**. The 4,4′-bipyridine moieties are aligned with the *ac* plane and therefore preclude porosity or interpenetration in this direction. The α-C-H moieties of the 4,4′-bipyridine ligands are hydrogen-bonded to the fluorine atoms of the SiF_6^{2-} ions.

disposed such that the pyridine moieties are almost coplanar with each other[16] and the crystallographic *ac* and *bc* planes, respectively. The former is quite unusual since such a conformation for 4,4′-bipyridine is sterically disfavored, and the latter is important since it precludes porosity and interpenetration along either the crystallographic *a* or *b* directions. We attribute this conformation and orientation to the existence of C-H···F hydrogen bonds between α-C-H hydrogen atoms and fluorine atoms of the SiF_6^{2-} ions.[17]

Although **2** does not compare to other zeolitic solids in terms of stability in aqueous environments or potential catalytic activity, we consider the following features of this study to be particularly salient: 1) Compound **2** represents, to our knowledge, the first example of a neutral octahedral coordination polymer and, therefore, there are no counterions occupying the microchannels.[18] 2) Compound **2** is inherently modular and all three components are in principle interchangeable. 3) The dimensions of the channels are precisely what one would expect based upon the geometric features of the three components. 4) The channels in **2** are hydrophobic. 5) The space group of **2** can be regarded as a direct manifestation of the point group symmetry (i.e. the structure of **2** can be regarded as having been "crystal engineered" even from the perspective of space group symmetry). We consider **2** to be the prototype of a potentially wide range of porous octahedral structures and are actively investigating the generality of this class of solid and its ability to incorporate medium-sized hydrophobic molecules of cross-sectional area consistent with the dimensions observed in **2**.

Experimental Procedure

2: $[Zn(OH_2)_6]SiF_6$ (0.31 g, 1.0 mmol) was suspended in 1,4-dioxane (25 mL) and benzene (25 mL), and the mixture was heated to reflux in a Dean–Stark apparatus to azeotropically remove the water. The powder of $ZnSiF_6$ thus formed was dissolved by adding DMF (25 mL) to the above mixture. Most of the benzene and 1,4-dioxane were removed by rotoevaporation at this point. The mixture was cooled and a solution of 4,4′-bipyridine (0.31 g, 2.0 mmol) in 1,4-dioxane (10 mL) was added. The solution was heated to reflux for 30 min. The resulting pale gold/yellow solution was cooled and allowed to stand at room temperature for 12 h. This afforded colorless crystals of **2** (0.48 g). Crystals appear to lose solvent and crystallinity within minutes if left to stand exposed to a solvent-free atmosphere and dissolve readily in water. IR (nujol mull): $\tilde{\nu}$ = 2985, 2872 (bpy C-H); 1668 (DMF C=O); 1609, 1457, 1379, 1236, 1086, 833, 770, 635 cm^{-1}.

Received: May 30, 1995 [Z8046IE]
German version: *Angew. Chem.* **1995**, *107*, 2295–2297

Keywords: crystal engineering · hydrogen bonds · porous materials · zinc compounds

[1] C. B. Aakeroy, K. R. Seddon, *Chem. Soc. Rev.* **1993**, 397; G. R. Desiraju, *Crystal Engineering. The Design of Organic Solids*, Elsevier, Amsterdam, **1989**; M. C. Etter, *Acc. Chem. Res.* **1990**, *23*, 120.

[2] M. Fujita, Y. J. Kwon, S. Washizu, K. Ogura, *J. Am. Chem. Soc.* **1994**, *116*, 1151; R. W. Gable, B. F. Hoskins, R. Robson, *J. Chem. Soc. Chem. Commun.* **1990**, 1677.

[3] L. R. MacGillivray, S. Subramanian, M. J. Zaworotko, *J. Chem. Soc. Chem. Commun.* **1994**, 1325; L. Carlucci, G. Ciani, D. M. Proserpio, A. Sironi, *J. Am. Chem. Soc.* **1995**, *117*, 4562.

[4] M. J. Zaworotko, *Chem. Soc. Rev.* **1994**, 23, 284; X. Wang, M. Simard, J. D. Wuest, *J. Am. Chem. Soc.* **1994**, *116*, 12119.

[5] For the purpose of this study, we define an octahedral polymer as an infinite 3D framework that is sustained by octahedral metal centers that are cross-linked by linear bifunctional ligands. We exclude infinite frameworks which consist of both octahedral metal centers and those with a different coordination geometry.

[6] H. J. Buser, D. Schwarzenbach, W. Petter, A. Ludi, *Inorg. Chem.* **1977**, *16*, 2704, and references therein

[7] B. F. Abrahams, M. J. Hardie, B. F. Hoskins, R. Robson, E. E. Sutherland, *J. Chem. Soc. Chem. Commun.* **1994**, 1049.

[8] T. Soma, H. Yuge, T. Iwamoto, *Angew. Chem.* **1994**, *33*, 1746; *Angew. Chem. Int. Ed. Engl.* **1994**, 33, 1665.

[9] a) Although Hoffmann type clathrates contain octahedral metal centers their architecture is based upon 2D μ-cyano sustained grids: T. Iwamoto, *Inclusion Compounds, Vol. 1* (Eds.: J. L. Atwood, J. E. D. Davies, D. D. MacNicol), Academic Press, London, **1984**, Chap. 2, p. 29; b) L. Carlucci, G. Ciani, D. M. Proserpio, A. Sironi, *Angew. Chem.* **1995**, *107*, 2037–2040; *Angew. Chem. Int. Ed. Engl.* **1995**, *34*, 1895–1898.

[10] R. A. J. Driessen, F. B. Hulsbergen, W. J. Vermin, J. Reedijk, *Inorg. Chem.* **1982**, *21*, 3594.

[11] F. S. Keij, R. A. G. de Graaff, J. H. Haasnoot, J. Reedijk, E. Pedersen, *Inorg. Chim. Acta* **1989**, *156*, 65.

[12] X-ray structure of **2**·*x*DMF: $C_{20}H_{16}F_6N_4SiZn \cdot x$DMF, colorless cubes (0.30 × 0.30 × 0.40 mm), tetragonal, space group *P4/mmm*, with a = 11.3959(11), c = 7.6775(9) Å, V = 997.05(15) Å^3, Z = 1, ρ = 0.87 Mg m^{-3} (octahedral polymer only) or 1.27 Mg m^{-3} (including disordered solvent). Data were collected on an Enraf-Nonius CAD-4 diffractometer with $Mo_{K\alpha}$ radiation (λ = 0.71073 Å). Non-hydrogen atoms of the coordination polymer were refined with anisotropic thermal parameters. The solvent molecules were observed to be disordered in a manner that could not be readily resolved. Solvent atoms were therefore treated as carbon atoms and refined with fixed isotropic thermal parameters and variable site occupancy. Values of R = 0.063 and R_w = 0.061 were obtained for 426 out of 569 reflections with $I > 2.5\sigma(I)$ and 48 parameters. Hydrogen atoms of the 4,4′-bipyridine moieties were placed in calculated positions with d_{C-H} = 1.00 Å. Further details of the crystal structure investigation may be obtained from the Director of the Cambridge Crystallographic Data Centre, 12 Union Road, Cambridge CB2 1EZ (UK) on quoting the full journal citation.

[13] Self-inclusion by interpenetration invariably occurs when cavities would be larger than 50% of the volume in 3D or 2D frameworks. For example, in diamondoid systems up to sevenfold interpenetration has been observed: K. Sinzger, S. Hunig, M. Jopp, D. Bauer, W. Bietsch, J. U. von Schutz, H. C. Wolf, R. K. Kremer, T. Metzenthin, R. Bau, S. I. Khan, A. Lindbaum, C. L. Lengauer, E. Tillmanns, *J. Am. Chem. Soc.* **1993**, *115*, 7696.

[14] W. M. Meier, D. H. Olson, *Atlas of Zeolite Structure Types*, 3rd revised edition, Butterworth-Heinemann, Boston, **1992**.

 © VCH Verlagsgesellschaft mbH, D-69451 Weinheim, 1995 0570-0833/95/3419-2128 $ 10.00+.25/0

[15] The density of **2** in the absence of solvent is just 0.87 Mgm^{-3} compared to 1.856 Mgm^{-3} in the corresponding dihydrate **1**. The density was not determined experimentally because of the tendency of the crystals to lose solvent rapidly.
[16] As noted by a reviewer and revealed by Figure 1a, there is considerable distortion of the thermal ellipsoids associated with carbon atoms 2,3,5,6,2',3',5' and 6' of the 4,4'-bipyridine ligands. This observation is consistent with slight twisting of the the pyridine moieties and either static or dynamic disorder between two orientations.
[17] C-H···F and C···F contacts, 2.342 and 3.429(9) Å, respectively, are well within ranges expected for significant C-H···F interactions: L. Shimoni, H. L. Carrell, J. P. Glusker, M. M. Coombs, *J. Am. Chem. Soc.* **1994**, *116*, 8162.
[18] Compounds with comparable or larger pores have recently been reported but either cations (T. J. McCarthy, T. A. Tanzer, M. G. Kanatzidis, *J. Am. Chem. Soc.* **1995**, *117*, 1294) or anions are necessarily present in the pores (B. F. Abrahams, B. F. Hoskins, D. M. Michall, R. Robson, *Nature*, **1994**, *369*, 727).

Rational Design of Orthogonal Receptor–Ligand Combinations**

Peter J. Belshaw, Joseph G. Schoepfer, Karen-Qianye Liu, Kim L. Morrison, and Stuart L. Schreiber*

Signal transduction in cells occurs primarily by two mechanisms, one involving allostery and the other involving proximity.[1] The role of ligand-induced allosteric change in proteins has been appreciated for many years, and has led to the synthesis of numerous molecules that either promote or inhibit the allosteric change required to transduce information in cells. More recently, cell biological studies have illuminated the role of regulated protein dimerization or oligomerization as a means of information transfer. Such an event can promote a proximal relationship between an enzyme and its substrate or a receptor and its ligand, thereby facilitating a molecular interaction leading to a signaling event. Examples include the dimerization of growth factor receptors,[2] oligomerization of antigen receptors,[3] and dimerization of transcription factors.[4] These insights have created new opportunities for chemists to synthesize molecules with two protein-binding surfaces and thereby to induce protein association. Such chemical inducers of dimerization (CIDs) have the potential to activate many cellular processes, including ones of biological and medical significance. We recently described a method to inducibly control the association of proteins in cells.[5, 6] This was accomplished through the expression of chimeric proteins in mammalian cells, consisting of a dimerization domain fused to a protein or protein domain of interest. By treating these cells with a synthetic, cell-permeable CID that binds to the dimerization domain, self-association of the protein occurs and a signal is transmitted (Fig. 1).

Although in theory many receptor–ligand systems can be used, the immunophilins FKBP12 and cyclophilin A (CyP) and their ligands FK506 and cyclosporin A (CsA) were selected for this purpose. The ligands are cell permeable and can be modified

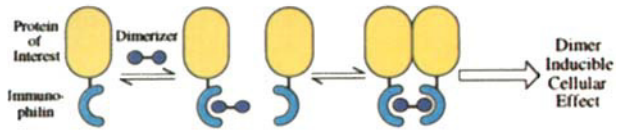

Fig. 1. Regulated intracellular dimerization with cell-permeable synthetic ligands named CIDs.

synthetically in a rational way to remove their intrinsic immunosuppressive and toxic properties. This requires modifying the calcineurin-binding (but not the immunophilin-binding) domain of these naturally occurring CIDs. FKBP12 and CyP bind their ligands with high affinity (K_d = 0.5 nM and 5 nM, respectively), are monomeric, have no discernible effect when expressed in cells, and their small size (12 kDa and 18 kDa, respectively) facilitates the incorporation of their cDNA into expression vectors. A shortcoming is that the natural immunophilins are expressed at high levels in many cells and can therefore diminish the potency of CID ligands toward immunophilin fusion proteins by forming nonproductive receptor–ligand complexes (Fig. 2a). The resulting loss in specificity is expected to be especially troublesome in whole organisms, where cells expressing the fusion proteins may be relatively few in number, thus magnifying the buffering effect of natural immunophilins.

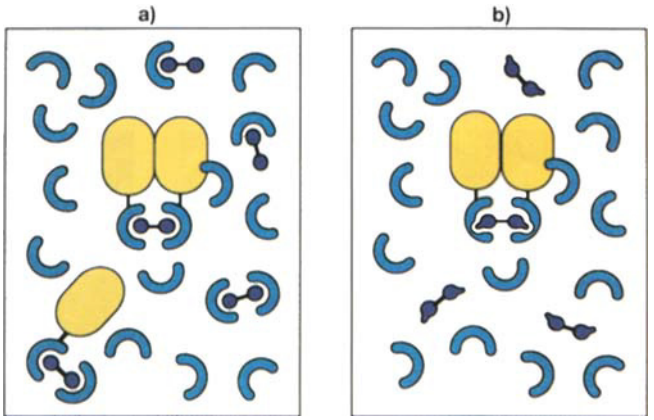

Fig. 2. Improved receptor–ligand pairs for the regulated intracellular protein association with synthetic ligands a) Possible protein associations occurring in cells expressing wild-type immunophilins as dimerization domains. b) Protein associations predicted to occur in cells by using modified CIDs and immunophilins with compensatory mutations.

To solve this problem we envisioned the creation of new receptor–ligand pairs with interacting surfaces that ensure a high degree of specificity. Immunophilin ligands were designed to contain substituents that clash sterically with amino acid sidechains in the immunophilin receptor, thereby abolishing their interaction with endogenous immunophilins. Compensatory mutations in the receptor were sought that would remove the offending interaction, thereby creating a unique receptor that would be used as a dimerization domain (Fig. 2b). Herein, we report the implementation of this strategy using CyP-CsA as a test system. In addition to providing an effective solution to the specific research problem outlined above, we propose that the creation of new receptor–ligand pairs in this manner will result in new experimental systems for testing our understanding of molecular recognition involving protein receptors.

[*] Prof. S. L. Schreiber, P. J. Belshaw, Dr. J. G. Schoepfer, K-Q. Liu, K. L. Morrison
Howard Hughes Medical Institute, Department of Chemistry
Harvard University, Cambridge, MA 02138 (USA)
Telefax: Int. + (617) 495-0751
e-mail: belshaw@slsiris.harvard.edu

[**] This research was supported by a grant from the National Institute of General Medical Sciences (GM-52067). We thank the NSERC for a postgraduate scholarship awarded to P. J. B., and the Swiss National Science Foundation, the Roche Research Foundation, and Ciba-Geigy Jubiläums Stiftung for fellowships to J. G. S.

The high-resolution X-ray structure of the CyP-CsA complex[7, 8] served as the starting point for the design of modified ligands. The primary hydrophobic interaction between CyP and CsA involves the sidechain of MeVal11 of CsA and a deep pocket on the receptor that is lined with the hydrophobic residues Phe60, Met61, Ala101, Phe113, and Leu122 (Fig. 3A). Several CsAs with modifications at residue 11 have been synthesized previously.[9] Binding assays showed that an increase in the size of the MeVal11 sidechain abrogated binding to CyP (MeIle11, Me-allo-Ile11), and conversely that compounds with smaller sidechains (MeAla11) still bind with substantial affinity. Our approach would lead to an increase in buried hydrophobic surface, and as hydrophobic interactions can provide a significant contribution to the free energy of binding,[10] this pocket was selected for modification.

For simplicity, the first target selected was MeIle11CsA. A hypothetical model of MeIle11CsA bound to CyP (Fig. 3B) suggests there should be a steric clash between the strategic methyl group of the modified ligand and the phenyl ring of Phe113 of the receptor. Removal of this ring (Phe113 to Ala) should relieve the steric clash (Fig. 3C), yet it should also create a considerable volume of unoccupied space. To minimize these voids and maximize binding energy, two secondary mutations were designed wherein nearby sidechains were increased in size. A Ser99 to Thr mutation (Fig. 3D) adds an extra methylene group and a Cys115 to Met mutation (Fig. 3E) adds two methylenes. Computer models were generated with MacroModel 4.0 by performing Monte Carlo substructure minimizations with all torsions specified for the sidechains of residues MeIle11, Phe60, Met61, Met115, and Thr99. All other atoms within 6 Å of these atoms were considered but were assigned a 100 kJ Å^{-1} movement penalty. These calculations indicated that the conformer required for efficient packing was the one least frequently observed for threonine residues in protein X-ray structures.[11] These modeling studies also predicted that the two secondary mutants could simultaneously assume their preferred conformations, thus the triple mutant was also investigated (Fig. 3F). These mutant proteins were prepared by PCR mutagenesis using the megaprimer method[12] and verified by sequencing.

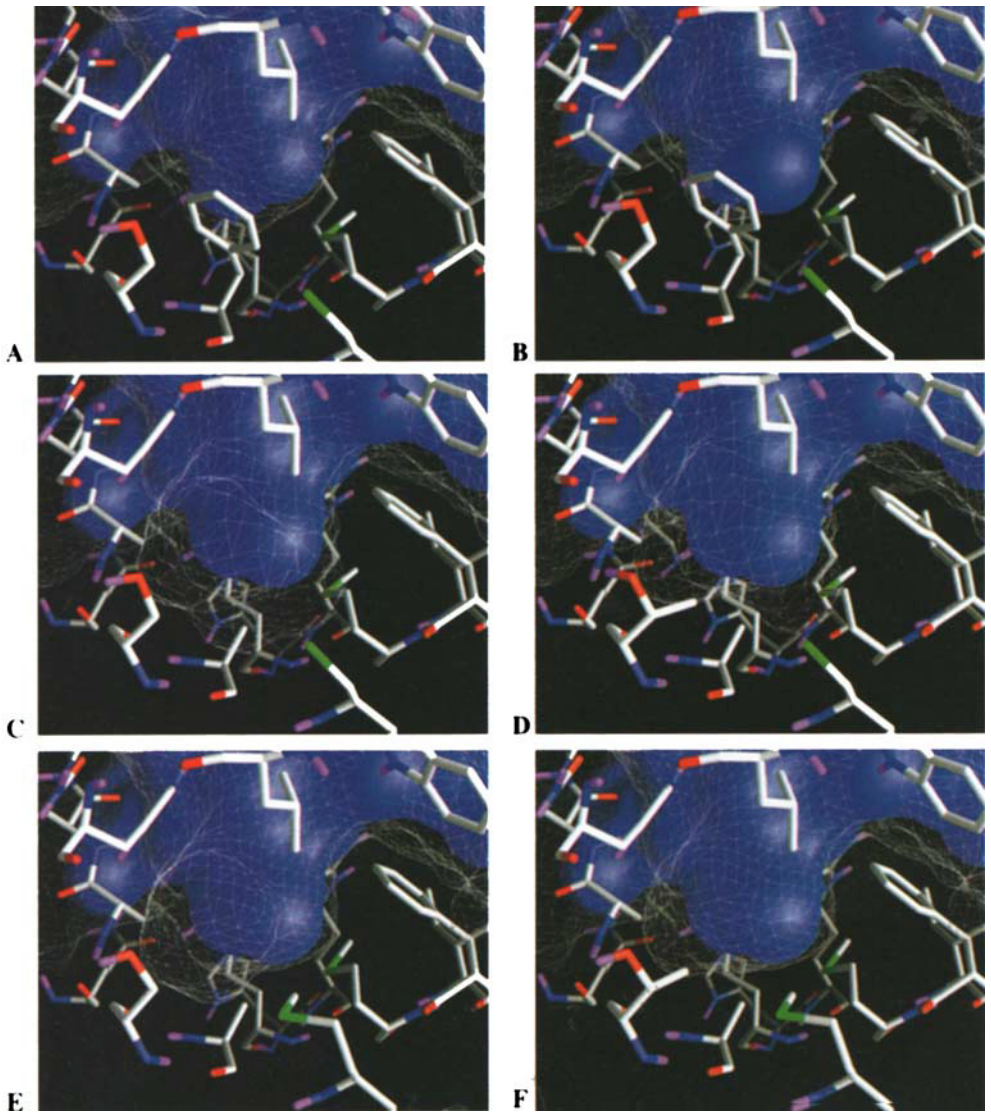

Fig. 3. Graphical representation of the binding interfaces between Cyp and CsA and variants. The solid blue surface and white mesh represent the solvent-accessible surfaces of CsA and Cyp, respectively (nonpolar hydrogens omitted). The contact sidechains of Cyp are represented as tubular bonds and viewed from the inside of the protein; the lowest protrusion of solid blue corresponds to the sidechain of residue 11 of CsA. A) Cyp-CsA crystal structure. B) Hypothetical model of Cyp-MeIle11CsA complex. C) Cyp(F113A)-MeIle11CsA complex. D) Cyp(S99T, F113A)-MeIle11CsA complex. E) Cyp(F113A, C115M)-MeIle11CsA complex. F) Cyp(S99T, F113A, C115M)-MeIle11CsA complex. Graphical representations were created by using GRASP [23].

Our synthetic route begins with the readily available CsA, and produces a common intermediate for the synthesis of compounds with modifications at residues 1 and 11 (Scheme 1). This plan is particularly attractive since position 1 is the site we have used previously to prepare dimeric versions of CsA, named (CsA)2.[13] Thus, by using modified amino acids at positions 1 and 11, we should be able to simplify the synthesis of CIDs with greater specificity than (CsA)2. CsA was ring-opened and degraded by first converting it to iso-CsA[14] and then subjecting the resulting amine to a modified Edman degradation sequence.[15] This procedure excises the MeBmt amino acid, producing a linear peptide that was protected at its amino- and carboxy-termini. The selection of the MEM ester was essential for the subsequent reduction,[16] as all other combinations of common esters and reducing agents failed. Following reduction, another acid-catalyzed N to O shift and an N-acylation produced the target intermediate from which CsAs with modifications at residues 1 and/or 11 are accessible. Two cycles of deprotection and coupling

 © VCH Verlagsgesellschaft mbH, D-69451 Weinheim, 1995 0570-0833/95/3419-2130 $ 10.00+.25/0

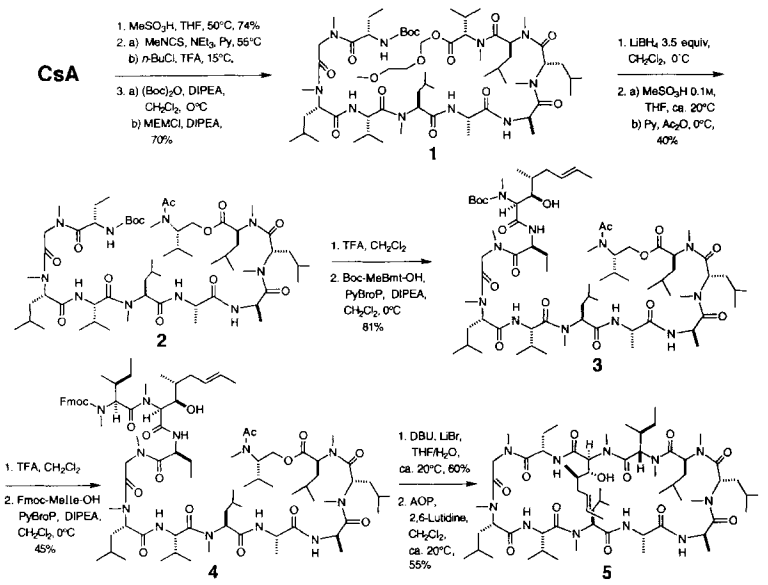

Scheme 1. Semi-synthesis of MeIle11CsA from CsA. For details see Experimental Procedure.

yielded a linear, protected undecapeptide that was deprotected and cyclized to give MeIle11CsA. This unprecedented cyclization between residues 10 and 11 proceeds with good yield and no detectable racemization. The choice of coupling agent and base proved to be critical for efficient cyclization.[17]

CyP experiences an approximate twofold enhancement in fluorescence upon binding CsA. This effect provides a convenient assay for the determination of K_d values.[18–20] Using this fluorescence assay, the binding constants for MeIle11CsA and CsA with the wild-type and mutant CyP proteins were determined and are shown in Table 1. The data show that the extra methyl group of MeIle11CsA dramatically decreases binding to CyP.

Table 1. Binding constants K_d [nM] of CsA-based ligands for wild-type and mutant CyPs.

Protein	MeIle11CsA	CsA
hCyP(wild-type)	> 3000 [a]	5 ± 1
hCyP(F113A)	53 ± 9	55 ± 15
hCyP(F113A, C115M)	75 ± 13	19 ± 7
hCyP(S99T, F113A)	2 ± 0.5	5 ± 1
hCyP(S99T, F113A, C115M)	4 ± 1	7 ± 1

[a] This value represents the lowest possible value, as precise determination is hindered by the solubility of the ligand.

Mutation of Phe113 to Ala has an even more dramatic effect, restoring the binding affinity to within an order of magnitude of the wild-type receptor. The double mutant CyP(S99T, F113A) binds MeIle11CsA with an affinity of 2 nM. Thus, by adding a substituent to CsA and by creating a binding pocket for it on its receptor using site-directed mutagenesis, a new receptor–ligand pair results that binds with two- to threefold greater affinity than the wild-type system. The other double mutant, CyP(F113A, C115M), has less affinity for MeIle11CsA than the F113A single mutant, indicating that this mutation is slightly destabilizing. This appears to be due to an interfering contact between the terminal methyl of M115 and the terminal methyl of the MeIle11 sidechain. Models show that this interaction is slightly closer than any other contact in the binding pocket, although we cannot rule out a disturbance of the local structure due to the Met. Interestingly, the triple mutant CyP(S99T, F113A, C115M) binds MeIle11CsA more poorly than the double mutant CyP(S99T, F113A), and the free energy difference between these two mutants is approximately the same as the difference between CyP(F113A) and CyP(F113A, C115M). This indicates that the destabilizing effect of the C115M mutation is independent of the S99T mutation. All of the mutants show good binding to CsA with affinity generally increasing as the predicted void volume decreases.

We have successfully generated new high affinity receptor–ligand pairs through structure-guided rational design. By selecting other residues with large, hydrophobic, conformationally constrained sidechains as replacements for MeIle11 and by judicious introduction of point mutations, we may be able to extract even greater free energy gains from the hydrophobic effect. In addition to this goal, we intend to synthesize dimeric versions of these new ligands in order to induce the dimerization of target proteins in vivo, thereby assessing the effect of endogenous immunophilins in these types of experiments. The generation of "bumps" and compensatory "holes" provides a controlled system for studying molecular recognition involving protein receptors. Through the iterative interplay of synthesis, molecular and structural biology, and calorimetry and/or other physical methods, the contribution of specific molecular interactions to the free energy of binding can be assessed.

Experimental Procedure

Fluorescence measurements were made on a Hitachi F2000 fluorescence spectrometer following a 10 min incubation with ligand at 20 °C. Excitation was at 280 nm, 10 nm bandwidth and 33/100 filter. Emissions were scanned at 300–400 nm, 10 nm bandwidth. Proteins were diluted to 3 mL in Tris-buffered saline pH 7.4 at about 100 nM (for $K_d > 10$ nM) or 200–500 nM (for $K_d < 10$ nM). Small aliquots of ligand in 50% ethanol were added between successive measurements such that the total volume added was < 1.5%.

An equation relating the observed fluorescence change (ΔF_{obs}), the total fluorescence change at saturation (ΔF_{sat}), the protein concentration (E_o), the ligand concentration (I_o), and the K_d can be derived from consideration of tight binding kinetics and the assumption that $F_{obs} = (EI)F_{sat}/E_o$ [Eq. (a)].

$$\Delta F_{obs} = [(E_o + I_o + K_d) - \{(E_o + I_o + K_d)^2 - 4(E_o)(I_o)\}^{1/2}]\,(\Delta F_{sat})/2) \qquad (a)$$

The fluorescence change at 338 nm (after adjustment for fluorescence of the ligand solution alone) was plotted vs the concentration of the ligand. The data for each determination of K_d (≥ 14 measurements) were fitted to Equation (a) with Kaleidagraph 3.0. All fits have $r > 0.99$.

Physical data for all compounds are in accord with the expected structures and are available upon request from the authors.

1: To a solution of IsoCsA [14] (2.886 g, 2.401 mmol) in pyridine, (144 mL) triethylamine (7.2 mL) and methyl isothiocyanate (7.2 mL) were added. The solution was heated under nitrogen at 50 °C for 30 min. More triethylamine (2.9 mL) and methyl isothiocyanate (2.9 mL) were added and the reaction mixture was heated for an additional 30 min. Following evaporation at room temperature (RT), the residue was dissolved in chorobutane/trifluoroacetic acid (TFA) (9/1), stirred at 10 °C for 1 h, evaporated, and the residue was precipitated three times from EtOAc/hexane to give the crude precursor of **1**. To this crude product (2.4 g) in dichloromethane (DCM) (100 mL) was added *tert*-butyoxycarbonyl (Boc) anhydride (654 mg, 3.0 mmol) and diisopropylethylamine (DIPEA) (1.4 mL, 8.00 mmol). After 4h at RT, MEMCl (570 μL, 5 mmol) was added and the mixture was stirred overnight. The solution was diluted with DCM (200 mL), washed with sodium bisulfate (1 M), water, sodium bicarbonate (sat.), water, and brine (50 mL each). The organic layer was dried (Na_2SO_4), filtered, and evaporated. The residue was chromatographed (silica gel, DCM/MeOH (98/2, 95/5) to afford **1** (1.933 g, 66 % from IsoCsA).

2: To a solution of **1** (975 mg, 0.795 mmol) in DCM (10 mL), 1 mL of 2 M lithium borohydride in THF was added dropwise at 0 °C. The reaction mixture was stirred overnight at room temperature and an additional 0.5 mL of lithium borohydride solution was added. After 24 h the reaction mixture was cooled to 0 °C and

quenched with a solution of citric acid. The mixture was diluted with DCM (100 mL) and washed with sodium bicarbonate (sat.), water, and brine (25 mL each). The organic layer was dried (Na_2SO_4), evaporated, and the residue was dissolved in DCM/MeOH (98/2) and filtered through a plug of silica gel. Evaporation gave the crude precursor of **2** (773 mg). To this crude product (746 mg) in dry THF (40 mL) was added methanesulfonic acid (300 μL). After stirring the mixture at RT for 72 h under nitrogen, pyridine (400 μL), DIPEA (1.5 mL), and acetic anhydride were added at 0 °C. After 2 h the solution was diluted with DCM (100 mL), washed with sodium bisulfate (1 M), water, sodium bicarbonate (sat.), water, and brine (25 mL each). The organic layer was dried (Na_2SO_4), filtered, evaporated, and chromatographed (silica gel, DCM/MeOH (98/2)) to afford **2** (360 mg, 40 % based on **1**).

3: To **2** (60 mg, 0.051 mmol) in DCM (1 mL), TFA (0.5 mL) was added dropwise and stirred for 1 h at 0 °C. The reaction mixture was diluted with DCM (50 mL) and washed three times with sodium bicarbonate (sat.) then water and brine (10 mL each). The organic layer was dried (Na_2SO_4), evaporated, and redissolved in DCM (0.5 mL). Boc-(2*S*,3*R*,4*R*,6*E*)-3-hydoxy-4-methyl-2-(methylamino)-6-octenoic acid (Boc-MeBmt)[21] (18.7 mg, 0.062 mmol), bromotripyrrolidinophosphonium hexafluorophosphate (PyBroP)[22] (27 mg, 0.060 mmol) and DIPEA (27 μL) were added at 0 °C under nitrogen. After 2 h at 0 °C the reaction was allowed to warm to RT, diluted with DCM (50 mL), washed with sodium bisulfate (1 M), water, sodium bicarbonate (sat.), water, and brine (20 mL each). The organic layer was dried (Na_2SO_4), filtered, evaporated and chromatographed (flash silica gel, EtOAc/acetone (9/1)) to give **3** (56 mg, 81 %).

4: To **3** (27 mg, 0.022 mmol) in DCM (1 mL), TFA (0.5 mL) was added dropwise and stirred for 1 h at 0 °C, diluted with DCM (50 mL) and washed three times with with sodium bicarbonate (sat.), water and brine (10 mL each). The organic layer was dried (Na_2SO_4), filtered and evaporated. To the residue in DCM (30 μL), Fmoc-N-MeIle (12 mg, 0.032 mmol), PyBroP (14 mg, 0.032 mmol) and DIPEA (15 μL) were added and the mixture was stirred for 6 h at 0 °C and 30 min at RT. Fmoc-N-MeIle (5 mg, 0.013 mmol), PyBroP (5 mg, 0.011 mmol) were added again at 0 °C and allowed to warm to RT overnight. The mixture was diluted with DCM (50 mL), washed with sodium bisulfate (1 M), water, sodium bicarbonate (sat.), water, brine (20 mL each). The organic layer was dried (Na_2SO_4), filtered, evaporated, and chromatographed (silica gel, EtOAc/acetone 9:1) to afford **4** (19 mg, 60 %).

5: To **4** (4.6 mg, 0.0028 mmol) in THF/water (10:1, 200 μL), DBU (3 μL) and lithium bromide (2 mg) were added. After stirring overnight at RT, DBU (4 μL) and lithium bromide (3 mg) were added again. After 5 h, the reaction was quenched with acetic acid (20 μL) and purified by reverse-phase HPLC (Beckman ODS ultrasphere 5 μ 10 mm × 25 cm, 0.1 % TFA/MeCN 70/30 → 10/90 in 30 min, 70 °C, 3 runs) to yield the peptide precursor of **5** (2.1 mg, 60 %). A solution of this peptide precursor (1.2 mg, 970 nmol), AOP[17] (4 mg, 0.009 mmol) and 2,6-lutidine (4 μL) in DCM (1.2 mL) was stirred for 48 h at RT. The reaction mixture was quenched with acetic acid (30 μL), the DCM evaporated, and the residue dissolved in acetonitrile and purified by reverse-phase HPLC (Beckman ODS ultrasphere 5 μ 10 mm × 25 cm, 0.1 % TFA/MeCN 70/30 → 10/90 in 30 min. 70 °C) to afford the pure cyclic peptide **5** (0.65 mg, 55 %).

Received: June 9, 1995 [Z 80801E]
German version: *Angew. Chem.* **1995**, *107*, 2313–2317

Keywords: cyclophilin · cyclosporin · immunophilins · protein dimerization

[1] D. J. Austin, G. R. Crabtree, S. L. Schreiber, *Chem. & Biol.* **1994**, *1*, 131.
[2] M. A. Lemmon, J. Schlessinger, *Trends Biochem. Sci.* **1994**, *19*, 459.
[3] A. C. Chan, D. M. Desai, A. Weiss, *Annu. Rev. Immunol.* **1994**, *12*, 555.
[4] W. H. Landschulz, P. F. Johnson, S. L. McKnight, *Science* **1988**, *240*, 1759.
[5] D. M. Spencer, T. J. Wandless, S. L. Schreiber, G. R. Crabtree, *Science* **1993**, *262*, 1019.
[6] M. N. Pruschy, D. M. Spencer, T. M. Kapoor, H. Miyaki, G. R. Crabtree, S. S. L. Schreiber, *Chem. & Biol.* **1994**, *1*, 163.
[7] H. Ke, D. Mayrose, P. J. Belshaw, D. G. Alberg, S. L. Schreiber, Z. Y. Chang, F. A. Etzkorn, S. Ho, C. T. Walsh, *Structure (London)* **1994**, *2*, 33.
[8] G. Pflugl, J. Kallen, T. Schirmer, J. N. Jansonius, M. G. Zurini, M. D. Walkinshaw, *Nature* **1993**, *361*, 91.
[9] V. F. Quesniaux, M. H. Schreier, R. M. Wenger, P. C. Hiestand, M. W. Harding, M. H. V. Van Regenmortel, *Eur. J. Immunol.* **1987**, *17*, 1359.
[10] T. Clackson, J. A. Wells, *Science* **1995**, *267*, 383.
[11] J. S. Richardson, D. C. Richardson in *Prediction of protein structure and the principles of protein conformation, Vol. XIII*; (Ed. G. D. Fasman), Plenum, New York, **1989**.
[12] G. Sarkar, S. S. Sommer, *BioTechniques* **1990**, *8*, 404.
[13] P. J. Belshaw, S. L. Schreiber, *Chem. & Biol.*, submitted.
[14] R. Oliyai, V. J. Stella, *Pharm. Res.* **1992**, *9*, 617.
[15] A. Ruegger, M. Kuhn, H. Lichti, H. R. Loosli, R. Huguenin, C. Quiquerez, W. A. Von, *Helv. Chim. Acta.* **1976**, *59*, 1075.
[16] R. E. Ireland, W. J. Thompson, *Tetrahedron Lett.* **1979**, 4705.
[17] L. A. Carpino, F. A. El, *J. Org. Chem.* **1994**, *59*, 695.
[18] R. E. Handschumacher, M. W. Harding, J. Rice, R. J. Drugge, D. W. Speicher, *Science* **1984**, *226*, 544.
[19] H. Husi, M. Zurini, *Anal. Biochem.* **1994**, *222*, 251.
[20] L. D. Zydowsky, F. A. Etzkorn, H. Y. Chang, S. B. Ferguson, L. A. Stolz, S. I. Ho, C. T. Walsh, *Protein Sci.* **1992**, *1*, 1092.
[21] W. D. Lubell, T. F. Jamison, H. Rapoport, *J. Org. Chem.* **1990**, *55*, 3511.
[22] J. Coste, E. Frerot, P. Jouin, *J. Org. Chem.* **1994**, *59*, 2437.
[23] A. Nicholls, K. A. Sharp, B. Honig, *Prot. Struct. Funct. Genet.* **1991**, *11*, 283.

Strong Binding of Paraquat and Polymeric Paraquat Derivatives by Basket-Shaped Hosts**

Albertus P. H. J. Schenning, Bas de Bruin, Alan E. Rowan,* Huub Kooijman, Anthony L. Spek, and Roeland J. M. Nolte

Clip-shaped host molecules of type **1** can bind uncharged aromatic guest molecules, for example resorcinol, by π–π stacking and hydrogen bonding interactions.[1] Basket-shaped derivates of **1** containing crown ether moieties (compounds of type **2**) are, in addition, able to bind alkali metal ions and protonated amines.[2] We report here on the binding affinities of these host molecules towards charged aromatic compounds, such as paraquat **3** and the polymeric paraquat derivatives **4** and

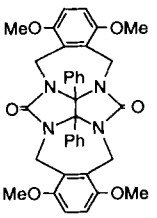

1

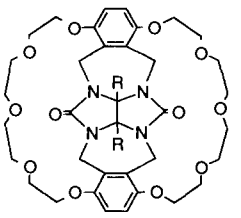

2 a, R = C_6H_5
b, R = $CH_3C_6H_4$

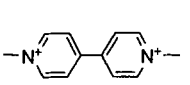

3

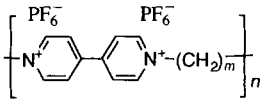

4 a, *m* = 5
b, *m* = 8

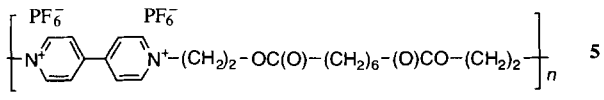

5

5. There is currently a great deal of interest in paraquat-binding, which has resulted in the design and construction of new molecular structures, as exemplified by the elegant work by Stoddart et al. on catenands and rotaxanes.[3] We describe here that com-

[*] Dr. A. E. Rowan, Dipl.-Chem. A. P. H. J. Schenning, Dipl.-Chem. B. de Bruin, Prof. Dr. R. J. M. Nolte
Department of Organic Chemistry, NSR Center
University of Nijmegen
Toernooiveld, NL-6525 ED Nijmegen (The Netherlands)
Telefax: Int. code +(80) 553450
Dr. H. Kooijman, Dr. A. L. Spek
Bijvoet Center for Biomolecular Research, Crystal and Structural Chemistry
Utrecht University (The Netherlands)

[**] This work was supported by the Netherlands Foundation for Chemical Research (SON) with financial aid from the Netherlands Organization for Scientific Research (NWO).

pound **2** is an exceptionally good host for paraquat. This opens the possibility of clipping host molecules of type **2** to polymeric chains containing paraquat units. The X-ray structure and properties of the complex between **2** and paraquat are also presented.

Compounds **1** and **2** were synthesized as described previously.[1, 2] For the synthesis of **2b**, 4,4'-dimethylbenzil was used as the starting material. Compounds **3** and **4** were prepared by using literature procedures.[3, 4] Compound **5** was prepared by the condensation of *N*,*N*'-bis(2-hydroxyethyl)-4,4'-bipyridinium hexafluorophosphate in acetonitrile with one equivalent of adipoyl chloride with triethylamine as the base,[5] and purified by precipitation from ethyl acetate.

Addition of **3**-Cl_2 to a solution of host **2b** in for example methanol/chloroform led to an immediate color change from colorless to yellow-orange, indicative of the formation of a charge-transfer complex.[3] ^{1}H NMR spectroscopic studies revealed that in this complex the paraquat guest is located in the cleft of the cavity.[6] Fast atom bombardment mass spectrometry (FAB MS) showed a peak at *m*/*z* 1094 (matrix: nitrobenzyl alcohol), which corresponds to the mass of the host–guest complex. Crystals of the complex between **2b** and **3**-$(PF_6)_2$ suitable for X-ray analysis were grown from a mixture of **2b** and tetrabutylammonium hexafluorophosphate dissolved in chloroform, which was layered with **3**-Cl_2 dissolved in methanol. The X-ray structure of complex is shown in Figure 1 (top).[7] It reveals a

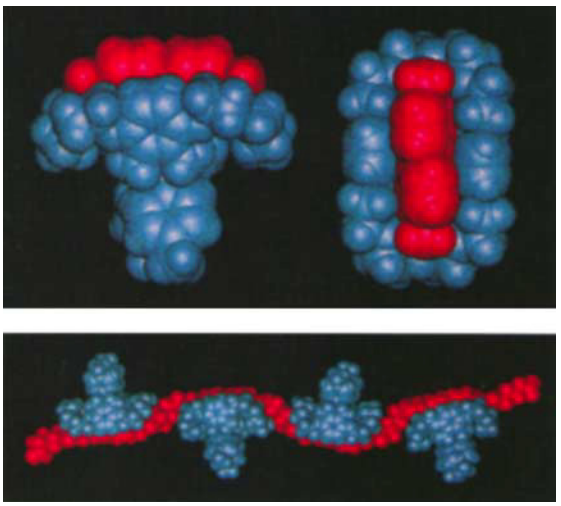

Fig. 1. Top: Crystal structure of the complex between **2b** and **3**-$(PF_6)_2$. Left top view, right side view [14]. Bottom: Computer-generated model of the complex between **2b** and **5**.

perfect complementarity between host and guest. The paraquat guest sits symmetrically within the walls of the basket; the methyl substituents are partially encapsulated by the crown ether rings. The crystal structure is different from that of the complex of paraquat with "bis(paraphenylene)-[34]crown-10" (the same macrocycle as compound **2a**, but without the diphenylglucoluril unit), as published by Stoddart et al.[3] In the case of the latter the bipyridinium guest is flat, whereas in the crystal structure described herein the two bipyridinium units are twisted by an angle of 22.5(3)°. This is a consequence of being less sterically constrained by the aromatic side walls of the basket. In Stoddart's compound the bipyridinium is tilted at an angle of about 28° with respect to the O–O axis of the paraphenylene unit; in our case the bipyridinium guest in the basket is not tilted. The binding constant of the bis(paraphenylene)-[34]crown-10 macrocycle with **3**-$(PF_6)_2$ in acetone is 730 M^{-1}. The binding properties of **1** and **2** were evaluated by recording the intensity of the charge-transfer absorption band at approximately 425 nm at different host–guest ratios. The results for different solvents are presented in Table 1. The basket-shaped host molecules **2** bind paraquat approximately 25–75 times stronger than the bis(paraphenylene)-[34]crown-10 macrocycle.[3] This result can be explained from the fact that compounds **2** are more preorganized for binding than Stoddart's compound.[8] Only a very small K_a of 80 M^{-1} was found for the binding of **3** in the cavity of clip molecule **1**. This clearly demonstrates the importance of the crown ether moieties in **2** for the complexation of paraquat.

Table 1. Binding constants [a] of the complexes between hosts **1** and **2** and guests **3**, **4**, and **5**.

Host	Guest	K_a [M^{-1}]
1	**3**-Cl_2	80 [b]
2a	**3**-$(PF_6)_2$	57000 [c]
2a	**3**-$(PF_6)_2$	20000 [d]
2b	**3**-Cl_2	22000 [b]
2a	**4a** [f]	1800 [c, e]
2a	**4b** [g]	4500 [c, e]
2a	**5** [h]	19000 [c, e]

[a] Association constants were calculated using the Benesi–Hildebrand equation [13]. Good correlations ($R > 0.995$) were obtained for all titration curves assuming a 1:1 host–guest complexation. Estimated error in K_a is 10%. For the K_a measured in acetone, the error is 50% due to the poor solubility of the host molecule in this solvent. [b] Methanol-chloroform (1:1, v/v). [c] Acetonitrile. [d] Acetone. [e] Per polymer repeat unit. [f] Intrinsic viscosity of polymer $[\eta] = 0.006$ dL g^{-1} (acetonitrile, 25 °C). [g] Intrinsic viscosity of polymer $[\eta] = 0.293$ dL g^{-1} (acetonitrile, 25 °C). [h] Average degree of polymerization = 4 (NMR, endgroup analysis).

The electrochemical behavior of the complex between **3**-$(PF_6)_2$ and compound **2a** was studied in acetonitrile. In this solvent the guest showed two reversible one-electron transfers: $E_{1/2}(2+/1+) = -0.423$ V, $E_{1/2}(1+/0) = -0.840$ V (vs. SCE, for both transitions $\Delta E_p = 60$ mV). Upon the addition of one equivalent of **2a** the first redox transfer shifted 100 mV to more negative potential, whereas the second electron transfer potential remained unaffected. These data indicate that **2a** binds and stabilizes the doubly charged paraquat species, which results in a more negative redox potential for the first redox transfer. It is well known that in this type of host–guest system the guest reduced by one electron dissociates form the host, and this explains the unaltered second redox potential.[3]

Polymeric paraquat derivatives have previously been investigated as redox-active films and more recently as optical data storage materials and show a wide variety of electrochromic and thermochromic behavior.[4, 9, 10] The polymeric paraquat derivative with tosylate counterions has been shown to possess liquid crystalline properties.[11, 12] We felt that host–guest complexation might be an interesting way to modify and control the physical properties of this interesting class of polymers. The results of binding studies carried out in acetonitrile, showed that **2a** can be clipped to polymeric paraquat derivatives **4a**, **4b**, and **5** with association constants of 1800 M^{-1}, 4500 M^{-1}, and 19000 M^{-1}, respectively (per polymer repeat unit, see Table 1, Fig. 1). The binding constants of **4a** and **4b** are lower than those observed for paraquat itself. Molecular modeling studies have revealed that in the case of **4a** and **4b**, complexation of a basket to a paraquat unit in the polymer is sterically hindered by baskets complexed to adjacent paraquat units. The overall lower binding constants reflect this steric hindrance, which is less for

the polymer with a longer spacer (**4b**) than for the one with the smaller spacer (**4a**). Viscosity measurements showed that the specific viscosity of the polymers solubilized in acetonitrile increases upon the addition of 0.03 equivalents of the host molecule **2a** per repeat unit: for example, **4a**: $\eta_{sp} = 0.006$, **4a** + **2a** $\eta_{sp} = 0.008$; **4b**: $\eta_{sp} = 0.068$, **4b** + **2a** $\eta_{sp} = 0.070$. These results indicate that the average molecular mass of the polymers increases on complexation with **2a**. The redox potentials of the polymers were also influenced by the hosts. Polymer **4a** displayed the following redox transitions in acetonitrile: $E_{1/2}(2+/1+) = -0.387$ V, $E_{1/2}(1+/0) = -0.840$ V (vs. SCE, for both transitions $\Delta E_p = 60$ mV). Upon the addition of one equivalent of **2a** per repeat unit the first redox transfer shifted 20 mV to more negative potential, whereas the second redox transfer remained unchanged. Addition of three equivalents of **2a** resulted in a 35 mV shift in the negative direction. These shift values are smaller than the 100 mV shift measured for paraquat (**3**) which may be the result of the lower binding affinity of **2a** for the polymeric paraquat derivatives. These preliminary results indicate that the electrochemical behavior of polymeric paraquat derivatives can easily be tuned by the addition of basket molecules. This may be of interest for future application of these polymers as optical data storage systems or as molecular switches, etc.

In conclusion, we have shown that host molecules of the type **2** strongly bind paraquat **3** and that it is possible to clip these molecules to polymeric paraquat derivatives. Further studies are underway.

Received: March 14, 1995 [Z 7792 IE]
German version: *Angew. Chem.* **1995**, *107*, 2288 - 2289

Keywords: crown ethers · paraquat · supramolecular chemistry

[1] R. P. Sijbesma, A. P. M. Kentgens, E. T. G. Lutz, J. H. van der Maas, R. J. M. Nolte, *J. Am. Chem. Soc.* **1993**, *115*, 8999.
[2] J. W. H. Smeets, R. P. Sijbesma, L. van Dalen, A. L. Spek, W. J. J. Smeets, R. J. M. Nolte, *J. Org. Chem.* **1989**, *54*, 3710.
[3] a) B. L. Allwood, N. Spencer, H. Shahriari-Zavareh, J. F. Stoddart, D. J. Williams, *J. Chem. Soc. Chem. Commun.* **1987**, 1064; b) P. L. Anelli, P. R. Ashton, R. Ballardini, V. Balzani, M. Delgado, M. T. Gandolfi, T. T. Goodnow, A. E. Kaifer, D. Philp, M. Pietraszkiewicz, L. Prodi, M. V. Reddington, A. M. Z. Slawin, N. Spencer, J. F. Stoddart, C. Vicent, D. J. Williams, *J. Am. Chem. Soc.* **1992**, *114*, 193.
[4] T. Ohsaka, M. Nakanishi, O. Hatozaki, N. Oyama, *Electrochim. Acta* **1990**, *35*, 63.
[5] P. R. Ashton, D. Philp, M. V. Reddington, A. M. Z. Slawin, N. Spencer, J. F. Stoddart, D. J. Williams, *J. Chem. Soc. Chem. Commun.* **1991**, 1680.
[6] The following ^{1}H NMR signals of **2a** are shifted by complexation with **3**-$(PF_6)_2$ (1:1): (200 MHz, $CD_3CN/CDCl_3$ (7/3, v/v), 25 °C): $\Delta\delta = -0.81$ (s, 4H, Ar-H), +0.07 (AB quartet, 4H, CH_2-N), −0.87 (m, 8H, CH_2O-Ar); likewise for **3**-$(PF_6)_2$ by complexation with **2a**: $\Delta\delta = -1.08$ (d, 4H, Ar-H), +0.12 (d, 4H, Ar-H), +0.22 (s, 6H, CH_3).
[7] Crystal data for [(**2b**) · (**3**) · $2PF_6$ · $2CHCl_3$]: $C_{64}H_{74}N_6O_{12}P_2F_{12}Cl_6$, $M_r = 1622.0$, monoclinic, space group $C2/c$, $a = 32.968(5)$, $b = 13.6135(14)$, $c = 17.875(2)$ Å, $\beta = 118.375(11)°$, $V = 7058.6(17)$ Å^3, $Z = 4$, $\rho_{calcd} = 1.5263(4)$ g cm^{-3}, $Mo_{K\alpha}$ radiation (graphite monochromator), $\mu = 3.9$ cm^{-1}, 7352 intensity data collected at 150 K, 6778 unique, Lp correction, no absorption correction. The structure was solved by direct methods (SHELXS-86) and refined on F^2 (SHELXL-93), no observance criterion applied during refinement. Final $wR2 = 0.226$, $R1 = 0.099$ (for 3162 $I > 2\sigma(I)$), $S = 1.00$. Residual electron density was in the range −0.34, 0.50 (near PF_6). Further details of the crystal structure investigation may be obtained from the Director of the Cambridge Crystallographic Data Centre, 12 Union Road, GB-Cambridge CB2 1EZ (UK), on quoting the full journal citation.
[8] E. P. Kyba, R. C. Helgeson, K. Madan, G. W. Gokel, T. L. Tarnowski, S. S. Moore, D. J. Cram, *J. Am. Chem. Soc.* **1977**, *99*, 2564.
[9] T. Nagumura, Y. Isoda, *J. Chem. Soc. Chem. Commun.* **1991**, 72.
[10] L. P. Yu, E. T. Samulski in *Oriented Fluids and Liquid Crystals, Vol. 4* (Eds.: A. C. Griffin, J. F. Johnson), Plenum, New York, **1984**, p. 697.
[11] P. K. Bhowmik, W. Xu, H. Han, *J. Polym. Sci. Part A: Polym. Chem.* **1994**, *32*, 3205.
[12] P. K. Bhowmik, H. Han, *J. Polym. Sci. Part A: Polym. Chem.* **1995**, *33*, 1745.
[13] J. A. Hildebrand, H. A. Benesi, *J. Am. Chem. Soc.* **1949**, *71*, 2703.

Formation of a "*meso*-Helicate" by Self-Assembly of Three Bis(catecholate) Ligands and Two Titanium(IV) Ions

Markus Albrecht* and Sirpa Kotila

Double- or triple-helical oligonuclear coordination compounds that are formed spontaneously by self-assembly of two or three oligodentate ligands and several metal ions are called helicates. Due to their helicity, such molecules are chiral.[1] On the other hand, *meso*-helicates are analogous metal complexes with two differently configurated helical units and are thus achiral. In a topological sense, the *meso*-helicates are helices that inverse their helical twist.[2]

An octahedral complex formed by one metal center and three bidentate ligands is the most simple helical unit. It can have two configurations (Δ or Λ).[3] Triple bridging between the ligands of two such octahedrons results in the formation of three different coordination compounds: the enantiomeric Δ,Δ- and Λ,Λ-helicates, and the diasteromeric Δ,Λ-form—the most simple triple-stranded *meso*-helicate (Fig. 1).

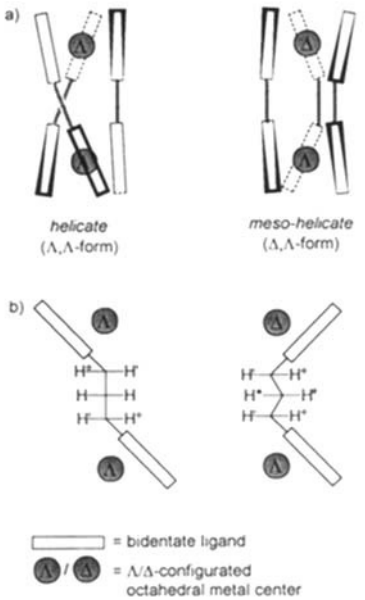

Fig. 1. Schematic representation of a) a helicate (here: Λ,Λ-form) and the corresponding *meso*-helicate (Δ,Λ-form) and b) a binuclear C_3-bridged helicate and *meso*-helicate (only one of the ligand strands is shown).

The coordination chemistry of linear oligodentate nitrogen donor ligands with soft metal ions has recently become the focus of a great deal of attention. To our knowledge, investigations towards the metal-directed self-assembly of helicates have resulted only in the characterization of double-[1, 4] and triple-helical[5] and double-stranded non-helical metal complexes, which do not possess units with helical chirality.[6] In this context, the triple-stranded *meso*-helicate is a missing structural motif.

This stimulated our interest in self-assembly processes based on oxygen donor ligands in combination with hard metal ions.[7, 8] The use of early transition metals should provide access to new supramolecular aggregates, whose properties should differ from those of the "traditional" compounds.

Catechol ligands seem to be ideal bidentate chelating units for this purpose.[8] Initially we chose the $(CH_2)_3$ group as a spacer

[*] Dr. M. Albrecht
Institut für Organische Chemie der Universität
Richard-Willstätter-Allee, D-76131 Karlsruhe (Germany)
Telefax: Int. code + (721)698529
Dr. S. Kotila
Organisch-Chemisches Institut der Universität Münster (Germany)

[**] This work was supported by the Fonds der Chemischen Industrie (Liebig Stipendium), the Deutsche Forschungsgemeinschaft, and the Academy of Finnland. Dr. H. Röttele is thanked for the NMR measurements. Mrs. B. Wibbeling's and Dr. R. Fröhlich's help with the X-ray structure analysis is gratefully acknowledged.

between the aromatic moieties. Additional work concerns the combination of oxygen and nitrogen donor systems in order to obtain sequential ligand strands for use in the formation of oligonuclear metal complexes with a high content of information.[9]

Figure 1b shows a schematic representation of the ligand orientation in triple-stranded helicates and *meso*-helicates with C_3 spacers between the chelating units. In both cases the benzylic protons (H°/H′) are diastereotopic. However, the protons of the central methylene group of the C_3 spacer only show diastereotopic behavior in the *meso*-helicate (H*/H#). In the case of the helicate, these protons (H/H) are enantiotopic. Thus, it should be possible to readily assign the structure in solution by ^{1}H NMR spectroscopy.

The C_3-bridged catechol ligand **6-H$_4$** was synthesized in a reaction sequence starting with a palladium-catalyzed Stephens–Castro coupling reaction of 1-bromo-2,3-dimethoxybenzene (**1**)[10] with trimethylsilylacetylene. Subsequent removal of the silyl group gave the terminal alkyne **3**, which was coupled in the critical step of the reaction with 2,3-dimethoxybenzyl bromide[9] to give 1,3-bis(2,3-dimethoxyphenyl) propyne (**4**). Catalytic hydrogenation of the triple bond and cleavage of the methyl ether of the resulting bis(veratrole) **5** yielded 3,3′-propane-1,3-diylbis(1,2-benzenediol) [1,3-bis(2,3-dihydroxyphenyl)propane] (**6-H$_4$**) (Scheme 1).[11]

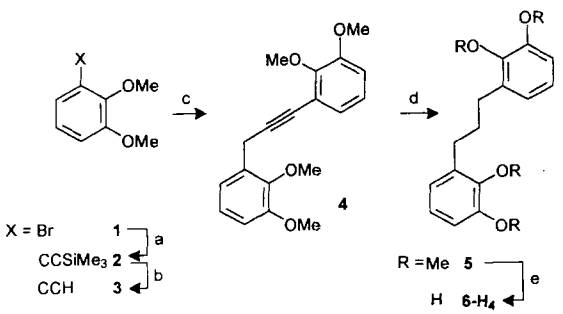

Scheme 1. Synthesis of **6-H$_4$**: a) $[Ph_3P)_2PdCl_2]$, CuI, piperidine, trimethylsilyl acetylene (70%); b) K_2CO_3, methanol (96%); c) *n*BuLi, 2,3-dimethoxybenzyl bromide (21%); d) H_2, Pd/C (96%); e) BBr_3 (99%).

The reaction of three equivalents of **6-H$_4$** with two equivalents of titanoyl bis(acetylacetonate) in the presence of two equivalents of potassium or sodium carbonate as a base afforded quantitative yields of red-orange metal complexes. The compounds are highly soluble in methanol or water, indicating that not an unspecific coordination polymer but a well-defined metal complex is formed by self-assembly. The stoichiometry of the potassium salt $K_4[(\mathbf{6})_3Ti_2]$ was determined by elemental analysis, FAB(+) mass spectrometry, and measurement of the molar weight in solution.[11]

The reaction of three equivalents of **6-H$_4$** with only one equivalent each of titanoyl bis(acetylacetonate) and potassium carbonate resulted in the formation of the binuclear metal complex in "positive cooperativity".[1] In the crude product only $K_4[(\mathbf{6})_3Ti_2]$ and ligand **6-H$_4$** were detected (^{1}H/^{13}C NMR).

The ^{13}C NMR spectrum of $K_4[(\mathbf{6})_3Ti_2]$ ([D$_4$]methanol, 100 MHz) shows one set of aromatic resonances at $\delta = 159.2$, 157.3, 127.3 (3 C), 120.5, 118.6, and 110.8 (3 CH), and two signals of methylene groups at $\delta = 34.1$ and 33.3 (double intensity). Thus, the binuclear coordination compound has a high symmetry with six magnetically equivalent catecholate units. This is in accordance with both structures shown in Figure 1 (helicate and *meso*-helicate). It is possible to distinguish between the two structures by ^{1}H NMR spectroscopy in [D$_4$]methanol (400 MHz). At 296 K the resonances of the aromatic moiety are detected at $\delta = 6.38$ (4 H) and 6.23 (2 H) and those of the $(CH_2)_3$ spacer at $\delta = 2.85$ and 2.18 (2 H each, diastereotopic benzylic protons) and 2.15 and 1.57 (1 H each, diastereotopic protons of the central methylene group). The observation of two sets of diastereotopic alkyl protons clearly shows that the complex has two differently configurated metal centers in solution (*meso*-helicate; see Fig. 1).

The corresponding sodium salt $Na_4[(\mathbf{6})_3Ti_2]$ was characterized by an X-ray crystal structure analysis.[12] The crystal contained several partially disordered solvent molecules (six DMF, five water) resulting in a relatively high *R* value of $R = 0.130$. However, comments about the structure of the tetraanion and the positions of the sodium ions can be made unambiguously.

In the crystal, the $[(\mathbf{6})_3Ti_2]^{4-}$ ion adopts the same *meso*-helicate structure as observed in solution. Figure 2 shows the

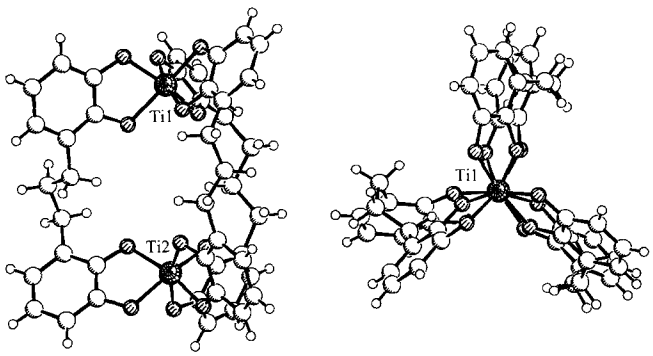

Fig. 2. Molecular structure (SCHAKAL) of the tetraanion $[(\mathbf{6})_3Ti_2]^{4-}$; side view (left) and view along the Ti–Ti axis (right).

two differently configurated pseudo-octahedral titanium(IV) tris(catecholate) moieties.[13] The two complex units are connected through three $(CH_2)_3$ groups. The length of the alkyl spacer might be the reason for the unusual *meso*-helicate structure of this triple-stranded binuclear metal complex. The most favorable conformation that a linear alkyl chain can adopt is a zigzag structure, as observed for two of the bridges in the crystal (the third spacer seems to deviate from this conformation because of interaction with a DMF molecule). This leads in the case of a C_3 chain to the observed *meso*-helicate. In contrast, a chain with an even number of members should favor the formation of helicates. Whether this is true requires further investigation.

Another unusual feature of the structure of the sodium salt are the positions adopted by the cations. Na4 is the only cation to be separated from the anion by coordination to solvent molecules (Fig. 3). Na1 and Na3 are exohedrally bound to the terminal oxygen functionalities of the *meso*-helicate anion. The remaining free valences of these two cations are saturated by solvent molecules. Na1, Na3, and Na4 are surrounded by ligands in a distorted octahedral fashion (Na–O = 219(2)–268(3) pm). However, the most striking position is taken by Na2. It is bound endohedrally in the cavity which is formed by the three ligands **6** and the two titanium(IV) centers. Interactions are observed with three oxygen atoms of the catecholates, one DMF, and one water molecule. The next closest contact to an O atom is observed at 340 pm. Similar to Na2, the water molecule is located inside the cavity and interacts through hydrogen

$m/z = 1021$ $[HK_4[(\mathbf{6})_3Ti_2]^+]$, 1059 $[K_5[(\mathbf{6})_3Ti_2]^+]$; $C_{43}H_{36}K_4O_{12}Ti_2 \cdot 7H_2O$ (1147.1): calcd. C 47.12, H 4.39, found C 47.07, H 4.13; molecular weight determination of $C_{45}H_{36}K_4O_{12}Ti_2 \cdot 7H_2O$ (vapor pressure osmometry, H_2O): calcd. 1147, found 1108. $Na_4[(\mathbf{6})_3Ti_2]$: FAB(+)-MS (glycerine): $m/z = 935$ $[H_2Na_3[(\mathbf{6})_3Ti_2]^+]$, 957 $[HNa_4[(\mathbf{6})_3Ti_2]^+]$, 980 $[Na_5[(\mathbf{6})_3Ti_2]^+]$.

[12] Crystals of $Na_4[(\mathbf{6})_3Ti_2] \cdot 6DMF \cdot 5H_2O$ were obtained by slow diffusion of ether in a solution of the compound in DMF/water (ca. 10:1). Crystal data for $Na_4[(\mathbf{6})_3Ti_2] \cdot 6DMF \cdot 5H_2O$: Formula $C_{63}H_{88}N_6Na_4O_{23}Ti_2$, formula weight 1485.15, red prisms ($0.90 \times 0.60 \times 0.25$ mm^3), triclinic, space group $P\bar{1}$ (no. 2), $a = 1278.7(1)$, $b = 1363.8(1)$, $c = 2236.7(3)$ pm, $\alpha = 75.12(1)$, $\beta = 82.03(1)$, $\gamma = 78.65(1)^\circ$, $V = 3680 \times 10^6$ pm^3, $Z = 2$, $F(000) = 1560$, $T = -140\,^\circ$C, $\rho_{calcd.} = 1.340$ g cm^{-3}, $\mu = 3.17$ cm^{-1}, empirical absorption correction from psi-scans ($C_{min/max} = 0.965/0.999$), Enraf-Nonius-CAD4 diffractometer, $\lambda = 71.073$ pm, ω-2θ scan, 10089 reflections measured ($\pm h, +k, \pm l$, $2\theta_{max} = 45^\circ$) of which 9605 were independent and 4105 observed [$I \geq 2\sigma(I)$], 1021 refined parameters, $Rw = 0.130$, $wR^2 = 0.341$, the largest peaks in the residual electron density map [max. 2.00(−0.72) eÅ^{-3}] were located near the disordered solvent molecules. The structure was solved by direct methods (SHELXS-86) and refined against F^2 (SHELXL-93), hydrogens were introduced in their calculated positions and refined isotropically as riding atoms, hydrogens of the crystalline water molecules were not located from the difference Fourier map. Three out of six DMF molecules were disordered and the main orientation was 53% for each. The disordered DMF molecules were refined by using geometrical restraints, where one non-disordered DMF molecule served as a structural model. The figures were drawn with the SCHAKAL program. Further details of the X-ray crystal structure analysis are available upon request from the Fachinformationszentrum Karlsruhe, D-76344 Eggenstein-Leopoldshafen (Germany), on quoting the depository number CSD-401879.

[13] For the structure of mononuclear [(catecholate)$_3$Ti]$^{2-}$ see: B. A. Borgias, S. R. Cooper, Y. B. Koh, K. N. Raymond, *Inorg. Chem.* **1984**, *23*, 1009.

[14] R. W. Saalfrank, R. Burak, A. Breit, D. Stalke, R. Herbst-Irmer, J. Daub, M. Porsch, E. Bill, M. Müther, A. X. Trautwein, *Angew. Chem.* **1994**, *106*, 1697; *Angew. Chem. Int. Ed. Engl.* **1994**, *33*, 1621; E. Graf, M. W. Hosseini, R. Ruppert, N. Kyritsakas, A. De Cian, J. Fischer, C. Estournès, F. Taulelle, *ibid.* **1995**, *107*, 1204; and **1995**, *34*, 1115.

[15] Attempts to observe the racemization of helicates are already described: J.-M. Lehn, A. Rigault, J. Siegel, J. Harrowfield, B. Chevrier, D. Moras, *Proc. Natl. Acad. Sci. USA* **1987**, *84*, 2565; D. E. Fenton, R. W. Matthews, M. McPartlin, B. P. Murphy, I. J. Scowen, P. A. Tasker, *J. Chem. Soc. Chem. Commun.* **1994**, 1391.

[16] K. E. Drexler, *Engines of Creation*, 2nd ed., Anchor Books, New York, 1990.

Radical C–C Bond Formation by Photoinduced Electron Transfer Addition of α-Silyl Carbamates to Acceptor-Substituted Alkenes**

Eric Meggers, Eberhard Steckhan,* and Siegfried Blechert

Light-induced reactions between donor and acceptor molecules form an important chapter in radical ion chemistry.[1] Among these, photoinduced electron transfer (PET) is the basis of a modern method for the formation of radicals under mild conditions.[2] One-electron oxidation generates an intermediate radical cation, which fragments to split off an electrofuge. We have now developed a new method based on this principle for electron transfer catalyzed intermolecular C–C bond formation. On irradiation with UV/Vis light and in the presence of catalytic amounts of 9,10-anthracenedicarbonitrile (ADC) and biphenyl (BP), α-silyl carbamates add to acceptor-substituted alkenes. In this way, γ-acceptor-substituted amino derivatives are formed (Scheme 1).[3]

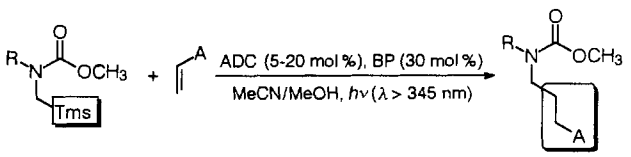

Scheme 1. PET-catalyzed reaction of α-silyl carbamates with acceptor-substituted alkenes. A = acceptor, Tms = trimethylsilyl. For A and R see Table 1.

We accomplished this transformation using the starting materials listed in Table 1.[4] The results of additional reactions with acceptor-substituted alkenes indicate that this reaction is general. Electron-rich alkenes like cyclohexene and 1-hexene, however, are unreactive.

The following mechanism can be assumed for the reaction: ET quenching between the primary electron donor BP ($E_{ox} = 1.98$ V vs. SCE) and photochemically excited ADC* (E_{red} (S1) = 2.0 V vs. SCE)[5] generates the biphenyl radical cation

Table 1. Addition reactions conducted.

α-Silyl carbamate	Alkene	Addition product [a]		Yield [%]
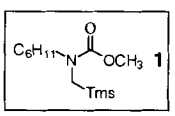 **1**	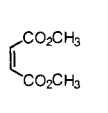	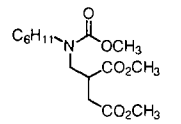	**4**	62 [b]
	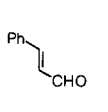	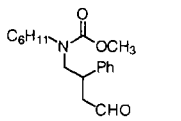	**5**	25 [b]
	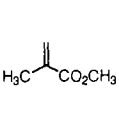	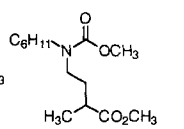	**6**	46 [b]
	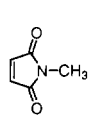	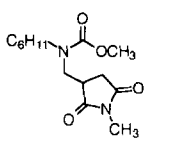	**7**	60–67 [c]
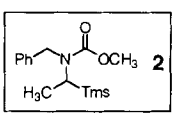 **2**	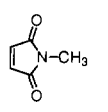	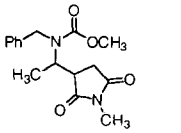	**8**	32 [c, e]
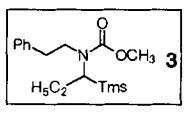 **3**	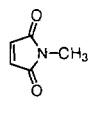	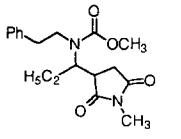	**9**	ca. 75 [d, e]

[a] All addition products were fully characterized by ^{13}C NMR (DEPT), ^{1}H NMR, and IR spectroscopy, MS and high-resolution MS, and CHN elemental analyses. Because of the instability of **9**, an elemental analysis could not be obtained. For typical data see Experimental Procedure. [b] Yields of isolated products. [c] Yields determined by gas chromatography. [d] The yield was estimated by gas chromatography using the calibration curve for **8**. [e] **9** is formed in a diastereomeric ratio of ca. 2:1, while for **8** only one diastereoisomer could be found.

[*] Prof. Dr. E. Steckhan, E. Meggers
Institut für Organische Chemie und Biochemie der Universität
Gerhard-Domagk-Strasse 1, D-53121 Bonn (Germany)
Telefax: Int. code +(228) 735683
e-mail: steckhan@uni-bonn.de
Prof. Dr. S. Blechert
Institut für Organische Chemie der Technischen Universität Berlin
Sekreteriat TC 2

[**] This work was supported by the Volkswagen-Stiftung (I/69415), the Fonds der Chemischen Industrie, and the BASF AG. E. M. thanks the Theodor-Laymann-Stiftung for a fellowship.

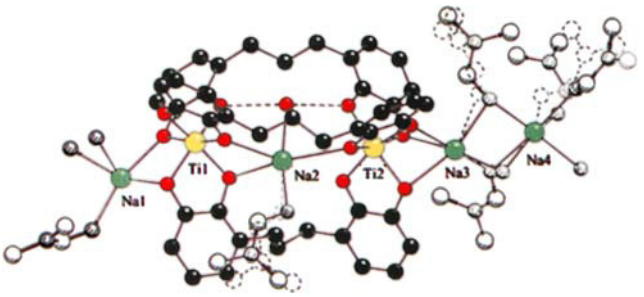

Fig. 3. Molecular structure (SCHAKAL) of the monomeric unit of $Na_4[(\mathbf{6})_3Ti_2]\cdot 6DMF\cdot 5H_2O$. Black: carbon, red: oxygen, yellow: titanium, green: sodium; H atoms are omitted for clarity; solvent molecules are not colored; disorder is indicated by dotted lines. The red-brown dashed lines denote hydrogen bonds.

bonds with two internal oxygen atoms of one of the ligands **6** (Fig. 3, the hydrogen bonds are indicated by dashed lines; $O_{water}\cdots O_{ligand} = 270(2)$ or 277(2) pm, respectively). Na2 shows a distorted trigonal bipyramidal geometry. Thus, $Na_4[(\mathbf{6})_3Ti_2]$ is a further example for a supramolecular device formed by self-assembly, which itself can act as a receptor (*exo* as well as *endo*) towards small ions.[14] The receptor properties of this molecule in solution are currently under investigation.

$Na_4[(\mathbf{6})_3Ti_2]\cdot 6DMF\cdot 5H_2O$ dimerizes in the solid state through bridging of DMF molecules between Na1 and Na1′. The resulting rodlike C_i-symmetric supramolecular species exhibits nanometer scale dimensions (length: 4 nm) and a nearly linear sequence of 12 metal ions (4 Ti and 8 Na) with well-defined intermetallic distances.

The results of ^{1}H NMR spectroscopic investigations of $K_4[(\mathbf{6})_3Ti_2]$ (D_2O, 400 MHz) at variable temperature are shown in Figure 4. At room temperature, the spectrum is similar to that

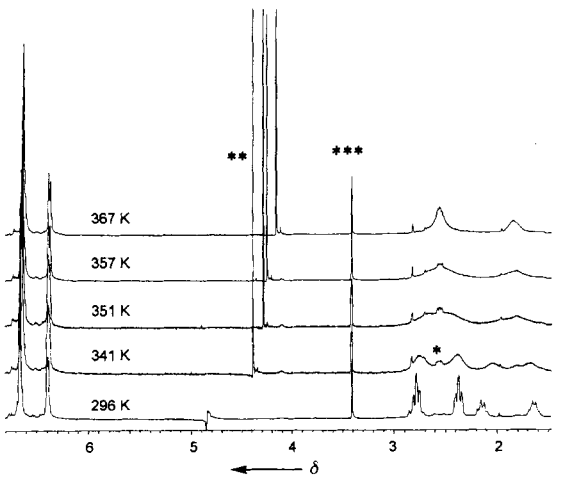

Fig. 4. ^{1}H NMR spectra of $K_4[(\mathbf{6})_3Ti_2]$ at variable temperature in D_2O (*impurity, **DOH, ***methanol).

measured in [D_4]methanol. On heating the sample in the NMR machine, a broadening of the alkyl resonances can be observed. The coalescence temperature of the central methylene group is reached at 356 K, that of the benzylic protons at 357 K ($\Delta G^{\ddagger} = 16.6$ kcal mol^{-1}). Two broad multiplets at $\delta = 2.50$ (4 H, benzylic protons) and 1.88 (2 H, central methylene group) are detected at 367 K. The signals of the aromatic protons do not show any significant changes on warming. The reason for the observed symmetrization of the diastereotopic protons is the inversion of the chiral centers, which are hidden in the achiral *meso*-helicate $[(\mathbf{6})_3Ti_2]^{4-}$ (Λ_1,Λ_2 inverts to Δ_1,Λ_2).[15] The use of the diastereotopic protons as a stereochemical probe allows the inversion of the configuration of the two titanium(IV) centers to be observed directly.

The above-mentioned results clearly reveal that metal-directed self-assembly is not limited to nitrogen donor ligands in combination with soft metal centers. Use of the C_3-bridged bis(catechol) system **6** and hard titanium(IV) ions leads in a highly diastereoselective reaction to the cooperative formation of a binuclear metal complex. This complex does not form the helicate structure, but the *meso*-helicate. With its two differently configurated metal centers, it represents a missing structural motif in the chemistry of helicates. The inclusion of helicate and *meso*-helicate domains in one linear oligonuclear coordination compound might lead to helices containing parts in which the helical twist inverts. This enables a fine tuning of the self-assembly of supramolecular architectures, which can undergo further supramolecular interactions (e.g. with small guest molecules), and therefore is a further step towards a working nanotechnology.[16]

Received: February 9, 1995
Revised version: June 20, 1995 [Z 7705 IE]
German version: *Angew. Chem.* **1995**, *107*, 2285–2287

Keywords: catechol · self-assembly · titanium compounds

[1] J.-M. Lehn, *Angew. Chem.* **1988**, *100*, 92; *Angew. Chem. Int. Ed. Engl.* **1988**, *27*, 90; *ibid.* **1990**, *102*, 1347 and **1990**, *29*, 1304; W. Zarges, J. Hall, J.-M. Lehn, C. Bolm, *Helv. Chim. Acta* **1991**, *74*, 1843; R. Krämer, J.-M. Lehn, A. Marquis-Rigault, *Proc. Natl. Acad. Sci. USA* **1993**, *90*, 5394.

[2] The terminology "*meso*" relates to the different configurations of two helical units in one molecule and corresponds to the nomenclature that was introduced for compounds with two chiral centers and one mirror plane (see: *meso*- and *rac*-tartaric acid).

[3] F. A. Cotton, G. Wilkinson, *Anorganische Chemie*, 3rd ed., VCH, Weinheim **1974**, p. 621.

[4] E. C. Constable, *Tetrahedron* **1992**, *48*, 10013, and references therein; E. C. Constable, A. J. Edwards, P. R. Raithby, J. V. Walker, *Angew. Chem.* **1993**, *105*, 1486; *Angew. Chem. Int. Ed. Engl.* **1993**, *32*, 1465; K. T. Potts, M. Keshavarz-K, F. S. Tham, H. D. Abruna, C. Arana, *Inorg. Chem.* **1993**, *32*, 4450. For an example with P donor ligands see: A. L. Airey, G. F. Swiegers, A. C. Willis, S. B. Wild, *J. Chem. Soc. Chem. Commun.* **1995**, 695.

[5] E. C. Constable, *Angew. Chem.* **1991**, *103*, 1482; *Angew. Chem. Int. Ed. Engl.* **1991**, *30*, 1450, and references therein; A. F. Williams, C. Piguet, G. Bernardinelli, *ibid.* **1991**, *103*, 1530 and **1991**, *30*, 1490; G. Bernardinelli, C. Piguet, A. F. Williams, *ibid.* **1992**, *104*, 1626 and **1992**, *31*, 1622; R. Krämer, J.-M. Lehn, A. De Cian, J. Fischer, *ibid.* **1993**, *105*, 764 and **1993**, *32*, 703; K. T. Potts, C. P. Horwitz, A. Fessak, M. Keshavarz-K, K. E. Nash, P. J. Toscano, *J. Am. Chem. Soc.* **1993**, *115*, 10444; D. Zurita, P. Baret, J.-L. Pierre, *New J. Chem.* **1994**, *18*, 1143; C. Piguet, G. Hopfgartner, A. F. Williams, J.-C. G. Bünzli, *J. Chem. Soc. Chem. Commun.* **1995**, 491.

[6] S. Rüttimann, C. Piguet, G. Bernardinelli, B. Bocquet, A. F. Williams, *J. Am. Chem. Soc.* **1992**, *114*, 4230; A. Bilyk, M. M. Harding, P. Turner, T. W. Hambley, *J. Chem. Soc. Dalton Trans.* **1994**, 2783; C. O. Dietrich-Buchecker, J.-P. Sauvage, J.-P. Kintzinger, P. Maltese, C. Pascard, J. Guilhem, *New. J. Chem.* **1992**, *16*, 931.

[7] For exceptional examples of helicates with oxygen donor ligands see: R. C. Scarrow, D. L. White, K. N. Raymond, *J. Am. Chem. Soc.* **1985**, *107*, 6540; J. Libman, Y. Tor, A. Shanzer, *J. Am. Chem. Soc.* **1987**, *109*, 5880; E. J. Corey, C. L. Cywin, M. C. Noe, *Tetrahedron Lett.* **1994**, *35*, 69.

[8] Recently chiral catecholamide ligands were used for the formation of binuclear gallium(III) helicates: E. J. Enemark, T. D. P. Stack, *Angew. Chem.* **1995**, *107*, 1082; *Angew. Chem. Int. Ed. Engl.* **1995**, *34*, 996.

[9] M. Albrecht, C. Riether, *Synlett* **1995**, 309.

[10] R. V. Stevens, G. S. Bisacchi, *J. Org. Chem.* **1982**, *47*, 2393.

[11] **6-H$_4$**: M.p. 137 °C; ^{1}H NMR (400 MHz, [D_4]methanol, 296 K): $\delta = 6.63$ (m, 2 H), 6.60 (m, 4 H), 2.65 (t, ^3J(H,H) = 7.7 Hz, 4 H), 1.88 (quin, ^3J(H,H) = 7.7 Hz, 2 H); ^{13}C NMR (100 MHz, BB, DEPT 90°/135°, [D_4]methanol, 296 K): $\delta = 145.7$ (C), 144.0 (C), 130.5 (C), 121.9 (CH), 120.2 (CH), 113.6 (CH), 31.2 (CH_2), 30.9 (CH_2, double intensity); MS (70 eV): *m/z* (%): 260 (90) [M^+], 124 (100) [$C_7H_8O_2^+$]; HRMS, $C_{15}H_{16}O_4$: calcd. 260.1049, found 260.1072. $K_4[(\mathbf{6})_3Ti_2]$: M.p. >160 °C (decomp.); UV/Vis (methanol): λ_{max} (ε) = 209 (165000), 275 (38000), 372 nm (18000); FAB(+)-MS (glycerine):

 © VCH Verlagsgesellschaft mbH, D-69451 Weinheim, 1995 0570-0833/95/3419-2136 $ 10.00+.25/0

$m/z = 1021$ $[HK_4[(\mathbf{6})_3Ti_2]^+]$, 1059 $[K_5[(\mathbf{6})_3Ti_2]^+]$; $C_{43}H_{36}K_4O_{12}Ti_2 \cdot 7H_2O$ (1147.1): calcd. C 47.12, H 4.39, found C 47.07, H 4.13; molecular weight determination of $C_{45}H_{36}K_4O_{12}Ti_2 \cdot 7H_2O$ (vapor pressure osmometry, H_2O): calcd. 1147, found 1108. $Na_4[(\mathbf{6})_3Ti_2]$: FAB(+)-MS (glycerine): $m/z = 935$ $[H_2Na_3[(\mathbf{6})_3Ti_2]^+]$, 957 $[HNa_4[(\mathbf{6})_3Ti_2]^+]$, 980 $[Na_5[(\mathbf{6})_3Ti_2]^+]$.

[12] Crystals of $Na_4[(\mathbf{6})_3Ti_2] \cdot 6DMF \cdot 5H_2O$ were obtained by slow diffusion of ether in a solution of the compound in DMF/water (ca. 10:1). Crystal data for $Na_4[(\mathbf{6})_3Ti_2] \cdot 6DMF \cdot 5H_2O$: Formula $C_{63}H_{88}N_6Na_4O_{23}Ti_2$, formula weight 1485.15, red prisms ($0.90 \times 0.60 \times 0.25$ mm^3), triclinic, space group $P\bar{1}$ (no. 2), $a = 1278.7(1)$, $b = 1363.8(1)$, $c = 2236.7(3)$ pm, $\alpha = 75.12(1)$, $\beta = 82.03(1)$, $\gamma = 78.65(1)^\circ$, $V = 3680 \times 10^6$ pm^3, $Z = 2$, $F(000) = 1560$, $T = -140\,^\circ$C, $\rho_{calcd.} = 1.340$ g cm^{-3}, $\mu = 3.17$ cm^{-1}, empirical absorption correction from psi-scans ($C_{min/max} = 0.965/0.999$), Enraf-Nonius-CAD4 diffractometer, $\lambda = 71.073$ pm, ω-2θ scan, 10089 reflections measured ($\pm h, +k, \pm l$, $2\theta_{max} = 45^\circ$) of which 9605 were independent and 4105 observed [$I \geq 2\sigma(I)$], 1021 refined parameters, $Rw = 0.130$, $wR^2 = 0.341$, the largest peaks in the residual electron density map [max. 2.00(−0.72) eÅ^{-3}] were located near the disordered solvent molecules. The structure was solved by direct methods (SHELXS-86) and refined against F^2 (SHELXL-93), hydrogens were introduced in their calculated positions and refined isotropically as riding atoms, hydrogens of the crystalline water molecules were not located from the difference Fourier map. Three out of six DMF molecules were disordered and the main orientation was 53% for each. The disordered DMF molecules were refined by using geometrical restraints, where one non-disordered DMF molecule served as a structural model. The figures were drawn with the SCHAKAL program. Further details of the X-ray crystal structure analysis are available upon request from the Fachinformationszentrum Karlsruhe, D-76344 Eggenstein-Leopoldshafen (Germany), on quoting the depository number CSD-401879.

[13] For the structure of mononuclear [(catecholate)$_3$Ti]$^{2-}$ see: B. A. Borgias, S. R. Cooper, Y. B. Koh, K. N. Raymond, *Inorg. Chem.* **1984**, *23*, 1009.

[14] R. W. Saalfrank, R. Burak, A. Breit, D. Stalke, R. Herbst-Irmer, J. Daub, M. Porsch, E. Bill, M. Müther, A. X. Trautwein, *Angew. Chem.* **1994**, *106*, 1697; *Angew. Chem. Int. Ed. Engl.* **1994**, *33*, 1621; E. Graf, M. W. Hosseini, R. Ruppert, N. Kyritsakas, A. De Cian, J. Fischer, C. Estournès, F. Taulelle, *ibid.* **1995**, *107*, 1204; and **1995**, *34*, 1115.

[15] Attempts to observe the racemization of helicates are already described: J.-M. Lehn, A. Rigault, J. Siegel, J. Harrowfield, B. Chevrier, D. Moras, *Proc. Natl. Acad. Sci. USA* **1987**, *84*, 2565; D. E. Fenton, R. W. Matthews, M. McPartlin, B. P. Murphy, I. J. Scowen, P. A. Tasker, *J. Chem. Soc. Chem. Commun.* **1994**, 1391.

[16] K. E. Drexler, *Engines of Creation*, 2nd ed., Anchor Books, New York, 1990.

Radical C–C Bond Formation by Photoinduced Electron Transfer Addition of α-Silyl Carbamates to Acceptor-Substituted Alkenes**

Eric Meggers, Eberhard Steckhan,* and Siegfried Blechert

Light-induced reactions between donor and acceptor molecules form an important chapter in radical ion chemistry.[1] Among these, photoinduced electron transfer (PET) is the basis of a modern method for the formation of radicals under mild conditions.[2] One-electron oxidation generates an intermediate radical cation, which fragments to split off an electrofuge. We have now developed a new method based on this principle for electron transfer catalyzed intermolecular C–C bond formation. On irradiation with UV/Vis light and in the presence of catalytic amounts of 9,10-anthracenedicarbonitrile (ADC) and biphenyl (BP), α-silyl carbamates add to acceptor-substituted alkenes. In this way, γ-acceptor-substituted amino derivatives are formed (Scheme 1).[3]

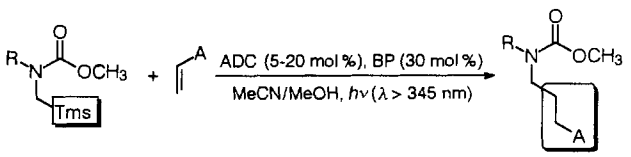

Scheme 1. PET-catalyzed reaction of α-silyl carbamates with acceptor-substituted alkenes. A = acceptor, Tms = trimethylsilyl. For A and R see Table 1.

We accomplished this transformation using the starting materials listed in Table 1.[4] The results of additional reactions with acceptor-substituted alkenes indicate that this reaction is general. Electron-rich alkenes like cyclohexene and 1-hexene, however, are unreactive.

The following mechanism can be assumed for the reaction: ET quenching between the primary electron donor BP ($E_{ox} = 1.98$ V vs. SCE) and photochemically excited ADC* (E_{red} (S1) = 2.0 V vs. SCE)[5] generates the biphenyl radical cation

Table 1. Addition reactions conducted.

α-Silyl carbamate	Alkene	Addition product [a]		Yield [%]
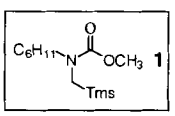 **1**	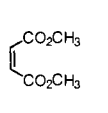	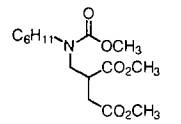	**4**	62 [b]
	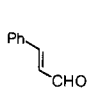	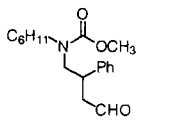	**5**	25 [b]
	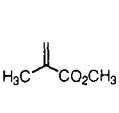	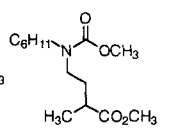	**6**	46 [b]
	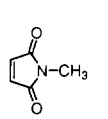	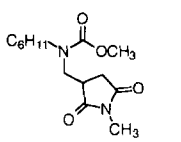	**7**	60–67 [c]
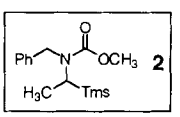 **2**	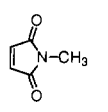	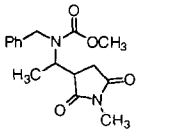	**8**	32 [c, e]
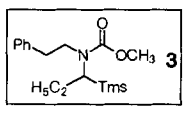 **3**	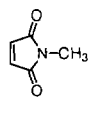	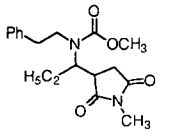	**9**	ca. 75 [d, e]

[a] All addition products were fully characterized by ^{13}C NMR (DEPT), ^{1}H NMR, and IR spectroscopy, MS and high-resolution MS, and CHN elemental analyses. Because of the instability of **9**, an elemental analysis could not be obtained. For typical data see Experimental Procedure. [b] Yields of isolated products. [c] Yields determined by gas chromatography. [d] The yield was estimated by gas chromatography using the calibration curve for **8**. [e] **9** is formed in a diastereomeric ratio of ca. 2:1, while for **8** only one diastereoisomer could be found.

[*] Prof. Dr. E. Steckhan, E. Meggers
Institut für Organische Chemie und Biochemie der Universität
Gerhard-Domagk-Strasse 1, D-53121 Bonn (Germany)
Telefax: Int. code +(228) 735683
e-mail: steckhan@uni-bonn.de
Prof. Dr. S. Blechert
Institut für Organische Chemie der Technischen Universität Berlin
Sekreteriat TC 2

[**] This work was supported by the Volkswagen-Stiftung (I/69415), the Fonds der Chemischen Industrie, and the BASF AG. E. M. thanks the Theodor-Laymann-Stiftung for a fellowship.

(Scheme 2), which subsequently oxidizes the α-silyl carbamate ($E_{ox} \approx 1.45$ V vs. Ag/AgCl)[6] to give its radical cation through a one-electron transfer reaction (redox photosensitization).[7] After cleavage of the silyl group,[8] the resulting nucleophilic radical is trapped by a compound having an electron-poor

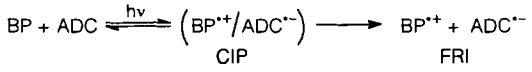

Scheme 2. Redox photosensitization with ADC and BP. CIP = contact radical ion pair, FRI = free radical ions.

double bond. Back electron transfer from an ADC radical anion to the radical addition product and protonation complete the electron transfer catalytic cycle (Scheme 3). An alternative hydrogen abstraction from the solvent at the stage of the α-carbonyl radical cannot be excluded.

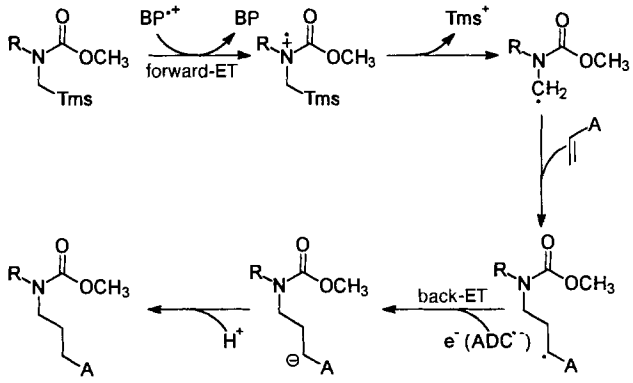

Scheme 3. Proposed mechanism for the ET-catalyzed replacement of the silyl group.

As a side product, a Tms/H substitution product is formed in small amounts.[9] The extent of this side reaction depends on the reactivity of the alkene and the alkene concentration. The reactivity of the alkenes towards the intermediate, strongly nucleophilic α-*N*-substituted radical correlates with the electron density at the double bond.[10] With very reactive alkenes oligo- and polymerization occurs. In these cases the reaction can be accomplished by modifying the reaction procedure. When the alkene is added continuously during the course of the irradiation, the yield of the reaction between **1** and *N*-methyl maleimide depends strongly on the rate of addition (Fig. 1).[11]

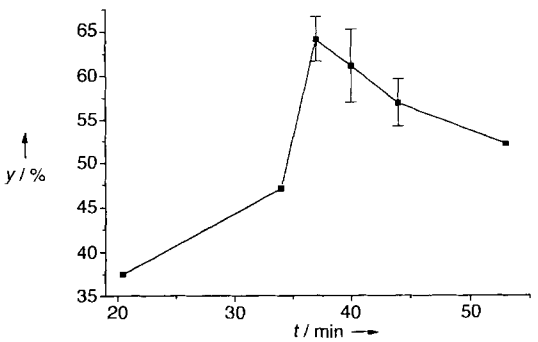

Fig. 1. Dependence of the yield y of **7** on the rate of addition t of the reactive *N*-methyl maleimide. Addition rate = time after which 1.1 equivalents of alkene had been added by continuous addition.

We conducted the reaction with other photosensitizers besides ADC and BP. The reaction between **1** and dimethyl maleate was applied as a test system.[12] Only with 2,4,6-triphenyl-*N*-methylpyridinium tetrafluoroborate (TPNMP)[13] as sensitizer could we obtain results comparable with those of the cosensitization by ADC/BP (Fig. 2). All of the tested excited

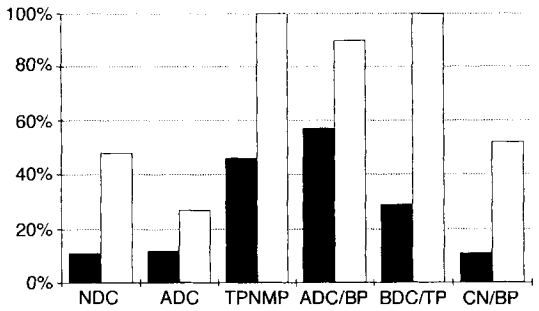

Fig. 2. Comparison of the results obtained with different sensitizers for the photosensitized reaction of **1** and dimethyl maleate giving **4**. NDC = 1,4-naphthalenedicarbonitrile, BDC = 1,4-benzenedicarbonitrile, TP = triphenylene, CN = 1-naphthalenecarbonitrile, black bar = yield, white bar = conversion.

sensitizers are thermodynamically capable of oxidizing the α-silyl carbamates.[14] However, the usually very fast back electron transfer within the intermediate solvated radical ion pair CIP is a substantial and often limiting problem (Scheme 2). In contrast, the sensitizer pair ADC/BP provides a very high quantum yield for the formation of the free radical ions after induction by SET.[15] The resulting free biphenyl radical cation is then able to oxidize the α-silyl carbamate under diffusion control. In this way, BP acts as a very efficient mediator for the PET reaction between ADC and a secondary electron donor.

The reaction described here obviously offers a general and mild method for PET-catalyzed intermolecular C–C bond formation. Presently we are studying the application of this reaction to other substrates like α-silyl ethers and α-silyl sulfides.

Experimental Procedure

A 450 W Xenon lamp with a wavelength filter was used as a light source. The solutions were degassed with argon prior to and during irradiation and thermostated in a water bath.

4 (analogous for **5** and **6**): α-Silyl carbamate **1** (122 mg, 0.5 mmol), dimethyl maleate (140 mg, 1 mmol), BP (23.1 mg, 0.15 mmol), ADC (11 mg, 0.05 mmol), and 6 mL of MeCN/MeOH (2:1) were mixed in a Duran glass test tube and irradiated with stirring and water cooling for 7 h (filter for $\lambda > 345$ nm). After one-half of the irradiation time another portion (11 mg) of ADC was added. Subsequently, the solvent was removed by distillation. The residue was dissolved in a small amount of diethyl ether and filtered to remove the precipitated ADC. Flash chromatography on silica gel using petroleum ether (40/60)/ethyl acetate (10:3) ($R_f = 0.25$) provided a light yellow oil (98.5 mg, 62%). ^{1}H NMR (200 MHz, $CDCl_3$): $\delta = 0.95$–1.85 (m, 10H), 2.5 (dd, $J = 17$, 4.8 Hz, 1H), 2.7 (dd, $J = 17$, 8.7 Hz, 1H), 3.1 (br., 1H), 3.4 (m, 2H), 3.66 (s, 6H), 3.68 (s, 3H), 3.7 (br., 1H); ^{13}C NMR (50.3 MHz, $CDCl_3$): $\delta = 25.14$, 25.76, 30.55, 33.32, 41.68, 44.84, 51.55, 51.74, 52.22, 56.89, 156.28, 171.91, 173.49; IR (NaCl): $\tilde{\nu} = 2934$, 2857, 1741, 1701, 1439, 1167, 1010, 895, 774 cm^{-1}; MS (180 °C, EI/DE): *m/z* (%): 315 (2), 272 (21), 256 (35), 202 (22), 200 (12), 170 (93), 159 (20), 127 (17), 114 (11), 88 (100), 83 (14), 71 (10), 59 (16), 55 (24); High-resolution MS (70 °C, EI/DE): calcd for $C_{15}H_{25}NO_6$) 315.1682, found 315.1682; CHN analysis: calcd C 57.11, H 7.99, N 4.44; found C 57.43, H 7.97, N 4.38.

7: Compound **1** (10 mg, 0.041 mmol), BP (2.5 mg, 0.016 mmol), and ADC (ca. 1 mg, 0.004 mmol) were mixed in 5 mL of MeCN/MeOH (3:2) in a Duran glass test tube. A solution of *N*-methyl maleimide (5 mg, 0.045 mmol) in 3 mL of MeCN/MeOH (3:2) was added dropwise and continuously while the reaction mixture was irradiated for 40 min ($\lambda > 345$ nm) (see Fig. 1). After flash chromatography on silica gel using cyclohexane/ethyl acetate (5:1), the addition product was obtained.

8: A solution of **2** (10 mg, 0.038 mmol), *N*-methyl maleimide (2.5 mg), BP (1.85 mg, 0.012 mmol) and ADC (ca. 1 mg, 0.004 mmol) in 5 mL of MeCN/MeOH (3:2) was

irradiated over 2 h ($\lambda > 345$ nm), during which additional *N*-methyl maleimide (3×2.5 mg, altogether 0.09 mmol) was added at 30 min intervals. The addition product was isolated by flash chromatography on silica gel with ether/cyclohexane (2:1).

9: A solution of **3** (15 mg, 0.051 mmol), *N*-methyl maleimide (4 mg), BP (2.3 mg, 0.015 mmol), and ADC (ca. 2 mg, 0.009 mmol) in 5 mL of MeCN/MeOH (3:2) was irradiated over a period of 2.25 h ($\lambda > 345$ nm). In analogy to the synthesis of **8** more *N*-methyl maleimide was added at 45 min intervals (2×4 mg, altogether 0.11 mmol).

The reactions were scaled up successfully; however, when the very reactive *N*-methyl maleimide was used (addition compounds **7**, **8**, and **9**), the reaction conditions had to be reoptimized.

Received: April 5, 1995
Revised version: July 5, 1995 [Z 7871 IE]
German version: *Angew. Chem.* **1995**, *107*, 2317–2319

Keywords: cosensitization · oxidative fragmentations · photoelectron transfer · radical additions · sensitization

[1] For a review on PET: J. Mattay, *Angew. Chem.* **1987**, *99*, 849; *Angew. Chem. Int. Ed. Engl.* **1987**, *26*, 825; *Synthesis* **1989**, 233.

[2] PET-induced oxidative fragmentation: A. Albini, M. Mella, M. Freccero, *Tetrahedron* **1994**, *50*, 575.

[3] Until now, only ADC- and NDC-sensitized radical cyclizations have been successful: W. Xu, Y. T. Jeon, E. Hasegawa, U. C. Yoon, P. S. Mariano, *J. Am. Chem. Soc.* **1989**, *111*, 406; Y. T. Jeon, C.-P. Lee, P. S. Mariano, *ibid.* **1991**, *113*, 8847; S. K. Khim, P. S. Mariano, *Tetrahedron Lett.* **1994**, *35*, 999; G. Pandey, G. D. Reddy, G. Kumaraswamy, *Tetrahedron* **1994**, *50*, 8185. The ADC-sensitized addition of *N*-(trimethylsilyl)methyl-*N*,*N*-diethyl amine to cyclohexenone and 4,4-dimethylcyclohexenone was reported; however, no yields were given. The authors report that this reaction yields a Tms-containing and a Tms-free addition product: E. Hasegawa, W. Xu, P. S. Mariano, U.-C. Yoon, J.-U. Kim, *J. Am. Chem. Soc.* **1988**, *110*, 8099; siehe auch X.-M. Zhang, P. S. Mariano, *J. Org. Chem.* **1991**, *56*, 1655.

[4] α-Silyl carbamates were prepared by alkylation of primary amines with α-haloalkane silanes and subsequent reaction with methyl chloroformate.

[5] Reduction potentials of the most important sensitizers: H. D. Roth, *Top. Curr. Chem.* **1992**, *163*, 131.

[6] Oxidation of α-silyl carbamates: J. Yoshida, S. Isoe, *Tetrahedron Lett.* **1987**, *28*, 6621.

[7] Redox photosensitization: S. Tazuke, N. Kitamura, *J. Chem. Soc. Chem. Commun.* **1977**, 515; T. Majima, C. Pac, A. Nakasone, H. Sakurai, *J. Am. Chem. Soc.* **1981**, *103*, 4499.

[8] The desilylation of amine radical cations can be accelerated by silophiles like MeOH: X. Zhang, S.-R. Yeh, S. Hong, M. Freccero, A. Albini, D. E. Falvey, P. S. Mariano, *J. Am. Chem. Soc.* **1994**, *116*, 4211.

[9] This reaction is also useful for desilylation and, for example, for the introduction of deuterium atoms. The ADC/BP-sensitized irradiation of **1** in MeCN yields the Tms-H-exchange compound as the main product.

[10] Addition of radicals to alkenes: B. Giese, *Angew. Chem.* **1983**, *95*, 771; *Angew. Chem. Int. Ed. Engl.* **1983**, *22*, 753.

[11] The rate of the addition of a solution of *N*-methyl maleimide in MeCN/MeOH was varied and the yields were determined by gas chromatography (see Experimental Procedure).

[12] Solutions of **1** (10 mg, 0.04 mmol), dimethyl maleate (12 mg, 0.08 mmol), and ca. 0.1 mmol of the sensitizer in 4 mL of MeCN/MeOH (3:1) were irradiated over 3 h and the yields determined by gas chromatography.

[13] Pyrylium and pyridinium salts as sensitizers for PET reactions: M. Martiny, E. Steckhan, T. Esch, *Chem. Ber.* **1993**, *126*, 1671.

[14] 2,4,6-Trianisylpyrylium tetrafluoroborate (TAP) is not suitable. This sensitizer in its ground state is able to oxidize the intermediate primary radical. Thus, the exchange of the silyl group by a methoxy group during irradiation of **1** in MeCN/MeOH was the main reaction.

[15] Efficient ET with ADC/BP: I. R. Gould, D. Ege, J. E. Moser, S. Farid, *J. Am. Chem. Soc.* **1990**, *112*, 4290.

Synthesis of the First Adducts of the Dimetallofullerenes $La_2@C_{80}$ and $Sc_2@C_{84}$ by Addition of a Disilirane**

Takeshi Akasaka,* Shigeru Nagase,* Kaoru Kobayashi, Toshiyasu Suzuki, Tatsuhisa Kato, Koichi Kikuchi, Yohji Achiba, Kazunori Yamamoto, Hideyuki Funasaka, and Takeshi Takahashi

Endohedral monometallofullerenes, fullerenes with a metal inside the carbon cage, have long attracted special interest because they could give rise to new species or materials with novel properties.[1] Considerable interest is now directed toward the characterization of dimetallofullerenes containing two metal atoms inside the cage.[2–6] Recent important progress is marked by the successful isolation and purification of $La_2@C_{80}$[3] and $Sc_2@C_{84}$[4a, 5] in large quantities. Little is known about the physical properties[3] of these dimetallofullerenes and there are no reports concerning the chemical properties of these species. Very recently, we succeeded in the chemical derivatization of the monometallofullerenes $La@C_{82}$[7] and $Gd@C_{82}$,[8] giving exohedral adducts. This has prompted us to investigate how the reactivities of fullerenes change when two metal atoms are inside the cage. We report here the first exohedral functionalization of $La_2@C_{80}$ and $Sc_2@C_{84}$.

A solution of $La_2@C_{80}$ and an excess of 1,1,2,2-tetramesityl-1,2-disilirane (**1**)[9] in 1,2-dichlorobenzene was irradiated ($\lambda > 400$ nm) at 20 °C. The positive-ion FAB mass spectrum of the product verifies the formation of the 1:1 adduct, $La_2@C_{80}(Mes_2Si)_2CH_2$ (*m/z* 1784–1788) (Fig. 1). No molecular ion peaks ascribable to the multiple-addition products such as $La_2@C_{80}[(Mes_2Si)_2CH_2]_2$ were observed. The ion peak at *m/z* 1238–1242 due to $[La_2@C_{80}]^+$ is a base peak similar to the $[La@C_{82}]^+$ base peak of the exohedral adduct $La@C_{82}(Mes_2Si)_2CH_2$.[7] In both cases strong fragmentation peaks result due to loss of the exohedral functional group $(Mes_2Si)_2CH_2$ from the adduct. The observed ion intensity ratio of a group of molecular peaks for $La_2@C_{80}(Mes_2Si)_2CH_2$ agrees with the ^{13}C isotope distribution.[10] Very similar results were also obtained with $Sc_2@C_{84}$. It is noteworthy that the dimetallofullerenes $La_2@C_{80}$ and $Sc_2@C_{84}$ are also functionalized by photochemical reaction with **1** to give the adducts $La_2@C_{80}(Mes_2Si)_2CH_2$ and $Sc_2@C_{84}(Mes_2Si)_2CH_2$, respectively. These successful exohedral derivatizations of endohedral dimetallofullerenes should open the way to new organodimetallofullerenes which may have applications in materials science and biochemistry.

[*] Prof. T. Akasaka
Department of Chemistry, University of Tsukuba
Tsukuba, Ibaraki 305 (Japan)
Telefax: Int. code + (298) 53-6503

Prof. S. Nagase, K. Kobayashi
Department of Chemistry, Faculty of Science, Tokyo Metropolitan University
Hachioji, Tokyo 192-03 (Japan)

Dr. T. Suzuki
NEC Corporation, Tsukuba (Japan)

Prof. T. Kato
Institute for Molecular Science, Okazaki (Japan)

Prof. K. Kikuchi, Prof. Y. Achiba
Tokyo Metropolitan University (Japan)

Dr. K. Yamamoto, Dr. H. Funasaka, Dr. T. Takahashi
Power Reactor & Nuclear Fuel Development Corporation
Tokai (Japan)

[**] This work was supported by the grant from the Iketani Science and Technology Foundation and a Grant-in-Aid for Scientific Research on Priority Area (No. 06224204) from the Ministry of Education, Science, and Culture in Japan.

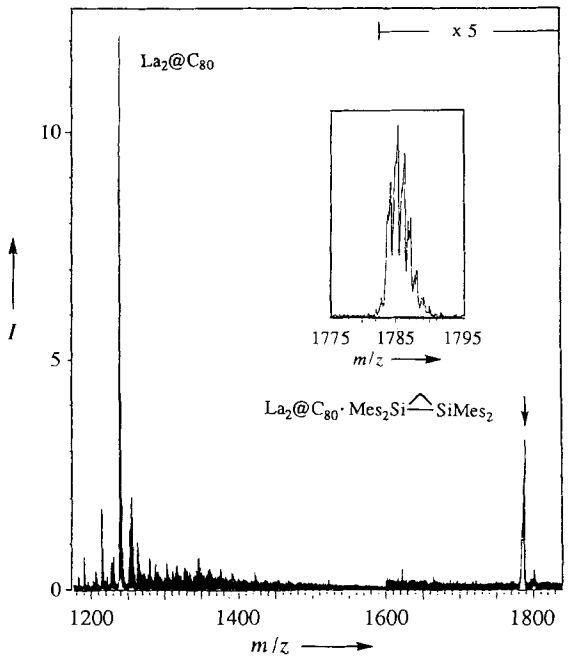

Fig. 1. FAB mass spectrum of the adduct $La_2@C_{80}(Mes_2Si)_2CH_2$ in the range m/z 1200–1850. Inset: Expanded view of the region m/z 1775–1795.

To disclose further interesting properties of dimetallofullerenes, we examined the thermal reaction with **1**. $La_2@C_{80}$ was revealed to have a remarkable feature not found for the empty fullerenes C_{60}, C_{70}, C_{76}, C_{78}, C_{82}, and C_{84} (Table 1). The empty fullerenes reacted with **1** only photochemically, whereas $La_2@C_{80}$ was also thermally reactive toward **1**. When a solution of $La_2@C_{80}$ and **1** in 1,2-dichlorobenzene was heated at 80 °C for 1 h, an adduct formed which was verified by FAB mass spectrometry. The thermal reaction of $La_2@C_{80}$ with **1** can be explained by its strong electron-acceptor character. Ab initio molecular orbital calculations show that the LUMO level of $La_2@C_{80}$ is 1–2 eV lower than those of the empty fullerenes. This is consistent with the fact that the reduction potential of $La_2@C_{80}$ (−0.31 V)[3] is lower than those of the empty fullerenes (Table 1).[11] Even though the oxidation potential of $Sc_2@C_{84}$ is almost as same as that of $La_2@C_{80}$, thermal addition of **1** onto $Sc_2@C_{84}$ is restrained, as in the empty fullerenes, due to its higher reduction potential. This can be also confirmed by the higher LUMO level of $Sc_2@C_{84}$.[12] In this context, it is not surprising that both $La@C_{82}$[7] and $Gd@C_{82}$[8] react thermally with **1**, since they have low reduction potentials comparable to that of $La_2@C_{80}$ (Table 1). This suggests that the thermal additions of **1** are initiated by electron transfer from **1** to metallofullerenes with strong electron-acceptor character.

Table 1. Reactivities, redox potentials [V], and HOMO and LUMO levels [eV] of selected metallofullerenes and empty fullerenes.

Cmpd.	Reactivity light	Reactivity heat	E_{ox} [b]	E_{red} [b]	HOMO	LUMO
$La_2@C_{80}$	+	+	+0.56 [c]	−0.31 [c]	−7.18	−2.55
$Sc_2@C_{84}$	+	−	+0.53	−0.97 [d, e]	−6.77	−1.38
C_{60}	+	−	+1.21 [d, e, f]	−1.12 [f]	−8.33	−0.63
C_{70}	+	−	+1.19 [f]	−1.09 [f]	−7.97	−0.84
C_{76}	+	−	+0.81 [c]	−0.94 [c]	−7.42	−1.13
C_{78}	+	−	+0.85	−0.73	−7.44	−1.49
C_{82}	+	−	+0.72	−0.69	−7.36	−1.52
C_{84}	+	−	+1.04 [d, e]	−0.75	−7.79	−1.34
$La@C_{82}$	+	+	+0.07 [f]	−0.42 [f]		
$Gd@C_{82}$	+	+	+0.09 [g]	−0.39 [g]		

[a] +: formation of a 1:1 adduct; −: no formation of a 1:1 adduct and also no change of the starting fullerene. [b] Half-cell potentials obtained by cyclic voltammetry unless otherwise stated. [c] Ref. [3b]. [d] Values were obtained by differential pulse voltammetry. [e] Irreversible. [f] Ref. [16]. [g] Ref. [8].

The details of the structures of these adducts remain to be resolved, yet this successful chemical derivatization of dimetallofullerenes is an important stepping-stone on the way to a variety of new chemical entities with novel properties, and should enrich the chemistry of metallofullerenes. Especially interesting for future applications is the strong electron-accepting power of $La_2@C_{80}$,[13] since its reactivity should differ significantly from that of empty fullerenes.

Experimental Procedure

$La_2@C_{80}$ [3], $Sc_2@C_{84}$ [14], and the empty fullerenes [15] were produced and purified according to our recently developed method. A degassed solution of $La_2@C_{80}$ (0.1 mg, 10^{-4} M) and an excess of 1,1,2,2-tetramesityl-1,2-disilirane (**1**) [9] in 1,2-dichlorobenzene in a sealed tube was photoirradiated at 20 °C with a tungsten–halogen lamp ($\lambda > 400$ nm). The color of the solution did not change from dark brown. The reaction product was isolated by flash chromatography on silica gel using toluene as eluent and analyzed by positive-ion FAB mass spectrometry (JEOL SX-102) using *m*-nitrobenzyl alcohol as matrix. Redox potentials were measured according to the method reported before [3,8,16]. The FAB mass spectrum of $Sc_2@C_{84}(Mes_2Si)_2CH_2$, and the cyclic voltammograms and differential pulse voltammograms of $Sc_2@C_{84}$ are available from the author (T. A.) upon request.

Calculations were carried out at the Hartree-Fock level using the Gaussian 92/DFT program [17]. The effective core potentials were described by the basis sets (5s5p5d)/[4s4p3d] for Sc and by (5s5p3d)/[4s4p3d] for La in standard notation [18]. The split-valence 3-21G basis set was used for C [19]. The geometries were fully optimized for C_{60} (I_h), C_{70} (D_{5h}), C_{76} (D_2), C_{78} (C_{2v}), C_{82} (C_2), C_{84} (D_{2d}), $La_2@C_{80}$ (D_{2h}), and $Sc_2@C_{84}$ (D_{2d}). The initial geometries of $La_2@C_{80}$ [3] and $Sc_2@C_{84}$ [6], in which two metal atoms are placed inside the I_h and D_{2d} cages of C_{80} and C_{84}, respectively, were taken from our previous studies. The resultant optimized structures of $La_2@C_{80}$ and $Sc_2@C_{84}$ are shown in Figure 2. The frontier orbitals indicate that the disilirane can add at several positions.

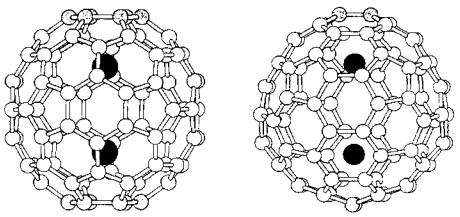

$La_2@C_{80}$ $Sc_2@C_{84}$

Fig. 2. The optimized structures of $La_2@C_{80}$ (D_{2h}) and $Sc_2@C_{84}$ (D_{2d}). In $La_2@C_{80}$ the La-La distance is 3.655 Å, and the La atoms (black) are 2.567–2.598 Å away from the carbon atoms that are shaded gray in the representation (C–C = 1.453–1.479 Å). In $Sc_2@C_{84}$ the Sc–Sc distance is 4.029 Å, and the Sc atoms are 2.358 Å away from the carbon atoms that are shaded gray in the representation (C–C = 1.434 Å). The electronic structures in the singlet ground states are formally described as $(La^{3+})_2C_{80}^{6-}$ and $(Sc^{2+})_2C_{84}^{4-}$.

Received: May 22, 1995 [Z 8016 IE]
German version: *Angew. Chem.* **1995**, *107*, 2303–2304

Keywords: fullerenes · lanthanide compounds · scandium compounds

[1] a) J. R. Heath, S. C. O'Brien, Q. Zhang, Y. Liu, R. F. Curl, H. W. Kroto, K. Tittle, R. E. Smalley, *J. Am. Chem. Soc.* **1985**, *107*, 7779; b) Y. Chai, T. Guo, C. Jin, R. E. Haufler, P. F. Chibante, J. Fure, L. Wang, J. M. Alford, R. E. Smalley, *J. Phys. Chem.* **1991**, *95*, 7564; c) For a recent review on metallofullerenes, see: D. S. Bethune, R. D. Johnson, J. R. Salem, M. S. de Vries, C. S. Yannoni, *Nature (London)* **1993**, *366*, 123.

[2] a) M. M. Alvarez, E. G. Gillan, K. Holczer, R. B. Kaner, K. S. Min, R. L. Whetten, *J. Phys. Chem.* **1991**, *95*, 10561; b) C. Yeretzian, K. Hansen, M. M. Alvarez, K. S. Min, E. G. Gillan, K. Holczer, R. B. Kaner, R. L. Whetten, *Chem. Phys. Lett.* **1992**, *196*, 337.
[3] T. Suzuki, Y. Maruyama, T. Kato, K. Kikuchi, Y. Nakao, Y. Achiba, K. Kobayashi, S. Nagase, *Angew. Chem.* **1995**, *107*, 1228; *Angew. Chem. Int. Ed. Engl.* **1995**, *34*, 1094.
[4] a) H. Shinohara, H. Yamaguchi, N. Hayashi, H. Sato, M. Ohkohchi, Y. Ando, Y. Saito, *J. Phys. Chem.* **1993**, *97*, 4259; b) H. Shinohara, N. Hayashi, H. Sato, Y. Saito, X.-D. Wang, T. Hashizume, T. Sakurai, *ibid.* **1993**, *97*, 13438.
[5] R. Beyers, C.-H. Kiang, R. D. Johnson, J. R. Salem, M. S. de Vries, C. S. Yannoni, D. S. Bethune, H. C. Dorn, P. Burbank, K. Harich, S. Stevenson, *Nature (London)* **1994**, *370*, 196.
[6] S. Nagase, K. Kobayashi, *Chem. Phys. Lett.* **1994**, *231*, 319.
[7] T. Akasaka, T. Kato, K. Kobayashi, S. Nagase, K. Yamamoto, H. Funasaka, T. Takahashi, *Nature (London)* **1995**, *374*, 600.
[8] T. Akasaka, S. Nagase, K. Kobayashi, T. Suzuki, T. Kato, K. Yamamoto, H. Funasaka, T. Takahashi, *J. Chem. Soc. Chem. Commun.* **1995**, 1343.
[9] a) T. Akasaka, W. Ando, K. Kobayashi, S. Nagase, *J. Am. Chem. Soc.* **1993**, *115*, 10366; b) T. Akasaka, E. Mitsuhida, W. Ando, K. Kobayashi, S. Nagase, *ibid.* **1994**, *116*, 2627.
[10] H. Shinohara, H. Sato, Y. Saito, A. Izuoka, T. Sugawara, H. Ito, T. Sakurai, T. Matsuo, *Rapid Commun. Mass Spectrom.* **1992**, *6*, 413.
[11] For the redox potentials of C_{84}, see: a) M. S. Meier, T. F. Guarr, J. P. Selegue, V. K. Vance, *J. Chem. Soc. Chem. Commun.* **1993**, 63; b) P. Boulas, M. T. Jones, K. M. Kadish, R. S. Ruoff, D. C. Lorents, D. S. Tse, *J. Am. Chem. Soc.* **1994**, *116*, 9393.
[12] According to the non-local density functional calculations ("3-parameter" exchange functional [12a] with the gradient correlation [12b], the electron affinity of $Sc_2@C_{84}$ is 1.48 eV smaller than that of $La_2@C_{80}$ (4.44 eV): a) A. D. Becke, *J. Chem. Phys.* **1993**, *98*, 5648; b) J. P. Perdew, *Phys. Rev. B* **1986**, *33*, 8822.
[13] Although not yet isolated, $Sc_2@C_{80}$ might also act as a strong electron acceptor with a low LUMO level of −3.73 eV.
[14] Isolation of $Sc_2@C_{84}$ was carried out by the two-step HPLC method: K. Kikuchi, S. Suzuki, Y. Nakao, N. Nakahara, T. Wakabayashi, H. Shiromaru, K. Saito, I. Ikemoto, Y. Achiba, Y. *Chem. Phys. Lett.* **1993**, *216*, 67.
[15] The empty fullerenes were obtained from the extracts of the soot using an HPLC system with a 2-(1-pyrenyl)ethyldimethylsilylated silica column (Cosmosil 5PYE, 20 mm inner diameter, 250 mm in length, Nakalai Tesque Co.) with toluene as eluent: K. Yamamoto, H. Funasaka, T. Takahashi, T. Akasaka, *J. Phys. Chem.* **1994**, *98*, 2008.
[16] T. Suzuki, Y. Maruyama, T. Kato, K. Kikuchi, Y. Achiba, *J. Am. Chem. Soc.* **1993**, *115*, 11006.
[17] GAUSSIAN 92/DFT: M. J. Frisch, G. W. Trucks, H. B. Schlegel, P. M. W. Gill, B. G. Johnson, M. W. Wong, J. B. Foresman, M. A. Robb, M. Head-Gordon, E. S. Replogle, R. Gomperts, J. L. Andres, K. Raghavachari, J. S. Binkley, C. Gonzalez, R. L. Martin, D. J. Fox, D. J. DeFrees, J. Baker, J. J. P. Stewart, J. A. Pople, Gaussian, Inc., Pittsburgh, **1993**.
[18] P. J. Hay, W. R. Wadt, *J. Chem. Phys.* **1985**, *82*, 299.
[19] J. S. Binkley, J. A. Pople, W. J. Hehre, *J. Am. Chem. Soc.* **1980**, *102*, 939.

The First Dinuclear Low-Valent Samarium Complex with a Short Sm–Sm Contact**

Jae-Inh Song and Sandro Gambarotta*

The impressive variety of transformations discovered during the last decade for divalent samarium[1] has acted as a potent stimulus for the synthesis of further Sm^{II} complexes. In this paper, we describe the preparation and characterization of the dimer $[(OEPG)Sm_2(Et_2O)_2]$ (OEPG-H_4 = octaethylporphyrinogen). To our knowledge this is the first crystal structure of a dinuclear complex of a divalent lanthanide with a short intermetallic distance. Two aspects of our study are of particular interest.

Firstly, the remarkable chemical behavior of this divalent metal can be well-rationalized by assuming that samarium(II) has a radical-like nature[2] which, however, cannot be explained on the basis of its f^6 electronic configuration. No information is available for divalent lanthanides, but the f electrons are deep within the electron cloud and subjected to a small crystal field. Theoretical work has recently suggested that f orbitals may play an important role in forming metal–metal bonds in bridged actinide complexes.[3] Therefore, we became interested in probing the ability of low-valent lanthanides to form dimers with short M–M contacts.

Secondly, the reaction of OEPG-Li_4 with $[SmCl_3(THF)_3]$ forms a complex which, upon reduction, yielded a dinuclear complex with a side-on bound dinitrogen ligand.[4] In this structure, the dinitrogen ligand is encapsulated inside a Sm_2Li_4 octahedron (Scheme 1). The very long N–N distance (1.525 Å),

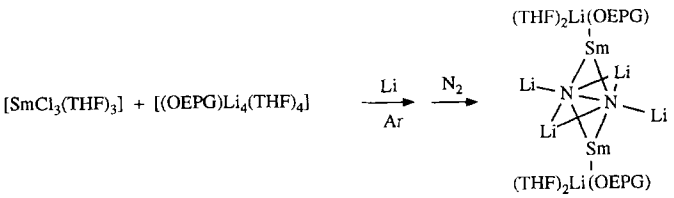

Scheme 1. OEPG-H_4 = Octaethylporphyrinogen.

indicative of a significant reduction of dinitrogen, is in sharp contrast to that found in $[(Cp^*_2Sm)_2(N_2)]$ ($Cp^* = C_5Me_5$), which also contains a side-on dinitrogen ligand but with a very short N–N distance (1.088 Å).[5] In addition, the recently reported reversible side-on coordination of dinitrogen to a cationic dilithium unit[6] suggested to us that the four lithium atoms of $[\{(OEPG)Sm[Li(THF)_2]\}_2(N_2Li_4)]$ may play an important role, not only for the assembly of the dinuclear structure through a network of bridging interactions, but also for the stabilization of the dinitrogen moiety itself. To evaluate the role of the lithium atoms in the stabilization of the dinitrogen units, it was important to attempt the preparation of a samarium(II) OEPG complex in the absence of alkali cations.

The reaction of $[(\{Me_3Si)_2N\}_2Sm(tmeda)]$,[7] conveniently prepared in situ, with 0.5 equiv of OEPG-H_4 proceeded at room temperature under either N_2 or Ar atmosphere. When the reactants were mixed the color changed from purple-blue to intense red, and well-formed, deep-red, very air-sensitive crystals formulated as **1** were isolated in reasonable yield (57%) upon crystallization from ether. While the IR spectrum of **1** shows the characteristic absorptions of the OEPG ligand at 3075, 1035, and 570 cm^{-1}, the ^1H NMR spectrum is uninformative, showing broad resonances spread over a rather large range. The formula of **1** was therefore inferred from the analytical data. The complex was EPR-silent in both the solid state and in solution, and showed unusually low paramagnetism[9] in the solid state ($\mu_{eff} = 1.95\ \mu_B$ per dimer, at room temperature),[9] possibly indicating the presence of a rather strong magnetic coupling. However, variable-temperature measurements of the magnetic susceptibility (162–288 K) carried out in toluene gave a plot in

[*] Prof. Dr. S. Gambarotta, J.-I. Song
Department of Chemistry, University of Ottawa
Ottawa, ON K1N 6N5 (Canada)
Telefax: Int. code +(613) 562-5170
e-mail: SGAMBARO@OREO.CHEM.UOTTAWA.CA

[**] This work was supported by the Natural Sciences and Engineering Research Council of Canada.

good agreement with the Curie–Weiss law, with a large negative intercept ($\theta = -153$ K).

The molecular structure of **1**, as determined by X-ray diffraction methods,[10] consists of an almost linear $Sm_2(Et_2O)_2$ unit surrounded by an OEPG tetraanion ligand (Fig. 1). The porphyrinogen ligand is centered on the Sm–Sm vector and adopts an almost symmetric conformation; each pair of pyrrole rings at the opposite positions of the macrocycle are nearly parallel to

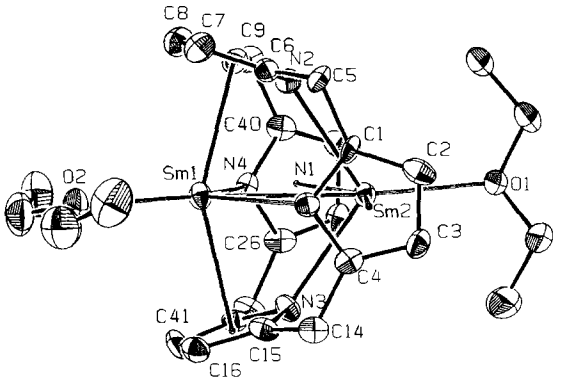

Fig. 1. Crystal structure of **1** (ORTEP representation; ethyl groups have been omitted for clarity). Selected bond lengths [Å] and angles [°]: Sm1-Sm2 3.3159(5), Sm1-N1 2.703(5), Sm1-N4 2.705(5), Sm2-N2 2.707(5), Sm2-N3 2.707(5), Sm1-N2 2.847(5), Sm1-C6 2.957(6), Sm1-C7 3.063(6), Sm1-C8 3.062(5), Sm1-C9 2.948(5), Sm1-O2 2.586(5), Sm2-O1 2.588(4); Sm1-Sm2-O1 173.5(1), Sm2-Sm1-O2 173.9(1), N1-Sm1-N4 109.8(1), N1-Sm1-O2 119.7(2), O2-Sm1-N4 130.4(1).

each other. Each pair of rings coordinates one of the two Sm atoms in an η^5 fashion, ultimately forming a bent samarocene-like structure. The two N atoms of each pair of parallel pyrrole rings are also σ-bonded to the second samarium atom, which is therefore connected to the four pyrrole rings in an η^1,η^5-bonding fashion. The second set of pyrrole rings displays an identical arrangement with the second samarium atom. The coordination environment around each samarium may be considered as severely distorted trigonal bipyramidal; the two σ-bonded nitrogens and the oxygen atom of the ether define the equatorial plane, and the two centroids of the two η^5-bonded rings occupy the axial positions.

Although complex **1** has two samarium(II) centers and the OEPG ligand, it has a short Sm–Sm contact and does not coordinate dinitrogen, thus indicating that Li cations indeed play a crucial role in N_2-fixing systems. Short intermetallic contacts are encountered only rarely in lanthanide chemistry even though these metals tend to form polynuclear aggregates.[11] Yet a Sm–Sm distance as short as 3.49 Å[13] and a Yb–Yb distance of 3.0 Å[12] have been found in two trivalent complexes. Conversely, complexes with divalent lanthanides are mainly mononuclear,[13] and the few dinuclear complexes reported in the literature have fairly long intermetallic distances.[7, 14] The Sm–Sm distance of complex **1** (Sm1–Sm2 = 3.3159(5) Å) is quite short, and given the size of the $Sm^{(II)}$ atom,[15] might be considered within the bonding range. For example, dinuclear and diamagnetic complexes of trivalent zirconium (with a covalent radius significantly smaller than that of samarium(II)[15] show intermetallic distances ranging from 3.2 to 3.6 Å[16] and are believed to have a Zr–Zr bond.[17] By analogy, the short Sm–Sm distance in **1** along with its low paramagnetism (consistent with one unpaired electron per dinuclear complex) suggest the presence of a Sm–Sm interaction.

Experimental Procedure

1: Upon addition of $(Me_3Si)_2NLi$ (6.0 g, 36.0 mmol) to an emerald-green suspension of $[SmI_2(tmeda)_2(THF)]$ (12.7 g, 17.9 mmol) in THF (100 mL) at room temperature the reaction mixture turned purplish-blue. The mixture was allowed to stir for 2 h at room temperature. Solid OEPG-H_4 (4.7 g, 8.8 mmol) was added to the suspension upon which it turned intense red. The mixture was stirred ca. 12 h at room temperature. The solvent was evaporated in vacuo and the residual solid resuspended in Et_2O (100 mL). The resulting intense red solution was filtered and cooled to −15 °C to give dark red crystals of **1** (5.1 g, 5.0 mmol, 57% based on OEPG). Anal. for $C_{44}H_{68}N_4Sm_2O_2 \cdot 0.5(Et_2O)$: calcd (found): C 54.02 (53.96), H 7.19 (7.17), N 5.48 (5.43). IR (Nujol): $\tilde{\nu}$ [cm^{-1}] = 3075 (w), 1593 (w), 1261 (s), 1159 (m), 1091 (vs), 1035 (s), 1018 (s), 927 (w), 889 (m), 796 (s), 755 (s).

Received: May 3, 1995 [Z 7954 IE]
German version: *Angew. Chem.* **1995**, *107*, 2319–2321

Keywords: complexes with macrocyclic ligands · metal–metal interactions · porphyrinoids · samarium compounds

[1] a) W. J. Evans, G. Kociok-Köhn, V. S. Leong, J. W. Ziller, *Inorg. Chem.* **1992**, *31*, 3592; b) W. J. Evans, D. K. Drummond, *J. Am. Chem. Soc.* **1988**, *110*, 2772; c) *ibid.* **1986**, *108*, 7440; d) N. S. Radu, T. D. Tilley, A. L. Rheingold, *ibid.* **1992**, *114*, 8293; e) W. J. Evans, L. A. Hughes, D. K. Drummond, H. Zhang, J. L. Atwood, *ibid.* **1986**, *108*, 1722; f) W. J. Evans, J. W. Grate, L. A. Hughes, H. Zhang, J. L. Atwood, *ibid.* **1985**, *107*, 3728; g) W. J. Evans, D. K. Drummond, H. Zhang, J. L. Atwood, *Organometallics* **1988**, *7*, 797; h) A. Recknagel, D. Stalke, H. W. Roesky, F. T. Edelmann, *Angew. Chem.* **1989**, *101*, 496; *Angew. Chem. Int. Ed. Engl.* **1989**, *28*, 445.

[2] a) W. J. Evans, G. W. Rabe, J. W. Ziller, *J. Organomet. Chem.* **1994**, *483*, 21; b) A. J. Arduengo, M. Tamm, S. J. McLain, J. C. Calabrese, F. Davidson, W. J. Marshall, *J. Am. Chem. Soc.* **1994**, *116*, 7927; c) W. J. Evans, D. K. Drummond, *ibid.* **1989**, *111*, 3329; d) W. J. Evans, T. A. Ulibarri, J. W. Ziegler, *ibid.* **1990**, *112*, 2314; e) W. J. Evans, R. A. Keyer, H. Zhang, J. L. Atwood, *J. Chem. Soc. Chem. Commun.* **1987**, 837; f) W. J. Evans, D. K. Drummond, S. G. Bott, J. L. Atwood, *Organometallics* **1986**, *5*, 2389.

[3] R. H. Cayton, K. J. Novo-Gradac, B. E. Bursten, *Inorg. Chem.* **1991**, *30*, 2265.

[4] J. Jubb, S. Gambarotta, *J. Am. Chem. Soc.* **1994**, *116*, 4477.

[5] W. J. Evans, T. A. Ulibarri, J. W. Ziller, *J. Am. Chem. Soc.* **1988**, *110*, 6877.

[6] J. Ho, R. J. Drake, D. W. Stephan, *J. Am. Chem. Soc.* **1993**, *115*, 3792.

[7] J. I. Song, S. Gambarotta, unpublished results.

[8] W. J. Evans, M. A. Hozbor, *J. Organomet. Chem.* **1987**, *326*, 299.

[9] $\chi_g = 1.36$ cgsu measured at room temperature with a Johnson Matthey magnetic susceptibility balance.

[10] Crystal data for **1**: $C_{46}H_{73}O_{2.5}Sm_2N_4$, $M_r = 1022.91$, triclinic, $P\bar{1}$, $a = 11.810(1)$, $b = 18.817(1)$, $c = 11.122(1)$ Å, $\alpha = 92.214(9)$, $\beta = 103.88(1)$, $\gamma = 101.82(1)°$, $V = 2338.3(8)$ Å^3, $Z = 2$, $\rho_{calcd} = 1.453$ g cm^{-1}, $\mu = 25.35$ cm^{-1}, $F(000) = 1041$, $R = 0.028$ ($R_w = 0.047$), GOF = 2.31 for 485 parameters and 5289 unique reflections. Positions of non-hydrogen atoms were refined anisotropically. All the hydrogen atom were located in the difference Fourier maps. Absorption corections (DIFABS) were applied to the data. A half molecule of ether was found in the lattice. The two α-carbons (C46 and C47) were found disordered over two positions. The disorder was modeled by arbitrarily attributing a 50% occupancy to each disordered atom. The significant improvement of the convergence confirmed the goodness of the model. Further details of the crystal structure investigation may be obtained from the Director of the Cambridge Crystallographic Data Centre, 12 Union Road, GB-Cambridge CB2 1EZ (UK), on quoting the full journal citation.

[11] See for example: a) D. L. Clark, J. C. Gordon, J. C. Huffman, R. L. Vincent-Hollis, J. C. Watkin, B. D. Zwick, *Inorg. Chem.* **1994**, *33*, 5903; b) W. J. Evans, G. W. Rabe, J. W. Ziller, *ibid.* **1994**, *33*, 3072; c) D. M. Barnhart, D. L. Clark, J. C. Gordon, J. C. Huffman, J. G. Watkin, B. D. Zwick, *J. Am. Chem. Soc.* **1993**, *115*, 8461; d) C. J. Burns, D. J. Berg, R. A. Andersen, *J. Chem. Soc. Chem. Commun.* **1987**, 272.

[12] W. J. Evans, D. K. Drummond, R. L. Chamberlain, R. J. Doedens, S. G. Bott, H. Zhang, J. L. Atwood, *J. Am. Chem. Soc.* **1988**, *110*, 4983.

[13] a) V. Chebolou, R. R. Whittle, A. Sen, *Inorg. Chem.* **1985**, *24*, 3082; b) J. P. White, H. Deng, E. P. Boyd, J. Gallucci, S. G. Shore, *ibid.* **1994**, *33*, 1683; c) T. D. Tilley, R. A. Andersen, A. Zalkin, *ibid.* **1984**, *23*, 2271; d) W. J. Evans, I. Bloom, W. E. Hunter, J. L. Atwood, *Organometallics* **1985**, *4*, 112; e) G. W. Watt, E. W. Gillow, *J. Am. Chem. Soc.* **1969**, *91*, 775; f) A. Recknagel, A. Steiner, S. Brooker, D. Stalke, F. T. Edelmann, *J. Organomet. Chem.* **1991**, *415*, 315; g) A. Recknagel, A. Steiner, M. Noltemeyer, S. Brooker, D. Stalke, F. T. Edelmann, *ibid.* **1991**, *414*, 327.

[14] a) W. J. Evans, J. W. Grate, H. W. Coi, I. Bloom, W. E. Hunter, J. L. Atwood, *J. Am. Chem. Soc.* **1985**, *107*, 941; b) J. Takats, X. W. Zhang, V. W. Day, T. A. Eberspacher, *Organometallics* **1993**, *12*, 4286; c) M. Wedler, A. Recknagel, J. W. Gilje, F. T. Edelmann, *J. Organomet. Chem.* **1992**, *426*, 295; d) W. J. Evans, H. Anwander, M. A. Ansari, J. W. Ziller, *Inorg. Chem.* **1995**, *34*, 5; e) L. Lee, D. J. Berg, G. W. Bushnell, *ibid.* **1994**, *33*, 5302.

[15] a) R. D. Shannon, *Acta Crystallogr. Sect. A* **1976**, *32*, 751; b) F. A. Cotton, G. Wilkinson, *Advanced Inorganic Chemistry*, 5th ed., Wiley Interscience, New York, **1988**.

[16] a) J. H. Wengrovius, R. R. Schrock, C. S. Day, *Inorg. Chem.* **1981**, *20*, 184; b) F. A. Cotton, M. Shang, W. A. Wojtczak, *ibid.* **1991**, *30*, 3670; c) F. A. Cotton, M. P. Diebold, P. A. Kibala, *ibid.* **1988**, *27*, 799; d) M. Y. Chiang, S. Gambarotta, F. van Bolhuis, *Organometallics* **1988**, *7*, 1864; e) Y. Wielstra, S. Gambarotta, M. Y. Chiang, *ibid.* **1988**, *7*, 1866; f) Y. Wielstra, S. Gambarotta, A. Meetsma, J. deBoer, *ibid.* **1989**, *8*, 250; g) Y. Wielstra, S. Gambarotta, A. L. Spek, *ibid.* **1989**, *8*, 2948; h) Y. Wielstra, S. Gambarotta, A. L. Spek, W. J. J. Smeets, *ibid.* **1990**, *9*, 2142; i) Y. Wielstra, S. Gambarotta, A. Meetsma, S. Khan, *ibid.* **1990**, *9*, 876.

[17] a) M. Benard, M. M. Rohmer, *J. Am. Chem. Soc.* **1992**, *114*, 4785; b) *Organometallics* **1991**, *10*, 157; c) R. L. DeKock, M. A. Teterson, L. E. L. Reynolds, L. H. Chen, J. Baerends, P. Vernooijs, *ibid.* **1993**, *12*, 2794.

An Yttrium-Based Strong Lewis Acid for the Heterogeneous Catalysis of the Diels–Alder Reaction**

Alive Keshavaraja, Vishnumurthy R. Hegde, Bipin Pandey,* Arumugamangalam V. Ramaswamy,* Pradeep Kumar, and T. Ravindranathan*

While yttrium has gained considerable prominence in superconductivity research in recent times,[1] very little is known about its application in organic chemistry.[2] Indeed, recent efforts by Evans et al.[3] to use YI_3 as a catalyst for stereoselective reduction in the presence of a suitable auxiliary and by Kobayashi et al.[4] to use $Y(OTf)_3$ (Tf = trifluoromethanesulfonyl) as a Diels–Alder catalyst were unsuccessful. Since yttrium with its vacant d orbitals offers opportunities for forming strong Lewis acid sites in a heterogeneous catalyst, development of such a catalyst is highly desirable for organic synthetic transformations. Here, we report on the synthesis and characterization of the first yttrium-based strong Lewis acid catalyst and its applications mainly in Diels–Alder reactions and one example of a hetero-Diels–Alder reaction. The acidity of the catalyst has been demonstrated by FTIR studies,[5] potentiometric titration,[6] and temperature-programmed desorption (TPD)[7] of ammonia, whereas its surface area has been determined by the N_2 adsorption (BET) method.[8]

The catalyst was prepared by treating a mixture of aqueous solutions of yttrium nitrate and zirconyl nitrate (molar ratio 16:84) with aqueous ammonia (28%) under vigorous stirring until a pH value of 8.5 was achieved and a precipitate was formed. This precipitate was washed with deionized water, dried at 110 °C, treated with 2 N sulfuric acid, dried again at 120 °C for 24 h, and subsequently was heated to 500 °C at a programmed heating rate of 2 °C min^{-1} and then calcined for 3 h. This resulted in a highly acidic catalytic material, whose chemical composition (determined by X-ray fluorescence) was found to be 82.6 mol % Zr, 15.6 mol % Y, and 1.8 mol % S. The physicochemical characterization of the catalyst was carried out by X-ray powder diffraction, FTIR, potentiometric titrations, temperature-programmed desorption (TPD), scanning electron microscopy (SEM), and N_2 adsorption techniques. The X-ray powder diffraction profile of the catalyst shows the formation of a cubic phase (Fig. 1). The IR spectra of pyridine adsorbed on the catalyst show absorption bands at 1640, 1605, 1577, 1542, 1490, and 1444 cm^{-1} (Fig. 2). The strong absorption bands at

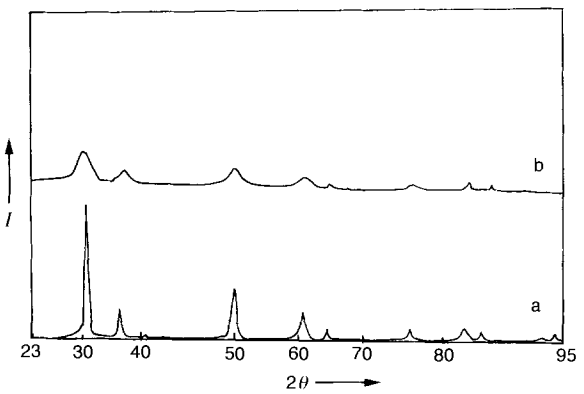

Fig. 1. X-ray powder diffraction pattern of the yttrium-based catalyst prior to (a) and after (b) sulfation. The diffractogram was recorded on a Rigaku diffractometer, model D/Max, IIIVC, with Ni-filtered Ca_{K_α} radiation. I = intensity (arbitrary units).

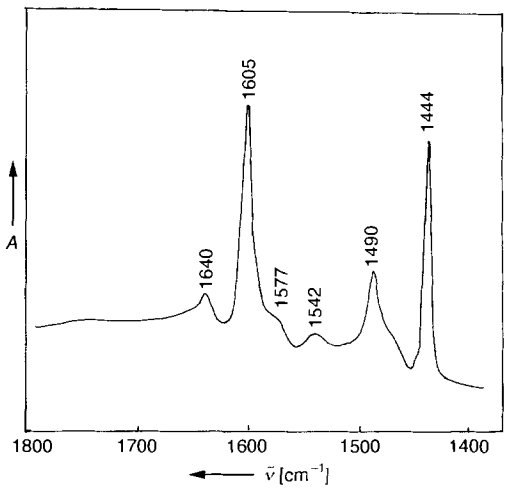

Fig. 2. FTIR spectrum of pyridine adsorbed on the yttrium-based catalyst, recorded on a Nicolet 60 SXB FTIR spectrometer. A = absorption (arbitrary units).

1605 and 1444 cm^{-1} indicate the presence of coordinated pyridine at the Lewis acid sites of the catalyst. The weak absorption at 1542 cm^{-1}, attributed to the pyridinium ion,[5] indicates the presence of a few Brönsted acid sites. The potentiometric titration of the acid sites with *n*-butylamine in nonaqueous medium (Fig. 3) shows the influence of yttrium in enhancing the number of acid sites. The amount of *n*-butylamine consumed was 7.7 mol equiv g^{-1} for the yttrium-based catalyst compared to 5.8 mol equiv g^{-1} for the yttrium-free catalyst. The presence of very strong acid sites in the catalyst is indicated by the peak maxima at 530 °C in the TPD profile (Fig. 4).[7] The scanning electron micrograph of the sample shows the presence of uni-

[*] Dr. A. V. Ramaswamy, A. Keshavaraja
Catalysis Division
National Chemical Laboratory
Pune 411008 (India)
Telefax: Int. code + (212) 330 233

Dr. B. Pandey, Dr. T. Ravindranathan, V. R. Hegde, Dr. P. Kumar
Organic Chemistry, Technology Division
National Chemical Laboratory

[**] NCL Communication No. 6049. A. K. and V. R. H. thank the Council of Scientific and Industrial Research, New Delhi, Government of India for Senior Research Fellowships. The authors are thankful to Dr. S. G. Hegde for FTIR studies and fruitful discussion.

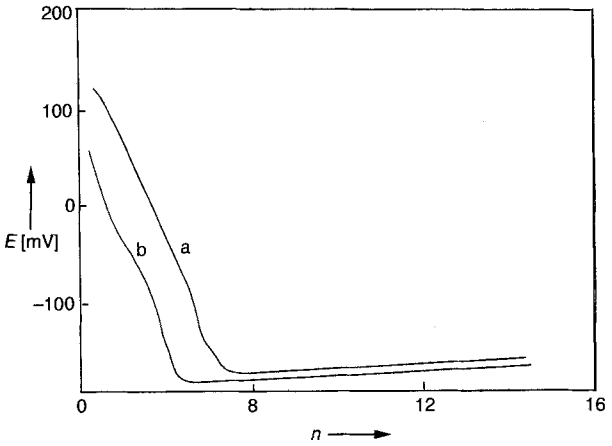

Fig. 3. Potentiometric titration curves of the sulfated catalyst with yttrium (curve a) and without yttrium (curve b) in CH_3CN. For details see ref. [7]. n = number of molar equivalents of n-butylamine per g.

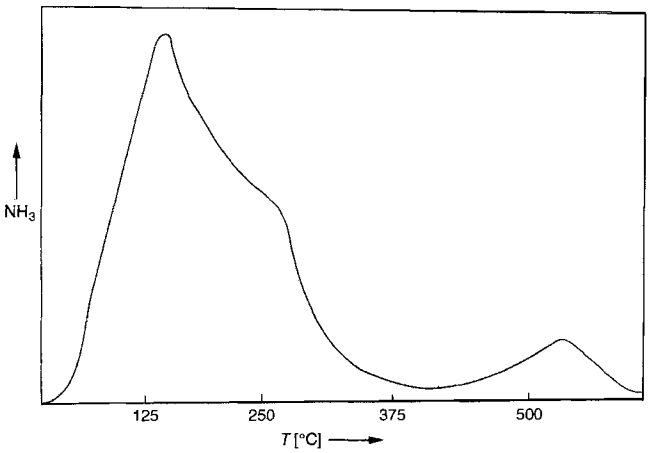

Fig. 4. TPD profile (ammonia) of the yttrium-based catalyst, recorded on a Sorbstar apparatus, Institute of Isotopes, Hungary, with He as the carrier gas, a flow rate of 50 mL min^{-1}, and a heating rate of 10 K min^{-1} from room temperature to 625 °C. NH_3 = amount of ammonia desorbed (arbitrary units).

form-sized (around 0.3 μm) particles (Fig. 5). The surface area[8] of the sample determined by the BET method was 150 m^{2}g^{-1}. The lattice defects caused by the incorporation of yttrium in the Zr^{4+} sites appear to enhance the number and strength of the Lewis acid sites of the catalyst.

The Diels–Alder reaction and its variants like the intramolecular, hetero-, inverse-electron demand, and asymmetric Diels–Alder reactions offer considerable opportunities to organic chemists for the construction of complex structures. In last few years there has been a tremendous upsurge in the interest in

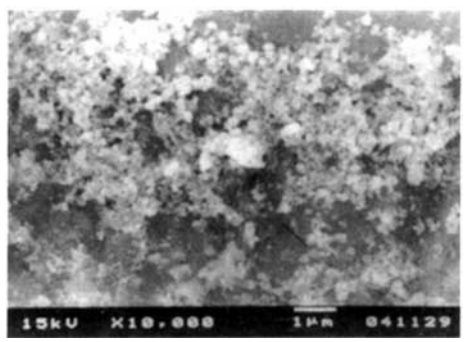

Fig. 5. Scanning electron micrograph of the catalyst.

increasing the reactivity[9] and altering the selectivity of Diels–Alder reactions.[10] Indeed, acceleration of the Diels–Alder reaction is one of the testing grounds for newly discovered Lewis acids.[11] One of the recent arrivals on the scene is $LiClO_4$ in ether,[12] where the strong Lewis acidity of the lithium ion is presumably responsible for the acceleration of the Diels–Alder reaction.[13] Since Kobayashi et al.[4] reported that $Y(OTf)_3$ was unable to accelerate the Diels–Alder reaction between cyclopentadiene **1** and 1,4-naphthoquinone **2a** (Scheme 1), we examined the reaction of this system with our catalyst as a test case. As shown in Table 1, stirring the reaction mixture (including our catalyst) at room temperature for 5 h gave exclusively the *endo* (100% *endo* selectivity) product in 93% yield (entry 1). For comparison, the reaction without the catalyst under identi-

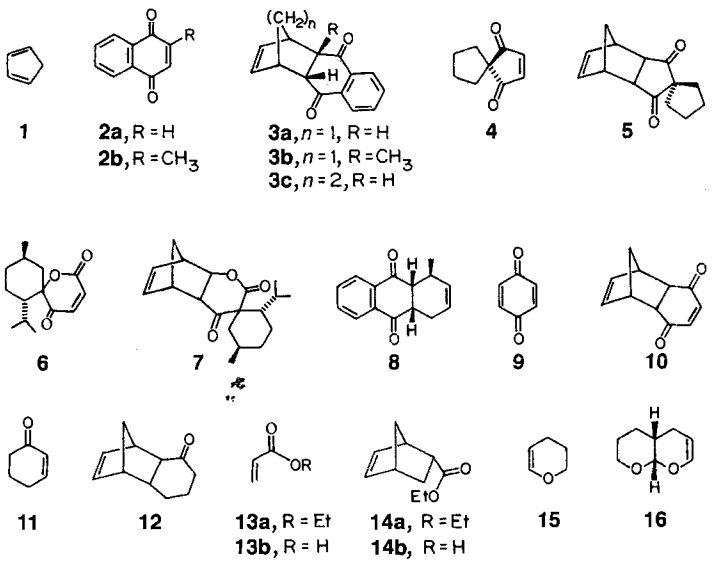

Scheme 1. Formulae of the dienes, dienophiles, and Diels–Alder products from Table 1.

Table 1. Diels–Alder reactions [a] catalyzed by an yttrium-based Lewis acid.

Entry	Diene	Dienophile	Molar ratio [b]	Time [h] [c]	Conversion [%] [d]	Product [e]	Yield [f]	Ratio *endo*:*exo* [g]	Ref.
1	**1**	**2a**	2:1	5	100	**3a**	93	100:0	[4]
2	**1**	**2b**	2:1	10	100	**3b**	85	96:4	[15]
3	**1**	**4**	2:1	6	100	**5**	92	95:5	[14]
4	**1**	**6**	2:1	8	90	**7** [h]	80	98:2	[14]
5	[i]	**2a**	1.2:1	20	85	**8**	65	–	[4]
6	[j]	**2a**	1.2:1	48	50	**3c**	45	98:2	[4]
7	**1**	**9**	1.2:1	8	100	**10**	92	99:1	[12]
8	**1**	**11**	10:1	10	45	**12**	66	–	[17]
9	**1**	**13a**	2:1	5	100	**14a**	94	95:5	[12]
10	**1**	**13b**	2:1	20	–	**14b**	–	–	–
11 [k]	[l]	**15**	1:2	20	85	**16** [m]	66	–	[16]

[a] Unless otherwise indicated, all reactions were performed in CH_2Cl_2 (approx. 100 mg of dienophile in 10 mL of CH_2Cl_2) at room temperature under stirring. The amount of catalyst taken was half the weight of the dienophile. [b] The molar ratio of diene to dienophile. [c] Sampling time or duration in hours. [d] The % conversion of the dienophile, based on recovered material. No destruction of dienophile was observed. [e] The structure of major isomer is given. All the products were characterized by spectral and analytical data or by comparison with authentic samples. [f] Yield [%] of products after column chromatography based on the recovered starting material. [g] *Endo-exo* ratio was determined by GC by comparison with authentic samples of both isomers [10a–c]. [h] See ref. [14]. [i] (*E*)-1,3-Pentadiene. [j] 1,3-cyclohexadiene. [k] The reaction was carried out without any solvent. [l] Acrolein. [m] Only one regio- and stereoisomer was obtained.

 © VCH Verlagsgesellschaft mbH, D-69451 Weinheim, 1995 0570-0833/95/3419-2144 $ 10.00+.25/0

cal conditions gave only 4% of the *endo* product **3a**. Under usual thermal Diels–Alder reaction conditions, that is heating to reflux in benzene, an *endo* to *exo* product ratio of 95:5 was obtained.[14] The enhanced *endo* selectivity and the reaction rate with our catalyst prompted us to examine the Diels–Alder reaction of **1** with 2-methylnaphthoquinone **2b**, which is known to be a troublesome reaction;[15] however, **2b** was converted quantitatively into **3b** and isolated in 85% yield (entry 2). The reaction of **1** with other demanding and structurally different dienophiles such as the spiro compounds **4** and **6** gave **5** (92%) and **7** (80%), respectively (entries 3 and 4). Mention must be made here that **6** reacts with **1** under a variety of Diels–Alder conditions such as, heating to reflux in high boiling solvents, neat heating, sealed tube heating, or ultra sound acceleration, with or without various well-known Lewis acids like BF_3, $TiCl_4$, etc., to give **7** in not more than 10% yield.[14] The generality of the Diels–Alder catalysis with the yttrium-based reagent has been demonstrated with other dienes and dienophiles (entries 5–9). However, our attempts to use our catalyst also for carboxylic acids as dienophile, instead of the corresponding esters have not been successful (entries 9, 10). The yttrium-based catalyst has also been found to be useful for hetero-Diels–Alder reactions (entry 11).[16]

A control experiment has shown that for the reactions 6, 7, and 11 without the catalyst, the reaction does not go at all under identical conditions. Literature evidence is also available for the failure of the Diels–Alder reactions of 2,[15] 3,[14] 4,[14] 6,[14] 8,[17] and 11[16] without Lewis acid. The catalyst can be recovered after the reaction and can be reused; comparable results for the Diels–Alder reaction were obtained in second runs.

As discussed earlier based on the results from the TPD studies and potentiometric titrations, the lattice defects introduced due to yttrium increase the number and strength of the active Lewis acidic sites. Furthermore the oxophilic nature of yttrium enhances the reactivity of oxygen-containing dienophiles, thereby lowering the LUMO and decreasing the gap between the HOMO of diene and LUMO of dienophile.[18] Surprisingly, in our reaction, only 20 mol % excess of diene is sufficient for the efficient Diels–Alder reaction, which is usually not the case. Indeed, the diene dimerization of either **1** or 1,3-cyclohexadiene was not observed with the catalyst.

In conclusion, a yttrium-based catalyst has been prepared by a novel methodology and has been fully characterized by XRD, SEM, and BET surface area studies. Its Lewis acidity has been demonstrated by the FTIR spectrum of adsorbed pyridine, the desorption of ammonia, and potentiometric titration studies. The general applicability of the new Lewis acid catalyst for Diels–Alder reactions has been established with several models. We are currently investigating its application as a strong Lewis acid in other organic reactions.

Experimental Procedure

In a typical experiment (Table 1, entry 1), cyclopentadiene **1** (0.198 g, 0.003 mol), 1,4-naphthoquinone (0.158 g, 0.001 mol) **2a**, and catalyst (0.075 g, 50% by weight with respect to dienophile) in dichloromethane (10 mL) was stirred at room temperature for 5 h. The progress of the reaction was monitored by TLC. The catalyst was filtered off, the solvent removed by rotary evaporation, and the residue chromatographed over a silica gel column by eluting with 5% acetone/petroleum ether to give 0.2083 g of the *endo* adduct **3a** (93% yield).

Received: April 29, 1995 [Z 7942 IE]
German version: *Angew. Chem.* **1995**, *107*, 2333–2336

Keywords: Diels–Alder reactions · heterogeneous catalysis · Lewis acids · yttrium compounds

[1] S. M. Zahurak, D. Werder, *Nature (London)* **1987**, *329*, 423.
[2] Recently selective oxidation of isobutane by Y_2O_3-$CeFe_3$ has been reported: W. D. Zhang, D. L. Tang, X. P. Zhou, H. L. Wan, K. R. Tsai, *J. Chem. Soc. Chem. Commun.* **1994**, 771.
[3] D. A. Evans, S. G. Nelson, M. R. Gagne, A. R. Muci, *J. Am. Chem. Soc.* **1993**, *115*, 9800.
[4] S. Kobayashi, I. Hachiya, M. Araki, H. Ishitani, *Tetrahedron Lett.* **1993**, *34*, 3755.
[5] N. Mizuno, H. Fujii, H. Igarashi, M. Misono, *J. Am. Chem. Soc.* **1992**, *114*, 7151.
[6] R. Cid, G. Pecchi, *Appl. Catal.* **1985**, *14*, 15.
[7] M. J. F. M. Verbaak, A. J. van Dillen, J. W. Geus, *Appl. Catal.* **1993**, *105*, 251.
[8] Determination of specific surface area was carried out by BET (Brunner–Emmett–Teller) N_2 adsorption using a Omnisorp 100 CX apparatus.
[9] Review on the catalysis of Diels–Alder reactions, see U. Pindur, G. Lutz, C. Otto, *Chem. Rev.* **1993**, *93*, 741.
[10] a) B. Pandey, P. V. Dalvi, *Angew. Chem.* **1993**, *105*, 1724; *Angew. Chem. Int. Ed. Engl.* **1993**, *32*, 1612; b) W. R. Roush, B. B. Brown, *J. Org. Chem.* **1992**, *57*, 3380; c) B. Pandey, P. V. Dalvi, A. A. Athawale, B. G. Pant, P. P. Kewale, *J. Chem. Soc. Chem. Commun.* **1990**, 1505.
[11] See Section VI-B and X in ref. [9].
[12] P. A. Grieco, J. J. Nunes, M. D. Gaul, *J. Am. Chem. Soc.* **1990**, *112*, 4595.
[13] a) A. Casasch, G. Desimoni, G. Faita, A. G. Invernizzi, S. Laneti, P. P. Righetti, *J. Am. Chem. Soc.* **1993**, *115*, 8002; b) R. M. Pagni, G. W. Kabalka, S. Bains, M. Presco, J. Wilson, J. Bartmess, *J. Org. Chem.* **1993**, *58*, 3130.
[14] B. Pandey, C. U. Dinesh, R. S. Reddy, V. R. Hegde, unpublished results.
[15] V. K. Singh, B. N. Raju, P. T. Deota, *Synth. Commun.* **1988**, *18*, 567.
[16] S. Danishefsky, M. Bednarski, *Tetrahedron Lett.* **1984**, *25*, 721.
[17] E. C. Angell, F. Fringuelli, M. Guo, L. Minuti, A. Taticchi, E. Wenkert, *J. Org. Chem.* **1988**, *53*, 4325.
[18] Lewis acids are known to lower the LUMO of dienophiles: a) K. N. Houk, R. W. Strozier, *J. Am. Chem. Soc.* **1973**, *95*, 4094; b) D. M. Birney, K. N. Houk, *ibid.* **1990**, *112*, 4127.

Enantioselective Reduction of Ketones with Sodium Borohydride, Catalyzed by Optically Active (β-Oxoaldiminato)cobalt(II) Complexes

Takushi Nagata, Kiyotaka Yorozu, Tohru Yamada, and Teruaki Mukaiyama*

Dedicated to Professor Ivar Ugi on the occasion of his 65th birthday

A wide variety of asymmetric reducing agents have been developed for the enantioselective reduction of prochiral ketones.[1] An asymmetric reduction of prochiral ketones catalyzed by chiral oxazaborolidines is noteworthy in this context.[2] Numerous successful applications taking advantage of the catalytic reduction have been shown: for example, various optically active secondary alcohols such as prostaglandin intermediates,[3a] agonists,[3b] potassium channel blockers,[3c] and the like were prepared by the enantioselective reduction with oxazaborolidine catalysts. On the contrary, few examples on the use of sodium borohydride with chiral metal complex catalysts in enantioselective reduction have been reported.[4, 5] It was recently shown that optically active β-oxoaldimines form a new class of effective ligand for aerobic enantioselective epoxidation

[*] Prof. Dr. T. Mukaiyama
Department of Applied Chemistry, Faculty of Science
Science University of Tokyo
Kagurazaka, Shinjuku-ku, Tokyo 162 (Japan)
T. Nagata, Dr. K. Yorozu, Dr. T. Yamada
Basic Research Laboratories for Organic Synthesis
Mitsui Petrochemical Industries
Nagaura, Sodegaura-shi, Chiba 299-02 (Japan)
Telefax: Int. code + 438/625395

of simple alkenes with manganese(III) complexes as catalysts.[6] In this communication we report a novel method for the enantioselective reduction of ketones with a cobalt hydride species[7] generated from sodium borohydride and catalytic amounts of optically active cobalt(II) complexes having the β-oxoaldimine ligand, *N,N'*-bis(3-oxobut-2-enylidene)ethylenediamine.[6]

The optically active cobalt(II) complexes **1**–**4** were prepared by heating the corresponding β-oxoaldimine ligand with sodium

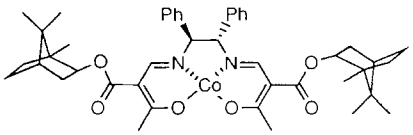

1

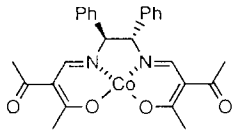

2

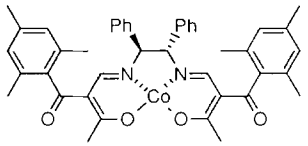

3

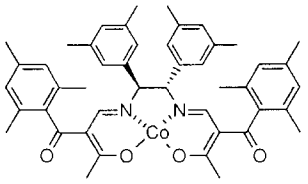

4

hydroxide and cobalt(II) chloride hexahydrate in methanol/water solution at 60 °C.[8] First the effectiveness of the ligand in the enantioselective reduction was examined relative to the reduction of 2,2-dimethylchroman-4-one with sodium borohydride [Eq. (a) and entries 1, 2, and 3 in Table 1]. The reduction was

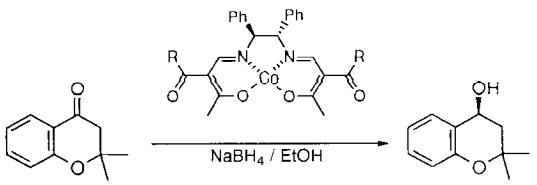

(a)

carried out at −20 °C in the presence of a small amount of ethanol in chloroform solution, and the optical yield was determined by HPLC analysis. Catalyst system **3** containing bulkier acyl groups showed sufficient asymmetric induction (88% *ee*). An aldimine sterically hindered at the chiral C_2-symmetric diamine unit (**4**) was more efficient (92% ee, Table 1 entry 4).

In this catalytic system, a small amount of alcohol was indispensable for achieving a high enantiofacial differentiation.

Table 1. Effect of catalysts on yield and optical yield in the asymmetric reduction of 2,2-dimethylchroman-4-one (**5**) [a].

Entry	Catalyst	Yield [%]	*ee* [%] [b]
1	**1**	95	51
2	**2**	90	51
3	**3**	98	88
4	**4**	94	92

[a] Reaction conditions: 0.50 mmol **5**, 0.025 mmol (5 mol%) cobalt(II) complex, 0.75 mmol $NaBH_4$, 250 μL ethanol in $CHCl_3$ (9 mL), −20 °C. [b] Determination by HPLC (Daicel Chiralpak AD).

Ethanol was the most suitable alcohol with respect to both enantioselectivities and chemical yields. Other borohydride reagents ($LiBH_4$, KBH_4, $Ca(BH_4)_2$, and R_4NBH_4 (R = Me, Et, Bu) were also suitable for the asymmetric reduction catalyzed by the cobalt(II) complex. However, in general, sodium or potassium borohydride gave better results.

The catalyst system **4** was successfully applied in the asymmetric reduction of several aromatic ketones[9] (Table 2). High enantiomeric excesses were observed in the asymmetric reduction of chromanone derivatives having alkyl groups in 2-position (compounds **5**, **6**, and **7**). In the case of 2,2-dimethyltetralone (**10**), the catalyst system **3** with sodium borohydride afforded a higher optical purity (90% *ee*) than system **4** (66% *ee*). The use of potassium borohydride instead of sodium borohydride with this system gave an even better result (94% *ee*, Table 2 entry 6).

Table 2. Enantioselective reduction of prochiral ketones catalyzed by **4** [a].

Entry	Ketone		Yield [%]	*ee* [%] [b]
1	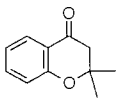	**5**	94	92 [c]
2	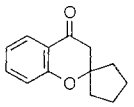	**6**	95	89 [c]
3	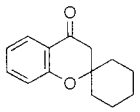	**7**	96	87 [c]
4	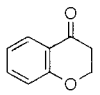	**8**	92	70 (*S*) [d]
5	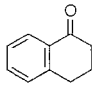	**9**	99	73 (*S*) [e]
6 [f]	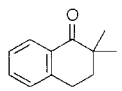	**10**	76	94 [d]
7	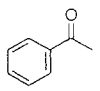	**11**	95	68 (*S*) [d]

[a] For reaction conditions see Experimental Procedure. [b] Absolute configurations are in parentheses and are based on the optical rotation; for **8** see Ref. [10], for **9** Ref. [11]; **11**: comparison with an authentic sample obtained from TCI. [c] HPLC on Chiralpak AD. [d] HPLC on Daicel Chiralcel OD-H. [e] HPLC on Chiralcel OB. [f] The catalyst **3** and KBH_4 was used instead of **4** and $NaBH_4$.

Both enantiomers of the optically active diarylethylenediamine ((*S,S*) and (*R,R*)) are commercially available or can be readily prepared by literature methods.[12] Since the enantiomers of the cobalt(II) complexes can be prepared from the corresponding diarylethylenediamine, the use of the present catalytic reducing system enables us to synthesize both enantiomers of the alcohols. The enantioselective reduction of prochiral aro-

 © VCH Verlagsgesellschaft mbH, D-69451 Weinheim, 1995 0570-0833/95/3419-2146 $ 10.00+.25/0

matic ketones with sodium borohydride catalyzed by optically active *N,N'*-bis(3-oxobut-2-enylidene)ethylenediaminatocobalt(II) thus provides a practical method for the preparation of optically active secondary alcohols with good or very good enantiomeric excess. Further investigations into the design of chiral cobalt(II) complexes and their applications are now in progress.

Experimental Procedure

A typical procedure for the enantioselective reduction of **5** (Table 2 entry 1) using the cobalt complex **4** as catalyst is performed as follows: To a suspension of sodium borohydride (29 mg, 0.75 mmol) in chloroform (5.0 mL) was added ethanol (250 mL) under an argon atmosphere. After stirring for 1.0 h at room temperature, a solution of the (*S,S*)-cobalt(II) complex **4** (19 mg, 0.025 mmol, 5 mol%) in chloroform (2.0 mL) was poured into the mixture. Then it was cooled to −20 °C and **5** (88 mg, 0.50 mmol) in chloroform (2.0 mL) was added. The mixture was stirred for 120 h before the reaction was quenched by adding 1 M hydrochloric acid (2 mL). The reaction mixture was poured into a saturated aqueous solution of sodium hydrogen carbonate and extracted with ether. The organic layer was then washed with brine and dried over anhydrous sodium sulfate. Concentration in vacuo and purification by column chromatography on silica gel (hexane/ethyl acetate) afforded the corresponding optically active alcohol **2**: 98% yield, 87 mg; white crystals; 92% *ee* by HPLC analysis (Chiralpak AD, Daicel Ltd., Co.). $[\alpha]_D^{28} = +49.0$ ($c = 1.0$ in $CHCl_3$).

Received: May 15, 1995 [Z 7986 IE]
German version: *Angew. Chem.* **1995**, *107*, 2309–2311

Keywords: asymmetric syntheses · catalysis · chiral auxiliaries · cobalt compounds · reductions

[1] a) Reviews: K. Harada, T. Munegumi in *Comprehensive Organic Synthesis*, *Vol. 8* (Eds.: B. M. Trost, I. Fleming), Pergamon, Oxford, **1991**, p. 139; M. Nishizawa, R. Noyori, *ibid.*, p. 159; V. K. Singh, *Synthesis* **1992**, 605–617. Recent developments in the area of asymmetric metal-catalyzed reductions: b) of ketones: X. Zhang, T. Taketomi, T. Yoshizumi, H. Kumobayashi, S. Akutagawa, K. Mashima, H. Takaya, *J. Am. Chem. Soc.* **1993**, *115*, 3318–3319; X. Zhang, H. Kumobayashi, H. Takaya, *Tetrahedron: Asymmetry* **1994**, *5*, 1179–1182; T. Ohkuma, H. Ooka, S. Hashiguchi, T. Ikariya, R. Noyori, *J. Am. Chem. Soc.* **1995**, *117*, 2675–2676; c) of imines: C. A. Willoughby, S. L. Buchwald, *J. Org. Chem.* **1993**, *58*, 7627–7629; C. A. Willoughby, S. L. Buchwald, *J. Am. Chem. Soc.* **1994**, *116*, 8952–8965; d) of olefins: K. Wan, M. E. Davis, *Tetrahedron: Asymmetry* **1993**, *4*, 2461–2468; M. Kitamura, Y. Hsiao, M. Ohta, M. Tsukamoto, T. Ohta, H. Takaya, R. Noyori, *J. Org. Chem.* **1994**, *59*, 297–310; T. Ohta, T. Miyake, N. Seido, H. Kumobayashi, H. Takaya, *ibid.* **1995**, *60*, 357–363, and references therein.

[2] S. Itsuno, K. Ito, A. Hirao, S. Nakahama, *J. Chem. Soc. Chem. Commun.* **1983**, 469–470; E. J. Corey, R. K. Bakshi, S. Shibata, *J. Am. Chem. Soc.* **1987**, *109*, 5551–5553; M. Nakagawa, T. Kawate, T. Kakikawa, H. Yamada, T. Matsui, T. Hino, *Tetrahedron* **1993**, *49*, 1739–1748; G. J. Quallich, J. F. Blake, T. M. Woodall, *J. Am. Chem. Soc.* **1994**, *116*, 8516–8525; P. Delair, C. Einhorn, J. L. Luche, *Tetrahedron* **1995**, *51*, 165–172; reviews: S. Wallbaum, J. Martens, *Tetrahedron: Asymmetry* **1992**, *3*, 1475–1504; L. Deloux, M. Srebnik, *Chem. Rev.* **1993**, *93*, 763–784.

[3] a) E. J. Corey, R. K. Bakshi, S. Shibata, C.-P. Chen, V. K. Singh, *J. Am. Chem. Soc.* **1987**, *109*, 7925–7926; b) Y. Hong, Y. Gao, X. Nie, C. M. Zepp, *Tetrahedron Lett.* **1994**, *35*, 5551–5554; c) Y.-J. Shi, D. Cai, U.-H. Dolling, A. W. Douglas, D. M. Tschaen, T. R. Verhoeven, *ibid.* **1994**, *35*, 6409–6412.

[4] For stoichiometric reductions with chiral metal borohydrides see: "Reductions with Chiral Boron Reagents": M. M. Midland in *Asymmetric Synthesis*, *Vol. 2*, *Part A* (Ed.: J. D. Morrison), Academic Press, New York, **1983**, p. 45; K. Soai, H. Oyamada, T. Yamanoi, *J. Chem. Soc. Chem. Commun.* **1984**, 413–414; H. Okawa, T. Katsuki, M. Nakamura, N. Kumagai, Y. Shuin, T. Shinmyozu, S. Kida, *ibid.* **1989**, 139–140; S. Itsuno, Y. Sakurai, K. Shimizu, K. Ito, *J. Chem. Soc. Perkin Trans. 1* **1990**, 1859–1863.

[5] Cobalt-semicorrin catalysts gave high enantiomeric excesses in asymmetric 1,4-reductions of α,β-unsaturated carbonyl compounds with sodium borohydride: U. Leutenegger, A. Madin, A. Pfaltz, *Angew. Chem.* **1989**, *101*, 61–62; *Angew. Chem. Int. Ed. Engl.* **1989**, *28*, 60–61.

[6] a) T. Mukaiyama, T. Yamada, T. Nagata, K. Imagawa, *Chem. Lett.* **1993**, 327–330; b) *Inorg. Chim. Acta* **1994**, *220*, 283–287; c) *Chem. Lett.* **1994**, 1259–1262; d) *Bull. Chem. Soc. Jpn.* **1995**, *68*, 1455–1465.

[7] S.-K. Chung, *J. Org. Chem.* **1979**, *44*, 1014–1016.

[8] The synthesis of β-oxoaldimines was reported in [6d]. For the complexation of the ligands by cobalt(II) chloride, see K. Kato, T. Mukaiyama, *Chem. Lett.* **1990**, 1917–1920.

[9] The ketones **5**, **6**, **7**, and **10** were prepared according to literature methods. Compounds **5**, **6**, and **7**: R. Bergmann, R. Gericke, *J. Med. Chem.* **1990**, *33*, 492–504; **10**: J. G. Garcia, J. D. Enas, F. R. Fronczek, H. F. VanBrocklin, *J. Org. Chem.* **1994**, *59*, 8299–8301. The ketones **8**, **9**, and **11** were purchased from Tokyo Kasei Kogyo.

[10] H. L. Holland, T. S. Manoharan, F. Schweizer, *Tetrahedron: Asymmetry* **1991**, *2*, 335–338.

[11] R. Wiedmann, J.-P. Guetté, M. H. Normant, *C. R. Acad. Sci. Ser. C* **1969**, *268*, 2225–2227.

[12] (*R,R*)- and (*S,S*)-diphenylethylendiamine were purchased from Aldrich; for details on the synthesis see S. Pikul, E. J. Corey, *Org. Synth.* **1992**, *71*, 22–29; H. Sasaki, R. Irie, T. Hamada, K. Suzuki, T. Katsuki, *Tetrahedron* **1994**, *50*, 11827–11838.

Octacationic Cyclophanes: Binding of ATP and Other Anionic Guests in Water**

Fredric M. Menger* and Kelly K. Catlin

Chloroform and methylene chloride, rather than aqueous solvents, have been the media of choice for most host–guest studies. This is because many types of associative forces (for example, hydrogen-bonding and cation/polyether attraction) are unfavorable in water where the solvent competes for the binding sites. Of course, in notable exceptions synthetic hosts have been designed to incorporate small guest molecules in water.[1] Hydrophobic bonding is often a major stabilizing factor in such complexes. Host–guest chemistry has also favored the use of neutral or cationic guests. Anionic guests are known[2] but, as with aqueous solvents, they are relatively uncommon despite their importance to biology. It was the purpose of the present foray into supramolecular chemistry[3] to bind anions in water. The hope was to accomplish this electrostatically with DABCO-based cyclophanes (**1**, DABCO = 1,4-diazabicyclo[2.2.2]octane) whose cavities are lined with eight positive charges. NMR and X-ray data show that the cyclophanes do indeed adsorb anions, including ATP, in aqueous media.

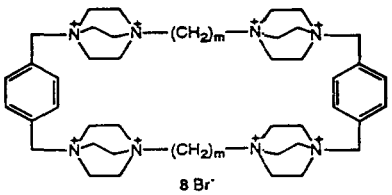

1, $m = 3,5,7$

The synthesis of the cationic cyclophanes is given in Scheme 1. Purification was the major obstacle. In fact, a previously reported DABCO-based macrocycle[4] was later taken to be a linear ionene (a polyquaternary polymer).[5] Published syntheses of water-soluble cyclophanes are commonly carried out with neutral polyamino macrocycles that are purified prior to quaternization of the nitrogen atoms. This strategy was obviously impossible with cyclophanes **1**. Ultimate success in securing pure compounds was achieved by observing the following

[*] Prof. F. M. Menger, Dr. K. K. Catlin
Department of Chemistry, Emory University
Atlanta, GA 30322 (USA)
Telefax: Int. code + (404) 727-6586

[**] This work was supported by the National Science Foundation.

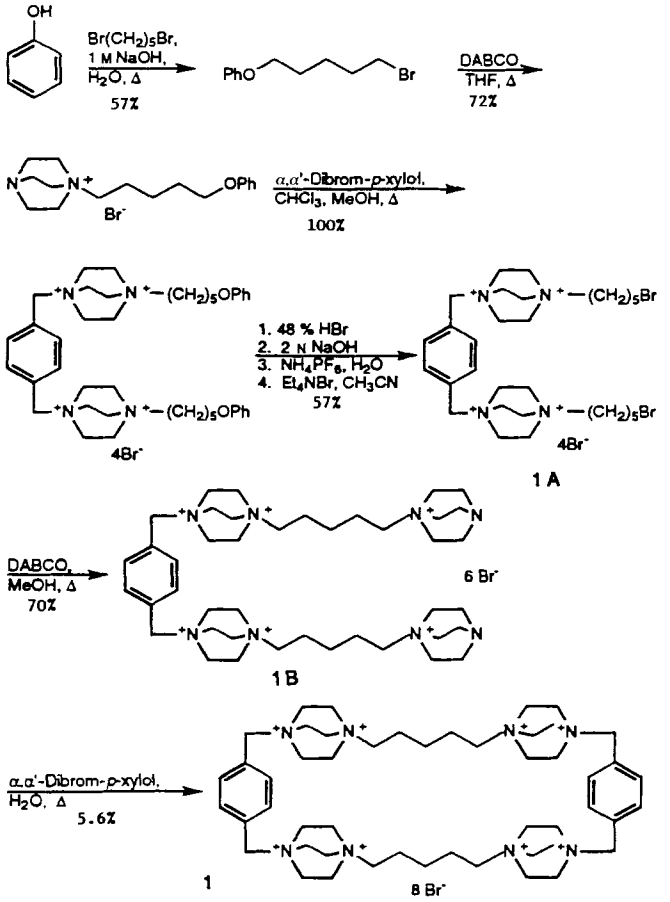

Scheme 1. Synthesis of octacationic cyclophanes **1** ($m = 5$). Host molecules with three and seven methylene units ($m = 3, 7$) were prepared in an identical manner.

details: a) Great care was taken to define conditions that minimized unwanted side-reactions (for example, substitution reactions at the benzylic sites). b) Intermediate **1A**, being unpurifiable by crystallization or chromatography, was precipitated from water by addition of NH_4PF_6. The resulting tetra-PF_6 salt was filtered, dried, and dissolved in CH_3CN. Addition of Et_4NBr then reformed the tetrabromide salt, which fell out of solution and was collected by filtration and used for the next step. c) Intermediate **1B** was used without further purification except for trituration with hot EtOH. d) The final step, cyclization of **1B** to **1**, was run with either the hexabromide salt in water or the hexa-PF_6 salt in CH_3CN. In the former case, slow dissolution of α,α'-dibromo-*p*-xylene in water over several days ensured high dilution. In the latter case, high dilution was effected with the aid of a syringe pump. Product was then converted back into the octabromide or octachloride salts on an ion-exchange column.

Several methods were attempted to purify **1**. Chromatography on silica columns or preparative plates, with MeOH/aqueous NH_4OH as an eluent, gave reasonably pure material but in poor yields. Ion-exchange chromatography could not separate cyclic product from linear impurities. Size-exclusion chromatography, dialysis, and reverse phase chromatography were not successful. In the end, we contented ourselves with simple crystallization carried out three times from water or aqueous ethanol. This gave **1** with satisfactory ^1H and ^{13}C NMR spectra, elemental analyses, MS (FAB-MS with low resolution) and, in one case, an X-ray structure. Attempts to prepare several analogs of **1** (namely, compounds with even m values or with biphenyl and diphenylmethane spacers) failed owing to purification difficulties.

Figure 1 shows the dimensions of our three cyclophanes **1** ($m = 3$, 5, and 7) as modeled with Sybyl (Tripos force-field including electrostatic interactions). The cavity size for the $m = 3$ compound corresponds closely to that later determined by X-ray structural analysis. The cavity is about 4 Å deep. Note that the DABCO rings partially shield the aromatic spacers from the cavity, thereby reducing the possibility of $\pi-\pi$ stacking with an aromatic guest molecule. Nonetheless, ion–dipole interactions between an aromatic guest molecule and the quaternary nitrogen atoms, of a type described previously,[6, 7] could conceivably contribute to the binding of aromatic anions.

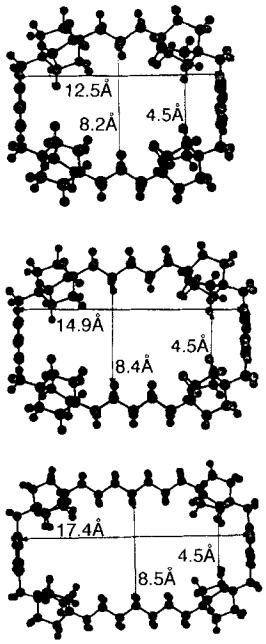

Fig. 1. Dimensions of the cyclophane cavities of **1** ($m = 3$, 5, 7, from top to bottom), determined by molecular mechanics simulations.

It was initially necessary to test for the possible aggregation of the cyclophanes in the absence of any guest.[8] Changes in the chemical shifts as large as $\delta = 0.04$ were observed when the concentration of **1** in pure water was increased from 1.3×10^{-5} to 2.4×10^{-3} M (GN-500 MHz spectrometer at 30 °C with CH_3CN as external reference). Since in 0.20 NaBr the NMR chemical shifts did not depend on concentration, these changes are probably caused by binding phenomena between the cyclophanes and their bromide counterions.[9] To obviate this complication, we operated exclusively at 5×10^{-5} M cyclophane in deionized water (a compromise between minimal counterion binding and a suitable signal-to-noise ratio).

Association constants for the cyclophanes and the guests in Scheme 2 were determined (somewhat unusually) by holding the host concentration constant while varying the concentration of excess guest. Accordingly, it was the chemical shift of the host that was monitored. The low concentration of host (5×10^{-5} M) required that the HDO peak be suppressed by a 1331 experiment or presaturation.[10] Host–guest complexation typically gave a $\Delta\delta = 0.1-0.2$ change in chemical shift as the guest reached mM levels. The shift vs. concentration data were converted into association constants with the aid of the Benesi–

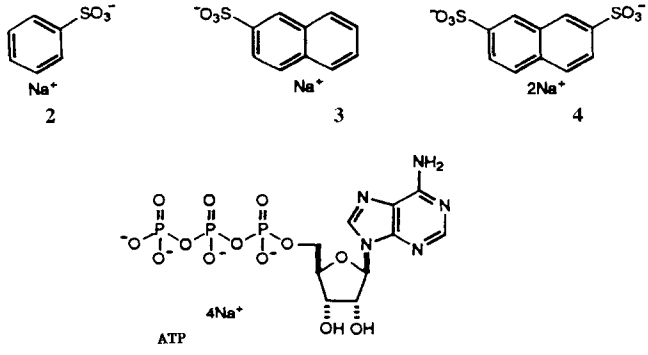

Scheme 2. Guest molecules that were used in binding studies with the octacationic host molecules.

Hildebrand equation.[11] Agreement among K_a values determined from different protons of a given host–guest system was satisfactory (±6%).

The following summarizes the key observations: a) Neutral aromatic guests (such as benzene, catechol, and 2,7-naphthalenediol) do not bind to the cyclophanes ($K_a < 100\ M^{-1}$). b) According to Job plots,[12] complexes between the cyclophanes and the anions in Scheme 2 all have 1:1 stoichiometries. c) $K_a = 61$, 447, and 3390 M^{-1} for complexation of **1** ($m = 3$) to **2**, **3**, and **4**, respectively. Coulombic forces clearly dominate the interactions. d) ATP (self-buffered at pH 8.0–8.5 where the compound exists as a tetraanion) binds to **1** ($m = 3,5,7$) with K_a values of 13300, 15900, and 12100 M^{-1}, respectively. Cavity size is, therefore, not critical. The numbers are much less than that measured for ATP and a macrocycle with six ammonium hydrogen-bonding sites,[13] but slightly larger than that reported for a tetraquaternary ammonium host.[14] K_a for ATP plus **1** ($m = 5$) diminishes to less than 100 M^{-1} in the presence of 0.2 N NaBr.

Detection of host–guest association does not, in and of itself, require that the guest resides *inside* the host's cavity. Since external binding was a possibility in our system, we examined the complexation of ATP with linear analogs of the cyclophanes. ATP will not associate with doubly N-alkylated DABCO salts, but will indeed bind efficiently ($K_a = 22200\ M^{-1}$) to the acyclic tetracation **5**. This is a strong indication that ATP never directly enters the cavity. Association between the ATP and cyclophanes appears to be a type of ion-exchange with the bromide counterions. Long-chain tetracationic DABCO derivatives have been shown by others to form 1:1 complexes with ATP in CH_2Cl_2.[15]

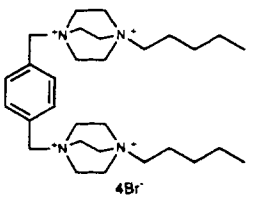

5

X-ray crystallographic studies are a particulary informative means of probing supramolecular complexes,[16, 17] the possible disparity between solution and solid-state structures notwithstanding. In the X-ray structure of **1** ($m = 3$), where chlorides were used as the counterions in order to minimize X-ray absorption, three water molecules were found to occupy the center of the cyclophane (Fig. 2). The cyclophane cavities line up to form parallel channels. Water molecules and chloride, sandwiched between the cyclophanes, may be responsible for this channel formation. The columns of cyclophanes lie side-by-side, and the distance between the neighboring aromatic rings is approximately 3.5–3.8 Å. The X-ray structure of the complex between **1** ($m = 3$) and **4** (Fig. 3) shows the formation of a 1:3 clathrate

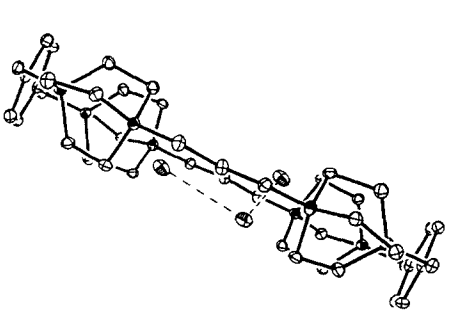

Fig. 2. The crystal structure of the octacationic host molecule **1** ($m = 3$) shows three water molecules within the cavity. The external counterions are not shown.

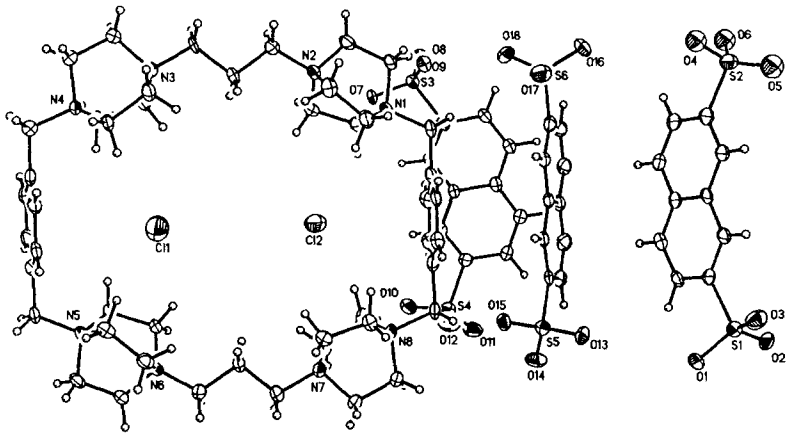

Fig. 3. The crystal structure of the complex of **1** ($m = 3$) and **4** shows three "guest" molecules outside the cavity. Two chloride counterions are present within the cavity.

between host and guest. No intracavity encapsulation of the guest was exhibited; only two chloride counterions reside within the cavity of the cyclophane. The three "guests" are considered to interact externally with the host through π–π stacking and/or electrostatic interactions. Thus, X-ray data further substantiate our NMR studies, which suggest that the guests do not enter the cavities. Association arises exclusively by an ion exchange between host and guest, a remarkably effective process considering the nonpolymeric nature of the host.[18]

Received: April 26, 1995 [Z 7931 IE]
German version: *Angew. Chem.* **1995**, *107*, 2330–2333

Keywords: ATP · cyclophanes · macrocycles · supramolecular chemistry

[1] Representative articles: D. R. Carcanague, C. B. Knobler, F. Diederich, *J. Am. Chem. Soc.* **1992**, *114*, 1515; T. H. Webb, H. Suh, C. S. Wilcox, *ibid.* **1991**, *113*, 8554; R. Shimazawa, Y. Hashimoto, S. Iwasaki, *Tetrahedron Lett.* **1992**, *33*, 7197; P. C. Kearney, L. S. Mizoue, R. A. Kumpf, J. E. Forman, A. McCurdy, D. A. Dougherty, *J. Am. Chem. Soc.* **1993**, *115*, 9907; E. Fan, S. A. Van Arman, S. Kincaid, A. D. Hamilton, *J. Am. Chem. Soc.* **1993**, *115*, 369; H-J. Schneider, K. Philippi, J. Pöhlmann, *Angew. Chem.* **1984**, *96*, 907; *Angew. Chem. Int. Ed. Engl.* **1984**, *23*, 908; Y. Murakami, J. Kikuchi, T. Hirayama, *Chem. Lett.* **1987**, 161.

[2] Representative articles: K. Worm, F. P. Schmidtchen, A. Schier, A. Schäfer, M. Hesse, *Angew. Chem.* **1994**, *106*, 360; *Angew. Chem. Int. Ed. Engl.* **1994**, *33*, 327; M. T. Reetz, C. M. Niemeyer, K. Harms, *ibid.* **1991**, *103*, 1515 and **1991**, *30*, 1472; J. L. Sessler, T. D. Mody, D. A. Ford, V. Lynch, *ibid.* **1992**, *104*, 461 and **1992**, *31*, 452; A. Bencini, A. Bianchi, M. I. Burguete, A. Domenech, E. Garcia-Espan < Ü = > a, S. V. Luis, M. A. Niño, J. A. Ramirez, *J. Chem. Soc. Perkin Trans. 2* **1991**, 1445; J-M. Lehn, R. Méric, J-P. Vigneron, I. Bkouche-Waksman, C. Pascard, *J. Chem. Soc. Chem. Commun.* **1991**, 62; M. W. Hosseini, A. J. Blacker, J-M. Lehn, *J. Am. Chem. Soc.* **1990**, *112*, 3896; H-J. Schneider, I. Theis, *Angew. Chem.* **1989**, *101*, 757; *Angew. Chem. Int. Ed. Engl.* **1989**, *28*, 753; M. P. Mertes, K. B. Mertes, *Acc. Chem. Res.* **1990**, *23*, 413; Y. Murakami, J. Kikuchi, T. Ohno, O. Hayashida, M. Kojima, *J. Am. Chem. Soc.* **1990**, *112*, 7672; F. Vögtle, H. Sieger, W. M. Müller, *Topics Curr. Chem.* **1981**, *98*, 107.

[3] For a "systems approach" to supramolecular chemistry, see F. M. Menger, *Angew. Chem.* **1991**, *103*, 1104; *Angew. Chem. Int. Ed. Engl.* **1991**, *30*, 1086.

[4] T. P. Abbiss, F. G. Mann, *J. Chem. Soc.* **1964**, 2248.

[5] J. C. Salamone, B. Snider, *J. Polym. Sci. Polym. Chem. Ed.* **1970**, *8*, 3495.

[6] M. A. Petti, T. J. Sheppodd, R. E. Barrans, Jr., D. A. Dougherty, *J. Am. Chem. Soc.* **1988**, *110*, 6825.

[7] H.-J. Schneider, T. Blatter, *Angew. Chem.* **1988**, *100*, 1211; *Angew. Chem. Int. Ed. Engl.* **1988**, *27*, 1163.

[8] F. Diederich, K. Dick, *J. Am. Chem. Soc.* **1984**, *106*, 8024.

[9] F. P. Schmidtchen, G. Müller, *J. Chem. Soc. Chem. Commun.* **1984**, 1115.

[10] A. E. Derome, *Modern NMR Techniques for Chemistry Research*, Pergamon, New York, **1987**, chap. 7.

[11] H. A. Benesi, J. H. Hildebrand, *J. Am. Chem. Soc.* **1949**, *71*, 2703.

[12] K. A. Conors, *Binding Constants, The Measurement of Complex Stability*, Wiley, Chichester, **1987**.

[13] B. Dietrich, M. W. Hosseini, J. M. Lehn, R. B. Sessions, *J. Am. Chem. Soc.* **1981**, *103*, 1282.
[14] H. J. Schneider, T. Blatter, B. Palm, U. Pfingstag, W. Rüdiger, I. Theis, *J. Am. Chem. Soc.* **1992**, *114*, 7704.
[15] T. Li, S. J. Krasne, B. Persson, H. R. Kaback, F. Diederich, *J. Org. Chem.* **1993**, *58*, 380.
[16] J.-M. Lehn, R. Méric, J.-P. Vigneron, I. Bkouche-Waksman, C. Pascard, *J. Chem. Soc. Chem. Commun.* **1991**, 62.
[17] A. D. Hamilton, N. Pant, A. Muehldorf, *Pure Appl. Chem.* **1988**, *60*, 533.
[18] Single-crystal structural data for $C_{46}H_{76}N_8 \cdot (H_2O)_{20} \cdot Cl_8$: monoclinic space group $P2_1/n$, $a = 6.922(2)$, $b = 30.655(2)$, $c = 15.962(2)$ Å, $\beta = 92.83(2)°$, $V = 3383.0(3)$ Å^3, $Z = 2$. Of 6044 measured reflections 4459 were symmetry-independent, of which 3862 ($I > 6\sigma(I)$) were used in the refinement. $R = 0.053$. Determination of the lattice parameters and measurement of the intensities were carried out with a Siemens P4RA diffractometer ($Cu_{K\alpha}$ radiations $\mu = 3.641$ cm^{-1}, $2\theta_{max} = 113°$). Empirical absorption correction and structure determination were carried out with SHELXS-86 and structure refinement with SHELXTL IRIS. Single-crystal structural data for $(C_{46}H_{76}N_8 \cdot Cl_2)(C_{10}H_6O_6S_2)_3(CH_3OH)_3(H_2O)_{13}$: triclinic space group $P\bar{1}$, $a = 15.995(3)$, $b = 17.263(3)$, $c = 17.405(3)$ Å, $\alpha = 94.55(3)$, $\beta = 99.67(3)$, $\gamma = 107.50(3)°$, $V = 4475.0(14)$ Å^3, $Z = 2$. Of 13502 measured reflections 11960 were symmetry-independent, of which 11960 ($I > 2\sigma(I)$) were used in the refinement, $R = 0.1045$. Determination of the lattice parameters and measurement of the intensities were carried out with a Siemens P4RA diffractometer ($Cu_{K\alpha}$ radiation, $\mu = 2.505$ cm^{-1}, $2\theta_{max} = 113.5°$). Empirical absorption correction and structure determination were carried out with SHELXS-86 and structure refinement with SHELXTL-93 IRIS. Further details of the crystal structure determinations are available on request from the Director of the Cambridge Crystallographic Data Centre, 12 Union Road, GB-Cambridge, CB2 1EZ (UK), on quoting the full journal citation.

Temperature and Solvent Effect on the Nucleophilic Addition of *n*-Butyllithium to the *N*-(Trimethylsilyl)imine of (2*S*)-Lactal**

Gianfranco Cainelli,* Daria Giacomini, and Martin Walzl

Studies of the diastereoselective conversion of a trigonal carbon center into a tetrahedral one under the stereochemical influence of a nearby chiral center have provided valuable mechanistic and synthetic information for organic chemists. Among such studies, investigations of 1,2-asymmetric induction in additions of organometallic reagents to carbonyl compounds have been most intensive and fruitful.[1] The stereochemical outcome of these reactions is a critical issue, and models have been proposed to help to rationalize and predict the observed diastereoselectivity. Through experimental and theoretical analysis, Cram's original rules[2] have been reformulated and are now referred to as the Felkin–Anh model[3] and Cram's chelation model.[4] In the former, the argument is based mainly on steric and/or stereoelectronic considerations, in the latter, primarily on the substrate's bidentate ligation to the metal countercation. But all the models proposed suffer from the lack of any consideration of temperature and solvent effects.

Recently, we have demonstrated that the diastereoselectivity of the addition of organomagnesium compounds to O-protected (2*S*)-lactal at −78 °C, is highly dependent on the nature of the ethereal solvent.[5] Particularly in the case of the *O*-triisopropylsilyl derivative and MeMgBr, the diastereomeric excess could be completely reversed on going from THF (*syn*:*anti* = 36:64) to *tert*-butyl methyl ether (*syn*:*anti* = 84:16).

Stimulated by our interest in understanding and controlling the π-facial selectivity of α-hydroxymetalloimines,[6] we report here on the influence of temperature and solvent on the diastereoselectivity of *n*BuLi addition to *N*-(trimethylsilyl)imine **1** of (2*S*)-*O*-(*tert*-butyldimethylsilyl)lactal[7] (Scheme 1).

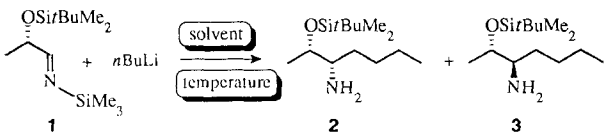

1 **2** **3**

Scheme 1. Solvents: THF, *n*-hexane, *t*BuOMe.

The addition reaction was performed by introducing a stoichiometric amount of *n*BuLi (1.6 M in *n*-hexane) to pure **1** in different solvents (tetrahydrofuran, *tert*-butyl methyl ether, *n*-hexane). The temperature was varied over a range of about 130 °C.

The diastereomeric excess of the products **2** and **3** was determined on the crude reaction mixture by ^{1}H NMR analysis.[8] Results are reported in Table 1.

Table 1. Influence of temperature and solvent on the diastereoselectivity of the nucleophilic addition of *n*-butyllithium to the *N*-(trimethylsilyl)imine of (2*S*)-*O*-(*tert*-butyldimethylsilyl)lactal. The *de* values were determined from ^{1}H NMR spectra.

Solvent	*T* [°C]	*t* [h]	*syn*/*anti*	*de* [%]	Yield [%]
THF	−90	2	98:2	96	61
THF	−78	2	94:6	88	41
THF	−70	2	93:7	86	64
THF	−65	2	92:8	84	57
THF	−60	2	84:16	68	53
THF	−55	2	84:16	68	78
THF	−50	2	78:22	56	57
THF	−40	2	73:27	46	76
THF	−35	2	72:28	44	57
THF	−30	2	66:34	32	65
THF	−20	2	67:33	34	65
THF	−10	1.5	65:35	30	61
THF	0	1.5	65:35	30	86
THF	16	1	65:35	30	49
THF	25	0.5	65:35	30	50
THF	31	0.5	65:35	30	45
*t*BuOMe	−90	2	73:27	46	79
*t*BuOMe	−70	2	73:27	46	78
*t*BuOMe	−50	2	73:27	46	89
*t*BuOMe	−20	2	67:33	34	80
*t*BuOMe	0	2	68:32	36	81
*t*BuOMe	30	0.5	64:36	28	80
n-hexane	−90	2	28:72	−44	70
n-hexane	−70	2	45:55	−10	65
n-hexane	50	2	44:56	−12	68
n-hexane	−30	2	68:32	36	74
n-hexane	0	2	75:25	50	70
n-hexane	32	0.5	78:22	56	75
n-hexane	54	0.1	78:22	56	72

Analysis of the data show that at low temperature the *syn*/*anti* ratio is dramatically dependent on the nature of the solvent, ranging from 98:2 in THF to 28:72 in *n*-hexane. In contrast, at higher temperature the three solvents show a similar behavior giving rise to a *syn*/*anti* ratio ranging only from 65:35 (THF) to 78:22 (*n*-hexane). The highest diastereoselectivity differences

[*] Prof. Dr. G. Cainelli, Dr. D. Giacomini
Dipartimento di Chimica "G. Ciamician"
Via Selmi, 2, I-40126 Bologna (Italy)
Telefax: Int. code + (51)25-9456
e-mail: cainelli@ciam01.ciam.unibo.it
Dr. M. Walzl
Du Pont de Nemours Italiana
Via Siemens, 12, I-39100 Bolzano (Italy)

[**] This work was supported by MURST (Fondi 40% and 60%) and the CNR.

with temperature were observed with THF and *n*-hexane, while in *tert*-butyl methyl ether as solvent, temperature shows little influence on the *syn*/*anti* ratio.

The temperature dependence of the *de* values was analyzed according to the modified Eyring[9] equation: $\ln P = -(\Delta\Delta H^{\ddagger}/RT) + (\Delta\Delta S^{\ddagger}/R)$, where $P = k(syn\text{-aminol})/k'(anti\text{-aminol}) = I(syn\text{-aminol})/I'(anti\text{ aminol})$, k and k' are the overall rate constants, and I and I' are the intensity of signals in the ^{1}H NMR spectra of **2** and **3**. The results are summarized in Figure 1.

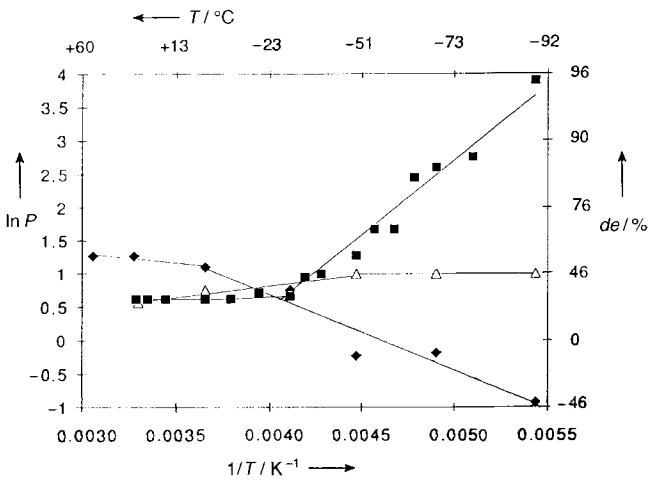

Fig. 1. Eyring plots for the diastereomeric excess obtained in the nucleophilic addition of *n*-butyllithium to **1** at various temperatures in THF (■), *t*BuOMe (△), *n*-hexane (◆)

In the Eyring plot each imine/solvent combination shows two linear regions with a characteristic inversion temperature, the inversion point T_{inv}. Inversion points have been observed in stereoselective processes,[10] but this is the first case for nucleophilic addition. According to Scharf et al.,[11] this indicates the presence of at least two selection steps in the reaction mechanism. Consequently two sets of activation parameters ($\Delta\Delta H_1^{\ddagger}$, $\Delta\Delta S_1^{\ddagger}$ for $T > T_{inv}$ and $\Delta\Delta H_2^{\ddagger}$, $\Delta\Delta S_2^{\ddagger}$ for $T < T_{inv}$) are obtained.

Considerable attention has been paid to the significance of the difference $\delta\Delta\Delta H^{\ddagger} = \Delta\Delta H_1^{\ddagger} - \Delta\Delta H_2^{\ddagger}$ values.[12] A plot of $\delta\Delta\Delta H^{\ddagger}$ against the corresponding entropy term $\delta\Delta\Delta S^{\ddagger}$ is linear. From the slope of this plot (Fig. 2) we can determine the isoinversion temperature $T_i = +252$ K (-21 °C). As stated by

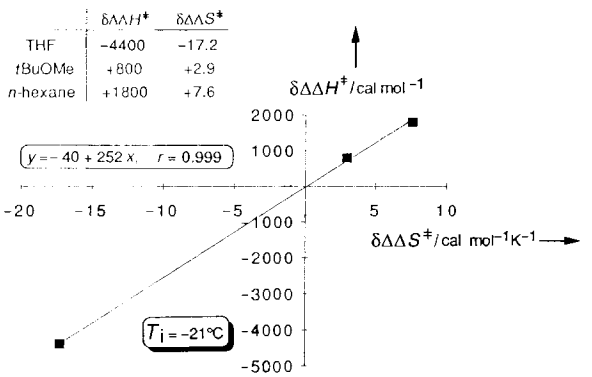

Fig. 2. $\delta\Delta\Delta H^{\ddagger}$ $\delta\Delta\Delta S^{\ddagger}$ plot for the determination of the isoinversion temperature T_i.

Scharf et al., systems show high stereoselectivity when T_{inv} is close to T_i. Indeed, the diastereoselectivity of our addition reaction with silylimine **1** is high in THF, for which T_{inv} is close to T_i, whereas in *n*-hexane and *t*BuOMe, with T_{inv} relatively far from T_i, low values of *de* are observed. Remarkably, in our case for a temperature corresponding to T_i, we observe a minimum in the diastereoselectivity.[13] Our results are consistent with a stepwise process with at least two diastereoselective steps that are affected differently by temperature and solvent. At this stage it is not easy to formulate a detailed mechanism, although it is apparent that the solvent should have a dramatic influence on the structure of the intermediates.[14] In view of the high charge density of the lithium cation, it is very reasonable, at least at low temperature, that the stereochemistry of this addition reaction should be controlled by lithium chelation. So lactic imine **1**, bearing two potentially chelating ancillary ligands,[15] could form chelates with *n*-butyllithium. In the high temperature region where the solvent appears to have little influence and entropy control is operative, the reaction mechanism could favor open intermediates with a higher degree of freedom. Nevertheless, in the absence of experimental evidence for the structures of the intermediates, our results emphasize the limits of current models for the interpretation of the 1,2-asymmetric induction observed in this kind of reactions. As a matter of fact, none of the classical models consider either temperature or solvent effects at all.

Experimental Procedure

In a typical experiment, **1** (0.259 g, 1.00 mmol) was dissolved in anhydrous solvent (5 mL, THF or *t*BuOMe or *n*-hexane) under inert atmosphere, and the solution cooled to the desired temperature; then *n*-butyl lithium (1.20 mmol, 0.75 mL of a 1.6 M solution in *n*-hexane) was added. After the stipulated reaction time (Table 1), the reaction was quenched at 0 °C with a saturated aqueous solution of NH_4Cl, extracted with CH_2Cl_2 (3×50 mL), and dried with $MgSO_4$. From the ^{1}H NMR analysis of the crude product the *syn*/*anti* ratio and the *de* value were obtained. Chromatography of the residue on a silica gel column afforded the mixture of the two aminols **2** and **3** so that the chemical yield could be calculated.

Received: May 17, 1995 [Z 8000 IE]
German version: *Angew. Chem.* **1995**, *107*, 2336–2338

Keywords: hydroxyaldehydes · imines · nucleophilic additions

[1] J. M. Coxon, K. N. Houk, R. T. Luibrand, *J. Org. Chem.* **1995**, *60*, 418 and references cees therein.
[2] D. J. Cram, F. A. A. Elhafez, *J. Am. Chem. Soc.* **1952**, *74*, 5828.
[3] a) M. Cherest, H. Felkin, N. Prudent, *Tetrahedron Lett.* **1968**, 2199; b) N. T. Anh, O. Eisenstein, *Nouv. J. Chim.* **1977**, *1*, 61; c) N. T. Anh, *Top. Curr. Chem.* **1980**, *88*, 145.
[4] a) D. J. Cram, K. R. Kopecky, *J. Am. Chem. Soc.* **1959**, *81*, 2748; b) M. T. Reetz, *Angew. Chem.* **1984**, *96*, 542; *Angew. Chem. Int. Ed. Engl.* **1984**, *23*, 556; c) E. L. Eliel, S. V. Frye, E. R. Hortelano, X. Chen, X. Bai, *Pure Appl. Chem.* **1991**, *63*, 1591; d) M. T. Reetz, B. Raguse, T. Seitz, *Tetrahedron* **1993**, *49*, 8561; e) S. Mori, M. Nakamura, E. Nakamura, N. Koga, K. Morokuma, *J. Am. Chem. Soc.* **1995**, *117*, 5055.
[5] G. Cainelli, D. Giacomini, F. Perciaccante, A. Trerè, *Tetrahedron: Asymmetry*, **1994**, *5*, 1913.
[6] a) G. Cainelli, M. Panunzio, D. Giacomini, G. Martelli, G. Spunta, *J. Am. Chem. Soc.* **1988**, *110*, 6879; b) G. Cainelli, D. Giacomini, E. Mezzina, M. Panunzio, P. Zarantonello *Tetrahedron Lett.* **1991**, *32*, 2967; c) G. Cainelli, D. Giacomini, M. Panunzio, P. Zarantonello, *Tetrahedron Lett.* **1992**, *33*, 7783.
[7] The imine **1** was prepared according Ref. [6a], but to separate **1** from Me_3SiOLi, the imine was distilled at +44 °C ($2.4 \cdot 10^{-4}$ mm Hg) to give a clear oil.
[8] The diastereoselectivity of the aminol formation is characterized by the *de* value of the *syn* adduct, which was determined by integration of the $CHNH_2$ signals in the ^{1}H NMR spectrum of the crude product.
[9] a) H. Eyring, *J. Phys. Chem.* **1935**, *3*, 107; b) S. Glasstone, K. J. Laidler, H. Eyring, *The Theory of Rate Processes* McGraw-Hill, New York, **1941**, Chap. 4.

 © VCH Verlagsgesellschaft mbH, D-69451 Weinheim, 1995 0570-0833/95/3419-2151 $ 10.00+.25/0

[10] a) H. Buschmann, H.-D. Scharf, N. Hoffmann, M. W. Plath, J. Runsink, *J. Am. Chem. Soc.* **1989**, 111, 5367; b) T. Göbel, K. B. Sharpless, *Angew. Chem.* **1993**, *105*, 1417; *Angew. Chem. Int. Ed. Engl.* **1993**, *32*, 1329; c) I. Toth, I. Guo, B. E. Hanson, *Organometallics* **1993**, *12*, 848; d) J. Brunne, N. Hoffmann, H.-D. Scharf, *Tetrahedron* **1994**, *50*, 6819; e) J. Muzart, F. Hénin, J.-P. Pète, A. M'Boungou-M'Passi, *Tetrahedron: Asymmetry* **1993**, *4*, 2531; f) M. Palucki, P. J. Pospisil, W. Zhang, N. Jacobsen, *J. Am. Chem. Soc.* **1994**, *116*, 9333.
[11] Review: H. Buschmann, H.-D. Scharf, N. Hoffmann, P. Esser, *Angew. Chem.* **1991**, *103*, 480; *Angew. Chem. Int. Ed. Engl.* **1991**, *30*, 477.
[12] For a recent contribution see, for instance, K. J. Hale, J. H. Ridd, *J. Chem. Soc. Chem. Comm.* **1995**, 357.
[13] The observed minimum value of *de* near the T_i appears to be rare. As reported in Ref. [11], most of the reactions examined show a maximum.
[14] The solvent effect observed could be attributed to a different aggregation state of the reactants and intermediates involved, and to the difference in the capacity of the solvent to coordinate the activated complexes of the process.
[15] N-Li-O chelation: E. M. Arnett, M. A. Nichols, A. T. McPhail, *J. Am. Chem. Soc.* **1990**, 112, 7059.

Influence of Lewis Base Complexation and the Degree of Aggregation of Alkyllithium Compounds on the Ratio in Which They Form Addition Products and Enolates with Ketones

Hendrikus Luitjes, Marius Schakel, Robert F. Schmitz, and Gerhard W. Klumpp*

Although the importance of the σ-organolithium compounds (σ-RLi) in synthetic chemistry can hardly be overstated, empirical observations and the rules of thumb still play an important role in their application. For instance, for one of their most important reactions, the reaction with aldehydes and ketones, it has been stated that[1] "Enolization is favoured by steric hindrance in either the carbonyl compound or the organometallic reagent[2]... Addition is favoured ... by non-polar solvents". Detailed reaction mechanisms, the real guidelines when reactions are planned, can only be obtained with difficulty due to the dynamic nature of σ-RLi: In the presence of frequently used Lewis bases [LB (ethers, tertiary amines)], these reagents are found as a mixture of several complexes $R_mLi_m \cdot n\,LB$ (*m,n*: 4, 1–4; 2, 4; 1, 3).[3] As the establishment of the equilibria between these complexes is often faster than the reaction under investigation, the individual contributions of the various particles towards the reaction rate and the chemo-, regio-, and stereoselectivity cannot be determined; proportions of the various complexes in the mixture are constant throughout the experiment.[4]

In our studies of the organolithium compounds **1**–**3**,[6] **4**, and *tert*-butyllithium, we have now obtained data for the first time regarding the influence of the LB-dependent aggregation of σ-RLi on the ratios in which they form addition products and enolates with ketones.

The NMR spectra of **1** (Li/N = 1/1) and **2** (Li/N = 1/2) show that they are tetrameric $\mathbf{1}_4$ and dimeric $\mathbf{2}_2$, respectively, under

1-4: $LiCH_2Si(Me)_2CH_2N(CH_2X)CH_2Y$

1: X = Y = H **2**: X = CH_2NMe_2, Y = H **3**: X = Y = CH_2NMe_2

4: X = $CH_2N(Me)CH_2CH_2NMe_2$, Y = H

[*] Prof. Dr. G. W. Klumpp, Dr. Ing. H. Luitjes, Dr. M. Schakel, R. F. Schmitz
Scheikundig Laboratorium Vrije Universiteit
De Boelelaan 1083, NL-1081 HV Amsterdam (The Netherlands)
Telefax: Int. code + (20) 444 7488

the reaction conditions (−70 °C, pentane), and at the very most take part only slowly (on the NMR time scale) in exchange processes with undetectable amounts of other species.[6] In contrast, **3**[6] and very probably **4** (Li/N = 1/3) as well are present as equilibrium mixtures of rapidly exchanging monomers **3a** and **3b** (**4a** and **4b**) and dimers $\mathbf{3}_2$ ($\mathbf{4}_2$) at −70 °C.[7]

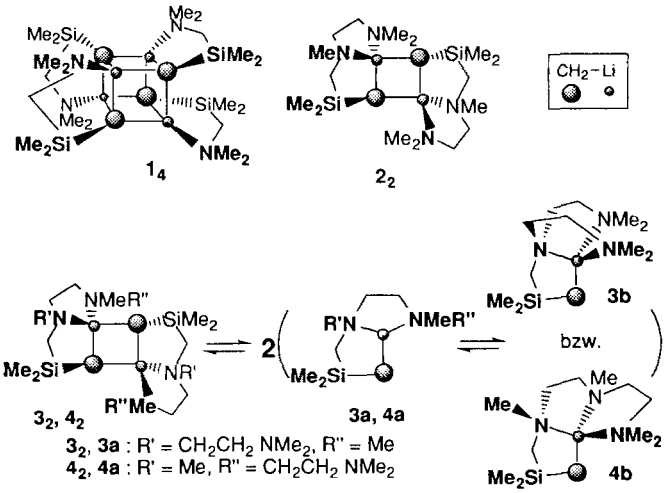

Since the structural differences between **1**, **2**, **3**, and **4** are located far from the anionic carbon atom, on the nitrogen end of the common building block $^-CH_2Si(Me)_2CH_2N(CH_2-)_2$, we assume that differences in the reactivity can be attributed (almost) exclusively to differences in the degree of aggregation.

When one molar equivalent of ketone $R^1R^2C{=}O$ was added to each of the slightly yellow solutions of **1**–**4** in pentane at −70 °C, instantaneous decolorization occurred. After 30 min an excess of chlorotrimethylsilane was added; the mixture was allowed to reach room temperature and then worked up in the usual way. The ratio of the enolate to the addition product (E/A) was determined by gas chromatographic measurement of **5**:{**6** (R = H) + **6** (R = $SiMe_3$)}. The quantitative results of the reactions are shown in Table 1.

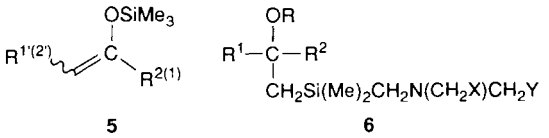

Table 1. The ratio of enolate to addition product (E/A) in the reactions of **1**, **2**, **3**, and **4** with ketones $R^1R^2C{=}O$ in pentane at −70 °C.

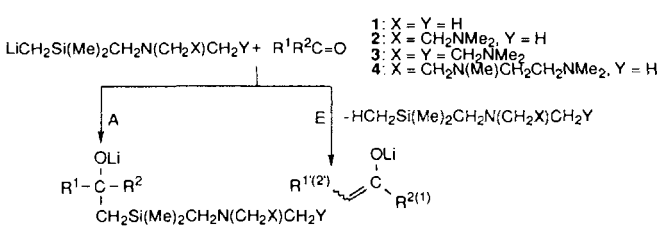

$R^1R^2C{=}O$	**1**	**1** [a]	**2**	**3**	**4**
pinacolone	5:95	68:32	44:56	45:55	96:4
cyclohexanone	29:71 [18]	56:44	40:60	69:31	94:6
3-hexanone [b]	5:95	50:50	35:65	48:52	86:14
2-hexanone [b]	5:95	46:54	5:95 [18]	46:54	62:38 [18]

[a] In THF/pentane (3:1). [b] Several enolates were formed with all lithium compounds. The structures were not determined.

In keeping with our suppositions, we interpret the different E/A profiles of **1**, **2**, and **4** in pentane as indications of the reacting tetramer $\mathbf{1}_4$, dimer $\mathbf{2}_2$,[8] and monomer **4**. The E/A profiles of **1** in THF/pentane (3:1) and **3** are similar to that of $\mathbf{2}_2$ ($1:2 < E/A < 2:1$) and thus indicate the reaction of dimers $\mathbf{3}_2$ and $\mathbf{1}_2 \cdot n$THF, as confirmed (for THF) by cryoscopic and NMR methods.[9] It is not known why, in contrast to **4**, which reacts as a monomer, dimeric $\mathbf{3}_2$ is the most reactive component in the $\mathbf{3}_2 \rightleftarrows 2(\mathbf{3a} \rightleftarrows \mathbf{3b})$ system. In the reaction with triphenylmethane, however, we found that monomeric **3** is only slightly more reactive than $\mathbf{2}_2$.[10] From this we deduce that slight differences, possibly of steric origin, can be decisive in determining which particle forms the most favorable transition state in dynamic dimer/monomer/LB equilibria. We also found similar E/A ratios for reactions of *tert*-butyllithium with cyclohexanone (−70 °C): *t*BuLi·TMTAN (TMTAN = 1,4,7-trimethyl-1,4,7-triazacyclononane), THF:[10] 88:12 (reaction of the monomer); *t*BuLi, THF: 46:54 (reaction of the dimer);[11] *t*BuLi, hexane: 0:100 (reaction of the tetramer).[3b, 12] The similarity of the E/A profiles of $\mathbf{1}_2 \cdot n$THF and $\mathbf{2}_2$ (pentane), and the cyclohexanone E/A values of *t*BuLi·TMTAN and $t\mathrm{Bu}_2\mathrm{Li}_2 \cdot n$THF and of **4** and $\mathbf{2}_2$, respectively, would seem to indicate that the E/A values of σ-RLi are aggregate-specific (tetramer: ca. 1:20, dimer: 1:2 – 2:1, monomer: > 6:1) and are only influenced by the Lewis base and R to a relatively small extent.[15, 17, 18] It is clear that high E/A values are not linked to the steric effects of the R group as one might have supposed from the rules of thumb mentioned at the beginning—it is rather improbable that the steric effects in the transition states of the additions of the monomer **4** and *t*BuLi·TMTAN are stronger than in those of the additions of $\mathbf{1}_4$ and $t\mathrm{Bu}_4\mathrm{Li}_4$—but rather mainly to the type of the aggregates, as might be surmised from the statement of the rule of thumb concerning the solvent (see ref. [3]).[18] Considerations of possible causes point to the character of the carbon–lithium bonds in the monomers and in the σ-RLi aggregates.[19] Theoretical investigations must answer the following questions: 1) Which bonding properties form the basis of the shift of the preferred reaction pathway from deprotonation in the case of monomers with C–Li two-center bonds to addition to the C=O bond in the case of aggregates with C–Li multiple-center bonds? 2) Of what type are the corresponding transition states?[20, 21]

Received: March 31, 1995
Revised version: July 6, 1995 [Z 7853 IE]
German version: *Angew. Chem.* **1995**, *107*, 2324 – 2325

Keywords: lithium compounds · reaction mechanisms

[1] B. J. Wakefield in *Comprehensive Organometallic Chemistry*, *Vol. 7* (Eds.: G. Wilkinson, F. G. A. Stone, E. W. Abel), Pergamon, Oxford, **1982**, pp. 24–25.

[2] Mesityllithium: A. K. Beck, M. S. Hoekstra, D. Seebach, *Tetrahedron Lett.* **1977**, 1187; 2,4,6-Tris(*tert*-butyl)phenyllithium: M. Yoshifuji, T. Nakamura, N. Inamoto, *ibid.* **1987**, *28*, 6325; 2,4,6-Tris[bis(trimethylsilyl)methyl]phenyllithium: R. Okazaki, M. Umo, N. Imamoto, *Chem. Lett.* **1989**, 791.

[3] a) K. C. Williams, T. L. Brown, *J. Am. Chem. Soc.* **1966**, *88*, 4134; b) H. L. Lewis, T. L. Brown, *ibid.* **1970**, *92*, 4664; c) J. Heinzer, J. F. M. Oth, D. Seebach, *Helv. Chim. Acta* **1985**, *68*, 1848; d) T. F. Bates, M. T. Clarke, R. D. Thomas, *J. Am. Chem. Soc.* **1988**, *110*, 5109; e) G. Fraenkel, A. Chow, W. R. Winchester, *ibid.* **1990**, *112*, 6190, and references 1–12 therein.

[4] Only in a few cases was it possible to determine the relative reactivities of several coexisting aggregates or their model compounds [5]: a) P. West, R. Waak, P. I. Purmont, *J. Am. Chem. Soc.* **1970**, *92*, 840; b) T. Holm, *Acta Chem. Scand. B* **1978**, *32*, 162; c) J. F. McGarrity, C. A. Ogle, Z. Brich, H.-R. Loosli, *J. Am. Chem. Soc.* **1985**, *107*, 1810; d) H. J. Reich, D. P. Green, N. H. Phillips, *ibid.* **1991**, *113*, 1414; see also ref. [3d].

[5] a) W. H. Glaze, C. H. Freeman, *J. Am. Chem. Soc.* **1969**, *91*, 7198; b) M. Vos, F. J. J. de Kanter, M. Schakel, N. J. R. van Eikema Hommes, G. W. Klumpp, *ibid.* **1987**, *109*, 2187; c) B. O. T. Kammermeier, G. W. Klumpp, K. Kolthof, M. Vos, *Tetrahedron Lett.* **1991**, *32*, 3111.

[6] H. Luitjes, F. J. J. de Kanter, M. Schakel, R. F. Schmitz, G. W. Klumpp, *J. Am. Chem. Soc.* **1995**, *117*, 4179.

[7] The complicated low-temperature ^{13}C NMR spectra of **4** (containing ^{6}Li) in pentane show no splitting of the C_α signal (presumably due to the rapidity of the intermolecular exchange processes), but cryoscopic investigations in benzene showed the degree of aggregation to be 1.

[8] The following indicate that $\mathbf{2}_2$ is the only reactive species. 1) The order of reaction (0.83) of $\mathbf{2}_2$ with triphenylmethane (benzene, 23 °C) [6] rules out a reaction via rapidly regenerated, nondetectable, potentially more reactive **2** and $\mathbf{2}_4$. It therefore seems improbable that these particles play a role in the significantly faster reaction with ketones at −70 °C. 2) Based on the splitting of the NMR signal of the protons in the diastereotopic dimethylsilyl groups in $\mathbf{2}_2$ [$\Delta\nu$(22 °C) = 16 Hz] [6] and on known activation parameters [$\Delta H^{\neq}$, $\Delta S^{\neq}$ {$\mathbf{3}_2 \rightarrow 2(\mathbf{3a} \rightleftarrows \mathbf{3b})$}: 39 kJ mol^{-1}, 50 J K^{-1} mol^{-1}; H. Luitjes, unpublished), it is estimated that the average lifetime of $\mathbf{2}_2$ in the $\mathbf{2}_2 \rightleftarrows 2\,\mathbf{2}$ system at −70 °C is more than 40 s. 3) The mass spectrum of $\mathbf{2}_2$ shows no indication of dissociation into the monomer.

[9] Two dimers of unknown structure are apparent. $\mathbf{1}_2$, ^{13}C NMR (62.88 MHz, THF:[D$_8$]THF 10:1, −119 °C, TMS): δ = −11.51 (septet, $^1J(^7\mathrm{Li}, ^{13}\mathrm{C})$ = 14.6 Hz, CH_2Li), 3.41 + 3.56 (ca. 2:1, $SiCH_3$), ca. 5.49 + 5.59 (overlapping, ca. 1:2, $SiCH_3$), 47.88 + 48.64 (ca. 2:1, NCH_3), 52.23 (NCH_3), 56.20 + 56.53 (ca. 2:1, NCH_2).

[10] *t*Bu^{n}Li·TMTAN, ^{13}C NMR (62.88 MHz, [D$_8$]THF, −108 °C, TMS): δ = 17.49 (t, $^1J(^6\mathrm{Li}, ^{13}\mathrm{C})$ = 14.3 Hz, CLi), 39.85 (CH_3), 45.45 (NCH_3), 50.60 (NCH_2), 56.40 (NCH_2).

[11] For the occurrence of ether adducts of $t\mathrm{Bu}_2\mathrm{Li}_2$, see: T. Kottke, D. Stalke, *Angew. Chem.* **1993**, *105*, 619; *Angew. Chem. Int. Ed. Engl.* **1993**, *32*, 580, and [3d, 16].

[12] For similar data for cyclohexanone and other ketones, see: J. D. Buhler, *J. Org. Chem.* **1973**, *38*, 904; for 4-*tert*-butylcyclohexanone: E. Juaristi, J. S. Cruz-Sánchez, F. R. Ramos-Morales, *ibid.* **1984**, *49*, 4912. Additional E/A values that correspond to those of $\mathbf{1}_4$: EtLi/LiBr, Et_2O, 20 °C, 2-octanone: 1.6:98.4 [13]; PhLi/LiBr, Et_2O, 20 °C, acetophenone: 4:96 [14].

[13] T. Holm, *Acta Chem. Scand.* **1994**, *48*, 362.

[14] W. I. O'Sullivan, F. W. Swamer, W. J. Humphlett, C. R. Hauser, *J. Org. Chem.* **1961**, *26*, 2306.

[15] The exclusive formation of enolates by "crown ether complexation" of alkyllithium compounds (J. L. Pierre, H. Handel, R. Perraud, *Tetrahedron Lett.* **1977**, 2013) may, in reality, be the reaction of lithium alkoxide, which is formed by the decomposition of the crown ether [16].

[16] W. Bauer, W. R. Winchester, P. von R. Schleyer, *Organometallics* **1987**, *6*, 2371.

[17] The experiments described here were conducted with normal working methods from preparative chemistry. Our dimer and tetramer E/A values are thus the results of the reactions of families of complexes $R_m{}_nR'O_nLi_m{}_{-n}$·*n* LB (m = 2, 4; $n \leq m$), which are gradually formed during an experiment by incorporation of the reaction products into the reacting aggregates. Detailed mechanistic conclusions require the determination of *initial* reaction rates of both the transformations (E, A) (relating solely to the $R_mLi_m \cdot n$ LB reagent used), and the corresponding *initial molecularities*. The role of precomplexes of ketone and reagent will also become apparent from the latter (D. R. Hay, S. G. Song, S. G. Smith, P. Beak, *J. Am. Chem. Soc.* **1988**, *110*, 8145 and references therein).

[18] The extreme positions of cyclohexanone and 2-hexanone on certain E/A profiles (e.g. $\mathbf{1}_4$ or $\mathbf{2}_2$ and **4**, see also ref. [21]) cannot be interpreted at this time.

[19] G. Graham, S. Richtsmeier, D. A. Dixon, *J. Am. Chem. Soc.* **1980**, *102*, 5759; E. Kaufmann, K. Raghavachari, A. E. Reed, P. von R. Schleyer, *Organometallics* **1988**, *7*, 1597.

[20] In addition to the polar addition of RLi to ketones (E. Kaufmann, P. von R. Schleyer, K. N. Houk, Y.-D. Wu, *J. Am. Chem. Soc.* **1985**, *107*, 5560), the possibility of addition by means of single electron transfer is discussed [13].

[21] Postscript (July 6, 1995): In the meantime, we have found that **2** and **4** are monomeric in THF at −100 °C and show monomer E/A profiles in THF/pentane (3:1) at −70 °C: pinacolone, cyclohexanone, 3-hexanone, 2-hexanone (see Table 1): for **2**, respectively, 95:5, 65:35 [18], 77:23, 84:16; for **4**, respectively, 95:5, 25:75 [18], 95:5, 95:5. These results confirm our suppositions. Slight variations in the E/A profiles are the result of the replacement of Li–N with Li–THF.

A Concise Synthetic Route to Cyclopentenes by [3+2] Cycloaddition of Dipolar Trimethylenemethane to Alkynes**

Shigeru Yamago, Satoshi Ejiri, and Eiichi Nakamura*

Alkynes are known to be relatively unreactive dienophiles in Diels–Alder reactions.[1] Their performance as 2π-electron reactants is even poorer in isoelectronic cycloadditions with 4π-trimethylenemethane species (TMM, cf. **2**), giving the expected [3+2] cycloaddition products only under special conditions (i.e. with a large excess of a highly reactive alkyne).[2] The [3+2] cycloadditions of metal-complexed TMM[3] and related species[4] have also proven to be of rather restricted scope. This current situation is particularly unfortunate since this type of cycloaddition reaction would allow us to achieve an efficient single-step synthesis of substituted cyclopentenes, for which only a few reactions of some synthetic significance exist.[5] We report herein the first effective trapping of a TMM species with an alkyne, as demonstrated for the reaction of a dipolar TMM **2** generated reversibly by thermolysis of **1**.[6] Heating an equimolar mixture of an electron-deficient alkyne (EWG = electron-withdrawing group) and the readily available TMM precursor **1** (see Experimental Procedure)[7] at 80–100 °C afforded the cyclopentene carboxylic acid ester **5** after hydrolysis of the ketene acetal **3** with aqueous AcOH in CH_3CN. The reaction is purely thermal and proceeds under neutral conditions.

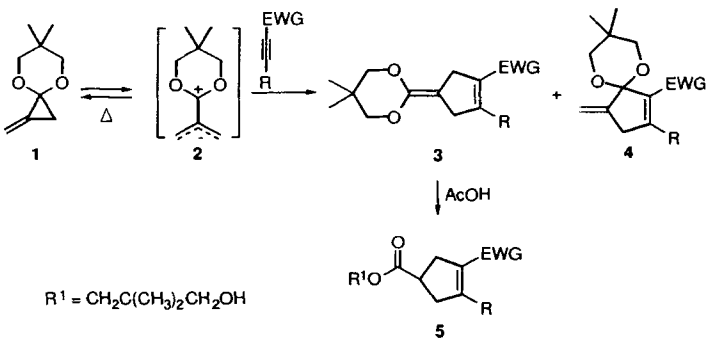

1 2 3 4 5

In the early stages of our studies we recognized that alkynes are indeed less reactive toward **2** than the structurally related alkenes.[7a, 8] Thus, the reaction of **1** with methyl 2-heptynoate in toluene proceeded only at 100 °C (56 h), while methyl (*E*)-2-hexenoate reacted at 80 °C.[9] Nonetheless, the cycloaddition to an acetylenic ester proceeded efficiently at 80–100 °C to afford the acid-labile ketene acetal **3** (EWG = CO_2Me or CO_2iPr), which was converted to the dicarboxylic ester **5** and isolated in good yield (Table 1, entries 1–4). A small amount of exo-methylene isomer **4** was also formed, suggesting the intervention of a single-electron transfer cycloaddition pathway.[10] The reaction rate increased as the polarity of the solvent was increased: octane < toluene < dimethoxyethane < CH_3CN < dimethylsulfoxide. This is in part due to faster formation of **2** in polar solvents.[6] The reaction was complete after 5 h at 80 °C when DMSO was used as a solvent. The ratio of **3** to **4** was not solvent dependent.

In line with the nucleophilic nature of **2**, the reaction rate increases as the electron demand of the alkyne increases. 1-Alkoxyalkyl and trimethylsilyl groups (which lower the LUMO

Table 1. Cycloaddition of **1** with electron-deficient alkynes[a].

Entry	Alkyne (equiv)	*T* [°C]	*t* [h]	Major product	Yield of **5** [%][b]	**3**:**4**[c]
1		(1.2)	100	56	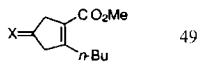	49	(82:18)[d]
2	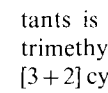	(0.91)	80	44	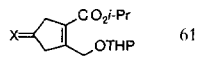	61	(82:18)
3	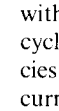	(1.2)	80	18	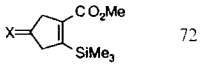	72	(93:7)[e]
4		(0.91)	80	29	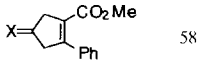	58	(68:32)[f]
5	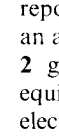	(1.0)	100	36	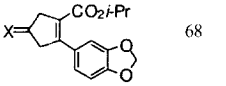	68	(83:17)
6	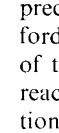	(1.0)	100	10	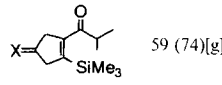	59 (74)[g]	(> 97:3)
7		(0.83)	80	27	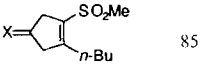	85	(> 95:5)
8		(0.91)	80	26	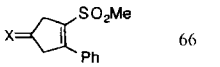	66	(82:18)
9		(1.1)	80	14	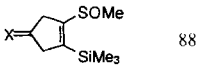	88	(> 98:2)
10		(1.2)	100	27	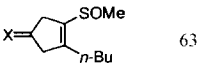	63	(> 95:5)

[a] The reactions were carried out in CH_3CN or CD_3CN, except that in entry 6 which was carried out in toluene. [b] Yield of isolated product. The ketene acetal **3** (X = $OCH_2C(CH_3)_2CH_2O$) was not isolated but converted into the ester **5**. The yields are based on **1** except in entries 7 and 8 where they are based on the alkyne. The yield of the cycloaddition was found to concentration independent (up to 1.5 M). [c] Determined by capillary GLC and/or by ^1H NMR for the equivalent reaction carried out in CD_3CN. [d] The cycloadduct due to the cycloaddition to carbonyl group is also formed in ca. 10% yield. [e] The cycloadduct due to the cycloaddition to carbonyl group is also formed is ca. 3% yield. [f] The cycloadduct due to the cycloaddition to carbonyl group is also formed is ca. 3% yield. [g] Yield when 3 equiv of **1** is used.

[*] Prof. E. Nakamura
Department of Chemistry, The University of Tokyo
Hongo, Tokyo 113 (Japan)
Telefax: Int. code + (3) 5800-6889
e-mail: nakamura@chem.s.u-tokyo.ac.jp
Dr. S. Yamago
Department of Synthetic Chemistry and Biological Chemistry
Kyoto University, Kyoto 606-01 (Japan)
S. Ejiri (deceased)
Department of Chemistry, Tokyo Institute of Technology
Meguro, Tokyo 152 (Japan)

[**] We thank the Ministry of Education, Science and Culture, Japan, for financial support.

of acetylene)[11] accelerate the cycloaddition of acetylenic esters (entries 2 and 3). In contrast, an electron-donating *p*-alkoxyphenyl group retards the cycloaddition reaction (cf. entries 4 and 5).

The cycloaddition to acetylenic ketones revealed an interesting dichotomy. When ketone **6a** was allowed to react with **1** in toluene, we found that the cycloaddition reaction occurs exclusively on the carbonyl group to give the exomethylene product **7a**.[12] Only when the carbonyl group was deactivated electronically and sterically as in **6b**, did the desired cycloaddition in toluene take place on the acetylenic bond to give the ketene acetal **8b**.[13] The selectivity toward **8b**, however, decreased in a polar solvent (CH_3CN) and a significant amount of the exomethylene product **7b** also formed. This solvent effect suggests that the cycloaddition to the carbonyl group occurs through a polar (stepwise) reaction pathway,[14] which, in a polar solvent, is faster than the (presumably concerted) cycloaddition to the C≡C bond.

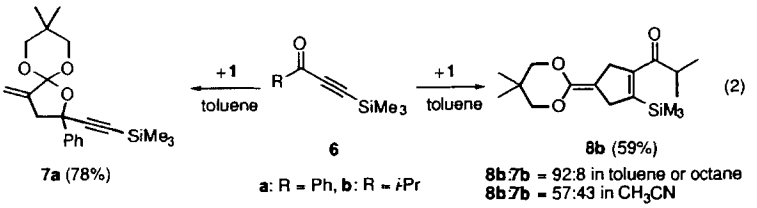

A drawback of the present cycloaddition for application in synthesis is the failure of unactivated alkynes to act as 2π-electron partners. For instance, phenylacetylene and hexyne are totally inert under these reaction conditions. We found however that sulfur-substituted alkynes can be used as synthetic equivalents of simple alkynes. Acetylenic sulfones and sulfoxides were found to be very reactive TMM acceptors at 80–100 °C; in fact, the former are the most reactive substrates examined in these studies (entries 7–10). After the cycloaddition, the vinyl sulfone cycloadduct **9** could be readily desulfurized under mild conditions; treatment of **9** with $Na_2S_2O_4$ in the presence of a phase transfer catalyst (Aliquat 336) in a water/toluene mixture afforded the cyclopentene **10**.[15]

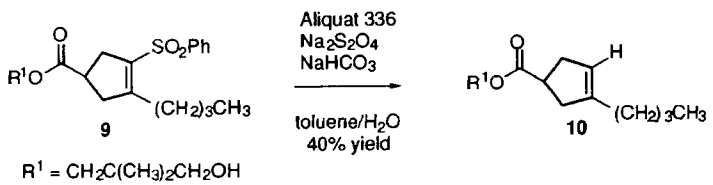

Finally, preliminary studies on the regiochemistry of the cycloaddition of a substituted TMM, which was generated from an ethylidene homologue of **1**, with methyltrimethylsilylpropynoate showed rather poor regioselectivity; a 77:23 mixture of two regioisomeric ketene acetal cycloadducts formed.[16]

In summary, we found that alkynes are relatively poor acceptors of dipolar TMM species but can still be used as a useful two-carbon unit in the [3+2] cycloaddition with **2** to provide a new synthetic route to cyclopentene derivatives. We attribute the success of the cycloaddition to the well-defined singlet character of the dipolar TMM molecule,[6] which undergoes either the desired cycloaddition or the ring closure back to the starting material **1**. The other known TMM species,[2] on the other hand, tend to undergo side reactions (irreversible ring closure to unreactive methylenecyclopropane, intersystem crossing to the triplet state and subsequent rapid dimerization)[17] rather than reacting with unreactive acceptors.

Experimental Procedure

6,6-Dimethyl-4,8-dioxa-1-methylenespiro[2.5]octane (**1**): To a solution of solid $NaNH_2$ (minimum assay 95%; 57.60 g, maximum 1.48 mol) in ca. 650 mL of liq. NH_3 in a dry ice/acetone bath was added 2,2-bis-(chloromethyl)-5,5-dimethyl-1,3-dioxane [7b] (102.3 g, 0.48 mol) in 200 mL of dry Et_2O over 30 min. The mixture was warmed to the reflux temperature of NH_3, and after 2 h the mixture was cooled again to −78 °C. Methyl iodide (33.0 mL, 0.53 mol) in 200 mL of dry Et_2O was added over 1.5 h, and after 15 min the cooling bath was removed. After 30 min solid NH_4Cl (20 g) was added in several portions at −78 °C over 30 min. Ammonia was allowed to evaporate at room temperature, while a 1:1 mixture of ether and pentane (500 mL) was added. Inorganic salt was removed by filtration and **1** was obtained by distillation (53.2 g, 72%; b.p. 37–40 °C/1.7 Torr). This material contained 9% of unsubstituted cyclopropenone acetal and 3% of 2,3-dimethyl cyclopropenone acetal as judged by GLC.

A solution of potassium *tert*-butoxide (1.32 g, 12 mmol) in *t*BuOH (7.11 g, 96 mmol) and 40 mL of ether was added under nitrogen over 5 min to a solution of **1** (46.3 g, 0.30 mol) in ether (100 mL) at −78 °C. After 5 min the mixture was warmed to room temperature and stirred for 4 h. 1 N Hydrochloric acid (15 mL) was added and the mixture was subjected to extractive workup and distillation to obtain **1** (36.49 g, 79% yield, b.p. 57–59 °C/7.3 Torr).

General procedure for the cycloaddition illustrated by the preparation of 2,2-dimethyl-3-hydroxypropyl 4-butyl-3-methylsulfonylcyclopent-3-enecarboxylate (entry 7 in Table 7): A solution of **1** (0.113 mL, 111 mg, 0.72 mmol), and methyl hex-1-ynyl sulfone (96 mg, 0.6 mmol) in 0.5 mL of CD_3CN was heated in a sealed NMR tube at 80 °C for 27 h. ^1H NMR monitoring indicated the formation of an (acid-labile ketene) acetal **3** in high yield: ^1H NMR (200 MHz, $CDCl_3$, TMS): δ = 0.92 (t, J = 7.0 Hz, 3H), 1.00 (s, 6H), 1.24–1.57 (m, 4H), 2.59 (br. t, J = 7.4 Hz, 2H), 2.89 (s, 3H), 3.24 (br s, 2H), 3.34 (br s, 2H), 3.8 (br s, 4H). This primary cycloadduct was hydrolyzed to the corresponding ester **5** for further characterization. The crude $CDCl_3$ solution was treated with 35 mg of Amberlyst 15 and 40 mg of water and the mixture was stirred for 30 min. The resin was removed to give crude cyclopentenecarboxylic acid ester **5** (270 mg). Purification by chromatography (silica gel 8 g, 45% ethyl acetate/hexane) afforded the desired compound (169 mg, 85% yield). ^1H NMR (200 MHz, $CDCl_3$): δ = 0.92 (t, J = 6.9 Hz, 3H), 0.94 (s, 6H), 1.26–1.54 (m, 4H), 2.05 (br t, J = 6.1 Hz, 1H), 2.59 (br t, J = 7.4 Hz, 2H), 2.86–2.96 (m, 2H), 3.03–3.11 (m, 2H), 3.13–3.29 (m, 1H), 3.31 (br d, J = 6.1 Hz, 2H), 3.98 (s, 2H); IR (neat): $\tilde{\nu}$ = 3520, 1730, 1635, 1320, 1300, 1140, 1055 cm^{-1}; Anal. calcd. for $C_{16}H_{28}SO_5$: C 57.80, H 8.49; found C 57.58, H 8.28.

Received: March 21, 1995
Revised version: July 3, 1995 [Z7818IE]
German version: *Angew. Chem.* **1995**, *107*, 2338–2340

Keywords: cycloadditions · cyclopentenes · methylenecyclopropane · trimethylenemethane

[1] a) H. S. Holmes, *Org. React.* **1948**, *4*, 60–173, b) J. M. Coxon, S. T. Grice, R. G. A. R. Maclagan, D. Q. McDonald, *J. Org. Chem.* **1990**, *55*, 3804–3807.

[2] L. R. Corwin, D. M. McDaniel, R. J. Bushby, J. A. Berson, *J. Am. Chem. Soc.* **1980**, *102*, 276–287; A. D. Sabatelli, R. F. Salinaro, J. A. Mondo, J. A. Berson, *Tetrahedron Lett.* **1985**, *26*, 5851–5855; R. D. Little, H. Bede, K. J. Stone, O. Wallquist, R. Dannecker, *J. Org. Chem.* **1985**, *55*, 2401–2402.

[3] B. M. Trost, J. M. Balkovec, S. R. Angle, *Tetrahedron Lett.* **1986**, *27*, 1445–1149.

[4] P. Binger, Q.-H. Lü, P. Wedemann, *Angew. Chem.* **1985**, *97*, 333–334; *Angew. Chem. Int. Ed. Engl.* **1985**, *24*, 316–317; S. A. Bapuji, W. B. Motherwell, M. Shipman, *Tetrahedron Lett.* **1989**, *30*, 7107–7110.

[5] T. S. Abram, R. Baker, C. M. Exon, V. B. Rao, *J. Chem. Soc. Perkin I* **1982**, 285–294; B. D. Gray, C. M. McMillan, J. A. Miller, G. M. Ullah, *Tetrahedron Lett.* **1987**, *28*, 689–692; M. T. Crimmins, P. G. Nantermet, *J. Org. Chem.* **1990**, *55*, 4235–4237.

[6] E. Nakamura, S. Yamago, S. Ejiri, A. E. Dorigo, K. Morokuma, *J. Am. Chem. Soc.* **1991**, *113*, 3183–3184.

[7] a) S. Yamago, E. Nakamura, *ibid.* **1989**, *111*, 7285, b) M. Isaka, S. Ejiri, E. Nakamura, *Tetrahedron* **1992**, *48*, 2045–2057; c) Reviews: E. Nakamura in *Organic Synthesis in Japan. Past, Present and Future*, (Ed.: R. Noyori), Tokyo, Kagaku Dojin, **1992**, pp. 275–282; E. Nakamura, *J. Synth. Org. Chem. Jpn.* **1994**, *52*, 935–945.

[8] M. Prato, T. Suzuki, H. Foroudian, Q. Li, K. Khemani, F. Wudl, J. Leonetti, R. D. Little, T. White, B. Rickborn, S. Yamago, E. Nakamura, *J. Am. Chem. Soc.* **1993**, *115*, 1594.
[9] Since TMM **2** is formed reversibly at temperatures lower than 60 °C [6], the observed rate difference reflects the relative rate of the cycloaddition.
[10] S. Yamago, S. Ejiri, M. Nakamura, E. Nakamura, *J. Am. Chem. Soc.* **1993**, *115*, 5344–5345.
[11] E. Nakamura, Y. Miyachi, N. Koga, K. Morokuma, *J. Am. Chem. Soc.* **1992**, *114*, 6686–6692.
[12] S. Yamago, E. Nakamura, *J. Org. Chem.* **1990**, *55*, 5553–5555.
[13] Notably, a small amount of **7** formed even with a methyl ester (R = MeO, Table 1, entries 1, 3, and 4). The formation of this side product was suppressed when R was *i*PrO (entries 2 and 5).
[14] Two stepwise pathways are possible. One is a single-electron transfer pathway, and another is a two-electron nucleophilic mechanism. The former has been shown to operate in the reaction with highly electron-deficient olefins [10].
[15] J. Bremner, M. Julia, M. L. J.-P. Stacino, *Tetrahedron Lett.* **1982**, *23*, 3265–3266.
[16] S. Ejiri, S. Yamago, E. Nakamura, *J. Am. Chem. Soc.* **1992**, *114*, 8707–8708.
[17] J. A. Berson, *Acc. Chem. Res.* **1978**, *11*, 446–453.

N-Hydroxypyridinethiones as Photochemical Hydroxyl Radical Sources for Oxidative DNA Damage**

Waldemar Adam, Daniel Ballmaier, Bernd Epe, Günther N. Grimm, and Chantu R. Saha-Möller*

For about five years it has been known that *N*-hydroxypyridine-2-thione (**1**) generates hydroxyl radicals on irradiation with visible light,[1] and that this reaction also takes place in aqueous buffer solution.[2] Thione **1** is a versatile antibacterial and antifungal reagent; furthermore, it exhibits in vitro cytotoxic activity in leukemia cells and is therefore a potential chemotherapeutic agent.[3] The biological activity of this reagent is probably due to the photochemical formation of hydroxyl radicals. Recently the genotoxicity of *N*-hydroxypyridinethiones has been investigated in cellular systems.[4] The preliminary results reveal that these reagents are indeed cytotoxic in mouse cells and Chinese hamster fibroblasts only in the presence of light.[4]

Among reactive oxygen species, hydroxyl radicals play a particularly important role in oxidative damage of biomolecules (for example, DNA, proteins, and lipids) in cellular systems.[5] Since the conventional methods for the generation of hydroxyl radicals are of limited scope for biochemical investigations,[6] in the last few years new, photochemical hydroxyl radical sources, the so-called photo-Fenton reagents, were developed.[7] In this context we have investigated the genotoxicity of the thiones **1** and **2** and observed significant DNA damage.

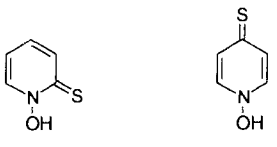

1 **2**

[*] Dr. C. R. Saha-Möller, Prof. Dr. W. Adam, Dipl.-Chem. G. N. Grimm
Institut für Organische Chemie, Universität Würzburg
Am Hubland, D-97074 Würzburg (Germany)
Telefax: Int. code + (931)888-4756
e-mail: Adam@chemie.uni-wuerzburg.d400.de
Dipl.-Chem. D. Ballmaier, Prof. Dr. B. Epe
Institut für Pharmakologie und Toxikologie, Universität Würzburg (Germany)

[**] This work was supported by the Deutsche Forschungsgemeinschaft (SFB 172 "Molekulare Mechanismen kanzerogener Primärveränderungen") and the Fonds der Chemischen Industrie.

The damage profiles that are characteristic for hydroxyl radicals, namely, oxidation of DNA bases (mainly guanine) and single strand breaks, are shown in Figure 1. Analogous to 2-thiopyridone (**1**), which is an established photochemical hydroxyl radical source,[1,2] 4-thiopyridone (**2**) efficiently forms hydroxyl radicals on irradiation. Here we present our preliminary results.

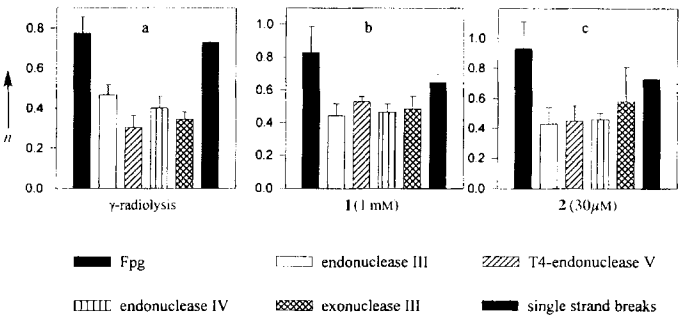

Fig. 1. DNA damage profiles after treating PM2 DNA with ionizing γ radiation (a), or light and **1** (1 mM) (b), or light and **2** (30 μM) (c). The columns show the number n of single-strand breaks and various repair endonuclease-sensitive modifications per 10000 base pairs [17].

The irradiation of the *N*-hydroxy compound **2** (60.0 mg, 4.70 mmol) at 350 nm (Rayonet photoreactor) in water (10 mL) and acetonitrile (3 mL) yielded, after silica gel chromatography, the products **2a** (17%), **2b** (32%), and **2c** (42%) (Scheme 1).

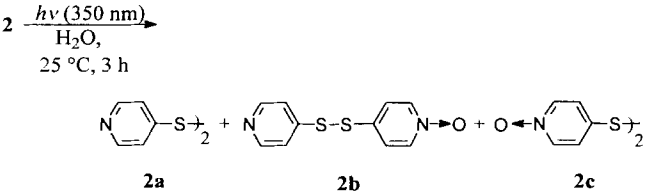

Scheme 1.

Additional products, which might be formed by incorporation of acetonitrile radicals generated by the reaction of hydroxyl radicals with acetonitrile,[8] were not observed. The formation of the photoproducts **2a–c** can be rationalized by the reported mechanism[1] postulated for the photolysis of *N*-hydroxypyridine-2-thione (**1**), which implies that the photoproducts are formed not only by N–O bond cleavage, but also through a radical chain reaction initiated by H abstraction from the thiol tautomer of the starting material. In the latter case, acetonitrile radicals may also be involved.

The following results confirm the formation of hydroxyl radicals by irradiation of thione **2**. In the photolysis (λ = 350 nm) of the *N*-hydroxypyridinethiones **1**[9] and **2** (40 mmol) in degassed, pure acetonitrile (4 mL) and benzene (5 mL) under inert atmosphere (nitrogen), phenol was detected by gas chromatography[10] (5.1 and 9.5%, relative to the amount of *N*-hydroxy derivative employed). In comparison, about five times higher amounts of phenol were formed in oxygen-saturated solutions. The lower yield of phenol in the absence of oxygen may readily be explained in terms of preferential dimerization of the initially formed hydroxycyclohexadienyl radicals, and consequently only a small fraction of the initial hydroxyl radicals produce phenol.[11]

To confirm the generation of hydroxyl radicals in aqueous solution, thiones **1** or **2**[9] (5.40 mg, 42.5 μmol) were irradiated in aqueous solution of benzoic acid (51.2 mg, 419 μmol in 20 mL), and the reaction products were quantified by HPLC analysis. In both cases, the 2-, 3- and 4-hydroxybenzoic acids were formed in a total yield of 6.2 and 8.8%.[12]

The direct spectral evidence for the formation of hydroxyl radicals in the photolysis of *N*-hydroxypyridine-4-thione (**2**) was obtained by ESR analysis through spin trapping with 5,5-dimethyl-1-pyrroline-*N*-oxide (DMPO) in aqueous solution. The characteristic quartet for the hydroxyl radical adduct[13, 14] was observed ($a_N = a_H = 14.8$ G, $g = 2.0054$), while the trapping product of thiyl radicals was not detected under these reaction conditions. Recently, the detailed ESR spectral study of the photolysis of thione **1** has appeared,[14, 15] and our data agree well with the reported ones. These results confirm unequivocally that, like the *N*-hydroxypyridine-2-thione (**1**), the regioisomeric 4-thione **2** is also an efficient photochemical hydroxyl radical source.

As an indicator for the oxidative DNA damage, the formation of 7,8-dihydro-8-oxoguanine (**3**) by thiones **1** and **2** on UVA irradiation ($\lambda = 350$ nm) was examined in isolated DNA. For this purpose a solution of calf thymus DNA (0.1 μg μL^{-1}) and thione **1** or **2** in 5 mM phosphate buffer was irradiated at 6 °C for 20 to 60 min. Subsequently the modified DNA was precipitated, hydrolyzed with HF/pyridine, and submitted to HPLC analysis (electrochemical detection at 350 mV); the results are shown in Table 1. The *N*-hydroxypyridine-4-thione (**2**) formed more 8-OxoGua (**3**) than thione **1** after irradiation for 20 min. The addition of the hydroxyl radical scavenger *tert*-butyl alcohol[16] (2%) decreased the 8-OxoGua yield significantly in both cases (about 40%) (Table 1, entries 2 and 6). In the presence of 40 mM mannitol, which is also a hydroxyl radical scavenger,[2] the yield of 8-OxoGua was reduced as well (Table 1, entries 3 and 7). The moderate scavenging effect may emanate from the association of *N*-hydroxypyridinethiones with DNA.

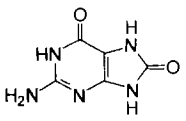

3

Besides the scavenging experiments with *tert*-butyl alcohol and mannitol, additional control reactions were carried out, which confirm that hydroxyl radicals are responsible for the oxidative DNA damage. Thus, in the absence of light, the thiones **1** and **2** did not form any 8-OxoGua. Furthermore, at longer irradiation times the amount of 8-OxoGua did not increase, which indicates that the photoproducts of thiones **1** and **2** do not induce significant DNA oxidation.

Table 1. Photoinduced formation of 8-OxoGua by the *N*-hydroxypyridinethiones **1** and **2** in calf thymus DNA [a].

No.	Thione[b]	*t*BuOH[Vol.%]	Mannitol[mM]	*t*[min][c]	Yield (**3**)[%][d]
1	**1**	-	-	20.0	0.19±0.03
2	**1**	2.00	-	20.0	0.11±0.03
3	**1**		40.0	20.0	0.13±0.02
4	**1**		-	60.0	0.46±0.06
5	**2**	-	-	20.0	0.42±0.09
6	**2**	2.00	-	20.0	0.26±0.02
7	**2**		40.0	20.0	0.16±0.06

[a] 200 μL solutions of DNA and *N*-hydroxypyridinethiones in 5 mM phosphate buffer (pH 7.0) were irradiated at 6 °C (*t* = duration of irradiation). [b] The thione concentration was 62.5 μM (one equivalent, based on the guanine concentration in DNA). [c] Irradiation at $\lambda = 350$ nm in a Rayonet photoreactor. [d] Quantification by HPLC (electrochemical detection at 350 mV), yield relative to guanine (after subtraction of blank), this corresponds to the yield relative to 1 equiv *N*-hydroxypyridinethione.

Further evidence that hydroxyl radicals cause the damage was obtained by a relaxation assay with PM2 DNA and specific repair endonucleases.[17] The irradiation of superhelical PM2 DNA in the presence of *N*-hydroxypyridine-2-thione (**1**) or *N*-hydroxypyridine-4-thione (**2**) led to single strand breaks, apurinic sites (AP lesions), and numerous base oxidation products.[18] The damage profiles for the thiones **1** and **2** show the characteristic pattern (Fig. 1) for hydroxyl radicals (formed by γ radiolysis of water). The 4-thione **2** exhibited a significantly higher reactivity than the 2-thione **1**. For example, during the same irradiation time (10 min), the thione **2** caused the same extent of DNA damage at a concentration of 30 μM (Fig. 1c) as thione **1** formed at 1 mM (Fig. 1b). For comparison, the damage profile of hydroxyl radicals generated by γ radiolysis (Fig. 1a) is significantly different from that of photosensitizers.[17c] In the latter process the DNA is damaged predominantly through type II (singlet oxygen) and type I photooxidation (radical and electron transfer processes). While singlet oxygen causes mainly Fpg-sensitive[19] base modifications, hydroxyl radicals also form considerable amounts of single strand breaks and AP lesions.[17b, c 20, 21]

That other active oxygen species are not involved in the reaction of DNA with the *N*-hydroxypyridinethiones **1** or **2** was established through control experiments. Both the additives superoxide dismutase and catalase did not show any significant effects. In contrast, *tert*-butyl alcohol decreased the formation of single strand breaks and Fpg-sensitive modifications remarkably. This suggests that neither superoxide anions nor hydrogen peroxide appear to be involved, and consequently, hydroxyl radicals are the only DNA-damaging species in the photolysis of the thiones **1** and **2**.

Our study confirms that *N*-hydroxypyridine-2-thione (**1**), and even more its *para* regioisomer **2**, are efficient photochemical sources for hydroxyl radicals. For the first time their DNA-damaging activity was demonstrated. Their favorable properties, such as water solubility, availability, and absorption in the visible region, make them particularly suited as hydroxyl radical sources for the investigation of biochemically and biologically important reactions. Of relevance in the potential application of the *N*-hydroxypyridinethiones **1** and **2** as chemotherapeutics is their expected cytotoxity elicited through the specific oxidative alteration of biomolecules by the photochemically generated reactive oxygen species. Such applications require highest priority.

Received: April 1, 1995
Revised version: July 13, 1995 [Z 7861 IE]
German version: *Angew. Chem.* **1995**, *107*, 2326–2328

Keywords: DNA oxidations · hydroxyl radical · *N*-hydroxypyridinethione

[1] a) J. Boivin, E. Crépon, S. Z. Zard, *Tetrahedron. Lett.* **1990**, *31*, 6869–6872; b) *Bull. Soc. Chim. Fr.* **1992**, *129*, 145–150.
[2] K. M. Hess, T. A. Dix, *Anal. Biochem.* **1992**, *206*, 309–314.
[3] a) J. Blatt, S. R. Taylor, G. J. Kontoghiorghes, *Cancer Res.* **1989**, *49*, 2925–2927; b) G. J. Kontoghiorghes, A. Piga, A. V. Hoffbrand, *Hermatol. Oncol.* **1986**, *4*, 195–204.
[4] B. Epe, D. Ballmaier, W. Adam, G. N. Grimm, C. R. Saha-Möller, Universität Würzburg, unpublished results.
[5] a) *Oxidative Stress* (Ed.: H. Sies), Academic Press, London, **1985**; b) *Oxidative Stress: Oxidants and Antioxidants* (Ed.: H. Sies), Academic Press, London, **1991**.
[6] a) C. Walling, *Acc. Chem. Res.* **1975**, *8*, 125–131; b) D. Schulte-Frohlinde, C. von Sonntag in Chap. 1, Ref. [5b].
[7] a) I. Saito, M. Takayama, T. Matsuura, S. Matsugo, S. Kawanishi, *J. Am. Chem. Soc.* **1990**, *112*, 883–884; b) W. Adam, J. Cadet, F. Dall'Acqua, B. Epe, D. Ramaiah, C. R. Saha-Möller, *Angew. Chem.* **1995**, *107*, 91–94, *Angew. Chem. Int. Ed. Engl.* **1995**, *34*, 107–110.

[8] G. V. Buxton, C. L. Greenstock, W. P. Helman, A. B. Ross, *J. Phys. Chem. Ref. Data* **1988**, *17*, 513–886.
[9] For comparison, in each case the thione **1**, which is described in the literature as photochemical source of hydroxyl radicals, was also investigated.
[10] The yields of phenol refer to the amount of *N*-hydroxy compound consumed. The quantification was carried out by GC analysis with naphthalene as standard (added after reaction); the error was ±10% of the stated values.
[11] G. W. Klein, R. H. Schuler, *Radiat. Phys. Chem.* **1978**, *11*, 167–171.
[12] These experiments were carried out in the absence of an additional oxidant, and no oxygen gas was bubbled through the reaction mixture, which may account for the low yields of the hydroxylation products.
[13] E. Finkelstein, G. M. Rosen, E. J. Rauckmann, *Arch. Biochem. Biophys.* **1980**, *200*, 1–16.
[14] Recently an ESR spectral study of the photolytic formation of hydroxyl radicals from thione **1** was reported: K. J. Reszka, C. F. Chignell, *Photochem. Photobiol.* **1995**, *61*, 269–275.
[15] K. J. Reszka, C. F. Chignell, *Photochem. Photobiol.* **1994**, *60*, 442–449.
[16] B. Epe, M. Häring, D. Ramaiah, H. Stopper, M. M. Abou-Elzahab, W. Adam, C. R. Saha-Möller, *Carcinogenesis* **1993**, *4*, 2271–2276.
[17] a) S. Boiteux, *J. Photochem. Photobiol. B* **1993**, *19*, 87–96; b) B. Epe, J. Hegler, *Methods Enzymol.* **1994**, *234*, 122–131; c) B. Epe, M. Pflaum, M. Häring, J. Hegler, H. Rüdiger, *Tox. Lett.* **1993**, *67*, 57–72.
[18] a) C. von Sonntag, *The Chemical Basis of Radiation Biology*, 1st ed., Taylor & Francis, London, **1987**; b) N. Paillous, P. Vicendo, *J. Photochem. Photobiol. B* **1993**, *20*, 203–209; c) A. J. S. C. Vieira, S. Steenken, *J. Am. Chem. Soc.* **1990**, *112*, 6986–6994; d) S. Steenken, *Chem. Rev.* **1989**, *89*, 503–520.
[19] Fpg protein: repair endonuclease formamidopyrimidine DNA-glycosylase from *Escherichia coli*.
[20] E. Müller, S. Boiteux, M. R. P. Cunningham, *Nucleic Acid Res.* **1990**, *18*, 5969–5973.
[21] AP lesion: base-free (apurinic/apyrimidinic) site in DNA.

Generation of Enantiomerically Enriched Lithium Indenides by Means of (−)-Sparteine: Structure, Stereoselective Substitution, and Solvent Effects**

Inga Hoppe, Michael Marsch, Klaus Harms, Gernot Boche,* and Dieter Hoppe*

Dedicated to Professor Manfred Regitz on the occasion of his 60th birthday

A number of enantiomerically enriched carbanionic building blocks that are stereogenic at the metal-carrying C atom have in the past been synthesized by deprotonation and substituted stereospecifically by electrophiles.[1] This has been achieved by four methods: 1) stereoselective deprotonation of chiral precursors to give configuratively stable ion pairs;[2] 2) asymmetric deprotonation of achiral precursors by a chiral base that differentiates between the enantiotopic protons;[3] 3) asymmetric deprotonation under kinetically controlled resolution of a racemic mixture;[4] 4) thermodynamically controlled equilibrium between configuratively labile, diastereomeric ion pairs in the presence of a chiral cation such as $Li^+ \cdot (-)$-sparteine ($Li^+ \cdot$ **2**),[5] often combined with the crystallization of the most favorable diastereoisomer[5a,b] ("second-order asymmetric transformation"[6]). The crystal structure of an allyllithium complex synthesized by this method has been solved.[7]

Alkali metal indenides are important intermediates in the construction of chiral metallocene catalysts.[8] Although the rates of the interconversion of the enantiomers of trialkylammonium–indenide ion pairs and the protonation of the anions are of the same order of magnitude,[9,10] enantiomerically enriched metal indenides have not been known until now. We report on the highly stereoselective, but strongly solvent-dependent, generation of lithium 1-alkylindenides by method 4, their structure, and their stereoselective substitution with electrophiles.

1-Methylindene (**1a**) was deprotonated by *n*-butyllithium/(−)-sparteine[11] (*n*BuLi·**2**) in *ether/hexane* at −70 °C. Crystallization began on warming to room temperature. Addition of acylchlorides or -in the presence of tetra(isopropoxy)titanium (TIPT)—aldehydes and ketones, yielded the 1-substituted indenes **5a–g,i** with >95% *ee* as major products, and generally favored by more than 97:3 over the 3-regioisomer **6** (Scheme 1,

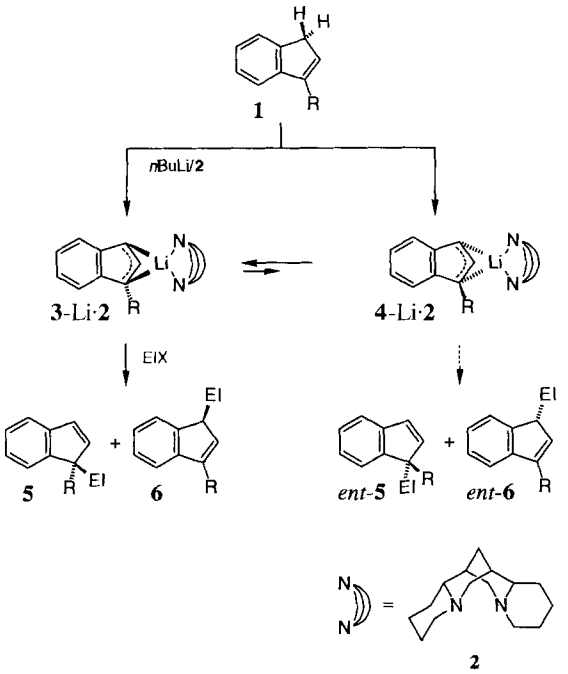

Scheme 1. Synthesis of the functionalized indenes **5** and **6** in the presence of the chiral ligand (−)-sparteine (**2**) For **1a**, **3a**, and **4a**, R = Me. For **1b**, **3b**, and **4b**, R = nC_4H_9. For **5** and **6**, R and El are given in Table 1.

Table 1). The products **5** have the (1*R*) configuration, as shown by the X-ray crystal structure of the (*R*)-1-phenylethylamide formed from the ester **5a**[12] and by the chemical correlation of this amide with **5c**, **5i**, and **5m**.[13] Like **5a**, **5c**, **5i**, and **5m**, the other compounds **5** also have a high negative specific rotation $[\alpha]_D$. Thus it is highly probable that they belong to the same stereochemical series. In contrast, the α-branched aldehydes 2-methylpropanal and 2,2-dimethylpropanal give predominantly the regioisomeric adducts **6k** and **6l**. Due to the strongly positive optical rotation we ascribe to them the (1*S*) configuration (at the former C3 center).

[*] Prof. Dr. D. Hoppe, Dr. I. Hoppe
Organisch-chemisches Institut der Universität
Corrensstrasse 40, D-48149 Münster (Germany)
Telefax: Int. code + (251)83-9772
Prof. Dr. G. Boche, M. Marsch, Dr. K. Harms
Fachbereich Chemie der Universität
D-35032 Marburg (Germany)
Telefax: Int. code +(6421)28-8917
e-mail: Boche@ps1515.chemie.unimarburg.de

[**] This work was supported by the Volkswagen-Stiftung, the Fonds der Chemischen Industrie, and the Deutschen Forschungsgemeinschaft (G. Boche, SFB 260).

Table 1. Reactions of lithium indenides **3**-Li·**2** and **4**-Li·**2** with electrophiles EIX.

Product	R	El	EIX	Yield[%][a]	**5**:**6**	*ee*[%][b]	$[\alpha]_D^{20}$	*c*[c]
5a	Me	MeOCO	$MeCO_2Cl$	64	>97:3	>95	−80	1.3
5b	Me	MeCO	MeCOCl	63	>97:3	>95	−128	2.1
5c	Me	H_2C=CHCO	H_2C=CHCOCl	67	>97:3	>95	−137	1.8
5d	Me	PhCO	PhCOCl	74	>97:3	>95	−289	1.7
5e	Me	4-BrC_6H_4CO	4-BrC_6H_4COCl	79	>97:3	>95	−304	1.5
5f	Me	R^1CO[l]	R^1COCl[l]	52	>97:3	>95	−193	1.0
5g	*n*Bu	PhCO	PhCOCl	79	>97:3	>95	−157	1.6
5h	*n*Bu	PhCHOH[d,e]	PhCHO	52	35:65	[f]	+82[g]	1.3
5i	Me	PhCHOH[d,h]	PhCHO	67	>97:3	>95	−117[g]	1.1
6k	Me	*t*BuCHOH[d,i]	*t*BuCHO	55	<3:97	>95	+133	1.1
6l	Me	*i*PrCHOH[d,j]	*i*PrCHO	59	3:97	[f]	+79[g]	1.2
5m + **6m**	Me	Me_2COH[d]	Me_2C=O	36	31:69	>95[k]	−12[k]	0.7

[a] Yield after chromatographic separation. [b] Determined by ^{1}H NMR spectroscopy with Eu(hfc)$_3$. [c] In CH_2Cl_2. [d] Addition of tetra(isopropoxy)titanium to the reaction mixture. [e] Mixture of diastereomers. [f] The enantiomeric excess could not be determined. [g] Optical rotation of the mixture of diastereomers. [h] Diastereomeric mixture 55:45. [i] Diastereomeric ratio greater than 95:5. [j] Diastereomeric ratio of 61:39. [k] Data for **5m** (yield 11%); **6m** (25%), $[\alpha]_D^{20}$ = +16 (*c* = 1) for 10%*ee*. [l] R^1 = 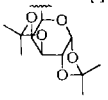

From **1b**, which like **1a** was deprotonated in *ether/hexane*, we obtained lithium/(−)-sparteine 1-butylindenide **3b**-Li·**2**, which also has a (1*R*) configuration at the C1 position according to the X-ray crystal structure (Fig. 1).[14] The distance from Li1 to C1 (243.2 pm) is longer than that to C3 (233.4 pm). Li1 forms only weak interactions to the C4 and C9 atoms of the annulated benzene ring (C4–Li1 251.0 pm; C9–Li1 254.5 pm). The distance to C2 is 229.9 pm.

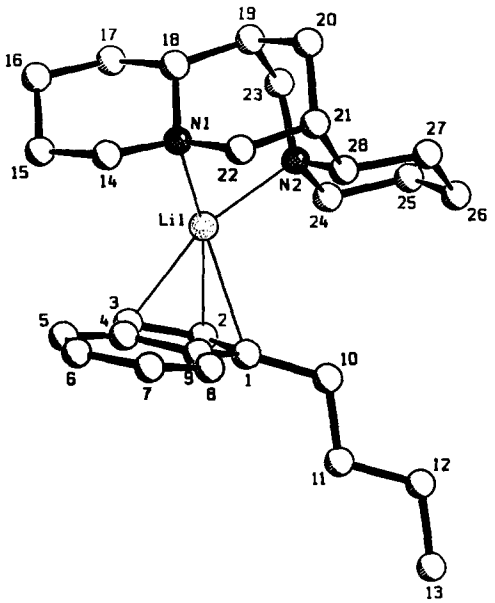

Fig. 1. Crystal structure of **3b**-Li·**2**. Some important bond lengths [pm]: Li1-C1 243.2(6), Li1-C2 229.9(6), Li1-C3 233.4(6), Li1-N1 209.5(6), Li1-N2 214.0(6), C1-C2 139.2(5), C2-C3 140.9(5).

The reaction of **3b**-Li·**2** with benzoyl chloride gives the 1-adduct **5g**, which also has a strongly negative optical rotation (Scheme 1, Table 1). This implies that the crystallized lithium indenide complexes **3a**-Li·**2** and **3b**-Li·**2** have the same (1*R*) configuration at C1, and their reactions with carbonyl compounds give **5a**–**i** with retention of configuration. Diastereomeric complexes of the type **4**-Li·**2** appear to be of no great importance. Probably the Li cation captures the carbonyl compound through complexation, which is then inserted into the longer and therefore weaker C1–Li1 bond. Only for bulky electrophiles, for example 2-methylpropanal, is attack at the sterically less hindered 3-position favored. We do not have any evidence that TIPT reacts with the **3**-Li·**2** complexes. Presumably it merely prevents reversibility of the aldehyde addition.[20]

The importance of the choice of solvent is highlighted by the reaction of 1-methylindene (**1a**) with *n*BuLi/(−)-sparteine at −70 °C in *tetrahydrofuran/hexane* instead of in *ether/hexane*. Addition of benzaldehyde yields the racemic 3-adduct **6i** as a 1:1 mixture of diastereomers. Consequently (−)-sparteine (**2**) in THF solution seems to have no influence on the stereoselectivity of this reaction, probably because it is displaced from Li^+ by THF. This is in accord with the structure of crystals isolated from such a solution:[21] 1-methyl-3-lithioindene crystallizes with three THF molecules (**3a**-Li·3THF) (Fig. 2).[25] Due to the threefold coordination of Li1 by THF there is only η^1-bonding (C3–Li1 230.9 pm) to the "allyl anion" part of **3a**.

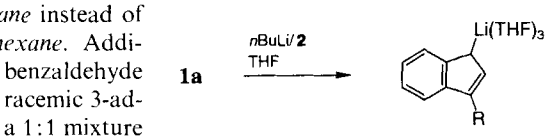

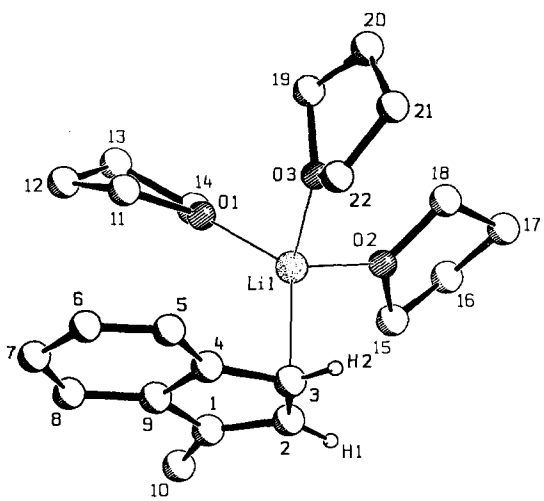

Fig. 2. Crystal structure of **3a**-Li·3THF. Some important bond lengths [pm]: Li1-C3 230.9(6), Li1-C2 252.6(6), Li1-C1 303.1(7), Li1-O1 193.8(5), Li1-O2 197.4(5), Li1-O3 197.7(5), C1-C2 139.3(5), C2-C3 139.2(5).

In this paper we have not only developed an easy and efficient method of preparing virtually enantiomerically pure, functionalized indenes, but have also demonstrated for the first time the solvent-dependent structures of the participating lithiated intermediates and the stereochemistry of their reactions with electrophiles.

Experimental Procedure

Successively, *n*-butyllithium (2.0 mmol, about 1.5 N in hexane), (−)-sparteine (2.0 mmol, dissolved in 3 mL diethyl ether), and 1-methyl-(3*H*)-indene (2.0 mmol in 2 mL diethyl ether) were added dropwise to diethyl ether (6 mL) below −70 °C. The reaction mixture was stirred and allowed to warm to 20 °C. After a further 30 min stirring it was cooled to −70 °C, and tetra(isopropoxy)titanium (4.0 mmol) and the acyl chloride or aldehyde (2.0 mmol) was added. The mixture was stirred for a further 2–6 h at this temperature. After addition of 2 N HCl (10 mL) to the reaction mixture the product was isolated and purified by chromatography on silica gel with ether/pentane.

3a-Li·3THF: 1-methyl-indene (100 mg, 0.77 mmol) was dissolved in THF (1 mL) followed by (−)-sparteine (**2**, 215 mg, 0.92 mmol). To this solution was added dropwise at −78 °C *n*BuLi (0.92 mmol, 1.6 M in hexane). After 12 h at −26 °C crystals had formed, which were good enough for X-ray analysis. Yield: 222 mg (82%).

3b-Li·**2**: To diethyl ether (2.5 mL) was added at −78 °C *n*BuLi (0.5 mmol, 1.6 M in hexane) and subsequently a solution of (−)-sparteine (**2**, 117 mg, 0.5 mmol) in diethyl ether (1 mL). After 15 min 1-butylindene (86 mg, 0.5 mmol) in diethyl ether (1.3 mL) was added. On warming to room temperature single crystals, good enough for X-ray analysis, were formed within 1 hour. Yield: 163 mg (79%).

Received: June 14, 1995 [Z 8099 IE]
German version: *Angew. Chem.* **1995**, *107*, 2328–2330

Keywords: asymmetric syntheses · chiral auxiliaries · indenes · lithium compounds

[1] Reviews: a) D. Hoppe, F. Hintze, P. Tebben, M. Paetow, H. Ahrens, J. Schwerdtfeger, P. Sommerfeld, J. Haller, W. Guarnieri, S. Kolczewski, T. Hense, I. Hoppe, *Pure Appl. Chem.* **1994**, *66*, 1479–1486; b) D. Hoppe, T. Krämer, J.-R. Schwark, O. Zschage, *ibid.* **1990**, *62*, 1999–2006; c) P. Beak, S. T. Kerrick, S. Wu, J. Chu, *J. Am. Chem. Soc.* **1994**, *116*, 3231–3239.

[2] a) D. Hoppe, T. Krämer, *Angew. Chem.* **1986**, *98*, 171–173; *Angew. Chem. Int. Ed. Engl.* **1986**, *25*, 160–162; b) D. Hoppe, A. Carstens, T. Krämer, *ibid.* **1990**, *102*, 1455–1456 and **1990**, *29*, 1424–1425; c) A. Carstens, D. Hoppe, *Tetrahedron* **1994**, *50*, 6097–6108.

[3] a) D. Hoppe, F. Hintze, P. Tebben, *Angew. Chem.* **1990**, *102*, 1457–1459; *Angew. Chem. Int. Ed. Engl.* **1990**, *29*, 1422–1423; b) S. T. Kerrick, P. Beak, *J. Am. Chem. Soc.* **1991**, *113*, 9708–9710.

[4] O. Zschage, D. Hoppe, *Tetrahedron* **1992**, *48*, 5657–5666.

[5] a) D. Hoppe, O. Zschage, *Angew. Chem.* **1989**, *101*, 67–69; *Angew. Chem. Int. Ed. Engl.* **1989**, *28*, 69–70; b) O. Zschage, D. Hoppe, *Tetrahedron* **1992**, *48*, 8389–8392; c) P. Beak, H. Du, *J. Am. Chem. Soc.* **1993**, *115*, 2516–2518; d) S. Thayumanavan, S. Lee, C. Liao, P. Beak, *ibid.* **1994**, *116*, 9755–9756; e) B. Kaiser, D. Hoppe, *Angew. Chem.* **1995**, *107*, 344–346; *Angew. Chem. Int. Ed. Engl.* **1995**, *34*, 323–325.

[6] a) R. Kuhn, *Chem. Ber.* **1932**, *65*, 49–51; b) M. M. Harris, *Prog. Stereochem.* **1958**, *2*, 157–195.

[7] M. Marsch, K. Harms, O. Zschage, D. Hoppe, G. Boche, *Angew. Chem.* **1991**, *103*, 338–339; *Angew. Chem. Int. Ed. Engl.* **1991**, *29*, 296–297.

[8] a) F. R. W. P. Wild, L. Zsolnai, G. Huttner, H.-H. Brintzinger, *J. Organomet. Chem.* **1982**, *232*, 233–247; b) reveiw: H.-H. Brintzinger, D. Fischer, R. Mülhaupt, B. Rieger, R. Waymouth, *Angew. Chem.* **1995**, *107*, 1255–1283; *Angew. Chem. Int. Ed. Engl.* **1995**, *34*, 1143–1170; c) C. A. Willoughby, S. L. Buchwald, *J. Am. Chem. Soc.* **1994**, *116*, 11703–11714; d) G. Erker, M. Aulbach, M. Knickmeier, D. Wingbermühle, C. Krüger, M. Nolte, S. Werner, *ibid.* **1993**, *115*, 4590–4601; e) A. H. Hoveyda, J. J. Morken, *J. Org. Chem.* **1993**, *58*, 4237–4244; f) R. L. Haltermann, T. M. Ramsey, Z. Chen, *ibid.* **1994**, *59*, 2642–2644; g) M. Bochmann, S. J. Lancaster, *Angew. Chem.* **1994**, *106*, 1715–1718; *Angew. Chem. Int. Ed. Engl.* **1994**, *34*, 1634–1637.

[9] K. Bott, *Tetrahedron Lett.* **1965**, 4569–4572.

[10] a) G. Bergson, A. M. Weidler, *Acta Chem. Scand.* **1963**, *17*, 862–864, 1798–1799, 2691–2700; b) A. Weidler, *ibid.* **1963**, *17*, 2724–2734; c) M. Aune, A. Gogoll, O. Matsson, *J. Org. Chem.* **1995**, *60*, 1356–1364.

[11] First application of (−)-sparteine in carbanionic chemistry: a) H. Nozaki, T. Aratani, T. Toraya, *Tetrahedron Lett.* **1968**, 4097–4098; b) H. Nozaki, T. Aratani, T. Toraya, R. Noyori, *Tetrahedron* **1971**, *27*, 905–913.

[12] I. Hoppe, M. Marsch, K. Harms, G. Boche, D. Hoppe, *Z. Kristallogr.*, in press.

[13] (*R*)-(−)-**5m** was obtained in 87% yield by methylation of (*R*)-(−)-**5a** with MeMgI and (*R*)-(−)-**5d** in 57% yield by oxidation of [1*R*,1(*R*,*S*)]-(−)-**5i** with PDC.

[14] Crystallographic data of **3b**-Li·**2** ($C_{28}H_{41}LiN_2$, $M_r = 412.57$): orthorhombic, space group $P2_12_12_1$, $a = 1096.6(1)$, $b = 1159.7(1)$, $c = 1901.5(1)$ pm, $V = 2418.2(2) \times 10^{-30}$ m^3, $Z = 4$, $\rho_{ber.} = 1.133$ Mg m^{-3}, $\mu(Cu_{K\alpha}) = 0.479$ mm^{-1}. Enraf-Nonius CAD4 diffractometer, graphite monochromated $Cu_{K\alpha}$ radiation, $T = 193(2)$ K, 5428 reflections ($4 < \theta < 75°$), of which 4927 independent ($R_{int} = 0.058$). Solution with direct methods (SHELXTL-PLUS), refined on F^2 with all reflections (SHELXL-93). The nonhydrogen atoms were refined anisotropically, the H atoms isotropically. Parameters of the weighting scheme: 0.0589, 0.8644; extinction coefficient $x = 0.0029(3)$; *wR*2 (*R*1 for 3429 reflections with $I > 2\sigma(I)$): 0.145 (0.055), 445 refined parameters. All calculations were carried out on a Micro-VAX II and a DEC 3000-300X [15–19].

[15] Siemens SHELXTL-PLUS (VMS) V4.21, Siemens Analytical X-Ray Instruments, Inc., Madison, **1990**.

[16] G. M. Sheldrick, SHELXL-93, Program for the Refinement of Crystal Structures, Göttingen, **1993**.

[17] A. L. Spek, Platon92, Program for the geometric analysis of Crystal Structures, Utrecht, **1992**.

[18] E. Keller, SCHAKAL-88B, a FORTRAN Program for the Graphic Representation of Molecular and Crystallographic Models, Freiburg, **1988**.

[19] Further details of the crystal structure determinations can be obtained from the Director of the Cambridge Crystallographic Data Centre, 12 Union Road, GB-Cambridge CB2 1EZ, on quoting the full journal citation.

[20] For reveiws on the application of titanium compounds in organic synthesis see, for example, a) M. T. Reetz, *Organotitanium Reagents in Organic Synthesis*, 1st ed., Springer, Berlin, **1986**; b) B. Weidmann, D. Seebach, *Angew. Chem.* **1983**, *95*, 12–26; *Angew. Chem. Int. Ed. Engl.* **1983**, *22*, 31–44; c) M. T. Reetz in *Organometallics in Synthesis* (Ed. M. Schlosser), Wiley, Chichester, **1994**, p. 195.

[21] We have not yet examined (for example, with ^{6}Li^{1}H-HOESY experiments) whether a (small) equilibrium coucentration of a complex **3b**-Li·**2** (Fig. 1) analogous to **3a**-Li·**2** is present. Beak et al.[22] have shown by NMR spectroscopy that an isopropyllithium·(−)-sparteine complex exists in diethyl ether solution. Also the Li cation in [^{6}Li]-α-lithiobenzylphenylsulfide is coordinated by (−)-sparteine in THF/[D_8]THF (1/1)[23·24].

[22] D. J. Gallagher, S. T. Kerrick, P. Beak, *J. Am. Chem. Soc.* **1992**, *114*, 5872–5873.

[23] S. Schade, Dissertation, Universität Marburg, **1995**.

[24] There is no uniform picture on extent to which amine ligands are bound to the Li cation in THF solutions, since it is obviously dependent on the nature of the anion. Tetramethylethylendiamine (TMEDA), the most examined ligand, can be attached to Li^+ in THF solution or can be replaced by THF. A review of this topic is found in the article of D. B. Collum, *Acc. Chem. Res.* **1993**, *26*, 227–234.

[25] Crystallographic data for **3a**-Li·3THF ($C_{22}H_{33}LiO_3$, $M_r = 352.42$): monoclinic, space group $P2_1/n$, $a = 895.6(1)$, $b = 1832.5(1)$, $c = 1278.8(1)$ pm, $\beta = 93.53(1)°$, $V = 2093.6(3) \times 10^{-30}$ m^3, $Z = 4$, $\rho_{calcd} = 1.118$ Mg m^{-3}, $\mu(Cu_{K\alpha}) = 0.557$ mm^{-1}. Enraf-Nonius CAD4 diffractometer, graphite monochromated $Cu_{K\alpha}$ radiation, $T = 193(2)$ K, 2781 reflections ($4 < \theta < 55°$), of which 2582 independent ($R_{int} = 0.029$). Solved by direct methods (SHELXTL-PLUS), refined on F^2 with all reflections (SHELXL-93). The non-hydrogen atoms were refined anisotropically, the hydrogen atoms isotropically. Parameters for the weighting scheme: 0.1088, 1.5505; *wR*2 (*R*1 for 2238 reflections with $I > 2\sigma(I)$): 0.194 (0.065), 242 refined parameters. The data were corrected with the programm DIFABS. All calculations were carried out on a Micro-VAX II and a DEC 3000-300X [15–19,26].

[26] N. Walker, S. Stewart, *Acta Crystallogr. Sect. A.* **1993**, *39*, 158.

Additions of Carbanions to a Cationic Cyclopentadienyl(naphthalene)iron Complex**

Ernst Peter Kündig,* Patrick Jeger, and Gérald Bernardinelli

Arenes bound to electrophilic transition metal complex fragments are activated for nucleophilic addition reactions.[1] When this type of complex contains a second unsaturated ligand, nucleophiles add to the more electron-deficient unit. In cationic arene(cyclopentadienyl)iron complexes, addition thus takes place on the arene rather than on the cyclopentadienyl ligand.[2] Some years ago, Davies, Green, and Mingos formulated concise rules for nucleophilic addition to cationic complexes having unsaturated organic ligands:[3] the selectivity in these reactions is based on charge control and the irreversibility of the addition. The predictions hold well for cationic complexes, because addition to this class of compounds generally proceeds under kinetic control. However, for complexes containing an electrophilic metal center, single electron transfer resulting in reduction of the metal center can be a competitive process. This can severely limit the scope of this C–C bond forming method. The reactivity of iron complex **1** (Cp = cyclopentadienyl) serves as an

$[(\eta^5\text{-Cp})(\eta^6\text{-naphthalene})\text{Fe}]PF_6$ **1**

example.[4] Unlike the benzene analogue, which reacts with carbanions to give η^5-cyclohexadienyl complexes,[5] complex **1** reacts with alkyllithium and Grignard reagents to give dark green solutions of the unstable 19e complex $[(\eta^5\text{-Cp})(\eta^6\text{-naphthalene})\text{Fe}^I]$.[6] We found that **1** is also reduced by stabilized carbon nucleophiles ($LiCMe_2CN$, $LiCH_2CN$, $LICH_2CO_2tBu$), and we did not succeed in isolating benzocyclohexadienyl complexes from the reaction mixtures. The naphthalene complex **1** behaves differently from the benzene complex in these reactions because complexes with condensed arenes as ligands are more easily reduced than those with monocyclic arenes. Cyclic voltammetry shows the naphthalene complex **1** to undergo one-electron reduction at -1.04 V,[7] whereas complexes with monocyclic arenes are reduced at more negative potentials (range -1.3 to -1.4 V).[7] We anticipated that methoxy substituents on naphthalene would make reduction more difficult and hopefully change the reaction pattern of the complex.

In this article we report on the synthesis of complex **2a** and on the observation that this complex, unlike **1**, reacts with

$[(\eta^5\text{-Cp})\text{-}\{(1\text{-}4,4a,8a\text{-}\eta)\text{-}5,8\text{-dimethoxynaphthalene}\}\text{Fe}]PF_6$ **2a**

carbanions by addition. Remarkably, depending on the nature of the carbanion, addition occurs to either or both of the ligands (arene and/or the cyclopentadienyl ring).

First attempts to synthesize complex **2a** and/or its (4a,5-8,8a-η) regioisomer **2b** by Lewis acid mediated ring exchange in ferrocene (**3**)[8] or by photolytic arene exchange[9] were not successful. We therefore turned to the thermal arene exchange reaction[10] and were pleased to obtain **2** from complex **4**[11] in

$[(\eta^5\text{-Cp})(\eta^6\text{-pyrene})\text{Fe}]PF_6$ **4**

nearly quantitative yield (ratio **2a**:**2b** = 19:1). Crystallization gave pure **2a** in 87% yield. Although the difference in reduction potential between **2a** ($E_1^0 = -1.11$ V) and **1** is only 70 mV,[7] the simple modification of substituting the noncomplexed ring is enough to change the reaction pathway from reduction to nucleophilic addition. Complex **2a** reacts readily with carbanions at low temperature. This was indicated by the formation of a red homogeneous solution when solid **2a** (insoluble in THF) was added to a solution of the organolithium reagent in THF at $-78\,^\circ$C. Neutral benzocyclohexadienyl complexes **5**–**7** were isolated from these reactions in high yield. The results are listed in Table 1 and they also include the reaction with $NaBH_4$.

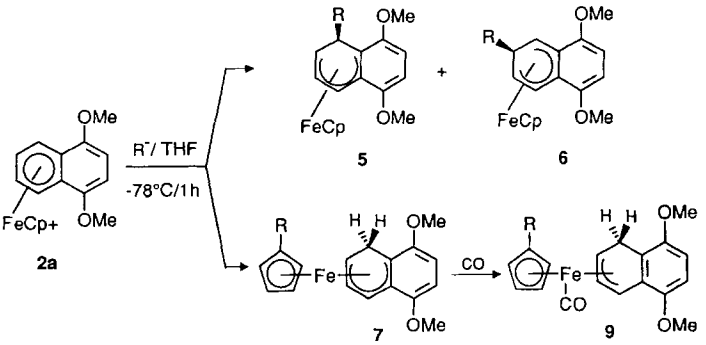

Table 1. Chemo- and regioselectivity of nucleophilic additions to complex **2a**.

Entry	Nucleophile R^- as salt	Products (and ratios) of addition to arene	to Cp	Yield [%]
1	$LiCH_2CN$	**5a** (91) : **6a** (9)	: **7a** (0)	85
2	$LiCH_2CO_2tBu$	**5b** (80) : **6b** (20)	: **7b** (0)	97
3	$NaBH_4$	**5c** (69) : **6c** (31)	: **7c** (0)	92
4	MeLi	**5d** (72) : **6d** (17)	: **7d** (11)	91
5	PhLi	**5e** (61) : **6e** (26)	: **7e** (13)	92
6	AllylLi	**5f** (75) : **6f** (7)	: **7f** (18)	98
7	$LiCMe_2CN$	**5g** (36) : **6g** (35)	: **7g** (29)	84
8	$LiCHS(CH_2)_3S$	**5h** (0) : **6h** (66)	: **7h** (34)	92
9	*t*BuLi	**5i** (0) : **6i** (0)	: **7i** (100)	77

Stabilized primary carbon nucleophiles and also hydride ions added exclusively to the naphthalene ligand to give the *exo* addition products **5** and **6**, where addition to C5 is favored over addition to C6. These results are analogous to those obtained previously with complex **8**.[12] Addition to C6 predominates

$[\{(1\text{-}4,4a,8a\text{-}\eta)\text{-}5,8\text{-dimethoxynaphthalene}\}\text{Cr}(CO)_3]$ **8**

with more reactive and/or more bulky nucleophiles. Again, there is precedence for this in reactions of the Cr complex **8**, with the difference that in the reactions reported here regioselectivity is independent of reaction time and temperature (-70 to $25\,^\circ$C), and we therefore assume that additions to **2a** are under kinetic control. The formation of **7** was unexpected. There is scarce precedence for addition to the Cp ring in this class of compounds.[13] Table 1 shows that the proportion of **7** increases with increasing size and reactivity of the nucleophile. *t*BuLi added selectively to the Cp ring.

[*] Prof. Dr. E. P. Kündig, Dr. P. Jeger
Département de Chimie Organique, Université de Genève
30 Quai Ernest Ansermet, CH-1211 Genève 4 (Switzerland)
Telefax: Int. code + (22)328-7396
Dr. G. Bernardinelli
Laboratoire de Crystallographie, Université de Genève

[**] We thank the Swiss National Science Foundation for support of this work (FNS grant 20-39118.93).

η^5-Benzocyclohexadienyl ligands can undergo facile haptotropic rearrangement to an η^3-enyl coordination mode.[14] Complex **7i**, when subjected to a CO atmosphere, gave product **9**, whose structure is shown in Figure 1.[15]

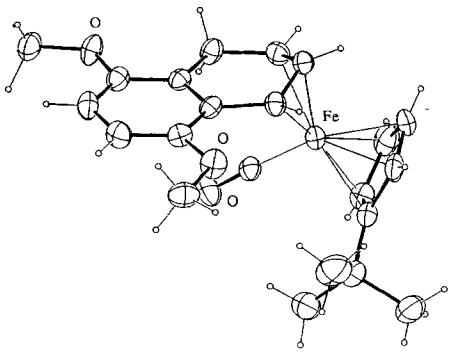

Fig. 1. Perspective view of the crystal structure of **9i**. Ellipsoids are at the 40% probability level.

The pathway for the the formation of **7** was probed using [D_5]-**2a**. In accord with ^{1}H NMR data we deduce a pathway which involves nucleophilic addition to the Cp ring, followed by D^- transfer from the Cp to the C5 *endo* position of the naphthalene ligand.[21] In agreement with the proposed stereochemistry, $[Ph_3C]PF_6$ reacts with [D_5]-**7i** by abstracting the *exo* H atom from C1 to give the cationic arene complex [D_5]-**10i**.[22]

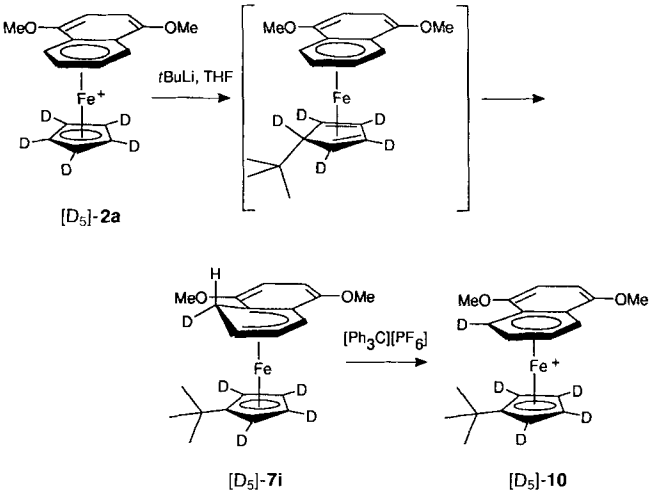

Experimental Procedure

2a: Under N_2, complex **4** [11] (11.6 g, 24.8 mmol) was added to liquid 1,4-dimethoxynaphthalene (23.3 g, 0.124 mol) at 130 °C. After stirring for 2.5 h at this temperature, the reaction mixture was cooled to room temperature and dissolved in CH_2Cl_2 (20 mL). On addition of hexane (100 mL) a dark precipitate formed which was collected by filtration and washed with toluene (3 × 20 mL). Extraction with CH_2Cl_2, filtration, and solvent removal yielded the crude complex, which consisted of **2a** and **2b** in a ratio of 19:1, according to the ^{1}H NMR spectrum. Recrystallization from CH_2Cl_2/toluene (5:1) gave red **2a** (9.83 g, 87%). M.p. 166 °C. ^{1}H NMR (200 MHz, [D$_6$]DMSO, 22 °C): δ = 7.29–7.33 (m, 2H; H_{Ar}), 7.06 (s, 2H; H-C(6,7)), 6.44–6.49 (m, 2H; H_{Ar}), 4.69 (s, 5H; H_{Cp}), 4.03 (s, 6H, H_{OMe}). ^{13}C NMR (50 MHz, [D$_6$]DMSO, 22 °C): δ = 149.2, 106.4, 88.6, 86.5, 79.4, 76.3, 56.6. ES-MS: *m/z* = 309 (M^+, 100). Anal. calc for $C_{17}H_{17}O_2FePF_6$ (454.1): C 44.96, H 3.77; found: C 44.87, H 3.80.

7i: Under N_2, complex **2a** (400 mg, 0.88 mmol) was added in one portion to a stirred, cold (−78 °C) solution of *t*BuLi (0.90 mmol) in THF (10 mL). A brown solution formed within minutes. The reaction mixture was stirred at −78 °C for 1 h and then hexane (50 mL) was added. After warming to ambient temperature, the reaction mixture was filtered over Celite. The ^{1}H NMR spectrum of the crude product showed 1,4-dimethoxynaphthalene and **7i**. During chromatography on Alox V (*n*-hexane/ether = 20/1) first the arene (33 mg, 20%), then **7i** (brown oil, 250 mg, 77%) eluted. ^{1}H NMR (C_6D_6, 200 MHz, 22 °C): δ = 7.47 (d, *J* = 5.3 Hz, 1H; H-C(4)), 5.79 (AB, *J* = 7.9 Hz, 2H; H-C(6,7)), 4.51–4.55 (*m*, 1H; H_{Cp}), 4.44 (dd, *J* = 6.3, 5.3 Hz, 1H; H-C(3)), 3.89 (dd, *J* = 13.2, 6.6 Hz; 1H, H_{endo}-C(1)), 3.67–3.70 (m, 1H; H_{Cp}), 3.59–3.62 (m, 1H; H_{Cp}), 3.53 (s, 3H; H_{OMe}), 3.49 (s, 3H; H_{OMe}), 2.74–2.77 (m, 1H; H_{Cp}), 2.65 (t, *J* = 6.5 Hz, 1H; H-C(2)), 1.86 (dd, *J* = 13.2, 1.2 Hz, H_{exo}-C(1)), 1.26 (*s*, 9H; H_{Me}). ^{13}C NMR (C_6D_6, 50 MHz, 22 °C): δ = 159.6, 151.5, 104.2, 98.7, 96.4, 91.0, 80.1, 76.1, 69.1, 68.9, 68.4, 55.0, 41.1, 31.6, 31.0, 24.1, 23.9. EI-MS (70 eV): *m/z*: 366 (M^+, 1), 309 (12), 188 (89), 173 (100).

9i: A solution of complex **7i** (250 mg, 0.68 mmol) in toluene (10 mL) was placed under CO (4.5 bar). After stirring for 5 h at 22 °C, the reaction mixture was filtered over Celite and the solvent removed in vacuo. Chromatography on Alox V (*n*-hexane/ether = 20/1) gave **9i** (170 mg, 63%), which was recrystallized from *n*-hexane. M.p. 113 °C. ^{1}H NMR (C_6D_6, 200 MHz, 22 °C): δ = 6.30 (AB, *J* = 8.8 Hz, 2H; H-C(6,7)), 5.26 (d, *J* = 6.1 Hz, 1H; H-C(4)), 4.76 (dd, *J* = 6.7, 6.1 Hz, 1H; H-C(3)), 4.49–4.58 (m, 1H; H-C(2)), 3.97–4.05 (m, 2H; H_{Cp}), 3.72–3.81 (m, 2H; H_{Cp}), 3.54 (s, 3H; H_{OMe}), 3.32 (s, 3H; H_{OMe}), 2.88–3.24 (m, 2H, H-C(1)), 1.22 (s, 9H; H_{Me}). ^{13}C NMR (C_6D_6, 50 MHz, 22 °C): δ = 222.9, 151.7, 149.0, 134.5, 119.1, 109.5, 108.8, 105.5, 79.6, 78.9, 78.6, 77.3, 67.9, 55.7, 55.0, 51.2, 44.1, 31.9, 30.8, 30.4. EI-MS (70 eV): *m/z* = 366 (M^+−CO, 4), 309 (100). Anal. calc for $C_{22}H_{26}O_3Fe$ (394.3): C 67.02, H 6.65; found: C 67.02, H 6.57.

Received: May 12, 1995 [Z 79801E]
German version: *Angew. Chem.* **1995**, *107*, 2305–2307

Keywords: arene complexes · iron compounds · haptotropic rearrangements · nucleophilic additions

[1] M. F. Semmelhack in *Comprehensive Organic Chemistry Vol. 4* (Eds.: B. M. Trost, I. Fleming), Pergamon, Oxford, **1991**, pp. 517–549.
[2] For a review of nucleophilic additions to cationic arene(cyclopentadienyl)iron complexes see: D. Astruc, *Tetrahedron* **1983**, *39*, 4027–4095.
[3] S. G. Davies, M. L. H. Green, D. M. P. Mingos, *Tetrahedron* **1978**, *34*, 3047–3077.
[4] R. G. Sutherland, S. C. Chen, W. J. Pannekoek, C. C. Lee, *J. Organomet. Chem.* **1975**, *101*, 221–229.
[5] A. N. Nesmeyanov, N. A. Vol'kenau, L. S. Shilovtseva, V. A. Petrakova, *J. Organomet. Chem.* **1975**, *85*, 365–373.
[6] A. N. Nesmeyanov, S. P. Solodovnikov, N. A. Vol'kenau, L. S. Kotova, N. A. Sinitsyna, *J. Organomet. Chem.* **1978**, *148*, C5–C8.
[7] D. Astruc, *Chem. Rev.* **1988**, *88*, 1189–1216.
[8] A. N. Nesmeyanov, N. A. Vol'kenau, I. N. Bolesova, *Tetrahedron Lett.* **1963**, 1725–1729. For an improved procedure see: H. O. Doggweiler, V. Desobry (Ciba-Geigy AG) *Eur. Pat. Appl.* 0270490A1, **1988** [*Chem. Abstr.* **1988**, *109*, 129310z].
[9] T. P. Gill, K. R. Mann, *Inorg. Chem.* **1980**, *19*, 3007–3010.
[10] Thermal arene exchange in [(naphthalene)Cr(CO)$_3$] is a mild and selective method that has found wide application. For recent reports see: a) E. P. Kündig, A. Ripa, R. Liu, D. Amurrio, G. Bernardinelli, *Organometallics* **1993**, *12*, 3724; b) M. Uemura, R. Miyake, K. Nakayama, M. Shiro, Y. Hayashi, *J. Org. Chem.* **1993**, *58*, 1238; c) A. Alexakis, P. Mangeney, I. Marek, F. Rose-Munch, E. Rose, A. Semra, F. Robert, *J. Am. Chem. Soc.* **1992**, *114*, 8288; d) H.-G. Schmalz, B. Millies, J. W. Bats, G. Dürner, *Angew. Chem.* **1992**, *104*, 640; *Angew. Chem. Int. Ed. Engl.* **1992**, *31*, 631. A patent report shows that the method has potential also in the synthesis of cationic arene(cyclopentadienyl)iron complexes: K. Meier (Ciba-Geigy AG) *Eur. Pat. Appl.* 0207889B1, [*Chem. Abstr.* **1987**, *107*, 23505k].
[11] M. Lacoste, H. Rabaa, D. Astruc, A. Le Beuze, J.-Y. Saillard, G. Précigoux, C. Courseille, N. Ardoin, W. Bowyer, *Organometallics* **1989**, *8*, 2233–2242.
[12] E. P. Kündig, V. Desobry, D. P. Simmons, E. Wenger, *J. Am. Chem. Soc.* **1989**, *111*, 1804–1814.
[13] Previous examples involve peralkylarenes: I. U. Khand, P. L. Pauson, W. E. Watts, *J. Chem. Soc. C* **1969**, 2024–2029; see also ref. [7].
[14] K. Jonas, *Pure Appl. Chem.* **1990**, *62*, 1169–1174.
[15] Crystallographic data for **9** (crystals were grown from a *n*-hexane solution): $Fe(C_{12}H_{13}O_2)(C_9H_{13})(CO)$, M_r = 394.3; μ = 0.811 mm^{-1}, $F(000)$ = 1664, ρ_{calcd} = 1.38 gcm^{-3}, monoclinic, *C2/c*, *Z* = 8, *a* = 20.758(3), *b* = 10.966(1), *c* = 16.934(2) Å, β = 99.239(7)°, *V* = 3804.7(8) Å^3, from 30 reflections (20° < 2θ < 25°). A violet prism of dimensions 0.16 × 0.18 × 0.20 mm was mounted in a capillary to prevent degradation. Cell dimensions and intensities were measured at room temperature on a Stoe STADI4 diffractometer with graphite-monochromated $Mo_{K\alpha}$ radiation (λ = 0.71069 Å), ω – 2θ scans, scan width 1.05 + 0.35 *tg*θ. Two reference reflections measured every 45 min showed variation less than 3.1σ(*I*). −23 < *h* < 23; 0 < *k* < 12; 0 < *l* < 19; 3136 measured reflections, 3016 unique reflections, of which 2091 were observed ($|F_o| > 4\sigma|F_o|$). Data were corrected for Lorentz and polarization effects and for absorption [16]. The structure was solved by direct methods using MULTAN 87 [17]; all other calculations used XTAL [18] system and ORTEP [19] programs. Atomic scattering factors and anomalous dispersion terms were

taken from ref. [20]. Full-matrix least-squares refinement based on $|F|$ using the weighting $1/\sigma^2(F_o)$ gave final values $R = 0.043$, $wR = 0.023$, and $S = 1.78$ for 313 variables and 2091 contributing reflections. The maximum shift/error on the last cycle was 0.003. All coordinates of the hydrogen atoms were observed and refined with a fixed value of isotropic displacement parameters ($U = 0.05$ Å^2), and the 26 other atoms were refined with anisotropic displacement parameters. The final difference electron density map showed a maximum of $+0.45$ and a minimum of -0.50 e Å^{-3}. Further details of the crystal structure investigation may be obtained from the Director of the Cambridge Crystallographic Data Centre, University Chemical Laboratory, 12 Union Road, GB-Cambridge CB2 1EZ (UK), on quoting the full journal citation.

[16] E. Blanc, D. Schwarzenbach, H. D. Flack, *J. Appl. Crystallogr.* **1991**, *24*, 1035–1041.

[17] P. Main, S. J. Fiske, S. E. Hull, L. Lessinger, G. Germain, J.-P. Declercq, M. M. Woolfson, *A System of Computer Programs for the Automatic Solution of Crystal Structures from X-Ray Diffraction Data*, University of York, England, and Louvain-la-Neuve, Belgium, **1991**.

[18] S. R. Hall, H. D. Flack, J. M. Stewart, *XTAL3.2 User's Manual*, Universities of Western Australia and Maryland, **1992**.

[19] C. K. Johnson, *ORTEP II*; Report ORNL-5138; Oak Ridge National Laboratory: Oak Ridge, TN, **1976**.

[20] *International Tables for X-ray Crystallography, Vol. IV*, Birmingham, Kynoch, **1974**.

[21] Interannular H-transfer is frequent in polyene–metal complexes. For a recent example in ferrocene chemistry see: A. Cunningham, Jr., *Organometallics*, **1994**, *13*, 2480–2485. In the reaction of [D_5]-**2a** with *t*BuLi, the product [D_5]-**7i** does not display the ^{1}H NMR signal associated with the *endo* H atom at C1 of the benzocyclohexadienyl ligand ($\delta = 3.89$).

[22] Trityl cations have been used extensively to remove *exo* hydride from organometallic complexes: For an example in Fe chemistry see: D. Mandon, L. Toupet, D. Astruc, *J. Am. Chem. Soc.* **1986**, *108*, 1320–1322.

Highly Effective Hydrogen-Bonding Receptors for Guanine Derivatives**

Thomas W. Bell,* Zheng Hou, Steven C. Zimmerman,* and Paul A. Thiessen

Many artificial receptors have been designed and synthesized for the purpose of recognizing nucleobases.[1–4] Hydrogen-bonding receptors can bind nucleobase derivatives tightly in nonpolar organic solvents,[1, 2] but ionic or solvophobic interactions are usually needed for strong complexation of nucleosides and nucleotides in polar solvents.[1a, b, 3, 4] Hydrogen bonds are critical to biomolecular recognition of guanosine phosphates[5] and other nucleotides, but they are greatly weakened in polar solvents. Herein we show that receptors having hydrogen bonding sites positioned on a hexagonal lattice (hexagonal lattice receptors)[6] can bind guanine derivatives tightly through hydrogen bonds alone, even in a highly competitive solvent such as DMSO. Decreasing the preorganization or number of hydrogen bond donor or acceptor sites in the receptor weakens the complex.

Guanine derivatives **1**–**3**[7] were chosen as guests for the current study, and hosts **4**–**7** were designed to form hydrogen bonded complexes, as shown for **4** in structure **I**. Receptors **4**–**7** have varying degrees of flexibility and numbers of hydrogen-bonding sites, enabling estimation of enthalpic and entropic contributions to the binding free energy.[8] The design of **4** and **5** combines the fused pyridine framework of hexagonal lattice receptors for urea,[6e, f] guanidinium,[6d, e] and benzamidinium[6c] with *o*-aminonitrile hydrogen bond donors[6a] that are complementary to acceptor sites on guanine. Preorganized receptors **4** and **5** were synthesized from benzylidene ketone **8**[6b, e] by the methods shown in Scheme 1, and flexible analogue **6** was

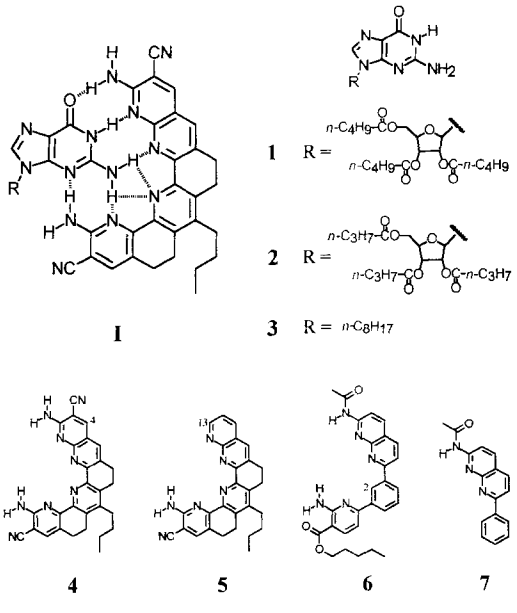

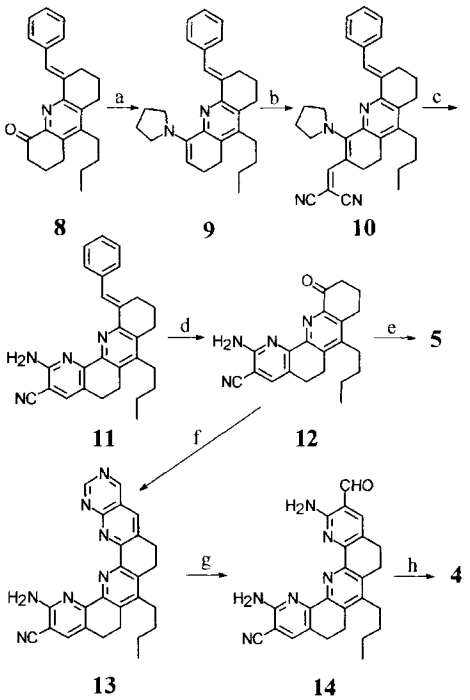

Scheme 1. Synthesis of preorganized receptors **4** and **5**. a) Pyrrolidine, benzene, reflux, 24 h (64%); b) $CH_3CH_2OCH{=}C(CN)_2$, THF, −20 °C, 0.5 h; c: conc. aq. NH_3, THF, reflux, 4 h (61% from **9**) [9]; d) CH_2Cl_2/CH_3OH, O_3, −78 °C (76%); e) 2-aminonicotinaldehyde [10], CH_3OH/toluene (5:3, v/v), 1,8-diazabicyclo[5.4.0]undec-7-ene (DBU), reflux, 24 h (73%); f) 4-amino-1,3-pyrimidine-5-carboxaldehyde [11], CH_3OH/toluene (3:2, v/v), 15% KOH/CH_3OH, reflux, 30 h (36%); g) 0.2 N HCl, reflux, 12 h (100%); h) $CH_2(CN)_2$, CH_3OH/toluene (3:2, v/v), piperidine, reflux, 24 h (79%) [12].

[*] Prof. T. W. Bell,[+] Z. Hou
Department of Chemistry, State University of New York
Stony Brook, NY 11794-3400 (USA)

[+] New address: Department of Chemistry/216, University of Nevada
Reno, NV 89557-0020 (USA)
Telefax: Int. code + (702) 784-6804

[*] Prof. S. C. Zimmerman, P. A. Thiessen
Department of Chemistry, University of Illinois at Urbana-Champaign
600 South Mathews Avenue, Urbana, IL 61801 (USA)
e-mail: Zimmerma@aries.scs.uiuc.edu

[**] This work was funded by the National Institutes of Health (GM 32937 and GM 38010).

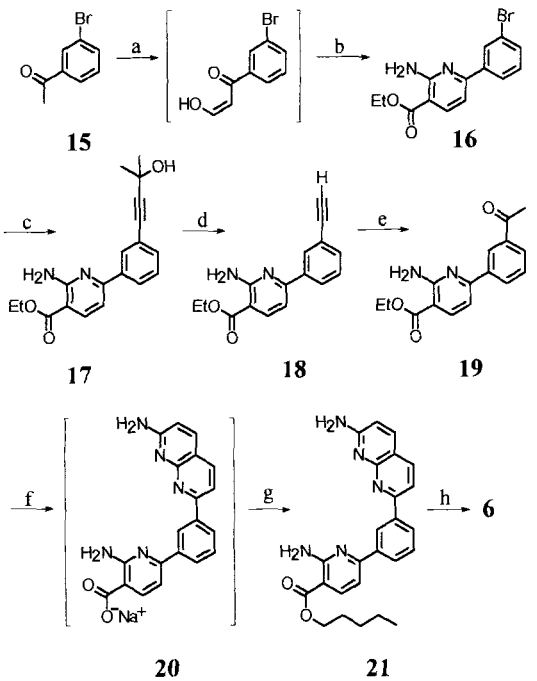

Scheme 2. Synthesis of flexible receptor **6**. a) HCO_2Et, NaH, ethanol/benzene, reflux, 22 h; b) ethyl 3,3-diamino-2-propenoate hydrochloride [13], ethanol (50% from **15**); c) 2-methyl-3-butyn-2-ol, $[(PPh_3)_2PdCl_2]$, CuI, PPh_3, Et_3N, reflux, 2 h (92%) [14]; d) NaH, toluene, distillation (80%) [15]; e) conc. HCOOH, sealed tube, 150 °C, 10 h (92%) [16]; f) 2,6-diamino-3-pyridinecarboxaldehyde [17], 20% NaOH/MeOH, toluene, reflux, 1 h; g) *n*-pentanol, H_2SO_4, reflux, 15 h (67% from **19**); h) $(CH_3CO)_2O$, CH_2Cl_2, room temperature, 15 min (67%).

prepared as shown in Scheme 2. Receptor **7** was prepared from acetophenone and 2,6-diamino-3-pyridinecarboxaldehyde[17] by analogy with the synthesis of **6**.[18]

Binary mixtures of $CDCl_3$ and [D_6]DMSO served as convenient solvents for ^{1}H NMR studies of complexation for the following reasons: 1) guests **1**–**3** and hosts **4**–**7** are soluble over wide concentration ranges; 2) the [D_6]DMSO/$CDCl_3$ ratio can be decreased to observe host and guest aggregation,[19] then increased to conduct binding studies without competing aggregation; and 3) the [D_6]DMSO/$CDCl_3$ ratio can be increased to weaken 1:1 complexes, enabling measurement of stability constants (K_a) by titration and dilution methods.[20] The stability constants of complexes listed in Table 1 were determined by addition of the guanine guests to solutions of the hosts or by addition of the hosts to solutions of the guests. The chemical shifts of the compound with the fixed concentration were used to model complexation equilibria. The stability constants were checked by dilution of the 1:1 complexes or by multiple titrations. A 1:4 mixture of [D_6]DMSO and $CDCl_3$ was found to be the best solvent for comparing the binding abilities of all four receptors, though only the lower limit of the stability constant could be estimated for the strongest complex (**4**·**2**) in this solvent.

The complexation shifts and relative stability constants in Table 1 are all consistent with the binding model shown in structure **I**. For example, extending receptor **5** to **4** or receptor **7** to **6** markedly increases the K_a value, indicating that the aminopyridine units contribute to the binding. Furthermore, stability constants are inversely related to the amount of [D_6]DMSO in the solvent mixture, showing that desolvation of host and guest is a significant factor. Finally, the K_a values for complexes between receptors **4**–**6** and **1** measured at Illinois were identical to those for the analogous complexes of **4**–**6** and **2** measured at

Table 1. Stability constants [M^{-1}] and free energies of association [kcal mol^{-1}], in parentheses) for 1:1 complexes of receptors **4**–**7** with guanine derivatives **1**–**3** (298 K) [a], as calculated from changes in ^{1}H NMR chemical shifts ($\Delta\delta$) on complexation.

Complex	Solvents	([D_6]DMSO/$CDCl_3$, v/v)		
$\Delta\delta_{max}$ [b]	1:0	1:1	1:4	1:19
4·**2**	140 ± 20	3800 ± 300	>190000 [d]	
0.14 [c]	(− 2.9)	(− 4.8)	(< − 7.1)	
5·**2**		380 ± 50	19000 ± 3000	
0.47 [e]		(− 3.5)	(− 5.7)	
5·**3**			9000 ± 1000	
0.47 [e]			(− 5.3)	
6·**1**			180	4600
0.19, − 0.25, − 0.21 [f]			(− 3.0)	(− 4.9)
6·**2**			170 ± 10	
1.57 [g]			(− 3.0)	
6·**3**			190	5000
2.21 [h]			(− 3.1)	(− 5.0)
7·**1**			ca. 14	360
2.52, 1.33 [i]			(− 1.5)	(− 3.4)

[a] Errors given are σ values for the averages of K_a values calculated for each data point; duplicate measurements by nonlinear regression were within 20% of the K_a values, for which no errors are given. [b] Unless stated otherwise, chemical shifts on complexation for the species at a fixed concentration were calculated from analysis of the results of titrations in [D_6]DMSO/$CDCl_3$ (1:4); positive $\Delta\delta_{max}$ value for downfield shift. [c] H4 in **4**, [D_6]DMSO/$CDCl_3$ (1:1). [d] Estimated by assuming that the difference between the binding energies of **4**·**2** and **5**·**2** should be larger in 1:4 [D_6]DMSO/$CDCl_3$ than in the 1:1 solvent mixture. [e] H13 in **5**. [f] H1′, H2′, and H3′, respectively, in **1**. [g] H2 in **6**. [h] NH in **3**. [i] NH and NH_2, respectively, in **1**.

Stony Brook. These results indicate both that the minor structural difference between guests **1** and **2** is irrelevent to binding strength and that experimental variations between the different laboratories negligibly affect the binding analyses.

The most striking result shown in Table 1 is that receptor **4** binds triacylated guanosine **2** in 1:1 [D_6]DMSO/$CDCl_3$ with a K_a value of greater than 3000 M^{-1} by means of hydrogen bonding alone. Even in pure DMSO the complex **4**·**2** is moderately stable. Flexible receptor **6** can form the same number of primary hydrogen bonds with guanosine **2**, but in 1:4 [D_6]DMSO/$CDCl_3$ the complex **6**·**2** is at least 4.1 kcal mol^{-1} weaker than **4**·**2**. The source of the difference in the stabilities of these two complexes cannot be elucidated completely because receptors **4** and **6** have several structural differences. Nevertheless, it is instructive to consider the factors that may be responsible.[8] Two degrees of rotational freedom must be lost in **6** upon complexation. In a related host–guest study the energy cost of freezing an aryl–aryl bond was determined to be 0.9 kcal mol^{-1},[21] in line with Jencks's estimate of 0.5–1.4 kcal mol^{-1} per restricted rotation.[8d] This loss in entropy accounts for less than half of the difference between the stabilities of complexes **4**·**2** and **6**·**2**. The remainder can be attributed to enthalpic factors, including secondary electrostatic interactions[22] that stabilize **4**·**2** (structure **I**) and conformational strain in **6**·**2** caused by steric interactions involving the aromatic hydrogens (structure **II**). Additionally, the convergence of nonbonded electrons shown in structure **III** may weaken solvation of the host cleft per hydrogen bond acceptor, enhancing hydrogen bond strengths in complex **4**·**2**. The large increase in binding energy observed upon ligand extension from **5** to **4** apparently reflects the "intrinsic energy" described by Jencks[8d] and shows that much of the entropy cost in **4**·**2** is already paid upon formation of **5**·**2**.

Although acetamido, *o*-aminoester, and *o*-aminonitrile groups are all expected to be good hydrogen bond donors, host series **4**–**7** does not allow comparison of relative donor abilities. To determine if **4**·**2** and **5**·**2** might be stabilized by an additional interaction between the 2′-ester group of **2** and the *o*-aminoni-

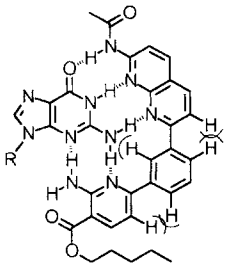

II

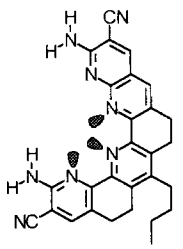

III

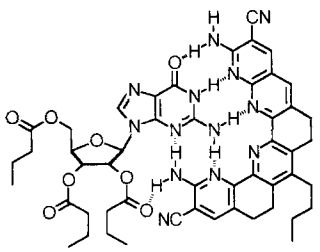

IV

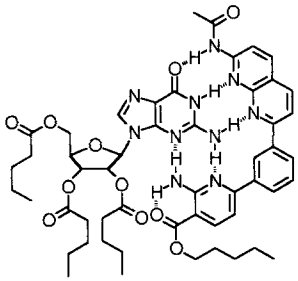

V

trile group (cf. structure **IV**), the complexation studies were repeated using 9-octylguanine (**3**). Interestingly, **5·2** is 0.8 kcal mol^{-1} more stable than **5·3**, whereas **6** binds 9-octylguanine (**3**) as strongly as it does **1** or **2**. It is possible that intramolecular hydrogen bonding in the *o*-aminoester group of **6** (see structure **V**) weakens this additional interaction, which represents a final contribution to the remarkable stability of **4·2**.

This comparison of synthetic receptors for guanosine derivatives demonstrates that hydrogen-bonded complexes between neutral organic molecules can be stable in highly competitive solvents if some of the energy costs of binding are paid in advance during the synthesis of highly preorganized receptors. The synthetic price of preorganized receptors is comparable to that of flexible analogues explored in this study. Questions that remain are whether such hosts can select between different nucleosides and whether chromogenic or fluorogenic groups can be incorporated into their structures to optically signal the binding event.[6a, 23]

Received: March 20, 1995
Revised version: May 29, 1995 [Z 7812 IE]
German version: *Angew. Chem.* **1995**, *107*, 2321–2324

Keywords: hydrogen bonds · molecular recognition · nucleosides

[1] Reviews: a) S. C. Zimmerman, *Top. Curr. Chem.* **1993**, *165*, 71–102; b) A. D. Hamilton *Adv. Supramol. Chem.* **1991**, *1*, 1–64; c) J. Rebek, Jr., *Acc. Chem. Res.* **1990**, *23*, 399–404.

[2] a) M. Inouye, K. Kim, T. Kitao, *J. Am. Chem. Soc.* **1992**, *114*, 778–780; b) F. Vögtle, *Angew. Chem.* **1991**, *103*, 433–436; *Angew. Chem. Int. Ed. Engl.* **1991**, *30*, 442–444; c) S. C. Zimmerman, Z. Zeng, W. Wu, D. E. Reichert, *J. Am. Chem. Soc.* **1991**, *113*, 196–201; d) K. S. Jeong, T. Tjivikua, A. Muehldorf, G. Deslongchamps, M. Famulok, J. Rebek, Jr., *ibid.* **1991**, *113*, 201–209.

[3] a) V. Král, J. L. Sessler, *Tetrahedron* **1995**, *51*, 539–554; b) M. M. Conn, G. Deslongchamps, J. de Mendoza, J. Rebek, Jr., *J. Am. Chem. Soc.* **1993**, *115*, 3548–3557; c) E. B. Schwartz, C. B. Knobler, D. J. Cram, *ibid.* **1992**, *114*, 10775–10784; d) H. Furuta, D. Magda, J. L. Sessler, *ibid.* **1991**, *113*, 978–985.

[4] a) P. Schiessl, F. P. Schmidtchen, *J. Org. Chem.* **1994**, 509–511; b) A. V. Eliseev, H.-J. Schneider, *J. Am. Chem. Soc.* **1994**, *116*, 6081–6088; c) M. Dhaenens, J.-M. Lehn, J.-P. Vigneron, *J. Chem. Soc. Perkin Trans. 2* **1993**, 1379–1381; d) V. M. Rotello, E. A. Viani, G. Deslongchamps, B. A. Murray, J. Rebek, Jr., *J. Am. Chem. Soc.* **1993**, *115*, 797–798.

[5] a) T. S. McConnell, T. R. Cech, *Biochemistry* **1995**, *34*, 4056–4067; b) E. F. Pai, W. Kabsch, U. Krengel, K. C. Holmes, J. John, A. Wittinghofer, *Nature* **1989**, *341*, 209–214.

[6] a) D. Beckles, J. Maioriello, V. J. Santora, T. W. Bell, E. Chapoteau, B. P. Czech, A. Kumar, *Tetrahedron* **1995**, *51*, 363–376; b) T. W. Bell, Y.-M. Cho, A. Firestone, K. Healy, J. Liu, R. Ludwig, S. D. Rothenberger in *Organic Syntheses, Collective Vol. VIII* (Ed.: J. P. Freeman), Wiley, New York, **1993**, 87–93; c) T. W. Bell, V. J. Santora, *J. Am. Chem. Soc.* **1992**, *114*, 8300–8302; d) T. W. Bell, J. Liu, *Angew. Chem.* **1990**, *102*, 931–933; *Angew. Chem. Int. Ed. Engl.* **1990**, *29*, 923–925; e) T. W. Bell, A. Firestone, J. Liu, R. Ludwig, S. D. Rothenberger in *Inclusion Phenomena and Molecular Recognition* (Ed.: J. L. Atwood), Plenum, New York, **1990**, pp. 49–56; f) T. W. Bell, J. Liu, *J. Am. Chem. Soc.* **1988**, *110*, 3673–3674.

[7] For the synthesis of **1** and **2**, see A. Matsuda, M. Shinozaki, M. Suzuki, K. Watanabe, T. Miyasaka, *Synthesis* **1986**, 385–386. For the synthesis of **3**, see F. Seela, A. Kehne, H.-D. Winkeler, *Liebigs Ann. Chem.* **1983**, 137–146; J. Kjellberg, M. Liljenberg, N. G. Johansson, *Tetrahedron Lett.* **1986**, *27*, 877–880.

[8] a) D. H. Williams, M. S. Searle, P. Groves, J. P. Mackay, M. S. Westwell, D. A. Beauregard, M. F. Cristofaro, *Pure Appl. Chem.* **1994**, *66*, 1975–1982; b) D. H. Williams, M. S. Searle, J. P. Mackay, U. Gerhard, R. A. Maplestone, *Proc. Natl. Acad. Sci. USA* **1993**, *90*, 1172–1178; c) A. R. Fersht, *Trends Biochem. Sci.* **1987**, *12*, 301–304; d) W. P. Jencks, *Proc. Natl. Acad. Sci. USA* **1981**, *78*, 4046–4050.

[9] H. Kurihara, H. Mishima, *J. Heterocycl. Chem.* **1977**, *14*, 1077–1079.

[10] T. G. Majewicz, P. J. Caluwe, *J. Org. Chem.* **1974**, *39*, 720–721.

[11] J. Baddiley, B. Lythgoe, A. R. Todd, *J. Chem. Soc.* **1943**, 386–387.

[12] E. W. Hawes, D. K. J. Gorecki, D. D. Johnson, *J. Med. Chem.* **1973**, *16*, 849–853.

[13] S. M. McElvain, B. E. Tate, *J. Am. Chem. Soc.* **1951**, *73*, 2760–2764; H. Meyer, F. Bossert, H. Horstmann, *Liebigs Ann. Chem.* **1977**, 1895–1908.

[14] E. T. Sabourin, A. Onopchenko, *J. Org. Chem.* **1983**, *48*, 5135–5137.

[15] S. J. Havens, P. M. Hergenrother, *J. Org. Chem.* **1985**, *50*, 1763–1765.

[16] N. Menashe, Y. Shvo, *J. Org. Chem.* **1993**, *58*, 7434–7439.

[17] E. E. Fenlon, T. J. Murray, M. H. Baloga, S. C. Zimmerman, *J. Org. Chem.* **1993**, *58*, 6625–6628.

[18] All new compounds gave elemental analyses and spectra in accord with assigned structures.

[19] Variable-concentration ^{1}H NMR experiments indicated that **1** and **2** aggregate in [D$_6$]DMSO/CDCl$_3$ mixtures containing less than 5% [D$_6$]DMSO by volume. Guanosine dimerizes weakly in pure DMSO: R. A. Newmark, C. R. Cantor, *J. Am. Chem. Soc.* **1968**, *90*, 5010–5017.

[20] a) C. S. Wilcox in *Frontiers of Supramolecular Organic Chemistry and Photochemistry* (Eds.: H.-J. Schneider, H. Dürr), VCH, Weinheim, **1990**, pp. 123–143; b) T. Wang, J. S. Bradshaw, R. M. Izatt, *J. Heterocycl. Chem.* **1994**, *31*, 1097–1114.

[21] S. C. Zimmerman, M. Mrksich, M. Baloga, *J. Am. Chem. Soc.* **1989**, *111*, 8528–8530.

[22] a) S. C. Zimmerman, T. J. Murry, in *Computational Approaches in Supramolecular Chemistry*, (Ed.: W. Wipff), (*NATO ASI Ser.* **1994**, *426*, 109–115); b) W. L. Jorgensen, J. Pranata, *J. Am. Chem. Soc.* **1990**, *112*, 2008–2010.

[23] T. W. Bell, D. L. Beckles, P. J. Cragg, J. Liu, J. Maioriello, A. T. Papoulis, V. J. Santora in *Fluorescent Chemosensors of Ion and Molecule Recognition*, (Ed.: A. W. Czarnik), (*ACS Symp. Ser.* **1993**, *538*, 85–103).

Corrigendum

In the communication "1,5-Anhydrohexitol Nucleic Acids, a New Promising Antisense Construct" by Arthur Van Aerschot,* Ilse Verheggen, Chris Hendrix, and Piet Herdewijn (*Angew. Chem. Int. Ed. Engl.* **1995**, *34*, 1338–1339) the curves of Figure 3 were inadvertently exchanged in the legend. The dashed curve was determined at 260 nm (A_1) and the solid curve at 284 nm (A_2).

Compromises: Quality, Quantity, and Cost

Biographical Encyclopedia of Scientists. 2nd Edition. Edited by *J. Daintith, S. Mitchell, E. Tootill* and *D. Gjertsen.* Institute of Physics, Bristol and Philadelphia, 1994. Two-volume set, 1075 pp., hardcover £ 95.00.—ISBN 0-7503-0287-9

Whereas book reviews are usually written by request of editors of learned journals, the present report has been prompted by my experiences while using this recently purchased two-volume encyclopedia. First I have to make a confession: I did not read the encyclopedia from cover to cover. I only perused it in the course of some work I am doing, which led me to consult only about 100 of its 2000 short biographies. Secondly, being a chemist with some physical leanings, my 5% sample concerns mainly chemistry and could therefore be a biased one. A mathematician or an astronomer may well get a different impression from that reported below.

According to the masthead, no fewer than seven proofreaders have read the encyclopedia's 1075 pages, compiled by 15 contributors. Despite this, the name of one of my teachers, Nobel prize winner Leopold Ruzicka, is consistently (eight times) misspelled "Ruicka", and that of another one, Christopher Longuet-Higgins, is always graced with a second "t" i.e. "Longuett". Heyrovsky is shortened to "Heyrovsk" and Benjamin Thompson, later Lord Rumford, has been renamed "Thomson". Gerd Binnig, who shared the Nobel prize for the invention of the scanning tunneling electron microscope, is renamed "Bining", Conrad Gessner becomes "Gesner", and in Newton's biography his mathematical rival is called "Liebnitz". Von Laue's coworker in the discovery of X-ray diffraction is named "Kipping" instead of Knipping. We are told that Professor Wittig worked in "Heidelberg", that Chaim Weizmann obtained his doctorate in "Freiburg, Germany" instead of Fribourg, Switzerland, and that Richard Stock died in 1946 "in Karlsruhe, now in Germany". Albert Einstein's biography mentions his four fundamental papers published in 1905 in *Annalen der Physik*. However, the one on Brownian movement, claimed to be the first one, was in fact the second (pp. 549–560 of Vol. 17) and its German title is quoted with four mistakes in it, whereas the paper on the photoelectric effect, said to be the second paper, was in fact the first one (pp. 132–148 of the same volume).

The two volumes are so very sparsely illustrated that the reader feels drawn almost automatically to look at the few figures. Leaving aside the fact that the reasons for the particular choice of some of these illustrations are not always obvious, it seems strange that they are not referred to in the text and that they lack a detailed explanatory caption, in particular with respect to the symbols used. One of these illustrations purports to show a two-dimensional section through the ground-state electron cloud of the hydrogen atom according to Schrödinger. Instead of having a maximum at the origin and falling off with increasing distance, the electron density is zero at the origin with a maximum at some unspecified distance r from it. Obviously the authors have confused the density function $\Psi\Psi^*$ with the radial distribution $4\pi r^2\Psi\Psi^*$. Augustin Fresnel's biography is followed by a figure allegedly showing the section through a Fresnel lens. If this were true, the lens would be about as effective as a window pane, the inner and outer faces of the individual rings being parallel to each other.

The work of Biot, who discovered in 1815 that certain liquids (e.g. turpentine, solutions of camphor) rotate the plane of polarized light, is illustrated by showing—without comment—the stereo-formulas of the enantiomers of tartaric acid! However, Pasteur's work on ammonium tartrate dates from 1848, and the two formulas shown were not known until Van't Hoff's and Le Bel's publications in 1874. Unfortunately, Le Bel's biography in the encyclopedia is accompanied by a linear formula for water, H–O–H, and by planar (!) formulas for methane, ethanol, and dimethylether with 90° HCH bond angles and a linear C–O–C bond. But these pale into insignificance compared with the following two formulas for methylene chloride, which are presumably supposed to illustrate the phenomenon of enantiomerism:

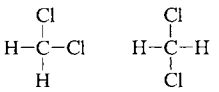

The account of Ziegler's Nobel prize winning research is illustrated by portions of isotactic and syndiotactic polypropylene chains. These should, of course, have accompanied the biography of Giulio Natta, who shared the Nobel prize with Ziegler. Also, the two formulas depicting Alfred Werner's coordination complexes lack a central metal atom. The author consortium's lack of appreciation of chemistry (see also the comment on "Chronology" below) is amusingly obvious from statements such as "[Willstaetter's] work on chlorophyll was justified in 1960 when Robert Woodward succeeded in synthesizing the compounds described by his formulae and came up with chlorophyll". You can almost see Woodward's surprised reaction.

The most remarkable illustration is that following the biography of Copernicus. To counter possible disbelief, this figure is reproduced directly from the encyclopedia:

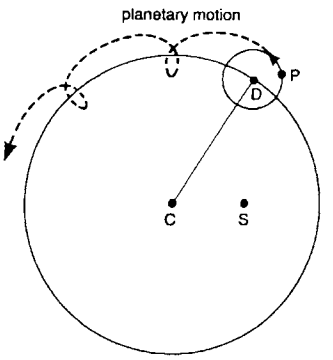

COPERNICAN SYSTEM The epicyclic motion of a planet.

This section contains book reviews and a list of new books received by the editor. Book reviews are written by invitation from the editor. Suggestions for books to be reviewed and for book reviewers are welcome. Publishers should send brochures or (better) books to Dr. Ralf Baumann, Redaktion Angewandte Chemie, Postfach 101161, D-69451 Weinheim, Federal Republic of Germany. The editor reserves the right of selecting which books will be reviewed. Uninvited books not chosen for review will not be returned.

 © *VCH Verlagsgesellschaft mbH, D-69451 Weinheim, 1995* *0570-0833/95/3419-2167 $ 10.00+.25/0*

The whirring sound you hear is Copernicus rotating in his grave.

In the preface the editors discuss their selection criteria. With regard to 20th century candidates, many of them still living, they are "guided by lists of prizes and awards made by scientific societies..." and in addition the "compilers and editors have used their own judgement in choosing what is important or useful". However, it is sometimes rather difficult to appreciate the basis of such judgements. Whereas one will look in vain for chemists such as H. Meerwein, A. Katchalsky, S. Winstein, G. Olah, J. A. Pople, E. Wiberg, W. Reppe, T. Nozoe, G. Schwarzenbach, or G. Wilke—to name but a few at random—we are told at great length about F. Hurter whose only claim to fame (according to the authors) is that he became chief chemist at Holbrook Gaskell & Henry Deacon's alkali factory. Or take Lyon Playfair, 1st Baron, on whom I stumbled by accident. "As a politician he was reasonably successful" we are told, but as a scientist he was obviously a failure, nothing of relevance being reported. Even some physicists, such as W. Kossel, G. Wenzel, T. Koopmans (who, admittedly, gained his Nobel prize in economics), or even such an important contributor to the quantum theory as Friedrich Hund (!) were not considered worthy of inclusion, in contrast to Ernö Rubik (his first name is given as "Erno") whose invention of a toy, the Rubik cube, earns him a longer entry than those of many living scientists.

In a section entitled "Chronology" the authors have compiled year by year what they consider the most important discoveries in the fields of mathematics, physics, chemistry, biology, and medicine. During the last 40 years, roughly the span of an academic lifetime, chemists and in particular organic chemists must have been sound asleep. Whereas scientists working in other fields seem to have produced noteworthy results practically every year, chemistry is mentioned only ten times. Of these ten entries, three refer to fullerenes and three to the depletion of the ozone layer by chlorofluorohydrocarbons. The remaining four mentions concern the discovery of crown ethers by Pedersen, the preparation of rare gas compounds by Bartlett, Prigogine's work on irreversible thermodynamics, and the discovery of quasi-crystals by Shechtman. The latter's name is misspelled "Schectman", and although his important work is deemed worthy of mention in the chronology, a biographical note devoted to Shechtman is lacking.

These shortcomings may be regarded as nothing but nagging criticism of points of minor importance, but they do not inspire confidence in the reliability of biographies of scientists you know little or nothing about. In this connection, my major criticism is that the encyclopedia does not contain a single reference to primary or secondary literature. Not only are we not told the sources of the information given, but the reader is offered no help at all if he or she wants to follow up or complement—and check!!—the short biographies provided. Thus, if you want additional information, you must do what you would have done anyway without the encyclopedia, namely go to the library to search for reliable works of reference and biography.

Edgar Heilbronner
Herrliberg (Switzerland)

The Biographical Dictionary of Scientists. Second Edition. Edited by *R. Porter*. Oxford University Press, New York, 1994. LVII, 891 pp., hardcover $ 85.00 (also published in Great Britain as The Hutchinson Dictionary of Scientific Biography, Helicon, Oxford, 1994, £ 50.00).—ISBN 0-19-521083-2

In the mid-1980s Peter Bedrick (New York) published and Harper & Row (New York) distributed a six-volume set, *The Biographical Dictionary of Scientists,* edited by David Abbott, with volume titles *Astronomers* (1984), *Biologists* (1984), *Chemists* (1984), *Physicists* (1984), *Mathematicians* (1986), and *Engineers and Inventors* (1986). Now Roy Porter, Associate Director of the Wellcome Institute of the History of Medicine, London, and 34 other contributors have produced the second edition of this reference work in one convenient volume, which includes entries on men and women from ancient times to the present day in the above fields of science plus geology, ranging in length from seven lines (al-Sufi) to three pages (Sir Isaac Newton). Arranged alphabetically from Abbe to Zworykin, the entries not only provide basic biographical information in a historical and scientific context but also discuss the significance of the scientist's contribution and show how the scientist's personal, social, political, religious, and artistic concerns affected his or her life. The work also contains a short general introduction and succinct (6–7 page) historical reviews of the seven fields (in the case of chemistry, a panorama recounting highlights from contributions of the ancient Egyptians to the discovery of buckyballs), along with 107 illustrations (but unfortunately no portraits). Useful but unusual features for a biographical dictionary are an extensive (77-page) glossary of about 2000 items, and appendices listing Nobel laureates for chemistry, physiology or medicine, and physics through 1993 and the grounds for their awards. A detailed 47-page index (3 columns per page), with names of the biographees in capitals, facilitates quick access to information. British spelling is used consistently, and although the coverage is international, a surprisingly large amount of space is devoted to British scientists, some of whom are only minor figures.

Some closely associated scientists, 25 in all, are grouped together and discussed in single entries, e.g., Beadle, Tatum, and Lederberg; Crick, Watson, and Wilkins; Fischer and Wilkinson; Hall and Héroult. Many, but by no means all, Nobel laureates are the subjects of entries. Psychiatrists and psychologists such as Adler, Eysenck, Freud, Jung, and Piaget are included, as is Nicolas Bourbaki, the collective pseudonym for the group of mathematicians who have been publishing collectively and anonymously since the late 1930s. Although almost a third of the contributors to this volume are women, only 19 women are discussed, including well-known scientists such as Rachel Carson, Goeppert-Mayer, Hodgkin, Meitner, McClintock, and Yalow, and lesser-known ones such as Hyman and Morgan. Obviously, additional efforts are required to include women scientists in biographical dictionaries such as this and others.

Unlike the 18-volume *Dictionary of Scientific Biography* (DSB), which is the standard in this genre, the volume under review here includes living subjects such as science popularizers David Attenborough, Jacques Cousteau, Richard Dawkins, Stephen Jay Gould, Stephen Hawking, and Carl Sagan. Although Lysenko, Mendeleev, and Pavlov are included, Russian scientists such as Borodin, Butlerov, Chugaev, Kurnakov, Lomonosov, Vernadsky and Zinin are missing, as are some important chemists of other nationalities. The extent of coverage is still not always commensurate with the scientist's contributions, a defect noted by at least one reviewer of the "Mathematicians" volume of the first edition (D. V. Feldman, *Choice* **1986**, *23*, 1651). For example, Lavoisier rates only a page, while lesser figures, in chemistry and other fields, receive equal or greater coverage. Although touted as "updated and expanded," the entry on Henry Gilman (p. 277), who died in 1986, and the passing mention of Robert Mullikan, who died in 1986 (p. 440), do not reflect this fact.

 © VCH Verlagsgesellschaft mbH, D-69451 Weinheim, 1995 0570-0833/95/3419-2168 $ 10.00+.25/0

With its coverage of 1178 scientists, this volume compares favorably with its primary competitors, e.g., Asimov's *Biographical Dictionary of Science and Technology* (2nd revised edition, Doubleday, Garden City, NY 1982—1510 entries, $ 39.95 paperback); David, Ian, John, and Margaret Millar's *Chambers Concise Dictionary of Scientists* (W. & R. Chambers Ltd., Edinburgh, Scotland, 1989—882 entries, $ 29.95), and John Daintith, Sara Mitchell, Elisabeth Tootill, and Derek Gjertsen's *Biographical Encyclopedia of Scientists* (2nd ed., 2 vols., Institute for Physics Publishing, Bristol, England and Philadelphia, PA,1994—ca. 2000 entries, $ 190). However, the hallmark of an encyclopedia is not only coverage but accuracy, and it is here that Porter's dictionary possesses serious deficiencies. A reviewer of the "Engineers and Inventors" volume of the first edition noted: "Proofreading is rather uneven," citing errors which have still not been corrected in the second edition (R. J. Havlik, *Choice* **1986**, *24*, 78). In the new edition the English chemist Nevil Vincent Sidgwick's name is consistently misspelled Sidgewick (pp. 486, 621), and the first names of Bosch (pp. 86, 293) and Scheele (p. 168) are given as Karl, not Carl. Other misspellings include "Marcelin" for Marcellin (Berthelot) (p. 62), "diamene" for diamine (p. 119), "Encyclopedia Britannica" for Encyclopaedia Britannica (p. 224), "CL" for Cl (pp. 233, 715), "Bresslau" for Breslau (p. 293), "van Neumann" for von Neumann (p. 317), "Handwortenbuch" for Handwörterbuch, and "practische" for praktische (p. 395), and the cross-reference for Count Rumford lists him as "Thomson" not Thompson. Diacritical marks are sometimes missing, as in Väversunda (p.65), Traité élémentaire (p. 167), and Ružička (p. 564). Several chemists are consistently referred to by their first names rather than by their more familiar names, e.g., Johann (not Adolf) von Baeyer (p. 382), Friedrich (not August) Kekulé (pp. 37, 232, 381, 685), Friedrich (not Wilhelm) Ostwald (p. 686), and Pierre (not Marcellin) Berthelot (p. 715).

However, the volume also contains errors of fact. The formula for adipic acid contains two N atoms instead of C atoms; that for nylon has a C–O bond missing (p. 119); those for 1-methylphenylhydrazone and an indole derivative lack N atoms (p. 233); that for benzene has a double bond missing (p. 382); and one of the Lewis structures for NO lacks formal charges (p. 429). Benzene was discovered in 1825 not 1835 (p. 224); Heisenberg was born in Sanderau, a suburb of Würzburg, not in Duisberg, a mistake also made by Asimov (p. 317); gallium was discovered in 1875, not 1871, and Moseley's work on atomic numbers as a basis for the Periodic System dates from the 1910s, not the 1920s (p. 477); Alfred Werner was too ill to work on coordination compounds after the end of World War I (p. 621); Guldberg and Waage announced their law of mass action in 1864, not 1867 (p. 686); and Werner considered only organic compounds, not coordination compounds, in his Habilitationsschrift (p. 715). Both inorganic and organic nomenclature and formulas do not adhere to IUPAC recommendations (e.g., pp. 119, 715). These errors among the chemist entries cast doubt on the accuracy of the entries on practitioners of the other fields, a point corroborated for biologists by another reviewer (J. Altman, *New Scientist*, 30 July **1994**, *143*, 41).

Finally, as reviewers of the first edition have stated, the lack of any citations to sources of biographical information is a serious flaw in this dictionary and makes it of little use to the historian of science. Yet this charge could be leveled at its competitors listed above, which also do not contain references. Furthermore, Professor Edgar Heilbronner, a respected chemist colleague, found Daintith et al.'s *Biographical Encyclopedia of Scientists* to contain numerous errors (for review see *Angew. Chem.* **1995**, this issue). Thus, the relatively modest price of Porter's *Biographical Dictionary* makes it a handy one-volume first-step reference work for the general public and for high school, college, and university students as well as practicing scientists with an interest in the history of their fields. However, the frequency of errors will make it necessary for the user to visit a library to consult other more authoritative sources such as the *Dictionary of Scientific Biography*, both to check specific facts and spellings and for additional, more detailed information.

George B. Kauffman
California State University
Fresno, CA (USA)

Volatile Metal Alkoxides according to the Concept of Donor Functionalization

Wolfgang A. Herrmann,* Norbert W. Huber, and Oliver Runte

Dedicated to Professor Henri Brunner on the occasion of his 60th birthday

Since the fundamental works of D. C. Bradley and R. C. Mehrotra, metal alkoxides have attracted attention because of the diversity of their low- and high-molecular-weight structures; they are also generating increasing interest as precursor compounds for solving technical materials problems. The understanding of the hydrolytic nucleation behavior is a prerequisite for the optimization of materials from sol–gel processes. For metal alkoxides to be precursors in *c*hemical *v*apor *d*eposition (CVD) processes in the preparation of inorganic oxidic materials, they should be sufficiently volatile, and sublimation should occur without decomposition at as low a temperature as possible ($< 150\,^{\circ}C$). Only recently, using the "donor functionalization" concept, was a ligand type systematically developed that unifies the advantages of both steric demands and σ-donor stabilization and so stabilizes low-molecular-weight metal alkoxides. Even large metal ions of low charge (for example Ba^{2+}) can thus form volatile alkoxides. O- and N-donor functions in bidentate and multidentate alkoxo ligands are particularly advantageous; hence, for example, the vanadium derivative $[V(OCMe_2CH_2OMe)_3]$ is one of the most volatile metal alkoxides known to date. The first alkoxides of the alkaline earth metals calcium, strontium, and barium, which sublime without decomposition, have the formula $[M_2\{OC(CH_2OiPr)_2tBu\}_4]$. This article presents a critical inventory of the metal alkoxides with particular regard to the aspect of volatility. It also describes successes of the donor functionalization concept and shows—in perspective—how alkoxo ligands can be "tailor made" for metals according to their charge-to-radius ratio by further development of the concept.

Keywords: coordination chemistry · CVD precursors · donor functionalization · metal oxides

1. Introduction

It was more than 30 years ago that man learned how to prepare high purity oxides of the refractory metals by pyrolysis of metal alkoxides.[1, 2] Nowadays simple binary and ternary metal oxides of high purity are of considerable importance in the development of materials. Thin oxide layers are in demand particularly in electronic materials, and since the development of the high-temperature superconductors (for example $YBa_2Cu_3O_{7-\delta}$),[3] efforts to synthesize volatile metal alkoxide precursors have increased.[4] CVD techniques also promise the preparation of more complex inorganic materials by the gas-phase thermal decomposition of volatile (molecular) precursors.[5] Emphasis is being placed on defined decomposition routes and on the conservation of the given metal stoichiometry of the precursor molecule ("single-source precursor") in the deposition product.[6] As far as oxidic materials are concerned, a replacement is being sought for the β-diketonato metal complexes, which though partially volatile, often lead to considerable carbon contamination of the deposited products (or to the incorporation of fluorine in the case of the particularly volatile fluorinated β-diketonato metal complexes).[7] A special need exists here for rare earth metals that by doping can reduce the electronic work function for light bulb wires (tungsten) by orders of magnitudes, and thus improve the light yield (thorium substitutes). For this purpose carbidic materials (mixed carbides, "compulsory carbides") are feasible. The molecular precursor must therefore always be attuned to the desired materials result. In this respect, the strengths of inorganic molecular chemistry lie in its great constitutional variety.

Alkoxides are known for practically every element of the s, p, d, and f blocks of the Periodic Table. The standard work "Metal Alkoxides" from 1978 provides a first encompassing overview of the topic.[8] A series of relevant review articles followed.[1, 4, 9] *Aggregation*, that is, the formation of multinuclear structures—often polymeric—dominates the structural chemistry of the alkoxides. Whereas the concept of steric overcrowding had been favored for the verification of low-molecular-weight compounds, the donor functionalization concept now finds itself on the road to success: Mehrotra and Singh noted that "the bulky ligand

[*] Prof. Dr. W. A. Herrmann, Dr. N. W. Huber,[+] O. Runte
Anorganisch-chemisches Institut der Technischen Universität München
Lichtenbergstrasse 4, D-85747 Garching (Germany)
Telefax: Int. code + (89) 3209-3473
e-mail: herrmann@zaphod.anorg.chemie.tu-muenchen.de
[+] Present address: SKW Piesteritz AG, Wittenberg (Germany)

with side chains capable of donor functionality ... appears to combine the advantages of steric crowding as well as coordinative saturation within the same species"[10a] in reference to the preparation of the first volatile barium alkoxide $[Ba_2\{OC(CH_2OiPr)_2tBu\}_4]$.[10b]

A prerequisite for CVD applications is volatility. Other areas, however, are increasingly reported in which the use is dependent on the solubility. Hence the zinc alkoxide **1** can be transformed into very pure zinc oxide by using acetone as a condensation reagent in accordance with Equation (a).[11] In this area of research great emphasis is being placed on the kinetics of the nucleation in sol–gel reactions.[12]

$$\underset{\mathbf{1}}{[Zn\{OC(C_2H_5)_3\}_2]} + (CH_3)_2C{=}O \longrightarrow ZnO + (CH_3)_2C[OC(C_2H_5)_3]_2 \quad (a)$$

2. The Aims of Ligand Design

Volatility is based, in essence, on weak attractive interactions between molecules. Polar groups or polarizable groups and high molecular masses tend to reduce volatility. Metal alkoxides contain by definition at least one M–O–C structural unit. Because of the high effective nuclear charge of oxygen, alkoxides of metal elements have highly polar M–O bonds. The polarity of the alkoxides of the distinctly electropositive alkali, alkaline earth, lanthanide, and actinide metals (Pauling electronegativity = 0.9–1.2) is the highest; the proportion of ionic bonding can be as much as 80 %. The low volatility—or even the lack of volatility—of the alkoxides of these metals is mainly due to this fact. As a result most of these alkoxides have oligomeric and polymeric structures and are insoluble even in polar solvents such as ethers and amines. Other dimensions that can have an important influence are the size and the charge of the central metal ion. The steric and electronic shielding of the metal by the ligands have to be optimized taking these characteristics into account. A low charge on a metal ion combined with a large ionic radius (for example Ba^{2+}) causes considerable problems when attempting to achieve volatility. The strategies that are employed are introduced in the following sections.

3. Preparation and Structure of Metal Alkoxides

3.1. Synthetic Methods

From a synthetic point of view, metal alkoxides have been well documented since the works of Bradley and Mehrotra.[8] Metal halides and metal halide complexes are most often the starting materials, as the standard method is salt metathesis [Eq. (b)]. The chlorides and bromides, but above all the iodides, are generally preferred (X = Cl, Br, I; L_n = other ligands). Complications can arise for metals in high oxidation states due to redox reactions and coordination reactions, because saltlike alcoholates act as (weak) reducing agents. In addition, they can lead to ionic (that is, nonvolatile) ate-complexes [Eq. (c)] by increasing the coordination number. This problem can be avoided by using the so-called amide route [Eq. (d)], which only requires a sufficiently acidic but not especially bulky alcohol to give the target product by elimination of an amine (usually a volatile amine, for example $HNMe_2$ or $HN(SiMe_3)_2$). The method is most potent when acidity and bulk—also as regards the metal amide—are mutually optimized (for example $SiHMe_2$ instead of $SiMe_3$).[13] This route is often pursued when quantitative yields are imperative, for example for workup reasons.

$$L_nM{-}X + Li(Na,K)OR \longrightarrow L_nM{-}OR + Li(Na,K)X \quad (b)$$

$$L_nM{-}OR + LiOR \longrightarrow Li^+[L_nM(OR)_2]^- \quad (c)$$

$$L_nM{-}NR_2 + HOR \longrightarrow L_nM{-}OR + HNR_2 \quad (d)$$

Metallocene chemistry has recently provided convincing examples of the amide route that also have practical importance. Whereas the classical salt metathesis causes unclear redox processes in this context, the metal amides lead to 75 % yields (Mo) or quantitative yields (Zr) of the alkoxo complexes **2a** and **2b** (X = hydrocarbon bridge) according to Equation (e). Analogously, the derivative **3** with forced C_2-symmetry ("helical shape") is accessible from $[Zr(NMe_2)_4]$ and two equivalents of the ligand.[14] The neodymium complexes **4a** and **4b** were prepared by salt metathesis;[15] the details of their constitution

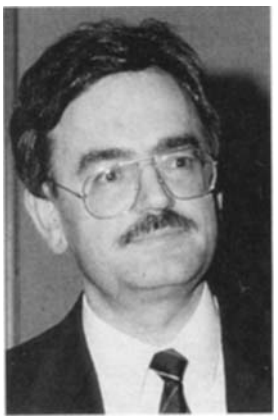

Wolfgang A. Herrmann was born in 1948 in Kelheim on the Danube (Bavaria). After studying chemistry (Diplom: Technische Universität München) and completing a research thesis with E. O. Fischer in 1971, he obtained his doctorate in 1973 on a topic dealing with organometallic stereochemistry under H. Brunner at the Universität Regensburg. From 1975–1976 he carried out research with P. S. Skell at the Pennsylvania State University, and in 1978 completed his habilitation with a thesis titled "Organometallic Syntheses with diazoalkanes". He was appointed professor at the Universität Regensburg (1979), and full professor at the Universität Frankfurt (1982). In 1985 he accepted a chair at the Technische Universität München as the successor to E. O. Fischer. His area of research is synthetic and catalytic chemistry, primarily in organometallic chemistry. He is the author of 380 publications, and holds 30 patents. His work has frequently been the subject of special recognition, including the German–French Alexander-von-Humboldt Award (1988), the Otto-Bayer Award (1990), and the Max Planck Research Award (1991). He is a member of the Akademie der Wissenschaften und der Literatur zu Mainz (1990) and the Deutsche Akademie der Naturforscher Leopoldina (1995). He received honorary doctorates from the University of Lyon (1990) and the University of Veszprèm (1995). He is at present President of the Technische Universität München.

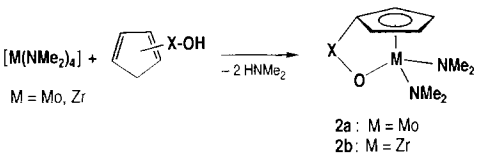

(e)

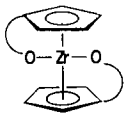

3

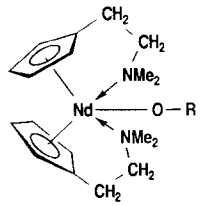

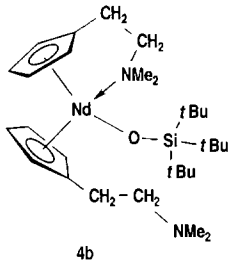

indicate the consequences of the spatial requirements of coordinated alkoxo ligands (cf. Section 5). The structural type **4a** is also observed for other types of small ligands (for example, Cl instead of OR).[115]

Finally, the deoxygenation of oxometal complexes (higher oxidation states; for example Mo^{VI}, W^{VI}, Re^{VII}) according to Equation (f) has also been employed. A variant, the defluorination route, is also known [Equation (g)]. As metal oxides mainly have to be prepared by hydrolysis of the halides, and metal fluorides from the chlorides or bromides, the metal halides are usually the primary precursors in metal alkoxide syntheses [Eq. (h), X = halogen]. For electropositive metals direct synthesis in accordance with Equation (i) can be carried out,[9e, 16] provided the alcohol is sufficiently acidic and the metal is finely divided (where appropriate, metal vapor in a "cocondensation reactor" or a freshly reduced metal iodide must be used).

$$L_nM{=}O + 2\,ROSiMe_3 \longrightarrow L_nM(OR)_2 + Me_3SiOSiMe_3 \quad (f)$$

$$L_nM{-}F + ROSiMe_3 \longrightarrow L_nM{-}OR + Me_3SiF \quad (g)$$

$$MX_n + m\,ROH \rightarrow M(OR)_mX_{n-m} + m\,HX \quad (h)$$

$$M + n\,ROH \rightarrow M(OR)_n + n/2\,H_2 \quad (i)$$

Heteronuclear alkoxides are accessible through acid–base and salt metathesis reactions.[9e] Chelate complexes such as **5a, b** can thus typically be obtained in accordance with Equations (j) or (k).[123, 18]

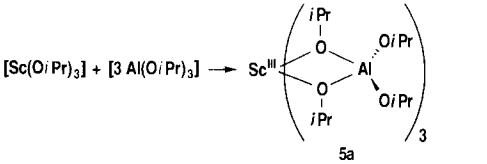

(j)

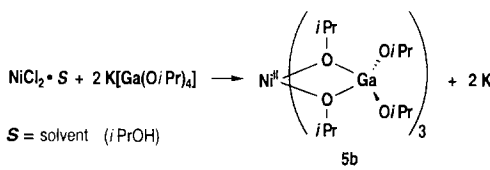

(k)

Like alkoxo ligands OR, amides NR_2 are hard ligands according to the definition of Pearson. For this reason they are particularly in demand as precursors in the chemistry of the rare earth metals ("one of the most prolific ligands"[128]), and numerous synthetic methods are now known, including those described in Equations (l)–(n) for divalent lanthanides.

$$LnI_2 + 2\,NaNR_2 \longrightarrow Ln(NR_2)_2 + 2\,NaI \quad (l)$$

$$Ln + M[N(SiMe_3)_2]_2 \longrightarrow Ln[N(SiMe_3)_2]_2 + M \quad (M = Sn, Hg) \quad (m)$$

$$Ln + 2\,Hg(C_6F_5)_2 + 2\,HNR_2 \longrightarrow Ln(NR_2)_2 + 2\,Hg + 2\,C_6F_5H \quad (n)$$

As a result of the three-connectivity of nitrogen, amido ligands can provide a more efficient spatial screening of the metal atom by the introduction of two groups at the β-position to the metal center (larger cone angle for NR_2 than for OR). The metal atom is thus more effectively protected (and usually has a higher stability with respect to oxygen and water).

3.2. Coordination Chemistry

The structural diversity of the metal alkoxides is based on the coordination chemistry of the OR ligand and the numerous possibilities that this provides. These can even be brought to bear when no other R groups capable of coordination with the metal are present. In the isovalence electronic series alkyl - amide - alkoxide - halide with increasing number of "lone electron pairs" (with the exception of alkyl groups **I**, which rather rarely are bridging ligands), the heteroatomic ligands **II**–**IV** are often bound to between two and six metal atoms (for example $[Nd_6(OiPr)_{17}Cl]$[19]). Intermolecular bridging produces aggregated systems, which are to be avoided in particular in the preparation of volatile metal alkoxides.

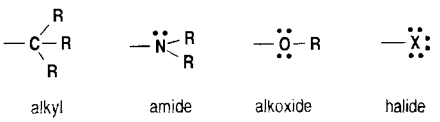

Terminal binding of the alkoxo ligand results in the bent structural type **A** (M–O–R < 170°). The standard type for bridge-forming, σ-donor interactions with other metals is less often available in the case of perfluorinated substituents R (for example $OCH(CF_3)_2$) with their reduced O-basicity. The frequently encountered structural type **B** has a linear M-O-R sequence primarily because of steric effects, but cases are known that can only be explained by electronic effects.[120] The bond angles of between 170 and 180° determined by X-ray diffraction methods on single crystals should be interpreted with caution; it is often crystal packing effects that lead to almost linear structures, as is the case in $[Yb(O\text{-}2,6\text{-}tBu_2\text{-}4\text{-}R\text{-}C_6H_2)_2]\cdot 3THF$ (R = Me, *t*Bu).[121] In the (edge-)bridging constitution **C**, the oxy-

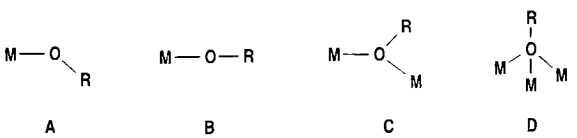

gen atom takes on a pyramidal, or much more often a trigonal-planar configuration. With oxophilic metals, the structural type **D** exhibiting triply bridging alkoxo ligands is often encountered.

During the preparation of alkoxometal complexes it is not uncommon for side products containing "lone" oxo ligands to be formed, which are encapsulated in ensembles of between three and six metal atoms. Examples of these are the metal complexes **6a, b** (Fig. 1). The oxo ligands originate, as a rule, from spurious moisture in the reaction mixture. In rare individual cases, they have been confirmed to originate from OR ligands by cleavage of the O–R bond.[22, 44] As the determination of such complicated structures is dependent on X-ray diffraction methods on single crystals, attention must be drawn to the danger of confusing oxo with hydroxo ligands (O and OH).

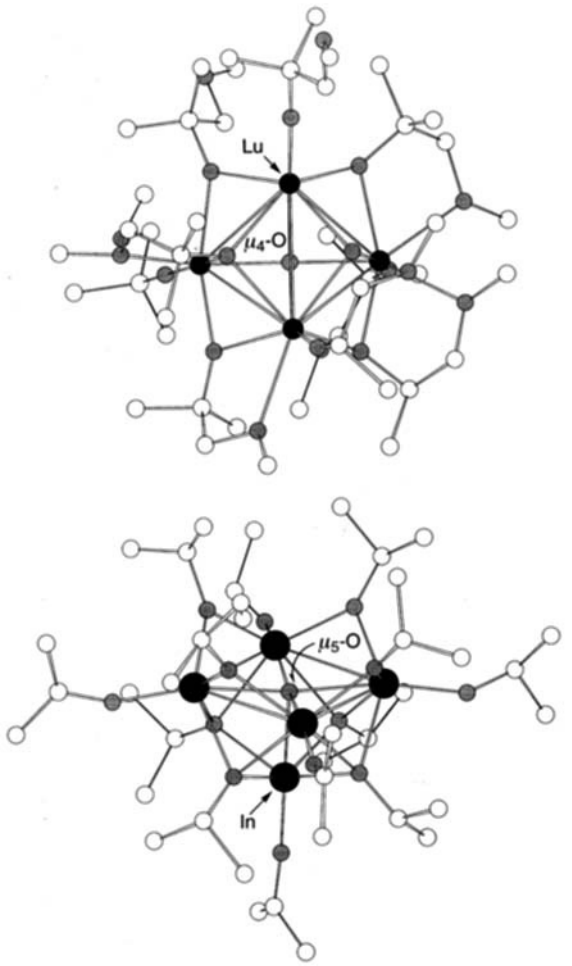

Fig. 1. Alkoxides of metals with "lone" oxo ligands. Top: Structure of the compound $[Lu_4(\mu_4\text{-}O)(OH)(OR)_9]$ (**6a**), R = CMe_2CH_2OMe, with Lu_4O_{15} substructure [184]. Bottom: Structure of the compound $[In_5(\mu_5\text{-}O)(O\mathit{i}Pr)_{13}]$ (**6b**) with In_5O_{14} substructure [172a]. Here as in all other structural diagrams carbon atoms are represented by white spheres, oxygen, nitrogen, and phosphorus atoms by gray spheres, and metal ions by black spheres.

4. Sterically Demanding Ligands—Volatility Versus Lability of the Complexes

The importance of steric ligand effects is just as well known in coordination chemistry (phosphanes, Tolman cone angle, dissociation equilibria, catalysis) as in the chemistry of main-group elements with low coordination numbers (for example silaolefins, phosphaalkynes, phosphaalkenes). Figure 2 shows ligands with increasing spatial requirements ranging from *tert*-butyl alcohol to the bulkiest alcohol "tris(*tert*-butyl)methanol" (tritox-H, molecular mass 200 u).[23] Tritox-H was introduced into coordination chemistry by Power et al. and Wolczanski et al.[24]

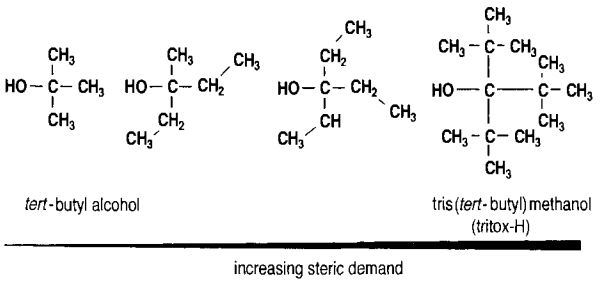

Fig. 2. Increasing spatial demands of nonfunctionalized alcohols from *tert*-butyl alcohol to tritox-H.

As was exemplified by $[Ce(tritox)_3]$, steric overcrowding of the ligand periphery entails an increasing fragility of the compound as a whole.[25] The grouping of 39 C atoms, 81 H atoms, 36 CC bonds and 81 CH bonds (!) in the closest of neighborhoods lowers the thermolysis temperature to such an extent that CC bonds are cleaved merely on sublimation of the metal complexes under vacuum (Scheme 1).

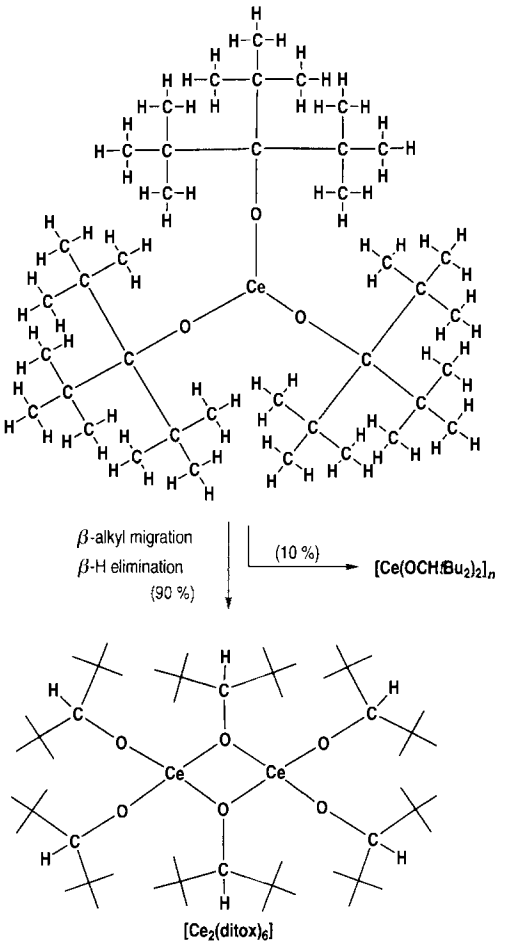

Scheme 1. Thermal decomposition of the sterically congested tritox complex $[Ce(tritox)_3]$ to the ditox complex $[Ce_2(ditox)_6]$; ditox-H = "bis(*tert*-butyl)-methanol".

4.1. Unproblematic Cases and the Limits of Steric Demands

In order to obtain volatile metal alkoxides $M_x(OR)_n$, the nuclearity x must be low—this is not typical for this class of molecular compounds. If possible, the complexes $M(OR)_n$ should be monomeric and the R group should not be too large in order to ensure that the molecular mass is low. These demands of large ligands and low molecular masses are conflicting and cannot, therefore, be easily satisfied simultaneously, in particular in the case of large low-valent metal ions (for example Ba^{2+}).

In contrast, the class of compounds $M(OR)_6$ of the hexavalent metals (W, Re) presents no problems. Even uranium, the largest representative, forms (like tungsten) a monomeric methoxide $[M(OMe)_6]$ in the solid state and in the gas phase.[117] Nevertheless, in as far as they are known for M = Nb, Ta, W and Re, the pentacoordinated M^V methoxides $[M(OCH_3)_5]$ exist as dimers and, in the case of uranium, as a trimer.[26, 27] $[U(OEt)_5]$, on the other hand, is dimeric, and the nuclearity for the analogous Pa^V derivative in solution is given as $x = 5.7$.[29, 30] For R = *i*Pr monomeric and dimeric Nb^V and Ta^V derivatives $[M(OiPr)_5]$ are obtained.[31] $[Nb(OiPr)_5]$ has a dimeric structure in the solid state.[32] For the larger uranium this occurs only with a ligand the size of R = *t*Bu ($x = 1.35$ in solution).[29] The importance of the extent of the ligand periphery can be seen here in convincing clarity.

Whereas $Si(OMe)_4$ and $Ge(OEt)_4$ already have monomeric structures even with their small ligands,[8] this first occurs for the higher congener $Sn(OR)_4$ when R = *t*Bu.[33] The same behavior can be observed for the Zr^{IV} and Hf^{IV} analogues, whereas $[M(OiPr)_4]$ monomers exist for Ti and V, at least in the gas phase.[34] For large ions (M = Th, U), the $[M(OR)_4]$ alkoxides are oligomeric even for R = *t*Bu.[35, 36] Monomeric thorium alkoxides are only obtained with larger groups such as $CMeEt_2$ and CMeEt*i*Pr.[35]

For the alkoxides of the trivalent elements, only the semimetals and nonmetals B, P, and As with methoxy or ethoxy substituents are monomeric and markedly volatile.[8] Even the *t*Bu derivatives of Al and Ga are dimeric,[39, 40, 84, 88] and those of Y and La form alcohol adducts with the formula $[M(OtBu)_3]_3 \cdot 2\,tBuOH$.[41] The bismuth derivative $Bi(OtBu)_3$ is monomeric in the gas phase.[42] The nuclearity of $In(OtBu)_3$ is unknown,[43] yet $In(OiPr)_3$—like the corresponding derivatives of Sc and Y, as well as of the rare earth metals La, Nd, and Yb—forms a pentameric oxo cluster.[44–46] The alkoxides that form dinuclear complexes with lanthanide metals range from $OCMe_2iPr$ to $OCiPr_2tBu$.[41] If monomeric alkoxides of the rare earth metals are desired, however, the synthetic chemist has to resort to bulky organic groups: tritox ($OCtBu_3$) and silox ($OSitBu_3$) produce mononuclear complexes. A mononuclear structure was attributed to the yttrium alkoxide $[Y(OCtBu_2iPr)_3]$ because of its volatility.[47]

The preparation of monomeric metal aryloxo complexes is generally simpler. These complexes are, however, normally much less volatile. For the 2,6-disubstituted phenoxides of the type $[M(O\text{-}2,6\text{-}tBu_2\text{-}4\text{-}R\text{-}C_6H_2)_3]$ (R = H, Me, *t*Bu) for example, monomeric formulas have been assigned to all trivalent metal ions: the Al,[48] Sc,[49] Y,[50] and Ce[38] derivatives have been structurally characterized. A perfect shielding of the metal is not achieved in this class of substances either, however, as can be deduced from the occurrence of adduct formation: $[Al(O\text{-}2,6\text{-}tBu_2\text{-}4\text{-}MeC_6H_2)_3]\cdot O{=}C(C_5H_{11})tBu$[37] and $[Ce(O\text{-}2,6\text{-}tBu_2C_6H_3)_3]\cdot 2\,tBuNC$[38] (cf. $[Nd(OCtBu_3)_3]\cdot 2\,NCMe$[47] and $[V(OSitBu_3)_3]\cdot THF$[51]).

The limits of steric shielding are reached with the ligands mentioned above. Only a few remaining $[M(OR)_2]$ complexes of divalent metals can be obtained in monomeric form and free of solvent: the aryloxo complexes $[M(O\text{-}2,6\text{-}tBu_2\text{-}4\text{-}Me\text{-}C_6H_2)_2]$ (M = Be,[52] Ge, Sn, Pb[53]) and the alkoxo complexes $[M(OCtBu_3)_2]$ (M = Ge, Sn).[54] In addition, as the (unstable) lead complex $[Pb(OCtBu_3)_2]\cdot tBu_3COH$ is known and structurally characterized,[85] there is a tendency to ascribe to the phenoxo ligand a somewhat higher steric shielding factor than to the alkoxo ligands; nevertheless, from considering models, Sen et al. deduce that the opposite is true.[25] All in all, the topic is not relevant for CVD studies because of the poor volatility of metal aryloxo complexes. Incidentally, the selected ligands shown in Figure 3 exist mostly either as dimeric species or as monomers with an additional two or three donor molecules coordinated to the metal.

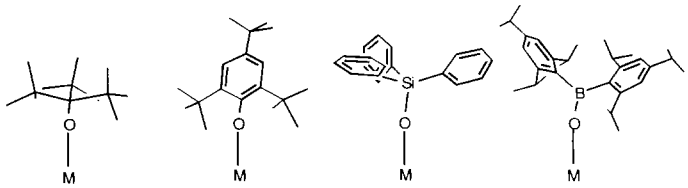

tris(*t*-butyl)methoxo tris-2,4,6-*t*-butylphenoxo triphenylsiloxo bis(2,4,6-isopropylphenyl)-boryloxo

Fig. 3. Some metal complexes containing sterically highly demanding oxo ligands.

Wolczanski et al. reported a cone angle of 125° for the tritox ligand. This angle is also regarded as valid for silox and thus analogously for "silaz" ($NHSitBu_3$).[57] A comparison of silaz with the $N(SiMe_3)_2$ and $N(SiMe_2H)_2$ ligands demonstrates the relatively low steric requirements of ligands *without* α-branching (Fig. 4). Other ligands are significantly "smaller": Roesky et al. estimated a cone angle of 94° for the M-O-[2,4,6-$(CF_3)_3C_6H_2$] group.[59]

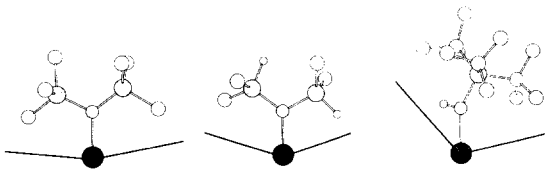

Fig. 4. A comparison of the steric requirements of the silylamido ligands $N(SiMe_3)_2$ (left) and $N(SiMe_2H)_2$ (middle), and the silaz ligand $NH(SitBu_3)$ (right), which is analogous to the tritox/silox ligands [58].

From the structural chemistry discussed for coordination numbers greater than or equal to 2, it follows that monoalkoxides can only be obtained in the form of oligomers or polymers. Lithium methoxide thus forms a layered lattice in the crystal.[60] $LiOtBu$ [61] exists as a hexamer in the gas phase as does $LiOCMe_2Ph$ in the condensed phase.[62] Hexameric and nonameric units have been found together in the crystal structure of $NaOtBu$.[63a] whereas $Na[OCH(CF_3)_2]$ forms a cubane-like

tetramer.[64] The larger alkali metal ions K^+, Rb^+, and Cs^+ are less acidic in the Lewis sense than Li^+ or Na^+ because of their smaller charge-to-radius ratios; their *tert*-butoxide derivatives are tetrameric.[56] Solvent-free dimers have as yet only been structurally characterized for lithium derivatives Li(OR) with the particularly bulky groups R = C*t*Bu$_3$ and B[CH(SiMe$_3$)$_2$]$_2$.[66] The Tl^I and In^I complexes [{M(O-2,4,6-{CF$_3$}$_3$C$_6$H$_2$)$_2$}$_2$][72, 74] are also binuclear, whereas the remaining Tl^I alkoxides—like the parent compound [{TlOMe}$_4$]—form cubane tetramers.[8] The Cu^I alkoxides such as [{(Cu(O*t*Bu)}$_4$] are also tetrameric, but of square-planar structure.[69] The planar, tetrameric [CuX]$_4$ unit can only be broken with sterically extremely demanding ligands such as N(SiMePh$_2$)$_2$: the resulting Cu^I amide is then trimeric.[70] Homoleptic,[*] solvent-free alkoxides of other monovalent elements are not known.

4.2. Thermal Stability and Decomposition Reactions

Alkoxo ligands are sterically rather undemanding because there is no possibility of α-branching—in this they differ from alkyl ligands. Hardly any steric interactions between ligands are therefore known. An example is [W(O*t*Bu)$_6$], which decomposes only in benzene under reflux to relieve the steric strain and forms [WO(O*t*Bu)$_4$].[71] In the analogous complex of the (larger) uranium, the metal center is shielded so well, that [U(O*t*Bu)$_6$] is stable to air and water (ionic radii: 60 pm, W^{VI}; 73 pm, U^{VI}).[8]

Steric intraligand interactions of alkoxo ligands, on the other hand, are known for complexes of mono-, di-, and trivalent metals. Aryloxides often lead to monomeric and dimeric metal complexes of high thermal stability but low volatility (see Section 4.1). Si(OPh)$_4$ can be distilled under normal pressure at 417–420 °C (!) without decomposition. In contrast, [Ln-{O-2,6-*t*Bu$_2$-4-MeC$_6$H$_2$}$_3$] (Ln = Sc, Y, La–Lu)[49, 50, 73] and [{M(O-2,4,6-*t*Bu$_3$C$_6$H$_2$)$_2$}$_4$] (M = Ca, Sr, Ba)[75] only sublime above 200–250 °C in vacuum (10^{-4} Torr). In spite of their thermal stability, aryloxo metal complexes are not nearly volatile enough for CVD purposes. This is due mainly to the polarizing character of the aryl groups, which reduces the volatility by means of intermolecular π–π interactions.

Against expectations, complexes of the silox ligand (OSi*t*Bu$_3$) are also nonvolatile,[51, 57, 76, 77] with the exception of the rare heteroleptic oxo complexes: [CrO$_2$(OSi*t*Bu$_3$)$_2$] (160 °C/1 Torr)[**] and [ReO$_3$(OSi*t*Bu$_3$)] (100 °C/0.5 Torr).[78] Unusually favorable volatility data were reported for [Ba$_2$(OSi*t*Bu$_3$)$_4$]·THF (80 °C/1 Torr),[79] but the ligand (60–90 °C/1 Torr[80]) sublimed here and not the metal complex.[68]

Silox and tritox complexes differ considerably in their thermal stabilities. The homoleptic Nd^{III} derivatives permit a comparison to be made: Whereas [Nd(OSi*t*Bu$_3$)$_3$] is still nonvolatile and thermally stable at 250 °C/10^{-3} Torr (sublimation) and decomposes at temperatures above 340 °C, [Nd(OC*t*Bu$_3$)$_3$] decomposes at 150 °C to give the dinuclear derivative [{Nd(OCH*t*Bu$_2$)$_3$}$_2$], which sublimes at 175 °C/10^{-3} Torr.[47] The particular strength of the Si–O bond and the less favorable cleavage of silyl cations than of carbocations are responsible for these differences. Table 1 shows that decomposition reactions of tritox complexes are not restricted to the example given for neodymium.[25, 81, 83, 85]

Table 1. Tritox complexes and their thermal decomposition products (R = C*t*Bu$_3$, R′ = CH*t*Bu$_2$).

Metal alkoxide	Conditions	Product	Ref.
[{Li(OR)}$_2$] [a]	$t_{1/2}$ (85 °C) = 80 min	[{Li(OR′)}$_n$]	[25]
[{Ca(OR)$_2$}$_2$] [a]	185 °C/10^{-3} Torr	[{Ca(OR′)$_2$}$_3$]	[81]
[Pb(OR)$_2$] · ROH	>0 °C	Pb	[85]
[Li(thf)$_2$][CrCl(OC*t*Bu$_3$)$_2$]	*n*-hexane/60 °C	[{Cr(OR′)(OR)}$_2$]	[24a]
[Ce(OR)$_3$]	150 °C	[{Ce(OR′)$_3$}$_2$]	[25]
[Nd(OR)$_3$]	150 °C	[{Nd(OR′)$_3$}$_2$]	[47]

[a] Due to the low temperatures of decomposition (approximately 120 °C), similar decomposition processes are also presumed for the Na and Mg derivatives mentioned only in a footnote [83].

Isobutene was found by Power et al. to be the main degradation product of the complex [Li(thf)$_2$][CrCl(OC*t*Bu$_3$)$_2$].[24a] This was confirmed by Sen et al. for the Li and Ce complexes.[25] In addition, a small amount of di-*tert*-butyl ketone was identified. The authors assume that the cleavage of ketone as a result of γ-H-migration plays only a minor role at best, because the kinetic isotope effect (k_H/k_D = 1.5 (Ce) and 1.8 (Li)) is relatively high. A possible β-alkyl migration is also regarded as improbable, because the rate of decomposition increases by two orders of magnitude when [12]crown-4 is added to [{Li(OC*t*Bu$_3$)}$_2$]. However, due to the increase in the Li···ligand distance caused by complexation by the crown ether, the rate of decomposition as a result of β-alkyl migration ought to decrease. The authors therefore favor homolytic cleavage of the OC–CMe$_3$ bond with subsequent abstraction of an H atom to give isobutene and a ditox fragment (Scheme 2).

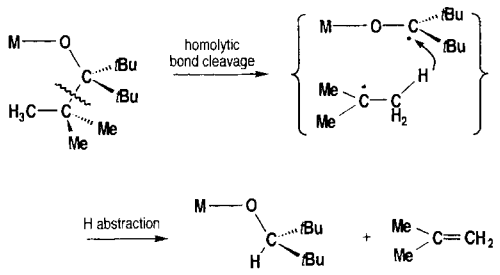

Scheme 2. Mechanism of decomposition of metal tritox complexes according to Sen et al. [25].

This decomposition route has been experimentally confirmed, in as far as *tert*-butyl radicals have been captured with benzophenone. Whether the light-sensitive solvent adduct [Pb(OC*t*Bu$_3$)$_2$]·HOC*t*Bu$_3$ takes the same decomposition path as other tritox derivatives is not clear.[85] The formation of lead radicals could not be determined on irradiation of [Pb{N(SiMe$_3$)$_2$}$_2$], [Pb{CH(SiMe$_3$)$_2$}$_2$], and [Pb(S-2,4,6-*t*Bu$_3$C$_6$H$_2$)$_2$] at any rate, as was the case for the analogous Ge and Sn compounds. The ˙S-2,4,6-*t*Bu$_3$C$_6$H$_2$ radical was identified in the case of the lead thiolate; however, its occurrence indicates

[*] We use the term homoleptic (as introduced into coordination chemistry by Lappert et al. for metal alkoxides when just *one* type of metal and *one* type of alkoxo ligand are present (P. J. Davidson, M. F. Lappert, R. Pearce, *Acc. Chem. Res.* **1974**, *7*, 209–217).

[**] Unless stated otherwise, the data in parentheses indicate the temperature of sublimation and the pressure.

a Pb–ligand bond cleavage instead of a C–C bond cleavage.[86] For the tritox complexes of other more electropositive metals, the C–C bond cleavage clearly dominates.[25]

According to some authors, the instability of the tritox complexes is caused by a relatively weak $OC-CMe_3$ bond that itself results from intramolecular repulsion of the *t*Bu groups. These CC bonds are indeed unusually long (>160 pm). The effect can be studied for $[\{Cr(ditox)(tritox)\}_2]$ (**7**, Fig. 5), the only compound which has been structurally characterized and in which both these ligands are present.[24b]

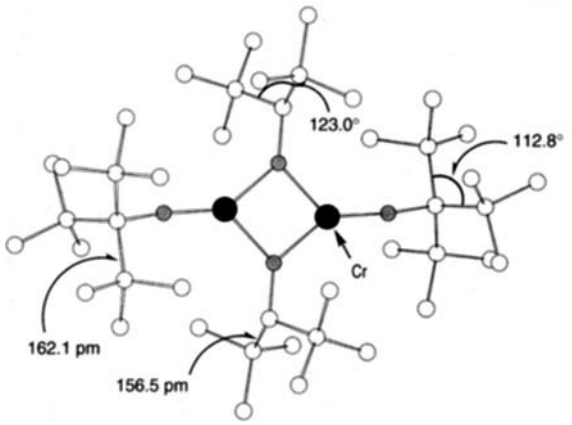

Fig. 5. Long (and therefore weak?) $C-CMe_3$ bonds in sterically congested metal complexes as exemplified by the Cr^{II} complex **7** with bridging ditox and terminal tritox ligands. Average values are given [24a].

In our group, Anwander et al. used this knowledge to lower the steric strain by replacing just one *i*Pr group with a *t*Bu group. The yttrium complex with the proditox ligand, $[Y(OCtBu_2iPr)_3]$ (**8b**), is indeed so thermally stable that it can be sublimed at 160 °C/10^{-3} Torr without decomposition.[47] The tritox complex **8a** (Fig. 6) is unstable. Power et al. observed the formation of methanol during the preparation of $[\{Co(OCCy_3)_2\}_2]$ (Cy = cyclohexyl), which might indicate a thorough decomposition of this special alkoxo ligand.[89]

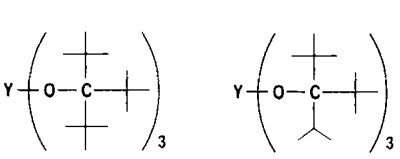

[Y(tritox)$_3$] **8a** [Y(proditox)$_3$] **8b**

Fig. 6. Comparison between complexes containing tritox and proditox ligands.

Summary: a) Even the most sterically demanding of the conventional alkoxo ligands cannot stabilize complexes of metal ions such as Ca^{2+} in a monomeric form, let alone the much larger Ba^{2+} ion (ionic radius 135 pm). b) Alkoxo ligands usually form complexes of low volatility with strongly oxophilic metals. c) Silox complexes are nonvolatile. Most tritox complexes decompose to give decomposition products of higher nuclearity (mainly binuclear) with ditox ligands.

A sound concept for volatile alkoxides of electropositive mono-, di-, and trivalent metals can, therefore, not be based solely on steric requirements.

5. Fluorinated Ligands

(Per)fluorinated or highly fluorinated ligands are a special case. The substitution of H, CH_3, or CR_3 groups with fluorine ligands causes intermolecular repulsion due to the resulting negative "charge envelope"—and thus an increase in the volatility. This effect is well known, for example from the chemistry of the metal β-diketonato complexes.[7, 90, 94] A comparison of the boiling points of $HOC(CF_3)_3$ (45 °C/760 Torr, $M_r = 236$) and $HOC(CMe_3)_3$ (85 °C/1.5 Torr, $M_r = 200$) speaks for itself. On the other hand, the van der Waals radius of fluorine is only approximately 10 % larger than that of hydrogen (135 vs. 120 pm),[67] which is why the CF_3 group is considerably less sterically demanding than the *t*Bu group. $[La_3\{OCMe(CF_3)_2\}_9]$[91] is thus trimeric like $[La_3(OCMe_3)_9]\cdot 2HOCMe_3$,[92] yet much more volatile (130 °C/10^{-2} Torr as against 240 °C/10^{-3} Torr). Similarly, Na and Cu alkoxides with fluorinated ligands are more volatile than the nonfluorinated analogues.[93, 64] $[Tl_4\{OCH(CF_3)_2\}_4]$ is in fact the only vaporizable alkoxide of the monovalent metal known to date (85 °C/10^{-2} Torr).[64] The examples $[Ba\{OC(CF_3)_3\}_2]$ (280 °C/<10^{-5} Torr) and $[Ba\{OCMe_3\}_2]$ (270 °C/<10^{-5} Torr) as well as $[Bi\{OCH(CH_3)_2\}_3]$ (90 °C/<10^{-4} Torr)[101] and $[Bi\{OCH(CF_3)_2\}_3]$ (110 °C/<10^{-2} Torr)[87] show quite clearly, however, that the expected increases in volatility are not always achieved.[95]

Alkoxides with fluorinated ligands often have short M···F contacts. These interactions are responsible for the undesired fluorine content that is found now and then in thin layers generated from fluorinated alkoxides by CVD techniques. Pure sodium fluoride layers have been prepared from $[Na_4\{OCH(CF_3)_2\}_4]$ by deposition onto SiO_2 at 285 °C.[64]

Summary: As a rule, metal (per)fluoroalkoxo complexes are extremely volatile. The incorporation of fluorine into decomposition products prepared by thermal and plasma-chemical methods is a disadvantage that can hardly be avoided, however. The concept is therefore no longer being intensively pursued in current materials research.

6. Donor Functionalized Alkoxo Ligands

The use of polyetheralcohols both as solvent and as ligand for sol–gel processes has become standard practice. Ligands of this type are assumed to be less easily separated from the metal center by hydrolysis than monodentate ligands because of the chelate effect. The resulting improved solubility of the growing oxo cluster delays its gel point[*]. Alcoholysis reactions probably give rise to the same result when alcohols are used as solvent.[96]

Based on this experience, donor groups—preferably ether and amino functions—are taken into consideration for use in materials science applications, at least when the molecular chemistry approach is being applied. The first volatile metal alkoxide of this type was reported by Horowitz et al. in 1989: the blue-green compound $[Cu(OCH_2CH_2NEt_2)_2]$, volatile at 100 °C in a high vacuum.[97] This and the compound $[Cu(OCH_2CH_2OnBu)_2]$, which was also prepared, dissolve well in toluene.[97]

[*] The *gel point*, a term used in macromolecular chemistry, is defined as the point at which insolubility starts due to molecular cross-linking (for example polymerization, polycondensation).

Complexes of the metals relevant to oxidic ceramics (Ca, Ba, Pb, Bi, Cu, Zn, Cd, Y, and Ce) were prepared containing donor functionalized alkoxo ligands, especially in the groups around Buhro (St. Louis, USA), Caulton (Bloomington, USA) and Hubert-Pfalzgraf (Nice, France). The ligand most often used was 2-methoxyethanol $HOCH_2CH_2OCH_3$, the simplest in the series. After the molecular structures of the Ca,[98] Ba,[99] Pb,[100] Bi,[101] Cd,[102] and Y[103, 112] derivatives were known, the expectations were dashed to a large extent: a) Homoleptic metal complexes of these ligands are nonvolatile, which is explicitly acknowledged in most cases. A (rather improbable[68]) low sublimation temperature of 160 °C/10^{-1} Torr has been reported only in the case of the barium–solvent complex $[Ba_6O(OCH_2CH_2OMe)_{10}]\cdot 4HOCH_2CH_2OMe$.[99] b) The structural chemistry in the solid is characterized by infinite chains (Pb, Bi, Cu), oligomeric rings (Y), and units with nonmolecular structures (for example, CdI_2 type for Ca, Cd). c) Because of the frequently good solubility in nonpolar organic solvents, these special alkoxide complexes are of interest as variants in sol–gel processes, in particular in the case of Ca, Ba, Bi, and Y.

As regards solubility, it should be noted that derivatives with free ether functions, that is, not coordinated to the metal ("dangling ligands"), can be insoluble in aprotic organic solvents (Pb and Cu derivatives). The structures of the likewise insoluble Be and Zn derivatives are not known. In contrast, in case of the Bi derivative, Bi···O interactions ranging from 290 to 310 pm have been found; these are comparable with the Bi···THF bond lengths of 295 pm in $[Bi(OSiPh_3)_3]\cdot 3THF$ (**9**).[104]

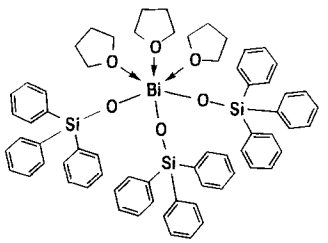

9

In 1990 Buhro et al. quite clearly stated the view on alkoxo ligands that prevailed at that time:[98] "However, group 2 alkoxides with conventional, monodentate alkoxide ligands are generally nonvolatile and poorly soluble in nondonor solvents, probably as a result of nonmolecular structures. Bidentate alkoxide ligands may reduce molecularities sufficiently to allow soluble derivatives to be obtained. A simple extension of this reasoning above suggests that appropriate tridentate alkoxide ligands may produce molecularities as low as $n = 2$, perhaps inducing volatility as well."

As Rees et al. were able to show a little later for the complex $[Ba\{O(CH_2CH_2O)_nMe\}_2]$ ($n = 2, 3$) that the expectations placed in an increase in volatility were not fulfilled here either.[105] Cryoscopic molecular mass determinations in solution suggested that monomers were indeed present, but nevertheless, no increase in volatility was achieved. The copper and zinc derivatives $[M\{O(CH_2CH_2O)_2Me\}_2]$ are also nonvolatile (M = Cu,[106] Zn[107]). Primary polyetheralkoxo ligands all form nonvolatile metal complexes, in contrast to some metal alkoxides with the more strongly basic amino functions (Table 2). The Pauling electronegativities[67] for those metals for which volatile amino-functionalized alkoxides are known lie in the upper region [1.65 (Zn), 1.87 (Pb), 2.00 (Cu), 2.02 (Bi)]. To a first approximation, the volatility is also found to increase in the same order. Volatile alkoxides of electropositive metals such as barium with such ligands are not known, nor are they to be expected.

Table 2. Properties of metal alkoxides whose ligands are functionalized by amino groups.

Ligand/Metal	Structure (degree of aggregation)	Sbl. [°C]/Yield [%] [a] (Solubility)	Ref.
$OCH_2CH_2NMe_2$			
Be^{2+}	(8–11)	(slightly in benzene)	[139]
Bi^{3+}	(1.5)	85/38	[101]
Cu^{2+}	(1)	80/85	[161]
Zn^{2+}	oligomer	170/53	[107]
Cd^{2+}	–	(slightly in *n*-hexane)	[102]
$OCH_2CH_2NEt_2$			
Cu^{2+}		100/75	[97]
$OCHMeCH_2NMe_2$			
Pb^{2+}	(1.3)	106/80	[100]
Bi^{3+}	(1.1)	90/54	[104]
Cu^{2+}	$Cu(\mu_2\text{-}OR)_2$	60/85	[161]
Zn^{2+}	(3)	170/80	[107]
Cd^{2+}		(slightly in *n*-hexane)	[102]
$OC_2H_4N(CH_3)C_2H_4NCH_3$			
Cu^{2+}	$Cu(\mu_3\text{-}OR)(\mu_2\text{-}OR)$	110–112/85	[161]
Zn^{2+}	(2.4) $Zn(\mu_3\text{-}OR)_2\text{-}2H_2$	170/55	[107]

[a] The yield is the sublimation yield significant for practical purposes (for example CVD applications) at 10^{-4} Torr and the given temperature.

With the exception of the Cu complex, the sublimation yields of complexes with primary alcoholate ligands are less than 60 %. The secondary alcoholate ligand $OCH(CH_3)CH_2NMe_2$ often forms more volatile, but at any rate thermally more stable, metal complexes.

No volatilities are reported for the $[M(OCtBu_2CH_2PMe_2)_3]$ complexes (M = Y, Nd) with phosphino-substituted alkoxo ligands.[108] The ligand $HOCMe_2CH_2PPh_2$ has also been used in Pd^{II} chemistry. Whereas $[Pd(OCH_2CH_2PPh_2)_2]$ slowly decomposes at 0 °C with deposition of metallic palladium, $[Pd(OCMe_2CH_2PPh_2)_2]$ is stable under these conditions.[109] Seemingly unimportant constitutional details of the chelate ligand thus seem to influence the properties of the complex considerably.

Summary: Alkoxo ligands that have more than one ether function at their disposal tend to yield nonvolatile alkoxides, whereas amino groups in the alkoxide lead to sublimable complexes, at least for the less electropositive metals. The thermal stability of the complexes containing O,N-ligands is not quite as desired, however, which can clearly be seen in the poor sublimation yields.

6.1. Combination of Steric Demands and Donor Functionalization

Metal alkoxide bonds in metal oxo complexes have predominantly ionic character due to the mainly large differences in the electronegativities between metal and oxygen. This often results in saltlike solid-state structures. To achieve volatility, the strength of the polar interactions have to be minimized. This can be achieved by either increasing the distance between polar M–O units by means of large organic groups ("concept of steric shielding"), or reducing the polarizing strength of the metal ion by charge transfer from donor ligands (concept of donor functionalization). As neither of these principles alone leads to

optimal volatility and thermal stability, the approach followed in our group since the doctoral work of Anwander[110] therefore consists of the combination of steric demand and donor functionalization in one and the same ligand (Scheme 3).

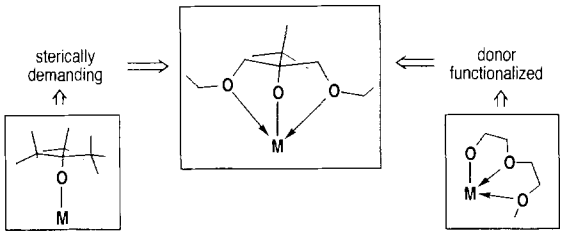

Scheme 3. Concept of the combination of sterically and electronically shielding alkoxo ligands.

The Cr^{III} complex **10** (Fig. 7) prepared in this manner enters the gas phase at 65 °C/1.5 Torr without decomposition it is the most volatile compound of trivalent chromium known to date.[10b, 111] Bismuth exemplifies how delicate the balance of the exact ligand constitution really is: The nonvolatile chelate complex **11a** has a polymeric structure in the solid state,[169] whereas its β-dimethyl derivative **11b** is a monomer (60 °C/10^{-3} Torr).[68]

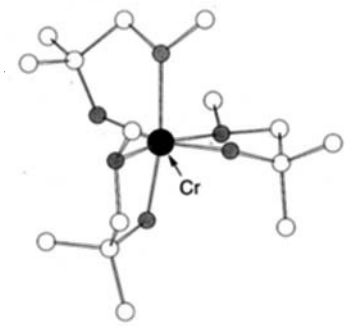

Fig. 7. Crystal structure of the Cr^{III} complex $[Cr(OCMe_2CH_2OMe)_3]$ (**10**) [10b, 111].

Donor-functionalized alkoxy ligands can perfectly surround large metals even with relatively small steric bulk, because they have at least two coordination sites at their disposal: an alcoholate function for charge neutralization, and a donor function to compensate the steric and electronic demands of the metal ion. The synthesis of the metal complex is thus easier, and the disadvantageous results of steric overcrowding (see tritox, above) are avoided. In addition, the chelate effect contributes to the stability, also with respect to moisture. The commercially available alcohols that are also predominantly used even in the newer literature do not fulfill these requirements. The concept cannot, therefore, fall back on commercially available ligands as yet, but well-elaborated syntheses have become available in the meantime.[68, 110] The constitution of the ligands can be tailor-made for the coordination chemistry of the metals under consideration, for example, with respect to electronegativity, charge, and ionic radius.

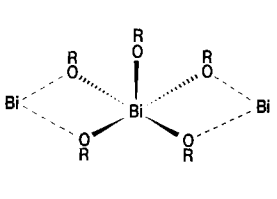

11a, R = CH_2CH_2OMe

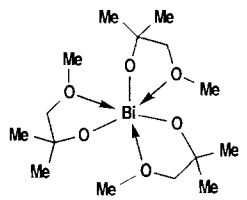

11b

6.2. Heteronuclear Alkoxides

The extension of this approach to include metal alkoxides that contain different metals ("heteronuclear alkoxides") seems realistic. Alkoxide ligands here fulfill not only their donor function, but also act as a tether between the metal atoms. The volatile Mg/Co alkoxide **12** was obtained at the first attempt and its structure is shown in Figure 8.[113] Heteronuclear alkoxides with the element combinations La^{III}/Co^{II}, Li^{I}/Nb^{V}, Fe^{II}/Mg^{II}, K^{I}/Co^{II}, Na^{I}/Ce^{IV}, Li^{I}/Co^{II}, and Fe^{II}/Zn^{II} were also prepared according to this concept.[113]

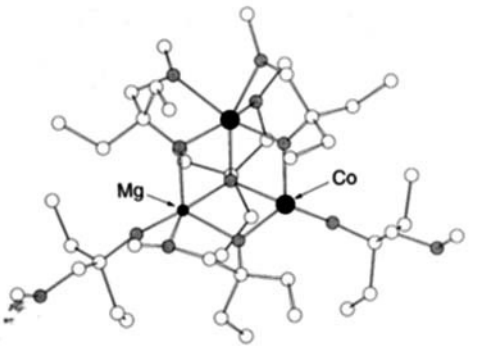

Fig. 8. Crystal structure of $[MgCo_2(OCEt_2CH_2OMe)_6]$ (**12**).

The first systematic investigations into the synthesis of heteronuclear alkoxides were performed by Meerwein and Bersin in 1929.[116] The double oxides ("Doppeloxide"), as they referred to the compounds, go back to the works of Copaux and Cambi, who synthesized the first boron alcoholate complexes at the turn of the century.[117] The technical importance of the heteronuclear alkoxides is indisputable today. The area of possible applications ranges from the synthesis of ferroelectric ($KTaO_3$) and dielectric materials ($SrTiO_3$) to the preparation of multimetallic "high-tech ceramics" ($YBa_2Cu_3O_{7-\delta}$).

Volatile molecular precursors are admittedly still rare. The heteronuclear transition metal complexes $[M\{Al(OiPr)_4\}_2]$ (M = Be, Zn, Cd, Hg[118]), $[Zn\{Al(OiPr)_4\}_2]$, $[Zn\{Al(OiPr)(OR)_3\}_2]$ (R = Me, Et, *n*Pr, *n*Bu, *i*Bu, *s*Bu, amyl[119]) and $[M^1(OiPr)_{5-x}\{M^2(OiPr)_4\}_x]$ (M^1 = Nb, Ta; M^2 = Al, Ga; $x = 1$, 2[121]), the alkaline earth metal complexes $[Be\{Al(OiPr)_4\}_2]$,[118] $[M\{Al(OtBu)_4\}_2]$ (M = Mg, Ca, Sr), $[M\{Al(OnBu)_4\}_2]$ (M = Mg, Ca), $[Mg\{Al(OEt)_4\}_2]$,[120] and the lanthanide complexes $[Ln\{Al(OiPr)_4\}_3]$ (Ln = Sc, Y, La, Pr, Nd, Sm, Gd, Dy, Ho, Er, Yb, Lu[122, 123]) described by Mehrotra et al. are some of the few examples known.

This class of compounds is naturally characterized by its great variety in terms of composition and structure. At this point only the aspect of the donor functionalization will be explored. Among the synthetic methods for 1:1-heterodimetallic systems, the ate-reaction [Eqns. (o) and (p)] are the most important. The difference in electronegativity between the metals involved and the steric demands of the alcohol influence the formation of the heterodinuclear alkoxide.

$$2\,LiO\mathit{t}Bu + 2\,Sn(O\mathit{t}Bu)_2 \rightarrow [Li_2Sn_2(O\mathit{t}Bu)_6] \quad \text{(o)}$$

$$2\,LiO\mathit{i}Pr + 2[Ti(O\mathit{i}Pr)_4] \rightarrow [Li_2Ti_2(O\mathit{i}Pr)_{10}] \quad \text{(p)}$$

The target of the synthesis is usually a "monomeric" 1:1-heterodimetallic alkoxide. This is not easy to achieve, because a difference in electronegativity and use of the individual components in stoichiometric ratios are rarely sufficient to guarantee its formation. A 1:1 mixture of $[Ba(OR)_2]$ and $[Ti(OR)_4]$ (R = Et, *i*Pr, Bu) thus does not lead to the expected $[BaTi(OR)_6]$, but to $[BaTi_4(OR)_{18}]$ (R = Et, C_6H_5). The solvent adducts $[BaTi_2(OEt)_{10}]\cdot 5EtOH$ and $[Ba_4Ti_2O(OEt)_{14}]\cdot 8EtOH$ have also been detected in solution.[124] None of these compounds is volatile, but instead they release $[Ti(OEt)_4]$ on heating. Similar problems are encountered in the synthesis of $[Sr_2Ti(OiPr)_8]\cdot 5HOiPr$ and $[NaW_2H(OR)_8]_8$ (R = *i*Pr, CH_2tBu).[125]

Donor-functionalized alcohols have had no importance as yet for the heterobinuclear complexes; at best they served to increase the solubility. The transfer of our ligand concept to complexes such as these should ensure volatility and thermal stability. We considered the alcoholysis of equimolar amounts of metal amides with subsequent ate-complex formation according to Equation (q) as synthetic method.[113]

$$[Fe\{N(SiMe_3)_2\}_2] + [Zn\{N(SiMe_3)_2\}_2] + 4HOCEt_2CH_2OMe \longrightarrow [FeZn(OCEt_2CH_2OMe)_4] + 4HN(SiMe_3)_2 \quad (q)$$

As metal amides are known for virtually all metals, this method promises wide access to the heteronuclear complexes. The element combinations Mg^{II}/Co^{II} and Fe^{II}/Zn^{II} were investigated first as model systems to sound out the influence of the electronegativities on the formation and thermal stability of heterodinuclear alkoxides. After reaction of $[M\{N(SiMe_3)_2\}_2]\cdot x$THF with $HOCEt_2CH_2OMe$ ($M = Mg^{II}$, $x = 2$; Co^{II}, $x = 0$), only the heteronuclear species could be identified by mass spectroscopy. In contrast, after treatment of the iron and zinc amides $[M\{N(SiMe_3)_2\}_2]\cdot x$THF with $HOCEt_2CH_2OMe$ ($M = Fe^{II}$, $x = 1$; Zn^{II}, $x = 0$), signals for the homodinuclear alkoxides were identified in addition to those for the heterodinuclear species. As the difference in electronegativities for the element combination Fe/Zn ($\Delta\chi = 0.18$) is considerably smaller than for Mg/Co ($\Delta\chi = 0.57$), it is assumed that large differences in electronegativity favor the exclusive formation of the heterodinuclear alkoxide. Based on this assumption we were able to synthesize the compounds **13**–**16**.[113]

$[LiCo\{OC(CF_3)(OiPr)_2\}_3]$ **13** (95 °C/10^{-2} Torr)

$[Na_2Ce(OCEt_2CH_2OMe)_6]$ **14** (95 °C/10^{-2} Torr)

$[KCo(OCEt_2CH_2OMe)_3]$ **15** (110 °C/10^{-3} Torr)

$[LaCo(OCEt_2CH_2OMe)_5]$ **16** (115 °C/10^{-3} Torr)

The K/Co complex **15** is dimeric (Fig. 9) and has great structural similarity with the K/Zn derivative $[\{KZn(OCMe_3)_3\}_2]$.[127] Attempts to prepare volatile heterodinuclear indium/tin and strontium/calcium alkoxides failed. We put this down to the relatively small differences in the electronegativities ($\Delta\chi = 0.1$ and <0.1, respectively[67]).

The synthetic method does not necessarily demand the use of "basic" and "acidic" alkoxides as a matter of course, however. In the reaction of $[Nb(OMe)_5]$ with $[Ta(OMe)_5]$ also the *heterodinuclear* alkoxide $[NbTa(OMe)_{10}]$ is formed ($\Delta\chi$(Nb/Ta) = 0.1).[128] Nevertheless, the electronegativity rule has proved to be a useful rule-of-thumb.

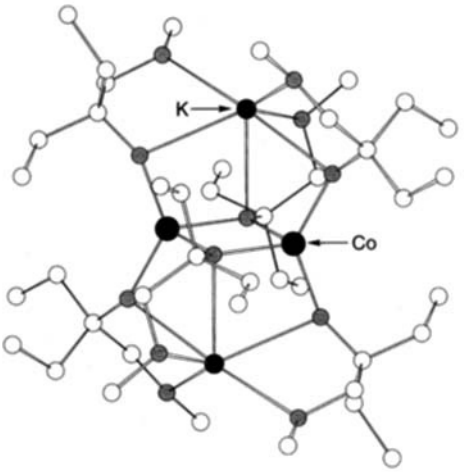

Fig. 9. Crystal structure of $[K_2Co_2(OCEt_2CH_2OMe)_6]$ (**15**). All alkoxo ligands are bridging.

6.3. Lithium/Niobium Alkoxides

Lithium niobate ($LiNbO_3$) is an interesting heterodinuclear metal oxide from a materials science point of view due to its piezoelectrical and pyroelectrical properties as well as its nonlinear optical (NLO) properties. Molecularly defined precursors for the MOCVD (MOCVD = metal-organic chemical vapor deposition) and sol–gel processes have thus always been a priority synthetic goal. The first route providing access to lithium/niobium alkoxides was found by Mehrotra et al. in 1968 with the ate-reaction of niobium alkoxides $[Nb(OR)_5]$ (R = Me, Et, *i*Pr) with lithium alkoxides LiOR (R = Me, Et, *i*Pr).[115] On workup, however, these lithium/niobium alkoxides decomposed under the conditions of vacuum sublimation in the back reaction of their formation [Eq. (r)]. Bradley et al. confirmed this for

$$[LiNb(OR)_6] \overset{\Delta,\ \text{vacuum}}{\rightleftharpoons} LiOR + [Nb(OR)_5] \quad (r)$$

$[LiNb(OtBu)_6]$ (**17a**).[1] This "demixing" ("dismutation") is structure-related: lithium/niobium alkoxides, for example $[LiNb(OEt)_6]$ (**17b**), have chain structures in which lithium is tetracoordinated and niobium hexacoordinated.[129]

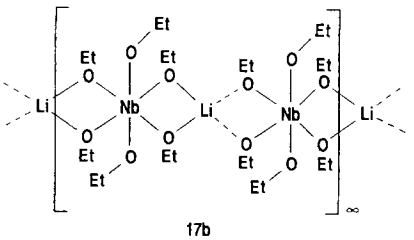

17b

The dinuclear precursor $[Li_2Nb_2O_2(OEt)_8]\cdot 2HOEt$ (**18**), originally formulated as the tetrameric hydroxo cluster $[Li_2Nb_2(OH)_2(OEt)_{10}]$,[142] is a structurally characterized (Fig. 10) intermediate on the way to **17b**. For this reason, multicomponent CVD precursors such as lithium-β-diketonate/niobium(v) ethoxide had to be used until now.[130] However, this route gave only amorphous $LiNbO_3$ layers that had to be made

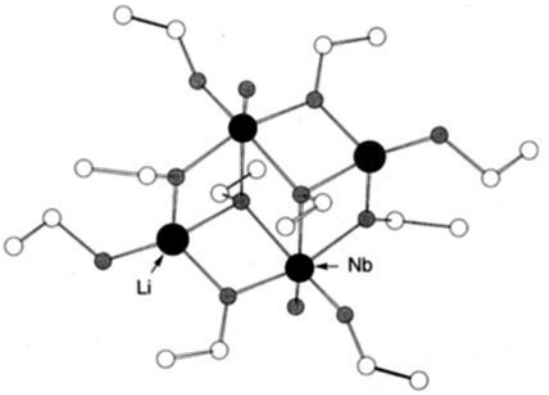

Fig. 10. Crystal structure of $[Li_2Nb_2(OEt)_{10}]\cdot 2\,HOEt$ (**18**).

crystalline by tempering at 1000 °C. $[LiNb(OEt)_6]$ is said to give monocrystalline layers in the spray-CVD process at 400 °C. Equation (r) arouses doubt about the integrity of the molecular precursor under these experimental conditions.[131] The reaction is therefore based on the concept of donor functionalization [Eq. (s)]. At 90 °C/10^{-3} Torr, **19** (Fig. 11) is volatile and does

$$Li^+[OCMe_2CH_2OMe]^- + NbOCl_3 \longrightarrow \underset{\mathbf{19}}{[Li_2Nb_2O_3(OCMe_2CH_2OMe)_6]} + \ldots \quad (s)$$

not decompose. At 600 °C it produces lithium niobate films that have the correct Li:Nb:O ratio of 1:1:3 (Fig. 12) after tempering at 700 °C in an oxygen plasma.[126] The alkoxide **19** does not, therefore, "demix" on vaporizing—an important criterion for every precursor philosophy that aims at predetermining the composition of the CVD product from the metal ratio in the molecular precursor.[114]

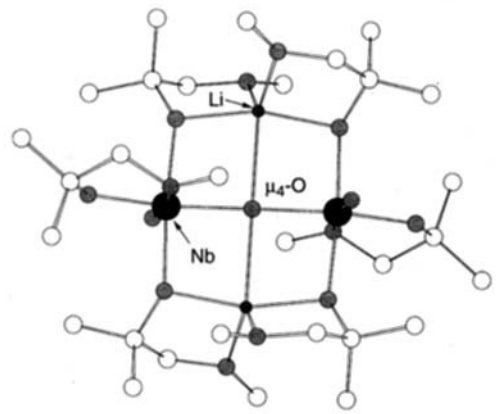

Fig. 11. Crystal structure of the Li_2Nb_2 alkoxo cluster compound **19** with a central ("lone") oxo ligand.

Fig. 12. $LiNbO_3$ from the molecular precursor **19**, deposited on steel at 350 °C and tempered at 650 °C in an O_2 plasma; scanning electron micrograph magnified 1000×. (The layer has caved in due to the different thermal expansion coefficients.)

Steel, glass, glass coated with vaporized gold, silicon, and lithium tantalate $LiTaO_3$ can be used as substrates. According to XPS data, the proportion of carbidic carbon is less than 5%.[126] The newer strategy for success for the introduction of donor functionalization is demonstrated by the reactions according to Equations (s) and (t). The heterodinuclear alkoxide **20** sublimes at 110 °C/10^{-2} Torr without decomposition and is monomeric according to EI-MS data.[126]

$$Li^+[OCHMeCH_2NMe_2]^- + [Nb(OiPr)_4(OCHMeCH_2NMe_2)] \longrightarrow \underset{\mathbf{20}}{[LiNb(OCHMeCH_2NMe_2)_2(OiPr)_4]} \quad (t)$$

7. Further Strategies

The polarity in metal alkoxides arising from M–O bonds can be reduced by the (partial) exchange of alkoxides with, for example, alkyl groups. $[Be_3(OtBu)_6]$ thus sublimes at 110 °C/10^{-3} Torr,[138] and $[Be_2tBu_2(OtBu)_2]$ at 50 °C/10^{-2} Torr.[149] Such compounds are not a subject of this article because of their homoleptic character, but this aspect will require more attention for CVD in the future.

If a metal center in M–O(R)–M units is replaced by one of higher electronegativity, the polarity of the M–O bond is reduced due to a decrease in the electron density on the alkoxide oxygen atom. The pentanuclear complex $[Sc_5O(OiPr)_{13}]$ (**21**) can be vaporized only above 210 °C/10^{-2} Torr,[44] the tetranuclear dinuclear complex $[Sc\{Al(OiPr)_4\}_3]$ (**5a**) (Section 3) under conditions as mild as 140 °C/0.5 Torr.[123]

8. Volatile Metal Alkoxides

As most metals within a period or group have neighbors whose alkoxides have similar properties, these will be summarized in the following discussion. In the context of volatile compounds, the limitation to homoleptic metal alkoxides is justifiable.

8.1. Alkoxides MOR of Monovalent Metals

Volatile alkoxides of the alkali and coinage metals, as well as those of thallium, are little known, mainly as a result of the unfavorable charge-to-radius ratio. Consequently, sterically undemanding ligands give rise to oligomeric, nonvolatile compounds.

8.1.1. Alkali Metal Alkoxides

Hexameric $[Li_6(OtBu)_6]$ sublimes at 110 °C/10^{-1} Torr.[8] The tetrameric K, Rb, and Cs derivatives can be vaporized at 140–195 °C/10^{-2} Torr.[8, 132] $[Li_6(OCMe_2Ph)_6]$ is less volatile (165 °C/10^{-3} Torr) than the *tert*-butoxide derivative $[Li_6(OtBu)_6]$ because of the phenyl group (cf. Section 4.1).[62] The O-donor-function-

alized $[Li_6(OMe_2CH_2OMe)_6]$, which sublimes at 110 °C/10^{-3} Torr, is also hexameric based on CI-MS data.[113] $[Na_4\{OCH(CF_3)_2\}_4]$ sublimes slowly at 75 °C/10^{-2} Torr,[64] $[Na\{OCtBu(CH_2OiPr)_2\}]$ quickly at 155 °C/10^{-3} Torr.[113] No volatility data were reported for the P-donor-functionalized complexes $[M_2\{OCtBu_2CH_2PR_2\}_2]$ (M = Li, Na; R = Me, Ph).[133]

8.1.2. Thallium(I) and Copper(I) Alkoxides

The heterocubane $[Tl_4\{OCH(CF_3)_2\}_4]$ is the only known vaporizable alkoxide of this metal (85 °C/10^{-2} Torr).[64] For monovalent copper only $[Cu_4\{OtBu\}_4]$ (110 °C/10^{-3} Torr) is known.[134] Fluorinated alcohols give more volatile derivatives such as $[Cu_4\{OtBu\}_2][\{OCR_{3-n}(CF_3)_n\}_2]$ (R = H, n = 2: 90 °C/10^{-3} Torr; R = Me, n = 2: 70 °C/10^{-3} Torr; R = Me, n = 1: 95 °C/10^{-3} Torr) on partial alcoholysis.[135] Other volatile homoleptic metal alkoxides are not known if the adduct $Me_3P\cdot[Au(OSiMe_3)]$ (which is described as being partially sublimable, although no details are given[136]) is disregarded.

8.2. Alkoxides $M(OR)_2$ of Divalent Metals

The heavy alkaline earth and the divalent rare earth metals are to be discussed together because of their large ionic radii (Fig. 13) and their electropositive character. Similar properties link magnesium (ionic radius Mg^{2+}: 72 pm) with divalent first row transition metals (69–80 pm), and the "soft" divalent main group metals Ge, Sn, and Pb form an additional unit. The current literature only justifies special consideration for Be^{II} (27 pm) and Cu^{II} (57 pm). Homoleptic alkoxides of Pd^{II}, Pt^{II}, and Hg^{II} are known but they are all nonvolatile.[118, 137, 152]

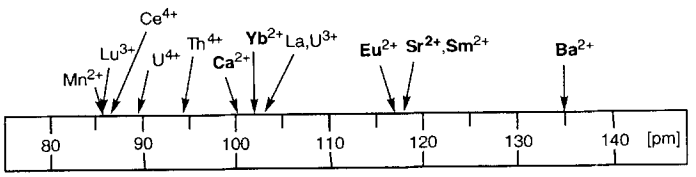

Fig. 13. Radii of large metal ions (C.N. 6) according to Shannon; data from Ref. [154].

8.2.1. Beryllium Alkoxides

The alkoxides of beryllium, $Be(OR)_2$, are dimeric or trimeric even with bulky substituents such as R = CEt_3, CEt_2Me, $CEtMe_2$, and $CtBu$ and $C_2H_4NMe_2$[138, 139] because of the extremely high Lewis acidity in spite of the very small ionic radius. The only monomeric exception is $[Be(O\text{-}2,6\text{-}tBuC_6H_3)_2]$.[138] Besides $[Be_3Cl_2(OtBu)_4]$ and $[Be_2Br_2(OtBu)_2]\cdot 2OEt_2$,[139] in 1993 Power et al. reported $[Be(O\text{-}2,4,6\text{-}tBu_3C_6H_2)_2]\cdot OEt_2$, one of the few tricoordinate, structurally characterized beryllium complexes.[140] The reactions of $[Be\{N(SiMe_3)_2\}_2]$ with $HOCMe_2CH_2OMe$ and $HOCEt_2CH_2OMe$ led to volatile products (72 °C/10^{-2} Torr and 78 °C/10^{-3} Torr respectively)—products that show no fluxional behavior in their ^1H NMR spectra. As they are as volatile as $[\{Be(OCEt_3)_2\}_2]$, they are probably dimeric structures. The beryllium alkoxides thus belong to the few examples where the additional donor functionality does not produce an increase in volatility. As the coordination number 4 typical for beryllium is only rarely exceeded, the structure of the molecules is comparable to that of $[\{Sn(OCMe_2CH_2OMe)_2\}_2]$ (Section 8.2.3).

8.2.2. Calcium, Strontium, Barium, and Ytterbium(II) Alkoxides

Immediately after the discovery of the oxidic high-temperature superconductors, research into the alkoxides of the heavy alkaline earth metals experienced a dramatic upswing; no solution was forthcoming for the notorious lack of volatility, however. The following ligands were used: OMe, OEt,[141] OiPr,[8] OtBu,[144] OPh,[144b] $OCPh_3$, $OSitBu_3$, $OSiPh_3$,[143] $O(CH_2CH_2O)_nMe$ (n = 1, 2, 3)[98, 99, 105], $O(C_2H_4O)_2nBu$,[145] $OCH_2CH_2NMe_2$,[146] $OCH_2CHO(CH_2)_3$ (= 2-tetrahydrofurfuryl),[95] $OCH_2CH_2N(C_2H_4OH)_2$,[147] O-2,6-tBu_2-4-Me-C_6H_3,[148] O-2,4,6-$(Me_2NCH_2)_3C_6H_2$,[146] O-2,4,6-$(F_3C)_3C_6H_2$,[150] and $OSiPh_2OSiPh_2O$.[151] Little effort was expended on the synthesis of new alcohol derivatives: even today, the greater part of the alcohols used as ligand precursors come from the shelf and are not tailor-made for the particular metal concerned.

The difficulties in obtaining volatile Ca, Sr, and Ba alkoxides are as follows: a) The large size of these metal ions (100–135 pm, Fig. 13) makes the construction of a perfect ligand shell (only *one* alcoholate ligand can be bound per metal charge!) very difficult in view of the relatively low charge (+ 2). Decomposition processes arising from intermolecular interactions are often the result. The low charge-to-radius ratios require donor-functionalized ligands. b) The polarizability of the metal ions is low. Apart from Ca, Sr, and Ba, only the divalent rare earth metals Sm, Eu, and Yb have this property profile to such an extreme degree.

For this reason, volatile alkoxides of these metals have only been obtained in exceptional cases: 1) Purdy et al. were able to obtain barium alkoxides with standard ligands such as OtBu, which were volatile under drastic conditions (270 °C/$<10^{-5}$ Torr).[95] 2) The homoleptic aryl oxides $[M_2(O\text{-}2,4,6\text{-}tBu_3C_6H_2)_4]$ of calcium, strontium, and barium sublime at 250 °C/10^{-4} Torr with partial decomposition.[75] The monomeric THF adducts are thermally more labile; for example $[Ca(O\text{-}2,6\text{-}tBu_2\text{-}4\text{-}MeC_6H_2)_2]\cdot 2THF$ already decomposes at 90 °C, presumably releasing the solvent molecule THF.[155] 3) The siloxo complex $[Ba_3(OSiPh_3)_6]\cdot THF$ sublimes at 225 °C/10^{-2} Torr with cleavage of THF.[143a] The analogous Ca and Sr complexes were also described as sublimable, though no data was specified. In contrast, according to thermogravimetric data, the ammonia adduct $[Ca_2(OSiPh_3)_4]\cdot 4NH_3$ is nonvolatile and only expels NH_3 on heating.[156] 4) Dimeric $[\{Ca(OCtBu_3)_2\}_2]$ (**22**) decomposes like tritox derivatives of other metals, under cleavage of isobutene. Trimeric $[Ca_3(OCHtBu_2)_6]$ (**23**) is formed according to Equation (u). This sublimes in small yield at

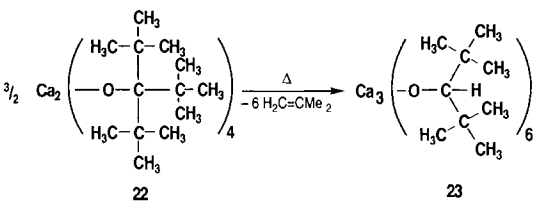

22 23 (u)

185 °C/10^{-3} Torr. The analogous Yb^{II} derivative $[\{Yb(OCtBu_3)_2\}_2]$ was described recently, but nothing is known about its thermal properties.

The volatile alkoxides $[M_2\{OC(CH_2OiPr)_2tBu\}_4]$ (M = Ca, **24a**; Sr, **24b**; Ba, **24c**) were obtained in our laboratory according to Equation (v) from the THF adducts of the amides $[M\{N(SiMe_3)_2\}_2]$ and structurally characterized (Fig. 14). These

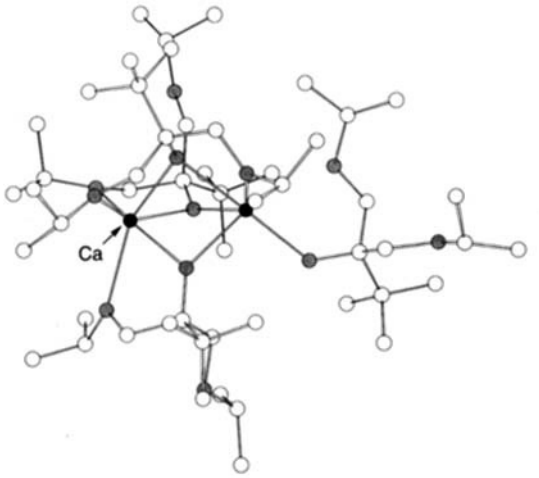

Fig. 14. Crystal structure of the first calcium alkoxide that sublimes without decomposition: $[Ca_2\{OC(CH_2OiPr)_2tBu\}_4]$ **24a** [68, 81].

complexes sublime in vacuum (10^{-2} Torr) without decomposition at 150 °C (Ca), 170 °C (Sr), and 185 °C (Ba).[68] The barium derivative $[Ba_2\{OC(CH_2OiPr)_2tBu\}_4]$ (**24d**) [Eq. (w)] sublimes at 150 °C/10^{-2} Torr. Compounds **24a**–**d** are the first alkoxides of these alkaline earth metals that fully sublime without any decomposition.

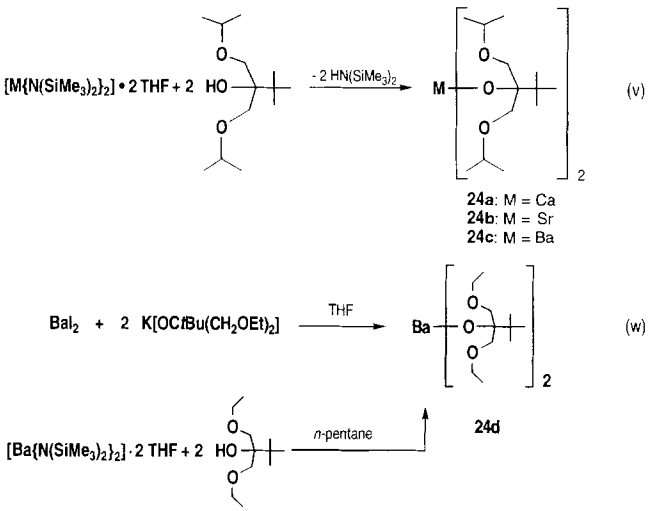

Triple bridging, as shown in Fig. 14, is not at all unusual for the alkaline earth alkoxides. This structural characteristic has been determined for the complexes $[Ca_2(OSiPh_3)_4]\cdot 4NH_3$,[156] $[Ba_2(OSitBu_3)_6]\cdot THF$,[79] and $[Ba_3(OSiPh_3)_4]\cdot THF$.[143a] Apart from the alkaline earth metals, this coordination has only been observed for $[Y_2\{(cyclo\text{-}C_5H_9Si)_7O_{11}\}_2]\cdot OPPh_3$ and $[Lu_2(OCMe_2CH_2OMe)_6]$ as yet.[82]

The divalent lanthanides (Yb, Sm, Eu) display the same properties profile (ionic radius, electronegativity) as the alkaline earth ions. For this reason, no volatile alkoxide complexes of these elements are known as yet. Taking the smallest and "heaviest" of the lanthanide ions Yb^{2+} as an example, we were able to obtain the first volatile alkoxide complex by reaction of $[Yb\{N(SiMe_3)_2\}_2]\cdot DME$ with $HOC(CH_2OiPr)_2tBu$: $[\{Yb[OC(CH_2OiPr)_2tBu]_2\}_2]$ (115 °C/10^{-3} Torr). As can be seen from Fig. 13, the ionic radii of Yb^{2+} and Ca^{2+} are equally large. The somewhat higher volatility of the ytterbium alkoxide is likely to arise from its lower Lewis acidity.

8.2.3. Germanium, Tin, and Lead Alkoxides

From a coordination chemistry point of view, germanium(II), tin(II), and lead(II) usually form a group.[8] This does not apply for the alkoxides: $[M(OCtBu_3)_2]$ (M = Ge, Sn) and $[M_2(OtBu)_4]$ (M = Ge, Sn) have dimeric structures,[54] whereas the complexes $[Pb(OCtBu_3)_2]\cdot HOCtBu_3$[85] and $[Pb_3(OtBu)_6]$ (**25**)[55, 96, 100] are known (Fig. 15).

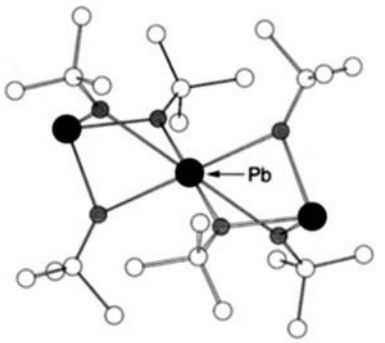

Fig. 15. Crystal structure of the trimeric lead(II) alkoxide $[Pb(OtBu)_2]$ (**25**).

The O-functionalized derivatives $[\{M(OCMe_2CH_2OMe)_2\}_2]$ (M = Sn, Pb) are quantitatively volatile.[113] The tin alkoxide **26a** (Fig. 16, top) sublimes completely and without decomposition at 70 °C/1.5 Torr. The only other volatile tin alkoxide is $[\{Sn(OtBu)_2\}_2]$ **26b** (Fig. 16, bottom), for which Veith et al. reported sublimation conditions of 60 °C/10^{-3} Torr[160] and Lappert et al. 103 °C/10^{-1} Torr.[157]

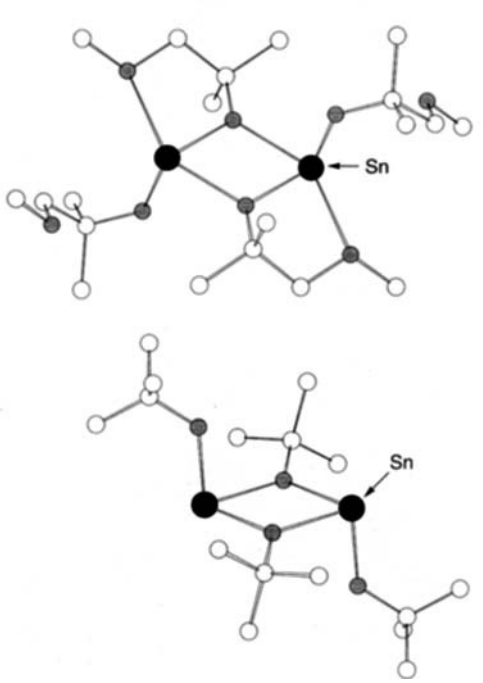

Fig. 16. Crystal structures of (dimeric) tin(II) alkoxides $[Sn_2(OCMe_2CH_2OMe)_4]$ (**26a**, top) and $[Sn_2(OtBu)_4]$ (**26b**, bottom).

These values are consistent with one another and correspond approximately to 140 °C/1.5 Torr, which demonstrates again the positive effect of alcoholate chelates on volatility. The lead alkoxide analogous to **26a** is less volatile, subliming at 80 °C/10^{-2} Torr. Although a dimeric formula has been confirmed for the gas phase, the lower volatility of the lead alkoxide (relative to the Sn derivative) would seem to indicate a higher nuclearity in the solid phase. Lead alkoxides do indeed have a greater tendency to aggregate. Freshly prepared $Pb(OiPr)_2$ is trimeric, for example, but rapidly ages and polymerizes. The same coordination was found for $[Pb(OCH_2CH_2OMe)_2]_\infty$ (**27**, Fig. 17).[100] To

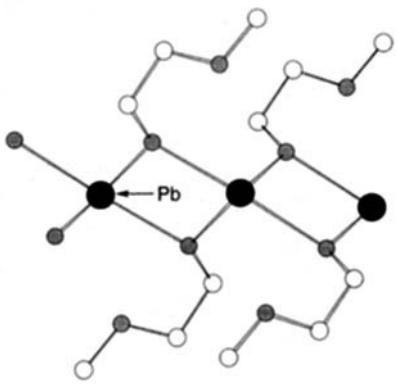

Fig. 17. Crystal structure of the polymeric Pb^{II} alkoxide $[Pb(OCH_2CH_2OMe)_2]_\infty$ (**27**).

increase the volatility, the chiral alcohol $HOCMe_2CHMeOMe$ was employed. Using the racemate should reduce the melting point of the resulting metal complex and increase the volatility. Moreover, the steric interligand interaction should facilitate the approach of the ligand to the metal and the coordination of the donor function.

The sublimation conditions of 95–115 °C/10^{-2} Torr contradict these considerations, but simultaneously reinforce the notion that the alkoxides $[Pb(OCMe_2CHMeOMe)_2]$ and $[Pb(OCMe_2CH_2OMe)_2]$ are isostructural. Attempts to prepare the analogous germanium(II) alkoxide surprisingly led to the oxo cluster compound $[Ge_6O_4(OCMe_2CH_2OMe)_4]$ (**28**, Fig. 18).[68] Presumably, this is the product of partial hydrolysis, as is expressly emphasized by the authors in the case of the structural analogue $[Sn_6O_4(OMe)_4]$.[158] Moreover, this structural type was also found for $[Pb_6O_4(OiPr)_4]$,[159] in which the origin of the oxo ligand is unknown.

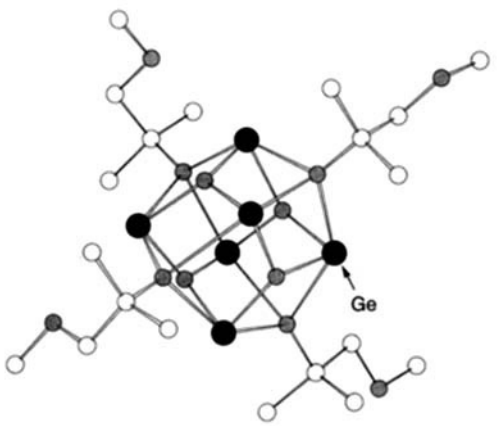

Fig. 18. Crystal structure of the hexameric alkoxo(oxo)germanium cluster $[Ge_6O_4(OCMe_2CH_2OMe)_4]$ (**28**).

8.2.4. Copper(II) Alkoxides

Just as for the alkaline earth metals, the development of the copper(II) alkoxides was influenced by the discovery of the high-temperature superconductors. Until 1989, the only known volatile copper alkoxide was the already mentioned $[Cu_4(OtBu)_4]$.[134] Horowitz et al., and later Buhro et al., were able to obtain monomeric volatile copper(II) alkoxides by using amino-functionalized ligands.[97, 161] The idea of using of O-functionalized ligands was discarded, because the ether function does not coordinate to the metal.[162] For this reason, $[Cu(OC_2H_4OMe)_2]$ is insoluble,[163] as are the simple homoleptic alkoxides of the type $[Cu(OR)_2]$ (R = Me, Et, *i*Pr, *t*Bu); it presumably has a polymeric chain structure as has already been confirmed for $[Pb(OC_2H_4OMe)_2]_\infty$ (**27**, Fig. 17). The $[Cu(OCMe_2CH_2OMe)_2]$ prepared by alcoholysis of $[Cu(OMe)_2]$ with $HOCMe_2CH_2OMe$ was sublimed at 85 °C/10^{-4} Torr in 40 % yield. In terms of volatility it is thus comparable to the monomeric $[Cu(OCMeHCH_2NMe_2)_2]$, but thermally much less stable. The observations made by Buhro and Horowitz on the O-functionalized ligands were thus confirmed.

8.2.5. Magnesium, Manganese(II), Iron(II), Cobalt(II), Zinc(II), and Cadmium Alkoxides

The synthesis of volatile divalent transition metal alkoxides is no less complicated than the preparation of volatile alkaline earth or lanthanide alkoxides. This becomes especially apparent when making the comparison with the lanthanides (Section 8.3.2). The complexes with simple ligands such as OMe and O*t*Bu are polymeric and nonvolatile,[8] whereas the lanthanide alkoxides already form volatile complexes with isopropoxide ligands.[28] Ditox complexes of the lanthanides are all dimeric,[47] whereas the corresponding manganese compound is trimeric.[24b] The 2,6-tBu_2-substituted phenoxo lanthanide complexes are monomeric;[49, 50] the corresponding analogues of manganese, iron,[201] and zinc[165] are dimeric. The synthesis of volatile alkoxides of the above-mentioned metal ions thus requires the use of bischelating ligands that were also required for the alkaline earth metals [Eq. (x)].[199] In addition to the electronegativity, the ionic radius (Table 3) is also crucial for the volatility. The

Table 3. Sublimation temperatures *T* [a] of the alkoxides **30a–d**, the ionic radii *r* of the M^{2+} ions [b], and the electronegativities EN of the metals M.

Cmpd.	M	*T* [°C]	*r* [pm]	EN
30d	Cd	95	78	1.69
30a	Mn	90	66	1.55
30c	Zn	80	60	1.65
30b	Co	72	58	1.88
30e	Mg	80 [c]	57	1.31

[a] At 10^{-2} Torr. [b] Effective ionic radius according to Shannon. [c] At 10^{-3} Torr, which corresponds to 90 °C/10^{-2} Torr.

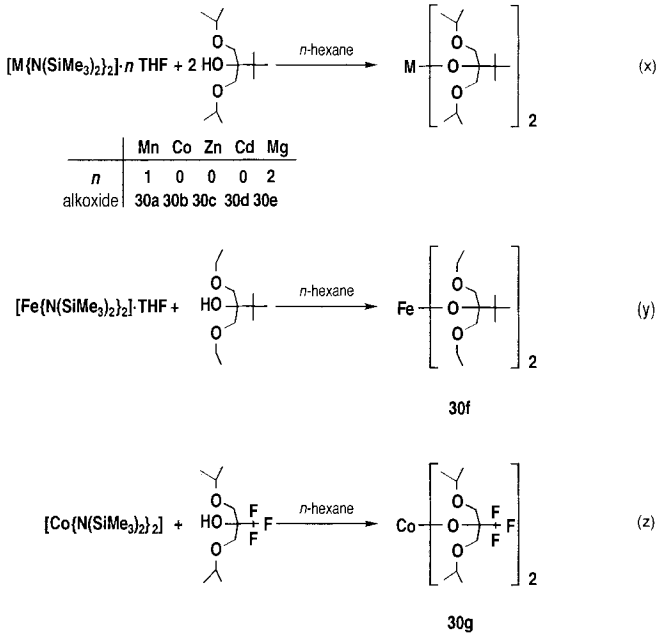

exchange of the *tert*-butyl group in **30b** for the sterically less demanding CF_3 group in **30g** leads to the dimeric cobalt alkoxide $[\{Co[OC(CH_2OiPr)_2CF_3]\}_2]$ (115 °C/10^{-3} Torr) [Eq. (z)]. The cadmium alkoxide **30d** has been structurally characterized (Fig. 19).[81]

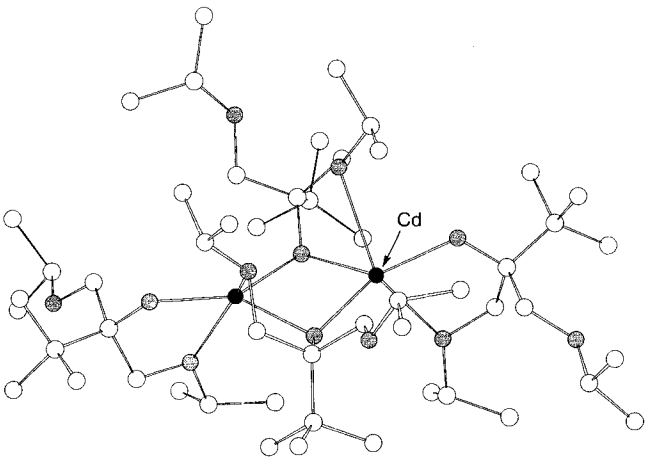

Fig. 19. Crystal structure of the (dimeric) volatile cadmium alkoxide $[\{Cd[OC(CH_2OiPr)_2OtBu]_2\}_2]$ (**30**).

The simple zinc(II) alkoxides $[Zn(OR)_2]$ (R = Me, Et, *i*Pr, *n*Bu, *t*Bu, *n*-octyl) are insoluble and nonvolatile.[8, 164] The first readily soluble homoleptic zinc(II) aryloxides $[Zn(OAr)_2]$ (Ar = 2,4,6-$tBu_3C_6H_2$) were reported in 1986.[165] The use of sterically demanding groups (R = CEt_3, CEt_2Me) made it possible to synthesize sublimable alkoxozinc complexes.[100, 166] Whereas the $[Zn(OR)_2]$ complexes (R = C_2H_4OMe, $C_2H_4OC_2H_4OMe$) are nonvolatile and only slightly soluble even in donor solvents such as THF, the complexes $[Zn(OCH_2CH_2NMe_2)_2]$ and $[Zn(OCHMeCH_2NMe_2)_2]$ with amino-substituted ligands can be partially sublimed at 170 °C/10^{-4} Torr. The greater volatility of the copper(II) complexes arises from the monomeric structure (both in solution and in the crystal). The chelating alcohol $HOCtBu(OiPr)_2$ allows a significant increase in the volatility, while at the same time improving the stability.

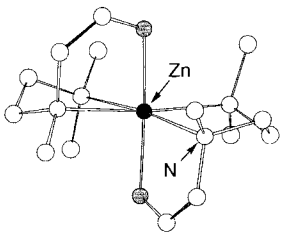

Fig. 20. Crystal structure of the zinc alkoxide **29** contaning the N-functionalized alkoxo ligand $OCHCHNMeCH_2CH_2NMe_2$.

The complex with an O,N,N-ligand, $[Zn(OCHCHNMeCH_2CH_2NMe_2)_2]$ (**29**), is a special case. The analytical data and the crystal structure of the sublimate show (Fig. 20) that hydrogen is eliminated during the sublimation. This was also observed for $[Y(OiPr)_3]$ by Mazdiyasni et al.[167]

8.3. Alkoxides $M(OR)_3$ of Trivalent Metals

The transition metals, the rare earth metals, and the metals of the third main group of the Periodic Table form their own classes of compounds, but only few structurally well-defined examples are known.

8.3.1. Bismuth, Vanadium, and Chromium Alkoxides

Bismuth oxides are components of the ceramic high-temperature superconductors. In contrast to $YBa_2Cu_3O_{7-\delta}$ systems, those containing bismuth, such as $Bi_2(Sr,Ca)_4Cu_3O_{10-\delta}$ are ductile and can be cast. Alkoxides of the type $[Bi(OR)_3]$ (R = Me, Et, *i*Pr) [168, 169] have been known since 1966 and were first used in sol–gel and MOCVD processes in 1988.[170, 188] $[Bi(OtBu)_3]$ was prepared[175] by Evans et al. and Hubert-Pfalzgraf et al. and is monomeric in the gas phase according to an electron diffraction analysis;[171a] the crystal structure has not yet been solved.[171b] A characteristic of all homoleptic bismuth alkoxides is their low thermal stability; they decompose partially during sublimation.[169] This problem was eliminated in the preparation of $[Bi(OCMe_2CH_2OMe)_3]$ (**11b**, see Section 6.1).[68] The compound can be sublimed without decomposition at 60 °C/10^{-2} Torr and is thus significantly more volatile and thermally more stable than the N-donor-functionalized complexes $[Bi(OR)_3]$ (R = $CHMeCH_2NMe_2$, 90 °C/10^{-4} Torr, R = $C_2H_4NMe_2$, 85 °C/10^{-4} Torr).[169] The complexes $[Cr(OCMe_2CH_2OMe)_3]$ (**10**, 65 °C/1.5 Torr; see Fig. 6 in Section 6.1) and $[V(OCMe_2CH_2OMe)_3]$ (**11**, 55 °C/1.5 Torr), originating from our Munich laboratory, are also considerably more volatile and thermally more stable than simple alkoxides of the composition $M^{III}(OR)_3$. The extraordinarily low sublimation points of both compounds are remarkable. The vanadium compound is the most volatile metal alkoxide yet known. Similar volatilities are only displayed by the methoxides and ethoxides of some nonmetals and semimetals. Compound **10** is the first monomeric homoleptic chromium(III) alkoxide with a known molecular structure.

8.3.2 Rare Earth Metal Alkoxides

The spectrum of the simple lanthanide alkoxides $Ln(OR)_3$ (R = Me, Et, *i*Pr) ranges from oligomeric structures to cluster-like structures.[8, 173] The selection of the ligand system for the synthesis of volatile lanthanide alcoholates is less troublesome than that of the alkaline earth metals for the following reasons: a) Even the largest (trivalent) lanthanide ion has an ionic radius only insignificantly larger than calcium (La^{3+} 103 pm, Ca^{2+} 100 pm). b) The rare earth metals are somewhat more electronegative than the alkaline earth metals [EN(Ln) ≈ 1.1, EN (Ca, Sr, Ba) = 0.8–1.0]. c) Three valences are available for the saturation of the ligand sphere instead of just two. Sterically demanding CH alcohols are therefore sufficient for the synthesis of volatile alkoxides (Table 4).

Table 4. Volatile rare earth alkoxides.

Ligand	Alkoxide	M	T [°C] [a]	Ref.
Alkoxo ligand				
$OCHMe_2$	$[M(OiPr)_3]$	Sc, Y, Yb	>215 [b]	[44–46]
$OCMe_3$	$[M_3(OR)_3]\cdot 2HOR$	Y	235 [b]	[92]
		La	240	
$OCMe_2Et$	$[Y_3(OR)_9]\cdot 2HOR$	Y	150	[92]
$OCMe_2iPr$	$[M_2(OR)_6]$	Y	170	[92]
		La	135	
$OCMeEtiPr$	$[M_2(OR)_6]$	Y	170	[92]
		La	150	
$OCEt_3$	$[Y_2(OR)_6]$	Y	225 [b]	[92]
$OCHtBu_2$	$[M_2(OR)_6]$	Nd	170	[47]
		Dy	240	
		Tm	220	
$OCiPr_3$	$[M_2(OR)_6]$	Nd	220	[174]
		Tb	200	
$OCiPr_2tBu$	$[Nd_2(OR)_6]$	Nd	160	[174]
$OCiPrtBu_2$	$[Y(OR)_3]$	Y	160	[47b]
Aryloxo ligand				
O-2,6-$tBu_2C_6H_3$	$[Y(OAr)_3]$	Y	250–255	[49]
O-2,6-tBu_2-4-MeC_6H_2	$[M(OAr)_3]$	Sc, Y, La, Pr, Nd, Dy, Ho, Er, Yb	250–260	[49]
O-2,6-tBu_2-4-RC_6H_2 (R = H, Me, *t*Bu)	$[Ce(OAr)_3]$	Ce	180 190 [c]	[50]
Donor-functionalized ligand				
$OCMe_2CH_2OMe$	$[Sc_2(OR)_6]$	Sc	140 [b]	
	$Lu_4O(OH)(OR)_{11}]$	Lu	220	[110, 177]
$OCEt_2CH_2OMe$	$[Sc(OR)_3]$	Sc	60	
	$[Y_2(OR)_6]$	Y	160	
$OCHtBuCH_2OEt$	$[Nd(OR)_3]$	Nd	175	[110, 177]
$OCHtBuCH_2NEt_2$	$[Nd(OR)_3]$	Nd	150	[110, 177]
$OCtBu_2CH_2OEt$	$[Nd(OR)_3]$	Nd	125	[110, 177]
$OCiPr_2CH_2OEt$	$[M(OR)_3]$	Y	95	[110, 177]
		Nd	115	
$OCiPr_2CH_2OC_2H_4OMe$	$[Nd(OR)_3]$	Nd	138	[178]
$OCtBu(CH_2OiPr)_2$	$[Nd(OR)_3]$	Nd	142	[178]
	$[Yb_2(OR)_4]$	Yb	115	

[a] Sublimation temperature at 10^{-3} Torr. [b] 10^{-2} Torr. [c] 10^{-4} Torr.

Fluorinated alkoxo ligands can increase the volatility of the lanthanide complexes considerably. Due to the incorporation of fluorine in pyrolytically formed layers as already mentioned, this type of ligand no longer seems attractive for the preparation of purely oxidic materials.[91, 179] Simple chelating ligands (OC_2H_4OR; R = Me, *i*Pr,[180] *n*Bu,[181] C_2H_4OMe, C_2H_4OnBu, $OC_2H_4NMe_2$, $OC_2H_4NMeC_2H_4NMe_2$[181–183]) do not offer significant advantages either. Ligands of this type lead to nonvolatile oligomeric compounds, for example the cyclic decamer $[\{Y(OC_2H_4OMe)_3\}_{10}]$.[103a]

Volatile, thermally stable lanthanide alkoxides can only be prepared by the use of tailor-made, donor-functionalized, sterically demanding alcohols. $[Nd(OCHiPr_2CH_2OEt)_3]$ already sublimes at 115 °C in a vacuum (approximately 10^{-3} Torr). The exchange of neodymium (Nd^{3+}, ionic radius 98 pm) for the smaller, lighter yttrium (Y^{3+}, 90 pm) causes a further drop in sublimation temperature (95 °C/10^{-3} Torr). Taking the information known about the structure of $[M(OCtBu_2CH_2PMe_2)_3]$ (M = Nd, **31a**; Y, **31b**) into account, both alkoxides probably occur as monomers in both the gas and solid phases (Fig. 21). $[\{Lu(OCMe_2CH_2OMe)_3\}_2]$ (**32**, Fig. 22) has the lowest sublimation temperature yet known for a lanthanide alkoxide complex (90 °C/10^{-3} Torr).[184]

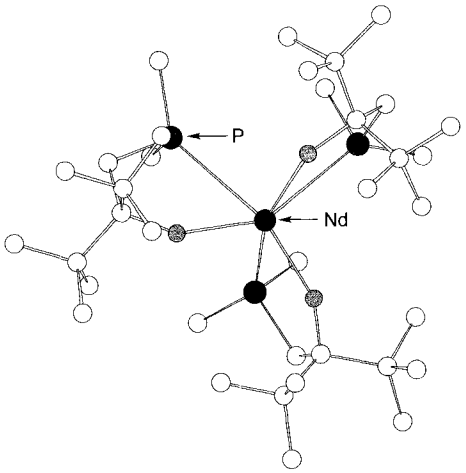

Fig. 21. Crystal structure of the P-functionalized alkoxoneodymium complex $[Nd(OCtBu_2CH_2PMe_2)_3]$ (**31a**).

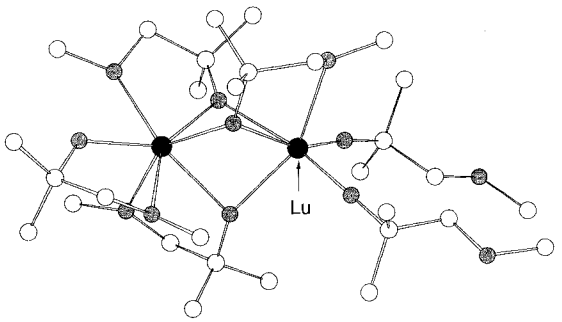

Fig. 22. Crystal structure of the (dimeric) volatile lutetium alkoxide $[\{Lu(OCMe_2CH_2OMe_3\}_2]$ (**32**).

8.3.3. Aluminium, Gallium, Indium, and Thallium Alkoxides

In contrast to aluminum,[185] gallium,[186] and thallium[187] alkoxides, homoleptic alkoxides of indium first became known in 1976.[43] In addition to some heteronuclear compounds of the type $[In\{M(OiPr)_4\}_3]$ (M = Al, Ga)[189] and dialkylindium alkoxides of the formula R_2InOR' (R = Me, *t*Bu; R' = Me,[190] Et,[191] *t*Bu,[192] $CMe(CF_3)_2$[193]), the alkoxide chemistry of indium is limited to simple, commercially available alcohols. Moreover, it occupies a special position in the third group of the Periodic Table: indium methoxides and ethoxides are insoluble in the usual solvents, and there are no volatile indium alkoxides.

The tendency to form cluster compounds, which is attributed to the larger ionic radius (In^{3+} 80 pm; Ga^{3+} 62 pm; Al^{3+} 54 pm) can best be illustrated by the isopropoxides: Bradley et al. isolated the pentameric oxo cluster with the formula $[In_5(OiPr)_5(\mu_2\text{-}OiPr)_4(\mu_3\text{-}OiPr)_4(\mu_5\text{-}O)]$ (cf. Fig. 1b),[172] whereas the corresponding Al and Ga derivatives are trimeric and dimeric, respectively.[189, 195] Sterically demanding donor-functionalized alcohols should reduce the nuclearity of the indium alkoxides and thus permit their synthesis. We were indeed able to obtain the first volatile indium alkoxides in the form of $[In(OCR_2CH_2OMe)_3]$ (R = Me: **33a**, 110 °C/10^{-3} Torr; R = Et: **33b**, 110 °C/10^{-3} Torr).[113] These are dimeric in the gas phase according to CI-MS.

8.4. Alkoxides of Tetravalent Metals and Metals of Higher Valency

The preparation of volatile alkoxides becomes easier with increasing oxidation number (increase in the coordination number). As was exemplified in Section 4.1, metal complexes that can be vaporized without decomposition can even be obtained with alkoxo ligands that are sterically relatively undemanding. This topic seems to be rounded off now, and we therefore refer the reader to the relevant literature.[1, 2, 4, 8, 196]

9. Conclusion and Perspectives

What have we learned? Putting increasingly larger ligands on metal centers is not a patent solution for achieving mononuclear metal complexes with sufficient volatility. Steric crowding also leads to fragility of the ligand sphere in terms of nonspecific bond cleavage. The concept of donor functionalization is a much more reliable strategy. It is satisfied with moderately bulky ligands and relies on the electronic σ-donor saturation of the metal centers through suitably positioned, electron-rich substituents (heteroatoms). This concept verified by using alkoxo ligands with ether and dialkylamino groups in β-positions is particularly important in the context of the preparation of oxidic materials, for which metal alkoxides are of great importance. As far as the volatility that can be attained by donor functionalization is concerned, the monomeric chromium and vanadium alkoxides $[M(OCMe_2CH_2OMe)_3]$ and the barium alkoxide $[Ba_2\{OC(CH_2OiPr)_2tBu\}_4]$, which sublime under vacuum at temperatures lower than 60 °C without leaving a residue, are convincing examples.[199]

The concept of the combination of donor functionalization and steric demand is proving itself not only in alkoxide chemistry: monomeric lanthanide complexes with amino-functionalized siloxy ligands have also now become accessible.[194] The "problem case" of barium in the β-diketonato series was countered with monomeric volatile β-ketoiminates that are ether-functionalized.[197] P-functionalized silylamide ligands now enrich the coordination chemistry of transition metal amides.[198] Topical works from the field of cyclopentadienyl chemistry, to which our laboratory has contributed,[110] confirm this trend. A breakthrough for this concept in the coordination chemistry of the alkyl[201] and hydroboranate complexes is to be expected.

Now that the preparation of volatile metal alkoxides seems to be feasible on all fronts, the future task is to bring in deliberately targeted "cleavage points" with a view to bringing about an orderly thermolytic (or, more rarely, photolytic) decomposition of these compounds. Experience to date would seem to indicate that plasma-chemical methods are insufficiently selective as regards definite decomposition paths. The decomposition methods coming into consideration from the materials science point of view have to be tuned to the chemical constitution of the molecularly defined precursors. Kinetic studies into their chemical decomposition should provide insight into the degradation and rearrangement mechanisms of metal alkoxides. This presents an open- and probably very fruitful- field of cooperation between synthetic chemistry and the material sciences.

The roots of this article are to be found in Dr. Rainer Anwander's pioneering Ph.D. thesis submitted to the Technische Universität München in 1992. We are deeply obliged to him for his stimulating discussions and persistent experimental results in the field of rare earth chemistry. Our thanks also go to doctoral students Florian Munck and Thomas Priermeier, and to Dr. Wolfgang Scherer for synthetic and structural chemical contributions to the "concept of donor functionalization", as well as to Wolfgang Wachter for the gas phase depositions and the scanning electron microscope photos. The correspondence author thanks the numerous supporters of his research work, in particular the Freistaat Bayern for equipment from the Bavarian long-term program "Neue Werkstoffe", the Fonds der Chemischen Industrie for equipment and a doctoral grant (N. W. H.), as well as the Bundesministerium für Forschung und Technologie, which supported us in the group project "MOCVD für Hartstoffschichten". We would also like to thank the research group of Dr. Roland Fischer for discussions on the application of organometallic chemistry in material sciences. Thanks also to Hoechst AG (Zentralforschung II), Frankfurt am Main, for generous support in the team project "Molekulare Supraleiter-Alkoxidvorstufen".

Received: June 2, 1995 [A 1181E]
German version: *Angew. Chem.* **1995**, *106*, 2371–2390

[1] D. C. Bradley, *Chem. Rev.* **1989**, *89*, 1317–1322.
[2] L. G. Hubert-Pfalzgraf, *Appl. Organomet. Chem.* **1992**, *6*, 627–643.
[3] J. G. Bednorz, K. A. Müller, *Z. Phys. B* **1986**, *64*, 189–193; Nobel lecture: J. G. Bednorz, K. A. Müller, *Angew. Chem.* **1988**, *100*, 757–770; *Angew. Chem. Int. Ed. Engl.* **1988**, *27*, 735–748
[4] K. G. Caulton, L. G. Hubert-Pfalzgraf, *Chem. Rev.* **1990**, *90*, 969–995.
[5] a) J. Vossen, *Thin Film Processes*, Academic Press, New York, **1978**; b) *Microelectronics Processing: Chemical and Engineering Aspects* (Eds.: G. Haas) (*Adv. Chem. Ser.*), Am. Chem. Soc., Washington, **1989**; c) *The Chemistry of Metal CVD* (Eds.: T. Kodas, M. Hampden-Smith), VCH, Weinheim, **1994**.
[6] D. C. Bradley, *Polyhedron* **1994**, *13*, 1111–1121.
[7] a) A. P. Purdy, A. D. Berry, R. T. Holm, M. Fatemi, D. K. Gaskill, *Inorg. Chem.* **1989**, *28*, 2799–2803; b) J. Zhao, K. H. Dahmen, H. O. Marcy, L. M. Tonge, T. J. Marks, B. M. Wessels, C. R. Kannewurf, *Appl. Phys. Lett.* **1989**, *53*, 1750–1752.
[8] D. C. Bradley, R. C. Mehrotra, D. P. Gaur, *Metal Alkoxides*, Academic Press, New York, **1978**.
[9] a) C. D. Chandler, C. Roger, M. J. Hampden-Smith, *Chem. Rev.* **1993**, *93*, 1205–1241; b) L. G. Hubert-Pfalzgraf, *Polyhedron* **1994**, *13*, 1181–1195; c) W. G. Van der Sluys, A. P. Sattelberger, *Chem. Rev.* **1990**, *90*, 1027–1040; d) R. C. Mehrotra, A. Singh, S. Sogiani, *ibid.* **1994**, *94*, 1643–1660; e) *Chem. Soc. Rev.* **1994**, 215–225; f) R. C. Mehrotra, A. Mehrotra, *Inorg. Chim. Acta* **1971**, *5*, 127–136.
[10] a) R. C. Mehrotra, A. Singh, *Chemtracts Inorg. Chem.* **1994**, *6*, 27–30; b) W. A. Herrmann, N. W. Huber, R. Anwander, T. Priermeier, *Chem. Ber.* **1993**, *126*, 1127–1130.
[11] S. C. Goel, M. Y. Chiang, P. C. Gibbons, W. E. Buhro, *Mater. Res. Soc. Symp. Proc.* **1992**, 271–273.
[12] L. G. Hubert-Pfalzgraf, *New J. Chem.* **1987**, *11*, 663–675.

[13] W. A. Herrmann, R. Anwander, F. C. Munck, W. Scherer, V. Dufaud, N. W. Huber, G. R. J. Artus, *Z. Naturforsch. B* **1994**, *49*, 1789–1797.

[14] a) W. A. Herrmann, M. J. A. Morawietz, T. Priermeier, *Angew. Chem.* **1994**, *106*, 2025–2028; *Angew. Chem. Int. Ed. Engl.* **1994**, *33*, 1944–1946; b) W. A. Herrmann, M. J. A. Morawietz, *J. Organomet. Chem.* **1994**, *482*, 169–181; c) *ibid.* **1995**, *486*, 291–295.

[15] W. A. Herrmann, R. Anwander, F. C. Munck, *Inorg. Chem.* **1995**, in press.

[16] R. C. Mehrotra, A. Singh, U. M. Tripathi, *Chem. Rev.* **1991**, *91*, 1287–1303.

[17] a) B. E. Bursten, M. Casarin, D. E. Ellis, I. Fragala, T. Marks, *Inorg. Chem.* **1986**, *25*, 1257–1261; b) E. A. Cuelar, S. S. Miller, T. J. Marks, E. Weitz, *J. Am. Chem. Soc.* **1983**, *105*, 4580–4589; c) S. S. Miller, D. D. DeFord, T. J. Marks, E. Weitz, *J. Am. Chem. Soc.* **1979**, *101*, 1036–1037; d) A. Haaland, K. Rypdal, H. V. Volden, E. Jacob, J. Wudda, *Acta Chem. Scand.* **1989**, *43*, 911–913.

[18] R. C. Mehrotra, R. Jain, A. K. Rai, *Wuji Huaxue* **1987**, *3*, 96.

[19] R. A. Andersen, D. H. Templeton, A. Zalkin, *Inorg. Chem.* **1978**, *17*, 1962–1965.

[20] G. B. Deacon, T. Feng, B. W. Skelton, A. H. White, *Aust. J. Chem.* **1995**, *48*, 741–756.

[21] a) G. B. Deacon, P. B. Hitchcock, S. A. Holmes, M. F. Lappert, P. MacKinnon, R. H. Newnham, *J. Chem. Soc. Chem. Commun.* **1989**, 935–937; b) G. B. Deacon, T. Feng, P. MacKinnon, R. H. Newnham, S. Nickel, B. W. Skelton, A. H. White, *Aust. J. Chem.* **1993**, *46*, 387–399.

[22] a) B. A. Vaartstra, W. E. Streib, K. G. Caulton, *J. Am. Chem. Soc.* **1990**, *112*, 8593–8595; b) N. Y. Turova, V. G. Kessler, S. I. Kucheiko, *Polyhedron* **1991**, *10*, 2617–2628.

[23] a) L. Syper, *Rocz. Chem.* **1973**, *47*, 433–439; b) P. D. Bartlett, E. B. Lefferts, *J. Am. Chem. Soc.* **1955**, *77*, 2804–2805.

[24] a) B. D. Murray, H. Hope, P. P. Power, *J. Am. Chem. Soc.* **1985**, *107*, 169–173; b) J. Hvoslef, H. Hope, B. D. Murray, P. P. Power, *J. Chem. Soc. Chem. Commun.* **1983**, 1438–1439; c) B. D. Murray, P. P. Power, *J. Am. Chem. Soc.* **1984**, *106*, 7011–7015; d) M. M. Olmstead, P. P. Power, G. Sigl, *Inorg. Chem.* **1986**, *25*, 1027–1033; e) T. V. Lubben, P. T. Wolczanski, *J. Am. Chem. Soc.* **1987**, *109*, 424–435; f) *ibid.* **1985**, *107*, 701–703; g) T. V. Lubben, P. T. Wolczanski, G. D. Van Dyne, *Organometallics* **1984**, *3*, 977–983.

[25] H. A. Stecher, A. Sen, A. L. Rheingold, *Inorg. Chem.* **1989**, *28*, 3280–3282.

[26] a) A. A. Pinkerton, D. Schwarzenbach, L. G. Hubert-Pfalzgraf, J. G. Riess, *Inorg. Chem.* **1976**, *15*, 1196–1199; b) D. C. Bradley, B. N. Chakravarti, W. Wardlaw, *J. Chem. Soc.* **1956**, 4439–4442; c) I. M. Thomas, *Can. J. Chem.* **1961**, *39*, 1386–1388; d) D. C. Bradley, C. E. Holloway, *J. Chem. Soc. A* **1968**, 219–223.

[27] J. Bryan, D. R. Wheeler, D. L. Clark, J. C. Huffman, A. P. Sattelberger, *J. Am. Chem. Soc.* **1991**, *113*, 3184–3186.

[28] M. F. Lappert, P. P. Power, A. R. Sanger, R. C. Sanger, R. C. Srivastava, *Metal and Metalloid Amides*, Wiley, New York, **1980**.

[29] D. C. Bradley, A. K. Chatterjee, *J. Inorg. Nucl. Chem.* **1957**, *4*, 279–282.

[30] A. G. Maddock, A. Pires de Matos, *Radiochim. Acta* **1972**, *18*, 71–73.

[31] D. C. Bradley, B. N. Chakravarti, W. Wardlaw, A. Whitley, A. K. Chatterjee, *J. Chem. Soc.* **1958**, 99–101.

[32] E. P. Turevskaya, N. Y. Turova, A. V. Korovlev, A. I. Yanovsky, Y. T. Struchkov, *Polyhedron* **1995**, *14*, 1531–1542.

[33] M. J. Hampden-Smith, T. A. Wark, A. Rheingold, J. C. Huffman, *Can. J. Chem.* **1991**, *69*, 121–129.

[34] D. C. Bradley, C. E. Holloway, *Proc. Paint Res. Inst.* **1965**, *37*, 487.

[35] D. C. Bradley, M. A. Saad, W. J. Wardlaw, *J. Chem. Soc.* **1954**, 3488–3490.

[36] R. G. Jones, G. Karmas, G. A. Martin, H. Gilman, *J. Am. Chem. Soc.* **1956**, *78*, 4258–4260.

[37] M. D. Healy, M. R. Mason, P. W. Gravelle, S. G. Bott, A. K. Baron, *J. Chem. Soc. Dalton Trans.* **1993**, 441–454.

[38] H. A. Stecher, A. Sen, A. L. Rheingold, *Inorg. Chem.* **1988**, *27*, 1130–1132.

[39] R. H. Cayton, M. H. Chisholm, E. R. Davidson, V. F. DiStasi, P. Du, J. C. Huffman, *Inorg. Chem.* **1991**, *30*, 1020–1024.

[40] J. G. Oliver, J. J. Worrall, *J. Chem. Soc. A* **1970**, 845–848.

[41] D. C. Bradley, H. Chudzynska, M. B. Hursthouse, M. Motevalli, *Polyhedron* **1991**, *10*, 1049–1059.

[42] A. Haaland, H. P. Verne, H. V. Volden, R. Papiernik, L. G. Hubert-Pfalzgraf, *Acta Chem. Scand.* **1993**, *47*, 1043–1045.

[43] S. Chatterjee, S. R. Bindal, R. C. Mehrotra, *J. Indian Chem. Soc.* **1976**, 867–869.

[44] D. C. Bradley, H. Chudzynska, D. M. Frigo, M. E. Hammond, M. B. Hursthouse, M. A. Mazid, *Polyhedron* **1990**, *9*, 719–726.

[45] O. Poncelet, W. J. Sartain, L. G. Hubert-Pfalzgraf, K. Folting, K. G. Caulton, *Inorg. Chem.* **1989**, *28*, 263–267.

[46] G. Helgesson, S. Jagner, O. Poncelet, L. G. Hubert-Pfalzgraf, *Polyhedron* **1991**, *10*, 1559–1564.

[47] a) W. A. Herrmann, R. Anwander, M. Kleine, W. Scherer, *Chem. Ber.* **1992**, *125*, 1971–1979; b) W. A. Herrmann, R. Anwander, W. Scherer, *Chem. Ber.* **1993**, *126*, 1533–1539.

[48] M. D. Healy, A. R. Barron, *Angew. Chem.* **1992**, *104*, 939–941; *Angew. Chem. Int. Ed. Engl.* **1992**, *31*, 921–922.

[49] P. B. Hitchcock, M. F. Lappert, A. Singh, *J. Chem. Soc. Chem. Commun.* **1983**, 1499–1501.

[50] P. B. Hitchcock, M. F. Lappert, R. G. Smith, *Inorg. Chim. Acta* **1987**, *139*, 183–184.

[51] K. J. Covert, D. R. Neithammer, M. C. Zonnevylle, R. E. LaPointe, C. P. Schaller, P. T. Wolczanski, *Inorg. Chem.* **1991**, *30*, 2494–2508.

[52] R. A. Andersen, N. A. Bell, G. E. Coates, *J. Chem. Soc. Dalton Trans.* **1972**, 577–582.

[53] B. Cetinkaya, I. Gümrükcü, M. F. Lappert, L. J. Atwood, D. R. Rogers, M. J. Zaworotko, *J. Am. Chem. Soc.* **1980**, *102*, 2088–2089.

[54] a) T. Fjeldberg, P. B. Hitchcock, M. F. Lappert, S. J. Smith, A. J. Thorne, *J. Chem. Soc. Chem. Commun.* **1985**, 939–941; b) M. J. Geary, R. H. Cayton, K. Folting, J. C. Huffman, K. G. Caulton, *Polyhedron* **1992**, *11*, 1369–1373.

[55] R. Papiernik, L. G. Hubert-Pfalzgraf, M. C. Massiani, *Inorg. Chim. Acta* **1989**, *165*, 1–2.

[56] E. Weiss, H. Alsdorf, H. Kühr, *Angew. Chem.* **1967**, *79*, 816; *Angew. Chem. Int. Ed. Engl.* **1967**, *6*, 801.

[57] R. E. LaPointe, P. T. Wolczanski, G. D. Van Duyne, *Organometallics* **1985**, *4*, 1810–1818.

[58] The portrayal is exaggerated in that the silaz ligand, in contrast to the other ligands, has a relatively isotropic spatial behavior. The graduation is still retained, however.

[59] H. W. Roesky, M. Scholz, M. Noltemeyer, *Chem. Ber.* **1990**, *123*, 2303–2309.

[60] P. J. Wheatly, *J. Chem. Soc.* **1960**, 4270–4274.

[61] a) H. Huml, *Czech. J. Phys.* **1965**, *15*, 699; b) V. Halaska, L. Lochmann, D. Lim, *Collect. Czech. Chem. Commun.* **1968**, *33*, 3245–3253.

[62] M. H. Chisholm, S. R. Drake, A. A. Naiini, W. E. Streib, *Polyhedron* **1991**, *10*, 805–810.

[63] T. Greiser, E. Weiss, *Chem. Ber.* **1977**, *110*, 3388–3396.

[64] J. A. Samuels, E. B. Lobkovsky, W. E. Streib, K. Folting, J. C. Huffman, J. W. Zwanziger, K. G. Caulton, *J. Am. Chem. Soc.* **1993**, *115*, 5093–5104.

[65] L. F. Dahl, G. L. Davies, D. L. Wampler, R. West, *J. Inorg. Nucl. Chem.* **1962**, *24*, 357–363.

[66] G. Beck, P. B. Hitchcock, M. F. Lappert, I. A. McKinnon, *J. Chem. Soc. Chem. Commun.* **1989**, 1312–1314.

[67] L. Pauling, *Die Natur der chemischen Bindung*, 3rd ed., Verlag Chemie, Weinheim, **1968**.

[68] N. W. Huber, Dissertation, Technische Universität München, **1994**.

[69] T. Greiser, E. Weiss, *Chem. Ber.* **1976**, *109*, 3142–3146.

[70] H. Chen, M. M. Olmstead, S. C. Shoner, P. P. Power, *J. Chem. Soc. Dalton Trans.* **1992**, 451–457.

[71] D. C. Bradley, M. H. Chisholm, M. W. Extine, M. E. Stager, *Inorg. Chem.* **1977**, *16*, 1794–1801.

[72] M. Scholz, M. Noltemeyer, H. W. Roesky, *Angew. Chem.* **1989**, *101*, 1419–1420; *Angew. Chem. Int. Ed. Engl.* **1989**, *28*, 1383–1384.

[73] a) H. A. Stecher, A. Sen, A. L. Rheingold, *Inorg. Chem.* **1988**, *27*, 1130–1132; b) G. B. Deacon, T. Feng, S. Nickel, M. I. Ogden, A. H. White, *Aust. J. Chem.* **1992**, *45*, 671–683.

[74] H. W. Roesky, M. Scholz, M. Noltemeyer, F. T. Edelmann, *Inorg. Chem.* **1989**, *28*, 3829–3830.

[75] S. R. Drake, D. J. Otway, M. B. Hursthouse, K. M. A. Malik, *Polyhedron* **1992**, *11*, 1995–2007.

[76] a) R. Toreki, R. E. LaPointe, P. T. Wolczanski, *J. Am. Chem. Soc.* **1987**, *109*, 7558–7560; b) R. E. LaPointe, P. T. Wolczanski, *ibid.* **1986**, *108*, 6382–6384; c) C. C. Cummins, G. D. Van Duyne, C. P. Schaller, P. T. Wolczanski, *Organometallics* **1991**, *10*, 164–170.

[77] a) D. R. Neithamer, L. Parkanyi, J. F. Mitchell, P. T. Wolczanski, *J. Am. Chem. Soc.* **1988**, *110*, 4421–4423; b) D. F. Eppley, P. T. Wolczanski, G. D. Van Duyne, *Angew. Chem.* **1991**, *103*, 616–617; *Angew. Chem. Int. Ed. Engl.* **1991**, *30*, 584–585.

[78] M. Weidenbruch, C. Pierrard, H. Pesel, *Z. Naturforsch. B* **1978**, *33*, 1468–1471.

[79] S. R. Drake, W. E. Streib, K. Folting, M. H. Chisholm, K. G. Caulton, *Inorg. Chem.* **1992**, *31*, 3205–3210.

[80] M. Weidenbruch, H. Pesel, W. Peter, R. Steichen, *J. Organomet. Chem.* **1977**, *141*, 9–21.

[81] W. A. Herrmann, N. W. Huber, T. Priermeier, *Angew. Chem.* **1994**, *106*, 102–104; *Angew. Chem. Int. Ed. Engl.* **1994**, *33*, 105–107.

[82] W. A. Herrmann, R. Anwander, V. Dufaud, W. Scherer, *Angew. Chem.* **1994**, *106*, 1338–1340; *Angew. Chem. Int. Ed. Engl.* **1994**, *33*, 1285–1286.

[83] G. Beck, P. B. Hitchcock, M. F. Lappert, I. A. MacKinnon, *J. Chem. Soc. Chem. Commun.* **1989**, 1312-1314.

[84] V. J. Shiner, Jr., D. Whittaker, V. P. Fernandez, *J. Am. Chem. Soc.* **1963**, *85*, 2318–2322.

[85] R. Papiernik, L. G. Hubert-Pfalzgraf, M. C. Massiani, *Polyhedron* **1991**, *10*, 1657–1662.

[86] J. D. Cotton, C. S. Cundy, D. H. Harris, A. Hudson, M. F. Lappert, P. W. Lednor, *J. Chem. Soc. Chem. Commun.* **1974**, 651–652.

[87] C. M. Jones, M. D. Burkart, R. E. Bachmann, D. L. Serra, S.-J. Hwu, K. H. Whitmire, *Inorg. Chem.* **1993**, *32*, 5136–5144.

[88] S. R. Bindal, V. K. Mathew, R. C. Mehrotra, *J. Inorg. Phys. Theor.* **1969**, 863–867.
[89] G. A. Sigel, R. A. Bartlett, D. Decker, M. M. Olmstead, P. P. Power, *Inorg. Chem.* **1987**, *26*, 1773–1780.
[90] R. Gardiner, D. W. Brown, P. S. Kirlin, A. Rheingold, *Chem. Mater.* **1991**, *3*, 45–50.
[91] D. C. Bradley, H. Chudzynska, M. B. Husthouse, M. Motevalli, R. Wu, *Polyhedron* **1994**, *13*, 1–6.
[92] D. C. Bradley, H. Chudzynska, M. B. Husthouse, M. Motevalli, *Polyhedron* **1991**, *10*, 1049–1059.
[93] P. M. Jeffries, S. R. Wilson, G. S. Girolami, *Inorg. Chem.* **1992**, *31*, 4503–4509.
[94] a) W. S. Rees, K. A. Dippel, M. W. Carris, C. R. Caballero, D. A. Moreno, W. Hesse, *Better Ceramics Through Chemistry, Mat. Res. Soc. Symp. Proc.*, in press; b) K. Timmer, C. I. Spee, A. Mackor, H. Meinema, EP 405 634 A2 **1991**.
[95] A. P. Purdy, C. F. George, J. H. Callahan, *Inorg. Chem.* **1991**, *30*, 2812–2819.
[96] M. Veith, *Chem. Rev.* **1990**, *90*, 3–16.
[97] H. S. Horowitz, S. J. McLane, A. W. Sleight, J. D. Druliner, P. L. Gai, M. J. VanKavelaar, J. L. Wagner, B. D. Biggs, S. J. Poon, *Science* **1989**, *243*, 66–69.
[98] S. C. Goel, M. A. Matchett, M. Y. Chiang, W. E. Buhro, *J. Am. Chem. Soc.* **1991**, *113*, 1844–1845.
[99] K. G. Caulton, M. H. Chisholm, S. R. Drake, J. C. Huffman, *J. Chem. Soc. Chem. Commun.* **1990**, 1498–1499.
[100] S. C. Goel, M. Y. Chiang, W. E. Buhro, *Inorg. Chem.* **1990**, *29*, 4640–4646.
[101] M. A. Matchett, M. Y. Chiang, W. E. Buhro, *Inorg. Chem.* **1990**, *29*, 358–360.
[102] S. Boulmaaz, R. Papiernik, L. G. Hubert-Pfalzgraf, *Polyhedron* **1992**, *11*, 1331–1336.
[103] O. Poncelet, L. G. Hubert-Pfalzgraf, J. C. Daran, R. Astier, *J. Chem. Soc. Chem. Commun.* **1989**, 1846–1848.
[104] M.-C. Massiani, R. Papiernik, L. G. Hubert-Pfalzgraf, *Polyhedron* **1991**, *10*, 437–445.
[105] W. S. Rees, Jr., D. A. Moreno, *J. Chem. Soc. Chem. Commun.* **1991**, 1759–1760.
[106] S. C. Goel, K. S. Kramer, P. C. Gibbons, W. E. Buhro, *Inorg. Chem.* **1989**, *28*, 3619–3620.
[107] S. C. Goel, M. Y. Chiang, W. E. Buhro, *Inorg. Chem.* **1990**, *29*, 4646–4652.
[108] P. B. Hitchcock, M. F. Lappert, I. A. MacKinnon, *J. Chem. Soc. Chem. Commun.* **1988**, 1557–1558.
[109] A. W. G. Platt, P. G. Pringle, *J. Chem. Soc. Dalton Trans.* **1989**, 1193–1196.
[110] R. A. Anwander, Dissertation, Technische Universität München, **1992**.
[111] See Ref. [68], p. 128.
[112] O. Poncelet, L. G. Hubert-Pfalzgraf, J. C. Daran, *Inorg. Chem.* **1990**, *29*, 2883–2885.
[113] W. A. Herrmann, O. Runte, *J. Organomet. Chem.* **1995**, in press.
[114] R. A. Fischer, J. Behm, T. Priermeier, W. Scherer, *Angew. Chem.* **1993**, *105*, 776–778; *Angew. Chem. Int. Ed. Engl.* **1993**, *32*, 746–748.
[115] R. C. Mehrotra, M. M. Agrawal, P. N. Kapoor, *J. Chem. Soc. A* **1968**, 2673–2676.
[116] H. Meerwein, T. Bersin, *Justus Liebigs Ann. Chem.* **1929**, *475*, 113–150.
[117] a) G. Copaux, *Compt. Rend.* **1898**, *127*, 721; b) C. Cambi, *ibid.* **1924**, 1412–1417.
[118] M. M. Aggrawal, R. C. Mehrotra, *Synth. React. Inorg. Met. Org. Chem.* **1983**, *13*, 571–583.
[119] M. M. Aggrawal, C. K. Sharma, R. C. Mehrotra, *Synth. React. Inorg. Met. Org. Chem.* **1988**, *18*, 9–19.
[120] S. Govil, R. C. Mehrotra, *Synth. React. Inorg. Met. Org. Chem.* **1975**, *5*, 267–277.
[121] S. Govil, P. N. Kapoor, R. C. Mehrotra, *Inorg. Chim. Acta* **1975**, *15*, 43–46.
[122] R. C. Mehrotra, M. M. Aggrawal, *J. Chem. Soc. Chem. Commun.* **1968**, 469–470.
[123] R. C. Mehrotra, M. M. Aggrawal, A. Mehrotra, *Synth. React. Inorg. Met. Org. Chem.* **1973**, *3*, 181–191.
[124] M. I. Yanovskaya, E. P. Turvskaya, V. G. Kessler, I. E. Obvintseva, N. Y. Turova, *Integr. Ferroelectr.* **1992**, *1*, 343.
[125] a) W. K. Kirby, *Mater. Res. Bull.* **1988**, *23*, 881; b) M. H. Chisholm, J. C. Huffman, C. A. Smith, *J. Am. Chem. Soc.* **1986**, *108*, 222–230.
[126] W. A. Herrmann, O. Runte, W. Wachter, *J. Organomet. Chem.* **1995**, in press.
[127] A. P. Purdy, C. F. George, *Polyhedron* **1994**, *13*, 709–712.
[128] L. G. Hubert-Pfalzgraf, J. G. Riess, *Inorg. Chem.* **1975**, *14*, 2854–2856.
[129] D. J. Eichhorst, D. A. Payne, S. R. Wilson, *Inorg. Chem.* **1990**, *29*, 1458–1459.
[130] B. J. Curtis, H. R. Brunner, *Mat. Res. Bull.* **1975**, *10*, 515.
[131] a) A. A. Wernberg, H. J. Gysling, *J. Cryst. Growth* **1994**, *140*, 57–64; b) A. A. Wernberg, H. J. Gysling, A. J. Filo, T. N. Blanton, *Appl. Phys. Lett.* **1993**, *62*, 946–948.
[132] E. Weiss, H. Alsdorf, H. Kühr, H. F. Grützmacher, *Chem. Ber.* **1968**, *101*, 3777–3786.
[133] L. M. Engelhardt, J. M. Harrowfield, M. F. Lappert, I. A. McKinnon, B. H. Newton, C. L. Raston, B. W. Skelton, A. J. White, *J. Chem. Soc. Chem. Commun.* **1986**, 846–848.
[134] P. M. Jeffries, G. S. Girolami, *Chem. Mater.* **1989**, *1*, 8–10.
[135] M. E. Gross, *J. Electrochem. Soc.* **1991**, *138*, 2422–2426.
[136] H. Schmidbaur, J. Adlkofer, A. Shiotani, *Chem. Ber.* **1972**, *105*, 3389–3396.
[137] R. T. Boere, C. D. Montgomery, N. C. Payne, C. J. Willis, *Inorg. Chem.* **1985**, *24*, 3680–3687.
[138] R. A. Andersen, G. E. Coates, *J. Chem. Soc. Dalton Trans.* **1972**, 2153–2155.
[139] a) N. A. Bell, *J. Chem. Soc. A* **1966**, 542–544; b) N. A. Bell, G. E. Coates, H. M. M. Shearer, J. Twiss, *J. Chem. Soc. Chem. Commun.* **1983**, 840–841.
[140] K. Ruhlandt-Senge, R. A. Bartlett, M. M. Olmstead, P. P. Power, *Inorg. Chem.* **1993**, *32*, 3724–3728.
[141] a) H. D. Lutz, *Z. Anorg. Allg. Chem.* **1967**, *353*, 207–215; b) *ibid.* **1968**, *356*, 132–139; c) H. Staeglich, E. Weiss, *Chem. Ber.* **1978**, 901–905; d) N. Y. Turova, B. A. Popovkin, A. V. Novoselova, *Dokl. Akad. Nauk. SSSR* **1966**, *167*, 604; e) N. Y. Turova, E. P. Turevskaya, V. G. Kessler, A. I. Yanovsky, Y. T. Struchkov, *J. Chem. Soc. Chem. Commun.* **1993**, 21–23.
[142] A. I. Yanovsky, E. P. Turevskaya, N. Y. Turova, *Soviet J. Coord. Chem.* **1985**, *11*, 63–68.
[143] a) K. G. Caulton, M. H. Chisholm, S. R. Drake, W. E. Streib, *Angew. Chem.* **1990**, *102*, 1492–1493; *Angew. Chem. Int. Ed. Engl.* **1990**, *29*, 1483–1485; b) K. G. Caulton, M. H. Chisholm, S. R. Drake, K. Folting, J. C. Huffman, W. E. Streib, *Inorg. Chem.* **1993**, *32*, 1970–1976; c) S. R. Drake, W. E. Streib, K. Folting, M. H. Chisholm, K. G. Caulton, *ibid.* **1992**, *31*, 3205–3210; d) K. F. Tesh, T. P. Hanusa, J. C. Huffman, C. J. Huffman, *ibid.* **1992**, *31*, 5572–5579.
[144] a) H. Bock, T. Hauck, C. Nähter, N. Rösch, M. Staufer, O. D. Häberlein, *Angew. Chem.* **1995**, *107*, 1353–1355; *Angew. Chem. Int. Ed. Engl.* **1995**, *34*, 1355–1357; b) K. G. Caulton, M. M. Chisholm, S. R. Drake, K. Folting, *J. Chem. Soc. Chem. Commun.* **1990**, 1349–1351.
[145] W. G. Fahrenholtz, D. M. Millar, D. A. Payne, *Research Update* **1988** (*Ceramic Superconductors II*), Am. Ceramic Soc., Westerville, USA, **1988**, p. 141.
[146] K. G. Caulton, M. H. Chisholm, S. R. Drake, K. Folting, *Inorg. Chem.* **1991**, *30*, 1500–1503.
[147] J. C. Daran, L. Toupet, O. Poncelet, L. G. Hubert-Pfalzgraf, *Polyhedron* **1991**, *10*, 2045–2050.
[148] K. F. Tesh, T. P. Hanusa, *J. Chem. Soc. Chem. Commun.* **1991**, 879–881.
[149] G. E. Coates, A. H. Fishwick, *J. Chem. Soc. A* **1968**, 477–483.
[150] H. W. Roesky, M. Scholz, M. Noltemeyer, *Chem. Ber.* **1990**, *123*, 2303–2309.
[151] J. A. Darr, S. R. Drake, D. J. Williams, A. M. Z. Slawin, *J. Chem. Soc. Chem. Commun.* **1993**, 866–868.
[152] C. D. Montgomery, N. C. Payne, C. J. Willis, *Inorg. Chem.* **1987**, *26*, 519–526.
[153] G. Beck, P. B. Hitchcock, M. F. Lappert, I. A. McKinnon, *J. Chem. Soc. Chem. Commun.* **1989**, 1312–1314.
[154] R. D. Shannon, *Acta Crystallogr. A* **1976**, *32*, 751–767.
[155] M. J. McCormick, K. B. Moon, S. R. Jones, T. P. Hanusa, *J. Chem. Soc. Chem. Commun.* **1990**, 778–779.
[156] J. A. Darr, S. R. Drake, M. B. Hursthouse, K. M. A. Malik, *Inorg. Chem.* **1993**, *32*, 5704–5708.
[157] R. W. Chorley, P. B. Hitchcock, M. F. Lappert, W. P. Leung, P. P. Power, M. M. Olmstead, *Inorg. Chim. Acta* **1992**, *198–200*, 203–209.
[158] P. G. Harrison, B. J. Haylett, T. J. King, *J. Chem. Soc. Chem. Commun.* **1978**, 112–113.
[159] A. I. Yanovskii, N. Y. Turova, E. P. Turevskaya, Y.T. Struchkov, *Koord. Khim. (Engl. Transl.)* **1982**, *8*, 153.
[160] M. Veith, F. Töllner, *J. Organomet. Chem.* **1983**, *246*, 219–226.
[161] S. C. Goel, K. S. Kramer, M. Y. Chiang, W. E. Buhro, *Polyhedron* **1990**, *9*, 611–613.
[162] S. C. Goel, K. S. Kramer, P. C. Gibbons, W. E. Buhro, *Inorg. Chem.* **1989**, *28*, 3619–3620.
[163] a) J. V. Singh, B. P. Baranwal, R. C. Mehrotra, *Z. Anorg. Allg. Chem.* **1981**, *477*, 235–240; b) C. H. Brubaker, M. Wicholas, *J. Inorg. Nucl. Chem.* **1965**, 59–62.
[164] R. C. Mehrotra, M. Arora, *Z. Anorg. Allg. Chem.* **1969**, *370*, 300–309.
[165] R. L. Geerts, J. C. Huffman, K. G. Caulton, *Inorg. Chem.* **1986**, *25*, 1803–1805.
[166] S. C. Goel, M. Y. Chiang, W. E. Buhro, *Inorg. Chem.* **1990**, *29*, 4640–4646.
[167] K. S. Mazdiyasni, C. T. Lynch, J. S. Smith, *Inorg. Chem.* **1966**, *5*, 342–346.
[168] R. C. Mehrotra, A. K. Rai, *Indian J. Chem.* **1966**, *4*, 537–540.
[169] M. A. Matchett, M. Y. Chiang, W. E. Buhro, *Inorg. Chem.* **1990**, *29*, 358–360.
[170] T. Kobabayashi, K. Nomura, F. Uchikawa, T. Masumi, Y. Uehara, *Jpn. J. Appl. Phys.* **1988**, *27*, 1880.
[171] a) A. Haaland, H. P. Verne, H. V. Volden, R. Papiernik, L. G. Hubert-Pfalzgraf, *Acta Chem. Scand.* **1993**, *47*, 1043–1045; b) M. C. Massiani, R. Papiernik, L. G. Hubert-Pfalzgraf, J. C. Daran, *J. Chem. Soc. Chem. Commun.* **1990**, 301–302.
[172] D. C. Bradley, H. Chudzynska, D. M. Frigo, M. B. Hursthouse, M. A. Mazid, *J. Chem. Soc. Chem. Commun.* **1988**, 1258–1259.
[173] L. M. Brown, K. S. Mazdiyasni, *Inorg. Chem.* **1970**, *9*, 2783–2786.
[174] F. Munk, Diplomarbeit, Technische Universität München, **1993**.

[175] a) W. J. Evans, J. H. Hain, J. W. Ziller, *J. Chem. Soc. Chem. Commun.* **1989**, 1628–1629; b) M. C. Massiani, R. Papiernik, L. G. Hubert-Pfalzgraf, J. C. Daran, *ibid.* **1990**, 301–302.
[176] O. Poncelet, W. J. Sartain, L. G. Hubert-Pfalzgraf, K. Folting, K. G. Caulton, *J. Chem. Soc. Chem. Commun.* **1989**, 263–267.
[177] W. A. Herrmann, R. Anwander, M. Denk, *Chem. Ber.* **1992**, *125*, 2399–2405.
[178] W. A. Herrmann, R. Anwander, F. Munck, N. Huber, unpublished results.
[179] a) D. C. Bradley, H. Chudzynska, M. B. Hursthouse, M. Motevalli, R. Wu, *Polyhedron* **1993**, *12*, 2955–2960; b) D. C. Bradley, H. Chudzynska, M. B. Hursthouse, M. Motevalli, *ibid.* **1994**, *13*, 7–14; c) *ibid.* **1993**, *12*, 1907–1918; d) D. C. Bradley, H. Chudzynska, M. E. Hammond, M. B. Hursthouse, M. Motevalli, R. Wu, *ibid.* **1992**, *11*, 375–379.
[180] C. Sirio, O. Poncelet, L. G. Hubert-Pfalzgraf, J. C. Daran, J. Vaissermann, *Polyhedron* **1992**, *11*, 177–184.
[181] P. J. Hampson, T. J. Leedham, *Chemtronics* **1991**, 5, 115–116.
[182] P. S. Gradeff, M. Mauermann, F. G. Schreiber, *J. Less-Common Met.* **1989**, *11*, 177–184.
[183] L. G. Hubert-Pfalzgraf, N. E. Khokh, J. C. Daran, *Polyhedron* **1992**, *11*, 59–63.
[184] W. A. Herrmann, R. Anwander, F. C. Munck, W. Scherer, T. Priermeier, *Inorg. Chem.* **1995**, in press.
[185] J. H. Gladstone, A. Tribe, *J. Chem. Soc.* **1876**, *29*, 158–162.
[186] R. C. Mehrotra, *J. Am. Chem. Soc.* **1954**, *74*, 2266–2271.
[187] A. Lamy, *Ann. Chim. Phys.* **1864**, *3*, 373.
[188] H. Yamane, H. Kurzawa, T. Hirai, *Chem. Lett.* **1988**, 1515–1516.
[189] A. Mehrotra, R. C. Mehrotra, *Inorg. Chem.* **1972**, *11*, 2170–2174.
[190] G. E. Coates, R. A. Whitcombe, *J. Chem. Soc.* **1956**, 3351–3354.
[191] D. C. Bradley, D. M. Frigo, M. B. Hursthouse, B. Hussain, *Organometallics* **1988**, *7*, 1112–1115.
[192] H. Schmidbaur, W. Findeiss, E. Gast, *Angew. Chem.* **1965**, *77*, 169; *Angew. Chem. Int. Ed. Engl.* **1965**, *4*, 152.
[193] H. C. Clark, A. L. Pickard, *J. Organomet. Chem.* **1968**, *13*, 61–71.
[194] a) P. Shao, D. J. Berg, G. W. Bushnell, *Inorg. Chem.* **1994**, *33*, 3452–3458; b) *ibid.* **1994**, *33*, 6334–6339.
[195] a) N. Y. Turova, V. A. Kazunov, A. I. Yanovskii, Y. T. Boskii, Y. T. Struchkov, T. Yu. B. L. Tamopolskii, *J. Inorg. Nucl. Chem.* **1979**, *41*, 5–11; b) K. Folting, W. E. Streib, K. G. Caulton, O. Poncelet, L. G. Hubert-Pfalzgraf, *Polyhedron* **1991**, *10*, 1639–1646.
[196] D. C. Bradley, *Adv. Inorg. Chem. Radiochem.* **1972**, *15*, 259–322.
[197] a) D. L. Schulz, B. G. Hinds, C. L. Stern, T. J. Marks, *Inorg. Chem.* **1993**, *32*, 249–250; b) D. L. Schulz, B. G. Hinds, D. A. Neumayer, C. L. Stern, T. J. Marks, *Chem. Mater.* **1993**, *5*, 1605–1617.
[198] M. P. Fryzuk, X. Gao, S. J. Rettig, *J. Am. Chem. Soc.* **1995**, *117*, 3106–3117.
[199] W. A. Herrmann, N. W. Huber, *Chem. Ber.* **1994**, *127*, 821–824.
[200] D. Steinborn, *Angew. Chem.* **1992**, *104*, 392–412; *Angew. Chem. Int. Ed. Engl.* **1992**, *31*, 401–421.
[201] R. A. Bartlett, J. J. Elison, P. P. Power, S. C. Shoner, *Inorg. Chem.* **1991**, *30*, 2888–2894.

Carbon Dioxide as a Raw Material: The Synthesis of Formic Acid and Its Derivatives from CO_2

Walter Leitner*

Dedicated to Professor Henri Brunner on the occasion of his 60th birthday

The use of carbon dioxide as a raw material for chemical syntheses is an ecologically and economically valuable extension to the carbon sources used at the present time. In order to convert the thermodynamically stable and comparatively unreactive CO_2 molecule into the desired product in an efficient manner, suitable reaction conditions and activation mechanisms must be found. The catalytic reduction of CO_2 to formic acid and its derivatives has been intensively studied in recent years. A number of new approaches to the synthesis of formic acid from CO_2 have reached such a state of knowledge that continuing development may well lead to industrial-scale operation in the near future. This can to a large extent be attributed to the fruitful interaction between investigative work into reaction mechanisms and the development of new catalytic systems.

Keywords: CO_2 activation · formic acid · homogeneous catalysis · reductions · transition metal complexes

Then what can be done on the Day of Judgement, when human deeds are weighed, with three essays on formic acid, or with thirty?
On the other hand, what do we know of the Day of Judgement if we do not know everything that might come out of formic acid by that time?

Robert Musil, The Man without Qualities

1. Carbon Dioxide as a Raw Material

1.1. CO_2 as an Environmentally Friendly C_1 Building Block

The number of different chemical compounds produced worldwide at the present time is roughly in the range 20000–30000.[1] This large number of substances is produced from only a very few basic chemical raw materials, the source of carbon being almost exclusively fossilized matter, namely mineral oil, natural gas, and coal (Fig. 1). The fact that these resources are limited has led to a growth of scientific efforts to find alternative carbon sources since the early 1970s. Carbon dioxide has always attracted the greatest interest,[2, 3] as Nature uses this compound so successfully as a synthetic building block in photosynthesis—the basis of life on earth.

The carbon reserves on our planet in the form of CO_2 and CO_3^{2-} are for practical purposes inexhaustible, exceeding the carbon content of the deposits of fossil raw materials many times over. Since the beginning of industrialization in the second half of the last century, mankind has "produced" CO_2 in increasing amounts and released it into the atmosphere. The most important source of anthropogenic CO_2 emission is the combustion of fossil fuels for energy production. The destruction of biomasses also contributes indirectly to the increase in the concentration of atmospheric CO_2. In 1989, the total amount of CO_2 added to the atmosphere due to human activity was approximately 7×10^9 t carbon. The possible connections between anthropogenic CO_2 emission, the increasing CO_2 content of the atmosphere, and the global climate have for some years been exhaustively investigated[4] and discussed.[2g, 5, 6]

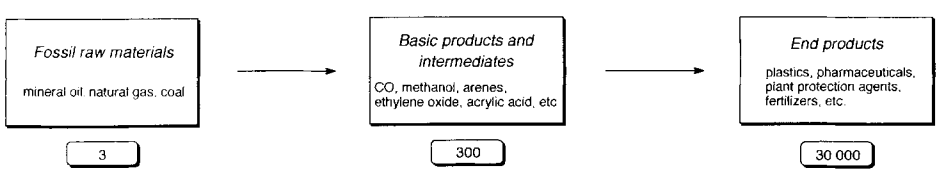

Fig. 1. The raw material basis of the chemical industry.

Estimating the risks that would follow from a global climatic change and developing strategies for the prevention of further increase in the atmospheric CO_2 concentration are undoubtedly important tasks. In this context, the use of CO_2 as a raw material for chemical synthesis can only make a very small contribution. Realistically, only a responsible use of primary energy and a greater utilization of nonfossil and ideally renewable energy carriers will ever be able to achieve a major reduc-

[*] Priv.-Doz. Dr. W. Leitner
Max-Planck-Institut für Kohlenforschung
Kaiser-Wilhelm-Platz 1, D-45470 Mülheim an der Ruhr (Germany)
Telefax: Int. code + (208)306-2980
e-mail: leitner@mpi-muelheim.mpg.d400.de

tion in the release of CO_2. At the same time, this also means that enough "waste CO_2" will be produced to provide a carbon source sufficient for a multitude of chemical requirements, even allowing for large reductions in anthropogenic carbon dioxide emissions. For example, a typical coal-fired power station with desulfurization of the exhaust gas produces 830 kg CO_2 per MWh electric power, and a power station fired with natural gas produces 400 kg CO_2 per MWh. In the exhaust gases from coal-fired power stations, the CO_2 concentration can reach 14%.[6]

In principle, an "anthropogenic CO_2 cycle" could therefore be achieved without making additional demands on the natural reservoir of carbon. However, most of the CO_2 bought and sold on the world market does not come from this over-abundance, but from hydrogen production [Eqs. (a) and (b)].[7] It is possible

$$CO + 3H_2 + H_2O(g) \longrightarrow CO_2 + 4H_2 \quad (a)$$

$$CH_4 + 2H_2O(g) \longrightarrow CO_2 + 4H_2 \quad (b)$$

in principle to extract CO_2 from power station exhaust gases by the same methods that have been developed for extracting it from process gases of hydrogen production.[2g, 6] The method that is growing most rapidly in importance in this context is absorption in aqueous solutions of amines. The trend towards recovery of CO_2 will probably greatly intensify in the future, leading to the increasing availability of large quantities of this cheap raw material.

Table 1. Properties of various C_1 building blocks [a].

	CO	$COCl_2$	CO_2
MAK value	30 ppm	0.1 ppm	5000 ppm
toxicology	affinity for hemoglobin 210 times that of O_2	war gas	danger of asphyxiation at 10 vol% in air
LC_{50} (inhal. mouse)	2444 ppm (4 h)	110 ppm (30 min)	-
environmental hazard	yes	high	"negative"
flammability	12–74 vol%	no	no
boiling point	−192 °C	8 °C	−78 °C (subl.)
storage	only at pressure ≤3.5 MPa	very difficult, to be avoided	no problem
transport	gas bottles or tanks	only possible for kilogram quantities	gas bottles or tanks
solubility in 1 mL toluene at 20 °C	0.17 mL	miscible in all proportions	3.45 mL

[a] Data taken from refs. [8–10].

From the safety aspect, carbon dioxide is an ideal raw material, as can be seen from a comparison of its properties with those of the widely used C_1 starting compounds carbon monoxide (CO) and phosgene ($COCl_2$) (Table 1). For example, CO_2 is practically nontoxic, and can be stored, transported, and handled without problems.

1.2. Why Formic Acid?

Most current applications of carbon dioxide are based on its physical or physico-chemical properties.[7, 9] However, CO_2 is already being used as a raw material in some industrially important chemical reactions.[2b] For example, the direct hydrogenation of CO_2 plays an important role in the industrial synthesis of methanol from $H_2/CO/CO_2$ mixtures (ICI process).[11] In principle, the reduction of CO_2 also provides a potential approach to a number of other important products as shown in Scheme 1. The reduction equivalents required for the individual transformations can be made available by addition of hydrogen as shown in Scheme 1 or by electron transfer processes. The

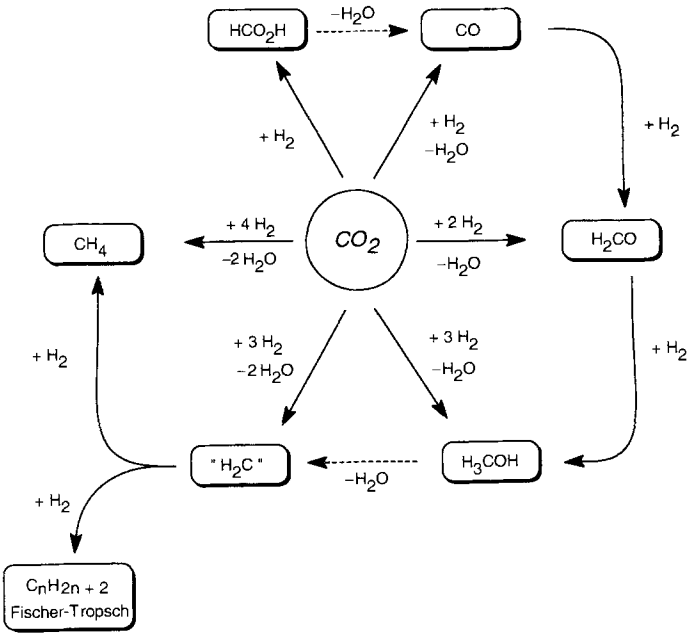

Scheme 1. Reduction of CO_2 as a source for industrially important products.

Walter Leitner was born in 1963, studied chemistry in Regensburg, where he obtained his Doctorate under Prof. H. Brunner in 1989. After a period of post-doctorate research with John M. Brown at the Dyson Perrins Laboratory at the University of Oxford he returned to Regensburg in 1991 as a Liebig Fellow, and began his research into the catalytic hydrogenation of carbon dioxide. In 1992, he moved to the research unit "CO_2 chemistry" of the Max-Planck-Gesellschaft led by Prof. E. Dinjus at the University of Jena, where he habilitated in the Inorganic Chemistry Department. Since June 1995, he has been active at the Max-Planck-Institut für Kohlenforschung in Mülheim an der Ruhr. His special field of research is the use of transition metal compounds in homogeneous catalysis and the understanding of their mode of action.

very first product of the reduction of CO_2 in this scheme is formic acid.

Approximately 300000 t formic acid is produced annually worldwide,[12] most of which is consumed in silage for animal feeds. Large amounts are also used in the leather and textile industries for tanning and dyeing. Formic acid is also employed as a coagulating agent in the production of latex rubber, and it is sometimes used as a food preservative (E236). The reducing properties of formic acid are often exploited in preparative synthetic chemistry, (Leuckart–Wallach reaction, Eschweiler–Clark methylation, transfer hydrogenolysis,[13] and transfer hydrogenation[14]). Nitro compounds can be reduced to amines batchwise in large-scale processes by catalyzed reduction with formic acid or ammonium formate. Many derivatives of formic acid, such as sodium formate (a component of de-icing salts and photographic fixing baths), methyl formate (DMF production), ethyl formate (flavoring), and dimethyl formamide (solvent) are also of considerable economic importance.

Formic acid was isolated in the pure state for the first time in 1749 by Markgraf by dry distillation of red ants. On an industrial scale, formic acid was for many years produced exclusively by the reaction of CO with hot sodium hydroxide solution at high pressure and subsequent acidification with dilute sulfuric acid. Large quantities of the unwanted by-product sodium sulfate are formed in this process. Considerable quantities of formic acid are obtained as the by-product of the oxidation of low boiling mineral oil fractions during the synthesis of acetic acid.

At present, the most widely used method of producing formic acid is based on the two-stage process of Equation (c).[12] In the

$$CH_3OH + CO \xrightarrow[NaOMe\ (cat.)]{80^\circ C,\ 45\ atm} HCO_2CH_3 \xrightarrow[-CH_3OH]{+H_2O} HCO_2H \qquad (c)$$

first stage, methyl formate is formed by the carbonylation of methanol, and this is then hydrolyzed to formic acid and methanol in the second stage. The methanol is recovered and returned to the first stage. The net process is therefore the addition of water to CO. This reaction can also be carried out directly under comparatively severe conditions in the presence of certain amines.[15]

The synthesis of formic acid by the reduction of CO_2 is an interesting alternative to these processes; the energy balance of the addition of H_2O to CO and the reduction of CO_2 with H_2 are very similar [Eqs. (d) and (e)].[10] The synthesis of formic

$$CO(g) + H_2O(l) \underset{}{\overset{\Delta H^0_{298} = -28.4\ kJ\ mol^{-1}}{\rightleftharpoons}} HCO_2H(l) \qquad (d)$$

$$CO_2(g) + H_2(g) \underset{}{\overset{\Delta H^0_{298} = -31.6\ kJ\ mol^{-1}}{\rightleftharpoons}} HCO_2H(l) \qquad (e)$$

acid from CO_2 offers the possibility of using carbon dioxide as a raw material to the extent of approximately 10^5 tonnes carbon per year. The state of development of the various approaches to the synthesis of formic acid and its derivatives from CO_2 is discussed below, with a strong emphasis on systems in which transition metal complexes are used as catalysts in a homogeneous phase.

2. Reduction of CO_2 by Electron Transfer

2.1. Electrochemical Reduction of CO_2 to Formate

The one-electron reduction of CO_2 to the radical anion $CO_2^{\bullet -}$ [Eq. (f)] requires a reduction potential of -1.9 V.[16] The high energy species $CO_2^{\bullet -}$ reacts readily with $H^\bullet$ sources to give the formate ion, but other possible reaction routes such as disproportionation, dimerization with formation of oxalate, or further reduction are difficult to suppress.

$$CO_2 + 1e^- \longrightarrow CO_2^{\bullet -} \qquad E^\circ = -1.9\ V \qquad (f)$$

An alternative and very promising approach to the electrochemical reduction of CO_2 involves the production of a suitable catalyst at the electrode to enable formate or formic acid to be formed directly from CO_2, H^+ ions, and two electrons [Eq. (g)]. Since the two-electron reduction to formic acid requires a considerably lower potential than the one-electron reduction, the electrolyses in the presence of catalysts can be carried out at considerably lower voltages. However, it is still a problem to control the selectivity between the various two-electron reductions [Eqs. (g)–(i)]. A general discussion of electrocatalytic CO_2 reduction can be found in reports and reviews of the original research.[16, 17]

$$CO_2 + 2H^+ + 2e^- \longrightarrow HCO_2H \qquad E^\circ = -0.61\ V \qquad (g)$$

$$CO_2 + 2H^+ + 2e^- \longrightarrow CO + H_2O \qquad E^\circ = -0.53\ V \qquad (h)$$

$$2H^+ + 2e^- \longrightarrow H_2 \qquad E^\circ = -0.41\ V \qquad (i)$$

Characteristic parameters of the electrocatalytic systems used to produce formates by this principle include the overvoltage required for the electrolysis, the current yield, and the number of catalytic cycles (turnover number (TON)) for the formate formation. For many years, the use of transition metal complexes as electrocatalysts has attracted much attention, and typical systems that form significant amounts of formate are listed in Table 2. In addition to the catalysts used in homogeneous phase or bonded in polymeric matrices, the use of metal complexes adsorbed directly onto an electrode surface to produce formate and formic acid has also been described.[18, 29]

With a number of catalysts, reaction conditions have a remarkable influence on product distribution of the two-electron reductions (g)–(i). In the case of the complex $[Ru(bpy)_2(CO)_2]^{2+}$, CO and H_2 are formed almost exclusively in the ratio 1:1 in H_2O/DMF at pH 6.0, whereas, at pH 9.5 and under otherwise identical conditions, all three possible products are formed in the molar ratio $CO/H_2/HCO_2^- = 2:3:3$.[32] In acetonitrile, the same catalyst causes formate to be produced in 44 catalytic cycles with a current yield of more than 80% (Table 2, entry 3),[23] and the formation of DMF by the electrocatalytic reduction of CO_2 in the presence of Me_2NH has also been reported.[33a] On the other hand, the structure of the nitrogen ligand has a relatively small influence on the product distribution.[33b] The highly selective reduction of CO_2 with the mono(bipyridine)complex $[Ru(bpy)(CO)_2Cl_2]$ results from the formation of a polymeric film of $[\{Ru^0(bpy)(CO)_2\}_n]$ at the surface of the electrode.[33c]

Similar observations were made with complexes of the type $[Re(L)(CO)_2X]$ (L = derivatives of bpy, X = halide). They lead

Table 2. Transition metal complexes in a homogeneous phase or a polymer matrix for the electrocatalytic formation of formate from CO_2.

Entry	Catalyst	Solvent	Electrode	Current yield [%]	U [V]	TON [a]	t [h]	Other products [b]	Ref.
1	$[Fe_4S_4(SR)_4]^{2-}$	DMF	Hg	40	−2.0	10	–	CO (<1), RCO_2^- (2)	[19–21]
2	$[Fe_6Mo_2S_8(SEt)_9]^{3-}$	CH_3CN	C	11	−1.5		–	$CH_3C(O)CO_2^-$ (27)	[22]
3	$[Ru(bpy)_2(CO)_2(PF_6)_2$ [c]	CH_3CN	Hg	84.3	−1.30	43.7		CO (2.4), H_2 (6.8)	[23]
4	$[Os(bpy)_2(CO)H]PF_6$ [c]	CH_3CN/H_2O	Pt	25	−1.5	1.8	–	CO, H_2	[24]
5	$[Rh(dppe)_2Cl]$ [c]	CH_3CN	Hg	41.6	−1.5	1.6		$NCCH_2CO_2^-$	[25]
6	$[Rh(bpm)_2Br_2]Br$ [c]	CH_3CN	C	63.3	−1.7	4.8	2	[d]	[26]
7	$[Rh(bpy)_2(CF_3SO_3)_2]CF_3SO_3$ [c]	CH_3CN	C	64.3	−1.55	6.1	1	H_2 (12.6)	[27]
8	$[Re(terpy)(CO)_3Br]$ [c] in Nafion 117	H_2O, pH 7	C	14.5	−1.6	401	3.2	CO (<1), H_2 (50)	[28]
9	$[Co(tpery)_2](PF_6)_2$ [c] polymeric film	DMF	C	ca. 100	−1.2	>500	4		[30]
10	$[Co(terpy)_2](PF_6)_2$ [c] in Nafion 117	H_2O, pH 7	C	51.4	−1.10	11	4.8	H_2 (13)	[31]

[a] Maximum total number of mols formic acid or formate per mol complex in the given reaction time. [b] Current yield in parentheses where known. [c] bpy = bipyridine, dppe = $Ph_2P(CH_2)_2PPh_2$, bpm = 2,2′-bipyrimidine, terpy = 2,2′:6′,2″-terpyridine. [d] No information.

mainly to CO production by electrocatalytic reduction of CO_2 in organic solvents both in the homogeneous phase[17a, 34] and in polymer films.[35] They cannot be used for CO_2 reduction in aqueous solution as hydrogen is liberated preferentially. However, production of formate can successfully compete with the formation of H_2 in water, if the complexes are incorporated in a polymer matrix of Nafion and fixed to the electrode.[28]

2.2. Photochemical Reduction of CO_2 to Formate

The fundamental principles of the photochemical reduction of CO_2 to formate are largely identical to those described in Section 2.1. The one-electron reduction to $CO_2^{\bullet-}$ requires extremely strong reducing agents that are difficult to produce by photochemical means.[36] Kubiak et al. recently reported that irradiation even by diffuse daylight enables the trinuclear cluster $[Ni_3(\mu_3\text{-}I)_2(dppm)_3]$ to reduce CO_2 to the radical anion $CO_2^{\bullet-}$, whose presence was demonstrated inter alia by its subsequent reaction to give formate.[36b] However, the two-electron reduction [Eq. (g)] also represents the most energetically favorable route from CO_2 to formate in photochemistry. An approach closely related to electrocatalysis consists of using a photoactive system to convert light into electrical energy, which is then used with the help of a catalyst to reduce CO_2.[16, 37]

Semiconductor materials in the form of electrodes, colloids, or powders are able to reduce CO_2 to formate as the principal product when photochemically irradiated, even without catalysts.[38] Systems reported to catalyze the formation of formate in combinations with semiconductors include formate dehydrogenase,[39a] methylviologen,[39b] metals,[39c–i] and a ruthenium complex.[40] The formation of formic acid by photocatalytic reduction of CO_2 in a supercritical phase has recently been reported.[39h]

Organic photoactive systems also enable the direct[41] and catalyzed[42, 43] photochemical reduction of CO_2 to formate to be carried out in the presence of suitable reducing agents such as triethylamine. However, if *p*-terphenyl is used as the photosensitizer with cobalt(III) complexes as catalysts, there is an increase in the amount of CO produced relative to that of formate compared to the catalyst-free system.[43]

The most thoroughly investigated molecular photosensitizer for the photochemical reduction of CO_2 to formate is the complex cation $[Ru(bpy)_3]^{2+}$.[16, 44–47] In the preliminary experiments, $[Ru(bpy)_3]^{2+}$ was used with methylviologen, which was intended to perform the electron transfer.[45] However, it was found that the electron transfer was brought about by $[Ru(bpy)_2]$ species produced by photolabilization of the bpy ligands from $[Ru(bpy)_3]^{2+}$.[46a, 47a] Then, over a period of time, several systems for the photoreduction of CO_2 to formate were developed based on the combination $[Ru(bpy)_3]^{2+}/[Ru(bpy)_2(CO)(L)]^{n+}$ (L = CO, $n = 2$; L = H·Cl, $n = 1$).[46, 47] Triethanolamine in DMF is usually used as the reducing agent, and quantum yields of up to 15% are obtained. Irradiation of these systems with visible light ($\lambda > 320$ nm) produces up to 3700 mol formate per mol catalyst within 20 h.[47b] The formation of small amounts of formate has also been reported for the combination of $[Ru(bpy)_3]^{2+}$ with macrocyclic nickel complexes[48] and for photosensitizers based on vanadium complexes.[49]

2.3. Mechanistic Aspects of the Catalytic Formation of Formate by Electron Transfer

As shown schematically in Figure 2, the electrocatalytic and photocatalytic reductions of CO_2 to formate differ only in the method of producing the electrons required for the reduction. The catalytic cycle leading to formate is the same in both cases,

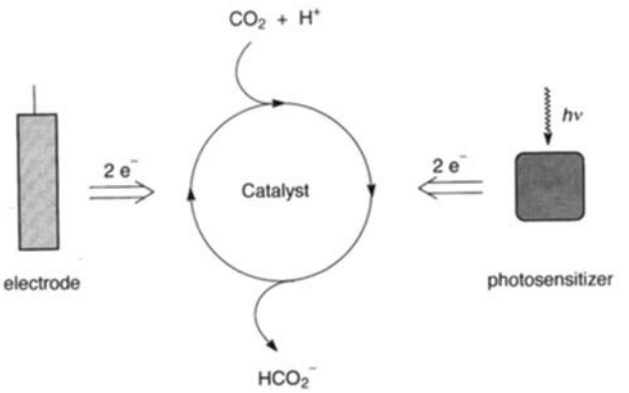

Fig. 2. Principle of the electrocatalytic and photocatalytic reduction of CO_2 to formate.

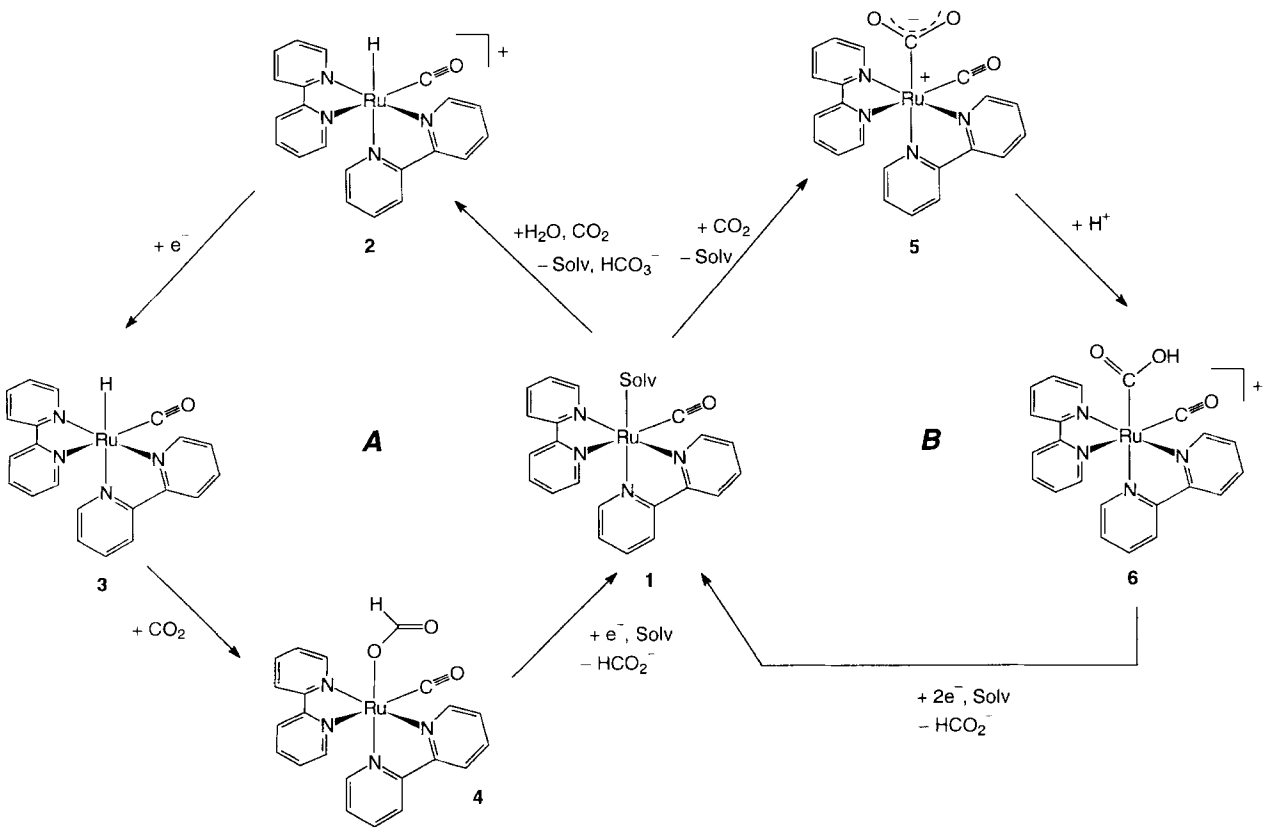

Scheme 2. Catalytic cycles in formate formation by electron transfer with Ru^{II}(bpy) catalysts $[Ru(bpy)_2(CO)(L)]^{n+}$ (L = CO, $n = 2$; L = H, $n = 1$) according to refs. [50, 51]; Solv = solvent.

and, in fact, the same catalysts can often be employed. However, a complex sequence of electron transfer steps and changes in the coordination sphere is necessary to build such a catalytic cycle[16, 17] and the understanding of these combinations is a field of great current interest.

The most extensively investigated catalysts for the electrochemical and photochemical reduction of CO_2 are of the type $[Ru(bpy)_2(CO)(L)]^{n+}$ (L = CO, $n = 2$; L = H, $n = 1$), and the mechanisms for the electron transfer in formate formation illustrated in Scheme 2 have been elaborated in recent years regardless of the type of excitation. Both cycles include a common catalytically active intermediate, namely the twice reduced solvent complex $[Ru^0(bpy)_2(CO)(Solv)]$ **1**.

In Cycle A, the formate group is formed by the insertion of CO_2 into the Ru–H bond of the hydrido complex **3**[50] in analogy to the hydrogenation of CO_2 (see Section 3.4). It was possible to detect all the individual steps of this cycle, which leads to the selective formation of formate, under catalytic conditions. However, it was found in this study that an additional cycle was responsible for the reduction of CO_2 to CO *and* formate. This becomes the dominant reaction route with $[Os(bpy)_2(CO)H]^+$.[24]

This second route presumably involves Cycle B in which formate is liberated from a metal carboxylic acid formed by protonation of the η^1-CO_2 complex **5**. Complex **5** was recently synthesized by an independent route and characterized by X-ray structural analysis.[51] The formation of **5** under the conditions of electrocatalysis was detected spectroscopically. The pH-dependent simultaneous formation of HCO_2^- *and* CO in the electrocatalytic reduction of CO_2 can be explained by the protonation equilibrium **5**/**6**.[47] Intermediates analogous to **5** and **6** have also been suggested for the electrochemical reduction of CO_2 to CO with $[Re(L)(CO_2)X]$ as catalysts, based on the results of an in situ IR investigation.[34d]

Two comparable cycles were recently shown to be responsible for the cobalt-catalyzed photochemical reduction of CO_2 with *p*-terphenyl as the photosensitizer.[43] In this case, formate is formed exclusively by a route analogous to A,[43c] while the formation of a CO_2 adduct eventually leads to CO only.[43d]

In addition to the difficulty of controlling the product selectivity, there is a further problem in the electrocatalytic and photocatalytic reduction of CO_2 to formate. The concentration of catalyst must be kept as low as possible to prevent deactivation processes. Even with the most active known catalysts, the concentrations of reduction products in the reaction solution are therefore usually only in the millimolar range. In contrast, the methods of catalytic hydrogenation of CO_2 to formic acid and its derivatives described in the following Section, can lead to product concentrations of up to several mol per liter.

3. Transition Metal Catalyzed Formation of Formic Acid and Its Derivatives from CO_2 and H_2

3.1. General Considerations

In the early 1970s, the pioneering work of several research groups showed that formic acid, its salts, esters, or amides are

accessible from hydrogen, carbon dioxide, and a possible third component in the presence of homogeneous transition metal catalysts [Eqs. (j)–(m)].

$$CO_2 + H_2 \rightarrow HCO_2H \quad (j)$$
$$CO_2 + H_2 \rightarrow HCO_2^- + H^+ \quad (k)$$
$$CO_2 + H_2 + HNR_2 \rightarrow HC(O)NR_2 + H_2O \quad (l)$$
$$CO_2 + H_2 + HOR \rightarrow HC(O)OR + H_2O \quad (m)$$

Since the synthesis of formic acid derivatives, unlike the formation of HCO_2H or HCO_2^-, requires not only the formation of the C–H bond but also the breaking and reforming of another covalent bond during the reaction, these processes will be dealt with separately.

3.2. Synthesis of Formic Acid and Formates from CO_2 and H_2

Table 3 summarizes typical catalytic systems used for the hydrogenation of CO_2 to formic acid and formates. The maximum total number of catalytic cycles per metal center (turnover number (TON)), and, where available, the maximum rate at which the catalytic cycles can take place at the beginning of the reaction (turnover frequency (TOF)) are also given. Further examples can be found in the original research cited.

3.2.1. *Hydrogenation of CO_2 in Organic Solvents*

The Catalytic Systems

In 1974, a Polish research group reported that a homogeneous titanium(II) catalyst produced from $TiCl_4$ and magnesium in THF promoted the catalytic formation of $Mg(HCO_2)_2$ by treatment with H_2 and CO_2 alternately.[52] Up to 15 equivalents of CO_2 per equivalent Ti^{II} could be fixed this way.

A little time later, Y. Inoue et al. reported the catalytic hydrogenation of CO_2 with phosphane complexes of transition metals of Groups 9 and 10.[53a] A yield of 22 mol formic acid per mol rhodium was obtained with Wilkinson's catalyst $[Rh(PPh_3)_3Cl]$ under the conditions detailed in Table 3 (entry 2). At the end of the reaction, there is approximately a 50-fold excess of amine relative to the concentration of the newly formed formic acid. The presence of small amounts of water favors the hydrogenation of CO_2. Later modifications to the process described in a series of patents gave only small improvements to the original system.[54a–e] The highest TON (314) was reported with $[Rh(PPh_3)_3Cl]$ in a mixture of isopropyl alcohol, water, and NEt_3.[54e] Very recently a complex with nitrogen ligands has been reported to act as an effective catalyst for CO_2 hydrogenation in alcoholic solution.[54f] Up to 5000 turnovers are observed with the complex *cis*-$[Ru(6,6'\text{-}Cl_2bpy)_2(H_2O)_2](CF_3SO_3)_2$ in EtOH/NEt_3. In the absence of amine, the drastic reaction conditions (60 atm, 150 °C) lead to formation of ethyl formate (see Section 3.3.3).

In 1992, Nicholas and Tsai discovered that the hydrogenation of CO_2 could also be carried out in the absence of bases.[55] However, with the catalyst $[Rh(PMe_2Ph)_3(nbd)]BF_4$ (nbd = norbornadiene) in THF under similar high pressures, only 64 mol HCO_2H per mol catalyst per day are formed. Again, the presence of small amounts of water increases the activity of the catalyst (Table 3, entry 6).

At about the same time, we were able for the first time to report a system for transition metal catalyzed hydrogenation of CO_2 to formic acid in which TONs greater than 1000 and TOFs of approximately 40 h^{-1} can be obtained under mild conditions (Scheme 3).[56a] The catalyst is produced in situ from the dimer-

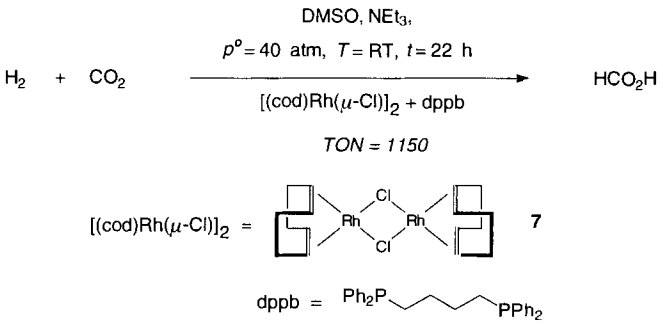

Scheme 3. Hydrogenation of CO_2 to formic acid according to ref. [56a].

Table 3. Catalytic systems for the synthesis of formic acid or formates by the hydrogenation of CO_2. RT = room temperature.

Entry	Catalyst	Solvent	Additive	$p(H_2)/p(CO_2)$ [bar]	T [°C]	TON [a]	t [h]	TOF [b] [h^{-1}]	Ref.
1	$TiCl_4/Mg$	THF	Mg	1/1	RT	15	24	–	[52]
2	$[Ru(PPh_3)_3(H)_2]$	benzene	NEt_3, H_2O	25/25	RT	87	20	–	[53a]
3	$[Pd(PPh_3)_2Cl_2]$	benzene	NEt_3, H_2O	50/50	RT	15	–	–	[53b]
4	$[Rh(PPh_3)_3Cl]$	*i*PrOH	NEt_3, H_2O	50/30	40	314	–	–	[54e]
5	*cis*-$[Ru(6,6'\text{-}Cl_2bpy)_2(H_2O)_2](CF_3SO_3)_2$	EtOH	NEt_3	30/30	150	5000	8	–	[54f]
6	$[Rh(PMe_2Ph)_3(nbd)]BF_4$ [c]	THF	H_2O	48/48	40	128	48	ca. 3	[55]
7	$[\{Rh(cod)(\mu\text{-}Cl)\}_2]$/dppb [c]	DMSO	NEt_3	20/20	RT	1150	22	39	[56]
8	$[\{Rh(cod)(\mu\text{-}H)\}_4]$/dppb [c]	DMSO	NEt_3	20/20	RT	2200	18	375	[57]
9	[Rh(dcpb)(hfacac)] [c]	DMSO	NEt_3	20/20	25	3005 [d]	31 [d]	1335	[58]
10	$PdCl_2$	H_2O	KOH	106/40	240	340	3	–	[67]
11	Pd/C	H_2O	Na_2CO_3	1.7/– [e]	RT	113	46	35	[68]
12	[Rh(TPPTS)$_3$Cl] [c]	H_2O	$HNMe_2$	20/20	25	3440	12	1365 [d]	[71]
13	$[Ru(PMe_3)_3(H)_2]$	$CO_{2(sc)}$	NEt_3, H_2O	85/120 [f]	50	7200	–	1400	[73]

[a] Turnover number is the maximum total number of mols formic acid or formate per metal center in the given reaction time. [b] From the maximum initial rates of reaction; the TON and TOF are usually derived from different experiments. [c] nbd = norbornadiene, cod = cyclooctadiene, dppb = $Ph_2P(CH_2)_4PPh_2$, dcpb = $Cy_2P(CH_2)_4PCy_2$, hfacac = hexafluoroacetylacetonate, TPPTS = $P(C_6H_4SO_3Na)_3$. [d] Unpublished results. [e] 1.0 mol L^{-1} Na_2CO_3 without added CO_2 atmosphere. [f] At reaction temperature.

ic rhodium complex $[\{(cod)Rh(\mu\text{-}Cl)\}_2]$ **7** (cod = 1,5-cyclooctadiene) and the bidentate phosphane $Ph_2P(CH_2)_4PPh_2$ (dppb). A mixture of DMSO and NEt_3 is used as the reaction medium. The final concentration of formic acid, under the conditions given in Scheme 3, is 2.1 mol L^{-1} and *exceeds* the concentration of the amine by 65%. In contrast to all other systems, water has a detrimental effect on the performance of this catalytic system. In the absence of amine, only small amounts of formic acid are formed, similar to those observed in THF.[57]

The Thermodynamics of CO_2 Hydrogenation

The drastic effect of the reaction medium on the maximum yield of formic acid can be explained by the thermodynamic balance[10] in the addition of H_2 to CO_2 [Eq. (n)]. Under stan-

$$H_2(g) + CO_2(g) \underset{\Delta G^0_{298} = +32.9\ kJ\ mol^{-1}}{\overset{\Delta H^0_{298} = -31.6\ kJ\ mol^{-1}}{\rightleftharpoons}} HCO_2H(l) \qquad (n)$$

dard conditions, this reaction is exothermic (approximately $-32\ kJ\ mol^{-1}$), but strongly endoergic ($+33\ kJ\ mol^{-1}$) because of the unfavorable entropy conditions (two gases reacting to form a liquid with strong intermolecular hydrogen bonds). To obtain high yields of formic acid, the entropy difference between the starting materials and the product must be reduced by a suitable choice of reaction conditions.

Full reversibility of formic acid formation was demonstrated experimentally for the first time for the catalytic system shown in Scheme 3. This enabled the effect of reaction conditions and the reaction medium on the yields and hence on the position of the equilibrium to be systematically investigated.[57] As expected for an exothermic reaction between two gaseous reactants, the equilibrium concentration increases as temperature decreases and pressure increases.

The solvent is very important for the yield of formic acid, as it can strongly influence the entropy difference by solvation of both the reactants and the product. The main reason for the special suitability of dipolar aprotic solvents for the hydrogenation of CO_2 to formic acid was shown to be the solvation of the product with cleavage of the hydrogen bonds. At the same time, it is assumed that these solvents also affect the catalytic activity by stabilizing intermediate stages of the catalytic cycle (see Section 3.4).

As mentioned above, the addition of trialkylamine is not absolutely necessary for the catalytic hydrogenation of CO_2 under the conditions given in Scheme 3, although it too leads to cleavage of the hydrogen bonds and hence to a drastic increase in the equilibrium concentration. With formic acid, trialkylamines do not form true 1:1 salts, but form liquid azeotropes with the composition $HCO_2H/NR_3 = 1.5\text{–}2:1$.[59] The final concentration of formic acid only exceeds the concentration of the amine when such azeotropes can be formed and ratios of approximately 1:1 are observed with secondary amines.[57] In contrast to the reactions described in Section 3.3, the use of dimethylamine as the amine component does not lead to further reaction of the formic acid to give dimethylformamide under the mild conditions indicated in Scheme 3.

The catalytic systems for the hydrogenation of CO_2 (Table 3) are, of course, not only characterized by the total number of possible catalytic cycles, but also by the rate at which these take place. Systematic studies of catalyst optimization have so far only been reported for the rhodium-catalyzed hydrogenation of CO_2 to formic acid in $DMSO/NEt_3$.[57, 58, 60]

Catalyst Optimization in the Rhodium-Catalyzed Hydrogenation of CO_2 to Formic Acid

Variation of the phosphane component has a considerable effect on the activity of the catalyst formed with **7** (Scheme 3).[60] When in situ catalysts are formed from **7** and monodentate phosphane ligands PR_3 (Rh:P = 1:4), the observed ligand effects can be explained by classical ligand concepts such as basicity[61, 62] and steric demand[62] of the PR_3 groups. For PR_3 ligands of comparable size, the most active catalysts are obtained with phosphanes of medium basicity ($pK_a(HPR_3^+) \approx 4$). The activity of such catalysts corresponds approximately to that of the system **7**/dppb. Both more strongly acidic and more strongly basic phosphanes lead to rapid decrease in the activity. With similar basicity, the activity decreases with increasing bulkiness of the ligands, and phosphanes PR_3 with a cone angle[62a] greater than 180° are not suited as cocatalysts for in situ systems **7**/PR_3 in the hydrogenation of CO_2.

These rules cannot be applied to in situ catalysts with bidentate phosphanes, as with these ligands the size of the chelate ring formed on the metal center has a very important effect on the activity of the catalyst.[60, 63] However, even with constant chain length, the trends observed with monodentate phosphanes no longer apply, as can be seen from the increase in the activity of the in situ catalysts **7**/$R_2P(CH_2)_2PR_2$ in the sequence R = Ph < Me < Cy < *i*Pr.

When the in situ catalyst **7**/dppb is used, the catalytically active species is formed slowly compared with the rate of the actual catalytic cycle, as proved by the marked induction period on the first use of a catalyst solution.[57] This induction period can be avoided by treating the catalyst solution with H_2 or HCO_2H before reaction. However, even under these conditions, only some of the rhodium complex appears to be converted into the catalytically active species, as indicated by the effect of activation on the turnover frequency. It is therefore impossible to know to what extent the observed ligand effects are associated with the influence of the phosphanes on the course of the catalytic cycle or on the formation of the catalytically active intermediate.

As explained in detail in Section 3.4, it is highly probable that electronically and coordinatively unsaturated molecules of $[(P_2)RhH]$ **11** (Scheme 4; P_2 = bidentate phosphane) represent the catalytically active intermediate in the rhodium-catalyzed hydrogenation of CO_2 in $DMSO/NEt_3$. The aim of the development of catalysts must therefore be to produce these species under catalytic conditions in a rapid and well-defined reaction. At the same time, a stable and easily produced precursor should be used and wide variation in the phosphane component is desirable.

To avoid the reduction stage in the formation of the catalytically active intermediate **11**, the hydrido complex $[\{(cod)Rh(\mu\text{-}H)\}_4]$ **8** was tested as a precursor for in situ catalysts (Table 3, entry 8), which proved to be considerably more effective than systems formed with **7**.[57] A lower limit for the maximum

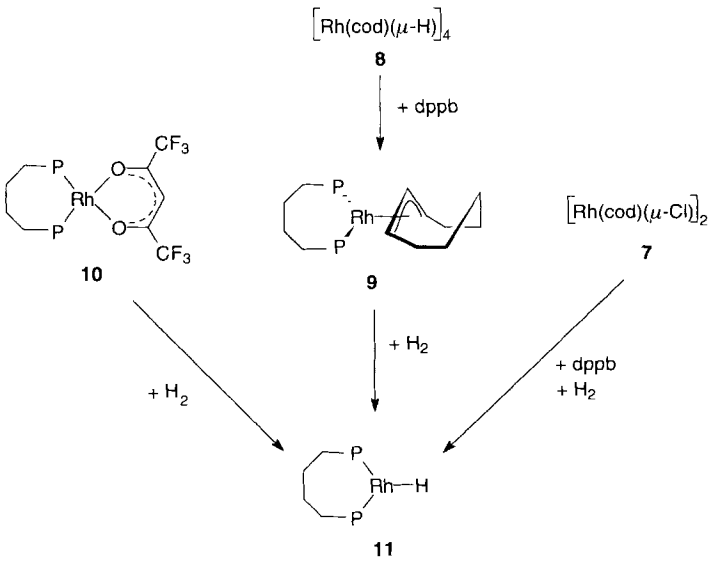

Scheme 4. Formation of the active intermediate **11** from the various catalyst precursors in the catalytic hydrogenation of CO_2 to formic acid in DMSO/NEt_3. P = PPh_2; maximum TOF: **7**/dppb: 39 h^{-1} [56a]; **8**/dppb: 370 h^{-1} [57]; **10**: 565 h^{-1} [58].

turnover frequency of the system **8**/dppb has been estimated to be 370 h^{-1} under the conditions indicated in Scheme 3, that is, it was possible to increase the activity of the catalyst by a factor of 10 compared with that of the system **7**/dppb (Scheme 4).

As shown in recent research,[64] and contrary to earlier opinion,[57] the catalytically active intermediate **11** is not formed directly from **8** and dppb (Scheme 4). Instead, the η^3-cyclooctenyl complex **9** is formed by the reaction of **8** with dppb by hydride transfer. Complex **9** was identified unambiguously by NMR spectroscopy and X-ray structural analysis (Fig. 3). Complex **9** is the actual catalyst precursor, reacting readily in a hydrogen atmosphere to form the neutral monohydride **11**.[64b, 65]

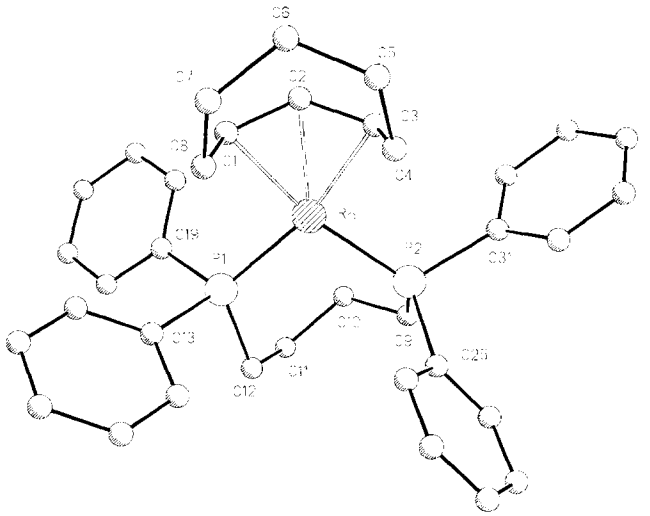

Fig. 3. Molecular structure of the η^3-cyclooctenyl complex **9** in the solid state. Selected interatomic distances [Å] and angles [°]: Rh–C(1) 2.219(10), Rh–C(2) 2.122(10), Rh–C(3) 2.209(10), Rh–P(1) 2.237(3), Rh–P(2) 2.228(3); C(1)-Rh-C(3) 68.8(4), P(1)-Rh-P(2) 98.63(10), C(2)-C(1)-C(3) 124.0(10), θ[P(1)-Rh-P(2)]/[C(1)-Rh-C(3)] 6.

Like allylrhodium complexes, acetylacetonatorhodium complexes are able to form neutral monohydrides by hydrogenolysis,[66] and in fact the hexafluoroacetylacetonatorhodium complexes of type **10** prove to be ideal catalyst precursors for the hydrogenation of CO_2 to formic acid.[58] The formation of formic acid starts at maximum velocity without an induction period, and the complex shows its full catalytic activity even at concentrations of 5×10^{-4} mol L^{-1}. The turnover frequency of 565 h^{-1} obtained with complex **10** corresponds to the lower limit of catalytic activity estimated for the in situ system **8**/dppb.

Interestingly, in complexes of type **10**, relationships are found between the P-Rh-P angles in the solid state, the ^{103}Rh NMR shifts in solution, and the catalytic activities in CO_2 hydrogenation.[58] The cyclohexyl derivative [{$Cy_2P(CH_2)_4PCy_2$}-Rh(hfacac)] (Table 3, entry 9), with a maximum TOF of 1335 h^{-1} under mild conditions (40 bar, 25 °C), is the most active catalyst so far reported for direct hydrogenation of CO_2 to formic acid or formates in organic solvents. Under comparatively mild conditions, similar high TOFs are obtained only in aqueous solution. The complex $[Ru(PMe_3)_4(H)_2]$ enables a TOF of 1400 h^{-1} to be obtained only at pressures exceeding 200 bar (Table 3, entry 13).

3.2.2. *Hydrogenation of CO_2 in Aqueous Solution*

The hydrogenation of CO_2 to formic acid in aqueous solution is a particularly attractive approach to the utilization of carbon dioxide as a raw material, as water is the usual solvent for the recovery of CO_2 from process flue gases (Section 1.1). Thus, aqueous solutions of amines could be used as both absorber and reaction solutions.

It has been known for some time that at temperatures above 200 °C in an atmosphere of CO_2 and hydrogen, potassium formate is formed in aqueous potassium hydroxide solution, $PdCl_2$ being the catalyst (Table 3, entry 10).[67] The formation of sodium formate from Na_2CO_3 and hydrogen in aqueous solution in the presence of a heterogeneous Pd/C catalyst can also be regarded as an example of CO_2 hydrogenation (Table 3, entry 11).[68] With K[Ru(EDTA-H)Cl]·H_2O as a catalyst for the water gas shift reaction in neutral aqeous solution, formic acid was observed as a possible intermediate in a stoichiometric and catalytic reaction.[69]

Phosphane complexes of transition metals successfully used as catalysts in organic solvents cannot be used in aqueous solution owing to their insolubility in water. Alcohol/water mixtures have been used as reaction media for phosphane-containing catalysts, although they have no particular advantages compared with purely organic solvents.[54e] We have been able to demonstrate that aqueous solutions of rhodium complexes of the water-soluble phosphane (C_6H_4-*m*-$SO_3^-Na^+)_3P$-(TPPTS)[70] give homogeneous catalytic systems that can lead to even higher activities and yields than obtained in organic solvents (Scheme 5).[71]

In situ catalysts can be employed for the hydrogenation of CO_2 in aqueous solution using TPPTS and the same rhodium precursors as in organic solvents. However, the most effective catalyst was found to be the water-soluble analogue of Wilkinson's catalyst [$(TPPTS)_3RhCl$] **12**, yielding up to 3440 mol formic acid per mol catalyst (Table 3, entry 12).[71a] The hydro-

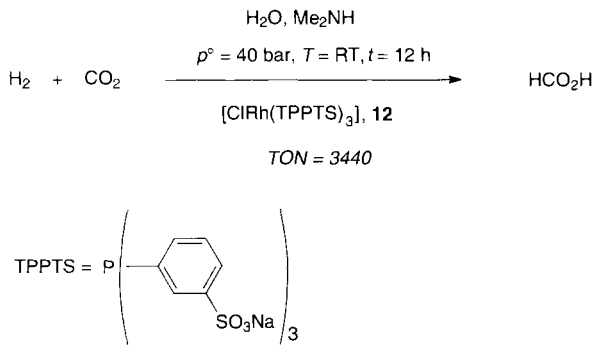

Scheme 5. Hydrogenation of CO_2 to formic acid in aqueous solution according to ref. [71a].

genation of CO_2 begins without an induction period at maximum velocity, TOFs of up to 1365 h^{-1} being reached.[71b] In contrast to the reaction in organic solvents, the concentration of the amine is never exceeded in aqueous systems, and no reaction occurs in the absence of amine.[71a] Formation of the free formate anion was confirmed by ^{13}C NMR spectroscopic measurements on the reaction product, and in agreement with thermodynamic considerations the formate anion was shown to be stable towards decomposition even in the presence of an active catalyst.[71b]

3.2.3. *Hydrogenation of CO_2 in the Supercritical Phase*

Carbon dioxide in its supercritical state is an interesting reaction medium,[72a, 72b] and the possibility of transition metal catalyzed CO_2 activation in the supercritical phase was demonstrated by Reetz et al., taking as an example the known synthesis of pyrones from alkynes and CO_2.[72c] Jessop, Noyori, and Ikariya recently reported that an efficient transition metal catalyzed hydrogenation of CO_2 to formic acid can take place in a supercritical mixture of H_2, CO_2, and NEt_3 without any additional solvent (Scheme 6).[73] With the ruthenium complexes

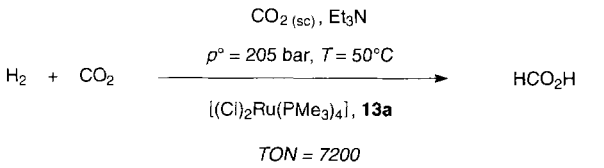

Scheme 6. Hydrogenation of CO_2 to formic acid in the supercritical phase according to ref. [73a].

$[(X)_2Ru(PMe_3)_4]$ (X = Cl, H) **13a** and **13b**, 7200 mol formic acid are formed per mol Ru with TOFs up to 1400 h^{-1}. The reaction rate in the supercritical phase is 18 times that in THF under comparable conditions. The authors assign this beneficial effect to special properties of the supercritical phase with respect to the miscibility and mass transport of the reactants.[73a]

To ensure a homogeneous supercritical phase during the reaction, comparatively drastic reaction conditions are necessary (205 bar total pressure, 50 °C). Rhodium(I) catalysts of the type used successfully in organic solvents and aqueous solution do not seem to be stable under these conditions,[73a] possibly because of the formation of inactive carbonate species.[57, 74]

The presence of triethylamine and small amounts of water is a necessary precondition for the production of formic acid by the hydrogenation of CO_2 in a supercritical phase.[73] After the equilibrium concentration has been reached, the HCO_2H/NEt_3 ratio is approximately 1.6:1, just as when DMSO is used as the solvent. In the presence of dimethylamine, HCO_2H reacts further to form DMF (see Section 3.3.2),[75a] whereas in the absence of an amine, no formic acid is formed at all. Other bases, such as K_2CO_3, which are immiscible with the supercritical phase, lead to TOFs of less than 10 h^{-1}.

3.2.4. *Isolation of Formic Acid Produced by the Hydrogenation of CO_2*

Thus, a series of extremely effective catalytic systems for the synthesis of formic acid from CO_2 and H_2 is now available. High yields of formic acid in the homogeneous transition metal catalyzed hydrogenation of CO_2 can be achieved if the equilibrium of Equation (n) can be shifted by minimizing the entropy difference between the starting materials and the product in favor of formic acid. Independently of the reaction conditions, the best method of achieving this seems to be the addition of amines to form either the corresponding azeotropes or ammonium formates.

From the reaction solutions of the rhodium-catalyzed hydrogenation of CO_2 in $DMSO/NEt_3$, the formic acid formed can be recovered as sodium formate, with the noble metal being recovered in catalytically active form.[56a] The liberation of formic acid from sodium formate is a well-known process, but involves ecological and economic problems that are intolerable today.

Free formic acid can also be recovered from mixtures with amines by a number of processes based on reamination of the formates and azeotropes to give thermally labile formic acid/amine adducts followed by distillative separation.[76] However, these methods can usually only be used on reaction solutions after deactivation of the catalyst,[76c] as formic acid would otherwise decompose under the workup conditions. The loss of costly noble metal that occurs and the laborious multistage workup and recycling processes are severe disadvantages of these methods. In addition to the search for even more effective catalysts it seems therefore essential to develop economic methods for the recovery of the formic acid from the reaction solutions from CO_2 hydrogenation processes in order to be able to operate the process on an industrial scale.

3.3. Synthesis of Formic Acid Derivatives by the Hydrogenation of CO_2

3.3.1. *General Considerations*

Under suitable reaction conditions, the hydrogenation of CO_2 in the presence of amines or alcohols can lead to amides or esters of formic acid, respectively (Table 4). In most cases where experimental data are available, it is found that the formation of derivatives proceeds by the intermediate formation of free formic acid,[75, 77] although other reaction routes are possible.[77c, 78, 79] The derivatization usually leads to products that

Table 4. Catalytic systems for the synthesis of formic acid derivatives by the hydrogenation of CO_2.

Entry	Catalyst	Solvent	Reagent	$p(H_2)/p(CO_2)$ [bar]	T [°C]	Yield [a] [%]	TON [b]	t [h]	Ref.
1	$[Ir(PPh_3)_2(CO)Cl]$	benzene	Me_2NH	28/28	125	–	1200	17	[78]
2	$PdCl_2$	NMP [c]	Me_2NH	80/40	170	99	34	1.5	[79]
3	$[Ru(PPh_3)_4(H)_2]$	hexane	Me_2NH	30/30	130	57	2645	6	[80]
4	$[Pt_2(\mu\text{-dppm})_3]$ [c]	toluene	Me_2NH	114 (total) [d]	100	–	1375	24	[81b]
5	$[Ir(PPh_3)_2(CO)Cl]$	MeOH	NH_3	122 (total) [d]	125	–	1145	240	[81c]
6	$[Ru(PMe_3)_4Cl_2]$	$CO_{2(sc)}$	Me_2NH [e]	80/130 [d]	100	76	370000	37	[75a]
7	$PdCl_2$	MeOH	MeOH	30/30	100	–	38	10	[83]
8	$[Pd(dppe)_2]$ [c]	EtOH	EtOH	30/70	160	2	58	20	[84]
9	$[Fe_3(CO)_{11}H]^-$	MeOH	MeOH	20/20	175	–	5.8	96	[85]
10	$[Ru_4(CO)_{12}(H)_3]^-$	MeOH	MeOH	17/17	125	–	7.3	24	[77a]
11	$[(HCO_2)W(CO)_5]^-$	MeOH	MeOH	17/17	125	–	16.4	24	[77b]
12	$[Ru(PMe_3)_4Cl_2]$	$CO_{2(sc)}$	MeOH	80/125 [d]	80	12	3500	64	[75b]

[a] Yield of amide or ester based on amine or alcohol. [b] Maximum total number of mols formamide or ester per mol catalyst in the given reaction time. [c] NMP = *N*-methylpyrrolidone, dppm = $Ph_2P(CH_2)PPh_2$, dppe = $Ph_2P(CH_2)PPh_2$. [d] At reaction temperature. [e] Used as dimethylammonium carbamate.

are stable in the presence of the catalyst at normal pressure, although the thermodynamics for the formation of, for example, formamides are similar to those of formic acid.

3.3.2. *Synthesis of Formamides*

As early as 1970, Haynes et al. synthesized dimethylformamide (DMF) from H_2, CO_2, and $HNMe_2$ by using transition metal phosphane complexes as the catalysts.[78] Using the complex $[(Ph_3P)_2(CO)IrCl]$, they were able to obtain a total of 1200 mol DMF per mol catalyst by repeated use of the reaction solution. In the years following, a number of other systems for producing formamides from CO_2, H_2, and the corresponding amines under similar conditions were described (Table 4).[79–81] The complex $[(\mu\text{-dppm})_3Pt_2]$ (Table 4, entry 4) is exceptional, as it catalyzes not only formation, but also cleavage of DMF, depending on the reaction conditions.[81b] Various other secondary amines can be used, and the formation of formamide itself in the presence of ammonia has also been reported.[81c]

A very efficient method of synthesizing DMF is to use dimethylamine as the amine component under conditions suitable for hydrogenating CO_2 in a supercritical phase.[75a] Using the catalyst $[Ru(PMe_3)_4Cl_2]$ **13a** (Table 4, entry 6), up to 370000 mol DMF per mol catalyst is formed in less than 37 h (Scheme 7).

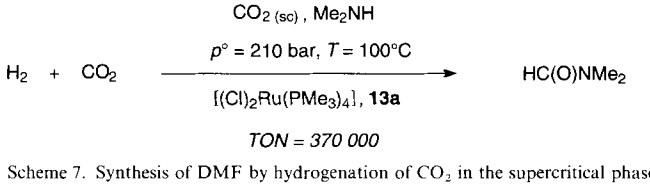

Scheme 7. Synthesis of DMF by hydrogenation of CO_2 in the supercritical phase according to ref. [75a].

The solubility of the components of the mixture, which consists of two phases during the reaction, is of great importance for the high turnover numbers that are achieved with this system. The liquid adduct of dimethylamine and CO_2 (dimethylammonium carbamate, "Dimcarb"[82]), which acts as the dimethylamine source in the reaction in Scheme 7, is practically insoluble in supercritical CO_2 because of its high polarity. In the supercritical phase, which contains CO_2, H_2, Me_2NH, and the catalyst, HCO_2H is formed in analogy to the system using trialkylamines (Section 3.2.3).[73] Under the comparatively drastic reaction conditions (100 °C, 210 atm), condensation of dimethylammonium formate to DMF takes place in the liquid phase. Most of the DMF formed then dissolves in the supercritical phase, while the water content of the liquid phase increases. In this way, all the dimethylamine used is converted into DMF quantitatively and with high selectivity. Small amounts of formic acid and trimethylamine (formed by further reduction of DMF[81b,c]) are formed as by-products.

3.3.3. *Synthesis of Formic Acid Esters*

The transition metal catalyzed formation of alkyl formates from CO_2, H_2, and alcohols was first described by the Russian research group of Vol'pin and Kolomnikov.[83] Not only phosphane complexes of transition metals of Groups 8–10[54a,75b,83,84], but also the carbonyl metalates of Groups 8[85,77a] and 6[77b] show catalytic activity (Table 4). In many cases, amines or other basic additives have a positive effect on the course of the reaction.

The anionic ruthenium carbonyl clusters used by Darensbourg et al. show considerably higher catalytic activity in the formation of alkyl formates by carbonylation of alcohols than in the reaction of CO_2 with H_2.[77a] However, a possible reaction route via the intermediate reduction of CO_2 to CO was ruled out. In the presence of CO_2 and hydrogen, formic acid is formed initially, and then esterified under the reaction conditions.

The formation of methyl formate by esterification of formic acid obtained from CO_2 hydrogenation also takes place in the supercritical phase if methanol is added to the reaction mixture under conditions comparable to those in Scheme 6.[75b] Because of the high efficiency of the CO_2 hydrogenation under these conditions, the yield of methyl formate exceeds the yields obtained by the other methods. However, the esterification is incomplete, and the reaction product consists of a 2:1 mixture of formic acid and methyl formate.

Alkyl halides can be used instead of alcohols as the source of the alkyl groups for the formation of formic acid esters.[83,77c] In this case, the derivatization most likely takes place directly on an intermediate formate complex without the liberation of formic acid.[77c]

3.4. Mechanistic Aspects of the Addition of Hydrogen to CO_2 with Formation of Formic Acid

3.4.1. General Considerations

The key step in the catalytic formation of formic acid or its derivatives from CO_2 and H_2 is the formation of the formyl C–H bond. In all cases in which catalytically active intermediates in the CO_2 hydrogenation to formic acid were characterized spectroscopically, the formation of formate complexes was detected in this step.[55, 63, 77] Carbonate species[53, 67] and metallacarboxylic acids[69] were also suggested as possible intermediates of CO_2 hydrogenation, and the formation of the C–H bond by hydrolysis or hydrogenolysis of such intermediates cannot be excluded a priori in spite of the lack of experimental proof.

The formation of the formate group on the metal center can take place either by the insertion of CO_2 into a M–H bond or by hydride transfer to coordinated CO_2. A large number of stoichiometric examples confirm the general validity of the CO_2 insertion,[2b, 3g, 86] and its exact mechanism is well understood in the light of experimental[86a, 86b, 88] and theoretical[89, 90] investigations. Experimental evidence for the alternative pathway for the formation of a formate ligand, that is hydride transfer to coordinated CO_2, has emerged only most recently in the oxidation of $[(\eta^5\text{-}C_5H_4Me)_2M(CO)H]$ (M = Nb, Ta) to $[(\eta^5\text{-}C_5H_4Me)_2M(O_2CH)]$[87a] and in the formation of $[(\eta^5\text{-}C_5H_4Me)(PCy_3)Ru(\eta^2\text{-}O_2CH)]$.[87b] It should be noted, however, that CO_2 insertion cannot be definitely excluded to account for formate formation in both cases.

In this context, it is somewhat surprising that the insertion of CO_2 into a Rh–H bond could not be realized for a long time[74a, b, 91] despite the excellent catalytic activities observed in CO_2 hydrogenation using rhodium phosphane catalysts. It is only most recently that detailed information on the catalytic cycle of the rhodium-catalyzed hydrogenation of CO_2 to formic acid under various conditions has been collected.

3.4.2. The Mechanism of the Rhodium-Catalyzed Hydrogenation of CO_2 in Organic Solvents

Nicholas and Tsai used IR and NMR spectroscopy at elevated pressure to investigate the mechanism of formation of formic acid from H_2 and CO_2 in THF with the catalyst $[Rh(Me_2PPh)_3(nbd)]BF_4$ in the absence of amines.[55] They were able to demonstrate the formation of the cationic dihydrido complex **14** and the subsequent insertion of CO_2 into the Rh–H bond to give complexes **15** and **17** with respectively η^1- or η^2-bonded formato ligands (Scheme 8). Only the η^1 complex **15** appears to be actively involved in the catalytic cycle. The subsequent step of reductive elimination of formic acid to give the square-planar cation **16** and regeneration of the dihydride **14** by oxidative addition of H_2 were postulated in analogy to known reactions.

It would appear likely at first sight that this mechanism could also be applied to the considerably more effectively catalyzed hydrogenation of CO_2 to formic acid by rhodium phosphane complexes in DMSO/NEt_3. However, cationic dihydrido complexes like **14** are deprotonated in the presence of amines, and

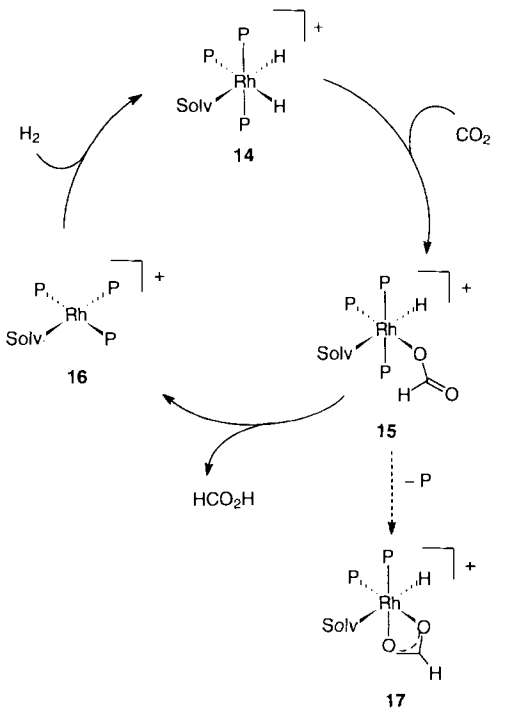

Scheme 8. Catalytic cycle of the hydrogenation of CO_2 with cationic rhodium complexes in THF according to ref. [55]. P = Me_2PPh, Solv = solvent.

the monohydrido complexes formed are usually the more active catalysts in hydrogenation reactions.[92] Interestingly, the first example of an insertion of CO_2 into M–H bonds, discovered in 1968, involved a *neutral* monohydridocobalt complex, the homologous 3d metal to rhodium.[93] However, the reaction of neutral monohydridorhodium complexes with CO_2 in conventional organic solvents has been reported to lead to the formation of carbonato or bicarbonato complexes.[74a, 74b, 91] Only in the solvent DMSO, which is very suitable for catalytic hydrogenation, was it possible to observe by NMR spectroscopy not only the CO_2 insertion but also for the first time all subsequent steps of a catalytic cycle for CO_2 hydrogenation with the neutral hydrido complex $[(Ph_2P(CH_2)_3PPh_2)_2RhH]$ **18** (Scheme 9).[63]

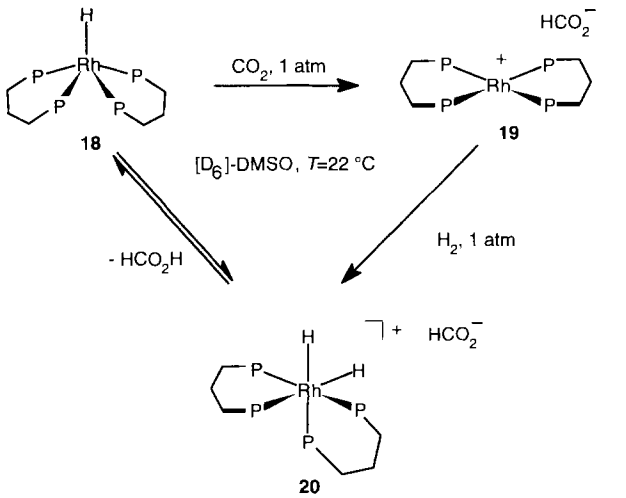

Scheme 9. Reaction of $[(Ph_2P(CH_2)_3PPh_2)_2RhH]$ **18** with CO_2 and H_2 in $[D_6]$DMSO according to ref. [63]. P = PPh_2.

Formal insertion of CO_2 into the Rh–H bond of **18** leads to the complex **19**, which, unlike all other known transition metal formato complexes exists in dissociated form in solution. Nevertheless, the insertion is reversible, as shown by the rapid CO_2 exchange and incorporation of deuterium in the formate unit. Interestingly, the rates of these exchange reactions with complex **19** and its analogue bearing the phosphane ligand $Ph_2P(CH_2)_2PPh_2$ reflect the catalytic activity of the corresponding hydrido complexes in the hydrogenation of CO_2.[63] The oxidative addition of H_2 to the cation of **19** yields the dihydride **20**, which is in equilibrium with the monohydride **18** and free formic acid under the reaction conditions given in Scheme 9.

However, complex **18** is only a moderately active catalyst for the hydrogenation of CO_2, as it contains two chelating phosphane ligands per rhodium center.[57, 63] The catalytic cycle of Scheme 9 can be applied, however, in an analogous manner to the most active catalyst systems in which the ratio Rh/P_2 is 1:1 (Scheme 10).[57] The starting point for the catalytic cycle is now the hydrido complex **11**, which can be formed from all the catalyst precursors so far used under these conditions (Scheme 4).[57, 58]

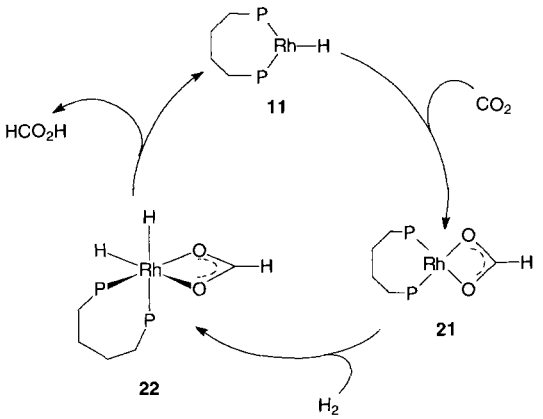

Scheme 10. Application of the cycle in Scheme 9 to the most active catalyst system dppb/Rh with a ligand–metal ratio of 1:1 according to ref. [57]. P = PPh_2.

Electronically unsaturated 14e complexes like **11** were studied in detail by Muetterties et al.[94] and by Fryzuk et al.[65] They tend to form hydride-bridged clusters $[\{(P_2)Rh(\mu\text{-}H)\}_n]$ (n = 2–4), and both the monomers and the intact clusters can take part in catalytic reactions.[65d] The participation of bridged hydridorhodium clusters has to be taken into account for CO_2 hydrogenation, as insertion of CO_2 into a Rh–H bridge is a known process.[95] However, there is so far no experimental evidence for the involvement of oligomeric species in the catalytic cycle of the rhodium-catalyzed hydrogenation of CO_2.[64a] It is reported that for the rhenium complexes $[Re(bpy)(CO)_3H]$ and $[(\mu\text{-}H)\{Re(bpy)(CO)_3\}_2]^+$, CO_2 is inserted into the Re–H bond of the monomeric complex only, the reaction being stoichiometric.[17a]

Insertion of CO_2 into the Rh–H bond of **11** can produce a formate group in analogy to the model complex **18**, but the formate group acts as a coordinating ligand in **21** owing to the electron deficiency of the catalyst center. The η^2-carboxylato complex $[(iPr_3P)_2Rh(\eta^2\text{-}O_2CCH_3)]$ analogous to **21** was recently prepared and characterized by X-ray crystal analysis by Werner et al.[96] Starting from **21**, the catalytic cycle in Scheme 10 can be closed by the oxidative addition of hydrogen and reductive elimination. The bicarbonato complex $[(H)_2Rh(iPr_3P)_2(\eta^2\text{-}O_2COH)]$ related to **22** was characterized by Ibers et al. by X-ray structural analysis.[74b]

Sakaki et al. have have carried out theoretical studies on the CO_2 insertion into the Rh–H bond of $[(PH_3)_3RhH]$ and found that coordinated formate is formed and bound in a η^1 fashion owing to the presence of three additional phosphorus ligands.[90f] Very recent ab initio calculations by Dedieu et al. show that the η^2 formate group represents the most stable coordination form in the presence of only two P donor atoms as depicted for complexes **21** and **22** (Scheme 10).[97] However, it appears from this latter work that the η^1 form is the more reactive species which sustains the catalytic cycle. Most intriguingly, the study by Dedieu et al. points to an interesting alternative for the liberation of formic acid from formate complexes like **15** and **21**.[97] A σ-bond metathesis between the η^1 formate group and nonclassically coordinated H_2[98] seems feasible to by-pass the oxidative addition/reductive elimination sequence. The Rh–H bond required for the insertion of CO_2 is regenerated without changing the oxidation state of the metal center, and the calculated energy barriers for the σ-bond metathesis are considerably less than those of the mechanisms shown in Schemes 8 and 10. It should be noted that the oxidative addition of H_2 has so far only been demonstrated experimentally in the catalytic cycle of Scheme 9, where a σ-bond metathesis is impossible.

Furthermore, it is interesting to note that the two mechanisms of Scheme 8 and Scheme 10 differ not only in the charge and coordination number of the intermediate species, but also quite fundamentally in the order of events. Whereas in Scheme 8 the product-forming step takes place immediately after reaction with CO_2, in Scheme 10, product formation follows the reaction with hydrogen. One might speculate on the impact of this situation on the large difference observed in the activity of the two catalytic systems. Although questions of detail require further experimental investigation, we may conclude that the two mechanisms depicted in Schemes 8 and 10 present a clear and reliable picture of the actual catalytic cycle of the rhodium-catalyzed hydrogenation of CO_2 to formic acid under the individual reaction conditions. Building on the reaction mechanism proposed in Scheme 10, it was already possible to develop catalysts whose activity exceeds that of the original in situ systems by more than an order of magnitude (Scheme 4).[57, 58] Catalytic cycles for formic acid formation from CO_2 and H_2 involving metal centers other than rhodium have not yet been studied in great detail and it will be interesting to see what kind of general pattern will arise from future studies.

4. Summary and Outlook

The reduction of CO_2 to formic acid and its derivatives can be carried out by photochemical and electrochemical processes as well as by the direct addition of H_2. Transition metal complexes have been found to catalyze all these routes. With regard to the reduction of CO_2 by electron transfer, recent years have seen a growing understanding of the catalytic cycles that comprise the

competing reduction processes that lead to the formation of HCO_2^-, CO, and H_2. Taken in conjunction with the enormous number of possible combinations of catalysts with electron sources, this should lead to a rapid and fruitful growth in this area.

However, in the medium term, the use of hydrogen for the reduction of CO_2 to formic acid is certainly a more easily realized approach, as it is based on existing technical know-how. Even more so because even today very effective catalytic systems for this reaction are already available. This is partly a result of a judicious use of "thermodynamic tricks", which enable high yields of reduction products to be obtained in spite of the endoergic nature of this reaction under standard conditions. Equally important is the rapid progress in our understanding of the fundamental mechanisms of catalysis based on experimental and theoretical studies that has a continuing influence on the development of new and powerful catalysts. Both the turnover numbers and turnover frequencies of these catalytic systems can compete with those of other homogeneous transition metal catalysts that are already used on an industrial scale.

The principles explained in this review for the hydrogenation of CO_2 can also be applied in full analogy to the simultaneous activation of CO_2 and any X–H bonds. As can be seen from Equation (o), the thermodynamic conditions that apply, for ex-

$$CH_4(g) + CO_2(g) \underset{\Delta G^0_{298} = +55.2\ kJ\ mol^{-1}}{\overset{\Delta H^0_{298} = -16.2\ kJ\ mol^{-1}}{\rightleftharpoons}} CH_3CO_2H(l) \qquad (o)$$

ample, to the reaction of methane with CO_2 to form acetic acid are comparable to those for the formation of formic acid according to Equation (n). Possible single steps in a potential catalysis cycle such as oxidative addition of C–H bonds[99] or insertion of CO_2 into M–C bonds[2b, 3, 86a] are also known. The creativity and inventiveness of many dedicated chemists will be needed to put together the pieces of the mosaic, but achievement of the ultimate aim will fully justify the effort involved.[100]

My special thanks are due to Prof. H. Brunner for his generous support in the beginning, and for his constant interest as this work has progressed. I also thank the leader of the research unit "CO_2 Chemistry" of the Max-Planck-Society at the University of Jena, Prof. E. Dinjus, for the outstanding facilities provided by his laboratory, and for many interesting discussions. I must also extend sincere thanks to the co-authors of the publications cited, and especially to Drs. F. Gassner, R. Fornika, and H. Görls for their fruitful cooperation. Very special thanks are due to Dr. A. Dedieu, CNRS Strasbourg, for a stimulating exchange of ideas. Finally, I thank the Fonds der Chemischen Industrie (Liebig Stipendium), the Max-Planck-Gesellschaft, the BMBF and the DAAD for financial support, and Degussa AG and Hoechst AG for the donation of chemicals.

Received: March 13, 1995 [A 109 IE]
German version: *Angew. Chem.* **1995**, *107*, 2391–2405
Translated by R. G. Leach, Basingstoke, UK

[1] a) K. Weissermel, H.-J. Arpe, *Industrielle Organische Chemie*, 3rd ed., VCH, Weinheim, **1988**; b) B. Blumenberg, *Nachr. Chem. Tech. Lab.* **1994**, *42*, 480.

[2] a) *Organic and Bio-Organic Chemistry of Carbon Dioxide* (Eds.: S. Inoue, N. Yamazaki), Wiley, New York, **1982**; b) A. Behr, *Carbon Dioxide Activation by Metal Complexes*, VCH, Weinheim, **1988**; c) *Catalytic Activation of Carbon Dioxide* (*ACS Symp. Ser.* **1988**, *363*); d) *Enzymatic and Model Carboxylation and Reduction Reactions for Carbon Dioxide Utilization* (*NATO ASI Ser. C* **1990**, *314*); e) *Electrochemical and Electrocatalytic Reactions of Carbon Dioxide* (Eds.: B. P. Sullivan, K. Krist, H. E. Guard), Elsevier, Amsterdam, **1993**; f) M. M. Halmann, *Chemical Fixation of Carbon Dioxide*, CRC, Boca Raton, **1993**; g) *Carbon Dioxide Chemistry: Environmental Issues* (Eds.: J. Paul, C.-M. Pradier), Royal Society of Chemistry, London, **1994**.

[3] a) D. J. Darensbourg, R. A. Kudaroski, *Adv. Organomet. Chem.* **1983**, *22*, 129; b) D. R. Palmer, R. van Eldik, *Chem. Rev.* **1983**, *83*, 651; c) D. Walther, *Coord. Chem. Rev.* **1987**, *79*, 135; d) A. Behr, *Angew. Chem.* **1988**, *100*, 681; *Angew. Chem. Int. Ed. Engl.* **1988**, *27*, 661; e) *Aspects Homogeneous Catal.* **1988**, *6*, 59; f) P. Braunstein, D. Matt, D. Nobel, *Chem. Rev.* **1988**, *88*, 747; g) I. S. Kolomnikov, T. V. Lysak, *Russ. Chem. Rev. (Engl. Transl.)* **1990**, *59*, 344; h) D. Walther, *Nachr. Chem. Tech. Lab.* **1992**, *40*, 1214; i) M. Aresta, E. Quartana, I. Tommasi, *New J. Chem.* **1994**, *18*, 133; k) P. G. Jessop, T. Ikariya, R. Noyori, *Chem. Rev.* **1995**, *95*, 259; l) W. Leitner, *Coord. Chem. Rev.* in press.

[4] See for example: a) E. T. Sundquist, *Science* **1993**, *259*, 934; b) P. S. Zurer, *Chem. Eng. News* **1991**, *69*(13), 7; c) J. L. Sarmiento, *ibid.* **1993**, *71*(22), 30; d) U. Siegenthaler, J. L. Sarmiento, *Nature* **1993**, *365*, 119; e) D. Dyrssen, D. R. Turner in ref. [2g], p. 317.

[5] See for example: a) *The Handbook of Environmental Chemistry, Vol. 1, Part A* (Ed.: O. Hutzinger), 1st ed., Springer, Berlin, **1980**; b) R. Kümmel, S. Papp, *Umweltchemie*, 2nd ed., VEB Deutscher Verlag for Grundstoffindustrie, Leipzig, **1990**; c) C.-D. Schönwiese, B. Diekmann, *Der Treibhauseffekt. Der Mensch verändert das Klima*, Rowohlt, **1990**; d) W. Seifritz, *Der Treibhauseffekt*, Hanser, München, **1991**.

[6] a) *Greenhouse Gas Emissions from Power Stations*, IEA Greenhouse Gas R & D Programme, Cheltenham, **1993**; b) *Carbon Dioxide Capture From Power Stations*, IEA Greenhouse Gas R & D Programme, Cheltenham, **1994**.

[7] *Kirk-Othmer Encyclopedia of Chemical Technology, Vol. 5*, 4th ed., Wiley, New York, **1993**, p. 35.

[8] *Merkblätter gefährliche Arbeitsstoffe (Kühn-Birett), Vol. 8*, 9th ed., ecomed, Landsberg/Lech, **1990**.

[9] *Römpp Chemie Lexikon* (Eds.: J. Falbe, M. Regitz), 9th edition, Thieme, Stuttgart, **1990**, p. 2277.

[10] *Handbook of Chemistry and Physics*, (Ed.: R. C. Weast), CRC, 65th ed., Boca Raton, **1984**.

[11] a) A. Y. Rozovsky, *Kinet. Catal.* **1980**, *21*, 97; b) G. C. Chinchen, P. J. Denny, D. J. Parker, M. S. Spencer, D. Whan, *Appl. Catal.* **1987**, *30*, 333; c) G. C. Chinchen, K. Manfield, M. S. Spencer, CHEMTECH **1990**, 692; d) K. C. Waugh, *Catal. Today* **1992**, *15*, 51.

[12] *Ullmann's Enzyclopedia of Industrial Chemistry*, 5th ed., VCH, Weinheim, **1986**.

[13] S. Rajagopal, M. K. Anwer, A. F. Spatola, *Peptides* **1994**, 11.

[14] For the application of formic acid as hydrogen donor in enantioselective hydrogenation see a) H. Brunner, W. Leitner, *Angew. Chem.* **1988**, *100*, 1231; *Angew. Chem. Int. Ed. Engl.* **1988**, *27*, 1180; b) W. Leitner, J. M. Brown, H. Brunner, *J. Am. Chem. Soc.* **1993**, *115*, 152.

[15] F. Lippert, A. Höhn (BASF AG), EP 583695, **1994** [*Chem. Abstr.* **1994**, *120*, 216715f].

[16] I. Willner, B. Willner, *Top. Curr. Chem.* **1991**, *159*, 153.

[17] a) J. Hawecker, J-M. Lehn, R. Ziessel, *Helv. Chim. Acta* **1986**, *69*, 1990; b) J. P. Collin, J. P. Sauvage, *Coord. Chem. Rev.* **1989**, *93*, 245; c) M. Hammouche, D. Lexa, M. Momenteau, J.-M. Savéant, *J. Am. Chem. Soc.* **1991**, *113*, 8455; d) G. Silvestri, S. Gambino, G. Filardo in ref. [2d], p. 101; e) F. R. Keene, B. P. Sullivan in ref. [2e], p. 118.

[18] J.-P. Collin, A. Jouati, J.-P. Sauvage, *Inorg. Chem.* **1988**, *27*, 1986.

[19] M. Tezuka, T. Yajima, A. Tsuchija, Y. Matsumoto, Y. Uchida, M. Hidai, *J. Am. Chem. Soc.* **1982**, *104*, 6834.

[20] M. Nakazawa, Y. Mizobe, Y. Matsumoto, Y. Uchida, M. Tezuka, M. Hidai, *Bull. Chem. Soc. Jpn.* **1986**, *59*, 809.

[21] T. Tomohiro, K. Uoto, H. Y. Okuno, *J. Chem. Soc. Chem. Commun.* **1990**, 194.

[22] K. Tanaka, T. Matsui, T. Tanaka, *J. Am. Chem. Soc.* **1989**, *111*, 3765.

[23] H. Ishida, H. Tanaka, K. Tanaka, T. Tanaka, *J. Chem. Soc. Chem. Commun.* **1987**, 131.

[24] a) M. R. M. Bruce, E. MeGehee, B. P. Sullivan, H. Thorp, T. R. O'Toole, A. Downard, T. J. Meyer, *Organometallics* **1988**, *7*, 238; b) M. R. M. Bruce, E. MeGehee, B. P. Sullivan, H. H. Thorp, T. R. O'Toole, A. Downard, J. R. Pugh, T. J. Meyer, *Inorg. Chem.* **1992**, *31*, 4864.

[25] a) S. Slater, J. H. Wagenknecht, *J. Am. Chem. Soc.* **1984**, *106*, 5367; b) A. Szymaszek, F. P. Pruchnik, *J. Organomet. Chem.* **1989**, *376*, 133.

[26] S. Rasmussen, M. M. Richter, E. Yi, H. Place, K. J. Brewer, *Inorg. Chem.* **1990**, *29*, 3926.

[27] a) C. M. Bolinger, B. P. Sullivan, D. Conrad, J. A. Gilbert, N. Story, T. J. Meyer, *J. Chem. Soc. Chem. Commun.* **1985**, 796; b) C. M. Bolinger, N. Story, B. P. Sullivan, T. J. Meyer, *Inorg. Chem.* **1988**, *27*, 4582.

[28] T. Yoshida, K. Tsutumida, S. Teratani, K. Yasufuku, M. Kaneko, *J. Chem. Soc. Chem. Commun.* **1993**, 631.

[29] a) S. Kapusta, N. Hackerman, *J. Electrochem. Soc.* **1984**, *131*, 1511; b) M. N. Mahmood, D. Masheder, C. J. Harty, *J. Appl. Electrochem.* **1987**, *17*, 1233; c) N. Furuya, K. Matsui, *J. Electroanal. Chem. Interfacial Electrochem.* **1989**, *271*, 181; d) N. Furuya, S. Koide, *Electrochim. Acta* **1991**, *36*, 1309.

[30] H. C. Hurrell, A. L. Mogstad, D. A. Usifer, K. T. Potts, H. D. Abruña, *Inorg. Chem.* **1989**, *28*, 1080.

[31] T. Yoshida, T. Iida, T. Shirasagi, R.-J. Lin, M. Kaneko, *J. Electroanal. Chem. Intrafacial Electrochem.* **1993**, *344*, 355.

[32] H. Ishida, K. Tanaka, T. Tanaka, *Organometallics* **1987**, *6*, 181.

[33] a) H. Ishida, H. Tanaka, K. Tanaka, T. Tanaka, *Chem. Lett.* **1987**, 597; b) H. Ishida, K. Fujiki, T. Ohba, K. Ohkubo, K. Tanaka, T. Terada, *J. Chem. Soc. Dalton Trans.* **1990**, 2155; c) M.-N. Collomb-Dunand-Sauthier, A. Deronzier, R. Ziessel, *Inorg. Chem.* **1994**, *33*, 2961.

[34] a) J. Hawecker, J.-M. Lehn, R. Ziessel, *J. Chem. Soc. Chem. Commun.* **1984**, 328; b) B. P. Sullivan, C. M. Bolinger, D. Conrad, W. J. Vining, T. J. Meyer, *ibid.* **1985**, 1414; c) G. Calzaferri, K. Hädener, J. Li, *J. Photochem. Photobiol. A* **1992**, *64*, 259; d) P. Christensen, A. Hamnett, A. V. G. Muir, J. A. Timney, *J. Chem. Soc. Dalton Trans.* **1992**, 1455.

[35] a) C. R. Cabrera, H. D. Abruña, *J. Electroanal. Chem. Intrafacial Electrochem.* **1986**, *209*, 101; b) S. Cosnier, A. Deronzier, J.-C. Moutet, *J. Mol. Catal.* **1988**, *45*, 381; c) T. R. O'Toole, B. P. Sullivan, M. R. M. Bruce, L. D. Margerum, R. W. Murray, T. J. Meyer, *J. Electroanal. Chem. Intrafacial Electrochem.* **1989**, *259*, 217.

[36] a) N. D. Silavwe, A. S. Goldman, R. Ritter, D. R. Tyler, *Inorg. Chem.* **1989**, *28*, 1231; b) D. A. Morgenstern, R. E. Wittrig, P. E. Fanwick, C. P. Kubiak, *J. Am. Chem. Soc.* **1993**, *115*, 6470.

[37] N. S. Lewis, G. Shreve in ref. [2e], p. 263.

[38] a) M. Halmann, *Nature* **1978**, *275*, 115; b) A. Henglein, M. Gutierrez, H. Fischer, *Ber. Bunsen-Ges. Phys. Chem.* **1984**, *88*, 170; recent examples: c) H. Inoue, T. Torimoto, T. Sakata, H. Mori, H. Yoneyama, *Chem. Lett.* **1990**, 1483; d) H. Noda, A. Yamamoto, S. Ikeda, M. Maeda, K. Ito, *ibid.* **1990**, 1757; e) H. Kisch, G. Twardzik, *Chem. Ber.* **1991**, *124*, 1161; f) J. F. Liu, C. Y. Baozhu, *J. Electroanal. Chem. Intrafacial Electrochem.* **1992**, *324*, 191; g) M. Kanemoto, T. Shiragami, C. Pac, S. Yanagida, *J. Phys. Chem.* **1992**, *96*, 3521; h) M. Kanemoto, M. Nomura, Y. Wada, T. Akano, S. Yanagida, *Chem. Lett.* **1993**, 1687; i) S. Ikeda, A. Yamamoto, H. Noda, M. Maeda, K. Ito, *Bull. Chem. Soc. Jpn.* **1993**, *66*, 2473; k) M. Halmann, B. Aurian-Blajeni, *J. Electroanal. Chem. Intrafacial Electrochem.* **1994**, *375*, 379; l) C. Furuya (Tanaka Ind.), JP 6158374, **1994** [*Chem. Abstr.* **1994**, *121*, 182382y].

[39] a) B. A. Parkinson, P. F. Weaver, *Nature* **1984**, *309*, 148; b) S. M. Aliwi, I. Al-Daghstani, *J. Sol. Energy Res.* **1989**, *7*, 49; c) S. Chao, C. J. Stadler, D. P. Summers, M. S. Wrighton, *J. Am. Chem. Soc.* **1984**, *106*, 2732; d) M. Wrighton, *J. Vac. Sci. Tech. A* **1984**, *2*, 795; e) Z. Goren, I. Willner, *J. Phys. Chem.* **1990**, *94*, 3784; f) P. Albers, J. Kiwi, *New J. Chem.* **1990**, *14*, 135; g) K. Hirano, K. Inoue, T. Yatsu, *J. Photochem. Photobiol. A* **1992**, *64*, 255; h) M. Takayuki, H. Tsutumi, K. Ohta, A. Saji, H. Noda, *Chem. Lett.* **1994**, 1533; i) V. Heleg, I. Willner, *J. Chem. Soc. Chem. Commun.* **1994**, 2113.

[40] M. T. Khan, N. N. M. Rao, D. Chatterjee, *J. Photochem. Photobiol. A* **1991**, *60*, 311.

[41] S. Matsuoka, T. Kohzuki, C. Pac, A. Ishida, S. Takamuku, M. Kusaba, N. Nakashima, S. Yanagida, *J. Phys. Chem.* **1992**, *96*, 4437.

[42] a) D. Mandler, I. Willner, *J. Am. Chem. Soc.* **1987**, *109*, 7884; b) I. Willner, D. Mandler, *ibid.* **1989**, *111*, 1330.

[43] a) S. Matsuoka, K. Yamamoto, C. Pac, S. Yanagida, *Chem. Lett.* **1991**, 2099; b) S. Matsuoka, K. Yamamoto, T. Ogata, M. Kusaba, N. Nakashima, E. Fujita, S. Yanagida, *J. Am. Chem. Soc.* **1993**, *115*, 601; c) T. Ogata, Y. Yamamoto, Y. Wada, K. Murakoshi, M. Kusaba, N. Nakashima, A. Ishida, S. Takamuku, S. Yanagida, *J. Phys. Chem.* **1995**, *9*, 11916; d) T. Ogata, S. Yanagida, B. S. Brunschwig, E. Fujita, *J. Am. Chem. Soc.* **1995**, *117*, 6708.

[44] M.-N. Collomb-Dunand-Sauthier, A. Deronzier, R. Ziessel, *J. Organomet. Chem.* **1993**, *444*, 191.

[45] N. Kitamura, S. Tazuke, *Chem. Lett.* **1983**, 1109.

[46] a) J. Hawecker, J.-M. Lehn, R. Ziessel, *J. Chem. Soc. Chem. Commun.* **1985**, 56; b) R. Ziessel in ref. [2g], p. 79; c) J.-M. Lehn, R. Ziessel, *J. Organomet. Chem.* **1990**, *382*, 157.

[47] a) H. Ishida, K. Tanaka, T. Tanaka, *Chem. Lett.* **1987**, 1035; b) *ibid.* **1988**, 339; c) H. Ishida, T. Terada, K. Tanaka, T. Tanaka, *Inorg. Chem.* **1990**, *29*, 905.

[48] C. A. Craig, L. O. Spreer, J. W. Otvos, M. Calvin, *J. Phys. Chem.* **1990**, *94*, 7957.

[49] a) S. M. Aliwi, *J. Photochem. Photobiol. A* **1992**, *67*, 67; *ibid.* **1992**, *67*, 329.

[50] J. R. Pugh, M. R. M. Bruce, B. P. Sullivan, T. J. Meyer, *Inorg. Chem.* **1991**, *30*, 86.

[51] H. Tanaka, H. Nagao, S.-M. Peng, K. Tanaka, *Organometallics* **1992**, *11*, 1450.

[52] B. Jezowska-Trzebiatowska, P. Sobota, *J. Organomet. Chem.* **1974**, *80*, C27.

[53] a) Y. Inoue, H. Izumida, Y. Sasaki, H. Hashimoto, *Chem. Lett.* **1976**, 863; b) M. Sakamoto, I. Shimizu, A. Yamamoto, *Organometallics* **1994**, *13*, 407.

[54] a) Y. Hashimoto, Y. Inoue (Mitsubishi Co.), JP 138 614, **1976** [*Chem. Abstr.* **1977**, *87*, 67853v]; b) T. Yamaji (Teijin Ltd.), JP 166 146, **1981** [*Chem. Abstr.* **1982**, *96*, 122211x]; c) T. Yamaji (Teijin Ltd.), JP 140 948, **1981** [*Chem. Abstr.* **1982**, *96*, 68352d]; d) D. J. Drury, J. E. Hamlin (BP Ltd.), EP 95321, **1983** [*Chem. Abstr.* **1984**, *100*, 174262k]; e) A. G. Kent (BP Ltd.), EP 151510, **1985** [*Chem. Abstr.* **1986**, *104*, 109029h]; f) C. P. Lau, Y. Z. Chen, *J. Mol. Catal. A Chem.* **1995**, *101*, 33.

[55] J.-C. Tsai, K. M. Nicholas, *J. Am. Chem. Soc.* **1992**, *114*, 5117.

[56] a) E. Graf, W. Leitner, *J. Chem. Soc. Chem. Commun.* **1992**, 623; b) W. Leitner, *GIT Fachz. Lab.* **1992**, *36*, 912.

[57] W. Leitner, E. Dinjus, F. Gassner, *J. Organomet. Chem.* **1994**, *475*, 257.

[58] a) R. Fornika, Dissertation, Universität Jena, **1994**; b) R. Fornika, H. Görls, B. Seemann, W. Leitner, *J. Chem. Soc. Chem. Commun.* **1995**, 1479.

[59] a) K. Wagner, *Angew. Chem.* **1970**, *82*, 73; *Angew. Chem. Int. Ed. Engl.* **1970**, *9*, 50; b) K. Narita, M. Sekiya, *Chem. Pharm. Bull.* **1977**, *25*, 135.

[60] a) W. Leitner, *Proc. II. Int. Conf. Carbon Dioxide Utilization*, Bari **1993**, p. 111; b) E. Graf, W. Leitner, *Chem. Ber.* in press.

[61] a) M. M. Rahman, H. Y. Liu, A. Prock, W. P. Giering, *Organometallics* **1987**, *6*, 650; b) R. C. Bush, R. J. Angelici, *Inorg. Chem.* **1988**, *27*, 681; c) J. R. Sowa, R. J. Angelici, *ibid.* **1991**, *30*, 3534.

[62] a) C. A. Tolman, *Chem. Rev.* **1977**, *77*, 312; b) T. L. Brown, *Inorg. Chem.* **1992**, *31*, 1286.

[63] T. Burgemeister, F. Kastner, W. Leitner, *Angew. Chem.* **1993**, *105*, 781; *Angew. Chem. Int. Ed. Engl.* **1993**, *32*, 739.

[64] a) R. Fornika, E. Dinjus, H. Görls, W. Leitner, *J. Organomet. Chem.* in press; b) F. Gassner, E. Dinjus, H. Görls, W. Leitner, unpublished results.

[65] a) M. D. Fryzuk, *Can. J. Chem.* **1983**, *61*, 1347; b) M. D. Fryzuk, T. Jones, F. W. B. Einstein, *Organometallics* **1984**, *3*, 185; c) M. D. Fryzuk, W. E. Piers, S. J. Rettig, F. W. B. Einstein, T. Jones, T. A. Albright, *J. Am. Chem. Soc.* **1989**, *111*, 5709; d) M. D. Fryzuk, W. E. Piers, F. W. B. Einstein, T. Jones, *Can. J. Chem.* **1989**, *67*, 883.

[66] a) A. A. Oswald, D. E. Hendriksen, R. V. Kastrup, K. Irikura, E. J. Mozeleski, D. A. Young, *Phosphorus Sulfur* **1987**, *20*, 237; b) A. A. Oswald, D. E. Hendriksen, R. V. Kastrup, E. J. Mozeleski in *Homogeneous Transition Metal Catalyzed Reactions* (*Adv. Chem. Ser.* **1992**, *230*, 395).

[67] K. Kudo, N. Sugita, Y. Takezaki, *Nippon Kagaku Kaishi* **1977**, 302.

[68] C. J. Stadler, S. Chao, D. P. Summers, M. S. Wrighton, *J. Am. Chem. Soc.* **1983**, *105*, 6318.

[69] a) M. M. Taqui Khan, S. B. Halligudi, S. Shukla, *J. Mol. Catal.* **1989**, *53*, 305; b) *ibid.* **1989**, *57*, 47.

[70] a) R. Gärtner, B. Cornils, H. Springer, P. Lappe (Ruhrchemie AG), DE 3235030, **1982** [*Chem. Abstr.* **1984**, *101*, 55331t]; b) L. Bexten, B. Cornils, D. Kupies (Ruhrchemie AG), DE 3431643, **1984** [*Chem. Abstr.* **1986**, *105*, 117009n]; c) W. A. Herrmann, C. W. Kohlpaintner, *Angew. Chem.* **1993**, *105*, 1588; *Angew. Chem. Int. Ed. Engl.* **1993**, *32*, 1524.

[71] a) F. Gassner, W. Leitner, *J. Chem. Soc. Chem. Commun.* **1993**, 1465; b) F. Gassner, Dissertation, Universität Jena, **1994**.

[72] a) G. Kaupp, *Angew. Chem.* **1994**, *106*, 1519; *Angew. Chem. Int. Ed. Engl.* **1994**, *33*, 1452; b) M. Poliakoff, S. G. Kazarian, S. Howdle, *ibid.* **1995**, *107*, 1409 and **1995**, *34*, 1275; c) M. T. Reetz, W. Könen, T. Strack, *Chimia* **1993**, *47*, 493.

[73] a) P. G. Jessop, T. Ikariya, R. Noyori, *Nature* **1994**, *368*, 231; b) T. Ikaraiya, P. G. Jessop, R. Noyori EP 652202, **1994**.

[74] a) S. Krogsrud, S. Komiya, T. Ito, J. A. Ibers, A. Yamamoto, *Inorg. Chem.* **1976**, *15*, 2798; b) T. Yoshida, D. L. Thorn, T. Okano, J. A. Ibers, S. Otsuka, *J. Am. Chem. Soc.* **1979**, *101*, 4212; c) L. Dahlenburg, C. Prengel, *J. Organomet. Chem.* **1986**, *308*, 63; d) L. Dahlenburg, C. Prengel, N. Höck, *Z. Naturforsch. B* **1986**, *41*, 718.

[75] a) P. G. Jessop, Y. Hsiao, T. Ikariya, R. Noyori, *J. Am. Chem. Soc.* **1994**, *116*, 8851; b) *J. Chem. Soc. Chem. Commun.* **1995**, 707.

[76] a) J. J. Anderson, J. E. Hamlin (BP Ltd.), EP 126524, **1984** [*Chem. Abstr.* **1985**, *102*, 95259c]; b) J. J. Anderson, D. J. Drury, J. E. Hamlin, A. G. Kent (BP Ltd.), WO 2066, **1986** [*Chem. Abstr.* **1986**, *105*, 210757q]; c) M. J. Green, A. R. Lucy, M. Kitson, S. J. Smith (BP Ltd.), EP 329337, **1989** [*Chem. Abstr.* **1990**, *112*, 58742r]; d) R. G. Beevor, D. J. Gulliver, M. Kitson, R. M. Sorrell (BP Ltd.), EP 357243, **1989** [*Chem. Abstr.* **1990**, *113*, 114638w]; e) D. C. Engel, W. P. van Swaji, G. F. Versteeg (University Twente), EP 597151, **1994** [*Chem. Abstr.* **1995**, *122*, 58814x].

[77] a) D. J. Darensbourg, C. Ovalles, M. Pala, *J. Am. Chem. Soc.* **1983**, *105*, 5937; b) *ibid.* **1984**, *106*, 3750; c) *ibid.* **1987**, *109*, 330.

[78] P. Haynes, L. H. Slaugh, J. F. Kohnle, *Tetrahedron Lett.* **1970**, 365.

[79] a) K. Kudo, H. Phala, N. Sugita, Y. Takezaki, *Chem. Lett.* **1977**, 1495; b) H. Phala, K. Kudo, N. Sugita, *Bull. Inst. Chem. Res. Kyoto Univ.* **1981**, *59*, 88.

[80] Y. Kiso, K. Saeki (Mitsui Ltd.), JP 36617, **1977** [*Chem. Abstr.* **1977**, *87*, 84562s].

[81] a) S. Schreiner, J. Y. Yu, L. Vaska, *J. Chem. Soc. Chem. Commun.* 1988, 602; b) *Inorg. Chim. Acta* **1988**, *147*, 139; c) L. Vaska, S. Schreiner, R. A. Felty, J. Y. Yu, *J. Mol. Catal.* **1989**, *52*, L11.

[82] a) J. A. Mitchell, E. E. Reid, *J. Am. Chem. Soc.* **1931**, *53*, 1879; b) W. Schroth, J. Andersch, H.-D. Schädler, R. Spitzner, *Chem. Ztg.* **1989**, *113*, 9.

[83] a) I. S. Kolomnikov, T. S. Lobeeva, M. E. Vol'pin, *Izv. Akad. Nauk. Ser. Khim.* **1970**, 2650; b) T. S. Lobeeva, M. E. Vol'pin, *ibid.* **1972**, 2329.

[84] Y. Inoue, Y. Sasaki, H. Hashimoto, *J. Chem. Soc. Chem. Commun.* **1975**, 718.

[85] G. O. Evans, C. J. Newell, *Inorg. Chim. Acta* **1978**, *31*, L387.

[86] a) J. D. Miller in *Reactions of Coordinated Ligands, Vol. 2* (Ed.: P. S. Braterman), Plenum, New York, **1989**, p. 1; b) D. J. Darensbourg in Lit. [2d], p. 43; recent examples: c) ref. [50]; d) K. K. Pandey, K. H. Garg, S. K. Tiwari, *Polyhedron* **1992**, 947; e) J. C. Berthet, M. Ephritikhine, *New J. Chem.* **1992**, *16*, 767; f) D. Nietlispach, H. W. Bosch, H. Berke, *Chem. Ber.* **1994**, *127*, 2403.

[87] a) P.-F. Fu, A. K. Fazlur-Rahman, K. M. Nicholas, *Organometallics* **1994**, *13*, 413; b) C. S. Yi, N. Lin, *ibid.* **1995**, *14*, 2616.

[88] a) B. P. Sullivan, T. J. Meyer, *Organometallics* **1986**, *5*, 1500; b) D. J. Darensbourg, M. Y. Darensbourg, L. Y. Goh, M. Ludvig, P. Wiegreffe, *J. Am. Chem. Soc.* **1987**, *109*, 7539; c) D. J. Darensbourg, H. P. Wiegreffe, P. W. Wiegreffe, *ibid.* **1990**, *112*, 9252.

[89] a) A. Dedieu, C. Bo, F. Ingold in ref. [2d], p. 23; b) N. Koga, K. Morokuma, *Chem. Rev.* **1991**, *91*, 283.

[90] a) S. Sakaki, K. Ohkubo, *Inorg. Chem.* **1988**, *27*, 2020; b) C. Bo, A. Dedieu, *ibid.* **1989**, *28*, 304; c) E. Kaufmann, S. Sieber, P. von R. Schleyer, *J. Am. Chem. Soc.* **1989**, *111*, 4005; d) S. Sakaki, K. Ohkubo, *Organometallics* **1989**, *8*, 2973; e) *Inorg. Chem.* **1989**, *28*, 2583; f) S. Sakaki, Y. Musahi, *J. Chem. Soc. Dalton Trans.* **1994**, 3047.

[91] The reported formato complex in ref. [25a] is probably a hydrogencarbonate or carbonate compound [63].

[92] a) R. R. Schrock, J. A. Osborn, *J. Am. Chem. Soc.* **1976**, *98*, 2134; b) P. A. Chaloner, M. A. esteruelas, F. Joó, L. A. Oro, *Homogeneous Hydrogenation*, Kluwer, Dordrecht, **1994**, Chap. 2.

[93] a) L. S. Pu, A. Yamamoto, S. Ikeda, *J. Am. Chem. Soc.* **1968**, *90*, 3896; b) A. Misono, Y. Uchida, M. Hidai, T. Kuse, *J. Chem. Soc. Chem. Commun.* **1968**, 981.

[94] a) V. W. Day, M. F. Fredrich, G. S. Reddy, A. J. Sivak, W. R. Pretzer, E. L. Muetterties, *J. Am. Chem. Soc.* **1977**, *99*, 8091; b) A. J. Sivak, E. L. Muetterties, *ibid.* **1979**, *101*, 4878.

[95] C. P. Kubiak, C. Woodcock, R. Eisenberg, *Inorg. Chem.* **1982**, *21*, 2119.

[96] a) M. Schäfer, J. Wolf, H. Werner, *J. Chem. Soc. Chem. Commun.* **1991**, 1341; b) H. Werner, M. Schäfer, O. Nürnberg, J. Wolf, *Chem. Ber.* **1994**, *127*, 27.

[97] F. Hutschka, A. Dedieu, W. Leitner, *Angew. Chem.* **1995**, *107*, 1905; *Angew. Chem. Int. Ed. Engl.* **1995**, *34*, 1742.

[98] P. G. Jessop, R. H. Morris, *Coord. Chem. Rev.* **1992**, *121*, 155.

[99] a) R. H. Crabtree, *Chem. Rev.* **1985**, *85*, 245; b) *Selective Hydrocarbon Activation* (Eds.: J. A. Davies, P. C. Watson, J. F. Liebman, A. Greenberg), VCH, Weinheim, **1990**; c) B. A. Arndtsen, R. G. Bergman, T. A. Nobley, T. H. Peterson, *Acc. Chem. Res.* **1995**, *28*, 154.

[100] A first little piece is found in R. Wesendrup, H. Schwarz, *Angew. Chem.* **1995**, *107*, 2176; *Angew. Chem. Int. Ed. Engl.* **1995**, *34*, 2033.

Transition Metal Catalyzed Synthesis of Seven-Membered Carbocyclic Rings**

Gerald Dyker*

The Diels–Alder reaction is the most important method for the preparation of functionalized cyclohexenes and is characterized by an almost inexhaustible range of possible variations: numerous functional groups and even heteroatoms can be tolerated and both diastereoselective and enantioselective syntheses are possible. Thus, there has been no shortage of attempts to develop homologous variants and to extend the range of application to the synthesis of seven-membered carbocyclic rings. In specific cases it has been possible to employ vinylcyclopropanes as "homodienes" and to carry out a cycloaddition with appropriate alkenes.[1] However, the mild reaction conditions of the example shown in Scheme 1 are an exception. This special case apparently profits from the fixed, favorable geometry of the heterocyclic-bridged vinylcyclopropane **1**, from the high reactivity of the dienophile **2**, and from the initial association of the reactants in the form of a charge–transfer complex.

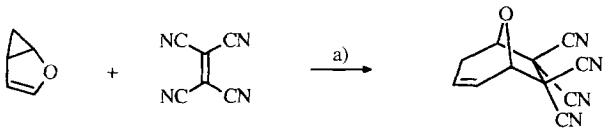

1 **2** **3**

Scheme 1. a) CH_2Cl_2, 20 °C, quantitative yield.

For a few combinations of less reactive dienes and dienophiles, transition metal catalyzed variants have been developed. An example is the cycloaddition of an apolar diene and an unactivated alkyne; however, except when the reaction is catalyzed with iron, nickel, cobalt, or rhodium(I) complexes, the temperature required often causes competing decomposition, even for the intramolecular version.[2] Wilkinson's catalyst[3]—tris(triphenylphosphane)rhodium(I) chloride—frequently used for hydrogenations and for decarbonylations, permits the cyclization of **4** to the annelated cyclohexadiene **5** in excellent yield in only 15 minutes at 55 °C in trifluoroethanol as solvent (Scheme 2).[2e]

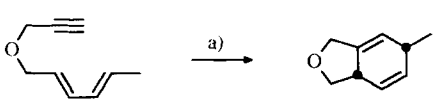

4 **5**

Scheme 2. a) 10 mol % $[(PPh_3)_3RhCl]$, trifluoroethanol, 55 °C, 15 min, yield 96%.

[*] Prof. Dr. G. Dyker
FB6 - Organische Chemie der Universität-Gesamthochschule
Lotharstrasse 1, D-47048 Duisburg (Germany)

Recently, Wender, Takahashi, and Witulski[4] found that this rhodium complex also catalyzes the homologous Diels–Alder reaction[5] of vinylcyclopropanes with alkynes, leading to formation of cyclohepta-1,4-trienes. By this method, hitherto used exclusively as an intramolecular process, annelated and functionalized seven-membered carbocycles such as **7** have been synthesized simply and efficiently (Scheme 3).

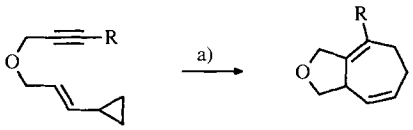

6 **7**

Scheme 3. R = H, Me, Ph, trimethylsilyl (TMS), CO_2Me; a) 10 mol% $[(PPh_3)_3RhCl]$, toluene, 110 °C, 1.5 h, yield 50–88%.

Acceleration of the reaction has been achieved by the use of the polar solvent trifluoroethanol and also by the addition of silver triflate; thus, it can be assumed that cationic rhodium complexes act as the active catalyst. Eight-membered metallacycles such as **9** are probably key intermediates.[6] Cyclopropyl-substituted five-membered metallacycles **8** and homoallyl complexes **10** can be considered as precursors of **9**[7] (Scheme 4).

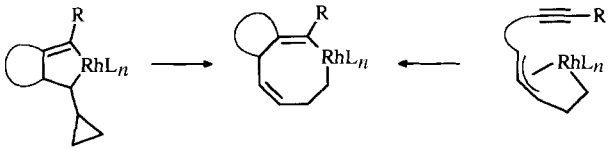

8 **9** **10**

Scheme 4. Metallacycles as possible reactive intermediates of the reaction in Scheme 3. L = ligand.

Rhodium catalysis is also of crucial importance in the conceptually new type of synthesis of cyclohepta-2,4-dien-1-ones (e.g. **12**) by Huffman and Liebeskind.[8] The rearrangement of 4-cyclopropyl-2-cyclobutenones such as **11**, which are accessible in a few steps from squaric acid,[9] is similarly achieved with Wilkinson's catalyst (Scheme 5). This concept is particularly

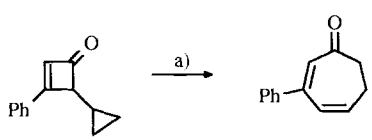

11 **12**

Scheme 5. a) 10 mol% $[(PPh_3)_3RhCl]$, toluene, 60 °C, yield 84%.

flexible in that the corresponding reaction of 4-cyclobutyl-2-cyclobutenones opens a route to eight-membered carbocyclic rings.

The new rhodium-catalyzed processes appear as competition to known and thoroughly tested methods for the synthesis of seven-membered carbocyclic rings, such as [4 + 3] cycloadditions catalyzed or induced by transition metals (Scheme 6).

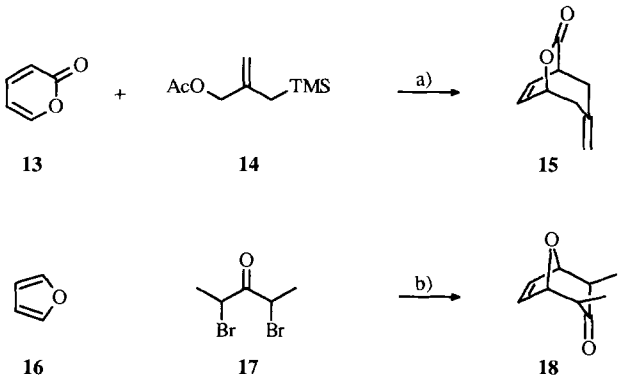

13 **14** **15**

16 **17** **18**

Scheme 6. a) 5 mol% $Pd(OAc)_2$, $P(OiPr)_3$, benzene, 80 °C, yield 70%; TMS: b) NaI, Cu, CH_3CN, 4 h, 50 °C, yield 40–48%.

According to Trost et al.,[10] trimethylenemethane palladium complexes, which undergo cycloaddition with suitable dienes, can be prepared from the allylsilane **14** under catalytic conditions. Thus, the bridged cycloheptene **15**, containing an exocyclic methylene group, can be obtained from α-pyrone **13**. Cycloheptanones such as **18** can be prepared according to Hoffmann[11a–c] with α,α′-dibromoketones as coupling component.[11d,e] The preparative potential of such compounds for the diastereoselective synthesis of highly functionalized cycloheptanes and also of open-chain compounds has been demonstrated impressively quite recently.[12] It will be interesting to see whether the new rhodium-catalyzed processes also offer opportunities for enantioselective induction.[13]

German version: *Angew. Chem.* **1995**, *107*, 2407–2408

Keywords: catalysis · cycloadditions · Diels–Alder reactions · rhodium compounds · carbocycles

[1] R. Herges, I. Ugi, *Angew. Chem.* **1985**, *97*, 596–597; *Angew. Chem. Int. Ed. Engl.* **1985**, *24*, 594–596, and references therein.

[2] a) P. A. Wender, T. E. Jenkins, S. Suzuki, *J. Am. Chem. Soc.* **1995**, *117*, 1843–1844; b) L. McKinstry, T. Livinghouse, *Tetrahedron* **1994**, *50*, 6145–6154; c) R. S. Jolly, G. Luedtke, D. Sheehan, T. Livinghouse, *J. Am. Chem. Soc.* **1990**, *112*, 4965–4966; d) P. A. Wender, T. Jenkins, *ibid.* **1989**, *111*, 6432–6434; e) I. Matsuda, M. Shibata, S. Sato, Y. Izumi, *Tetrahedron Lett.* **1987**, *28*, 3361–3362; f) K. Mach, H. Antropiusova, L. Petrusova, F. Turecek, V. Hanus, P. Sedmera, J. Schraml, *J. Organomet. Chem.* **1985**, *289*, 331–339; g) H. tom Dieck, R. Diercks, *Angew. Chem.* **1983**, *95*, 801–802; *Angew. Chem. Int. Ed. Engl.* **1983**, *22*, 778–779; h) J. P. Genet, J. Ficini, *Tetrahedron Lett.* **1979**, 1499–1502; i) A. Carbonaro, A. Greco, G. Dall'Asra, *J. Org. Chem.* **1968**, *33*, 3948–3950.

[3] L. S. Hegedus, *Organische Synthese with Übergangsmetallen*, VCH, Weinheim, **1995**.

[4] P. A. Wender, H. Takahashi, B. Witulski, *J. Am. Chem. Soc.* **1995**, *117*, 4720–4721.

[5] The cycloaddition of norbornadiene with alkynes to give deltacyclenes has also been described as a homo-Diels–Alder reaction: M. Lautens, J. C. Lautens, A. C. Smith, *J. Am. Chem. Soc.* **1990**, *112*, 5627–5628.

[6] For an eight-membered metallacycle as reactive intermediate in the formation of a cycloheptadiene, see J. W. Herndon, G. Chatterjee, P. P. Patel, J. J. Matasi, S. U. Turner, J. J. Harp, M. D. Reid, *J. Am. Chem. Soc.* **1991**, *113*, 7508–7509.

[7] Topical examples of ring opening of cyclopropyl-substituted transition metal complexes with formation of homoallyl metal compounds: a) R. I. Khusnutdinov, U. M. Dzhemilev, *J. Organomet. Chem.* **1994**, *471*, 1–18; b) I. Ryu, K. Ikura, Y. Tamura, J. Maenaka, A. Ogawa, N. Sonoda, Synlett 1994, 941–942; c) S. Bräse, A. de Meijere, *Angew. Chem.* **1995**, *107*, in press; *Angew. Chem. Int. Ed. Engl.* **1995**, *34*, in press.

[8] M. A. Huffman, L. S. Liebeskind, *J. Am. Chem. Soc.* **1993**, *115*, 4895–4896.

[9] L. S. Liebeskind, R. W. Fengl, K. R. Wirtz, T. T. Shawe, *J. Org. Chem.* **1988**, *53*, 2482–2488.

[10] a) B. M. Trost, S. Schneider, *Angew. Chem.* **1989**, *101*, 215–217; *Angew. Chem. Int. Ed. Engl.* **1989**, *28*, 213–215; b) B. M. Trost, D. T. MacPherson, *J. Am. Chem. Soc.* **1987**, *109*, 3483–3484.

[11] a) H. M. R. Hoffmann, *Angew. Chem.* **1984**, *96*, 29–48; *Angew. Chem. Int. Ed. Engl.* **1984**, *23*, 1–32; b) *ibid.* **1973**, *96*, 877–894 and **1973**, *12*, 819–835; c) M. R. Ashcroft, H. M. R. Hoffmann, *Org. Synth.* **1978**, *58*, 17–23; d) R. Noyori, *Acc. Chem. Res.* **1979**, *12*, 61–66; e) J. Mann, *Tetrahedron* **1986**, *42*, 4611–4659.

[12] a) M. Lautens, S. Kumanovic, *J. Am. Chem. Soc.* **1995**, *117*, 1954–1964; b) M. Lautens, *Pure Appl. Chem.* **1992**, *64*, 1873–1882.

[13] For other recent contributions to the synthesis of seven-membered carbocyclic rings see: a) H. M. L. Davies, *Tetrahedron* **1993**, *49*, 5203–5223; b) A. Padwa, S. F. Hornbuckle, G. E. Fryxell, Z. J. Zhang, *J. Org. Chem.* **1992**, *57*, 5747–5757; c) P. A. Wender, H. Y. Lee, R. S. Wilhelm, P. D. Williams, *J. Am. Chem. Soc.* **1989**, *111*, 8954–8957; d) K. E. Schwiebert, J. M. Stryker, *ibid.* **1995**, *117*, 8275–8276.

 © VCH Verlagsgesellschaft mbH, D-69451 Weinheim, 1995 0570-0833/95/3420-2224 $ 10.00+.25/0

Control of the Reactivity of Double Bonds through Their Fixed Geometrical Arrangement

J. Jens Wolff*

Chemists of all disciplines have always strived to maximize selectivities in their chemical reactions. From early on, they speculated that the mutual geometrical arrangement of the reactants might have a decisive influence on the rate and the outcome of a particular reaction. From this point of view, it is obvious to try to constrain the reactants to a well-defined geometrical arrangement before the actual reaction which—ideally—will then proceed only through a single reaction channel, predictable from the arrangement chosen. In a close to ideal way, such an arrangement exists in a molecular crystal. While the idea to peruse the high molecular order of crystals for directed chemical reactions in the solid phase seems logical enough, systematic investigations on reactions in the crystalline phase began quite late in the history of chemistry, namely only after the methods of X-ray structure analysis had been perfected to a degree that allowed the elucidation of the structures of even complex molecular crystals within a short time.

G. M. J. Schmidt and coworkers[1a] developed the concept of topochemical reaction control, using as an example the stereocontrolled [2+2]photodimerization of several cinnamic acid derivatives in the crystal.[1b] According to this principle, requirements for a successful reaction are minimum dislocations of the molecules with respect to the initial lattice, and—in the cases investigated—a maximum distance of about 4.2 Å for the reacting double bonds. Even though a fair number of research teams have focussed their research on this and related topics—the topotactical polymerization should be given extra credit[1c, 2]—only quite a small number of reactions can be realized in the crystalline phase proper. This limitation is aggravated by a still unresolved problem of solid-state organic chemistry:[3] how to predict the structures of molecular crystals from the molecular structure, or even more demanding, how to modify it at will—the term "crystal engineering", stressed far too often, should not gloss over this unfortunate situation. Thin films (like Langmuir–Blodgett films) or clathrates which are easier to control with respect to their stoichiometries and structures may be solutions to this problem.[4]

Therefore, by far the most attempts aimed at "geometrical reaction control" were directed towards reactions in solution. A well-known example for the use of this concept is given by the reduction in molecularity achieved through assembly of the reactants within the same molecule. Very recently, Hopf et al.[5] tried to combine this approach with the topochemical, or topotactical concept of solid-state chemistry in order to take advantage from both. To this end, two cinnamic acid esters and their vinylogous derivatives were grafted on a paracyclophane to give **1**. The rigid backbone of the cyclophane controls to a high degree the mutual arrangement of the double bonds in the form of a "microcrystal". Irradiation of a solution of **1** leads to dimerization in exceptionally high chemical and quantum yields to give compounds **2** with ladderlike structures.[6] The rigid σ-skeleton of the products may, for example, be used as a rigid spacer in studies of through-bond intramolecular electron transfer reactions.[7]

The choice of the system presented by Hopf et al. may not have been fortuitous: H. Meier's group[8] succeeded in the intermolecular dimerization of the divinylbenzene **3** to give **4**, and also obtained **5** in an analogous fashion; Japanese chemists[9] performed the intramolecular photoreaction of **6** to give **7**. In all these cases the arrangement of the reactant centers is probably

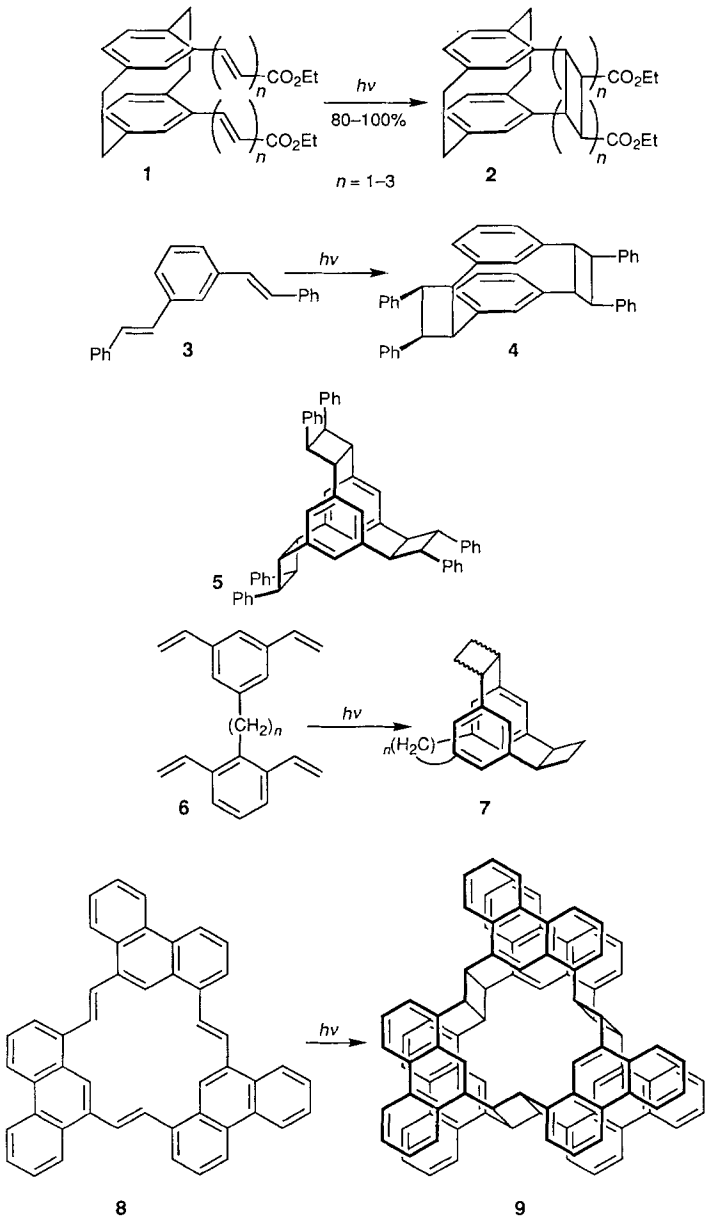

[*] Dr. habil. J. J. Wolff
Organisch-chemisches Institut der Universität
Im Neuenheimer Feld 270, D-69120 Heidelberg (Germany)
Telefax: Int. code +(6221) 564205

 © VCH Verlagsgesellschaft mbH, D-69451 Weinheim, 1995 0570-0833/95/3420-2225 $ 10.00+.25/0

determined by the formation of excimers. Very recently, along the same line, H. Meier and coworkers dimerized derivatives of an analogous [18]annulene **8** to give substituted beltlike hydrocarbons of type **9**, thus demonstrating the broad applicability of this method.[10]

The proximity and geometrical fixation of two double bonds on its own is, however, not always sufficient to effect the desired [2 + 2]cycloaddition. Criegee et al.[11] previously attempted in vain to synthesize octamethylcubane (**11**) starting from the *syn*-dimer **10** of tetramethylcyclobutadiene. According to recent reinvestigations, a small amount of cubane may be isolated nevertheless,[12a] but the reaction **12** → **13** proceeds much better. The additional handles not only shorten the distance between the double bonds from 3.05 Å in **10** to 2.65 Å, but also effect a favorable change in the sequence of the π-molecular orbitals.[12b]

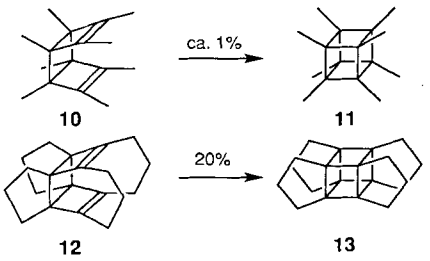

The placement of two double bonds in close spatial proximity also allows for unusual transannular reactions without the use of light. Of the great number of examples, the reactions of tetradehydrodianthracene (**14**)—for example, those affording **15**—are mentioned,[13] in which the distance between the two

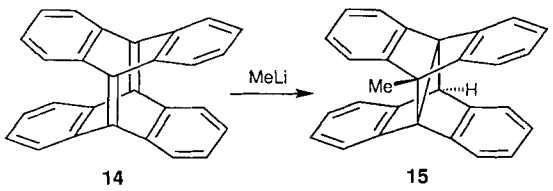

double bonds (2.4 Å) is shorter than the sum of the van der Waals radii. The stabilization of otherwise reactive structures with four-center–three-electron bonds is also possible through cage structures: the unstable cyclobutyl cation, whose structure corresponds to the geometry of the symmetry-forbidden [2+1]addition of ethylene to ethylene cation, can be stabilized in the closed and the open form within the constraints of pagodane and isopagodane radical cations.[14]

The geometrical constraint, put in effect by many different methods, is still the most effective method to improve the selectivity of chemical reactions, but also to stabilize unusual structures. Many achievements in the development of catalytic processes are also based on this concept. Future research will probably be directed towards the understanding of self-assembly mechanisms in molecular crystals, clathrates, and thin layers, in order to make use of the enormous synthetic potential of these ordered structures.

German version: *Angew. Chem.* **1995**, *107*, 2409–2410

Keywords: alkenes · cycloadditions · geometrical reaction control · topochemical principle

[1] a) G. M. J. Schmidt, *Pure Appl. Chem.* **1971**, *27*, 647; a short survey on photochemistry in the crystalline state is given therein (for further reading, see: H.-D. Roth, *Angew. Chem.* **1989**, *101*, 1220; *Angew. Chem. Int. Ed. Engl.* **1989**, *28*, 1193); b) V. Ramamurthy, K. Venkatesan, *Chem. Rev.* **1987**, *87*, 433; c) Reactions at surfaces of crystallites may not be called a topochemical reaction; however, a single crystal of the starting material need not be converted to a single crystal of the product. A single crystal–single crystal conversion is successful in some cases if light of longer wavelength is used for the irradiation: V. Enkelmann, G. Wegner, K. Novak, K. B. Wagener, *J. Am. Chem. Soc.* **1993**, *115*, 10390; further examples and extensive discussion in: K. Saigo, M. Hasegawa in *Reactivity in Molecular Crystals* (Ed.: Y. Ohashi), Kodanska/VCH, Tokyo/Weinheim, **1993**, p. 203–236; G. Kaupp, M. Haak, *Angew. Chem.* **1993**, *105*, 727; *Angew. Chem. Int. Ed. Engl.* **1993**, *32*, 694.

[2] G. Wegner, *Pure Appl. Chem.* **1977**, *49*, 443.

[3] A. Gavezzotti, *Acc. Chem. Res.* **1994**, *27*, 309, and references therein.

[4] Cf. *Photochemistry in Organized and Constrained Media* (Ed.: V. Ramamurthy), VCH, Weinheim, **1991**.

[5] H. Hopf, H. Greiving, P. G. Jones, P. Bubenitschek, *Angew. Chem.* **1995**, *107*, 742; *Angew. Chem. Int. Ed. Engl.* **1995**, *34*, 685.

[6] Unsubstituted ladderanes have been obtained recently by a different route: G. Mehta, M. B. Viswanath, A. C. Kunwar, *J. Org. Chem.* **1994**, *59*, 6131; *J. Chem. Soc. Chem. Commun.* **1994**, 739; see also H.-D. Martin, B. Mayer, M. Pütter, H. Höchstetter, *Angew. Chem.* **1981**, *93*, 695; *Angew. Chem. Int. Ed. Engl.* **1981**, *20*, 677.

[7] K. D. Jordan, M. N. Paddon-Row, *Chem. Rev.* **1992**, *92*, 395; S. F. Nelsen, J. Adamus, J. J. Wolff, *J. Am. Chem. Soc.* **1994**, *116*, 1589.

[8] H. Meier, *Angew. Chem.* **1992**, *104*, 1425; *Angew. Chem. Int. Ed. Engl.* **1992**, *31*, 1399.

[9] J. Nishimura, H. Doi, E. Ueda, A. Obayashi, A. Oku, *J. Am. Chem. Soc.* **1987**, *109*, 5293; Further examples see: J. Nishimura, *Cyclophanes from Vinylarenes* in *Carbocyclic Cage Compounds: Chemistry and Applications* (Eds.: E. Osawa, O. Yonemitsu), VCH, New York, **1992**, Chap. 6.2.

[10] H. Meier, K. Müller, *Angew. Chem.* **1995**, *107*, 1598; *Angew. Chem. Int. Ed. Engl.* **1995**, *34*, 1437.

[11] R. Criegee, *Angew. Chem.* **1962**, *74*, 703; *Angew. Chem. Int. Ed. Engl.* **1962**, *1*, 519.

[12] a) R. Gleiter, S. Brand, *Tetrahedron Lett.* **1994**, *35*, 4969; b) R. Gleiter, K.-H. Pfeifer, W. Koch, *J. Comput. Chem.* **1995**, *16*, 31.

[13] R. Herges, H. Neumann, F. Hampel, *Angew. Chem.* **1994**, *106*, 1024; *Angew. Chem. Int. Ed. Engl.* **1994**, *33*, 993; see also: D. Hellwinkel, H.-J. Hasselbach, F. Lämmerzahl, *Angew. Chem.* **1984**, *96*, 713; *Angew. Chem. Int. Ed. Engl.* **1984**, *23*, 705.

[14] H. Prinzbach, K. Weber, *Angew. Chem.* **1994**, *106*, 2329; *Angew. Chem. Int. Ed. Engl.* **1994**, *33*, 2239; H. Prinzbach, M. Wollenweber, R. Herges, H. Neumann, G. Gescheidt, R. Schmidlin, *J. Am. Chem. Soc.* **1995**, *117*, 1439.

 © VCH Verlagsgesellschaft mbH, D-69451 Weinheim, 1995 0570-0833/95/3420-2226 $ 10.00+.25/0

Selective Syntheses of 1,3-Diphosphacyclobutadiene, Dewar-1,3,5-triphosphabenzene, 1,3,5-Triphosphabenzene, and 1,3,5,7-Tetraphosphabarrelene by Cyclooligomerization of Phosphaalkynes**

Paul Binger,* Stefan Leininger, Jörg Stannek, Barbara Gabor, Richard Mynott, Joachim Bruckmann, and Carl Krüger

Dedicated to Professor Manfred Regitz on the occasion of his 60th birthday

The recently described synthesis of the 1,3,5,7-tetraphosphabarrelene complex **3** from *tert*-butylphosphaacetylene **1** and bis(cyclooctatetraene)zirconium $[Zr(cot)_2]$[1] led to the assumption that the 12-valence electron fragment [cotM], formed as an intermediate by elimination of one of the two cot ligands, is an ideal template for cyclooligomerizations of phosphaalkynes. Phosphaalkynes are known to cyclodimerize on the 14-valence electron fragments $[Cp_2M']$ (M = Zr, Hf) to give the 1,3-diphosphabicyclo[1.1.0]butanediyl metallocenes such as **2**.[2]

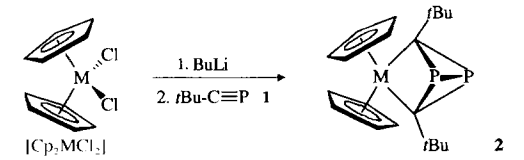

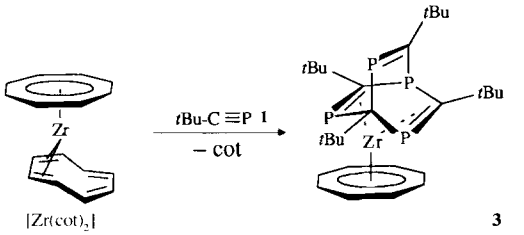

In the coordination sphere of electron-rich transition metals (M = Ni, Co, Rh, Fe), phosphaalkynes prefer to cyclodimerize to give 1,3-diphosphacyclobutadiene metal complexes.[3, 4] Only two examples are known for the cyclotrimerization of phosphaalkynes on transition metal complexes: a η^6-1,3,5-triphosphabenzenemolybdenum complex is formed with tricarbonyl(η^6-cycloheptatriene)molybdenum,[5] which, however, was unsatisfactorily characterized and whose synthesis we could not follow.[6] In contrast, the structure of the dewar-1,3,5-triphosphabenzenevanadium complex, prepared from naphthalene(pentamethylcyclopentadienyl)vanadium and **1**, has been confirmed by an X-ray crystal structure analysis.[7]

A better access to coordinatively unsaturated transition metal templates [cotM] is provided by the known η^4-butadiene complexes of zirconium (**4a**) and hafnium (**5a**)[8] as well as their η^8-bis(trimethylsilyl)cyclooctatetraene derivatives **4b** and **5b**. Indeed, complexes **5a** and **5b** did react with the phosphaalkyne **1**[9] at room temperature. In these reactions **1** was cyclotetramerized in a few hours to give almost quantitative yields of the tetraphosphabarrelene complexes **7a** and **7b**, respectively (Scheme 1). The zirconium complex **4a** analogous to **5a** does

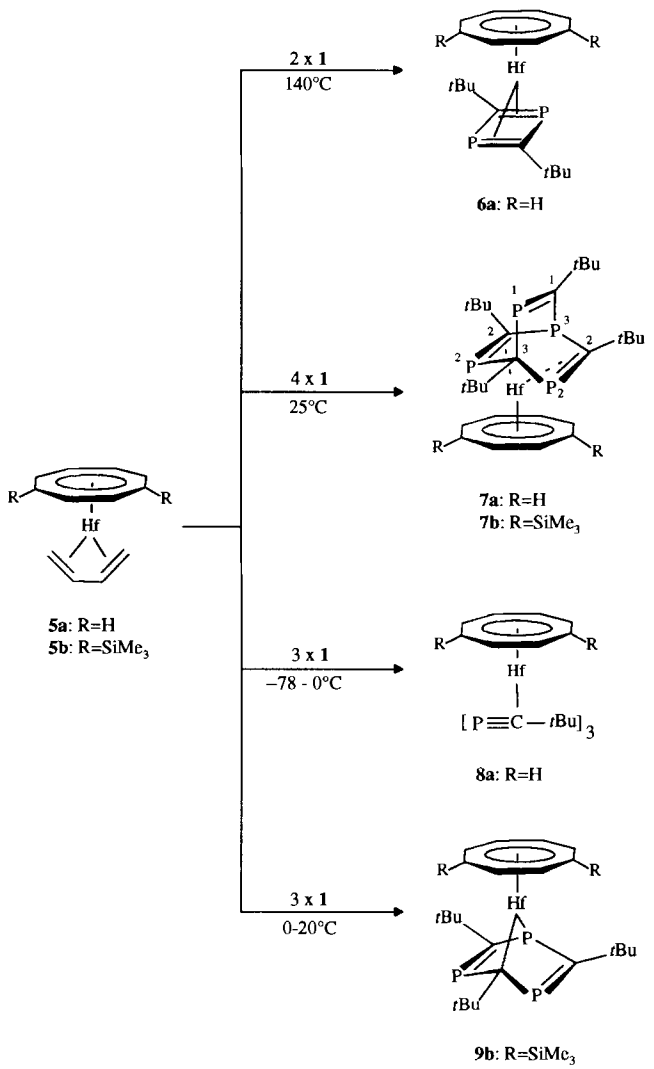

Scheme 1. Cyclooligomerization of **1** at the hafnium complexes **5a**, **b**.

[*] Prof. Dr. P. Binger, Dipl.-Chem. J. Stannek, B. Gabor, Dr. R. Mynott, Dipl.-Min. J. Bruckmann, Prof. Dr. C. Krüger
Max-Planck-Institut für Kohlenforschung
Kaiser-Wilhelm-Platz 1, D-45470 Mülheim an der Ruhr (Germany)
Telefax: Int. code + (208)306-2980
Dipl.-Chem. S. Leininger
Fachbereich Chemie der Universität Kaiserslautern (Germany)

[**] This work was supported by the Deutsche Forschungsgemeinschaft (Graduiertenkolleg "Phosphor als Bindeglied verschiedener chemischer Disziplinen").

not react with **1** under these conditions, in contrast, **4b** reacts with **1** to give the zirconium complex analogous to **7b**.

An investigation of the temperature dependence of this cyclotetramerization of **1** with the hafnium complexes **5a, b** revealed that **1** reacts already at low temperatures with **5a** or **5b** to give new hafnium complexes. From this finding the postulated stepwise course of the cyclotetramerization of **1**[1] can be partly experimentally understood. Thus, even at $-78\,^{\circ}C$, the hafnium complex **8a** is the sole product of the reaction of **5a** and **1**. It is formed as a green powder in 83% yield; in **8a**, three molecules of **1** are bound to the metal atom (*m/z* 584 (M^+)).

The ^1H NMR spectrum of **8a** recorded at $-30\,^{\circ}C$ shows two sharp singlets at $\delta = 1.35$ and 0.81 (ratio of intensities 2:1) for the three *tert*-butyl groups. These signals broaden significantly at 20 °C and collapse to one singlet at 60 °C at $\delta = 1.17$. In contrast, the position and multiplicity of the signal at $\delta = 6.60$ (s) for the H atoms of the cot ring are almost independent of the temperature. In the ^{31}P NMR spectrum of **8a** at $-30\,^{\circ}C$, there are only two signals at $\delta = 17.3$ and 357.1 ($J_{P,P} = 43.7$ Hz; ratio 2:1) for the three phosphorus atoms; these signals do not separate further down to temperatures of $-80\,^{\circ}C$; at 60 °C these signals are broadened. In the ^{13}C NMR spectrum at $-30\,^{\circ}C$, the weak signals of the P-bound C atoms could only be identified clearly under INEPT conditions[10] (a doublet of triplets at $\delta = 139.3$ and a triplet at $\delta = 93.8$ (half intensity)). The signals of the C atoms of the *tert*-butyl groups show a similar splitting pattern (Table 1). Together with the result of the ligand liberation with hexachloroethane, which affords the free 1,3,5-triphosphabenzene **13** (see below), the spectroscopic findings only allow the conclusion that a cyclic trimer of **1** is bound in the complex **8a**.

If the hafnium complex **5b** is allowed to react with **1** at 0 °C, the reaction likewise does not proceed further than the stage of a cyclotrimeric complex of **1**. The bonding between the metal atom and the phosphaalkyne trimer in the new hafnium complex **9b** evidently differs from that in complex **8a**, since two broad signals at $\delta = 263$ and 140 appear in the ^{31}P NMR spectrum of **9b** in the temperature range $-40\,^{\circ}C$ to 30 °C; the coupling constants, however, could not be determined. In the ^1H NMR spectrum of **9b**, the signals for the *tert*-butyl groups are resolved only at $-40\,^{\circ}C$; two singlets are observed at $\delta = 1.32$ and 1.34 in the ratio 2:1 (Table 1). A meaningful ^{13}C NMR spectrum of **9b** has not been obtained yet. According to the analytical results gathered to date, **9b** has the structure given in Scheme 1; the metal atom possibly interacts in a rapid exchange with one of the two P=C bonds. This proposed structure is supported by the liberation reaction with hexachloroethane, which affords the dewar-1,3,5-triphosphabenzene **14** (see below).

The course of the reaction between **5a** and **1** at higher temperatures is surprising. An approximate 1:1 mixture of the tetraphosphabarrelene complex **7a** and the 1,3-diphosphete complex **6a** is formed at about 80 °C, whereas at about 140 °C only **6a** is formed in 68% yield. The spectroscopic data of **6a** indicate that the π electrons are not completely delocalized in the η^4-bound 1,3-diphosphete ligand, as in the corresponding 1,3-diphosphete complexes of Co, Rh, or Fe.[4] In the ^{31}P and ^{13}C NMR spectra of **6a**, the signals of the phosphorus and carbon atoms of the four-membered ring are considerably shifted downfield in comparison to those in the spectra of the 1,3-diphosphacyclobutadienecobalt and -rhodium complexes (^{31}P: $\delta = 38-50 \rightarrow 201.7$; ^{13}C: $\delta = 108-113 \rightarrow 149.7$). Similar shifts were determined in the recently synthesized η^8-cyclooctatetraene(η^4-di-*tert*-butyl-1,3-diphosphete)titanium complex.[11] Our assumptions were confirmed by a crystal structure analysis of this compound: in the complex-bound 1,3-diphosphete, the P–C bond lengths alternate (1.748 and 1.828 Å).[11] A localization of the π electrons in the 1,3-diphosphete ligand of **6a** should result in a weaker interaction with the metal atom.

Table 1. Selected physical data of **6a**, **7a**, **8a**, **9b**, **13**, and **14** [a, b].

6a: ^1H NMR: $\delta = 1.20$ (s, 18H, *t*Bu), 6.89 (s, 8H, cot); ^{13}C NMR: $\delta = 149.7$ (t, J(C,P) = 55.4 Hz, ring-C), 37.7 (t, J(C,P) = 8.2, *t*Bu), 34.5 (q, t, J(C,H) = 125, J(C,P) = 5.0 Hz, *t*Bu), 91.6 (d, ^1J(C,H) = 171, cot); ^{31}P NMR: $\delta = 201.7$ (s); MS (70 eV): *m/z* [%]: 484 (M^+) [80], 469 ($M^+ - CH_3$) [100], 346 ($M^+ - C_2tBu_2$) [51], 284 ($M^+ - 2P{\equiv}CtBu$) [17]

7a [1]: ^1H NMR: $\delta = 1.13$ (s, 18H, *t*Bu), 1.35 (s, 9H, *t*Bu), 1.50 (s, 9H, *t*Bu), 6.39 (s, 8H, cot); ^{13}C NMR: $\delta = 216.6$ (J(C,P1) = 99.8, J(C,P2) = 6.9, J(C,P3) = 59.8 Hz, C1), 43.6 (J(C,P1) = 25.2, J(C,P3) = 22.7 Hz, *t*Bu at C1), 35.4 (^1J(C,H) = 126, J(C,P1) = 14.8, J(C,P3) = 8.7 Hz, *t*Bu at C1), 74.1 (J(C,P2A) + J(C,P2B) = 101.9, J(C,P3) = 46.1 Hz, C2), 37.3 (J(C,P2A) + J(C,P2B) = 20.9, J(C,P3) = 12.6 Hz, *t*Bu at C2), 35.7 (^1J(C,H) = 125, J(C,P2A) + J(C,P2B) = J(C,P3) = 10.0 Hz, *t*Bu at C2), 34.9 (J(C,P1) = 84.9, J(C,P2) = 71.4, J(C,P3) = 3.8 Hz, C3), 37.2 (J(C,P1) = 21.2, J(C,P2) = 12.0, J(C,P3) = 3.1 Hz, *t*Bu at C3), 31.2 (^1J(C,H) = 126, J(C,P1) = 12.0, J(C,P2) = 4.8 Hz, *t*Bu at C3); ^{31}P NMR: $\delta = 283.2$ (J(P1,P2) = 8.1, J(P1,P3) = 7.3 Hz, P1), −134.2 (J(P2,P3) = 23.4, J(P2,P1) = 8.1, J(P2,P3) = 23.4 Hz, P2), −140.7 (J(P3,P1) = 7.3, J(P3,P2) = 23.4 Hz, P3); MS (70 eV): *m/z* [%]: 684 (M^+) [15], 627 ($M^+ - tBu$) [14], 402 ($(P{\equiv}CtBu)_4^+ + H_2$) [70], 262 [46], 231 [86], 169 [87], 131 [58], 41 [100]

8a: ^1H NMR (−30 °C): $\delta = 0.81$ (s, 9H, *t*Bu), 1.35 (s, 18H, *t*Bu), 6.60 (s, 8H, cot); ^1H NMR (+60 °C): $\delta = 1.17$ (s, 27H, *t*Bu), 6.5 (s, 8H, cot); ^{13}C NMR (−30 °C): $\delta = 139.3$ (dt, J(C,P) = 74, J(C,P) + J(C,P′) = 69.4 Hz, ring-C), 93.8 (t, J(C,P) = 59.4 Hz, ring-C), 40.1 (J(C,P) = 18.9, J(C,P) + J(C,P′) = 22.0 Hz, *t*Bu), 35.1 (^1J(C,H) = 125 Hz, *t*Bu), 38.7 (J(C,P) = 9.5 Hz, *t*Bu), 30.8 (^1J(C,H) = 125, J(C,P) = 7.4 Hz, *t*Bu), 95.5 (^1J(C,H) = 171 Hz, cot); ^{31}P NMR (−30 °C): $\delta = 357.1$ (t, J(P,P) = 43.8, 2P), 17.3 (d, 1P); MS (70 eV): *m/z* [%]: 584 (M^+) [38], 515 ($M^+ - CtBu$) [19], 469 ($M^+ - P{\equiv}CtBu - Me$) [19], 446 ($M^+ - C_2tBu_2$) [100], 346 [68], 299 [26]

9b: ^1H NMR (−40 °C): $\delta = 0.49$ (s, 18H, $SiMe_3$), 1.32 (s, 18H, *t*Bu), 1.34 (s, 9H, *t*Bu), 6.46 and 6.72 (m, 4H, AA′BB′ spin system, ^3J(H,H) = 11.3, 11.1, ^4J(H,H) = 1.2 Hz, cot), 6.84 (s, 2H, cot); ^{31}P NMR: $\delta = 263$ (br., 2P), 140 (br., 1P); MS (70 eV): *m/z* [%]: 728 (M^+) [1], 590 ($M^+ - tBu_2C_2$) [6], 300 ($P_3C_3tBu_3^+$) [84], 175 ($cotSiMe_3$) [89], 73 ($SiMe_3^+$) [100]

13: ^1H NMR: $\delta = 1.71$ (s, *t*Bu); ^{13}C NMR{^1H}: $\delta = 211.8$ (X component of an A_2BX spin system, $|J(P,P)| = 8.0$, ^1J(P,C) = ±77.0, ^3J(P,C) = ±15.2, ($\nu_A - \nu_B$) = ±10.2 Hz (from iteration), ring-C), 44.5 (A_2BX spin system, $|J(P,P)| = 8.1$, ^2J(P,C) = ±24.5, ^4J(P,C) = ±1.6, ($\nu_A - \nu_B$) = ±0.7 Hz (from iteration), *t*Bu), 36.1 (^1J(P,P) = 8.0, ^3J(P,C) = ±14.5, ^5J(P,C) = ±1.1, ($\nu_A - \nu_B$) = ±0.1 Hz (from iteration), *t*Bu); ^{31}P NMR: $\delta = 232.6$ (s); MS (70 eV): *m/z* [%]: 300 (M^+) [39], 169 ($PC_2tBu_2^+$) [100], 100 ($P{\equiv}CtBu^+$) [32]

14: ^1H NMR: $\delta = 1.34$ (s, 18H, *t*Bu), 1.40 (s, 9H, *t*Bu); ^{13}C NMR: $\delta = 236.7$ (ddd, ^1J(C,P) = 55.9, 47.5, ^3J(C,P) = 20.0 Hz, C1), 39.5 (dt, ^2J(C,P) = 6.8, ^4J(C,P) = 3.4 Hz, *t*Bu at C1), 32.1 (dt, ^3J(C,P) = 5.4, ^5J(C,P) = 4.4 Hz, *t*Bu at C1), 46.6 (dt, ^1J(C,P) = 39.8, 28.0, C2), 35.3 (dt, ^2J(C,P) = 6.7, 1.8 Hz, *t*Bu at C2), 28.5 (pseudo-q, ^3J(P,C) = 7.2 Hz, *t*Bu at C2); ^{31}P NMR: $\delta = 336.8$ (d, ^2J(P,P) = 23.5 Hz, P1), 93.6 (t, ^2J(C,P) = 23.5 Hz, P2); MS (70 eV): *m/z* [%]: 300 (M^+) [42], 200 ($M^+ - P{\equiv}CtBu$) [30], 169 ($PC_2tBu_2^+$) [100], 100 ($P{\equiv}CtBu^+$) [30]

[a] ^1H NMR (TMS): 300 MHz (**6a**–**8a**), 400 MHz (**9b**, **13**, **14**); ^{13}C NMR (TMS): 100.6 MHz; ^{31}P NMR (85% H_3PO_4): 162.0 MHz; solvent: [D_8]THF (**6a**, **8a**, **13**), [D_8]toluene (**7a**, **14**), CD_2Cl_2 (**9b**); MS: Varian-CH5. [b] For the numbering of the C and P atoms see Scheme 1 and 2.

An experimental test of the reactivity of **6a** towards hexachloroethane revealed that the 1,3-diphosphete **10** can be liberated from **6a** even at room temperature by a redox reaction. To date this has not been achieved with any of the other known η^4-1,3-diphosphete complexes.[3, 4, 11] However, as expected, **10** is so unstable that it cannot be isolated or detected by spectroscopy. The only isolable reaction product is the tetraphosphacubane **11**, [12] which is formed from **10** in 34% yield through a sequence of [4 + 2]- and [2 + 2]cycloadditions[2b] (Scheme 2).

Thus, **6a** shows the same reactivity towards hexachloroethane as the recently described cyclooctatetraene(tetraphosphabarrelene)zirconium complex **3**[1] and the two tetraphosphabarrelenehafnium complexes **7a** and **7b** described here for the first time. In all three cases two of the double bonds π-bound to the metal atom were liberated under oxidation of the metal to [(cot)MCl_2] and reduction of the hexachloroethane to give the tetrachloroethylene. In this way, as described recently for the

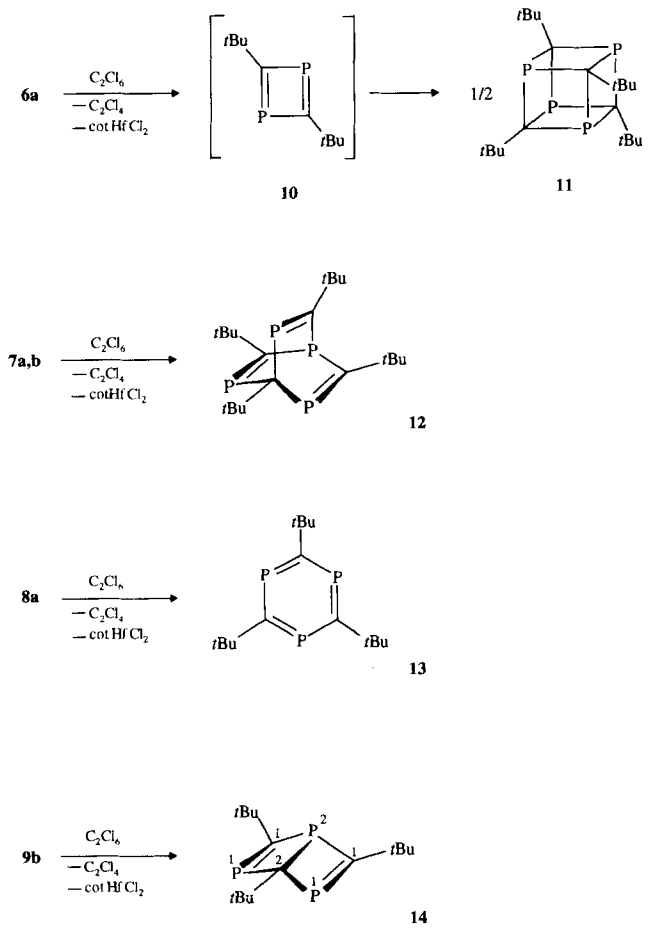

Scheme 2. Liberation of the phosphorus heterocycles **10**–**14**.

tetraphosphabarrelenezirconium complex **3**,[11] the 1,3,5,7-tetraphosphabarrelene **12** was obtained in over 80% yield from **7a** and **7b** (Scheme 2).

The structure of **12**, which had already been identified unambiguously on the basis of its spectroscopic data,[11] was confirmed by an X-ray structure analysis (Fig. 1).[13]

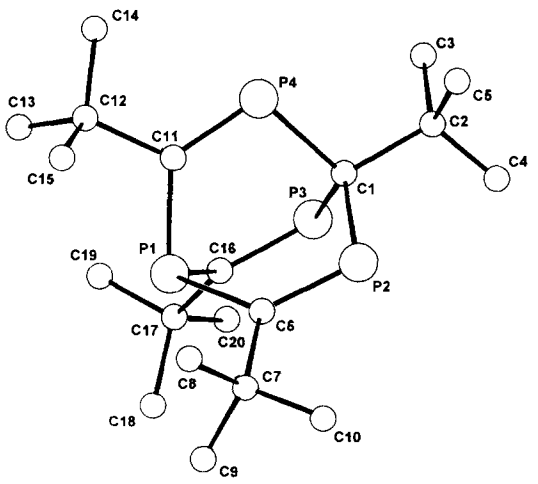

Fig. 1. Crystal structure of **12**. Selected bond lengths [Å] and angles [°]: P1-C6 1.862(1), P1-C11 1.851(1), P1-C16 1.858(1), P2-C1 1.877(1), P2-C6 1.671(1), P3-C1 1.871(1), P3-C16 1.667(1), P4-C1 1.869(1), P4-C11 1.668(1); C16-P1-C11 100.1(1), C16-P1-C6 98.8(1), C11-P1-C6 99.9(1), C6-P2-C1 104.7(1), C16-P3-C1 104.4(1), C11-P4-C1 104.5(1), P4-C1-P3 110.6(1), P4-C1-P2 110.0(1), P3-C1-P2 109.1(1), P2-C6-P1 122.3(1), P4-C11-P1 122.8(1), P3-C16-P1 122.8(1).

The two trimer complexes **8a** and **9b** also react readily with hexachloroethane at room temperature. Thus, in this way one example from the class of 1,3,5-triphosphabenzenes (**13**) and one from the class of dewar-1,3,5-triphosphabenzenes (**14**) could be synthesized and characterized for the first time. The triphosphabenzene **13** was obtained in 53% yield from **8a** in the form of a pale yellow, microcrystalline powder by stirring with hexachloroethane at room temperature for 12 h. Under similar conditions, the dewar-triphosphabenzene derivative **14** is formed in 70% yield from **9b** in the form of orange microcrystals. Both compounds are stable at room temperature under exclusion of air and moisture. An isomerization of **14** to **13** can be achieved by heating to 90 °C; after 5 h 20% of **14** had rearranged into **13**. For the parent compounds, the triphosphabenzene is 25 kcal mol^{-1} more stable than the dewar-triphosphabenzene.[14]

The structures of the two new compounds **13** and **14** were established unambiguously by mass spectrometry and ^1H, ^{13}C, and ^{31}P NMR spectroscopy. The mass spectra of the two compounds exhibit a molecular ion peak at m/z 300; the spectra of **13** and **14** differ only slightly in the intensities of the fragment ion signals (Table 1). The different structures of **13** and **14** are clearly evident in their ^{31}P NMR spectra; in the spectrum of **13** a singlet appears at $\delta = 232.6$ for all three phosphorus atoms, whereas in the spectrum of **14** a doublet appears at $\delta = 336.8$ ($J_{P,P} = 23.5$ Hz) for the two unsaturated phosphorus atoms P1 and a triplet appears at $\delta = 93.6$ for the bridgehead phosphorus atom P2 (for atom numbering see Scheme 2). All the NMR signals lie in the expected range.[1, 6, 15] The structure determinations of **13** and **14** were completed by their ^{13}C NMR spectra: the ring carbon atoms of **13** give rise to one signal at $\delta = 211.8$, whose coupling pattern corresponds to the X component of an A_2BX spin system (Table 1). A multiplet for the two sp^2 carbon atoms C1 at $\delta = 236.7$ ($^1J_{C,P} = 55.9, 47.5$ Hz, $^3J_{C,P} = 20$ Hz), which can be roughly analyzed as a first order signal (ddd), and a triplet of doublets at $\delta = 46.6$ ($^1J_{C,P} = 39.8, 28.0$ Hz) for the bridgehead carbon atom C2 appear in the spectrum for the differently bound carbon atoms of the bicycle **14**. The chemical shifts of the C atoms of the *tert*-butyl groups do not require an explanation. Neither do their signals in the ^1H NMR spectra (one signal for **13** and two singlets in the ratio 2:1 for **14**; Table 1).

According to its NMR spectra (^1H, ^{13}C, ^{31}P), the free 1,3,5-triphosphinine **13** is a π^6-heteroarene. Its relationship to the many known phosphinines[16] and the two recently synthesized 1,3-diphosphinines[15] is unmistakable. A 1,4-diphosphinine, 2,3,5,6-tetrakis(trifluoromethyl)-1,4-diphosphinine has so far only been detected in solution; NMR spectroscopic data of this compound are not known.[17] The spectroscopic data of a well-known $1\lambda^5,3\lambda^5,5\lambda^3$-triphosphinine differ considerably from those of the compound **13**.[18]

The NMR spectra of the dewar-1,3,5-triphosphabenzene (dewar-1,3,5-triphosphinine) **14** resemble those of dewar-1-phosphinine[19] and of dewar-2-phosphinine.[20] The only notable difference between the spectra is the position of the signal of the bridgehead phosphorus atom P2, which is considerably shifted downfield in **14**. However, the corresponding phosphorus atom in a dewar-1,3,5-triphosphabenzenevanadium complex adopts a similar position ($\delta = 84.4$).[6]

With the successful synthesis of the 1,3,5-triphosphabenzene **13** and its dewar benzene valence isomer **14**, we are now in the position to investigate the reactivity of these new phosphorus heterocycles. Our priorities in this respect are the study of the cycloaddition behavior and the properties of these compounds as complex ligands in transition metal chemistry.

Experimental Procedure

6a: **1** (1.12 g, 11.2 mmol) in xylene (10 mL) was added dropwise over 0.5 h to a boiling solution of **5a** (2.0 g, 5.6 mmol) in xylene (40 mL). The mixture was stirred for a further 0.5 h at about 140 °C and then the solvent was removed at 0.5 mbar. The resulting brown solid was suspended in pentane (20 mL), filtered with a D3 frit, washed with pentane, and dried at 10^{-3} mbar. Recrystallization from toluene afforded **6a** (1.83 g, 68%) as brown microcrystals; m.p. 163 °C (decomp.).

8a: **1** (3.4 g, 34 mmol) was added dropwise to a solution of **5a** (4.0 g, 11.2 mmol) in toluene (10 mL) and pentane (10 mL) at −78 °C and stirred for 18 h at −78 °C. The green-brown suspension was filtered at −78 °C and the residue washed twice with pentane (2 × 20 mL). Recrystallization from THF (10 mL) afforded **8a** (5.39 g, 83%) as green microcrystals; m.p. ca. 138 °C (decomp.).

9b: **1** (1.3 g, 13 mmol) was added dropwise to a solution of **5b** (2.08 g, 4.32 mmol) in Et_2O (30 mL) at 0 °C. After 1 h the reaction solution was cooled to −30 °C, the green crystals of **9b** which precipitated were filtered off and dried at 10^{-3} mbar; **9b** (2.8 g, 89%); m.p. 107 °C (decomp.).

13: Hexachloroethane (0.2 g, 0.86 mmol) was added to a suspension of **8a** (0.5 g, 0.86 mmol) in toluene (30 mL) at −78 °C. The reaction mixture was allowed to warm to room temperature over the course of 12 h, filtered, and the filtrate was evaporated to dryness at 0.5 mbar. The residue was dissolved in pentane (20 mL) and small amounts of insoluble material were removed by filtration. The yellow filtrate was concentrated to 5 mL and cooled to −78 °C. After 8 h, 0.14 g of **13** (53%) had precipitated in the form of a yellow solid; m.p. 88 °C (decomp.).

14: Hexachloroethane (425 mg, 1.8 mmol) was added to a solution of **9b** (1.3 g, 1.8 mmol) in toluene (10 mL) at room temperature and the mixture was stirred for 2 h. The solvent was removed at 0.5 mbar, the residue was taken up in pentane (40 mL) and filtered over Celite to remove insoluble material. On cooling to −30 °C small amounts of [bis(trimethylsilyl)cyclooctatetraene]hafnium dichloride precipitated, which was likewise filtered off. The clear filtrate was concentrated to 20 mL, and subsequent cooling to −30 °C led to the precipitation of **14** (380 mg, 70%) in the form of orange microcrystals; m.p. about 128 °C (decomp.).

Received: June 16, 1995 [Z 8104 1E]
German version: *Angew. Chem.* **1995**, *107*, 2411–2414

Keywords: cyclooligomerizations · hafnium compounds · heterocycles · phosphaalkynes · phosphorus compounds

[1] P. Binger, G. Glaser, B. Gabor, R. Mynott, *Angew. Chem.* **1995**, *107*, 114–115; *Angew. Chem. Int. Ed. Engl.* **1995**, *34*, 81–83.

[2] a) P. Binger, B. Biedenbach, C. Krüger, M. Regitz, *Angew. Chem.* **1987**, *99*, 798–799; *Angew. Chem. Int. Ed. Engl.* **1987**, *26*, 764–765; b) T. Wettling, B. Geissler, R. Schneider, S. Barth, P. Binger, M. Regitz, *ibid.* **1992**, *104*, 761–762 and **1992**, *31*, 758–759.

[3] Review: a) J. F. Nixon, *Chem. Rev.* **1988**, *88*, 1327–1362; b) M. Regitz, P. Binger, *Angew. Chem.* **1988**, *100*, 1541–1565; *Angew. Chem. Int. Ed. Engl.* **1988**, *27*, 1484–1508; c) P. Binger in *Multiple Bonds and Low Coordination in Phosphorus Chemistry*, 1st ed. (Eds.: M. Regitz, O. J. Scherer), Thieme, Stuttgart, **1990**, pp. 90–111; d) M. Regitz in *Organic Synthesis via Organometallics (OSM 4, Aachen)* (Eds.: D. Enders, H.-J. Gais, W. Keim), Vieweg, Wiesbaden, **1993**, pp. 93–113.

[4] a) P. Binger, R. Milczarek, R. Mynott, M. Regitz, W. Rösch, *Angew. Chem.* **1986**, *98*, 645–646; *Angew. Chem. Int. Ed. Engl.* **1986**, *25*, 644–645; b) P. Binger, R. Milczarek, R. Mynott, C. Krüger, Y.-H. Tsay, E. Raabe, M. Regitz, *Chem. Ber.* **1988**, *121*, 637–645; c) P. Binger, B. Biedenbach, R. Mynott, C. Krüger, P. Betz, M. Regitz, *Angew. Chem.* **1988**, *100*, 1219–1221; *Angew. Chem. Int. Ed. Engl.* **1988**, *27*, 1158–1160; d) P. B. Hitchcock, M. J. Maah, J. F. Nixon, *J. Chem. Soc. Chem. Commun.* **1986**, 737–738.

[5] A. R. Barron, A. H. Cowley, *Angew. Chem.* **1987**, *99*, 956; *Angew. Chem. Int. Ed. Engl.* **1987**, *26*, 907–908.

[6] R. Milczarek, W. Rüsseler, P. Binger, K. Jonas, K. Angermund, C. Krüger, M. Regitz, *Angew. Chem.* **1987**, *99*, 957–958; *Angew. Chem. Int. Ed. Engl.* **1987**, *26*, 908–909.

[7] J. Haas, Diplomarbeit, Universität Bonn, **1988**.

[8] a) G. Wilke, L. Stehling, unpublished; b) G. Wilke in *Fundamental Research in Homogeneous Catalysis, Vol. 3* (Ed.: M. Tsutsui), Plenum, New York, **1979**, pp. 1–24; c) Experimental procedures: J. Wicher, Dissertation, Universität Bochum, **1983**; d) ^{1}H NMR-spectra: R. Benn, G. Schroth, *J. Organomet. Chem.* **1982**, *228*, 71–85.

[9] a) G. Becker, G. Gresser, W. Uhl, *Z. Naturforsch. B* **1981**, *36*, 16–19; b) Optimized procedure: W. Rösch, V. Hees, M. Regitz, *Chem. Ber.* **1987**, *120*, 1645–1652.

[10] INEPT (optimized for ^nJ(C,H) = 5 Hz, in order to transfer the magnetization from the protons of the *tert*-butyl group): the experiment was carried out with ^{1}H decoupling. Because of the shorter delays [1/4 J(C,H) instead of 1/2 J(C,H)], the INEPT pulse sequence was preferred over the DEPT pulse sequence.

[11] P. Binger, G. Glaser, S. Albus, C. Krüger, *Chem. Ber.*, in press.

[12] a) T. Wettling, J. Schneider, O. Wagner, C. G. Kreiter, M. Regitz, *Angew. Chem.* **1989**, *101*, 1035–1037; *Angew. Chem. Int. Ed. Engl.* **1989**, *28*, 1013–1014; b) B. Geissler, T. Wettling, S. Barth, P. Binger, M. Regitz, *Synthesis* **1994**, 1337–1343.

[13] Data for the crystal structure analysis of **12**: $C_{20}H_{36}P_4$, $M_r = 400.4$, crystal dimensions: $0.16 \times 0.30 \times 0.37$ mm^3, $a = 9.434(2)$, $b = 17.130(3)$, $c = 14.256(1)$ Å, $\beta = 91.38(1)°$, $V = 2303.2$ Å^3, $T = 100$ K, $\rho_{calcd} = 1.15$ g cm^{-3}, $\mu = 3.22$ cm^{-1}, $Z = 4$, monoclinic, space group $P2_1/n$ (no. 14), Enraf-Nonius CAD4 diffractometer, $\lambda = 0.71069$ Å, ω-2θ scan, 32698 measured reflections ($\pm h$, $\pm k$, $\pm l$), (different Ψ values), $[(\sin\theta)/\lambda]_{max} = 0.83$ Å^{-1}, 10628 independent and 7427 observed reflections [$I \geq 2\sigma(I)$], 361 refined parameters, direct methods. H atom positions found and refined, $R = 0.043$, $R_w = 0.035$ [$w = 1/\sigma^2(F_o)$], max. residual electron density 0.60 e Å^{-3}. Further details of the crystal structure investigation may be obtained from the Fachinformationszentrum Karlsruhe, D-76344 Eggenstein-Leopoldshafen (Germany) on quoting the depository number CSD-59068.

[14] M. Hofmann, P. von R. Schleyer, unpublished; V. Caliman, P. B. Hitchcock, J. F. Nixon, M. Hofmann, P. von R. Schleyer, *Angew. Chem.* **1994**, *106*, 2284–2286; *Angew. Chem. Int. Ed. Engl.* **1994**, *33*, 2202–2204.

[15] D. Böhm, F. Knoch, S. Kummer, V. Schmidt, U. Zenneck, *Angew. Chem.* **1995**, *107*, 251–254; *Angew. Chem. Int. Ed. Engl.* **1995**, *34*, 198–201.

[16] G. Märkl in *Multiple Bonds and Low Coordination in Phosphorus Chemistry*, 1st ed. (Eds.: M. Regitz, O. J. Scherer), Thieme, Stuttgart, **1990**, pp. 220–257.

[17] Y. Kobayashi, J. Kumadaki, A. Ohsawa, W. Hamana, *Tetrahedron Lett.* **1976**, 3715–3716.

[18] E. Fluck, G. Becker, B. Neumüller, R. Knebl, G. Heckmann, H. Riffel, *Z. Naturforsch. B* **1987**, *42*, 1213–1221.

[19] J. Fink, W. Rösch, V.-J. Vogelbacher, M. Regitz, *Angew. Chem.* **1986**, *98*, 265–266; *Angew. Chem. Int. Ed. Engl.* **1986**, *25*, 280–281.

[20] K. Blatter, W. Rösch, V.-J. Vogelbacher, J. Fink, M. Regitz, *Angew. Chem.* **1987**, *99*, 67–68; *Angew. Chem. Int. Ed. Engl.* **1987**, *26*, 85–86.

meso-Tetrakis[4-(diphenylphosphino)-phenyl]porphyrin and a Water-Soluble Octakis-(phosphonium salt) Porphyrin Double-Decker with a Cage Structure

Gottfried Märkl,* Martin Reiss, Peter Kreitmeier, and Heinrich Nöth

Dedicated to Professor Rolf Huisgen on the occasion of his 75th birthday

Water-soluble porphyrins are important because of their potential interactions with biological systems (e.g. double-stranded cleavage of DNA, photochemical oxidations, photodynamic tumor therapy, photoinduced intramolecular electron- and energy transfer).[1–3] As a result, a series of ammonio-substituted porphyrins,[4–6] porphyrinyl uridines,[7] and sugar-substituted porphyrins[8] have been reported. So far there are no reports of phosphinoporphyrins; we are only aware of complexes of octaethylporphyrin (OEP) and tri- or pentavalent phosphorus as the "metallic" central atom, $([P(OEP)]^+X^-$ and $([P[OEP)-(OH)_2]^+ClO_4^-)$.[9] Here, we describe a phosphino-substituted porphyrin for the first time, the tetrakis[4-diphenylphosphino)phenyl]porphyrin **2a**, whose cationic form represents a new type of water-soluble porphyrin.

[*] Prof. Dr. G. Märkl, Dipl.-Chem. M. Reiss, Dr. P. Kreitmeier
Institut für Organische Chemie der Universität
Universitätsstrasse 31, D-93040 Regensburg (Germany)
Telefax: Int. code + (941)943-4504
Prof. Dr. H. Nöth
Institut für Anorganische Chemie der Universität
Meiserstrasse 1, D-80333 München (Germany)
Telefax: Int. code + (89)590-2451

The synthesis of **2a** was achieved by using the universal method of A. D. Adler et al. [10], from (4-diphenylphosphino)benzaldehyde **1** and pyrrole.

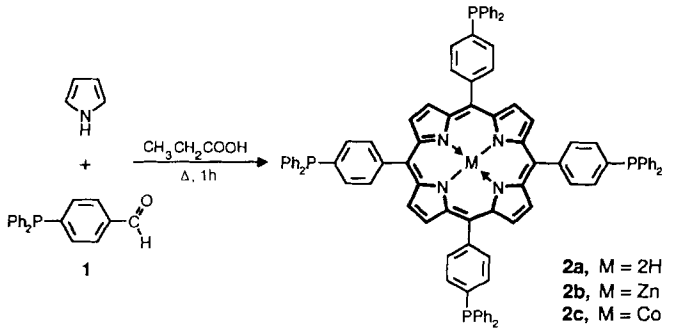

In accordance with the method of G. Schiemenz et al.,[11] **1** is obtained from 4-bromobenzaldehyde-ethyleneglycolacetal via the Grignard compound, by reaction with chlorodiphenylphosphane[12a] and subsequent hydrolysis.[12b] The Adler condensation of **1** with pyrrole affords **2a** in 21% yield (purification by recrystallization from CH_2Cl_2/MeOH, m.p. >350 °C, black-red, shiny needles). The characteristic Soret band at 423 nm (benzene, $\varepsilon = 490000$) undergoes a bathochromic shift of 18 nm in the diprotonated species **2a** (solution of **2a** in benzene/HCl g; $\varepsilon = 412000$). The fluorescence spectrum of **2a** ($CHCl_3$)[13] shows absorption maxima at 650, 707, and 760 nm (the longest wavelength band is only weakly defined); the Stokes shift of 4 nm is very small due to the rigid structure of the system.

It is surprising that the tervalent phosphorus atoms in compound **2a** are slightly oxidizable, even though this is formally a triphenylphosphane unit. IR spectroscopic monitoring of the autooxidation of **2a** in $CHCl_3$ in daylight by oxygen in air—which leads to the tetraoxide **3a** (Table 1)—shows that formation of the phosphane oxide is about 1000 times faster than for triphenylphosphane. This apparent autocatalyzed oxidation of **2a** by the porphyrin system could be due to intramolecular, photoinduced activation of oxygen in air.[14] However, since triphenylphosphane is also rapidly oxidized by oxygen in air in the presence of catalytic amounts of *meso*-tetraphenylporphyrin (TPP) under the same conditions, an intermolecular catalysis cannot be ruled out for **2a**. Due to this extreme autooxidizability, reactions with **2a** must be performed under strict exclusion of oxygen. In the crystal structure of the oxide **3a**,[15] the *meso*-phenyl substituents are arranged propeller-like on the porphyrin and the $P(O)Ph_2$-oxygen atoms are oriented *syn*, *anti*, *syn*, *anti* to each other (Fig. 1a,b).

Porphyrin **2a** is also converted by H_2O_2/acetone into the tetraoxide **3a** and by sulfur in benzene to the tetrasulfide **4a** (Table 1). Compounds **3a** and **4a** can also be obtained by Adler condensation of the oxide (m.p. 104–106 °C) or the sulfide (m.p. 82–84 °C) of **1** with pyrrole (yields 12 and 16%, respectively).

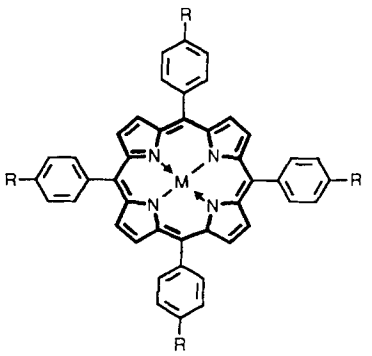

3, R = $-\overset{\overset{O}{\|}}{P}Ph_2$, **3a**, M = 2 H; **3b**, M = Co **3c**, M = Zn

4a, R = $-\overset{\overset{S}{\|}}{P}Ph_2$, M = 2H

5, R = $-\overset{\overset{CH_3}{|}}{\overset{\oplus}{P}}Ph_2\ I^{\ominus}$, **5a**, M = 2H; **5b**, M = Zn

6a, R = $-\overset{H_2C}{\underset{PPh_2}{\overset{|}{\overset{\oplus}{|}}}}-C_6H_4-COOH\ Br^{\ominus}$, M = 2H

The formation of quaternary ions of **2a** in dimethylformamide can be achieved at room temperature, for example, with

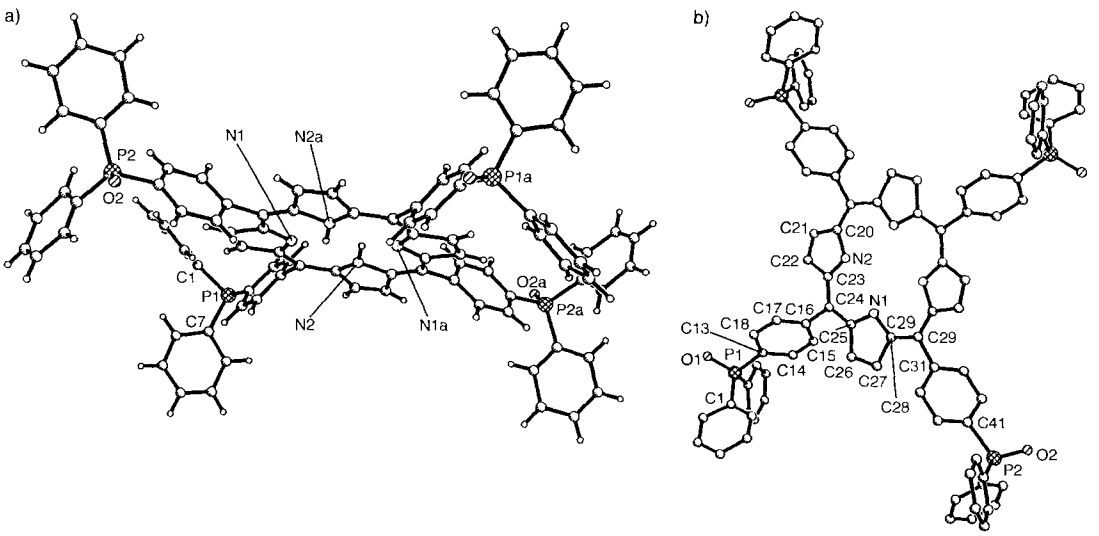

Fig. 1. Crystal structure of **3a**. a) Side view. b) Plan view. Selected bond lengths [Å] and angles [°], standard deviations are in parentheses: P1-C1 1.80(2), P1-C13 1.77(2), P1-O1 1.491(10), P2-C41 1.77(2), P2-O2 1.484(12), N1-C28 1.37(2), C27-C28 1.48(2), C26-C27 1.38(2), C24-C25 1.40(2), C23-C24 1.39(2), N2-C23 1.38(2), C22-C23 1.45(2), C21-C22 1.34(2); C25-N1-C28 106.7(11), N1-C25-C24 126.5(12), N2-C23-C24 125.3(13), C23-N2-C20 106.9(11), N2-C20-C21 108.1(13), C21-C22-C23 107.6(14), C25-C24-C23 126.7(13), C23-C24-C16 116.4(12).

 © VCH Verlagsgesellschaft mbH, D-69451 Weinheim, 1995 0570-0833/95/3420-2231 $ 10.00+.25/0

Table 1. Spectroscopic data of **2b**, **3a**, **3b**, **4a**, **5a**, **5b**, **6a**, **8a**, and **8b**.

Compd.	UV/Vis [solvent] unprotonated species $\lambda_{max}(\varepsilon)$	UV/Vis [solvent] diprotonated species $\lambda_{max}(\varepsilon)$	*m/z*	$\delta(^{31}P)$ [solvent]
oxide **3a**	[benzene] 421 (482000) 519 (20900) 554 (10900) 595 (7300) 647 (5450)	[benzene] 361 (25400) 442 (430000) 609 (10900) 651 (44500)	(toluene, PI-FDMS): 1416.1	+30.00 (s) [$CHCl_3$]
sulfide **4a**	[$CHCl_3$] 420 (536500) 515 (24400) 550 (12500) 586 (7750) 643 (5700)	[$CHCl_3$] 373 (25000) 444 (505000) 619 (13100) 653 (62800)	(CH_2Cl_2, PI-FDMS): 1479.2	+44.53 (s) [$CHCl_3$]
phosphonium salt **5a**	[MeOH] 416 (420000) 514 (20000) 548 (9600) 590 (7000) 653 (3500)	[MeOH] 378 (26000) 445 (337000) 653 (35700)	–	+23.24 (s) [$CDCl_3$]
phosphonium salt **6a**	[MeOH] 417 (392500) 512 (19400) 550 (8300) 586 (5500) 641 (3200)	[MeOH] 365 (19400) 447 (353000) 594 (8300) 651 (38700)	–	+24.96 (s) [$CDCl_3$]
Zn complex **2b**	[THF] 405 (49900) 425 (570000) 556 (22900) 583 (9400)	–	(MNBA/CH_2Cl_2, PI-LISIMS): 1416.3	−5.61 (s) [$CDCl_3$]
Zn complex **5b** (from MeOH/ether) [a]	[MeOH] 425 (550100) 553 (23800) 592 (9500) 405 (58700)	–	–	+23.88 (s) [CD_3NO_2]
Co complex **3b**	[$CHCl_3$] 413 (475000) 533 (21600)	–	(MNBA/CH_2Cl_2, PI-LISIMS): 1472.2	
$W(CO)_5$ complex **8a**	[THF] 420 (507000) 514 (23700) 547 (13700) 588 (6800) 652 (6000)	[THF] 456 (399000) 609 (11400) 667 (66400)	(MNBA/CH_2Cl_2, PI-LISIMS): 2647.0	+21.66 (s) [[D_8]THF] IR (KBr): $\tilde{\nu}$ = 1900–1955 (vs, br., CO)
$W(CO)_5Zn$ complex **8b**	[THF] 406 (54200) 427 (544000) 556 (26300) 596 (11700)	–	(MNBA/CH_2Cl_2, PI-LISIMS): 2712.2	21.75 (s) [$CDCl_3$] IR (KBr): $\tilde{\nu}$ = 1900–1955 (vs, br., CO)

[a] ^{1}H NMR (400 MHz, CD_3NO_2): δ = 3.21 (d, ^3J(P,H) = 13.64 Hz, CH_3), 7.92–8.23 (m, 48H), 8.64 (d, 8H), 8.96 (s, 8H).

methyl iodide to give **5a** and with (4-bromomethyl)benzoic acid to give **6a** (Table 1). The phosphonium salts show normal Soret bands (**5a**, λ_{max} = 416 nm (ε = 420000), **6a**, λ_{max} = 417 nm (ε = 392500)). The salts do not precipitate from solutions in a little ethanol (**5a**) or DMF (**6a**) on dilution with water.

The reaction of **2a** with *para*-xylylene dibromide in the molar ratio 1:2 (DMF 100 °C, dilution method, dropwise addition of the bromide over 24 h, total reaction time 48 h) gives the octakis(phosphonium salt) **7**. Compound **7** can be isolated by precipitation with ether, leading to a dark violet crystalline powder, without by-products and in almost quantitative yield, which is readily soluble in DMF, alcohol, and water. The appearance of

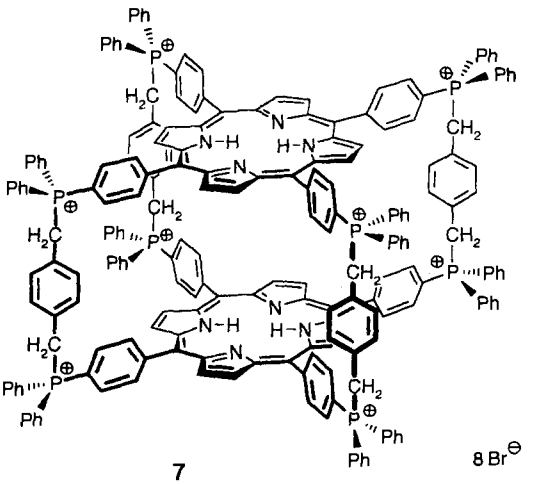

7

a single signal in the ^{31}P NMR spectrum at δ = 25.0 indicates that all phosphorus atoms are in the same chemical and magnetic environment. The UV/Vis spectrum of **7** (MeOH: λ_{max}[nm] (ε) = 408 (468500), Soret bands, Q bands: 516 (21000), 547 (12000), 584 (7000), 650 (5600); MeOH/HCl: 428 (430000), 598 (14700), 649 (55300)) does not show any electronic interactions resulting from the porphyrin rings; however, a drastic increase in the ε value of the longwave Q bands at 649 nm is noteworthy. The extreme high-field shift of the NH signals in the ^{1}H NMR spectrum (from $\delta \approx -2.5$–3.0 to −6.5) clearly indicates that the NH protons in each ring are influenced by the ring currents of the other porphyrin ring.[16]

The mass spectrum ("TSQ/SSQ 7000 Atmospheric Pressure Ionization (API) System, Electrospray Ionization (ESI) process", Finnigan MAT[17]) establishes the structure of **7**.[18] The ions appearing in the ESI spectrum are listed in Table 2.

The octakis(phosphonium salt) **7** is the first example of an ionic, vertically stacked porphyrin. It can be classed as a "porphyrin double-decker" (separation of the porphyrin rings ca. 7 Å) with a cage structure. So far, to the best of our knowledge, only two neutral systems with two vertically stacked, covalently bound porphyrins are known.[19, 20] Depending on the length of the α,ω-dibromides, it should be possible to adjust the height of the porphyrin cage so that different guest molecules (organic molecules, complex fragments) can form stable host–guest complexes. Similarly, stacking of porphyrins which contain metal ions could enable formation of "molecular" metals.[21]

The reaction of **2a** with $Zn(OAc)_2$ in $CHCl_3$ gives the zinc complex **2b** (Table 1). The cobalt complex **2c** (reaction of **2a** with $Co(OAc)_2$ in $CHCl_3$) is much more readily autooxidizable than the metal-free phosphinoporphyrin **2a**, which has meant that until now, only the corresponding phosphane oxide **3b** could be isolated. This is plausible since cobalt complexes with nitrogen donor ligands readily react with molecular oxygen to form peroxo- and superoxo complexes. Some of these complexes can function as reversible oxygen carriers and may be used as models for biological oxygen transport systems.[22] (μ-O_2)-Cobalt complexes could therefore trigger the extremely facile intra- or intermolecular autooxidation of the phosphorus atoms in **2c**.

The zinc complex **2b** can be converted smoothly to the phosphonium salt **5b**, by using methyl iodide (DMF, 20 h, room temperature), and with careful exclusion of oxygen and light (Table 1).

Table 2. Electrospray ionization (ESI) mass spectrum of **7** [a].

7, Cation	*m/z* (Assignment)
M^{8+}	389.93 ($[M^{8+}]/8$)
M^{7+}	445.50 ($[M^{8+} - H^+]^{7+}/7$); 457.06 ($[M^{8+} + Br^-]^{7+}/7$)
M^{6+}	519.59 ($[M^{8+} - 2H^+]^{6+}/6$), 533.07 ($[M^{8+} + Br^- - H^+]^{6+}/6$), 546.55 ($[M^{8+} + 2Br^-]^{6+}/6$)
M^{5+}	623.30 ($[M^{8+} - 3H^+]^{5+}/5$), 639.48 ($[M^{8+} + Br^- - 2H^+]^{5+}/5$), 655.67 ($[M^{8+} + 2Br^- - H^+]^{5+}/5$), 671.845 ($[M^{8+} + 3Br^-]^{5+}/5$)
M^{4+}	778.89 ($[M^{8+} - 4H^+]^{4+}/4$), 799.11 ($[M^{8+} + Br^- - 3H^+]^{4+}/4$), 819.33 ($[M^{8+} + 2Br^- - 2H^+]^{4+}/4$), 839.56 ($[M^{8+} + 3Br^- - H^+]^{4+}/4$), 859.78 ($[M^{8+} + 4Br^-]^{4+}/4$)
M^{3+}	1038.17 ($[M^{8+} - 5H^+]^{3+}/3$), 1065.14 ($[M^{8+} + Br^- - 4H^+]^{3+}/3$), 1092.11 ($[M^{8+} + 2Br^- - 3H^+]^{3+}/3$), 1119.08 ($[M^{8+} + 3Br^- - 2H^+]^{3+}/3$), 1146.04 ($[M^{8+} + 4Br^- - H^+]^{3+}/3$), 1173.01 ($[M^{8+} + 5Br^-]^{3+}/3$)
M^{2+}	1556.76 ($[M^{8+} - 6H^+]^{2+}/2$), 1597.21 ($[M^{8+} + Br^- - 5H^+]^{2+}/2$), 1637.66 ($[M^{8+} + 2Br^- - 4H^+]^{2+}/2$), 1678.11 ($[M^{8+} + 3Br^- - 3H^+]^{2+}/2$), 1718.57 ($[M^{8+} + 4Br^- - 2H^+]^{2+}/2$), 1759.02 ($[M^{8+} + 5Br^- - H^+]^{2+}/2$), 1799.47 ($[M^{8+} + 6Br^-]^{2+}/2$)
M^{+}	3112.52 ($[M^{8+} - 7H^+]^+$), 3193.42 ($[M^{8+} + Br^- - 6H^+]^+$), 3274.32 ($[M^{8+} + 2Br^- - 5H^+]^+$), 3355.23 ($[M^{8+} + 3Br^- - 4H^+]^+$), 3436.13 ($[M^{8+} + 4Br^- - 3H^+]^+$), 3517.03 ($[M^{8+} + 5Br^- - 2H^+]^+$), 3597.94 ($[M^{8+} + 6Br^- - H^+]^+$), 3678.84 ($[M^{8+} + 7Br^-]^+$)

[a] $C_{216}H_{164}Br_8N_8P_8$, $M_r = 3758.75$ ($C_{216}H_{164}N_8P_8)^{8+}$, $M_r = 3119.52$; measurement conditions: solution in methanol/water (1/1), heated capillary (180 °C), 196 eV acceleration potential.

Compound **2a** reacts with $W(CO)_5 \cdot THF$ in THF at room temperature (reaction time 20 h) to form the tetrakis(pentacarbonyltungsten) complex **8a** (Table 1); the mass spectrum (PI-LISIMS, MNBA/CH_2Cl_2, MNBA = *m*-nitrobenzyl alcohol) confirms the chemical composition $C_{112}H_{66}N_4O_{20}P_4W_4$. The complex molecule peak observed[23] agrees with calculated values for the given isotope ratios.

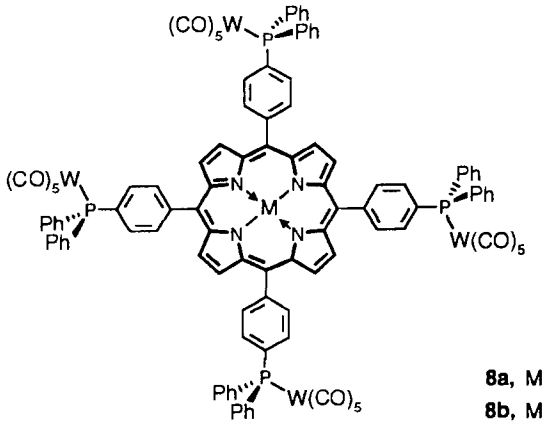

8a, M = 2H
8b, M = Zn

Modeling studies show that the *meso*-phenyl substituents are perpendicular to the plane of the porphyrin ring and the $PPh_2W(CO)_5$ substituents are free to rotate. The molecule has a spatial expansion of about 20 Å.

Analogous to **2a**, the zinc complex **2b** can also react at room temperature with $W(CO)_5 \cdot THF$ in THF. This produces complex **8b** (Table 1), which can also be obtained from **8a** using $Zn(OAc)_2$ in boiling methanol (reaction time 1 h).[24] As far as we know, **8b** is the only porphyrin reported which contains a σ-bound transition metal complex fragment[25] (mono- and bis-$Cr(CO)_3$-π complexes of TPP were reported by N. J. Gogan et al.[26]).

Received: June 1, 1995 [Z 8052 IE]
German version: *Angew. Chem.* **1995**, *107*, 2439–2442

Keywords: cage compounds · macrocycles · phosphorus compounds · porphyrinoids · tungsten compounds

[1] E. J. Gibbs, R. F. Pasternack, *Semin. Hematol.* **1989**, *26*, 77; R. J. Fiel, *J. Biomol. Struct. Dyn.* **1989**, *6*, 1259; ref. [14].
[2] B. Garcia, C.-H. Lee, A. Blaskó, T. C. Bruice, *J. Am. Chem. Soc.* **1991**, *113*, 8118; A. Robert, B. Loock, M. Momenteau, B. Meunier, *Inorg. Chem.* **1991**, *30*, 706; T. C. Bruice, *Acc. Chem. Res.* **1991**, *24*, 243; H. van den Bergh, P. Cornaz, *Nachr. Chem. Techn. Lab.* **1985**, *33*, 582.
[3] a) T. Nagata, A. Osuka, K. Maruyama, *J. Am. Chem. Soc.* **1990**, *112*, 3054; b) R. J. Fiel, M. R. Munson, *Nucleic Acids Res.* **1980**, *8*, 2835; J. M. Kelly, M. J. Murphy, D. J. McConnell, C. Oh Uigin, *ibid.* **1985**, *13*, 167.
[4] R. F. Pasternack, E. J. Gibbs, J. J. Villafranca, *Biochemistry* **1983**, *22*, 2406; ref. [3b].
[5] M. J. Carvlin, N. Datta-Gupta, R. J. Fiel, *Biochem. Biophys. Res. Commun.* **1982**, *108*, 66.
[6] N. Robic, C. Bied-Charreton, M. Perrée-Fauvet, C. Verchère-Béaur, L. Salmon, A. Gaudemer, R. F. Pasternack, *Tetrahedron Lett.* **1990**, *31*, 4739.
[7] L. Czuchajowski, J. Habdas, H. Niedbala, V. Wandrekar, *Tetrahedron Lett.* **1991**, *32*, 7511.
[8] N. Ono, M. Bougauchi, K. Maruyama, *Tetrahedron Lett.* **1992**, *33*, 1629; P. Maillard, C. Huel, M. Momenteau, *ibid.* **1992**, *33*, 8081; K. Driaf, P. Krausz, B. Verneuil, M. Spiro, J. C. Blais, G. Bolbach, *ibid.* **1993**, *34*, 1027; H. Li, L. Czuchajowski, *ibid.* **1994**, *35*, 1629.
[9] P. Sayer, M. Gouterman, C. R. Connell, *J. Am. Chem. Soc.* **1977**, *99*, 1082.
[10] A. D. Adler, R. F. Longo, J. D. Finarelli, J. Goldmacher, J. Assour, L. Korsakoff, *J. Org. Chem.* **1967**, *32*, 476.
[11] G. P. Schiemenz, H. Kaack, *Liebigs Ann. Chem.* **1973**, 1494.
[12] a) Acetal, yield 70%, m.p. 86–87 °C (methanol); b) **1**, yield 80–90%, m.p. 69–71 °C (methanol).
[13] We thank Prof. Dr. Langhals, Institut for Organische Chemie der Universität München, for recording the fluorescence spectra; see also: M. Gouterman, *The Porphyrins, Vol. III*, Academic Press, New York, **1978**; D. J. Quimby, F. Longo, *J. Am. Chem. Soc.* **1975**, *97*, 5111.
[14] J. Moan, E. Boye, *Photobiochem. Photobiophys.* **1981**, *2*, 301; D. Praseuth, A. Gaudemer, J. B. Verlhac, I. Kraljic, I. Sissöeff, E. Guillé, *Photochem. Photobiol.* **1986**, *44*, 717.
[15] X-ray structure analysis: Siemens P4 diffractometer, $Mo_{K\alpha}$ irradiation, graphite monochromator, measurements at 293 K, single crystal size: 0.7 × 0.6 × 0.5 mm, red-black rhombus. Crystal data: $C_{92}H_{66}N_4O_3P_4$, $M_r = 1415.37$, $a = 20.414(12)$, $b = 7.914(5)$, $c = 25.671(12)$ Å, $\beta = 104.51(1)°$, $V = 4015.0(39)$ Å^3, $Z = 2$, monoclinic, space group $P2_1/n$, $\rho_{calcd} = 1.171$ Mg m^{-3}, $\mu = 0.126$ mm^{-1}, $F(000) = 1476$. Data collection: ω-scan, 2θ range 2.28–47.0° in h, k, $\pm l$, measuring speed: 6–60° per min. Reflection width: 2.0°, 6758 measured reflections, 5611 observed [$> 4\sigma(F)$]. Structure solution: direct methods (SHELXL93). Further details of the crystal structure determination can be obtained from the Fachinformationszentrum Karlsruhe, D-76344 Eggenstein-Leopoldshafen, on quoting depository number CSD-58965.
[16] H. Scheer, J. J. Katz in *Porphyrins and Metalloporphyrins* (Ed.: K. M. Smith), Elsevier, Amsterdam, **1975**, p. 430–437; see also ref. [24].
[17] We would like to thank Doz. Dr. R. Deutzmann, Universität Regensburg, for accurate recording of the ESI spectrum of **7**.
[18] The reliability of the method is confirmed by the ESI spectrum of the methylphosphonium salt **5a** ($M_r = 1411.64$). Here, the ions *m/z* 352.9 ($[M^{4+}]/4 = 352.51$) and 512.9 ($[M^{4+} + I^-]^{3+}/3 = 512.85$) are observed almost exclusively.
[19] N. E. Kagan, D. Mauzerall, R. B. Merrifield, *J. Am. Chem. Soc.* **1977**, *99*, 5484; F. R. Longo, *Porphyrin Chemistry Advances*, Ann Arbor Science Publishers, **1979**, p. 44–48.

[20] H. A. Staab, T. Carell, *Angew. Chem.* **1994**, *106*, 1534; *Angew. Chem. Int. Ed. Engl.* **1994**, *33*, 1466.
[21] B. M. Hoffmann, J. A. Ibers, *Acc. Chem. Res.* **1983**, *16*, 15; M. Hanack, *Chimia* **1983**, *37*, 238.
[22] See for example F. A. Cotton, G. Wilkinson, *Advanced Inorganic Chemistry*, 5th ed., Wiley, New York, **1988**, p. 735ff. and 1343ff.; M. Kikkawa, Y. Sasaki, S. Kawata, Y. Hatakeyama, F. B. Ueno, K. Saito, *Inorg. Chem.* **1985**, *24*, 4096; L. Casella, M. Gullotti, *ibid.* **1986**, *25*, 1293; D. Chen, A. E. Martell, *ibid.* **1987**, *26*, 1026; D. Mansuy, *Pure Appl. Chem.* **1990**, *62*, 741.
[23] Isotope distribution of the molecular peak of **8a** (*m/z* 2638.9, 2639.9, 2641.1, 2642.2, 2643.1, 2644.1, 2645.1, 2648.1, 2649.0, 2650.1, 2651.2, 2652.2, 2653.0, 2656.2). We would like to thank Dr. K. Mayer, Universität Regensburg, for recording the mass spectra.
[24] After reaction of **2a** with $W(CO)_5 \cdot THF$ in THF at 25 °C (60 h) and subsequent reaction with a saturated solution of $Zn(OAc)_2$ in refluxing methanol, a mixture of the tris-, di-, and mono-$W(CO)_5$ complexes of the mono-, di- and trioxides of **2a** and the zinc complex **3c** of the tetraoxide are obtained, in addition to the zinc complex **8b**. Chromatographic separation can be achieved on silica gel without problem.
[25] See for example M. Tsutsui, G. A. Taylor in *Porphyrins and Metalloporphyrins* (Ed.: K. M. Smith), Elsevier, Amsterdam, **1975**, p. 279ff.
[26] N. J. Gogan, Z. U. Siddiqui, *Can. J. Chem.* **1972**, *50*, 720.

Tetracarboxylic Bisimide–Lactam Ring Contraction: A Novel Type of Rearrangement**

Heinz Langhals* and Petra von Unold

Dedicated to Professor Rolf Huisgen on the occasion of his 75th birthday

Six-membered ring dicarboximides **1** with aromatic substituents are commonly viewed as chemically very inert.[1] Strong hydrolyzing reagents such as hot, concentrated sulfuric acid or KOH/*tert*-butyl alcohol are required for their saponification to **2a** or **2b** as, for example, in the case of perylene-3,4-dicarboximides[2, 3] or perylene-3,4:9,10-tetracarboxylic bisimides **7**.[1] A completely different reaction pathway is observed if, under much milder conditions, alkali metal hydroxides in alcohol react with bisimides **3**: In this case, the loss of a C_1 fragment from one of the carboximide substructures leads to the formation of the corresponding ring-contracted lactamimides **4**. This reaction occurs with naphthalene-1,8:4,5-tetracarboxylic bisimides **5**[4] and with the related perylene bisimides **7**[5] and is discussed in more detail herein.

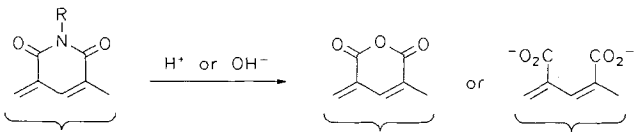

1 **2a** **2b**

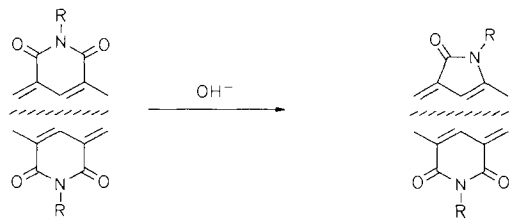

3 **4**

The reaction of **5** or **7** with KOH in *tert*-butanol leads to the corresponding lactamimides in only small amounts as by-products. However, in ethanol and especially in methanol ring contraction is the dominant reaction pathway. Addition of dimethyl sulfoxide (DMSO) further increases the yield and shortens reaction times, so that now the lactamimides **6** and **8**, of which only few derivatives are known,[3–7] are obtained in high yield, and only trace amounts of hydrolysis products are formed (Scheme 1).[8]

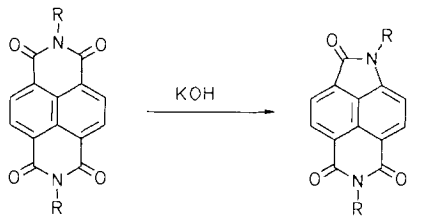

5 **6**

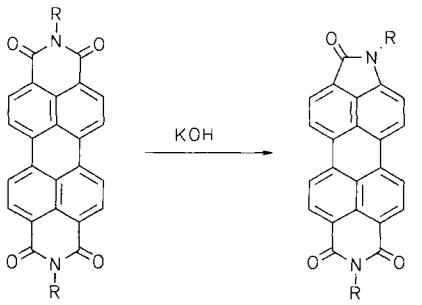

7 **8**

Scheme 1. Reaction of the bisimides **5** and **7** with KOH; **a**, R = 2,5-di-*tert*-butylphenyl; **b**, R = 4-*tert*-butylphenyl; **c**, R = 2-*tert*-butylphenyl; **d**, R = 5-*tert*-butyl-2-methylphenyl; **e**, R = 2,2-dimethylheptyl; **f**, R = (1-propylcyclohexyl)methyl.

Interestingly, ring contraction proceeds quite easily for R = aryl, but is more difficult for R = alkyl. In bisimides bearing aromatic and aliphatic substituents contraction of the aryl-substituted ring is favored. In both, **5** and **7** only one of the imide ring systems is transformed to the lactam, leaving the second one unchanged even under more vigorous conditions. Evidently, the second imide subunit is essential for the reaction to occur. In agreement with this conclusion is the finding that monoimide **1** does not undergo ring contraction.

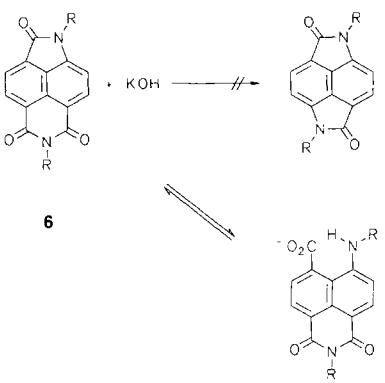

6 **9**

Lactamimides **6** and **8** (and also the bisimides **5** and **7**) reversibly add OH^- in the presence of a large

[*] Prof. Dr. H. Langhals, Dipl.-Chem. P. von Unold
Institut für Organische Chemie der Universität
Karlstrasse 23, D-80333 München (Germany)
Telefax: Int. code + (89)5902-483
e-mail: ui26101@sunmail.lrz-muenchen.de

[**] This work was supported by the Deutsche Forschungsgemeinschaft and the Fonds der Chemischen Industrie.

excess of alkaline metal hydroxide in alcohol to form either orange-red or blue salts **9**,[12] in which the lactam rings are hydrolyzed.

On the basis of these experimental findings, the following rearrangement mechanism is proposed (Scheme 2): The reaction is initiated by the addition of one equivalent of OH^- to one of the imide carbonyl groups. Subsequent ring contraction leads to the formation of a lactam followed by decarboxylation.[9, 10] In this step, the adjacent carbonyl group, possibly after the attack of another equivalent of OH^-, may function as an intramolecular base and accept the proton of the carboxylic acid group. In light of the present experimental data, however, this postulate can be neither supported nor excluded. The decarboxylated product is a dihydroaromatic species that is oxidized to the aromatic lactamimide. Presumably, the presence of air is enough to achieve this oxidation, but it is also possible that the cosolvent DMSO is involved.

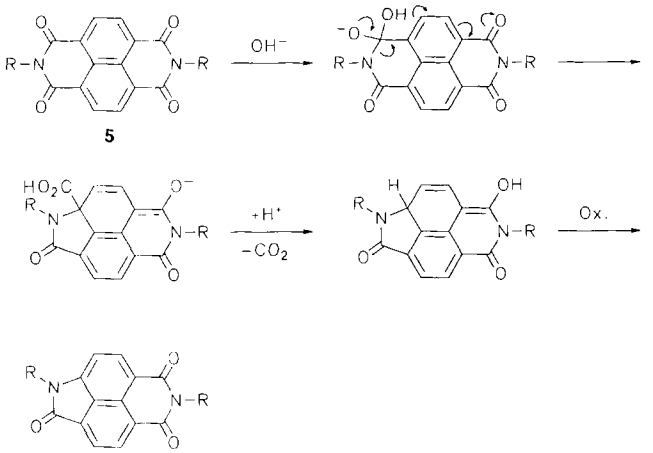

5

Scheme 2. Mechanism of the ring contraction of **5**.

The proposed dihydroaromatic intermediates are difficult to characterize. If the ring contraction of **6c** (R = 2-*tert*-butylphenyl) is conducted under inert gas (argon), one can observe a transient, violet color of the reaction mixture that only persists under rigorous exclusion of oxygen[11] but otherwise instantly changes to pale yellow. In the presence of air, oxidation in the alkaline reaction medium is complete, and after aqueous workup (with 2–6 N HCl for example) the protonated aminocarboxylate **9c** (R = 2-*tert*-butylphenyl) can be isolated.[12] After treatment of a solution of **5c** in ethanol with concentrated HCl or refluxing glacial acetic acid one obtains, in addition to 50% unchanged starting material, lactam **6c** in 31% yield. Furthermore and in contrast to reactions performed in the presence of air, one can isolate the product formed by hydrolysis of one imide ring, namely *N*-(2-*tert*-butylphenyl)naphthalene-1,8:4,5-tetracarboxylic-1,8-anhydride-4,5-imide in 7% yield. If a corresponding reaction mixture starting from **5a** is treated with concentrated sulfuric acid,[14] the phenyl group on the lactam-nitrogen loses its *tert*-butyl group in position 2.

On the basis of these experimental findings it is clear that the base-induced ring contraction of bisimides constitutes a novel type of rearrangement. The first step of the reaction is similar to the benzilic rearrangement to which it is vinylogous. Preliminary experiments show that the reaction can be successfully extended to other bisimides and hence appears to be a general reaction principle.

The naphthalene-lactamimides **6** absorb in the visible region of the UV spectrum with absorption bands significantly shifted to longer wavelengths compared to the pale-yellow to colorless naphthalene-bisimides **5**. In the solid state and in solution compounds **6** exhibit strong fluorescence (quantum yields > 80%) that is described here for the first time. A characteristic UV/Vis absorption and fluorescence spectrum of **6** is depicted in Figure 1;

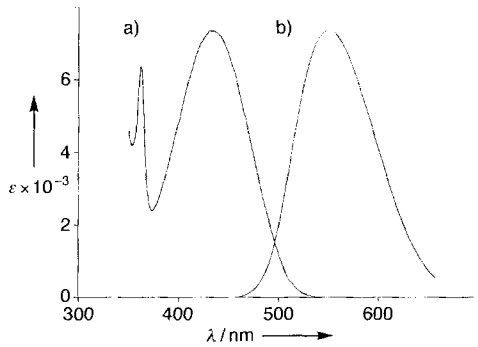

Fig. 1. Absorption (a) and fluorescence spectrum (b) of **6a** (R = 2,5-di-*tert*-butylphenyl) in $CHCl_3$.

further spectroscopic data are listed in Table 1. The photostability of the lactamimides **6** is considerable (at least 30% of the photostability of the corresponding derivatives of **7**)[14] typifying them as a novel class of fluorescent dyes. Remarkable are their large Stokes-shifts (112 nm for **6a**) rendering them promising compounds for dye lasers and other fluorescence applications.

Table 1. Yields, melting points, absorption (A) and fluorescence maxima (F) of lactams **6** [8].

Lactam	Yield [%]	M.p. [°C]	λ_{max} [nm] (ε) ($CHCl_3$)
6a	68[a] 47[b]	275	A: 432.5(7370), 361.9(6380); F: 545.8
6b	47[b]	301	A: 446.5(5480), 361.9(7420), 343.4(8500), 273(22700)
6c	79[a] 67[b]	247	A: 431.8(7000), 361.7(6330), 343.9(5240), 314.2(5780), 265.2(21700); F: 544.5
6d	89[a] 68[b]	211	A: 432.2(7350), 361.1(6790), 343.4(5720), 310.2(6550), 264.7(22800); F: 559.3
6e	18[a] 8[b]	94	A: 439.0(6210), 361.8(5170), 343.4(5480), 328.0(6380), 311.7(6790), 267.8(21320); F: 540.8
6f	10[b]	187–191	A: 435.7, 361.9, 342.4, 316.7 sh, 268.4; F: 541.5
6g	74[a]	163	A: 439(6230), 361.9(7780)

[a] KOH/MeOH/DMSO, 90 °C, 3 h. [b] KOH/EtOH, 90–100 °C, 8–18 h.

The nitrogen atoms of the naphthalene- and perylenetetracarboxylic bisimides **5** and **7** have nodes or at least very small coefficients.[13] This electronic structure has two important consequences: First, their UV/Vis spectra are influenced only little by substituents on the nitrogen and second, flexible substituents at this site do not lead to fluorescence quenching[13, 14] by the Loose–Bolt mechanism.[15, 16] The symmetry of the lactamimides, however, is sufficiently low so that larger atomic coefficients on the nitrogens result.[17] Hence, the Loose–Bolt mechanism can be readily studied for this class of compounds.

The lactamimides **6** with aliphatic substituents, for example **6e** and **6f**, show large fluorescence quantum yields without exception. This suggests that there is no electronic coupling between the flexible parts of the molecular skeleton and the π system of the chromophore. However, phenyl substituents on the nitrogen atoms of **6** couple their π systems with that of the chromophore. Fluorescence quenching by the Loose–Bolt mechanism can now occur after rotation about the $N-C_{Ph}$ bond. This applies, for example, to dye **6b**, for which no fluorescence can be observed (the *tert*-butyl groups in the 4-positions of the phenyl substituents serve to improve the solubility of the dye[18]). A *tert*-butyl group in the 2-position of the phenyl substituent (**6c**) completely obstructs rotation about the $N-C_{Ph}$ bond and leads to high fluorescence quantum yields. Similar conclusions can be drawn for **6a** with a 2,5-di-*tert*-butylphenyl substituent that efficiently hinders free rotation and gives rise to a strongly fluorescent dye. The requirement of hindered rotation is already met with a methyl substituent in position 2, as can be seen from dye **6d**, which shows intense fluorescence. Interestingly, complete fluorescence quenching is observed in the case of **6g**, in which only the $N-C_{Ph}$ bond of the lactam unit freely rotates, whereas that of the imide substructure is blocked. Free rotation in the lactam unit is therefore sufficient to induce fluorescence quenching.

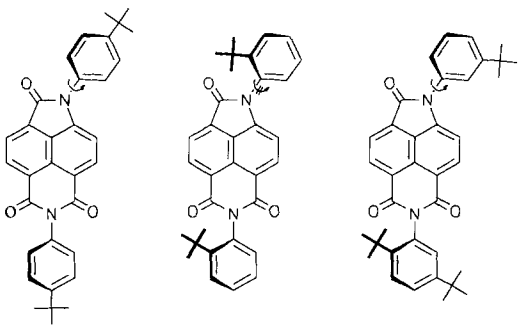

6b **6c** **6g**

These results suggest that it should be possible to develop fluorescent dyes based on **6** with aromatic R or other π substituents in which free rotation about the $N-C_{Ph}$ bond is hindered. If, however, fluorescence is not a desired property of these systems, free rotation about this bond is a prerequisite.

Experimental Procedure

6a: A solution of **5a** (590 mg, 0.90 mmol) in aqueous KOH (85%, 1.4 g), DMSO (6 mL), and MeOH (8 mL) was heated at reflux (100 °C) for 3 h. The hot reaction mixture was stirred into distilled water (200 mL), further diluted with water to 300 mL, and, after treatment with conc. HCl (100 mL), left standing at room temperature for 16 h. The resulting precipitate was dissolved in ethanol (100 mL), the solution treated with conc. HCl (15 mL) and heated at reflux until the color changed from light red to orange-yellow. After dilution with water (300 mL) a precipitate was obtained that was chromatographed on silica with $CHCl_3$ and recrystallized from ethanol/water to yield **6a** (380 mg, 62%). IR (KBr): $\tilde{\nu}$ = 2962 cm^{-1} m, 2926 s, 1733 m, 1714 s, 1683 s, 1661 s, 1503 m, 1467 m, 1426 m, 1364 m, 1340 m, 1245 m, 1169 m, 765 m; ^1H NMR ($CDCl_3$): δ = 8.71 (d, J = 7.3 Hz, 1H, naph.), 8.44 (2d, J = 7.6 Hz, 1H, naph.), 8.32 (d, J = 7.3 Hz, 1H, naph.), 6.76 (d, J = 7.6 Hz, 1H, naph.), 7.61 (d, J = 8.5 Hz, 1H, Ph), 7.56 (2d, J = 8.5 Hz, 1H, Ph), 7.49 (dd, J = 8.6, J' = 2.2 Hz, 1H, Ph), 7.42 (dd, J = 8.6, J' = 2.2 Hz, 1H, Ph), 7.09 and 7.02 (2d, J = 2.2 Hz, 1H, Ph), 6.95 and 6.94 (2d, J = 2.2 Hz, 1H, Ph), 1.32 (s, 9H, *t*Bu), 1.31 (s, 9H, *t*Bu), 1.30 (s, 9H, *t*Bu), 1.26 (s, 9H, *t*Bu); ^{13}C NMR ($CDCl_3$): δ = 168.4, 164.4, 151.1, 150.0, 147.0, 146.0, 144.2, 135.0, 132.1, 131.7, 130.0, 128.9, 128.8, 127.9, 127.2, 126.6, 126.2, 125.8, 125.3, 117.0, 107.7, 35.6, 35.4, 34.4, 34.2, 31.8, 31.8, 31.2, 31.2; MS (70 eV): m/z (%): 614 (0.3) [M^+], 557 (100) [$M^+ - t$Bu].

Received: May 5, 1995 [Z 7916 IE]
German version: *Angew. Chem.* **1995**, *107*, 2436–2439

Keywords: fluorescence · imides · lactams · rearrangements

[1] The synthesis of 7 molten alkali metal hydroxides are sometimes used. For a review see H. Langhals, *Heterocycles* **1995**, *40*, 477–500.
[2] Y. Nagao, T. Misono, *Shikizai Kyokaishi* **1976**, *49*, 29–34 [*Chem. Abstr.* **1976**, *85*, 20928s].
[3] In the reaction of perylene-3,4-dicarboximides with alkali metal hydroxides the carboxamide carboxylic acids can be isolated as intermediates in the hydrolysis. See L. Feiler, H. Langhals, K. Polborn, *Liebigs Ann.* **1995**, 1229–1244.
[4] E. F. Bondarenko, V. A. Shigalevskii, *J. Org. Chem. USSR (Engl. Transl.)* **1986**, *22*, 1155–1159.
[5] H. Kaiser, J. Lindner, H. Langhals, *Chem. Ber.* **1991**, *124*, 529–535.
[6] G. I. Bystritskii, S. V. Ovsyannikova, *J. Org. Chem. USSR (Engl. Transl.)* **1979**, *15*, 2329–2333.
[7] S. S. Dalvi, S. Seshadri, *Indian J. Chem. Sect. B* **1985**, *24*, 377–382.
[8] Correct elemental analyses were obtained for **6a**–**6c** and **6e**. Other derivatives of **6** were contaminated by small amounts of starting material **5** that were not removed because they did not interfere with spectroscopic investigations.
[9] In contrast to ref. [4], the formation of CO could not be observed (MS). Instead, stoichiometric amounts of CO_2 were detected.
[10] Yields of CO_2 (adsorbed on a mixture of NaOH and CaO, after acidification with HCl and purification of the gaseous products with conc. H_2SO_4, relative to starting material): 117.5 mg **5c** furnished 9.38 mg (7.98%) CO_2 (calcd. 9.74 mg, 8.29%).
[11] Broad, unstructured absorption bands at 542 nm in a mixture of ethanol (2 mL), DMSO (1 mL) and KOH (0.2 g).
[12] In contrast to reports in ref. [4] the reaction of **5a** and **5c** did not yield the fully hydrolyzed products, but rather **9a** and **9c** with one intact carboximide ring (**9c**: yield 96%, R_f (silica, $CHCl_3$) = 0.5). For example, the remaining carboximide ring can be identified for **9a** by IR spectroscopy (KBr; 3429 cm^{-1} m, 1700 s, 1653 s, 1605 m) and in the FAB-MS recorded in the negative-ion-mode ($C_{33}H_{31}N_2O_4^-$: m/z: calcd. 519, found 519). UV/Vis ($CHCl_3$): λ_{max} = 451.4 nm.
[13] H. Langhals, S. Demmig, H. Huber, *Spectrochim. Acta Part A* **1988**, *44*, 1189–1193.
[14] A. Rademacher, S. Märkle, H. Langhals, *Chem. Ber.* **1982**, *115*, 2927–2934.
[15] H. A. Staab, *Einführung in die theoretische organische Chemie*, VCH, Weinheim, **1975**.
[16] T. Förster, *Fluoreszenz Organischer Verbindungen*, 1. ed., Vandenhoeck & Ruprecht, Göttingen, **1951**.
[17] HMO calculations on **6** employing standard heteroatom coefficients gave a HOMO coefficient of 0.24 for the lactam-nitrogen and −0.03 for the imide-nitrogen atom. The corresponding coefficients of the LUMO were −0.03 and −0.33, respectively.
[18] H. Langhals, DE-A 3016764, **1980** [*Chem. Abstr.* **1982**, *96*, P70417x].

First Reaction of 1,2-Dimethyl-*o*-silaborane: Nucleophilic Degradation**

Lars Wesemann,* Ulli Englert, and Dietmar Seyferth

1,2-Dimethyl-1,2-disila-*closo*-dodecaborane(12) (**1**)[1] is to date the only reported group 14 element analogue of the intensively investigated 1,2-dicarba-*closo*-dodecaborane(12) $C_2B_{10}H_{12}$[2] (more commonly known as *o*-carborane). From the fundamental work by Hawthorne et al.[3] it is known that the 1,2-dicarba-*closo*-dodecaborane(12) can be degraded by strong bases in the presence of a protic solvent to give 7,8-dicarba-*nido*-undecaborate(1−) $C_2B_9H_{12}^-$. We report here on the attack of bases on the icosahedral skeleton of 1,2-dimethyl-1,2-disila-*closo*-dodecaborane(12) (**1**).

[*] Dr. L. Wesemann, Dr. U. Englert
Institut für Anorganische Chemie der Technischen Hochschule
Professor-Pirlet-Strasse, D-52056 Aachen (Germany)
Telefax: Int. code + (241)8888-288
Prof. Dr. D. Seyferth
Department of Chemistry
Massachusetts Institute of Technology
Cambridge, MA 02139 (USA)

[**] This work was supported by the Deutsche Forschungsgemeinschaft (DFG-Schwerpunktprogramm "Polyeder").

Treatment of 1,2-dimethyl-*o*-silaborane (**1**) in the two-phase mixture of diethyl ether/water with one equivalent of sodium hydroxide containing $[NMe_4]Cl$ as a precipitating agent leads to the degradation product $[NMe_4]$-**2** in 89% yield [Eq. (a)].

$$\underset{\mathbf{1}}{Me_2Si_2B_{10}H_{10}} \xrightarrow[-\,NaCl\ -\,[MeSi(OH)_3]]{+\,NaOH\ +\,2\,H_2O\ +\,[NMe_4]Cl} \underset{[NMe_4]\text{-}\mathbf{2}}{[NMe_4][MeSiB_{10}H_{12}]} \quad (a)$$

The immediate precipitation of the degraded silaborane from the aqueous solution is essential for high yields of $[NMe_4]$-**2**. If the anion **2** remains in water for only a few minutes, it is degraded further to the pentadecahydrodecaborate(1−) $B_{10}H_{15}^-$.[4] Compound **1** can also be degraded by the nucleophile methanolate in tetrahydrofuran at 50 °C, and in the presence of *N*,*N*,*N*′,*N*′-tetramethylethylenediamine (TMEDA) the salt [Li(TMEDA)]-**2** can be isolated in 46% yield [Eq.(b)].

$$\mathbf{1} \xrightarrow[-\,MeSi(OMe)_3]{+\,LiOMe\ +\,2\,MeOH\ +\,TMEDA} [Li(TMEDA)]\text{-}\mathbf{2} \quad (b)$$

$MeSi(OMe)_3$ formed by the extrusion of a MeSi cluster vertex from **1** can, after separation by vacuum distillation, be clearly detected by mass spectrometry. In analogy to this result $MeSi(OH)_3$ should be formed from the degradation by OH^- [Eq.(a)]. This, however, has not been proven since the product condenses to give polymeric methylsiloxanes.[5]

The spectroscopic data of the hitherto unknown 8,9:10,11-di-μ-hydrodecahydro-7-methyl-7-sila-*nido*-undecaborate(1−) **2** confirm the constitution of this *nido*-cluster anion shown in Figure 1. Six signals with an intensity ratio of 1:2:2:2:2:1 are observed for the ten B atoms in the ^{11}B NMR spectrum. Thus, the anion **2** has C_s symmetry in solution; the B atoms B1 and B5 lie on the mirror plane. All B atoms reveal a B–H coupling with a terminal H atom.

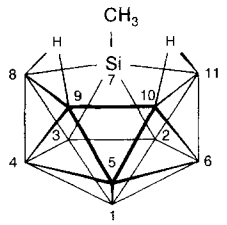

Fig. 1. Constitution of **2**.

The connectivities in the B_{10} framework can be established clearly from the 2D-^{11}B-^{11}B NMR spectrum. The lack of the cross peak between the B atoms B8–B9 and B10–B11 is a known phenomenon in bridging by H atoms.[6] Contrary to the expectations all cross peaks for the B–B edges bridged by the heteroatom silicon are visible.[7] The assignment of the signals in the ^1H NMR spectrum to the appropriate B atoms follows unambiguously from the 2D-^{11}B-^1H NMR spectrum; the cross peaks between the signal for the bridging H atoms and the signals for the B atoms B8,11 and B9,10 are particulary noteworthy.

The constitution of the anion **2** in solution determined from the spectroscopic data is consistent with the results of the crystal structure analysis (Fig. 2).[8] All B–B distances lie in the expected range of 1.74 to 1.90 Å; the three distances in the opened five-membered ring are the longest (1.86, 1.87, and 1.90 Å). The Si–B distances, which lie between 2.04 and 2.07 Å, correspond to those in 1,2-$Me_2Si_2B_{10}H_{10}$,[1] *commo*-3,3′-Si(3,1,2-$SiC_2B_9H_{11})_2$,[12] and $[(Me_3Si)_2C_2B_4H_4]_2Si$.[13] The Si atom lies 0.22 Å above the best plane through B8, B9, B10, and B11.

The anion **2** with 26 framework electrons is both isoelectronic and isostructural to 7-Me-7-$PB_{10}H_{12}$.[14] Other compounds of this structural type, all of which carry two bridging H atoms on the open, heteroatom-substituted pentagonal faces, are $CB_{10}H_{13}^-$[15] and $(NB_2tBu_3H)NB_{10}H_{12}$.[16] A corresponding silaborane of the composition $Me_2SiB_{10}H_{12}$ was claimed to be formed in the reaction of $Na_2B_{10}H_{12}$ with Me_2SiCl_2, but this compound has only been characterized unsatisfactorily.[17]

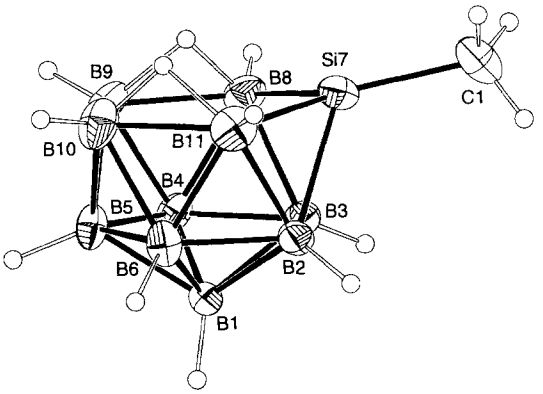

Fig. 2. Crystal structure of the anion **2** (PLATON representation [11]; thermal ellipsoids for 30% probability). Selected distances [Å], standard deviation in parentheses: B1-B2 1.762(4), B1-B3 1.762(5), B1-B4 1.782(5), B1-B5 1.742(6), B1-B6 1.781(6), B2-B3 1.783(5), B2-B6 1.773(6), B2-B11 1.843(6), B3-B4 1.773(5), B3-B8 1.840(5), B4-B5 1.751(6), B4-B8 1.796(5), B4-B9 1.796(6), B5-B6 1.783(5), B5-B9 1.747(5), B5-B10 1.758(6), B6-B10 1.801(7), B6-B11 1.778(5), B8-B9 1.870(7), B9-B10 1.857(7), B10-B11 1.895(7), Si7-C1 1.877(4), Si7-B2 2.048(3), Si7-B3 2.069(4), Si7-B8 2.045(4), Si7-B11 2.036(5).

1,2-Dimethyl-*o*-silaborane is attacked by nucleophiles with the loss of a MeSi vertex, whereas in *o*-carborane a B atom adjacent to the two C atoms reacts with the nucleophiles. A plausible explanation for this different pattern of reactivity follows from the consideration of the electronegativities of the participating elements. In the series carbon, boron, and silicon, the electronegativity decreases continually. Thus, the polarities in the examined heteroboranes are different, and this is the reason for the different nucleophilic degradation. As expected for the nucleophilic degradation of 1,2-diphospha-*closo*-dodecaborane(12) $P_2B_{10}H_{10}$, both degradation variants (that is, both the loss of a B atom and that of a P atom from the icosahedral framework) are known.[18]

In additional experiments we will study the reactivity of the anion **2**. These experiments will focus on the cluster formation by suitable main group element compounds and investigations on the coordination of **2** to transition metal complex fragments.

Experimental Procedure

2: **1** (306 mg, 1.50 mmol) [1] dissolved in Et_2O (70 mL) was treated with 0.1 N NaOH (15 mL), in which $[NMe_4]Cl$ (0.25 g, 2.3 mmol) was dissolved. $[NMe_4]$-**2** precipitated immediately as a white solid at the phase boundary. Et_2O was removed in vacuum from the two-phase mixture, $[NMe_4]$-**2** was filtered and washed (2 × 5 mL) with water. After drying, tetramethylammonium 8,9:10,11-di-μ-hydrodecahydro-7-methyl-7-sila-*nido*-undecaborate(1−) ($[Me_4N]$-**2**) was obtained in 89% yield (317 mg) [19]. MS (SIMS in 3,4-dimethoxybenzyl alcohol): *m/z* (%): 163 (29, M^-); NMR spectra at 25 °C in $[D_8]$THF; ^1H NMR (500 MHz, TMS): δ = 3.22 (s, Me_4N), 1.69 (H5), 1.52 (H8/11), 1.37 (H2/3), 0.95 (H4/6), 0.86 (H1/9/10), 0.51 (s, SiMe), −5.67 (broad, μ-H8/9, μ-H10/11), measurement and assignment of the B–H signals as cross peaks in the 2D-^{11}B-^1H NMR spectrum; ^{11}B NMR spectrum (160 MHz, $Et_2O{\cdot}BF_3$): δ = −12.3 (d, J = 140 Hz, B5), −14.7 (d, J = 134 Hz, B2/3), −21.9 (d, J = 140 Hz, B8/11), −23.8 (d, J = 140 Hz, B9/10), −25.3 (d, J = 140 Hz, B4/6), −32.5 (d, J = 140 Hz, B1); ^{13}C NMR (125 MHz, TMS): δ = 55.8 (s, NMe_4), −6.8 (s, SiMe); ^{29}Si NMR (100 MHz, TMS): δ = −36.4 (s).

Received: May 19, 1995 [Z 8008 IE]
German version: *Angew. Chem.* **1995**, *107*, 2435–2436

Keywords: boron compounds · silaboranes · silicon compounds

[1] a) D. Seyferth, K. Büchner, W. S. Rees, Jr., W. M. Davis, *Angew. Chem.* **1990**, *102*, 911–913; *Angew. Chem. Int. Ed. Engl.* **1990**, *29*, 918–920; b) D. Seyferth, K. Büchner, W. S. Rees, Jr., L. Wesemann, W. M. Davis, S. S. Bukalov, L. A. Leites, H. Bock, B. Solouki, *J. Am. Chem. Soc.* **1993**, *115*, 3586–3594.
[2] V. I. Bregadze, *Chem. Rev.* **1992**, *92*, 209–223.
[3] R. A. Wiesboeck, M. F. Hawthorne, *J. Am. Chem. Soc.* **1964**, *86*, 1642–1643.
[4] R. R. Rietz, A. R. Siedle, R. Schaeffer, L. J. Todd, *Inorg. Chem.* **1973**, *12*, 2100–2102.
[5] S. W. Kantor, *J. Am. Chem. Soc.* **1953**, *75*, 2712–2714.
[6] D. F. Gaines, G. M. Edvenson, T. G. Hill, B. R. Adams, *Inorg. Chem.* **1987**, *26*, 1813–1816.
[7] T. L. Venable, W. C. Hutton, R. N. Grimes, *J. Am. Chem. Soc.* **1984**, *106*, 29–37.
[8] a) Crystals of the $[Ph_3PMe]$ salt of **2** suitable for the X-ray structure analysis were obtained from THF/diethyl ether at room temperature. b) Crystal structure analysis: ENRAF-Nonius-CAD4 diffractometer; $Cu_{K\alpha}$ radiation, graphite monochromator; intensity data collected with ω-Θ scan at 203 K. $[Ph_3PMe]$-**2**: colorless, transparent rod $0.6 \times 0.3 \times 0.3 \times$ mm, orthorhombic space group $P2_12_12_1$ (no. 19); $a = 11.385(2)$, $b = 14.794(3)$, $c = 15.446(2)$ Å, $V = 2601.7(8)$ Å^3, $Z = 4$, $\rho_{calcd} = 1.212$ g cm^{-3}, $\mu(Cu_{K\alpha}) = 14.0$ cm^{-1}, $F(000) = 928$; 3088 reflections with $4 < \theta < 70°$, 2688 symmetry independent with $I > \sigma(I)$ in structure solution [9] and refinement [10] for 337 parameters; $R = 0.045$, $Rw = 0.056$, $w^{-1} = 1/\sigma^2$ (F_o); hydrogen atoms bound to carbon were refined as riding atoms, those bound to boron were isotropically refined. c) Further details of the crystal structure investigation may be obtained from the Fachinformationszentrum Karlsruhe, D-76344 Eggenstein-Leopoldshafen (Germany) on quoting the depository number CSD-404032.
[9] G. M. Sheldrick, SHELXS-86, Universität Göttingen, **1988**.
[10] B. A. Frenz, ENRAF-Nonius, SDP, Version 5.0, **1989**.
[11] A. L. Spek, *Acta Crystallogr. Sect. A* **1990**, *46*, C34.
[12] W. S. Rees, Jr., D. M. Schubert, C. B. Knobler, M. F. Hawthorne, *J. Am. Chem. Soc.* **1986**, *108*, 5369–5370.
[13] N. S. Hosmane, P. de Meester, U. Siriwardane, M. S. Islam, S. C. C. Chu, *J. Chem. Soc. Chem. Commun.* **1986**, 1421–1422.
[14] T. D. Getman, H. Deng, L. Hsu, S. G. Shore, *Inorg. Chem.* **1989**, *28*, 3612–3616.
[15] C. R. Whitaker, A. Romerosa, F. Teixidor, J. Rius, *Acta Crystallogr. Sect. C* **1995**, *51*, 188–190.
[16] M. Müller, U. Englert, P. Paetzold, *Inorg. Chem.*, in press.
[17] R. E. Loffredo, A. D. Norman, *Inorg. Nucl. Chem. Lett.* **1977**, *13*, 599–601.
[18] a) J. L. Little, M. A. Whitesell, R. W. Chapman, J. G. Kester, J. C. Huffman, L. J. Todd, *Inorg. Chem.* **1993**, *32*, 3369–3372; b) J. L. Little, J. G. Kester, J. C. Huffman, L. J. Todd, *ibid.* **1989**, *28*, 1087–1091.
[19] Correct C,H analysis for $[Ph_3PMe]$-**2** has been carried out.

The β-Lactam-Nucleoside Chimera

Alexander Dömling, Manfred Starnecker, and Ivar Ugi*

Dedicated to Professor Hubert Schmidbaur on the occasion of his 60th birthday

Multicomponent reactions (MCRs) have played a very important role since the beginning of organic chemistry.[1] The emergence of combinatorial chemistry[2] has revived the interest in these reactions. Furthermore, their applicability has been extensively broadened by the introduction of new MCRs[3] as well as novel concepts for the generation of MCRs.[1] Compared to conventional reactions, MCRs offer numerous advantages. For the rapid construction of large substance libraries, it is crucial that all compounds of a given component set can be combined with each other. In the case of the Ugi reaction (U-4CR), these libraries are prepared from a variety of commercially available compounds that represent all archetypes of chemical reactivity: oxo components, diverse acids, amines, and isocyanides. Building blocks that contain appropriate functional groups can be employed for the design of intelligent systems.

Nucleoside analogues are among the few agents that can be used against viral infections[4] and have therefore gained significance since the appearance of AIDS. β-Lactams, on the other hand, belong to the most efficient drugs for the treatment of bacterial infections by virtue of their ability to stop the cell-wall biosynthesis. An acylation by the β-lactam portion of the antibiotic deactivates the dipeptidase which effects the cross-linking of murein.[5] In addition, β-lactams have become a major focus in medicinal chemistry due to their ability to inhibit human leucocyte elastase (HLE).[6] Immunoconjugates consisting of monoclonal antibodies and β-lactam agents are discussed as very promising anticancer drugs.[7] The combination of the acylating activity of β-lactam antibiotics and the recognition ability of nucleoside bases results in a novel class of nucleoside analogues, which can be referred to as a chimera consisting of both classes of compounds.[8]

A concept called dual action drugs, which combines substance groups with different types of activity into a new drug, has been successfully applied by several research groups. For example, the combination of classical β-lactam antibiotics and gyrase inhibitors gives rise to extremely potent antibiotics.[9]

The reaction of β-amino acids with oxo components and isocyanides results in the formation of strained four-membered β-lactams by a ring contraction of the intermediate, nonisolable seven-membered rings (Scheme 1). When employing aldehydes

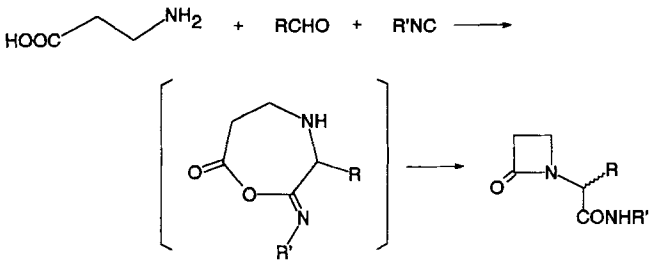

Scheme 1. β-Amino acids, oxo components, and isocyanides react to form intermediate, nonisolable seven-membered ring compounds that collapse to yield strained four-membered β-lactams.

based on nucleobases as oxo components, the chimeric nucleoside analogues **1**–**3** (Table 1) can be obtained in good yields (>80%). The aldehydes are readily available in two steps from the corresponding bases.[10] *O*,*N*-acetal **4** (Table 1) is formed

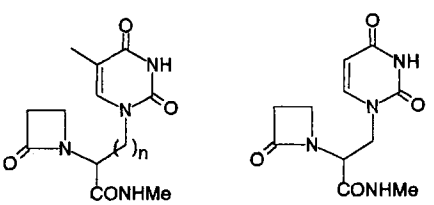

exclusively when 3-amino-4,4-dimethyl-5-hydroxyvaleric acid is used as the β-amino acid,[11] the expected β-lactam **5**, however, is not observed (Scheme 2). The relative configuration of **4** could be confirmed by NOESY experiments. All compounds

[*] Prof. Dr. I. Ugi, Dr. A. Dömling, Dipl.-Chem. M. Starnecker
Institut für Organische Chemie und Biochemie
der Technischen Universität München
Lichtenbergstrasse 4, D-85747 Garching (Germany)
Telefax: Int. code + (89)3209-3290

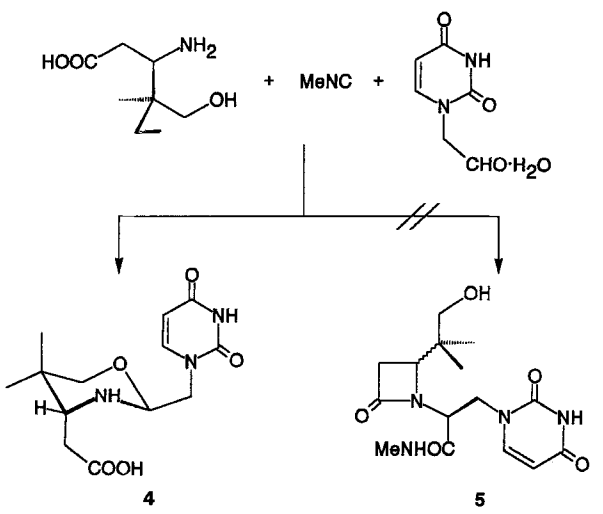

4 5

Scheme 2. 3-amino-4,4-dimethyl-5-hydroxyvaleric acid reacts with methylisocyanide and 1-uracilacetaldehyde hydrate to form the *N,O*-acetal **4** instead of the expected chimera **5**

Table 1. Selected physical data of compounds **1**, **2**, and **4** [a].

1: $C_{12}H_{16}N_4O_4$, M = 280.28 g mol^{-1}; colorless powder; m.p. 224 °C (decomp.); R_F ($CHCl_3$/MeOH 4/1 v/v) = 0.69; ^{1}H NMR ([D$_6$]DMSO, 360 MHz): δ = 1.72 (s, 3H), 2.54 (m, 1H), 2.59 (d, 3H, ^3J = 4.5 Hz), 2.60–2.85 (m, 2H), 3.18 (m, 1H), 3.43 (m, 1H), 3.87 (m, 2H), 4.51 (dd, 1H, ^3J = 5.3, ^3J = 9.2 Hz), 8.26 (q, 1H, ^3J = 4.6 Hz), 11.26 (br.s, 1H); ^{13}C NMR ([D$_6$]DMSO, 90 MHz): δ = 11.6, 25.3, 35.8, 37.3, 46.4, 52.5, 108.4, 140.4, 150.7, 163.9, 166.5, 167.0

2: $C_{13}H_{18}N_4O_4$, M = 294.31 g mol^{-1}; colorless powder; m.p. 170 °C (decomp.); R_F ($CHCl_3$/MeOH, 4/1, v/v) = 0.85; ^{1}H NMR (D_2O, 360 MHz): δ = 1.78 (s, 3H), 2.19 (m, 2H), 2.61 (d, 3H, ^2J = 10.8 Hz), 2.88 (m, 2H), 3.35 (m, 2H), 3.76 (m, 2H), 4.16 (m, 1H), 7.38 (s, 1H), 8.06 (br.q, 1H, ^2J = 10.8 Hz), the NH proton of thymine apparently exchanges and therefore does not give a signal; ^{13}C NMR ([D$_6$]DMSO, 90 MHz): δ = 11.8, 25.4, 28.3, 35.8, 37.3, 44.6, 51.9, 108.3, 141.5, 150.7, 164.3, 167.1, 169.1

4: $C_{13}H_{19}N_3O_5$, M = 297.31 g mol^{-1}; colorless powder; m.p. 220 °C (decomp.); R_F (ethyl acetate/hexane 1/1 v/v) = 0.46; ^{1}H NMR ([D$_6$]DMSO, 360 MHz): δ = 0.66 (s, 3H), 0.86 (s, 3H), 1.89 (dd, 1H, ^2J = 14.9, ^3J = 10.7 Hz), 2.36 (dd, 1H, ^2J = 14.9, ^3J = 2.6 Hz), 2.91 (dd, 1H, ^2J = 10.4, ^3J = 2.6 Hz), 3.24 (d, 1H, ^3J = 11.0 Hz), 3.42 (d, 1H, ^3J = 11.0 Hz), 3.69 (d, 2H, ^3J = 5.8 Hz), 4.14 (t, 1H, ^3J = 5.8 Hz), 5.47 (d, 1H, ^3J = 7.8 Hz), 7.49 (d, 1H, ^3J = 7.8 Hz), 11.24 (br.s, 1H), two acidic protons do not give a signal; ^{13}C NMR ([D$_6$]DMSO, 90 MHz): δ = 17.9, 22.4, 31.6, 35.4, 50.3, 59.4, 77.6, 85.1, 100.2, 146.7, 151.0, 163.7, 173.4

[a] All compounds described in this communication were characterized by ^{1}H NMR and ^{13}C NMR spectroscopy (C-H correlation, NOESY, COSY), mass spectrometry and combustion analysis (C, H, N).

introduced herein are currently being screened for antiviral and antibacterial activity.

The described transformation provides a general access to a novel class of nucleoside analogues called β-lactam nucleoside chimera. The starting materials, which include natural and non-naturally-substituted nucleobase aldehydes and β-amino acids, are readily available in few steps and in a wide variety from commercially available compounds.[10, 12] We could furthermore establish that slightly modified β-lactam nucleoside chimera can also be used for the rapid and efficient construction of PNA-analogous (PNA = peptide nucleic acid) oligomers.[13] This work will be reported shortly.

Experimental Procedure

1 (1 mmol scale): Methyl isocyanide (0.1 mL) was added to a suspension of β-alanine (89 mg) and 1-thyminyl acetaldehyde hydrate (186 mg) in anhydrous methanol (20 mL) at 0 °C, and the reaction mixture was subsequently stirred for 72 h at room temperature. The solution became clear after several hours, and turned cloudy after 48 h. After 72 h, half of the solvent was removed, and the remaining solution placed into a refrigerator. The precipitated product was filtered and dried to obtain 270 mg of a colorless powder. Compounds **2**–**4** were prepared analogously.

Received: December 27, 1994
Revised version: July 27, 1995 [Z7576IE]
German version: *Angew. Chem.* **1995**, *107*, 2465–2467

Keywords: lactams · multicomponent reactions · nucleoside analogues

[1] "Multicomponent Reactions in Organic Chemistry": I. Ugi, A. Dömling, W. Hörl, *Endeavour* **1994**, *18*, 115.
[2] Review article on combinatorial chemistry: "Drug Discovery on the Assembly Line": J. Alper, *Science* **1994**, *264*, 1399; M. A. Gallop, R. W. Barett, W. J. Dower, S. P. A. Fodor, E. M. Gordon, *J. Med. Chem.* **1994**, *37*, 1233, 1385; see also: R. M. J. Liskamp, *Angew. Chem.* **1994**, *106*, 661; *Angew. Chem. Int. Ed. Engl.* **1994**, *33*, 633; P. Eckes, *ibid.* **1994**, *106*, 1649 and **1994**, *33*, 1573.
[3] In our research group we have recently developed a novel urethane synthesis from amino acids, oxo components, and isocyanides (W. Hörl, I. Ugi, unpublished), as well as a novel synthesis for iminodicarboxylic acids (A. Demharter, W. Hörl, I. Ugi, unpublished); pyrrole derivatives by Ugi reaction (U-4CR): R. Bossio, S. Marcaccini, R. Pepino, T. Torroba, *Synthesis* **1993**, 783; imidazole by U-4CR and selenocyanate (HSeCN) as thirteenth acid component in the U-4CR: R. Bossio, S. Marcaccini, R. Pepino, *Liebigs Ann. Chem.* **1993**, 1229; *N,N'*-diarylpeptides by U-4CR: R. Bossio, S. Marcaccini, P. Paoli, R. Pepino, *Synthesis* **1994**, 672; extension of the Asinger condensation (A-4CR) to 5,6-dihydro-2*H*-oxazines: A. Dömling, I. Ugi, *Tetrahedron* **1993**, *49*, 9495; 4-hydroxymethyl-2,5-dihydro-1,3-oxazoles by A-4CR: A. Dömling, A. Bayler, I. Ugi, *Tetrahedron* **1995**, *51*, 755; hydrochlorides of amino acids, di-, and tripeptides as acid components in the U-4CR: M. Hatam, D. Tehranfar, J. Martens, *Synthesis*, **1994**, 619.
[4] G. J. Koomen, *Recl. Trav. Chim. Pays-Bas* **1993**, *112*, 51.
[5] J. M. Frere, M. Nguyen-Disteche, J. Coyette, B. Joris in *Chemistry of β-Lactams* (Ed.: M. I. Page), Chapman & Hall, Cambridge, **1992**, p. 148.
[6] Symposia in Print No. 8: *Recent Advances in the Chemistry and Biology of β-Lactams and β-Lactam Antibiotics* (*BioMed. Chem. Lett.* **1993**, *3*, 2135).
[7] Review: L. N. Jungheim, T. A. Shepherd, *Chem. Rev.* **1994**, *94*, 1553.
[8] Nucleoside analogues containing at azetidine unit have recently been described: F. Hosono, S. Nishiyama, S. Yamamura, T. Izawa, K. Kato, *Biomed. Chem. Lett.* **1994**, *4*, 2083; chimera of a β-lactam unit and a steroid unit will be described elsewhere: K. Kehagia, A. Dömling, I. Ugi, *Tetrahedron* **1995**, *51*, 9519.
[9] C. H. O'Callaghan, R. B. Sykes, S. E. Stanforth, *Antimicrob. Agents Chemother.* **1976**, *10*, 254; D. Greenwood, F. O'Grady, *ibid.* **1976**, *10*, 249; A. J. Corraz, S. L. Dax, N. K. Dunlap, N. H. Georgopapadakou, D. D. Keith, D. L. Pruess, P. L. Rossman, R. Then, J. Unowsky, C.-C. Wei, *J. Med. Chem.* **1992**, *35*, 1828, and references therein.
[10] A. P. Martinez, W. W. Lee, *J. Org. Chem.* **1965**, *30*, 317; M. Yu. Lidak, R. A. Paegle, M. G. Plata, Yu. P. Shvachkin, *Chem. Heterocycl. Compd.* **1971**, 494.
[11] K. Kehagia, D. Dömling, I. Ugi, *Tetrahedron* **1995**, *51*, 139.
[12] β-Amino acid syntheses: J. G. Rivo, *Tetrahedron Lett.* **1994**, *35*, 6599; Review: D. C. Cole, *Tetrahedron* **1994**, *50*, 9517.
[13] A. Dömling, M. Starnecker, M. Mayer, I. Ugi, unpublished results.

 © VCH Verlagsgesellschaft mbH, D-69451 Weinheim, 1995 0570-0833/95/3420-2239 $ 10.00+.25/0

A New Method for the Preparation of Nanostructured Metal Clusters

Manfred T. Reetz* and Stefan A. Quaiser

Nanostructured metal clusters and colloids are of interest as catalysts for organic and inorganic reactions, as electrocatalysts in fuel cells, and as components for materials with special electronic, optical, or magnetic properties.[1, 2] They are usually prepared by chemical reduction of metal salts. In order to prevent undesired agglomeration with formation of either large metal particles in the micrometer range or metal powders, stabilizers such as special ligands,[3] polymers,[4] or tetraalkylammonium salts[5] generally need to be used. Nevertheless, high yields, simple isolation and purification, and control of the cluster size is only seldom possible.[6] Recently we described an electrochemical process by which metal foils are anodically dissolved, and the metal salts formed as intermediates are cathodically reduced with quantitative formation of metal clusters stabilized by tetraalkylammonium salts.[7, 8] Besides the simple isolation and the high purity of the clusters, another advantage is the control of particle size (1–10 nm) by adjusting the current density, that is, the overpotential. Tetraalkylammonium salts serve simultaneously as supporting electrolyte and stabilizer for the cluster. Though this method can be employed for relatively easily oxidizable metals (for example, Pd, Ni, Cu, Au, etc.),[7, 8] for anodically less readily soluble metals like Pt, Rh, Ru, and Mo it functions poorly or not at all. This is unfortunate, because precisely these metals are of interest as potential catalysts.

We now report a solution to this problem based on the use of metal salts.[9] Initially a mixture of $PtCl_2$ and $(NR_4)Br$ in acetonitrile/THF (1:3) was electrolyzed in a simple electrolysis cell[10] consisting of a Pt anode and a Pt cathode. Unfortunately, only a small amount of Pt-containing material was formed, which was difficult to isolate. Because the oxidation process at the anode (for example, $Br^- \rightarrow Br^{\cdot}$) possibly caused problems, in a renewed attempt we used $PtCl_2$ as the metal source and $(NR_4)OAc$ as the supporting electrolyte and stabilizer, in the hope that the Kolbe electrolysis would ensure the chemical "disposal" at the anode (Scheme 1).

Cathode: $Pt^{2+} + 2e^- \longrightarrow Pt^0$

Anode: $2\,CH_3CO_2^- \longrightarrow 2\,CH_3CO_2^{\cdot} + 2e^-$

Scheme 1.

Indeed, this strategy led to the successful electrochemical reduction of $PtCl_2$, with nearly quantitative formation of Pt clusters. The average size of the clusters was determined by high resolution transmission electron microscopy (HRTEM) on 100 to 200 particles (Table 1). The same result was achieved with $RhCl_3/(Bu_4N)OAc$. Under these conditions, the $(Bu_4N)OAc$-stabilized Pt clusters precipitate as solids that can be conveniently isolated by decantation and washing (for example with ether), and when required, redispersed in DMF (up to 1 M solution). Other metals that are not easily oxidized can also be employed, for example, salts of osmium or ruthenium (Table 1). Furthermore, if metal carboxylates are used as the metal source, completely halide-free, stabilized metal clusters are obtained. Because the electrolysis also works with easily oxidizable metals like palladium, this new method is more general than our first process based on sacrificial metal anodes.[7, 8] If the betain 3-(dimethyldodecylammonio)propanesulfonate[7] is used as stabilizer (solvent H_2O or H_2O/THF), a very readily water-soluble metal cluster results (Fig. 1), which is of great industrial interest. For example, 6 nm large, betain-stabilized Pt clusters can be prepared as 1 M solutions in water.

Table 1. Metal clusters prepared by electrochemical reduction of metal salts (electrolyte: 0.1 M $(n\mathrm{Bu_4N})OAc$/THF). d = average diameter, EA = elemental analysis.

Metal salt	d [nm]	EA [a]
$PtCl_2$	2.5 [b]	51.21% Pt
$PtCl_2$	5.0 [c]	59.71% Pt
$RhCl_3 \cdot x\,H_2O$	2.5	26.35% Rh
$RuCl_3 \cdot x\,H_2O$	3.5	38.55% Ru
$OsCl_3$	2.0	37.88% Os
$Pd(OAc)_2$	2.5	54.40% Pd
$Mo_2(OAc)_4$	5.0	36.97% Mo
$PtCl_2 + RuCl_3 \cdot x\,H_2O$	2.5	41.79% Pt + 23.63% Rh [d]

[a] Based on stabilizer-containing material. [b] Current density: 5.00 mA cm^{-2}. [c] Current density: 0.05 mA cm^{-2}. [d] Pt–Rh dimetallic cluster.

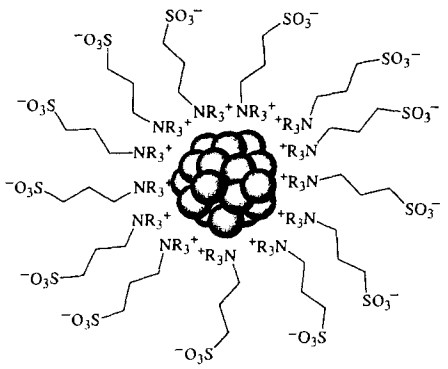

Fig. 1. Schematic view of a betain-stabilized, water-soluble metal cluster.

Preliminary experiments to control the cluster size by means of current density[7] were also successful. The higher the current density, the smaller the cluster (Table 1). The structure of the metal clusters is a spherical "metal core" surrounded by tetraalkylammonium salt that functions as a stabilizing mantle. Recently we were able to visualize such protective mantles of differently sized Pd clusters for the first time by means of the combination of HRTEM and scanning tunneling microscopy (STM).[11, 12]

If two metal salts are employed, for instance $PtCl_2$ and $RhCl_3$, dimetallic clusters are obtained (Table 1). Dimetallic clusters are also accessible by a combination of both electrochemical methods. In this synthetically useful variation the oxidative process at the anode corresponds to the dissolution of the metal sheet (Table 2).

Table 2. Dimetallic clusters prepared by electrochemical reduction of metal salts at sacrificial anodes (electrolyte: 0.1 M $(n\mathrm{Bu_4N})OAc$/THF). d = average diameter, Stoich. = stoichiometry.

Anode	Metal salt	d [nm]	Stoich. (EDX)
Sn	$PtCl_2$	3.0	$Pt_{50}Sn_{50}$
Cu	$Pd(OAc)_2$ [a]	2.5	$Cu_{44}Pd_{56}$
Pd	$PtCl_2$	3.5	$Pd_{50}Pt_{50}$

[a] Electrolyte: 0.1 M $(n\text{-octyl}_4\mathrm{N})OAc$/THF.

[*] Prof. Dr. M. T. Reetz, Dipl.-Chem. S. A. Quaiser
Max-Planck-Institut für Kohlenforschung
Kaiser-Wilhelm-Platz 1, D-45470 Mülheim/Ruhr (Germany)
Telefax: Int. code + (208) 306-2985

 © VCH Verlagsgesellschaft mbH, D-69451 Weinheim, 1995 0570-0833/95/3420-2240 $ 10.00+.25/0

The use of a sacrificial tin electrode, for example, and $PtCl_2$ as the second metal component, in the presence of $(Bu_4N)Br$ as electrolyte and stabilizer, yields 3 nm large Pt–Sn clusters, whose Pt:Sn ratio is shown to be about 1:1 by the *e*nergy *d*ispersive *X*-ray (EDX) spot analysis of individual particles (Fig. 2). To prove the crystalline character of the dimetallic particles, a solution of the sample was first dip-coated onto a holey carbon grid on a copper net. Some clusters remain hanging on the edge of the grid and enable distinct visualization by a high-resolution TEM image (Fig. 3). The diffraction planes are clearly recognizable.

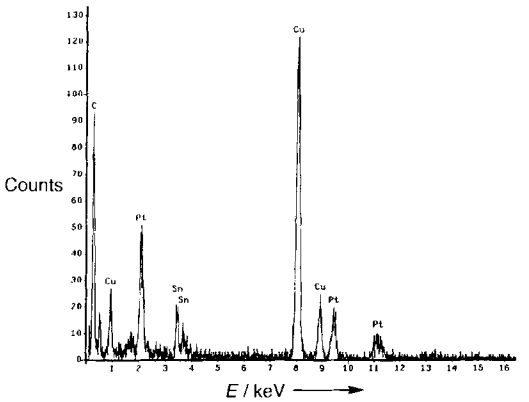

Fig. 2. EDX spectrum of a Pt–Sn dimetallic cluster (copper signals originate from the support net, carbon signals from the carbon grid and stabilizer).

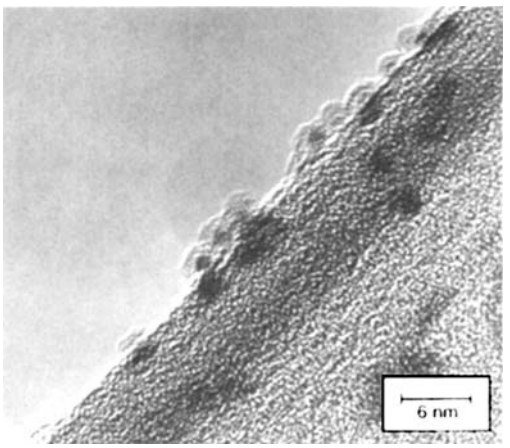

Fig. 3. HRTEM image of Pt–Sn dimetallic clusters (on the edge of a carbon grid).

To prepare supported metal clusters, solids like activated carbon or SiO_2 can be used as suspensions in the electrolysis cell. The clusters are immobilized in situ. Significantly, the size of the metal clusters is not affected by the process. Alternatively, the metal clusters can be conveniently immobilized on solid supports after synthesis: for example, if activated carbon is treated with the black aqueous solution of betain-stabilized Pt clusters (about 6 nm diameter), the metal clusters deposit quantitatively on the solid support within five hours. Simple decantation of the water and washing of the solid material affords the carrier-supported clusters and a colorless, metal-free, aqueous phase that contains about 90% of the betain. The adhesion between carrier and metal cluster is very strong, but no undesirable particle agglomeration occurs. Besides the conventional solid supports, materials like electrically conducting SnO_2 layers are also suitable for coating.

Experimental Procedure

Typical procedure: A solution of tetra-*n*-butylammonium acetate (0.1 M) in THF (90 mL) was placed in a universal electrolysis cell capable of holding 20–100 mL electrolyte. Two pure platinum sheets (3×3 cm^2 surface area, 0.5 mm thickness) about 5 mm apart served as electrodes. All operations were performed under inert atmosphere (argon or nitrogen). Palladium acetate (500 mg) was dissolved in the electrolyte with stirring, and a current of 5 mA was applied and increased to 30 mA within 10 min. The electrolysis cell was kept at 20 °C by means of a cooling mantle. During the course of the electrolysis the electrolyte became dark brown, and a black precipitate formed. After a current flux of 450 C the electrolysis was stopped, and the light brown supernatant was removed by pressure of inert gas. The precipitate was washed with two portions (10 mL each) of diethyl ether and dried under oil pump vacuum. A gray-black solid (406 mg) was obtained; particle size 2.5 nm; metal content according to elemental analysis: 54% palladium, based on stabilizer-containing material.

Received: April 12, 1995 [Z 7886 IE]
German version: *Angew. Chem.* **1995**, *107*, 2461–2463

Keywords: catalysis · clusters · electrolysis · metal salts · transmission electron microscopy

[1] a) *Clusters and Colloids* (Ed.: G. Schmid), VCH, Weinheim, **1994**; b) A. Henglein, *J. Phys. Chem.* **1993**, *97*, 5457; c) S. C. Davis, K. J. Klabunde, *Chem. Rev.* **1982**, *82*, 153; d) L. N. Lewis, *ibid.* **1993**, *93*, 2693; e) G. Schmid, *ibid.* **1992**, *92*, 1709; f) B. C. Gates, L. Guczi, H. Knözinger, *Metal Clusters in Catalysis*, Elsevier, Amsterdam, **1986**; g) G. Schön, U. Simon, *Coll. Polym. Sci.* **1995**, *273*, 101.

[2] B. Conway, B. Tilak in *Adv. Catalysis, Vol. 38* (Eds.: D. Eley, H. Pines, P. Weisz), Academic Press, New York, **1992**; H. Wendt, *Electrochemical Hydrogen Technology*, Elsevier, Amsterdam, **1990**.

[3] G. Schmid, B. Morun, J.-O. Malm, *Angew. Chem.* **1989**, *101*, 772; *Angew. Chem. Int. Ed. Engl.* **1989**, *28*, 778; M. N. Vargaftik, V. P. Zagorodnikov, I. P. Stolarov, I. I. Moiseev, *Mol. Catal.* **1989**, *53*, 315.

[4] J. S. Bradley, J. M. Millar, E. W. Hill, *J. Am. Chem. Soc.* **1991**, *113*, 4016; F. Porta, F. Ragaini, S. Cenini, G. Scari, *Gazz. Chim. Ital.* **1992**, *122*, 361.

[5] J. Kiwi, M. Grätzel, *J. Am. Chem. Soc.* **1979**, *101*, 7214; J. Blum, Y. Sasson, A. Zoran, *J. Mol. Catal.* **1981**, *11*, 293; M. Boutonnet, J. Kizling, P. Stenius, G. Maire, *Colloids Surf.* **1982**, *5*, 209; N. Toshima, T. Takahashi, H. Hirai, *Chem. Lett.* **1985**, 1245; M. Boutonnet, J. Kizling, R. Touroude, G. Maire, P. Stenius, *Appl. Catal.* **1986**, *20*, 163; K. Meguro, M. Toriyuka, K. Esumi, *Bull. Chem. Soc. Jpn.* **1988**, *61*, 341; J. Wiesner, A. Wokaun, H. Hoffmann, *Prog. Coll. Polym. Sci.* **1988**, *76*, 271; N. Satoh, K. Kimura, *Bull. Chem. Soc. Jpn.* **1989**, *62*, 1758; H. Bönnemann, W. Brijoux, R. Brinkmann, E. Dinjus, T. Joussen, B. Korall, *Angew. Chem.* **1991**, *103*, 1344; *Angew. Chem. Int. Ed. Engl.* **1991**, *30*, 1312; N. Toshima, T. Takahashi, *Bull. Chem. Soc. Jpn.* **1992**, *65*, 400.

[6] J. S. Bradley in [1a], Chap. 6.

[7] M. T. Reetz, W. Helbig, *J. Am. Chem. Soc.* **1994**, *116*, 7401.

[8] M. T. Reetz, W. Helbig, S. A. Quaiser, application for patent **1994**.

[9] M. T. Reetz, W. Helbig, S. A. Quaiser, in *Active Metals– Preparation, Characterization, Applications* (Ed.: A. Fürstner), VCH, Weinheim, **1995**, 279–297.

[10] The electrochemical reduction of metal salts used for decades by industry in acidic, aqueous medium affords only powders: N. Ibl, *Chem.-Ing. Tech.* **1964**, *36*, 601; R. Walker, *Chem. Ind.* **1980**, 260.

[11] M. T. Reetz, W. Helbig, S. A. Quaiser, U. Stimming, N. Breuer, R. Vogel, *Science* **1995**, *267*, 367.

[12] The present results do not exclude the presence of an oxidized layer.

A Novel Hexanuclear Fe^{III}-*cis*-Inositolato Complex as a Model for Fe^{III}–Polyol Interactions in Aqueous Solution**

Kaspar Hegetschweiler,* Lorenza Hausherr-Primo, Willem H. Koppenol, Volker Gramlich, Léon Odier, Wolfram Meyer, Heiner Winkler, and Alfred X. Trautwein

It has been known for some time now that sugars, sugar alcohols, and sugar acids can effectively prevent the precipitation of only slightly soluble metal hydroxides in aqueous solution.[1] If alkali is added to a solution of a metal salt in the presence of a polyol, depending on the selected conditions, soluble polyolato metalates or solid metal polyolates can be obtained.[2] The hydrolytic polymerization of the metal cations can often be observed as a competitive reaction, although a combination of both reactions (that is, the formation of oxo- or hydroxo-bridged multinuclear polyolato complexes) can take place.[3] These compounds are of great interest, in particular with regard to the synthesis of new materials (sol–gel technology).[4]

The structures of many of the metal polyolates are not known as these compounds often crystallize poorly and are amorphous. We have now been able to obtain crystals of the potassium salt of the polyolato(oxo)iron complex **1** (which is stable in water) with the composition K_5-**1**$\cdot 14.5H_2O$ and to characterize it by

$K_5[OFe_6\{(ino)_6\text{-}2\,1H\}]\cdot 14.5H_2O$ $\quad$ K_5-**1**$\cdot 14.5H_2O$ (ino = *cis*-inositol)

means of X-ray structure analysis[5] and by magnetic susceptibility measurements.[6] The complex anion **1** containing the sorbitol ligand (depicted in Scheme 1) fits into a continually growing series of multinuclear Fe^{III} complexes, which are of interest as model compounds for proteins, such as ferritin.[7]

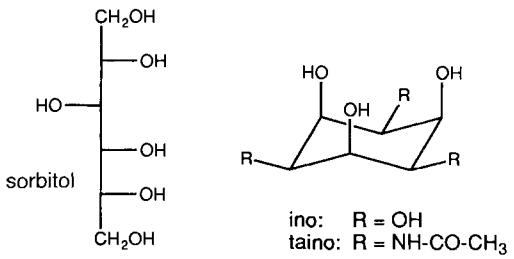

Scheme 1. Structural formulas of the ligands used here.

[*] Dr. K. Hegetschweiler, Dipl.-Chem. L. Hausherr-Primo, Prof. Dr. W. H. Koppenol
Laboratorium für Anorganische Chemie
ETH Zentrum, CH-8092 Zurich (Switzerland)
Telefax: Int. code + (1)632-1090
Dr. V. Gramlich
Institut für Kristallographie
ETH Zentrum, CH-8092 Zurich (Switzerland)
Dr. L. Odier
CEA DRFMC/SESAM/MV, CENG
F-38054 Grenoble Cedex 9 (France)
Dipl.-Phys. W. Meyer, Dr. H. Winkler, Prof. Dr. A. X. Trautwein
Institut für Physik der Medizinischen Universität
Ratzeburger Allee 160, D-23538 Lübeck (Germany)

[**] Metal Complexes of Polyalcohols, Part 3. This work was supported by the company Vifor (International), St. Gallen, Switzerland, and by the BMFT (Project 05 5FLAXI4). We would like to thank Prof. S. J. Angyal, Sydney, Australia, for valuable suggestions, and Dr. H.-F. Nolting from the EMBL-Aussenstelle Hamburg for his helpful support. Part 2: L. Hausherr-Primo, K. Hegetschweiler, H. Rüegger, L. Odier, R. D. Hancock, H. W. Schmalle, V. Gramlich, *J. Chem. Soc. Dalton Trans.* **1994**, 1689–1701.

If two equivalents of *cis*-inositol are added to an aqueous solution of $FeCl_3$, and the mixture is subsequently neutralized with KOH, a pale yellow and barely soluble solid is initially obtained at pH = 7. This redissolves in alkaline medium to give a deep brown solution. We assume that the yellow compound is an uncharged mononuclear dipolyolato complex,[8] which then slowly reacts to give the hydrolysis product **1** described. The complex **1** is stable in water between pH 8 and 10.

The structure of **1** has no point symmetry, and the Fe_6O_{22} core can be considered a random netlike aggregate of FeO_x polyhedra (x = 5, 6). Though edge-bridged octahedra dominate in the structure, polyhedra with common faces or common apices also occur (Fig. 1). The pentacoordinate Fe(1) atom is located at the center of a distorted square pyramid;[9] the other Fe atoms are in a distorted octahedral environment. The central μ_3-oxo ligand bridges three of the six Fe centers. The remaining bridges are exclusively the eleven μ_2-alkanolato groups of the peripheral *cis*-inositol ligands, which provide an additional ten oxygen atoms for terminal coordination. All the hydroxy groups deprotonate on coordination.

The interactions between the metal ions and the ligands do not allow the recognition of a consistent coordination principle either. Binding of the iron ions to the *syn*-triaxial coordination site of the inositol ligand dominates, but a series of other structural elements can also be observed. It is striking that all the ligands are bound to several iron ions; two, three, and even four iron ions are simultaneously coordinated to a single ligand. Conversely, *cis*-inositol can act as a mono-, bi-, or tridentate ligand. In one case one ligand is coordinated in a tridentate fashion to two iron ions simultaneously; one iron center occupies the *syn*-triaxial binding site and the other the axial–equatorial–axial binding site.

The six *cis*-inositol ligands obviously shield the periphery of the complex so efficiently that no further aggregation can occur. When treated with Fe^{III} ions, the open-chain sugar alcohol sorbitol (Scheme 1) forms only low-molecular-weight complexes when the solution is strongly alkaline. If the pH is lowered to about 8, a continuous aggregation results, which finally leads to the formation of brown gels.[10] An EXAFS measurement[11] on the sorbitol complex **2**—which has a similar hydrodynamic radius[10]

$Na_x[Fe_xO_{2x}(sor)_x]$ **2**, sor = sorbitol $(5 \le x \le 8)$

to **1**—shows, however, that the two complexes have analogous local structures (Table 1). The magnetic properties of **1** and **2** are also similar between 10 and 250 K.[6]

When 1,3,5-triacetamido-1,3,5-trideoxy-*cis*-inositol (taino, Scheme 1) is treated with Fe^{III} ions in aqueous solution, the mononuclear complex **3** is formed exclusively. This complex was

$[Fe\{(taino)_2\text{-}3H\}]$ **3**

insoluble at pH = 7, and was isolated and structurally characterized.[8] The complex **3** can be readily dissolved in alkaline media; the pale yellow solutions are stable. The formation of multinuclear hydrolysis products has not been observed. In the series **3** → **1** → **2**, the number of the possible metal–ligand interactions increases drastically. The *cis*-inositol ligand is obviously just rigid enough to form a definite, stable hexanuclear complex. In the case of polyol ligands with a greater number of degrees of freedom, a large number of energetically almost equivalent structures can form; this hinders the crystallization process considerably.

In previous publications the Fe-(μ-OH)$_2$-Fe complex fragment has been postulated as a bridging unit for multinuclear polyolatoiron complexes.[12] The short Fe–Fe distance of 285(3) pm[13] in **2** is incompatible with this structural unit.[14] However, it falls within the same region as the Fe(3)–Fe(6)

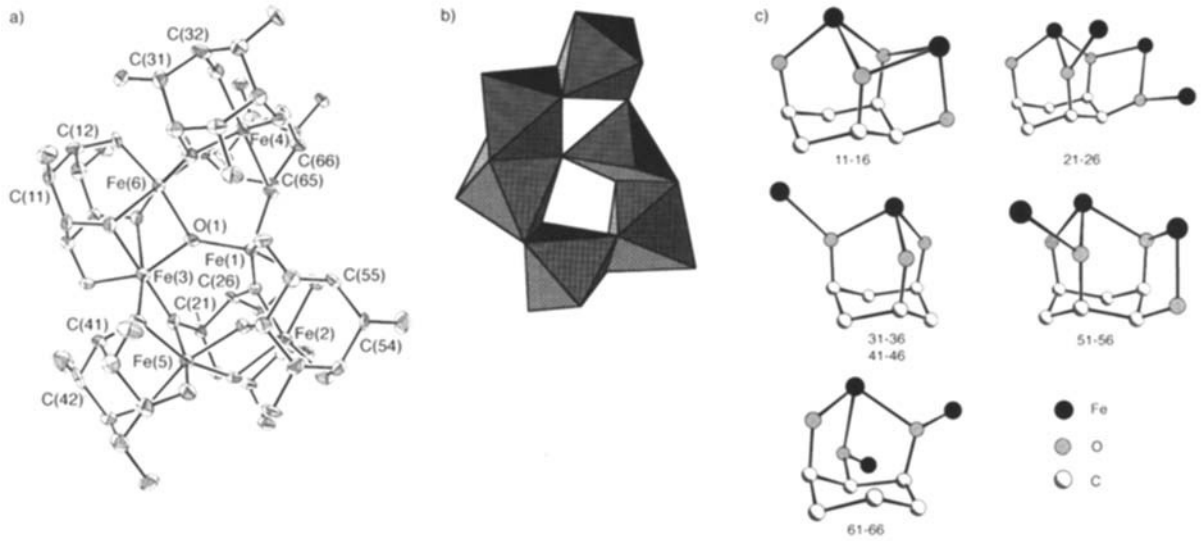

Fig. 1. Structure of $[OFe_6\{(ino)_6-2\,H\}]^{5-}$ (**1**). a) ORTEP representation of the complex anion with numbering scheme. The oxygen atoms of the inositol ligands are labeled O(11) O(66) in accordance with the C atoms of the cyclohexane ring to which they are bound. The thermal ellipsoids represent 50 % probabilities of occupation. b) Representation of the cyclic Fe_6O_{22} core. c) Individual Fe-inositol interactions (noncoordinated hydroxy groups are not shown). The numbering of the ligands is as in a). The average Fe–O distance is 197 pm at the pentacoordinate Fe(1), considerably shorter than at the hexacoordinate iron centers (202 pm). Fe–Fe distances [pm]: Fe(1)-Fe(2) 298.3(2), Fe(1)-Fe(3) 350.5(2), Fe(1)-Fe(4) 367.0(2), Fe(1)-Fe(6) 350.4(2), Fe(2)-Fe(5) 324.2(2), Fe(3)-Fe(5) 310.8(2), Fe(3)-Fe(6) 280.4(2), Fe(4)-Fe(6) 313.8(2). Average Fe–O bond lengths [pm]: $Fe-O_{oxo}$ 192.4, $Fe-O_{term}$ 192.9, $Fe-O_{br}$ 206.6.

Table 1. Averaged coordination numbers of the Fe atoms (N), mean Fe–O and Fe–Fe distances (R), and mean static and dynamic displacement parameters (σ) from the X-ray structure analysis of **1** and the EXAFS measurements [11, 13] of **2**. The average standard deviations are 1 pm for the Fe–O distances and 0.2 pm for the Fe–Fe distances in **1** (X-ray diffraction), and 2 pm and 3 pm respectively for the corresponding distances in **2** (EXAFS measurement).

Sample	**1**			**2**	
Fe-O					
N	2.0	3.83 [a]		2	4
R (pm)	192	206		194	202
σ (pm)	3	8		6	11
Fe-Fe					
N	0.67	1.0	1.0	1	1
R (pm)	290	316	356	285	312
σ (pm)	8	6	8	8	8

[a] This value results from an average of five hexacoordinate Fe centers and one pentacoordinate Fe center.

distance of 280.4(2) pm in **1** (octahedra with common face) and thus could indicate a multiple μ-alkanolato bridging mode in which the Fe atoms are bound to the same ligand. The structural properties of **1** thus permit a valuable insight into the build-up of polyolatoiron compounds.

Received: February 20, 1995
Revised version: August 1, 1995 [Z 7727IE]
German version: *Angew. Chem.* **1995**, *107*, 2421–2423

Keywords: chelate ligands · iron compounds · complexes with oxygen ligands · polyols

[1] P. Goldschmidt, E. Weingardt, W. Bachmann, *Kolloid-Z.* **1929**, *47*, 49–55.
[2] P. Klüfers, J. Schuhmacher, *Angew. Chem.* **1994**, *106*, 1925; *Angew. Chem. Int. Ed. Engl.* **1994**, *33*, 1863.
[3] K. Hegetschweiler, H. Schmalle, H. M. Streit, W. Schneider, *Inorg. Chem.* **1990**, *29*, 3625–3627.
[4] a) L. G. Hubert-Pfalzgraf, *New J. Chem.* **1987**, *11*, 663; b) C. J. Brinker, G. W. Scherer, *Sol-gel science: the physics and chemistry of sol-gel processing*, Academic Press, San Diego, **1990**.
[5] The dark brown triclinic crystals were obtained at pH = 9 by covering an aqueous solution with a layer of ethanol. Water of crystallization was lost on contact with air, so the crystals were measured in a glass capillary: space group $P\bar{1}$ (No. 2), $a = 1273.0(3)$, $b = 1385.0(3)$, $c = 1974.3(4)$ pm, $\alpha = 90.65(3)$, $\beta = 93.29(3)$, $\gamma = 112.34(3)$°, $V = 3212(1) \times 10^6$ pm^3, $Z = 2$, $Mo_{K\alpha}$ radiation, graphite monochromator, four-circle diffractometer Picker-Stoe, $2\theta = 3$–40°, **6019 reflections measured, 5982 independent, of which 4305 with $I > 2\sigma(I)$ were used for the refinement of 901 parameters. Structure solution using direct methods, numerical absorption correction. All non-hydrogen atoms were refined anisotropicically (least-squares, full matrix). The H(–C) positions were taken from the difference Fourier map, but not refined, however. $R = 0.0471$, $R_w = 0.0520$. Residual electron density + 0.68/–0.80 e A^{-3}. Further details of** the crystal structure investigation may be obtained from the Director of the Cambridge Crystallographic Data Centre, 12 Union Road, GB-Cambridge CB2 1EZ, on quoting the full literature citation.
[6] The magnetic susceptibility measurements were carried out on a polycrystalline sample of the inositol complex **1** and on a frozen solution of the sorbitol complex **2** using a SQUID magnetometer. For **1** it was found that $\mu_{eff} = 10.8\ \mu_B$ (250 K) and $10.0\ \mu_B$ (10 K). This result indicates at $S = 5$ ground state. Analogously, it was found for **2** that $\mu_{eff} = 11.8\ \mu_B$ (250 K) and $10.0\ \mu_B$ (10 K). The magnetic moments given are based on iron hexamers. This assumption is confirmed in the case of **1** by the crystal structure determination, whereas in the case of **2** it is supported by laser light scattering measurements [10]. It is quite possible that the sorbitol solution contains a great variety of species; the agreement of the two sets of results, however, indicates an analogy in the magnetic coupling structure too.
[7] S. J. Lippard, *Angew. Chem.* **1988**, *100*, 353–371; *Angew. Chem. Int. Ed. Engl.* **1988**, *27*, 344–361; J. K. McCusker, C. A. Christmas, P. M. Hagen, R. K. Chadha, D. F. Harvey, D. N. Hendrickson, *J. Am. Chem. Soc.* **1991**, *113*, 6114–6124; S. L. Heath, A. K. Powell, *Angew. Chem.* **1992**, *104*, 191–192; *Angew. Chem. Int. Ed. Engl.* **1992**, *31*, 191–193; V. S. Nair, K. S. Hagen, *Inorg. Chem.* **1992**, *31*, 4048; K. L. Taft, C. D. Delfs, G. C. Papaefthymiou, S. Foner, D. Gatteschi, S. J. Lippard, *J. Am. Chem. Soc.* **1994**, *116*, 823–832; V. S. Nair, K. S. Hagen, *Inorg. Chem.* **1994**, *33*, 185–186.
[8] K. Hegetschweiler, M. Ghisletta, L. Hausherr-Primo, T. Kradolfer, H. W. Schmalle, V. Gramlich, *Inorg. Chem.* **1995**, *34*, 1950.
[9] The pyramid is transformed into a severely distorted octahedron by the addition of O(51). The distance between Fe(1) and O(51) is 2.47 Å, however, which means that they cannot be regarded as having bonding interactions.
[10] H. W. Rich, K. Hegetschweiler, H. M. Streit, I. Erni, W. Schneider, *Inorg. Chim. Acta* **1991**, *187*, 9–15.
[11] H. Winkler, W. Meyer, A. X. Trautwein, K. Hegetschweiler, H.-F. Nolting, *Physica B* **1995**, *208–209*, 733.
[12] P. Saltman, *J. Chem. Educ.* **1965**, *42*, 682–687; W. Schneider, *Chimia* **1988**, *42*, 9–20; L. Nagy, H. Ohtaki, T. Yamaguchi, M. Nomura, *Inorg. Chim. Acta* **1989**, *159*, 201–207.
[13] The determination of the Fe–Fe distances is difficult, because several C atoms are situated at similar distances as those of the Fe neighbors. Differentiation between the different types of atoms is possible, however, because the amplitude of the back scattering as a function of the wave number k passes through a maximum at about $k = 0.08$ pm^{-1} in the case of Fe, whereas it decreases continuously in the case of C.
[14] A series of dinuclear Fe^{III} complexes with a μ-oxo bridge (Fe–Fe: 339–356 pm) or a μ-dihydroxo bridge (Fe–Fe: 308–316 pm) were structurally characterized. See for example: D. M. Kurtz, *Chem. Rev.* **1990**, *90*, 585.

Bis(trifluoromethyl)trioxide: First Structure of a Straight-Chain Trioxide**

Karina I. Gobbato, Martin Frank Klapdor, Dietrich Mootz, Wolfgang Poll, Sonia E. Ulic, Helge Willner, and Heinz Oberhammer*

Dedicated to Professor Herbert W. Roesky on the occasion of his 65th birthday

Straight-chain polyoxygen compounds of the type R_2O_n ($n = 1, 2, 3, 4 \ldots$) become less stable with increasing chain length. The parent compounds H_2O_n are of general and theoretical interest.[1] Numerous compounds of the type R_2O_2 are known, but polyoxygen compounds with $n \geq 3$ were reported almost exclusively with R = F, SF_5, alkyl, or perfluoroalkyl groups. At room temperature only trioxides with perfluoroalkyl groups can be isolated. The simplest derivative of this class of compounds, bis(trifluoromethyl) trioxide, CF_3OOOCF_3, which was reported for the first time in 1963[2] and isolated as pure substance shortly after,[3] is the best characterized trioxide. The colorless gas with a boiling point of $-16\,^{\circ}C$ and melting point of $-138\,^{\circ}C$ decomposes at room temperature within months to give CF_3OOCF_3 and oxygen.[3] Vibrational,[3,4] NMR,[3] mass,[3] and X-ray photoelectron spectra (XPS)[5] of this interesting compound are known, but the molecular structures of this and any other covalent straight-chain trioxide[6] have not been determined unequivocally. The result of an electron diffraction study of a mixture of CF_3OOCF_3 and CF_3OOOCF_3 appears to be uncertain,[7] as demonstrated by a later investigation of CF_3OOCF_3.[8] We therefore decided to synthesize this trioxide again and to determine its structure in the gas phase by electron diffraction and in the crystalline state by X-ray diffraction. The experimental studies are supplemented by ab initio calculations. The derived structural parameters are listed in Table 1.

Analysis of the radial distribution curve of CF_3OOOCF_3 (Fig. 1), calculated by Fourier transform of the molecular intensities, yields a skew structure with *trans* orientation of the two CF_3 groups (C_2 symmetry). This result agrees with the interpretation of Raman spectra,[4b] but is in contrast to the interpretation of IR spectra, which indicate C_1 symmetry.[4c] In the least-squares refinement local C_{3v} symmetry was assumed for the CF_3 groups with a possible tilt angle between the C_3 axis and the O–C bond. The fit of the experimental molecular intensities improves slightly if a small amount of impurity (5% CF_3OOCF_3), which was observed immediately after the synthesis, is taken into account in the structure analysis.

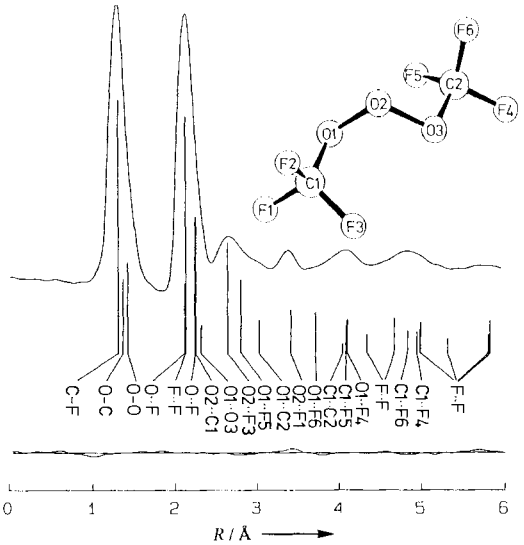

Fig. 1. Experimental radial distribution function and difference between experimental and calculated curve. The positions of interatomic distances are indicated by vertical bars.

Table 1. Experimentally and theoretically determined structural parameters of CF_3OOOCF_3.

	Gas [a]	Crystal [b]	HF/3-21G
C-F	1.326(3)	1.315(2)	1.327
O-C	1.378(12)	1.389(2)	1.393
O-O	1.452(5)	1.437(2)	1.453
O-O-O	106.7(20)	106.4(1)	104.4
O-O-C	105.8(6)	106.5(1)	107.4
F-C-F	108.3(4)	109.3(7)	109.6
$\alpha(CF_3)$ [c]	5.4(7)	5.0(2)	4.0
O-O-O-C	96.0(38)	95.9(8)	97.6

[a] Electron diffraction; r_a [Å] and α [°], 3σ values in parentheses. [b] X-ray diffraction; mean parameters; σ values in parentheses. [c] Tilt angle between the C_3 axis of the CF_3 group and O–C bond.

[*] Prof. Dr. H. Oberhammer, K. I. Gobbato
Institut für Physikalische und Theoretische Chemie der Universität
D-72076 Tübingen (Germany)
Telefax: Int. code + (7071) 296910
e-mail: heinz.oberhammer@uni-tuebingen.de
M. F. Klapdor, Prof. Dr. D. Mootz, Dr. W. Poll
Institut für Anorganische Chemie und Strukturchemie
der Universität Düsseldorf (Germany)
Dr. S. E. Ulic
Facultad de Ciencas Exactas, Universidad Nacional de La Plata (Argentina)
Prof. Dr. H. Willner
Institut für Anorganische Chemie der Universität Hannover (Germany)

[**] K. I. G. and S. E. U are grateful for fellowships from the DAAD and CONICET (República Argentine), respectively. H. W. and H. O. acknowledge financial support by the DFG.

In the crystal (unit cell in Fig. 2), the asymmetric unit comprises a whole molecule, twisted as in the gas phase and with a *trans* orientation of the CF_3 groups. Deviations from C_2 symmetry are only small. As an example, the dihedral angles C1-O1-O2-O3 and O1-O2-O3-C2 have been determined independently, but the obtained values of 96.8(1) and 95.1(1)° are quite similar. The same holds for the individual values of other geometric parameters (only their averages are listed in Table 1), as well as for the dihedral angles F1-C1-O1-O2 and O2-O3-C2-F4 of 178.1(1) and 176.7(1)°. These dihedral angles show that the *trans* position (antiperiplanar orientation) of the F atoms with respect to the central O2 is almost ideal. The distinct widening of all bond

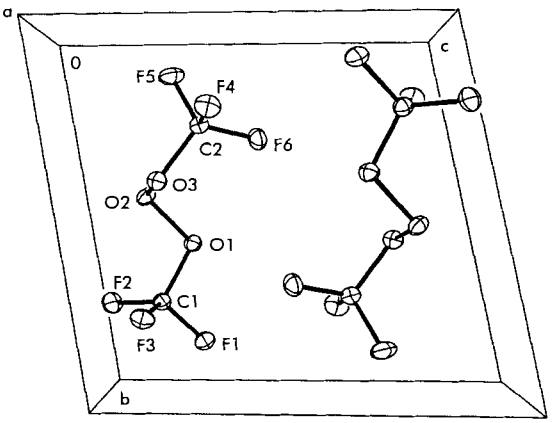

Fig. 2. Unit cell of a crystal of $CF_3COOOCF_3$ with two molecules (ellipsoids represent 25% probability; viewed down the x axis).

angles F-C-O when the F atom is *gauche* rather than *trans* (mean values 112.1(1) and 104.7(1)°, tilt angle $\alpha(CF_3) = 5.0(2)°$) correlates with the smallness of the nonbonding intramolecular distances: F(*gauche*) $\cdots$ O2 mean value: 2.65(3) Å; for F(*trans*) $\cdots$ O2: 3.399(2) Å.

Although systematic differences exist between structural parameters for the gaseous and crystalline state, the agreement of the results obtained with electron and X-ray diffraction is very good. In particular the bond angles and the O-O-O-C dihedral angle, which are most easily affected by packing effects in the crystal,[9] possess identical values within experimental uncertainties in both phases. The good agreement of the geometric parameters optimized with the HF/3-21G method with the experimental values is most likely due to a fortuitous compensation of several inadequacies of this method. Ab initio calculations for HOOOH with different basis sets result in O–O bond lengths between 1.373 and 1.539 Å.[10] The HF/3-21G calculations for CF_3OOOCF_3 predict the existence of a second stable conformer with *cis* orientation of the two CF_3 groups (C_s symmetry), 3.3 kcal mol^{-1} higher in energy.

The O–O bond in CF_3OOOCF_3 is slightly shorter than that in hydrogen peroxide (1.464 Å[10]), but longer than that in CF_3OOCF_3 (1.419(20) Å[8]). As expected, this distance is longer than in ozone (1.2716(2) Å[11]) or in the O_3^- ion (1.29–1.35 Å[12]). The O-O-O bond angle in the trioxide is smaller than a tetrahedral angle and considerably smaller than in O_3 (117.79(3)°) or in O_3^- (113–119°). The O-O-O-C dihedral angle is larger than the predicted value for HOOOH of about 80°,[11] but distinctly smaller than the C-O-O-C angle in CF_3OOCF_3 (123.3(40)°[8]). A value similar to that in the trioxide was observed for the S-S-S-C angle in CF_3SSSCF_3 (89(3)° in the gas[13] and 88.5(1)° in the crystal[14]).

Experimental Procedure

Caution: CF_3OOOCF_3 is potentially explosive, especially in the presence of organic or oxidizable materials. It should be handled only in millimolar quantities and with proper safety precautions. The synthesis was performed according to a modified literature method [15]. A 4 L round-bottomed flask, equipped with a water-cooled high-pressure mercury lamp (TQ150, Heraeus) at its center, was filled with a mixture of 100 mbar $CF_3C(O)CF_3$ (ca. 16 mmol), 200 mbar F_2, and 300 mbar O_2. After 24 hours photolysis, excess F_2 and O_2 was pumped off at −196 °C, and the residue fractionated in vacuo through a series of traps held at −80, −120, and −196 °C. In the trap at −120 °C CF_3OOOCF_3 was collected, which after repeated fractionation contained as the only impurity 5% CF_3OOCF_3, as determined by IR and ^{19}F NMR spectroscopy. Yield 1.2 g (6.5 mmol).

The electron diffraction intensities were recorded with a Gasdiffraktograph KD-G2 at nozzle-to-plate distances of 25 and 50 cm and with an accelerating voltage of ca. 60 kV. The electron wavelength was calibrated with ZnO powder. The temperature of the sample reservoir was −90 °C, that of the inlet nozzle 15 °C. The photographic plates were analyzed with the usual methods [16] and scattering intensities in the s ranges 2–18 and 8–35 Å^{-1} ($s = (4\pi/\lambda)\sin\theta/2$, λ = electron wavelength, θ = scattering angle) were used in the structure analysis.

Crystal growth was performed from the melt in a thin-walled quartz glass capillary. The sample was cooled at a rate of 1 °C min^{-1} in the cold gas stream of a diffractometer (Siemens/Stoe AED2) equipped for work at low temperatures; $Mo_{K\alpha}$ radiation ($\lambda = 0.71073$ Å), graphite monochromator, Ω-θ scan, $2\theta_{max} = 65°$, $T = -170$ °C; space group $P\bar{1}$, $Z = 2$; $a = 4.810(2)$, $b = 7.477(4)$, $c = 7.993(4)$ Å, $\alpha = 78.91(3)$, $\beta = 86.12(3)$, $\gamma = 83.49(3)°$, $V = 280.0(2)$ Å^3. The structure was solved by direct methods with SHELXS-86 [17], and refined with 2026 independent $|F_o|^2$ values (of these 1763 with $|F_o| > 4\sigma_F$ were classified as observed) with SHELXL-93 [18]: $R(F^2) = 0.146$ with all and $R(F) = 0.048$ only with the observed reflections. The residual electron density was between −0.33 and 0.48 e Å^{-3}. The program SHELXTL PLUS [19] was used to draw the crystal structure (Fig. 2). Further details of the crystal structure investigation are available on request from Fachinformationszentrum Karlsruhe, D-76344 Eggenstein-Leopoldshafen (Germany) by quoting the depository number CSD-401780.

Received: May 29, 1995 [Z 8033 IE]
German version: *Angew. Chem.* **1995**, *107*, 2433–2434

Keywords: electron diffraction · oxygen compounds · structure elucidation · trioxides

[1] D. Cremer, *J. Chem. Phys.* **1978**, *69*, 4456.
[2] V. A. Ginsburg, E. S. Vlasva, N. M. Vasil'eva, N. S. Mirzabekova, S. P. Makarov, A. I. Schchekotikhin, A. Ya. Yakubovich, *Dokl. Akad. Nauk SSSR.* **1963**, *149*, 97; *Dokl. Chem. (Engl. Transl.)* **1963**, *149*, 188.
[3] a) P. G. Thompson, *J. Am. Chem. Soc.* **1967**, *89*, 4316; b) L. R. Anderson, W. B. Fox, *ibid.* **1967**, *89*, 4313.
[4] a) R. A. De Marco, R. R. Smardzewski, *J. Fluorine Chem.* **1976**, *7*, 347; b) J. D. Witt, J. R. Durig, D. D. DesMarteau, R. M. Hammaker, *Inorg. Chem.* **1973**, *12*, 807; c) R. P. Hirschmann, W. B. Fox, L. R. Anderson, *Spectrochim. Acta A* **1969**, *25*, 811.
[5] P. Brant, J. A. Hashmall, F. L. Carter, R. A. De Marco, W. B. Fox, *J. Am. Chem. Soc.* **1981**, *103*, 329.
[6] Only one crystal structure of a cyclic compound has been reported, namely, that of the transannular primary ozonide of *tert*-butyl-10-methyl-anthracene: Y. Ito, A. Matsuura, R. Otani, T. Matsuura, *J. Am. Chem. Soc.* **1983**, *105*, 5699. Moreover, the central oxygen atom appears to be disordered.
[7] A. Yokozeki, S. H. Bauer, *Top. Curr. Chem.* **1974**, *53*, 71; R. L. Hilderbrandt, S. H. Bauer, *Third Austin Symposium on Gas Phase Molecular Structure*, Austin, Texas, **1970**.
[8] C. J. Marsden, L. S. Bartell, F. P. Diodati, *J. Mol. Struct.* **1977**, *39*, 253.
[9] No intermolecular distance in the crystal is shorter than the sum of the respective van der Waals radii. The shortest contact (2.956(2) Å) occurs between an F2 and an O2 atom.
[10] J. Koput, *J. Mol. Spectrosc.* **1986**, *115*, 438.
[11] J. C. Depannemaecker, J. Bellet, *J. Mol. Spectrosc.* **1977**, *66*, 106.
[12] W. Hesse, M. Jansen, W. Schnick, *Prog. Solid State Chem.* **1989**, *19*, 47.
[13] M. Gaensslen, R. Minkwitz, W. Molzbeck, H. Oberhammer, *Inorg. Chem.* **1992**, *31*, 4147.
[14] C. Meyer, Dissertation, Universität Düsseldorf, **1994**.
[15] E. L. Varetti, P. J. Aymonino, *Ann. Asoc. Quim. Argent.* **1970**, *23*, 58.
[16] H. Oberhammer, W. Gombler, H. Willner, *J. Mol Struct.* **1981**, *70*, 273.
[17] G. M. Sheldrick, *Acta Crystallogr. Sect. A* **1990**, *46*, 467.
[18] G. M. Sheldrick, *Program for the Refinement of Crystal Structures*, Universität Göttingen, **1993**.
[19] SHELXTL PLUS, Structure Determination Systems, Revision 4.21, Siemens Analytical X-Ray Instruments Inc., Madison, WI, **1990**.

Electronically Tuned *trans* Labilization Controls the Substitution Behavior of Rhodoximes**

Carlos Dücker-Benfer, Renata Dreos, and Rudi van Eldik*

Substitutions of axial ligands of alkyl(aqua)bis(dimethylglyoximato)rhodium(III) complexes were studied in earlier reports [Eq. (a); Hdmg = dimethylglyoximate anion].[1–6] The reactivity of the rhodium complexes shows a strong dependence on the nature of the alkyl substituent R. The lability of these complexes is affected by the size of the alkyl group and the electronic

$$trans\text{-}[Rh(Hdmg)_2(R)(H_2O)] + L \underset{k_2}{\overset{k_1}{\rightleftharpoons}} trans\text{-}[Rh(Hdmg)_2(R)L] + H_2O \quad (a)$$

state of the nonlabile ligands. In all cases the reaction rate is nearly independent of the nucleophilicity of the incoming ligand. This observation as well as the thermal activation parameters suggest a dissociative interchange mechanism. The high lability of these complexes results from two effects, namely, the *trans* in-

[*] Prof. Dr. R. van Eldik, Dipl.-Chem. C. Dücker-Benfer
Institut für Anorganische Chemie der Universität Erlangen-Nürnberg
Egerlandstrasse 1, D-91058 Erlangen (Germany)
Telefax: Int. code + (9131) 85-7387
e-mail: vaneldik@anorganik.chemie.uni-erlangen.de
Prof. Dr. R. Dreos
Universitá di Trieste
I-34127 Trieste (Italy)

[**] The authors acknowledge financial support from the Deutsche Forschungsgemeinschaft, Fonds der Chemischen Industrie, MURST, and the Max Buchner Forschungsstiftung.

fluence of the R group and the labilizing effect of the equatorial chelating ligands.

In an effort to obtain more insight into the transition state and the intimate mechanism of reaction (a), we have studied the pressure dependence of the substitution process for different substituents R and ligands L. The results demonstrated an unexpected changeover in mechanism controlled by the nature of the alkyl group R.

The kinetics of reaction (a) were studied at ambient pressure before.[1-3] The observed rate constants did not show a significant dependence on the nature of the entering ligand. In all cases the calculated activation entropies were significantly negative. We found a linear dependence of k_{obs} on ligand concentration in the presence of an excess of ligand for all reactions studied [Eq. (b)]. Only in the case of $L = I^-$ could a significant y-inter-

$$k_{obs} = k_1[L] + k_2 \qquad (b)$$

cept, k_2, due to the back reaction be observed. The rate constants at ambient conditions were in good agreement with those reported before.[1-3]

The pressure dependence of k_1 was estimated from the pressure dependence of k_{obs} at constant ligand concentration, except for $L = I^-$, where the dependence of the rate on the ligand concentration was studied in detail as a function of pressure. In the

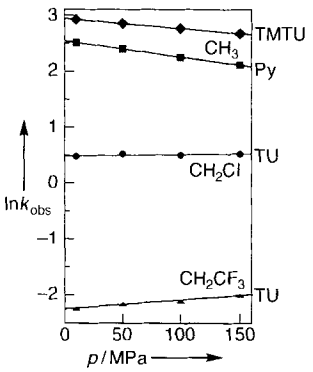

Fig. 1. Pressure dependence of k_{obs} for reaction (a). TU = thiourea, TMTU = tetramethylthiourea, py = pyridine, p = pressure. Experimental conditions: $[Rh] = (2-4) \times 10^{-4}$ M, $[L] = (5-10) \times 10^{-3}$ M, pH = 7.0 (phosphate buffer), ionic strength $I = 1.0$ M ($NaNO_3$), $T = 293$ K.

latter case k_1 and k_2 were determined from plots of k_{obs} versus $[I^-]$ [see Eq. (b)] as a function of pressure. Plots of $\ln k_1$ and $\ln k_2$ versus pressure were linear in all cases (see some typical examples in Fig. 1). The volumes of activation $\Delta V^{\neq}$, calculated from these plots in the usual way, are summarized in Table 1 together with the rate constants at ambient pressure and thermal activation parameters.

There is a definite trend in the $\Delta V^{\neq}$ data: the values are significantly positive for the faster substitution reactions ($R = CH_3$), but significantly negative for the slower substitution reactions ($R = CH_2CF_3$). This trend correlates well with the *trans* influence of the R groups in the ground state as observed for a series of pyridine (py) complexes.[4, 6] The Rh–py bond length decreased (222, 217.8, 214.5 pm) for $R = CH_3$, CH_2Cl, and CH_2CF_3.[4, 6] A similar trend is expected for the Rh–O bond in the corresponding aqua complexes studied here: faster reactions are thus associated with the stronger *trans* effect of the methyl group, and slower reactions with the weaker *trans* effect of CH_2Cl and CH_2CF_3. Furthermore, the *trans* labilization by R directly determines the nature of the ligand substitution mechanism. The stronger donor properties of CH_3 result in a dissociative substitution process as characterized by the significantly positve $\Delta V^{\neq}$ values. Similary, the weaker donor properties of CH_2CF_3 favor a more associative substitution mechanism as shown by the significantly negative $\Delta V^{\neq}$ data. The absolute magnitude of $\Delta V^{\neq}$ is such that the reactions are most probably of the interchange (I_d versus I_a) type, respectively.[7] Thus the transition state for such a ligand substitution process can be visualized as in Figure 2. Here both the degree of bond breakage ($Rh-OH_2$) and the degree of bond formation (Rh–L) are controlled by the donor properties of R.

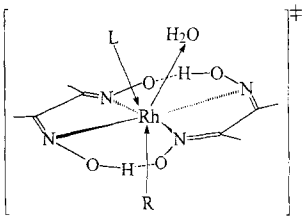

Fig. 2. A closer view of the transition state. R = CH_3, CH_2Cl, CH_2CF_3.

For the substitution reaction with iodide it was possible to measure $\Delta V^{\neq}$ for the forward and the reverse reactions [Eq. (c)],

$$trans\text{-}[Rh(Hdmg)_2(CH_3)(H_2O)] + I^- \rightleftharpoons trans\text{-}[Rh(Hdmg)_2(CH_3)(I)]^- + H_2O \qquad (c)$$

and these data enabled us to construct a volume profile for the overall process (Fig. 3).

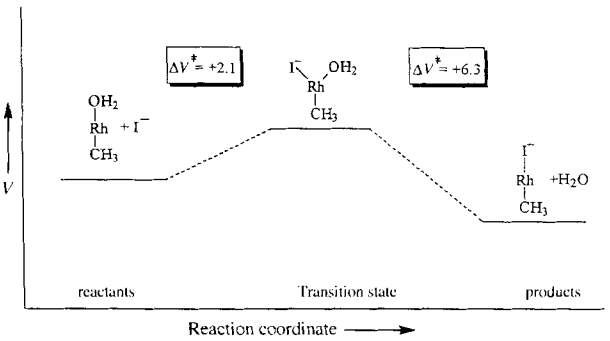

Fig. 3. Volume profile for reaction (c). V = relative partial molar volume in $cm^3\ mol^{-1}$. Experimental conditions: $[Rh] = 2 \times 10^{-4}$ M, $[L] = (5-10) \times 10^{-3}$ M, pH = 7.0 (phosphate buffer), $I = 1.0$ M ($NaNO_3$), $T = 282$ K.

Table 1. Rate constants and activation parameters for the reaction (a) [a].

R	L	k_1 [b] $[M^{-1}s^{-1}]$	k_2 [b] $[s^{-1}]$	$\Delta H^{\neq}$ $[kJ\,mol^{-1}]$	$\Delta S^{\neq}$ $[JK^{-1}mol^{-1}]$	$\Delta V^{\neq}$ [c] $[cm^3\,mol^{-1}]$
CH_3	N_3^-	9590	27.2			
	SCN^-	6760	4.36			
	I^-	4660		42 ± 1 [d]	−32 ± 3 [d]	2.1 ± 0.4 (282)
			32.0	52 ± 2 [d]	−41 ± 7 [d]	6.3 ± 0.3 (282)
	Py	4230		45 ± 3 [d]	−22 ± 11 [d]	7.16 ± 0.01 (293)
	TMTU	4600 [d]		43 ± 2 [d]	−30 ± 6 [d]	4.3 ± 0.04 (293)
	TU	7000		32 ± 1 [b]	−61 ± 4 [b]	
CH_2Cl	TU	312		42 ± 2 [b]	−51 ± 16 [b]	−0.6 ± 0.5 (293)
CH_2CF_3	TU	13.2		60 ± 1 [b]	−16 ± 4 [b]	−4.0 ± 0.3 (293)

[a] $[Rh] = (2-4) \times 10^{-4}$ M, $[L] = (5-10) \times 10^{-3}$ M, $I = 1.0$ M ($NaNO_3$), pH = 7 (phosphate). For abbreviations of the ligands see the legend of Fig. 1. [b] Data taken from ref. [1–5, 7]. k_1 and k_2 were determined at 293 K. [c] Temperature is quoted in brackets in K. [d] This work.

 © VCH Verlagsgesellschaft mbH, D-69451 Weinheim, 1995 0570-0833/95/3420-2246 $ 10.00+.25/0

The profile clearly demonstrates that the partial molar volume of the transition state is significantly larger than that of either the reactant or the product states. The *trans* labilization by the methyl group controls the dissociative nature of both the forward and reverse reactions. The more positive volume of activation for the release of I^- relative to the release of H_2O is probably related to the significantly larger partial molar volume of I^- and to the effect of electrostriction on the complex due to the charged ligand. The $\Delta V^{\neq}$ values support the assumption of an I_d mechanism.[7, 8]

A comparison of the activation parameters in Table 1 clearly shows that the $\Delta S^{\neq}$ values are all negative and suggest the operation of an interchange (I) mechanism, but they do not allow a further distinction to be made between an I_a or I_d mechanism. It is generally known that entropies of activation are intrinsically subject to large error limits due to the extrapolation required to determine these values. In contrast, volumes of activation are determined from the initial slope of a plot of $\ln k$ versus pressure and are in general subject to significantly smaller error limits.[7] Thus a too detailed interpretation of activation entropy data can be rather misleading. Similar conclusions have been reached in earlier kinetic studies dealing with the evaluation of thermal and pressure activation parameters.[7] The mechanistic changeover only shows up clearly in the $\Delta V^{\neq}$ data, and can be directly correlated with the donor properties of R, which in turn control the magnitude of the rate constants.

Volume of activation data have only been measured for a limited number of reactions that involve activation of metal–carbon bonds. In the case of square-planar Pt^{II} complexes, the introduction of a single Pt–C bond increases the lability of the metal center by five orders of magnitude, but does not cause a changeover in mechanism.[9] The introduction of a CMe_5 ligand onto the metal center leads to a tremendous labilization in the case of Rh^{III} and evidence for an I_d mechanism was reported.[10] For comparison, solvent exchange and ligand substitution reactions of $[Rh(NH_3)_5(OH_2)]^{3+}$ are extremely slow and follow an I_a mechanism.[11] Thus the introduction of the carbon bond in *trans* position (ligand R), as well as the dimethylglyoximate chelates in the present system, cause a significant labilization of Rh^{III} and even leads to a mechanistic changeover from I_a to I_d.

The mechanistic fine tuning caused by the nature of the R group is rather surprising. It is generally known that such groups labilize the *trans* position, and it was therefore logical to suggest the operation of an I_d mechanism previously.[1–3] However, our present results demonstrate very clearly that the labilization effect strongly depends on the donor properties of R. These properties are, for instance, controlled by electron-withdrawing substituents on R and can control the nature of the substitution mechanism. We conclude on the basis of these results that the substitution behavior of rhodoximes and related complexes is controlled by an electronically tuned labilization effect.

Experimental Procedure

All complexes were prepared by published methods [1–3]. Millipore water was used in the preparation of all solutions. All other materials were p.a. grade and used without further purification, except for pyridine, which was distilled before use. Kinetic measurements at ambient pressure were performed on a Durrum D 110 or a Biologic SFM-3 stopped flow instrument and those at elevated pressure on a homemade high-pressure stopped flow [11]. The temperature of all instruments was controlled to within 0.1 °C. For the analysis of the kinetic data we used the OLIS KINFIT set of programs [12].

The kinetic measurements were performed under pseudo-first-order conditions at 1 M *ionic strength* ($NaNO_3$). Solutions of the ligand and the complexes were buffered with phosphate at pH = 7. The rate of the reaction is independent of the pH in this range [2]. The pK_a values for the different complexes are 9.78 (R = CH_3), 9.06 (R = CH_2Cl), and 8.85 (R = CF_3CH_2); consequently a possible change in pH due to the effect of pressure on the buffer will not affect the measured data or the mechanism of the reaction [3]. The initial complex concentration was $(2–4) \times 10^{-4}$ M, and the initial ligand concentration varied between 5×10^{-3} and 10×10^{-3} M. The reactions were followed by the change in absorbance in the visible spectrum between 340 and 380 nm [1–3].

Received: May 11, 1995 [Z 7974 IE]
German version: *Angew. Chem.* **1995**, *107*, 2414–2416

Keywords: kinetics · reaction mechanisms · rhodium compounds · substitutions

[1] R. Dreos-Garlatti, G. Tauzher, M. Blaschich, G. Costa, *Inorg. Chim. Acta* **1984**, *86*, L63.
[2] R. Dreos-Garlatti, G. Tauzher, M. Blaschich, G. Costa, *Inorg. Chim. Acta* **1985**, *105*, 129.
[3] R. Dreos-Garlatti, G. Tauzher, G. Costa, *Inorg. Chim. Acta* **1986**, *121*, 27.
[4] N. B. Pahor, R. Dreos-Garlatti, S. Geremia, L. Randaccio, G. Tauzher, E. Zangrando, *Inorg. Chem.* **1990**, *29*, 3437.
[5] R. Dreos-Garlatti, G. Tauzher, *Polyhedron* **1990**, *9*, 2047.
[6] L. Randaccio, S. Geremia, R. Dreos-Garlatti, G. Tauzher, F. Asano, G. Pellizer, *Inorg. Chim. Acta* **1992**, *194*, 1.
[7] a) R. van Eldik, A. E. Merbach, *Comments Inorg. Chem.* **1992**, *12*, 341; b) R. van Eldik in *Perspectives in Coordination Chemistry*, (Eds. A. F. Williams, C. Floriani, A. E. Merbach), VCH, Weinheim, **1992**, p. 55.
[8] J. G. Leipoldt, R. van Eldik, H. Kelm, *Inorg. Chem.* **1983**, *22*, 4147.
[9] M. Schmülling, A. Ryabov, R. van Eldik, *J. Chem. Soc. Dalton Trans.* **1994**, 1257.
[10] L. Dadci, H. Elias, U. Frey, A. Hörnig, U. Koelle, A. E. Merbach, H. Paulus, J. S. Schneider, *Inorg. Chem.* **1995**, *34*, 306.
[11] R. van Eldik, W. Gaede, S. Wieland, J. Kraft, M. Spitzer, D. A. Palmer, *Rev. Sci. Instrum.* **1993**, *64*, 1355.
[12] OLIS KINFIT, On-Line Instruments Systems Inc., Bogart, GA 30622.

On the Mechanism of Catalysis by a Metal-Free Hydrogenase from Methanogenic Archaea: Enzymatic Transformation of H_2 without a Metal and Its Analogy to the Chemistry of Alkanes in Superacidic Solution**

Albrecht Berkessel* and Rudolf K. Thauer*

Hydrogenases are enzymes that catalyze reactions with molecular hydrogen (H_2) either as substrate or as product. All hydrogenases investigated so far are metalloenzymes: they all contain iron–sulfur clusters, and most of them also contain nickel.[1] Presumably the activation of the H_2 molecule takes place at one of the redox-active transition metal ions. The detailed structure of the active site is still unknown. Although an X-ray crystal structure of a nickel–iron hydrogenase exists,[2] it was performed on an inactive sample of the enzyme.[2] On the other hand, both the binding and the activation of molecular hydrogen effected by low molecular weight transition metal complexes is comparatively well understood.[3] Most likely, the mechanisms known from organometallic chemistry[3] will soon be proven valid for transition metal hydrogenases, too.

[*] Prof. Dr. A. Berkessel
Organisch-chemisches Institut der Universität
Im Neuenheimer Feld 270, D-69120 Heidelberg (Germany)
Telefax: Int. code + (6221) 56-4205
e-mail: gz7@ix.urz.uni-heidelberg.de
Prof. Dr. R. K. Thauer
Max-Planck-Institut für terrestrische Mikrobiologie
Karl-von-Frisch-Strasse, D-35043 Marburg (Germany)
Telefax: Int. code + (6421) 28-5833

[**] This work was supported by the Bundesministerium für Forschung und Technologie (Förderprogramm "Biologische Wasserstoffgewinnung") and by the Fonds der Chemischen Industrie.

About five years ago, a new hydrogenase was found in methanogenic archaea that catalyzes the reversible reduction of N^5,N^{10}-methenyl tetrahydromethanopterin (methenyl-H_4MPT, **1**) with molecular hydrogen to N^5,N^{10}-methylene tetrahydromethanopterin (methylene-H_4MPT, **2**) and a proton (Scheme 1). This hydrogenase apparently contains neither nickel nor iron–sulfur clusters and can thus be considered metal-free.[4–8]

The reaction shown in Scheme 1 represents one step in the production of methane from CO_2 and H_2 by methanogenic archaea.[9, 10] Its stereochemical course was elucidated by NMR ("magnetic labeling") studies:[11–13] a) The substrate **1** is reduced stereoselectively. Hydride is formally transferred to or abstracted from the pro-*R* position of methylene-H_4MPT (**2**). The pro-*S* hydrogen atom remains unaffected. b) Furthermore, there is an exchange of the pro-*R* hydrogen atom of methylene-H_4MPT (**2**) with the solvent water. The rate of exchange with the solvent is approximately 2.4 times that of the reaction **2** → **1**.

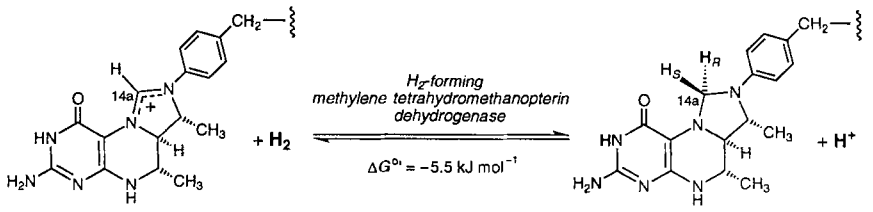

Scheme 1. For complete structural formulas for **1** and **2**, including side chains, see refs. [11, 12].

This result indicates that the proton exchange with the solvent takes place directly and is not a secondary reaction via initially formed hydrogen. These findings are in good agreement with other experiments showing that the dehydrogenation of methylene-H_4MPT (**2**) in D_2O results in the simultaneous formation of HD and D_2.[14, 15]

H_2-Forming methylene tetrahydromethanopterin dehydrogenase—as the enzyme is called—differs from all other hydrogenases not only by the absence of nickel and iron–sulfur centers, but also by the following features: CO, NO, cyanide, azide, nitrite, or acetylene are not inhibitors; H_2/H^+ exchange is not catalyzed in the absence of substrate; the enzyme does not catalyze the reversible reduction of dyes such as methylene blue or viologens with H_2; the enzyme shows a pure protein UV/VIS spectrum.

The absence of a redox-active transition metal clearly distinguishes H_2-forming methylene tetrahydromethanopterin dehydrogenase from all other hydrogenases: activation of the H_2 molecule by binding to a transition metal cannot account for its catalytic activity. Thus, the enzyme appears extremely interesting both from a mechanistic and a preparative point of view: the reduction of an organic substrate with molecular hydrogen (Scheme 1) is catalyzed without employing a redox-active transition metal!

We propose that the reaction between methenyl tetrahydromethanopterin **1** and H_2 is effected by enzymatic activation of the substrate **1**. This is a new mechanism of catalysis for hydrogenases, because transition metal containing hydrogenases activate the H_2 molecule. We demonstrate how the reaction shown in Scheme 1 can be catalyzed by conformational locking and protonation of the substrate **1** when bound to the enzyme. Furthermore we show that this mode of reaction has analogies in the chemistry of alkanes in superacidic solutions.[16–19]

First, we shall consider the back reaction, that is, the formal elimination of hydride from methylene-H_4MPT (**2**) (Scheme 1). Similar transformations are known from the structurally related ortho amides like, for example, **3** (perhydro-3a,6a,9a-triazaphenalene).[20–22] As shown in Equation (a), the guanidinium

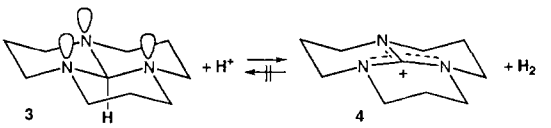

(a)

salt **4** and molecular hydrogen are formed quantitatively from the ortho amide **3** upon treatment with tetrafluoroboric acid or hydrochloric acid at 110 °C within 23 h.[20] The unusual reactivity of the ortho amide **3** can be explained by the interaction of the σ* orbital of the central C–H bond with the three antiperiplanar lone pairs of the nitrogen atoms. The weakening of this bond is manifested by its C–H stretching band in the IR at unusually high wavelength (4.0 μm, Bohlmann band[23]). As shown in Scheme 2, the five-membered imidazolidine ring of methylene-H_4MPT (**2**) can easily adopt a conformation in which the lone pairs of the neighboring nitrogen atoms are oriented antiperiplanar to the bond C–H_R (**A**, Scheme 2). An acidic functional group within the enzyme's active site, like the carboxyl group of an aspartate or glutamate residue, is assumed to provide the proton. The antiperiplanar arrangement of the nitrogen lone pairs and the C–H bond facilitates the protolysis (stereoelectronic effect). The stereoselectivity of the formal elimination of hydride from **2** is explained by this conformational locking of the five-membered ring upon binding at the enzyme's active site. Finally, in the free formamidinium ion methenyl-H_4MPT (**1**), the positive charge at C14a is optimally stabilized in the now flattened five-membered imidazolidine ring.

Whereas the "ortho amide analogy" explains the formal elimination of hydride from methylene-H_4MPT (**2**), as well as its

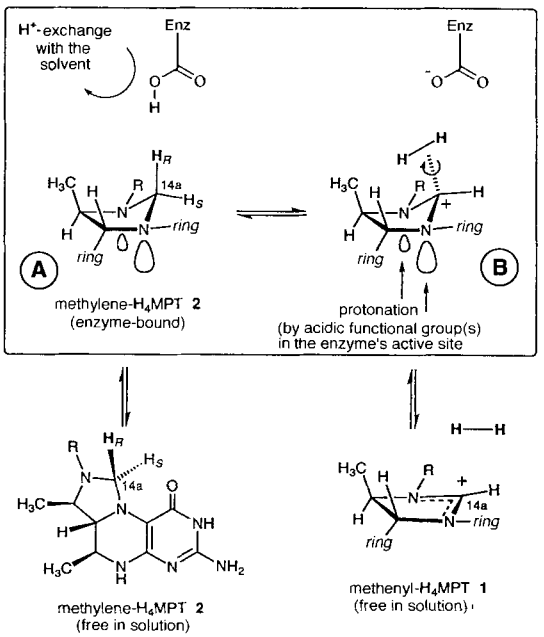

Scheme 2.

stereoselectivity, this analogy fails with respect to two further important aspects of the enzyme-catalyzed transformation shown in Scheme 1. a) As mentioned above, the exchange of the pro-*R* hydrogen atom of methylene-H_4MPT (**2**) with the solvent is about 2.4 times faster than its elimination with concomitant formation of methenyl-H_4MPT (**1**).[13] However, an analogous H/D exchange at the central C–H bond of ortho amides of type **3**, for example upon treatment with DBF_4 instead of HBF_4, has never been observed.[20–22] b) In contrast to the *reversible* enzymatic reduction of methenyl-H_4MPT (**1**) (Scheme 1), a reaction of guanidinium cations with molecular hydrogen to form ortho amides does not take place [Eq. (a)]; in other words, the ortho amide reaction in tetrafluoroboric acid or hydrochloric acid is irreversible. This dilemma is solved by the assumption that the stabilization of the cationic center at C14a of methenyl-H_4MPT (**1**) by the lone pairs of the neighboring nitrogen atoms can be turned off by binding to the enzyme. In Scheme 2, this hypothesis is indicated as the transition from free methenyl-H_4MPT (**1**) to the enzyme-bound state **B**; in the unbound state, the positive charge at C14a is stabilized by the two neighboring nitrogen atoms in the planar conformation of the five-membered ring. Upon binding of methenyl-H_4MPT (**1**) to the enzyme (**B**, Scheme 2), the lone pairs at the nitrogen atoms could be protonated, again by acidic residues in the enzyme's active site. An envelope conformation of the imidazolidine ring results. Because of this turning off of conjugative stabilization, the electrophilicity of the cationic center at C14a should be dramatically increased relative to that of the formamidinium ion **1** or the guanidinium ion **4** [Eq. (a)]. The reactivity of the resulting cation should more closely resemble that of carbocations that can be generated in solution under superacidic conditions.[16–19] The similarities are indeed striking. As shown by Olah et al.[24, 25] and by Hogeveen et al.,[26] alkanes can undergo H/D exchange in superacidic solution with retention of configuration and without carbocation formation or before the corresponding carbocations are formed. For example, the tertiary hydrogen atom exchanges rapidly in the case of isobutane [**5**, Eq. (b)].[16–19, 27] This

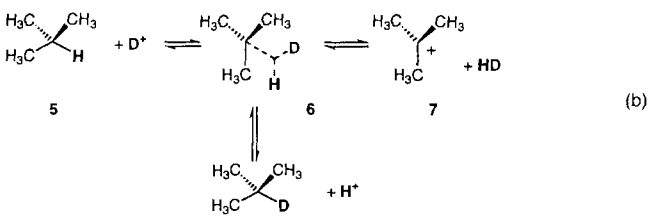

isotope exchange was explained by reversible protonation of the exchanging C–H bond, resulting in the formation of a transient 3-center, 2-electron bond[24] [**6**, Eq. (b)]. The reversible formation of an analogous species with a 3-center, 2-electron bond (**B**, Scheme 2) and the ability of the resulting "cation-bound H_2 molecule" to rotate, readily explain the rapid isotope exchange of the pro-*R* hydrogen atom of **2** with the solvent. Because in the course of the enzymatic reduction of **1** to **2**, the protons formed are given off to the solution, a proton path between the acidic functional group Enz-CO_2H in the enzyme's active site and the solvent must exist. Our hypothesis also explains why isotope exchange between the gas phase and the solution is catalyzed by H_2-forming methylene tetrahydromethanopterin dehydrogenase only in the presence of substrate (**1** or **2**).[12, 14] Hogeveen et al.[28] could show that molecular hydrogen reacts with carbocations like the *tert*-butyl cation, affording the corresponding saturated hydrocarbon [Eq. (b), reaction of **7** with hydrogen to **5**]. This transformation is analogous to the reaction of enzymatically activated methenyl-H_4MPT with hydrogen yielding methylene-H_4MPT and a proton. The latter proton would be accepted by the carboxylate anion in the enzyme's active site (**B** → **A**, Scheme 2). Walling and Bollyky achieved the reduction of benzophenone with H_2 in the presence of strong bases under drastic reaction conditions.[29a] This result indicates that heterolysis of the H_2 molecule may be further facilitated by the basic residue in the enzyme's active site. Hogeveen et al. did not observe a kinetic isotope effect in the reaction of the *tert*-butyl cation with D_2 or H_2.[28] Interestingly, H_2-forming methylene tetrahydromethanopterin dehydrogenase does not show a significant isotope effect either: the reduction of methenyl-H_4MPT (**1**) was found to proceed at identical rates with H_2 and D_2 at all the substrate concentrations and pH values studied.[29b]

At first glance, the assumption of intermediates in an enzymatic transformation that are otherwise found only under superacidic conditions may appear somewhat risky. However, reaction patterns characteristic of organic molecules under superacidic conditions, for example the isomerization of alkanes, are also observed in the presence of solid ion exchangers or zeolites carrying sulfonic acid functional groups.[19, 30, 31] Consequently, "superacidic reactions" are also possible without the typical superacids of solution chemistry –provided that an adequate, nonbasic environment and properly positioned acidic functional groups are present (possibly by "bi-" or even "multifunctional catalysis"[32]). Thus, why not in the course of an enzymatic transformation? Proteases hydrolyze amide bonds at room temperature and at pH 7 within minutes, whereas the analogous acid-catalyzed reaction in solution requires some hours of heating at reflux in 6 M hydrochloric acid.

In view of the chemistry of carbocations in superacidic solution, the catalysis effected by H_2-forming methylene tetrahydromethanopterin dehydrogenase is not mysterious any longer, but merely appears as a logical alternative to the activation of the H_2 molecule by metal-containing hydrogenases. Could substrate activation by protonation, as proposed here, also be of importance for other enzymatic reactions? The transformation of the only very poorly nucleophilic hydrogen molecule without the aid of a transition metal requires the intermediacy of a highly reactive, that is, highly energetic, carbocation. Thus, H_2-forming methylene tetrahydromethanopterin dehydrogenase surely is an extreme case. It may well be, however, that the following methyl group transfer reactions that take place only when catalyzed by the appropriate enzyme and not spontaneously in solution may be catalyzed by intermediary selective protonation of the methyl group donors: a) methyl group transfer from methanol to coenzyme M (**8**) affording methyl-coenzyme M (**9**, Scheme 3) in methanogenic archaea,[33] or b) the

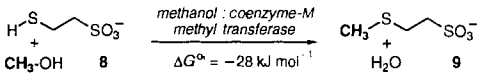

Scheme 3.

methylation of homocysteine by N^5-methyl tetrahydrofolate, affording methionine in all living organisms.[34] This hypothesis appears quite reasonable, since under superacidic conditions the electrophilicity of, for example, methanol is increased to such an extent that it can methylate benzene[31] or can undergo ionic hydrogenation affording methane.[35] Similar reactivity patterns apply for the activation of methylamine.[19]

Received: June 20, 1995 [Z8115IE]
German version: *Angew. Chem.* **1995**, *107*, 2418–2421

Keywords: Archaea bacteria · carbocations · enzymes · hydrogenases

[1] S. P. J. Albracht, *Biochim. Biophys. Acta*, **1994**, *1188*, 167–204.
[2] a) A. Volbeda, M.-H. Charon, C. Piras, E. C. Hatchikian, M. Frey, J. C. Fontecilla-Camps, *Nature* **1995**, *373*, 580–587; b) R. Cammack, *Nature* **1995**, *373*, 556–557; c) M. A. Halcrow, *Angew. Chem.* **1995**, *107*, 1307–1310; *Angew. Chem. Int. Ed. Engl.* **1995**, *34*, 1193–1195.
[3] R. H. Crabtree, *Angew. Chem.* **1993**, *105*, 828–845; *Angew. Chem. Int. Ed. Engl.* **1993**, *32*, 789–805.
[4] C. Zirngibl, R. Hedderich, R. K. Thauer, *FEBS Lett.* **1990**, *261*, 112–116.
[5] B. Schwörer, R. K. Thauer, *Arch. Microbiol.* **1991**, *155*, 459–465.
[6] K. Ma, C. Zirngibl, D. Linder, K. O. Stetter, R. K. Thauer, *Arch. Microbiol.* **1991**, *156*, 43–48.
[7] R. von Bünau, C. Zirngibl, R. K. Thauer, A. Klein, *Eur. J. Biochem.* **1991**, *202*, 1205–1208.
[8] C. Zirngibl, W. van Dongen, B. Schwörer, R. von Bünau, M. Richter, A. Klein, R. K. Thauer, *Eur. J. Biochem.* **1992**, *208*, 511–520.
[9] R. S. Wolfe, *Annu. Rev. Microbiol.* **1991**, *45*, 1–35.
[10] D. S. Weiss, R. K. Thauer, *Cell* **1993**, *72*, 819–822.
[11] J. Schleucher, B. Schwörer, C. Zirngibl, U. Koch, W. Weber, E. Egert, R. K. Thauer, C. Griesinger, *FEBS Lett.* **1992**, *314*, 440–444.
[12] J. Schleucher, C. Griesinger, B. Schwörer, R. K. Thauer, *Biochemistry* **1994**, *33*, 3986–3993.
[13] J. Schleucher, B. Schwörer, R. K. Thauer, C. Griesinger, *J. Am. Chem. Soc.* **1995**, *117*, 2941–2942.
[14] B. Schwörer, V. M. Fernandez, C. Zirngibl, R. K. Thauer, *Eur. J. Biochem.* **1993**, *212*, 255–261.
[15] A. Klein, M. Fernandez, R. K. Thauer, *FEBS Lett.* **1995**, in press.
[16] G. A. Olah, G. K. Surya Prakash, J. Sommer, *Superacids*, Wiley, New York, **1985**.
[17] P. Vogel, *Carbocation Chemistry*, Elsevier, Amsterdam, **1985**.
[18] G. A. Olah in *The Chemistry of Alkanes and Cycloalkanes* (Ed.: S. A. Patai), Wiley, New York, **1992**, pp. 609–652.
[19] a) G. A. Olah, *Angew. Chem.* **1993**, *105*, 805–827; *Angew. Chem. Int. Ed. Engl.* **1993**, *32*, 767–788; b) G. A. Olah, *Angew. Chem.* **1995**, *107*, 1519–1532; *Angew. Chem. Int. Ed. Engl.* **1995**, *34*, 1393–1405.
[20] J. M. Erhardt, J. D. Wuest, *J. Am. Chem. Soc.* **1980**, *102*, 6363–6364.
[21] T. J. Atkins, *J. Am. Chem. Soc.* **1980**, *102*, 6364–6365.
[22] J. M. Erhardt, E. R. Grover, J. D. Wuest, *J. Am. Chem. Soc.* **1980**, *102*, 6365–6369.
[23] F. Bohlmann, *Angew. Chem.* **1957**, *69*, 641–642.
[24] G. A. Olah, N. Hartz, G. Rasul, G. K. Surya Prakash, *J. Am. Chem. Soc.* **1995**, *117*, 1336–1343.
[25] G. A. Olah, G. Klopman, R. H. Schlosberg, *J. Am. Chem. Soc.* **1969**, *91*, 3261–3268.
[26] H. Hogeveen, C. J. Gaasbeek, *Recl. Trav. Chim Pays-Bas*, **1968**, *87*, 319–320.
[27] G. A. Olah, Y. Halpern, J. Shen, Y. K. Mo, *J. Am. Chem. Soc.* **1973**, *95*, 4960–4970.
[28] A. F. Bickel, C. J. Gaasbeek, H. Hogeveen, J. M. Oelderik, J. C. Platteeuw, *J. Chem. Soc. Chem. Commun.* **1967**, 634–635.
[29] a) C. Walling, L. Bollyky, *J. Am. Chem. Soc.* **1964**, *86*, 3750–3752; b) A. Klein, G. Hartmann, R. K. Thauer, *Eur. J. Biochem.* **1995**, in press.
[30] W. O. Haag, *Stud. Surf. Sci. Catal.* 1994, *84*, 1375–1394.
[31] J. Kaspi, D. D. Montgomery, G. A. Olah, *J. Org. Chem.* **1978**, *43*, 3147–3150.
[32] R. Breslow, *Acc. Chem. Res.* **1995**, *28*, 146–153.
[33] J. T. Keltjens, G. D. Vogels in *Methanogenesis: Ecology, Physiology, Biochemistry and Genetics* (Ed.: J. G. Ferry), Chapman & Hall, New York, **1993**, pp. 253–303.
[34] R. V. Banerjee, V. Frasca, D. P. Ballou, R. G. Matthews, *Biochemistry* **1990**, *29*, 11101–11109.
[35] G. A. Olah, A.-H. Wu, *Synlett*, **1990**, 599–600.

The Coexistence of the Reactivity–Selectivity Principle and of Linear Free Energy Relationships: A Diffusion Clock for Determining Carbocation Reactivities**

Michael Roth and Herbert Mayr*

Dedicated to Professor Günter Schäfer on the occasion of his 60th birthday

The rates of reactions of carbocations with uncharged nucleophiles are given by Equation (a), where electrophiles are represented by a single electrophilicity parameter E, while nucleophiles are characterized by the nucleophilicity parameter N and the slope parameter s, which is usually close to 1.[1] For the

$$\lg k = s(N + E) \qquad \text{(a)}$$

determination of the strengths of electrophiles, we usually measure the rates of the reactions ($\lg k$) of these electrophiles with nucleophiles of well-known s and N, and we then use Equation (a) to calculate the electrophilicity parameter E.[2, 3] However, this method is only applicable to well-stabilized carbocations, that is cations that can be produced in organic solvents as persistent entities with lifetimes of more than one hour. We now introduce a general method for the determination of absolute rate constants and electrophilicity parameters of short-lived carbocations. It is based on the selectivities of carbocations that are generated from suitable precursors by chemical ionization and thus does not depend on the presence of certain chromophores as, for example, in the case of the flash-photolytic generation of carbocations.

We observed a decrease of the relative reactivities of the allylsilanes **3a** and **3b** toward the benzhydryl chlorides **1a–e** (Scheme 1) from 208 to 2.6 with decreasing electron-releasing

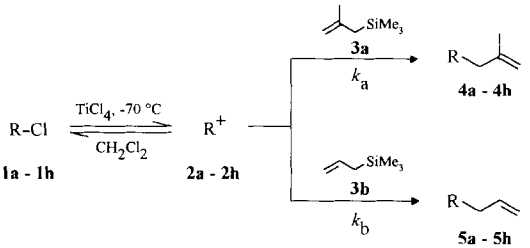

Scheme 1.

abilities of the aryl substituents (Table 1). The competition experiments were performed as described previously,[4–6] and yielded competition constants that were independent of the ratios of the nucleophiles **3a**:**3b**. Only in the case of **1a** (very large value which is difficult to determine) did the standard deviation exceed 10%. The agreement of the competition constants with the directly measured rate constants is shown by the entry for **1c**: While competition experiments yielded a value of $k_a/k_b = 42.7$ for the bis(*p*-chlorophenyl)carbenium ion **2c** (Table 1), a k_a/k_b value of 37 is calculated from the directly measured rate constants (CH_3CN, 20 °C).[7] As these reactions

[*] Prof. Dr. H. Mayr, Dipl.-Ing. M. Roth
Institut für Organische Chemie der Technischen Hochschule
Petersenstrasse 22, D-64287 Darmstadt (Germany)
Telefax: Int. code + (6151) 165591

[**] We thank the Bayer AG, Leverkusen, for financial support.

Table 1. Relative reactivities of carbocations toward allylsilanes (CH_2Cl_2, $-70\,^{\circ}C$) and electrophilicity parameters.

RCl		k_a/k_b	k_a/k_c	E
(*p*-MeC_6H_4)PhCHCl	**1a**	208 ± 32		4.33
Ph_2CHCl	**1b**	39.9 ± 2.6		6.15
(*p*-ClC_6H_4)$_2$CHCl	**1c**	42.7 ± 3.8		5.95
(*m*-ClC_6H_4)PhCHCl	**1d**	7.03 ± 0.23		6.5–7.0
(*m*-ClC_6H_4)$_2$CHCl	**1e**	2.61 ± 0.20		7.0–7.5
	1f	2.41 ± 0.25	140 ± 13.5	7.50
	1g	1.10 ± 0.10	8.31 ± 3.61	8.5–9.0
	1h	1.85 ± 0.12		8.0–8.5

do not have an enthalpy barrier,[8] the comparison of these reactivity ratios is possible without correcting for temperature. The decrease of the competition constants k_a/k_b with increasing reactivities of the benzhydryl cations (Table 1) is in accord with the postulate of the reactivity–selectivity principle[9–12] and opposes Equation (a) which predicts constant selectivities for competing nucleophiles with the same s parameter.

This apparent contradiction is resolved in Figure 1, where the results of direct kinetic measurements and of competition experiments are presented side by side. A noticeable decrease of the selectivity does not occur until the rate constant k of one of the parallel reactions exceeds 10^8 L mol^{-1} s^{-1}, that is, when the more reactive competitor approaches the diffusion limit.[13] Figure 1 now unambiguously corroborates the conclusion that constant selectivity relationships and the reactivity–selectivity principle hold in different ranges of reactivity, as previously derived from studies of relative reactivities.[14, 15]

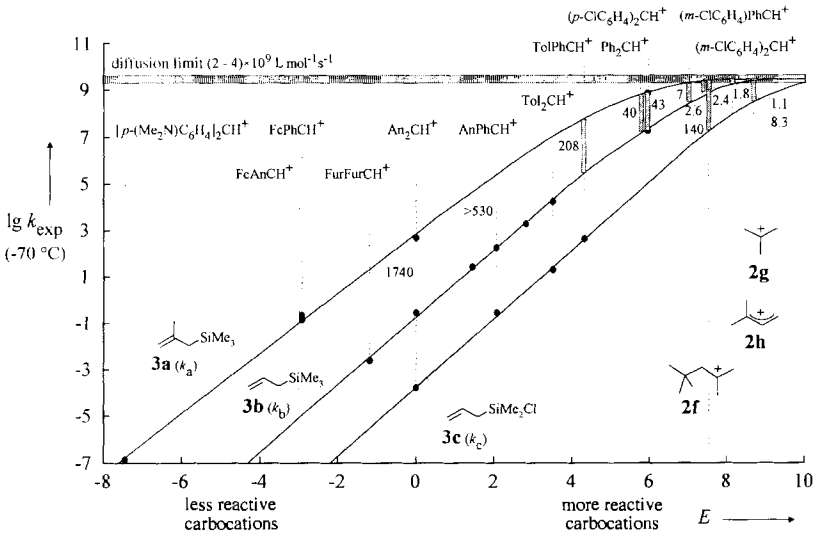

Fig. 1. Changeover from constant selectivity relationships to the reactivity–selectivity principle. An = *p*-$MeOC_6H_4$, Fc = ferrocenyl, Fur = 2,3-dihydrobenzofuran-5-yl, Tol = *p*-MeC_6H_4. Directly measured rate constants are marked by dots, results from competition experiments by shaded bars.

Kinetic investigations of laser-flash photolytically generated carbocations in acetonitrile at 20 °C showed that different types of highly reactive uncharged nucleophiles react with almost identical rate constants $k = (2–4) \times 10^9$ L mol^{-1} s^{-1},[7] indicating that this value corresponds to the diffusion limit. As acetonitrile and dichloromethane have almost identical viscosities at 20 °C ($\eta_{CH_3CN} = 0.39$ mPa s, $\eta_{CH_2Cl_2} = 0.43$ mPa s), one can expect the same diffusion rates in both solvents as a consequence of the Stokes–Einstein equation. The similar selectivities, which were determined for the carbenium ion **2c** by competition experiments at 20 °C ($k_a/k_b = 32.0$) and $-70\,^{\circ}C$ ($k_a/k_b = 42.7$), again demonstrate that an explicit treatment of temperature dependence is unnecessary.

It, therefore, becomes possible to determine absolute rate constants for reactions which cannot be followed directly. In the region where Equation (a) holds, that is, for "slow" reactions, k_a/k_b is generally greater than 1000. When the alkyl cation **2f** is generated from the alkyl chloride **1f** and titanium(IV) chloride in the presence of **3a** and **3b**, the products **4f** and **5f** are formed. Their ratio yields a competition constant of $k_a/k_b = 2.41$, indicating diffusion control of the faster reaction (**2f**+**3a**). Analogous generation of the carbocation **2f** in the presence of **3a** and **3c** yields the ratio $k_a/k_b = 140$, which can be combined with the diffusion-controlled $k_a \approx 3 \times 10^9$ L mol^{-1} s^{-1}, to give $k_c \approx 2.1 \times 10^7$ L mol^{-1} s^{-1}. Since this value of k_c is within the scope of the linear free energy relationships, the electrophilicity parameter E (**2f**) = 7.50 can be derived by substitution into Equation (a) or graphically from Figure 1. Analogously, for the *tert*-butyl cation **2g** the ratio $k_a/k_c = 8.31$ is obtained, and for the prenyl cation **2h** the ratio $k_a/k_b = 1.85$. Since none of these ratios refer to a reaction within the scope of the linear reactivity relationships, only approximate values of E for the corresponding cations can be derived from Figure 1.

The procedure presented herein basically corresponds to Jencks's diffusion clock,[16–19] which employs the fact that many carbocations undergo diffusion-controlled reactions with the azide ion in aqueous solution ($k \approx 5 \times 10^9$ L mol^{-1} s^{-1}).[20] Therefore, one can use the alkanol/alkyl azide ratio, which is obtained by solvolytic generation of carbocations in aqueous azide solution, for calculating the rate constant of the reaction of the carbocation with water. As the azide clock uses a single pair of competing nucleophiles, its scope for the determination of E parameters is limited, and it cannot be used to establish E values greater than 6.5 because of the large value of k_{H_2O} which then is outside the scope of the linear free energy relationships. Our previous investigations on the reactivities of π nucleophiles,[1] on the other hand, provide a large choice of reaction partners and allow the selection of suitable pairs of nucleophiles for determining the electrophilicity parameter E for any electrophile.

Received: May 13, 1995 [Z 7984IE]
German version: *Angew. Chem.* **1995**, *107*, 2428–2430

Keywords: carbocations · kinetics · linear free energy relationships · reactivity–selectivity principle

[1] H. Mayr, M. Patz, *Angew. Chem.* **1994**, *106*, 990–1010; *Angew. Chem. Int. Ed. Engl.* **1994**, *33*, 938–957.
[2] H. Mayr, D. Rau, *Chem. Ber.* **1994**, *127*, 2493–2498.
[3] H. Mayr, G. Gorath, *J. Am. Chem. Soc.* **1995**, *117*, 7862–7868.
[4] H. Mayr, R. Pock, *Chem. Ber.* **1986**, *119*, 2473–2496.
[5] R. Pock, H. Mayr, *Chem. Ber.* **1986**, *119*, 2497–2509.
[6] H. Mayr, R. Pock, *Tetrahedron* **1986**, *42*, 4211–4214.
[7] J. Bartl, S. Steenken, H. Mayr, *J. Am. Chem. Soc.* **1991**, *113*, 7710–7716.
[8] M. Patz, H. Mayr, J. Bartl, S. Steenken, *Angew. Chem.* **1995**, *107*, 519–521; *Angew. Chem. Int. Ed. Engl.* **1995**, *34*, 490–492.
[9] a) O. Exner, *J. Chem. Soc. Perkin Trans. 2* **1993**, 973–979; b) J. E. Leffler, E. Grunwald, *Rates and Equilibria of Chemical Reactions*, Wiley, New York, **1963**.

p. 162–168; c) S. J. Formosinho, *J. Chem. Soc. Perkin Trans. 2* **1988**, 839–846; d) E. M. Arnett, K. E. Molter, *Acc. Chem. Res.* **1985**, *18*, 339–346; e) W. P. Jencks, *Chem. Rev.* **1985**, *85*, 511–527; f) A. Pross, *Adv. Phys. Org. Chem.* **1977**, *14*, 69–132; g) I. Lee, *Chem. Soc. Rev.* **1990**, *19*, 317–333.

[10] C. D. Johnson, B. Stratton, *J. Chem. Soc. Perkin Trans. 2* **1988**, 1903–1907.

[11] B. Giese, *Angew. Chem.* **1977**, *89*, 162–173; *Angew. Chem. Int. Ed. Engl.* **1977**, *16*, 125–136.

[12] E. Buncel, H. Wilson, *J. Chem. Educ.* **1987**, *64*, 475–480.

[13] The decrease of the competition constants cannot exclusively be due to diffusion control of one of the parallel reactions. There are indications that in this region the position of the transition state on the reaction coordinate is shifted (Hammond effect), that is the classical rationalization of the reactivity–selectivity principles may hold in this range [15].

[14] R. Ta-Shma, Z. Rappoport, *J. Am. Chem. Soc.* **1983**, *105*, 6082–6095.

[15] J. P. Richard, *Tetrahedron* **1995**, *51*, 1535–1573.

[16] J. P. Richard, M. E. Rothenberg, W. P. Jencks, *J. Am. Chem. Soc.* **1984**, *106*, 1361–1372.

[17] J. P. Richard, W. P. Jencks, *J. Am. Chem. Soc.* **1984**, *106*, 1373–1383.

[18] J. P. Richard, W. P. Jencks, *J. Am. Chem. Soc.* **1982**, *104*, 4689–4691.

[19] J. P. Richard, W. P. Jencks, *J. Am. Chem. Soc.* **1982**, *104*, 4691–4692.

[20] R. A. McClelland, V. M. Kanagasabapathy, N. S. Banait, S. Steenken, *J. Am. Chem. Soc.* **1991**, *113*, 1009–1014.

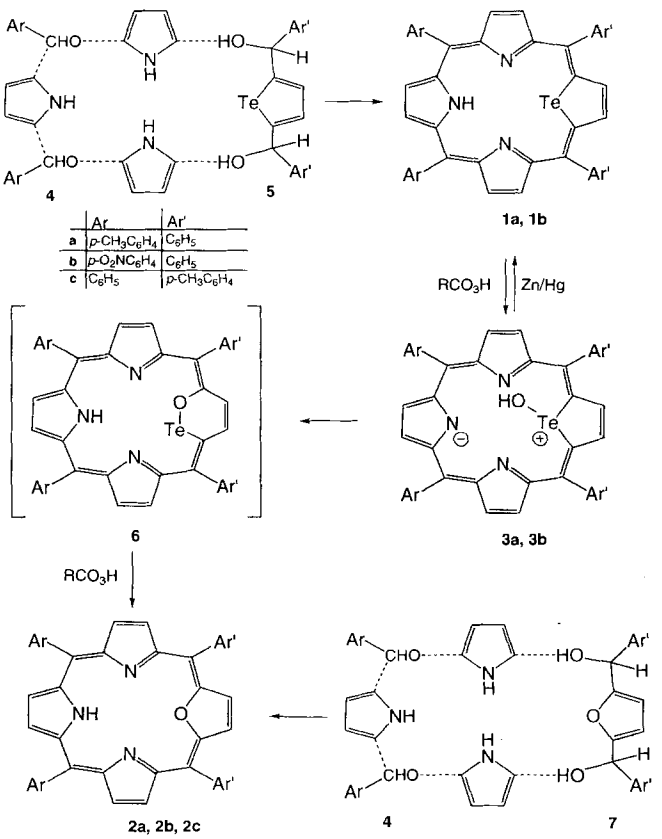

Scheme 1. Summary of the reactions of the core-modified porphyrins discussed in the text.

Alteration of the Reactivity of a Tellurophene Within a Core-Modified Porphyrin Environment: Synthesis and Oxidation of 21-Telluraporphyrin**

Lechosław Latos-Grażyński,* Ewa Pacholska, Piotr J. Chmielewski, Marilyn M. Olmstead, and Alan L. Balch*

Recent work on core-modified porphyrins, in which one or more heteroatoms O, S, Se, or CH replace some of the four nitrogen atoms, has produced new macrocycles with altered core sizes and metal ion binding properties.[1–4] The 21-thiaporphyrin has been utilized to produce η^1 coordination of the thiophene ring to a variety of transition metal ions.[2] Other studies have been concerned with the effect of heteroatom substitution on the aromaticity of the macrocycle.[3] Here we report on the synthesis of the 21-telluraporphyrins **1** and their conversion by oxidation into the 21-oxaporphyrins **2**,[5] which proceeds via the novel tellurium hydroxy compounds **3** as isolable intermediates. The reactions of the new macrocycle **1** demonstrate the remarkable ability of the porphyrin environment to alter the fundamental reactivity of the tellurophene portion.

The synthetic work is summarized in Scheme 1. The 21-telluraporphyrins **1a** and **1b** and the 21-oxaporphyrins **2a–c** have been synthesized by the condensation of pyrrole, a substituted benzaldehyde (**4a**, **4b**, or **4c**, respectively) and the appropriate α,α′-disubstituted tellurophene **5** or furan **6**. These procedures follow the methodology previously utilized for the preparation of 21-thiaporphyrin and 21-selenaporphyrin.[1, 3] After chromatographic workup, the macrocycles **1a** and **2a** were obtained in 20 and 15% yield, respectively. Both **1a** and **2c** have been characterized by X-ray crystallography (Figs. 1 and 2).[6, 7] The size of the tellurium atom (Te–C 2.083(9); Te–C4 2.065(9) Å) results in a distortion of the core of **1a** such that the non-

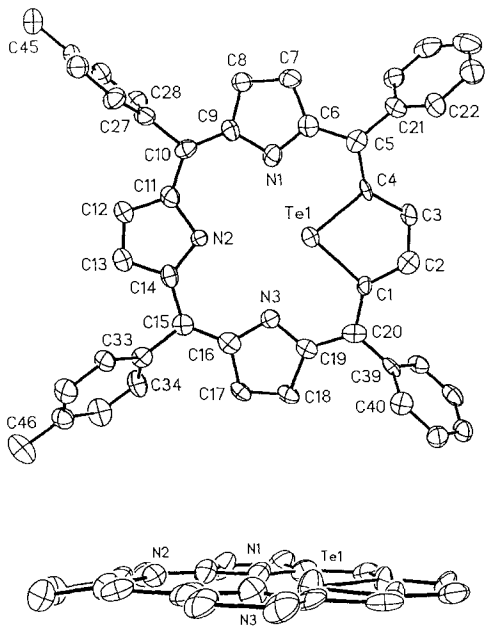

Fig. 1. Two views of the crystal structure of the 21-telluraporphyrin **1a** (thermal ellipsoids for all non-hydrogen atoms for 50% probability). The lower drawing, in which the aryl groups are omitted, emphasizes the deviations from planarity.

[*] Prof. Dr. L. Latos-Grażyński, E. Pacholska, Dr. P. J. Chmielewski
Institute of Chemistry
University of Wrocław
50383 Wrocław (Poland)
Telefax: Int. code +(71) 222-348
e-mail: llg@chem.uni.wroc.pl
Prof. Dr. A. L. Balch, Dr. M. M. Olmstead
Department of Chemistry
University of California, Davis, CA 95616 (USA)
Telefax: Int. code +(916) 752-8995
e-mail: albalch@ucdavis.edu

[**] This work was supported by the State Committee for Scientific Research KBN of Poland (Grant 2.0732 91 01) and the U.S. National Science Foundation (Grant INT-9114389).

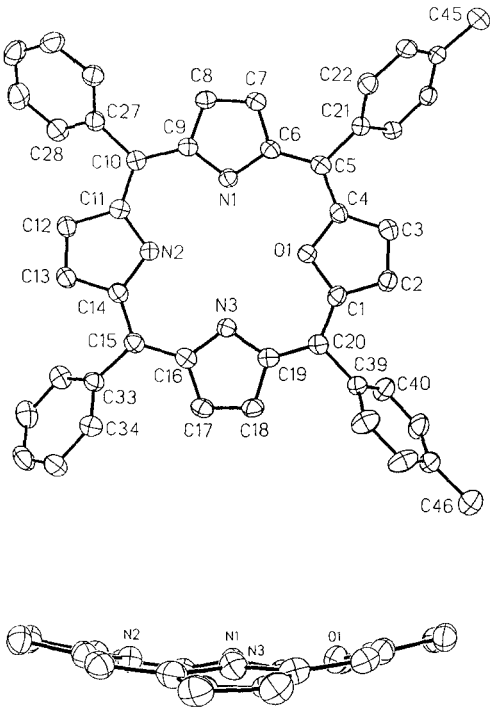

Fig. 2. Two views of the crystal structure of the 21-oxaporphyrin **2c** that correspond to those in Figure 1.

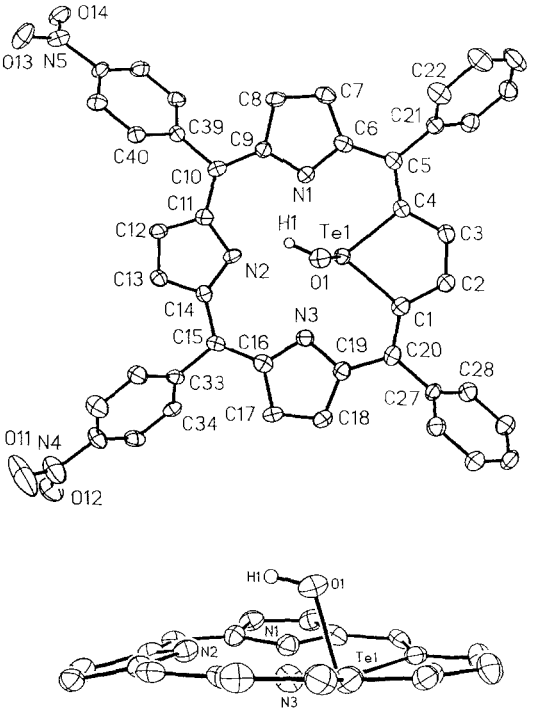

Fig. 3. Two views of the crystal structure of **3b** that correspond to those in Figure 1.

bonded N1 $\cdots$ N3 distance (4.65(2) Å) is elongated relative to that in a normal porphyrin. The nonbonded Te $\cdots$ N2 distance is 3.13(1) Å. Surprisingly, this macrocycle with the large core heteroatom is nearly planar, while the 21-oxaporphyrin **2c** is markedly nonplanar. However, similar nonplanarity is seen in one crystalline modification of tetraphenylporphyrin itself.[8] The C_β–C_β and C_α–C_β bond lengths in **1a** are 1.37(2) and 1.42(2) Å, respectively, in tellurophene 1.45(1) and 1.34(1) Å,[9] respectively, in **2c** 1.363(4) and 1.403(4) Å, respectively, and in furan 1.425 and 1.322 Å,[10] respectively. The reversal of the C_β–C_β and C_α–C_β bond lengths in **1a** and tellurophene as well as in **2c** and furan shows that the tellurophene or furan portions are involved in aromatic delocalization.

Unlike 21-thiaporphyrins and 21-selenaporphyrins, 21-telluraporphyrins are air sensitive. Red solutions of **1a** gradually turn green when exposed to the atmosphere for several minutes. This process is accelerated when **1a** is treated with *m*-chloroperoxybenzoic acid, and the reaction yields two products. With an excess of the peroxy acid, the red-brown 21-oxaporphyrin **2a** is formed. However, this process occurs through the formation of a green intermediate (**3a**) which can be isolated if the quantity of oxidant is limited. Treatment of **3a** with additional *m*-chloroperoxybenzoic acid or prolonged exposure to atmospheric dioxygen produces **2a**. The intermediate **3a** can also be reduced back to **1a** by treatment with either zinc amalgam or sodium dithionite. Green **3b** has been isolated in crystalline form. The results of an X-ray diffraction study are shown in Figure 3.[11] The new macrocycle consists of the telluraporphyrin with an oxygen atom attached to the tellurium atom and a proton transferred from the pyrrole nitrogen atom to the oxygen atom; this produces a zwitterion with a hydroxy group attached to the tellurium atom. The hydrogen atom of the hydroxy group was clearly located in a difference map and its position was subsequently refined with the O–H bond riding on the attached oxygen atom (bond length fixed at 0.92 Å and a $U = 0.03$ Å^2). Interestingly, the hydroxy substituent is positioned so that the Te–O bond passes through the porphyrin plane. The Te–O bond length (1.916(4) Å) is comparable to the shorter of the two Te–O bond lengths (1.890, 2.554 Å) in dimeric diphenyl telluroxide.[12] The hydroxy group attached to the tellurium atom interacts with the *trans*-pyrrole ring through a weak hydrogen bond. This *trans* pyrrole ring is tipped upward toward the hydroxy group so that the N $\cdots$ H distance is 2.243 Å.

The facile oxidation of the tellurium atom in the tellurophene unit in **1** and its eventual conversion into a furan upon treatment with a peroxy acid are unusual in tellurophene chemistry.[13] We suggest in Scheme 1 that the conversion of **3** to **2** proceeds via an intermediate in which the tellurophene ring is expanded to form the intermediate **6**. Related ring expansions of selenophene- and thiophene-containing compounds have been observed.[14] Organotellurium compounds with Te–O bonds are rare and difficult to obtain in pure crystalline form.[15] In the present case the porphyrin unit has served as a unique proton donor and stabilized a new form of tellurium coordination.

Experimental Procedure

1a: Boron trifluoride (1 mL) was added to a solution of 2,5-bis(phenylhydroxymethyl)tellurophene (**5a**) (1.1 g, 3 mmol), which was obtained according to the literature method [1], *p*-tolylaldehyde (**4a**) (2.0 g, 17 mmol), and pyrrole (1.3 g, 20 mmol) in dioxygen-free dichloromethane (0.5 mL). The mixture was stirred under dinitrogen in the dark for 1 h and then *p*-chloranil (4.0 g, 17 mmol) was added. The mixture was heated under reflux for 1 h. The solution was evaporated to dryness. The residue was dissolved in deoxygenated dichloromethane and chromatographed on basic alumina. The first red-brown fraction was collected and evaporated to dryness. The residue was then subjected to chromatography under dinitrogen on very fine silica under pressure with benzene/cyclohexane (3/1 v/v) as eluant. The first red band was collected and evaporated to dryness. The product was recrystallized from chloroform/methanol to give 425 mg, 20% yield of **1a**. MS(EI): *m/z* 756 (100%), 758 (95%). ^{1}H NMR (300 MHz, $CDCl_3$): $\delta = 10.421$ (s, 2H), 8.642 (d, 2H, $^4J(H,H) = 1.8$ Hz), 8.579 (s, 4H), 8.230 (d, 4H, $^3J(H,H) = 7.5$ Hz), 8.105 (d, 4H, $^3J(H,H) = 7.8$ Hz), 7.815 (m, 4H), 7.724 (m, 2H), 7.554 (d, 4H), $^3J(H,H) = 7.5$ Hz), 2.690 (s, 6H), -1.544 (s, 1H). UV/Vis: λ_{max} [nm] (ε, $M^{-1}cm^{-1}$) = 440 (1.5×10^4); 533 (1.6×10^4); 574 sh; 622 (6.6×10^3); 681

(6.6×10^3). A similar procedure that utilized 2,5-bis(phenylhydroxymethyl)furan (**6**, 300 mg) produced **2a** (100 mg, 15%). MS(EI): *m/z* 643 (100%). ^{1}H NMR (300 MHz, $CDCl_3$): $\delta = 9.132$ (s, 2H), 8.868 (s, 2H), 8.609 (d, 2H), 8.498 (d, 2H, $^3J(H,H) = 4.6$ Hz), 8.160 (m, 4H), 8.038 (d, 4H, $^3J(H,H) = 7.8$ Hz), 7.742 (m, 6H), 7.520 (d, 4H, $^3J(H,H) = 7.8$ Hz), 2.673 (s, 6H), −1.65 (s, 1H). UV/Vis, λ_{max} [nm] (ε, $M^{-1}cm^{-1}$) = 422 (9.3×10^4); 478 (2.1×10^3); 508 (9.9×10^3); 540 (2.2×10^3); 612 (1.7×10^3), 672 (1.8×10^3).

3a: A portion of **1a** (10 mg, 0.013 mmol) in chloroform (5 mL) was treated with two molar equivalents of *m*-chloroperoxybenzoic acid (11 mg of a 40% mixture with benzoic acid, 0.026 mmol) for 1 h. The green solution was subjected to chromatography on basic alumina with chloroform as eluant. The green band was collected and crystallized from chloroform/ethanol to produce dark green crystals of the compound **3a** (9 mg, 90%). MS(EI): *m/z* 774. ^{1}H NMR (300 MHz, $CDCl_3$): $\delta = 10.425$ (s, 2H), 8.469 (d, 2H), 8.400 (d, 2H, $^3J(H,H) = 4.6$ Hz), 8.318 (s, 2H), 8.214 (m, 4H), 8.050 (m, 4H), 7.535 (m, 4H), 7.736 (m, 2H), 7.485 (m, 4H), 2.687 (s, 6H). UV/Vis, λ_{max} [nm] (ε, $M^{-1}cm^{-1}$) = 465 (8.2×10^4); 485 (6.2×10^4); 564 (9.7×10^3); 629 sh; 659 (1.7×10^4). A similar procedure with five molar equivalents of *m*-chloroperoxybenzoic acid produces **2a**.

Compounds with different substituents were obtained by similar procedures.

Received: March 20, 1995 [Z 7814 IE]
German version: *Angew. Chem.* **1995**, *107*, 2467–2469

Keywords: oxidations · porphyrinoids · tellurium compounds

[1] a) A. Ulman, J. Manassen, *J. Am. Chem. Soc.* **1975**, *97*, 6540; b) A. Ulman, J. Manassen, F. Frolow, D. Rabinovich, *Tetrahedron Lett.* **1978**, 1855; c) A. Ulman, J. Manassen, *J. Chem. Soc. Perkin Trans. 1* **1979**, 1066; d) A. Ulman, J. Manassen, F. Frolow, D. Rabinovich, *Inorg. Chem.* **1981**, *20*, 1987; e) R. J. Abraham, P. Leonard, A. Ulman, *Org. Magn. Reson.* **1984**, *22*, 561.

[2] a) E. Vogel, W. Haas, B. Knipp, J. Lex, H. Schmickler, *Angew. Chem.* **1988**, *100*, 445; *Angew. Chem. Int. Ed. Engl.* **1988**, *27*, 406; b) E. Vogel, P. Röhring, M. Sicken, B. Knipp, A. Herrman, M. Pohl, H. Schmickler, J. Lex, *ibid.* **1989**, *101*, 1682 and **1989**, *28*, 1651.

[3] a) L. Latos-Grażyński, J. Lisowski, M. M. Olmstead, A. L. Balch, *J. Am. Chem. Soc.* **1987**, *109*, 4428–4429; b) J. Lisowski, M. Grzeszczuk, L. Latos-Grażyński, *Recl. Trav. Chim. Pays-Bas* **1987**, *106*, 319; c) L. Latos-Grażyński, J. Lisowski, M. M. Olmstead, A. L. Balch, *Inorg. Chem.* **1989**, *28*, 1183; d) J. Lisowski, M. Grzeszczuk, L. Latos-Grażyński, *Inorg. Chim. Acta* **1989**, *161*, 153; e) L. Latos-Grażyński, J. Lisowski, M. M. Olmstead, A. L. Balch, *Inorg. Chem.* **1989**, *28*, 3328; f) P. Chmielewski, M. Grzeszczuk, L. Latos-Grażyński, J. Lisowski, *ibid.* **1989**, *28*, 3546; g) L. Latos-Grażyński, M. M. Olmstead, A. L. Balch, *ibid.* **1989**, *28*, 4065; h) L. Latos-Grażyński, J. Lisowski, L. Szterenberg, M. M. Olmstead, A. L. Balch, *J. Org. Chem.* **1991**, *56*, 4043; i) J. Lisowski, L. Latos-Grażyński, L. Szterenberg, *Inorg. Chem.* **1992**, *31*, 1933; j) P. J. Chmielewski, L. Latos-Grażyński, *ibid.* **1992**, *31*, 5231; k) P. J. Chmielewski, L. Latos-Grażyński, E. Pacholska, *ibid.* **1994**, *33*, 1992.

[4] a) P. J. Chmielewski, L. Latos-Grażyński, K. Rachlewicz, T. Głowiak, *Angew. Chem.* **1994**, *106*, 805; *Angew. Chem. Int. Ed. Engl.* **1994**, *33*, 779; b) H. Furuta, T. Asano, T. Ogawa, *J. Am. Chem. Soc.* **1994**, *116*, 767.

[5] a) M. J. Broadhurst, R. Grigg, A. W. Johnson, *J. Chem. Soc. C* **1971**, 3681; b) A. W. Johnson in *Porphyrins and Metalloporphyrins* (Ed.: K. M. Smith), Elsevier, Amsterdam, **1975**, p. 279.

[6] Crystal data for **1a**: Dark purple parallelepipeds of $C_{46}H_{33}N_3Te$ that were obtained by diffusion of *n*-hexane into a dichloromethane solution of the compound under dioxygen-free conditions form in the monoclinic space group $P2_1$ with $a = 9.9640(10)$, $b = 8.6020(10)$, $c = 20.820(3)$ Å, $\beta = 98.26(1)°$, at 130 K with $Z = 2$ with the use of nickel monochromated $Cu_{K\alpha}$ ($\lambda = 1.54178$ Å) radiation. Refinement of 2486 reflections with 207 parameters yielded $wR2 = 0.1332$ and a conventional $R_1 = 0.053$ for 2431 reflections with $I > 2\sigma(I)$. Further details of the crystal structure investigations may be obtained from the Director of the Cambridge Crystallographic Data Centre, 12 Union Road, GB-Cambridge CB2 1EZ (UK), on quoting the full journal citation.

[7] Crystal data for **2c** · $CHCl_3$: Black parallelepipeds of $C_{47}H_{34}Cl_3N_3O$ that were obtained by diffusion of ethanol into a chloroform solution of the compound form in the monoclinic space group $P2_1/n$ with $a = 18.568(4)$, $b = 10.740(2)$, $c = 19.929(3)$ Å, $\beta = 107.731(13)°$ at 130 K with $Z = 4$ with the use of nickel monochromated $Cu_{K\alpha}$ ($\lambda = 1.54178$ Å) radiation. Refinement of 4954 reflections with 499 parameters yielded $wR2 = 0.096$ and a conventional $R_1 = 0.041$ for 4220 reflections with $I > 2\sigma(I)$ [6].

[8] S. J. Silvers, A. Tulinsky, *J. Am. Chem. Soc.* **1967**, *89*, 3331.

[9] J. Zukerman-Schpector, M. J. Dabdoub, M. A. Perira, *Acta Crystallogr. Sect. C* **1992**, *48*, 767.

[10] R. Fourme, *Acta Crystallogr. Sect. B* **1972**, *28*, 2984.

[11] Crystal data for **3b** · $2.5C_6H_6$: Dark green parallelepipeds of $C_{59}H_{42}N_5O_5Te$ that were obtained by diffusion of cyclohexane into a benzene solution of the compound form in the triclinic space group $P\bar{1}$ with $a = 10.2370(10)$, $b = 15.326(2)$, $c = 16.851(2)$ Å, $\alpha = 63.60(1)°$, $\beta = 88.53(1)°$, $\gamma = 81.23(1)°$ at 130 K with $Z = 2$ with the use of nickel monochromated $Cu_{K\alpha}$ ($\lambda = 1.54178$ Å) radiation. Refinement of 6104 reflections with 564 parameters yielded $wR2 = 0.132$ and a conventional $R_1 = 0.051$ for 5251 reflections with $I > 2\sigma(I)$ [6].

[12] N. W. Alcock, W. D. Harrison, *J. Chem. Soc. Dalton Trans.* **1982**, 709.

[13] F. Fringuelli, G. Marino, A. Taticchi, *Adv. Heterocyclic Chem.* **1977**, *21*, 120.

[14] a) C. J. White, R. J. Angelici, M.-G. Choi, *Organometallics* **1995**, *14*, 332; b) W. D. Jones, R. M. Chin, *J. Am. Chem. Soc.* **1992**, *114*, 9851.

[15] Y. Nishibayashi, N. Komatsu, K. Ohe, S. Uemura, *J. Chem. Soc. Perkin Trans. 1* **1993**, 1133.

Acyclic 1,4-Diastereoselectivity in γ-Substituted α-Enones: Transmission of Chiral Information through Conjugation

Tsuneo Sato, Masaru Kido, and Junzo Otera*

Diastereoselectivity arising from stereogenic centers in the vicinity plays a central role in acyclic stereoselectivity. In this context, high 1,2- and 1,3-diastereoselectivities have been achieved so far,[1] and in particular, the 1,2-stereochemical relationship is well documented as Cram's rule. On the other hand, asymmetric induction between more remote sites remains a challenge. The approaches that met with success for the 1,4-relationship basically relied on chelation of metal atoms or steric origins (π-complexation of transition metals, neighboring group participation, or *gauche* interactions).[2] In particular, Reetz et al.[3] and Nakamura et al.[4] disclosed that γ-amino or γ-alkoxy enals undergo nucleophilic addition of cuprates to the carbonyl groups with significant levels of the diastereoselectivity. π-Complexation of copper was suggested to be essential for these reactions since only stereorandom behavior was observed by use of alkyllithium or Grignard reagents. Consistent with these results, complete loss of diastereoselectivity in hydride reduction and alkylation of 2-ene-1,4-diones or γ-methoxy enones or enals led Fleming et al. to conclude that "Cram's rule diastereoselectivity is either largely steric in origin or that chiral information is very inefficiently transmitted by conjugation".[5] Very recently, however, cyclic substrates were successfully invoked by Wipf et al.: nucleophilic addition to 4,4-disubstituted cyclohexadienones occurred *anti* to the oxygen substituent at C4 with a considerable level of selectivity.[6] We report here on the surprisingly high diastereoselectivities in the carbonyl reduction and alkylation of γ-sulfenyl α-enones. Consequently, we substantiate unprecedented acyclic 1,4-diastereoselectivity for which neither chelation nor steric demands are invoked. In addition, we show that even γ-alkoxy α-enones undergo appreciably stereoselective reaction by proper design of the substrate structures.

The reaction of γ-sulfenyl-substituted α-enone **1**[7] with Li-*s*Bu_3BH (2 equiv.)[8] in THF at −78 °C results exclusively in reduction of the carbonyl group. (The equations for the reactions and the representations are given for only one enantiomer.) The diastereomer ratio of the allylic alcohols obtained is constantly high irrespective of R^1 (Table 1, entries 1–7).[9]

[*] Prof. Dr. J. Otera, Prof. Dr. T. Sato
Department of Applied Chemistry, Okayama University of Science
Ridai-cho, Okayama 700 (Japan)
Telefax: Int. code +(86) 252-6891
Dr. M. Kido
Otsuka Pharmaceutical Co.
463-10 Kagosuno, Kawauchi-cho, Tokushima 771-1 (Japan)

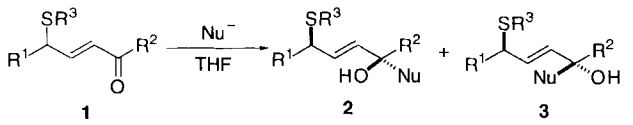

Table 1. Reactions of γ-substituted α-enones **1** and **7** with $LisBu_3BH$ [a].

Entry	R^1	R^2	R^3	R^4	R^5	Yield of **2** + **3** or **8** + **9** [%] [b]	**2**:**3** or **8**:**9** [c]
1	tC_4H_9	tC_4H_9	C_6H_5			96	97:3
2	iC_3H_7	tC_4H_9	C_6H_5			91	96:4
3	CH_3	tC_4H_9	C_6H_5			82	95:5
4	tC_4H_9	iC_3H_7	C_6H_5			82	94:6
5	tC_4H_9	CH_3	C_6H_5			98	91:9
6	nC_8H_{15}	nC_5H_{11}	C_6H_5			71	93:7
7	nC_6H_{13}	tC_4H_9	C_6H_5			100	93:7
8 [d]	tC_4H_9	tC_4H_9	C_6H_5			57 (71) [e]	85:15
9	nC_6H_{13}	tC_4H_9	CH_3			84	87:13
10 [f]				*cyclo*-C_6H_{11}	CH_2Ph	81	30:70
11 [g]				tC_4H_9	CH_2Ph	86	25:75
12 [f]				*cyclo*-C_6H_{11}	$SiMe_2tBu$	86	71:29
13 [f]				tC_4H_9	$SiMe_2tBu$	43	72:28

[a] All reactions were carried out in THF at −78 °C for 0.5 h unless otherwise noted. [b] Isolated yields. [c] Determined by HPLC. [d] MeMgBr as nucleophile (5 h). [e] Based on consumed starting material. [f] Reaction time 1 h. [g] Reaction time 1.5 h.

The hydride attacks from the opposite side of the sulfenyl group to give **2** as the major isomers. The selectivity slightly decreases with decreasing bulk of R^2, indicative of the importance of the ground state geometry of the α-enone moiety for the high selectivity. The *tert*-butyl derivative (entry 1) possesses almost pure s-*cis* configuration, while contribution of the s-*trans* counterpart increases as R^2 becomes smaller.[10] Attack of a methyl Grignard reagent also takes place in a similar manner (entry 8). A chelate-controlled mechanism is incompatible with the sense of the observed diastereoselectivities. The X-ray crystal structure analysis of the enone **1** (R^1,R^2 = *tert*-butyl; Fig. 1) reveals that the C–S bond is directed almost perpendicular to the plane of the enone moiety with the S-C-C=C dihedral angle of 106°. This is completely consistent with the results of ab initio calculations for γ-substituted α-enals by Morokuma et al.[11] An electron-donating group is favorably situated orthogonal to the enone face so that such an arrangement could stabilize the enal fragment through the σ-π* interaction.[12] One may assume that

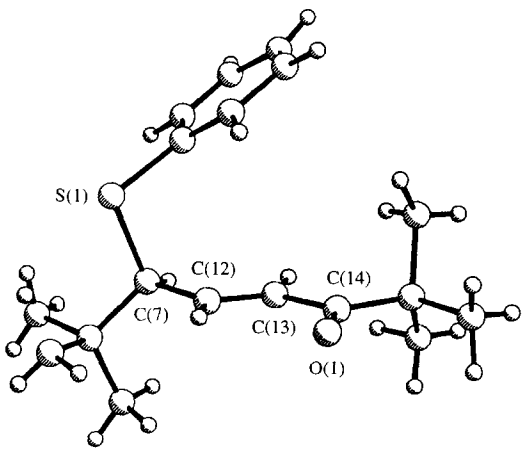

Fig. 1. Crystal structure of compound **1**. Selected bond lengths [Å] and angles [°]: S1-C7 1.83(1), O1-C14 1.19(1), C7-C12 1.50(1), C12-C13 1.34(1), C13-C14 1.53(1); S1-C7-C12 106.4(8), C7-C12-C13 123(1), C12-C13-C14 119(1), O1-C14-C13 121(1).

an aromatic ring of the phenylthio group sterically shields the "front side" of the carbonyl face to facilitate the "back-side" attack of the nucleophile. This assumption is proved invalid by the fact that a smaller methylthio-substituted derivative gives rise to the analogous outcome (Table 1, entry 9). It is apparent therefore that the asymmetric character is transmitted through the olefinic bond. The σ-π* interaction would perturb the electronic environments of the enone moiety, and hence the facial selectivity might be governed by this stereoelectronic effect.

The innate tendency of the back-side attack is further confirmed by the stereoselectivity of the nucleophilic addition to the γ-sulfenyl-α-enal **4**. Reduction of **4** with $LiEt_3BH$ affords **5** and **6** in a 77:23 ratio (Bz = PhCO) consistent with the above results.[9] Use of $LisBu_3BH$ leads to loss of the diastereoselectivity, and use of the more bulky Li(siamyl)$_3$BH (siamyl = 1,2-dimethylpropyl) results in the reversal of the selectivity. These results lend additional support to the rationalization that the back-side attack is not induced by the steric bulk of the sulfenyl group. These variations of the stereoselectivity are ascribed to the s-*trans* configuration of the enal **4**.[10] Since the α-enones **1** have basically an s-*cis* configuration, the Bürgi–Dunitz trajectory of the nucleophile[13] is not influenced by the R^1 group (**A**). On the other hand, the approach of the nucleophile towards the s-*trans* configurated enal **4** experiences steric hindrance from the *tert*-butyl group (**B**). Thus, the bulky reducing agent is forced to have a front-side access. In other words, nucleophiles discriminate the carbonyl face essentially in favor of the opposite side of the sulfenyl group in the absence of steric demands.

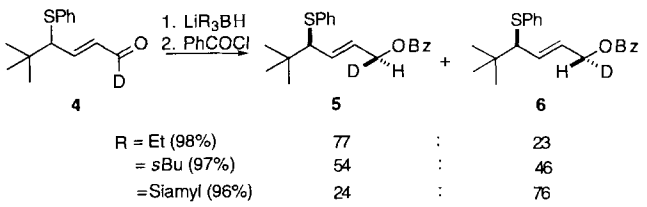

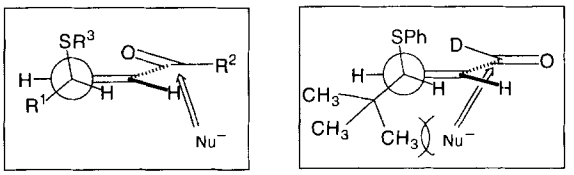

In contrast to previous results,[4,5,14] we have established that carbonyl additions to γ-alkoxy or -siloxy α-enones **7** exhibit a small degree of diastereoselectivity. Remarkably, the stereochemical outcome is dependent on the oxygen functions (Table 1, entries 10–13).[9] The benzyloxy derivatives **7** are reduced preferably to *anti* products, the siloxy analogues **7** to *syn* isomers. Again, the chelate-controlled mechanism is ruled out since chelation with (*E*)-γ-heteroatom-substituted enones is improbable because of the distant location of the two oxygen atoms.[15] The different stereochemical outcomes are attributable to the different ground state conformations of the

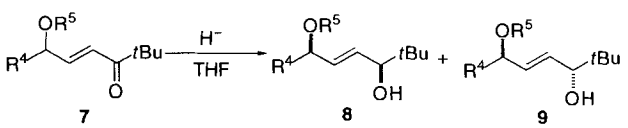

substrates. Gung et al. disclosed that γ-benzyloxy α,β-unsaturated carbonyl compounds prefer the CH eclipsed form, while the corresponding silyl ethers prefer the CO eclipsed form.[16] We therefore reasonably assume that the most electron-donating alkyl group is located perpendicular to the "front side" of the enone (Scheme 1), and the hydride attack from the opposite side leads to the *anti* isomer with the benzyl ethers and to the *syn* isomer with the siloxy ethers.

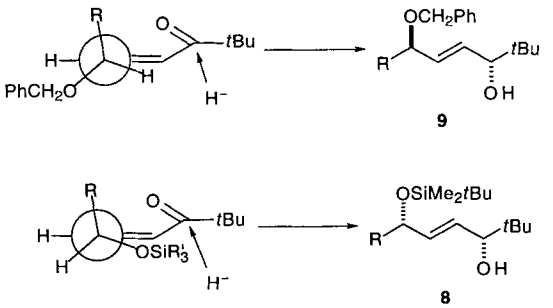

Scheme 1. Stereochemical consideration for the reduction of **7** ($R^5 = PhCH_2$, SiR'_3; $R^4 = R$).

This dependence of the diastereoselectivity on the heteroatom substituents contrasts sharply with the propensity in typical Felkin–Cram-type reactions where the alkoxy and alkylthio groups always work in the same manner as the largest substituents.[17] Apparently, the sulfur and oxygen functional groups exert electronic influences in different ways in the vinylogous Cram case. The superior selectivity and constant mode of diastereofacial discrimination of the sulfenyl starting materials can be attributed to the effective σ-π* interaction which fixes the C–S bond perpendicular to one side of the enone. On the other hand, the rotation of the C_β–C_γ bond in **7** cannot be completely suppressed by the weak hyperconjugative effect of the C–O, C–C, or C–H bond leading to the stereochemical fluctuation and lower diastereoselectivities.

In conclusion, the stereochemical sense of both γ-sulfenyl and -alkoxy substrates is consistently interpreted by situating the most electron-donating group[18] orthogonal to the enone face concurrent with the back-side attack of the nucleophiles. Although the back-side attack may possibly be induced simply by the steric bulk of the substituent in the orthogonal position, we rather advance that the stereoelectronic origin is more plausible on the basis of only a small difference between the phenylthio and methylthio derivatives as well as the results with α-enals. More significantly, the stereochemical outcome with γ-siloxy α-enones is not consistent with the steric argument because back-side attack should be hampered by the largest siloxy group and this should result in the opposite sense of the stereoselectivity if the steric origin is valid (see Scheme 1). Obviously, the precise picture of the mechanism would be drawn by dealing with transition states, not with the ground states. Studies along this line as well as synthetic applications are now in progress in our laboratories.

Experimental Procedure

To a solution of (*E*)-2,2,7,7-tetramethyl-6-phenylthio-4-octen-3-one (145 mg, 0.5 mmol) in THF (2 mL) was added $LisBu_3BH$ (1.0 M THF solution, 1 mL, 1 mmol) at −78 °C. After being stirred for 30 min, the reaction mixture was combined with MeOH (0.5 mL), 1 N NaOH (0.5 mL), and 30% H_2O_2 (0.5 mL). The resulting mixture was allowed to warm up to room temperature and stirred for 30 min. Extraction with ethyl acetate followed by evaporation provided an oil. HPLC analysis (Develosil Si 30, 3 mm, 4.6 × 250 mm, hexane/ethyl acetate (90/10), 1 mL min^{-1} showed that the crude product consisted of (3*S**,6*S**,*E*)- and (3*R**,6*S**,*E*)-3-hydroxy-2,2,7,7-tetramethyl-6-phenylthio-4-octene in a 97:3 ratio. Column chromatography on silica gel (hexane/ethyl acetate (95/5) provided (*E*)-3-hydroxy-2,2,7,7-tetramethyl-6-phenylthio-4-octene (140 mg, 96%): Anal. calcd. for $C_{18}H_{28}OS$: C 73.91, H 9.64; found: C 73.62, H 9.66. Preparative HPLC (Develosil Si 30, 10 mm, 20 × 250 mm, hexane/ethyl acetate (95:5)) afforded the pure isomers. (3*S**,6*S**,*E*)-3-Hydroxy-2,2,7,7-tetramethyl-6-phenylthio-4-octene: m.p. 67–69 °C; IR (CCl_4): 3680, 3460 cm^{-1}; ^{1}H NMR $CDCl_3$): δ = 0.66 (br.s, 1H), 0.75 (s, 9H), 1.07 (s, 9H), 3.36 (d, *J* = 10.3 Hz, 1H), 3.53 (d, *J* = 7.87 Hz, 1H), 5.05 (dd, *J* = 7.87, 15.1 Hz, 1H), 5.54 (dd, *J* = 10.3, 15.1 Hz, 1H), 7.2–7.4 (m, 5H); ^{13}C NMR ($CDCl_3$): δ = 25.5, 28.0, 34.3, 64.9, 80.4, 127.2, 128.5, 131.3, 131.8, 134.0, 135.4; MS: *m/z*: 292 (M^+); HRMS calcd for $C_{18}H_{28}OS$ (M^+) 292.1861, found 292.1818; HPLC: t_R = 7.5 min. The structure of this compound was confirmed by X-ray crystallography. (3*R**,6*S**,*E*)-3-Hydroxy-2,2,7,7-tetramethyl-6-phenylthio-4-octene: JR (CCl_4): 3500 cm^{-1}; ^{1}H NMR ($CDCl_3$): δ = 0.67 (s, 9H), 1.09 (s, 9H), 1.56 (br.s, 1H), 3.41 (d, *J* = 10.1 Hz, 1H), 3.58 (d, *J* = 7.33 Hz, 1H), 5.24 (dd, *J* = 7.33, 15.2 Hz, 1H), 5.64 (dd, *J* = 10.1, 15.2 Hz, 1H), 7.2–7.4 (m, 5H); ^{13}C NMR ($CDCl_3$): δ = 25.3, 28.0, 34.5, 34.6, 64.3, 80.4, 126.6, 128.6, 130.9, 131.5, 132.5, 135.6; MS: *m/z*: 292 (M^+); HRMS calcd for $C_{18}H_{28}OS$ (M^+) 292.1861, found 292.1863; HPLC: t_R = 11.1 min.

Received: May 24, 1995 [Z 8020 IE]
German version: *Angew. Chem.* **1995**, *107*, 2459–2461

Keywords: asymmetric syntheses · enones · nucleophilic additions · reductions

[1] P. A. Bartlett, *Tetrahedron* **1980**, *36*, 3.
[2] Recent, representative studies on 1,4-diastereoselecivity: R. Bloch, C. Brillet, *Tetrahedron: Asymmetry* **1992**, *3*, 333; H. Grennberg, A. Gogoll, J.-E. Bäckvall, *J. Org. Chem.* **1991**, *56*, 5808; J. S. Panek, M. Yang, *ibid.* **1991**, *56*, 5755; G. A. Molander, J. P. Haar, Jr., *J. Am. Chem. Soc.* **1991**, *113*, 3608; G. A. Molander, J. B. Etter, L. S. Harring, P.-J. Thorel, *ibid.* **1991**, *113*, 8036; G. A. Molander, K. O. Cameron, *J. Org. Chem.* **1991**, *56*, 2617.
[3] M. T. Reetz, F. Wang, K. Harms, *J. Chem. Soc. Chem. Commun.* **1991**, 1309.
[4] M. Arai, T. Nemoto, Y. Ohashi, E. Nakamura, *Synlett* **1992**, 309.
[5] I. Fleming, H. Kühne, K. Takaki, *J. Chem. Soc., Perkin Trans. 1* **1986**, 725.
[6] P. Wipf, Y. Kim, *J. Am. Chem. Soc.* **1994**, *116*, 11 678.
[7] α-Enones **1** were prepared by Wittig–Horner reaction of α-sulfenyl aldehyde. For the preparation of α-sulfenyl aldehydes, see T. Sato, H. Okazaki, J. Otera, *H.* Nozaki, *J. Am. Chem. Soc.* **1988**, *110*, 5209.
[8] Use of 1 equiv of $LisBu_3BH$ gave the same selectivity but a lower yield (68%).
[9] All compounds in this study were fully confirmed by ^{1}H and ^{13}C NMR, IR, HRMS, elemental analyses, or X-ray diffraction study, and comparison with authentic samples.
[10] F. H. Cottee, B. P. Straughan, C. J. Timmons, *J. Chem. Soc. B* **1967**, 1146; T. Liljefors, N. L. Allinger, *J. Am. Chem. Soc.* **1976**, *98*, 2745; H.-J. Oelichmann, D. Bougeard, B. Schrader, *Angew. Chem. Suppl.* **1982**, 1404.
[11] A. E. Dorigo, K. Morokuma, *J. Am. Chem. Soc.* **1989**, *111*, 6524.
[12] This is also compatible with rationalization for the inside alkoxy transition state model in electrophilic reaction toward chiral allylic ethers in which the C=C bond is electron-deficient: K. N. Houk, S. R. Moses, Y.-D. Wu, N. G. Rondan, V. Jäger, R. Schohe, F. R. Fronczek, *J. Am. Chem. Soc.* **1984**, *106*, 3880.
[13] H. B. Bürgi, *Angew. Chem.* **1975**, *87*, 461; *Angew. Chem. Int. Ed. Engl.* **1975**, *14*, 460; H. B. Bürgi, J. D. Dunitz, *Acc. Chem. Res.* **1983**, *16*, 153.
[14] It was reported that a diethyl acetal of a γ-siloxy α-enone underwent the 1,2-reduction with $LisBu_3BH$ with 67:33 diastereoselectivity, but the use of a chiral borane led to the high enantioselectivity (95:5): H. Dumartin, Y. Le Floc'h, R. Grée, *Tetrahedron Lett.* **1994**, *36*, 6681.
[15] By comparing (*E*)- and (*Z*)-γ-amino enals, Reetz concluded that the former reacted by a non-chelation mechanism, while reaction of the latter was chelate-controlled [3].
[16] B. W. Gung, M. A. Wolf, *J. Org. Chem.* **1993**, *58*, 7038; B. W. Gung, M. S. Gerdeman, R. A. Fouch, M. A. Wolf, *ibid.* **1994**, *59*, 4255; B. W. Gung, J. P. Melnick, M. A. Wolf, A. King, *ibid.* **1995**, *60*, 1947.
[17] For α-alkoxy carbonyl compounds see ref. [1]. For α-sulfenyl carbonyl compounds: M. Shimagaki, T. Maeda, Y. Matsuzaki, I. Hori, T. Nakata, T. Oishi, *Tetrahedron Lett.* **1984**, *25*, 4475; H. J. Reich, R. C. Holton, S. L. Borkowsky, *J. Org. Chem.* **1987**, *52*, 314; R. Annunziata, M. Cinquini, F. Cozzi, P. G. Cozzi, E. Consoland, *ibid.* **1992**, *57*, 456.
[18] The electron-donating power of σ-bonds increases in the following order: $\sigma_{CO} < \sigma_{CH} \approx \sigma_{CC} < \sigma_{CS}$: N. D. Epiotis, W. R. Cherry, S. Shaik, R. L. Yates, F. Bernardi, *Top. Curr. Chem.* **1977**, 70; A. S. Cieplak, *J. Am. Chem. Soc.* **1981**, *103*, 4540; D. Mukherjee, Y.-D. Wu, F. R. Fronczek, K. N. Houk, *ibid.* **1988**, *110*, 3328.

$C_{59}N^+$ and $C_{69}N^+$: Isoelectronic Heteroanalogues of C_{60} and C_{70}**

Iris Lamparth, Berthold Nuber, Georg Schick, Andreas Skiebe, Thomas Grösser, and Andreas Hirsch*

Dedicated to Professor Hans Jürgen Bestmann on the occasion of his 70th birthday

For the structural variation of fullerenes three strategies can in principle be considered: 1) the synthesis of exohedral adducts, 2) the formation of heterofullerenes in which one or several C atoms of the fullerene core are replaced by, for example, N or B atoms, and 3) the generation of endohedral complexes. Whereas both exohedral and endohedral derivatives can be synthesized and isolated by a variety of methods,[1] it has not been possible so far to produce macroscopic amounts of heterofullerenes.[2] Even the mass spectrometric detection of heterofullerenes was accomplished only for boron fullerenes $C_{60-n}B_n^+$ ($n = 1-6$), which were generated in situ by laser vaporization of boron/graphite composite rods.[3] We now report for the first time on the formation of the nitrogen heterofullerenes $C_{59}N^+$ and $C_{69}N^+$, which are isoelectronic with C_{60} and C_{70}. These ions are formed by fragmentation (FAB-MS) of regioselectively synthesized iminofullerene derivatives. The specific arrangement of the nitrogen addends facilitates the removal of a carbon atom from the fullerene core and the incorporation of a nitrogen atom.

Bisazafulleroid **3**[4] served as a precursor for compounds leading to $C_{59}N^+$, and we synthesized for the first time the bisadducts **2**, which directly fragment to form this heterofullerene ion (Scheme 1, Table 1). The C_s-symmetric compounds **2**, which are

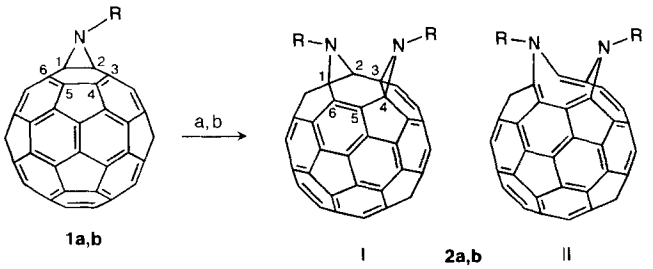

Scheme 1. **a**: R = COOEt; **b**: R = COO*t*Bu. Reaction conditions: a) N_3R, 1-chloronaphthalene, 60 °C; b) toluene, reflux.

green in solution, are the first examples of dicyclo adducts with addends bound *in cis-1* positions.[1] The adducts **2** are formed regioselectively from the reaction of **1**[5] with two equivalents of azidoformate in 1-chloronaphthalene at 60 °C and subsequent thermal extrusion of N_2 from the triazoline intermediate (Scheme 1). The structure of **2** was determined by ^{13}C NMR spectroscopy and was proven unambiguously by the use of 100% ^{15}N-labeled **2a** and **2a** in which only one imino bridge is ^{15}N-labeled (Table 1). The signals of C-1 and C-4 at $\delta = 128$ ($^1J_{(C,^{15}N)} = 14$ Hz) and of C-2 and C-3 at $\delta = 114$ ($^1J_{(C,^{15}N)} = 15$ Hz) exhibit a remarkable downfield shift. This shows that the bridged 6-6 bonds are open and that the 5-6 bonds in the corresponding six-membered ring have double-bond character. According to AM1 calculations the open structure II is 3 kcal mol^{-1} lower in energy even though a double bond has to be introduced formally into each of the three five-membered rings.

As a precursor for molecules suitable for the formation of $C_{69}N^+$ we synthesized for the first time the C_s-symmetric bisazafulleroid **4**. This C_{70} analogue of **3** is the major product from the

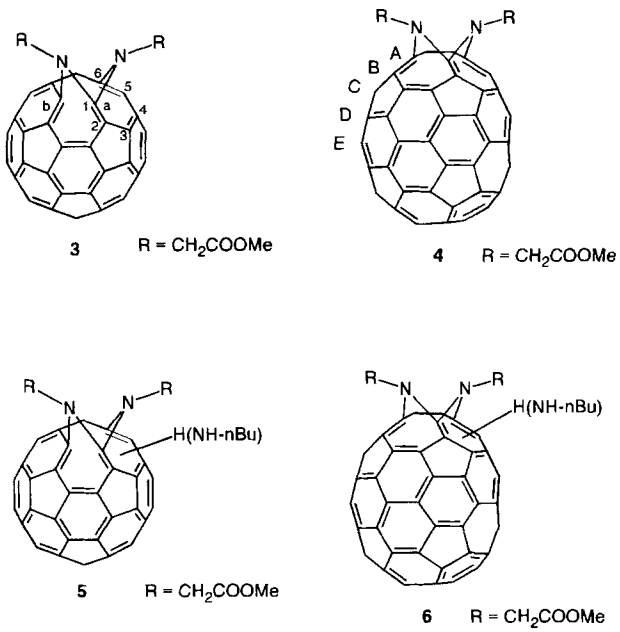

3 R = CH_2COOMe **4** R = CH_2COOMe

5 R = CH_2COOMe **6** R = CH_2COOMe

twofold reaction of C_{70} with azide. The preferred formation of **4** shows that the regioselective formation of bisazafulleroids[4] is also possible with C_{70}. In analogy to the ^1H NMR spectrum of **3**[4] we observe a quartet for the diastereotopic protons of the methylene groups in **4** (Table 1).

Whereas the mass spectra of the bisadducts **3** and **4** show the typical characteristics of fullerene adducts (a relatively small M^+ peak, the peak of the fullerene fragment ions C_{60}^+ or C_{70}^+ at $m/z = 720$ or 840 as the most intense signals), completely new behavior was observed with the bisadducts **2** (Fig. 1a). In this case the peak at $m/z = 722$ is the most intense signal, which is due to the formation of the heterofullerene ion $C_{59}N^+$.[6] The signal of $^{12}C_{60}^+$ at $m/z = 720$, which arises by the usual fragmentation, is less intense. After isotope correction, the spectrum of **2b** exhibits an intensity ratio of 5:4 for the ions $C_{59}N^+$ and C_{60}^+. The assignment of the peak at $m/z = 722$ to $^{12}C_{59}{}^{14}N^+$ is also confirmed by the observation that after the first "shrink-wrapping" the signal at $m/z = 698$ ($^{12}C_{57}{}^{14}N^+$) is still more intense than that at $m/z = 696$ ($^{12}C_{58}N^+$). Shrink-wrapping is the fragmentation of the fullerene core by successive elimination of C_2 units with retention of the fullerene structure.[3c, 7] This process requires such high energy (> 40 eV)[7b] that all exohedrally bound groups are removed first. Thus the peaks at $m/z = 722$ and 698 cannot be due to exohedral fullerene derivatives such as dihydrofullerenes. Trisadducts, which are formed by the reaction of azidoformates and **1** or of the corresponding 5-6-bridged azafulleroids having a mixed 5-6/6-6 addition pattern, show fragmentation behavior similar to that of **2**.[8]

The observation that heterofullerene ions are formed under these conditions from **2** and mixed 5-6/6-6 adducts but not from the bisadducts **3** and **4** or the 5-6 or 6-6 monoadducts such as **1**[4]

[*] Prof. Dr. A. Hirsch, I. Lamparth, B. Nuber, G. Schick, A. Skiebe, T. Grösser
Institut für Organische Chemie der Universität
Richard-Willstätter-Allee 2, D-76131 Karlsruhe (Germany)
Telefax: Int. code + (721)698-305

[**] This work was supported by the Bundesministerium für Bildung und Forschung (BMBF), Hoechst AG, and the Dr. Otto Röhm Gedächtnisstiftung.

Table 1. Selected spectroscopic data of the new compounds **2** and **4**.

[^{15}N]-**2a**: ^{1}H NMR (CS_2/10% $CDCl_3$, 250 MHz, 25 °C): δ = 4.11 (dq, J = 1.2, 7.0 Hz), 1.25 (t, J = 7.1 Hz); ^{13}C NMR (CS_2/10% $CDCl_3$, 62.9 MHz, 25 °C): δ = 152.57 (d, ^1J(C,N) = 27.6 Hz), 146.46 (1C), 145.91, 145.55, 145.33, 144.53, 144.42 (1C), 144.25, 143.73, 143.18, 143.09, 143.02, 142.84, 142.78, 142.76, 142.58, 140.96, 140.83, 140.76 (1C), 140.71, 140.28, 139.95, 139.31 (d, ^2J(C,N) = 2 Hz), 139.14 (1C), 138.96, 137.74, 137.18 (d, ^2J(C,N) = 1 Hz), 134.92 (d, ^2J(C,N) = 3 Hz), 128.09 (d, ^1J(C,N) = 14 Hz), 114.73 (dd, ^1J(C,N) = 15, ^2J(C,N) = 3 Hz), 62.65, 14.32; UV/Vis (CH_2Cl_2): λ_{max} [nm] (ε) = 260 (90000), 338 (26000), 549 (1000); FAB-MS (NBA): m/z: 896 (M^+, 25%), 723 ($C_{59}{}^{15}N^+$, 100%), 720 (C_{60}^+, 95%)

[^{14}N/^{15}N]-**2a** (C_{60}(^{15}NCOOEt)(^{14}NCOOEt)): ^{13}C NMR (CS_2/10% $CDCl_3$, 62.9 MHz, 25 °C): δ = 152.57 (s, d, ^1J(C,N) = 27.6 Hz), 146.46 (1C), 145.91, 145.55, 145.33, 144.53, 144.42 (1C), 144.25, 143.73, 143.18, 143.09, 143.02, 142.84, 142.78, 142.76, 142.58, 140.96, 140.83, 140.76 (1C), 140.71, 140.28, 139.95, 139.31 (b), 139.14 (1C), 138.96, 137.74, 137.18 (b), 134.92 (b), 128.09 (s, d, ^1J(C,N) = 14 Hz), 114.73 (d, d, ^1J(C,N) = 15, ^2J(C,N) = 3 Hz), 62.65, 14.32

2b: ^{1}H NMR (CS_2/10% $CDCl_3$, 250 MHz, 25 °C): δ = 1.44 (s); ^{13}C NMR (CS_2/10% $CDCl_3$, 62.9 MHz, 25 °C): δ = 151.43, 146.35 (1C), 145.81, 145.40, 145.26, 144.48, 144.31 (1C), 144.18, 143.62, 143.17, 142.99, 142.97, 142.93, 142.86, 142.76, 142.74, 142.48, 142.42, 140.93, 140.76, 140.58, 140.42 (1C), 140.31, 139.83, 139.83, 139.48 (1C), 139.41, 138.96, 137.58, 137.28, 134.74, 128.09, 114.60, 82.16, 27.62; UV/Vis (CH_2Cl_2): λ_{max} [nm] (ε) = 259 (90700), 337 (26000), 555 (1000); FAB-MS (NBA): m/z: 950 (M^+, 20%), 722 ($C_{59}N^+$, 100%), 720 (C_{60}^+, 95%), 698 ($C_{57}N^+$, 15%)

4: ^{1}H NMR (CS_2/20% $CDCl_3$, 250 MHz, 25 °C): δ = 5.34 (d), 4.57 (d), 3.93 (s); ^{13}C NMR (CS_2/20% $CDCl_3$, 62.9 MHz, 25 °C): δ = 169.61, 154.82, 152.23, 150.55, 150.50, 148.89, 148.66, 148.34, 148.01, 147.83, 147.29, 147.21, 146.85, 146.54, 146.38, 145.55, 145.25, 145.16, 144.66, 144.63, 144.21, 144.11, 143.54, 142.74, 140.93, 138.55, 136.98, 135.81, 134.45, 133.03, 132.53, 130.76, 129.85, 129.52, 128.61, 124.76, 52.79, 52.23 (b), 51.86, 51.70 (b); UV/Vis (cyclohexane): λ_{max} [nm] (ε) = 212 (71000), 237 (76000), 328 (17000), 393 (12600), 458 (11500); FAB-MS (NBA): m/z: 1015 (M^+, 20%), 928 ($M^+ - NCH_2COOMe$, 15%), 840 (C_{70}, 100%)

prompted us to further modify the fullerene core in **3** and **4** regioselectively and synthesize precursor molecules that are also able to fragment to give heterofullerene ions. According to AM1 calculations bonds *a* and *b* are the most polarized and attack of a nucleophile should take place there preferably. Hence, we treated **3** and **4** with one equivalent of butylamine in the presence of DBU. The initially formed precipitate became soluble upon the addition of acetic acid. The products are the monohydroamination products **5** and **6**, which are mixtures of regioisomers (attack at bond *a* or *b*) having identical R_f values. In analogy to dissolved **2** the solution of the hydroamination product **5** in $CHCl_3$ is green.

Under the conditions of FAB mass spectrometry **5** and **6** indeed fragment efficiently with formation of the ions $C_{59}N^+$ and $C_{69}N^+$ (Fig. 1b), which give rise to the most intense signals in the spectra. In the range of ions with cluster size 58, which are generated by shrink-wrapping, the same fragmentation features as those of **2** were observed. The signals of $C_{57}N^+$ and $C_{67}N^+$ are in general less intense than those of the corresponding ions with cluster size 60 and 70 (Fig. 1), which indicates that CN is eliminated more efficiently than C_2. The high-resolution signals of, for example, the fragment ions of **5** at 721.997 ($\pm$0.005) and of **6** at 841.997 ($\pm$0.006) clearly prove that these signals do not correspond to $^{12}C_{60}H_2^+$ (722.0157) and $^{12}C_{70}H_2^+$ (842.0157), because their calculated values are well outside the margin of error. The calculated masses of all possible combinations of $^{12}C_{58}{}^{13}C_2$ and $^{12}C_{59}{}^{14}N$ range between 722.0031 and 722.0067 and therefore very close to the range of the experimental values. The ions with cluster size 70 behave analogously. To finally prove unequivocally that a nitrogen atom is incorporated into the fullerene core under these conditions, we treated 100% ^{15}N-labeled **3** and **4** with unlabeled butylamine to convert them into the corresponding hydroamination products. Like in the FAB spectrum of [^{15}N]-**2a** the most intense fragmentation signals are

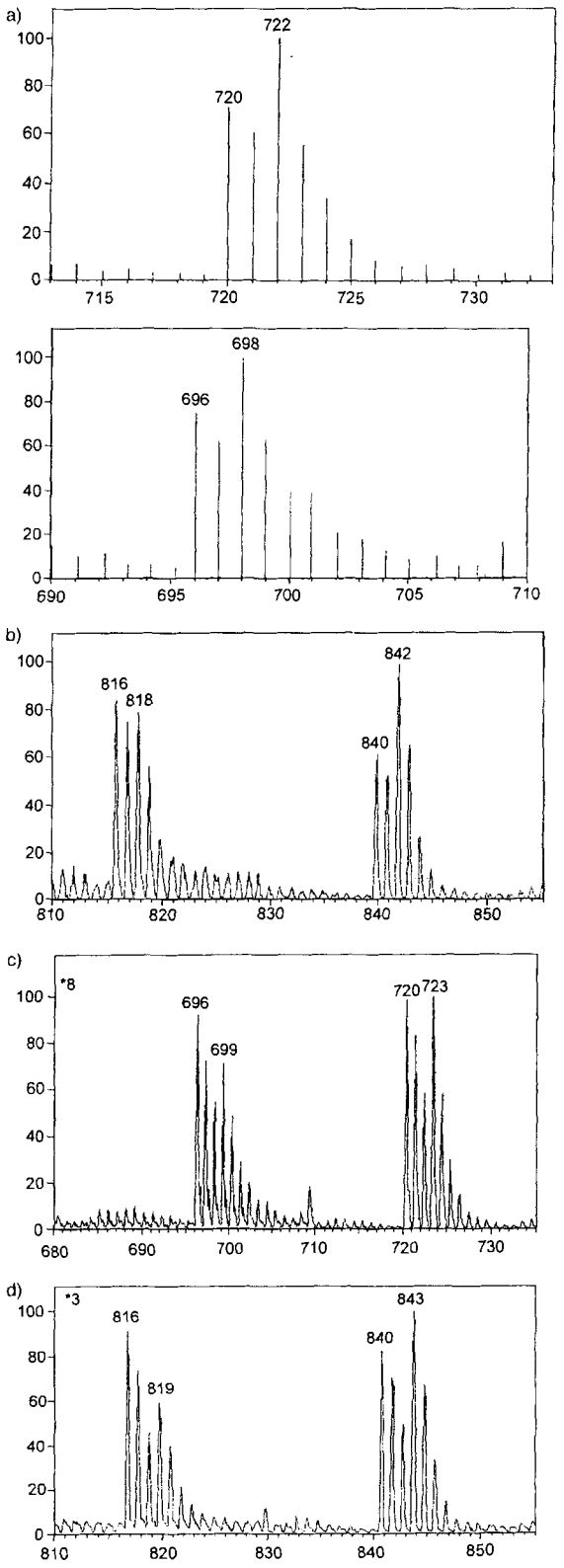

Fig. 1. FAB mass spectrum (Finnigan MAT 90; Cs gun, emission current 2 μA, acceleration voltage 20 kV, detection by secondary electron multiplier, matrix: 3-nitrobenzyl alcohol) in the range of the major fragmentation signals of a) **2b** (line spectrum), b) **6**, c) [^{15}N]-**5**, and d) [^{15}N]-**6** (profile mode).

due to the cluster ions $^{12}C_{59}{}^{15}N^+$ (m/z = 723) and $^{12}C_{69}{}^{15}N^+$ (m/z = 843) (Fig. 1c, 1d).

The parent ions $C_{59}N^+$ and $C_{69}N^+$ are isoelectronic with C_{60} and C_{70}. AM1 calculations show that $C_{59}N^+$ has almost the

 © VCH Verlagsgesellschaft mbH, D-69451 Weinheim, 1995 0570-0833/95/3420-2258 $ 10.00+.25/0

same structure as C_{60} (Fig. 2). Also in this case there is bond length alternation[1] between 5-6 and 6-6 bonds. Like all 6-6 bonds in the molecule, the 6-6 C–N bond in $C_{59}N^+$ has double-bond character (1.37 Å) and is even shorter than the C–C double bonds (1.38 Å). The pyramidalization at the N atom is slightly stronger than that at the C atoms. The highest positive charge density of 0.159 is located at C-2 and the next lowest at C-4 (C-11) and C-6 (C-9). Therefore, the resonance structures I–IV (Fig. 2), in particular I and II, are the most important.

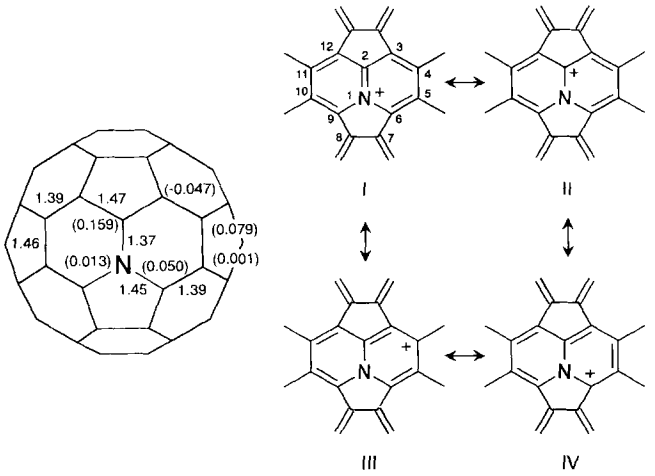

Fig. 2. Characteristic bond lengths in Å, Mulliken charges (in brackets), and the most important resonance structures of $C_{59}N^+$.

Based on this new observation on the generation of the free ions $C_{59}N^+$ and $C_{69}N^+$ we are now working on the synthesis and isolation of heterofullerene derivatives such as $C_{59}NR$ in macroscopic amounts.

Received: May 31, 1995 [Z8047IE]
German version: *Angew. Chem.* **1995**, *107*, 2473–2476

Keywords: fullerenes · heterofullerenes · mass spectrometry

[1] A. Hirsch, *The Chemistry of the Fullerenes*, Thieme, Stuttgart, **1994**.
[2] a) H. R. Karfunkel, T. Dressler, A. Hirsch, *J. Comp. Aid. Mol. Des.* **1992**, *6*, 521; b) N. Kurita, K. Kobayashi, H. Kumahora, K. Tago, K. Ozawa, *Chem. Phys. Lett.* **1992**, *198*, 95; c) W. Andreoni, F. Gygi, M. Parrinello, *ibid.* **1992**, *190*, 159.
[3] a) T. Guo, C. Jin, R. E. Smalley, *J. Phys. Chem.* **1991**, *95*, 4948; b) V. Chai, T. Guo, C. Jin, R. E. Haufler, L. P. F. Chibante, I. Fure, L. Wang, J. M. Alford, R. E. Smalley, *ibid.* **1991**, *95*, 7564; c) R. E. Smalley in *Fullerenes: Synthesis, Properties, and Chemistry of Large Carbon Clusters* (*ACS Symp. Ser.* **1992**, *481*, 141–159).
[4] T. Grösser, M. Prato, V. Lucchini, A. Hirsch, F. Wudl, *Angew. Chem.* **1995**, *107*, 1462; *Angew. Chem. Int. Ed. Engl.* **1995**, *34*, 1341.
[5] M. R. Banks, J. I. G. Cadogan, I. Gosney, P. K. G. Hodgson, P. R. R. Langridge-Smith, D. W. H. Rankin, *J. Chem. Soc. Chem. Commun.* **1994**, 1365.
[6] Independent of our investigations Mattay et al. recently showed that the azamono- and azadihydrofullerenes $C_{59}NH^+$ and $C_{59}NH_2^+$, respectively, can be generated from the 1,2-bridged aziridinofullerene $C_{60}NH$ by using DCI (desorptive chemical ionization) mass spectrometry and ammonia as reagent gas. Further functionalization by nitrogen through the reagent gas seems to be the decisive step in this case, too. But this method does not provide direct access to the parent compounds $C_{59}N^+$ and $C_{69}N^+$, which we achieved by fragmentation of systematically designed oligoadducts under conditions of FAB mass spectrometry. J. Averdung, H. Luftmann, I. Schlachter, J. Mattay, *Tetrahedron* **1995**, *51*, 6977.
[7] a) S. C. O'Brien, J. R. Heath, R. F. Curl, R. E. Smalley, *J. Chem. Phys.* **1988**, *88*, 220; b) H. Schwarz, T. Weiske, D. Böhme, J. Hrusak in *Buckminsterfullerenes* (Eds.: W. E. Billups, M. A. Ciufolini), VCH, Weinheim, **1993**.
[8] The FAB mass spectrum of a polyimino adduct of C_{60}, which we obtained by exhaustive addition of azide and subsequent extrusion of N_2, shows the incorporation of at least three nitrogen atoms into the fullerene core; this is particularly evident from the fragment ions of cluster size 58.

Synthesis of the Palmitoylated and Farnesylated C-Terminal Lipohexapeptide of the Human N-*Ras* Protein by Employing an Enzymatically Removable Urethane Protecting Group**

Herbert Waldmann* and Edgar Nägele

Dedicated to Professor Franz Effenberger on the occasion of his 65th birthday

Ras proteins form a class of membrane-bound lipoproteins that play a central role in the growth-factor-mediated transduction of extracellular signals across the cell membrane into the interior of the cell. By the so-called *Ras* pathway of signal transduction, organisms as diverse as mammals, flies, worms, and yeast regulate cell growth and proliferation.[1] If this regulation is disturbed or interrupted an uncontrolled proliferation may occur, which ultimately may result in the establishment of cancer. This is highlighted by the fact that point mutations in the respective *ras*-oncogenes may result in malignant transformation of the cell. A remarkable observation is that in about 40% of all human cancers such a point mutation is found, and in some of the major malignancies like lung, colon, and pancreas cancer this figure rises to 85%.[2] To study the biological phenomena associated with the functions of the *Ras* proteins, model peptides that embody the characteristic structural elements of their parent lipoproteins are urgently needed.[3] All *Ras*-proteins terminate in an S-farnesylated cysteine methyl ester and, except for Ki-*Ras*, towards the N-terminus one or more S-palmitoylated cysteines are present (see, for instance, the C-terminal lipohexapeptide part **1** of the human N-*Ras* protein; Fig. 1).[4]

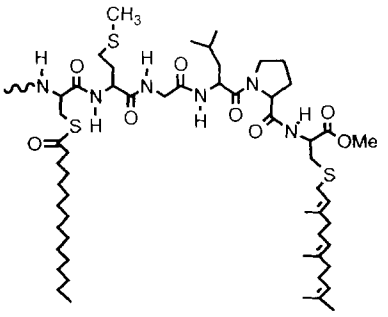

-Cys(Pal)-Met-Gly-Leu-Pro-Cys(Far)OMe **1**

Fig. 1. Structure of the characteristic C-terminal lipohexapeptide (**1**) of the human N-*Ras* protein.

The presence of these sensitive side-chain functionalities excludes the use of classical acid- and base-labile protecting groups in the assembly of *Ras*-related lipopeptides. Thus, we found that upon acid-mediated removal of the Boc protecting group from S-farnesylated cysteinyl peptides, an attack of the acid on the double bonds of the farnesyl residue always occurs, and that the thioesters present in S-palmitoylated lipopeptides hydrolyze spontaneously even at pH 6–7 in aqueous solution.[5] Due to this pronounced lability, up to now a successful synthesis of a fully functionalized (that is, an S-farnesylated and S-palmitoylated) *Ras*-lipopeptide could not be achieved. For this purpose blocking functions have to be employed that can be selectively removed under the mildest, preferably neutral conditions. Previously we reported the development of enzyme-labile protecting groups[6] that fulfill these criteria. In particular, the phenyl-

[*] Prof. Dr. H. Waldmann, Dipl.-Chem. E. Nägele
Institut für Organische Chemie der Universität
Richard-Willstätter-Allee 2, D-76128 Karlsruhe (Germany)
Telefax: Int. code + (0721) 608-4825

[**] This work was supported by the Deutsche Forschungsgemeinschaft and the Fonds der Chemischen Industrie.

acetamide (PhAc), which is cleaved by the enzyme penicillin G acylase, was introduced as an enzymatically removable blocking function for the N-terminal amino group of peptides.[7]

However, a major drawback of this non-urethane protecting group is that its application results in 2–5% racemization of the PhAc-masked amino acids upon activation by established peptide coupling reagents.[7] Therefore, in order to make full use of the attractive features of enzyme-mediated transformations in the construction of complex peptide conjugates like **1**, enzymatically removable urethane blocking functions have to be used.

Although in a few cases biocatalyzed hydrolyses of urethane-protected amino acids were observed,[8] to the best of our knowledge the selective enzymatic removal of simple urethane protecting groups from peptides and related compounds has not been reported yet. Therefore, a new strategy for the development of enzymatically removable urethane blocking groups for peptides and peptide conjugates had to be developed.

We now report that *p*-acetoxybenzyloxycarbonyl(AcOZ)-urethanes can be cleaved enzymatically under mildest conditions (pH 7, 45 °C) from peptides and that this protecting group technique can be advantageously applied for the construction of complex and sensitive, biologically relevant peptide conjugates like the characteristic S-farnesylated and S-palmitoylated C-terminal lipohexapeptide of the human N-*Ras* protein.

To develop a general class of enzyme-labile urethane blocking groups a strategy was chosen in which the urethanes embody a) a functional group that is recognized by the biocatalyst and that is bound by an enzyme-labile linkage to b) a functional group that undergoes a spontaneous fragmentation upon cleavage of the enzyme-sensitive bond (Fig. 2). In the fragmentation process, a carbamic acid derivative is liberated, which decarboxylates to give the desired deprotected peptide.[9] As a protecting function that might fulfill these criteria the *p*-acetoxybenzyloxycarbonyl (AcOZ) group was chosen.[10]

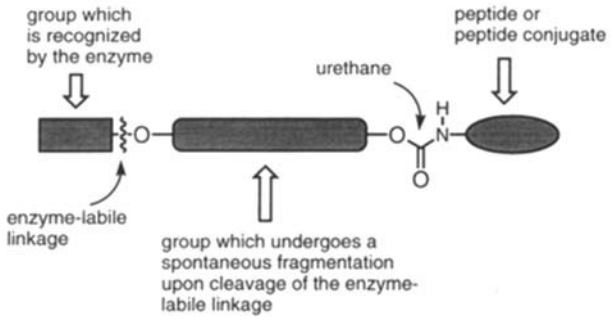

Fig. 2. Strategy for the development of a general class of enzyme-labile urethane protecting groups.

The AcOZ-protected peptide allyl esters **2** (Scheme 1) are readily synthesized from AcOZ-protected amino acids and amino acid allyl esters by employing established peptide coupling reagents like *N,N'*-diisopropylcarbodiimide/*N*-hydroxybenzotriazole. Contrary to the observations made for phenylacetamido-protected peptides[7] (vide supra) no racemization of the N-terminal amino acid of the AcOZ-blocked compounds **2** could be detected by high-field NMR techniques and HPLC investigations. The AcOZ-protected amino acids required are obtained in a straightforward manner from *p*-acetoxybenzyl chloroformate and *N,O*-bis(trimethylsilyl) amino acids.[11] Since the compounds **2** contain two esters (an acetic acid phenyl ester at the N-terminus and a peptide allyl ester at the C-terminus), for the desired N-terminal deprotection a biocatalyst had

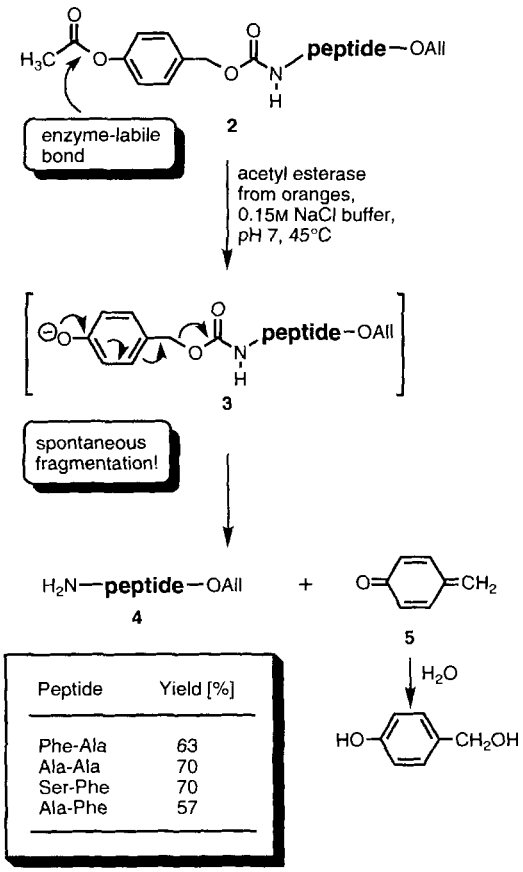

Peptide	Yield [%]
Phe-Ala	63
Ala-Ala	70
Ser-Phe	70
Ala-Phe	57

Scheme 1. Enzymatic cleavage of the *p*-acetoxybenzyloxycarbonyl (AcOZ) protecting group by means of acetyl esterase from oranges.

to be applied that can discriminate between these ester groups. For the hydrolysis of the acetates in **2** and the induction of the subsequent fragmentation, the enzyme acetyl esterase from the *flavedo* of oranges was chosen, because this biocatalyst attacks acetates but not longer acyl chains.[12] In addition, it does not display any amidase activity at all, so an undesired attack on the peptide bonds need not be feared. Upon treatment of the protected peptides **2** with acetyl esterase in aqueous buffer at pH 7 and 45 °C, the acetates in the N-terminal urethane protecting group are smoothly hydrolyzed to give the phenolates **3**. Under the reaction conditions these intermediates undergo a spontaneous fragmentation and thereby liberate the desired peptides **4**, which are isolated in analytically pure form in 60–70% yields. The quinone methide **5**, which is formed from the phenolate, is trapped by water and converted to *p*-hydroxybenzyl alcohol (Scheme 1). In this process no undesired attack of the enzyme on the allyl esters present or on the peptide bonds was observed; that is, the enzymatic transformations proceed with complete chemoselectivity. It was not a foregone conclusion that the fragmentation would occur at neutral pH, since in the previously reported nonenzymatic cleavage of the AcOZ group the pH had to be raised to 10–11 to deprotonate the phenol and induce its subsequent conversion into a quinone methide.[10] The enzyme-triggered removal of the AcOZ-group from peptides is not restricted to the use of acetyl esterase. The AcOZ-urethanes are also substrates for acetyl choline esterase from electrical eel and, in particular, for the lipases from *Mucor miehei* and *Rhizopus arrhizus*, which, for instance, selectively remove the N-terminal blocking group from the protected sterically demanding phenylalanyl peptide **6** in high yield (Scheme 2).

 © VCH Verlagsgesellschaft mbH, D-69451 Weinheim, 1995 0570-0833/95/3420-2260 $ 10.00+.25/0 Angew. Chem. Int. Ed. Engl. 1995, 34, No. 20

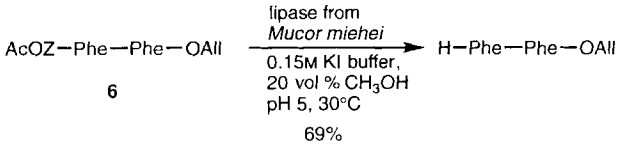

Scheme 2. Lipase-mediated cleavage of the *p*-acetoxybenzyloxycarbonyl (AcOZ) protecting group.

A particularly advantageous feature of the AcOZ protecting function is that the enzyme used can recognize the same structural element in all cases. The variable peptide part of the substrates is remote from the site of the biocatalyst's attack. Thus, possible sterically or electronically unfavorable interactions of the enzyme with the substrates (caused, for example, by bulky amino acid side chains) are guaranteed not to limit the substrate tolerance of the enzyme.

The AcOZ protecting group is orthogonally stable to the allyl ester function. Thus, from the dipeptides **2** the allyl ester can be selectively removed, for example, by treatment with $[(Ph_3)P]_3RhCl$ at 70 °C or with $[(Ph_3)P]_4Pd^0$/morpholine at room temperature.[13]

To demonstrate the full capacity of the enzymatic protecting group technique described above, the characteristic C-terminal lipohexapeptide **1** of the human N-*Ras* protein was constructed. To this end, S-farnesylated cysteine methyl ester **7**[14] was coupled with the C-terminally deblocked, AcOZ-protected peptide **8** (Scheme 3) by carbodiimide-mediated activation of the carboxylic acid to give the lipotripeptide **9** in high yield. From **9** the AcOZ urethane blocking group was removed quantitatively, and without any attack on the farnesyl residue and the C-terminal methyl ester, by treatment with lipase from *Mucor miehei*. The N-terminally deprotected farnesylated peptide **10** was isolated in analytically pure form in 65% yield. A further elongation of the peptide chain by the dipeptide **11** yielded the AcOZ-protected lipopentapeptide **12**. From **12** the N-terminal urethane could again be removed enzymatically without any detectable attack on the farnesyl residue or the C-terminal methyl ester. The enzymatic deprotection of the fairly hydrophobic lipopeptides **9** and **12** required the presence of 20 vol% of methanol to solubilize the organic substrate and make it accessible to the biocatalyst. Since acetyl esterase is unstable under these conditions[12] the removal of the protecting groups from **9** and **12** was carried out with lipase from *Mucor miehei*. To avoid an undesired attack of the amines **10** and **13**, liberated in these transformations, on the formed quinone methide, the enzymatic reactions were carried out at pH 5 (conditions under which the amines are protonated) and in the presence of NaHS and/or KI (reagents that trap the quinone methide by nucleophilic attack). The synthesis of the Aloc-protected *Ras* peptide **15** was finally completed by coupling the selectively deprotected peptide conjugate **13** to the S-palmitoylated cysteine **14** to give the fully functionalized lipopeptide **15**, which carries both a base-labile palmitic acid thioester and an acid-labile farnesyl thioether.

In conclusion we have developed a strategy for the enzymatic removal of urethane protecting groups from peptides and labile peptide conjugates and demonstrated its usefulness in the first synthesis of the sensitive C-terminal lipohexapeptide of the human N-*Ras* protein. By this technique further S-palmitoylated and S-farnesylated peptide conjugates are potentially accessible, which may open up new avenues of research in bioorganic chemistry and biology.

Received: May 16, 1995 [Z 7993 IE]
German version: *Angew. Chem.* **1995**, *107*, 2425–2428

Keywords: bioorganic chemistry · enzymes · protecting groups · *Ras* proteins

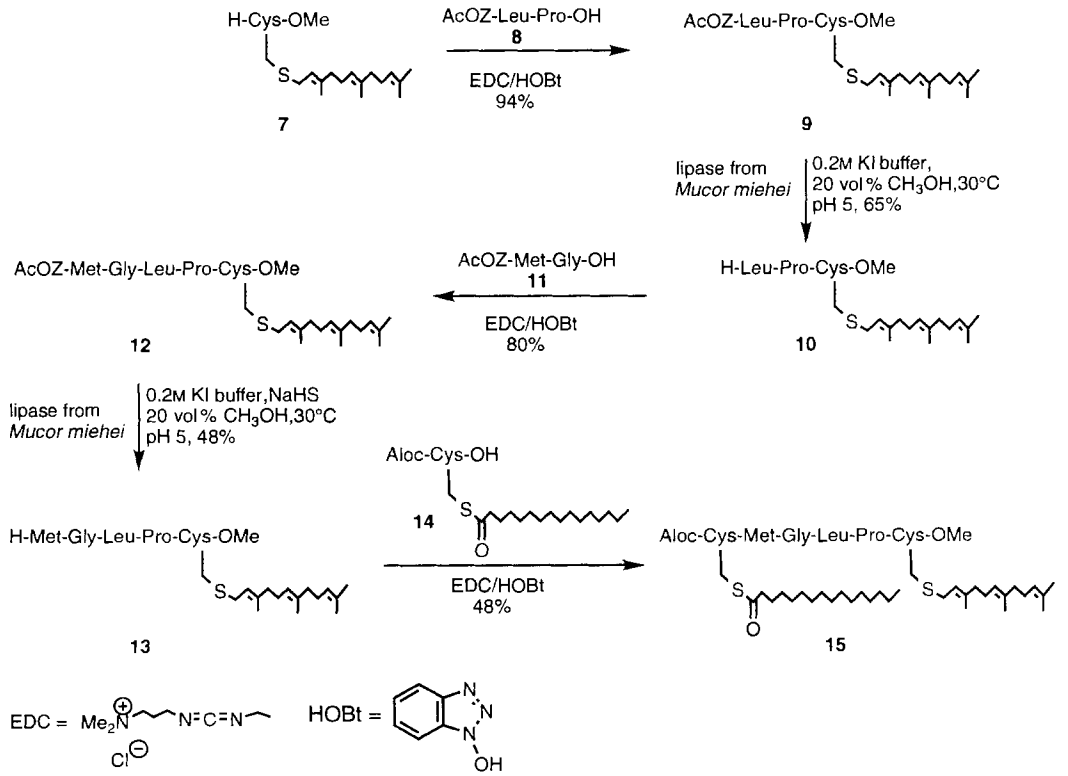

Scheme 3. Synthesis of the fully functionalized characteristic C-terminal lipohexapeptide of the human N-*Ras* protein by enzymatic removal of the N-terminal *p*-acetoxybenzyloxycarbonyl (AcOZ) protecting group. Aloc = allyloxycarbonyl.

[1] Reviews: a) S. E. Egan, R. A. Weinberg, *Nature* **1993**, *365*, 781; b) M. S. Boguski, F. McCormick, *ibid.* **1993**, *366*, 643; c) J. L. Bos, *Mutat. Res.* **1988**, *195*, 255.

[2] Review: A. Levitsky, *Eur. J. Biochem.* **1994**, *226*, 1.

[3] For applications of S-farnesylated peptides, see, for instance: a) M. D. Schaber, M. B. O'Hara, V. M. Garsky, S. D. Mosser, J. D. Bergstrom, S. L. Moores, M. S. Marshall, P. A. Friedman, R. A. F. Dixon, J. B. Gibbs, *J. Biol. Chem.* **1990**, *265*, 14701; b) S. L. Moores, M. D. Schaber, S. D. Mosser, E. Rands, M. B. O'Hara, V. M. Garsky, M. S. Marshall, D. L. Pompliano, J. B. Gibbs, *ibid.* **1991**, *266*, 14603; c) D. L. Pompliano, E. Rands, M. D. Schaber, S. D. Mosser, N. J. Anthony, J. B. Gibbs, *Biochemistry* **1992**, *31*, 3800; d) D. L. Pompliano, R. P. Gomez, N. J. Anthony, *J. Am. Chem. Soc.* **1992**, *114*, 7945.

[4] W. A. Maltese, *FASEB J.* **1990**, *4*, 3319, and references therein.

[5] H. Waldmann, P. Stöber, M. Schelhaas, unpublished.

[6] Reviews: a) H. Waldmann, D. Sebastian, *Chem. Rev.* **1994**, *94*, 911; b) H. Waldmann in *Enzyme Catalysis in Organic Synthesis – A Comprehensive Handbook, Vol. II* (Eds.: K. Drauz, H. Waldmann), VCH, Weinheim, **1995**, p. 851.

[7] a) H. Waldmann, *Tetrahedron Lett.* **1988**, *29*, 1131; b) *Liebigs Ann. Chem.* **1988**, 1175.

[8] a) C. Sambale, M.-R. Kula, *Appl. Biochem.* **1987**, *9*, 251; b) *J. Biotechnol.* **1988**, *7*, 49; c) E. Matsumura, T. Shin, S. Murao, M. Sakaguchi, T. Kawano, *Agric. Biol. Chem.* **1985**, *49*, 3643.

[9] This principle has successfully been used to develop a prodrug concept: L. N. Jungheim, T. A. Shepherd, *Chem. Rev.* **1994**, *94*, 1553.

[10] The AcOZ group was used in peptide chemistry before (G. Le Corre, E. Guibé-Jampel, M. Wakselman, *Tetrahedron* **1978**, *34*, 3105). It can be removed non-enzymatically by treatment with hydrazine, Na_2CO_3, or H_2O_2/NH_3, that is, conditions that cannot be applied for the construction of sensitive peptide conjugates like the N-*Ras* peptide **1**.

[11] D. R. Bolin, I.-I. Sytwu, F. Humiec, J. Meienhofer, *Int. J. Pept. Res.* **1989**, *33*, 353, and references therein.

[12] H. Waldmann, A. Heuser, *Bioorg. Med. Chem.* **1994**, *2*, 477, and references therein.

[13] a) H. Waldmann, H. Kunz, *Liebigs Ann. Chem.* **1983**, 1712; b) S. Friedrich-Bochnitschek, H. Waldmann, H. Kunz, *J. Org. Chem.* **1989**, *54*, 751.

[14] M. Liakopoulou-Kyriakides, *Phytochemistry* **1985**, *24*, 1593.

$CsPr_9NbBr_{15}N_6$: A New Type of Interstitially Stabilized Cluster Compound**

Michael Lulei and John D. Corbett*

Synthetic research conducted with some knowledge of electronic and structural principles has led to the discovery of a large variety of interstitially stabilized rare earth metal cluster halides.[1, 2] A characteristic structural feature of the vast majority of these compounds is rare earth element octahedra M_6 which occur either isolated (e.g. in $Pr_6Br_{10}Co$[3]) or condensed through common metal edges to oligomers (e.g. in $Y_{16}I_{20}Ru_4$[4]) or infinite chains (e.g. in Pr_4I_5Ru[5]). A smaller number of halides contain tetrahedra M_4 which may also be isolated from each other (e.g. in Yb_4OCl_6[6]) or formed into either edge-sharing dimers (e.g. in Gd_3Cl_6N[7]) or infinite chains (e.g. in $Na_2Pr_4Br_9NO$[8]). Except for the Gd_2Cl_3 structure type,[9] the foregoing octahedral and tetrahedral cluster units exist only with a centered (interstitial) heteroatom. While octahedra may be centered by either transition metals (e.g. Mn, Ru, Ir) or main group elements (e.g. B, C, N), the tetrahedra known so far only form with N or O as interstitial atoms, probably because of the size of the void. In all cases, the centered atoms provide not only central bonding to the cluster, but in the reduced examples, valence electrons as well that aid in fulfilling certain minimal electron counts necessary for metal–metal bonding of the electron-poor rare earth metals. As the recent examples of $Na_2Pr_4Cl_9O_2$[10] versus $Na_2Pr_4Br_9NO$ nicely illustrate, it appears possible to change the chemical and physical properties (e.g. conductivity, magnetic susceptibility, and color of the compound) by varying the interstitial atoms. Crystals of $Na_2Pr_4Cl_9O_2$ with the formulation $(Na^+)_2(Pr^{3+})_4(Cl^-)_9(O^{2-})_2(e^-)$ are black because of the surplus electron, and the compound can therefore be viewed as "reduced", while $Na_2Pr_4Br_9NO$ with the precise electron count $(Na^+)_2(Pr^{3+})_4(Br^-)_9(N^{3-})(O^{2-})$ crystallizes as green, transparent crystals and is an insulator or "simple" salt. However, the two compounds are isostructural with similar metal–metal distances within chains formed by edge-sharing tetrahedra centered by either O or disordered O and N, respectively. Instead of changing the interstitial atom, we have found that it is also possible to introduce heterometal atoms in the rare earth metal cluster framework to modify the structure and physical properties.

We report here the first example of a rare earth metal halide in which one rare earth metal atom has been substituted by a transition metal atom, leading to a new structure and cluster type. $CsPr_9NbBr_{15}N_6$ crystallizes as large, green, transparent crystals.[11] As shown in Figure 1,[15] the core of the new structure $[Pr_9NbN_6]$ consists of a niobium atom centering a tricapped trigonal prism of praseodymium atoms (six Pr1 as trigonal prism, three Pr2 as caps; distances: Pr1–Nb 3.405, Pr2–Nb 3.380, Pr1–Pr1 3.917, Pr1–Pr2 3.921 Å). Nitrogen atoms center the six tetrahedral Pr_3Nb cavities in this metal array (distances: Pr1–N 2.32, Pr2–N 2.25, Nb–N 2.13 Å). The $[Pr_9NbN_6]$ unit can therefore also be regarded as the condensation product of six $Pr_3Nb(N)$ tetrahedra that share three edges and the niobium atom with each other to form a trigonal prism of tetrahedra. Evidently, niobium substitution is responsible for this arrangement since M_4N tetrahedra usually form chains, as mentioned earlier. The reason might be the high formal ionic charge or oxidation state of niobium relative to the praseodymium atoms. According to Coulomb's Law, the gain for the Madelung part of the lattice energy[16] is maximized when each of the (formally) highly charged anions N^{3-} are bonded to Nb^{5+} but also have $3Pr^{3+}$ as nearest neighbors. This is efficiently achieved in the new cluster arrangement; of course, the real charges are doubtlessly lower but somewhat proportional.

All 18 Pr–Pr edges on the surface of this cluster are bridged by one of three crystallographically distinct bromine atoms (Fig. 2),

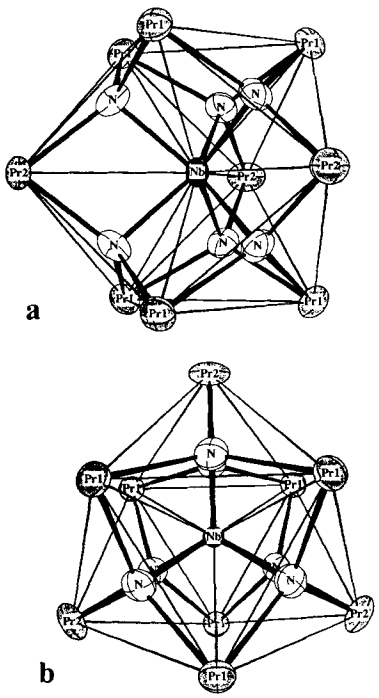

Fig. 1. Crystal structure of $CsPr_9NbBr_{15}N_6$: Views of the $[Pr_9NbN_6]$ unit approximately along [110] (a) and along [001] (b) ($\bar{6}(S_3)$ symmetry, ellipsoids at 99% probability; the lines between the metal atoms represent only geometric relationships).

[*] Prof. J. D. Corbett, Dr. M. Lulei
Department of Chemistry
Iowa State University, Ames, IA 50011 (USA)
Telefax: Int. code + (515) 294-5718

[**] This research was supported by the National Science Foundation—Solid State Chemistry– under DMR-9207361 and was carried out in the facilities of Ames Laboratory, U. S. Department of Energy. M. L. thanks the Alexander-von-Humboldt Foundation for a Feodor-Lynen Fellowship.

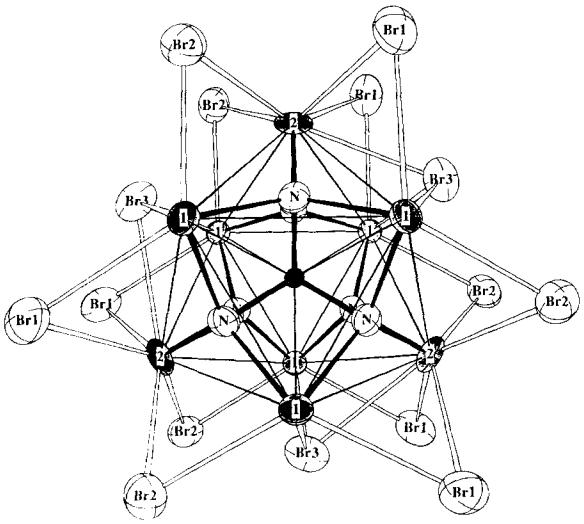

Fig. 2. Crystal structure of $CsPr_9NbBr_{15}N_6$: [001] view of the cluster unit with its bromine environment (99% ellipsoids, the Br1 atoms that bridge the Pr1–Pr1 edges normal to c have been omitted for clarity).

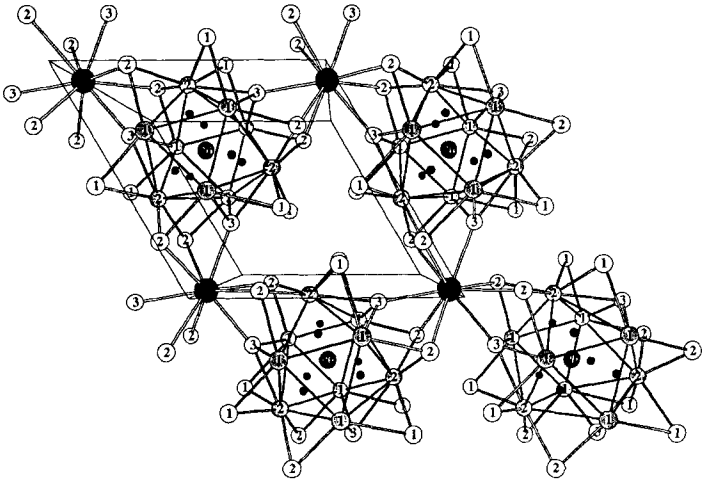

Fig. 4. Crystal structure of $CsPr_9NbBr_{15}N_6$: View of the unit cell along [001] with one layer about $z = 1/4$ to show the connectivity of Br2 and Br3 around Cs (atoms coded as in Figure 3, Cs: large black circles ($\bar{6}(S_3)$ symmetry).

which also serve to connect the clusters into a three-dimensional network. Br1 bridges both the Pr1–Pr1 edges that lie parallel to [110] and half of the Pr1–Pr2 edges and serves to link the clusters as $Br1^{i-i}$[11] only along the c axis (Fig. 3). Br2 bridges the remaining Pr1–Pr2 edges, while Br3 is located over the Pr1–Pr1 edge parallel to c and is also 0.4 Å more distant to Pr2 (Fig. 2). Both Br2 and Br3 connect the clusters through the cesium atom to form layers about (0, 0, 1/4) (Fig. 4) and (0, 0, 3/4) in the unit cell. The two layers are rotated 180° relative to each other around [001]. The result is a $Pr_9NbN_6(Br1^{i-i})_{12/2}(Br2^i)_6(Br3^i)_3 = [Pr_9NbN_6Br_{15}]^-$ complex unit (Fig. 2) complemented by only one Cs^+ ion which centers a tricapped trigonal prism of bromine atoms (six Br2 in the trigonal prism, three Br1 as caps).

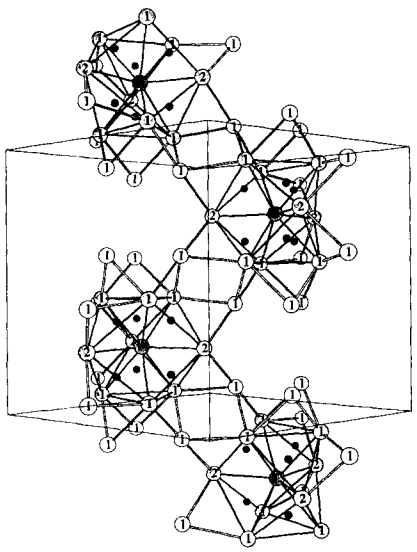

Fig. 3. Crystal structure of $CsPr_9NbBr_{15}N_6$: View of the unit cell approximately along [110] showing the $Br1^{i-i}$ connectivity (N: black; metal atoms: gray; Br1: white; Br2, Br3; Cs atoms are omitted).

The assumed oxidation state formulation $(Cs^+)(Pr^{3+})_9(Nb^{5+})(Br^-)_{15}(N^{3-})_6$ shows that there are no electrons left for metal–metal bonding, and $CsPr_9NbBr_{15}N_6$ can be regarded as a "non-reduced" closed-shell cluster compound or "simple" salt. However, the structure exhibits many features common to the traditional "reduced" cluster compounds: The Pr–Pr distances in the $[Pr_9NbN_6]$ unit (3.92 Å) are very similar to those in $Pr_6Br_{10}Ru$[3] ($\bar{d} = 3.94$ Å) and in Pr_3I_3Ru[17] ($\bar{d} = 3.93$ Å) with isolated Pr_6Ru octahedra and infinite chains of the same type of octahedra, respectively. The short Nb–Pr separations within the cluster are evidently caused by a matrix effect[18] from nitrogen and are therefore mainly determined by the Nb–N and Pr–N distances. This effect can also be observed in the shared edges of the *trans*-edge-sharing Pr_4 tetrahedra chain in $Na_2Pr_4Br_9NO$ and the isotypic but slightly reduced $Na_2Pr_4Cl_9O_2$. Furthermore, the connectivity of the bromines in $CsPr_9NbBr_{15}N_6$ is reminiscent of that in many other rare earth metal cluster compounds.

The discovery of this surprising cluster may therefore forecast still more novel chemistry and structures. The introduction of other high-valent heteroatoms like zirconium or molybdenum instead of niobium into the rare earth element network, or a change of all or some of the interstitial nitrogen atoms to oxygen (or other) atoms should be considered as a route to new (and perhaps "reduced") variants with different chemical and physical properties.

Experimental Procedure

The synthetic and sublimation techniques for $PrBr_3$ and the reaction procedures utilizing welded Nb tubing have been described before [19,20]. CsBr (Baker, 99.9%) was dried by slow heating under dynamic vacuum and then sublimed, while NaN_3 (Aldrich, 99.9%) was used as received as a source of nitrogen and as the oxidizing agent for the Nb container. Reaction mixtures with the overall stoichiometry $CsNaPr_3Br_{10}N_3$ were heated at 750 °C for 28 days. According to Guinier powder diffraction, the products were crystals of $CsPr_9NbBr_{15}N_6$ (70%) and NaBr (10%) besides an unknown phase ($\approx 20\%$). After the formula and structure were determined by single crystal diffraction, two crystals were analyzed by energy-dispersive X-ray spectroscopy to confirm the niobium content and the stoichiometry.

Received: May 24, 1995 [Z80211E]
German version: *Angew. Chem.* **1995**, *107*, 2463–2465

Keywords: halides · lanthanide compounds · niobium compounds · nitrides · solid-state structures

[1] J. D. Corbett in *Modern Perspectives in Inorganic Crystal Chemistry* (Ed. E. Parthé), Kluwer, Dordrecht, **1992**, p. 27.
[2] A. Simon, H. Mattausch, G. J. Miller, W. Bauhofer, R. K. Kremer in *Handbook on the Physics and Chemistry of Rare Earths, Vol. 15* (Eds.: K. A. Gschneider Jr., L. Eyring), Elsevier, Amsterdam, **1991**, p. 191.
[3] R. Llusar, J. D. Corbett, *Inorg. Chem.* **1994**, *33*, 849.

[4] M. W. Payne, M. Ebihara, J. D. Corbett, *Angew. Chem.* **1991**, *103*, 842; *Angew. Chem. Int. Ed. Engl.* **1991**, *30*, 856.
[5] M. W. Payne, P. K. Dorhout, J. D. Corbett, *Inorg. Chem.* **1991**, *30*, 1467.
[6] T. Schleid, G. Meyer, *Z. Anorg. Allg. Chem.* **1987**, *554*, 118.
[7] A. Simon, T. Koehler, *J. Less-Common Met.* **1986**, *116*, 279.
[8] M. Lulei, S. J. Steinwand, J. D. Corbett, *Inorg. Chem.* **1995**, *34*, 2671.
[9] J. E. Mee, J. D. Corbett, *Inorg. Chem.* **1965**, *4*, 88; D. A. Lokken, J. D. Corbett, *J. Am. Chem. Soc.* **1970**, *92*, 1799; A. Simon, N. Holzer, H. Mattausch, *Z. Anorg. Allg. Chem.* **1979**, *456*, 207
[10] H. Mattfeld, G. Meyer, *Z. Anorg. Allg. Chem.* **1994**, *620*, 85.
[11] Crystal structure analysis of $CsPr_9NbBr_{15}N_6$: lattice constants for the hexagonal cell (space group $P6_3/m$), $a = 12.070$ (2), $c = 13.801$ (4) Å, were obtained from Guinier powder patterns ($\lambda = 1.540562$ Å), $V = 1741.2$ (8) Å^3, $Z = 2$, $\rho = 5.31$ g cm^{-1}. 13042 data ($\pm h, -k, \pm l$; $2\theta < 65°$) were collected with the aid of a CAD4 diffractometer (23 °C, $Mo_{K\alpha}$ radiation, $\mu = 307.6$ cm^{-1}, crystal dimensions $0.2 \times 0.1 \times 0.3$ mm, min./max. transmission: 0.865/1.091). The structure was solved by direct methods (SHELXS) [12]. Programs utilized were those in the instrument package TEXSAN [13]. The residuals for the anisotropic refinement were $R(F) = 0.029$, $R_w = 0.030$ with 2020 independent reflections ($I_0 < MG > 3\sigma(I_0)$), empirical absorption correction by 4 Ψ scans followed by DIFABS [14]) and 54 variables. Further details of the crystal structure investigation and results may be obtained from the authors (J.D.C) or from the Fachinformationszentrum Karlsruhe, D-76344, Eggenstein-Leopoldshafen (Germany), on quoting the depository number CSD-59021.
[12] G. M. Sheldrick, SHELXS-86, Universität Göttingen, Germany, **1986**.
[13] TEXSAN, version 6.0, Molecular Structure Corp., The Woodlands, Texas, **1990**.
[14] N. Walker, D. Stuart, *Acta Crystallogr. Sect. A*, **1983**, *39*, 159.
[15] All drawings were produced with ATOMS, Shape Software, Kingsport, Tennessee.
[16] R. Hoppe, *Angew. Chem.* **1966**, *78*, 52; *Angew. Chem. Int. Ed. Engl.* **1966**, *5*, 95; *ibid.* **1970**, *82*, 7 and **1970**, *9*, 20.
[17] M. W. Payne, P. K. Dorhout, S. J. Kim, T. R. Hughbanks, J. D. Corbett, *Inorg. Chem.* **1992**, *31*, 1389.
[18] J. D. Corbett, *J. Solid State Chem.* **1981**, *37*, 335.
[19] M. W. Payne, J. D. Corbett, *Inorg. Chem.* **1990**, *29*, 2246.
[20] J. D. Corbett, *Inorg. Synth.* **1983**, *22*, 15, 31.

$[\{Ti(\mu\text{-}CH_3)_5(\mu\text{-}CH_2)\}\{(tmeda)Li\}_3] \cdot THF$: An Unusual and Highly Fluxional Titanium Organometallic Compound**

Pietro Berno, Hilary Jenkins, Sandro Gambarotta,* Johan Blixt, Glenn A. Facey, and Christian Detellier

The ability of transition and main group metal amides to function as precursors in the preparation of metal nitrides[1] with useful physical properties is one of the key points in the current revival of interest in the synthesis and characterization of these species. Our interest in the utilization of organic amides to support low-valent early transition metal complexes[2] has been prompted by the observation that these ligands may be directly involved in a variety of transformations, which include C–H σ-bond metathesis,[3] hydrogenolysis,[4] dehydrogenation,[5] hydrogen transfer reactions,[6] and the stabilization of methylidene functions.[7] In view of the relevance of this type of reactivity in the Ziegler–Natta process, we became interested in studying the chemical behavior of medium-valent titanium amides. In this paper we describe the unexpected formation of a rare example of an alkyl(alkylidene) titanium species from a homoleptic titanium(III) amide starting material.

[*] Prof. S. Gambarotta, P. Berno, H. Jenkins, J. Blixt, G. A. Facey, C. Detellier
Department of Chemistry, University of Ottawa
Ottawa, Ont K1N 6N5 (Canada)
Telefax: Int. code +(613) 562-5170
e-mail: SGAMBARO@OREO.CHEM.UOTTAWA.CA

[**] This work was supported by the Natural Sciences and Engineering Research Council of Canada (operating and strategic grants). tmeda = *N,N,N',N'*-tetramethylethylenediamine.

In the attempt to prepare a titanaazacyclobutane complex by C–H σ-bond metathesis, the toluene solution obtained from the reaction of $[TiCl_3(thf)_3]$ with an excess of $[(Me_3Si)_2NLi]$ was thermolyzed (Scheme 1).[8] The initially intense blue color of $[Ti\{N(SiMe_3)_2\}_3]$ rapidly changed to green. After evaporation

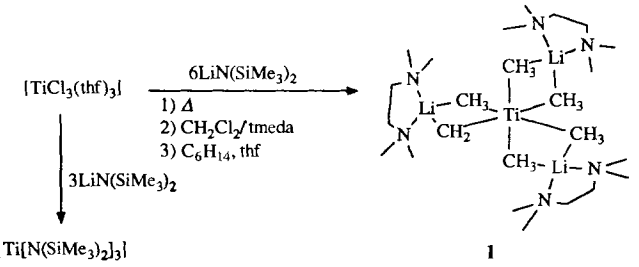

Scheme 1. Synthesis of **1**.

of solvent, the residual waxy solid was treated with a mixture of CH_2Cl_2 and TMEDA and subsequently recrystallized from hexane to yield well-formed, extremely air-sensitive, colorless needles of a new compound (**1**). Surprisingly, the IR spectrum did not display the characteristic absorptions of the silazanide group. The complex tested negatively for chlorine and positively for lithium and combustion analysis data were in good agreement with the formulation $[\{Ti(\mu\text{-}CH_3)_5(\mu\text{-}CH_2)\}\{(tmeda)Li\}_3] \cdot THF$. Chemical degradation experiments with gaseous HCl carried out with a Toepler pump yielded about 77% of the expected amount of gas which was identified by gas chromatography as CH_4 (99.5% with small amounts of ethane, traces of propane, and no ethylene). Magnetic measurements in both the solid state and solution showed the complex to be diamagnetic and therefore either oxidation to the tetravalent state or reduction to the divalent state had to have occurred (see below). Compound **1** is stable at room temperature in both the solid state and solution but does react violently with moisture and air.

The molecular structure of **1** was elucidated by X-ray analysis[9] and consists of a monomeric $[Ti(\mu\text{-}CH_3)_5(\mu\text{-}CH_2)]$ unit in which the titanium atom resides in an octahedral environment surrounded by six carbon atoms, the position of only one having been determined, while the positions of the others were generated by the symmetry operators of the $R\bar{3}c$ space group (Fig. 1).

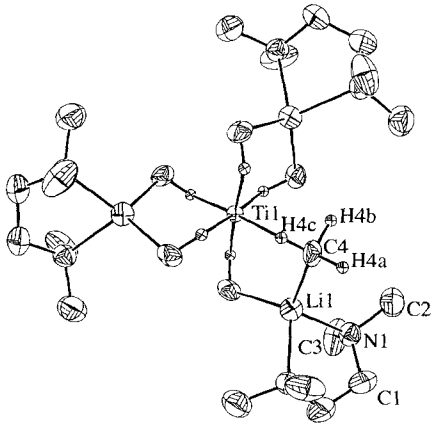

Fig. 1. Crystal structure of **1**. Selected bond lengths [Å] and angles [°]: Ti1-C4 2.615(4), C4-Li1 2.195(8), Li1-N1 2.137(9), Ti1-Li1 3.027(9), Ti1-H4c 2.229, C4-H4c 1.072, Ti1-H4c-C4 98.7, H4c-C4-H4b 110.8, H4a-C4-H4c 109.9, H4c-C4-Li1 108.7. Only two the hydrogen atoms not participating in hydrogen bonds are shown.

The Ti–C distance is remarkably long (Ti–C4 2.615(4) Å) and probably outside the bonding range. A tetrahedrally surrounded Li atom is bound to the two nitrogens of one TMEDA molecule and two carbon atoms (Li1–C4 2.195(8) Å). The positions of all the hydrogen atoms were revealed by the difference Fourier maps but were not refined. The C atoms surrounding Ti are placed in the center of a regular tetrahedron defined by three H atoms and the Li atom which occupies the fourth position. One of the three H atoms points toward the Ti atom, forming a rather short Ti–H distance (Ti1–H4c 2.229 Å). Therefore the connection between Ti and the six C atoms appears to have been realized through six hydrogen bonds. A disordered molecule of THF was also found in the lattice.

In order to account for the observed diamagnetism, one of the methyl groups must actually be a methylene disordered over the six C atom positions. The complex was found to be fluxional in solution, and the methylene resonance was not conclusively located in either the ^{1}H (500.1 MHz) or ^{13}C NMR (125.8 MHz) spectra. In fact, in addition to the THF and TMEDA resonances, the ^{1}H NMR spectrum showed only one resonance at $\delta = -3.2$. Variable-temperature experiments resulted in a broadening of this singlet on lowering the temperature from 298 K (8 Hz) to 180 K (20 Hz). However, the solid-state ^{13}C NMR (CP-MAS) spectrum (50.3 MHz) shows a resonance at $\delta = 125$, which is in the expected range for a methylene group,[7] in a ratio of approximately 1:5 with the methyl group resonance observed at $\delta = -12.3$. Conversely, the ^{13}C NMR spectrum of the solution shows only the resonances of TMEDA and THF. No resonances attributable to either methyl or methylene groups were detected. This can reasonably be explained by the large difference in chemical shift for the interconverting methyl ($\delta = -12.3$) and methylene ($\delta = 125$) groups which gives only a flattened resonance over a range of more than 137 ppm. The TMEDA methyl resonances were also found to be fluxional with a coalescence temperature T of 189 K.[14] The singlet at $\delta = 47.19$ split at 180 K into two resonances at $\delta = 45$ and $\delta = 50$ ($\Delta H^{\neq} = 19(3)$ kJ mol^{-1}, $\Delta S^{\neq} = -82(13)$ JK^{-1} mol^{-1}) attributed to rotational isomers of coordinated TMEDA. Interestingly, the signal of free TMEDA also appears at 180 K as a sharp resonance at $\delta = 46.5$. This resonance broadens at higher temperatures as a result of a fast dissociation/recombination equilibrium of TMEDA from the coordination sphere of lithium ($\Delta H^{\neq} = 17(3)$ kJ mol^{-1}, $\Delta S^{\neq} = -121(16)$ JK^{-1} mol^{-1}). The similarity of the activation parameters for the two independently measured processes (dissociation/recombination of TMEDA and internal rotation of the methyl groups) indicates that the two fluxionality trends belong to the same process. In other words, the internal rotation of TMEDA methyl groups proceeds through dissociation and is controlled by the cleavage of the Li–N bond. Moreover, the large negative activation entropies are plausibly indicative of a rather large reorganization of the solvent cage during the dissociation process.

It is difficult to envision at this stage a possible mechanism or rationalization for the formation of complex **1**. One possibility is that the methyl and methylene groups might originate from the silazanide groups similar to the previously reported cases of Al[10] and Pt.[11] However, the fact that treatment of the reaction mixture with CH_2Cl_2 is a necessary step for the successful isolation of **1**, possibly indicates that CH_2Cl_2 may also act as a source of both methyl or methylene groups. The structure, bonding, and spectroscopic features of complex **1** are unique not only in the organometallic chemistry of Ti but also with respect to closely related structures of tetravalent Zr and Hf complexes,[12] for which a non-octahedral coordination geometry is preferred. Even in the chemistry of trivalent lanthanides, which possess similar structures,[13] the bonding of the methyl groups to the metal is achieved through direct M–C bonds. Finally, we find remarkable that any attempt to form complex **1** in a more straightforward manner, for example by reaction of either $TiCl_4(L)_2$ [L = thf, 0.5 tmeda] or $TiCl_3(thf)_3$ with MeLi with or without TMEDA, and by using several different stoichiometric ratios and different reaction temperatures, invariably led to decomposition and an intractable mixture.

Received: May 22, 1995
Revised version: July 22, 1995 [Z 8012 IE]
German version: *Angew. Chem.* **1995**, *107*, 2457–2458

Keywords: complexes with carbon ligands · titanium compounds

[1] R. L. LaDuca, P. T. Wolczanski, *Inorg. Chem.* **1992**, *31*, 1311; L. E. Toth, *Transition Metal Carbides and Nitrides*, Academic Press, New York, **1971**; Recent Development in the Chemistry of Transition Metal Carbides and Nitrides, H. A. Johansen, in *Survey of Progress in Chemistry, Vol. 8* (Ed.: F. A. Scott), Academic Press, New York, **1977** 57; A. F. Wells, *Structural Inorganic Chemistry*, Clarendon, Oxford, England, **1975**; C. H. Jaggers, J. N. Michaels, A. M. Stacy, *Chem. Mater.* **1990**, *2*, 150.

[2] D. C. Bradley, M. B. Hursthouse, K. M. A. Malik, R. Moseler, *Transition Met. Chem. (London)* **1978**, *3*, 253, and references therein; M. F. Lappert, P. P. Power, A. R. Sanger, R. C. Srivastava, *Metal and Metalloid Amides*, Ellis Horwood, Chichester, England, **1980** and references therein; M. H. Chisholm, D. C. Bradley, *Acc. Chem. Res.* **1976**, *9*, 273; W. E. Buhro, M. H. Chisholm, K. Folting, J. C. Huffman, J. D. Martin, W. E. Streib, *J. Am. Chem. Soc.* **1992**, *114*, 557, and references therein; W. E. Buhro, M. H. Chisholm, J. D. Martin, J. C. Huffman, K. Folting, W. E. Streib, *ibid.* **1989**, *111*, 8149, and references therein; T. P. Blatchford, M. H. Chisholm, J. C. Huffman, *Inorg. Chem.* **1987**, *26*, 1920; D. C. Bradley, *Chem. Br.* **1975**, *11*, 393; R. A. Bartlett, H. Chen, P. P. Power, *Angew. Chem.* **1989**, *101*, 325; *Angew. Chem. Int. Ed. Engl.* **1989**, *28*, 316; J. J. H. Edema, S. Gambarotta, A. L. Spek, *Inorg. Chem.* **1989**, *28*, 811; J. J. H. Edema, S. Gambarotta, A. Meetsma, A. L. Spek, W. J. J. Smeets, M. Y. Chang, *J. Chem. Soc. Dalton Trans.* **1993**, 789; H. Hope, M. M. Olmstead, B. D. Murray, P. P. Power, *J. Am. Chem. Soc.* **1985**, *107*, 712; B. D. Murray, P. P. Power, *Inorg. Chem.* **1984**, *23*, 4584; H. Chen, R. A. Bartlet, M. M. Olmstead, P. P. Power, S. C. Shoner, *J. Am. Chem. Soc.* **1990**, *112*, 1048, and references therein; R. A. Andersen, K. Faegri, J. C. Green, A. Haaland, M. F. Lappert, W. P. Leung, K. Rypdal, *Inorg. Chem.* **1988**, *27*, 1782; R. Duchateau, N. Beydhoun, S. Gambarotta, C. Bensimon, *J. Am. Chem. Soc.* **1991**, *113*, 8986; *J. Chem. Soc. Chem. Commun.* **1992**, 244.

[3] S. J. Simpson, R. A. Andersen *J. Am. Chem. Soc.* **1981**, *103*, 4063; R. P. Planalp, R. A. Andersen, A. Zalkin, *Organometallics* **1983**, *2*, 16; P. Berno, R. Minhas, S. Hao, S. Gambarotta, *ibid.* **1994**, *13*, 1052.

[4] P. Berno, S. Gambarotta, *Angew. Chem.* **1995**, *107*, 871; *Angew. Chem. Int. Ed. Engl.* **1995**, *34*, 822.

[5] J. Song, P. Berno, S. Gambarotta, *J. Am. Chem. Soc.* **1994**, *116*, 6927.

[6] P. Berno, S. Gambarotta, *Organometallics* **1994**, *13*, 2569.

[7] L. Scoles, R. Minhas, R. Duchateau, J. Jubb, S. Gambarotta, *ibid.* **1994**, *13*, 4978.

[8] Freshly sublimed [$(Me_3Si)_2NLi$] (50.1 g, 0.3 mol) was added to a stirred greenish suspension of [$TiCl_3(thf)_3$] (17.40 g, 47.0 mmol) in toluene (120 mL). The suspension slowly turned blue. The mixture was then boiled and filtered hot. The green–red solution was evaporated to dryness giving an orange oil which slowly solidified. The solid was redissolved in CH_2Cl_2 (30 mL) and treated with TMEDA (4.5 mL). The addition of hexane (110 mL) and of a very small amount of THF to the solution initialized the crystallization. The solution was left to stand at −30 °C which yielded pale yellow crystals of **1** (4.20 g, 17%). Elemental analysis calcd for $C_{28}H_{73}N_6Li_3OTi$ (found): C 58.02 (57.66), H 12.87 (12.21), N 14.50 (14.44). IR [nujol mull, cm^{-1}]: $\tilde{\nu}$ = 1357 (sp), 1291 (s), 1251 (m), 1180 (w), 1160 (m), 1129 (sp), 1106 (s), 1063 (s), 1038 (vs), 1021 (vs), 949 (vs), 909 (w), 838 (m), 790 (s), 770 (sh), 456 (vs, br.); ^{1}H NMR (C_6D_6, 500 MHz): δ = 3.60 (m, 4H, THF), 2.94 (s, 36H, TMEDA), 2.64 (s, 12H, TMEDA), 1.40 (m, 4H, THF), −3.00 (s, 17H); ^{13}C NMR (C_6D_6, 125.8 MHz): δ = 67.85 (THF), 58.08 (TMEDA), 47.19 (TMEDA), 27.52 (THF); ^{13}C NMR (CP-MAS, 50.3 MHz): δ = 64.5 (THF), 57.7 (TMEDA), 46.8 (TMEDA), 23.2 (THF), −13.4 (CH_3).

[9] Crystal data of **1**: $C_{28}H_{73}N_6Li_3TiO$, M_r = 578.64, trigonal, $R\bar{3}c$, a = 16.654(1), c = 24.959(1) Å, V = 5995.3(6) Å^3, Z = 6, ρ_{calcd} = 0.962 g cm^{-1}, μ = 2.34 cm^{-1}, $F(000)$ = 1932, R = 0.034 (R_w = 0.048), GoF = 1.39 for 61 parameters and 843 unique reflections. The positions of the non-hydrogen atoms were located and refined anisotropically. The hydrogen atom positions were located

from difference Fourier maps but not refined. One disordered molecule of THF was found in the lattice and the oxygen atom could not conclusively be identified. Further details of the crystal structure investigation may be obtained from the Fachinformationszentrum Karlsruhe, D-76344 Eggenstein-Leopoldshafen (Germany), on quoting the depository number CSD-59063.

[10] H. H. Karsch, K. Zellner, G. Müller, *J. Chem. Soc. Chem. Commun.* **1990**, 1621.

[11] P. Hoffmann, H. Heiss, P. Neiteler, G. Müller, J. Lachmann, *Angew. Chem.* **1990**, *102*, 935; *Angew. Chem. Int. Ed. Engl.* **1990**, *29*, 880.

[12] P. M. Morse, S. G. Girolami, *J. Am. Chem. Soc.* **1989**, *111*, 4114.

[13] H. Schumann, J. Pickardt, N. Bruncks, *Angew. Chem. Int. Ed. Engl.* **1981**, *20*, 120.

[14] Detailed information on the structure determination and on the NMR experiments are available on request from the authors.

Stereoselective Synthesis of Chiral Zirconocenes from Doubly Substituted, Donor Functionalized Cyclopentadienes via Helical Chelate Complexes**

Jens Christoffers and Robert G. Bergman*

Metallocenes that carry two different substituents on one or both of their cyclopentadienyl rings exhibit "planar chirality".[1] Certain systems of this type (the *ansa*-metallocenes) are valuable catalysts for stereoregular Ziegler–Natta polymerization.[2] A second, and at present more unusual, way to produce chiral metallocenes is to connect each cyclopentadienyl ring to the metal center with a chelating chain, producing a helical structure.[3] However, in the latter case, breaking the metal–chelate bonds in the complexes known so far destroys the system's chirality. We report here on a simple, stereospecific conversion of a donor-substituted cyclopentadiene[4] into a doubly bridged metallocene **4a**, in which *both* planar chirality and helicity are present. Instead of eliminating the chirality of the system, cleavage of the metal–chelate bonds converts the planar chiral and helical starting material **4a** into single diastereomers of doubly planar chiral complexes **5** and **6**.

The two new cyclopentadiene derivatives **1** and **3** have been prepared from lithiated *tert*-butylcyclopentadiene[5] and *p*-$MeC_6H_4SO_2OCH_2CH_2OMe$[6] (**1**, yield 67%) or oxirane-$BF_3 \cdot OEt_2$ (**3**, yield 87%), respectively. Both compounds are isolated as mixtures of isomeric 1,3-disubstituted products (only one isomer of each compound is shown in Scheme 1). Upon reaction of either singly deprotonated **1** or doubly deprotonated **3** with $ZrCl_4$ in THF followed by removal of the solvent and redissolving in toluene to remove LiCl, the two metallocenes **2** and **4** are formed and isolated by crystallization from toluene/hexane at −40 °C.

Complex **2** is formed as a 3:1 mixture of two diastereomers **2a** and **2b** (Scheme 2), which have not been separated. In the *rac* isomer **2a** the C_5 ligands are homotopic and therefore one signal

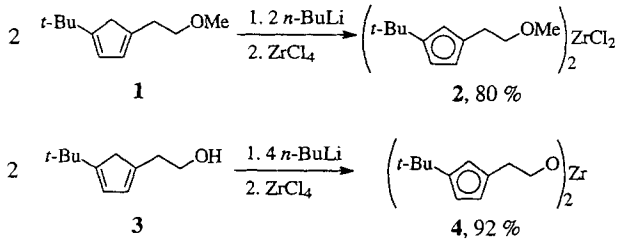

Scheme 1. Synthesis of the zirconocenes **2** and **4**. ^{1}H NMR data see Table 1.

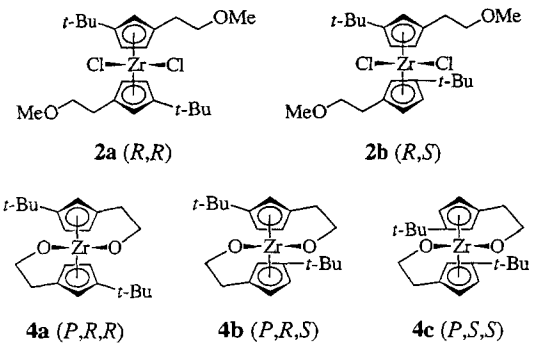

Scheme 2. Stereoisomers of the zirconocenes **2** and **4**. Only one enantiomer of each pair is shown.

set is observed in the ^{1}H NMR spectrum (Table 1). The ^{1}H NMR spectrum for the *meso* compound **2b** shows two independent sets of resonances for each C_5 ligand, although we expected that they might be enantiotopic. We believe that the doubling of resonances is due to the steric bulk of the *t*Bu substituents, preventing free rotation about the Zr–C_5 bond and leading to a relatively stable conformation of molecule **2b** in which the two ligands are diastereotopic. Although the zirconium center in **2** is electron deficient, we see no evidence for coordination of the MeO groups to the metal center in this case.[7]

Table 1. ^{1}H NMR data (300 MHz, C_6D_6) for **2a**, **2b**, **4a**, **5**, and **6**.

2a: δ = 1.32 (s, 9H; *t*Bu), 2.82–2.98 (m, 1H; CH_2CH_2O), 3.06–3.13 (m, 1H; CH_2CH_2O), 3.15 (s, 3H; OCH_3), 3.36–3.52 (m, 2H; CH_2CH_2O), 5.80 (t, J = 2.7 Hz, 1H; =CH), 5.93 (t, J = 2.7 Hz, 1H; =CH), 6.45 (t, J = 2.5 Hz, 1H; =CH)

2b: δ = 1.40 (s, 9H; *t*Bu), 1.51 (s, 9H; *t*Bu), 2.82–2.98 (m, 2H; CH_2CH_2O), 3.06–3.13 (m, 2H; CH_2CH_2O), 3.16 (s, 3H; OCH_3), 3.22 (s, 3H; OCH_3), 3.36–3.52 (m, 4H; CH_2CH_2O), 5.83 (t, J = 2.7 Hz, 1H; =CH), 5.94 (t, J = 2.8 Hz, 1H; =CH), 6.01 (t, J = 2.8 Hz, 1H; =CH), 6.13 (t, J = 2.8 Hz, 1H; =CH), 6.16 (t, J = 2.8 Hz, 1H; =CH), 6.24 (t, J = 2.7 Hz, 1H; =CH)

4a: δ = 1.39 (s, 9H; *t*Bu), 2.49 (ddd, ^3J = 7.2, ^3J = 11.0, ^2J = 13.0 Hz, 1H; $CHHCH_2O$), 2.65 (ddd, ^3J = 1.3, ^3J = 5.5, ^2J = 13.0 Hz, 1H; $CHHCH_2O$), 4.77 (ddd, ^3J = 1.5, ^3J = 7.3, ^2J = 10.0 Hz, 1H; CH_2CHHO), 5.10 (ddd, ^3J = 5.5, ^3J = 11.0, ^2J = 10.0 Hz, 1H; CH_2CHHO), 5.71–5.76 (m, 2H; =CH), 6.11 (t, ^4J = 2.5 Hz, 1H; =CH)

5: δ = 1.18 (s, 9H; *t*Bu), 1.20 (s, 9H; *t*Bu), 2.18 (ddd, ^2J = 13.2, ^3J = 9.0, ^3J = 7.5 Hz, 1H; $CHHCH_2O$), 2.58–2.69 (m, 2H; $CHHCH_2O$ and $CHHCH_2OCH_3$), 3.03 (dt, ^2J = 14.8, ^3J = 5.4 Hz, 1H; $CHHCH_2OCH_3$), 3.10 (s, 3H; OCH_3), 3.26–3.37 (m, 2H; $CH_2CH_2OCH_3$), 4.65 (ddd, ^2J = 10.6, ^3J = 7.4, ^3J = 3.3 Hz, 1H; CH_2CHHO), 5.40 (t, J = 2.7 Hz, 1H; =CH), 5.43 (ddd, ^2J = 10.6, ^3J = 9.1, ^3J = 6.7 Hz, 1H; CH_2CHHO), 5.75 (t, J = 2.7 Hz, 1H; =CH), 5.77 (t, J = 2.6 Hz, 1H; =CH), 6.00 (t, J = 2.6 Hz, 1H; =CH), 6.32 (t, J = 2.6 Hz, 1H; =CH), 6.43 (t, J = 2.5 Hz, 1H; =CH)

6: δ = 0.10 (s, d, $^2J(^1H,^{29}Si)$ = 3.3 Hz, 9H; $Si(CH_3)_3$), 1.29 (s, 9H; *t*Bu), 2.77–2.81 (m, 1H; $CHHCH_2O$), 3.00 (dt, ^2J = 14.6, ^3J = 5.9 Hz, 1H; $CHHCH_2O$), 3.64–3.73 (m, 2H; CH_2CH_2O), 5.77 (t, J = 2.7 Hz, 1H; =CH), 5.91 (t, J = 2.7 Hz, 1H; =CH), 6.37 (t, J = 2.5 Hz, 1H; =CH)

[*] Prof. Dr. R. G. Bergman, Dr. J. Christoffers
Department of Chemistry
University of California at Berkeley
Berkeley, CA 94720-1460 (USA)
Telefax: Int. code +(510)642-7714
e-mail: rgberg@violet.berkeley.edu

[**] We acknowledge the United States National Science Foundation (Grant No. CHE-91134261) for generous financial support of this work, the Alexander-von-Humboldt-Stiftung for a fellowship for J. C., and Dr. F. Hollander, Director of the University of California at Berkeley X-ray diffraction facility, for the determination of the X-ray structure. We are also grateful to Prof. C. H. Heathcock for helpful discussions on the stereochemistry of complex **4** and to Prof. J. Okuda for disclosure of results prior to publication.

In contrast to the two stereogenic elements in the planar chiral complex **2**, complex **4** bears three stereogenic elements: one helix represented by the (*t*BuCp)-CH_2-CH_2-O···O-CH_2-CH_2-(*t*BuCp) moiety and two planes of chirality represented by the two C_5 ligands. Of the four potential pairs of enantiomers for such a system, only three exist in this case (**4a**, **4b**, and **4c** in Scheme 2), because the two chiral planes in **4b** have a *meso* relationship with respect to one another. Complex **4** is formed completely stereospecifically: only one of the diastereomers, which by single-crystal X-ray diffraction analysis[8] is shown to be **4a** (Fig. 1), is observed. We believe the quantitative stereoselectivity is caused by a high degree of steric strain in the unseen isomers **4b** and **4c** attributed to the bulky *t*Bu substituents. Reduction of strain by rotation (as is possible in compound **2b**) is prevented by the conformational rigidity enforced by the chelating side chains.

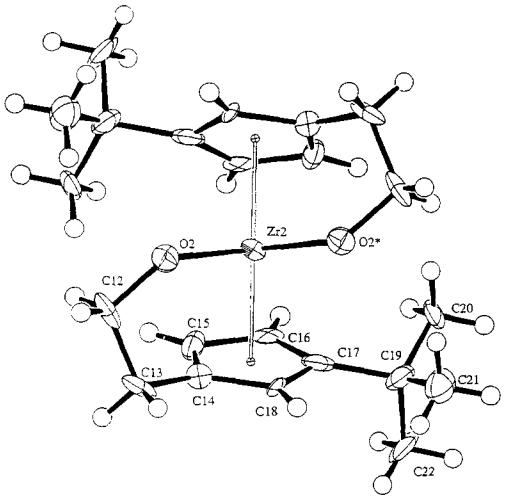

Fig. 1. ORTEP diagram illustrating the solid-state molecular structure of **4a** (one of two independent molecules in the unit cell). Selected bond lengths [Å] and angles [°]: Zr2–O2 2.006(6), Zr2–C102 2.237, C12–O2 1.44(1); O2-Zr2-O2* 103.6(4), Zr2-O2-C12 126.1(6), O2-C12-C13 109.4(8), C12-C13-C14 107.3(8), C102-Zr2-C102* 131.88 (C102 and C102* are the centroids of the Cp rings).

The oxygen atoms in **4a** are homotopic. Therefore, room temperature alkylation with excess methyl triflate at either alkoxy ligand of **4** gives only complex **5**; it is formed in quantitative yield (Scheme 3). The observation of the M^+ signal (85% rel. intensity at 70 eV) in the EI mass spectrum and of a very strong band at $\tilde{\nu} = 1384\ cm^{-1}$ in the IR spectrum[9] indicates that the triflate ligand is covalently bound to the Zr center. The replacement of an alkoxy with a sulfonato ligand increases the electrophilicity at the Zr center in **5**, resulting in a reduction of electron density at the attached oxygen atom compared with that in **4a**.[7] This makes the remaining chelate arm less reactive towards a second equivalent of methyl triflate. The ability to carry out cleavage of only one Zr–O bond in **4a** permits the helicity of this molecule to be stereospecifically converted into central chirality at the Zr atom in complex **5**, and thus this material is formed as only one diastereomer.

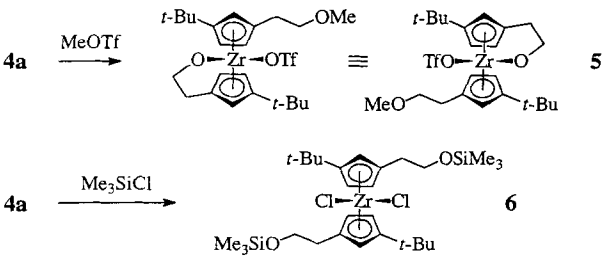

Scheme 3. Ring opening reactions of **4** (Tf = F_3CSO_2). ^1H NMR data see Table 1.

Reaction of complex **4** with excess Me_3SiCl at room temperature opens both chelate arms and yields the zirconocene dichloride **6** quantitatively. Only the *rac* compound is formed; no *meso* isomer is detectable by ^1H NMR spectroscopy. We conclude that the reaction proceeds with retention of stereochemical configuration at the planar chiral substituted cyclopentadienyl ligands.

The simple and diastereospecific preparation of complexes **5** and **6** in high yield in only two steps from $ZrCl_4$ exemplifies the useful synthetic potential of 1,3-disubstituted cyclopentadienes with a donor functionalized side chain and the novel stereochemical properties that arise when helical and planar chirality are combined in the same complex. Further chemical properties of these new chiral materials are being explored in our laboratory.

Received: July 3, 1995 [Z8160IE]
German version: *Angew. Chem.* **1995**, *107*, 2423–2425

Keywords: chelate complexes · chirality · cyclopentadiene derivatives · helicity · zirconium compounds

[1] M. Uemura in *Stereochemistry of Organometallic and Inorganic Compounds Vol. 5* (Ed.: P. Zanello), Elsevier, Amsterdam, **1994**, p. 507–558.

[2] a) W. Kaminsky, K. Külper, H. H. Brintzinger, F. R. W. P. Wild, *Angew. Chem.* **1985**, *97*, 507–508; *Angew. Chem. Int. Ed. Engl.* **1985**, *24*, 507–508; b) M. Bochmann, A. J. Jaggar, J. C. Nicholls, *ibid.* **1990**, *102*, 830–832; and **1990**, *29*, 780–782; c) J. A. Ewen, *J. Am. Chem. Soc.* **1984**, *106*, 6355–6364; d) J. A. Ewen, R. L. Jones, A. Razavi, J. D. Ferrara, *ibid.* **1988**, *110*, 6255–6256; e) P. G. Gassmann, M. R. Callstrom, *ibid.* **1987**, *109*, 7875–7876.

[3] a) W. A. Herrmann, M. J. A. Morawietz, T. Priermeier, *Angew. Chem.* **1994**, *106*, 2025–2028; *Angew. Chem. Int. Ed. Engl.* **1994**, *33*, 1946–1949; b) K. E. du Plooy, U. Moll, S. Wocadlo, W. Massa, J. Okuda *Organometallics* **1995**, *14*, 3129–3131. Such doubly chelated metallocenes are also stereochemically analogous to spirocyclic organic compounds: see Eliel, E. L.; Wilen, S. H. *Stereochemistry of Carbon Compounds*, Wiley, NY, 1994, Chapter 14.

[4] Cyclopentadiene derivatives with donor functionalized side chains have been prepared and used as chelating ligands in a variety of metal complexes: a) T.-F. Wang, T.-Y. Lee, J.-W. Chou, C.-W. Ong, *J. Organomet. Chem.* **1992**, *423*, 31–38; b) P. Jutzi, J. Dahlhaus, M. O. Kristen, *ibid.* **1993**, *450*, C1–C3; c) P. Van de Weghe, C. Bied, J. Collin, J. Marcalo, I. Santos, *ibid.* **1994**, *475*, 121–126; d) P. Jutzi, J. Dahlhaus, *Synthesis* **1993**, 648–686; e) P. Jutzi, M. O. Kristen, B. Neumann, H.-G. Stammler, *Organometallics* **1994**, *13*, 3854–3861; f) I. Lee, F. Dahan, A. Maisonnat, R. Poilblanc, *ibid.* **1994**, *13*, 2743–2750; g) J. Okuda, *Comments Inorg. Chem.* **1994**, *16*, 185–205.

[5] a) R. Riemschneider, R. Nehring, *Monatsh. Chem.* **1959**, *90*, 568–570; b) S. Schönholzer, M. Slongo, C. Rentsch, M. Neuenschwander, *Makromol. Chem.* **1980**, *181*, 37–45.

[6] a) J. Dale, S. B. Fredriksen, *Acta. Chem. Scand. Ser. B* **1985**, *B39*, 511–512; b) R. A. Schultz, B. D. White, D. M. Dishong, K. A. Arnold, G. W. Gokel, *J. Am. Chem. Soc.* **1985**, *107*, 6659–6668.

[7] Coordination to the zirconium center causes a downfield shift of the signals of the CH_2O protons of 1.5 ppm in **4** compared with the corresponding signals in complex **2**. The higher electrophilicity of the Zr center and thus the reduced electron density at the oxygen atom results in another downfield shift of the signal of the CH_2O protons of 0.8 ppm in **5** compared with the corresponding signals in compound **4**.

[8] Further details of the crystal structure investigation may be obtained from the Director of the Cambridge Crystallographic Data Centre, 12 Union Road, GB-Cambridge CB2 1EZ (UK), on quoting the full journal citation.

[9] a) G. A. Lawrance, *Chem. Rev.* **1986**, *86*, 17–33; b) D. H. Johnston, D. F. Shriver, *Inorg. Chem.* **1993**, *32*, 1045–1047.

 © VCH Verlagsgesellschaft mbH, D-69451 Weinheim, 1995 0570-0833/95/3420-2267 $ 10.00+.25/0

Detection and Reactions of Radical Cations Generated by Photolysis of Aromatic Compounds with Tetranitromethane in 1,1,1,3,3,3-Hexafluoro-2-propanol at Room Temperature**

Lennart Eberson,* Michael P. Hartshorn, and Ola Persson

Dedicated to Professor Ivar Ugi on the occasion of his 65th birthday

Radical cations of aromatic compounds ($ArH^{\bullet+}$) generated in 1,1,1,3,3,3-hexafluoro-2-propanol (HFP) are extremely persistent, their half-lives in HFP often exceeding those found in trifluoroacetic acid by a factor of more than 100.[1] We have previously[2] generated and detected (by EPR spectroscopy) radical cations of moderately high reactivity by photolysis of ArH with tetranitromethane in dichloromethane at $-60\,^{\circ}C$ [Eq.(a)], most often with trifluoroacetic acid present in order to suppress the reactivity of trinitromethanide ion by protonation [Eq.(b)].[3] Under the conditions defined by Equation (a), the further course of the reaction is largely determined by the reactivity of the radical cation $ArH^{\bullet+}$ toward trinitromethanide ion. In Equation (b), this reaction has been ruled out and replaced by other, slower processes.

$$ArH\cdots C(NO_2)_4 \xrightarrow{h\nu} ArH^{\bullet+}NO_2(NO_2)_3C^- \quad (a)$$

$$ArH\cdots C(NO_2)_4 \xrightarrow{H^+,\,h\nu} ArH^{\bullet+}NO_2(NO_2)_3CH \quad (b)$$

In view of the extreme deactivation of radical cation reactivity towards nucleophiles found in HFP, we expected that the tetranitromethane method might be applicable at room temperature in HFP. In the event, we demonstrated that otherwise readily reacting radical cations can persist at room temperature in HFP in the presence of trinitromethanide ion.

When 1-methoxynaphthalene, **1**-H, is photolyzed with tetranitromethane in dichloromethane at temperatures below $-48\,^{\circ}C$, the radical cation of its 4,4'-connected dehydrodimer $(\mathbf{1})_2$ can be detected.[2b] Irradiation of solutions of **1**-H and tetranitromethane (0.4 mol dm^{-3}) in HFP at 22 °C, using light of $\lambda > 430$ nm gives rise to a broad singlet ($\Delta H_{pp} \approx 0.7$ mT; Fig. 1a) in the resulting EPR spectrum at relatively high concentrations of **1**-H (70 mmol dm^{-3}). The line broadening probably results from electron exchange of $(\mathbf{1})_2^{\bullet+}$ with **1**-H or $(\mathbf{1})_2$. The signal could be resolved at [**1**-H] = 5 mmol dm^{-3} (Fig. 1b). This spectrum was the same as that obtained by treatment of the dehydrodimer $(\mathbf{1})_2$ under similar conditions (Fig. 1c). Thus it appears that the reactivity of trinitromethanide ion has been strongly suppressed in HFP, permitting observation of $(\mathbf{1})_2^{\bullet+}$ in the presence of this nucleophile. This conclusion was supported by results from a preparative run in HFP ([**1**-H] = 0.5, [tetranitromethane] = 1.0 mol dm^{-3}, light of $\lambda > 430$ nm) at 20 °C which gave after 40% conversion a 72% yield of dehydrodimer $(\mathbf{1})_2$ and 28% yield of **1**-H with a nitro group in the 4-position (**1**-NO_2). A comparison with runs in dichloromethane[2b] reveals that no products derived from an initial reaction between trinitromethanide ion and $\mathbf{1}\text{-H}^{\bullet+}$ are formed in HFP. In dichloromethane, the same effect was obtained by conducting the photolysis in the presence of trifluoroacetic acid (0.4 mol dm^{-3}).[2b]

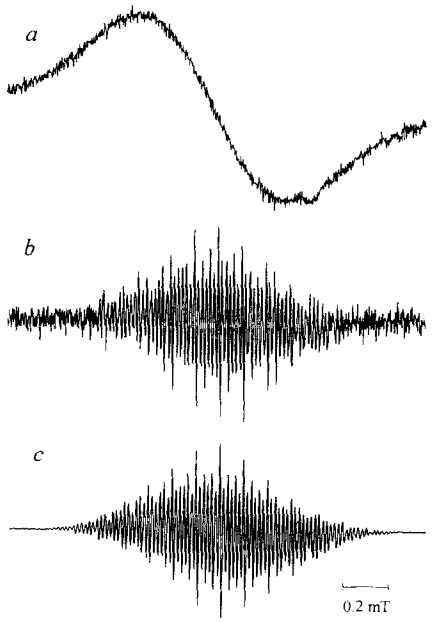

Fig. 1. EPR spectrum of the sample solutions from the photolysis ($\lambda > 430$ nm) of tetranitromethane (0.4 mol dm^{-3}) and a) 1-methoxynaphthalene (**1**-H, 70 mmol dm^{-3}), b) **1**-H (5 mmol dm^{-3}) and c) 4,4'-dimethoxy-1,1'-binaphthalene [$(\mathbf{1})_2$, 5 mmol dm^{-3}] in HFP.

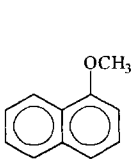

1-H

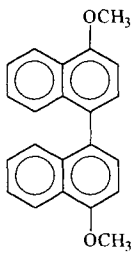

$(\mathbf{1})_2$

1,4-Dimethoxybenzene (**2**-H), the radical cation of which could not be detected by photolysis with tetranitromethane in dichloromethane at $-60\,^{\circ}C$,[2a] on photolysis with tetranitromethane in HFP at 22 °C gave a strong, well-resolved EPR spectrum corresponding to $\mathbf{2}\text{-H}^{\bullet+}$. The authentic dehydrodimer of **2**-H, 2,2',5,5'-tetramethoxybiphenyl $(\mathbf{2})_2$, was prepared in order to allow the reactions analogous to those of **1** and $(\mathbf{1})_2$ to be studied. The EPR spectrum recorded for $(\mathbf{2})_2^{\bullet+}$ (obtained by photolysis of a solution of $(\mathbf{2})_2$ and tetranitromethane in HFP)

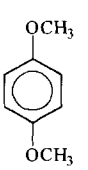

2-H

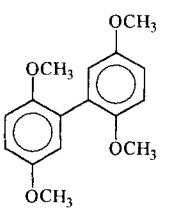

$(\mathbf{2})_2$

[*] Prof. L. Eberson, O. Persson
Chemical Center, Lund University
P. O. Box 124, S-221 00 Lund (Sweden)
Telefax: Int. code + (46) 222 41 19
e-mail: Lennart.Eberson@maxkemi.lu.se
Prof. M. P. Hartshorn
University of Canterbury, Christchurch (New Zealand)

[**] Photochemical Nitration by Tetranitromethane. Part 28. This work was supported by the Swedish Natural Science Research Council and the Knut and Alice Wallenberg Foundation. Part 27: C. P. Butts, L. Eberson, M. P. Hartshorn, W. T. Robinson, *Acta Chem. Scand.* in press.

was distinctly different from the spectrum of **2**-H$^{\bullet+}$. Under preparative conditions, the photolysis of **2-H** with tetranitromethane in HFP at 20 °C gave after 2 h a 19% (after 4 h, 33%) conversion into 1,4-dimethoxy-2-nitrobenzene (**2**-NO_2) as the only product; the analogous reaction in dichloromethane gave under identical conditions a 47% (after 4 h, 82%) conversion into **2**-NO_2. Since the product in the two solvents is the same, one can only conclude that the higher efficiency of the conversion in dichloromethane points to a trinitromethanide ion initiated pathway, possibly leading to a transient adduct,[4] which is eventually transformed into **2**-NO_2. The markedly lower efficiency in HFP would then be caused by HFP blocking this pathway, leaving the fairly slow reaction between **2**-H$^{\bullet+}$ and NO_2 as a feasible route to **2**-NO_2.

1,4-Dimethylnaphthalene (**3**), which gave no EPR signal upon photolysis with tetranitromethane in dichloromethane at −60 °C,[2a] in HFP under the same conditions but at 5 °C gave a broad unresolved signal. A preparative run in HFP ([**3**] = 0.5, [tetranitromethane] = 1.0 mol dm^{-3}) at 20 °C after 40% conversion showed essentially quantitative formation of 1,4-dimethyl-2-nitro-naphthalene. Again it is evident that the formation of the **3**$^{\bullet+}$-trinitromethanide ion derived products obtained in dichloromethane at 20 °C,[5] namely the adducts **4** and **5** (in total 49% yield) and the side chain nitro substitution product **6** (48%), have been completely suppressed.

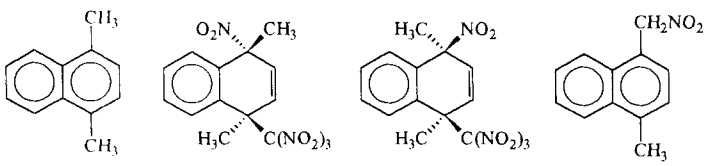

3 **4** **5** **6**

These examples demonstrate the unique high persistency of radical cations in HFP, which allows these radical cations to be observed in the presence of a nucleophile such as trinitromethanide ion even at room temperature. The reactivity of the radical cations that remain leads to dehydrodimer formation and/or radical coupling with NO_2 to give the "normal" product(s) of the reactions of ArH$^{\bullet+}$ with NO_2. Thus it appears that HFP will discriminate decisively between the radical and electrophilic reactivity of radical cations.

Received: June 8, 1995 [Z 8071 IE]
German version: *Angew. Chem.* **1995**, *107*, 2417–2418

Keywords: hexafluoropropanol · nitro compounds · photochemistry · radical cations · tetranitromethane

[1] L. Eberson, M. P. Hartshorn, O. Persson, *J. Chem. Soc. Chem. Commun.* **1995**, 1131–1132; *J. Chem. Soc. Perkin Trans. 2*, in press.

[2] a) L. Eberson, M. P. Hartshorn, F. Radner, J. O. Svensson, *J. Chem. Soc. Perkin Trans. 2* **1994**, 1719–1730; b) C. P. Butts, L. Eberson, M. P. Hartshorn, O. Persson, W. T. Robinson, *Acta Chem. Scand.* **1995**, *49*, 253–264.

[3] A similar mechanism operates in the generation of ArH$^{\bullet+}$ from the photolysis of ArH with 2,3-dichloro-4,5-dicyanobenzoquinone in trifluoroacetic acid: A. G. Davies, K.-M. Ng, *Aust. J. Chem.* **1995**, *48*, 167–173.

[4] Most products from the photolysis of ArH and tetranitromethane in dichloromethane or acetonitrile are derived by elimination of nitroform or nitrous acid from initially formed nitro-trinitromethyl or nitrito-trinitromethyl 1,2- and/or 1,4-adducts to the aromatic ring system. The persistency of the adducts range from isolable to transient. See earlier papers of this series and two reviews: L. Eberson, M. P. Hartshorn, F. Radner, *Acta Chem. Scand.*, **1994**, *48*, 937–950; *Advances in Carbocation Chemistry*, *Vol 2* (Ed.: J. M. Coxon), JAI, **1995**, in press.

[5] L. Eberson, M. P. Hartshorn, F. Radner, *J. Chem. Soc. Perkin Trans. 2* **1992**, 1799–1806.

Molecular Recognition between Chemically Modified β-Cyclodextrin and Dec-1-ene: New Prospects for Biphasic Hydroformylation of Water-Insoluble Olefins**

Eric Monflier,* Georges Fremy, Yves Castanet, and André Mortreux

The development of water-soluble catalysts for the hydroformylation of olefins in a two-phase system has attracted a great deal of attention during the last years. The application of this concept to the hydroformylation of propylene has been developed industrially by Hoechst AG using a water-soluble rhodium catalyst containing triphenylphosphane trisulfonate as ligand.[1] Although hydroformylation of long-chain olefins can be achieved in good yields in the presence of organic solvent, these olefins are generally hydroformylated slowly with low selectivities in two-phase systems owing to their poor solubility in water.[2] To solve these problems, surfactants,[3] catalyst-binding ligands,[4] amphiphilic phosphanes,[5] supported aqueous-phase catalysts,[6] and/or cosolvents[7] have been used. However, despite these numerous efforts, the hydroformylation of water-insoluble olefins remains a challenge, and research in this field is still being pursued.

We have previously reported in this journal that the Wacker oxidation of higher α-olefins could be achieved in high yields (up to 95%) in an aqueous two-phase system in the presence of β-cyclodextrins functionalized with hydrophilic or lipophilic groups.[8] In this reaction, the chemically modified β-cyclodextrins behaved mainly as inverse phase-transfer catalysts. Indeed, owing to the formation of inclusion complexes, the chemically modified cyclodextrins can transfer the higher olefins into the aqueous phase and so improve the mass transfer between aqueous and organic layers. We wish now to report that these chemically modified β-cyclodextrins were also very effective for the hydroformylation of water-insoluble olefins in an aqueous two-phase system free of organic solvent (Scheme 1).[9]

The typical results obtained with and without chemically modified cyclodextrins are given in Table 1. The catalytic activ-

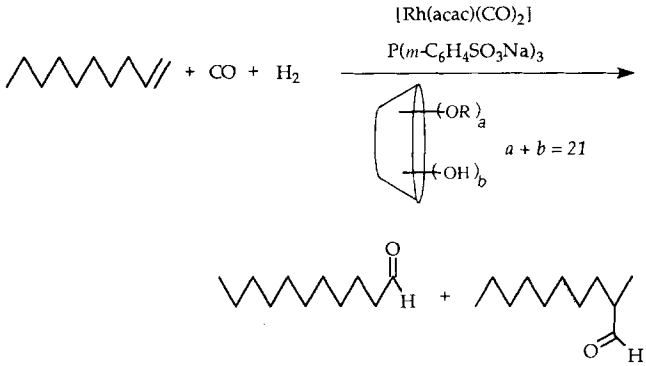

Scheme 1. Rhodium-catalyzed hydroformylation of dec-1-ene in a two-phase system. The chemically modified cyclodextrins are schematically represented by a hollow truncated cone. R = CH_3, $CH_2CH(OH)CH_3$, $COCH_3$.

[*] Dr. E. Monflier
Université d'Artois, Faculté des Sciences J. Perrin
Rue Jean Souvraz, Sac postal 18, F-62307 Lens (France)
Telefax: Int. code + 21791717
Dipl.-Chem. G. Fremy, Prof. Dr. A. Mortreux, Prof. Dr. Y. Castanet
Laboratoire de Catalyse Hétérogène et Homogène
Villeneuve d'Ascq Cedex (France)

[**] This work was supported by the CNRS.

Table 1. Hydroformylation of dec-1-ene in the presence of chemically modified cyclodextrins [a].

No.	Cyclodextrin[b] type	R	a	b	M_r[c]	Conversion (dec-1-ene) [mol %]	Yield [mol%]	n/iso-ratio [d]	Selectivity (aldehyde formation) [e][mol %]
1	-	-	-	-		10	6	2.7	60
2	α	-	0	18	973	10	8.5	3.2	85
3	γ		0	24	1297	9	6	2.5	66
4	β	-	0	21	1135	19	15	2.1	78
5	β	CH_3	12.6	8.4	1310	76	69	1.8	91
6[f]	β	CH_3	12.6	8.4	1310	100	95	1.9	95
7	β	CH_3	21	0	1428	30	17	2.5	57
8	β	$COCH_3$	21	0	2017	6	4	2.6	66
9	β	$COCH_3$	14	7	1724	46	26	2.6	57
10	β	$CH_2CH(OH)CH_3$	6.3	14.7	1500	32	27	2	84
11	β	SO_3Na	9	12	1253	7	5	2.8	69

[a] Reaction conditions: $[Rh(acac)(CO)_2]$ (0.16 mmol), $P(m\text{-}C_6H_4SO_3Na)_3$ (0.8 mmol), cyclodextrin (1.12 mmol), H_2O (45 mL), dec-1-ene (80 mmol), undecane (4 mmol); $p(CO/H_2) = 50$ atm, $T = 80\,^{\circ}C$, $t = 8$ h. [b] For the structures of cyclodextrins see ref. [14]. a = no. of hydrophilic or hydrophobic groups R; b = no. of free OH groups (Schemes 1 and 2). The chemically modified cyclodextrins were supplied by Cyclolab (Budapest, Hungary) and Aldrich Chemical Co. and used without further purification. [c] Relative molecular mass of the cyclodextrin. [d] Ratio of linear (n) to branched aldehyde (iso). [e] (Yield aldehydes)/(dec-1-ene conversion); the side products were mainly dec-2-ene, dec-3-ene, and dec-4-ene. [f] Cyclodextrin (2.24 mmol); the time required for complete conversion was 6 h; at the end of the reaction the phase separation was excellent and the Rh and P content in the organic phase was <0.5 and 1.2 ppm, respectively; that is, the water-soluble catalysts can be easily and completely recovered after the reaction.

ities of the classical α-, β-, and γ-cyclodextrins are rather disappointing.[10] Actually, the only suitable cyclodextrin was the β-cyclodextrin, and the dec-1-ene conversion can only be enhanced by a factor of 2 (entry 4). Interestingly, the functionalization of this β-cyclodextrin with hydrophilic or hydrophobic groups such as methyl, acetyl, and 2-hydroxypropyl improved the dec-1-ene conversion greatly. The best results have been obtained with the dimethyl-β-cyclodextrin (entries 5 and 6). Indeed, in this case the dec-1-ene conversion reached 100%, and the aldehyde was formed with 95% selectivity (entry 6). However, the activity is strikingly dependent on the degree of substitution of the β-cyclodextrin. For example, the permethyl-β-cyclodextrin exhibited a much lower activity than the dimethyl-β-cyclodextrin. Acetylated cyclodextrins behaved similarly (entries 8 and 9).

As it has been suggested that hydroformylation under two-phase reaction conditions with water-insoluble olefins is limited by the rate of mass transfer,[11] we think that the beneficial effect of the chemically modified cyclodextrins on the dec-1-ene conversion can be mainly explained by an improvement of the transfer of material between aqueous and organic layers according to Scheme 2.

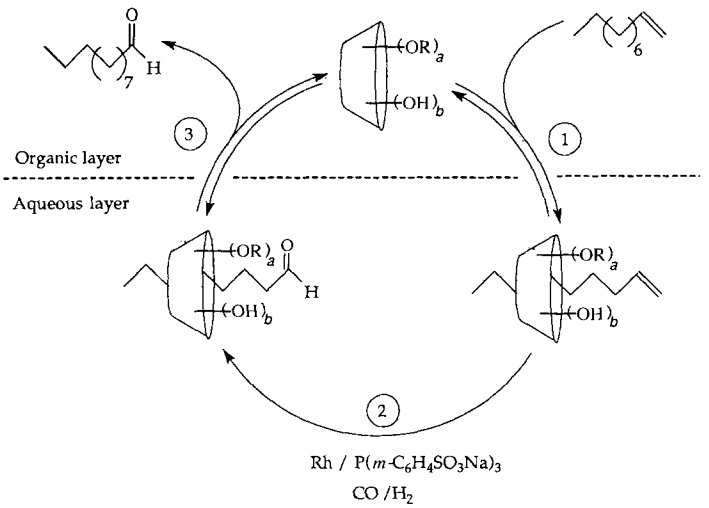

Scheme 2. Transfer of material between the aqueous and the organic phases in the presence of chemically modified cyclodextrin during the dec-1-ene hydroformylation.

The effectiveness of chemically modified cyclodextrins on the mass transfer is probably due to the solubility of these cyclodextrins in both the aqueous and organic layers. Indeed, in contrast to the β-cyclodextrin and the sulfonated β-cyclodextrin, which are totally insoluble in the organic phase, the dimethyl-β-cyclodextrin and the diacetylated-β-cyclodextrin dissolve well in water and partially in the organic layer, and can therefore transfer the olefin rapidly into the aqueous phase.[11] This hypothesis is in agreement with the results obtained with the peracetylated and the permethylated-β-cyclodextrins. These cyclodextrins are weakly soluble in aqueous layer and are preferably localized in the organic layer. Consequently, transfer of dec-1-ene into the aqueous layer is unlikely. Another possible explanation could be the lower stability of the host–guest complexes. The stability constant of the inclusion complex between the aldehyde and chemically modified cyclodextrin is probably weaker than that of the aldehyde–cyclodextrin complex (fewer hydrogen bonds). Therefore, the organic compounds and cyclodextrins would dissociate and associate more readily (step 1 and 3 in Scheme 2).

The unusually high selectivities (up to 90%) observed with the dimethyl-β-cyclodextrin could be explained by the deeper hydrophobic cavity in the host of this cyclodextrin, which would wrap the olefin efficiently and would so avoid isomerization by the rhodium catalyst.[12] Finally, the variations of the normal to branched aldehyde ratio (1.8 to 3.2) could be attributed to the ability of modified cyclodextrins to cause preorientation of the dec-1-ene in the host cavity and/or to interactions between the cyclodextrin and the catalyst. Indeed, interactions between transition metal complexes and cyclodextrins can give rise to the formation of inclusion compounds.[10, 13] To confirm this latter hypothesis, NMR investigations are now under way in our laboratory.

These results and our previous work on the Wacker oxidation of higher olefins support the idea that the beneficial effect of chemically modified cyclodextrins in an aqueous two-phase system is a phenomenon of general importance. As the chemically modified cyclodextrins are nontoxic, cheap, biodegradable, and bulk industrial chemicals, the use of these compounds in biphasic reactions catalyzed by transition-metal complexes should become general. Due to the chiral environment of cyclodextrins, some fruitful developments are possible, for example, in asymetric catalysis.

 © VCH Verlagsgesellschaft mbH, D-69451 Weinheim, 1995 0570-0833/95/3420-2270 $ 10.00+.25/0

Experimental Procedure

In a typical experiment, $[Rh(acac)(CO)_2]$ (0.16 mmol), P(*meta*-$C_6H_4SO_3Na)_3$ (0.8 mmol; this sulfonated phosphane was synthesized as reported by R. Gärtner et al. [15]), and chemically modified cyclodextrin (1.12 mmol) were dissolved in water (45 mL). A stainless steel autoclave (100 mL) was charged under an atmosphere of N_2 with the resulting aqueous phase and an organic phase composed of dec-1-ene (80 mmol) and undecane (4 mmol, GC internal standard), and then heated at 80 °C and pressurized with 50 atm of CO/H_2 (1/1). A mechanical stirrer (1000 rpm) equipped with a multipaddle unit was then started. The pressure was kept constant throughout the whole reaction by using a gas reservoir along with a pressure regulator. The reaction was monitored by quantitative gas chromatographic analysis (CP Sil 5-CB, 25 m, inner diameter 0.32 mm).

Received: June 3, 1995 [Z 7812IE]
German version: *Angew. Chem.* **1995**, *107*, 2450–2452

Keywords: cyclodextrins · hydroformylation · phase transfer catalysis · rhodium compounds · Wacker oxidation

[1] a) W. A. Herrmann, C. W. Kohlpaintner, *Angew. Chem.* **1993**, *105*, 1588; *Angew. Chem. Int. Ed. Engl.* **1993**, *32*, 1524; b) B. Cornils, E. Wiebus, *CHEMTECH* **1995**, *33*; c) *Chem. Ing. Tech.* **1994**, *66*, 916; d) W. A. Herrmann, C. W. Kohlpaintner, R. B. Manetsberger, H. Bahrmann, H. Kottmann, *J. Mol. Catal.* **1995**, *97*, 65.

[2] S. S. Divekar, B. M. Bhanage, R. M. Deshpande, R. V. Gholap, R. V. Chaudhari, *J. Mol. Catal.* **1994**, *91*, L1.

[3] a) M. J. H. Russel, B. A. Murrer (Johnson Matthey), US-A 4399312, **1983** [*Chem. Abstr.* **1982**, *97*, P23291n]; b) H. Bahrmann, P. Lappe (Hoechst AG), *Eur. Pat. Appl. 602463*, **1994** [*Chem. Abstr.* **1994**, *121*, P107982r]; c) T. Bartik, B. Bartik, B. E. Hanson, *J. Mol. Catal.* **1994**, *88*, 43.

[4] R. V. Chaudhari, B. M. Bhanage, R. M. Deshpande, H. Delmas, *Nature* **1995**, *373*, 501.

[5] a) H. Ding, B. E. Hanson, T. Bartik, B. Bartik, *Organometallics* **1994**, *13*, 3761; b) H. Ding, T. E. Glass, B. E. Hanson, *Inorg. Chem. Acta* **1995**, 229, 3289; c) B. Fell, G. Papadogianakis, *J. Mol. Catal.* **1991**, *66*, 143; d) H. Bahrmann, G. Deckers, W. Greb, P. Heymanns, P. Lappe, T. Mueller, J. Szameitat, E. Weibus (Hoechst AG), *Eur. Pat. Appl. 602442*, **1994** [*Chem. Abstr.* **1994**, *121*, P107978u].

[6] J. P. Arhancet, M. E. Davis, J. S. Merola, B. E. Hanson, *J. Catal.* **1990**, *121*, 327.

[7] F. Monteil, R. Queau, P. Kalck, *J. Organomet. Chem.* **1994**, *480*, 177.

[8] a) E. Monflier, E. Blouet, Y. Barbaux, A. Mortreux, *Angew. Chem.* **1994**, *106*, 2183; *Angew. Chem. Int. Ed. Engl.* **1994**, *33*, 2100; b) E. Monflier, S. Tilloy, G. Fremy, Y. Barbaux, A. Mortreux, *Tetrahedron Lett.* **1995**, *36*, 387.

[9] E. Monflier, Y. Castanet, A. Mortreux (Centre National de la Recherche Scientifique), FR-A 9500466, **1995**.

[10] The lack of activity of the α-cyclodextrin was also observed by W. R. Jackson during the biphasic hydroformylation but with hex-1-ene; J. R. Anderson, E. M. Campi, W. R. Jackson, *Catal. Lett.* **1991**, *9*, 55.

[11] a) D. Duchene, D. Wouessidjewe, *J. Coord. Chem.* **1992**, *27*, 223; b) H. Ikeda, R. Kojin, C. J. Yoon, T. Ikeda, *J. Inclusion Phenom. Mol. Recognit. Chem.* **1989**, *7*, 11; c) C. M. Spencer, J. F. Stoddart, R. Zarzycki, *J. Chem. Soc. Perkin Trans 2* **1987**, 1323; d) Y. Kubota, T. Tanimoto, S. Horiyama, K. Koizumi, *Carbohyd. Res.* **1989**, *192*, 159.

[12] M. Czugler, E. Ecke, J. J. Stezowski, *J. Chem. Soc. Chem. Commun.* **1981**, 1294.

[13] H. M. Colquhoun, J. F. Stoddart, D. J. Williams, *Angew. Chem.* **1986**, *98*, 483; *Angew. Chem. Int. Ed. Engl.* **1986**, *25*, 487.

[14] G. Wenz, *Angew. Chem.* **1994**, *106*, 851; *Angew. Chem. Int. Ed. Engl.* **1994**, *33*, 803.

[15] R. Gärtner, B. Cornils, H. Springer, P. Lappe (Ruhrchemie AG), DE-B 3235030, **1982** [*Chem. Abstr.* **1984**, *101*, P55331t].

Facial Diastereoselectivity in the Paternò–Büchi Reaction of Chiral Silyl Enol Ethers**

Thorsten Bach,* Kai Jödicke, Kristian Kather, and Jürgen Hecht

The [2 + 2] photocycloaddition of alkenes to carbonyl compounds commonly known as the Paternò–Büchi reaction provides an efficient and straightforward route to functionalized oxetanes.[1] By employing chiral auxiliaries it has become possible to photochemically produce enantiomerically pure oxetanes.[2] Studies by Scharf et al. impressively demonstrated that the two diastereotopic carbonyl faces can be well differentiated in phenyl glyoxylates of 8-phenylmenthol and related concave alcohols.[3] Besides the auxiliary-directed methodology there are several procedures that employ cyclic substrates to establish a stereoselective carbonyl photocycloaddition.[4] In these cases a stereogenic center within the ring system is responsible for a successful side differentiation. Contrary to the auxiliary-directed method, the chiral information is not removed after the reaction but is utilized for further synthetic operations. Analogously acyclic chiral substrates have not yet been employed for the preparation of enantiomerically pure oxetanes. Chiral aldehydes, which showed a remarkable Cram selectivity in nucleophilic addition reactions, proved less selective as carbonyl substrates in Paternò–Büchi reactions and yielded an unsatisfactory mixture of diastereoisomers.[5]

In connection with our studies on the regio- and stereoselective photocycloaddition of silyl enol ethers to aromatic aldehydes,[6] we were intrigued by a possible synthesis of enantiomerically pure oxetanes according to the principles of acyclic stereoselection. We started our investigations with a single carbonyl compound (benzaldehyde) and left the α-substituent on the silyl enol ether unchanged.[7] The only parameter varied was the γ-substituent on the silyl enol ether. The starting materials *rac*-**1** were readily accessible in racemic form by addition of the appropriate cuprates to 2,2-dimethyl-4-hexen-3-one and subsequent silylation. Upon irradiation of these substrates in the presence of benzaldehyde the desired oxetanes were produced as one of four possible pairs of diastereoisomers *rac*-**2**/*rac*-**3** (the formula of only one enantiomer is shown in each case). Based on our previous studies[6c, d] it appears likely that the relative configuration of the three substituents within the oxetane ring is fixed. The ratio of the two diastereoisomers found therefore reflects the facial diastereoselectivity which is induced by the stereogenic center. This ratio increases with increasing size of the substituent R and is considerably high for some examples (Table 1).

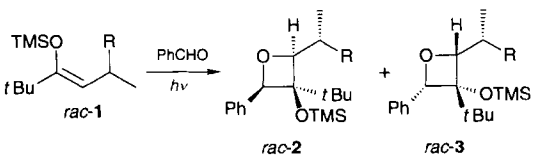

[*] Dr. T. Bach, Dipl.-Chem. K. Jödicke, Dipl.-Chem. K. Kather, Dipl.-Chem. J. Hecht[+]
Organisch-chemisches Institut der Universität
Orléansring 23, D-48149 Münster (Germany)
Telefax: Int. code + (251)83-9772
e-mail: bacht@uni-muenster.de

[+] X-ray crystallography

[**] This project was generously supported by the Deutsche Forschungsgemeinschaft, the Fonds der Chemischen Industrie, the Gesellschaft zur Förderung der Westfälischen Wilhelms-Universität, and the Dr. Otto Röhm-Gedächtnisstiftung. We thank Mrs. B. Wibbeling for her help with the X-ray crystallographic measurement. The continuing support of Prof. Dr. D. Hoppe is gratefully acknowleged.

Table 1. Yields and diastereomeric ratios (*d.r.*) observed in the photocycloaddition of benzaldehyde to the silyl enol ethers *rac*-**1** with benzene as solvent.

Alkene	R	*T*[°C]	*t*[h][a]	Yield[%][b]	*d.r.*(**2**:**3**)[c]
1a	Et	30	4	61	61:39
1b	*i*Pr	30	4	57	70:30
1c	*t*Bu	30	4	64	92:8
1d	Ph	30	4	72	69:31
1d	Ph	−30[d]	6	51	58:42
1e	$SiMe_2Ph$	30	9	44	95:5

[a] Irradiation time. [b] Total yield of both diastereoisomers (*rac*-**2** and *rac*-**3**). [c] Diastereomeric ratios (*d.r.*) were determined by GLC analyses of the crude product mixture and were checked by ^{1}H NMR spectroscopy. [d] *n*-Hexane as solvent.

The 3-(silyloxy)oxetanes *rac*-**2** and *rac*-**3** are easy to identify by ^{1}H NMR spectroscopy because of their characteristic singlet (2-H of the oxetane). The detection and quantification of the regioisomeric 2-(silyloxy)oxetanes is difficult. In general, they are not produced stereoselectively in the examples under scrutiny and they are sensitive to hydrolysis. Based on the GLC data an upper limit for the amount of regioisomers formed may be estimated and one finds a decrease of regioselectivity with increasing size of the β-alkyl substituent. Silyl enol ether *rac*-**1e** gave the worst ratio (70:30), a result which explains at least partially the low yield obtained in this example.

In order to elucidate the configuration of the major diastereoisomers, we have studied compound *rac*-**2d** by X-ray crystallography.[8] The preferred attack of the photoexcited carbonyl compound on the silyl enol ether can be obviously explained by invoking the influence of 1,3-allylic strain.[9, 10] The conformational rigidity facilitates the differentiation of the diastereotopic alkene faces, and the approach of the electrophile takes place preferentially from the less shielded side. Stereoelectronic considerations lead to a similar result.[11] In the course of the reaction, after addition of the carbonyl triplet to a putative 1,4-triplet biradical (^{3}D) the relative configuration of the oxetane ring is directed by previously discussed phenomena (free rotation in ^{3}D, intersystem crossing,[12] cleavage vs. ring closure in a 1,4-singlet biradical).[6b, d]

Since there is a plethora of methods for the stereoselective 1,4-addition to Michael acceptors,[13] enantiomerically pure silyl enol ethers can be synthesized in a few steps. As an example we converted the previously described acid **4**[14] into the corresponding ketone **5** from which the silyl enol ether was readily obtained. Photocycloaddition gave oxetane **2d** as the major product; its enantiomeric purity was determined by shift experiments as >95% *ee*[15] (Scheme 1). The reaction proceeds without racemization at the stereogenic center responsible for the stereoselectivity.

As a substrate with a polar substituent R we chose the silyl enol ether *rac*-**1f** which displayed a good diastereoselectivity (*d.r.* = 85/15) upon irradiation in the presence of benzaldehyde. The major diastereoisomer *rac*-**2f** was isolated in 54% yield and

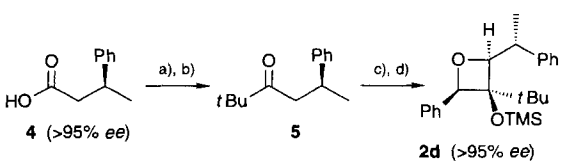

Scheme 1. Preparation of the enantiomerically pure oxetane **2d**. a) $SOCl_2$ (1.5 equiv), reflux, 6 h, 92%; b) *t*BuMgCl (1.5 equiv), CuCl (0.2 equiv) in Et_2O, −78 °C, 2 h, 93%; c) TMSCl, lithium diisopropylamide (LDA) in THF, −78 °C to RT, 65%; d) PhCHO in benzene, *hv*, 5 h, 51% (+ 22% **3d**).

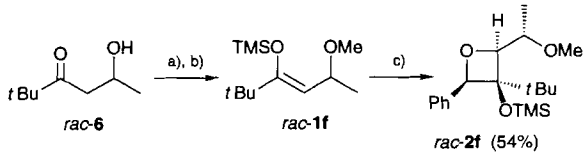

Scheme 2. Diastereoselective synthesis of the oxetane *rac*-**2f** from the ketone *rac*-**6**. a) Me_3OBF_4 (1.5 equiv), 1,8-bis(dimethylamino)naphthalene (2 equiv) in CH_2Cl_2, RT, 10 d, 58%; b) TMSCl, LDA in THF, −78 °C to RT, 72%; c) PhCHO in benzene, *hv*, 4 h, 54%.

has the depicted configuration (Scheme 2). To determine the relative configuration the noncrystalline product *rac*-**2f** was deprotected (K_2CO_3, MeOH) and the 3-oxetanol *rac*-**7** obtained in this way was crystallized from ether and characterized by a crystal structure analysis (Fig. 1).[16]

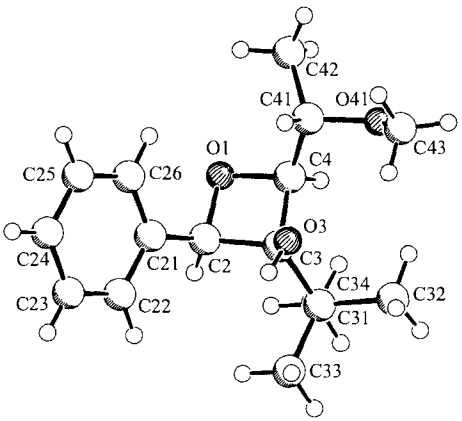

Fig. 1. Crystal structure of the 3-oxetanol *rac*-**7** obtained by desilylation from the 3-(silyloxy)oxetane *rac*-**2f**.

As a possible explanation for the mode of attack the "inside alkoxy" model first suggested by Houk may be invoked.[17] The steric difference between a methyl group and a hydrogen atom attached to the stereogenic center is responsible for the facial diastereoselectivity.

Two examples were used to demonstrate that the oxetanes which are available according to the methodology described herein may also be employed for the stereoselective construction of acyclic molecules. The hydrogenolytic ring opening[18] of oxetane *rac*-**2f** (cleavage of the bond between O and C-2) leads to a partially protected triol *rac*-**8** and the new fluoride-promoted fragmentation[19] of *rac*-**2e** (cleavage of the bond between O and C-4) to the (*E*)-alkenediol *rac*-**9**.

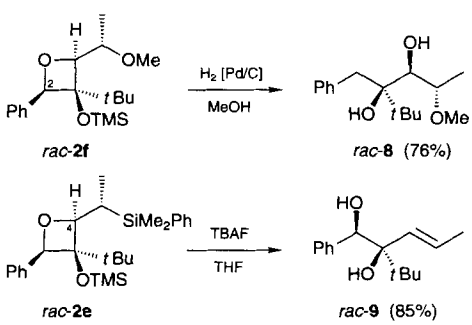

Experimental Procedure

Silyl enol ether (4.5 mmol) was dissolved in benzene (8 mL) in a quartz tube. The irradiation was started (300 nm; light source: Rayonet RPR 3000) and a solution of benzaldehyde (159 mg, 1.5 mmol, 152 μL) in benzene (2 mL) was slowly added to the reaction mixture by a syringe (within ca. 2 h). As soon as the aldehyde was fully consumed (TLC) the irradiation was stopped and the solvent evaporated in vacuo. The diastereomeric ratio was determined by GLC and ^{1}H NMR analyses. Excess silyl enol ether and the desired oxetane were obtained by column chromatography (flash chromatography; eluent: cyclohexane/ethyl acetate as a gradient 200/1 → 95/5). For oxetanes *rac*-**2d**/*rac*-**3d** and *rac*-**2f**/*rac*-**3f** a complete separation of diastereoisomers was possible. In the other examples only an enrichment of the major diastereoisomers could be achieved. All compounds not yet reported were characterized by spectroscopic methods (^{1}H, ^{13}C, IR, MS) and gave correct elemental analyses (C, H ± 0.3%).

Received: May 9, 1995 [Z7968IE]
German version: *Angew. Chem.* **1995**, *107*, 2455–2457

Keywords: asymmetric syntheses · cycloadditions · oxetanes · Paternò–Büchi reactions · photochemistry

[1] a) J. A. Porco, S. L. Schreiber in *Comprehensive Organic Synthesis Vol. 5* (Eds.: B. Trost, I. Fleming, L. A. Paquette), Pergamon, Oxford, **1991**, pp. 151–192; b) H. A. J. Carless in *Synthetic Organic Photochemistry* (Ed.: W. M. Horspool), Plenum, New York, **1984**, pp. 425–487; c) G. Jones II in *Organic Photochemistry Vol. 5* (Ed.: A. Padwa), Dekker, New York, **1981**, pp. 1–123; d) D. A. Arnold, *Adv. Photochem.* **1968**, *6*, 301–423.

[2] Review: Y. Inoue, *Chem. Rev.* **1992**, *92*, 741–770.

[3] H. Buschmann, H.-D. Scharf, N. Hoffmann, P. Esser, *Angew. Chem.* **1991**, *103*, 480–518; *Angew. Chem. Int. Ed. Engl.* **1991**, *30*, 477–515 and references therein.

[4] Examples: a) D. R. Morton, R. A. Morge, *J. Org. Chem.* **1978**, *43*, 2093–2101; b) Y. Araki, K. Senna, K. Matsuura, Y. Ishido, *Carbohydr. Res.* **1978**, *60*, 389–395; c) S. Vasudevan, C. P. Brock, D. S. Watt, H. Morita, *J. Org. Chem.* **1994**, *59*, 4677–4679.

[5] S. L. Schreiber, *Science* **1985**, *227*, 857–863.

[6] a) T. Bach, *Tetrahedron Lett.* **1991**, *32*, 7037–7038; b) T. Bach, K. Jödicke, *Chem. Ber.* **1993**, *126*, 2457–2466; c) T. Bach, *Tetrahedron Lett.* **1994**, *35*, 5845–5848; d) T. Bach, *Liebigs Ann.* **1995**, 855–866.

[7] Since the silyl enol ethers *rac*-**1** all have (*Z*)-configuration the size of the α-substituent has presumably no influence on the facial diastereoselectivity. The choice of the *tert*-butyl group proved advantageous in view of the desired determination of the enantiomeric purity for oxetane **2d**.

[8] T. Bach, K. Jödicke, M. Grehl, R. Fröhlich, unpublished.

[9] Review: R. W. Hoffmann, *Chem. Rev.* **1989**, *89*, 1841–1860.

[10] The course of radical additions to a prostereogenic C=C double bond is often directed by a neighboring stereogenic center in a related way. However, almost any of these additions include a nucleophilic attack on an electron deficient double bond, see a) W. Smadja, *Synlett* **1994**, 1–26; b) T. Morikawa, Y. Washio, S. Harada, R. Hanai, T. Kayashita, H. Nemoto, M. Shiro, T. Taguchi, *J. Chem. Soc. Perkin Trans. 1* **1995**, 271–281 and references therein.

[11] G. J. McGarvey, J. M. Williams, *J. Am. Chem. Soc.* **1985**, *107*, 1435–1437 and references therein.

[12] For a comprehensive review on the various intersystem crossing geometries related to oxetane formation, see: A. G. Griesbeck, H. Mauder, S. Stadtmüller, *Acc. Chem. Res.* **1994**, *27*, 70–75.

[13] B. E. Rossiter, N. M. Swingle, *Chem. Rev.* **1992**, *92*, 771–806.

[14] T. Mukaiyama, N. Iwasawa, *Chem. Lett.* **1981**, 913–916.

[15] The shift experiments were conducted with tris-[3-(heptafluoropropylhydroxymethylene)-D-camphorato]europium [Eu(hfc)$_3$], and the *ee* values were determined by integration of the separated signals obtained for the *tert*-butyl group at C-3 of the oxetane. Base line separation was achieved by employing 10 mg of the reagent for 15 mg of *rac*-**2d** in 1 mL $CDCl_3$. Under these conditions **2d** displayed a single line only.

[16] Crystal data for 3-oxetanol *rac*-**7** ($C_{16}H_{24}O_3$, M_r = 264.35): crystal size 0.25 × 0.2 × 0.05 mm, a = 10.278(2), b = 18.493(4), c = 8.458(1) Å, β = 108.40(2)°, V = 1530.3(5) Å^3, ρ_{calcd} = 1.147 g cm^{-3}, μm = 6.2 cm^{-1}, Z = 4, monoclinic, space group Cc (No. 9), Enraf-Nonius-CAD4 diffractometer, λ = 1.54178 Å, ω-2θ scan, 1648 reflections ($-h$, $+k$, $\pm l$), $[\sin\theta/\lambda]_{max}$ 0.62 Å^{-1}, 1647 independent and 1235 observed reflections [$F \geq 4\sigma(F)$], refinement of 178 parameters, R = 0.051, wR^2 = 0.131, direct methods, hydrogen atoms calculated. Further details of the crystal structure investigation may be obtained from the Fachinformationszentrum Karlsruhe, D-76344 Eggenstein-Leopoldshafen (Germany), on quoting the depository number CSD-401769.

[17] K. N. Houk, M. N. Paddon-Row, N. G. Rondan, Y.-D. Wu, F. K. Brown, D. C. Spellmeyer, J. T. Metz, Y. Li, R. J. Loncharich, *Science* **1986**, *231*, 1108–1117.

[18] a) T. Bach, *Tetrahedron Lett.* **1994**, *35*, 1855–1858; b) T. Bach, *Liebigs Ann.* **1995**, 1045–1053.

[19] For a projected ring opening of this type, see: T. Bach, K. Kather, *Tetrahedron* **1994**, *50*, 12319–12328.

A Tailor-Made Metallocene for the Copolymerization of Ethene with Bulky Cycloalkenes**

Walter Kaminsky,* Rüdiger Engehausen, and Jürgen Kopf

Dedicated to Professor Joachim Klein on the occasion of his 60th birthday

Metallocenes in combination with methylaluminoxane (MAO) have gained great prominence as catalysts for the polymerization of olefins. Remarkable is their ability to polymerize cycloolefins such as cyclopentene, norbornene, and dimethanooctahydronaphthalene (DMON) to give homo- and copolymers in which only the double bond is opened and not the ring.[1] This distinguishes catalysis with metallocenes from that with common Ziegler–Natta catalysts or metathesis catalysts which are known to produce polymers containing ring-opened structures and elastomeric polymers by ring-opening polymerization.[2] Polycycloolefins prepared with metallocene catalysts exhibit extraordinarily high melting points of 400 °C and above due to their rigid, tactic structures. The high melting points prevent melt processing of these polymers. However, the copolymerization of cycloolefins with ethene results in cycloolefin copolymers (COC) with interesting properties. These copolymers are amorphous if more than 15 mol% of cycloolefin is incorporated, feature glass transition temperatures exceeding 200 °C, have high mechanical strength, and are stable towards common solvents. Since they contain no aromatic groups or double bonds their interaction with light waves is modest. Therefore they are well suited for optoelectronic applications in data transfer and storage (polymer optical fibers, compact discs); other possible applications have been discussed recently.[3] C_2- and C_s-symmetric metallocenes perform much better in the homopolymerization of cycloolefins and their copolymerization with ethene than compounds with higher symmetry like bis(cyclopentadienyl)zirconium dichloride which shows only low polymerization activities.

Zirconocenes like **1**[4] and **2**[5] containing unequally sized π ligands incorporate sterically demanding cycloolefins at high speeds into the polymer chain. The best copolymerization results are obtained with the C_1-symmetric **3** which up to now has not been characterized in detail and has only been applied in the polymerization of styrene.[6]

[{Me_2C(fluo)(Cp)}$ZrCl_2$] **1**

[{Ph_2C(fluo)(Cp)}$ZrCl_2$] **2**

[{Ph_2C(ind)(Cp)}$ZrCl_2$] **3**

The structure of **3**, which crystallizes as yellow needles, was elucidated by single-crystal X-ray diffraction studies (Fig. 1).[8] The zirconium atom resides in a tetrahedral environment surrounded by two chlorine atoms and the centroids (Cen) of the five-membered rings of the indenyl and the cyclopentadienyl groups. The centroid-Zr-centroid angle (117.14°) in **3** which is

[*] Prof. Dr. W. Kaminsky, Dr. R. Engehausen
Institut für Technische und Makromolekular Chemie der Universität
Bundesstrasse 45, D-20146 Hamburg (Germany)
Telefax: Int. code +(40) 41236008
Dr. J. Kopf
Institut für Anorganische und Angewandte Chemie der Universität
Martin-Luther-King-Platz, D-20146 Hamburg (Germany)

[**] This work was financially supported by the Bundesministerium für Forschung und Technologie, the Hoechst AG, and the Fonds der chemischen Industrie.

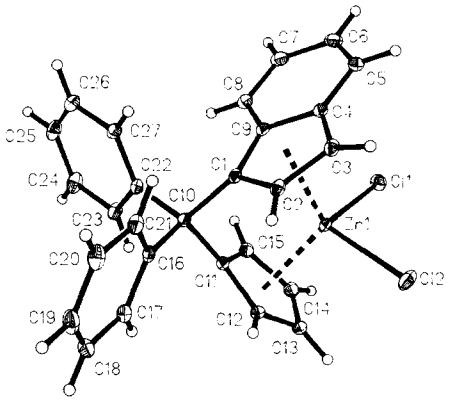

Fig. 1. Crystal structure of **3**. Selected bond lengths [Å] and angles [°]: Zr1-Cl1 2.404(1), Zr1-Cl2 2.433(1), Zr1-C1 2.436(2), Zr1-C2 2.425(2), Zr1-C3 2.551(2), Zr1-C4 2.631(2), Zr1-C9 2.536(2), Zr1-C11 2.446(2), Zr1-C12 2.451(2), Zr1-C13 2.523(2), Zr1-C14 (2.536(2), Zr1-C15 2.459(2), C1-C10 1.536(2), C10-C11 1.534(2), C10-C16 1.533(3), C10-C22 1.534(2); Cl1-Zr1-Cl2 102.63(2), Cen-Zr1-Cen 117.14(2), C1-C10-C11 99.1(1), C16-C10-C22 107.3(2), C1-C10-C16 112.9(2), C1-C10-C22 111.8(2), C11-C10-C16 111.5(2), C11-C10-C22 114.3(2).

important for the polymerization of sterically demanding cycloalkenes, exactly matches that of the isopropyl-bridged analogue [{Me_2C(ind)(Cp)}$ZrCl_2$], while the Cl-ZrCl angle of 102.63° in **3** is 2.5° larger. Compared to the corresponding angle in **1**, this angle is 5° larger. This somewhat more open angle should facilitate the polymerization of sterically demanding cycloalkenes. This effect is strengthened by the presence of electron-rich phenyl groups in the bridge, since they cause an increased activity which probably originates from enhanced stabilization of a cationic active species.[7]

Metallocene **3** is well-suited for the copolymerization of ethene with bulky cycloolefins like 1,4,5,8-dimethano-1,2,3,4,4a,5,8,8a-octahydronaphthalene (DMON) and 1,4,5,8,9,10-trimethano-1,2,3,4,4a,5,8,8a,9,9a,10,10a-dodecahydroanthracene (TMDA) which are prepared from the Diels–Alder reaction of cyclopentadiene and norbornene. Table 1 summarizes the results of the copolymerization of ethene and DMON by selected metallocene/MAO catalysts. A comparison of the activities achieved by **3** to those attained by the fluorenyl-cyclopentadienyl systems (structures **1** and **2**) shows the latter to be more active at low temperatures, while at high temperatures **3** is superior.

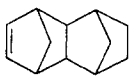

DMON

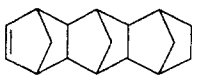

TMDA

Table 1. Comparison of the copolymerization of ethene and DMNO with different metallocene/MAO catalysts at various temperatures (metallocene concentration: 10^{-5} mol L^{-1}; MAO: 300 mg in 100 mL toluene) [a].

Catalyst	T [°C]	C_D/C_E	A	M_n	Incorp. [mol%]	T_g [°C]
[{Me_2C(fluo)(Cp)}$ZrCl_2$] **1**	50	6.58	940	82000	28	125.1
[{Ph_2C(fluo)(Cp)}$ZrCl_2$] **2**	50	13.16	230	60000	50	155.2
	70	16.3	330	23000	58	171.6
	90	20.49	24	n.d.	68	187.5
[{Ph_2C(ind)(Cp)}$ZrCl_2$] **3**	50	13.16	60	n.d.	59	162.4
	70	16.3	65	11000	68	194.3
	90	20.49	78	16000	84	201.5
	90	30.73	31	13000	85	215.7
[{Me_2C(fluo)(Cp)}$HfCl_2$] **4**	50	13.16	6	n.d.	57	155.1
	70	16.03	32	44000	67	182.2
	90	20.49	16	25000	73	203

[a] C_D/C_E: Molar ratio DMNO:ethene, A: Activity in kg copolymer per mol metallocene per hour, M_n: Average molecular weight determined from viscosity, calculated as polyethylene; n.d. = not determined, Incorp.: Incorporation of DMON in the copolymer, T_g: Glass transition temperature.

The hafnocene **4**[4] is less active than the zirconocenes by one order of magnitude. The average molecular mass of the polymer decreases with increasing temperature of polymerization, but interpretation is hindered by different copolymer compositions. Compound **3** behaves differently in the catalysis: The overall low molecular mass of the copolymer increases with rising temperature and only decreases at very high DMON/ethene ratios. The metallocene **3** always incorporates higher proportions of DMON in the copolymer under comparable conditions.

The copolymers have melting points of 60–70 °C at low DMON incorporation, if the incorporation rate exceeds 15 mol% only a glass transition is observed. Metallocene **3** is able to incorporate more than 80 mol% of DMON, forming a copolymer with a glass transition temperature of 215 °C. The various catalysts produce copolymers with different microstructures as revealed by ^{13}C NMR spectroscopy and WAXS.[9] The copolymers produced by catalysis with **3** exhibit a less-ordered structure; they are less crystalline than copolymers produced by C_s-symmetric metallocenes **1** and **2**.

The copolymerization is characterized by the copolymerization parameter r_1. This expresses how much faster ethene is incorporated than DMON in the copolymer. The parameter r_2 was also determined which gives the ratio of DMON to ethene incorporation. Further interpretation is not possible due to the lack of a model for the mechanism of insertion. The calculations were done according to Mayo–Lewis and Finemann–Ross models[10] from kinetic data and copolymer composition as detected by ^{13}C NMR spectroscopy. Table 2 gives the results for the three catalysts.

Table 2. Copolymerization parameters of the ethene/DMON copolymerization at 50 °C.

Catalyst	r_1	r_2	$r_1 \times r_2$
[{Ph_2C(fluo)(Cp)}$ZrCl_2$] **2**	7.0	0.02	0.14
[{Ph_2C(ind)(Cp)}$ZrCl_2$] **3**	6.4	0.10	0.64
[{Me_2C(fluo)(Cp)}$HfCl_2$] **4**	7.1	0.04	0.28

The zirconocene **3** inserts ethene only 6.4 times faster than DMON and therefore has the lowest r_1 value. Thus, it inserts the bulky cycloolefin better than the two C_s symmetric catalysts **1** and **2**. C_2-symmetric metallocenes like *rac*-[en(ind)$_2$]$ZrCl_2$ or *rac*-[en(indH_4)$_2$]$ZrCl_2$ give r_1 parameters of 15 and 50, respectively.[11] The product $r_1 \times r_2$ is less than 1 for all metallocenes tested. For the metallocene **3** this product is 0.63, which is closest to that of a statistical copolymer (1). The smaller $r_1 \times r_2$ values observed in case of the C_s-symmetric metallocenes indicate a tendency to alternation.

Analogous copolymerizations of ethene with the even more bulky TMDA were carried out using zirconocenes **2** and **3** as catalysts. Table 3 summarizes the results. As already observed for the DMON/ethene system, the activity and molecular mass decreases as the cycloolefin/ethene ratio and thereby the incorporation of cycloolefin increases. Again **3** incorporates more TMDA than the metallocene **2**. The observation of melting points by DSC measurements indicates a higher amount of crystalline polyethylene domains in these copolymers. The glass transition temperature of copolymers containing the same amount of cyclic monomer units is higher for TMDA/ethene

Table 3. Copolymerization of TMDA and ethene with two zirconocene/MAO catalysts at 50 °C [a].

Catalyst	C_T/C_E	A	M_n	Incorp. [mol %]	T_g [°C]
[{Ph_2C(fluo)(Cp)}$ZrCl_2$] **2**	0	1800	400000	0	(134.4)
	1.64	780	59000	9	65.5 (132.1)
	3.29	232	30000	18	96.1 (128.0)
	6.58	41	22000	27	110 (124.4)
[{Ph_2C(ind)(Cp)}$ZrCl_2$] **3**	3.29	33	17000	20	(128.2)

[a] C_T/C_E: Molar ratio of TMDA:ethene. A: Activity in kg polmyer per mol metallocene per hour. M_n: Average molecular weight determined from viscosity, Incorp.: Incorporation of TMDA in the copolymer. T_g: Glass transition temperature, melting point in parentheses.

copolymers than for DMON/ethene copolymers. At 50 °C the r_1 value for the TMDA/ethene copolymerization is 15.6, the r_2 value is 0.06, and $r_1 \times r_2$ is 0.94 (cf. Table 3).

The results presented here indicate that the performance of different metallocenes in the copolymerization of ethene and cycloolefins strongly depends on the metallocene used. The copolymers produced by the zirconocene **3** feature the highest incorporation rates of bulky comonomers.

Received: April 7, 1995 [Z 7875 IE]
German version: *Angew. Chem.* **1995**, *107*, 2469–2471

Keywords: catalysis · copolymerizations · cycloolefin copolymers · Sandwich complexes

[1] W. Kaminsky, R. Spiehl, *Makromol. Chem.* **1989**, *190*, 515–526; W. Kaminsky, A. Bark, R. Steiger, *J. Mol. Catal.* **1992**, *74*, 109–119; S. Collins, D. G. Ward, *J. Am. Chem. Soc.* **1992**, *114*, 5460–5462; S. Collins, W. M. Kelly, D. A. Holden, *Macromolecules* **1992**, *25*, 1780–1785; W. Kaminsky, A. Noll, *Polym. Bull.* **1993**, *31*, 175–182; H. Cherdron, M.-J. Brekner, F. Osan, *Angew. Makromol. Chem.* **1994**, *223*, 121–133.

[2] G. Dall'Asta, *Makromol. Chem.* **1972**, *154*, 1–19; G. Natta, G. Dall'Asta, G. Mazzanti, *Angew. Chem.* **1964**, *76*, 765–772; *Angew. Chem. Int. Ed. Engl.* **1964**, *3*, 723–729; T. Sagane, A. Mizuno, T. Takata, *Makromol. Chem.* **1992**, *193*, 2697–2711; C. Mehler, W. Risse, *Makromol. Chem. Rapid Commun.* **1992**, *13*, 455–459; D. S. Breslow, *Prog. Polym. Sci.* **1993**, *18*, 1141–1195; Ref. [9a].

[3] W. Spaleck, *Hoechst High Chem.* **1993**, *14*, 44–48; R. Mülhaupt, *Nachr. Chem. Tech. Lab.* **1993**, *41*, 1341–1351.

[4] J. A. Ewen, L. Haspeslagh, J. L. Atwood, H. Zhang, *J. Am. Chem. Soc.* **1987**, *109*, 6544–6545; A. Razavi, J. Ferrara, *J. Organomet. Chem.* **1992**, *435*, 299–310.

[5] A. Winter, J. Rohrmann, M. Antberg, V. Dolle, W. Spaleck (Hoechst AG), DE-B 3907965, **1990** [*Chem. Abstr.* **1991**, *114*, 165103].

[6] M. L. H. Green, N. Ishihara, *J. Chem. Soc. Dalton Trans.* **1994**, 657–665; N. Ishihara, *Macromol. Symp.* **1995**, *89*, 553–562.

[7] W. Kaminsky, *Catal. Today* **1994**, *20*, 257–271; H.-H. Brintzinger, D. Fischer, R. Mülhaupt, B. Rieger, R. Waymouth, *Angew. Chem.* **1995**, *107*, 1255–1283; *Angew. Chem. Int. Ed. Engl.* **1995**, *34*, 1143–1170.

[8] Crystallographic details for **3**: crystallization from toluene; monoclinic; space group $P2_1/n$, $Z = 4$, $a = 12.358(2)$, $b = 13.969(3)$, $c = 13.482(3)$, $\beta = 111.74(2)$, $V = 2161.8(8)$ Å^3, $\varrho_{calcd.} = 1.556$ gcm^{-3}; 5377 reflections measured; 4985 of them independent, range $\theta = 2.30–27.55$°; temperature 153 K; number of refined parameters 292, reflection to parameter ratio 17.07, least squares method $R = 0.0361$; diffractometer Hilger & Watts (Y 290). Further details of the crystal structure investigation may be obtained from the Fachinformationszentrum Karlsruhe, D-76344 Eggenstein-Leopoldsbafen (Germany), on quoting the depository number CSD-401676.

[9] a) G. M. Benedikt, B. L. Goodall, N. S. Marchant, L. F. Rhodes, *New J. Chem.* **1994**, *18*, 105–114; b) G. H. Llinas, R. O. Day, M. D. Rausch, J. C. W. Chien, *Organometallics* **1993**, *12*, 1283–1288.

[10] F. R. Mayo, F. M. Lewis, *J. Am. Chem. Soc.* **1944**, *66*, 1594–1601; M. Finemann, S. D. Ross, *J. Polym. Sci.* **1950**, *5*, 259–262.

[11] W. Kaminsky, A. Bark, M. Arndt, *Makromol. Chem. Macromol. Symp.* **1991**, *47*, 83–93.

Antibody-Catalyzed Phosphate Triester Hydrolysis**

Jonathan S. Rosenblum, Lee-Chiang Lo, Tingyu Li, Kim D. Janda,* and Richard A. Lerner*

Dedicated to the memory of James D. Bain

Phosphate ester hydrolysis has challenged biologists and chemists for many years. While attention has focused on phosphate mono- and diesters since these have the best understood biological properties, phosphate triesters are also biologically relevant. The significance of phosphotriesters in biology ranges from their essential role in the adaptive response in *E. coli*[1] to their use as prodrugs for nucleoside analog pharmaceuticals.[2, 3] Derivatives of phosphate triesters are used as insecticides and are potent biological warfare agents. This class of compounds includes sarin, isopropyl(methyl)phosphonofluoridate, which was recently used in a deadly bombing in a Japanese subway.[4] Although there are phosphotriesterases in nature, their natural substrates are not known.[5]

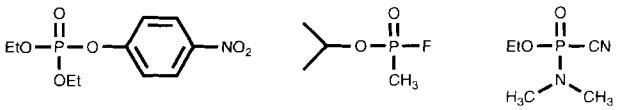

Paraoxon Sarin Tabun

In addition to their biological importance, phosphate esters present fundamental chemical issues relating to their unique hydrolytic stability[6] and involvement of a pentacoordinate transition state for hydrolysis. Antibodies catalyzing the hydrolysis of phosphate triesters would be interesting from biological and chemical points of view. Such antibodies could be used to interfere with the response of *E. coli* to mutagenic methylating agents, activate prodrugs (carboxylate ester prodrugs have been hydrolyzed by catalytic antibodies[7, 8]) or treat or prevent organophosphate neurotoxin poisoning.[9, 10] Such catalysts should also help define the structural and electrostatic requirements of the transition states for phosphate ester hydrolysis. Herein we describe an antibody capable of catalyzing phosphate triester hydrolysis.

The pentacoordinate transition state for base-promoted phosphate di- and triester hydrolysis arises from attack of hydroxide and leaving group extrusion in-line on the apical axis (Scheme 1). Whereas the tetrahedral intermediate of carboxylate ester hydrolysis is accurately mimicked by many functionalities,[11, 12] pentavalent centers are rare in organic chemistry (for recent exceptions see refs. [13,14]). Additionally, many pentavalent species are either toxic or unstable, decreasing their utility as haptens for immunization. Conversely, the unique electrostatic features of the transition state anticipated on the

[*] Prof. Dr. K. D. Janda, Prof. Dr. R. A. Lerner, J. S. Rosenblum, Dr. L.-C. Lo, Dr. T. Li
The Scripps Research Institute
Departments of Chemistry and Molecular Biology
10666 N. Torrey Pines Road, La Jolla, CA 92037 (USA)
Telefax: Int. code + (619)554-6068

[**] We acknowledge support from the Alfred P. Sloan Foundation, the National Institutes of Health (GM48351 to K. D. J.), and the National Science Foundation (predoctoral fellowship to J. S. R.). We thank Ping Fan and Tami Danon for expert technical support and Dr. Dee-Hua Huang for assistance with obtaining ^{31}P NMR spectra.

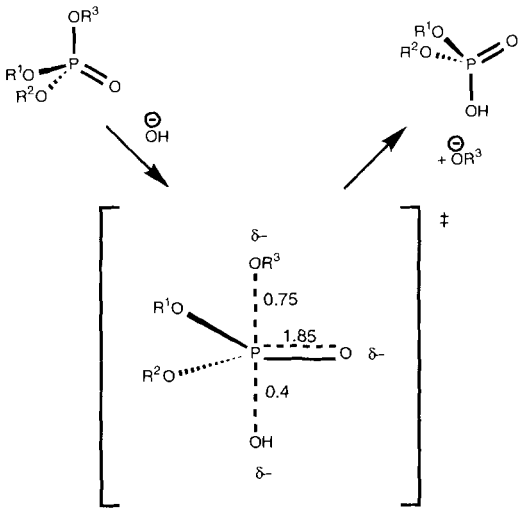

Scheme 1. Mechanism of phosphate triester hydrolysis emphasizing structure and electrostatics of the transition state. Numbers refer to bond order in the case of base-catalyzed paraoxon hydrolysis [27].

reaction coordinate are more easily mimicked. As such it is of interest to determine if a pentavalent species is a necessary feature of the hapten, or if addressing the electrostatic features of the transition state alone are sufficient to yield an efficient catalyst.

We have screened antibodies which recognize either an amine oxide-containing hapten or a quaternary amine-containing hapten for phosphotriesterase activity. Charged haptens are expected to induce antibodies that affect catalysis by either stabilization of a polar transition state or by elicitation of a reactive side chain that may act as a general base.[15-17] Hapten **1** contains an amine oxide whose dative bond overlaps with the scissile bond of **3** and the P=O bond of **4**. Any positive charge developing at the phosphorus center would be stabilized by anionic functionalities in the antibody combining site, induced by the positive pole of the amine oxide hapten **1**. The negative pole of the amine oxide corresponds to the developing negative charge on the oxygen atom of the leaving group in the transition state for the hydrolysis of **3**, or to a partial negative charge on the phosphoryl oxygen atom in the transition state for the hydrolysis of **4** (Scheme 2). As a result of regiospecific induction of countercharge, it may be possible, by comparing the hydrolysis of **3** and **4** by antibodies to **1**, to determine which of the partial negative charges in the transition state need to be stabilized.

Hapten **2** is a close analog of **1**, differing only in the substitution of a quaternary amine for the amine oxide functionality of **1**.[18] This hapten is expected to induce anionic but not cationic character in the antibody binding site and as such may help to further deconstruct the important charge parameters for transition state stabilization.

Twenty-five antibodies to **1** and 17 antibodies to **2**[19] were screened for their ability to catalyze the hydrolysis of **3** and **4**. Five antibodies to each hapten were catalytic. One antibody to **1**, Tx1-4C6,[19] was particularly efficient and was studied further. Reaction of Tx1-4C6 with **3** and **4** followed Michaelis–Menten kinetics (Fig. 1, Table 1). Antibody-catalyzed reactions were stoichiometrically inhibited by the hapten, could be saturated by substrate and displayed turnover. Antibody Tx1-4C6 bound hapten **1** with a K_d of 0.67 μM as determined by quenching of intrinsic antibody fluorescence by the hapten.

The rate of the uncatalyzed hydrolysis of **3** is slower than that of **4**, since **3** is stabilized by the generalized anomeric effect.[20]

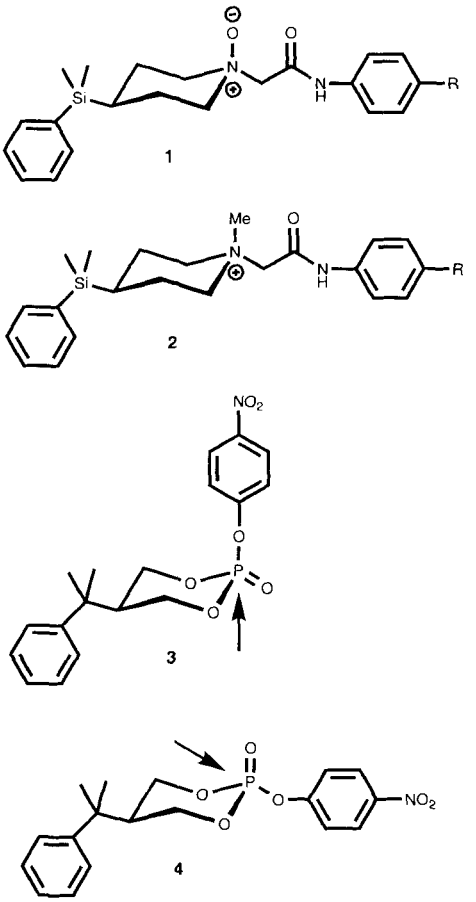

Scheme 2. Structural formulas of the haptens **1** and **2** and substrates **3** and **4**. Arrows indicate orientation of attacking hydroxide for in-line triester hydrolysis. R = linkage to protein (for immunization). R = $NHCOCH_3$ (for inhibition studies).

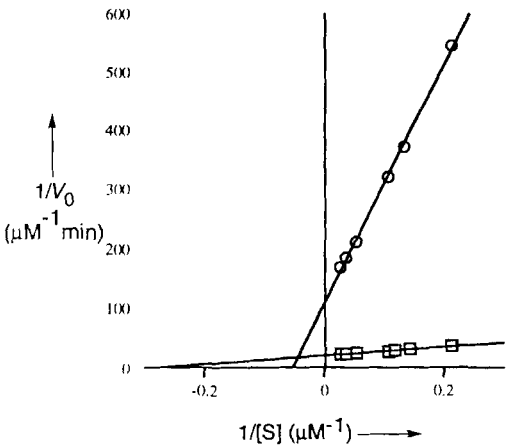

Fig. 1. Lineweaver–Burke plot of antibody Tx1-4C6 hydrolysis of **3** (□) and **4** (○). S = substrate, V_0 = initial rate.

Table 1. Kinetic parameters for Tx1-4C6-catalyzed hydrolysis of compounds **3** and **4**.

Substrate	k_{uncat} [min^{-1}]	k_{cat} [min^{-1}]	K_M [μM]
3	2.77×10^{-5}	1.01×10^{-2}	3.57
4	8.77×10^{-5}	1.85×10^{-3}	18.7

Interestingly, Tx1-4C6 was able to effect a reversal of intrinsic reactivity, catalyzing the hydrolysis of **3** more so than **4**, $k_{uncat}(\mathbf{3})/k_{uncat}(\mathbf{4}) = 0.316$; $k_{cat}(\mathbf{3})/k_{cat}(\mathbf{4}) = 5.46$. This reversal may be derived from either ground-state stabilization[21] or a tighter geometrical fit of the transition state for the hydrolysis of **3** than that of **4**. This differential accomodation can be rationalized in light of the structure of the eliciting hapten **1** (Scheme 2). For substrate **3**, the apical axis of the pentavalent phosphorus at the transition state overlaps with the axial orientation of the N–O bond in **1**.[19] thus stabilizing a mechanism in which the leaving group departs from a subtended angle of 180° relative to the three interacting atoms. By contrast, antibodies to amine oxide hapten **1** would be expected to polarize the P=O bond for substrate **4**. As **3** is a better substrate for Tx1-4C6, we suggest that polarization of the scissile bond for a concerted reaction is more profitable than polarization of the P=O bond which may favor a two-step reaction involving pseudorotation.[22]

Antibody Tx1-4C6 has a limited substrate range. It does not bind, and therefore does not hydrolyze, paraoxon. Likewise, Tx1-4C6 is not able to hydrolyze carboxylate esters related to **3** and **4**.

One of the powerful aspects of antibody catalysis is the ability to address selected features of the transition state of any chemical reaction. Here, we have demonstrated this principle and achieved phosphate ester hydrolysis by an antibody that was programmed to accomodate only the electrostatics of the transition state of the reaction. The best antibody catalysts were induced by amine oxide **1**, yet **2** also induced several catalysts, indicating that catalysis may be achieved by the singular event of lowering the energy of a developing positive charge in the transition state. But, as expected, better catalysis is achieved when additional features of the transition state, such as the developing negative charge at the leaving-group oxygen is addressed. In order to generate more efficient catalysts it will now be necessary to keep the electrostatic features of the antibody in place and address the more difficult geometric parameters. In this way we can learn about catalysis by building an enzyme piece by piece. Furthermore, through the development of antibodies we could explore whether the hydrolysis of phosphate diesters can be facilitated through a "triester-like" mechanism,[23, 24] in which the initial step is the protonation of the phosphate anion oxygen.

Experimental Procedure

3, **4**: *Alkylation of diethyl isopropylidenemalonate* [25]: To a solution of diethyl isopropylidenemalonate (10.0 g, 50 mmol) in anhydrous ether (20 mL) was slowly added phenylmagnesium bromide (50 mL, 50 mmol, 1.0 M in THF) at 0 °C. The reaction was kept at 0 °C for 30 min, then heated to reflux for 1 h. The reaction mixture was concentrated, poured into ice-cold diluted H_2SO_4, and extracted three times with EtOAc. The combined EtOAc solution was concentrated and the 1,4-addition product purified (3.8 g, 28%) by silica gel column chromatography eluted with hexane/EtOAc (8/1).

$LiAlH_4$ reduction of the diester: The diester (1.34 g) obtained was dissolved in anhydrous ether (42 mL), followed by slow addition of $LiAlH_4$ (0.37 g). The reaction was kept at room temperature overnight. Usual workup offered diol in 35% yield. ^1H NMR (300 MHz, $CDCl_3$): $\delta = 7.34$–7.27 (m, 4 H; aromatic), 7.21–7.16 (m, 1 H; aromatic), 3.78 (dd, $J = 10.4$, 3.7 Hz, 2 H), 3.70 (dd, $J = 10.4$, 9.8 Hz, 2 H), 2.15 (m, 1 H), 2.00 (bs, 2 H; *OH*).

Phosphorylation of the diol: The diol (145 mg) in THF (2 mL) was added dropwise to a solution of pyridine (133 μL) and *p*-nitrophenylphosphorodichloridate (210 mg) in THF (5 mL). The mixture was stirred at room temperature for 2 h, then concentrated. The desired products **3** (70 mg, 25%) and **4** (72 mg, 26%) were separated by silica gel column chromatography eluted with hexane/EtOAc (2/1). Compound **3**: $R_f = 0.27$. ^1H NMR (300 MHz, $CDCl_3$): $\delta = 8.22$ (d, $J = 9.2$ Hz, 2 H; aromatic), 7.39–7.24 (m, 7 H; aromatic), 4.32 (dd, $J = 10.9$, 4.9 Hz, 2 H), 4.26 (dd, $J = 10.9$, 4.9 Hz, 2 H), 2.68 (m, 1 H), 1.38 (s, 6 H; CH_3); ^{31}P NMR (300 MHz, $CDCl_3$, heteronuclear decoupled): $\delta = -13.37$. Compound **4**: $R_f = 0.20$, ^1H NMR (300 MHz, $CDCl_3$): $\delta = 8.22$ (d, $J = 9.2$ Hz, 2 H; aromatic), 7.38–7.22 (m, 7 H; aromatic), 4.48–4.36 (m, 4 H), 2.31 (m, 1 H), 1.47 (s, 6 H; CH_3); ^{31}P NMR (300 MHz, $CDCl_3$, heteronuclear decoupled): $\delta = -12.29$.

The stereochemistry of **3** and **4** was determined by comparing their R_f values, ^1H and ^{31}P NMR spectra with those of similar compounds from the literature [26].

Assays: All reactions were followed spectrophotometrically at 30 °C, following *p*-nitrophenolate production at 402 nm. The extinction coefficient determined under the reaction conditions was $1.80 \times 10^4\,M^{-1}\,cm^{-1}$. Typically, solutions of 50 mM Bicine, pH 8.5 with or without 5 μM 4C6 were equilibrated at the reaction conditions for 30 min. Reactions were initiated by addition of a constant volume of various concentrations of the substrate in DMSO. The final DMSO concentration was 0.375%. The reactions were followed for approximately 2 h, after which time less than ten percent of the substrate had been consumed.

Received: May 2, 1995
Revised version: July 24, 1995 [Z 7949 IE]
German version: *Angew. Chem.* **1995**, *107*, 2448–2450

Keywords: catalytic antibodies · electrostatic interactions · hydrolyses · phosphates · transition states

[1] B. M. Saget, G. C. Walker, *Proc. Natl. Acad. Sci. USA* **1994**, *91*, 9730–9734.
[2] C. Perigaud, A. M. Aubertin, S. Benzaria, H. Pelicano, J. L. Girardet, G. Maury, G. Gosselin, A. Kirn, J. L. Imbach, *Biochem. Pharmacol.* **1994**, *48*, 11–14.
[3] A. Namane, C. Gouyette, M. P. Fillion, G. Fillion, T. Huynh-Dinh, *J. Med. Chem.* **1992**, *35*, 3039–3044.
[4] N. D. Kristof, *The New York Times*, **1995**, A1, A6.
[5] S. R. Caldwell, J. R. Newcomb, K. A. Schlecht, F. M. Raushel, *Biochemistry* **1991**, *30*, 7438–7444.
[6] F. H. Westheimer, *Science* **1987**, *235*, 1173–1178.
[7] H. Miyashita, Y. Karaki, M. Kikuchi, I. Fujii, *Proc. Natl. Acad. Sci. USA* **1993**, *90*, 5337–5340.
[8] D. A. Campbell, B. Gong, L. M. Kochersperger, S. Yonkovich, M. A. Gallop, P. G. Schultz, *J. Am. Chem. Soc.* **1994**, *116*, 2165–2166.
[9] Y. Ashani, N. Rothschild, Y. Segall, D. Levanon, L. Raveh, *Life Sciences* **1991**, *49*, 367–374.
[10] E. Kaliste-Korhonen, P. Ylitalo, O. Hanninen, F. M. Raushel, *Toxicol. Appl. Pharm.* **1993**, *121*, 275–278.
[11] R. A. Lerner, S. J. Benkovic, P. G. Schultz, *Science* **1991**, *252*, 659–667.
[12] K. D. Janda, Y.-C. J. Chen, *The Pharmacology of Monoclonal Antibodies, Vol. 113*, Springer, Berlin, **1994**, p. 209–241.
[13] R. M. Moriarty, J. Hiratake, K. Liu, *J. Am. Chem. Soc.* **1990**, *112*, 8575–8577.
[14] Y.-C. J. Chen, K. D. Janda, *J. Am. Chem. Soc.* **1992**, *114*, 1488–1489.
[15] K. D. Janda, *Abstr. Pap. 198th National Meeting Am. Chem. Soc.*, American Chemical Society, Washington, DC, **1987**; ORGN 196.
[16] K. M. Shokat, C. J. Leumann, R. Sugasawara, P. G. Schultz, *Nature* **1989**, *338*, 269–271.
[17] K. D. Janda, M. I. Weinhouse, T. Dannon, K. A. Pacelli, D. M. Schloeder, *J. Am. Chem. Soc.* **1991**, *113*, 5427–5434.
[18] T. Li, S. Hilton, K. D. Janda, *J. Am. Chem. Soc.* **1995**, *117*, 3308–3309.
[19] Hapten synthesis and antibody production are detailed in: T. Li, K. D. Janda, J. A. Ashley, R. A. Lerner, *Science* **1994**, *264*, 1289–1293.
[20] A. J. Kirby, *The Anomeric Effect and Related Stereoelectronic Effects at Oxygen*, Springer, Berlin, **1983**, p. 20–32.
[21] W. P. Jencks, *Catalysis in Chemistry and Enzymology*, Dover, New York, **1987**, p. 51.
[22] J. R. Knowles, *Annu. Rev. Biochem.* **1980**, *49*, 877–919; C. R. Hall, T. D. Finch, *Tetrahedron* **1980**, *36*, 2059–2095.
[23] R. Breslow, R. Xu, *Proc. Natl. Acad. Sci. USA* **1993**, *90*, 1201–1207.
[24] D. Herschlag, *J. Am. Chem. Soc.* **1994**, *116*, 11631–11635.
[25] F. S. Prout, E. P.-Y. Huang, R. J. Hartman, C. J. Korpics, *J. Am. Chem. Soc.* **1954**, *76*, 1911–1913.
[26] L. D. Hall, R. B. Malcolm, *Can. J. Chem.* **1972**, *50*, 2102–2110.
[27] S. R. Caldwell, F. M. Raushel, P. M. Weiss, W. W. Cleland, *Biochemistry* **1991**, *30*, 7444–7450.

Diastereo- and Enantioselective Synthesis of Polyfunctional Ketones with Adjacent Quaternary and Tertiary Centers by Asymmetric Carroll Rearrangement**

Dieter Enders,* Monika Knopp, Jan Runsink, and Gerhard Raabe

Dedicated to Professor Hans Jürgen Bestmann on the occasion of his 70th birthday

The diastereo- and enantioselective generation of adjacent quaternary and tertiary stereogenic centers by C–C bond formation is a challenge in natural product and drug synthesis.[1] Recently, numerous methods for the introduction of quaternary stereogenic centers in highly functionalized building blocks have been developed.[2–7] But only a few variants allow the simultaneous preparation of an adjacent tertiary stereogenic center.[8] Intramolecular transformations such as sigmatropic rearrangements appear to be highly suited for this purpose. The [3,3]-sigmatropic Carroll rearrangement is an appropriate synthetic tool. Although discovered in 1940,[9] this reaction was first applied in drug synthesis only recently.[10] Many different variations of the Carroll rearrangement are known but most of them proceed with decarboxylation of the initially formed β-keto-acid.[11–13] Decarboxylation can be avoided by esterification or intramolecular lactonization of the β-keto acids at low temperatures, leading to the rearranged products with excellent *syn*/*anti* diastereoselectivities.[10, 14] Whereas so far only one diastereoselective variant, starting from (*S*)-pulegone, has been described for the preparation of optically active rearrangement products,[15] we have succeeded in the development of an asymmetric variant of the Carroll rearrangement.

We report here on a highly diastereo- and enantioselective synthesis of sterically demanding, functionalized ketones **A** with adjacent quaternary and tertiary centers starting from β-hydrazonoesters **B**. The key step is the stereoselective [3,3]-sigmatropic Carroll rearrangement of the hydrazonoester dienolate **C**. The ketones **A** are obtained after reductive workup and oxidative cleavage of the auxiliary.

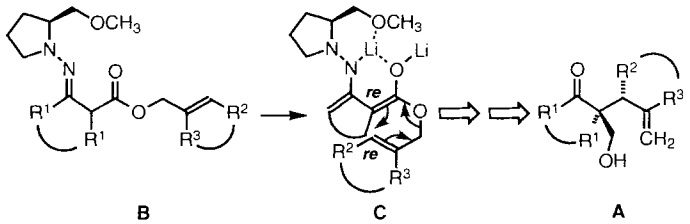

As depicted in Scheme 1, reaction of β-ketoesters **1**[16] with the chiral auxiliary (*S*)-1-amino-2-methoxymethylpyrrolidine (SAMP) yields the corresponding SAMP hydrazones (*S*)-**2**. These are doubly deprotonated with 2.6 equivalents of lithium diisopropylamide at −100 °C in THF/TMEDA, allowed to rearrange, and then directly reduced with 5 equivalents of lithium

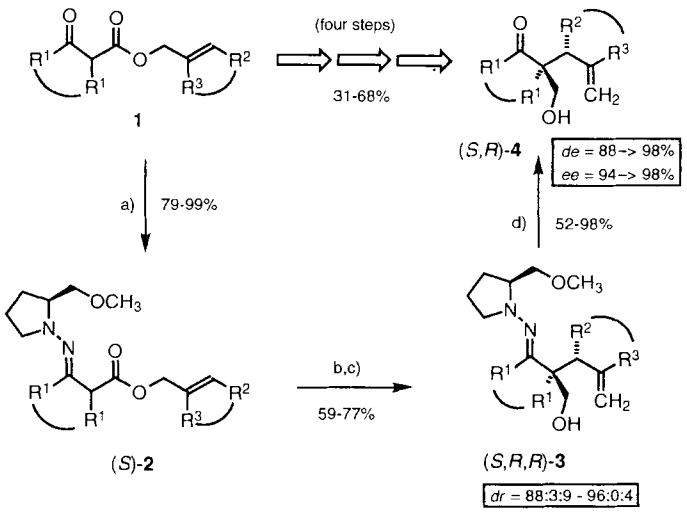

Scheme 1. Asymmetric Carroll rearrangement of allyloxycarbonyl ketones to polyfunctional ketones in four steps: a) 1.2 equiv SAMP, toluene, 5 mol% *p*-TosOH, molecular sieves, 110 °C, 1–2 h; column chromatography (silica gel, ether/petroleum ether/triethylamine 1/10/0.2); b) 2.6 equiv LDA, THF/TMEDA (8/1), −100 °C → 25 °C, 20 h; c) 5 equiv $LiAlH_4$, ether, 25 °C, 2 h; column chromatography (silica gel, ether/petroleum ether 1/2); d) ozone (2–3 min mmol^{-1}) pentane, −78 °C; column chromatography (silica gel, ether/petroleum ether 1/6). TMEDA = *N*,*N*,*N*′,*N*′-tetramethylethylenediamine.

aluminium hydride in ether to give the β-hydroxy hydrazones (*S*,*R*,*R*)-**3**.[17] Upon column chromatography the rearranged products are obtained in good yields (59–77%) as pale yellow oils (**3a–d, f, i**) or colorless crystals (**3e, g, h**). The hydrazone **3h** could be diastereomerically enriched by column chromatography to give the diastereomerically pure product. The ketone function was regenerated by ozonolysis of the rearranged products (*S*,*R*,*R*)-**3** at −78 °C in pentane, giving compounds **4a–g** in very good yields (89–99%). The ozonolysis occurred without racemization and chemoselectively without oxidation of the C=C bond. For the ketones **4h, i** the yields were only 52–57%, since in these cases the exocyclic C=C bond was partially oxidized.

The ratios of the diastereomeric products **3** resulting from the asymmetric Carroll rearrangement are very good [(*S*,*R*,*R*):(*S*,*S*,*S*):(*S*,*S*,*R*):(*S*,*R*,*S*) = 88:3:9:0 to 96:0:4:0] and were determined by ^{13}C NMR spectroscopy (Table 1).

The diastereomeric excesses of the ketones **4** were determined by ^{13}C NMR spectroscopy. The enantiomeric excesses were measured by ^{1}H NMR spectroscopy of the α-methoxyphenylacetic acid esters (MTPA esters) by comparison with the corresponding racemates.[18] The racemates were prepared by submitting

Table 1. Hydrazones (*S*,*R*,*R*)-**3** prepared by Carroll rearrangement of SAMP hydrazones (*S*)-**2** [27].

Cmpd.	R^1	R^2	R^3	Yield [%]	*dr* [a]	$[\alpha]_D^{20}$ (*c*, $CHCl_3$)	Config.
3a	$-(CH_2)_3-$	*i*Pr	H	73	95:2:3	+284.9 (1.0)	(*S*,*R*,*R*)
3b	$-(CH_2)_3-$	*i*Bu	H	62	94:2:4	+227.5 (1.0)	(*S*,*R*,*R*)
3c	$-(CH_2)_3-$	*i*Pe [b]	H	66	96:0:4	+211.2 (1.0)	(*S*,*R*,*R*)
3d	$-(CH_2)_4-$	*i*Pr	H	69	94:0:6	+181.7 (1.0)	(*S*,*R*,*R*)
3e	$-(CH_2)_4-$	*i*Bu	H	59	91:3:6	+123.4 (1.2)	(*S*,*R*,*R*)
3f	$-(CH_2)_4-$	*i*Pe [b]	H	64	93:1:6	+133.9 (0.9)	(*S*,*R*,*R*)
3g	$-(CH_2)_4-$	*c*Hex [c]	H	77	94:0:6	+154.6 (1.0)	(*S*,*R*,*R*)
3h	Me	$-(CH_2)_4-$		63	88:3:9	+212.0 (0.9)	(*S*,*R*,*R*)
3i	$-(CH_2)_3-$	$-(CH_2)_4-$		75	93:2:5	+199.0 (0.5)	(*S*,*R*,*R*)

[a] The ratio of diastereomers (*S*,*R*,*R*):(*S*,*S*,*S*):(*S*,*S*,*R*) were determined by ^{13}C NMR spectroscopy. The diastereoisomer (*S*,*R*,*S*) was not formed. [b] *i*Pe = isopentyl. [c] *c*Hex = cyclohexyl.

[*] Prof. Dr. D. Enders, Dipl.-Chem. M. Knopp, Dr. J. Runsink, Dr. G. Raabe
Institut für Organische Chemie der Technischen Hochschule
Professor-Pirlet-Strasse 1, D-52074 Aachen (Germany)
Telefax: Int. code + (241)8888-127

[**] This work was supported by the Deutsche Forschungsgemeinschaft (Leibniz award) and the Fonds der Chemischen Industrie. We are grateful to the companies Degussa AG, BASF AG, Bayer AG, and Hoechst AG for the donation of chemicals.

Table 2. Polyfunctional ketones **4** prepared by oxidative cleavage of the hydrazone (*S,R,R*)-**3** [27].

Cmpd.	Yield [%]	*de* [a] [%]	*ee* [a] [%]	$[\alpha]_D^{20}$ (*c*, $CHCl_3$)	Config.
4a	89	96	94	−4.3 (0.2)	(*S,R*)
4b	91	91	96	−55.0 (0.2)	(*S,R*)
4c	96	94	>98	−27.7 (0.2)	(*S,R*)
4d	95	89	>98	−67.9 (0.3)	(*S,R*)
4e	92	88	94	−89.0 (0.2)	(*S,R*)
4f	98	88	98	−121.9 (0.3)	(*S,R*)
4g	99	88	>98	−48.2 (0.4)	(*S,R*)
4h	57	>98 [b]	>96	−45.2 (0.3)	(*S,R*)
4i	52	90	96	−38.6 (0.4)	(*S,R*)

[a] Determined by ^1H NMR spectroscopy. [b] The enriched hydrazone was used in the cleavage reaction.

the respective *N,N*-dimethylhydrazones to the rearrangement (Table 2).

The absolute configuration of the rearranged hydrazones was determined to be (*S,R,R*) by means of the X-ray structure of the hydrazone **3e** (Fig. 1).[19] The absolute configuration of the hydrazones **3a**–**d**, **f**–**i**, and thus consequently of the final products **4**, was assigned accordingly based on the assumption that the

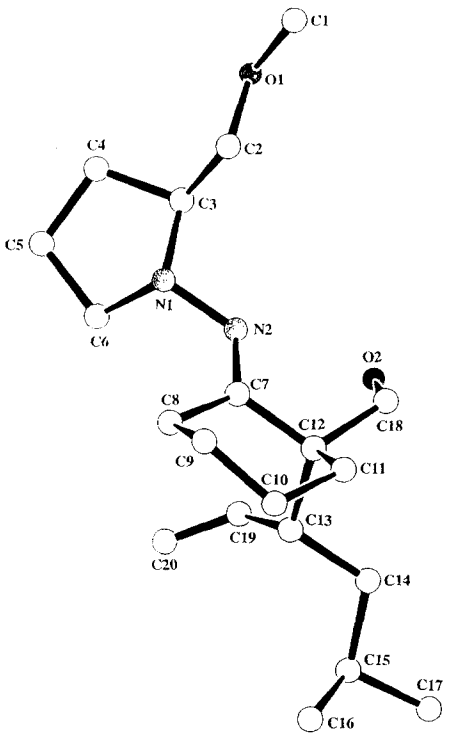

Fig. 1. Crystal structure of hydrazone **3e** [19] (SCHAKAL presentation [26]).

reaction proceeds analogously in all cases. For hydrazone **3h** the configuration of the major diastereomer and one minor diastereomer was investigated by NMR spectroscopy using NOE measurements (Fig. 2).[20]

The absolute configuration (*R*) at the quaternary stereogenic center, assigned by X-ray structure determination,[21] is in accordance with results concerning intermolecular electrophilic substitutions of β-hydrazonoesters.[22] As depicted for hydrazonoester dienolate **C**, we postulate an intramolecular chelation of the lithium by the methoxymethyl group and consequently, the

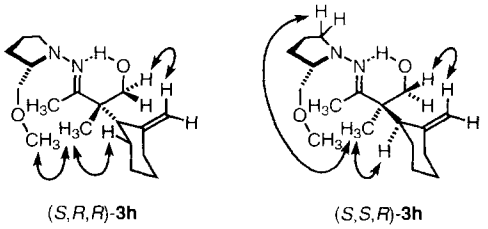

(*S,R,R*)-**3h** (*S,S,R*)-**3h**

Fig. 2. NOE measurements for hydrazone **3h**.

allylic moiety approaches from the sterically less hindered side[23] (*re–re* attack) with formation of a new σ bond. The configuration of the tertiary stereogenic center is easily assigned under the assumption that the [3,3]-sigmatropic rearrangement occurs via a chairlike transition state.[24]

The synthetic value of this [3,3]-sigmatropic rearrangement is due to the high flexibility possible through variation of the residues (R^1, R^2, and R^3). Not only cyclopentanone SAMP and cyclohexanone SAMP hydrazones (**2a–g, i**) but also acyclic hydrazones (e.g. **2h**) can be employed. The allylic alcohol moiety can be varied significantly too. Use of alcohols with an endocyclic double bond (**2h, i**) leads to rearranged products with exocyclic double bonds (**3h, i**).

The [3,3]-sigmatropic rearrangement presented here is, to the best of our knowledge, the first asymmetric Carroll rearrangement. It makes possible the C–C bond forming, intramolecular generation of two adjacent stereogenic centers in good yield with high diastereoselectivity and extremely high enantioselectivity. The γ,δ-unsaturated β′-hydroxyketones accessible with this method have a stereogenic center in the α position and variable substitution at the tertiary stereogenic center in the β position, and may serve as chiral building blocks in natural product and drug synthesis.

Experimental Procedure

SAMP hydrazones **2**: β-Ketoester **1** was heated to reflux for 1–2 h in toluene (1 mL mmol^{-1}) with 1.2 equivalents of SAMP in the presence of 5 mol% *p*-toluenesulfonic acid and molecular sieves. The reaction was monitored by thin-layer chromatography. Upon removal of the solvent, the residue was dissolved in ether (3 mL mmol^{-1}), washed twice with saturated aqueous NaCl solution, and dried over magnesium sulfate. Purification of the yellow crude products by column chromatography (silica gel, ether/petroleum ether/triethylamine 1:10:0.2) provided colorless liquids.

Hydrazones **3**: To 5.2 mmol of diisopropylamine in 8 mL of anhydrous THF was added dropwise 3.25 mL of a 1.6 N solution of *n*-butyllithium in hexane at 0 °C under an atmosphere of argon. After 5 min, 1 mL of TMEDA was added dropwise. Then 2 mmol of the hydrazone **2**, dissolved in 1 mL of THF, was added dropwise at −100 °C. The reaction mixture was allowed to warm to room temperature over 12 h. The reduction was carried out by dropwise addition of the reaction mixture to a suspension of 10 mmol of $LiAlH_4$ in 50 mL of ether at room temperature using a cannula. After 3 h the reaction mixture was hydrolyzed with 10 mL of 1% HCl solution, the aluminium hydroxide precipitate filtered, and the filtrate dried over magnesium sulfate. Upon purification by column chromatography (silica gel, ether/petroleum ether 1:2) pale yellow liquids (**3a–d, f, i**) or colorless crystals (**3e, g, h**) were obtained.

Ketones **4**: 1 mmol of hydrazone **3** was dissolved in 20 mL of pentane and cooled to −78 °C. Ozone was bubbled through the reaction mixture (flow rate 40 L h^{-1}) [25]. The reaction was interrupted by bubbling argon through the solution in order to monitor by thin-layer chromatography. Upon completion the reaction mixture was allowed to warm to room temperature whilst argon was bubbled through. After removal of the solvent, the residue was purified by column chromatography (silica gel, ether/petroleum ether 1:6).

Received: May 17, 1995 [Z 7999 IE]
German version: *Angew. Chem.* **1995**, *107*, 2442–2445

Keywords: asymmetric syntheses · Carroll rearrangement · ketones · SAMP hydrazones

[1] Review articles: S. F. Martin, *Tetrahedron* **1980**, *36*, 419; A. I. Meyers, D. Romo, *ibid.* **1991**, *47*, 9503; K. Fuji, *Chem. Rev.* **1993**, *93*, 2037.
[2] S. Hashimoto, K. Koga, *Tetrahedron Lett.* **1978**, 573; K. Tomioka, Y. Cho, F. Sato, K. Koga, *J. Org. Chem.* **1988**, *53*, 4094; A. Ando, Y. Takemasa, K. Tomioka, K. Koga, *Tetrahedron* **1993**, *49*, 1579; K. Ando, K. Yasuda, K. Tomioka, K. Koga, *J. Chem. Soc. Perkin Trans. 1* **1994**, *277*; B. Westermann, H. Grosse Scharmann, I. Kortmann, *Tetrahedron Asymmetry* **1993**, *4*, 2119.
[3] U. Schöllkopf, W. Hartwig, U. Groth, *Angew. Chem.* **1979**, *91*, 922; *Angew. Chem. Int. Ed. Engl.* **1979**, *18*, 863; U. Schöllkopf, *Top. Curr. Chem.* **1983**, *109*, 65.
[4] A. I. Meyers, M. Harre, R. Garland, *J. Am. Chem. Soc.* **1984**, *106*, 1146; A. I. Meyers, K. T. Wanner, *Tetrahedron Lett.* **1985**, *26*, 2047; A. I. Meyers, B. A. Lefker, K. T. Wanner, R. A. Aitken, *J. Org. Chem.* **1986**, *51*, 1936; A. I. Meyers, B. A. Lefker, *Tetrahedron Lett.* **1987**, *28*, 1745; *Tetrahedron* **1987**, *43*, 5663; A. I. Meyers, T. Wunsch, *J. Org. Chem.* **1990**, *55*, 4233; A. I. Meyers, W. R. Leonard, J. L. Romine, *Tetrahedron Lett.* **1991**, *32*, 597; L. J. Westrum, A. I. Meyers, *ibid.* **1993**, *34*, 7701; *ibid.* **1994**, *35*, 973; T. G. Gant, A. I. Meyers, *ibid.* **1993**, *34*, 3707; J. E. Resek, A. I. Meyers, *Synlett*, **1995**, 145.
[5] D. Seebach, J. D. Aebi, R. Naef, T. Weber, *Helv. Chim. Acta* **1985**, *68*, 144; D. Seebach, J. Zimmermann, *ibid.* **1986**, *69*, 1147; D. Seebach, J. Zimmermann, U. Gysel, R. Ziegler, T. Ha, *J. Am. Chem. Soc.* **1988**, *110*, 4763; S. Blank, D. Seebach, *Angew. Chem.* **1993**, *104*, 1780; *Angew. Chem. Int. Ed. Engl.* **1993**, *32*, 1765; B. Weber, D. Seebach, *Tetrahedron*, **1994**, *50*, 6117.
[6] K. Hiroi, J. Abe, K. Suya, S. Sato, *Tetrahedron Lett.* **1989**, *30*, 1543; K. Hiroi, J. Abe, *Heterocycles* **1990**, 283; K. Hiroi, T. Koyama, K. Anzai, *Chem. Lett.* **1990**, 235; K. Hiroi, J. Abe, K. Suya, S. Sato, T. Koyama, *J. Org. Chem.* **1994**, *59*, 203.
[7] D. Enders in *Asymmetric Synthesis Vol. 3*, (Ed.: J. D. Morrison), Academic Press, Orlando, FL, **1984**, p. 275; D. Enders, *Chem. Scr.* **1985**, *25*, 139; D. Enders, P. Fey, H. Kipphardt, *Org. Synth.* **1987**, *65*, 173, 183; D. Enders, A. Zamponi, G. Raabe, *Synlett* **1992**, 897; D. Enders, A. Zamponi, J. Runsink, G. Raabe, *Synthesis* **1993**, 725.
[8] H. Kogen, K. Tomioka, S. Hashimoto, K. Koga, *Tetrahedron Lett.* **1980**, *21*, 4005; U. Schöllkopf, W. Hartwig, U. Groth, *Angew. Chem.* **1980**, *92*, 205; *Angew. Chem. Int. Ed. Engl.* **1980**, *19*, 212; H. Kogen, K. Tomioka, S. Hashimoto, K. Koga, *Tetrahedron* **1981**, *37*, 3951; U. Schöllkopf, *Pure Appl. Chem.* **1983**, *55*, 1799; K. Tomioka, H. Kawasaki, K. Koga, *Tetrahedron Lett.* **1985**, *26*, 3027; K. Tomioka, K. Yasuda, K. Koga, *J. Chem. Soc. Chem. Commun.* **1987**, 1345; M. Nakajima, K. Tomioka, Y. Iitaka, K. Koga, *Tetrahedron* **1993**, *49*, 10793; T. Gees, W. B. Schweizer, D. Seebach, *Helv. Chim. Acta* **1993**, *76*, 2640; L. Snyder, A. I. Meyers, *J. Org. Chem.* **1993**, *58*, 7507; A. N. Hulme, A. I. Meyers, *ibid.* **1994**, *59*, 952; G. P. Brengel, C. Rithner, A. I. Meyers, *ibid.* **1994**, *59*, 5144; M. Tanaka, K. Tomioka, K. Koga, *Tetrahedron*, **1994**, *50*, 12829, 12843; P. N. Devine, A. I. Meyers, *J. Am. Chem. Soc.* **1994**, *116*, 2633; N. Shimano, A. I. Meyers, *ibid.* **1994**, *116*, 6437; L. H. Baptistella, A. M. Alexio, *Liebigs Ann. Chem.* **1994**, 785.
[9] M. F. Carroll, *J. Chem. Soc.* **1940**, 704, 1266; *ibid.* **1941**, 507.
[10] A. M. Echavarren, J. de Mendoza, P. Prados, A. Zapata, *Tetrahedron Lett.* **1991**, *32*, 6421.
[11] J. Tsuji, *Tetrahedron* **1986**, *42*, 4361; *Pure Appl. Chem.* **1982**, *54*, 197; S. I. Pogrebnoi, Y. B. Kalyan, M. Z. Krimer, *Tetrahedron Lett.* **1987**, *28*, 4893; *Bull. Acad. Sci. USSR* **1991**, 733.
[12] S. R. Wilson, M. F. Price, *J. Org. Chem.* **1984**, *49*, 722.
[13] J. F. Genus, D. D. Peters, J. F. Ding, T. A. Bryson, *Synlett* **1994**, 209.
[14] J. C. Gilbert, T. A. Kelly, *Tetrahedron* **1988**, *44*, 7587.
[15] N. Ouvard, J. Rodriguez, M. Santelli, *Tetrahedron Lett.* **1993**, *34*, 1149; N. Ouvard, A. Baldy, J. Rodriguez, J. Feneaudupond, J. P. Declerque, *Acta Crystallogr. Sect. C* **1994**, *50*, 624.
[16] Preparation of β-ketoesters **1**: D. F. Taber, J. C. Amedio, Y. K. Patel, *J. Org. Chem.* **1985**, *50*, 3618; J. C. Gilbert, T. A. Kelly, *ibid.* **1988**, *53*, 449; R. J. Clemens, J. A. Hyatt, *J. Org. Chem.* **1985**, *50*, 2431.
[17] The diastereoselectivity of the [3,3]-sigmatropic rearrangement could be improved by transmetalation in the presence of the cosolvent HMPA only insignificantly (Al) or with considerable losses of yield (Si): R. E. Ireland, P. Wipf, J. D. Armstrong, *J. Org. Chem.* **1991**, *56*, 650; H. Yamamoto, K. Hattori, *ibid.* **1993**, *58*, 5301; K. Hattori, H. Yamamoto, *Tetrahedron* **1994**, *50*, 3099; J. Otera, Y. Fujita, S. Fukuzumi, *Synlett* **1994**, 213; Transmetalation with B, P, Ti gave no improvement in the selectivity: E. J. Corey, D. H. Lee *J. Am. Chem. Soc.* **1991**, *113*, 4026; R. L. Funk, J. B. Stallman, J. A. Wos, *ibid.* **1993**, *115*, 8847; U. Katzmaier, *Angew. Chem.* **1994**, *106*, 1046, *Angew. Chem. Int. Ed. Engl.* **1994**, *33*, 998; K. Mikami, O. Takahashi, K. Fujimoto, T. Nakai, *Synlett* **1991**, 629; M. Ushikawa, T. Kiatsuki, M. Yamagushi, *Tetrahedron Lett.* **1986**, *27*, 4581; M. Yamagushi, *Pure Appl. Chem.* **1989**, *61*, 413.
[18] J. A. Dale, D. L. Dull, H. S. Mosher, *J. Org. Chem.* **1969**, *34*, 2543.
[19] Suitable single crystals were obtained from ether at −20 °C. The compound crystallizes in the orthorhombic space group $P2_12_12_1$ (No. 19), $a = 6.7328(3)$, $b = 13.9095(6)$, $c = 22.3704(7)$ Å. For a cell volume of 2095.0 Å^3, $Z = 4$ and $M_{calcd} = 336.5$ the density is 1.067 g cm^{-3}. Total number of electrons per element unit F(000) = 744. Enraf-Nonius CAD4 diffractometer, graphite monochromator, $Cu_{K\alpha}$ radiation ($\lambda = 1.54179$ Å). The structure was solved by direct methods (GENSIN, GENTAN aus XTAL3.2 [21]). Some of the positions of the hydrogen atoms could be located, the others were calculated. 1915 observed reflections ($I > 2\sigma(I)$), 218 parameters refined, $R = 0.055$ ($R_w = 0.051$). Maximum residual electron density ±0.2 e Å^{-3}. The Absolute configuration was assigned using the known configuration at C3. Further details of the crystal structure investigation may be obtained from the Fachinformationszentrum Karlsruhe, D-76344 Eggenstein-Leopoldshafen (Germany), on quoting the depository number CSD-59067.
[20] Both isomers are conformationally rigid due to hydrogen bonding of the alcohol proton to the sp^2-hybridized nitrogen atom. For the major diastereoisomer (*S,R,R*)-**3h** an NOE between the methyl group at the quaternary center and the methyl protons of the SAMP methoxy group is observed. For the minor diastereoisomer (*S,S,R*)-**3h** an NOE between the methyl group and the NCH_2 protons of the chiral auxiliary is found. Thus the two isomers differ from each other with regard to the configuration of the quaternary center. Further NOE measurements show that both isomers are substituted at the equatorial positions of the six-membered ring. The relative configurations of the two stereogenic centers were determined by means of the following NOEs: Firstly, both diastereoisomers show a strong NOE between one of the two protons of the exocyclic double bond and one of the two diastereotopic hydroxymethylene protons. Secondly, an NOE is observed between the protons of the methyl group at the quaternary stereogenic center and the equatorial proton of the CH_2 group in the six-membered ring in the α position to the tertiary stereogenic center in the major diastereoisomer, whereas in the minor diastereoisomer an interaction of the methyl group at the quaternary stereogenic center with the axial ring proton at the tertiary stereogenic center is found (Fig. 2).
[21] S. R. Hall, H. D. Flack, J. M. Steward, *XTAL3.2 Reference Manual*, Universities of West Australia, Geneva, and Maryland, **1992**; V. Subramanian, S. R. Hall in *XTAL3.2 Reference Manual: GENSIN* (Eds.: S. R. Hall, H. D. Flack, J. M. Stewart), Universities of West Australia, Geneva, and Maryland, Perth, **1992**, p. 131; S. R. Hall in *XTAL3.2 Reference Manual: GENTAN* (Eds.: S. R. Hall, H. D. Flack, J. M. Stewart), Universities of West Australia, Geneva, and Maryland, Perth, **1992**, p. 139.
[22] D. Enders, A. Zamponi, T. Schäfer, C. Nübling, H. Eichenauer, A. S. Demir, G. Raabe, *Chem. Ber.* **1994**, *127*, 1707.
[23] D. Enders, G. Bachstädter, K. A. M. Kremer, M. Marsch, K. Harms, G. Boche, *Angew. Chem.* **1988**, *100*, 1580; *Angew. Chem. Int. Ed. Engl.* **1988**, *27*, 1522.
[24] K. N. Houk, *J. Am. Chem. Soc.* **1994**, *116*, 12047.
[25] For higher flow rates partial oxidation of the C=C bond is also observed for ketones **4a–g**.
[26] E. Keller, *Chem. Unserer Zeit* **1988**, *20*, 178.
[27] All new compounds gave correct elemental analyses and suitable spectroscopic data (NMR, IR, MS).

Optimization of the Biological Activity of Combinatorial Compound Libraries by a Genetic Algorithm**

Lutz Weber,* Sabine Wallbaum, Clemens Broger, and Klaus Gubernator

Dedicated to Professor Ivar Ugi on the occasion of his 65th birthday

The key task in the initial phase of the discovery of biological effectors is to identify a tightly binding ligand for a given biological target molecule. Exploiting molecular diversity with combinatorial compound libraries has been proposed as a method to speed up the development of such new prototype ligands. Compound libraries are synthesized either as complex mixtures by the "split and combine" methodology (mainly by solid-phase syntheses) or as single compounds by "array" syntheses carried out in solution.[1] Whereas the "split and combine" method

[*] Dr. L. Weber, Dr. S. Wallbaum, Dr. C. Broger, Dr. K. Gubernator
Präklinische Forschung, Pharma Division
F. Hoffmann-La Roche AG, CH-4002 Basel (Switzerland)
Telefax: Int. code + (41)61 6888714
e-mail: lutz.weber@roche.com

[**] We wish to thank Dr. David Weininger, Daylight Chemical Information Systems, Inc., Irvine CA, for fruitful discussions.

uses sequential synthesis schemes to generate a large number of compounds, synthesis of many compounds in an array ideally uses versatile one-pot reactions. Cycloadditions or reactions with even more components like the Asinger or Ugi cascade reactions provide diverse products in a one-pot procedure and are therefore especially suitable for parallel synthesis.[2, 3] Thus, the Ugi reaction allows the rapid set-up of many reactions in parallel by mixing an isocyanide, an aldehyde, an amine, and a carboxylic acid in methanol at room temperature (Scheme 1). The combination of 10 isocyanides (**1**), 40 aldehydes (**2**), 10 amines (**3**), and 40 carboxylic acids (**4**) results in 160000 different Ugi-type reactions. We present here a search and synthesis procedure that can be used to find biologically active compounds from this library of 160000 reactions by synthesizing and testing only a small fraction of all possible reaction products.

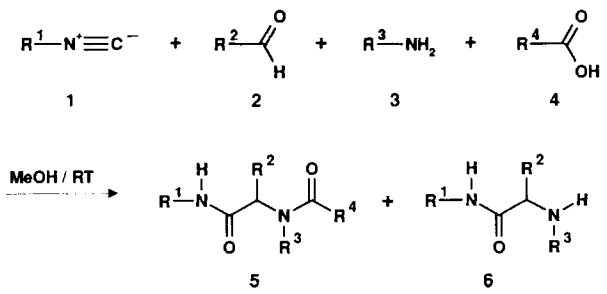

Scheme 1. The four-component Ugi reaction. RT = room temperature.

Genetic algorithms have proven to be extraordinarily efficient in optimizing complex, multidimensional problems. Adopting the rules of genetics (replication, crossover, and mutation), new generations of molecules that may show more favorable properties than their parents are synthesized in parallel.[4] Using an enzymatic assay to test the biological activity, this evolutionary feedback loop will search for those starting materials in the Ugi reactions whose reaction products have high inhibitory activity against the given enzyme. The serine protease thrombin was chosen as the target biochemical system.[5] Its pivotal role in the blood coagulation cascade and related pathogenic thrombotic processes makes the identification of thrombin inhibitors an attractive goal for therapeutic anticoagulants. Commercially available reagents **1** (10), **2** (40), **3** (10), and **4** (40 compounds) were selected to obtain a diverse set for each component **1**–**4** with respect to size, hydrophobicity, and donor and acceptor properties. This general library was limited only in that amine **3** has a donor-rich basic side chain (Scheme 2), which is known to mediate trypsin-like serine protease inhibitory activity.[6]

Experimental conditions were chosen after performing a series of test reactions and thrombin chromogenic assays of the crude reaction mixtures.[7] Weak nucleophilic amines like 4-aminobenzamidine afforded two main products upon dilution of the reaction mixture with the aqueous buffer assay medium, the four-component adduct **5** and a three-component product **6** lacking the carboxylic acid residue (Scheme 1).[8] Interference with residual unreacted reagents, which show only weak inhibitory activities in the enzyme assay, could be excluded by control experiments.

A simple genetic algorithm was implemented.[9] Individual reagents were encoded by an arbitrary bit pattern, for example 0010 for benzylisocyanide. The length of bit patterns was chosen to encode each of the possible substituents (or reagents) at each of the four positions R^1–R^4. Thus, the combined bit pattern encodes the reaction mixture of four specified reagents **1**, **2**, **3**, and **4**, for example, 0010 011100 0111 010011 for the starting materials benzylisocyanide, salicylaldehyde, agmatine [(4-amino-*n*-butyl)guanidine], and propionic acid. Survival of patterns, "replication", is ensured in our experiment by storing all experimental results in a database. Crossover and mutation however, are allowed only for those bit patterns (reactions) which showed high inhibitory activity in the thrombin assay. Crossover is performed by intersecting two bit patterns at a random position and exchanging the intersected parts, resulting in two new patterns. A mutation results in reversal of a bit at a random position of a given bit pattern. Reactions are then carried out if a new bit pattern corresponds to real starting materials otherwise the procedure is repeated. The adjustable parameters of the genetic algorithm, population size (number of reactions to be performed in parallel) and mutation rate, were chosen in a series of test runs against a database of 160000 virtual compounds, whose activities were calculated with different test functions, such as superimposed sinusoidal functions in four dimensions. For the four-component problem presented here the most active individual was obtained with a population size of 20, a crossover probability of 100%, and a mutation rate of 1% in 20 to 50 generations.

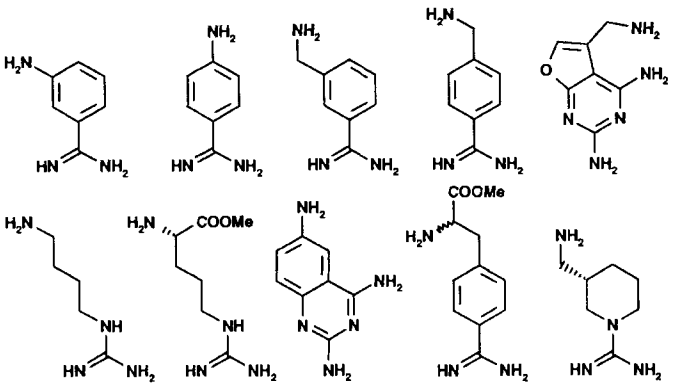

Scheme 2. The ten amines **3** used in the genetic algorithm.

The experiment was started by selecting the first 20 bit patterns randomly. The corresponding reactions were performed and the crude products were tested. The resulting data were entered into the genetic algorithm that calculated the next 20 bit patterns by crossover and mutation. From these 40 reaction products, the 20 most active were used as parents for the calculation and synthesis of the next generation. This was repeated for 20 generations such that a total of 400 different Ugi reactions were carried out.

Already after 16 cycles, the average effective inhibitory activity (EC_{50}) of the 20 best products at each generation was submicromolar in the thrombin assay (Fig. 1). The most active

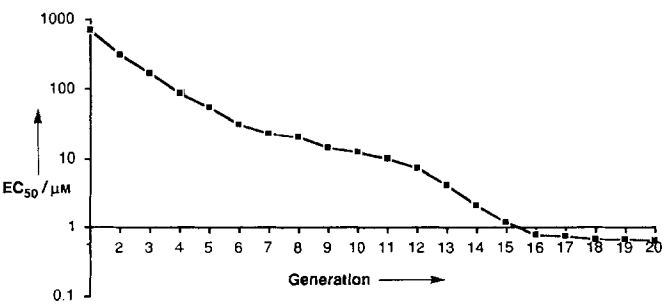

Fig. 1. Average inhibitory activity of the 20 best Ugi reaction products in the thrombin chromogenic assay. Effective inhibitory concentrations (EC_{50}) are given in micromolar concentrations.

reaction product out of these 400 reactions was found in generation 18. This reaction was repeated on a larger scale and the expected products were isolated and purified. The inhibitory activities (K_i) of the novel racemic four-component adduct **7** and the three-component compound **8** were 1.4 and 0.22 μM, respectively. Both compounds exhibit structural features of already known thrombin inhibitors[5] and might be regarded as prototypic compounds which could be further optimized by classical medicinal chemistry methods.

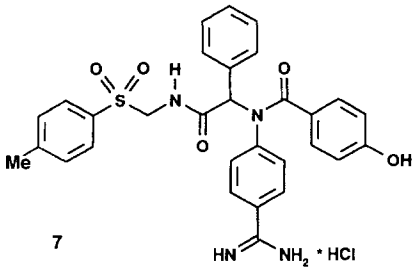

7

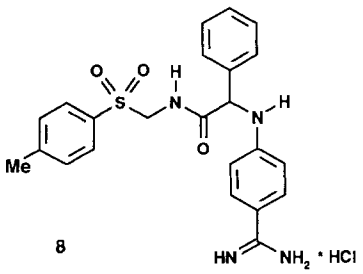

8

We may not necessarily have discovered the most active compound out of all 160000 possible reactions by the described method. However, the method can easily be modified by synthesizing more generations, by varying the population size and/or mutation rate, or by introduction of other useful starting materials. Modern robotic bioassay systems may allow the easy implementation of this method including both automatic synthesis and testing. As a consequence, the design of multicomponent reactions and limited starting material libraries based on biostructural information will become an important tool in pharmaceutical research.

Experimental Procedure

General procedure: 25 μL of 0.1 M solutions of an isocyanide, aldehyde, amine, and a carboxylic acid in methanol were allowed to react at room temperature for 20 h. The crude reaction product was then dissolved in dimethyl sulfoxide (50 μL) and diluted with Britt–Robinson buffer (pH = 7.8) to obtain the desired concentration for the thrombin assay [7].

7: Solutions (each 1 mmol) of benzaldehyde, 4-amino-benzamidine dihydrochloride, 4-hydroxybenzoic acid, toluene-4-sulfonylmethyl isocyanide as well as triethylamine (2 mmol) in methanol were allowed to react at room temperature for 24 h. After addition of several drops of 25% HCl to the reaction mixture, the solvent was evaporated in vacuo and the resulting residue was separated on reversed-phase silica (RP18) using a water/methanol gradient. Yield 28%; yellow powder; ^{1}H NMR (250 MHz, [D$_6$]DMSO, 25 °C, TMS): δ = 2.41 (s, 3H), 3.72 (s, 2H), 5.61 (s, 1H), 6.72-8.01 (m, 18H), 8.82 (s, broad, 2H), 8.98 (s, broad, 2H); electrospray-MS: *m/z* 557.7 ([*M* + H]$^+$, 100%).

8: Using the same procedure as for compound **7** but without 4-hydroxybenzoic acid, **8** was obtained in 22% yield as a yellow amorphous powder. ^{1}H NMR (250 MHz, [D$_6$]DMSO, 25°C, TMS): δ = 2.37 (s, 3H), 3.67 (s, 2H), 5.50 (s, 1H), 6.83-7.69 (m, 13H), 8.88 (s, broad, 2H), 9.00 (s, broad, 2H); electrospray-MS: *m/z* 437.6 ([*M* + H]$^+$, 100%).

Received: May 31, 1995 [Z 8050 IE]
German version: *Angew. Chem.* **1995**, *107*, 2452–2454

Keywords: combinatorial chemistry · compound libraries · enzyme inhibitors · genetic algorithm · multicomponent reactions

[1] a) B. A. Bunin, M. J. Plunkett, J. A. Ellman, *Proc. Natl. Acad. Sci. USA* **1994**, *92*, 4708–4712; b) M. A. Gallop, R. W. Barrett, W. J. Dower, S. P. A. Fodor, E. M. Gordon, *J. Med. Chem.* **1994**, *37*, 1233–1251.

[2] U. Obst, V. Gramlich, F. Diederich, L. Weber, D. W. Banner, *Angew. Chem.* **1995**, *107*, 1874–1877; *Angew. Chem. Int. Ed. Engl.* **1995**, *34*, 1739–1742.

[3] I. Ugi, S. Lohberger, R. Karl in *Comprehensive organic synthesis: Selectivity for synthetic efficiency, Vol. 2*, (Eds. B. M. Trost, I. Fleming, C. H. Heathcock), Pergamon Press, Oxford, **1991**, p. 1083–1109.

[4] a) D. E. Goldberg, *Genetic Algorithms in Search Optimization and Machine Learning*, Addison Wesley, Reading MA, **1989**; b) R. P. Sheridan, S. K. Kearsley, *J. Chem. Inf. Comput. Sci.* **1995**, *35*, 310–320; c) V. Venkatasubramanian, K. Chan, J. M. Caruthers, *ibid* **1995**, *35*, 188–195.

[5] K. Hilpert, J. Ackermann, D. W. Banner, A. Gast, K. Gubernator, P. Hadvá ry, L. Labler, K. Müller, G. Schmid, T. B. Tschopp, H. van de Waterbeemd, *J. Med. Chem.* **1994**, *37*, 3889–3901.

[6] In an alternative approach, biostructural information like the three-dimensional structure of the target protein [5] may be used to limit the compound library at all substituents.

[7] R. Lottenberg, J. A. Hall, J. W. Fenton, G. M. Jackson, *Thromb. Res.* **1982**, *28*, 313 (chromogenic substrate S-2238).

[8] Product **6** is formed in the presence of water which either replaces the acid as the fourth component or by its reaction with the imino ester precursor of **5**.

[9] A daylight database, Daylight Chemical Information Systems, Inc., Irvine, CA, was used on a Silicon Graphics Onyx computer for storing chemical structures and biological activities. A C-program for the genetic algorithm was written which uses this database.

Mechanism of the Fe^+ Mediated C–C and C–H Bond Activations in Ethane from a Theoretical Viewpoint**

Max C. Holthausen, Andreas Fiedler, Helmut Schwarz, and Wolfram Koch*

Dedicated to Professor Paul von Ragué Schleyer on the occasion of his 65th birthday

The activation of C–H and C–C bonds in hydrocarbons by transition metals is of paramount interest in organic chemistry, biochemistry, and catalytic research.[1] A sound understanding of the crucial steps and the complete characterization of the central intermediates are prerequisites, for example, for the de novo design of catalysts. However, the synergistic cooperation of experiment and theory, so successful in many areas of research, has had only limited impact in this field as of yet. The description of complicated electronic structures of open-shell transition metal compounds requires a very sophisticated treatment which, in the framework of conventional ab initio MO theory, usually exceeds nowadays computational capabilities, even for only moderately sized systems.[2] As promising alternative for an accurate and yet efficient computational treatment of such species, density functional theory (DFT)[3] and, in particular, DFT/Hartree-Fock (HF) hybrid methods[4] have recently attracted considerable attention.

The reaction of Fe^+ with ethane is a prototype for the activation of C–H and C–C bonds by transition metal cations, and extensive studies employing various mass spectrometric tech-

[*] Prof. Dr. W. Koch, Dipl.-Chem. M. C. Holthausen, Dipl.-Chem. A. Fiedler, Prof. Dr. H. Schwarz
Institut für Organische Chemie
Strasse des 17. Juni 135, D-10623 Berlin (Germany)
Telefax: Int. code + (30) 314 21102

[**] This work was supported by the Deutsche Forschungsgemeinschaft, the Volkswagen-Stiftung, and the Fonds der Chemischen Industrie. Computer time was generously provided by the Konrad-Zuse-Zentrum für Informationstechnik Berlin. We thank Prof. P. B. Armentrout and Dr. D. Schröder for helpful discussions and Prof. K. Morokuma for a preprint of ref. [12].

niques have been carried out.[5] While rather accurate thermochemical information on the entrance and exit channels of the potential energy surface (PES) are available,[5] very little is known about the actual reaction mechanisms, that is which elementary steps are involved and what are the geometries and relative energies of the corresponding saddle points and intermediates. In the following, we describe the stationary points on the $[Fe,C_2,H_6]^+$ PES relevant for the C–C and C–H bond activations at the DFT/HF hybrid level.[6] This study is not only the first attempt to employ quantum chemical calculations to this important reaction sequence,[7] but—at least to the best of our knowledge -also the first application of DFT/HF hybrid methods for elucidating mechanistic details involving open-shell transition metal compounds.

First of all, the level of accuracy that can be expected from our computational strategy has to be established. Tables 1 and 2 contain a comparison between the experimentally determined[8] and the theoretically predicted bond dissociation energies (BDEs) and energies of the exit channels relative to the separated system $Fe^+(^6D) + C_2H_6$.[9] While the data in Table 1 reveal a rather systematic (and, for transition metal complexes, DFT-typical[10]) overestimation of the computed BDEs by up to 18 kcal mol^{-1} for weakly bound complexes, the description of relative energies (Table 2) is much less problematic with a maximum deviation of only 6 kcal mol^{-1}. Thus, we are confident that the chosen DFT/HF approach correctly describes the qualitative features of the potential energy surfaces, which are based on relative energies.

Table 1. Experimental and calculated BDE values in kcal mol^{-1}.

Species	exp. [a]	calcd.	Species	exp. [a]	calcd.
$Fe(C_2H_6)^+$	16	27	H-H	104	113
Fe^+-C_2H_5	56	65	CH_3-H	105	113
$Fe(C_2H_4)^+$	35	53	CH_3-CH_3	90	92
Fe^+-CH_3	55	65	H_2C=CH_2	174	175
Fe^+=CH_2	82	86	C_2H_5-H	100	108
Fe^+-H	49	61			
$Fe(H_2)^+$	5	19			

[a] Taken from ref. [8].

Table 2. Experimental and calculated energies of the exit channel relative to separated $Fe^+(^6D) + C_2H_6$ in kcal mol^{-1}.

Exit channel	exp. [a]	calcd.
$Fe^+ + C_2H_6$	0	0
$FeCH_3^+ + CH_3^\bullet$	31	27
$FeCH_2^+ + CH_4$	13	12
$Fe(H_2)^+ + C_2H_4$	27	23
$Fe(C_2H_4)^+ + H_2$	−5	−11
$FeH^+ + C_2H_5^\bullet$	51	47
$FeC_2H_5^+ + H^\bullet$	44	43

[a] Taken from ref. [8].

The course of the C–C and C–H bond activation on the $[Fe,C_2,H_6]^+$ PES is shown in Scheme 1. It should be noted that the initial interaction of the iron cation in the $Fe^+(^6D)$ ground state with ethane occurs on the sextet surface, while the remainder of the $[Fe,C_2,H_6]^+$ PES has only three unpaired electrons, that is it has quartet spin multiplicity. However, spin-orbit interaction is most probably large enough in this system to allow for efficient conversion to the energetically most favorable surface along the reaction coordinate.[11]

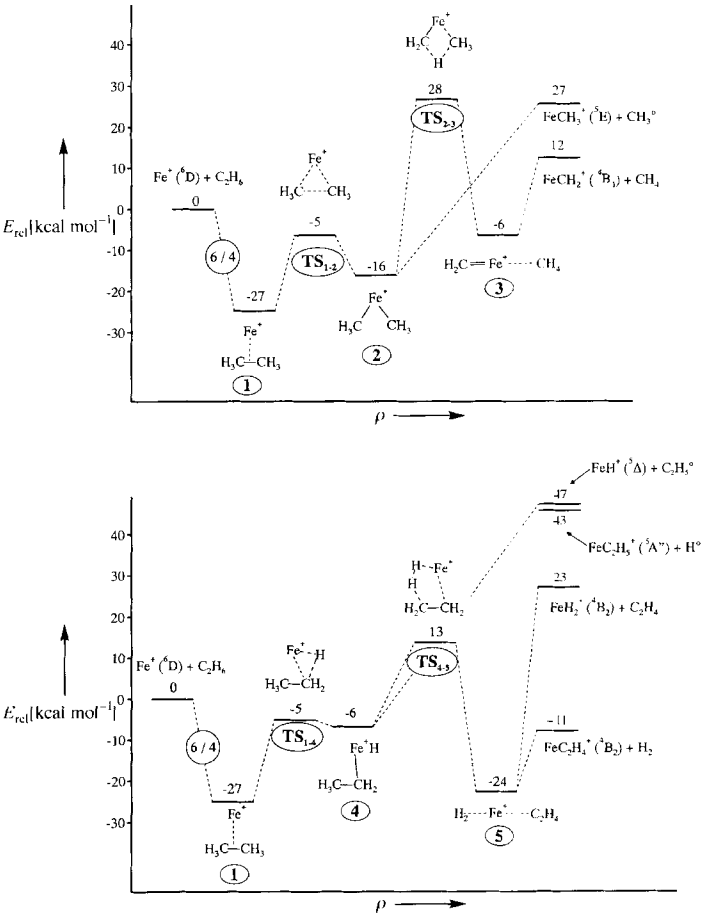

Scheme 1. Calculated course of the C–C bond activation (top) and C–H bond activation in the $[Fe,C_2,H_6]^+$ system (bottom). ρ = reaction coordinate.

No exothermic reaction of Fe^+ with ethane was observed in threshold collisional activation experiments.[5] At thermal energies, the only reaction that takes place is formation of the $Fe(C_2H_6)^+$ adduct ion. At higher kinetic energies, the reverse reaction, that is the loss of ethane, is the major process in competition with two minor processes which lead to the formation of $FeH^+ + C_2H_5^\bullet$ and $FeCH_3^+ + CH_3^\bullet$. Elimination of H_2 and methane observed in similar reactions for higher alkanes as exothermic processes does not occur, although these products are thermodynamically favored (Table 2). Thus, there must be sizable activation barriers along the reaction coordinate of these processes which prevent their occurrence. It is conceivable that these barriers are connected to the primary C–C and C–H insertion processes, and it is one of the major goals of the present investigation to shed more light on those parts of the PES decisive for the observed fragmentation patterns.

We commence the in-depth analysis of the computed stationary points for the C–C bond activation branch (Scheme 1 top). Here, the experiments point to the existence of two distinct $Fe(C_2H_6)^+$ minima, an iron–ethane complex **1** and a C–C inserted dimethyl structure **2**, the former being 3 kcal mol^{-1} lower in energy than the latter and separated by a barrier which is probably somewhat below the entrance channel.[5] In complete qualitative accord with these results, we find the iron–ethane encounter complex **1** and the C–C inserted structure **2** as initial products of the $Fe^+ + C_2H_6$ interaction. Complex **1** is 27 kcal mol^{-1} below the entrance channel, while **2** is 11 kcal mol^{-1} less stable. The activation barrier separating the two minima (transition state $\mathbf{TS_{1-2}}$ is located 5 kcal mol^{-1} be-

low the $Fe^+(^6D) + C_2H_6$ asymptote. Thus, TS_{1-2} is low in energy and cannot be responsible for the lack of observing the $FeCH_2^+ + CH_4$ fragmentation reaction. Rather, we find the saddle point TS_{2-3} of the [1,3]-H shift, which joins **2** with the complex of methane and the iron-carbene cation **3**, as the energetic bottleneck for the methane loss. TS_{2-3}, whose structure and transition vector are depicted in Figure 1, is located

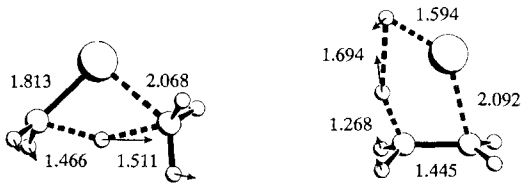

TS_{2-3} (i1502) TS_{4-5} (i642)

Fig. 1. Optimized structures (bond lengths in Å), transition vectors, and imaginary frequencies (in cm^{-1}) of TS_{2-3} and TS_{4-5}.

28 kcal mol^{-1} above the starting materials and thus prevents methane elimination. Instead, the direct fragmentation process cleaving a C–Fe bond in **2** and leading to $FeCH_3^+ + CH_3^{\bullet}$ occurs at this energy threshold, which is energetically similar (27 kcal mol^{-1} above $Fe^+(^6D) + C_2H_6$) but entropically much less demanding than TS_{2-3}. We note in passing that the threshold for this fragmentation from isomer **2** was measured as 43 kcal mol^{-1}, in perfect agreement with the calculated energy difference between **2** and $FeCH_3^+ + CH_3^{\bullet}$.

Turning to the second part of the PES, that is the C–H bond activation branch (Scheme 1 bottom), we first note that even less is known experimentally on intermediates and transition structures here than for its C–C bond activation counterpart. Structure **1** is common to both branches which then fork into the C–C bond activation route via TS_{1-2} and the C–H bond activation domain through TS_{1-4}. The computed height of the activation barrier TS_{1-4} is identical to that of TS_{1-2} (-5 kcal mol^{-1} relative to isolated $Fe^+ + C_2H_6$); thus from an energetical point of view both pathways have equal probability. Another consequence of the low activation energy of TS_{1-4} is that the absence of the exothermic H_2 elimination in the experiments cannot be explained by the assumption of an energetically demanding primary C–H insertion barrier. Structure **4** following the TS_{1-4} transition state is energetically less favorable than the C–C inserted product **2**. The PES in the vicinity of **4** is extremely shallow and located only a few kcal mol^{-1} below the saddle point. Actually, two distinct rotamers of **4** resulted from the geometry optimizations. The barrier for this rotation is, however, negligibly small and hence, the rotation around the C–Fe bond is virtually free. In most previous experimental studies on C–H bond activation of alkanes, a stepwise reaction pathway starting from the C–H-inserted species **4** has often been proposed.[1b] Coming from **4**, this mechanistic scenario would involve a transition structure for a β-H-shift resulting in a dihydrido species such as that schematically depicted in Scheme 2. This would be followed by a reductive elimination of molecular hydrogen which often has been considered as the rate-determining step.

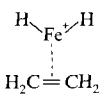

Scheme 2. Previously postulated dihydrido species for the explanation of the activation of C–H bonds by Fe^+ ions.

However, all our attempts to locate an inserted dihydrido minimum for the $[Fe,C_2,H_6]^+$ system failed and rather led to the dihydrogen complex **5**. This result is corroborated by a careful and systematic evaluation of the H-Fe-H bending potentials of both, the parent system $Fe(H_2)^+$ as well as complex **5**, which gave no indication of a dihydrido minimum, regardless of the spin state (quartet or sextet) or the electronic configuration. A similar conclusion was recently drawn by Musaev and Morokuma[12] in the context of the reaction of $FeCH_2^+$ with H_2. Thus it seems to be a general feature that, in spite of being often proposed, the dihydrido species $(H)_2FeL^+$ does not exist as a stable intermediate. Instead, we located a transition structure TS_{4-5}, whose structure and transition vector are also depicted in Figure 1, directly connecting one of the rotamers of **4** and the complex of Fe^+ with molecular hydrogen and ethylene (**5**). The barrier for this four-centered H_2 activation lies 13 kcal mol^{-1} above the entrance channel and thus prevents the exothermic H_2 elimination at thermal energies in this system.[13] In the higher kinetic energy regime of the experiments, FeH^+ but not $Fe(C_2H_4)^+$ is generated, although the latter process is much more favorable on pure energetic grounds. It should, however, be kept in mind that at these energies, the observed fragmentation patterns are not solely determined by the energetics of the PES, but also by the dynamic behavior of the collision processes. While its interpretation is beyond the domain of the present quantum chemical approach, already from a qualitative point of view it seems very plausible that a direct bond cleavage producing $FeH^+ + C_2H_5^{\bullet}$ should be easier to accomplish on the time scale of the experiment than the complicated rearrangement via TS_{4-5} necessary for H_2 loss to produce $Fe(C_2H_4)^+$.

The preceding discussion of the relevant points on the $[Fe,C_2,H_6]^+$ potential energy surfaces is an important first step en route to an understanding of the basic reaction sequence of alkane activation by Fe^+. The DFT/HF hybrid method has not only proven to be a suitable tool for this purpose but also opened new vistas on the crucial mechanistic details of the C–C and C–H bond activations. Its application to the interaction of Fe^+ with larger, chemically more relevant alkanes seems to be in reach and is currently being pursued in our laboratory.

Received: April 1, 1995 [Z 7858 IE]
German version: *Angew. Chem.* **1995**, *107*, 2430–2432

Keywords: ab initio calculations · bond activation · density functional theory

[1] a) J. C. Weisshaar, *Acc. Chem. Res.* **1993**, *26*, 213; b) K. Eller, H. Schwarz, *Chem. Rev.* **1991**, *91*, 1121; c) J. A. Martinho Simões, J. L. Beauchamp *ibid.* **1990**, *90*, 629; d) D. Schröder, H. Schwarz, *Angew. Chem.* **1995**, *107*, 2126; *Angew. Chem. Int. Ed. Engl.* **1995**, *34*, 1973.

[2] See for example. *The Challenge of d and f Electrons, Theory and Computation* (Eds.: D. R. Salahub, M. C. Zerner) (*ACS Symp. Ser.* **1989**, *394*).

[3] See for example. *Density Functional Methods in Chemistry* (Eds.: J. K. Labanowski, J. W. Andzelm), Springer, Heidelberg, **1991**.

[4] a) M. C. Holthausen, C. Heinemann, H. Cornehl, W. Koch, H. Schwarz, *J. Chem. Phys.* **1995**, *102*, 4931; b) M. C. Holthausen, M. Mohr, W. Koch, *Chem. Phys. Lett.* **1995**, *240*, 245; c) D. Schröder, A. Fiedler, H. Schwarz, *Int. J. Mass Spectrom. Ion Processes* **1994**, *134*, 239.

[5] a) R. H. Schultz, P. B. Armentrout, *J. Phys. Chem.* **1992**, *96*, 1662; b) R. Tonkyn, M. Ronan, J. C. Weisshaar, *ibid.* **1988**, *92*, 92; c) R. Tonkyn, J. C. Weisshaar, *ibid.* **1986**, *90*, 2305; d) L. F. Halle, P. B. Armentrout, J. L. Beauchamp, *Organometallics* **1982**, *1*, 963.

[6] The Becke3LYP functional [14] was combined with the Wachters/Hay [15] and Dunning/Huzinaga [16] DZP basis sets on Fe and C and H, respectively. All calculations were performed with Gaussian92/DFT [17]. For a detailed discussion of the used functional, see ref. [4a].

[7] For work on related problems see: a) J.-Y. Saillard, R. Hoffmann, *J. Am. Chem. Soc.* **1984**, *106*, 2006; b) J. K. Perry, G. Ohanessian, W. A. Goddard III, *Organometallics* **1994**, *13*, 1870; c) M. A. Blomberg, P. E. M. Siegbahn, U. Nagashima, J. Wennerberg, *J. Am. Chem. Soc.* **1991**, *113*, 424; as well as ref. [12].

 © VCH Verlagsgesellschaft mbH, D-69451 Weinheim, 1995 0570-0833/95/3420-2284 $ 10.00+.25/0

[8] a) P. B. Armentrout, B. L. Kickel in *Organometallic Ion Chemistry* (Ed.: B. S. Freiser), submitted; b) S. G. Lias, J. E. Bartmess, J. F. Liebman, J. L. Holmes, R. D. Levin, W. G. Mallard, *J. Phys. Chem. Ref. Data* **1988**, *17*, Suppl. 1.
[9] At the employed level of theory, the $Fe^+(^4F)$ state is computed to be 2.3 kcal mol^{-1} more stable than the $Fe^+(^6D)$ state. The experimental splitting is 5.8 kal mol^{-1} in favor of the sextet state (*J* averaged value from C. E. Moore, *Atomic Energy Levels (NBS Handb. (U.S.)* **1949**, Circular 467).
[10] See for example T. Ziegler, J. Li, *Can. J. Chem.* **1994**, *72*, 783.
[11] For other examples of spin-orbit coupled transition metal mediated reactions see a) A. Fiedler, D. Schröder, S. Shaik, H. Schwarz, *J. Am. Chem. Soc.* **1994**, *116*, 10734; b) H. H. Cornehl, C. Heinemann, D. Schröder, H. Schwarz, *Organometallics* **1995**, *14*, 992.
[12] D. G. Musaev, K. Morokuma, *J. Chem. Phys.*, submitted. For related studies on H_2 activation with transition metals see for example D. G. Musaev, K. Morokuma, *Isr. J. Chem.* **1993**, *33*, 307.
[13] The experimental finding that larger alkanes react more efficiently has been attributed to the increasing stability of the encounter complex. This shifts the relative height of the central barrier to lower energies.
[14] A. D. Becke, *J. Chem. Phys.* **1993**, *98*, 1372.
[15] a) A. J. H. Wachters, *J. Chem. Phys.* **1970**, *52*, 1033; b) P. J. Hay, *ibid.* **1977**, *66*, 4377.
[16] T. H. Dunning, P. J. Hay in *Modern Theoretical Chemistry, Vol. II* (Ed.: H. F. Schaefer III), Plenum, New York, **1977**.
[17] Gaussian92/DFT, Revision F2: M. J. Frisch, G. W. Trucks, H. B. Schlegel, P. M. W. Gill, B. G. Johnson, M. W. Wong, J. B. Foresman, M. A. Robb, M. Head-Gordon, E. S. Replogle, R. Gomperts, J. L. Andres, K. Ragavachari, J. S. Binkley, C. Gonzales, R. L. Martin, D. J. Fox, D. J. DeFrees, J. Baker, J. A. Pople, Pittsburgh, PA, **1993**.

(*S*)-Selective Retroaldol Reaction and (*R*)-Selective β-Elimination with an Aldolase Catalytic Antibody**

Jean-Louis Reymond*

By virtue of microscopic reversibility, a catalytic pathway linking two chemical states can be used in both directions. This is well known for enzymes that catalyze reversible processes in vivo. By contrast, microscopic reversibility is rarely verified with designed biocatalysts because reactions tend to be highly exothermic and/or irreversible.[1] The reversible catalysis reported here for an aldolase catalytic antibody leads to an unexpected stereochemical consequence: the (*S*) selectivity of the catalyst in the aldol addition and cleavage is matched by a complementary (*R*) selectivity in the β-elimination.[2] An interpretation is advanced in terms of conformational control.

We recently reported the first aldolase catalytic antibody, which was obtained by linking primary amine **1** with an antibody against hapten **2**. This artificial aldolase catalyzed the aldol addition of acetone to aldehydes by an enzyme-like enamine mechanism, with rate-limiting formation of intermediate **I** within the antibody binding pocket.[3, 4] Starting with racemic aldehyde **3**, the reaction was *si* selective and produced the Cram aldol (4*S*,5*S*)-**4** in >95% *de* from (*S*)-**3** and the anti-Cram aldol (4*S*,5*R*)-**4** in 65% *de* from (*R*)-**3** in a ratio of 1:2.8 (Scheme 1).

The aldol addition, which is favored at high concentrations of acetone (1–10% v/v), can be reversed readily by removing acetone from the medium.[5] The retroaldol reaction of aldol **4** giving aldehyde **3** is catalyzed by the antibody–amine complex under these conditions. As in aldol addition, catalysis requires both amine **1** and the antibody (Ab 72D4, anti-**2**), with an apparent dissociation constant $K_D = 100$ μM for the dissociation of amine **1** from the antibody. Catalysis is quantitatively inhibited by addition of the hapten, ensuring that the reaction takes place in the antigen combining site. The stereoselectivity was determined by assaying the four stereoisomeric aldols **4** individually. As in the aldol addition,[3] preequilibrium binding of the aldols is weak, and the specificity constants k_{cat}/K_M were obtained as a measure of catalysis (Fig. 1). The substrate specificity for retroaldol reaction reproduced the enantioselectivity of the aldol addition (Table 1).

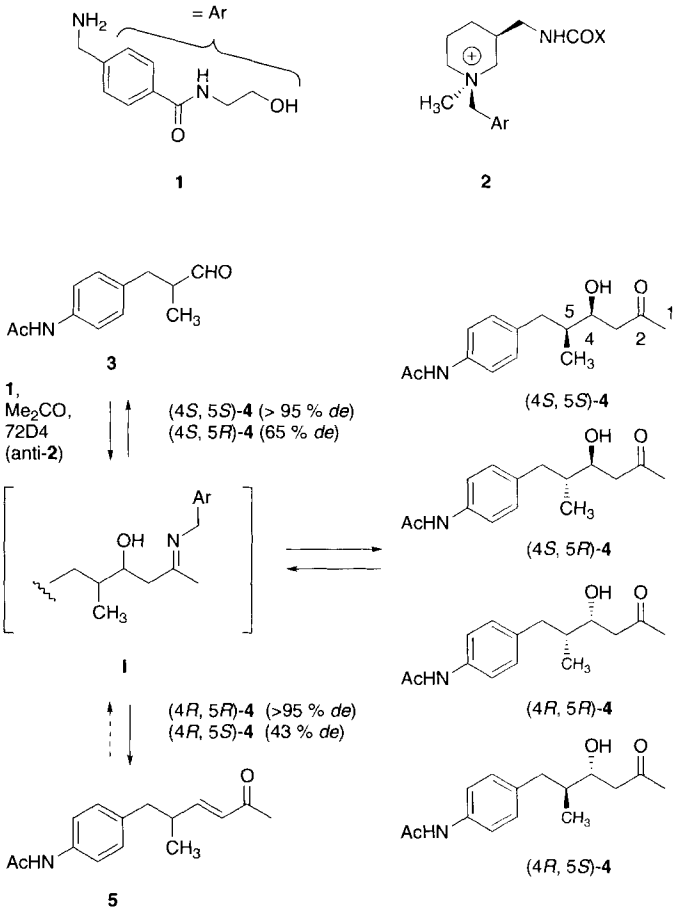

Scheme 1. The artificial aldolase assembled from antibody 72D4 (anti-**2**) and amine **1** catalyzes a (4*S*)-selective aldol cleavage from **4** giving **3** and a (4*R*)-selective β-elimination of **4** giving **5**.

Most interestingly, catalysis of the elimination of water from **4** to form (*E*)-enone **5** was also observed as a concurrent reaction. It was in fact the preferred reaction under hydroxide catalysis, with a 5:1 preference over retroaldol reaction for (4*R**,5*R**)-**4** and 2:1 for (4*R**,5*S**)-**4**.[6, 7] There the antibody–amine complex displayed a completely different stereoselectivity. For the pair of diastereomers of **4** derived from aldehyde (*R*)-**3**, the selectivity was complete for elimination in favor of (4*R*,5*R*)-**4** (>95% *de*), compared to an opposite 8:1 selectivity for (4*S*,5*R*)-**4** (77% *de*) over (4*R*,5*R*)-**4** in the retroaldol reaction. For the adducts stemming from aldehyde (*S*)-**3**, there was a 2.5:1 preference for (4*R*,5*S*)-**4** over (4*S*,5*S*)-**4** in the elimination (43% *de*), versus a complete selectivity for (4*S*,5*S*)-**4** (>95% *de*) in the retroaldol reaction. Thus a (4*S*) configuration at the β-carbon induces aldol cleavage, while a (4*R*) configuration results in β-elimination.

[*] Prof. J.-L. Reymond
Department of Molecular Biology, The Scripps Research Institute
10666 North Torrey Pines Road, La Jolla, CA 92037 (USA)
Telefax: Int. code + (619) 554-6778
e-mail: jlouis@scripps.edu

[**] This work was supported financially by the U. S. National Institutes of Health (GM 49736).

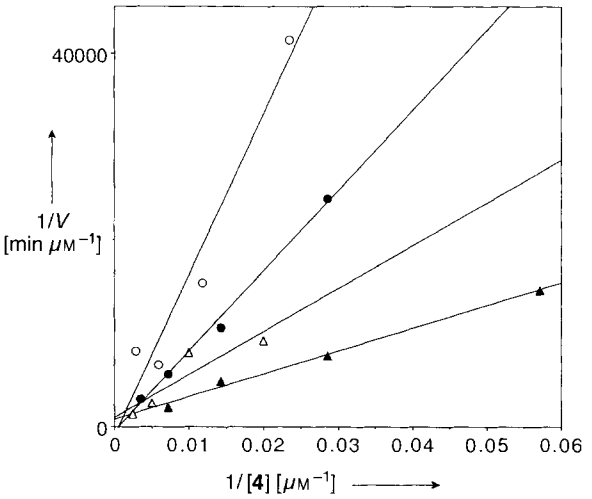

Fig. 1. Lineweaver Burk plot of the initial reaction rates V for catalysis by the complex of antibody 72D4 (anti-**2**) and amine **1**. $k_{cat}/K_M = 1/(\text{slope [anti-2]})$. Retroaldol reaction of isomer (4*S*,5*R*)-**4** (▲), β-elimination of water from isomer (4*R*,5*S*)-**4** (△), retroaldol reaction of isomer (4*S*,5*S*)-**4** (●), retroaldol reaction of isomer (4*R*,5*R*)-**4** (○). Conditions: 20 °C, 50 mM bicine, 100 mM NaCl, pH 9.2, [**1**] = 800 μM, [Ab72D4] = 18 μM. There is no apparent catalysis by amine **1** alone. The rate constants of the background reactions are 2.0×10^{-7} min^{-1} and 3.0×10^{-7} min^{-1} for the retroaldol reactions of (4*R**,5*S**)-**4** and (4*R**,5*R**)-**4**, respectively, and 1.0×10^{-6} min^{-1} and 7.0×10^{-7} min^{-1} for subsequent β-elimination giving enone **5**.

Table 1. Apparent specificity constants for catalysis by antibody 72D4 (anti-**2**) + amine **1** at pH 9.2, 20 °C (50 mM bicine, 100 mM NaCl).

Substrate	Aldol [a] [M^{-2} min^{-1}]	Retroaldol [b] [M^{-1} min^{-1}]	β-Elimination [b] [M^{-1} min^{-1}]
(4*S*,5*S*)-**4**	2.1	0.078	0.044
(4*S*,5*R*)-**4**	5.0	0.22	–
(4*R*,5*S*)-**4**	-	-	0.11
(4*R*,5*R*)-**4**	1.1	0.028	0.022

[a] Addition of acetone to the corresponding enantiomer of aldehyde **3**. From two-dimensional kinetics with respect to acetone and **3** at saturation with **1** ([**1**] = 1 mM), $k_{cat} = 4.1$ M^{-1} min^{-1} for the specificity constant [3b]. For catalysis by amine **1** alone, $k(\mathbf{1}) = 0.011$ M^{-2} min^{-1} and $k_{app}(OH^-) = 2.8 \times 10^{-7}$ M^{-1} min^{-1}, both with a Cram-sense stereoselectivity of 1.5:1. [b] Each constant is derived from saturation kinetics with respect to amine **1** ([**1**] = 100, 200, 400, 800 μM) at four concentrations of the aldol **4** isomer.

The conformations of aldol **4** leading to aldol cleavage ($\theta(N{=}C\text{-}C_\alpha\text{-}C_\beta) = 90°$) and to β-elimination ($\theta = 180°$) are very different. Therefore the chemoselectivity of the antibody–amine **1** catalyst probably results from conformational control. For example a localized hydrogen bonding residue assisting proton transfer at the 4-OH group could enforce complementary conformations on a pair of enantiomeric aldols (Scheme 2).

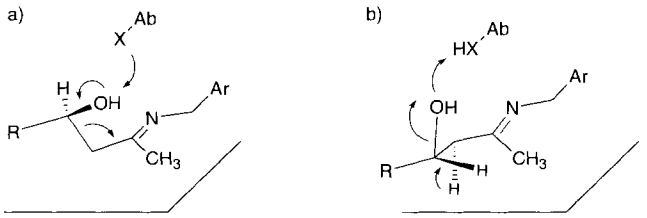

Scheme 2. Conformations favorable for aldol cleavage (a, (4*S*)) or β-elimination (b, (4*R*)) modeled by a hydrogen bonding interaction of a single group X of the antibody Ab with the C_β-OH group of the key intermediate **1**.

As a consequence of this chemoselectivity, the catalysis favoring the (4*S*)-configurated aldols in the aldol reaction is reinforced by selective removal of the (4*R*)-configurated aldols in the β-elimination. If this double induction follows the conformational model proposed here, it could also exist in other aldolase biocatalysts. Such a mechanism might have contributed to the emergence of optical activity for simple carbohydrates in the prebiotic era.[8]

In summary, the first investigation of antibody catalysis with a reversible process has been reported. The (*S*)-selectivity of the aldol cleavage is matched by an (*R*)-selectivity in the β-elimination, probably as a result of conformational control. The reactivity profile of the aldol product is not only straightforward to investigate, but also turns out to be more informative than the aldol addition in terms of enantio- and chemoselectivity of the catalyst. In general, following the reverse reaction with isolated stereoisomers is an attractive method for investigating new enantioselective catalysts, particularly if a large numbers of small-scale assays are required.[9] Future research will address the application of this principle to the aldol reaction and other reversible synthetic reactions.

Experimental Procedure

Isomer separation: A sample of chemically synthesized [3] aldol **4** (4 × 250 μg) was separated on a Chiralcel OJ column (Daicel) (0.45 × 22 cm, 1.0 mL min^{-1}, 2-propanol/hexane (3:1), detection at $\lambda = 250$ nm), giving three fractions: $t_R = 10$–12 min (F1, containing (4*S*,5*S*)-**4**), $t_R = 14$–15 min (F2), and $t_R = 15$–17 min (F3). Repurification of each fraction on a Chiralpak AS column (Daicel), gave $t_R = 23.3$ min ((4*R*,5*S*)-**4**), $t_R = 25.0$ min ((4*S*,5*R*)-**4**), $t_R = 28.5$ min ((4*S*,5*S*)-**4**), and $t_R = 29.3$ min ((4*R*,5*R*)-**4**). Pooled fractions for $t_R = 25.0$ min ((4*S*,5*R*)-**4**) were repurified once on the same column. Each stereoisomer was >95% pure (no other stereoisomer was detected on chiral column). After solvent removal, each isomer was dissolved in 100 μL of acetonitrile/water (1:1). These solutions contained >99.5% pure aldol **4** by RP-HPLC at concentrations of 1.5–2.5 mM, and were used in the kinetic assays.

Assay conditions: 50–350 μM **4**, 100–800 μM **1**, 18 μM Ab 72D4 in 100 mM NaCl, 50 mM bicine (bis(hydroxyethyl)glycine) pH 9.2, 20 °C. Product formation was followed by RP-HPLC (Microsorb-MV C-18, 0.45 × 22 cm, 1.5 mL min^{-1}, H_2O/CH_3CN (3:1), 0.1% CF_3COOH, t_R(**4**) = 3.9 min, t_R(**3**) = 4.8 min, t_R(**5**) = 11.6 min).

Received: May 24, 1995 [Z 8024 IE]
German version: *Angew. Chem.* **1995**, *107*, 2471–2473

Keywords: aldolases · aldol reactions · catalysis · catalytic antibodies

[1] Catalytic antibodies: a) R. A. Lerner, S. J. Benkovic, P. G. Schultz, *Science* **1991**, *252*, 659–667; b) P. G. Schultz, R. A. Lerner, *Acc. Chem. Res.* **1993**, *26*, 391. Catalytic peptides: c) K. Johnsson, R. K. Allemann, H. Widmer, S. A. Benner, *Nature* **1993**, *365*, 530; d) B. Imperiali, R. S. Roy, *J. Am. Chem. Soc.* **1994**, *116*, 12083. Other biomimetic approaches: e) L. G. Mackay, R. S. Wylie, J. K. M. Sanders, *ibid.* **1994**, *116*, 3141, and references therein.

[2] The absolute configurations are not known and are assigned arbitrarily to facilitate discussion. For determination of the relative configuration see ref. [3].

[3] a) J.-L. Reymond, Y. Chen, *Tetrahedron Lett.* **1995**, *36*, 2575; b) *J. Org. Chem.* **1995**, in press.

[4] Leading reference for aldolase enzymes: D. J. Hupe, *Enzyme Mechanisms* (Eds.: M. I. Page, A. Williams), **1987**, pp. 317–344; C.-H. Wong, G. Whitesides, *Enzymes in Synthetic Organic Chemistry*, Pergamon, **1994**. For a recent example of applications of aldolases: H. J. M. Gijsen, C.-H. Wong, *J. Am. Chem.* **1994**, *116*, 8422.

[5] For a detailed discussion of the aldol equilibrium, see: a) J. P. Guthrie, *J. Am. Chem. Soc.* **1991**, *113*, 7249; b) *Can. J. Chem.* **1978**, *56*, 962. The equilibrium constant reported for the reaction acetone + acetaldehyde ⇌ 4-hydroxy-2-pentanone is 25 M^{-1}. In the present paper the equilibrium constant for the reaction (*R*)-**3** + acetone ⇌ (4*S*,5*R*)-**4** under chemoselective catalysis by Ab 724D4 + **1** is 23 M^{-1}.

[6] Studies on imine-mediated aldol β-eliminations: a) T. A. Spencer, M. C. R. Kendall, D. J. Hupe, *J. Am. Chem. Soc.* **1972**, *94*, 1254; *ibid.* **1973**, *95*, 2272; b) T. A. Spencer, M. J. Gula, H. E. Ferran, R. D. Roberts, *ibid.* **1980**, *102*, 7054; see also: c) P. G. Gassman, J. A. Gerlt, *ibid.* **1993**, *115*, 11552.

[7] Antibody-catalyzed aldol eliminations: a) T. Uno, P. G. Schultz, *J. Am. Chem. Soc.* **1992**, *114*, 6573; b) T. Koch, J.-L. Reymond, R. A. Lerner, *ibid.*, in press. Antibody-catalyzed β-fluoro eliminations: c) K. M. Shokat, C. J. Leumann, R. Sugasawara, P. G. Schultz, *Nature* **1989**, *338*, 269; d) K. Shokat, T. Uno, P. G. Schultz, *J. Am. Chem. Soc.* **1994**, *116*, 2261; e) B. Cravatt, J. Ashley, K. D. Janda, D. L. Boger, R. A. Lerner, *ibid.* **1994**, *116*, 6013.

[8] For carbohydrate syntheses with aldolases see ref. [4c]. Leading reference for prebiotic aspects of carbohydrate chemistry: S. S. Pitsch, S. Pombo-Villar, A. Eschenmoser, *Helv. Chim. Acta* **1995**, *77*, 2251.

[9] Screening methods for catalysis: a) D. S. Tawfik, B. S. Green, R. Chap, M. Sela, Z. Eshhar, *Proc. Natl. Acad. Sci. USA* **1993**, *90*, 373; b) G. MacBeath, D. Hilvert, *J. Am. Chem. Soc.* **1994**, *116*, 6101; c) J. W. Lane, X. Hong, A. W. Schwabacher, *ibid.* **1993**, *115*, 2078; d) H. Fenniri, K. D. Janda, R. A. Lerner, *Proc. Natl. Acad. Sci. USA* **1995**, *92*, 2278, and references therein.

Asymmetrization of *meso* 1,4-Enediol Ethers by Isomerization with a Chiral binap–Rh^I Catalyst**

Kou Hiroya, Yuko Kurihara, and Kunio Ogasawara*

We recently reported a highly efficient enantioselective synthesis[1] of both enantiomers of the optically pure tetrahydro-*endo*-1,4-methano- and tetrahydro-*endo*-1,4-ethanonaphthalenones (**4a**, **b**) by lipase-mediated asymmetrization of the corresponding *meso* 1,4-enediols (**1a**, **b**), followed by a novel palladium-mediated rearrangement[2] of the resulting optically pure monoacylated intermediates (**2a**, **b**) and (**3a**, **b**) (Scheme 1). Owing to

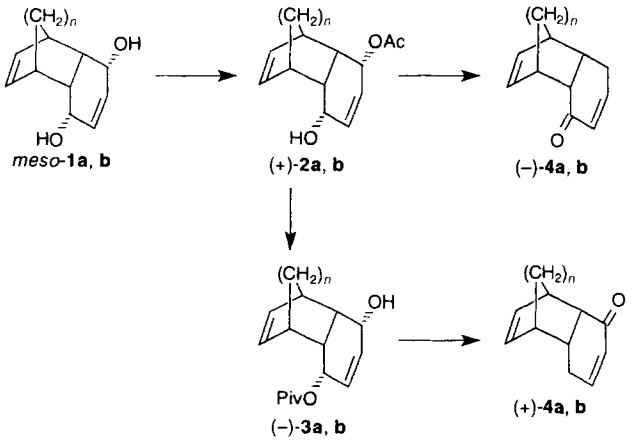

Scheme 1. Piv = pivaloyl. **1a**–**4a**: $n = 1$; **1b**–**4b**: $n = 2$.

its molecular bias, its α,β-unsaturated ketone functionality, and its facile thermal extrusion of cyclopentadiene, the naphthalenone **4a** allows stereoselective introduction of both nucleophiles and electrophiles from the convex face. Since the the masked double bonds can be regenerated **4a** may serve as a chiral synthon of 2,5-cyclohexadienone.[3] Because we have been interested in obtaining this highly versatile chiral synthon by a nonenzymatic procedure and because the catalytic asymmetric isomerization of a *meso* allylic 1,4-enediols such as **1** is not known, we examined the asymmetric isomerization of **1** and the related *meso* substrates using [Rh{(*S*)-binap}(cod)]ClO_4 (cod = 1,5-cyclooctadiene).[4] This catalyst has been successfully employed in the catalytic asymmetric isomerization of allylic amines.[5] Although use of this catalyst for the analogous reaction of allylic alcohols and other allylic oxygen substrates previously met with only limited success,[5–7] in the present study asymmetric isomerization of our *meso* substrates occurred with high enantioselectivity.

The products obtained can be transformed easily into the highly versatile, chiral 2,5-cyclohexadienone synthon **4**[1–3] as well as synthetically useful, chiral 4-*tert*-butyldimethylsilyloxy-2-cyclohexenone (**14**)[8] and 4-hydroxy-2-cyclohexenone (**15**),[8] which serve as starting materials for the synthesis of the medicinally important compounds ML-236A and FK-506, respectively.

We first treated the *meso* diol **1** (0.1 M in THF) with a catalytic amount of (*S*)-binap/Rh^I (5 mol%). At room temperature **1** isomerized cleanly giving the hydroxyketone (+)-**5a** in quantitative yield after 40 h (Scheme 2); its optical purity was deter-

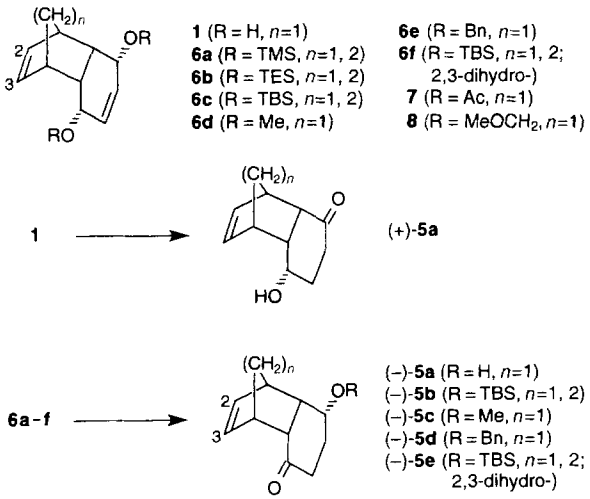

Scheme 2. TMS = trimethylsilyl, TES = triethylsilyl, TBS = *tert*-butyldimethylsilyl.

mined to be 43.3% *ee* by hplc analysis of its benzoate derivative using a chiral column (Table 1, entry 1). Because **1** is insoluble in most solvents, further examination at lower temperature was not possible, and the reactions at higher temperatures in 1,2-dichloroethane (DCE) displayed decreased selectivity (Table 1, entries 2 and 3). Though **1** is soluble in acetonitrile, the reaction did not proceed at all. We therefore transformed **1** into the ethers **6a**–**f**; these were treated with the same chiral catalyst at concentrations of 0.1–0.2 M in DCE, because the reaction in this solvent was found to be more selective than that in THF. Of the examined substrates the silyl ethers showed the best results: after desilylation with aqueous HCl or nBu_4NF,[9] the products were obtained with 93–98% *ee* and in high yields[10] (Table 1, entries 4–9, 12, 13). The dimethyl and the dibenzyl ethers (Table 1, entries 10 and 11) also showed high selectivity; however, bisacetate **7** (R = Ac) and bis(methoxymethyl) ether **8** (R = $MeOCH_2$) did not form any isolable product. Similar results were obtained with the 1,4-ethano counterparts ($n = 2$) (Table 1, entries 5, 7, and 9). The best substrate was the bis-TBS ether **6c** ($n = 1$), which afforded the crystalline silyloxyketone **5b** (m.p. 32 °C, $[\alpha]_D^{29} = -27.0$ ($c = 1.08$ in $CHCl_3$)) on brief expo-

[*] Prof. Dr. K. Ogasawara, Prof. Dr. K. Hiroya, Y. Kurihara
Pharmaceutical Institute, Tohoku University
Aobayama, Sendai 980-77 (Japan)
Telefax: Int. code + (22) 217-6845
e-mail: c21799@cctu.cc.tohoku.ac.jp

[**] binap = *P*,*P*'-(1,1'-binaphthyl-2,2'-diyl)bis(dipbenylphosphane).

 © VCH Verlagsgesellschaft mbH, D-69451 Weinheim, 1995 0570-0833/95/3420-2287 $ 10.00+.25/0

Table 1. Asymmetrization of *meso* diol **1** and ethers **6a–f** by (*S*)-binap/Rh^{I} in DCE [a].

Entry	Substr.	Cat. [mol%]	T	t	Product	Yield [%]	Selectivity [% *ee*]
1	**1** ($n=1$)	5.0	25 °C	15	(+)-**5a** ($n=1$)	≈100	43.3 [e]
2	**1** ($n=1$)	2.0	25 °C	100	(+)-**5a** ($n=1$)	28.0	38.3 [e]
3	**1** ($n=1$)	2.0	reflux	15	(+)-**5a** ($n=1$)	99.6 [b]	16.9 [e]
4	**6a** ($n=1$)	2.0	reflux	14	(−)-**5a** ($n=1$)	≈100 [b]	93.5 [e]
5	**6a** ($n=2$)	2.0	reflux	11	(−)-**5a** ($n=2$)	96.8 [b]	93.6 [e]
6	**6b** ($n=1$)	2.0	reflux	16	(−)-**5a** ($n=1$)	85.8 [b]	97.5 [e]
7	**6b** ($n=2$)	2.0	reflux	12	(−)-**5a** ($n=2$)	94.0 [b]	96.0 [e]
8	**6c** ($n=1$)	2.0	reflux	17	(−)-**5b** ($n=1$)	94.9 [c]	96.1 [e]
9	**6c** ($n=2$)	2.0	reflux	12	(−)-**5b** ($n=2$)	78.6 [c]	96.0 [e]
10	**6d** ($n=1$)	2.0	50 °C	12	(−)-**5c** ($n=1$)	91.4	73.0 [f]
11	**6e** ($n=1$)	2.0	50 °C	40	(−)-**5d** ($n=1$)	66.6 [d]	72.8 [f]
12	**6f** ($n=1$)	2.0	reflux	20	(−)-**5e** ($n=1$)	88.7 [c]	93.7 [e]
13	**6f** ($n=2$)	2.0	reflux	16	(−)-**5e** ($n=2$)	85.2 [c]	93.9 [e]

[a] DCE = 1,2-dichloroethane; in entry 1 THF was used instead of DCE. [b] Yield after conversion of the product into hydroxyketone **5a** by desilylation (dil. HCl in THF or nBu$_4$NF in THF). [c] Yield after conversion of the product into the silyloxyketone **5b** by treatment with dilute HCl. [d] About 30% of **6e** was recovered unchanged. [e] Enantiomeric excess was determined by converting the product into its benzoate derivative and analyzing by HPLC using a chiral column (CHIRALCEL OD; elution, *i*PrOH/hexane, 1:99 v/v). [f] Enantiomeric excess was estimated by comparison of the optical rotation values with those of authentic material.

sure (ca. 5 min) to nBu$_4$NF in THF at 0 °C (Table 1, entry 8). Interestingly, the enantioselectivity exerted by diol **1** and ethers **6a–d** is inverted. Moreover, the asymmetrization occurred with excellent selectivity with the 2,3-dihydro substrates (**6f**: $n=1$, 2), indicating the 2,3-olefin functionality is not critical for the reaction. It is particularly significant that this first successful asymmetrization of the *meso* allylic oxygen substrates proceeded with yields and selectivities comparable to those of the enzymatic reaction (Scheme 2 and Table 1).

The absolute configuration of the 1,4-methano-bridged hydroxyketone **5a** ($n=1$) was determined by transforming (−)-**5a** ($n=1$) into the chiral 2,5-cyclohexadienone synthon (+)-**4a**[1, 2] via the monoacetate (−)-**2a**; (−)-**5b** ($n=1$) was converted into the known chiral 4-*tert*-butyldimethylsilyl-2-cyclohexenone (*R*)-**14**[11] and 4-hydroxy-2-cyclohexenone (*R*)-**15** (Scheme 3). Thus, (−)-**5a** (96% *ee*) was first treated with NBS[12] to give bromo ether **9** in 92% yield, which then was dehydrogenated to give enone **11** in 80% overall yield via the silyl enol ether **10** by employing the Saegusa conditions.[13] Further transformation of **11** into allyl acetate **13** via allyl alcohol **12**, followed by reductive cleavage of the bromo ether functionality[12] yielded monoacetate (−)-**2a** (m.p. 86.5–87.5 °C, $[\alpha]_D^{27} = -68.78$ ($c = 0.96$ in CHCl$_3$)), whose enantiomer (+)-**2a** (m.p. 87–88 °C, $[\alpha]_D^{30} = +70.05$ ($c = 1.02$ in CHCl$_3$)) was previously obtained by enzymatic transesterification of **1**.[1a] Quite similarly, the configuration of 1,4-ethano-bridged hydroxyketone (−)-**5a** ($n=2$) was determined by conversion into (−)-**4b**, which was identical with an authentic material obtained by the enzymatic procedure.[1b]

On the other hand, a solution of the ketosilyl ether (−)-**5b** (96% *ee*) in freshly distilled diphenyl ether was refluxed for 20 min to afford (*R*)-4-*tert*-butyldimethylsilyloxy-2-cyclohexenone [(*R*)-**14**][8] ($[\alpha]_D^{29} = +109.0$ ($c = 1.15$ in CHCl$_3$) (96.4% *ee* by hplc); literature value for the (*S*) enantiomer:[11a] $[\alpha]_D = -115.9$ ($c = 1.06$ in CHCl$_3$)) in 95% yield. The absolute configuration of (*R*)-**14** was confirmed by further transformation into (*R*)-4-hydroxy-2-cyclohexenone [(*R*)-**15**][8] ($[\alpha]_D^{29} = +109.0$ ($c = 1.29$, CHCl$_3$); literature value for the (*S*) enantiomer:[11a] $[\alpha]_D = -110$ ($c = 0.92$ in CHCl$_3$)) in 94% yield on exposure to hydrofluoric acid (48%) in acetonitrile[14] (1:19) (Scheme 3).

Although we could not explain the inversion of enantioselectivity on going from the free diol **1** to the bisethers **6a–f** in the presence of the same catalyst, the isomerization of the *meso* bisethers may be rationalized by a mechanism involving a suprafacial 1,3-hydrogen shift.[15] This hypothesis was supported by a deuterium labeling experiment using [D$_2$]**6c**. This 5β,8β-deuterium-labeled compound afforded the rearranged product 7β,8β-deuterium-labeled hydroxyketone [D$_2$]**5a** cleanly after desilylation without scrambling or loss of the original deuterium atoms. As shown in Scheme 4, oxidative addition occurs first to form the Rh^{III} complex **16**, which in turn is isomerized by 1,3-metal migration to give the alternative Rh^{III} complex **17** carrying a silyl enol ether functionality. Subsequent reductive elimination produces the Rh^{I} complex **18** and release of the Rh^{I} catalyst yields the disilyl ether **19**.

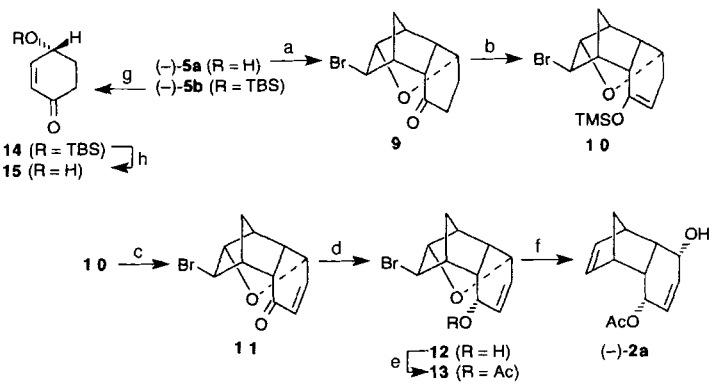

Scheme 3. a) *N*-Bromosuccinimide (1.1 equiv), CH_2Cl_2, 0 °C, 1 h; 91.5%; b) *i*Pr-NEt$_2$ (11 equiv), TMSOTf (2 equiv), CH_2Cl_2, 0 °C, 2.5 h; c) Pd(OAc)$_2$ (1.1 equiv), MeCN, room temperature (RT), 26 h; 80% based on **9**; d) $NaBH_4$ (1.5 equiv), $CeCl_3 \cdot 7H_2O$ (1.5 equiv), −78 °C, 4.5 h; 92%; e) Ac_2O (2 equiv), Et_3N (3 equiv), 4-dimethylaminopyridine (cat.), CH_2Cl_2, 0–25 °C, 12 h; f) Zn (8 equiv), AcOH (15 equiv), MeOH, reflux, 7 h; 76% based on **12**; g) 260 °C, diphenyl ether, 20 min; 95%; h) HF (45%)/MeCN (1:5 v/v), 0 °C, 4 h; 96%.

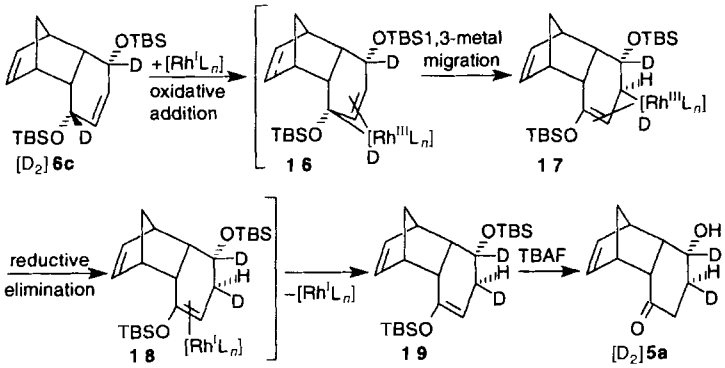

Scheme 4.

In conclusion, we have established a new highly efficient, enantioselective entry to the versatile chiral building blocks tetrahydro-*endo*-1,4-methano- and tetrahydro-*endo*-1,4-ethano-naphthalenones by isomerization of the bissilyl ethers of *meso* allylic 1,4-enediols using a cationic chiral binap-Rh^{I} catalyst. This result is remarkable for a number of reasons: 1) This is the first application of a catalytic asymmetric isomerization to an allyl ether substrate that reaches a practical level of enantioselectivity. 2) This is the first successful asymmetrization of a *meso* substrate by a catalytic isomerization. 3) The chemical and

enantiomeric efficiencies of this method are fully comparable to those of the enzymatic procedure. 4) This method can provide highly versatile cyclohexenone chiral synthons very efficiently. 5) The reaction mechanism has been proven to include a suprafacial 1,3-hydrogen migration pathway.

Experimental Procedure

Transformation of **6c** into **5b**: To a stirred solution of **6c** (405 mg, 1.0 mmol) in 1,2-dichloroethane (4.6 mL) was added [Rh{(*S*)-binap}(cod)]ClO_4 (18.6 mg, 19.9 mmol) in 1,2-dichloroethane (0.5 mL) dropwise at room temperature under argon and the mixture was refluxed for 17 h. The solvent was evaporated, the residue dissolved in THF (5 mL), and the resulting solution stirred with nBu$_4$NF (1.0 M in THF, 1.0 mL) at 0 °C for 5 min. The solution was diluted with ether and washed successively with water and brine, dried over $MgSO_4$, and concentrated under reduced pressure. The residue was chromatographed on silica gel (EtOAc/hexane 1:9) to give **5b** as colorless crystals (276 mg, 94.9%) (96.1% *ee*). A single recrystallization from hexane gave the optically pure material (99.5% *ee*) as colorless prisms, m.p. 32 °C, $[\alpha]_D^{29} = -27.0$ ($c = 1.08$ in $CHCl_3$).

Received: June 9, 1995 [Z8073IE]
German version: *Angew. Chem.* **1995**, *107*, 2445–2448

Keywords: asymmetric syntheses · catalysis · isomerizations · rhodium compounds

[1] a) For **4a**, see: S. Takano, Y. Higashi, T. Kamikubo, M. Moriya, K. Ogasawara, *Synthesis* **1993**, 948–950; b) for **4b**, see: M. Moriya, T. Kamikubo, K. Ogasawara, *ibid.* **1995**, 187–190.

[2] S. Takano, M. Moriya, T. Kamikubo, K. Hiroya, K. Ogasawara, *Tetrahedron Lett.* **1993**, *34*, 8485–8488.

[3] Some representative examples, see: a) K. Ogasawara, *Pure Appl. Chem.* **1994**, *66*, 2119–2122; b) S. Takano, M. Moriya, Y. Higashi, K. Ogasawara, *J. Chem. Soc. Chem. Commun.* **1993**, 177–178; c) S. Takano, M. Moriya, K. Ogasawara, *ibid.* **1993**, 614–615; d) S. Takano, Y. Higashi, T. Kamikubo, M. Moriya, K. Ogasawara, *ibid.* **1993**, 788–789; e) S. Takano, M. Moriya, K. Ogasawara, *Synlett* **1993**, 601–602; f) S. Takano, T. Kamikubo, M. Moriya, K. Ogasawara, *Synthesis* **1994**, 601–604; g) T. Kamikubo, K. Ogasawara, *Chem. Lett.* **1995**, 95–96; h) T. Kamikubo, K. Ogasawara, *Tetrahedron Lett.* **1995**, *36*, 1685–1688.

[4] a) A. Miyashita, A. Yasuda, H. Takaya, K. Toriumi, T. Ito, T. Souchi, R. Noyori, *J. Am. Chem. Soc.* **1980**, *102*, 7932–7934; b) A. Miyashita, H. Takaya, T. Souchi, R. Noyori, *Tetrahedron* **1984**, *40*, 1245–1253; c) M. Takaya, K. Mashima, K. Koyano, M. Yagi, H. Kumobayashi, T. Taketomi, S. Akutagawa, R. Noyori, *J. Org. Chem.* **1986**, *51*, 629–635.

[5] Pertinent reviews, see: a) S. Otsuka, K. Tani in *Asymmetric Synthesis, Vol. 5* (Ed.: J. D. Morrison), Academic Press, New York, **1985**, pp. 171–191; b) R. Noyori, M. Kitamura in *Modern Synthetic Methods, Vol. 5* (Ed.: R. Schefford), Springer, Heidelberg, **1989**, pp. 115–198; c) S. Otsuka, K. Tani, *Synthesis* **1991**, 665–680.

[6] M. Kitamura, K. Manake, R. Noyori, H. Takaya, *Tetrahedron Lett.* **1987**, *28*, 4719–4720.

[7] Efficient catalytic production of achiral enols using Rh^I–diphosphane complexes, see: S. H. Bergens, B. Bosnich, *J. Am. Chem. Soc.* **1991**, *113*, 958–967.

[8] a) S. J. Danishefsky, B. Simoneau, *J. Am. Chem. Soc.* **1989**, *111*, 2599–2604; b) A. B. Jones, M. Yamaguchi, A. Patten, S. J. Danishefsky, J. A. Ragan, D. B. Smith, S. L. Schreiber, *J. Org. Chem.* **1989**, *54*, 17–19.

[9] Attempts to isolate the products as the silyl enol ethers in pure form failed since a considerable amount of the ketones (>20%) always formed before the reaction was quenched.

[10] I. Kuwajima, E. Nakamura, M. Shimizu, *J. Am. Chem. Soc.* **1982**, *104*, 1025–1030.

[11] a) J. E. Audia, L. Boisvert, A. D. Patten, A. Villalobos, S. J. Danishefsky, *J. Org. Chem.* **1989**, *54*, 3738–3740; b) M. C. Carreno, J. L. Ruano, M. Garrido, M. P. Ruiz, G. Solladie, *Tetrahedron Lett.* **1990**, *31*, 6653–6656.

[12] Cf. S. Takano, K. Inomata, K. Ogasawara, *Chem. Lett.* **1989**, 359–362.

[13] Y. Ito, T. Hirao, T. Saegusa, *J. Org. Chem.* **1978**, *43*, 1011–1013.

[14] R. F. Newton, D. P. Reynolds, M. A. Finch, F. D. Kelly, S. M. Roberts, *Tetrahedron Lett.* **1979**, 3981–3982.

[15] Cf. R. Noyori, *Tetrahedron* **1994**, *50*, 4259–4292.

Radiofrequency Encoded Combinatorial Chemistry**

K. C. Nicolaou,* Xiao-Yi Xiao,* Zahra Parandoosh, Andrew Senyei, Michael P. Nova*

Combinatorial chemistry[1] has recently been recognized as a powerful tool in drug discovery[2] and materials science.[3] Although the potential of this method in these areas is enormous, its current scope is limited by several factors.[1] Particularly prohibitive is the lack of a general encoding system for following the synthetic sequence leading to the chemical constructs so that structural characterization can be facilitated. Despite the introduction of several encoding,[4] physical,[5] and deconvolution[6] techniques for identification of members in a chemical library, serious practical issues still remain and a more general and practical solution to this problem is needed.

We introduce here a new concept for encoding combinatorial chemical libraries based on radiofrequency signals and semiconductor memory devices using a multifunctional Microreactor. Radiofrequency Encoded Combinatorial (REC™) chemistry, as this new method is termed, combines recent advances in microelectronics, sensors, and chemistry and uses a Single or Multiple Addressable Radiofrequency Tag (SMART™) semiconductor unit[7] to record encoding and other relevant information along the synthetic pathway. This allows identification of library members by retrieval of the recorded history and other specific information relating to the construction of each compound. The practicability of the concept and the validity of the principles of REC chemistry are demonstrated here with a small peptide library generated by the "split and pool" method.[8]

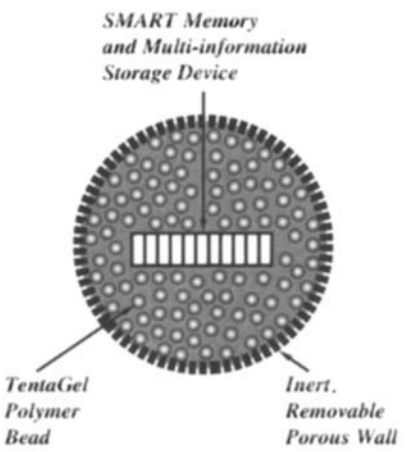

Fig. 1. Schematic cross-section of a Microreactor used in REC chemistry relying on SMART multi-information storage devices.

A SMART Microreactor™ (Fig. 1) was constructed from the following units: 1) a small (8 × 1 × 1 mm) semiconductor SMART memory device capable of receiving, storing, and emitting radiofrequency signals instantaneously from a distance of 75–150 mm; 2) several TentaGel-like polymer beads carrying an acid-cleavable linker; and 3) a chemically inert, surrounding porous support. A representative REC chemistry

[*] Prof. Dr. K. C. Nicolaou[+]
Department of Chemistry, The Scripps Research Institute
10666 N. Torrey Pines Road, La Jolla, CA 92037 (USA)
and
Department of Chemistry and Biochemistry
University of California, San Diego
9500 Gilman Drive, La Jolla, CA 92093 (USA)
Telefax: Int. code + (619) 554-6738
e-mail: knicolaou@ucsd.edu
Dr. M. P. Nova, Dr. X.-Y. Xiao, Dr. Z. Parandoosh, Dr. A. Senyei
IRORI Quantum Microchemistry
11025 N. Torrey Pines Road, La Jolla, CA 92037 (USA)
Telefax: Int. code + (619) 546-1300
e-mail: NOVAIRORI@AOL
[+] K. C. N. is an advisor to IRORI Quantum Microchemistry.

[**] We thank Chris Claiborne for the computer-generated drawings.

sequence is shown in Scheme 1. A pool of Microreactors is split into two groups. Each group is then addressed by write-encoding[9] with a unique radiofrequency signal (i.e. **a** or **b**) corresponding to the building block to be added to that group (i.e. **A** or **B**). The reactions are carried out separately with each group.

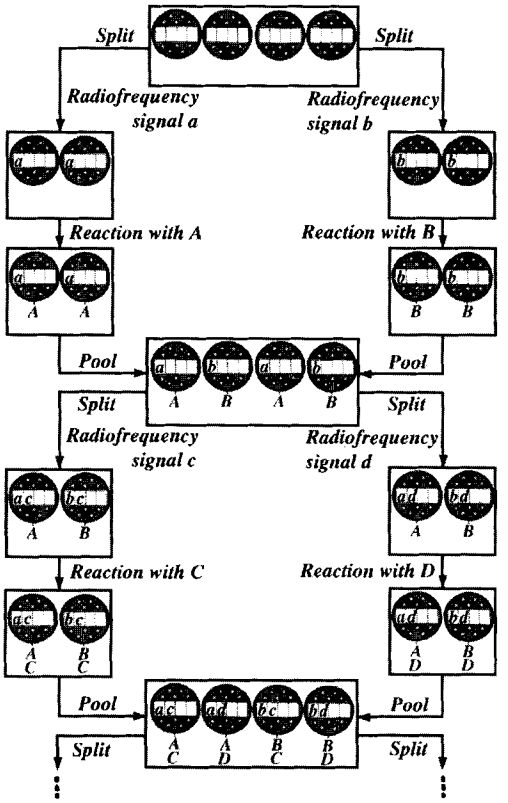

Scheme 1. A REC chemistry sequence using SMART semiconductor memory devices in Microreactors and the "split and pool" method. The order of the encoding and the chemical steps can be interchanged. The pool can be split into more than two groups.

The Microreactors are then pooled together, and common reactions and manipulations such as deprotections, washing, and drying are performed at this stage. The pool is then split again into two groups and encoded with a second set of radiofrequency signals (i.e. **c** or **d**) corresponding to the next set of building blocks to be introduced (i.e. **C** or **D**), and the reactions are performed accordingly. This process is repeated until the synthesis is completed. It should be noted that the large memory capacity of the SMART devices allows multiple splits at each stage of the combinatorial synthesis as well as multistep sequences to be carried out. Furthermore, the semiconductor devices record the temperature for each synthetic step and could potentially sense and store other important information relating to reaction conditions and compounds.

A specific example of the REC method is detailed in Scheme 2. Ninety-six Microreactors were used to construct a 24-member REC peptide library using a $3 \times 2 \times 2 \times 2$ "split and pool" strategy.[10] Each Microreactor of the final 96-member pool was decoded using a specially designed radiofrequency memory retrieving device to reveal the identity of the peptide on each Microreactor (Table 1). The identity of each peptide was confirmed by both mass spectrometry and ^{1}H NMR spectroscopy.[11] Peptide purity was shown by HPLC to be high in each crude sample even prior to purification (Table 1) and could be increased further by standard chromatographic techniques.

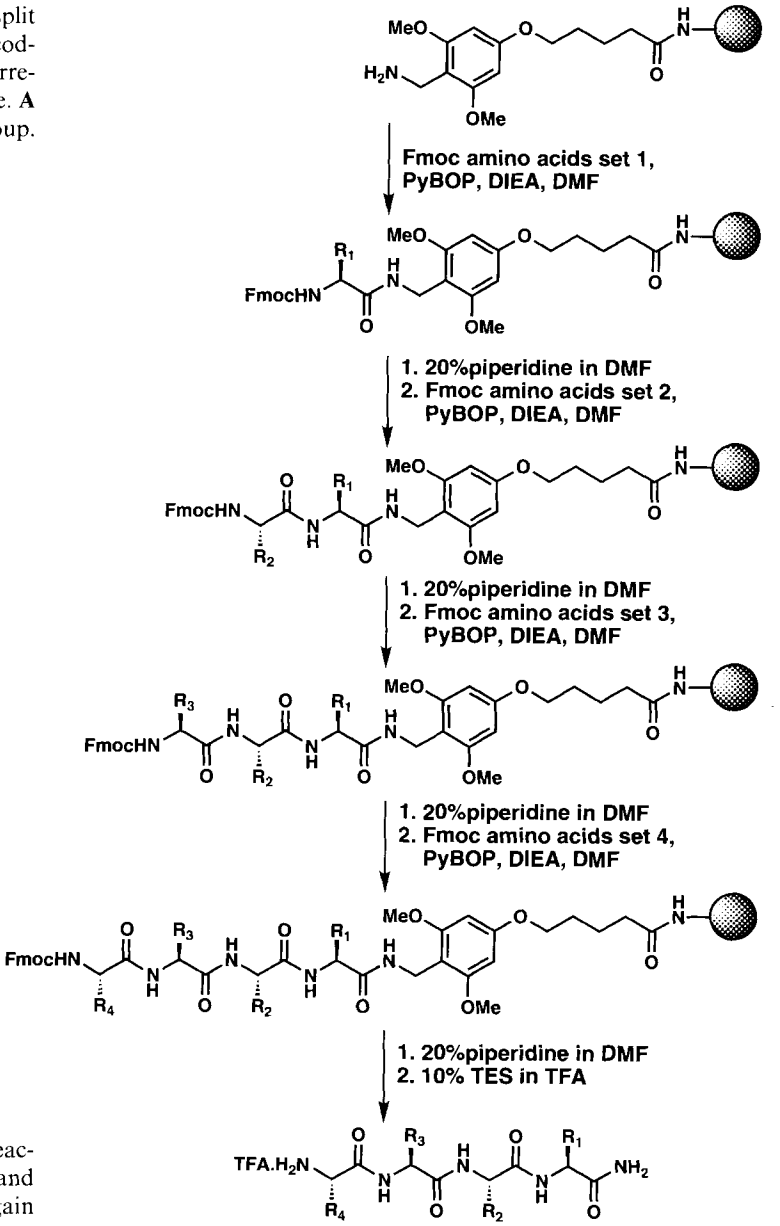

Scheme 2. Synthesis of a 24-member peptide library using REC chemistry. Fmoc = 9-fluorenylmethoxycarbonyl; DIEA = diisopropylethylamine; TES = triethylsilane; TFA = trifluoroacetic acid; PyBOP = benzotriazol-1-yloxy(trispyrrolidino)phosphonium hexafluorophosphate; amino acids set 1 = Asp(O*t*Bu)-OH (code D), Phe-OH (code F), or Lys(Boc)-OH (code K); amino acids set 2 = Gly-OH (code G), or Val-OH (Code V); amino acids set 3 = Glu(O*t*Bu)-OH (code E), or Ala-OH (code A); amino acids set 4 = Leu-OH (code L) or Ser(O*t*Bu)-OH (code S). All reactions were carried out at ambient temperature. Reaction times: Fmoc deprotection, 0.5 h; coupling, 1 h (two couplings per amino acid); cleavage, 2 h.

The Microreactor shown in Figure 1 is highly flexible and can be used in various sizes, shapes, and forms, including platforms in which the polymer support is coated directly on the SMART chips; other mobile and fixed reaction vehicles are also possible.[12] The feasibility of Microreactors consisting of directly polymer-coated SMART devices has already been demonstrated.

We have developed a new method of encoding combinatorial chemical libraries using a novel multifunctional platform for synthetic chemistry, relying entirely on chemically benign radiofrequency signals and semiconductor memory microchips for information storage. The obvious advantages of this method include: a) easy and rapid encoding, b) very large encoding

 © VCH Verlagsgesellschaft mbH, D-69451 Weinheim, 1995 0570-0833/95/3420-2290 $ 10.00+.25/0

Table 1. REC peptide library consisting of 24 compounds. Rf code = radiofrequency code.

Entry	Rf code	Peptide sequence	n [a, b]	*m/z* [c]	HPLC purity [%] [d]
1	LAGD	Leu-Ala-Gly-Asp	3	372 (373)	85
2	LEGD	Leu-Glu-Gly-Asp	4	432 (431)	94
3	SAGD	Ser-Ala-Gly-Asp	5	348 (347)	83
4	SEGD	Ser-Glu-Gly-Asp	5	406 (405)	88
5	LAVD	Leu-Ala-Val-Asp	4	416 (415)	97
6	LEVD	Leu-Glu-Val-Asp	6	474 (473)	98
7	SAVD	Ser-Ala-Val-Asp	2	390 (389)	89
8	SEVD	Ser-Glu-Val-Asp	3	446 (447)	92
9	LAGF	Leu-Ala-Gly-Phe	5	406 (405)	92
10	LEGF	Leu-Glu-Gly-Phe	5	464 (463)	93
11	SAGF	Ser-Ala-Gly-Phe	5	380 (379)	91
12	SEGF	Ser-Glu-Gly-Phe	6	438 (437)	91
13	LAVF	Leu-Ala-Val-Phe	6	448 (447)	72
14	LEVF	Leu-Glu-Val-Phe	2	506 (505)	92
15	SAVF	Ser-Ala-Val-Phe	2	422 (421)	94
16	SEVF	Ser-Glu-Val-Phe	1	480 (479)	94
17	LAGK	Leu-Ala-Gly-Lys	2	387 (386)	67
18	LEGK	Leu-Glu-Gly-Lys	1	445 (444)	85
19	SAGK	Ser-Ala-Gly-Lys	4	361 (360)	71
20	SEGK	Ser-Glu-Gly-Lys	3	419 (418)	82
21	LAVK	Leu-Ala-Val-Lys	4	429 (428)	72
22	LEVK	Leu-Glu-Val-Lys	6	487 (486)	79
23	SAVK	Ser-Ala-Val-Lys	6	403 (402)	71
24	SEVK	Ser-Glu-Val-Lys	6	461 (460)	85

[a] Number of Microreactors containing the same peptide sequence. [b] The ambient temperature was recorded by the sensor device of the SMART chip in the Microreactors at various points during the synthesis. [c] *m/z* refers to $[M + H]^+$ or (for entries 1 and 8) $[M - H]^-$ (Electrospray MS); since each peptide has a unique mass (the calculated values are given in parentheses), the mass spectra confirm all peptide structures. [d] HPLC conditions: Shimadzu SCL 10A with a Microsorb-MV C-18 column (5 μm, 100 Å); isocratic elution with acetonitrile/water (1:1).

capacity, c) non-interference with chemical steps, d) storage of numerous types of information at each step, e) delivery of large libraries in amounts ranging from nano- to multimilligram quantities per compound, f) synthesis of pure compounds whose structures can be identified by decoding and confirmed by spectroscopic means, and g) versatility in both reactor configuration and scope of chemistry. The potential for automation and integration of such Microreactors for synthetic chemistry with assay platforms for high-throughput biological screening and data storage devices should make this technology the method of choice for many future combinatorial and other chemistry applications. Further applications of this basic technology in other areas of chemistry, biology, and medicine are also envisioned.

Received: September 15, 1995 [Z 8402IE]
German version: *Angew. Chem.* **1995**, *107*, 2476–2479

Keywords: combinatorial chemistry · microreactors · peptides · radiofrequency encoding

[1] a) M. A. Gallop, R. W. Barret, W. J. Dower, S. P. A. Fodor, E. M. Gordon, *J. Med. Chem.* **1994**, *37*, 1233; b) E. M. Gordon, R. W. Barret, W. J. Dower, S. P. Fodor, M. A. Gallop, *ibid.* **1994**, *37*, 1385; c) J. A. Ellman, *Chemtracts: Org. Chem.* **1995**, *8*, 5; d) A. W. Czamik, *ibid.* **1995**, *8*, 13; e) M. R. Pavia, T. K. Sawyer, W. H. Moos, *Bioorg. Med. Chem. Lett.* **1993**, *3*, 387, and other articles in that issue; f) H. M. Geysen, R. H. Meloen, S. J. Barteling, *Proc. Natl. Acad. Sci. USA* **1984**, *81*, 3998; g) B. A. Bunin, J. A. Ellman, *J. Am. Chem. Soc.* **1992**, *114*, 10997.

[2] R. Hirschmann, *Angew. Chem.* **1991**, *103*, 1305; *Angew. Chem. Int. Ed. Engl.* **1991**, *30*, 1278.

[3] X.-D. Xiang, X. Sun, G. Briceño, Y. Lou, K.-A. Wang, H. Chang, W. G. Wallace-Freedman, S.-W. Chen, P. G. Schultz, *Science* **1995**, *268*, 1738.

[4] a) S. Brenner, R. A. Lerner, *Proc. Natl. Acad. Sci. USA* **1992**, *89*, 5381; b) M. C. Needels, D. G. Jones, E. H. Tate, G. L. Heinkel, L. M. Kochersperger, W. J. Dower, R. W. Barret, M. A. Gallop, *ibid.* **1993**, *90*, 10700; c) J. Nielsen, S. Brenner, K. D. Janda, *J. Am. Chem. Soc.* **1993**, *115*, 9812; d) V. Nikolaiev, A. Stierandova, V. Krchnak, B. Seligmann, K. S. Lam, S. E. Salmon, M. Lebl, *Peptide Res.* **1993**, *6*, 161; e) J. M. Kerr, S. C. Banville, R. N. Zuckermann, *J. Am. Chem. Soc.* **1993**, *115*, 2529; f) M. H. J. Ohlmeyer, R. N. Swanson, L. W. Dillard, J. C. Reader, G. Asouline, R. Kobayashi, M. Wigler, W. C. Still, *Proc. Natl. Acad. Sci. USA* **1993**, *90*, 10922; g) A. Borchardt, W. C. Still, *J. Am. Chem. Soc.* **1994**, *116*, 373; h) H. P. Nester, P. A. Bartlett, W. C. Still, *J. Org. Chem.* **1994**, *59*, 4723.

[5] a) G. Jung, A. G. Beck-Sickinger, *Angew. Chem.* **1992**, *104*, 375; *Angew. Chem. Int. Ed. Engl.* **1992**, *31*, 367; b) C. L. Brummel, I. N. W. Lee, Y. Zou, S. J. Benkovic, N. Winograd, *Science* **1994**, *264*, 399; c) B. J. Egner, G. J. Langley, M. Bradley, *J. Org. Chem.* **1995**, *60*, 2652; d) R. S. Youngquist, G. R. Fuentes, M. P. Lacey, T. Keough, *J. Am. Chem. Soc.* **1995**, *117*, 3900; e) Y.-H. Chu, D. P. Kirby, B. L. Karger, *ibid.* **1995**, *117*, 5419; f) G. C. Look, C. P. Holmes, J. P. Chinn, M. A. Gallop, *J. Org. Chem.* **1994**, *59*, 7588.

[6] a) R. A. Houghten, C. Pinilla, S. E. Blondelle, J. R. Appel, C. T. Dooley, J. H. Cuervo, *Nature* **1991**, *354*, 84; b) H. Han, M. M. Wolfe, S. Brenner, K. D. Janda, *Proc. Natl. Acad. Sci. USA* **1995**, *92*, 6419.

[7] M. L. Beigel US-A 5266926; 5257011 and 5214409.

[8] a) A. Furka, F. Sebestyén, M. Asgedom, G. Dibó, *Abstr. 14th Int. Congr. Biochem. (Prague, Czechoslovokia)* **1988**, *Vol. 5*, 47; b) *Abstr. 10th Int. Symp. Med. Chem. (Budapest, Hungary)* **1988**, *Vol. 5*, 288; c) *Int. J. Pept. Protein Res.* **1991**, *37*, 487; d) K. S. Lam, S. E. Salmon, E. M. Hersh, V. J. Hruby, W. M. Kazmierski, R. J. Knapp, *Nature* **1991**, *354*, 82.

[9] Encoding and decoding was accomplished using radiofrequency pulse signals (100–400 kHz) whose generation, transmission, and retrieval was assisted by appropriate computer hardware and software.

[10] The number selected for the construction of this combinatorial library was chosen to virtually ensure the statistical formation of a 24-member library, see: K. Burgess, A. I. Liaw, N. Wang, *J. Med. Chem.* **1994**, *37*, 2985. Of course, sorting out the Microreactors precisely prior to each "split" converts this statistical method into an exact approach with one compound per Microreactor.

[11] Selective ^{1}H NMR data (500 MHz, [D$_6$]DMSO). **LAGD** (entry 1, Table 1): δ = 8.68 (d, J = 7.3 Hz, 1H, NH), 8.24 (t, J = 5.5 Hz, 1H, NH), 8.01–8.13 (m, 3H, NH), 7.24 (s, 1H, NH), 7.14 (s, 1H, NH), 4.45–4.52 (m, 1H, CH), 4.35–4.42 (m, 1H, CH), 3.67–3.82 (m, 3H, H), 2.67 (dd, J = 5.5, 16.0 Hz, 1H, CH*H*COO), 2.45–2.52 (m, 1H, CH*H*COO), 1.48–1.70 (m, 3H, CH, CH$_2$), 1.27 (d, J = 6.5 Hz, 3H, CH$_3$), 0.91 (d, J = 6.3 Hz, 3H, CH$_3$), 0.86 (d, J = 6.6 Hz, 3H, CH$_3$). **SAVF** (entry 15, Table 1): δ = 8.59 (d, J = 7.5 Hz, 1H, NH), 8.05–8.15 (m, 3H, NH), 7.88 (dd, J = 8.5, 22.4 Hz, 1H, NH), 7.36 (s, 1H, NH), 7.14–7.26 (m, 5H, Ph), 7.06 (s, 1H, NH), 4.38–4.48 (m, 2H, CH), 4.09 (dd, J = 7.2, 8.4 Hz, 1H, CH), 3.82–3.88 (m, 1H, CH), 3.4–3.6 (m, 2H, CH$_2$O), 2.98 (dd, J = 5.0, 13.8 Hz, 1H, PhCH*H*), 2.80 (dd, J = 8.9, 13.8 Hz, 1H, PhCH*H*), 1.89–1.95 (m, 1H, CH), 1.19 (d, J = 7.0 Hz, 3H, CH$_3$), 0.77 (d, J = 6.8 Hz, 6H, CH$_3$).

[12] The SMART chips are equipped with a standard EEPROM (Electrically Erasable, Programmable, Read-Only Memory) unit and temperature-sensing probe; they are passive devices deriving their required energy directly from the radiofrequency pulses used for encoding. These devices are enclosed in glass and are therefore completely inert to most reagents and conditions used in organic synthesis and can withstand temperatures between −78 °C and 150 °C. These devices will be available from IRORI Quantum Microchemistry.

A Fitting Legacy for All Time

The Lock and Key Principle. The State of the Art—100 Years on. Edited by *J.-P. Behr*. Wiley, Chichester, 1994. 325 pp., hardcover £ 85.00.—ISBN 0-471-93902-1

All scientists who work in the field of enzymology, or on its fringes, are familiar with the "Lock and Key" (L & K) principle of Emil Fischer. It is the foundation upon which the understanding of enzyme action still rests, despite having evolved significantly since first proposed approximately 100 years ago.

The new insights into, as well as the modern interpretations of this principle are the focus of the first volume in the series "Perspectives in Supramolecular Chemistry". One issue which must have concerned the founder and editor of this series (J.-M. Lehn and J.-P. Behr, respectively) is how to achieve the proper mix of enzymologists, molecular biologists, material scientists, and organic chemists to contribute chapters to this perspective.

Their answer has resulted in a text that is truly interdisciplinary, covering aspects of immunology, enzymology, molecular recognition, protein and nucleic acid structure, solid state chemistry, and molecular biology. This book impresses upon the reader the remarkable contribution from Emil Fischer, to whom all these fields must pay homage after 100 years for his original L & K notion.

The chapters vary widely in topic. The first one gives an imaginative analogy between several kinds of "locks", and the modern interpretation of the L & K principle. It analyzes cyclodextrin as a "classical lock", aminoacyl tRNA synthetases as "safety locks", and antisense gene therapy as a "magnetic lock". Chapter 2 discusses thermodynamic considerations for the L & K principle, including the mathematics of specificity and affinity distributions. It also focuses on the geometric fit between proteins and ligands, and the additivity and nonadditivity of protein–ligand interactions. Chapter 3 gives an excellent overview of chemical modification of enzyme active sites as a means of altering the shape of the "lock" to fit new "keys". A discussion of chemical mutagenesis, and an introduction to cofactors and site-specific nucleases are included. Chapter 4 gives a detailed analysis of the strategies for nucleic acid recognition using synthetic nucleic acids. The structure of nucleic acids is covered as an introduction to the design of receptors. The effectiveness of oligonucleotide analogs and derivatives is also presented. The chapter ends by introducing nucleic acid molecular devices, affinity modification, and the inhibition of gene expression. Chapter 5 is focused primarily on antibody catalysis, but gives some attention to catalysis by macrocycles. The similarities and differences between artificial enzymes and catalytic antibodies are well developed. Chapter 6 presents a fascinating description of the L & K principle as it applies to the solid state and crystalline interfaces. In this chapter the generation and amplification of chirality at surfaces is described in detail. Several well drawn diagrams, as well as photographs of crystals, allow the reader to easily understand the forces that drive molecular packing and aligning of neighboring molecules. The lessons are then extended to the packing of amphiphiles at air–water interfaces. Chapter 6 concludes with a discussion of the guiding principles for molecular recognition and molecular inclusion during crystal formation.

There are two remaining chapters, the first of which is concerned with the origin of life and concentrates on models for self-replicating and templating molecules. The lessons from the models are extended to DNA and proteins, and the chapter ends with strategies that chemists may use to develop molecular devices. The last chapter is an overview of the entire field of supramolecular chemistry, its new directions, and the interrelationships of recognition, catalysis, information storage, organization, and assembly.

In summary, this book is a truly fascinating perspective that ties together many fields under the L & K guiding principle. Particular chapters which stand out as unique are those dealing with nucleic acid structure, molecular devices, crystalline interfaces, and the origin of life.

The book will be useful to any scientist concerned with supramolecular chemistry, since it covers several new directions of this field and, as stated in the preface, "unlocks our thought" with regard to intramolecular interactions.

Eric V. Anslyn
Department of Chemistry
and Biochemistry
The University of Texas at Austin
Austin, TX (USA)

This section contains book reviews and a list of new books received by the editor. Book reviews are written by invitation from the editor. Suggestions for books to be reviewed and for book reviewers are welcome. Publishers should send brochures or (better) books to Dr. Ralf Baumann, Redaktion Angewandte Chemie, Postfach 101161, D-69451 Weinheim, Federal Republic of Germany. The editor reserves the right of selecting which books will be reviewed. Uninvited books not chosen for review will not be returned.

Supramolecular Synthons in Crystal Engineering—A New Organic Synthesis

Gautam R. Desiraju*

Dedicated to Professor David Y. Curtin and Professor Iain C. Paul

A crystal of an organic compound is the ultimate supermolecule, and its assembly, governed by chemical and geometrical factors, from individual molecules is the perfect example of solid-state molecular recognition. Implicit in the supramolecular description of a crystal structure is the fact that molecules in a crystal are held together by noncovalent interactions. The need for rational approaches towards solid-state structures of fundamental and practical importance has led to the emergence of crystal engineering, which seeks to understand intermolecular interactions and recognition phenomena in the context of crystal packing. The aim of crystal engineering is to establish reliable connections between molecular and supramolecular structure on the basis of intermolecular interactions. Ideally one would like to identify substructural units in a target supermolecule that can be assembled from logically chosen precursor molecules. Indeed, crystal engineering *is* a new organic synthesis, and the aim of this article is to show that rather than being only nominally relevant to organic chemistry, this subject is well within the mainstream, being surprisingly similar to traditional organic synthesis in concept. The details vary because one is dealing here with intermolecular interactions rather than with covalent bonds; so this article is divided into two parts. The first is concerned with strategy, highlighting the conceptual relationship between crystal engineering and organic synthesis and introduces the term *supramolecular synthon*. The second part emphasizes methodology, that is, the chemical and geometrical properties of specific intermolecular interactions.

Keywords: crystal engineering · hydrogen bonding · molecular recognition · organic synthesis · supramolecular chemistry

Par ma foi! il y a plus de quarante ans
que je dis de la prose sans que j'en susse rien.[**]
Molière

1. Introduction

Chemistry constantly seeks analogies and connections and supramolecular chemistry has grown into a distinct field around Lehn's analogy that "supermolecules are to molecules and the intermolecular bond what molecules are to atoms and the covalent bond".[1] This analogy represents a departure from classical chemical thought in that it discards the notion that the molecular structure of an organic substance embodies all of its chemical and physical properties.[2–4] Supermolecules are not just collections of molecules; their structure and characteristic properties are distinct from the aggregate properties of the constituent molecular species.[5] Of course, the hydrogen bond has always been recognized by organic chemists as being significant, especially in biomolecular structures,[6] and it is known that the strongest intermolecular interactions are stronger than the weakest of covalent bonds.[7] However, in general it has been felt that the aims of supramolecular chemistry fall somewhat outside the mainstream of organic chemistry.[8]

Structural chemists and crystallographers have, however, been quick to realise that a crystal of an organic compound is the perfect supermolecule,[9, 10] according to Dunitz "a supermolecule par excellence", an assembly of literally millions of molecules self-crafted by mutual recognition at an "amazing level of precision".[11] If molecules are built by connecting atoms with covalent bonds, solid-state supermolecules (crystals) are built by connecting molecules with intermolecular interactions. So, the supramolecular equivalents of structural isomers are crystalline polymorphs, and the solid-state topochemical photodimerization of cinnamic acids a very good example that relates polymorphism (in the reactant) with structural isomerism (in the product).[12] Continuing the analogy further, a molecular isomerization may be compared with a phase transition and stereoisomers with enantiomorphous crystals. Again, disorder in a topochemically reactive crystal finds a molecular parallel in alternative reaction pathways.[13] Homology is not a

[*] Prof. G. R. Desiraju
School of Chemistry, University of Hyderabad
Hyderabad 500046 (India)
Telefax: Int. code + (40)258-145
e-mail: grdch@uohyd.ernet.in

[**] With regard to organic synthesis, the practitioner of crystal engineering today seems to be in the position of M. Jourdain in "Le Bourgeois Gentilhomme" when he exclaims, "I've been talking prose for the last forty years and have never known it!"

 © VCH Verlagsgesellschaft mbH, D-69451 Weinheim, 1995 0570-0833/95/3421-2311 $ 10.00+.25/0

property restricted to molecules alone, and crystalline homologous series have been identified in which patterns of intermolecular interactions (rather than patterns of covalent bonds) are systematically graded; typical examples are benzene, naphthalene and anthracene, or alternatively, benzene, biphenyl, terphenyl.[14]

Given this background, it is instructive to consider the subject of crystal engineering, which has been defined as "the understanding of intermolecular interactions in the context of crystal packing and in the utilisation of such understanding in the design of new solids with desired physical and chemical properties".[15] Crystal engineering is concerned with the systematic architecture of crystal structures.[16] This architecture is governed by the rules of supramolecular valence, that is, by the chemistry and geometry of the intermolecular interactions, which are, in effect, the supramolecular cement.[17] Therefore, if crystals are the supramolecular equivalents of molecules, crystal engineering is the supramolecular equivalent of organic synthesis.

2. General Principles and Strategies

> *... structural units within molecules which can be formed and/or assembled by known or conceivable synthetic operations.*[*]
> Corey's definition of a synthon

Targets in organic synthesis are defined in terms of the connectivity of covalent bonds (that is, a molecular structural formula). At a supramolecular level, it should be recognized that targets in crystal engineering are defined in terms of interaction connectivity, that is, in geometrical and topological terms. One aims, for example, at particular patterns such as ribbons, sheets, layers, channels, tubes, and cavities, which may be appropriately functionalized to yield materials that act as templates for subsequent chemical transformations (catalysts, nanostructures, organic zeolites). Alternatively, the desired geometrical pattern may itself be of inherent significance, because it defines a useful physical property (electronic or proton conductivity, ferromagnetism, nonlinear optics).

[*] This and succeeding quotations are taken from Refs. [18, 19].

All crystal structures of organic compounds may be formally depicted as networks with the molecules being the nodes and the intermolecular interactions representing node connections.[5] Therefore, the predictable self-organization of molecules into one-, two-, or three-dimensional networks is of the utmost importance in crystal engineering. For such rational design, hydrogen bonding of the conventional OH···O and NH···O variety has been the most commonly used supramolecular cement, yet weaker forces such as CH···O, CH···N, I···I, O···I, N···Cl, or even C···H and C···C can be used. All these interactions, be they strong or not so strong, are directional—anyway directional enough in combination that the orientation of molecules in the solid can be predicted with a reasonable degree of accuracy. These interactions can be combined by a designed placement of functional groups in the molecular skeleton to generate *supramolecular synthons*, examples of which are shown in Scheme 1.

The term "synthon" was introduced by Corey in 1967 in an article entitled "General Methods for the Construction of Complex Molecules".[18] This article was of extraordinary importance in shaping the course of organic synthesis. Corey's definition of a synthon is stated above, and the term was traditionally used to represent key structural features in a target molecule in organic synthesis. In later years the term fell into disuse as explained by Corey himself in 1988[19] and Seebach in 1990,[20] because it degenerated into a descriptor of synthetic intermediates. However, since crystal engineering and an appreciation of the properties of intermolecular interactions are probably today at that stage of sophistication that organic synthesis and an appreciation of the properties of covalent bonds were in the fifties and sixties, and also because the term synthon is so useful in the context of retrosynthetic analysis,[20] the supramolecular counterpart of which is crystallographic database analysis, the term "synthon" has been retained here and used in the manner originally intended. In keeping with modern organic synthetic parlance the term "retron" might have been more appropriate[21] but this is a subjective matter. Corey's definition of a synthon is so general and flexible that more than twenty-five years later it can be used with almost the same connotations but in a supramolecular sense. Thus *supramolecular synthons are structural units within supermolecules which can be formed and/or assembled by known or conceivable synthetic operations involving intermolecular interactions*, and crystal engineering is the new

Gautam R. Desiraju was born in Madras, India, in 1952 and received his B. Sc. at the University of Bombay in 1972. He was awarded his Ph.D. from the University of Illinois at Urbana-Champaign in 1976 under the supervision of Professor David Y. Curtin and Professor Iain C. Paul. From 1976–1978 he was a member of the research staff in the laboratories of Eastman Kodak Company in Rochester, New York. He joined the faculty at the University of Hyderabad as Lecturer in 1979, being appointed Reader in 1984 and Professor in 1990. He has published more than 100 research papers in the area of crystal engineering and solid-state supramolecular chemistry, and his interests include the study of weak hydrogen bonding and other intermolecular forces. He is the author of a book entitled "Crystal Engineering—The Design of Organic Solids" published in 1989 and the editor of multiauthor volumes on organic solid-state chemistry (1987) and supramolecular chemistry (1996). He is currently coeditor of Acta Crystallographica.

organic synthesis. To summarize, supramolecular synthons are spatial arrangements of intermolecular interactions and play the same focusing role in supramolecular synthesis that conventional synthons do in molecular synthesis. In effect, the goal of crystal engineering is to recognize and design synthons that are robust enough to be exchanged from one network structure to another, which ensures generality and predictability. Such structural predictability leads, in turn, to the anticipation of one-, two-, and three-dimensional patterns formed with intermolecular interactions. There is a particular relevance of the solid state to this kind of supramolecular chemistry, because many of the weaker interactions are probably deformed if not destroyed in solution. However, the persistent recurrence of patterns mediated by weak forces in crystals indicates that such interactions might still be important in solution for transient processes such as those associated with biomolecular structure and conformation.

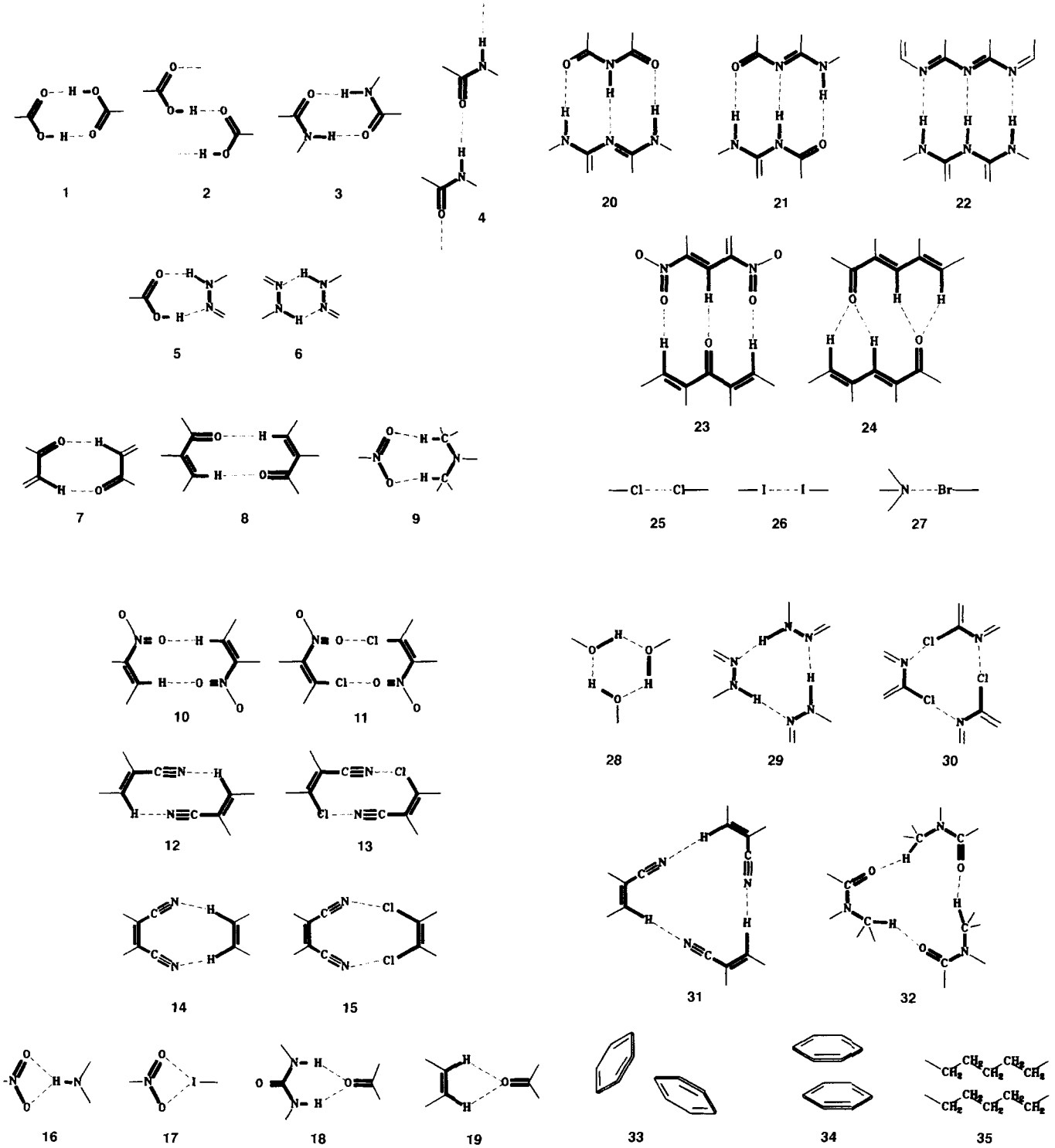

Scheme 1. Representative supramolecular synthons.

2.1. Solid-State Architecture with Supramolecular Synthons

...recognition of some synthons (usually the larger or major synthons) normally is more useful in analysis than that of others.

Scheme 1 shows a variety of supramolecular synthons **1**–**35**, culled from the recent literature. A supramolecular synthon is an identifiable design element and should be, strictly speaking, distinguished from an intermolecular interaction. It must be emphasized that synthons are *derived* from designed combinations of interactions and are *not identical* to the interactions. For example, the carboxyl dimer synthon **1** is assembled with two centrosymmetrically related C=O···HO hydrogen bonds. In still other synthons, for example **33**–**35**, the involvement of the interactions is implicit. Though subtle, this distinction between an interaction and a synthon is real, because supramolecular synthons incorporate *both* chemical and geometrical recognition features of molecular fragments, in other words both explicit and implicit involvement of intermolecular interactions. On occasion, however, when chemistry and geometry are inextricably linked, a single interaction may be regarded as a synthon, for instance Cl···Cl, **25** or N···Br, **27**.

The supramolecular synthon concept is conveniently illustrated in the crystal structures of some aromatic carboxylic acids. Scheme 2 shows how the structures of benzoic, terephthalic, isophthalic, trimesic, and adamantane-1,3,5,7-tetracarboxylic acids (**36**) are built with phenyl rings and dimer synthons **1** in a logical progression. The benzoic acid dimer is zero-dimensional, the linear or crinkled ribbons in the dibasic acid structures are one-dimensional patterns, while the sheet structure in trimesic acid is two-dimensional.[22] The three-dimensional extension of these structures is the diamondoid structure of acid **36**, where synthons **1** are disposed tetrahedrally about the adamantyl nucleus to yield a network that is topologically similar to diamond, in which **1** replaces C–C bonds, and the adamantyl nucleus becomes a super-C atom.[23]

Weaker hydrogen bonding of the CH···X variety may now be considered. Although these bonds have energies only in the 2–20 kJ mol^{-1} range, their effects on crystal structure and packing are just about as predictable as the effects of conventional hydrogen bonding.[24] Scheme 1 includes several CH···X-mediated synthons, and Scheme 3 shows some typical crystal structures based on these synthons. In crystalline 1,4-benzoquinone, the symmetrical disposition of functional groups results in a linear ribbon pattern linked by synthon **7**. This pattern is carried over largely unscathed into the crystal structure of 2-methoxy-1,4-benzoquinone, while the CH···N≡C analogue **12** is observed in 1,4-dicyanobenzene.[25] Another common CH···O synthon **24** is seen in the crystal structure of α-benzylidene-γ-butyrolactone.[26]

A comparison of the crystal structures of solid chlorine and the monoclinic form of 1,4-dichlorobenzene (Fig. 1) is revealing and shows how the supramolecular synthon concept may be extended to lesser known intermolecular interactions.[15] The contacts between the halogen atoms define the Cl···Cl synthon **25** and are virtually identical in the two structures. The aromatic rings in 1,4-dichlorobenzene fulfill a spacer function.

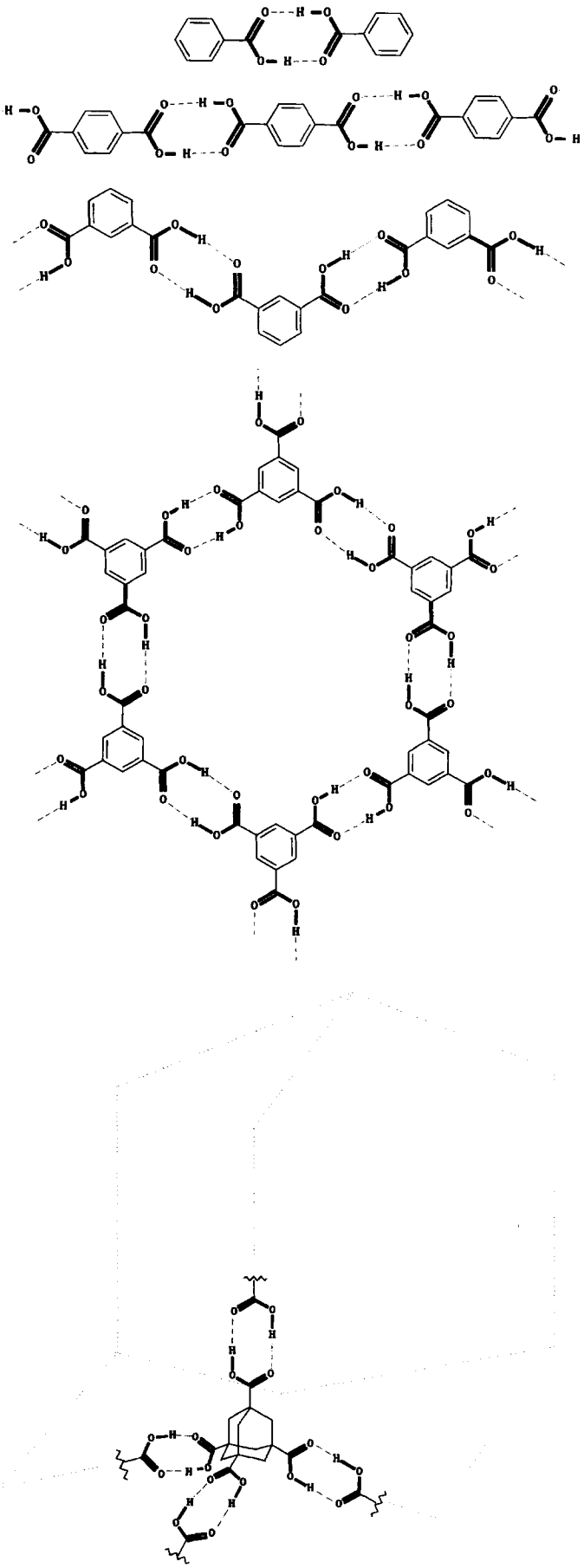

Scheme 2. Construction of aromatic carboxylic acid crystal structures with synthon **1**.

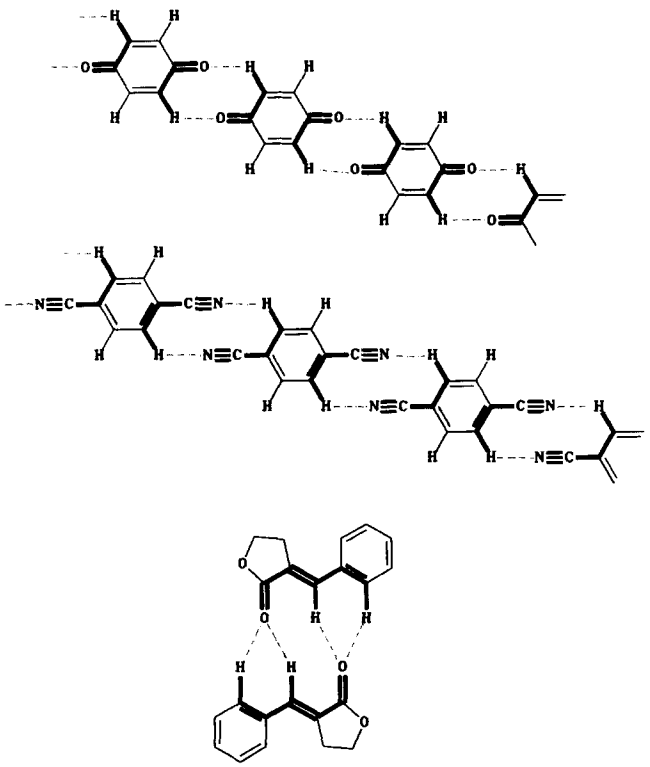

Scheme 3. Construction of crystal packing patterns with CH···X synthons **7**, **12**, and **24**.

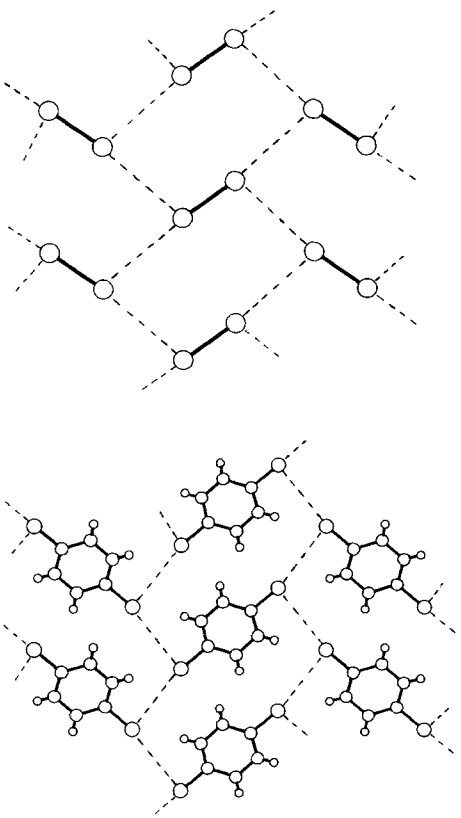

Fig. 1. Similarity between the crystal structures of chlorine (top) and 1,4-dichlorobenzene (bottom). Note the identical disposition of the Cl···Cl synthons **25** in the two cases.

The above examples cannot be exhaustive, but they illustrate the importance of being able to identify structurally significant synthons in a supermolecule. Such identification helps in the analysis of more complex crystal packings and the design of new target structures. These examples also highlight two other important features that should be noted in systematic crystal engineering. These are the following:

1) Consideration of a crystal structure in terms of supramolecular synthons can effect a simplification, which facilitates comparison with other seemingly different crystal structures. Accordingly, different molecular functionalities can result in similar crystal structures provided synthons in the various crystal structures possess shape or topological similarity.

2) The interference between the significant supramolecular synthons should be a minimum. Alternatively, the nature of such interference should be understood so that it may be exploited in the engineering strategy. These features will now be discussed in greater detail.

2.2. Simplification of Crystal Structures

...even in the earliest stages of the process of simplification of a synthetic problem, the chemist must make use of a particular form of analysis which depends on the interplay between structural features that exist in the target molecule...

Kitaigorodskii's close-packing principle implies that molecules undergo a shape simplification as they progress towards dimers, higher aggregates, and ultimately crystals.[27] Shape is a very powerful agent of molecular recognition that in crystals generally proceeds in a way such that supramolecular fragments of a crystal structure have simpler shapes than the constituent molecular species. Accordingly their packing patterns may be easier to predict (see Section 2.8). Molecules in organic crystals are surrounded typically by twelve to fourteen near-neighbors to define quasi-spherical clusters.[28] Similar shape-simplifying effects are seen in Rebek's "tennis ball" dimer,[29] and the tertiary structural features in globular proteins are responsible for converting an exceedingly complicated molecular structure into a nearly spherical unit.[30]

These geometrical consequences of shape recognition can be employed in crystal engineering. A comparison of the crystal structures of benzoic acid and *p*-terphenyl (Fig. 2) is pertinent. Because of the parallel hydrogen bonds in synthon **1**, the shape and size of the benzoic acid dimer mimics that of *p*-terphenyl. The two crystal structures are not identical but reasonably similar with the same space group $P2_1/n$, comparable cell dimensions and volumes, and most importantly, the benzoic acid dimers are packed together using the same herringbone C···H interactions that exist in *p*-terphenyl.[31] To be sure, there are differences in the two structures but these can be understood and rationalized. For example, *p*-terphenyl molecules are tilted along their molecular lengths to optimize herringbone interactions and form slabs that are themselves aligned parallel to optimize other herringbone interactions. In benzoic acid, the dimers are stacked rather than tilted to form slabs, which are then inclined in a herringbone fashion. Stacking rather than

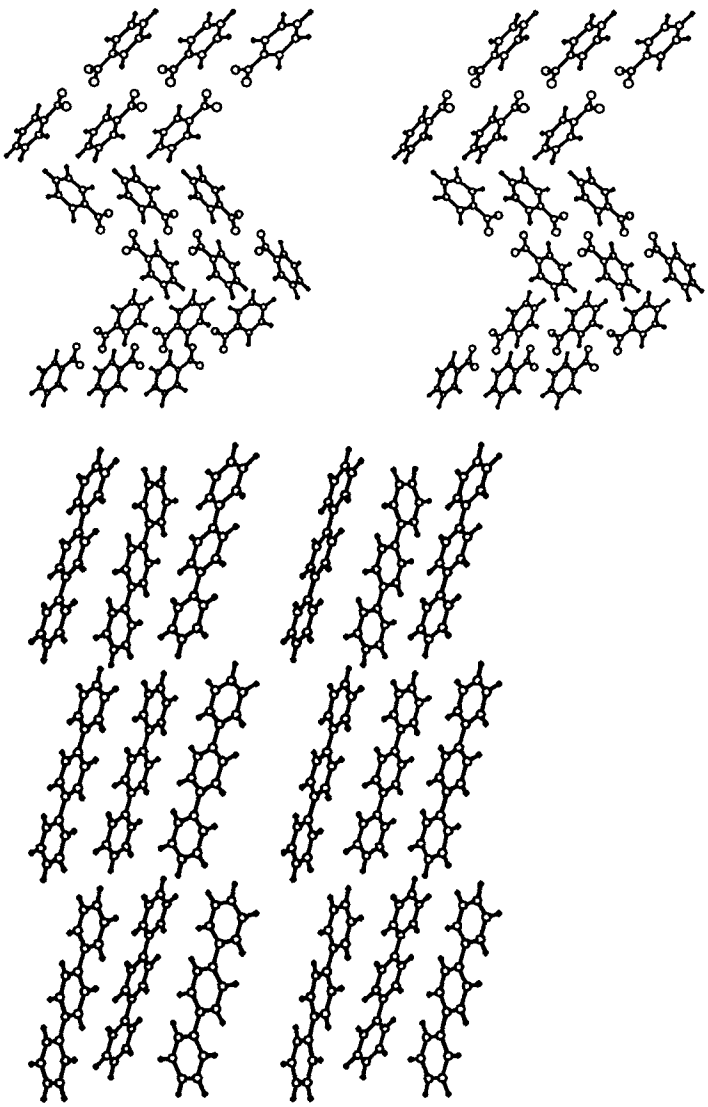

Fig. 2. Stereoviews of the crystal structures of benzoic acid (top) and *p*-terphenyl (bottom), each showing three slab sections. Notice that the benzoic acid dimer mimics the shape of the terphenyl molecule and also the similar herringbone dovetailing between slabs in the two structures.

tilting occurs within the benzoic acid slabs because of the tendency of a phenyl ring to be overlaid on a carboxyl dimer ring.[32] However, the main message is clear—the carboxyl dimer synthon **1** can be used as a surrogate for a 1,4-disubstituted phenyl ring, and it is pertinent to compare this dissection of the benzoic acid dimer supramolecular skeleton with that of the squalene molecular skeleton by Corey.[18]

This strategy can now be used in the design of crystal structures. We found that halogen atoms, especially iodine, tend to form short polarization-induced contacts with nitro groups (synthon **17**) where the oxygen atoms of the nitro group grip the iodine atom in a two-pronged fashion.[33] This synthon was initially introduced in the crystal structure of 4-iodonitrobenzene, where it alternates with the phenyl rings to give a ribbon as expected (Scheme 4).[34] In fact, this molecule has few other crystallization options. The strategy was then extended to the crystal structure of the 1:1 complex of 1,4-dinitrobenzene and 1,4-diiodobenzene where again **17** alternates, but in opposite senses with phenyl rings.[35] At this stage the hydrocarbon spacer between the **17** synthons was extended by crystallizing a 2:1 complex of 4-iodocinnamic acid with 1,4-dinitrobenzene.[34] The carboxyl synthon **1** elongates the (now supramolecular) diiodo moiety, which is then able to link with the nitro moiety through synthon **17**. These results are surprising—acids are known to complex with bases or with other acids but not with neutral compounds; however, in this case the acid dimer behaves effectively like a neutral diiodohydrocarbon because the hydrogen bonding requirements of the monomers are completely satisfied by dimer formation.

A very similar exercise may be carried out with CH···O hydrogen bonds. Nitro and dimethylamino groups form a CH···O-mediated synthon **9**, and the crystal structure of *N*,*N*-dimethylnitramine is unique in that it consists exclusively of infinite ribbons of this synthon (Scheme 5).[36] The crystal structure of the 1:1 complex of 4-nitrobenzoic acid and 4-(*N*,*N*-dimethylamino)benzoic acid may now be anticipated as a ribbon consisting of synthon **9** alternating with an extended terphenyl surrogate formed by a linking of acid molecules with synthon **1**.[37] To summarize, the crystal packing properties of an aromatic carboxylic acid dimer are distinct from those of the monomer and are more reminiscent of an aromatic hydrocarbon.

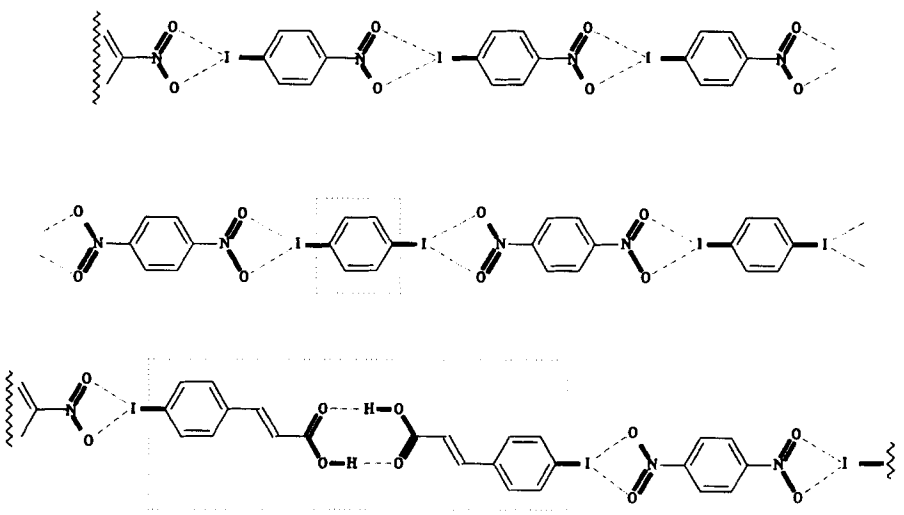

Scheme 4. Use of the iodo···nitro synthon **17** in crystal engineering. Note how the 1,4-disubstituted phenyl ring and the extended carboxylic dimer are similarly employed.

Inherent in structural simplification is a reduction of a crystal structure to its interaction network information. The crystal structure of tetraacid **36** has been described in Section 2.1 in terms of a diamond network with synthons **1** tetrahedrally disposed about the adamantyl skeleton.[23] It is therefore possible to substitute other synthons for **1** on adamantyl or other tetrahedral templates and generate similar diamondoid structures (Fig. 3). Typical examples of such alternative synthons are metal···NC,[38] I···I **26**,[39,40] O–H···N,[41] and the *cis*-amide dimer synthon **3**.[42] We have

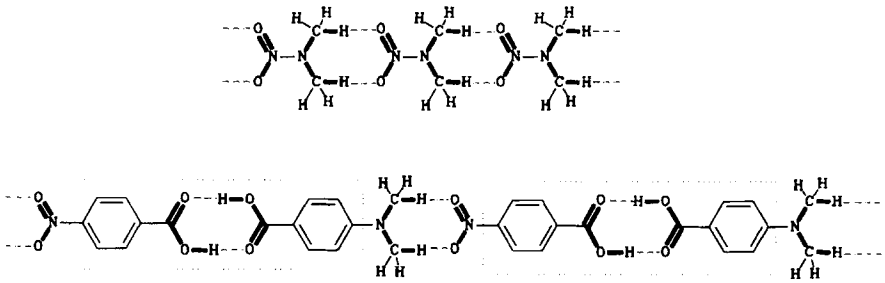

Scheme 5. Use of the dimethylamino···nitro synthon **9**. The strategy for the design of these structures is similar to that employed for the design of the structures in Scheme 4.

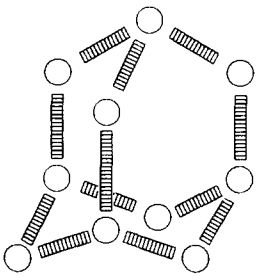

Fig. 3. Archetypical diamondoid network structure. ○ represents a tetrahedral molecular template (for example, adamantyl) and ▥ an appropriate supramolecular synthon.

used the same strategy with the much weaker N···Br synthon **27**;[43] the crystal structure of the 1:1 complex of hexamethylenetetramine (**42**) and CBr_4 contains a tetrahedral arrangement of synthon **27** resulting in a super-ZnS type structure (Fig. 4). That the N···Br and similar interactions are polarization-induced is well-known from the work of Hassel,[44] but their use in crystal engineering strategies is relatively new.[45]

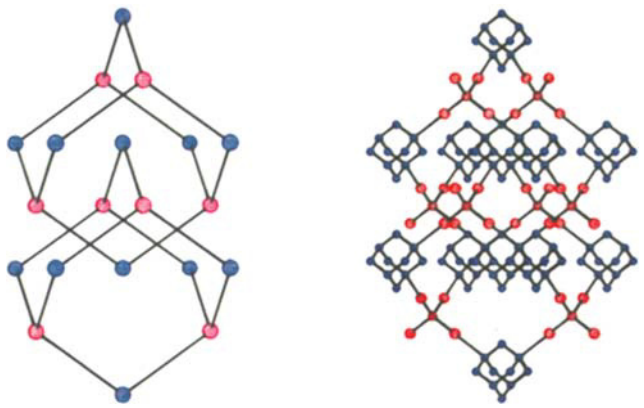

Fig. 4. Schematic (left) and complete (right) representations of the diamondoid network structure of the 1:1 complex hexamethylenetetramine (**42**, blue) and CBr_4 (red). Both intra- and intermolecular bonds are shown as solid lines. The N···Br synthon **27** connects molecules. Notice the catenation of networks and the similarity to Fig. 3.

A recurring theme in crystal engineering is that quite different covalent bond frameworks and chemical functionalities in the monomer building blocks can still result in similar supramolecular (crystal) structures. It has long been known that molecules with similar sizes, shapes, and functionalities have similar crystal structures; this principle of structural mimicry explains, for instance, phenomena such as solid-solution formation.[46] However, a more powerful generalization in the crystal engineering context is that *supramolecular fragments with similar sizes, shapes, and topologies have similar crystal structures*. Such a generalization is more useful, because it recognizes the interchangeability of supramolecular synthons within a particular family of crystal structures.

2.3. Synthon Interference and Structural Robustness

Proximity of reactive functional groups is of major importance in synthesis.

The examples discussed above might imply that supramolecular synthons are completely modular, capable of being introduced, removed, or replaced at will to generate new crystal structures. This would be an ideal, indeed a Utopian situation. However, chemistry is not geometry, and the major challenge in the practice of crystal engineering is that a crystal structure is a compromise, at times quite uneasy, between interactions of varying strengths, directionalities, and distance-dependence properties (see Section 2.9). Indeed, interference between synthons is *the* critical problem in crystal engineering, and structural robustness or the ability to use the same supramolecular synthon in a variety of situations is the key to a successful practice of the subject. A thorough understanding of the several ways in which intermolecular interactions interfere with one another is essential for a predictive control over crystal packing. Interactions in an organic crystal are numerous and weak. At a basic level, one attempts to insulate various types of interactions from one another so that their individual (geometrical) features are manifested more effectively. At a higher level, one can exploit the interfering effects of one interaction type on another to realize a supramolecular target structure very much as a synthetic chemist would use a neighboring or proximal group effect.

A discussion of structural robustness begins again with the carboxyl dimer synthon **1**. Generally, aliphatic and aromatic carboxylic acids RCO_2H adopt this dimer pattern in crystals, because its stability and packing efficiency are largely unaffected by the nature of the R group.[32] The robustness of **1** is revealed by considering the packing preferences of the patterns in Scheme 2. In benzoic, isophthalic, and terephthalic acids, the dimers and ribbons can close-pack without complications. In trimesic acid, however, the "holes" in the hexagonal hydrogen-bonded patterns pose a packing problem, which is solved by inclusion of a second molecular species (a guest).[22] This problem of voids is seemingly worse in acid **36**, but Nature solves it in a fascinating way by the catenation of as many as five distinct diamondoid networks.[23] Significantly, the close-packing problems caused by awkwardly shaped networks do not perturb the **1** synthons. However, even such a seemingly robust supramolecular synthon has limits on its use, and we have, in recent years, described four anomalous situations (Fig. 5) in which the centrosymmetric dimer synthon **1**, though expected, is not observed: 1) 4-Chloro- and 4-bromophenylpropiolic acids adopt a variation of the carboxyl catemer synthon **2** (actually 50:50 *syn:anti* O=C–OH conformations), while the corresponding cinnamic and benzoic acids adopt synthon **1**. This occurs because the phenylpropiolic acids cannot form CH···O hydrogen bonds.[47] 2) 3,5-Dinitrocinnamic acid forms a carboxylic dimer, but this pattern has two-fold rather than inversion symmetry. This occurs because of the dominance of CH···O bonding.[48] 3) In the 1:1 complex between

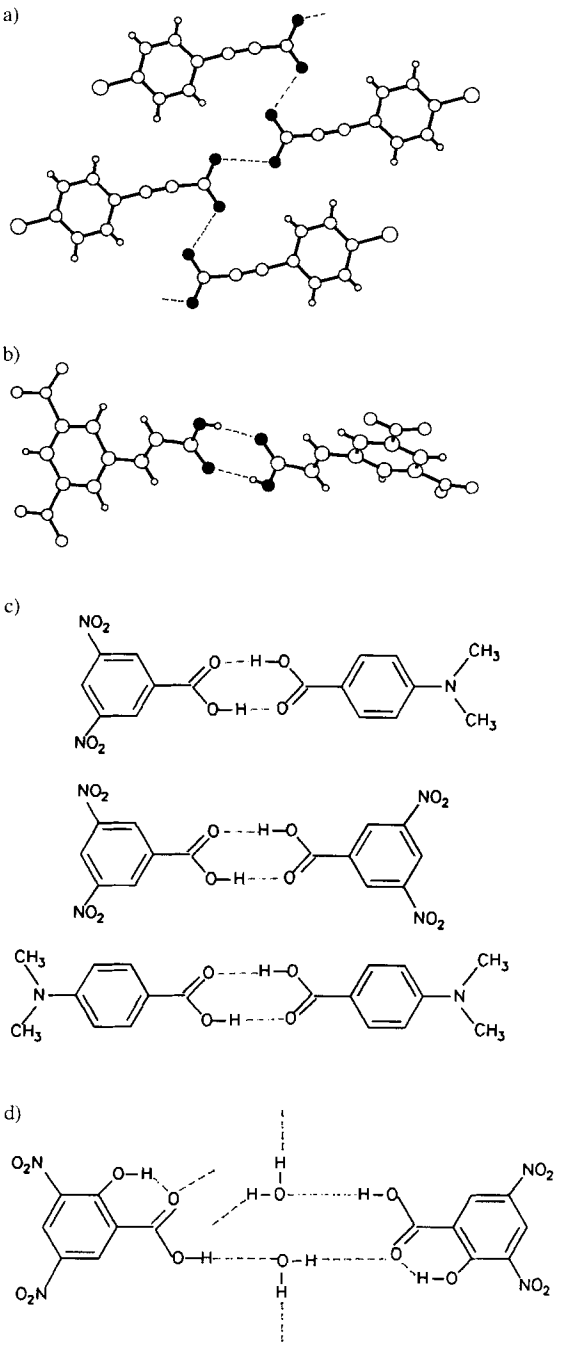

Fig. 5. Anomalously hydrogen-bonded carboxylic acid structures: a) modified catemer synthon **2** in 4-chlorophenylpropiolic acid; b) dimer located on a twofold axis in 3,5-dinitrocinnamic acid; c) observed homodimers (bottom) and unobserved, though expected, heterodimer (top) in the 1:1 complex 3,5-dinitrobenzoic acid and 4-(*N*,*N*-dimethylamino)benzoic acid; d) 3,5-dinitrosalicylic acid monohydrate with interrupting water molecules. In all cases, OH ··· O hydrogen bonds are shown as dashed lines.

3,5-dinitrobenzoic acid and 4-(*N*,*N*-dimethyl)aminobenzoic acid, homodimers are formed between like acids rather than the expected heterodimers between unlike acid monomers. This occurs because of the importance of $\pi \cdots \pi$ interactions.[49] 4) Unlike other salicylic acids, which adopt the dimer pattern, 3,5-dinitrosalicylic acid crystallizes as a hydrate in which hydrogen-bonded water molecules interrupt the dimer network.[50]

Multipoint recognition of functional groups is expected to improve synthon robustness as in the triply hydrogen-bonded synthon **20**, which has been used by Lehn, Whitesides, Kunitake, Ringsdorf, and others.[51] The relationship of **20** to recognition patterns between nucleotide bases in DNA is unmistakable. The existence of three hydrogen bonds in **20** (rather than two bonds in, say, synthon **1**) means that it can be used to construct more intricate supramolecular structures. For example, **20** is a constituent of the rosette structures **37**–**39** in Scheme 6. Such rosettes themselves occur within the proposed infinite network structure of the 1:1 complex of cyanuric acid and melamine.[52] Rosettes **37**–**39** are supermolecules of intermediate hierarchy (see Section 4) in that they consist of a finite number of molecules and have become attractive goals in what is perhaps one of the first examples of a target-oriented supramolecular synthesis. While synthon **20** is quite robust, it can align with itself through further hydrogen bonding in at least three distinct ways to yield, in Whitesides's terminology, a linear tape, a crinkled tape, and the desired rosette.[53] Two possible approaches to the rosette have been described. Lehn et al. found that the molecular complex of 5,5-diethylbarbituric acid and 5-*n*-butylpyrimidine-2,4,6-triamine contains a linear tape pattern rather than **37**. Cocrystallization of unsymmetrical precursors was expected to yield rosette **38**, but the compounds crystallized separately instead.[54] Whitesides and co-workers, on the other hand, employed bulky *tert*-butyl substituents on the amine component. The buttressing effects of these groups disfavor linear and crinkled patterns for steric reasons, leading successfully to rosette **39**.[55] Further attempts to synthesize similar rosette structures based on hydrogen bonding[56] and other types of interactions are anticipated, but already a certain sophistication in the manipulation of supramolecular synthons is apparent, and the resemblance to logic-directed organic synthesis is clearly discernible.[57] As our knowledge about intermolecular forces increases, there can be no doubt that complex supramolecular structures will be synthesized with increasing reliability and regularity.

2.4. Subjectivity in Synthon Choice

The recognition of synthons within molecules is purely a utilitarian device; the derivation of all possible synthons in a molecule may never be required.

The dissection of a crystal structure and the identification of particular supramolecular synthons within it is entirely subjective. A variety of patterns may be derived from any given structure and none of these are fundamentally more significant than the others. Rather, all of them assist in what is hopefully a better comprehension of the crystal structure and better methods for the systematic design of related structures. The same intermolecular interaction may be a constituent of several overlapping supramolecular synthons. Assessments of the "significance" of a particular supramolecular synthon are related to the question of structure simplification and could be quite arbitrary. For instance, in the iodo–nitro structures discussed in Section 2.2, it is arguable whether synthon **1** or **17** is the more significant.

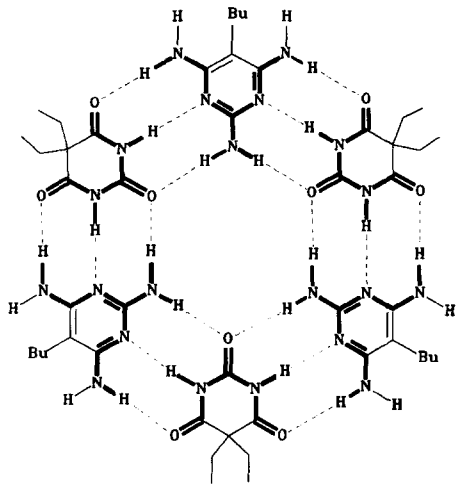

37

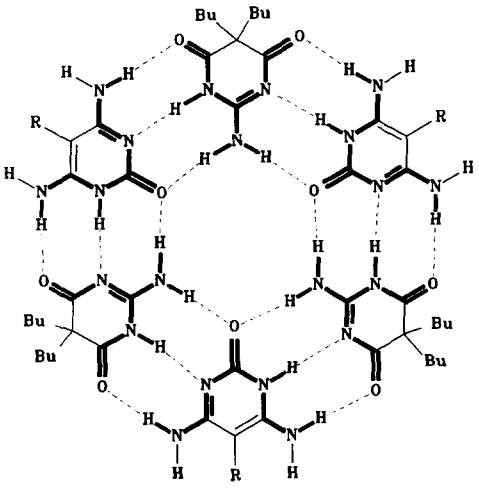

38 (R = C_8H_{17})

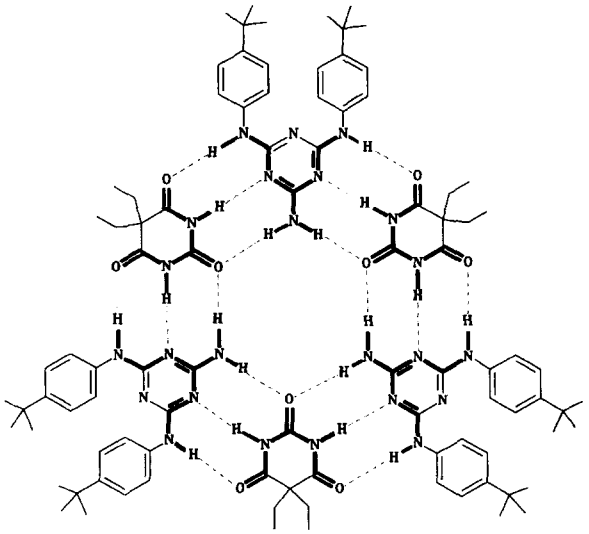

39

Scheme 6. Target rosette structures: **37**, **38** (not observed); **39** (observed). The synthons are highlighted. Notice the slightly different synthon structure in **38**.

It is particularly appropriate here to discuss the aryl···aryl synthons **33** and **34**, which are based, respectively, on herringbone and stacking modes of association of aromatic rings,[58] and the hydrophobic synthon **35**. The geometries of **33** and **34** are well-defined and occur in thousands of structures. If one were to assign significance to supramolecular synthons on the basis of specific interaction strengths, these synthons might not rank very high. However, it is known that they play an important role in determining stable crystal packing arrangements characterized by sparing solubility and high crystallinity.[59] Figure 6 shows the crystal structures of benzene and 2-aminophenol. The latter structure contains alternating polar and apolar bilayers. The structure of the apolar layer is almost identical to the benzene structure with aromatic rings mutually perpendicular. The identification of synthon **33** in both these structures confirms their close relationship.[60] The nature of aryl···aryl stacking interactions, as manifested in synthon **34**, has also been the subject of intensive studies, and their utilization in crystal engineering depends on the well-known proclivity of planar π donors and acceptors to form overlapped layered structures.[61] Hydrophobic effects are revealed by the appearance of synthons such as **35** and have been exploited in the design of monolayer structures.

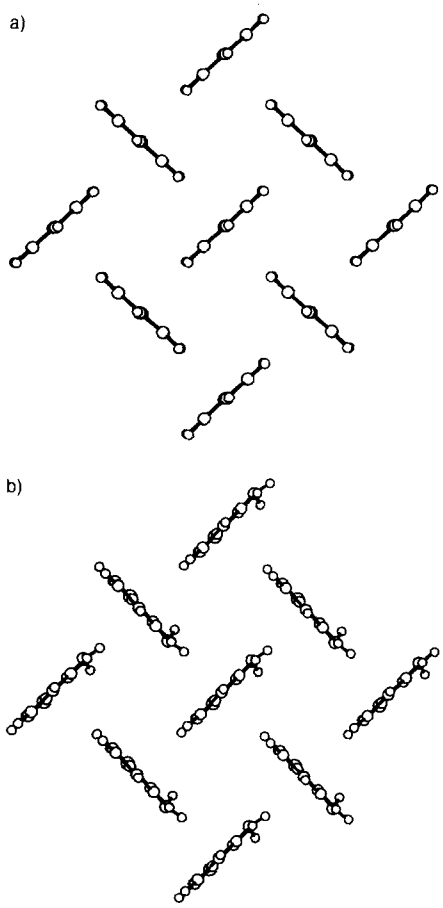

Fig. 6. Comparison of the crystal structures of benzene (top) and 2-aminophenol (bottom). Note the almost identical arrangement of phenyl rings (synthon **33**) in the two structures.

2.5. Conventional and Exotic Interactions

...it may be desirable to attempt a synthesis by the use of new reactions if a great simplification can result or if there is simply no alternative.

Reactions are used in organic synthesis to make covalent bonds, and if structural transformations are to be reliable and efficient, such reactions should evidently be of known mechanism and scope. In the supramolecular context, one would like to use interactions of known directionalities, which can be combined to give structurally robust synthons. Not surprisingly, many current studies in crystal engineering are centered around conventional hydrogen bonding of the OH···O or the NH···O type. But just as organic synthesis progressed by the study of new and (at the time) exotic reaction types, crystal engineering is also amenable to the use of lesser known or weaker and possibly less directional interactions. Gratifyingly, it appears that these weaker interactions are just as effective, especially if they are used in multipoint recognition.

A recent example of the use of CH···O interactions in supramolecular design is provided by the complexation of 1,3,5-trinitrobenzene with dibenzylidene ketones.[62] The target synthon **23** is obtained by replacing the conventional hydrogen bonds in **20** with CH···O hydrogen bonds. The precursor molecular components suggest themselves naturally, and **23** is obtained in the crystal structures of the molecular complexes formed by either 1,3,5-trinitrobenzene or picryl chloride with either dibenzylideneacetone or 2,5-dibenzylidenecyclopentanone (Fig. 7). Reference has already been made to diamondoid structures assembled with I···I synthons (**26**) and N···Br synthons (**27**, Section 2.2, Fig. 4).[39, 40, 43] The scope of ionic interactions in crystal engineering studies is only just beginning to be realized. The structures of organic malates and tartrates, for example, contain strongly hydrogen-bonded networks that are robust in two dimensions, permitting other structural variations in the third dimension.[63]

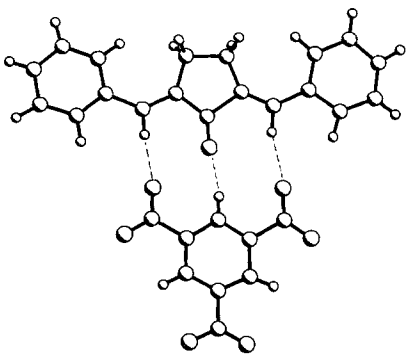

Fig. 7. CH···O-mediated recognition (synthon **23**) in the 1:2 molecular complex formed between 2,5-dibenzylidenecyclopentanone and 1,3,5-trinitrobenzene. Only one of the two symmetry-independent trinitrobenzene molecules is shown.

Conventional hydrogen bonding continues to be used in new and ingenious ways.[64] Two recent reports are based on the complementarity of the hydrogen-bonding capabilities of the OH and NH_2 groups. Ermer and Eling have pointed out that while an OH group has one hydrogen bond donor and two acceptors, an NH_2 group has two donors and one acceptor.[65] Accordingly, compounds or complexes that contain equal stoichiometric amounts of these groups are likely to have highly organized hydrogen-bonded networks with a tetrahedral environment about the O and N atoms. Ermer and Eling have utilized this fact in the design of several diphenol–diamine complexes. Hanessian et al. have discussed the crystal structure of the 1:1 complex between *trans*-1,2-cyclohexanediol and *trans*-1,2-diaminocyclohexane while recognizing again that half of the heteroatoms are fully tetracoordinated.[66]

In general, one may expect to witness several new and exciting developments in the systematic engineering of crystal structures based on interactions with boron, sulfur, and halogen atoms,[67, 68] on hydrogen bonding of the CH···X[24] and XH···π[69] type (in which X can also perhaps be C), and metal–atom interactions, the latter being, of course, exclusive to organometallic clusters and complexes.[70] These constitute the supramolecular reaction methodologies of the future.

2.6. Knowledge of Other Crystal Structures

Knowledge or enlightened speculation as to the way in which a molecule to be synthesized has previously been brought into existence can be extremely helpful in simplifying a synthetic problem.

As far back as 1961 Hassel commented on the hexagonal, layered network of weak N···Cl interactions (synthon **30**) in the crystal structure of cyanuric chloride,[71] which had been previously reported by Hoppe, Lenné, and Morandi in 1957.[72] More recently we noted that synthons such as **12** are common in cyanoaromatic compounds.[73] These ideas and the knowledge of the linearity of CH···N hydrogen bonds led to the identification of 1,3,5-tricyanobenzene as a potential candidate for the formation of similar hexagonal networks. Cocrystallization with hexamethylbenzene proved serendipitous, for the 1:1 complex of these two compounds contains the desired hexagonal network (synthon **31**; Fig. 8).[74] A comparison of **30** and **31** shows that they are interchangeable with a substitution of the N···Cl interaction by the CH···N interaction.

A knowledge of the 1,3,5-tricyanobenzene–hexamethylbenzene crystal structure leads to the possibility of obtaining similar hexagonal networks with related molecules. Trimethylisocyanurate (**40**) was identified, because it contains only CH···O donor and acceptor groups in its symmetrical framework, and the crystal structure of its 1:1 complex with 1,3,5-trinitrobenzene con-

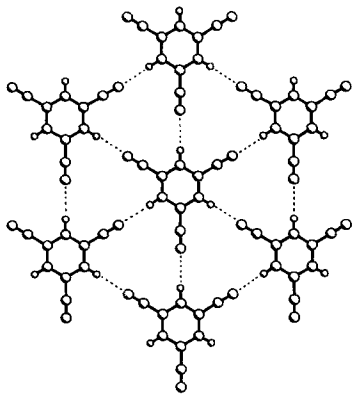

Fig. 8. CH···N network of 1,3,5-tricyanobenzene molecules (synthon **31**) in the crystal structure of the 1:1 complex formed by this substance with hexamethylbenzene. The interleaving hexamethylbenzene network is not shown.

sists of discrete molecular layers.[75] The layers of **40** are networked into a hexagonal pattern (synthon **32**), while the trinitrobenzene molecules are close-packed in two dimensions to yield another hexagonal pattern (Fig. 9).[76] Most interestingly,

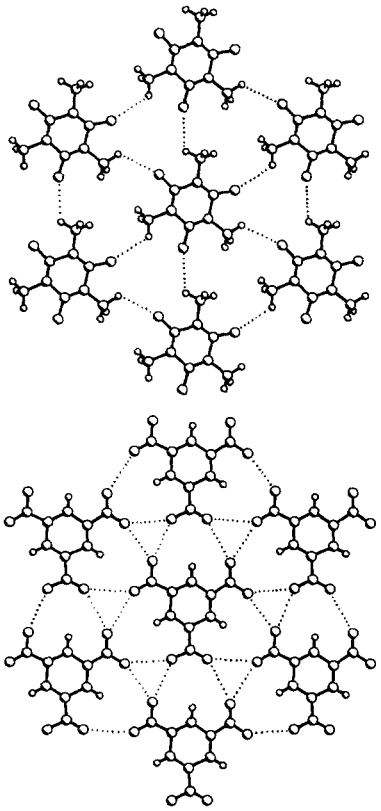

Fig. 9. Hexagonal CH···O network of trimethylisocyanurate (**40**, synthon **32**) (top) and O···O-mediated network of 1,3,5-trinitrobenzene (bottom) in the layered structure of the 1:1 complex formed by these substances.

and unlike the 1,3,5-tricyanobenzene–hexamethylbenzene complex, which is monoclinic, this complex crystallizes in the hexagonal space group $P\bar{6}$; in other words the molecular symmetries have been fully retained in the crystal, a rare and exceptional event (see also Section 2.8). Why this happens is not clear—perhaps it has to do with a certain amount of structural insulation of the layers of **40** and trinitrobenzene, thereby reducing three-dimensional interference.

We have observed recently that tetrabromoadamantane (**41**) and hexamethylenetetramine (**42**) form a 1:2 complex in which the molecules of **41** and half those of **42** form a CH···N-mediated diamondoid network related topologically to that in tetraacid **36** (Fig. 10).[77] Instead of catenation as in acid **36**,[23] the other half of the molecules of **42** are clathrated within the

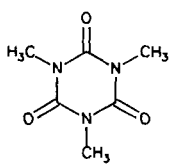

40

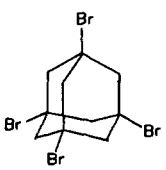

41

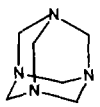

42

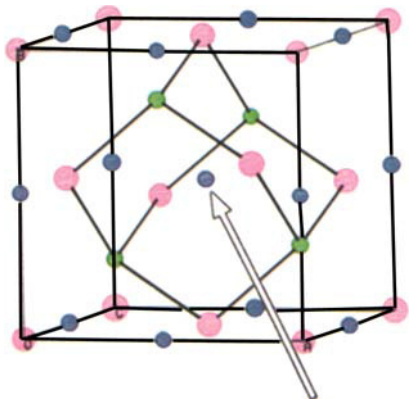

Fig. 10. Organic alloys; a molecule of hexamethylenetetramine (**42**, blue) may be replaced (arrow) by a CBr_4 molecule, leaving the diamondoid CH···N network of **42** (green) and 1,3,5,7-tetrabromoadamantane (**41**, pink) intact.

diamondoid cavities and are disordered. We therefore felt that these clathrated molecules of **42** could be replaced by another molecule of similar shape and size. Accordingly we cocrystallized a 1:1:1 complex of **41**, **42**, and CBr_4. The structure of this ternary complex was exactly as expected. The diamondoid network is retained and the CBr_4 molecules enter the cavities formerly occupied by the disordered molecules of **42**. Interestingly, the CBr_4 molecules are ordered, because they participate in auxiliary Br···Br interactions with the molecules of **41**.

2.7. Supramolecular Retrosynthesis—The Cambridge Structural Database

This is the oldest and most traditional of all synthetic strategies ...

Retrosynthetic analysis in organic synthesis associates synthons, the substructural units in the target structure, with precursor structures in a sequential pathway. This process eventually leads to an identification of one or more potential starting materials.[19, 21] In crystal engineering, target structures are geometrically and topologically defined, and so the equivalent thought process should associate these target networks with precursor molecules that when crystallized will yield appropriate supramolecular synthons that are compatible with the target network structure. Retrosynthetic analysis is at the heart of organic synthesis, because it uses what is known (target structure) to heuristically derive what is unknown (precursor structure). Supramolecular retrosynthesis is of equal importance in crystal engineering and for the same reason. It uses a particular target network and works backwards to identify molecules that by using their intermolecular interactions will crystallize in the target structure.

Traditional retrosynthetic analysis is based on the bedrock of knowledge of the various reactions (covalent bond-making processes) available to the synthetic chemist. This knowledge has been built up through the endeavors of generations of organic chemists.[20] The practice of supramolecular retrosynthesis must analogously depend on an intimate knowledge of the myriad ways in which intermolecular interactions are manifested in crystals. This knowledge has come to us through the endeavors

of generations of crystallographers who have bequeathed to us around 125000 accurate crystal structures of organic and organometallic small-molecules. To a large extent, the assimilation and digestion of the organic synthetic repertoire is still a manual, individual effort.[78] However, because of the peculiarly geometrical nature of intermolecular forces, supramolecular synthetic methodology is suited to computer storage and retrieval techniques, and the essential tool for retrosynthetic analysis in crystal engineering already exists in the form of the Cambridge Structural Database (CSD).[79]

The CSD is now more than ever suited to the purpose of supramolecular retrosynthesis, because it may be searched for patterns of intermolecular forces. Till very recently, the search protocols in the CSD were molecular in their bias; only questions based on covalent bond connectivity could be posed. In studies of interaction geometry, the hits that were thus obtained through molecular-type searches were manipulated with geometrical calculation programs. Today it is possible to code the supramolecular synthon structure directly (as shown in Scheme 1) *inclusive of geometrical attributes* in the search question and obtain all crystal structures that contain the chosen synthon. As a typical example, in attempting to extract all structures that contain dimer synthon **1**, one might typically, in former times, have retrieved all carboxylic acid structures using in the search question a molecular fragment such as CO_2H. This search would have yielded not only compounds that contain the desired **1**, but also acids that adopt the alternative catemer **2**. Yet, structurally related synthons like **3** would not have been obtained. In contrast, the distinctly supramolecular bias of the latest versions of the CSD surely takes into account its ever-increasing relevance in systematic crystal engineering.

The CSD is extremely useful in the study of intermolecular forces weaker than conventional hydrogen bonding. For any given interaction there is an ideal intermolecular orientation. However, this ideal geometry is deformed to a greater or lesser extent in crystals, because the crystal geometry is the result of interaction interference (see Section 2.3). Therefore a statistical analysis of crystal structures is mandatory when studying weak interactions. These statistical techniques minimize the crystallographic noise, that is, the effects of the various deformations, which are inevitable when the interactions are weak. The greater the sampling of crystal structures, the weaker the interaction that may be analyzed. It is reasonable to expect that the present size of the CSD is sufficient to permit an analysis of most types of intermolecular interactions that have been used in crystal engineering or are likely to be used in the foreseeable future.

2.8. Supramolecular Symmetry

...any synthetic scheme which does not take full cognizance of stereochemical possibilities or problems will have a correspondingly low expectation of success.

Stereochemistry is an expression of molecular topology, and its supramolecular equivalent is expressed in terms of the spatial and geometrical relationships between supramolecular fragments in the crystal. For instance, how does one obtain particular dispositions and arrangements *between* ribbons, layers and networks within a crystal structure? This is a matter of considerable importance in crystal engineering, because it results in the manifestation or disappearance of physical effects such as Second Harmonic Generation (SHG) or chemical effects such as host–guest complexation. For instance, crystallization in an enantiomorphous space group of an SHG-active material may be likened to a supramolecular asymmetric synthesis. Such considerations are closely linked to questions concerning symmetry. In general, three sorts of symmetry need to be considered: molecular symmetry, the symmetry of supramolecular fragments (tapes, helices, knots, sheets, channels, voids), and crystal symmetry. The first and the third kinds of symmetry are matters of fact, while the second is subject to individual interpretation.

The carry-over of molecular symmetry into the crystal is not a trivial matter, and in no aspect of crystal engineering is the practitioner of the subject quite so helpless today as in establishing connections between molecular and crystal symmetry. Indeed, Kitaigorodskii's laws of close-packing almost dictate that molecular symmetry is a very poor guide to the molecular site-symmetry in the crystal. The inversion center is the only molecular symmetry element that is routinely carried over into the crystal, because it is the only crystal symmetry element that does not entail loss of packing efficiency by its presence.[27, 80] In practice this means that higher symmetry molecules almost always do not adopt higher crystal symmetries. However, the shape factor is also important and when the molecular shape exceeds a certain awkwardness, which is still not really quantifiable, close-packing is problematic leading to the formation of open networks in which the full molecular symmetry is retained, and a second molecular species is included as a guest to improve packing efficiency. For example, 1,3,5-triphenylbenzene forms 1:3 host–guest complexes with benzene, whereas mesitylene, 1,3,5-trichlorobenzene, and 1,3,5-trinitrobenzene form single-component crystals.[10] The presence of high molecular symmetry coupled with a symmetrical interaction pattern is a more powerful combination for the engineering of host networks. In such cases, there is a pronounced conflict between close-packing and directional factors. Such a situation often arises when groups capable of hydrogen bonding are symmetrically disposed in a symmetrical molecular framework. The rigid scaffolding of hydrogen bonds is also compelled to be symmetrical, because the directionality of the hydrogen bonds cannot be compromised. Gross violations of the close-packing principle may sometimes result leading to guest-molecule inclusion (hydroquinone-C_{60}), catenation of networks (acid **36**), or simultaneous inclusion and catenation (hydroquinone with small guests, trimesic acid).

Consideration of spatial relationships between supramolecular fragments in a crystal reveal the following alternatives: 1) Translation versus inversion stacking of two-dimensional fragments such as ribbons and sheets.[81] 2) Packing of fragments of similar and opposite chiralities, for example helices.[82] 3) Alternative topologies of catenation of two- and three-dimensional networks.[83] 4) Segregated versus mixed stacks of planar donor and acceptor molecules in organic metal structures.[84] Many of these possibilities are influenced by extremely weak interactions and are not only poorly understood at present, but also not very amenable to computational techniques. Since the final outcome of crystallization is often governed by a combination of kinetic

and thermodynamic factors, stereoselective supramolecular synthesis remains a difficult though achievable goal for the future.

2.9. Polymorphism

...the possibility of competing reaction paths should be minimized...

No discussion of crystal engineering can sidestep the problem of polymorphism. This phenomenon is as mysterious and vexing as when a wrong isomer is obtained in a reaction sequence in spite of the best planning and effort. As in traditional synthesis, our inability to grapple with such a problem stems from an incomplete or incorrect knowledge of the factors that affect structure. On occasion it also appears to arise because of outright bad luck, a commodity that is probably as prevalent in crystal engineering as in organic synthesis.

Much has been said about the frequency of occurrence of polymorphism among small-molecule substances, on whether the proportion of polymorphic structures in the CSD is representative of the global proportion of polymorphs in all possible crystal structures (if such details could be ascertained reliably), or even if the number of polymorphs of a given substance increases with the amount of time and effort spent on studying the compound.[85] Many of these questions are rhetorical and quasi-philosophical and are not very helpful in solving the practical problems of crystal engineering. However, a few generalizations may be made: 1) The frequency of occurrence of polymorphic modifications is not uniform in all categories of substances. The phenomenon is probably more common among molecules that have flexible conformations or many different groups capable of hydrogen bonding. By the same token, rigid, flat molecules such as condensed aromatic hydrocarbons are unlikely to have many polymorphic modifications under normal conditions of temperature and pressure. Again, the likelihood of polymorphism may be greatest in an intermediate molecular weight range, approximately C_{10} to C_{20}. 2) Ingenious methods of crystal engineering that create several sites for (three-dimensional) multipoint recognition of molecules will probably decrease the likelihood of polymorphism. In such cases, the general strategy would be to ensure that there is a unique pattern of supramolecular synthons. 3) For the particular application under consideration, it may not really matter whether polymorphs exist, because the critical, property-defining supramolecular fragment (that is, the particular synthon) may be found intact in all the polymorphs. 4) Polymorphism is strongly solvent-dependent in some cases, and computer simulation of crystal structures with and without adhering solvent molecules may provide guidelines for the crystallization of a particular polymorph.

The study of polymorphism in organic crystals is still in a process of evolution, and much more data will be required before firm and general conclusions can be drawn. Recent computational approaches based on molecular dynamics calculations seem to show considerable promise. The Monte-Carlo-based Polymorph Predictor technique has been implemented in the Cerius^2 package from BIOSYM/Molecular Simulations to obtain ab initio predictions of a number of polymorphs.[85] Yet, crystallization almost certainly does not depend exclusively on energetics and may proceed through discrete stages with the result that multimolecular clusters are trapped in higher energy minima in the final crystal structure. A better understanding of polymorphism will depend on a better understanding of the crystallization process itself, and this in turn will rely on advances in spectroscopy (detection of crystal nuclei), physical chemistry (thermodynamics, chaos theory), and biophysics (protein folding). These are difficult issues, and only better experimental and theoretical insights will lead to any measure of control over the problem of polymorphism.

3. Methodology—Intermolecular Interactions

A number of intermolecular interactions, the nuts and bolts of crystal engineering, have been discussed implicitly in the preceding sections, and several detailed and definitive experimental CSD-based and theoretical studies of these interactions have been the subject of recent publications.[6–10, 13, 15, 24, 40, 58, 59, 67–70, 85, 86] The purpose of this section is therefore only to enumerate these forces and to very briefly highlight some of our own results especially those pertaining to the weaker interactions.

The most meaningful criteria for the classification of intermolecular forces from the crystal engineering standpoint are distance-dependence and directionality. Typically, the medium-range forces are isotropic in character and define molecular shape, size, and close-packing (implicit involvement of interactions). Generally, these forces are limited to C···H, C···C and H···H interactions. The long-range forces on the other hand are electrostatic and anisotropic and involve heteroatom interactions, that is, interactions among N, O, S, Cl, Br, I (rarely B, F, P, Se) or between any of these elements and C or H (explicit involvement of interactions). Ionic forces are extremely long-range in nature and are quite specific, directing supramolecular structure effectively.

3.1. Nondirectional Forces

Nondirectional forces (2–10 kJ mol^{-1}) traditionally, though not necessarily exclusively, include C···C, C···H and H···H interactions.[87] The relative importance of these interactions in any particular crystal depends on the C:H stoichiometry. Aromatic compounds (high C:H ratios) have a much stronger tendency to stack, since this would increase the number of C···C interactions. The coulombic character of the C···H interaction could account for its prevalence in a wide variety of aromatic and aliphatic compounds (Section 2.4). For planar aromatic compounds these interactions result in the characteristic T-shaped herringbone synthon **33**. Crystal structures are also known where an unusually acidic C–H group (alkyne) makes close contacts with conjugated π systems.[88] Whether these contacts are to be termed CH···π hydrogen bonds, like the recently studied OH···π hydrogen bonds (see Section 3.2.1), or whether they are merely extreme manifestations of the C···H herringbone interaction is an open question.

3.2. Hydrogen Bonding

Hydrogen bonding, the master key for molecular recognition, is the most reliable directional interaction in supramolecular construction, and its significance in crystal engineering can scarcely be underestimated. As a vast amount of work has been carried out on the various aspects of hydrogen bonding, it would be futile to attempt even a brief review of these efforts here. Hydrogen bonds of the type OH···O and NH···O may be termed "strong" or "conventional" (energies 20–40 kJ mol^{-1})[89] to distinguish them from the weaker CH···O and OH···π interactions (energies 2–20 kJ mol^{-1}), which share many of their characteristics and which are discussed in greater detail in Section 3.2.1.

The distinctive geometrical attributes of a hydrogen bond D–H···A–X (D = donor, A = acceptor) are the D···A and H···A lengths, the hydrogen bond angle D-H-A or θ, the H-A-X angle or ϕ and the planarity of the DHAX system. All these features have been discussed extensively.[6, 15] Typical values for the H···A distance are 1.80 to 2.00 Å for NH···O bonds and 1.60 to 1.80 Å for OH···O bonds. More relaxed definitions of these distance criteria permit a consideration of the slightly longer three-centered and four-centered bonds, which seem to be very common in several hydrogen-bonded structures. Ranges for θ and ϕ occur around 150–160° and around 120–130°, respectively. This marked directionality of hydrogen bonds is well-established and is the basis for efficient and reliable supramolecular construction using supramolecular synthons that contain groups such as –OH, $-CO_2H$, –CONHR, and $-CONH_2$. Synthon **28**, for instance, occurs in several phenols and in the water trimer and is related to other synthons such as $(OH)_4$ and $(OH)_6$.[90] We have found recently that many hydrogen-bonded synthons containing carboxyl and hydroxyl groups in organic crystals are retained largely intact in organometallic crystals.[91]

3.2.1. CH···O and OH···π Hydrogen Bonds

This discussion is also valid for the related CH···N and NH···π[69, 92] interactions. Furthermore, while there is some question whether the CH···Cl interaction is a viable one, recent reports provide evidence for CH···F[94] and CH···Se[95] hydrogen bonds.

There is little doubt that CH···O hydrogen bonds are important, even if subtle, determinants of crystal packing, especially when strong OH···O and NH···O hydrogen bonds are absent.[24, 96] As has been discussed in Section 2.3, CH···O hydrogen bonds may distort the geometry and topology of even the strong hydrogen-bond network in specific instances. Anomalies and puzzles in the strong hydrogen-bond patterns of certain crystal structures are explained on the basis of the interplay of strong and weak hydrogen bonds. In general, the strength and effectiveness of a CH···O hydrogen bond depends on C–H carbon acidity[97] and on O-atom basicity,[98] which is enhanced by cooperative effects. We have shown for instance that CH···O distances in crystals correlate so well with solution C–H group pK_a values that it is even possible to define a crystallographic scale of carbon acidity.[99]

The criteria for the significance of a particular CH···O geometry have also been the subject of some discussion. Recent analysis has shown that the angular characteristics of many longer CH···O contacts (C···O 3.50–4.00 Å) and their effects on crystal structures resemble those of the shorter contacts (3.10–3.50 Å).[24] It should be emphasized that the CH···O bond is not really a van der Waals contact but is primarily electrostatic; as its strength therefore falls off much more slowly with distance, it is viable at distances equal to or longer than the van der Waals limit. Therefore, even long C···O separations (about 4.00 Å) have to be considered seriously, and these weak hydrogen bonds are expected to have orienting effects on molecules prior to nucleation and crystallization. This underlines the important role of these bonds in crystal engineering especially in orchestration.

While CH···O hydrogen bonds are widespread, the complementary OH···π interactions are rare, because C is not as electronegative as O and also because unsaturated carbon atoms are not often situated in sterically unhindered positions, unlike carbonyl and ethereal O atoms, which permit easy access for C–H groups to form CH···O bonds. In spite of these limitations, a sufficiently electron-rich C atom (alkyne, alkene, aromatic) has a propensity to form a hydrogen-bond-like interaction with O–H groups thus contributing to crystal stability.[100] We have studied these interactions systematically with the CSD: around 50 unambiguous cases of intermolecular OH···π and NH···π hydrogen bonding were found in the 1993 update.[69]

3.3. Halogen Atom Interactions

It has long been known that the halogens Cl, Br, and I form short nonbonded contacts in crystals.[15] Not only are these contacts (synthons **25**, **26**) clearly manifested in the crystal structures of the elements themselves; they are also of historical importance in crystal engineering, because they form the basis of the so-called "4 Å chloro rule" enunciated by Schmidt for planar dichloroaromatic compounds.[101] The nature of these interactions is still somewhat obscure. Nyburg and Wong-Ng,[102] and more recently, Price et al.,[86] have held that these short contacts are the result of elliptically shaped atoms (anisotropy), while others including ourselves have maintained that there are specific attractive forces between halogen atoms in crystals.[40, 103] Certainly atomic polarization is an important factor here, because there are clear distinctions between Cl···Cl, Br···Br and I···I interactions and between these symmetrical interactions on the one hand and unsymmetrical interactions such as I···Cl, Br···F and I···F on the other. Directional interactions formed by the halogens with O and N atoms are also polarization-induced and have been used by us and others in systematic crystal engineering (Section 2.1).[33–35, 45]

3.4. Other Interactions: Hardness and Softness

As in the case of halogens, polarization effects are important for sulfur, which is known to form short directional contacts of the type S···N, S···S, and S···Cl. These contacts have been thoroughly studied in the crystal chemistry of the TTF–TCNQ family of compounds.[104] Intermolecular interactions that are

specific to organometallic compounds have only been the subject of very recent study.[105] Our systematic survey of Au···Au interactions has shown that they affect molecular conformation and crystal packing.[106] Hydrogen-bonding patterns in organometallic crystals are, in general, similar to those in simple organic compounds. However, the CO ligand is a base unique to organometallic compounds, and our results indicate that it is more important for CH···O bonding than for OH···O bonding.[91, 107] A possible explanation for such an observation considers the hardness and softness of intermolecular interactions. It appears that the hard and soft acid and base (HSAB) principle may be profitably extended to supramolecular chemistry. For instance, NH···O and OH···O could be considered hard hydrogen bonds, CH···O and CH···π soft hydrogen bonds, and NH···N have perhaps intermediate character.[107] Accordingly, it might be argued that the soft acceptor CO prefers to form a hydrogen bond with the soft donor C–H, or alternatively the hard donor O–H prefers to form bifurcated or solvated hydrogen bonds with hard acceptors rather than waste itself on the soft acceptor CO. Along these lines, the unexpected formation of the CH···Se may be understood in terms of the relative softness of both donor and acceptor species.[95] Again, Scheme 3 shows how the hard synthon **1** and the soft synthon **17** operate independently, but equally effectively, in the crystal.

4. Summary and Outlook

...although chemistry is a science of vast scope and countless specialties, it has no real boundaries...

In writing this article and drawing an analogy between crystal engineering and organic synthesis, I have tried to address two groups of chemists whose concerns and goals might at the outset appear to be somewhat unrelated. Yet, crystal engineering today seems to be poised at the point where organic synthesis was in the fifties and sixties. Empirical, largely intuitive strategies or manipulations within narrowly defined structural families dominate the scene even as one already discerns glimmers of a more logic-driven approach. All these developments have generated a substantial body of data on intermolecular interactions and crystal packing. It is from this corpus that more systematic strategies of crystal engineering will appear. I have attempted to show that the kernel of such strategies already exists in synthetic organic chemistry, and that with this foreknowledge, solid-state supramolecular chemists might well be able to create patterns of extraordinary finesse in crystals. On the other hand, it is hoped that synthetic organic chemists will recognize in crystal engineering a natural extension of so many principles in their canon and realize that with an appreciation of the properties of intermolecular interactions, they may be equally well-equipped to undertake research in this challenging discipline. In either case, crystal engineering, which has been recognized as the central issue in organic materials chemistry, is well set to become the breakthrough technology for industrial research and development.

The term "supermolecule" has been used synonymously with "crystal" in this article, and as mentioned at the very outset, a crystal is the *ultimate* example of a supermolecule in that it consists of an infinity of molecules divergently bound. Hierarchies of supramolecular species may accordingly be recognized, and the synthesis of lower hierarchy supermolecules consisting of two or more convergently bound molecular components has become an extremely attractive and competitive area of research combining molecular synthetic methodology with supramolecular ideas of molecular association.[108] However, such efforts must logically progress towards crystal engineering in the quest for complex three-dimensional networks based on complex polyfunctional molecules.

At one level it is remarkable that concepts and models which were developed in the sixties for organic synthesis can be so readily reapplied today, and in such minute and faithful detail, to a research area which was barely conceived at that time. This parallelism has continued to unfold itself for me even during the writing of this article—I have little doubt that other structural and synthetic chemists will be able to uncover more relationships between these two fascinating areas of chemistry. Yet, at another level such a striking resemblance only reaffirms the oneness or nonduality in the chemical thought process. Though I have quoted only a few sentences from Corey's 1967 article here,[18] almost the entire Part I can be reread and reassimilated in the context of crystal engineering and solid-state supramolecular chemistry, and perhaps even such an eventuality was foreseen, for it is stated while justifying the quest for a general strategy of synthesis that *"such an effort surely is more than an intriguing theoretical exercise; it is a prerequisite to a deeper comprehension of Synthesis and the methodologies which are fundamental to it, and it is likely to be the keystone in the rational development of Synthesis* ***to still higher forms.***"[*]

It is a pleasure to acknowledge the enthusiasm, hard work, and support of my former and present students and postdoctoral associates. Among these, the following have assisted me greatly during the preparation of this manuscript: C. V. K. Sharma, D. S. Reddy, B. S. Goud, K. Biradha, V. R. Thalladi. Much of the work described here would not have been possible without the skillful assistance of several crystallographic collaborators, especially H. L. Carrell and D. E. Zacharias (Fox Chase Cancer Center, Philadelphia), D. C. Craig (University of New South Wales, Sydney), J. A. K. Howard (University of Durham), T. Pilati (Università di Milano), W. T. Robinson (University of Canterbury, Christchurch), Y. T. Struchkov (Nesmeyanov Institute of Organoelement Compounds, Moscow), and others whose names appear as coauthors in the appropriate publications. I would like to thank G. Klebe (BASF AG, Ludwigshafen) for initial discussions, A. Nangia (University of Hyderabad) for many useful comments during the writing of this article, and C. B. Aakeröy (Queen's University, Belfast) for his willingness to prepare the cover illustration. The Cerius² software from BIOSYM/Molecular Simulations provides computational methods cited in this article and modeling tools used to produce some of the accompanying illustrations, and I wish to thank BIOSYM/Molecular Simulations for their support. Financial assistance from the Department of Science and Technology, Government of India, is gratefully acknowledged.

Received: November 15, 1994 [A 931E]
German version: *Angew. Chem.* **1995**, *107*, 2541–2558

[*] The emphasis is mine.

[1] J.-M. Lehn, *Angew. Chem.* **1988**, *100*, 91; *Angew. Chem. Int. Ed. Engl.* **1988**, *27*, 89; *ibid.* **1990**, *102*, 1347 and **1990**, *29*, 1304.

[2] J.-M. Lehn, *Supramolecular Chemistry*, VCH, Weinheim, **1995**.

[3] F. Vögtle, *Supramolecular Chemistry: An Introduction*, Wiley, Chichester, **1991**.

[4] G. M. Whitesides, J. P. Mathias, C. T. Seto, *Science* **1991**, *254*, 1312.

[5] However, inorganic crystal chemists have always appreciated the collective properties of molecules and ions and have traditionally viewed a crystal in terms of its network connectivity. See, for example, A. F. Wells, *Structural Inorganic Chemistry*, Oxford University Press, Oxford, 1975. Yet, these "organic" and "inorganic" perceptions are only parts of the whole! For an example which illustrates that organic and inorganic crystal structures are governed by the same grammar, see D. S. Reddy, D. C. Craig, G. R. Desiraju, *J. Chem. Soc. Chem. Commun.* **1995**, 339.

[6] G. A. Jeffrey, W. Saenger, *Hydrogen Bonding in Biological Structures*, Springer, Berlin, **1991**.

[7] C. B. Aakeröy, K. R. Seddon, *Chem. Soc. Rev.* **1993**, *22*, 397.

[8] M. Mascal, *Contemp. Org. Syn.* **1994**, 31; see, however, J. S. Moore, S. Lee, *Chem. Ind.* **1994**, 556.

[9] *Perspectives in Supramolecular Chemistry: The Crystal as a Supramolecular Entity, Vol. 2* (Ed.: G. R. Desiraju), Wiley, Chichester, **1996**.

[10] G. R. Desiraju in *Comprehensive Supramolecular Chemistry, Vol. 6* (Eds.: D. D. MacNicol, F. Toda, R. Bishop), Pergamon, Oxford, **1996**.

[11] J. D. Dunitz, *Pure Appl. Chem.* **1991**, *63*, 177.

[12] M. D. Cohen, G. M. J. Schmidt, *J. Chem. Soc.* **1964**, 1996; M. D. Cohen, G. M. J. Schmidt, F. I. Sonntag, *ibid.* **1964**, 2000; G. M. J. Schmidt, *ibid.* **1964**, 2014.

[13] G. R. Desiraju, V. R. Pedireddi, *J. Chem. Soc. Chem. Commun.* **1989**, 1112.

[14] G. R. Desiraju, A. Gavezzotti, *J. Chem. Soc. Chem. Commun.* **1989**, 621; *Acta Crystallogr. Sect. B* **1989**, *45*, 473.

[15] G. R. Desiraju, *Crystal Engineering: The Design of Organic Solids*, Elsevier, Amsterdam, **1989**.

[16] See, for example, the preface in the organic solid-state chemistry special issue: *Chem. Mater.* **1994**, *6*, 1087–1462, and references therein; see also J. C. MacDonald, G. M. Whitesides, *Chem. Rev.* **1994**, *94*, 2383.

[17] In the limit it is impossible to strictly separate chemical and geometrical effects, because the geometrical preferences of intermolecular associations follow from chemical factors; see also A. Gavezzotti, *J. Am. Chem. Soc.* **1991**, *113*, 4622.

[18] E. J. Corey, *Pure Appl. Chem.* **1967**, *14*, 19.

[19] E. J. Corey, *Chem. Soc. Rev.* **1988**, *17*, 111.

[20] D. Seebach, *Angew. Chem.* **1990**, *102*, 1363; *Angew. Chem. Int. Ed. Engl.* **1990**, *29*, 1320.

[21] E. J. Corey, X.-M. Cheng, *The Logic of Chemical Synthesis*, Wiley, New York, **1989**.

[22] F. H. Herbstein, *Top. Curr. Chem.* **1987**, *140*, 107.

[23] O. Ermer, *J. Am. Chem. Soc.* **1988**, *110*, 3747.

[24] G. R. Desiraju, *Acc. Chem. Res.* **1991**, *24*, 290.

[25] 2-Methoxy-1,4-benzoquinone: E. M. D. Keegstra, A. L. Spek, J. W. Zwikker, L. W. Jenneskens, *J. Chem. Soc. Chem. Commun.* **1994**, 1633; 1,4-dicyanobenzene: H. Guth, G. Heger, U. Drück, *Z. Kristallogr.* **1982**, *159*, 185.

[26] S. K. Kearsley, G. R. Desiraju, *Proc. R. Soc. London A* **1985**, *397*, 157.

[27] A. I. Kitaigorodskii, *Molecular Crystals and Molecules*, Academic Press, New York, **1973**.

[28] P. M. Zorkii, *Russ. J. Phys. Chem. Engl. Transl.* **1994**, *68*, 870.

[29] R. Wyler, J. de Mendoza, J. Rebek, Jr., *Angew. Chem.* **1993**, *105*, 1820; *Angew. Chem. Int. Ed. Engl.* **1993**, *32*, 1699.

[30] A. L. Lehninger, D. L. Nelson, M. M. Cox, *Principles of Biochemistry*, 2nd ed., Worth, New York, **1993**, pp. 160–197; J. P. Glusker, M. Lewis, M. Rossi, *Crystal Structure Analysis for Chemists and Biologists*, VCH, Weinheim, **1994**.

[31] Volumes of the unit cells: benzoic acid, 617 Å^3; *p*-terphenyl, 619 Å^3; for an example of a much larger though similarly shaped molecule that packs like the benzoic acid dimer and *p*-terphenyl, see P. R. Ashton, D. Joachimi, N. Spencer, J. F. Stoddart, C. Tschierske, A. J. P. White, D. J. Williams, K. Zab, *Angew. Chem.* **1994**, *106*, 1563; *Angew. Chem. Int. Ed. Engl.* **1994**, *33*, 1503.

[32] L. Leiserowitz, *Acta Crystallogr. Sect. B* **1976**, *32*, 775.

[33] V. R. Pedireddi, J. A. R. P. Sarma, G. R. Desiraju, *J. Chem. Soc. Perkin Trans. 2* **1992**, 311; G. R. Desiraju, V. R. Pedireddi, J. A. R. P. Sarma, D. E. Zacharias, *Acta Chim. Hung.* **1993**, *130*, 451.

[34] 4-Iodobenzoic acid might just as effectively be used in such a strategy: B. S. Goud, V. R. Thalladi, V. J. Hoy, F. H. Allen, J. A. K. Howard, G. R. Desiraju, unpublished results.

[35] F. H. Allen, B. S. Goud, V. J. Hoy, J. A. K. Howard, G. R. Desiraju, *J. Chem. Soc. Chem. Commun.* **1994**, 2729.

[36] C. V. K. Sharma, G. R. Desiraju, *J. Chem. Soc. Perkin Trans. 2* **1994**, 2345.

[37] C. V. K. Sharma, K. Panneerselvam, T. Pilati, G. R. Desiraju, *J. Chem. Soc. Chem. Commun.* **1992**, 832.

[38] B. F. Abrahams, B. F. Hoskins, D. M. Michall, R. Robson, *Nature (London)* **1994**, *369*, 727, and references therein; the crystal structure of succinatodisilver(I) also exemplifies the architecture of a diamondoid network structure through ionic $CO_2^- \cdots Ag^+$ interactions; see A. Michaelides, V. Kiritsis, S. Skoulika, A. Aubry, *Angew. Chem.* **1993**, *105*, 1525; *Angew. Chem. Int. Ed. Engl.* **1993**, *32*, 1495; for a more recent report, see L. Carlucci, G. Ciani, D. M. Proserpio, A. Sironi, *J. Chem. Soc. Chem. Commun.* **1994**, 2755.

[39] M. Bremer, P. S. Gregory, P. von R. Schleyer, *J. Org. Chem.* **1989**, *54*, 3796.

[40] V. R. Pedireddi, D. S. Reddy, B. S. Goud, D. C. Craig, A. D. Rae, G. R. Desiraju, *J. Chem. Soc. Perkin Trans. 2* **1994**, 2353.

[41] M. Zaworotko, *Chem. Soc. Rev.* **1994**, *23*, 283, and references therein.

[42] M. Simard, D. Su, J. D. Wuest, *J. Am. Chem. Soc.* **1991**, *113*, 4696.

[43] D. S. Reddy, D. C. Craig, A. D. Rae, G. R. Desiraju, *J. Chem. Soc. Chem. Commun.* **1993**, 1737.

[44] O. Hassel, C. Rømming, *Quart. Rev.* **1962**, 16, 1; classical review on polarization-induced interactions: H. Bent, *Chem. Rev.* **1968**, *68*, 587.

[45] For recent reports on the use of cyano $\cdots$ chloro and aza $\cdots$ chloro interactions in structural design, see respectively, D. S. Reddy, K. Panneerselvam, T. Pilati, G. R. Desiraju, *J. Chem. Soc. Chem. Commun.* **1993**, 661 and K. Xu, M. Ho, R. A. Pascal, Jr., *J. Am. Chem. Soc.* **1994**, *116*, 105.

[46] W. Jones, C. R. Theocharis, J. M. Thomas, G. R. Desiraju, *J. Chem. Soc. Chem. Commun.* **1983**, 1443.

[47] G. R. Desiraju, B. N. Murty, K. V. R. Kishan, *Chem. Mater.* **1990**, *2*, 447; B. S. Goud, G. R. Desiraju, *Acta Crystallogr. Sect. C* **1993**, *49*, 292. For a discussion of *syn-anti* carboxyl group conformations in cubane-1,4-dicarboxylic acid, see O. Ermer, J. Lex, *Angew. Chem.* **1987**, *99*, 455; *Angew. Chem. Int. Ed. Engl.* **1987**, *26*, 447.

[48] G. R. Desiraju, C. V. K. Sharma, *J. Chem. Soc. Chem. Commun.* **1991**, 1239.

[49] C. V. K. Sharma, K. Panneerselvam, T. Pilati, G. R. Desiraju, *J. Chem. Soc. Perkin Trans. 2* **1993**, 2209.

[50] G. R. Desiraju, *J. Chem. Soc. Chem. Commun.* **1991**, 426.

[51] J.-M. Lehn, M. Mascal, A. DeCian, J. Fischer, *J. Chem. Soc. Chem. Commun.* **1990**, 479; J. A. Zerkowski, C. T. Seto, D. A. Wierda, G. M. Whitesides, *J. Am. Chem. Soc.* **1990**, *112*, 9025; N. Kimizuka, T. Kawasaki, T. Kunitake, *ibid.* **1993**, *115*, 4387; R. Ahuja, P.-L. Caruso, D. Möbius, W. Paulus, H. Ringsdorf, G. Wildburg, *Angew. Chem.* **1993**, *105*, 1082; *Angew. Chem. Int. Ed. Engl.* **1993**, *32*, 1033; D. A. Bell, E. V. Anslyn, *J. Org. Chem.* **1994**, *59*, 512; A. Houlton, D. M. P. Mingos, D. J. Williams, *J. Chem. Soc. Chem. Commun.* **1994**, 503; M. Kotera, J.-M. Lehn, J.-P. Vigneron, *ibid.* **1994**, 197.

[52] C. T. Seto, G. M. Whitesides, *J. Am. Chem. Soc.* **1993**, *115*, 905.

[53] J. A. Zerkowski, C. T. Seto, G. M. Whitesides, *J. Am. Chem. Soc.* **1992**, *114*, 5473.

[54] J.-M. Lehn, M. Mascal, A. DeCian, J. Fischer, *J. Chem. Soc. Perkin Trans. 2* **1992**, 461.

[55] J. P. Mathias, E. E. Simanek, J. A. Zerkowski, C. T. Seto, G. M. Whitesides, *J. Am. Chem. Soc.* **1994**, *116*, 4316.

[56] V. A. Russell, M. C. Etter, M. D. Ward, *J. Am. Chem. Soc.* **1994**, *116*, 1941.

[57] For another recent example, see A. Marsh, E. G. Nolen, K. M. Gardinier, J.-M. Lehn, *Tetrahedron Lett.* **1994**, *35*, 397.

[58] For recent reports on $\pi \cdots \pi$ interactions in crystal engineering and molecular recognition, see C. A. Hunter, J. K. M. Sanders, *J. Am. Chem. Soc.* **1990**, *112*, 5525; D. Philp, J. F. Stoddart, *Synlett* **1991**, 445; P. L. Anelli, P. R. Ashton, R. Ballardini, V. Balzani, M. Delgado, M. T. Gandolfi, T. T. Goodnow, A. E. Kaifer, D. Philp, M. Pietraszkiewicz, L. Prodi, M. V. Reddington, A. M. Z. Slawin, N. Spencer, J. F. Stoddart, C. Vicent, D. J. Williams, *J. Am. Chem. Soc.* **1992**, *114*, 193; J. Zhang, J. S. Moore, *ibid.* **1992**, *114*, 9701; J. E. Kickham, S. J. Loeb, S. L. Murphy, *ibid.* **1993**, *115*, 7031; S. Paliwal, S. Geib, C. S. Wilcox, *ibid.* **1994**, *116*, 4497; C. A. Hunter, *Chem. Soc. Rev.* **1994**, *23*, 101.

[59] I. G. Dance in [9].

[60] I am indebted to Dr. O. Zorkaya (Moscow State University) for drawing my attention to the similarity between these crystal structures. For another striking manifestation of synthon **33**, see G. Klebe, F. Diederich, *Phil. Trans. R. Soc. London A* **1993**, *345*, 37.

[61] C. V. K. Sharma, K. Panneerselvam, L. Shimoni, H. Katz, H. L. Carrell, G. R. Desiraju, *Chem. Mater.* **1994**, *6*, 1282.

[62] K. Biradha, C. V. K. Sharma, K. Panneerselvam, L. Shimoni, H. L. Carrell, D. E. Zacharias, G. R. Desiraju, *J. Chem. Soc. Chem. Commun.* **1993**, 1473.

[63] C. B. Aakeröy, G. S. Bahra, P. B. Hitchcock, Y. Patell, K. R. Seddon, *J. Chem. Soc. Chem. Commun.* **1993**, 152; C. B. Aakeröy, P. B. Hitchcock, *J. Chem. Mater.* **1993**, *3*, 1129; C. B. Aakeröy, M. Nieuwenhuyzen, *J. Am. Chem. Soc.* **1994**, *116*, 10983.

[64] Recent examples of the use of conventional hydrogen bonding in crystal engineering: Y.-L. Chang, M. A. West, F. W. Fowler, J. W. Lauher, *J. Am. Chem. Soc.* **1993**, *115*, 5991; K. D. M. Harris, N. M. Stainton, A. M. Callan, R. A. Howie, *J. Mater. Chem.* **1993**, *3*, 947; C.-Y. Hung, T. Höpfner, R. P. Thummel, *J. Am. Chem. Soc.* **1993**, *115*, 12602; E. E. Fenlon, T. J. Murray, M. H. Baloga, S. C. Zimmerman, *J. Org. Chem.* **1993**, *58*, 6625; H. Bock, R. Dienelt, H. Schodel, Z. Havlas, E. Herdtweck, W. A. Herrmann, *Angew. Chem.* **1993**, *105*, 1826; *Angew. Chem. Int. Ed. Engl.* **1993**, 32, 1758; J. C. Beeson, L. J. Fitzgerald, J. C. Gallucci, R. E. Gerkin, J. T. Rademacher, A. W. Czarnik, *J. Am. Chem. Soc.* **1994**, *116*, 4621; J. Yang, J.-L. Marendaz, S. J. Geib, A. D. Hamilton, *Tetrahedron Lett.* **1994**, 35, 3665; E. Fan, C. Vicent, S. J. Geib, A. D. Hamilton, *Chem. Mater.* **1994**, *6*, 1113; A. T. Ung, R. Bishop, D. C. Craig, I. G. Dance, M. L. Scudder, *ibid.* **1994**, *6*, 1269.

[65] O. Ermer, A. Eling, *J. Chem. Soc. Perkin Trans. 2* **1994**, 925; the relationship between organic and inorganic crystal chemistry is lucidly demonstrated here.

[66] S. Hanessian, A. Gomtsyan, M. Simard, S. Roelens, *J. Am. Chem. Soc.* **1994**, *116*, 4495.

[67] For a report on B···O interactions in triethylcyclotriboroxane, see R. Boese, M. Polk, D. Bläser, *Angew. Chem.* **1987**, *99*, 239; *Angew. Chem. Int. Ed. Engl.* **1987**, *26*, 245; for a summary of S-atom interactions see. G. R. Desiraju, V. Nalini, *J. Mater. Chem.* **1991**, *1*, 201.

[68] Review of the use of Cl···Cl interactions in crystal engineering: J. A. R. P. Sarma, G. R. Desiraju, *Acc. Chem. Res.* **1986**, *19*, 222.

[69] M. A. Viswamitra, R. Radhakrishnan, J. Bandekar, G. R. Desiraju, *J. Am. Chem. Soc.* **1993**, *115*, 4868, and references therein.

[70] D. Braga, *Chem. Rev.* **1992**, *92*, 633; A. G. Orpen, *Chem. Soc. Rev.* **1993**, *22*, 191.

[71] O. Hassel, *Tidsskr. Kjemi Bergves. Metall* **1961**, *21*, 60; for a summary, see R. Foster, *Organic Charge Transfer Complexes*, Academic Press, London, **1969**, p. 299.

[72] W. Hoppe, H. U. Lenné, U. Morandi, *Z. Kristallogr.* **1957**, *108*, 321.

[73] M. S. K. Dhurjati, J. A. R. P. Sarma, G. R. Desiraju, *J. Chem. Soc. Chem. Commun.* **1991**, 1702.

[74] D. S. Reddy, B. S. Goud, K. Panneerselvam, G. R. Desiraju, *J. Chem. Soc. Chem. Commun.* **1993**, 663.

[75] V. R. Thalladi, K. Panneerselvam, C. J. Carrell, H. L. Carrell, G. R. Desiraju, *J. Chem. Soc. Chem. Commun.* **1995**, 341.

[76] Interestingly, the trinitrobenzene layers are held together by O···O van der Waals interactions without CH···O hydrogen bonds. See Ref.[27], p. 14.

[77] D. S. Reddy, D. C. Craig, G. R. Desiraju, *J. Chem. Soc. Chem. Commun.* **1994**, 1457.

[78] However, it has long been recognized that synthetic pathways for organic reactions may also be derived computationally. See, for example, E. J. Corey, W. T. Wipke, *Science* **1969**, *166*, 178; J. B. Hendrickson, *Angew. Chem.* **1990**, *102*, 1328; *Angew. Chem. Int. Ed. Engl.* **1990**, *29*, 1286; and references therein.

[79] F. H. Allen, J. E. Davies, J. J. Galloy, O. Johnson, O. Kennard, C. F. Macrae, D. G. Watson, *J. Chem. Inf. Comput. Sci.* **1991**, *31*, 204; F. H. Allen, O. Kennard, R. Taylor, *Acc. Chem. Res.* **1983**, *16*, 146; F. H. Allen, O. Kennard, D. G. Watson in *Structure Correlation, Vol. 1* (Eds.: H.-B. Bürgi, J. D. Dunitz), VCH, Weinheim, **1994**, p. 71. These papers deal with the CSD structure and database methodology per se, but also contain references to work in which the CSD is employed to obtain information about intermolecular interactions.

[80] C. P. Brock, J. D. Dunitz, *Chem. Mater.* **1994**, *6*, 1118.

[81] G. R. Desiraju, K. V. R. Kishan, *J. Am. Chem. Soc.* **1989**, *111*, 4838; G. R. Desiraju, R. L. Harlow, *ibid.* **1989**, *111*, 6757; J. K. Whitesell, R. E. Davis, L. L. Saunders, R. J. Wilson, J. P. Feagins, *ibid.* **1991**, *113*, 3267; G. Filippini, A. Gavezzotti, *Chem. Phys. Lett.* **1994**, *231*, 86.

[82] C. P. Brock, W. B. Schweizer, J. D. Dunitz, *J. Am. Chem. Soc.* **1991**, *113*, 9811; S. J. Geib, C. Vicent, E. Fan, A. D. Hamilton, *Angew. Chem.* **1993**, *105*, 83; *Angew. Chem. Int. Ed. Engl.* **1993**, 32, 119.

[83] J. Konnert, D. Britton, *Inorg. Chem.* **1966**, *5*, 1193.

[84] M. R. Bryce, L. C. Murphy, *Nature (London)*, **1984**, 309, 119; Ref.[16] contains an update on the literature on crystal engineering of TTF–TCNQ type materials.

[85] Review: Ref.[15], pp. 285–299. For a recent, excellent summary of the various computational approaches to crystal engineering, including a brief description of the Cerius^2 package, see A. Gavezzotti, *Acc. Chem. Res.* **1994**, *27*, 309. For a description of the methods based on Monte-Carlo techniques for the prediction of polymorphism, see H. R. Karfunkel, F. J. J. Leusen, R. J. Gdanitz, *J. Comput. Mater. Des.* **1993**, *1*, 177; H. R. Karfunkel, F. J. J. Leusen, *Speedup* **1992**, *6*, 43; Cerius^2 Program, BIOSYM/Molecular Simulations, 9685 Scranton Road, San Diego, CA 92121-3752 (USA) and 240/250 The Quorum, Barnwell Road, Cambridge CB5 8RE (UK).

[86] a) Ref.[15] describes several types of intermolecular interactions in the crystal engineering context. For more recent work see the special issue of *Acta Chim. Hung.* **1993**, *130*, 151–577; b) G. Gilli, F. Bellucci, V. Ferretti, V. Bertolasi, *J. Am. Chem. Soc.* **1989**, *111*, 1023; c) L. Turi, J. J. Dannenberg, *J. Phys. Chem.* **1993**, *97*, 7899; d) *Chem. Mater.* **1994**, *6*, 1313; e) S. L. Price, A. J. Stone, J. Lucas, R. S. Rowland, A. Thornley, *J. Am. Chem. Soc.* **1994**, *116*, 4910; f) J. Perlstein, *ibid.* **1994**, *116*, 455; g) P. Gilli, V. Bertolasi, V. Ferretti, G. Gilli, *ibid.* **1994**, *116*, 909.

[87] However, it is important to note that van der Waals contacts of the type N···N and O···O are just as feasible: see, for example, Ref.[27, 76].

[88] J. E. Cochran, T. J. Parrott, B. J. Whitlock, H. W. Whitlock, *J. Am. Chem. Soc.* **1992**, *114*, 2269; P. E. Eaton, E. Galoppini, R. Gilardi, *ibid.* **1994**, *116*, 7588; R. Hunter, R. H. Haueisen, A. Irving, *Angew. Chem.* **1994**, *106*, 588; *Angew. Chem. Int. Ed. Engl.* **1994**, 33, 566; D. A. Leigh, P. Linnane, R. G. Pritchard, G. Jackson, *J. Chem. Soc. Chem. Commun.* **1994**, 389; T. E. Muller, D. M. P. Mingos, D. J. Williams, *ibid.* **1994**, 1787; T. Steiner, *ibid* **1995**, 95.

[89] For an interesting report on a hydrogen-bonded complex that may be sublimed intact, see D. R. Armstrong, S. Bennett, M. G. Davidson, R. Snaith, D. Stalke, D. S. Wright, *J. Chem. Soc. Chem. Commun.* **1992**, 262.

[90] N. W. Thomas, G. R. Desiraju, *Chem. Phys. Lett.* **1984**, *110*, 99; O. Ermer, C. Röbke, *Angew. Chem.* **1994**, *106*, 1832; *Angew. Chem. Int. Ed. Engl.* **1994**, *33*, 1755.

[91] D. Braga, F. Grepioni, P. Sabatino, G. R. Desiraju, *Organometallics*, **1994**, *13*, 3532.

[92] L. R. Hanton, C. A. Hunter, D. H. Purvis, *J. Chem. Soc. Chem. Commun.* **1992**, 1134.

[93] R. Taylor, O. Kennard, *J. Am. Chem. Soc.* **1982**, *104*, 5063.

[94] L. Shimoni, H. L. Carrell, J. P. Glusker, M. M. Coombs, *J. Am. Chem. Soc.* **1994**, *116*, 8162.

[95] M. Iwaoka, S. Tomoda, *J. Am. Chem. Soc.* **1994**, *116*, 4463.

[96] P. Seiler, J. D. Dunitz, *Helv. Chim. Acta* **1989**, 72, 1125; T. Suzuki, H. Fujii, T. Miyashi, *J. Org. Chem.* **1992**, 57, 6744; T. Steiner, W. Saenger, *J. Am. Chem. Soc.* **1992**, *114*, 10146; *ibid.* **1993**, *115*, 4540; *Acta Crystallogr. Sect. D* **1993**, *49*, 592; B. D. Smith, K. H. Haller, M. Shang, *J. Org. Chem.* **1993**, 58, 6905; T. Steiner, *J. Chem. Soc. Chem. Commun.* **1994**, 101.

[97] G. R. Desiraju, *J. Chem. Soc. Chem. Commun.* **1989**, 179; *ibid.* **1990**, 454.

[98] T. Steiner, *J. Chem. Soc. Chem. Commun.* **1994**, 2341.

[99] V. R. Pedireddi, G. R. Desiraju, *J. Chem. Soc. Chem. Commun.* **1992**, 988.

[100] D. Mootz, A. Deeg, *J. Am. Chem. Soc.* **1992**, *114*, 5887.

[101] G. M. J. Schmidt, *Pure Appl. Chem.* **1971**, *27*, 647.

[102] S. C. Nyburg, W. Wong-Ng, *Proc. R. Soc. London Ser. A* **1979**, *367*, 29.

[103] D. E. Williams, L.-Y. Hsu, *Acta Crystallogr. Sect. A* **1985**, *41*, 296; G. R. Desiraju, R. Parthasarathy, *J. Am. Chem. Soc.* **1989**, *111*, 8725.

[104] T. Suzuki, H. Fujii, Y. Yamashita, C. Kabuto, S. Tanaka, M. Harasawa, T. Mukai, T. Miyashi, *J. Am. Chem. Soc.* **1992**, *114*, 3034; T. Jørgensen, T. H. Hansen, J. Becher, *Chem. Soc. Rev.* **1994**, *23*, 41.

[105] D. Braga, F. Grepioni, *Acc. Chem. Res.* **1994**, *27*, 51; L. Brammer, D. Zhao, *Organometallics*, **1994**, *13*, 1545.

[106] S. S. Pathaneni, G. R. Desiraju, *J. Chem. Soc. Dalton Trans.* **1993**, 2505.

[107] D. Braga, F. Grepioni, K. Biradha, V. R. Pedireddi, G. R. Desiraju, *J. Am. Chem. Soc.* **1995**, *117*, 3156.

[108] E. C. Constable, A. J. Edwards, P. R. Raithby, J. V. Walker, *Angew. Chem.* **1993**, *105*, 1486; *Angew. Chem. Int. Ed. Engl.* **1993**, *32*, 1465; C. Dietrich-Buchecker, B. Frommberger, J. Lüer, J.-P. Sauvage, F. Vögtle, *ibid.* **1993**, *105*, 1526 and **1993**, *32*, 1434; F. Vögtle, W. M. Müller, U. Müller, M. Bauer, K. Rissanen, *ibid.* **1993**, *105*, 1356 and **1993**, *32*, 1295; E. A. Wintner, M. M. Conn, J. Rebek, Jr., *Acc. Chem. Res.* **1994**, *27*, 198; P. R. Ashton, D. Philp, N. Spencer, J. F. Stoddart, D. J. Williams, *J. Chem. Soc. Chem. Commun.* **1994**, 181; M. J. Gunter, D. C. R. Hockless, M. R. Johnston, B. W. Skelton, A. H. White, *J. Am. Chem. Soc.* **1994**, *116*, 4810; H. L. Anderson, A. Bashall, K. Henrick, M. McPartlin, J. K. M. Sanders, *Angew. Chem.* **1994**, *106*, 445; *Angew. Chem. Int. Ed. Engl.* **1994**, *33*, 429.

Supramolecular Inorganic Chemistry: Small Guests in Small and Large Hosts

Achim Müller,* Hans Reuter,* and Stephan Dillinger

Dedicated to Professor Jean-Marie Lehn

A key reaction in the biological and material world is the controlled linking of simple (molecular) building blocks, a reaction with which one can create mesoscopic structures, which, for example, contain cavities and display specifically desired properties, but also compounds that exhibit typical solid-state structures. The best example in this context is the chemistry of host–guest interactions, which spans the entire range from three- and two-dimensional to one- and "zero-dimensional", discrete host structures. Members of the class of multidimensional compounds have been classified as such for a long time, for example, clathrates and intercalation compounds. Thus far, however, there are no classifications for discrete inorganic host–guest compounds. The first systematic approach can be applied to novel polyoxometalates, a class of compounds which has only recently become known. Molecular recognition; tailor-made, molecular engineering; control of fragment linkage of spin organization and crystallization; cryptands and coronands as "cages" for cations, anions or anion–cation aggregates as sections of ionic lattices; anions within anions, receptors; host–guest interactions; complementarity, as well as the dialectic terms reduction and emergence are important terms and concepts of supramolecular inorganic chemistry. Of particular importance for future research is the comprehension of the mesoscopic area (molecular assemblies) –that between individual molecules and solids ("substances") –which acts in the biological world as carrier of function and information and for which interesting material properties are expected. This area is accessible through certain variations of "controlled" self-organization processes, which can be demonstrated by using examples from the chemistry of polyoxometalates. The comprehension of the laws that rule the linking of simple polyhedra to give complex systems enables one to deal with numerous interdisciplinary areas of research: crystal physics and chemistry, heterogeneous catalysis, bioinorganic chemistry (biomineralization), and materials science. In addition, conservative self-organization processes, for example template-directed syntheses, are of importance for natural philosophy in the context of the question about the inherent properties of material systems.

Keywords: clathrates · clusters · layer compounds · polyoxometalates · supramolecular chemistry

Only the Whole is the Truth.
G. W. F. Hegel

1. Introduction and the Current State of the Art

1.1. Supramolecular Chemistry:[1] Definitions

After the accidental discovery of crown ethers by Pedersen[2] nearly 30 years ago, the field of supramolecular organic chemistry, due to its close relationship with bioorganic chemistry and its research topics, such as receptors, enzymes, and carrier molecules,[3a] has not only brought forth a plethora of new classes of compounds (cryptands,[3b, c] spherands,[4] siderands[5]) with unusual structure–property relationships but has also developed an independent terminology to describe supramolecular phenomena. Consequently, this area of research has a quite homogeneous appearance, despite its wide span of activities. In contrast to this, the field of inorganic host–guest chemistry presents a rather more inhomogeneous picture. This stems in part from the lack of commonly accepted definitions and concepts and the fact that this field differs noticeably from its organic counterpart due to dissimilar notions of bonding and syntheses.

Supramolecular compounds (supermolecules and complexes) in organic chemistry are, specifically, aggregates of well-defined composition and structure, consisting of two or more different building blocks (see Fig. 1); host–guest compounds are a subgroup, hydrogen-bonded donor–acceptor aggregates another. These building blocks are –like those of molecular materials[6]– molecules or ions, which are stable in the pure or dissolved state and have well-defined physical and chemical properties. The intermolecular interactions between the host species

[*] Prof. Dr. A. Müller, Dipl.-Chem. S. Dillinger
Fakultät für Chemie der Universität
Postfach 100131, D-33501 Bielefeld (Germany)
Telefax: Int. code + 521-106-6003
Prof. Dr. H. Reuter
Institut für Chemie der Universität
Postfach 4469, D-49069 Osnabrück (Germany)
Telefax: Int. code + (541) 969-2370

 © VCH Verlagsgesellschaft mbH, D-69451 Weinheim, 1995 0570-0833/95/3421-2328 $ 10.00+.25/0 Angew. Chem. Int. Ed. Engl. 1995, 34, 2328–2361

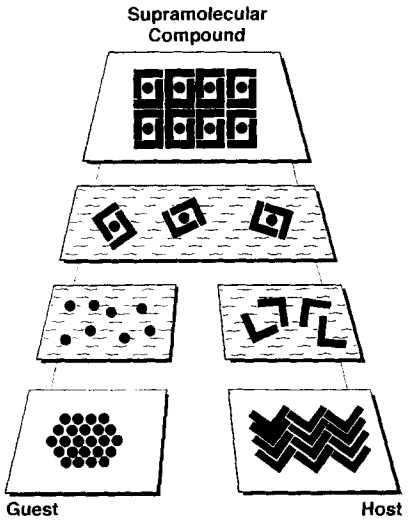

Fig. 1. Flow scheme depicting the construction of supramolecular compounds from molecular host and guest species. Beginning with well-defined starting materials (for which the crystalline state was chosen in this example), the reaction in solution leads to the supramolecular species. In general, it is desirable to isolate and characterize the compound in the crystalline form. Depending on the actual host–guest compound, some of the steps shown may be skipped or performed in a different order.

or between host and guest species as well as between donor and acceptor compounds—electrostatic attraction, van der Waals forces, hydrogen bonds—are strong enough to ensure the integrity of the supramolecular aggregates in solution. These forces, however, are in general still weak enough to enable the reversible decomposition of the aggregates into their primary building units under only slightly modified conditions.

As the important steps in the formation of organic host–guest compounds, as well as their reactions, occur in general in solution, supramolecular organic chemistry long limited itself to this phase. Only in borderline cases, for example, for structural determinations, was the solid phase included in studies. This tendency has recently been reversed in the context of "crystal engineering", that is, by studying the systematic creation of organic crystal structures, too.[7] In contrast, inorganic host–guest compounds were until recently[8] almost exclusively observed in the solid state. Today, there are indications that many zero-dimensional aggregates are also stable in solution. Therefore, for supramolecular inorganic chemistry not only stable (i.e., actually existing) discrete species as primary building blocks, but also hypothetical ones and even single atoms have to be considered and strong interactions (covalent or ionic bonds) between host fragments must also be taken into account. In this last case, however, it is necessary that the host–guest interactions are weak in order to constitute a "real" supramolecular compound, although deviations from this rule should be discussed in special cases, based on the experimental data on hand.

This somewhat modified definition leads to a conceptual change in the synthetic strategies for the construction of multidimensional inorganic host–guest compounds. In many cases, the host is synthesized first, after which the guest is allowed to interact with it. Conversely, sometimes the guest is utilized as the template for the synthesis of the host. The host structures in supramolecular inorganic compounds are often metastable phases, which could not have been created without the aid of the guest.

The entire field is best subdivided according to topological/structural aspects,[9] independent of the specific nature of the chemical bonds and the host-specific synthesis. This approach, formally, leads to four categories (see Fig. 2) of host–guest compounds, corresponding to the relevant dimensionality of the *three-*, *two-*, *one-*, or *"zero-dimensional" host structure.*

The host structure is determined primarily by the connectivity (e.g., two, three, four, or six bonds), by the geometric requirements (e.g., linear, square-pyramidal, tetrahedral, or octahedral linkage points), and by the type of linkage (corner-, edge-, or face-sharing) of the *molecular subunits.*

Achim Müller, born in 1938 in Detmold, studied chemistry and physics as the University of Göttingen and received his Ph.D. (1965) and his Habilitation (1967) there under the supervision of O. Glemser. He is now Professor of Inorganic Chemistry at the University of Bielefeld and is a member of several scientific academies, including the Deutsche Akademie für Naturforscher (Leopoldina) and the Polish Academy of Sciences. His research interests range from problems of molecular physics (theory of mass influence on molecular constants), vibrational spectroscopy (matrix isolation spectroscopy, band contour analysis, resonance Raman effect, metal isotope effects), bioinorganic chemistry (model compounds and biological nitrogen fixation by free-living organisms), and molecular metal chalcogenide complexes and clusters (synthesis, geochemical relevance, electronic and molecular structure, topological and supramolecular aspects, and their use in heterogeneous catalysis) to aspects of natural philosophy. He has published, besides numerous original papers, more than 30 reviews and is coeditor of eight books.

H. Reuter

A. Müller

Hans Reuter was born in 1952 in Niederoberweiler, a small community in the German region of the Vulkaneifel. He studied chemistry at the University of Bonn, where he completed his Ph.D. in 1987 working under the supervision of H. Puff on the hydrolysis of organotin halides. His Habilitation in the field of inorganic chemistry also took place in Bonn, in 1992. His research interests lie in the area of preparative solid-state chemistry, with emphasis on syntheses from molecular precursors at low temperatures, particularly the solution-sol–gel process. In 1990, Hans Reuter was awarded the Bennigsen-Foerder Award of the German state of Nordrhein-Westfalen for a research project on supramolecular organometallic chemistry. After a temporary appointment at the University of Münster, he received an offer for a chair at the Institute for Chemistry at the University of Osnabrück at the end of 1993.

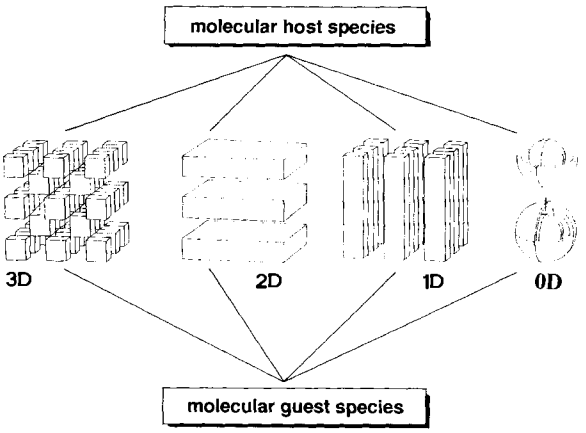

Fig. 2. Schematic representation of the four categories of host–guest compounds as a function of the dimensionality of the host. In the case of zero-dimensional hosts, one has to distinguish between closed (bottom) and open (top) hosts.

1.2. Retrosynthesis and Preliminary Synthetic Strategies

Upon analyzing the existing data, one finds that many basic building blocks form similar, if not identical structures, that is, their behavior is topologically/structurally equivalent, in spite of the different types of bonding and atomic distances involved (see Section 2.1.4). Using retrosynthesis, one often finds molecular building blocks in the host structures that are unknown as isolated species. These must, therefore, have formed from the starting materials by complex reaction mechanisms and reaction pathways.

In order to avoid potential linguistic confusion stemming from the constant switching between actually existing and hypothetical subunits, and to build a connection between the starting materials and the structural characteristics of the host species, it appears useful to comment on some basic aspects of retrosynthesis and synthetic strategies. Using the concept of retrosynthesis as a guide, which has been quite successful in organic chemistry,[10] an agreement on the definition and usage of terms should be reached that is appropriate for inorganic host–guest phenomena.

It is a frequent desire in preparative chemistry to tailor a host for a specific guest. In these cases, the chemist acts as the designer. If size, polarity, charge, etc. of the guest are given, it is possible to design a host with a matching surface topology and polarity. The actual synthetic strategy will be guided by this design and by the pool of known relevant reactions, reagents, and starting materials.

1.3. Tectons

The starting point of a successful synthesis of a host or a host–guest compound is its rational retrosynthesis. In the first step, the structural building blocks are reduced to simple geometric "figures", such as squares, tetrahedra, or cubes, with the corners acting as linkage points to other corresponding figures. In analogy to the term synthon in organic chemistry, these entities will be called *tectons*.[11] Just as in Corey's[12] original definition of synthon, the term tecton applies to basic structural units of the host that can be formed by known or presumed synthetic operations.[13]

Among the tectons shown in Figure 3, the T_1 tecton represents a certain exception in that it stands for an end group, which terminates the structure at this linkage point. Similarly, the T_2 tecton is less often used as a structure-forming element than as a spacer, that is, as a building block that increases the distance between two tectons and yields another linkage point, which can formally be viewed as a "ball joint" that freely rotates in all three spatial dimensions.

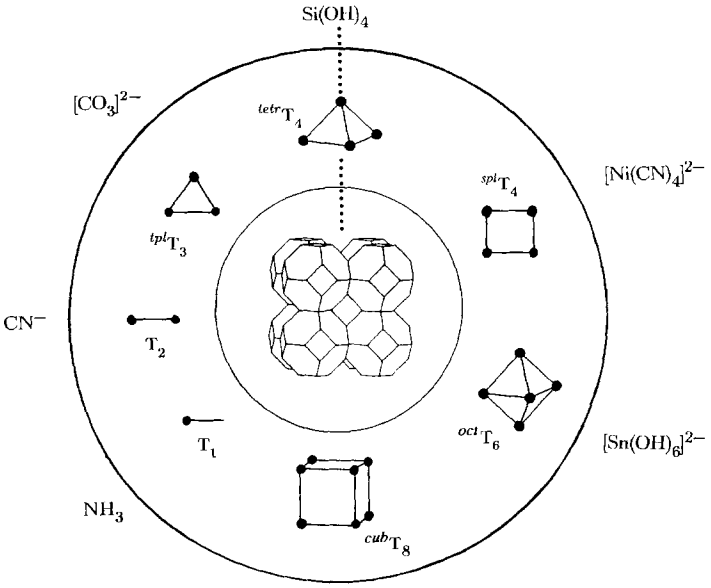

Fig. 3. Summary of common (basic) tectons and tecton equivalents in inorganic host–guest chemistry. The target compound (center) is decomposed by retrosynthesis into tectons (middle ring) which, in turn, should be accessible by simple reactions from either known stable inorganic tecton equivalents or from those that are postulated as intermediates (outer ring).

1.4. Tecton Equivalents

After these abstract considerations regarding the formation of a host structure, the next step includes the first fundamental considerations regarding their chemical realization, which crucially influence all further planning. We have to look for actually existing or hypothetical compounds for the tectons in the host structure. These are called *tecton equivalents*, based on the term synthetic equivalents in the retrosynthesis of organic molecules. The tecton equivalents should either contain the necessary tectons or they should be readily obtainable from them by simple reactions.

1.5. Reagents and Reaction Conditions

Once these planning steps are completed, the appropriate preparative conditions, that is, the *reagents*, *starting materials*, and *reaction conditions*, must be chosen so that they yield the desired tecton equivalents.

The above-mentioned considerations can be clarified by referring to the formation of two-dimensional host structures such as those shown in Figure 4. The layer topology of these host structures is known from α-tin(II) oxide which has the same layer structure as red PbO, and hence, is composed of edge-sharing

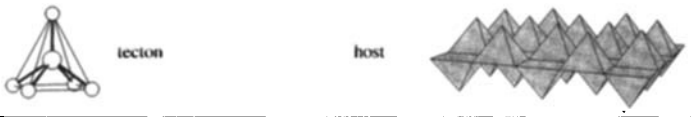

host topology	*alpha-SnO layers*		
layer formula	SnO	$[RSnO]^-$	$[RSnO]^+$
structural unit	spy-$\{SnO_4\}$	spy-$\{RSnO_4\}$	spy-$\{RSnO_4\}$
tecton	$^{scon}T_4$-4E		
	⇧ *condensation*		
tecton equivalent	$H_2[Sn^{II}(OH)_4]$	$H_3[RSn^{II}(OH)_4]$	$H[RSn^{IV}(OH)_4]$
	⇧ *hydrolysis*		
reagent	$SnCl_2$	?	$RSnCl_3$
reaction conditions	$SnCl_{2(aq)} + 2\ NaOH_{(aq)}$ $SnO_{2(s)} + 2\ NaCl_{(aq)}$	?	?

Fig. 4. Schematic representation of the retrosynthesis of planar, two-dimensional host structures with the topology of an α-SnO layer, based on a square-pyramidal, quadruply linked (edge-sharing) tecton. The position at the tip of the pyramid is occupied by a lone pair of electrons or an organic residue.

square-pyramidal (spy) $\{SnO_4\}$ units. The tin atoms at the tip of the pyramids occupy alternate positions above and below the central plane of oxygen atoms, in a chessboard-like manner. The corresponding tecton for this structural unit is, therefore, a square-concave (*scon*) one labeled as a $^{scon}T_4$-4E tecton, according to its linkage pattern (number of linkages/type of linkage: face = F, edge = E, point (corner) = P).

During the search for a suitable tecton equivalent, one first has to decide which chemical elements should build up the host. Those combinations of elements should be contemplated of which it is known or at least assumed that, under the right conditions, they can form the building blocks corresponding to the desired tecton. If we consider the elements tin and oxygen, a possible tecton equivalent for the purely inorganic SnO layer would be the hypothetical acid $H_2[Sn(OH)_4]$, which could form the desired product by a condensation reaction, cleaving off three H_2O molecules. The search for a possible starting material and a rational synthesis leads to tin(II) chloride as the cheapest tin(II) halide and to its reaction with sodium hydroxide. And, as we know, this approach turns out to be successful.

The layers of our target host can, at least formally, be modified by replacing the lone pair of electrons on the tin atoms by an organic residue R and by "manipulating" the oxidation state of the tin atoms. Both cases strongly affect the polarity and charge of our target host, as negatively ($[RSn^{II}O]^-$) and positively ($[RSn^{IV}O]^+$) charged layers must be formulated. These host layers should now exhibit very different (supramolecular) properties compared to the original, neutral ones. Possible relevant tectons are shown in Fig. 4. While, as yet, a rational starting material for the tin(II) case is not known, suitable starting materials for the tetravalent tin species in the form of alkyl- or aryltin trichlorides and related compounds are readily available.[14]

In the following discussions, some inorganic host–guest compounds will be presented, most of which have been discovered accidentally, some of which, however, are the result of successful, controlled synthetic strategies. This will demonstrate that inorganic chemistry has at its disposal a near inexhaustible supply of "materials", which can be used according to unit construction, a fact which has often fueled the imagination of chemists in the past, and will, indeed, provide future generations with countless opportunities for new developments.

Nevertheless, it remains the privilege of nature to determine—based on her numerous options regarding self-organization[1, 15]—whether the planned structure can be realized or whether a different reaction course is preferred, leading, due to kinetic constraints, to a different minimum on the energy hypersurface.

2. Multidimensional Host Structures

2.1. Three-Dimensional Host Structures

The host–guest compounds most readily understood with respect to primary building blocks and their linkage are the *clathrates*. This class encompasses crystalline lattice inclusion compounds with host structures that are composed of separate molecules. These are linked by hydrogen bonds in such a manner as to form cavities, connected by pores and channels, some or all of which contain small guest species. Since the interactions between the host matrix and the guest molecules are, by definition, limited to weak van der Waals forces, it is frequently observed that the guest species are very mobile and, as a result, disordered. Hence, the overall composition of clathrates varies within a certain range and different guest species can replace each other. In principle, the formation of clathrate-type host–guest compounds is not limited to three-dimensional host structures.

2.1.1. Clathrate Hydrates[16a]

Among the earliest known clathrate-type host–guest compounds in inorganic chemistry are the *gas* and *liquid hydrates* which in the formulation as "host·guest", have limiting compositions of **1** and **2**, respectively. The formation of a chlorine

$46H_2O{\cdot}8G$ **1** $136H_2O{\cdot}8G$ **2**

hydrate was first observed by Davy in 1811,[17] and its approximate composition determined by Faraday as early as 1823.[18] The structural details, however, were elucidated only in the middle of this century by the studies of von Stackelberg and Müller.[19] It was found that the water molecules form the primary building blocks in these classic examples of inorganic host–guest chemistry. Every water molecule functions, as shown in Figure 5, as a donor and an acceptor each for two

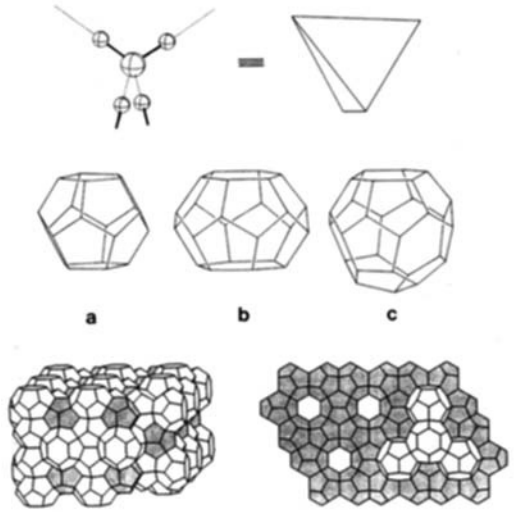

Fig. 5. Sections from the crystal structures of gas and liquid hydrates. The H_2O molecules (top) act as donor and acceptor for two hydrogen bonds each and, hence, are tetrahedrally connected to four other molecules. The polyhedra (center) thus formed are a) the pentagonal dodecahedron, b) the tetrakisdodecahedron, and c) the hexakisdodecahedron. The crystal structures (bottom) of the gas (left) and liquid (right) hydrates exhibit pentagonal dodecahedra which are either isolated or linked in a layer-type manner.

hydrogen bonds, and, thus, is surrounded by four other water molecules in a nearly tetrahedral manner. Similar arrangements are found for the various modifications of ice.[20]

Gas Hydrates

In the *gas hydrates* **1**, which crystallize in a cubic lattice, the 46 clathrand molecules form two cavities of different size: two smaller pentagonal dodecahedra [5^{12}] and six slightly larger 14-faced-polyhedra, which are formed by twelve pentagons and two hexagons [$5^{12}6^2$]. Oxygen atoms occupy the 20 or 24 corners of these polyhedra, respectively, while the hydrogen atoms are disordered along the edges of the polyhedra. The tetrakisdecahedra create, through common hexagonal faces, a system of three mutually perpendicular pipes which, in turn, are connected by common pentagonal faces. Finally, three pairs of these pipes enclose the smaller pentagonal dodecahedra which, therefore, are not interconnected.

Within the structures of gas hydrates the cavities are available in different numbers (2/6 per unit formula) and sizes (pentagonal dodecahedra/tetrakisdecahedra) for inclusion of guest species, which can be expressed by the description $46\,H_2O \cdot 2G^{12} \cdot 6G^{14}$. The limiting factor for the occupancy of these cavities by guest species is the ratio of steric requirements of the guest to the available volume in the host. The latter factor is not very flexible, according to the constant length of the hydrogen bonds of 280 pm. The van der Waals radii of the guests must of course be smaller than those of the cavities. These conditions are fulfilled by noble gases (G = Ar, Kr, Xe), gaseous elements of nonmetals (G = Cl_2, O_2, N_2), various inorganic molecules (G = CO_2, H_2S, PH_3, SO_2), and even by some organic species (G = CH_4, CH_3Cl, C_2H_6, C_2H_4O). Ethylene oxide[21] is a special case due to its three-membered-ring structure. Hydrogen, helium, and neon cannot be incorporated, most probably due to their weak interactions with the host and because, on account of their small size, they can readily diffuse out of the cavities by way of the small pentagonal and hexagonal polyhedral "windows".

Liquid Hydrates

The *liquid hydrates* **2**, which also crystallize in a cubic lattice, exhibit, in addition to pentagonal dodecahedra, polyhedral building blocks with sixteen faces and twenty-eight corners, which create twelve pentagons and four hexagons [$5^{12}6^4$]. In contrast to the isolated twelve-faced polyhedra in the gas hydrates, these units are linked through common faces to layers which exhibit the [ABC] sequence typical of cubic closest packing (ccp). The hexakisdecahedra fill the gaps between the layers and are linked to each other by their hexagonal faces, forming a diamond-like lattice.

The number and size of cavities leads to the formula $136\,H_2O \cdot 16G^{12} \cdot 8G^{16}$; only the larger cavities are occupied. The preferred guests are organic molecules (G = *n*-propane, nitromethane, cyclopentane, cyclobutanone), with one known exception (G = SF_6).

Double Hydrates

In the liquid hydrates, only the eight larger cavities are filled with guest species. In the *double hydrates*, for which the H_2S double hydrates can serve as example, one finds that hydrogen sulfide molecules, acting as "host helpers", occupy the 16 smaller cavities as well. This yields the limiting composition of **3**. Among the guests observed within these compounds are

$$136\,H_2O \cdot 16\,H_2S \cdot 8G \quad \mathbf{3}$$

chloroform, carbon tetrachloride, iodine, carbon disulfide, as well as larger organic molecules such as tetrahydrofuran[22] and benzene.

The clathrate hydrates are formed during the freezing of water in the presence of the corresponding guest species. Apart from steric considerations, electronic effects play a crucial role, as only those guest species will yield real clathrates that form relatively weak—if any—hydrogen bonds.[23]

Structurally, clathrates strongly resemble the ice modifications known to date. The guest-free hosts, however, are not known, which indicates that the guests are required as templates. The ambient-pressure modifications of ice exhibit smaller cavities, while the high-pressure modifications display much larger ones. This leads, in a formal sense, to mutually penetrating hosts, due to their high degree of "openness".

2.1.2. *Clathrasils, Zintl-Phases, and Polycations*

Even though gas and liquid hydrates are, from a chemical viewpoint, rather unimportant, they have gained a lot of prominence as prototypes for the structures of quite a large number of different compounds. This is surprising insofar as these compounds, often rather stable species, minerals, or metallic conductors, do not chemically resemble the labile hydrates.

The mineral melanophlogite, **4** (MEP),[25] and the synthetic zeolite ZSM-39, **5** (MTN)[24] exhibit a structural relationship to the liquid and gas hydrates that is not so surprising insofar as

the ice modifications—normal hexagonal ice (I_h) and cubic ice (I_c) are isostructural to the SiO_2 modifications β-tridymite and β-cristobalite, respectively.

$46SiO_2 \cdot nG$ **4** $136SiO_2 \cdot nG$ **5**

It has been known for some time that several alkali metal stannides, germanides,[26] and silicides such as Na_8Si_{46} **6** or $Na_{11}Si_{136}$ **7**[27], which belong to the class of *Zintl phases*, are topologically/structurally equivalent to the gas and liquid hydrates. These compounds exhibit nearly the same Si–Si distances (237 pm) as elemental silicon (235 pm). The alkali metals, in contrast to earlier assumptions, are most likely to be present as cations and are disordered over the two polyhedral cavities.

The compound $Ge_{38}P_8Cl_8$ **8**[28] shows that the inclusion of anions of suitable size and charge in *polycations* is also feasible. In this species, eight tetravalent germanium atoms of a Ge_{46} lattice have been replaced by pentavalent phosphorus atoms, making the host a polycation. In order to maintain electroneutrality, a corresponding number of chloride ions are incorporated as guests within the cavities.

Na_8Si_{46} **6** $Na_{11}Si_{136}$ **7** $Ge_{38}P_8Cl_8$ **8**

The formation of identical structural characteristics in the four classes of compounds listed in Table 1 can be understood in the following way: The primary building blocks (H_2O, SiO_4, Ge) are tetrafunctional, that is, they each form four "bonds" to neighboring blocks with tetrahedral orientation. These geometric factors are primarily responsible for the creation of the structures, while all other effects, such as distances between the building blocks and the type of linkage are only of secondary importance.

Table 1. Summary of the classes of compounds belonging to the structural families of the gas and liquid hydrates and of the average values of the observed distances $\bar{d}$ between tetrahedral centers.

Structure type	Gas hydrates	Liquid hydrates	$\bar{d}$(X–X) [pm]
clathrates	$46H_2O \cdot 8Cl_2$	$136H_2O \cdot 8CHCl_3$	280
framework silicates	$(SiO_2)_{46} \cdot nG$	$(SiO_2)_{136} \cdot nG$	306
Zintl phases	$Si_{46} \cdot 8Na$	$Si_{136} \cdot 11Na$	237
polycations	$[Ge_{38}P_8]^{8+} \cdot 8Cl^-$		

The existence of these compounds is critically determined by the ratio of cavity volume to guest size, as well as by the interaction between host matrix and guests. The drawings shown in Figure 6, which depict the position of some guest species in the different cavities of melanophlogite **4**, give an impression of the size relationships involved. This kind of knowledge regarding the nature and the orientation of the guest molecules, which are often statically/dynamically disordered, can only be gleaned from single-crystal X-ray structure analyses. These yield an interpretable distribution of the electron density throughout the various host cavities.[30]

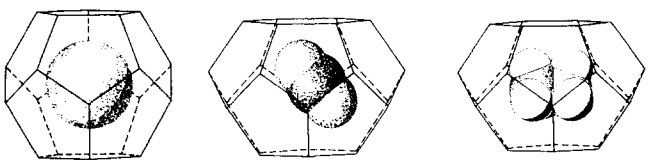

Fig. 6. Position of some guest species in the cavities of synthetic melanophlogite **4**: Left: xenon in a $[5^{12}]$ polyhedron; middle: carbon dioxide in a $[5^{12}6^2]$ polyhedron, and right: methylamine also in a $[5^{12}6^2]$ polyhedron. The guest species are shown as space-filling models to give an approximate impression of the van der Waals volumes of the atoms and molecules (from ref. [29]).

2.1.3. Silicates with Framework Structures

As mentioned above, compounds **4** and **5** belong to the class of clathrasils. Based on their composition and structural characteristics, these compounds belong—according to the "family tree" shown in Scheme 1—to the class of porous tectosilicates.[31] Compounds of this class with the general formula $mSiO_2 \cdot nG$ **9** are called porosils. The term *clathrasils*[32a] describes all host structures with pores and cavities whose dimensions are such that an exchange of the guests is not possible. The term *zeosils*, on the other hand, is used for compounds such as silica-ZSM-11 (MEL) **10**[33] or decadodecasil 3R (DDR) **11**[34] that exhibit channel-like pores with openings that are large enough to allow guest exchange.

$mSiO_2 \cdot nG$ **9** $96SiO_2 \cdot nG$ **10** $120SiO_2 \cdot nG$ **11**

The frameworks of clathrasil hosts are neutral, so that only neutral species—in general, solvent molecules or more or less solvated ion pairs—can function as guests. As the guests in clathrasils cannot leave the host without destroying it, and as guests cannot enter the host once it is formed, the host structure must, correspondingly, be formed under some kind of template control by the guest.

A class of compounds that is closely related to porosils is that of the porolites. In these porolites some of the silicon atoms have been replaced by aluminum atoms; electroneutrality leads to the general formula **12**. Moreover, one can distinguish between

$M^{x+}_{x/y}[Al_xSi_{1-x}O_2] \cdot mH_2O \cdot nG$ **12**

open and closed porolite hosts. These are called *clathralites* and *zeolites*,[35] respectively, and exhibit properties similar to those of the corresponding classes of porosils. As their host lattices, however, are negatively charged, cations are incorporated into the host cavities, which in turn means that there are additional electrostatic interactions between guest and host system. In general, however, these interactions are rather weak, as the negative charges are "smeared" over the inner surface of the host, and because the cations are solvated. Therefore, the cationic guests can still be exchanged in these compounds.

The porous tectosilicates must be contrasted with the dense ones. In this sense, the family of pyknosils can, according to Scheme 1, be represented by the various modifications of SiO_2, such as quartz, coesite, or crystobalite, while the pyknolites are correspondingly represented, for example, by the feldspars. All these compounds are built primarily from $\{SiO_4\}$ or $\{AlO_4\}$

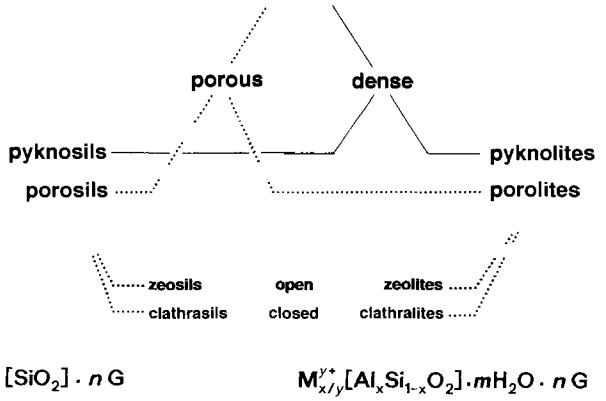

Scheme 1. Family tree of the classes of compounds belonging to the tectosilicates, showing the classification of clathrasils and zeolites. Only the porous tectosilicates can participate in supramolecular processes.

units, which are linked by shared corners. The structural variety arises from the various ways in which these units can be linked three-dimensionally. But this variety can be systematically ordered because the type of linkage is controlled by strict rules. Thus, it is only necessary to distinguish between a few small, so-called secondary building units (SBUs) and larger polyhedral blocks, which can be linked according to certain rules.

The mentioned classes of compounds have been described extensively with respect to syntheses,[36] structures,[37] properties (catalysis, ion exchange, host–guest chemistry, etc.), and industrial applications.[38] Therefore this review will be limited—apart from the systematic classification—to a few details, which illuminate the structural variety and, in particular, the host–guest phenomena. A relatively new branch of the host–guest chemistry of nanoporous tectosilicates and related compounds deals with the incorporation of dye molecules and molecules with high molecular hyperpolarizability.[39] The latter case refers to supramolecular compounds which are capable of doubling the frequency of incident laser radiation, making them attractive as potential materials for nonlinear optical applications.

The number of three-dimensional host structures has significantly increased over the last few years owing to the discovery of novel, zeolite-type classes of compounds. While these do not formally belong to the tectosilicates, they exhibit similar or new structures with comparable properties. *Aluminophosphates*[40] also belong to this group in which alternating phosphorous and aluminum atoms occupy the positions in the tetrahedral centers of the "primary building blocks", thus yielding the general formula for this class of compounds as **13**. The host structures of

$[AlPO_4] \cdot mH_2O \cdot nG$ **13**

these microporous materials, which are used as molecular sieves, are neutral, that is, they are organophilic. In contrast, the host structures of *silicoaluminophosphates*[41] are negatively charged, as some of the phosphorus atoms have been replaced by silicon atoms, corresponding to the general formula **14**. These compounds show a certain ability for cation exchange.

$M^{y+}_{x/y}[AlP_{1-x}Si_xO_4] \cdot mH_2O \cdot nG$ **14**

The structure of sodalite (SOD) occupies a special place within the multitude of structures of zeolites, as it formally serves as prototype for a number of other classes of compounds in nature (cf. Fig. 7). The mineral sodalite itself has the composition $Na_8Al_6Si_6O_{24}Cl_2$; the formulation as **15** indicates that it be-

$Na_6[Al_6Si_6O_{24}] \cdot 2NaCl$ **15**

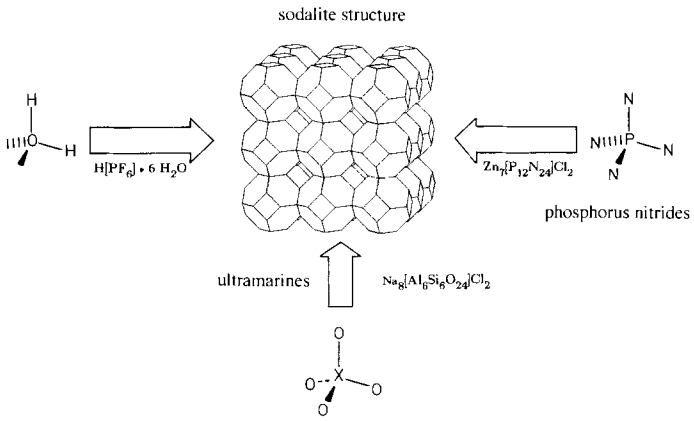

Fig. 7. Schematic summary of those classes of compounds with structures related to the sodalite structure.

longs to the class of zeolites. Sodalite is the only tectosilicate that is built from a single polyhedral unit; all other tectosilicates contain at least a second, often even a third polyhedral building block. The characteristic building unit is the sixfold truncated octahedron $[4^66^8]$, which is linked through the square faces in a three-dimensional and space-filling manner. The cations required for compensating the charges of the host, as well as additional cations and anions, are statistically distributed over the cavities. Not only the cations, but also the anions are susceptible to ion exchange reactions. In molten sodium sulfate, sodalite can be transformed into the mineral noselite **16**.

$Na_6[Al_6Si_6O_{24}] \cdot Na_2SO_4$ **16**

The same structural type is exhibited by the mineral lapis lazuli, and its synthetic equivalent, ultramarine. Both substances contain an S_3^- ion within their sodalite cages. The guest radical is responsible for the blue color of these species, which are highly valued as pigments.

Surprisingly, the structural characteristics of sodalite are also found in *phosphorus nitrides*, as exemplified by the compound **17**, which has only recently become known.[42] The primary

$Zn_7[P_{12}N_{24}]Cl_2$ **17**

building blocks are $\{PN_4\}$ tetrahedra. The pentavalent phosphorus atoms occupy the positions of the silicon and aluminum atoms, while the trivalent nitrogen atoms take the positions of the oxygen atoms. A chloride ion, which is tetrahedrally surrounded by four zinc ions, is located in the center of each so-

dalite cage. The positions of the zinc ions are statistically disordered with an occupancy of 7/8.

Apart from the *neutral* water clathrates just described, *cationic* water clathrates are known as well. An example is the hexahydrate of hexafluorophosphoric acid, **18**,[43] which has a crystal structure that also shows sodalite-like structural elements.

$H[PF_6]\cdot 6H_2O$ **18**

Based on the results known thus far, it is assumed that a PF_6^- ion is incorporated into a cage, while a proton is integrated into the lattice of water molecules, so that the formulation $[(H_2O)_5(H_3O)]^+[PF_6]^-$ describes the actual structure much better than the simple chemical formula given above.[44] The pentahydrate of tetramethylammonium hydroxide, **19**,[45] belongs to the *anionic* water clathrates. The hydroxide ion is part

$[Me_4N][OH]\cdot 5H_2O$ **19**

of the sodalite-like host lattice, into which the tetramethylammonium ion is incorporated, yielding the formulation $[(H_2O)_5(OH)]^-[Me_4N]^+$. The cation is a little too large for the sodalite cage, therefore the cage is slightly expanded at the site of incorporation.

2.1.5. Reaction Sites

One of the greatest challenges of modern chemistry is to perform transformations as efficiently and selectively as possible, primarily for environmental and monetary reasons. As transformations in biological systems are especially characterized by structurally organized reaction media and reactions that in general yield only *one* product, namely the desired one, nature itself is often used as a guide.[46] It should, needless to say, also be a goal of supramolecular chemistry to provide and utilize organized reaction sites.[47]

In inorganic chemistry, compounds that largely correspond to the ideas about structurally organized reaction sites exist, namely the zeolites. They possess cavities that are essentially isolated from each other and have a specific shape, a defined size, and inner surfaces with a given polarity. These cavities form ideal reaction sites, for instance, to stabilize unusual particles like certain radicals (e.g., in the case of ultramarine) or metal clusters. This requires that it is possible to incorporate these species, which are not accessible (or only with difficulty) by conventional means, into the lattice of the zeolite, or to create them within it. Once this difficulty has been overcome, the zeolite acts like a refrigerator that keeps its perishable contents "palatable" for some period of time.

Indeed, attempts are being made to solve this fundamental problem. For example, silver clusters have been created within zeolites.[48] Another example concerns the incorporation of CdS clusters in zeolites.[49] The starting point for the synthesis of these host–guest compounds is, among others, the commercially available zeolite Y, (FAU) **20**. This compound is built from sodalite cages with a pore size of 500 pm which are linked by hexagonal prisms as the second polyhedral building unit in such a way as to create a supercage at their center, exhibiting pores of 1.3 nm diameter (Fig. 8 left). After an ion exchange and loading with Cd^{2+}, this zeolite was first dried at high temperatures and subsequently treated at 100 °C with hydrogen sulfide gas.

$Na_{56}[(AlO_2)_{56}(SiO_2)_{136}]\cdot 250H_2O$ **20**

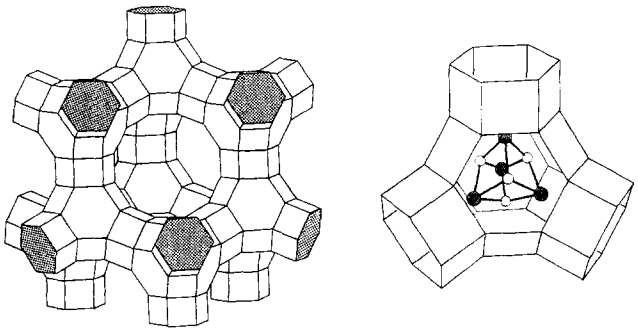

Fig. 8. Left: Section of the crystal structure of zeolite Y (FAU) **20** showing the view into one of the supercages. This supercage is formed by eight sodalite cages, which are linked by twelve hexagonal prisms. Right: Orientation of the cubane-type $(CdS)_4$ cluster encapsulated within the sodalite cages of the host–guest species FAU·CdS.

The X-ray crystallographic and optical data are interpreted to indicate that during the above-mentioned process at low loading, cubane-type $(CdS)_4$ clusters, with Cd–S bond lengths of 247 pm, are formed in the sodalite cages (Fig. 8 right). In each cage of the host structure, these cubes are arranged so that cadmium atoms of neighboring clusters point at each other through the hexagonal prism. The corresponding Cd–Cd distance here is about 600 pm.

In order to use zeolites as catalysts, for example, for catalytic cracking, it is essential that a better understanding of those chemical processes and relationships is reached that occur during the catalysis within the relevant inorganic reaction sites. As expected, the structure and properties of the reaction product are governed by the architecture of the zeolite. This role of the zeolite is not limited to the spatial arrangement and extent of the reaction sites (by limiting them to the nanodimensional area), but is also observed with respect to potential host–guest and guest–guest type interactions. In this case, the host creates or at least influences the structure of the guests.

The generation of a zeolite catalyst—suitable for a desired range of products—is, in turn, controlled by template-directed syntheses, that is, in this case the guest generates the host structure according to its own size, shape, charge, or polarity. For instance, the use of monomeric, oligomeric, or polymeric quaternary ammonium ions leads to the formation of lattice structures, which are complementary to the form of the template employed. Thus, it may be possible to create host structures with large cavities by employing spherical templates, or channel-like structures with the aid of cylindrical or rod-shaped guests.[50]

The dualism that characterizes the host–guest relationships of zeolites now becomes clear: On the one hand, a given guest controls the synthesis of the zeolite host, on the other hand, this zeolite later directs the synthesis of another guest type within its reaction cavities. The host itself, however, does not act as guest for the formation of an even larger host (cf. Sections 3.6 and

3.7). Instead, according to its size, it induces, for example in the context of a host–guest catalysis, the synthesis of smaller guest species; the host acts as template and controlling agent. The complexity of these reactions is currently nearly impossible to oversee. It is therefore not surprising that the development of zeolite catalysts up to now has primarily proceeded by trial-and-error methods.

2.1.6. *Molybdenum and Vanadium Phosphates*

Zeolite-type host structures are also observed when octahedra, square pyramids, or cubes are introduced as structure-determining units in addition to tetrahedra, as is the case in the numerous *molybdenum*[51] and *vanadium phosphates*. The multitude of possible combinations of the primary building blocks significantly increases the variety of structures observed for these classes of compounds as compared to zeolites. In addition, the structures are not limited to three-dimensional host edifices.[52] The anionic three-dimensional host structure in the compound **21**[53] consists of $\{[Mo_4O_8]^{4+}\}$ cubes and $\{PO_4^{3-}\}$

$(Me_4N)_{1.3}(H_3O)_{0.7}[Mo_4O_8(PO_4)_2]\cdot 2H_2O$ **21**

tetrahedra. These are linked such that a porous structure results, in which cation-occupied voids represent 25% of the total volume. Hence, this compound can reversibly incorporate water. The compound **22**[54] has similar properties. Its host structure,

$[Mo_8O_{12}(PO_4)_4(HPO_4)_2]\cdot 13H_2O$ **22**

however, is neutral, in contrast to its counterpart in **21**. The vanadium phosphates **23** and **24**[55] are built up from corner-sharing $\{VO_6\}$ octahedra and $\{PO_4\}$ units. This leads—similar to the case for **21**—to three-dimensional lattice structures with cavities that incorporate the alkali metal cations.

$Cs[V^{III}_2(PO_4)(HPO_4)_2(H_2O)_2]$ **23**

$K[(V^{IV}O)V^{III}(HPO_4)_3(H_2O)_2]$ **24**

Large cavities that are occupied by organic cations are also found in the compound **25**.[56] The crystal structure of the host, depicted in Figure 9, consists of undulating layers, which in turn are made up of rings formed by four square $\{OVO_4\}$ pyramids, two phosphate and two hydrogenphosphate units. The vanadium and phosphorus atoms of these eight-membered rings form a plane, with the vanadyl groups on one side and the phosphorus–oxygen units on the other. Two of the latter are P–OH groups, while the other two are linked to the $\{(H_2O)_2V^{III}O_4\}$ octahedra which connect the layers. This creates large ellipsoidal cavities between the layers. These cavities measure approximately 620–720 pm (O–O distance) along the short axis and about 1840 pm (V^{III}–V^{III} separation) along the long axis.

$(H_3NCH_2CH_2NH_3)_2(H_3NCH_2CH_2NH_2)$

$\cdot[V^{III}(H_2O)_2(V^{IV}O)_8(OH)_4(HPO_4)_4(PO_4)_4(H_2O)_2]\cdot 2H_2O$ **25**

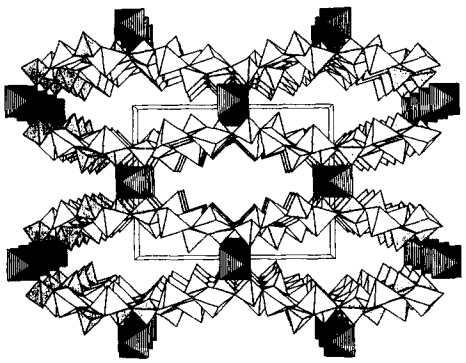

Fig. 9. View into the ellipsoidal cavities of compound **25**. The square $\{VO_5\}$ pyramids are shown as open polyhedra, the $\{PO_4\}$ tetrahedra are lightly shaded, and the octahedral $\{VO_6\}$ units are shown hatched.

2.1.7. *Cadmium Cyanide Compounds*[57]

A relatively new area of supramolecular inorganic chemistry deals with the three-dimensional lattice structures based on cadmium cyanide, $Cd(CN)_2$ (**26**). In the crystalline, guest-free state, this compound—like $Zn(CN)_2$—exhibits two mutually penetrating diamond-type networks. Formally, the metal ions occupy the positions of the carbon atoms, while the cyanide ions occupy the sites of the bonds (Fig. 10 left).[58] Each cadmium ion is, therefore, tetrahedrally coordinated, which means that **26**, in agreement with its AX_2 basic stoichiometry, structurally resembles H_2O and SiO_2. This similarity is quite far-reaching: Each of the two lattices is isostructural to β-crystobalite.

$Cd(CN)_2$ **26** $Cd(CN)_2\cdot$neopentane **27**

Starting with the host, supramolecular compounds can be readily prepared by bringing the desired guest into contact with an aqueous solution containing equimolar amounts of cadmium cyanide and potassium tetracyanocadmiate. In this manner a large number of host–guest compounds can be prepared.[59] The example $Cd(CN)_2\cdot$neopentane **27**[60] shows that the structure of the host–guest compound (Fig. 10 right) is derived from the guest-free host structure by completely removing one of the two networks. The adamantanoid voids thus created are occupied by the guests.

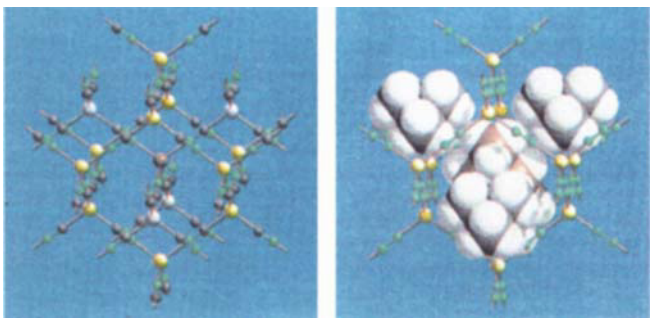

Fig. 10. Perspective views of the crystal structures of $Cd(CN)_2$ **26** (left) and its host–guest compound **27** with neopentane (right). The $Cd(CN)_2$ partial structures are shown as ball-and-stick models in both cases, the organic guest molecules are shown as space-filling models. The cadmium atoms are shown in yellow and white in the different networks of the host. The CN groups in the "pure" host are ordered (N green, C gray), while they are disordered in the host–guest compound (N, C green).

The incorporation of guests as large as neopentane molecules only becomes possible by the increase in the distance between the cadmium centers of the tetrahedra to about 550 pm. In contrast, the Si–Si distance in tectosilicates is only about 306 pm, the O–O distance in hydrate clathrates about 280 pm. The cyanide ion functions as a sterically undemanding spacer between the tetrahedrally coordinated cadmium ions, thus leading to the formation of the large voids within the host structure.

2.2. Two-Dimensional Host Structures

A comparison of the number of different compound classes and related compounds shows that there are far more two-dimensional host–guest species than their three-dimensional counterparts. The number of potential hosts, that is, compounds with layer structures, is comparatively large.[61]

Compared to three-dimensional hosts, many layer structures exhibit features that significantly simplify the synthesis of corresponding host–guest compounds as well as their subsequent modifications. The most important characteristic in this context is the ability of many two-dimensional hosts to vary their interlayer distance within wide boundaries according to the steric requirements and structure of any particular guest. In addition, some classes of compounds show strong tendencies not only to incorporate neutral species, but also ionic guests, with charges complementary to those of the host. Some of the hosts have electronic properties that allow them to accept electrons from the guest species in a redox reaction, thus leading to changes in the charges of the host layers and the incorporation of a corresponding number of cations in the space between the host layers.[9]

Correspondingly, the synthesis of two-dimensional host–guest compounds starts in most cases with the already completely preformed host. Topotactic reactions then, apparently, insert the guest species between the layers, which has led to the common acceptance of the term *intercalation compounds* as generic label for these supramolecular species. The synthesis concept requires a high mobility of the guest species in the interlayer space, as they have to diffuse from the edges into the interior of the host matrix in order to find the "free lattice sites" located there. This means, in turn, that the potential wells between the host layers must be rather shallow, otherwise the diffusion rate would be reduced too much. Usually there are strong covalent or ionic bonds within the layers, while between them there are only weak van der Waals interactions, at least in the case of neutral layers.

In the case of electrically charged hosts, in which ions and/or solvent molecules are incorporated between the layers, there are, of course, additional electrostatic interactions. In general, however, these are rather weak, and supramolecular chemistry, that is, an exchange of ions or solvent molecules is still possible. The high mobility of the guest species stemming from the shallow potential wells between the layers leads not only to the reversibility of their intercalation reactions, but frequently to nonstoichiometric compounds with a wide range of compositions. If the potential wells are relatively deep, or if the access to the interior of the host matrix is sterically encumbered, the corresponding intercalation compounds must be synthesized by the reaction of the molecular building units of the host with the guest species in homogeneous solution.

In the following, these principles, developed for two-dimensional host–guest species, will be demonstrated by using different classes of compounds, taking some recent developments into account. The selection of the compound classes presented herein is rather subjective, hence it cannot claim to be complete either with respect to the details presented or the number of classes examined. For instance, the classic textbook example for inorganic host–guest species, namely *graphite intercalation compounds*,[62] is not dealt with. This is justified because the entire area of two-dimensional host–guest compounds is fairly well documented.[63]

2.2.1. *Clays*[64]

Clays are among the host–guest species that are most important culturally and historically (manufacture of ceramics and porcelain) as well as of intense interest to modern and also prebiotic chemistry. A number of different groups of silicates and aluminosilicates with layered structures belong to this class. In spite of the nearly endless variety exhibited by clay minerals with respect to their chemical composition, it is possible to relate their layer structures to two fundamental types. These two basic phyllosilicate types are characterized by their layered structures, in which layers of corner-sharing $\{SiO_4\}$ tetrahedra are linked with layers of edge-sharing $\{M(O,OH)_6\}$ octahedra. One of the fundamental structures consists of one layer of octahedra and one layer of tetrahedra (TO type), while the other one consists of one layer of octahedra surrounded by two layers of tetrahedra (TOT type).

Typical examples for the TO structural type are serpentine (**28**) and caolinite (**29**). In serpentine, the magnesium ions occupy all available octahedral holes, while in caolinite the aluminum ions occupy only 2/3 of these holes. This composition results in individual layers that are neutral. No ions are incorporated between the layers, hence their host–guest chemistry is limited to the incorporation and release of neutral molecules.

$Mg_3[Si_2O_5](OH)_4$ **28** $Al_2[Si_2O_5](OH)_4$ **29**

$Mg_3[Si_2O_5]_2(OH)_2$ **30** $Al_2[Si_2O_5]_2(OH)_2$ **31**

Characteristic examples for the TOT structural type are talcum (**30**) and pyrophyllite (**31**). Except for the different ordering of the layers of octahedra and tetrahedra, these compounds correspond to serpentine and caolinite, respectively. The layers, which are wider in these cases, are still neutral, which means that the supramolecular activities also correspond to those exhibited by the two compounds of the TO structural type.

A completely different behavior is found for the class of *micas*, which comprises the layered aluminosilicates. Within these structures, as for example in biotite, **32**, and muscovite **33**, some of the tetravalent silicon atoms of the "tetrahedral layers" are replaced by trivalent aluminum atoms. This leads to negatively

$KMg_3[AlSi_3O_{10}](OH)_2$ **32** $KAl_2[AlSi_3O_{10}](OH)_2$ **33**

charged layers, and additional cations must be incorporated between them in order to reach electroneutrality. As these ions are bound to the layers by only relatively weak electrostatic interactions, they are subject to cation exchange reactions.

The interest in clays stems from their ease of modification and their excellent catalytic properties. Recent developments also deal with the incorporation of chiral molecules into such hosts with the aim of employing the resulting supramolecular materials in asymmetric syntheses or in the area of nonlinear optics.

Catalysts based on layered aluminosilicates with exchangeable cations between the layers are often not particularly thermally stable due to the fact that the cations in these species are generally solvated. When the solvent molecules evaporate from the interlayer space at higher temperatures, the layers move closer together, thus reducing the catalytic activity. Recent experiments have focused on incorporating supporting pillars in an effort to prevent the layers from coming closer together (Fig. 11). The later incorporation of such pillars is made possible by first introducing cations of suitable size (e.g., polycations such as the Keggin-type ion $[Al_{13}O_4(OH)_{24}(H_2O)_{12}]^{7+}$, or other multinuclear species such as $Si_8O_{12}(OH)_8$) by ion exchange reactions, followed by "sintering". The increased thermal stability achieved this way is significant.[65]

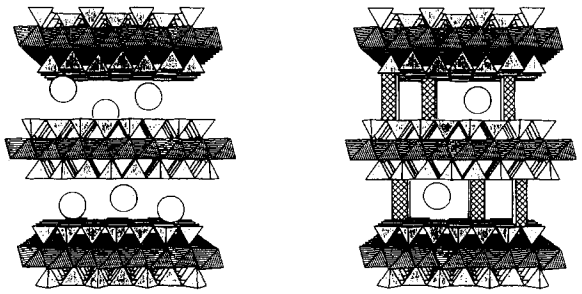

Fig. 11. Schematic representation of clay layers without (left) and with support structures (right). Ion exchange reactions build up the potential pillars, in the form of cations between the layers. These pillars are later made permanent by "sintering".

2.2.2. Transition Metal Dichalcogenides[66]

The early *transition metal dichalcogenides* MX_2 with readily polarizable chalcogen atoms (M = element of group 4, 5, or 6, X = S, Se) can also act as hosts due to their layered structures. These compounds have, therefore, been the subject of studies to this end for some time. Within the layers of these dichalcogenides, the metal atoms M occupy octahedral (e.g., in TiS_2 **34**) or trigonal-prismatic holes (e.g., in $TaSe_2$ **35** and MoS_2 **36**) between two planar, hexagonally closest packed layers of chalcogen atoms X, which are arranged either with holes stacked on top of holes (**35**, **36**) or on top of atoms (**34**). While there are very strong ionic/covalent bonds between the metal and chalcogen atoms within a layer, only weak van der Waals interactions exist between the layers. This explains why these compounds exhibit many variations of layer ordering (stacking variations) and, hence, many polymorphic modifications. The layers, about 600 pm wide, are neutral and their surfaces show little electronic or steric fluctuations.

TiS_2 **34** $TaSe_2$ **35** MoS_2 **36**

The incorporation of alkali metals between such packets of layers was first observed by Rüdorff in 1965, when he allowed alkali metals to react with the dichalcogenide in liquid ammonia.[67] This represents the prototype of a reversible, topotactic redox reaction, during which each alkali metal A injects one electron into the conduction band of the host MX_2. This dramatically changes the electronic properties of the host and causes the host layers to be negatively charged. The resulting compound must be described as the incorporation of alkali metal ions A^+ into the (now) anionic transition metal dichalcogenide $[MX_2]^-$. It is also possible to prepare many corresponding intercalation compounds by electrochemical means. The dichalcogenide acts as the cathode, the metal as the anode of an electrochemical cell. A solution of the corresponding alkali metal salt in a nonaqueous solvent (e.g., dioxolane, propylene carbonate) is employed as electrolyte.

The *alkali metal transition metal dichalcogenides* AMX_2 are true intercalation compounds. This is also demonstrated by the fact that the cations embedded between the layers are available for ion exchange and hydration or solvation reactions (e.g., with *N*-methylformamide, dimethyl sulfoxide). It is thus not surprising that during the synthetic process employed by Rüdorff ammonia molecules, which can later only be removed with difficulty, are incorporated into the reaction product. The capacity for ion exchange reactions can also be exploited to embed other, sometimes significantly larger, cations between the layers. This allows the controlled variation of the properties of these host–guest compounds. Out of a multitude of supramolecular compounds created by this type of reaction, the most remarkable examples, based on size and complexity of the guests, are those stemming from the metal clusters $[Fe_6S_8(PEt_3)_6]^{2+}$ and TaS_2[68] as well as from the species $[Co(\eta\text{-}C_5H_5)_2]^+$ and ZrS_2.[69] Even though the reaction products are often not well ordered, the crystallinity of samples of the first example was sufficient to determine the orientation of the Fe_6S_8 clusters between the layers by X-ray diffraction studies of oriented films (see Fig. 12).

Metallocene cations—as well as a number of other organic and organometallic compounds (*n*-alkyl amines, phosphanes)—can also be incorporated between the layers of alkali-metal-free dichalcogenides by the direct reaction of the components under anhydrous conditions at temperatures of up to 200 °C.

2.2.3. Metal Phosphorus Trisulfides[70]

Metal phosphorus trisulfides, MPS_3, represent a group of compounds that is closely related to the transition metal dichalcogenides. For many elements of the first transition metal series (M = V, Mn, Fe, Co, Ni, Zn), compounds of this composition exhibit layered structures. Within the layers of these trichalcogenides, the metal atoms M—as shown by the example of the cadmium compound[71] in Figure 13—occupy two thirds of the octahedral holes between two planar, hexagonally close packed layers of sulfur atoms, while the remaining third is occupied by the P_2 "dumbbells". These two structural elements are arranged in such a way that the $\{MS_6\}$ octahedra form a honeycomb-like network, in which the voids are filled by single $\{P_2S_6\}$ octahedra. Hence, each $\{P_2S_6\}$ octahedron is edge-linked (i.e., shares edges) with six $\{MS_6\}$ octahedra, while each $\{MS_6\}$ octa-

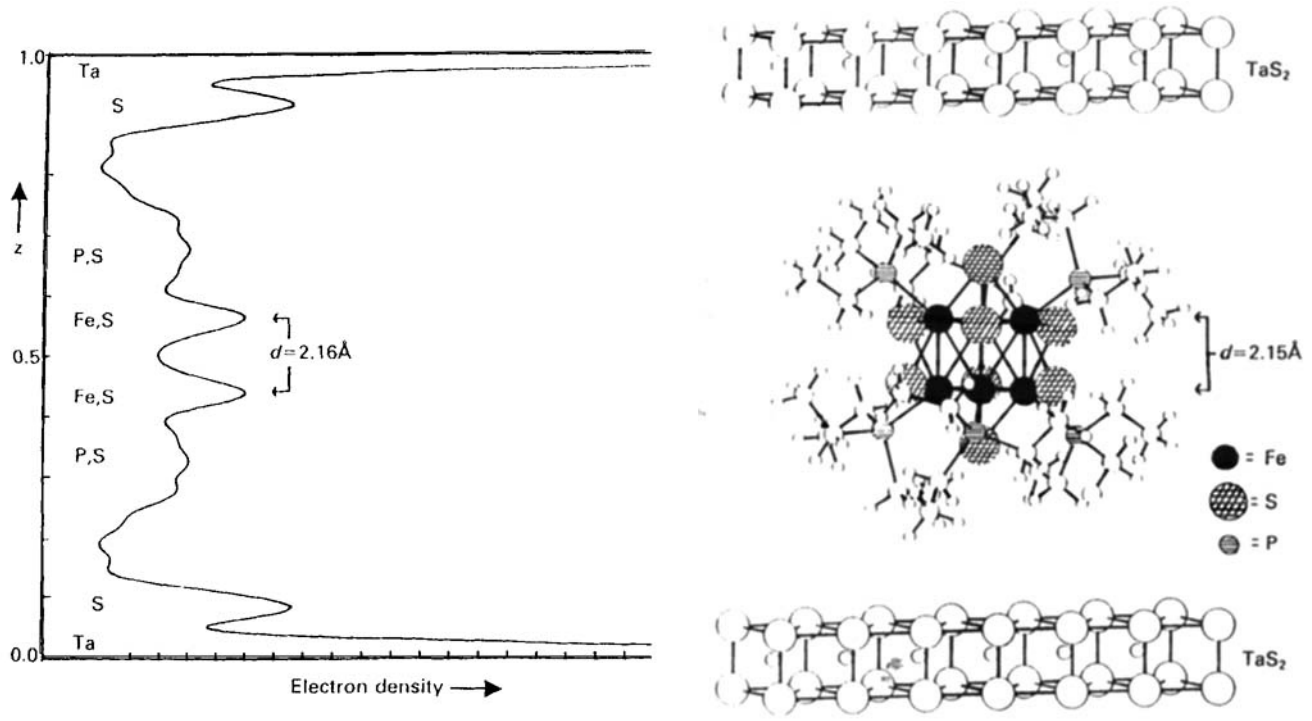

Fig. 12. Left: Experimentally determined electron density of oriented films of the inclusion compound of $[Fe_6S_8(PEt_3)_6]^{2+}$ in TaS_2; right: the thus deduced orientation of the guest between the layers of the host (from ref.[68]).

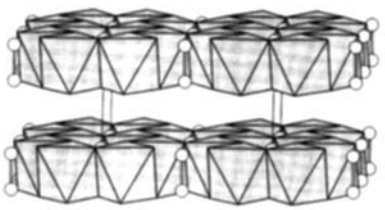

Fig. 13. Schematic representation of the layer structure of the potential host species $CdPS_3$; the $\{CdS_6\}$ octahedra are shaded and the P_2 "dumbbells" are shown as ball-and-stick models; the octahedra form a type of honeycomb network, with the phosphorus embedded into the voids; there are only weak van der Waals interactions between the layers.

hedron shares edges with three others of its kind and three $\{P_2S_6\}$ units. The ordering of the layers of sulfur atoms corresponds to cubic closest packing.

Similar to transition metal dichalcogenides, these metal phosphorus trisulfides are capable of incorporating alkali metals or their cations by reversible redox reactions. Typical for the host species described here is their ability to undergo unusual ion exchange reactions, in which some of the metal cations M^+ are dissolved out of the host layers, which, in turn, then do not only exhibit voids, but are also negatively charged. This necessarily requires that positively charged guest species are incorporated between the layers of the anionic host in order to achieve charge compensation. As is the case for ZrS_2, there is a cobaltocenium "adduct" of $MnPS_3$ (**37**), which in contrast to the disulfide, can also be prepared by a direct reaction of the host with a solution containing the cobaltocenium ion.[72]

$[Mn_{1-x}PS_3][CoCp_2]_{2x} \cdot nH_2O$ **37**

2.2.4. *Hofmann Clathrates*[57, 73]

The prototype of this class is a compound with the composition **38**. Its synthesis was first reported in 1897 by Hofmann and

$Ni(CN)_2 \cdot NH_3 \cdot C_6H_6$ **38**

Küspert,[74] but its structure was only determined more than half a century later by Rayner and Powell.[75] The structure (Fig. 14) consists of planar layers which are stacked in a parallel manner. The layers are based on a chessboard pattern of square-planar and octahedrally coordinated nickel(II) ions ligated by cyanide ions and ammonia molecules. The carbon atoms of the cyanide ions are bound to the four-coordinate metal ions, the

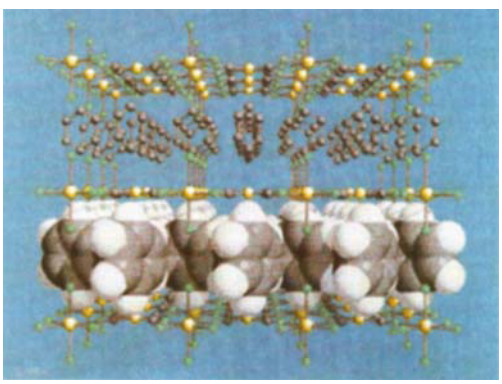

Fig. 14. Perspective view of the crystal structure of $Ni(CN)_2 \cdot NH_3 \cdot C_6H_6$ **38**. The top half of the figure depicts the benzene molecules as ball-and-stick models without hydrogen atoms, the bottom half shows them with the hydrogen atoms as space-filling models. The CN groups link the nickel atoms, while the ammine ligands are oriented perpendicular to the plane of the layers (N green, C gray, Ni yellow).

nitrogen atoms to the six-coordinate ones, which also have a pair of *trans*-located ammine ligands completing the coordination sphere. The ammine ligands stick out above and below each layer, thus segregating the space between the layers into block-shaped voids. The benzene molecules are incorporated into these voids in a clathrate-type manner.

The ammine ligands form steric obstacles to the diffusion of guest species. In addition, their strong electronic interactions with the arenes cause relatively deep potential wells. This compound can therefore only be prepared from solution and the guest-free host is not known.

After the structure was solved, a large number of further representatives of this structural type were prepared and examined by X-ray structure analysis. Based on these results, the general formula for clathrate compounds of the Hofmann type is **39**.

$M(NH_3)_2M'(CN)_4 \cdot 2C_6H_6$ **39**

Within the last few years, there have been studies to systematically modify the basic structure of Hofmann clathrates. Apart from, for example, the use of other guests, the terminal NH_3 groups were replaced by NH_2R ligands. One of the primary characteristics of the thus obtained structural types is that the layers are no longer planar, but more or less puckered. Similar layers are also found in the recently reported derivative **40** of a Hofmann clathrate.[76] The puckered layers in this compound serve to stabilize a very unusual two-dimensional network of water molecules. The water molecules in these layers are linked by hydrogen bonds. The oxygen atoms form a puckered network of edge-sharing, boat-shaped six-membered rings of the type also found in the hexagonal modification of ice. These layers are in effect a two-dimensional variation of three-dimensional clathrates, even though they are hitched to the cadmium ions.

$Cd(H_2O)_2Ni(CN)_4 \cdot 4H_2O$ **40**

2.2.5. *Alkali Metal Halide Intercalation Compounds*

This class of compounds is unusual at first glance. It has only recently become known by the structure determination of **41**.[77] This compound is generated by the reaction of cesium fluoride

$CsF \cdot Br_2$ **41**

with excess halogen at room temperature. The tetragonal structure (Fig. 15) consists of planar CsF layers in which each cesium and fluoride ion is surrounded by the respective counterion in a square-planar arangement. The layers, therefore, correspond to sections of the cesium fluoride with the NaCl-type structure. The Cs–F distances, however, are somewhat shorter (294.0 pm) than in the unmodified compound (300 pm). The layers are stacked directly on top of each other, with an interlayer distance of 736.4 pm. The Br_2 "dumbbells" are located between two fluoride ions and are oriented perpendicular to the layers. Their distance to the two neighboring fluoride ions is equal (252.1 pm) and significantly longer than a normal covalent fluorine–bromine bond. Therefore, the electronic interactions between the host system and guests are apparently rather weak. The

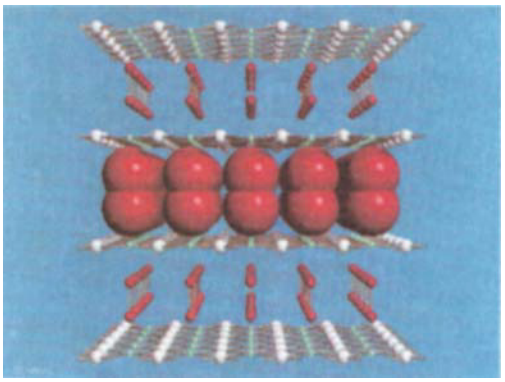

Fig. 15. Perspective view of the crystal structure of $CsF \cdot Br_2$ **41**. The embedded bromine molecules are shown in the middle layer as space-filling models to demonstrate the degree of space usage, while they are shown as ball-and-stick models in the upper and lower layers (Br = red, F = green, Cs = white).

Br–Br distance (232.4 pm) is, correspondingly, only slightly longer than in elemental bromine (228 pm). The surprising stability stems, apart from electronic effects, certainly also from steric reasons. The van der Waals surface of the host layers must be quite puckered due to the different sizes of cesium and fluoride ions, thus causing the bromine molecules to be tightly held and well ordered between the layers, like eggs in an egg carton.

2.2.6. *Metal(IV) Phosphates and Organoelement Derivatives*

Compounds of the type $Zr(RPO_3)_2$[78] lead into the area of organoelement layer structures, as they can formally be considered as organometallic derivatives of the zirconium phosphate in which an OH group has been replaced by an organic residue R. The layer organization of these *zirconium phosphonates* is analogous to that of α-zirconium phosphate **42**.[79]

$Zr(HPO_4)_2 \cdot H_2O$ **42**

The crystal structure of this compound, a section of which is shown in Figure 16, reveals nearly flat layers of $\{ZrO_6\}$ octahedra which are linked by corners to $\{PO_3(OH)\}$ tetrahedra. Three of these tetrahedra are located above, three of them below the plane of octahedra. As each tetrahedron is linked to three octahedral units, the OH groups jut out into the interlamellar space, perpendicular to the layer. The layers are stacked in such a way as to create small block-shaped voids between the phosphorus

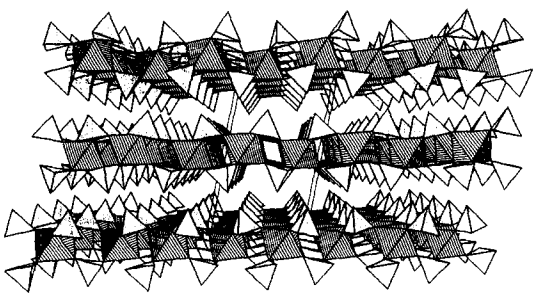

Fig. 16. Perspective view of the structure of α-$Zr(HPO_4)_2 \cdot H_2O$ **42**. The polyhedra are shaded as indicated in Figure 9.

and zirconium atoms of neighboring layers, in which water molecules are encapsulated. Since, relatively small windows represent the only access to these spaces, the mobility of the guests is rather restricted. It appears feasible to utilize some of these compounds as catalysts or proton conductors.

In this context, further very promising variations for supramolecular applications are offered by the use of diphosphonates as space-controlling columns between the layers and the construction of "organometallic layers" of the type of γ-zirconium phosphate **43**.[80] The combination of both concepts is realized, for example, in the zirconium phosphates phosphonates[81] and zirconium phosphite diphosphonates.[82]

γ-$Zr(H_2PO_4)(PO_4)\cdot 2H_2O$ **43**

2.2.7. *Molybdenum and Vanadium Phosphates*

The description of the three-dimensional host structures has already shown that the use of additional structural units (cubes, pyramids) leads to a significant increase in structural variety, and thereby also creates new potential applications. The same holds for two-dimensional host structures. For instance, the anionic host lattice of the *molybdenum phosphate* **44**[83] consists

$[N(C_3H_7)_4(NH_4)][(MoO)_4O_4(PO_4)_2]$ **44**

of layers of $\{Mo_4O_8\}$ cubes, which are linked by corner-sharing phosphate tetrahedra. The space between the layers is occupied by tetrapropylammonium ions as guests, while the NH_4^+ ions are encapsulated inside voids located within the layers.

A stair-shaped layer structure is found for the mixed-valence *vanadium phosphate* **45**.[84] The host structure, depicted in Figure 17, consists of parallel bands, in which corner-sharing

$K_2[(V^{IV}O)_2V^{III}(PO_4)_2(H_2PO_4)(HPO_4)(H_2O)_2]$ **45**

$\{VO_6\}$ octahedra, square $\{VO_5\}$ pyramids, and phosphate tetrahedra alternate. The potassium ions acting as guests are found within the individual steps as well as between them.

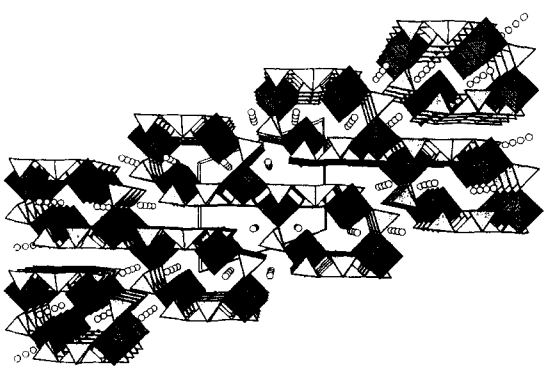

Fig. 17. Section of the crystal structure of compound **45** showing the view along the stair-shaped layers. The polyhedra are shaded as indicated in Figure 9.

2.2.8. *Diamond- and Carpet-Like Networks*

An aesthetic delight is presented by the structural aspects of compounds in which the host also functions as its own guest. This concept appears unproblematic at first glance. However, its full complexity only becomes apparent through a consideration of the requirements attached to the term supramolecular compound, namely, that in the crystalline state no translational relationship between host and guest species is allowed and only weak interactions, such as van der Waals forces may act between them. Both requirements taken together imply that host and guest structures must penetrate each other.

Indeed, such structural characteristics are not only laboratory oddities, but are also found in nature, as shown by the minerals cuprite (Cu_2O)[85] and neptunite, $(LiNa_2K(Fe,Mg,Mn)_2Ti_2[Si_8O_{22}]O_2)$.[86] The former exhibits two three-dimensional diamond-type networks, which penetrate each other—analogous to the situation in $Cd(CN)_2$ (See section 2.1.7).

In the case of two-dimensional hosts, this concept requires that the host shells are not closed within themselves. They must possess pores or openings that are large enough to allow the guest species to pass through. An interesting example which demonstrates this principle is Hittorf's phosphorus, which has a double layer structure formed by pentagonal tubes.[87]

The first attempts to create such three- and two-dimensional structures stem from organic chemistry.[88] However, inorganic chemists have started picking up on this idea as well. One of the highlights achieved thus far is the recently reported compound $Zn[Au_2(CN)_4]$ **46**, in which no less than six identical, but independent networks interpenetrate.[89] In each of the six networks, tetrahedrally coordinated zinc atoms occupy the positions of the silicon atoms, while linear $[Au(CN)_2]$ units have replaced the oxygen atoms in quartz.

$Zn[Au_2(CN)_4]$ **46**

$[M(CO)_3(\mu_3\text{-}OH)]_4$ **47**, M = Mn; **48**, M = Re

A second development stems from the cubane-like molecules **47** and **48**, which, by virtue of their four rigid hydrogen bond donors, can function retrosynthetically as tetrahedral T_4 tectons.[90] Together with linear bifunctional hydrogen bond acceptors as spacers, such as 1,4-diaminobenzene, 1,2-diaminoethane, or 4,4'-dipyridine, these building blocks form doubly, triply, or quadruply interpenetrating diamond-like networks.[91] In combination with nonlinear spacers, such as 1,3-diaminopropane (DAP) or hexamethylenediamine (HMTA), the compounds **47**·2DAP or **47**·1.5HMTA, respectively are formed, which exhibit two-dimensional, wire-mesh-like lattices.

In addition, spontaneous and strict self-organization of compound **48** in the presence of methanol and 4,4'-dipyridine (Dipy) leads to **48**·2Dipy·2MeOH, which exhibits two carpet-like intertwined networks (see Fig. 18). The dipyridine units act as linear bifunctional hydrogen bond acceptors, while methanol acts as a bent donor/acceptor unit.[90]

2.3. One-Dimensional Host Structures

In contrast to three- and two-dimensional host structures, *real* one-dimensional host–guest compounds are relatively rare, even though a number of potential hosts are known, which,

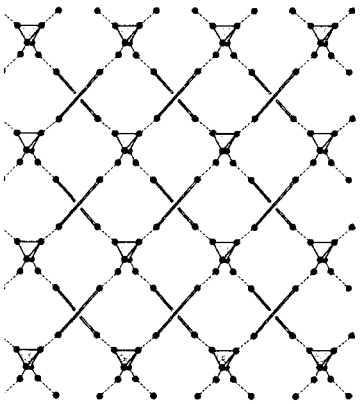

Fig. 18. Top view of the two intertwined networks of compound **48**·2Dipy·2MeOH; in this schematic representation, the cubane-type $[\{Mn(CO)_3(\mu_3\text{-}OH)\}_4]$ molecules are shown as tetrahedra based on the tetrahedral orientation of the OH groups, the 4,4'-dipyridine molecules are shown as sticks, and the methanol molecules are represented by black dots; the dashed lines indicate the hydrogen bonds between the different building blocks of the network.

based on their structure should display a high degree of structural flexibility with respect to the incorporation of guest species of different shape and size. Compounds with chain structures "suffer" from the disadvantage that they tend to show disorders or defects much more frequently than the higher dimensional hosts. In addition, the guest molecules within them "enjoy" a significantly higher mobility, which is only decreased if the host–guest interactions are significantly stronger than simple van der Waals interactions.

2.3.1. *Chevrel Phases*

Among the few one-dimensional host–guest compounds are ternary molybdenum chalcogenides of the type AMo_3X_3 (X = S, Se; A = alkali metal, In, Tl), which belong to the group of *Chevrel phases*, and, therefore, exhibit semiconductor properties. An example is the compound **49** [92] (see Fig. 19),

$TlMo_3Se_3$ **49**

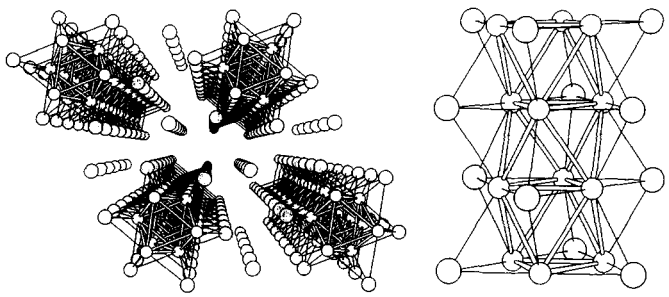

Fig. 19. Left: Perspective view of the crystal structure of $TlMo_3Se_3$ **49** (thallium atoms = large open spheres); the enlarged detail (right) shows that the Mo atoms (small open spheres) form face-sharing octahedral $\{Mo_6\}$ clusters. The edges of the common triangular faces are bridged by three Se atoms (large shaded spheres).

which consists of parallel columns of face-sharing molybdenum octahedra, which are surrounded by selenium atoms on the basis of $^1_\infty\{Mo_{6/2}X_{6/2}\}$ clusters. The monovalent metal ions are incorporated as guests between these columns, where they effect the stability of the crystal lattice by means of comparatively weak interactions, which still permit ion exchange reactions.

2.3.2. *Molybdenum and Vanadium Phosphates*

Molybdenum and *vanadium phosphates* form not only three- and two-dimensional host species, but also species in which the host exhibits only a chain structure. An example is found in the compound **50**,[93] which shows strands formed by cubane-type $\{Mo_4O_8\}$ units and tetrahedral $\{PO_4\}$ ones. The strands, however, are interlinked by hydrogen bonds in such a way that sheets result. The organic cations occupy positions between the chains.

$(Et_4N)_2[Mo_4O_8(PO_4)_{2/2}(H_{1.5}PO_4)_2]\cdot 2H_2O$ **50**

The fact that inorganic species can also mimic biologically relevant structures is demonstrated by compound **51**.[94] This species contains chiral double helices consisting of interpenetrating spirals, which, in turn, are formed by $\{VO_5\}$ units and tetrahedral phosphate groups. The double helices are arranged in such a manner as to create tunnels and cavities within the structure that are occupied by the organic and inorganic cations.

$(Me_2NH_2)K_4[V_{10}O_{10}(H_2O)_2(OH)_4(PO_4)_7]\cdot 4H_2O$ **51**

2.3.3. *The Compound 2 HgS·SnBr$_2$*

In contrast to linear host structures, helical chain arrangements have the advantage that guest molecules are not only held between the chains, but that they can also get jammed, springlike, within the turns of the helix. A remarkable example displaying this feature was recently found by Blachnik et al.[95] in the species **52**.

$2HgS\cdot SnBr_2$ **52**

As can be gleaned from Figure 20, this compound consists of Hg–S chains that have a nearly square cross section. "Dimeric $SnBr_2$ molecules" are incorporated into these chains in such a way that the bonds to the *exo* bromine atoms penetrate into the interior of the helix. The interaction between guest and host is essentially limited to an increase in the pitch of the turns, as the three-sided helices of the guest-free host (cinnabar[96]) are apparently too small to accommodate the guest. The increase stems from the decrease of the bond angle at sulfur from 105° to 95.1°. The bond lengths (235.6 pm vs. 236 pm in HgS) and the bond angles at the Hg center (172.5°/180°) are nearly unaffected

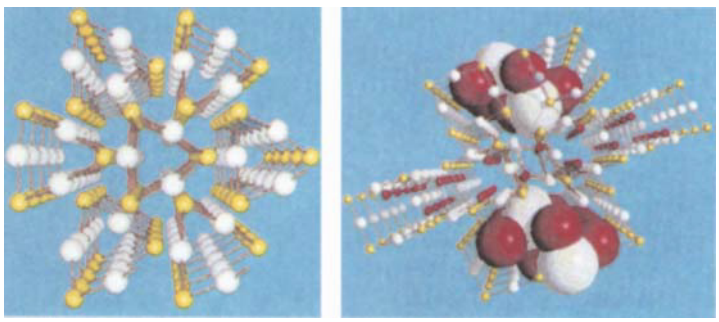

Fig. 20. Perspective view of the crystal structure of mercuric sulfide, HgS: guest-free (left) and loaded with molecular $SnBr_2$ dimers (right); some of the guest molecules are shown as space-filling, some as ball-and-stick models (Hg white, S yellow, Br red, Sn white); in the cinnabar modification, the Hg–S helices have a triangular cross section, in $2HgS\cdot SnBr_2$ **52** these helices have a nearly square cross section.

by this interaction. In the gas phase, the guest tin(II) bromide consists of monomeric molecules displaying a bent structure. In the crystalline state, $SnBr_2$ exhibits a polymeric chain structure.[97] From these chains the host "cuts" dimeric blocks, which correspond to edge-sharing units of trigonal-pyramidally coordinated tin atoms; no important changes in bond lengths and angles result.

3. "Zero-Dimensional" Host Structures

3.1. Definition of Terms

Until now the discussion has focused on one-, two-, or three-dimensional hosts, in which the guests are characteristically incorporated within extended column, layer, or lattice structures. If, however, only uniform, spatially restricted units are present, the resulting discrete host structures are formally defined as zero-dimensional. As will be shown in the following sections, the template-controlled linking of inorganic building blocks can lead to a wholly unexpected number and variety of zero-dimensional hosts, in which one finds various ways by which a small molecule or ion is embedded as guest within a larger one. The host–guest compounds discussed herein, many of which are of a mesoscopic nature,[98] can be classified according to their geometry and topology as either "closed" or "open" (see Fig. 2). Both terms are applied to species that contain cavities of the appropriate dimensions to hold the corresponding guests or ions in place. If such a guest species is located within a cavity formed by a spherical shell-like molecular aggregate in which the guest is permanently enclosed, this "host cage" is termed *closed*. Systems are termed *open* if the host function[99] is performed by a zero-dimensional structure that contains certain "portals" large enough to allow the guest to "leave" the host.

A further criterion for the formal classification of host structures is, according to historical terminology, the division into *electronically normal* and *electronically inverse hosts*. Electronic normality is present if the charge relationships in the host–guest system under consideration are the same as those in the classic crown ether/alkali metal systems. An electronically inverse system displays the inverse relationships which opens up the possibility of incorporating anions as guests. Host structures that incorporate neutral species are termed *electronically neutral hosts*, whereas host structures that can possess nucleophilic as well as electrophilic character are termed *electronically bifunctional hosts*.

3.2. Electronically Normal and Inverse Hosts

3.2.1. *Electronically Normal Hosts*

Closed Hosts

The mixed-valent (Mo^V/Mo^{VI}) complex anion **53a**[100] is a closed inorganic host. It exhibits a central ε-Keggin unit[101] with the composition $\{Mo_{12}O_{40}\}^{20-}$, which has as its basis a truncated Mo^V_{12} tetrahedron. Four facial $\{MoO_3\}$ "anti-Lipscomb" units (cf. the definition in ref. [101]) cap the four Mo_6O_6 faces of the ε-Keggin unit.[102] The flexibility of the anionic host **53a** is demonstrated by the existence of the two compounds **54**[100] and **55**[100] (see Fig. 21): The host **53a** possesses a tetrahedral cavity which can accept cations with very different coor-

$[(Mo^{VI}O_3)_4Mo^V_{12}O_{28}(OH)_{12}]^{8-}$ **53a**

$[Me_2NH_2]_6[H_2Mo_{16}O_{40}(OH)_{12}]$ **54**

$[H_2Mo_{16}O_{40}(OH)_{12}]^{6-}$ **54a**

$(NH_4)_7[NaMo_{16}O_{40}(OH)_{12}]\cdot 4H_2O$ **55**

$[NaMo_{16}O_{40}(OH)_{12}]^{7-}$ **55a**

$[Na(H_2O)_3Mo_{42}H_{15}O_{109}\{(OCH_2)_3(CCH_2OH)\}_7]^{7-}$ **56a**

$[Na(i\text{PrSn})_{12}O_4(OH)_{24}][Ag_7I_{11}]Cl\cdot 10\,DMSO\cdot H_2O$ **57**

$[Na(i\text{PrSn})_{12}O_4(OH)_{24}]^{5+}$ **57a**

dination requirements, such as protons and Na^+. Similar host–guest relationships are found in **56a**[103] (see Sections 3.5 and 3.7) and **57**.[104] The crystal lattice of the latter species contains the isopolycation **57a**. The tin–oxygen framework of this cation exhibits the γ-Keggin structure[101] and contains a cavity formed by four nucleophilic μ_3-O units, which holds a sodium ion, similar to **55a**. The condensation reactions leading to the formation of **54a** (see Fig. 21), **55a**, and **57a** appear to be under some kind of template control, where the host framework forms around the guest in solution.[105–109]

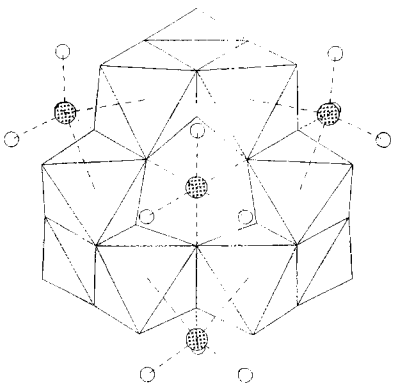

Fig. 21. Structure of the cluster anion $[H_2Mo_{16}O_{40}(OH)_{12}]^{6-}$ **54a** in crystals of **54**, viewed along the crystallographic threefold axis to clearly show the capping of the hexagonal faces of the $\{Mo_{12}O_{40}\}^{20-}$-ε-Keggin fragment (shown as a polyhedral representation) by the facial "anti-Lipscomb" trioxomolybdenum(VI) units (shown as ball-and-stick models) [102].

An interesting structural principle is found in the anion **58a**[110] (Fig. 22a) which exhibits an electronically normal, thirty-membered $[Pd_2S_{28}]^{4-}$ host framework; the closed structure is formed by the linking of two Pd^{II} atoms and four polysulfide chains. Hence, a relatively large cavity with an NH_4^+ ion at its center is formed (Pd–Pd distance 630 pm).

$[(NH_4)Pd_2(S_7)_4]^{3-}$ **58a**

α-$[Na_2Fe_{18}S_{30}]^{8-}$ **59a**

β-$[Na_2Fe_{18}S_{30}]^{8-}$ **59b**

$[Na_9Fe_{20}Se_{38}]^{9-}$ **60a**

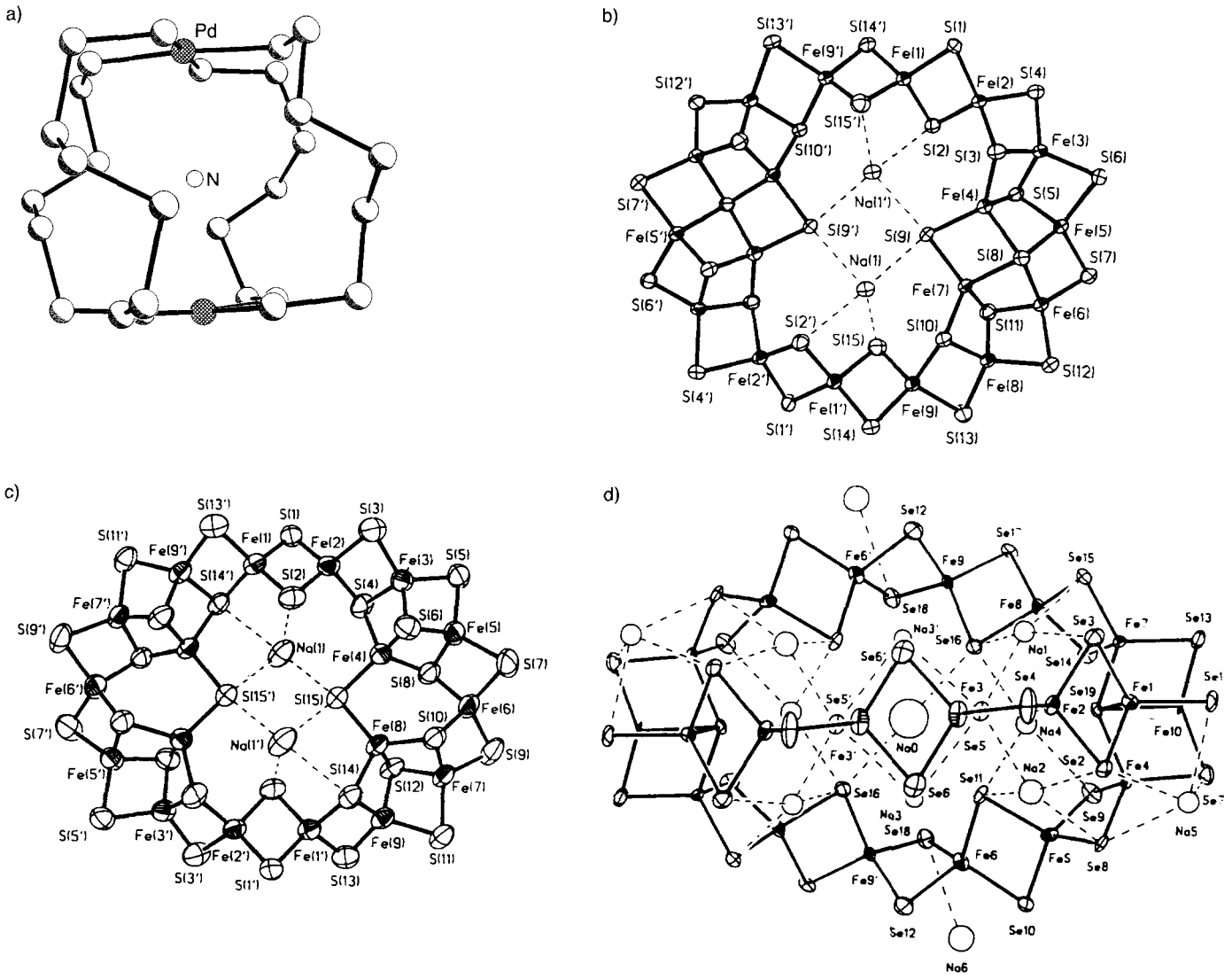

Fig. 22. Structures of the host–guest systems a) $[(NH_4)Pd_2(S_7)_4]^{3-}$ **58a**, b) α-$[Na_2Fe_{18}S_{30}]^{8-}$ **59a**, c) β-$[Na_2Fe_{18}S_{30}]^{8-}$ **59b**, and d) $[Na_9Fe_{20}Se_{38}]^{9-}$ **60a**.

Interesting host–guest relationships are found for the slice-shaped anions **59a**[111a] and **59b**[111b], as well as for the bicyclic anion **60a**.[111b] Compounds **59a** and **59b** (Figs. 22b,c) are formed by twenty-four nonplanar, corner- and edge-sharing Fe_2S_2 rhombi, respectively, such that all iron centers are localized in distorted tetrahedral FeS_4 units. Within the interior of **59a** and **59b**, there are two sodium ions coordinated to sulfur atoms of the Fe–S cage. Hence, the monocyclic species **59a** and **59b** can be considered as inorganic crown thioethers. The cluster structure of the α-isomer **59a** (Fig. 22b) contains two (linear) Fe_3S_4 and two Fe_6S_9 fragments. Fe_3S_4 and Fe_6S_9 units are linked to each other by a total of twenty μ_2-S, eight μ_3-S, and two μ_4-S atoms. In contrast, the structure of the β-isomer **59b** (Fig. 22c) consists of two Fe_2S_2, four cubic Fe_3S_4, and two tetrahedral FeS_4 units linked by eighteen μ_2-S and twelve μ_3-S atoms. The elliptical bicyclic species **60a** (Fig. 22d) is formed by twenty-one nonplanar Fe_2Se_2 rhombi, fifteen of which share corners through common iron centers, leading to three $Fe_6(\mu_2\text{-}Se)_{10}$ chains. This anion therefore exhibits thirty-six μ_2-Se atoms, two μ_4-Se centers, fifteen corner-sharing, and six edge-sharing Fe_2Se_2 rhombi. All iron atoms are grouped into distorted tetrahedral $FeSe_4$ units. The selenium-rich cavity of **60a** contains nine sodium ions, demonstrating that this nano-sized species is a host–guest system. The assignment to the closed hosts is provisional, since the host–guest behavior has not yet been studied in detail.

Open Hosts

The chemistry of polyoxotungstates yields several examples of electronically normal, open inorganic cryptands which can encapsulate electrophilic guest species. A representative of this host category is the anion **61a** (Fig. 23a),[112] which has a cyclic structure formed by the linking of four $\{AsW_9O_{33}\}$ subunits through WO_6 octahedra. If, for example, a sodium cation is located at the center of the aggregate **61a**, it can be replaced with other alkali and earth alkaline metals, as well as silver and ammonium ions. The host **61a** also possesses a lacunary structure and can incorporate transition metal centers into its framework.[113] For example, in the presence of Co^{2+} ions, the supramolecular host–guest structure **62a** is formed.[114] In

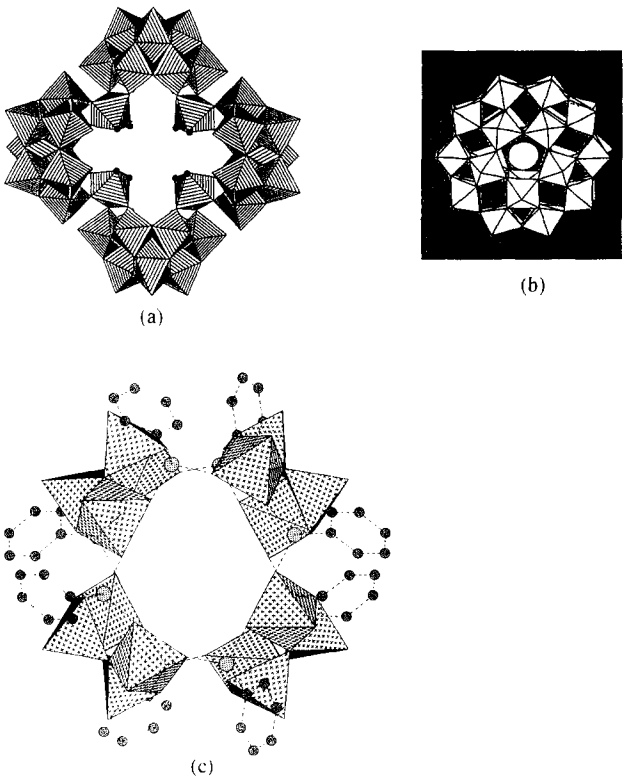

Fig. 23. a) Polyhedral representation of the cryptand $[As_4W_{40}O_{140}]^{28-}$ **61a**, viewed along the S_4 axis. The black circles mark those oxygen atoms that border the cavity of the host [114]. b) The structure of the host–guest system $[NaP_5W_{30}O_{110}]^{14-}$ **64a** (WO_6 octahedra shown as polyhedra; the five PO_4 tetrahedra are hidden), viewed along the C_5 axis. The exchangeable Na^+ ion inside the cavity is depicted by a circle [116]. c) Structure of the host of $[(Me_2NH_2)H_{11}(V^{IV}O_2)_{16}(PhAsO_3)_8]^{4-}$ **65a** with four units each of which is built up by four edge-sharing VO_5 pyramids [117].

the open host(–guest) structure **63a**[115], the nucleophilic coronand consists of two $\{Sb_3O_7\}$ and three $\{SbW_7O_{28}\}$ subunits, which are linked by oxygen atoms. The electrophilic guest (the sodium ion) is located at the center of the host, in an environment formed by eight oxygen atoms, which formally form a double-capped trigonal prism. Na^+ can be exchanged with earth alkaline metal and other alkali metal cations. The cryptate **64a**[116] consists of a ring of five $\{PW_6O_{22}\}$ units and encapsulates a sodium ion, which is located on the fivefold axis (Fig. 23b). Under relatively drastic conditions (aqueous solution, 140–180 °C), this Na^+ ion can be exchanged with other cations such as Ca^{2+} and Y^{3+}, and also with most trivalent lanthanide ions (all except La^{3+}, Ce^{3+}, and Pr^{3+}), as well as with Ce^{4+} and U^{4+}.

$[As_4W_{40}O_{140}]^{28-}$ **61a**

$[(NH_4)(Co\text{-}H_2O)_2As_4W_{40}O_{140}]^{23-}$ **62a**

$[NaSb_9W_{21}O_{86}]^{18-}$ **63a**

$[NaP_5W_{30}O_{110}]^{14-}$ **64a**

Open nucleophilic host structures with enclosed electrophiles are also known from the chemistry of oxovanadium phenylarsonates. This category of host–guest systems includes, for instance, the species **65a** (Fig. 23c).[117]

$[(Me_2NH_2)H_{11}(V^{IV}O_2)_{16}(PhAsO_3)_8]^{4-}$ **65a**

3.2.2. *Electronically Inverse Hosts*

Attraction and Repulsion (...) as principles of a natural system.
F. W. J. Schelling[118]

Closed Hosts

In our opinion, isopolyoxovanadates currently present the most instructive examples for the inorganic chemistry of host–guest species. The cluster anions of the type **66a–c**[119] and **67a**[107, 120] (Fig. 24) will be discussed in some detail. Similar host–guest systems include the complex anions **68a**[105–107, 120], **69a**,[107, 120] **70a**,[105, 120] and **71a**[125a], as well as the anion of the compound $[Et_4N]_6[HV_{22}O_{54}(HMoO_4)]$.[125b] The host shells are formed by using the template function of the (preferably) anionic guest and are dependent on its shape and size.[105–107, 121] The use of suitable basic fragments allows the formation of host–guest compounds which exhibit a cavity enclosing the template. *These closed hosts are only electronically inverse with respect to the observed "incarceration" of anions*: Studies of the electrostatic

$[H_4V_{18}O_{42}(X)]^{9-}$
66a X = Cl
66b X = Br
66c X = I

$[H_2V_{18}O_{44}(N_3)]^{5-}$ **67a**

$[HV_{18}O_{44}(NO_3)]^{10-}$ **68a**

$[HV_{22}O_{54}(ClO_4)]^{6-}$ **69a**

$[HV_{22}O_{54}(SCN)]^{6-}$ **70a**

$[V_{18}O_{42}(HCOO)]^{11-}$ **71a**

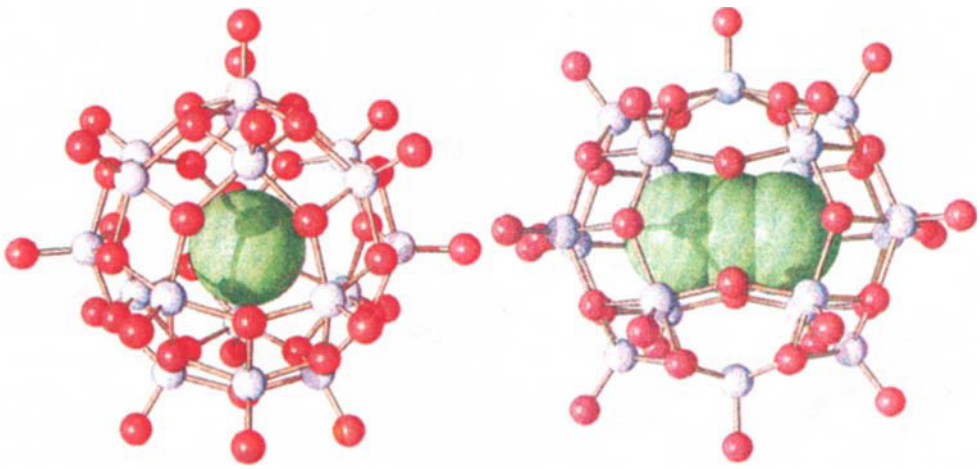

Fig. 24. Representation of host–guest relationships: structures of the cluster anions **66a–c** [119] (left) and **67a** [107, 120] (right) (V blue, O red, the central template green is shown as a space-filling model).

interactions in the hypothetical cluster anion $[V^{IV}_{18}O_{42}(Cl)]^{13-}$, based on extended Hückel calculations, have shown that the resulting electrostatic energy E_{res} is positive, indicating a destabilization and, hence, a repulsion in the case of the interactions of the Cl^- guest with the negatively charged oxygen–vanadium sphere.[122a] On the other hand, the significantly lower charge density on the encapsulated Cl^- ion indicates the presence of (only according to the calculation very weak) attractive interactions between the electrophilic vanadium centers and the chloride ion.[122b] The calculation of the charge distribution for $[V^{IV}_{18}O_{42}(Cl)]^{13-}$ (for a relevant unit cell) using the charge equilibration model with subsequent calculation of the electrostatic energies, suggests that attractive interactions with the cationic lattice are necessary to stabilize this host–guest system. This means, however, that the classification that ascribes an electronically inverse behavior to the isopolyoxovanadates is a consecutio ex eventu: Based on the above-mentioned dualism of attractive and repulsive interactions, one should talk about a primarily pseudo-mechanical incorporation of the guest by the host.[119–123] This point of view is supported by the fact that neutral molecules can be incorporated into cluster shells of appropriate size.[123] As expected the corresponding extended Hückel calculations indicate that the interaction of the H_2O guest in **72a**[124, 125] with the polyoxovanadate shell is infinitely small ($E_{res} \approx 0$).[122a]

$[V^{IV}_{18}O_{42}(H_2O)]^{12-}$ **72a**

Open Hosts and a Remarkable Synergism

The rigid electrophilic macrocycle "[12]-mercuracarborand-4" **73** is an example of such host compounds, as is demonstrated by the structure of the lithium salt **74** (Fig. 25).[126] The anion

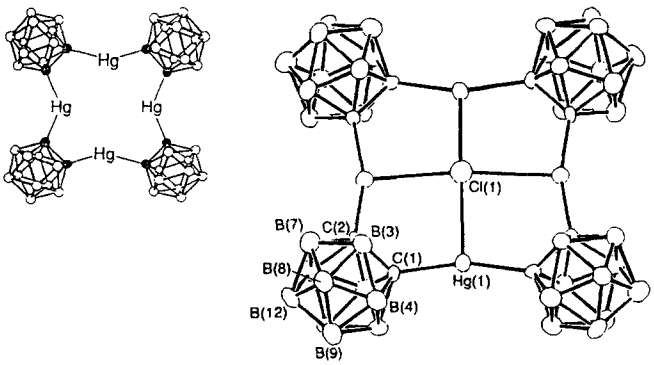

Fig. 25. Left: The electrophilic host "[12]-mercuracarborand-4" $(HgC_2B_{10}H_{10})_4$ **73**; the C atoms are denoted by black circles, the BH groups by white circles. Right: The structure of the anion $[(HgC_2B_{10}H_{10})_4Cl]^-$ in crystals of **74** (hydrogen atoms omitted) [126].

of **74** consists of four divalent 1,2-$C_2B_{10}H_{10}$ "cages" which are linked by four mercury atoms to form a cyclic tetramer with the chloride ion at the center. The related compounds **75**[127]

$(HgC_2B_{10}H_{10})_4$ **73**

$Li[(HgC_2B_{10}H_{10})_4Cl]$ **74**

$Li[(HgC_2B_{10}H_{10})_4I]$ **75**

$Li_2[(HgC_2B_{10}H_{10})_4I_2]$ **76**

and **76**[127] are known as well. The X-ray crystal structure analysis of **76** shows that the iodide ions are located above and below the plane formed by the four mercury atoms (average distance to this plane is 196 pm).[127] It is remarkable that the reaction of an ethanol solution of **76** with silver acetate yields, in addition to silver iodide and lithium acetate, the "template-free" host **73**.[127, 128]

An unusual type of inorganic host–guest system is represented by the cluster anion **78a** (Fig. 26).[129] This species is formed

$[(SCN)_9W_3S_4SnCl_3]^{6-}$ **78a**

through weak interactions between the *anionic* $[(SCN)_9W_3S_4]^{5-}$ receptor and also the *anionic* guest $[SnCl_3]^-$. In this context,

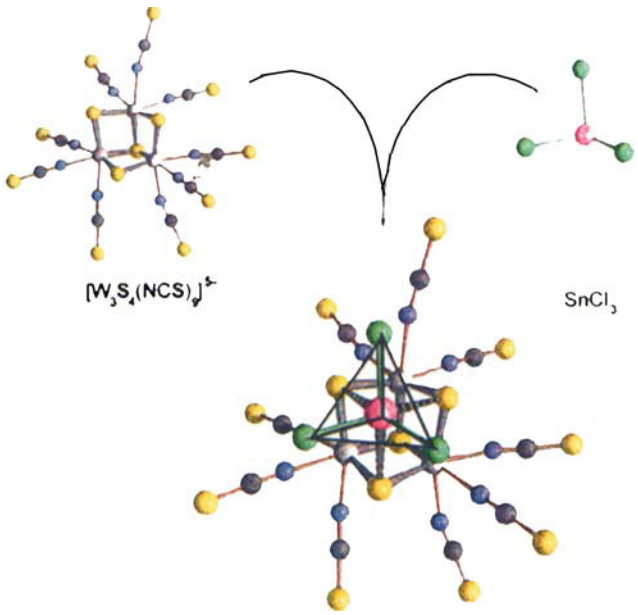

Fig. 26. The formation and structure of the cluster anion **78a**, a novel type of inorganic host–guest system (Sn pink, Cl green, W light gray, S yellow, C dark gray, N blue). Its formation is based on a synergistic effect (see text).

it should be noted that the two complementary anions are independently stable. This complementarity is reminiscent of a lock-and-key mechanism (lone pair of electrons of $[SnCl_3]^-$ as key, missing corner in the W_3S_4 cube as lock). The Sn^{2+} "reduction" of the $[W_3(\mu_3\text{-}S)(\mu_2\text{-}S)_3]^{4+}$ fragment that is contained within the $[(SCN)_9W_3S_4]^{5-}$ ion increases the nucleophilicity of the three coordinatively unsaturated μ_2-S atoms. The affinity of the $[W_3(\mu_3\text{-}S)(\mu_2\text{-}S)_3]^{4+}$ ligand for cations like Sn^{2+} increases with its increasing electron donor strength (i.e., according to the electron density at the S atoms), which is caused by the "reducing power" of the cation itself. The cluster aggregate **78a** is therefore to be viewed as an unusual host–guest system. Its guest and host components can exist independent of each other as stable anions, but they are nevertheless capable of forming host–guest structures, due to this *special* synergistic effect (special within the field of supramolecular chemistry).

3.2.3. $[As_4Mo_6V_7O_{39}(SO_4)]^{4-}$: A Model System for the Different Host–Guest Properties of Polyoxomolybdates and Polyoxovanadates

As a final example in this category the inorganic host–guest system **79a** will be discussed.[130] It consists formally of the "host" **79b** and the "guest" SO_4^{2-} and combines the pseudo-clathrate properties[131a] of some polyoxomolybdate shells (e.g., **80a**, see below) and the electrophilic character of polyoxovanadate host structures (cf. Section 3.2.2) within a single cluster species (Fig. 27).[131b] The host–guest species **79a** shows two special characteristics: The six Mo^{VI} centers are exclusively present as MoO_6 octahedra, while the seven V^{IV} atoms are found in the form of four VO_6 octahedra and three square VO_5 pyramids (Fig. 28). This indicates the remarkable property of V^{IV} centers to form octahedral as well as square-pyramidal coordination spheres. The second characteristic is that the shortest distances between a metal atom and $O(SO_3)$ are found between O42 and O43 of the central oxoanion and the molybdenum atoms Mo5 and Mo6 (only 238 and 244 pm), and not, as would have been expected, between the O atoms of the sulfate ion and the (closest) vanadium atoms V2, V3, V6, and V7 (cf. Fig. 27). This apparently indicates that at least these two molybdenum atoms interact more strongly with the sulfate oxygen atoms. These host–guest relationships, basically, reflect the various possibilities of interactions between electronically inverse polyoxovanadate host shells and their enclosed guest species on the one hand and polyoxomolybdate structures with a central oxoanion that are only capable of forming pseudo-clathrates on the other hand. The most "extreme" examples are anions like $[H_4V_{18}O_{42}(X)]^{9-}$ **66a–c**[119] and $[Mo_{12}O_{36}(PO_4)]^{3-}$ **80a**.[133]

$[As_4^{III}Mo_6^{VI}V_7^{IV}O_{39}(SO_4)]^{4-}$ **79a**

$[As_4Mo_6V_7O_{30}]^{2-}$ **79b**

$[Mo_{12}O_{36}(PO_4)]^{3-}$ **80a**

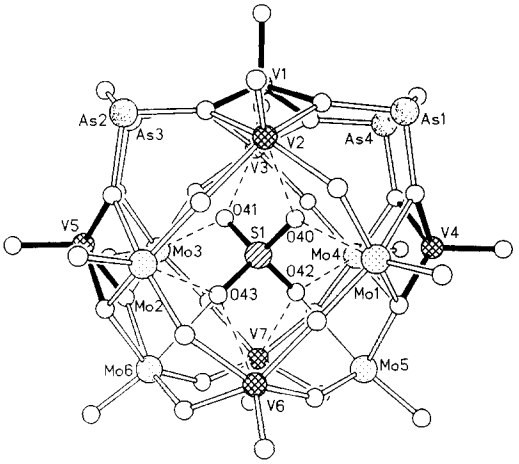

Fig. 27. The structure of the cluster anion **79a**. Metal atom–$O(SO_3)$ distances: $V\cdots O(SO_3)$ (V1, V4, and V5, square VO_5 pyramids): 325–333 pm, $M-O(SO_3)$ (M = Mo1–4, V2, V3, V6, and V7, MO_6 octahedra): 256–267 pm; $Mo-O(SO_3)$ (Mo5 and Mo6, MoO_6 octahedra): 238 and 244 pm.

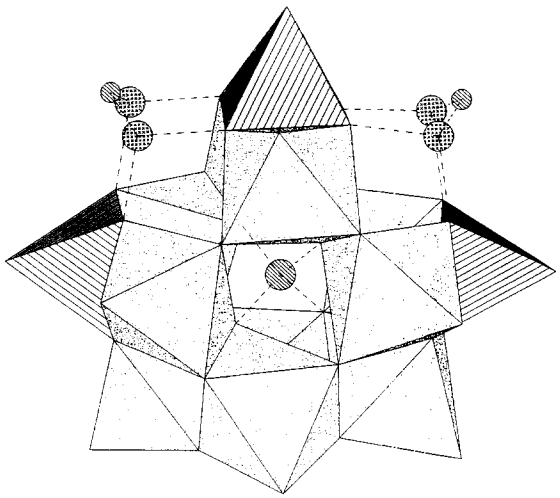

Fig. 28. Representation of the different characteristic polyhedra (octahedra and square pyramids) of the cluster anion **79a**. These polyhedra underline the model character of this compound for the electrophilic behavior of V^{IV} centers and the pseudo-clathrate properties of Mo^{VI}–oxygen aggregates, as well as for the hybrid behavior of V^{IV} centers discussed in the main text (randomly dotted: the six $OMoO_5$ and four OVO_5 octahedra; hatched: the three square OVO_4 pyramids; large circle with diagonal lines: the sulfur atom of the central SO_4^{2-} ion; small circles with diagonal lines: the oxygen atoms of the As_2O^{4+} units; cross-hatched circles: As^{III} centers of the As_2O^{4+} groups).

A comparison of the relevant chemistry of *reduced* polyoxomolybdates and -vanadates clearly shows, correspondingly, the different properties of *host–guest systems* that are exclusively built from MoO_6 octahedra or square OVO_4 pyramids, respectively: In the case of polymolybdates under reducing conditions, one obtains a nucleophilic, electronically normal host like **53a** in which sodium ions can be encapsulated (see Section 3.2.1). In contrast, square OVO_4 pyramids can be employed to construct "electrophilic", and thus electronically inverse host systems of the type **66a** (Section 3.2.2).

3.3. Electronically "Neutral" and Bifunctional Hosts

The large distances between guest species and the atoms in the cluster shell in isopolyvanadates (see Section 3.2.2) that contain an encapsulated anion with low charge density allow only weak interactions between the anionic guest and the surrounding host structure. This correlates with the idea that repulsive ($O\cdots$anion) and attractive ($V^{n+}\cdots$anion) forces are in an *approximate* balance[105, 109, 122] (with regard to the synthesis see also ref. [123]). These considerations also explain why the neutral solvent itself can take on the role as template during syntheses in aqueous and nonaqueous media where no anions are added to the reaction mixture. In this context, the formation of the remarkable basket-shaped open dodecavanadate **81a**[8] or closed isopolyvanadates such as $[V_{18}^{IV}O_{42}(H_2O)]^{12-}$ **72a**[124, 125a] may be recalled. Both are cluster species that consist of an "electronically neutral" host shell and an enclosed CH_3CN or H_2O molecule as guest.

$[V_{12}O_{32}(CH_3CN)]^{4-}$ **81a**

The relevance of the mentioned attraction/repulsion concept for the resulting weak interactions between a host and a weakly

nucleophilic as well as weakly basic guest is supported by additional observations. For example, the $\{V_4O_{16}\}$ unit is capable of coordinating cations as well as anions, as demonstrated by the syntheses of the compounds **82**[134, 135] and **83**[136] (see Fig. 29).

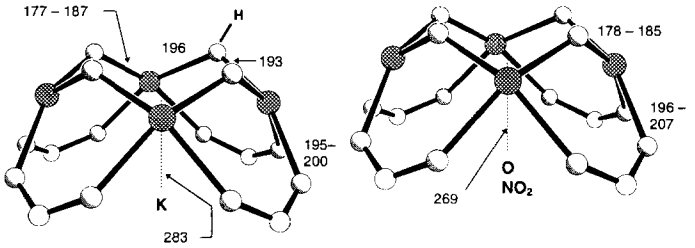

Fig. 29. A receptor for cations and anions: Left: Part of the structure of the cation $[K\{V_4O_7(OH)(O_2CR)_4\}]^+$ **82a**; right: Part of the structure of the anion $[(NO_3)\{V_4O_8(O_2CR')_4\}]^{2-}$ **83a**. (For **82a**: R = neopentyl; counterion: $[RCO_2]^-$; central unit: $V^{IV}(OH)V^V_3O_3$. For **83a**: R' = 2-thienyl; counterion: $[Et_4N]^+$; central unit $V^{IV}V^V_3O_4$.) The vanadium atoms are represented as cross-hatched circles and the oxygen atoms as shaded circles; some bond lengths are shown. All figures are according to ref. [135].

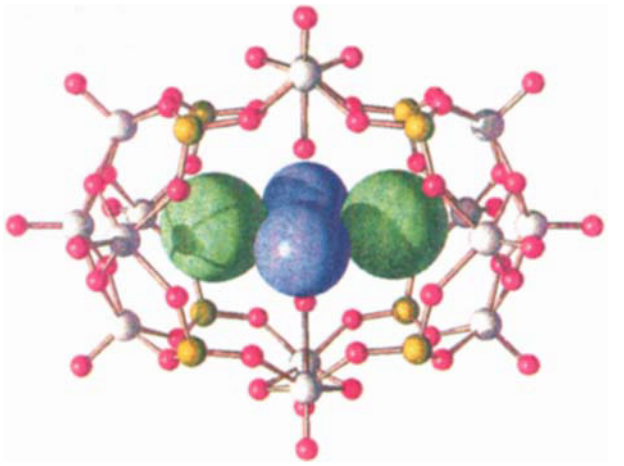

Fig. 30. Structure of the central cage of the cluster anion **84a**, viewed along one of the idealized C_2 axes (V gray, P yellow, O red, NH_4^+ blue, Cl^- green; central guest system shown as a space-filling model), demonstrating the host–guest relationship (see text). The phenyl rings of the phenylphosphonate units have been omitted for clarity.

Hence, this electronically bifunctional $\{V_4O_{16}\}$ unit can be formally submitted to a reversal of polarity by the judicious choice

$[K\{V_4O_7(OH)(O_2CCH_2tBu)_4\}][O_2CCH_2tBu]\cdot 2\,tBuCH_2CO_2H$ **82**

$[Et_4N]_2[(NO_3)\{V_4O_8(tca)_4\}]\cdot H_2O$ **83** (tca = thiophene-2-carboxylate)

of reaction conditions, even in the case of a constant degree of reduction (identical electron populations in **82** and **83**, one V^{IV} and three V^V centers). But, it must be noted that the electronic properties of the $\{V_4O_{16}\}$ host are also slightly influenced by the choice of organic ligands and by minor modifications of the basic host (e.g., the protonation of the $V^{IV}V^V_3O_4$ unit in **82** in contrast to that in **83**): Electronically normal or inverse charge conditions in our formal approach are properties of the *same* basic host structure in *different* host–guest systems (not in the *same* host–guest system, a topic that will be discussed in Section 3.4). The tendency of isopolyvanadates to incorporate anions is expected to increase with an increase in the number of Lewis acidic vanadium centers.

3.4. Hosts Comprising Electronically Normal and Inverse Subhosts

The coupling of electronically normal and inverse subhosts, as demonstrated by the synthesis of the host–guest species **84**,[109] opens up a new dimension in inorganic host–guest

$[Me_2NH_2]_5(NH_4)[2NH_4^+, 2Cl^-\subset V_{14}O_{22}(OH)_4(H_2O)_2(PhPO_3)_8]$
$\cdot 5H_2O\cdot 4DMF$ **84** (DMF = dimethylformamide)

chemistry. The cage of the cluster anion **84a** (Fig. 30) consists of two half-shells, which are formed from isopolyvanadate and phenylphosphonate units. The central neutral guest system $(2NH_4^+, 2Cl^-)$ is a cation/anion aggregate that can be interpreted as a section of the NH_4Cl ionic lattice. Thus anions and cations are both encapsulated within the same cavity, which is formally separated into two segments by two water molecules bound to V^{IV} centers. These water molecules apparently stabilize the $(2NH_4^+, 2Cl^-)$ guest system by hydrogen bonds. The formation of the host shell **84b** is possibly based on a conservative self-organization process.[137] During this process, the two chloride ions could induce the generation of the corresponding

$[V_{14}O_{22}(OH)_4(H_2O)_2(PhPO_3)_8]^{6-}$ **84b**

electrophilic isopolyvanadate fragments, while the ammonium ions could induce the formation of the nucleophilic coronands.

The (formal) removal of the two water ligands from **84b** yields the host shell **84c**. This transformation converts the initially octahedral coordination sphere of the vanadium atoms in the bridging $\{V_2O_2(OH)_2(H_2O)(PhPO_3)_4\}^{6-}$ units[109] into a square-

$[V_{14}O_{22}(OH)_4(PhPO_3)_8]^{6-}$ **84c**

pyramidal one. This creates further possibilities regarding the encapsulation of other guest species or guest systems. The syntheses of the cluster compounds **85**[138] and **86**[139] provide an impressive demonstration of that principle. The careful choice

$[PhCH_2NEt_3]_2[PhCH_2NMe_3]_4[(CH_3CN)_2\subset V_{14}O_{22}(OH)_4(PhPO_3)_8]$
$\cdot 2CH_3CN\cdot 2CH_3OH\cdot 2H_2O$ **85**

$[Et_3NH]_3[tBuNH_3]_2Na_2[(H_2O)_2, N_3^-\subset V_{14}O_{22}(OH)_4(PhPO_3)_8]$
$\cdot 6H_2O\cdot 2DMF$ **86**

of *reaction conditions* can lead to the controlled formation of a multitude of zero-dimensional host–guest structures, when combined with knowledge about the complex host–guest relationships that form the basis of these oxovanadiumphenylphosphonate systems and determine the genesis of the host lattices **84b** and **84c**.

It is remarkable that the organization of particles within the closed cavity of $V/O/PhPO_3^{2-}$ host–guest systems can be controlled from the "outside". For example, the addition of a thir-

teenfold excess of rubidium bromide to an aqueous DMF solution of **86** yields the species **87** (see Fig. 31).[139] During the

$[Et_3NH][tBuNH_3]_2(0.5\,Rb/0.5\,Na)_2$
$\cdot Rb_2[(H_2O)_2 \cdot N_3 \subset V_{14}O_{22}(OH)_4(PhPO_3)_8] \cdot 10\,H_2O \cdot 2\,DMF$ **87**

transformation of **86** to **87**, an exchange of the guests located in the truncated-cone-shaped ion channels takes place (see Fig. 31) which, in turn, leads to a reorganization of the guest system ($2\,H_2O$, N_3^-) within the closed cavity.[139] This shows how the organization of species within a closed host can be remotely controlled.

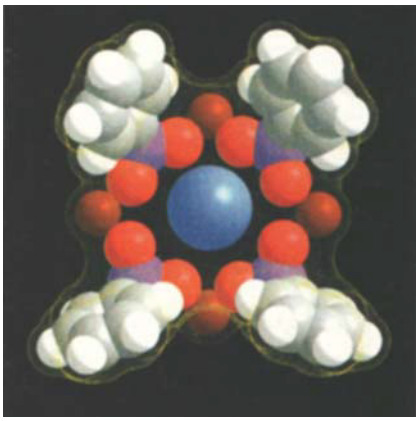

Fig. 31. Space-filling plot with a weakly outlined "Connolly surface" [140], of the ion channel of **87a**, built from four $PhPO_2$ units and four V atoms, showing the embedded Rb^+ cation in the coronand (viewing direction as in Figure 30; V brown, P violet, O bright red, Rb large central blue sphere, C gray, H white).

In these examples of host–guest systems, it appears to be irrelevant in terms of the control over the reaction whether the host forms around a guest template or whether the host is formed without a template effect and then itself stabilizes the guest system such as ($2\,NH_4^+$, $2\,Cl^-$). The detection of *rules* that underlie the reactions in question makes it possible to plan and control syntheses, even without an understanding of the fundamental principles that govern the formation of these V/O/Ph-PO_3^{2-} systems. This also allows the researcher to "play" with the host–guest relationships inherent to these cluster species. There are obvious potential applications of this kind of host–guest chemistry, for instance the template-controlled formation of oligomers from anions and cations. It also allows the study of intermolecular interactions within nano-sized aggregates.

3.5. "Cluster Within Cluster"—A Model for Nucleation Processes and Some Relevant Comments about the (Template) Conductor Principle

"Nothing originates by chance, but everything is due to a specific reason and the force of necessity."
Democritus[141]

Compounds that show "a cluster encapsulated within a cluster" are of particular interest.[142] These species can only be formally viewed as host–guest systems, as strong covalent interactions between the "guest template" and the "host shell" must be "ignored". But, this procedure is justified due to the general validity of the principles of molecular construction and organization that have been discussed thus far. The principles responsible for the formation of relevant nano-sized structures resemble the structure-determining schemes that result from the dominance of weak host–guest interactions in the area of "normal" host–guest systems.[142]

An example for such "cluster within cluster" compounds is the mixed-valent nano-sized polyoxovanadate **90a**.[105–108] It consists of a $V_{30}O_{74}$ shell formed by the linking of 30 tetragonal

$[V_{34}O_{82}]^{10-}$ **90a**

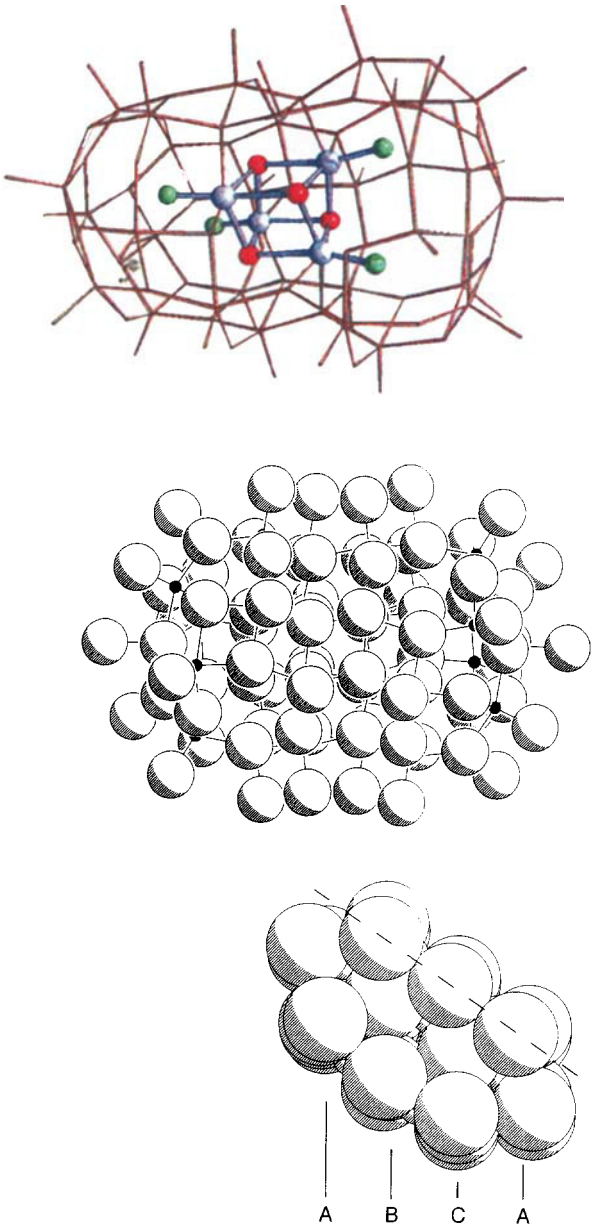

Fig. 32. Top: "Host shell" (brown stick model) of the cluster anion $[V_{34}O_{82}]^{10-}$ **90a** showing the central $\{V_4O_4\}(O_{term})_4$ cube as a ball-and-stick model (V blue, μ_3-O red, O_{term} green). Middle: The vanadium–oxygen system represents a section from a distorted and defect NaCl lattice; the layers of oxygen atoms in **90a** are shown as viewed perpendicular to the approximate S_4 axis. Bottom: View of the cubic closest packing of oxygen atoms, indicating the ABCA layer structure (one of the layers shown in the middle figure perpendicular to the approximate S_4 axis is indicated by the dashed line).

VO_5 pyramids and an incorporated central $\{V_4O_4\}(O_{term})_4$ cube that exhibits four V=O groups (Fig. 32 top). This cube, which is probably formed as an intermediate in the vanadate solution, acts as template and generates the structure of the $V_{30}O_{74}$ shell in a conservative self-organization process[137] according to its "own" shape and size. This $\{V^{IV}_4O_4\}(O_{term})_4$ unit, which has the same stoichiometry as amphoteric $V^{IV}O_2$ (and, hence, can be precipitated), in effect initiates the construction of the $[V_{34}O_{82}]^{10-}$ ion by acting as the "crystallization nucleus". The anion formed shows similarities to a segment of a disordered cubic solid-state structure of the NaCl type (see Fig. 32 middle and bottom). The process just described is important because the initial steps of crystal formation, for which it can serve as a model, are not yet properly understood.

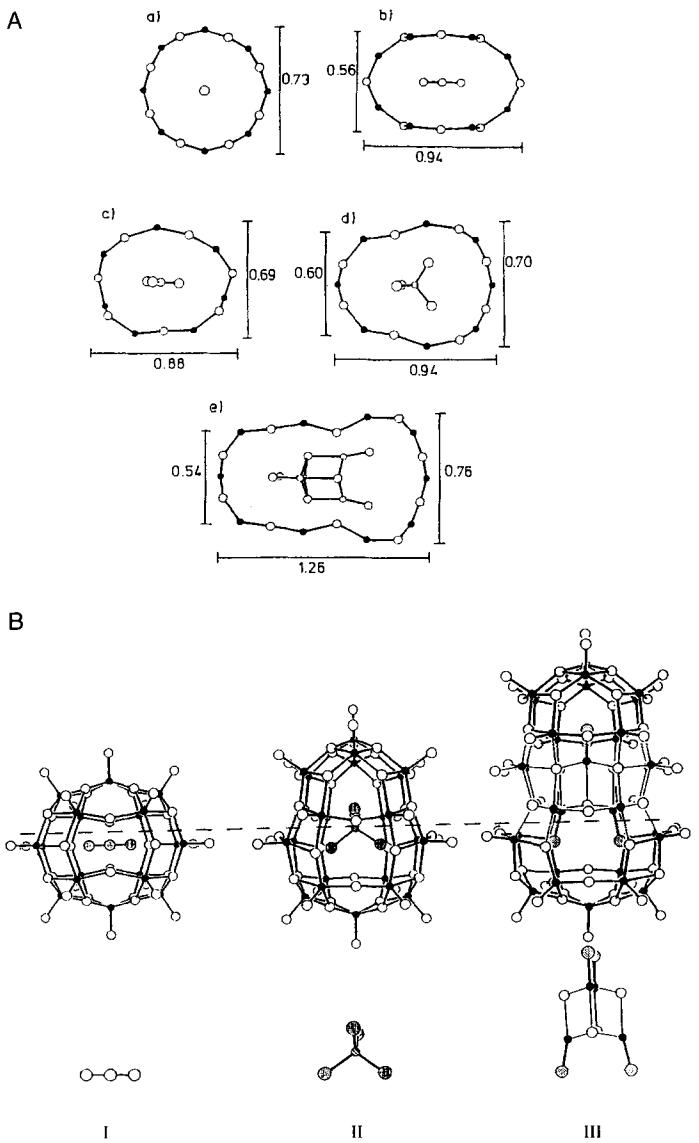

Fig. 33. Depiction of the template effect/conductor principle (see text) A) by a simplified representation of the shape and size of several different V–O cluster shells, showing measurements in nm. a) $[H_4V_{18}O_{42}(X)]^{9-}$ **66** (X = Cl, Br, I), b) $[H_2V_{18}O_{44}(N_3)]^{5-}$ **67a**, c) $[HV_{18}O_{44}(NO_3)]^{10-}$ **68a**, d) $[HV_{22}O_{54}(ClO_4)]^{6-}$ **69a**, e) $[V_{34}O_{82}]^{10-}$ **90a** (shown without the covalent V–O bonds between the central $\{V_4O_4\}(O_{term})_4$ cube and the cluster shell) and by B) structural comparison between $[H_2V_{18}O_{44}(N_3)]^{5-}$ **67a** (I), $[HV_{22}O_{54}(ClO_4)]^{6-}$ **69a** (II), and $[V_{34}O_{82}]^{10-}$ **90a** (III) and their central templates (V black; O white, for the shells; see text).

This method of constructing inorganic host–guest systems is "in effect" based on a type of *conductor principle*: The controlled linking of inorganic basic units for the purpose of generating larger stable mesoscopic structures is directed by *templates*. These can, essentially act as "seedlings" for the architectures to be created and are either added to the reaction mixture or are formed in it. Such templates regulate the mobility of the basic building blocks and guide, like a conductor, these usually freely mobile fragments into a well-defined order (cf. Figs. 33 and 34). A completely new supramolecular ensemble of different particles is thus formed, often displaying exceptional properties (a comparison with the term "slaving principle" in the terminology of Hermann Haken's synergetics is certainly worthwhile). The "conducting" influence of weak interactions in "cluster within cluster" type compounds such as **90a** even in the presence of strong covalent interactions becomes evident from the following comparison (see Fig. 33B): The formal removal of the two middle layers in **90a** (a $\{V_{12}O_{28}\}$ fragment containing the central $\{V_4O_4\}(O_{term})_4$ cube, Fig. 33 B III)), followed by the linking of the remaining $\{V_{11}O_{27}\}$ half-shells yields the shell of $[HV_{22}O_{54}(ClO_4)]^{6-}$ **69a** (Fig. 33 B II). The formation of the half-shells in **69a** and **90a**, together with their rotation by 90°, occurs in both cases after the recognition of the "$(O-O)_2$ unit": The arrangement of the four shape-determining terminal O atoms in the cube of **90a** (a tetragonal disphenoid) corresponds to that of the four O atoms in the ClO_4^- unit of **69a**. The cluster shell of $[H_2V_{18}O_{44}(N_3)]^{5-}$ **67a** can formally be created in a similar way by fusing two $\{V_{11}O_{27}\}$ half-shells (see Fig. 33 B I[107]). The linear azide ion with its $D_{\infty h}$ symmetry acts as template in this case and assures that the two shells are arranged as mirror images, that is, without the rotation observed in **69a** and **90a**. The entire cluster shell thus obtains an oblong shape with D_{2h} symmetry, which is complementary to the azide ion (D_{2h} is a subgroup of $D_{\infty h}$). With respect to these arguments, it must be noted that in the case of V–O inclusion compounds the apparently only weak interactions allow the central units to act as matrices or templates that determine the symmetry, the shape, and the structure of their respective shells (Fig. 33 A and B).

The weak part of the interaction between the $\{V_4O_4\}(O_{term})_4$ cluster and the shell of the $[V_{34}O_{82}]^{10-}$ anion ($O{=}V(shell)\cdots(O_{term}){=}V(cluster) > 254$ pm) can be compared to those that exist between the layers of the V_2O_5 lattice.[105, 143] Using the template principle, the V_2O_5 layers are "systematically arranged" in such a way as to "imagine" the layer $n+1$ on top of layer n according to the weak interactions $O{=}V\cdots O{=}V$

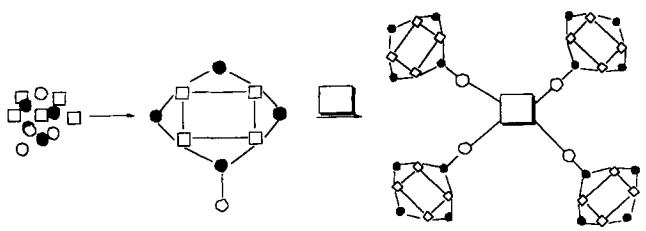

Fig. 34. Schematic representation of a reaction that could take place in solution during a self-organization process (see text). This scheme shows a possible template-directed synthesis (the large symbol □ represents a template) of supramolecular structures from prefabricated basic aggregates, which, in turn, are formed in primary reaction steps.

(distance between the layers $d = 279$ pm, layer n considered as template for layer $n+1$).

The giant cluster anion **91a**, which contains the $\{Mo_{16}O_{52}\}$ group of **54a** as central structural element,[100, 144] is another

$[Mo_{43}H_{15}O_{112}\{(OCH_2)_3CCH_3\}_5]^{8-}$ **91a**

example for a "cluster within a cluster" system. The four facial $\{Mo^{VI}O_3\}$ trioxomolybdenum units of **54a** function as *inorganic protecting groups* (with simultaneous protonation of twelve μ_2-O atoms) for the highly unstable negatively charged $\{Mo_{12}O_{40}\}^{20-}$ cluster fragment forming the reactive $\{Mo_{16}\}$ intermediate. This species can be "utilized" for the synthesis of cluster systems with higher nuclearities, such as **91a**.[100] It is, therefore, reasonable to view this $\{Mo_{16}\}$ unit as a structure-determining agent, which is formed as an intermediate in solution, and which enables the template-controlled synthesis of the complex cluster anion **91a**.[144]

3.6. Cavities in Giant Clusters and Molecular Models for Clathrates

The principle of the formation of ordered structures by template-controlled self-organization processes leads directly to the concept of syntheses of "large" systems as intermediates in the reaction solution. Under the structure-determining influence of host–guest relationships, these preorganized units have a "strengthening" and controlling effect on subsequent steps. Larger and larger molecular building blocks are formed by conservative self-organization processes. The aggregates formed by the intermediate steps are in effect linked to giant cluster species in a controlled manner. In certain cases, such structures also contain nano-sized cavities.

Examples for such novel host–guest systems are the highly symmetric, torus-shaped giant cluster anions **93a** and **94a**

$[\{Z(H_2O)\}_6\{Mo(\mu_2\text{-}H_2O)_2(\mu_2\text{-}OH)Mo\}_3\{Mo_{15}(MoNO)_2^{3+}O_{58}(H_2O)_2\}_3]^{n-}$

93a: Z = VO, $n = 21$

94a: Z = Fe(H_2O), $n = 15$

(Fig. 35 top).[146–150] These nano-sized or mesoscopic structures contain $\{Mo_{15}(MoNO)_2^{3+}O_{58}(H_2O)_2\}^{20-}$ units ($\{Mo_{17}\}$) (Fig. 35 middle) that formally function as ligands and are linked and stabilized by coordination to cationic species such as $\{(H_2O)V^{IV}O\}^{2+}$, $\{Fe^{III}(H_2O)_2\}^{3+}$ and $\{Mo^{V}(\mu_2\text{-}H_2O)_2(\mu_2\text{-}OH)Mo^{V}\}^{9+}$ (Fig. 35). The aggregation variability behavior of these $\{Mo_{17}\}$ units is also demonstrated by the synthesis of the polyoxomolybdate **95a**.[147, 154] It consists of two $\{Mo_{17}\}$

$[\{MoO_2\}_2\{H_{12}Mo_{15}(MoNO)_2^{3+}O_{58}(H_2O)_2\}_2]^{12-}$ **95a**

units, which are linked by two *cis*-MoO_2^{2+} groups, two NH_4^+ ions, and two H_2O molecules (Fig. 35 bottom). These ammonium ions and water molecules are located in a "space" formed by the two $\{Mo_{17}\}$ units which cannot be considered as a cavity. (The $\{Mo_{17}\}$ units are "formed" by the linking of two $\{Mo_8\}$ units by an Mo atom) (see also the incorrect formulas in refs. [151–153]).

This aggregation leads to the generation of a host, which contains a relatively large cavity (diameter perpendicular to the

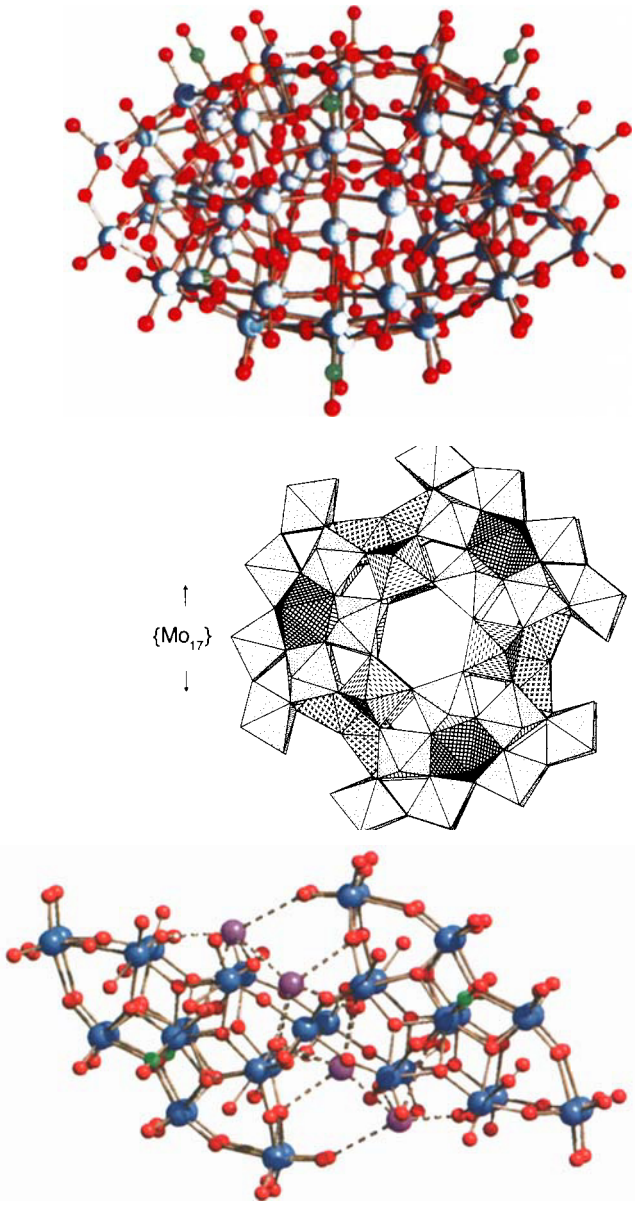

Fig. 35. Top: Ball-and-stick model of the cluster anions **93a** and **94a**, viewed approximately along the 2-(C_2) axis (Mo blue, V/Fe orange, O red, N green). Middle: Polyhedral representation of the cluster anions **93a** and **94a** (dashed polyhedra: $V^{IV}O_5(OH_2)$ and $Fe^{III}O_4(OH_2)_2$ octahedra, crossed polyhedra: $\{Mo(\mu_2\text{-}H_2O)_2(\mu_2\text{-}OH)Mo\}$ units, square-filled polyhedra: pentagonal $Mo(NO)O_6$ bipyramids, dotted polyhedra: MoO_6 octahedra). Bottom: Structure of the cluster anion **95a** (Mo blue, O red, N(NO) light green; in between the $\{Mo_{17}\}$ units NH_4^+ and H_2O violet).

$\bar{6}$-(S_3) axis approximately 0.9 nm, parallel to it approximately 0.5 nm (ignoring the H atoms)). This cavity in the interior of the cluster anions **93a** and **94a** is formed by a central O_{33} polyhedron and is bordered at both poles by alternating M-O-Mo-O twelve-membered rings (M = V, Fe), which are perpendicular to the $\bar{6}$-(S_3) axis (Fig. 36). Remarkably, the O_{33} polyhedron contains two six-membered H_2O rings, which are located between the planes of the twelve-membered M-O-Mo-O rings. Hence, the cavities of **93a** and **94a** are bordered by H_2O molecules, which are interlinked by hydrogen bonds. The question whether "some water" is present as disordered guest in the cavity cannot be answered conclusively either by X-ray crystallography (no significant residual electron density was found within

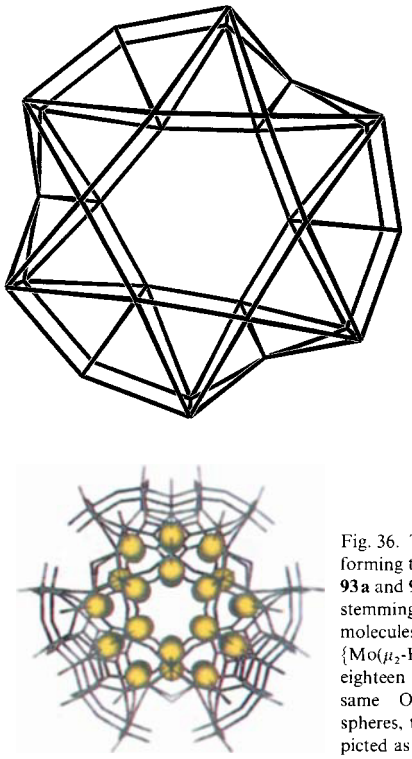

Fig. 36. Top: Central polyhedron forming the cavity in the cluster anions **93a** and **94a**, built up from 33 O atoms stemming from twelve terminal H_2O molecules, three μ_2-OH groups of $\{Mo(\mu_2\text{-}H_2O)_2(\mu_2\text{-}OH)Mo\}$ units, and eighteen μ_2-O atoms. Bottom: The same O_{33} polyhedron (O yellow spheres, the "rest" of the cluster is depicted as the blue-gray stick model).

the cavity) or by thermogravimetric data (the mass fraction per H_2O molecule is only approximately 0.2%). Such a disorder of guest species in the sense of the clathrate definition (see Section 2.1), however, would correlate with the expectation of weak van der Waals interactions between host structures and guests. This interpretation implies the conclusion that the giant cluster anions **93a** and **94a** are molecular models for clathrate hydrates.[155a] The H_2O molecules of the above-mentioned six-membered rings form a subhost $\{(H_2O)_6\}_2$. This subhost provides an "extramolecular cavity"[47] within the proper cavity of **93a** and **94a**, which serves as additional guest space for "further water" $(H_2O)_x$. This clathrate $[(H_2O)_x\{(H_2O)_6\}_2]$ is, in turn, incorporated as guest into the host $[Z_6\{Mo(\mu_2\text{-}H_2O)_2(\mu_2\text{-}OH)Mo\}_3\{Mo_{15}(MoNO)_2^{3+}O_{58}\}_3]^{n-}$ ($Z = VO$, $n = 21$; $Z = Fe(H_2O)$, $n = 15$). In this context, the giant cluster anions **93a** and **94a** can be viewed as double host–guest systems[155b] (the relevance of double host–guest systems for bioinorganic chemistry is discussed in Section 5).

3.7. The Shell Aufbau Principle

"Nature is to be considered as a system of steps, each of which is born out of the previous one."
G. W. F. Hegel[156]

The increasing complexity in the series of $\{Mo_7\}/\{Mo_8\}$, $\{Mo_{17}\}$, $\{Mo_{36}\}$, and $\{Mo_{57}\}$ units, as well as that of $\{Mo_2\}$, $\{Mo_6\}$, $\{Mo_{12}\}$, $\{Mo_{16}\}$, and $\{Mo_{42}\}/\{Mo_{43}\}$ units demonstrates a *shell Aufbau principle*: compare the change in complexity in **54a** → **91a** and in **54a** → **56a** (see Section 3.5). The shell Aufbau principle demonstrates the growth principle of complex systems in the antagonism "growth by accumulation and limitation of growth".

This concept is not limited to spherical compounds and applies to the category of compounds with weak host–guest interactions as well as to that of compounds with strong covalent and metal–metal interactions. It is, for instance, possible to describe the systematic construction of metal clusters of higher nuclearities on the basis of the shell Aufbau principle. Examples with idealized metal content include **96**,[157] **97**[158] (Phen* = 4,7-di(*p*-sulfophenyl)-1,10-phenanthroline), and **98**[159] (Phen = 1,10-phenanthroline)—species that have, however, not yet been

$[Au_{55}(PPh_3)_{12}Cl_6]$ **96** $[Pt_{309}Phen^*_{36}O_{30\pm10}]$ **97** $[Pd_{561}Phen_{36}O_{190\pm10}]$ **98**

characterized by X-ray structure analysis. Thus, a sequence of "magic numbers" is produced when a closed outer shape (a cuboctahedron for ccp and an anticuboctahedron for hcp) is reached in each case for a cubic closest packing (ccp) or hexagonal closest packing (hcp) of the metal atoms.[160] The Aufbau principle that forms the basis of this shell model states that a central metal atom is surrounded by n shells each with $(10n^2 + 2)$ atoms. The successful syntheses of *ligand-stabilized* single shell $\{M_{13}\}$, double shell $\{M_{55}\}$ (**96**), quadruple shell $\{M_{309}\}$ (**97**), and quintuple shell $\{M_{561}\}$ clusters (**98**) provide a striking demonstration of this principle.[160, 161] The ligands and the low nucleophilicity of the terminal oxygen atoms in the case of polyoxometalates serve to interrupt the growth processes, which lead to the formation of high-nuclearity clusters at a given aggregation level. In this manner, one obtains cluster aggregates of a defined level of complexity not only for metal–oxygen clusters (e.g., **56** and **91**) but also for metal clusters (e.g., **96**–**98**). The latter species, in turn, contain cluster fragments as subunits, which are known as stable, isolated compounds or as components of other, previously synthesized clusters. Examples include the three $\{Mo_{17}\}$ units in the giant anions **93a** and **94a**, the $\{Mo_{16}\}$ groups in **56** and **91**, as well as the $\{M_{13}\}$, $\{M_{55}\}$, $\{M_{147}\}$, and $\{M_{309}\}$ units in **98**. This general shell Aufbau principle does not prescribe the exact way in which the specific subunits are to be linked: The $\{Mo_{17}\}$ unit, for example, can be "used" to form the "double shell" $\{Mo_{17}\}_2$ species **95a** or the triple shell $\{Mo_{17}\}_3$ anions **93a** and **94a**. By suitable variation of the reaction conditions it is also possible to use the $\{M_{13}\}$ cores of $\{M_{55}\}$ clusters as building blocks for the generation of $\{M_{13}\}_{13}$ giant clusters.[161] The shell Aufbau principle is therefore by no means limited to spherical "cluster within cluster" compounds. Nature has apparently utilized such a principle for a long time in order to reduce the necessary amount of "genetic information" to a minimum, a principle exemplified by the tobacco mosaic virus.[162]

4. Potential Applications

4.1. Molecular Magnets: Controlling the Spin Organization in Host Molecules

The template syntheses of new cluster compounds utilizing intrinsic host–guest relationships open up new possibilities for chemists to create nano-sized host or cluster structures with novel magnetic properties. This is the case when the relative number of paramagnetic centers (e.g., the V^{IV}/V^{V} ratio) and,

hence, the type of exchange interactions can be influenced (in general, exchange interactions become stronger when, in clusters of the same size, the number of V^{IV} atoms is increased, due to the accompanying reduction in interatomic distances).[163] The cluster anion **99a**[164-166] is an example for such a "high-nuclearity spin cluster" with magnetic properties reminiscent of

$[V_{15}As_6O_{42}(H_2O)]^{6-}$ **99a**

those of extended two and three-dimensional inorganic solids, as it consists of a unique multilayer magnetic structure (Fig. 37). The host-guest system of **99a** exhibits 15 paramagnetic $V^{IV}(d^1)$

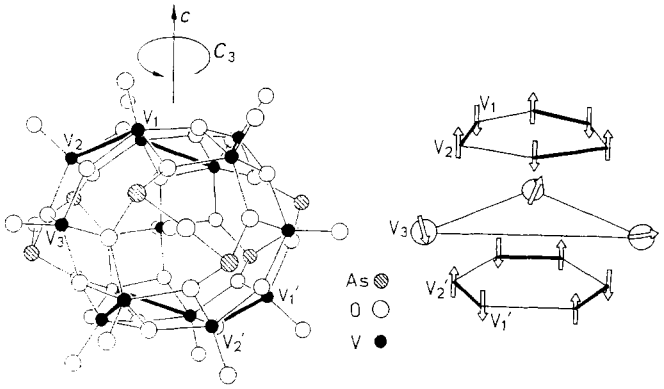

Fig. 37. Left: Structure of the cluster anion $[V_{15}As_6O_{42}(H_2O)]^{6-}$ **99a** showing the crystallographic C_3 axis. Right: Schematic representation of the spin organization at low temperatures ($T < 100$ K). The circled arrows indicate uncoupled spins (the phenomenon of spin frustration). The distance between coupled vanadium centers of V^{IV} V^{IV} pairs is 287 pm, other V···V distances are 302-305 pm (cf. ref. [165, 168]).

centers, which are grouped in such a way as to form two distorted, nonplanar hexagons with six V^{IV} atoms, between which a central triangle of three V^{IV} centers is located. This arrangement results in a sandwich-like structure with three planes of different magnetization at low temperatures ($T < 100$ K). While spin pairing occurs among the V^{IV} atoms of the two V_6 hexagons, the spins in the central V_3 plane are uncorrelated and exhibit—as expected—the interesting phenomenon of spin frustration. The spins of the host-guest system **99a** are, therefore, *formally* subject to a kind of self-organization process.[165, 168]

In this context it is important to note that by the combined synthetic strategy of a controlled V^{IV}/V^{V} ratio *and* the use of a template it is not only possible to adjust the ratio of paramagnetic to diamagnetic centers (this enables the planning of spin frustration effects by using an odd number of V^{IV} centers) but also to predetermine the topology and structure of the cluster in question. This possibility of controlling the magnetic properties of high-nuclearity spin clusters can be exploited in order to create host-guest systems displaying very different nuances in their magnetic behavior.[165-170]

Of particular importance in this context are large cluster surfaces that can be loaded with various paramagnetic centers. Examples for this procedure include the giant clusters **93a** and **94a** and their derivatives: Not only unusually strong antiferromagnetic exchange interactions have been observed in these species, but also an abundance of ferrimagnetic properties;[150b] the possibility of "tuning" these properties remains as well.

4.2. Molecular Anion Cages

The properties of ions in the solid state as well as in solution can only be evaluated in the presence of appropriate perturbing counterions due to the governing principle of electroneutrality. It is a very difficult undertaking to derive the properties of the free ion from spectroscopic data obtained in this manner. However, this dilemma can be avoided by encapsulating such a charged species, for example an anion, as guest within a rigid host that is also negatively charged, for example an isopolyvanadate. In this particular host structure, with a central weakly nucleophilic/basic anion as guest, repulsive (O···anion) and attractive (V^{n+}···anion) forces balance each other out, at least approximately (cf. the discussion in Section 3.2.2). This leads to relatively weak interactions and, hence, to rather large distances between the anion and the cluster shell. The resulting pseudomechanical fixation of the guest by the host offers the opportunity

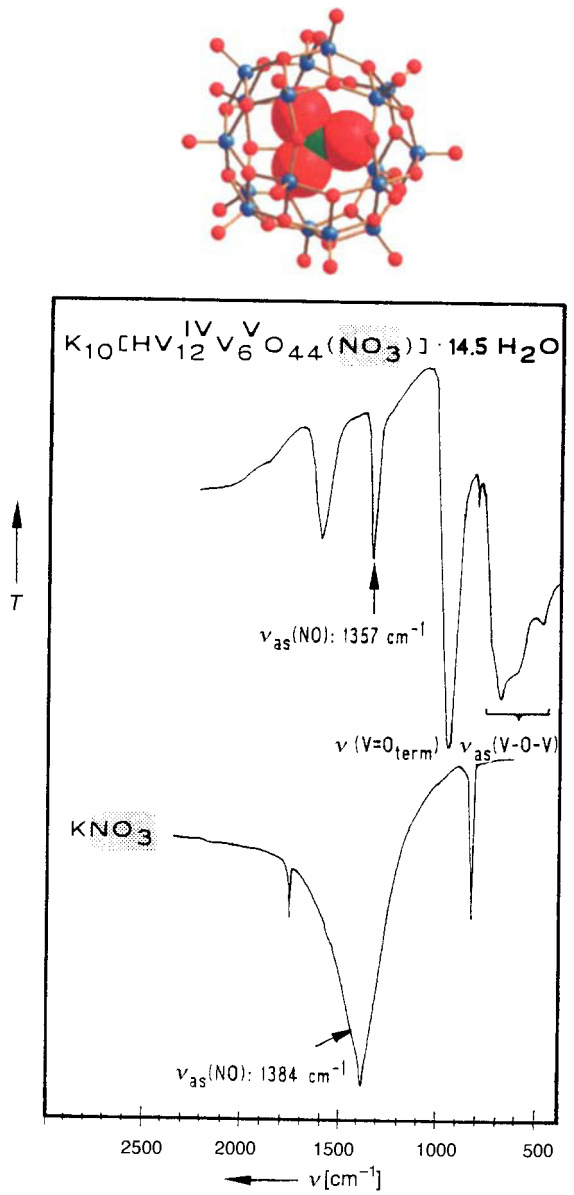

Fig. 38. Top: Structure of the cluster anion **68a**. Bottom: IR spectra of the cluster species $K_{10}[HV_{18}O_{44}(NO_3)] \cdot 14.5H_2O$ **68** and KNO_3 (both as KBr pellets). T = transmission.

to make an almost isolated anion, which is formally "floating" in the center of its cryptand, the object of scientific curiosity. The "corresponding counterion" in this case is located far away, outside the host–guest system, that is in the cationic lattice and has, therefore, no noticeable effect on the anion, which, while encapsulated, is nevertheless nearly "free" with respect to the above-mentioned interaction.

An example for this type of host–guest compound is the cluster species $[HV_{18}O_{44}(NO_3)]^{10-}$ **68a** (Fig. 38 top).[105–107, 120] With the aid of vibrational spectroscopy studies of the host–guest system **68a**, the weak interactions between guest and host shell can be confirmed. For this purpose, the IR band stemming from the asymmetric N–O stretching vibration of the NO_3^- ion was examined in different environments (in the host shell of **68a** and in crystalline KNO_3). The measured half width of this band in **68a** is smaller by a factor of about five than the corresponding $\nu_{as}(NO)$ stretching vibration band of the nitrate ion in KNO_3 (Fig. 38 bottom). This clearly shows the mentioned weak interactions between the NO_3^- ion and the cluster shell in **68a**.[120]

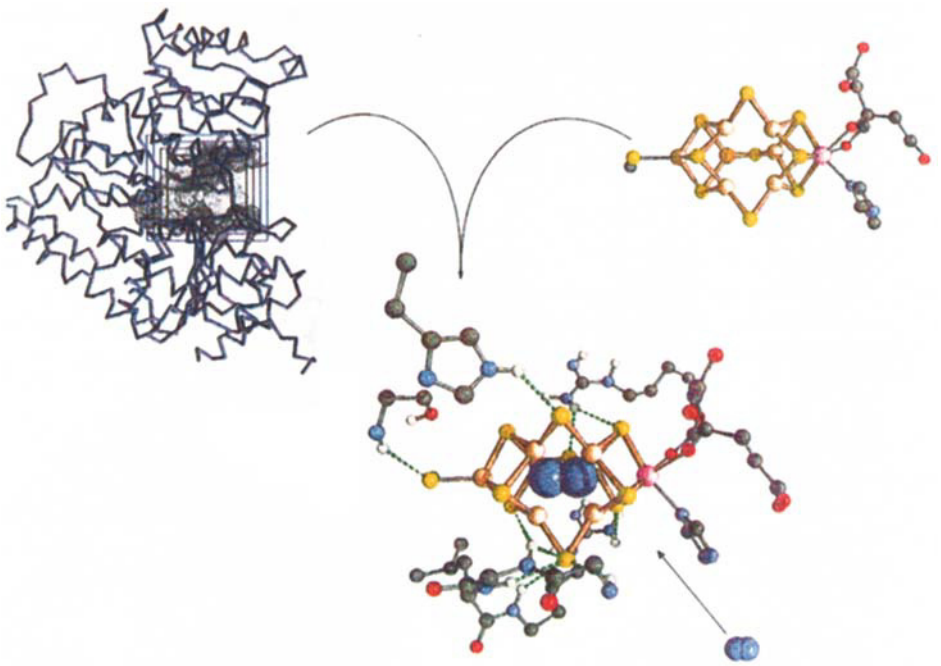

Fig. 39. Depiction of the host–guest relationships in the nitrogenase enzyme system, an "inorganic" double host–guest structure: the FeMo cofactor (i.e., the $MoFe_7S_9$/homocitrate cluster) acts as host for N_2 and simultaneously is formally incorporated as "guest" into the apoprotein.

5. Inorganic Host–Guest Chemistry and Bioinorganic Chemistry

Double host–guest systems, which have already been briefly mentioned in Section 3.6, also exist in the area of bioinorganic chemistry, for example in the form of the MoFe protein of the nitrogenase enzyme system with "fixed" nitrogen at the FeMo cofactor.[171] The principles governing the host–guest relationships of giant clusters apply likewise to these supramolecular aggregates, but in a somewhat modified form: The iron–molybdenum cofactor in the above-mentioned enzyme is synthesized by proteins using template-controlled syntheses. These proteins function to a certain extent as intermediate hosts. In the final step (formally speaking), the cofactor is incorporated as guest into the MoFe apoprotein.[171] This intermediary simple host–guest system, in turn, acts as host towards N_2, thus forming a bioinorganic double host–guest system: The protein hosts the cofactor, which contains a cavity, into which a guest can be incorporated, in this case the substrate N_2 (Fig. 39).[171] In contrast to the inorganic host–guest systems **56a**, **90a**, **91a**, **93a**, and **94a** (see Sections 3.2.1, 3.5, and 3.6), the components of this double bioinorganic host–guest structure can exist independently. In terms of the synergistic effects underlying the host–guest interactions, the nitrogenase system most likely resembles simple host–guest systems of the type $[(SCN)_9W_3S_4SnCl_3]^{6-}$ **78a** (see Section 3.2.2; the covalent bonds between the FeMo cofactor and the apoprotein by cystein and histidine have not been considered in this context). It is apparent that the concepts developed for inorganic host–guest chemistry through their application to biochemically relevant reaction processes can lead to first insights into the behavior of bioinorganic host–guest systems.

It is remarkable that the isolated cofactor, in contrast to the complete nitrogenase enzyme system, is not capable of reducing molecular nitrogen to NH_4^+ ions. But, once incorporated back into the apoprotein, the cofactor regains its full catalytic activity (cf. reconstitution test). The ability to reduce N_2 is, therefore, a new characteristic of the nitrogenase enzyme host–guest system, and not a property of its individual isolated components. The interaction of biosynthetic information carriers in the context of self-organization processes based on the initial properties of the individual components can lead, in the sense of emergent phenomena, to more complex host–guest systems with novel properties and new information content.

Another interesting example of a relevant bioinorganic host–guest system is ferritin,[172] an iron-storage protein that occurs in many higher organisms. Ferritin contains a core of about 4500 iron atoms and has a diameter of approximately 7.5 nm (its structure resembles the metastable mineral ferrihydrite and its stoichiometric composition that of an Fe^{III} hydroxydihydrogenphosphate $Fe_9O_9(OH)_8(H_2PO_4)$). This iron-containing core is enclosed by a protein shell that consists of 24 identical subunits (the whole structure has a diameter of about 12 nm). The subunits set up a spatial arrangement which is lined with channels. These channels serve to transport the iron atoms and, hence, have a *selective function* like their counterparts in zeolites. The nucleus formation (i.e. the nucleation phase) is most likely catalyzed by specific amino acid residues in the subunits of apoferritin and could start from an Fe^{III} oxide/hydroxide aggre-

gate.[172] Thus, this hypothetical "iron nucleus" would assume the *template function*. The subsequent growth phase, which leads to the formation of a quasi-crystalline assembly by a conservative self-organization process, is "terminated" by the finite size of the cavity. Formally speaking, ferritin is, therefore, an unusual host–guest system consisting of an organic host (the apoprotein) and a variable inorganic guest or guest system (the "iron" core). Depending on the external demand, "iron" can either be removed from this system or incorporated into it.

6 From Topology to Design of Supramolecular Compounds

The template-controlled linking of the simplest inorganic units can lead to a multitude of structures as is the case for the host–guest systems discussed in this article. In order to fully appreciate this variety of shapes, it is not enough to have an extensive knowledge of all interactions that regulate the concerted actions of host and guest fragments. During the analysis of structures, the boundary conditions that stem from metric and non-metric properties must also be considered. The methods of combinatorial topology and group theory should be utilized to determine which structures and shell formations (neglecting the terminal O atoms) are principally possible and which are not.[132b, 173] It was thus possible to demonstrate that the α-Keggin structure of the shell of the $[Mo_{12}O_{36}(PO_4)]^{3-}$ anion **80a** (Fig. 40 left) represents the only cluster shell which is

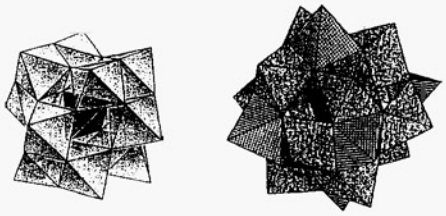

Fig. 40. Polyhedral representation of cluster anions with high symmetries which are built from MO_6 octahedra and exhibit a central O_4 tetrahedron: Left: $[Mo_{12}O_{36}(PO_4)]^{3-}$ **80a**; right: $[H_9V_{18}O_{42}(VO_4)]^{6-}$ **100a**.

formed by six octagons and eight hexagons *and* has tetrahedral symmetry.[174] A further example is given by the existence of a single polyhedron with tetrahedral symmetry and built up by eight hexagons and twenty-four rectangles, a structure that is found in the cluster shell of the anion **100a** (Fig. 40 right).[174, 175] On the other hand six rectangles, fourteen hexagons, and three octagons can form 539 different polyhedra with the lower D_{3h} symmetry.[174]

$[H_9V_{18}O_{42}(VO_4)]^{6-}$ **100a**

Evidently, such a combination of chemical knowledge, mathematical thinking, and computer methodology is also of significance for a synthetic strategy. For instance, the remarkable relationship between certain segments of the V_2O_5 layer structure and the surfaces of cluster shells of several polyoxovanadates (Fig. 41)[105, 143] can be used to gain an insight into the surface organization of host–guest systems, thus enabling the development of new ideas with respect to the prediction and

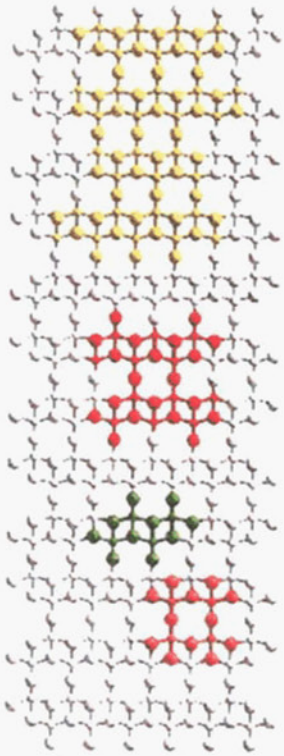

Fig. 41. Section of a layer of the V_2O_5 lattice; the terminal oxygen atoms are omitted (V small spheres, O large spheres). The $\{V_{30}O_{74}\}^{10-}$ cluster shell of **90a** can be derived from the yellow marked segment by removing the segment from one layer of the crystal lattice and linking these V–O segments in the appropriate manner (cf. ref. [143]). The same is valid for the $\{V_4O_{16}\}^{13-}$ shell of **82** and **83** (orange segment), the $\{V_{12}O_{32}\}^{4-}$ shell of **81** (red increment), and the $\{V_4O_{14}\}^{11-/12-}$ grouping [177] (green increment). The cluster shells $\{V_{15}O_{21}\}$, $\{V_{18}O_{24}\}$, and $\{V_{18}O_{28}\}$ of corresponding anions can also be interpreted as segments of the V_2O_5 layer structure [105].

discovery of novel supramolecular compounds. The application of the appropriate mathematical methods will not only contribute to the better understanding of the formation of metal–oxygen polyhedra, but also of other surface structures such as fullerenes.

Fullerenes are networks of sp^2-carbon atoms which are formed by 12 pentagons and n hexagons ($n > 1$; e.g., C_{60}: $n = 20$, C_{70}: $n = 25$). They resemble polyoxovanadates with respect to structure and cryptand functions. It is apparent that fullerenes, due to their large cavities, represent a promising starting point for a thus far largely unknown, but *preparatively accessible*, host–guest chemistry. The synthesis and characterization of endohedral fullerene complexes such as $Na_{12}C_{60}$, MC_{60}, MC_{70}, MC_{74}, (MC_{82}) (M = Y, Sc, La; Ce and other lanthanides), or La_2C_{82} indicate a rich potential for further developments.[176]

The variety of shapes that can be formed from oxygen atoms and/or metal centers is immense.[132b, 174] It is particularly remarkable that the 24 bridging oxygen atoms of two cluster shells with exactly the same stoichiometric composition $\{V_{18}O_{42}\}$ can appear either in the form of an Archimedean body (the O_{24} rhombicuboctahedron in $[H_9V_{18}O_{42}(VO_4)]^{6-}$ **100a**) or in that of the so-called "14th Archimedean body" (the O_{24} pseudo-rhombicuboctahedron in $[H_4V_{18}O_{42}(X)]^{9-}$ **66a–c** (see also ref. [8]).[119] Both cluster shells can formally be interconverted by the rotation of one half of the shell by 45° (see Fig. 42). Both types of polyhedra can also be formed, correspondingly by a Japanese cookie jar.[132a]

Topological considerations play an important role in the investigation of the template functions of multidimensional host structures that catalyze the generation of specific guest species such as zeolites (cf. Section 2.1.5). It would be advantageous to

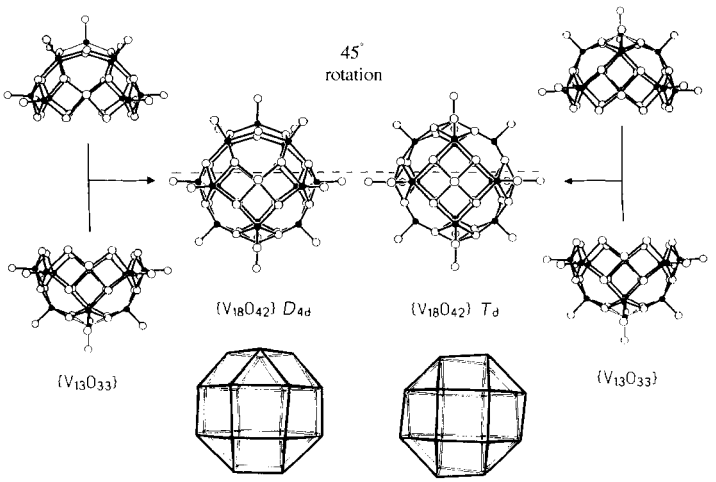

Fig. 42. Depiction of the $\{V_{18}O_{42}\}$ cluster shells in $[H_9V_{18}O_{42}(VO_4)]^{6-}$ in **100a** (right) and $[H_4V_{18}O_{42}(X)]^{9-}$ **66a–c** (left) using stick bonds (V black spheres, O white spheres) [119, 132a]. A rotation by 45° of one of the shell halves (the top part of the Japanese cookie jar mentioned in the main text) transforms the O_{24} rhombicuboctahedron (an Archimedean body) of the bridging oxygen atoms in **100a** into the O_{24} pseudo-rhombicuboctahedron (the so-called "14th Archimedean body") of the bridging oxygen atoms in **66a** (**81a** contains one VO group less than the $\{V_{13}\}$ fragment [8]).

know exactly how and why these reactions occur, and on what host–guest relationships they are based. This would enable the construction of a tailor-made host for the synthetic problem at hand.

7. Epilogue

"The sole task of the natural scientist is: to construct matter. (...) If the intent of a general theory of Nature would be to bring the infinite variations and depth of natural phenomena (...) to consciousness, it would have to be classified among the impossibilities."
F. W. J. Schelling[178]

The fundamental importance of chemistry for nearly all areas of science and even for society in general is nowadays rarely appreciated. However, the lack of appreciation for the importance of the sciences, and chemistry in particular, also appears to be a historical phenomenon, which can assume enormous significance in the context of a "rebelión de las masas". On May 8, 1794, Jean Baptiste Coffinhal, Vice-President of the Revolutionary Tribunal, decided on the fate of the chemist Antoine Laurent Lavoisier, who died on the guillotine the same day, with the following words: *"La République n'a besoin ni de savants ni de chimistes. Le cours de la justice ne sera pas interrompu."*[*] It therefore seems appropriate, along with the absolutely necessary intensive work in the laboratory, to recall the importance of the ideas of such men as Aristotle, Schelling, and Heisenberg. If the general public were to become aware of the importance and ubiquity of chemistry, the lack of acceptance, with which this science has to cope nowadays, would gradually disappear. Thus, let us recall the hylomorphism[180a] of Aristotle and the related scholastics, as well as Schelling's and others' romantic concepts of nature; this statement should, of course, be viewed within the context of the (contemporary) level of scientific knowledge at the particular time.[180b] We should attempt to find potentialities, propensities, or principles of material systems (e.g., in the sense of the results presented herein) in order to achieve a better understanding of how complex diversity arises from the linking of interacting basic structures (e.g., on the basis of reaction types that are of crucial relevance for both the (pure) material and biological world). Chemical research should consider principles and concepts that are of fundamental importance for events in the biosphere and also for the discovery of their primary causes; it should also consider terms of general importance such as complementarity,[181] emergence versus reduction,[182] intrinsic information, inherent properties of material systems, control, maybe even autopoiesis. Chemists have tended to forget that chemistry is a basic science. "He who has dedicated his life to the determination of individual connections and relations in nature is again and again, automatically, confronted by the question of how these individual connections fit harmoniously into the whole picture that is presented to us by *life* or the *world*."[183] We thus can and must (want to) learn from natural processes, also with respect to the development of new materials. In demand are substances with mesoscopic and supramolecular structures that exhibit novel complex interactions between their individual building blocks, which, in turn, can principally lead to ("unpredictable") emergent properties. In contrast to the "molecule-by-molecule" syntheses, these do not entail reactions that simply follow each other like a ceremonious changing of the guards, but rather which evolve one from the other in the sense of emerging developmental phenomena. The scientist is then challenged with respect to the possibility of reduction. The *dialectical unit of emergence and reduction* represents a guiding principle, which ought to be accepted as the essential basis for research, thinking, and comprehension in the area of empirical and semiempirical sciences. Even in our present special case of the formation and intentional creation of supramolecular inorganic host–guest systems, this "unit" can act as guiding principle: Small basic fragments with known properties can lead in the course of their reaction processes to very large complex (host–guest) aggregates with unexpected properties. We should realize that the mesoscopic area is relevant for information and functional carriers in nature.

The term *information*, according to the definition by Carl Friedrich von Weizsäcker ("Information is the measure of a certain amount of form. (...) Matter has form (...)."[184a]) can be used in this context to classify self-organization processes. In principle, reactions (processes) are based on the information that is stored —as previously noted by Monod[184b] —in the starting materials and on the type of interaction between these information carriers. Existing information thus creates new information: In chemical reactions, a growth phase can occur after a nucleation phase (as is the case, e.g., for the tobacco mosaic virus). This entails the opportunity to apply synthetic tricks or suitable strategies, depending on the information content, to further link large intermediates that have formed in the solution so as to finally yield giant systems such as those described in **93a** and **94a** (see Section 3.6). A simultaneous increase in the information content and the complexity as well as

[*] "The republic needs neither scholars nor chemists. The course of justice will not be halted" [179].

the differentiation on a nanoscale is observed. In terms of the validity of the algorithm "small becomes large and simple becomes complex", this corresponds to evolutionary processes in nature.

Conservative self-organization processes[137] play a major role during ontogenesis as non-gene-controlled reactions. Only a "clever" combination of dissipative and conservative self-organization, based on chance and necessity, could have initiated evolution within the possibility field of material systems. All real possibilities result from the preceding developments. This implies that there is no absolute, but only a relative chance.[185] The enormous importance of conservative processes, which in the final analysis lead to the multitude of appearances, has thus far not been realized in this context. For instance, the excellent writings of Eigen, Haken, and Prigogine lack detailed statements concerning the interacting dualism of conservative and dissipative self-organization.[186]

The ubiquity of chemical processes in our (pure) material and biological world is relevant for all areas of science. This fact must be acknowledged not only by the natural scientist, who, in the meantime, is in danger of becoming a slave to the modern trend towards specialization, but also by individuals concerned with the social sciences and humanities. It is, indeed, not surprising that on the one hand chemists ignore (or would like to do so) philosophical problems arising from the term matter, while on the other hand philosophers believe themselves to be able to investigate matter without any knowledge of chemistry whatsoever. (The philosophy of constructivism is of course in this context of no use.) An *extensive philosophy of chemistry* as companion to experimental chemistry which is itself always concerned with different kinds of interactions—maybe as causa finalis—would help to alleviate these deficiencies. (In fact, similar ideas were expressed by Boltzmann with respect to the necessary dialogue between philosophy and science.[187]) Only mutual interactions create that what could only be demonstrated here using a few simple examples, namely, the complexity of nature which is far from being understood in spite of the enormous growth of knowledge over the past few decades.

Dialogue poli entre un énergumène et un philosophe.[188]
L'Énergumène: *Qu'est-ce que la matière?*
Le Philosophe: *Je n'en sais pas grand'chose. Je la crois étendue, solide, résistante, gravitante, divisible, mobile; Dieu peut lui avoir donné mille autres qualités que j'ignore.*[*]
Voltaire

The financial support of the Fonds der Chemischen Industrie, the Deutsche Forschungsgemeinschaft, the Bundesministerium für Forschung und Technologie, and the state of Nordrhein-Westfalen (Bennigsen-Foerder Award; H. R.) is gratefully acknowledged. H. R. is indebted to Dr. R. Hundt (Bonn) for numerous discussions concerning the graphic depiction of crystal structures[190] *and his constant efforts to adapt his program KPLOT according to the results of these discussions. A. M. and S. D. thank Dipl.-Chem. H.-J. Westphal for preparing several of the figures, Dipl.-Chem. E. Krahn for his valuable assistance in preparing Section 5, as well as all co-workers mentioned in the references.*

Received: October 28, 1994
Revised version: June 22, 1995 [A 921E]
German version: *Angew. Chem.* **1995**, *107*, 2505–2539
Translated by Dr. W. C. Wilisch, Ansbach, Germany

[*] Polite discourse between a possessed man and a philosopher.
The possessed: *What is matter?*
The philosopher: *I do not know much about it, either. In my opinion it is spread out, firm, resistant, heavy, divisible, and mobile. The Lord might have given it a thousand further properties, of which I know nothing* [189].

[1] J.-M. Lehn, *Supramolecular Chemistry, Concepts and Perspectives*, VCH, Weinheim, **1995**.
[2] a) C. J. Pedersen, *J. Am. Chem. Soc.* **1967**, *89*, 2495, 7017; b) C. J. Pedersen, H. K. Frensdorff, *Angew. Chem.* **1972**, *84*, 16; *Angew. Chem. Int. Ed. Engl.* **1972**, *11*, 16.
[3] a) J.-M. Lehn, *Science* **1985**, *227*, 849; b) *Acc. Chem. Res.* **1978**, *11*, 49; c) *Pure Appl. Chem.* **1978**, *50*, 871.
[4] a) D. J. Cram, *Angew. Chem.* **1986**, *98*, 1041; *Angew. Chem. Int. Ed. Engl.* **1986**, *25*, 1039; b) *Host Guest Complex Chemistry I* (*Top. Curr. Chem.*, **1981**, *98*; Ed.: F. Vögtle); c) *Host Guest Complex Chemistry - Macrocycles - Synthesis, Structures, Applications* (Eds.: F. Vögtle, E. Weber) Springer, Berlin, **1985**.
[5] W. Kiggen, F. Vögtle, *Angew. Chem.* **1984**, *96*, 712; *Angew. Chem. Int. Ed. Engl.* **1984**, *23*, 714.
[6] J. Simon, J.-J. André, A. Skoulios, *New J. Chem.* **1986**, *10*, 295.
[7] Cf. G. R. Desiraju, *Angew. Chem.* **1995**, *107*, 2541; *Angew. Chem. Int. Ed. Engl.* **1995**, *34*, 2311.
[8] V. W. Day, W. G. Klemperer, O. M. Yaghi, *J. Am. Chem. Soc.* **1989**, *111*, 5959.
[9] This is an extension of the concept proposed by R. Schöllhorn, *Angew. Chem.* **1980**, *92*, 1015; *Angew. Chem. Int. Ed. Engl.* **1980**, *19*, 983.
[10] E. J. Corey, *Angew. Chem.* **1991**, *103*, 469; *Angew. Chem. Int. Ed. Engl.* **1991**, *30*, 455; S. Warren, *Designing Organic Syntheses – A Programmed Introduction to the Synthon Approach*, Wiley, Chichester, **1978**.
[11] This term was initially developed by Simard et al. to designate molecules that have the ability to form networks similar to H_2O (M. Simard, D. Su, J. D. Wuest, *J. Am. Chem. Soc.* **1991**, *113*, 4696). The definition proposed here implies that H_2O is the equivalent for a $^{[en]}T_4$-4P tecton, which is stable and can, therefore, also be utilized as an actual reagent.
[12] E. J. Corey, *Pure Appl. Chem.* **1967**, *14*, 19. While this term was initially used in its original meaning (cf. D. Seebach, *Angew. Chem.* **1979**, *91*, 259; *Angew. Chem. Int. Ed. Engl.* **1979**, *18*, 239), it was later applied in a more general sense (cf. E. J. Corey, *Chem. Soc. Rev.* **1988**, *17*, 111; D. Seebach, *Angew. Chem.* **1990**, *102*, 1363; *Angew. Chem. Int. Ed. Engl.* **1990**, *29*, 1320).
[13] Many tectons will be recognizable as building blocks known from structural chemistry. It is important, however, to distinguish here between the two terms: Tecton should only be used in the area of retrosynthesis, while building block (or structural unit) should only be used in the context of structural descriptions. But the term tecton could not be consequently used in this review, since the relevant description of most of the structures, in the context of planning the synthesis, is not possible according to current knowledge.
[14] One of the authors (H. R.) is currently conducting studies to clarify this question.
[15] a) G. M. Whitesides, J. P. Mathias, C. T. Seto, *Science* **1991**, *254*, 1312; b) J. S. Lindsey, *New J. Chem.* **1991**, *15*, 153.
[16] a) G. A. Jeffrey in ref. [16b], Chap. 5, p. 135; b) *Inclusion Compounds, Vol. 1, Structural Aspects of Inclusion Compounds Formed by Inorganic and Organometallic Host Lattices* (Eds.: J. L. Atwood, J. E. D. Davies, D. D. MacNicol), Academic Press, London, **1984**.
[17] H. Davy, *Philos. Trans. R. Soc. (London)* **1811**, *101*, 155 (from ref [16a]).
[18] M. Faraday, *Quart. J. Sci. Lit. Arts* **1823**, *15*, 71 (from ref [16a]).
[19] a) M. von Stackelberg, H. R. Müller, *Naturwissenschaften* **1951**, *38*, 456; b) H. R. Müller, M. von Stackelberg, *ibid.* **1952**, *39*, 20.
[20] A. F. Wells, *Structural Inorganic Chemistry*, 5th ed. Clarendon, Oxford, **1991**, p. 653ff.
[21] a) R. K. McMullan, G. A. Jeffrey, *J. Chem. Phys.* **1965**, *42*, 2725; b) F. Hollander, G. A. Jeffrey, *ibid.* **1977**, *66*, 4699.
[22] T. C. W. Mak, R. K. McMullan, *J. Chem. Phys.* **1965**, *42*, 2732.
[23] The *alkylamine hydrates* $m H_2O \cdot n$amine are closely related, both chemically and topologically, to the gas and liquid hydrates. In the few compounds that have been structurally characterized thus far, the host structure can be described within wide boundaries in analogy to the gas and liquid hydrates, that is, with the concept of face-linked water polyhedra. However, these polyhedra are very much more varied in the case of the alkylamine hydrates and the pentagonal dodecahedron, which is characteristic for the two other classes of compounds, is not found at all. There are only a few cases, such as the *tert*-butylamine hydrate $156\,H_2O \cdot 16\,t\mathrm{BuNH_2}$ (R. K. McMullan, T. H. Jordan, G. A. Jeffrey, *J. Chem. Phys.* **1967**, *47*, 1218), of real clathrates with only weak van der Waals interactions between guest and host. In most cases, the amine within a void is bound by hydrogen bonds to the framework of water molecules (e.g., propylamine hydrate $26\,H_2O \cdot 4\,n\mathrm{PrNH_2}$; cf. C. S. Brickenkamp, D. Panke, *J. Chem. Phys.* **1973**, *58*, 5284).

[24] J. L. Schlenker, F. G. Dwyer, E. E. Jenkins, W. J. Rohrbaugh, G. T. Kokotailo, W. M. Meier, *Nature* **1981**, *294*, 340.
[25] B. Kamb, *Science* **1965**, *148*, 232.
[26] J. Gallmeier, H. Schäfer, A. Weiss, *Z. Naturforsch. B* **1969**, *24*, 665.
[27] a) J. S. Kasper, P. Hagenmuller, M. Pouchard, C. Cros, *Science* **1965**, *150*, 1713; b) C. Cros, M. Pouchard, P. Hagenmuller, *J. Solid State Chem.* **1970**, *2*, 570.
[28] H. Menke, H. G. von Schnering, *Z. Anorg. Allg. Chem.* **1973**, *395*, 223.
[29] F. Liebau, *Structural Chemistry of Silicates – Structure, Bonding, and Classification*, Springer, Berlin, **1985**, p. 243.
[30] a) H. Gies, *Z. Kristallogr.* **1983**, *164*, 247; b) H. Gerke, H. Gies, *ibid.* **1984**, *166*, 11.
[31] F. Liebau, H. Gies, R. P. Gunawardane, B. Marler, *Zeolites* **1986**, *4*, 373.
[32] a) H. Gies in ref. [32b], Chap. 1, p. 1; b) *Inclusion Compounds, Vol. 5, Inorganic and Physical Aspects of Inclusion* (Eds.: J. L. Atwood, J. E. D. Davies, D. D. MacNicol), Oxford University Press, Oxford, **1991**.
[33] C. A. Fyfe, H. Gies, G. T. Kokotailo, C. Pasztor, H. Strobl, D. E. Cox, *J. Am. Chem. Soc.* **1989**, *111*, 2470.
[34] H. Gies, *Z. Kristallogr.* **1986**, *175*, 93.
[35] J. M. Newsam in *Solid State Chemistry – Compounds* (Eds.: A. K. Cheetham, P. Day), Clarendon, Oxford, **1992**, Chap. 7, p. 234.
[36] A. Tissler, U. Müller, K. K. Unger, *Nachr. Chem. Tech. Lab.* **1988**, *36*, 624.
[37] a) W. M. Meier, D. A. Olson, *Atlas of Zeolite Structure Types*, Butterworths, London, **1987**; b) J. V. Smith, *Chem. Rev.* **1988**, *88*, 149.
[38] a) L. Puppe, *Chem. Unserer Zeit* **1986**, *20*, 117; b) F. Schüth, *ibid.* **1995**, *29*, 42.
[39] J. Caro, F. Marlow, M. Wübbenhorst, *Adv. Mater.* **1994**, *6*, 413.
[40] S. T. Wilson, B. M. Lok, C. A. Messina, T. R. Cannan, E. M. Flanigen, *J. Am. Chem. Soc.* **1982**, *104*, 1146.
[41] B. M. Lok, C. A. Messina, R. L. Patton, R. T. Gajek, T. R. Cannan, E. M. Flanigen, *J. Am. Chem. Soc.* **1984**, *106*, 6092.
[42] W. Schnick, J. Lücke, *Angew. Chem.* **1992**, *104*, 208; *Angew. Chem. Int. Ed. Engl.* **1992**, *31*, 213.
[43] H. Bode, G. Teufer, *Acta Crystallogr.* **1955**, *8*, 611.
[44] New studies on ionic compounds of the type A_3X with large cations A (A. Müller, E. Diemann, E. Krickemeyer, H. Bögge, C. Menke, C. Kuhlmann, *Monatsh. Chem.*, in press) have shown that these ions form densely packed host structures which are mainly held together by van der Waals interactions. While these host structures cannot be compared topologically/structurally to classic clathrates, they do force the comparatively small anion into adapting its geometry to the cationic host matrix.
[45] a) W. Hesse, M. Jansen, *Z. Anorg. Allg. Chem.* **1991**, *595*, 115; b) R. K. McMullan, T. C. W. Mak, G. A. Jeffrey, *J. Chem. Phys.* **1966**, *44*, 2338.
[46] J.-H. Fuhrhop, *Bio-organische Chemie*, Thieme, Stuttgart, **1982**.
[47] F. Vögtle, *Supramolekulare Chemie*, 2nd ed., Teubner, Stuttgart, **1992**.
[48] M. D. Baker, J. Godber, G. A. Ozin, *J. Phys. Chem.* **1985**, *89*, 2299.
[49] N. Herron, Y. Wang, M. M. Eddy, G. D. Stucky, D. E. Cox, K. Moller, T. Bein, *J. Am. Chem. Soc.* **1989**, *111*, 530.
[50] G. A. Ozin, *Adv. Mater.* **1992**, *4*, 612.
[51] R. C. Haushalter, L. A. Mundi, *Chem. Mater.* **1992**, *4*, 31.
[52] An even more varied structural multitude is obtained when phosphonates or diphosphonates are employed instead of phosphates: V. Soghomonian, Q. Chen, R. C. Haushalter, J. Zubieta, *Angew. Chem.* **1995**, *107*, 229; *Angew. Chem. Int. Ed. Engl.* **1995**, *34*, 223.
[53] R. C. Haushalter, K. G. Strohmaier, F. W. Lai, *Science* **1989**, *246*, 1289.
[54] L. A. Mundi, K. G. Strohmaier, D. P. Goshorn, R. C. Haushalter, *J. Am. Chem. Soc.* **1990**, *112*, 8182.
[55] R. C. Haushalter, Z. Wang, M. E. Thompson, J. Zubieta, *Inorg. Chem.* **1993**, *32*, 3700.
[56] V. Soghomonian, Q. Chen, R. C. Haushalter, J. Zubieta, *Angew. Chem.* **1993**, *105*, 601; *Angew. Chem. Int. Ed. Engl.* **1993**, *32*, 610.
[57] T. Iwamoto in ref. [32b], Chap. 6, pp. 177.
[58] B. F. Hoskins, R. Robson, *J. Am. Chem. Soc.* **1990**, *112*, 1546.
[59] a) T. Kitazawa, S. Nishikiori, R. Kuroda, T. Iwamoto, *Chem. Lett.* **1988**, 1729; b) *ibid.* **1988**, 459.
[60] T. Kitazawa, S. Nishikiori, A. Yamagishi, R. Kuroda, T. Iwamoto, *J. Chem. Soc. Chem. Commun.* **1992**, 413.
[61] Cf. F. Hulliger in *Physics and Chemistry of Materials with Layered Structures, Vol. 5* (Ed.: F. Lévy), Reidel, Dordrecht, **1976**.
[62] Cf. recent review articles on this class of compounds: R. Csuk, B. I. Glänzer, A. Fürstner, *Adv. Organomet. Chem.* **1988**, *28*, 85; H. Selig, L. B. Ebert, *Adv. Inorg. Radiochem.* **1980**, *23*, 281.
[63] a) D. O'Hare in *Inorganic Materials* (Eds.: D. W. Bruce, D. O'Hare), Wiley, Chichester, **1992**, Chap. 4, p. 165; b) A. J. Jacobson in *Solid State Chemistry – Compounds* (Eds.: A. K. Cheetham, P. Day), Clarendon, Oxford, **1992**, Chap. 6, p. 182; c) R. Schöllhorn in ref. [16b], Chap. 7, p. 249.
[64] a) J. M. Thomas, C. R. Theocharis in ref. [32b], Chap. 4, p. 104; b) R. W. McCabe in *Inorganic Materials* (Eds.: D. W. Bruce, D. O'Hare), Wiley, Chichester, **1992**, Chap. 6, p. 295.
[65] J. M. Thomas, *Angew. Chem.* **1988**, *100*, 1735; *Angew. Chem. Int. Ed. Engl.* **1988**, *27*, 1673.
[66] a) M. S. Whittingham, *Prog. Solid State Chem.* **1978**, *12*, 41; b) G. V. Subba Rao, M. W. Shafer in ref. [66d], p. 99; c) J. Rouxel in ref. [66d], p. 201; d) *Physics and Chemistry of Materials with Layered Structures, Vol. 6, Intercalated Layered Materials* (Ed.: F. Lévy), Reidel, Dordrecht, **1979**.
[67] W. Rüdorff, *Chimia* **1965**, *19*, 489.
[68] L. F. Nazar, A. J. Jacobson, *J. Chem. Soc. Chem. Commun.* **1986**, 570.
[69] a) M. B. Dines, *Science* **1975**, *188*, 1210; b) R. P. Clement, W. B. Davies, K. A. Ford, M. L. H. Green, A. J. Jacobson, *Inorg. Chem.* **1978**, *17*, 2754.
[70] R. Brec, *Solid State Ionics* **1986**, *22*, 3.
[71] G. Ouvrard, R. Brec, J. Rouxel, *Mater. Res. Bull.* **1985**, *20*, 1181.
[72] a) R. Clement, M. L. H. Green, *J. Chem. Soc. Dalton Trans.* **1979**, 1566; b) R. Clement, *J. Chem. Soc. Chem. Commun.* **1980**, 647; c) *J. Am. Chem. Soc.* **1981**, *103*, 6998; d) R. Clement, O. Garnier, J. Jegoudez, *Inorg. Chem.* **1986**, *25*, 1404; e) R. Clement, J.-P. Audiere, J.-P. Renard, *Rev. Chim. Miner.* **1982**, *19*, 560.
[73] a) T. Iwamoto in ref. [32b], Chap. 6, p. 177; b) T. Iwamoto in ref. [16b], Chap. 2, p. 29.
[74] K. A. Hofmann, F. Küspert, *Z. Anorg. Chem.* **1897**, *15*, 204.
[75] J. H. Rayner, H. M. Powell, *J. Chem. Soc.* **1952**, 319.
[76] K.-M. Park, R. Kuroda, T. Iwamoto, *Angew. Chem.* **1993**, *105*, 939; *Angew. Chem. Int. Ed. Engl.* **1993**, *32*, 884.
[77] D. D. DesMarteau, T. Grelbig, S.-H. Hwang, K. Seppelt, *Angew. Chem.* **1990**, *102*, 1519; *Angew. Chem. Int. Ed. Engl.* **1990**, *29*, 1448.
[78] G. Alberti, U. Costantino in ref. [32b], Chap. 5, p. 136.
[79] a) A. Clearfield, G. D. Smith, *Inorg. Chem.* **1969**, *8*, 431; b) J. M. Troup, A. Clearfield, *Inorg. Chem.* **1977**, *16*, 3311.
[80] A. Nørlund Christensen, E. Krogh Andersen, I. G. Krogh Andersen, G. Alberti, M. Nielsen, M. S. Lehmann, *Acta Chem. Scand.* **1990**, *44*, 865.
[81] G. Alberti, M. Casciola, R. Vivani, R. K. Biswas, *Inorg. Chem.* **1993**, *32*, 4600.
[82] G. Alberti, U. Costantino, F. Marmottini, R. Vivani, P. Zappelli, *Angew. Chem.* **1993**, *105*, 1396; *Angew. Chem. Int. Ed. Engl.* **1993**, *32*, 1357.
[83] E. W. Corcoran, Jr., *Inorg. Chem.* **1990**, *29*, 157.
[84] R. C. Haushalter, Z. Wang, M. E. Thompson, J. Zubieta, C. J. O'Connor, *Inorg. Chem.* **1993**, *32*, 3966.
[85] T. Okada, *Proc. Phys. Soc. Japan* **1949**, *4*, 140 [*Chem. Abstr.* **1950**, *44*, 10434].
[86] E. Cannillo, F. Mazzi, G. Rossi, *Acta Crystallogr.* **1966**, *21*, 200.
[87] H. Thurn, H. Krebs, *Acta Crystallogr. Sect. B* **1969**, *25*, 125.
[88] Cf.: O. Ermer, L. Lindenberg, *Helv. Chim. Acta* **1991**, *74*, 825.
[89] B. F. Hoskins, R. Robson, N. V. Y. Scarlett, *Angew. Chem.* **1995**, *107*, 1317; *Angew. Chem. Int. Ed. Engl.* **1995**, *34*, 1203.
[90] S. B. Copp, S. Subramanian, M. J. Zaworotko, *Angew. Chem.* **1993**, *105*, 755; *Angew. Chem. Int. Ed. Engl.* **1993**, *32*, 706.
[91] S. B. Copp, S. Subramanian, M. J. Zaworotko, *J. Am. Chem. Soc.* **1992**, *114*, 8719.
[92] M. Potel, R. Chevrel, M. Sergent, *Acta Crystallogr. Sect. B* **1980**, *36*, 1545.
[93] L. A. Mundi, R. C. Haushalter, *J. Am. Chem. Soc.* **1991**, *113*, 6340.
[94] V. Soghomonian, Q. Chen, R. C. Haushalter, J. Zubieta, C. J. O'Connor, *Science* **1993**, *259*, 1596.
[95] R. Blachnik, M. Lytze, H. Reuter, unpublished results.
[96] K. L. Aurivillius, *Acta Chem. Scand.* **1950**, *4*, 1413.
[97] J. Andersson, *Acta Chem. Scand. Ser. A* **1975**, *29*, 956.
[98] Cf. the definition for "mesoscopic", to be found in, for example, R. W. Siegel, *Physics Today* **1993**, *46*, *no.10*, 64.
[99] Cf. the definitions of terms, such as *container*, *carcerand*, and *cavitand*, that have recently been introduced into supramolecular host–guest chemistry by D. J. Cram, *Nature* **1992**, *356*, 29 and F. Vögtle (see ref. [47]). Here, however, definitions of terms based on the classification by Vögtle (ref. [47], p. 48) of neutral organic ligands according to topological aspects are sufficient: Monocyclic ligands should be called *coronands* (*crown ethers* are coronands that exclusively contain ether-type oxygen atoms), while oligocyclic, spherical ligands should be called *cryptands*.
[100] M. I. Khan, A. Müller, S. Dillinger, H. Bögge, Q. Chen, J. Zubieta, *Angew. Chem.* **1993**, *105*, 1811; *Angew. Chem. Int. Ed. Engl.* **1993**, *32*, 1780.
[101] M. T. Pope, A. Müller, *Angew. Chem.* **1991**, *103*, 56; *Angew. Chem. Int. Ed. Engl.* **1991**, *30*, 34.
[102] The calculated sum of the bond valences indicates that the twelve μ_2-O atoms, each of which bridges two Mo^V centers of two neighboring Mo_2^V dumbbells are, in fact, μ_2-bridging hydroxyl groups. These form hydrogen bonds (270 pm) to the oxygen atoms of the $\{Mo^{VI}O_3\}$ moieties. This shows that the highly negatively charged, nucleophilic central $\{Mo_{12}O_{40}\}^{20-}$ unit is stabilized by both protonation and aggregation with electrophilic $\{Mo^{VI}O_3\}$ groups. The hydrogen bonds apparently play a crucial role in this stabilization.
[103] M. I. Khan, J. Zubieta, *J. Am. Chem. Soc.* **1992**, *114*, 10058.
[104] H. Reuter, *Angew. Chem.* **1991**, *103*, 1487; *Angew. Chem. Int. Ed. Engl.* **1991**, *30*, 1482; *ibid.* **1992**, *104*, 1210 and **1992**, *31*, 1185.
[105] A. Müller, R. Rohlfing, E. Krickemeyer, H. Bögge, *Angew. Chem.* **1993**, *105*, 916; *Angew. Chem. Int. Ed. Engl.* **1993**, *32*, 909. This article also discusses the limitations of the complementarity principle.
[106] A. Müller, *Nature* **1991**, *352*, 115; P. C. H. Mitchell, *ibid.* **1991**, *348*, 15.

[107] A. Müller, E. Krickemeyer, M. Penk, R. Rohlfing, A. Armatage, H. Bögge, *Angew. Chem.* **1991**, *103*, 1720; *Angew. Chem. Int. Ed. Engl.* **1991**, *30*, 1674.

[108] A. Müller, R. Rohlfing, J. Döring, M. Penk, *Angew. Chem.* **1991**, *103*, 575; *Angew. Chem. Int. Ed. Engl.* **1991**, *30*, 588.

[109] A. Müller, K. Hovemeier, R. Rohlfing, *Angew. Chem.* **1992**, *104*, 1214; *Angew. Chem. Int. Ed. Engl.* **1992**, *31*, 1192.

[110] A. Müller, K. Schmitz, E. Krickemeyer, M. Penk, H. Bögge, *Angew. Chem.* **1986**, *98*, 470; *Angew. Chem. Int. Ed. Engl.* **1986**, *25*, 453.

[111] a) J.-F. You, B. S. Snyder, G. C. Papaefthymiou, R. H. Holm, *J. Am. Chem. Soc.* **1990**, *112*, 1067; b) J.-F. You, G. C. Papaefthymiou, R. H. Holm, *J. Am. Chem. Soc.* **1992**, *114*, 2697. It might be interesting to study intensively the possible exchange of the encapsulated Na^+ ions in the anions **59a**, **59b**, and **60a** in order to verify our classification of "closed" hosts.

[112] M. Leyrie, G. Hervé, *New J. Chem.* **1978**, *2*, 233.

[113] M. Leyrie, R. Thouvenot, A. Tézé, G. Hervé, *New J. Chem.* **1992**, *16*, 475.

[114] F. Robert, M. Leyrie, G. Hervé, A. Tézé, Y. Jeannin, *Inorg. Chem.* **1980**, *19*, 1746.

[115] J. Fischer, L. Ricard, R. Weiss, *J. Am. Chem. Soc.* **1976**, *98*, 3050.

[116] M. H. Alizadeh, S. P. Harmalker, Y. Jeannin, J. Martin-Frère, M. T. Pope, *J. Am. Chem. Soc.* **1985**, *107*, 2662; I. Creaser, M. C. Heckel, J. R. Neitz, M. T. Pope, *Inorg. Chem.* **1993**, *32*, 1573.

[117] A. Müller, H.-J. Westphal, K. Hovemeier, E. Krickemeyer, H. Bögge, unpublished results. Cf. the similar oxovanadiumphenylphosphonate in ref. [177].

[118] F. W. J. Schelling, *Ideen zu einer Philosophie der Natur (1797)* in *Schellings Werke* (Ed.: M. Schröter), Erster Ergänzungsband zur Naturphilosophie 1792–1803, Beck'sche Verlagsbuchhandlung, München, **1956**, p. 77.

[119] A. Müller, M. Penk, R. Rohlfing, E. Krickemeyer, J. Döring, *Angew. Chem.* **1990**, *102*, 927; *Angew. Chem. Int. Ed. Engl.* **1990**, *29*, 926.

[120] A. Müller, F. Diemann, E. Krickemeyer, S. Che, *Naturwissenschaften* **1993**, *80*, 77.

[121] The increase of the proportion of V^V centers leads principally to a larger attraction between shell and central anion and can even lead to the formation of smaller shells like $\{V^V_2V^{IV}_8O_{36}\}^{5-}$ with an incorporated Cl^- or Br^- ion; cf. A. Müller, E. Krickemeyer, M. Penk, H.-J. Walberg, H. Bögge, *Angew. Chem.* **1987**, *99*, 1060; *Angew. Chem. Int. Ed. Engl.* **1987**, *26*, 1045.

[122] a) A. Müller, F. Diemann, C. Menke, unpublished; b) A. Müller, D. Sölter, unpublished.

[123] The reaction conditions employed are of prime importance. For instance, the cluster anions $[V^{IV}_{18}O_{42}(H_2O)]^{12-}$ **72a** [124, 125] and $[H_4V_{18}O_{42}(X)]^{9-}$ **66a–c** [119] (X = Cl, **66a**; Br, **66b**; I, **66c**) are formed at different pH values: While **66a** is formed as the sole product at a pH value of 8, at pH = 14 only **72a** is formed from the same reaction mixture (i.e., despite the presence of chloride ions). This result raises, principally, the question whether **72** might not be the mixed-valent species $K_{12}[V^{IV}_{17}V^{V}O_{42}(OH)]\cdot 15H_2O$ with an encapsulated OH^- ion rather than $K_{12}[V^{IV}_{18}O_{42}(H_2O)]\cdot 15H_2O$ **72**. In this context, it must be noted that neither X-ray crystal structure analyses, nor elemental analyses including manganometric titrations can distinguish for example between $\{V^{IV}_{18}O_{42}\}$ and $\{V^{IV}_{17}V^{V}O_{42}\}$ host shells (it has to be assumed that the incorporation of a negatively charged guest into a $\{V_{18}O_{42}\}$ shell is inhibited when only V^{IV} centers are present). Compounds which contain different numbers of disordered H atoms but otherwise have identical stoichiometries, such as $K_9[H_4V^{IV}_{18}O_{42}(Cl)]$, $K_9[H_3V^{IV}_{17}V^{V}O_{42}(Cl)]$, and $K_9[H_2V^{IV}_{16}V^{V}_2O_{42}(Cl)]$ can, according to current knowledge, predominantly be distinguished by ESR and magnetic susceptibility measurements. (This gives evidence for the abundance of $\{V^{IV}_{16}V^{V}_2\}$ shells in the case of **66a–c**). In the meantime, we have been able – in contrast to earlier work (cf. ref. [124])—to determine the exact number of cations in the compound with the anion **72a** by X-ray crystallography, a prerequisite to solve the problem at hand. The (correct) formula of **72** was estimated in ref. [124] and only recently proven in ref. [125] (see comments in ref. [131a], p. 39).

[124] G. K. Johnson, E. O. Schlemper, *J. Am. Chem. Soc.* **1978**, *100*, 3645.

[125] a) A. Müller, H.-J. Westphal, J. Meyer, H. Bögge, D. Gatteschi, unpublished; b) A. Müller, E. Krickemeyer, H. Bögge, unpublished.

[126] X. Yang, C. B. Knobler, M. F. Hawthorne, *Angew. Chem.* **1991**, *103*, 1519; *Angew. Chem. Int. Ed. Engl.* **1991**, *30*, 1507.

[127] X. Yang, C. B. Knobler, M. F. Hawthorne, *J. Am. Chem. Soc.* **1992**, *114*, 380.

[128] The reaction of **76** with $[(C_6H_5)_4As]Cl$ does not lead to a halide ion exchange but to the formation of the compound **77** [127]. ^{199}Hg NMR studies, however, indicate that in acetone the anion **74a** can be transformed into anion **76a** by the addition of $[nBu_4N]I$.

$[(C_6H_5)_4As]_2[(HgC_2B_{10}H_{10})_4I_2]$ **77**

[129] A. Müller, V. P. Fedin, E. Diemann, H. Bögge, E. Krickemeyer, D. Sölter, A. M. Giuliani, R. Barbieri, P. Adler, *Inorg. Chem.* **1994**, *33*, 2243.

[130] A. Müller, E. Krickemeyer, S. Dillinger, H. Bögge, A. Stammler, *J. Chem. Soc. Chem. Commun.* **1994**, 2539.

[131] a) Cf. M. T. Pope, *Heteropoly and Isopoly Oxometalates*, Springer, Berlin, **1983**; *Nature* **1992**, *355*, 27; b) The cluster anion **79a** can be derived from an O_{24} rhombicuboctahedron, one of the 13 Archimedean bodies (see also ref. [132]), by capping its twelve [110]-O_4 faces with four VO^{2+}, six MoO^{4+}, and two As_2O^{4+} units, and three of its six [100]-O_4 faces with a VO^{2+} group (Fig. 27). Formally speaking, the highly negatively charged pseudo-α-Keggin ion **79c** is stabilized in solution by the VO^{2+} moieties occupying the [100]-O_4 faces (see also ref. [133]).

$\{Mo^{VI}_6V^{IV}_4(As^{III}_2O)_2O_{34}(SO_4)\}^{10-}$ **79c**

[132] a) A. Müller, M. Penk, *Chem. Unserer Zeit* **1990**, *24*, 258; b) A. Müller, M. Penk, J. Döring, *Inorg. Chem.* **1991**, *30*, 4935; see also ref. [8].

[133] It should be noted in this context that in the host–guest systems $[H_4V_{18}O_{42}(X)]^{9-}$ **66a–c** [119] the V^{IV} centers exclusively form square VO_5 pyramids, while in the cluster anion $[Mo_{12}O_{36}(PO_4)]^{3-}$ **80a**, the Mo^{VI} atoms are all present in the form of MoO_6 octahedra. In addition, in **80a**, the interaction of the oxygen atoms of the formally encapsulated PO_4^{3-} tetrahedron with the neighboring Mo^{VI} centers is so strong that one can no longer talk about a host–guest interaction. On this basis, the encapsulated sulfate ion of **79a** occupies an intermediate position with respect to its nucleophilicity and basicity between the halide ions of **66a–c** and the phosphate ion of **80a**. This correlates with the fact that the extremely different interactions present in the host–guest system **66a–c** and the anion **80a** cannot fully develop between the isopolyoxometalate shell and the central unit in the cluster anion **79a**. Hence, **79a** occupies an intermediate position between the anions **66a** and **80a**. The strong interaction of the Mo^{VI} centers Mo5 and Mo6 with the oxygen atoms O42 and O43 (see Fig. 27) of the central sulfate ion causes the electron density at the two other oxygen atoms O40 and O41 to be reduced. Thus O40 and O41 can—even for this reason –only weakly interact with the V^{IV} centers which is evident from the corresponding distances. Only this combination of weak and strong interactions appears to enable the formation of **79a**, with its unusually low C_2 symmetry.

[134] W. Priebsch, D. Rehder, M. von Oeynhausen, *Chem. Ber.* **1991**, *124*, 761. In this report, compound **82** was incorrectly described as a $(V^V)_4$ cluster with a $V_4(\mu_2\text{-}O)_4$ central core. However, **82**, in fact, is a $V^{IV}(V^V)_3$ cluster with a central $V_4(\mu_2\text{-}O)_3(\mu_2\text{-}OH)$ group. Cf. the authors' correction in ref. [135].

[135] D. Rehder in *Polyoxometalates: From Platonic Solids to Anti-Retroviral Activity* (Eds.: M. T. Pope, A. Müller), Kluwer, Dordrecht, **1994**.

[136] D. D. Heinrich, K. Folting, W. E. Streib, J. C. Huffman, G. Christou, *J. Chem. Soc. Chem. Commun.* **1989**, 1411.

[137] In this case, the term "self-organization" is applied to the phenomenon of the spontaneous formation of "ordered" structures in or close to equilibrium conditions. This is generally termed "conservative self-organization". During the syntheses of the cluster anions **84a** or $[V_{34}O_{82}]^{10-}$ **90a** (see Section 3.5) the "ordered" cluster structures are presumably formed by the influence of an initially formed moiety (possible examples are the cation/anion aggregate $(2NH_4^+, 2Cl^-)$ of **84a** or the central $\{V_4O_4\}(O_{term})_4$ cube in **90a**), which directs and "reinforces" the subsequent condensation processes. Because of weak interactions the central cores act as templates which determine, by a process of "molecular recognition", the symmetry, form, and structure of the cluster shells (see Sections 3.2.2, 3.3, and 3.5). This special case of a conservative self-organization process can thus be called a template-directed or "induced self-organization". The term "conservative self-organization" can also be formally applied to magnetic systems, such as the host–guest system $[V_{15}As_6O_{42}(H_2O)]^{6-}$ **99a** (see Section 4.1) which at low temperatures, exhibit layers of different magnetization. Another interesting aspect in the context of conservative self-organization processes is the following: The directing agent correlates the fragments, or "enslaves" them by forcing them into a certain system or order. But the term "correlation" is generally applied to dissipative structures by Prigogine: "The equilibrium state is a singular condition, in which the correlation between different parts of the system is zero." (cited from: I. Prigogine, I. Stengers in *Selbstorganisation, Bd. I*, (Eds.: U. Niedersen, L. Pohlmann) Duncker & Humblot, Berlin, **1990**, p. 3). In contrast to conservative self-organization processes, the term "dissipative self-organization" is applied to nonlinear, irreversible processes, which operate far from equilibrium and lead through the cooperative interactions of subsystems to the complex structures of the final system. A well-known example for such a dissipative self-organization process in chemistry is the Belousov–Zhabotinsky reaction.

[138] M. I. Khan, J. Zubieta, *Angew. Chem.* **1994**, *106*, 784; *Angew. Chem. Int. Ed. Engl.* **1994**, *33*, 760.

[139] The exchange of the contents of the two truncated cones occurs in the following manner: **86** has a closed, nano-sized cavity with two attached open truncated cones (or ion channels), formed by the phenyl rings. Within each of the two truncated cones, there is a sodium ion with two coordinated water molecules and one dimethylformamide molecule. The distorted octahedral environment of the Na^+ ion is completed by two oxygen atoms of the coronand (a nucleophilic shell fragment of the [16]crown-8 type, built from four $(Ph\text{-}PO_2)$ units and four vanadium atoms) as well as by a water molecule positioned in the center of the coronand. If **86** is treated with an approximately thirteenfold excess of rubidium bromide in a 1:1.3 mixture of water and dimethylformamide, one obtains the compound **87**. In the center of the coronand of **87** there is now, instead of the water molecule in **86**, a Rb^+ ion which in contrast to the Na^+ ion, fits exactly into the coronand. This exchange of guests in the truncated cones of **86** leads to a significant reorganization and migration of the particles in the central cavity: During the reaction a water

molecule "migrates" from its position in **86** to the new position in **87**, where it serves as a bridging function between two vanadium centers. The azide ion "orients" itself between the electrophilic centers (the V^V atom of the $\{V_5O_9\}^{3+}$ unit and the Rb^+ ion in the center of the coronand). Hence, the reaction **86** → **87** occurs under retention of the host lattice (A. Müller, K. Hovemeier, E. Krickemeyer, H. Bögge, *Angew. Chem.* **1995**, *107*, 857; *Angew. Chem. Int. Ed. Engl.* **1995**, *34*, 779). A further proof for the stability of the cluster anions derived from $[V_{14}O_{22}(OH)_4(H_2O)_2(PhPO_3)_8]^{6-}$ **84b** lies in the isolation of the oxidized anion **88a**. One obtains **88a** by the air oxidation of the species **89a**; all V^{IV} atoms of the electrophilic $\{V_5O_9\}^{3+}$ unit of **89a** are oxidized to V^V

$[2\,Rb^+, 2\,Cl^- \subset V_{12}O_{20}(OH)_4(H_2O)_2(PhPO_3)_8]^{4-}$ **88a**
$[2\,Rb^+, 2\,Cl^- \subset V_{14}O_{22}(OH)_4(H_2O)_2(PhPO_3)_8]^{6-}$ **89a**

centers and the $\{V^V{=}O\}^{3+}$ caps contained in **89a** are cleaved off (A. Müller, K. Hovemeier, H. Bögge, unpublished results). (The symbol ⊂ from set theory is only used for guests which represent aggregates.)

[140] M. L. Connolly, *Science* **1983**, *221*, 709; M. L. Connolly, *J. Appl. Cryst.* **1983**, *16*, 548.

[141] Cited by Aristotle, *De generatione animalium*, V 8. 789b, 2f. See also F. Jürss, *Griechische Atomisten*, Reclam, Leipzig, **1977**, p. 129, with respect to the Aristotelian works *De generatione animalium* and *Physica* (cf. in particular II 4, 195b 36ff.).

[142] The term "cluster within a cluster" appears justified to us in the case of **90a** due to the presence of $V{=}O_{term}$ groups in the central $\{V_4^{IV}O_4\}(O_{term})_4$ cube (with the stoichiometry of $V^{IV}O_2$; cf. ref. [108]). (The cluster definition used here corresponds to the usual procedure with respect to the topological and electronic requirements; the metal–metal interactions can vary from weak to strong.) The dark blue amphoteric VO_2 can be precipitated from the aqueous solution (cf. ref. [108]).

[143] W.G. Klemperer, T. A. Marquart, O. M. Yaghi, *Angew. Chem.* **1992**, *104*, 51; *Angew. Chem. Int. Ed. Engl.* **1992**, *31*, 49.

[144] Similar arguments are valid for the anion $[Na(H_2O)_3Mo_{42}H_{15}O_{109}\{(OCH_2)_3(CCH_2OH)\}_7]^{7-}$ **56a** [103], which has a structure that differs from that of **91a** in that all seven $[(CH_2)_3CCH_3]^{3+}$ groups have been replaced by the corresponding number of $[(CH_2)_3CCH_2OH]^{3+}$ units and that the facial $\{Mo^{VI}O_3\}$ group, which is a remnant of the original $\{Mo_{16}O_{52}\}$ framework of **54a**, has been substituted with a $\{Na(H_2O)_3\}^+$ group (see also H. K. Chae, W. G. Klemperer, T. A. Marquart, *Coord. Chem. Rev.* **1993**, *128*, 209). The cluster anions **54a** and **55a** are, in turn, built up of $\{Mo_2^V\}_3$ hexagons. These can be "intercepted" under the right reaction conditions (given the required template *and* the appropriate Mo^V/Mo^{VI} ratio), as is demonstrated by the synthesis of **92**. Compounds **54**, **55**, and **92** contain formally the same $\{(Mo_2^VO_4)_3(\mu_2\text{-}OH)_3\}^{3+}$ units [145].

$Na_7(N_2H_4)_2[Na\{(Mo_2^V)_3O_{12}(\mu_2\text{-}OH)_3(PhPO_3)_3(PhPO_3H)\}_2]\cdot 26\,H_2O$ **92**

[145] A. Müller, S. Dillinger, H. Bögge, unpublished results. The cluster aggregate **92a** contained in **92** exhibits two $(Mo_2^V)_3$ units, which are linked by a

$[Na\{(Mo_2^V)_3O_{12}(\mu_2\text{-}OH)_3(PhPO_3)_3(PhPO_3H)\}_2]^{7-}$ **92a**

Na^+ ion in the crystal; cf. the similarly structured, sandwich-type compound $Na_3(H_3O)_4[NEt_4]_2[Na\{(Mo_2^V)_3O_{15}(PhPO_3)(PhPO_3H)_3\}_2]\cdot 14\,H_2O$ in G. Cao, R. C. Haushalter, K. G. Strohmaier, *Inorg. Chem.* **1993**, *32*, 127. In this direct self-organization process, the phenylphosphonic acid (component 1) directs the synthesis of **92** in concert with Na^+ ions (component 2). The reaction occurs under reducing conditions ($Mo^V/Mo^{VI} = 12{:}0$). If one of those two components is lacking, the anion **54a** is formed when the Mo^V/Mo^{VI} ratio is adjusted appropriately (3:1).

[146] A. Müller, H. Bögge, E. Krickemeyer, S. Dillinger, *Bull. Pol. Acad. Sci. (Chem.)* **1994**, *42*, 291.

[147] A. Müller, E. Krickemeyer, S. Dillinger, H. Bögge, W. Plass, A. Proust, L. Dloczik, C. Menke, J. Meyer, R. Rohlfing, *Z. Anorg. Allg. Chem.* **1994**, *620*, 599.

[148] A. Müller, W. Plass, E. Krickemeyer, S. Dillinger, H. Bögge, A. Armatage, A. Proust, C. Beugholt, U. Bergmann, *Angew. Chem.* **1994**, *106*, 897; *Angew. Chem. Int. Ed. Engl.* **1994**, *33*, 849.

[149] A. Müller, W. Plass, E. Krickemeyer, S. Dillinger, H. Bögge, A. Armatage, C. Beugholt, U. Bergmann, *Monatsh. Chem.* **1994**, *125*, 525.

[150] a) A. Müller, W. Plass, *J. Mol. Struct.* **1994**, *321*, 215; b) D. Gatteschi, R. Sessoli, W. Plass, A. Müller, E. Krickemeyer, D. Sölter, P. Adler, *Inorg. Chem.*, in press.

[151] S.-W. Zhang, G.-Q. Huang, M.-S. Shao, Y.-Q. Tang, *J. Chem. Soc. Chem. Commun.* **1993**, 37 (incorrect data).

[152] G.-Q. Huang, S.-W. Zhang, M.-S. Shao, *Polyhedron* **1993**, *12*, 2067 (incorrect data).

[153] S.-W. Zhang, D.-Q. Liao, M.-S. Shao, Y.-Q. Tang, *J. Chem. Soc. Chem. Commun.* **1986**, 835 (incorrect data).

[154] In a formal sense, the $\{Mo_{17}\}$ units can be derived either from heptamolybdate-like $\{Mo_7\}$ fragments, which contain two $(MoNO)^{3+}$ groups instead of $(MoO)^{4+}$ units or from two $\{Mo_8\}$ units linked by an Mo atom.

[155] a) The six-membered H_2O rings located in the cavity of **93a** and **94a** represent structural elements that are similar to those found in one of the modifications of ice. These six-membered rings might, therefore, in principle, act as templates for the formation of the cluster shells of these giant anions. b) Cf. also the [12]crown-4 complex of LiSCN in the cavity of γ-cyclodextrin (S. Kamitori, K. Hirotsu, T. Higuchi, *J. Am. Chem. Soc.* **1987**, 109, 2409).

[156] G. W. F. Hegel, *Gesammelte Werke*, *Vol. 20*, Meiner, Hamburg, **1992**, p. 238.

[157] G. Schmid, R. Pfeil, R. Boese, F. Bandermann, S. Meyer, G. H. M. Calis, J. W. A. van der Velden, *Chem. Ber.* **1981**, *114*, 3634; G. Schmid, W. Huster, *Z. Naturforsch. B* **1986**, *41*, 1028.

[158] G. Schmid, B. Morun, J.-O. Malm, *Angew. Chem.* **1989**, *101*, 772; *Angew. Chem. Int. Ed. Engl.* **1989**, *28*, 779.

[159] M. N. Vargaftik, V. P. Zagorodnikov, I. P. Stolyarov, I. A. Moiseev, V. A. Likholobov, D. I. Kochubey, A. L. Chuvilin, V. I. Zaikovsky, K. I. Zamaraev, G. I. Timofeeva, *J. Chem. Soc. Chem. Commun.* **1985**, 937; G. Schmid, *Nachr. Chem. Tech. Lab.* **1987**, *34*, 249.

[160] G. Schmid, *Chem. Unserer Zeit* **1988**, *22*, 85; *Endeavour, New Ser.* **1990**, *14*, 172; *Chem. Rev.* **1992**, *92*, 1709.

[161] G. Schmid, N. Klein, *Angew. Chem.* **1986**, *98*, 910; *Angew. Chem. Int. Ed. Engl.* **1986**, *25*, 922.

[162] H. Fraenkel-Conrat, R. C. Williams, *Proc. Natl. Acad. Sci. USA* **1955**, *41*, 690.

[163] A. Müller, J. Döring, *Z. Anorg. Allg. Chem.* **1991**, *595*, 251.

[164] A. Müller, J. Döring, *Angew. Chem.* **1988**, *100*, 1789; *Angew. Chem. Int. Ed. Engl.* **1988**, *27*, 1721.

[165] D. Gatteschi, L. Pardi, A.-L. Barra, A. Müller, J. Döring, *Nature* **1991**, *354*, 463.

[166] A. Müller, J. Döring, H. Bögge, *J. Chem. Soc. Chem. Commun.* **1991**, 273.

[167] A.-L. Barra, D. Gatteschi, B. Tsukerblatt, J. Döring, A. Müller, L.-C. Brunel, *Inorg. Chem.* **1992**, *31*, 5132.

[168] A.-L. Barra, D. Gatteschi, L. Pardi, A. Müller, J. Döring, *J. Am. Chem. Soc.* **1992**, *114*, 8509.

[169] D. Gatteschi, B. Tsukerblatt, A.-L. Barra, L.-C. Brunel, A. Müller, J. Döring, *Inorg. Chem.* **1993**, *32*, 2114.

[170] A. Müller, R. Rohlfing, A.-L. Barra, D. Gatteschi, *Adv. Mater.* **1993**, *5*, 915.

[171] D. C. Rees, M. K. Chan, J. Kim, *Adv. Inorg. Chem.* **1993**, *40*, 89, and references therein. Cf. also A. Müller, E. Krahn, *Angew. Chem.* **1995**, *107*, 1172; *Angew. Chem. Int. Ed. Engl.* **1995**, *34*, 1071.

[172] W. Kaim, B. Schwederski, *Bioanorganische Chemie*, Teubner, Stuttgart, **1991**, p. 171.

[173] *Geometry* deals with the congruity of metric parameters, such as angles or distances. *Topology*, on the other hand, is another branch of mathematics that deals with non-metric properties, which remain invariant under bijective and continuous mappings.

[174] O. Delgado, A. Dress, A. Müller, M. T. Pope in *Polyoxometalates: From Platonic Solids to Anti-Retroviral Activity* (Eds.: M. T. Pope, A. Müller), Kluwer, Dordrecht, **1994**.

[175] A. Müller, M. Penk, E. Krickemeyer, H. Bögge, H.-J. Walberg, *Angew. Chem.* **1988**, *100*, 1787; *Angew. Chem. Int. Ed. Engl.* **1988**, *27*, 1719. In the meantime, there are new findings that indicate that the previously published formula $[H_9V_{18}O_{42}(VO_4)]^{6-}$ **100a** (with 18 V^{IV} centers and a tetrahedrally coordinated central V^V atom) is not correct with respect to the actual degree of protonation. Even when all data are known, it is very difficult—and in the presence of significant disorder of the different anions in the crystal even impossible—to distinguish between the species $[H_{9-x}V_{18}^{IV}{}_xV_x^VO_{42}(V^VO_4)]^{6-}$ ($x = 0$–2) (cf. the comments in ref. [123]).

[176] F. T. Edelmann, *Angew. Chem.* **1995**, *107*, 1071; *Angew. Chem. Int. Ed. Engl.* **1995**, *34*, 981; T. Yildirim et al. *Nature* **1992**, *360*, 568; T. Suzuki, Y. Maruyama, T. Kato, K. Kikuchi, Y. Achiba, *J. Am. Chem. Soc.* **1993**, *115*, 11006; A. Hirsch, *Chem. Unserer Zeit* **1994**, *28*, 79.

[177] G. Huan, A. J. Jacobson, V. W. Day, *Angew. Chem.* **1991**, *103*, 426; *Angew. Chem. Int. Ed. Engl.* **1991**, *30*, 422.

[178] F. W. J. Schelling, *Allgemeine Deduktion des dynamischen Prozesses oder der Kategorien der Physik (1800)* in *Schellings Werke* (Ed.: M. Schröter), 2nd main volume (Schriften zur Naturphilosophie 1799–1801), Beck'sche Verlagsbuchhandlung, München, **1927**, p.635. According to Schelling "to construct" implies a "rational catching up with the evolutionary process".

[179] For the judicial murder of the chemist Lavoisier see: J. B. von Weiss, *Die Französische Revolution, Vol. 4*, Styria, Graz, **1930**, p.294. Together with 31 other landlords, Lavoisier stood accused of alleged fraud during his term as supervisor of the regions of Lorraine and Flanders. He "foresaw the verdict and requested only a stay of execution for 14 days, in order to complete an important study on which he had worked for many years; he then would gladly die as he had sacrificed his life for his country" (*ibid.*, p.295). Coffinhal had no sympathy for this request and gave the cited response.

[180] a) Hylomorphism is based on the assumption that every natural object is composed in some manner of (unstructured) matter (Greek *hylè*) and form (Greek *morphé*); b) important are the Arabian natural scientists of the Middle Ages Averroës and Avicenna (Aristolian leftists).

[181] The principle of complementarity controls many important biological processes (e.g. immunological ones). With the help of computer models, it was, for instance, possible to confirm the complementarity between the fullerene C_{60} and the protease which is essential for the replication of the HI-virus. Cf. S. H. Friedman, D. L. DeCamp, R. P. Sijbesma, G. Srdanov, F. Wudl, G. L. Kenyon, *J. Am. Chem. Soc.* **1993**, *115*, 6506.

[182] In philosophy, the appearance of new qualities and developmental levels due to evolutionary processes is termed emergence (Latin *emergere* = to surface, to become visible, to come out, to come into being). Emergent developmental phenomena are characterized by the either sudden or slow generation of something new in the sense of the appearance of new qualities. Emergent properties of complex systems can no longer be described solely by those theories that apply to the isolated components that make up the complex system. The concept of emergence encompasses not only dissipative, but also conservative self-organization processes. This may be the case when the aggregation of small building blocks (e.g., MoO_4^{2-} and VO_4^{3-} ions) leads, by conservative self-organization, to the generation of extremely large cluster species (e.g., **93a**) which have new characteristics that can no longer be explained (or at least not be predicted) by the properties of the isolated components, but only exist due to the mutual interactions (e.g., magnetic exchange interactions) of these system components (cf. A. Müller, *J. Mol. Struct.* **1994**, *325*, 13).

[183] W. Heisenberg, *Gesammelte Werke. Abtlg. C. Bd. 1* (Eds.: W. Blum, H.-P. Dürr, H. Rechenberg), Piper, München, **1984**, p. 218.

[184] a) C. F. von Weizsäcker, *Aufbau der Physik* (*Structure of Physics*), 1st ed., dtv, Stuttgart, **1988**, p.167; b) see also Monod's comments "Comme dans un cristal, c'est la structure même des molécules assemblées qui constitue la source d'*information* pour la construction de l'ensemble." (J. Monod, *Le Hasard et la Nécessité*, Éditions du Seuil, Paris, **1970**, p. 102).

[185] Cf. for example H. Hörz, *Zufall. Eine philosophische Untersuchung*, Akademie Verlag, Berlin, **1980**.

[186] See for example H. Haken, A. Wunderlin, *Die Selbststrukturierung der Materie*, Vieweg, Braunschweig, **1991**. Fundamental questions we have to ask are whether complex near-equilibrium systems were a necessary basis for the formation of dissipative structures during evolution and whether it is possible to create molecular complexity stepwise by a conservative growth process corresponding to the following schematic description:

$$\begin{array}{ccccccc} \mathbf{I} & \Rightarrow & \mathbf{III} & \Rightarrow & \mathbf{V} & \Rightarrow & \mathbf{VII} \qquad (2N-1) \\ \Updownarrow & & \Updownarrow & & \Updownarrow & & \\ \mathbf{2} & & \mathbf{4} & & \mathbf{6} & & \qquad (2n) \end{array}$$

Here, the uneven Roman numerals, $2N-1$, represent a series of maturation steps of a molecular system in growth or development and even Arabic numerals $2n$ stand for ingredients of the solution which react only with the relevant "preliminary" or intermediate product, $2N-1$. The species $2n$ can themselves be products of self-assembly processes. The target molecule at the "end" of the growth process would be formed by some kind of (near-equilibrium) symmetry breaking steps. The information it carries could, in principle, be transferred to other systems (A. Müller et al. unpublished).

[187] a) A. Müller, H. Hörz in *From Simplicity to Complexity in Chemistry and Beyond* (Eds.: A. Müller, A. Dress, F. Vögtle), Vieweg, Wiesbaden, **1995**; b) A. Müller, H. Hörz, S. Dillinger, *Brit. J. Phil. Sci.*, submitted.

[188] Voltaire, *Questions sur l'Encyclopédie, VIIIe partie (1771)* (Œuvres Complètes de Voltaire, Vol. 20, Dictionnaire Philosophique IV), Garnier Frères, Paris, **1879**, p. 49. See also ref. [189].

[189] Voltaire in *Aus dem Philosophischen Wörterbuch* (Ed.: K. Stierle), Insel, Frankfurt am Main, **1967**, p. 128.

[190] For this purpose, we have used the following graphic programs: a) "KPLOT" by R. Hundt—a program to depict and study crystal structures, Bonn, **1969**; b) "ORTEP" by C. K. Johnson—a FORTRAN thermal ellipsoid plot program for crystal structures, Oak Ridge, USA, **1965**; c) "SCHAKAL 92" by E. Keller—a computer program for the graphic representation of molecular and crystallographic models, Freiburg, **1993**.

New Brain Lipids that Induce Sleep

Thomas Kolter and Konrad Sandhoff*

In search of endogenous factors with sleep-inducing properties, Lerner et al. isolated a substance from the cerebrospinal fluid of cats that had been deprived of sleep for 22 hours.[1] In a further publication the unknown compound was characterized as the amide **1** of an ω-9-unsaturated fatty acid with a (*Z*) double bond.[2] The substance, which could not be detected in cats under control conditions, was isolated by reversed-phase HPLC in amounts of 0.1 to 5 pmol per 100 µL of cerebrospinal fluid. Mass spectrometric analysis revealed *m/z* 304.2614 for the $[M + Na]^+$ ion, which best fits the formula $C_{18}H_{35}NO$ having two double-bond equivalents. The ready loss of a neutral 17 Da fragment from the $[M + H]^+$ ion suggests the cleavage of a primary amino group as ammonia. Based on these and further spectroscopic data (UV, ^{1}H NMR), the substance was initially proposed to be a "cerebrodiene", for example **2**.[1] The postulated structure suggested that **2** may arise biosynthetically from sphingosine **3** or other sphingolipids and thus attracted considerable attention,[3] since several intermediates of sphingolipid metabolism are currently discussed as potential signaling molecules.[4]

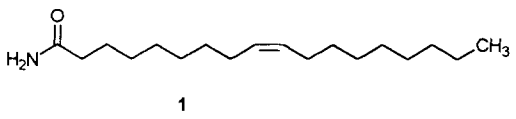

1

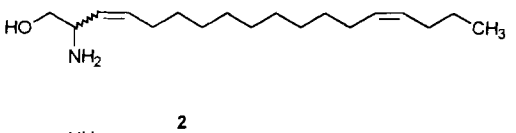

2

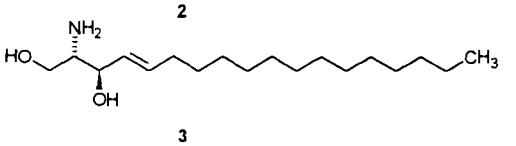

3

The final assignment of structure **1** to the unknown compound succeeded by comparison of the spectroscopic data to those of model substances.[2] The position of the double bond was determined after ozonolysis and its configuration by IR and ^{1}H NMR spectroscopy. Moreover, it could be shown in a functional assay that intraventricular injection of 10 nmol (2.8 µg) of synthetic **1** induced sleep in laboratory animals. Variation of double-bond configuration, position, and alkyl chain length resulted in decreasing extent and duration of the observed effect. Further, it was shown that membrane fractions isolated from brain rapidly degrade **1** into oleic acid.

The crucial assumption in this study is an idea that originated at the beginning of our century. Henri Piéron[5] postulated the existence of a sleep-inducing substance that is formed in the course of the day, accumulates, and is destroyed during sleep. To verify this hypothesis, Piéron collected cerebrospinal fluid from dogs that had been deprived of sleep for several days. He injected the fluid into the ventricles of other dogs, which then promptly fell asleep for two to six hours.

In recent years several substances with sleep-promoting factors have been discovered,[6] including the delta sleep inducing peptide,[7] which was isolated from the blood of sleeping rabbits and led to sleeplike behavior after intraventricular infusion into rabbit brain (δ-slow wave sleep). Prostaglandin D_2[8, 9] also meets most of the requirements of a sleep substance:[10] 1) The substance must induce sleep. 2) The induced sleep must be natural. 3) A dose–response curve must be demonstrated. 4) Sleep must be followed by appropriate wakefulness. 5) The substance must be present in the brain. 6) There should be binding sites for the substance in the central nervous system. 7) Receptor blockers should prevent sleep induction. 8) Direct application to regions of high binding should induce sleep. 9) The substance should have appropriate circadian changes. 10) Inhibition of synthesis of the substance should reduce sleep. 11) Metabolic pathways should be known. 12) Relevant enzymes should be present in appropriate regions. 13) The substance should accumulate with prolonged wakefulness. 14) Its concentration should decrease with prolonged sleep. 15) The substance should be present in several species. Additional substances[6, 12] discussed as potential sleep promoting factors include interleukin 1, interferon α2, lipopolysaccharides, muramyl peptides, serotonin, tumor necrosis factor, and vasoactive intestinal peptide. The relationship between substances apparently acting as neurotransmitters and neuromodulators and the phenomenon of sleep is far from clear.

Sleep is one of several circadian rhythms, which, genetically controlled, are synchronized with the change of day and night as the most important environmental factors.[11] Several stages of sleep can be distinguished, which follow each other in a predictable manner and appear to be controlled by different neurochemical systems.[12] The stages of sleep (and of other circadian

[*] Prof. Dr. K. Sandhoff, Dr. T. Kolter
Institut für Organische Chemie und Biochemie der Universität
Gerhard-Domagk-Strasse 1, D-53121 Bonn (Germany)
Telefax: Int. code + (228) 737778

 © VCH Verlagsgesellschaft mbH, D-69451 Weinheim, 1995 0570-0833/95/3421-2363 $ 10.00+.25/0

processes) are affected differently by drugs in pharmacological intervention.[13]

During a typical night's sleep, the adult human progresses through different sleeping periods in a predictable manner, which can be distinguished electrophysiologically (slow wave sleep) and by the occurrence of rapid eye movements (REM sleep). Slow wave sleep and REM sleep alternate four to six times a night with increasing duration of REM sleep but decreasing duration and depth of slow wave sleep.[12]

Slow wave sleep is characterized by progressively longer wavelengths and amplitudes in the electroencephalogram (EEG). During slow wave sleep, humans pass through up to four levels, which are accompanied by successive lower heart frequency, decreasing blood pressure, and deeper sleep. After about 45 minutes these levels are retraced in the opposite order. After a total of about 90 minutes several abrupt physiological changes occur, and the EEG becomes similar but not identical to that of the waking state. Different names are used for this state: REM sleep, paradoxical sleep, active sleep, and desynchronized sleep. The active EEG patterns are coupled with a loss of muscle tone and rapid eye movements occur. According to the criterion of arousability by external influences, REM sleep is the deepest; however, spontaneous waking occurs most easily. When humans are awakened from REM sleep, dreams are much more easy remembered than when they are awakened from slow wave sleep. On the other hand, definite nightmares occur predominantly in stages three and four of slow wave sleep, the so-called delta sleep.[12] Barbiturates and ethanol suppress REM sleep, while benzodiazepines, for instance, reduce the fourth and deepest stage of slow wave sleep to a much greater extent than REM sleep.

Just as unsuccessful as the search for a universal sleep-inducing substance was the search for a single sleep center in the brain.[12] Stimulation of neurons at different anatomical locations induced sleep. Selective destruction of these cells led to insomnia in laboratory animals. Neurons of the brain stem that use serotonin as neurotransmitter seem to responsible for induction and maintenance of slow wave sleep. Injection of serotonin into these regions induces sleep, and application of *para*-chlorophenylalanine, an inhibitor of serotonin biosynthesis, causes insomnia as expected. However, after one week of daily injection of the inhibitor it is observed that in spite of low serotonin levels sleeping behavior normalizes and reaches 70% of the control values.

Let us return to the relatively simple structure of **1**, which might play a role in the complex phenomenon of sleep. Several questions are still unanswered. It remains to be clarified how the substance is metabolized, how the metabolism is regulated, and whether it can be attributed to regions of the brain that are responsible for the induction and maintenance of sleep.[10] The isolation of another long-chain carboxylic acid amide with biological function from brain has attracted attention to this class of compounds. In a screening process, anandamide **4**, tee ethanol amide of arachidonic acid has been identified as an endogenous ligand of the cannabinoid receptor (K_i = 52 nM).[14] In a functional assay it gave the same physiological response and behavior as Δ^9-tetrahydrocannabinol (**5**), the active con-

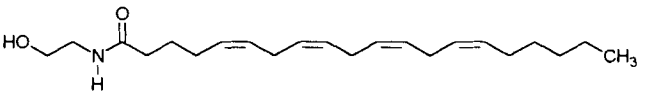

4

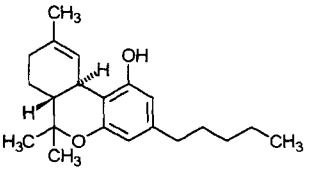

5

stituent of hashish and marijuana. Brain membranes are able to synthesize **4** from ethanolamine and arachidonic acid, which should be accessible from phospholipids of the plasma membrane on action of phospholipase D or A2.[15] It remains to be seen whether more than a structural similarity exists between **1** and **4**, and further, whether the findings of the authors[1, 2] will contribute to the answer of the still-open question of how sleep "functions". Since nature, and maybe also sleep, is organized hierarchically, the question of why we need to sleep at all can presumably not be answered on the molecular level alone.

German version: *Angew. Chem.* **1995**, *107*, 2559–2560

Keywords: brain lipids · neurotransmitters · sphingosines

[1] R. A. Lerner, G. Siuzdak, O. Prospero-Garcia, S. J. Henriksen, D. L. Boger, B. F. Cravatt, *Proc. Natl. Acad. Sci. USA* **1994**, *91*, 9505–9508.
[2] B. F. Cravatt, O. Prospero-Garcia, G. Siuzdak, N. B. Gilula, S. J. Henriksen, D. L. Boger, R. A. Lerner, *Science* **1995**, *268*, 1506–1509.
[3] L. Jaenicke, *Chemie Unserer Zeit* **1995**, *29*, 21.
[4] Reviews: a) A. Olivera, S. Spiegel, *Nature* **1993**, *365*, 557–560; b) R. Kolesnick, *Mol. Chem. Neuropathol.* **1994**, *21*, 287–297; c) R. H. Michell, M. J. O. Wakelam, *Curr. Biol.* **1994**, *4*, 370–373; d) R. Kolesnick, D. W. Golde, *Cell* **1994**, *77*, 325–328; e) Y. A. Hannun, *J. Biol. Chem.* **1994**, *269*, 3125–3128; f) Y. A. Hannun, L. M. Obeid, *Trends Biochem. Sci.* **1995**, *20*, 73–77.
[5] H. Piéron, *Le Problème Physiologique du Sommeil*, Paris, Masson, **1913**, cited in ref. [6, 12].
[6] A. B. Borbély, I. Tobler, *Physiol. Rev.* **1989**, *69*, 605–670.
[7] G. A. Schoenenberger, M. Monnier, *Proc. Natl. Acad. Sci. USA* **1977**, *74*, 1282–1286.
[8] R. Ueno, Y. Ishikawa, T. Nakayama, O. Hayashi, *Biochem. Biophys. Res. Commun.* **1982**, *109*, 576–582.
[9] O. Hayaishi, *FASEB J.* **1991**, *5*, 2575–2581.
[10] W. C. Dement, presented at the International Symposium on Endogenous Sleep Factors, Honolulu, HI, November 7–11, **1988**; see also S. Nishino, E. Migot, B. Fruhstorfer, W. C. Dement, O. Hayaishi, *Proc. Natl. Acad. Sci. USA* **1989**, *86*, 2483–2487, cited in ref. [9].
[11] J. S. Takahashi, *Annu. Rev. Neurosci.* **1995**, *18*, 531–553.
[12] D. D. Kelly in *Principles of Neural Science* (Eds.: E. R. Kandel, J. H. Schwarz, T. M. Jessel), Elsevier, New York, **1991**, Chapter 51, pp. 792–804.
[13] J. D. Miller, *Annu. Rep. Med. Chem.* **1992**, *27*, 11–19.
[14] W. A. Devane, L. Hanuš, A. Breuer, R. G. Pertwee, L. S. Stevenson, G. Griffin, D. Gibson, A. Mandelbaum, A. Etinger, R. Mechoulam, *Science* **1992**, *258*, 1946–1949.
[15] W. A. Devane, J. Axelrod, *Proc. Natl. Acad. Sci. USA* **1994**, *91*, 6698–6701.

Aligning and Trapping Molecules with Light

Lothar Kador*

The investigation of absorbing particles (atoms, ions, or molecules) trapped in various environments has yielded important insight into the fundamental structure of matter and has opened the door to exciting new fields of spectroscopy. Trapping in vacuum is most easily accomplished for ionized atoms, which, due to their charge, can be confined in radio-frequency electromagnetic traps (Paul traps). In this way quantum-optical effects such as quantum jumps[1] and photon antibunching[2] were observed on single ions. Photon antibunching is the phenomenon of a two-level system's inability to emit two photons arbitrarily fast after one another. Neutral atoms can be trapped by a tightly focused laser beam, since the electric field of the light induces a dipole moment, which, in the classical picture, pulls the atom towards the region of the highest field strength. Results of quantum-mechanical calculations show that this works only if the laser frequency lies below the resonance frequency of an atomic transition.[3, 4] Typical numbers of stored atoms in such dipole force traps are on the order of 10^3; consequently, cold atomic collisions or collective effects, for instance, can be studied. The storage time of the atoms (around seconds) is usually limited by collisions with the residual gas.

For molecules the situation is less favorable. Ionizing molecules is often problematic, because the ionization tends to make them less stable and, hence, favors dissociation. Moreover, molecules have far more internal degrees of freedom than atoms. Thus, in addition to the electronic states, vibrations and rotations and combinations thereof can be excited. As a consequence, cooling molecules to below 1 K in vacuum is difficult, since all these possible excitations must be frozen out, in addition to drastically reducing the translational temperature.

A way around this problem is to investigate molecules that are not in vacuum but are embedded in a solid at liquid-helium temperatures. In the solid environment, rotations are usually not possible, and the molecule is spatially confined. The optical spectroscopy of single, large organic dye molecules in transparent crystals or glasses has almost become a standard technique.[5, 6] In a crystalline environment, the phase relaxation of the electronic transition is often negligible at low temperatures, with the result that the spectral linewidth can be very narrow and can reach the limit determined by the lifetime of the excited state. Nevertheless, the spectroscopic characteristics of the dopant molecules are still influenced by interaction with the solid environment to a large degree. A simple example is the spectral position of the absorption line, which differs from its value in vacuum by a solvent shift or gas-to-crystal shift. Therefore, trapping and cooling molecules in a vacuum chamber to avoid these interactions is still a challenging goal.

[*] Dr. L. Kador
Universität Bayreuth
Lehrstuhl für Experimentalphysik IV
and
Bayreuther Institut für Makromolekülforschung (BIMF)
D-95440 Bayreuth (Germany)
Telefax: Int. code +(921) 55-3250
e-mail: lothar.kador@uni-bayreuth.de

A recent theoretical article[7] showed that this should indeed be possible. A prerequisite for spatial trapping of molecules is a means to provide a localized region where an attractive potential exceeds the molecular kinetic energy. In principle, this might be done with a very strong static electric or magnetic field, provided that the molecules have permanent dipole moments. The remarkable new scheme proposed by Friedrich and Herschbach,[7] however, utilizes the high oscillating electric field strength of intense laser radiation to attract the molecules by means of induced dipole moments. Since all molecules are polarizable, this technique has a much wider applicability. When, as in most cases, the molecular polarizability is anisotropic, the interaction with the laser field will also align the molecules. In diatomic molecules, for instance, the polarizability along the molecular axis will always be larger than perpendicular to it. Friedrich and Herschbach's study was motivated by a previous experiment,[8] which provided evidence that CO molecules of thermal energy can be aligned by a strong pulsed laser field of intensity $I \approx 10^{14}\ \mathrm{Wcm^{-2}}$ and pulse duration between 1 and 30 ps. Yet, the calculation shows that even an intense, tightly focused continuous-wave (cw) infrared laser of a few kW power (with an intensity around $10^{11}\ \mathrm{Wcm^{-2}}$ in the focus) should be sufficient for trapping as well as alignment. Permanent electric dipole moments are not a factor, because the electric light field oscillates too fast to reorient a molecule according to its permanent moment. (Molecular rotational frequencies are located in the microwave spectral region.) The induced dipole moment causes a molecule to be pulled along the gradient of increasing field strength; consequently, in the focal region of the laser there is a conservative trapping potential, as in the case of neutral atoms.[4] Hence, the proposed method is extremely simple: both aligning and trapping of the molecules is performed by a single focused laser beam.

The Schrödinger equation of a linear molecule in a strong laser field is described by Equation (a),[7] where B denotes the rotational constant, $\boldsymbol{J}^2$ the squared angular momentum operator, and the angular potential is given by Equation (b).

$$[B\boldsymbol{J}^2 + V_a(\theta)]\,\Psi = E\Psi \qquad \text{(a)}$$

$$V_a(\theta) = -\tfrac{1}{2}\varepsilon^2(\alpha_{\parallel}\cos^2\theta + \alpha_{\perp}\sin^2\theta) \qquad \text{(b)}$$

The polarizabilities $\alpha_{\parallel}$ and $\alpha_{\perp}$ are the components parallel and perpendicular to the molecular axis, respectively, and θ is the angle between this axis and the polarization direction of the light. The electric field ε oscillates according to $\varepsilon = \varepsilon_0 \cos(2\pi\nu t)$. Note that its frequency ν must be off-resonant so that neither electronic nor vibrational transitions can be induced. Equation (a) cannot be solved in closed form. However, accurate numerical solutions are readily obtained, and analytical perturbation expansions are possible for the limiting cases of low and high field strength. For $\varepsilon = 0$, the problem reduces to that of a free rotor whose eigenfunctions Ψ are spherical harmonics and

 © VCH Verlagsgesellschaft mbH, D-69451 Weinheim, 1995 0570-0833/95/3421-2365 $ 10.00+.25/0

whose eigenenergies are given by $E = J(J+1)B$ with the rotational quantum number $J = 0, 1, 2, \ldots$

Equation (b) shows that the angular potential of the light field is purely attractive, since the polarizabilities $\alpha_{\parallel}$ and $\alpha_{\perp}$ are always positive. For $\alpha_{\parallel} \neq \alpha_{\perp}$, it has the form of a double-well potential with two minima and two maxima in a full circle of 360°. Hence, the molecular states that are bound by the wells occur in pairs, split by the tunneling matrix element. Apart from this tunneling splitting, the lowest states in the wells feel a potential that strongly resembles that of a harmonic oscillator. They were therefore dubbed "pendular states" by the authors.[7] The corresponding wave functions have their highest amplitudes in the vicinity of the potential minima. This means that the molecules are aligned (not oriented, though) along the polarization direction and perform nearly harmonic two-dimensional librations about it; the amplitude of the librations depends on the energy (or temperature) of the molecules. The free-rotor states are adiabatically transformed into these bound pendular states as the laser is turned on, and at sufficiently high intensities and low temperatures only the lowest states will be populated.

In the focus of a high-power cw laser, the calculated binding energy of the molecular trap corresponds to thermal energies of about 1 K for small molecules (CO and CS_2). Substantially deeper traps (50 K or more) can be obtained for larger molecules (for example, C_{60}). To be confined in the trap, the molecules must be cooled to temperatures below the trap depth. This can be accomplished by the interaction with a cold buffer gas, for instance the gas evaporating from liquid ^{3}He (240 mK).[9] The density of the trapped molecules can reach values between 10^8 and 10^{11} cm^{-3}, depending on the molecular polarizabilities, light intensity, and temperature of the buffer gas. These densities are comparable to those obtainable in atom traps.[4] They are high enough for thermal equilibration of the molecules to take place by collisions. This opens up the fascinating possibility of lowering the temperature of the trapped molecules much further by "evaporative cooling":[10] The binding energy of the trap is temporarily reduced by attenuating the laser power, and the molecules of highest energy are released. After removing the ^{3}He buffer gas and increasing the trap depth again, a new thermal equilibrium at a lower temperature will be established. Applied to trapped atoms, iteration of this cooling technique enabled the recent achievement of a macroscopic quantum state by Bose–Einstein condensation[11] (see also Ref. [12]). Such states, as well as many less exotic phenomena,[13] are among prospects that now may be envisioned for molecules trapped by light.

German version: *Angew. Chem.* **1995**, *107*, 2561–2562

Keywords: evaporative cooling · lasers · polarizability · vacuum traps

[1] W. M. Itano, J. C. Bergquist, D. J. Wineland, *Science* **1987**, *237*, 612, and references therein.
[2] F. Diedrich, H. Walther, *Phys. Rev. Lett.* **1987**, *58*, 203.
[3] S. Chu, J. E. Bjorkholm, A. Ashkin, A. Cable, *Phys. Rev. Lett.* **1986**, *57*, 314.
[4] J. D. Miller, R. A. Cline, D. J. Heinzen, *Phys. Rev. A* **1993**, *47*, R4567.
[5] Review: W. E. Moerner, T. Basché, *Angew. Chem.* **1993**, *105*, 537; *Angew. Chem. Int. Ed. Engl.* **1993**, *32*, 457.
[6] Review: L. Kador, *Phys. Status Solidi B* **1995**, *189*, 11.
[7] B. Friedrich, D. Herschbach, *Phys. Rev. Lett.* **1995**, *74*, 4623.
[8] D. Normand, L. A. Lompre, C. Cornaggia, *J. Phys. B* **1992**, *25*, L497.
[9] J. M. Doyle, *Bull. Am. Phys. Soc.* **1994**, *39*, 1166.
[10] J. M. Doyle, J. C. Sandberg, I. A. Yu, C. L. Cesar, D. Kleppner, T. J. Greytak, *Physica (Amsterdam) B* **1994**, *194*, 13.
[11] M. H. Anderson, J. R. Ensher, M. R. Matthews, C. E. Wieman, E. A. Cornell, *Science* **1995**, *269*, 198.
[12] W. Petrich, *Phys. Bl.* **1995**, *51*, 592.
[13] J. Maddox, *Nature* **1995**, *375*, 531.

 © VCH Verlagsgesellschaft mbH, D-69451 Weinheim, 1995 0570-0833/95/3421-2366 $ 10.00+.25/0

para- and *ortho*-Quinodimethane Intermediates with Cumulative Double Bonds**

Henning Hopf,* Peter G. Jones, Peter Bubenitschek, and Christian Werner

In the construction of complex molecular structures *para*- and *ortho*-quinodimethanes **1** and **4** and countless of their derivatives play an important role, both in hydrocarbon[1] and natural product chemistry.[2] We were interested in whether the exocyclic double bonds of these parent compounds could be "extended" by the deliberate insertion of sp-hybridized carbon atoms, and also in the chemical behavior of the presumably highly reactive quinodimethanes **2**,[3] **3**, **5**, and **6**, which contain cumulative double bonds (Scheme 1). We report here on the synthesis of the intermediates **3** and **6** and their respective inter- and intramolecular cyclizations.

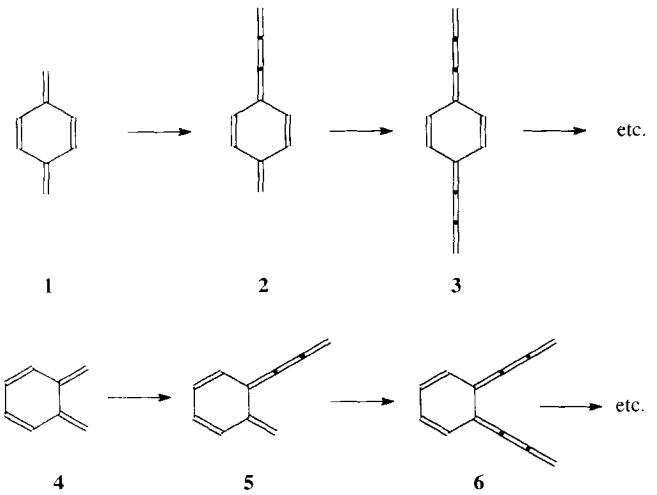

Scheme 1. Construction of quinodimethanes with cumulative double bonds from the parent *para*- and *ortho*-quinodimethanes **1** and **4**.

Coupling of *p*-dibromobenzene (**7**) with propargyl alcohol (for conditions see Scheme 2) afforded diol **8**,[4] which was converted into dibromide **9**[4] by standard procedures. In the reaction of **9** with the debromination reagent $Bu_3SnSiMe_3$/CsF described by Mori et al.[5] a hydrocarbon was formed (yield 7.5%), which is assigned the dimeric structure **10** on the basis of spectroscopic and analytical data.[6] The isomeric tetraallene **11**, which could equally have been formed by the dimerization of **3**, is not accessible by this method. The driving force of the dimerization is clearly the gain in resonance energy brought about by the formation of the cyclophane and the conversion of the thermodynamically unfavorable cumulene units into isolated triple bonds.[7]

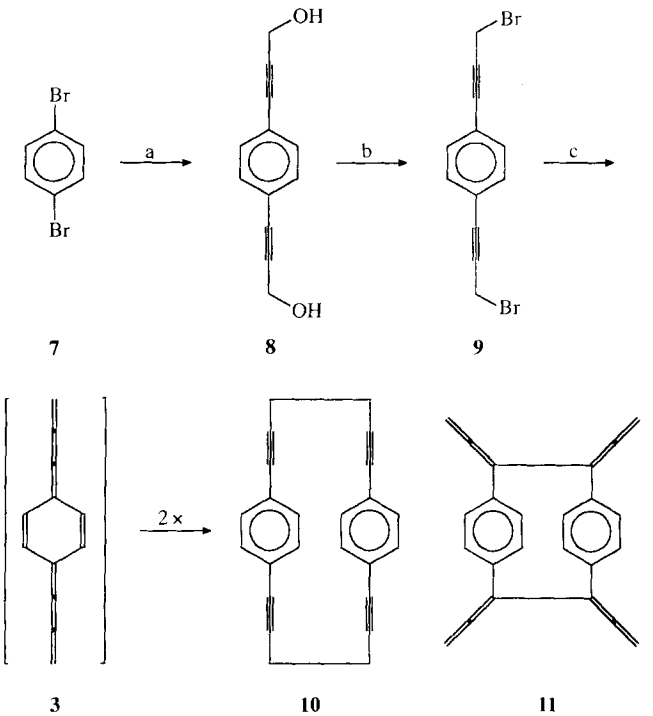

Scheme 2. Preparation and dimerization of *para*-quinodimethane **3**. a) 2-Propynol, $[Pd(PPh_3)_4]$, *n*-propylamine, 72 h at reflux, 93%. b) PBr_3, diethyl ether, 30 min at 0 °C, 30 min at reflux, 68%. c) $Bu_3SnSiMe_3$/CsF, DMF, 6 h at 0 °C, 16 h at 25 °C, 7.5%.

To confirm the postulated structure unambiguously, **10** was recrystallized from methanol and the resulting crystals were analyzed by X-ray diffraction.[8] [6.6]Paracyclophanetetrayne **10** crystallizes as two independent inversion-symmetric molecules with different conformations. In molecule 1 (Fig. 1a) the C_6 rings are eclipsed (torsion angle C2-C1-C12-C11 10°) and the distance between the ring planes is 384 pm. In contrast, in molecule 2 (Fig. 1b) the rings are displaced laterally (torsion angle C2′-C1′-C12′-C11′ 42°) and separated by 343 pm. The aromatic rings are all planar (mean deviation < 2 pm). As a consequence of ring strain the substituents (cyclophane bridges) lie significantly out of the ring plane: C3 by 22, C10 by 21, C3′ by 25, and C10′ by 28 pm. For the same reason, the bond angles of the triple bonds deviate from the ideal value of 180° (169–172°).

[*] Prof. Dr. H. Hopf, Dipl.-Chem. P. Bubenitschek, C. Werner
Institut für Organische Chemie der Technischen Universität
Hagenring 30, D-38106 Braunschweig (Germany)
Telefax: Int. code + (531)391-5388
Prof. Dr. P. G. Jones
Institut für Anorganische und Analytische Chemie
der Technischen Universität Braunschweig (Germany)

[**] New Planar π-Systems, Part 5. We thank the Deutsche Forschungsgemeinschaft and the Fonds der Chemischen Industrie for supporting this work. – Part 4: H. Hopf, U. Hamman, G. Zimmerman, D. Rammler, *J. Pure Appl. Pyrolysis* **1994**, *29*, 57–63.

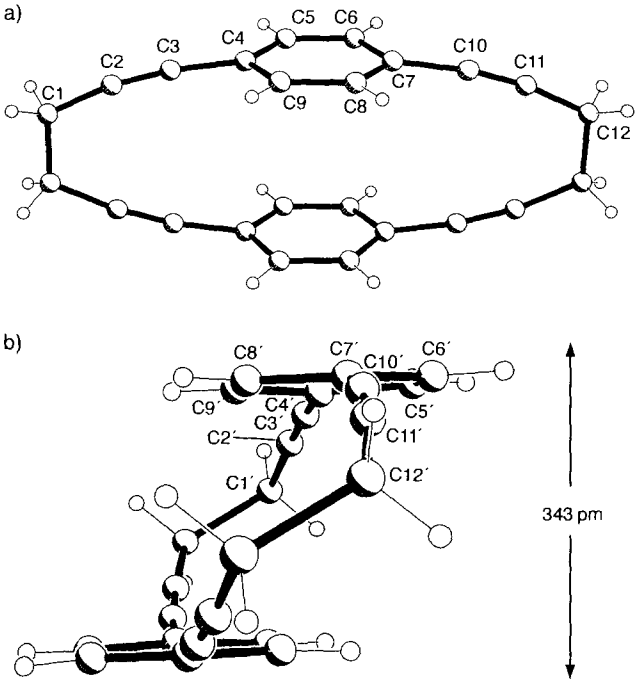

Fig. 1. Crystal structure of compound **10**: a) molecule 1; b) molecule 2. Radii are arbitrary.

To prepare the *ortho*-quinodimethane **6**, *ortho*-dibromobenzene (**12**) was transformed into the dibromide **13**[4] by reaction with propargyl alcohol and subsequent bromination (Scheme 3). Compound **13** was debrominated as described above and a hydrocarbon, recrystallizable from methanol, was obtained in

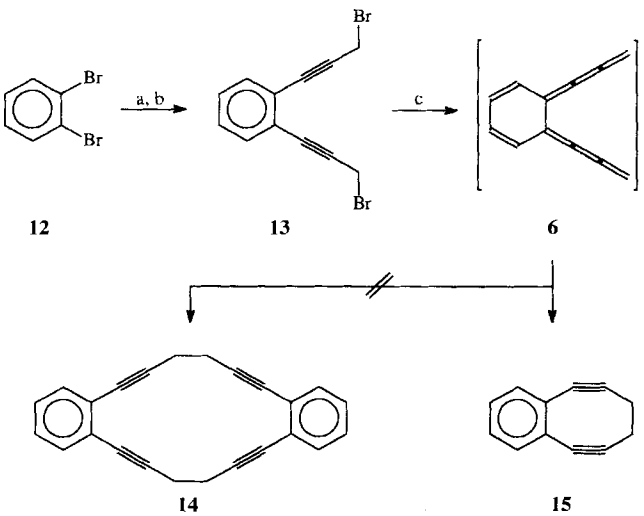

Scheme 3. Preparation and dimerization of *ortho*-quinodimethane **6**. a) 2-Propynol, $[Pd(PPh_3)_4]$, *n*-propylamine, 5 d at reflux, 47%. b) PBr_3, diethyl ether, 1 h at 0 °C, 1 h at reflux, 60%. c) $Bu_3SnSiMe_3$/CsF, DMF, 1 h at 0 °C, 16 h at 25 °C, 61%.

good yield (61%), to which we assign the structure 3,4-benzocycloocten-1,5-diyne (**15**) on the basis of its spectroscopic properties.[9] The cyclophane dimer **14** was not formed. Presumably the termini of biscumulene **6** are in such close proximity that intramolecular ring closure is preferred. After recrystallization, compound **15** was obtained as colorless needles, which rapidly discolor and darken on standing. The structure of this decomposition product is as yet unknown. To the best of our knowledge, **15** is the first derivative of the highly strained C_8H_6 hydrocarbon cycloocta-3-en-1,9-diyne.[10]

Received: May 18, 1995 [Z8005IE]
German version: *Angew. Chem.* **1995**, *107*, 2592–2594

Keywords: cumulenes · cyclophanes · quinodimethanes

[1] V. Boekelheide in *Strategies and Tactics in Organic Synthesis, Vol. 1* (Ed.: T. Lindberg), Academic Press, Orlando, **1984**, pp. 1–19.
[2] W. Carruthers, *Some Modern Methods of Organic Synthesis*, 3rd ed., Cambridge University Press, **1986**, Chapter 3, pp. 207–221.
[3] For a report on the preparation of a structural isomer of **2**, 3,6-bisethenylidene-1,4-cyclohexadiene using flash vacuum pyrolysis, see: M. C. Lasne, J. L. Ripoll, J. D. Denis, *Tetrahedron* **1981**, *37*, 503–508. Unfortunately the chemical behavior of this substance was not investigated.
[4] The structures of these compounds were determined by spectroscopic (IR, ^1H and ^{13}C NMR, and UV spectroscopy) and analytical methods (MS, elementary analysis).
[5] H. Sato, N. Isono, K. Okamura, T. Date, M. Mori, *Tetrahedron Lett.* **1994**, *35*, 2035–2038.
[6] Spectroscopic data for **10**. ^1H NMR ($CDCl_3$, int. TMS, 400 MHz): $\delta = 2.69$ (s, 8H, 1-, 12-, 13-, 24-H) 6.92 (s, 8H, 5-, 6-, 8-, 9-, 17-, 18-, 21-, 22-H); ^{13}C NMR ($CDCl_3$, 100 MHz): $\delta = 19.32$ (t, C-1, -12, -13, -24), 85.58 (s, C-2, -11, -14, -23), 91.96 (s, C-3, -10, -15, -22), 123.0 (s, C-4, -7, -16, -19), 130.7 (d, C-5, -6, -8, -9, -17, -18, -20, -21); IR (KBr): $\tilde{\nu} = 3034$ (vw), 2928 (w), 2909 (w), 2835 (vw), 2217 (w), 1503 (s), 834 (vs) cm^{-1}; UV (*n*-hexane): λ_{max} (lgε) = 194 (4.56), 212 (4.45), 264 (4.76), 286 nm (4.30); MS (70 eV): *m/z* (%): 304 [M^+] (100), 276 (16), 152 (62).
[7] The dimerization of 1,2,3-butatriene to 1,5-cyclooctadiyne can be regarded as the prototype of the dimerization of **3** to **10**: E. Kloster-Jenson, J. Wirz, *Angew. Chem.* **1973**, *85*, 723; *Angew. Chem. Int. Ed. Engl.* **1973**, *12*, 671; see also *Helv. Chim. Acta.* **1975**, *58*, 162–177.
[8] Crystal data for compound **10**: $C_{24}H_{16}$, triclinic, $P\bar{1}$, $a = 865.2(3)$, $b = 918.6(3)$, $c = 1162.3(3)$ pm, $\alpha = 90.41(2)$, $\beta = 98.09(2)$, $\gamma = 112.03(2)°$, $V = 0.8459$ nm^3, $Z = 2$ (two independent inversion-symmetric molecules), $T = -100$ °C. Colorless tablet, $0.4 \times 0.4 \times 0.15$ mm, Siemens P4 diffractometer, 2962 independent reflections to $2\theta_{max}$ 50°. Structure solution: direct methods. Structure refinement: anisotropically against F^2 (program SHELXL-93, G. M. Sheldrick, Universität Göttingen, **1993**); H atoms with a riding model: $wR(F^2)$ 0.191, conventional $R(F)$ 0.063, for 217 parameters and 196 restraints: max. $\Delta\rho$ 163 e nm^3. Further details of the crystal structure determination may be obtained from the Fachinformationszentrum Karlsruhe, D-76344 Eggenstein-Leopoldshafen (Germany) on quoting the depository number CSD-401565.
[9] Spectroscopic data for **15**: ^1H NMR ($CDCl_3$, int. TMS, 400 MHz): $\delta = 2.99$ (s, 4H, 7-, 8-H), 7.27 (AA'BB'-m, 4H, C-9, -10, -11, -12); ^{13}C NMR ($CDCl_3$, 100 MHz): $\delta = 20.98$ (t, C-7, -8), 96.14 (s, C-1, -6), 110.99 (s, C-2, -5), 126.59 (d, C-10, -11), 127.42 (d, C-9, -12), 131.74 (s, C-3, -4); IR (KBr): $\tilde{\nu} = 3079$ (w), 2922 (w), 2830 (w), 2159 (s), 1555 (vs), 1540 (m), 1536 (m), 1450 (vs), 1438 (vs), 1420 (vs), 1282 (s), 1033 (s), 751 (vs), 447 (vs) cm^{-1}; UV (acenonitrile): λ_{max} (lgε) = 200 (4.38), 222 (4.28), 232 (4.43), 250 nm (sh, 3.86); MS (70 eV): *m/z* (%): 152 [M^+] (100), 126 (18).
[10] The energy of formation of **15** calculated by using MNDO methods is 592.7 kJ mol^{-1}. Thus this substance, whose minimum energy conformer is planar, is about 400 kJ mol^{-1} higher in energy than 3,4-benzocycloocta-1,3,5-triene ($\Delta H_f = 195.4$ kJ mol^{-1}). We thank Prof. Dr. H. Meier (Universität Mainz) for these calculations and for valuable discussions. The even more highly unsaturated hydrocarbon 5,6,9,10-tetrahydrobenzocyclooctene, a bisdehydro derivative of **15**, has been described in the literature as an oily substance stable for only a few minutes at 0 °C: H. N. C. Wong, F. Sondheimer, *Angew. Chem.* **1976**, *88*, 126–127; *Angew. Chem. Int. Ed. Engl.* **1976**, *15*, 117.

A Simple Route to the 1-Aza-3-Phosphaallyl System: Structure of a Dimeric Lithium Complex and Protonation to Give the First NH_2-Substituted Phosphaalkene**

Karin Paasch, Martin Nieger, and Edgar Niecke*

Dedicated to Professor Herbert Roesky on the occasion of his 60th birthday

N-Silylated derivatives of 1,3-diazaallyl anions[1] **I** are important chelate ligands for main group and transition metals[1] and have recently gained significance as cocatalysts for olefin polymerization.[1, 2] Compounds of the 1,3-diphosphaallyl system[3] (**II**) homologous to **I** are versatile complex ligands (σ and π coordination),[4] and activities in the olefin polymerization were detected for a nickel complex.[5] As an extension of our studies on 1-phosphaallyl anions,[6] we became interested in the 1-aza-3-phosphaallyl system[7] (**III**) which combines the reactivity of

I **II** **III**

both due to the presence of a "soft" (phosphorus) and a "hard" reaction center (nitrogen). We report herein on a simple route to this heteroallyl system, the crystal structure of a lithium complex, and its reaction with electrophiles.

The reaction of equimolar amounts of lithium phenyl phosphanide **1a** with acetonitrile in THF leads smoothly to the lithium complex of the 1-aza-3-phosphaallyl anion **2**, which was

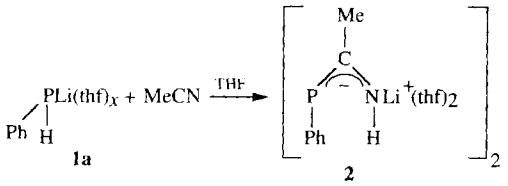

1a **2**

isolated in the form of yellow, air- and moisture-sensitive crystals. According to the results of an X-ray structure analysis[8] **2** is dimeric in the crystal (Fig. 1). The two heteroallyl anions are linked through a planar Li_2N_2 unit; the lithium atoms attain a distorted tetrahedral geometry by the additional coordination of two THF molecules. The Li–N distances lie in the expected range[10] (203.1(8), 209.0(8) pm). The acute Li-N-Li angle (75.6(4)°), which results in the two lithium atoms (253(2) pm) approaching one another, is particularly noteworthy. The coplanar arrangement of the atoms H1-N1-C1-C2-P1-C11 (average deviation from the best plane: 0.5 pm) indicates the formation of a delocalized 4electron–3center-pπ system. This assumption is also supported by the short N1–C1 and C1–P1 distances (132.0(5) and 174.0(4) pm, respectively), which lie between those of a single and a double bond for these element

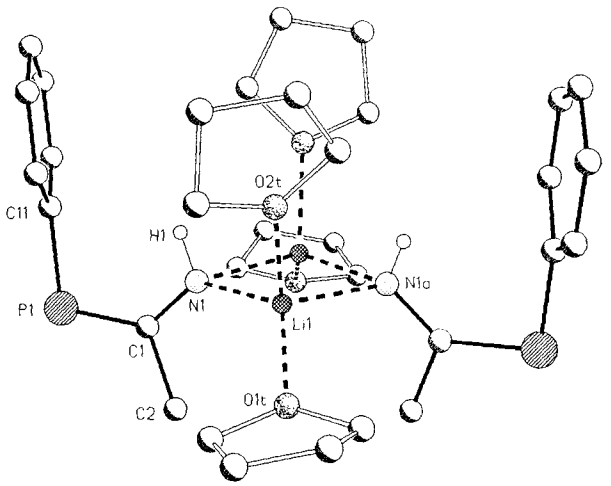

Fig. 1. Crystal structure of **2**. Selected bond lengths [pm] and angles [°]: P1–C1 174.0(4), C1–N1 132.0(5), N1–Li1 203.1(8), P1–C11 182.9(5), C1–C2 152.0(6), N1a-Li1 209.0(8); C1–P1–C11 100.3(2), N1–C1–P1 132.0(3), C1–N1–Li1 132.3(4), Li1–N1–Li1a 75.6(4), N1–C1–C2 113.6(4), C2–C1–P1 114.4(3), C1–N1–Li1a 119.0(4).

combinations. The phenyl substituent at the phosphorus atom is twisted out of the P-C-N plane by 116° and as in the 1-phosphaallyl system[6a, d] is located in the energetically favored[11] *endo* position.

The *trans* arrangement of the phosphorus substituent with respect to the methyl group in **2** confirmed in the solid state, is supported in solution by the large value for ^2J(C,P) (60.7 Hz). The ^{31}P chemical shift (δ = 34.3) resembles the shifts of similarly substituted 1-phosphaallyl anions.[6a, d] In contrast, the allyl carbon atom in **2** is more strongly deshielded by the nitrogen atom (δ = 201.3, ^1J(C,P) = 76.3 Hz). The strong deshielding of the NH proton (δ = 7.9) is indicative of a "tetrahedral" environment for the nitrogen atom and thus the presence of a dimeric structure in solution.[12]

The chemical behavior of **2** towards hard electrophiles reflects the higher basicity of the nitrogen center in comparison to the phosphorus center. Therefore, protonation and silylation of **2** lead smoothly to the phosphaalkenes **3** and **4**, respectively, which can be isolated as thermally stable products. To date an aminophosphaalkene of type **3** is unprecedented, and could be suitable as a starting material in the formation of heteropolyenes. The lithium complex of the *N*-silylated heteroallyl

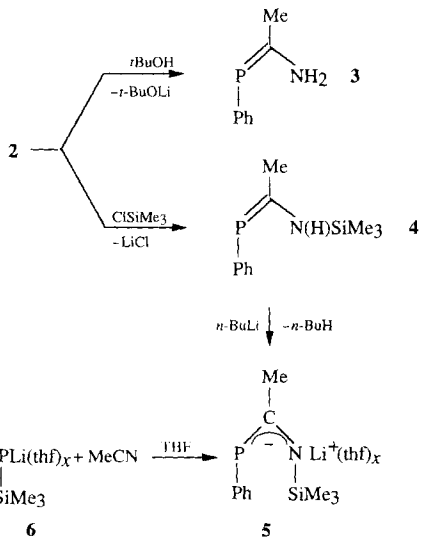

6 **5**

[*] Prof. Dr. E. Niecke, Dipl.-Chem. K. Paasch, Dr. M. Nieger
Anorganisch-chemisches Institut der Universität
Gerhard-Domagk-Strasse 1, D-53121 Bonn (Germany)
Telefax: Int. code + (228)73-5327

[**] This work was supported by the Deutsche Forschungsgemeinschaft and the Fonds der Chemischen Industrie. K. P. thanks the Fonds der Chemischen Industrie for a doctoral grant.

system **5** is accessible from lithium (phenyl)(trimethylsilyl)phosphanide **6** and acetonitrile or by metalation of the phosphaalkene **4**.

Compounds **3** and **4** were characterized on the basis of their elemental analysis, mass spectra (molecular ion peak) as well as ^{1}H, ^{13}C, and ^{31}P NMR experiments. Protonation as well as silylation of **2** lead to a significant deshielding of the phosphorus nucleus (δ = 74.7 (**3**), 94.7(**4**)), whereas the allyl carbon atom only experiences a slight shielding ($\delta(^{13}C)$ = 189.0, ^1J(C,P) = 63.3 Hz (**3**); 193.6, ^1J(C,P) = 64.1 Hz (**4**)). The *cis* position of the methyl group to the lone pair of electrons on the phosphorus atom is proven by the unchanged large value of ^2J(C,P) (**3**:43.5 Hz; **4**: 48.6 Hz). A configuration of this sort is also exhibited by the aminomethylenephosphane **7** in the crystal

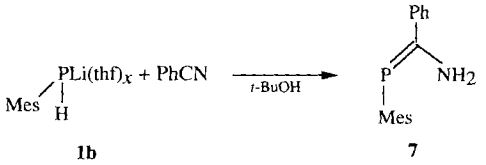

1b **7**

(Fig. 2);[8] compound **7** is accessible in the same way from lithium mesityl phosphanide **1b** and benzonitrile.

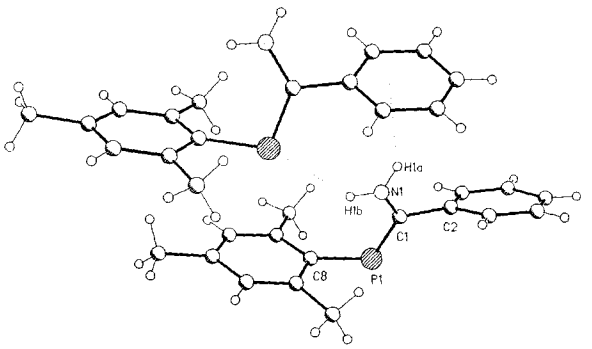

Fig. 2. Crystal structure of **7**. Selected bond lengths [pm] and angles [°]: P1–C1 170.4(2), P1–C8 183.9(2), C1–N1 135.7(3), C1–C2 148.7(2); C1–P1–C8 101.8(1), P1–C1–C2 116.6(1), P1–C1–N1 128.0(2), N1–C1–C2 115.2(2).

The molecules form a chain structure, in which the shortest intermolecular distances (H1 ··· C2–C7 272–316 pm) lie in the range of the sum of the van der Waals radii. An additional van der Waals contact (284 pm) occurs between the second hydrogen atom of the amino group and the phosphorus atom of a neighboring molecule. The C-P-C and P-C-N bond angles (101.8(1)° and 128.0(2)°, respectively) correspond to those in the anion of **2** (100.3.(2)° and 132.0(3)°, respectively). The bond lengths C1–N1 (135.7(3) pm) and P1–C1 (170.4(2) pm) corresponding to those in **2** indicate the presence of a pπ system delocalized over three centers also for **7**.

Experimental Procedure

2: Phenylphosphane (0.26 g, 2.4 mmol) dissolved in THF (6 mL) was treated with *n*BuLi (1.5 mL, 1.6 M in *n*-hexane) at 25 °C under constant stirring. After the reaction mixture had been stirred for 15 min, it was cooled to −30 °C and a solution of acetonitrile (0.1 g, 2.4 mmol) in THF (1.5 mL) was added dropwise. The reaction solution was allowed to warm to 25 °C over 30 min and then left for 16 h. During this time **2** had separated from the orange solution as a yellow microcrystalline solid. Filtration and cooling of the filtrate to −20 °C yielded additional product in the form of yellow extremely air- and moisture-sensitive crystals. Yield: 0.63 g (87%), m.p. 90–92 °C (decomp.); ^{31}P NMR (121.5 MHz, THF): δ = 34.3 (q, ^3J(P,H) = 11.4 Hz); ^{1}H NMR (300 MHz, THF, ext. ref., without Ph group): δ = 2.3 (d, ^3J(P,H) = 11.6 Hz, CH_3, 3H), 7.9 (b, NH, 1H); ^{13}C NMR (75.5 MHz, THF, ext. ref., without PH group): δ = 201.3 (d, ^1J(C,P) = 76.3 Hz, P-C-NH), 27.1 (d, ^2J(C,P) = 60.7 Hz, CH_3).

3, 4: *tert*-Butyl alcohol (**3**) (and trimethylsilyl chloride (**4**), respectively) was added dropwise to a solution of **2** (0.48 g, 1.6 mmol) in THF (10 mL) under ice cooling until decoloration; LiO*t*Bu (and LiCl, respectively) precipitated as a white solid. The solution was stirred again for 1 h at 25 °C, the volatile components were removed in vacuum, the residue was taken up in pentane and filtered through Celite. After removal of the pentane in vacuum, the phosphaalkene **3** was obtained as a white solid, **4** as a yellow oil.

3: Yield 0.20 g (83%); ^{31}P NMR (121.5 MHz, *n*-pentane): δ = 74.7 (q, ^3J(P,H) = 16.5 Hz); ^{1}H NMR (300 MHz, C_6D_6, without Ph group): δ = 2.0 (d, ^3J(P,H) = 16.8 Hz, CH_3, 3H), 4.7 (b, NH_2, 2H); ^{13}C NMR (75.5 MHz, C_6D_6, without Ph group): δ = 24.4 (d, ^2J(C,P) = 43.5 Hz, CH_3), 189.0 (d, ^1J(C,P) = 63 Hz, Ph-P=C); MS (EI, 70 eV): *m/z* (%): [M^+] 151 (100), [M^+−CH_3−H] 135 (9), [M^+−NH_3] 124 (4), [PhP^+] 108 (30), [CH_3CNH^+] 42 (70).

4: Yield 0.26 g (72%); ^{31}P NMR (121.5 MHz, *n*-pentane): δ = 94.7 (q, ^3J(P,H) = 18.3 Hz); ^{1}H NMR (300 MHz, C_6D_6, without Ph group): δ = 0.0 (s, $SiMe_3$, 9H), 2.3 (d, ^3J(P,H) = 18.3 Hz, CH_3, 3H), 5.8 (b, NH, 1H); ^{13}C NMR (75.5 MHz, C_6D_6, without Ph group): δ = 1.7 (s, $SiMe_3$), 24.7 (d, ^2J(C,P) = 48.1 Hz, CH_3), 193.6 (d, ^1J(C,P) = 64.1 Hz, P=C); MS (EI, 70 eV): *m/z* (%): [M^+] 223 (38), [M^+−$SiMe_3$ + H] 151 (13), [M^+−PhP−H] 114 (26), [$SiMe_3^+$] 73 (100).

5: *n*BuLi (1 mL, 1.6 mmol, 1.6 M in *n*-hexane) was added dropwise to a solution of phosphaalkene **4** (0.36 g, 1.6 mmol) in DME (10 mL) at −30 °C. The solution turned red-orange. The solution was slowly allowed to warm to 25 °C and then the solvent was removed in vacuum. The product was obtained in pure form as a yellow oil. Alternatively **5** was afforded in a less pure form (^{31}P NMR: ca. 80%) by reaction of **6** with acetonitrile. ^{31}P NMR (121.5 MHz, DME, −40 °C): δ = 28.5; ^{1}H NMR (300 MHz, DME, ext. ref., −40 °C, without PH group): δ = 0.83 (s, $SiMe_3$, 9H), 1.7 (d, ^3J(P,H) = 6.9 Hz, CH_3, 3H); ^{13}C NMR (75.5 MHz, DME, ext. ref., −40 °C, without Ph group): δ = 4.6 (s, $SiMe_3$), 15.3 (d, ^2J(C,P) = 21.6 Hz, CH_3), 199.1 (d, ^1J(C,P) = 57.4 Hz, P-C-N$SiMe_3$).

7: *n*BuLi (1 mL, 1.6 mmol, 1.6 M in *n*-hexane) was added to a solution of mesitylphosphane (0.24 g, 1.6 mmol) in DME (10 mL) and stirred for 15 min at 25 °C. Subsequently the solution was cooled to −30 °C and treated with a solution of benzonitrile (0.17 g, 1.6 mmol) in DME (1.5 mL). The solution was allowed to warm to 25 °C under constant stirring and then *tert*-butyl alcohol was added dropwise under ice cooling until decoloration. After the solution had been allowed to warm to 25 °C the volatile components were removed in vacuum, the residue was taken up in pentane and filtered through Celite. The product crystallized from the concentrated filtrate at −20 °C in the form of colorless crystals. Yield: 0.37 g (91%), m.p. 70–71 °C; ^{31}P NMR (121.5 MHz, *n*-pentane): δ = 64.4; ^{1}H NMR (300 MHz, C_6D_6, without aryl group): δ = 4.4 (NH_2, 2H); ^{13}C NMR (75.7 MHz, C_6D_6, without aryl groups): δ = 186.6 (d, ^1J(C,P) = 60.3 Hz, P=C); MS (70 eV): *m/z* (%): 255 (68.0) [M^+], 238 (75.2) [M^+-NH_3], 223 (21.9) [M^+-NH_3-CH_3], 119 (49.0) [Mes^+] 104 (100) [Mes-Me^+]; high resolution (M^+): 255.1176 (255.1177 calcd. for $C_{16}H_{18}NP$).

Received: May 30, 1995 [Z 8045 IE]
German version: *Angew. Chem.* **1995**, *107*, 2600–2602

Keywords: heteroallyl anions · lithium compounds · phosphaalkenes · phosphorus compounds

[1] F. T. Edelmann, *Coord. Chem. Rev.* **1994**, *137*, 403–481.
[2] a) A. Chernega, R. Gomez, M. L. H. Green, *J. Chem. Soc. Chem. Commun.* **1993**, 1415–1417; b) R. Gomez, R. Duchateau, A. Chernega, J. H. Teuben, F. T. Edelmann, M. L. H. Green, *J. Organomet. Chem.* **1995**, *491*, 153–158; c) J. C. Flores, J. C. W. Chien, M. D. Rausch, *Organometallics* **1995**, *14*, 1827–1833.
[3] H. H. Karsch, A. Appelt, H.-U. Reisacher, G. Müller, *Phosphorus, Sulfur Relat. Elem.* **1987**, *30*, 417–420; H. H. Karsch, H.-U. Reisacher, A. Schneider, T. Rupprich in *Synthetic Methods of Inorganic and Organometallic Chemistry, Vol. 3* (Eds.: G. Brauer, W. A. Herrmann) Thieme, Stuttgart, **1995**, in press.
[4] R. Appel in *Multiple Bonding and Low Coordination in Phosphorus Chemistry* (Eds.: M. Regitz, O. J. Scherer), Thieme, Stuttgart **1990**, pp. 157–219.
[5] W. Keim, R. Appel, S. Gruppe, F. Knoch, *Angew. Chem.* **1987**, *99*, 1042–1043; *Angew. Chem. Int. Ed. Engl.* **1987**, *27*, 1012–1013.
[6] a) E. Niecke, M. Nieger, P. Wenderoth, *J. Am. Chem. Soc.* **1993**, *115*, 6989–6990; b) *Angew. Chem.* **1994**, *106*, 362–363; *Angew. Chem. Int. Ed. Engl.* **1994**, *33*, 353–354; c) *ibid.* **1994**, *106*, 2045–2046 and **1994**, *33*, 1953–1954; d) K. Paasch, M. Nieger, P. Wenderoth, E. Niecke, unpublished.

[7] There is little known about the 1-aza-3-phosphaallyl anion, cf.: a) K. Issleib, H. Schmidt, H. Meyer, *J. Organomet. Chem.* **1978**, *160*, 47–57. b) [PhPC(Ph)NSiMe$_3$Li(dme)], a monomeric lithium complex of an 1-aza-3-phosphaallyl anion, has also been prepared: G. Becker, Stuttgart, personal communication. G. Becker, G. Ditten, K. Hübler, K. Merz, M. Niemeyer, N. Seidler, M. Westermann in *Organosilicon Chemistry II* (Eds.: N. Auner, J. Weiss), VCH, Weinheim, in press.

[8] X-ray structure analysis of **2** [7]: yellow [colorless] crystals, crystal dimensions $0.05 \times 0.13 \times 0.20$ mm [$0.08 \times 0.23 \times 0.58$ mm]; $M_r = 602.6$ [255.3]; monoclinic [monoclinic], space group $C2/c$ (no. 15) [$P2_1/c$ (no. 14)], $a = 23.835(4)$ [14.077(1)], $b = 8.818(2)$ [9.937(1)], $c = 18.786(2)$ Å [10.635(1) Å], $\beta = 116.07(1)$ [108.36(1)°], $V = 3547(1)$ Å^3 [1411.9(2) Å^3], $Z = 4$ [4], $\mu(Cu_{K\alpha}) = 1.38$ [1.56] mm^{-1}, $T = 200$ [208] K, $F(000) = 1296$ [544]. 1851 [2787] intensities up to $2\theta_{max} = 100°$ [140°] were measured on an Enraf-Nonius-CAD4-diffractometer with $Cu_{K\alpha}$ radiation, of which 1778 [2671] were independent and were used for all calculations. The structure was solved with direct methods and refined on F^2 anisotropically, the H atoms were refined with a riding model (program: SHELXL-93 [9]). The final quality coefficient $wR2$ (F^2) was 0.165 [0.145] with a conventional $R(F) = 0.056$ [0.049] for 223 [173] parameters and 139 [2] restraints. The THF ligands in **2** are disordered. For **7** an extinction correction and an empirical absorption correction was carried out on the basis of Ψ scans. Further details of the crystal structure investigation may be obtained from the Fachinformationszentrum Karlsruhe, D-76344 Eggenstein-Leopoldshafen (Germany) on quoting the depository number CSD-59144.

[9] G. M. Sheldrick, SHELXL-93, Universität Göttingen. **1993**.

[10] W. N. Setzer, P. von R. Schleyer, *Adv. Organomet. Chem.* **1985**, *24*, 354–450.

[11] Quantum chemical calculations on the configuration isomers of the parent compound [HPC(H)NH]$^-$ show the *endo*/*endo* form to be energetically favored. Relative energies of the different configuration isomers of [HPC(H)NH]$^-$ (relative to *endo*/*endo* form) [kcal mol^{-1}]: *exo*(PH)/*endo*(NH): + 0.6; *endo*(PH)/*exo*(NH): + 4.4; *exo*(PH)/*exo*(NH): + 5.1. We thank Prof. Dr. W. W. Schoeller, Bielefeld, for providing us with the results.

[12] This was confirmed by a molecular weight determination.

Metal Complexes of N-Heterocyclic Carbenes—A New Structural Principle for Catalysts in Homogeneous Catalysis**

Wolfgang A. Herrmann,* Martina Elison, Jakob Fischer, Christian Köcher, and Georg R. J. Artus

A basic functional principle in homogeneous complex catalysis is based on the fact that phosphane and phosphite ligands not only protect low-valent metal centers from aggregation (stabilization effect), but also create coordination sites in dissociation equilibria at which the catalytic elementary steps proceed (activation effect).[1] Examples of industrial importance are hydrocyanation ($Ni^0/P(OR)_3$) and hydroformylation (Co^I/PR_3, Rh^I/PR_3). Generally, as a result of the notorious phosphane degradation by P–C bond cleavage,[2] an excess of the ligand—often 100 times more than the metal—is required to control the equilibrium in the activation and propagation steps in homogeneous catalysis. This excess increases the running costs of technical plants.[3] Phosphane and phosphite complexes are also often water- and air-sensitive. Using the Heck coupling as example,[1c, 4] we now describe a new catalyst principle that does not have these disadvantages. It relies on the special ligand properties of N-heterocyclic carbenes and stands out because of its simplicity and efficiency.

[*] Prof. Dr. W. A. Herrmann, M. Elison, J. Fischer, C. Köcher, G. R. J. Artus
Anorganisch-chemisches Institut der Technischen Universität München
Lichtenbergstrasse 4, D-85747 Garching (Germany)
Telefax: Int. code + (89)3209-3473

[**] Coordination Chemistry and Mechanisms of Metal-Catalyzed CC Coupling Reactions, Part 9. Part 8: W. A. Herrmann, C. P. Reisinger, K. Öfele, C. Brossmer, M. Beller, H. Fischer, *J. Mol. Catal.*, in press.

The carbene–palladium complexes **1** and **2** of the imidazole series were prepared from $[Pd(OAc)_2]$ and 1,3-dimethylimidazolium iodide or 3,3′-dimethyl-1,1′-methylenediimidazolium diiodide in more than 70 and 40% yield, respectively [Eq. (a) and (b)]. They are extraordinarily stable to heat, oxygen, and

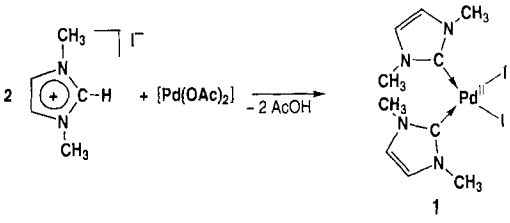

(a)

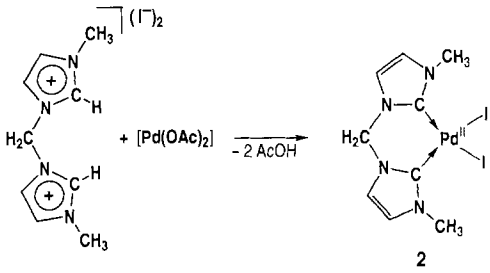

(b)

moisture. Catalyst **1** melts at temperatures as high as 299 °C with partial decomposition and resists several days treatment with O_2 in boiling THF. The complex **2** melts at 280 °C, but decomposes noticably in solution (*N*,*N*-dimethylacetamide) at temperatures above 70 °C.

Besides the expected square-planar core geometry, a crystal structure analysis of **1** (Fig. 1)[5] shows that the two carbene

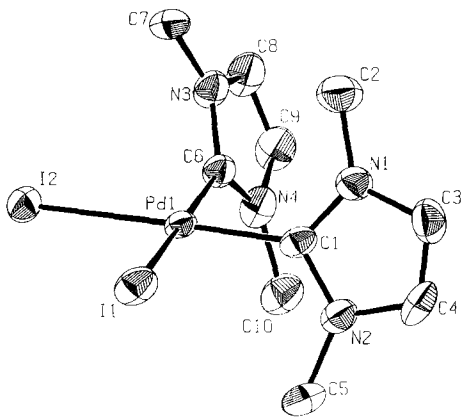

Fig. 1. PLATON representation of the crystal structure of the "carbene" complex **1**. The ellipsoids represent 50% probability; H atoms are omitted for clarity. Selected distances [Å] and angles [°]: Pd1-I1 2.6479(3), Pd1-I2 2.6572(3), Pd1-C1 1.990(3), Pd1-C6 1.997(3), N1-C1 1.347(4), N2-C1 1.363(4), N3-C6 1.357(4), N4-C6 1.336(4); I2-Pd1-I1 93.590(9), C1-Pd1-I1 87.32(8), C1-Pd1-I2 178.08(8), C6-Pd1-I1 175.52(9), C6-Pd1-I2 88.97(8), C6-Pd1-C1 90.2(1).

ligands are in a *cis* arrangement and twisted relative to the PdI_2 plane (70.5 and 69.4°). The $[(PR_3)_2PdX_2]$ (X = halogen) complexes with monodentate phosphane ligands that were known previously and characterized by crystal structure analyses have *trans* configurations, which reflects the greater steric demand of the phosphane ligand. In contrast to the planar carbene ligands, the phosphane ligands cannot relieve the steric congestion by rotation about the metal–ligand bond (Pd–P instead of Pd–C).

The Pd–C bond lengths (1.990(3)/1.997(3) Å) lie in the range of those of known carbene complexes (1.95–2.07 Å)[6]– true Pd–C single bonds (Pd–C(alkyl), Pd–C(benzyl)) are, however, hardly longer: 1.99–2.05 Å.[7] In accord with results from vibrational spectroscopy,[8] it is therefore certainly valid that heterocyclic carbenes of the imidazole type have pronounced donor properties similar to the electron-rich phosphanes and that π-backbonding is insignificant. The formal depiction of this class of compounds as **A** (σ-donor) and **B** (π-donor) probably most closely represents the bonding; on the contrary, the conventional, formal notation **C** is certainly inaccurate in that it does not reflect the apparent analogy between these "carbenes" and other donor ligands.

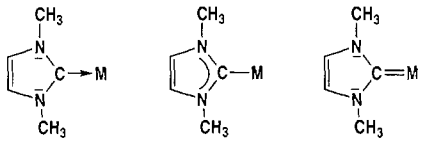

The Pd complexes **1** and **2** catalyze the Heck coupling of aryl halides [Eq. (c)].[9a] The higher turnovers are obtained with **1**

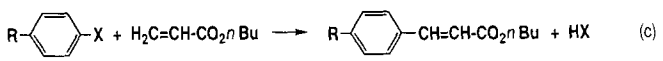

X	Br	Br, Cl	Br	Cl
R	CH_3O	C(=O)H	$C(=O)CH_3$	NO_2

because of its pronounced thermal stability in solution (see Table 1). As shown by kinetic measurements (see Fig. 2), the activity at the beginning of the reaction of bromoarenes (for example 4-bromobenzaldehyde) is lower than that of the particularly active palladacycles,[7b, 9b] but the advantages of the new catalyst **1** lie in the formation of stable active species and in the length of time it remains stable *even at high temperatures*, a property that is still essential for the activation of chloroarenes.

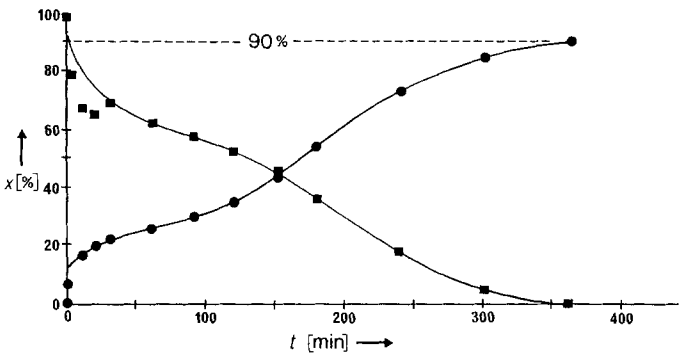

Fig. 2. Concentration/time diagram (amount of substance x[%], time t [min]) for the Heck olefination of 4-bromobenzaldehyde (■) with n-butyl acrylate to form n-butyl (*E*)-4-formylcinnamate (●); for reaction conditions see Experimental Procedure and Table 1. 0.5 mol% **1**. The loss of the starting material (approximately 10%) immediately after the start of the reaction is attributed to the formation of the Heck coupling product and appears to be correlated to the activation of the catalyst, for example by reduction through the aldehyde.

The sigmoidal turnover characteristics (concentration/time diagram; Fig. 2) result in an initially sluggish product formation. As the reaction proceeds the turnover per time increases markedly. An activating conversion step must thus be assumed for the catalytic activity of **1**. No inductive phase is observed for **1** after treatment with reducing agents: whereas 4-bromoacetophenone is converted only very slowly with **1** under mild conditions and no other additives (Fig. 3), the concentration of the starting material decreases suddenly and exponentially after addition of hydrazine (after 67 min). Sodium formate is a particularly advantageous reducing agent in this context (no metal complexation, nontoxic).

Table 1. Heck olefination of chloro- and bromoarenes with carbene–palladium catalysts [a].

Substrate	Catalyst	Amount of catalyst [mol%]	t[h]	Turnover[%]
$4\text{-BrC}_6\text{H}_4\text{CHO}$	**1**	0.5	10	>99
$4\text{-BrC}_6\text{H}_4\text{CHO}$	**2**	0.5	10	>99
$4\text{-BrC}_6\text{H}_4\text{CHO}$	**3**	0.1	3	>99
$4\text{-BrC}_6\text{H}_4\text{C(=O)CH}_3$	**1**	0.5	10	>99
$4\text{-BrC}_6\text{H}_4\text{C(=O)CH}_3$	**2**	0.5	10	>99
$4\text{-BrC}_6\text{H}_4\text{C(=O)CH}_3$	**3**	0.1	3	>99
$4\text{-BrC}_6\text{H}_4\text{C(=O)CH}_3$	**3**	2×10^{-3}	19	>99
$4\text{-BrC}_6\text{H}_4\text{C(=O)CH}_3$	**3**	4×10^{-4}	43	>99
$4\text{-BrC}_6\text{H}_4\text{C(=O)CH}_3$	**3**	2×10^{-4}	96	66
$4\text{-BrC}_6\text{H}_4\text{OCH}_3$	**1**	0.67	50	60
$4\text{-BrC}_6\text{H}_4\text{OCH}_3$	**2**	0.67	50	20
$4\text{-BrC}_6\text{H}_4\text{OCH}_3$	**3**	2×10^{-3}	8	78
$4\text{-ClC}_6\text{H}_4\text{CHO}$	**1**	1	24	12
$4\text{-ClC}_6\text{H}_4\text{CHO}$	**1**[b]	1	24	>99
$4\text{-ClC}_6\text{H}_4\text{NO}_2$	**1**[b]	0.1	36	>99

[a] For reaction conditions, see Experimental Procedure. The catalyst **3** is the carbene complex $[Pd^0L_2]$ formed in situ from $[Pd(dba)_2]$ and free carbene L (see text). [b] With addition of $[N(n\text{-}C_4H_9)_4]Br$ (50 mmol).

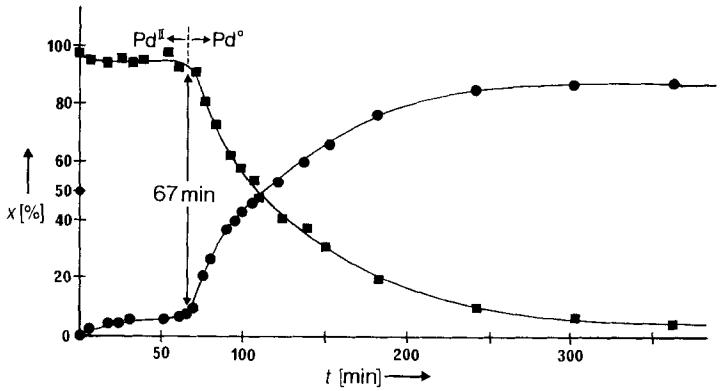

Fig. 3. Concentration/time diagram (amount of substance x[%], time t [min]) for the Heck olefination of 4-bromoacetophenone (■) with n-butyl acrylate to form n-butyl (*E*)-4-acetylcinnamate (●); for reaction conditions see Experimental Procedure and Table 1. 0.5 mol% **1**, addition of 85 μL hydrazine hydrate after 67 min.

The conversions of 4-chlorobenzaldehyde and 4-chloronitrobenzene with n-butyl acrylate [Eq. (c)] proceed quantitatively at 130 °C with **1** (1 and 0.1 mol%, respectively) on addition of $[N(n\text{-}C_4H_9)_4]Br$ (Fig. 4, Table 1). Here too, the usual induction period is absent. We conclude that the formyl group of the chloroarene or $[N(n\text{-}C_4H_9)_4]Br$ acts as reducing agent.

The results raise the expectation that a carbene complex $[Pd(carbene)_2]$ (**3**) with a zerovalent palladium center prepared in situ should be immediately active without induction period. $[Pd(dba)_2]$ (dba = dibenzylidene acetone) was therefore treated

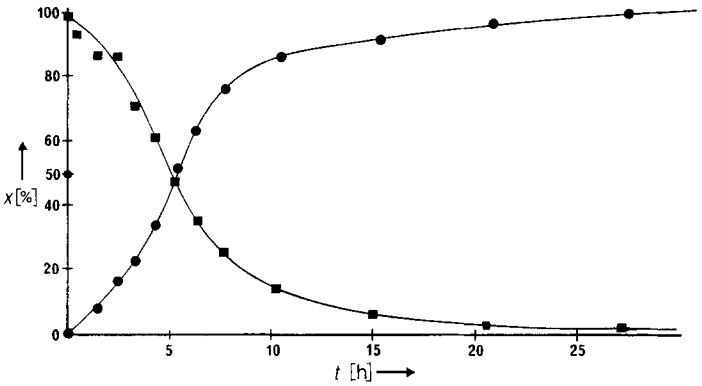

Fig. 4. Concentration/time diagram (amount of substance x[%], time t [h]) for the Heck olefination of 4-chlorobenzaldehyde (■) with *n*-butyl acrylate to form *n*-butyl (*E*)-4-formylcinnamate (●); for reaction conditions see Experimental Procedure and Table 1, 1 mol% 1, 50 mmol $[N(n\text{-}C_4H_9)_4]Br$.

with two equivalents of free 1,3-dimethyldihydroimidazole-2-ylidene (L) in toluene at room temperature. The coordination of the metal center by the carbene can be monitored by the color change from violet to red, as well as by ^1H and ^{13}C NMR spectroscopy ($\delta_{C(carbene)} = 180.2$, [D$_8$]toluene). The Pd^0–carbene catalyst **3** does indeed have an extremely large initial activity with long-term stability in the Heck olefination (Table 1): with only 4×10^{-4} mol% (!) catalyst, 50 mmol 4-bromoacetophenone can be completely converted in 43 h without palladium deposition. Because of the absence of an induction period and of the high activity, turnover numbers (TON) of more than 250000 can be achieved with **3** for activated bromoarenes, whereas with $[Pd(dba)_2]$ without the stabilizing carbene ligands turnovers are only low in the same time. In the catalytic conversion of 4-bromoanisol with $[Pd(dba)_2]$, inactive palladium separates quantitatively at room temperature already. Even with these deactivated bromoarenes the stabilizing influence of the carbene ligands is obvious: here the turnover numbers per hour (TOF = 15000) reach higher values than with all classical phosphane complexes.

The "carbenes" derived from imidazole appear to stabilize Pd^{II} and Pd^0 complexes because of their pronounced donor properties. This picture also encompasses the existence of the recently described complexes $[BeCl \cdot L_3]^+Cl^-$, $[TiCl_4 \cdot L_2]$, and $[MoO_2Cl \cdot L_3]^+Cl^-$, in which the carbene ligand L replaces conventional solvent ligands like acetonitrile, tetrahydrofuran, and *N*,*N*-dimethylformamide by formation of a stable dative bond, or breaks dimeric and polymeric structures.[10] In contrast to the common Pd/phosphane catalysts, in the new Pd/carbene systems the ligands do not undergo deactivating degradation reactions.[11] No deposition of (catalytically inactive) palladium can be detected.

The new catalyst type described here has a series of advantageous properties and potential for development: a) high thermal and hydrolytic durability resulting from exceptionally stable M–C bonds (long shelf-life, stability to oxidation); b) easy accessibility, and c) no need for an excess of the ligand. The prospects for derivatization to water-soluble catalysts (two-phase catalysis), immobilization, and chiral modification seem promising because of the constitution of the ligands.

Experimental Procedure

1: A solution of $[Pd(OAc)_2]$ (2.00 g, 8.9 mmol) and 1,3-dimethylimidazolium iodide (4.20 g, 18.7 mmol) in THF (150 mL) was heated for 30 min under reflux, during which time the initially brown solution bleached to yellow. After evaporation to dryness under vacuum, the residue was washed with diethyl ether (three 50 mL portions), taken up in CH_2Cl_2 (100 mL), and the solution layered with *n*-pentane (200 mL). At 25 °C **1** crystallized as a yellow solid that was very soluble in $CHCl_3$, and slightly soluble in THF and toluene. Yield: 3.70 g (75%). ^1H NMR (400 MHz, $CDCl_3$, 20 °C): $\delta = 7.24$ (s, 4H, NCH), 3.92 (s, 12H, CH_3); ^{13}C NMR (100.1 MHz, $CDCl_3$, 20 °C): $\delta = 168.2$ (carbene-C), 122.3 (NCH), 38.2 (CH_3); correct C,H,N analysis.

2: $[Pd(OAc)_2]$ (200 mg, 0.89 mmol) was treated at 170 °C with 3,3'-dimethyl-1,1'-methylenediimidazolium diiodide (400 mg, 0.89 mmol). After heating for 5 min under vacuum the residue was extracted with THF and filtered over a frit covered with a layer of silica gel. The solvent was removed under vacuum, the residue washed with absolute diethyl ether (three 20 mL portions), taken up in CH_2Cl_2 (10 mL), and the solution carefully layered with *n*-pentane (30 mL). The yellow crystals of **2** were dried under vacuum. They dissolve well in $CHCl_3$, CH_2Cl_2, THF, and toluene, to give a yellow solution. Yield: 190 mg (40%). ^1H NMR (400 MHz, $CDCl_3$, 20 °C): $\delta = 3.92$ (s, 6H, NCH_3), 6.61 (s, 2H, CH_2), 7.41, 7.43 (s, 4H, NCH); ^{13}C NMR (100.1 MHz, $CDCl_3$, 20 °C): $\delta = 36.31$ (NCH_3), 53.60 (CH_2), 121.87, 124.35 (NCH), 185.50 (carbene-C); correct C,H,N analysis.

General procedure for Heck olefination of chloro- and bromoarenes: In a 100 mL three-necked flask fitted with a septum, thermometer, and reflux condenser (with mercury overpressure valve) were placed the haloarene (50 mmol), anhydrous sodium acetate (4.51 g, 55 mmol) and diethyleneglycol di-*n*-butyl ether (GC standard, 1000 mg) in 50 mL *N*,*N*-dimethylacetamide. After repeated degassing under oil pump vacuum and flushing with argon, *n*-butyl acrylate (10 mL, 70 mmol) was injected through the septum. The charge was heated to 100 °C, whereupon the freshly prepared catalyst mixture or the solution of the Pd^{II}–carbene complex was added through the septum, and the mixture heated to the reaction temperature (125 °C with bromoarenes, 140 °C with chloroarenes). To monitor the reaction, 500 μL samples were taken at regular intervals, washed with 5 mL dilute hydrochloric acid (5%), and extracted with 3.5 mL CH_2Cl_2. The organic phases were analyzed by gas chromatography (GC-FID, GC-MS, GC-IR-MS). For quantitative analysis and the recording of concentration/time diagrams a gas chromatograph GC 5980A with flame ionization detector (FID), automatic sampler, and an HP-1 capillary column (12.5 m) from Hewlett Packard was used.

Received: June 26, 1995 [Z8131IE]
German version: *Angew. Chem.* **1995**, *107*, 2602–2605

Keywords: carbenes · catalysis · Heck reactions · palladium compounds

[1] a) J. P. Collman, L. S. Hegedus, J. R. Norton, R. G. Finke, *Principles and Applications of Organotransition Metal Chemistry*, University Science Books, Mill Valley, CA, USA, **1987**; b) G. W. Parshall, S. D. Ittel, *Homogeneous Catalysis*, 2nd ed., Wiley, New York, **1992**; c) *Applied Homogeneous Catalysis by Organometallic Complexes* (Eds.: B. Cornils, W. A. Herrmann), VCH, Weinheim, **1996**, in press.

[2] P. E. Garrou, *Chem. Rev.* **1985**, *85*, 171–185.

[3] A well documented example of this problem is the hydroformylation (annual world capacity 6–8 million metric tons): a) B. Cornils in *New Syntheses with Carbon Monoxide* (Ed.: J. Falbe), Springer, Berlin, **1980**, Chap. 1; b) W. A. Herrmann, C. W. Kohlpaintner, *Angew. Chem.* **1993**, *105*, 1588–1609; *Angew. Chem. Int. Ed. Engl.* **1993**, *32*, 1524–1544.

[4] Reviews: a) V. V. Grushin, H. Alper, *Chem. Rev.* **1994**, *94*, 1047–1062; b) A. de Meijere, F. E. Meyer, *Angew. Chem.* **1994**, *106*, 2473–2506; *Angew. Chem. Int. Ed. Engl.* **1994**, *33*, 2379–2411.

[5] The complex **1** ($C_{10}H_{16}I_2N_4Pd$, 552.49 g mol^{-1}, $F(000) = 1024$) crystallizes in the form of yellow crystals of X-ray quality at 25 °C after layering a CH_2Cl_2 solution with *n*-pentane. Space group $P2_1/n$ (no. 14), cell constants by least-squares refinement of 25 reflections in the angle range $32.6 < 2\theta < 41.5°$ ($\lambda = 0.70930$ Å, $Mo_{K\alpha 1}$): $a = 8.875(3)$, $b = 16.375(2)$, $c = 11.216(3)$ Å, $\beta = 94.87(2)°$, $V = 1624.0$ Å^3, $Z = 4$, $\rho_{calcd} = 2.26$ g cm^{-3}. CAD4-Enraf-Nonius diffractometer, graphite monochromator ($\lambda = 0.71073$ Å, $Mo_{K\alpha}$), $T = -50 \pm 3$ °C, measurement range: $1.0° < \theta < 25.0°$, mode: ω scan, scan time max. 60 s, scan width $(1.0 + 0.2 \tan\theta)°$, every 3600 s three reflections used to check the intensity, every 100 reflections three used to check orientation; 5923 measured reflections, 232 systematic absences, 447 with negative intensity ($I/\sigma(I) < 0.01$), 4583 reflections averaged, of 2758 independent reflections 2461 ($I > 2.0\sigma(I)$) used in the refinement, structure solution by Patterson methods (SHELXS-86), refinement with the program CRYSTALS. All H positions were calculated by assuming ideal geometry, but not refined, weighting scheme according to Tukey and Prince with three parameters, 154 parameters refined, 16 reflections per parameter, shift/err < 0.0001. $R = \Sigma(||F_o| - |F_c||)/\Sigma|F_o| = 0.027$, $R_w = [\Sigma w(|F_o| - |F_c|)^2/\Sigma w F_o^2]^{1/2} = 0.026$. Refined: $\Sigma w(|F_o| - |F_c|)_2$. Residual electron density: max. $+1.13$ e Å^{-3} at a distance of 0.82 Å from a Pd atom, min. -0.94 e Å^{-3}. Further details of the crystal structure investigation may be obtained from the Fachinformationszentrum Karlsruhe, D-76344 Eggenstein-Leopoldshafen (Germany) on quoting the depository number CSD-59066.

[6] Examples: a) R. D. Wilson, Y. Kamitori, H. Ogoshi, Z.-I. Yoshida, J. A. Ibers, *J. Organomet. Chem.* **1979**, *173*, 199–209; b) A. Modinos, P. Woodward, *J. Chem. Soc. Dalton Trans.* **1974**, 2065–2069; c) P. Domiano, A. Musatti, M. Nardelli, G. Predieri, *J. Chem. Soc. Dalton Trans.* **1975**, 2165–2168; d) H. C. Clark, C. R. C. Milne, N. C. Payne, *J. Am. Chem. Soc.* **1978**, *100*, 1164–1169; e) W. M. Butler, J. H. Enemark, *Inorg. Chem.* **1971**, *10*, 2416–2419; f) O. P. Anderson, A. B. Packard, *ibid.* **1978**, *17*, 1333–1337.

[7] Examples: a) P. K. Beyers, A. J. Canty, L. M. Engelhardt, A. H. White, *J. Chem. Soc. Dalton Trans.* **1986**, 1731–1734; b) W. A. Herrmann, C. Broßmer, K. Öfele, C.-P. Reisinger, T. Priermeier, M. Beller, H. Fischer, *Angew. Chem.* **1995**, *107*, 1989–1992; *Angew. Chem. Int. Ed. Engl.* **1995**, *34*, 1844–1848; c) A. L. Rheingold, W. C. Fultz, *Organometallics* **1984**, *3*, 1414–1417; d) W. De Graaf, J. Boersma, W. J. J. Smeets, A. L. Spek, G. van Koten, *Organometallics*, **1989**, *8*, 2907–2917.

[8] K. Öfele, W. A. Herrmann, D. Mihalios, M. Elison, E. Herdtweck, W. Scherer, J. Mink, *J. Organomet. Chem.* **1993**, *459*, 177–184.

[9] a) W. A. Herrmann, M. Elison, J. Fischer, C. Köcher (Hoechst AG), DE-4447068, **1994**; b) W. A. Herrmann, C. Brossmer, M. Beller, H. Fischer (Hoechst AG), DE-4421730, **1994** and DE-4421753, **1994**.

[10] a) W. A. Herrmann, K. Öfele, M. Elison, F. E. Kühn, P. W. Roesky, *J. Organomet. Chem.* **1994**, *480*, C7–C9; b) W. A. Herrmann, O. Runte, G. Artus, *ibid.* **1995**, *501*, C1–C4; c) W. A. Herrmann, M. Elison, J. Fischer, C. Köcher, G. R. J. Artus, *Chem. Eur. J.*, in press; d) W. A. Herrmann, G. M. Lobmaier, M. Elison, *J. Organomet. Chem.*, in press.

[11] W. A. Herrmann, C. Brossmer, K. Öfele, M. Beller, H. Fischer, *J. Organomet. Chem.* **1995**, *491*, C1–C4.

Self-Assembly of Polyanions at a Metal Cation Template: Syntheses and Structures of $[\{Ag([18]aneS_6)\}I_7]_n$ and $[Ag([18]aneS_6)]I_3$**

Alexander J. Blake, Robert O. Gould, Simon Parsons, Christian Radek, and Martin Schröder*

The formation and stability of extended polyiodide species has been found to be dependent on the size of the accompanying cation.[1] We have been interested over the past few years in the coordination chemistry of transition metal ions with homoleptic macrocyclic S-donor ligands.[2] In the context of this work we were interested in ascertaining whether metal macrocyclic cations could be used to template-synthesize extended polyiodide arrays. While numerous examples of small polyiodides such as I_3^-, I_4^{2-}, and I_5^- have been reported,[3, 4] only a few large and very large polyiodide species such as I_7^-, I_8^{2-}, I_9^-, I_{12}^{2-}, I_{14}^{2-}, I_{15}^{3-}, and I_{16}^{4-} are known.[5–10] We report herein the synthesis of a new polymeric $(I_7^-)_n$ polyiodide species assembled around a central macrocyclic cation, $[Ag([18]aneS_6)]^+$.

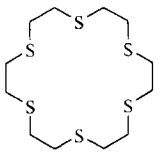

[18]anS$_6$

Reaction of $[Ag([18]aneS_6)]BF_4$ with I_2 afforded, after evaporation of the solvent in vacuo, a dark blue powder. No precipitation of AgI was observed, confirming the effective encapsulation of the Ag^+ ions by [18]aneS$_6$. The elemental analysis data are consistent with the stoichiometry $[Ag([18]aneS_6)]I_5$, while the FAB mass spectrum shows a peak at m/z 469 with an isotopic distribution consistent with $[^{109}Ag([18]aneS_6)]^+$. The ESR spectrum is featureless, showing that the dark blue color cannot be due to the formation of a radical Ag^{II} complex.[11] Recrystallization of the initial blue product from MeCN and EtOH affords lustrous red crystals of **1** and brown crystals of **2**, respectively. Analytical and spectroscopic data are consistent with these formulations. In order to fully establish the structure of these products, single-crystal X-ray determinations were undertaken.

$[\{Ag([18]aneS_6)\}I_7]_n$ **1**

$[Ag([18]aneS_6)]I_3$ **2**

The single-crystal structure of **1**[12] shows the $[Ag([18]aneS_6)]^+$ ions embedded in a three-dimensional polymeric polyiodide matrix (Fig. 1). The structure of the $(I_7^-)_n$ polyiodide network in the crystal lattice can best be described as

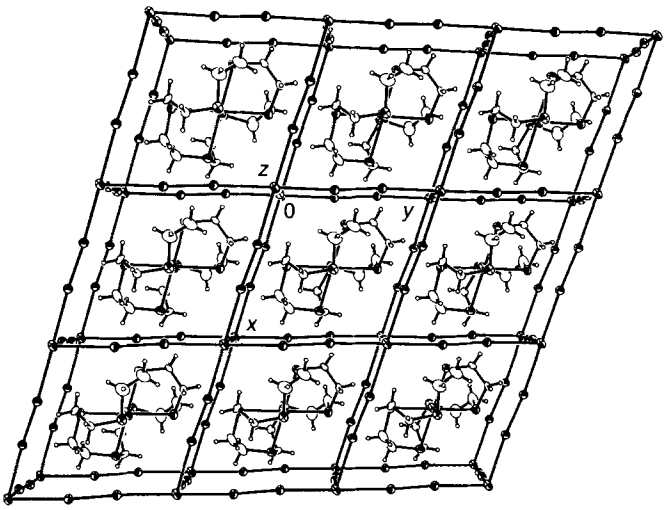

Fig. 1. View of the polymeric matrix of **1**.

a distorted cubic structure in which I^- ions occupy the lattice points of a primitive rhombohedral lattice with one I_2 molecule [I–I 2.7519(14) Å] placed along each edge, bridging two I^- ions, $I^- \cdots I$ 3.3564(15) Å. The I–I bond length in the I_2 molecule in **1** is longer than that in I_2 in the vapor [2.667(2) Å][17] and in the solid state [2.715(6) Å].[18] This elongation is attributable to donation of electron density from I^- into the σ^*-antibonding LUMO of the I_2 molecule. The structure is completed by an $[Ag([18]aneS_6)]^+$ ion sitting inside each rhombohedral interstice (Fig. 2).

I_7^- polyiodide species have been reported previously although none with the current cubic structure. The structures of $(Et_4N)I_7$[5] and $[(py)_2I]I_7$[6] (py = pyridine) show a three-dimensional network of symmetrical I_3^- anions and I_2 molecules and these are therefore better described as an adduct of $[(I_3^-)\cdot(I_2)_2]$. The two compounds $(Hpy)_2I_3I_7$[7] and $[(N\text{-methylbenzothiazole-2(3}H)\text{-thione})_2I]I_7$[8] feature I_7^- ions which are to a first approximation isolated species but linked through long-range $I \cdots I$ interactions of 3.545(13) and 3.502(1) Å, respectively, to give one-dimensional infinite chain structures. The I_7^- ion in these two structures can be described as adducts of $[(I^-)\cdot(I_2)_3]$. The structure of $(PPh_4)I_7$, however, does show discrete I_7^- units.[9]

The single-crystal structure determination of **2**[12] shows discrete metal macrocyclic cations $[Ag([18]aneS_6)]^+$ and symmetrical I_3^- ions [I–I 2.9137(3) Å] in the crystal lattice. The packing

[*] Prof. Dr. M. Schröder, Dr. A. J. Blake
Department of Chemistry, The University of Nottingham
University Park, Nottingham NG7 2RD (UK)
Telefax: Int. code + (115)9513563
Dr. R. O. Gould, Dr. S. Parsons, Dr. C. Radek
Department of Chemistry, The University of Edinburgh
West Mains Road, Edinburgh, EH9 3JJ (UK)

[**] This work was supported by the Engineering and Physical Sciences Research Council, UK. [18]aneS$_6$ = 1,4,7,10,13,16-hexathiacyclooctadecane.

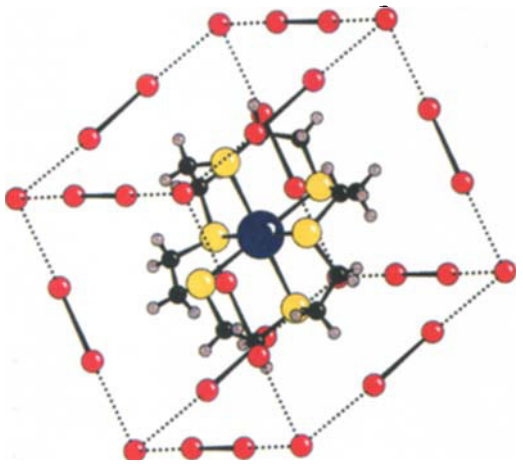

Fig. 2. Section of the structure of **1**. I⁻···I 2.7519(14) Å, I···I 3.3564(15) Å.

diagram (Fig. 3) shows a columnar stacking arrangement with parallel stacks of macrocycles and I_3^- ions. It is noticeable that the orientation of the long Ag–S(1) bond length in the cation of **2** is parallel to the axis of the I_3^- ion.

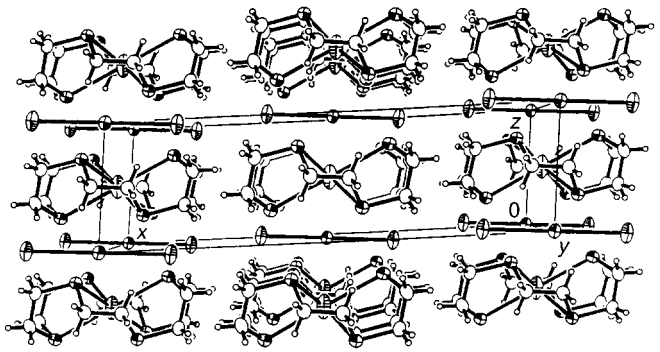

Fig. 3. Crystal structure of **2**.

As in $[Ag([18]aneS_6)]PF_6$,[11] the macrocyclic cations in **1** and **2** both adopt trigonally compressed octahedral coordination geometries; the S-Ag-S chelate angles are about 80° and non-chelate angles are about 100°. In the I_7^- salt **1**, however, all Ag–S distances are equivalent [2.754(2) Å], while the PF_6^- salt shows a tetragonal compression [$Ag-S_{ax} = 2.697(5)$, $Ag-S_{eq} = 2.753(4)$ Å][11] and the I_3^- salt **2** a tetragonal elongation [$Ag-S_{ax} = 2.8007(10)$, $Ag-S_{eq} = 2.7255(7)$ Å]. The template effect of the macrocyclic cation on the structure of the polymeric I_7^- anion in **1** may be demonstrated by comparing the diagonals of the unit cell with the spacing of the S_3 triangles making up the faces of the coordination polyhedron around Ag. The cell diagonal along the threefold axis is 11.850(5) Å, while the other diagonals are 17.635(7) Å. The thickness of the cation may be estimated as the separation of the S_3 triangles (2.48 Å) plus twice the van der Waals radius of sulfur (1.85 Å), giving 6.18 Å. Its mean diameter may be estimated as twice the mean distance of the carbon atoms from the threefold axis (3.55 Å) plus twice the van der Waals radius of carbon (1.50 Å), making 10.1 Å. Thus, the $[Ag([18]aneS_6)]^+$ cation represents a good fit within the cubic second-sphere framework formed by the I_7^- polyanion.

The structures of the anions in **1** and **2** can be compared to that observed in $(Me_4N)I_5$.[4] Thus, the structures of these I_3^-, I_5^-, and I_7^- polyanions can be considered as one-, two-, and three-dimensional structures of the adducts of I^- with one, two, and three I_2 molecules, respectively, with (I_2)-I-(I_2) angles of 90°. We are currently investigating the reaction pathway to the formation of the initial dark blue product assigned tentatively as $[Ag([18]aneS_6)]I_5$ and its conversion to other polyanionic species. The mechanism of formation of these polyanions around the macrocyclic complex cation is so far unclear. "Spontaneous" heterolytic cleavage of the I–I bond has, however, been reported in the gas phase preparation of the dark blue I_2-amylose complex which contains I_5^- ions.[19]

Experimental Procedure

$[18]aneS_6$ (90 mg, 0.25 mmol) was dissolved in $CHCl_3$ (3 cm^3) and a solution of $AgBF_4$ (48.6 mg, 0.25 mmol) in $MeNO_2$ (5 cm^3) added. The colorless solution was stirred vigorously for 15 min and a solution of I_2 (190 mg, 0.75 mmol) in $CHCl_3$ (5 cm^3) added, after which the reaction solution changed color to orange and then violet. The solution was filtered and solvent removed in vacuo to afford a dark blue solid. The product was soluble in DMF, DMSO, EtOH, and $MeNO_2$ to give yellow-brown solutions, and in CH_2Cl_2 to give a purple solution. Recrystallization of the blue product from EtOH afforded brown crystals of **2** (elemental analysis [%]: found C 17.34, H 2.77; calcd. C 16.97, H 2.85), while recrystallization in MeCN gave red **1** (elemental analysis [%]: found C 11.11, H 1.76; calcd. C 10.62, H 1.78). An amorphous green product could also be isolated from MeCN solution; the precise nature of this species was unclear although it seemed reasonable to assume that it was an alternative polyiodide adduct of $[Ag([18]aneS_6)]^+$. Compound **2** can be prepared more directly by addition of I_3^- to $[Ag([18]aneS_6)]PF_6$.

Received: June 16, 1995 [Z.8106IE]
German version: *Angew. Chem.* **1995**, *107*, 2563–2565

Keywords: crown thioethers · macrocycles · polyiodides · self-assembly · silver compounds

[1] R. E. Rundle, *Acta Crystallogr.* **1961**, *14*, 585; N. V. Sidgwick, *Chemical Elements and Their Compounds*, Oxford University Press, **1950**, *Vol. II*, pp. 1190–1200; see also T. Klapötke, J. Passmore, *Acc. Chem. Res.* **1989**, *22*, 234.

[2] A. J. Blake, M. Schröder, *Adv. Inorg. Chem.* **1990**, *35*, 1.

[3] See for example: R. Thomas, F. H. Moore, *Acta Crystallogr. Sect. B* **1980**, *36*, 2869 and references therein; F. H. Herbstein, M. Kapon, W. Schwotzer, *Helv. Chim. Acta* **1983**, *66*, 35; M. F. Belicci, G. G. Fava, C. Pelizzi, *Acta Crystallogr. Sect. B* **1981**, *37*, 924; E. Dubler, L. Linowsky, *Helv. Chim. Acta* **1978**, *58*, 2604; A. Rabenau, H. Schulz, W. Stoeger, *Naturwissenschaften* **1976**, *63*, 245; R. Thomas, F. H. Moore, *Acta Crystallogr. Sect. B*, **1981**, *37*, 2156; F. H. Herbstein, M. Kapon, *Acta Crystallogr. Sect. A* **1972**, *28*, S74; F. H. Herbstein, M. Kapon, G. M. Reisner, *Acta Crystallogr. Sect. B* **1985**, *41*, 348; F. H. Herbstein, M. Kapon, G. M. Reisner, *Proc. Roy. Soc. (London) Ser. A* **1981**, *376*, 301; K. Neupert-Laves, M. Dobler, *Helv. Chim. Acta* **1975**, *58*, 432; M. A. Beno, U. Geiser, K. L. Kostka, H. H. Wang, K. S. Webb, M. A. Firestone, K. D. Carlson, L. Nuñez, M.-H. Whangbo, J. M. Williams, *Inorg. Chem.* **1987**, *26*, 1912.

[4] J. Broekema, E. E. Havinga, E. H. Wiebenga, *Acta Crystallogr.* **1957**, *10*, 596; R. J. Hach, R. E. Rundle, *J. Am. Chem. Soc.* **1951**, *73*, 4321.

[5] E. E. Havinga, E. H. Wiebenga, *Acta Crystallogr.* **1958**, *11*, 733.

[6] O. Hassel, H. Hope, *Acta Chem. Scand.* **1961**, *15*, 407.

[7] T. L. Hendrixson, M. A. ter Horst, R. A. Jacobson, *Acta Crystallogr. Sect. C* **1991**, *47*, 2141.

[8] F. Demartin, P. Deplano, F. A. Devillanova, F. Isaia, V. Lippolis, G. Verani, *Inorg. Chem.* **1993**, *32*, 3694.

[9] R. Poli, J. C. Gordon, R. K. Khanna, P. E. Fanwick, *Inorg. Chem.* **1992**, *31*, 3165.

[10] See for example: E. E. Havinga, K. H. Boswijk, E. H. Wiebenga, *Acta Crystallogr.* **1954**, *7*, 487; R. Thomas, F. H. Moore, *Acta Crystallogr. Sect. B* **1981**, *37*, 2153; W. J. James, R. J. Hach, D. French, R. E. Rundle, *Acta Crystallogr.* **1955**, *8*, 814; F. H. Herbstein, W. Schwotzer, *Angew. Chem.* **1982**, *94*, 222; *Angew. Chem. Int. Ed. Engl.* **1982**, *21*, 219; J. Passmore, P. Taylor, T. Whidden, P. S. White, *Can. J. Chem.* **1979**, *57*, 968; F. H. Herbstein, M. Kapon, *Phil. Trans. Roy. Soc. Lond.* **1979**, *A291*, 199; F. Bigoli, M. A. Pellinghelli, G. Crisponi, P. Deplano, E. F. Trogu, *J. Chem. Soc., Dalton Trans.* 1985, 1349; K.-F. Tebbe, A. Kavoosian, *Z. Naturforsch. B* **1993**, *48B*, 438.

[11] A. J. Blake, R. O. Gould, G. Reid, M. Schröder, *J. Chem. Soc. Chem. Commun.* **1990**, 974; A. J. Blake, R. O. Gould, A. J. Holder, T. I. Hyde, M. Schröder, *Polyhedron* **1989**, *8*, 513.

[12] Crystal data for $C_{12}H_{24}AgS_6I_7$: $M = 1356.84$, trigonal, space group $R\bar{3}m$, $a = 9.458(4)$ Å, $\alpha = 103.79(3)°$, $V = 758$ Å^3 [from 2θ values of 18 reflections measured at $\pm\omega$ ($2\theta = 30$–$32°$, $\lambda = 0.71073$ Å), $T = 150.0(1)$ K], $Z = 1$, $\rho_{calcd} = 2.972$ g cm^{-3}, $\mu(Mo_{K\alpha}) = 8.207$ mm^{-1}. Deep red block ($0.23 \times 0.15 \times 0.12$ mm^3). 1332 absorption-corrected reflections ($2\theta_{max}$ 45°, T_{min} 0.299, T_{max}

 © VCH Verlagsgesellschaft mbH, D-69451 Weinheim, 1995 0570-0833/95/3421-2375 $ 10.00+.25/0

0.368), of which 383 unique data ($R_{int} = 0.060$) were used in all calculations. Individual cations are chiral with D_3 (32) point symmetry but are randomly distributed to give apparent D_{3d} ($\bar{3}m$) symmetry. At final convergence, R[380 data with $F \leq 4\sigma(F)$] = 0.0192, $wR[F^2$, all data] = 0.0390 and $S[F^2] = 1.112$ for 37 parameters and the final ΔF synthesis showed no feature above 1.07 e Å^{-3}. Crystal data for $C_{12}H_{24}AgS_6I_3$: $M = 849.29$, monoclinic, space group $C2/m$, $a = 18.5767(11)$, $b = 11.9188(7)$, $c = 5.2714(5)$ Å, $\beta = 95.634(9)°$, $V = 1162$ Å^3 [from 2θ values of 32 reflections measured at $\pm\omega$ ($2\theta = 29$–$32°$, $\lambda = 0.71073$ Å), $T = 280.0(1)$ K], $Z = 2$, $\rho_{calcd} = 2.428$ g cm^{-3}, $\mu(Mo_{K\alpha}) = 5.389$ mm^{-1}. Brown columnar block ($0.38 \times 0.16 \times 0.16$ mm^3). 2740 absorption-corrected reflections ($2\theta_{max}$ 50°, T_{min} 0.131, T_{max} 0.164) of which 1074 unique data ($R_{int} = 0.0130$) were used in all calculations. At final convergence, R[988 data with $F \leq 4\sigma(F)$] = 0.0181, $wR[F^2$, all data] = 0.0422 and $S[F^2] = 1.081$ for 58 parameters and the final ΔF synthesis showed no feature above 0.58 e Å^{-3}. Both crystals were mounted on a Stoë Stadi-4 four-circle diffractometer in the stream of an Oxford Cryosystems low-temperature device [13]. Data collection used $Mo_{K\alpha}$ X-radiation ($\lambda = 0.71073$ Å), ω-2θ scans and the learnt profile method [14]. Patterson synthesis [15] was used to locate the iodine and silver atoms in each structure, from which point the structures were developed by iterative cycles of least squares refinement and difference Fourier synthesis. The structures were refined by full-matrix least squares (on F^2) with anisotropic thermal parameters for all fully occupied non-H atoms. H atoms were included in fixed calculated positions with U_{iso} 1.2 times U_{eq} for the parent C atom [16]. Further details of the crystal structure investigations may be obtained from the Director of the Cambridge Crystallographic Data Centre, 12 Union Road, GB-Cambridge CB2 1EZ (UK).

[13] J. Cosier, A. M. Glazer, *J. Appl. Crystallogr.* **1986**, *19*, 105.
[14] W. Clegg, *Acta Crystallogr., Sect. A* **1981**, *37*, 22.
[15] SHELXS-86: G. M. Sheldrick, *Acta Crystallogr., Sect. A* **1990**, *46*, 467.
[16] SHELXL-93: G. M. Sheldrick, Universität Göttingen, 1993.
[17] I. L. Karle, *J. Chem. Phys.* **1955**, *23*, 1739.
[18] F. van Bolhuis, P. B. Koster, T. Migchelsen, *Acta Crystallogr.* **1967**, *23*, 90.
[19] R. C. Teitelbaum, S. L. Ruby, T. J. Marks, *J. Am. Chem. Soc.* **1980**, *102*, 3322.

Alkali Metallocene Anions: Syntheses and Structures**

Jens Wessel, Enno Lork, and Rüdiger Mews*

Dedicated to Professor Herbert Schumann on the occasion of his 60th Birthday

Recently Harder and Prosenc reported on the synthesis of $[CpLiCp]^-$, the simplest metallocene, which is obtained from the reaction of $(LiCp)_n$ with $Ph_4P^+Cl^-$ in THF at room temperature [Eq. (a)].[1]

$$2/n\,(LiCp)_n + Ph_4P^+Cl^- \xrightarrow[RT]{THF} Ph_4P^+[CpLiCp]^- + LiCl \quad (a)$$

$$2\,CpSiMe_3 + 2(TAS)F \xrightarrow[-30\,°C]{CH_3CN} [(TAS)Cp(TAS)]^+Cp^- + 4\,Me_3SiF \quad (b)$$

Concurrently, we synthesized tris(dimethylamino)sulfonium cyclopentadienide, $(Me_2N)_3S^+Cp^-$, [(TAS)Cp] [Eq. (b)],[2] whose solid-state structure can be described as $[(TAS)Cp(TAS)]^+Cp^-$. The cation is present as an "inverse" sandwich complex, lying alongside the "naked" Cp^- ion. The aim of our studies was to generate cyclopentadienide anions in the presence of weakly interacting cations which are not coordinated by interfering auxiliary bases. With these systems we hoped to observe novel reactions, not normally seen for typical metallocyclopentadiene reagents. Herein we report the first unusual reactions of (TAS)Cp in the currently topical area of alkali metallocenes.[3, 4] The important results from the work of Harder and Prosenc and from our own work[1, 2] are that on the one hand, alkali metallocene anions are stable in the presence of weakly coordinating cations, but on the other hand "naked" Cp^- ions are extremely reactive, decomposing in organic solvents between -30 and $-10\,°C$. Thus, $Ph_4P^+Cp^-$ can be obtained from the reaction of $(LiCp)_n$ with $Ph_4P^+Cl^-$ in CH_3CN only at temperatures below $-30\,°C$[5].

Because of its thermal instability in solution, (TAS)Cp is only a useful synthetic reagent if the desired reaction occurs at low temperature. Breakdown of the polymeric ("supersandwich") structures of the alkali metal cyclopentadienides[6, 7] occurs rapidly at $-35\,°C$ in a (TAS)Cp-acetonitrile solution. On addition of diethyl ether, the salts **1a–c** precipitate quantitatively at this temperature [Eq. (c)].

$$2/n\,(MCp)_n + [(TAS)_2Cp]^+Cp^- \longrightarrow \underset{\mathbf{1a\text{–}c}\ (M = Li, Na, K)}{2\,TAS^+[CpMCp]^-} \quad (c)$$

$$1/n\,(NaCp)_n + n[(TAS)_2Cp]^+Cp^- \longrightarrow \underset{\mathbf{2}}{[(TAS)_2Cp]^+[CpNaCp]^-} \quad (d)$$

By changing the stoichiometry, the salt **2**, in which a sandwich and inverse-sandwich complex lie side by side, was obtained in quantitative yield [Eq. (d)]. Reactions of (TAS)Cp with polymeric alkali metal cyclopentadienide fragments of the type $[M_nCp_{n+1}]^-$, (e.g. the recently reported thallium system $[Cp_3Tl_2]^-$[8]) remain to be studied.

Single crystals of **1a** (M = Li) and **2** suitable for X-ray crystal structure analyses were obtained by recrystallization from CH_3CN/ether at $-30\,°C$. Complex **1a** crystallizes in the space group $P\bar{1}$ with two independent Cp_2Li units[9] in the unit cell (Fig. 1); the data were collected at $-100\,°C$. The structures of

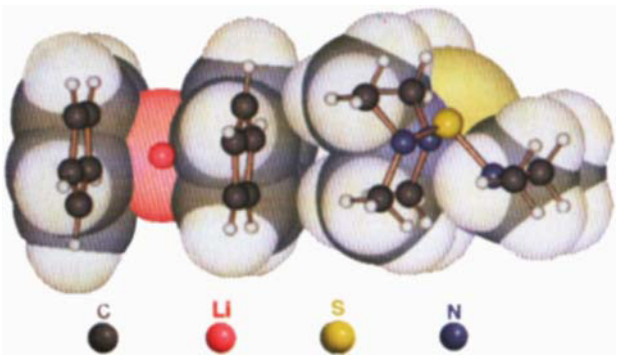

Fig. 1. Crystal structure of $TAS^+[CpLiCp]^-$ **1a** (SCHAKAL drawing).

the $[Cp_2Li]^-$ ions in **1a** are almost identical to those in $Ph_4P^+[Cp_2Li]^-$[1]; the cation appears to have no influence on the anion. The small variation in bond lengths can be rationalized in terms of thermal effects, since our data for **1a** were collected at lower temperature. In the lithocene unit with Li(1), the Li–C distances lie between 226.0 (2) and 233.4 (2) pm (average 229.7 pm), the average C–C bond length is 138.9 (3) pm, and the Li–Cp (ring centroid) distance is 196.9 pm. In the lithocene unit with Li(2), the corresponding values are 226.2 (3)–235.9 (2) pm (average 231.4 pm), 139.0 (8), and 198.9 pm, respectively (reported values for $Ph_4P^+[Cp_2Li]^-$[1] are: 226.2 (3)–236.6 (4) pm (average 231.8 pm), 136.2, and

[*] Prof. Dr. R. Mews, Dipl.-Chem. J. Wessel, Dr. E. Lork
Institut für Anorganische und Physikalische Chemie der Universität
Postfach 33 04 40, D-28334 Bremen (Germany)
Telefax: Int. code + (4 21)-2 18 42 67

[**] This work was supported by the Fonds der Chemischen Industrie. We thank Prof. Dr. U. Behrens, Hamburg, for helpful discussions.

200.8 (4) pm, respectively). In both centrosymmetric units $[Cp_2Li\ (1)]^-$ and $[Cp_2Li\ (2)]^-$ the rings are tilted away from the normal by 2.1° and 2.9°, respectively; these values are also in agreement with that of the Ph_4P compound (2.9 (3)°).[1] Isotropic refinement of the Cp-hydrogen atoms showed eight hydrogen atoms inclined toward the lithium atom in molecule 1, whereas only two are inclined toward the lithium atom in molecule 2, the other eight hydrogen atoms however are bent away.

Figure 2 shows the structure of compound **2**[10] and Figure 3 a section of the crystal lattice clearly showing the presence of sandwich and inverse-sandwich units. The distances between the sulfonium centers and the enclosed Cp ring (311.8 and 317.0 pm) are only marginally shorter than those in $[(TAS)_2Cp]^+Cp^-$.[2] The enclosed Cp ring in **2** is also disordered; the refinement as a perfect pentagon gave a C–C distance of 138.1 (3) pm.

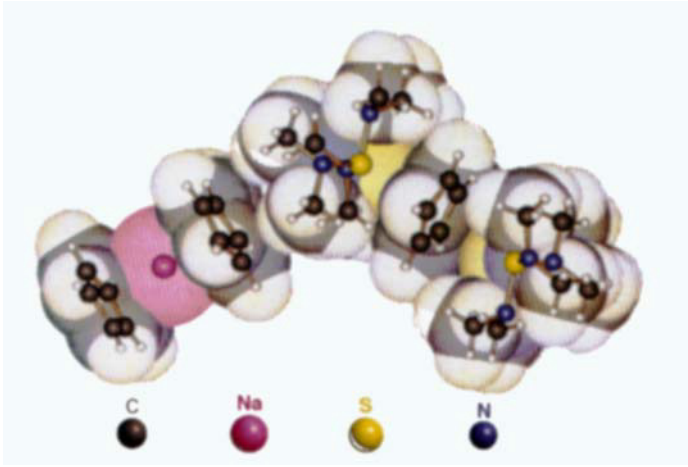

Fig. 2. Crystal structure of $[(TAS)Cp(TAS)]^+[CpNaCp]^-$ **2** (SCHAKAL drawing).

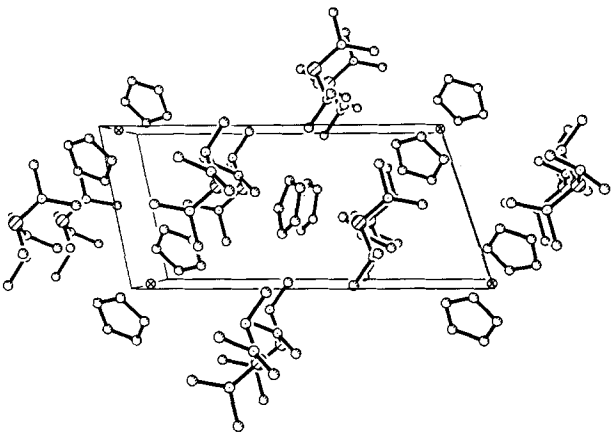

Fig. 3. View of the crystal lattice of **2**.

The natrocene (sodocene) anion in **2** has almost ideal D_{5d} symmetry. The tilt angle of the rings from the normal through the Na atom is only 1.1°. Correspondingly Na–C distances vary relatively little (259.6 (3)–263.9 (3) pm). In contrast to the Li–Cp compound **1a**, where the average Li–C distance is relatively large in comparison with other examples, the average Na–C distance in the $[Na_2Cp]^-$ unit of **2** of 261.6 pm is the shortest, crystallographically characterized Na–C distance reported.[11–15] Distances of 268 pm (in $Me_5C_5Na \cdot 3\ py$)[14] to 292 pm (in $NaCp \cdot TMEDA)_n$[12] are reported in the literature. This difference in behavior to that of the Li–Cp compound is rationalized by the fact that the considerably larger central atom in $[Cp_2Na]^-$ hinders intramolecular repulsion of the two Cp rings.

Experimental Procedure

1a: In a N_2-filled dry box, (TAS)Cp (2.5–3 mmol) and the corresponding stoichiometric amount of LiCp were weighed into a λ-shaped Schlenk tube, fitted with a Teflon valve. Subsequently CH_3CN (30 mL) was condensed onto this mixture through a vacuum line at −196 °C. The reaction vessel was allowed to warm to −40 °C and the reaction mixture was stirred at this temperature for 2 h. After removal of volatiles under vacuum, **1a** remained in quantitative yield as a red solid, m.p. 107 °. Single crystals for X-ray analysis were grown by slow diffusion of Et_2O into a CH_3CN solution of **1a** at −30 °C. ^1H NMR (CD_3CN, 233 K): δ = 5.49 (s, 10 H, Cp), 2.85 (s, 18 H, $(Me_2N)_3S^+$); ^{13}C NMR: δ = 104.6 (Cp), 38.5 ($(Me_2N)_3S^+$).

NaCp and KCp were treated in an analogous manner to **1a** to give **1b** (m.p. 109 °C) and **1c** (m.p. 113 °C), respectively, in quantitative yield. The ^1H NMR spectra (**1b**: δ = 5.56 **1c**: δ = 5.50 (Cp)) showed few differences to those of **1a**.

2: Compound **2** was prepared by an analogous route to **1a** from (TAS)Cp and NaCp in a molar ratio 2:1. After removal of volatiles, **2** remained in the reaction vessel as a violet solid (m.p. 85 °C), which decomposed at room temperature. Single crystals suitable for X-ray structure analysis were obtained at −30 °C by diffusion of Et_2O into solution of **2** in CH_3CN. ^1H NMR (CH_3CN, 233 K): δ = 5.50 (s, 10 H, Cp), 2.85 (s, 36 H, $Me_2N)_3S^+$).

Received: June 27, 1995 [Z 81411E]
German version: *Angew. Chem.* **1995**, *107*, 2565–2567

Keywords: alkali metal compounds · metallocene anions · sandwich complexes

[1] S. Harder, M. H. Prosenc, *Angew. Chem.* **1994**, *106*, 1830; *Angew. Chem. Int. Ed. Engl.* **1994**, *33*, 1744.
[2] J. Wessel, U. Behrens, E. Lork, R. Mews, *Angew. Chem.* **1995**, *107*, 516; *Angew. Chem. Int. Ed. Engl.* **1995**, *34*, 443.
[3] D. Stalke, *Angew. Chem.* **1994**, *106*, 2256; *Angew. Chem. Int. Ed. Engl.* **1994**, *33*, 2168.
[4] The first reactions of the "naked" Cp^- ion (by $[Cp_2Ta(\mu\text{-}CH_2)_2Pd(dmpe)]^+$-$Cp^-$) as a nucleophile were reported by: M. D. Butts, R. G. Bergman, *Organometallics* **1993**, *12*, 4269; *ibid.* **1994**, *13*, 1899.
[5] J. Wessel, R. Mews, unpublished results.
[6] Review: P. Jutzi, *Adv. Organomet. Chem.* **1986**, *26*, 217; *Pure Appl. Chem.* **1989**, *61*, 1731.
[7] Review: E. Weiss, *Angew. Chem.* **1993**, *105*, 1565; *Angew. Chem. Int. Ed. Engl.* **1993**, *32*, 1501.
[8] D. R. Armstrong, A. J. Edwards, D. Moncrieff, M. A. Paver, P. R. Raithby, M.-A. Rennie, C. A. Russell, D. S. Wright, *J. Chem. Soc. Chem. Commun.* **1995**, 927; see also: M. A. Paver, C. A. Russell, D. S. Wright, *Angew. Chem.* **1995**, *107*, 1679, *Angew. Chem. Int. Ed. Engl.* **1995**, *34*, 1545.
[9] X-ray crystal structure analysis of **1a** ($C_{16}H_{28}LiN_3S$). M = 301.41; crystal dimensions 1.2 × 0.6 × 0.4 mm³; triclinic, space group $P\bar{1}$. a = 775.40 (10), b = 870.50 (10), c = 1640.0 (2) pm, α = 81.980 (10), β = 85.460 (10), γ = 63.090 (10)°, V = 0.9178 (2) nm³, Z = 2, ρ_{calcd} = 1.091 Mg m⁻³, μ = 0.173 mm⁻¹. A crystal suitable for X-ray analysis was fixed to a glass fiber with Kel-F oil and measured on a Siemens P4 four-circle diffractometer at −100 °C (graphite monochromator, $Mo_{K\alpha}$ radiation, $\omega/2\,\theta$ scan). Of the 5201 measured reflections ($2.5° < \theta < 27.5°$), 2560 independent reflections remained after averaging. The structure was solved by direct methods. The refinement calculations converged at wR_2 = 0.0823 (refined against F^2) for all 2560 reflections and 241 variables [R_1 = 0.0364 for 1809 reflections with $I > 2\sigma(I)$]; heavy atoms were assigned individual anisotropic deflection parameters. The Cp-H atom positions were taken from the difference Fourier map and isotropically refined, the methyl H atoms were treated by using a riding model with a common isotropic temperature factor. A difference Fourier synthesis indicated no residual electron density beyond +165 e nm⁻³ and −307 e nm⁻³. Calculations were carried out using the SHELXTL program package [16], the refinements with the program SHELXL-93 [17], and the drawings with SCHAKAL [18, 19].
[10] X-ray crystal structure analysis of **2** ($C_{27}H_{51}N_6NaS_2$). M = 546.84; crystal dimensions 0.6 × 0.4 × 0.3 mm³; triclinic, space group $P\bar{1}$. a = 806.70 (10), b = 828.30 (10), c = 1447.0 (2) pm, α = 92.480 (10), β = 104.400 (10), γ = 119.120 (10)°, V = 0.8026 (2) nm³, Z = 2, ρ_{calcd} = 1.131 Mg m⁻³, μ = 0.204 mm⁻¹. A crystal suitable for X-ray analysis was fixed to a glass fiber with Kel-F oil and measured on a Siemens P4 four-circle diffractometer at −100 °C (graphite monochromator, $Mo_{K\alpha}$ radiation, $\omega/2\,\theta$ scan). Of the 4513 measured reflections ($2.9° < \theta < 27.5°$), 3667 independent reflections remained after averaging. The structure was solved by direct methods. The solution indicated

 © VCH Verlagsgesellschaft mbH, D-69451 Weinheim, 1995 0570-0833/95/3421-2377 $ 10.00+.25/0

that the two Cp units of the $[(TAS)Cp(TAS)]^+$ cation almost lie on the centers of symmetry in the space group; thus they are disordered. The Cp rings were therefore refined as perfect pentagons. The refinement calculations converged at $wR_2 = 0.1831$ (refined against F^2) for all 3667 reflections and 211 variables [$R_1 = 0.0642$ for 2945 reflections with $I > 2\sigma(I)$]; heavy atoms were assigned individual anisotropic deflection parameters. The Cp-H atom positions were taken from the difference Fourier map and isotropically refined, the methyl H atoms were treated by using a riding model with a common isotropic temperature factor. A difference Fourier synthesis indicated no residual electron density beyond $+1037$ e nm^{-3} and -874 e nm^{-3}. Calculations were carried out using the SHELXTL program package [16], the refinements with the program SHELXL-93 [17] and the drawings with SCHAKAL [18] and SHELXTL [19].

[11] O. Mundt, G. Becker, *Z. Anorg. Allg. Chem.* **1983**, *496*, 58.

[12] T. Aoyagi, H. M. M. Shearer, K. Wade, G. Whitehead, *J. Organomet. Chem.* **1979**, *175*, 21. TMEDA = *N,N,N',N'*-tetramethylethylenediamine.

[13] R. D. Rogers, J. C. Atwood, M. D. Rausch, D. W. Macomber, W. P. Hart, *J. Organomet. Chem.* **1982**, *238*, 79.

[14] G. Rabe, H. W. Roesky, D. Stalke, F. Pauer, G. M. Sheldrick, *J. Organomet. Chem.* **1991**, *403*, 11. py = pyridine.

[15] M. G. Davidson, D. Stalke, D. S. Wright, *Angew. Chem.* **1992**, *104*, 1265; *Angew. Chem. Int. Ed. Engl.* **1992**, *31*, 1226.

[16] Siemens SHELXTL-Plus: Release for Siemens R3 Crystallographic Research Systems, Siemens Analytical X-Ray Instruments Inc., Madison, WI, **1989**.

[17] G. M. Sheldrick, SHELXL-93, Universität Göttingen, **1993**.

[18] E. Keller, SCHAKAL-92, Universität Freiburg, **1992**.

[19] Further details of the crystal structure investigations may be obtained from the Director of the Cambridge Crystallographic Data Centre, 12 Union Road, GB-Cambridge CB2 1EZ, on quoting the full literature citation.

their interlocked molecular structures. Specifically, we have examined the relative templating abilities of 1,5-dinaphtho[38]crown-10 (DN38C10)[9] and bis(*para*-phenylene)[34]crown-10 (BPP34C10)[10] for catenation by the components of the tetracationic cyclophanes[11–14] **A**, **B**, **C**, and **D**, which incorporate 4,4'-bipyridinium and/or bis(4-pyridinium)ethylene dications, linked by either *meta*- or *para*-xylyl spacer units

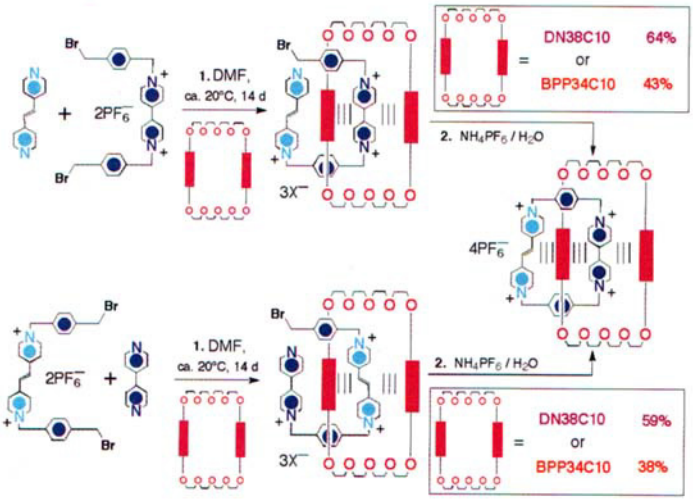

Fig. 1. The competitive self-assembly experiments involving the formation of the tetracationic cyclophanes **A**, **B**, **C**, and **D** in the presence of the template macrocyclic polyether DN38C10 and BPP34C10 to form [2]catenanes, showing the ratio of products formed. The components of the tetracationic cyclophanes used in these experiments can be deduced by disconnecting the covalent bonds indicated and adding a bromine atom to the methylene group.

Kinetic Selection in the Template-Directed Self-Assembly of [2]Catenanes**

David B. Amabilino, Peter R. Ashton, Lluïsa Pérez-García, and J. Fraser Stoddart*

Since natural systems employ the self-assembly[1, 2] of chemical components in a selective manner when they grow and regenerate themselves, it is a realistic challenge for the synthetic chemist to design entirely unnatural systems that will mimic the remarkable selection displayed in the construction of biological systems. Already, the groups led by Lehn[3, 4] and Whitesides[5] have described synthetic systems which self-assemble under equilibrium control by a mechanism of strict self-assembly.[1] Recently, we reported[6] the self-assembly of a wide range of catenanes containing between two and five interlocked rings. These wholly synthetic molecular compounds consist of macrocyclic polyethers incorporating π-electron-rich aromatic units, which act as templates[7] for the formation of tetracationic cyclophanes incorporating π-electron-deficient aromatic units.[8] The self-assembly mechanism that creates these catenanes operates[1] with intermittent processing: that is, a covalent bond is formed, followed by a binding event in volving molecular recognition before a second covalent bond is formed.

We describe here a series of competitive self-assembly experiments in which the precursors of [2]catenanes are given some choice as to which components they ultimately incorporate into

The competitive catenations were all carried out under identical conditions with equimolar amounts of BPP34C10, DN38C10, and the components of either **A**, **B**, **C**, or **D** (see Experimental Procedure). The mixture of [2]catenanes was then isolated quantitatively from the other materials present in the reaction mixture and analyzed quantitatively with ^{1}H NMR spectroscopy. All the [2]catenanes formed in the competitive reactions have at least one proton resonance that is unique and well-resolved relative to proton resonances in the other [2]catenanes. Integration of these resonances gave the ratio of the products from the competitive self-assembly processes. The ratio of the [2]catenanes, incorporating either BPP34C10 or DN38C10, reveals a pronounced preference for the the naphthalene-containing polyether. Furthermore, this preference depends on the nature of the tetracationic cyclophane to be templated. The tetracationic cyclophane **A**[12] self-assembles in the presence of the two macrocyclic polyethers with least selectivity, the ratio of the [2]catenanes incorporating DN38C10 and BPP34C10 being 62:38. The highest selectivity is observed when the components of the tetracationic cyclophane **C**[13] are treated in the presence of the two macrocyclic polyethers. Remarkably, 99% of the [2]catenane molecules formed in the reaction mixture contain DN38C10 and only 1% incorporate BPP34C10.[16]

Interestingly, the most efficient catenation performed under noncompetitive conditions (80% yield) involves[17] the templating of **B** by DN38C10. However, the competition experiment involving the components of **B** and the two macrocyclic polyethers is not the most selective. More important for the selectivities are the relative rates of reactions templated by the two macrocyclic polyethers present in the reaction mixtures.

The [2]catenanes incorporating the tetracationic cyclophanes **A** and **C** were self-assembled by two different routes. The efficiencies of the reactions leading to the [2]catenanes incorporating

[*] Prof. J. F. Stoddart, Dr. D. B. Amabilino, P. R. Ashton, Dr. L. Pérez-García
School of Chemistry, University of Birmingham
Edgbaston, Birmingham B15 2TT (UK)
Telefax: Int. code + (121)414-3531

[**] This research was supported by the Ministerio de Educación y Ciencia in Spain (Fleming Postdoctoral Fellowship for L. P.-G.) and by the Engineering and Physical Sciences Research Council (EPSRC) in the United Kingdom.

A are sensitive to the constitutions of the tetracationic cyclophane precursors.[12] In addition the [2]catenane incorporating **C** can be self-assembled (Fig. 2) from two alternative starting materials—one with a bis(4-pyridinium)ethylene dication and the other with a 4,4′-bipyridinium dication. Despite the much lower association constants[13] for the complexation of

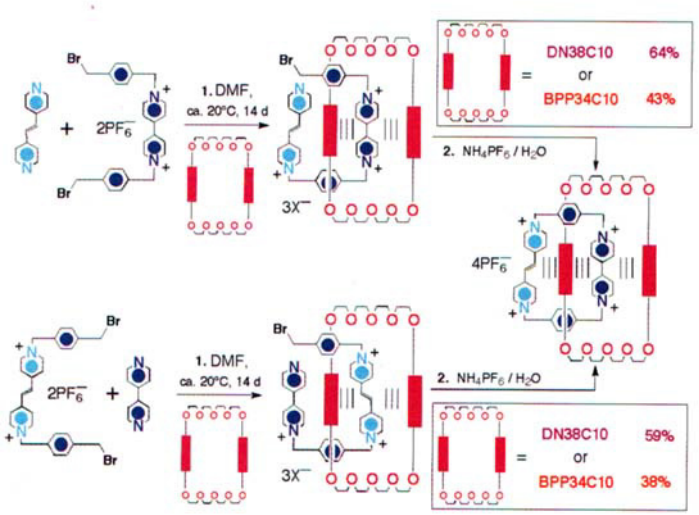

Fig. 2. The two routes to the [2]catenane incorporating cyclophane **C** with either DN38C10 or BPP3410 as template.

the ethylene-substituted bipyridinium dications with BPP34C10 relative to those for the bipyridinium dications, only a modest difference in chemical yields is observed between the two routes, irrespective of whether the template is BPP34C10 or DN38C10. These observations suggest very strongly that the factor governing the relative efficiencies of the self-assembly processes is predominantly a kinetic one.

In an attempt to shed further light on the selectivities observed in the competition studies, the components of the tetracationic cyclophane **A** were treated in an NMR tube under identical conditions to the competition experiments described already, except that [D_7]DMF (plus a drop of D_2O) was used as the solvent. To explain the results of this NMR experiment, it is first necessary to consider the course of the self-assembly processes responsible for the catenations. In principle, self-assembly can occur under either kinetic or thermodynamic control. The situation is illustrated in Figure 3 for the case of the templated self-assembly of **A**. One would expect that the binding (K and K') of the initially formed (k_1) tricationic intermediates would be approximately the same for a given macrocyclic polyether across the range of tetracationic cyclophanes **A** to **C**, since all possess at least one 4,4′-bipyridinium dicationic unit that is bound strongly by the macrocyclic polyethers. The initial precursors to the tetracationic cyclophanes, which contain two pyridyl–pyridinium moieties, are bound extremely weakly by the receptor.[13] The important factors are the rates (k_2 and k_3) of ring closure of the tricationic intermediates once they have been complexed. These rates will be dependent upon the abilities of the respective macrocyclic polyethers to lower the Gibbs free energies of the transition states associated with the ring-closure steps. The reactions, which were followed by ^{1}H NMR spectroscopy, showed that the rate of the ring closure of **A** is much slower than that of **B** under the same reaction conditions.[18] In the competitive ^{1}H NMR experiment, when a bipyridinium dication is formed, the chemical shifts of the resonances arising

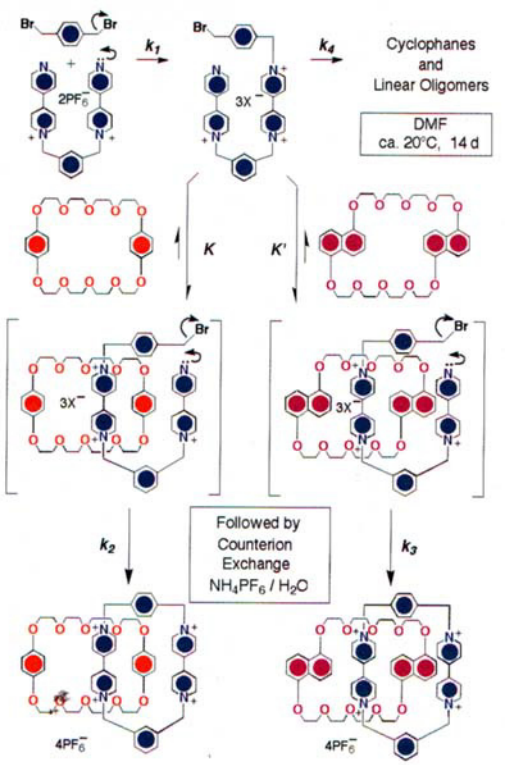

Fig. 3. The kinetically (k_1, k_2, k_3, k_4) and thermodynamically (K and K') controlled steps en route to the [2]catenanes incorporating the tetracationic cyclophane **A** and either BPP34C10 or DN38C10.

from both macrocyclic polyethers are shifted to high field, indicating molecular recognition. The presence of both the complexes of the tricationic intermediates **G** and **H** was also confirmed by FAB mass spectrometry (Fig. 4, FAB = fast atom bombardment),[19] which revealed peaks corresponding to the two [2]catenanes—containing BPP34C10 (**E**) and DN38C10 (**F**)—as well as the complexes of the tricationic intermediate with the two macrocyclic polyethers.

The results presented here suggest strongly that the preferences observed for the DN38C10 macrocyclic polyether over the

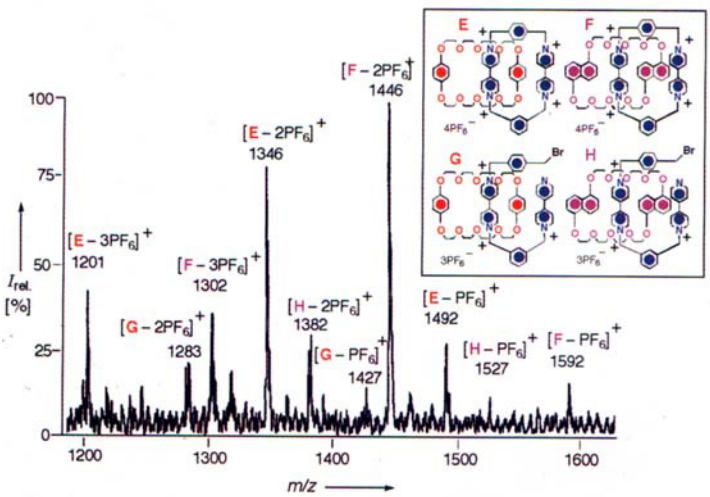

Fig. 4. The FAB mass spectrum of the reaction mixture relating to the scheme outlined in Fig. 3. The peaks that can be identified are attributable to the products of the self-assembly process—the [2]catenanes **E** and **F**, as well as the intermediates **G** and **H**. There was no evidence in the spectrum of the unbound tricationic intermediate to the tetracationic cyclophane **A**.

analogous BPP34C10 are a result of the greater ability of the former to stabilize the transition state for the tetracationic cyclophane ring closure. If the self-assembly was governed solely by the thermodynamics of the noncovalent binding, approximately the same selectivities would be expected for the [2]catenanes incorporating **A**, **B**, and **C**—since they are not, the Curtin-Hammett principle[20] is apparently valid. This hypothesis is supported by the observation of both the tricationic intermediates, namely the intermediates to the [2]catenanes with BPP34C10 and with DN38C10. The selection is dependent on the dimensions of the cyclophane formed.[15] A similar kinetic situation has also been observed in the formation of macrocycles assisted by metal ion templates—termed the *kinetic template effect*[21, 22]—as well as in the templated formation of carceplexes[23] and the self-assembly of monolayers.[24] The ratio of the products formed is determined by the relative stabilization of transition states.[25] The effective molarities[26, 27] of the reactive termini in the acyclic precursors are greater in complexed forms than they are in uncomplexed forms.

Lehn[4] and Whitesides[5] have demonstrated selection in self-assembly as a result of the thermodynamics of binding in solution. The selectivities associated with the self-assembly processes presented here are apparently not governed by the thermodynamics[28] of noncovalent interactions, but rather by the relative rates of covalent bond formation in the final cyclization steps to give the [2]catenanes. As such, the formation of [2]catenanes containing complementary recognition sites in their component rings provides a fascinating and rare example of kinetic selection operating during the intermittently processed self-assembly[1] of unnatural products.

Experimental Procedure

The components of the competition reactions (the two components of the tetracationic cyclophane and the two macrocyclic polyethers, initial concentrations of 20 mM in dry DMF) were introduced into a round-bottomed flask, and the solution was stirred at room temperature and ambient pressure for 14 days. The mixture of [2]catenanes incorporating the tetracationic cyclophane **A** was purified by column chromatography [SiO_2, MeOH/NH_4Cl (2 M)/$MeNO_2$ (7:2:1)]. All fractions containing [2]catenanes were worked up according to a previously described procedure [12]. The mixtures of [2]catenanes incorporating the cyclophanes **B**, **C**, and **D** were isolated by successive precipitation from Et_2O and washing with Et_2O and CH_2Cl_2 in order to obtain *all* the catenated compounds. The ^1H NMR spectra (CD_3CN, 400 MHz) of the mixtures of catenanes were run at temperatures at which all the relevant resonances in the spectra were least broadened by exchange processes and processed without line broadening. Comparisons were made with the spectra for the pure [2]catenanes—containing the tetracationic cyclophanes **A**, **B**, **C**, or **D**, severally, and either BPP34C10 or DN38C10—all of which had already been self-assembled separately under noncompetitive conditions and fully characterized.

Received: June 3, 1995 [Z 8057 IE]
German version: *Angew. Chem.* **1995**, *107*, 2569–2572

Keywords: catenanes · Curtin-Hammett principle · molecular recognition · self-assembly · template effect

[1] J. S. Lindsey, *New J. Chem.* **1991**, *15*, 153–180.
[2] G. M. Whitesides, J. P. Mathias, C. T. Seto, *Science* **1991**, *254*, 1312–1319.
[3] R. Krämer, J.-M. Lehn, A. Marquis-Rigault, *Proc. Nat. Acad. Sci. USA* **1993**, *90*, 5394–5398.
[4] J.-M. Lehn, *Science* **1993**, *260*, 1760–1763; see also J.-M. Lehn, *Supramolecular Chemistry*, VCH, Weinheim, **1995**.
[5] G. M. Whitesides, E. E. Simanek, J. P. Mathias, C. T. Seto, D. N. Chin, M. Mammen, D. M. Gordon, *Acc. Chem. Res.* **1995**, *28*, 37–44.
[6] D. B. Amabilino, P. R. Ashton, C. L. Brown, E. Córdova, L. A. Godínez, T. T. Goodnow, A. E. Kaifer, S. P. Newton, M. Pietraszkiewicz, D. Philp, F. M. Raymo, A. S. Reder, M. T. Rutland, A. M. Z. Slawin, N. Spencer, J. F. Stoddart, D. J. Williams, *J. Am. Chem. Soc.* **1995**, *117*, 1271–1293, and references therein.
[7] a) S. Anderson, H. L. Anderson, J. K. M. Sanders, *Acc. Chem. Res.* **1993**, *26*, 469–475; b) R. Hoss, F. Vögtle, *Angew. Chem.* **1994**, *106*, 389–398; *Angew. Chem. Int. Ed. Engl.* **1994**, *33*, 375–384.
[8] P. L. Anelli, P. R. Ashton, R. Ballardini, V. Balzani, M. Delgado, M. T. Gandolfi, T. T. Goodnow, A. E. Kaifer, D. Philp, M. Pietraszkiewicz, L. Prodi, M. V. Reddington, A. M. Z. Slawin, N. Spencer, J. F. Stoddart, C. Vicent, D. J. Williams, *J. Am. Chem. Soc.* **1992**, *114*, 193–218.
[9] P. R. Ashton, E. J. T. Chrystal, J. P. Mathias, K. P. Parry, A. M. Z. Slawin, N. Spencer, J. F. Stoddart, D. J. Williams, *Tetrahedron Lett.* **1987**, *28*, 6367–6370.
[10] a) R. C. Helgeson, T. L. Tarnowski, J. M. Timko, D. J. Cram, *J. Am. Chem. Soc.* **1977**, *99*, 6411–6418; b) B. L. Allwood, N. Spencer, H. Shahriari-Zavareh, J. F. Stoddart, D. J. Williams, *J. Chem. Soc. Chem. Commun.* **1987**, 1061–1064.
[11] P. R. Ashton, R. Ballardini, T. T. Goodnow, A. E. Kaifer, M. V. Reddington, A. M. Z. Slawin, N. Spencer, J. F. Stoddart, C. Vicent, D. J. Williams, *Angew. Chem.* **1989**, *101*, 1404–1408; *Angew. Chem. Int. Ed. Engl.* **1989**, *28*, 1396–1399.
[12] D. B. Amabilino, P. R. Ashton, M. S. Tolley, J. F. Stoddart, D. J. Williams, *Angew. Chem.* **1993**, *105*, 1358–1362; *Angew. Chem. Int. Ed. Engl.* **1993**, *32*, 1297–1301.
[13] a) P. R. Ashton, R. Ballardini, V. Balzani, M. T. Gandolfi, D. J.-F. Marquis, L. Pérez-García, J. F. Stoddart, M. Venturi, *J. Chem. Soc., Chem. Commun.* **1994**, 177–180; b) P. R. Ashton, R. Ballardini, V. Balzani, A. Credo, M. T. Gandolfi, S. Menzer, L. Pérez-García, L. Prodi, J. F. Stoddart, M. Venturi, A. J. P. White, D. J. Williams, *J. Am. Chem. Soc.*, in press.
[14] P. R. Ashton, L. Pérez-García, J. F. Stoddart, A. J. P. White, D. J. Williams, *Angew. Chem.* **1995**, *107*, 607–610; *Angew. Chem. Int. Ed. Engl.* **1995**, *34*, 571–574.
[15] The tetracationic cyclophanes **A**, **B**, **C**, and **D** have approximately the same depths, but have different lengths and breadths. The approximate cross-sectional areas of **A**, **B**, **C**, and **D** are 69, 72, 81, and 88 Å^2, respectively. The values have been obtained from X-ray structural data (refs.: **A** [11], **B** [12], **C** [14]; **D**: [13b]) for [2]catenanes which incorporate them.
[16] We estimate that the total errors in the product ratios are no more than 2%. This value is a combination of the small uncertainty (<1%) in the NMR integration and errors associated with experimental manipulation.
[17] D. B. Amabilino, L. Pérez-García, J. F. Stoddart, unpublished.
[18] C. L. Brown, D. Philp, N. Spencer, J. F. Stoddart, *Isr. J. Chem.* **1992**, *32*, 61–67.
[19] A drop of the reaction mixture was removed and mixed with the FAB mass spectrometric matrix (3-nitrobenzyl alcohol). This mixture was then subjected to bombardment with fast atoms of krypton in a Kratos MS 80 mass spectrometer.
[20] E. L. Eliel, S. H. Wilen, *Stereochemistry of Carbon Compounds*, Wiley, New York, **1994**, pp. 647–655.
[21] M. C. Thompson, D. H. Busch, *J. Am. Chem. Soc.* **1964**, *86*, 3651–3656.
[22] L. F. Lindoy, *The Chemistry of Macrocyclic Ligand Complexes*, Cambridge University Press, New York, **1989**.
[23] a) R. G. Chapman, N. Chopra, E. D. Cochien, J. C. Sherman, *J. Am. Chem. Soc.* **1994**, *116*, 369–370; b) J. R. Fraser, B. Borecka, J. Trotter, J. C. Sherman, *J. Org. Chem.* **1995**, *60*, 1207–1213.
[24] D. A. Offord, J. H. Griffin, *Langmuir* **1993**, *9*, 3015–3025.
[25] Y. Hung, D. H. Busch, *J. Am. Chem. Soc.* **1977**, *99*, 4977–4984.
[26] A. J. Kirby, *Adv. Phys. Org. Chem.* **1980**, *17*, 183–278.
[27] A. D. Cort, G. Ercolani, A. L. Iamiceli, L. Mandolini, P. Mencarelli, *J. Am. Chem. Soc.* **1994**, *116*, 7081–7087.
[28] Building controlled reversibility into the self-assembly processes, such as those described in this communication, would allow thermodynamics to control the nature of catenane formation. Such developments would introduce error checking into the self-assembly processes leading to mechanically interlocked molecular compounds. We are now addressing this challenge.

A Molecular Composite Containing Organic and Inorganic Components—A Complex from β-Cyclodextrin and Hydrated Magnesium Chloride

Ioannis Nicolis, Anthony W. Coleman, Pierrette Charpin, and Colette de Rango*

Two distinct structural motifs are essential for biomineralization, namely, the crystalline systems of insoluble alkaline earth metal salts and the bioorganic matrix that directs the orientation of the crystalline inorganic components.[1] Two processes occur in biomineralization and these are crystallization, which is directed into the interior of vesicles,[2] and growth in the form of a columnar matrix, as is the case for collagen.[3]

Recently, S. J. Mann[4] considered, and subsequently correctly rejected, cyclodextrins (CDs) as models for host compounds for inward biomineralization. However, the strong tendency of CDs to form columnar (herringbone-like) structures bridged by hydrate zones suggested that they may serve as models for the second form of biomineralization mentioned above.[5] Since the salts usually found in biominerals—carbonates, phosphates, and sulfates—are only sparingly soluble, we chose to use chlorides in our studies. In the first β-CD composite containing a salt of a divalent cation ($CaCl_2$), modulation of the herringbone β-CD motif was observed;[6] however, a distinct structural motif for the mineral components was lacking.

We report here the crystal structure of a compound of the composition β-CD. $2[Mg(H_2O)_6]Cl_2$, and $3.5\,H_2O$,[7] a β-CD/$MgCl_2$ composite, which shows distinct, interlocking organic and inorganic matrices. The nature of the structure is such that it is difficult to say which substructure, organic or inorganic, determines the overall packing.

The Mg^{2+} ions are octahedrally coordinated by water molecules to form complex $[Mg(H_2O)_6]^{2+}$ cations, as normally observed in hydrated magnesium salt structures.[8] These $[Mg(H_2O)_6]^{2+}$ ions display a well-ordered arrangement and interact with the β-CD organic matrix in two distinct ways. On the two independent cations, Mg1 forms intermolecular bridges (see Fig. 4); the O atom of the aqua ligands link up to six β-CD units. In contrast, Mg2 displays second-sphere interactions essentially with mineral elements, through hydrogen bonding with its aqua ligands, and may be considered as undergoing partial inclusion. The chloride ions show different types of coordination; one of them, Cl4 (see Fig. 4), is the first free anion included within β-CD in a solid-state structure.

The intermeshing substructures from β-CDs and mineral elements form a unique organic–inorganic assembly (Fig. 1 left) comprising two distinct and interlocking networks: a novel chainlike arrangement of β-CD monomers held together by intermolecular hydrogen bonds and an infinite inorganic matrix passes through the cavities of the β-CDs (Fig. 1 right).

The $[Mg(H_2O)_6]^{2+}$ ions are arranged in a very regular geometry; part of the unit cell may be described as a pseudo face-centered orthorhombic lattice (Fig. 2), in which all octahedra are slightly displaced (< 0.9 Å) from the ideal positions. The majority of the inorganic components are arranged in layers, perpendicular to the *b* axis (Fig. 3). Within these inorganic layers, Mg1 and Mg2 octahedra are bridged by Cl3 anions to form a cluster. The anion Cl4, located between the inorganic layers, links two

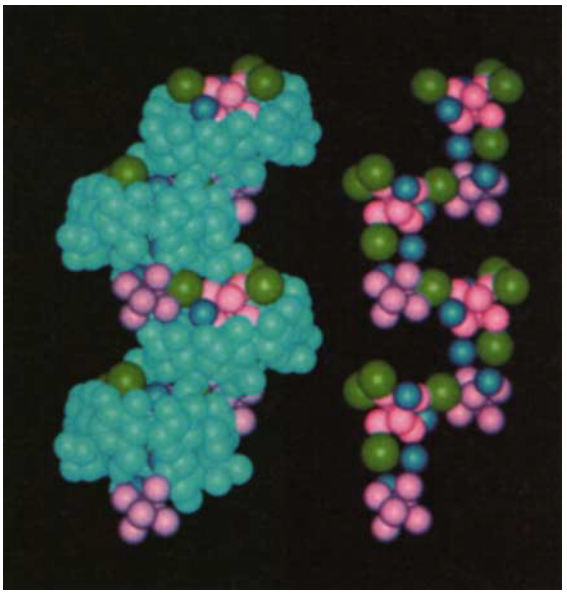

Fig. 1. Space-filling model of a section of the structure of the composite parallel to the *ab* plane (*a* horizontal). Left: The infinite intermeshing pattern of the β-CD monomer/inorganic matrix networks. Right: The infinite chain of the inorganic components separated from its β-CD environment for clarity (aqua ligands at Mg1 dark violet, those at Mg2 violet, Cl green, water of crystallization dark blue).

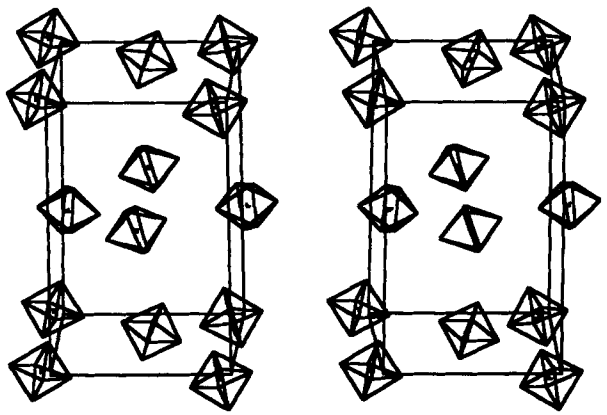

Fig. 2. Stereoview of the Mg^{2+} octahedra (*c* horizontal, *b* vertical) in a part of the unit cell (*a*, *b*, *c*/2); Mg1 are at *z* = 0 or 1/2 and Mg2 at *z* = 1/4 or 3/4. In an ideal arrangement, a cation would be surrounded by twelve neighbors; of the eight closest neighbors four are at 9.88 Å and four at 10.98 Å. Small distortions lead one neighbor of each group to be closer to the cation (Mg1 ··· Mg2 and Mg2 ··· Mg1′: 8.75 and 9.85 Å, compared to 10.35 and 11.40 Å, respectively).

symmetry-related clusters from adjacent layers, through the water molecule W14 (water of crystallization), to give infinite chains of Mg cations Mg1-Mg2-Mg1′-Mg2′. The mineral units are anchored along this basic structural motif (Fig. 4) and form, owing to the twofold screw axis parallel to the *b* axis, infinite chainlike structural motifs of inorganic units (see Fig. 1 right). Two antiparallel inorganic chains of this kind related by symmetry are alternately packed along the *c* axis (Fig. 3).

The two independent Mg cations possess quite different second coordination spheres. The Mg1 ion, located in the intermolecular CD interstices, has predominantly CD hydroxy groups as second neighbors: apart from the aqua ligand W4, which is hydrogen bonded to Cl3 and W14, the other five O atoms of aqua ligands are each directly hydrogen bonded to two hydroxy groups (ten interactions), thus simultaneously cross-

[*] Dr. C. de Rango, Dr. I. Nicolis, Dr. A. W. Coleman, Dr. P. Charpin
UPR180 CNRS, Centre Pharmaceutique
Université Paris Sud
F-92296 Châtenay Malabry (France)
Telefax: Int. code + (1)46831303

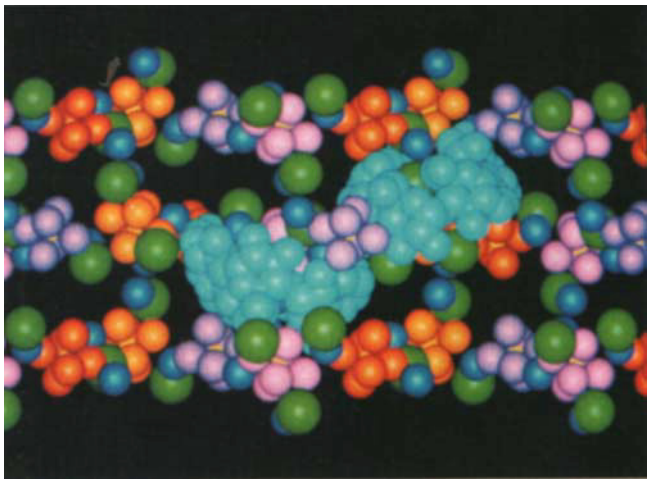

Fig. 3. View along the a axis (c horizontal) showing the packing of the inorganic layers parallel to the ac plane ($y = 0$ or $1/2$), the chloride ion Cl4 between the layers at $y = 1/4$ or $3/4$, and the β-CD monomers between adjacent inorganic layers. The chains of inorganic components run parallel to the vertical b axis (Mg^{2+}, yellow, barely visible) at $0 < z < 1/2$ (aqua ligands of Mg^{2+}, violet) and $1/2 < z < 1$ (aqua ligands of Mg^{2+}, orange). For clarity only one β-CD monomer is represented along each of the two antiparallel interlocking organic/inorganic chains in the unit cell.

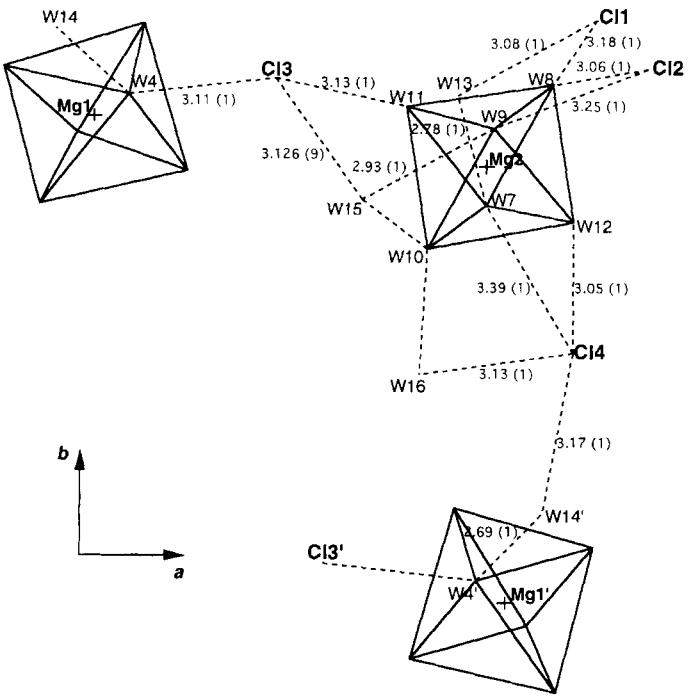

Fig. 4. A view of the inorganic structural motif indicating short contacts between the elements. It shows the intralayer Cl3 in the cluster formed by Mg1 and Mg2 octahedra (distance Mg1 $\cdots$ Mg2, 8.75 Å), and the interlayer Cl4 between clusters from adjacent layers (distances Mg2 $\cdots$ Mg(1'), 9.85 Å).

linking six β-CD monomers. These hydrogen bonds contribute to the three-dimensional cohesion of the structure. The environment about the Mg2 centers is particularly interesting, since these centers lie approximately at the level of the secondary O2/O3 hydroxy groups with a second-sphere coordination involving, through its hydration sphere, the four anions, three water molecules of crystallization, and only three O atoms from two different β-CD monomers. Three aqua ligands of the Mg2 octahedra are located in a β-CD cavity. This partial inclusion of the complex cation is stabilized by interactions through the anions: apart from Cl3, each chloride ion forms bridges to the aqua ligands coordinated to Mg2 and the secondary hydroxy groups of the host β-CD at hydrogen bonding distances.

The organic and inorganic parts of the structure interact through Cl anions, which form hydrogen bonds both with water molecules and with hydroxy groups of CDs: Cl1 and Cl2 form bridges between two or three β-CD monomers, the others, Cl3 and Cl4, have only one CD hydroxy group at hydrogen bonding distances. The chloride ion Cl3 links the Mg1 and Mg2 octahedra through W4 and W11 to give a cluster (Mg $\cdots$ Cl distances, 4.22 and 4.26 Å, respectively). Unexpectedly, the anion Cl4, which is located between the layers and forms part of the inorganic chain passing through the β-CDs, is in a real inclusion site within the cyclodextrin cavity.

The packing of the β-CD molecules likewise is a novel pattern of two "antiparallel" head-to-tail monomer helical chains related by symmetry. However, the β-CD monomers are embedded between two adjacent inorganic layers (Fig. 3), and the basic inorganic structural motifs pass through intramolecular CD cavities (Fig. 5).

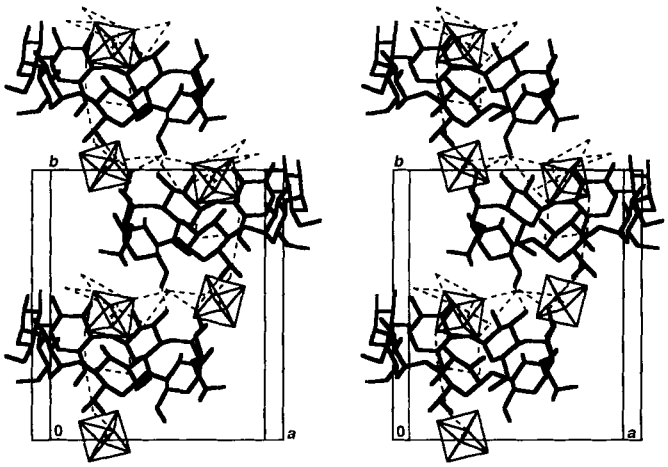

Fig. 5. Stereoview along the c axis showing the head-to-tail chain of β-CD monomers, through whose cavities the chain of inorganic components passes.

Indeed, the basic structure comprises two distinct and interlocking infinite helical chains running parallel to the b axis, one of β-CD monomers, the other involving the inorganic components (Fig. 1 left). The whole structure consists of two of these antiparallel "organic/inorganic chains" arranged alternately along the c axis (Fig. 3).

The structure may be considered in two ways: first, a novel arrangement of β-CD monomers into which an inorganic motif is inserted or second, a space-fitting arrangement of a β-CD assembly within an inorganic lattice.

Received: October 14, 1994
Revised version: August 2, 1995 [Z 7402 IE]
German version: *Angew. Chem.* **1995**, *107*, 2567–2569

Keywords: composites · cyclodextrins · hydrogen bonds · structure elucidation

[1] J. J. R. Frausto da Silva, R. J. P. Williams, *The Biological Chemistry of the Elements*, Clarendon, Oxford, **1991**.
[2] A. Veis, B. Sabsay, C. B. Win, *ACS Symp. Ser.* **1991**, *444*, Chapter 1.
[3] G. C. Ford, P. M. Harriso, D. W. Rice, J. M. A. Smith, A. Treffy, J. L. White, *Philos. Trans. R. Soc. London B* **1984**, *304*, 551.
[4] S. J. Mann, *J. Chem. Soc. Dalton Trans.* **1993**, 1–9.

[5] W. Saenger in *Hydrogen Bonding in Biological Structures*, (Eds.: G. A. Jeffrey, W. Saenger), Springer, Berlin, Chapter 18, p. 309–350; K. Harata, *Inclusion Compd.* **1991**, 5, Chapter 9, p. 311–344; P. Charpin, I. Nicolis, F. Villain, C. de Rango, A. W. Coleman, *Acta Crystallogr. Sect. C* **1991**, *47*, 1829–1833; K. Gessler, T. Steiner, G. Koellner, W. Saenger, *Carbohydr. Res.* **1993**, *249*, 327–344.

[6] I. Nicolis, A. W. Coleman, P. Charpin, C. de Rango, *Acta Crystallogr. Sect. B* **1995**, in press.

[7] Suitable crystals for X-ray analysis were grown by slow evaporation of a saturated $MgCl_2$/β-CD solution; crystal data: formula $C_{42}H_{70}O_{35}\cdot 2[Mg(H_2O)_6]Cl_2\cdot 3.5(H_2O)$; $P2_12_12_1$, $a = 15.947(3)$, $b = 18.610(1)$, $c = 23.361(6)$ Å, $V = 6933(2)$ Å^3; $Z = 4$; $R_F = 0.052$ for 6458 unique observed reflections with $I > 3\sigma(I)$. A full description of the structure will be given elsewhere.

[8] P. A. Agron, W. R. Busing, *Acta Crystallogr. Sect. C* **1985**, *41*, 8–10; K. Waizumi, H. Masuda, H. Ohtaki, K. A. Burkov, Y. Scripkin, ibid. **1991**, *C47*, 251–254; X. Solans, M. Font-Altaba, M. Aguilo, J. Solans, V. Domenech, *ibid.* **1983**, *C39*, 1488–1490.

Radical Additions to (η^6-Arene)(tricarbonyl)-chromium Complexes: Diastereoselective Synthesis of Hydrophenalene and Hydrobenzindene Derivatives by Samarium(II) Iodide Induced Cyclization**

Hans-Günther Schmalz,* Stephan Siegel, and Jan W. Bats

Arene–$Cr(CO)_3$ complexes have frequently proven their value for organic synthesis,[1] and the chemistry of this class of compounds has been the subject of intense investigations for many years.[2] In connection with our own work on the use of chiral tetralin–$Cr(CO)_3$ complexes as building blocks for the enantioselective total synthesis of compounds of biological relevance,[3] and with the intention of further exploring and developing the synthetic potential of this class of compounds, we wondered whether radical cyclizations[4] of the type shown in Scheme 1 can be utilized for the preparation of hydrophenalene derivatives.[5] We here report on the successful realization of such transformations and on the first examples of radical additions to arene–$Cr(CO)_3$ complexes.[6]

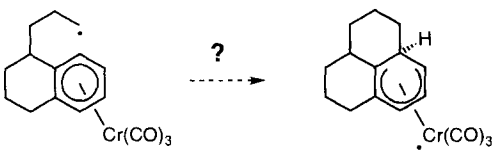

Scheme 1.

Due to the general sensitivity of Cr^0 complexes towards oxidation, we generated the radicals under reductive conditions. For this purpose the samarium(II) iodide mediated conversion of keto groups into ketyl radicals[7] appeared especially suitable to us. The first substrates we examined, 4-(3-oxobutyl)-1,2-dihydronaphthalene complexes of type **3**, are accessible from tetralone–$Cr(CO)_3$ derivatives **1**[8] in only two steps (Scheme 2).[9] The side chain was introduced by reaction with an organocerium reagent.[10] Treatment of the resulting alcohol intermediate **2** with *p*-toluenesulfonic acid on silica gel[11] led to (completely regioselective!) dehydration and deketalization.

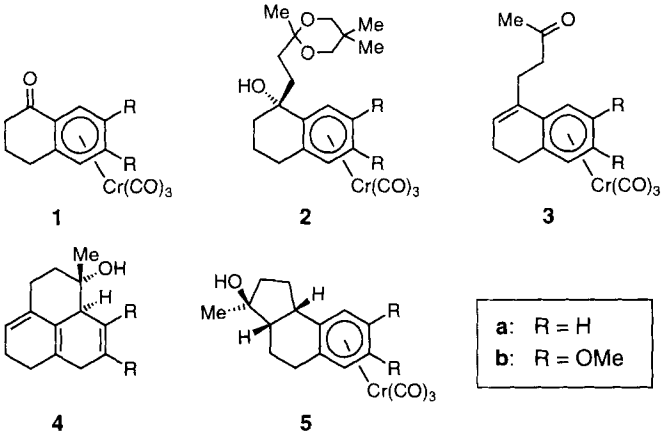

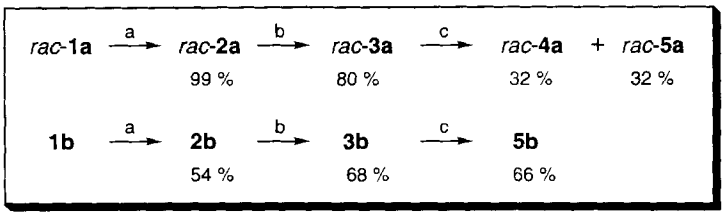

Scheme 2. Preparation and cyclization of complexes of type **3**. a) 2-(2-Bromoethyl)-2,5,5-trimethyl-1,3-dioxane, Mg, THF, then $CeCl_3$·THF, 0 °C, 1.5 h, then addition of **1**, 0 °C, 45 min; b) *p*TsOH/SiO_2, benzene, 20 °C, 2 h; c) 2.5 equiv SmI_2, THF, HMPT, *t*BuOH, −78 °C, 2 h, then room temperature, 1 h. Characteristic data for compounds **4** and **5** are given in Table 1.

When complex *rac*-**3a** was treated with 2.5 equivalents of samarium(II) iodide in THF with hexamethyl phosphoric acid triamide (HMPA) as a cosolvent and *t*-butyl alcohol as a proton source at −78 °C,[12] the tricyclic compounds *rac*-**4a** and *rac*-**5a** were obtained (both as pure diastereomers[13]), together with some recovered starting material (Scheme 2). Under the same conditions, the (optically active) dimethoxy-substituted substrate **3b** selectively afforded complex **5b** in good yield; the structure of **5b** was established by X-ray crystallography (Fig. 1).[14]

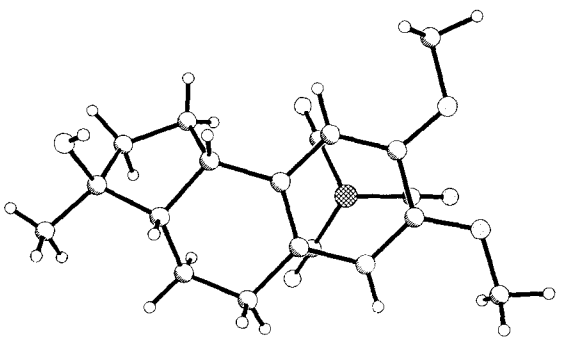

Fig. 1. X-ray crystal structure of **5b**.

[*] Prof. Dr. H.-G. Schmalz, Dipl.-Chem. S. Siegel
Institut für Organische Chemie der Technischen Universität
Strasse des 17. Juni 135, D-10623 Berlin (Germany)
Telefax: Int. code + (30)314-21105
Dr. J. W. Bats
Institut für Organische Chemie der Universität Frankfurt am Main (Germany)

[**] This work was supported by the Volkswagen-Stiftung, the Fonds der Chemischen Industrie, and Schering AG. We thank Prof. Dr. H. Schumann, Berlin, for a gift of samarium metal.

The formation of the hydrophenalene derivative *rac*-**4a** (formally the product of an alkylative Birch reduction[15]) can be rationalized as resulting from attack of the initially generated (relatively nucleophilic) ketyl radical **6** at the coordinated arene ring[16] according to Scheme 1 (see also Scheme 5). In contrast, the (unexpected) formation of the hydrobenzindenes *rac*-**5a** and **5b** can only be explained in terms of a (generally very unfavorable) 5-*endo-trig* cyclization[17, 18] of **6** to give the benzyl radical **7** (Scheme 3). We suspect that this cyclization is reversible (as is the formation of the ketyl radical **6**[19]) and that the second electron transfer (**7** → **8**) is actually the product-determining step.

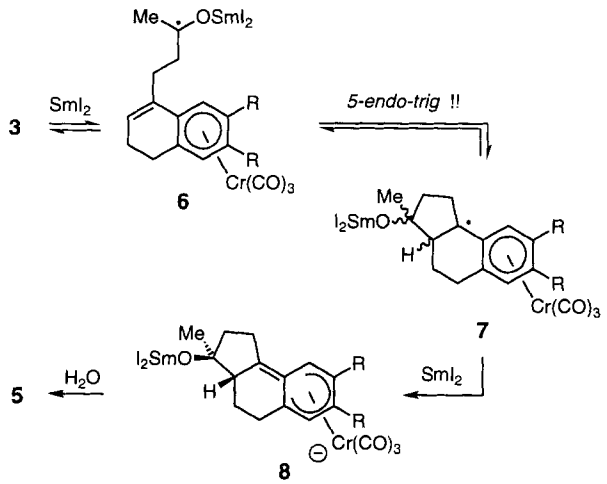

Scheme 3. Mechanism of the formation of hydrobenzindenes of type **5**.

In this context, the diastereoselectivity (≥99% *de*) of the formation of *rac*-**5a** and **5b** can be explained as follows: During the cyclization step the bulky (HMPA-solvated) $OSmI_2$ group points into free space (e.g. **6A**). Of the two possible diastereoisomeric benzylic radicals **7** that could result, only one (**7A**) reacts further with samarium(II) iodide. In radical **7A** the unpaired electron at the radical center (which should be pyramidalized due to the preferred *cis* fusion of the rings) points away from the bulky $Cr(CO)_3$ fragment (Fig. 2). The resulting anionic complex

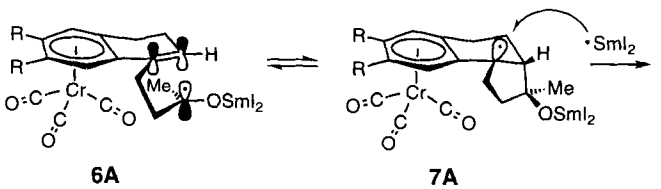

Fig. 2. Explanation of the diastereoselectivity of the formation of the hydrobenzindene derivative **5**.

8 is then finally protonated from the *exo* face[20] (→ **5**). All in all, three new chiral centers are generated with virtually complete diastereoselectivity under the influence of the chiral metal complex substructure.

In the case of substrate **3b** only the hydrobenzindene derivative **5b** is formed, implying that the attack of the (nucleophilic) ketyl radical at the arene ring is suppressed as a consequence of the increased electron density of the methoxy-substituted aromatic ring. This is in accordance with the observation that the cyclization of the uncomplexed ketone, prepared by decomplexation of *rac*-**3a**, affords predominantly a single hydrobenzindene derivative (56% isolated yield), which proved to be identical with decomplexed *rac*-**5a**. At this point, the activating effect of the (electron-withdrawing) $Cr(CO)_3$ fragment for the addition of ketyl radicals to arene rings becomes evident. The advantage of complexed substrates (of type **3**) is that, in contrast to the free ligands, they are chiral and readily available in enantiomerically pure form, such that the absolute configuration of the cyclization products can be controlled.

The formation of a hydrophenalene derivative becomes the major cyclization pathway, when a tetralin complex is employed instead of a dihydronaphthalene complex (**3**) (Scheme 4). Thus, complex **9**,[21] obtained from the readily accessible complex *rac*-**10** by benzylic deprotonation, Michael addition, and desilylation, affords the hydrophenalene–$Cr(CO)_3$ derivative *rac*-**11** in high yield under the standard cyclization conditions (Table 1).

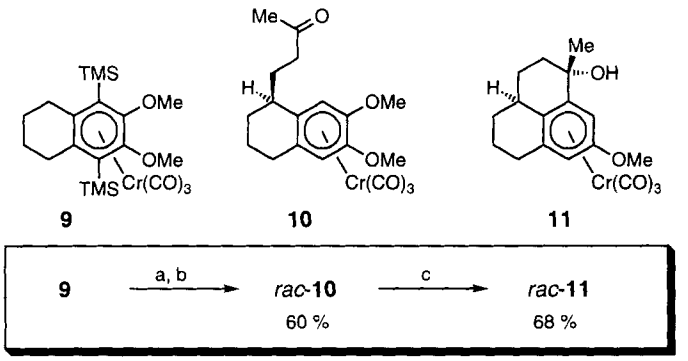

Scheme 4. Preparation and cyclization of *rac*-**10**. a) *n*BuLi, THF, HMPT, 0 °C, then $H_2C{=}C(SiMe_3)$-C(O)CH_3, then 2 N HCl; b) nBu_4NF, THF, H_2O; c) 2.5 equiv SmI_2, THF, HMPT, *t*BuOH, −78 °C, 2 h, then room temperature, 1 h. TMS = $SiMe_3$.

Table 1. Characteristic data for compounds *rac*-**4a**, *rac*-**5a**, **5b**, and *rac*-**11**. ^{1}H NMR (400 MHz, $CDCl_3$); ^{13}C NMR (67.7 MHz, $CDCl_3$, with DEPT experiments as well).

rac-**4a**: IR (KBr): $\tilde{\nu}$ [cm^{-1}] = 3432, 1653, 1448, 1437; ^{1}H NMR: δ = 1.31 (s, 3H), 1.33–1.44 (m, 1H), 1.64–1.74 (m, 1H), 1.78–1.93 (m, 3H), 2.13–2.23 (m, 4H), 2.25–2.37 (m, 2H), 2.37–2.51 (m, 1H), 5.58 (pseudo-triplet, 1H, ^3J = 4 Hz), 5.88 (ddd, 1H, ^3J = 10 Hz, ^3J = 7 Hz, ^3J = 2 Hz), 6.31 (dd, 1H, ^3J = 10 Hz, ^4J = 3.5 Hz); ^{13}C NMR: δ = 25.35 (CH_2), 27.38 (CH_3), 27.44 (CH_2), 30.39 (CH_2), 30.84 (CH_2), 34.28 (CH), 38.72 (CH_2), 70.04, 124.09 (CH), 125.01 (CH), 126.80 (CH), 130.03, 132.17, 132.45.

rac-**5a**: M.p. 136 °C; IR (KBr): $\tilde{\nu}$ [cm^{-1}] = 3422, 1955, 1868, 1863, 1852, 1627; ^{1}H NMR: δ = 1.36 (s, 3H), 1.35–1.45 (m, 1H), 1.66–1.77 (m, 1H), 1.8–1.9 (m, 3H), 1.9–2.03 (m, 1H), 2.48–2.7 (m, 3H), 3.37 (ddd, 1H, ^3J = 7.5 Hz, ^3J = 10 Hz, ^3J = 8 Hz), 5.06 (d, 1H, ^3J = 6 Hz), 5.12 (pseudo-triplet, 1H, J = 6 Hz), 5.42 (pseudo-triplet, 1H, ^3J = 6 Hz), 5.44 (d, 1H, ^3J = 6 Hz); ^{13}C NMR: δ = 22.3 (CH_2), 24.5 (CH_3), 29.3 (CH_2), 35.6 (CH_2), 37.9 (CH), 38.4 (CH_2), 50.2 (CH), 82.5, 88.7 (CH), 89.5 (CH), 95.0 (CH), 96.1 (CH), 113.2, 115.6, 212.2.

5b: M.p. 160–162 °C; $[\alpha]_D^{20}$ = −91.3 (c = 0.115 in $CHCl_3$); IR (CCl_4): $\tilde{\nu}$ [cm^{-1}] = 3612, 1958, 1883, 1493; ^{1}H NMR: δ = 1.34 (s, 3H), 1.65–1.74 (m, 2H), 1.76–1.87 (m, 2H), 1.87–2.0 (m, 2H), 2.45–2.62 (m, 3H), 2.29 (pseudo-quartet, 1H), 3.77 (s, 3H), 3.81 (s, 3H), 5.03 (s, 1H), 5.4 (s, 1H); ^{13}C NMR: δ = 22.5 (CH_2), 24.5 (CH_3), 29.0 (CH_2), 35.0 (CH_2), 37.6 (CH), 38.4 (CH_2), 50.3 (CH), 56.3 (CH_3), 58.3 (CH_3), 74.7 (CH), 82.4 (CH), 82.5, 107.1, 108.1, 129.1, 134.7, 234.1.

rac-**11**: M.p. 128 °C; IR (CCl_4): $\tilde{\nu}$ [cm^{-1}] = 3592, 1959, 1893, 1866, 1535, 1459; ^{1}H NMR: δ = 1.13–1.28 (m, 1H), 1.33–1.47 (m, 1H), 1.55 (s, 3H), 1.72–1.90 (m, 3H), 1.93–2.13 (m, 3H), 2.14 (s, OH), 2.52 (pseudo-triplet, 1H, ^3J = 12 Hz), 2.8–2.9 (m, 2H), 3.68 (s, 3H), 4.99 (d, 1H, ^4J = 1 Hz), 5.38 (d, 1H, ^4J = 1 Hz), ^{13}C NMR: δ = 22.0 (CH_2), 28.8 (CH_2), 29.3 (CH_2), 29.8 (CH_2), 32.6 (CH_3), 37.0 (CH), 39.0 (CH_2), 55.5 (CH_3), 71.2, 74.7 (CH), 78.5 (CH), 100.9, 111.1, 121.6, 142.3, 234.3.

The formation of the demethoxylated complexes *rac*-**11**, which seems unexpected at first glance, resembles in some ways a nucleophilic aromatic (*cine*) substitution with methoxide as the leaving group.[22] Mechanistically, this reaction can be rationalized as follows (Scheme 5): In the first step the ketyl radical

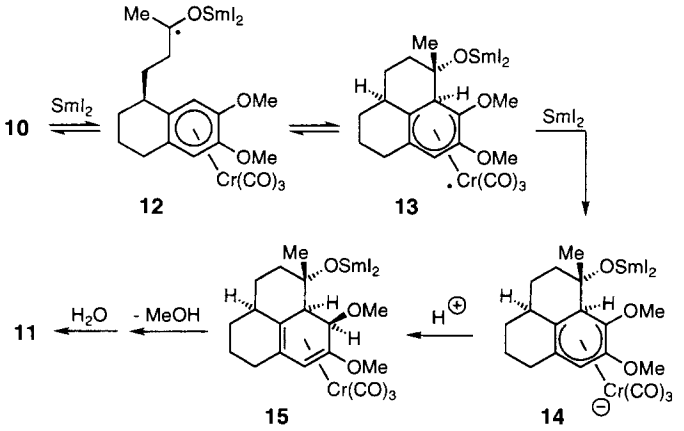

Scheme 5. Mechanism of the formation of *rac*-**11** from *rac*-**10** (only one enantiomer shown).

12 is generated, which adds to the arene ring from the face opposite to the $Cr(CO)_3$ fragment (→**13**). The transfer of a further electron by samarium(II) iodide then leads to the anionic η^5-complex **14**, which is initially protonated at the chromium atom.[23] Rapid isomerization then gives the *endo*-protonated η^4 intermediate **15**, from which the stable (η^6-arene)–$Cr(CO)_3$ substructure is obtained by elimination of methanol.

We have shown that radical additions to arene–$Cr(CO)_3$ complexes can be employed in a preparatively attractive and mechanistically understandable fashion for the regio- and stereoselective synthesis of interesting products. Considering the 5-*endo-trig* cyclizations of ketyl radicals of type **6** observed during our investigations, one wonders whether analogous reactions (against all expectations) can eventually be realized in other cases.

Received: July 7, 1995 [Z 8190 IE]
German version: *Angew. Chem.* **1995**, *107*, 2597–2599

Keywords: arene complexes · chromium compounds · cyclizations · ketyl radicals · samarium compounds

[1] a) L. S. Hegedus, *Transition Metals in the Synthesis of Complex Organic Molecules*, University Science Books, Mill Valley, CA, **1994**, Chapter 10; b) M. Uemura in *Advances in Metal-Organic Chemistry*, Vol. 2 (Ed.: L. S. Liebeskind), JAI Press, London, **1991**, p. 195; c) V. N. Kalinin, *Russ. Chem. Rev.* **1987**, *56*, 682.

[2] Selected recent work: a) S. G. Davies, O. M. L. R. Furtado, D. Hepworth, T. Loveridge, *Synlett* **1995**, 69; b) E. P. Kündig, A. Ripa, R. Liu, G. Bernardinelli, *J. Org. Chem.* **1994**, *59*, 4773; c) M. Uemura, K. Kamikawa, *J. Chem. Soc. Chem. Commun.* **1994**, 2697; d) J. P. Djukic, F. Rose-Munch, E. Rose, F. Simon, Y. Dromzee, *Organometallics* **1995**, *14*, 2027.

[3] a) H.-G. Schmalz, J. Hollander, M. Arnold, G. Dürner, *Tetrahedron Lett.* **1993**, *34*, 6259; b) H.-G. Schmalz, M. Arnold, J. Hollander, J. W. Bats, *Angew. Chem.* **1994**, *106*, 77; *Angew. Chem. Int. Ed. Engl.* **1994**, *33*, 109; c) H.-G. Schmalz, A. Schwarz, G. Dürner, *Tetrahedron Lett.* **1994**, *35*, 6861; d) H.-G. Schmalz, A. Majdalani, T. Geller, J. Hollander, J. W. Bats, *ibid.* **1995**, *36*, 4777; e) H.-G. Schmalz, K. Schellhaas, *ibid.* **1995**, *36*, 5515.

[4] a) B. Giese, *Radicals in Organic Synthesis: Formation of Carbon-Carbon Bonds*, Pergamon, Oxford, **1986**, and references therein; b) D. P. Curran in *Comprehensive Organic Synthesis, Vol. 4* (Eds.: B. M. Trost, I. Fleming), Pergamon, Oxford, **1991**, p. 779, and references therein; for some recent work, see: c) G. A. Molander, J. A. McKie, *J. Org. Chem.* **1995**, *60*, 872, and references therein.

[5] Hydrophenalenes of pharmacological interest occur, for instance, in corals: a) J.-I. Tanaka, N. Ogawa, J. Liang, T. Higa, D. G. Gravalos, *Tetrahedron* **1993**, *49*, 811; b) V. Roussis, Z. Wu, W. Fenical, S. A. Strobel, G. Van Duyne, J. Clardy, *J. Org. Chem.* **1990**, *55*, 4916.

[6] To our knowledge, only the kinetics of radical additions to the double bond of styrene–$Cr(CO)_3$ were investigated (B. Giese, personal communication).

[7] Reviews: a) H. B. Kagan, *New J. Chem.* **1990**, *14*, 453; b) G. A. Molander, *Chem. Rev.* **1992**, *92*, 26.

[8] Tetralone complexes of type **2** are easily accessible in optically active form by diastereoselective complexation of the temporarily chirally modified ligands: H.-G. Schmalz, B. Millies, J. W. Bats, G. Dürner, *Angew. Chem.* **1992**, *104*, 640; *Angew. Chem. Int. Ed. Engl.* **1992**, *31*, 631.

[9] All new compounds were characterized by the usual spectroscopic methods (see also Table 1) and gave correct microanalytical data.

[10] a) T. Imamoto, N. Takiyama, K. Nakamura, *Tetrahedron Lett.* **1985**, *26*, 4763; b) T. Imamoto, *Pure Appl. Chem.* **1990**, *62*, 747.

[11] F. D'Onofrio, A. Scettri, *Synthesis* **1985**, 1159.

[12] G. A. Molander, J. A. McKie, *J. Org. Chem.* **1994**, *59*, 3186.

[13] The relative configurations of *rac*-**4a** and *rac*-**5a** were assigned by correlation of the NMR data and also by NOE measurements.

[14] X-ray crystal structure of **5b**: Enraf-Nonius CAD4 diffractometer, $Cu_{K\alpha}$ irradiation, $2\theta_{max} = 120°$; structure determination with direct methods (SHELXS). $C_{19}H_{22}CrO_6$, orthorhombic, space group $P2_12_12$, $a = 10.327(3)$, $b = 13.208(4)$, $c = 13.536(4)$ Å, $V = 1846(2)$ Å^3, $Z = 4$, $\rho_{calcd} = 1.433$ g cm^{-3}, $\mu = 54.5$ cm^{-1}; 2740 independent reflections, of which 2730 with $I > 0$ were used; $R = 0.030$, $R_w = 0.034$. The residual electron density ranged from −0.19 to 0.34 e Å^{-3}. The absolute configuration of **5b** was confirmed by refinement of the Flack-*x* parameter ($x = -0.004$ (5)). Further details of the crystal structure investigation may be obtained from the Director of the Cambridge Crystallographic Centre, 12 Union Road, GB-Cambridge CB21EZ (UK), on quoting the full journal citation.

[15] The Birch-type reduction of benzophenone by SmI_2 in the presence of phenol was recently described: a) Z. Hou, T. Yoshimura, Y. Wakatsuki, *J. Am. Chem. Soc.* **1994**, *116*, 11169; for the preparation of cyclohexadienes by (electrochemical) reductive alkylation of arenes, see: b) T. Shono, N. Kise, T. Suzumoto, T. Morimoto, *J. Am. Chem. Soc.* **1986**, *108*, 4676.

[16] For the addition of nucleophiles to arene–$Cr(CO)_3$ complexes, see: M. F. Semmelhack in *Comprehensive Organic Synthesis, Vol. 4* (Eds.: B. M. Trost, I. Fleming), Pergamon, Oxford, **1991**, p. 517, and references therein.

[17] a) J. E. Baldwin, *J. Chem. Soc. Chem. Commun.* **1976**, 734; b) J. E. Baldwin, *ibid.* **1976**, 736.

[18] To our knowledge, the only examples for 5-*endo-trig* radical cyclizations are: a) T. Sato, N. Nakamura, K. Ikeda, M. Okada, H. Ishibashi, M. Ikeda, *J. Chem. Soc. Perkin Trans. 1* **1992**, 2399; b) H. Ishibashi, N. Nakamura, T. Sato, M. Takeuchi, M. Ikeda, *Tetrahedron Lett.* **1991**, 1725; for two recent papers, see: c) D. L. J. Clive, M. Cantin, *J. Chem. Soc. Chem. Commun.* **1995**, 319; d) T. Sato, N. Chono, H. Ishibashi, M. Ikeda, *J. Chem. Soc. Perkin Trans. 1* **1995**, 1115.

[19] E. Hasegawa, D. P. Curran, *J. Org. Chem.* **1993**, *58*, 5008.

[20] S. G. Davies, S. J. Coote, C. L. Goodfellow in *Advances in Metal-Organic Chemistry, Vol. 2* (Ed.: L. S. Liebeskind), JAI Press, London, **1991**, p. 1, and references therein.

[21] A. Schwarz, Dissertation, Universität Frankfurt am Main, **1994**.

[22] There are several examples for nucleophilic *tele* and *cine* substitutions to $Cr(CO)_3$-complexed arenes [16] but only in very few cases does a methoxy group act as a leaving group: See, for instance, refs. [3b, 2d], as well as: a) F. Rose-Munch, O. Bellot, L. Mignon, A. Semra, F. Robert, Y. Jeannin, *J. Organomet. Chem.* **1991**, *402*, 1; b) H.-G. Schmalz, K. Schellhaas, *Tetrahedron Lett.* **1995**, *36*, 5511, and references therein.

[23] a) M. F. Semmelhack, H. T. Hall, Jr., R. Farina, M. Yoshifuji, G. Clark, T. Bargar, K. Hirotsu, J. Clardy, *J. Am. Chem. Soc.* **1979**, *101*, 3535; b) J.-C. Boutonnet, F. Rose-Munch, E. Rose, *Tetrahedron Lett.* **1985**, *26*, 3989.

A New Platform for Designing Ligands for Asymmetric Induction in Allylic Alkylations**

Barry M. Trost,* Bernhard Breit, Stefan Peukert, Jorge Zambrano, and Joseph W. Ziller

The design of ligands for asymmetric induction in transition metal catalyzed reactions has made great strides in reduction and oxidation processes. Success for the metal-catalyzed alkylation of allylic compounds by stabilized nucleophiles has been slower presumably because the bond-making or -breaking event in which the chirality is created occurs outside the coordination sphere of the metal and therefore distal to the chiral ligands.[1-5] Chiral phosphinoaryloxazoline ligands have had limited success; the best results are restricted to substrates that form π-allylpalladium complexes bearing bulky substituents like phenyl or isopropyl in the 1- and 3-positions.[1] Ligands based upon amides prepared from chiral diamines have proven more versatile.[2] Thus, cyclic allylic esters gave excellent results with a broad range of nucleophiles.[2b,c] In the desymmetrization of *meso* 1,4-enediol esters, which depended upon the nature of the ester, benzoates gave satisfactory results.[2a] However, the problem of the dependence of the enantiomeric discriminating step on leaving group became evident during cyclization of the biscarbamates to form oxazolidinones, which gave less satisfactory results.[1a] Enhancement of the process for asymmetric synthesis requires resolving those examples that have proven resistant to giving high *ee*'s with existing ligands. Designing new platforms chiral ligands should maintain a simplicity of synthesis. Based upon the model depicted in Figure 1, we now have developed a new platform for application to some of the systems that were previously less successful; our studies also revealed a most interesting dependence of the sense of chirality on the nature of the linker.

The availability of dicarboxylic acids in enantiomerically pure form, which could serve as the chiral scaffold, led to our consideration of a linker with an appropriate binding post. The success of amides in our first-generation ligands led to our choice of 2-diphenylphosphinoaniline (**1**) for the new linker, which is readily available in two steps from 2-chloroaniline and triphenylphosphane.[6] Acylation of **1** with the carboxylic acid chlorides derived from dicarboxylic acids **2a**–**5a**[7] gave the new diamindes **2b**–**5b** (see Table 2).[8] We began our tests of these ligands with the cyclization of the glycosidase precursor **6** [Eq. (a)].[2a] In each case, the diol **6a** was treated with *p*-toluenesulfonylisocyanate (*p*TsNCO) in THF at room temperature and then warmed to 60 °C. The resulting solution was added to a solution of the catalyst prepared from 2.5 mol% $[Pd_2(dba)_3]\cdot CHCl_3$ (**8**) (dba = dibenzylidenacetone) and 5–10 mol% of the ligand at 0 °C. The reaction was typically complete within 2–3.5 h. The results of the experiments with ligands **2b**, **3b**, and **5b** are given in Table 1 and compared to the results obtained with ligands **9**[2a] and **10**.[2a]

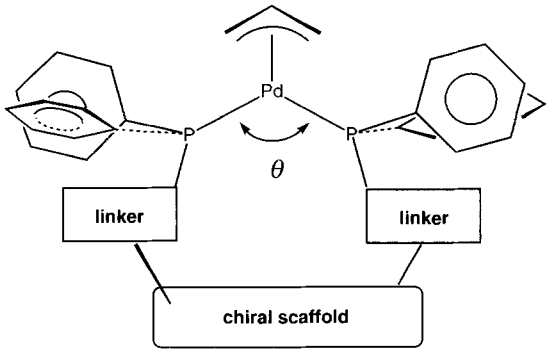

Fig. 1. Model of the ligand design.

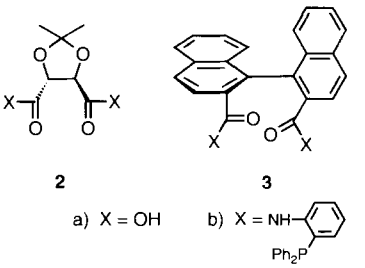

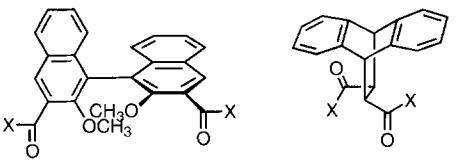

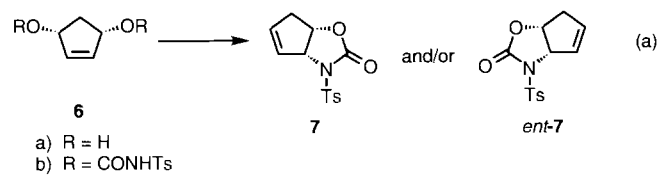

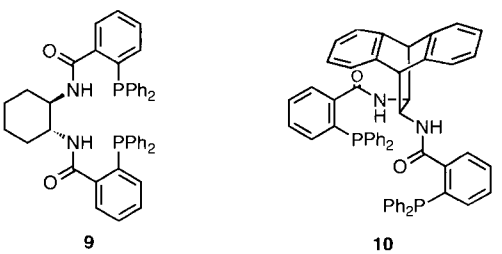

Table 1. Asymmetric induction in the Pd-catalyzed formation of oxazolidin-2-ones **7** and *ent*-**7**.

Entry	Ligand	Yield [%]	**7**:*ent*-**7** [a] (*ee*)
1	**2b**	29	56:44 (12)
2	**3b**	81	65:35 (30)
3	**5b**	99	6:94 (88)
4	**9**	97	11:89 (78)
5	**10**	94	94:6 (88)

[a] Determined as described in ref. [2a].

[*] Prof. B. M. Trost, B. Breit, S. Peukert, J. Zambrano
Department of Chemistry, Stanford University
Stanford, CA 94305-5080 (USA)
Telefax: Int. code +(415) 725-0259
J. W. Ziller
Department of Chemistry, University of California–Irvine (USA)

[**] We thank the National Science Foundation and the National Institutes of Health, General Medical Sciences, for their generous support of our programs. A postdoctoral fellowship for B. B. was provided by the BASF Aktiengesellschaft, a stipend for S. P. by the Studienstiftung des Deutschen Volkes, and a predoctoral fellowship for J. Z. by INTEVEP (Venezuela). Mass spectra were provided by the Mass Spectrometry Facility, University of California–San Francisco, which is supported by the NIH Division of Research Resources. Johnson Matthey Alfa Aesar provided palladium salts under a loan program.

Several interesting points are to be noted. Of the new ligands, only **5b** gave the product with acceptable levels of enantiomeric excess.[19] We previously suggested that the bite angle θ in the Pd complex (see Fig. 1) should be made as large as possible for higher selectivity; this bite angle may be related to the dihedral angle between the anchoring groups at the stereogenic centers of the chiral scaffold.[2a] Only in **5b** is the dihedral angle between the two carboxylate groups forced to be large. Completely surprising is the absolute configuration of the product. Comparing entries 3 and 5 (Table 1) show that maintaining the same sense of chirality of the chiral scaffold and only changing the orientation of the amide function reverses the sense of chirality in the product. Thus, from the same enantiomer of the dicarboxylic acid **5a**, which is the precursor of both **5b** and **10**, either enantiomer of the product is available with high *ee*.

The effectiveness of this new class of ligands in discriminating enantiotopic urethane leaving groups is revealed in examining examples with six- and seven-membered rings [Eq. (b)]. Following the same protocol as previously described, the bisurethanes

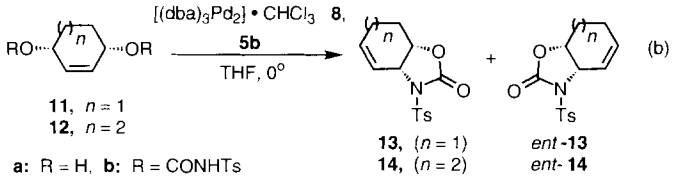

11b[2a] and **12b**[8] derived from diols **11a** and **12a** gave *ent*-**13**[8] and *ent*-**14**[8] in 97% *ee* (82% yield) and 95% *ee* (82% yield), respectively (Table 2).[9] By comparison, when ligand **10** was employed in these reactions, enantiomers **13** and **14** were obtained in 81% *ee* and 35% *ee*, respectively.

Table 2. Data for **5b**, *ent*-**13**, and *ent*-**14**.

5b: M.p. 118–121 °C; $[\alpha]_D^{25} = +117.9$ ($c = 1.25$, CH_2Cl_2); IR (film): $\tilde{\nu} = 3300$, 1694, 1575, 1504, 1435 cm^{-1}; ^1H NMR ($CDCl_3$, 400 MHz): $\delta = 8.54$ (d, $J =$ 6.72 Hz, 2H), 8.02 (m, 2H), 7.41–6.92 (m, 30H), 6.82 (m, 2H), 4.19 (s, 2H), 2.82 (s, 2H); ^{13}C NMR ($CDCl_3$, 100 MHz): $\delta = 170.37$, 142.21, 140.52 (d, $J_{PC} =$ 18.3 Hz), 139.75, 134.57 (d, $J_{PC} = 19.3$ Hz), 134.50 (d, $J_{PC} = 19.2$ Hz), 134.06, 133.80 (d, $J_{PC} = 13.9$ Hz), 133.51 (d, $J_{PC} = 7.1$ Hz), 129.96, 129.34 (d, $J_{PC} = 5.6$ Hz), 128.93 (d, $J_{PC} = 7.0$ Hz), 128.75 (d, $J_{PC} = 6.8$ Hz), 126.03 (d, $J_{PC} = 10.7$ Hz), 125.38, 124.86, 123.0, 122.75, 49.65, 46.65; ^{31}P NMR ($CDCl_3$, 161 MHz): $\delta = -19.3$; Anal. calcd for $C_{54}H_{42}N_2O_2P_2$: C 79.79, H 5.21, N 3.45; found: C 79.84, H 5.28, N 3.19

ent-**13**: M.p. 122 °C; $[\alpha]_D^{25} = +87.5$ ($c = 2.27$, CH_2Cl_2); IR (film): $\tilde{\nu} = 1778$, 1597, 1367, 1348 cm^{-1}; ^1H NMR ($CDCl_3$, 300 MHz): $\delta = 7.95$ (d, $J = 8.3$ Hz, 2H), 7.34 (d, $J = 8.3$ Hz, 2H), 6.08 (m, 1H), 5.95 (m, 1H), 4.85 (m, 2H), 2.44 (s, 3H), 2.3–2.0 (m, 3H), 1.8 (m, 1H); HR-MS: calcd for $C_{14}H_{16}NO_3S$ ($M^+ + H$): 294.0800; found: 294.0791

ent-**14**: M.p. (racemate) 158 °C; $[\alpha]_D^{25} = +70.2$ ($c = 2.68$, CH_2Cl_2); IR (film): $\tilde{\nu} = 1767$, 1597, 1364, 1311 cm^{-1}; ^1H NMR ($CDCl_3$, 300 MHz): $\delta = 7.97$ (d, $J = 8.4$ Hz, 2H), 7.35 (d, $J = 8.4$ Hz, 2H), 5.97 (dddd, $J = 11.1$, 6.6, 5.7, 2.0 Hz, 1H), 5.67 (ddd, $J = 11.1$, 3.4, 1.7 Hz, 1H), 5.21 (br.d, $J = 8.5$ Hz, 1H), 4.66 (ddd, $J = 9.9$, 8.5, 4.4 Hz, 1H), 2.45 (s, 3H), 2.18–1.83 (m, 4H), 1.70–1.53 (m, 2H); ^{13}C NMR ($CDCl_3$, 75 MHz): $\delta = 151.7$, 145.4, 135.3, 130.6, 129.7, 128.4, 125.8, 76.6, 58.7, 27.2, 26.6, 21.7, 17.6; Anal. calcd for $C_{15}H_{17}NO_4S$: C 58.62, H 5.57, N 4.56; found: C 58.53, H 5.71, N 4.53

We also examined 4-acetoxy-2-pentene as a substrate since, in contrast to 1,3-diphenylallyl acetate, the highest selectivity observed was only 71% *ee*.[1e] Using the sodium salt of dimethyl malonate in THF at room temperature gave the alkylated product **15**[1] in 74% *ee* (90% yield) [Eq. (c)] as determined by [Eu(hfc)$_3$] (hfa = heptafluoropropylhydroxymethylenecamphorato) NMR shift experiments. The *ee* jumped to 87% (93% yield) for the alkylation with the sodium salt of dimethyl

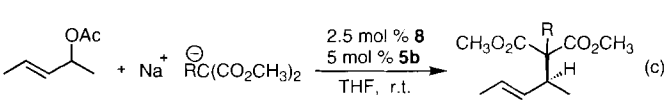

15 (R = H)
16 (R = CH_3)

methylmalonate to give **16**.[4] Thus, this new ligand gave the best results to date for asymmetric alkylation of the dimethylallyl system.

In trying to understand the contrasting chiral recognition of our normal carboxamide ligand **10** and our carboxamide "invertomer" ligand **5b**, we sought to obtain a crystal structure of one of the π-allyl complexes. The π-allylpalladium chloride dimer was mixed with **5b** and the anion was exchanged with perchlorate to give crystals suitable for X-ray analysis. Several striking features are revealed (Fig. 2).[11] The ligand moiety of

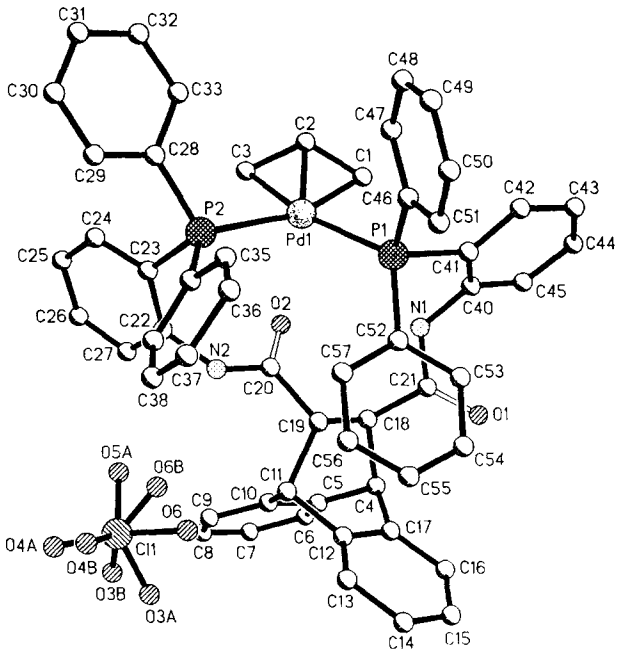

Fig. 2. Crystal structure of the Pd–allyl complex of the invertomer ligand.

the complex does not have C_2 symmetry even though it is feasible. NMR spectroscopy also indicates that the ligand lacks C_2 symmetry when bound to the π-allylpalladium unit in solution.[10] This clearly raises questions about the relevance of such symmetry for ligands designed for the Pd-catalyzed alkylation of allylic compounds. The bite angle indeed has opened from the typical 90° in square-planar palladium complexes to 110.5° in accord with our explanation of the enhanced selectivity of the reaction. As shown in Figure 3, these ligands, wherein the "chiral space" is defined by the grooves of the propellers formed by the bis(triarylphosphane) moieties, offer two types of cavities in which the palladium and substrate will reside, one flanked by Ar′ and Ar (the spaces labeled a and a*) and one flanked by only Ar groups (spaces b and b*). The X-ray structure for the complex formed from **5b** indicates that the π-allyl unit sits in a groove of the former kind. Based upon our molecular modeling, we have proposed that our normal ligands place the substrate in a groove of the latter type. While any definite conclusions must await an X-ray structure determination of a complex from **10**, the different positions of the π-allylpalladium in the two grooves

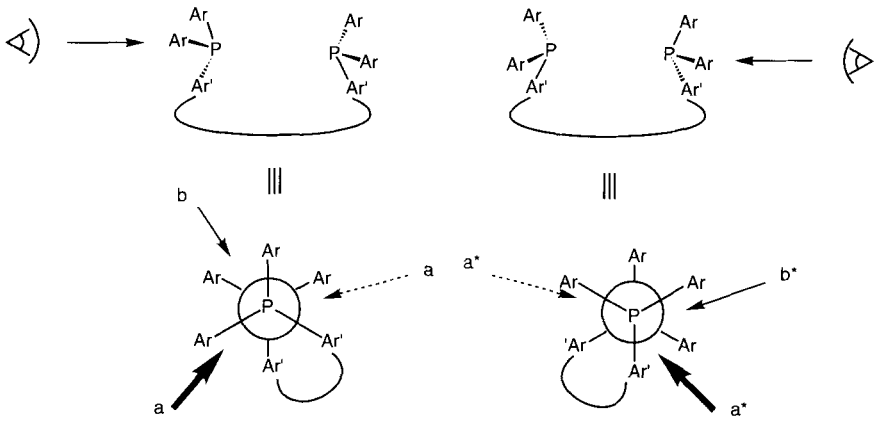

Fig. 3. Model of the different chiral spaces of the ligand.

may account for the change in chiral recognition. A rationalization traces back to the different properties of the linker aryl group, which is electron rich in **5b** and electron poor in **10**. Complexes of the latter would achieve some electronic stabilization by placing the π-allylpalladium cationic moiety closer to the more electron-rich aryl rings of the propeller. This new family of ligands provides a nice complement to our previous series and offers a new platform for further development.[12]

Received: May 16, 1995 [Z 7995 IE]
German version: *Angew. Chem.* **1995**, *107*, 2577–2579

Keywords: alkylations · asymmetric syntheses · chiral auxiliaries · palladium compounds

[1] a) G. J. Dawson, J. M. J. Williams, S. J. Coote, *Tetrahedron Lett.* **1995**, *36*, 461; b) P. von Matt, O. Loiseleur, G. Koch, A. Pfaltz, C. Lefeber, T. Feucht, G. Helmchen, *Tetrahedron: Asymmetry* **1994**, *5*, 573; c) P. Sennhenn, B. Gabler, G. Helmchen, *Tetrahedron Lett.* **1994**, *35*, 8595; d) J. Sprinz, M. Kiefer, G. Helmchen, M. Reggelin, G. Huttner, O. Walter, L. Zsolnai, *ibid.* **1994**, *35*, 1523; e) P. von Matt, A. Pfaltz, *Angew. Chem.* **1993**, *105*, 614; *Angew. Chem. Int. Ed. Engl.* **1993**, *32*, 566; f) G. J. Dawson, C. G. Frost, J. M. J. Williams, S. J. Coote, *Tetrahedron Lett.* **1993**, *34*, 3149; g) J. Sprinz, G. Helmchen, *ibid.* **1993**, *34*, 1769; h) U. Lütenegger, G. Umbricht, C. Fahrni, P. von Matt, A. Pfaltz, *Tetrahedron* **1992**, *48*, 2143.

[2] A) B. M. Trost, D. L. Van Vranken, C. Bingel, *J. Am. Chem. Soc.* **1992**, *114*, 9327; b) B. M. Trost, R. C. Bunt, *ibid.* **1994**, *116*, 4089; c) B. M. Trost, M. G. Organ, *ibid.* **1994**, *116*, 10320; d) B. M. Trost, B. Breit, M. G. Organ, *Tetrahedron Lett.* **1994**, *35*, 5817.

[3] H. Kubota, K. Koga, *Tetrahedron Lett.* **1994**, *35*, 6689; T. Hayashi, A. Ohno, S. Lu, Y. Matsumoto, E. Fukuyo, K. Yanagi, *J. Am. Chem. Soc.* **1994**, *116*, 4221; A. Togni, C. Breutel, A. Schnyder, F. Spindler, H. Landert, A. Tijina, *ibid.* **1994**, *116*, 4062; M. Massacret, C. Goux, P. Lhoste, D. Sinou, *Tetrahedron Lett.* **1994**, *35*, 6093; J. Y. Legros, J. C. Fraud, *Tetrahedron* **1994**, *50*, 465; J. V. Allen, S. J. Coote, G. J. Dawson, C. G. Frost, C. J. Martin, J. M. J. Williams, *J. Chem. Soc. Perkin Trans. 1* **1994**, 2065; C. G. Frost, J. M. J. Williams, *Synlett* **1994**, 551; J. M. Brown, D. I. Hulmes, P. J. Guiry, *Tetrahedron* **1994**, *50*, 4493; J. Kang, W. O. Cho, H. G. Cho, *Tetrahedron: Asymmetry* **1994**, *5*, 1347; D. Tanner, P. G. Andersson, A. Harden, P. Somfai, *Tetrahedron Lett.* **1994**, *35*, 4631; P. Gamez, B. Dunjic, F. Fache, M. Lemaire, *J. Chem. Soc. Chem. Commun.* **1994**, 1417; G. Brenchley, E. Merifield, M. Wills, M. Fedouloff, *Tetrahedron Lett.* **1994**, *35*, 2791; M. Yamaguchi, T. Shima, T. Yamagishi, M. Hida, *ibid.* **1990**, *31*, 5049; T. Hayashi, A. Yamamoto, Y. Ito, *ibid.* **1988**, *29*, 99; T. Hayashi, A. Yamamoto, T. Hagihara, Y. Ito, *ibid.* **1986**, *27*, 191; B. M. Trost, D. J. Murphy, *Organometallics* **1985**, *4*, 1143.

[4] B. M. Trost, P. E. Strege, *J. Am. Chem. Soc.* **1977**, *99*, 1649; B. M. Trost, T. J. Dietsche, *ibid.* **1973**, *95*, 8200.

[5] For reviews, see: G. Consiglio, R. M. Waymouth, *Chem. Rev.* **1989**, *89*, 257; S. A. Godleski in *Comprehensive Organic Synthesis, Vol. 4* (Eds.: B. M. Trost, I. Fleming, M. F. Semmelhack), Pergamon, Oxford, **1991**, Chapter 3.3; G. C. Frost, J. Howarth, J. M. J. Williams, *Tetrahedron: Asymmetry* **1992**, *3*, 1089; T. Hayashi in *Catalytic Asymmetric Synthesis* (Ed.: I. Ojima), VCH, New York, **1993**, pp. 325–365.

[6] M. K. Cooper, J. M. Downes, P. A. Duckworth, M. C. Kerby, R. J. Powell, M. D. Soucek, *Inorg. Synth.* **1988**, 129.

[7] **3a**: R. Kuhn, O. Albrecht, *Justus Liebigs Ann. Chem.* **1928**, *465*, 282; D. M. Hall, E. E. Turner, *J. Chem. Soc.* **1955**, 1242; **4a**: W. M. Stanley, R. Adams, *Rec. Trav. Chim. Pays Bas* **1928**, *48*, 1035; K. Weil, W. Kuhn, *Helv. Chim. Acta* **1944**, *27*, 1648; H. J. Barber, K. Gaimster, *J. Appl. Chem.* **1952**, *2*, 565; **5a**: ref. [2a].

[8] New compounds were characterized spectroscopically and elemental composition established by high-resolution mass spectroscopy or combustion analysis.

[9] The enantiomeric excesses and absolute configurations of the products were determined by hydrolysis to the hydroxyamide and derivatization with (*S*)-*O*-methylmandelic acid. See: B. M. Trost, J. M. Belletire, S. A. Godleski, P. G. McDougal, J. M. Balkovec, J. J. Baldwin, M. E. Christy, G. S. Ponticello, S. L. Varga, J. P. Springer, *J. Org. Chem.* **1986**, *51*, 2370.

[10] Distortion of the preferred conformation of π-allylpalladium complexes with C_2-symmetric ligands in solution has been recently discussed: P. G. Andersson, A. Harden, D. Tanner, P.-D. Norrby, *Chem. Eur. J.* **1995**, *1*, 12.

[11] X-ray data were collected at 296 K using a 0-2θ scan technique with $Mo_{K\alpha}$ radiation. All 3578 reflections were corrected for Lorentz and polarization effects and were placed on an approximately absolute scale. The diffraction symmetry was *mmm* with systematic absences $h00$ for $h = 2n+1$, $0k0$ for $k = 2n+1$ and $00l$ for $l = 2n+1$. The noncentrosymmetric orthorhombic space group $P2_12_12_1$ is therefore uniquely defined, $a = 12.2672$), $b = 17.735(2)$, $c = 23.861(9)$ Å, $V = 5191(3)$ Å^3, $Z = 4$, $\rho_{calcd} = 1.356$ g cm^{-3}. All crystallographic calculations were carried out using either our locally modified version of the UCLA Crystallographic Computing Package or the SHELXTL PLUS program package. The analytical scattering factors for neutral atoms were used throughout the analysis; both the real ($\Delta f'$) and imaginary ($i\Delta f''$) components of anomalous dispersion were included. The quantity minimized during least-squares analysis was $\sum w(F_o - F_c)^2$ where $w^{-1} = \sigma^2(F) + 0.0009^2$. The structure was solved by direct methods and refined by full-matrix least-squares techniques. Hydrogen atoms were included using a riding model with d(C–H) = 0.96 Å, d(N–H) = 0.90 Å, and U(iso) = 0.08 Å^2. Those hydrogens associated with the allyl unit could not be located and were not included. The perchlorate anion is disordered. Refinement of positional and thermal parameters led to convergence with $R_F = 0.069$; $R_{wF} = 0.077$ and GOF = 1.62 for 325 variables refined against those 2575 reflections with $F > 4.0\sigma(F)$. The absolute structure was determined by refinement of the Rogers' h-parameter. A final difference-Fourier synthesis yielded ρ(max) = 0.61 e Å^{-3}. Further details of the crystal structure investigation may be obtained from the Director of the Cambridge Crystallographic Data Centre, 12 Union Road, GB-Cambridge CB2 1EZ (UK) on quoting the full journal citation.

Peripherally Substituted Cobaloximes; X-ray Crystal Structure Analysis of σ-Hexylbis[1,8-di(*N*-morpholino)octane-4,5-dioximato]pyridinecobalt(III)**

Berthold Köhler, Martin Knauer, William Clegg, Mark R. J. Elsegood, Bernard T. Golding,* and János Rétey*

During our ongoing attempts to mimic the functions of the B_{12} coenzyme (5'-deoxyadenosylcobalamin, AdoCbl),[1,2] we synthesized several bridged, intramolecularly alkylated cobaloximes.[2] The homolysis of their Co–C σ bond is reversible, like that of the natural cofactor when bound to an enzyme. The development of supramolecular cobaloximes that exhibit molecular recognition and modeling the main features[3] of adenosylcobalamin-dependent enzymatic reactions requires the synthesis of bridged alkylcobaloximes with peripheral substituents to enable substrate binding. We have found that alkylcobaloximes bearing aminoalkyl substituents on the 1,2-dioxime units can be synthesized, provided the amino groups are γ-substituents, but not α- or β-substituents.

Most cobaloximes contain two dimethylglyoxime units.[4] Our attempts to synthesize alkylcobaloximes bearing α-amino substituents on methyl groups attached to the dioxime unit failed because of elimination of these substituents during the attempted preparation of an intermediate cobaloxime(I) species required for alkylation of the cobalt. Thus, oxime formation with 1,4-dibenzoyloxybutane-2,3-dione[5] gave the dioxime ligand **1a**, which was combined with cobalt(II) chloride

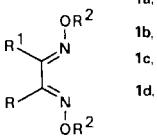

1a, R = R^1 = $PhCO_2CH_2$, R^2 = H
1b, R = Br, R^1 = Cl, R^2 = Tetrahydropyran-2-yl
1c, R = R^1 = $ClCH_2CH_2$, R^2 = H
1d, R = R^1 = $tBuPh_2SiOCH_2CH_2$, R^2 = H
1e, R = R^1 = 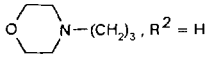 , R^2 = H

and pyridine in alkaline ethanol in the standard manner.[6] Addition of sodium borohydride followed by 2-bromopropane unexpectedly gave σ-isopropylbis(butane-2,3-dioximato)pyridinecobalt(III) (**2**) in 90% yield. Presumably, after cobalt is reduced to oxidation state 1, ejection of an α-substituent is triggered, and this is faster than reaction of the cobalt with the alkylating agent. The elimination is facilitated by conjugation of the filled d_{z^2} orbital on cobalt with the p orbitals of the dioxime, provided the bond to the leaving group is nearly perpendicular to the dioxime π system (Scheme 1). An analogous elimination occurred with a nitrogen function occupying the α-positions in the dioxime ligand.[7] In the corrin system reductive elimination of a peripheral bromine atom has been described[8a] and later interpreted[8b] as intramolecular electron transfer from the Co^I center. We therefore directed our attention to β-amino- and γ-amino-substituted alkylcobaloximes.

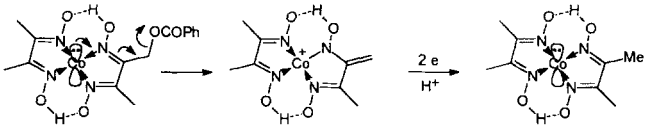

Scheme 1. Postulated mechanism for elimination of α-substituents during reduction of cobaloximes.

Protection of the hydroxy groups of 1-bromo-2-chloroglyoxime[9] as tetrahydropyranyl ethers gave **1b**, which was treated with ethene in the presence of aluminum trichloride to afford dioxime **1c**. The very low yield obtained in this Friedel–Crafts acylation (<5%) led us to investigate an alternative route to β-substituted dioximes based on the method of Criegee and Lederer.[5] This gave 1,6-dihydroxyhexane-3,4-dione bis-*t*-butyldiphenylsilyl ether, which was easily converted into the dioxime **1d**. However, all attempts to replace the β-oxygen functions of **1d** with amino functions failed.

In another approach we prepared 1,6-bis(*N*,*N*-diethylamino)-3,4-bis(trimethylsilyloxy)hex-3-ene (**3**) (TMS = trimethylsilyl) by sodium-induced acyloin condensation[10,11] of ethyl 3-(*N*,*N*-diethylamino)propanoate[12] in the presence of chlorotrimethylsilane. Numerous attempts to convert the bis(silyl) ether into the corresponding diketone (using bromine in dichloromethane,[11] thiocyanogen in chloroform,[11] or copper(II) acetate[13]) or derived 1,2-dioxime (for example using hydroxylamine hydrochloride in pyridine/ethanol[14] or dimethyl formamide[15]) failed. Methanolysis of **3** gave the very labile 1,6-bis(*N*,*N*-diethylamino)-4-hydroxyhexan-3-one (**4**), which could not be oxidized

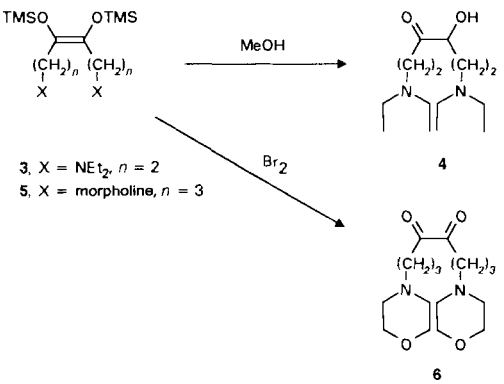

(dimethyl sulfoxide/acetic anhydride[16]) to the corresponding diketone and did not give an isolable 1,2-dioxime on direct reaction with hydroxylamine. The lability of **4** (and **1d**) is ascribed to a tendency to undergo β-elimination. In contrast, the homologous system 1,8-di(*N*-morpholino)-4,5-bis(trimethylsilyloxy)oct-4-ene (**5**),[17] obtained by acyloin condensation[10,11] of ethyl 4-(*N*-morpholino)butanoate,[18] could be smoothly converted into the corresponding dioxime **1e**,[19] a relatively

[*] Prof. Dr. B. T. Golding, Prof. Dr. W. Clegg, Dr. M. R. J. Elsegood
Department of Chemistry, Bedson Building
University of Newcastle upon Tyne
GB-Newcastle upon Tyne NE1 7RU (UK)
Telefax: Int. code + (191) 222-7070
e-mail: b.t.golding@newcastle.ac.uk
Prof. Dr. J. Rétey, B. Köhler, Dr. M. Knauer
Institut für Organische Chemie der Universität
Richard-Willstätter Allee, D-76128 Karlsruhe (Germany)
Telefax: Int. code + (721) 608 4823
e-mail: biochem@ochhades.chemie.uni-karlsruhe.de

[**] This research was supported by the Commission of European Communities, the Deutsche Forschungsgemeinschaft, the Fonds der Chemischen Industrie, and the Engineering and Physical Sciences Research Council.

stable compound, from which the alkylcobaloxime 7[20] could be prepared by standard methodology.[6] Thus, reaction of ethyl 4-(*N*-morpholino)butanoate with four equivalents of sodium powder/chlorotrimethylsilane in diethyl ether afforded 1,8-di(*N*-morpholino)-4,5-bis(trimethylsilyloxy)oct-4-ene (**5**, 67%).

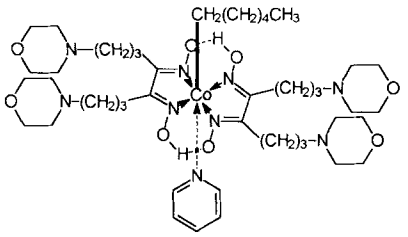

7

Oxidation of **5** with bromine[11] gave 1,8-di(*N*-morpholino)octane-4,5-dione (**6**), and the crude product was directly converted into the corresponding dioxime **1e** (49% overall yield) with hydroxylamine. The dioxime was treated with cobalt(II) bromide in methanol containing pyridine and sodium hydroxide to afford an intermediate cobaloxime(II) complex, which was reduced to cobaloxime(I) by addition of sodium borohydride. Alkylation with 1-iodohexane gave, after chromatogaphic purification, the crystalline alkylcobaloxime σ-hexylbis[1,8-di(*N*-morpholino)octane-4,5-dioximato]pyridinecobalt(III) (**7**, 40% yield). The ^{1}H and ^{13}C NMR spectra of **7** were consistent with the structure proposed, which was confirmed by X-ray analysis of single crystals[21] obtained from a solution of the complex in petroleum ether (Fig. 1). It is interesting that all the alkyl side chains contain one or two *gauche* elements. The Co–hexyl group exhibits the following arrangement for the major disorder component: Co-C1-C2-C3 *anti*, C1-C2-C3-C4 *gauche*, with C2-C3-C4-C5 and C3-C4-C5-C6 both *anti*. The Co–C1 bond length is 2.011(6) Å and the Co-C1-C2 bond angle is 123.6(6)°, which is unusually large[22] for a relatively unhindered Co–alkyl group.

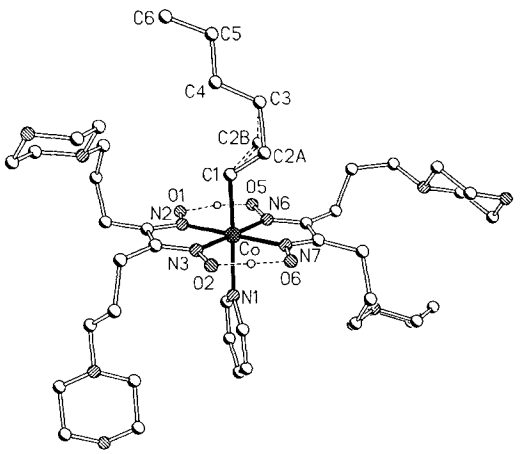

Fig. 1. Crystal structure of 7.

Received: May 30, 1995 [Z80401E]
German version: *Angew. Chem.* **1995**, *107*, 2580–2581

Keywords: acyloin condensation · cobaloxime · eliminations · vitamin B_{12} model compounds

[1] R. J. Anderson, S. Ashwell, R. M. Dixon, B. T. Golding, *J. Chem. Soc. Chem. Commun.* **1990**, 70–72.
[2] J. A. Robinson, H. Flohr, U. M. Kempe, W. Pannhorst, J. Rétey, *Liebigs Ann. Chem.* **1983**, 181–203, and references therein.
[3] B. T. Golding, *Chem. Br.* **1990**, *26*, 950–954, and references therein.
[4] G. N. Schrauzer, J. Kohnle, *Chem. Ber.* **1964**, *97*, 3056–3064; G. N. Schrauzer, *Angew. Chem.* **1976**, *88*, 465–474; *Angew. Chem. Int. Ed. Engl.* **1976**, *15*, 417–426.
[5] R. Criegee, M. Lederer, *Justus Liebigs Ann. Chem.* **1953**, *583*, 29–36.
[6] G. N. Schrauzer, *Inorg. Synth.* **1968**, *11*, 61–70.
[7] M. Knauer, Dissertation, Universität Karlsruhe, **1986**.
[8] a) F. Wagner, *Proc. R. Soc. (London) A* **1965**, *288*, 344–347; b) R. Bonnett in *B_{12} Vol. 1* (Ed.: D. Dolphin), Wiley, New York, **1982**, p. 220.
[9] A. Hantzsch, *Chem. Ber.* **1892**, *25*, 705–712; G. Ponzio, *Gazz. Chim. Ital.* **1930**, *60*, 429–436.
[10] U. Schräpler, K. Rühlmann, *Chem. Ber.* **1963**, *96*, 2780–2785; K. Rühlmann, H. Seefluth, H. Becker, *ibid.* **1967**, *100*, 3820–3824.
[11] K. Rühlmann, *Synthesis* **1971**, 236–253.
[12] C. A. Weisel, R. B. Taylor, H. S. Mosher, F. C. Whitmore, *J. Am. Chem. Soc.* **1945**, *67*, 1071–1072.
[13] A. T. Blomquist, A. Goldstein in *Org. Synth., Vol. IV*, 2nd ed. (Ed.: N. Rabjohn), Wiley, New York, **1967**, pp. 838–839.
[14] N. J. Leonard, R. C. Fox, M. Ōki, *J. Am. Chem. Soc.* **1954**, *76*, 5708–5714; R. L. Shriner, R. C. Fuson, *The Systematic Identification of Organic Compounds*, 6th ed., Wiley, New York, **1980**, pp. 181–182.
[15] J. Parrick, J. W. Rasburn, *Can. J. Chem.* **1965**, *43*, 3453–3456.
[16] J. D. Albright, L. Goldman, *J. Am. Chem. Soc.* **1967**, *89*, 2416–2423; M. VanDyke, N. D. Pritchard, *J. Org. Chem.* **1967**, *32*, 3204–3205.
[17] **5**: b.p. 160 °C (0.1 Torr); ^{1}H NMR (200 MHz, $CDCl_3$, 25 °C): δ = 0.0 (s, 18H, 2 × TMS), 1.49 (q, 4H, 2 × $CH_2CH_2CH_2$), 1.93 (t, 4H, 2 × CH_2C(OTMS)), 2.17 (t, 4H, 2 × CH_2NCH_2), 2.28 (t, 8H, 2 × NCH_2), 3.58 (t, 8H, 4 × OCH_2); ^{13}C NMR (200 MHz, $CDCl_3$, 25 °C): δ = 0.8 (2 × TMS), 24.1 (2 × $CH_2CH_2CH_2$), 28.8 (2 × CH_2C(OTMS)), 53.5 (2 × NCH_2), 58.1 (2 × CH_2NCH_2), 67.1 (4 × OCH_2), 133.7 (C=C).
[18] P. Canonne, M. Belley, G. Fytas, J. Plamondon, *Can. J. Chem.* **1988**, *66*, 168–173; W. V. Drake, S. M. McElvain, *J. Am. Chem. Soc.* **1934**, *56*, 697–700.
[19] **1e**: m.p. 258 °C (decomposition); ^{1}H NMR (200 MHz, CD_3OD/D_2O, 25 °C): δ = 2.14 (q, 4H, 2 × $CH_2CH_2CH_2$), 2.92 (t, 4H, 2 × CH_2C=NOH), 3.27 (t, 4H, 2 × NCH_2), 3.41 (m, 8H, 2 × CH_2NCH_2), 4.10 (t, 8H, 4 × OCH_2); ^{13}C NMR (200 MHz, D_2O, 25 °C): δ = 21.72 (2 × $CH_2CH_2CH_2$, 2 × CH_2C=NOH), 53.14 (2 × CH_2NCH_2), 58.19 (2 × NCH_2), 65.35 (4 × OCH_2), 157.9 (2 × C=NOH).
[20] **7** (orange crystals): ^{1}H NMR (500 MHz, $CDCl_3$, 25 °C): δ = 0.78 (t, 3H, CH_3), 0.92 (br., 2H, $CoCH_2$), 1.14 (m, 6H, $CH_2CH_2CH_2CH_3$), 1.51 (m, 2H, $CoCH_2CH_2$), 1.59 (m, 8H, 4 × CH_2CH_2C=N), 2.16 (m, 8H, 4 × CH_2CH_2C=N), 2.29 (br., 16H, 4 × CH_2NCH_2), 2.58 (t, 8H, 4 × NCH_2), 3.63 (t, 16H, 8 × OCH_2), 7.27 (t, 2H, 2 × *m*-Py), 7.69 (t, 1H, *p*-Py), 8.55 (d, 2H, 2 × *o*-Py), 18.19 (br. s, 2H, 2 × NOH); ^{13}C NMR (500 MHz, $CDCl_3$, 25 °C): δ = 14.11 (CH_3), 22.71 (CH_2CH_3), 22.99 (4 × CH_2CH_2C=N), 23.56 (4 × CH_2C=N), 30.56 ($Co(CH_2)_3CH_2$), 30.60 ($Co(CH_2)_2CH_2$), 31.75 ($CoCH_2CH_2$), 32.87 (br., $CoCH_2$), 53.57 (4 × CH_2NCH_2), 57.90 (4 × NCH_2), 66.94 (8 × OCH_2), 124.98 (2 × *m*-Py), 137.45 (1 × *p*-Py), 149.87 (2 × *o*-Py), 153.06 (4 × C=N).
[21] **7** ($C_{43}H_{76}CoN_9O_8$, M_r = 906.06): triclinic, space group $P\bar{1}$, a = 8.924(2), b = 15.982(3), c = 16.713(4) Å, α = 100.328(13), β = 93.70(2), γ = 92.46(2)°, V = 2336.7(10) Å^3, Z = 2, ρ_{calcd} = 1.288 g cm^{-3}, $F(000)$ = 976, $Mo_{K\alpha}$ radiation, λ = 0.71073 Å, μ = 0.427 mm^{-1}. The structure was determined by heavy-atom methods and refined on F^2 for all 6602 independent, absorption-corrected reflections from a total of 9302 reflections measured at 160 K with a Siemens SMART area-detector diffractometer ($2\theta_{max.}$ = 46.5°), with anisotropic atomic displacement parameters, constrained isotropic H atoms, except for H1 and H6 where the coordinates were refined, and two-fold disorder (68:32) of the hexyl β-carbon atom C2: $R' = [\Sigma w(F_o^2 - F_c^2)^2/\Sigma w(F_o^2)^2]^{\frac{1}{2}}$ = 0.1577 for all data, conventional R [on F values for 6343 reflections with $F_o^2 > 2\sigma(F_o^2)$] = 0.0739, goodness of fit = 1.325 on F^2 for 568 parameters. Programs: SHELXTL, Siemens Analytical *X*-ray Instruments Inc., Madison, Wi., USA. Further details of the crystal structure investigation can be obtained from the director of the Cambridge Crystallographic Data Centre, 12 Union Road, GB-Cambridge CB2 1EZ (UK), on quoting the full journal citation.
[22] L. Randaccio, N. Bresciani Pahor, E. Zangrando, L. G. Marzilli, *Chem. Soc. Rev.* **1989**, *18*, 225–250.

Synthesis of D-(+)-Biotin through Selective Ring Closure of *N*-Acyliminium Silyl Enol Ethers**

Marinus J. Moolenaar, W. Nico Speckamp,*
Henk Hiemstra, Eike Poetsch, and Michael Casutt

Over the years both the synthesis[1] and biosynthesis[2] of the nutritional cofactor D-(+)-biotin (**1**)[3, 4] have aroused continuing interest. As a result of its commercial value and increasing applications in medicine,[5] new syntheses continue to be published,[6] several of which are based on the ready availability of L-cysteine or L-cystine as a chiral starting material.[1c, 6d–f, h, i]

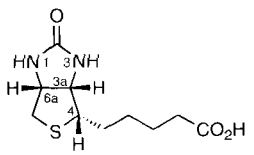

1

The condensation of silyl enol ethers with *N*-acyliminium intermediates is efficient not only in intermolecular reactions,[7] but also in intramolecular processes, as exemplified by our total synthesis of gelsemine,[8] where this reaction is the key transformation. Applying a similar strategy for (+)-biotin (**1**) leads to a retrosynthetic route as illustrated in Scheme 1, in which the

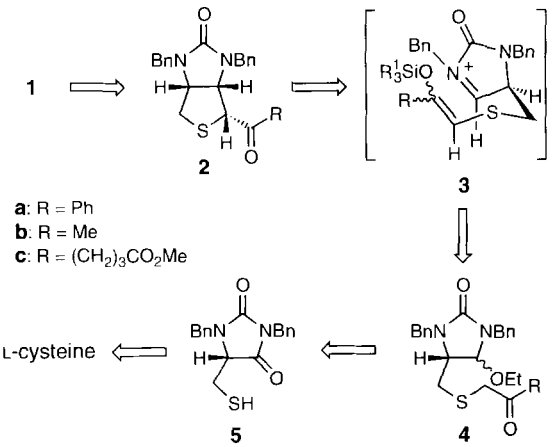

Scheme 1. Retrosynthesis of D-(+)-biotin (**1**). R^1 = protecting group.

essential carbon–carbon bond-forming step is realized through cyclization of the intermediate **3c** (R = $(CH_2)_3CO_2Me$). The latter species is expected to be generated in a few steps from the known imidazolidinone **5**.[6d, 9] The following prerequisites must be met if such a cyclization process is to occur with maximum efficiency: 1) competing proton loss from intermediate **3c** has to be strictly avoided, 2) formation of the silyl enol ether from the appropriate ketone has to be regioselective, and 3) the presence of the adjacent stereogenic center has to direct the formation of the desired (6a*R*,3a*S*,4*R*) isomer via the shown chairlike transition state. To probe the feasibility of such a ring closure of iminium species **3c**, identical annulations through analogs **3a** (R = Ph) and **3b** (R = Me) were investigated first.

The preparation of the cyclization precursors **4a–c** starts from the readily available imidazolidinone **5** (Scheme 2). Reduction with diisobutylaluminum hydride (DIBALH) in THF gave the corresponding hydroxyimidazolidinone **6** in quantitative yield (*cis*:*trans* ≈ 10:1 according to ^{1}H NMR spectroscopy), which after coupling with the appropriate α-chloroketones was converted into thioethers **7a–c** in 85–90% yield. Conversion of these compounds into their ethoxy counterparts **4a–c** was achieved in 78–91% yields under carefully controlled conditions. This result already indicated the possibility of generating a cationic intermediate without affecting the adjacent sensitive stereocenter.[10]

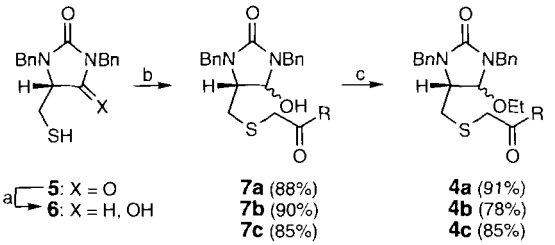

Scheme 2. a) 2.2 equiv DIBALH, −70 °C, THF, 1 h, 99%; b) 1.05 equiv $RC(O)CH_2Cl$, 1.5 equiv Et_3N, 0 → 25 °C, 4 h; c) H_2SO_4/EtOH, methyl orange, pH = 3.1, 0 °C, 2 h.

Formation of the stable triisopropylsilyl (TIPS) enol ether **8** (Scheme 3) proceeded upon treatment of **4a** with an excess of TIPSOTf (Tf = SO_2CF_3) to give an 81% yield of a 46:54 mixture of *E*/*Z* isomers. The isomers of the readily separable *E*/*Z* mixture were subjected to the cyclization reaction separately to afford in each case the crystalline product **2a** (m.p. 143–144 °C, $[\alpha]_D^{25} = -77.6$ ($c = 1.1$, $CHCl_3$)) in 91% yield as a single isomer with the configuration corresponding to D-(+)-biotin (**1**) according to several ^{1}H NMR techniques (NOE-difference, COSY, NOSY). The formation of only one diastereoisomer is rationalized by assuming that both isomers cyclize via the aforementioned chairlike conformation, regardless of the geometry of the double bond.

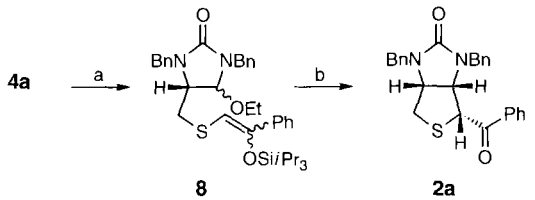

Scheme 3. a) 5.5 equiv TIPSOTf, 6.0 equiv Et_3N, CH_2Cl_2, 25 °C, 18 h, 81% (*E*:*Z* = 46:54); b) 1.5 equiv TMSOTf, CH_2Cl_2, −78 °C, 1 h, 91%.

Prompted by this encouraging result, the methyl derivative **4b** was studied (Scheme 4) to investigate the effect of the enolizable methyl protons in the enol ether formation. Both the regio- and stereoselectivity of the enol ether formation varied dramatically with minor changes of the reaction conditions, to give *E*/*Z* mixtures of **9** and its regioisomer **10** in ratios that could not be sufficiently controlled. After it was found that cyclization of the pure (*Z*)-TIPS enol ether of **9**, as well as cyclization of *in situ* prepared trimethylsilyl (TMS) enol ethers, invariably produced mixtures of **2b** and **11**, our further efforts were only focused on the cyclization of **4c** and the synthesis of D-(+)-biotin (**1**) itself (Scheme 5).

It was anticipated that the presence of the ester side chain might favor the formation of the desired silyl enol ether by lowering the acidity of the α-methylene protons. Most gratifyingly, treatment of **4c** with TMSOTf (1 equiv, 1.05 equiv Et_3N,

[*] Prof. Dr. W. N. Speckamp, M. J. Moolenaar, Dr. H. Hiemstra
Laboratory of Organic Chemistry, University of Amsterdam
Nieuwe Achtergracht 129, NL-1018 WS Amsterdam (The Netherlands)
Telefax: Int. code + (20) 525-5670
Dr. E. Poetsch, Dr. M. Casutt
E. Merck, Darmstadt (Germany)

[**] We thank J. R. Frowijn for his experimental work.

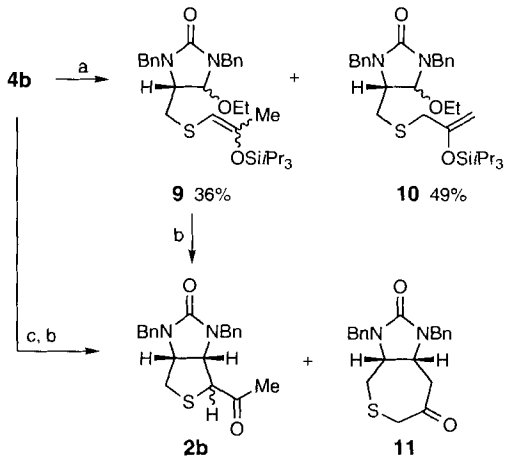

Scheme 4. a) 3.0 equiv TIPSOTf, 3.3 equiv Et_3N, CH_2Cl_2, 25 °C, 18 h; b) 1.5 equiv TMSOTf, CH_2Cl_2, −78 °C, 1 h; c) 2.2 equiv TMSOTf, 2.5 equiv Et_3N, CH_2Cl_2, −20 → 10 °C, 2 h.

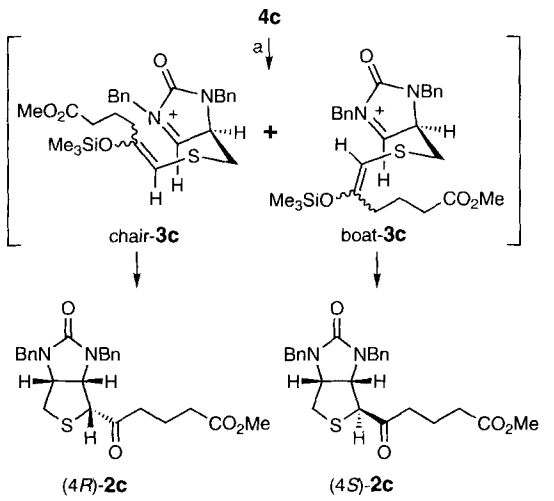

Scheme 5. a) 2.1 equiv $TMSCH_2CO_2Et$, 0.03 equiv TBAF, THF, −78 → 25 °C, 18 h, then 1.5 equiv TMSOTf, CH_2Cl_2, −78 °C, 1 h, 78% (3:2 mixture of 4*R*:4*S* diastereomers).

CH_2Cl_2, −20 → 10 °C, 2 h) to form the enol ether in situ, followed by addition of a second equivalent of TMSOTf (CH_2Cl_2, −70 °C, 1 h) gave (4*R*)-**2c** and its 4*S* diastereoisomer in a 2:1 ratio and 69% yield. Optimization of the reaction conditions did not lead to an improvement of this ratio, but the use of $TMSCH_2CO_2Et$/TBAF (TBAF = tetra-*n*-butylammonium fluoride)[11] for the in situ enol ether formation and addition of TMSOTf to induce cyclization did lead to a slightly better yield (78%) for (4*R*)-**2c** and its 4*S* diastereoisomer (3:2 ratio). Apparently, this cyclization also proceeds partly through a boatlike conformation to give the 4*S* diastereoisomer. A single crystallization afforded pure (4*R*)-**2c** (m.p. 101.5–102.5 °C, $[\alpha]_D^{25} = -10.7$ ($c = 0.2$, $CHCl_3$)); the conformation was confirmed by ^1H NMR spectroscopy. These one-pot/two-step techniques constitute a novel extension of the useful applications of *N*-acyliminium intermediates in natural product synthesis.[12]

The loss of control of the stereochemistry at C4 did not influence the conversion of the diastereomeric mixture of **2c** into D-(+)-biotin (**1**) (Scheme 6). The sequence involved standard reactions: 1) reduction of the ketone with $NaBH_4$ to give the alcohol **12**, 2) formation of the mesylate **13**, 3) elimination of the

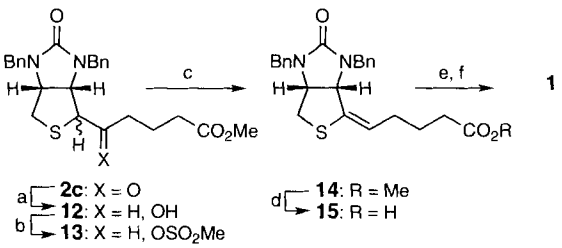

Scheme 6. a) 1.0 equiv $NaBH_4$, MeOH, 25 °C, 1 h; b) 5.0 equiv $MeSO_2Cl$, Et_3N/CH_2Cl_2 1/1, 0 → 35 °C, 1.5 h; c) DBU, 60 °C, 2 h; d) KOH/MeOH, 2 h, 87% (four steps); e) H_2 (10 bar), 10% Pd/C, 2-propanol, 50 °C, 18 h; f) 48% HBr, 100 °C, 2 h, 85% (two steps).

mesylate with 1,8-diazabicyclo[5.4.0]undec-7-ene (DBU) to give the olefin **14**, 4) hydrolysis of the methyl ester, 5) hydrogenation of the double bond of the carboxylic acid **15**, and finally 6) deprotection of the imidazolidinone moiety to give D-(+)-biotin (**1**) in 74% yield over the last six steps.

In this contribution we describe a novel, eleven-step total synthesis of the vitamin D-(+)-biotin (**1**) that proceeds in 42% overall yield starting from the imidazolidinone **5**.[9b] Particularly noteworthy is the regioselective, in situ enol ether formation, directly followed by an *N*-acyliminium ion cyclization producing the desired *cis*-fused bicyclic framework. Although there is some lack of selectivity with respect to the C4 center, the efficiency of the sequence as a whole is not affected.

Experimental Procedure

6: A solution of **5** (9.80 g, 30.0 mmol) in THF (200 mL) was treated dropwise with DIBALH (66.0 mL of a 1.0 M solution in CH_2Cl_2, 66.0 mmol) at −70 °C. After stirring at −70 °C for 1 h, water (50 mL), 10% NaOH (50 mL), and again water (150 mL) were added dropwise, and the mixture was stirred for 1 h at 25 °C. The organic layer was separated, washed with brine (3 × 100 mL), dried (Na_2SO_4), filtered, and concentrated to give the hydroxyimidazolidinone **6** (9.82 g, 99%) as a viscous colorless oil. **6**: $R_f = 0.40$ (ethyl acetate/petroleum ether 50/50); $[\alpha]_D^{25} = -14.8$ ($c = 0.87$ in $CHCl_3$); ^1H NMR (250 MHz, $CDCl_3$): $\delta = 7.40-7.10$ (m, 10H, ArH), 5.00 (d, $J = 6.2$ Hz, 1H, C*H*OH), 4.86 (d, $J = 15.0$ Hz, 1H, CH_2Ph), 4.82 (d, $J = 15.4$ Hz, 1H, CH_2Ph), 4.23 (d, $J = 15.0$ Hz, 1H, CH_2Ph), 4.04 (d, $J = 15.3$ Hz, 1H, CH_2Ph), 3.43–3.33 (m, 1H, C*H*CH_2), 2.85 (br.t, $J = 10.0$ Hz, 1H, C*H*$_2$SH), 2.64 (br.d, $J = 10.5$ Hz, 1H, C*H*$_2$SH), 2.37 (s, 1H, SH); IR ($CHCl_3$): $\tilde{\nu} = 3520-3170$, 1690 cm^{-1}.

7c: A solution of **6** (2.30 g, 7.00 mmol) in THF (15 mL) was treated at 0 °C with Et_3N (1.4 mL, 10.0 mmol), followed by methyl 6-chloro-5-oxohexanoate (1.31 g, 7.35 mmol), and stirred at 0 °C for 2 h. After stirring at 25 °C for 2 h, the mixture was filtered, concentrated, and filtered through silica (pretreated with ammonia, ethyl acetate/petroleum ether 60/40) to give **7c** (2.79 g, 85%) as a viscous colorless oil that was used directly for the next step.

4c: A solution of **7c** (4.70 g, 10.0 mmol) in EtOH (200 mL) was acidified dropwise at 0 °C with a H_2SO_4 (2 N)/EtOH solution to pH 3.1 (indicator methyl orange). After stirring at 0 °C for 2 h, the pH of the solution was raised carefully to pH 5.5 by adding a 2% solution of KOH in EtOH, and the mixture was concentrated. The residue was dissolved in EtOAc (100 mL), washed with water (100 mL), dried (Na_2SO_4), concentrated, and purified by flash column chromatography (silica, pretreated with ammonia, ethyl acetate/petroleum ether 50/50) to give **4c** (4.24 g, 85%, *trans*:*cis* = 9:1) as a viscous colorless oil. *trans*-**4c**: $R_f = 0.62$ (ethyl acetate/petroleum ether 50/50); ^1H NMR (250 MHz, $CDCl_3$): $\delta = 7.32-7.22$ (m, 10H, ArH), 4.92 (d, $J = 15.0$ Hz, 1H, CH_2Ph), 4.88 (d, $J = 14.9$ Hz, 1H, CH_2Ph), 4.50 (s, 1H, C*H*OEt), 4.12 (d, $J = 15.0$ Hz, 2H, CH_2Ph), 3.65 (s, 3H, OCH_3), 3.50–3.10 (m, 3H, C*H*CH_2S, OCH_2), 3.07 (s, 2H, $SCH_2C(O)$), 2.75–2.25 (m, 6H, $CH_2CO_2CH_3$, $CH_2C(O)$, CH_2S), 1.85 (quintet, $J = 7.5$ Hz, 2H, $CH_2CH_2CH_2$), 1.05 (t, $J = 7.5$ Hz, 3H, CH_2CH_3); IR ($CHCl_3$): $\tilde{\nu} = 1725$, 1700 cm^{-1}.

2c: A mixture of **4c** (249 mg, 0.500 mmol) and ethyl (trimethylsilyl)acetate (189 µL, 1.05 mmol) in THF (1 mL) was treated dropwise at −78 °C with TBAF (150 µL of a 0.1 M solution in THF, 15 µmol) over 20 min. After stirring at −78 °C for 20 min and at 25 °C for 18 h, the mixture was concentrated, and the residue dissolved in CH_2Cl_2 (2 mL). The solution was cooled to −78 °C, TMSOTf (135 µL, 0.750 mmol) added dropwise, and the mixture stirred at −78 °C for 1 h. The reaction was quenched with aqueous saturated ammonium chloride (5 mL) and diluted with CH_2Cl_2 (50 mL). The organic layer was washed with water (40 mL) and brine (40 mL), dried ($MgSO_4$), concentrated, and purified by flash column chromatography (ethyl acetate/petroleum ether 80/20) to give the imidazolidinone **2c** (175 mg,

78%) as a 3:2 mixture of isomers. Both isomers could be obtained in pure form as white solids by recrystallization from ethyl acetate/hexane. (4*R*)-**2c**: $R_f = 0.65$ (ethyl acetate/petroleum ether 60/40); m.p. 101.5–102.5 °C; $[\alpha]_D^{25} = -10.7$ ($c = 0.2$ in $CHCl_3$); ^{1}H NMR (250 MHz, $CDCl_3$): $\delta = 7.32-7.22$ (m, 10H, ArH), 4.78 (d, $J = 15.2$ Hz, 1H, CH_2Ph), 4.57 (d, $J = 15.0$ Hz, 1H, CH_2Ph), 4.22 (d, $J = 15.2$ Hz, 1H, CH_2Ph), 4.05 (d, $J = 15.0$ Hz, 1H, CH_2Ph), 4.04–4.02 (m, 2H, H6a, H3a), 3.65 (s, 3H, CH_3), 3.59 (d, $J = 5.7$ Hz, 1H, H4), 2.82–2.71 (m, 2H, H6), 2.56 (dt, $J = 17.5$, 7.5 Hz, 1H, $CH_2C(O)$), 2.25 (dt, $J = 1.7$, 7.5 Hz, 2H, $CH_2C(O)$), 1.95 (dt, $J = 17.5$, 7.5 Hz, 1H, $CH_2C(O)$), 1.78 (quintet, $J = 7.5$ Hz, 2H, $CH_2CH_2CH_2$); IR ($CHCl_3$): $\tilde{\nu} = 1725$, 1700, 1680 cm^{-1}; HRMS (EI, 70 eV) calcd for $C_{25}H_{28}N_2O_4S$ 452.1770, found 452.1766. (4*S*)-**2c**: $R_f = 0.70$ (ethyl acetate/petroleum ether 60/40); m.p. 82.5–83 °C; $[\alpha]_D^{25} = -21.2$ ($c = 1.3$ in $CHCl_3$); ^{1}H NMR (400 MHz, $CDCl_3$): $\delta = 7.35-7.25$ (m, 10H, ArH), 4.75 (d, $J = 15.4$ Hz, 1H, CH_2Ph), 4.50 (d, $J = 15.2$ Hz, 1H, CH_2Ph), 4.45 (d, $J = 15.2$ Hz, 1H, CH_2Ph), 4.29 (d, $J = 7.9$ Hz, 1H, H3a), 4.21 (d, $J = 15.4$ Hz, 1H, CH_2Ph), 4.20 (dd, $J = 4.6$, 7.9 Hz, 1H, H6a), 3.65 (s, 3H, CH_3), 3.58 (s, 1H, H4), 2.75 (d, $J = 12.9$ Hz, 1H, H6), 2.69 (dt, $J = 7.5$, 17.3 Hz, 1H, $CH_2C(O)$), 2.56 (dd, $J = 4.8$, 12.9 Hz, 1H, H6), 2.26–2.19 (m, 3H, $CH_2C(O)$), 1.78 (quintet, $J = 7.3$ Hz, 2H, $CH_2CH_2CH_2$); IR ($CHCl_3$): $\tilde{\nu} = 1725$, 1700, 1680 cm^{-1}; HRMS (EI, 70 eV) calcd for $C_{25}H_{28}N_2O_4S$ 452.1770, found 452.1760.

Received: June 9, 1995 [Z 8078 IE]
German version: *Angew. Chem.* **1995**, *107*, 2582-2584

Keywords: acyliminium ions · biotin · cyclizations · silyl enol ethers · total syntheses

[1] For early syntheses of D-(+)-biotin, see a) M. W. Goldberg, L. H. Sternbach, US-A Patent 2489232, **1949** [*Chem. Abstr.* **1951**, *45*, 184b]; b) H. Ohrui, S. Emoto, *Tetrahedron Lett.* **1975**, 2765; c) P. N. Confalone, G. Pizzolato, E. G. Baggiolini, D. Lollar, M. R. Uskokovic, *J. Am. Chem. Soc.* **1977**, *99*, 7020; d) T. Ogawa, T. Kawano, M. Matsui, *Carbohydr. Res.* **1977**, *57*, C31; e) H. Ohrui, N. Sueda, S. Emoto, *Agric. Biol. Chem.* **1978**, *42*, 865; f) J. Vasilevskis, J. A. Gualtieri, S. D. Hutchings, R. C. West, J. W. Scott, D. R. Parrish, F. T. Bizzarro, G. F. Field, *J. Am. Chem. Soc.* **1978**, *100*, 7423; g) F. G. M. Vogel, J. Paust, A. Nürrenbach, *Liebigs Ann. Chem.* **1980**, 1972.

[2] Biosynthesis of D-(+)-biotin, see a) R. J. Parry, *Tetrahedron* **1983**, *39*, 1215; b) A. Marquet, *Pure Appl. Chem.* **1993**, *65*, 1249; c) P. Baldet, H. Gerbling, S. Axiotis, R. Douce, *Eur. J. Biochem.* **1993**, *217*, 479.

[3] For the first isolation, see V. du Vigneaud, D. B. Melville, J. Rachele, *J. Biol. Chem.* **1941**, *140*, 763.

[4] a) Special issue: *Ann. N. Y. Acad. Sci.* **1985**, *447*, 1–441; b) M. R. Uskokovic, *Kirk-Othmer Encycl. Chem. Technol.* 3rd ed., **1978–1984**, *24*, 41.

[5] For some applications, see a) M. Ahlers, W. Müller, A. Reichert, H. Ringsdorf, J. Venzmer, *Angew. Chem.* **1990**, *102*, 1310; *Angew. Chem. Int. Ed. Engl.* **1990**, *29*, 1269; b) O. Livnah, E. A. Bayer, M. Wilchek, J. L. Sussman, *Proc. Natl. Acad. Sci. USA* **1993**, *90*, 5076; c) H. Martini, J. Rétey, *Angew. Chem.* **1993**, *105*, 287; *Angew. Chem. Int. Ed. Engl.* **1993**, *32*, 278; d) I. Sanyal, S.-L. Lee, D. H. Flint, *J. Am. Chem. Soc.* **1994**, *116*, 2637.

[6] For more recent syntheses of D-(+)-biotin, see a) R. R. Schmidt, M. Maier, *Synthesis* **1982**, 747; b) R. A. Volkmann, J. T. Davis, C. N. Meltz, *J. Am. Chem. Soc.* **1983**, *105*, 5946; c) T. Ravindramathan, S. V. Hiremath, D. Reddy, A. V. R. Rao, *Carbohydr. Res.* **1984**, *134*, 332; d) E. Poetsch, M. Casutt, *Chimia* **1987**, *41*, 148; e) H. L. Lee, E. G. Baggiolini, M. R. Uskokovic, *Tetrahedron* **1987**, *43*, 4887; f) E. J. Corey, M. M. Mehrotra, *Tetrahedron Lett.* **1988**, *29*, 57; g) R. Bihovsky, V. Bodepudi, *Tetrahedron* **1990**, *46*, 7667; h) T. Fujisawa, M. Nagai, Y. Koike, M. Shimizu, *J. Org. Chem.* **1994**, *59*, 5865; i) F. D. Deroose, P. J. De Clercq, *ibid.* **1995**, *60*, 321.

[7] a) R. Kober, K. Papadopoulos, W. Miltz, D. Enders, W. Steglich, H. Reuter, H. Puff, *Tetrahedron* **1985**, *41*, 1693; b) T. Allmendinger, G. Rihs, H. Wetter, *Helv. Chim. Acta* **1988**, *71*, 395; c) R. M. Williams, P. J. Sinclair, D. Zhai, D. Chen, *J. Am. Chem. Soc.* **1988**, *110*, 1547; d) H. H. Mooiweer, K. W. A. Ettema, H. Hiemstra, W. N. Speckamp, *Tetrahedron* **1990**, *46*, 2991; e) E. C. Roos, H. Hiemstra, W. N. Speckamp, B. Kaptein, J. Kamphuis, H. E. Schoemaker, *Recl. Trav. Chim. Pays-Bas* **1992**, *111*, 360.

[8] N. J. Newcombe, Y. Fang, R. J. Vijn, H. Hiemstra, W. N. Speckamp, *J. Chem. Soc. Chem. Commun.* **1994**, 767.

[9] a) A. Schöberl, R. Hamm, *Chem. Ber.* **1948**, *81*, 210; b) M. Casutt, E. Poetsch, W. N. Speckamp (Merck GmbH), DE-A 3926690, **1991** [*Chem. Abstr.* **1991**, *115*, 8429k].

[10] The hydroxy- and ethoxyimidazolidinones were purified by flash column chromatography after pretreating the silica gel with ammonia to avoid elimination of water or ethanol. All reported products were appropriately characterized by IR, NMR, and mass spectroscopy.

[11] E. Nakamura, T. Murofushi, M. Shimizu, I. Kuwajima, *J. Am. Chem. Soc.* **1976**, *98*, 2346.

[12] a) H. Hiemstra, W. N. Speckamp in *The Alkaloids, Vol. 32* (Ed.: A. Brossi), Academic Press, San Diego, **1988**, pp. 271–239; b) H. de Koning, M. J. Moolenaar, H. Hiemstra, W. N. Speckamp in *Studies in Natural Products Chemistry, Vol. 13* (Ed.: Atta-ur-Rahman), Elsevier, Amsterdam, **1993**, pp. 473–518.

Lactendiynes: A New Class of Triggered Cyclic Enediynes**

Luca Banfi and Giuseppe Guanti*

After the recent discovery of the potent anticancer activity of naturally occurring cyclic enediynes, great efforts are now being made in the design and synthesis of analogues of these compounds characterized by a similar mode of action, but, at the same time, by low molecular complexity.[1] Ideally, these mimics should be endowed with a chemical "trigger", a structural element that locks the enediyne system in a stable form, but that can be removed in a controlled fashion, unveiling the DNA-damaging power of the enediyne unit. Moreover, to increase selectivity and effectiveness, these mimics should also preferably possess suitable handles for appending DNA-binding agents.[1c, 2]

With this aim we are exploring a new class of synthetic enediynes of general formula **5**, which we have christened "lactendiynes", and which are characterized by a β-lactam *trans*-fused to a ten-membered cyclic enediyne. These compounds are analogues of the known parent compounds **1**[3] and **2**,[4] which have been shown to undergo Bergman cycloaromatization at a moderate rate at 37 °C, affording the highly reactive aryl diradicals **3** and **4**, respectively. We reasoned that lactendiynes should be

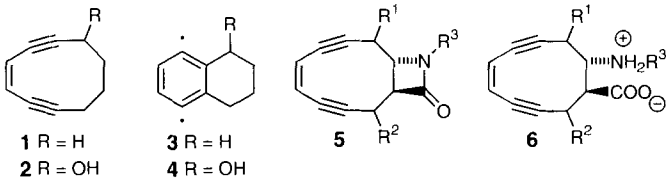

1 R = H
2 R = OH

3 R = H
4 R = OH

5

6

completely stable toward cycloaromatization, whereas their hydrolysis products **6** should be even more reactive than the parent compounds **1** and **2**. The first prediction was based: a) on the previous work of Nicolaou, Bergman, et al.,[5] who demonstrated that a ten-membered enediyne *trans*-fused to a dioxolanone is not reactive; and b) on molecular mechanics calculations,[6] which indicated that the cycloaromatized product is highly strained. The second less obvious prediction was based on MM calculations,[6] which indicated that **6** should have a very short lifetime at 37 °C. Therefore, in vivo β-lactam opening could serve as the triggering event for transforming potential enediyne prodrugs **5** into the actually active species **6**. Further advantages of compounds **5** are their simple structure, which facilitates their total synthesis, and the possibility of appending DNA-binding agents by using the substituents R^1, R^2, and R^3 as handles.

To verify these assumptions we have now prepared the first compounds of this class. Scheme 1 shows the synthetic route, which starts from known 2-azetidinone **7**, prepared in six steps by reported procedures[7] from D,L-aspartic acid.[8] After protection of the nitrogen function,[9] the side chain at position 3 was introduced by condensation of the lithium enolate derived from **8** with 3-bromo-1-(trimethylsilyl)propyne. This reaction

[*] Prof. G. Guanti, Dr. L. Banfi
Istituto di Chimica Organica
e CNR, Centro di Studio per la Chimica
dei Composti Cicloalifatici ed Aromatici
corso Europa 26, I-16132 Genoa (Italy)
Telefax: Int. code + (10)3538218

[**] We thank Andrea Basso for his valuable collaboration. This work was supported by the CNR and MURST.

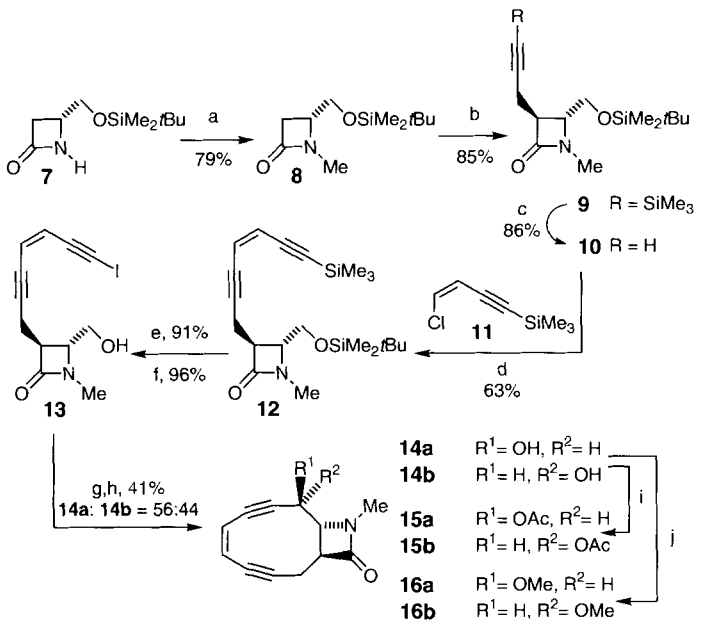

Scheme 1. a) nBu$_4$NBr, MeI, KOH (pellets), THF, 0 °C; b) LDA, then BrCH$_2$C≡CSiMe$_3$; c) AgNO$_3$, NaCN, EtOH/H$_2$O; d) CuI, [(PhCN)$_2$PdCl$_2$], piperidine/THF; e) AgNO$_3$, NIS, DMF; f) HF, H$_2$O, CH$_3$CN, −20 °C → 0 °C; g) (COCl)$_2$, DMSO, Et$_3$N, CH$_2$Cl$_2$, −78 °C; h) CrCl$_2$, NiCl$_2$, THF; i) Ac$_2$O, pyridine/CH$_2$Cl$_2$ (76% for **15a**, 66% for **15b**); j) NaH, MeI, DMF (85% for **16a**; 76% for **16b**).

proceeded with complete stereoselectivity, affording only the desired *trans* product **9**. After selective removal of the trimethylsilyl group,[10] the stage was set for the construction of the enediyne system by Castro–Stephens coupling with chloroenyne **11**.[11] However, under standard conditions with [Pd(PPh$_3$)$_4$] as catalyst, the reaction was sluggish and **12** was obtained in at most 25–30% yield. In contrast, good yields were achieved by employing [(PhCN)$_2$PdCl$_2$] in THF/piperidine, according to a procedure by Alami and Linstrumelle.[12] One-pot transformation of enediyne **12** into the corresponding iodoacetylene using a method developed by Isobe et al.,[13] followed by deprotection of the primary alcohol, gave **13**. Oxidation and Nozaki cyclization[6, 14] afforded the diastereomeric mixture of alcohols **14a,b** in satisfactory yield (41%, 13% overall from **7**), which are easily separable by silica gel chromatography.

Alcohols **14a,b** are remarkably stable both in solution and in the solid state,[15] and have been smoothly transformed into the corresponding acetyl and methyl derivatives **15a,b** and **16a,b** (Table 1). Heating the methyl ethers **16a,b** at 100 °C for several hours in the presence of 1,4-cyclohexadiene gave no reaction. On the other hand, when **16a** was treated with 1 N NaOH in MeOH in the presence of 1,4-cyclohexadiene for two hours, complete transformation into the cycloaromatized products **18a** took place (Scheme 2). The product formed as a mixture of two

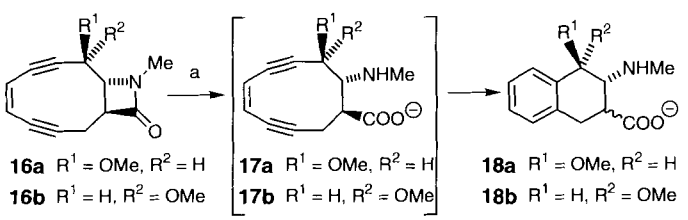

Scheme 2. a) 1–1.5 N NaOH in abs. MeOH, 1,4-cyclohexadiene, 50 °C, 2–5 h.

diastereoisomers (Table 1), presumably because of epimerization at the carbon α to the carboxylate group.[16] The reaction was monitored by ^{1}H NMR spectroscopy; no signals attributable to the intermediate enediynic amino acids **17a,b** were observed. Thus cycloaromatization seems to take place immediately after the β-lactam opens, in line with the theoretical predictions.[17] Under the same conditions **16b** is converted into **18b** (Table 1).[18]

Table 1. Physical data for **16a,b** and **18a,b**.

16a: ^{1}H NMR (200 MHz, CDCl$_3$, 25 °C, TMS): δ = 2.66 (dd, ^2J(H, H) = 17.9 Hz, ^3J(H, H) = 12.2 Hz, 1 H, C*H*HC≡), 2.88 (dd, ^2J(H, H) = 17.9 Hz, ^3J(H, H) = 3.9 Hz, 1 H, CH*H*C≡), 2.92 (s, 3 H, CH$_3$N), 3.24–3.38 (m, 1 H, CHC=O), 3.46 (s, 3 H, CH$_3$O), 3.73 (dd, ^3J(H, H) = 2.3, 9.1 Hz, 1 H, CHN), 4.25 (d, ^3J(H, H) = 9.1 Hz, 1 H, C*H*OMe), 5.91 (s, 2 H, C*H*=CH); ^{13}C NMR (50 MHz, CDCl$_3$, 25 °C, TMS): δ = 19.50 (*C*H$_2$C≡), 28.90 (CH$_3$N), 54.93, 56.87, 63.76, 64.19 (CH and OCH$_3$), 83.93, 88.30, 95.18, 100.00 (C≡C), 122.20, 124.57 (C=C), 167.45 (C=O); MS (70 eV): *m/z* (%): 215 (29) [*M*$^+$], 200 (76) [*M*$^+$−CH$_3$], 184 (14.6), 172 (21.9), 156 (43), 144 (25.5), 143 (32.5), 129 (21.2), 128 (17.6), 115 (66), 105 (100), 63 (39), 42 (82); IR (CHCl$_3$): $\tilde{\nu}$ = 2200 (very weak), 1747 cm^{-1}

16b: ^{1}H NMR (200 MHz, CDCl$_3$, 25 °C, TMS): δ = 2.59 (dd, ^2J(H, H) = 17.9 Hz, ^3J(H, H) = 13.1 Hz, 1 H, C*H*HC≡), 2.81 (s, 3 H, CH$_3$N), 2.89 (ddd, ^2J(H, H) = 17.9 Hz, ^3J(H, H) = 3.8 Hz, ^5J(H, H) = 1.7 Hz, 1 H, CH*H*C≡), 3.46 (s, 3 H, CH$_3$O), 3.64–3.80 (m, 2 H, CHC=O and CHN), 4.37 (t, ^3J(H, H), ^5J(H, H) = 1.8 Hz, 1 H, C*H*OCH$_3$), 5.96, 5.89 (br., AB system, ^2J(H, H) = 9.7 Hz, 2 H, CH=CH); ^{13}C NMR (50 MHz, CDCl$_3$, 25 °C, TMS): δ = 19.36 (*C*H$_2$C≡), 26.60 (CH$_3$N), 52.19, 57.20, 63.25, 67.72 (CH and OCH$_3$), 83.58, 87.28, 95.66, 100.79 (C≡C), 122.02, 126.26 (C=C), 167.82 (C=O); MS (70 eV): *m/z* (%): 215 (42) [*M*$^+$], 200 (100) [*M*$^+$−CH$_3$], 184 (15.7), 172 (24), 156 (45), 144 (31), 143 (32), 129 (22.5), 128 (19.4), 115 (67), 105 (94), 63 (40), 42 (83); IR (CHCl$_3$): $\tilde{\nu}$ = 2240, 2205, 1750 cm^{-1}

18a: ^{1}H NMR (200 MHz, CD$_3$OD, NaOD, 25 °C, TMS): δ = 2.42 and 2.49 (s, 3 H, CH$_3$N), 2.80–3.40 (m, 4 H, CH$_2$Ar, CHCOO, CHN), 3.23 and 3.49 (s, 3 H, CH$_3$O), 4.23 (d, ^3J(H, H) = 2.6 Hz, 1/2 H, C*H*OMe), 4.41 (d, ^3J(H, H) = 5.8 Hz, 1/2 H, CHOMe), 7.10–7.25 (m, 3 H, arom.), 7.25–7.35 (m, 1 H, arom.)

18b: ^{1}H NMR (200 MHz, CD$_3$OD, NaOD, 25 °C, TMS): δ = 2.44 and 2.49 (s, 3 H, CH$_3$N), 2.70–3.60 (m, 4 H, CH$_2$Ar, CHCOO, CHN), 3.33 and 3.38 (s, 3 H, CH$_3$O), 4.36 (br. s, 2/3 H, C*H*OMe) 4.43 (d, ^3J(H, H) = 4.0 Hz, 1/3 H, CHOMe), 7.05–7.30 (m, 4 H, arom.).

This study demonstrates the feasibility of employing lactendiynes as enediyne prodrugs. Although hydrolysis of inactivated β-lactams **14**–**16** is probably difficult to achieve in vivo, modification of the same synthetic scheme should lead to more reactive analogues of **5**, bearing suitable activating groups R^3 for facilitating azetidinone opening.

Received: June 16, 1995 [Z8109IE]
German version: *Angew. Chem.* **1995**, *107*, 2613–2615

Keywords: antitumor agents · azetidinones · cycloaromatizations · enediynes

[1] Reviews: a) M. E. Maier, *Synlett* **1995**, 13–26; b) L. Banfi in *Seminars in Organic Synthesis* (Ed.: B. Danieli), S. C. I., Rome, **1994**, pp. 253–277; c) K. C. Nicolaou, W.-M. Dai, S.-C. Tsay, V. A. Estevez, W. Wrasidlo, *Science* **1992**, *256*, 1172–1178; d) K. C. Nicolaou, A. L. Smith, E. W. Yue, *Proc. Natl. Acad. Sci., USA* **1993**, *90*, 5881–5888; e) K. C. Nicolaou, A. L. Smith, *Acc. Chem. Res.* **1992**, *25*, 497–503.

[2] M. F. Semmelhack, J. J. Gallagher, W. D. Ding, G. Krishnamurthy, R. Babine, G. A. Ellestad, *J. Org. Chem.* **1994**, *59*, 4357–4359.

[3] At 37 °C, $t_{1/2}$ = 18 h: K. C. Nicolaou, G. Zuccarello, Y. Ogawa, E. J. Schweiger, T. Kumazawa, *J. Am. Chem. Soc.* **1988**, *110*, 4866–4868.

[4] The half-life of the acetyl derivative of **2** at 37 °C is 28 h: C. Crévisy, J.-M. Beau, *Tetrahedron Lett.* **1991**, *32*, 3171–3174; see also ref. [2].

[5] K. C. Nicolaou, E. J. Sorensen, R. Discordia, C.-K. Hwang, R. E. Minto, K. N. Bharucha, R. G. Bergman, *Angew. Chem.* **1992**, *104*, 1094–1096; *Angew. Chem. Int. Ed. Engl.* **1992**, *31*, 1044–1046.

[6] We used the simplified approach proposed by Maier [1a], based on calculation of the difference of the strain energies (E_S) of the final product (the hydrogenated diradical) and the substrate. Performing the calculations with Chem3D Plus

(CSC, Cambridge, MA), we obtained for **14a,b**–**16a,b** values of ΔE_s that are 15–17 kcal mol^{-1} higher than for models compounds **1** and **2**. In contrast, calculated ΔE_s valued for **6** (R^1 = OH, OMe, OAc) are lower than those obtained for **1** and **2** by about 2–4 kcal mol^{-1}. (In general the ΔE_s values of the all-*trans* isomers were lower.)

[7] a) Y. Takahashi, H. Yamashita, S. Kobayashi, M. Ohno, *Chem. Pharm. Bull.* **1986**, *34*, 2732–2742; b) Y. Takahashi, H. Yamashita, T. Izawa, S. Kobayashi, M. Ohno, *ibid.* **1986**, *34*, 3020–3024.

[8] All the compounds used in this work were racemic, but, for clarity, one enantiomer is arbitrarily shown in the schemes.

[9] D. Reuschling, H. Pietsch, A. Linkies, *Tetrahedron Lett.* **1978**, 615–618.

[10] H. M. Schmidt, J. F. Arens, *Rec. Trav. Chim. Pays Bas* **1967**, *86*, 1138–1142.

[11] D. Chemin, G. Linstrumelle, *Tetrahedron* **1994**, *50*, 5335–5344.

[12] M. Alami, G. Linstrumelle, *Tetrahedron Lett.* **1991**, *32*, 6109–6112.

[13] T. Nishikawa, S. Shibuya, S. Hosokawa, M. Isobe, *Synlett* **1994**, 485–486.

[14] T. Brandstetter, M. E. Maier, *Tetrahedron* **1994**, *50*, 1435–1448, and references therein.

[15] In contrast, the related alcohol **2** is unstable at room temperature and even at 20 °C in neat form, undergoing side reactions other than cycloaromatization (see ref. [4]).

[16] This epimerization takes place only after β-lactam opening, since the *cis* β-lactam is not evident by either NMR spectroscopy or by TLC. Moreover, the relative amount of the two epimers increases with time, reaching a final ratio of ca. 1:1.

[17] As a comparison: at 50 °C, $t_{1/2}$ (**1**) = 3.6 h [3]. The reason for the higher reactivity of **17a,b** compared to **1** or **2** probably lies in the more unfavorable steric interactions between the carboxylate and NHMe groups in the cyclic enediyne (dihedral angle ca. 25°) than in the tetrahydronaphthalenes **18** (dihedral angle ca. 50°). Snyder has calculated that placing two *trans* methyl groups at positions 8 and 9 of **1** should decrease the activation energy for cycloaromatization of about 1.1 kcal mol^{-1}: J. P. Snyder, *J. Am. Chem. Soc.*, **1990**, *112*, 5367–5369.

[18] In this case, however, β-lactam opening was slower, and was complete only after 5 h with 1.5 N NaOH in MeOH. The ratio of the two epimers of **18b** (initially ca. 1:3) was inverted to ca. 3:1 by the end of reaction.

Highly Enantioselective Opening of Cyclic *meso*-Anhydrides to Isopropyl Hemiesters with Diisopropoxytitanium TADDOLates**

Dieter Seebach,* Georg Jaeschke, and Yan Ming Wang

Based on the enormous structural diversity of readily accessible C_s-symmetrical anhydrides of dicarboxylic acids with enantiotopic carbonyl groups, a catalytic, enantioselective opening to give the corresponding hemiesters is of great significance for organic synthesis [Eq. (1a)]. The usefulness of such hemiesters becomes quite clear when the vast amount of literature dealing with the enantioselective enzymatic hydrolysis of the analogous diesters is considered [Eq. (1b)].[1]

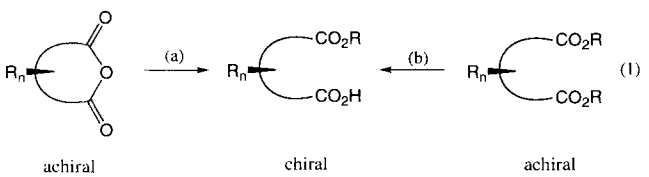

In this publication, we describe the reactions of anhydrides in THF to give isopropyl hemiesters (mono-isopropyl esters) of high enantiopurity; the reactions were initially carried out with stoichiometric amounts of chiral Lewis acids, namely the diisopropoxytitanium TADDOLates **1**.[2] The reaction conditions were optimized with the *endo*-Diels–Alder product **2** of maleic anhydride and cyclopentadiene, by using the β-naphthyl derivative **1a**.[2] After a reaction time of several days at a temperature of −30 °C, we obtained the hemiester **3** in a virtually enantiopure form (see Experimental Procedure) with yields exceeding 90%. Also, the hexaphenyl derivative **1b**,[2] as well as the original titanium TADDOLate **1c**[3] and **1d** (unsymmetrically substituted at the acetal center),[2] produced comparable selectivities (see Table 1). The isolation of the hemiester is quite simple; during work up, the carboxylic acid is extracted into an aqueous alkaline solution, this separates it from the TADDOL, which is subsequently quantitatively recovered from the organic phase. The configuration (1*R*,2*S*,3*R*,4*S*) of the dextrorotatory[4] monoester **3** was determined through reduction with $LiBEt_3H$ and lactonization to the known compound **4**.[5] Thus, the isopropoxy group has attacked the *Re*-carbonyl group of the anhydride **2** (Scheme 1).

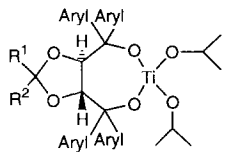

1a ($R^1 = R^2 = CH_3$, Aryl = β-$C_{10}H_7$)
1b ($R^1 = R^2$ = Aryl = C_6H_5)
1c ($R^1 = R^2 = CH_3$, Aryl = C_6H_5)
1d ($R^1 = C_6H_5$, R^2 = H, Aryl = C_6H_5)

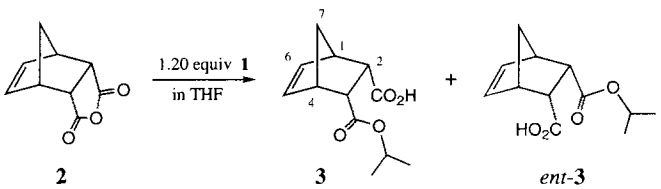

2 **3** *ent*-**3**

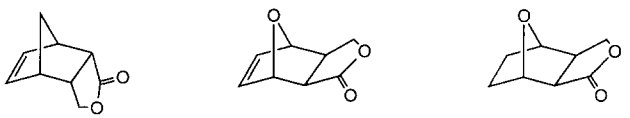

4 **5** **6**

Scheme 1. Opening of the anhydride **2** with titanium TADDOLates **1** to the isopropyl hemiesters **3** and *ent*-**3** and also lactones **4**–**6** obtained from **2**, **10**, and **11**, respectively, via the appropiate hemiesters.

Other tricyclic (**7**–**11**), bicyclic (**12**–**13**), and monocyclic (**14**) anhydrides react analogously, yielding hemiesters of high enantiopurity (Table 1). Only the anhydride **15** with a methyl substituent in the β-position to the carbonyl groups is opened with a moderate 3:1 selectivity. In all cases, the enantiomer ratio was determined by using CSP-GC (details see Table 1 and Experimental Procedure). Also, the absolute configuration (1*S*,2*R*,3*S*,4*R*) of the hemiesters obtained from **10** and **11** was determined by comparison of the sense of rotation from the corresponding lactones **5** and **6**,[6] while that of the hemiesters resulting from the reactions of the other substrates has not yet been established.[7] With two exceptions (products obtained from **14** and **15**) all hemiesters are dextrorotatory.

[*] Prof. Dr. D. Seebach, Dipl.-Chem. G. Jaeschke, Dr. Y. M. Wang
Laboratorium für Organische Chemie der
Eidgenössischen Technischen Hochschule
ETH-Zentrum, Universitätstrasse 16, CH-8092 Zürich (Switzerland)
Telefax: Int. code + (1)632-1144

[**] We thank the Stiftung Stipendien-Fonds des Verbandes der Chemischen Industrie for a Kekulé-Fellowship (G. J.).

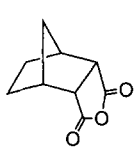
7

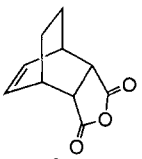
8

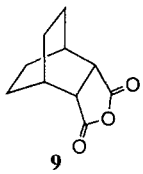
9

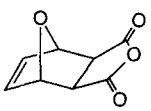
10

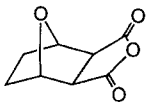
11

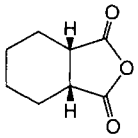
12

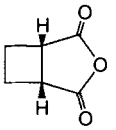
13

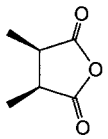
14

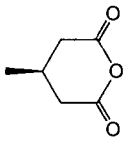
15

Table 1. Reaction conditions, yields and enantioselectivities of the isopropyl hemiesters obtained from the anhydrides **2** and **7**–**14** with 1.20 equiv diisopropoxytitanium TADDOLate **1**. Except with the products from **10** and **11** [a], all enantiomer ratios were determined by GC analysis (on various cyclodextrin columns) of the methylisopropyl esters obtained from the hemiesters and diazomethane.

anhydride	**1**	Reaction conditions time [d]	T [°C]	Hemiester yield [%]	enantiomer ratio
2	**1a**	7	−30	88	99:1
2	**1b**	6	−30	87	99:1
2	**1c**	5	−30	91	97:3
2	**1d**	5	−30	88	96:4
7	**1a**	6	−30	91	99:1
8	**1b**	6	−30	91	99:1
9	**1a**	6	−30	92	97:3
10	**1a**	6	−30	63	99:1 [a]
11	**1a**	6	−30	82	98:2 [a]
12	**1a**	5	−15	87	>95:5
13	**1a**	5	−15	76	97:3
14	**1a**	5	−18	73	98:2

[a] In these two cases the enantiomer ratio was determined by GC analysis of **6** (to which **5** was also hydrogenated).

Earlier experiments by other research groups on enantioselective ring-opening of suitable anhydrides were less successful.[8, 9] Preliminary tests with the anhydride **2** have shown that an enantioselective ring-opening is also possible using substoichiometric amounts of the titanium TADDOLate **1** and stoichiometric amounts of titanium tetraisopropoxide. Analogous reactions of other carboxylic acid derivatives such as phenolic esters[10] and *N*-sulfonylimides and the use of other chiral Lewis acids in these reactions will be reported in the near future. We believe it should be possible to use chiral titanium Lewis acids such as **1** in many other reactions, in which so-called hydrolytic enzymes[1b] are currently being employed.

Experimental Procedure

Hemiester **3**: $Ti(OCHMe_2)_4$ (2.4 mmol, 0.707 mL) was added dropwise to a solution of β-naphthyl-TADDOL (2.50 mmol, 1.67 g) in ether (20 mL) under argon and the mixture was stirred for 3 h at room temperature (RT) to produce **1a**. The solvent was removed under vacuum and the residue was dried for 30 min. The residue was dissolved in THF (10 mL) (distilled from K) and the solution was cooled to −30 °C. A cold solution (ca. −30 °C) of the anhydride **2** (2.0 mmol, 328 mg) in THF (5 mL) was added. The homogeneous solution was sealed and stored for 7 d in a freezer (−30 °C). Subsequently, the reaction mixture was poured into 0.5 N NaOH (80 mL), ether (ca. 100 mL) was added, and the aqueous phase was separated. The organic phase was extracted with further 0.5 N NaOH (80 mL), and the combined aqueous phases were washed with ether. Acidification with 1 N HCl to pH 1–2, followed by extraction with ether (2 × 100 mL), drying with $MgSO_4$, and evaporation of the solvent yielded 394 mg of **3** (88%); m.p. 89–90 °C, $[\alpha]_D^{RT}$ +7.5 (c = 2.5, $CHCl_3$); ratio of enantiomers = 99:1 (determined by GC-analysis on a β-3P-cyclodextrin column of the methylisopropyl ester obtained by reaction of **3** with diazomethane).

Received: May 22, 1995 [Z8014IE]
German version: *Angew. Chem.* **1995**, *107*, 2605–2606

Keywords: anhydrides · asymmetric syntheses · hemiesters · TADDOL · titanium compounds

[1] a) D. H. G. Crout, M. Christen, *Mod. Synth. Methods* **1989**, *5*, 1; b) C.-H. Wong, G. M. Whitesides, *Enzymes in Synthetic Organic Chemistry*, Pergamon, London, **1994**, p. 41; c) B. Danieli, G. Lesma, D. Passarella, S. Riva in *Advances in the Use of Synthons in Organic Chemistry, Vol. 1* (Ed.: A. Dondoni), Jai, London, **1993**, p. 143; d) enantioselective enzymatic opening of cyclic anhydrides: K. Yamamoto, T. Nishioka, J. Oda, Y. Yamamoto, *Tetrahedron Lett.* **1988**, *29*, 1717.

[2] For synthesis of TADDOLs and the most recent applications of titanium TADDOLates in enantioselective catalysis see: a) A. K. Beck, B. Bastani, D. A. Plattner, W. Petter, D. Seebach, H. Braunschweiger, P. Gysi, L. La Vecchia, *Chimia* **1991**, *45*, 238; b) Y. N. Ito, X. Ariza, A. K. Beck, A. Bohác, C. Ganter, R. E. Gawley, F. N. M. Kühnle, J. Tuleja, Y. M. Wang, D. Seebach, *Helv. Chim. Acta* **1994**, *77*, 2071; c) D. Seebach, R. Dahinden, R. E. Marti, A. K. Beck, D. A. Plattner, F. N. M. Kühnle, *J. Org. Chem.* **1995**, *60*, 1788; and references therein.

[3] D. Seebach, B. Weidmann, L. Widler, *Mod. Synth. Methods* **1983**, *3*, 217.

[4] Interestingly the hemiester **3** is dextrorotatory, whilst the corresponding methyl ester is levorotatory [5a].

[5] a) P. Storme, L. Quaeghebeur, M. Vandewalle, *Bull. Chem. Soc. Chim. Belg.* **1984**, *93*, 999; b) T. Harada, I. Wada, A. Oku, *J. Org. Chem.* **1989**, *54*, 2599.

[6] R. Bloch, E. Guibe-Jampel, C. Girard, *Tetrahedron Lett.* **1985**, *26*, 4087.

[7] The isopropyl hemiesters from **2** and **7**–**14** are, to the best of our knowledge, not described in the literature.

[8] a) J. Hiratake, Y. Yamamoto, J. Oda, *J. Chem. Soc. Chem. Commun.* **1985**, 1717; b) M. Shimizu, K. Matsukawa, T. Fujisawa, *Bull. Chem. Soc. Jpn.* **1993**, *66*, 2128.

[9] For the enantioselective synthesis of derivatives of C_2-symmetric dicarboxylic acids with covalently bound auxiliares see: a) Y. Nagao, Y. Hagiwara, Y. Hasegawa, M. Ochiai, T. Inoue, M. Shiro, E. Fujita, *Chem. Lett.* **1988**, 381; b) T. Ishizuka, T. Kunieda, *J. Synth. Org. Chem. Jpn.* **1995**, *53*, 95. Compare also the "Two-Directional Chain Synthesis": C. S. Poss, L. Schreiber, *Acc. Chem. Res.* **1994**, *27*, 9.

[10] Compare the kinetic resolution of the racemic pyridinethiol esters of 2-phenylbutanoic acid with a titanium TADDOLate: K. Narasaka, F. Kanai, M. Okudo, N. Miyoshi, *Chem. Lett.* **1989**, 1187 and the mechanistic discussion in ref. [2c].

Total Synthesis of Natural (+)-SF2315A and Determination of the Absolute Configuration**

Kyungjin Kim and Gary A. Sulikowski*

The antibiotic SF2315A (**1**) was identified during the course of screening for new antibiotics from soil microorganisms.[1] Spectral analysis of **1** established a benz[*a*]anthracene core structure leading to the classification of SF2315A (**1**) as a member of the angucycline family of antibiotics.[2] The relative configuration of **1** was assigned based on a single-crystal X-ray analysis, while the absolute configuration was not assigned.[1b] Antibiotic SF2315A (**1**) exhibits weak activity against Gram-

[*] Prof. G. A. Sulikowski, K. Kim
Department of Chemistry, Texas A & M University
College Station, TX 77843-3255 (USA)
Telefax: Int. code + (409)845-4719

[**] This work was supported in part by the Welch Foundation (A-1230) and Texas A & M University. We thank Dr. Toru Sasaki (Meiji Seika Kaisha, Ltd.) for kindly providing an authentic sample of SF2315A. G. A. S. thanks the American Cancer Society for a Junior Faculty Research Award and the American Cyanamid Company for a Cyanamid Faculty Award.

positive bacteria and inhibits the reverse transcriptase of avian myeloblastosis virus (IC_{50} 100 $\mu g mL^{-1}$).[1a]

Efforts directed towards the total synthesis of angucycline antibiotics have led to the completion of angucyclinones of the benz[*a*]anthraquinone subclass.[3, 4] In contrast, no synthesis of a family member that possesses an angular oxygen, such as SF 2315A (**1**), has been reported.[5] Herein, we describe the first total synthesis of (+)-SF 2315A (**1**), which establishes the absolute configuration and represents the first synthesis of an angucycline antibiotic that bears an angular oxygen (that is, a nonaromatic B ring).

Our approach to SF 2315A (**1**) is outlined in a retrosynthetic sense in Scheme 1. Various derivatives of diene **3** are available

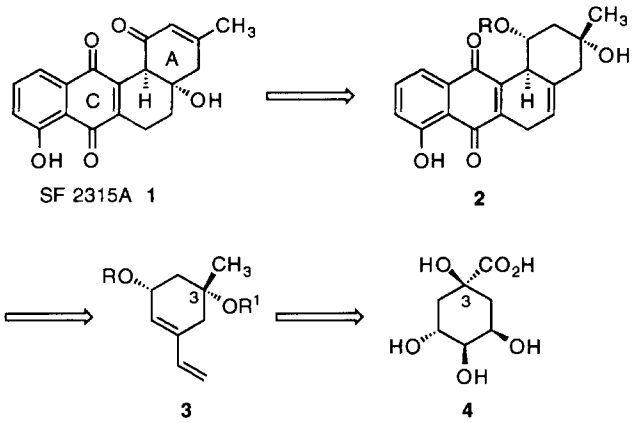

Scheme 1. Retrosynthetic analysis of SF 2315A (**1**).

starting from (−)-quinic acid (**4**).[6] The Diels–Alder cycloaddition of **3** and 5-acetoxy-2-bromojuglone (**7**) followed by minor functional group transformations would deliver quinone **2**.[7] The stereochemical course of the cycloaddition would be determined by the C1 allylic ether within the diene component.[8] Finally, oxidation of the C4a–C5 double bond of **2** from the α face, *cis* to the angular C12b hydrogen, would establish the *cis* AB ring fusion.

We recently described the preparation of dienol **5** starting from (−)-quinic acid.[4d, 6] Silylation of **5** under standard conditions afforded the silyl ether **6** in quantitative yield. Diels–Alder cycloaddition between **6** and 5-acetoxy-2-bromojuglone (**7**)[13] proceeded smoothly to deliver a single diastereomer (**8**). In this way the absolute configuration of the C12b stereocenter as well as the correct regiochemical arrangement between the A ring and the aryl substituent at C8 were established. Brief hydrogenation of **8** over palladium in ethanol followed by the introduction of a catalytic amount of K_2CO_3 effected the cleavage of the C3 benzyl ether, dehydrobromination, and the removal of the C8 acetyl group to give rise to quinone **9** in quantitative yield. Examination of molecular models revealed that oxidants would attack alkene **9** preferably from the α face (that is, *cis* to the C12b hydrogen). Indeed, epoxidation of **9** provided, exclusively, α-epoxide **10**. Epoxide **10** underwent rearrangement to the corresponding allylic alcohol upon treatment with 0.5 equivalents of tetrabutylammonium fluoride (TBAF) in THF. Peracetylation of this allylic alcohol then provided diacetate **11**. Reduction of the C5–C6 double bond proved problematic due presumably to the intermediacy of the dihydro(semi)quinone oxidation state of **11**. For example, competing elimination of the angular hydroxyl group or decomposition was observed when **11** was directly hydrogenated over Adam's catalyst. However, brief hydrogenation over 5% palladium–carbon generated the corresponding dihydroquinone, which following removal of the palladium catalyst, further hydrogenation over Adam's catalyst, and final oxidation with cerium ammonium nitrate (CAN), afforded **12** in 73% yield.

The remaining synthetic operations involved manipulation of the A ring functionality. To this end, removal of the C1 triisopropylsilyl (TIPS) group followed by Dess–Martin oxidation of the resultant alcohol provided ketone **13**.[14] Treatment of **13** with lithium hydroxide in THF produced an approximately equal mixture of **14** and SF 2315A (**1**). The former was again subjected to lithium hydroxide to afford SF 2315A (**1**). Synthetic **1** was identical in all respects to natural material (according to the 400 MHz ^1H and 50 MHz ^{13}C NMR spectra). The sign of optical rotation of synthetic SF 2315A (**1**) $\{[\alpha]_D^{25} = +112$ (*c* 0.05 in $CH_3OH)\}$ was also identical with that of natural **1** $\{[\alpha]_D^{25} = +106$ (*c* 0.05 in $CH_3OH)\}$. Thus the absolute configuration of (+)-SF 2315A is assigned as 4a*S*-(4aα,12bα). (Selected physical and spectroscopic data of compounds **8**–**13** and **1** are summarized in Table 1.)

In summary, we have completed the first total synthesis of SF 2315A (**1**), which constitutes the first assembly of an angucycline antibiotic possessing an angular hydroxyl group and de-

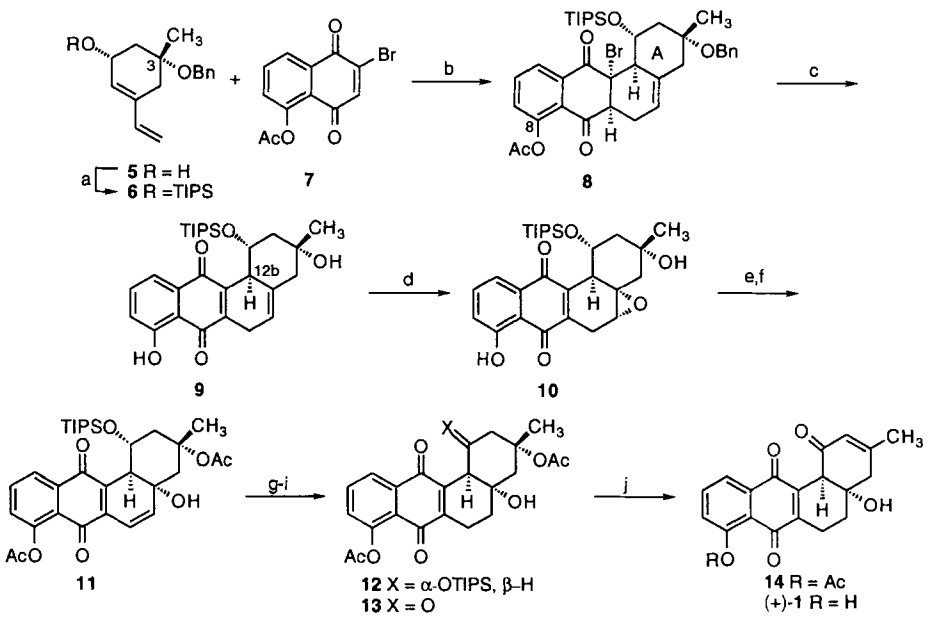

Scheme 2. a) Triisopropylsilyl chloride (TIPSCl), imidazole, 4-dimethylaminopyridine (DMAP), CH_2Cl_2, 100%; b) toluene, reflux, 66%; c) H_2, 20% $Pd(OH)_2/C$, EtOH, then K_2CO_3, 20 °C, 100%; d) dimethyldioxirane, Me_2CO, 20 °C, 100%; e) Ac_2O, pyridine, DMAP, CH_2Cl_2, 20 °C; f) TBAF (0.5 equiv), THF, 0 °C, 86%; g) 1: H_2, 5% Pd/C, EtOAc, 20 °C; 2: H_2, PtO_2, EtOAc then CAN, 20 °C, 73%; h) HF·pyridine, CH_3CN, 0 → 20 °C, 89%; i) Dess–Martin periodine, CH_2Cl_2, 20 °C, 93%; j) 0.1 M LiOH, EtOH, 0 °C, 29% **14** and 33% **1**.

 © VCH Verlagsgesellschaft mbH, D-69451 Weinheim, 1995 0570-0833/95/3421-2397 $ 10.00+.25/0

Table 1. Selected physical and spectroscopic data for compounds **8**–**13** and **1**.

8: M.p. 103–104 °C; $[\alpha]_D^{25} = -34.5$ ($c = 0.5$ in $CHCl_3$); IR ($CDCl_3$): $\tilde{\nu} = 1769$, 1707 cm^{-1}; ^1H NMR (200 MHz, $CDCl_3$): $\delta = 0.8$–1.1 (m, 21H), 1.29 (s, 3H), 1.85–1.95 (m, 1H), 2.3–2.6 (m, 5H), 2.39 (s, 3H), 3.0–3.15 (m, 1H), 3.61 (t, $J = 7.2$, 1H), 4.50 (s, 2H), 4.7–4.8 (m, 1H), 5.5–5.6 (m, 1H), 7.2–7.4 (m, 6H), 7.73 (t, $J = 7.8$ Hz, 1H), 8.0 (dd, $J = 7.8$, 1.2 Hz, 1H); ^{13}C NMR (50 MHz, $CDCl_3$): $\delta = 13.5$, 18.2, 18.4, 21.0, 22.8, 46.1, 46.2, 56.8, 59.3, 63.6, 70.0, 74.5, 120.6, 126.2, 127.2, 127.3, 128.3, 129.3, 133.8, 134.8, 135.5, 139.5, 149.0, 169.2, 189.7, 193.5; HR-MS (FAB) *m/z*: 651.1802 $[(M-C_3H_7)^+]$; calcd for $C_{34}H_{40}O_6BrSi$ 651.1778

9: M.p. 51–53 °C; $[\alpha]_D^{25} = +71.3$ ($c = 1.5$ in $CHCl_3$); IR ($CDCl_3$): $\tilde{\nu} = 3599$, 1664, 1636, 1614, 1459 cm^{-1}; ^1H NMR (200 MHz, $CDCl_3$): $\delta = 0.8$–1.0 (m, 21H), 1.23 (s, 3H), 1.8–2.4 (m, 5H), 3.0–3.8 (m, 4H), 5.61 (br. s, 1H), 7.18 (dd, $J = 7.3$, 2.3 Hz, 1H), 7.5–7.7 (m, 2H), 12.0 (s, 1H); ^{13}C NMR (50 MHz, $CDCl_3$): $\delta = 12.8$, 17.8, 17.9, 25.1, 26.9, 45.0, 49.2, 51.7, 71.0, 74.8, 114.7, 118.4, 119.0, 123.3, 133.0, 133.7, 136.0, 140.8, 146.1, 161.0, 183.1, 189.3; HR-MS (FAB) *m/z*: 483.2555 $[(M+H)^+]$, calcd for $C_{28}H_{39}O_5Si$ 483.2567

10: M.p. 159–160 °C; $[\alpha]_D^{25} = +63.8$ ($c = 1.0$ in $CHCl_3$); IR ($CDCl_3$): $\tilde{\nu} = 3599$, 1667, 1642, 1618, 1459 cm^{-1}; ^1H NMR (200 MHz, $CDCl_3$): $\delta = 0.75$–0.95 (m, 21H), 1.35 (s, 3H), 1.5–1.7 (m, 2H), 1.8–2.0 (m, 1H), 2.1–2.4 (m, 2H), 2.6–2.7 (m, 1H), 3.26 (s, 1H), 3.5–3.7 (m, 1H), 3.75–3.85 (m, 2H), 7.15–7.25 (m, 1H), 7.5–7.7 (m, 2H), 12.0 (s, 1H); ^{13}C NMR (50 MHz, $CDCl_3$): $\delta = 12.9$, 17.8, 17.9, 23.9, 27.9, 44.6, 46.9, 50.0, 56.2, 59.0, 69.5, 72.7, 114.6, 119.2, 123.6, 132.6, 136.1, 137.6, 145.9, 161.1, 182.2, 189.1; HR-MS (FAB) *m/z* 499.2527 $[(M+H)^+]$, calcd for $C_{28}H_{39}O_6Si$ 499.2516

11: M.p. 73–75 °C; $[\alpha]_D^{25} = -168.8$ ($c = 0.5$ in $CHCl_3$); IR ($CDCl_3$): $\tilde{\nu} = 3591$, 1769, 1728, 1664, 1597 cm^{-1}; ^1H NMR (400 MHz, $CDCl_3$): $\delta = 0.7$–1.0 (m, 21H), 1.57 (s, 3H), 1.8 (s, 1H), 1.9–2.0 (m, 1H), 2.02 (s, 3H), 2.6–2.7 (m, 1H), 2.35–2.45 (m, 1H), 2.45 (s, 3H), 2.65 (dd, $J = 13.1$, 1.4 Hz, 1H), 3.51 (d, $J = 9.7$ Hz, 1H), 3.72 (td, $J = 10.5$, 2.4 Hz, 1H), 6.27 (dd, $J = 9.6$, 1.0 Hz, 1H), 6.94 (d, $J = 9.6$ Hz, 1H), 7.34 (dd, $J = 8.1$, 1.0 Hz, 1H), 7.73 (t, $J = 7.8$ Hz, 1H), 8.05 (dd, $J = 7.8$, 1.1 Hz, 1H); ^{13}C NMR (50 MHz, $CDCl_3$): $\delta = 12.9$, 17.7, 17.8, 21.1, 22.4, 23.7, 45.7, 46.8, 47.7, 68.5, 70.8, 79.7, 120.1, 122.7, 124.8, 129.0, 134.5, 135.3, 139.8, 142.0, 149.4, 169.3, 170.2, 181.2, 182.7; HR-MS (FAB) *m/z* 584.2813 $[(M+2H)^+]$, calcd for $C_{32}H_{44}O_8Si$ 584.2806]

12: M.p. 75–77 °C; $[\alpha]_D^{25} = +335$ ($c = 0.2$ in $CHCl_3$); IR ($CDCl_3$): $\tilde{\nu} = 1769$, 1728, 1662, 1596 cm^{-1}; ^1H NMR (400 MHz, $CDCl_3$): $\delta = 1.0$–1.3 (m, 21H), 1.4–1.6 (m, 4H), 1.5 (s, 3H), 1.6–1.7 (m, 1H), 1.75–1.85 (m, 1H), 2.0 (s, 3H), 2.35–2.6 (m, 2H), 2.4 (s, 3H), 2.75–2.85 (m, 1H), 3.29 (br. s, 1H), 4.9 (br. s, 1H), 7.33 (dd, $J = 8.0$, 1.2 Hz, 1H), 7.70 (t, $J = 8.0$ Hz, 1H), 7.98 (dd, $J = 7.8$, 1.2 Hz, 1H); ^{13}C NMR (50 MHz, $CDCl_3$): $\delta = -1.27$, 12.4, 16.1, 21.1, 22.7, 22.8, 27.3, 32.7, 47.8, 70.3, 70.8, 79.5, 123.0, 125.0, 129.0, 134.4, 134.8, 143.5, 146.5, 149.1, 169.5, 170.4, 182.9, 183.9; HR-MS (FAB) *m/z* 586.2962 $[(M+2H)^+]$, calcd for $C_{32}H_{46}O_8Si$ 586.2962

13: M.p. 84–86 °C; $[\alpha]_D^{25} = -94.3$ ($c = 0.3$ in $CHCl_3$); IR ($CDCl_3$): $\tilde{\nu} = 3590$, 1764, 1723, 1665, 1596 cm^{-1}; ^1H NMR (200 MHz, $CDCl_3$): $\delta = 1.4$–1.6 (m, 2H), 1.62 (s, 3H), 1.8–2.1 (m, 2H), 2.09 (s, 3H), 2.23 (br. s, 1H), 2.45 (s, 3H), 2.47–2.75 (m, 2H), 2.83 (dd, $J = 15.2$, 2.6 Hz, 1H), 3.32 (dd, $J = 16.7$, 2.3 Hz, 1H), 4.2 (br. s, 1H), 7.34 (dd, $J = 8.0$, 1.2 Hz, 1H), 7.71 (t, $J = 8.0$ Hz, 1H), 8.02 (dd, $J = 7.7$, 1.2 Hz, 1H); ^{13}C NMR (50 MHz, $CDCl_3$): $\delta = 19.9$, 21.1, 22.6, 26.1, 33.0, 47.5, 50.9, 54.5, 71.0, 81.9, 123.3, 125.1, 129.5, 133.7, 134.6, 138.3, 146.6, 149.4, 169.5, 170.6, 182.7, 183.0, 204.8; HR-MS (FAB) *m/z* 367.1173 $[(M-OAc)^+]$, calcd for $C_{21}H_{19}O_6$ 376.1181

1: $[\alpha]_D^{25} = +112$ ($c = 0.05$ in MeOH) {$[\alpha]_D^{25} = +106$ ($c = 0.05$ in MeOH); natural SF 2315A}; IR ($CDCl_3$): $\tilde{\nu} = 3600$, 1660, 1643, 1621, 1458, 1296 cm^{-1}; ^1H NMR (400 MHz, $CDCl_3$): $\delta = 1.7$–1.8 (m, 2H), 1.85–1.95 (m, 1H), 2.04 (s, 3H), 2.55 (d, $J = 18.3$ Hz, 1H), 2.65–2.97 (m, 2H), 2.93 (br. d, $J = 20$ Hz, 1H), 4.14 (br. d, $J = 4.0$ Hz, 1H), 5.89 (br. s, 1H), 7.23 (dd, $J = 8.2$, 1.2 Hz, 1H), 7.59 (t, $J = 8.2$ Hz, 1H), 7.68 (dd, $J = 8.2$, 1.2 Hz, 1H), 12.1 (s, 1H); ^{13}C NMR (50 MHz, $CDCl_3$): $\delta = 20.0$, 23.8, 27.7, 45.7, 51.9, 68.9, 114.5, 118.7, 123.0, 123.8, 131.8, 136.6, 142.4, 143.4, 160.3, 161.0, 182.8, 189.1, 196.0; HR-MS (FAB) *m/z* 325.1086 $[(M+H)^+]$, calcd for $C_{19}H_{17}O_5$ 325.1076

void of an anthraquinone chromophore. Progress towards the synthesis of more structurally complex angucycline antibiotics will be reported in due course.

Received: June 12, 1995 [Z 8085 IE]
German version: *Angew. Chem.* **1995**, *107*, 2587–2589

Keywords: antibiotics · Diels–Alder reactions · natural products · total syntheses

[1] a) T. Sasaki, J. Yoshida, M. Itoh, S. Gomi, T. Shomura, M. Sezaki, *J. Antibiot.* **1988**, *41*, 835–842; b) T. Sasaki, S. Gomi, M. Sezaki, Y. Takeuchi, Y. Kodama, K. Kawamura, *ibid* **1988**, *41*, 843–848.

[2] For a comprehensive review of angucycline antibiotics, see J. Rohr, R. Thiericke, *Nat. Prod. Rep.* **1992**, *9*, 103–137.

[3] a) A. Guingant, M. M. Barreto, *Tetrahedron Lett.* **1987**, *28*, 3107–3110; b) K. Katsuura, V. Snieckus, *Can. J. Chem.* **1987**, *65*, 124–130; c) K. Krohn, K. Khanababaee, *Liebigs Ann. Chem.* **1994**, 1109–1112; d) D. S. Larsen, M. D. O'Shea, *Tetrahedron Lett.* **1993**, *34*, 1373–1376; e) F. L. Andrews, D. S. Larsen, *ibid* **1994**, *35*, 8693–8696; f) K. Kim, J. Reibenspies, G. Sulikowski, *J. Org. Chem.* **1992**, *57*, 5557–5559.

[4] Total syntheses of benz[*a*]anthraquinone angucyclines: a) Y. Yamaguchi, T. Okuma, A. Horiguchi, C. Ikeura, T. Minami, *J. Org. Chem.* **1992**, *57*, 1647–1649; b) K. Krohn, K. Khanbabaee, *Angew. Chem.* **1994**, *106*, 100–102; *Angew. Chem. Int. Ed. Engl.* **1994**, *33*, 99–100; c) T. Matsumoto, T. Sohma, H. Yamaguchi, S. Kurata, K. Suzuki, *Synlett* **1995**, 263–266; d) V. A. Boyd, G. A. Sulikowski, *J. Am. Chem. Soc.* **1995**, *117*, 8472–8473.

[5] For a novel synthetic approach to SF 2315A, see D. M. Gordon, S. J. Danishefsky, G. M. Schulte, *J. Org. Chem.* **1992**, *57*, 7052–7055.

[6] a) Diene **5** is available in 13 steps starting from (−)-quinic acid (**4**). The preparation of **5** and its utility in the total synthesis of the benz[*a*]anthraquinone angucyclines urdamycinone B and 104-2 are described in ref. [4d]; b) for a conceptually related reaction sequence starting from (−)-quinic acid, see G. Billen, U. Karl, T. Scholl, K. D. Stroech, W. Steglich in *Natural Products Chemistry 3* (Eds.: Atta-Ur-Rahman, P. W. Le Quesne), Springer, Berlin, **1988**, pp. 305–315.

[7] a) J. G. Bauman, R. C. Hawley, H. Rapoport, *J. Org. Chem.* **1985**, *50*, 1569–1573; b) J. M. McNamara, Y. Kishi, *Tetrahedron* **1984**, *40*, 4685–4691.

[8] S. C. Datt, R. W. Franck, R. Tripathy, G. J. Quigley, L. Huang, S. Chen, A. Sihaid, *J. Am. Chem. Soc.* **1990**, *112*, 8472–8478.

[9] B. M. Trost, A. G. Romero, *J. Org. Chem.* **1986**, *51*, 2332–2342.

[10] W. P. Griffith, S. V. Ley, *J. Chem. Soc. Chem. Commun.* **1987**, 1625–1627.

[11] a) J. R. Behling, K. A. Babiak, J. S. Ng, A. L. Campbell, R. Morettie, M. Koerner, B. H. Lipshutz, *J. Am. Chem. Soc.* **1988**, *110*, 2641–2643. Reviews: b) B. H. Lipshutz, R. S. Wilhelm, J. A. Kozlowski, *Tetrahedron* **1984**, *40*, 5005–5038; c) B. H. Lipshutz, *Synlett* **1990**, 119–128.

[12] E. J. Corey, A. Guzman-Perez, T.-P. Loh, *J. Am. Chem. Soc.* **1994**, *116*, 3611–3612.

[13] a) S. W. Heinzman, J. R. Grunwell, *Tetrahedron Lett.* **1980**, *21*, 4305–4308; b) M. E. Jung, J. A. Hagenah, *J. Org. Chem.* **1983**, *48*, 5359–5361.

[14] D. B. Dess, J. C. Martin, *J. Org. Chem.* **1983**, *48*, 4155–4156.

Evidence for a Mechanism Involving Transient Fragmentation in Carbon Skeleton Rearrangements Dependent on Coenzyme B_{12}**

Birgitta Beatrix, Oskar Zelder, Friedrich K. Kroll, Gissur Örlygsson, Bernard T. Golding,* and Wolfgang Buckel*

Dedicated to Professor Albert Eschenmoser on the occasion of his 70th birthday

We propose a new mechanistic hypothesis for the remarkable rearrangements of carbon skeletons catalyzed by adenosylcobalamin (coenzyme B_{12}) dependent glutamate mutase [EC 5.4.99.1] from *Clostridium tetanomorphum* and *C. cochlearium*, 2-methyleneglutarate mutase [EC 5.4.99.4] from *C. barkeri*, and methylmalonyl-CoA mutase [EC 5.4.99.2] from humans,

[*] Prof. Dr. W. Buckel, Dr. B. Beatrix, Dr. O. Zelder, G. Örlygsson
Laboratorium für Mikrobiologie
Fachbereich Biologie der Universität
Karl-von-Frisch Strasse, D-35032 Marburg (Germany)
Telefax: Int. code + (6421) 285833
e-mail: buckel@mailer.uni-marburg.de
Prof. Dr. B. T. Golding, Dr. F. K. Kroll
Department of Chemistry, Bedson Building, University of Newcastle
GB-Newcastle upon Tyne NE1 7RU (UK)
Telefax: Int. code + (191) 222-7070
e-mail: B. T. Golding@Newcastle.ac.uk

[**] This research was supported by the Commission of European Communities, the Deutsche Forschungsgemeinschaft, and the Fonds der Chemischen Industrie.

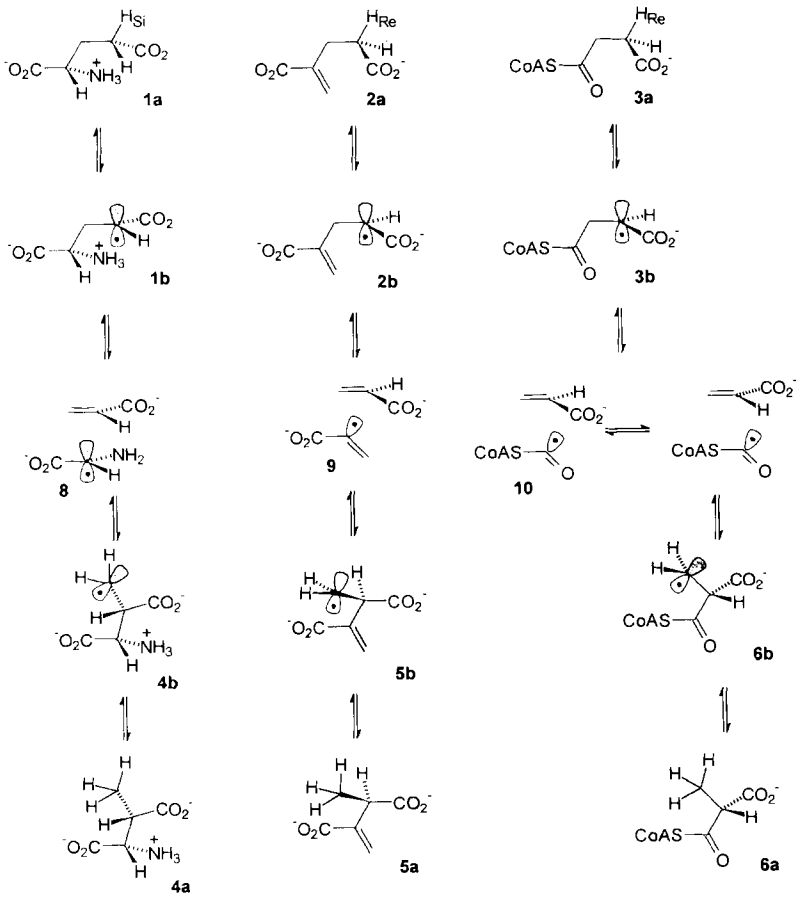

Scheme 1. Proposed reaction pathways for coenzyme B_{12} dependent reactions catalyzed by glutamate mutase (**1**⇔**4**), 2-methyleneglutarate mutase (**2**⇔**5**), and methylmalonyl-CoA mutase (**3**⇔**6**).

animals, and bacteria.[1] The substrate for glutamate mutase is (*S*)-glutamate (**1a**, Scheme 1), which is in equilibrium with the branched isomer (2*S*,3*S*)-3-methylaspartate (**4a**); with 2-methyleneglutarate mutase, 2-methyleneglutarate (**2a**) is converted into the more highly branched (*R*)-3-methylitaconate (**5a**); with methylmalonyl-CoA mutase, succinyl-CoA (**3a**) is in equilibrium with (*R*)-methylmalonyl-CoA (**6a**). Each of the substrates **1a**–**3a** contains a propionate residue within which the rearrangement occurs. A hydrogen atom migrates *inter*molecularly from C2 to C3 of the propionate residue via the 5′-carbon of the 5′-deoxyadenosyl moiety of coenzyme B_{12}, to form the methyl groups of the products **4a**–**6a**. The substituents at C3 of the propionate residues—glycinyl, ethenyl-1-carboxylate (2-acrylate), or formyl-CoA—migrate *intra*molecularly in the opposite direction. Determinations of the stereochemistry of each rearrangement have revealed that for substrate **1a**, H_{Si} is removed from the methylene group adjacent to the carboxyl function, whereas for substrates **2a** and **3a**, H_{Re} is removed. The migrating groups for substrates **1a** and **2a** move with inversion of configuration at the carbon atom from which the hydrogen atom is removed, whilst for substrate **3a** the migration occurs with retention of configuration. The methyl groups in products **4a**–**6a** appear to be formed with racemization.[2]

Despite the stereochemical differences, it is attractive to consider a unifying mechanism for the coenzyme B_{12} dependent rearrangements. It is generally accepted that the reactions are initiated by abstraction of the migrating hydrogen atom from the C2 atom of the propionate residue by the 5′-deoxyadenosyl radical, generated by homolysis of the Co–C σ bond of the coenzyme.[3] This process affords a substrate-derived radical, deoxyadenosine, and cob(II)alamin. Little is known, however, about the mechanism of the conversion of the substrate-derived radical into the product radical, to which a hydrogen atom from deoxyadenosine is donated to yield the product, with regeneration of the coenzyme. Chemical modeling[4] of the interconversion of 2-methyleneglutarate and (*R*)-3-methylitaconate suggested that the 1-methylenecyclopropane-1,2-dicarboxylate radical **7** is possibly an intermediate. This species could be formed by intramolecular addition at the double bond of the initially generated radical **2b**. Cleavage of the original 2,3-bond would lead to the product radical **5b**. Difficulties arise in the application of this mechanism to the rearrangement of glutamate to 3-methylaspartate, because neither amino acid contains a double bond at which a radical could add. It has been suggested[5] that glutamate may form a Schiff's base with a carbonyl group present in the enzyme. Isomerization of the Schiff's base to the ketimine of 2-oxoglutarate would yield an intermediate similar to 2-methyleneglutarate, and enable a rearrangement via an azacyclopropylcarbinyl radical.[6] However, attempts to trap such a Schiff's base by reduction with sodium borohydride have been unsuccessful.[7a] Moreover, microbiological and genetic experiments indicate the absence of a reactive carbonyl group in glutamate mutase.[8] A unifying mechanism valid for all three rearrangements is obtained by postulating the fragmentation of the substrate-derived radical (**1b**, **2b**, or **3b**) into acrylate and either the glycinyl radical **8**, the 2-acrylate radical **9**, or the formyl-CoA radical **10**. Readdition of the radical (**8**, **9**, or **10**) at C2 of acrylate would lead to the product radical **4b**–**6b**.[3a] We present data in favor of this hypothesis and show that it can readily explain the stereochemical details described above.

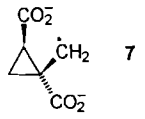

7

Glutamate mutase from *C. cochlearium* is composed of two components: E, a dimer (ε_2, $M = 100$ kDa); and S, a monomer (σ, 14.7 kDa).[7] The genes coding for the polypeptide chains ε (*glmE*) and σ (*glmS*) have been cloned and separately overexpressed in *Escherichia coli*.[9] Upon addition of coenzyme B_{12} to a mixture of the purified components, an enzymatically active complex, $\varepsilon_2\sigma_2$, is spontaneously formed, containing one mole of adenosylcobalamin per mole of tetramer.[9b] Component S alone is also able to bind the coenzyme, but much more weakly than the complex. On addition of the substrate glutamate to the complex, a paramagnetic species is formed, yielding a signal in the EPR (electron paramagnetic resonance) with a spin concentration of up to 50% of that of the enzyme concentration (Fig 1). Similar but not identical signals are generated by addition of either of the inhibitors 2-methyleneglutarate or (2*S*,4*S*)-fluoroglutamate,[7b] with spin concentrations up to 150%.[9b] The *g*-values ($g_{xy} \approx 2.15$) of these signals are different from those of free or enzyme-bound cob(II)alamin ($g_{xy} \approx 2.3$), but clearly attributable to Co^{II} compounds, as shown by the overall shape and the eightfold hyperfine splitting of the g_z-line. The signals have been interpreted as a coupling between Co^{II} and an organic radical, at least partly localized on the substrate or inhibitor.[9b] Less well resolved EPR signals have been obtained with methylmalonyl-CoA mutase[10] and 2-methyleneglutarate mutase[11]

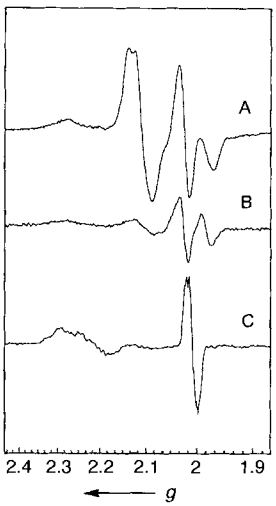

Fig. 1. EPR spectra of glutamate mutase. Component S (670 μM), 1.1 mM component E, and 4 mM coenzyme B_{12} were incubated with 13.3 mM 2-mercaptoethanol, 33 mM Tris/HCl (pH 8.3), and either 16.7 mM glycine (B) or 16.7 mM acrylate (C) or a mixture of both (A) to give a total volume of 300 μL [26]. All three spectra were obtained at identical instrument settings.

in the presence of coenzyme B_{12} and their corresponding substrates or inhibitors.

2-Methyleneglutarate mutase from *C. barkeri* is composed of only one polypeptide chain (α, 70 kDa).[12] The gene coding for the α-chain (*mgm*) has been cloned and overexpressed in *E.coli*.[13] The specific activity of the purified apo-enzyme was assayed after addition of an excess of coenzyme B_{12}, whereby active 2-methyleneglutarate mutase was immediately reconstituted. The activity of this reconstituted enzyme was twice as high as the best preparation from *C. barkeri*, which in addition to correctly bound coenzyme B_{12} also contains incorrectly bound coenzyme and air-stable cob(II)alamin.[11b] Upon gel filtration on a Superose 6 column the reconstituted enzyme was eluted with an apparent molecular mass of 180 kDa containing 1 mol coenzyme B_{12}, which suggests a homodimeric structure (α_2). Hence, the enzyme is of a size similar to glutamate mutase.

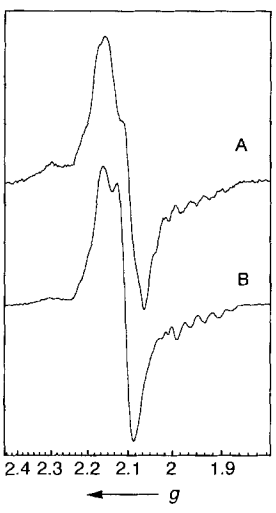

Fig. 2. EPR spectra of 2-methyleneglutarate mutase. The apoenzyme (270 μM) and 4 mM coenzyme B_{12} were incubated with 7 mM 2-mercaptoethanol, 33 mM potassium phosphate (pH 6.4), and either 16.7 mM 2-methyleneglutarate (A) or 16.7 mM acrylate (B) to give a total volume of 300 μL [26]. Spectrum A was recorded at a four times higher receiver gain than spectrum B.

We have found that in the presence of 2-methyleneglutarate the reconstituted enzyme gives rise to an EPR signal (Fig. 2A) exhibiting the same high resolution as glutamate mutase with glutamate. The C-terminus of 2-methyleneglutarate mutase (about 100 amino acids) shows significant sequence homology to component S of glutamate mutase, to the C-termini of the methylmalonyl–CoA mutases, and to the cobalamin-binding domain of the methionine synthase (MetH) from *E.coli*.[13] X-ray analysis of this MetH domain revealed the coordination of the only conserved histidine residue to the cobalt atom of the coenzyme at the same position that in free coenzyme B_{12} is occupied by dimethylbenzimidazole.[14a] EPR experiments with ^{15}N-labeled component S indicated that this was also true for glutamate mutase.[14b] Finally, the H486Q mutant of 2-methyleneglutarate mutase, in which this histidine has been converted into glutamine, is completely inactive since it is not able to bind even a trace of coenzyme B_{12}.[14c]

In order to examine the hypothesis of fragmentation of glutamate during catalysis of glutamate mutase, acrylate and glycine were tested as inhibitors of the enzyme. Neither acrylate nor glycine *alone* at concentrations up to 20 mM influenced the enzymatic reaction significantly. However, the combination of the two efficiently inhibited the conversion of (2*S*,3*S*)-3-methylaspartate into (*S*)-glutamate as assayed with the auxiliary enzymes glutamate oxaloacetate aminotransferase (aspartate aminotransferase, [EC 2.6.1.1]) and (*R*)-2-hydroxyglutarate dehydrogenase (NADH, [EC 1.1.1.-]). The initial rate of this reaction decreased to 60, 42, and 20% in the presence of equimolar mixtures of acrylate and glycine (5, 10, and 15 mM each, respectively). A dramatic effect was observed by EPR spectroscopy: A mixture of component E, S, and coenzyme B_{12} with glycine or acrylate alone gave only weak signals around $g = 2$, (Figs. 1B and C; spin concentration less than 5% of the enzyme concentration), whereas the combination of both yielded an intense signal at $g = 2.15$ (Fig. 1A). Interestingly, the shape of this signal closely resembles those observed with other coenzyme B_{12} dependent enzymes and their substrates[15] rather than those observed with glutamate mutase and glutamate[9b] or with 2-methyleneglutarate mutase and 2-methyleneglutarate (Fig. 2A). Especially in the case of the coenzyme B_{12} dependent ribonucleotide reductase, the signal was successfully simulated as that of an interaction of an organic radical with cob(II)alamin.[15] The synergistic effect of acrylate and glycine suggests that together the compounds mimic the intermediate state (see Scheme 1) and are able to induce homolytic cleavage of the Co–C bond of the coenzyme.

We were intrigued by the reported inhibition[16] of 2-methyleneglutarate mutase by *trans*-1-methylcyclopropane-1,2-dicarboxylates **11a**/**11b**, but less so by the corresponding *cis* isomers **11c**/**11d**. Assumption of a pathway via radical **7** leads to

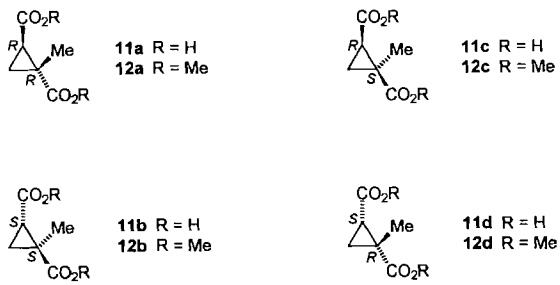

the conclusion that a particular stereoisomer of 1-methylcyclopropane-1,2-dicarboxylate should inhibit 2-methyleneglutarate mutase. Since the product of the rearrangement of 2-methyleneglutarate is (*R*)-3-methylitaconate[2c] and considering the above-mentioned report,[16] it can be concluded that the most active inhibitory 1-methylcyclopropane-1,2-dicarboxylate should be the (*R*,*R*)-isomer **11a**, which correlates with the configuration of **7**. However, no significant inhibition of 2-methyleneglutarate mutase was observed with any of the isomers at concentrations up to 20 mM.[17] Furthermore, a mixture of the two *trans* enantiomers of 1-methylcyclopropane-1,2-dicarboxylate did not induce an EPR signal with 2-methyleneglutarate mutase. However, acrylate alone inhibited 2-methyleneglutarate mutase. Interestingly, a plot of $1/v$ versus the square of the acrylate concentration rather than acrylate concentration itself gave a straight line (Dixon plot,[18] v = initial velocity). This linear correlation indicates that two acrylate molecules are involved in the inhibition of the enzyme. Assuming

competitive inhibition, at 2 and 10 mM acrylate the apparent K_i was 2 and 0.5 mM, respectively. Furthermore, acrylate induced a similar EPR signal, but with a higher spin concentration, than that obtained with 2-methyleneglutarate (Fig. 2b). This is consistent with a fragmentation of the 2-methyleneglutarate radical into acrylate and the 2-acrylate radical **9** (see Scheme 1). Based on the results described, we speculate that during catalysis of methylmalonyl-CoA mutase, acrylate and a formyl-CoA radical **10** are obtained by fragmentation of the succinyl-CoA or methylmalonyl-CoA radical (**3b** or **6b**, Scheme 1). Hence, a combination of acrylate and formyl-CoA should inhibit the enzyme and induce an EPR signal.

In Scheme 1 we present a unifying mechanism for the coenzyme B_{12} dependent mutases. Following binding of the substrate to the enzyme, homolytic fission of the Co-C bond of coenzyme B_{12} releases the 5'-deoxyadenosyl radical, which abstracts the nearest available hydrogen atom (slight differences in protein structure would suffice to place either H_{Re} or H_{Si} in position for hydrogen abstraction). In the conformation that permits maximal overlap of the radical center (π orbital) with the 2,3- (substrates **1a** and **2a**) or 1,2-σ bond (substrate **3a**), fragmentation to acrylate and a radical occurs (glycinyl radical **8** from **1b**, 2-acrylate radical **9** from **2b**, and formyl-CoA radical **10** from **3b**). Recombination of the radical with acrylate can generate product radicals **4b**–**6b**, which leads to product **4a**–**6a** by hydrogen abstraction from 5'-deoxyadenosine. The inversion of the configuration for the migratory step is in accord with this mechanism for substrates **1a** and **2a**, but the retention of configuration observed for **3a** requires a special explanation. We propose that two conformations of the acrylate formed from **3a** can equilibrate (see Scheme 1), for example by rotation about the 1,2-bond. The movement of the relatively small acrylate could be accommodated by the protein. This proposal can explain "the error in the cryptic stereochemistry of methylmalonyl-CoA mutase".[19] It was shown that in addition to the expected migration of H_{Re} at C3 of succinyl-CoA to the methyl group of methylmalonyl-CoA, the "exchangeable hydrogen" at C2 of methylmalonyl-CoA migrated to C3 of succinyl-CoA. This result was explained by invoking a 1,2-hydrogen shift in the intermediate succinyl-CoA radical, but can also be due to the occasional removal of H_{Si} from C3, leading *directly* to the correct acrylate conformation for further elaboration to (*R*)-methylmalonyl-CoA.

Some of the radicals proposed as the migrating entities in Scheme 1, or analogues thereof, have been characterized in other systems. The 2-acrylate radical is believed to have a structure (**13**) in which the three carbon atoms are colinear and the C2 atom is *sp* hybridized.[20] The glycinyl radical has been calculated[21] to be the glycine carbon radical with the lowest energy, stabilized in a captodative manner: the carboxylate withdraws electrons, whilst the amino group is an electron donor. The stability of the glycine radical at position 734 of the polypeptide chain of pyruvate formate lyase from *E.coli* has also been attributed to a captodative effect.[22]

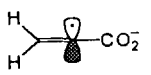

13

In summary, the data presented here strongly support the fragmentation mechanism of coenzyme B_{12} dependent carbon skeleton rearrangements and are a basis for further experiments, especially with isotopically labeled substrates and inhibitors, which may help to elucidate the nature of the intermediate radicals. The most striking aspect of our proposal is that glutamate mutase, long considered to be the least explicable coenzyme B_{12} dependent mutase,[23] emerges as the paradigm![25]

Received: June 16, 1995 [Z 8107 IE]
German version: *Angew. Chem.* **1995**, *107*, 2573–2576

Keywords: coenzyme B_{12} · enzyme catalysis · rearrangements

[1] a) H. A. Barker, H. Weissbach, R. D. Smyth, *Proc. Natl. Acad. Sci. USA* **1958**, *44*, 1093; b) R. L. Switzer, *B_{12}* **1982**, *2*, 289–305; c) H. F. Kung, S. Cederbaum, L. Tsai, T. C. Stadtman, *Proc. Natl. Acad. Sci. USA* **1970**, *65*, 978–984; d) J. Rétey in *B_{12}* **1982**, *2*, 357-379.

[2] a) M. Sprecher, R. L. Switzer, D. B. Sprinson, *J. Biol. Chem* **1966**, *241*, 864–867; b) G. Hartrampf, W. Buckel, *FEBS Lett.* **1984**, *171*, 73–78; c) G. Hartrampf, W. Buckel, *Eur. J. Biochem.*, **1986**, *156*, 301–304; d) M. Sprecher, M. J. Clark, D. B. Sprinson, *J. Biol. Chem.* **1966**, *241*, 872–877; e) J. Rétey, J. A. Robinson, *Stereospecificity in Organic Chemistry and Enzymology*, Verlag Chemie, Weinheim, **1982**, pp. 183–207; f) G. Hartrampf, W. Buckel, *FEBS Lett.* **1984**, *171*, 73–78.

[3] a) B. T. Golding in *B_{12}* **1982**, *1*, 543–582; b) J. Halpern, *Science (Washington, D. C.)* **1985**, *227*, 869; c) B. M. Babior, *Bio Factors* **1988**, *1*, 21–26; d) B. T. Golding, *Chem. Br.* **1990**, 950–954. See also U. von Arx, Ph.D. Thesis, University of Bern, Switzerland **1985**.

[4] S. Ashwell, A. G. Davies, B. T. Golding, R. Hay-Motherwell, S. Mwesigye-Kibende, *J. Chem. Soc. Chem. Commun.* **1989**, 1483–1485.

[5] a) P. Dowd, S.-C. Choi, F. Duah, C. Kaufman, *Tetrahedron* **1988**, *44*, 2137; b) S.-C. Choi, P. Dowd, *J. Am. Chem. Soc.* **1989**, *111*, 2313.

[6] M. D. Balinger, G. H. Reed, P. A. Frey, *Biochemistry* **1992**, *31*, 949-953.

[7] a) U. Leutbecher, R. Böcher, D. Linder, W. Buckel, *Eur. J. Biochem.* **1992**, *205*, 759–765; b) U. Leutbecher, S. P. J. Albracht, W. Buckel, *FEBS Lett.* **1992**, *307*, 144–146.

[8] a) F. Suzuki, H. A. Barker, *J. Biol. Chem.* **1966**, *241*, 878–888; b) E. N. G. Marsh, D. E. Holloway, *FEBS Lett.* **1992**, *310*, 167–170; c) D. E. Holloway, E. N. G. Marsh, *ibid.* **1993**, *317*, 44–48; d) M. Brecht, J. Kellermann, A. Plückthun, *ibid.* **1993**, *319*, 84–89.

[9] a) O. Zelder, B. Beatrix, W. Buckel, *FEMS Microbiol. Lett.* **1994**, *118*, 15–22. b) O. Zelder, B. Beatrix, U. Leutbecher, W. Buckel, *Eur. J. Biochem.* **1994**, *226*, 577–585.

[10] a) Y. Zhao, P. Such, J. Rétey, *Angew. Chem.* **1992**, *104*, 212–213. *Angew. Chem. Int. Ed. Engl.* **1992**, *31*, 215–216; b) Y. Zhao, A. Abend, M. Kunz, P. Such, J. Rétey, *Eur. J. Biochem.* **1994**, *225*, 891–896.

[11] a) C. Michel, S. P. J. Albracht, W. Buckel, *Eur. J. Biochem.* **1992**, *205*, 767–773; b) O. Zelder, W. Buckel, *Biol. Chem. Hoppe Seyler* **1993**, *374*, 85–90; c) R. Padmakumar, R. Banerjee, *J. Biol. Chem.* **1995**, *270*, 9295–9300.

[12] C. Michel, G. Hartrampf, W. Buckel, *Eur. J. Biochem.* **1989**, *184*, 103–107.

[13] B. Beatrix, O. Zelder, D. Linder, W. Buckel, *Eur. J. Biochem.* **1994**, *221*, 101–109.

[14] a) C. Luschinsky-Drennan, S. Huang, J. T. Drummond, R. G. Matthews, M. L. Ludwig, *Science* **1994**, *266*, 1669–1674; b) O. Zelder, B. Beatrix, F. Kroll, W. Buckel *FEBS Lett.* **1995**, *369*, 252–254; c) F. Kroll, B. Beatrix, O. Zelder, W. Buckel, unpublished.

[15] J. A. Hamilton, Y. Tamao, R. L. Blakley, R. E. Coffman, *Biochemistry*, **1972**, *11*, 4696–4705; K. L. Schepler, W. R. Dunham, R. H. Sands, J. A. Fee, R. H. Abeles, *Biochim. Biophys. Acta* **1975**, *397*, 510–518; G. R. Buettner, R. E. Coffman, *ibid.* **1977**, *480*, 495–505.

[16] H.-F. Kung, T. C. Stadtman, *J. Biol. Chem.* **1971**, *246*, 3378–3388.

[17] L. L. McCoy, *J. Am. Chem. Soc.* **1958**, *80*, 6568–6572. The dimethyl ester of **11** was prepared by sodium methoxide induced condensation of methyl acrylate with methyl 2-chloropropionate. The *cis* isomers formed preferentially at 17–25 °C, whereas the *trans* isomers required more than 50 °C. Saponification and resolution of the enantiomers gave: **11a**, m.p. 173 °C, $[\alpha]_D^{20}$ −232; **11b**, m.p. 174 °C, $[\alpha]_D^{20}$ + 213; **11c**, m.p. 150 °C, $[\alpha]_D^{20}$ −70; **11d**, m.p. 149 °C; $[\alpha]_D^{20}$ + 62. Further details will be published elsewhere.

[18] M. Dixon, E. C. Webb, *Enzymes*, 2nd ed., Longmans, London **1964**, pp. 327–331.

[19] a) M. Michenfelder, W. E. Hull, J. Rétey, *Eur. J. Biochem.* **1987**, *168*, 659–667. b) W. E. Hull, M. Michenfelder, J. Rétey, *ibid.* **1988**, *173*, 191–201.

[20] G. W. Neilson, M. C. R. Symons, *J. Chem. Soc. Perkin Trans. 2* **1973**, 1405–1410.

[21] D. Yu, A. Rauk, D. A. Armstrong, *J. Am. Chem. Soc.* **1995**, *117*, 1789–1796.

[22] A. F. V. Wagner, M. Frey, F. A. Neugebauer, W. Schäfer and J. Knappe, *Proc. Natl. Acad. Sci. USA*, **1992**, *89*, 996–1000.

[23] Y. Murakami, Y. Hisaeda, X.-M. Song, T. Ohno, *J. Chem. Soc. Perkin Trans. 2* **1992**, 1527–1528.

[24] The components were mixed in an EPR tube in the dark, and the reaction was started by addition of the acids followed by incubation under N_2 at 30 °C for 5 min. The reaction was stopped by freezing in a mixture of liquid nitrogen and pentane. X-band EPR spectra were recorded with a Varian E-3 EPR spectrometer at a temperature of 77 K, microwave frequency 9.1 GHz, microwave power 2 mW (Fig. 1) or 20 mW (Fig. 2), modulation frequency 100 kHz, modulation amplitude 0.4 mT.

[25] Note added in proof: Reaction of diethyl 2-bromomethyl-2-methylmalonyl-monothiolate with cob(I)alamin yields, among other products, ethyl methacrylate. It was suggested that the latter is derived by the β-scission of intermediate radicals analogous to **3b** and **6b** [A. J. Scott, P. Karuso, H. J. Williams, J. Lally, J. Robinson, G. P. Nayar, *J. Am. Chem. Soc.* **1994**, *116*, 777–778].

Asymmetric Pictet–Spengler Reactions Employing *N,N*-Phthaloyl Amino Acids as Chiral Auxiliary Groups**

Herbert Waldmann,* Gunther Schmidt, Henning Henke, and Michael Burkard

Dedicated to Professor Ivar Ugi on the occasion of his 65th birthday

The Pictet–Spengler reaction is one of the most important methods in heterocyclic and natural product chemistry.[1] In particular, it has proven to be a very powerful tool for the construction of complex alkaloids, for example those belonging to the tetrahydroisoquinoline and β-carboline classes. Therefore, the development of methods that allow this transformation to be performed asymmetrically by employing a removable chiral auxiliary group is of great importance to organic synthesis. However, in only a few cases has this problem been addressed, and the techniques developed so far either remained restricted to a special application in a particular total synthesis, or they suffer from being not generally applicable.[2, 4] The purpose of this paper is to report that high levels of stereoselectivity (diastereomeric ratio can be greater than 99:1) are reached in Pictet–Spengler reactions employing both aliphatic and aromatic Schiff bases by using *N,N*-phthaloyl amino acids (Pht amino acids) as chiral auxiliary groups.

During a research program directed at the use of the readily available amino acid esters as chiral auxiliary groups,[3] we recently showed that asymmetric steering of the Pictet–Spengler reaction can be achieved by generating intermediate *N*-alkyliminium salts derived from amino acid esters.[4] But, because of the low reactivity of these Schiff base derivatives, only aromatic aldehydes could be converted into the desired products with preparatively useful yields. However, chiral nitrogen heterocycles derived from aliphatic aldehydes, which are much more relevant to the synthesis of alkaloids and their analogs, cannot be obtained by this method. In addition, the chiral auxiliaries can only be removed from the resulting N-alkylated Pictet–Spengler adducts by a laborious multistep procedure. We reasoned that these serious limitations might be overcome by the intermediacy of *N-acyl*iminium salts like **3** rather than *N-alkyl*-iminium salts. Because of the electron-withdrawing influence of the N-acyl group, these electrophiles should be more susceptible to a nucleophilic attack of aromatic residues on the C=N bond, and the resulting Pictet–Spengler adducts would be linked to the chiral auxiliary by an amide rather than an N-alkyl bond, thereby allowing for a straightforward removal of the mediator of chirality.

If the Schiff bases **1**, which are derived from tryptamine, are treated with the *N,N*-phthaloyl-protected amino acid chlorides **2**[5] in the presence of titanium alkoxides like $Ti(OnPr)_4$ and $Ti(OiPr)_4$ in CH_2Cl_2 at room temperature, the desired tetrahydro-β-carbolines **4** and **5** are formed in a smooth reaction in satisfactory yields and with excellent diastereoselectivity (Table 1). If imines of aliphatic aldehydes are employed the cyclization is complete within 5 min to 1 h; in the case of aromatic Schiff bases, however, several days are required. Presumably the reaction proceeds by attack of the acid chlorides on the nitrogen of the C–N double bond to give rise to the *N*-acyliminium intermediates **3**, which then are subject to a cyclization by attack of the electron-rich nucleophilic indole on the electrophilic carbon of the C=N bond. With aromatic Schiff bases, the diastereomer ratio increases with increasing steric demand of the amino acid side chain R^2 (Pht-alanine and Pht-valine are clearly less favorable auxiliaries than Pht-*tert*-leucine; Table 1, compare nos. 1, 2, and 4 as well as 5 and 6). The same observation is made for aliphatic Schiff bases if the aliphatic group R^1 is small (for example methyl: Table 1, nos. 9 and 10). However, with increasing steric demand of R^1 this trend may be reversed (Table 1, nos. 11 and 12) and for R^1 = *i*Pr, *N,N*-Pht-valine is an excellent auxiliary group, which makes the desired Pictet–Spengler adduct available in 99% yield in diastereomerically

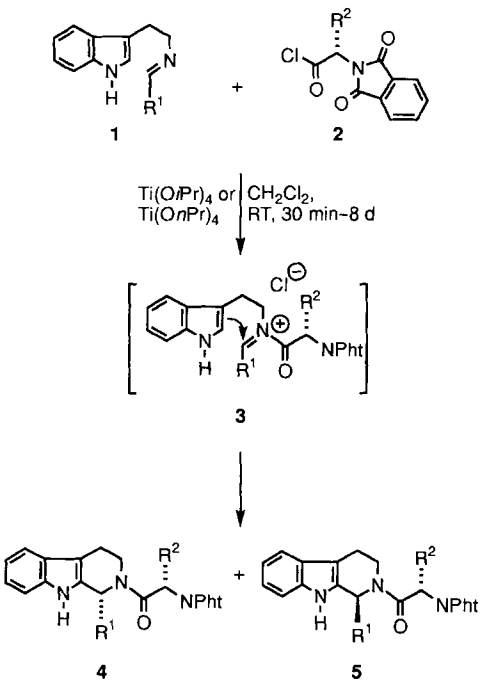

1 **2** **3** **4** **5**

Table 1. Results of the Pictet–Spengler reactions of **1** employing *N,N*-phthaloyl amino acids as chiral auxiliary groups yielding **4** and **5**.

No.	4	R^1	R^2	Lewis acid	$[\alpha]_D^{25}$ [°] (c = 1, $CHCl_3$)	M.p. [°C]	Yield [%] [a]	4:5 [b]
1	**a**	Ph	Me	$Ti(OnPr)_4$	−102 [c]	247–250	30	84:16
2	**b**	Ph	*i*Pr	$Ti(OnPr)_4$	−150	265	52	90:10
3	**b**	Ph	*i*Pr	$Ti(OiPr)_4$			58	96:4
4	**c**	Ph	*t*Bu	$Ti(OnPr)_4$	−209	298	60	>99:1
5	**d**	4-$NO_2C_6H_4$	*i*Pr	$Ti(OnPr)_4$	−185 [d]	284	56	86:14
6	**e**	4-$NO_2C_6H_4$	*t*Bu	$Ti(OnPr)_4$	−232	283	54	93:7
7	**f**	4-ClC_6H_4	*t*Bu	$Ti(OnPr)_4$	−205	250–252	44	89:11
8	**f**	4-ClC_6H_4	*t*Bu	$Ti(OiPr)_4$			60	96:4
9	**g**	Me	*i*Pr	$Ti(OnPr)_4$	−154	300	31	83:17
10	**h**	Me	*t*Bu	$Ti(OnPr)_4$	−267	274	66	96:4
11	**i**	Et	*i*Pr	$Ti(OnPr)_4$	−131	228	57	97:3
12	**k**	Et	*t*Bu	$Ti(OnPr)_4$	−194	262	59	95:5
13	**l**	*i*Pr	*i*Pr	$Ti(OnPr)_4$	−111	254	99	>99:1

[a] The yields are based on pure diastereomer **4**. All tetrahydro-β-carbolines **4** were identified from 250- or 400-MHz ^1H NMR spectra ($CDCl_3$) and gave correct elemental analyses. [b] Determined from the crude reaction mixture by HPLC. [c] c = 0.5. [d] c = 0.27.

[*] Prof. Dr. H. Waldmann, Dipl.-Chem. G. Schmidt
Institut für Organische Chemie der Universität
Richard-Willstätter-Allee 2, D-76128 Karlsruhe (Germany)
Telefax: Int. code +(721) 608-4825
Dr. H. Henke, M. Burkard
Institut für Anorganische Chemie der Universität Karlsruhe

[**] This work was supported by the Deutsche Forschungsgemeinschaft and the Fonds der Chemischen Industrie. We thank Degussa AG for the donation of amino acids.

form (Table 1, no. 13; the second diastereomer could not be detected by 400 MHz NMR spectroscopy or by HPLC). The steric demand of the alkyl groups of the titanium Lewis acids employed may have a marked influence on the diastereoselectivity. Thus, although high diastereomer ratios can, in general, be induced with titanium tetra-*n*-propylate (see, for instance, Table 1, nos. 4, 6, 10–13), the stereoselectivity in some cases is more efficient in the presence of titanium tetra-*iso*-propylate (Table 1, compare no. 2 with 3 and 7 with 8).

The best results are obtained if the amino acid chlorides **2**, the titanium alkoxide, and the imines **1**. Lowering the temperature to −40 °C reduces the rate of reaction, but does not improve the diastereoselectivity. The presence of the phthaloyl protecting group is important. If 9-fluorenylmethoxycarbonyl- (Fmoc) or benzyloxycarbonyl (*Z*)-protected Pht amino acid chlorides are used, the levels of stereoselectivity are consistently lower. In addition, *N*,*N*-phthaloyl amino acid chlorides are not prone to racemization[5] and, in contrast to the Fmoc- or Z analogs, the Pht-protected Pictet–Spengler adducts **4** and **5** are highly crystalline compounds from which the major isomers **4** are obtained in analytically and enantiomerically pure form by a single recrystallization (in general from a mixture of ethyl acetate and hexane or diethyl ether and hexane). These advantageous physical properties also enabled a rigorous determination of the absolute configuration of the major diastereomers by crystal structure analysis of the tetrahydro-β-carboline (**4d**).[6]

To explain the high stereoselectivity attained through the Pictet–Spengler reactions detailed above, we assume that the reaction proceeds preferentially via transition states **A**. In **A** the titanium atom coordinates to the carbonyl oxygen atoms of the amino acid and the phthaloyl group. An octahedral complex is thereby formed in which the top-side of the C=N bond is shielded by a substituent of the activating Lewis acid. This is in accord with a related finding for $TiCl_4$ mediated Diels–Alder reactions of α,β-unsaturated proline ester amides.[7] In this arrangement the bulky amino acid side chain points away from the ethylene bridge between the indole nucleus and the iminium nitrogen; consequently, unfavorable steric interactions are avoided. Furthermore, by analogy with the configuration of α,β-unsaturated amides,[7] substituent R^1 of the C–N double bond and the amino acid carbonyl function are in an *s-cis* orientation. If these two groups were in an s-*trans* orientation, R^1 would come close to the α-carbon of the amino acid , a situation which for steric reasons would also be unfavorable. In the 3-indolylethyl-substituted iminium intermediate **A**, the imine substituent R^1 is *trans* to the ethylene bridge. This is the favored configuration because a 1,3-interaction between R^1 and the protons of a CH_2 group would develop upon ring closure if R^1 was *cis* to the ethylene bridge.[4] Potential involvement of the transition states **A** also explains why stereoselectivity in the Pictet–Spengler cyclizations is more efficient if a bulkier alkyl residue is present in the titanium Lewis acid (for example, *i*-Pr vs. *n*-Pr): one of the diastereotopic faces of the C=N bond is more efficiently shielded.

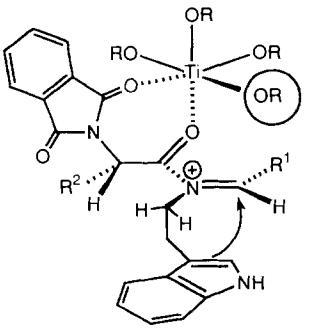

A

From the Pictet–Spengler adducts **4** the chiral auxiliary can readily be removed by cleavage of the amide bond with reducing reagents like $LiAlH_4$. The enantiomerically pure tetrahydro-β-carboline **6**, for instance, is readily obtained from **4c** by this straightforward procedure.[8]

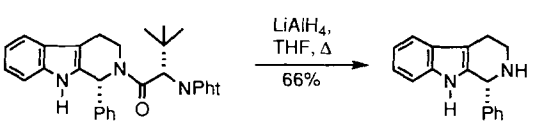

4c **6**

In conclusion, *N*,*N*-phthaloyl amino acids are the first generally applicable chiral auxiliary groups for the Pictet–Spengler reaction that efficiently control the stereochemical course of this important transformation of alkaloid chemistry.

Received: June 30, 1995 [Z 8153 IE]
German version: *Angew. Chem.* **1995**, *107*, 2608–2610

Keywords: amino acids · asymmetric syntheses · chiral auxiliaries · Pictet–Spengler reactions · tetrahydrocarbolines

[1] W. M. Whaley, T. R. Govindachari, *Organic Reactions*, Vol. 6, Wiley, New York, **1951**, pp. 151–206.

[2] a) C. Bohlmann, R. Bohlmann, E. G. Rivera, C. Vogel, M. D. Manandhar, E. Winterfeldt, *Liebigs Ann. Chem.* **1985**, 1752–1763; b) D. L. Comins, M. M. Badawi, *Tetrahedron Lett.* **1991**, *32*, 2995–2996; c) R. Amann, D. Spitzner, *Angew. Chem.* **1991**, *103*, 1373–1374; *Angew. Chem. Int. Ed. Engl.* **1991**, *103*, 1320–1321; d) T. Soe, T. Kawate, N. Fukui, M. Nakagawa, *Tetrahedron Lett.* **1995**, *36*, 1857–1860.

[3] Review: H. Waldmann, *Synlett* **1995**, 133–141.

[4] H. Waldmann, G. Schmidt, M. Jansen, J. Geb, *Tetrahedron* **1994**, *50*, 11865–11884.

[5] a) J. Sheehan, D. W. Chapman, R. W. Roth, *J. Am. Chem. Soc.* **1952**, *74*, 3822–3825; b) C. R. McArthur, P. M. Worster, A. U. Okon, *Synth. Comm.* **1983**, *13*, 311–318.

[6] Crystal structure determination of **4d** ($C_{30}H_{26}N_4O_5$): noncentrosymmetric, monoclinic, $P2_1$ (no. 4), $a = 1201.3(1)$, $b = 987.4(1)$, $c = 1238.1(1)$ pm, $\beta = 114.48(2)°$, $Z = 2$, $\rho_{calcd} = 1.298(1)\,g\,cm^{-3}$, $T = -85$ °C, 3256 unique reflections, ω/θ scans (Stoe four-circle diffractometer, graphite monochromator, $Mo_{K\alpha}$ radiation, $2\theta_{max} = 55°$), learnt profiles fit. The structure was solved by direct methods (SHELXS-86), and refined on F_o^2 data (SHELXL-93) with anisotropic temperature factors for C, N and O. All H atoms were localized by a difference Fourier synthesis. $R_1 = 0.030$ for 2713 $F_o > 4\sigma(F_o)$ and $wR_2 = 0.079$, 431 structure parameters. The absolute configuration of **4d** was assessed possible on the basis that the chirality of thevaline derived chiral auxiliary group is known. Further details of the crystal structure determination may be obtained from the Fachinformationszentrum Karlsruhe, D-76344 Eggenstein-Leopoldshafen (Germany), on quoting the depository number CSD-59081.

[7] H. Waldmann, *Liebigs Ann. Chem.* **1990**, 671–680, and references therein.

[8] **6**: $[\alpha]_D^{22} = -4.3$ ($c = 1.0$, $CHCl_3$); m.p. 186 °C; published values: a) $[\alpha]_D^{22} = -4.4$ ($c = 1.0$, $CHCl_3$); m.p. 167 °C [4]; b) (*R*)-**6**: $[\alpha]_D^{25} = +4.37$ ($c = 1.19$, EtOH), 27% *ee*; (*S*)-**6**: $[\alpha]_D^{24} = -16.4$ ($c = 0.38$, EtOH) (M. Nakagawa, T. Kawate, T. Kakikawa, H. Yamada, T. Matsui, T. Hino, *Tetrahedron* **1993**, *49*, 1739–1748).

A Comparison of Enthalpies of Formation in Solution and Enthalpies for HPLC Retention for Hydrogen-Bonded Host–Guest Complexes**

Steven C. Zimmerman* and Wing-Sum Kwan

New methods that rapidly and accurately measure the stability of molecular complexes can greatly assist molecular recognition studies. Enthalpies of complexation, in particular, have proven valuable in understanding the origin of stabilities of host–guest compounds.[1] We recently reported that enthalpies of retention of nitroaromatic analytes—conveniently determined by their temperature-dependent retention (vide infra) by tweezer molecules attached to HPLC stationary phases—were within experimental error of the analogous complexation enthalpies measured in free solution.[2, 3] This result required both a minimal amount of retention by nonspecific interactions and a similar molecular recognition event in solution and on the silica surface. To test the generality of this method, we have now examined host–guest systems in which complexation is driven by hydrogen bonding or a combination of hydrogen bonding and π-stacking. In contrast to the earlier study, the current hosts are more exposed for potential interaction with the silica surface, and nonspecific retention of the more polar heterocyclic analytes is more likely. A broad range of such host–guest systems has been examined, and we report herein a comparison of enthalpies determined in solution and by HPLC; the latter were determined on **1**–**3**, stationary phases containing chemically bonded hosts.

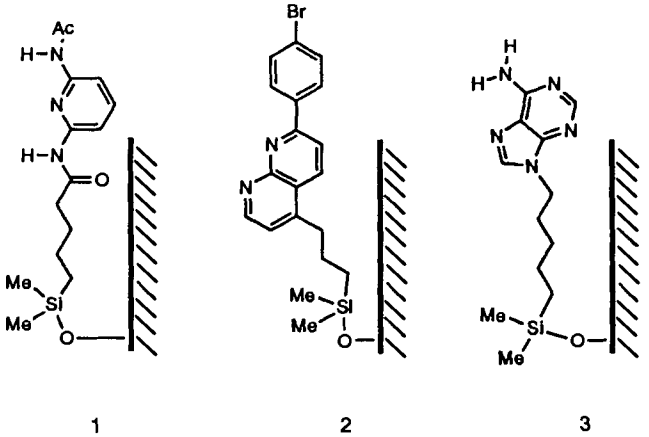

1 **2** **3**

Chemically bonded stationary phase **1** (CBSP **1**) is related to a 2,6-diamidopyridine phase studied by Feibush et al.[4] The diamidopyridine unit contains a donor–acceptor–donor array of hydrogen-bonding sites that is complementary to the acceptor-donor-acceptor array found in certain imides and thymine derivatives (see Scheme 1, **4**·**5**, **4**·**6**, **4**·**7**, **4**·**8**).[4, 5] To prepare **1**, 2,6-diaminopyridine (**9**) was monoacetylated with acetic anhydride and then treated with 4-pentenoyl chloride to produce

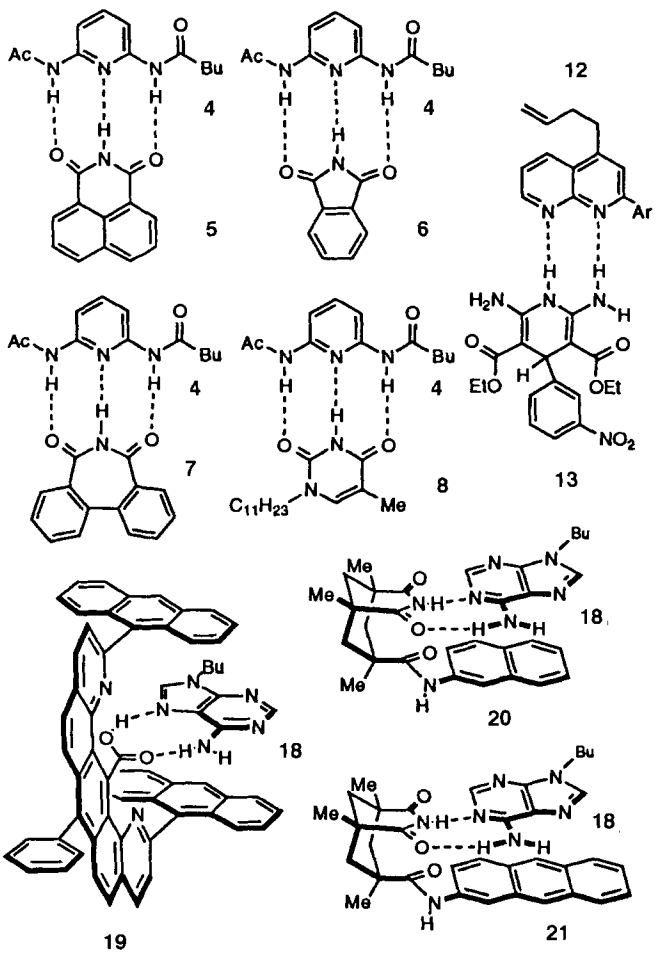

Scheme 1.

diamide **10** in 52% yield (Scheme 2).[6] Regioselective hydrosilylation with dimethylchlorosilane followed by treatment with ethanol and triethylamine afforded ethoxysilane **11**, which was purified by chromatography (33% yield). In order to test the

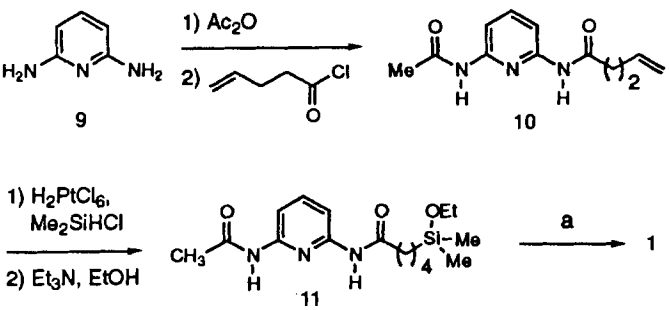

Scheme 2. Synthesis of CBSP **1**. a) 5 μM HPLC silica gel.

effect of loading, bonding to 5 μM Spherisorb silica was carried out twice to produce phases **1a** and **1b** that contained 0.11 and 0.055 mmol of host per gram of silica gel, respectively. The loadings were determined by elemental analysis and represent the average of carbon and nitrogen content.

Two more lightly loaded phases, **1c** and **1d**, were produced by capping **1a** with a 10% solution of hexamethyldisilazane in chloroform (50–60 °C) and diluting it (1:4 and 1:12 w/w, respectively) with trimethylsilyl-capped silica gel. These phases

[*] Prof. S. C. Zimmerman, Dr. W.-S. Kwan
Department of Chemistry, 600 S. Mathews Avenue
University of Illinois, Urbana, IL 61801 (USA)
Telefax: Int. code + (217)244-9919
e-mail: zimmerma@aries.scs.uiuc.edu

[**] Quantitative Host–Guest Complexation Studies Using Chemically Bonded Stationary Phases, Part 2. Part 1: Ref. [2]. This work was supported by the National Institutes of Health (GM38010).

were designed both to provide convenient retention times with more highly retained analytes, and to investigate whether the physical dilution of the bonded phases with a nonretaining phase would affect the thermodynamics of retention. Phase **1a** was slurry-packed into a 250 mm × 4.6 mm O. D. stainless steel column, and **1b–d** into shorter columns with narrower bores (dimensions: 100 mm × 2.1 mm). In the case of **1a** and **1b**, the residual silanol groups were capped by passing a solution of hexamethyldisilazane in methylene chloride through the column.

CBSP **2** contained the 1,8-naphthyridine chromophore that was shown to bind dihydrodiaminopyridines (for example, **12·13**) with an association constant about an order of magnitude higher than that for the diamidopyridine–imide type complexes described above.[5b] The synthesis of this CBSP began with the ortho-lithiation of **14** followed by treatment with **15** and deprotection to aminoketone **16** in 65% overall yield (Scheme 3). Friedländer condensation of **16** and 4-bromoacetophenone gave **17** in 76% yield (the bromine substituent serves to increase the crystallinity of the product). The hydrosilylation of **17** (34% yield) and subsequent bonding and capping steps were performed as described for **10** in Scheme 1. A column with a loading of 0.05 mmol of host per gram of silica gel (CBSP **2**), retained analytes too strongly, so it was diluted ca. 1:2 and 1:9 (w/w) with trimethylsilyl-capped silica gel to produce CBSPs **2a** and **2b**, respectively, which were slurry-packed into 100 mm × 2.1 mm O. D. stainless steel columns.

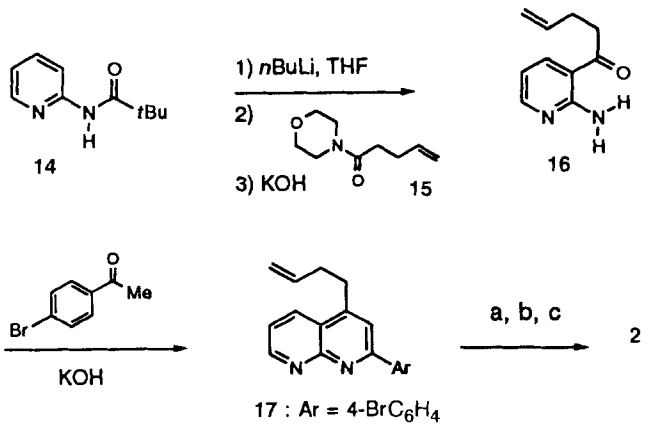

Scheme 3. Synthesis of CBSP **2**. a) H_2PtCl_6/Me_2SiHCl; b) Et_3N, EtOH; c) 5 μM HPLC silica gel.

The last chemically bonded stationary phase, **3**, was of interest because of the availability of adenine hosts with a broad range of affinities (for example, **18·19**, **18·20**, **18·21**, Scheme 1) and very large enthalpies of complexation.[7, 8] The synthesis of CBSP **3** began by alkylating 6-chloropurine with 5-bromo-1-pentene to afford **22** in 76% yield (Scheme 4). As described for the previous CBSPs, regioselective hydrosilylation and treatment with ethanol and triethylamine gave the corresponding ethoxysilane (**23**, 73% yield). Heating **23** with ammonia converted it into the 9-substituted adenine in 94% yield, which was bonded to silica as described previously. The resultant CBSP **3**, with a loading of 0.11 mmol of host per gram of silica gel, was diluted 1:1, 1:9, and 1:99 (w/w) with trimethylsilyl-capped silica gel to produce CBSPs **3a**, **3b**, and **3c**, respectively. These CBSPs were slurry-packed into 100 mm × 2.1 mm O. D. stainless steel columns and capped as previously described.

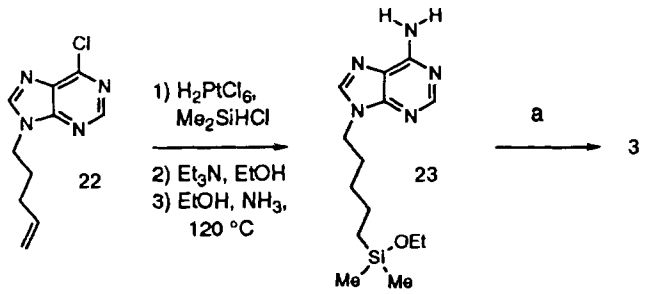

Scheme 4. Synthesis of CBSP **3**. a) 5 μM HPLC silica gel.

Enthalpies of the retention process were measured on these HPLC columns with the general method described previously.[2] Retention times of most analytes were measured over temperature ranges greater than or equal to 50 °C in about 10 °C intervals. The peaks for host **19** on CBSP **3** showed significant tailing below 45 °C, limiting the range of temperatures studied. For all runs the t_M (t_0) was measured at each temperature as the retention time of 1,3,5-tri-*tert*-butylbenzene.[9] Using the relationship, $\ln k' = \Delta H^\circ/RT + \Delta S^\circ/R + \ln(\Phi)$, Van't Hoff plots were constructed by plotting $\ln k'$ against $1/T$.[10] Enthalpies of complexation in solution were determined by the van't Hoff method for which changes in the ^{1}H NMR spectrum at four to six temperatures indicated the extent of saturation. For the ^{1}H NMR technique, the chemical shift of the imide N–H proton in **5–8** and **20–21** (NH_2 in **13**) was followed to evaluate the association constants with the method described by Dougherty.[11a] Binding isotherms were generated so as to cover a saturation range of 20–80% with seven or more points. In chloroform and carbon tetrachloride, K_{assoc} and ΔH° values for complex **18·19** were so high that microcalorimetry had to be employed.[11]

Altogether, three types of CBSPs were studied and eight complexes (Scheme 1) were analyzed (Table 1). The eighteen comparisons made between solution complexation enthalpies and enthalpies of HPLC retention are represented graphically in Figure 1. Most significantly, a linear correlation was found; regression analysis gives a slope of 1.0 ± 0.2 and a y intercept of 0.14 ± 0.61 kJ mol^{-1}. Thus, the HPLC retention enthalpies for a

Table 1. Enthalpy of retention for analytes on CBSPs **1–3** and corresponding complexation enthalpies for host–guest complexes of Scheme 1 in the solvents S.

		Complexation in solution				HPLC		
Host	Guest	S	ΔT [a]	K_{assoc} [b]	$-\Delta H^\circ$ [c]	CBSP	ΔT [a]	$-\Delta H^\circ$ [c]
4	**5**	CH_2Cl_2	−50–20	144	24.8	**1a**	0–65	24.3
						1b	0–55	25.5
	6	CH_2Cl_2	−40–20	16	20.6	**1a**	0–65	17.2
						1b	13–55	16.7
	7	CH_2Cl_2	−55–20	114	26.8	**1a**	0–75	27.5
						1b	0–55	27.7
		CCl_4	0–55	785	47.9	**1b**	20–55	45.8
						1d	65–95	42.0
	8	CCl_4	20–68	12.000 [d]	45.2	**1a**	35–75	45.8
						1d	65–95	47.7
		CCl_4:CH_2Cl_2 9:1 (v/v)	0–35	16.750	35.6	**1c**	25-65	37.3
						1d	35–84	40.0
12	**13**	CH_2Cl_2	−40–20	1.234	18.8	**2a**	0–55	23.2
						2b	0–55	20.1
18	**20**	CH_2Cl_2	−40–30	86	25.7	**3a**	0–65	26.3
	21	CH_2Cl_2	−40–20	131	28.5	**3a**	0–65	29.1
	19	$CHCl_3$		55.675	48.8 [e]	**3b**	45–95	47.6
	19	CCl_4		366.000	58.2 [e]	**3c**	55–95	57.3

[a] Temperature range in °C. [b] M^{-1} determined at 293 K. [c] kJ mol^{-1}, duplicate runs within 20% (solution) and 10% (HPLC). [d] Determined at 318 K. [e] Determined by microcalorimetry at 303 K.

 © VCH Verlagsgesellschaft mbH, D-69451 Weinheim, 1995 0570-0833/95/3421-2405 $ 10.00+.25/0

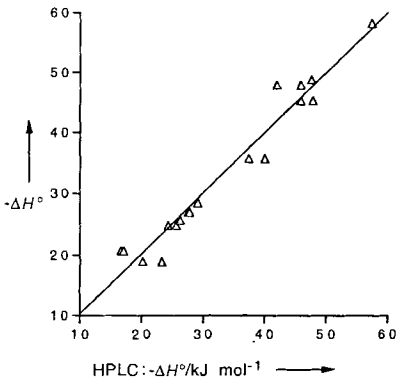

Fig. 1. Correlation between enthalpies of complexation in solution and enthalpies of retention on CBSPs **1**–**3**.

broad range of host–guest complexes are within experimental error of the corresponding complexation enthalpies measured in solution. The effect of loading of the CBSPs on the ΔH° values was negligible, suggesting that the change in enthalpy with loading seen by Pirkle[12] originates in the nature of the attachment to the silica surface. CBSPs **1**–**3** were prepared from monofunctional silanes that generate "brush phases", whereas the Pirkle CBSPs were derived from trifunctional silanes that produce polymeric phases.[12]

Our results suggest that enthalpies of complexation of host–guest systems that use hydrogen bonding, alone or with π-stacking, can be determined from normal-phase HPLC. Even very stable host–guest complexes (for example, **18**·**19**) can be evaluated without unreasonably long retention times, because the CBSP can be diluted without affecting the enthalpy of retention. Indeed, a wide range of enthalpies (about 40 kJ mol^{-1}) were determined. The method does have limitations, including the need for more than one column loading for complexes of very different stabilities and the obvious requirement for covalent linkage to silica. In addition, as the kinetics of complexation become slow (for example for very tight binding), band broadening or tailing can become a problem. In spite of these limitations, we believe the method will be of considerable value in assaying stabilities of several host–guest complexes, perhaps even for combinatorial host or guest libraries, or in investigating a single complex in a range of solvents.

Received: May 23, 1995 [Z 8022 IE]
German version: *Angew. Chem.* **1995**, *107*, 2589–2592

Keywords: heterocycles · HPLC · hydrogen bonding · supramolecular chemistry · thermodynamics

[1] Recent examples: a) D. A. Stauffer, R. E. Barrans, Jr., D. A. Dougherty, *J. Org. Chem.* **1990**, *55*, 2762–2767; b) F. N. Diederich, D. B. Smithrud, E. M. Sanford, T. B. Wyman, S. B. Ferguson, D. R. Carcanague, I. Chao, K. N. Houk, *Acta. Chem. Scand.* **1992**, *46*, 205–215; c) J. C. Adrian, Jr., C. S. Wilcox, *J. Am. Chem. Soc.* **1992**, *114*, 1398–1403.

[2] S. C. Zimmerman, K. W. Saionz, *J. Am. Chem. Soc.* **1995**, *117*, 1175–1176.

[3] Other HPLC methods to detect and measure binding interactions: a) T. Cserháti, K. Valkó, *Chromatographic Determination of Molecular Interactions*, CRC Press, Boca Raton, **1994**; b) G. Fassina, I. M. Chaiken, *Adv. Chromatogr.* **1987**, *27*, 247–297; c) *Handbook of Affinity Chromatography* (Ed.: T. Kline), Dekker, New York, **1993**.

[4] B. Feibush, M. Saha, K. Onan, B. Karger, R. Giese, *J. Am. Chem. Soc.* **1987**, *109*, 7531–7533.

[5] a) A. D. Hamilton, D. Van Engen, *J. Am. Chem. Soc.* **1987**, *109*, 5035–5036; b) S. C. Zimmerman, T. J. Murray, *Philos. Trans. R. Soc. London Series A* **1993**, *345*, 49–56.

[6] All new compounds gave correct elemental analyses and had spectral data in accord with their structures. Details of the syntheses will be published in a full paper.

[7] S. C. Zimmerman, W. Wu, Z. Zeng, *J. Am. Chem. Soc.* **1991**, *113*, 196–201.

[8] K. Williams, B. Askew, P. Ballester, C. Buhr, K. S. Jeong, S. Jones, J. Rebek, Jr., *J. Am. Chem. Soc.* **1989**, *111*, 1090–1094.

[9] W. H. Pirkle, R. S. Readnour, *Anal. Chem.* **1990**, *63*, 16–20.

[10] a) The retention factor k' is defined by $k' = (t_r - t_M)/t_M$. Note that t_M is the mobile-phase hold-up time (t_0); b) L. R. Snyder, *J. Chromatogr. Libr.* **1992**, *51A*, Chap. 1.

[11] For the method used see T. Wiseman, S. Williston, J. F. Brandts, L.-N. Lin, *Anal. Chem.* **1989**, *179*, 131–137.

[12] W. H. Pirkle, C. J. Welch, *J. Liq. Chromatogr.* **1991**, *14*, 1–8.

Phosphorothioates: β-Fragmentation versus β-Silicon Effect**

Achim H. Krotz,* Patrick Wheeler, and Vasulinga T. Ravikumar

Modified oligonucleotides are efficient antisense therapeutic agents.[1] Among the DNA modifications reported to date, phosphorothioates are the first class of compounds to undergo clinical trials in humans.[2] To maximize the efficiency of large-scale oligonucleotide synthesis we are currently investigating novel phosphorus-protecting groups.[3, 4] The most widely used approach in automated DNA synthesis employs β-cyanoethyl-3′-phosphoramidites.[5] Selective deprotection occurs through β-elimination.[6] The possibility of cleaving β-silylethyl-protected oligonucleotides selectively with nucleophiles through β-fragmentation[4, 7] (Scheme 1) prompted us to investigate a series of alkyl- and alkyl/aryl-substituted β-silylethyl phosphoramidites with regard to their applicability in oligonucleotide synthesis.

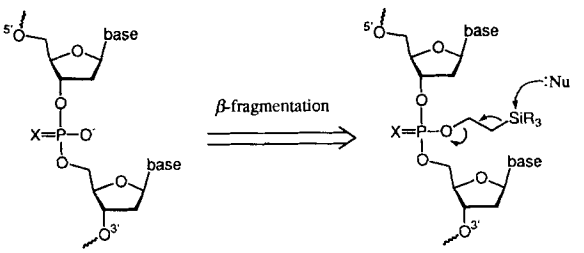

Scheme 1. Selective deprotection of β-silylethyl-protected oligonucleotides through β-fragmentation.

The synthesis of four 5′-*O*-(4,4′-dimethoxytrityl)thymidinyl-3′-[2-(trialkyl/arylsilyl)ethyl-*N*,*N*-diisopropyl] phosphoramidites **3a**–**d** (**a**–**d**: $R_3 = Me_3$, Et_3, Me_2tBu, Ph_2Me, respectively) is depicted in Scheme 2. The requisite β-(silyl)ethanols are either commercially available (**1a**, **1d**) or were synthesized from trialkylvinylsilane precursors (**1b**, **1c**).[8] In the case of **1c**, we first prepared *tert*-butyl(1-methoxyvinyl)dimethylsilane from

[*] Dr. A. H. Krotz, P. Wheeler, Dr. V. T. Ravikumar
Isis Pharmaceuticals
2292 Faraday Avenue, Carlsbad, CA 92008 (USA)
Telefax: Int. code + (619) 929-0528
e-mail: achim_krotz@isisph.com

[**] The authors wish to thank Dr. T. K. Wyrzykiewicz and Dr. D. L. Cole for helpful discussions.

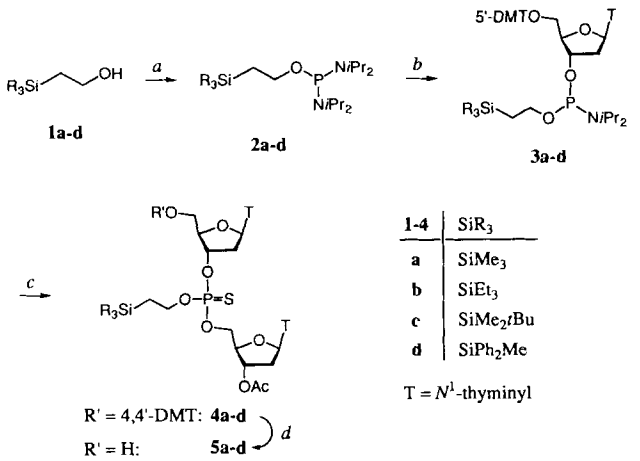

Scheme 2. Synthesis of β-silylethyl-protected phosphorothioates. a: PCl_3 (4 equiv), Et_2O, room temperature (r.t.), 2 h, then $HNiPr_2$ (7 equiv), Et_2O, r.t., 24 h, 85–95%; b: 1*H*-tetrazole, 5′-*O*-DMT-thymidine, CH_3CN, r.t., 2–3 h, 65–85%; c: 1*H*-tetrazole, 3′-*O*-Ac-thymidine, 3*H*-1,2-benzodithiol-3-one-1,1-dioxide, CH_3CN, r.t., 5 h, 77–88%; d: 2% DCA in CH_2Cl_2, r.t., 5 min, 95%. DMT = 4,4′-dimethoxytrityl; DCA = dichloroacetic acid.

*t*BuMe$_2$SiCl and (1-methoxyvinyl)lithium (76%). Subsequent regioselective hydroboration/oxidation with 9-borabicyclo-[3.3.1]nonane (9-BBN, 2 equiv)/H_2O_2 provided **1c** (92%). Following the standard procedure (see Experimental Procedure), PCl_3 (4 equiv) was first treated with **1a–d**, and, after a brief workup, treated with dry $HNiPr_2$ (7 equiv) to furnish bis(*N*,*N*-diisopropylamino)-2-trialkyl/arylsilylethoxyphosphanes **2a–d** in near quantitative yield. In the subsequent phosphitylation step, **2a–d** (2 equiv) in dry CH_3CN was first activated with 1*H*-tetrazole (0.8 equiv) for 20 min, and this mixture was added to 5′-*O*-DMT-thymidine (DMT = 4,4′-dimethoxytrityl). The hydrophobic reaction products were stable to both aqueous workup (0.5 M $NaHCO_3$) and flash chromatography on silica. Phosphoramidites **3a–d**, as mixtures of R_p/S_p diastereomers (ratio about 1:1), were obtained in good yield (65–85%; colorless glasslike solids). To evaluate the compatibility of the protecting groups with the conditions commonly employed in DNA automated synthesis (coupling, oxidation, 5′-deprotection, P-deprotection), we prepared homo-thymidinephosphorothioate dimers as model substrates. Coupling of **3a–d** (2 equiv) with 3′-*O*-acetylthymidine in the presence of 1*H*-tetrazole (4 equiv) in dry CH_3CN, followed by oxidation of the resulting trialkylphosphite with 3*H*-1,2-benzodithiol-3-one-1,1-dioxide[9] (5 equiv) afforded the protected phosphorothioates **4a–d** in high yield (77–88%) after column chromatography (^{31}P NMR δ = 67–68, two signals, R_p/S_p isomers).

Since one of the key steps in DNA synthesis involves cleavage of the 5′-*O*-DMT protecting group with organic acids, acid stability of the phosphorus protecting group is an important requirement. 5′-Deprotection of **4a–d** with 2% dichloroacetic acid (DCA) in CH_2Cl_2 for 5 min afforded **5a–d** in high yield. Prolonged exposure (several hours) of *O*,*O*,*O*-trialkylphosphorothioates **4a–d** or **5a–d** to the reaction conditions resulted in very efficient and selective O to S migration of the protecting group to furnish *O*,*O*,*S*-trialkylphosphorothioates **6a–d** (Scheme 3). Treatment of **5c** with 2% DCA/CH_2Cl_2 for 22 h afforded **6c** in 88% yield. The TOCSY spectrum of **6c** showed a strong coupling between the multiplet at δ = 3 (CH_2S) and δ = 1 (SiCH_2), confirming that the $R_3SiCH_2CH_2$ group and not any of the nucleosides was now attached to the sulfur atom. Treatment of **6c** under the same reaction conditions showed that the isomerization was irreversible. The O to S migration of alkyl

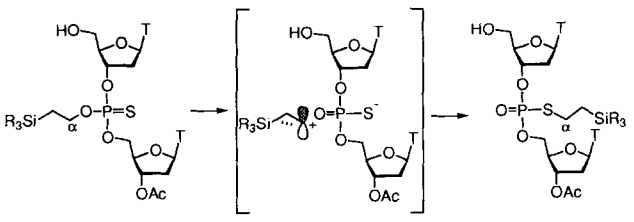

Scheme 3. Rearrangement of *O*,*O*,*O*-trialkylphosphorothioates. Hyperconjugative stabilization of the intermediate β-silyl-substituted cation may be provided through $(\sigma-p)_\pi$ overlap (β-silicon effect). Pseudo-first-order rate constants k_2 [10^{-5} s^{-1}] ($t_{1/2}$ [h]) for the rearrangement **5** → **6** in 2% DCA/CD_2Cl_2 at 20 °C are 3.3 (5.8) (**a**), 21 (0.9) (**b**), 3.5 (5.5) (**c**), and 0.05 (385) (**d**).

groups of *O*,*O*,*O*-trialkylphosphorothioates, commonly referred to as the thiono–thiolo rearrangement, is brought about thermally, by electron impact, by alkyl halides, or by Lewis or Brønsted acids.[10] Mechanistic studies provided good evidence that an (alkyl$^+$)(thiophosphate$^-$) ion pair is formed along the reaction pathway. Internal shift of the cation to the more nucleophilic sulfur of the ambident phosphorothioate anion then leads to formation of the thermodynamically more stable *O*,*O*,*S*-trialkylphosphorothioate.[10c, d] To assess the relative stability of the four β-silylethyl groups under 5′-DMT-deprotection conditions quantitatively, we analyzed the distribution of phosphorus-containing compounds in solutions of **5a–d** (0.01 mmol) in 2% DCA/CD_2Cl_2 (0.24 M, 0.6 mL) by ^{31}P NMR spectroscopy. The time course of the isomerizaton of **5b** is shown in Figure 1. Fast isomerization of **5a–c** (δ = 67) to **6a–c** (δ = 32) is observed (Scheme 3). Under the same conditions, **5d** isomerizes only very slowly ($t_{1/2}$ = 385 h). The unusually high isomerization rates of **5a–c** support an acid-catalyzed isomerization mechanism through an ion-pair intermediate (Scheme 3), as silyl substituents stabilize positive charges in the β position through $(\sigma-p)_\pi$ overlap (β-silicon effect).[11] In the case of **5d**, a decreased electron density of the C–Si σ bond caused by the electron-withdrawing phenyl groups and/or steric hindrance may be responsible for the lower isomerization rate.[12] Solutions of 2-(diphenylmethylsilyl)ethyl-protected phosphorothioates in $CDCl_3$, CD_2Cl_2, [D_6]acetone,

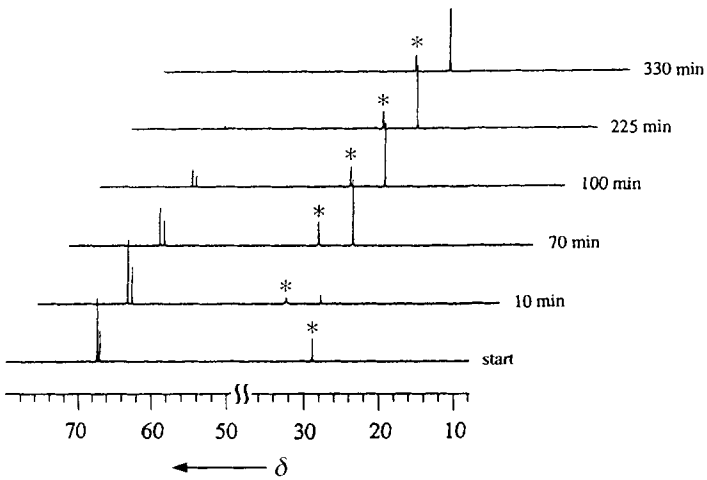

Fig. 1. ^{31}P NMR spectra (161.9 MHz) showing the thiono–thiolo rearrangement of **5b** in 2% DCA/CD_2Cl_2. The intensity of the signals for the two R_p/S_p diastereomers of *O*,*O*,*O*-trialkylphosphorothioate **5b** (δ = 67, 67.5) decreases, whereas that of the signal for the *O*,*O*,*S*-trialkylphosphorothioates **6b** increases (δ = 32) with time. The initial spectrum is taken in CD_2Cl_2. The peaks marked * are from triphenylphosphine oxide (δ = 36.7), which was used as internal standard for quantification.

[D_3]acetonitrile, [D_7]DMF, [D_6]DMSO, [D_4]MeOH, EtOH, and 1,2-dichloroethane did not show any rearrangement product after four weeks at 20 °C. In 80% acetic acid, solvolysis as well as rearrangement was observed.

The final step in oligonucleotide synthesis is the removal of protecting groups from the backbone and the bases. Treatment of **5a–d** with 30% NH_4OH/D_2O/ethanol 63:7:30 (v/v/v) resulted selectively in formation of phosphorothioates **7a–d** (^{31}P NMR $\delta = 56$) and appreciable quantities of phosphodiesters **8a–d** (3–40%, $\delta = 0.1$). This was especially surprising, since **5a–d** did not contain *O,O,O*-trialkylphosphate impurities. Following the time course of the deprotection by ^{31}P NMR shed light in this unexpected result (Fig. 2, bottom). Deprotection of **5a–d** furnishes **7a–d** through β-fragmentation, but in a competing reaction rearrangement of **5a–d** to **6a–d** also takes place (Fig 2, bottom). The disappearance of **5a–d** follows first-order kinetics, and pseudo-first-order rate constants (k_d) were calculated from the decrease in intensities of the ^{31}P signals of **5a–d** (Table 1). The constant k_d comprises the rate constant for hydrolysis of **5a–d** k_1 and the rate constant for rearrangement k_2 [Eq. (a)]. A higher electrophilicity of the phosphorothioate group of **6a–d** accelerates hydrolysis (k_3) at the phosphorus center to afford the corresponding phosphodiesters **8a–d** [Eq. (b)].[13] The maximum concentration (24%) of intermediate **6c** is observed after about 8 h and then decreases to 0%, while the dialkyl phosphate content approaches its final concentration. The ratio of phosphorothioate **7a–d** to dialkyl phosphate **8a–d** plus *O,O,S*-trialkylphosphorothioate **6a–d** reflects directly the relative rates of hydrolysis and rearrangement [Eq. (c)].

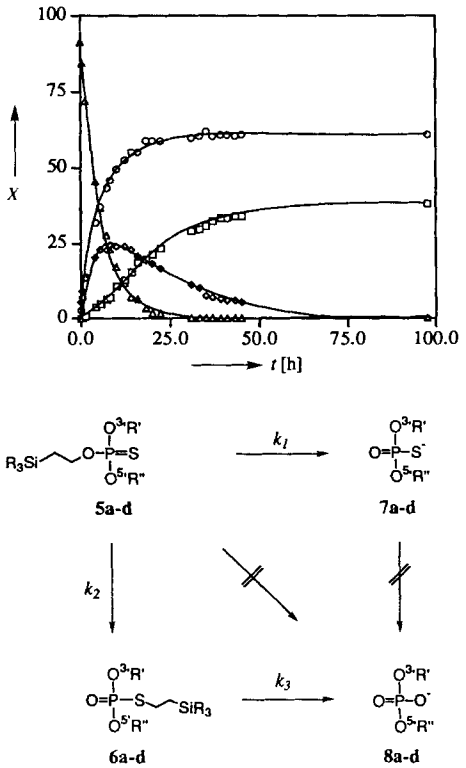

Fig. 2. Deprotection of **5c** in 30% ammonium hydroxide/D_2O/ethanol (63:7:30 *v/v/v*). Top: The relative abundance *X* (monitored by ^{31}P NMR spectroscopy) of *O,O,O*-trialkylphosphorothioate (**5c**, Δ, $\delta = 67.67.3, 67.4$), *O,O,S*-trialkylphosphorothioate (**6c**, $\diamond$, $\delta = 31.7, 31.8$), *O,O*-dialkylphosphorothioate (**7c**, $\circ$, $\delta = 56.07, 56.13$) and dialkylphosphate (**8c**, $\square$, $\delta = 0.1$) as a function of time. Bottom: The competing reactions under the conditions outlined above.

$$k_d = k_1 + k_2 \quad \text{(a)}$$

$$d[\mathbf{6}]/dt = k_2[\mathbf{5}] - k_3[\mathbf{6}] \quad \text{(b)}$$

Table 1. Pseudo-first-order rate constants ($\times 10^{-5}$) [s^{-1}] for the deprotection/rearrangement of **5a–d** in NH_4OH/ethanol at 20 °C.

	5a	5b	5c	5d
k_d	11.7	10.2	5.1 10[a]	0.23 fast[a, b]
k_1	10.2	7.5	3.1 10[a]	0.22 fast[a, b]
k_2	1.5 3.3[c]	2.7 21[c]	2.0 3.5[c]	0.007 0.05[c]

[a] Deprotection with Bu_4NF in THF (2 equiv, 25mM, r.t.). [b] Complete deprotection within minutes. [c] Rearrangement in 2% DCA/CH_2Cl_2.

$$[\mathbf{7a-d}]/[\mathbf{8a-d} + \mathbf{6a-d}] = k_1/k_2 \quad \text{(c)}$$

Equations (a) and (c) allow us to calculate the pseudo-first-order rate constants k_1 and k_2 (Table 1). The constant k_1 decreases with increasing steric demand of the substituents at the silicon [k_1(**5a**) > k_1(**5b**) > k_1(**5c**) > k_1(**5d**)]. Whereas k_2 is in the same order of magnitude for **5a–c**, it decreases dramatically for **5d**. In the case of **5d**, we did not observe intermediate **6d** in the ^{31}P NMR spectrum. The inverse proportionality between NH_4OH concentration and dialkyl phosphate content (Fig. 3) is consistent with the notion that **6d** is indeed formed as an intermediate, but is more rapidly hydrolyzed ($k_3 > k_2$). Lowering the NH_4OH concentration decreases the rate of hydrolysis, but does not affect k_2 to a great extent. Deprotection of **5d** in methylamine/water is about 20 times faster than in NH_4OH, and in 40% methylamine the formation of dialkylphosphates is completely suppressed. Deprotection with even more nucleophilic reagents, like $Bu_4N^+F^-$, is complete within minutes.

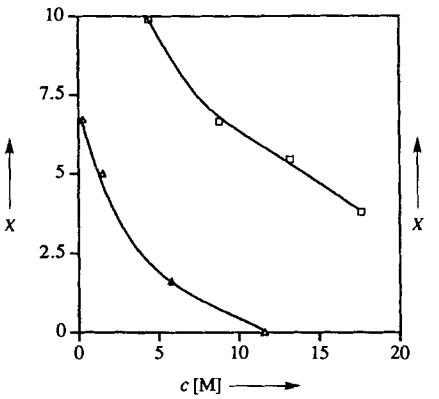

Fig. 3. Deprotection of **5d** in 30% ammonium hydroxide and aqueous methylamine solution at 62 °C. The dialkylphosphate-to-phosphorothioate ratio *X* depends upon the concentration and nucleophilicity of the base. In 40% aqueous methylamine, dialkylphosphate formation is not observed.

In conclusion, we have demonstrated that β-silylethyl protected *O,O,O*-trialkylphosphorothioates can be efficiently synthesized from phosphoramidites **3a–d**. Deprotection with nucleophilic agents (ammonium hydroxide, methylamine, fluoride[4, 7]) affords phosphorothioates **7a–d** through β-fragmentation. The phosphorus-protecting groups of **4/5a–c** are suscepti-

ble to a rapid thiono–thiolo rearrangement supported by the β-silicon effect with formation of *O,O,S*-trialkylphosphorothioates **6a–c**, which, under the deprotection conditions, form dialkylphosphates **8a–c**. The properties of the 2-(diphenylmethyl)silylethyl group in **5d**, however, are compatible with oligophosphorothioate synthesis, that is, the thiono–thiolo rearrangement driven by the β-silicon effect is largely suppressed under acidic as well as under basic conditions, while selective deprotection under mild conditions through a β-fragmentation mechanism is preserved.

Experimental Procedure

2a–d: All operations were performed under exclusion of moisture (Ar atmosphere). To a cold (ice bath) solution of PCl_3 (27.5 g, 200 mmol) in dry Et_2O (100 mL) was added dropwise a solution of the β-silylethanol derivatives **1a–d** (50 mmol) in dry Et_2O (50 mL). The ice bath was removed, and after 2 h the solution was concentrated in vacuo (20 Torr, then 1 Torr). Dry Et_2O (200 mL) was added, followed by dropwise addition of $HNiPr_2$ (50 mL). After stirring for 24 h at room temperature the mixture was filtered, and the solvent removed in vacuo to afford **2a–d** as colorless oils in near quantitative yield. ^{31}P NMR (81 MHz, $CDCl_3$): $\delta = 123.7$ (**2a**), 124.4 (**2b**), 123.9 (**2c**), 123.4 (**2d**).

3a–d: Under exclusion of moisture, 1*H*-tetrazole (12 mmol) was added to a stirred solution of **2a–d** (30 mmol) in dry CH_3CN (600 mL). After 20 min this solution was added to 5′-*O*-(4,4′-dimethoxytrityl)thymidine (15 mmol) within 30 min. After 2–3 h, triethylamine (30 mL) was added, and the solution was stored at −20 °C for 12 h. After filtration the solution was concentrated in vacuo. The oily residue was dissolved in ethyl acetate, and the solution extracted with $NaHCO_3$ (1 M) and H_2O. The organic phase was dried (Na_2SO_4), concentrated, and the remaining oil purified by flash chromatography on silica (eluent: *n*-hexanes/ethyl acetate/NEt_3 90/10/0.1 to 50/50/0.1) to furnish **3a–d**. ^{31}P NMR (81 MHz, $CDCl_3$): d = 145.9, 146.1 (**3a**), 145.8, 146.0 (**3b**), 145.9, 146.1 (**3c**), 146.0, 146.3 (**3d**).

4a–d: Under exclusion of moisture 1*H*-tetrazole (6 mmol) was added to a stirred solution of **3a–d** (2 mmol) and 3′-*O*-acetylthymidine (1 mmol) in dry CH_3CN (10 mL). After 2 h a solution of 3*H*-1,2-benzodithiol-3-one-1,1-dioxide (5 mmol) in dry CH_3CN (5 mL) was added. After 30 min triethylamine (1 mL) was added, and the mixture filtered. The filtrate was concentrated in vacuo. The residue was dissolved in ethyl acetate, and the solution extracted with aqueous $NaHCO_3$ (0.5 M) and H_2O. The organic phase was dried (Na_2SO_4), concentrated, and the residue purified by flash chromatography on silica (eluent: *n*-hexanes/ethyl acetate/NEt_3 50/50/0.1 to 20/80/0.1) to furnish **4a–d**. ^{31}P NMR (81 MHz, $CDCl_3$): $\delta = 67.5$, 67.6 (**4a**), 67.6, 67.7 (**4b**), 67.2, 67.5 (**4c**), 67.4, 67.5 (**4d**).

Received: May 3, 1995 [Z 7953 IE]
German version: *Angew. Chem.* **1995**, *107*, 2584–2587

Keywords: antisense systems · neighboring-group effects · nucleotides · phosphorus compounds · rearrangements

[1] S. T. Crooke in *Burger's Medicinal Chemistry and Drug Discovery, Vol. 1* (Ed.: M. E. Wolff), Wiley, **1995**, pp. 863–900 and references therein.
[2] S. T. Crooke, *Annual Meeting of the Federation of the American Society of Experimental Biology (FASEB)*, April **1994**, Anaheim, CA, USA.
[3] A homo-thymidine dialkylphosphate dodecamer (T_{12}) was synthesized on CPG using 2-(diphenylmethylsilyl)ethylphosphoramidite (**3d**) with an average coupling efficiency of 98.5%. a) V. T. Ravikumar, H. Sasmor, D. L. Cole, *Bioorg. Med. Chem. Lett.* **1993**, *3*, 2637–2640. b) V. T. Ravikumar, T. K. Wyrzykiewicz, D. L. Cole, *Tetrahedron* **1994**, *50*, 9255–9266.
[4] A homo-thymidine phosphorothioate heptamer (T_7) was synthesized on CPG using **3d** with an average coupling efficiency of 99%: V. T. Ravikumar, D. L. Cole, *Gene* **1994**, *149*, 157–161.
[5] S. L. Beaucage, M. H. Caruthers, *Tetrahedron Lett.* **1981**, *22*, 1859–1862.
[6] N. D. Sinha, J. Biernat, H. Köster, *Tetrahedron Lett.* **1983**, *24*, 5843–5846.
[7] S. Honda, T. Hata, *Tetrahedron Lett.* **1981**, *22*, 2093–2096.
[8] J. A. Soderquist, I. Rivera, A. Negron, *J. Org. Chem.* **1989**, *54*, 4051–4055.
[9] R. P. Iyer, L. R. Phillips, W. Egan, J. B. Regan, S. L. Beaucage, *J. Org. Chem.* **1990**, *55*, 4693–4699.
[10] a) H. Teichmann, G. Hilgetag, *Angew. Chem.* **1967**, *79*, 1077–1088; *Angew. Chem. Int. Ed. Engl.* **1967**, *6*, 1013–1023; b) R. G. Cooks, A. F. Gerrard, *J. Chem. Soc. B* **1968**, 1327–1333; c) K. Bruzik, W. J. Stec, *J. Org. Chem.* **1981**, *46*, 1625–1630; (d) C. D. Poulter, D. S. Mautz, *J. Am. Chem. Soc.* **1991**, *113*, 4895–4903.
[11] J. B. Lambert, *Tetrahedron* **1990**, *46*, 2677–2689 and references therein.
[12] N. Shimizu, S. Watanabe, F. Hayakawa, S. Yasuhara, Y. Tsuno, T. Inazu, *Bull. Chem. Soc. Jpn.* **1994**, *67*, 500–504.
[13] In a control experiment we deprotected **6c** under the same conditions. Compound **8c** was the exclusive product (^{31}P NMR $\delta = 0.02$), $k_3 = 1.4 \times 10^{-5}\ s^{-1}$ ($t_{1/2} = 13.4$ h).

Direct Electrochemical Coupling of Components of the Biological Electron Transfer Chain to Modified Surfaces: Molecular Recognition between Cytochrome c Peroxidase and Cytochrome c**

Li Jiang, Calum J. McNeil, and Jonathan M. Cooper*

The modification of surfaces with proteins is established as a method for preparing analytical devices capable of biomolecular recognition. For example, research on ligand binding at interfaces has focused on the immobilization of both antibody–antigen and avidin–biotin couples,[1, 2] resulting in commercial biosensing methods[3] as well as in techniques for controlling molecular architectures.[2] Likewise, the immobilization of enzymes at electrodes has enabled the study of heterogeneous biocatalysis, and has produced an attractive sensing technology through the *indirect* measurement of either a cofactor associated with the biochemical activity,[4] or of an immobilized inorganic redox mediator in electrochemical communication with a protein.[5]

Over the last decade, there has been a large body of literature exploring direct electron transfer (ET) between immobilized proteins and conducting surfaces. To date, however, research has been limited to small model proteins,[6, 7] and it is now known that suitable modification of an electrode provides an appropriate environment for studying facile, quasi-reversible bioelectrochemistry. A particular example involves using a film of self-assembled ω-mercaptocarboxylic acid on gold to measure ET kinetics of cytochrome c (cyt c) across a "zero-length" carbodiimide coupling.[7] These architectures have proved exciting for those involved in biosensor research, as they offer the possibility of electrochemically "wiring" larger proteins to electrodes without ET mediators.

We now present a development of these ideas to produce more complex assemblies at which biomolecular recognition between redox proteins can be studied. We show the immobilization of components of the biological ET chain and demonstrate the direct electron transfer between the modified gold electrode and the immobilized heme proteins. We also measure the enhanced electrocatalytic response due to heterogeneous biomolecular recognition at the protein-modified surface.

Cytochrome c peroxidase (CcP, [EC 1.11.1.5]) is a heme-containing enzyme (35 kDa) that acts as an alternative terminal electron acceptor (complex IV) in anaerobic yeast (*Saccharomyces cerevisiae*). Its interaction with cyt c (12.6 kDa), another heme protein, has provided a model upon which an understanding of protein–protein ET has been established.[8] CcP reacts rapidly with H_2O_2 to form a doubly oxidized form of the enzyme containing a bound radical (compound II). This intermediate compound reacts further with two molecules of reduced cyt c ($cyt c_{red}$) to regenerate the reduced form of CcP (Fe^{III}). Long range ET between the two heme centers occurs across the cyt c–CcP complex, itself stabilized by ion-pairing between lysine groups in cyt c and a ring of acidic amino acid residues

[*] Dr. J. M. Cooper, Dr. L. Jiang
Department of Electronics and Electrical Engineering
University of Glasgow, Glasgow G12 8LT (UK)
Telefax: Int. code + (141) 330-4907
e-mail: jmcooper@elec.gla.ac.uk
Dr. C. J. McNeil
Department of Clinical Biochemistry
University of Newcastle upon Tyne (UK)

[**] We thank Prof. J. E. Erman, Northern Illinois University, USA, for the original sample of CcP, and EPSRC (Grant GR/J30189) for support.

around the heme edge of CcP.[8] The study of cyt c–CcP is of particular interest to us as it contains pathways along which electrons flow as a direct result of the interaction between the two proteins.

The proteins were immobilized using 3,3′-dithiobissulfosuccinimidyl propionate (DTSSP). DTSSP assembles spontaneously on a bare gold electrode with a surface coverage, estimated by integration of its oxidation peak at 150 mV vs. Ag/AgCl, of 1.5×10^{-10} mol cm^{-2}. In order to study the cyt c–CcP interaction electrochemically, in the first instance, cyt c was immobilized in a single-step reagentless procedure involving the reaction of its (surface) lysines with DTSSP. The biomolecular film assembles at a gold surface, providing electrochemical access to the heme redox center of cyt c, apparent in deoxygenated electrolyte (the experimentally measured half wave potential $E^{\circ}_{1/2} = -153$ mV vs Ag/AgCl, $\Delta E_p = 70$ mV, $v = 10$ mVs^{-1}, Fig. 1). Integration of the reduction current of the immobilized cyt c indicated that the surface concentration was 4.1×10^{-11} mol cm^{-2}. This value is generally in agreement with those obtained by others who have immobilized proteins at self-assembled monolayers.[5]

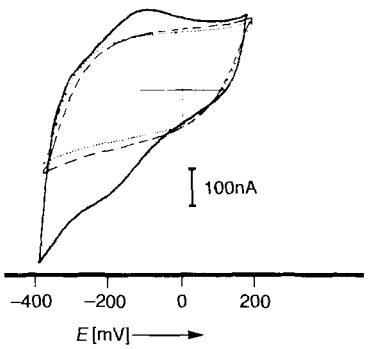

Fig. 1. DC cyclic voltammogram ($v = 10$ mVs^{-1}) depicting the direct electrochemistry of immobilized cyt c (Au\DTSSP\cyt c ——) in a degassed solution (0.1 mol dm^{-3} sodium phosphate buffer, pH 6.3). Also shown are control experiments: the DTSSP monolayer alone (Au\DTSSP ···), and Au\DTSSP\apo-cyt c in the presence of 0.5 μM CcP (– – –).

Cyt c has eighteen surface lysine groups able to bind to DTSSP. The ET route within the biomolecular film can be considered as a statistically averaged pathway, depending upon the probability of binding of particular primary amines on the protein surface. A weighted rate constant $k^{\circ\prime}_{ET}$ for ET between the protein and the electrode was estimated with Laviron's model as 0.18 s^{-1}.[9] The linear dependence of the peak currents on the potential scan rate, measured between 10 and 50 mVs^{-1} (data not shown), indicated that cyt c exists as a surface-bound species, [for example, for i_{pa}, y(/nA) = 9.7 x(/mVs^{-1}) + 0.8 (/nA)]. This fact was further confirmed by the persistence of the protein redox signal after exhaustive washing.

Upon addition of H_2O_2 to the Au–cyt c electrode, the reduction current is enhanced, consistent with previously characterized electrochemical reactions involving the reduction of hydroperoxide (Fig. 2b).[10] Subsequently, additions of CcP (Fig. 2c–f) resulted in substantial increases in the reduction currents due to enzymatic regeneration of immobilized cyt $c_{(ox)}$ and its electrocatalytic reduction at the electrode surface. The reaction scheme is illustrated in Figure 2.

The same Au–cyt c assembly was also used to study protein–protein recognition in the absence of H_2O_2. To this end, ET reactions between soluble $CcP_{(ox)}$ and the modified electrode

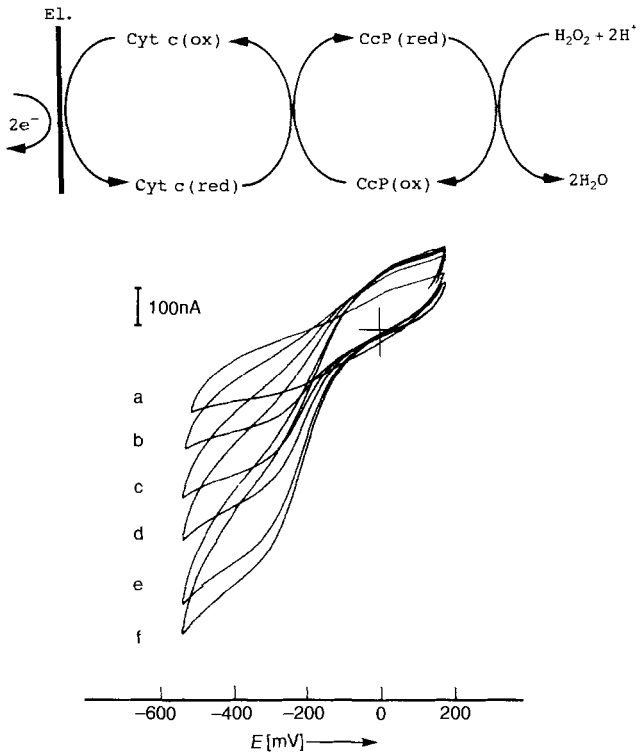

Fig. 2. Top: Scheme of the electrocatalytic reactions for the reduction of immobilized cyt c with enzymatic regeneration of cyt $c_{(ox)}$ by solution phase CcP in the presence of H_2O_2. Bottom: DC cyclic voltammograms of immobilized cyt c (vs. Ag/AgCl electrode): a) in 0.1 mol dm^{-3} sodium phosphate buffer, pH 6.3; b) on addition of 30 μM H_2O_2; and c)–f) in the presence of successive additions of 0.43, 0.86, 1.29, and 1.72 μM CcP, respectively ($v = 5$ mVs^{-1}). The reduction current for immobilized cyt c is enhanced, because the inter-protein ET rate is about 1000 s^{-1}, which is nearly four orders of magnitude faster than that at the electrode surface [16]. El. = electrode.

were measured (Fig. 3). As expected from its biological function, and due to the relatively free accessibility of the immobilized heme redox center, CcP serves to regenerate immobilized cyt $c_{(ox)}$ (via compound I), resulting in an enhanced reduction current at the electrode, as illustrated schematically in Figure 3.

In a series of complimentary experiments, CcP was immobilized using DTSSP, and its direct electrochemistry was characterized in deoxygenated electrolyte (Fig. 4). The weighted $k^{\circ\prime}_{ET}$ was calculated as 0.04 s^{-1}. The lower value for the ET rate constant for CcP (with respect to cyt c) is attributable to the longer probable ET pathway between the heme and the gold surface. Assignment of such a pathlength is, however, difficult as there are 23 lysines on the surface of CcP, available to bind with DTSSP.

Plots of i_{pa} or i_{pc} vs. v were linear [for example, for i_{pa}, y (/nA) = 9.1 x(/mVs^{-1}) + 2.7 (/nA), data not shown], thus confirming that the electrochemical reactions were confined to the surface. The $E^{\circ}_{1/2}$ for immobilized CcP was estimated as −254 mV vs. Ag/AgCl at $v = 10$ mVs^{-1}, relative to the reduction potential of CcP in solution (compound II containing Fe^{III} ions), estimated as 848 mV vs. Ag/AgCl.[11] This large shift in the enzyme's redox character is attributed to the substantial change in the local physical and chemical environment of the immobilized heme redox center. Integration of the reduction peak of CcP demonstrated that the surface coverage of the enzyme was 2.8×10^{-11} mol cm^{-2}, a lower apparent value than that measured for cyt c.

On addition of soluble cyt c to the Au–CcP electrode, the CcP reduction current is enhanced (Fig. 4). The redox conditions

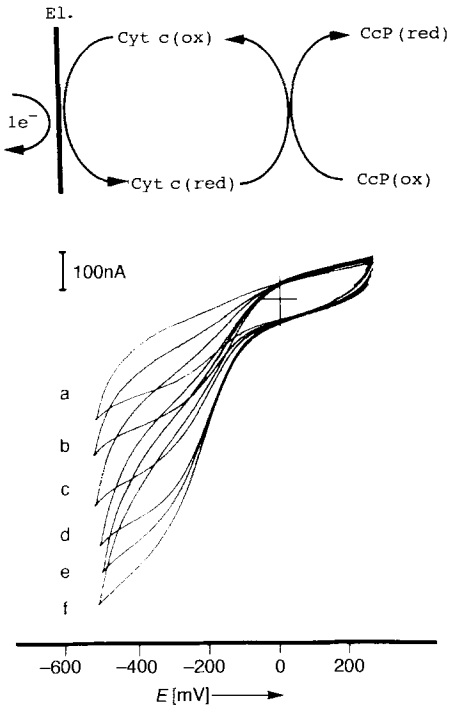

Fig. 3. Top: Scheme of the electrocatalytic reaction showing the one-electron enzymatic oxidation of immobilized cyt c by solution phase CcP, with subsequent electrochemical reduction. Bottom: DC cyclic voltammograms of immobilized cyt c (a), enhanced by the successive addition of 0.30 μM (b), 0.60 μM (c), 0.90 μM (d), 1.8 μM (e), and 2.4 μM (f) CcP, in the absence of H_2O_2 ($v = 5\ mV s^{-1}$, all the other conditions as in Fig. 2).

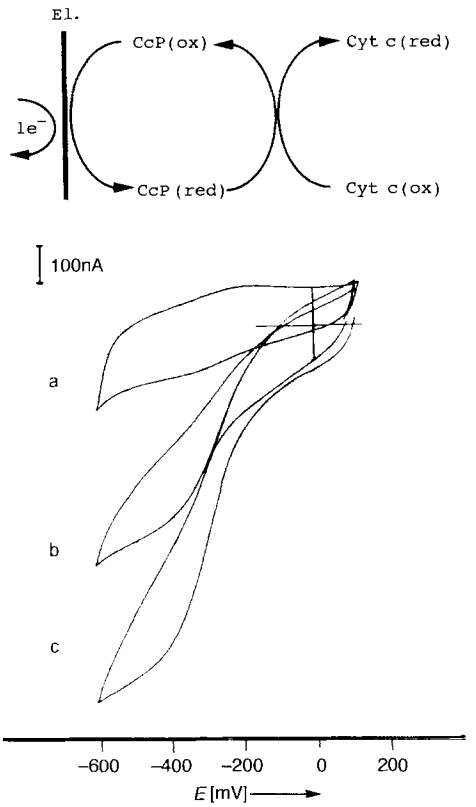

Fig. 4. Top: Scheme showing the one-electron enzymatic oxidation of immobilized CcP by solution phase cyt c, with subsequent electrochemical reduction. Bottom: DC cyclic voltammograms ($v = 5\ mV s^{-1}$) of immobilized CcP in 0.1 mol dm^{-3} sodium phosphate buffer, pH 6.3 (a) and after successive additions of 7.0 μM (b) and 42 μM cyt c (c).

within the electrochemical cell are such that the reaction is reversed from that in nature, where CcP acts as a terminal electron acceptor during the oxidation of $cyt\,c_{(red)}$ ($E_{1/2}$ cyt c = + 40 mV vs. Ag/AgCl).[12] This reverse reaction has been studied, for example by means of laser radiolysis.[8]

Previously, solution-phase components of the ET chain have been shown to communicate with monolayers at an electrode surface.[13–15] The novel electrode arrangement that we describe here for the electrochemical investigation of immobilized components of the ET chain offers potential advantages over such homogenous models. Not only does the system mimic that of nature, where different protein interactions occur at different phase interfaces, but from an experimental viewpoint, problems of solution resistance are negligible. Two aspects of the study are of particular interest: the work provides an example of direct faradaic signal transduction due to protein recognition at a protein modified surface; in addition, the techniques used can to manipulate the redox character of biological molecules through immobilization.

Experimental Procedure

Horse heart cyt c and CcP was immobilized by mixing 10 mg mL^{-1} of the protein within an excess of DTSSP (10 mM solution in 100 mM sodium phosphate buffer, pH 6.3) for 30 min. Alternatively, DSP was used (10 mM solution in dimethylsulfoxide, diluted 1:5 with water). A gold electrode ($A = 0.031\ cm^2$, polished with 0.05 μm alumina, treated with 25% H_2O_2 in H_2SO_4, and sonicated in water for 15 min) was incubated in the enzyme cross-linker solution overnight at 4 °C. All electrochemical measurements were made with a BAS CV-37 potentiostat and were collected either as digital or analog data sets. DC cyclic voltammetric experiments were performed in a sealed two-chamber electrolytic cell, which had a working solution volume of 500 μL.

The direct electrochemical measurements on protein were carried out in 0.1 mol dm^{-3} sodium phosphate buffer, pH 6.3, which was deoxygenated for 15 min with nitrogen prior to measurement. The solution was maintained under a nitrogen blanket during the experiment. Likewise, all stock solutions of reagents, prior to addition to the electrochemical cell, were treated in a similar fashion.

Exclusion of dioxygen from degassed solutions was confirmed independently with an unmodified gold electrode, poised at −300 mV vs. Ag/AgCl. Control experiments in which the heme redox center of the proteins were removed (by incubating the electrode in 4.0 M guanidine·HCl, pH 6.0 overnight followed by washing) were carried out for both electrodes, and are shown for cyt c in Figure 1.

Received: April 28, 1995
Revised version: August 14, 1995 [Z 7939 IE]
German version: *Angew. Chem.* **1995**, *107*, 2610–2613

Keywords: bioelectrochemistry · cytochromec peroxidase · electron transfer · immobilization

[1] H. Ebato, J. N. Herron, W. Müller, Y. O. Kahata, H. Ringsdorf, P. Suci, *Angew. Chem.* **1992**, *104*, 1064–1067; *Angew. Chem. Int. Ed. Engl.* **1992**, *31*, 1087–1090.
[2] D. J. Pritchard, H. Morgan, J. M. Cooper, *Angew. Chem.* **1995**, *107*, 84–86; *Angew. Chem. Int. Ed. Engl.* **1995**, *34*, 91–93.
[3] D. Altshuh, M. C. Dubs, E. Weiss, G. Zederlutz, M. H. V. Vanregenmortel, *Biochemistry* **1992**, *31*, 6298–6304.
[4] L. C. Clark, C. Lyons, *Ann. NY Acad. Sci.* **1962**, *102*, 29–45.
[5] I. Willner, N. Lapidot, A. Riklin, R. Kasher, E. Zahavy, E. Katz, *J. Am. Chem. Soc.* **1994**, *116*, 1428–1441.
[6] J. M. Cooper, K. Greenough, C. J. McNeil, *J. Electroanal. Chem.* **1993**, *347*, 267–275.
[7] M. Collinson, E. F. Bowden, M. J. Tarlov, *Langmuir* **1992**, *8*, 1247–1250.
[8] E. Cheung, K. Taylor, J. A. Kornblatt, A. M. English, G. McLendon, A. Miller, *Proc. Nat. Acad. Sci. USA* **1986**, *83*, 1330–1333.
[9] E. Laviron, *J. Electroanal. Chem.* **1979**, *101*, 19–28.
[10] J. Wilshire, D. T. Sawyer, *Acc. Chem. Res.* **1979**, *12*, 105–110.
[11] W. L. Purcell, J. E. Erman, *J. Am. Chem. Soc.* **1976**, *98*, 7033–7037.
[12] D. C. Rees, *Proc. Nat. Acad. Sci. USA* **1985**, *82*, 3082–3085.
[13] F. A. Armstrong, A. M. Lannon, *J. Am. Chem. Soc.* **1987**, *109*, 7211–7212.
[14] M. Lion-Dagan, E. Katz, I. Willner, *J. Chem. Soc. Chem. Commun.* **1994**, 2741.
[15] S. Bagby, P. D. Barker, L. H. Guo, H. A. O. Hill, *Biochemistry* **1990**, *29*, 3213–3219.
[16] A. F. Corin, R. A. Hake, G. McLendon, J. T. Hazzard, G. Tollin, *Biochemistry* **1993**, *32*, 2756–2762.

Hydrolysis of a Phosphate Diester Doubly Coordinated to a Dinuclear Cobalt(III) Complex: A Novel Mechanism**

Daphne Wahnon, Anne-Marie Lebuis, and Jik Chin*

Metal ions play enormously important roles in both enzymic and nonenzymic[1] hydrolysis of phosphate diesters including DNA and RNA. Some enzymes such as 3′-5′ exonuclease from the Klenow fragment of DNA polymerase I,[2] RNAse H from the HIV reverse transcriptase,[3] Group I intron from *Tetrahymena* ribozyme,[4] P1 nuclease,[5] phospholipase C,[6] purple acid phosphatase,[7] and alkaline phosphatase[8] are activated by two or more metal ions. Functional models of phosphoesterases with two metal atoms in the active site may provide mechanistic insights into the role of the metal ions in the enzymes. We have shown that dinuclear copper(II) complexes, in which both Cu atoms reversibly coordinate the two phosphoryl oxygens of a bridging phosphate diester simultaneously, can be highly reactive for cleaving the ester.[9] Here we report on the hydrolysis of a phosphate diester that is doubly coordinated to a dinuclear cobalt(III) complex. Since this complex does not undergo rapid substitution, it is possible to examine the effect of the dinuclear complex alone on the hydrolysis of the coordinated phosphate diester.

The perchlorate salts of the dinuclear cobalt(III) complex cations **1** and **2**[10] with bridging dimethyl phosphate and

$[Co_2([9]aneN_3)_2(OH)_2\{O_2P(OCH_3)_2\}]^{3+}$ **1**

$[Co_2([9]aneN_3)_2(OH)_2\{O_2P(OCH_3)\}(OC_6H_4NO_2)]^{3+}$ **2**

bridging methyl *p*-nitrophenyl phosphate ligands, respectively, were synthesized by treating $[([9]aneN_3)_2Co_2(OH)_3](NO_3)_3$ ([9]aneN$_3$ = 1,4,7-triazacyclononane) (25 mM) with the sodium salt of the phosphate diester (25 mM) in aqueous $HClO_4$ (1 M).[11] ^{31}P NMR spectroscopy is a useful method for characterizing the bridging phosphate diester in **1** and **2**.[10] Monodentate coordination of dimethyl phosphate to mononuclear Co^{III} complexes results in a downfield shift of the phosphorus signal by about 7 ppm.[12] The phosphorus signals of the bridging phosphates in **1** and **2** are shifted about 14 ppm downfield relative to the signals of the corresponding free phosphates. Over the years many interesting dinuclear metal complexes structurally related to **1** and **2** that contain bridging carboxylate[11] rather than bridging phosphate groups have been reported. Many structures of substitutionally labile dinuclear metal complexes with bridging phosphate diesters have also been reported.[9, 13] Figure 1 shows the crystal structure of trication **1**.[14] This is the first structure of a complex in which a phosphate diester ligand bridges two substitutionally inert metal centers. The distance between the two cobalt(III) centers in **1** (2.9 Å) is somewhat shorter than intermetallic distances in dinuclear phosphodiesterases (ca. 4 Å)[2, 3] but comparable to that recently reported for a purple acid phosphatase (ca. 3.1 Å).[7d] The distances between the phosphorus and the bridging oxygen atoms (P1–O5, P1–O6 3.230(7) Å) are slightly shorter than the P–O van der Waals distance (3.3 Å).

[*] Prof. J. Chin, D. Wahnon, A.-M. Lebuis
Department of Chemistry, McGill University
801 Sherbrooke Street West, Montreal, Quebec H3A 2K6 (Canada)
Telefax: Int. code + (514) 398-3797
e-mail: JikChin@maclan.mcgill.ca

[**] Financial support was provided by the National Science and Engineering Council of Canada, Pioneer Hi-Bred International Inc., and the U. S. Army Research Office.

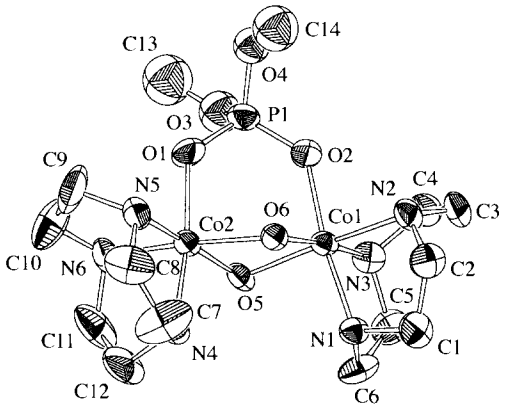

Fig. 1. X-ray structure of cation **1** (ORTEP representation; ellipsoids at the 40% probability level). Selected distances [Å] and angles [°]: Co1-Co2 2.903(2), Co1-O2 1.935(6), P1-O2 1.469(7), P1-O5 3.230(7), P1-O6 3.230(7), Co1-O6 1.927(6); O5-Co1-O6 79.5(3), Co1-O6-Co2 97.1(3), O6-Co1-O2 94.1(3), O6-Co1-N1 91.3(3), Co1-O2-P1 127.1(4), O2-P1-O1 117.4(4).

Hydrolysis of the phosphate diester in **2** was monitored by UV/Vis methods. The half-life for the hydrolysis reaction is about 6 s at pH 8. The pH–rate profile (Fig. 2) for the hydrolysis reaction was approximated with a linear equation having a slope of unity (intercept = −8.89; correlation coefficient = 0.996). The products of the hydrolysis reaction are *p*-nitrophenol and the dinuclear cobalt(III) complex $[Co_2([9]aneN_3)_2(OH)_2\{O_3P(OCH_3)\}]^{3+}$ having the bridging methyl phosphate, as confirmed by the ^{1}H and ^{31}P NMR spectra.[15] Methyl *p*-nitrophenyl phosphate does not dissociate from **2** to any observable extent, according to ^{31}P NMR spectroscopy.

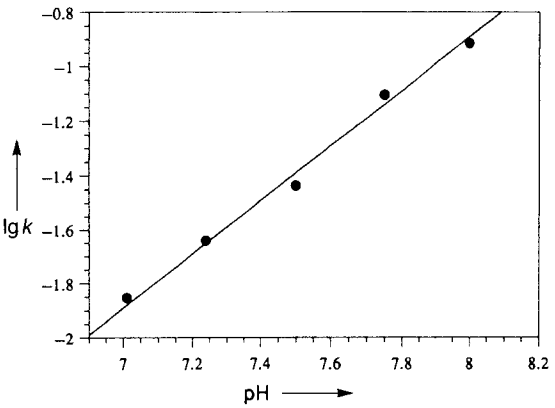

Fig. 2. Plot of the logarithm of the observed rate constants vs. pH for hydrolysis of the phosphate diester unit in **2** at 25 °C.

The second-order rate constant for hydroxide-catalyzed hydrolysis of the phosphate diester in **2** is 1.3×10^5 M^{-1}s^{-1} at 25 °C (Fig. 2), and the pseudo-first-order rate constant at pH 7.0 and 45 °C is 1.1×10^{-1} s^{-1}. The pseudo-first-order rate constant for the analogous hydrolysis of methyl *p*-nitrophenyl phosphate at pH 7.0 and 45 °C is 1.9×10^{-13} s^{-1}.[16] Hence, the phosphate diester in **2** is hydrolyzed about 6×10^{11} times more rapidly than the corresponding free phosphate diester. This is the greatest rate acceleration reported to date for the hydrolysis of phosphate diesters with a cobalt(III) complex. For comparison, ethyl *p*-nitrophenyl phosphate coordinated to a pentaamine–cobalt(III) moiety is hydrolyzed about 10^6 times faster than the free phosphodiester.[17] (*cis*-Diaqua)cobalt(III) com-

plexes (10 mM) provide up to 10^8-fold rate accelerations for the hydrolysis of phosphate diesters with good[18] or poor[19] leaving groups.

Under acidic conditions one of the four-membered rings in $[([9]aneN_3)_2Co_2(OH)_3]^{3+}$ is known to open to give **3**, which isomerizes to give **4**.[11b] Although the value of the equilibrium constant for the isomerization is not known, the *trans* isomer is favored ($K_1 \gg 1$, Scheme 1). Dimethylphosphate dissociates

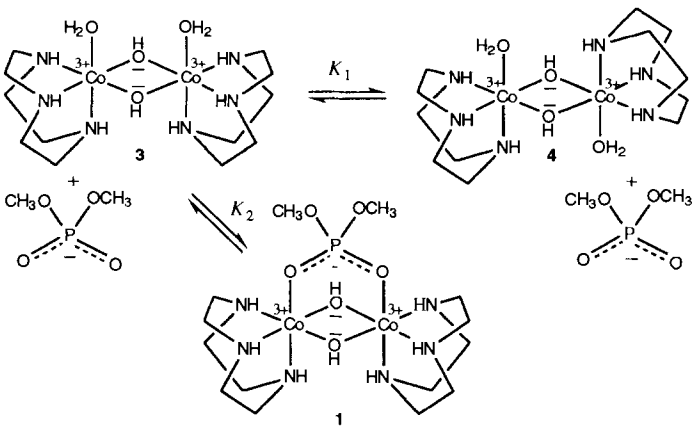

Scheme 1. Equilibrium between and isomerization of **3** and **4**, and coordination of dimethyl phosphate.

from **1** without hydrolysis of the diester group. The equilibrium constant for the binding of dimethyl phosphate to **4** to form **1** (K_2/K_1) as determined by ^1H and ^{31}P NMR spectroscopy[10, 15] is approximately 330 M^{-1}. The equilibrium constant (K_2) for the binding of dimethyl phosphate to **3** must be even greater than 330 M^{-1}, since $K_1 \gg 1$.[11b] In contrast, the equilibrium constant for the monodentate coordination of dimethyl phosphate to a mononuclear cobalt(III) complex is only about 4 M^{-1}.[12, 18, 19] Hence, there is significant cooperativity between the two metal centers in **3** for binding dimethyl phosphate.

In an interesting study, Hendry and Sargeson reported on the reactivity of a dinuclear cobalt(III) complex with two bridging phosphate monoesters.[20] They showed that one of the two bridging phosphate monoesters hydrolyzes rapidly by initial formation of a metal–hydroxide intermediate (Scheme 2). A rate acceleration of approximately 10^8-fold has been observed for hydrolysis of the phosphate monoester.[20]

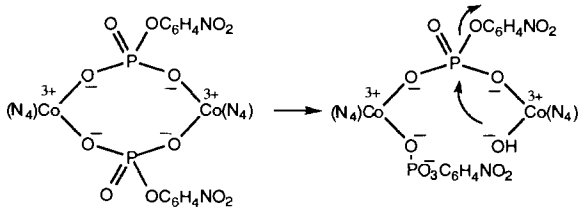

Scheme 2. Initial step in the hydrolysis of a phosphoate monoester [20]. N_4 = 2 tn, tn = 1,3-diaminopropane.

The mechanism for hydrolysis of **2** may also involve initial dissociation of the bridging phosphate diester to form the monodentate phosphate diester followed by intramolecular attack of a metal-bound hydroxo ligand much like shown in Scheme 2. In order to investigate this possibility, ^{18}O-labeling experiments were performed (Scheme 3).

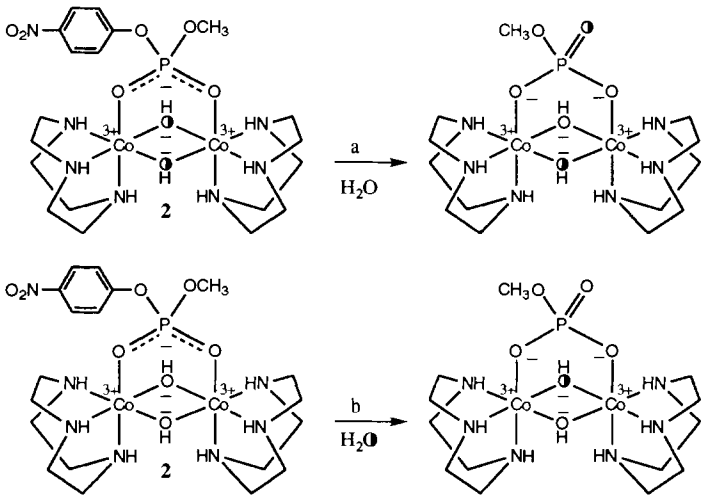

Scheme 3. ^{18}O-labeling experiments. a) Hydrolysis of **2**, in which 50% of the hydroxo ligand is labeled with ^{18}O, in unlabeled H_2O; b) hydrolysis of unlabeled **2** in 50% ^{18}O-labeled H_2O. ◑: 50% ^{18}O label (statistical distribution).

The incorporation of ^{18}O into phosphates can be detected by ^{31}P NMR spectroscopy since it results in an upfield shift of the phosphate signal by about 0.02 ppm.[21] We synthesized **2** in which the two bridging hydroxo ligands were labeled with 50% ^{18}O. Hydrolysis of labeled **2** with unlabeled water gave a product having two ^{31}P NMR peaks[22] (Scheme 3a, Fig. 3a). In contrast, hydrolysis of the unlabeled dinuclear complex **2** with 50% ^{18}O-labeled water gave a product with only one ^{31}P NMR peak (Scheme 3b, Fig. 3b). The mechanism for hydrolysis of **2** does not involve initial dissociation of the bridging phosphate diester to form the monodentate phosphate diester followed by intramolecular attack of a hydroxo ligand (see Scheme 2).[20] Such a mechanism would result in incorporation of ^{18}O in the phosphate from the solvent. A mechanism in which external hydroxide attacks the doubly coordinated phosphate in **2** is also eliminated by the labeling experiment. The ^{18}O-labeling studies together with the pH–rate profile (Fig. 2) clearly indicate that the bridging hydroxo ligand in **2** is first deprotonated to give the bridging oxo ligand, which then attacks the bridging phosphate diester (Scheme 4). The pK_a of the bridging hydroxo ligand in **2** is expected to be about 14.[23]

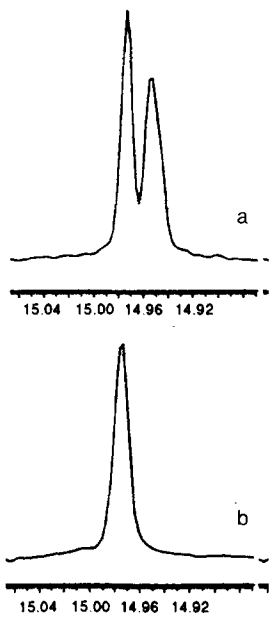

Fig. 3. ^{31}P NMR signal of the product formed from the hydrolysis of **2**·$(ClO_4)_3$. a) See Scheme 3a; b) see Scheme 3b).

In conclusion, substitutionally inert dinuclear cobalt(III) complexes with bridging phosphate diesters (**1** and **2**) have been synthesized for the first

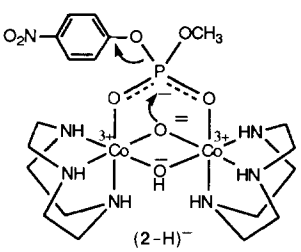

Scheme 4.

time. The distance between the two Co^{III} centers in **1** (2.9 Å) is roughly 1 Å shorter that that in dinuclear phosphodiesterases.[2, 3] The equilibrium constant for coordination of dimethyl phosphate to the dinuclear cobalt(III) complex **3** to form **1** ($K > 330\ M^{-1}$) is at least two orders of magnitude greater than that found for coordination of the diester to mononuclear cobalt(III) complexes ($K \approx 4\ M^{-1}$). Finally, the phosphate diester unit in the dinuclear cobalt(III) complex **2** is hydrolyzed by a novel mechanism involving double Lewis acid activation and the attack of a bridging, nucleophilic oxo ligand, which together lead to an unprecedented 10^{12}-fold rate accleration for the hydrolysis reaction.

Experimental Procedure

The perchlorate salts of **1** and **2** were synthesized by reacting $[([9]aneN_3)_2Co_2(OH)_3](NO_3)_3$ (25 mM) with the sodium salt of the phosphate diester (25 mM) in aqueous $HClO_4$ (1 M) [11]. The perchlorate salt of **1** was recrystallized from water yielding red block-shaped crystals.

Hydrolysis of the phosphate diester ligand in **2** was monitored by UV/Vis methods. In a typical experiment 10 µL of a stock solution of **2** (10 mM in DMSO) was injected into 2 mL of a buffered solution (5 mM *N*-2-hydroxyethylpiperazine-*N'*-2-ethanesulfonic acid (HEPES), pH 7 to 8, 25 °C), and the reaction was monitored by following the increase in the absorbance at 400 nm due to the release of *p*-nitrophenoxide. The rate constants were obtained by fitting the first three half-lives of the reaction according to a first-order kinetics equation.

Received: June 14, 1995 [Z 8092 IE]
German version: *Angew. Chem.* **1995**, *107*, 2594–2597

Keywords: cobalt compounds · enzyme models · hydrolyses · phosphorus compounds

[1] a) K. A. Browne, T. C. Bruice, *J. Am. Chem. Soc.* **1992**, *114*, 4951; b) B. K. Takasaki, J. Chin *ibid.* **1994**, *116*, 1121; c) M. W. Göbel, J. W. Bats, G. Dürner, *Angew. Chem.* **1992**, *104*, 217; *Angew. Chem. Int. Ed. Engl.* **1992**, *31*, 207; d) Y. Matsumoto, M. Komiyama, *J. Chem. Soc. Chem. Commun.* **1990**, 1050; e) J. R. Morrow, L. A. Buttrey, V. M. Shelton, K. A. Berback, *J. Am. Chem. Soc.* **1992**, *114*, 1903; f) R. Breslow, D. L. Huang, *Proc. Natl. Acad. Sci. USA* **1991**, *88*, 4080; g) J. K. Bashkin, E. I. Frolova, U. S. Sampath, *ibid.* **1994**, *116*, 5981; h) D. Magda, R. A. Miller, J. L. Sessler, B. Iverson, *ibid.* **1994**, *116*, 7439; i) H.-J. Schneider, J. Rammo, R. Hettich, *Angew. Chem.* **1993**, *105*, 1773; *Angew. Chem. Int. Ed. Engl.* **1993**, *32*, 1716; j) K. Matsumura, M. Endo, M. Komiyama *J. Chem. Soc. Chem. Commun.* **1994**, 2019; k) S. Amin, J. R. Morrow, C. H. Lake, M. R. Churchill *Angew. Chem.* **1994**, *106*, 824; *Angew. Chem. Int. Ed. Engl.* **1994**, *33*, 773; l) J. Hall, D. Hüsken, U. Pieles, H. E. Moser, R. Häner *Chem. Biol.* **1994**, *1*, 185.

[2] L. S. Beese, T. A. Steitz, *EMBO J.* **1991**, *10*, 25.

[3] J. F. Davies, Z. Hostomska, Z. Hostomsky, S. R. Jordan, D. A. Mathews, *Science*, **1991**, *252*, 88.

[4] J. A. Piccirilli, J. S. Vyle, M. H. Caruthers, T. R. Cech, *Nature (London)* **1993**, *361*, 85.

[5] A. Volbeda, S. Lahm, F. Sakiyama, D. Suck, *EMBO J.* **1991**, *10*, 1607.

[6] E. Hough, L. K. Hansen, B. Birknes, K. Jynge, S. Hansen, A. Hordirk, C. Little, E. J. Dodson, Z. Derenwenda, *Nature (London)* **1989**, *338*, 357.

[7] a) L. Que, Jr., R. C. Scarrow *ACS Symp. Ser.* **1988**, *372*, 152; b) J. T. Sage, Y. M. Xia, P. G. Debrunner, D. T. Keough, J. de Jersey, B. Zerner, *J. Am. Chem. Soc.* **1989**, *111*, 7239 and references therein; c) W. H. Armstrong, S. J. Lippard, *J. Am. Chem. Soc.* **1987**, *109*, 3730; d) T. Klabunde, N. Strater, P. Tucker, H. Witzel, B. Krebs, *Science* **1995**, *268*, 1489.

[8] E. E. Kim, H. W. Wyckoff, *J. Mol. Biol.* **1991**, *218*, 449.

[9] a) M. Wall, R. C. Hynes, J. Chin, *Angew. Chem.* **1993**, *105*, 1696; *Angew. Chem. Int. Ed. Engl.* **1993**, *32*, 1633; b) D. Wahnon, R. C. Hynes, J. Chin, *J. Chem. Soc. Chem. Commun.* **1994**, 1441.

[10] ^{31}P and ^{1}H NMR spectra were recorded in D_2O on a Varian XL-300 and a Gemini 200 spectrometer, respectively. The chemical shifts are reported relative to 10% trimethylphosphate and sodium [D_6]3-trimethylsilyl-1-propanesulfonate (DSS), respectively. ^{31}P NMR: **1**·$(ClO_4)_3$: $\delta = 14.3$; sodium dimethylphosphate: −0.3; **2**·$(ClO_4)_3$: 7.0; sodium methyl *p*-nitrophenylphosphate: −6.8. ^{1}H NMR: **1**·$(ClO_4)_3$: $\delta = 2.7$ (12H, m) 3.25 (12H, m) 3.72 (6H, d, J(P-H) = 10.9 Hz); **2**·$(ClO_4)_3$: 2.7 (12H, m), 3.25 (12H, m), 3.76 (3H, d, J(P-H) = 11.4 Hz), 7.41 (2H, d, $J = 9.1$ Hz), 8.31 (2H, d, $J = 9.1$ Hz). Anal. cald. for $C_{19}H_{39}N_7O_{20}PCo_2Cl_3$ (**2**·$(ClO_4)_3$: C 24.26, H 4.18, N 10.42. Found: C 23.99, H 4.32, N 10.18.

[11] a) A. Werner, *Justus Liebigs Ann. Chem.* **1910**, *375*, 114; b) K. Wieghardt, W. Schmidt, B. Nuber, J. Weiss, *Chem. Ber.* **1979**, *112*, 2220; c) H. Siebert, G. Tremmel, *Z. Anorg. Allg. Chem.* **1972**, *390*, 292.

[12] J. A. Connolly, J. H. Kim, M. Banaszczyk, M. Drouin, J. Chin, *Inorg. Chem.* **1995**, *34*, 1094.

[13] a) K. Schepers, B. Bremer, B. Krebs, G. Henkel, E. Althous, B. Mosel, W. Müller-Warmuth, *Angew. Chem.* **1990**, *102*, 582; *Angew. Chem. Int. Ed. Engl.* **1990**, *29*, 531; b) S. Uhlenbrock, B. Krebs, *ibid.* **1992**, *104*, 1631 and **1992**, *31*, 1647; c) M. Suzuki, H. Kanatomi, I. Murase, *Chem. Lett.* **1983**, 185; d) T. Tomoaki, S. P. Watton, S. J. Lippard, *J. Am. Chem. Soc.* **1994**, *116*, 9401.

[14] Crystal structural data for **1**·$(ClO_4)_3$: monoclinic, $P2_1/c$, $a = 13.084(3)$, $b = 11.222(3)$, $c = 22.784(5)$ Å, $\beta = 103.87(2)°$, $V = 3248(1)$ Å^3, $Z = 4$; 6043 unique reflections, 2647 with $I > 2.5\sigma(I)$, 447 refined parameters, $R = 0.057$, $R_w = 0.068$. Further details of the crystal structure investigation may be obtained from the Fachinformationszentrum Karlsruhe, Gesellschaft für wissenschaftlich-technische Information mbH, D-76344 Eggenstein-Leopoldshafen (Germany), on quoting the depository number CSD-59069.

[15] $[Co_2([9]aneN_3)_2(OH)_2\{O_3P(OCH_3)\}](ClO_4)_3$: ^{31}P NMR: $\delta = 14.97$ (at pH 8.0); ^{1}H NMR: $\delta = 2.65$ (12H, m), 3.20 (12H, m), 3.53 (3H, d, J(P-H) = 10.2 Hz).

[16] Extrapolated to pH 7 from data obtained at pH 11 by A. C. Hengge, W. W. Cleland, *J. Org. Chem.* **1991**, *56*, 1972.

[17] P. Hendry, A. M. Sargeson, *Inorg. Chem.* **1990**, *29*, 92.

[18] a) J. Chin, M. Banaszczyk, V. Jubian, X. Zou, *J. Am. Chem. Soc.* **1989**, *111*, 186; b) J. Chin *Acc. Chem. Res.* **1991**, *24*, 145.

[19] J. H. Kim, J. Chin, *J. Am. Chem. Soc.* **1992**, *114*, 9792.

[20] P. Hendry, A. M. Sargeson, *Prog. Inorg. Chem.* **1990**, *38*, 201.

[21] a) M. Cohn, A. Hu, *Proc. Natl. Acad. Sci. USA* **1978**, *75*, 200; b) G. Lowe, B. S. Sproat, *J. Chem. Soc. Chem. Commun.* **1978**, 565.

[22] The ^{31}P NMR spectra were recorded on a Unity 500 FT spectrometer.

[23] H. C. Käler, G. Geier, G. Schwarzenbach, *Helv. Chim. Acta* **1974**, *57*, 802.

A Framework Containing Ga-O-Ga Links: The Synthesis and Structure of Gallobicchulite $Ca_8(Ga_2SiO_6)_4(OH)_8$

Sandra E. Dann, Philip J. Mead, and Mark T. Weller*

The majority of framework structures formed from linked tetrahedral units are aluminosilicates with an upper limit on the Al to Si ratio of 1:1. Gallium may replace aluminum to various extents in these structures but again the systems are always silicon-rich. We have now prepared the gallium-rich silicate $Ca_8(Ga_2SiO_6)_4(OH)_8$ **1**, a framework material of the sodalite family containing Ga-O-Ga links, and report here its structure as investigated by powder neutron diffraction and MAS-NMR spectroscopy (MAS = magic angle spinning). The hydroxide groups trapped in the sodalite type cages show disordering with a weak hydrogen-bonded interaction with the framework.

The majority of framework structures constructed from linked TO_4 tetrahedra synthesized to date have been aluminosilicates, though more recently a large number of aluminophosphates have been discovered. However, frameworks may be formed from other tetrahedral oxoanions specifically BO_4, GaO_4, GeO_4, ZnO_4, BeO_4, and AsO_4. Examples of compounds containing these units include the sodalites $Na_8(GaSiO_4)_6(OH)_2$[1] and $Li_8(BeAsO_4)_6Cl_2$.[2] Aluminosilicates synthesized hydrothermally invariably obey Löwenstein's

[*] Prof. M. T. Weller, Dr. S. E. Dann, P. J. Mead
Department of Chemistry
University of Southampton
Southampton, SO17 1BJ (UK)
Telefax: Int. code + (1703) 593592

[**] This work was supported by the Engineering and Physical Sciences Research Council under Grant GR/H 94900. We thank Dr A. Hewat (Institut Laue-Langevin Grenoble) for his help in collecting the neutron diffraction data.

rule of aluminum avoidance[3] in that Al-O-Al linkages are prohibited and the Si:Al ratio reaches 1:1 at best. However, some frameworks containing directly linked AlO_4 groups are known. The best characterized materials are the pure aluminate sodalites of the general composition $M_8(AlO_2)_{12}X_2$, where M is a divalent cation for example Ca^{2+}, Sr^{2+}, Cd^{2+}, and X is a divalent anion such as SO_4^{2-}, CrO_4^{2-}, WO_4^{2-}, O^{2-}, S^{2-}, Se^{2-}, and Te^{2-}.[4-6] These materials are prepared under dry, high-temperature conditions by direct reaction of alumina with metal oxides/salts. The only other well-authenticated framework structure containing Al-O-Al linkages is bicchulite, $Ca_8(Al_2SiO_6)_4(OH)_8$.[7, 8] This compound is synthesized under hydrothermal conditions at 540 °C and 2 kbar, rather higher temperatures and pressures than most framework-forming reactions. The successful synthesis of these high aluminium frameworks at elevated temperature indicates that obeyance of Löwenstein's rule is kinetic in origin; that is, formation of Al-O-Al units is possible under the correct synthetic conditions. Attempts to prepare gallium analogues of the pure aluminate sodalites have been unsuccessful: reactions of gallia at high temperatures with metal salts form a variety of complex products. This may be related to the preference of gallium for coordination geometries higher than fourfold in complex oxides, and until now no framework structure containing a GaO_3-O-GaO_3 link was known.

In the course of the investigation of the structure of bicchulite we have successfully synthesized the gallobicchulite $Ca_8(Ga_2SiO_6)_4(OH)_8$ **1**, in which the aluminum of the aluminum sodalite has been totally replaced by gallium in the framework (crystallographic data see Table 1). Compound **1** has

Table 1. Crystallographic data [a] and atomic parameters for $Ca_8(Ga_2SiO_6)_4(OH)_8$ (esd's are given in parentheses).

Atom	x	y	z	$U_i/U_e \times 10^2$	Site/ Occupancy
Ga/Si	0.25	0.5	0	0.95(9)	12/1.0
O	0.13958(16)	0.13958(16)	0.41296(20)	1.89(6)	24/1.0
Ca	0.14147(21)	0.14147(21)	0.14147(21)	1.47(5)	8/1.0
O(H)	0.38344(17)	0.38344(17)	0.38344(17)	1.27(9)	8/1.0
H	0.3106(5)	0.3106(5)	0.3525(7)	1.8(3)	24/0.3333

[a] $a = 8.93213(4)$ Å, $V = 712.632(6)$ Å^3, space group $I\bar{4}3m$

a sodalite type structure but unusually has four anions per β-cage. The calcium and hydroxide ions form two interpenetrating tetrahedral units in the β-cages (Fig. 1 left). The calcium ion is coordinated to three hydroxide oxygens plus three oxide ions of the framework, producing a roughly octahedral environment. Weaker interactions exist to a fourth hydroxide ion and three further framework oxygens. The hydroxide ions are not aligned directly along the threefold axis of the unit cell, which would produce an extremely unusual symmetrical trifurcated hydrogen bond. Displacement from the threefold axis occurs to produce one stronger interaction to just one of the framework oxygens (Fig. 1 right). The O–H···O bond angle of 149.3° is typical of such an environment with a weak hydrogen bond as found in hydrates.[9]

The gallobicchulite framework consists of a long-range disordered arrangement of the gallium and silicon atoms. The average bond length between the tetrahedrally coordinated atoms and oxygen atoms of 1.77 Å (Table 2) is close to that expected from the weighted average of typical Si–O and Ga–O distances in tetrahedral environments (Si–O 1.62 Å, Ga–O 1.85 Å).

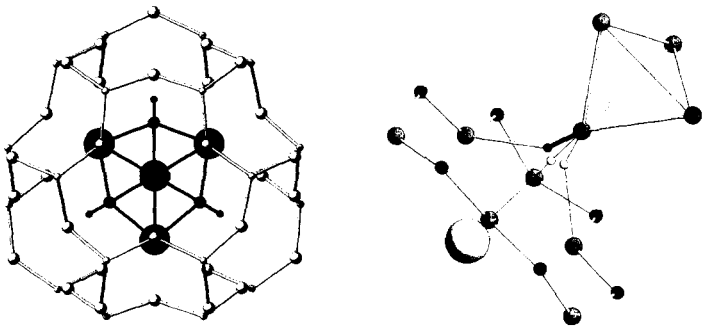

Fig. 1. The structure of $Ca_8(Ga_2SiO_6)_4(OH)_8$ **1**. Left: View along [111] with the cage contents highlighted; the cube formed from the four calcium and four hydroxide ions is shown. Right: The interaction of the hydroxide ion with a six ring of the cage (Ca: large spheres, O: medium-sized grey spheres, Ga/Si: small dark spheres in the six ring, H: small sphere). One of the three possible hydroxide ion orientations is shown in bold.

Table 2. Bond lengths [Å] and selected bond angles [°] in **1** (esd's are given in parentheses).

Bond	Bond length	n [a]	Bond	Bond angle	n [a]
Ga-O/Si-O:	1.770(1)	4	O-Ga(Si)-O:	108.10(7)	4
Ca-O:	2.425(3)	3	O-Ga(Si)-O:	112.25(14)	2
Ca-O(H):	2.326(3)	4	Ga/Si-O-Ga/Si	126.32(11)	
O-H:	0.960(7)	1	O-H···O:	149.3(6)	
HO-O:	2.227(7)				

[a] n shows how often the bond or angle occurs.

However, the ^{29}Si MAS-NMR data essentially consists of a single resonance ($\delta = -77.1$), which indicates that the distribution of the silicon and gallium atoms is not wholly random and which is consistent with the silicon atoms solely in $Si(OGa)_4$ environments. If the distribution of the silicon and gallium atoms were random, a number of Si environments $Si(\text{-}OSi)_n(\text{-}OGa)_{4-n}$ would occur, producing the characteristic multiline spectrum ($n = 0-4$; relative intensities 16:32:24:8:1, representing the probability of each $Si(\text{-}OSi)_n(\text{-}OGa)_{4-n}$ environment derived from binomial theorem with a Si:Ga ratio of 1:2). This indicates that in the gallium-rich framework of **1** that Si-O-Si and Ga-O-Ga links are avoided as far as possible. The latter can be derived from the fact that distributing the silicon such that each has an immediate environment of $Si(OGa)_4$ also minimizes the number of Ga-O-Ga links; distribution of the silicon in a gallium-rich framework such as that any Si-O-Si links are formed necessarily means that more Ga-O-Ga units remain elsewhere. The weak resonance at $\delta = -82$ in the ^{29}Si MAS-NMR spectrum indicates that this minimization is not perfect; a low level of $Si(OGa)_3(OSi)$ environments still remains in **1**. The ^{1}H chemical shift of $\delta = 6.89$ is typical of a free or weakly bound OH group.

The synthesis of gallobicchulite has shown that the formation of framework structures containing high levels of gallium and hence direct tetrahedral Ga-O-Ga links is possible. Within the framework the level of these Ga-O-Ga links is minimized as far as possible in accordance with a Löwenstein type rule.

Experimental Procedure

Gallobicchulite was prepared hydrothermally following the literature method for the synthesis of aluminobicchulite from gehlenite [10]. $CaCO_3$, Ga_2O_3, and SiO_2 in the correct molar ratios were fired at initially at 800 °C for two periods of 24 h and then 1330 °C for 48 h. Powder X-ray diffraction of the product was consistent with formation of $Ca_2Ga_2SiO_7$ which has a gehlenite type structure [10]. $Ca_2Ga_2SiO_7$ (2 g) was placed in a gold capsule with H_2O (0.5 mL) and sealed; the capsule was

heated to 538 °C under 1 kbar hydrothermal pressure for 7 days and then slowly cooled to room temperature. The product was dried at 160 °C and transferred to a dry box. The powder X-ray diffraction pattern of the product was consistent with the formation of cubic gallobicchulite. Whilst deuteration can be achieved under these synthetic conditions, bicchulite samples undergo extremely rapid proton exchange with moisture making preservation of full deuteration extremely difficult. However, with the relatively low overall level of hydrogen in the material, collection and refinement of powder neutron diffraction data from $Ca_8(Ga_2SiO_6)_4(OH)_8$ was possible (Fig. 2). Powder neutron diffraction data were collected on the D2B instrument at the Institut Laue-Langevin (ILL), Grenoble ($\lambda = 1.594$ Å, measurement time: 6 h, step size: 0.05°, angular range: 5–160°). The data were of good quality and only very minor amounts of impurity (reactant gallogehlenite) produced reflections which could not be indexed on the cubic unit cell gallobicchulite. These additional reflections were ignored in the subsequent refinement. Structure refinement was undertaken in the space group $I\bar{4}3m$ by using the structure of aluminobicchulite as the starting model [8]. Scattering lengths were taken as 7.29, 5.81, 4.90, and −3.74 fm for Ga, O, Ca, and H, respectively. No evidence was seen for ordering of the framework species and a mixed occupancy site with a scattering power equivalent to 2/3:1/3 Ga:Si was assigned to the framework. The large scattering power difference between Ga and Si would produce reasonably intense additional reflections if ordering occurred. The refinement was carried out with the GSAS package [11], and initial cycles involved instrumental parameters and positional parameters for all atoms. Refinement of temperature factors produced reasonable values for all atoms with the exception of hydrogen for which a value of 6 Å^2 was obtained. The O–H bond length with the hydrogen on (*x*,*x*,*x*) was also somewhat short at 0.84 Å. This indicated that the hydrogen atom distribution was poorly described by the (*x*,*x*,*x*) position, and disordering of this atom onto an (*x*,*x*,*z*) site (1/3 occupancy) was permitted. Refinement produced a small lowering in R_{wp} (from 0.0369 to 0.0365) and more significantly a marked reduction in temperature factor and a more reasonable O–H distance. Final refined atomic coordinates and derived bond lengths and angles are given in Tables 1 and 2.

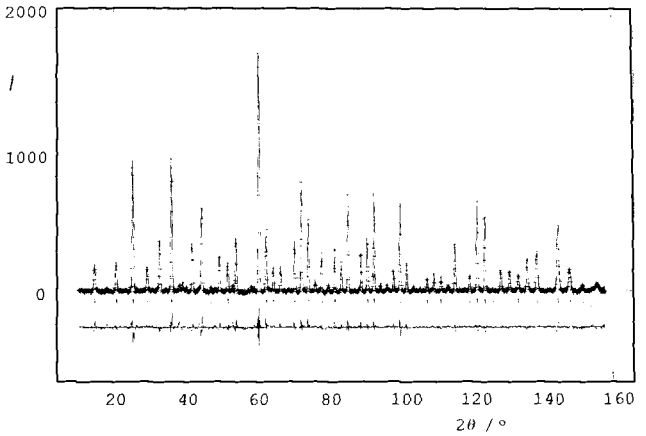

Fig. 2. Final fit to the powder neutron diffraction data. Observed powder diffraction (crosses), calculated (full line), and difference plot (lower line) for $Ca_8(Ga_2SiO_6)_4(OH)_8$ **1** ($\lambda = 1.594$ Å; the tick marks show the positions of the reflections).

The ^{1}H and ^{29}Si MAS-NMR spectra of gallobicchulite were collected with a Bruker AM300 spectrometer. Sample spin speeds were 4.5 KHz for ^{1}H and 4 KHz for ^{29}Si. The proton NMR spectrum consisted of a single resonance at $\delta = 6.89$ relative to TMS. The ^{29}Si NMR spectrum showed a strong resonance at $\delta = -77.1$ relative to TMS with a weak shoulder (5%) at $\delta = -82.0$. The IR spectrum of gallobicchulite was recorded on a Perkin Elmer FT-IR 1710 spectrometer equipped with a PE 3600 data station on a pressed KBr disc. In the OH stretching region a strong sharp band was observed centered at 3662 cm^{-1} consistent with a free or very weakly hydrogen-bonded hydroxide ion.

Received: May 19, 1995 [Z8009IE]
German version: *Angew. Chem.* **1995**, *107*, 2606–2608

Keywords: gallium compounds · solid-state spectroscopy · neutron diffraction · silicon compounds · sodalites

[1] J. W. Newsam, J. D. Jorgensen, *Zeolites* **1987**, *7*, 569.
[2] W. T. A. Harrison, T. E. Gier, G. D. Stucky, *Acta Crystallogr. Sect. C.* **1994**, *50*, 471.
[3] W. Löwenstein, *Am. Miner.* **1954**, *39*, 92.
[4] R. Kondo, *Yogyo Kyokaishi* **1965**, *71*, 1
[5] M. E. Brenchley, M. T. Weller, *Angew. Chem.* **1993**, *105*, 1726; *Angew. Chem. Int. Ed. Engl.* **1993**, *32*, 1663.
[6] G. Engelhardt, H. Koller, P. Sieger, W. Depmeier, A. Samoson, *Solid State Nucl. Magn. Reson.*, **1992**, *1*, 127.
[7] A. K. Gupta, N. D. Chatterjee, *Am. Miner.* **1978**, *63*, 58.
[8] K. Sahl, *Z. Kristallogr.* **1980**, *152*, 13–21.
[9] G. Chiari, G. Ferraris, *Acta Crystallogr. Sect. B.* **1982**, *38*, 2331
[10] T. S. Toporov, *Russ. J. Inorg. Chem.* **1960**, *5*, 1194.
[11] GSAS: Generalised Structure Analysis System. (A. C. Larson, R. B. Von Dreele, **1990**, MS-H805, Los Alamos, NM 87545, USA).

The Nonaaquabismuth(III) Cation**

Walter Frank,* Guido J. Reiss, and Jürgen Schneider

Almost 100 years ago, within the scope of his "Coordinationstheorie der hydratisierten Salze", Alfred Werner for the first time described water in its function as an aqua ligand for metal ions.[1] Today, more than 60 years after the first X-ray crystallographic characterization of an aqua complex,[2] there is conclusive evidence for the existence of $M(H_2O)_n^{m+}$ ions in solution[3] or in the solid state[4] for the sufficiently metallic elements, with only a few exceptions. The last of the main group metals for which knowledge is lacking in this respect, as has been indicated repeatedly,[5] is the element bismuth. From acid solutions containing Bi^{III}, which are supposed to contain aqua ions at Bi concentrations of less than 10^{-5} mol L^{-1} and pH values of less than 2,[6] only basic salts with polynuclear cations[7] or mononuclear cations with coordinated anions[8] could be isolated to date. In studies on the solvation behavior of bismuth(III) trifluoromethanesulfonate, we have now been able to isolate a compound containing a hydrated Bi^{3+} ion, to determine its solid-state structure including the positions of the hydrogen atoms, and hence to close the last gap in the systematics of aqua complexes of main group metals.

From a saturated solution of bismuth(III) trifluoromethanesulfonate (triflate) in aqueous trifluoromethanesulfonic acid (ca. 0.5 M), a colorless material **1** crystallizes at room temperature which has been shown by vibrational spectroscopy to contain no hydroxo groups and has been identified as an enneahydrate of bismuth(III) triflate by elemental analysis. It can already be concluded directly from the fact that **1** is isotypic to compounds of the type $[Ln(H_2O)_9](SO_3CF_3)_3$ (Ln = lanthanide)[9] that all of the water molecules are bound to the metal, that is **1** is a compound containing a homoleptic complex cation with nine monodentate ligands, unique in the chemistry of main group elements.

$[Bi(H_2O)_9](SO_3CF_3)_3$ **1**

Figure 1 shows the structure of the nonaaquabismuth(III) cation of **1** in the crystal at −140 °C.[10] It has crystallographic C_{3h} symmetry; the oxygen atoms, in good approximation, occupy the corner positions of a tricapped trigonal prism so that the symmetry of the coordination polyhedron of the bismuth atom

[*] Prof. Dr. W. Frank, Dipl.-Chem. G. J. Reiss, Dipl.-Chem. J. Schneider
Fachbereich Chemie der Universität
Postfach 3049, D-67653 Kaiserslautern (Germany)
Telefax: Int. code + (631)205-2187

[**] This work has been supported by the Fonds der Chemischen Industrie. We thank Prof. Dr. R. Eujen, Universität-Gesamthochschule Wuppertal, Germany, for recording the Raman spectrum

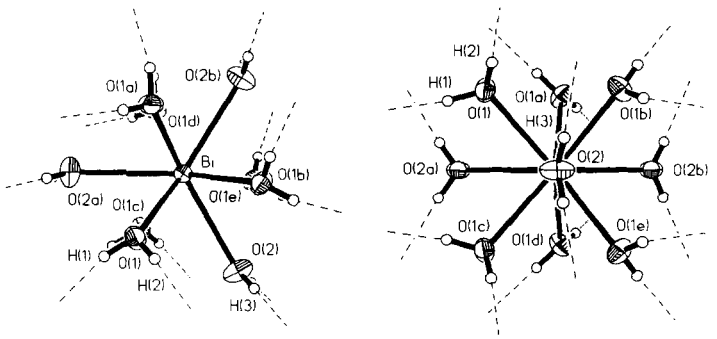

Fig. 1. The nonaaquabismuth(III) cation of **1**, view along [001] (left) and along [−1 −1 0] (right). The atoms were refined with anisotropic thermal parameters (ellipsoids at the 70% probability level); the radii of the H atoms were chosen arbitrarily, only the symmetry independent H atoms are labeled. The directions of the linkage of the cation in the crystal are illustrated. Bond lengths [Å] and angles [°]: Bi–O(1) 2.448(2), Bi–O(2) 2.577(2), O(1)–H(1) 0.85(3), O(1)–H(2) 0.82(2), O(2)–H(3) 0.81(2); O(1)-Bi-O(2) 73.4(1), O(1)-Bi-O(1a) 73.3(1), O(1)-Bi-O(1c) 92.9(1), O(1)-Bi-O(1d) 139.7(1), O(1)-Bi-O(2a) 66.4(1), O(1)-Bi-O(2b) 133.3(1) H(1)-O(1)-H(2) 111(3), H3-O(2)-H(3c) 109(2), Bi-O(1)-H(1) 114(2), Bi-O(1)-H(2) 125(2), Bi-O(2)-H(3) 124(2).

approaches D_{3h}. Thus, the molecular structure represents that which would be expected for a complex with coordination number 9 without recognizable stereochemical activity of the lone pair of electrons. The Bi–O distances lie in the expected range for a ratio of Bi–O(2) to Bi–O(1) of 1.05[11] and a sum of Brown bond orders of 3.12.[12] Each of the cations that are stacked along [001] in the crystal is linked to nine triflate anions through O–H···O hydrogen bonds of medium strength (O(1)···O 2.811(3) and 2.762(2) Å, respectively, O(2)···O 2.755(2) Å). The conformation-determining action of solid-state association on the ligand shell of the complex can be understood directly from the direction of the hydrogen bonds to the oxo functions of the anions (Fig. 1). The orientation of the hydrogen atoms at the O1 center, which is determined by hydrogen bonds, causes (for the entire complex) a significant deviation from the most similar of the conceivable arrangements with D_{3h} symmetry. By comparing the unit cell volume of **1** at room temperature[10] with the corresponding data of the isotypic lanthanide compounds,[9] the effective ionic radius (IR^{IX})[13] of the Bi^{3+} ion in **1** can be estimated to 1.15 Å. Thus, it may be arranged, with regard to its size, between Nd^{3+} (IR^{IX} = 1.163 Å) and Sm^{3+} ions (IR^{IX} = 1.132 Å). The $IR^{IX}(La^{3+})/IR^{IX}(Bi^{3+})$ ratio of radii (1.05) is typical of Bi^{III} compounds with no pronounced lone pair activity.[13]

The surprisingly low tendency of hydrated Bi^{3+} ions to undergo condensation in HSO_3CF_3 solution becomes more evident by the fact that even from the oily, highly supersaturated solutions which are sometimes obtained when the solvent is quickly evaporated, only **1** can be isolated, whereas compounds with hexanuclear "bismuthyl ions" $[Bi_6O_n(OH)_{12-2n}]^{6+}$ crystallize from correspondingly acidic $HClO_4$ or HNO_3 solutions already at very much lower Bi^{III} concentrations.[7] This suggests that the corresponding anions have a considerable influence on complex condensation.

The knowledge of **1**, in principle, offers the chance to study from the outset the basic hydrolysis and the condensation reactions of the Bi^{III} ion in aqueous solution. Investigations in this direction have already been initiated.

Experimental Procedure

1: To a suspension of bismuth(III) oxide (2.6 g, 5.58 mmol) in trifluoromethanesulfonic acid anhydride (5.0 g, 17.72 mmol), trifluoromethanesulfonic acid (5.0 g, 33.32 mmol) was added dropwise at 0 °C. Upon heating at room temperature, the reaction mixture solidified to give a yellowish substance which was dissolved in water (65 mL). Crystallization from this highly acidic solution at room temperature yielded a total of 7.4 g (81.0%, based on Bi_2O_3) of **1** in the form of colorless rods. Elemental analysis (M_r = 818.31): C 4.59 (4.40), H 1.99 (2.22), Bi 26.3 (25.54)%; IR (nujol, BaF_2): $\tilde{\nu}$ [cm^{-1}] = 3365 (sb), 3210 (shb), 1624 (m), 1246 (sb), 1172 (m), 1029 (s); (nujol, ZnSe): $\tilde{\nu}$ [cm^{-1}] = 1033 (s), 769 (m), 638 (s), 574 (w); Raman (powder): $\tilde{\nu}$ [cm^{-1}] = 1232 (w), 1195 (w), 1050 (s), 1030 (w), 775 (s), 580 (m), 522 (w), 358 (s), 320 (m), 237 (w).

Received: June 30, 1995 [Z8146IE]
German version: *Angew. Chem.* **1995**, *107*, 2572–2573

Keywords: aqua complexes · bismuth compounds · hydrogen bonds

[1] A. Werner, *Justus Liebigs Ann.* **1902**, *322*, 261.
[2] R. B. Corey, R. W. G. Wyckoff, *Z. Kristallogr.* **1933**, *84*, 477.
[3] H. Ohtaki, T. Radnai, *Chem. Rev.* **1993**, *93*, 1157.
[4] J. Burgess in *Comprehensive Coordination Chemistry, Vol.2* (Eds. G. Wilkinson, R. D. Gillard, J. A. McCleverty), Pergamon, Oxford, **1987**, p. 305.
[5] See for example a) Holleman-Wiberg, *Lehrbuch der Anorganischen Chemie*, 91.-100 ed., de Gruyter, Berlin, **1985**, p. 694; b) F. A. Cotton, G. Wilkinson, *Advanced Inorganic Chemistry*, 5th ed., Wiley, New York, **1988**, p. 420; c) J. Burgess, *Ions in Solution: Basic Principles of Chemical Interactions*, Horwood, Chichester, **1988**, p. 68.
[6] C. F. Baes, R. E. Messmer, *The Hydrolysis of Cations*, Wiley, New York, **1976**, p. 382.
[7] a) F. Lazarini, *Acta Crystallogr. Sect. B* **1979**, *35*, 448; *Cryst. Struc. Commun.* **1979**, *8*, 69; b) B. Sundvall, *Acta. Chem. Scand. Ser. A* **1979**, *33*, 219.
[8] F. Lazarini, *Acta Crystallogr. Sect. C* **1985**, *41*, 1144.
[9] J. McB. Harrowfield, D. L. Kepert, J. M. Patrick, A. H. White, *Aust. J. Chem.* **1983**, *36*, 483.
[10] $C_3H_{18}BiF_9O_{18}S_3$, M_r = 818.31; crystal dimensions: 0.07 × 0.25 × 0.80 mm^3, hexagonal, space group $P6_3/m$, a = 13.855(2), c = 7.313(2) Å, Z = 2, V = 1215.7(4) $Å^3$ ($V_{18\,C}$ = 1234.5(4) $Å^3$), ρ_{calcd} = 2.235 Mgm^{-3}, T = −140 ± 1 °C, $2\theta_{max}$ = 83.9°, four-circle diffractometer, $Mo_{K\alpha}$ radiation (λ = 0.71073 Å), ω scan, 4211 reflections measured, 1586 independent reflections, 1472 reflections observed with $F > 4\sigma(F_o)$, LP and numerical absorption corrections (μ = 7.648 mm^{-1}, T_{min} = 0.121, T_{max} = 0.602), heavy atom method, $\Sigma w(F_o - F_c)^2$ minimized with $w = \sigma^{-1}$, 73 parameters refined, R = 0.023, wR = 0.014; $\Delta\rho_{max}/\Delta\rho_{min}$ = + 0.9/−1.6 e $Å^{-3}$. Further details of the crystal structure investigation may be obtained from the Fachinformationszentrum Karlsruhe, D-76344 Eggenstein-Leopoldshafen, on quoting the depository number CSD-59065.
[11] M. C. Favas, D. L. Kepert, *Progr. Inorg. Chem.* **1981**, *28*, 309.
[12] I. D. Brown, D. Altermatt, *Acta Crystallogr. Sect. B* **1985**, *41*, 441. The value of r_0(Bi–O) has been established without distinguishing between compounds with or without stereochemical lone pair activity. Therefore, for a compound with no lone pair action, Σs(Bi–O) > 3 is to be expected.
[13] R. D. Shannon, *Acta Crystallogr. Sect. A* **1976**, *32*, 751.

Fascinating Alchemical History—A Labor of Love

Nucleophilic Aromatic Substitution of Hydrogen. By *O. N. Chupakhin, V. N. Charushin* and *H. C. van der Plas*. Academic Press, San Diego, 1994. 367 pp., hardcover $ 95.00.—ISBN 0-12-174640-2

The chemistry of aromatic compounds is presently not in the mainstream of organic chemistry research, although a substantial proportion of the products of the fine chemicals industry contain aromatic moieties, and there are still many challenging and important questions concerning reactions of aromatic compounds. Therefore the monograph *Nucleophilic Aromatic Substitution of Hydrogen* by O. N. Chupakhin, V. N. Charushin, and H. C. van der Plas is a very welcome and needed contribution.

The book is divided into four chapters: 1. Introduction (16 pp.), 2. Nucleophilic Substitution of Hydrogen in Arenes (70 pp.), 3. Nucleophilic Substitution of Hydrogen in Heteroaromatics (152 pp.), and 4. Reactivity of Arenes and Heteroarenes and Mechanisms of the S_N^H Reactions (40 pp.). The length of the third chapter, which forms more than half of the book, reflects the personal interest of the authors who are very active in the chemistry of azines. In the first chapter the authors formulate the theme of the book, present basic concepts of the reactions between nucleophilic agents and electrophilic arenes, and briefly discuss possible ways in which the σ^H adducts of nucleophilic agents to electrophilic arenes can be converted into products. In the second chapter these possibilities are discussed in detail for the reactions of nucleophiles with carbocyclic nitroarenes and complexes of arenes with transition metals. The third and longest chapter describes analogous reactions with electrophilic heteroarenes. This is mostly devoted to the various possibilities of nucleophilic amination, mainly the Chichibabin reaction—particularly its oxidative variant. The fourth chapter deals with mechanistic aspects of the nucleophilic substitution of hydrogen, formation of the σ^H adducts, and their conversion to the final products.

The book is well written and also contains examples of experimental procedures. It will be of great value to chemists working in research laboratories in academia and industry who need to be acquainted with possibilities of introducing substituents into aromatic rings via this process. The experimental procedures enable the reader to evaluate the practical usefulness of a variety of reactions without the necessity to consult the original literature. An additional advantage of this book, written partly by Russian chemists, is that it contains many references to the Russian literature, often not available in Western libraries and therefore somewhat neglected.

I also have some critical remarks about this book. First of all, in promoting the usefulness of nucleophilic substitution of hydrogen the authors should stress in a more unambiguous way that where there is competition from the S_NAr reaction of halogen this is just a secondary process. Also it seems that sigmatropic rearrangement reactions such as the Hauser–Sommelet rearrangement or the Gassmann reaction, which are included in the book, are close analogs of the Claisen aryl–allyl ethers rearrangement and should not be considered as the nucleophilic substitution of hydrogen. Also nucleophilic aromatic substitutions via arynes can hardly be considered as examples of nucleophilic substitution of hydrogen. The titles of the chapters are somewhat inconsistent because the general term "arenes" also embraces "heteroarenes". In the list of contents the title of Chapter 4 should be "Heteroarenes", not "Hetarenes". The mechanistic discussions in Chapter 4 are sometimes superficial. There are some rather questionable opinions; for example, orientation effects in nucleophilic addition to derivatives of nitrothiophene, nitrofuran, etc. (p. 256) should be explained as due to efficient conjugation, not as an anomeric effect. Also the preceding discussion concerning site selectivity (p. 255) appears doubtful. There is only a subject index, which is not sufficiently comprehensive. These minor flaws do not spoil my general positive impression of the book, which due to its great value should find a place not only in libraries but also in individual collections.

Mieczysław Mąkosza
Institute of Organic Chemistry
Polish Academy of Sciences
Warsaw (Poland)

The Jewish Alchemists. A History and Source Book. By *R. Patai*. Princeton University Press, Princeton, NJ, 1994. XVI, 617 pp., hardcover $ 35.00.—ISBN 0-691-03290-4

When I taught Sunday School at Fresno's Temple Beth Israel during the late 1950s and early 1960s, the consensus was that mysticism had never occupied more than a minor position in Judaism. This denigration of the Zohar and the Kabbalah was probably due to the earlier influence of the Jewish Enlightenment (Haskalah) and its attempt to distance Judaism from "unenlightened" superstition. Similarly, as Professor Raphael Patai, the eminent Hungarian-born octogenarian Jewish anthropologist, folklorist, Biblical scholar, and prolific author, points out, contemporary Jewish scholars have asserted that the participation of Jews in alchemy was likewise insignificant. Although there exists no inventory of alchemical manuscripts written by Jews, nor even a study of references to alchemy found in books written by Jews, and although the number of Jewish alchemists was small in comparison to the number of non-Jewish alchemists in the countries of the Jewish Diaspora, Jewish alchemists exerted an important influence on the origin, development, transmission, and spread of alchemy.

In fact, as Professor Patai's book effectively demonstrates, throughout much of

This section contains book reviews and a list of new books received by the editor. Book reviews are written by invitation from the editor. Suggestions for books to be reviewed and for book reviewers are welcome. Publishers should send brochures or (better) books to Dr. Ralf Baumann, Redaktion Angewandte Chemie, Postfach 101161, D-69451 Weinheim, Federal Republic of Germany. The editor reserves the right of selecting which books will be reviewed. Uninvited books not chosen for review will not be returned.

the history of alchemy, in order to provide a legitimation and respectable family tree for the "Great Art," there was a persistent tendency to attribute a Jewish or even biblical origin to alchemy as a whole, and numerous biblical figures, from Adam through the prophets (with Moses considered its greatest master), were regarded by later alchemists as adepts or recipients of its secrets by divine revelation. Alchemical efficacy was attributed to Hebrew divine, angelic, and demonic names, to Hebrew words, and even to the 22 letters of the Hebrew alphabet; and Hebrew was more important for the alchemist than was Latin for the physician. This overvaluation by gentiles of the Jewish role in the origin and development of alchemy survived the European Enlightenment and continued through the 18th and 19th centuries.

In order to counteract the negative attitude of Jewish scholars toward Jewish contributions to alchemy, Professor Patai has written this meticulously documented book, which is clearly a labor of love. In it he opens up a previously unexplored field in cultural history by tracing Jewish alchemy from Hellenistic times through the 19th century. Despite the book's length, broad scope, and the number of years spent and the number of archives consulted in writing it, the author modestly states: "it should not be considered more than a prolegomenon to the history of the Jewish work in alchemy and the role of Jews in contributing to its theory and practice." Patai cites two reasons for this limitation. First, he admits that he was unable to consult all existing Jewish alchemical writings, especially those still in manuscript and scattered throughout the world's libraries and archives. Many of these are probably in various languages, and the impression obtained from the vast amount of material in this book, viz., that Jews wrote most of their alchemical works in Hebrew characters, is probably incorrect. Second, Patai was able to refer only occasionally to the personal relationships between Jewish and non-Jewish alchemists and the literary influences between Jewish alchemical writings and the more numerous writings produced in the Moslem and Christian worlds.

The book, which is graced by 35 illustrations, consists of 40 chapters (ranging in length from $2\frac{1}{2}$ to 30 pages), arranged in 10 sections (ranging from 31 to 88 pages), each prefaced by a summarizing introduction. The material is arranged chronologically, which is sometimes problematic because authorship of manuscripts is often pseudepigraphic, e.g., Pseudo-Maimonides. Patai begins his first section (Prelude) with a careful explication of the multifaceted aspects of alchemy, both exoteric and esoteric, proceeds to show that the major biblical figures were considered as alchemists for centuries, and presents the very few occurrences of alchemical topics in the Bible and Talmud. In his second section (The Hellenistic Age) he devotes two chapters to Maria the Jewess (sometimes identified with Miriam, the sister of Moses), one of the earliest nonfictional alchemists of the Western world, who constructed and described various ovens and alchemical apparatus (her name is preserved in the Latin, French, and German terms for the water bath—balneum Mariae, bain Marie, and Marienbad, respectively). Zosimus the Panopolitan, the first Greek alchemical author whose writings have survived and who was the greatest authority among the Hellenistic alchemists, considered Maria the greatest authority among all the alchemists who preceded him. After a section on the early Arab world, and one on the 11th to 13th centuries (the golden age of Arab culture in general and Arab alchemy in particular), the remaining six sections consider individually the 14th to 19th centuries. The 14th century saw a marked increase in the number of alchemists as a shortage of precious metals for coinage produced a greater demand for alchemical gold and silver. Most Jewish alchemists were Sephardim (those who lived in the Mediterranean area), while Ashkenazim (the Jews of Northern Europe) did not participate in the art until the 18th century.

Patai presents exegetic translations of original Hebrew and Arabic documents and includes biographies not only of Jewish alchemists but of non-Jews who learned their secret art from Jewish masters, e.g., Nicholas Flamel from "Abraham the Jew" and Solomon Trismosin from an unnamed "Jew who knew German." Some Jewish alchemists combined alchemy with magic or kabbalistic practices, while others became forerunners of modern chemistry. Patai's book contains many facts and anecdotes of which I was unaware. Although I had written an article on the Comte de Saint-Germain with a student from my alchemy course, I did not know of the count's Jewish origins, for which Patai cogently argues. The book concludes with an 18-page alchemical vocabulary (Hebrew, Arabic, and Italian), the most valuable part of a manuscript from the Tunisian island of Jerba (Djerba) discussed in Chapter 39, followed by 45 pages of detailed notes and references and a 29-page (2 columns per cage) index, which adds to the utility of the volume.

According to Patai, Jewish alchemy possessed a number of specific characteristics. Because almost all the adepts were religiously observant, they considered their art closely interwoven with religious practice. They were scrupulously honest, for to be otherwise would be a religious transgression. Their search for the philosophers' stone was more associated with the humanitarian purpose of healing the sick than was the case among non-Jewish alchemists. Based on extant sources, Jewish alchemists were more concerned with practice than with theory and made few contributions to the latter. Their technical directions were precise and detailed. Also, the Kabbalah and its concomitant gematria (calculations based on the numerical values of Hebrew letters) helped transform medieval alchemy into the more mystically and religiously orientated discipline of the Renaissance.

This highly recommended book is a rich storehouse of information on a grossly neglected field of alchemical history. It demonstrates that from its earliest origins alchemy was a Jewish occupational specialization, comparable to the better known Jewish work on medicine. It shows that Jewish alchemists introduced new apparatus, techniques, and procedures, were employed as court alchemists, and achieved a high reputation in the Muslim and Christian worlds in which alchemy was practiced. Let us hope that it fulfills the author's hope that it "will stimulate younger scholars to devote their attention to this subject, and to carry on this fascinating task that time no longer permits me to undertake."

George B. Kauffman
Department of Chemistry
California State University
Fresno, CA (USA)

 © VCH Verlagsgesellschaft mbH, D-69451 Weinheim, 1995 0570-0833/95/3421-2420 $ 10.00+.25/0

Dynamics of Environmental Bioprocesses. Modelling and Simulation. (discette enclosed). By **J. B. Snape, I. J. Dunn, J. Ingham, J. E. Prenosil.** VCH, Weinheim/New York, **1995.** 492 pp., hardcover, DM 258.00/$ 165.00.—ISBN 3-527-28705-1

Foods and Packaging Materials - Chemical Interactions. Edited by **P. Ackermann, M. Jägerstad, T. Ohlsson.** The Royal Society of Chemistry, Cambridge, **1995.** 232 pp., hardcover, £ 45.00.—ISBN 0-85404-720-4

Environmental Chemistry. By **C. Baird.** Freeman, New York, **1995.** 484 pp., hardcover, £ 24.95.—ISBN 0-7167-2404-9

Enzyme Catalysis in Organic Synthesis, Vol. 1 and 2. A Comprehensive Handbook. Edited by **K. Drauz, H. Waldmann.** VCH, Weinheim, **1995.** 1050 pp., hardcover, DM 498.00/$ 475.00.—ISBN 3-527-28479-6

Electron-Atom Collisions. (Cambridge Monographs on Atomic, Molecular and Chemical Physics, 5). By **I. E. McCarthy, E. Weigold.** Cambridge University Press, Cambridge, **1995.** 328 pp., hardcover, £ 50.00.—ISBN 0-521-41359-1

An Introduction to Medicinal Chemistry. By **G. L. Patrick.** Oxford University Press, Oxford, **1995.** 336 pp., paperback, £ 17.50.—ISBN 0-19-855871-6

Waste Treatment and Disposal. Issues in Environmental Science and Technology, 3. Edited by **R. E. Hester, R. M. Harrison.** The Royal Society of Chemistry, Cambridge, **1995.** 158 pp., paperback, £ 15.00.—ISBN 0-85404-210-5

Fluorine-containing Amino Acids. Synthesis and Properties. Edited by **V. P. Kukhar', V. A. Soloshonok.** Wiley, Chichester, **1995.** 411 pp., hardcover, £ 90.00.—ISBN 0-471-95203-6

Guidelines for Achieving Quality in Trace Analysis. Edited by **M. Sargent, G. MacKay.** The Royal Society of Chemistry, Cambridge, **1995.** 48 pp., paperback, £ 12.50.—ISBN 0-85404-402-7

Organische Chemie II. Spezielle Verbindungsklassen, Naturstoffe, Synthesen, Strukturaufklärung, 2. Aufl. By **E. Breitmaier.** Thieme, Stuttgart, **1995.** 292 pp., hardcover, DM 79.00.—ISBN 3-13-541602-X

Analytische Chemie und Qualitätssicherung. Proceedings des GSF-Symposiums "Qualitätssicherung in der Analytischen Chemie". Edited by **A. Kettrup, E. Flammenkamp.** Ecomed Verlag, Landsberg, **1995.** 196 pp., paperback, DM 68.00.—ISBN 3-609-69200-6

Coordination Chemistry. Structure and Bonding, Vol. 82. Edited by **M. J. Clarke, J. B. Goodenough, C. K. Jorgensen, D. M. P. Mingos, J. B. Neilands, G. A. Palmer, P. J. Sadler, R. Weiss, R. J. P. Williams.** Springer, Berlin, **1995.** 200 pp., hardcover, DM 168.00.—ISBN 3-540-58761-6

Coordination Chemistry: A Century of Progress. Symposium Series 565. Edited by **G. B. Kauffman.** American Chemical Society, Washington, **1994.** 480 pp., hardcover, $ 99.95.—ISBN 0-8412-2950-3

Chemistry of the Amazon: Biodiversity, Natural Products, and Environmental Issues. (ACS Symposium Series No. 588). Edited by **P. R. Seidl, O. R. Gottlieb, M. A. Coelho Kaplan.** American Chemical Society, Washington, **1995.** 328 pp., hardcover, $ 89.95.—ISBN 0-8412-3159-1

Synthetische Fasern. Herstellung, Maschinen und Apparate, Eigenschaften. Handbuch für Anlagenplanung, Maschinenkonstruktion und Betrieb. By **F. Fourné.** Carl Hanser Verlag, München, **1995.** 910 pp., hardcover, DM 480.00.—ISBN 3-446-16058-2

Techniques and Practice of Chromatography. (Chromatographic Science Series, 70). By **R. P. W. Scott.** Marcel Dekker, New York, **1995.** 400 pp., hardcover, $ 85.00.—ISBN 0-8247-9460-5

Supramolecular Chemistry II. Host Design and Molecular Recognition. Edited by **E. Weber.** Springer, Berlin, **1995.** 164 pp., hardcover, DM 178.00.—ISBN 3-540-58800-0

Lebensmittelchemie. By **W. Baltes.** Springer, Berlin, **1995.** 474 pp., paperback, DM 49.80.—ISBN 3-540-58986-4

Analytiker-Taschenbuch, Bd. 13. Edited by **H. Günzler.** Springer, Berlin, **1995.** 273 pp., hardcover, DM 148.00.—ISBN 3-540-58424-2

Forschung mit Röntgenstrahlen. Bilanz eines Jahrhunderts (1895-1995). Edited by **F. H. W. Heuck, E. Macherauch.** Springer, Berlin, **1995.** 682 pp., hardcover, DM 98.00.—ISBN 3-540-57718-1

Radicals on Surfaces. (Topics in Molecular Organization and Engineering, Vol. 13). Edited by **A. Lund, C. J. Rhodes.** Kluwer, Dordrecht (Netherlands), **1995.** 260 pp., hardcover, $ 154.00.—ISBN 0-7923-3108-7

Nuclear Magnetic Resonance of Paramagnetic Macromolecules. NATO Advanced Science Institutes Series: C. Mathematical and Physical Sciences 457. Edited by **G. N. La Mar.** Kluwer, Dordrecht (Netherlands), **1995.** 416 pp., hardcover, $ 185.50.—ISBN 0-7923-3348-9

Mineralogie. Grundlagen und Methoden. By **G. Strübel.** Enke, Stuttgart, **1995.** 336 pp., hardcover, DM 60.00.—ISBN 3-432-88922-4

Molecular Engineering for Advanced Materials. NATO Advanced Science Institutes Series: C. Mathematical and Physical Sciences 456. Edited by **J. Becher, K. Schaumburg.** Kluwer, Dordrecht (Netherlands), **1995.** 400 pp., hardcover, $ 189.00.—ISBN 0-7923-3347-0

Ziegler Catalysts. Recent Scientific Innovations and Technological Improvements. Edited by **G. Fink, R. Mülhaupt, H. H. Brintzinger.** Springer, Berlin, **1995.** 511 pp., hardcover, DM 198.00.—ISBN 3-540-58225-8

Physikalische Chemie und Biophysik. By **G. Adam, P. Läuger, G. Stark.** Springer, Berlin, **1995.** 532 pp., paperback, DM 59.00.—ISBN 3-540-58849-3

Low-Level Environmental Radioactivity: Sources and Evaluation. By **R. Tykva, J. Sabol.** Technomic, Basel, **1995.** 335 pp., paperback, SFr. 110.00.—ISBN 1-56676-189-1

Fundamentals of Grain and Interphase Boundary Diffusion. 3rd Edition. By **I. Kaur, Y. Mishin, W. Gust.** Wiley, Chichester, **1995.** 536 pp., hardcover, £ 85.00.—ISBN 0-471-93819-X

Xenobiotics and Inflammation. Edited by **L. B. Schook, D. L. Laskin.** Academic Press, London, **1994.** 361 pp., hardcover, £ 76.00.—ISBN 0-12-628930-1

The Metabolism of Drugs and Other Xenobiotics. Biochemistry of Redox Reactions. Edited by **B. Testa, J. Caldwell.** Academic, Press, London, **1994.** 471 pp., hardcover, £ 75.00.—ISBN 0-12-685391-6

Allgemeine Chemie: Theorie und Praxis. By **G. Baars, H. R. Christen.** Diesterweg, Frankfurt, **1995.** 326 pp., paperback, DM 49.80.—ISBN 3-425-05413-9

Industry's Future: Changing Patterns of Industrial Research. By **H. L Fusfeld.** American Chemical Society, Washington, **1994.** 370 pp., hardcover/paperback, $ 39.95/$ 24.95.—ISBN 0-8412-2983-X/0-8412-2984-8

Mikroskopie in Forschung und Praxis. Edited by **H. Robenek.** GIT-Verlag, Darmstadt, **1995.** 399 pp., hardcover, DM 68.00.—ISBN 3-928865-18-8

Enzymatic Conversion of Biomass for Fuels Production. (Symposium Series 566). Edited by **M. E. Himmel, J. O. Baker, R. P. Overend.** American Chemical Society, Washington, **1994.** 512 pp., hardcover, $ 109.95.—ISBN 0-8412-2956-2

Structure and Reactivity in Aqueous Solution: Characterization of Chemical and Biological Systems. (Symposium Series 568). Edited by **C. J. Cramer, D. G. Truhlar.** American Chemical Society, Washington, **1994.** 448 pp., hardcover, $ 99.95.—ISBN 0-8412-2980-5

Modeling the Hydrogen Bond. (Symposium Series 569). Edited by **D. A. Smith.** American Chemical Society, Washington, **1994.** 312 pp., hardcover, $ 74.95.—ISBN 0-8412-2981-3

Fluid Catalytic Cracking III: Materials and Processes. (Symposium Series 571). Edited by **M. L. Occelli, P. O'Connor.** American Chemical Society, Washington, **1994.** 400 pp., hardcover, $ 99.95.—ISBN 0-8412-2996-1

Inorganic and Organometallic Polymers II: Advanced Materials and Intermediates. Symposium Series 572. Edited by **P. Wisian-Neilson, H. R. Allcock, K. J. Wynne.** American Chemical Society, Washington, **1994.** 552 pp., hardcover, $ 129.95.—ISBN 0-8412-3036-6

Polymers from Agricultural Coproducts. (Symposium Series 575). Edited by **M. L. Fishman, R. B. Friedman, S. J. Huang.** American Chemical Society, Washington, **1994.** 262 pp., hardcover, $ 69.95.—ISBN 0-8412-3041-2

Carbohydrate Modifications in Antisense Research. (Symposium Series 580). Edited by **Y. S. Sanghvi, P. D. Cook.** American Chemical Society, Washington, **1994.** 240 pp., hardcover, $ 69.95.—ISBN 0-8412-3056-0

Computer-Aided Molecular Design: Applications in Agrochemicals, Materials, and Pharmaceuticals. (Symposium Series No. 589). Edited by C. **H. Reynolds, M. K. Holloway, H. K. Cox.** American Chemical Society, Washington, **1995.** 448 pp., hardcover, $ 109.95.—ISBN 0-8412-3160-5

Introduction to Biocatalysis Using Enzymes and Microorganisms. By **S. M. Roberts, N. J. Turner, A. J. Willetts, M. K. Turner.** Cambridge University Press, Cambridge, **1995.** 195 pp., hardcover, £ 11.95.—ISBN 0-521-43070-4

Interpretation von Massenspektren. By **F. W. McLafferty, F. Turecek.** Spektrum Akademischer Verlag, Heidelberg, **1995.** 380 pp., hardcover, DM 78.00.—ISBN 3-86025-148-1

Organosulfur Chemistry. Synthetic Aspects. Edited by **P. Page.** Academic Press, London, **1995.** 277 pp., hardcover, £ 55.00.—ISBN 0-12-543560-6

Lehrbuch der Pharmazeutischen Chemie. 13., new edition. By **H. Auterhoff, J. Knabe und H.-D. Höltje.** Wissenschaftliche Verlagsgemeinschaft, Stuttgart, **1994.** 894 pp., hardcover, DM 118.00.—ISBN 3-8047-1356-4

Reaktionskinetische Auswertung spektroskopischer Meßdaten. By **J. Polster.** Vieweg, Wiesbaden, **1995.** 320 pp., softcover, DM 68.00.—ISBN 3-528-06577-X

New Gmelin Volumes:
Gmelin Handbook of Inorganic and Organometallic Chemistry. 8th Ed.

Re, Organorhenium Compounds, Part 5. Edited by **A. Slawisch.** Springer, Berlin, **1994.** 542 pp., hardcover, DM 3200.00.—ISBN 3-540-93695-5

Ge, Organogermanium Compounds, Part 4. Compounds with Germanium-Hydrogen Bonds. Edited by **U. Krüerke.** Springer, Berlin, **1994.** 364 pp., hardcover, DM 2200.00.—ISBN 3-540-93696-3

Si, Supplement Vol. B5e. Non-Electronic Applications of Silicon Nitride. SiN_x, SiN_x: H. Edited by **F. Schröder.** Springer, Berlin, **1994.** 386 pp., hardcover, DM 2375.00.—ISBN 3-540-93693-9

Au, Supplement Vol. B2. Compounds with Br, I, the Chalcogens (S,Se,Te,Po), B, and C. Edited by **R. Keim.** Springer, Berlin, **1994.** 367 pp., hardcover, DM 2290.00.—ISBN 3-540-93694-7

Synthetic Aspects of Metal-Catalyzed Oxidations of Amines and Related Reactions

Shun-Ichi Murahashi*

The metabolism of amines is governed by a variety of enzymes such as amine oxidase, flavoenzyme, and cytochrome P-450. A wide variety of compounds are produced such as ammonia and alkaloids in selective and clean oxidation reactions that proceed under mild reaction conditions. Simulation of the functions of these enzymes with simple transition metal complex catalysts may lead to the discovery of biomimetic, catalytic oxidations of amines and related compounds. Indeed, metal complex catalyzed oxidations have been found to proceed with high efficiency. The first section of this review discusses the dehydrogenative oxidations of amines with transition metal catalysts by transition metal catalysts that simulate amine oxidase. The second section highlights the catalytic oxidation of secondary amines to nitrones by simulation of flavoenzymes. The third section describes the simulation of the function of cytochrome P-450 with low-valent ruthenium complexes and peroxides. Biomimetic ruthenium-catalyzed oxidations of tertiary amines, secondary amines, and other substrates such as amides, β-lactams, nitriles, alcohols, alkenes, ketones, and even nonactivated hydrocarbons can be performed selectively under mild conditions. These three general approaches provide highly useful strategies for synthesis of fine chemicals and biologically active compounds such as alkaloids, amino acids, and β-lactams.

Keywords: catalysis · oxidations · synthetic methods

1. Introduction

Oxidation is one of the most fundamental reactions in organic synthesis.[1] Owing to the current need to develop forward-looking technology that is environmentally acceptable with respect to, for example, negligible formation of inorganic salts and efficient, highly selective formation of products, many aspects must be considered in the search for new catalytic oxidation reactions. The most attractive approaches are biomimetic oxidation reactions that are closely related to the metabolism of living things.

The metabolism of amines is promoted by various enzymes such as amine oxidase, hepatic flavoenzyme (**1**), and cytochrome P-450 (**2**). The metabolic routes of oxidation of a wide variety of amine compounds are of importance from both biological and synthetic points of view. Simulation of the functions of the enzymes catalyzing such metabolic routes with metal complex catalysts should provide novel biomimetic methods for catalytic oxidation of amines and related compounds, and hence highly useful strategies for organic synthesis can be explored.[2]

The catalytic systems used in practical organic synthesis and industrial processes are very simple and sometimes require high reaction temperatures of over 100 °C. But these conditions are a long way from those of biomimetic and/or enzymatic reactions, which occur at room temperature within a specific, complex reaction system. We laid our emphasis on exploring *simple*, *convenient*, and *general* catalytic reactions by using principles similar to those of enzymes, although the resulting catalytic reactions are in some cases far from enzymatic reactions.

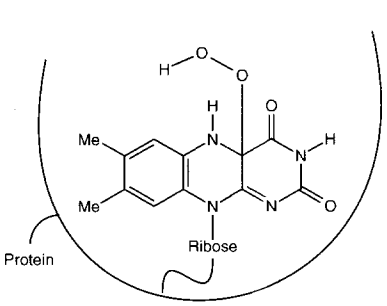

Flavoenzyme
1

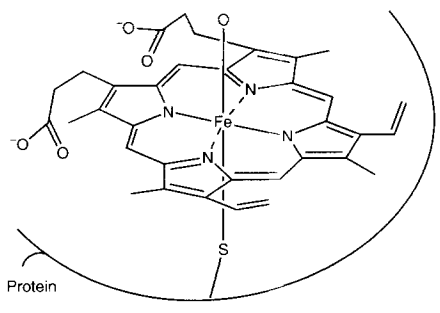

Cytochrome P-450
2

[*] Prof. Dr. S.-I. Murahashi
Department of Chemistry
Faculty of Engineering Science, Osaka University
Machikaneyama, Toyonaka, Osaka 560 (Japan)
Telefax: Int. code + (6)850-6224

2. Amine Oxidase Type Oxidation Catalysts

Mitochondrial monoamine oxidase (MAO) is a flavin-dependent enzyme that catalyzes the oxidative deamination of biogenic monoamines to give the corresponding aldehydes.[3] MAO catalyzes the oxidation of amines by two one-electron transfers from the substrate to the flavin. Simulation of the function of MAO with metal complex catalysts can lead to the discovery of new types of transformations of amines. We have found that activation of amines with low-valent transition metal catalysts generally gives two types of key intermediates. The reaction of an amine that has a N–H bond gives an imine metal complex **3** [Eq. (1a)],[4] while that of an amine without a N–H bond gives an iminium ion complex **4** [Eq. (1b)].[5] Using these intermediates, various catalytic transformations of amines can be explored.

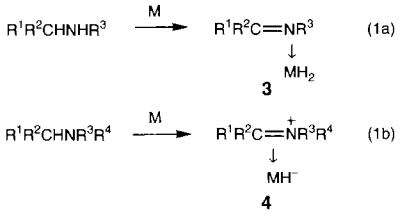

(1a)

(1b)

2.1. Catalytic Oxidation of Primary and Secondary Amines

MAO catalyzes the oxidation of monoamines by two one-electron transfers from the substrate to the flavin. The first one-electron transfer from the amine to flavin (Fl_{ox}) gives the amine radical cation. Loss of a proton and the second transfer of one electron to the flavin yields the iminium ion and the reduced flavin FlH_2 [(Eq. (2a)].[3]

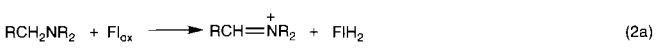

(2a)

The study of the generation of iminium ions by activating amines with metal complexes led to the discovery of catalytic alkyl group exchange reactions of amines [Eq.(2b)].[4] The reaction is simple to carry out and can be applied to the preparation of various nitrogen compounds. Palladium black, prepared by a modification of Willstätter's method, is an excellent catalyst, although the reaction is also catalyzed by other heterogeneous and homogeneous transition metal catalysts. Variation of the exchange reaction can open new processes for the synthesis of tertiary amines, diamines, polyamines, and heterocyclic amines. Typically, the palladium-catalyzed reaction of *N*-methylbenzylamine with *N*-methylbutylamine gives *N*-butyl-*N*-methylbenzylamine (95%). The treatment of azetidine (**5**) with the palladium catalyst in the presence of 1,3-propanediamine (**6**) gives *N*-(3-aminopropyl)-1,3-propanediamine (**7**), which undergoes a further palladium-catalyzed reaction with **5** at 120 °C to give the tetramine **8** (75%). Apparently, 1,*n*-diamines ($n = 2, 3$) are less reactive than azetidine towards palladium, because they are stabilized by bidentate chelation. Further, a new process for the synthesis of heterocyclic compounds can be explored. The palladium-catalyzed reaction of **6** with allylamine at 25 °C gives 2-ethylhexahydropyrimidine (**9**) (95%), which is a highly efficient hydrogen donor for selective hydrogenations.[6]

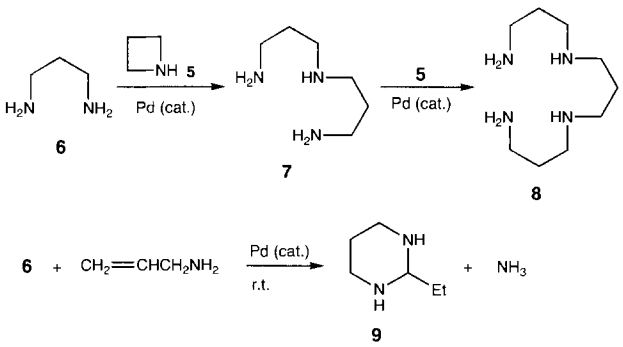

The reaction involves general, fundamental steps. The oxidative addition of a low-valent metal atom to the N–H bond and subsequent β-MH elimination gives the imine hydride complex **10**, which reacts with nucleophiles such as additional amines to give **11** (Scheme 1). Intramolecular reductive cleavage of **11**

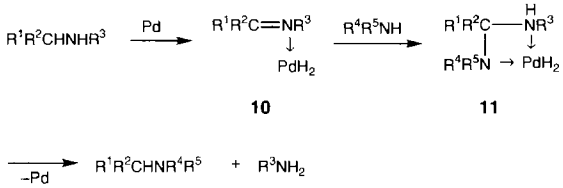

Scheme 1. Catalytic transalkylation of primary and secondary amines.

S.-I. Murahashi was born in Osaka, Japan, in 1937. He received his Ph.D. degree under the supervision of Professor Ichiro Moritani with a thesis on the structure and reactivity of carbenes. In 1963 he was appointed assistant professor at Osaka University. He spent two years (1968–1970) at Columbia University as a postdoctoral fellow under the supervision of Professor Ronald Breslow. Since 1979 he has been a full professor at Osaka University. His research interests include organometallic chemistry directed towards organic synthesis, homogeneous catalysis, biomimetic oxidation, and carbene chemistry.

with the metal hydride provides amines with exchanged substituents. This is the crucial step for the activation of primary and secondary amines with metal catalysts and homogeneous metal complex catalysts.

2.2. Catalytic Oxidation and Hydrolysis of Tertiary Amines

Tertiary amines can be activated in the same way as primary and secondary amines.[5] Thus, the palladium-catalyzed amine exchange reaction of tertiary amines occurs at 200 °C with high efficiency [Eq. (3a)]. In a typical case, a mixture of dibutylhexylamine and a catalytic amount of palladium black was heated in

$$R^1R^2CHNR^3R^4 + R^5R^6R^7N \xrightarrow{Pd} R^1R^2CHNR^5R^6 + R^7NR^3R^4 \qquad (3a)$$

an autoclave at 200 °C for 16 h. After distillation a mixture of tributylamine (26%), dibutylhexylamine (37%), butyldihexylamine (26%), and trihexylamine (3%) was obtained; the alkyl groups are distributed statistically in these tertiary amines. This process may provide a convenient method for the synthesis of unsymmetrical tertiary amines because the desired products can be prepared simply and with high efficiency, and isolation is straightforward. These reactions can be rationalized by assuming that palladium coordinates to nitrogen and inserts into the adjacent C–H bond to give **13**, which is in equilibrium with a key intermediate, the iminium ion complex **14** (Scheme 2).[5]

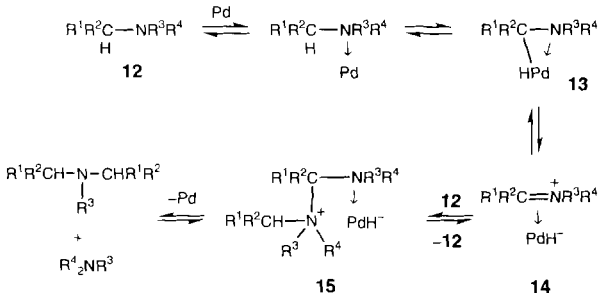

Scheme 2. Catalytic transalkylation of tertiary amines.

Since an iminium ion presents an extremely electrophilic carbon for nucleophilic attack, the second tertiary amine attacks **14** to give **15**, from which the exchange amines are produced. This mechanism is supported by control experiments, loss of optical activity, deuterium distribution, and studies of metal complexes.[5, 7] Consequently, the reaction mechanism of tertiary amines contrasts that of primary and secondary amines, in which a complex of imine **10** is formed by insertion of palladium into the N–C bond.

The rhodium-catalyzed isomerization of allylamines **16** to enamines **18**, which is one of the key steps of the industrial

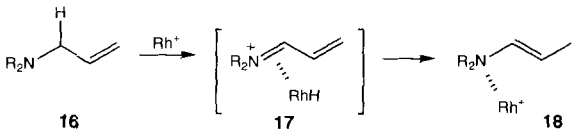

synthesis of menthol, is initiated by C–H activation to form a transient iminium–RhH π-complex **17**.[8]

In attempts to trap the iminium ion metal complexes **14** with an external nucleophile, we examined the effect of water. We hoped to achieve catalytic hydrolysis of tertiary amines, because this procedure is of principal importance with respect to biological deamination processes. Indeed, we discovered a novel palladium-catalyzed hydrolysis of tertiary amines [Eq. (3b)],[9] which is superior in certain cases to the current procedures that require stoichiometric quantities of oxidizing agents.

$$R^1CH_2NR^2R^3 + H_2O \xrightarrow{cat.} R^1CHO + R^2R^3NH + H_2 \qquad (3b)$$

A mechanism that may explain these results is shown in Scheme 3. The metal atom initially coordinates the nitrogen lone pair and then inserts into the adjacent carbon–hydrogen bond to form **20**, which is in equilibrium with the iminium ion

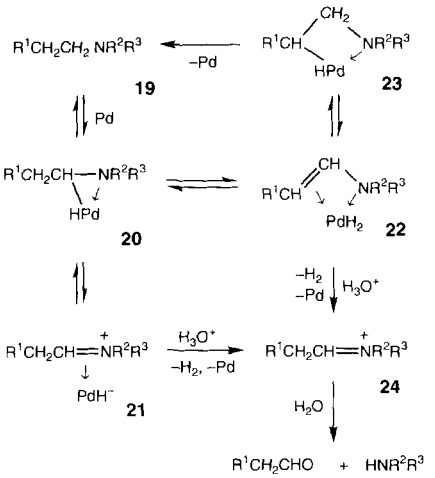

Scheme 3. Catalytic hydrolysis of tertiary amines.

21 and the enamine intermediate **22**. In the absence of protons, the interconversions **20** ⇌ **21** and **20** ⇌ **22** ⇌ **23** proceed rapidly without change of configuration at the β-position of the amine. Under the hydrolysis conditions, protonolysis of complexes **21** and **22** gives the uncomplexed iminium ion **24**, which undergoes the acid-catalyzed hydrolysis steps typical for enamines to produce carbonyl compounds and secondary amines. It is noteworthy that a similar catalytic reaction proceeds in the presence of the homogeneous cluster catalyst $[Rh_6(CO)_{16}]$,[10] although a small distinction is observed between the palladium and $[Rh_6(CO)_{16}]$ catalysts.[9] (η^1-Ylide)palladium complexes[11] and unusual amino–carbene cluster complexes[7] have been isolated as key intermediates in these reactions.

This principle of activating amines by oxidative dehydrogenation can be extended to the activation of alcohols. Insertion of low-valent metal complexes into the oxygen–hydrogen bonds of alcohols followed by β-elimination gives an aldehyde metal hydride species **25** [Eq. (4a)], which reacts with nucleophiles in various catalytic transformations. The $[RuH_2(PPh_3)_4]$-catalyzed oxidative transformation of alcohols proceeds efficiently

and cleanly to give esters and molecular hydrogen [Eq. (4b)].[12] This reaction may thus be important in solving environmental and energy problems. In this reaction, the second molecule of alcohol acts as a nucleophile to trap **25**. If an amine serves as the

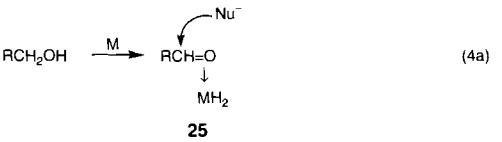

25 (4a)

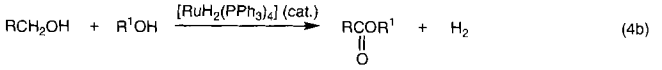

(4b)

nucleophile, palladium(0)- or ruthenium(II)-catalyzed amination reactions can be used, for example for constructing heterocyclic nitrogen compounds like **27a** and **27b**.[13, 14] Importantly, when the $[RuH_2(PPh_3)_4]$-catalyzed reaction of amino alcohols such as **26** is performed under similar reaction conditions, in the presence of a hydrogen acceptor such as benzalacetone, lactams like **27c** are formed instead of piperidines.[15]

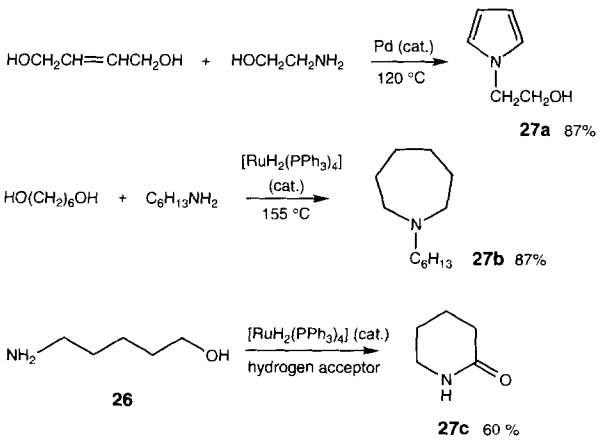

3. Hepatic Flavoenzyme Type Oxidation Catalysts

Mammalian liver contains microsomal FAD-containing monooxygenase (EC 1.14.13.8, FADMO), which oxygenates various amines.[16] The enzymatic oxygenation seems to involve the following catalytic cycle.[17] Oxygenation of enzyme-bound reduced flavin (Enz(FlH_2)) with molecular oxygen gives 4a-hydroperoxyflavin (Enz[4a-Fl(H)OOH]), which monooxygenates the substrates and is converted into 4a-hydroxyflavin (Enz[4a-Fl(H)OH]). Dehydration of Enz[4a-Fl(H)OH] gives oxidized flavin (Enz(Fl_{ox})),[17] which is reduced to Enz(FlH_2). The mechanism of FADMO has been studied extensively by use of 4a-hydroperoxyisoalloxazines (4a-FlOOH) and much has been learned;[18] however, the catalytic recycling step was ambiguous. We found that 4a-hydroxy-5-alkylflavins are readily transformed into 4a-hydroperoxyflavins upon treatment with hydrogen peroxide. This result led to the discovery of a novel biomimetic flavin-catalyzed oxidation with hydrogen peroxide.[19] Typically, the reaction of secondary amines with hydrogen peroxide in the presence of flavin catalysts such as flavinium perchlorate **28** gives nitrones **29** with high efficiency [Eq.(5)].

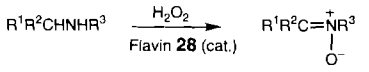

29 (5)

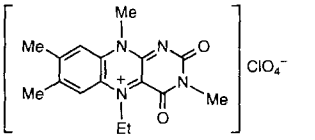

28

This biomimetic catalytic oxidation of secondary amines may correspond to the metabolism of amines. The application of this oxidation leads to new types of catalytic oxidation reactions using organic molecules.

Chiral flavins are attractive catalysts for asymmetric oxidation of sulfides and other substrates.[20] For example, oxidation of naphthyl sulfide **30** catalyzed by capped flavin **32** gives **31** with 72% *ee*.

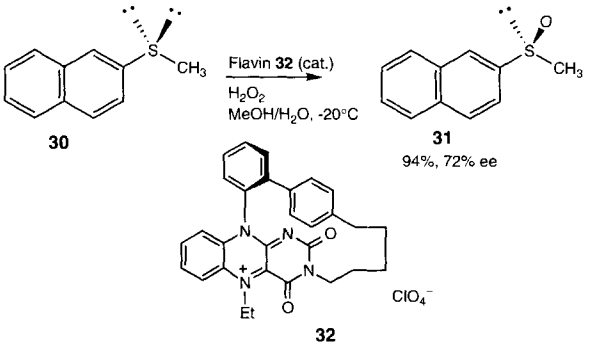

30 **31** 94%, 72% ee

32

3.1. Catalytic Oxidation of Secondary Amines

Previously, little attention was paid to metal hydroperoxides (MOOH). But since their reactivity is expected to be similar to that of hydroperoxyflavins (FlOOH), the reactivity of metal hydroperoxides towards amines has been examined extensively. Metal hydroperoxides are formed either by treatment of metals (M) with hydrogen peroxide[21] or by oxidation of metal hydrides (MH) with molecular oxygen.[22]

In attempts to simulate the function of hydroperoxyflavin (FlOOH) with metal hydroperoxide (MOOH), the reactivity of metal hydroperoxides towards the oxidation of secondary amines was examined. We found that the hydroperoxytungstate, which is generated by the first method (reaction of H_2O_2 with tungstate), is an excellent reagent.[23] This biomimetic single-step synthesis of nitrones from secondary amines is extremely useful, since the products are highly valuable synthetic intermediates[24] and spin-trapping reagents.[25] Nitrones are difficult to prepare by other methods; they have been obtained by HgO-induced stoichiometric oxidation of hydroxylamines, themselves derived by tedious methods, and by condensation of hy-

droxylamines with aldehydes. When solutions of secondary amines in either methanol or water are treated with three molar equivalents of a 30% hydrogen peroxide solution in the presence of 4 mol% sodium tungstate under nitrogen, the corresponding nitrones are produced in good to moderate yields [Eq.(6); Table 1].[23] Usually methanol can be used as a solvent,

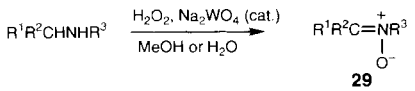

(6)

but water is the only solvent suitable for the preparation of cyclic nitrones. 2-Methylpiperidine was converted into the thermodynamically stable nitrone in 76% yield.

Table 1. Oxidation of secondary amines with H_2O_2 in the presence of $Na_2WO_4 \cdot 2H_2O$ and SeO_2 catalysts in MeOH.

Amine	Nitrone	Yield [%] Na_2WO_4 (cat.)	Yield [%] SeO_2 (cat.)
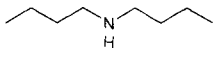	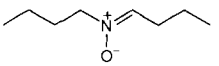	89	80
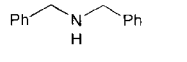	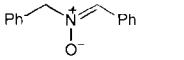	85	
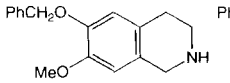	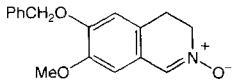	86	91
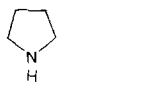	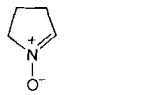	44[a]	73[b]
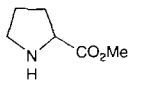	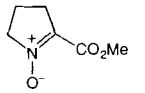	42[a]	57[b]
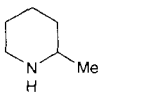	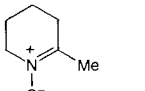	76[a]	79[b]

[a] Solvent: water. [b] Solvent: acetone.

This reaction can be rationalized by the mechanism shown in Scheme 4. The oxidation of secondary amines with tungstate hydroperoxide wOOH (w = WO_3^-, WO_4^-, WO_6^-) gives *N*-hydroxylamines **33**, which undergo further oxidation followed by dehydration to give nitrones **29**.[23]

The tungstate-catalyzed reaction can be used to oxidize various substrates. Typically, the oxidation of tetrahydroquinolines provides a convenient method for the synthesis of cyclic hydroxamic acids.[26] The mechanism is rationalized by assuming the formation of nitrones and subsequent addition of third molecule of H_2O_2 to give 2-hydroperoxy-*N*-hydroxylamines, which undergo dehydration to give hydroxamic acids. For example, treatment of 4-methyl-1,2,3,4-tetrahydroquinoline (**35**) with H_2O_2 gives pure **36**, an antibacterial agent, in 83% yield after recrystallization. It should be pointed out that substrate **35** was obtained selectively in 98% yield from the $[Rh_6(CO)_{16}]$-catalyzed water–gas shift reaction of **34**.[27]

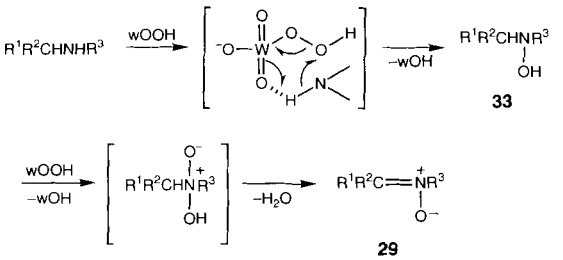

Scheme 4. Tungstate-catalyzed oxidation of secondary amines.

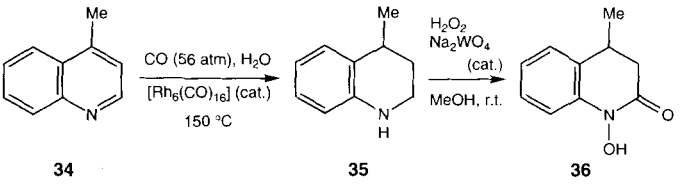

The yields of isolated cyclic nitrones are sometimes low because the extraction from water is difficult. In such cases, oxidation of secondary amines catalyzed by selenium dioxide is more convenient [Eq.(7); Table 1].[28] The oxidation seems to be induced by peroxyselenious acid, HOSe(O)OOH, which is derived from SeO_2 and H_2O_2.

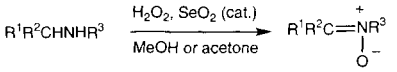

(7)

In an important variation of this nitrone synthesis, decarboxylative oxidation of *N*-alkyl-α-amino acids proceeds smoothly under similar conditions to give the corresponding nitrones regioselectively [Eq.(8)]. As a typical example, (*4R*)-4-

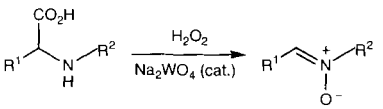

(8)

(*tert*-butyldimethylsiloxy)-1-pyrroline *N*-oxide (**38**), which is a versatile intermediate for the synthesis of optically active pyrrolidines, can be prepared simply in 70% yield by treating a solution of *trans*-4-(*tert*-butylsiloxy)-L-proline (**37**) in dichloromethane with hydrogen peroxide in the presence of Na_2WO_4

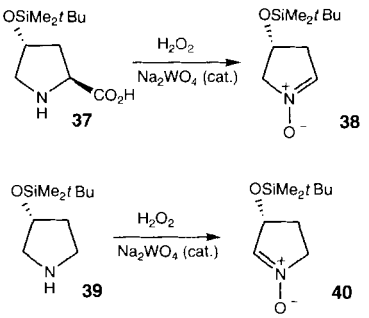

catalyst and tetraethylammonium chloride.[29] On the other hand, (3*R*)-3-(*tert*-butyldimethylsiloxy)-1-pyrroline *N*-oxide (**40**), a regioisomer of **38**, was obtained from amine **39** in 61% yield upon similar oxidation followed by chromatographic separation.

3.2. Substitution at the α-Position of Secondary Amines

The oxidation discussed in Section 3.1 opens up powerful strategies for organic syntheses. The most important synthetic application of this oxidation is substitution at the position α to the nitrogen in secondary amines. Introduction of α-substituents has hitherto been performed by using electrophilic reagents. The N-protected secondary amine **41** with an electron-withdrawing group (Z) undergoes lithiation with an organolithium reagent to give carbanion **42**. Treatment of **42** with an electrophile (E) and removal of the protecting group (Z) gives the α-substituted amine **44** [Eq.(9)].[30] Our reaction provides an alternative method for substitution α to the nitrogen of amines. Catalytic oxidation followed by reaction of the resulting nitrone **29** with a nucleophile (Nu) leads to *N*-hydroxylamine **45**, which can be reduced catalytically [Eq.(10)].[23] Various nucleophiles

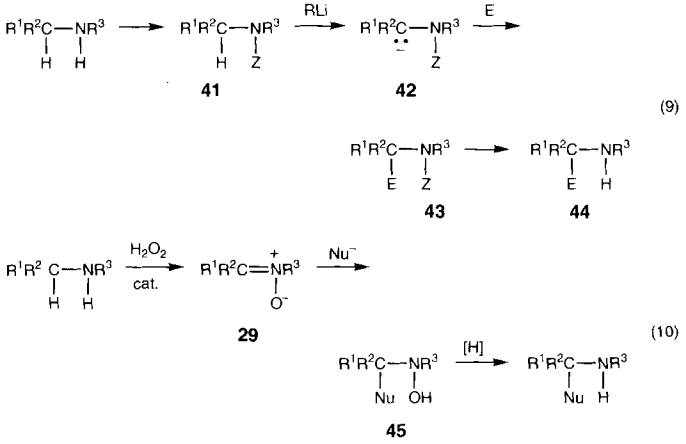

(9)

(10)

can be used to introduce substituents. Firstly, formation of the carbon–carbon bond at the α-position of secondary amines should be described. The usefulness of this reaction was demonstrated by the synthesis of nitrogen-containing, biologically active compounds from secondary amines. Nicotine (**48**) was prepared from pyrrolidine via nitrone **46**.[23]

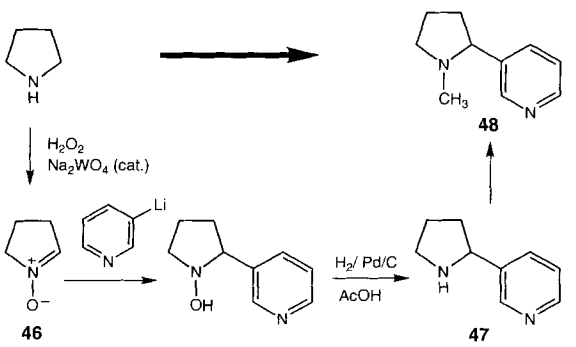

The nucleophiles employed are not limited to organolithium and Grignard reagents. Cyanide is used in a short synthesis of *N*-hydroxyamino acids and α-amino acids from secondary amines.[31] In one example *N*-hydroxyproline (**50**), which is only poorly accessible by conventional methods, is readily prepared from pyrrolidine in two steps without isolation of the nitrone. The yield of **49** (72%) is much higher than the yield of the isolated nitrone itself (44%), since extraction of the product in the workup is easier. Hydrolysis of **49** with dilute hydrochloric acid solution gives *N*-hydroxyproline (**50**) (93%), which undergoes catalytic hydrogenation over Pd/C to give proline (**51**)

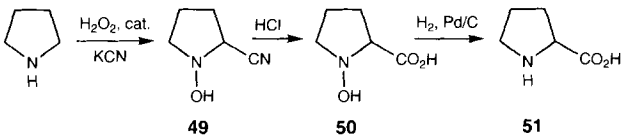

(93%). Thus, *N*-hydroxyproline (**50**) and proline (**51**) can be prepared simply by sequential transformations with inexpensive reagents. Further, various [1-^{14}C]-labeled amino acids, which are important in tracer experiments for the study of metabolism and biosynthesis, can be readily prepared by using the present reactions and labeled K^{14}CN.[31, 32]

3.2.1. *Asymmetric Synthesis of α-Substituted Amines and β-Amino Acids*

Asymmetric induction at the α-position of amines is important for the synthesis of biogenic amines as well as chiral amine ligands. Various optically active nucleophiles can be utilized to introduce chirality through the enantiofacial differentiation of nitrones [Eq.(11)]. Optically active α-sulfinyl carbanions are

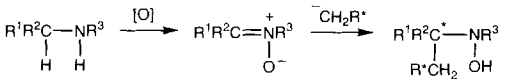

(11)

particularly attractive nucleophiles; they can be obtained by catalytic asymmetric oxidation of sulfides with, for example, chiral titanium catalysts[33] or our chiral flavin catalysts.[20a] The diastereoselective addition of an α-sulfinyl carbanion gives the optically active *N*-hydroxylamine **52**. The α-sulfinyl group can be removed under reducing conditions to give the optically active α-methyl-substituted amine **53**. The optically active nitrone **54** can be prepared by further oxidation of **52**. Diastereoselective addition of a nucleophile results in the introduction of the asymmetric quarternary carbon α to the nitrogen atom in secondary amine **56** (Scheme 5A).[34] Simple examples are the syntheses of (*R*)-(+)-salsolidine (**60**) and (*R*)-homolaudonosine (**63**) (Scheme 5B). The reaction of nitrone **57** with the α-sulfinyl carbanion **58** in the presence of quinidine in THF at −78 °C gave pure, crystalline sulfoxide **59** (68%). Treatment of **59** with Raney-Ni yielded **60**. Furthermore, benzylation of **59** followed by treatment with triphenyltin hydride afforded *N*-benzyl α-(sulfinyl)methylamine (**61**), which is a precursor of **63**.

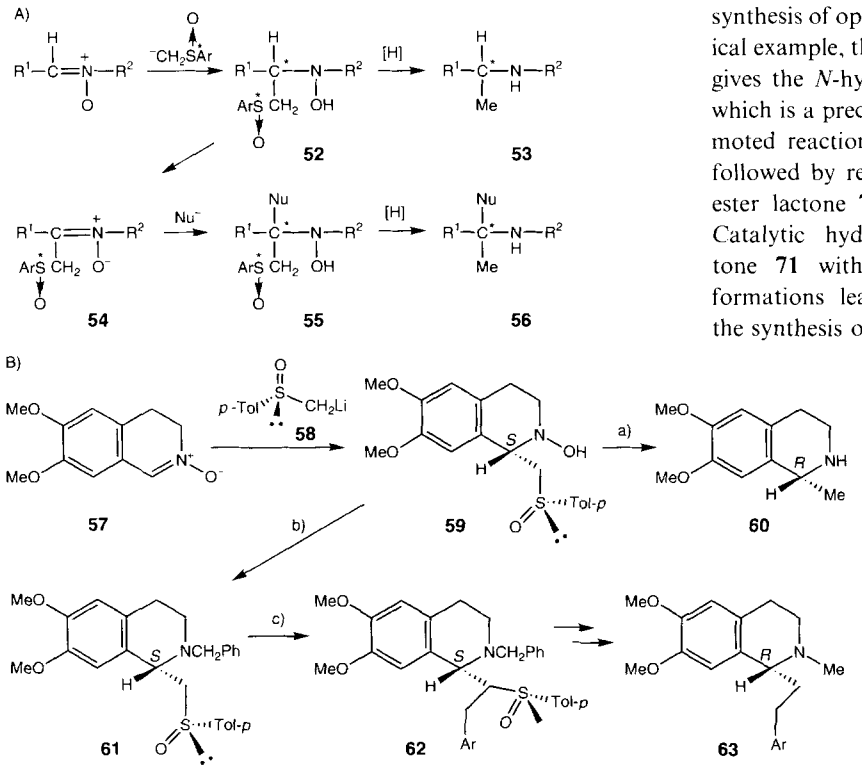

Scheme 5. A) Synthesis of optically active α-substituted amines. B) Synthesis of (*R*)-(+)-salsolidine (**60**) and (*R*)-homolaudanosine (**63**) (*p*-Tol = *p*-tolyl). a) Raney-Ni; b) $PhCH_2Br$, Ph_3SnH; c) LDA, $ArCH_2Br$, Ar = 3,4-$(MeO)_2C_6H_3$.

Chiral enolates are also attractive nucleophiles because they are readily accessible with high enantiomeric purity by asymmetric catalytic hydrogenation of β-ketoesters.[35] Optically active β-amino acids are important key intermediates for the synthesis of β-lactams and various antagonists.

Lewis acid promoted reactions of nitrones with the optically active ketene silyl acetal **65** provide a convenient method for the synthesis of optically active *N*-hydroxy-β-amino acids. In a typical example, the ZnI_2-promoted reaction of nitrone **64** with **65** gives the *N*-hydroxy-β-amino acid **66** selectively (<99% *de*), which is a precursor of β-lactam **67**.[36] Further, the ZnI_2-promoted reaction of nitrone **68** with **65** in CH_2Cl_2 at −78 °C followed by reduction with zinc in acetic acid gives β-amino ester lactone **70** as a single isomer (99.5% *de*, 60% yield). Catalytic hydrogenation and acetylation then gives lactone **71** with high diastereoselectivity; subsequent transformations lead to compound **72**, a key intermediate for the synthesis of carbapenems.[37]

Next, we aimed at generating oxyiminium ions in order to increase the reactivity of nitrones. If oxyiminium ions can be generated by treatment of nitrones with acid chlorides, then α-substituted amino compounds can be obtained readily. Nitrone **73** was treated with racemic 2-acetoxy-2-phenylacetyl chloride at −78 °C, and the resulting oxyiminium ion was allowed to react with chiral titanium enolate **74** to give the *anti* isomer **75** with high selectivity.[38] This compound can be converted into the known precursor **77** of indolizidine alkaloids **78**, which are skin alkaloids of the neotropical dart-poison frog and inhibitors of the acetyl choline receptor.

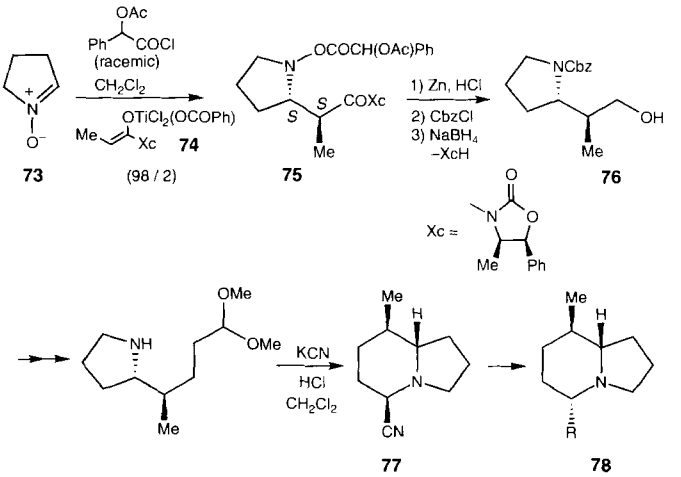

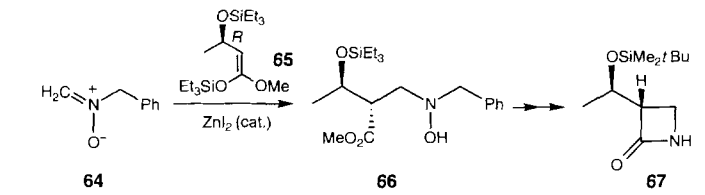

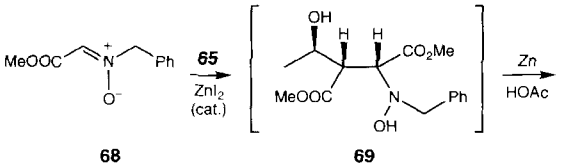

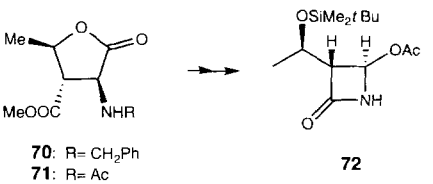

3.2.2. *Catalytic Asymmetric Synthesis of N-Hydroxylamines*

The catalytic asymmetric addition of nucleophiles to nitrones is the most attractive method for synthesizing optically active *N*-hydroxylamines bearing an asymmetric center α to the nitrogen function. These compounds are important since they are biologically active and may serve as precursors of chiral ligands for asymmetric synthesis. We found that the catalytic asymmetric hydrosilylation of nitrones proceeds with high efficiency. The catalytic oxidation of secondary amines and the subsequent asymmetric hydrosilylation of the resulting nitrones opens up a general and powerful strategy for the synthesis of optically active *N*-hydroxylamines from secondary amines (Scheme 6). The

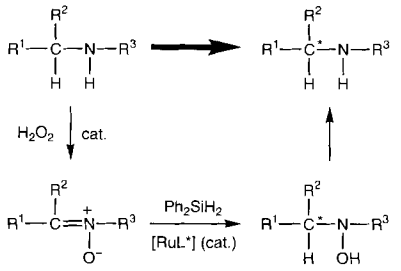

Scheme 6. Two-step asymmetric synthesis of *N*-hydroxylamines.

optically active secondary amines can be prepared by catalytic hydrogenation.

When (*E*)-*N*-[1-(4′-chlorophenyl)ethylidene]methylamine *N*-oxide (**79**), which was obtained from the catalytic oxidation of *N*-[1-(4′-chlorophenyl)ethyl]methylamine, was hydrosilalated with diphenylsilane in the presence of $[Ru_2Cl_4[(S)\text{-}(-)p\text{-tolbinap}]_2 \cdot NEt_3]$ (*p*-tolbinap = 1,1′-binaphthalene-2,2′-diylbis(di-*p*-tolylphosphane) in dioxane at 0 °C, (−)-hydroxylamine **80** was produced in 85% *ee*.[39] Furthermore, *N*-hydroxymethylalanine ethyl ester (**82**), an antimetabolite of the α-amino acid, was also prepared efficiently. Asymmetric hydrosilylation of **81** under similar conditions followed by hydrolysis afforded *N*-hydroxyamino acid **82** in 89% *ee*.

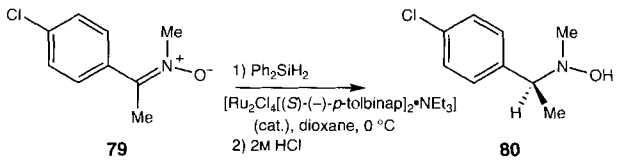

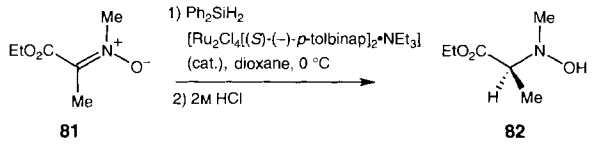

The asymmetric synthesis of *N*-hydroxy-β-amino acids is possible by treatment of nitrones with achiral ketene silyl acetals in the presence of chiral Lewis acid catalysts.[40] In a typical example, reaction of **83** with **84** in the presence of the titanium complex catalyst **85** furnished *N*-hydroxy-β-amino acid derivative **86** in 95% yield and with 62% *ee*.

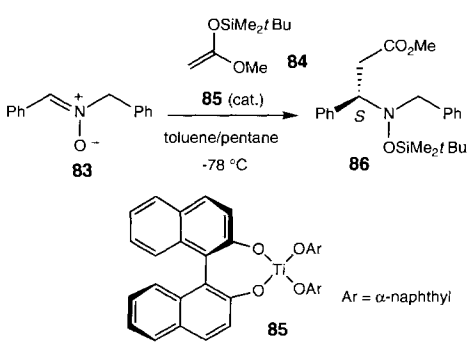

4. Cytochrome P-450 Type Oxidation Catalysts

Cytochrome P-450 (**2**) has two major functions. One is the activation of molecular oxygen by iron porphyrin to generate oxoiron(IV) porphyrin; the other is the transfer of an oxygen atom to substrates.[41] The porphyrin moiety is required for the generation of a hydroperoxyiron(III) species, which undergoes cleavage to give an oxoiron(IV) species (Scheme 7). However a "shunt process" is often used for the oxidation of organic substrates, because oxoiron(IV) species can be formed readily upon treatment with oxygen donors such as iodosylbenzene.[42] In this shunt process, oxometal complexes can be generated without using porphyrins. Various catalysts such as those with salen ligands[43, 44] (salen = bis(salicylidene)ethylenediamine) and organometallic oxides[45, 46] have been examined and found to be successful.

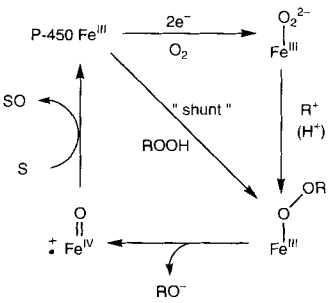

Scheme 7. Oxidation with cytochrome P-450. S = substrate.

Our approach for generating oxometal complexes, which may correspond to the oxoiron(IV) species of cytochrome P-450, is the oxidation of low-valent ruthenium complexes with the intention of generating of $L_nRu{=}O$ species. One important aspect that was focused on at the beginning of this review is the generation of middle-valent oxoruthenium species by using low-valent rather than high-valent ruthenium species.

4.1. Ruthenium-Catalyzed Oxidation of Tertiary Amines

4.1.1. *Oxidation with tert-Butyl Hydroperoxide*

The oxidative N-demethylation of amines is one of the important reactions specific to cytochrome P-450,[41] and several model reactions using iron porphyrins have been reported.[47] We found novel cytochrome P-450 type oxidation behavior with tertiary amines in reactions without porphyrin catalysts. Thus, ruthenium-catalyzed oxidation of tertiary amines with *tert*-butyl hydroperoxide gives the corresponding α-(*tert*-butyldioxy)alkylamines **87** with high efficiency [Eq. (12a)].[48] This is in contrast to the usual catalytic oxidation of tertiary amines with peroxides to give *N*-oxides.[49] In a typical case, a solution of *t*BuOOH (2.1 equiv) in dry benzene was added dropwise to a mixture of *N*,*N*-dimethylaniline and $[RuCl_2(PPh_3)_3]$ (3 mol%)

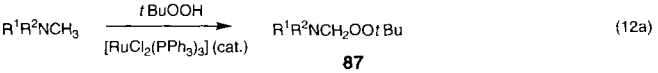

(12a)

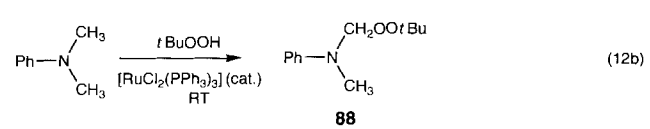

(12b)

in benzene at room temperature (r.t.). *N*-(*tert*-Butyldioxymethyl)-*N*-methylaniline (**88**) was obtained in 93% yield [Eq. (12b)]. Benzylic and allylic positions and carbon–carbon double bonds tolerate the oxidation.

To gain insight into the mechanism of the oxidation, the relative reaction rates of the oxidation of five substituted *N*,*N*-dimethylanilines ($XC_6H_4NMe_2$, X = *p*-MeO, *p*-Me, H, *p*-Cl, *m*-Cl) with *t*BuOOH in benzene were determined.[48] The rate data correlate well ($\gamma = 0.974$) with the Hammett linear free energy relationship with use of σ values. The ρ value is -0.84 (Table 2), which indicates a cationic intermediate in the rate-

Table 2. Kinetics and isotope effects on the catalytic oxidation of *N*,*N*-dimethylanilines.

Catalyst	Oxidizing agent	ρ	k_H/k_D [a]	[b]	Ref.
cytochrome P-450		−0.74	1.6–3.1	1.0–1.1	[50, 51]
$[RuCl_2(PPh_3)_3]$	*t*BuOOH	−0.84	3.53	1.64	[48]
$RuCl_3 \cdot n H_2O$	H_2O_2	−3.26	3.47	3.72	[58]

[a] Intramolecular. [b] Intermolecular.

determining step. The intramolecular deuterium isotope effect (k_H/k_D) in the ruthenium-catalyzed oxidation of *N*-methyl-*N*-(trideuteriomethyl)aniline was determined to be 3.53. Furthermore, the intermolecular isotope effect in the oxidation of *N*,*N*-dimethylaniline was determined to be 1.64 by NMR analysis of the demethylated products of the competitive reaction of *N*,*N*-dimethylaniline and *N*,*N*-bis(trideuteriomethyl)aniline. The observed intra- and intermolecular isotope effects (3.53 and 1.64) are larger than the values observed for N-demethylation with cytochrome P-450 (1.6–3.1[50] and 1.0–1.1[51]), suggesting that in the present reaction cleavage of the C–H bond proceeds via an intermediate having more radical character.

The reaction can be rationalized by assuming the cytochrome P-450 type mechanism[51, 52] shown in Scheme 8. A ruthenium(II) complex reacts with *t*BuOOH to give an oxoruthenium(IV) species.[53] Thus, the reaction of the Ru^{II} complex with *t*BuOOH yields $Ru^{II}OO$*t*Bu **89**, which is transformed into the $Ru^{IV}{=}O$ complex **90** by cleavage of the O–O bond. Electron transfer and subsequent proton transfer results in the iminium ion complex **91**. Nucleophilic attack of *t*BuOOH on **91** gives the product **92**, water, and the Ru^{II} species to complete the catalytic cycle.[48]

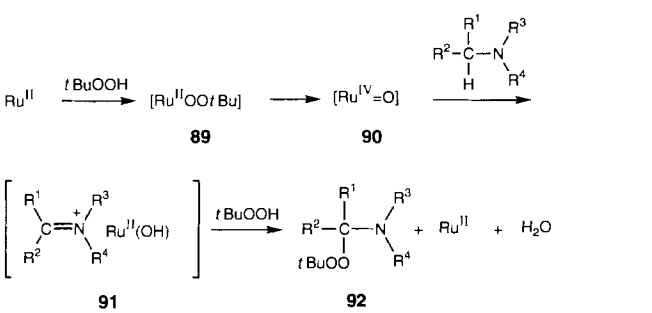

Scheme 8. Reaction pathway for the ruthenium-catalyzed oxidation of tertiary amines with *t*BuOOH.

4.1.2. *Selective N-Demethylation of Tertiary Methylamines*

The N-demethylation of tertiary amines is a typical function of cytochrome P-450. The selective N-demethylation of tertiary methylamines is performed by the ruthenium-catalyzed oxidation previously described to give α-*tert*-butyldioxymethylamines **87**, and subsequent hydrolysis with an aqueous HCl solution yields the secondary amines via iminium ion **93**.[48] This is the first synthetically practical method for the N-demethylation of tertiary methylamines, although several other catalytic and stoichiometric reactions have been reported.[47] Catalytic oxidation of *N*-ethyl-*N*-methylaniline followed by treatment of the reaction mixture with 2 M HCl solution gives *N*-ethylaniline. The methyl group is removed chemoselectively in the presence of various alkyl groups. The reaction seems to involve protonation, removal of *tert*-butyl hydroperoxide, and hydrolysis of the iminium ion to give the secondary amine and formaldehyde [Eq. (13)].

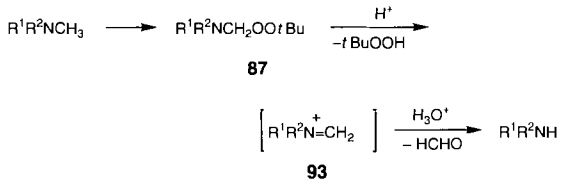

(13)

4.1.3. *Biomimetic Synthesis of Piperidines*

N-Demethylation of tertiary amines provides a novel, biomimetic method for the construction of piperidine skeletons from *N*-methylhomoallylamines by means of an olefin/iminium ion cyclization reaction.[54] The ruthenium-catalyzed oxidation of *N*-methyl-*N*-(3-heptenyl)aniline (**94**) gives peroxide **95** (87%), which can be converted into *trans*-4-chloro-1-phenyl-3-propylpiperidine (**96**) (77%) by treatment with 2 M HCl at room temperature.[48] It is noteworthy that homoallylamines are

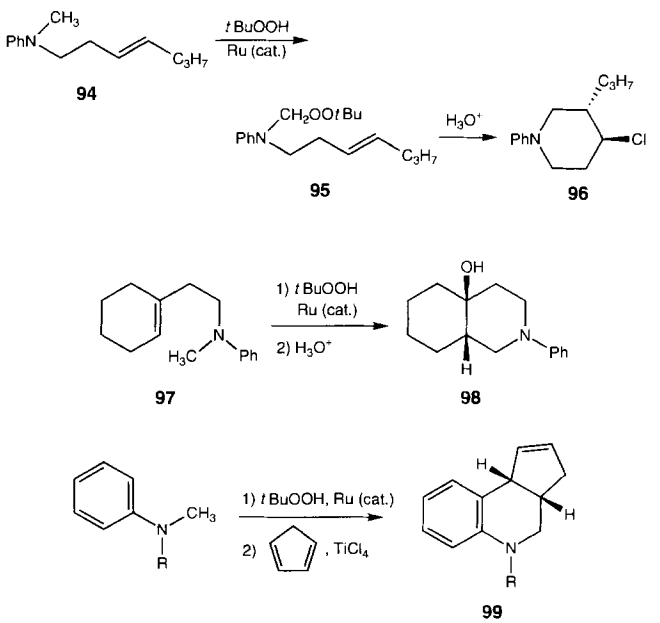

readily obtained by either palladium-catalyzed carbonylation of allylamines[55] or carboamination of allyl esters[56] and subsequent $LiAlH_4$ reduction of the resulting amides.

Reactions with cyclic amines give *cis*-fused bicyclic amines. Thus, *cis*-4α-hydroxy-2-phenyldecahydroisoquinoline (**98**) was obtained selectively in 85% yield from *N*-methyl-*N*-2-(1-cyclohexenyl)ethyl aniline (**97**) by treating the corresponding peroxide with an aqueous CF_3CO_2H solution.

The intermolecular reaction of the iminium ions with olefins or dienes provides a convenient method for synthesizing quinoline derivatives. Thus, the ruthenium-catalyzed oxidation of *N*-methyl-*N*-alkylanilines with *t*BuOOH, followed by treatment with cyclopentadiene in the presence of titanium tetrachloride, affords **99** highly efficiently.[57] These biomimetic reactions provide a second method for introducing a substituent at the α-position of amines by using nucleophiles [see Eq.(10)].

4.1.4. Oxidation of N-Methyl Tertiary Amines with Hydrogen Peroxide

Based on Scheme 8, generation of the oxoruthenium species **90** by using other oxidizing reagents and trapping the iminium ion intermediate **91** with other nucleophiles can be expected. Indeed, a catalytic system that satisfies these two points has been found. The ruthenium-catalyzed oxidation of tertiary methylamines with hydrogen peroxide in the presence of methanol gives the corresponding α-methoxymethylamines with high efficiency [Eq.(14)].[58] The reaction provides an efficient

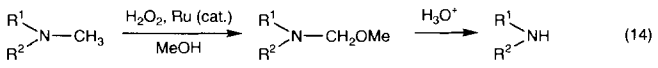

(14)

method for the selective N-demethylation of tertiary methylamines and construction of quinoline skeletons from tertiary methylamine. As an example, p-$MeOC_6H_4NMe_2$ can be converted into p-$MeOC_6H_4N(Me)CH_2OMe$ in 87% yield by treatment with a 30% H_2O_2 solution in methanol in the presence of 5 mol% $RuCl_3 \cdot nH_2O$ at room temperature.

Considering the kinetic data and isotope effects shown in Table 2, the present reaction can be rationalized by assuming a cytochrome P-450 type mechanism. The ruthenium(II) complex reacts with H_2O_2 to give an oxoruthenium species, which undergoes electron transfer followed by proton transfer to afford an iminium ion complex. Nucleophilic attack of methanol then gives the methoxylated amines (Scheme 9).

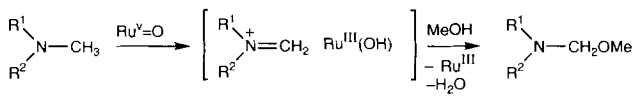

Scheme 9. Ruthenium-catalyzed oxidation of *N*-methylamines.

4.2. Oxidation of Secondary Amines

The mechanism of the ruthenium-catalyzed oxidation of tertiary amines with *t*BuOOH can be rationalized as shown in Scheme 8. If secondary amines are subjected to the same reaction conditions, they can be oxidized to give imines. Electron transfer from secondary amines to oxoruthenium(IV) species leads to the iminium ion complex **91** (R^4 = H), which decomposes to give the product imines, the Ru^{II} species, and water to complete the catalytic cycle (Scheme 10). Indeed, the same catalytic system can be used to convert secondary amines into the corresponding imines (**100**) with high efficiency [Eq.(15)].[59] This is the first catalytic oxidative transformation of secondary

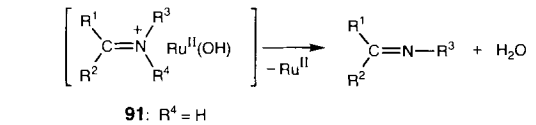

91: R^4 = H

Scheme 10. Reaction pathway for the catalytic oxidation of secondary amines to imines.

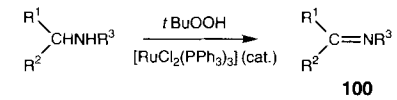

(15)

100

R^1 = Ph, R^2 = H, R^3 = CH_2Ph	80%
R^1 = Ph, R^2 = H, R^3 = Ph	85%
R^1 = PhCH = CH, R^2 = H, R^3 = p-$MeOC_6H_4$	80%

amines into imines. Treatment of a secondary amine with two equivalents of *t*BuOOH in benzene in the presence of 2 mol% $[RuCl_2(PPh_3)_3]$ at room temperature gives the corresponding imines in high yields. The present reaction is particularly useful for the preparation of 1-azadienes and 3,4-dihydroisoquinolines **101**, which are important precursors of isoquinoline alkaloids. Similar catalyst systems such as $[RuCl_2(PPh_3)_3]$/PhIO,[60] [Schiff base·Co]/*t*BuOOH,[61] and $[Pr_4NRuO_4]$[62]/*N*-methylmorpholine *N*-oxide[63] have been reported.

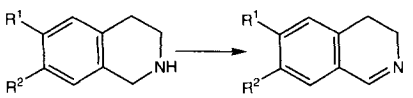

101

R^1 = R^2 = H	73%
R^1 = R^2 = -OCH_2O-	56%
R^1 = R^2 = OMe	82%
R^1 = OCH_2Ph, R^2 = OMe	98%

The catalytic oxidation of secondary amines provides the third key method for nucleophilic substitution α to the nitrogen of amines; the oxidation affords imines, which react with various nucleophiles [Eq.(16)]. Even the asymmetric catalytic addition of nucleophiles to imines has been explored.[64]

We have already shown that flavoenzyme-type oxidation of secondary amines gives nitrones. Thus, secondary amines can be converted into either imines or nitrones depending on the catalytic system employed. For example, the ruthenium-catalyzed oxidation of amine **102** gives imine **103** in 93% yield.[59] In contrast, the tungstate-catalyzed oxidation of the same amine with hydrogen peroxide gives nitrone **104** in 86% yield.[23] We are able to prepare either imines or nitrones from secondary amines by simply changing the catalyst.

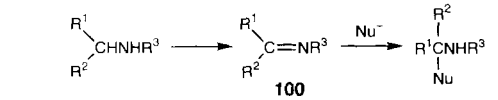

(16)

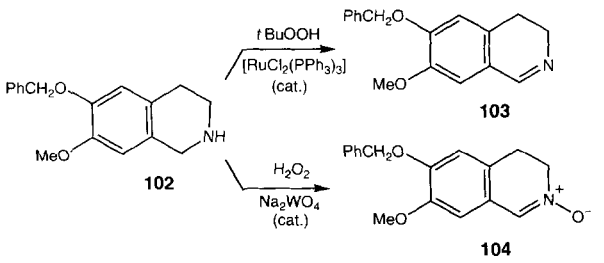

It is worthwhile to comment on the catalytic species. The contrasting formation of nitrones and imines depends on the oxidizing agent. The oxidation of secondary amines with hydroperoxymetal complexes (MOOH) gives nitrones, while the oxidation with oxometal complexes (M=O) gives imines. This is the first demonstration that the MOOH and M=O species have different reactivities [Eq.(17)]. Detection of the oxidation prod-

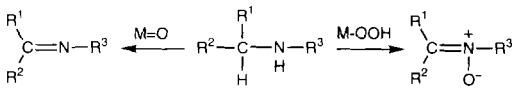

(17)

ucts of a secondary amine may be a convenient means of distinguishing the active species, that is, metal hydroperoxide (MOOH) or oxometal species (M=O).

4.3. Oxidation of Amides

Cytochrome P-450 catalyzes the specific oxygenation of amides;[50a,65] however, the only practical oxidation of amides is an electrochemical process.[66] We have found that the ruthenium-catalyzed oxidation of amides and lactams **105** with *t*BuOOH under mild conditions gives the corresponding *tert*-butyldioxyamides **106** in high yields [Eq.(18), Table 3].[67] The

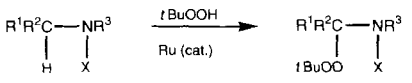

(18)

105 **106**

X = Ac, CO_2CH_3

tert-butyldioxyamides of isoquinolines **108** and indoles **109** thus obtained are important synthetic intermediates. The oxidation of γ-substituted γ-lactams gives γ-(*tert*-butyldioxy)lactams **110**. The oxidation of ω-substituted lactams such as δ-valerolactam gives the corresponding cyclic imide (80% yield).

Application of this catalytic system for oxidations of drugs, peptides, and other compounds provides a powerful method for

Table 3. Ruthenium-catalyzed oxidation of amides and lactams.

Substrate	Product	Yield [%]
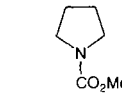	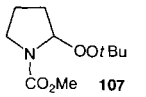 **107**	60
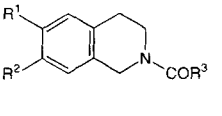	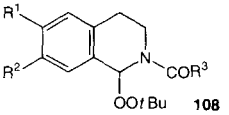 **108**	
	R^1, R^2 = H; R^3 = OMe	91
	R^1 = OCH_2Ph; R^2 = OMe; R^3 = Me	98
	R^1 = OCH_2Ph; R^2, R^3 = OMe	97
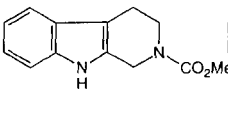	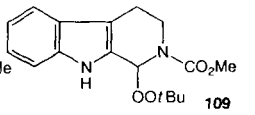 **109**	92
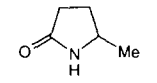	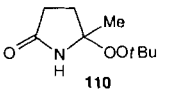 **110**	80

studying metabolic pathways. In one study the ruthenium-catalyzed oxidation of *N*-methoxycarbonylalanylglycine ethyl ester (**111**) with peracetic acid gave *N*-pyruvoylglycine ethyl ester (**112**) (48% yield), which is derived from oxidation of the C–H bond followed by hydrolysis.[68]

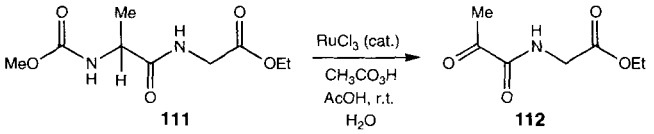

111 **112**

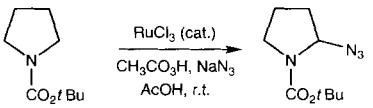

113 **114**

It is very important that the intermediate iminium ions generated by the oxidation of amides can be trapped by other nucleophiles such as N_3^-. As an example, the ruthenium-catalyzed oxidation of *N-tert*-butoxycarbonylpyrrolidine (**113**) with peracetic acid in acetic acid in the presence of sodium azide gave α-azido-*N-tert*-butoxycarbonylpyrrolidine (**114**) in 57% yield.[69]

4.3.1. Substitution at the α-Position of Amides

tert-Butyldioxyamides **106** [see Eq.(18)] undergo substitution reactions with various nucleophiles to give α-substituted amides **115**. Therefore, we now have a fourth method for the transformation of amines into the corresponding α-substituted amines.[70] The catalytic oxidation of an N-protected amine with *t*BuOOH gives α-*tert*-butyldioxyamide **106**, which undergoes nucleophilic substitution to give the α-substituted amide

115. Hydrolysis of the amide yields the corresponding α-substituted amine **116** [Eq. (19)].

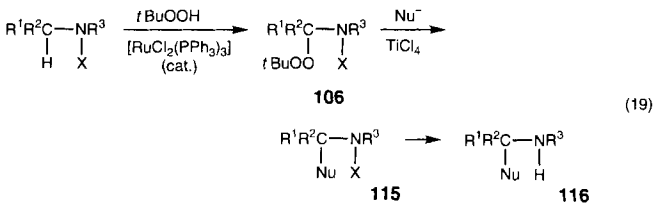

(19)

The most important transformation of α-*tert*-butyldioxyamides is the formation of a carbon–carbon bond at the position α to the nitrogen atom. A typical example is the transformation of pyrrolidines into the α-substituted derivatives. Titanium(IV)-promoted reactions of α-*tert*-butyldioxypyrrolidine **107** with a silyl enol ether, a ketene silyl acetal, and a silylated cyanide gave keto amide **117** (81%), β-amino ester **118** (55%), and α-cyano amide **119** (77%), respectively. These reactions clearly show the efficiency of the present oxidation reaction for the synthesis of various key synthetic intermediates.

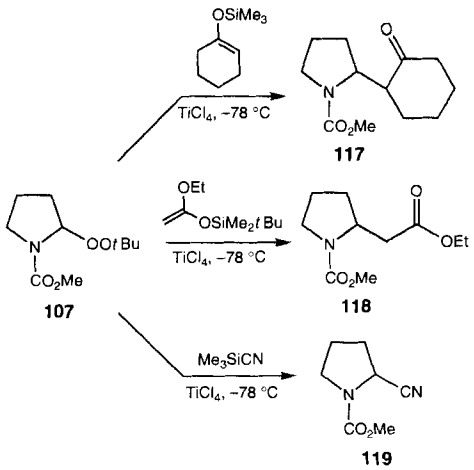

4.4. Oxidation of β-Lactams

4.4.1. Oxidation with Peracetic Acid

One of the most interesting oxidations of amides is the catalytic oxidation of β-lactams. Specific reaction conditions are required because of the higher strain of the four-membered acyliminium ion intermediates. Direct β-acetoxylation of β-lactams can be achieved by ruthenium-catalyzed oxidation with peracetic acid in acetic acid. Thus, the ruthenium-catalyzed oxidation of 2-azetidinones **120** with CH_3CO_3H in acetic acid in the presence of sodium acetate at room temperature gives 4-acetoxy-2-azetidinones **121** [Eq. (20)].[67] Importantly, (1′*R*,3*S*)-3-[1′-(*tert*-butyldimethylsilyloxy)ethyl]azetidin-2-one (**67**) can be converted into the corresponding 4-acetoxyazetidinone **72** with extremely high diastereoselectivity (99% yield, 99% *de*). The latter is a versatile and key intermediate for the synthesis of thienamycin and carbapenems **122**, which are important antibiotics.[71]

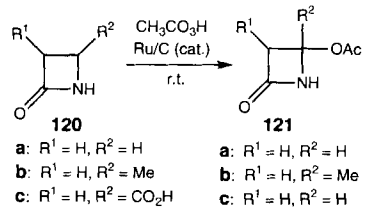

(20)

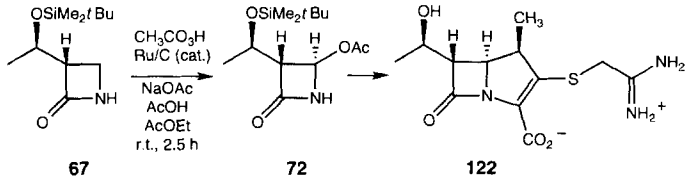

The oxidation can be rationalized as proceeding by a cytochrome P-450 type mechanism (Scheme 11). However, in the oxidation of β-lactams with CH_3CO_3H, more reactive oxoruthenium(IV) species may be formed. The nucleophilic attack

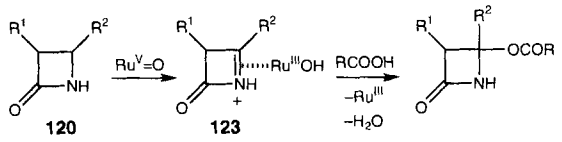

Scheme 11. Ruthenium-catalyzed oxidation of β-lactams.

of acetic acid dominates because it is much more nucleophilic than CH_3CO_3H. Formation of a four-membered acyliminium ion **123** has been confirmed by exclusive formation of the corresponding dichloroacetate upon oxidation of **120** in a mixture of CH_3CO_2H and Cl_2CHCO_2H (1:1).

The osmium-catalyzed oxidation of β-lactams with peracetic acid proceeds efficiently to give 4-acetoxyazetidinone in excellent yield [Eq. (21)].[72] This is the first example of an osmium-

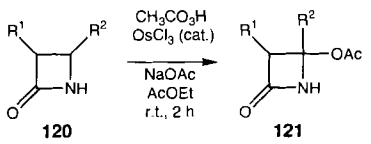

(21)

catalyzed oxidation of C–H bonds, although osmium-catalyzed reactions involving vicinal hydroxylation and vicinal oxyamination of alkenes have been reported.[73] The oxidations of **120a** (R^1, R^2 = H) and **67** in the presence of $OsCl_3$ and anhydrous sodium acetate in ethyl acetate at room temperature gave **121a** and **72** in 78% and 92% yields, respectively.[72] Suitable oxidizing agents for the oxidation of **67** are CH_3CO_3H (92%), *m*CPBA (73%), methyl ethyl ketone peroxide (70%), PhI(OAc)$_2$ (70%), and PhIO (67%). This oxidation is different from the OsO_4-catalyzed oxidation and can be rationalized by assuming the intermediacy of oxoosmium(V) species $L_nOs{=}O$ **124**, which seems to function in the same way as the oxoruthenium species **90**. Cobalt salts such as $CoCl_2$, Co(OAc)$_2$, and Co(acac)$_2$ (acac = acetylacetonate) can also be utilized as catalysts.

4.4.2. Oxidation with Molecular Oxygen

The ruthenium-catalyzed oxidation of β-lactams requires peroxides such as peracetic acid and methyl ethyl ketone peroxide; however, these peroxides are not always available and sometimes contain undesirable materials. We therefore examined the catalyzed formation of peroxides in situ from aldehydes and molecular oxygen. It is well known that peracetic acid can be prepared by treating acetaldehyde with molecular oxygen in the presence of catalysts such as cobalt salts.[74] We discovered that the ruthenium-catalyzed oxidation of β-lactams with molecular oxygen can be performed in the presence of acetaldehyde, an acid, and sodium acetate with high efficiency.[75] For example, 4-acetoxy- and 4-cyanoacetoxy-β-lactams (**126**, $R^2 = CH_2CN$) were obtained in 91% and 81% yields, respectively [Eq. (22)].

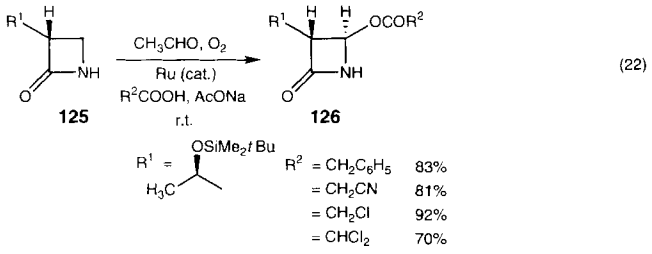

(22)

The active species in this oxidation seems to be oxoruthenium(v) species **90** (Scheme 12). The reaction of ruthenium with either peracetic acid or acetaldehyde and molecular oxygen leads to **90**, which abstracts the H atom from C4 of the β-lactam, and subsequent electron transfer gives acyliminium ion **123**. Nucleophilic reaction of **123** with an acid gives 4-acyloxyazetidinones.

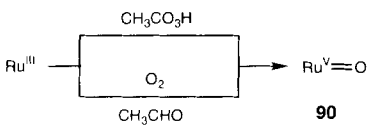

Scheme 12. Formation of oxoruthenium species.

The trimethylsilyltriflate (TMSOTf) promoted reaction of 4-cyanoacetoxy β-lactam (**126**, $R = CH_2CN$) with ketene silyl acetal gives 4-methoxycarbonylmethyl β-lactam (**127**) (92%) stereoselectively.

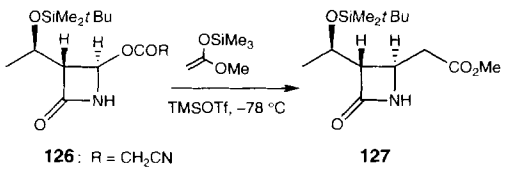

4.5. Oxidation of Hydrocarbons

The selective oxidation of hydrocarbons is an important topic in view of the economical and ecological use of natural raw materials. Direct oxidation of nonactivated hydrocarbons is one of the typical and important reactions of cytochrome P-450,[76] and model monooxygenases based on cytochrome P-450 have been thoroughly investigated.[41b,77-80] In analogy to the use of (tetraphenylporphyrinato)iron(III) chloride/PhIO for the oxidation of alkanes by a shunt process,[42a] many similar oxidation systems based on metalloporhyrins and various reactive oxygen donors have been explored, including iodosylbenene,[81] hypochlorites and chlorites,[82] H_2O_2,[83] $KHSO_5$,[84] alkylperoxides and peracids,[85] and amine *N*-oxide.[86] An alternative method is the metalloporphyrin-catalyzed oxidation with molecular oxygen in combination with reducing agents such as dihydrogen,[87] sodium ascorbate,[88] and zinc powder[89] (Table 4).

Table 4. Metalloporphyrin-catalyzed oxidations of alkanes with reactive oxygen donors or with molecular oxygen and a reducing agent.

Substrate	Catalyst[a]	Oxidizing agent	Product (ratio)	Yield [%]	Ref.
cyclohexane	[Fe(tpp)Cl]	PhIO	cyclohexanol, cyclohexanone (10:1)	26[b]	[81a]
cyclohexane	[Mn(tfpp)Cl]	NaOCl	cyclohexanol, cyclohexanone, cyclohexyl chloride (1:1.3:3.8)	24[c]	[82a]
cyclohexane	[Mn(tdcpp)Cl] + Im	H_2O_2	cyclohexanol, cyclohexanone (3:1)	40[c]	[83]
cyclohexane	[Mn(tdcpp)Cl] + 4-*t*BuPy	$KHSO_5$	cyclohexanol, cyclohexanone (8:1)	90[c]	[84]
cyclohexane	[Fe(tpp)Cl]	$PhCMe_2OOH$	cyclohexanol, cyclohexanone (2:1)	60[c]	[81a]
adamantane	[Ru(tmp)(O_2)] + HCl	2,6-$Cl_2C_5H_4NO$[e]	1-adamantanol, 1,3-adamantanediol, 2-adamantanone	94[c]	[86a]
cyclooctane	[Mn(tpp)Cl] + *N*-Me-Im	O_2/Zn, AcOH	cyclooctanol, cyclooctanone (1.8:1)	0.5[d]	[89]

[a] tpp = Tetraphenylporphyrinato; tfpp = tetrakis(pentafluorophenyl)porphyrinato; tdcpp = tetrakis(2,6-dichlorophenyl)porphyrinato; tmp = tetramesitylporphyrinato; Im = imidazole. [b] Based on oxidizing agent consumed. [c] Based on substrate. [d] Rate in cycles per minute. [e] 2,6-dichloropyridine *N*-oxide.

The unique structural characteristics of metalloporphyrins have been used for the regioselective and/or asymmetric oxidations of hydrocarbons. Thus, remote oxidation of steroids can be performed with the synthetic porphyrins covalently attached to steroidal substrates.[90] Asymmetric hydroxylations at the benzylic position of ethylbenzene and indane have been achieved with PhIO in the presence of a vaulted binaphthyl iron porphyrin catalyst and give (*R*)-phenylethanol and (*R*)-1,2,3,4-tetrahydro-1-naphthol in 41% and 72% *ee*, respectively.[91]

Simple and practical catalyst systems based on non-metalloporphyrins and various reactive oxygen donors such as H_2O_2[92] and alkylperoxides[93] have been explored. The oxidation of cyclohexane with *t*BuOOH and molecular oxygen catalyzed by soluble iron(III) tris(2,2,2-trimethylacetate) [Fe(tma)$_3$] proceeds efficiently to give cyclohexanol and cyclohexanone [Eq. (23)].[94]

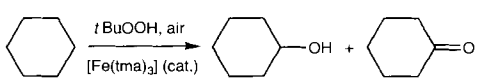

(23)

4.5.1. Oxidation with Peroxides

As described in the preceding sections, we are now able to generate oxoruthenium species without using porphyrins by 1) *t*BuOOH/[$RuCl_2(PPh_3)_3$], 2) H_2O_2/$RuCl_3$, 3) peracetic acid/Ru, and 4) aldehyde/O_2/Ru. These catalyst systems are expected

to promote cytochrome P-450 type oxidations of hydrocarbons efficiently.

First, the oxidation of hydrocarbons using the *t*BuOOH/ruthenium system was examined. Treatment of hydrocarbons with *t*BuOOH in benzene at room temperature in the presence of 3 mol% $[RuCl_2(PPh_3)_3]$ under argon gives the corresponding alcohols or ketones in good yields [Eq. (24)] (Table 5).[95]

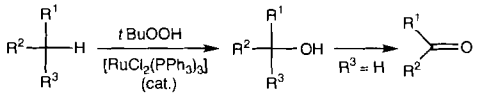

(24)

The oxidation of fluorene gives fluorenone (**128**) in 86% yield. It is noteworthy that the oxidation of 9-methylfluorene gives 9-*tert*-butyldioxy-9-methylfluorene (**129**) selectively (98%). These reactions are very simple and clean. The oxidation of cyclohexane gives cyclohexanol and cyclohexanone. Control experiments show that the ketones are derived from the alcohols under the reaction conditions. The oxidation of adamantane affords the corresponding tertiary alcohols predominantly. The selectivity for the oxidation of tertiary C–H bonds over that of secondary C–H bonds is 6.7:1. For the oxidation of heptane the selectivity for the oxidation of the secondary C–H bonds over that of primary C–H bonds is 13:1 (Table 5).

Table 5. Ruthenium-catalyzed oxidations of alkanes using *tert*-butyl hydroperoxide and peracetic acid.

Substrate	Conversion [%]		Product	Yield [%]	
	[a]	[b]		[a]	[b]
fluorene	–	–	fluorenone (**128**)	86	–
9-methylfluorene	–	–	**129**	98	–
cyclohexane	49	62	cyclohexanol	5	1
			cyclohexanone	23	67
adamantane	79	67	1-adamantanol	40	49
			2-adamantanol	4	9
			2-adamantanone	14	9
n-heptane	26	49	heptanols	3 [c]	71 [e]
			heptanones	19 [d]	4 [f]

[a] $[RuCl_2(PPh_3)_3]$, *t*BuOOH. [b] Ru/C, peracetic acid. [c] Ratio of the 2-, 3-, 4-heptanols 50:33:17. [d] Ratio of the 2-, 3-, 4-heptanones 49:36:15. [e] Ratio of the 2-, 3-, 4-heptanols 40:40:20. [f] Ratio of the 2-, 3-, 4-heptanones 36:44:22.

The data from kinetic and isotope effect studies (see Table 7) support the intermediacy of oxoruthenium(IV) species.[53] Hydrogen abstraction by an oxoruthenium(IV) species to give **130** is the rate-determining step. Subsequent coupling gives alcohols. Further electron transfer from **130** results in cation **131**, which undergoes nucleophilic attack by *tert*-butyl hydroperoxide to give the *tert*-butyldioxy compound, water, and a ruthenium(II) species (Scheme 13).

The ruthenium-catalyzed oxidation of nonactivated hydrocarbons can be also performed with other peroxides such as peracetic acid, cumene hydroperoxide, and *m*-chloroperbenzoic acid. The oxidations are dependent on the peroxides used. Apparently, more reactive peroxides produce highly reactive oxoruthenium species. Representative results of the ruthenium-

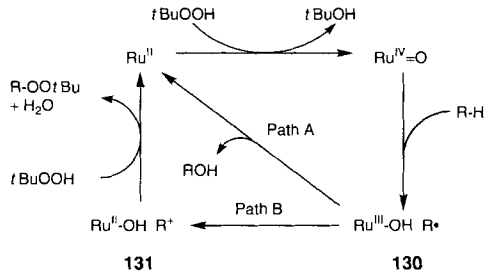

Scheme 13. Ruthenium-catalyzed oxidation of alkanes with *t*BuOOH.

catalyzed oxidation with peracetic acid [Eq. (25a)] are shown in Table 5.

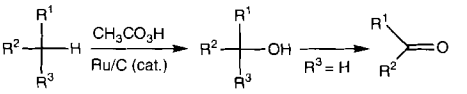

(25a)

The intra- and intermolecular isotope effects are smaller than those obtained for the oxidation of the same substrates with *t*BuOOH (see Table 7), indicating that the oxoruthenium species in the present reaction is more reactive than that produced by *t*BuOOH and cytochrome P-450.[96] It is noteworthy that a more reactive species seems to be generated when the oxidation with peracetic acid is carried out in the presence of trifluoroacetic acid, and the corresponding alcohol products are trapped by trifluoroacetylation. As an example, the $RuCl_3$-catalyzed oxidation of cyclohexane in trifluoroacetic acid and dichloromethane (5:1) with 30% peracetic acid (2 equiv) in ethyl acetate gave cyclohexyl trifluoroacetate (**132**) in 69% yield based on cyclohexane, along with cyclohexanone (12%) (90% conversion of cyclohexane) [Eq. (25b)].[96] Rhodium-catalyzed oxidation of alkanes with peracetic acid gives similar results.[97]

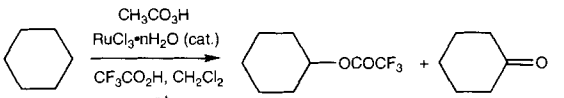

(25b)

132

4.5.2. Oxidation with Molecular Oxygen

The catalytic oxidation of alkanes has been explored by using various oxidizing agents,[81–86,92,93] and oxidations with molecular oxygen under mild conditions are especially rewarding goals.[87–89,98,99] Ruthenium- and iron-catalyzed oxidations of alkanes at room temperature with molecular oxygen (1 atm) in the presence of an aldehyde and a catalytic amount of an acid give the corresponding ketones and alcohols with high efficiency [Eq. (26)].[100] Iron powder has proved to be an effective catalyst, although $Fe(OAc)_3$, $FeCl_3 \cdot 6H_2O$, $RuCl_3 \cdot nH_2O$, and $[RuCl_2(PPh_3)_3]$ can also be used. An aldehyde such as heptanal,

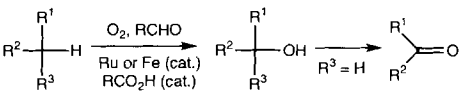

(26)

Table 6. Iron- [100], ruthenium- [100], and copper-catalyzed [105] aerobic oxidations of alkanes in the presence of an aldehyde [a].

Substrate	Conversion [%]			Product	Yield [%]		
	Fe[b]	$RuCl_3 \cdot nH_2O$[b]	$Cu(OH)_2$[c]		Fe[b]	$RuCl_3 \cdot nH_2O$[b]	$Cu(OH)_2$[c]
cyclohexane	11	3.1	4.5	cyclohexanol	29	36	38
				cyclohexanone	66	53	58
cyclooctane	15	8.4	9.9	cyclooctanol	12	21	9
				cyclooctanone	76	63	88
adamantane	36	28	29	1-adamantanol	75	71	86
				2-adamantanol	6	3	5
				2-adamantanone	5	3	3
n-decane	4.8	2.0	4.6	decanols	24[d]	41[f]	15[h]
				decanones	63[e]	44[g]	83[i]
ethylbenzene	20	6.5	8.1	1-phenylethanol	16	64	29
				acetophenone	79	29	70

[a] Under O_2 (1 atm) at room temperature. [b] With heptanal. [c] With acetaldehyde. [d] Ratio of the 2-, 3-, (4- + 5-)decanols 28:22:50. [e] Ratio of the 2-, 3-, (4- + 5-)decanones 24:24:52. [f] Ratio of the 2-, 3-, (4- + 5-)decanols 20:20:60. [g] Ratio of the 2-, 3-, (4- + 5-)decanones 27:27:46. [h] Ratio of the 2-, 3-, (4- + 5-)decanols 35:24:41. [i] Ratio of the 2-, 3-, (4- + 5-)decanones 21:26:53.

2-methylpropanal, or acetaldehyde is effective. A weak acid such as acetic acid is suitable for the iron-catalyzed oxidation. Representative results for the iron- and ruthenium-catalyzed oxidations of various alkanes and alkylated arenes with molecular oxygen (1 atm) in dichloromethane, in the presence of heptanal and a catalytic amount of acetic acid at room temperature, are listed in Table 6.

The kinetic results of these reactions and other related systems are listed in Table 7. These data indicate the following pathway. The reaction of an aldehyde with molecular oxygen[74] in the presence of either ruthenium complexes or iron acetate (derived from iron powder and acetic acid) leads to a peracid, which subsequently reacts with the metal complex to afford an oxometal species[67,101,102] along with a carboxylic acid. The oxometal species abstracts a hydrogen from the alkane, and a hydroxy ligand is transferred to the resulting radical giving an alcohol. Alcohols can be converted into ketones under the same reaction conditions.

The oxidative transformation of cyclohexane into cyclohexanone is of industrial importance. The cobalt-catalyzed aerobic oxidation of cyclohexane has been used commercially; however, the total yield of cyclohexanone and cyclohexanol is quite low.[103] Our oxidation method provides a powerful industrial strategy for the synthesis of cyclohexanone, since the Wacker oxidation of ethylene [Eq. (27a)] can be combined with the iron-catalyzed oxidation of cyclohexane. Another practical point: the oxidation of cyclohexane can be performed without a solvent under slightly modified conditions. The oxidation of cyclohexane in the presence of iron powder catalyst, acetic acid, and acetaldehyde at 70 °C under 8 atm of molecular oxygen gave cyclohexanone (60%) and cyclohexanol (40%) with a high turnover number (146) [Eq. (27b)]. The combined yield of cyclohexanone and cyclohexanol is almost 100%.[100] Cyclohexanol can be converted into cyclohexanone under the same reaction conditions.

$$CH_2{=}CH_2 + O_2 \xrightarrow{\text{Pd-Cu (cat.)}} CH_3CHO \qquad (27a)$$

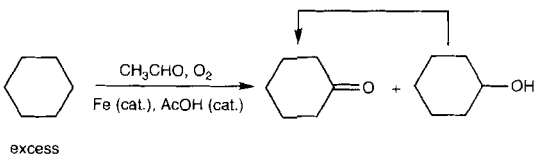

(27b)

4.5.3. Copper-Catalyzed Oxidation

Model studies for the copper-containing monooxygenases such as peptidylglycine α-amidating monooxygenase, which catalyze the oxidation of aliphatic C–H bonds, are limited to a few

Table 7. Kinetics and isotope effects for the catalytic oxidation of hydrocarbons.

Catalyst	Substrate [a]	Oxidizing agent	ρ [b]	k_H/k_D [c]	k_H/k_D [d]	3°:2° [e]	Ref.
cytochrome P-450	T, D		−1.6 [f], −0.42 [g]		11		[76]
[Fe(tpp)]Cl	T	PhIO	−1.69				[101]
$[RuCl_2(PPh_3)_3]$	C, D	*t*BuOOH		8.4	9.0	3.4	[95]
Ru/C	C, D	AcOOH		4.8	2.0	5.4	[96]
$[Ru(dmp)_2(CH_3CN)_2](PF_6)_2$	C	H_2O_2		4.0		7.1	[92g]
Fe	T, C, D	$C_6H_{13}CHO/O_2$	−1.69	5.5	5.0	6.8	[100]
$Cu(OH)_2$	T, C, D	CH_3CHO/O_2	−1.21	1.8	3.6	10	[105]
$Fe(ClO_4)_2 \cdot 6H_2O$		*t*BuOOH pyridine/AcOH		8.0		4.2	[93d]
$Fe(PA)_2$ [h]	C	H_2O_2/O_2 pyridine/AcOH		2.1			[92f]

[a] T = substituted toluene, D = 1,1-dideuterio-1,3-diphenylpropane, C = cyclohexane, and $[D_{12}]$cyclohexane. [b] Hammett linear free energy relationship. [c] Intermolecular kinetic isotope effect. [d] Intramolecular kinetic isotope effect. [e] Ratio of tertiary and secondary oxygenated products from the oxidation of adamantane. [f] *para*-Substituted toluenes. [g] *meta*-Substituted toluenes. [h] PA = picolinic acid.

cases.[104] As part of our study on the simulation of enzymes, we have found that novel copper salt catalyzed oxidations of alkanes and alkenes with molecular oxygen (1 atm) proceed efficiently at room temperature in the presence of aldehydes [Eq. (28)].[105] $Cu(OH)_2$ is an effective catalyst for this aerobic

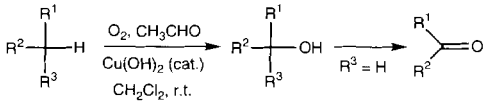

(28)

oxidation of alkanes (Table 6). The reaction of an aldehyde with molecular oxygen in the presence of $Cu(OH)_2$ yields a peracid,[74] which subsequently reacts with the copper salt to afford the active species Cu=O,[106,107] and a carboxylic acid. Hydrogen abstraction from the alkane and electron transfer leads to the cationic intermediate $[Cu^{II}(OH)(R^+)]$, which is converted into the alcohol and Cu^{II}. Importantly, addition of [18]crown-6 to the catalyst system results in higher turnover numbers and selectivities.[108]

4.6. Oxidation of Nitriles

The ruthenium-catalyzed oxidation of α-substituted nitriles **133**, with two equivalents of *t*BuOOH at room temperature gives 2-(*tert*-butyldioxy)alkanenitriles **134** (42–97% yield) [Eq. (29a)]. In contrast, oxidation of nitriles **136** having an α-substituent gives acyl cyanides **137** (89–97% yield) [Eq. (29b)].[109]

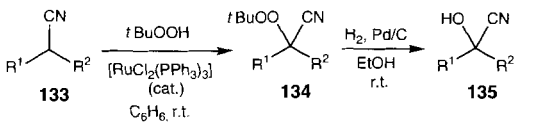

(29a)

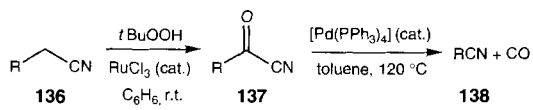

(29b)

The reaction provides a convenient method for transforming nitriles into either cyanohydrins **135** or nitriles **138** whose chain length decreases by one carbon. Catalytic hydrogenation of **134** over Pd/C catalyst in ethanol gives the corresponding cyanohydrins **135** (97–98% yield).[109] Interestingly, treatment of aromatic and heteroaromatic acyl cyanides **137** with $[Pd(PPh_3)_4]$ catalyst (3 mol%) in toluene at 120 °C, gives the shortened nitrile **138** (94–99% yield).[110]

4.7. Oxidation of Alcohols

4.7.1. Oxidation with Peroxides

Ruthenium-catalyzed oxidation of alcohols has been conducted with various oxidizing agents.[111] In particular, the oxidative transformation of primary and secondary alcohols by tetrapropylammonium perruthenate (TPAP)/*N*-methylmorpholine *N*-oxide (NMO) is an excellent method.[62] The $[RuCl_2(PPh_3)_3]$-catalyzed reaction of secondary alcohols with *t*BuOOH gives ketones in 50–90% yield under mild conditions [Eq. (30a)].[112,113] This oxidation can be also applied to the transformation of cyanohydrins (**135**, $R^2 = H$) into acyl cyanides **137** (65–99% yield),[112] which are versatile synthetic intermediates [Eq. (30b)].[114] It is worth noting that acyl cyanides are excellent reagents for the chemoselective acylation

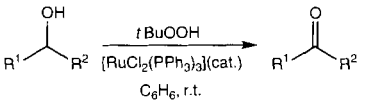

(30a)

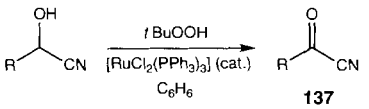

(30b)

of amino alcohols[112] and polyamines.[112b,115] The selective protection and functionalization of polyamines are particularly important for the synthesis of naturally occurring polyamines such as spermidine and spermine alkaloids,[115,116] which have potent antibiotic and antineoplastic properties. The efficiency of this oxidation is illustrated by the synthesis of maytenine (**141**),[117] which was isolated from *Maytenus chuchuhuasha*. Thus, the $[RuCl_2(PPh_3)_3]$-catalyzed oxidation of *trans*-cinnamaldehyde cyanohydrin (**139**) with *t*BuOOH gives *trans*-cinnamoyl cyanide (**140**) in 92% yield. Spermidine reacts with two equivalents of **140** in dry CH_2Cl_2 at room temperature to afford **141** in 92% yield. The Ru-catalyzed oxidation is also highly

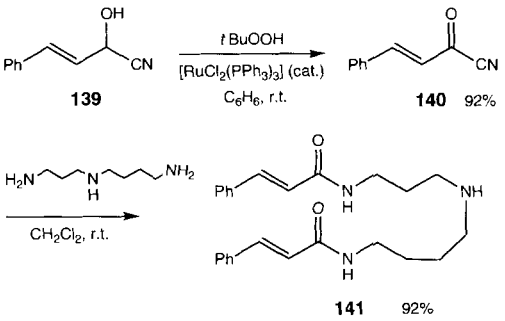

useful for a single-step synthesis of macrocyclic polyamides, which have received considerable attention because of their cation- and anion-binding properties. Indeed, the reactions of iso- and terephthaloyl cyanides with 3,3′-diaminopropylamine in acetonitrile, followed by treatment with hydrogen chloride, gave **142** and **143** in 46 and 42% yields, respectively.

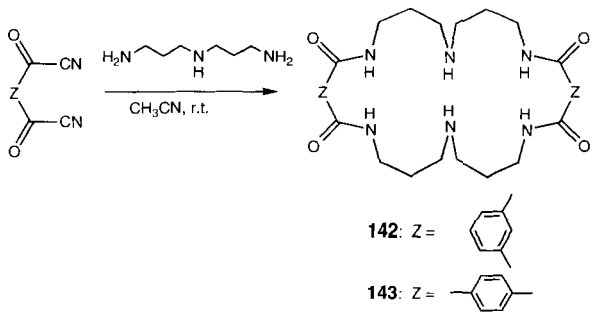

4.7.2. Oxidation with Molecular Oxygen

The aerobic oxidation of alcohols with metal catalysts is highly attractive for economical and environmental reasons. However, most of the reported methods are applicable only to activated alcohols such as benzylic[118] and allylic alcohols.[119] General methods are limited to a few reactions catalyzed by Pt,[120] $[Ru_3O(O_2CR)_6L_3]^-$,[111h] and $PdCl_2 \cdot NaOAc$,[121] and these require rather high reaction temperatures, high O_2 pressures, or long reaction times.

Considering the high reactivity of oxoruthenium complexes towards alcohols, the aerobic oxidation of alcohols in the presence of aldehydes under mild conditions seems feasible. Unfortunately, under these conditions, the oxidation does not occur because the formation of peracids seems to be prevented by the strong coordination of alcohols to the ruthenium. Therefore, we examined catalysts that are effective for the formation of peracids from molecular oxygen and aldehydes and do not coordinate alcohols strongly. $Co(OAc)_2$ is an efficient catalyst for the formation of peracetic acid from acetaldehyde and molecular oxygen, and seems to have no strong affinity to alcohols.[74] We discovered that a ruthenium–cobalt catalyst is excellent for the oxidation [Eq. (31)].[122] When a solution of acetaldehyde

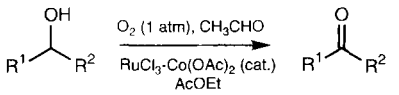

(31)

(4 equiv) in ethyl acetate at room temperature is added to a mixture of an alcohol, $RuCl_3 \cdot nH_2O$ (1 mol%), and $Co(OAc)_2 \cdot 4H_2O$ (1 mol%) in ethyl acetate under an oxygen atmosphere (1 atm), the corresponding ketone is produced with high efficiency. The workup, extraction with a small amount of water to remove the catalyst, is very simple. As typical examples, **144** and **146** gave ketones **145** and **147**, respectively, in 97–98% yield.

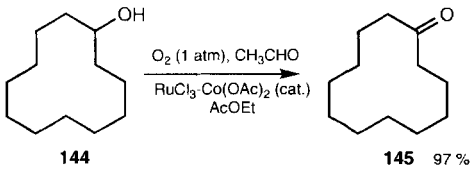

144 **145** 97%

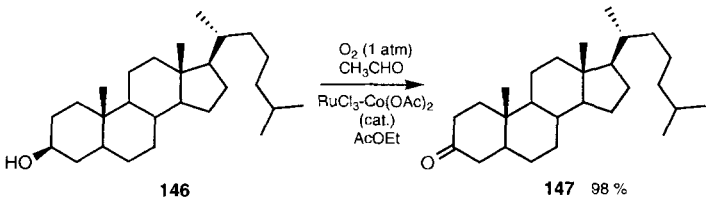

146 **147** 98%

The mechanism of this aerobic oxidation can be rationalized by assuming the following two sequential transformations: 1) formation of peracids by a cobalt-mediated radical chain reaction of aldehydes with molecular oxygen (Scheme 14),[74a] 2) ruthenium-catalyzed oxidation of alcohols[112] with the peracids thus formed. Thus, the reaction of an aldehyde with the

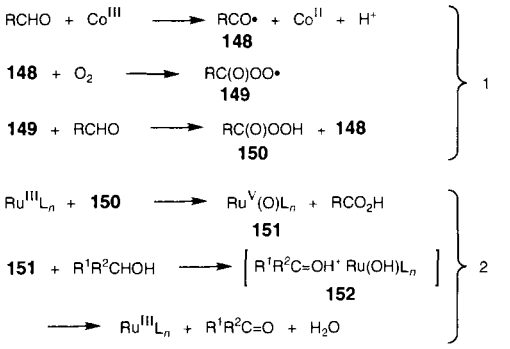

Scheme 14. Aerobic oxidation of alcohols with Co–Ru catalysts.

Co^{III} complex, derived from a Co^{II} complex,[74a] gives acyl radical **148**, which reacts with molecular oxygen to afford acylperoxy radical **149**. This radical abstracts hydrogen from the aldehyde to give peracid **150** and radical **148**. Reaction of the Ru^{III} complex with the peracid **150** leads to $Ru^{III}OOCOR$, which undergoes cleavage of the O–O bond to give the oxoruthenium(v) intermediate **151**.[53,100] Abstraction of a hydrogen atom and subsequent electron transfer provides intermediate **152**, which collapses to give Ru^{III}, a carbonyl compound, and water to complete the catalytic cycle.

4.8. Oxidation of Phenols

The catalytic oxidation of phenols usually gives complex oxygenated products[123] and coupling products,[124] except when the substrate has bulky substituents such as *tert*-butyl and isopropyl groups at the 2- and 4-positions or 2- and 6-positions. We found that oxidation of *p*-substituted phenols **153** with *t*BuOOH in the presence of $[RuCl_2(PPh_3)_3]$ catalyst gives 4-(*tert*-butyldioxy)-4-substituted cyclohexadienones **154**, which are versatile synthetic intermediates [Eq. (32)].[125] Treatment of phenols with four equivalents of *t*BuOOH in benzene at room temperature in the presence of 3 mol% $[RuCl_2(PPh_3)_3]$ catalyst

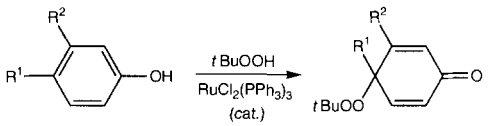

(32)

153 **154**

a: R^1 = Me, R^2 = H 85%
b: R^1 = Ph, R^2 = H 76%
c: R^1, R^2 = -$(CH_2)_4$- 85%

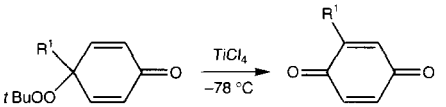

(33)

154a, b **155**

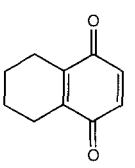

156

affords **154** in good yields. The reaction is an efficient method for the selective oxidation of the phenols that have no substituents at the 2- and 6-positions. Interestingly, when the hexadienones **154** thus obtained are treated with $TiCl_4$ at $-78\,^{\circ}C$, a novel rearrangement occurs. Thus, 2-substituted quinones **155** can be prepared highly efficiently from phenol **153a, b** via **154a, b** [Eq. (33)],[125] and peroxide **154c** can be converted into quinone **156** very efficiently (99%).

4.9. Oxidation of Ketones

The Baeyer–Villiger oxidation of ketones to lactones or esters is a widely used synthetic method.[126] This oxidative transformation has been performed with various peroxides such as peracids,[127] hydrogen peroxide,[128] and bis(trimethylsilyl)peroxide.[129] However, the catalytic Baeyer–Villiger oxidation of ketones with molecular oxygen has been limited to only a few cases.[130] A precise mechanistic study on the iron-catalyzed oxidation of alkanes led to the discovery of a highly efficient Baeyer–Villiger oxidation of ketones with molecular oxygen (1 atm), in the presence of Fe_2O_3 catalyst and benzaldehyde [Eq. (34)].[131] When a solution of cyclohexanone in benzene is

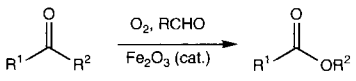

(34)

treated with benzaldehyde at room temperature in the presence of Fe_2O_3 catalyst (1 mol%) under oxygen (1 atm), ε-caprolactam (**157**) is produced in 92% yield. The Fe_2O_3-catalyzed aerobic oxidation of 4-benzoyl β-lactam **158** gives 4-benzoyloxy β-lactam **159** with complete retention of configuration in 93% yield.

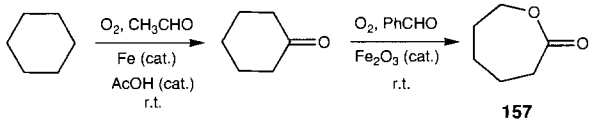

157

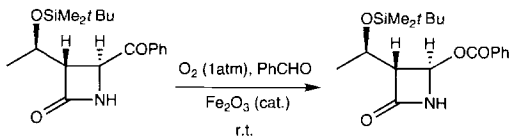

158 **159**

$Cu(OAc)_2$[132] and heteropolyoxometalates[133] have also been shown to be good catalysts, although Baeyer–Villiger oxidation of ketones using molecular oxygen and benzaldehyde can occur in the absence of metal catalysts,[134] and its mechanism has been reported.[135] Recently, an asymmetric Baeyer–Villiger oxidation of **160** with molecular oxygen was reported with the Cu^{II} catalyst **162**.[136]

As described in Section 4.5.2, the iron(0)-catalyzed oxidation of cyclohexane with molecular oxygen in the presence of acetaldehyde gives cyclohexanone with high efficiency. In contrast, the oxidation of cyclohexane does not occur with the Fe_2O_3 catalyst. We wish to emphasize that both transformations, the aerobic oxidation of hydrocarbons to ketones (or alcohols) and the aerobic oxidation of ketones to lactones, were explored by using iron catalysts, though the catalyst systems differed.

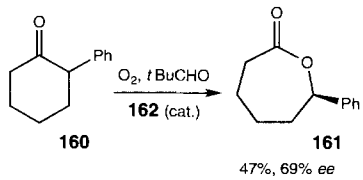

160 **161**

47%, 69% *ee*

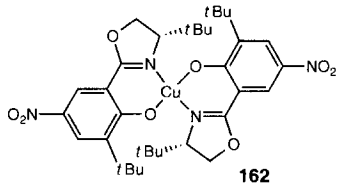

162

The oxidation giving lactones can be rationalized by assuming the pathways shown in Scheme 15. The Fe_2O_3-catalyzed reaction of an aldehyde with molecular oxygen[74] gives the acylperoxy radical **149**, which is a key intermediate in the autoxidation of an aldehyde. The radical **149** abstracts hydrogen from the aldehyde to afford peracid **150**, which reacts readily with the ketone to yield **163**. Alternatively, the radical **149** reacts first with the ketone and then with the aldehyde to give **163**. The intermediate **163** thus formed rearranges to give the ester and the carboxylic acid.

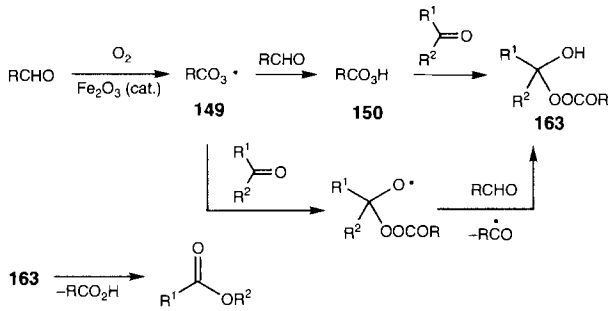

Scheme 15. Fe_2O_3-catalyzed aerobic Baeyer–Villiger oxidation of ketones.

4.10. Oxidation of Alkenes

The epoxidation of alkenes is one of the typical reactions of cytochrome P-450.[41] Metalloporphyrin-catalyzed epoxidation of alkenes with various oxidizing agents have been investigated extensively.[41b,137,138] One of the most important aspects is asymmetric epoxidation. A variety of characteristic, synthetic Fe^{III} complexes of chiral porphyrins such as (*R*)-$\alpha,\beta,\alpha,\beta$-tetrakis(*o*-hydratoamidophenyl)porphyrin,[139] vaulted chiral binaphthyl porphyrin,[91] and "basket-handle",[140] "picnic basket",[141] "twin-coronet",[142] "strapped",[143] and "chiral wall" porphyrins[144] have been designed and used successfully for epoxidation.

Of the catalysts not based on porphyrins, the chiral catalyst in the Sharpless epoxidation of allylic alcohols, which is prepared from $[Ti(OiPr)_4]$ and diethyl tartrate, is particularly important. This reaction is the first practical method for asymmetric epoxidation.[145] In this catalytic system, the substrate should bear

specific polar groups in order to precoordinate the active metal center. The success here stimulated the development of enantioselective catalysts for the epoxidation of unfunctionalized alkenes. The enantioselective epoxidation of these substrates described by Jacobsen, Katsuki, Berkessel, and Mukaiyama have greatly expanded the synthetic scope of metal-catalyzed asymmetric oxidations.[44] In these approaches oxygen transfer to the olefin is effected by chiral manganese(III) complexes with chiral salen ligands,[43] and iodosylbenene or hypochlorite,[146-149] hydrogen peroxide,[150] and even molecular oxygen/aldehydes is used.[151] As a typical example, the epoxidation of **164** with NaOCl in the presence of catalyst **166** gave **165** with 98% *ee* in 72% yield. These catalytic epoxidations have become very important reactions in synthetic organic chemistry.

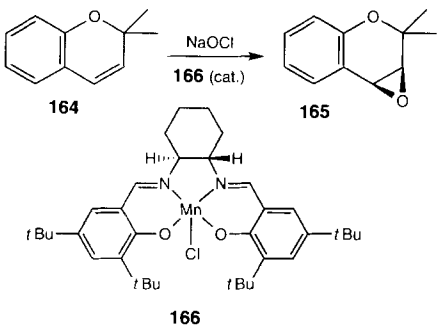

We wish to discuss another aspect of the cytochrome P-450 type oxidation of alkenes, namely, the catalytic oxidative transformation of alkenes into α-ketols. According to the proposed mechanism of cytochrome P-450 epoxidations, cationic intermediate **167** is formed before ring closure leading to epoxides (Scheme 16).[152] If **167** could be trapped with nucleophiles such

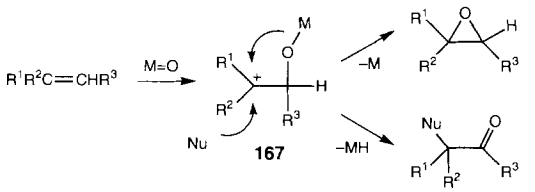

Scheme 16. Oxidation of alkenes catalyzed by a metal oxide.

as water before the ring closure, a new type of catalytic oxidation of alkenes would be possible. Indeed, the novel oxidative transformation of alkenes into α-ketols has been found to proceed very efficiently. Thus, the oxidation with peracetic acid in an aqueous solution catalyzed by low-valent ruthenium under mild conditions yields the corresponding α-ketols **168** [Eq. (35)].[153] The methods for the preparation of α-ketols from enol ethers[154] and enolates[155] have been studied extensively; however, the synthesis from alkenes is limited to oxidations with

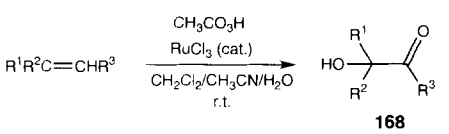

(35)

$KMnO_4/CuSO_4$[156] and with isobutyraldehyde/O_2 in the presence of OsO_4 and bis(3-methyl-2,4-pentanedioate)nickel catalysts.[157] This oxidation is quite different from that promoted by ruthenium tetraoxide.[111a] Indeed, the oxidation of 1-methylcyclohexene (**169**) under the present reaction conditions gives 2-hydroxy-2-methylcyclohexanone (**170**) (67%), while the oxidation of the same substrate under the conditions in which

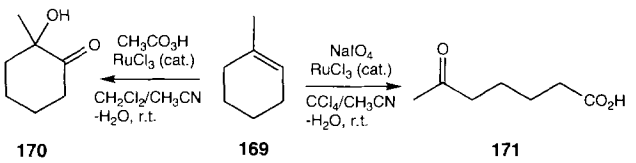

ruthenium tetraoxide is generated catalytically gives 6-oxoheptanoic acid (**171**) (91%). Importantly, allylic acetates can be oxidized to give the corresponding acetoxy α-ketols in good to excellent yields.

Table 8. Ruthenium-catalyzed oxidation of alkenes to α-ketols with peracetic acid.

Substrate	Product	Yield [%]
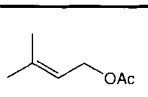	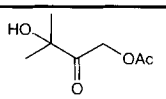	78
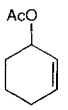	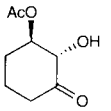	70
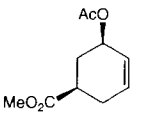	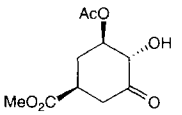	55
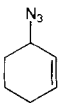	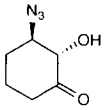	65
	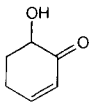	41
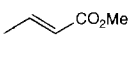	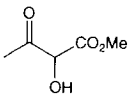	56

α-Ketols are important synthetic intermediates and partial structures of various biologically active compounds such as cortisone acetate (**172**) and adriamycin acetate (**173**). The efficiency of the present reaction has been demonstrated by the synthesis

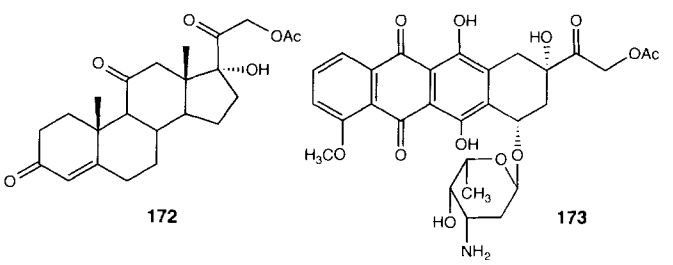

of cortisone acetate (**172**), which is a valuable antiinflammatory agent. Our synthesis started with the conversion of epiandrosterone (**174**), which is commercially available, into 3β,17ξ-diacetoxy-5α-pregn-20-ene (**175**) (Scheme 17). Rearrangement of **175** with $[PdCl_2(CH_3CN)_2]$ catalyst[158] in THF at room temperature gave 3β,21-diacetoxy-5α-pregn-17-ene (**176**) in 92% yield. The ruthenium-catalyzed oxidation of **176** proceeded stereoselectively to give 20-oxo-5α-pregnane-3β,17α,21-triol 3,21-diacetate (**177**) in 57% yield. Conventional treatment of **177** followed by microbial oxidation with *Rhizopus nigricans* gave **172**.

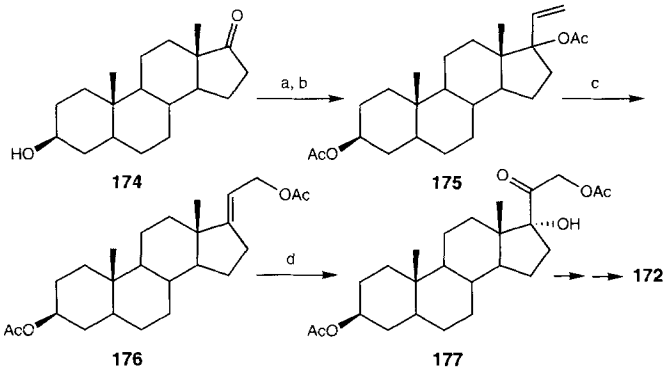

Scheme 17. Synthesis of cortisone acetate (**172**): a) $CH_2{=}CHMgBr$; b) Ac_2O, 4-*N*,*N*-dimethylaminopyridine/pyridine; c) $[PdCl_2(CH_3CN)_2]$ (cat.); d) $RuCl_3$ (cat.), CH_3CO_3H.

The oxidation leading to **177** can be rationalized by assuming the pathway shown in Scheme 18. The reaction of the Ru^{III} complex with peracetic acid gives a $Ru^V{=}O$ species,[67] which reacts with alkenes to give the cationic species **167**. Nucleophilic attack of water, before ring closure to give epoxide, and subsequent β-elimination of a ruthenium hydride species from **178** affords the α-ketol.

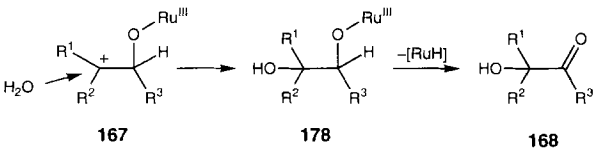

Scheme 18. Reaction process for the catalytic oxidation of alkenes to give α-ketols.

As described in Section 4.4.1, the osmium-catalyzed oxidation of β-lactams with peracetic acid proceeds smoothly. In this reaction a non-porphyrin oxoosmium species seems to play a key role, and hence we extended the catalytic system to the oxidation of alkenes. The $OsCl_3$-catalyzed oxidation of alkenes with peracetic acid in an aqueous solution gives the corresponding α-ketols [Eq. (36)].[159] This reaction is quite different from the OsO_4-catalyzed oxidation of alkenes. The catalytic asymmetric Sharpless dihydroxylation of unfunctionalized *trans*-alkenes with osmium tetraoxide/alkaloid complexes has now become a very powerful method for organic synthesis because of its extremely high enantioselectivity.[73b]

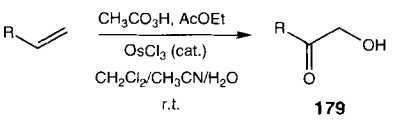

(36)

Both cyclic and acyclic alkenes are converted into the corresponding α-ketols conveniently in the presence of 1–3 mol% $OsCl_3$. Oxidation of 1-octene with peracetic acid in the presence of 1 mol% $OsCl_3$ in $CH_2Cl_2/CH_3CN/H_2O$ (1:1:1) at room temperature gave 1-hydroxy-2-octanone **179** ($R = C_6H_{13}$) in 88% yield. Importantly, the oxidation of monosubstituted alkenes proceeds smoothly to give α-ketols with high regioselectivity, although the reactivity is low. Electron-deficient alkenes are also converted into the corresponding α-ketols. The high reactivity towards less reactive 1-alkenes is due to the high electrophilicity of the $Os^V{=}O$ species.

For the aerobic epoxidation of alkenes a nickel(II) 1,3-diketone catalyst system[160] in the presence of an aldehyde is extremely efficient. Bis[1,3-bis(*p*-methylphenyl)-1,3-propanedionato]nickel(II) $[Ni(dmp)_2]$ was used in the aerobic oxidation of alkene **180** in 1,2-dichloroethane in the presence of 2-methylpropanal to give epoxide **181** in 100% yield; the turnover number was 10^7.[160a] Under similar conditions, cobalt(III)–salen systems[151,161] and heteropolyoxometalate systems[133] can be used. $RuCl_3$,[100] Fe,[100] and $Cu(OH)_2$[105] have been explored as simple catalytic systems for oxidations of alkenes in the presence of acetaldehyde.

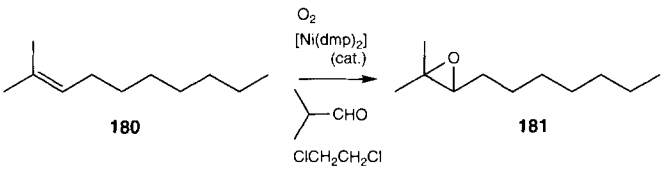

Methyltrioxorhenium (MTO, **182**) can be used to catalyze the oxidation of alkenes with hydrogen peroxide to give epoxides very efficiently.[46] This reaction is particularly interesting since the intermediates have been well defined by trapping experiments. Thus, treatment of **182** with hydrogen peroxide gives Re^{VII} peroxo complex **184** via **183**. Complex **184**, which surprisingly could be isolated in the solid state, is the active species in the olefin epoxidation catalyzed by **182** [Eq. (37)]. Compound **183** is formed rapidly from **184** in the presence of olefins. Since the chemistry of organometallic oxides is compatible with that of classical inorganic oxides, chemists from both areas of chemistry will soon be working together closely.[46]

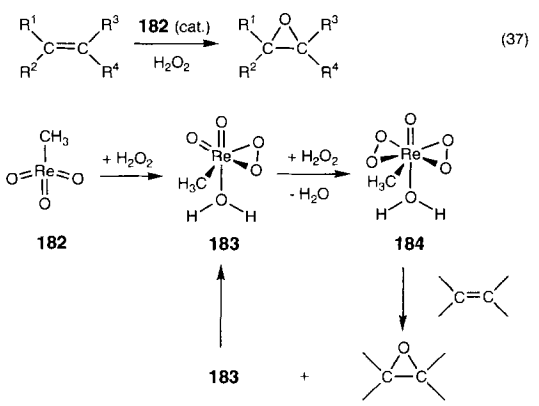

(37)

5. Summary and Outlook

Simulation of the functions of amine oxidase, hepatic flavoenzyme, and cytochrome P-450 with transition metal catalysts has resulted in the discovery of novel and selective catalytic reactions that are simple, clean, and practical. In addition, a variety of related reactions, including four new methods to introduce a substituent at the α-position of amines, using nucleophiles, have been explored.

For oxidations in the laboratory sodium dichromate or potassium permanganate may be used. But when these reactions are scaled up, they are costly and produce large volumes of effluent containing toxic metal salts that must be treated. For this reason more environmentally friendly oxidizing agents such as hydrogen peroxide, *tert*-butyl hydroperoxide, and acetaldehyde/O_2 (peracetic acid) have been examined for oxidations catalyzed by trace amounts of transition metal catalysts. The biomimetic oxidation reactions presented here can be worked up easily and result in only water, *tert*-butanol, or acetic acid as by-products, and, hence, will be widely used in the future. *tert*-Butanol can be consumed as a precursor of the gasoline additive methyl *tert*-butyl ether, in place of aromatic hydrocarbons.

I thank the Ministry of Education, Science and Culture, Japan, for financial support. It is a pleasure to acknowledge the experimental and intellectual contributions of the authors whose names are cited in the references.

Received: July 4, 1994
Revised version: February 21, 1995 [A 731E]
German version: *Angew. Chem.* **1995**, *107*, 2670–2693

[1] a) R. A. Sheldon, *Top. Curr. Chem.* **1993**, *164*, 20; b) R. A. Sheldon, J. K. Kochi, *Metal Catalyzed Oxidations of Organic Compounds*, Academic Press, New York, **1981**; c) M. Hudlicky, *Oxidations in Organic Chemistry*, American Chemical Society, Washington (*ACS Monogr.* **1990**, *186*).
[2] S.-I. Murahashi, *Pure Appl. Chem.* **1992**, *64*, 403.
[3] a) D. R. Patek, H. Y. K. Chuang, L. Hellerman, *FASEB J.* **1972**, *31*, 420; b) R. B. Silverman, S. J. Hoffman, W. B. Catus III, *J. Am. Chem. Soc.* **1980**, *102*, 7126.
[4] a) S.-I. Murahashi, N. Yoshimura, T. Tsumiyama, T. Kojima, *J. Am. Chem. Soc.* **1983**, *105*, 5002; b) N. Yoshimura, I. Moritani, T. Shimamura, S.-I. Murahashi, *ibid.* **1973**, *95*, 3038; c) *J. Chem. Soc. Chem. Commun.* **1973**, 307.
[5] S.-I. Murahashi, T. Hirano, T. Yano, *J. Am. Chem. Soc.* **1978**, *100*, 348.
[6] S.-I. Murahashi, T. Yano, K. Hino, *Tetrahedron Lett.* **1975**, 4235.
[7] R. D. Adams, H.-S. Kim, S. Wang, *J. Am. Chem. Soc.* **1985**, *107*, 6107.
[8] a) S. Inoue, H. Takaya, K. Tani, S. Otsuka, T. Sato, R. Noyori, *J. Am. Chem. Soc.* **1990**, *112*, 4897; b) R. Noyori, *Asymmetric Catalysis in Organic Synthesis*, Wiley, New York, **1994**, p. 95.
[9] S.-I. Murahashi, T. Watanabe, *J. Am. Chem. Soc.* **1979**, *101*, 7429.
[10] a) R. M. Laine, D. W. Thomas, L. W. Cary, S. E. Buttrill, *J. Am. Chem. Soc.* **1978**, *100*, 6527; b) Y. Shvo, R. M. Laine, *J. Chem. Soc. Chem. Commun.* **1980**, 753; c) R. B. Wilson, Jr., R. M. Laine, *J. Am. Chem. Soc.* **1985**, *107*, 361.
[11] R. McCrindle, G. Ferguson, G. J. Arsenault, A. J. McAlees, *J. Chem. Soc. Chem. Commun.* **1983**, 571.
[12] a) S.-I. Murahashi, T. Naota in *Advances in Metal-Organic Chemistry*, *Vol. 3* (Ed.: L. S. Liebeskind), JAI, London, **1994**, p. 225; b) S.-I. Murahashi, T. Naota in *Heteroatom Chemistry*, *Vol. 1* (Ed.: S. Oae), MYU, Tokyo, **1988**, p. 257; c) S.-I. Murahashi, T. Naota, K. Ito, Y. Maeda, H. Taki, *J. Org. Chem.* **1987**, *52*, 4319; d) S.-I. Murahashi, K. Ito, T. Naota, Y. Maeda, *Tetrahedron Lett.* **1981**, *22*, 5327.
[13] S.-I. Murahashi, T. Shimamura, I. Moritani, *J. Chem. Soc. Chem. Commun.* **1974**, 931.
[14] S.-I. Murahashi, K. Kondo, T. Hakata, *Tetrahedron Lett.* **1982**, *23*, 229.
[15] T. Naota, S.-I. Murahashi, *Synlett* **1991**, 693.
[16] a) L. L. Poulsen in *Reviews in Biochemical Toxicology* (Eds.: E. Hodogson, J. E. Bend, E. M. Philpot), Elsevier, New York, **1981**, pp. 33–49; b) D. M. Ziegler, *Enzym. Basis of Detoxication* **1970**, *1*, 201–207.
[17] a) L. L. Poulsen, D. M. Ziegler, *J. Biol. Chem.* **1979**, *254*, 6449; b) N. B. Beaty, D. P. Ballou, *ibid.* **1980**, *255*, 3817.
[18] a) S. Ball, T. C. Bruice, *J. Am. Chem. Soc.* **1980**, *102*, 6498; b) *ibid.* **1979**, *101*, 4017.
[19] S.-I. Murahashi, T. Oda, Y. Masui, *J. Am. Chem. Soc.* **1989**, *111*, 5002.
[20] a) S.-I. Murahashi, Y. Masui, H. Obuse, M. Fujiwara, S. Takatsuka, S. Matsuda, unpublished results; see also, b) S. Shinkai, T. Yamaguchi, O. Manabe, F. Toda, *J. Chem. Soc. Chem. Commun.* **1988**, 1399.
[21] G. Strukul, *Catal. Met. Complexes*, **1992**, *9*.
[22] T. Hosokawa, S.-I. Murahashi, *Acc. Chem. Res.* **1990**, *23*, 49.
[23] a) S.-I. Murahashi, H. Mitsui, T. Shiota, T. Tsuda, S. Watanabe, *J. Org. Chem.* **1990**, *55*, 1736; b) S.-I. Murahashi, T. Shiota, Y. Imada, *Org. Synth.* **1991**, *70*, 265; c) H. Mitsui, S. Zenki, T. Shiota, S.-I. Murahashi, *J. Chem. Soc. Chem. Commun.* **1984**, 874.
[24] For reviews, see: a) G. Tennant, *Compr. Org. Chem.* **1979**, *2*, 500; b) E. Breuer, *Chem. Amino, Nitroso, Nitro Compds. Their Deriv.* **1982**, *1*, 459; c) J. J. Tufariello in *1,3-Dipolar Cycloaddition Chemistry*, *Vol. 2* (Ed.: A. Padwa), Wiley, New York, **1984**, p. 83; d) K. B. G. Torssell, *Nitrile Oxides, Nitrones, and Nitronates in Organic Synthesis*, VCH, New York, **1988**.
[25] a) E. G. Janzen, *Acc. Chem. Res.* **1971**, *4*, 31; b) C. A. Evans, *Aldrichimica Acta* **1979**, *12*, 182.
[26] a) S.-I. Murahashi, T. Oda, T. Sugahara, Y. Masui, *J. Org. Chem.* **1990**, *55*, 1744; b) S.-I. Murahashi, Y. Imada, S. Watanabe, *Org. Synth.* submitted.
[27] a) S.-I. Murahashi, Y. Imada, Y. Hirai, *Tetrahedron Lett.* **1987**, *28*, 77; b) *Bull. Chem. Soc. Jpn.* **1989**, *62*, 2968.
[28] S.-I. Murahashi, T. Shiota, *Tetrahedron Lett.* **1987**, *28*, 2383.
[29] S.-I. Murahashi, Y. Imada, H. Ohtake, *J. Org. Chem.* **1994**, *59*, 6170.
[30] For reviews, see: a) A. I. Meyers, *Aldrichimica Acta* **1985**, *18*, 59; b) P. Beak, W. J. Zajdel, D. B. Reitz, *Chem. Rev.* **1984**, *84*, 471.
[31] S.-I. Murahashi, T. Shiota, *Tetrahedron Lett.* **1987**, *28*, 6469.
[32] A. Murray, D. L. Williams, *Organic Synthesis with Isotopes*, Interscience, New York, **1958**.
[33] a) H. B. Kagan, F. Rebière, *Synlett* **1990**, 643; b) H. B. Kagan in ref. [33c], p. 203; c) *Catalytic Asymmetric Synthesis* (Ed.: I. Ojima), VCH, Weinheim, **1993**.
[34] S.-I. Murahashi, J. Sun, T. Tsuda, *Tetrahedron Lett.* **1993**, *34*, 2645.
[35] H. Takaya, T. Ohta, R. Noyori in ref. [33c], p. 1.
[36] S.-I. Murahashi, H. Ohtake, Y. Imada, unpublished results.
[37] a) E. Hungerühler, M. Biollaz, I. Ernst, J. Kalvoda, M. Lang, P. Schneider, G. Sedelmeier in *New Aspects of Organic Chemistry I* (Eds.: Z. Yoshida, T. Shiba, Y. Ohshiro), Kodansha, Tokyo, **1989**, pp. 419–451; b) G. Sedelmeier, J. Bersier, EP-A 279781, **1988** [*Chem. Abstr.* **1988**, *113*, 237911.
[38] S.-I. Murahashi, H. Ohtake, T. Kawakami, H. Arakawa, unpublished results.
[39] S.-I. Murahashi, S. Watanabe, T. Shiota, *J. Chem. Soc. Chem. Commun.* **1994**, 725.
[40] T. Kawakami, S.-I. Murahashi, unpublished results.
[41] a) R. Sato, T. Omura, *Cytochrome P-450*, Kodansha, Tokyo, **1978**; b) T. J. McMurry, J. T. Groves, *Cytochrome P-450: Structure, Mechanism and Biochemistry*, (Ed.: P. R. Ortiz de Montellano), Plenum, New York, **1986**, p. 3.
[42] a) J. T. Groves, T. E. Nemo, R. S. Myers, *J. Am. Chem. Soc.* **1979**, *101*, 1032; b) J. T. Groves, *J. Chem. Educ.* **1985**, *62*, 928; c) T. C. Bruice, *Proc. Robert A. Welch Found Conf. Chem. Res.* **1987**, *31*, 37; d) J. P. Collman, T. Kodadek, J. I. Brauman, *J. Am. Chem. Soc.* **1986**, *108*, 2588; e) T. G. Traylor, F. Xu, *ibid.* **1988**, *110*, 1953; f) B. Meunier, *Bull. Soc. Chim. Fr.* **1986**, 578; g) D. Mansuy, *Pure Appl. Chem.* **1987**, *59*, 759.
[43] a) K. Srinivasan, P. Michaud, J. K. Kochi, *J. Am. Chem. Soc.* **1986**, *108*, 2309; b) E. G. Samsel, K. Srinivasan, J. K. Kochi, *ibid.* **1985**, *107*, 7606.
[44] E. N. Jacobsen in ref. [33c], p. 159.
[45] H. Mimoun, *Angew. Chem.* **1982**, *94*, 750; *Angew. Chem. Int. Ed. Engl.* **1982**, *21*, 734.
[46] a) W. A. Herrmann, R. W. Fischer, D. W. Marz, *Angew. Chem.* **1991**, *103*, 1706; *Angew. Chem. Int. Ed. Engl.* **1991**, *30*, 1638; b) W. A. Herrmann, R. W. Fischer, W. Scherer, M. U. Rauch, *ibid.* **1993**, *105*, 1209 and **1993**, *32*, 1157.
[47] a) P. Shannon, T. C. Bruice, *J. Am. Chem. Soc.* **1981**, *103*, 4580; b) C. M. Dicken, F.-L. Lu, M. W. Nee, T. C. Bruice, *ibid.* **1985**, *107*, 5776; c) D. Ostović, C. B. Knobler, T. C. Bruice, *ibid.* **1987**, *109*, 3444; d) T. Santa, N. Miyata, M. Hirobe, *Chem. Pharm. Bull.* **1984**, *32*, 1252; e) K. Fujimori, S. Fujiwara, T. Takata, S. Oae, *Tetrahedron Lett.* **1986**, *27*, 581; f) J. R. Lindsay Smith, D. N. Mortimer, *J. Chem. Soc. Chem. Commun.* **1985**, 64.
[48] S.-I. Murahashi, T. Naota, K. Yonemura, *J. Am. Chem. Soc.* **1988**, *110*, 8256.
[49] Ref. [1b], p. 387.
[50] a) T. Shono, T. Toda, N. Oshino, *J. Am. Chem. Soc.* **1982**, *104*, 2639; b) G. T. Miwa, W. A. Garland, B. J. Hodshon, A. Y. H. Lu, D. B. Northrop, *J. Biol. Chem.* **1980**, *255*, 6049; c) G. T. Miwa, J. S. Walsh, G. L. Kedderis, P. F. Hollenberg, *ibid.* **1983**, *258*, 14445.
[51] D. C. Heimbrook, R. I. Murray, K. D. Egeberg, S. G. Sligar, M. W. Nee, T. C. Bruice, *J. Am. Chem. Soc.* **1984**, *106*, 1514.
[52] L. T. Burka, F. P. Guengerich, R. J. Willard, T. L. Macdonald, *J. Am. Chem. Soc.* **1985**, *107*, 2549.
[53] a) M. E. Marmion, K. J. Takeuchi, *J. Am. Chem. Soc.* **1986**, *108*, 510; b) *ibid.* **1988**, *110*, 1472; c) L. Roecker, T. J. Meyer, *ibid.* **1987**, *109*, 746; d) R. A. Leising, J. S. Ohman, J. H. Acquaye, K. J. Takeuchi, *J. Chem. Soc. Chem. Commun.* **1989**, 905.

[54] Condensation of primary amines with carbonyl compounds: a) S. D. Larsen, P. A. Grieco, W. F. Fobare, *J. Am. Chem. Soc.* **1986**, *108*, 3512; b) R. J. Doedens, G. P. Meier, L. E. Overman, *J. Org. Chem.* **1988**, *53*, 685. Reaction of imines with acetyl chloride: c) H. Hiemstra, H. P. Fortgens, W. N. Speckamp, *Tetrahedron Lett.* **1985**, *26*, 3155. Protonolysis of reduced cyclic imides: d) C. J. Flann, L. E. Overman, *J. Am. Chem. Soc.* **1987**, *109*, 6115; e) W. N. Speckamp, *Recl. Trav. Chim. Pays-Bas* **1981**, *100*, 345.

[55] a) S.-I. Murahashi, Y. Imada, K. Nishimura, *Tetrahedron*, **1994**, *50*, 453; b) *J. Chem. Soc. Chem. Commun.* **1988**, 1578.

[56] a) S.-I. Murahashi, Y. Imada, Y. Taniguchi, S. Higashiura, *Tetrahedron Lett.* **1988**, *29*, 4945; b) *J. Org. Chem.* **1993**, *58*, 1538.

[57] S.-I. Murahashi, T. Naota, T. Nakato, *Synlett* **1992**, 835.

[58] S.-I. Murahashi, T. Naota, N. Miyaguchi, T. Nakato, *Tetrahedron Lett.* **1992**, *33*, 6991.

[59] S.-I. Murahashi, T. Naota, H. Taki, *J. Chem. Soc. Chem. Commun.* **1985**, 613.

[60] P. Müller, D. M. Gilabert, *Tetrahedron* **1988**, *44*, 7171.

[61] K. Maruyama, T. Kasukawa, Y. Higuchi, A. Nishinaga, *Chem. Lett.* **1991**, 1093.

[62] a) S. V. Ley, J. Norman, W. P. Griffith, S. P. Marsden, *Synthesis* **1994**, 639; b) W. P. Griffith, S. V. Ley, *Aldrichimica Acta* **1990**, *23*, 13.

[63] A. Goti, M. Romani, *Tetrahedron Lett.* **1994**, *35*, 6567.

[64] a) S. E. Denmark, N. Nakajima, O. J.-C. Nicaise, *J. Am. Chem. Soc.* **1994**, *116*, 8797, and references therein; b) K. Soai, T. Hatanaka, T. Miyazawa, *J. Chem. Soc. Chem. Commun.* **1992**, 1097; c) K. Tomioka, I. Inoue, M. Shindo, K. Koga, *Tetrahedron Lett.* **1991**, *32*, 3095; d) C. A. Willoughby, S. L. Buchwald, *J. Am. Chem. Soc.* **1994**, *116*, 11703.

[65] N-Dealkylation of amides: a) L. K. Low, N. Castagnoli, Jr. in *Burger's Medical Chemistry, Part I*, 4th ed. (Ed.: M. E. Wolff), Wiley, New York, **1980**, pp. 163–167; b) P. Kestell, M. D. Threadgill, A. Gescher, A. P. Gledhill, A. J. Shaw, P. B. Farmer, *J. Pharmacol. Exp. Ther.* **1987**, *240*, 265.

[66] For an excellent review, see: a) T. Shono, *Tetrahedron* **1984**, *40*, 811. Acetoxylation of β-lactams: b) P. Schneider, D. Ramos, J. Bersier (Ciba-Geigy), EP 290385, **1988** [*Chem. Abstr.* **1988**, *110*, 192526; c) M. Mori, K. Kagechika, K. Tohjima, M. Shibasaki, *Tetrahedron Lett.* **1988**, *29*, 1409.

[67] S.-I. Murahashi, T. Naota, T. Kuwabara, T. Saito, H. Kumobayashi, S. Akutagawa, *J. Am. Chem. Soc.* **1990**, *112*, 7820.

[68] A. Mitani, S.-I. Murahashi, unpublished results.

[69] N. Hirai, T. Naota, S.-I. Murahashi, unpublished results.

[70] T. Naota, T. Nakato, S.-I. Murahashi, *Tetrahedron Lett.* **1990**, *31*, 7475.

[71] a) T. Shibata, K. Iino, T. Tanaka, T. Hashimoto, Y. Kameyama, Y. Sugimura, *Tetrahedron Lett.* **1985**, *26*, 4739; b) Y. Nagao, T. Kumagai, S. Tamai, T. Abe, Y. Kuramoto, T. Taga, S. Aoyagi, Y. Nagase, M. Ochiai, Y. Inoue, E. Fujita, *J. Am. Chem. Soc.* **1986**, *108*, 4673; c) L. M. Fuentes, I. Shinkai, T. N. Salzmann, *ibid.* **1986**, *108*, 4675; d) A. I. Meyers, T. J. Sowin, S. Scholz, Y. Ueda, *Tetrahedron Lett.* **1987**, *28*, 5103; e) Y. Ito, S. Terashima, *ibid.* **1987**, *28*, 6625; f) F. Shirai, T. Nakai, *J. Org. Chem.* **1987**, *52*, 5491; g) R. Deziel, M. Endo, *Tetrahedron Lett.* **1988**, *29*, 61; h) Y. Nagao, T. Abe, H. Shimizu, T. Kumagai, Y. Inoue, *J. Chem. Soc. Chem. Commun.* **1989**, 821.

[72] S.-I. Murahashi, T. Saito, T. Naota, H. Kumobayashi, S. Akutagawa, *Tetrahedron Lett.* **1991**, *32*, 2145.

[73] a) M. Schröder, *Chem. Rev.* **1980**, *80*, 187; b) R. A. Johnson, K. B. Sharpless in ref. [33c], p. 227.

[74] a) C. E. H. Bawn, J. B. Williamson, *Trans. Faraday Soc.* **1951**, *47*, 721, 735; b) C. E. H. Bawn, J. E. Jolley, *Proc. R. Soc. London Ser. A.* **1956**, *237*, 297; c) ref. [1b], p. 140.

[75] S.-I. Murahashi, T. Saito, T. Naota, H. Kumobayashi, S. Akutagawa, *Tetrahedron Lett.* **1991**, *32*, 5991.

[76] a) R. C. Blake, II, M. J. Coon, *J. Biol. Chem.* **1981**, *256*, 12127; b) L. M. Hjelmeland, L. Aronow, J. R. Trudell, *Biochem. Biophys. Res. Commun.* **1977**, *76*, 541.

[77] A. E. Shilov, E. I. Karasevich, *Metalloporphyrins Catalyzed Oxidations* (Eds.: F. Montanari, L. Casella), Kluwer Academic, Dordrecht, **1994**, pp. 87–120.

[78] B. Meunier, *Chem. Rev.* **1992**, *92*, 1411.

[79] a) A. E. Shirov in ref. [79f], p. 1; b) D. Mansuy in ref. [79f], p. 195; c) K. S. Kuslick in ref. [79f], p. 219; d) C. H. Hill in ref. [79f], p. 243; e) C. A. Tolman, J.-D. Druliner, M. J. Nappa, N. Herron in ref. [79f], p. 267; f) *Activation and Functionalization of Alkanes* (Ed.: C. L. Hill), Wiley, New York, **1989**.

[80] D. Mansuy, P. Battioni, J.-P. Battioni, *Eur. J. Biochem.* **1989**, *184*, 267.

[81] a) D. Mansuy, J. F. Bartoli, M. Momenteau, *Tetrahedron Lett.* **1982**, *23*, 2781; b) J. T. Groves, T. E. Nemo, *J. Am. Chem. Soc.* **1983**, *105*, 6243; c) J. A. Smegal, C. L. Hill, *ibid.* **1983**, *105*, 3515; d) T. G. Traylor, Y. S. Byun, P. S. Traylor, P. Battioni, D. Mansuy, *ibid.* **1991**, *113*, 7821; e) P. Hoffmann, A. Robert, B. Meunier, *Bull. Soc. Chim. Fr.* **1992**, *129*, 85.

[82] a) B. De Poorter, M. Ricci, O. Bortolini, B. Meunier, *J. Mol. Cat.* **1985**, *31*, 221; b) J. P. Collman, H. Tanaka, R. T. Hembre, J. I. Brauman, *J. Am. Chem. Soc.* **1990**, *112*, 3689; c) A. B. Sorokin, A. M. Khenkin, *J. Chem. Soc. Chem. Commun.* **1990**, 45.

[83] D. Mansuy, *Pure Appl. Chem.* **1990**, *62*, 741.

[84] B. Meunier, *New J. Chem.* **1992**, *16*, 203.

[85] B. R. Cook, T. J. Reinert, K. S. Suslick, *J. Am. Chem. Soc.* **1986**, *108*, 7281.

[86] a) H. Ohtake, T. Higuchi, M. Hirobe, *J. Am. Chem. Soc.* **1992**, *114*, 10660; b) M. W. Nee, T. C. Bruice, *ibid.* **1982**, *104*, 6123.

[87] I. Tabushi, A. Yazaki, *J. Am. Chem. Soc.* **1981**, *103*, 7371.

[88] M. Fontecave, D. Mansuy, *Tetrahedron* **1984**, *40*, 4297.

[89] W. Y. Lu, J. F. Bartoli, P. Battioni, D. Mansuy, *New J. Chem.* **1992**, *16*, 621.

[90] a) P. A. Grieco, T. L. Stuk, *J. Am. Chem. Soc.* **1990**, *112*, 7799; b) T. L. Stuk, P. A. Grieco, M. M. Marsh, *J. Org. Chem.* **1991**, *56*, 2957.

[91] J. T. Groves, P. Viski, *J. Org. Chem.* **1990**, *55*, 3628.

[92] a) D. H. R. Barton, D. Doller, *Acc. Chem. Res.* **1992**, *25*, 504, and references therein; b) D. H. R. Barton, S. D. Béviére, W. Chavasiri, E. Csuhai, D. Doller, W.-G. Liu, *J. Am. Chem. Soc.* **1992**, *114*, 2147; c) D. H. R. Barton, E. Csuhai, D. Doller, Y. V. Geletti, *Tetrahedron* **1991**, *47*, 6561; d) C. Sheu, S. A. Richert, P. Cofré, B. Ross, Jr., A. Sobkowiak, D. T. Sawyer, J. R. Kanofsky, *J. Am. Chem. Soc.* **1990**, *112*, 1936; e) H.-C. Tung, C. Kang, D. T. Sawyer, *ibid.* **1992**, *114*, 3445; f) D. T. Sawyer, C. Kang, A. Llobet, C. Redman, *ibid.* **1993**, *115*, 5817; g) A. S. Goldstein, R. H. Beer, R. S. Drago, *ibid.* **1994**, *116*, 2424, and references therein.

[93] a) L. Saussine, E. Brazi, A. Robine, H. Mimoun, J. Fischer, R. Weiss, *J. Am. Chem. Soc.* **1985**, *107*, 3534; b) D. H. R. Barton, W. Chavasiri, *Tetrahedron* **1994**, *50*, 19; c) D. H. R. Barton, T.-L. Wang, *ibid.* **1994**, *50*, 1011; d) C. Bardin, D. H. R. Barton, B. Hu, R. Rojas-Wahl, D. K. Taylor, *Tetrahedron Lett.* **1994**, *35*, 5805; e) J. B. Vincent, J. C. Huffman, G. Christou, Q. Li, M. A. Nanny, D. N. Hendrickson, R. H. Fong, R. H. Fish, *J. Am. Chem. Soc.* **1988**, *110*, 6898; f) R. A. Leising, J. Kim, M. A. Perez, L. Que, Jr., *ibid.* **1993**, *115*, 9524; g) T.-C. Lau, C.-M. Che, W.-O. Lee, C.-K. Poon, *J. Chem. Soc. Chem. Commun.* **1988**, 1406; h) M. Faraj, C. L. Hill, *ibid.* **1987**, 1487.

[94] D. H. R. Barton, S. D. Béviére, D. R. Hill, *Tetrahedron* **1994**, *50*, 2665.

[95] S.-I. Murahashi, Y. Oda, T. Naota, T. Kuwabara, *Tetrahedron Lett.* **1993**, *34*, 1299.

[96] S.-I. Murahashi, Y. Oda, N. Komiya, T. Naota, *Tetrahedron Lett.* **1994**, *35*, 7953.

[97] K. Nomura, S. Uemura, *J. Chem. Soc. Chem. Commun.* **1994**, 129.

[98] a) D. H. R. Barton, *Aldrichimica Acta* **1990**, *23*, 3; b) D. H. R. Barton, J. Boivin, M. Gastiger, J. Morzycki, R. S. Hay-Motherwell, W. B. Motherwell, N. Ozbalik, K. M. Schwartzentruber, *J. Chem. Soc. Perkin Trans. 1* **1986**, 947; c) N. Kitajima, M. Ito, H. Fukui, Y. Moro-oka, *J. Chem. Soc. Chem. Commun.* **1991**, 102.

[99] J. F. Bartoli, P. Battioni, W. R. De Foor, D. Mansuy, *J. Chem. Soc. Chem. Commun.* **1994**, 23, and references therein.

[100] S.-I. Murahashi, Y. Oda, T. Naota, *J. Am. Chem. Soc.* **1992**, *114*, 7913.

[101] R. K. Khanna, T. M. Pauling, D. Vajpayee, *Tetrahedron Lett.* **1991**, *32*, 3759.

[102] R. A. Leising, B. A. Brennan, L. Que, Jr., B. G. Fox, E. Münck, *J. Am. Chem. Soc.* **1991**, *113*, 3988.

[103] a) J. W. M. Steeman, S. Kaarsemaker, P. J. Hoftyzer, *Chem. Eng. Sci.* **1961**, *14*, 139; b) S. A. Miller, *Chem. Process Eng. (London)* **1969**, *50*, 63.

[104] a) K. V. Reddy, S.-J. Jin, P. K. Arora, D. S. Sfeir, S. C. Feke Maloney, F. L. Urbach, L. M. Sayre, *J. Am. Chem. Soc.* **1990**, *112*, 2332; b) P. Capdevielle, M. Maumy, *Tetrahedron Lett.* **1991**, *32*, 3831.

[105] S.-I. Murahashi, Y. Oda, T. Naota, N. Komiya, *J. Chem. Soc. Chem. Commun.* **1993**, 139.

[106] D. H. R. Barton, S. D. Béviére, W. Chavasiri, É. Csuhai, D. Doller, *Tetrahedron* **1992**, *48*, 2895.

[107] a) P. Capdevielle, M. Maumy, *Tetrahedron Lett.* **1990**, *31*, 3891; b) N. Kitajima, T. Koda, Y. Iwata, Y. Moro-oka, *J. Am. Chem. Soc.* **1990**, *112*, 8833.

[108] S.-I. Murahashi, N. Komiya, T. Naota, unpublished results.

[109] S.-I. Murahashi, T. Naota, T. Kuwabara, *Synlett* **1989**, 62.

[110] S.-I. Murahashi, T. Naota, N. Nakajima, *J. Org. Chem.* **1986**, *51*, 898.

[111] Sodium periodate: a) P. H. J. Carlsen, T. Katsuki, V. S. Martin, K. B. Sharpless, *J. Org. Chem.* **1981**, *46*, 3936. Natriumbromat: b) Y. Yamamoto, H. Suzuki, Y. Moro-oka, *Tetrahedron Lett.* **1985**, *26*, 2107; c) S. Kanemoto, H. Tomioka, K. Oshima, H. Nozaki, *Bull. Chem. Soc. Jpn.* **1986**, *59*, 105. *N*-Methylmorpholine: d) K. B. Sharpless, K. Akashi, K. Oshima, *Tetrahedron Lett.* **1976**, 2503; e) ref. [62]. Iodosylbenzene: f) P. Müller, J. Godoy, *Tetrahedron Lett.* **1981**, *22*, 2361. Bis(trimethylsilyl)peroxide: g) S. Kanemoto, K. Oshima, S. Matsubara, K. Takai, H. Nozaki, *ibid.* **1983**, *24*, 2185. Oxygen: h) C. Bilgrien, S. Davis, R. S. Drago, *J. Am. Chem. Soc.* **1987**, *109*, 3786; i) J.-E. Bäckvall, R. L. Chowdhury, U. Karlsson, *J. Chem. Soc. Chem. Commun.* **1991**, 473, and references therein.

[112] a) S.-I. Murahashi, T. Naota, N. Nakajima, *Tetrahedron Lett.* **1985**, *26*, 925; b) S.-I. Murahashi, T. Naota, *Synthesis* **1993**, 433.

[113] a) Y. Tsuji, T. Ohta, T. Ido, H. Minbu, Y. Watanabe, *J. Organomet. Chem.* **1984**, *270*, 333; b) M. Tanaka, T. Kobayashi, T. Sakakura, *Angew. Chem.* **1984**, *96*, 519; *Angew. Chem. Int. Ed. Engl.* **1984**, *23*, 518.

[114] S. Hünig, R. Schaller, *Angew. Chem.* **1982**, *94*, 1; *Angew. Chem. Int. Ed. Engl.* **1982**, *21*, 36.

[115] S.-I. Murahashi, T. Naota, N. Nakajima, *Chem. Lett.* **1987**, 879.

[116] a) R. J. Bergeron, *Acc. Chem. Res.* **1986**, *19*, 105; b) B. Ganem, *ibid.* **1982**, *15*, 290.

[117] G. Englert, K. Klinga, Raymond-Hamet, E. Schlittler, W. Vetter, *Helv. Chim. Acta* **1973**, *56*, 474.

[118] CuCl/amine/K_2CO_3: a) C. Jallabert, H. Riviere, *Tetrahedron Lett.* **1977**, 1215. $[Cu(bpy)_2(OH)_2]$ (bpy = 2,2'-bipyridine); b) X. Liu, A. Qiu, D. T. Sawyer, *J. Am. Chem. Soc.* **1993**, *115*, 3239. $[RuCl(OAc)(PPh_3)_3]$/hydroquinone/$[Co(salophen)(PPh_3)]$ (salophen = bis(salicylidene)phenylenediamine); c) ref. [111i].
[119] RuO_2: M. Matsumoto, N. Watanabe, *J. Org. Chem.* **1984**, *49*, 3435.
[120] K. Heyns, L. Blazejewicz, *Tetrahedron* **1960**, *9*, 67.
[121] T. F. Blackburn, J. Schwartz, *J. Chem. Soc. Chem. Commun.* **1977**, 157.
[122] S.-I. Murahashi, T. Naota, N. Hirai, *J. Org. Chem.* **1993**, *58*, 7318.
[123] W. H. Richardson, *J. Am. Chem. Soc.* **1966**, *88*, 975.
[124] a) E. C. Horswill, K. U. Ingold, *Can. J. Chem.* **1966**, *44*, 269; b) L. H. Vogt, Jr., J. G. Wirth, H. L. Finkbeiner, *J. Org. Chem.* **1969**, *34*, 273.
[125] S.-I. Murahashi, N. Miyaguchi, S. Noda, T. Naota, unpublished results.
[126] For reviews, see: a) G. R. Know, *Org. React.* **1993**, *43*, 251; b) W. Carruthers, *Some Modern Methods of Organic Synthesis*, Cambridge University Press, New York, **1986**, pp. 403–407.
[127] Peracetic acid: a) P. S. Starcher, B. Phillips, *J. Am. Chem. Soc.* **1958**, *80*, 4079. Peroxytrifluoroacetic acid: b) W. D. Emmons, G. B. Lucas, *ibid.* **1955**, *77*, 2287. Perbenzoic acid: c) S. L. Friess, *ibid.* **1949**, *71*, 2571. *m*-Chloroperbenzoic acid: d) R. R. Sauers, R. W. Ubersax, *J. Org. Chem.* **1965**, *30*, 3939. Magnesium monoperoxyphthalate hexahydrate: e) P. Brougham, M. S. Cooper, D. A. Cummerson, H. Heaney, N. Thompson, *Synthesis* **1987**, 1015.
[128] a) P. A. Grieco, Y. Yokoyama, S. Gilman, Y. Ohfune, *J. Chem. Soc. Chem. Commun.* **1977**, 870; b) S. E. Jacobson, F. Mares, P. M. Zambri, *J. Am. Chem. Soc.* **1979**, *101*, 6938; c) L. Syper, *Synthesis* **1989**, 167; d) M. Del Todesco Frisone, F. Pinna, G. Strukul, *Organometallics* **1993**, *12*, 148; e) A. Gusso, C. Baccin, F. Pinna, G. Strukul, *ibid.* **1994**, *13*, 3442.
[129] M. Suzuki, H. Takada, R. Noyori, *J. Org. Chem.* **1982**, *47*, 902.
[130] a) R. G. Howard, W. K. Ben (Union Carbide Corp.) US-A 3025306, **1962** [*Chem. Abstr.* **1962**, *56*, 15368]; b) A. G. Knapsack, NL-A 6516355 [*Chem. Abstr.* **1966**, *65*, 15237]; c) T. Maki, K. Mineta (Mitsubishi Kasei Co.), JP-B 77100402 [*Chem. Abstr.* **1978**, *88*, 89122]; d) T. Yamada, K. Takahashi, K. Kato, T. Takai, S. Inoki, T. Mukaiyama, *Chem. Lett.* **1991**, 641.
[131] S.-I. Murahashi, Y. Oda, T. Naota, *Tetrahedron Lett.* **1992**, *33*, 7557.
[132] C. Bolm, G. Schlingloff, K. Weickhardt, *Tetrahedron Lett.* **1993**, *34*, 3405.
[133] M. Hamamoto, K. Nakayama, Y. Nishiyama, Y. Ishii, *J. Org. Chem.* **1993**, *58*, 6421.
[134] K. Kaneda, S. Ueno, T. Imanaka, E. Shimotsuma, Y. Nishiyama, Y. Ishii, *J. Org. Chem.* **1994**, *59*, 2915.
[135] K. R. Lassila, F. J. Waller, S. E. Werkheiser, A. L. Wressell, *Tetrahedron Lett.* **1994**, *35*, 8077.
[136] C. Bolm, G. Schlingloff, K. Weickhardt, *Angew. Chem.* **1994**, *106*, 1944; *Angew. Chem. Int. Ed. Engl.* **1994**, *33*, 1848.
[137] K. A. Jørgensen, *Chem. Rev.* **1989**, *89*, 431.
[138] B. Meunier, *Metalloporphyrins Catalyzed Oxidations* (Eds.: F. Montanari, L. Casella), Kluwer Academic, Dordrecht, **1994**, p. 1.
[139] J. T. Groves, R. S. Myers, *J. Am. Chem. Soc.* **1983**, *105*, 5791.
[140] D. Mansuy, P. Battioni, J. P. Renaud, P. Guerin, *J. Chem. Soc. Chem. Commun.* **1985**, 155.
[141] J. P. Collman, X. Zhang, R. T. Hembre, J. I. Brauman, *J. Am. Chem. Soc.* **1990**, *112*, 5356.
[142] Y. Naruta, F. Tani, N. Ishihara, K. Maruyama, *J. Am. Chem. Soc.* **1991**, *113*, 6865.
[143] K. Konishi, K.-I. Oda, K. Nishida, T. Aida, S. Inoue, *J. Am. Chem. Soc.* **1992**, *114*, 1313.
[144] S. O'Malley, T. Kodadek, *J. Am. Chem. Soc.* **1989**, *111*, 9116.
[145] a) R. A. Johnson, K. B. Sharpless in ref. [33c], p. 103; b) A. Pfenninger, *Synthesis*, **1986**, 89; c) K. B. Sharpless, *Chemtech* **1985**, *15*, 692; d) M. G. Finn, K. B. Sharpless, *Asymmetric Synth.* **1985**, *5*, 247; e) B. Rossiter, *ibid.* **1985**, *5*, 193; f) C. H. Behrens, K. B. Sharpless, *Aldrichimica Acta* **1983**, *16*, 67.
[146] W. Zhang, J. L. Loebach, S. R. Wilson, E. N. Jacobsen, *J. Am. Chem. Soc.* **1990**, *112*, 2801.
[147] W. Zhang, E. N. Jacobsen, *J. Org. Chem.* **1991**, *56*, 2296.
[148] E. N. Jacobsen, W. Zhang, A. R. Muci, J. R. Ecker, L. Deng, *J. Am. Chem. Soc.* **1991**, *113*, 7063.
[149] a) R. Irie, K. Noda, Y. Ito, N. Matsumoto, T. Katsuki, *Tetrahedron Lett.* **1990**, *31*, 7345; b) H. Sasaki, R. Irie, T. Hamada, K. Suzuki, T. Katsuki, *Tetrahedron* **1994**, *50*, 11827.
[150] a) T. Schwenkreis, A. Berkessel, *Tetrahedron Lett.* **1993**, *34*, 4785; b) R. Irie, N. Hosoya, T. Katsuki, *Synlett* **1994**, 255.
[151] a) T. Yamada, K. Imagawa, T. Nagata, T. Mukaiyama, *Chem. Lett.* **1992**, 2231; b) *Bull. Chem. Soc. Jpn.* **1994**, *67*, 2248.
[152] a) D. Ostović, T. C. Bruice, *J. Am. Chem. Soc.* **1989**, *111*, 6511; b) A. J. Castellino, T. C. Bruice, *ibid.* **1988**, *110*, 158, 7512; c) ref. [41e]; c) T. G. Traylor, A. R. Miksztal, *ibid.* **1987**, *109*, 2770.
[153] S.-I. Murahashi, T. Saito, H. Hanaoka, Y. Murakami, T. Naota, H. Kumobayashi, S. Akutagawa, *J. Org. Chem.* **1993**, *58*, 2929.
[154] T. Hashiyama, K. Morikawa, K. B. Sharpless, *J. Org. Chem.* **1992**, *57*, 5067, and references therein.
[155] F. A. Davis, A. C. Sheppard, B.-C. Chen, M. S. Haque, *J. Am. Chem. Soc.* **1990**, *112*, 6679, and references therein.
[156] S. Baskaran, J. Das, S. Chandrasekaran, *J. Org. Chem.* **1989**, *54*, 5182.
[157] T. Takai, T. Yamada, T. Mukaiyama, *Chem. Lett.* **1991**, 1499.
[158] a) L. E. Overman, F. M. Knoll, *Tetrahedron Lett.* **1979**, *4*, 321; b) P. A. Grieco, T. Takigawa, S. L. Bongers, H. Tanaka, *J. Am. Chem. Soc.* **1980**, *102*, 7587.
[159] S.-I. Murahashi, T. Naota, H. Hanaoka, *Chem. Lett.* **1993**, 1767.
[160] a) T. Yamada, T. Takai, O. Rhode, T. Mukaiyama, *Chem. Lett.* **1991**, 1; b) *Bull. Chem. Soc. Jpn.* **1991**, *64*, 2109.
[161] a) T. Punniyamurthy, B. Bhatia, J. Iqbal, *J. Org. Chem.* **1994**, *59*, 850; b) M. M. Reddy, T. Punniyamurthy, J. Iqbal, *Tetrahedron Lett.* **1995**, *36*, 159.

Cyclopentadienyl-Free Organolanthanide Chemistry

Frank T. Edelmann*

Dedicated to Professor Herbert W. Roesky on the occasion of his 60th birthday

During the past ten years the organometallic chemistry of the lanthanides has witnessed enormous growth. One of the main reasons for this development was the finding that lanthanide metallocenes can exhibit an unusually high catalytic activity. Considerable advances have also been achieved in the chemistry of organolanthanide complexes that are not stabilized by cyclopentadienyl ligands. For example, the successful synthesis of the first unsolvated homoleptic trialkyllanthanides, $[Ln\{CH(SiMe_3)_2\}_3]$, has recently been reported. Anionic allyl complexes of the lanthanides show promising catalytic properties and cyclooctatetraene complexes of these elements are also under active investigation. This review is intended to provide an overview of this rapidly developing area of research.

Keywords: cyclooctatetraene complexes · homogeneous catalysis · lanthanides · organolanthanide compounds

1. Introduction

Organolanthanide chemistry is currently one of the most rapidly developing areas of organometallic chemistry. This is even more surprising, as only twenty years ago it was stated in inorganic chemistry textbooks that the lanthanide elements do not form stable organometallic compounds. Meanwhile it has become quite clear that organolanthanide chemistry follows its own rules and often differs significantly from organometallic chemistry of the 3d transition metals. In recent years numerous unprecedented reaction pathways and novel molecular structures have been discovered, which demonstrate the unique character of organolanthanide chemistry. The impressive advance in this area has already been documented in several reviews.[1–6] The current research in the field of homogeneous catalysis with organolanthanide complexes is particularly exciting. It is now well established that certain lanthanide metallocenes can exhibit an unusually high catalytic activity. This is particularly true for olefin transformations such as hydrogenations, cyclizations, polymerizations, and addition reactions. Traditionally, for these purposes attention focused on cyclopentadienyl complexes of the lanthanides. Approximately 90% of all previously described organometallic complexes of the 4f elements are compounds containing cyclopentadienyl ligands.[4–6] Anionic π ligands are ideally suited for stabilizing highly reactive alkyl- and hydridolanthanide complexes. More recently, however, increasing use has been made of other ligand systems in organolanthanide chemistry. Among these ligands are bulky σ-alkyl groups and allyl ligands as well as pentadienyl anions ("open cyclopentadienyl"), neutral arenes, and anionic heterocycles. η^8-Cyclooctatetraene complexes of the lanthanides are a particularly large class of compounds. This review is intended to provide an overview of the current developments by illustrating synthetic and structural aspects as well as possible applications. Without trying to be fully comprehensive, it will present the most interesting results and show the main objectives.

Table 1 shows the assignment of the various lanthanide elements in the numbering of the compounds. As usual, scandium and yttrium have been included because of their chemical similarity with the lanthanides. The radioactive element promethium has been omitted as no organometallic compound without cyclopentadienyl ligands has so far been reported.[6] Compounds in which the formal oxidation state of the lanthanide is zero have also been excluded.

Table 1. Numbering scheme of the lanthanide elements in this article.

Sc	Y	La	Ce	Pr	Nd	Sm	Eu	Gd	Tb	Dy	Ho	Er	Tm	Yb	Lu
a	**b**	**c**	**d**	**e**	**f**	**g**	**h**	**i**	**j**	**k**	**l**	**m**	**n**	**o**	**p**

2. Carbonyl Complexes

In sharp contrast to the organometallic chemistry of the 3d transition metals, binary carbonyllanthanide compounds are unstable under normal conditions.[5] Ln^{3+} ions are considered good σ acceptors but poor π donors. Simple lanthanide carbonyls $[Ln(CO)_n]$ have so far only been detected in matrix inves-

[*] Prof. Dr. F. T. Edelmann
Chemisches Institut der Universität
Universitätsplatz 2, Gebäude M
D-39106 Magdeburg (Germany)
Telefax: Int. code + (391)67-12933

 © VCH Verlagsgesellschaft mbH, D-69451 Weinheim, 1995 0570-0833/95/3422-2466 $ 10.00+.25/0

tigations.[11] The only structurally characterized compound, for which coordination of a CO ligand to a lanthanide element was proven, is the heteronuclear erbium complex **1m** (Fig. 1).[7] Weak

$[Er(EtOH)(H_2O)_4\{Mo(CO)_3(C_5H_5)\}_3]$ **1m**

metal–metal interactions and semibridging carbonyl ligands between molybdenum and erbium characterize this compound, which resembles the previously described heterobimetallic complexes with isocarbonyl bridges between lanthanides and transition metals.[8] Even today there is still a long way to go before the main goal is reached, namely, the synthesis of "true" carbonyl complexes of the lanthanides with C-bonded CO.

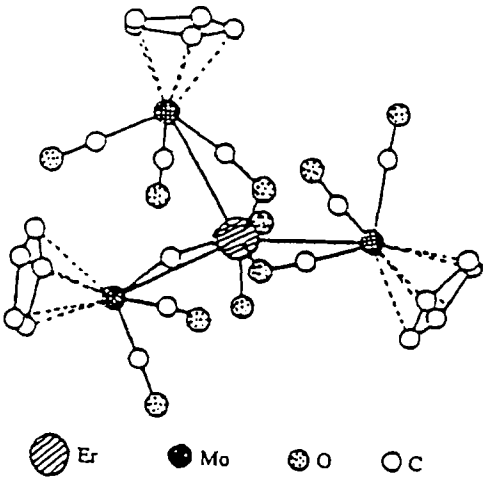

Fig. 1. Molecular structure of $[Er(EtOH)(H_2O)_4\{Mo(CO)_3(C_5H_5)\}_3]$ **1m** in the crystal.

3. Alkyl and Aryl Complexes

Once again in contrast to the countless π complexes of 3d transition metals, the lanthanides exhibit virtually no tendency to coordinate neutral alkenes, dienes, allenes, or alkynes.[1–6] The reasons for this behavior are the limited radial extension of the 4f orbitals and the fact that the Ln–C bond in organolanthanide complexes is predominantly ionic. Thus early attempts to prepare lanthanide complexes of unsaturated hydrocarbons were mostly unsuccessful. Likewise, the synthesis of simple organolanthanide complexes containing only σ-bonded ligands is quite problematic. One of the major challenges in the field of organolanthanide chemistry was (and continues to be) the synthesis of unsolvated, homoleptic trialkyl- and triaryllanthanides LnR_3. The main reason for the instability of such compounds is the tendency of the lanthanide to adopt high coordination numbers. Because of the large ionic radii of the Ln^{3+} ions, three-coordinate compounds with simple alkyl or aryl ligands are sterically highly unsaturated. Normally this leads to the formation of solvent adducts, "ate" complexes, or oligomeric species. A significant breakthrough was achieved only very recently through the use of sterically demanding alkyl ligands such as $CH(SiMe_3)_2$.

3.1. Neutral Homoleptic Compounds

In addition to neutral, unsolvated compounds of the composition LnR_2 and LnR_3, solvent adducts thereof will also be discussed in this section, although per definition these materials are heteroleptic complexes. The most thoroughly investigated lanthanide(II) compound in this group is bis(pentafluorophenyl)ytterbium(II), $[Yb(C_6F_5)_2]$ **2o**, which was described by Deacon et al.[8–10] This compound is easily accessible by a

$[Yb(C_6F_5)_2]$ **2o** $[Yb(o\text{-}C_6F_4H)_2]$ **3o** $[Yb(p\text{-}C_6F_4H)_2]$ **4o**

transmetalation reaction between metallic ytterbium and bis(pentafluorophenyl)mercury. The corresponding europium(II) compound **2h** can be obtained analogously [Eq. (1)].

$$Ln + [Hg(C_6F_5)_2] \longrightarrow \underset{\mathbf{2},\ Ln = Eu,\ Yb}{[Ln(C_6F_5)_2]} + Hg \qquad (1)$$

The comparably high stability of the pentafluorophenyl derivatives has been explained by the formation of metal–fluorine interactions. Partially fluorinated derivatives such as **3o** and **4o** are significantly less stable than **2o**. Compounds **2h** and **2o** are both very useful intermediates in various subsequent reactions, for example, as starting materials for the preparation of lanthanide(II) amides and phenoxides.[11] Furthermore, the σ-bonded pentafluorophenyl groups in **2o** can be transferred to

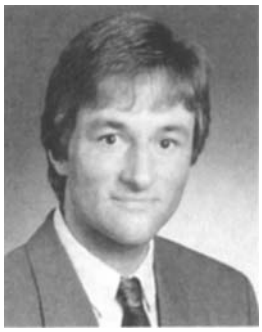

Frank T. Edelmann, born 1954 in Hamburg, studied chemistry from 1974–1979 at the University of Hamburg. He received his doctorate in 1983 under the supervision of U. Behrens with a Ph. D. thesis entitled "Die Chemie der Tricarbonyl(fulven)chrom-Komplexe" (The Chemistry of Tricarbonyl(fulvene)chromium Complexes). This was followed by two years of postdoctoral research as a Feodor Lynen Fellow of the Alexander-von-Humboldt-Stiftung in the groups of J. Takats (University of Alberta, Edmonton, Canada), J. W. Gilje (University of Hawaii, Honolulu, USA), and T. Chivers (University of Calgary, Calgary, Canada). In 1991 he finished his Habilitation in the group of H. W. Roesky at the University of Göttingen and in 1995 he was appointed a full professor of Inorganic Chemistry at the Otto-von-Guericke-University in Magdeburg. His research interests include the organometallic and coordination chemistry of the lanthanides, the development of novel metallocene catalysts and organometallic precursors for new materials, as well as fluorine chemistry.

transition metals.[10, 12] Recently Lappert et al. reported on an interesting new representative of this small class of compounds.[13] The first well-characterized dialkyllanthanide(II) compound **5o**, was prepared according to Equation (2). The

$[Yb\{CH(SiMe_3)_2\}_2(Et_2O)_2]$ **5o**

coordinated diethyl ether can be replaced by the chelating phosphane ligand 1,2-bis(dimethylphosphino)ethane (DMPE) [Eq. (3)]. Subsequent reactions with pivalonitrile or anionic azaallylic ligands indicate that **5o** is a very promising starting material for the preparation of novel organolanthanide(II) complexes.

$$YbI_2 + 2\,NaCH(SiMe_3)_2 \xrightarrow[-2\,NaI]{Et_2O} \underset{\mathbf{5o}}{[Yb\{CH(SiMe_3)_2\}_2(Et_2O)_2]} \quad (2)$$

$$\mathbf{5o} + DMPE \longrightarrow \underset{\mathbf{6o}}{[Yb\{CH(SiMe_3)_2\}_2(dmpe)]} + 2\,Et_2O \quad (3)$$

By using the sterically more demanding tris(trimethylsilyl)methyl ligand it was even possible to isolate an unsolvated homoleptic dialkyllanthanide(II) compound. The reaction of YbI_2 with two equivalents of $KC(SiMe_3)_3$ in benzene afforded **7o** in the form of orange, sublimable crystals, which were

$[Yb\{C(SiMe_3)_3\}_2]$ **7o**

characterized by X-ray structure analysis (Fig. 2).[14] A particularly surprising and interesting structural feature of **7o** is the C-Yb-C angle of 137°. All other bis[tris(trimethylsilyl)methyl] metal species, for example $[Mg\{C(SiMe_3)_3\}_2]$[15] and $[Na\{C(SiMe_3)_3\}_2]^-$[16], have been reported to be linear. Just a few years ago an unsolvated dialkyllanthanide(II) compound like **7o** was considered to be impossible to isolate.

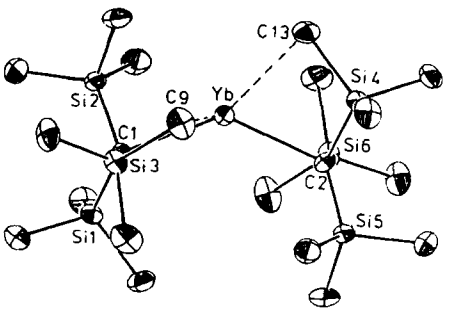

Fig. 2. Molecular structure of $[Yb\{C(SiMe_3)_3\}_2]$ **7o** in the crystal.

Organolanthanide(II) complexes can also be stabilized by σ-bonded carborane ligands.[17] The compound **8o** was synthesized by a transmetalation reaction [Eq. (4)], but an unambiguous structural characterization is still lacking.

$$Yb + [Hg(o\text{-}C_2H_2B_{10}H_9)_2] \xrightarrow[-Hg]{THF} \underset{\mathbf{8o}}{[Yb(o\text{-}C_2H_2B_{10}H_9)_2]} \quad (4)$$

Attempts at synthesizing homoleptic trialkyllanthanides were made some 50 years ago.[1] The first indications that such compounds might form came from the observation that lanthanum reacts with methyl radicals.[18] However, it was not possible to isolate a product of the composition $LaMe_3$. Early reports on the synthesis of $ScEt_3$ and YEt_3 have also never been verified.[19] It is anticipated that the reported triphenyl derivatives $ScPh_3$ **9a** and YPh_3 **10b** are oligomeric or polymeric materials.[20, 21] The reason for the inherent instability of all such compounds is that the formally three-coordinate central atom is sterically unsaturated. Only recently a well-defined σ-phenyl derivative of ytterbium became available in which the metal atoms attain the formal coordination number 6 through formation of a dinuclear complex. The highly remarkable mixed-valent Yb^{II}/Yb^{III} compound **11o** was obtained by treatment of "naphthaleneytterbium" **12o** with either diphenylmercury or triphenylbismuth.[22, 23] The crystal structure analysis revealed the presence of an asymmetric complex, in which both ytterbium atoms are coordinated in a distorted octahedral fashion (Fig. 3). Three phenyl groups act as bridging ligands by forming σ bonds to the first ytterbium atom, while being η^2-coordinated to the second ytterbium atom.

$ScPh_3$	YPh_3	$[Ph_2(thf)Yb(\mu\text{-}Ph)_3Yb(thf)_2]$	$[(C_{10}H_8)Yb(thf)_2]$
9a	**10b**	**11o**	**12o**

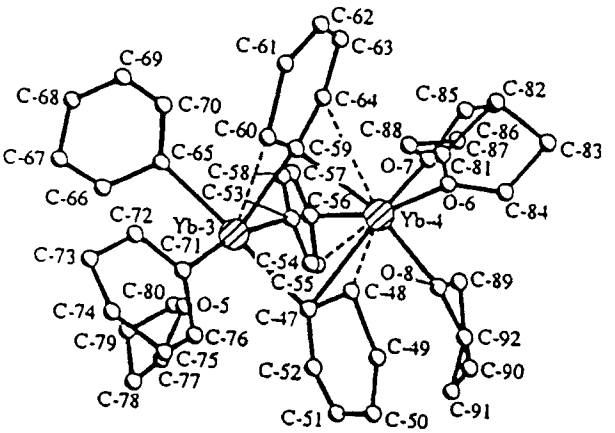

Fig. 3. Molecular structure of $[Ph_2(thf)Yb(\mu\text{-}Ph)_3Yb(thf)_2]$ **11o** in the crystal.

Recently the first structural characterization of two triphenyllanthanide complexes was reported by Bochkarev et al.[24] The THF adducts **13** were obtained according to Equation (5) by

$$2\,Ln + 3\,Ph_2Hg \xrightarrow[]{THF,\ LnI_3} \underset{\mathbf{13},\ Ln = Er,\ Tm}{2[Ph_3Ln(thf)_3]} + 3\,Hg \quad (5)$$

treatment of elemental lanthanides with diphenylmercury in the presence of small amounts of LnI_3. After reaction times of approximately 120–150 h, the products were isolated as pink (**13m**) or colorless (**13n**) highly air-sensitive crystals. Monomeric, distorted octahedral molecules with a facial arrangement of the ligands are present in the erbium derivative **13m** (Fig. 4).

Generally, however, low-coordinate organolanthanide complexes with simple σ-bound alkyl or aryl ligands are unstable. Compounds with a significantly higher stability are obtained by

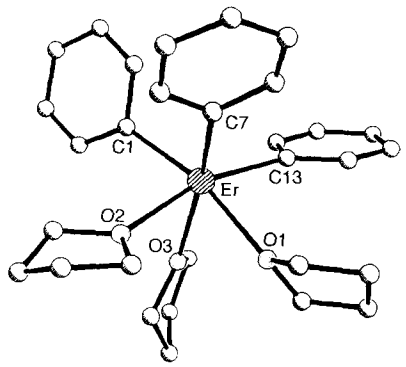

Fig. 4. Molecular structure of $[Ph_3Er(thf)_3]$ **13m** in the crystal.

using chelating ligands. Especially useful for this purpose are chelating ligands that contain an additional donor function and thus allow a coordinative saturation of the central metal atom. In this way homoleptic lanthanide complexes containing the chelating *o*-dimethylaminomethylphenyl substituent and related ligands were prepared in the 1970s. The six-coordinate complexes **14** and **15** can be isolated without any additional donor

$[Ln(o\text{-}Me_2NCH_2C_6H_4)_3]$ **14** $[Ln(o\text{-}Me_2NC_6H_4CH_2)_3]$ **15**

Ln = Sc, Y, La, Nd, Er, Yb, Lu

ligands such as THF.[25-27] Methoxy groups function as the additional donors in the complexes **16**.[28] A novel development

$[Ln(o\text{-}MeOC_6H_4)_3]$ **16**, Ln = Ce, Pr, Nd

in this area is the use of the chelating 2-dimethylaminomethylferrocenyl (FcN) ligands. FcN compounds contain cyclopentadienyl ligands, but these are not *pentahapto* coordinated to the lanthanide central atoms. Among the hitherto described organolanthanide complexes with σ-bonded FcN ligands are the compounds **17c**, **18**, and **19o**,[29] which were obtained by treatment of anhydrous lanthanide trichlorides with Li(FcN) [Eqs. (6)-(8)].

$$LaCl_3 + 2\,Li(FcN) \longrightarrow \underset{\mathbf{17c}}{[(FcN)_2LaCl]} + 2\,LiCl \quad (6)$$

$$LnCl_3 + 3\,Li(FcN) \xrightarrow{THF} \underset{\mathbf{18},\ Ln = Ce, Pr, Nd}{[(FcN)_3Ln \cdot LiCl \cdot THF]} + 2\,LiCl \quad (7)$$

$$YbCl_3 + 3\,Li(FcN) \longrightarrow \underset{\mathbf{19o}}{[Yb(FcN)_3]} + 3\,LiCl \quad (8)$$

The crystallographically characterized ytterbium "ate"-complex **20o** was obtained by reacting anhydrous ytterbium trichloride with two equivalents of Li(FcN) [Eq. (9)].[30] The product

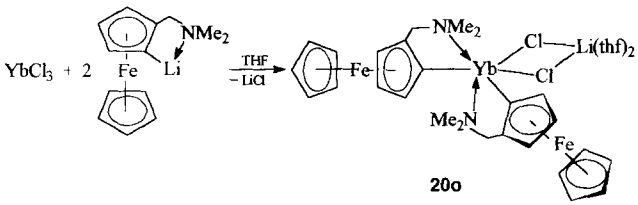

(9)

20o is the first bis(organo)lanthanide(III) halide containing only σ-bonded ligands (Fig. 5, Yb-C 265.1, 237.2 pm). This compound resembles the lanthanide metallocenes $[(C_5Me_5)_2Ln(\mu\text{-}Cl)_2Li(thf)_2]$[1-6] and thus an interesting derivative chemistry is also expected in this case.

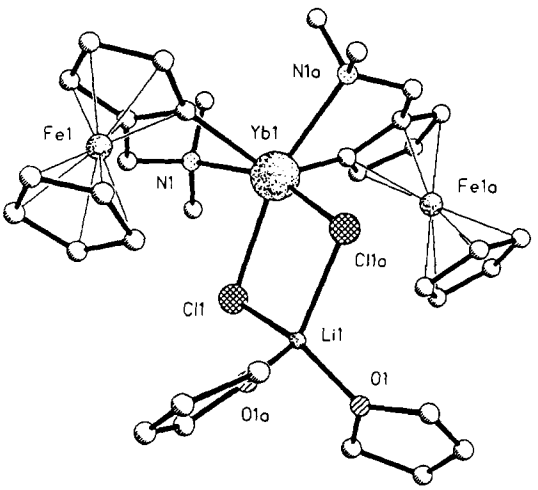

Fig. 5. Molecular structure of $[(FcN)_2Yb(\mu\text{-}Cl)_2Li(thf)_2]$ **20o** in the crystal.

Chelating phosphorus ylide anions should also be suitable for the synthesis of six-coordinate organolanthanide complexes. However, the products made according to Scheme 1 were polymeric and no structural characterization could be achieved. Even with the sterically demanding ligand $[(CH_2)_2PtBu_2]^-$ only oligomeric products were obtained.[31]

$$LnCl_3 + 3\,Me_3P{=}CH_2 \longrightarrow [Ln\{CH_2PMe_3Cl\}_3] \xrightarrow[-3\,C_4H_{10}\ -3\,LiCl]{+3n\,BuLi} \underset{\mathbf{21},\ Ln = La, Pr, Nd, Sm, Gd, Ho, Er, Lu}{[Ln\{(CH_2)_2PMe_2\}_3]}$$

Scheme 1. Synthesis of $[Ln\{(CH_2)_2PMe_2\}_3]$ **21**.

Allyl-like diphosphinomethanide ligands have been demonstrated to be much better suited for the synthesis of homoleptic organolanthanide complexes. The lanthanum derivative **22c** was structurally characterized in 1986.[32]

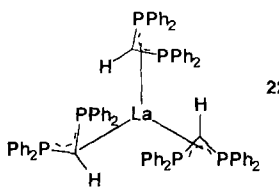

22c

With samarium as the central atom mono- or dinuclear diphosphinomethanide complexes can be isolated depending on the nature of the substituents on phosphorus [Eqs. (10) and (11), respectively].[33, 34] Both products have been unequiv-

$$[SmCl_3(thf)_3] + 3\,LiCH(PPh_2)_2 \xrightarrow[-3\,THF]{-3\,LiCl} \underset{\mathbf{23g}}{[Sm\{CH(PPh_2)_2\}_3]} \quad (10)$$

$$2\,Sm(O_3SCF_3)_3 + 6\,LiCH(PMe_2)_2 \xrightarrow[-6\,LiO_3SCF_3]{} \underset{\mathbf{24g}}{[\{\mu\text{-}\eta^2\text{-}CH(PMe_2)_2\}_2\{Sm[CH(PMe_2)_2]_2\}_2]} \quad (11)$$

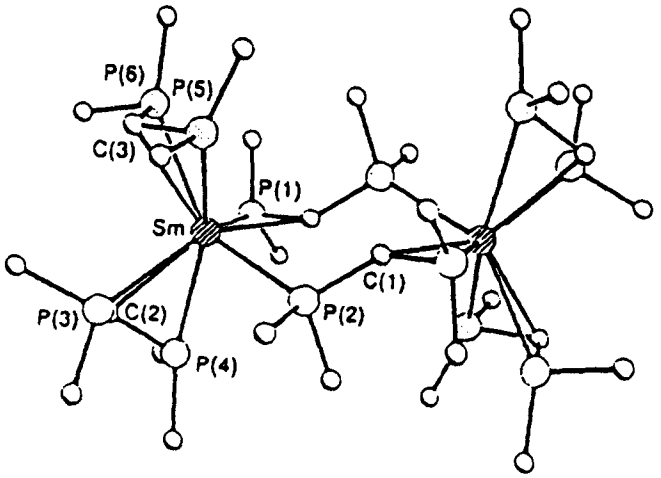

Fig. 6. Molecular structure of $[\{\mu\text{-}\eta^2\text{-}CH(PMe_2)_2\}_2\{Sm[CH(PMe_2)_2]_2\}_2]$ **24g** in the crystal.

ocally characterized by crystal structure analyses. In the centrosymmetric dimer **24g** the two samarium atoms are bridged by two diphosphinomethanide ligands through a carbon and a phosphorus atom (Fig. 6).

A second strategy for stabilizing lanthanide compounds with low coordination numbers (3–6) is the use of sterically demanding alkyl ligands. However, for this, alkyl groups such as *tert*-butyl, neopentyl, or trimethylsilylmethyl are not sufficiently bulky to allow the isolation of unsolvated trialkyllanthanides.[1] For example, treatment of lanthanide trichlorides with $LiCH_2SiMe_3$ in THF solution affords the THF adducts **25** as the final products [Eq. (12)], from which the coordinated solvent cannot be removed without decomposition.[35–39] The products are thermolabile and decompose upon heating under elimination of THF and tetramethylsilane. It was proposed that the resulting pyrophoric and presumably polymeric materials are lanthanide carbene complexes, although nothing is known about the molecular structure of these products.

$$LnCl_3 + 3\,LiCH_2SiMe_3 \xrightarrow{THF} [(Me_3SiCH_2)_3Ln(thf)_2] + 3\,LiCl \qquad (12)$$

25, Ln = Er, Tm, Yb, Lu

The results discussed above make quite clear that base-free homoleptic alkyllanthanide compounds are accessible only with the use of very bulky alkyl substituents. The synthesis of the trialkyl compounds $[Ln\{CH(SiMe_3)_2\}_3]$ **26** by Lappert et al. can be considered a milestone in organolanthanide chemistry.[40–42] Their successful preparation was made possible by a combination of two favorable factors: First, the bis(trimethylsilyl)methyl substituent was employed as a sterically highly demanding alkyl ligand. In addition, by using the low-coordinate phenoxides $[Ln(2,4,6\text{-}tBu_3C_6H_2O)_3]$ as starting materials it was possible to avoid the formation (and incorporation) of alkali metal halides. When the reactions are carried out in pentane, the lithium phenoxide by-product precipitates quantitatively and can be separated readily from the highly soluble trialkyllanthanide **26** [Eq. (13)].

$$[Ln(2,4,6\text{-}tBu_3C_6H_2O)_3] + 3\,LiCH(SiMe_3)_2 \xrightarrow[-3\ 2,4,6\text{-}tBu_3C_6H_2OLi]{pentane} [Ln\{CH(SiMe_3)_2\}_3] \qquad (13)$$

26, Ln = Y, La, Sm, Lu

The molecular structures of the lanthanum (Fig. 7) and samarium derivative have been determined by X-ray diffraction.[40–42] Like the homoleptic silylamides $[Ln\{N(SiMe_3)_2\}_3]$ the trialkyl compounds **26** adopt a flat pyramidal coordination geometry. The average metal–carbon distances for **26c** and **26g** are 251.5(9) (La–C) and 233(2) (Sm–C) pm, respectively.

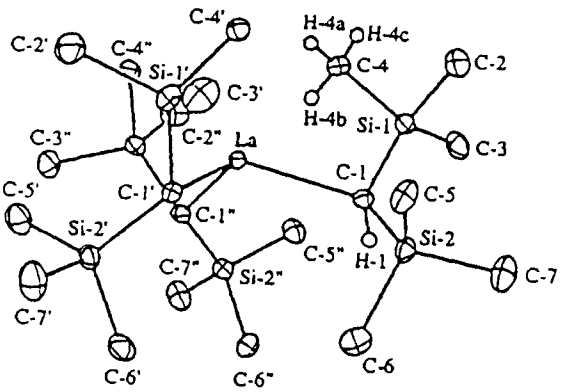

Fig. 7. Molecular structure of $[La\{CH(SiMe_3)_2\}_3]$ **26c** in the crystal.

The deviation from trigonal-planar coordination in the complexes **26** is somewhat surprising. Several explanations have been proposed for this unexpected coordination geometry. Initially, it was proposed that interligand repulsion would be minimized in a pyramidal structure. More important, however, is the possibility of forming agostic Ln-H-C interactions. In fact, short γ-agostic Ln···Me interactions have been found in both structurally characterized compounds (La···C 312.1 pm, Sm···C 285 pm). In this way, the extreme electronic and coordinative unsaturation can be diminished. A different, yet just as plausible, explanation would be the creation of a dipole moment in the pyramidal geometry which would then result in a higher lattice energy in the crystal.

Interestingly, the complexes **26** are not accessible directly from lanthanide trichlorides by conventional reactions. Instead of homoleptic trialkyl compounds, products containing incorporated lithium chloride are formed in these reactions [Eq. (14); PMDETA = *N*,*N*,*N*′,*N*″,*N*″-pentamethyldiethylenetriamine].[40]

$$LaCl_3 + 3\,LiCH(SiMe_3)_2 \xrightarrow[-2\,LiCl]{PMDETA} [\{(Me_3Si)_2CH\}_3La(\mu\text{-}Cl)Li(pmdeta)] \qquad (14)$$

27c

The LiCl adduct **27c** contains a nearly linear La-Cl-Li unit (La-Cl-Li 165.1°, La–Cl 276.2 pm, Li–Cl 228 pm). In comparison with the neutral compound **26c**, the $[Ln\{CH(SiMe_3)_2\}_3]$ fragment in **27c** exhibits no significant structural changes. An analogous reaction with ytterbium trichloride affords the salt-like product **28o**, which consists of separated ions in the solid

$[Li(thf)_4][YbCl\{CH(SiMe_3)_2\}_3]$ **28o**

state.[35] Evidently, the formation of the various types of complexes depends on a subtle balance of certain factors. These factors include the nature of the alkali metal, the presence of

halide ions, and the ionic radius of the lanthanide element. A similar situation was recently described for some low-coordinate lanthanide alkoxides and amides.[43] For example, the chloro-bridged **27c** is closely related to the neodymium compounds **29f** and **30f**, whereas **28o** is comparable to the compound **31f**.

$[\{(Me_3Si)_2N\}_3Nd(\mu\text{-}Cl)Li(thf)_3]$ **29f**

$[(tBu_3CO)_3Nd(\mu\text{-}Cl)Li(thf)_3]$ **30f**

$[Li(thf)_4][NdOSiMe_3\{N(SiMe_3)_2\}_3]$ **31f**

Recent papers by Schaverien et al. provided additional evidence on how minor changes of the reaction conditions or the choice of the reagents can influence the product formation.[44,45] In this case instead of $LiCH(SiMe_3)_2$, the more reactive $KCH(SiMe_3)_2$ was allowed to react with the lanthanide trichlorides. Owing to the enhanced solubility of the potassium compound it was possible to perform the reaction with lutetium trichloride in diethyl ether instead of THF (Scheme 2).

$$LuCl_3 + 3\,KCH(SiMe_3)_2 \xrightarrow{\text{ether}} [Lu\{CH(SiMe_3)_2\}_3(\mu\text{-}Cl)K(Et_2O)]$$
32p

ether ↑↓ −ether

$$[Lu\{CH(SiMe_3)_2\}_3(\mu\text{-}Cl)K(\eta^6\text{-}C_7H_8)] \xleftarrow{\text{toluene}} [Lu\{CH(SiMe_3)_2\}_3(\mu\text{-}Cl)K]$$
34p **33p**

Scheme 2. Interconversion of alkyllutetium compounds.

In contrast to the analogous LiCl adduct **27c**, the coordinated diethyl ether in **32p** can easily be removed under vacuum to produce the complex **33p**. In this compound the potassium is coordinatively unsaturated and readily adds solvent molecules such as diethyl ether or even toluene.[44,45]

Very little is known about heavier homologues of the alkyllanthanides such as homoleptic silyl and germyl derivatives or their solvent adducts. In the case of divalent ytterbium the preparation of such compounds was achieved by reacting metallic ytterbium with Ph_3ECl (E = Si, Ge) [Eq. (15)].[46] In both

$$2\,Yb + 2\,Ph_3ECl \xrightarrow{THF} [(Ph_3E)_2Yb(thf)_4] + [YbCl_2(thf)_2] \quad (15)$$
34o, E = Si
35o, E = Ge

cases the crystal structure determination showed the presence of centrosymmetric octahedral molecular structures, in which the Ph_3E ligands are arranged in the axial positions.

A small number of σ-stannyl complexes are also known. The ytterbium(II) compound **36o** was prepared by treatment of YbI_2 with the stannylpotassium reagent $K[Sn(CH_2tBu)_3]$ and structurally characterized by X-ray diffraction.[47] The structures were determined also for the stannyl complexes **37** (DME = 1,2-dimethoxyethane);[48,49] however, thus far no further reactions of these interesting products have been reported.

$[Yb\{Sn(CH_2tBu)_3\}_2(thf)_2]$ **36o**

$[Ln\{Sn(CH_2SiMe_3)_3\}_3(dme)]$ **37**, Ln = Pr, Nd

3.2. Anionic Homoleptic Compounds

As a result of the desire of the lanthanide ions to achieve high coordination numbers in their complexes, simple alkyllanthanide(III) complexes very easily add solvent molecules or anionic ligands and form so-called "ate" complexes. Such anionic alkyl complexes are often the only isolable products, when anhydrous lanthanide trichlorides are treated with alkyl- or aryllithium reagents. Quite often the anionic ate complexes are formed preferentially, regardless of the stoichiometric ratio of the starting materials. In a series of fundamental papers, Schumann et al. described the most simple compounds of this type, which formally contain $[LnMe_6]^{3-}$ ions.[50,51] The octahedral complexes **38** and **39** are formed when anhydrous lanthanide trichlorides are treated with six equivalents of methyllithium in the presence of a coordinating solvent. It was possible to prepare the complexes **38** for the entire lanthanide series except promethium and europium.(Owing to the subsequent facile reduction to undefined europium(II) species, the europium derivative **38h** cannot be isolated.) The chelate ligands TMEDA (TMEDA = *N,N,N′,N′*-tetramethylethylene-1,2-diamine) and DME serve to coordinatively saturate the lithium ion.

$$LnCl_3 + 6\,MeLi + 3\,TMEDA \xrightarrow[-3\,LiCl]{Et_2O} [Li(tmeda)]_3[LnMe_6] \quad (16)$$
38, Ln = Sc, Y, La, Sm, Gd–Lu

$$LnCl_3 + 6\,MeLi + 3\,DME \xrightarrow[-3\,LiCl]{Et_2O} [Li(dme)]_3[LnMe_6] \quad (17)$$
39, Ln = Ce, Pr, Gd, Tb, Dy, Er, Lu

The crystalline compounds are extremely air sensitive and reveal the characteristic colors of the respective lanthanide ions. The X-ray crystal structures were determined for the complexes **38l** (Fig. 8), **38m**, and **39p**.[50,51] Six methyl groups surround

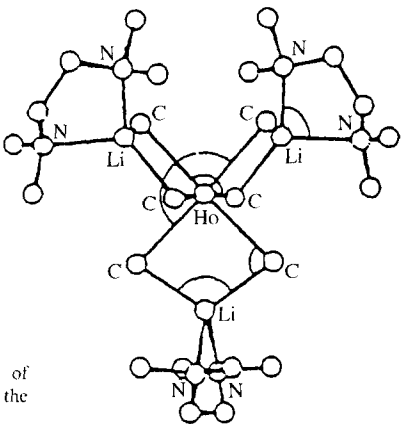

Fig. 8. Molecular structure of $[Li(tmeda)]_3[HoMe_6]$ **38l** in the crystal.

the central lanthanide ion in a slightly distorted octahedral arrangement. Two methyl ligands form bridges between the lanthanide ion and each lithium ion, which, in turn, is coordinatively saturated by chelating TMEDA or DME. All Ln–C bonds are the same length.

Very little has been reported about the reactivity of the complexes **38** and **39**. The first applications in organic synthesis were the reactions with α,β-unsaturated aldehydes and ketones. The

reaction of the samarium derivative **38g** with *tert*-butyl alcohol in diethyl ether afforded the alkoxide $[Li_5Sm(OtBu)_8]$.[52]

$[Li(tmeda)]_3[SmMe_6]$ **38g**

Lower coordination numbers than those in the $[LnMe_6]^{3-}$ ions can be achieved with sterically demanding alkyl ligands such as *tert*-butyl or trimethylsilymethyl. The synthesis of anionic tetra-*tert*-butyl complexes was achieved in a conventional way by reaction of $LnCl_3$ or $Ln(OtBu)_3$ with four equivalents *t*BuLi [Eqs. (18)–(20)]. Diethyl ether, THF, or TMEDA can be used as the coordinating solvent in these reactions.[50, 53, 54] An X-ray crystal structure determination of the lutetium compound **40p** revealed the presence of solvent-separated ions in the crystal.[55]

$$LnCl_3 + 4\,tBuLi \xrightarrow[-3\,LiCl]{pentane/Et_2O} \underset{\mathbf{40},\ Ln = Tb,\ Er,\ Lu}{[Li(Et_2O)_4][LntBu_4]} \quad (18)$$

$$LnCl_3 + 4\,tBuLi \xrightarrow[-3\,LiCl]{THF} \underset{\mathbf{41},\ Ln = Er\ (n = 4),\ Yb\ (n = 3)}{[Li(thf)_n][LntBu_4]} \quad (19)$$

$$Ln(OtBu)_3 + 4\,tBuLi \xrightarrow[-3\,LiOtBu]{pentane/TMEDA} \underset{\mathbf{42},\ Ln = Er,\ Lu}{[Li(tmeda)_2][LntBu_4]} \quad (20)$$

Four-coordinate anionic lanthanide(III) complexes are also accessible with σ-aryl ligands.[21] A typical example is the reaction of anhydrous lanthanide trichlorides with excess phenyllithium, which affords the tetraphenyl complexes **43** [Eq. (21)]. The proposed tetrahedral coordination geometry has been confirmed unambiguously by a crystal structure analysis of the ring-substituted derivative **44p**.[56]

$$LnCl_3 + 4\,PhLi \xrightarrow[-3\,LiCl]{THF} \underset{\mathbf{43},\ Ln = La,\ Pr}{Li[LnPh_4]} \quad (21)$$

$[Li(thf)_4][Lu(2,6\text{-}C_6H_3Me_2)_4]$ **44p**

The structurally characterized lutetium compound **45p** has recently been reported and is an unprecedented example of an anionic diene complex of a lanthanide element.[57] In **45p** two η^4-diphenylbutadiene ligands and two THF molecules are coordinated to the central lutetium ion; the diphenylbutadiene is bonded in its s-*cis* conformation. In the crystal, a polymeric chain structure results from additional η^6-coordination of two phenyl rings to potassium.

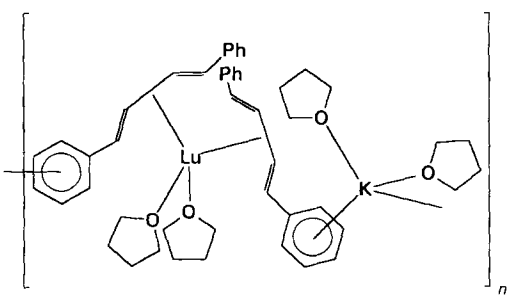

45p

3.3. Heteroleptic Compounds

Although THF adducts of alkyllanthanide compounds are formally heteroleptic complexes, only organolanthanide compounds containing additional anionic ligands will be discussed in this section. Until just a few years ago this class of compounds was fairly obscure; however, more recently a substantial number of highly interesting results in this area have been reported. Well-defined lanthanide(II) derivatives are still virtually unknown. The dimeric alkylytterbium(II) ethoxide **46o** was made by treatment of ytterbium(II) iodide with $KC(SiMe_3)_3$ in diethyl ether and characterized by X-ray crystallography.[13] Alternatively, **46o** is also accessible from **7o** by an ether cleavage reaction [Eq. (22)].[14]

$$2[Yb\{(Me_3Si)_3C\}_2] + 4\,Et_2O \xrightarrow[-(Me_3Si)_3CH,\ -CH_2=CH_2]{\mathbf{7o}} \underset{\mathbf{46o}}{[(Me_3Si)_3CYb(OEt)(OEt_2)]_2} \quad (22)$$

$[(Me_3Si)_2CHYb(OAr)(thf)_3]$ **47o**

The monomeric phenoxide **47o** is formed in the reaction of $[Yb(OAr)_2(thf)_3]$ with $KCH(SiMe_3)_2$. In this case the very bulky ArO ligand prevents the formation of a phenoxide-bridged dinuclear complex (Ar = 2,6-tBu_2-4-MeC_6H_2).[13]

Grignard-type organolanthanide complexes represent a synthetically important though structurally not fully understood class of compounds. Grignard analogues of the type RLnX (R = alkyl, aryl; Ln = Sm, Eu, Yb; X = halogen) have been thoroughly investigated since 1970 and are now widely used in organic synthesis.[5] The ytterbium compounds RYbI, in particular, are easily accessible from RI and elemental ytterbium in THF. The resulting deeply colored THF solutions are usually used in situ for subsequent reactions. These organolanthanide(II) compounds behave somewhat like typical Grignard compounds, although there are several interesting differences in reactivity. Until recently compounds of the type RLnX had never been isolated as pure materials nor had they been characterized spectroscopically or by X-ray diffraction. In 1994 Eaborn et al. reported the first preparation and structural characterization of such compounds.[14] The homoleptic dialkylytterbium(II) complex $[Yb\{(Me_3Si)_3C\}_2]$ **7o** reacts with iodomethane or 1,2-diiodoethane to give the ytterbium Grignard compound **48o**, which can be isolated in the form of greenish-yellow, exceedingly air-sensitive crystals. In complete analogy to normal Grignard compounds, **48o** could be prepared by direct reaction of elemental ytterbium with the corresponding silyl-substituted alkyl iodide [Eq. (23)].[14, 58] The crystal structure determination of **48o** revealed that the central Yb_2I_2 ring is planar (Fig. 9).

$$2\,Yb + 2(Me_3Si)_3CI \xrightarrow{Et_2O} \underset{\mathbf{48o}}{[\{[(Me_3Si)_3C]Yb(\mu\text{-}I)(Et_2O)\}_2]} \quad (23)$$

Several other compounds of this class were synthesized by varying the substituents.[58] The ytterbium complexes **49o**

$[\{[(Me_3Si)_2(Me_2XSi)C]Yb(\mu\text{-}I)(Et_2O)\}_2]$ **49o**, X = OMe, Ph, $CH{=}CH_2$

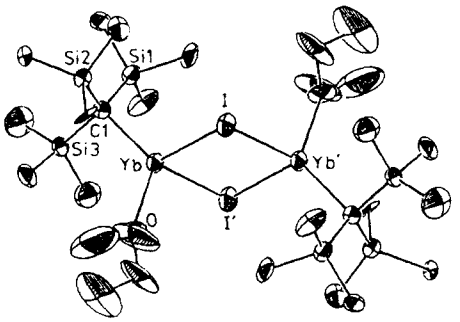

Fig. 9. Molecular structure of $[\{[(Me_3Si)_3C]Yb(\mu\text{-}I)(Et_2O)\}_2]$ **48o** in the crystal.

have been prepared according to Equation (23). Figure 10 depicts the unusual molecular structure of **49o** (X = $CH{=}CH_2$), in which the very rare lanthanide-vinyl π interaction occurs.

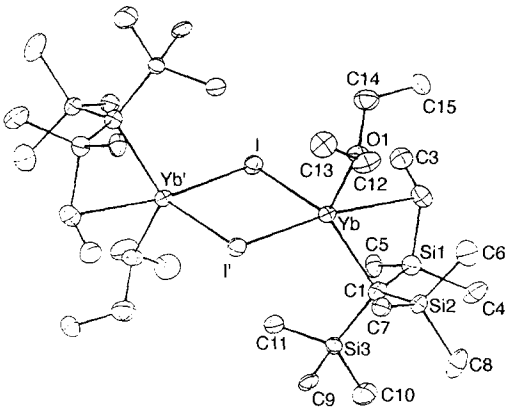

Fig. 10. Molecular structure of $[\{[(Me_3Si)_2(Me_2SiCH{=}CH_2)C]Yb(\mu\text{-}I)(Et_2O)\}_2]$ **49o** (X = $CH{=}CH_2$) in the crystal.

A typical Schlenk-equilibrium could be detected for all Grignard-type ytterbium(II) complexes in nonpolar organic solvents such as toluene [Eq. (24)].

$$[RYbI]_2 \rightleftharpoons R_2Yb + YbI_2 \qquad (24)$$

Until recently monoorganolanthanide(III) dihalides, $RLnX_2$, were still only poorly characterized. These compounds can likewise be considered as Grignard-type analogous compounds. They can be easily prepared in situ by alkylation of $LnCl_3$ or LnI_3 with organolithium compounds.[5] A remarkable result from an organometallic viewpoint was the first crystal structure determination of a "lanthanide(III) Grignard compound" of this type, which was reported by Chen et al.[59] Anhydrous gadolinium trichloride reacts with phenyllithium in a 1:1 molar ratio to give the well-defined seven-coordinate phenyl complex **50i**. The length of the gadolinium–carbon σ bond is 242(2) pm (Fig. 11).

$[PhGdCl_2(thf)_4]$ **50i**

Organolanthanide complexes containing different σ-alkyl ligands are still virtually unknown. A structurally characterized example is the heteroleptic anionic samarium complex **51g** with

$[\{(Me_3Si)_2CH\}_3Sm(\mu\text{-}Me)Li(pmdeta)]$ **51g**

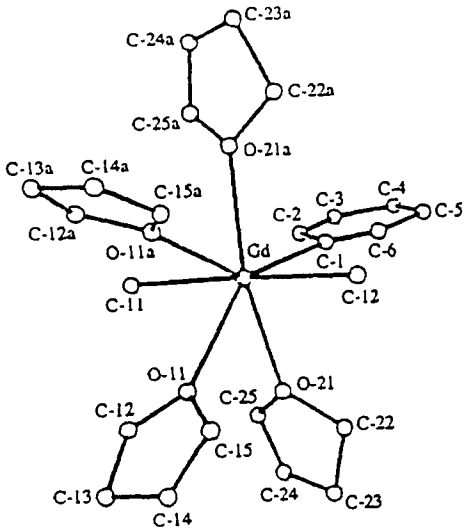

Fig. 11. Molecular structure of $[PhGdCl_2(thf)_4]$ **50i** in the crystal.

a methyl group bridging samarium and lithium.[60] Likewise, metallacycles containing a lanthanide atom in the ring are very rare species. Five-membered "lanthanols" such as **52f** and **52i** have been described, but are insufficiently characterized.[61]

$[Ph_4C_4Ln(\mu\text{-}Cl)_2Li(thf)_n]$, **52f**, Ln = Nd; **52i**, Ln = Gd

The same was true until recently for the metallacyclic products obtained by reacting anhydrous lanthanide tribromides with *o*-dilithiobiphenyl. The compounds **53** isolated as THF adducts were initially thought to be five-membered metallacycles [Eq. (25)].[62]

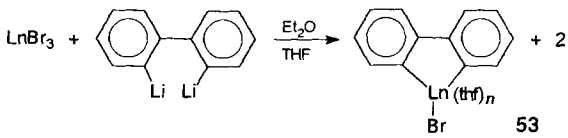

(25)

The reaction of $SmBr_3$ with *o*-dilithiobiphenyl $Li_2C_{12}H_8$ was recently reinvestigated and the true nature of the reaction product **54g** elucidated.[63] Contrary to the originally proposed structure, the product does not contain a five-membered metallacycle. Instead, a dimetalated *o*-quaterphenyl ligand is formed through dimerization [Eq. (26), Fig. 12], which with samarium

$$6SmBr_3 + 6Li_2C_{12}H_8 \xrightarrow[-H_2,\ -12\,LiBr]{-2\,Sm,\ -2\,SmBr_3} [(C_{24}H_{16})Sm(\mu\text{-}Br)(thf)_2]_2 \cdot C_{24}H_{14} \qquad (26)$$

54g

forms a nine-membered metallacycle. Dimerization through bromide ligands leads to the formation of the dinuclear product. The hydrocarbon dibenzonaphthacene ($C_{24}H_{14}$), which is formed as a by-product during the reaction, is intercalated in the crystal lattice.

Alkyllanthanide(III) alkoxides form a small, though very promising class of compounds. Such compounds are of great interest as intermediates in the lanthanide-catalyzed polymerization of 1,3-dienes. A typical multicomponent catalyst system

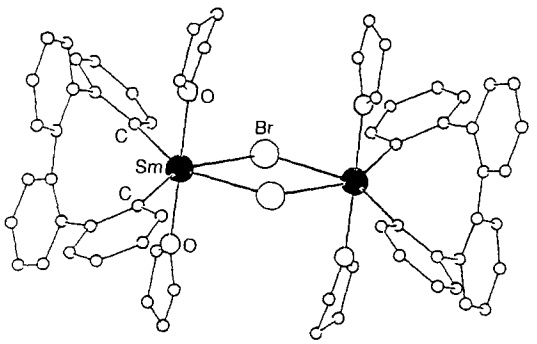

Fig. 12. Molecular structure of $[(C_{24}H_{16})Sm(\mu\text{-}Br)(thf)_2]_2 \cdot C_{24}H_{14}$ **54g** in the crystal (intercalated $C_{24}H_{14}$ omitted).

for diene polymerization is $Nd(OiPr)_3/AlEt_3/Et_2AlCl$. The heterobimetallic alkyllanthanide(III) alkoxide **55f** could be isolated

$[\{Nd_6Al_3(\mu\text{-}Cl)_6(\mu\text{-}Et)_9Et_5(OiPr)\}_2]$ **55f**

from this system and characterized by X-ray crystallography.[64] The complex structure of this catalytically active intermediate underlines the fact that lanthanide alkoxides tend to aggregate as clusters. Only in very rare cases is the constitution of lanthanide alkoxides as simple as implied by the formula $Ln(OR)_3$.[65] A series of heterobimetallic alkyllanthanide(III) alkoxides has been synthesized in a simple way by alkylation of lanthanide alkoxides [Eq. (27)].[66] The yttrium compound **56b** is also obtained by alkylation of the alkoxide cluster $[Y_3(OtBu)_9(thf)]$ with excess $AlMe_3$.[67]

$$Ln(OtBu)_3 + 3\,AlMe_3 \longrightarrow [Ln\{(\mu\text{-}OtBu)(\mu\text{-}Me)AlMe_2\}_3] \quad (27)$$

56, Ln = Y, Pr, Nd

The stabilization of monomeric alkyllanthanide(III) alkoxides was first achieved by employing the sterically demanding chelate ligand 3,3′,5,5′-tetra-*tert*-butyl-biphenyl-2,2′-diolate. In this case unsolvated $[La\{CH(SiMe_3)_2\}_3]$ **26c** served as a useful starting material (Scheme 3).[68]

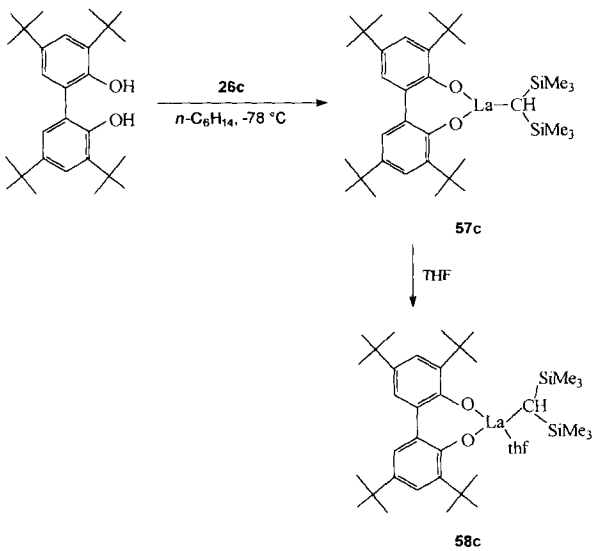

Scheme 3. Synthesis of alkyllanthanum(III) diolates.

Special nitrogen ligands are also suitable for stabilizing heteroleptic alkyllanthanide compounds. In recent years porphyrin ligands have been successfully employed. For example, treatment of $[ScCl_3(thf)_3]$ with $[Li(thf)_4][Li(oep)]$ or $[Li_2(OEP)(thf)_2]$ affords the chloro complex [ScCl(oep)] **59a** (oep = octaethylporphyrin dianion). Substitution of the chloride ligand in **59a** leads to the corresponding scandium amides, alkoxides, or σ-alkyl derivatives. Alkylation affords the unsolvated alkyl complexes [ScR(oep)] **60**.[69, 70] Evidently, the small ionic radius

[ScCl(oep)] **59a** [ScR(oep)] **60**, R = Me, CH_2tBu, $CH(SiMe_3)_2$

of the respective lanthanide facilitates the synthesis of porphyrin derivatives. Thus porphyrin-stabilized alkyllanthanide compounds can also be obtained with yttrium and lutetium as central atoms.[41] The thermal reaction of the homoleptic alkyl complexes $[Ln\{CH(SiMe_3)_2\}_3]$ with H_2oep in toluene has been demonstrated to be an elegant and effective access to such complexes [Eq. (28)]. This method completely circumvents compli-

$$[Ln\{CH(SiMe_3)_2\}_3] + H_2oep \xrightarrow[-2\,CH_2(SiMe_3)_2]{} [(oep)LnCH(SiMe_3)_2] \quad (28)$$

(26b, p) **61**, Ln = Y, Lu

cations that may arise from the formation of solvent adducts and/or incorporation of halide ions. The lutetium derivative **61p** has been characterized by an X-ray crystal structure analysis. Figure 13 depicts the square-planar coordination geometry.

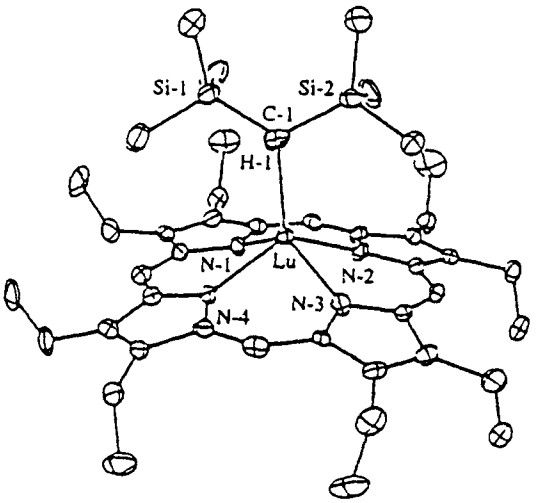

Fig. 13. Molecular structure of $[(oep)LuCH(SiMe_3)_2]$ **61p** in the crystal.

Alternatively, the porphyrin-stabilized alkyllanthanide(III) compounds **61** are accessible by a two-step synthetic procedure, in which the presence of coordinating solvent or alkali metal halides can also be avoided [Eqs. (29) and (30)].[41]

$$[Ln(2,6\text{-}tBu_2C_6H_3O)_3] + H_2oep \xrightarrow[-2\,2,6\text{-}tBu_2C_6H_3OH]{} [(oep)LnOC_6H_3tBu_2] \quad (29)$$

62 **63**

$$\mathbf{63} + LiCH(SiMe_3)_2 \xrightarrow[-2,6\text{-}tBu_2C_6H_3OH]{} [(oep)LnCH(SiMe_3)_2] \quad (30)$$

61, Ln = Y, Lu

Just like other highly reactive alkyllanthanide(III) compounds, the complexes **61** are interesting starting materials for subsequent reactions, which are summarized in Scheme 4.[41] The very facile hydrolysis leads to the dimeric hydroxo complexes **64**, and the σ-alkyl groups are easily substituted in reactions

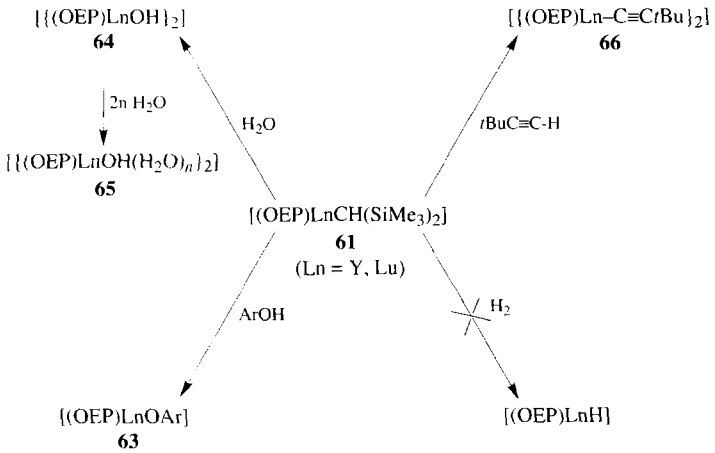

Scheme 4. Derivative chemistry of the complexes **61**.

with phenols or terminal alkynes. In contrast, hydrogenolysis to the corresponding hydrides cannot be achieved even under a hydrogen pressure of 20 bar. This unexpected result is in marked contrast to the chemistry of the related metallocenes $[(C_5Me_5)_2LnCH(SiMe_3)_2]$, which readily react with hydrogen at normal pressure to give the dimeric hydrides $[\{(C_5Me_5)_2Ln(\mu\text{-}H)\}_2]$.[71–73]

The heteronuclear alkyl complexes **68b** can be prepared by stepwise reaction of the yttrium alkoxide **63b** with methyllithium and trimethylaluminum (Scheme 5).[41]

$$[(oep)YOC_6H_3tBu_2] + 2\,MeLi \xrightarrow[-LiOC_6H_3tBu_2]{Et_2O} [(oep)Y(\mu\text{-}Me)_2Li(Et_2O)]$$
63b **67b**

$$\xrightarrow{Al_2Me_6} [(oep)Y(\mu\text{-}Me)_2AlMe_2]$$
68b

Scheme 5. Synthesis of $[(oep)Y(\mu\text{-}Me)_2AlMe_2]$ **68b**.

The reaction sequence shown in Scheme 5 parallels the multistep synthesis of $[(C_5Me_5)_2LuMe]$[74] with the only exception that the final step, that is the elimination of trimethylaluminum with Lewis bases, cannot be reproduced in the porphyrin series. Treatment of **68b** with Lewis bases such as pyridine only leads to the formation of adducts and not to unsolvated [YMe(oep)]. O_2 selectively attacks the bridging methyl groups in **68b** leading to the formation of the YAl alkoxide **69b**.

$[(oep)Y(\mu\text{-}OMe)_2AlMe_2]$ **69b**

More recently several other auxiliary ligands have been found that are capable of stabilizing σ-alkyllanthanide(III) complexes. These ligands include sterically demanding amido ligands as well as benzamidinate and pyrazolylborate ions. For example, an alkyllanthanide(III) amide is formed upon treatment of

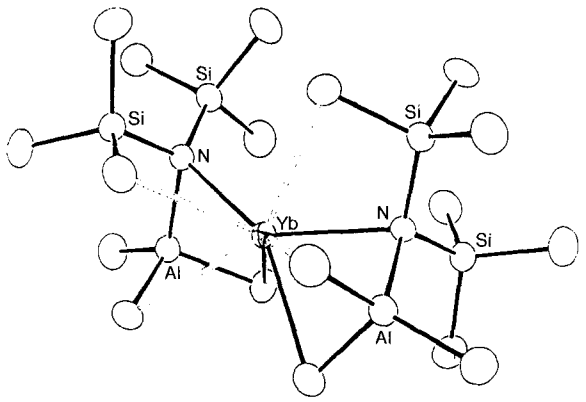

Fig. 14. Molecular structure of $[Yb\{N(SiMe_3)_2\}_2(AlMe_3)_2]$ **70o** in the crystal.

$[Yb_2\{N(SiMe_3)_2\}_4]$ with two equivalents of Al_2Me_6.[75] The reaction product **70o** contains four Yb-Me-Al and two Yb-Me-Si bridges (Fig. 14).

$[Yb\{N(SiMe_3)_2\}_2(AlMe_3)_2]$ **70o**

The potentially tridentate silylamide ion $[N(SiMe_2CH_2PMe_2)_2]^-$ developed by Fryzuk et al. has also been successfully employed in organolanthanide chemistry.[76–78] The stepwise preparation of heteroleptic alkyllanthanide(III) amides is illustrated in Scheme 6. The σ-alkyl complexes **72** are fluxional in solution and decompose upon heating under elimination of the hydrocarbon RH.

$$LnCl_3 + 2\,KN(SiMe_2CH_2PMe_2)_2 \xrightarrow[-2\,KCl]{} [LnCl\{N(SiMe_2CH_2PMe_2)_2\}_2]$$
71

$$\xrightarrow[-LiCl]{RLi} [LnR\{N(SiMe_2CH_2PMe_2)_2\}_2]$$
72

(Ln = La, Lu)

Scheme 6. Synthesis of $[LnR\{N(SiMe_2CH_2PMe_2)_2\}_2]$ **72**.

The synthesis of bis-σ-alkyllanthanide complexes containing only one chelating ligand proved to be more difficult. Such complexes have only become available by combining the very bulky silylamide ion $[N(SiMe_2CH_2PiPr_2)_2]^-$ with the small Sc^{3+} ion.[79] The complexes **73a** and **74a** have

$[\{N(SiMe_2CH_2PiPr_2)_2\}ScEt_2]$
73a

$[\{N(SiMe_2CH_2PiPr_2)_2\}Sc(CH_2SiMe_3)_2]$
74a

been prepared (cf. Scheme 6) and structurally characterized by X-ray diffraction (Fig. 15). A high reactivity and catalytic activity can be expected for these 10-electron complexes.

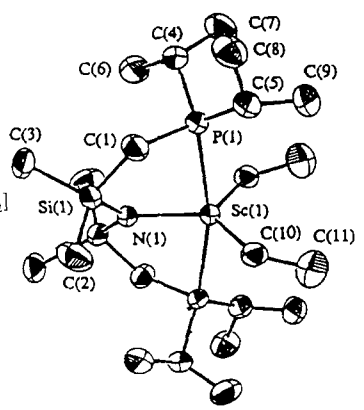

Fig. 15. Molecular structure of $[\{N(SiMe_2CH_2PiPr_2)_2\}ScEt_2]$ **73a** in the crystal.

Hydrotris(pyrazol-1-yl)borate ligands are enjoying increased popularity in the organometallic chemistry of lanthanides. By using the sterically demanding anion $[HB(3\text{-}t\text{Bu-}5\text{-Me-pz})_3]^-$, Takats et al. recently succeeded in preparing soluble, monosubstituted ytterbium(II) alkyl complexes.[80] The compounds **76o** (Fig. 16) and **77o** have been made by treatment of the precursor

$[\{HB(3\text{-}t\text{Bu-}5\text{-Me-pz})_3\}YbI(thf)]$ **75o**

$[\{HB(3\text{-}t\text{Bu-}5\text{-Me-pz})_3\}YbCH(SiMe_3)_2]$ **76o**

$[\{HB(3\text{-}t\text{Bu-}5\text{-Me-pz})_3\}Yb\{CH(SiMe_3)_2\}(Et_2O)]$ **77o**

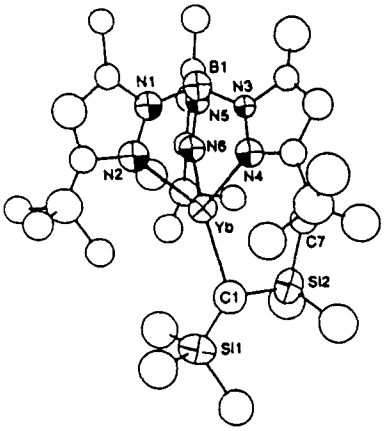

Fig. 16. Molecular structure of $[\{HB(3\text{-}t\text{Bu-}5\text{-Me-pz})_3\}YbCH(SiMe_3)_2]$ **76o** in the crystal.

75o with alkyllithium reagents. These compounds are rare examples of organolanthanide(II) complexes with σ-bonded alkyl ligands.

Bulky heteroallylic ligands such as the benzamidinate ions $[RC_6H_4C(NSiMe_3)_2]^-$ have recently been established as useful alternatives to the cyclopentadienyl ligands. Thus, the yttrium(III) benzamidinates **80b** can be regarded as analogues of the metallocene $[(C_5Me_5)_2YCH(SiMe_3)_2]$. All these compounds exhibit comparable catalytic activities, for example, in olefin polymerizations. The alkyl derivatives **80b** are easily accessible by alkylation of the corresponding chloride or triflate precursors [Eq. (31)].[81–83]

$$[\{RC_6H_4C(NSiMe_3)_2\}_2YX(thf)_n] + LiCH(SiMe_3)_2$$
78b, X = Cl, $n = 1$
79b, X = O_3SCF_3, $n = 0$
$$\xrightarrow[-LiX]{} [\{RC_6H_4C(NSiMe_3)_2\}_2YCH(SiMe_3)_2] \quad (31)$$
80b, R = H, OMe, CF_3

In contrast to the organometallic chemistry of the d-block transition metals, diene complexes are particularly rare in the case of the lanthanides.[1–6] This is especially true for complexes without supporting cyclopentadienyl ligands. The first successful approaches in this direction have been reported in two recent papers: The diene-bridged dilanthanum complex **81c** was obtained by reacting finely divided elemental lanthanum with 1,4-diphenylbutadiene and iodine in THF [Eq. (32)].[84] The samarium analogue **81g** had already been made earlier using a similar synthetic procedure.[85]

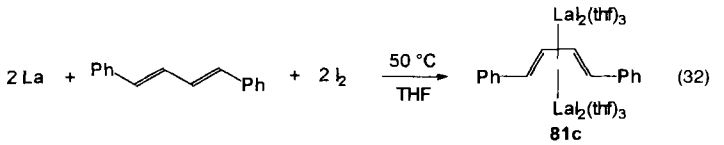

81c (32)

An X-ray structure determination of the isolated red crystals of **81c** revealed the presence of an "inverse sandwich complex" in which the two lanthanum atoms are symmetrically bridged by the $\eta^4:\eta^4$-coordinated diene ligand.[84] Structurally related "inverse sandwich complexes" have been prepared according to Equations (33) and (34) from naphthalene ($C_{10}H_8$).[86]

$$2[LaI_3(thf)_3] + 2Li + C_{10}H_8 \xrightarrow[-2LiI]{THF} [(\mu_2\text{-}\eta^4\text{:}\eta^4\text{-}C_{10}H_8)\{LaI_2(thf)_3\}_2] \quad (33)$$
82c

$$2[EuI_2(thf)_2] + 2C_{10}H_8Li \xrightarrow[-2LiI\ -C_{10}H_8]{DME} [(\mu_2\text{-}\eta^4\text{:}\eta^4\text{-}C_{10}H_8)\{EuI(dme)_2\}_2] \quad (34)$$
83h

The complexes **82c** (Fig. 17) and **83h** have been characterized by X-ray structure analyses. In both cases the lanthanide atoms are bridged by nonplanar naphthalene units bonded in diene-like fashion.

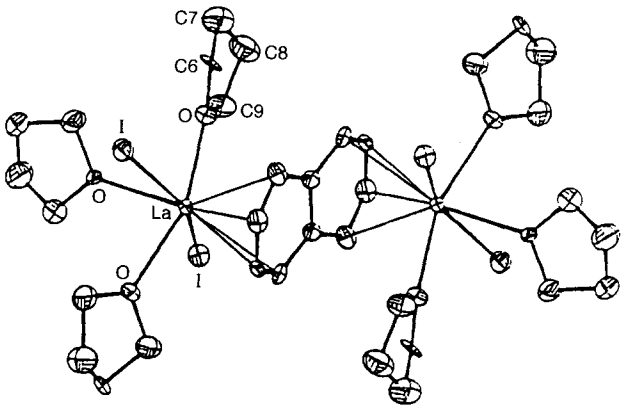

Fig. 17. Molecular structure of $[(\mu_2\text{-}\eta^4\text{:}\eta^4\text{-}C_{10}H_8)\{LaI_2(thf)_3\}_2]$ **82c** in the crystal.

4. Alkenyl and Alkynyl Complexes

Well-characterized alkenyl- and alkynyllanthanide complexes remain a relatively unexplored class of compounds. Ytterbium reacts with $Hg(CH{=}CHCl)_2$ to give the insufficiently characterized bis(β-chlorovinyl)ytterbium **84o**.[87] However, a well-defined alkynyl complex of divalent ytterbium could be synthesized by using the sterically demanding hydrotris(3,5-dimethylpyrazol-1-yl)borate ligand. The dark red phenylacetylide **86o** was obtained in good yield by reaction of the amide **85o** with phenylacetylene.[80]

$[Yb(CH{=}CHCl)_2]$ **84o**

$[\{HB(3,5\text{-}Me_2pz)_3\}Yb\{N(SiMe_3)_2\}]$ **85o**

$[\{HB(3,5\text{-}Me_2pz)_3\}YbC{\equiv}CPh]$ **86o**

It was reported that the blue solutions of elemental europium or ytterbium in liquid ammonia react with alkynes with terminal triple bonds to give bis(alkynyl)lanthanide(II) complexes. Alkynyl derivatives of divalent europium and ytterbium are also available by transmetalation of $Hg(C{\equiv}CR)_2$ with the respective metals [Eq. (35)].[88, 89]

$$Ln + Hg(C{\equiv}CR)_2 \xrightarrow{THF} [Ln(C{\equiv}CR)_2] + Hg \quad (35)$$
87h, o
R = *n*Bu; Ln = Eu, Yb
R = Ph; Ln = Yb

In the case of trivalent lanthanides the tris(alkynyl) complexes **88p**[27] and **89**[90, 91] have been described. Virtually nothing is known about the molecular structures of all these compounds; however, it is likely that the unsolvated complexes $[Ln(C{\equiv}CR)_2]$ and $[Ln(C{\equiv}CR)_3]$ are polymeric materials with bridging alkynyl ligands.

$[Lu(C{\equiv}CtBu)_3]$ **88p**

$[Ln(C{\equiv}CPh)_3]$ **89**, Ln = Pr, Sm, Eu, Gd, Tb, Er, Yb

A well-defined μ-ethynyl complex of yttrium is formed by protolysis of the alkyl derivative **80b** (R = H) with acetylene [Eq. (36)]. Figure 18 shows the dimeric structure of **90b** with bridging ethynyl ligands.

$$2[\{PhC(NSiMe_3)_2\}_2YCH(SiMe_3)_2] \quad \textbf{80b} \xrightarrow[-2\,CH_2(SiMe_3)_2]{2\,HC{\equiv}CH} [\{[PhC(NSiMe_3)_2]_2Y(\mu\text{-}C{\equiv}CH)\}_2] \quad \textbf{90b} \qquad (36)$$

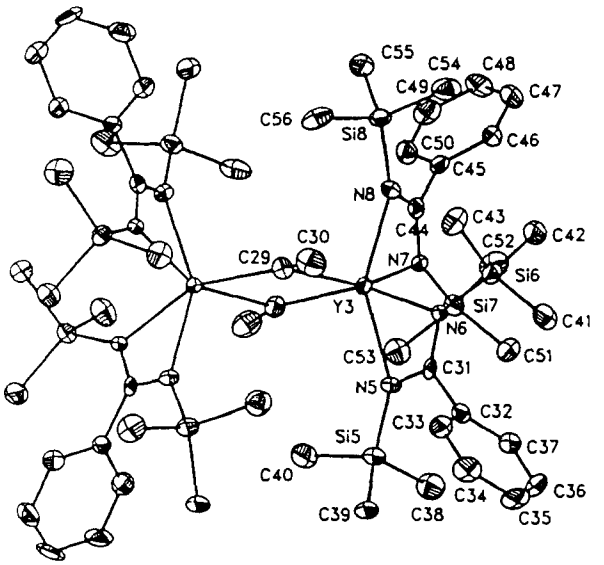

Fig. 18. Molecular structure of $[\{[PhC(NSiMe_3)_2]_2Y(\mu\text{-}C{\equiv}CH)\}_2]$ **90b** in the crystal.

5. Allyl Complexes

Homoleptic tris(η^3-allyl)lanthanides are unknown. Evidently, the steric bulk of three relatively small allyl ligands is not sufficient to coordinatively saturate the large lanthanide ions. Instead, reactions of anhydrous lanthanide trichlorides with allyllithium have produced a series of interesting anionic allyl complexes. The complexes **91**–**93** have been obtained depending on the reaction conditions and the solvents used.[92–94] Only recently it has been shown that such complexes are also available by a one-pot reaction in which the allyllithium reagent is prepared in situ from tetraallyltin and *n*-butyllithium [Eq. (37)].[92]

$[Li(dioxane)_n][Ln(\eta^3\text{-}C_3H_5)_4]$ **91**, Ln = Ce, Pr, Nd, Sm, Gd, $n = 2$; Ln = Y, $n = 2.5$; Ln = La, $n = 3$

$[Li_2(thf)_n][Ln(\eta^3\text{-}C_3H_5)_5]$ **92**, Ln = Y, La, $n = 2.5$; Ln = Ce, Pr, Nd, Sm, $n = 3$

$[Li_2(dioxane)_n][Ln(\eta^3\text{-}C_3H_5)_5]$ **93**, Ln = Ce, Nd, Sm, Gd, Dy, Ho, Er; $n = 1,3$

$$LaCl_3 + 2Sn(C_3H_5)_4 + 4n\text{BuLi} \xrightarrow[2.\ Et_2O/\text{dioxane}]{1.\ \text{toluene}} [Li(\mu\text{-dioxane})_{3/2}][La(\eta^3\text{-}C_3H_5)_4] + 3\,LiCl + 2n\text{Bu}_2Sn(C_3H_5)_2 \qquad (37)$$

In compound **94c** the central lanthanum atom is surrounded by the four η^3-allyl ligands in a distorted tetrahedral fashion (Fig. 19). The bridging dioxane molecules and the lithium ions form a two-dimensional sheet in the crystal lattice.

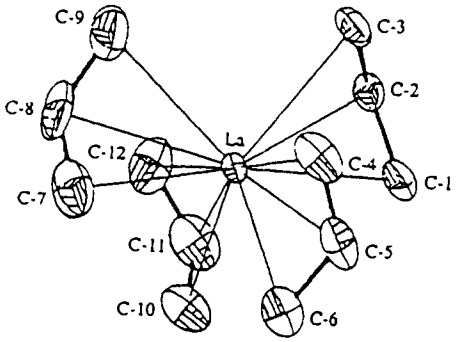

Fig. 19. Structure of the anion in $[Li(\mu\text{-dioxane})_{3/2}][La(\eta^3\text{-}C_3H_5)_4]$ **94c** in the crystal.

By partial protolysis one allyl ligand in **94c** can be selectively replaced by a cyclopentadienyl derivative, and in this way, the complexes **95c** can be isolated.[95] Such anionic allyllanthanide(III) complexes are valuable homogeneous catalysts for diene polymerizations.[5] More complicated coordination compounds containing η^3-allyl ligands have been obtained by reactions of anhydrous lanthanide trichlorides with allyl-Grignard reagents in the presence of TMEDA.[96] Among the structurally characterized products are **96d** and **97**.

$[Li(dioxane)_2][CpLa(C_3H_5)_3]$ **95c**, Cp = C_5H_5, C_5Me_5, indenyl, fluorenyl

$[(\eta^3\text{-}C_3H_5)_2Ce(\mu_3\text{-}Cl)_2(\mu\text{-}Cl)_3Mg_2(tmeda)_2]$ **96d**

$[(\eta^3\text{-}C_3H_5)_2Ln(\mu_3\text{-}Br)_2(\mu\text{-}Br)_3Mg_2(Et_2O)_4]$ **97**, Ln = Ce, Nd

The use of the tridentate amido ligand $[N(SiMe_2CH_2PMe_2)_2]^-$ also allowed the synthesis of a heteroleptic allyllanthanide complex.[77, 78] Treatment of **71b** with $(C_3H_5)MgCl$ led to elimination of one chelating amido ligand and formation of the chloro-bridged binuclear complex **98b**.

$[(\eta^3\text{-}C_3H_5)Y\{N(SiMe_2CH_2PMe_2)_2\}(\mu\text{-}Cl)]_2$ **98b**

6. Complexes Containing Cyclopentadienyl Analogues as Ligands

Cyclopentadienyl-analogous ligands are increasingly being employed in organolanthanide chemistry. Among these ligands are pentadienyl anions as well as five-membered anionic hetero-

cycles containing nitrogen, phosphorus, or arsenic in the ring. η^5-Cyclohexadienyl ligands, which have been reported to form interesting coordination compounds with uranium,[97,98] have so far not been used in organolanthanide chemistry.

6.1. Pentadienyl Complexes

In many cases transition metal complexes with pentadienyl ligands closely resemble the corresponding cyclopentadienyl complexes. Due to this relationship bis(pentadienyl) metal complexes are often termed "open metallocenes". One lanthanide derivative with "open cyclopentadienyl ligands" was synthesized as long ago as 1982. Bright green tris(2,4-dimethylpentadienyl)neodymium **99f** is formed when anhydrous neodymium trichloride is treated with three equivalents of potassium 2,4-dimethylpentadienide (KC_7H_{11}) in THF [Eq. (38)].[99]

$$NdCl_3 + 3KC_7H_{11} \xrightarrow{THF} \underset{\mathbf{99f}}{[Nd(C_7H_{11})_3]} + 3KCl \qquad (38)$$

A crystal structure analysis of the homoleptic complex **99f** revealed the presence of three equivalent η^5-coordinated 2,4-dimethylpentadienyl ligands. Meanwhile several other pentadienyllanthanide complexes have been reported, including the compounds **99**–**101**.[100,101] The tris(η^5-2,4-dimethylpentadienyl) complexes **99f**, **99i**, and **99p** have been structurally characterized. While the gadolinium complex adopts the same molecular structure as the neodymium compound, an interesting structural difference is found for the coordination mode of the three pentadienyl ligands in **99p**. Due to the smaller ionic radius of lutetium only two 2,4-dimethylpentadienyl ligands in this molecule are η^5-coordinated, while the third ligand is η^3-bonded (Fig. 20). This example nicely illustrates how the flexible pentadienyl ligands are able to adapt to the different ionic radii of the lanthanides.[101]

$[Ln(C_7H_{11})_3]$ **99**, Ln = La, Sm, Gd, Tb, Lu

$[(C_7H_{11})LnCl_2(thf)_3]$ **100**, Ln = Nd, Sm, Gd

$[(C_7H_{11})_2LnCl(thf)]$ **101**, Ln = Nd, Sm, Gd

A novel way of modifying pentadienyl ligands involves the connection of two of these anions through a hydrocarbon chain.[102] A bridged bis(pentadienyl) dianion (bpd) of this kind could be generated by deprotonation of two methyl groups in 2,4,7,9-tetramethyl-1,3,7,9-decatetraene. Subsequent reaction of the resulting potassium salt with ytterbium diiodide afforded the "open" ytterbium(II) metallocene **102o** (Fig. 21), which can be regarded as a pentadienyl analogue of $[(C_5Me_5)_2Yb(thf)_2]$. Thus far nothing has been reported about the reactivity of **102o**.

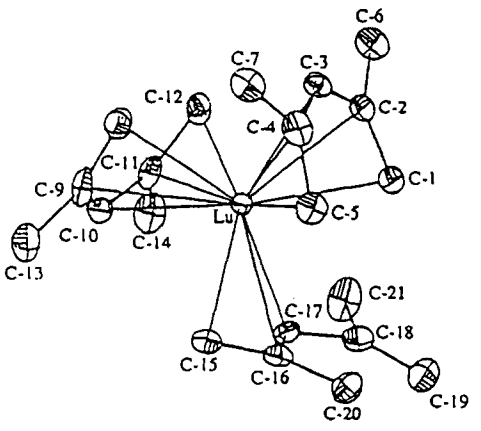

Fig. 20. Molecular structure of $[Lu(C_7H_{11})_3]$ **99p** in the crystal.

$[(bpd)Yb(thf)_2]$ **102o**

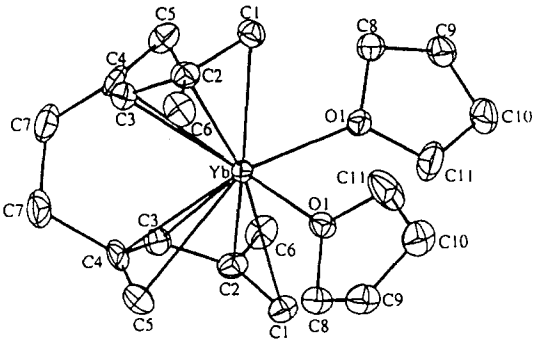

Fig. 21. Molecular structure of $[(bpd)Yb(thf)_2]$ **102o** in the crystal.

6.2. Complexes Containing Five-Membered Heterocycles as Ligands

A completely new development in organolanthanide chemistry is the use of anionic nitrogen, phosphorus, or arsenic heterocycles as ligands. Substituted pyrrolyl, phospholyl, or arsolyl ligands may turn out to be interesting alternatives to the ubiquitous pentamethylcyclopentadienyl ligands. Furthermore, the additional donor function could open up new possibilities for the construction of heteronuclear complexes.

At first glance nitrogen heterocycles appear to be less suited as π ligands for lanthanide complexes. Since the Ln^{3+} ions are known to be hard Lewis acids one would expect a preferred σ-coordination through the nitrogen atom. By introducing suitable substituents at the ring Schumann et al. succeeded in the first synthesis of organolanthanide complexes with π-bonded pyrrolyl ligands. Pyrrolyl-analogues of the known bis(pentamethylcyclopentadienyl)lanthanide(II) complexes are easily accessible according to Equation (39).[103]

$$[LnI_2(thf)_x] + 2Na[2,5\text{-}tBu_2C_4H_2N] \xrightarrow[-2NaI]{} \underset{\mathbf{103},\ Ln = Sm,\ Yb}{[(2,5\text{-}tBu_2C_4H_2N)_2Ln(thf)]} \qquad (39)$$

Mono- and bis(2,5-di-*tert*-butylpyrrolyl) complexes have been synthesized starting from anhydrous lanthanide trichlorides [Eqs. (40) and (41), respectively].[103,104] Complex **104o**

$$[YbCl_3(thf)_2] + Na[2,5\text{-}tBu_2C_4H_2N] \xrightarrow[-NaCl]{} \underset{\mathbf{104o}}{[(2,5\text{-}tBu_2C_4H_2N)YbCl_2(thf)_2]} \qquad (40)$$

$$2NdCl_3 + 4Na[2,5\text{-}tBu_2C_4H_2N] \xrightarrow[-2NaCl]{THF} \underset{\mathbf{105f}}{[(2,5\text{-}tBu_2C_4H_2N)_2Nd(\mu\text{-}Cl)_2\{Na(thf)\}_2(\mu\text{-}Cl)_2Nd(2,5\text{-}tBuC_4H_2N)_2]} \qquad (41)$$

is monomeric in the crystal (Fig. 22); in **105f** two [2,5-tBu$_2$C$_4$H$_2$N]$_2$NdCl "molecules". These results demonstrate that *N*-coordination of pyrrolyl ligands can be successfully avoided by introduction of bulky substituents, thus allowing the preparation of η^5-azacyclopentadienyl complexes of the lanthanides.

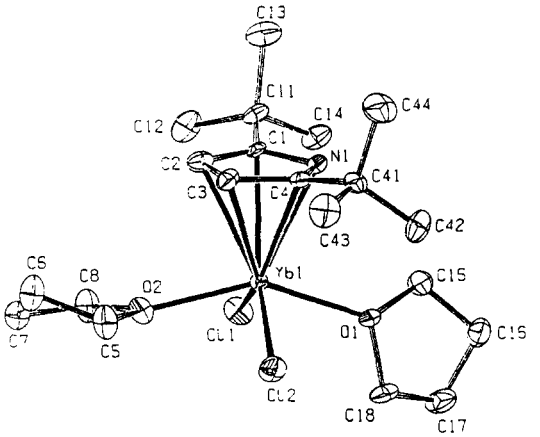

Fig. 22. Molecular structure of [(2,5-tBu$_2$C$_4$H$_2$N)YbCl$_2$(thf)$_2$] **104o** in the crystal.

Lanthanide(II) complexes containing tetrasubstituted phospholyl and arsolyl ligands have been obtained by treatment of lanthanide diiodides with two equivalents of K(C$_4$Me$_4$E) (E = P,As) [Eq. (42)].[105, 106]

$$[LnI_2(thf)_2] + 2K(C_4Me_4E) \xrightarrow[-2KI]{} [(C_4Me_4E)_2Ln(thf)_2] \quad (42)$$

106, **107**, Ln = Sm, Yb; E = P, As

[(2,5-Ph$_2$C$_4$H$_2$P)$_2$Yb(thf)$_2$] **108o**

Reductive cleavage of the E–E bond in the corresponding biphospholyl or biarsolyl derivatives by ytterbium affords the same products. The molecular structure of **108o** (Fig. 23) was determined by X-ray diffraction and illustrates the close relationship to analogous lanthanide(II) metallocenes such as [(C$_5$Me$_5$)$_2$Sm(thf)$_2$].[105]

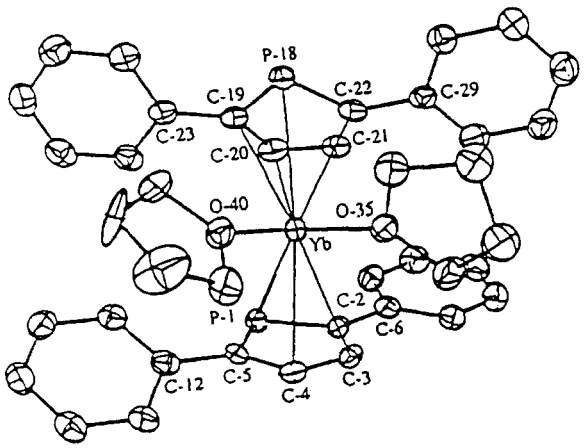

Fig. 23. Molecular structure of [(2,5-Ph$_2$C$_4$H$_2$P)$_2$Yb(thf)$_2$] **108o** in the crystal.

Of special interest with regard to derivative chemistry and possible catalytic applications are phospholyl analogues of the well-known bis(pentamethylcyclopentadienyl)lanthanide(III) halides [(C$_5$Me$_5$)$_2$Ln(μ-Cl)$_2$Li(solv.)$_2$] (solv. = solvent). First examples of such complexes have already been reported.[107] Thus, Li(C$_4$Me$_4$P) was generated in situ from bis(tetramethylphospholyl)butane, and subsequent treatment with LnCl$_3$ in a 2:1 molar ratio afforded the disubstituted products **109** in moderate yields [Eq. (43)].

$$LnCl_3 + 2Li(C_4Me_4P) \xrightarrow[-LiCl]{solv.} [(C_4Me_4P)_2Ln(\mu\text{-}Cl)_2Li(solv.)_2] \quad (43)$$

109b, Ln = Y; solv. = 1/2 DME
109p, Ln = Lu; solv. = Et$_2$O

These reactions are not always as straightforward as implied by Equation (43). This was demonstrated by the recently reported reaction of SmCl$_3$ with three equivalents of K(C$_4$Me$_4$P) in toluene, which led to the polymeric product **110g** (Fig. 24).[108]

[(C$_4$Me$_4$P)$_6$Sm$_2$(KCl)$_2$(C$_7$H$_8$)$_3$]$_n$ **110g**

A different result was obtained when the sterically less demanding 3,4-dimethylphospholyl ligand was used. The reaction of SmCl$_3$ with K(C$_4$Me$_2$H$_2$P) in a 1:3 molar ratio yielded a red crystalline material which was shown by X-ray diffraction to be dimeric **111g**.[108]

[(η^5-C$_4$Me$_2$H$_2$P)$_4$\{μ-(η^5,η^1)-(C$_4$Me$_2$H$_2$P)\}$_2$Sm$_2$] **111g**

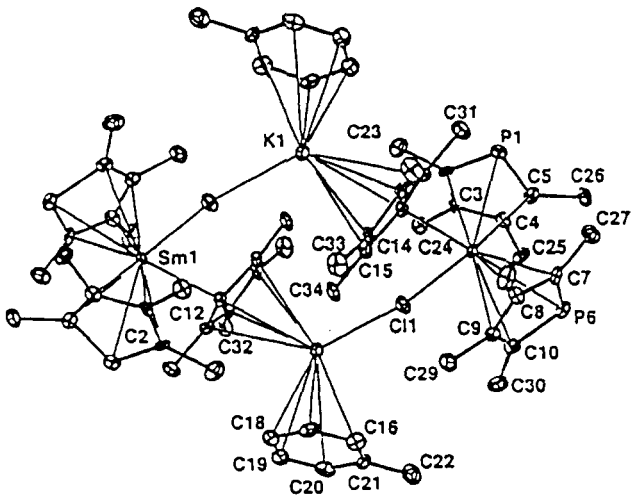

Fig. 24. Molecular structure of [(C$_4$Me$_4$P)$_6$Sm$_2$(KCl)$_2$(C$_7$H$_8$)$_3$]$_n$ **110g** in the crystal.

7. Arene Complexes

Lanthanide ions can participate in η^6 interactions with benzene derivatives, although the number of well-characterized arene complexes is still fairly small. The most important and best-known compounds are bimetallic arene complexes of the type [(η^6-arene)Ln(AlCl$_4$)$_3$] **112**–**114**.[109–114] In contrast to the anhydrous lanthanide trichlorides, these substances are soluble in hydrocarbons. The synthetic route involves treatment of anhydrous lanthanide trichlorides with AlCl$_3$ in the presence of

the arene ligand. Most conveniently these preparations are carried out in the appropriate benzene derivative as solvent [Eq. (44)].

$$LnCl_3 + 3AlCl_3 + C_6R_6 \longrightarrow [(\eta^6\text{-}C_6R_6)Ln(AlCl_4)_3] \quad (44)$$

112, **113**, Ln = La, Nd, Sm, Gd, Yb; R = H, Me

The bonding in these arene complexes can be described as an ion–dipole interaction between the Ln^{3+} ion and the π-electron system of the aromatic ring. Preferably electron-rich arenes such as benzene, toluene, and hexamethylbenzene are used. Among the well-characterized and in some cases structurally analyzed examples are the complexes **112**–**114**, which are usually monomeric in the crystal.[111, 112] The compounds **112f** and **112g** are isostructural with the uranium(III) analogue $[(\eta^6\text{-}C_6H_6)U(AlCl_4)_3]$. An exception is the tetramer $[\{(\eta^6\text{-}C_6H_6)Er(AlCl_4)_3\}_4]$ **112m**, in which the erbium ions are bridged by η^2-tetrachloroaluminate ligands.[115]

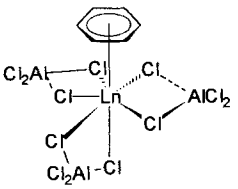

112

$[(\eta^6\text{-}C_6H_6)Ln(AlCl_4)_3]$ **112**, Ln = Nd, Sm, Yb

$[(\eta^6\text{-}C_6Me_6)Ln(AlCl_4)_3]$ **113**, Ln = Sm, Er, Yb

$[(\eta^6\text{-}C_6H_5Me)Ln(AlCl_4)_3]$ **114**, Ln = Y, Pr, Nd, Sm, Gd

Recently the first derivatization reactions of the arene complexes were reported. Addition of AlR_3 (R = Me, Et) to a toluene suspension of **114** results in the formation of clear solutions from which the alkylated products **115** and **116** can be isolated in good yields [Eq. (45)]. The synthesis of the complexes

$$[(\eta^6\text{-}C_6H_5Me)Ln(AlCl_4)_3] + 3AlR_3 \xrightarrow[-3AlCl_2R]{} [(\eta^6\text{-}C_6H_5Me)Ln(AlCl_3R)_3] \quad (45)$$

114 → **115**, R = Me; Ln = Y, Nd, Sm
116, R = Et; Ln = Pr, Nd

$[(\eta^6\text{-}C_6H_2Me_4)Nd(AlCl_3R)_3]$ **117f**, R = Me, Et

117f has been achieved in a similar way.[116] The neodymium complex **115f** was characterized by an X-ray crystal structure determination (Fig. 25). Initial experiments show that the complexes **115** and **116** catalyze the polymerization of ethylene and butadiene.

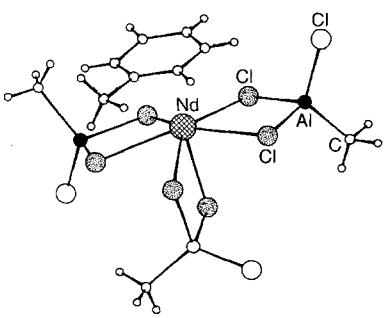

Fig. 25. Molecular structure of $[(\eta^6\text{-}C_6H_5Me)Nd(AlCl_3Me)_3]$ **115f** in the crystal.

In several recent papers some interesting cases of η^6-arene coordination between lanthanide ions and phenyl groups of certain phenoxide ligands have been reported. Thus far two types of this novel bonding have been described.[117, 118] Treatment of lanthanide metal powders with $[Hg(C_6F_5)_2]$ and 2,6-diphenylphenol in THF affords the lanthanide(III) phenoxides **118** and their THF adducts **119**. No unusual structural features were noted in the crystallographically characterized THF adduct **119o**. However, in the unsolvated compound **118o** one phenyl substituent is in a geometrically favorable position which allows this ring to engage in a novel π-interaction with the central ytterbium atom. The reason for this additional η^6-arene coordination most likely lies in the sterically unsaturated character of the three-coordinate species $[Ln(2,6\text{-}OC_6H_3Ph_2)_3]$.

$[Ln(2,6\text{-}OC_6H_3Ph_2)_3]$ **118**, Ln = Nd, Sm, Er, Yb, Lu

$[Yb(2,6\text{-}OC_6H_3Ph_2)_3(thf)_2]$ **119o**

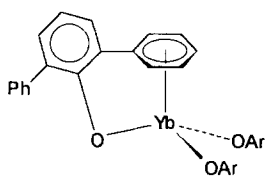

118o, Ar = $2,6\text{-}Ph_2C_6H_3$

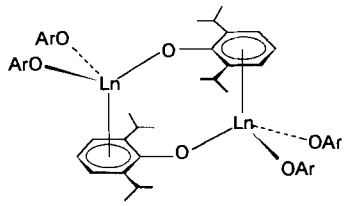

120, Ar = $2,6\text{-}iPr_2C_6H_3$

Another variant was found in the lanthanide derivatives **120** (Ln = Nd, Sm, Er, Yb) of 2,6-diisopropylphenol, which have been synthesized in an analogous manner.[118] Centrosymmetric dimers are present in the crystal; the monomeric units are each linked through a Ln–O bond and η^6-arene coordination. These results demonstrate that the formation of lanthanide arene complexes occurs more frequently than originally anticipated.

8. Cyclooctatetraene Complexes

The first cyclooctatetraene lanthanide complexes were reported in 1969.[1–6] These materials were lanthanide(II) compounds of the type $[Ln(C_8H_8)]$ **121** (Ln = Eu, Yb). Initial synthetic achievements in this area were followed by a period of stagnation, which in recent years has been replaced by a significant increase in the research activity. Today it is generally accepted that the large, flat cyclooctatetraene ligand is an especially valuable alternative to the cyclopentadienyl ligands. This is an area of organolanthanide chemistry where numerous interesting results can be expected in the future.[119]

8.1. Lanthanide(II) Complexes

Well-defined lanthanide(II) complexes with cyclooctatetraene ligands are rare. Cyclooctatetraene reacts with the dark blue solutions of europium or ytterbium in liquid ammonia to give $[Ln(C_8H_8)]$ **121** [Eq. (46)].[1] The orange products are extremely

$$Ln + C_8H_8 \xrightarrow{NH_3(l)} [Ln(C_8H_8)] \quad (46)$$

121, Ln = Eu, Yb

$[(C_8H_8)Yb(C_5H_5N)_3]$ **122o**

air sensitive and insoluble in organic solvents. This behavior suggests a polymeric structure of the compounds. Polymeric $[Sm(C_8H_8)]$ **121g** is more easily available by reacting $[SmI_2(thf)_2]$ with $K_2C_8H_8$.[120]

The polymeric structure can be broken up by treatment of **121o** with pyridine. This results in the formation of soluble, monomeric **122o**, for which a crystal structure determination has been reported (Fig. 26).[121] The structural characterization of the anionic sandwich complexes **123o** and **124o** revealed that

$[K(diglyme)]_2[Yb(C_8H_8)_2]$ **123o** $[K(dme)]_2[Yb(C_8H_8)_2]$ **124o**

in these compounds cyclooctatetraene dianions act as bridging ligands between ytterbium and potassium.[122]

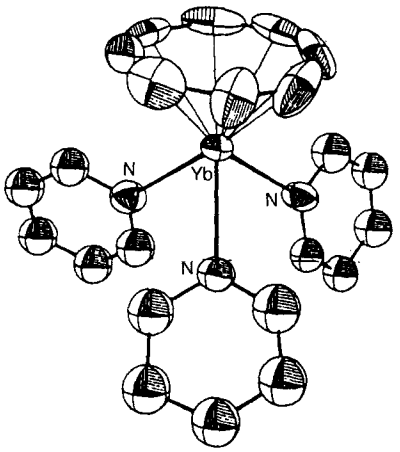

Fig. 26. Molecular structure of $[(C_8H_8)Yb(C_5H_5N)_3]$ **122o** in the crystal.

8.2. Lanthanide(III) Complexes

The first mono(cyclooctatetraene)lanthanide(III) halides were reported in 1971.[119, 123, 124] They are still among the most important starting materials for the preparation of other half-sandwich complexes of the lanthanides with cyclooctatetraene ligands. The complexes **125** are easily accessible by reaction of anhydrous lanthanide trichlorides with $K_2C_8H_8$ in a molar ratio of 1:1 [Eq. (47)].[125]

$$2LnCl_3 + 2K_2C_8H_8 \longrightarrow [\{(C_8H_8)Ln(\mu\text{-}Cl)(thf)_2\}_2] + 4KCl \quad (47)$$

125

Purification of the crystalline, intensely colored products can be achieved by Soxhlet extraction with THF. A crystal structure determination of the cerium compound **125d** revealed the presence of centrosymmetric, Cl-bridged dimers with η^8-coordinated cyclooctatetraene ligands.[1, 2, 119, 123, 124] The coordinated THF cannot be removed from the compounds without extensive decomposition.

An interesting change in the molecular structure is observed when the sterically highly demanding 1,4-bis(trimethylsilyl)-cyclooctatetraene ligand is used.[126, 127] The THF adducts $[LnCl_3(thf)_3]$ (Ln = Y, Sm, Ho, Lu) react with equimolar amounts of the dilithium salt $[Li(thf)]_2[1,4\text{-}(Me_3Si)_2C_8H_6]$ to afford the dimeric mono(cyclooctatetraene)lanthanide(III) chlorides **126**, of which the holmium derivative **1261** was characterized by X-ray crystallography. The single-crystal X-ray structural analysis of the scandium complex **127a** revealed the presence of an

$[\{Ln[1,4\text{-}(Me_3Si)_2C_8H_6](\mu\text{-}Cl)(thf)\}_2]$ **126**, Ln = Y, Sm, Ho, Lu

$[(\mu\text{-}Cl)_2(\mu\text{-}thf)\{Sc[1,4\text{-}(Me_3Si)_2C_8H_6]\}_2]$ **127a**

unusual semibridging THF ligand (Fig. 27). Evidently, the reason for the coordination of only one THF molecule is the increased steric demand of the substituted cyclooctatetraene ligands.[126]

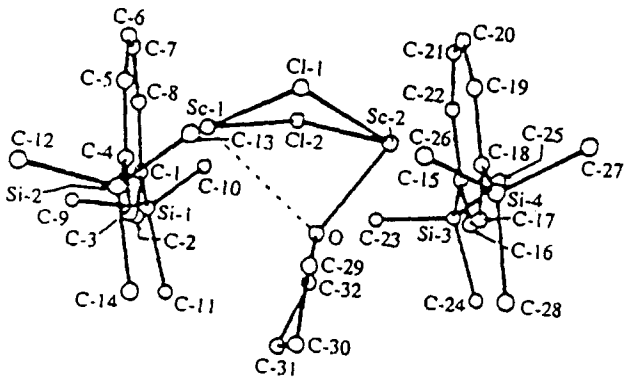

Fig. 27. Molecular structure of $[(\mu\text{-}Cl)_2(\mu\text{-}thf)\{Sc[1,4\text{-}(Me_3Si)_2C_8H_6]\}_2]$ **127a** in the crystal.

The complexes **125** are often used as starting materials for subsequent reactions because the bridging chloro ligands are easily replaced by other anions.[119] A certain disadvantage, however, is the very low solubility of these compounds even in THF. In the search for more soluble alternatives, preparative routes to mono(cyclooctatetraene)lanthanide(III) iodides and triflates have been developed. Mononuclear iodo complexes **128** are accessible in two ways [Eqs. (48) and (49)].[128–130] The

$$LnI_3 + K_2C_8H_8 \longrightarrow [(C_8H_8)LnI(thf)_n] + 2KI \quad (48)$$

128, Ln = Nd, Sm

$$Ln + C_8H_8 + 1/2I_2 \xrightarrow{THF} [(C_8H_8)LnI(thf)_n] \quad (49)$$

128

Ln = La, Ce, Pr, Nd, Sm,
$n = 1, 2, 3$

second procedure offers the advantage that the metal powders can be directly used as starting materials.[129, 130] Depending on the ionic radius of the lanthanide, the complexes are coordinated by a different number of THF molecules. The molecular structures of **128d** and **128f** have been determined by X-ray diffraction.

In contrast to the dimeric chloro complexes **125**, the iodides **128** are highly soluble in THF. The same is true for the recently described triflates. Schumann et al. and Fischer et al. had already shown that triflates are valuable alternatives to the previously used chloro complexes in the cyclopentadienyl chemistry of the lanthanides.[131, 132] Dimeric organolanthanide triflates **129** [Eq. (50)] are obtained in good yields in a smooth reaction between anhydrous lanthanide(III) triflates and equimolar

$$2\,K_2C_8H_8 + 2\,Ln(O_3SCF_3)_3 \xrightarrow[-4\,KO_3SCF_3]{THF} 2 \quad (50)$$

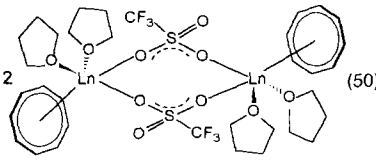

129, Ln = Ce, Pr, Nd, Sm

amounts of $K_2C_8H_8$.[128, 133] The intensely colored products which crystallize well are also highly soluble in THF. With yttrium as central atom the bis(tetrahydrofuran) complex **130b** is isolated due to the smaller ionic radius of the metal.[133]

$[\{(C_8H_8)Y(\mu\text{-}O_3SCF_3)(thf)\}_2]$ **130b**

The molecular structures of **129d** (Fig. 28) and **129f** have been determined by X-ray diffraction. A central eight-membered $Ln_2O_4S_2$ ring is formed by bridging of the lanthanide ions

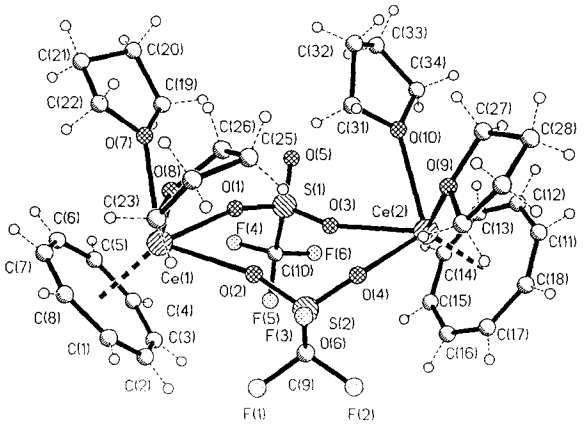

Fig. 28. Molecular structure of $[\{(C_8H_8)Ce(\mu\text{-}O_3SCF_3)(thf)_2\}_2]$ **129d** in the crystal.

by bidentate triflate ligands. Thus, the compounds **129** are structurally closely related to the bis(cyclopentadienyl)lanthanide(III) triflates $[\{(C_5H_5)_2Ln(\mu\text{-}O_3SCF_3)\}_2]$.[132] As expected, the cyclooctatetraene ligands are η^8-coordinated. Besides the improved solubility, the triflate complexes **129** and **130b** offer additional preparative advantages. First, the triflate anion is a good leaving group and thus facilitates substitution reactions with other ligands, second, LiO_3SCF_3 and NaO_3SCF_3 are more easily removed by filtration than finely divided LiCl or NaCl. Most of the subsequent reactions of the chloro complexes **125** described below have already been carried out with the corresponding triflates, and in many cases higher yields have been obtained.

In a series of recent papers an impressive number of mono(cyclooctatetraene)lanthanide(III) complexes has been reported. For example, the synthesis of some dinuclear complexes with bridging alkoxide ligands has been achieved according to Equation (51). The derivatives **131b** and **133k** have been structurally characterized.[134, 135] The compounds **134** and **135** were prepared with sterically more demanding alkoxide and siloxide ligands. These compounds are monomeric in the solid state,[134] as are the 1,4-bis(trimethylsilyl)cyclooctatetraene complexes $[Ln\{1,4\text{-}(Me_3Si)_2C_8H_6\}(2,6\text{-}tBu_2\text{-}4\text{-}MeOC_6H_2)(thf)]$ (Ln = Sc, Y).[127]

$$[\{(C_8H_8)Ln(\mu\text{-}Cl)(thf)_2\}_2] \xrightarrow[-2\,NaCl]{2\,NaOR} [\{(C_8H_8)Ln(\mu\text{-}OR)(thf)\}_2] \quad (51)$$

125

131, R = Ph; Ln = Y, Lu
132, R = 2,6-$Me_2C_6H_3$; Ln = Y, Lu
133k, R = $(CH_2)_3CH{=}CH_2$; Ln = Dy

$[(C_8H_8)Ln(OCtBu_3)(thf)]$ **134**, Ln = Y, Lu

$[(C_8H_8)Ln(OSiPh_3)(thf)]$ **135**, Ln = Y, Lu

The heterodinuclear alkoxide **136d** is formed in the reaction of $Ce(OiPr)_4$ with triethylaluminum in the presence of cyclooctatetraene [Eq. (52)].[11] During the course of this reaction Ce^{IV} is reduced to Ce^{III}. In the product, isopropoxide ligands act as bridges between cerium and aluminum.

$$Ce(OiPr)_4 \xrightarrow{AlEt_3,\ C_8H_8} [(C_8H_8)Ce(\mu\text{-}OiPr)_2AlEt_2] \quad (52)$$

136d

The synthesis of mono(cyclooctatetraene)lanthanide(III) thiolates and selenolates has been reported very recently.[130] Their preparation was achieved by using a procedure similar to that in Equation (49); diaryldisulfides or diaryldiselenides were used as oxidizing agents instead of iodine [Eq. (53)]. Catalytic amounts

$$2\,Sm + C_8H_8 + ArEEAr \xrightarrow{THF} [\{(C_8H_8)Sm(\mu\text{-}EAr)(thf)_n\}_2] \quad (53)$$

137g, n = 1, EAr = 2,4,6-$iPr_3C_6H_2S$
138g, n = 2, EAr = SPh, 2,4,6-$Me_3C_6H_2S$, SePh

of iodine accelerate the reactions by activating the metal surface. The X-ray structure analysis of $[\{(C_8H_8)Sm(\mu\text{-}SePh)(thf)_2\}_2]$ **138g** (EAr = SePh) revealed the presence of a dimer with phenylselenolate bridges (Fig. 29).

Nitrogen donor ligands are also increasingly used in connection with lanthanide cyclooctatetraene complexes. For example, interesting results were obtained with the sterically demanding

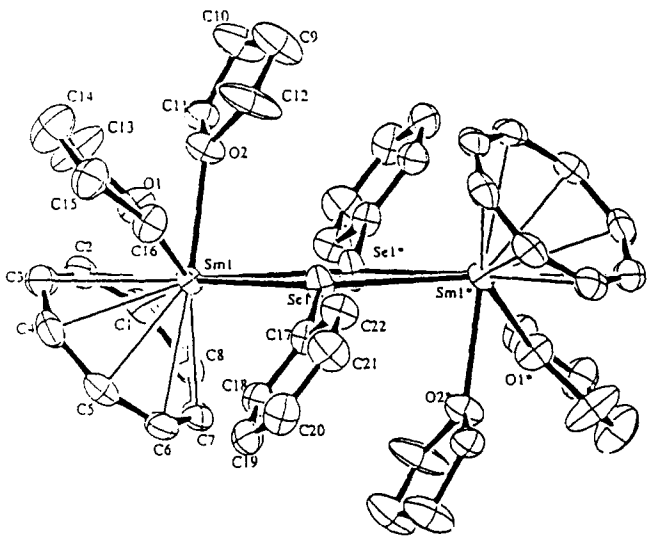

Fig. 29. Molecular structure of $[\{(C_8H_8)Sm(\mu\text{-}SePh)(thf)_2\}_2]$ **138g** (EAr = SePh) in the crystal.

bis(trimethylsilyl)amido ligand. The monomeric amido complexes **139** were isolated for yttrium and the "late" lanthanides [Eq. (54)].[136]

$$[\{(C_8H_8)Ln(\mu\text{-}Cl)(thf)_2\}_2] + 2\,NaN(SiMe_3)_2 \xrightarrow[-2\,NaCl]{} 2[(C_8H_8)Ln\{N(SiMe_3)_2\}(thf)] \quad (54)$$

125 → **139**, Ln = Y, Gd, Er, Lu

When the same reaction is carried out with the samarium derivative **125g** [Eq. (55)], an unusual "inverse sandwich complex" is formed, in which two $Sm[N(SiMe_3)_2]_2$ units are symmetrically bridged by a cyclooctatetraene ligand (Fig. 30).[136]

$$3[\{(C_8H_8)Sm(\mu\text{-}Cl)(thf)_2\}_2] + 8\,NaN(SiMe_3)_2 \xrightarrow[-6\,NaCl]{\text{toluene}} [(\mu\text{-}C_8H_8)\{Sm[N(SiMe_3)_2]_2\}_2] + 2[Na(thf)_n][Sm(C_8H_8)_2] \quad (55)$$

125g → **140g**

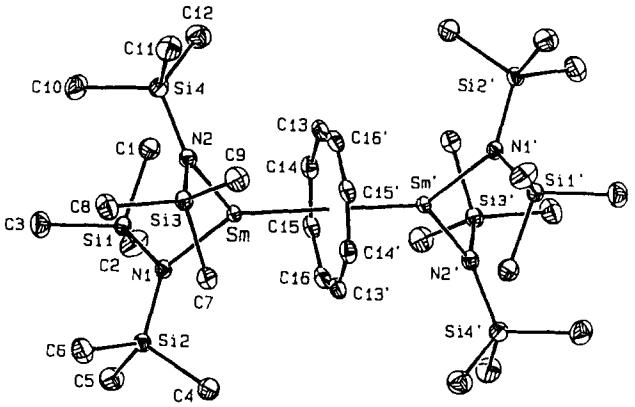

Fig. 30. Molecular structure of $[(\mu\text{-}C_8H_8)\{Sm[N(SiMe_3)_2]_2\}_2]$ **140g** in the crystal.

Mono(cyclooctatetraene)lanthanide(III) complexes containing polydentate nitrogen ligands are also currently being investigated. These include silylated benzamidinate and diiminophosphinate anions as well as tridentate pyrazolylborate ligands.[133, 137–140] Typical preparations are outlined in the Equations (56)–(58).

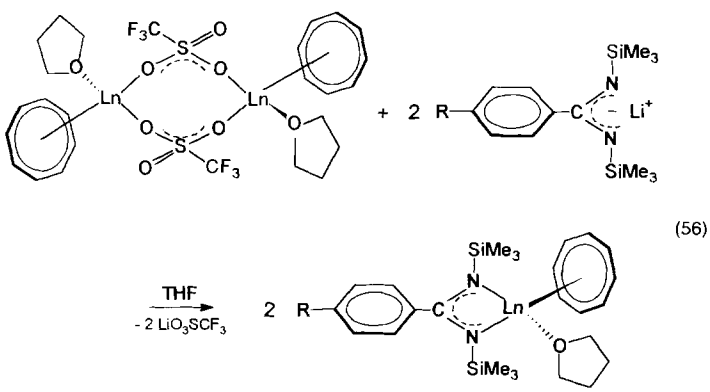

(56)

141, R = H; **142**, R = MeO; **143**, R = CF_3
Lw = Y, Ce, Pr, Nd, Sm, Tm, Lu

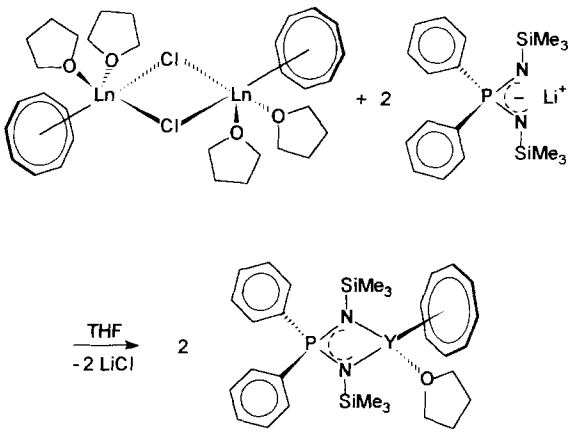

(57)

144, Ln = Ce, Pr, Nd, Sm

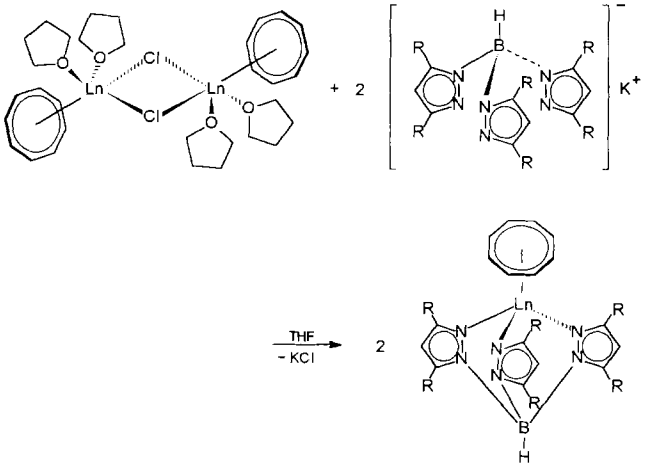

(58)

145, R = H; **146**, R = Me,
Ln = Ce, Pr, Nd, Sm

The first pyrazolylborate complexes of the type **145** had already been synthesized some years ago by Takats et al.[138] Depending on the ionic radius of the lanthanide element, these compounds can either be unsolvated or may contain a coordinated THF molecule. The complexes **145** and **146** are formed as highly crystalline, intensely colored substances and several representatives have already been characterized by crystal structure analyses.[140] Figure 31 shows the molecular structure of the THF adduct of the cerium compound **146d**.

The first σ-alkyl complexes with η^8-cyclooctatetraene ligands were isolated starting from the lutetium compound **125p** [Eq. (59)].[141, 142] The formation of mononuclear complexes is facilitated by the small ionic radius of lutetium as well as the high steric demand of the organic ligands.

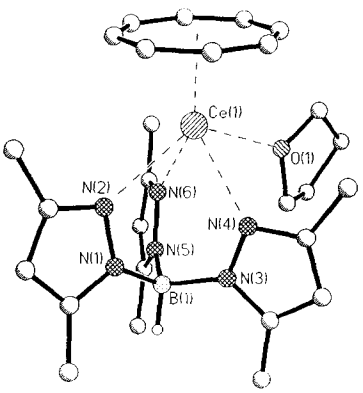

Fig. 31. Molecular structure of $[(C_8H_8)Ce\{HB(3,5\text{-}Me_2pz)_3\}(thf)]$ **146d** in the crystal.

$$[\{(C_8H_8)Lu(\mu\text{-}Cl)(thf)_2\}_2] + 2\,LiR \xrightarrow[-2\,THF]{-2\,LiCl} 2[(C_8H_8)LuR(thf)] \quad (59)$$

125p → **147p**, R = CH_2SiMe_3; **148p**, R = *o*-$Me_2NCH_2C_6H_4$

Similar alkylations of **125** (Ln = Y, Sm, Lu) with $LiCH(SiMe_3)_2$ did not lead to the expected neutral σ-alkyl complexes.[143] Instead, the "inverse sandwich complexes" **149** were

$[Li(thf)_2\{\mu\text{-}\eta^2,\eta^8\text{-}C_8H_8\}Ln\{CH(SiMe_3)_2\}]$ **149**

formed. Figure 32 shows the unusual zwitterionic structure of the samarium compound **149g** with a bridging cyclooctatetraene ligand which is η^2-coordinated to a $Li(thf)_2$ unit. The question of whether σ-alkyl complexes containing η^8-cyclooctatetraene ligands such as **147**, **148**, and **149** exhibit catalytic activities still remains to be answered.

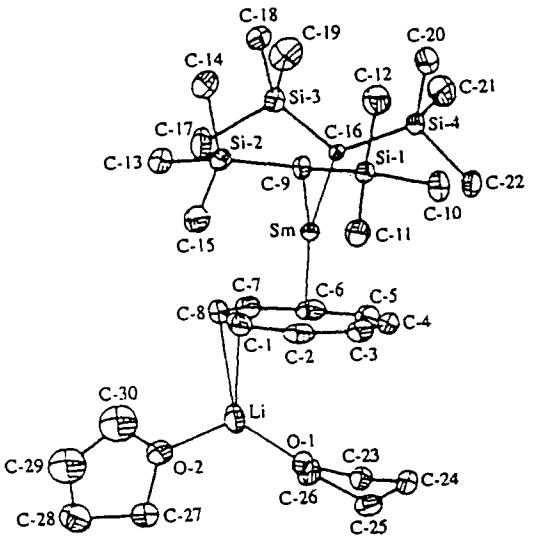

Fig. 32. Molecular structure of $[Li(thf)_2\{\mu\text{-}\eta^2,\eta^8\text{-}C_8H_8\}Sm\{CH(SiMe_3)_2\}]$ **149g** in the crystal.

The formation of neutral σ-alkyl complexes should be facilitated by the increased steric demand of the cyclooctatetraene ligand. This was recently verified by Cloke et al. with the 1,4-bis(trimethylsilyl)cyclooctatetraene complexes. Alkylation of the dimeric chloro complexes **126** with $LiCH(SiMe_3)_2$ afforded the monomeric σ-alkyl derivatives **150**.[127]

$[Ln\{1,4\text{-}(Me_3Si)_2C_8H_6\}\{CH(SiMe_3)_2\}(thf)]$ **150**, Ln = Sc, Y

Symmetrical sandwich complexes containing $[Ln(C_8H_8)_2]^-$ ions have been described previously for a series of lanthanides.[119, 123, 124] Potassium salts of these anions are easily accessible by treatment of anhydrous lanthanide trichlorides with two equivalents of $K_2C_8H_8$ [Eq. (60)]. The products are readily soluble in THF and can be isolated by extraction with this solvent. The potassium salts **151** are thermally very robust, but decompose almost explosively upon contact with traces of oxygen.

$$LnCl_3 + 2\,K_2C_8H_8 \xrightarrow[-3\,KCl]{} K[Ln(C_8H_8)_2] \quad (60)$$

151, Ln = Sc, Y, La, Ce, Pr, Nd, Sm, Gd, Tb

All structurally characterized compounds of this series contain coordinated solvent molecules. The structural chemistry of the cerium(III) anion $[Ce(C_8H_8)_2]^-$ has been investigated in detail. The crystallographically characterized lithium salt of this anion (**152d**) was obtained in the form of needlelike, bright green crystals as a by-product in the reaction of **125d** with $LiCH(SiMe_3)_2$.[144] The crystal structure reveals the presence of separated ions; the Li^+ ion is coordinated by four THF molecules (Fig. 33).

$[Li(thf)_4][Ce(C_8H_8)_2]$ **152d** $[Na(thf)_3][Ce(C_8H_8)_2]$ **153d** [K(diglyme)][$Ce(C_8H_8)_2$] **154d**

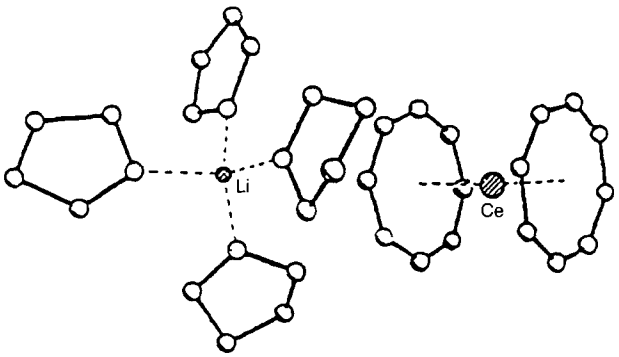

Fig. 33. Molecular structure of $[Li(thf)_4][Ce(C_8H_8)_2]$ **152d** in the crystal.

The sodium salt forms a sort of "double sandwich" **153d** (Fig. 34).[144] Two cyclooctatetraene ligands and the two metal ions are arranged as a linear unit. In this case three THF ligands are sufficient for the coordinative saturation of the sodium. A very similar structure was reported for the potassium salt **154d**.[145]

The stacking of cyclooctatetraene ligands in organolanthanide complexes can be further extended, as has been demonstrated by the structure determination of the unusual erbium complex **155m** (Fig. 35).[146] However, compounds of this type are not accessible by rational syntheses. The compound **155m** was isolated serendipitously from a reaction of $[(C_5H_4CH_2Ph)ErCl_2(thf)_3]$ with $K_2C_8H_8$.

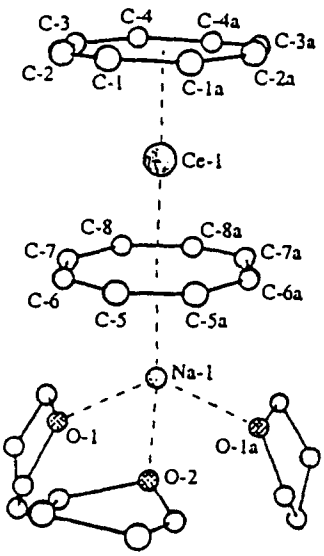

Fig. 34. Molecular structure of $[Na(thf)_3][Ce(C_8H_8)_2]$ **153d** in the crystal.

$[(C_8H_8)Er(\mu\text{-}C_8H_8)K(\mu\text{-}C_8H_8)Er(\mu\text{-}C_8H_8)K(thf)_4]$ **155m**

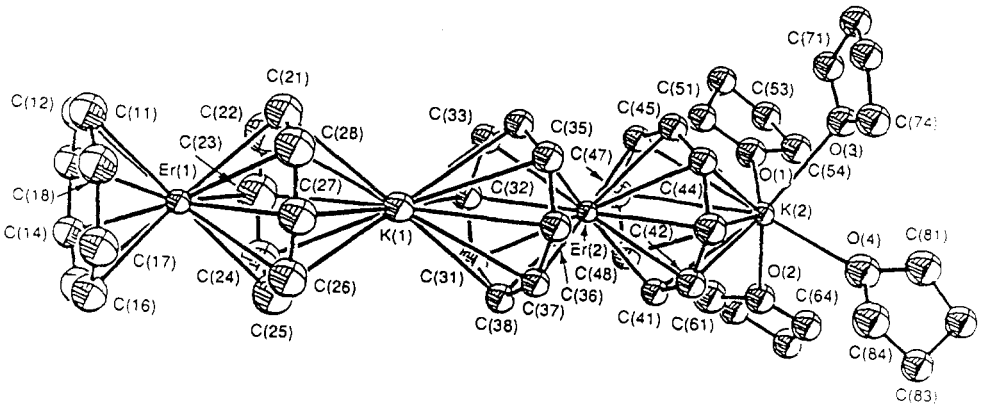

Fig. 35. Molecular structure of $[\{(C_8H_8)Er(\mu\text{-}C_8H_8)K(\mu\text{-}C_8H_8)Er(\mu\text{-}C_8H_8)K(thf)_4]$ **155m** in the crystal.

8.3. Lanthanide(IV) Complexes

Cerium is the only lanthanide that has been shown to form stable organometallic complexes in the formal oxdation state + IV; however, even well-defined organocerium(IV) compounds are very rare.[119, 123, 124] Many organic ligands are simply oxidized in the presence of Ce^{IV} ions. The longest known compound of this type is the so-called cerocene **156d**.[145–147]

$[Ce(C_8H_8)_2]$ **156d** $[Ce(MeC_8H_7)_2]$ **157d**

Cerocene was first made by the reaction of $Ce(OiPr)_4$ with cyclooctatetraene in the presence of triethylaluminum and isolated as a black-red, pyrophoric product.[1, 119] An improved synthetic route to cerocene involves controlled oxidation of the anionic sandwich complex with silver iodide or allyl iodide.[150] A thorough investigation of this interesting complex was complicated by its difficult accessibility as well as by its low solubility and pyrophoric nature. Except for the reduction by alkali metals, which leads to known derivatives of the cerium(III) anion $[Ce(C_8H_8)_2]^-$, no further reactions of cerocene have been reported. A novel development in the organometallic chemistry of tetravalent cerium was recently initiated through the use of substituted cyclooctatetraene ligands. The introduction of suitable substituents leads to an improved solubility as well as a significantly higher stability of the products toward oxygen. For instance, with the 1,1′-dimethyl compound **157d** Streitwieser et al. succeeded in the first structural characterization of a cerocene derivative; the result clearly established the proposed sandwich structure.[145] The angle between the central cerium atom and the ring centroids is 176.03°. Even better results can be obtained with the sterically demanding ligand 1,4-bis(trimethylsilyl)cyclooctatetraene as well as the novel 1,3,6-tris(trimethylsilyl) derivative.[151] Schemes 7 and 8 illustrate the syntheses of the silyl-substituted cerocene derivatives **159d** and **161d**. In both cases silver iodide has proven successful as the mild oxidizing agent. The compound **159d** is isolated as a dark purple oil,

$$CeCl_3 + 2[Li(thf)_n]_2[1,4\text{-}(Me_3Si)_2C_8H_6] \xrightarrow[-3\,LiCl]{THF}$$

$$Li[Ce\{1,4\text{-}(Me_3Si)_2C_8H_6\}_2] \xrightarrow[-Ag,\,-LiI]{+AgI} [Ce\{1,4\text{-}(Me_3Si)_2C_8H_6\}_2]$$

158d **159d**

Scheme 7. Synthesis of $[Ce\{1,4\text{-}(Me_3Si)_2C_8H_6\}_2]$ **159d**.

$$Ce(O_3SCF_3)_3 + 2[K(thf)_n]_2[1,3,6\text{-}(Me_3Si)_3C_8H_5]$$

$$\xrightarrow[-3\,KO_3SCF_3]{THF} K[Ce\{1,3,6\text{-}(Me_3Si)_3C_8H_5\}_2]$$

160d

$$\xrightarrow[-Ag,\,-KI]{+AgI} [Ce\{1,3,6\text{-}(Me_3Si)_3C_8H_5\}_2]$$

161d

Scheme 8. Synthesis of $[Ce\{1,3,6\text{-}(Me_3Si)_3C_8H_5\}_2]$ **161d**.

while **161d** forms permanganate-colored crystals. The two cerocenes are highly soluble in nonpolar organic solvents due to the presence of the trimethylsilyl substituents.

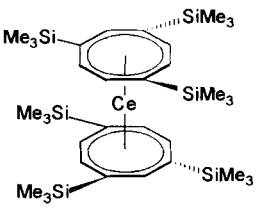

161d

The crystalline hexakis(trimethylsilyl)cerocene **161d** was characterized by a crystal structure analysis (Fig. 36);[151] the angle between cerium and the ring centroids is 176.1°. The compounds **159d** and **161d** are the first cerocene derivatives that are reproducibly accessible in synthetically useful amounts; thus, they allow the study of what is expected to be interesting derivative chemistry.[152]

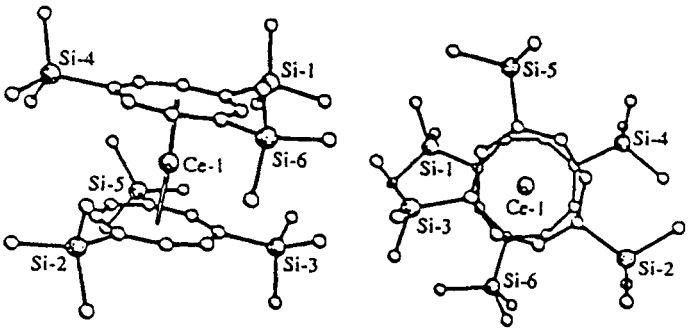

Fig. 36. Molecular structure of $[Ce\{1,3,6\text{-}(Me_3Si)_3C_8H_5\}_2]$ **161d** in the crystal.

9. Organolanthanides in Homogeneous Catalysis

Applications of organolanthanide complexes in homogeneous catalysis have been initiated by the observation that some of these complexes exhibit high catalytic activities in olefin polymerizations.[5, 74, 153] In the preliminary experiments in that di-

rection the catalytically active species were generated by activating lanthanide oxides, halides, or alkoxides with co-catalysts such as alkyllithium or alkylaluminum compounds. The intermediately formed σ-alkyl complexes were capable of catalyzing the cracking of hydrocarbons as well as oligomerizations and polymerizations of olefins. Since then well-defined organolanthanide complexes have become available, and many other cases of interesting catalytic activities have been discovered. It was found, for example, that (cyclooctatetraene)cerium complexes catalyze the polymerization of ethylene and butadiene.[153] Anionic tetrakis(η^3-allyl)lanthanide complexes are also highly active catalysts for the production of polybutadiene. In the meantime, however, it has become quite clear that catalytic activity is almost generally limited to cyclopentadienyl complexes of the lanthanides. Metallocene derivatives of trivalent lanthanides such as $[(C_5Me_5)_2LnCH(SiMe_3)_2]$ or $[\{(C_5Me_5)_2Ln(\mu\text{-}H)\}_2]$, in particular, have been found to display very high activities.[5] In contrast, the number of catalytically useful organolanthanide complexes without cyclopentadienyl ligands is still very limited.

The majority of the hitherto investigated reactions that are catalyzed by organolanthanide complexes are olefin transformations such as hydrogenations, polymerizations, or addition reactions. For example, a catalyst for the hydrogenation of ethylene was prepared from a samarium/magnesium alloy.[1] $SmMg_3$ reacts with anthracene in THF to afford a complex of unknown structure. This product absorbs hydrogen and is then able to catalyze the hydrogenation of ethylene.

The main field of application for organolanthanide catalysts without cyclopentadienyl ligands is diene polymerization. In earlier reports on the polymerization of butadiene, catalyst systems such as "$Ph_3Nd_2/Al_2Et_2Cl_3$",[154] neodymium-2-ethylhexanoate/$AlEt_2Cl/AlEt_3$,[155] or $LnCl_3/n$BuLi[156] were used. However, very little is known about the nature of the intermediately formed σ-alkyllanthanide species. Only in one case, that is the catalyst system $Nd(OiPr)_3/AlEt_3/AlEt_2Cl$, could a defined intermediate be "fished out" and structurally characterized.[64, 157] It was shown to be the heteronuclear alkyllanthanide(III) alkoxide **55f** (see Section 3.3). Promising results have been obtained in recent years with anionic allyl complexes of the type $[Ln(\eta^3\text{-}C_3H_5)_4]^-$.[95] Lithium salts of these anions catalyze the polymerization of butadiene and alkylbutadienes with moderate to high activity and high *trans* selectivity. Highly active catalysts for the production of *cis*-1,4-polybutadiene have been obtained by combining tris(2,4-dimethylpentadienyl)-neodymium **99f** with Lewis acids such as $AlEtCl_2$, $AlBr_3$, $SnCl_4$, or Ph_2SnCl_2. In this case the crystal structure analysis provided valuable insight about the constitution of an active pre-catalyst, since the hexanuclear complex **162f** could be isolated and characterized by X-ray diffraction.[158] Figure 37 shows the molecular structure of this unusual cluster, in which two hexagonal-bipyramidal Nd_3Cl_5 units are linked through two chloro bridges. All 2,4-dimethylpentadienyl ligands are η^5-coordinated to neodymium.

$[Nd_6Cl_{12}(C_7H_{11})_6(thf)_2]$ **162f** (C_7H_{11} = 2,4-dimethylpentadienyl)

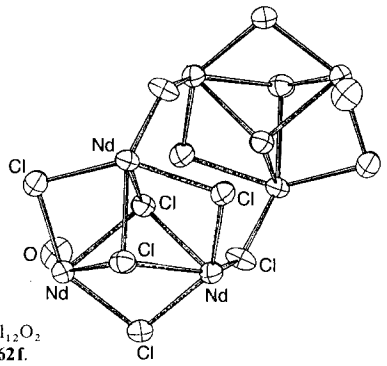

Fig. 37. Structure of the $Nd_6Cl_{12}O_2$ unit in $[Nd_6Cl_{12}(C_7H_{11})_6(thf)_2]$ **162f**.

10. Future Outlook

In the past 10–15 years organolanthanide chemistry has been developed into a highly dynamic area of research that continues to produce fascinating novel results. Until recently most of the research was focused mainly on the discovery of new types of structures and reaction pathways. Indeed, organolanthanide chemistry is characterized by a great diversity of novel and unusual molecular structures, and the extraordinarily high reactivity of certain organolanthanide complexes is without precedent in the chemistry of the d-block transition metals. Today an increased interest in possible applications of organolanthanides is apparent. For example, an enormous potential lies in the use of organolanthanide complexes in homogeneous catalysis. Lanthanide catalysts combine several favorable aspects such as very high activities, excellent environmental compatibility, and low costs. Possible applications in the area of materials science are also apparent and it should be worthwhile to consider future work in that direction. A conceivable application, for example, is the use of organolanthanide complexes in the doping of semiconductor materials, which has already been successful in the case of cyclopentadienyl lanthanide complexes.[5] There is a good chance that volatile organocerium compounds will turn out to be useful precursors for the vapor deposition of cerium dioxide. In addition, many interesting questions of a more academic nature still warrant further investigation: To what degree do f-orbitals participate in the bonding in (cyclooctatetraene)lanthanide complexes? Is it possible to construct multidecker sandwich complexes with cyclooctatetraene ligands? Will it ever be possible to synthesize organometallic complexes containing a direct Ln–Ln bond or to realize unusual oxidation states (e.g. Nd^{II}, Pr^{IV}, Tb^{IV}, Tm^{II}) in organolanthanide complexes? What are the structures of "Grignard-like" complexes RLnX with simple alkyl substituents? In any case, research in the area of "lanthanide chemistry without cyclopentadienyl" will continue to be exciting.

Our own investigations which have been carried out in Göttingen would not have been possible without the enthusiasm of my highly talented co-workers, whose names appear in the list of references. To them I owe my sincere gratitude. Special thanks are also due to Prof. Dr. H. W. Roesky for his continuing generous support. I have learned a lot from him. I also thank Prof. Dr. Josef Takats (University of Alberta, Edmonton, Canada) for initiating my interest in organo-f-element chemistry. Many stimulating discus-

sions with Prof. Dr. John W. Gilje (James Madison University, Harrisonburg, USA) are also gratefully acknowledged. I thank the Deutsche Forschungsgemeinschaft and the Fonds der Chemischen Industrie for the financial support of our research.

Received: June 16, 1995 [A 120 IE]
German version: *Angew. Chem.* **1995**, *107*, 2647–2669

[1] H. Schumann, *Angew. Chem.* **1984**, *96*, 475; *Angew. Chem. Int. Ed. Engl.* **1984**, *23*, 474.
[2] H. Schumann, *NATO ASI Ser. C*, **1985**, *155*, 1.
[3] R. D. Köhn, G. Kociok-Köhn, H. Schumann in *Encyclopedia of Inorganic Chemistry* (Ed.: R. B. King), Wiley, **1994**.
[4] C. J. Schaverien, *Adv. Organomet. Chem.* **1994**, *36*, 283.
[5] F. T. Edelmann in *Comprehensive Organometallic Chemistry II* (Eds.: E. W. Abel, F. G. A. Stone, G. Wilkinson), Pergamon, **1995**.
[6] H. Schumann, J. A. Meese-Marktscheffel, L. Esser, *Chem. Rev.* **1995**, *95*, 865.
[7] I. P. Beletskaya, A. Z. Voskoboinikov, E. B. Chuklanova, N. I. Kirillova, A. K. Shestakova, I. N. Parshina, A. I. Gusev, G. K.-I. Magomedov, *J. Am. Chem. Soc.* **1993**, *115*, 3156.
[8] G. B. Deacon, D. G. Vince, *J. Organomet. Chem.* **1976**, *112*, C1.
[9] G. B. Deacon, W. D. Raverty, D. G. Vince, *J. Organomet. Chem.* **1977**, *135*, 103.
[10] G. B. Deacon, A. J. Koplick, W. D. Raverty, D. G. Vince, *J. Organomet. Chem.* **1979**, *182*, 121.
[11] G. B. Deacon, C. M. Forsyth, R. H. Newnham, *Polyhedron* **1987**, *6*, 1143.
[12] G. B. Deacon, P. I. MacKinnon, T. D. Tuong, *Aust. J. Chem.* **1983**, *36*, 43.
[13] P. B. Hitchcock, S. A. Holmes, M. F. Lappert, S. Tian, *J. Chem. Soc. Chem. Commun.* **1994**, 2691.
[14] C. Eaborn, P. B. Hitchcock, K. Izod, J. D. Smith, *J. Am. Chem. Soc.* **1994**, *116*, 12071.
[15] S. S. Al-Juaid, C. Eaborn, P. B. Hitchcock, K. Izod, M. Mallien, J. D. Smith, *Angew. Chem.* **1994**, *106*, 1336; *Angew. Chem. Int. Ed. Engl.* **1994**, *33*, 1268.
[16] S. S. Al-Juaid, C. Eaborn, P. B. Hitchcock, C. A. McGeary, J. D. Smith, *J. Chem. Soc. Chem. Commun.* **1989**, 273.
[17] G. Z. Suleimanov, V. I. Bregadze, N. A. Kovalchuk, I. P. Beletskaya, *J. Organomet. Chem.* **1982**, *235*, C17.
[18] F. O. Rice, K. K. Rice, *The Aliphatic Free Radicals*, John Hopkins, Baltimore, **1935**, 58.
[19] W. M. Plets, *Dokl. Akad. Nauk SSSR* **1938**, *20*, 27; B. N. Afanasev, P. A. Tsyganova, *Zh. Obshch. Khim.* **1948**, *18*, 306.
[20] F. A. Hart, M. S. Saran, *J. Chem. Soc. Chem. Commun.* **1968**, 1614.
[21] F. A. Hart, A. G. Massey, M. S. Saran, *J. Organomet. Chem.* **1970**, *21*, 247.
[22] M. N. Bochkarev, V. V. Khramenkov, Y. F. Rad'kov, L. N. Zakharov, Y. T. Struchkov, *Metalloorg. Khim.* **1990**, *3*, 1438.
[23] M. N. Bochkarev, V. V. Khramenkov, Y. F. Rad'kov, L. N. Zakharov, Y. T. Struchkov, *J. Organomet. Chem.* **1992**, *429*, 27.
[24] L. N. Bochkarev, T. A. Stepantseva, L. N. Zakharov, G. K. Fukin, A. I. Yanovsky, Y. T. Struchkov, *Organometallics* **1995**, *14*, 2127.
[25] L. E. Manzer, *J. Am. Chem. Soc.* **1978**, *100*, 8068.
[26] L. E. Manzer, *J. Organomet. Chem.* **1977**, *135*, C6.
[27] A. L. Wayda, J. L. Atwood, W. E. Hunter, *Organometallics* **1984**, *3*, 939.
[28] Z. Huang, X. Wu, *Wuji Huaxue Xuebao* **1990**, *6*, 353.
[29] K. Jacob, W. Kretschmer, K.-H. Thiele, H. Gornitzka, F. T. Edelmann, I. Pavlik, A. Lycka, J. Holecek, *J. Organomet. Chem.* **1992**, *436*, 231.
[30] H. Gornitzka, A. Steiner, D. Stalke, U. Kilimann, F. T. Edelmann, K. Jacob, K.-H. Thiele, *J. Organomet. Chem.* **1992**, *439*, C6.
[31] H. Schumann, F. W. Reier, *J. Organomet. Chem.* **1982**, *235*, 287.
[32] H. H. Karsch, A. Appelt, G. Miller, *Angew. Chem.* **1986**, *98*, 832; *Angew. Chem. Int. Ed. Engl.* **1986**, *25*, 823.
[33] S. Hao, J.-I. Song, H. Aghabozorg, S. Gambarotta, *J. Chem. Soc. Chem. Commun.* **1994**, 157.
[34] H. H. Karsch, G. Ferazin, P. Bissinger, *J. Chem. Soc. Chem. Commun.* **1994**, 505.
[35] J. L. Atwood, W. E. Hunter, R. D. Rogers, J. Holton, J. McMeeking, R. Pearce, M. F. Lappert, *J. Chem. Soc. Chem. Commun.* **1978**, 140.
[36] H. Schumann, J. Müller, *J. Organomet. Chem.* **1978**, *146*, C5.
[37] H. Schumann, J. Müller, *J. Organomet. Chem.* **1979**, *169*, C1.
[38] M. F. Lappert, R. J. Pearce, *J. Chem. Soc. Chem. Commun.* **1973**, 126.
[39] A. A. Trifonov, M. N. Bochkarev, G. A. Razuvaev, *Zh. Obshch. Khim.* **1988**, *58*, 931.
[40] P. B. Hitchcock, M. F. Lappert, R. G. Smith, R. A. Bartlett, P. P. Power, *J. Chem. Soc. Chem. Commun.* **1988**, 1007.
[41] C. J. Schaverien, A. G. Orpen, *Inorg. Chem.* **1991**, *30*, 4968.
[42] J. L. Atwood, M. F. Lappert, R. G. Smith, H. Zhang, *J. Chem. Soc. Chem. Commun.* **1988**, 1308.
[43] F. T. Edelmann, A. Steiner, D. Stalke, J. W. Gilje, S. Jagner, M. Håkansson, *Polyhedron* **1994**, *13*, 539.
[44] C. J. Schaverien, J. B. van Mechelen, *Organometallics* **1991**, *10*, 1704.
[45] C. J. Schaverien, G. J. Nesbitt, *J. Chem. Soc. Dalton Trans.* **1992**, 157.
[46] L. N. Bochkarev, V. M. Makarov, Y. N. Hrzhanovskaya, L. N. Zakharov, G. K. Fukin, A. L. Yanovsky, Y. T. Struchkov, *J. Organomet. Chem.* **1994**, *467*, C3.
[47] F. G. N. Cloke, C. I. Dalby, P. B. Hitchcock, H. Karamallakis, G. A. Lawless, *J. Chem. Soc. Chem. Commun.* **1991**, 779.
[48] E. A. Fedorova, G. S. Kalinina, M. N. Bochkarev, G. A. Razuvaev, *J. Gen. Chem. USSR* **1983**, *52*, 1041.
[49] M. N. Bochkarev, E. A. Fedorova, Y. F. Rad'kov, S. Y. Khorshev, G. Kalinina, G. A. Razuvaev, *J. Organomet. Chem.* **1983**, *258*, C29.
[50] H. Schumann, J. Müller, N. Bruncks, H. Lauke, J. Pickardt, H. Schwarz, K. Eckart, *Organometallics* **1984**, *3*, 69.
[51] H. Schumann, H. Lauke, E. Hahn, J. Pickardt, *J. Organomet. Chem.* **1984**, *263*, 29.
[52] H. Schumann, G. Kociok-Köhn, A. Dietrich, F. H. Görlitz, *Z. Naturforsch. B* **1990**, *46*, 896.
[53] W. J. Evans, S. C. Engerer, P. A. Piliero, A. L. Wayda, *Fundam. Res. Homogeneous Catal.* **1979**, *3*, 941.
[54] A. L. Wayda, W. J. Evans, *J. Am. Chem. Soc.* **1978**, *100*, 7119.
[55] H. Schumann, W. Genthe, E. Hahn, J. Pickardt, H. Schwarz, K. Eckart, *J. Organomet. Chem.* **1986**, *306*, 215.
[56] S. A. Cotton, F. A. Hart, M. B. Hursthouse, A. J. Welch, *J. Chem. Soc. Chem. Commun.* **1972**, 1225.
[57] N. S. Emel'yanova, A. A. Trifonov, L. N. Zakharov, M. N. Bochkarev, A. F. Shestakov, Y. T. Struchkov, *Metalloorg. Khim.* **1993**, *6*, 363.
[58] C. Eaborn, P. B. Hitchcock, K. Izod, Z.-R. Lu, J. D. Smith, *3rd Int. Conf. Inorg. Chem.* Brighton, **1995**, Poster 113 (Abstr. p. 113).
[59] G. Lin, Z. Jin, Y. Zhang, W. Chen, *J. Organomet. Chem.* **1990**, *396*, 307.
[60] P. B. Hitchcock, M. F. Lappert, R. G. Smith, *J. Chem. Soc. Chem. Commun.* **1989**, 369.
[61] X. Bao, W. Chen, *Chin. Sci. Bull.* **1989**, *34*, 207.
[62] O. P. Syutkina, L. F. Rybakova, E. N. Egorova, A. B. Sigalov, I. P. Beletskaya, *Izv. Akad. Nauk SSSR* **1983**, 648; *Bull Acad. Sci. USSR* **1983**, 586.
[63] B. Boje, J. Magull, *Z. Anorg. Allg. Chem.* **1994**, *620*, 703.
[64] Z. Shen, *Inorg. Chim. Acta* **1987**, *140*, 7.
[65] R. C. Mehrotra, A. Singh, U. M. Tripathi, *Chem. Rev.*, **1991**, *91*, 1287.
[66] P. Biagini, G. Lugli, L. Abis, R. Millini, *J. Organomet. Chem.* **1994**, *474*, C16.
[67] W. J. Evans, *New J. Chem.* **1995**, *19*, 525.
[68] C. J. Schaverien, N. Meijboom, A. G. Orpen, *J. Chem. Soc. Chem. Commun.* **1992**, 124.
[69] J. Arnold, C. G. Hoffman, *J. Am. Chem. Soc.* **1990**, *112*, 8620.
[70] J. Arnold, C. G. Hoffman, D. Y. Dawson, F. J. Hollander, *Organometallics* **1993**, *12*, 3645.
[71] P. J. Fagan, J. M. Manriquez, T. J. Marks, V. W. Day, S. H. Vollmer, C. S. Day, *J. Am. Chem. Soc.* **1980**, *102*, 5393.
[72] K. H. den Haan, J. L. De Boer, J. H. Teuben, A. L. Spek, B. Kojic-Prodic, G. R. Hays, R. Huis, *Organometallics* **1986**, *5*, 1726.
[73] H. J. Heeres, J. Renkema, M. Booij, A. Meetsma, J. H. Teuben, *Organometallics* **1988**, *7*, 2495.
[74] P. L. Watson, G. W. Parshall, *Acc. Chem. Res.* **1985**, *18*, 51.
[75] J. M. Boncella, R. A. Andersen, *Organometallics* **1985**, *4*, 205.
[76] M. D. Fryzuk, T. S. Haddad, *J. Chem. Soc. Chem. Commun.* **1990**, 1088.
[77] M. D. Fryzuk, T. S. Haddad, S. J. Rettig, *Organometallics* **1992**, *11*, 2967.
[78] M. D. Fryzuk, T. S. Haddad, S. J. Rettig, *Organometallics* **1991**, *10*, 2026.
[79] M. D. Fryzuk, G. R. Giesbrecht, S. J. Rettig, *3rd Int. Conf. Inorg. Chem.* Brighton, **1995**, Poster 12 (Abstr. p. 12).
[80] L. Hasinoff, J. Takats, X. W. Zhang, A. H. Bond, R. D. Rogers, *J. Am. Chem. Soc.* **1994**, *116*, 8833.
[81] R. Duchateau, C. T. van Wee, A. Meetsma, J. H. Teuben, *J. Am. Chem. Soc.* **1993**, *115*, 4931.
[82] F. T. Edelmann, *J. Alloys Compd.* **1994**, *207/208*, 182.
[83] F. T. Edelmann, *Coord. Chem. Rev.* **1994**, *137*, 403.
[84] K. Mashima, H. Sugiyama, A. Nakamura, *J. Chem. Soc. Chem. Commun.* **1994**, 1581.
[85] K. Mashima, H. Takaya, *Tetrahedron Lett.* **1989**, *30*, 3697.
[86] I. L. Fedushkin, M. N. Bochkarev, H. Schumann, L. Esser, G. Kociok-Köhn, *J. Organomet. Chem.* **1995**, *489*, 145.
[87] G. Z. Suleimanov, Y. S. Bogachev, P. V. Petrovskii, Y. K. Grishin, I. L. Zhuravleva, I. P. Beletskaya, *Izv. Akad. Nauk SSSR Ser. Khim.* **1984**, 471.
[88] G. B. Deacon, A. J. Koplick, T. D. Tuong, *Aust. J. Chem.* **1982**, *35*, 941.
[89] G. B. Deacon, A. J. Koplick, *J. Organomet. Chem.* **1978**, *146*, C43.
[90] L. N. Bochkarev, S. B. Shustov, T. V. Guseva, S. F. Zhil'tsov, *Zh. Obshch. Khim.* **1988**, *58*, 923.
[91] S. B. Shustov, L. N. Bochkarev, S. F. Zhil'tsov, *Metalloorg. Khim.* **1990**, *3*, 624.
[92] R. Taube, H. Windisch, F. H. Görlitz, H. Schumann, *J. Organomet. Chem.* **1993**, *445*, 85.
[93] M. Brunelli, S. Poggio, U. Pedretti, G. Lugli, *Inorg. Chim. Acta* **1987**, *131*, 281.
[94] Z. Huang, M. Chen, W. Qiu, W. Wu, *Inorg. Chim. Acta* **1987**, *139*, 203.
[95] R. Taube, H. Windisch, *J. Organomet. Chem.* **1994**, *472*, 71.
[96] W. Wu, M. Chen, P. Zhou, *Organometallics* **1991**, *10*, 98.

[97] D. Baudry, E. Bulot, M. Ephritikhine, *J. Chem. Soc. Chem. Commun.* **1988**, 1369.
[98] D. Baudry, E. Bulot, M. Ephritikhine, *J. Organomet. Chem.* **1990**, *397*, 169.
[99] R. D. Ernst, T. H. Cymbaluk, *Organometallics* **1982**, *1*, 708.
[100] X. Qiu, J. Liu, *Chin. J. Chem.* **1991**, *9*, 10.
[101] H. Schumann, A. Dietrich, *J. Organomet. Chem.* **1991**, *401*, C33.
[102] W. Weng, K. Kunze, A. M. Arif, R. D. Ernst, *Organometallics* **1991**, *10*, 3643.
[103] H. Schumann, J. Winterfeld, H. Hemling, N. Kuhn, *Chem. Ber.* **1994**, *126*, 1657.
[104] H. Schumann, E. C. E. Rosenthal, J. Winterfeld, G. Kociok-Köhn, *J. Organomet. Chem.* **1995**, *495*, C12.
[105] F. Nief, L. Ricard, F. Mathey, *Polyhedron* **1993**, *12*, 19.
[106] F. Nief, F. Mathey, *Synlett* **1991**, 745.
[107] F. Nief, F. Mathey, *J. Chem. Soc. Chem. Commun.* **1989**, 800.
[108] H.-J. Gosink, F. Nief, L. Ricard, F. Mathey, *Inorg. Chem.* **1995**, *34*, 1306.
[109] B. Fan, Q. Shen, Y. Lin, *J. Organomet. Chem.* **1989**, *377*, 51.
[110] B. Fan, S. Jin, Q. Shen, Y. Lin, *Chin. Sci. Bull.* **1991**, *36*, 84.
[111] H. Liang, Q. Shen, J. Guan, Y. Lin, *J. Organomet. Chem.* **1994**, *474*, 113.
[112] F. A. Cotton, W. Schwotzer, *J. Am. Chem. Soc.* **1986**, *108*, 4657.
[113] B. Fan, Q. Shen, Y. Lin, *J. Organomet. Chem.* **1989**, *376*, 61.
[114] F. A. Cotton, W. Schwotzer, *Organometallics* **1987**, *6*, 1275.
[115] H. Liang, Q. Shen, S. Jin, Y. Lin, *J. Chem. Soc. Chem. Commun.* **1992**, 480.
[116] P. Biagini, G. Lugli, L. Abis, R. Millini, *New J. Chem.* **1995**, *19*, 713.
[117] G. B. Deacon, S. Nickel, P. MacKinnon, E. R. T. Tiekink, *Aust. J. Chem.* **1990**, *43*, 1245.
[118] D. M. Barnhart, D. L. Clark, J. C. Gordon, J. C. Huffman, R. L. Vincent, J. G. Watkin, B. D. Zwick, *Inorg. Chem.* **1994**, *33*, 3487.
[119] F. T. Edelmann, *New J. Chem.* **1995**, *19*, 535.
[120] A. L. Wayda, S. Cheng, I. Mukerji, *J. Organomet. Chem.* **1987**, *330*, C17.
[121] A. L. Wayda, I. Mukerji, J. L. Dye, R. D. Rogers, *Organometallics* **1987**, *6*, 1328.
[122] S. A. Kinsley, A. Streitwieser, Jr., A. Zalkin, *Organometallics* **1985**, *4*, 52.
[123] A. Streitwieser, Jr., *NATO ASI Ser. C*, **1985**, *155*, 77.
[124] A. Streitwieser, T. R. Boussie, *Eur. J. Solid State Inorg. Chem.* **1991**, *28*, 399.
[125] F. Mares, K. O. Hodgson, A. Streitwieser, Jr. *J. Organomet. Chem.* **1971**, *28*, C24.
[126] N. C. Burton, F. G. N. Cloke, P. B. Hitchcock, H. C. de Lemos, A. A. Sameh, *J. Chem. Soc. Chem. Commun.* **1989**, 1462.
[127] N. C. Burton, F. G. N. Cloke, P. B. Hitchcock, S. C. P. Joseph, H. de Lemos, *J. Chem. Soc. Dalton Trans.*, in press.
[128] U. Kilimann, M. Schäfer, R. Herbst-Irmer, F. T. Edelmann, *J. Organomet. Chem.* **1994**, *469*, C10.
[129] K. Mashima, H. Takaya, *Tetrahedron Lett.* **1989**, *30*, 3697.
[130] K. Mashima, Y. Nakayama, A. Nakamura, N. Kanehisa, Y. Kai, H. Takaya, *J. Organomet. Chem.* **1994**, *473*, 85.
[131] H. Schumann, J. A. Meese-Marktscheffel, A. Dietrich, *J. Organomet. Chem.* **1989**, *377*, C5.
[132] J. Stehr, R. D. Fischer, *J. Organomet. Chem.* **1992**, *430*, C1.
[133] U. Kilimann, F. T. Edelmann, *J. Organomet. Chem.* **1994**, *469*, C5.
[134] H. Schumann, J. Winterfeld, R. D. Köhn, L. Esser, J. Sun, A. Dietrich, *Chem. Ber.* **1993**, *126*, 907.
[135] S. Zhang, G. Wei, W. Chen, J. Liu, *Polyhedron* **1994**, *13*, 1927.
[136] H. Schumann, J. Winterfeld, L. Esser, G. Kociok-Köhn, *Angew. Chem.* **1993**, *105*, 1212; *Angew. Chem. Int. Ed. Engl.* **1993**, *32*, 1208.
[137] U. Kilimann, F. T. Edelmann, *J. Organomet. Chem.* **1993**, *444*, C15.
[138] A. Masino, *Ph. D. Thesis*, University of Alberta, **1978**.
[139] H. Schumann, J. Winterfeld, H. Hemling, F. E. Hahn, P. Reich, K.-W. Brzezinka, F. T. Edelmann, U. Kilimann, M. Schäfer, R. Herbst-Irmer, *Chem. Ber.* **1995**, *128*, 395.
[140] U. Kilimann, H.-D. Amberger, J. Takats, F. T. Edelmann, unpublished.
[141] A. L. Wayda, *Organometallics* **1983**, *2*, 565.
[142] A. L. Wayda, R. D. Rogers, *Organometallics* **1985**, *4*, 1440.
[143] H. Schumann, J. Winterfeld, F. H. Görlitz, J. Pickardt, *Organometallics* **1987**, *6*, 1328.
[144] U. Kilimann, M. Schäfer, R. Herbst-Irmer, F. T. Edelmann, *J. Organomet. Chem.* **1994**, *469*, C15.
[145] T. R. Boussie, D. C. Eisenberg, J. Rigsbee, A. Streitwieser, Jr., A. Zalkin, *Organometallics* **1991**, *10*, 1922.
[146] J. Xia, Z. Jin, W. Chen, *J. Chem. Soc. Chem. Commun.* **1991**, 1214.
[147] N. Rösch, *Inorg. Chim. Acta* **1984**, *94*, 297.
[148] A. Streitwieser, Jr., S. A. Kinsley, J. T. Rigsbee, I. L. Fragalà, E. Ciliberto, N. Rösch, *J. Am. Chem. Soc.* **1985**, *107*, 7786.
[149] M. Dolg, P. Fulde, W. Küchle, C.-S. Neumann, H. Stoll, *J. Chem. Phys.* **1991**, *94*, 3011.
[150] A. Streitwieser, Jr., S. A. Kinsley, J. T. Rigsbee, I. L. Fragalà, E. Ciliberto, N. Rösch, *J. Am. Chem. Soc.* **1985**, *107*, 641.
[151] U. Kilimann, R. Herbst-Irmer, D. Stalke, F. T. Edelmann, *Angew. Chem.* **1994**, *106*, 1684; *Angew. Chem. Int. Ed. Engl.* **1994**, *33*, 1618.
[152] R. D. Fischer, *Angew. Chem.*, **1994**, *106*, 2253; *Angew. Chem. Int. Ed. Engl.* **1994**, *33*, 2165.
[153] M. Bruzzone, *NATO ASI Ser. C*, **1985**, *155*, 387.
[154] S. Qi, X. Gao, S. Xiao, W. Chen, *Yingyong Huaxue* **1986**, *3*, 63.
[155] A. Oehme, U. Gebauer, K. Gehrke, *J. Mol. Catal.* **1993**, *82*, 83.
[156] S. B. Gol'shtein, V. A. Yakovlev, G. N. Bondarenko, Y. P. Yampol'skii, B. A. Dolgoplosk, *Dokl. Akad. Nauk SSSR* **1986**, *289*, 657.
[157] C. Shan, Y. Lin, J. Ouyang, Y. Fan, G. Yang, *Makromol. Chem.* **1987**, *188*, 629.
[158] J. Sieler, A. Simon, K. Peters, R. Taube, M. Geitner, *J. Organomet. Chem.* **1989**, *362*, 297.

New Surprises in Metal Carbonyl Chemistry**

John E. Ellis* and Wolfgang Beck*

Anionic and *cationic* metal carbonyls[1, 2] have been the focus of much attention for the past several years, however, recent exciting developments involving *neutral* metal carbonyls have again placed the spotlight on this historically rich and vital area of chemistry. The first study on the reaction of a metal, namely potassium, with carbon monoxide was reported by Justus von Liebig in 1834.[3] On the basis of this seminal study and later extensions by others,[4] it was widely believed in the 19th and early 20th centuries that alkali and alkaline earth metals reacted with CO under standard conditions to form binary metal carbonyls. Although all of these substances were later shown by E. Weiss et al. to be ionic in nature and to contain reductively coupled CO units, such as the acetylenediolate dianion, $^{-}O-C\equiv C-O^{-}$[5] and related oxocarbon anions $[C_nO_n]^{2-}$ ($n = 3-6$),[6] the idea that the reactions of carbon monoxide with metals could be quite interesting was firmly established. However, to the best of our knowledge until 1993, there were no reports in the literature on the existence of relatively stable neutral main group metal or metalloidal carbonyls.

Bona fide neutral metal carbonyls have been known since Schützenberger's synthesis of $[Pt(CO)_2Cl_2]$ in 1868.[7] Quite interestingly, this "classic" complex, and related platinum(II) carbonyl compounds (e.g. $[Pt(CO)_4]^{2+}$) are now considered to be examples of "nonclassical" carbonyl complexes, in which the CO ligand functions exclusively as a σ-donor.[8] The first examples of "classical" carbonyls in which the CO group simultaneously functions as both a σ-donor *and* π-acceptor ligand were Mond's $[Ni(CO)_4]$ and $[Fe(CO)_5]$ reported in 1890 and 1891, respectively.[9]. These first examples of metal carbonyls were all made by the direct combination of metallic compounds (e.g. $PtCl_2$) or pure metals (e.g., Ni and Fe) with carbon monoxide, a route which is still of key importance in the syntheses of new types of metal carbonyl complexes.

The chemical properties of metal carbonyls were first investigated in detail by Walter Hieber, who is deservedly known as the "father of metal carbonyl chemistry". Primarily through Hieber's and his students' extensive and systematic research,[10, 11] metal carbonyls ultimately were transformed from mainly laboratory curiosities into precursors of key importance throughout science, engineering, and commerce. Metal carbonyl chemistry represents an excellent, although not uncommon example of where pure or "curiosity-driven" scientific research has eventually led to many and largely unanticipated rewards for mankind (e.g. for homogenous catalysis).

Until very recently, all isolable examples of pure neutral metal carbonyls required stabilization by d-block transition metals (through formation of strong metal $\rightarrow$ CO back bonds). As shown in Figure 1, *neutral* binary or substituted metal carbonyl compounds have been isolated for all d-block metals, except Sc, Y, and Ag and for the f-elements La–Lu; however stable carbonyl cations of silver are now known.[12] For other metals or metalloids, except uranium, vide infra, only exceedingly unstable matrix-isolated carbonyls were reported before 1993. For example, binary carbonyls of uranium, several lanthanides,[13] alkali metals,[14] and recently beryllium[15] have been prepared by condensation of appropriate metal atoms with CO and inert gases such as argon or krypton. All of these compounds decom-

1	2	3	4	5	6	7	8	9	10	11	12	13	14	15	16	17	18
Li[a,b]	Be[b]																
Na[a,b]	Mg[b]																
K[a]	Ca[a,d]	Sc[b]	Ti[c]	V[c]	Cr[c]	Mn[c]	Fe[c]	Co[c]	Ni[c]	Cu[c]	Zn[b]	Ga[c]	Ge[b]	As[c]	Se[c]		
Rb[a]	Sr[a,d]	Y[b]	Zr[c]	Nb[c]	Mo[c]	Tc[c]	Ru[c]	Rh[c]	Pd[c]	Ag[c]	Cd[c]	In[c]	Sn[b]	Sb[c]	Te[c]		
Cs[a]	Ba[a,b]	La/Lu[b]	Hf[c]	Ta[c]	W[c]	Re[c]	Os[c]	Ir[c]	Pt[c]	Au[c]	Hg[c]	Tl[c]	Pb[b]	Bi[c]	Po[c]		
Fr[c]	Ra[c]	Ac/Lr[c]															

Ce[c]	Pr[b]	Nd[b]	Pm[c]	Sm[c]	Eu[b]	Gd[b]	Tb[c]	Dy[c]	Ho[b]	Er[c]	Tm[c]	Yb[b]
Th[c]	Pa[c]	U[c]	Np[c]	Pu[c]	Am[c]	Cm[c]	Bk[c]	Cf[c]	Es[c]	Fm[c]	Md[c]	No[c]

NON METALS

Fig. 1. Survey of metal and metalloid carbonyls. [a] Metals combine with CO under normal conditions to produce salts of oxocarbon anions [3–6]. [b] Only known as thermally unstable matrix-isolated species ($T \leq 77$ K) with metal atoms, halides or oxides. [c] No known carbonyls in condensed phases. [d] $[(C_5Me_5)_2M]$ form labile monocarbonyls in solution under CO atmosphere (>1 bar). [e] Isolable binary and/or substituted carbonyls known; Ag, Hg as cations only [2, 8, 12].

[*] Prof. Dr. J. E. Ellis
Department of Chemistry
University of Minnesota
Minneapolis, MN 55455 (USA)
Telefax: Int. code +(612) 626-7541
Prof. Dr. W. Beck
Institut für Anorganische Chemie der Universität
Meiserstrasse 1, D-80333 München (Germany)
Telefax: Int. code +(89) 5902-451

[**] J. E. E. thanks the Alexander-von-Humboldt-Stiftung for a Senior U.S. Scientist Research Award which made it possible to write this article jointly with W. B. while in residence at the Ludwig-Maximilians-Universität.

pose above 45 K and thus seem unlikely to ever be useful as reagents in conventional synthetic chemistry. Somewhat more stable are $Al(CO)_2$ and Me_2SiCO which survive at 77 K in an adamantane[16] or other frozen hydrocarbon matrices,[17] respectively. It is of interest to compare Me_2SiCO with similar organic compounds. Although carbenes are well known to combine with CO to give relatively stable ketenes $R_2C{=}C{=}O$ (Scheme 1), vibrational spectra of the formally analogous dimethylsilene-CO adduct indicated relatively little Si–C multiple bonding to be present.[7] Thus, ketenes prefer to adopt a "normal" structure containing trigonal-planar carbon and a strong C=C double bond, while the silicon analogues are likely to contain pyramidal silicon with a weak Si–CO interaction.

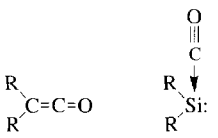

Scheme 1. R = Me.

All of this is understandable in terms of the reluctance of silicon to participate in p_π–p_π multiple bonding, along with the great strength of the CO triple bond in carbon monoxide. So the "silaketene" is really best described as being a silicon carbonyl. While these simple silylene–carbonyl adducts are only stable in solid matrices at low temperature, recently the first solutions of such a compound have been reported by Tacke and coworkers.[18] The reaction of Jutzi's stable silene, $[Cp^*_2Si]$ ($Cp^* = C_5Me_5$), with CO (1.5 bar) in liquid xenon at -20 to $-30\,^\circ C$ provides small amounts of $[Cp^*_2Si(CO)]$ [Eq. (a)]. An

$$[Cp^*_2Si] + CO \xrightleftharpoons{\text{LXe/253 K/1.5 bar}} [Cp^*_2Si(CO)] \qquad \text{(a)}$$

indication of the relatively weak Si–CO bond in this species is the observed $\tilde{\nu}$(CO) stretch at 2065 cm^{-1} in the IR spectrum; the corresponding CO stretching frequency in the related 16-electron titanium complex $[(C_5H_5)_2Ti(CO)]$ is 1890 cm^{-1}. While the coordinated CO is easily lost from $[Cp^*_2SiCO]$, binding of the CO to the titanocene unit is quite strong, in accord with the greater degree of back bonding from titanium to CO compared to the situation in the silicon carbonyl.

Equally impressive was the recent report by Selg, Brintzinger, Andersen, and Horvath of an alkaline earth metal carbonyl stable in solution.[19] All previously known alkaline earth metal carbonyl complexes were exceedingly unstable matrix-isolated species.[20] The reaction of $[Cp^*_2Ca]$ with CO (>2.5 bar) in toluene at -30 to $+30\,^\circ C$ led to the formation of $[Cp^*_2Ca(CO)]$ [Eq. (b)]. This substance was unambiguously characterized in

$$[Cp^*_2Ca] + CO \xrightleftharpoons{\text{toluene/246–305 K/2.5–70 bar}} [Cp^*_2Ca(CO)] \qquad \text{(b)}$$

toluene by IR and ^{13}C NMR spectroscopy. The rather high $\tilde{\nu}$(CO) value of 2158 cm^{-1} observed for $[Cp^*_2Ca(CO)]$ compared to that of free CO, 2134 cm^{-1} in toluene, as well as the upfield shift in the ^{13}CO resonance ($\delta = 180.4$) of the complex compared to that of free ^{13}CO ($\delta = 184.7$) justifies the authors' assertion that this Ca^{2+} complex is a σ-only carbonyl compound, in contrast to the aforementioned $[Cp^*_2Si(CO)]$, $\tilde{\nu}(CO) = 2065\ cm^{-1}$, in which some degree of back bonding from Si to CO is indicated. The relative weakness of Ca–CO binding is suggested by the inability of CO to displace ether from $[Cp^*_2Ca(OEt_2)]$ even at high pressures (120 bar). Selg et al. also found that a similar strontium carbonyl $[Cp^*_2Sr(CO)]$ was accessible under the same conditions employed for the calcium reaction, while no evidence could be obtained for the interaction of $[Cp^*_2Mg]$ with CO.

These reports on the first relatively stable metalloidal and main group metal carbonyls constitute remarkable advances and give hope that isolation of related materials may be possible in the near future with judicious choice of ligands. Most certainly they will also stimulate additional research in a totally new area of main group carbonyl chemistry! The results emphasize the continued importance of the pentamethylcyclopentadienyl ligand in helping to establish new and exciting chemistry since its main introduction in the research of King, Bercaw and Brintzinger more than 20 years ago.[21]

Nearly ten years ago, Andersen et al. reported the synthesis of the first relatively stable actinide carbonyl, $[(Me_3SiC_5H_4)_3U(CO)]$.[22] Under an atmosphere of carbon monoxide this substance was remarkably robust near ambient temperatures in solution and in the solid state, although it could not be isolated as a pure substance. This discovery was an important event in metal carbonyl chemistry, since it engendered much new interest in the prospects for developing f-block carbonyl chemistry. Now, quite remarkably Parry, Carmona, Coles, and Hursthouse have obtained the first isolable uranium carbonyl, $[(C_5Me_4H)_3U(CO)]$,[23] by the same direct synthesis procedure employed by Schützenberger for $[Pt(CO)_2Cl_2]$, more than 125 years ago![7] Treatment of the cherry red-brown solutions of $[U(C_5Me_4H)_3]$ with CO at 1 bar and 20 °C immediately resulted in the formation of a purple carbonyl adduct, which was isolated as an analytically pure substance [Eq. (c)]. One

$$[(C_5Me_4H)_3U] + CO \xrightarrow{\text{toluene/293 K/1 bar}} [(C_5Me_4H)_3U(CO)] \qquad \text{(c)}$$

striking feature is that the ν(CO) value in the IR spectrum for this complex, 1900 cm^{-1} in petroleum ether, is 76 cm^{-1} lower than that of Andersen's presumably analogous complex. Thus, the seemingly simple change from a trimethylsilylcyclopentadienyl group to the tetramethylcyclopentadienyl unit in this case had profound effects on the stability of the complex, possibly for both electronic *and* steric reasons. The coup de grace in the present study, however, was the X-ray structural characterization of the complex, which showed an essentially linear uranium–carbonyl unit and a quite short U–C distance of 2.383(6) Å, compared to a corresponding U–C(isonitrile) distance of 2.57(3) Å previously observed in $[(Me_3SiC_5H_4)_3U(CNEt)]$.[22, 24] This information, the low ν(CO) value, and a long C–O distance of 1.142(7) Å indicate that uranium in the proper ligand environment can participate in backbonding to carbonyl groups as effectively as d-block transition metals! Clearly Parry et al. have uncovered a potentially rich new area of chemistry filled with many treasures in the form of 5f- and possibly even 4f-block metal carbonyl chemistry.

Whether this newly discovered stable f-block metal carbonyl chemistry will be limited to neutral monocarbonyls only is a question of substantial interest. However, an even more interesting issue is whether the chemistry of 5f-block carbonyls will

differ in any substantial way from that of the familar d-block species except for the obvious fact that the 18-electron rule will be flagrantly violated!

Carbonyls of the transuranium elements are unknown presently; however, Nash and Bursten have recently predicted that the hexacarbonyl of zerovalent element 106, a member of the chromium family, should electronically resemble $[W(CO)_6]$ much more than the extremely unstable $[U(CO)_6]$.[25]

In summary, over the past two years our knowledge of relatively stable neutral carbonyl complexes has been dramatically enriched by the synthesis of the first metalloidal and alkaline earth metal carbonyls in solution, namely $[Cp^*_2Si(CO)]$ and $[Cp^*_2Ca(CO)]$, respectively, and by the isolation and X-ray structural characterization of the first f-block carbonyl complex, $[(C_5Me_4H)_3U(CO)]$. Undoubtedly, these remarkable new results will stimulate much new basic "curiosity-driven" research in a field that continues to provide excitement and drama!

Keywords: calcium compounds · carbonyl complexes · silicon compounds · uranium compounds

German version: *Angew. Chem.* **1995**, *107*, 2695–2697

[1] a) J. E. Ellis, *Adv. Organomet. Chem.* **1990**, *31*, 1–52; b) W. Beck, *Angew. Chem.* **1991**, *103*, 173–174; *Angew. Chem. Int. Ed. Engl.* **1991**, *30*, 168–169.
[2] L. Weber, *Angew. Chem.* **1994**, *106*, 1131–1133; *Angew. Chem. Int. Ed. Engl.* **1994**, *33*, 1077.
[3] J. Liebig, *Ann. Chem. Pharm.* **1834**, *11*, 182.
[4] a) A. C. Joannis, *C. R. Acad. Sci.* **1893**, *116*, 1518; b) M. M. Gunz, M. Mentrel, *Bull. Soc. Chem.* **1903**, *29*(3), 585; c) M. G. Roederer, *ibid.* **1906**, *35*, 715; d) T. G. Pearson, *Nature (London)* **1933**, *131*, 166–167.
[5] a) E. Weiss, W. Büchner, *Z. Anorg. Allg. Chem.* **1964**, *330*, 251–258; b) *Chem. Ber.* **1965**, *98*, 126–130.
[6] G. Seitz, P. Imming, *Chem. Rev.* **1992**, *92*, 1227–1260.
[7] M. P. Schützenberger, *Annales (Paris)* **1868**, *15*, 100.
[8] F. Aubke, C. Wang, *Coord. Chem. Rev.* **1994**, *137*, 483–524.
[9] L. Mond, C. Langer, F. Quincke, *J. Chem. Soc.* (London) **1890**, 749–753; facsimile thereof: *J. Organomet. Chem.* **1990**, *383*, 1–10; W. A. Herrmann, *J. Organomet. Chem.* **1990**, *383*, 21–44, and references therein.
[10] W. Hieber, *Adv. Organomet. Chem.* **1970**, *8*, 1–28.
[11] W. Hieber, W. Beck, G. Braun, *Angew. Chem.* **1960**, *72*, 795–801.
[12] P. K. Hurlbut, J. J. Rack, S. F. Dec, O. P. Anderson, S. W. Strauss, *Inorg. Chem.* **1993**, *32*, 373–374.
[13] R. K. Sheline, J. L. Slater, *Angew. Chem.* **1975**, *87*, 332–337; *Angew. Chem. Int. Ed. Engl.* **1975**, *14*, 309.
[14] O. Ayed, A. Loutellier, L. Manceron, J. P. Perchard, *J. Am. Chem. Soc.* **1986**, *108*, 8138.
[15] L. Andrews, T. J. Tague, Jr., G. P. Kushto, R. D. Davy, *Inorg. Chem.* **1995**, *34*, 2952–2961.
[16] J. H. B. Chenier, C. A. Hampson, J. A. Howard, B. Mile, *J. Chem. Soc. Chem. Commun.* **1986**, 730–732.
[17] a) C. A. Arrington, J. T. Petty, S. E. Payne, W. C. K. Haskins, *J. Am. Chem. Soc.* **1988**, *110*, 6240–6241; b) M. A. Pearsall, R. West, *ibid.* **1988**, *110*, 7228–7229.
[18] M. Tacke, C. Klein, D. J. Stufkens, A. Oskam, P. Jutzi, E. A. Bonte, *Z. Anorg. Allg. Chem.* **1993**, *619*, 865.
[19] P. Selg, H. H. Brintzinger, R. A. Andersen, I. T. Horvath, *Angew. Chem.* **1995**, *107*, 877–879; *Angew. Chem. Int. Ed. Engl.* **1995**, *34*, 791–793.
[20] a) R. H. Hauge, S. E. Gransden, J. L. Margrave, *J. Chem. Soc. Dalton Trans.* **1979**, 745–748; b) I. R. Beattie, P. J. Jones, N. A. Young, *J. Am. Chem. Soc.* **1992**, *114*, 6146–6152.
[21] M. B. Bisnette, R. B. King, *J. Organomet. Chem.* **1967**, *8*, 287–297; J. E. Bercaw, H. H. Brintzinger, *J. Am. Chem. Soc.* **1971**, *93*, 2045–2046.
[22] J. G. Brennan, R. A. Andersen, J. L. Robbins, *J. Am. Chem. Soc.* **1986**, *108*, 335–336.
[23] J. Parry, E. Carmona, S. Coles, M. Hursthouse, *J. Am. Chem. Soc.* **1995**, *117*, 2649–2650.
[24] J. G. Brennan, S. P. Stults, R. A. Andersen, *Organometallics* **1988**, *7*, 1329–1334.
[25] C. S. Nash, B. E. Bursten, *New J. Chem.* **1995**, *19*, 669–675.

Sunlight-Damaged DNA Repaired with Sunlight

Thomas Carell*

DNA, the carrier of genetic information, is continuously subjected to damaging environmental influences. As a consequence, genetic information is lost and the reliable function of cells is threatened.[1] To counter these potentially deadly effects, organisms have developed a number of sophisticated DNA repair mechanisms.[2] Since the discovery that errors in the repair process contribute directly to carcinogenesis, the investigation of the molecular events of damage removal inside the genome have attracted widespread interest.[3] Currently, DNA repair is one of the hottest topics in biochemical research.

Very recently H. W. Park, S.-T. Kim, A. Sancar, and J. Deisenhofer solved the X-ray structure of one of the most unusual DNA repair enzymes, the *Escherichia coli* DNA photolyase.[4] This accomplishment represents a landmark in an interdisciplinary effort to gain deeper insight into one of the major genome repair processes in nature. Photolyases are enzymes capable of repairing major DNA lesions introduced into the genome by irradiation of cells with sunlight (UV light with $\lambda = 200-300$ nm).[5] They are unusual because the repair reaction is also driven by sunlight ($\lambda = 300-500$ nm). In this way the repair reaction is similar to photosynthesis, where sunlight is transformed into chemical energy.[6] Photolyases are found in a variety of organisms including archaebacteria, amphibians, goldfish, rattlesnakes, and marsupials but are absent from others including man.[7] In many species the photolyase repair reaction (photoreactivation) is the only known mechanism for repairing the deleterious effects of sunlight.

The DNA lesions incurred upon UV irradiation of cells have been widely studied and are now well understood.[5] Through irradiation of double-helical DNA two neighboring pyrimidine bases undergo a photochemically allowed $[2\pi_s + 2\pi_s]$ cycloaddition of their C5–C6 double bonds, resulting in the formation of *cis-syn* cyclobutane pyrimidine dimers (Scheme 1). The major

[*] Dr. T. Carell
Laboratorium für Organische Chemie
Eidgenössische Technische Hochschule Zürich
Universitätsstrasse 16, CH-8046 Zürich (Switzerland)
Telefax: Int. code + (1)632-1109

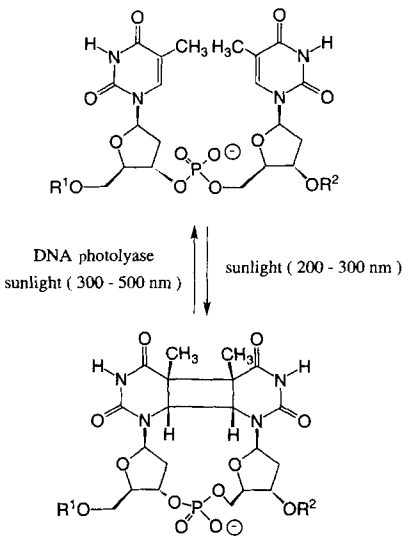

Scheme 1. Formation of a *cis-syn* cyclobutane thymine dimer upon UV irradiation (200–300 nm) of DNA containing a TpT segment. R_1 = 5′-terminus, R_2 = 3′-terminus.

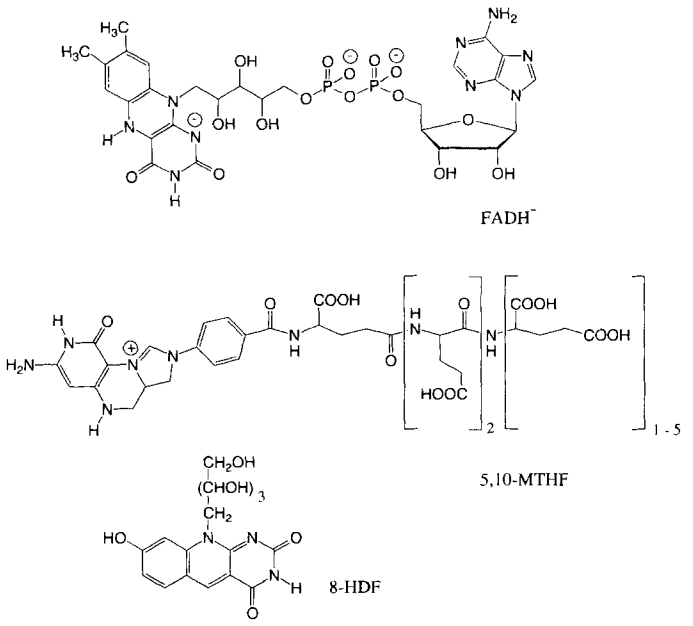

Scheme 2. Structures of photolyase cofactors. The folate class of photolyases contains one $FADH^-$ and one 5,10-MTHF unit; the deazaflavin class of photolyases contains one $FADH^-$ and one 8-HDF unit.

photolesions are *cis-syn* thymine photodimers, which cause structural distortion of the corresponding DNA region.[8] This DNA structure alteration blocks replication and transcription, and thus leads to cell death. The high frequency of skin cancer in patients with *Xeroderma pigmentosum*, a condition characterized by deficient capabilities for repairing UV-damaged DNA, show dramatically that UV-induced lesions are also directly involved in cancer development.[9]

Normal cells have developed sophisticated methods for repairing pyrimidine dimer lesions either by excision repair, whereby the damaged nucleotides are removed and replaced by new bases, or by photoreactivation.[3] Whereas excision repair requires several enzymes in a complicated multistep repair process, photoreactivation is exceptional, relying on only one enzyme, DNA photolyase.[10, 11] In recent years, research on photoreactivation has focused on the elucidation of the enzyme's repair mechanism by studying various photolyases, their cofactors, and specifically designed model compounds that mimic certain aspects of the repair process. A variety of techniques including time-resolved absorption and fluorescence spectroscopy have been used to this end.[12, 13] The sequencing of photolyases from various organisms, subsequent cloning, and overexpression together with mutagenesis studies are milestones on the way to a more detailed understanding of the enzyme's mode of action.[5]

The results have established that photolyases are monomeric enzymes with molecular weights between 55000 and 60000 Da. They contain two noncovalently bound chromophores as cofactors (Scheme 2). One of these is a flavin adenine dinucleotide in the unusual $FADH^-$ form, which is tightly bound to the enzyme ($K_d < 10^{-11}$ M).[5] All photolyases known to date contain as the second chromophore either 8-hydroxy-5-deazariboflavin (8-HDF) or 5,10-methenyltetrahydrofolylpolyglutamate (5,10-MTHF). Accordingly, photolyases are divided into two subgroups, the deazaflavin group, for example from *Methanobacterium thermoautotrophicum*, and the folate group, for example from *Escherichia coli*.

The recently published X-ray crystallographic analysis of a DNA photolyase reveals a number of interesting structural features.[4] The $FADH^-$ cofactor is bound to the enzyme in a surprising U-shaped conformation, and the flavin and adenine rings are in close proximity inside the protein pocket; both are partially solvent accessible. Responsible for the tight binding of $FADH^-$ are a network of hydrogen bonds around the riboflavin moiety and eight ionic interactions with the phosphates. The fact that the residues that participate in the binding of the flavin cofactor are conserved in eight of the ten known photolyase sequences demonstrates the importance of the $FADH^-$ binding site for the enzyme's function. The second chromophore is much more weakly bound inside a shallow protein groove, and in general a considerable amount of this second cofactor is lost during purification of the enzyme. In the *Escherichia coli* photolyase, the 5,10-MTHF molecule is bound at the periphery of the enzyme approximately 16.8 Å away from the flavin unit.

The peptide chain of the *Escherichia coli* photolyase is folded into five β-strands, twenty α-helices, five 3_{10} helices, and connecting segments.[4] Sequence and structure homology studies revealed that bacterial photolyases bear close resemblance only to the blue photoreceptors, a class of proteins analyzed in detail just recently.[14] No other sequence similarities were observed with other flavin binding proteins or animal photolyases. A characteristic feature of all photolyases is their *nonsequence*-specific binding to damaged DNA. In contrast to proteins involved in gene regulation, which are highly sequence specific, photolyases bind DNA in a *structure*-specific manner: they recognize defect sites. More puzzling is the fact that photolyases bind equally strongly to single- and double-stranded DNA ($K_d = 10^{-8}$ M and 10^{-9} M, respectively).[15] Based on the overall structure of the *Escherichia coli* photolyase, a plausible explanation for this phenomenon can now be proposed. The folding of the peptide chain results in the formation of a cavity that has the

correct size, shape, and polarity distribution for accommodating a thymine dimer. It is now speculated that after the binding of the photolyase to the damaged DNA strand, the thymine dimer "flips out" of the double helix into the photolyase cavity, where it is in van der Waals contact with the flavin. It is widely accepted that the hydrogen bonds between the thymine photodimer and their opposing adenines within the double helix are weaker than those in undamaged DNA. The reduced strength of the hydrogen bonds at the damaged site is thought to facilitate the flipping process. Further support for the flipping-out process was recently obtained through X-ray crystallographic analysis of four other proteins. Exonuclease III[15] and two uracil-DNA glycosylases,[16, 17] all three involved in DNA repair, have cavities potentially capable of binding the DNA lesions in a flipped-out conformation. In the case of the uracil-DNA glycosylase from *Herpes simplex* virus, a co-crystal structure of the protein with uracil bound in the proposed active site cavity strongly supports the flipping-out mechanism. Recently the X-ray crystal structure of HhaI methyltransferase, a protein not involved in DNA repair, was solved.[18] Here a modified substrate was used to trap a reaction intermediate covalently bound to the enzyme. Surprisingly the substrate was flipped out from the DNA double-helix and directed into the active site of the enzyme. All these investigations seem to indicate that DNA lesions within the double helix may be recognized by various repair enzymes and factors in a flipped-out conformation.

The proposed mechanism for the repair of thymine photodimers through the action of DNA photolyase is shown in Scheme 3. Upon irradiation of the photolyase–DNA complex, a quantum of light is captured either directly by the flavin moiety or more likely by the second chromophore, a folate or deazaflavin, due to their higher molar extinction coefficients in the spectral region between 300 and 500 nm. The second chromophore relays the excitation energy to the flavin, which subsequently transfers an electron to the thymine dimer. Computational studies (Hückel molecular orbital calculations) show that the activation barrier for the thermal, concerted collapse of the cyclobutane substructure into its radical anion is significantly reduced. Thus the electron transfer leads to efficient cleavage of the C5–C5′ and C6–C6′ σ bonds of the thymine dimer and restoration of the two thymines.[19] Indeed, recent observations confirm that the dimer is cleaved in a concerted fashion.[20] An electron is then transferred back to the flavin and the photolyase–DNA complex dissociates, presumbly due to the higher steric requirements of the two thymines in the active site.

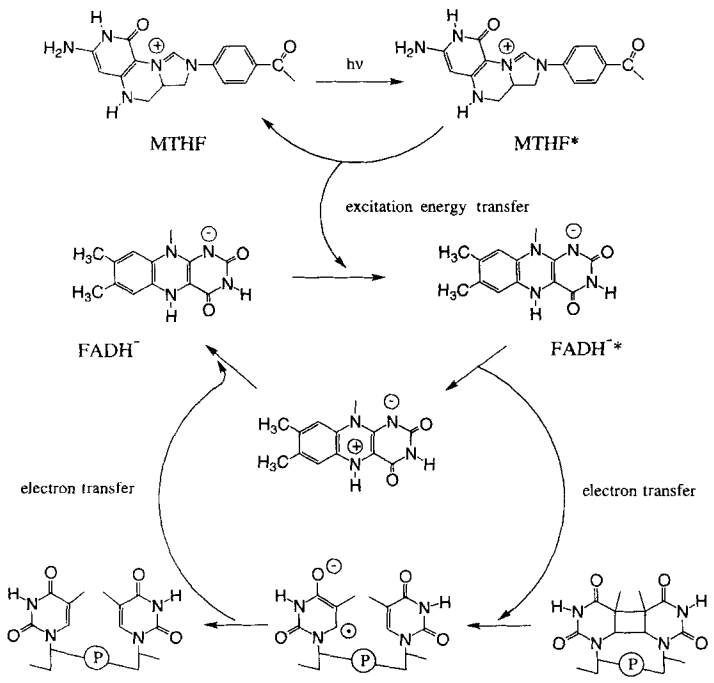

Scheme 3. Schematic representation of the proposed DNA repair mechanism for the *Escherichia coli* photolyase [5,12].

Time-resolved spectroscopic measurements on *Escherichia coli* photolyase yielded a rate constant for the energy transfer from the 5,10-MTHF to the flavin of $k = 4.6 \times 10^9\ s^{-1}$ and an efficiency of 62%.[5, 13] The process occurs by the radiationless resonant mechanism described by the Förster theory.[21] In the deazaflavin-containing photolyases, the energy transfer is significantly faster ($k = 1.9 \times 10^{10}\ s^{-1}$) and more efficient (100%). The rate constant for the electron transfer between the flavin and the thymine dimer was measured as $k = 5.5 \times 10^9\ s^{-1}$. The electron transfer efficiency is similar in both enzyme classes (90%).

Two other residues within the photolyase are directly involved in the repair process. Trp277 has been identified as the essential substructure for the repair function at 280 nm in a modified photolyase with an inactive flavin.[22] Model studies showed that indoles are indeed capable of splitting pyrimidine dimers in solution and in covalently linked indole–pyrimidine dimer systems at this wavelength.[23] The X-ray structure offers an explanation for the Trp277-mediated photorepair. Trp277 is located inside the proposed thymine dimer binding site and would come into van der Waals contact with the bound substrate with its flipped-out conformation. The role of Trp306, which is essential for the photoreduction of the excited FADH (a process required for the conversion of the flavin into its reduced state), is still unclear. It is widely assumed that the reduction of the flavin involves an electron transfer from Trp306 to the excited flavin. Since the Trp306 residue is located near the protein surface 13 Å away from the flavin, an efficient electron transfer between these chromophores is unlikely. Further studies are necessary to establish the function of Trp306 in the repair process.

The X-ray crystal structure of the *Escherichia coli* photolyase allows a deeper understanding of one of the most unusual processes in nature, the use of sunlight for the efficient repair of DNA.[4] The single events involved are the specific recognition of a photodamaged DNA region, possibly through the flipped-out conformation of the damaged bases, and the subsequent cleavage of the pyrimidine dimers employing energy and electron transfers steps. The mechanism of this repair reaction is comparable only with that of photosynthesis, where light-harvesting chromophores situated around an active center funnel their excitation energy to a specific chromophore, the "special pair". This special pair transfers a single electron to a special acceptor chromophore as the first event in an electron transfer cascade.[6] It is remarkable that a very similar reaction sequence is used in the photoreactivation process to maintain the genome, a problem presumably as old as life. The exciting finding that the peptide sequences of bacterial photolyases and the newly found blue photoreceptors, which are essential for the early

development of plants, show strong homologies fuels widespread speculation. Perhaps energy and electron transfer steps are not only used to convert sunlight into chemical energy (photosynthesis) and to protect organisms from the deleterious effects of far-UV light (photoreactivation), but are also involved in the induction of an early development signal in green plants (photoreceptors) by a yet unknown mechanism.[4, 14]

German version: *Angew. Chem.* **1995**, *107*, 2697–2700

Keywords: DNA repair · electron transfer · energy transfer · photolyases

[1] T. Lindahl, *Nature* **1993**, *362*, 709–715.
[2] E. C. Friedberg, G. C. Walker, W. Siede in *DNA Repair and Mutagenesis*, ASM Press, Washington DC, **1995**.
[3] P. Modrich, *Science* **1994**, *266*, 1959–1960; A. Sancar, *ibid.* **1994**, *266*, 1954–1956; *J. Biol. Chem.* **1995**, *27*, 15915–15918.
[4] H. W. Park, S.-T. Kim, A. Sancar, J. Deisenhofer, *Science* **1995**, *268*, 1866–1872.
[5] For a recent review, see: S.-T. Kim, A. Sancar, *Photochem. Photobiol.* **1993**, *57*, 895–904.
[6] For a recent review, see: H. Kurreck, M. Huber, *Angew. Chem.* **1995**, *107*, 929–947; *Angew. Chem. Int. Ed. Engl.* **1995**, *34*, 849–866.
[7] T. Kato, Jr., T. Todo, H. Ayaki, K. Ishizaki, T. Morita, S. Mitra, M. Ikenaga, *Nucleic Acids Res.* **1994**, *22*, 4119–4124.
[8] F. N. Hayes, D. L. Williams, R. L. Ratliff, A. J. Varghese, C. S. Rupert, *J. Am. Chem. Soc.* **1971**, *93*, 4940–4942; J. Kemmink, R. Boelens, T. Koning, G. A. van der Marel, J. H. van Boom, R. Kaptein, *Nucleic Acids Res.* **1987**, *15*, 4645–4653; J.-S. Taylor, D. S. Garrett, I. R. Brockie, D. L. Svoboda, J. Telser, *Biochemistry* **1990**, *29*, 8858–8866.
[9] L. Daya-Grosjean, N. Dumaz, A. Sarasin, *J. Photochem. Photobiol. B.* **1995**, *28*, 115–124.
[10] A. Sancar, *Biochemistry* **1994**, *33*, 2–9.
[11] C. S. Rupert, S. H. Goodgal, R. M. Herriott, *J. Gen. Physiol.* **1958**, *41*, 451.
[12] For a recent review, see: P. F. Heelis, S.-T. Kim, T. Okamura, A. Sancar, *J. Photochem. Photobiol. B.* **1993**, *17*, 219–228.
[13] S. T. Kim, P. F. Heelis, T. Okamura, Y. Hirata, N. Mataga, A. Sancar, *Biochemistry* **1991**, *30*, 11262–11270; S.-T. Kim, P. F. Heelis, A. Sancar, *ibid.* **1992**, *31*, 11244–11248.
[14] M. Ahmad, A. R. Cashmore, *Nature* **1993**, *366*, 162–166; K. Malhotra, S.-T. Kim, A. Batschauer, L. Dawut, A. Sancar, *Biochemistry* **1995**, *34*, 6892–6899.
[15] C. D. Mol, C.-F. Kuo, M. M. Thayer, R. P. Cunningham, F. A. Tainer, *Nature* **1995**, *374*, 381–386.
[16] R. Savva, K. McAuley-Hecht, T. Brown, L. Pearl, *Nature* **1995**, *373*, 487–493.
[17] C. D. Mol, A. S. Arvai, G. Slupphaug, B. Kavli, I. Alseth, H. E. Krokan, J. A. Tainer, *Cell*, **1995**, *80*, 869–878.
[18] S. Klimasauskas, S. Kumar, R. J. Roberts, X. Cheng, *Cell* **1994**, *76*, 357–369; R. J. Roberts, *Angew. Chem.* **1994**, *106*, 1285–1292; *Angew. Chem. Int. Ed. Engl.* **1994**, *33*, 1222–1228.
[19] R. F. Hartman, J. R. VanCamp, S. D. Rose, *J. Org. Chem.* **1987**, *52*, 2684–2689.
[20] R. Austin, S. McMorgie, T. P. Begley, *J. Am. Chem. Soc.* **1992**, *114*, 1886–1887; J. R. Jacobsen, A. G. Cochran, J. C. Stephans, D. S. King, P. G. Schultz, *ibid.* **1995**, *117*, 5453–5461.
[21] T. Förster, *Discuss. Faraday Soc.* **1959**, *27*, 7–17.
[22] D. A. Pearlman, S. R. Holbrook, D. H. Pirkle, S.-H. Kim, *Science* **1985**, *227*, 1304–1308.
[23] S. T. Kim, R. F. Hartman, S. D. Rose, *Photochem. Photobiol.* **1990**, *52*, 789–794; M. S. Goodman, S. D. Rose, *J. Org. Chem.* **1992**, *57*, 3268–3270.

 © VCH Verlagsgesellschaft mbH, D-69451 Weinheim, 1995 0570-0833/95/3422-2494 $ 10.00+.25/0

Reactions of Neopentyl 2,2,2,-Trifluoroethanesulfonate (Tresylate) with Nucleophiles: A Model Study for the Coupling of Nucleophiles with Tresyl Agarose

Comment by Herbert P. Jennissen*

In their paper[1] the authors confirm our general findings on agarose beads[2] that certain tresylates exhibit hitherto unexpected reactions without SO scission: a) the tresyl sulfur remains in the reaction product, b) fluoride is the main leaving group, and c) alkaline hydrolysis generates an acidic product. At the time of our work we had no possibility of stringently analyzing our solid-phase reaction products, and consequently, the proposed structures of the products under the assumption that S–C scission takes place (sulfates, sulfamates, and thiosulfates)[2] were of preliminary nature and other alternatives were discussed.[3]

In their interesting paper[1] King and Gill show that neopentyl tresylate reacts with butylamine, diethylamine, and phenylmethanethiol yielding amides, fluoromonosulfides, and a ketene dithioacetal. However, we feel that it has not been proved that these reactions (especially for thiols) can be generalized and assumed to be identical in all respects in a homogeneous phase as well as a heterogeneous phase system.

In independent work[3,4] we have done structural studies of tresyl agarose, tresyl silica, and the coupling products obtained with the nucleophiles butyl amine and butane thiol. Solid phase CP/MAS ^{13}C NMR and IR spectra (DRIFTS) of butyl-*NS*-agarose (coupling of butylamine with tresyl agarose) in conjunction with GC-MS analysis of the liquid phase obtained by alkaline hydrolysis of tresyl agarose led to the conclusion of a β-sulfonyl amide bond structure without S–C scission[4] in agreement with the structure of King and Gill. Besides butyl amide, a small amount of β-sulfonyl carboxylic acid was also detected, which from our elemental and ^{14}C-tracer analysis[2] was estimated to be no more than 5–10% (side reaction). β-Sulfonyl carboxylic acid (acetic acid-*S*-agarose) could also be identified as the above-mentioned acidic product[2] of alkaline hydrolysis.

In contrast, our CP/MAS ^{13}C NMR spectra of the butane thiol coupling products (butyl-*SS*-agarose, butyl-*SS*-silica) a) failed to turn up any signals resulting from an ethylenic group or of the α- and β-sulfonyl carbon atoms as suggested by King and Gill. In addition b) it is difficult to follow the conclusions of King and Gill, who explain our quantitative data as a result of 50% acid (due to hydrolysis of tresyl agarose) and 50% dithio derivative, since this is at variance to their own statement: "With three equivalents of the thiol the product was mainly **7** (i.e. dithio derivative, 80% yield)". Since under our coupling conditions[2] we had a large excess of thiol over immobilized tresyl groups, the main reaction product should have been the dithio derivative for which the molar ratio *sulfur in product* to *sulfur in tresyl agarose* is 3.0 (for 100% yield) or 2.4 (for 80% yield). A small calculation based on our elemental analysis and ^{14}C-tracer studies,[2] however, gives for this molar ratio $2.04 \pm 0.10(6)$ (instead of 2.4–3.0). The molar ratio of *^{14}C-butyl residue in product* to *sulfur in tresyl agarose* is $1.14 \pm 0.22(6)$ instead of 2.0. If a 50% yield (in spite of thiol excess) is accepted, a correspondingly strong signal for carboxyl groups should have been observed in our ^{13}C NMR spectra in agreement with the postulated 50% *carboxyl groups* per *sulfur in tresyl agarose*. However, only small signals (in butyl-*SS*-agarose) or no signals (in butyl-*SS*-silica) from carboxyl groups were observed, indicating a minor reaction. These two main discrepancies either indicate a different reaction sequence[2,3] or possibly a mixture of reaction products in the case of thiol coupling in heterogeneous phase.

[*] Prof. Dr. H. P. Jennissen
Institut für Physiologische Chemie
Universität Gesamthochschule
Hufelandstrasse 55, D-45122 Essen (Germany)
Telefax: Int. code + (201) 723-4694

[1] J. F. King, M. S. Gill, *Angew. Chem.* **1995**, *107*, 1778–1780; *Angew. Chem. Int. Ed. Engl.* **1995**, *34*, 1612–1613.
[2] A. Demiroglou, C. Bandel-Schlesselmann, H. P. Jennissen, *Angew. Chem.* **1994**, *106*, 126–128; *Angew. Chem. Int. Ed. Engl.* **1994**, *33*, 120–123.
[3] H. P. Jennissen, *J. Mol. Recogn.* **1995**, *8*, 116–124.
[4] T. Zumbrink, A. Demiroglou, H. P. Jennissen, *J. Mol. Recogn.* **1995**, *8*, in press.

Reply by James F. King* and Manjinder Singh Gill

We are pleased to learn that Professor Jennissen accepts two-thirds of our structural revisions. For the third species, butyl-*SS*-agarose, it would appear that the matter is not yet settled. In view of the fact that seven species, $ROSO_2CH_2COOH$, $ROSO_2CH{=}CF(SR')$ (two stereoisomers), $ROSO_2CH{=}C(SR')_2$, $ROSO_2CH_2C(SR')_3$, $ROSO_2CH_2CO{-}SR$, and RSR', have been identified as products in our model reactions, it would not be surprising if the butyl-*SS*-agarose were to prove to be structurally complex, as we have already suggested in the final sentence of our footnote 9. The lack of strong signals pointing to particular structural features in butyl-*SS*-agarose could arise either because a) butyl-*SS*-agarose is structurally complex, and (or) b) CP/MAS ^{13}C NMR spectra of polymers do not always show clear signals for all carbons. Further experimentation is clearly required.

[*] Prof. J. F. King, M. S. Gill
Department of Chemistry, University of Western Ontario
London, Ontario N6A 5B7 (Canada)
Telefax: Int. code + (519) 661-3022
e-mail: scijfk@uwoadmin.uwo.ca

A Novel Method for the Synthesis of Isocyanates Under Mild Conditions**

Hans-Joachim Knölker,* Tobias Braxmeier, and Georg Schlechtingen

Isocyanates are important commercial precursors for the synthesis of polyurethanes and polyureas. Moreover, they are frequently used as intermediates in the synthesis of biologically active compounds.[1] The most widely utilized method for the synthesis of isocyanates, the phosgenation of amines, uses highly toxic phosgene as a reagent and therefore involves environmental and safety problems. Alternative methods, such as the thermolysis of carbamates (urethanes), very often require rather drastic reaction conditions.[1] We now describe a procedure that converts alkyl- and arylamines into isocyanates in high yields by reaction with activated carbonates (for example, di-*tert*-butyl dicarbonate) in the presence of a catalytic amount of a nucleophilic nitrogen base at room temperature.[2]

Di-*tert*-butyl dicarbonate, $(Boc)_2O$, is a widely used protecting group reagent in peptide synthesis.[3] We have discovered that the reaction of substituted anilines with $(Boc)_2O$ in the presence of a stoichiometric amount of 4-dimethylaminopyridine (DMAP)[4] in an inert solvent (acetonitrile, dichloromethane, ethyl acetate, tetrahydrofuran, toluene) at room temperature leads to aryl isocyanates within 10 min in almost quantitative yields (Table 1).

With this strategy 2,6-disubstituted arylamines can be converted almost quantitatively into aryl isocyanates (see synthesis of **2a–d**). The application of the method is particularly straightforward when performed in acetonitrile followed by an acidic workup with sulfuric acid (see Table 1 and Experimental Section). When starting with 2-monosubstituted, 2,4-disubstituted, or 2,3,4-trisubstituted arylamines, the yields of the aryl isocyanates range between 40 and 90% (**2e–k**). In order to obtain 2,6-unsubstituted aryl isocyanates, such as **2l**, in moderate yields, the products have to be isolated by column chromatography on silica gel at −30 to −45 °C. The lower yields obtained with sterically less hindered arylamines arise from reaction of the isocyanates with the simultaneously formed *tert*-butanol affording an *N*-Boc derivative (urethane) and from product loss during workup.

When the arenediamines 2,4,6-trimethylbenzene-1,3-diamine and 2,2′,6,6′-tetramethyl-4,4′-methylenediphenylamine were treated under the same reaction conditions with 1.4 equivalents of $(Boc)_2O$ and 1.0 equivalent of DMAP per amino group in acetonitrile at room temperature (method A, workup with sulfuric acid), 2,4,6-trimethylbenzene-1,3-diisocyanate (**3**) and 2,2′,6,6′-tetramethyl-4,4′-methylenediphenyl isocyanate (**4**) were obtained in 84% and 93% yield, respectively. Arenediyl diisocyanates play a very important role as monomers for the industrial synthesis of polyurethanes and polyureas.[5]

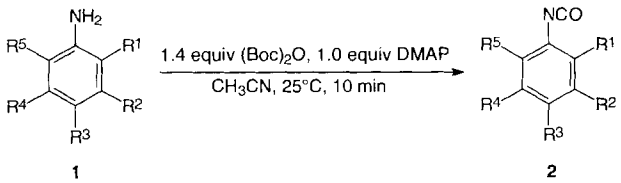

1 2

Table 1. Synthesis of aryl isocyanates **2** from arylamines **1** with $(Boc)_2O$ and a stoichiometric amount of DMAP.

	R^1	R^2	R^3	R^4	R^5	Method [a]	**2** Yield [%]
a	Me	H	Me	H	Me	A (B)	96 (93)
b	Me	H	H	H	Me	A	94
c	*i*Pr	H	H	H	*i*Pr	A	99
d	OMe	H	OMe	H	OMe	A	97
e	Me	H	H	H	H	A	44
f	OMe	H	H	H	H	A	86
g	OMe	H	Me	H	H	A	88
h	Me	H	OMe	H	H	A	58
i	OMe	H	OMe	H	H	A	76
j	Me	Me	OMe	H	H	A	89
k	$-(CH{=}CH)_2-$		OMe	H	H	A	42
l	H	H	OMe	H	H	B	41

[a] Method A: workup with sulfuric acid (reaction in CH_3CN at 25 °C, 10 min; workup by addition of H_2SO_4 (7.0 equiv) in CH_3CN [40%] and subsequent extraction with hexane). Method B: low-temperature chromatographic workup (reaction in CH_2Cl_2 at 25 °C, 10 min; purification by column chromatography on silica gel at −30 °C to −45 °C).

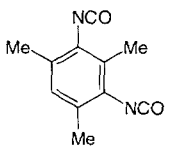

3

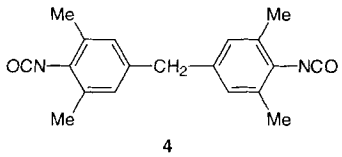

4

The reaction of sterically hindered alkylamines, such as *tert*-butylamine and 1,1,3,3-tetramethylbutylamine, performed in dichloromethane under the same reaction conditions (method B, low-temperature chromatography), afforded the alkyl isocyanates *tert*-butyl isocyanate (**5**) and 1,1,3,3-tetramethylbutyl isocyanate (**6**) in 49% and 97% yield, respectively. Isopropylamine can also be converted into the isocyanate by this method. As with *tert*-butyl isocyanate, isopropyl isocyanate has to be

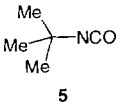

5

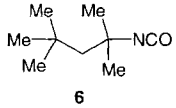

6

[*] Prof. Dr. H.-J. Knölker, Dipl.-Chem. T. Braxmeier, Dipl.-Chem. G. Schlechtingen
Institut für Organische Chemie der Universität
Richard-Willstätter-Allee, D-76131 Karlsruhe (Germany)
Telefax: Int. code + (721)698-529
e-mail: knoe@ochhades.chemie.uni-karlsruhe.de

[**] This work was supported by the Fonds der Chemischen Industrie and by the BASF AG, Ludwigshafen (donation of chemicals). We thank Dr. Werner Hoffmann and his coworkers of the ammonia laboratory at BASF, Ludwigshafen, for helpful and stimulating discussions.

separated from the *tert*-butanol formed simultaneously. Consequently, its yield is reduced. In contrast, higher branched alkyl isocyanates, like **6**, can be isolated in quantitative yields.

Some time ago Steglich et al. recognized early on the high efficiency of 4-dimethylaminopyridine (DMAP) as a catalyst in acylation reactions.[4] The reactive intermediates of these acylation reactions are *N*-acylpyridinium ions. Upon reaction of acetic anhydride with DMAP it could be proven that 1-acetyl-4-dimethylaminopyridinium acetate is spontaneously formed in equilibrium.[4] Based on spectroscopic studies and additional experiments, we postulate the reaction mechanism depicted in Scheme 1 for the novel isocyanate synthesis. The reaction mixture initially forms an equilibrium between the two starting reagents, DMAP and $(Boc)_2O$, and 1-*tert*-butoxycarbonyl-4-dimethylaminopyridinium-*tert*-butyl carbonate (**7**). Nucleophilic attack of the amine at the *tert*-butoxycarbonyl group of the pyridinium system **7** presumably leads to the tetrahedral intermediate **8**, which is converted into **9** by a transprotonation. In principle, the regeneration of the carbonyl group could also occur by loss of the pyridinium species (pathway B), which would provide *tert*-butanol, carbon dioxide DMAP, and urethane **10** (*N*-Boc derivative of the amine). However, the products we found indicate that intermediate **9** decomposes into *tert*-butanol and **11** (pathway A). Deprotonation of **11** by *tert*-butyl carbonate affords intermediate **12**. The rapid and irreversible decarboxylation of the resulting *tert*-butyl monoester of carbonic acid, which generates *tert*-butanol, shifts the equilibrium towards the intermediate **12**. Finally, loss of the pyridinium leaving group in **12** provides the isocyanate along with regenerated DMAP.

All spectroscopic and experimental results support the mechanism depicted in Scheme 1. 1-*tert*-Butoxycarbonyl-4-dimethylaminopyridinium-*tert*-butyl carbonate (**7**) is the key reagent in this novel isocyanate synthesis. Wakselman et al. described the corresponding chloride[6] and tetrafluoroborate[7] as reagents for the transfer of the Boc group in aqueous medium. Comparison of the ^{1}H NMR and ^{13}C NMR spectra of the tetrafluoroborate prepared as described by Wakselman et al. and of potassium *tert*-butyl carbonate[8] with the spectra of the equilibrium mixture of $(Boc)_2O$ with DMAP (1.1:1) in $[D_3]$acetonitrile proved unequivocally the existence of intermediate **7** in solution. The ^{1}H NMR and ^{13}C NMR spectra also revealed that DMAP and **7** exist in a ratio of 1:1.4 in this equilibrium mixture at room temperature. In agreement with Ragnarsson et al.,[9] we did not find any evidence for the formation of the [Boc-OCO-DMAP]$^+$ adduct postulated by Kemp and Curran.[10] In contrast to this report, the reagent mixture is stable for 1 h in anhydrous acetonitrile and decomposes only slowly to *tert*-butanol, isobutene, carbon dioxide, and di-*tert*-butyl carbonate.

Our mechanistic studies also emphasize the key role of intermediates analogous to **7** in the DMAP-catalyzed reaction of dialkyl dicarbonates and carboxylic acids, which was recently reported for the preparation of esters.[11] Control experiments showed that the reaction of the above-mentioned tetrafluoroborate with mesitylamine (**1a**) in acetonitrile does not give isocyanate **2a**. This shows the necessity of a counteranion that can function as an efficient base. Addition of potassium *tert*-butyl carbonate to this solution leads to immediate formation of *tert*-butanol, carbon dioxide, DMAP, and mesityl isocyanate, which can subsequently be isolated in more than 90% yield. Two equivalents of *tert*-butanol (detection and quantification by ^{1}H NMR) as well as one equivalent of carbon dioxide (gas-phase IR spectroscopy, quantification by gas volumetric analysis) are formed in the DMAP-mediated isocyanation of amines. The reaction of an arylamine with $(Boc)_2O$ in the absence of a nucleophilic nitrogen base exclusively affords the *N*-Boc derivative (urethane), as well established in protecting group chemistry. The urethane is not an intermediate of the isocyanate synthesis described here, since it does not undergo a reaction with either $(Boc)_2O$ or DMAP alone. The reaction of the urethane with $(Boc)_2O$ in the presence of DMAP, however, results in a nucleophilic reaction with **7** in which the *N*,*N*-bis-Boc derivative is formed.[12] The synthesis of *N*,*N*-bis-Boc derivatives can be explained by the formation of the [Boc-DMAP]$^+$ cation resulting from the activation of $(Boc)_2O$ by DMAP (Scheme 1).

The regeneration of DMAP as postulated in the mechanism outlined in Scheme 1 suggests the use of this component in catalytic amounts. This assumption was extensively investigated in the synthesis of mesityl isocyanate (**2a**) (Table 2). When employing low concentrations of DMAP, we isolated increasing amounts of the by-product *N*,*N*′-dimesitylurea (**14**) (see Table 2), arising from the reaction of the isocyanate with mesitylamine.[13] Nevertheless, the isocyanate was obtained in 92% yield when using 1 mol% of DMAP as the catalyst. With 0.1 mol% of DMAP, the reaction is incomplete after 10 min as a result of the low catalyst concentration. The yields, however, increased with increasing reaction times. 4-Pyrrolidinopyridine (PPY), which was used as an acylation catalyst by Steglich et al.,[4] was found to be another efficient catalyst for the isocyanation reaction described here. In contrast to the situation for acylation reactions, PPY did not prove to be a superior catalyst

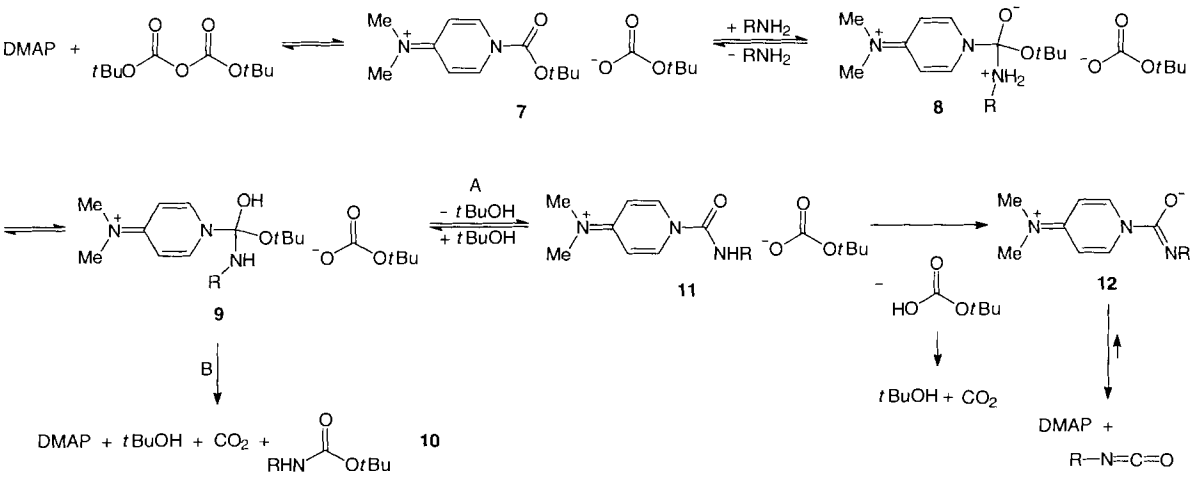

Scheme 1.

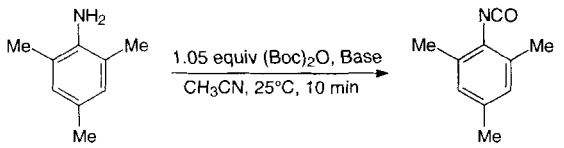

1a **2a**

Table 2. Synthesis of mesityl isocyanate (**2a**) from mesitylamine (**1a**) with $(Boc)_2O$, varying the nature and concentration of the base (reaction conditions and workup according to method A).

Base [a]	Equiv	**2a**, Yield [%]
DMAP	1.0	96
DMAP	0.1	97 [b]
DMAP	0.01	92 [b, c]
DMAP	0.001	32 [b, c]
PPY	1.0	94 [b]
PPY	0.1	91 [b]
PPY	0.01	92 [b]
PPY	0.001	14 [b, c]
4-MeOPy	1.0	51 [b, d]
Py	1.0	43 [b, d]
Et_3N	1.0	17 [b, d]

[a] Abbreviations: DMAP = 4-dimethylaminopyridine, PPY = 4-pyrrolidinopyridine, 4-MeOPy = 4-methoxypyridine, Py = pyridine. [b] Formation of *N*,*N*′-dimesitylurea (**14**) as a by-product (see Table 3). [c] Incomplete reaction. [d] Formation of *tert*-butyl-*N*-mesityl carbamate (**10**) (R = mesityl) as a by-product.

for this transformation. Along with isocyanate **2a**, urethane **10** (which most likely arises from the direct, uncatalyzed reaction of mesitylamine with $(Boc)_2O$) and urea **14**, which is a secondary product of isocyanate **2a**, were found when less nucleophilic pyridine bases such as 4-methoxypyridine (4-MeOPy), pyridine itself, or triethylamine were used.

For ecological reasons it seemed particularly important to achieve the isocyanation of amines with C1 building blocks that, unlike $(Boc)_2O$, can be synthesized without the use of phosgene. In fact, other activated carbonates can be used for the isocyanation of amines in the presence of DMAP (Table 3). However,

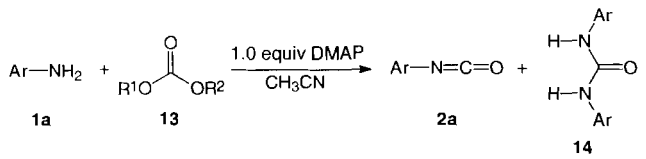

1a **13** **2a** **14**

Ar = Mesityl

Table 3. DMAP-mediated synthesis of mesityl isocyanate (**2a**) from mesitylamine (**1a**) with the activated carbonates **13** as the C1 building blocks. **13a** = $(Boc)_2O$.

13	R^1	R^2	T [°C]	t	**2a** Yield [%]	**14** Yield [%]
a	*t*BuOCO	*t*Bu	25	10 min	96	0
b	*t*BuCO	*t*Bu	25	4 h	17	64
c	C_6H_5	C_6H_5	82	15 d	0	29
d	4-$NO_2C_6H_4$	4-$NO_2C_6H_4$	25	18 h	19	64
d	4-$NO_2C_6H_4$	4-$NO_2C_6H_4$	82	18 h	9	86

due to its extreme reactivity, $(Boc)_2O$ (**13a**) provides the highest yields in a very rapid reaction. As an alternative to $(Boc)_2O$, we first synthesized *tert*-butoxycarbonyl pivalate (**13b**), which is readily available by successive transformation of *tert*-butanol with potassium and carbon dioxide followed by an in situ acylation with pivaloyl chloride. The reaction of **13b** with mesitylamine (**1a**) in the presence of DMAP provided isocyanate **2a** in 17% yield, along with 64% of urea **14**. In this context it is important to note that the urea is formed exclusively from the isocyanate under these reaction conditions and not from the corresponding urethane. The reaction of the mesitylamine-*N*-Boc derivative **10** (R = mesityl) in the presence of an equimolar amount of mesitylamine and DMAP afforded only 0.9% of *N*,*N*′-dimesitylurea (**14**) after 14 d in acetonitrile at 82 °C. Consequently, the urethane formed by the direct transformation of $(Boc)_2O$ with mesitylamine (**1a**) does not provide an isocyanate-free way to urea **14**. Thus, the isolation of larger amounts of urea gives direct evidence for the intermediate isocyanate as shown in the pathway outlined above. While dimethyl carbonate, di-*tert*-butyl carbonate, and ethylene carbonate did not react, the reaction of diphenyl carbonate (**13c**) with mesitylamine and DMAP in acetonitrile under reflux yielded urea **14** in a moderate 29% yield after 15 d. Under these reaction conditions, complete conversion of the isocyanate into the respective urea derivative is not unexpected. Because of the milder reaction conditions, when bis(4-nitrophenyl) carbonate (**13d**) is used, isocyanate **2a** could be isolated along with the secondary product **14**. The combined yield of 95% at 82 °C indicates that the DMAP-catalyzed reaction pathway involving the isocyanate is virtually the exclusive route in this case.

In conclusion, the DMAP-catalyzed reaction with activated carbonates as C1 building blocks constitutes a convenient laboratory method for the phosgene-free isocyanation of amines. The application of this method in the synthesis of symmetrical and unsymmetrical ureas as well as of heterocycles is currently under investigation.

Experimental Procedure

All reactions were performed in anhydrous solvents.

General procedure for the synthesis of alkyl and aryl isocyanates with stoichiometric amounts of DMAP: A solution of di-*tert*-butyl dicarbonate (1.4 equivalents) in acetonitrile was treated successively with a solution of 4-dimethylaminopyridine (1.0 equiv) in acetonitrile and a solution of the arylamine (1.0 equiv) in acetonitrile. The resulting mixture was stirred for 10 min at room temperature (dichloromethane was used as the solvent for workup according method B). Workup, method A: The reaction mixture was treated with sulfuric acid (7 equiv) as a 40% solution in acetonitrile ($\rho = 1.03\ g\,cm^{-3}$), and was stirred for 2 min. The mixture was then extracted three times with hexane. The combined hexane layers were dried over magnesium sulfate, and the solvent was removed in vacuo. Workup, method B: The solvent (dichloromethane) was completely removed, and the residue is extracted several times with small amounts of eluent (for example, hexane/ethyl acetate 4/1). The resulting suspension was subjected to silica gel chromatography at −30 °C to −45 °C.

Synthesis of mesityl isocyanate (**2a**) with a catalytic amount of DMAP: A solution of di-*tert*-butyl dicarbonate (619 mg, 2.84 mmol) in acetonitrile (2 mL) was treated successively with a solution of 4-dimethylaminopyridine (33 mg, 0.27 mmol) in acetonitrile (2 mL) and a solution of **1a** (365 mg, 2.7 mmol) in acetonitrile (2 mL). The reaction mixture was vigorously stirred for 10 min. After the addition of concentrated sulfuric acid in acetonitrile (40% solution, $\rho = 1.03\ g\,cm^{-3}$, 0.47 mL), the resulting mixture was stirred for 5 min. Water (0.47 mL) was then added, and the mixture was stirred for an additional 5 min. The reaction mixture was then poured into an equal amount of water, the solution was extracted three times with hexane, and the combined hexane layers were dried over magnesium sulfate. Removal of the solvent in vacuo afforded **2a** (420 mg, 97%) as colorless crystals, m.p. 42 °C; IR (KBr): $\tilde{\nu} = 2281$ (NCO), 1592, 1509 cm^{-1}; ^{13}C NMR and DEPT (100 MHz, $CDCl_3$): $\delta = 135.06$ (C), 132.68 (2C), 128.73 (2CH), 128.54 (C), 124.24 (NCO), 20.79 (CH_3), 18.62 ($2CH_3$); analysis for $C_{10}H_{11}NO$: calcd C 74.51, H 6.88, N 8.69; found C 74.38, H 6.79, N 8.71.

Received: July 19, 1995 [Z82291E]
German version: *Angew. Chem.* **1995**, *107*, 2746–2749

Keywords: arenes · di-*tert*-butyl dicarbonate · isocyanates

[1] S. Ozaki, *Chem. Rev.* **1972**, *72*, 457; K. Findeisen, K. König, R. Sundermann in *Methoden Org. Chem. (Houben-Weyl), 4th ed. 1952 – Band E4*, **1983**, p. 738.
[2] H.-J. Knölker, T. Braxmeier, G. Schlechtingen, German patent application P 19526081.3, **1995**.
[3] T. W. Greene, P. G. M. Wuts, *Protective Groups in Organic Synthesis*, 2nd ed., Wiley, New York, **1991**, Chap. 7, p. 309; P. J. Kocienski, *Protecting Groups*, Thieme, Stuttgart, **1994**, Chap. 6, p. 185.
[4] W. Steglich, G. Höfle, H. Vorbrüggen, *Angew. Chem.* **1978**, *90*, 602; *Angew. Chem. Int. Ed. Engl.* **1978**, *17*, 569.
[5] H. G. Schmelzer, R. M. Mafoti, J. Sanders, W. E. Slack, *J. Prakt. Chem.* **1994**, *336*, 483.
[6] E. Guibé-Jampel, M. Wakselman, *J. Chem. Soc. Chem. Commun.* **1971**, 267.
[7] E. Guibé-Jampel, M. Wakselman, *Synthesis* **1977**, 772.
[8] Potassium *tert*-butyl carbonate was synthesized analogous to potassium methyl carbonate and potassium ethyl carbonate: W. Behrendt, G. Gattow, M. Dräger, *Z. Anorg. Allg. Chem.* **1973**, *397*, 237.
[9] A. Könnecke, L. Grehn, U. Ragnarsson, *Tetrahedron Lett.* **1990**, *31*, 2697.
[10] D. S. Kemp, T. P. Curran, *J. Org. Chem.* **1988**, *53*, 5729.
[11] K. Takeda, A. Akiyama, H. Nakamura, S. Takizawa, Y. Mizuno, H. Takayanagi, Y. Harigaya, *Synthesis* **1994**, 1063.
[12] L. Grehn, U. Ragnarsson, *Angew. Chem.* **1985**, *97*, 519; *Angew. Chem. Int. Ed. Engl.* **1985**, *24*, 510.
[13] C. S. Dean, D. S. Tarbell, *J. Org. Chem.* **1971**, *36*, 1180.

P–H-Functionalized Phosphenium Complexes $[C_5R_5(OC)_2W{=}P(H)R']$ (R′ = *t*Bu, sMes): Synthesis, Isomerization, and Transformation into Hydrido Complexes Containing a *t*BuP(H)OH Ligand**

Wolfgang Malisch,* Ulrich-Andreas Hirth, Klaus Grün, Martin Schmeusser, Oliver Fey, and Udo Weis

Dedicated to Professor Hubert Schmidbaur on the occasion of his 60th birthday

The metal–phosphorus double bond in phosphenium complexes of the type $[Cp(OC)_2M{=}PR_2]$ (M = Mo, W) is employed increasingly in cycloaddition reactions,[1] which represent a first step towards the application of these compounds in the synthesis of organophosphorus compounds mediated by metal complexes. However, in the compounds known to date, bulky organo or heteroatom substituents on the phosphorus, which stabilize the double bond, limit the addition activity of the M=P unit quite considerably.[1] In this context promising candidates are hydrogen-substituted M=P units with an sp^2-hybridized phosphorus atom, which can be regarded as phosphorus analogues of primary carbene complexes.[2a, b] These units display increased potential for cycloaddition, but the possibility of isomerizations by hydrogen migration must also be taken into account.[2c] Furthermore, the possibility of exchange and insertion reactions involving the highly reactive P–H bond must be considered.[3]

The existence of these R(H)P=M complexes, which have been postulated repeatedly as intermediates in reactions of P–H-functionalized phosphido-osmium complexes,[4] has, to date, only been confirmed by the compound $[(Et_3P)_2(Me_3CC)Cl_2W{=}P(H)Ph]$ obtained by Schrock from a complex reaction.[5] The reason for the difficulty in isolating these compounds is the high reactivity of the insufficiently shielded M=P unit, which spontaneously dimerizes, as proved in the case of $[C_5R_5(OC)_2W{=}P(H)Mes]$ (R = H, Me) with the formation of phosphinidene complexes $[C_5R_5(OC)_2W{=}PMes\{W(PH_2Mes)(CO)_2C_5R_5\}]$.[6]

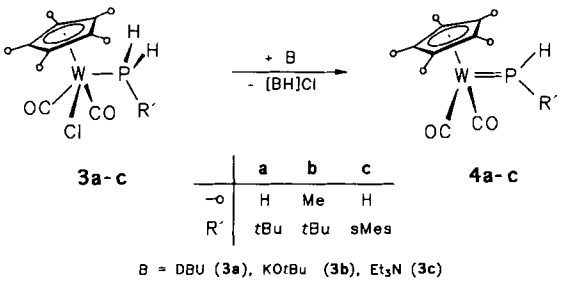

(a)

We have now been able to demonstrate that P–H-functionalized phosphenium complexes $[C_5R_5(OC)_2W{=}P(H)R']$ are accessible providing that the phosphorus carries a *tert*-butyl or a supermesityl (sMes) group. The synthesis is achieved by the dehydrochlorination of the complexes **3a–c**[7] obtained thermally from $[C_5R_5(OC)_3WCl]$ (**1**) and the primary phosphanes $R'PH_2$ (R′ = *t*Bu, sMes) **2** by reaction with 1,8-diazabicyclo[5.4.0]undec-7-ene (DBU) (**3a**, −78 °C), potassium *tert*-butyl alcoholate (**3b**, −10 °C), or triethylamine (**3c**, 25 °C) in toluene [Eq. (a)].

Whilst the supermesitylphosphenium complex **4c** can be isolated as a pale violet, air-stable crystalline powder, the *tert*-butyl-substituted compounds **4a** and **4b** only exist in toluene at −60 and 0 °C, respectively, for about three hours (spectroscopic data see Table 1). Compounds **4a–c** can be characterized unambiguously by the low-field shifts of the ^{31}P NMR resonance typical for W=P complexes (δ = 285.5 (**4a**), 275.1 (**4b**), 211.8 (**4c**)) and by the large $^1J(W,P)$ coupling (571.6 (**4a**), 575.5 (**4b**), 604.0 (**4c**) Hz).[8] At room temperature **4a,b** undergo rapid de-

Table 1. Selected spectroscopic data of the complexes **4a–c**, **5–8**, **9a,b**, and **10a,b**.

4a/4b: ^{31}P NMR (162 MHz, [D$_8$]toluene, −60 °C): δ = 285.5/275.6 (s, $^1J(W,P)$ = 571.6/575.5 Hz)

5: ^1H NMR (90 MHz, [D$_1$]chloroform): δ = 4.45 (d, $^1J(P,H)$ = 354.2 Hz, 1H, HP), −12.6 (d, $^2J(P,H)$ = 26 Hz, 1H, μ-H); ^{31}P NMR (36 MHz, [D$_1$]chloroform): δ = 276.6 (s, $^1J(W,P)$ = 221.8 Hz)

4c: ^1H NMR (200 MHz, [D$_6$]benzene): δ = 12.80 (d, $^1J(P,H)$ = 379.0 Hz, 1H, HP), 7.44 (d, $^4J(P,H)$ = 2.0 Hz, 2H, *m*-H), 5.08 (d, $^3J(P,H)$ = 0.3 Hz, 5H, H_5C_5), 1.37 (d, $^5J(P,H)$ = 0.7 Hz, 18H, *o*-$(H_3C)_3C$), 1.15 (s, 9H, *p*-$(H_3C)_3C$); ^{31}P NMR (162 MHz, [D$_6$]benzene): δ = 211.8 (s, $^1J(W,P)$ = 604.0 Hz); IR (pentane): $\tilde{\nu}$ = 1953 (vs), 1881 (s) (CO), 2299 (w) (PH) cm^{-1}

6/7: ^{31}P NMR (162 MHz, [D$_6$]benzene): δ = 201.8/262.8 (s, $^1J(W,P)$ = 711.6/617.8 Hz)

8: ^1H NMR (200 MHz, [D$_8$]toluene): δ = 7.04 (s, 1H, *m*-H), 6.92 (s, 1H, *m*-H), 5.24 (s, 5H, H_5C_5), 1.50 (s, 9H, *p*-$(H_3C)_3C$), 1.08 (s, 18H, *o*-$(H_3C)_3C$), −10.03 (d, $^2J(P,H)$ = 110.5 Hz, 1H, HW); ^{31}P NMR (162 MHz, [D$_6$]benzene): δ = 819.9 (s, $^1J(W,P)$ = 123.1 Hz); IR (benzene): $\tilde{\nu}$ = 1939 (vs), 1862 (s) (CO) cm^{-1}

9a/9b: ^{31}P NMR (162 MHz, [D$_6$]benzene): δ = −59.9/−9.4 (s, $^1J(W,P)$ = 64.5/71.5, $^2J(P,P)$ = 30.1/32.8 Hz), −12.9/−17.1 (s, $^1J(W,P)$ = 250.6/269.4 Hz, $^2J(P,P)$ = 30.1/32.8 Hz)

10a/10b: ^1H NMR (400 MHz, [D$_8$]toluene): δ = 7.32/7.23 (dd, $^1J(P,H)$ = 363.8/351.1, $^3J(H,H)$ = 2.7/3.4 Hz, 1H, HP), 1.23/2.67 (br.s/d, $^2J(P,H)$ = 8.8 Hz, 1H, HO), −8.49/−7.80 (dd, $^2J(P,H)$ = 88.3/79.6, $^3J(H,H)$ = 2.7/3.4 Hz, 1H, HW); ^{31}P NMR (162 MHz, [D$_8$]toluene): δ = 133.1/143.6 (s, $^1J(W,P)$ = 281.3/279.9 Hz).

[*] Prof. Dr. W. Malisch, Dr. U.-A. Hirth, Dipl.-Chem. K. Grün, Dr. M. Schmeusser, Dipl.-Chem. O. Fey, Dr. U. Weis
Institut für Anorganische Chemie der Universität
Am Hubland, D-97074 Würzburg (Germany)
Telefax: Int. code + (931)8884605
e-mail: anor075@rzbox.uni-wuerzburg.de

[**] Phosphenium Complexes, Part 27. This work was funded by SFB 347 ("Selektive Reaktionen Metall-aktivierter Moleküle"). Part 26: W. Malisch, K. Grün, N. Gunzelmann, S. Möller, R. Lankat, J. Reising, M. Neumayer, O. Fey in *Selective Reactions of Metal-Activated Molecules* (Eds.: H. Werner, J. Sundermeyer), Vieweg, Braunschweig, **1995**, pp. 183–190. sMes = supermesityl = 2,4,6-tBu$_3$C$_6$H$_2$.

composition in solution. In the case of **4a** this leads to the binuclear complex **5**, which is the product of the formal addition of the 16-electron complex fragment "$[Cp(OC)_2WH]$" to the W=P unit.

$[(\mu_2\text{-H})(\mu_2\text{-}t\text{BuHP})\{W(CO)_2Cp\}_2]$ **5**

Due to the greatly reduced reactivity of the M=P bond, **4c** preferentially undergoes reactions involving the P–H function (Scheme 1). Complex **4c** reacts with carbon tetrachloride by H/Cl exchange at the phosphorus atom to afford the extremely thermally stable PCl complex **6**.

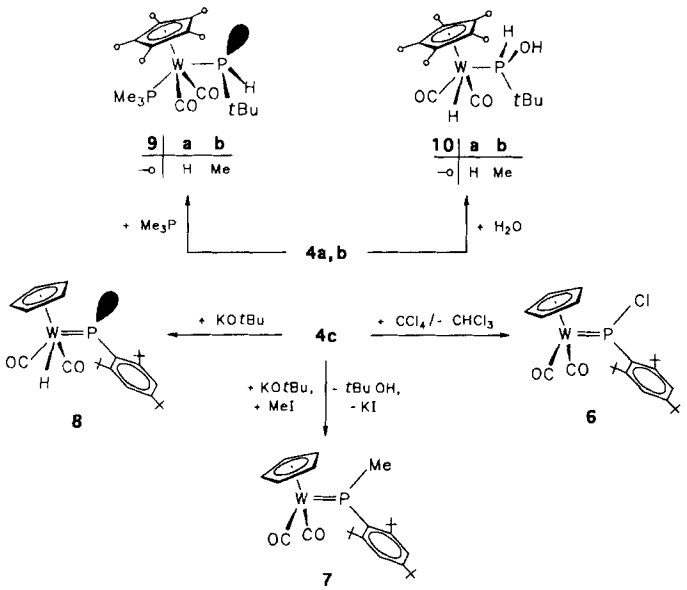

Scheme 1.

The reaction of **4c** with an equimolar amount of potassium *tert*-butyl alcoholate and excess methyl iodide in tetrahydrofuran yields the P-methylated phosphenium complex **7**. In the presence of the deprotonation reagent KO*t*Bu, isomerization of **4c** is evident by the change in color of the solution from violet to turquoise, during which a H atom migrates from the phosphorus center to the metal center, producing the phosphinidene complex **8**. This process is similar to the α-H abstraction in electron-rich Schrock carbene complexes[2a] and provides an explanation for the ready formation of phosphinidene–tantalum complexes.[9] Compound **8**, the first terminal phosphinidene complex with a functionalized metal center, is stable in solution up to 60 °C; however, it converts back into **4c** on attempted isolation. The structure of **8** was determined from a comparison of its ^{31}P NMR data [$\delta(^{31}P)$: 819.9 ($^1J(W,P) = 123.1$ Hz)] with those of the structurally characterized, bent phosphinidene complex $[Cp_2W{=}P(sMes)]$ [$\delta(^{31}P)$: 661.6 ($^1J(W,P) = 153.5$ Hz)].[10] The ^1H NMR resonance of the hydrido ligand at $\delta = -10.03$ splits into a doublet with an unusually large $^2J(P,H)$ coupling of 110.5 Hz.

The addition capacity of the M=P double bonds in complexes **4a,b**, which do not exhibit an analogous isomerization, exceed that of all the phosphenium complexes known to date (Scheme 1). Treatment of **4a** and **4b** with trimethylphosphane leads to the corresponding secondary metallophosphanes **9a** and **9b**. In tetrahydrofuran **4a** and **4b** react spontaneously with an excess of water at −78 and −10 °C, respectively, to yield the 1,2-addition products **10a** and **10b**. These contain complex-stabilized *t*Bu(H)P(OH), the tautomer of primary *tert*-butylphosphane oxide unknown in the free state.[11] As proven for **10a**,[12] the structure is characterized by the sterically determined *anti* arrangement of the *tert*-butyl ligand to the cyclopentadienyl unit (Z-W-P-C9 = 168°, Z = center of the cyclopentadienyl ring) and its eclipsed position relative to one of the two carbonyl groups (Fig. 1). The formation of intermolecular hydrogen bonds between the oxygen atom of the carbonyl group and the hydrogen atom of the hydroxyl group [d(O3–H31) = 1.13(3), d(O2–O3) = 2.820 Å[13]] leads to dimers with a puckered twelve-membered ring in the crystal.

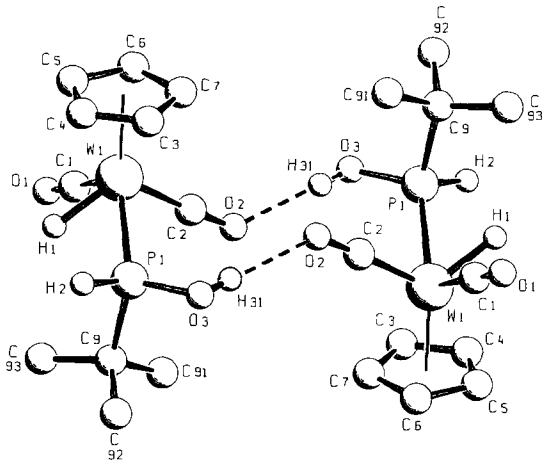

Fig. 1. Crystal structure of **10a**. All the hydrogen atoms except for H1, H2, and H31 have been omitted for the sake of clarity. Selected distances [Å], bond and dihedral angles [°]: W1-P1 2.371(1), W1-H1 1.65(5), P1-O3 1.642(5), P1-H2 1.40(5), O3-H31 1.13(3), O2-O3 2.820; C2-W1-C1 79.2(2), O3-P1-W1 116.7(2). O3-P1-H2 109.2(5), P1-O3-H31 113(7), Z-W-P-C9 167.9.

Experiments demonstrating the cycloaddition behavior of the P–H-functionalized phosphenium complexes presented here and subsequent reactions of the cycloadducts involving the P–H function will be reported in due course.

Experimental Procedure

All manipulations were performed in the absence of air and moisture.

4a/**4b**/**5**: A solution of **3a** (123 mg, 0.29 mmol)/**3b** (155 mg, 0.31 mmol) in toluene (10 mL) was treated at −78 °C/−10 °C with DBU (43 mg, 0.29 mmol)/KO*t*Bu (35 mg, 0.31 mmol) and stirred. This gave a violet solution of **4a** and **4b**, respectively, which was stable at −60 °C/0 °C for about 3 h. Workup of **4a** by column chromatography (column 8 × 1.5 cm, Al_2O_3, activity grade III, neutral, tetrahydrofuran, yellow zone) produced **5**. Yield: 49 mg (25%), orange-red crystalline powder, m.p. 166 °C (decomp.).

4c: A stirred solution of **3c** (80 mg, 0.13 mmol) in benzene (0.5 mL) was treated with triethylamine (79 mg, 0.78 mmol) at about 25 °C. After the mixture had been stirred for a further 10 min, it was centrifuged to remove the $(Et_3NH)Cl$ formed. The clear, violet solution was evaporated to dryness in vacuum. The residue, **4c**, was treated with pentane (2 mL) and dried in vacuum. Yield: 52 mg (69%), pale violet crystalline powder, m.p. 108 °C.

6: A solution of **4c** (85 mg, 0.15 mmol) in benzene (5 mL) was treated with carbon tetrachloride (22 mg, 0.15 mmol) and stirred for 22 h at about 25 °C. Yield: 86 mg (96%), red-violet crystalline powder, m.p. 120 °C.

7/**8**: A solution of **4c** (85 mg, 0.15 mmol) in tetrahydrofuran (10 mL) was treated with KO*t*Bu (19 mg, 0.15 mmol) at 0 °C; the color of the solution immediately changed from violet to turquoise indicating the spontaneous formation of **8**. After addition of methyl iodide (114 mg, 0.80 mmol), the mixture was stirred for 5 min at about 25 °C and then worked up by column chromatography (column 10 × 1.5 cm, Al_2O_3, activity grade IV, neutral, pentane). Yield: 69 mg (79%), violet crystalline powder, m.p. 135 °C (decomp.).

9a/**9b**: A solution of **3a** (168 mg, 0.39 mmol)/**3b** (240 mg, 0.48 mmol) and trimethylphosphane (30 mg, 0.39 mmol)/(37 mg, 0.48 mmol) in toluene (10 mL)

was treated at about 25 °C with DBU (59 mg, 0.39 mmol)/KO*t*Bu(57 mg, 0.48 mmol). After workup by column chromatography (column 10 × 2 cm, Al_2O_3, activity grade IV, neutral, diethyl ether) **9a**/**9b** was isolated from the light yellow fraction. Yield: 154 mg (84%)/182 mg (70%), lemon yellow crystalline powder/pale yellow crystalline powder, m.p. 126 °C/111 °C.

10a/**10b**: To a solution of **3a** (416 mg, 0.97 mmol)/**3b** (240 mg, 0.48 mmol) in tetrahydrofuran (20 mL) and H_2O (1 mL) was added DBU (147 mg, 0.97 mmol)/KO*t*Bu (54 mg, 0.48 mmol) at −78 °C/0 °C. After workup by column chromatography (column 15 × 2 cm, Al_2O_3, activity grade IV, neutral, toluene, tetrahydrofuran) **10a**/**10b** was isolated. Yield: 288 mg (72%)/100 mg (43%), pale yellow/light yellow crystalline powder, m.p. 97 °C/102 °C.

Received: May 9, 1995 [Z 7970 IE]
German version: *Angew. Chem.* **1995**, *107*, 2717–2719

Keywords: complexes with phosphorus ligands · phosphenium complexes · tungsten compounds

[1] a) *Selective Reactions of Metal-Activated Molecules* (Eds.: H. Werner, A. G. Griesbeck, W. Adam, G. Bringmann, W. Kiefer), Vieweg, Braunschweig, **1992**; b) A. Spörl, K. Kindahl, A. Fried, H. Pfister, W. Malisch in ref. [1a], pp. 191–194; A. Fried, C. Hahner, A. Spörl, W. Malisch in ref. [1a], pp. 195–196; c) A. Fried, W. Malisch, M. Schmeusser, U. Weis, *Phosphorus, Sulfur Silicon Relat. Elem.* **1992**, *65*, 75–78; d) H. Lang, M. Leise, L. Zsolnai, *Organometallics* **1993**, *12*, 2393–2397.

[2] a) W. A. Nugent, J. M. Mayer, *Metal-Ligand Multiple Bond*, Wiley, New York, **1988**; b) M. R. Churchill, H. J. Wasserman, H. W. Turner, R. R. Schrock, *J. Am. Chem. Soc.* **1982**, *104*, 1710–1716; c) H. Fischer, J. Hofmann, *Chem. Ber.* **1991**, *124*, 981–988.

[3] W. Wolfsberger, *Chem. Ztg.* **1986**, *109*, 317–332; *ibid.* **1988**, *112*, 53–68, 215–221.

[4] D. S. Bohle, T. C. Jones, C. E. F. Rickard, W. R. Roper, *J. Chem. Soc. Chem. Commun.* **1984**, 865–867; *Organometallics* **1986**, *5*, 1612–1619; D. S. Bohle, G. R. Clark, C. E. F. Rickard, W. R. Roper, *J. Organomet. Chem.* **1990**, *393*, 243–261.

[5] S. M. Rocklage, R. R. Schrock, M. R. Churchill, H. J. Wasserman, *Organometallics* **1982**, *1*, 1332–1334.

[6] W. Malisch, U.-A. Hirth, T. A. Bright, H. Käb, T. S. Ertel, S. Hückmann, H. Bertagnolli, *Angew. Chem.* **1992**, *104*, 1537–1539; *Angew. Chem. Int. Ed. Engl.* **1992**, *31*, 1525–1527.

[7] **3a**/**3b**/**3c**: orange crystalline powder; m.p. 124 °C (decomp.)/88 °C (decomp.)/161 °C. ^{31}P NMR (162 MHz, [D$_6$]benzene): $\delta = -22.0/-6.7/-71.4$ (s, $^1J(W,P) = 257.5/266.5/272.4$ Hz).

[8] E. Gross, K. Jörg, K. Fiederling, A. Göttlein, W. Malisch, R. Boese, *Angew. Chem.* **1984**, *96*, 705–706; *Angew. Chem. Int. Ed. Engl.* **1984**, *23*, 738–739; K. Jörg, W. Malisch, A. Meyer, W. Reich, U. Schubert, *ibid.* **1986**, *98*, 103–104 and **1986**, *25*, 92–93.

[9] C. C. Cummins, R. R. Schrock, W. M. Davis, *Angew. Chem.* **1993**, *105*, 758–761; *Angew. Chem. Int. Ed. Engl.* **1993**, *32*, 742–745.

[10] ^{31}P NMR data of further bent phosphinidene complexes: P. B. Hitchcock, M. F. Lappert, W. P. Leung, *J. Chem. Soc. Chem. Commun.* **1987**, 1282–1283 ($\delta(^{31}P)$ in [Cp$_2$Mo=P(sMes)]: 799.5); Z. Hou, T. L. Breen, D. W. Stephan, *Organometallics* **1993**, *12*, 3158–3167 ($\delta(^{31}P)$ in [Cp$_2$Zr(PMe$_3$)=P(sMes)]: 792). ^{31}P NMR data of linear phosphinidene complexes A. H. Cowley, B. Pellerin, J. L. Atwood, S. G. Bott, *J. Am. Chem. Soc.* **1990**, *112*, 6734–6735 ($\delta(^{31}P)$: 193); ref. [9] ($\delta(^{31}P$: 175.1–275.0).

[11] A. Marinetti, F. Mathey, *Organometallics* **1982**, *1*, 1488–1492.

[12] Crystal structure analysis of **10a** ($C_{11}H_{17}O_3PW$): $M = 412.08$; yellow crystal (0.3 × 0.3 × 0.4 mm); triclinic; space group $P\bar{1}$ (no. 2); $a = 8.04(1)$, $b = 8.38(8)$, $c = 10.60(5)$ Å, $\alpha = 99.60(7)$, $\beta = 99.22(9)$, $\gamma = 103.72(7)°$, $V = 669.9(2)$ Å^3, $Z = 2$, $\rho_{calcd} = 2.043$ g cm^{-3}, $\mu(Mo_{K\alpha}) = 87.31$ cm^{-1}; CAD4 Enraf-Nonius diffractometer (graphite monochromator, $Mo_{K\alpha}$), 1784 independent reflections ($2\theta_{max} = 44°$), of which 1604 with $I > 2\sigma(I)$ used for the structure solution with SHELXS-86 (direct methods) and refinement with SHELXL93 (179 parameters), absorption correction ψ scan (EAC in SDP), correction for decompositional decay in SDP (15.9%). The hydrogen atoms H1–H7 could be localized and were refined isotropically, the *tert*-butyl group and H31 were calculated from ideal geometry, fixed and included in the calculation of the structural factor. R = 0.019, Rw = 0.052, $w = 2.0672/[\sigma^2(F) + 0.000134F^2)$. Further details of the crystal structure investigation may be obtained from the Fachinformationszentrum Karlsruhe, D-76344 Eggenstein-Leopoldshafen (Germany) on quoting the depository number CSD-404302.

[13] The values were calculated with the program SCHAKAL 92.

Oxidative Transformations of a Pyrimidalized 1,5-Diene**

Gerald Dyker,* Jutta Körning, Peter G. Jones, and Peter Bubenitschek

In pyramidalized alkenes[1] the olefinic carbon atoms do not lie in the plane of the three atoms to which they are bonded. The deviation from the ideal geometry for CC double bonds may be remarkable. The pyramidalized 1,5-dienes **1**[2] and **2**[3] and the cage compound **3**[4] are of special interest: not only do they display the typical enhanced reactivity of pyramidalized alkenes, but they may also undergo other reactions due to the transannular interactions of the parallel-oriented π-orbitals. The shortest transannular distance in **2** is only 242 pm with a pyramidalization angle Φ of 35°;[1b, 3] this structure makes transannular addition reactions possible.[3c]

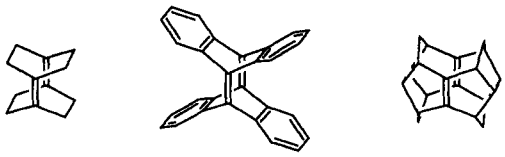

1 **2** **3**

For the synthesis of the pyramidalized diene **7** the recently described dienophilic character of the annelated pentalene **4** was exploited.[5] The Diels–Alder reaction with 9,10-dibromoanthracene (**5**) yielded the benzeno-bridged [4.3.3]propellane **6**, which is already suitably functionalized for conversion into the pyramidalized diene **7**. Monolithiation of **6** should lead to a 1,4-elimination of lithium bromide and cleavage of the strained central CC single bond of the propellane skeleton. The reagent of choice is the sterically hindered triphenylmethyllithium, and **7** was isolated in 79% yield in the form of colorless crystals (Scheme 1).[6] *n*-Butyllithium is not suitable as a lithiating agent in this case since it can add to diene **7**. Zinc dust in DMF at 150 °C, which are suitable conditions for the synthesis of **3** from the corresponding dibromide,[7] was less successful here because of the competing double dehalogenation.

In the X-ray structure analysis confirming the structure of **7** unusual structural features are evident (Fig. 1).[8] The length of the double bonds, 134 pm, is in the normal range, but in the side view (Fig. 1 right) distinct pyramidalization is apparent. The pyramidalization angle Φ on the benzeno-bridged side is 34.9° and corresponds to the value determined in the related compound **2**. On the naphthaleno-bridged side the pyramidalization angle Φ is 16.5°. The distances between the symmetrically positioned carbon atoms are 247.1 and 265.9 pm.

Whereas **1** is converted spontaneously by oxygen into its diepoxide,[2] diene **7**, in the dark, is kinetically stable towards oxygen. However, in sunlight a solution of **7** in $CDCl_3$ was completely oxidized within a few hours. The main products were

[*] Dr. G. Dyker,[+] Dipl.-Chem. J. Körning
Institut für Organische Chemie der Technischen Universität
Hagenring 30, D-38106 Braunschweig (Germany)
Telefax: Int. code + (531)391-5388
Prof. Dr. P. G. Jones, Dipl.-Chem. P. Bubenitschek
Institut für Anorganische und Analytische Chemie der Technischen Universität Braunschweig (Germany)

[+] New address:
FB6 - Organische Chemie, Universität Duisburg
Lotharstrasse 1, D-37048 Duisburg (Germany)

[**] This work was supported by the Deutsche Forschungsgemeinschaft and the Fonds der Chemischen Industrie.

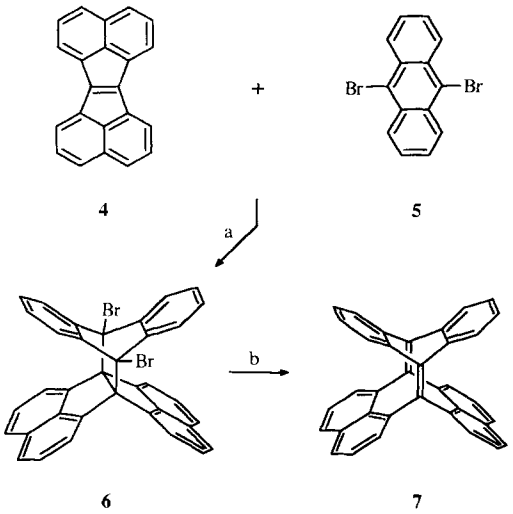

4 5 6 7

Scheme 1. Syntheses of **6** and **7**; a) 220 °C, 3 h, yield 78%; b) triphenylmethyllithium, THF, room temperature, 4 h, yield 79%.

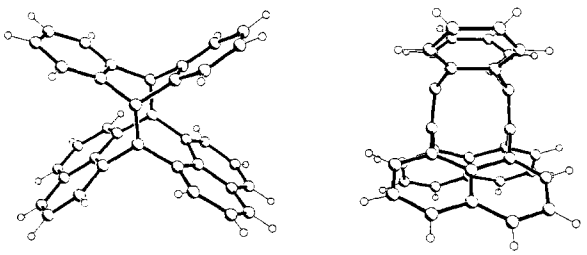

Fig. 1. Two views of the molecular structure of **7** in the crystal (arbitrary radii) [8].

identified by ^{1}H NMR spectroscopy as the annelated pentalene **4** and anthraquinone (**8**); the most likely oxidizing agent is singlet oxygen. In a reaction with rubrene endoperoxide[9] as a thermal source of singlet oxygen (xylene, 136 °C, 6 h) the fragmentation products **4** and **8** were also detected. The diepoxide **10** is not considered to be the reactive intermediate since solutions of **10** in $CDCl_3$ are stable even in sunlight. Only when heated in naphthalene at 285 °C for two hours (glass ampule) does **10** decompose almost completely into **4** and **8** (Scheme 2).

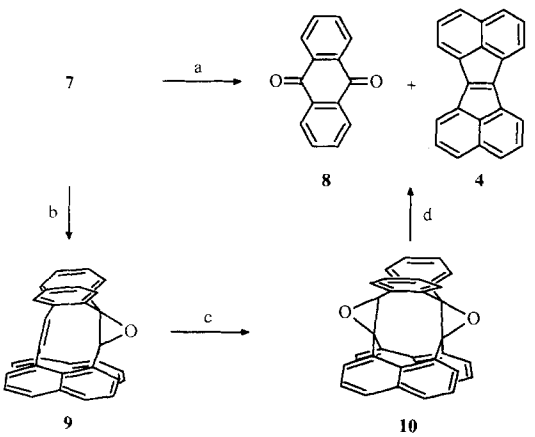

9 10

Scheme 2. Oxidative transformations of **7**: a) sunlight, aerial oxygen, $CDCl_3$; b) acetone/CH_2Cl_2/H_2O, $NaHCO_3$, oxone ($2KHSO_5 \cdot KHSO_4 \cdot K_2SO_4$, conditions for the formation of dimethyldioxirane in situ), 15 °C, 40 min, yield 55%; c) 0.05 M dimethyldioxirane in acetone, room temperature, 16 h, yield 80%; d) naphthalene, 285 °C, 2 h, glass ampule.

Diepoxide **10** was prepared by stepwise oxidation of **7** with dimethyldioxirane.[10] Monoepoxide **9** was isolated as an intermediate. In contrast to diepoxide **10**, which was purified without any problems by column chromatography on either silica gel or neutral alumina, the monoepoxide proved to be extremely labile on both of these stationary phases. A quantitative rearrangement of **9** giving the spiroannelated [3.3.1]propellane **11** occurred both when silica gel was loaded with a solution of **9** in dichloromethane at 40 °C, and when a toluene solution of **9** was passed through neutral alumina. We assume that the first reaction step is an acid-induced ring opening of the epoxide to give the carbenium ion **12**. Transannular ring closure provides the reactive intermediate **13**, and the cationotropic shift of an alkyl group leads finally to the formation of the cyclopropyl ring in **11** (Scheme 3).[11] According to semiempirical calculations (AM1), this process results in a gain of approximately 13 kcal mol^{-1}.

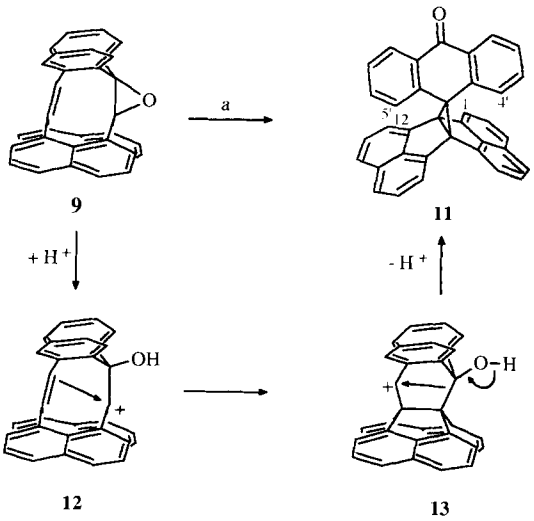

Scheme 3. Rearrangement of **9**; a) silica gel, 50 °C or neutral alumina/toluene, room temperature, yield 96%.

The X-ray structure analysis of **11** shows that the anthrone partial structure is present in a definite boat conformation due to the steric interactions of the hydrogen atoms H4′/H5′ in the "*peri*" positions of the naphthalene unit (Fig. 2). In contrast, the most stable conformer of spiro[anthracene-9,10′-cyclopropan]-10-one is planar.[12] The observation of six signals for different CH groups in the naphthalene unit in the NMR spectra of **11** agrees with this result (see Table 1). Apparently, inversion of the anthrone unit is not possible on the NMR time scale on steric grounds.[13] The H4′/H5′ doublet is shifted anisotropically to high field ($\delta = 6.34$).

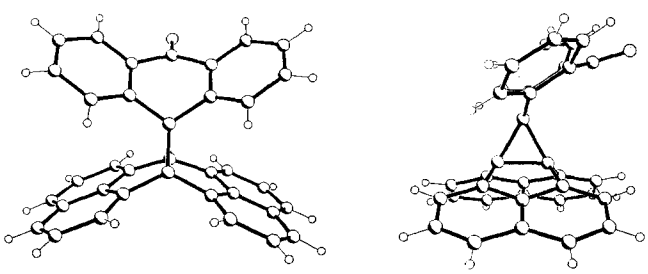

Fig. 2. Two views of the molecular structure of **11** in the crystal (arbitrary radii) [8].

Table 1. Selected physical and spectroscopic data for compounds **6**, **7**, **9**, **10**, and **11** [6]. ^{1}H NMR measurements: 400 MHz, $CDCl_3$, TMS; ^{13}C NMR measurements: 100.5 MHz, $CDCl_3$.

6: colorless crystals, m.p. 329 °C (decomp.); ^{1}H NMR: δ = 6.89 (m, 4 H), 7.35–7.44 (m, 8 H), 7.60 (m, 4 H), 8.22 ("d", "J" = 6.9 Hz, 4 H); MS (70 eV): m/z (%): 610/612/614 (0.3/0.6/0.3, M^+), 530/532 (0.3/0.3), 452 (3), 334/336/338 (2/4/2), 277 (26), 276 (100), 176 (5)

7: colorless crystals, rapid discoloration above 200 °C; ^{1}H NMR: δ = 6.76 (m, 4 H), 7.16 (m, 4 H), 7.30 (dd, J = 8.2, 7.0 Hz, 4 H), 7.46 (dd, J = 8.2, 1.1 Hz, 4 H), 7.52 (dd, J = 7.0, 1.1 Hz, 4 H); ^{13}C NMR: δ = 123.53 (d), 125.01 (d), 125.18 (d), 125.29 (d), 126.61 (s), 127.67 (d), 134.25 (s), 139.59 (s), 144.85 (s), 147.25 (s), 147.56 (s); UV/Vis (acetonitrile): λ_{max} (log ε) = 208 nm (4.940), 224 (sh, 4.736), 276 (3.926), 286 (3.984), 308 (3.991), 316 (3.971); MS (70 eV): m/z (%): 452 (9, M^+), 372 (8), 358 (7), 250 (10), 233 (10), 232 (15), 231 (94), 217 (16), 216 (100), 184 (35), 108 (20)

9: colorless crystals, decomp. above 190 °C; ^{1}H NMR: δ = 6.75–6.85 (m, 4 H), 7.10–7.16 (m, 4 H), 7.27–7.34 (m, 4 H), 7.44–7.50 (m, 4 H), 7.59 (dd, J = 7.0, 1.2 Hz, 2 H), 7.88 (dd, J = 7.1, 1.2 Hz, 2 H); MS (70 eV): m/z (%): 469 (41), 468 (100, M^+), 467 (21), 437 (26), 341 (23), 276 (51)

10: colorless crystals, decomp. above 240 °C; ^{1}H NMR: δ = 6.83 (m, 4 H), 7.14 (m, 4 H), 7.31 (dd, J = 8.2, 7.1 Hz, 4 H), 7.48 (dd, J = 8.2, 1.3 Hz, 4 H), 7.94 (dd, J = 7.1, 1.3 Hz, 4 H); MS (70 eV): m/z (%): 485 (7), 484 (17, M^+), 469 (12), 468 (31), 277 (23), 276 (100), 274 (16)

11: yellow crystals, rapid discoloration above 200 °C; ^{1}H NMR: δ = 6.34 ("d", "J" = 7.8 Hz, 2 H, H-4',5'), 6.56 (m, 2 H), 6.90 (m, 2 H), 7.20 (m, 2 H), 7.41–7.45 (m, 4 H), 7.63 (m, 2 H), 7.67–7.72 (m, 4 H), 8.15 ("d", "J" = 6.5 Hz, 2 H, H-1,12); ^{13}C NMR: δ = 57.77 (s), 60.95 (s), 65.26 (s), 121.89 (d), 122.05 (d), 123.86 (d), 124.91 (d), 125.70 (d), 125.98 (d), 126.67 (d), 127.73 (d), 127.98 (d), 129.33 (d), 131.53 (s), 136.50 (s), 140.40 (s), 142.25 (s), 142.51 (s), 142.61 (s), 188.46 (s); IR (KBr): $\tilde{\nu}$ = 3047 cm^{-1} (w), 3062 (w), 1672 (s), 1497 (s), 1301 (m), 933 (m), 784 (s), 773 (s), 703 (m); UV/Vis (acetonitrile): λ_{max} (log ε) = 220 nm (4.914), 228 (sh, 4.843), 276 (sh, 4.150), 296 (4.323), 306 (sh, 4.213), 314 (sh, 4.150), 320 (sh, 3.987), 330 (sh, 3.674); MS (70 eV): m/z (%): 469 (38), 468 (100, M^+), 439 (12), 437 (15), 341 (14), 276 (21)

We will continue to investigate dibromoanthracene **5** as a building block for the synthesis of alkenes with unusual structures and reactivities.

Experimental Procedure

6: A mixture of **4** (276 mg, 1.00 mmol) and **5** (1.01 g, 3.00 mmol) was ground to homogeneity, then allowed to react under nitrogen in a sealed ampule for 3 h at 220–225 °C (the melting point must be reached; at 200 °C no reaction takes place). Unreacted **5** was removed by sublimation at 220 °C/0.1 Torr, and the residue was purified by column chromatography (toluene/silica gel) and crystallization from $CHCl_3$. Yield: 477 mg (78%) **6**.

7: A solution of triphenylmethane (5.80 g, 19.0 mmol) in 50 mL of THF was treated at 0 °C with 7 mL of 15% *n*-butyllithium/*n*-hexane. After 2 h of stirring, a solution of **6** (986 mg, 1.60 mmol) in 100 mL of THF was added. Stirring was continued for a further 4 h at room temperature, and the mixture was then hydrolyzed with 5 mL of ethanol and 100 mL of water. After extraction with Et_2O (3 × 150 mL), the organic phase was adsorptively filtered through silica gel and the solvent removed by distillation. The crude product was digested with 400 mL of pentane, and the residue was dissolved in ethanol, adsorptively filtered through silica gel, and fractionally crystallized from ethanol. Yield: 572 mg (79%) **7**.

Received: May 30, 1995 [Z 8042 IE]
German version: *Angew. Chem.* **1995**, *107*, 2743–2745

Keywords: oxidations · propellanes · pyramidalized alkenes · rearrangements

[1] a) W. T. Borden, *Chem. Rev.* **1989**, *89*, 1095–1109; b) R. C. Haddon, *J. Am. Chem. Soc.* **1990**, *112*, 3385–3389; c) P. Camps, M. Font-Bardia, F. Perez, X. Solans, S. Vazquez, *Angew. Chem.* **1995**, *107*, 1011–1012; *Angew. Chem. Int. Ed. Engl.* **1995**, *34*, 912–914, and references therein.

[2] K. B. Wiberg, R. D. Adams, P. J. Okarma, M. G. Matturo, B. Segmuller, *J. Am. Chem. Soc.* **1984**, *106*, 2200–2206.

[3] a) R. L. Viavattene, F. D. Greene, L. D. Cheung, R. Majeste, L. M. Trefonas, *J. Am. Chem. Soc.* **1974**, *96*, 4342–4343; b) R. C. Haddon, *ibid.* **1990**, *112*, 8217; c) R. Herges, H. Neumann, F. Hampel, *Angew. Chem.* **1994**, *106*, 1024–1026; *Angew. Chem. Int. Ed. Engl.* **1994**, *33*, 993–995.

[4] H. Prinzbach, K. Weber, *Angew. Chem.* **1994**, *106*, 2329–2348; *Angew. Chem. Int. Ed. Engl.* **1994**, *33*, 2239–2257.

[5] G. Dyker, *Tetrahedron Lett.* **1991**, *32*, 7241–7242.

[6] The new compounds **6**, **7**, **9**, **10**, and **11** were characterized completely by spectroscopic methods (IR, UV, ^{1}H NMR, ^{13}C NMR, MS) (selected data in Table 1).

[7] W.-D. Fessner, B. A. R. C. Murty, P. R. Spurr, R. Pinkos, J.-P. Melder, H. Fritz, H. Prinzbach, *Chem. Ber.* **1992**, *125*, 1697–1717.

[8] Crystal structure data: **7**·$CHCl_3$ at −130 °C: monoclinic, $P2_1/n$, a = 1305.4(4), b = 941.5(3), c = 2189.2(6) pm, β = 92.05(3)°, V = 2.6889(14) nm^3, Z = 4, θ_{max} = 25°, $wR(F)^2$ = 0.309 for 4643 reflections, $R(F)$ = 0.096. Colorless prisms, 0.6 × 0.2 × 0.2 mm^3 (lower precision due to the presence of $CHCl_3$). **11** at −100 °C: monoclinic, $P2_1/c$, a = 1295.67(12), b = 1160.98(12), c = 1545.62(12) pm, β = 95.606(8)°, V = 2.3139(4) nm^3, Z = 4, θ_{max} = 25°, $wR(F)^2$ = 0.092 for 4073 reflections, $R(F)$ = 0.039. Yellowish tablets, 0.6 × 0.6 × 0.25 mm^3. The crystals were mounted in an inert oil; $Mo_{K\alpha}$ radiation, Stoe-Stadi-4 diffractometer for **7**, Siemens-P4 diffractometer for **11**. The structures were solved by direct methods and refined anisotropically against F^2 (Program SHELXL-93, G. M. Sheldrick, Universität Göttingen); H atoms were treated using a riding model. Further details of the crystal structure investigation may be obtained from the Fachinformationszentrum Karlsruhe, D-76344 Eggenstein-Leopoldshafen (Germany) on quoting the depository numbers CSD-401893 for **7** and CSD-401895 for **11**.

[9] W. Adam, *Chem. Unserer Zeit* **1981**, *15*, 190–196.

[10] a) R. W. Murray, *Chem. Rev.* **1989**, *89*, 1187–1201; b) W. Adam, L. Hadjiarapoglou, *Top. Curr. Chem.* **1993**, *164*, 45–62; c) W. Adam, J. Bialas, L. Hadjiarapoglou, *Chem. Ber.* **1991**, *124*, 2377; d) G. Dyker, *J. Prakt. Chem.* **1995**, *337*, 162–163.

[11] For the preparation of a cyclopropane by rearrangement of the monoepoxide of norbornadiene, see: J. Meinwald, S. S. Labana, M. S. Chadha, *J. Am. Chem. Soc.* **1963**, *85*, 582–585..

[12] S. Rosenfeld, C. W. Tingle, I. Abdelmoty, J. P. Jasinski, J. E. Whittum, R. C. Woudenberg, *J. Org. Chem.* **1995**, *60*, 751–753.

[13] According to semiempirical calculations (AM1) the activation barrier for the inversion of the anthrone unit is ca. 23.6 kcal mol^{-1}.

Soluble Aluminosilicates with Frameworks of Minerals**

Mavis L. Montero, Andreas Voigt, Markus Teichert, Isabel Usón, and Herbert W. Roesky*

Dedicated to Professor Edwin Hengge on the occasion of his 65th birthday

In the last century the American philosopher Ralph Waldo Emerson wrote that "it is a long way from granite to the oyster".[1, 2] An important component of granite is an aluminosilcate; the Al-O-Si fragment found therein is the most important unit of many natural and synthetic zeolites. Compounds of this type are used as ion-exchangers, acid-base catalysts, or as supports for metal catalysts.[3, 4]

We have been interested in the synthesis of aluminosilicates with different frameworks for a long time.[5, 6] We recently reported the details of a structural unit present in the mineral gismondine.[5] A large number of rocks and minerals comprise

[*] Prof. Dr. H. W. Roesky, Dipl.-Chem. M. L. Montero, Dipl.-Chem. A. Voigt, M. Teichert, Dr. I. Usón
Institut für Anorganische Chemie der Universität
Tammannstrasse 4, D-37077 Göttingen (Germany)
Telefax: Int. code + (551)393373

[**] This work was supported by the Deutsche Forschungsgemeinschaft, the Fonds der Chemischen Industrie, the Bundesministerium für Bildung and Forschung, and the Hoechst AG. I. U. thanks the European Union for a postdoctoral fellowship (ERB CHBG 930338).

alkali metal aluminosilicates. Among these are the feldspars, which often have a silicon–aluminum ratio close to one. Examples include the natural zeolites cancrinite ($Na_6Al_6Si_6O_{24}\cdot CaCO_3\cdot 2H_2O$) and sodalite ($Na_8Al_6Si_6O_{24}(OH)_2\cdot 2H_2O$) which are both used industrially.[7] Synthetic compounds belonging to this class are zeolites of the Linde type A (LTA) with the ideal composition $Na_{12}Al_{12}Si_{12}O_{48}\cdot 27H_2O$.[7] A characteristic structural feature of LTA is the cubic $Al_4Si_4O_{12}$ unit. We report here on the synthesis of $Al_4Si_4O_{12}$ and $Na_4Al_4Si_4O_{12}$ compounds that are soluble in organic solvents.

Molecular aluminosiloxanes, which function as model substances for zeolites, are known.[5, 6, 8–12] Feher et al. synthesized an aluminosilsesquioxane by the "corner-capping" reaction of $(cyclo\text{-}C_6H_{11})_7Si_7O_9(OH)_3$ with $AlMe_3$.[12] Aluminosiloxanes could also be synthesized from aqueous tetramethylammonium silicate and tetramethylammonium aluminate solutions.[8] In 1987 Smolin et al. described the compound $[(CH_3)_4N]_4[Si_4Al_4O_{12}(OH)_8]$.[9] Disadvantages of these reactions include the low flexibility with respect to the products that can be synthesized and the often uncontrollable course of the reaction.

We have previously synthesized various heterosiloxanes by using kinetically stable silanetriols.[5, 6, 13, 14] The silanetriols enable the synthesis of compounds with different skeletons. We report here on the reaction of the stable silanetriol **1** with alkylaluminum compounds. Elimination of alkane or hydrogen leads to **2a** and **2b**, respectively (Scheme 1). The reaction course

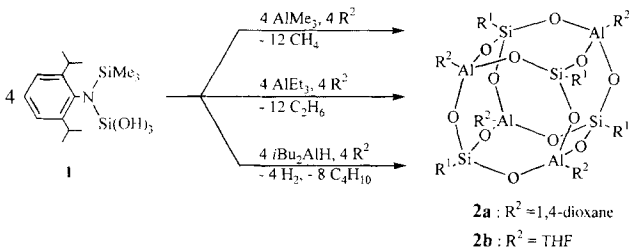

Scheme 1. Synthesis of **2a** and **2b**. $R^1 = (2,6\text{-}iPr_2C_6H_3)(SiMe_3)N$, R^2 = 1,4-dioxane or THF.

can be followed by monitoring the amounts of gas collected. The reaction is complete within about 2 min. The addition of a donor solvent, such as THF or 1,4-dioxane, is necessary to saturate the fourth coordination site on the aluminum atoms.

In contrast to this reaction, an organic group remains bound to aluminum when **1** is allowed to react with $Na[Et_2AlH_2]$ to form **3** (Scheme 2). Compound **3** is the first sodium aluminosilicate that is soluble in common organic solvents (diethyl ether, THF, toluene).

The structures of **2a** (Fig. 1), **2b**, and **3** (Fig. 2) comprise a cubic-shaped $Al_4Si_4O_{12}$ core built up of two eight-membered $Al_2Si_2O_4$ rings connected to each other by four oxygen

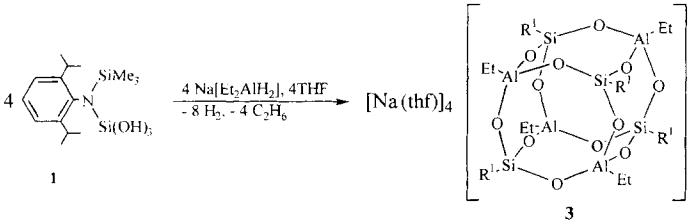

Scheme 2. Synthesis of **3**. $R^1 = (2,6\text{-}iPr_2C_6H_3)(SiMe_3)N$.

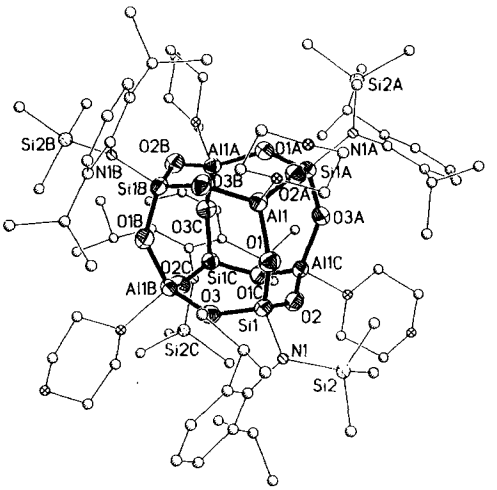

Fig. 1. Structure of **2a** in the crystal. Selected distances [pm] and angles [°]: Al1–O1 170.8 (3), Al1–O2 170.6 (3), Al1–O3 170.6 (3), Al1–O4 188.0 (3), Si1–O1 161.2 (3), Si1–O2 161.0 (3), Si1–O3 160.9 (3), Si1–N1 173.8 (3), O2–Al1–O1 113.9 (1), O2–Al1–O3 115.3 (1), O3–Al1–O1 117.6 (1), O3–Si1–O2 111.2 (2), O3–Si1–O1 109.8 (2), O2–Si1–O1 109.1 (2).

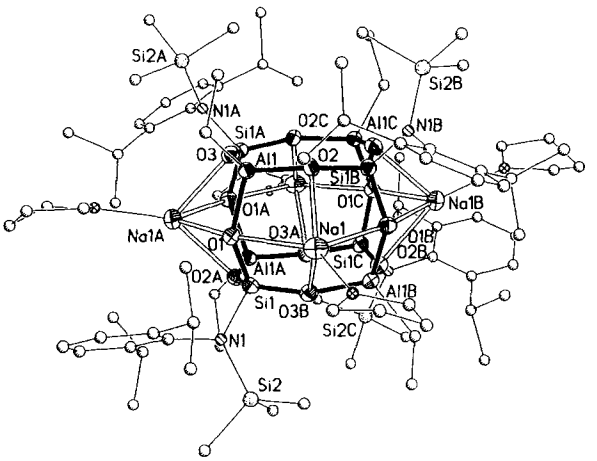

Fig. 2. Structure of **3** in the crystal. Selected distances [pm] and angles [°]: Al1–O1 178.4 (4), Al1–O2 175.4 (4), Al1–O3 175.3 (4), Al1–C1 196.0 (6), Si1–O1 162.8 (4), Si1–O2 160.3 (4), Si1–O3 161.1 (4), Si1–N1 174.0 (5), O3–Al1–O2 116.0 (2), O3–Al1–O1 104.5 (2), O2–Al1–O1 103.9 (2), O2–Si1–O3 112.9 (2), O2–Si1–O1 107.2 (2), O3–Si1–O1 110.1 (2).

atoms.[15] The same structural unit is also found in the zeolite of the Linde type A. The $Al_2Si_2O_4$ rings are in a chair–chair conformation. In **3**, four of the faces of the cube are capped by a sodium atom. The two remaining faces of the cube which have no contact with the sodium atoms are almost planar (7 pm deviation).[16] The coordination at the aluminum centers in **2a** is distorted tetrahedral; the bond angles range from 101.0(1)° to 117.6(1)°. The endocyclic Al–O bonds in **2a** are on average 171 pm long. As expected, the exocyclic Al–O bonds to the coordinated 1,4-dioxane are longer (188.0(3) pm). The silicon atoms of the core have almost ideal tetrahedral coordination; the bond angles range from 107.6(2)° to 111.2(2)°. The average Si–O bond length is 161 pm. The body diagonal of the Si_4Al_4 core in **2a** is about 540 pm, and the cubic-shaped core in **2b** is similar to that in **2a**. Owing to disorder in the core, a more detailed discussion of its structural parameters will be avoided. The coordination around the aluminum centers in **3** is distorted tetrahedral; the bond angles range from 103.9(2)° to 116.0(2)°. As expected, the endocyclic Al–O bonds (average 176 pm) are

longer than those in **2a** as a result of coordination to the fourth anionic ligand. The silicon atoms of the core also have distorted tetrahedral coordination (106.3(2)° to 112.9(2)°). The average Si–O bond length is 161 pm, and all experimentally determined Si–O bond lengths correspond well with those in aluminosilicates (ca. 160–161 pm).[17] Good agreement of the Al–O bond lengths with those in aluminosilicates (ca. 174–176 pm)[17] is only found for **3**. The sodium atoms in **3** are coordinated to the oxygen atoms of the cage through two shorter (240.5(4) and 241.5(4) pm) and two longer (257.4(4) and 267.1(4) pm) distances. The length of the bond between the Na atom and the oxygen of the coordinated THF molecule is 228.5(5) pm. Similar square-pyramidal environments for the Na atoms are found in the sodium zeolite A (Na–O distances of ca. 232–293 pm).[18, 19]

The syntheses of **2a** and **2b** show that cubane-like aluminosiloxanes can be obtained readily by choosing suitable reaction conditions. A large number of natural and synthetic zeolites have alkali metal counterions in addition to the anionic aluminosilicate framework. Earlier attempts to build an anionic lattice did not lead to the desired products.[12] Thus, reactions of $MOSiMe_3$ (M = alkali metal) with aluminosiloxanes resulted in the degradation of the aluminosiloxane framework. The reaction method leading to **3** seems to be suitable for a broad range of products of varying compositions. It remains to be seen, how many related, soluble compounds with Al-O-Si units can be synthesized. Products such as **3** could serve as precursors for novel solid-state syntheses under mild conditions.

Experimental Procedure

General procedure for **2a** and **2b**: A suspension of **1** (1.63 g, 5.00 mmol) in *n*-hexane (30 mL) and 1,4-dioxane or THF (5 mL) was treated with the aluminum compound (5.00 mmol) in *n*-hexane at room temperature. After about 2 min three equivalents of gas had been formed. The solution was concentrated to half its volume in vacuum. A white, microcrystalline solid was obtained at −21 °C (yield: 60–70%). Single crystals were obtained at 0 °C from *n*-hexane/1,4-dioxane and *n*-hexane/THF (10:1), respectively. **2a**: M.p. 127 °C; ^{1}H NMR (250 MHz, $CDCl_3$, TMS): $\delta = -0.05$(s, 9H, $Si(CH_3)_3$), 1.18 (d, 6H, $CH(CH_3)_2$), 1.26 (d, 6H, $CH(CH_3)_2$), 2.92 (m, 2H, $CH(CH_3)_2$), 3.53 (m, 4H, 1,4-dioxane), 3.60 (m, 4H, 1,4-dioxane), 6.92 (m, 3H, H_{arom}); ^{29}Si NMR (50 MHz, C_6D_6, TMS): $\delta = -80.3$ (SiO_3), 2.0 ($Si(CH_3)_3$); IR (KBr, nujol): $\tilde{\nu}$ = 1383, 1249, 1053, 958, 910, 804, 685, 543 cm^{-1}; MS (EI, *m/z* (%)): 1389 (10) $[C_{59}H_{101}Al_4N_4O_{12}Si_8]^+$, 162 (100) $[C_{12}H_{18}]^+$; correct elemental analysis. **2b**: M.p. > 200 °C (decomp.); ^{1}H NMR (250 MHz, C_6D_6, TMS): $\delta = 0.32$ (s, 9H, $Si(CH_3)_3$), 1.25 (m, 4H, THF), 1.35 (d, 6H, $CH(CH_3)_2$), 1.41 (d, 6H, $CH(CH_3)_2$), 3.45 (m, 4H, THF), 4.00 (m, 2H, $CH(CH_3)_2$), 7.02 (m, 3H, H_{arom}); ^{29}Si NMR (50 MHz, C_6D_6, TMS): $\delta = -75.0$ (SiO_3), 1.2 ($Si(CH_3)_3$); IR (KBr, nujol): $\tilde{\nu}$ = 1440, 1360, 1247, 1077, 943, 837, 544, 491 cm^{-1}; MS (EI, *m/z* (%)): 1069 (20) $[C_{45}H_{61}Al_4N_4O_{12}Si_4]^+$, 162 (100) $[C_{12}H_{18}]^+$; correct elemental analysis.

3: A solution of **1** (0.98 g, 3.00 mmol) in toluene (30 mL) was slowly added to a solution of $Na[Et_2AlH_2]$ (0.33 g, 3.00 mmol) in toluene/THF (15 mL/0.5 mL) at 0 °C. The solution was allowed to warm to room temperature and was then heated at reflux for 2 h. Afterwards, it was concentrated to half its volume in vacuum. Compound **3** was obtained as a white, microcrystalline solid at −21 °C (yield: 0.5 g, 35%). Single crystals were obtained at room temperature from toluene/THF (10:1). M.p. > 200 °C (decomp) ^{1}H NMR (250 MHz, [D$_8$]THF, TMS): $\delta = -0.32$ (m, 2H, CH_2CH_3), −0.10 (m, 3H, CH_2CH_3), 0.08 (s, 9H, $Si(CH_3)_3$), 1.21 (d, 12H, $CH(CH_3)_2$), 1.82 (m, 4H, THF), 3.00 (m, 2H, $CH(CH_3)_2$), 3.65 (m, 4H, THF), 7.13 (m, 3H, H_{arom}); ^{29}Si NMR (50 MHz, [D$_8$]THF, TMS): $\delta = -112$ (SiO_3), −1 ($Si(CH_3)_3$);); IR (KBr, nujol): $\tilde{\nu}$ = 1250, 1046, 936, 840, 767, 643, 547, 490 cm^{-1}; MS (EI, *m/z* (%)): 1479 (20) $[C_{61}H_{103}Al_4N_4Na_4O_{12}Si_4]^+$, 162 (100) $[C_{12}H_{18}]^+$; correct elemental analysis.

Received: June 26, 1995 [Z 8134 IE]
German version: *Angew. Chem.* **1995**, *107*, 2761–2763

Keywords: aluminosilicates · silanetriols · zeolites

[1] P. Ball, *Designing the Molecular World*, Princeton University Press, Princeton, USA, **1994**.

[2] The mineralization product from oysters is mainly calcium carbonate: H. Füchtbauer, *Sedimente und Sedimentgesteine*, E. Schweizerbart, Stuttgart, **1988**.

[3] R. L. Schneider, R. F. Howe, K. L. Watters, *J. Catal.* **1983**, *79*, 298.

[4] M. Ichikawa, L. R. Rao, A. Fukuoka in *Catalytic Science and Technology Vol. 1*, Proc. First Tokyo Conf. Adv. Catal. Sci. Technol. Tokyo, 1.–5. July 1990, VCH, Weinheim, **1991**.

[5] M. L. Montero, I. Usón, H. W. Roesky, *Angew. Chem.* **1994**, *106*, 2198; *Angew. Chem. Int. Ed. Eng.* **1994**, *33*, 2103.

[6] N. Winkhofer, U. Ritter, A. Voigt, D. Stalke, H. W. Roesky, unpublished.

[7] J. V. Smith, *Chem. Rev.* **1988**, *88*, 149.

[8] D. Hoebbel, G. Garzó, K. Ujszászi, G. Engelhardt, B. Fahlke, A. Vargha, *Z. Anorg. Allg. Chemie* **1982**, *484*, 7.

[9] Yu. I. Smolin, Yu. F. Shepelev, A. S. Ershov, D. Khobbel, *Dokl. Akad. Nauk SSSR* **1987**, *297*, 1377; *Chem. Abstr.* **1988**, *108*, 229950f.

[10] G. Fu, C. A. Fyfe, W. Schwieger, G. T. Kokotailo, *Angew. Chem.* **1995**, *107*, 1582; *Angew. Chem. Int. Ed. Eng.* **1995**, *34*, 1499.

[11] F. J. Feher, T. A. Budzichowski, K. J. Weller, *J. Am. Chem. Soc.* **1989**, *111*, 7288.

[12] F. J. Feher, K. J. Weller, *Organometallics* **1990**, *9*, 2638.

[13] N. Winkhofer, H. W. Roesky, M. Noltemeyer, W. D. Robinson, *Angew. Chem.* **1992**, *104*, 670; *Angew. Chem. Int. Ed. Engl.* **1992**, *31*, 599.

[14] N. Winkhofer, A. Voigt, H. Dorn, H. W. Roesky, A. Steiner, D. Stalke, A. Reller, *Angew. Chem.* **1994**, *106*, 1414; *Angew. Chem. Int. Ed. Engl.* **1994**, *33*, 1352.

[15] Crystal structure analysis of **2a**: $C_{76}H_{136}Al_4N_4O_{20}Si_8 + 4/3\,C_6H_{14}$, M_r = 1758.53 + 4/3 86.18, cubic, space group $I\bar{4}3d$, $a = b = c$ = 3147.8(2) pm, V = 31.1919(4) nm^3, Z = 12, ρ_{calcd} = 1.197 Mg m^{-3}, $F(000)$ = 12128, λ = 71.073 pm, T = 193 K, $\mu(Mo_{K\alpha})$ = 0.200 mm^{-1}, crystal dimensions: 0.75 × 0.50 × 0.35 mm, 7° < 2θ < 45°; of 6784 collected reflections 3396 were independent and 3394 were used for the structural refinement of 314 parameters with the help of 55 restraints. $R1 = \Sigma||F_o| - |F_c||/\Sigma|F_o| = 0.0431$ ($F > 4\sigma F$) and $wR2 = [\Sigma[w(F_o^2 - F_c^2)^2]/\Sigma[w(F_o^2)^2]]^{1/2} = 0.0961$ (complete data); minimum/maximum residual electron density: 174/−212 e nm^{-3}. Crystal structure analysis of **2b**: $C_{76}H_{136}Al_4N_4O_{16}Si_8 + 4C_4H_8O$, M_r = 1694.96 + 4 72.10, tetragonal, space group $I4_1/a$, $a = b$ = 2757.8(1), c = 1446.9(1) pm, V = 11.0039(9) nm^3, Z = 4, ρ_{calcd} = 1.197 Mg m^{-3}, $F(000)$ = 4288, λ = 71.073 pm, T = 153 K, $\mu(Mo_{K\alpha})$ = 0.192 mm^{-1}, crystal dimensions: 0.60 × 0.50 × 0.20 mm, 7° < 2θ < 45°; of 5689 collected reflections 3583 were independent and 3583 were used for the structural refinement of 359 parameters with the help of 283 restraints. $R1$ = 0.0951 ($F > 4\sigma F$) and $wR2$ = 0.2884 (complete data); minimum/maximum residual electron density: 408/−466 e nm^{-3}. Crystal structure analysis of **3**: $C_{84}H_{156}Al_4N_4Na_4O_{16}Si_8 + 4/3\,C_4H_8$, M_r = 1902.72 + 4/3 92.14, cubic, space group $P\bar{4}3n$, $a = b = c$ = 2675.6(2) pm, V = 19.1540(2) nm^3, Z = 6, ρ_{calcd} = 1.054 Mg m^{-3}, $F(000)$ = 6544, λ = 71.073 pm, T = 153 K, $\mu(Mo_{K\alpha})$ = 0.177 mm^{-1}, crystal dimensions: 0.60 × 0.55 × 0.45 mm, 5° > 2θ > 45°; of 14159 collected reflections 3651 were independent and 3646 were used for the structural refinement of 295 parameters with the help of 14 restraints. $R1$ = 0.0584 ($F > 4\sigma F$) and $wR2$ = 0.1867 (complete data); minimum/maximum residual electron density: 543/−341 e nm^{-3}. All data were collected on a Stoe–Siemens–Huber four-circle diffractometer. The reflections were measured on a cooled crystal in a drop of oil [20] by the Learnt-profile method [21]. The structures were solved by direct methods (SHELXS-90) [22] and refined versus F^2 by the least squares method [23]. All non-hydrogen atoms, excluding the carbon atoms in the free toluene molecule in **3**, were anisotropically refined. The hydrogen atoms were included in idealized positions. The disorder in the cages and the coordinated THF molecule in **2b** as well as all free solvent molecules in **2a**, **2b**, and **3** were refined with distance and ADP restraints. Further details of the crystal structure investigation may be obtained from the Director of the Cambridge Crystallographic Data Center, 12 Union Road, GB-Cambridge CB2 1EZ (UK), on quoting the complete journal citation.

[16] SHELXTL-PLUS *Software Package for the Determination of Crystal Structures*, Release 5.03; Siemens Analytical X-Ray Instruments, Inc., Madison, WI, USA, **1990**.

[17] J. B. Jones, *Acta Crystallogr. Sect. B* **1968**, *24*, 355.

[18] J. J. Pluth, J. V. Smith, *J. Am. Chem. Soc.* **1980**, *102*, 4704.

[19] J. M. Adams, D. A. Haselden, A. W. Hewat, *J. Solid State Chem.* **1982**, *44*, 245.

[20] T. Kottke, D. Stalke, *J. Appl. Crystallogr.* **1993**, *26*, 615.

[21] W. Clegg, *Acta Crystallogr. Sect. A* **1983**, *39*, 158.

[22] G. M. Sheldrick, *Acta Crystallogr. Sect. A* **1990**, *46*, 467.

[23] G. M. Sheldrick, SHELXL-93, program for crystal structure refinement, Göttingen, **1993**.

An Unconventional Intermolecular Three-Center N–H···H_2Re Hydrogen Bond in Crystalline $[ReH_5(PPh_3)_3]\cdot$indole$\cdot C_6H_6$

Jeremy Wessel, Jesse C. Lee, Jr., Eduardo Peris, Glenn P. A. Yap, Jeffrey B. Fortin, John S. Ricci, Gjergji Sini, Alberto Albinati,* Thomas F. Koetzle,* Odile Eisenstein,* Arnold L. Rheingold,* and Robert H. Crabtree*

In the hope of introducing ideas from molecular recognition into transition metal complexation and catalysis, we have been studying hydrogen bonding[1] in metal complexes. H-bonding is common between a weak acid A–H and one or two weak bases B, to give a 2-center (**1**) or three-center H-bond (**2**). In a number of recent cases,[2] for example **3**,[2a] intramolecular H-bonds of

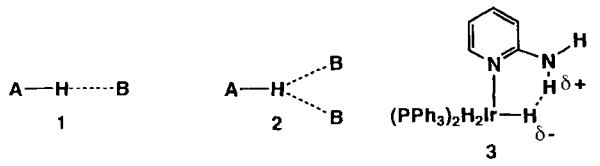

an unconventional kind have been discovered in which the weak base component is a metal hydride. Structural and spectroscopic data[2] suggest H···H distances of about 1.7–1.9 Å and H-bond strengths of 3–6 kcal mol^{-1}. If the Ir–H bond in **3** is replaced by Ir–X (X = F, Cl, Br, or I), conventional N–H···X H-bonds are formed, but surprisingly, these are weaker for X = Cl, Br, and I, and only marginally stronger for X = F.[3] We wanted to find out if intermolecular H-bonding was possible with a suitable H-bond donor AH, and if so, what geometry would be adopted in the absence of geometrical constraints such as those present in the chelate system **3**.

We chose indole because it is a good H-bond proton donor but does not self-associate significantly because it has no good H-bond proton acceptor site. We now find that the polyhydride $[ReH_5(PPh_3)_3]$ cocrystallizes with indole to give $[ReH_5(PPh_3)_3]\cdot C_8H_6NH\cdot C_6H_6$ (**4**) as large yellow crystals. An X-ray crystal structure clearly showed that the N–H hydrogen atom of indole is close to two of the rhenium hydrides, forming a three-center H-bond of type **2**. A subsequent neutron diffraction study (Fig. 1) confirmed this result, and both studies located the hydrogens in positions similar to those found[4] for free $[ReH_5(PMePh_2)_3]$ by neutron diffraction.

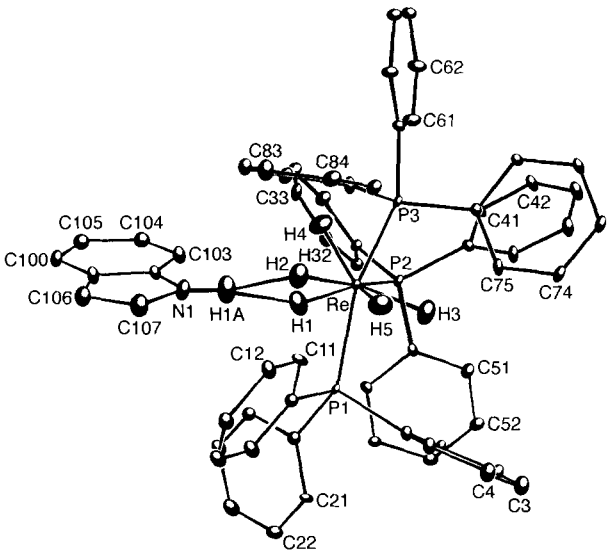

Fig. 1. The ORTEP diagram of the neutron diffraction structure (20 K) of **4** with ellipsoids drawn at 50% probability. The metric parameters of the N–H···H_2Re unit are given in Figure 2. Selected distances [Å] and angles [°]: Re–P1, 2.396(3); Re–P2, 2.387(4); Re–P3, 2.376(3); P1-Re-P2, 110.0(1); P2-Re-P3, 105.6(1); P1-Re-P3, 133.9(1); Re–H1, 1.683(6); Re–H2, 1.683(5); Re–H3, 1.686(5); Re–H4, 1.683(6); Re–H5, 1.681(6); H1-Re-H2, 79.2(3).

A similar compound $[ReH_5(Cyttp)]$ (Cyttp = $[Cy_2P(CH_2)_3]_2PPh$) can be protonated with $HSbF_6\cdot C_6H_6$ to give $[ReH_6(Cyttp)]SbF_6$.[5] In our case, $[ReH_5(PPh_3)_3]$ cocrystallizes with a much weaker acid, indole, to give crystals in which the $L_3H_3ReH_2\cdots H-NC_8H_6$ interaction is strong enough to hold the two components together in the crystal without complete proton transfer. A molecule of benzene was also found, but apart from the $ReH_2\cdots H-N$ interaction, there are no other close contacts in the structure.

The unusually precise neutron diffraction study[6] shows that the two short H···H distances in **4** are very asymmetric (H1A···H1, 2.212(9) Å; H1A···H2, 1.734(8) Å), the shorter being similar to the distances found[2] (1.7–1.9 Å) in the intramolecular N–H···H–M examples. Nonbonding H···H contacts are normally about twice the van der Waals radius[1] of H, or 2.4 Å; all other NH···HRe distances found here are greater than 2.6 Å. The finding that the NH proton lies at a distance of only 0.066(7) Å from the plane defined by N1, H1, and H2 fulfills the usual criteria[1c] for three-center H-bonding (**2**). The N–H bond points towards the closer metal hydride, H2 (N-H-H2 = 163.1(6), N-H-H1 = 130.9(5)°), which implies that the dominant interaction is with Re–H2 (Fig. 2). H2 is unique in that it is the only hydrogen in the structure occupying a B-site

[*] Prof. Dr. R. H. Crabtree, J. Wessel, Dr. J. Lee, Jr., Dr. E. Peris
Yale Chemistry Department
225 Prospect Street, New Haven, CT 06511 (USA)
Telefax: Int. code + (203)432-6144
e-mail: crabtree@minerva.cis.yale.edu

Prof. Dr. A. L. Rheingold, Dr. G. P. A. Yap
University of Delaware Chemistry Department
Newark, DE 19716 (USA)
Telefax: Int. code + (302)-831-6335
e-mail: arnrhein@strauss.udel.edu

Prof. Dr. A. Albinati
Institute of Pharmaceutical Chemistry
University of Milan, I-20131, Milan (Italy)

Dr. T. F. Koetzle
Brookhaven National Laboratory
Upton, NY, 11973 (USA)
Telefax: Int. code + (516)282-5815
e-mail: koetzle@chm.chm.bnl.gov

Prof. Dr. O. Eisenstein
Laboratoire de Chimie Théorique, (URA 506) Bât. 490
Université de Paris-Sud, 91405 Orsay (France)
Telefax: Int. code + (1)60-19-33-02
e-mail: odile.eisenstein@cth.u-psud.fr

J. B. Fortin, Prof. Dr. J. S. Ricci
BNL, Upton, and University of Southern Maine, Portland, ME (USA)

Dr. G. Sini
Université de Cergy-Pontoise (France)

[**] This work was supported by the NSF, the CNRS (URA 506) and Fellowships from the NSF and W. R. Grace & Co. to J. W. The neutron study was carried out at the High Flux Beam Reactor at Brookhaven National Laboratory under contract DE-AC02-76CH00016 with the US Department of Energy, Office of Basic Energy Sciences, Division of Chemical Sciences.

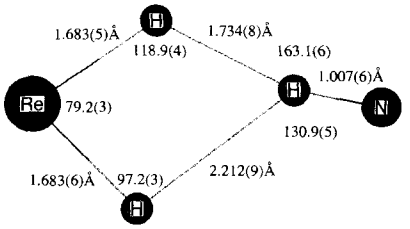

Fig. 2. The detailed structure of the $NH\cdots H_2Re$ unit from the neutron diffraction results.

of a dodecahedron (Fig. 3), and so is sterically the least hindered.

In order to eliminate the possibility that nonspecific crystal packing forces are responsible for the structure, we attempted to grow crystals using indene, which is isosteric with indole but lacking the NH bond. If the $N-H\cdots H$ interaction were not important for holding the supramolecule together, indene ought to cocrystallize just as well as indole. However, only small crystals could be grown under conditions identical to those used for **4** but substituting indene for indole, and these contain only $[ReH_5(PPh_3)_3]$ and no indene (from NMR and IR evidence). This suggests that the $N-H\cdots H$ interaction is indeed important in holding the assembly together and that the very short $H\cdots H$ distance is a result of the H-bonding. Weak aromatic stacking interactions between PPh_3 and indole may well also contribute to the stabilization of the supramolecular assembly, however.

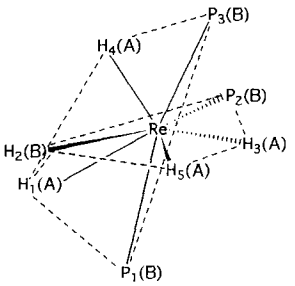

Fig. 3. The dodecahedral coordination geometry in the same molecular orientation as Figure 1 showing A and B sites and the two orthogonal BAAB trapezoids (dotted).

The IR spectrum (KBr pellet) shows a shift in the N–H band from 3437 cm^{-1} in free indole to 3242 cm^{-1} in crystals of **4**. According to the Iogansen equation,[7] which relates the bond strength to the shift in IR frequency, the H-bond strength in this case is 4.3 kcal mol^{-1}, close to the values (3–6 kcal mol^{-1}) determined for intramolecular $M-H\cdots H-N$ interactions.[2]

Figure 2 shows the structural details of the $ReH_2\cdots HN$ interaction. The $N-H\cdots H$ angles are comparable to those seen[1] in standard three-center H-bonds, but the $Re-H\cdots HN$ angles (97.2(3) and 118.9(4)°) are strongly bent. A nonlinear $M-H\cdots HN$ arrangement was already apparent[2a] in **3** ($Ir-H\cdots H = 132°$) and related species[2b] but could have been a result of the constraints of chelation. Now we see that in an unconstrained system like **4**, a strongly nonlinear $ReH\cdots HN$ arrangement is still preferred. This may be because an electrophile tends to attack a σ bond in a side-on manner.[8] In this view, **4** can be considered to represent the earliest stages of protonation of the Re–H2 hydride to give an H_2 complex, which would be bound side-on. This picture suggests other types of σ bonds should show H-bonding behavior; indeed, we have now found similar intramolecular $B-H\cdots H-N$ interactions, with bent $B-H\cdots H-N$ angles, in a number of amine–boranes.[9]

Theoretical work confirms that the interaction is attractive. The model compound $[ReH_5(PH_3)_3]\cdot NH_3$ was studied by ECP ab initio calculations with functional density theory.[10] Free ReH_5L_3 was first optimized and found to be in close agreement with the neutron structure.[4] It was then frozen, and NH_3 was placed in the vicinity of H1 and H2. Geometrical optimization, on a very flat potential surface, of the relative positions of the two molecules gives a structure similar to that of **4**. In particular, a three-center H-bond is preferred over the two- or four-center types, and the asymmetry of the experimental structure is reproduced ($H\cdots H$ distances: 1.92 Å (H2) and 2.48 Å (H1)). The interaction energy of 8 kcal mol^{-1} is in reasonable agreement with experiment (4.3 kcal mol^{-1}). In the theoretical study, the N–H is slightly closer to P1 than is found in **4**; steric effects may be responsible. As is well known,[11] the lone pair in a d^2 dodecahedral complex is perpendicular to both trapezoidal planes. Although in this complex it is not far from H2, it does not point towards the NH bond and so is unlikely to contribute much to the stabilization of the hydrogen bond. This emphasizes the electron donor power of the MH bond, which is also apparent in the ready formation of H_2 complexes by protonation of metal hydrides (even in competition with protonation at the metal),[8] in the ability of M–H in such complexes as $[Cp_2Zr(H)_2(CO)]$[12] to engage in back donation, and in the $M-H/H_2$ "cis effect".[13]

Our studies show that the presence of indole as crystallizing agent for $[ReH_5(PPh_3)_3]$ allows rapid formation of much larger (ca. 5 mm^3) crystals than in its absence, but that the structure of the complex is not significantly altered by H-bonding. Indole may be a useful agent whenever a compound that is a potential H-bond acceptor fails to crystallize satisfactorily for crystallographic or other single-crystal studies; it complements the Ph_3PO agent suggested by Etter[14] for compounds having H-bond donor groups.

Experimental Procedure

The general synthetic and spectroscopic methods were previously described [2a]. Pentahydrido(tristriphenylphosphane)Re^V·indole: A 0.8 mL aliquot of a filtered solution of the complex [15] $[ReH_5(PPh_3)_3]$ (1.1 g, 1.1 mmol) in benzene (10 mL) was added to a test tube containing indole (50 mg, 0.4 mmol). Hexanes were added to form a supernatant layer, and the sample tube refrigerated at 5 °C. After 1 day, large yellow crystals formed (18 mg, 21%).

Received: January 18, 1995
Revised version: August 1, 1995 [Z 7639 IE]
German version: *Angew. Chem.* **1995**, *107*, 2711–2713

Keywords: hydrogen bonding · hydrides · indoles · rhenium compounds

[1] a) G. A. Jeffrey, W. Saenger, *Hydrogen Bonding in Biological Structures*, Springer, Berlin, **1991**; b) ref.[1a], p. 110; c) ref.[1a], p. 22.

[2] a) J. C. Lee, E. Peris, A. L. Rheingold, R. H. Crabtree, *J. Am. Chem. Soc.* **1994**, *116*, 11014; G. P. A. Yap, A. L. Rheingold, P. Das, R. H. Crabtree, *Inorg. Chem.* **1995**, *34*, 3474; b) S. Park, R. Ramachandran, A. J. Lough, R. H. Morris, *J. Chem. Soc. Chem. Commun.* **1994**, 2201. c) A much weaker interaction of the same type is also known: R. C. Stevens, R. Bau, D. Milstein, O. Blum, T. F. Koetzle, *J. Chem. Soc. Dalton Trans.* **1990**, 1429.

[3] E. Peris, J. C. Lee, J. Rambo, O. Eisenstein, R. H. Crabtree, *J. Am. Chem. Soc.* **1995**, *117*, 3485.

[4] a) T. J. Emge, T. F. Koetzle, J. W. Bruno, K. G. Caulton, *Inorg. Chem.* **1984**, *23*, 4012; b) T. F. Koetzle, K. G. Caulton, *ibid.* **1984**, *23*, 4012.

[5] Y. Kim, H. Deng, D. W. Meek, A. Wojcicki, *J. Am. Chem. Soc.* **1990**, *112*, 2798.

[6] a) Neutron diffraction structure of **4** ($M_r = 1173.3$), triclinic, space group $P\bar{1}$; $T = 20$ K; $a = 13.037(3)$, $b = 13.410(4)$, $c = 19.221(5)$ Å, $\alpha = 91.67(2)$, $\beta = 107.79(2)$, $\gamma = 119.02(2)°$, $V = 2733(1)$ Å^3, $Z = 2$, $\varrho_{calcd} = 1.425$ g cm^{-3}, crystal dimensions $3.4 \times 1.9 \times 0.72$ mm^3; $2\theta_{max}$ 91°; $\mu = 1.952$ cm^{-1}; $\lambda_{neutrons} = 1.0462$ Å; scan mode $\omega:2\theta$, 12394 independent reflections observed, all of which were used for refinement; conventional $R(F)$, $[R > 3\sigma(F)] = 0.052$. Measurements carried out at the Brookhaven High Flux Beam Reactor. The crystal was sealed in an Al can under He, mounted in a DISPLEX refrigerator, and placed on the diffractometer. A hemisphere of reciprocal space was sampled, to a limit of $\sin\theta/\lambda = 0.67$ Å^{-1}. The $\omega/2\theta$ step-scan profiles were reduced to integrated intensities, assuming the first and last tenth of each scan to be background. Lorentz factors and absorption corrections (range $e^{-\mu t} = 0.702$–0.865), calculated by means of an analytical procedure [6b], were applied. The crystal was approximated by seven boundary planes, as follows: (010), (001), ($\bar{1}11$), ($\bar{1}1\bar{1}$), ($1\bar{1}2$), ($1\bar{1}0$). Initial coordinates for all atoms were taken from the

X-ray results. Refinements were carried out by a least-squares procedure [6c], minimizing $\Sigma w(F_o^2 - k^2F_c^2)^2$ using all independent data. Weights were assigned as $w = \sigma^{-2}$, where $\sigma^2 = (\sigma_{exp}^2 + (0.015)F_o^2)^2$. The structure model included adjustable positional and anisotropic thermal parameters for all 136 atoms, a scale factor k, and a parameter for an isotropic-type I extinction correction with Lorentzian mosaic spread [6c]. The maximum extinction correction was 10%, for the ($\bar{1}23$) reflection. Neutron scattering lengths were taken from a recent compilation by Sears [6b]: $b_C = 0.66484$, $b_H = -0.3741$, $b_N = 0.936$, $b_P = 0.513$, $b_{Re} = 0.920$ (all $\times 10^{-12}$ cm). Further details of the crystal structure investigation are available on request from the Director of the Cambridge Crystallographic Data Centre, 12 Union Road, GB-Cambridge CB2 1EZ (UK), on quoting the full journal citation. b) J. DeMeulenaer, H. Tompa, *Acta Crystallogr.* **1965**, *19*, 1014; L. K. Templeton, D. H. Templeton, *Am. Crystallogr. Assoc. Mtg.*, Storrs, CT Abstract E10, **1973**; c) J.-O. Lundgren, *Crystallographic Computer Programs* in Report UUIC-B13-4-05, Institute of Chemistry, University of Uppsala, Sweden, **1982**. d) P. Becker, P. Coppens, *Acta Crystallogr. Sect. A* **1974**, *30*, 129; *ibid.* **1975**, *31*, 417; e) V. F. Sears in *International Tables for Crystallography, Vol. C* (Ed.: A. J. C. Wilson), Kluwer, Academic Publishers, Dordrecht, **1993**.

[7] S. G. Kazarian, P. A. Hamley, M. Poliakoff, *J. Am. Chem. Soc.* **1993**, *115*, 9069.

[8] R. H. Crabtree, *Angew. Chem.* **1993**, *105*, 828; *Angew. Chem. Int. Ed. Engl.* **1993**, *32*, 789.

[9] T. Richardson, S. deGala, P. E. M. Siegbahn, R. H. Crabtree, *J. Am. Chem Soc.*, submitted.

[10] a) Gaussian 92/DFT, Revision F.4; M. J. Frisch, G. W. Trucks, H. B. Schlegel, P. M. W. Gill, B. G. Johnson, M. W. Wong, J. B. Foresman, M. A. Robb, M. Head-Gordon, E. S. Replogle, R. Gomperts, J. L. Andres, K. Raghavachari, J. S. Binkley, C. Gonzales, R. L. Martin, D. J. Fox, D. J. Defrees, J. Baker, J. J. P. Stewart, J. A. Pople, Gaussian Inc., Pittsburgh, PA, **1992** For further details of the calculation see ref.[10b]. b) For Re, a relativistic ECP [10c] was chosen. The valence shell of Re includes the 5s, 5p with a basis set of triple ζ quality. For P, the ECP of Stevens and Basch [10d] was chosen with a double ζ basis set plus polarization. Indole was represented by a planar NH_3. The hydrides are represeuted by a triple ζ basis set with polarization and the H of PH_3 by a single ζ basis set. For the functional density, we used the hybrid functions of Becke (B3LYP) [10e]. c) D. Andrae, U. Haussermann, M. Dolg, H. Stoll, H. Preuss, *Theor. Chim. Acta* **1990**, *77*, 123; d) W. J. Stevens, H. Bash, M. Krauss, *J. Chem. Phys.* **1984**, *12*, 6026. e) A. D. Becke, *J. Chem. Phys.* **1993**, *98*, 5648; P. J. Stevens, F. J. Devlin, C. F. Chablowski, M. J. Frish, *ibid.* **1994**, *98*, 11623.

[11] J. K. Burdett, R. Hoffmann, R. C. Fay, *Inorg. Chem.* **1978**, *17*, 2553.

[12] J. M. Manriquez, D. R. McAlister, R. D. Sanner, J. E. Bercaw, *J. Am. Chem. Soc.* **1978**, *100*, 2716; *ibid.* **1976**, *98*, 6733.

[13] L. S. Van der Sluys, J. Eckert, O. Eisenstein, J. H. Hall, J. C. Huffman, S. A. Jackson, T. F. Koetzle, G. J. Kubas, P. J. Vergamini, K. G. Caulton, *J. Am. Chem. Soc.* **1990**, *112*, 4831.

[14] M. C. Etter, *Acc. Chem. Res.* **1990**, *23*, 120.

[15] J. Chatt, R. S. Coffey, *J. Chem. Soc. A* **1969**, 1963.

Hydrothermal Synthesis of a Novel Se_{12} Ring in $[\{(NH_4)_2[Mo_3S_{11.72}Se_{1.28}]\}_2[Se_{12}]]$**

Richard A. Stevens, Casey C. Raymond, and Peter K. Dorhout*

Since their discovery,[1] the $[Mo_3S_{13}]^{2-}$ core clusters have spurred researchers on to further study. Electron-poor, trinuclear molybdenum chalcogenides, sulfides in particular, have aroused considerable interest because of their hydrodesulfurization activity.[2] New ventures into trinuclear molybdenum polychalcogenide chemistry have yielded several new "polymeric" materials: $[Mo_9Se_{40}]^{8-}$, $[Mo_3Se_{18}]^{2-}$, $[Mo_{12}Se_{56}]^{12-}$, $[Mo_3S_{15}]^{2-}$, and $[Mo_6Se_{27}]^{6-}$.[3,4] In this paper we report the formation of a novel puckered Se_{12} ring, stabilized by $[Mo_3S_{13}]^{2-}$ clusters through interchalcogen interactions. This new form of selenium fits into the Q_n sequence (Q = chalcogen) of homoatomic sulfur ring structures, S_8, S_{10}, S_{12}, ... S_{20}.[5]

Large ring systems of polyselenides and polytellurides have been examined as parts of metal complexes.[6,7] For example, it has been known that selenium and tellurium ions can form complex rings since the isolation of an Se_8^{2+} ring in $[Se_8][AlCl_4]_2$.[8] Kanatzidis has found isolated Se_{11}^{2-} rings in $(Ph_4P)_2[Se_{11}]$. These rings comprise two Se_5^{2-} ions and one Se^{2+} ion and link to form a cluster of corner-sharing "cyclohexane-like" rings of selenium.[9] Very recently, Sheldrick reported that the structure of Cs_3Te_{22} contains a two-dimensional 4^4 network of tellurium Te_6^{3-} ions as well as discrete Te_8 rings.[7]

The synthesis of the above-mentioned polychalcogenides has been achieved through moderate temperature reactions of the elements with oxidizing agents[8]—in the case of polyselenide ions with a mild oxidant[9]—or through methanothermal reactions with the elements.[10] We have had some success in preparing large polysulfide clusters by hydrothermal reactions,[4,11] and we used this synthetic route to prepare the title compound **1**.

$[\{(NH_4)_2[Mo_3S_{11.72}Se_{1.28}]\}_2[Se_{12}]]$ **1**

The hydrothermal reaction of $(NH_4)_2MoS_4$ with A_2S_x (A = Na, K; $x = 2-6$) generally resulted in the formation of a new phase of $(NH_4)_2[Mo_3S_{13}]$.[11] Replacing the polysulfide salt with A_2Se_x (A = Na, K; $x = 2-4$) yielded primarily selenium metal, molybdenum metal, and some soluble polychalcogenides. By preparing a new heteropolychalcogenide salt, $Na_2S_3Se_3$,[12] whose redox potential lies between the polysulfide and polyselenide,[13,14] we were able to tune the chemistry of the redox reaction and isolate compound **1**.

The solid-state structure of **1** is shown in Figures 1 and 2.[15,16] Double layers (AB packing) of trinuclear molybdenum

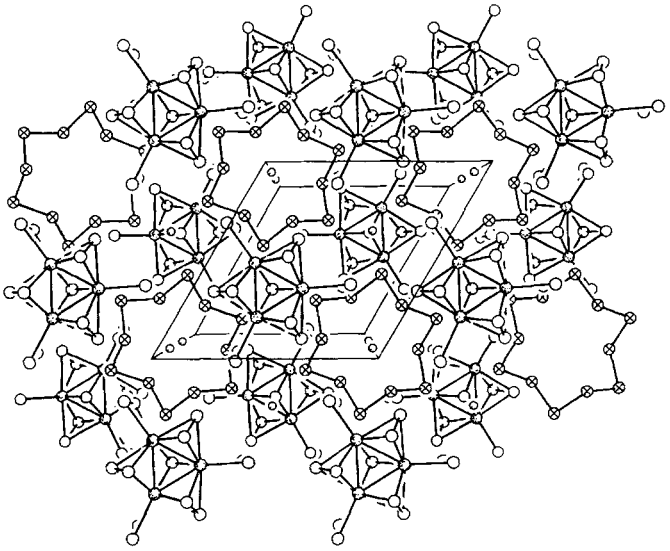

Fig. 1. Crystal structure of **1** viewed along the c axis [15]. Only half the cell is shown for clarity. ○: N atoms, ◍: Mo atoms, ○: S atoms, ⊗: Se atoms. The Se–Se bonds within the Se_{12} ring are nearly all identical: 2.335(2) and 2.327(2) Å. The internal Se-Se-Se ring angles are consistent with those found for Se_8 and Te_n [7], alternating between 105.14(4) and 102.94(7)°. Instead of $[Mo_3S_{11.72}Se_{1.28}]$ the simplified structure of $[Mo_3S_{13}]$ is shown.

[*] Prof. Dr. P. K. Dorhout, R. A. Stevens, C. C. Raymond
Department of Chemistry, Colorado State University
Fort Collins, Co 80523 (USA)
Telefax: Int. code + (303)491-1801
e-mail: PKD@LAMAR.COLOSTATE.EDU

[**] Financial support was provided by the American Chemical Society, Petroleum Research Foundation, and the Research Corporation, Cottrell Fellowship. Additional help provided by C. M. Zelenski (EDS), S. M. Miller (X-ray diffraction), and Dr. H. Murray, Exxon Research, for providing some molybdenum starting materials.

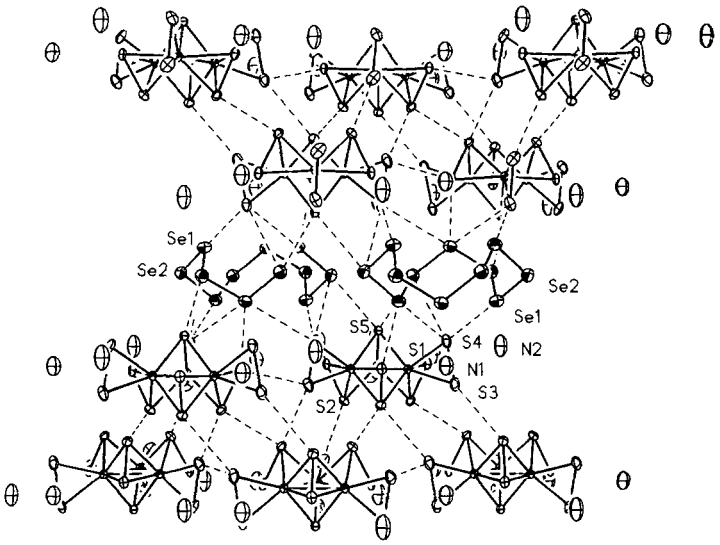

Fig. 2. Crystal structure of **1** viewed along the *a* axis and showing important Se–S intercluster interactions (dashed lines). Anisotropic thermal ellipsoids are shown: Mo and Se atoms are shaded, S and N atoms are principle axis ellipsoids. Selected chalcogen interaction distances [Å]: interactions between clusters from layer A and clusters from layer B: S2–S2, 3.207(3); S2–S3, 3.507(3); interactions between clusters within the same layer: S1–S3, 3.466(3); cluster–ring interactions: S1–Se1, 3.331(3); S4–Se1, 3.754(3) and 3.492(3); S4–Se2, 3.472(3); S5–Se2, 3.544(3). Instead of $[Mo_3S_{11.72}Se_{1.28}]$ the simplified structure of $[Mo_3S_{13}]$ is shown.

clusters of $[Mo_3S_{11.72}Se_{1.28}]^{2-}$ encircle D_{3d} rings of Se_{12}. One type of ammonium cation is located above and below the Se_{12} rings, located within the planes of the molybdenum clusters (N1, Fig. 2). A second ammonium cation (N2) is found centered on the other threefold axis in the cell, above and below the double layers. The packing forms a very intricate network of interactions between anionic clusters and neutral Se_{12} rings (Fig. 2). A summary of atomic coordinates is found in Table 1.

Table 1. Atomic coordinates. U(eq) ($Å^2 \times 10^3$), and site-occupancy factors SOF for **1**.

	x	y	z	U(eq)	SOF
N(1)	0.3333	0.6667	0.1236(7)	66(6)	
N(2)	0.0	0.0	0.1467(7)	54(5)	
Mo	0.6606(1)	0.1768(1)	0.1612(1)	15(1)	
S(1)	0.3799(2)	0.0572(2)	0.1570(1)	20(1)	
S(2)	0.8459(2)	0.3247(2)	0.2202(1)	22(1)	
S(3)	0.6386(14)	0.9295(14)	0.1850(4)	34(2)	0.786(7)
S(4)	0.6537(19)	0.9736(21)	0.1123(6)	29(3)	0.789(6)
S(5)	0.6667	0.3333	0.0978(1)	17(1)	
Se(1)	0.9616(1)	0.2332(1)	0.0451(1)	38(1)	
Se(2)	0.7372(1)	0.1506(1)	0.0030(1)	38(1)	
Se(3)	0.6579(19)	0.9417(22)	0.1905(6)	24(3)	0.214(7)
Se(4)	0.6683(29)	0.9788(34)	0.1099(9)	27(5)	0.211(7)

The neutral Se_{12} rings are reminiscent of the S_{12} allotrope of sulfur.[17] Until now, the largest known neutral selenium ring systems were only Se_8 rings[18] and heteropolychalcogenide, *n*-membered S_xSe_y rings (where $6 \le n \le 12$).[19] (Of course, gray selenium exists in the more common, "infinite" chain form.[20])

Unlike with our previous structures,[4, 11] the $[Mo_3Q_{13}]^{2-}$ portion of **1** (Q = S, Se) did not refine well. It was quite possible that both S_2^{2-} and Se_2^{2-} formed during the reaction of MoS_4^{2-} with the heteropolychalcogenide salt in aqueous solution.[14] The S3 and S4 atoms that comprise the "paddles" of the cluster were the only sulfur atoms that did not refine satisfactorily. This is consistent with the relative ease of substitution at this position of the $[Mo_3S_7]^{4+}$ core.[21] Using a correlated site-occupancy model,[22] we refined the site-occupancy factor of two related atoms (S and Se) on two different sites. The resulting refinement yielded a cluster best modeled as formula **2**.

$[Mo_3(\mu_3\text{-}S)(\mu_2\text{-}S_2)_3\{\eta_2\text{-}(S_{2-x}Se_x)\}_3]^{2-}$ **2** $x = 0.425$

The reactivity of our new heteropolychalcogenide anion $S_3Se_3^{2-}$ in hydrothermal reactions has proven to be unique. Hydrothermal synthesis has yielded a new form of neutral selenium that is intimately held within a network of molybdenum polychalcogenide clusters and ammonium ions.

Experimental Procedure

The title compound **1** was prepared by combining $(NH_4)_2MoS_4$ (0.131 g, 0.5 mmol) and $Na_2S_3Se_3$ (0.381 g, 1.0 mmol) with 500 μL degassed water in an evacuated, flame-sealed, fused silica ampoule. The reaction was complete under autogenous pressure at 150 °C after 100 h. The resulting solution was filtered, and the solids washed with deionized water until the filtrate was colorless. Since diffraction lines from any other compound were absent from the powder diffraction pattern of the product solids, the yield was nearly quantitative; selenium and molybdenum powders were, however, found. Elemental analysis (EDS) for $H_{16}N_4Mo_6S_{23.44}Se_{14.56}$ [%]: calcd. Mo 22.58, S 29.48, Se 45.11; found Mo 22.53, S 29.77, Se 44.71.

Received: June 14, 1995 [Z 8093 IE]
German version: *Angew. Chem.* **1995**, *107*, 2737–2739

Keywords: hydrothermal reactions · molybdenum compounds · polyselenides · polysulfides · selenium rings

[1] A. Müller, S. Sarkar, R. G. Bhattacharyya, S. Pohl, M. Dartmann, *Angew. Chem.* **1978**, *90*, 564–565; *Angew. Chem. Int. Ed. Engl.* **1978**, *17*, 535–536; A. Müller, R. G. Bhattacharyya, B. Pfefferkorn, *Chem. Ber.* **1979**, *112*, 778–780; A. Müller, S. Pohl, M. Dartmann, J. P. Cohen, J. Bennett, R. M. Kirchner, *Z. Naturforsch. B* **1979**, *34*, 434–436.

[2] A. Müller, *Polyhedron* **1986**, *5*, 323–340; A. Müller, E. Diemann, A. Branding, F. W. Baumann, M. Breysse, M. Vrinat, *Appl. Catal.* **1990**, *62*, L13–L17; A. Müller, R. Jostes, F. A. Cotton, *Angew. Chem.* **1980**, *92*, 921–929; *Angew. Chem. Int. Ed. Engl.* **1980**, *19*, 875–882.

[3] J.-H. Liao, M. G. Kanatzidis, *Inorg. Chem.* **1992**, *31*, 431–439; *J. Am. Chem. Soc.* **1990**, *112*, 7400–7402; J.-H. Liao, J. Li, M. G. Kanatzidis, *Inorg. Chem.* **1995**, *34*, 2658–2670.

[4] C. C. Raymond, P. K. Dorhout, S. M. Miller, *Inorg. Chem.* **1994**, *33*, 2703–2704.

[5] R. S. Laitinen, P. Pekonen, R. J. Suontamo, *Coord. Chem. Rev.* **1994**, *130*, 1–62.

[6] M. A. Ansari, J. A. Ibers, *Coord. Chem. Rev.* **1990**, *100*, 223–226; M. G. Kanatzidis, *Comments Inorg. Chem.* **1990**, *10*, 161–195.

[7] W. S. Sheldrick, M. Wachhold, *Angew. Chem.* **1995**, *107*, 490–491; *Angew. Chem. Int. Ed. Engl.* **1995**, *34*, 450–451.

[8] R. K. McMullen, D. J. Prince, J. D. Corbett, *Inorg. Chem.* **1971**, *10*, 1749–1753.

[9] M. G. Kanatzidis, S.-P. Huang, *Inorg. Chem.* **1989**, *28*, 4667–4669.

[10] W. S. Sheldrick, H. G. Braunbeck, *Z. Naturforsch. B* **1989**, *44*, 1397–1401.

[11] A new polytype of $(NH_4)_2[Mo_3S_{13}]$ has a monoclinic cell: *Pm*, $a = 5.694(2)$, $b = 18.907(7)$, $c = 9.899(4)$ Å, $\beta = 106.47(3)°$.

[12] $Na_2S_3Se_3$ was prepared from the elements in liquid ammonia. Differential scanning calorimetry confirmed that this new salt is a single phase with a congruent melting point of 330 °C. Chemically associated reduction/oxidation waves are seen at −0.74 V and −0.17 V vs. SHE.

[13] S. Licht, *J. Electrochem. Soc.* **1988**, *135*, 2971–2975.

[14] S. Licht, F. Forouzan, *J. Electrochem. Soc.* **1995**, *142*, 1546–1551.

[15] Crystal structure analysis of a black hexagonal plate of **1**: trigonal, $P\bar{3}c1$, $a = b = 10.207(1)$, $c = 28.351(3)$ Å, $V = 2558.0(4)$ Å^3, $Z = 3$, $\rho_{calcd} = 3.288$, $F(000) = 2300$, 3673 reflections were collected on a Siemens P4 diffractometer at 23 °C using $Mo_{K\alpha}$ radiation (θ-2θ scans, (4.6–50°, 2θ range), $\mu = 12.76$ mm^{-1}, semiempirical absorption correction using ψ-scans). 1496 unique reflections ($R_{int} = 0.0649$, 1103, $I \ge 2\sigma I$) were used to refine 83 parameters, refinement program SHELXL-93,[23] against $|F^2|$ to $R1 = 0.0401$, $wR2 = 0.0975$, and GOF = 1.005. Chalcogen atoms Q3 and Q4 were each refined at two distinct but correlated positions as Se and S based on appropriate bond distances. Further details of the crystal structure investigation may be obtained from the Fachinformationszentrum Karlsruhe, D-76344 Eggenstein-Leopoldshafen (Germany), on quoting the depository number CSD-59064.

[16] G. M. Sheldrick, unpublished.

[17] M. Schmidt, E. Wilhelm, *Angew. Chem.* **1966**, *78*, 1020, *Angew. Chem. Int. Ed. Engl.* **1966**, *5*, 964–965.
[18] P. Cherin, P. Unger, *Acta Crystallogr. B* **1972**, *28*, 313–317.
[19] J. Weiss, W. Bachtler, *Z. Naturforsch. B* **1973**, *28*, 523–524; R. Steudel, R. Laitinen, *Top. Curr. Chem.* **1982**, *102*, 177–198; R. Steudel, M. Pridöhl, H. Hartl, I. Brüdgam, *Z. Anorg. Allg. Chem.* **1993**, *619*, 1589–1596.
[20] N. N. Greenwood, A. Earnshaw *Chemistry of the Elements*, Pergamon, New York, **1984**, p. 887.
[21] V. P. Fedin, M. N. Sokolov, Y. V. Mironov, B. A. Kolesov, S. V. Tkachev, V. Y. Fedorov, *Inorg. Chim. Acta* **1990**, *167*, 39–45.
[22] J. C. Bollinger, J. A. Ibers, *Inorg. Chem.* **1995**, *34*, 1859–1867. A detailed description of the site-correlated model will be discussed: C. C. Raymond, P. K. Dorhout, unpublished.

From Porphyrin Isomers to Octapyrrolic "Figure Eight" Macrocycles

Emanuel Vogel,* Martin Bröring, Jürgen Fink, Daniel Rosen, Hans Schmickler, Johann Lex, Kyle W. K. Chan, Yun-Dong Wu,* Dietmar A. Plattner, Maja Nendel, and Kendall N. Houk*

Dedicated to Professor Rolf Huisgen on the occasion of his 75th birthday

The synthesis of porphycene **2**[1] marks the beginning of a promising new direction of research in porphyrin chemistry: the investigation of porphyrin isomers.[2] The formally simple construction principle of **2** involved the reorganization of the structural elements of porphyrin **1**—four pyrrole and four methine units—while maintaining the N_4 coordination site. This principle also led to the assembly of no less than six additional structural isomers, which contain one or two (as in **2**) (*Z*)-configured C···CH···CH···C units (arene fragments).

The structural isomers of [18]porphyrin-(1.1.1.1) resulting from this operation are depicted in order of increasing energy in Figure 1.[3] Presumably, there are even more candidates than shown, since the structural isomers of **1** might also occur as (*E*) forms due to the presence of the C=CH–CH=C group(s). While the existence of an (*E*) form of **2** can be safely excluded because of geometrical constraints, (*E*) forms are conceivable in the cases of the other isomers **3**–**8**. It should be noted that nonplanar isomers, regardless of their configuration (*E* or *Z*), may adopt chiral conformations, thus offering the possibility of separation of enantiomers.

For the synthesis of the porphyrin isomers **3**–**8**, it is useful to know their energies relative to that of **1**. These energies, calculated by the UHF/PM3 and BLYP/6-31G**//3-21G methods,[4] are given in Figure 1 (in kcal mol^{-1}) for the most stable NH tautomer. In each case, this particular tautomer has a diagonal

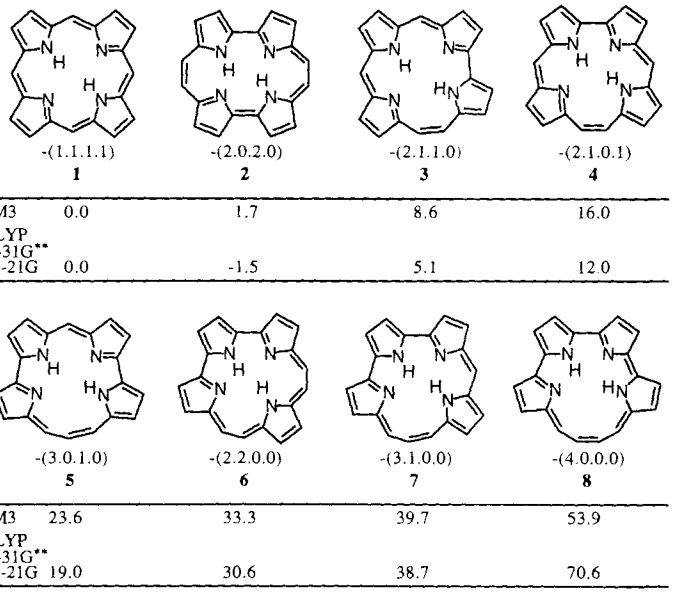

Fig. 1. Porphyrin and its isomers with an N_4 coordination site: [18]porphyrin-(*n.m.p.q*) (**1**–**8**). Data below the structural formulas: values of the relative energies (in kcal mol^{-1}) calculated by PM3 and BLYP/6-31G**//3-21G.

("trans") arrangement of the imino protons as shown in the formulas.[5] It is interesting to find that the stability of porphycene compares favorably with that of porphyrin; depending on the computational method employed, either **1** or **2** is predicted to be the more stable isomer. Evidently, the slightly strained porphycene is stabilized by the presence of strong NH ··· N hydrogen bonds. [18]Porphyrin-(2.1.1.0) (**3**, hemiporphycene) and [18]porphyrin-(2.1.0.1) (**4**, corrphycene) are predicted to be only moderately higher in energy. This prognosis is in accord with the observation that the hemiporphycenes[6] and corrphycenes[7] that have been synthesized recently have properties similar to porphyrins. The energies of the porphyrin isomers **6**–**8** relative to those of **1**–**5** increase so drastically that it is doubtful whether these species will be stable molecules.

These considerations turned our interests to (*E*)-corrphycene (**10**, Scheme 1). Inspection of the Briegleb–Stuart model indicat-

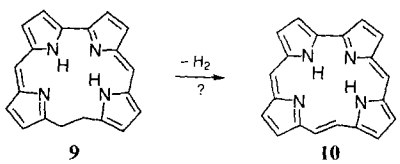

Scheme 1. The 3,4-diethyl substituents of the pyrrole rings are omitted for clarity.

ed that **10** is nearly unstrained but rigid, having the formal double bond in an orthogonal arrangement with respect to the tetrapyrrolic π system. Semiempirical UHF/PM3 calculations predict a similar geometry for **10** and an energy 8 kcal mol^{-1} above that of the (*Z*)-isomer **4**.[8] Consequently, **10** is likely to be a chiral, C_2 symmetric, and nonaromatic porphyrinoid. Porphyrinoid **10** can possibly be synthesized by dehydrogenation of dihydrocorrphycene **9**. According to models, the dihydro compound **9** has a conformation similar to that of **10** with the CH_2CH_2 group in a position conducive to the generation of an (*E*) double bond.

This synthetic strategy fell short of the original goal, since compound **9** never materialized. However, the search was success-

[*] Prof. Dr. E. Vogel, M. Bröring, J. Fink, D. Rosen, Dr. H. Schmickler, Dr. J. Lex
Institut für Organische Chemie der Universität
Greinstrasse 4, D-50939 Köln (Germany)
Telefax: Int. code + (221)470-5102
Prof. Dr. Y.-D. Wu, K. W. K. Chan
Department of Chemistry
The Hong Kong University of Science and Technology
Clear Water Bay, Kowloon (Hong Kong)
Telefax: Int. code + 2358-1594
Prof. Dr. K. N. Houk, M. Nendel, Dr. D. A. Plattner
Department of Chemistry and Biochemistry
University of California, Los Angeles
Los Angeles, CA 90095-1569 (USA)
Telefax: Int. code + (310)206-1843

ful in other respects in that it led to the serendipitous discovery of octapyrrolic "figure eight" macrocycles. These new substances are potential ligands for dinuclear metal complexes.[9]

Octaethyldihydrocorrphycene **9**, the key intermediate in the planned route to (*E*)-corrphycene **10**, was expected to be readily prepared by a MacDonald condensation[10] of the bipyrrole dialdehyde **13** with the dipyrrylethane dicarboxylic acid **12**

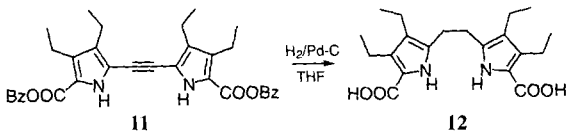

11 **12**

(Scheme 2). The previously unknown dicarboxylic acid **12** was obtained as a thermally labile compound by catalytic hydrogenation of the acetylenic dibenzyl ester **11**[11] (see Scheme 2, Table 1) with 10% palladium on carbon in tetrahydrofuran and in the presence of triethylamine (room temperature, 40 h). Because the acid decarboxylates rapidly in the solid state to form 1,2-dipyrrylethane (which then polymerizes readily), no attempts at isolation were undertaken. The MacDonald condensation was

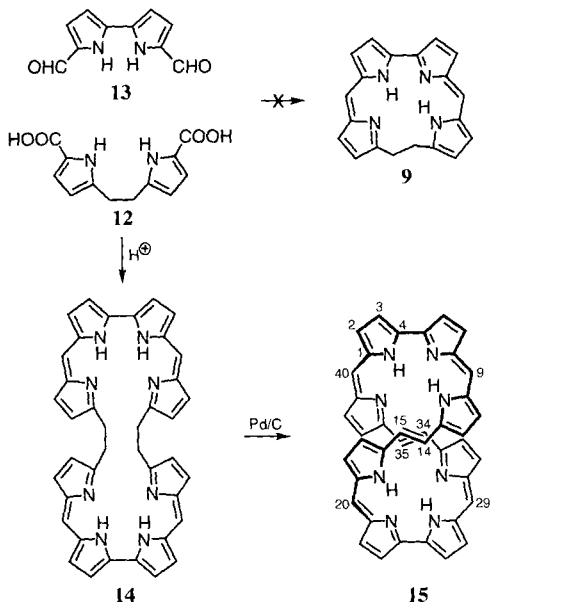

Scheme 2. Synthesis of the octapyrrolic macrocycle **15**. The 3,4-diethyl substituents of the pyrrole rings are omitted for clarity.

therefore carried out by the addition of dialdehyde **13** to a solution of hydrogenated **11**, followed by the dropwise addition of this mixture to a solution of methanol and 70% perchloric acid (30/1). To complete the reaction, the mixture was stirred for three hours, and then aqueous ammonia solution was added until the solution turned alkaline (color change from green to violet). Conventional workup afforded the crude product, which was chromatographed on aluminum oxide (activity II–III, hexane/toluene 2/1). From the brown-reddish main fraction a pure compound was isolated: black-violet crystals (needles) from dichloromethane/hexane (1/1); decomposition above 240 °C; yield 30%. Surprisingly, this compound turned out to be not the expected dihydrocorrphycene **9**, but the tetrahydrooctaphyrin-(2.1.0.1.2.1.0.1)[12] **14** (a formal dimer of **9**), resulting from the condensation of two molecules each of **12** and **13** (Scheme 2).

Initially, the ^{1}H NMR spectrum of **14** (300 MHz, $CDCl_3$, 217 K) was interpreted in terms of the presence of dihydrocorrphycene **9**, due to an absorption pattern compatible with the chiral, rigid, and C_2 symmetric structure expected for compound **9**. The following signals were observed: one singlet (*meso* protons), one AA'BB' system (CH_2CH_2 protons), four ABX_3 systems (ethyl groups with diastereotopic CH_2 protons), and a broad singlet (NH protons). On raising the temperature to 378 K ([D_8]toluene), the only significant change in the spectrum is the broadening and finally the disappearance of the NH signal. Complementary to the ^{1}H NMR spectrum, the ^{13}C NMR spectrum shows 18 signals. A reassignment of the spectra to compound **14**

Table 1. Selected physical data of the compounds **11**, **14**, **15**, and **19**. ^{1}H NMR: 300 MHz; ^{13}C NMR: 75.5 MHz; IR: CsI; UV/Vis: CH_2Cl_2.

11: m.p. 194 °C (ethyl acetate); ^{1}H NMR ($CDCl_3$): δ = 8.82 (br. s; NH), 7.37, 5.29, 2.73, 2.52,, 1.15, 1.11; ^{13}C NMR ($CDCl_3$): δ = 160.04, 133.12, 132.55, 128.58, 128.27, 118.95, 114.28, 85.09, 66.03, 18.19, 18.03, 15.63; IR: $\tilde{\nu}$ = 3298, 2974, 2933, 1659, 1501, 1462, 1445, 1280, 1180, 1134, 1100, 1017, 960, 907, 780, 740 cm^{-1}; UV/Vis: λ_{max} (ε) = 258 (13700 sh), 264 (14000), 318 (24600 sh), 332 (30400 sh), 344 (35900), 350 (33400 sh), 369 nm (30800); MS (EI, 70 eV): *m/z* (%): 536 (60) [M^+].

14: decomp. >240 °C (dichloromethane/hexane); ^{1}H NMR ($CDCl_3$, 298 K): δ = 6.57 (s, 4H; H-9,20,29,40), 2.92 (AA'BB' system, center, 8H; H-14,15,34,35), 2.66 (ABX_3 system, AB part, 8H; H-2a, 2a', 7a, 7a', 22a, 22a', 27a, 27a'), 2.62 (ABX_3 system, AB part, 8H; H-3a, 3a', 6a, 6a', 23a, 23a', 26a, 26a'), 2.39 (ABX_3 system, AB part, 8H; H-11a, 11a', 18a, 18a', 31a, 31a', 38a, 38a'), 1.95 (ABX_3 system, AB part, 8H; H-12a, 12a', 17a, 17a', 32a, 32a', 37a, 37a'), 1.21 (ABX_3 system, X_3 part, 12H, H-2b, 7b, 22b, 27b), 1.17 (ABX_3 system, X_3 part, 12H; H-3b, 6b, 23b, 26b), 1.07 (ABX_3 system, X_3 part, 12H; H-11b, 18b, 31b, 38b), 0.68 (ABX_3 system, X_3 part, 12H; H-12b, 17b, 32b, 37b), NH not detected; ^{1}H NMR ($CDCl_3$, 217 K): δ = 11.8 (br. s, 4H; NH), 6.6 (s, 4H; H-9, 20,29,40), 2.9 (AA'BB' system, 8H; H-14,15,34,35), 2.7 (br., 8H; H-2a,7a,22a,27a), 2.6 (br., 8H; H-3a,6a,23a,26a), 2.4 (br., 8H; H-11a,18a,31a,38a), 1.9 (br., 8H; H-12a,17a,32a,37a), 1.21 (br. t, 12H; H-2b,7b,22b,27b), 1.17 (br. t, 12H; H-3b,6b,23b,26b), 1.07 (br. t, 12H; H-11b,18b,31b,38b), 0.68 (br. t, 12H; H-12b,17b,32b,37b); ^{13}C NMR ($CDCl_3$): δ = 168.99, 145.01, 143.14, 135.70, 134.74, 133.05, 131.39, 125.72, 113.72, 26.17, 18.51, 17.93, 17.78, 17.57, 17.26, 17.15, 15.47, 14.88; IR: $\tilde{\nu}$ = 3274, 2964, 2930, 2869, 1617, 1463, 1408, 1263, 1201, 1139, 1108, 1058, 1009, 945, 682 cm^{-1}; UV/Vis: λ_{max} (ε) = 257 (28000), 397 (65300), 432 (62800), 567 nm (33000); MS (FAB): *m/z* (%): 1074 (70) [$(M+2H)^+$], 1072 (62) [M^+].

15: decomp. >310 °C (dichloromethane/hexane); ^{1}H NMR ($CDCl_3$, 298 K): δ = 7.19 (s, 4H; H-14,15,34,35), 6.60 (s, 4H; H-9,20,29,40), 2.68 (ABX_3 system, AB part, 8H; H-2a,2a',7a,7a',22a,22a',27a,27a'), 2.66 (ABX_3 system, AB part, 8H; H-3a,3a',6a,6a',23a,23a',26a,26a'), 2.51 (ABX_3 system, AB part, 8H; H-11a,11a',18a,18a',31a,31a',38a,38a'), 2.22 (ABX_3 system, AB part, 8H; H-12a,12a',17a,17a',32a,32a',37a,37a'), 1.24 (ABX_3 system, X_3 part, 12H; H-2b,7b,22b,27b), 1.18 (ABX_3 system, X_3 part, 12H; H-3b,6b,23b,26b), 1.14 (ABX_3 system, X_3 part, 12H; H-11b,18b,31b,38b), 0.87 (ABX_3 system, X_3 part, 12H; H-12b,17b,32b,37b), NH not detected; ^{1}H NMR ($CDCl_3$, 217 K): δ = 12.7 (br. s, 4H; NH), 7.19 (s, 4H; H-14,15,34,35), 6.60 (s, 4H; H-9,20,29,40), 2.7 (br., 8H; H-2a,7a,22a,27a), 2.6 (br., 8H; H 3a,6a,23a,26a), 2.5 (br., 8H; H-11a,18a,31a,38a), 2.2 (br., 8H; H-12a,17a,32a,37a), 1.24 (br. t, 12H; H-2b,7b,22b,27b), 1.18 (br. t, 12H; H-3b,6b,23b,26b), 1.14 (br. t, 12H; H-11b,18b,31b,38b), 0.87 (br. t, 12H; H-12b,17b,32b,37b); ^{13}C NMR ($CDCl_3$): δ = 150.80, 147.36, 141.57, 140.76, 139.99, 139.76, 134.04, 130.19, 121.39, 113.72, 18.76, 18.09, 17.74, 17.25, 17.20, 17.10, 16.23, 15.58; IR: $\tilde{\nu}$ = 3289, 2963, 2930, 2870, 1591, 1465, 1375, 1261, 1216, 1190, 1110, 1057, 1010, 950, 867 cm^{-1}; UV/Vis: λ_{max} (ε) = 276 (27800), 322 (34800), 410 (29400), 591 nm (54000); MS (FAB): *m/z* (%): 1070 (70) [$(M+2H)^+$], 1069 (100) [$(M+H)^+$], 1068 (60) [M^+].

19: decomp. 275 °C (dichloromethane/hexane); ^{1}H NMR ([D_8]toluene): δ = 12.1 (br. s, 4H; NH), 6.42 (s, 2H; H-5,24), 5.88 (s, 4H; H-10,19,29,38), 2.78 (ABX_3 system, A part, 4H; H-13a,16a,32a,35a), 2.52 (ABX_3 system, AB part, 8H; H-3a,3a',7a,7a',22a,22a',26a,26a'), 2.49 (ABX_3 system, AB part, 8H; H-2a,2a',8a,8a',21a,21a',27a,27a'), 1.86 (ABX_3 system, AB part, 8H; H-12a,12a',17a,17a',31a,31a',36a,36a'), 1.41 (ABX_3 system, B part, 4H; H-13a',16a',32a',35a'), 1.22 (ABX_3 system, X_3 part, 12H; H-3b,7b,22b,26b), 1.18 (ABX_3 system, X_3 part, 12H; H-2b,8b,21b,27b), 0.96 (ABX_3 system, X_3 part, 12H; H-12b,17b,31b, 36b), 0.80 (ABX_3 system, X_3 part, 12H; H-13b,16b,32b,35b); ^{13}C NMR ([D_8]toluene): δ = 149.47, 148.57, 148.57, 148.30, 139.77, 139.30, 139.16, 136.65, 101.96, 98.56, 18.34, 18.21, 18.10, 17.71, 17.02, 16.86, 16.67, 15.35; IR: $\tilde{\nu}$ = 3278, 2963, 2931, 2869, 1597, 1464, 1372, 1340, 1313, 1227, 1144, 1115, 826, 734, 669; UV/Vis: λ_{max} (ε) = 278 (30300), 291 (30700), 354 (52900), 378 (85200), 486 (15800), 503 (16600), 609 (40300), 656 (175900), 770 (23300), 899 nm (58300); MS (FAB): *m/z* (%): 1043 (100) [$(M+H)^+$].

became inevitable when the FAB mass spectrum (FAB = fast atom bombardment) indicated a molecular mass double that of **9** (*m/z* 1072, 62%). The new interpretation is consistent with the data if one assumes that **14**—as is the case for its derivative **15**, for which it was demonstrated by X-ray structure analysis—exhibits a figure-eight conformation. Chirality and the C_2 symmetry axis corresponding to the hypothetical **9** are maintained. In view of the small changes in the ^{1}H NMR spectrum upon varying the temperature (except for the NH protons), and particularly in view of the unchanged diastereotopic behavior of the ethyl-CH_2 protons, **14** must be a relatively rigid molecule.

Attempts to oxidize **14** with DDQ did not lead to a well defined product. However, upon heating, the compound (apart from experiencing some decomposition) is dehydrogenated to form the fully conjugated octaphyrin **15** with two (*E*)-configured double bonds. The thermal dehydrogenation of **14** by 10% palladium on carbon in toluene at reflux (48 h) takes place essentially without side reactions. Chromatographic filtration of the dehydrogenation product on aluminum oxide (activity II–III, hexane/toluene 1/1) and recrystallization from dichloromethane/hexane (1/1) gives **15** as bright golden, thin plates (solutions of **15** are deep blue); decomposition above 310 °C; yield 85%.

The ^{1}H NMR spectrum (300 MHz, $CDCl_3$, 217 K) reflects the transition from **14** to **15** by the replacement of the AA′BB′ system of the CH_2CH_2 protons with a singlet in the olefinic region ($\delta = 7.19$) for the four protons of the two (*E*) double bonds.[13] Thus, it appears that octaphyrin **15** adopts a figure-eight conformation as well. Special electronic effects that might have resulted from the cyclic conjugated π system (the main conjugation path has 36 [4*n*] π electrons; aromaticity is therefore excluded) have not been observed with **15**. Further, the data of the UV/Vis spectrum are not consistent with the presence of a porphyrinoid molecule. The diastereotopicity of the ethyl-CH_2 protons is maintained in the high temperature ^{1}H NMR spectrum (378 K) of **15**, thus indicating an inversion barrier larger than 20 kcal mol^{-1}. This suggests that the resolution of **15** into stable enantiomers should be possible. The same is true for the precursor **14**.

Upon treatment of **15** with 10% hydrochloric acid in dichloromethane, the tetrakis(hydrochloride) is formed, accompanied by small quantities of the bis(hydrochloride) **15a**. Treating it with perchloric acid, on the other hand, yields the tetrakis(hydroperchlorate) **15b** exclusively. In contrast to the free base **15**, its salts **15a** and **15b** could be analyzed by single crystal X-ray diffraction methods (Fig. 2).[14] Although both X-ray analyses need further refinement, it can be concluded unequivocally that the doubly protonated macrocycle **15a** (with chloride as counterion) forms a figure-eight loop with approximate D_2 symmetry. The same type of conformation applies to the tetraprotonated **15b**, even though in this case the incorporation of two more counterions stretches the skeleton like an accordion. Studies of whether **14** and **15** are able to form dinuclear complexes are currently under way.

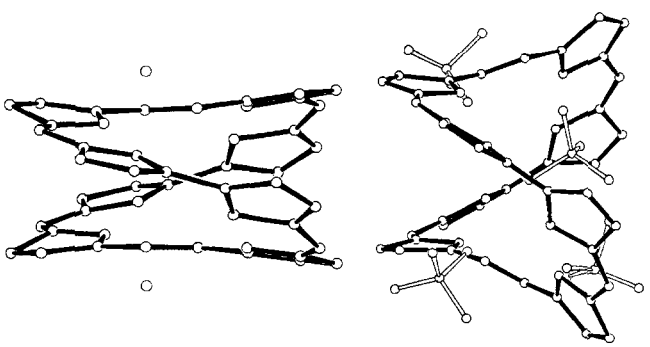

Fig. 2. Structures of the bis(hydrochloride) **15a** and tetrakis(hydroperchlorate) **15b** of **15** in the crystal (side views of **15a** (left) and **15b** (right); the ethyl substituents are omitted for clarity).

The thought that **14** and **15** might represent an entire class of octapyrrolic macrocycles prompted us to replace the dipyrrylethane by the dipyrrylmethane dicarboxylic acid **16** in the synthetic scheme of **14**. Initially we had thought that a MacDonald condensation of **13** with **16** would provide an improved access to corroles **17**.[15] As it turned out, the formation of the octapyrrolic macrocycle predominates over the formation of the cyclic tetrapyrrole in a condensation experiment performed as follows: dialdehyde **13** (300 mg, 1 mmol) and dicarboxylic acid **16** (346 mg, 1 mmol), dissolved in tetrahydrofuran (250 mL), are added dropwise under stirring to a solution of methanol (400 mL) and 70% perchloric acid (20 mL) at room temperature. After the addition is completed, the solution is allowed to stand for 30 minutes without stirring, and then concentrated aqueous ammonia solution is added until the reaction turns alkaline. The diethyl ether extract is worked up conventionally. Chromatography on aluminum oxide (activity II–III, hexane/toluene 2/1) provides a green fraction; after evaporation of the solvent and crystallization from dichloromethane/hexane the macrocycle **19**, an octaphyrin-(1.1.1.0.1.1.1.0), is obtained as red-golden cubes with a metallic luster; decomposition above 275 °C; yield 72 mg (10%) (see Scheme 3).

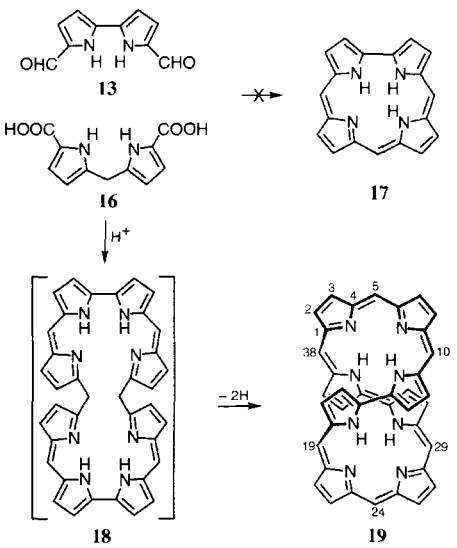

Scheme 3. Synthesis of the octapyrrolic macrocycle **19**. The 3,4-diethyl substituents of the pyrrole rings are omitted for clarity.

The ^{1}H NMR spectrum of **19** (300 MHz, [D_8]toluene, 298 K, thiophenol as radical trapping agent) consists of two singlets (*meso* protons), four ABX_3 systems (ethyl groups with diastereotopic CH_2 protons), and one more singlet (NH protons), indicating that the compound is chiral and D_2 symmetric. The position of the *meso* proton signals at relatively high field ($\delta = 5.88$ and 6.42) indicates that **19** is not aromatic, although the compound has a 34 π electron main conjugation path. As for the NH tautomerism in **19**, inverse ^{1}H–^{13}C long range experiments show that the major tautomer is the one depicted with the NH protons on both bipyrrole units. Similar to **14** and **15**, compound **19** is restricted in its conformational flexibility, and its enantiomers might be separable since the diastereotopicity of the ethyl-CH_2 protons encountered in the ^{1}H NMR spectrum is maintained over the entire temperature range studied (193 K to 378 K).

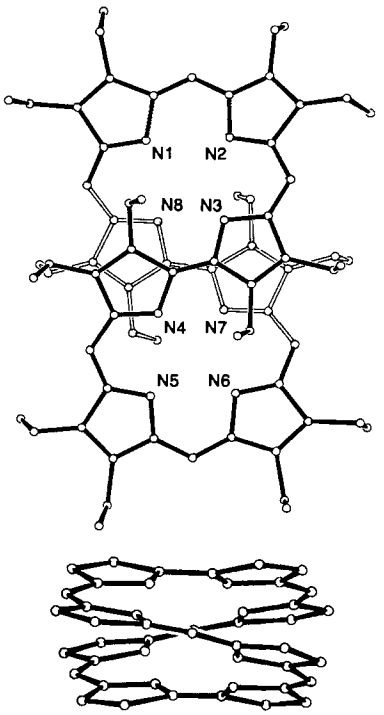

Fig. 3. Structure of the octapyrrolic macrocycle **19** in the crystal (top: top view; bottom: side view, with the ethyl groups omitted).

The X-ray crystal structure of **19** as free base[14] (Fig. 3) does not yet provide the accuracy necessary to assign molecular parameters for bond lengths, but it shows unequivocally that the figure-eight conformation of the molecule in solution is also present in the solid state.

The formation of the dehydrogenation product **19** in the course of the MacDonald condensation of **13** with **16** is surprising, since the fully conjugated tautomer of **18** with six imino protons would be anticipated to be the final product of the reaction. Because **19** is not aromatic, aromatization is ruled out as the driving force in the facile formation of **19** from **18**; the dehydrogenation of **18** (or its tautomer) is probably due to a decrease of conformational strain upon conversion to **19**.

A precedent for the synthesis of the figure-eight octaphyrins **14**, **15**, and **19** is found in the preparation of the blue-violet pigment turcasarin with ten pyrrole rings by J. L. Sessler et al.;[16] these discoveries will give new impetus to research on polypyrrolic macrocycles, molecules that show promise as versatile complexing agents (dinuclear and host–guest complexes).[17]

These latest developments notwithstanding, (*E*)-corrphycene **10** remains a synthetic goal worth pursuing. The hypothetical **10** is of particular significance, since, in conjunction with its (*Z*) isomer **4**, it demonstrates the close relationship existing between porphyrin and annulene chemistry. Most likely, the isomeric pair (*Z*)- and (*E*)-corrphycene parallels the known isomeric pair *syn*- and *anti*-bismethano[14]annulene[18] in representing a prime example of a geometrically induced loss of aromaticity in a cyclic conjugated $(4m + 2)$ π electron system.

Received: March 20, 1995 [Z 7813 IE]
German version: *Angew. Chem.* **1995**, *107*, 2705–2709

Keywords: macrocycles · octapyrroles · porphyrinoids

[1] E. Vogel, M. Köcher, H. Schmickler, J. Lex, *Angew. Chem.* **1986**, *98*, 262; *Angew. Chem. Int. Ed. Engl.* **1986**, *25*, 257; E. Vogel, *Pure Appl. Chem.* **1990**, *62*, 557; E. Vogel, *ibid.* **1993**, *65*, 143; E. Vogel, P. Koch, X.-L. Hou, J. Lex, M. Lausmann, M. Kisters, M. A. Aukauloo, P. Richard, R. Guilard, *Angew. Chem.* **1993**, *105*, 1670; *Angew. Chem. Int. Ed. Engl.* **1993**, *32*, 1600.

[2] A summary of porphyrin isomers including the recently discovered "inverted porphyrins" (H. Furata, T. Asano, T. Ogawa, *J. Am. Chem. Soc.* **1994**, *116*, 767; P. J. Chmielewski, L. Latos-Grazynski, K. Rachelwicz, T. Glowiak, *Angew. Chem.* **1994**, *106*, 805; *Angew. Chem. Int. Ed. Engl.* **1994**, *33*, 779) is found in a Highlight by J. L. Sessler, *ibid.* **1994**, *106*, 1410 and **1994**, *33*, 1348; for inverted porphyrins see also: A. Ghosh, *ibid.* **1995**, *107*, 1117 and **1995**, *34*, 1028.

[3] J. Waluk and J. Michl discussed the porphyrin isomers **2**–**8** in a study on the magnetic circular dichroism of porphyrin analogues, *J. Org. Chem.* **1991**, *56*, 2729.

[4] A. D. Becke, *Phys. Rev. A*, **1988**, *38*, 3098; C. Lee, W. Yang, R. G. Parr, *Phys. Rev. B*, **1988**, *37*, 785; B. G. Johnson, P. M. W. Gill, J. A. Pople, *J. Chem. Phys.* **1993**, *98*, 5612.

[5] The energy differences between the NH tautomers of **1**–**4** can be as much as 7 kcal mol^{-1} according to calculations with several different methods. The NH tautomers of **1** have been discussed in detail by J. R. Reimers, T. X. Lü, M. J. Crossley, N. S. Hush, *J. Am. Chem. Soc.* **1995**, *117*, 2855; A. Ghosh, J. Almlöf, *J. Phys. Chem.* **1995**, *99*, 1073.

[6] H. J. Callot, A. Rohrer, T. Tschamber, B. Metz, *New J. Chem.* **1995**, *19*, 155; E. Vogel, M. Bröring, J. Lex, J. L. Sessler, see ref. [11] in ref. [7a].

[7] a) J. L. Sessler, E. A. Brucker, S. J. Weghorn, M. Kisters, M. Schäfer, J. Lex, E. Vogel, *Angew. Chem.* **1994**, *106*, 2402; *Angew. Chem. Int. Ed. Engl.* **1994**, *33*, 2308; b) M. A. Aukauloo, R. Guilard, *New J. Chem.* **1994**, *18*, 1205. The knowledge of the properties of the octapyrrolic macrocycle **15** made it possible to show that **15** is also produced, albeit in very small quantities (less than 1%), during the synthesis of octaethylcorrphycene (experiments together with S. Pracht).

[8] An entirely different geometry for **10** (likewise a *trans*-tautomer) was subsequently obtained by calculations by the BLYP/6-31G**//3-21G method. Here, the result is a nonplanar, bowl-like structure in which the (*E*) double bond of the (CHCH) bridge is only slightly bent out of the mean plane of the adjacent pyrrole rings. The increase in energy with respect to (*Z*)-corrphycene **4** is found to be 16.1 kcal mol^{-1} (as compared to 8 kcal mol^{-1} by the UHF/PM3 method).

[9] J. P. Collman, P. S. Wagenknecht, J. E. Hutchison, *Angew. Chem.* **1994**, *106*, 1620; *Angew. Chem. Int. Ed. Engl.* **1994**, *33*, 1537; F. V. Acholla, K. B. Mertes, *Tetrahedron Lett.* **1984**, *25*, 3269; F. V. Acholla, F. Takusagawa, K. B. Mertes, *J. Am. Chem. Soc.* **1985**, *107*, 6902; H. Adams, N. A. Bailey, D. E. Fenton, S. Moss, C. O. Rodriguez de Barbarin, G. Jones, *J. Chem. Soc. Dalton Trans.* **1986**, 693.

[10] G. P. Arsenault, E. Bullock, S. F. MacDonald, *J. Am. Chem. Soc.* **1960**, *82*, 4384.

[11] The synthesis of the dibenzylic ester **11** was inspired by that of bis(3,4-diethyl-5-formyl-2-pyrryl)ethyne: N. Jux, P. Koch, H. Schmickler, J. Lex, E. Vogel, *Angew. Chem.* **1990**, *102*, 1429; *Angew. Chem. Int. Ed. Engl.* **1990**, *29*, 1385; D. O. Mártire, N. Jux, P. F. Aramendía, R. M. Negri, J. Lex, S. E. Braslavsky, K. Schaffner, E. Vogel, *J. Am. Chem. Soc.* **1992**, *114*, 9969.

[12] This name is proposed following Franck's porphyrin nomenclature; see: M. Gosmann, B. Franck, *Angew. Chem.* **1986**, *98*, 1107; *Angew. Chem. Int. Ed. Engl.* **1986**, *25*, 1100.

[13] The (*E*) configuration of the double bond can be deduced from the ^{1}H NMR spectrum (^{13}C satellites): the coupling constant ^3J (H14, H15) is 15.3 Hz, typical for an olefinic *trans* coupling constant.

[14] Enraf-Nonius CAD4 diffractometer (room temperature, $Mo_{K\alpha}$ radiation, $\lambda = 0.71069$ Å). The structure was solved by direct methods and refined with F^2 by using all observed reflections (heavy atoms with anisotropic temperature factors, H atoms have not yet been included); $wR2 = [\sum w(F_o^2 - F_c^2)^2 / \sum w(F_o^2)^2]^{1/2}$. Programs used: MolEN (Enraf-Nonius) for the structure determination and SHELXL-93 (G. M. Sheldrick, University of Göttingen, **1993**) for the refinement. The calculations were performed at the Regional Computational Center of the University of Cologne. Further details of the X-ray structure analysis can be requested from the Director of Cambridge Crystallographic Data Centre, 12 Union Road, GB-Cambridge, CB2 1EZ, on quoting the full journal citation. Preliminary X-ray structural data of **15a**: $C_{72}H_{94}N_8Cl_2$, crystallized from acetone; monoclinic, space group $C2/c$, $a = 14.065(3)$, $b = 26.425(8)$, $c = 19.783(5)$ Å, $\beta = 100.60(2)°$, $Z = 4$, $\rho_{calcd} = 1.050$ g cm^{-3}, $\mu_{Mo} = 1.33$ cm^{-1}; 4229 reflections measured; 1251 reflections observed ($F_o^2 > 2\sigma F_o^2$); $\theta_{max} = 22°$; $R1 = 0.12$, $wR2 = 0.25$. Preliminary X-ray data of **15b**: $C_{72}H_{96}N_8Cl_4O_{16}$, crystallized from dichloromethane/hexane (1/1); monoclinic, space group $P2_1/c$, $a = 28.004(8)$, $b = 10.138(4)$, $c = 28.014(9)$ Å, $\beta = 104.57(2)°$, $Z = 4$, $\rho_{calcd} = 1.27$ g cm^{-3}, $\mu_{Mo} = 2.22$ cm^{-1}; 6975 reflections measured; 2209 reflections observed ($F_o^2 > 2\sigma F_o^2$); $\theta_{max} = 21°$; $R1 = 0.13$, $wR2 = 0.24$. Preliminary X-ray data of **19**: $C_{70}H_{90}N_8$, crystallized from dichloromethane/hexane (1/1); triclinic, space group $P\bar{1}$, $a = 13.258(3)$, $b = 14.410(3)$, $c = 19.150(5)$ Å, $\alpha = 68.15(2)°$, $\beta = 84.97(2)°$, $\gamma = 66.67(2)°$, $Z = 2$, $\rho_{calcd} = 1.114$ g cm^{-3}, $\mu_{Mo} = 0.65$ cm^{-1}; 4487 reflections measured; 2525 reflections observed ($F_o^2 > 2\sigma F_o^2$); $\theta_{max} = 20°$; $R1 = 0.070$, $wR2 = 0.153$.

[15] The MacDonald condensation of 5,5'-diformyl-2,2'-bipyrroles with 5,5'-dicarboxy-2,2'-dipyrrylmethanes was reported to afford mainly linear hexapyrroles (M. Conlon, A. W. Johnson, W. R. Overend, D. Rajapaksa, C. M. Elson, *J. Chem. Soc. Perkin 1* **1973**, 2281), but for various reasons it seemed expedient to us to study the reaction again.

[16] J. L. Sessler, S. J. Weghorn, V. Lynch, M. R. Johnson, *Angew. Chem.* **1994**, *106*, 1572; *Angew. Chem. Int. Ed. Engl.* **1994**, *33*, 1509. In the case of the decapyrrolic turcasarin a figure-eight conformation is assumed, based on an X-ray crystallographic analysis of the tetrakis(hydrochloride) derivative.

[17] In the helicene and cyclophane field, molecules with a figure-eight topology are well-known; see B. Thulin, O. Wennerström, *Acta Chem. Scand., Ser. B* **1976**, *30*, 688; R. Schenk, K. Müllen, O. Wennerström, *Tetrahedron Lett.* **1990**, *31*, 7367.

[18] E. Vogel, J. Sombroek, W. Wagemann, *Angew. Chem.* **1975**, *87*, 591; *Angew. Chem. Int. Ed. Engl.* **1975**, *14*, 564.

Octaphyrin-(1.0.1.0.1.0.1.0)

Martin Bröring, Jörg Jendrny, Lars Zander, Hans Schmickler, Johann Lex, Yun-Dong Wu,* Maja Nendel, Jiangang Chen, Dietmar A. Plattner, Kendall N. Houk,* and Emanuel Vogel*

Dedicated to Professor Wolfgang R. Roth on the occasion of his 65th birthday

Polypyrrolic macrocycles with eight or more pyrrole units arouse interest as potential ligands for dinuclear metal complexes[1] and from various other points of view. The first representative of these macrocycles—turcasarin with ten pyrrole rings—was described recently by J. L. Sessler[2] in the course of work in the "expanded porphyrins"[3,4] area. Shortly thereafter, during an attempt—so far unsuccessful—to synthesize the porphyrin isomer (*E*)-corrphycene,[5] we discovered that a number of cyclooctapyrroles differing in structural type can be obtained relatively easily by MacDonald condensation reactions of appropriate dipyrrolic building blocks. Evidently, cyclooctapyrroles tend to form if the ring closure to cyclotetrapyrroles is hindered for mechanistic or conformational reasons. The cyclooctapyrroles known so far have a common geometrical feature – a chiral figure-eight topology with restricted conformational flexibility. Consequently, these molecules are potentially resolvable into enantiomers.[6]

The highly symmetric cyclooctapyrroles **1** and **2**, octaphyrin-(1.1.1.1.1.1.1.1) and octaphyrin-(1.0.1.0.1.0.1.0),[7] shown in planar representations, are particularly attractive targets among

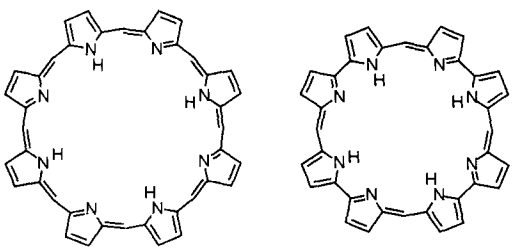

1 **2**

this class of compounds. Octaphyrin **1** is a homologue of porphyrin,[8] although it does not conform to the latter in its π electron structure.[9] Octaphyrin **2** derives from porphyrin by replacing the four pyrrole rings with four bipyrrole units. While **1** remains a synthetic challenge, **2** has now been prepared by two routes described here.

The simplest concept to approach octaphyrin-(1.0.1.0.1.0.1.0) is inspired by the Rothemund synthesis[10] of tetra-*meso*-substituted porphyrins, namely, the condensation of tetraalkyl-substituted bipyrroles (unsubstituted in the α and α′ positions) with aromatic aldehydes under acidic oxidizing conditions. This reaction, explored by J. L. Sessler et al. several years ago,[11] unexpectedly affords the hexapyrrolic "expanded porphyrin" rosarin [hexaphyrin-(1.0.1.0.1.0)] in high yield, rather than the octapyrrolic cyclic condensation product. Rosarin readily gives a tris(hydrochloride) with aqueous hydrochloric acid and was characterized as such by X-ray diffraction and NMR methods. Linear tetrapyrrole **3** and the α,ω-dialdehyde **4**, prepared by a Vilsmeier reaction of **3**, are both intermediates in our synthesis of isocorroles.[12] The availability of these intermediates invited the condensation of the two tetrapyrroles as an alternative synthetic route to octaphyrin-(1.0.1.0.1.0.1.0). When **3** and **4** are treated with trifluoroacetic acid in dichloromethane at room temperature, the octapyrrolic homologue **5** of rosarin is formed as the only well-defined product. Subsequently, it was found that **5** is obtained more expeditiously if two equivalents each of bipyrrole **6** and of bipyrrole dialdehyde **7**[13] are condensed with acid catalysis (see Experimental Procedure). In both cases, the chromatographically purified **5** is obtained after crystallization from dichloromethane/methanol as dark green rhombohedra with a metallic luster (yield 11% in the first case, 7% in the second).

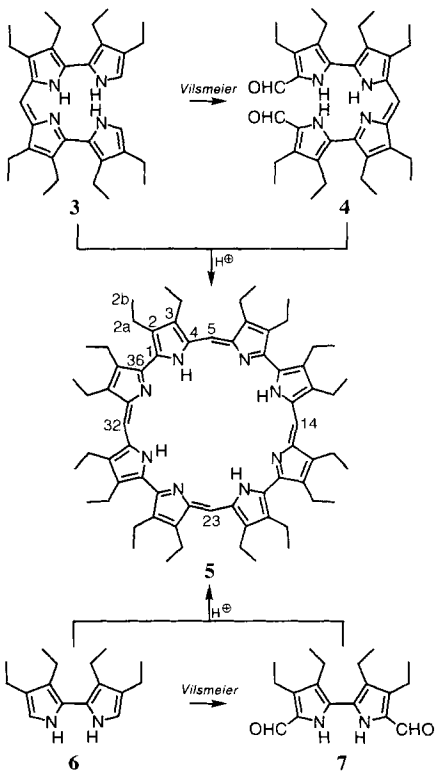

The ^{1}H NMR spectrum (300 MHz, $CDCl_3$, Al_2O_3 to remove traces of water) of **5** only consists of a singlet ($\delta = 6.57$, *meso* protons), a broad singlet ($\delta = 13.30$, NH protons), and two ABX_3 systems (ethyl groups with diastereotopic CH_2 protons). With [D_8]toluene as solvent no significant changes occur in the NMR spectrum in the temperature range between −100 °C and 100 °C. These NMR observations might best be explained by the two following scenarios, both of which are consistent with the constant diastereotopicity of the CH_2 protons: 1) Octaphyrin **5** exists in an achiral tub conformation resembling cycloocta-

[*] Prof. Dr. E. Vogel, M. Bröring, J. Jendrny, L. Zander, Dr. H. Schmickler, Dr. J. Lex
Institut für Organische Chemie der Universität
Greinstrasse 4, D-50939 Köln (Germany)
Telefax: Int. code + (221)470-5102
Prof. Dr. Y.-D. Wu
Department of Chemistry
The Hong Kong University of Science and Technology
Clear Water Bay, Kowloon (Hong Kong)
Telefax: Int. code + 2358-1594
Prof. Dr. K. N. Houk, M. Nendel, J. Chen, Dr. D. A. Plattner
Department of Chemistry and Biochemistry
University and Biochemistry
University of California, Los Angeles
Los Angeles, CA 90095-1569 (USA)
Telefax: Int. code + (310)206-1843

tetraene and does not invert on the NMR time scale. 2) **5** consists of two enantiomeric figure-eight conformers that are interconverting rapidly via a tub conformation.

To answer the question whether the molecule **5** is static (excluding the NH tautomerism) or dynamic, a force field conformational analysis was performed. Based upon this study, scenario 2 is most probable, and the barrier to racemization is too low to allow separation of enantiomers. Additionally, the study shows that the conformational change is coupled to NH tautomerism.[14]

In accordance with the presence of four basic nitrogen atoms, **5** is protonated by 70% perchloric acid in dichloromethane to form its tetrakis(hydroperchlorate). Since this perchlorate has the same splitting pattern in the ^{1}H NMR spectrum as **5**, it is improbable that salt formation has a profound effect on the conformation of the product.

The X-ray analysis of the free base **5** shows the figure-eight conformation in the solid state (Fig. 1).[15] As can be seen from

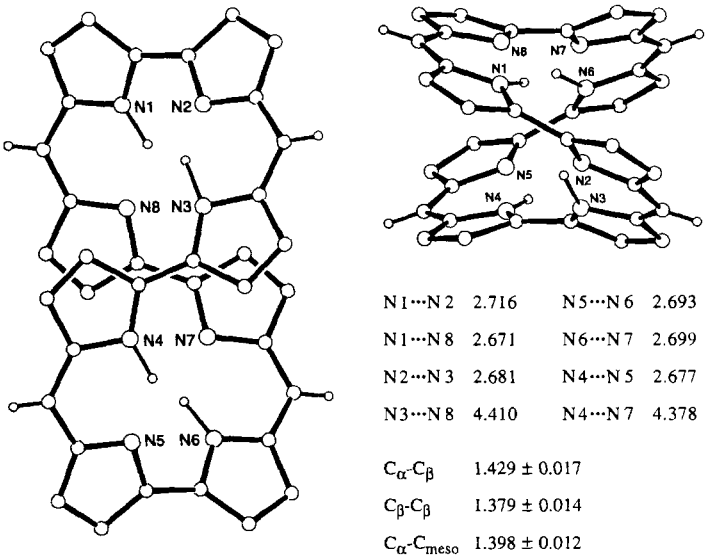

N1···N2	2.716	N5···N6	2.693
N1···N8	2.671	N6···N7	2.699
N2···N3	2.681	N4···N5	2.677
N3···N8	4.410	N4···N7	4.378

C_α-C_β	1.429 ± 0.017
C_β-C_β	1.379 ± 0.014
C_α-C_{meso}	1.398 ± 0.012

Fig. 1. Structure of octaphyrin **5** in the crystal (left: top view, right: side view). N···N contact distances and selected bond lengths are given in Å. Ethyl groups are omitted for clarity.

the structural parameters, **5** consists of four almost planar dipyrrin (pyrromethene) subunits (torsional angles between 1 and 10°) that maintain their individuality to a certain degree.[16] The conformation of the molecule arises mainly because the pyrrole rings of the bipyrrole units are rotated about their linking bond (the torsional angles are in the range of 43 to 52°). It was possible to assign the four imino hydrogen atoms to distinct nitrogen atoms. Evidently, as a result of the figure-eight conformation, the hydrogen atoms are located on N1, N3, N4, and N6 (Fig. 1) and not as shown in the drawing of **5**.

Octaphyrin **5**, made up of four dipyrrin units, is a remarkably stable yet chemically versatile compound. One is therefore tempted to "extrapolate" from **5** to the hitherto elusive polymers derived from the monobasic monomeric dipyrrin, specifically to the intriguing linear polypyrrole **8** and its helical variant.

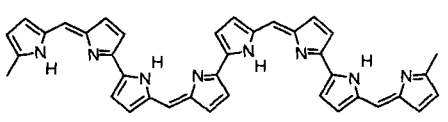

8

Experimental Procedure

5: 3,3',4,4'-Tetraethyl-5,5'-diformyl-2,2'-bipyrrole (**7**; 900 mg, 3 mmol) and 3,3',4,4'-tetraethyl-2,2'-bipyrrole (**6**; 732 mg, 3 mmol) dissolved in tetrahydrofuran (300 mL) are added dropwise to a solution of methanol (300 mL) and 70% perchloric acid (15 mL), followed by stirring at room temperature for 24 h. The solution is made basic with dilute sodium hydroxide, worked up by extraction into dichloromethane, and chromatographed on aluminum oxide (activity grade II–III according to Brockmann, column 10 × 2 cm) with hexane/toluene (2/1). Octaphyrin **5** is isolated as the only nonpolymeric product and was obtained after crystallization from dichloromethane/methanol (5/1) as dark green rhombohedric crystals with a metallic sheen; m.p. >300 C; yield 84 mg (7%). Selected physical data: ^{1}H NMR (300 MHz, $CDCl_3$, Al_2O_3): δ = 13.30 (br. s, 4H; NH), 6.57 (s, 4H; H-5,14,23,32), 2.57 (ABX_3 system, AB part, 16H; H-3a,3a',7a,7a',12a,12a',16a,16a',21a,21a', 25a,25a',30a,30a',34a,34a'), 2.57 (ABX_3 system, A part, 8H; H-2a,8a,11a, 17a,20a,26a,29a,35a), 2.45 (ABX_3 system, B part, 8H; H-2a',8a',11a',17a', 20a',26a',29a',35a'), 1.22 (ABX_3 system, X_3 part, 24H; H-3b,7b,12b,16b,21b, 25b,30b,34b), 1.13 (ABX_3 system, X_3 part, 24H; H-2b,8b,11b,17b,20b,26b, 29b,35b); ^{13}C NMR (75.5 MHz, $CDCl_3$, Al_2O_3): δ = 147.49, 140.40, 139.73, 132.12, 115.17, 18.32, 17.82, 17.33, 15.73; IR (CsI): $\tilde{\nu}$ = 3196, 2961, 2928, 2869, 1589, 1464, 1388, 1301, 1278, 1207, 1185, 1110, 1056, 1009, 950, 867, 764 cm^{-1}; UV/Vis (CH_2Cl_2): λ_{max} (ε) = 361 (28500), 548 nm (104000); MS (FAB): *m/z* (%): 1018 (98) [$(M+2H)^+$], 1017 (100) [$(M+H)^+$], 1016 (78) [M^+].

Received: June 3, 1995 [Z 8058 IE]
German version: *Angew. Chem.* **1995**, *107*, 2709–2711

Keywords: macrocycles · octaphyrin · porphyrinoids

[1] J. P. Collman, P. S. Wagenknecht, J. E. Hutchison, *Angew. Chem.* **1994**, *106*, 1620; *Angew. Chem. Int. Ed. Engl.* **1994**, *33*, 1537; J.-C. Chambron, C. Dietrich-Buchecker, J. P. Sauvage, *Top. Curr. Chem.* **1993**, *165*, 131; H. Adams, N. A. Bailey, D. E. Fenton, S. Moss, C. O. Rodriguez de Barbarin, G. Jones, *J. Chem. Soc. Dalton Trans.* **1986**, 693; F. V. Acholla, F. Takusagawa, K. B. Mertes, *J. Am. Chem. Soc.* **1985**, *107*, 6902; F. V. Acholla, K. B. Mertes, *Tetrahedron Lett.* **1984**, *25*, 3269.

[2] J. L. Sessler, S. J. Weghorn, V. Lynch, M. R. Johnson, *Angew. Chem.* **1994**, *106*, 1572; *Angew. Chem. Int. Ed. Engl.* **1994**, *33*, 1509. As noted in this work (footnote [14]), turcasarin forms a bis(uranyl) complex.

[3] J. L. Sessler, A. K. Burrell, *Top. Curr. Chem.* **1991**, *161*, 177; J. L. Sessler, S. J. Weghorn, Y. Hiseada, V. Lynch, *Chem. Eur. J.* **1995**, *1*, 56.

[4] T. Wessel, B. Franck, M. Müller, U. Rodewald, M. Läge, *Angew. Chem.* **1993**, *105*, 1201; *Angew. Chem. Int. Ed. Engl.* **1993**, *32*, 1148; H. König, C. Eickmeier, M. Müller, U. Rodewald, B. Franck, *ibid.* **1990**, *102*, 1437 and **1990**, *29*, 1393; G. Knübel, B. Franck, *ibid.* **1988**, *100*, 1203 and **1988**, *27*, 1170; M. Gosmann, B. Franck, *ibid.* **1986**, *98*, 1107 and **1986**, *25*, 1100.

[5] E. Vogel, M. Bröring, J. Fink, D. Rosen, H. Schmickler, J. Lex, K. W. K. Chan, Y.-D. Wu, M. Nendel, D. A. Plattner, K. N. Houk, *Angew. Chem.* **1995**, *107*, 2705; *Angew. Chem. Int. Ed. Engl.* **1995**, *34*, 2515.

[6] In the case of one chiral octaphyrin, the formal dimer of corrphycene [5], it has been established that the enantiomers can be separated (personal communication of Prof. O. Hofer and Dr. A. Werner, University of Vienna).

[7] Alternatively, cyclopolypyrroles consisting of *n* dipyrrin (pyrromethene) units can be named cyclo[*n*]dipyrrins. The first compound of this series is cyclo-[3]dipyrrin (rosarin [11]). Octaphyrin **2** would accordingly be named cyclo-[4]dipyrrin.

[8] The only homologues of porphyrin (tetraphyrin) known so far are pentaphyrin and hexaphyrin (each as derivatives): H. Rexhausen, A. Gossauer, *J. Chem. Soc. Chem. Commun.* **1983**, 275; A. Gossauer, *Bull. Soc. Chim. Belg.* **1983**, *92*, 793; *Chimia* **1983**, *37*, 341; *ibid.* **1984**, *38*, 45; A. K. Burrell, G. Hemmi, V. Lynch, J. L. Sessler, *J. Am. Chem. Soc.* **1991**, *113*, 4690.

[9] The main conjugation path of **1** consists of 36 ($4n$) π electrons, but this is probably insignificant because the conjugation is sterically hindered.

[10] P. Rothemund, *J. Am. Chem. Soc.* **1936**, *58*, 625; P. Rothemund, A. R. Menotti, *ibid.* **1941**, *63*, 267.

[11] J. L. Sessler, S. J. Weghorn, T. Morishima, M. Rosingana, V. Lynch, V. Lee, *J. Am. Chem. Soc.* **1992**, *114*, 8306.

[12] The McMurry-type reductive coupling of tetrapyrrolic α,ω-dialdehydes like **4** is a general method used to synthesize alkyl-substituted isocorroles; Y. Hellwig, *Dissertation*, University of Cologne, **1994**; B. Binsack, *Dissertation*, University of Cologne, **1995**. Isocorroles can also be prepared by a rearrangement of porphycenes with two substituents per pyrrole ring in basic media; S. Will, A. Rahbar, H. Schmickler, J. Lex, E. Vogel, *Angew. Chem.* **1990**, *102*, 1434; *Angew. Chem. Int. Ed. Engl.* **1990**, *29*, 1390; E. Vogel, *Pure Appl. Chem.* **1993**, *65*, 143.

[13] E. Vogel, P. Koch, X.-L. Hou, J. Lex, M. Lausmann, M. Kisters, M. A. Aukauloo, P. Richard, R. Guilard, *Angew. Chem.* **1993**, *105*, 1670; *Angew. Chem. Int. Ed. Engl.* **1993**, *32*, 1600.

[14] A detailed discussion of the conformational analysis of **5** by molecular mechanics, molecular dynamics, and quantum mechanical methods will be published in a separate account.

[15] Data of the crystal structure of **5**: $C_{68}H_{88}N_8$, crystallized from hexane; triclinic, space group $P\bar{1}$, $a = 12.851(3)$, $b = 14.341(3)$, $c = 18.879(5)$ Å, $\alpha = 77.51(2)$, $\beta = 70.45(2)$, $\gamma = 75.70(2)$, $Z = 2$, $\rho_{calc} = 1.074\ g\,cm^{-3}$; $\mu_{Mo} = 0.63\ cm^{-1}$; 13732 reflections measured; 6071 reflections observed ($F_o^2 > 2\sigma F_o^2$); $\theta_{max} = 28°$; $R1 = 0.075$, $wR2 = 0.151$. Enraf-Nonius CAD4 diffractometer (room temperature, $Mo_{K\alpha}$ radiation $\lambda = 0.71069$ Å). The structure was solved by direct methods and refined by F^2 using all observed reflections (heavy atoms with anisotropic, H atoms with isotropic temperature factors); $wR2 = [\sum w(F_o^2 - F_c^2)^2 / \sum w(F_o^2)^2]^{1/2}$. Programs used: structure determination by MolEN (Enraf-Nonius) and refinement by SHELXL-93 (G. M. Sheldrick, University of Göttingen). Calculations were performed at the regional computational center of the University of Cologne. Further details of the X-ray structure determination can be requested from the Director of Cambridge Crystallographic Data Centre, 12 Union Road, GB-Cambridge, CB21EZ, on quoting the full journal citation.

[16] For the structure and complexing properties of dipyrrins see the monograph: H. Falk, *The Chemistry of Linear Oligopyrroles and Bile Pigments*, Springer, Vienna, **1989**.

Coordination of Dioxygen in Three Representative Transition Metal Cations: FeO_2^+, CrO_2^+, and $[CH_3Re(O_2)_2O]^+$**

Detlef Schröder, Andreas Fiedler, Wolfgang A. Herrmann, and Helmut Schwarz*

Dedicated to Professor Herbert W. Roesky on the occasion of his 60th birthday

The activation of molecular oxygen for selective oxidations is important in numerous synthetic, industrial, and biological processes.[1] The transition metal mediated oxidation of hydrocarbons deserves special interest,[2] and here the use of dioxygen as the oxidant is chemically attractive. Activation of a dioxygen molecule by a mononuclear transition metal complex may involve three modes of coordination of the two oxygen atoms to "bare" or ligated metals [M] (Scheme 1):[3] 1) [M] may coordinate O_2 to yield the side-on complex **1**, which can also be described as a metal peroxide; 2) end-on coordination of O_2 to [M] leads to the linear or bent complex **2**, which may also be viewed as a metal superoxide; 3) if a high oxidation state is energetically possible for [M], cleavage of the O–O bond leads to the linear or bent metal dioxide **3**.

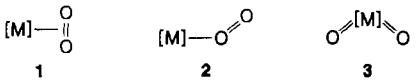

Scheme 1.

Gas-phase experiments reveal fundamental principles of binding for organometallic species, and reactivity studies can be used to evaluate the intrinsic properties of transition metals, thus uncovering the reaction mechanisms at a molecular level. In a few cases the information obtained has direct implications for applied chemistry.[4, 5] We describe here three prototypes of cationic $[M,O_2]^+$ systems in which the different types of bonding, as depicted in Scheme 1, are probed by experimental and theoretical methods. We have deliberately chosen iron and chromium compounds and a high-valent rhenium compound, since these metals are important in numerous oxidation processes.[1, 2, 6, 7] For the sake of brevity, we will focus on the structures of types **1**–**3** and will not discuss mechanistic or thermodynamic details of the oxidation reactions observed experimentally.[5]

Recently,[8] it was demonstrated that among the first-row transition metal cations only Fe^+ can mediate the coupled activation of molecular oxygen and that of C–H/C–C bonds in the ion/molecule reactions of $M(C_2H_4)^+$ complexes (M = Sc–Zn) with O_2. The cationic olefin complexes of Ru–Pd and Os–Pt are also unreactive in this respect.[9] As a possible explanation for the unique behavior of the iron system we proposed[10] a facile interconversion of structures **1** and **3** for [M] = Fe^+. As shown in Figure 1, the potential energy surface of $[Fe,O_2]^+$ does indeed permit the spin- and symmetry-allowed isomerization **1** ⇌ **3**, and the barrier associated with this process amounts to only a few kcal mol^{-1}. Consequently, one should expect that $[Fe,O_2]^+$ will react either as a dioxygen complex **1** or as the corresponding dioxide **3** in ion/molecule reactions. This is indeed observed experimentally (Scheme 2): Whereas $^{18}O_2$ and ethene simply replace the dioxygen ligand in $[Fe,O_2]^+$, propane reacts by hydride and methanide transfer to yield the corresponding carbocations and neutral OFeOH and $OFeOCH_3$, respectively. The fact that oxidation of the olefin does not occur when $[Fe,O_2]^+$ reacts with ethene but is observed[8] in the ion/molecule reaction of $Fe(C_2H_4)^+$ with O_2 can be attributed to

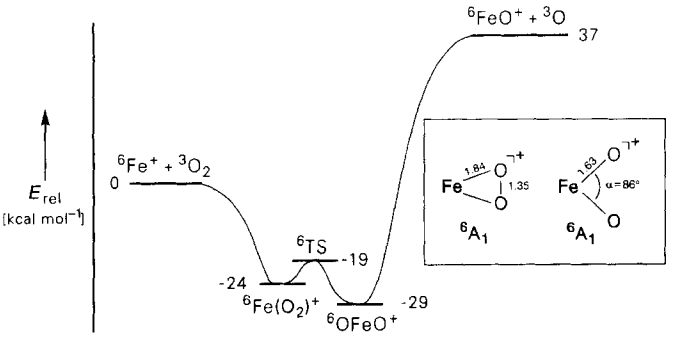

Fig. 1. Calculated sextet potential energy surface for $[Fe,O_2]^+$ ($^6A_1$); the exit channel leading to $FeO^+(^6\Sigma^+) + O(^3P)$ was taken from refs. [11, 13]. The inset shows the geometries of the minima (bond lengths in Å and angles in degrees). TS = transition structure.

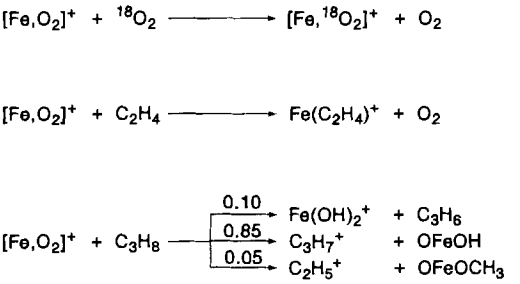

Scheme 2.

[*] Prof. Dr. H. Schwarz, Dr. D. Schröder, Dipl.-Chem. A. Fiedler
Institut für Organische Chemie der Technischen Universität
Strasse des 17. Juni 135, D-10623 Berlin (Germany)
Telefax: Int. code +(30) 314-21102
Prof. Dr. W. A. Herrmann
Anorganisch-chemisches Institut
der Technischen Universität München (Germany)
Telefax: Int. code +(89) 3209 3473

[**] Financial support from the Deutsche Forschungsgemeinschaft, the Volkswagen-Stiftung, and the Gesellschaft von Freunden der Technischen Universität Berlin is gratefully acknowledged. We thank Peter B. Armentrout for a preprint of ref. [11].

thermochemical properties. Since the bond dissociation energy $BDE(Fe^+-C_2H_4) = 34.5\ kcal\,mol^{-1}$[11] exceeds $BDE\ (Fe^+-O_2) \approx 25\ kcal\,mol^{-1}$, the energy gained in the association of C_2H_4 with $Fe(O_2)^+$ is great enough that the exothermicity leads to a rapid loss of the more weakly bound oxygen ligand prior to any C–H/C–C bond activation.

High-valent chromium compounds are widely applied as powerful oxidants in organic synthesis;[6] thus, it is not surprising that the $[Cr,O_2]^+$ cation generated by electron ionization of chromyl chloride CrO_2Cl_2 oxidizes ethene as well as propane (Scheme 3) through activation of both C–H and C–C bonds.[12] The absence of any isotope exchange of the $[Cr,O_2]^+$

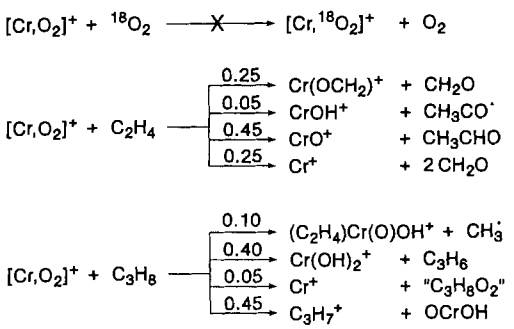

Scheme 3.

cation with $^{18}O_2$ supports the assignment of the chromium(V) dioxide cation with a connectivity like that in **3**. In line with this interpretation, computations reveal that the potential energy surface (PES) of the $[Cr,O_2]^+$ system differs greatly from that of $[Fe,O_2]^+$. For example, for the former, the global minimum corresponds to the low-spin chromium dioxide cation $Cr(O)_2^+(^2B_2)$. The calculated stability of $34\ kcal\,mol^{-1}$ for its dissociation into ground state $Cr^+(^6S)$ and $O_2\ (^3\Sigma_g^-)$ is in agreement with the literature value of $28 \pm 10\ kcal\,mol^{-1}$.[13] This dissociation, however, is spin-forbidden and an allowed, yet more energy-demanding pathway leads to the formation of singlet oxygen (Fig. 2). Nevertheless, spin-orbit coupling may render dissociation into the ground states possible by curve crossing. These calculated features of the PES explain why the $[Cr,O_2]^+$ cation generated from CrO_2Cl_2 is not capable of undergoing isotopic exchange with $^{18}O_2$ and instead acts as an oxidant in its reactions with C_2H_4 and C_3H_8 (Scheme 3). As far as the dioxygen complexes of Cr^+ are concerned, the lowest energy isomer $Cr(O_2)^+(^6B_2)$ is derived from the sextet surface and exhibits the (linear) end-on structure **2**; furthermore, the $BDE(Cr^+-O_2)$ amounts to only $10\ kcal\,mol^{-1}$, whereas that for bent $Fe^+-(O)_2$ is $24\ kcal\,mol^{-1}$. Both the thermochemical and the structural effects can be attributed to the spherical $3d^5$ configuration of the $Cr^+(^6S)$ ground state, since the large loss in exchange energy accompanying spin-pairing and the small radial extension of the d orbitals disfavor covalent bonding with oxygen.

In 1993[14] the aqua complex of $[CH_3Re(O_2)_2O]$ (**4**) was isolated and recognized as the active intermediate in the rhenium-catalyzed[15] epoxidation of olefins by H_2O_2. Our mass spectrometric experiments indicate that the cation 4^+ is also accessible. Further, no evidence was obtained for the occurrence of H/D or $^{16}O/^{18}O$ exchange in **4** in reactions with D_2O and $^{18}O_2$, thus indicating that the methyl as well as the peroxy groups in **4** remain intact upon ionization. With respect to the chemical reactivity towards hydrocarbons, the relatively high ionization energy (IE) of **4** (ca. 10.2 eV)[16] implies that electron-transfer chemistry dominates the ion/molecule reactions of 4^+ with electron-rich organic substrates. Indeed, with propene (IE = 9.7 eV)[13] rapid electron transfer from the alkene to 4^+ takes place to yield $C_3H_6^{+\cdot}$ and neutral **4**. In contrast, ethene (IE = 10.5 eV)[13] is hardly oxidized by 4^+. Furthermore, the fact that neither propene nor ethene can replace a dioxygen unit in 4^+ lends further support to the existence of intact peroxy units in 4^+, since for loosely coordinated dioxygen displacement by an alkene is expected. Interestingly, oxygen transfer of an atom from 4^+ to C_2H_4 and C_3H_6 does not take place in the gas phase.

Of interest in the rhenium case is the unimolecular dissociation of metastable 4^+. Loss of molecular oxygen yields the methyltrioxorhenium(VII) cation 5^+ (Scheme 4, Fig. 3). This process is accompanied by a kinetic energy release[17] of roughly 80 meV, pointing to the existence of a barrier for the reverse reaction, that is, addition of O_2 to 5^+. Subsequently, 5^+ undergoes unimolecular fragmentations of H_2 and CO ($\Delta m = 30$), as reported earlier for authentic 5^+.[18] Note that the large intensities of the signals for the consecutive dissociations point to a significant internal energy content in metastable 5^+, when it is

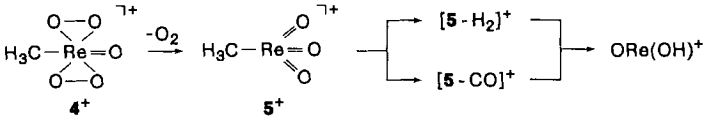

Scheme 4.

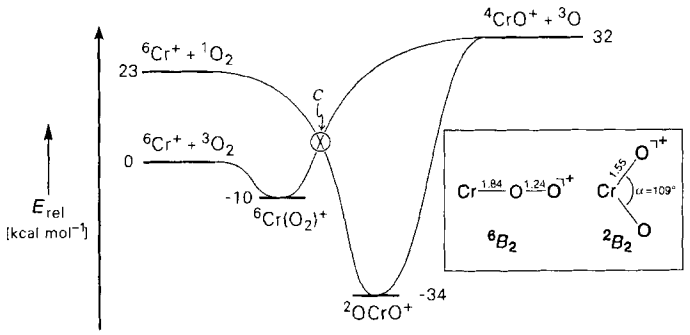

Fig. 2. Calculated potential energy surface for $[Cr,O_2]^+$; the exit channels leading to $CrO^+(^4\Sigma^+) + O(^3P)$ and $Cr^+(^6S) + O_2(^1\Delta_g)$ were taken from refs. [11, 13]. The inset shows the geometries of the minima (bond lengths in Å and angles in degrees). The encircled area is tentative and the point *C* denotes where curve crossing may occur.

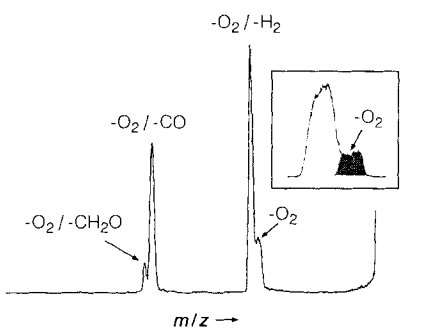

Fig. 3. Metastable-ion mass spectrum of $[CH_3Re(O_2)_2O]^+$ formed by electron ionization of neutral **4**. The inset shows the peak shape of the signals for O_2 and O_2/H_2 losses on an enlarged scale. The shaded area indicates the peak broadening due kinetic energy release; the inset was obtained by monitoring the unimolecular decay in the field-free region after B(2) by scanning E(2).

formed by unimolecular dissociation of $\mathbf{4}^+$. This result points to the existence of a substantial activation barrier for the process $\mathbf{4}^+ \rightarrow \mathbf{5}^+ + O_2$. In addition, for the $^{18}O_2$ complex of methyltrioxorhenium cation, $[CH_3ReO_3(^{18}O_2)]^+$ ($\mathbf{6}^+$), unimolecular loss of the coordinated $^{18}O_2$ is observed exclusively; this implies that the formation of $[CH_3Re(O_2)_2O]^+$ is not reversible. The existence of an activation barrier for dioxygen loss from **4** is essential (Fig. 4). Apparently, the additional ligands in **5** induce a significant barrier for the rearrangement of an incoming O_2 ligand. With respect to the condensed phase, these observations suggest that high-valent **4** is kinetically stable towards loss of dioxygen, since spin conservation would require the formation of singlet oxygen as both **4** and **5** have singlet ground states.

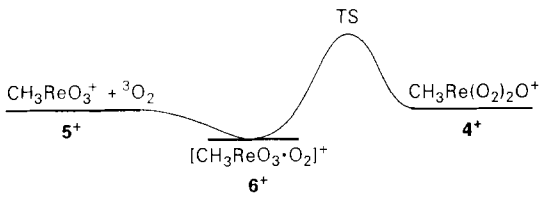

Fig. 4. Qualitative potential energy surface for the dissociation of $[CH_3Re(O_2)_2O]^+$ ($\mathbf{4}^+$) into $CH_3ReO_3^+$ (**5**) and O_2.

Finally, we would like to compare the present findings to the behavior of the transition metals chromium, iron, and rhenium towards hydrogen peroxide in the condensed phase. In general, two different reactivity patterns of a metal towards H_2O_2 are conceivable (Scheme 5): 1) The metal is oxidized to a high-

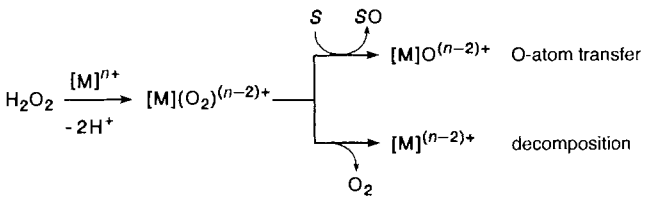

Scheme 5.

valent metaloxo species or it forms a peroxo complex, which can transfer an oxygen atom to an appropriate substrate *S*. 2) The metal may decompose hydrogen peroxide to yield dioxygen. Although the present gas-phase data cannot be compared directly to behavior in the condensed phase, the results parallel the observation that iron compounds, in general, catalyze the decomposition of H_2O_2 and can also serve as catalysts for the activation of dioxygen.[4, 5] In contrast, high-valent chromium and rhenium compounds may well mediate O-atom transfer rather than decompose peroxides. The particular role of the (formal) oxidation state of the metal in O_2 activation and H_2O_2 decomposition is the subject of ongoing studies.

Experimental Procedure

Most of the experiments were performed with a VG ZAB/HF/AMD 604 mass spectrometer of BEBE configuration (B stands for magnetic and E for electric sectors), which has been described elsewhere [19]. Ionization of the precursors or appropriate mixtures (i.e. $Fe(CO)_5/O_2$, CrO_2Cl_2, $CH_3Re(O_2)_2O \cdot H_2O$, $CH_3ReO_3/^{18}O_2$) was achieved in either an electron or a chemical ionization source, and the ions of interest, having 8 keV kinetic energy, were mass-selected using B(1)E(1) at a resolution of $m/\Delta m \approx 3000$. Unimolecular dissociations were monitored in the field-free region preceding B(2) and recorded by scanning this sector. Additional experiments were performed with a Spectrospin CMS 47X Fourier Transform ion cyclotron resonance (FTICR) mass spectrometer, which has been described previously [20]. In brief, ions were generated by electron ionization (12–100 eV electron energy) in the external ion source and transferred to the analyzer cell, which is located within a superconducting magnet (max. field strength 7.05 Tesla). For ion/molecule reactions the ions of interest were mass-selected using the FERETS technique [21]; in the case of $[CH_3Re(O_2)_2O^+]$, the mixture of ^{185}Re and ^{187}Re isotopes of $\mathbf{4}^+$ was mass-selected. In order to afford ion thermalization, argon and methane were pulsed in several times (ca. 200 collisions each) and pumped out; quenching with methane is essential for thermalization.

Although the vapor pressure of $\mathbf{4} \cdot H_2O$ is fairly high, the compound is somewhat difficult to handle and several precautions should be taken to prevent spontaneous decomposition in the inlet system of the mass spectrometer; full details will be described in a forthcoming paper [16]. Briefly, for the experiments using the tandem mass spectrometer, $\mathbf{4} \cdot H_2O$ was introduced through the solid probe; this procedure allows relatively constant ion currents for 3–7 min. The ion gauge and the vacuum protection system were switched off while **4** was present. As a consequence of these experimental conditions, the determination of the kinetic energy release (KER) for O_2 loss from $\mathbf{4}^+$ is less accurate than that by more standard experiments; however, within the context of this study the existence of a KER as such is of interest. Because the FTICR instrument has a different inlet system, the experimental difficulties are less severe. Here, a glass tube containing $\mathbf{4} \cdot H_2O$ was immersed into a water bath at ca. 15 °C and connected to the ion source.

The computational study of $[Cr,O_2]^+$ was performed in the same way as in our previous study of $[Fe,O_2]^+$, which is described in more detail in refs. [10, 22]; complete details of these calculations as well as the experimental characterization of other isomers will be published elsewhere [23]. In brief, geometries were optimized using the local density functional approach (LSD/DZP) of the DGAUSS 2.3 program [24]. Subsequently, the energies of the low-lying states in all spatial and spin symmetries were evaluated at the CASPT2D level of theory using the MOLCAS-2 package [25]. The results reported here were obtained with a (14s9p4d3f)/[5s4p3d2f] basis set for oxygen and a (21s15p10d6f4g)/[8s7p6d4f2g] basis set for chromium [26].

In the case of the $Cr(O_2)^+$ complex, geometry reoptimization of the bending mode at the CASPT2D level of theory reveals the linear structure to be a minimum, while this species exhibits an imaginary frequency in the LSD/DZP approach.

Received: June 10, 1995 [Z 8081 IE]
German version: *Angew. Chem.* **1995**, *107*, 2714–2717

Keywords: ab initio calculations · oxygen activation · mass spectrometry · transition metal oxides

[1] a) E. F. Elstner, *Der Sauerstoff: Biochemie, Biologie und Medizin*, Wissenschaftsverlag, Mannheim, **1990**; b) D. H. R. Barton, A. E. Martell, D. T. Sawyer, *The Activation of Dioxygen and Homogeneous Catalytic Oxidation*, Plenum, New York, **1993**.

[2] a) A. E. Shilov, *Activation of Saturated Hydrocarbons by Transition Metal Complexes*, Reidel, Boston, **1984**; b) *Cytochrome P-450: Structure, Mechanism and Biochemistry*, (Ed.: P. R. Ortiz de Montellano), Plenum, New York, **1986**; c) *Activation and Functionalization of Alkanes* (Ed. C. L. Hill), Wiley, New York, **1989**.

[3] E. C. Niederhoffer, J. H. Timmons, A. E. Martell, *Chem. Rev.* **1984**, *84*, 137; see also: P. E. M. Siegbahn, *J. Phys. Chem.* **1993**, *97*, 9096.

[4] Recent reviews: a) K. Eller, H. Schwarz, *Chem. Rev.* **1991**, *91*, 1121; b) K. Eller, *Coord. Chem. Rev.* **1993**, *126*, 93; c) B. S. Freiser, *Acc. Chem. Res.* **1994**, *27*, 353.

[5] Review on the reactions of oxometal cations in the gas phase: D. Schröder, H. Schwarz, *Angew. Chem.* **1995**, *107*, 2126; *Angew. Chem. Int. Ed. Engl.* **1995**, *34*, 1973.

[6] a) R. L. Augustine, D. J. Trecker, *Oxidation*, Dekker, New York, **1971**; b) M. Hudlicky, *Oxidations in Organic Chemistry* (*ACS Monogr.* **1990**, *186*). c) J. Muzart, *Chem. Rev.* **1992**, *92*, 113.

[7] a) W. A. Herrmann, *J. Organomet. Chem.* **1990**, *382*, 1; b) W. A. Herrmann, R. W. Fischer, W. Scherer, *J. Mol. Catal.* **1994**, *86*, 243.

[8] D. Schröder, H. Schwarz, *Angew. Chem.* **1993**, *105*, 1493; *Angew. Chem. Int. Ed. Engl.* **1993**, *32*, 1420.

[9] R. Wesendrup, Diplomarbeit, Technische Universität Berlin, **1994**.

[10] D. Schröder, A. Fiedler, J. Schwarz, H. Schwarz, *Inorg. Chem.* **1994**, *33*, 5094.

[11] P. B. Armentrout, B. L. Kickel in *Organometallic Ion Chemistry* (Ed. B. S. Freiser), Kluwer, Dordrecht, **1995**, p. 1.

[12] a) D. M. Walba, C. H. DePuy, J. J. Grabowski, V. M. Bierbaum, *Organometallics* **1984**, *3*, 498; b) see also: H. Kang, J. L. Beauchamp, *J. Am. Chem. Soc.* **1986**, *108*, 5663, 7502; c) M. F. Ryan, D. Stöckigt, H. Schwarz, *J. Am. Chem. Soc.* **1994**, *116*, 9565.

[13] Thermochemical data were taken from: a) K. P. Huber, G. Herzberg, *Molecular Spectra and Molecular Structure, Vol. 4*, Van Nostrand, New York, **1979**; b) S. G. Lias, J. E. Bartmess, J. F. Liebman, J. L. Holmes, R. D. Levin, W. G. Mallard, *J. Phys. Chem. Ref. Data* **1988**, *17*, Suppl. 1.

[14] W. A. Herrmann, R. W. Fischer, W. Scherer, M. U. Rauch, *Angew. Chem.* **1993**, *105*, 1209; *Angew. Chem. Int. Ed. Engl.* **1993**, *32*, 1157.

 © VCH Verlagsgesellschaft mbH, D-69451 Weinheim, 1995 0570-0833/95/3422-2519 $ 10.00+.25/0

[15] a) W. A. Herrmann, *Angew. Chem.* **1988**, *100*, 1269; *Angew. Chem. Int. Ed. Engl.* **1988**, *27*, 1297; b) W. A. Herrmann, R. W. Fischer, D. W. Marz, *ibid.* **1991**, *103*, 1706 or **1991**, *30*, 1638.
[16] R. W. Fischer, W. A. Herrmann, H. Bock, D. Schröder, H. Schwarz, unpublished.
[17] J. L. Holmes, J. K. Terlouw, *Org. Mass Spectrom.* **1980**, 5, 383.
[18] D. Schröder, W. A. Herrmann, R. W. Fischer, H. Schwarz, *Int. J. Mass. Spectrom. Ion Processes* **1992**, *122*, 99.
[19] a) R. Srinivas, D. Sülzle, T. Weiske, H. Schwarz, *Int. J. Mass Spectrom. Ion Processes* **1991**, *107*, 368; b) R. Srinivas, D. Sülzle, W. Koch, C. H. DePuy, H. Schwarz, *J. Am. Chem. Soc.* **1991**, *113*, 5970.
[20] a) K. Eller, H. Schwarz, *Int. J. Mass Spectrom. Ion Processes* **1988**, *83*, 23; b) K. Eller, W. Zummack, H. Schwarz, *J. Am. Chem. Soc.* **1990**, *112*, 621.
[21] R. A. Forbes, F. H. Laukien, J. Wronka, *Int. J. Mass Spectrom. Ion Processes* **1988**, *83*, 23.
[22] A. Fiedler, D. Schröder, S. Shaik, H. Schwarz, *J. Am. Chem. Soc.* **1994**, *116*, 10734.
[23] A. Fiedler, D. Schröder, H. Schwarz, unpublished.
[24] J. Andzelm, E. Wimmer, D. R. Salahub, Cray Research Inc., Pittsburg, **1991**.
[25] K. Andersson, M. P. Fülscher, R. Lindh, P. Å. Malmqvist, J. Olsen, B. O. Roos, A. J. Sadlej, MOLCAS version 2. University of Lund, Sweden. P.O. Widmark, IBM Sweden, **1992**.
[26] a) P.-O. Widmark, P.-A. Malmqvist, B. O. Roos, *Theor. Chim. Acta* **1990**, *77*, 291; b) R. Pou-Amerigo, M. Merchan, P.-O. Widmark, B. O. Roos, unpublished.

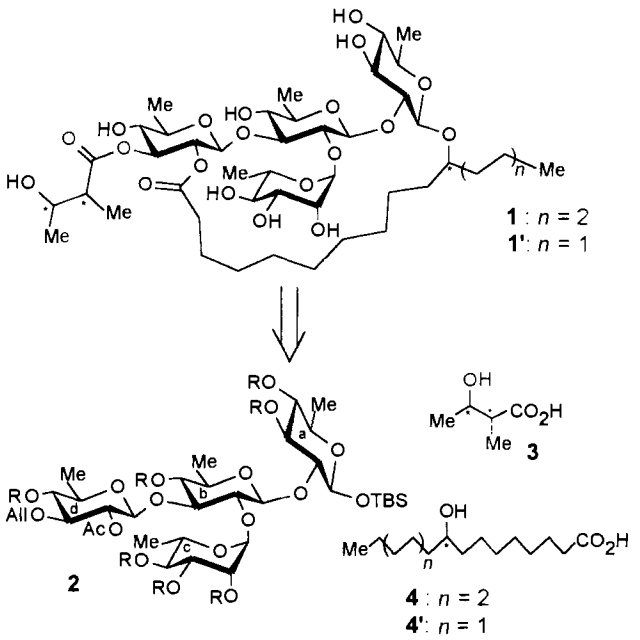

Scheme 1. Retrosynthesis of calonyctin A (**1**).

The Macrolidic Glycolipid Calonyctin A, a Plant Growth Regulator: Synthesis, Structural Assignment, and Conformational Analysis in Micellar Solution**

Zi-Hua Jiang, Armin Geyer, and Richard R. Schmidt*

Calonyctin A, extracted from *Calonyction aculeatum* L. House (moonlight flower), exhibits a strongly promoting effect on the growth and yield of various crops like peanuts, beans, and wheat.[1, 2] Calonyctin A consists of a mixture of the homologous 22-membered macrocycles **1** and **1'** (Scheme 1), which are assembled from the tetrasaccharide D-Quiβ(1-3)[L-Rhaα(1-2)]-D-Quiβ(1-2)D-Qui and the aglycons 3-hydroxy-2-methylbutyric acid (nilic acid, **3**) and 11-hydroxyhexadecanoic acid (jalapinolic acid, **4**) or 11-hydroxytetradecanoic acid (**4'**), respectively. The configurations of **3**, **4**, and **4'** have not been assigned. In addition, it was assumed that only the D isomer of quinovose (D-Qui) occurs in **1**, since it is the most common quinose isomer in nature.[1] Starting from the previously described tetrasaccharide intermediate **2**,[3] which has four orthogonal protecting groups in appropriate positions (*tert*-butyldimethylsilyl (TBS) at 1a, acetyl (Ac) at 2d, allyl (All) at 3d, and benzyl (Bn) at all other hydroxyl groups), we have now synthesized the unique macrolide calonyctin A (**1**) and determined its structure.[4] In addition, we performed a detailed conformational analysis of this 22-membered macrocyclic oligosaccharide in micellar solution. NMR methods (NOESY) were employed to derive proton–proton distances, and these were used in computer simulations of the glycolipid.[5] Based on these results, calonyctin A exhibits a well-defined conformation in the micellar environment. Rotational degrees of freedom of the tetrasaccharide moiety are reduced by the macrocyclic ring structure.

Assembled from one L-rhamnose and three D-quinovose units, the TBS-protected tetrasaccharide **2**[3] was desilylated with tetrabutylammonium fluoride (TBAF) in THF. Subsequent treatment with trichloroacetonitrile in the presence of 1,8-diazabicyclo[5.4.0]undec-7-ene (DBU) as base furnished trichloroacetimidate **5**, as a tetraosyl donor [^{1}H NMR: $\delta = 5.72$ (d, $J_{1a,2a} = 7.6$ Hz; 1a-H), 4.98 (dd, $J_{1d,2d} = 8.1$ Hz, $J_{2d,3d} = 9.5$ Hz; 2d-H)] (Scheme 2). 11-Hydroxyhexadecanoic acid (**4**), which was needed as an acceptor for the synthesis of **1**, was prepared as the racemic ethyl ester **7** from **6** according to a known procedure.[1] Racemic **7** was used in the glycoside synthesis; by adding $BF_3 \cdot OEt_2$ as catalyst in CH_2Cl_2 at $-8\,^\circ C$, we obtained a 1:1 mixture of two diastereomeric β-glycosides in 80% yield. The product mixture was treated with KOH in $MeOH/H_2O$ and purified by chromatography (SiO_2, petroleum ether/ethyl acetate 2.5:1 then 2:1) to provide the 2d-*O*-deprotected acids (*S*)-**8** [^{1}H NMR: $\delta = 4.24$ (d, $J_{1a,2a} = 7.1$ Hz; 1a-H); $[\alpha]_D^{20} = -2.5$ ($c = 1.0$ in $CHCl_3$)] and (*R*)-**8** [^{1}H NMR: $\delta = 4.27$ (d, $J_{1a,2a} = 7.5$ Hz; 1a-H); $[\alpha]_D^{20} = 2.0$ ($c = 1.0$ in $CHCl_3$)]. Hydrogenolytic debenzylation and total hydrolysis of (*S*)-**8** in 1 M H_2SO_4 at 100 °C gave 11-hydroxyhexadecanoic acid (*S*)-**4** in 60% yield. The (*S*) configuration was assigned by comparing optical rotations with literature data [$[\alpha]_D^{20} = 0.6$ ($c = 2.3$ in $CHCl_3$); ref. [7]: $[\alpha]_D^{20} = 0.7$ ($c = 0.9$ in $CHCl_3$)]. Since (*S*)-**4** was found previously as a component of structurally related, open-chain resin glycosides,[8] we performed the ring closure to give the 22-membered lactone with compound (*S*)-**8**. We employed a redox condensation with 2-pyridyl disulfide and triphenylphosphane, which was first described by Corey et al.[9] The intermediate 2-pyridylthioester was refluxed in toluene (4×10^{-4} M) to form macrolide (*S*)-**9** in 80% yield [^{1}H NMR: $\delta = 5.53$ (dd, $J_{1d,2d} = 8.2$ Hz, $J_{2d,3d} = 9.8$ Hz; 2d-H), 3.60 (dd, $J_{2d,3d} = 9.8$ Hz, $J_{3d,4d} = 9.1$ Hz; 3d-H); $[\alpha]_D^{20} = -4.2$ ($c = 1.0$ in $CHCl_3$)].

The allyl protecting group of quinovose d in (*S*)-**9** was isomerized with Wilkinson's catalyst[10] and then removed by addition of $HgO/HgCl_2$ in acetone/water giving (*S*)-**10** [^{1}H NMR: $\delta = 5.21$ ($J_{1d,2d} = 8.1$ Hz, $J_{2d,3d} = 9.8$ Hz; 2d-H); $[\alpha]_D^{20} = -9.1$

[*] Prof. Dr. R. R. Schmidt, Dr. Z.-H Jiang, Dr. A. Geyer
Fakultät Chemie der Universität
Postfach 5560 M725, D-78434 Konstanz (Germany)
Telefax: Int. code + (7531)883135

[**] This work was supported by the Deutsche Forschungsgemeinschaft and the Fonds der Chemischen Industrie.

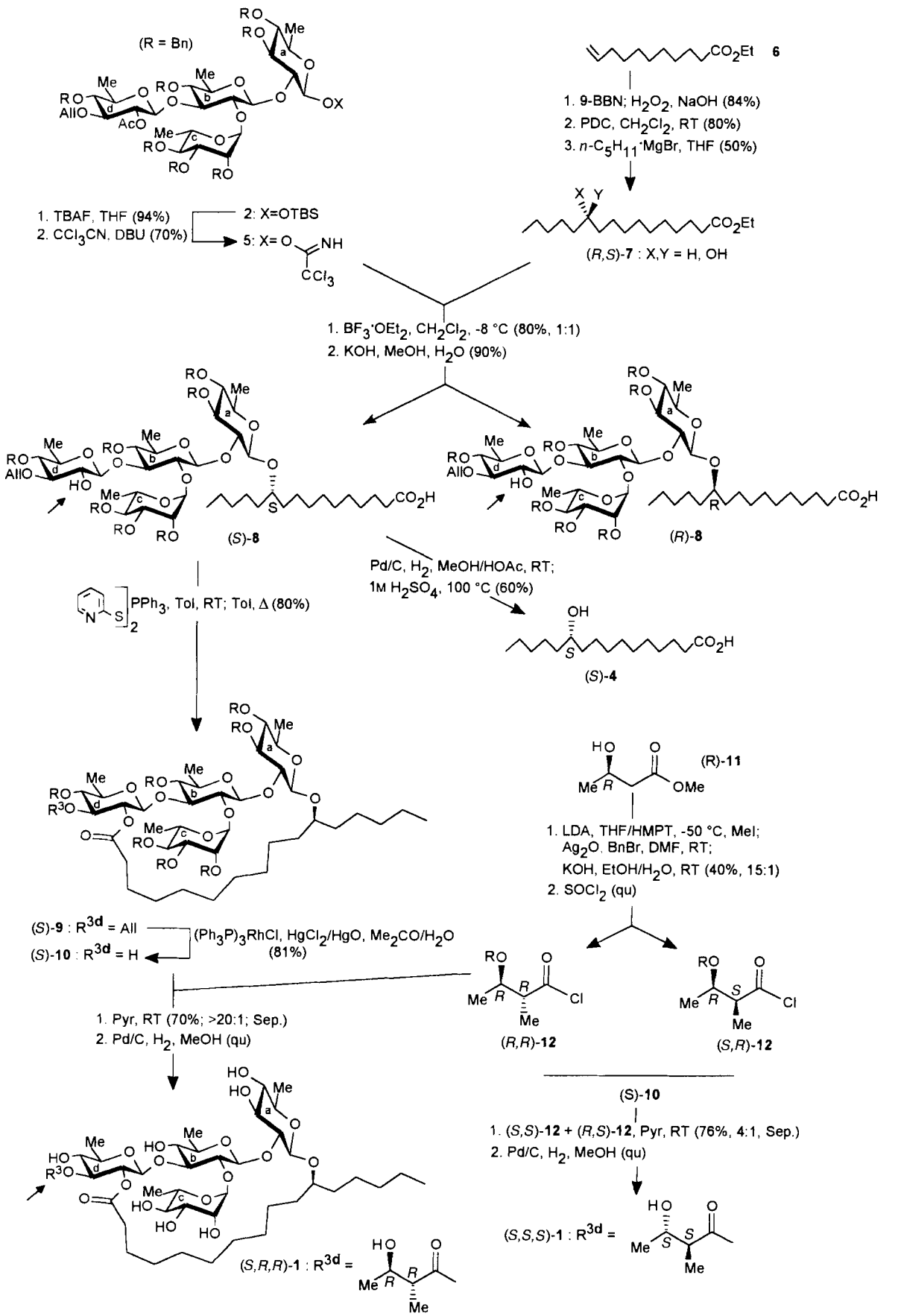

Scheme 2. Synthesis of calonyctin A (**1**). 9-BBN = 9-borabicyclo[3.3.1]nonane, DBU = 1,8-diazabicyclo[5.4.0]undec-7-ene, HMPT = hexamethylphosphoric triamide, LDA = lithium diisopropylamide, qu = quantitative, RT = room temperature, Sep. = separation, TBAF = tetrabutylammonium fluoride, TBS = *tert*-butyldimethylsilyl, Tol = toluene.

($c = 2.0$ in $CHCl_3$)]. Stereoselective synthesis of **12** was achieved by α-methylation of chiral β-hydroxyesters according to Fratér et al.[11] The commercially available methyl ester of 3-hydroxybutyric acid (*R*)-**11** was deprotonated at −50 °C and C-methylated. Subsequent O-benzylation with benzyl bromide/Ag_2O and saponification of the ester resulted in a 15:1 mixture of (*R,R*)- and (*S,R*)-3-hydroxy-2-methylbutyric acids. Further treatment with thionyl chloride gave the acid chlorides (*R,R*)-**12** and (*S,R*)-**12**. A 15:1 mixture of acid chlorides (*S,S*)-**12** and (*R,S*)-**12** was synthesized in an analogous way starting from (*S*)-**11**. 3-Hydroxy-2-methylbutyric acid is found in the (*R,R*) configuration in other natural substances,[12] therefore we concentrated on this compound. The reaction of (*S*)-**10** in pyridine with an excess of the 15:1 mixture of (*R,R*)-**12** and (*S,R*)-**12** (ca. 5 equiv) gave nearly exclusively the (*S,R,R*) diastereomer [(*S,R,R*)/(*S,S,R*) ≥ 20:1] in 70% yield as a result of diastereodifferentiation. Hydrogenolytic debenzylation in MeOH gave quantitatively the (*S,R,R*) diastereomer of **1**. In the same way, (*S*)-**10** was reacted with (*S,S*)-/(*R,S*)-**12**; diastereodifferentiation resulted in a 4:1 mixture of the (*S,S,S*) and the (*S,R,S*) diastereomers. (*S,S,S*)-**1** was obtained after chromatographic separation and hydrogenolytic debenzylation. Comparison of optical rotations [(*S,R,R*)-**1**: $[\alpha]_D^{20} = -55.0$ ($c = 1.0$ in EtOH); (*S,S,S*)-**1**: $[\alpha]_D^{20} = -51.2$ ($c = 1.0$ in EtOH)] and NMR data (Table 1) of these two compounds with those of isolated material [$[\alpha]_D^{20} = -55.0$ ($c = 1.0$ in EtOH)[11]] proved that calonyctin A and (*S,R,R*)-**1** are identical.[13] Intermediate compounds **5**, (*S*)-**8**, (*R*)-**8**, (*S*)-**9**, and (*S*)-**10** were structurally characterized by NMR (^1H, ^{13}C) and FAB-MS data. The ^1H and ^{13}C NMR signals of calonyctin A were fully assigned in [D_5]pyridine; a section of the HMBC spectrum[14] is shown in Figure 1.

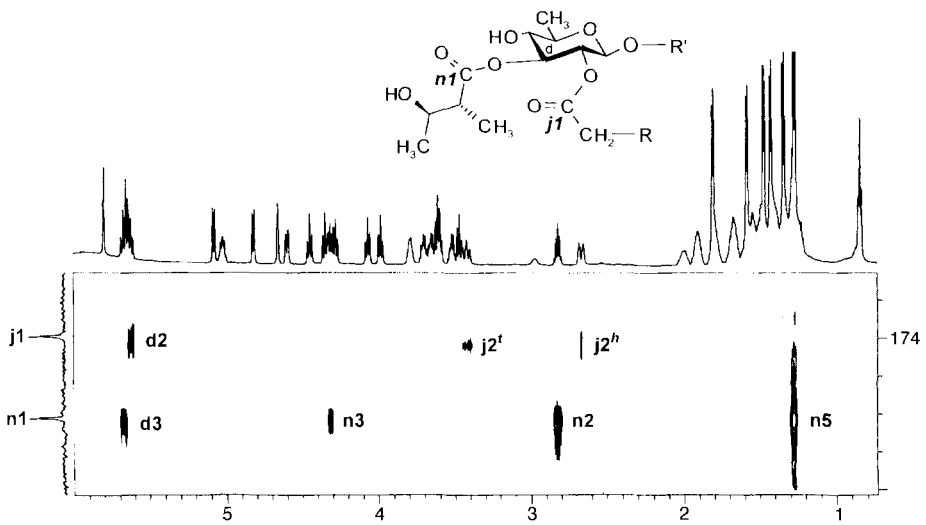

Fig. 1. Section from the low-pass filtered HMBC NMR spectrum of calonyctin A (1) (600 MHz, 300 K, [D_5]pyridine, linear prediction in F1). Proper connection of the aglycons is proven by the cross signals between the carbonyl carbons of jalapinolic acid (j1) and nilic acid (n1), and between the protons d2 and d3 of the carbohydrate chain.

Table 1. ^1H and ^{13}C chemical shifts [δ values] of the nilic acid aglycon of isolated calonyctin A and the synthetic analogues (*S,R,R*)-**1** and (*S,S,S*)-**1** in [D_5]pyridine. *Significant chemical shift differences were not observed for the other aglycons.*

	^1H NMR			^{13}C NMR		
	calonyctin A	(*S,R,R*)-**1**	(*S,S,S*)-**1**	calonyctin A	(*S,R,R*)-**1**	(*S,S,S*)-**1**
n1	–	–	–	175.06	175.02	175.16
n2	2.82	2.82	2.77	48.52	48.47	48.03
n3	4.33	4.31	4.36	69.13	69.10	68.50
n4	1.35	1.34	1.45	20.94	20.90	21.76
n5	1.27	1.27	1.46	13.24	13.20	12.90

Compounds **1** are amphiphilic substances; calonyctin A, which is nearly insoluble in water, is readily dissolved in a micellar solution of [D_{25}]sodium dodecylsulfate (SDS) in water (3 mg (*S,R,R*)-**1**, 46 mg [D_{25}]SDS in 0.5 mL D_2O). The glycolipid inserts into the SDS micelles, as indicated by clear increase in the intensity of the cross signals in the NOESY spectrum,[15] which was recorded with a mixing time of 150 ms at a ^1H resonance frequency of 600 MHz (Fig. 2). For such short mixing times the volume integrals of the NOE cross signals can be correlated to proton–proton distances (two-spin approximation). Cross signals of a geminal proton pair of the aglycon jalapinolic acid were calibrated at 178 pm. Proton–proton distances from Tables 2 and 3 were calculated according to the r^{-6} dependence of the NOE.[16] The clear signal separation allowed the quantification of 59 proton–proton distances, a remarkably high number for a tetrasaccharide. For both quinovose units b and d we could assign all ten possible proton–proton NOEs for each monosaccharide (intraglycosidic NOEs, Table 2). Quinovoses b and d exhibit $^4C_1$ conformation (^1H NMR: $J_{b1,b2} = 7.8$ Hz; $J_{d1,d2} = 7.9$ Hz[17]), and we could check the quality of the NOE data at these two hexoses. The average deviation of the NOE data from that of an idealized $^4C_1$ quinovose is less than 10% (Table 2). This is also true for the $^1C_4$ conformation of rhamnose c. Too little experimental data could be extracted for quinovose a due to signal overlap. The coupling constant $J_{Ha1,Ha2}$ of only 7.2 Hz indicates that quinovose a is distorted from $^4C_1$ conformation. An enhanced flexibility for this hexose is also found in computer simulations (vide infra).

The force field MM+ of the *HyperChem* program package was employed for the computer simulations of calonyctin A.[18] Binding parameters for the glycosidic bonds were adapted to experimental data.[19] Two intraglycosidic NOEs per hexose,

Table 2. Proton–proton distances [pm] for β-quinovose in $^4C_1$ conformation and α-rhamnose in $^1C_4$ conformation; average values from 50 ps of MD simulation without NOE distance restraints. Interproton distances for rings a–d were derived from a NOESY spectrum of (*S,R,R*)-**1** (Fig. 2). Due to signal overlap only three NOEs could be used for Qui a; the good quality of the interproton distances in rings b–d obtained from the NOE data is apparent. In all three cases the average deviation Δ is less than 10%.

H–H	$^4C_1$	Qui a	Qui b	Qui d	$^1C_4$	Rha c
1 2	*303*		283	297	*245*	229
1 3	*255*		255	261	*365*	320
1–4	*388*	332	333	353	*429*	–
1–5	*234*	221	220	220	*356*	351
2–3	*300*		268	246	*226*	233
2–4	*247*	–	255	248	*383*	–
2–5	*381*	–	334	313	*379*	334
3–4	*303*	–	268	290	*311*	–
3–5	*251*	–	253	254	*237*	228
4 5	*299*	265	272	271	*309*	–
Δ[%]		12	8	9		9

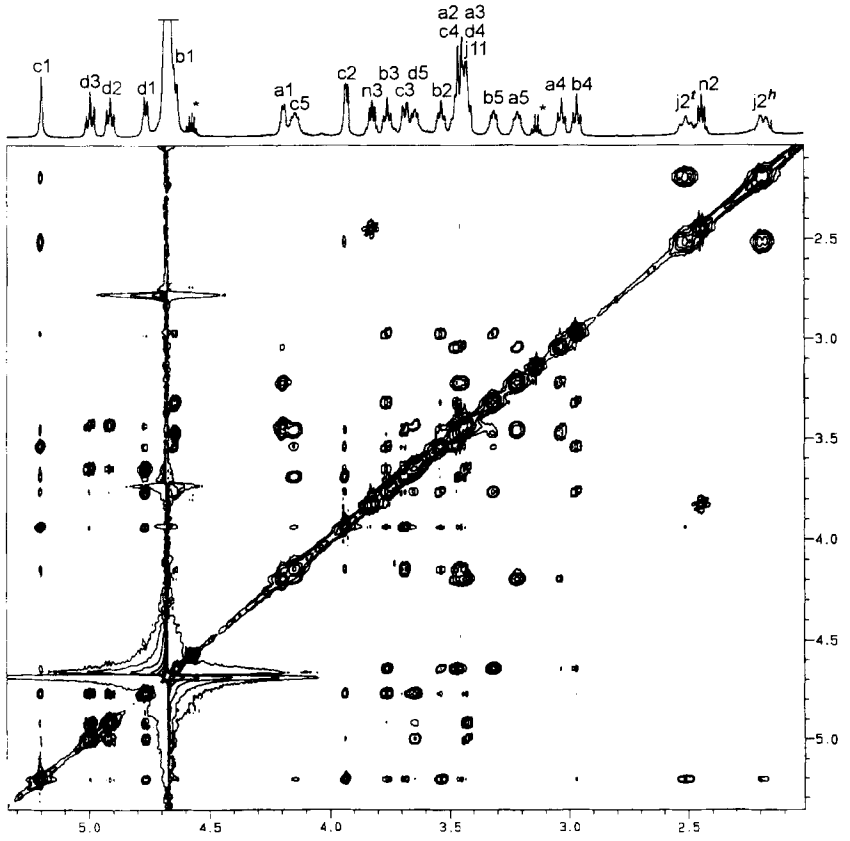

Fig. 2. Section from the NOESY spectrum of calonyctin A (**1**) (600 MHz, 300 K, 98.4% $[D_{25}]$SDS; micelle signals are marked with stars). The insertion of the glycolipid into the surface of the micelles slows down molecular tumbling and leads to intense NOE buildup rates in the NOESY spectrum.

four NOEs between quinovose c and jalapinolic acid, and 26 interglycosidic NOEs (total 38) served as experimental distance restraints in a molecular dynamics (MD) simulation. NOE distances were implemented as penalty terms in the computer simulation; a force constant of 7 kcal mol^{-1} Å^{-2} was used for the pseudo-potentials. Two starting structures converged after 50 ps of MD at 1000 K. During the following 75 ps at 300 K, 150 structures were stored; the average NOE violation is again less than 10% (Table 3). The ten superimposed structures shown in Figure 4 were determined in steps of 5 ps. A last simulation over 50 ps without NOE restraints shows no significant differences to the NOE structures. Thus, the structures in Figures 3 and 4 represent an energetic minimum in the physical force field independent of the experimental data.[20]

The glycosidic angles ϕ and ψ are within the expected ranges;[21] enhanced flexibility in the region of quinovose a is reflected by a wider fluctuation of glycosidic angles about their average values (Table 4).

The macrolide ring leads to a stabilization of the solution conformation of calonyctin A. Interproton distances determined in the biomimetic environment of SDS micelles are fulfilled by a single conformation of **1** recorded during the MD simulation. Apparently the amphiphilic glycolipid inserts its two hydrophobic fatty acid chains into the micelles. The tetrasaccharide moiety is aligned along the surface of the pseudo-membrane, and the hydroxyl groups form a network of hydrogen bonds with the polar head groups of the SDS membrane. Calonyctin A is clearly distinguished from other glycolipids, which have their carbohydrate chains oriented perpen-

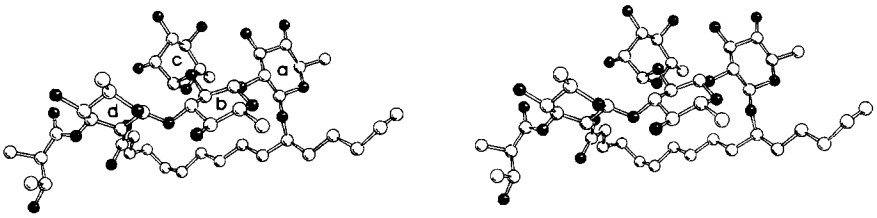

Fig. 3. Stereoplot of calonyctin A (**1**) (C: white, O: black). The glycolipid is shown after 75 ps of MD simulation at 300 K with NOE distance restraints.

Table 3. 26 Interproton distances [pm] in the four monosaccharide units of (*S,R,R*)-**1** in SDS micelles. The four distances between d and the geminal pair of protons in jalapinolic acid that is not diastereotopically assigned (numbering according to Fig. 1) were extended by 50 pm. The columns labeled MD contain the averaged distances from the MD simulation over 75 ps at 300 K. *l* and *h* denote the low-field or high-field signal in the ^{1}H NMR spectrum.

H-H	NOE	MD	H-H	NOE	MD
c1-d1	267	235	c5-b1	344	348
c1-d2	369	377	d1-b2	329	361
c1-d3	379	401	d1-b3	230	222
c1-d5	363	434	d1-b4	381	421
c1-b2	228	228	d1-b5	399	472
c1-b3	318	328	d2-b2	431	463
c1-b4	372	423	d2-b3	400	432
c1-b5	477	535	d2-b4	404	423
c2-d1	264	242	d5-b3	288	335
c2-d3	388	371	b1-a4	366	419
c2-b2	325	410	b2-a1	372	415
c2-b3	326	358	c1-2^l	350	
c2-d5	343	353	c1-2^h	350	
c3-b2	336	408	c2-2^l	400	
c5-b2	297	323	c2-2^h	400	

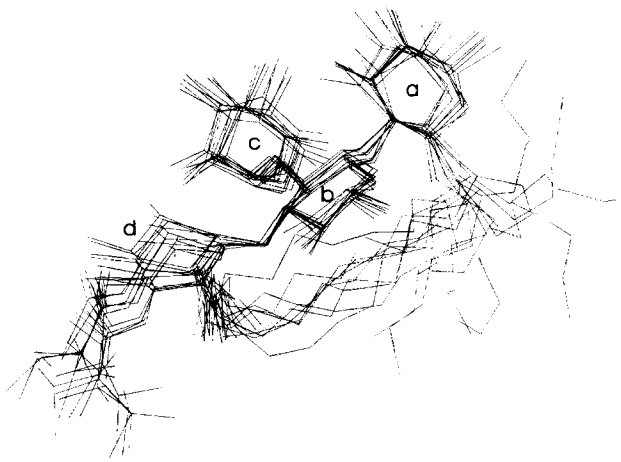

Fig. 4. Ten superimposed structures of calonyctin A (**1**) obtained in steps of 5 ps from MD simulation at 300 K. The conformation of the tetrasaccharide moiety is obviously less variable than those of the fatty acid chains [23].

Table 4. Average glycosidic angles ϕ and ψ [°] from an MD simulation over 75 ps at 300 K. The second column contains the root mean square deviation D [$D(x) = (x^2 - x^2)^{1/2}$].

	$\phi(H^1\text{-}C^1\text{-}O^x\text{-}C^x)$	$D(\phi)$	$\psi(C^1\text{-}O^x\text{-}C^x\text{-}H^x)$	$D(\psi)$
Qui (a)	45.6	*13.5*	28.0	*25.6*
Qui (b)	33.0	*12.7*	46.5	*21.4*
Rha (c)	43.4	*6.9*	26.3	*6.8*
Qui (d)	51.9	*7.1*	−5.3	*7.5*

dicular to the membrane surface; glycosphingolipids, for example, extend far into the periplasmic space.[22]

Reduction of the rotational degrees of freedom by ring formation is a well-known principle in nature and frequently found in peptides and macrolides; as a result their selectivity in ion or receptor binding and stability against enzymatic digestion is enhanced. Calonyctin A is the first cyclic plant glycolipid whose structure has been proved by total synthesis and whose configuration and conformation have been analyzed in detail. The development of new drugs derived from oligosaccharides can profit from studies of native glycolipids along this line.

Received: June 8, 1995 [Z 8072 IE]
German version: *Angew. Chem.* **1995**, *107*, 2730–2734

Keywords: calonyctin A · glycolipids · glycoside syntheses · macrolides · molecular dynamics simulation

[1] Y.-W. Fang, W.-R. Chai, S.-M. Chen, Y.-Z. He, L. Zhao, J.-H. Peng, H.-W. Huang, B. Xin, *Carbohydr. Res.* **1993**, *245*, 259–270.
[2] J. L. Ding, *Acta Nong Ye* **1952**, *3*, 17–24; Y. C. Hue, Q. Z. Guo, R. Pastor, G. Serratrice, A. Gambon, C. Bosso, *Youji Huaxue* **1989**, 146–150 [*Chem. Abstr.* **1989**, *111*, 214831f].
[3] Z.-H. Jiang, R. R. Schmidt, *Liebigs Ann. Chem.* **1994**, 645–651.
[4] Z.-H. Jiang, Dissertation, Universität Konstanz, **1995**.
[5] Structural data can be obtained from Dr. A. Geyer, Universität Konstanz.
[6] Y-H. Chen, Q.-Z. Guo, *Huaxue Xuebao* **1984**, *42*, 385–387 [*Chem. Abstr.* **1984**, *101*, 72253]; R. L. Danheiser, D. D. Cha, *Tetrahedron Lett.* **1990**, *31*, 1527–1530.
[7] H. Shibuya, K. Kawashina, N. I. Baetz, N. Narita, M. Yoshikawa, I. Kitagawa, *Chem. Pharm. Bull.* **1989**, *37*, 260–262.
[8] M. Ono, K. Kuwabata, T. Kawasaki, K. Miyahara, *Chem. Pharm. Bull.* **1992**, *40*, 2674–2680; M. Ono, F. Yamada, N. Noda, T. Kawasaki, K. Miyahara, *ibid.* **1993**, *41*, 1023–1026.
[9] E. J. Corey, K. C. Nicolaou, *J. Am. Chem. Soc.* **1974**, *96*, 5614–5616; E. J. Corey, D. J. Brunelle, *Tetrahedron Lett.* **1976**, *38*, 3409–3412.
[10] A. Marandubo, A. Veyrières, *Carbohydr. Res.* **1985**, *135*, 330–336.
[11] G. Fratér, U. Müller, W. Günther, *Tetrahedron* **1984**, *40*, 1269–1277.
[12] N. Noda, H. Kobayashi, K. Miyahara, T. Kawasaki, *Chem. Pharm. Bull.* **1988**, *36*, 627–633, 920–929; N. Noda, M. Ono, K. Miyahara, T. Kawasaki, *Tetrahedron* **1987**, *43*, 3889–3902.
[13] We thank Professor Y.-W. Fang for providing us with an authentic sample.
[14] M. F. Summers, L. G. Marzilli, A. Bax, *J. Am. Chem. Soc.* **1986**, *108*, 4285–4294.
[15] J. Jeener, B. H. Meier, P. Bachman, R. R. Ernst, *J. Chem. Phys.* **1979**, *71*, 4546–4553; C. Macura, Y. Huang, D. Suter, R. R. Ernst, *J. Magn. Res.* **1981**, *34*, 259–281.
[16] A. Kumar, G. Wagner, R. R. Ernst, K. Wüthrich, *J. Am. Chem. Soc.* **1981**, *103*, 3654–3658.
[17] C. Altona, C. A. G. Haasnoot, *Org. Magn. Reson.* **1980**, *13*, 417–429.
[18] *HyperChem* program package, Hypercube Inc., Waterloo, Ontario, Canada, **1994**.
[19] H. Kessler, H. Matter, G. Gemmecker, M. Kottenhahn, J. W. Bats, *J. Am. Chem. Soc.* **1992**, *114*, 4805–4818.
[20] J. Saulitis, D. F. Mierke, G. Byk, C. Gilon, H. Kessler, *J. Am. Chem. Soc.* **1992**, *114*, 4818–4827.
[21] M. C. Jarvis, *Carbohydr. Res.* **1994**, *259*, 311–318.
[22] S. Hakomori, *Sci. Am.* **1986**, *254*, 32–41.
[23] We thank Dr. Erich Graf von Roedern for the program *sup_multi.exe*.

Synthesis of Novel Tetrathiafulvalene-Based [3]Pseudocatenanes by Self-Assembly; Prevention of *trans/cis* Isomerization**

Zhan-Ting Li, Paul C. Stein, Niels Svenstrup, Kirsten H. Lund, and Jan Becher*

Dedicated to Professor Richard Neidlein on occasion of his 65th birthday

Catenanes, molecules consisting of interlocked rings, were prepared initially by the statistical threading method or by the Möbius strip approach, and the yields were usually very low.[1] During the past decade the applications of metal templating[2] and noncovalent interactions[3] have made such molecules preparatively accessible; the second strategy was developed by Stoddart et al. and has been utilized by other groups to synthesize different types of catenanes.[4]

Our studies on the synthesis of tetrathiafulvalene(TTF)-containing macrocyclic systems using the readily available 1,3-dithiole-2-thione-4,5-dithiolate[5–7] recently resulted in the development of a convenient method for their construction.[8] It is known that TTF forms a strong 1:1 electron-transfer complex with the π-electron-accepting, tetracationic cyclophane cyclobis(paraquat-*p*-phenylene),[9] and a molecular shuttle incorporating a TTF unit as an electron donor has also been reported.[10] We were therefore interested in exploring the possibility of synthesizing TTF-based catenanes by self-assembly. We expected that novel types of catenanes could be constructed,[11] because the TTF moiety is, in principle, tetravalent, while most building blocks hitherto used to construct macrocyclic and hence catenane systems, for example hydroquinone, phenylene-1,4-diamine, benzidine, and bipyridine, are divalent. In this report we describe the efficient preparation of two TTF-based bismacrocyclic compounds and subsequently the synthesis of a novel type of [3]pseudocatenanes by self-assembly. These new pseudocatenanes were characterized by electrospray mass spectrometry, NMR spectroscopy, and elemental analysis.

Biscycles **4** and **7** were chosen as the electron donors, because CPK models indicated that the triethylene glycol chains (albeit in a strained conformation) would lead to a separation between the TTF unit and hydroquinone or hydroanthroquinone units of approximately 7 Å. This distance had been identified as being optimal for the complexation of paraquat, because π–π charge-transfer stabilization is most effective when the interacting rings are 3.5 Å apart.[3a] The difference in the sizes and electrondonating abilities of the hydroquinone and hydroanthraquinone units might have a significant influence on the self-assembly and hence the structures and properties of the products. The synthesis of **4** from **1**[12] and **2**[13] by two-step macrocyclizations under high-dilution conditions in *N*,*N*-dimethylformamide (DMF) is shown in Scheme 1.[14] In a similar way, **7** was prepared from **1** and **5**[15] (Scheme 1).

Catenanes **10**·4PF$_6$, **11**·4PF$_6$, and **12**·4PF$_6$ self-assembled on treatment of the dication **8**·2PF$_6$[17] and 1,4-bis(bromomethyl)benzene (**9**) with an excess of **4** in DMF at room temperature and under atmospheric pressure (Scheme 2). Cate-

[*] Prof. Dr. J. Becher, Dr. Z.-T. Li, Dr. P. C. Stein, N. Svenstrup, K. H. Lund
Department of Chemistry, Odense University
Campusvej 55, DK-5230 Odense M (Denmark)
Telefax: Int. code + (66) 158780

[**] We thank the Forskerkademiet of Denmark for a Danvis postdoctoral fellowship (to Z.-T. L.).

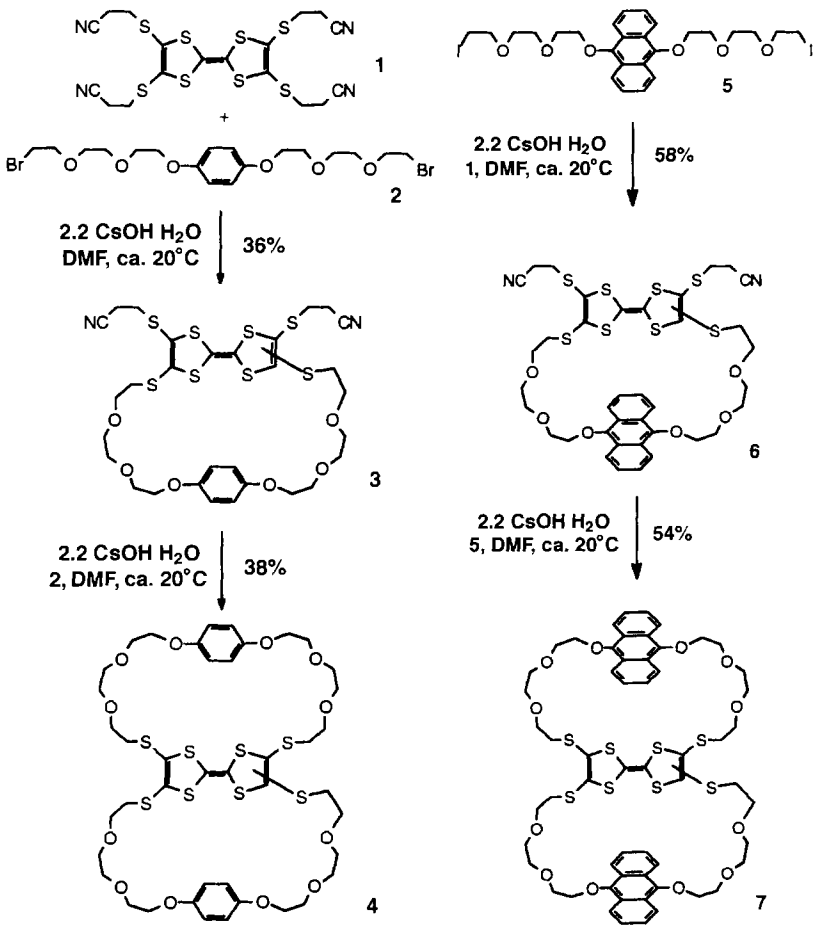

Scheme 1. The synthesis of **3**, **4**, **6**, and **7** under high-dilution conditions; **3**, **4**, **6**, and **7** are mixtures of *trans*/*cis* isomers [16].

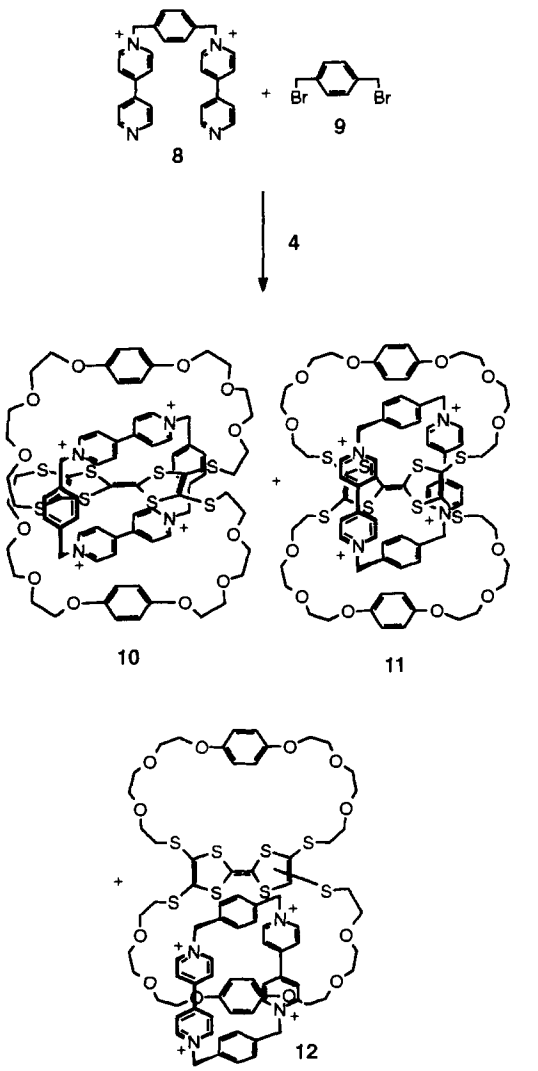

Scheme 2. Synthesis of [3]pseudocatenanes **10**·4PF$_6$, **11**·4PF$_6$, and **12**·4PF$_6$ by self-assembly. For details see the Experimental Procedure.

nanes **10**·4PF$_6$, **11**·4PF$_6$, and **12**·4PF$_6$ (a mixture of *trans* and *cis* isomers according to the ^{1}H NMR spectrum) were obtained in yields of 15, 10, and 4%, respectively. However, under similar conditions, the reaction of **7**, **8**·2PF$_6$, and **9** gave only one product, catenane **13**·4PF$_6$, in 4% yield [Eq.(a)]. We attribute

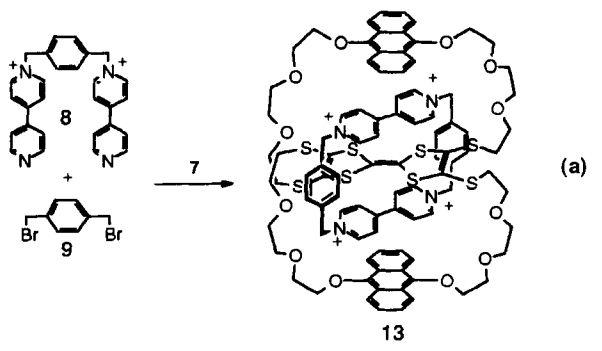

the low yield to the greater steric demand of the anthracene units. No catenane with *cis* structure like that of **11**·4PF$_6$ was detected. As expected, a product with a structure similar to that of **12**·4PF$_6$ was not produced because the anthracene units is too large to be encircled by the cyclobis(paraquat)-*p*-phenylene macrocycle. When this reaction was conducted under high pressure (10 kbar), **13**·4PF$_6$ was produced in 27% yield. We refer to these compounds as [3]pseudocatenanes because **4** and **7** consist of two macrocyclic units and one central TTF group.

All the catenanes were characterized by electrospray mass spectrometry.[18] It is worth noting that, in addition to other peaks, all the catenanes gave the ion peaks corresponding to the loss of four PF_6^- ions from three catenane species: *m*/*z* 1437 for **10**·4PF$_6$, **11**·4PF$_6$, and **12**·4PF$_6$, and *m*/*z* 1587 for **13**·4PF$_6$.[19]

The configurations of **10**·4PF$_6$, **11**·4PF$_6$, and **13**·4PF$_6$ were determined by ^{1}H NMR, ^{13}C NMR, DQ-COSY, and NOESY spectra.[20] The ^{1}H NMR spectra of **10**·4PF$_6$ and **11**·4PF$_6$ at room temperature are shown in Figure 1. Although the protons of the hydroquinone units of **10**·4PF$_6$ give rise to only a single signal (probably because of rapid rotation around the glycol chains), both the α- and the β-protons of the bipyridinium rings give rise to two signals with the same integrative strength (Fig. 1A). This proves that **10**·4PF$_6$ is D_2-symmetric and has a *trans* configuration. In contrast **11**·4PF$_6$ gives two simple doublets at $\delta = 8.95$ and 7.82, corresponding to the α- and β-protons of the bipyridinium rings and reflecting its D_{2h} symmetry and *cis* configuration (Fig. 1B). The α- and β-protons of the bipyridinium rings of **13**·4PF$_6$ are also each split into two signals, indicating its *trans* configuration and D_2 symmetry. The

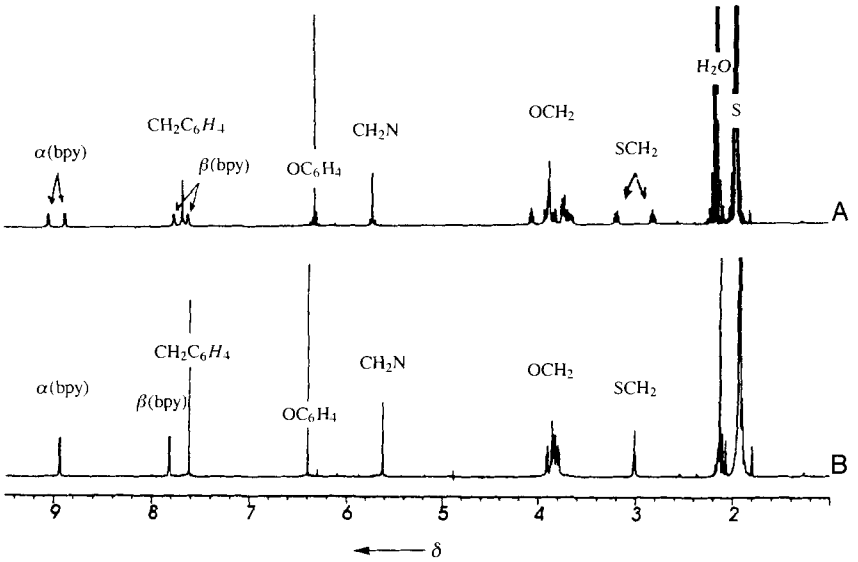

Fig. 1. 500 MHz ^{1}H NMR spectra of **10**·4PF$_6$ (A) and **11**·4PF$_6$ (B) in CD_3CN at room temperature.

resonances attributed to the polyether moieties are nonequivalent for **10**·4PF$_6$ and **13**·4PF$_6$ but equivalent for **11**·4PF$_6$. This proves that **10**·4PF$_6$ and **13**·4PF$_6$ exhibit a *trans* and **11**·4PF$_6$ a *cis* configuration. The symmetry of the polyether moiety in **11**·4PF$_6$ indicates that the polyether chains lie in the plane of the TTF unit. The ^{1}H NMR spectrum of **11**·4PF$_6$ is independent of temperature between -35 and 75 °C, whereas the signals of the aromatic protons of **10**·4PF$_6$ and **13**·4PF$_6$ show a strong temperature dependence. NOESY (chemical exchange) spectra prove that this temperature dependence is due to thermally activated exchange between sites on the aromatic rings. It seems that the rotational barrier is higher in **13**·4PF$_6$. The fact that the ^{1}H NMR spectrum of **11**·4PF$_6$ is temperature independent, and especially the fact that the observed scalar couplings between the protons of the polyether moiety are temperature independent, show that all motions of the polyether chains of **11**·4PF$_6$ are frozen out on the NMR time scale. The pyridine and hydroquinone or hydroanthraquinone rings are highly mobile in the *trans* compounds, **10**·4PF$_6$ and **13**·4PF$_6$. This indicates that the polyether moieties are configurated such that there is room enough for these ring systems to rotate around their axes. The hydroquinone rings of the *cis* compound **11**·4PF$_6$ do not show any sign of such motion. The only way to explain this result is that the position of the benzene rings of the tetracationic macrocycle stabilizes the hydroquinone rings by $\pi-\pi$ stacking. Such stacking is not possible in a *trans* configuration.

The redox behavior of the bicycles **4** and **7** and all the catenanes was investigated by cyclic voltammetry (CV) and their half-wave potentials are listed in Table 1. For **4** and **7** the first two redox waves result from the oxidation to the monocation and the dication of the TTF units, while the third redox waves are attributed to the oxidation of the hydroquinone and hydroanthraquinone units, respectively. All three oxidation steps of **7** are at significantly lower potentials than those of **4** because of the stronger electron-donating ability of the hydroanthraquinone units and their greater interactions with the TTF unit. The values of **10**·4PF$_6$ and **11**·4PF$_6$ show no significant difference, indicating that the change in configuration does not greatly affect the redox process. The first two oxidation steps of **12**·4PF$_6$, that is, the oxidation of the TTF unit to the mono- and dication, are very similar to those of **4** and apparently unaffected by the bipyridium macrocycle. This indicates that the interaction between the TTF unit and the bipyridium units in **12**·4PF$_6$ is weaker than in **10**·4PF$_6$ and in **11**·4PF$_6$. For pseudocatenane **13**·4PF$_6$ the last three waves correspond to the three processes described above; in addition a very low-energy redox process occurs as the first wave. We speculate that this process results from the intermolecular stacking interaction between two hydroanthraquinone units. UV/Vis spectra in acetonitrile reveal the charge-transfer absorption bands of **10**·4PF$_6$, **11**·4PF$_6$, **12**·4PF$_6$, and **13**·4PF$_6$ centered at 785 ($\varepsilon = 3100$), 807 (2900), 770 (900), and 773 nm (4200 $M^{-1}cm^{-1}$), respectively.

Table 1. Half wave-potentials [V] for the oxidation by cyclic voltammetry, determined in MeCN; electrolyte Bu_4NPF_6; electrolyte 100 mVs^{-1}, vs. Ag/AgCl [a].

Cmpd.	$E^1_{1/2}$	$E^2_{1/2}$	$E^3_{1/2}E^4_{1/2}$
4 [b]	0.50	0.79	1.38 (irrev.)
7 [b]	0.38	0.73	1.05 (irrev.)
10·4PF$_6$	0.63	0.94	1.34
11·4PF$_6$	0.62 (irrev.)	0.92 (irrev.)	1.34
12·4PF$_6$	0.58	0.82	1.28
13·4PF$_6$	0.21 (irrev.)	0.52 (irrev.)	0.87 (irrev.)1.19

[a] Reversible redox process unless noted otherwise. [b] Determined in CH_2Cl_2.

Addition of trifluoroacetic acid (0.1 M) to the solution of **10**·4PF$_6$ or **11**·4PF$_6$ in acetonitrile did not lead to any change that could be detected by TLC, indicating that *trans*/*cis* isomerization did not take place. This was also the case for **13**·4PF$_6$. These surprising observations seem to indicate that once the tetracationic macrocycle is interlocked around the TTF unit, it will efficiently prevent the protonation and hence isomerization of the TTF unit.[21] This observation may be important for the future use of TTF-derived macrocycles in supramolecular chemistry.[22]

Stoddart et al. originally developed the idea of using donor–acceptor interactions in the synthesis of catenanes. The template-directed synthetic strategy described here for inclusion of a TTF unit within catenanes is the first stage in the synthesis of a series of more elaborate and complex TTF-based catenanes. Replacing the hydroquinone and hydroanthraquinone units with other electron-rich systems such as hydronaphthoquinone and incorporating multiple TTF units into the macrocyclic polyether groups should lead to the construction of new types of catenanes.

Experimental Procedure

3: Under an atmosphere of nitrogen, **1** (1.09 g, 2.0 mmol) was stirred in DMF (40 mL). A solution of cesium hydroxide monohydrate (0.74 g, 4.4 mmol) in methanol (10 mL) was added dropwise with stirring within 10 min, and the resulting solution was stirred for 1 h. Then this solution and a solution of **2** (1.0 g, 2.0 mmol) in DMF (50 mL) were added simultaneously with a perfusor pump to 100 mL of DMF over 10 h at room temperature with stirring under high-dilution conditions. Stirring was continued for another 2 h and the reaction mixture concentrated in vacuo. The residue was then partly dissolved in dichloromethane (200 mL). The solution was washed with water (3 × 50 mL), dried ($MgSO_4$), and concentrated in vacuo to afford an oily residue, which was purified by column chromatography on silica gel using CH_2Cl_2/EtOAc (5:1) as an eluent. Compound **3** was obtained as an orange oil (0.56 g, 36%). ^{1}H NMR ($CDCl_3$): $\delta = 2.69$ (m, 4H), 3.04 (m, 8 H), 3.69 (m, 12H), 3.81 (m, 4H), 4.10 (m, 4H), 6.85 and 6.88 (s, 4H); EI-MS: *m/z* (%): 778 (4), 776 (11) [M^+], 537 (5), 436 (27), 404 (71), 172 (65), 54 (100), 32 (94); Anal. calcd. for $C_{30}H_{36}N_2O_6S_8$: C 46.36, H 4.68, N 3.61; found: C 46.12, H 4.49, N, 3.77.

4: Reaction of **3** and **2** in a similar way afforded **4** in 38% yield as an orange oil. ^{1}H NMR ($CDCl_3$): δ = 2.95 (m, 8H), 3.60 (m, 24H), 3.80 (s, 8H), 4.10 (m, 8H), 6.84 and 6.88 (s, 8H); EI-MS: m/z (%): 1008 (18) [M^+], 883 (10), 518 (28), 414 (40), 76 (100), 45 (77); Anal. calcd. for $C_{42}H_{56}O_{12}S_8$: C 49.97, H 5.60; found: C 49.89, H 5.72.

6: Orange oil, prepared from **1** and **5** in 58% yield according to a procedure similar to that used for the synthesis of **3**. ^{1}H NMR ($CDCl_3$): δ = 2.39 (t, 2H), 2.68 (t, 2H), 2.81 (t, 2H), 3.01 (t, 2H), 3.09 (m, 4H), 3.72–3.90 (m, 12H), 3.97 (m, 4H), 4.36 (m, 4H), 7.38 (m, 2H), 7.51 (m, 2H), 8.45 (m, 4H); EI-MS: m/z (%): 876 (8) [M^+], 208 (87), 76 (100); Anal. calcd. for $C_{38}H_{40}N_2O_6S_8$: C 52.02, H 4.61, N 3.19; found: C 52.14, H 4.60, N 3.40.

7: Orange oily solid, prepared from **5** and 6 in 54% yield. ^{1}H NMR ($CDCl_3$): δ = 2.84 (m, 4H), 2.92 (m, 4H), 3.05 (m, 8H), 3.75 (m, 24H), 3.97 (m, 8H), 4.34 (m, 8H), 7.39 (m, 4H), 7.49 (m, 4H), 8.39 (m, 8H); PD-MS: m/z: 1209.4 [M^+]. The compound was unstable and therefore used directly in the next step.

10·4PF_6, **11**·4PF_6, and **12**·4PF_6: A solution of **4** (200 mg, 0.2 mmol), **8**·2PF_6 (71 mg, 0.1 mmol), and **9** (29 mg, 1.1 mmol) in dry DMF (15 mL) was stirred under nitrogen at room temperature and under atmospheric pressure for 10 d. The solvent was then removed in vacuo and CH_2Cl_2 (20 mL) added. The resulting green solid was removed by filtration and washed with CH_2Cl_2 (2 × 10 mL). The organic phases were combined and concentrated in vacuo, giving 160 mg (80%) of starting material **4**. The solid residue was purified using column chromatography (silica gel) with MeOH/2 M aqueous NH_4Cl solution/$MeNO_2$ (7:2:1) as the eluent. Two blue fractions and one brown fraction were eluted from the column. The first fraction afforded a blue solid, which was partially dissolved in MeOH, filtered, and dried again. The residue was then dissolved in a minimum amount of water (about 8 mL), and a saturated aqueous NH_4PF_6 solution was added until precipitation was complete. The solid product was removed by filtration (Celite), washed with water, dried under vacuum, and then extracted with MeCN. After the solvent was removed under vacuum, 32 mg (15%) of **10**·4PF_6 was obtained as a dark blue solid. M.p. 220 °C (decomp); ^{1}H NMR (CD_3CN): δ = 2.80 (m, 4H; SCH_2), 3.21 (m, 4H; SCH_2), 3.71–4.12 (m, 40H; OCH_2), 5.66 (s, 8H; NCH_2), 6.32 (s, 8H; OC_6H_4), 7.63 (d, 4H; β-CH), 7.68 (s, 8H; $C_6H_4CH_2$), 7.80 (d, 4H; β-CH), 8.82 (d, 4H; α-CH), 9.01 (d, 4H; α-CH); ES-MS: m/z: 1437 [$(3M-4PF_6)^{4+}$], 1261 [$(2M-3PF_6)^{3+}$], 1008 [4^+], 909 [$(M-2PF_6)^{2+}$], 558 [$(M-3PF_6)^{3+}$], 382 [$(M-4PF_6)^{4+}$]; Anal. calcd. for $C_{78}H_{88}N_4O_{12}F_{24}P_4S_8 \cdot 2H_2O$: C 43.66, H 4.33, N 2.61; found: C 43.74, H 4.51, N 3.05.

Similarly, **11**·4PF_6 (21 mg, 10%) and **12**·4PF_6 (8 mg, 4%) were obtained after workup. **11**·4PF_6: Dark blue solid; m.p. 185 °C (decomp); ^{1}H NMR (CD_3CN): δ = 3.01 (t, 8H; SCH_2), 3.77–3.92 (m, 40H; OCH_2), 5.62 (s, 8H; NCH_2), 6.41 (s, 8H; OC_6H_4), 7.63 (s, 8H; $C_6H_4CH_2$), 7.82 (s, 8H; β-CH), 8.95 (s, 4H; α-CH); ES-MS: m/z: 1964 [$(M-PF_6)^+$], 1437 [$(3M-4PF_6)^{4+}$], 1261 [$(2M-3PF_6)^{3+}$], 909 [$(M-2PF_6)^{2+}$], 558 [$(M-3PF_6)^{3+}$], 382 [$(M-4PF_6)^{4+}$]; Anal. calcd. for $C_{78}H_{88}N_4O_{12}F_{24}P_4S_8 \cdot 2H_2O$: C 43.66, H 4.33, N 2.61; found: C 43.88, H 4.19, N 2.67.

12·4PF_6: Brown solid; m.p. 200 °C (decomp); ES-MS: m/z: 1964 [$(M-PF_6)^+$], 1437 [$(3M-4PF_6)^{4+}$], 1261 [$(2M-3PF_6)^{3+}$], 909 [$(M-2PF_6)^{2+}$], 558 [$(M-3PF_6)^{3+}$], 382 [$(M-4PF_6)^{4+}$]; Anal. calcd. for $C_{78}H_{88}N_4O_{12}F_{24}P_4S_8 \cdot H_2O$: C 44.03, H 4.27, N 2.63; found: C 44.42, H 4.52, N 2.73; Because **12**·4PF_6 is a mixture of *trans* and *cis* isomers, it is difficult to assign its ^{1}H NMR spectrum.

13·4PF_6: A solution of **7** (360 mg, 0.2 mmol), **8**·2PF_6 (71 mg, 0.1 mmol), and **9** (32 mg, 1.2 mmol) in dry DMF (40 mL) was stirred in the dark at room temperature and under atmospheric pressure for three weeks. The solvent was then removed under high vacuum without heating and CH_2Cl_2 (30 mL) added. The solid material was removed by filtration and washed with CH_2Cl_2 (2 × 20 mL). The organic phases were combined and, after concentration, gave 330 mg (92%) of starting material **7**. The solid residue was subjected to column chromatography. After workup, 9 mg (4%) of **13**·4PF_6 was obtained as a dark blue solid. **13**·4PF_6 was also obtained in 27% yield from a reaction conducted under ultrahigh pressure (10 kbar) at room temperature over 3 d. M.p. 250 °C (decomp); ^{1}H NMR (CD_3CN): δ = 2.70 (m, 4H; SCH_2), 3.13 (m, 4H; SCH_2), 3.55 (m, 8H; OCH_2), 4.04 (s, 8H; OCH_2), 4.13 (m, 4H; OCH_2), 3.82 (m, 16H; OCH_2), 4.47 (m, 4H; OCH_2), 5.59 (dd, 8H; NCH_2), 6.95 (d, 4H; 1-CH(anth)), 7.32 (d, 4H; 4-CH(anth)), 7.35 (t, 4H; 2-CH(anth)), 7.50 (t, 4H; 3-CH(anth)), 7.60 (s, 8H; $C_6H_4CH_2$), 7.86 (d, 4H; β-CH), 8.13 (d, 4H; β-CH), 8.50 (dd, 4H; α-CH), 8.87 (dd, 4H; α-CH); ES-MS: m/z: 1587 [$(3M-4PF_6)^{4+}$], 1395 [$(2M-3PF_6)^{3+}$], 1009 [$(M-2PF_6)^{2+}$], 625 [$(M-3PF_6)^{3+}$], 432 [$(M-4PF_6)^{4+}$]; Anal. calcd. for $C_{94}H_{96}N_4O_{12}F_{24}P_4S_8$: C 48.87, H 4.20, N 2.43; found: C 49.00, H 3.99, N 2.27.

Received: July 6, 1995 [Z8176IE]
German version: *Angew. Chem.* **1995**, *107*, 2719–2723

Keywords: catenanes · crown ethers · self-assembly · tetrathiafulvalenes

[1] G. Schill, *Catenanes, Rotaxanes, and Knots*, Academic Press, New York, **1971**.
[2] a) C. O. Dietrich-Buchecker, J.-P. Sauvage, *Chem. Rev.* **1987**, *87*, 795; b) A.-M. Albrecht-Gary, C.-O. Dietrich-Buchecker, Z. Saad, J.-P. Sauvage, *J. Chem. Soc. Chem. Commun.* **1992**, 280.
[3] a) P. L. Anelli, P. R. Ashton, R. Ballardini, V. Balzani, M. Delgado, M. T. Gandolfi, T. T. Goodnow, A. E. Kaifer, D. Philp, M. Pietraszkiewicz, L. Prodi, M. V. Reddington, A. M. Z. Slawin, N. Spencer, J. F. Stoddart, C. Vicent, D. J. Williams, *J. Am. Chem. Soc.* **1992**, *114*, 193; b) D. B. Amabillino, P. R. Ashton, C. L. Brown, E. Cordova, L. A. Godinez, T. T. Goodnow, A. E. Kaifer, S. P. Newton, M. Pietraszkiewicz, D. Philp, F. M. Raymo, A. S. Reder, J. F. Stoddart, D. J. Williams, *ibid.* **1995**, *117*, 1271; c) D. Philp, J. F. Stoddart, *Synlett* **1991**, 445; d) P. R. Ashton, J. A. Preece, J. F. Stoddart, M. S. Tolley, *ibid.* **1994**, 789; e) P. R. Ashton, L. Perez-Garcia, J. F. Stoddart, A. J. P. White, D. J. Williams, *Angew. Chem.* **1995**, *107*, 607; *Angew. Chem. Int. Ed. Engl.* **1995**, *34*, 571.
[4] a) F. Vögtle, W. M. Müller, U. Müller, M. Bauer, K. Rissanen, *Angew. Chem.* **1993**, *105*, 1356; *Angew. Chem. Int. Ed. Engl.* **1993**, *32*, 1295; b) M. J. Gunter, D. C. R. Hockless, M. R. Johnston, B. W. Skelton, A. H. White, *J. Am. Chem. Soc.* **1994**, *116*, 4810; c) T. Lu, L. Zhang, G. W. Gokel, A. E. Kaifer, *ibid.* **1993**, *115*, 2542.
[5] a) B. Girmay, J. D. Kilburn, A. E. Underhill, K. S. Varma, M. B. Hursthouse, M. E. Harman, J. Becher, G. Bojesen, *J. Chem. Soc. Chem. Commun.* **1989**, 1406; b) J. Becher, T. K. Hansen, N. Malhotra, G. Bojesen, S. Bøwadt, K. S. Varma, B. Girmay, J. D. Kilburn, A. E. Underhill, *J. Chem. Soc. Perkin Trans. 1* **1990**, 175; c) T. Jørgensen, B. Girmay, T. K. Hansen, J. Becher, A. E. Underhill, M. B. Hursthouse, M. E. Harman, J. D. Kilburn, *ibid.* **1992**, 2907; d) T. K. Hansen, T. Jørgensen, P. C. Stein, J. Becher, *J. Org. Chem.* **1992**, *57*, 6403; e) T. K. Hansen, T. Jørgensen, F. Jensen, P. H. Thygesen, K. Christiansen, M. B. Hursthouse, M. E. Harman, M. A. Malik, B. Girmay, A. E. Underhill, M. Begtrup, J. D. Kilburn, K. Belmore, P. Roepstorff, J. Becher, *ibid.* **1993**, *58*, 1359.
[6] For a review on TTF in supramolecular chemistry, see: T. Jørgensen, T. K. Hansen, J. Becher, *Chem. Soc. Rev.* **1994**, 41.
[7] For a review on the chemistry of 1,3-dithiole-2-thione-4,5-dithiolate, see: N. Svenstrup, J. Becher, *Synthesis* **1995**, 215.
[8] J. Becher, J. Lau, P. Leriche, P. Mørk, N. Svenstrup, *J. Chem. Soc. Chem. Commun.* **1994**, 2715.
[9] D. Philp, A. M. Z. Slawin, N. Spencer, J. F. Stoddart, D. J. Williams, *J. Chem. Soc. Chem. Commun.* **1991**, 1584.
[10] P. R. Ashton, R. A. Bissell, N. Spencer, J. F. Stoddart, M. S. Tolley, *Synlett* **1992**, 923. The TTF group used in this rotaxane was a mixture of diastereomers.
[11] For other types of catenanes, see: a) F. Vögtle, S. Meier, R. Hoss, *Angew. Chem.* **1992**, *104*, 1628; *Angew. Chem. Int. Ed. Engl.* **1992**, *31*, 1619; b) S. Ottens-Hildebrandt, S. Meier, W. Schmidt, F. Vögtle, *ibid.* **1994**, *106*, 1818 and **1994**, *33*, 1767; c) G. J. Gruter, F. J. J. Dekanter, P. R. Markies, T. Nomoto, O. S. Akkerman, F. Bickelhaupt, *J. Am. Chem. Soc.* **1993**, *115*, 12179; d) C. A. Hunter, *ibid.* **1992**, *114*, 5303; e) F. J. Carver, C. A. Hunter, R. J. Shannon, *J. Chem. Soc. Chem. Commun.* **1994**, 1277; f) M. Fujita, F. Ibukuro, H. Hagihara, *Nature (London)* **1994**, *367*, 720; g) T. Jørgensen, J. Becher, J.-C. Chambron, J.-P. Sauvage, *Tetrahedron Lett.* **1994**, *35*, 4339; h) D. Armspach, P. R. Ashton, R. Ballardini, V. Balzani, A. Godi, C. P. Moore, L. Prodi, N. Spencer, J. F. Stoddart, M. S. Tolley, T. J. Wear, D. J. Williams, *Chem. Eur. J.* **1995**, *1*, 33; i) S. Ottens-Hildebrandt, M. Nieger, K. Rissanen, J. Rouvinen, S. Meier, G. Harder, F. Vögtle, *J. Chem. Soc. Chem. Commun.* **1995**, 777; j) M. Bauer, W. M. Müller, U. Müller, K. Rissanen, F. Vögtle, *Liebigs Ann.* **1995**, 649; k) M. Fujita, F. Ibukuro, K. Yamaguchi, K. Ogura, *J. Am. Chem. Soc.* **1995**, *117*, 4175; l) J.-C. Chambron, V. Heitz, J.-P. Sauvage, *Bull. Soc. Chim. Fr.* **1995**, *132*, 340.
[12] N. Svenstrup, K. M. Rasmussen, T. K. Hansen, J. Becher, *Synthesis* **1994**, 809.
[13] A. Lüttringhaus, F. Cramer, H. Prinzbach, F. M. Henglein, *Justus Liebigs Ann. Chem.* **1958**, *613*, 185.
[14] TTF-containing macrocyclic compounds have been prepared in most cases using a coupling reaction with trialkyl phosphites from the corresponding thiones (see ref.[6]). There are only few reports to date describing the synthesis of TTF-derived macrocyclic systems starting directly from TTF-containing precursors (see ref.[8]).
[15] A. Castellan, M. Daney, J.-P. Desvergne, M.-H. Riffaud, H. Bouas-Laurent, *Tetrahedron Lett.* **1983**, *24*, 5215.
[16] The isomers could not be separated because they slowly interconverted in solution in the presence of trace amounts of acid; this was detected by thin layer chromatography (TLC). The first step (yielding **3** and **6**) did not afford 2,3-deprotected products (TLC indicated that no other important products formed except insoluble linear oligomers), although tetrathiafulvalene-2,3,6,7-tetrathiolate was produced quantitatively by treatment with eight equivalents of cesium hydroxide (see ref.[12]).
[17] P. R. Ashton, D. Philp, N. Spencer, J. F. Stoddart, *Makromol. Chem. Macromol. Symp.* **1992**, *54/55*, 441.
[18] All spectra were recorded with a Kratos MS50TC instrument operating at 4.7 kV accelerating voltage and fitted with an electrospray ion source.
[19] This type of fragmentation pattern has apparently not been observed before; however, ion peaks corresponding to the loss of three PF_6^- ions from a catenane dimer have been reported, see: P. R. Ashton, C. L. Brown, J. R. Chapman, R. T. Gallagher, J. F. Stoddart, *Tetrahedron Lett.* **1992**, *33*, 7771.

[20] NMR spectra were recorded on a Bruker 250 or a Varian unity 500 spectrometer. The temperature was maintained at 25 °C. ^{1}H, ^{13}C, DQ-COSY, and NOESY spectra were recorded using standard pulse sequences. All chemical shifts are referenced to TMS.

[21] Unsymmetric TTF compounds usually isomerize easily, catalyzed by trace amounts of acid. Two methods have been reported to be able to control the configurational interversion of TTF-based macrocyclic systems. The first utilizes the difference in ring strain between the *trans* and *cis* configurations, see ref.[5] and also F. Bertho-Thoraval, A. Robert, A. Souizi, K. Boubekeur, P. Batail, *J. Chem. Soc. Chem. Commun.* **1991**, 843. In the second approach, one-electron oxidation of [12]- and [14]tetrathiafulvalenophanes was employed to control their *trans/cis* isomerization, see K. Boubekeur, C. Lenoir, P. Batail, R. Carlier, A. Tallec, M.-P. Le Paillard, D. Lorcy, A. Robert, *Angew. Chem.* **1994**, *106*, 1448; *Angew. Chem. Int. Ed. Engl.* **1994**, *33*, 1379. However, in all these cases the planarity of the neutral TTF subunits was prevented by the short chains linking the opposite ends of the TTF groups. We found that the macrocyclic system incorporating a nonplanar TTF unit and a hydroquinone unit did not give catenanes by self-assembly in the presence of **8**·2PF$_6$ and **9** (Z.-T. Li, J. Becher, unpublished results).

[22] We have not yet studied the possibility of photochemical isomerization of these catenanes.

Selective Isomerization of Hydrocarbon Chains on External Surfaces of Zeolite Crystals**

Johan A. Martens,* Wim Souverijns, Wim Verrelst, Rudy Parton, Gilbert F. Froment, and Pierre A. Jacobs

It is generally assumed that the confinement of active sites within micropores is the key to the success of zeolites in a variety of petrochemical processes.[1-4] Although, it has been suggested that active sites present in interrupted cavities and pore mouths at the external surface of zeolite crystals are not merely responsible for selectivity loss, but are able to perform a significantly different catalytic chemistry,[5] the necessity to invoke the active participation of the external surface is still a matter of debate.[6-8] In order to rationalize detailed product distributions of the skeletal isomers produced by isomerization of long-chain *n*-alkanes and alkylcycloalkanes on ZSM-22 zeolite, selective pore mouth catalysis has to be invoked. An array of adjacent pore openings serves as a template for the branching; the spacing of the holes in the crystal surface determines the position of the chain branchings in the hydrocarbon skeletons.

Pore mouth catalysis occurs with bulky substrate molecules that cannot penetrate zeolite micropores and when intracrystalline counter diffusion of reactants and products within the zeolite is slow compared to the rate of the chemical reaction. The latter is typically the case in tubular pore zeolites in which the diameters of the pore openings approach those of the substrate molecules.[9]

To probe external surface catalysis, long-chain *n*-alkanes were allowed to react over ZSM-22 zeolite. The framework of ZSM-22 has parallel, uniform tubular pores with the smallest pore openings (0.55 × 0.45 nm) known for tubular pore zeolites.[10] As the pores run through the crystals in the [001] direction, arrays of pore mouths are available at crystal terminating [001] faces. ZSM-22 was synthesized according to an established recipe[11] and calcined to remove organic compounds. Then an ion exchange with ammonium ions (tenfold excess with respect to the ion exchange capacity) followed by impregnation in aqueous solution with $[Pt(NH_3)_4]^{2+}$ ions was carried out. The subsequent calcination and reduction in a hydrogen atmosphere at 673 K afforded the catalyst with 0.5 wt% of dispersed platinum metal. Scanning electron microscopy showed bundles of crystal needles of 1–2 × 0.1–0.5 μm. An ultrastable (US)-Y zeolite (USY:Si/Al ratio 4.0, prepared from NaY by ion exchange with ammonium ions, followed by steaming, and acid leaching) was included in the study as a reference large-pore zeolite catalyst. This catalyst was activated in the same way as ZSM-22. The reaction products were analyzed with high-resolution gas chromatography (GC) and GC/MS techniques (CPSil5 column with 150000 theoretical plates, length: 100 m).

The yields of specific product fractions from the isomerization of heptadecane over ZSM-22 and USY are plotted as a function of the reaction temperature in Figure 1. The isomeriza-

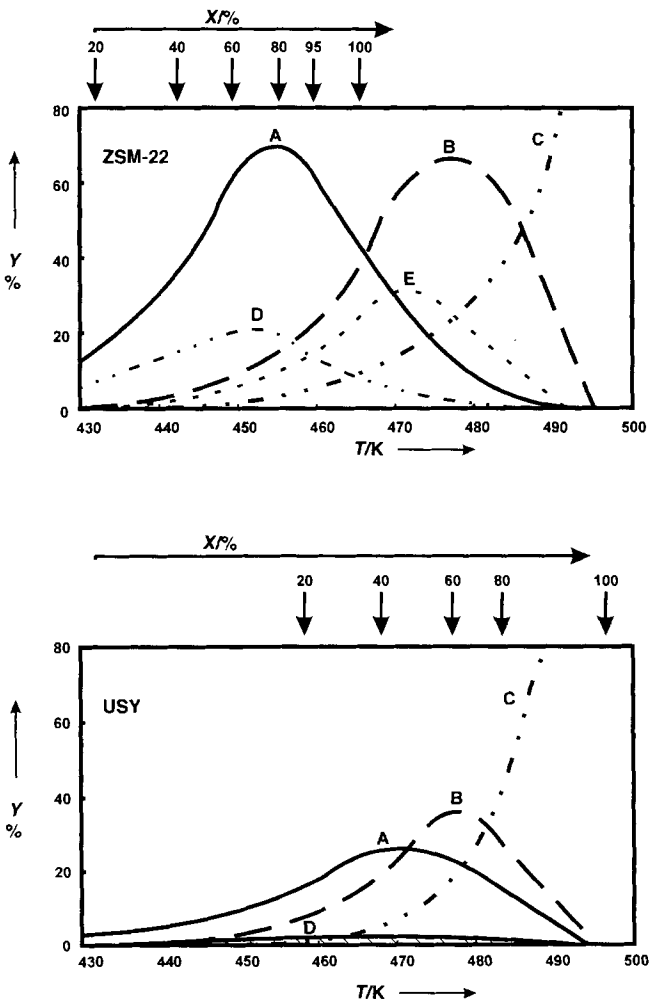

Fig. 1. Product yield (Y) of the heptadecane isomerization on ZSM-22 (top) and USY (bottom) zeolites. The conversion of heptadecane (X) is increased by increasing reaction temperature at constant space time. Monobranched products: curve A, multibranched products: curve B, cracked products: curve C, 2-methylhexadecane: curve D, sum of 2,7-, 2,8-, 2,9-, 2,10-, and 2,11-dimethylpentadecanes: curve E. Reaction conditions: H_2 pressure, 150 kPa; $C_{17}H_{34}$ pressure, 0.5 kPa; space time (W/F_0), 3.7 kg h mol^{-1}. (W is the catalyst weight and F_0 the molar flow rate at the reactor entrance.)

[*] Prof. Dr. Ir. J. A. Martens, Drs. Ir. W. Souverijns, Dr. Ir. W. Verrelst, Dr. Ir. R. Parton, Prof. Dr. Ir. P. A. Jacobs
Centre for Surface Science and Catalysis, KU Leuven
Kard. Mercierlaan 92, B-3001 Heverlee (Belgium)
Telefax: Int. code +(16) 321998
e-mail: Johan.Martens@agr.kuleuven.ac.be
Prof. Dr. Ir. G. F. Froment
Laboratorium von Petrochemische Technick, University of Gent (Belgium)

[**] This work is sponsored by the Belgian Federal Ministery of Science Policy in the frame of a UIAP-PAI programme and by the Flemish NFWO and LOTTO. J. A. M. acknowledges NFWO for a research position; R. P. and W. S. acknowledge NFWO and IWT, respectively, for a research fellowship.

tion to monobranched and multibranched compounds as well as hydrocracking of *n*-heptadecane are consecutive reaction steps on both zeolites. The reactivity of hydrocarbons increases with their degree of branching.[12] In the catalysis with USY the areas below the curves for monobranching, multibranching, and hydrocracking overlap considerably. For ZSM-22, the curve maxima of the consecutive steps are much better separated, and the maximum yields of monobranched and multibranched isomers are significantly higher.

On ZSM-22, monobranching of *n*-heptadecane results in the formation of methyl-branched isomers, and particularly of 2-methylhexadecane, while 4-, 5-, 6-, 7-, and 8-methylhexadecane formation is strongly suppressed (Fig. 2). In contrast for USY,

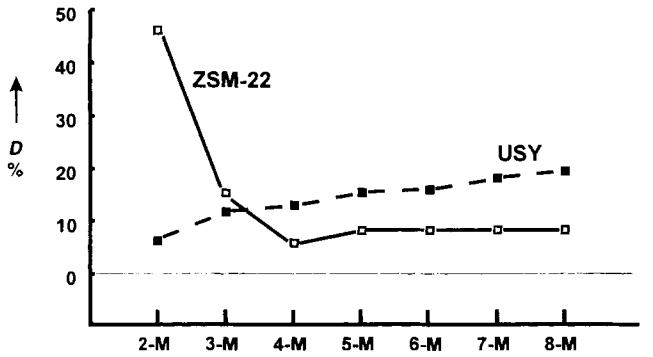

Fig. 2. Distribution (*D*) of methylhexadecane positional isomers at 15% conversion of heptadecane (for reaction conditions see legend to Fig. 1).

methyl branching at central positions in the chain is favored (Fig. 2). The isomerization of decane[11, 13] and dodecane[14] over ZSM-22 zeolites—like in the analogous reaction of heptadecane—was found to result in selective 2-methyl branching. The selectivity with which terminally branched alkane chains can be prepared on ZSM-22 has been ascribed to a pore mouth catalysis mechanism; isoalkanes with the longest possible linear chain are favored.[13]

Multibranching of monobranched isoheptadecanes proceeds only after almost complete conversion of the linear isomer (curve A in Fig. 1). Heptadecane can form 219 possible dibranched and 1171 tribranched isomers. The gas chromatographic analysis of the reaction products obtained on USY (Fig. 3 right) shows two envelopes of overlapping peaks that can be attributed to large numbers of di- and tribranched isoheptadecanes. The gas chromatogram of the compounds formed on ZSM-22, showed only signals for dibranched isoheptadecanes (Fig. 3 left, region B). Of the possible dimethyl-branched isomers, only five are obtained in significant quantities, namely 2,7-, 2,8-, 2,9-, 2,10-, and 2,11-dimethylpentadecane. These products contribute significantly to the overall yield of the multibranched isomers (curve E in Fig. 1). The formation of these specific isomers cannot be attributed to shape-selective reactions inside the uniform tubular micropores of ZSM-22. However, this behavior is readily rationalized when selective catalysis occurs at the [001] planes of the external crystal surface of the zeolite. When 2-methylhexadecane, the preferred monobranched isomer, is stretched across an external [001] crystal face such that the methyl group is pinned in one pore mouth, dibranching appears to occur when a neighboring pore mouth and its active site are in reach. The thickness of the pore wall, that is, the distance between two neighboring pore mouths, thus appears to determine the second branching position (Fig. 4).

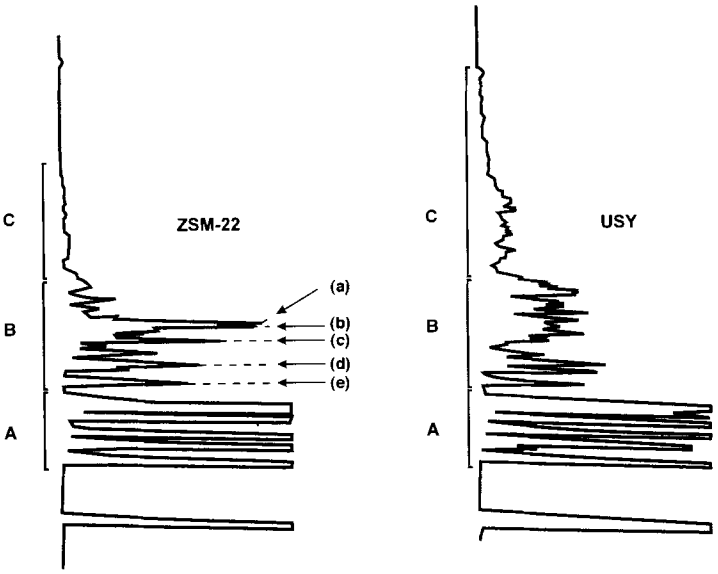

Fig. 3. Gas chromatogram of monobranched (A), dibranched (B), and tribranched (C) isoheptadecane isomers [(a) 2,9-, (b) 2,10-, (c) 2,8-, (d) 2,7-, (e) 2,11-dimethylpentadecane] obtained with ZSM-22 (left) and USY (right) (column: CP-Sil5CB, 60 m (Chrompack), film thickness: 1.31 μm, internal diameter 0.32 mm, 150000 theoretical plates).

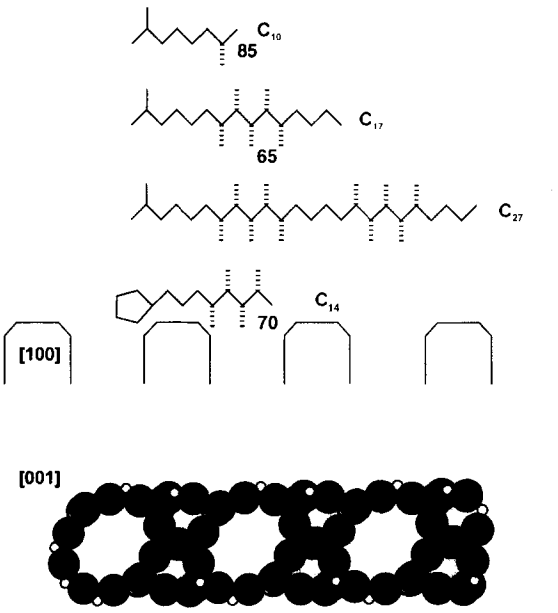

Fig. 4. Observed (for n-$C_{10}H_{22}$, n-$C_{17}H_{36}$, and 1-cyclopentylnonane) maximum product selectivities (%) of multi-methyl-branching of *n*-alkanes and *n*-alkylcycloalkanes by a selective lock-and-key mechanism at the [001] crystal faces of ZSM-22. For details see text.

The preferred isomers can maximize their van der Waals interactions with the zeolite surface; the two methyl substituents each penetrate neighboring pore mouths, and the hydrocarbon chain stretches across the framework oxygen atoms of the zeolite pore wall lying between them. The model also rationalizes why heptadecane forms virtually no tribranched isomers with ZSM-22 as catalyst: the hydrocarbon chain is too short to reach a third neighboring pore mouth (Fig. 4). Only with icosane (n-$C_{20}H_{42}$) or longer hydrocarbons are trimethyl-branched isomers accessible in large quantities. The high yield of 2,7-

dimethyloctane in the isomerization of *n*-decane on ZSM-22,[11] which was interpreted as methyl branching at both hydrocarbon chain ends,[11, 13] is another example of the same kind of selective catalysis at the external surface of the zeolite. This can be considered as a form of lock-and-key model in which the alkane (key) needs to fit in the pore opening of the catalyst (lock) (Fig. 4). The isomerization of *n*-dodecane on ZSM-22[14] in which 2,4-, 2,5-, 2,6-, 2,7-, 2,8-, 2,9-, 3,7-, and 3,8-dimethyldecane are formed in 6.0, 9.0, 8.8, 11.8, 26.6, 29.8, 1.8, and 3.1% yield, respectively, can now also be rationalized. This corresponds to the distribution required by the proposed lock-and-key model of selective branching at the [001] planes of the crystal surface.

The fate of 1-cyclopentylnonane on the ZSM-22 catalyst further supports the concept of shape-selective catalysis at the zeolite pore mouths (Fig. 4), as side-chain branching occurs preferentially at C atom positions remote from the ring. At 10% conversion more than 70% of the methyl-branched 1-cyclopentyloctanes have the methyl branching at positions 5-, 6-, or 7- in the alkyl chain. In these products and in the preferred dimethyl-branched isoheptadecanes, a minimum number of three or four methylene groups separates the respective tertiary carbon atoms (Fig. 4).

The proposed lock-and-key model for *n*-alkane isomerization seems to be valid for other 10-ring zeolites and long-chain alkanes as well. Waxes (n-$C_{26}H_{54}$ to n-$C_{34}H_{70}$) isomerized on a SAPO-11 catalyst were found to be multi-methyl-branched, with an average of three methyl branches per molecule.[15] Based on the proposed model and considering that the thickness of the pore wall for SAPO-11 and ZSM-22 materials is similar,[10b] it can be speculated that the waxes are branched at the carbon atoms C_2, C_7–C_{11}, C_{16}–C_{20}. For alkanes with more than 28 carbon atoms, an additional branching might be generated at positions C_{25}–C_{29}.

The present study demonstrates that external surfaces of zeolite crystals have to be considered as potential shape-selective environments. In particular, in view of the variety of available zeolite structure types, tailored multibranching of hydrocarbon skeletons should now be possible.

Received: July 3, 1995 [Z 8174 IE]
German version: *Angew. Chem.* **1995**, *107*, 2726–2728

Keywords: alkanes · catalysis · isomerizations · shape selectivity · zeolites

[1] a) N. Y. Chen, T. F. Degnan, C. M. Smith, *Molecular Transport and Reaction in Zeolites. Design and Application of Shape Selective Catalysts*, VCH, New York, **1994**, p. 202; b) I. E. Maxwell, W. H. J. Stork, *Stud. Surf. Sci. Catal.* **1991**, *58*, 57.
[2] a) N. Y. Chen, W. W. Keading, F. G. Dwyer, *J. Am. Chem. Soc.* **1979**, *101*, 6783; b) P. B. Weisz, *Pure Appl. Chem.* **1980**, *52*, 2091.
[3] W. O. Haag, R. M. Lago, P. B. Weisz, *Nature* **1984**, *309*, 589.
[4] S. M. Csicsery, *Pure Appl. Chem.* **1986**, *58*, 841.
[5] a) P. B. Venuto, *ACS Symp. Ser.* **1977**, *40*, 260; b) E. G. Derouane, *J. Catal.* **1986**, *100*, 541; c) E. G. Derouane, J. M. André, A. A. Lucas, *ibid.* **1988**, *110*, 58.
[6] D. Fraenkel, M. Cherniavsky, B. Ittah, M. Levy, *J. Catal.* **1986**, *101*, 273.
[7] J. Weitkamp, M. Neuber, *Stud. Surf. Sci. Catal.* **1991**, *60*, 291.
[8] J.-P. Gilson, E. G. Derouane, *J. Catal.* **1984**, *88*, 538.
[9] J. Kärger, M. Petzold, H. Pfeifer, S. Ernst, J. Weitkamp, *J. Catal.* **1992**, *136*, 283.
[10] a) S. A. I. Barri, G. W. Smith, D. White, D. Young, *Nature* **1984**, *312*, 534; b) M. M. Meier, D. H. Olson, *Atlas of Zeolite Structure Types*, Butterworth-Heinemann, Boston, **1992**, p. 178.
[11] S. Ernst, J. Weitkamp, J. A. Martens, P. A. Jacobs, *Appl. Catal.* **1989**, *48*, 137.
[12] F. G. Ciapetta, J. B. Hunter, *Ind. Eng. Chem.* **1953**, *45*, 147.
[13] J. A. Martens, R. F. Parton, L. Uytterhoeven, P. A. Jacobs, G. F. Froment, *Appl. Catal.* **1991**, *76*, 95.
[14] S. Ernst, G. T. Kokotailo, R. Kumar, J. Weitkamp, *Proc. 9th Int. Zeolite Conf. 1992*, Montreal, **1993**, p. 388.
[15] S. J. Miller, *Microporous Mater.* **1994**, *2*, 439.

Photochromism Dependent on Crystal Packing: Photoinduced and Thermal Proton-Transfer Processes in Single Crystals of 6-(2,4-Dinitrobenzyl)-2,2′-Bipyridine**

Yoav Eichen, Jean-Marie Lehn,* Michael Scherl, Dietrich Haarer, Jean Fischer, André DeCian, Anne Corval, and Hans Peter Trommsdorff

Thermo- and photoinduced inter- and intramolecular transformations provide means to control the physical properties of solid phases[1] such as polymeric films, glasses, and crystals. The development of such tunable materials is a key step for the design of new applications in optical data processing and storage[2] such as optical memories and all-optical processors. Proton-transfer (PT) and proton-mediated electron-transfer (PMET) processes are of particular interest, as they present a number of unique properties: a) they are in most cases reversible and can be used for many cycles; b) PT does not necessarily induce large structural changes and therefore can take place in the solid state, amorphous and crystalline, even at low temperatures; c) PT processes are in general electronically well shielded, and the coulombic interactions far from the reactive site need not be considered; d) the lifetimes of proton-transferred states range from the picosecond regime to seconds, hours, and even days at low temperatures.

A variety of molecular and supramolecular structures have been shown to undergo photo-, thermo-, and piezoinduced PT processes.[3–6] PT has been found to be strongly dependent on the topography of the reaction center. Thus, the differences in the PT properties of the polymorphs of salicylidene anilides were attributed to the variations in the free volume offered by the crystal packing.[5]

One of the most interesting solid-state photoactive PT processes is the photoinduced PT (PIPT) taking place in 2-(2,4-dinitrobenzyl)pyridine crystals (α-DNBP, **1**). Although the photochromism of **1**, was reported as early as 1925,[7] only little is known about this process in solid matrices and about the correlation between the structure (molecular and crystalline) and its PT properties. The phototautomerization of **1** to its "NH" tautomer **1a** may, in principle, proceed directly or via its metastable "OH" tautomer. Scheme 1 shows the proposed mechanism for the reaction in the crystalline state.[8] None of the other 2,4-dinitrobenzyl derivatives prepared to date was reported to be photochromic in the solid state.[9]

In order to prepare new PT systems exhibiting longer lifetimes for the proton-transferred tautomers and to understand the

[*] Prof. Dr. J. M. Lehn
Laboratoire de Chimie Supramoléculaire
URA 422 of the CNRS, Institut Le Bel, Université Louis Pasteur
4, Rue Blaise Pascal, F-67000 Strasbourg (France)
Telefax: Int. code +88 41 10 20
Dr. Y. Eichen
Department of Chemistry
Technion – Israel Institute of Technology
Technion City, Haifa 32000 (Israel)
M. Scherl, Prof. Dr. D. Haarer
Lehrstuhl für Experimentalphysik IV der Universität Bayreuth (Germany)
Prof. Dr. J. Fischer, Dr. A. DeCian
Laboratoire de Cristallochimie et de Chimie Structurale, Strasbourg (France)
Dr. A. Corval, Prof. Dr. H. P. Trommsdorff
Laboratoire de Spectrométrie Physique, Université Joseph Fourier
St Martin d'Hères Cedex (France)

[**] This work was supported by the EC ESPRIT program PROTIOS (No. 7238). Y. E. thank C.I.E.S. and the Israel Academy of Sciences and Humanities for post-doctoral fellowships.

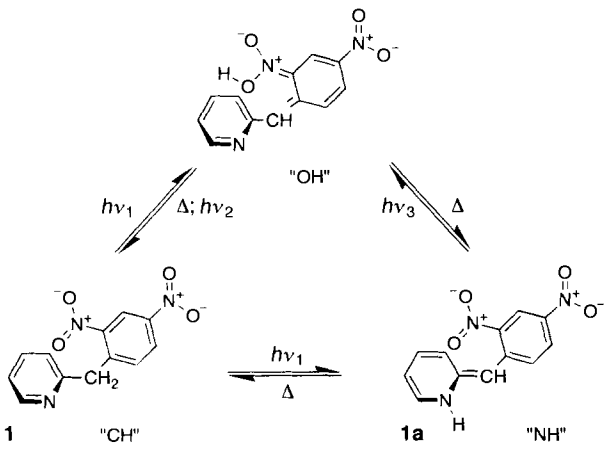

Scheme 1.

structure-PT dynamics relationship better, 6-(2,4-dinitrobenzyl)-2,2′-bipyridine (**2**) has been synthesized according to Scheme 2. After eluting **2** from the chromatographic column, two different forms of colorless crystals, **2I** and **2II**, are obtained. The intermolecular arrangements in the unit cells of **2I** (monoclinic) and **2II** (orthorhombic) are shown in Figure 1.[10]

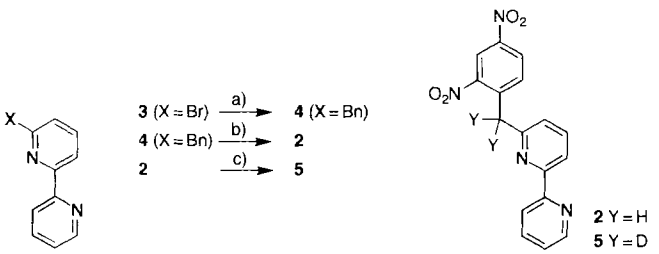

Scheme 2. a) BnZnBr, $[(Ph_3P)_4Pd]$, 50 °C, 2 h, 95%; b) HNO_3, H_2SO_4, 25 °C, 3 h, 75%; c) EtOD, Et_3N (cat.), 40 °C, 7 d, 92–95% D.

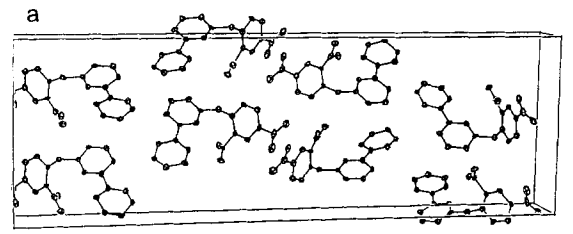

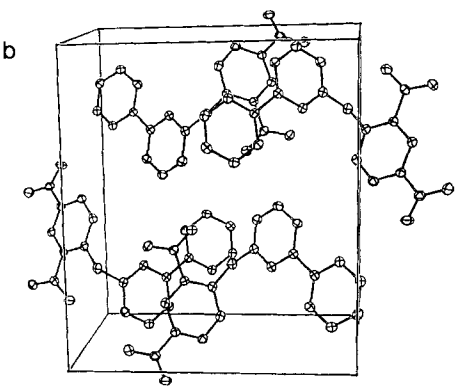

Fig. 1. a) Crystallographic unit cell of the photochromic phase **2I**; b) crystallographic unit cell of the nonphotochromic phase **2II**.

Table 1 presents some important intra- and intermolecular parameters; the numbering scheme is shown in Figure 2. In both crystals one benzylic proton is close to one oxygen atom of the *o*-nitrophenyl moiety; $d_{N-O\cdots H-C}$ is 2.4093 ± 0.0027 for **2I** and 2.3792 ± 0.0017 for **2II**. In the two polymorphs, the molecules of **2** are π-stacked, forming infinite chains.

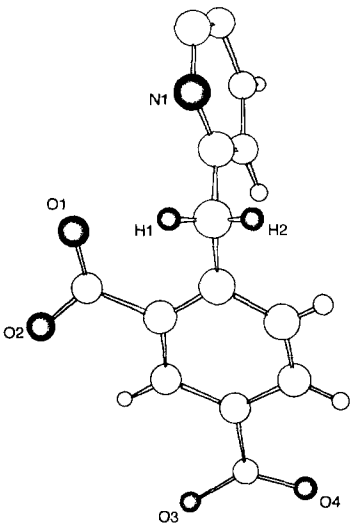

Fig. 2. Atomic numbering scheme for **2**.

Table 1. Selected intermolecular and intramolecular distances for **2** [Å] [a].

Pair of atoms	**2I** [b]	**2I** [b]	**2II**
N1-H1	2.936(6)	2.873(6)	>3
N1-H2	>3	>3	2.724(2)
O1-H1	2.409(3)	2.306(3)	2.379(2)
O1-H2	>3	>3	>3
N1-O1	3.155(6)	3.193(6)	4.004(6)
N1-H1′	>3	>3	>3
O2-H2′	2.363(3)	2.492(3)	2.406(2)
N3-H1′	>3	>3	2.850(2)
N3-H2′	>3	>3	2.830(2)

[a] For numbering see Fig. 2. [b] The values refer to the two different molecules in the **2I** phase.

Although structurally similar, **2I** was photochromic, whereas **2II** did not change its color upon illumination (the crystal did not show any photochromic properties between 330 and 800 nm at 4–300 K). Figure 3 shows the absorption spectrum of irradiated **2I**. The similarities in the intramolecular coordinates

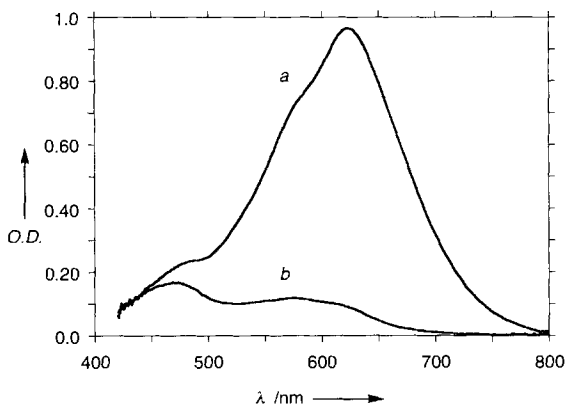

Fig. 3. Absorption spectra of **2I** that was partially converted into the "NH" form; the spectra were obtained with polarized light: a) 0°, b) 90°.

around the reaction center (the dinitrobenzyl group) and the negligible difference in the crystal density ($\rho_{2I} = 1.467\ g cm^{-3}$ and $\rho_{2II} = 1.460\ g cm^{-3}$) seems to rule out the possibility that the difference in reactivity originates from the differences in the crystal free volume, as was suggested for salicylidene anilides.[5] One would expect to observe at least the first PT step, the conversion of **2** from the "CH" form into the "OH" form, in **2I** and **2II**, as the O···H distances associated with this process are virtually the same. The differences in reactivity must therefore have another cause associated with the intermolecular arrangement of molecules of **2** in the different crystals.

In the photochromic crystal (**2I**) the molecules present π-stacking ($d_{center-center} = 3.77$ Å; $\alpha = 13.28°$) between the bipyridine rings in which one 2-pyridine ring interacts with its neighbors' 2′-pyridine ring, (Fig. 4a). This leaves the 2,4-dinitrobenzyl chromophore relatively isolated and with no close inter-ring contacts ($d_{center-center} > 5$ Å). On the other hand, in the nonphotochromic crystal (**2II**) the 2,4-dinitrobenzyl chromophore of one molecule is tightly sandwiched between a 2-pyridine and a 2′-pyridine ring of two adjacent molecules ($d^1_{center-center} = 3.79$ Å; $\alpha = 7.36°$; $d^2_{center-center} = 3.73$ Å; $\alpha = 5.56°$) (Fig. 4b). In this arrangement, deactivation pathways other then PT could be envisaged because of stronger electronic coupling between the excited chromophore and the π-systems of neighboring molecules.

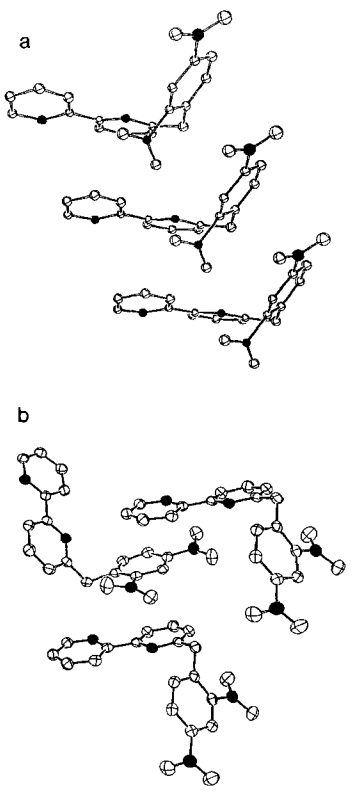

Fig. 4. Intermolecular arrangement of the molecules of **2** in the crystals of **2I** (a) and **2II** (b).

Unlike in salicylidene anilides, deuteration of **2** to give **5** (Scheme 2) resulted in a remarkably strong isotope effect on the photocoloration and the rate of thermal decoloration. This effect emphasizes that a PT is involved in the rate-determining steps of both processes. The blue color of irradiated **2I** and **5I**, attributed to their "NH" forms,[11a] fades slowly in the dark, and the molecules revert to the thermodynamically stable "CH" form. This thermal back reaction leads to a monoexponential decay of the "NH" form in both crystals.[11b] Figure 5 shows the temperature dependence of the "NH" to "CH" transformation for **2** and **5** relative to that of **1**. Each of the crystals shows a typical Arrhenius behavior indicating a uniform thermally activated process. The lifetime of the "NH" tautomer is significantly longer at all temperatures for **5I** than for **2I** and **1**, in spite of the insignificant difference in the activation barrier. For instance, the lifetimes of **5I**, **2I**, and **1** at 330 K are 17800 s, 3200 s, and 440 s, respectively. Extrapolating to room temperature (298 K) the "NH" lifetimes are expected to be 595000 s, 97200 s, and 15500 s (that is, 6.9 days, 27 h, and 4.3 h) for **5I**, **2I**, and **1**, respectively. The deuterated **5I** showed

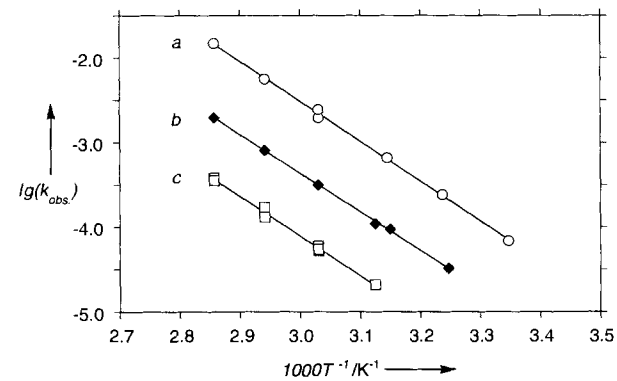

Fig. 5. Arrhenius plots for the "NH"-to-"CH" thermal backconversion: a) **1**; b) **2** in the **2I** phase; c) **5** in the **5I** phase.

a barrier of $90.0 \pm 2.9\ KJ mol^{-1}$ for the "NH" thermal decay to "CH" as compared to $87.5 \pm 0.8\ KJ mol^{-1}$ and $90.4 \pm 1.7\ KJ mol^{-1}$ for **2I** and **1** crystals, respectively.

In addition, deuteration had a marked effect on the formation ratio of the polymorphs. All crystallization conditions tried gave **5II** as the major product with variable minute amounts of **5I**, whereas for **2** the **2I** phase dominated under the same crystallization conditions.[11c] The strong influence of hydrogen/deuterium exchange at the benzylic position on the ratio of polymorph formation may indicate that intermolecular N–O···H–C interactions contribute to the crystal packing.

Other dinitrobenzyl derivatives are currently being prepared and studied to further elucidate the origins of the photocoloration process as well as the correlation between the molecular and crystal structure and PT dynamics. The control of these PIPT processes in the solid state may have promising prospects for the development of materials for optical data processing and storage.

Experimental Procedure

4: A suspension of zinc dust (1.1 g, 17 mmol) in dry THF, under argon, was activated with 0.1 mL HCl solution in dry 1,4-dioxan (4 M, Aldrich). When hydrogen evolution ceased, benzyl bromide (1.1 mL, 4.4 mmol) was added dropwise over 15 minutes. The solution was stirred at 20 °C for another 1 hour, and then filtered. A solution of 6-bromo-2,2′-bipyridine [12] (**3**, 1 g, 4.25 mmol) and $[(Ph_3P)_4Pd]$ (0.2 mmol) in THF (15 mL) was added to the benzyl zinc bromide solution. The mixture was stirred for 2 h at 50 °C, the solvent then removed under reduced pressure, and the product extracted into an acidic aqueous solution. The product was re-extracted after basification of the aqueous solution with dichloromethane. Chromatography (alumina; eluent 2% ethyl acetate in hexane, $R_f = 0.7$) afforded 0.98 g (95%) of pure **4**, m.p. (ether) 61–62 °C. Elemental analysis: calcd for $C_{17}H_{14}N_2$: C 82.90, H 5.73, N 11.37; found: C 83.06, H 5.78, N 11.19. ^{1}H NMR (200 MHz, $CDCl_3$, 25 °C, TMS): $\delta = 4.25$ (s, 3H), 7.11 (d, 1H), 7.36–721 (m, 5H), 7.70 (t, 1H), 7.81 (dt, 1H), 8.22 (d, 1H), 8.46 (d, 1H), 8.67 (dd, 1H).

2: **4** (0.9 g, 3.6 mmol) was dissolved in 97% cold sulfuric acid (11 mL). The solution temperature was set to −10 °C; then nitric acid (1.5 mL, 100%) was added drop by drop while stirring vigorously. The solution was stirred for another 3 h at room temperature, then poured on ice, neutralized with NH_4OH, and extracted with three portions of dichloromethane (100 mL each). The combined organic layers were concentrated under reduced pressure and chromatographed (alumina; eluent ether/hexane 1/1, $R_f = 0.7$) yielding 0.9 g (75%) of **2**. Recrystallization from ether/hexane gave **2I** (m.p. 110–110.5 °C), whereas from ethanol **2II** (m.p. 118–118.5 °C) was obtained. Elemental analysis: calcd for $C_{17}H_{12}N_4O_4$: C 60.71, H 3.60, N 16.66; found: C 60.81, H 3.60, N 16.50. ^{1}H NMR (200 MHz, $CDCl_3$, 25 °C, TMS): $\delta = 4.69$ (s, 2H), 7.30 (d, 1H), 7.82–763 (m, 4H), 8.11 (d, 1H), 8.28 (d, 1H), 8.41 (dd, 1H), 8.64 (d, 1H), 8.86 (d, 1H).

5: **2** (0.5 g, 1.5 mmol) was dissolved in dry THF (5 mL) under argon. To this solution were added two drops of dry triethylamine and 10 mL of [D$_1$]ethanol. The solution was heated at 40 °C for one week, and the solvent was subsequently removed under reduced pressure. The white crystals that separated from solution were filtered and dried. NMR characterization showed 92–95% deuteration, exclusively at the benzylic position.

Received: June 9, 1995 [Z 8075 IE]
German version: *Angew. Chem.* **1995**, *107*, 2753–2756

Keywords: nitro compounds · photochromism · proton transfer · solid-state structures · tautomerism

[1] M. Irie, R. Iga, *Macromolecules* **1986**, *19*, 2480; A. Mamada, T. Tanaka, D. Kungwatchakun, M. Irie, *ibid.* **1990**, *23*, 1517; F. P. Shvartsman, V. A. Krongauz, *J. Phys. Chem.* **1984**, *88*, 6448; J.-C. Anzai, K. Sakamura, T. Osa, *J. Chem. Soc. Chem. Commun.* **1992**, 888; I. Willner, S. Rubin, R. Shatzmiller, T. Zor, *J. Am. Chem. Soc.* **1993**, *115*, 8690.

[2] *Optical Processing and Computing* (Ed.: A. Arsenault), Academic Press, New York, **1989**; R. R. Birge, *Ann. Rev. Phys. Chem.* **1990**, *41*, 683; *Molecular Electronic Devices* (Eds.: F. L. Carter, R. E. Siatkowski, H. Wohltjen), North Holland, **1989**; *Supramolecular Photochemistry* (Eds.: V. Balzani, F. Scandola), Ellis Horwood, New York, **1991**; J. Friedrich, D. Haarer, *Angew. Chem.* **1984**, *96*, 96; *Angew. Chem. Int. Ed. Engl.* **1984**, *23*, 133.

[3] M. T. Reetz, S. Höger, K. Harms, *Angew. Chem.* **1994**, *106*, 193; *Angew. Chem. Int. Ed. Engl.* **1994**, *33*, 181.

[4] A. O. Patil, D. Y. Curtin, I. C. Paul, *J. Am. Chem. Soc.* **1984**, *106*, 4010.

[5] E. Hadjoudis, *Stud. Org. Chem. (Amsterdam)* **1990**, *40*, 685, and references therein.

[6] G. M. J. Schmidt in *Solid State Photochemistry* (Ed.: D. Ginsburg), Verlag Chemie, Weinheim, **1976**; T. Kawato, H. Koyama, H. Kanatomi, M. Isshiki, *J. Photochem.* **1985**, *28*, 103; T. Kawato, H. Kanatomi, H. Koyama, T. Igrashi, *ibid.* **1986**, *33*, 199; H. Koyama, T. Kawato, H. Kanatomi, H. Matsushita, K. Yonetani, *J. Chem. Soc. Chem. Commun.* **1994**, 579.

[7] A. E. Chichibabin, B. M. Kuindzhi, S. W. Benewolenskaja, *Ber. Dtsch. Chem. Ges.* **1925**, *58*, 1580.

[8] H. Sixl, R. Warta, *Chem. Phys.* **1985**, *94*, 147.

[9] See, for example: D. Margerum, J. L. Miller, E. Saito, M. S. Brown, H. S. Mosher, R. Hardwick, *J. Phys. Chem.* **1962**, *66*, 2434.

[10] Crystal data for **21** (and **21I**): $C_{34}H_{24}N_8O_8$ ($C_{17}H_{12}N_4O_4$), $M_r = 672.6$ (336.3), orthorhombic (monoclinic), space group $Pna2_1$ ($P2_1/c$), $a = 14.051(4)$ (8.340(3)), $b = 5.159(2)$ (12.740(4)), $c = 42.017(9)$ (14.408(4)) Å, $\beta = 90°$ (92.13(2)°), $V = 3045.8$ (1529.8) Å^3, $Z = 4$ (4), $\rho_{calcd.} = 1.467$ (1.46) g cm^{-3}, $\lambda(Cu_{K\alpha}) = 1.5418$ (1.5418) Å, $\mu = 8.602$ (8.563) cm^{-1}, $T = 173$ K, crystal dimensions $0.38 \times 0.12 \times 0.1$ ($0.32 \times 0.2 \times 0.18$). Crystallographic data were collected on a PHILIPS PW1100/16 diffractometer, $3° < 2\theta < 52°$ ($\theta/2\theta$ scans; 2053 (1903) independent reflections, 1270 (1381) with $I > 3\sigma(I)$ were observed and used for structure refinement. The structure was solved by direct methods and refined on $|F_0|$ to $R = 0.06$ (0.037), $Rw = 0.09$ (0.053) for 301 (226) variables. GOF = 1.723 (1.256). A difference map following convergence showed no peak higher than 0.1 (0.05) e Å^{-3}. Further details of the crystal investigation are available on request from the Director of Cambridge Crystallographic Data Centre, 12 Union Road, GB-Cambridge CB2 1EZ (UK) on quoting the full journal citation.

[11] a) Confirmed by differential FT IR measurements. b) The reaction was followed over at least five half-lives. For **5I** crystals, the thermal decay of the concentration of the "NH" form presented a biexponential decay composed of the monoexponential decay of the traces of the nondeuterated **2** and the monoexponential decay of **5**. c) The unit cell parameters of the two deuterated polymorphs have been found to be identical within experimental error (see ref. [10]) to the non-deuterated polymorphs.

[12] Prepared according to a modification of a published synthesis of 6-chloro-2,2'-bipyridine: D. B. Moran, G. O. Morton, J. D. Albright, *J. Heterocyclic Chem.* **1986**, *23*, 1071.

Oxybenziporphyrin, a Fully Aromatic Semiquinone Porphyrin Analog with Pathways for 18π-Electron Delocalization**

Timothy D. Lash*

Investigations into the synthesis of novel conjugated macrocycles related to the porphyrins have intensified in recent years, in part because these compounds are potentially useful in numerous, seemingly unrelated areas such as the development of novel materials (molecular wires, shape-selective catalysts, etc.)[1] and photodynamic therapy.[2] A number of approaches have been taken to modify the porphyrin chromophore, including the synthesis of structural variants (inverted porphyrins,[3] porphyrin linkage isomers[4]), expanded porphyrins,[5] heterocyclic analogs (macrocycles containing furan, thiophene, and other heterocyclic subunits),[6] and highly conjugated porphyrins bearing fused aromatic subunits.[7]

In a recent paper by Berlin and Breitmaier,[8] the synthesis of a benzene containing porphyrin analog **1a** (benziporphyrin) by the acid-catalyzed condensation of a tripyrrane dicarboxylic acid with isophthalaldehyde was reported. Although this system might exist as a fully aromatic macrocycle, aromatization would only be possible at the expense of losing the conjugative pathway of the benzene subunit and the associated resonance stabilization energy. Perhaps not surprisingly, this system did not exhibit aromatic properties as a whole, and the ^{1}H NMR data suggested that benziporphyrin existed as a mixture of two nonequivalent tautomers **1a** and **2a** (Scheme 1). Although this

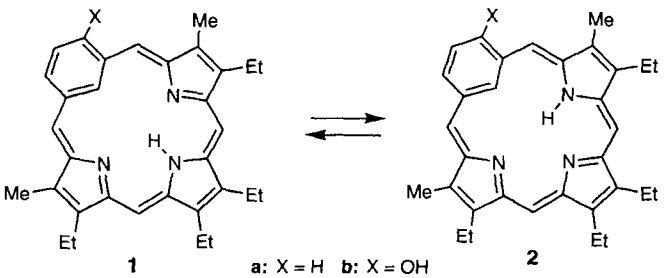

Scheme 1. Structures for the two nonequivalent tautomers for benziporphyrin.

is an intriguing system, fully aromatic structures related to benziporphyrin would be of far greater intrinsic interest. The reasoning that a suitably placed hydroxyl substituent, as in structures **1b** and **2b**, would allow access to the related keto tautomers **3** (Scheme 2), structures that should be able to support porphyrin-like aromatic 18π-electron pathways, led to the successful synthesis of this remarkable new system, termed oxybenziporphyrin, disclosed here.

[*] Prof. T. D. Lash
Department of Chemistry, Illinois State University
Normal, IL 61790-4160 (USA)
Telefax: Int. code + (309) 438-5538

[**] Conjugated Macrocycles Related to the Porphyrins, Part 5. This work was supported by the Donors of the Petroleum Research Fund, administered by the American Chemical Society, and the University Research Fund of Illinois State University. We also thank the National Science Foundation (CHE-9001175 and DUE-9452437) for providing partial funding for two 300 MHz NMR spectrometers. Mass spectral data were obtained from the Mass Spectral Laboratory, School of Chemical Sciences, University of Illinois at Urbana-Champaign, supported in part by a grant from the National Institute of General Medical Sciences (GM 27029). Part 4: T. D. Lash, *J. Org. Chem.* **1992**, *57*, 4312–4315.

 © VCH Verlagsgesellschaft mbH, D-69451 Weinheim, 1995 0570-0833/95/3422-2533 $ 10.00+.25/0

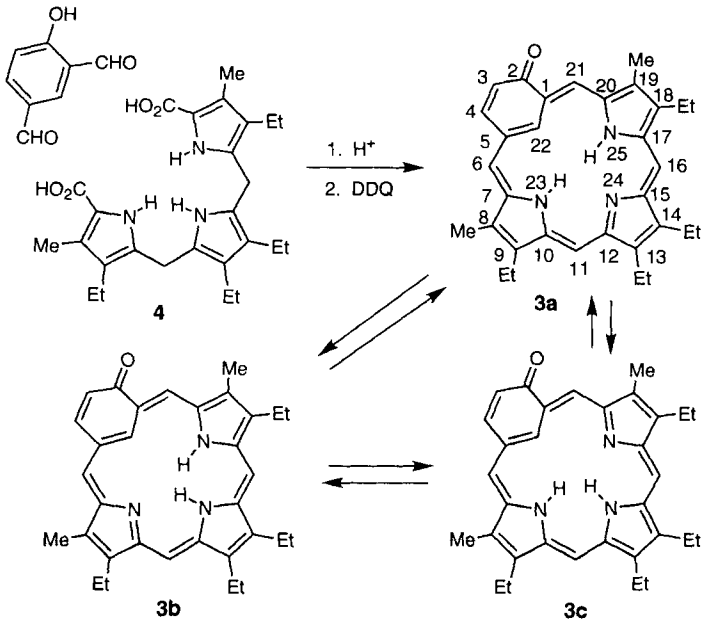

Scheme 2. Synthesis of oxybenziporphyrin **3**.

Tripyrrane dicarboxylic acid (**4**)[9] was decarboxylated with trifluoroacetic acid, diluted with dichloromethane, and condensed with 5-formylsalicylaldehyde (Scheme 2). After 2 h the mixture was neutralized with triethylamine and oxidized with 2,3-dichloro-5,6-dicyano-1,4-benzoquinone (DDQ) for a further 1 h. Chromatography of the reaction mixture on alumina yielded a green band, which was collected and recrystallized from chloroform/methanol to give the required porphyrin analog as lustrous purple crystals in 35% yield. The conjugated macrocycle gave deep green solutions in chloroform and dichloromethane.

The structure of oxybenziporphyrin was confirmed by using a variety of spectroscopic techniques. IR spectra showed an intense band at 1624 cm^{-1} that was consistent with the presence of a cross-conjugated carbonyl unit. Electronic spectra were also consistent with a porphyrinoid system, showing an intense Soret band at 426 nm with a molar extinction coefficient of over 1.6×10^5 $dm^3 mol^{-1} cm^{-1}$ and a series of smaller absorptions in the visible region (Fig. 1). The ^1H NMR spectrum of **3** confirmed the presence of a macrocyclic ring current, showing the signal attributable to the bridge methine protons downfield at $\delta = 8.8-10.3$ (Fig. 2). The internal CH group of the semiquinone subunit was extensively shielded, giving rise to a doublet coupled to the *meta* proton ($^4J_{H,H} = 2$ Hz) at $\delta = -7.2$, and the signal of the two NH protons appeared as a broad resonance near $\delta = -4$. As expected, the protons at positions 3 and 4 yielded a doublet ($\delta = 7.35$) and a doublet of doublets ($\delta = 8.49$), respectively, and their relative chemical shifts were in accord with an α,β-unsaturated ketone subunit. Several aromatic tautomers for **3** are possible (structures **3a–c**, Scheme 2), although the NMR data is consistent with a single structure at room temperature, probably due to rapid equilibration between these different species. The ^{13}C NMR spectrum of **3** was in complete agreement with the assigned structure: the chemical shift for the carbonyl unit was fairly typical ($\delta = 188$), and all 22 of the ring carbons for this asymmetrical macrocycle were observable as separate resonances. The 70 eV electron-impact mass spectrum for **3** (Fig. 3) revealed a very strong molecular ion, as expected for a stable aromatic system, and showed only a small amount of benzylic fragmentation ($M^+ - 15$).

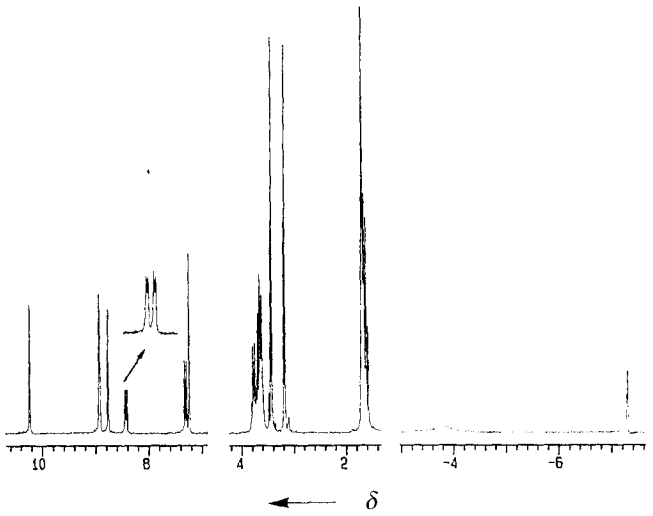

Fig. 2. 300 MHz ^1H NMR NMR spectrum of oxybenziporphyrin **3** in $CDCl_3$.

This study demonstrates a new approach to the synthesis of modified porphyrin-like chromophores, and application of this strategy should allow access to a number of other related aromatic systems including pyridine-containing macrocycles[10, 11] and expanded porphyrin systems. These possibilities are currently under investigation.

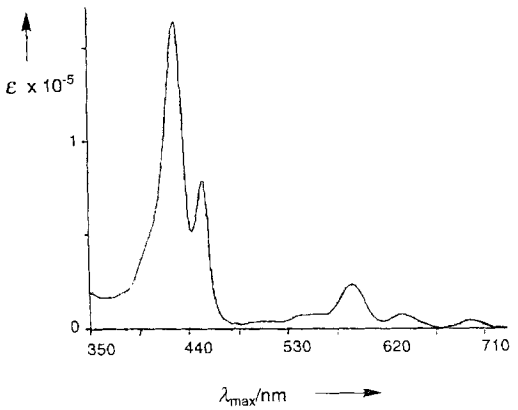

Fig. 1. Electronic absorption spectrum of oxybenziporphyrin **3** in dichloromethane.

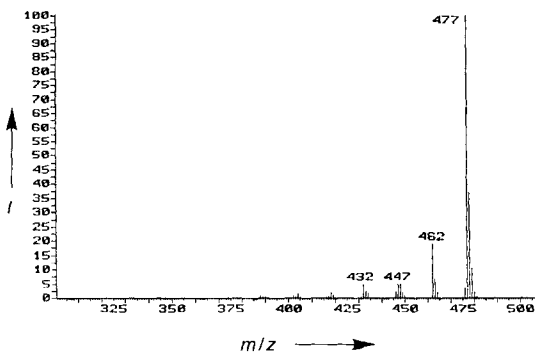

Fig. 3. 70 eV electron impact mass spectrum of oxybenziporphyrin **3**. *I* = intensity (arbitrary units).

 © VCH Verlagsgesellschaft mbH, D-69451 Weinheim, 1995 0570-0833/95/3422-2534 $ 10.00+.25/0

Experimental Procedure

Oxybenziporphyrin **3**: Tripyrranedicarboxylic acid (**4**) (200 mg) was stirred with trifluoroacetic acid (2 mL) under an atmosphere of nitrogen for 10 min. Dichloromethane (38 mL) was added, followed immediately by 5-formylsalicylaldehyde (66 mg), and the mixture was stirred under nitrogen for a further 2 h. The mixture was neutralized by the dropwise addition of triethylamine, DDQ (102 mg) was added, and the resulting solution was stirred for an additional 1 h. The mixture was washed with water and chromatographed on alumina (Grade 3) by eluting first with dichloromethane and then with chloroform. A deep green fraction was collected and recrystallized from chloroform/methanol to give the porphyrin analog (73 mg; 35%) as bright purple microneedles. Selected physical and spectroscopic data for **3**: m.p. 261–262 °C (decomp.); UV/Vis (CH_2Cl_2): λ_{max} (lg ε) = 426 (5.05), 452 (4.89), 507 (3.62), 547 (3.93), 588 (4.39), 635 (3.89), 698 nm (3.70); IR (KBr): $\tilde{\nu}$ = 3030, 2961, 2929, 2867, 1624, 1593, 1560, 1553, 1522, 1498, 1464, 1450, 1420, 1376, 1364, 1348, 1315, 1272, 1252, 1226, 1187, 1162, 1154, 1116, 1095, 1057, 1015, 976, 949, 876, 851, 828, 805, 768, 739, 681, 660, 620, 591, 560, 546, 517, 472 cm^{-1}; ^1H NMR (300 MHz, $CDCl_3$): δ = −7.17 (1H, d, J = 2 Hz, 22H), −3.8 (2H, br, 2 × NH), 1.61–1.73 (12H, 4 overlapping triplets, 4 × CH_2CH_3), 3.29 (3H, s), 3.65 (3H, s) (8,19-CH_3), 3.62-3.81 (8H, 4 overlapping quartets, 4 × CH_2CH_3), 7.35 (1H, d, J = 9 Hz, 3-H), 8.49 (1H, dd, ^3J = 9 Hz, ^4J = 2 Hz, 4-H), 8.85 (1H, s), 8.98 (1H, s), 8.99 (1H, s) (6,11,16-H), 10.29 (1H, s, 21-H); ^{13}C NMR ($CDCl_3$): δ = 11.39, 11.85, 17.08, 17.17, 18.25, 18.32, 19.31, 19.41, 19.74, 93.29, 94.92, 105.66, 111.07, 112.27, 121.35, 126.08, 130.15, 131.61, 134.14, 135.31, 136.28, 137.12, 137.90, 138.07, 140.07, 144.54, 145.07, 147.09, 154.64, 156.17, 187.94; MS (70 eV): *m/z* (%): 477 (100) [M^+], 462 (19) [$M^+ - CH_3$]; HR-MS: calculated for $C_{32}H_{35}N_3O$: *m/z* 477.2782; found: 477.2774. Correct C, H, N analysis for $C_{32}H_{35}N_3O \cdot 0.5\,H_2O$.

Received: June 29, 1995 [Z 8143 IE]
German version: *Angew. Chem.* **1995**, *107*, 2703–2705

Keywords: aromaticity · keto–enol tautomerism · porphyrinoids

[1] For example: M. J. Crossley, P. L. Burn, *J. Chem. Soc. Chem. Commun.* **1991**, 1569; M. J. Gunter, M. R. Johnston, *ibid.* **1992**, 1163; S. Anderson, H. L. Anderson, J. K. M. Sanders, *Acc. Chem. Res.* **1993**, *26*, 469; R. W. Wagner, J. S. Lindsey, *J. Am. Chem. Soc.* **1994**, *116*, 9759.

[2] S. B. Brown, T. G. Truscott, *Chem. Br.* **1993**, *29*, 955.

[3] P. J. Chmielewski, L. Latos-Grazynski, K. Rachlewicz, T. Glowiak, *Angew. Chem.* **1994**, *106*, 305; *Angew. Chem. Int. Ed. Engl.* **1994**, *33*, 779; H. Furuta, T. Asano, T. Ogawa, *J. Am. Chem. Soc.* **1994**, *116*, 767; P. J. Chmielewski, L. Latos-Grazynski, *J. Chem. Soc. Perkin Trans. 2* **1995**, 503.

[4] E. Vogel, M. Kocher, H. Schmickler, J. Lex, *Angew. Chem.* **1986**, *98*, 262; *Angew. Chem. Int. Ed. Engl.* **1986**, *25*, 257; J. L. Sessler, *Angew. Chem.* **1994**, *106*, 1410; *Angew. Chem. Int. Ed. Engl.* **1994**, *33*, 1348; J. L. Sessler, E. A. Brucker, S. J. Weghorn, M. Kisters, M. Schafer, J. Lex, E. Vogel, *Angew. Chem.* **1994**, *106*, 2402; *Angew. Chem. Int. Ed. Engl.* **1994**, *33*, 2308.

[5] J. L. Sessler, A. K. Burrell, *Top. Curr. Chem.* **1991**, *161*, 177–273.

[6] A. W. Johnson in *Porphyrins and Metalloporphyrins* (Ed.: K. M. Smith), Elsevier, Amsterdam, **1975**, pp. 729–754; M. J. Broadhurst, R. Grigg, A. W. Johnson, *J. Chem. Soc. C* **1971**, 3681; A. Ulman, J. Manassen, *J. Am. Chem. Soc.* **1975**, *97* 6540; *J. Chem. Soc. Perkin Trans. 1* **1979**, 1066; T. D. Lash, Y. G. Motta, *Heterocycles* **1983**, *20*, 2343; E. Vogel, W. Haas, B. Knipp, J. Lex, H. Schmickler, *Angew. Chem.* **1988**, *100*, 445; *Angew. Chem. Int. Ed. Engl.* **1988**, *27*, 406; W. Haas, B. Knipp, M. Sicken, J. Lex, E. Vogel, *ibid.* **1988**, *100*, 448 and **1988**, *27*, 409; E. Vogel, P. Rohrig, M. Sicken, B. Knipp, A. Herrmann, M. Pohl, H. Schmickler, J. Lex, *ibid.* **1989**, *101*, 1683 and **1989**, *28*, 1651; T. D. Lash, Y. L. S.-T. Armiger, *J. Heterocycl. Chem.* **1991**, *28*, 965.

[7] T. D. Lash, *Energy Fuels* **1993**, *7*, 166; T. D. Lash, T. J. Roper, *Tetrahedron Lett.* **1994**, *35*, 7715; T. D. Lash, C. P. Denny, *Tetrahedron* **1995**, *51*, 59; T. D. Lash, B. H. Novak, *Angew. Chem.* **1995**, *107*, 723; *Angew. Chem. Int. Ed. Engl.* **1995**, *34*, 683; *Tetrahedron Lett.* **1995**, *36*, 4381.

[8] K. Berlin, E. Breitmeier, *Angew. Chem.* **1994**, *106*, 1356; *Angew. Chem. Int. Ed. Engl.* **1994**, *33*, 1246.

[9] J. L. Sessler, M. R. Johnson, V. Lynch, *J. Org. Chem.* **1987**, *52*, 4394.

[10] See also: K. Berlin, E. Breitmaier, *Angew. Chem.* **1994**, *106*, 229; *Angew. Chem. Int. Ed. Engl.* **1994**, *33*, 219.

[11] For nonaromatic examples of benzene- and pyridine-containing conjugated macrocycles related to the phthalocyanines, see R. P. Linstead, *J. Chem. Soc.* **1953**, 2873.

A Dinuclear (μ-Carboxylato)manganese(II) Complex Derived from a Macrocyclic Ligand: A Structural Model for Active Sites in Natural Systems**

Harry Adams, Neil A. Bailey, Noele Debaecker, David E. Fenton,* Wakako Kanda, Jean-Marc Latour,* Hisashi Okawa, and Hiroshi Sakiyama

Active sites containing two manganese atoms have been implicated recently in a growing number of proteins with various redox or hydrolytic functions; representative examples are the catalases (H_2O_2 disproportionation),[1] arginase (L-arginine hydrolysis),[2] and the xylose isomerases (isomerization of β-hydroxyaldehydes to β-oxoalcohols such as glucose to fructose).[3]

D-Xylose isomerase catalyzes the isomerization of the aldose xylose to the ketose xylulose as the second step in the utilization of D-(+)-xylose as a food source by bacteria.[3a] Two metals (Mg^{II}, Mn^{II}, or Co^{II}) are required at the active site.[3b] The general features of this metal-containing active site are clearly shown in the structure of the D-xylose isomerase from *Arthrobacterr* strain B3728 (Fig. 1).[3d] One manganese atom is

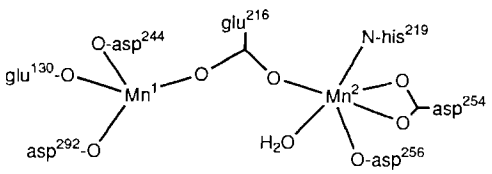

Fig. 1. The metal-containing binding site of D-xylose isomerase from *Arthrobacterr* strain B3728.

octahedrally coordinated and the second is four-coordinate; this second manganese atoms has two vacant sites that can be occupied by water molecules or by the incoming substrate. The manganese atoms are linked by a single bridging glutamate residue.

Two other structures have been solved for D-xylose isomerases. The metal-containing binding site in the enzyme from *Actinoplanes missouriensi*, with Mg^{II}, Co^{II}, or Mn^{II} as the metal, is very similar to that shown in Figure 1.[3e] The dinuclear site in D-xylose isomerase from *Streptomyces rubiginosus* also has a single glutamato bridge, this time between two manganese atoms separated by 4.9 Å.[3f] The two manganese atoms are both six-coordinate: Mn^1 binds to Glu217, Glu181, Asp245, Asp282, and two water molecules, whereas Mn^2 binds to Glu217, Asp255, Asp257, His220 (twice), and one water molecule.

[*] Prof. D. E. Fenton, H. Adams, Dr. N. A. Bailey
Department of Chemistry, Dainton Building
The University of Sheffield, GB-Sheffield S3 7HF (UK)
Telefax: Int. code + (1142) 738673

Dr. J.-M. Latour, Dr. N. Debaecker
Laboratoires DRFMC/SESM
Centre d'Études Nucleaires de Grenoble
F-85X 38041 Grenoble Cedex (France)

Dr. W. Kanda
Faculty of Education, Wakayama University (Japan)

Prof. H. Okawa, Dr. H. Sakiyama
Department of Chemistry, Faculty of Science
Kyushu University (Japan)

[**] We thank the SERC and the Royal Society for funds towards the purchase of the diffractometer. Dr. Kanda thanks Wakayama University for a leave of absence and the Japanese Ministry of Education, Science and Culture for support.

A common feature of these sites is the single bridging glutamate residue; to our knowledge this mode of single carboxylato bridging has not previously been simulated in model studies. Herein we report the isolation and characterization of a dinuclear manganese(II) complex containing only a single carboxylato bridge. This complex can be viewed, through its structural and physicochemical parameters, as providing a model for the occurrence of such a species at the metal-containing site in D-xylose isomerase.

Reaction of the diprotonated Schiff base cryptate $(L^1H_2)(BF_4)_2$ (**1**)[4] with manganese(II) acetate in methanol/acetonitrile (1:1), to which sodium tetrafluoroborate and triethylamine have been added, leads to complex **2**.[9] Recrystallization from acetonitrile/ethanol gives orange crystals of $2 \cdot CH_3CN \cdot 0.5CH_3CH_2OH$.

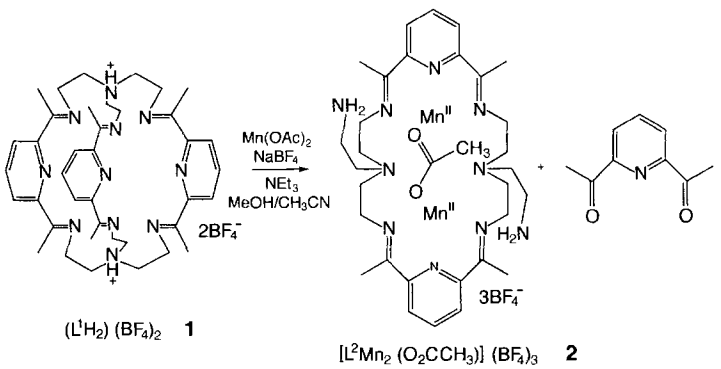

$(L^1H_2)(BF_4)_2$ **1**

$[L^2Mn_2(O_2CCH_3)](BF_4)_3$ **2**

The X-ray crystal structure (Fig. 2) confirms that a single ring-opening of the Schiff base cryptand has occurred to yield a carboxylato-bridged dinuclear manganese(II) complex of the bibracchial tetraimine Schiff base macrocycle L^2.[6] The macrocyclic trication accommodates two manganese(II) atoms, each of which is coordinated to five nitrogen atoms—three from a pyridine dicarbimine head unit, one from a tertiary amino group, and one from the pendant aminoethane residue. The two manganese atoms are thus located at opposite ends of the 24-membered macrocycle which has a semiopen, concertina-like conformation. The metal–metal separation of 4.82 Å may be compared with that of 4.9 Å found in the D-xylose isomerase from *Streptomyces rubiginosus*.[3f] The metal atoms in **2** are singly bridged in an unusual *syn-anti* manner by an acetato ligand. This is a relatively rare bridging bonding mode for the anion and leads to a greater metal–metal distance than that in other carboxylato-bridged dimetallic centers. This was previously noted in two structures containing dinuclear Mn^{II} centers bridged by two *syn-anti* carboxylates, $[Mn_2(OAc)_2(bpy)_4](ClO_4)_2$[7] and $[Mn_2(OAc)_2(bpen)_2](ClO_4)_2$ (bpen = *N,N'*-dimethyl-*N,N'*-bis(2-pyridylmethyl)ethane-1,2-diamine).[8] The metal separations in these two complexes are 4.58 and 4.29 Å respectively. More generally, dinuclear acetato-bridged species have been synthesized in which a single M-O-M bridge is also present.[9] This leads to a *syn-syn* bridging mode for the acetato ligand and a metal separation of roughly 3.5 Å. The absence of the one-atom bridge appears to lift any steric constraints imposing a *syn-syn* bridge and allows the achievement of the sterically less demanding *syn-anti* configuration. The Mn–Mn separation of 4.82 Å in **2** may also be contrasted with that of 5.6 Å found in a dinuclear Mn^{III} complex derived from salen and bearing a single bridging carboxylate anion.[10]

Figure 3 illustrates the dependence of the molar magnetic susceptibility of complex **2** with $1/T$ at two extreme fields (0.5 and 5 Tesla).[11] The curves follow linear Curie behavior only at temperatures above 10 K, which indicates the presence of a

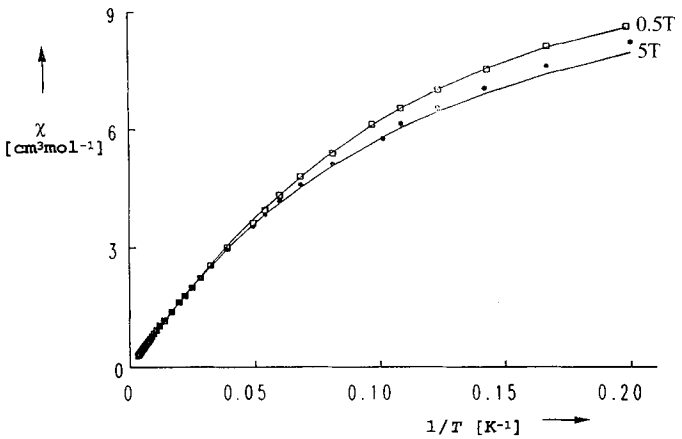

Fig. 3. Dependence of the magnetic susceptibility of **2** on the inverse temperature at two extreme field strengths; the solid lines correspond to calculated values.

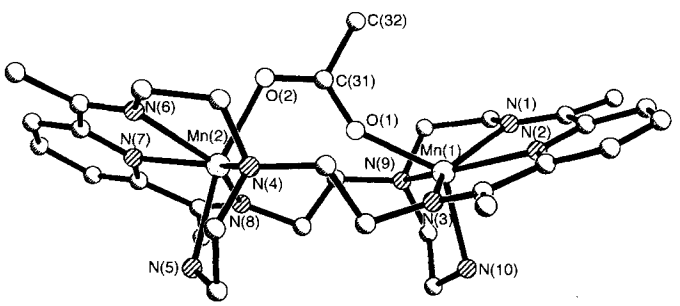

Fig. 2. The crystal structure of the cation in **2**. Selected bond lengths [Å]: Mn(1)-Mn(2) 4.82, Mn(1)-O(1) 2.10, Mn(1)-N(1) 2.29, Mn(1)-N(2) 2.26, Mn(1)-N(3) 2.35, Mn(1)-N(9) 2.47, Mn(1)-N(10) 2.54, Mn(2)-O(2) 2.16, Mn(2)-N(4) 2.40, Mn(2)-N(5) 2.28, Mn(2)-N(6) 2.30, Mn(2)-N(7) 2.28, Mn(2)-N(8) 2.36. Selected bond angles [°]: Mn(1)-O(1)-C(31) 145.7, Mn(2)-O(2)-C(31) 116.2, O(1)-C(31)-O(2) 122.1, O(2)-C(31)-C(32) 117.5, O(1)-C(31)-C(32) 120.3.

small exchange interaction. A slight field dependence at low temperature is evident, which points to the occurrence of some zero-field effects, albeit small. This behavior is clearly consistent with the simultaneous occurrence of a small exchange interaction and a small zero-field effect. These data were fitted with a Hamiltonian operator,[12] taking into account both the exchange coupling (J) and the anisotropic Zeeman interaction (zero-field splitting parameters D and E) of two identical ions of spin 5/2. The solid lines in the figures correspond to the theoretical values obtained with the following best fit parameters: $g_x = 2.07$, $g_y = 1.96$, $g_z = 2.02$, $J = -0.37\ cm^{-1}$. Approximations of comparable quality were obtained with $-0.1\ cm^{-1} < D < 0.1\ cm^{-1}$, and $E \neq 0$. Therefore while the exchange integral J is determined with good accuracy, the zero-field splittings cannot be estimated properly. This is not too astonishing since D values estimated through EPR experiments amount to a few hundredths of wavenumbers. Attention is drawn to the weakness of the antiferromagnetic exchange interaction mediated by the single bridging acetate group.

Figure 4 shows two EPR spectra of **2**. The spectrum measured at 4 K in a toluene/acetonitrile glass[13] consists of a broad line centered at $g = 1.96$ flanked by several features both at lower and higher fields. As described by Khangulov et al.,[14] such

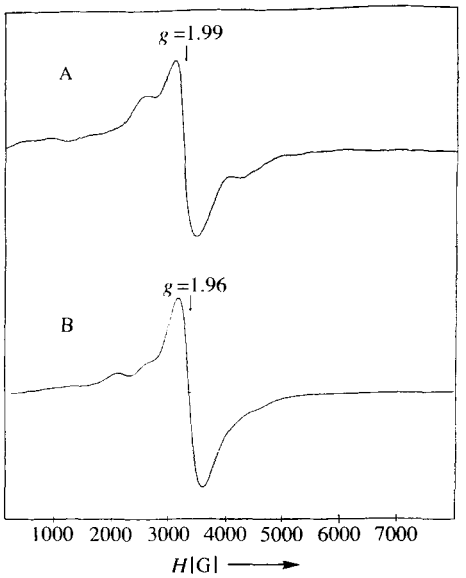

Fig. 4. X-Band EPR spectra of **2** in the solid state (A) and in a toluene/acetonitrile (1:1) glass (B) at 4 K. Operating conditions: microwave power 0.5 mW, modulation amplitude 1 G, gain 5000 (A) and 2000 (B), time constant 0.128 s.

spectra are very common for weakly coupled manganese(II) derivatives and correspond to the superposition of spectra of the various excited spin states ($s = 1-5$) of the manganese(II) pair modulated by a Boltzmann distribution. In the case of dimanganoproteins and complexes with exchange interactions of several wavenumbers, only the first excited state dominates with some contribution from the second. In the present case, however, owing to the very small exchange coupling ($J = -0.37\ cm^{-1}$), the situation is more complicated since more states are likely to be contributing, as shown by their respective populations p ($s = 0$, $p = 0.3989$; $s = 1$, $p = 0.3057$; $s = 2$, $p = 0.1795$; $s = 3$, $p = 0.0808$; $s = 4$, $p = 0.0278$; $s = 5$, $p = 0.0073$). Nevertheless, contributions from the first and second excited states can be clearly identified in the spectrum. It is noteworthy that the solution-state spectrum (Fig. 4B) is quite similar to that of the polycrystalline sample (Fig. 4A). This finding is a strong indication that the complex retains the acetato bridge in solution. It is therefore concluded that complex **2** can be viewed as a structural model for the metal-containing active site in D-xylose isomerase.

Received: July 7, 1995 [Z81821E]
German version: *Angew. Chem.* **1995**, *107*, 2749–2751

Keywords: complexes with nitrogen ligands · enzymes · manganese compounds · D-xylose isomerase

[1] a) Y. Kono, I. Fridovich, *J. Biol. Chem.* **1983**, *258*, 6015–6019; b) W. F. Beyer, I. Fridovich, *Biochemistry* **1985**, *24*, 6460–6467; c) S. V. Khangulov, V. V. Barynin, N. V. Voevodskaya, A. I. Grebenko, *Biochem. Biophys. Acta* **1990**, *1020*, 305–310; d) G. Schimpff-Weiland, H. Follman, G. Auling, *Biochem. Biophys. Res. Commun.* **1981**, *102*, 1276–1282; e) V. V. Barynin, A. A. Vagin, V. R. Melik-Adamyan, A. I. Grebenko, S. V. Khangulov, A. N. Popov, M. E. Andrianova, A. Vainshtein, *Dokl. Akad. Nauk. SSSR* **1986**, *228*, 877–880; f) M. Zheng, S. V. Khangulov, G. C. Dismukes, V. V. Barynin, *J. Inorg. Biochem.* **1993**, *51*, 510; g) G. S. Waldo, S. Yu, J. E. Penner-Hahn, *J. Am. Chem. Soc.* **1992**, *114*, 5869–5870.

[2] R. S. Reczkowski, D. E. Ash, *J. Am. Chem. Soc.* **1992**, *114*, 10992–10994.

[3] a) R. M. Hochster, R. W. Watson, *J. Am. Chem. Soc.* **1953**, *75*, 3284–3285; b) T. K. Kasumi, L. Hayashi, N. Tsumara, *Agric. Biol. Chem.* **1982**, *46*, 21–30; c) H. L. Carrell, J. P. Glusker, V. Burger, F. Manfre, D. Tritsch, J. F. Bieuman, *Proc. Natl. Acad. Sci. USA* **1989**, *86*, 4440–4444; d) C. A. Collyer, K. Henrick, D. M. Blow, *J. Mol. Biol.* **1990**, *212*, 211–235; e) J. Jenkins, J. Janin, F. Rey, M. Chiadmi, H. Vantilbeurgh, I. Lasters, M. Demaeyer, D. Vanbelle, S. J. Wodak, S. M. Lauwerey, P. Stanssens, N. T. Mrabet, J. Nauwaert, G. Matthyssens, A. M. Lambeir, *Biochemistry* **1992**, *31*, 5449–5458; f) M. Whitlow, A. J. Howard, B. C. Finzel, T. L. Foulos, E. Winborne, G. L. Gilliland, *Proteins* **1991**, *9*, 153–173; g) A. Lavie, K. N. Allen, G. A. Petsko, D. Ringe, *Biochemistry* **1994**, *33*, 5469–5480.

[4] H. Adams, N. A. Bailey, D. E. Fenton, C. Fukuhara, M. Kanesato, *Supramol. Chem.* **1993**, *2*, 325–330.

[5] Microanalytical data: calcd for $2 \cdot CH_3CN \cdot 0.5CH_3CH_2OH$: C 40.41, H 5.33, N 14.81%; found: C 40.49, H 5.36, N 14.83%. The fast atom bombardment mass spectrum has a peak of highest mass at m/z 889, which corresponds to $[L^2Mn_2(O_2CCH_3)(BF_4)_2]^+$, indicating that a ring-opening has occurred; there are further peaks at m/z 821 $[L^2Mn_2(O_2CCH_3)(BF_4)F]^+$, 802 $[L^2Mn_2(O_2CCH_3)(BF_4)]^+$, and 734 $[L^2Mn_2(O_2CCH_3)F)]^+$. No peaks are observed that can be assigned to a species retaining the intact Schiff base cryptand.

[6] Crystal structure data for $2 \cdot CH_3CN \cdot 0.5CH_3CH_2OH$ (empirical formula: $C_{35}H_{55}B_3F_{12}Mn_2N_{11}O_{2.5}$; $M = 1040.2$, orange blocks from acetonitrile/ethanol; crystal dimensions $0.60 \times 0.40 \times 0.2$ mm): monoclinic, $a = 11.883(14)$, $b = 15.731(8)$, $c = 26.148(13)$ Å, $\beta = 101.90(7)^\circ$, $V = 4783(7)$ Å^3, $Z = 4$, $\rho_{calcd} = 1.455\ g\,cm^{-3}$, space group $P2_1/n$ (a nonstandard setting of $P2_1/c$ (C_{2h}^5, No.14), $Mo_{K\alpha}$ radiation ($\lambda = 0.71073$ Å), $\mu(Mo_{K\alpha}) = 0.620\ mm^{-1}$, $F(000) = 2140$. Reflections were collected in the range $3.5 < 2\theta < 45$ on a Nicolet R3 diffractometer by the ω-scan method. The 3601 independent reflections (of 6649 measured) for which $|F|/\sigma(|F|) > 3.0$ were corrected for Lorentz and polarization effects, and for absorption (minimum and maximum transmission coefficients 0.568, 0.622). The structure was solved by direct methods and refined by blocked cascade least squares methods. Hydrogen atoms were included in calculated positions and refined in riding mode. Refinement converged at a final $R = 0.0817$ ($Rw = 0.0795$, 580 parameters, mean and maximum δ/σ 0.004, 0.039), with allowance for the thermal anisotropy of all non-hydrogen atoms. Minimum and maximum final electron density -0.49 and $0.62\ e\,Å^{-3}$. The weighting scheme $w^{-1} = \sigma^2(F) + 0.00156F^2$ was used in the latter stages of refinement. Complex scattering factors were taken from the program package SHELXTL/PC [15] as implemented on the Viglen 486dx computer. Further details of the crystal structure investigation may be obtained from the Director of the Cambridge Crystallographic Data Centre, 12 Union Road, GB-Cambridge, CB2 1EZ (UK), on quoting the full journal citation.

[7] R. L. Rardin, W. B. Tolman, S. J. Lippard, *New J. Chem.* **1991**, *15*, 417–430 (there: G. Christou, personal communication).

[8] C.-M. Che, W.-T. Tang, K. Y. Wong, W. T. Wong, T. F. Lai, *J. Chem. Res. S* **1991**, 30.

[9] a) L. Que, Jr., A. E. True, *Prog. Inorg. Chem.* **1990**, *38*, 97–200; b) K. Wieghardt, *Angew. Chem.* **1989**, *101*, 1179–1198; *Angew. Chem. Int. Ed. Engl.* **1989**, *28*, 1153–1172; c) "Polynuclear Manganese Enzymes": G. C. Dismukes, in *Bioinorganic Catalysis* (Ed.: J. Reedijk), Marcel Dekker, Amsterdam, **1993**.

[10] N. Aurangzeb, C. E. Holmes, C. A. McAuliffe, R. G. Pritchard, M. Watkinson, M. R. Bermejo, A. Sousa, *J. Chem. Soc. Chem. Commun.* **1994**, 2193–2195.

[11] Multifield saturation magnetization data were collected on crystals of the complex using a Quantum Design MPMS squid magnetometer. Measurements were performed in the 5–300 K temperature range at six field strengths (0.5, 1, 2, 3, 4, 5 Tesla). The magnetization of the sample holder (kel F bucket) was measured at the same temperatures and field strengths and subtracted from the sample measurements. The diamagnetic correction was estimated from Pascals constants.

[12] The Hamiltonian operator is given in Equation (a) and $\mathcal{H}_{iz}$ is defined in Equation (b). J is the isotropic exchange interaction and D and E are the axial

$$\mathcal{H} = -2JS_1S_2 + \sum_{i=1,2}[D(S_{iz}^2 - 2) + E_i(S_{ix}^2 - S_{iy}^2)] + \mathcal{H}_{iz} \quad \text{(a)}$$

$$\mathcal{H}_{iz} = \mu_B(g_xH_xS_{ix} + g_yH_yS_{iy} + g_zH_zS_{iz}) \quad \text{(b)}$$

and rhombic parameters of the zero-field splitting tensors. In agreement with the structural data, the two metal sites are assumed to be identical. The usual hypothesis is made that for each ion the zero-field splitting and g tensors can be diagonalized simultaneously.

[13] EPR spectra were measured in the range 4–20 K on a Varian E9 spectrometer operating at 9.2 GHz equipped with an Oxford cryostat.

Activation of Macrocyclic Biaryl-Enediynes by Metal Ion Coordination**

Burkhard König,* Helli Hollnagel, Birte Ahrens, and Peter G. Jones

Aromatic diradicals have been identified as the active species in several natural products with antitumor activity. The cytotoxic action is explained as being caused by hydrogen abstraction from DNA by the radical, leading to strand cleavage and cell death.[1] The reactive intermediates are formed by the cyclization of enediynes or enynallenes to arene diradicals. Pharmaceutical applications of these highly cytotoxic compounds depend on a selective trigger mechanism for radical formation. Several mechanisms have been investigated for triggering the activation of designed or natural prodrugs, including bioreduction and activation by light, bases, metal ions, or nucleophiles.[2] Conformational changes in the prodrug that increase the strain of the unsaturated cycle or lower the energy of the transition state for the cyclization can cause activation at the molecular level.[3] We describe here the synthesis of functionalized macrocyclic enediynes and the modulation of their chemical reactivity by metal ion coordination.

Compound **4** is a versatile building block in the synthesis of functionalized acyclic and cyclic enediynes by nucleophilic displacement of the bromine substituents. The basicity of the nucleophile is important in this process. Strong bases induce the formation of unstable enynallenes by propargyl–allene tautomerization.[4] The (*Z*) configuration of **4** favors the formation of cyclic compounds with suitable bisnucleophiles. High-dilution conditions are therefore not necessary to obtain the cyclic enediynes **5a–d** (Scheme 1, Table 1, Table 2). Palladium-catalyzed coupling[5] of (*Z*)-1,2-dichloroethene (**1**) with **2**, followed by OTHP/bromine[6] exchange (THP = tetrahydropyranyl) with PPh_3/Br_2 provides **4** in multigram quantities.

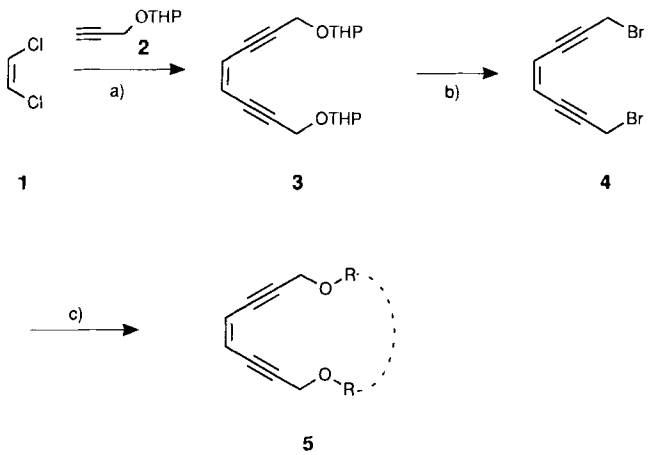

Scheme 1. Synthesis of the macrocyclic enediynes **5a–d**. a) 2 mol% $[Pd(PPh_3)_4]$, 15 mol% CuI, $nBuNH_2$, benzene, 12 h room temperature, 75%; b) PPh_3, Br_2, dichloromethane, 6 h room temperature, 77%; c) dimethylsulfoxide, ROH, KOH (for **5d**: K_2CO_3), room temperature, 8 h.

[*] Dr. B. König, H. Hollnagel
Institut für Organische Chemie der Technischen Universität
Hagenring 30, D-38106 Braunschweig (Germany)
Telefax: Int. code + (531)391-5388

B. Ahrens, Prof. Dr. P. G. Jones
Institut für Anorganische und Analytische Chemie
der Technischen Universität Braunschweig

[**] This work was supported by the Fonds der Chemischen Industrie and the Deutsche Forschungsgemeinschaft (grant KO1537/1-1). B. K. thanks the Fonds der Chemischen Industrie for a Liebig Stipendium and Prof. Dr. H. Hopf for his support. We thank Prof. Dr. C. Müller-Goymann and G. Hildebrandt, Institut für Pharmazeutische Technologie, Braunschweig, for the DSC measurements.

Table 1. Synthesis of the macrocyclic enediynes **5a–d**.

Product	HO-R- - -R-OH	Yield[%]	*T*[K][a]
5a	2,2′-biphenyldicarboxylic acid	46	445
5b	2,2′-dihydroxybiphenyl	35	435
5c	3,3′-dihydroxy-6,6′-dimethyl-2,2′-bipyridine	54	510
5d	1,3-*p*-*tert*-butylcalix[4]arene	55	>530

[a] Cyclization temperature.

Table 2. Selected spectroscopic data [a] for compounds **4**, **5**, and **6**.

4: oil; ^1H NMR: $\delta = 4.15$ (s, 4H), 5.92 (s, 2H); ^{13}C NMR: $\delta = 14.8$ (−), 83.5 (C_q), 92.2 (C_q), 120.1 (+); MS (70 eV): *m/z* (%): 260/262/264 (10/20/10) [M^+], 181/183 (60/60) [M^+ − Br], 102 (100)

5a: colorless crystals, m.p. 170 °C (decomp); ^1H NMR: $\delta = 4.70$ (d, $^2J = 15.1$ Hz, 2H), 4.94 (d, $^2J = 15.1$ Hz, 2H), 5.77 (s, 2H), 7.18 (dd, $^3J = 7.5$, $^4J = 1.1$ Hz, 2H), 7.44 (dt, $^3J = 7.4$, $^4J = 1.2$ Hz, 2H), 7.57 (dt, $^3J = 7.4$, $^4J = 1.2$ Hz, 2H), 8.16 (dd, $^3J = 7.4$, $^4J = 1.2$ Hz, 2H); ^{13}C NMR: $\delta = 52.2$ (−), 83.0 (C_q), 91.4 (C_q), 119.2 (+), 127.2 (+), 128.0 (C_q), 130.0 (+), 130.4 (+), 132.2 (+), 144.3 (C_q); MS (70 eV): *m/z* (%): 342 (16) [M^+], 225 (100); $C_{22}H_{14}O_4$ (342.4): calcd C 77.18, H 4.12; found C 76.82, H 4.04

5b: white solid, m.p. 160 °C (decomp); ^1H NMR: $\delta = 4.77$ (d, $^2J = 16.0$ Hz, 2H), 4.88 (d, $^2J = 16.0$ Hz, 2H), 5.84 (s, 2H), 6.92 (d, $^3J = 7.6$ Hz, 2H), 7.03 (dt, $^3J = 7.3$, $^4J = 1.1$ Hz, 2H), 7.22 (dd, $^3J = 7.2$, $^4J = 1.8$ Hz, 2H), 7.33 (m, 2H); ^{13}C NMR: $\delta = 56.4$ (−), 85.0 (C_q), 93.4 (C_q), 111.3 (+), 121.0 (+), 121.1 (+), 128.5 (C_q), 128.7 (+), 131.5 (+), 155.2 (C_q); HR-MS (EI): *m/z*: 286.099 [M^+, calcd for $C_{20}H_{14}O_2$: 286.099]

5c: white solid; ^1H NMR (C_6D_6): $\delta = 2.42$ (s, 6H), 4.18 and 4.19 (s, 4H), 5.39 (s, 2H), 6.50 (d, $^3J = 8.5$ Hz, 2H), 6.61 (d, $^3J = 8.5$ Hz, 2H); ^{13}C NMR: $\delta = 23.6$ (+), 56.5 (−), 85.4 (C_q), 92.6 (C_q), 119.5 (+), 121.2 (+), 123.4 (+), 147.3 (C_q), 150.0 (C_q), 150.6 (C_q); ^1H NMR ([D$_4$]methanol): $\delta = 2.50$ (s, 6H), 4.82 and 5.00 (d, $^2J = 16.2$ Hz, 4H), 5.94 (s, 2H), 7.31 (d, $^3J = 8.5$ Hz), 7.46 (d, $^3J = 8.5$ Hz); MS (CI, NH_3, negative): *m/z* (%): 316 (100) [M^+]; $C_{20}H_{16}N_2O_2$ (316.4): calcd C 75.93, H 5.10, N 8.85; found C 75.73, H 5.27, N 8.82

[**5c**·Hg(tfa)$_2$]: ^1H NMR ([D$_4$]methanol): $\delta = 2.74$ (s, 6H), 5.05 (br. s, 4H), 6.04 (s, 2H), 7.68 (d, $^3J = 8.7$ Hz), 7.84 (d, $^3J = 8.7$ Hz); ^{13}C NMR: $\delta = 26.6$ (+), 57.5 (−), 85.3 (C_q), 91.5 (C_q), 119.0 (+), 120.6 (+), 122.4 (+), 147.7 (C_q), 150.4 (C_q), 150.6 (C_q); MS (ESI): *m/z* (%): 631.07 (15) [**5c**·Hg(tfa)$^+$]; $C_{24}H_{16}N_2O_6F_6Hg$ (742.9): calcd C 38.80, H 2.17, N 3.77; found C 38.50, H 2.10, N 3.43

5d: white solid, m.p. >300 °C; ^1H NMR: $\delta = 1.19$ (br. s, 36H), 3.35 (d, $^2J = 12.7$ Hz, 4H), 4.39 (d, $^2J = 12.7$ Hz, 4H), 4.85 (s, 4H), 5.99 (s, 2H), 6.97 (s, 4H), 7.09 (s, 4H), 8.60 (s, 2H); ^{13}C NMR: $\delta = 31.2$ (+), 31.5 (+), 32.5 (−), 33.8 (C_q), 34.2 (C_q), 63.3 (−), 84.9 (C_q), 91.3 (C_q), 118.9 (+), 125.2 (+), 126.0 (+), 127.6 (C_q), 128.4 (C_q), 134.3 (C_q), 141.8 (C_q), 148.1 (C_q), 150.1 (C_q); MS (70 eV): *m/z* (%): 748 (0.5) [M^+], 648 (100); $C_{52}H_{60}O_4$ (748.4): calcd C 83.37, H 8.08; found C 83.24, H 8.10

6: white solid, m.p. 110 °C; ^1H NMR ($CDCl_3$, 400 MHz): $\delta = 2.49$ (s, 6H), 5.19 (br. s, 4H), 7.02 (d, $^3J = 8.3$ Hz), 7.29 (d, $^3J = 8.3$ Hz), 7.31 (m, 4H); ^{13}C NMR: ($CDCl_3$, 100 MHz): $\delta = 23.9$ (+), 71.5 (−), 123.2 (+), 123.3 (+), 129.2 (+), 131.3 (+), 135.5 (C_q), 147.4 (C_q), 151.3 (C_q), 152.4 (C_q); HR-MS (EI): *m/z*: 318.136 [M^+; calcd for $C_{20}H_{18}N_2O_2$: 318.136]

[a] ^1H NMR: 400 MHz, $CDCl_3$, TMS; ^{13}C NMR: 100 MHz, $CDCl_3$; the multiplicity of the ^{13}C NMR signals was determined by DEPT experiments and denoted as (+) for CH_3 and CH groups, (−) for CH_2 groups, and C_q for quarternary carbons.

Figure 1 shows the X-ray structure[7] of the 16-membered macrocyclic enediyne ester **5a**. The phenyl rings subtend an interplanar angle of 68°, while the carbon atoms of the enediyne moiety are almost coplanar (mean deviation 2.5 pm). Enantiomeric conformers of the molecule, which displays crystallographic twofold symmetry, are packed alternatingly in the crystal lattice.

The thermal stability of the cyclic enediynes **5a–d** was investigated by differential scanning calorimetry (DSC).[8] The DSC

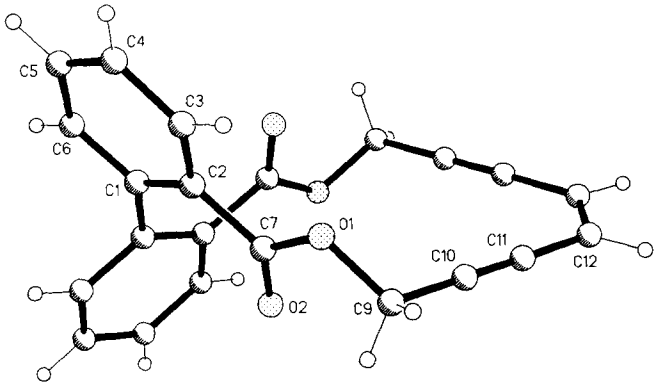

Fig. 1. X-ray crystal structure of **5a**. Selected bond lengths [pm] and angles [°]: C12-C12A 133.5(3), C10-C11 119.2(2), C1-C1A 149.6(2), C10-C10A 432.1(3), C11-C11A 294.2(3); C10-C11-C12 178.1(2), C12A-C12-C11 124.36(8), interplanar angle of the biaryl unit 68 .

trace of **5a** (Fig. 2) clearly indicates an exothermic, irreversible reaction at 445 K.[9] The 2,2′-bipyridine macrocycle **5c** shows an exothermic reaction at approximately 510 K.[9] The coordination of the 2,2′-bipyridine moiety by transition metal ions[10]

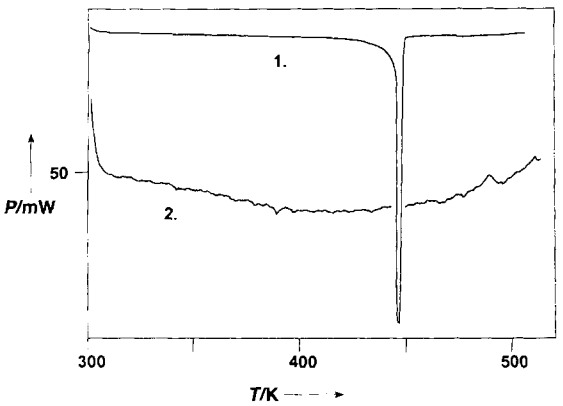

Fig. 2. DSC analysis of **5a**. The power input P (endothermic process) is plotted against the temperature T. Scan rate 10 K min^{-1}; 1. first heating cycle; 2. second heating cycle.

alters the conformation of the macrocycle. Without metal ion coordination, the less strained *transoid* orientation of the 2,2′-bipyridine should be favored, according to force field calculations (Scheme 2).[11] When $[Hg(tfa)_2]$ (tfa = O_2CCF_3) is added to a suspension of **5c** in methanol, a clear solution is formed instantaneously and significant changes in the ^{1}H NMR spectra indicate metal coordination. The preserved symmetry of the

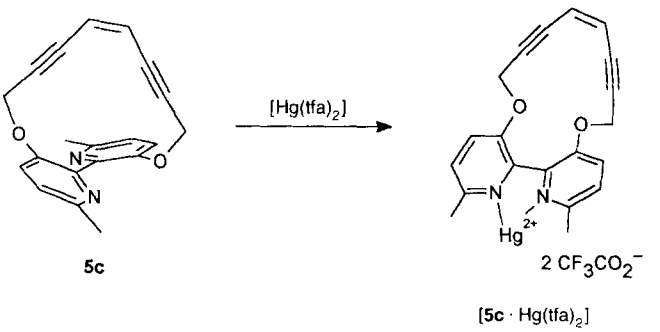

Scheme 2. Coordination of **5c** by $[Hg(CF_3CO_2)_2]$.

compound suggests that both nitrogen atoms are coordinated symmetrically. However, the metal ion must induce a change in the conformation of the 2,2′-bipyridine unit to a predominantly *cisoid* orientation for complex formation. In this conformation the macrocyclic enediyne is more strained,[11] which is reflected in a decrease of the cyclization temperature to 418 K as shown by DSC.[9] When a suitable 2,2′-bipyridine binding site for strong coordination of a metal is not available, the cyclization temperature is not affected by addition of $[Hg(tfa)_2]$. In DSC analyses mixtures of **5a** and $[Hg(tfa)_2]$ show the exothermic reaction at the same temperature as pure **5a**.[12]

In contrast to the results discussed here, a rigid conformation can stabilize an enediyne moiety against thermally induced cyclization. No exothermic reaction is observed when the compound **5d** is heated to 530 K.

Although elevated temperatures are still necessary to trigger the cyclization of the macrocycles **5a–d**, their reactivity can be significantly altered by noncovalent interactions that influence their conformation. The use of even more strained bicyclic enediynes[13] might lead to the development of compounds that can be selectively triggered by a chemical signal at room temperature.

Experimental Procedure

General procedure for the reaction of **4** with nucleophiles: Macrocycle **4** (262 mg, 1.0 mmol) was dissolved in 2 mL of DMSO and added to a solution of 2.0 mmol of the nucleophile (or 1.0 mmol of the bisnucleophile) and 4 mmol of KOH in 30 mL of DMSO at room temperature. The reaction mixture was stirred for 6 h, poured into 100 mL of saturated aqueous NH_4Cl, and extracted with dichloromethane. The organic phase was dried over $MgSO_4$ and concentrated in vacuo; the products were purified by column chromatography on silica gel.

Received: June 7, 1995
Revised version: August 7, 1995 [Z 8066 IE]
German version: *Angew. Chem.* **1995**, *107*, 2763–2765

Keywords: biaryls · conformation · enediynes · macrocycles · supramolecular chemistry

[1] a) For a review see: K. C. Nicolaou, W.-M. Dai, *Angew. Chem.* **1991**, *103*, 1453–1481; *Angew. Chem. Int. Ed. Engl.* **1991**, *30*, 1387–1416. b) For a recent review of nonenzymatic DNA cleavage see: G. Pratviel, J. Bernadou, B. Meunier, *Angew. Chem.* **1995**, *107*, 819–845; *Angew. Chem. Int. Ed. Engl.* **1995**, *34*, 746–769.

[2] Selected examples of various trigger mechanisms: bioreduction: a) M. F. Semmelhack, J. Gallagher, D. Cohen, *Tetrahedron Lett.* **1990**, *31*, 1521–1522; photochemical: b) K. Nakatani, S. Isoe, S. Maekawa, I. Saito, *ibid.* **1994**, *35*, 605–608; c) J. M. Nuss, M. M. Murphy, *ibid.* **1994**, *35*, 37–40; base-induced: d) S. M. Kerwin, *ibid.* **1994**, *35*, 1023–1026; e) M.-J. Wu, C.-F. Lin, J.-S. Wu, H.-T. Chen, *ibid.* **1994**, *35*, 1879–1882; metal ion induced: f) B. P. Warner, S. P. Millar, R. D. Broene, S. L. Buchwald, *Science* **1995**, *269*, 814–816.

[3] M. E. Maier, *Synlett* **1995**, 13–26.

[4] L. Brandsma, *Preparative Acetylenic Chemistry*, Springer, Berlin, **1988**, p. 79 ff.

[5] L. S. Hegedus in *Organometallics in Synthesis* (Ed.: M. Schlosser), Wiley, Chichester, **1994**, p. 383 ff.

[6] M. Schwarz, J. E. Oliver, P. E. Sonnet, *J. Org. Chem.* **1975**, *40*, 2410–2411.

[7] X-ray structure determination of compound **5a**: $C_{22}H_{14}O_4$, M = 342.33, orthorhombic, space group *Pnna*, a = 1966.9(3), b = 1024.5(2), c = 822.6(2) pm, V = 1.6576(6) nm^3, Z = 4, $\lambda(Mo_{K\alpha})$ = 0.71073 Å, T = 143 K. The final $wR(F^2)$-value was 0.095 for all 3712 reflections with $2\theta < 55°$, conventional $R(F)$-value of 0.037, 119 parameters. Diffractometer: Stoe STADI-4. Program: SHELXL-93 (G. M. Sheldrick, Universität Göttingen). Further details of the crystal structure determination may be obtained from the Fachinformationszentrum Karlsruhe, D-76344 Eggenstein-Leopoldshafen (Germany) on quoting the depository number CSD-401890.

[8] H.-G. Elias, *Makromoleküle, Bd. 1*, Hüthig & Wepf, Basel, **1990**, pp. 817–820.

[9] The thermally induced cyclization is accompanied by radical polymerization of the compounds. However, when the compounds were heated in decalin or ethylene glycol, the trapped product **6**

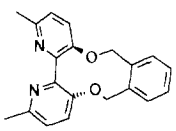

6

from the Bergman cyclization was identified by NMR, high-resolution mass spectra, and TLC (see Table 2). Compound **6** was synthesized independently for comparison from 3,3′-dihydroxy-6,6′-dimethyl-2,2′-bipyridine and α,α′-dibromo-*o*-xylylene.

[10] a) For a recent example of the control of conformation by metal ion coordination see: T. R. Kelly, M. C. Bowyer, K. V. Bhaskar, D. Bebbington, A. Garcia, F. Lang, M. H. Kim, M. P. Jette, *J. Am. Chem. Soc.* **1994**, *116*, 3657–3658. b) Hg^{2+} was used because it forms very stable 2,2′-bipyridine (bipy) complexes: $[Hg^{2+}(bipy)]$: $\lg k = 9.6$; $[Hg^{2+}(bipy)_2]$: $\lg k = 7.1$; F. Vögtle, *Supramolecular Chemistry*, Wiley, Chichester, **1991**, p. 18. c) The change in the conformation of a 2,2′-bipyridine unit on coordination by a transition metal ion has been used previously in an allosteric receptor to alter rates of metal ion transport: J. Rebek, Jr., R. V. Wattley, *J. Heterocycl. Chem.* **1980**, *17*, 749–751; d) J. Rebek, Jr., R. V. Wattley, *J. Am. Chem. Soc.* **1980**, *102*, 4853–4854.

[11] Calculations were performed with the program SPARTAN on a Silicon Graphics workstation. Sybil and MM2 force fields were used.

[12] To investigate the possible influence of the morphology of the solids on their reactivity, DSCs were recorded from single crystals and powders of **5a**. The observed temperatures of the exothermic cyclization are identical.

[13] The reactivity of [7.3.1]bicyclotridecenediynes is very sensitive to small conformational changes; ref. [3].

Synthesis and Structure of Bimetallic η^4,η^6-Naphthalene Complexes Containing a Mn–Mn Moiety Bonded in a *syn*-Facial Manner: A General Route to Homo- and Heteronuclear Bimetallic Complexes of Polyarenes**

Shouheng Sun, Conor A. Dullaghan, Gene B. Carpenter, Anne L. Rieger, Philip H. Rieger, and Dwight A. Sweigart*

Bimetallic organometallic complexes have long been investigated in order to probe the effect of electron delocalization and metal–metal interactions on physical properties such as charge transfer, conductivity, and nonlinear optical behavior. Equally interesting has been the chemical application of bimetallic systems to stoichiometric and catalytic reactions. There are three common types of bimetallic complexes. In type **A** complexes the metals are coordinated to separate π-hydrocarbon rings, which are attached directly to each other or are separated by a spacer.[1] The metals may have a *syn*-facial or *anti*-facial arrangement; in the former case there is sometimes a direct metal–metal interaction, whereas in the latter any such interaction is necessarily indirect through the ligand system. In type **B** complexes two metals are bound (*syn* or *anti*) to the same π-hydrocarbon ring,[2] and in type **C** systems the metals are bound to adjacent fused rings. Examples of type **C** systems include complexes with pentalene, azulene, indenyl, and naphthalene-type ligands;[3–6] most of the known examples contain indenyl ligands.[4] By comparison, bimetallic complexes with naphthalene-type ligands are rare and those known[5] have the metals in an *anti*-facial conformation.[7] In this paper we outline a general synthetic route to homo- and heteronuclear bimetallic naphthalene complexes that usually, but not always, yields products with a *syn*-facial arrangement of metal atoms and a metal–metal bond. Furthermore, it is demonstrated that the procedure can be extended to fused ring systems other than naphthalenes.

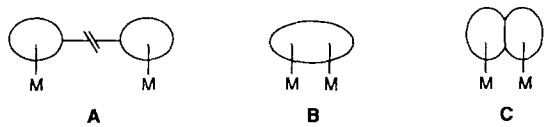

We recently reported[8] that $[Mn(\eta^6\text{-polyarene})(CO)_3]^+$ complexes such as **1** function as efficient manganese tricarbonyl transfer (MTT) reagents by rapidly and cleanly transferring the $[Mn(CO)_3]^+$ moiety to other arenes upon warming in dichloromethane. The facility of the MTT reaction was shown to correlate with the ease of $\eta^6 \rightarrow \eta^4$ ring slippage in **1**, which accompanies associative nucleophilic attack at the metal. In a similar vein, we find that two-electron chemical or electrochemical reduction of **1** (R = H, 1,4-Me_2, 2,6-Me_2) reversibly generates the anionic 18-electron η^4-diene complex **2**.[9, 10] The diene complex **2** with R = H was previously prepared by an alternative route and structurally characterized.[11] However, when only one equivalent of reducing agent (cobaltocene) is present, complexes **1** react not to give the η^4-diene complex, but rather the novel deeply colored ("black") bimetallic species shown in structures **3**–**7**. That the compounds **3**–**5** contain two *syn*-facial metal atoms was confirmed by single-crystal X-ray structure analyses. Figure 1 shows the structure of **3**; details of the structures of **4** and **5** will be published separately.[12] When the naphthalene ligand in **1** is the relatively rigid hexahydropyrene or acenaphthene, it was found that the bimetallic products **5** and **6**, respectively, are formed in good yield even when excess cobaltocene is used. It is likely that this is due to a structurally imposed barrier that inhibits slippage to the η^4-diene complex, which is a conclusion supported by electrochemical experiments.[9]

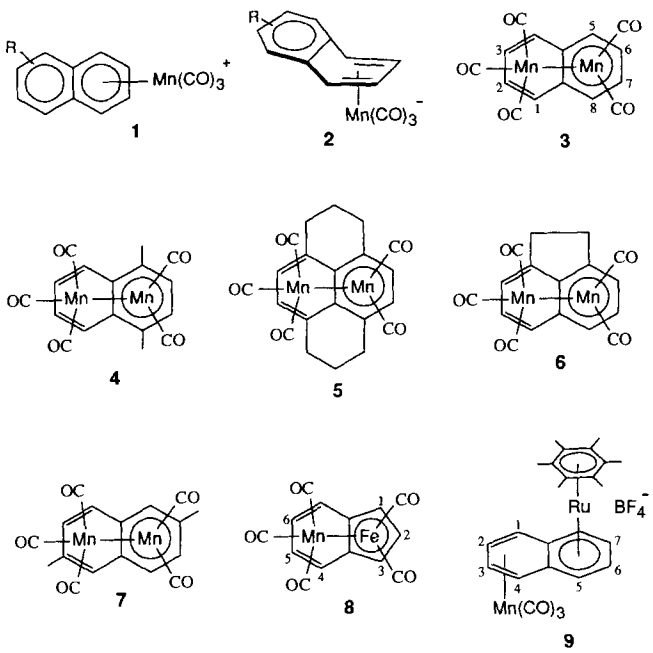

Complex **3** has a Mn–Mn bond length of 2.9231(7) Å, a value close to that in $[Mn_2(CO)_{10}]$.[13] The dihedral angle between

[*] Prof. D. A. Sweigart, S. Sun, C. A. Dullaghan, Prof. G. B. Carpenter, Dr. A. L. Rieger, Prof. P. H. Rieger
Department of Chemistry, Brown University
Providence, RI 02912 (USA)
Telefax: Int. code + (401)863-2594
e-mail: Dwight_Sweigart@Brown.edu

[**] This work was supported by a grant from the National Science Foundation (NSF) (CHE-9400800). The X-ray equipment was purchased with assistance from NSF (Grant CHE-8206423) and the National Institutes of Health (Grant RR-06462).

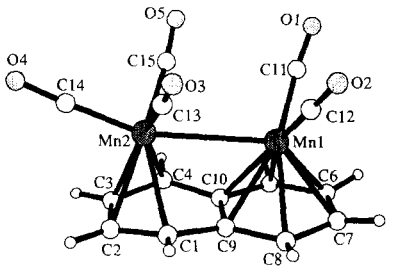

3

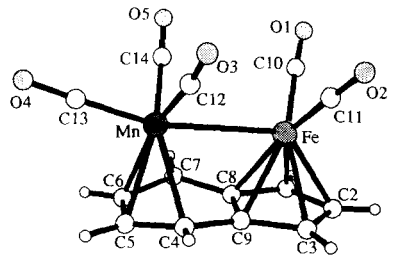

8

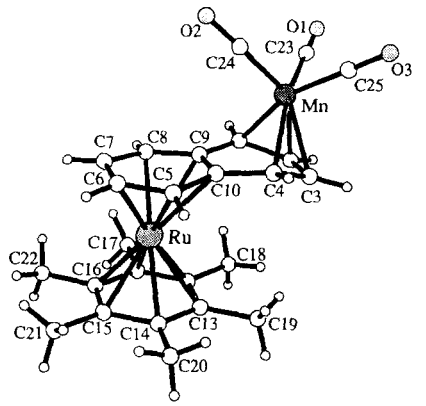

9

Fig. 1. Crystal structures of complexes **3**, **8**, and **9** (BF_4^- ion omitted for clarity). Selected bond lengths [Å] for **3**: Mn(1)-Mn(2) 2.9231(7), Mn(2)-C(1) 2.240(3), Mn(2)-C(2) 2.143(3), Mn(2)-C(3) 2.147(3), Mn(2)-C(4) 2.246(3), Mn(1)-C(5) 2.164(3), Mn(1)-C(6) 2.119(4), Mn(1)-C(7) 2.116(3), Mn(1)-C(8) 2.164(3), Mn(1)-C(9) 2.168(3), Mn(1)-C(10) 2.154(3); for **8**: Mn-Fe 2.8270(7), Mn-C(4) 2.267(3), Mn-C(5) 2.145(3), Mn-C(6) 2.150(3), Mn-C(7) 2.268(3), Fe-C(1) 2.085(3), Fe-C(2) 2.077(4), Fe-C(3) 2.103(4), Fe-C(8) 2.106(3), Fe-C(9) 2.117(3); for **9**: Mn-C(1) 2.183(6), Mn-C(2) 2.081(6), Mn-C(3) 2.104(6), Mn-C(4) 2.226(6), Ru-C(5) 2.230(6), Ru-C(6) 2.167(6), Ru-C(7) 2.179(6), Ru-C(8) 2.214(6), Ru-C(9) 2.412(5), Ru-C(10) 2.452(5).

planes C1-C2-C3-C4 and C1-C9-C10-C4 is 16.6°, which is considerably less than the values found in **2**[11] and other[14] monometallic η^4-naphthalene-type complexes. The obvious reason for this difference is the presence of the second metal, which is simultaneously η^6-bonded to the second naphthalene ring and bonded to the other metal atom. As far as we are aware, **3** is the first example of a bimetallic η^4,η^6-naphthalene complex with *syn*-facially bound metal atoms.

The pure dimanganese complexes **3**–**7** are moderately stable as solids and in solution. The IR spectra are simple and give no evidence for bridging CO ligands in solution. The ^{1}H NMR spectra between ambient temperature and −80 °C indicate that the environments of the manganese atoms in **3** and **5**–**7** are identical on the NMR timescale. For example, the four protons $H^{2,3}$ and $H^{6,7}$ in **3** give a single resonance as do the two methyl groups in **7**, suggesting very rapid $\eta^4,\eta^6 \rightarrow \eta^6,\eta^4$ interconversion (Scheme 1). This transformation probably occurs through an

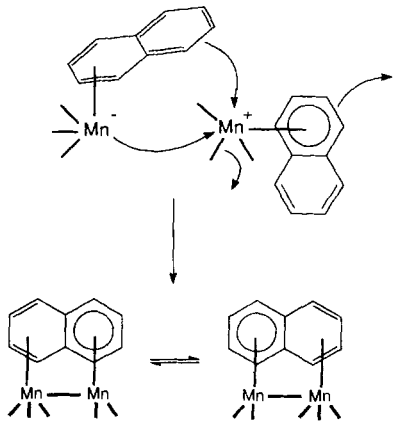

Scheme 1. Possible mechanism for the formation of *syn*-facial bimetallic complexes of naphthalenes.

intermediate with a bridging CO ligand. Voltammetric oxidation of **3**–**7** in CH_2Cl_2/TBAPF$_6$ (TBA = tetra-*n*-butylammonium) occurs as a one-electron, partially chemically reversible process (scan rate: 0.5 Vs^{-1}) at $E_{1/2} = 0.45$ V relative to ferrocene ($E_{1/2} = 0.50$ V). The intense color of **3**–**7** and the rather low redox potential suggests that the HOMO is essentially Mn–Mn σ-bonding. This was confirmed by measuring the ESR spectrum of $\mathbf{5}^+$ at 110 K in CH_2Cl_2/1,2-$C_2H_4Cl_2$. The spectrum consists of a broad envelope with eight resolved features at lower and higher fields; these are the outer members of the 1:2:3:4:5:6:5:4:3:2:1 multiplet expected for two *equivalent* ^{55}Mn nuclei ($I = 5/2$) and correspond to $g_1 = 2.067$, $A_1^{Mn} = 57.0 \times 10^{-4}$ cm^{-1}. The other two g components are approximately 2.0 and 2.1, but these have much smaller manganese couplings. Assuming that each Mn atom contributes a 3d orbital to the SOMO, the dipolar contribution to the coupling matrix is $A_{\parallel} = (4/7)P\rho^d$ where $P = 205 \times 10^{-4}$ cm^{-1}.[15] Since the two missing hyperfine components are small, $\langle A \rangle \approx A_{\parallel}/3$ and $\rho^d \approx 0.3$, and hence we may conclude that the HOMO is largely metal-based.

The mechanism of formation of **3**–**7** when a reducing agent is added to **1** probably involves initial formation of some η^4-diene anion **2**, which attacks remaining cation **1**. Scheme 1 shows a plausible pathway (for R = H), and in accordance with this, the addition of a solution of the η^4-diene to a separate solution of **1** (R = H) gave the bimetallic complex **3**. This scheme suggests that heteronuclear bimetallic complexes may be formed by the reaction of **1** with appropriate metal complexes that possess ambident nucleophilic behavior. In this manner, complex **8** was prepared from the reduction of a mixture of [Fe(indenyl)$(CO)_3$]$^+$ and **1**. Figure 1 shows the structure of **8**, which is a bimetallic complex with η^4,η^5-bonding. The dihedral angle between planes C4-C5-C6-C7 and C4-C9-C8-C7 is 18.1°, and the Mn–Fe bond length is 2.8270(7) Å. In a related experiment, the reaction of the nucleophilic complex [(η^4-naphthalene)-Ru(C_6Me_6)] with **1** (R = H) was found to give the bimetallic complex **9**, which is prevented for steric reasons from forming a Ru–Mn bond (Fig. 1). In this case the C1-C2-C3-C4 plane is folded about the C1-C9-C10-C4 plane by 22.9°.

In conclusion, we have shown that the ability of **1** to function as a facile manganese tricarbonyl transfer reagent provides a general synthetic route to homo- and heteronuclear bimetallic complexes of fused ring systems which, in the absence of steric constraints, adopt a *syn*-facial structure. Herein we have described homocyclic fused ring systems; preliminary results with the η^6-manganese tricarbonyl complexes of the fused ring hete-

rocycles *N*-methylindole and benzothiophene indicate that cobaltocene reduction also leads to bimetallic complexes in these cases.[16] The usefulness of the new bimetallic complexes in promoting/catalyzing chemical reactions is currently under investigation.

Experimental Procedure

3–**7**: Cobaltocene (0.2 mmol) was added to the appropriate manganese complex **1** (0.2 mmol) in CH_2Cl_2 (10 mL). The mixture was stirred under N_2 for 15 min and then chromatographed rapidly through a short column of deactivated neutral alumina with CH_2Cl_2 as the eluent. After solvent removal, the dark solid was washed with pentane and dried. Analytical and spectroscopic data showed the product to be pure. **3**: yield 40%; m. p. 74 °C; IR (CH_2Cl_2): ν_{CO} [cm^{-1}] = 2008(s), 1941(s), 1885(w); ^1H NMR (CD_2Cl_2): δ = 5.27 ($H^{2,3,6,7}$), 4.05 ($H^{1,4,5,8}$). **4**: yield 55%; m. p. 88 °C; IR (CH_2Cl_2): ν_{CO} [cm^{-1}] = 2004(s), 1937(s), 1875(w); ^1H NMR (CD_2Cl_2): δ = 5.43 ($H^{2,3}$), 5.20 ($H^{6,7}$), 4.06 ($H^{1,4}$), 1.77 (Me). **5**: yield 60%; m. p. 128 °C; IR (CH_2Cl_2): ν_{CO} [cm^{-1}] = 1996(s), 1935(s), 1869(w); ^1H NMR (CD_2Cl_2): δ = 5.18 ($H^{2,3,6,7}$), 1.80–2.55 (H^{9-14}). **6**: yield 43%; m. p. 112 °C; IR (CH_2Cl_2): ν_{CO} [cm^{-1}] = 2002(s), 1935(s), 1877(w); ^1H NMR (CD_2Cl_2): δ = 3.93 ($H^{2,3,6,7}$), 3.40 ($H^{1,8}$), 2.60–2.90 ($H^{9,10}$). **7**: yield 31%; m. p. 90 °C; IR (CH_2Cl_2): ν_{CO} [cm^{-1}] = 2004(s), 1935(s), 1877(w); ^1H NMR (CD_2Cl_2): δ = 5.24 ($H^{3,7}$), 3.95 ($H^{1,4,5,8}$), 2.26 (Me). Complexes **3** and **7** were also synthesized by an alternative method: cobaltocene (0.2 mmol) and **1** (0.1 mmol, R = H) were combined in CH_2Cl_2 (10 mL) and stirred under N_2 for 10 min. To this solution of the anion **2** (R = H), the cationic complex **1** (0.1 mol, R = H or 2,6-Me_2) was added. After stirring for 20 min, the reaction mixture was chromatographed as above. High-quality single crystals of **3**–**7** were readily grown by pentane diffusion into a solution of the respective compound CH_2Cl_2 at −20 °C.

8: Cobaltocene (0.42 mmol) was added to a mixture of [Mn(1-methylnaphthalene)$(CO)_3$]BF_4 (0.21 mmol) and [Fe(indenyl)$(CO)_3$]BF_4 (0.21 mmol) in CH_2Cl_2 (10 mL). The mixture was stirred under N_2 for 10 min, during which CO evolution was evident. Workup was as described above for **3**–**7**. Yield 72%; IR (CH_2Cl_2): ν_{CO} [cm^{-1}] = 2018(s), 1956(s, br); ^1H NMR (CD_2Cl_2): δ = 5.49 (dd, $H^{4,7}$), 5.09 (t, H^2), 4.34 (dd, $H^{5,6}$), 4.12 (d, $H^{1,3}$). X-ray quality crystals of **8** were grown by slow evaporation of a hexane solution at −20 °C.

9: Cobaltocene (0.2 mmol) was added to [(naphthalene)Ru(C_6Me_6)]$(BF_4)_2$ [1f,17] (0.1 mmol) in CH_2Cl_2 (10 mL) and the mixture stirred under N_2 for 1 h. Complex **1** (0.1 mmol, R = H) was then added and the stirring continued for 3 h. After most of the solvent had been removed, purification was effected by chromatography on deactivated neutral alumina by first eluting with CH_2Cl_2 to remove any neutral Mn–Mn complex and then CH_2Cl_2/acetone (2:1) to elute the product. Solvent removal gave **9** as a dark red solid. Yield 51%; IR (KCl): ν_{CO} [cm^{-1}] = 1985(s), 1920(s), 1886(s); ^1H NMR (CD_2Cl_2): δ = 5.90 ($H^{6,7}$), 5.74 ($H^{5,8}$), 3.47 ($H^{2,3}$), 3.14 ($H^{1,4}$), 2.16 (Me). Diffusion of diethyl ether into a solution of **9** in acetone at −20 °C afforded crystals suitable for X-ray diffraction.

Received: June 26, 1995 [Z81351E]
German version: *Angew. Chem.* **1995**, *107*, 2734–2737

Keywords: arene complexes · complexes with carbon ligands · naphthalenes · manganese compounds · metal–metal bonds

[1] a) W. H. Morrison, E. Y. Ho, D. N. Hendrickson, *J. Am. Chem. Soc.* **1974**, *96*, 3603; b) D. Seyferth, J. S. Merola, C. S. Eschbach, *ibid.* **1978**, *100*, 4124; c) R. Q. Bligh, R. Moulton, A. J. Bard, A. Piórko, R. G. Sutherland, *Inorg. Chem.* **1989**, *28*, 2652; d) U. Koelle, M. H. Wang, *Organometallics* **1990**, *9*, 195; e) N. Van Order, W. E. Geiger, T. E. Bitterwolf, A. L. Rheingold, *J. Am. Chem. Soc.* **1987**, *109*, 5680; f) K.-D. Plitzko, G. Wehrle, B. Gollas, B. Rapko, J. Dannheim, V. Boekelheide, *ibid.* **1990**, *112*, 6556; g) W. E. Geiger, N. Van Order, D. T. Pierce, T. E. Bitterwolf, A. L. Rheingold, N. D. Chasteen, *Organometallics* **1991**, *10*, 2403; h) J. W. Merkert, W. E. Geiger, M. N. Paddon-Row, A. M. Oliver, A. L. Rheingold, *ibid.* **1992**, *11*, 4109; i) D. T. Pierce, W. E. Geiger, *Inorg. Chem.* **1994**, *33*, 373; j) M. Tilset, K. P. C. Vollhardt, R. Boese, *Organometallics* **1994**, *13*, 3146; k) T. T. Chin, W. E. Geiger, *ibid.* **1995**, *14*, 1316.

[2] a) F. A. Cotton, M. D. LaPrade, *J. Am. Chem. Soc.* **1968**, *90*, 2026; b) M. J. Bennett, J. L. Pratt, K. A. Simpson, L. K. K. LiShingMan, J. Takata, *ibid.* **1976**, *98*, 4810; c) K. Jonas, G. Koepe, L. Schieferstein, R. Mynott, C. Krüger, Y.-H. Tsay, *Angew. Chem.* **1983**, *95*, 737; *Angew. Chem. Int. Ed. Engl.* **1983**, *22*, 620; d) A. W. Duff, K. Jonas, R. Goddard, H.-J. Kraus, C. Krüger, *J. Am. Chem. Soc.* **1983**, *105*, 5479; e) R. G. Ball, F. Edelmann, G.-Y. Kiel, J. Takats, *Organometallics* **1986**, *5*, 829; f) F. Edelmann, G.-Y. Kiel, J. Takats, A. Vasudevamurphy, M.-Y. Yeung, *J. Chem. Soc. Chem. Commun.* **1988**, 296; g) F. Edelmann, J. Takats, *J. Organomet. Chem.* **1988**, *344*, 351; h) S. T. Astley, J. Takats, *ibid.* **1989**, *363*, 167; i) J. Heck, G. Rist, *ibid.* **1988**, *342*, 45; j) M. Airoldi, G. Deganello, G. Gennaro, M. Moret, A. Sironi, *Organometallics* **1993**, *12*, 3964; k) J. J. Schneider, U. Denninger, O. Heinemann, C. Krüger, *Angew. Chem.* **1995**, *107*, 631; *Angew. Chem. Int. Ed. Engl.* **1995**, *34*, 592.

[3] a) M. R. Churchill, *Inorg. Chem.* **1967**, *6*, 190; b) M. R. Churchill, P. H. Bird, *Inorg. Chem.* **1968**, *7*, 1793; c) M. R. Churchill, J. Wormald, *ibid.* **1970**, *9*, 2239; d) D. F. Hunt, J. W. Russell, *J. Am. Chem. Soc.* **1972**, *94*, 7198; e) P. Mues, R. Benn, C. Krüger, Y.-H. Tsay, E. Vogel, G. Wilke, *Angew. Chem.* **1982**, *94*, 879; *Angew. Chem. Int. Ed. Engl.* **1982**, *21*, 868; f) E. E. Bunel, L. Valle, N. L. Jones, P. J. Carroll, C. Barra, M. Gonzalez, N. Munoz, G. Visconti, A. Aizman, J. M. Manriquez, *J. Am. Chem. Soc.* **1988**, *110*, 6596.

[4] a) K. Jonas, W. Rüsseler, C. Krüger, E. Raabe, *Angew. Chem.* **1986**, *98*, 905; *Angew. Chem. Int. Ed. Engl.* **1986**, *25*, 928; b) A. R. Kudinov, P. V. Petrovskii, Yu. T. Struchkov, A. I. Yanovskii, M. I. Rybinskaya, *J. Organomet. Chem.* **1991**, *421*, 91; c) C. Bonifaci, A. Ceccon, A. Gambaro, P. Ganis, S. Santi, G. Valle, A. Venzo, *Organometallics* **1993**, *12*, 4211; d) C. Bonifaci, A. Ceccon, A. Gambaro, P. Ganis, S. Santi, A. Venzo, *ibid.* **1995**, *14*, 2430; e) C. Bonifaci, A. Ceccon, A. Gambaro, P. Ganis, S. Santi, G. Valle, A. Venzo, *J. Organomet. Chem.* **1995**, *492*, 35; f) R. Winter, D. T. Pierce, W. E. Geiger, T. J. Lynch, *J. Chem. Soc. Chem. Commun.* **1994**, 1949.

[5] a) B. F. Rush, V. M. Lynch, J. J. Lagowski, *Organometallics* **1987**, *6*, 1267; b) B. F. Rush, J. J. Lagowski, *J. Organomet. Chem.* **1990**, *386*, 37; c) K. Jonas, *ibid.* **1990**, *400* 165.

[6] a) R. A. Bauer, E. O. Fischer, C. G. Kreiter, *J. Organomet. Chem.* **1970**, *24*, 737; b) M. J. Begley, S. G. Puntambekar, A. H. Wright, *J. Chem. Soc., Chem. Commun.* **1987**, 1251.

[7] Although not strictly of type **C**, mention should be made of the existence of *syn*-facial [$Fe_2(CO)_6(L)$] (L = anthracene, tetracene), in which each of the (equivalent) iron atoms is bound in an η^3 manner spanning two aromatic rings [6].

[8] S. Sun, L. K. Yeung, D. A. Sweigart, T.-Y. Lee, S. S. Lee, Y. K. Chung, S. R. Switzer, R. D. Pike, *Organometallics* **1995**, *14*, 2613.

[9] S. Sun, C. A. Dullaghan, D. A. Sweigart, unpublished.

[10] In contrast to the behavior of **1**, reduction of [Mn(monoarene)$(CO)_3$]$^+$ generally leads to irreversible formation of dimeric products, although a transient η^4-diene has been detected in one case. See: a) M. V. Gaudet, A. W. Hanson, P. S. White, M. J. Zaworotko, *Organometallics* **1989**, *8*, 286; b) R. L. Thompson, S. J. Geib, N. J. Cooper, *J. Am. Chem. Soc.* **1991**, *113*, 8961; c) C. C. Neto, C. D. Baer, Y. K. Chung, D. A. Sweigart, *J. Chem. Soc. Chem. Commun.* **1993**, 816.

[11] R. L. Thompson, S. Lee, A. L. Rheingold, N. J. Cooper, *Organometallics* **1991**, *10*, 1657.

[12] The crystal structures of **3**, **8**, and **9** were determined using a Siemens P4 diffractometer. Data collection was at 25 °C with $Mo_{K\alpha}$ radiation and refinements based on F^2 were carried out by using the SHELXL 93 package. For **3**: monoclinic, space group $P2_1/n$, a = 8.1706(10), b = 13.001(2), c = 13.5349(13) Å, β = 105.113(8)°, V = 1388.0(3) Å^3, Z = 4, ρ_{calcd} = 1.809 g cm^{-3}, μ = 1.839 mm^{-1}, θ range 2.21–25.99°, 200 variables refined with 2714 independent reflections ($I > 2\sigma(I)$) to R = 0.0378, $wR2$ = 0.0917, GOF = 0.968. For **8**: triclinic, space group $P\bar{1}$, a = 6.6830(10), b = 8.9370(10), c = 12.658(2) Å, α = 102.90(1)°, β = 101.15(1)°, γ = 109.62(1)°, V = 663.8(2) Å^3, Z = 2, ρ_{calcd} = 1.831 g cm^{-3}, μ = 2.060 mm^{-1}, θ range 2.55–30.00°, 190 variables refined with 3830 independent reflections ($I > 2\sigma(I)$) to R = 0.0417, $wR2$ = 0.0917, and GOF = 0.876. For **9**: monoclinic, space group $P2_1/n$, a = 13.225(2), b = 13.050(2), c = 14.495(2) Å, β = 97.857(12)°, V = 2478.1(6) Å^3, Z = 4, ρ_{calcd} = 1.654 g cm^{-3}, μ = 1.174 mm^{-1}, θ range 1.96–25.00°, 322 variables refined with 4363 independent reflections ($I > 2\sigma(I)$) to R = 0.0518, $wR2$ = 0.1244, and GOF = 0.919. Further details of the crystal structures investigations are available on request from the Director of the Cambridge Crystallographic Data Centre, 12 Union Road, GB-Cambridge CB2 1EZ (UK), on quoting the full journal citation.

[13] M. R. Churchill, K. N. Amoh, H. J. Wasserman, *Inorg. Chem.* **1981**, *20*, 1609.

[14] a) J. W. Hull, W. L. Gladfelter, *Organometallics* **1984**, *3*, 605; b) H. Schäufele, D. Hu, H. Pritzkow, U. Zenneck, *ibid.* **1989**, *8*, 396; c) R. Boese, A. Stanger, P. Stellberg, A. Shazar, *Angew. Chem.* **1993**, *105*, 1500; *Angew. Chem. Int. Ed. Engl.* **1993**, *32*, 1475; d) J. O. Albright, L. D. Brown, S. Datta, J. K. Kouba, S. S. Wreford, B. M. Foxman, *J. Am. Chem. Soc.* **1977**, *99*, 5518; e) J. D. Protasiewicz, P. A. Bianconi, I. D. Williams, S. Liu, C. P. Rao, S. J. Lippard, *Inorg. Chem.* **1992**, *31*, 4134.

[15] J. R. Morton, K. F. Preston, *J. Magn. Reson.* **1978**, *30*, 577.

[16] The bimetallic complex with benzothiophene is particularly interesting because the isolated product was found to contain a manganese atom inserted into the S–C(aryl) bond: C. A. Dullaghan, S. Sun, G. B. Carpenter, B. Weldon, D. A. Sweigart, *Angew. Chem.* **1996**, *108*, in press; *Angew. Chem. Int. Ed. Engl.* **1996**, *35*, in press.

[17] M. A. Bennett, T. W. Matheson, *J. Organomet. Chem.* **1979**, *175*, 87.

Commensurate Freezing of *n*-Alkanes in Silicalite**

Willy J. M. van Well, Jillus P. Wolthuizen, Berend Smit, Jan H. C. van Hooff, and Rutger A. van Santen*

Computer simulations recently suggested the occurrence of a kind of phase transition in the adsorption of *n*-alkanes in zeolites.[1] The described transition occurs as commensurate freezing of certain *n*-alkanes into the zigzag channels of silicalite. It was shown that *n*-alkanes that just fit in the zigzag channels, *n*-hexane and *n*-heptane, have to be first commensurately frozen in these channels before loadings higher than approximately half the maximum loading can be reached. Due to the additional loss of entropy, an increased pressure is needed to freeze the molecules into the channels. This increase in pressure is reflected as a step in the adsorption isotherms. The transition is also found in the adsorption isotherms of *n*-hexane and *n*-heptane in silicalite measured experimentally.[2-4] In agreement with the additional loss of entropy, the occurrence of the step in the adsorption isotherms of *n*-hexane shows a temperature dependence.[2, 3, 5] We have studied the behavior of *n*-alkanes as adsorbates in silicalite by temperature programmed desorption (TPD) and herein we discuss the results obtained; furthermore *n*-alkanes that have been predicted to show commensurate freezing behavior are compared with those that do not.

The synthesis of the silicalite sample was described in reference [6]. The elemental analysis revealed a Si/Al ratio greater than 4000 and a Si/Na ratio of 529. According to X-ray diffraction, the as-synthesized sample was highly crystalline. Calcination was performed in situ in a Setaram TG-DSC 111 apparatus (in which the adsorption and desorption measurements were also performed) in a mixture of helium and air (5% O_2) at 943 K for 1 h. The liquid sorbates, ranging from *n*-pentane to *n*-decane, were obtained from Janssen Chimica (Geel, Belgium). The purity of these sorbates was 99% or higher; *n*-butane 3.5 (purity 99.95%) was obtained from Hoek Loos (Schiedam, The Netherlands).

Adsorption into silicalite was achieved at room temperature by mixing the gaseous sorbate (*n*-butane) or a helium flow saturated with the vapor of the liquid sorbate in a pure helium flow of approximately 1.8 L h^{-1}. The rate of both the *n*-butane flow and the helium flow saturated with sorbate was about 0.6 L h^{-1}. Therefore, adsorption is achieved at a relative adsorbate pressure in the helium flow of at most 0.25. Saturation was reached within a few minutes for *n*-butane, while adsorption over 24 hours was needed to saturate the sample with *n*-decane. The obtained maximum loadings of the different sorbates and the micropore volumes calculated from these maximum loadings are given in Table 1. All loadings agree very well with the maximum loadings reported in literature, indicating that the crystallinity of the sample we studied was very good. However, the loadings reported by Flanigen,[7] 1.9 mmol g^{-1} for *n*-butane and 1.5 mmol g^{-1} for *n*-hexane, were not reached.

[*] Prof. Dr. R. A. van Santen, Ir. W. J. M. van Well, Ing. J. P. Wolthuizen, Prof. Dr. Ir. J. H. C. van Hooff
Schuit Institute of Catalysis
Laboratory of Inorganic Chemistry and Catalysis
Eindhoven University of Technology
P. O. Box 513, NL-5600 MB Eindhoven (The Netherlands)
Telefax: Int. code + (40)2455054
Dr. Ir. B. Smit
Shell Research B. V.
Koninklijke/Shell-Laboratorium, Amsterdam (The Netherlands)

[**] W. J. M. van Well is indebted to the Stichting Scheikundig Onderzoek in Nederland (SON).

Table 1. Maximum loadings of the *n*-alkanes on silicalite, and the micropore volume of silicalite calculated from these loadings. The micropore volume is calculated by using the density of the *n*-alkane at 20 °C relative to water at 4 °C. uc = unit cell.

n-Alkane	Maximum loading [molecule uc^{-1}]	Maximum loading [mmol g^{-1}]	Micropore volume [mL g^{-1}]
n-butane	9.3	1.8	0.16
n-pentane	8.7	1.5	0.17
n-hexane	8.1	1.4	0.18
n-heptane	7.3	1.3	0.18
n-octane	5.4	0.93	0.15
n-nonane	5.1	0.89	0.16
n-decane	5.1	0.87	0.17

Temperature programmed desorptions were performed at a heating rate of 5 K min^{-1} to a temperature of 723 K in a helium flow of 1.8 L h^{-1}. The temperature program was started immediately after the flow with sorbate was switched off. A blank run of the clean sample was subtracted from all TPD curves to correct for the temperature effect on the mass. All curves were measured on the same sample of activated silicalite with a mass of 10.39 mg.

A schematic drawing of silicalite (an all-silica zeolite) is given in Figure 1. As can be seen, it has a three-dimensional pore system consisting of intersecting straight and zigzag channels.

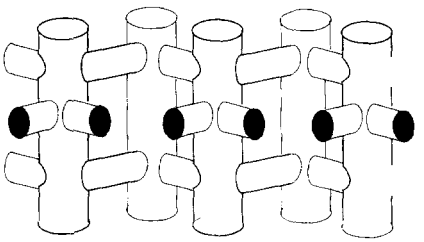

Fig. 1. Pore structure of silicalite.

In Figure 2, the TPD curves of the *n*-alkanes ranging from *n*-butane to *n*-decane are given. The differential mass loss (dm/dT) curves of *n*-pentane, *n*-hexane, *n*-heptane, and *n*-octane are

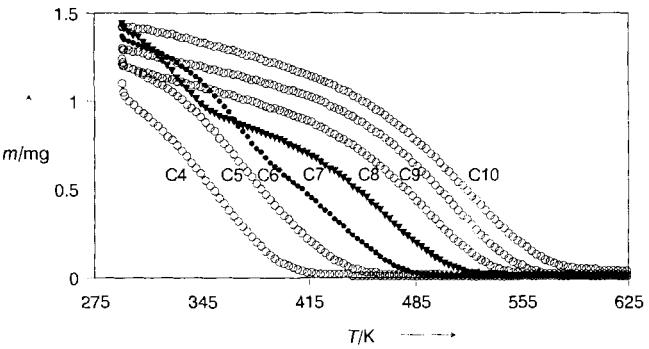

Fig. 2. Temperature programmed desorption curves of *n*-alkanes from silicalite; 10.39 mg silicalite; heating rate 5 K min^{-1}.

shown in Figure 3. For the sake of clarity in Figure 3, the differential mass curves are separated from each other. The curves of *n*-butane, *n*-nonane, and *n*-decane are similar to the curves of *n*-pentane and *n*-octane. Also for the sake of clarity, these curves are not displayed. The temperatures at which the maximum

 © VCH Verlagsgesellschaft mbH, D-69451 Weinheim, 1995 0570-0833/95/3422-2543 $ 10.00+.25/0

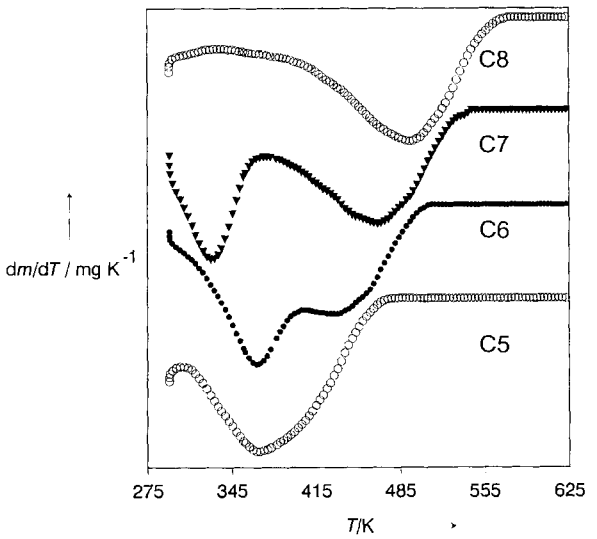

Fig. 3. Differential mass loss, dm/dT, during the TPD. The curves are separated from each other for the sake of clarity.

mass loss of the different sorbates occurred are given in Table 2. The reported results were verified by measurements on a different silicalite sample using a different heating rate (7 K min^{-1}).

Table 2. Temperatures at which the mass loss of the *n*-alkanes is at a maximum.

n-Alkane	*T* [K] of maximum mass loss	*T* [K] of maximum mass loss
n-butane	–	355
n-pentane	–	369
n-hexane	367	429
n-heptane	329	467
n-octane	–	493
n-nonane	–	512
n-decane	–	520

While *n*-butane, *n*-pentane, *n*-octane, *n*-nonane, and *n*-decane show a single desorption step, *n*-hexane and especially *n*-heptane show a two-step desorption profile. The second desorption peak of *n*-hexane and *n*-heptane, and the desorption peaks of the other *n*-alkanes occur at increasing temperatures in accordance with their increasing chain length. The first desorption peak of *n*-hexane and *n*-heptane occurs, however, at lower temperature than expected on the basis of the chain length of these two *n*-alkanes. Furthermore, it is remarkable that the first desorption step of *n*-heptane takes place at a lower temperature than that of *n*-hexane.

The results show that at high loadings some of the adsorbed *n*-hexane and *n*-heptane molecules desorb more easily from silicalite than the other *n*-alkanes. Since the first desorption step of *n*-heptane takes place before that of *n*-hexane, this first mass loss should be determined by entropic effects rather than by energetic effects. This means that the low temperature at which the first desorption peak occurs should be caused by a relative high gain in entropy upon desorption compared to the other *n*-alkanes. The relative high gain in entropy upon desorption can only be the result of a low entropy value, a constrained position of the adsorbed *n*-hexane and *n*-heptane molecules at high loadings.

The two-step desorption profile of *n*-hexane and *n*-heptane gives evidence for commensurate freezing of these two *n*-alkanes in silicalite. The commensurate freezing of some of the molecules in the zigzag channels at high loadings results in a particularly low entropy value for these molecules. Consequently, the desorption of these *n*-hexane and *n*-heptane molecules will result in a relative high gain in entropy causing the first desorption peak to occur at relatively low temperatures. Partial desorption then allows a rearrangement of the adsorbed *n*-hexane and *n*-heptane molecules, resulting in an ordering similar to the ordering of the other *n*-alkanes with a normal entropy value. The similarity in ordering is reflected in the second desorption peak of *n*-hexane and *n*-heptane and the desorption peak of the other *n*-alkanes. These peaks occur at temperatures that are in accordance with the chain length of the *n*-alkane. The occurrence of a rearrangement during the desorption of *n*-hexane and *n*-heptane is consistent with the earlier interpretation of Richards and Rees[8] of a two-step desorption of *n*-hexane from silicalite. The observation of a single-step desorption of the other *n*-alkanes agrees with the computational results, which indicated the absence of commensurate freezing for these molecules.

Furthermore, it can be concluded that the *n*-heptane molecules are much more constrained in the zigzag channels than the *n*-hexane molecules. This is indicated by the lower temperature of desorption, compared to that of *n*-hexane, at which the first *n*-heptane desorption peak occurs. The last result is supported by the simulated[1] and measured[2–5] adsorption isotherms of *n*-hexane and *n*-heptane. These show that the step in the adsorption isotherm of *n*-heptane is more pronounced than the step in the adsorption isotherm of *n*-hexane.

The temperature programmed desorption of *n*-alkanes from silicalite has provided evidence for the existence of a kind of phase transition during the filling of silicalite. Moreover, in agreement with the results from computer simulations, the occurrence of this transition is a subtle function of the *n*-alkane length and only occurs for molecules that just fit into the zigzag channels.

Received: July 7, 1995 [Z8180IE]
German version: *Angew. Chem.* **1995**, *107*, 2765–2767

Keywords: alkanes · catalysis · thermochemistry · zeolites

[1] B. Smit, T. L. M. Maesen, *Nature* **1995**, *374*, 42.
[2] U. Lohse, B. Fahlke, *Chem. Techn.* **1983**, *35*, 350.
[3] R. E. Richards, L. V. C. Rees, *Langmuir* **1987**, *3*, 335.
[4] M. M. Dubinin, G. U. Rakhmatkariev, A. A. Isirikyan, *Izv. Akad. Nauk SSSR, Ser. Khim.* **1989**, *10*, 2333.
[5] U. Lohse, M. Thamm, M. Noack, B. Fahlke, *J. Incl. Phenom.* **1987**, *5*, 307.
[6] B. Kraushaar, L. J. M. Van de Ven, J. W. De Haan, J. H. C. Van Hooff, *Stud. Surf. Sci. Catal.* **1988**, *37*, 167.
[7] E. M. Flanigen, J. M. Bennett, R. W. Grose, J. P. Cohen, R. L. Patton, R. M. Kirchner, J. V. Smith, *Nature* **1978**, *271*, 512.
[8] R. E. Richards, L. V. C. Rees, *Zeolites* **1986**, *6*, 17.

Unprecedented Intra- and Intermolecular Palladium-Catalyzed Coupling Reactions with Methylenecyclopropane-Type Tetrasubstituted Alkenes**

Stefan Bräse and Armin de Meijere*

Dedicated to Professor Rolf Huisgen on the occasion of his 75th birthday

In trying to elucidate the scope and limitations of a recently developed domino sequence consisting of an intramolecular Heck reaction and a subsequent intermolecular Diels–Alder reaction,[1] we have successfully used 2-bromo-1,6-dienes of type **1** with methylenecyclopropane end groups. Compounds **1** with R = H react in the usual way to give vicinal exodimethylenecycloalkanes, which cycloadd dienophiles like methyl acrylate to yield products of type **3** (Scheme 1).[1b] A different situation arises for **1** with R = Me, because the intermediate cyclopropylpalladium bromide **4** would probably be reluctant to undergo β-hydride elimination (to give a cyclopropene) and might prefer to couple with the methyl acrylate.

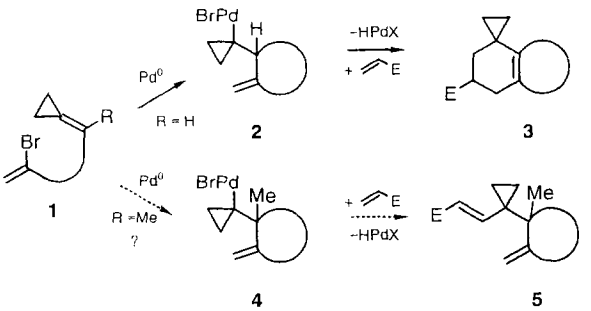

Scheme 1. E = CO_2Me.

To test this hypothesis, the bromodiene **8a**[2] was treated with methyl acrylate under the previously described conditions[1a] ($Pd(OAc)_2$, PPh_3, Ag_2CO_3). However, no coupling product of type **5** was observed; instead the reaction took a totally different course. Under typical Heck conditions ($Pd(OAc)_2$, PPh_3, NEt_3)[3] (A in Scheme 2) a new product was formed in 72% yield and identified as the cross-conjugated triene **9a**.[4] The homologous 2-bromo-1,7-diene **8b** reacted in the same way to give the seven-membered ring analogue **9b** in 53% yield. However, the corresponding 2-bromo-1,5-diene did not yield any cyclization product but underwent a Cope rearrangement even at 60 °C (in the absence of palladium).[5] Under the conditions of the Trost cycloisomerization reaction[6] (B in Scheme 2), the 1,6- and 1,7-enynes **10a** and **10b** gave the dendralenes[7] **9a** and **9b** in 78 and 100% yield, respectively. In the presence of iodobenzene under Heck conditions the enyne **10a** gave the phenyl-substituted (*Z*)-dendralene **6a** (45%) together with the phenyl-substituted enyne **7a** (42%).

[*] Prof. Dr. A. de Meijere, Dipl.-Chem. S. Bräse
Institut für Organische Chemie der Universität
Tammannstrasse 2, D-37077 Göttingen (Germany)
Telefax: Int. code +(551) 399475

[**] Cyclopropyl Building Blocks for Organic Synthesis, Part 32. This work was supported by the Deutsche Forschungsgemeinschaft, the Volkswagen-Stiftung, and the Fonds der Chemischen Industrie as well as by BASF, Bayer, Degussa, Hoechst, and Hüls AG (chemicals). S. B. is grateful to the Fonds der Chemischen Industrie for a graduate fellowship. Part 31: ref. [17e]. Part 30: ref. [17f].

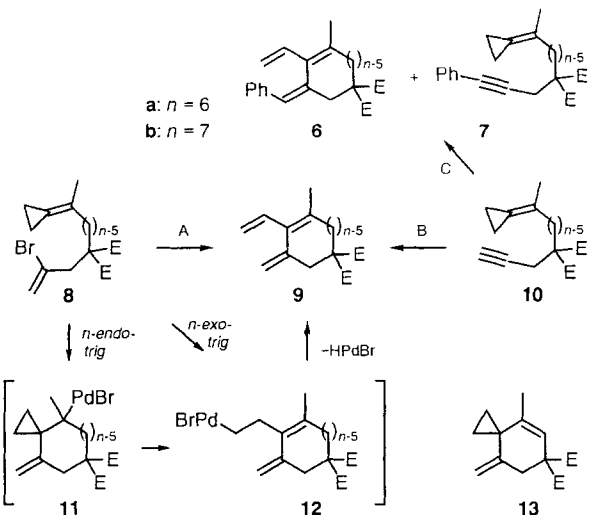

Scheme 2. A) $Pd(OAc)_2$, PPh_3, NEt_3, DMF, 100 °C, 12 h; B) $[Pd_2(dba)_3] \cdot CHCl_3$, $P(o\text{Tol})_3$, HOAc, PhH, 20 °C, 12 h; C) PhI, $Pd(OAc)_2$, PPh_3, NEt_3, DMF, 100 °C, 12 h; E = CO_2Me, CO_2Et.

This strikingly facile formation of cross-conjugated trienes **9** is also interesting mechanically. This type of product might result from the attack of an intermediate σ-alkenylpalladium species like **15** on the tetrasubstituted double bond of the strained methylenecyclopropane moiety[8] to yield the neopentyl-type σ-alkylpalladium intermediate **11** in an *n-endo-trig* cyclization.[9] A cyclopropylcarbinyl → homoallyl type rearrangement[10] would lead to **12** and subsequent β-hydride elimination would then yield **9** (Scheme 2). Alternatively, an *n-exo-trig* cyclization of the first intermediate with attack across the cyclopropyl σ-bond[1] could lead directly to **12**. A careful check of the reaction mixture from **8a** disclosed formation of the 8-methylenespiro[2.5]oct-4-ene derivative **13** as a by-product (22% yield), which must have been formed from intermediate **11a** rather than **12a** by direct β-hydride elimination. To further test this mechanism, the model enyne **14**[2] with an additional cyclopropyl group was subjected to cycloisomerization conditions B (Scheme 3). The fact that only product **20** (45% yield) was isolated along with a trace of dimeric intermolecular coupling product of two molecules of **14** (9%)[12] proved that no direct 7-*exo-trig*[9c] ring closure to intermediate **17** had oc-

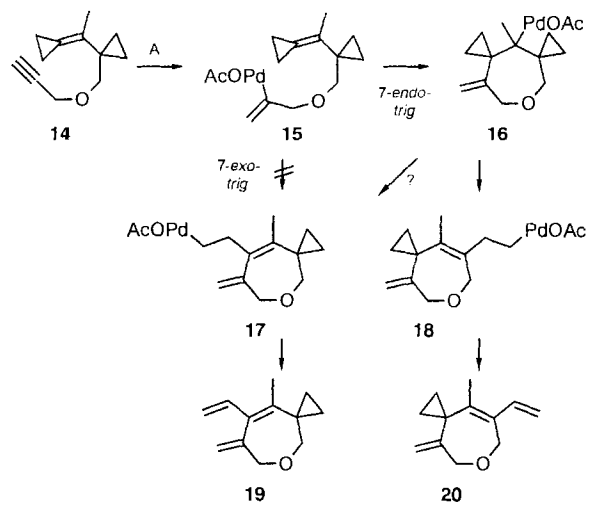

Scheme 3. A) $[Pd_2(dba)_3] \cdot CHCl_3$, $P(o\text{Tol})_3$, HOAc, PhH, 20 °C, 12 h.

curred, as that would have led to the dendralene **19**. It is not fully understood, however, why the intermediate **16** selectively opened one spirocyclopropane group to give **18** and not the other one to give **17**.

Dendralenes of type **9** ought to be useful intermediates for organic synthesis as they are good candidates for subsequent domino Diels–Alder reactions,[13] which can lead to complex skeletons in remarkably few steps. The scope of this new route to cross-conjugated systems can be substantially extended by applying the palladium-mediated sequential addition–rearrangement–elimination in an intermolecular fashion using bicyclopropylidene (**22**)[14] as an acceptor alkene. Thus in the intermolecular coupling of **22** and iodobenzene under Heck conditions the expected product **21** was obtained in 57% yield but tends to polymerize in neat form. When treated with various dienophiles, **21** gave the spiro[2.5]octenes **25** regioselectively in moderate to good yields (Table 1). The chiral, nonracemic *N*-acryloylcamphorsultame **24c**[15] gave a single diastereomer of the spirooctene **25c** ($dr > 20:1$). The reaction sequence can even be conducted as a one-pot operation. When a mixture of bicyclopropylidene (**22**), iodobenzene, and one of the dienophiles **24a–c** was subjected to Heck conditions (A in Scheme 4), the spiro[2.5]octenes **25a–c** could be isolated in good yields (61–65%); even with methyl acrylate **24a** only traces of methyl cinnamate resulting from direct coupling with iodobenzene were formed. This indicates that bicyclopropylidene (**22**), although it is a tetrasubstituted alkene, is more reactive (ca. 10 times) than an acrylate in the intermolecular Heck reaction.[16]

Table 1. A domino-type cascade of an intermolecular coupling of bicyclopropylidene (**22**) with aryl and alkenyl halides/sulfonates and Diels–Alder reaction(s).

Substrate	Dienophile	R^1	R^2	Product	Yield [a] [%]
PhI	**24a**	H	CO_2Me	**25a**	61 [b]
PhI	**24b**	CO_2Me	CO_2Me	**25b**	55 [c]
PhI	**24c**	H	COR* [d]	**25c**	49 [b]
C_6H_9ONf [e]	**24b**	CO_2Me	CO_2Me	**28b**/**29b**	41 [c]
C_2H_3I [f]	**24a**	H	CO_2Me	**27a**	63 [c]
C_2H_3I	**24a**	H	CO_2Me	**30a**	59 [b, g]
C_2H_3I	**24b**	CO_2Me	CO_2Me	**27b**	60 [c]
C_2H_3I	**24b**	CO_2Me	CO_2Me	**30b**	49 [b, h]
C_2H_3I	**24c**	H	COR* [d]	**27c**	35 [c]

[a] Isolated material. [b] One pot, one step. [c] One pot, two steps. [d] *N*-acryloyl-(*S*)-camphorsultame. [e] 1-Cyclohexenyl nonafluorobutanesulfonate. [f] Vinyl iodide. [g] Mixture of two regioisomers each consisting of four diastereomers. [h] Mixture of four diastereomers.

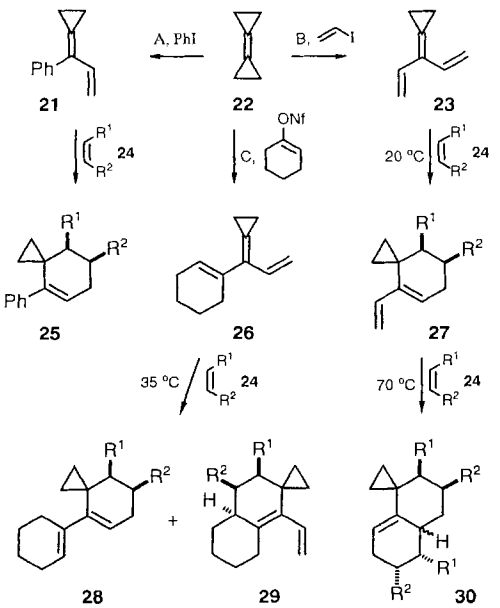

Scheme 4. A) $Pd(OAc)_2$, PPh_3, NEt_3, DMF, 80 °C, 4 h; B) $Pd(OAc)_2$, PPh_3, NEt_3, DMF, 75 °C, 20 h; C) $[Pd(PPh_3)_4]$, MeCN, 75 °C, 4 h; ONf = $OSO_2nC_4F_9$; for further details see Table 1.

Under appropriate conditions (C in Scheme 4), cyclohexenyl nonaflate reacted with **22** to give the expected dendralene **26** in 41% yield. The Diels–Alder reaction of **26** with dimethyl maleate at 35 °C led to both possible monoadducts **28** and **29** in a ratio of 2:1 (79% total yield based on **26**). It is remarkable that the more highly substituted diene moiety in **26** reacts at roughly the same rate as the other one. Vinyl iodide and bicyclopropylidene (**22**) gave the rather sensitive, novel dendralene **23** in 43% yield. When one of the dienophiles **24a–c** was added to the reaction mixture prior to workup, the monoadducts **27a–c** were isolated at ambient temperature. Heating a mixture of **22**, vinyl iodide, and one of the dienophiles **24a**, **b** in the presence of the palladium catalyst, resulted in bisadducts **30a**, **b** directly.

In conclusion, methylenecyclopropanes are not only favorable reaction partners in intramolecular [3 + 2] cycloadditions,[17a–c] Pauson–Khand,[17d, e] and Diels–Alder reactions,[17e, f] but also in cascade reactions consisting of a Heck-type coupling and subsequent Diels–Alder cycloaddition.

Received: June 23, 1995 [Z 8127 IE]
German version: *Angew. Chem.* **1995**, *107*, 2741–2743

Keywords: cyclopropanes · cascade reactions · dendralenes · palladium compounds

[1] a) F. E. Meyer, K. H. Ang, A. G. Steinig, A. de Meijere, *Synlett* **1994**, 191–193; b) K. H. Ang, S. Bräse, A. G. Steinig, F. E. Meyer, A. Llebaria, K. Voigt, A. de Meijere, unpublished.

[2] Methylenecyclopropanes **8**, **10**, and **14** were prepared by published procedures using either Wittig-type reactions: a) G. Fournet, G. Balme, J. J. Barieux, J. Gore, *Tetrahedron* **1988**, *44*, 5821–5832, or palladium-catalyzed substitutions of 1-ethenylcyclopropyl halides: b) G. McGaffin, S. Michalski, A. Stolle, S. Bräse, J. Salaün, A. de Meijere, *Synlett* **1992**, 558–560.

[3] a) R. F. Heck, *Acc. Chem. Res.* **1979**, *12*, 146–151; b) *Org. React.* **1982**, *27*, 345–390; c) *Palladium Reagents in Organic Synthesis*, Academic Press, London, **1985**; d) A. de Meijere, F. E. Meyer, *Angew. Chem.* **1994**, *106*, 2473–2506; *Angew. Chem. Int. Ed. Engl.* **1994**, *33*, 2379–2411.

[4] All new products were fully characterized by spectroscopic methods (IR, ^1H and ^{13}C NMR, MS). Molecular formulas were established by elemental analysis or HRMS.

[5] An accelerated Cope rearrangement of 1,5-hexadienes with methylenecyclopropane end groups has been reported earlier: D. Kaufmann, A. de Meijere, *Chem. Ber.* **1984**, *117*, 1128–1138.

[6] B. M. Trost, *Acc. Chem. Res.* **1990**, *23*, 34–42.

[7] Cross-conjugated trienes such as **7** are recognized as the lowest members of a family of cross-conjugated polyenes termed "dendralenes". For a review see: H. Hopf, *Angew. Chem.* **1984**, *96*, 947–958; *Angew. Chem. Int. Ed. Engl.* **1984**, *23*, 947–958.

[8] The reactivity of the double bond in methylenecyclopropanes is frequently exalted: a) P. Binger, H. M. Büch, *Top. Curr. Chem.* **1987**, *135*, 77–151, and references therein; b) A. Stolle, H. Becker, J. Salaün, A. de Meijere, *Tetrahedron Lett.* **1994**, *35*, 3517–3524.

[9] For this designation of cyclization types see: a) J. E. Baldwin, *J. Chem. Soc. Chem. Commun.* **1976**, 734–736; for a recent example of metal-promoted *endo-trig* cyclizations: b) V. H. Rawal, C. Michoud, *J. Org. Chem.* **1993**, *58*, 5583–5584. c) Since the quaternary carbon in a methylenecyclopropane moiety is closer to being sp- than sp^2-hybridized, the cyclization incorporating such a unit ought to be termed *n-exo-dig*.

[10] It is well-documented that cyclopropylcarbinylmetal intermediates easily undergo ring-opening to give homoallylmetal compounds: a) M. S. Silver, P. A. Shafer, J. E. Nordlander, C. Rüchardt, J. D. Roberts, *J. Am. Chem. Soc.* **1960**, *82*, 2646–2647; b) P. A. Wender, H. Takahashi, B. Witulski, *ibid.* **1995**, *117*, 4720–4721. For a recent review see: G. Dyker, *Angew. Chem.* **1995**, *107*, 2407–2408; *Angew. Chem. Int. Ed. Engl.* **1995**, *34*, 2223–2224.

[11] Additions to the proximal C–C σ-bond of methylenecyclopropanes have been observed under nickel(0) catalysis: see ref. [8a].

[12] Intermolecular coupling has been observed in palladium-catalyzed enyne cycloisomerizations in a few cases: B. M. Trost, C. Chan, G. Ruhter, *J. Am. Chem. Soc.* **1987**, *109*, 3486–3487.

[13] For a review on sequential reactions see: a) L.-F. Tietze, U. Beifuss, *Angew. Chem.* **1993**, *105*, 137–170; *Angew. Chem. Int. Ed. Engl.* **1993**, *32*, 131–164. Such domino Diels–Alder reactions have been termed "transmissive cycloadditions": b) O. Tsuge, E. Wada, S. Kanemasa, *Chem. Lett.* **1983**, 1525–1528.

[14] Bicyclopropylidene (**22**) is readily available in three simple steps: A. de Meijere, S. I. Kozhushkov, T. Späth, N. S. Zefirov, *J. Org. Chem.* **1993**, *58*, 502–505.

[15] W. Oppolzer, C. Chapuis, G. Bernardinelli, *Helv. Chim. Acta* **1984**, *67*, 1397–1401.

[16] For the first example of an intermolecular Heck reaction on a tetrasubstituted alkene see: G. Dyker, J. Körning, P. G. Jones, P. Bubenitschek, *Angew. Chem.* **1993**, *105*, 1805–1807; *Angew. Chem. Int. Ed. Engl.* **1993**, *32*, 1733–1735.

[17] a) R. T. Lewis, W. B. Motherwell, M. Shipman, *J. Chem. Soc. Chem. Commun.* **1988**, 948–950; b) S. A. Bapuji, W. B. Motherwell, M. Shipman, *Tetrahedron Lett.* **1989**, *30*, 7107–7710; c) H. Corlay, R. T. Lewis, W. B. Motherwell, M. Shipman, *Tetrahedron* **1995**, *51*, 3303–3318; d) ref. [8b]; e) S. Bräse, S. Schömenauer, G. McGaffin, A. Stolle, A. de Meijere, *Chem. Eur. J.* **1996**, in press; f) T. Heiner, S. Michalski, K. Gerke, G. Kuchta, M. Buback, A. de Meijere, *Synlett* **1995**, 355–357.

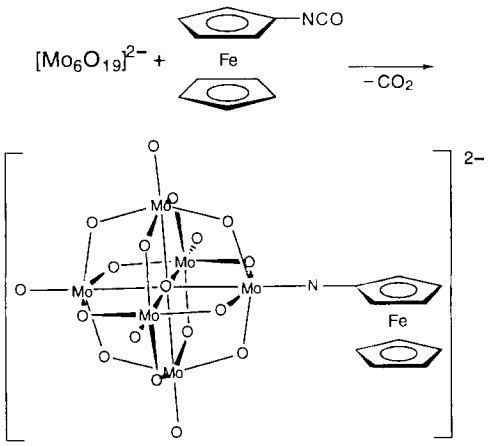

1

Scheme 1.

A Functionalized Polyoxometalate Bearing a Ferrocenylimido Ligand: Preparation and Structure of $[(FcN)Mo_6O_{18}]^{2-}$**

Joseph L. Stark, Victor G. Young, Jr., and Eric A. Maatta*

Charge-transfer interactions involving polyoxometalate anions[1] as acceptors form the basis of an intensifying research area with relevancy and applications in fields ranging from photocatalytic reactions of organic substrates[2] to the preparations of new types of magnetic[3] and electrically conducting[4] materials. Currently, polyoxometalate-based donor–acceptor systems are restricted to existence either in the solid state only[5] or in those solutions wherein the donor constitutes a significant fraction of the solvent.[6] It is therefore highly desirable to provide a means of enforcing and controlling the donor–acceptor interactions that occur in solution. Here we report on the preparation and structure of the ferrocenylimidohexamolybdate complex **1** (isolated as the tetrabutylammonium salt), which features the covalent attachment of an oxidizable donor to a reducible polyoxometalate acceptor system.

$[Bu_4N]_2[(FcN)Mo_6O_{18}]$
$[Bu_4N]_2$-**1**

Reaction of $[Bu_4N]_2[Mo_6O_{19}]$ with ferrocenyl isocyanate in pyridine (Scheme 1) affords a purple solution from which crystalline $[Bu_4N]_2$-**1** is obtained in 19% yield after workup and recrystallization. To our knowledge, **1** is the first example of a ferrocenylimido complex; since isocyanates are often employed as imido delivery reagents in metatheses with oxo–metal functions,[7] we expect that this methodology will be applicable to the preparations of various ferrocenylimido complexes $[FcN{\equiv}ML_n]$.

Cyclic voltammetry studies of $[Bu_4N]_2$-**1** (CH_3CN; 298 K; Pt electrode; $[Bu_4N][PF_6]$ supporting electrolyte; 100 mVs^{-1}) in the range +1.0 V to −1.5 V (vs. Ag/Ag^+) reveal a one-electron oxidation wave at 0.226 V ($\Delta E_p = 0.060$ V) and a one-electron reduction wave at −0.951 V ($\Delta E_p = 0.162$ V); under these conditions, the electrochemical couple of added ferrocene was observed at $E_{1/2} = 0.119$ V, and that of the $[Mo_6O_{19}]^{2-}$ ion at $E_{1/2} = -0.706$ V. These two processes for **1** are attributed to oxidation of the ferrocenyl $[Fe]^{2+}$ center and reduction of the $[(FcN)Mo_6O_{18}]^{2-}$ cluster,[8] respectively. Extending the scan to more negative potentials reveals a second, irreversible wave ($E_{pc} = -2.168$ V), and upon reversing the sweep a new reversible wave is observed at −0.248 V. The species and events responsible for this apparent EC process are not yet understood.

The structure[9] of the anionic cluster **1** is shown in Figure 1. The ferrocenylimido ligand is bound in a terminal position at

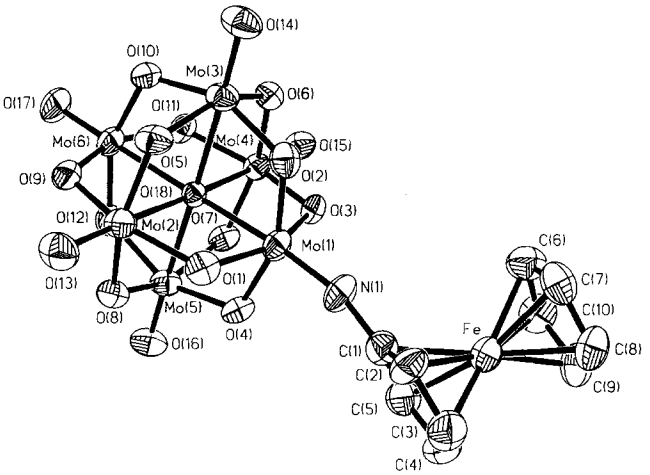

Fig. 1. Crystal structure of **1** (ORTEP drawing). Selected bond lengths [Å] and angle [°]: Mo(1)-N(1) 1.720(7), Mo(2)-O(13) 1.681(6), Mo(3)-O(14) 1.688(6), Mo(4)-O(15) 1.695(6), Mo(5)-O(16) 1.692(6), Mo(6)-O(17) 1.673(6), Mo(1)-O(18) 2.213(5), Mo(2)-O(18) 2.350(5), Mo(3)-O(18) 2.343(5), Mo(4)-O(18) 2.325(5), Mo(5)-O(18) 2.317(5), Mo(6)-O(18) 2.360(5); Mo(1)-N(1)-C(1) 164.8(7).

[*] Prof. E. A. Maatta, J. L. Stark
Department of Chemistry
Kansas State University, Manhattan, KS 66506 (USA)
Telefax: Int. code + (913) 532-6666
e-mail: eam@ksu.ksu.edu
Dr. V. G. Young, Jr.
X-Ray Crystallographic Laboratory
Department of Chemistry
University of Minnesota, Minneapolis, MN 55455 (USA)

[**] Organoimido Ligands with Remote Functionality, Part 2. We thank the National Science Foundation and the NSF-EPSCoR "KAN-SYN" program for supporting this work. Part 1: P. L. Hill, G. P. A. Yap, A. L. Rheingold, E. A. Maatta, *J. Chem. Soc. Chem. Commun.* **1995**, 737. FcN = $(\eta^5\text{-}C_5H_5)Fe\text{-}(\mu\text{-}\eta^5\text{:}\sigma\text{-}C_5H_4N)$.

the hexamolybdate and its metrical parameters (Mo(1)–N(1) = 1.720(7) Å; Mo(1)-N(1)-C(1) = 164.8(7)°) are consistent with the presence of a formal Mo≡NFc triple bond. As in other imidohexametalate structures, the bond between the imido-bearing Mo(1) atom and the central O(18) atom (2.213(5) Å) is substantially shorter than the remaining Mo–O(18) interactions, which range from 2.317(5)–2.360(5) Å. The cyclopentadienyl rings within the ferrocenylimido ligand deviate by only about 4.4° from an ideal eclipsed conformation. The Fe–Mo(1) distance is 4.78 Å.

Within the lattice of $[Bu_4N]_2$-**1**, $[(FcN)Mo_6O_{18}]^{2-}$ ions are organized into pairs displaying close intercluster approaches between cyclopentadienyl hydrogen atoms and μ_2-oxygen atoms (Fig. 2). The closest H···O separations observed are for

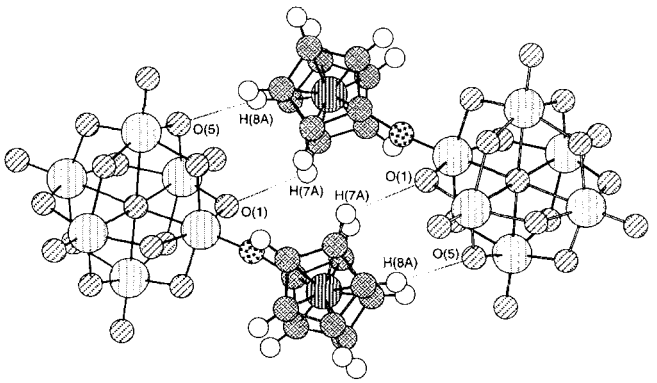

Fig. 2. Pairing of the anions **1** in the lattice of $[Bu_4N]_2$-**1**. Highlighted distances [Å]: H(8A)-O(5) 2.37, H(7A)-O(1) 2.62.

H(8A)–O(5) at 2.37 Å and for H(7A)–O(1) at 2.62 Å. These distances are similar to those observed between the methyl hydrogen atoms of the cationic ferrocene derivative $[(\eta^5\text{-}C_5H_5)Fe(\eta^5\text{-}C_5H_4CH_2N(CH_3)_3)]^+$ and oxygen atoms of $[Mo_6O_{19}]^{2-}$ (2.56–2.60 Å) in a recently reported 2:1 charge-transfer salt.[10] The "dimerization" observed for the anions **1** in the solid state is undoubtedly facilitated by the superior electron donation provided by the organoimido ligand,[8] which renders the μ_2-oxygen sites of **1** more basic than those in the $[Mo_6O_{19}]^{2-}$ ion.

The electronic spectrum of **1** is unique among all other monoimidohexamolybdates (Table 1). Apart from the transition at 337 nm, which is common to the systems shown in Table 1, the spectrum of **1** also contains a strong, broad absorption centered at 536 nm ($\varepsilon = 1500$). Based on its intensity, this band cannot be a d-d transition[12] within the ferrocenyl component of **1**, and we assign this feature as arising from an intramolecular charge transfer from the $\{Fe^{2+}\}$ center to the $\{(NMo_6O_{18})^{2-}\}$ cluster; the position of this band in **1** is similar to that observed in the (solid-state) diffuse reflectance spectrum

Table 1. Electronic spectra of $[Mo_6O_{18}(NR)]^{2-}$ systems (recorded in CH_3CN as $[Bu_4N]^+$ salts).

Complex	λ_{max} [nm]	ε [$M^{-1}cm^{-1}$]
$[Mo_6O_{18}(NBu)]^{2-}$ [a]	329	6.0×10^3
$[Mo_6O_{18}(NCy)]^{2-}$ [a]	325	7.0×10^3
$[Mo_6O_{18}(NPh)]^{2-}$ [b]	342	2.0×10^4
$[Mo_6O_{18}(NAr)]^{2-}$ [a, c]	351	1.9×10^4
$[Mo_6O_{18}(NFc)]^{2-}$ [d]	337	1.0×10^4
	536	1.5×10^3

[a] Ref. [8]. [b] Ref. [11]. [c] Ar = 2,6-iPr$_2$C$_6$H$_3$. [d] This work.

of the above-mentioned $[(\eta^5\text{-}C_5H_5)Fe(\eta^5\text{-}C_5H_4CH_2N(CH_3)_3)]^+$ charge-transfer salt of the $[Mo_6O_{19}]^{2-}$ ion [10] (λ_{max} = 550 nm). Studies of the photophysics and photochemistry of **1** are now underway.

In summary, we have demonstrated that a ferrocenyl donor can be bound covalently to a polyoxometalate acceptor, thereby ensuring that the integrity of the donor–acceptor system is maintained in solution. The simple methodology employed in this synthesis suggests that a variety of other donor/antenna groups may be similarly incorporated into polyoxometalates.

Experimental Procedure

Ferrocenyl isocyanate [13] (0.25 g, 1.1 mmol) and $[Bu_4N]_2[Mo_6O_{19}]$ [14] (1.50 g, 1.1 mmol) were stirred in dry pyridine (50 mL) at 25 °C for 48 h, which led to a purple solution. The solvent was evaporated under vacuum and the residue was extracted into CH_2Cl_2, filtered, taken to dryness, washed with Et_2O, and the resulting purple solid **1** was dried under vacuum (0.32 g, 19%). Analysis for $C_{42}H_{81}N_3O_{18}FeMo_6$: Calc. C 32.60, H 5.28, N 2.72; found: C 32.52, H 5.18, N 3.06. ^{1}H NMR (CD_3CN, 25 °C): δ = 4.66 (t, 2H, C_5H_4), 4.50 (s, 5H, C_5H_5), 4.22 (t, 2H, C_5H_4), 3.08 (m, 16H, N-CH_2), 1.60 (m, 16H, CH_2), 1.35 (m, 16H, CH_2), 0.96 (t, 24H, CH_3). Solvated crystals of $[Bu_4N]_2$-**1** were grown by diffusion of Et_2O vapor into a CH_3NO_2 solution of the salt at 25 °C and a suitable specimen for X-ray analysis was chosen under the mother liquor.

Received: June 30, 1995 [Z81521E]
German version: *Angew. Chem.* **1995**, *107*, 2751–2753

Keywords: complexes with ferrocenyl ligands · donor–acceptor systems · molybdenum compounds · polyoxometalates

[1] *Polyoxometalates: From Platonic Solids to Antiretroviral Activity*, (Eds.: M. T. Pope, A. Müller), Kluwer, Dordrecht, **1994**; M. T. Pope, A. Müller, *Angew. Chem.* **1991**, *103*, 56; *Angew. Chem. Int. Ed. Engl.* **1991**, *30*, 34; M. T. Pope, *Heteropoly and Isopoly Oxometalates*, Springer, New York, **1983**.
[2] For example, M. A. Fox, R. Cardona, E. Gaillard, *J. Am. Chem. Soc.* **1987**, *109*, 6347; M. M. Williamson, D. A. Bouchard, C. L. Hill, *Inorg. Chem.* **1987**, *26*, 1436; T. Yamase, R. Watanabe, *J. Chem. Soc. Dalton Trans.* **1986**, 1669.
[3] P. Le Maguerès, L. Ouahab, S. Golhen, D. Grandjean, O. Peña, J.-C. Jegaden, C. J. Gomez-Garcia, P. Delhaès, *Inorg. Chem.* **1994**, *33*, 5180, and references therein.
[4] S. Triki, L. Ouahab, J. Padiou, D. Grandjean, *J. Chem. Soc. Chem. Commun.* **1989**, 1068; E. Coronado, C. J. Gomez-Garcia, *Comments Inorg. Chem.* **1995**, *17*, 255.
[5] D. Attanasio, M. Bonamico, V. Fares, L. Suber, *J. Chem. Soc. Dalton Trans.* **1992**, 2523, and references therein.
[6] C. L. Hill, D. A. Bouchard, M. Kadkhodayan, M. M. Williamson, J. A. Schmidt, E. F. Hilinsky, *J. Am. Chem. Soc.* **1988**, *110*, 5471.
[7] D. E. Wigley, *Prog. Inorg. Chem.* **1994**, *42*, 239.
[8] J. B. Strong, R. Ostrander, A. L. Rheingold, E. A. Maatta, *J. Am. Chem. Soc.* **1994**, *116*, 3601.
[9] Summary of crystal structure data for $[Bu_4N]_2$-**1**·(disordered solvent). The crystals are stable only under the mother liquor and the identity of the solvate(s) could not be established; three carbon atoms of the disordered solvate(s) located near an inversion center were refined in the structural analysis and are included in the following density and empirical formula calculations: M = 1583.62, monoclinic, $P2_1/n$, a = 17.153(4), b = 17.095(3), c = 20.510(6) Å, β = 105.043(13)°, V = 5808(3) Å^3, Z = 4, ρ_{calcd} = 1.811 g cm^{-3}, T = 173(2) K, crystal dimensions = 0.50 × 0.25 × 0.10 mm, μ = 1.563 mm^{-1}, λ = 0.71073 Å; 23202 reflections (8986 independent) were collected on a Siemens SMART system ($2\theta_{max}$ = 48.3°) of which 8984 independent reflections with $I > 2\sigma(I)$ were used in refinement. The structure was solved by direct methods and refined by full-matrix least-squares (on F^2) and difference Fourier cycles (SHELXTL V5.0). A face-indexed analytical absorption correction was applied (T_{min}/T_{max} = 0.6153). All non-hydrogen atoms (except those of the disordered solvent) were refined anisotropically. H atoms were treated as idealized isotropic contributions. Final residuals were $R1$ = 0.0662 and $wR2$ = 0.1157 for 8984 data and 651 parameters. Largest difference peak and hole = 0.914 and −0.866 e Å^{-3}. GOF (F^2) = 1.183. Further details of the crystal structure investigation may be obtained from the Director of the Cambridge Crystallographic Data Centre, 12 Union Road, GB-Cambridge CB2 1EZ (UK) on quoting the full journal citation.
[10] P. L. Veya, J. K. Kochi, *J. Organomet. Chem.* **1995**, *488*, C4.
[11] A. Proust, R. Thouvenot, M. Chaussade, F. Robert, P. Gouzerh, *Inorg. Chim. Acta* **1994**, *224*, 81.
[12] Y. S. Sohn, D. N. Hendrickson, H. B. Gray, *J. Am. Chem. Soc.* **1971**, *93*, 3603.
[13] K. Schlögl, H. Seiler, *Naturwissenschaften* **1958**, *45*, 337.
[14] M. Che, M. Fournier, J. P. Launay, *J. Chem. Phys.* **1979**, *71*, 1954.

A $Te_2N_6Li_4$ Cage Containing the Tris(*tert*-butylimido)tellurite Dianion**

Tristram Chivers,* Xiaoliang Gao, and Masood Parvez

Dedicated to Professor Max Herberhold on the occasion of his 60th birthday

The development of tellurium–nitrogen chemistry has been impeded for many years on account of the explosive nature of simple compounds such as Te_3N_4[1, 2] and $K_2[Te(NH)_3]$.[2] Recently, however, significant progress has resulted from the discovery of Te–N reagents that are safe to handle. Many Te–N compounds exhibit structures and/or reactions that are either unique or significantly different from those of their lighter chalcogen analogues.[3] For example, the three tellurium atoms in the twelve-membered rings of $(XTeNSN)_3N$ (X = Cl, F) are connected by a μ_3-nitrido bridge,[4] the Te^{II} derivative $(Me_3Si)_2NTeN(SiMe_3)_2$ forms a monomeric cation radical upon oxidation with AsF_5,[5] the cation $Te_2S_2N_4^{2+}$ adopts a bicyclic structure,[6] and *N*,*N*′-di-*tert*-butyltellurium(IV) diimide exists as a thermally stable dimer (tBuN)Te(μ-NtBu)$_2$Te(NtBu) (**1**).[7]

A characteristic reaction of sulfur(IV) diimides RN=S=NR is the quantitative formation of sulfinimidamides [RNS(R)NR]Li on treatment with R′Li reagents;[8] the structures of these organolithium adducts have only been determined recently.[9] We report here on the reaction of the dimer **1** with phenyllithium or, preferably, tBuNHLi, which produces $[(tBuN)_3TeLi_2]_2$ (**2**) (Scheme 1). Complex **2** forms a $Te_2N_6Li_4$ cage which contains

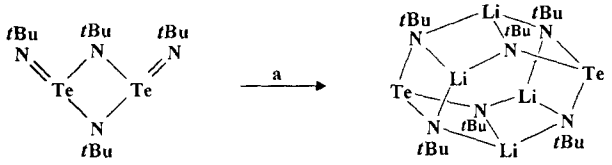

1 **2**

Scheme 1. a) + 4 tBuNHLi, −2 tBuNH$_2$.

the first structurally characterized tris(imido)tellurite ion $Te(NR)_3^{2-}$ (R = tBu). This dianion is isoelectronic with the recently described $Sb(NR)_3^{3-}$ (R = $PhCH_2CH_2$) trianion, which, as its trilithium derivative, exists as an $Sb_2N_6Li_6$ cage.[10] The reaction of **2** with two molar equivalents of $PhPCl_2$ or $PhBCl_2$ yields the spirocyclic tellurium(IV) derivative Ph(tBuN)P(μ-NtBu)$_2$Te(μ-NtBu)$_2$P(NtBu)Ph **3** or the four-membered ring compound PhB(μ-NtBu)$_2$Te(NtBu) **4**, respectively.

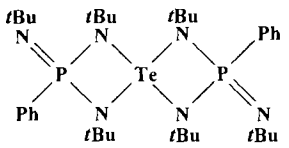

3

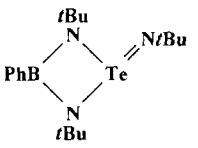

4

[*] Prof. Dr. T. Chivers, Dr. X. Gao, Dr. M. Parvez
Department of Chemistry
The University of Calgary
Calgary, Alberta, T2N 1N4 (Canada)
Telefax: Int. code + (403) 289-9488

[**] Financial support from the Natural Sciences and Engineering Research Council (Canada) is gratefully acknowledged.

Compound **2** was initially obtained unexpectedly in 35% yield, together with diphenyltelluride, as moisture-sensitive, colorless crystals from the reaction of **1** with phenyllithium. The dimeric structure of **2** was established by X-ray crystallography. Subsequently, it was found that **2** may be prepared in 91% yield by the treatment of **1** with four molar equivalents of tBuNHLi in toluene at −78 °C, followed by warming to room temperature.

A low-temperature X-ray structure determination confirmed the presence of a $Te_2N_6Li_4$ cage in **2** (Fig. 1).[11] All the lithium

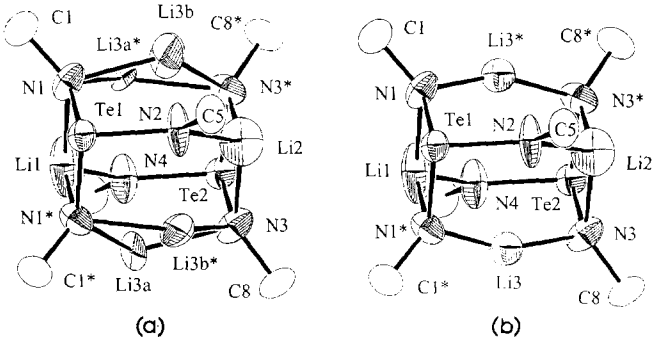

Fig. 1. Representations of the dimer **2** showing a) all lithium sites [with 50% occupancies for Li(3a) and Li(3b)] and b) an averaged structure with Li(3) and Li(3)* at the midpoint between two disordered sites. Only the α-carbon atoms of tBu groups attached to nitrogen atoms are shown for clarity. Selected bond lengths [Å] and bond angles [ ] are given in the text. Asterisks indicate atoms related by symmetry: x, 1/2−y, z.

atoms are unsolvated (recrystallization from toluene). The lithium atoms Li(3) and Li(3)* each inhabit two sites with 50% occupancies. Figure 1 shows both the disordered and averaged structures of the $Te_2N_6Li_4$ cage. In the dimer $[W(NtBu)_4Li_2]_2$, which also contains a $M_2N_6Li_4$ cage, disorder involving all four lithium atoms (with 2/3 occupancies) was observed.[12] In the context of the estimated values of 2.05 and 1.83 Å for Te^{IV}–N single and double bonds, respectively,[13] the mean Te–N distance of 1.980 Å and the distorted pyramidal geometry at the tellurium centers with mean N-Te-N bond angles of 93.6° are consistent with the description of **2** as the dilithium derivative of the tris(*tert*-butylimido)tellurite $Te(NtBu)_3^{2-}$ dianion, which may be represented as the resonance hybrid **5** (the lone pair on the Te atom has been omitted).

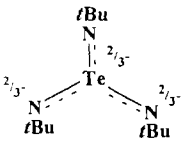

5

As a general rule Li–N bond lengths increase as the coordination number of Li increases;[14] however, both types of lithium atoms in the $Te_2N_6Li_4$ cage of **2** are three-coordinate. The mean Li–N distances for Li(1) and Li(2) are 1.93(2) Å and 2.07(2) Å, respectively, whereas the mean Li–N distances for Li(3a) and Li(3b) are 2.08(3), 2.14(3), and 2.20(2) Å, the longest of which lies across the "waist" of the cage (see Fig. 1a and Scheme 1). Thus the dimer **2** can be viewed as a distorted hexagonal prism (cf. $[(thf)Mg(NPh)]_6$[15a] and $(RAlN(R')_6$[15b]). The Li–Li contacts of 2.25(3)–2.35(3) Å are not considered to have bonding significance.[16]

The ^{1}H NMR and ^{7}Li NMR spectra of **2** in C_7D_8 both exhibit singlets at δ = 1.34 and 5.7, respectively, throughout the temperature range 185 to 298 K. In view of the tendency of organonitrogen–lithium compounds to have different degrees of association in solution than those observed in the solid state,[16] a full understanding of the structure of **2** in solution must await more detailed NMR studies and molecular weight measurements.

The novel cage compound **2** is the first structurally characterized triimidotellurite ion $Te(NR)_3^{2-}$. The compound $K_2[Te(NH)_3]$ **6**, which presumably contains the parent

$K_2[Te(NH)_3]$ **6**

$Te(NH)_3^{2-}$ ion, was obtained many years ago in unspecified yield as colorless crystals from the remarkable reaction of diphenyltelluride with potassium amide in liquid ammonia; it was identified on the basis of analytical data alone.[2] Compound **6** is *highly explosive*, however, whereas **2** can be handled without fear of explosion and is readily soluble in organic solvents such as toluene or THF. The $Te(NtBu)_3^{2-}$ ion is formally isoelectronic with the tellurite TeO_3^{2-} ion and is a potentially versatile building block for the construction of rings (or cages) involving other main group elements, as illustrated by the following examples.

The reaction of **2** with two molar equivalents of $PhPCl_2$ in hexane at $-100\,^{\circ}C$, followed by warming slowly to room temperature, produced orange crystals of the spirocyclic compound **3** and elemental tellurium. Complex **3** was characterized by ^1H, ^{31}P, and ^{125}Te NMR spectroscopic data (see Experimental Procedure) and by an X-ray crystallographic analysis.[17] The spirocyclic structure of **3** (Fig. 2) is comparable to that determined

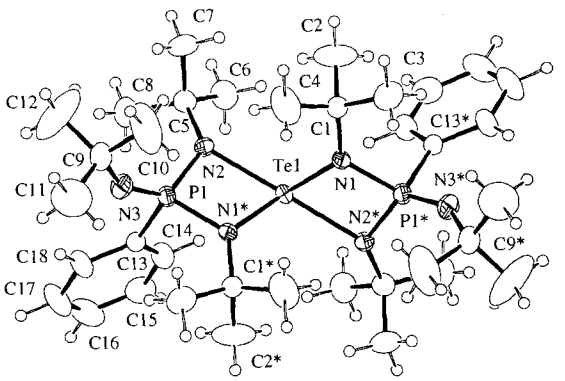

Fig. 2. Crystal structure of **3**. Selected bond lengths [Å] and bond angles [°]: Te(1)-N(1) 2.034(5), Te(1)-N(2) 2.212(5), P(1)-N(1) 1.736(5), P(1)-N(2) 1.646(5), P(1)-N(3) 1.498(6); N(1)-Te(1)-N(1)* 103.4(3), N(1)-Te(1)-N(2) 110.6(2), N(1)-Te(1)-N(2)* 68.2(2), N(2)-Te(1)-N(2)* 178.2(3), Te(1)-N(2)-P(1) 97.3(2), Te(1)-N(1)*-P(1) 101.3(3), N(1)*-P(1)-N(2) 89.7(2). Asterisks indicate atoms related by symmetry: $2-x, y, 1/2-z$.

recently for the related complex $PhB(\mu\text{-}NtBu)_2Te(\mu\text{-}NtBu)_2BPh$.[18] We note, however, that the boron complex is prepared from $TeCl_4$ and $PhB(NtBu)_2Li_2$ (1:2 molar ratio) in a straightforward metathesis reaction, whereas the formation of **3** involves a redox process with transfer of $NtBu$ groups from tellurium to phosphorus and the formation of elemental tellurium. For comparison, the reaction of **2** with two molar equivalents of $PhBCl_2$ produces the new four-membered BN_2Te ring **4** as yellow crystals in about 30% yield, together with the known cyclic tellurium(II) imide $(tBuNTe)_3$.[7] The structure of **4** was confirmed by a single-crystal X-ray analysis (Fig. 3).[19] The B–N bond lengths (1.45–1.46 Å) and the almost planar structure at the bridging nitrogens (sum of angles = 356.7°) are consistent with substantial multiple bonding.[20] The endocyclic and exocyclic Te–N bond lengths of 2.081 and 1.878 Å are identical to the values found for the tellurium diimide dimer **1**,[7] indicating single and double bonds, respectively.

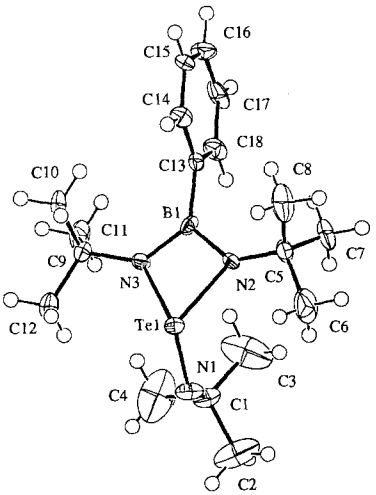

Fig. 3. Crystal structure of **4**. Selected bond lengths [Å] and bond angles [°]: B(1)–N(2) 1.46(1), B(1)–N(3) 1.45(1), Te(1)–N(1) 1.878(7), Te(1)–N(2) 2.081(7), Te(1)–N(3) 2.081(6); N(2)-B(1)-N(3) 104.1(8), B(1)-N(2)-Te(1) 93.6(6), B(1)-N(3)-Te(1) 94.1(5), N(2)-Te(1)-N(3) 67.0(3), N(1)-Te(1)-N(2) 113.0(3), N(1)-Te(1)-N(3) 111.8(3).

In view of the recently demonstrated ability of the trithiotellurite ion TeS_3^{2-} to form a variety of novel layer structures with transition metals,[21] investigations of the ligand behavior of **5** should be fruitful.

Experimental Procedure

2: A solution of $tBuNHLi$ (0.360 g, 4.49 mmol) in toluene (30 mL) was added to a stirred, orange solution of $Te_2(NtBu)_4$ (0.60 g, 1.11 mmol) in toluene (10 mL) at $-78\,^{\circ}C$. The mixture was allowed to warm to $23\,^{\circ}C$ to give an almost colorless solution. After 5 h, the volume of the solution was reduced to about 0.5 mL and the resulting colorless crystals were rinsed quickly with 5 mL of cold toluene ($-30\,^{\circ}C$). A second crop was obtained from the filtrate at $-20\,^{\circ}C$ when the volume was reduced to about 1 mL. The combined yield of **2** was 0.718 g (1.01 mmol, 91%). ^1H NMR (C_7D_8, 25 °C): $\delta = 1.34$(s); ^{125}Te NMR (C_7D_8, 25 °C, Ph_2Te): $\delta = 152.6$(s); ^7Li NMR (C_7D_8, 25 °C, 4.0 M $LiClO_4$ in D_2O): $\delta = 5.7$(s).

3: A solution of $PhPCl_2$ (0.050 g, 0.282 mmol) in hexane (10 mL) was added dropwise to a stirred, colorless solution of $[Li_2Te(NtBu)_3]_2$ (0.100 g, 0.141 mmol) in hexane (20 mL) at $-100\,^{\circ}C$ to give an orange solution. Upon warming to 23 °C, some black precipitate (elemental Te) was formed. The mixture was stirred for a further 10 h and then filtered. The volume of the orange filtrate was reduced to 3 mL and large platelets of **3** formed within a few hours. A second crop of **3** was obtained by cooling the concentrated mother liquor (ca. 0.5 mL) to $-20\,^{\circ}C$. The combined yield of **3** was 87 mg (0.113 mmol, 40%). ^1H NMR (C_6D_6, 25 °C): $\delta = 7.9$–8.1(m), 7.05–7.3 (m, 5H), 1.66 (d, $J = 1.46$ Hz, 9H), 1.60 (s, 9H), 1.35 (s, 9H); $^{31}P\{^1H\}$ NMR (C_6D_6, 25 °C, 85% H_3PO_4): $\delta = -37.9$ (s, $^2J(^{125}Te,^{31}P) = 121.5$ Hz); ^{125}Te NMR (C_6D_6, 25 °C, Ph_2Te): $\delta = -254.0$ (t, $^2J(^{125}Te,^{31}P) = 124.2$ Hz).

4: A solution of $PhBCl_2$ (0.118 g, 0.741 mmol) in pentane (5 mL) was added slowly to a solution of $[Li_2Te(NtBu)_3]_2$ (0.263 g, 0.371 mmol) in toluene (20 mL) at $-78\,^{\circ}C$. The colorless solution turned orange in 20 min. The reaction mixture was allowed to warm up to 23 °C, stirred for 2 h, and then filtered through a fine frit. Solvent was removed from the filtrate under vacuum and the residue was dissolved in diethyl ether (2 mL). This solution was cooled to $-20\,^{\circ}C$ and colorless crystals of **4** (0.092 g, 0.215 mmol, 29%) were isolated. ^1H NMR (C_6D_6, 25 °C): $\delta = 7.2$–7.6 (m, 5H), 1.70 (s, 9H), 1.11 (s, 18H); ^{11}B NMR (C_6D_6, 25 °C): $\delta = 36.0$(s) (ref. $NaBH_4$ in D_2O). Some orange crystals of $Te_3(NtBu)_3$ (identified by ^1H NMR and MS) [7] were obtained from a pentane solution of the residue after the isolation of **4**.

Satisfactory C, H, N analyses were obtained for **2**, **3**, and **4**.

Received: June 27, 1995 [Z8140IE]
German version: *Angew. Chem.* **1995**, *107*, 2756–2758

Keywords: heterocycles · lithium compounds · nitrogen compounds · tellurium compounds

[1] S. Strecker, C. Mahr, *Z. Anorg. Chem.* **1934**, *221*, 199.
[2] O. Schmitz-Dumont, B. Ross, *Angew. Chem.* **1967**, *79*, 1061; *Angew. Chem. Int. Ed. Engl.* **1967**, *6*, 1071.
[3] a) M. Björgvinsson, H. W. Roesky, *Polyhedron* **1992**, *10*, 2353; b) A. Haas, J. Kasprowski, M. Pryka, *Coord. Chem. Rev.* **1994**, *130*, 301.

[4] a) H. W. Roesky, J. Münzenberg, M. Noltemeyer, *Angew. Chem.* **1990**, *102*, 73; *Angew. Chem. Int. Ed. Engl.* **1990**, *29*, 61; b) J. Münzenberg, H. W. Roesky, S. Besser, R. Herbst-Irmer, G. M. Sheldrick, *Inorg. Chem.* **1992**, *31*, 2986.

[5] M. Björgvinsson, T. Heinze, H. W. Roesky, F. Pauer, D. Stalke, G. M. Sheldrick, *Angew. Chem.* **1991**, *103*, 1671; *Angew. Chem. Int. Ed. Engl.* **1991**, *30*, 1677.

[6] A. Haas, M. Pryka, *Chem. Ber.* **1995**, *128*, 11.

[7] T. Chivers, X. Gao, M. Parvez, *J. Am. Chem. Soc.* **1995**, *117*, 2359.

[8] a) J. Kuyper, K. Vrieze, *J. Chem. Soc. Chem. Commun.* **1976**, 64; b) J. Kuyper, P. C. Keijzer, K. Vrieze, *J. Organomet. Chem.* **1976**, *116*, 1.

[9] a) F. Pauer, D. Stalke, *J. Organomet. Chem.* **1991**, *418*, 127; b) S. Freitag, W. Kolodziejski, F. Pauer, D. Stalke, *J. Chem. Soc. Dalton Trans.* **1993**, 3479.

[10] A. J. Edwards, M. A. Paver, P. R. Raithby, M.-A. Rennie, C. A. Russell, D. S. Wright, *Angew. Chem.* **1994**, *106*, 1334; *Angew. Chem. Int. Ed. Engl.* **1994**, *33*, 1277.

[11] Crystal data for **2** $C_{12}H_{27}N_3Li_2Te$, $M = 354.85$, orthorhombic, space group *Pnma* (no. 62), $a = 19.380(3)$, $b = 17.551(4)$, $c = 10.341(2)$ Å, $V = 3517(1)$ Å^3, $Z = 8$, $\rho_{calcd} = 1.366$ g cm^{-3}, $F(000) = 1448$, $\lambda = 0.71069$ Å, $T = 220(1)$ K, $\mu(Mo_{K\alpha}) = 16.79$ cm^{-1}. Data were collected on a Rigaku AFC6S diffractometer on a colorless prism ($0.45 \times 0.30 \times 0.28$ mm) mounted in a glass capillary by the ω-2θ method. Of a total 3533 collected reflections, 2040 were observed [$I > 3.00\sigma(I)$]. The structure was solved by direct methods (SAPI91; Fan Hai-Fu, Rigaku Corp., Tokyo, **1991**) and expanded using Fourier techniques (DIRDIF92). The data were corrected for absorption, Lorentz and polarization effects. Non-hydrogen atoms were refined anisotropically. One of the lithium atoms was disordered over two sites (Li(3a) and Li(3b)) with equal populations. Hydrogen atoms were included but not refined. Refinement by full-matrix least-squares calculations converged at $R = 0.036$ and $R_w = 0.036$. All calculations for **2**, **3**, and **4** were performed by using the teXsan crystallographic package (Molecular Structure Corp.). See also [19b].

[12] A. A. Danopoulos, G. Wilkinson, B. Hussain, M. B. Hursthouse, *J. Chem. Soc. Chem. Commun.* **1989**, 896.

[13] a) J. Münzenberg, H. W. Roesky, M. Noltemeyer, S. Besser, R. Herbst-Irmer, *Z. Naturforsch. B* **1993**, *48b*, 199; b) H. W. Roesky, J. Münzenberg, R. Bohra, M. Noltemeyer, *J. Organomet. Chem.* **1991**, *418*, 339.

[14] M. Veith, S. Müller-Becker in *The Chemistry of Inorganic Ring Systems* (Ed.: R. Steudel), Elsevier, Amsterdam, **1992**, p. 132.

[15] a) T. Hascall, K. Ruhlandt-Senge, P. P. Power, *Angew. Chem.* **1994**, *106*, 35; *Angew. Chem. Int. Ed. Engl.* **1994**, *33*, 356; b) C. E. Housecroft, *Cluster Molecules of the p-Block Elements*, Oxford University Press, Oxford, **1994**, p. 24.

[16] K. Gregory, P. von R. Schleyer, R. Snaith, *Adv. Inorg. Chem.* **1991**, *37*, 58.

[17] Crystal data for **3** $C_{30}H_{64}N_6P_2Te$, $M = 770.49$, monoclinic, space group $C2/c$ (no. 15), $a = 26.598(4)$, $b = 9.195(1)$, $c = 17.799(3)$ Å, $\beta = 109.24(1)$°, $V = 4109(1)$ Å^3, $Z = 4$, $\rho_{calcd} = 1.245$ g cm^{-3}, $F(000) = 1616$, $\lambda = 0.71069$ Å, $T = 296(1)$ K, $\mu(Mo_{K\alpha}) = 8.32$ cm^{-1}. Data were collected on an orange plate ($0.40 \times 0.45 \times 0.07$ mm) mounted in a glass capillary. Of a total 3975 collected reflections, 2043 were observed [$I > 3.00\sigma(I)$]. The structure was solved by direct methods (SAPI91) and expanded by using Fourier techniques. The data were corrected for absorption, Lorentz and polarization effects. Non-hydrogen atoms were refined anisotropically. Hydrogen atoms were included but not refined. Refinement by full-matrix least-squares calculations converged at $R = 0.044$ and $R_w = 0.043$. See also [19b].

[18] H.-J. Koch, H. W. Roesky, S. Besser, R. Herbst-Irmer, *Chem. Ber.* **1993**, *126*, 571.

[19] Crystal data for **4** $C_{18}H_{32}BN_3Te$, $M = 428.88$, orthorhombic, space group *Pbca* (no. 61), $a = 19.845(2)$, $b = 17.799(2)$, $c = 11.656(2)$ Å, $V = 4117.1(8)$ Å^3, $Z = 8$, $\rho_{calcd} = 1.384$ g cm^{-3}, $F(000) = 1744$, $\lambda = 0.71069$ Å, $T = 150$ K, $\mu(Mo_{K\alpha}) = 14.48$ cm^{-1}. Data were collected on a colorless plate ($0.55 \times 0.30 \times 0.17$ mm) mounted on a glass fiber. Of a total of 5280 collected reflections, 2634 were observed [$I > 3.00\sigma(I)$]. The structure was solved by the heavy atom method (PATTY) and expanded by using Fourier techniques. The data were corrected for absorption, Lorentz and polarization effects. Non-hydrogen atoms were refined anisotropically. Hydrogen atoms were included but not refined. Refinement by full-matrix least-squares calculations converged at $R = 0.051$ and $R_w = 0.055$. b) Further details of the crystal structure investigations of **2**–**4** may be obtained from The Director of the Cambridge Crystallographic Data Centre, 12 Union Road, Cambridge CB2 1EZ (UK), on quoting the full journal citation.

[20] A. F. Wells, *Structural Inorganic Chemistry*, 5th edition, Clarendon Press, Oxford, **1984**, p. 1062.

[21] a) T. J. McCarthy, X. Zhang, M. G. Kanatzidis, *Inorg. Chem.* **1993**, *32*, 2944; b) X. Zhang, M. G. Kanatzidis, *J. Am. Chem. Soc.* **1994** *116*, 1890; c) X. Zhang, M. G. Kanatzidis, *Inorg. Chem.* **1994**, *33*, 1238.

Nucleophilic Attack on (π-Allyl)palladium Complexes: Direction of the Attack to the Central or Terminal Carbon Atom by Ligand Control**

Ana M. Castaño, Attila Aranyos, Kálmán J. Szabó, and Jan-E. Bäckvall*

Nucleophilic addition to (π-allyl)palladium complexes is an important step in a number of synthetically useful palladium-catalyzed reactions,[1] for example, allylic nucleophilic substitutions,[2] allylic acetoxylation,[3] and 1,4-oxidation of conjugated dienes.[4] In all these reactions the regiochemistry observed has been attack at either terminus (C1 or C3) of the π-allyl group. However, some time ago Hegedus reported an example of attack at the central carbon (C2),[5] and since then several examples of such unusual reactivity have been reported with (π-allyl)palladium complexes.[6] Recently for a number of other (π-allyl)metal complexes attack at the central carbon has also been observed,[7, 8] sometimes in a reversible reaction.[7b, 8]

Until now it has generally been assumed that only less stabilized carbon nucleophiles (pK_a 20–30) are able to attack the central carbon in (π-allyl)palladium complexes.[5, 6] In this communication we provide evidence that also more stabilized carbon nucleophiles (pK_a 14–15), such as diethyl methylmalonate, attack at the central carbon under certain conditions. We have studied the factors governing the regiochemistry of the attack (at the central or the terminal carbon) and explain the observed regiochemistry.

The (π-allyl)palladium complex **1a**, prepared in 90% yield by reaction of 2,3-dichloropropene with 1 equiv of $PdCl_2$ in the presence of CO,[9] was used as a substrate to study the effect of the ligand and other parameters in the regiochemistry of the nucleophilic attack.[10] Complex **1a** was allowed to react with sodium diethyl methylmalonate (2.0–2.5 equiv) in THF at −78 °C in the presence of different ligands (2–6 equiv) and left to warm up overnight to room temperature. Two products, the doubly alkylated product **3** and the monoalkylated product **4**, were obtained (Scheme 1, Table 1).

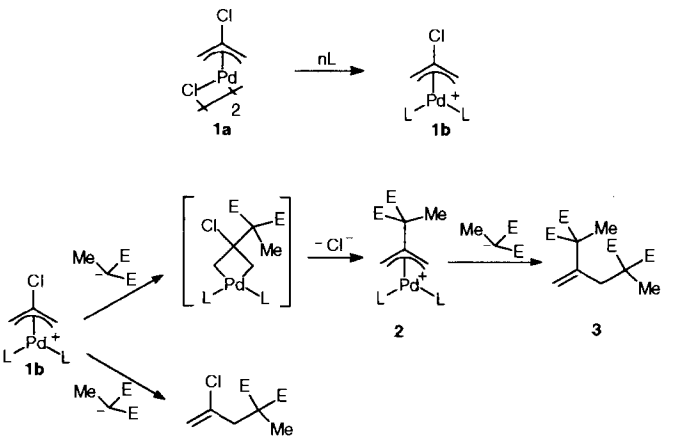

Scheme 1. Reaction of complex **1** with sodium diethyl methylmalonate. E = CO_2Et.

[*] Prof. Dr. J.-E. Bäckvall, Dr. A. M. Castaño, A. Aranyos, Dr. K. J. Szabó
Department of Organic Chemistry, University of Uppsala
Box 531, S-75121 Uppsala (Sweden)
Telefax: Int. code + (18) 508542
e-mail: Jeb@kemi.uu.se

[**] Financial support from the Swedish Natural Science Research Council, the Spanish Ministerio de Educación y Ciencia (fellowship to A. M. C.), and the National Supercomputer Centre in Sweden is gratefully acknowledged.

Table 1. Product distribution in the reaction of sodium diethyl methylmalonate with a series of allyl complexes **1** containing different ligands L [a].

Entry	L (equiv)	**3**:**4** [b]
1	PPh_3 (4) [c]	<2:>98
2	PBu_3 (4)	13:87
3	$P(OPh)_3$ (6)	<1:>99
4	dppf (2) [c]	<1:>99
5	dppe (2) [c]	25:75
6	dppe (4.5) [c]	23:77
7	dppb (2) [c]	10:90
8	bpy (2) [d]	>99:<1
9	tmeda (2) [d]	>99:<1

[a] Unless otherwise stated, the ligand was added to a solution of **1** in THF at −78 °C, followed by addition of sodium diethyl methylmalonate in THF. The reaction was allowed to warm to room temperature overnight. Conversion of **1** to products **3** and/or **4** was >95%. Abbreviations: dppf = 1,1′-bis(diphenylphosphino)ferrocene; dppe = 1,2-bis(diphenylphosphino)ethane; dppb = 1,4-bis(diphenylphosphino)butane; bpy = 2,2′-bipyridine; tmeda = *N*,*N*,*N*′,*N*′-tetramethylethylenediamine. [b] Ratio determined by ^{1}H NMR spectroscopy. [c] After adding the ligand, the cold bath was removed for a few minutes to facilitate the ligand exchange. [d] Variable amounts of diethyl (allyl)methylmalonate and diethyl 2-(2-propenyl)methylmalonate were also obtained.

Compound **3** is formed in a multistep process: addition of the nucleophile to the central carbon of the (π-allyl)palladium complex followed by elimination of Cl^- gives the substituted (π-allyl)palladium complex **2**, which subsequently undergoes a second nucleophilic attack at the terminal carbon atom.[11] Compound **4** is formed in a one-step attack by the nucleophile at the terminal carbon atom.

The ratio between products **3** and **4** is strongly dependent on the choice of the ligand (Table 1). π-Acceptor phosphorus ligands favor terminal attack, whereas strong σ-donor nitrogen ligands favor C2 attack. Thus, the use of triphenylphosphane as ligand afforded **4** highly selectively (>98%), indicating terminal attack by the nucleophile (entry 1). With the more electron-donating tributylphosphane some C2 attack took place, the ratio of **3** to **4** being 13:87 (entry 2). Interestingly, the bidentate phosphane ligand dppe gave significant amounts of C2 attack (entries 5 and 6). With bipyridine and tmeda as ligand only product **3** from initial C2 attack was observed (entries 8–9).

Reaction of **1a** with an even more stabilized carbon nucleophile, sodium methyl methylacetoacetate, afforded product **5** by terminal attack even if tmeda was used as a ligand [Eq. (a)].

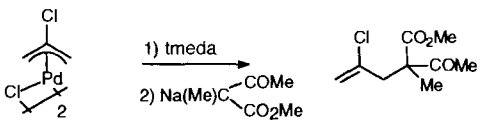

1a **5**

To gain further insight into the mechanism of this reaction, ab initio[12] calculations at the Hartree–Fock level as well as at the second and fourth order Møller–Plesset perturbation theory[13] were performed on (π-allyl)palladium complex **6**, which contains simple phosphorus and nitrogen ligands. Previous theoretical studies on C2 attack by nucleophiles on (π-allyl)palladium complexes have employed Extended Hückel MO (EHMO) calculations.[7b,14] From results one of the studies,[14] frontier orbital controlled nucleophilic attack at the central carbon atom was considered unlikely, whereas in the other study[7b] it was argued to be a possible pathway. Our calculations on **6** show that: 1) The orbital energies of the two lowest unoccupied MOs, $\varphi_{a'}$ and $\varphi_{a''}$, (Fig. 1) are rather similar and vary for different ligands.[15] 2) With NH_3 as ligand $\varphi_{a'}$ is the LUMO and approximately 0.4 eV below $\varphi_{a''}$. 3) With PH_3 as ligand the order is reversed, and $\varphi_{a''}$ has the lowest energy, although the energy difference between the two orbitals is small (<0.2 eV) and perhaps not significant.

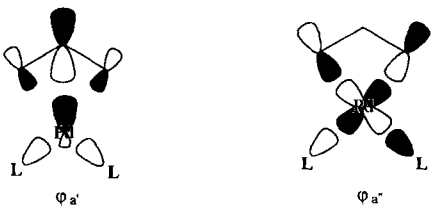

$\varphi_{a'}$ $\varphi_{a''}$

Fig. 1. Possible LUMOs in Pd(π-allyl) complexes.

There are two possible explanations for the ligand effects observed (Table 1): 1) There is a balance between charge controlled and orbital controlled reactions. 2) The reaction is frontier orbital controlled for all ligands, but the LUMO is different for different ligands ($\varphi_{a'}$ or $\varphi_{a''}$). According to the first explanation, an electron-accepting ligand such as triphenylphosphane would create significant carbenium ion character at the allyl moiety. The complex can be best described as an allyl cation coordinated to Pd^0, and therefore the positive charge in the allyl group is located more on the terminal carbon atoms. As a result, charge controlled attack at the terminal carbon would be favored. On the other hand, with more strongly electron-donating ligands such as tmeda, the positive charge will be smaller and frontier orbital control will become more important. When $\varphi_{a'}$, where the MO coefficient is large at the C2 carbon, is the LUMO, attack at this carbon will predominate. The fact that the methyl methylacetoacetate anion [Eq. (a)], which is more stabilized than the dialkyl methylmalonate anion, gives terminal attack in a reaction with the allylpalladium complex containing tmeda as ligand is consistent with the first explanation. The energy of the nucleophile orbital (HOMO) will be significantly lower in this case and therefore the rate of the frontier orbital controlled pathway, which is inversely dependent on the difference $E_{LUMO}-E_{HOMO}$, would decrease.[16]

On the other hand, if the reaction is completely governed by frontier orbital control (as in the second explanation) the terminal attack on allylic complexes with PPh_3 and $P(OPh)_3$ as ligands would be explained by a change of LUMO from $\varphi_{a'}$ to $\varphi_{a''}$ on changing from the strong σ-donor ligands to the π-acceptor phosphorus ligands. This is in agreement with the calculations. However, the reason for terminal attack by sodium methyl methylacetoacetate on **1** with tmeda as ligand [Eq. (a)] is not obvious with this explanation, but may be rationalized by repulsive HOMO(nucleophile)–HOMO(allyl) interactions as suggested by Musco et al.[7b]

Recently, Murai et al.[7c] showed that the nucleophile sodium diethyl methylmalonate attacks the C2 carbon atom of a (π-allyl)platinum intermediate corresponding to **1**. The (π-allyl)-platinum species was generated from 2-chloro-2-propenyl-acetate and $[Pt(CH_2{=}CH_2)(PPh_3)_2]$ in a catalytic reaction that afforded **3** as final product.

In summary, we have demonstrated for the first time that nucleophilic attack by a dialkyl malonate anion (a more stabilized carbon nucleophile) takes place at the central carbon atom of a (π-allyl)palladium complex. The regiochemistry of the reac-

tion is controlled by proper choice of ligand on the metal. The effect of temperature, chelation, and other reaction parameters are under investigation.

Received: July 6, 1995 [Z 8175 IE]
German version: *Angew. Chem.* **1995**, *107*, 2767–2769

Keywords: complexes with carbon ligands · ligand effects · nucleophilic attack · palladium compounds

[1] *Palladium in Organic Synthesis, Symposium in print No. 52* (Ed.: J. E. Bäckvall), *Tetrahedron* **1994**, *50*, 285–572.

[2] a) For a recent review, see: S. A. Godlesky in *Comprehensive Organic Synthesis, Vol. 4* (Eds.: B. M. Trost, I. Fleming, M. F. Semmelhack), Pergamon, Oxford, **1991**, p. 585; b) Y. M. Nilsson, P. G. Andersson, J. E. Bäckvall, *J. Am. Chem. Soc.* **1993**, *115*, 6609; c) B. M. Trost, T. R. Verhoeven in *Comprehensive Organometallic Chemistry, Vol. 8* (Eds.: G. Wilkinson, F. G. A. Stone, E. A. Abel), Pergamon, Oxford, **1982**, p. 799; d) J. Tsuji, *Acc. Chem. Res.* **1969**, *2*, 144.

[3] a) A. Heumann, B. Åkermark, *Angew. Chem.* **1984**, *96*, 443; *Angew. Chem. Int. Ed. Engl.* **1984**, *23*, 453; b) S. Hansson, A. Heumann, T. Rein, B. Åkermark, *J. Org. Chem.* **1990**, *55*, 975; c) J. E. Bäckvall, R. B. Hopkins, H. Grennberg, M. M. Mader, A. K. Awasthi, *J. Am. Chem. Soc.* **1990**, *112*, 5160.

[4] a) J. E. Bäckvall in *Organometallic Reagents in Organic Synthesis* (Eds.: J. H. Bateson, M. B. Mitchell), Academic Press, London, **1994**, p. 81; b) J. E. Bäckvall, *Adv. Met. Org. Chem.* **1989**, *1*, 135; c) J. E. Bäckvall, J. E. Nyström, R. E. Nordberg, *J. Am. Chem. Soc.* **1985**, *107*, 3676; d) A. M. Castaño, J. E. Bäckvall, *ibid.* **1995**, *117*, 560.

[5] L. S. Hegedus, W. H. Darlington, C. E. Russell, *J. Org. Chem.* **1980**, *45*, 5193.

[6] a) H. M. R. Hoffmann, A. R. Otte, A. Wilde, S. Menzer, D. J. Williams, *Angew. Chem.* **1995**, *107*, 73; *Angew. Chem. Int. Ed. Engl.* **1995**, *34*, 100; b) A. Wilde, A. R. Otte, H. M. R. Hoffmann, *J. Chem. Soc. Chem. Commun.* **1993**, 615; c) H. M. R. Hoffmann, A. R. Otte, A. Wilde, *Angew. Chem.* **1992**, *104*, 224; *Angew. Chem. Int. Ed. Engl.* **1992**, *32*, 234; d) C. Carfagna, L. Mariani, A. Musco, G. Sallese, R. Santi, *J. Org. Chem.* **1991**, *56*, 3924; e) C. Carfagna, R. Galarini, A. Musco, *J. Mol. Catal.* **1992**, *72*, 19.

[7] For a recent review on metallacyclobutane complexes of group 8 transition metals, see: a) P. W. Jennings, L. L. Johnson, *Chem. Rev.* **1994**, *94*, 2241; b) C. Carfagna, R. Galarini, K. Linn, J. A. López, C. Mealli, A. Musco, *Organometallics* **1993**, *12*, 3019; c) K. Ohe, H. Matsuda, T. Morimoto, S. Ogoshi, N. Chatani, S. Murai, *J. Am. Chem. Soc.* **1994**, *116*, 4125; d) M. Ephritikhine, M. L. H. Green, R. E. MacKenzie, *J. Chem. Soc. Chem. Commun.* **1976**, 619; e) M. Ephritikhine, B. R. Francis, M. L. H. Green, R. E. MacKenzie, M. J. Smith, *J. Chem. Soc. Dalton Trans.* **1977**, 1131; f) E. B. Tjaden, G. L. Casty, J. M. Stryker, *J. Am. Chem. Soc.* **1993**, *115*, 9814.

[8] a) E. B. Tjaden, J. M. Stryker, *J. Am. Chem. Soc.* **1990**, *112*, 6420; b) G. J. A. Adams, S. G. Davies, K. A. Ford, M. Ephritikhine, P. F. Todd, M. L. H. Green, *J. Mol. Catal.* **1980**, *8*, 15; c) Ref. [7b].

[9] P. R. Auburn, P. B. MacKenzie, B. Bosnich, *J. Am. Chem. Soc.* **1985**, *107*, 2033.

[10] Recently, Murai et al. generated homologous (π-allyl)palladium and -platinum complexes in situ in catalytic reactions from 2-chloro-2-propenylacetates to study the site of nucleophilic attack [7c].

[11] Complex **1** is indeed highly reactive and reacts even at −78 °C with stabilized carbon nucleophiles.

[12] a) The program GAUSSIAN 92 was employed. For hydrogens the primitive (4s) [12b] basis was used contracted to [2s]. For carbon, nitrogen, and chlorine atoms the (9s,5p) basis of Huzinaga [12b] was used, augmented with one d-function and contracted to [3s,2p,1d]; the chlorine core was replaced by an effective core potential (ECP) [12c]. For palladium a relativistic ECP according to Hay and Wadt [12d] was used. The 4s and 4p orbitals are described by a single zeta contraction, the valence 5s and 5p orbitals by a double zeta basis, and the 4d orbital by a triple zeta basis including one diffuse d-function. b) S. Huzinaga, *J. Chem. Phys.* **1965**, *42*, 1293; c) P. J. Hay, W. R. Wadt, *ibid.* **1985**, *82*, 270; d) P. J. Hay, W. R. Wadt, *ibid.* **1985**, *82*, 299.

[13] P. C. Hariharan, J. A. Pople, *Theor. Chim. Acta* **1973**, *28*, 213.

[14] M. D. Curtis, O. Eisenstein, *Organometallics* **1984**, *3*, 887.

[15] On the basis of EHMO results (based on the experimental geometry) Formica et. al. has stated that these two orbitals are similar in energy and reverse their relative position: M. Formica, A. Musco, R. Pontellini, K. Linn, C. Mealli, *J. Organomet. Chem.* **1993**, *448*, C6.

[16] a) G. Klopman, *J. Am. Chem. Soc.* **1968**, *90*, 2; b) *Chemical Reactivity and Reaction Paths*, (Ed. G. Klopman), Wiley, New York, **1974**; c) I. Fleming, *Frontier Orbitals and Organic Reactions*, Wiley, New York, **1978**.

6,7-Bis(methoxycarbonyl)-2,3-dimethyl-[5](1,4)naphthalenophane, the First Benzoannelated [5]Paracyclophane

Daniël S. van Es, Franciscus J. J. de Kanter, Willem H. de Wolf, and Friedrich Bickelhaupt*

The chemistry of small strained cyclophanes keeps fascinating chemists, both because of the remarkable physical and chemical properties of these compounds and because of the challenge posed by their synthesis.[1] In 1985, we reported the first synthesis of [5]paracyclophane, which was at that time the smallest known [*n*]paracyclophane.[2] In contrast to its next higher homologue [6]paracyclophane,[3] [5]paracyclophane is not stable at room temperature; it could only be stored in dilute solution at low temperatures.[2] Introduction of substituents at the benzene ring slightly increased the thermal stability.[4] Therefore, a further increase in stability could be expected on annelation of an additional benzene ring, especially since Tobe and co-workers had shown that [6](1,4)naphthalenophane is more stable than [6]paracyclophane.[5] Here we report the synthesis and characterization of a derivative of [5](1,4)naphthalenophane, which is the smallest known [*n*](1,4)naphthalenophane and the first benzoannelated [5]paracyclophane.

The Dewar benzene **1**[4b] was converted by known methods,[6, 7] as indicated in Scheme 1, via the corresponding diol

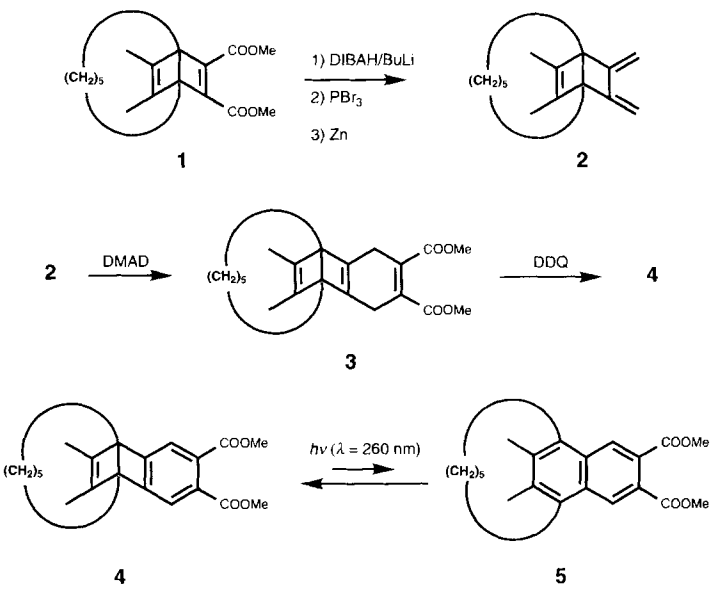

Scheme 1. Synthesis of **5** from **1**. DIBAH = Diisobutylaluminum hydride.

(step 1) and dibromide (step 2) to the triene **2** (step 3). In a Diels–Alder reaction with dimethyl acetylenedicarboxylate (DMAD), **2** yielded the adduct **3**, which in turn was oxidized with dichlorodicyanobenzoquinone (DDQ) to give **4**. After preparative thin layer chromatography, **4** was obtained in low yield, but pure.

Initial attempts to aromatize **4** photochemically to the naphthalenophane **5** with a white light source resulted in the forma-

[*] Prof. Dr. F. Bickelhaupt, Drs. D. S. van Es, Dr. F. J. J. de Kanter, Dr. W. H. de Wolf
Scheikundig Laboratorium, Vrije Universiteit
De Boelelaan 1083, NL-1081 HV Amsterdam (The Netherlands)
Telefax. Int. code + (20)4447488

tion of polymer only. By excitation with monochromatic light ($\lambda = 260$ nm) at low temperatures (248 K), we were able to obtain **5** in 35% yield in a photodynamic equilibrium with **4**.[8] Even after 280 hours of irradiation in [D$_8$]THF, the sample showed no degradation; in contrast, on irradiation at wavelengths longer than 350 nm, **5** underwent photoreversion to **4**. It should be pointed out that the yield of **5**, 35%, is the highest one recorded so far in the photochemical aromatization of any Dewar isomer of a small cyclophane.

The comparison of the ^{1}H NMR spectrum (400 MHz, [D$_8$]THF, 210 K) of **5** with that of the unstrained reference compound **6**[9] reveals that the aromatic protons of **5** (major isomer: $\delta(^1H\{5,8\}) = 8.29$; minor isomer: $\delta(^1H\{5,8\}) = 8.26$) show the shift typical for a naphthalene derivative (cf. **6**: $\delta = 8.43$; **4**: $\delta = 7.41$). Some of the methylene signals ($\delta = -0.37$, 2H, homobenzylic; $\delta = -0.61$, 1H, central methylene group) are characteristic for a substituted [5]paracyclophane;[4] these bridge protons are found in the shielding cone of the aromatic ring. It is remarkable that the shielding in **5** is stronger than that in monocyclic [5]paracyclophanes (homobenzylic: $\delta = 0.22$,[2] 0.33,[4b] central: $\delta = 0.01$,[2] -0.55,[4b]). This effect may be attributed to the increased ring current of a naphthalene system compared to that of a benzene ring.

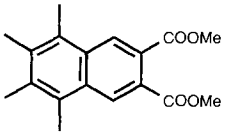

6

The fluorescence excitation spectrum of **5** shows a red shift for the first electronic transition in **5** ($\lambda = 390$ nm) of about 40 nm compared to that of the unstrained model **6**.[9] Thus, this shift is significantly smaller than those reported for monocyclic [5]paracyclophanes (70–90 nm[2, 4b]).

Like other unsymmetrically substituted [5]paracyclophanes, **5** occurs as an equilibrating mixture of two conformational isomers **5′** and **5″**. However, in contrast to other [5]paracyclophanes, one conformer strongly dominates in a ratio of 95:5, as

5′ **5″**

indicated by the arene signals at 210 K. Despite extensive NOE experiments, we have not been able to assign the conformations, as most signals of the minor conformer are obscured by those of the major one and of **4**.

The barrier for the conformational change of the pentamethylene bridge (**5′**⇌**5″**) was determined from variable temperature ^{1}H NMR measurements (206–244 K). Usually, this barrier decreases with decreasing strain in the molecular skeleton; thus, Tobe and co-workers found in the [6]paracyclophane series that the ring flip barrier does indeed decrease slightly with an increasing number of annelated rings.[5] However, the parameters of **5** ($\Delta H^{\neq} = 11.3 \pm 1.2$ kcal mol^{-1}, $\Delta S^{\neq} = -15.1 \pm 5.1$ cal K^{-1} mol^{-1}) are nearly identical to those of its monocyclic analogue.[4b]

Of all [5]paracyclophanes, **5** is the most stable one known to date. In the 2:1 mixture of **4** and **5**, **5** slowly decomposed at 298 K leading to the formation of a white insoluble polymer (half-life >80 h); for monocyclic [5]paracyclophanes, half-lives of 12[10] to 22 hours[4a] have been determined. In contrast, the chemical reactivity of **5** is still very high. The bright yellow solution of the 2:1 mixture of **4** and **5** mentioned above decolorized immediately on exposure to air; in the NMR spectrum the signals of **5** disappeared (formation of a white insoluble polymer), whereas those of **4** remained unchanged.

The synthesis of **5**, the first derivative of [5]paracyclophane with sufficient thermal stability, will form the basis of investigations of the chemical behavior of this class of highly strained aromatic compounds.

Experimental Procedure

2: The products of the first three steps of Scheme 1 were prepared by using known methods [6,7]; details of the syntheses are available on request from the authors. The yield of **2** as a transparent oil was about 0.18 g (0.90 mmol, ca. 82%); because of its sensitivity, it was only characterized by NMR spectroscopy and was directly used in the next reaction step. ^{1}H NMR (200.1 MHz, $CDCl_3$, 298 K): $\delta =$ 5.16 (br. s, 2H), 4.76 (br. s, 2H), 1.8–1.2 (m, 10H), 1.55 (s, 6H); ^{13}C NMR (50.32 MHz, $CDCl_3$, 298 K): $\delta = 153.1$ (s), 143.0 (s), 101.3 (t), 62.0 (s), 33.0 (t, central bridge-CH_2), 28.5 (t), 26.5 (t), 10.1 (q).

3: The bright yellow reaction mixture from **2** (0.14 g, 0.70 mmol) and four equivalents of DMAD (0.40 g) in benzene (20 mL) were stirred for 4 h at 80 °C. Then the benzene was removed at room temperature under reduced pressure, and the excess DMAD was removed under high vacuum. The residue was chromatographed (Kieselgel 60, pentane/ether 50/50)) to give a colorless oil **3** (0.22 g, 0.63 mmol, 90%). ^{1}H NMR (200.1 MHz, $CDCl_3$, 298 K): $\delta = 3.57$ (s, 6H), 3.04 (m, 2H), 2.99 (m, 2H), 1.67 (m, 4H), 1.60 (s, 6H), 1.52 (m, 6H); ^{13}C NMR (50.32 MHz, $CDCl_3$, 298 K): $\delta = 168.9$ (s), 144.5 (s), 143.0 (s), 134.0 (s), 63.6 (s), 52.0 (q), 33.4 (t, central bridge-CH_2), 28.1 (t), 27.2 (t), 26.3 (t), 11.4 (q).

4: To **3** (0.22 g, 0.63 mmol) in benzene (25 mL) was added 1.1 equivalents of DDQ. This mixture was stirred at 80 °C for 3 h, and then poured into ice-water and extracted with diethyl ether (three times). The combined organic phases were washed with water (four times), brine, and dried over $MgSO_4$. After the solvent was removed under reduced pressure, a brown oil remained containing largely **4**. Purification was finally achieved by preparative thin layer chromatography (Al_2O_3 on glass, pentane/ethyl acetate 90/10). Due to losses during attempted purification, meaningful yields could not be determined. **4** (colorless oil): ^{1}H NMR (200.1 MHz, $CDCl_3$, 298K): $\delta = 7.41$ (s, 2H), 3.87 (s, 6H), 2.04 (m, 4H), 1.56 (s, 6H), 1.47 (m, 6H); ^{13}C NMR (50.32 MHz, $CDCl_3$, 298K): $\delta = 168.8$ (s), 155.4 (s), 143.7 (s), 130.3 (s), 121.6 (d, J(C,H) = 164 Hz), 64.9 (s), 52.3 (q, J(C,H) = 147 Hz), 33.1 (t, J(C,H) = 121 Hz, central bridge-CH_2), 28.3 (t, J(C,H) = 125 Hz), 26.3 (t, J(C,H) = 125 Hz), 11.1 (q, J(C,H) = 126 Hz); high resolution MS: $C_{21}H_{24}O_4$ (M^+) calcd.: m/z 340.1674, observed 340.1677 ± 0.0005; fluorescence excitation/emission spectroscopy (THF, 298 K, Perkin Elmer LS-50); excitation spectrum: $\lambda_{em} = 430$, $\lambda_{max} = 260$, 325 nm; emission spectrum: $\lambda_{exc} = 260$ nm, $\lambda_{max} = 392$ nm.

5: A solution of **4** in [D$_8$]THF was filled into a quartz NMR tube, degassed by means of five freeze-pump-thaw cycles, and sealed in vacuo. The tube was irradiated at −25 °C with a Xenon-arc lamp (450 W) fitted with a monochromator set at 260 nm. After about 60 h of irradiation, a photodynamic equilibrium had been reached at 35% of **5** (^{1}H NMR). Major isomer (the signals of the minor isomer are largely obscured by other signals, with the exception of the arene signal at $\delta = 8.26$): ^{1}H NMR (400.1 MHz, [D$_8$]THF, 210 K): $\delta = 8.29$ (s, 2H), 3.85 (s, 6H, OMe), 3.22 (dd, ^2J(H,H) = 12.7 ± 0.3 Hz, ^3J(H,H) = 4.9 Hz, 2H, Ar-CHH), 2.63 (ddd, ^2J(H,H) = 12.4 ± 0.3 Hz, ^3J(H,H) = ^3J(H,H) = 5.2 Hz, 2H, Ar-CH*H*), 2.41 (s, 6H, Ar*Me*), 1.50 (m [11]), 1.20 (m [11]), −0.37 (m, 2H), −0.61 (ddd, ^2J(H,H) = 16.2 Hz, ^3J(H,H) = ^3J(H,H) = 7.3 Hz, 1H); ^{13}C NMR (100 MHz, [D$_8$]THF, 210 K): $\delta = 168.9$ (s), 143.8 (s), 140.4 (s), 137.7 (s), 128.8 (s), 125.7 (d), 53.0 (q), 36.8 (t), 34.9 (t), 20.3 (t), 19.3 (q); fluorescence excitation spectroscopy (THF, 298 K, Perkin Elmer LS-50): $\lambda_{em} = 500$ nm, $\lambda_{max} = 260$ nm, 330 nm, 390 nm.

Received: July 13, 1995 [Z 8209 IE]
German version: *Angew. Chem.* **1995**, *107*, 2728–2730

Keywords: cyclophanes · Dewar naphthalene · photochemistry · strained rings

[1] a) F. Bickelhaupt, *Pure Appl. Chem.* **1990**, *62*, 37; b) F. Bickelhaupt, W. H. de Wolf, *Adv. Strain Org. Chem.* **1993**, *3*, 185–227.

[2] L. W. Jenneskens, F. J. J. de Kanter, P. A. Kraakman, L. A. M. Turkenburg, W. E. Koolhaas, W. H. de Wolf, F. Bickelhaupt, Y. Tobe, K. Kakiuchi, Y. Odaira, *J. Am. Chem. Soc.* **1985**, *107*, 3716.

[3] a) V. V. Kane, A. D. Wolf, M. Jones, Jr., *J. Am. Chem. Soc.* **1974**, *96*, 2643; b) S. L. Kammula, L. D. Iroff, M. Jones, Jr., J. W. van Straten, W. H. de Wolf, F. Bickelhaupt, *ibid.* **1977**, *99*, 5815; c) Y. Tobe, K. Ueda, K. Kakiuchi, Y. Odaira, *Tetrahedron* **1986**, *42*, 1851.

[4] a) Y. Tobe, T. Kaneda, K. Kakiuchi, Y. Odaira, *Chem. Lett.* **1985**, 1301; b) G. B. M. Kostermans, W. H. de Wolf, F. Bickelhaupt, *Tetrahedron* **1987**, *43*, 2955.

[5] Y. Tobe, T. Takahashi, T. Ishikawa, M. Yoshimura, M. Suwa, K. Kobiro, K. Kakiuchi, R. Gleiter, *J. Am. Chem. Soc.* **1990**, *112*, 8889.
[6] A. U. Baldew, Dissertation, Vrije Universiteit, **1993**.
[7] a) R. Gleiter, B. Treptow, *J. Org. Chem.* **1993**, *58*, 7740; b) B. Treptow, Dissertation, Universität Heidelberg, **1992**. We thank Prof. Dr. Gleiter for communicating these results prior to publication.
[8] We thank Drs. S. J. Kok and Mr. H. Bulthuis for their technical assistance.
[9] Reference compound **6** was prepared from hexamethyl Dewar benzene in four steps. Steps 1 and 2: B. Freiermuth, J. Wirz, *Chimia*, **1985**, *39*, 22; steps 3 and 4 are analogous to the syntheses of **3** and **4**, respectively. **6**: white solid, m.p. 163–166 °C; ^{1}H NMR (400 MHz, [D$_8$]THF, 298 K): δ = 8.43 (s, 2H), 3.88 (s, 6H), 2.65 (s, 6H), 2.46 (s, 6H). ^{13}C NMR (100 MHz, [D$_8$]THF, 210 K): δ = 168.7 (s), 137.1 (s), 132.0 (s), 130.4 (s), 127.8 (d, J(C,H) = 161 Hz), 127.2 (s), 52.7 (q, J(C,H) = 147 Hz), 17.8 (q, J(C,H) = 126 Hz), 15.3 (q, J(C,H) = 126 Hz); high resolution MS: $C_{18}H_{20}O_4$ (M^+) calcd. m/z 300.1362, observed 300.1362 ± 0.0005; fluorescence excitation spectroscopy (THF, 298 K, Perkin Elmer LS-50): λ_{em} = 420 nm, λ_{max} = 260 nm, 310 nm, 351 nm.
[10] L. W. Jenneskens, Dissertation, Vrije Universiteit, **1986**.
[11] The signals were obscured by those of the solvent and/or of **4**.

Concave Reagents Based on Calixarenes**

Haymo Ross and Ulrich Lüning*

The high (stereo)selectivity of an enzyme is mainly caused by the concave environment of the active site. In comparison, reagents with simpler structures behave unselectively. According to the concept of concave reagents, the selectivity of standard reagents can be altered by placing them in a concave environment.[1, 2] Like a light bulb in a lamp shade, the functional group of the concave reagent is built into a bimacrocycle. Various synthetic pathways are used to prepare concave pyridines, phenanthrolines, benzoic acids, and thiolacetates.[2] The unit with the functional group, for example a pyridine ring,[1–3] is either first cyclized to give a monomacrocycle and then bridged to form a bimacrocycle, or it is converted directly into a bimacrocycle in a one-pot reaction. Often high-dilution conditions are necessary.

Our goal was to use a new strategy for the synthesis of concave reagents: An easily accessible macrocycle was to be bridged with a building block that contained the functional group. Calixarenes[4] are well suited for this purpose because they are easily accessible and can be bridged regioselectively. Examples for the bridging of *p-tert*-butylcalix[4]arene (**1**) have been known for quite some time,[5] and the bridging of the larger *p-tert*-butylcalix[6]arene (**2**) was reported recently.[6] Usually the bridges are either flexible aliphatic chains or polyether chains, or they are rigid units with geometries adjusted to the calixarenes **1** or **2**.[6–8] Acidic or basic functional groups in the bridges are the exception: an alkali metal complexing calix[4]arene containing a 2,6-dianisylpyridine bridge has been synthesized.[9] But it is not a concave base because its pyridine nitrogen atom is more accessible from the outside than from within the calixarene cavity.

Our attempts to bridge *p-tert*-butylcalix[4]arene with 2,6-bis(bromomethyl)pyridine (**3a**) led to a [2 + 2] cyclization product,

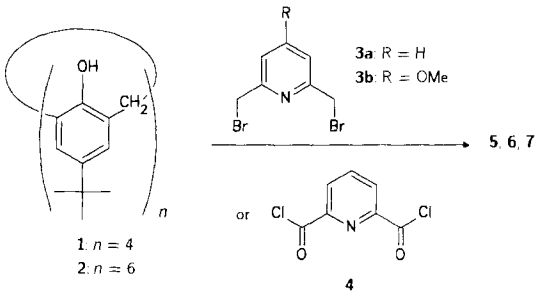

1: n = 4
2: n = 6

4

Scheme 1.

the biscalix[4]arene **5**. It is also not a concave base because the pyridine nitrogen atoms do not point exclusively into the calixarene cavity; they are also accessible from the sides.

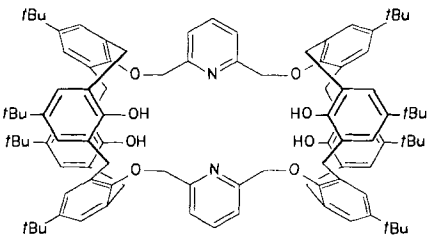

5

[1 + 1] Bridging with 2,6-bis(bromomethyl)pyridine (**3a**) and its methoxy derivative **3b** was successful when carried out with the larger *p-tert*-butylcalix[6]arene (**2**). The reactions of **2** and compounds **3** in the presence of an excess of potassium *tert*-butoxide gave the new concave bases **6** in initial yields of 36% (**6a**)

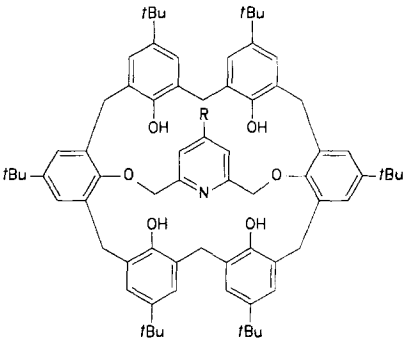

6a R = H
6b R = OMe

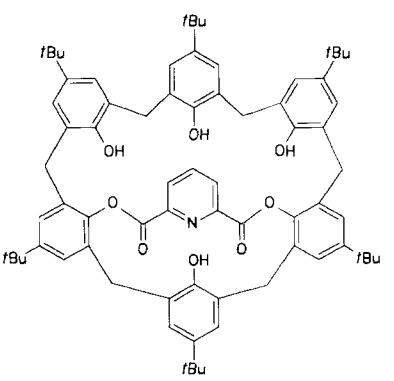

7

[*] Prof. Dr. U. Lüning, Dipl.-Chem. H. Ross
Institut für Organische Chemie der Universität
Olshausenstrasse 40, D-24109 Kiel (Germany)
Telefax: Int. code + (431)880-1558
e-mail: noc03@rz.uni-kiel.d400.de

[**] Concave Reagents, Part 16. We thank Mrs. G. Kohlmeyer-Yilmaz for carrying out the NMR titrations. Part 15: U. Lüning, M. Müller, M. Gelbert, K. Peters, H. G. von Schnering, M. Keller, *Chem. Ber.* **1994**, *127*, 2297–2306.

and 32% (**6b**) after several hours of stirring in THF at room temperature without high dilution. Better yields (55% and 51%, respectively) were obtained when the reaction was carried out in THF/DMF (9:1) at reflux with sodium hydride as base.

The ^{1}H NMR spectrum of **6a** indicates that it is an A,D-bridged[10] C_{2v}-symmetric calixarene. Since two conformers with this symmetry are conceivable, a NOESY spectrum was recorded to determine the conformation. The interactions H_a/H_d, H_b/H_d, H_c/H_f, and especially H_a/H_b show that all the phenyl rings of the calixarene are oriented *syn* (Fig. 1). The

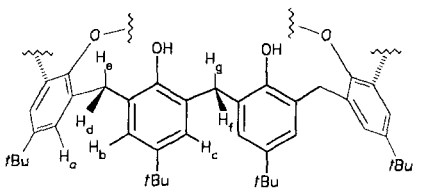

Fig. 1. Partial structure of **6a** to explain the NOE interactions.

differences in the chemical shifts ($\Delta\delta = 0.86$ and 0.61) of the AB doublets belonging to the methylene groups of the calixarene provide further support for the all-*syn* conformation.[11] The calixarene cavity is bridged by the pyridine moiety. The *tert*-butyl groups are located at the open side of the cavity; the nitrogen atom points into the cavity. Because the ^{1}H NMR data of **6b** are similar to those of **6a**, a concave geometry can also be assumed for **6b**.

In addition to the bromides **3a** and **3b**, pyridine-2,6-dicarboxylic acid dichloride (**4**) was also used to bridge *p-tert*-butylcalix[6]arene (Scheme 1). A solution of **2**, **4**, and potassium *tert*-butoxide was stirred for several days at room temperature to give the A,C-bridged calix[6]arene **7** in 24% yield. The yield could not be increased by altering the reaction conditions as was possible for **6a** and **6b**. To our knowledge, **7** is the first example of an A,C-bridged calix[6]arene obtained directly from **2**.[12] An A,D-bridged calix[6]arene could not be isolated after reaction with the dichloride **4**, and likewise no A,C-bridged calix[6]arene was obtained using the dibromides **3a** or **3b**. The low flexibility of **4** together with a change in reaction mechanism when the acid chloride **4** is used instead of an alkyl bromide **3** seems to be the reason for the difference in regioselectivity of the bridging process.

The addition of 4-nitrophenol to a solution of **6a** in [D$_1$]chloroform leads to shifts in the ^{1}H NMR signals, which can be explained by inclusion of the phenol in the cavity of **6a**. The singlet arising from the *tert*-butyl hydrogen atoms (54 H) at $\delta = 1.23$ splits into two singlets with a ratio of 2:1 at $\delta = 1.15$ and 1.23. This and shifts of the pyridine signals are in accordance with formation of a hydrogen bond. An association constant K_{ass} of 12 M^{-1} was determined by NMR titration ($CDCl_3$, 300 MHz, 25 °C) (Table 1). The more acidic, but bulkier 2-chloro-4-nitrophenol is bound less strongly, the phenols 2,6-dimethyl-4-nitrophenol and 2,4-dinitrophenol, which are even bulkier but have considerable differences in acidity, are not bound detectably. An excess of the latter two phenols leads to no significant changes in the ^{1}H NMR spectrum. The association constants can therefore only be estimated (< 1 M^{-1}); the exact values cannot be determined.

For comparison, the association of the nonconcave 2,6-dimethylpyridine with the phenols mentioned above was also investigated by NMR spectroscopy. The difference in the association constants of 2,6-dimethylpyridine with 4-nitrophenol and

Table 1. Association constants determined by NMR titration ($CDCl_3$, 300 MHz, 25 °C).

Phenol	K_{ass} [M^{-1}] with **6a**	K_{ass} [M^{-1}] with 2,6-dimethylpyridine
4-$NO_2C_6H_4OH$	12	13
2-Cl-4-$NO_2C_6H_3OH$	6	(2) [a]
2,4-$(NO_2)_2C_6H_3OH$	[b]	(3) [a]
2,6-$(CH_3)_2$-4-$NO_2C_6H_2OH$	[b]	5

[a] Larger shifts in the signals than in the other cases, probably due to partial protonation of 2,6-dimethylpyridine. [b] $K_{ass} < 1$; a more accurate value cannot be determined owing to the small shifts in the signals.

with 2,6-dimethyl-4-nitrophenol is smaller than in the case of **6a**. The association constants determined by titration of 2,6-dimethylpyridine with 2-chloro-4-nitrophenol and 2,4-dinitrophenol, however, cannot be compared with the others, because the detectable signal shifts are much larger ($\Delta\delta_{max}$ ca. 1.0 instead of 0.2) and indicate partial protonation of the 2,6-dimethylpyridine.

The differing behavior of **6a** with phenols with varying steric demand indicates that substrate specificity in base-catalyzed reactions may be possible. Calixarene **6a** was already used successfully as a catalyst in the base-catalyzed addition of alcohols to diphenylketene. To eliminate the influences of phenolic and therefore acidic hydroxyl groups of the calixarenes, investigations are now being carried out with tetra-*O*-alkyl derivatives of **6a** and **6b**.

Experimental Procedure

5: Under nitrogen, the *p-tert*-butylcalix[4]arene–toluene complex (**1** · toluene) [13b] (1.550 g, 2.092 mmol) was suspended with potassium carbonate (580.0 mg, 4.197 mmol) in 360 mL of acetonitrile. After addition of [18]crown-6 (27.6 mg, 0.104 mmol), the mixture was stirred for 30 min at 70 °C. Then a solution of **3a** (554.2 mg, 2.092 mmol) in 240 mL of acetonitrile was added dropwise over a period of 24 h, and the mixture was stirred for another 2 h at 70 °C. After evaporation of the solvents in vacuo, the residue was dissolved in 200 mL of dichloromethane. The solution was washed (60 mL of water, 60 mL of 1 N hydrochloric acid, 60 mL of water) and dried over magnesium sulfate. Column chromatography (silica gel 0.06–0.20 mm, dichloromethane) gave **5** in 52% yield as a colorless solid, m.p. > 350 °C (decomp). ^{1}H NMR (300 MHz, $CDCl_3$): $\delta = 1.08$ (s, 36 H, $C(CH_3)$), 1.28 (s, 36 H, $C(CH_3)_3$), 1.56 (br. s, < 6 H, H_2O), 3.37 (d, $J = 13.1$ Hz, 8 H, Ar-CH_2-Ar), 4.49 (d, $J = 13.1$ Hz, 8 H, Ar-CH_2-Ar), 5.16 (s, 8 H, -CH_2O-), 6.96 (s, 8 H, Ar*H*), 7.05 (s, 8 H, Ar*H*), 7.35 (t, $J = 7.9$ Hz, 2 H, 4-Py*H*), 7.97 (s, 4 H, O*H*), 8.33 (d, $J = 7.9$ Hz, 4 H, 3,5-Py*H*); IR (KBr): $\tilde{\nu} = 3406$ cm^{-1} (OH); MS (70 eV): *m/z* (%): 1502 (100, M^+); elemental analysis: $C_{102}H_{122}N_2O_8 \cdot 2H_2O$ (1504.09 + 36.02): calcd C 79.55, H 8.25, N 1.82; found C 79.84, H 8.02, N 1.80.

6a: Compound **2** [13a] (973 mg, 1.00 mmol) was added to a suspension of sodium hydride (250 mg, ca. 6.25 mmol; the dispersion in mineral oil (60%) was washed several times with *n*-pentane prior to use) in 100 mL of THF/DMF (9:1) under nitrogen. After 15 min of stirring at room temperature the mixture was heated at reflux. A solution of **3a** (318 mg, 1.20 mmol) in 30 mL of THF/DMF (9:1) was added dropwise, then the mixture was refluxed for another 15 h. After cooling, 5 mL of methanol and 40 mL of 0.1 N hydrochloric acid were added, and the mixture was extracted with 75 mL of chloroform. The aqueous layer was removed and the combined organic phases were dried with magnesium sulfate. Column chromatography (silica gel 0.06–0.20 mm, dichloromethane) of the crude product gave **6a** in 55% yield as a colorless solid, m.p. 215–219 °C (decomp). ^{1}H NMR (300 MHz, $CDCl_3$): $\delta = 1.23$ (s, 54 H, $C(CH_3)_3$), 1.61 (br. s, < 3 H, H_2O), 3.28 (d, $J = 14.4$ Hz, 2 H, Ar-CH_2-Ar), 3.57 (d, $J = 14.3$ Hz, 4 H, Ar-CH_2-Ar), 4.14 (d, $J = 14.4$ Hz, 2 H, Ar-CH_2-Ar), 4.18 (d, $J = 14.3$ Hz, 4 H, Ar-CH_2-Ar), 5.07 (s, 4 H, -CH_2-O-), 6.96 (d, $J = 2.4$ Hz, 4 H, Ar*H*), 7.09 (d, $J = 2.4$ Hz, 4 H, Ar*H*), 7.19 (s, 4 H, Ar*H*), 7.34 (d, $J = 7.7$ Hz, 2 H, 3,5-Py*H*), 7.71 (t, $J = 7.7$ Hz, 1 H, 4-Py*H*), 7.81 (s, 4 H, O*H*); IR (KBr): $\tilde{\nu} = 3344$ cm^{-1} (OH); MS (EI, 70 eV): *m/z* (%): 1075 (100, M^+); elemental analysis: $C_{73}H_{89}NO_6 \cdot H_2O$ (1076.51 + 18.01): calcd C 80.10, H 8.37, N 1.27; found C 79.93, H 8.20, N 1.21.

6b was obtained analogously: m.p. 284–288 °C (decomp); ^{1}H NMR (300 MHz, $CDCl_3$): $\delta = 1.22$ (s, 18 H, $C(CH_3)_3$), 1.23 (s, 36 H, $C(CH_3)_3$), 1.64 (< 6 H, H_2O), 3.29 (d, $J = 14.6$ Hz, 2 H, CH_2), 3.58 (d, $J = 14.2$ Hz, 4 H, CH_2), 3.86 (s, 3 H, CH_3), 4.12 (d, $J = 14.6$ Hz, 2 H, CH_2), 4.14 (d, $J = 14.2$ Hz, 4 H, CH_2), 4.97 (s, 4 H, -O-CH_2-), 6.87 (s, 2 H, Py*H*), 6.94 (d, $J = 2.5$ Hz, 4 H, Ar*H*), 7.09 (d, $J = 2.5$ Hz, 4 H, Ar*H*), 7.19 (s, 4 H, Ar*H*), 7.80 (s, 4 H, O*H*); IR (KBr): $\tilde{\nu} = 3384$ cm^{-1} (OH); MS

(EI, 70 eV): m/z (%): 1105.8 (100, M^+); elemental analysis: $C_{74}H_{91}NO_7 \cdot 0.5H_2O$ (1106.54 + 9.01): calcd C 79.67, H 8.31, N 1.26; found C 79.79, H 8.27, N 1.31.

7: Under nitrogen, **2** [13a] (973 mg, 1.00 mmol) and potassium *tert*-butoxide (741 mg, 6.60 mmol) were stirred for 20 min in 100 mL of THF. Then a solution of **4** (245 mg, 1.20 mmol) in 20 mL of THF was added dropwise. The mixture was stirred for 48 h at room temperature. The reaction was quenched by adding 10 mL of 1 N hydrochloric acid. After evaporation of the solvents in vacuo, the residue was dissolved in 150 mL of dichloromethane. The solution was washed with 60 mL of 1 N hydrochloric acid and twice with 50 mL of water, and was dried over magnesium sulfate. Column chromatography (silica gel 0.06–0.20 mm, dichloromethane) gave **7** in 24% yield as a colorless solid, m.p. 280–284 °C (decomp). ^{1}H NMR (300 MHz, $CDCl_3$): δ = 1.05 (s, 9H, $C(CH_3)_3$), 1.18 (s, 9H, $C(CH_3)_3$), 1.24 (s, 18H, $C(CH_3)_3$), 1.27 (s, 18H, $C(CH_3)_3$), 1.92 (s, ca. 6H, H_2O), 3.34 (d, J = 13.9 Hz, 2H, CH_2), 3.37 (d, J = 16.4 Hz, 2H, CH_2), 3.48 (d, J = 14.0 Hz, 2H, CH_2), 3.75 (d, J = 16.2 Hz, 2H, CH_2), 3.89 (d, J = 13.9 Hz, 2H, CH_2), 4.49 (d, J = 13.9 Hz, 2H, CH_2), 5.22 (s, 1H, OH), 6.68 (d, J = 2.4 Hz, 2H, Ar*H*), 6.77 (s, 2H, Ar*H*), 7.02 (d, J = 2.5 Hz, 2H, Ar*H*), 7.06 (s, 2H, Ar*H*), 7.18 (d, J = 2.4 Hz, 2H, Ar*H*), 7.41 (d, J = 2.4 Hz, 2H, Ar*H*), 7.81 (s, 2H, O*H*), 8.22 (t, J = 7.8 Hz, 1H, 4-Py*H*), 8.56 (d, J = 7.8 Hz, 2H, 3,5-Py*H*), 8.89 (s, 1H, O*H*); IR (KBr): $\tilde{\nu}$ = 3342 cm^{-1} (OH), 1750 (C=O); MS (EI, 70 eV): m/z (%): = 1103.6 (100, M^+); elemental analysis: $C_{73}H_{85}NO_8 \cdot 3H_2O$ (1104.48 + 54.03): calcd C 75.68, H 7.92, N 1.21; found C 75.38, H 7.61, N 1.19.

Received: April 12, 1995
Revised version: August 28, 1995 [Z 7889 IE]
German version: *Angew. Chem.* **1995**, *107*, 2723–2725

Keywords: calixarenes · concave reagents · macrocycles · supramolecular chemistry

[1] U. Lüning, *Liebigs Ann. Chem.* **1987**, 949–955.
[2] U. Lüning, *Top. Curr. Chem.* **1995**, *175*, 57–99, and references therein.
[3] a) U. Lüning, R. Baumstark, M. Müller, *Liebigs Ann. Chem.* **1991**, 987–998; b) U. Lüning, R. Baumstark, W. Schyja, *Tetrahedron Lett.* **1993**, *34*, 5063–5066.
[4] a) C. D. Gutsche, *Calixarenes*, The Royal Society of Chemistry, Cambridge, **1989**; b) *Calixarenes, a Versatile Class of Macrocyclic Compounds* (Eds.: J. Vicens, V. Böhmer), Kluwer Academic, Dordrecht, **1991**; c) V. Böhmer, *Angew. Chem.* **1995**, *107*, 785–818; *Angew. Chem. Int. Ed. Engl.* **1995**, *34*, 713–745.
[5] C. Alfieri, E. Dradi, A. Pochini, R. Ungaro, G. D. Andreetti, *J. Chem. Soc. Chem. Commun.* **1983**, 1075–1077.
[6] a) S. Kanamathareddy, C. D. Gutsche, *J. Am. Chem. Soc.* **1993**, *115*, 6572–6579; b) H. Otsuka, K. Araki, S. Shinkai, *J. Org. Chem.* **1994**, *59*, 1542–1547; c) A. Casnati, P. Jacopozzi, A. Pochini, F. Ugozzoli, R. Cacciapaglia, L. Mandolini, R. Ungaro, *Tetrahedron* **1995**, *51*, 591–598.
[7] D. N. Reinhoudt, P. J. Dijkstra, P. J. A. in't Veld, K. E. Bugge, S. Harkema, R. Ungaro, E. Ghidini, *J. Am. Chem. Soc.* **1987**, *109*, 4761–4762.
[8] J.-D. van Loon, D. Kraft, M. J. Ankoné, W. Verboom, S. Harkema, W. Vogt, V. Böhmer, D. N. Reinhoudt, *J. Org. Chem.* **1990**, *55*, 5176–5179.
[9] P. J. Dijkstra, J. A. J. Brunink, K.-E. Bugge, D. N. Reinhoudt, S. Harkema, R. Ungaro, F. Ugozzoli, E. Ghidini, *J. Am. Chem. Soc.* **1989**, *111*, 7567–7575.
[10] A,D-bridging is defined as the connection of two opposite phenol rings of a calix[6]arene. Thus A,C-bridging is the connection of the first and third rings. The terms 1,4-bridging and 1,3-bridging are often used but do not correspond to the numbering of the calix[6]arene oxygen atoms (37–42).
[11] S. Kanamathareddy, C. D. Gutsche, *J. Org. Chem.* **1994**, *59*, 3871–3879.
[12] The synthesis of A,C-bridged and A,C,E-capped calix[6]arenes was reported but they were not synthesized in a single step from *p-tert*-butylcalix[6]arene (**2**): a) H. Otsuka, K. Araki, H. Matsumoto, T. Harada, S. Shinkai, *J. Org. Chem.* **1995**, *60*, 4862–5867; b) K. Araki, K. Akao, H. Otsuka, K. Nakashima, F. Inokuchi, S. Shinkai, *Chem. Lett.* **1994**, 1251–1254; c) R. G. Janssen, W. Verboom, J. P. M. van Duynhoven, E. J. J. van Velzen, D. N. Reinhoudt, *Tetrahedron Lett.* **1994**, *35*, 6555–6558.
[13] a) C. D. Gutsche, B. Dhawan, M. Leonis, D. Stewart, *Org. Synth.* **1990**, *68*, 238–242; b) C. D. Gutsche, M. Iqbal, *ibid.* **1990**, *68*, 234–237.

Synthesis and Structure of the Three-Dimensional Coordination Polymers $[(Me_3Sn)_4M(CN)_8]$ (M = Mo, W)**

J. Lu, W. T. A. Harrison, and A. J. Jacobson*

Three-dimensional polymers formed by coordination between inorganic units and organic or organometallic ligands have been closely studied.[1–5] These materials can form porous structures with channels that are potentially tunable by changing the building unit sizes or functional groups. A large number of compounds with three-dimensional structures formed by connecting metal cyanide anions with organotin cations $(R_3Sn)^{3+}$ have been synthesized and studied in some detail;[1] however, limited structural information is available. The metal ions in these three-dimensional polymers are either octahedrally coordinated (e.g. $[M(CN)_6]^{3-}$, M = Co, Fe, Ru, Os; $[M(CN)_6]^{4-}$, M = Fe, Ru, Os)[1] or tetrahedrally coordinated (e.g. $[Cu(CN)_4]^{3-}$).[3] A previous attempt to use the $[Mo(CN)_8]^{4-}$ and $[W(CN)_8]^{4-}$ anions to form single crystals of the title compounds was apparently not successful.[2]

The structure of the building unit $[M(CN)_8]^{4-}$ can be either dodecahedral (e.g. $K_4[Mo(CN)_8]$) or square antiprismatic (e.g. $H_4[W(CN)_8]$) depending on the counterion.[6] Either geometry can lead to the formation of three-dimensional structures that differ considerably from those obtained with octahedrally or tetrahedrally coordinated metal cyanide ions. We report here on the synthesis, structure, and preliminary characterization of the coordination polymers **1**-*n*THF and **2**-*n*THF. The compounds **1** and **2** are formed in a straightforward way by the reaction given in Equation (a).

$$K_4M(CN)_8 + 4Me_3SnCl \xrightarrow{H_2O/THF} [(Me_3Sn)_4M(CN)_8] \quad \text{(a)}$$
1, M = Mo
2, M = W

Polymers of the type $[(R_3E)_nM(CN)_{2n}]$ (E = Sn or Pb) with n = 4 have been proposed previously but synthesis attempts led to the formation of layered compounds, for example, $[(Me_3Sn)_2MoO_4]$, presumably due to molybdenum oxidation in air.[2] When the reactions were carried out in sealed tubes, **1** and **2** formed without difficulty. In a comparison experiment carried out in an open tube, colorless crystals were formed that were shown by single-crystal X-ray diffraction to have the same unit cell as $[(Me_3Sn)_2MoO_4]$.

Infrared C–N stretches in compound **1** (2143 (s), 2105 (w, sh) cm^{-1}) and **2** (2141 (s), 2105 (w, sh) cm^{-1}) are blue shifted from those of $K_4[Mo(CN)_8]$ (2102 (s), 2125 (s) cm^{-1}) and $K_4[W(CN)_8]$ (2096 (s), 2127(s) cm^{-1}). Small weak shoulders are also observed at $\approx$2105 cm^{-1} in both **1** and **2**. Metal cyanide–organotin compounds typically show this behavior.[1] The Me_3Sn group is a Lewis acid and is unable to π back-bond and consequently the C–N stretching frequency increases on coordination.[7]

The structures of **1** and **2** were determined by single-crystal X-ray diffraction.[8] The compounds **1** and **2** are isostructural and have similar cell dimensions. Elemental analysis results in-

[*] Prof. A. J. Jacobson, Dr. J. Lu, Dr. W. T. A. Harrison
Department of Chemistry, University of Houston
Houston, TX 77204-5641 (USA)
Telefax: Int. code + (713)743-2787

[**] This material is based in part on work supported by the Texas Advanced Research Program under grant No. 003652-048. We also thank the Robert A. Welch Foundation for support of this work and Dr. James Korp for help with crystallography.

dicated that the disordered interstitial solvent molecules are THF.[9] In the structures of **1** and **2**, every $M(CN)_8$ group is connected through Me_3Sn bridges to eight $M(CN)_8$ groups which form the corners of a body-centered tetragonal unit cell (Fig. 1). The $M(CN)_8^{4-}$ unit rearranges from the dodecahedral structure of the starting $K_4M(CN)_8$ compounds[10] to square

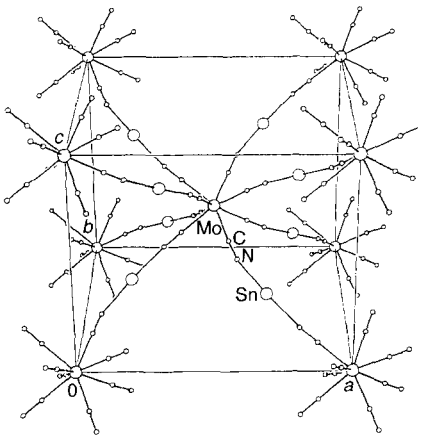

Fig. 1. A view of the unit cell of **1**. The methyl groups are omitted for clarity.

antiprismatic geometry in the final products. The M–C and C–N bond lengths remain the same within experimental error. The N–Sn distances (2.335(5) Å and 2.32(1) Å for **1** and **2**, respectively) are comparable to those in similar compounds such as $[(Me_3Sn)_3Co(CN)_6]$[1] (av. 2.32 Å) and $[(nBu_4N)(Et_3Sn)_2Cu(CN)_4]$[3] (av. 2.33 Å). The local coordinations of the $Mo(CN)_8$ and Me_3Sn units are shown in Figure 2.

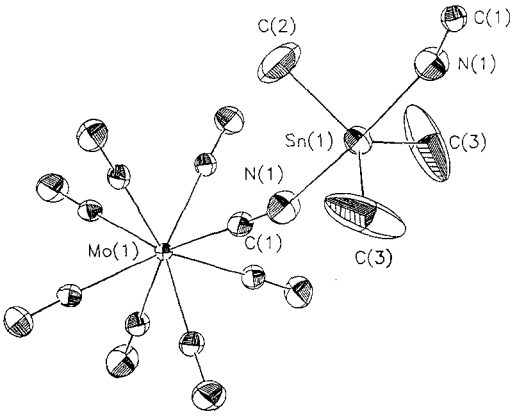

Fig. 2. ORTEP drawing of the local coordination environments of the molybdenum and tin atoms in **1**.

Compounds **1** and **2** crystallize in the chiral space group *I*422. Every Sn-$M(CN)_8$ unit is equivalent and has the same chirality. When one looks down the fourfold axis (Fig. 3 top), the tin atoms appear in pairs, with two tin atoms in each pair closer to each other in the projection. The top molybdenum to tin vectors rotate to the right to overlap with the corresponding vectors at the bottom of the projection. Thus, the chirality of the local arrangement around the molybdenum or tungsten atoms in **1** and **2** can be described as right-handed.

The structures of **1** and **2** can be compared with other compounds of this general type, $[(R_3E)_nM(CN)_{2n}]$ (E = Sn, Pb), where the metal coordination is tetrahedral ($n = 2$) or octahedral ($n = 3$). The structure of polymeric compound with $n = 2$,

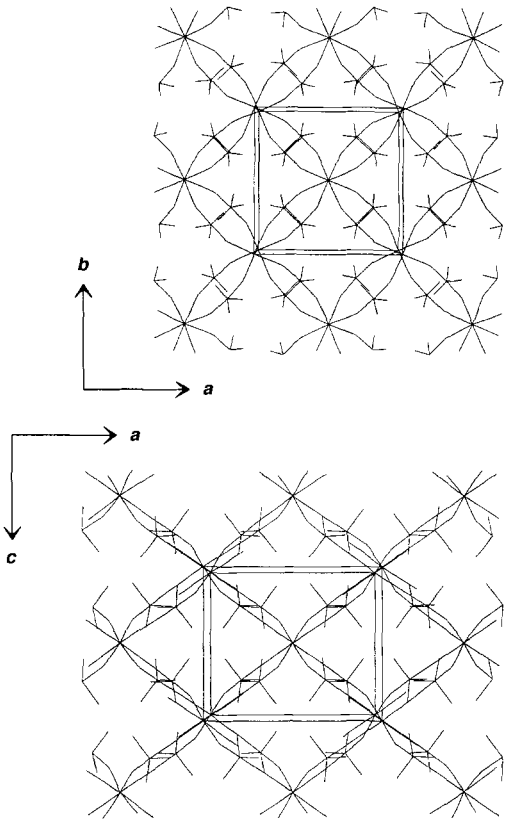

Fig. 3. Views of the structure of **1** along the crystallographic *c* axis (top) and along the crystallographic *b* axis (bottom).

$[(nBu_4N)(Et_3Sn)_2Cu(CN)_4]$, has a distorted diamond-type network but with a more compact lattice than the ideal diamondoid framework.[3] The compounds with $n = 3$, $[(Me_3E)_3Co(CN)_6]$ (E = Sn, Pb), have three-dimensional structures with cavities smaller than the ideal "super-Prussian-blue" structure and do not include guest molecules.[1] In both cases the networks condense by bending the E-N-C angles away from 180°. The minimum values of the E-N-C angle in the above-mentioned structures range from 125° to 149.3°. Similarly, the C-N-Sn angles in **1** and **2** (163.7(5)° and 166.0(9)°, respectively) also deviate from 180° but are closer to the ideal value. The views of the structure along the principal crystallographic axes (Fig. 3) show the channels in the network. A space-filling model shows that the methyl groups block the channels along the *a* and *b* axes, but along the *c* axis an open channel of about 2.8×2.8 Å^2 remains. If we regard the methyl groups as not rigidly fixed, the maximum size of the channel along *c* is about 6.0×6.0 Å^2 and the size of channels along *a* and *b* is about 7.1×5.2 Å^2. The channels are occupied by disordered THF solvent molecules.

Unlike the networks formed by porphyrin building blocks,[4] the framework is retained upon removing some of the solvent molecules. Thermogravimetric analysis of **1** showed a slow weight loss below 200 °C as the temperature was increased. The residues from heating samples of either **1** or **2** to 185 °C for 2 h retained the same structure as shown by X-ray powder diffraction. At temperatures above 225 °C, the rate of weight loss increased and a powder pattern for a tungsten sample heated to 250 °C indicated decomposition and loss of the original structure. No reabsorption of THF or absorption of *n*-hexane or dichloromethane was observed at room temperature by samples that had been outgassed at 185 °C indicating that even at this temperature some surface decomposition must occur.

Experimental Procedure

$K_4[Mo(CN)_8]$ (0.496 g, 1 mmol) or $K_4[W(CN)_8]$ (0.584 g, 1 mmol) was dissolved in distilled water (10 mL) and was placed in a 30 mL screw-capped culture tube. A 5 mL mixture of 1:1 water/THF was carefully layered onto this solution as a protection layer and 5 mL of a 1.0 M THF solution of Me_3SnCl was layered on the very top. The tube was left undisturbed and capped. Slow diffusion of Me_3SnCl into $K_4[M(CN)_8]$ (M = Mo, W) solutions resulted in the formation of yellow block-shaped crystals at the interface in about a week. When interdiffusion was allowed to procede to completion and the product washed and dried, yields of 0.8816 g of the molybdenum compound **1** (92% based on formula $[(Me_3Sn)_4Mo(CN)_8]$) or 1.0273 g of the tungsten compound **2** (98% based on formula $[(Me_3Sn)_4W(CN)_8]$) were obtained. The powder X-ray patterns of the bulk solids were the same as patterns simulated by using the single-crystal structure data. The products are insoluble in most common solvents and indefinitely stable in air.

Received: July 13, 1995 [Z82101E]
German version: *Angew. Chem.* **1995**, *107*, 2759–2760

Keywords: cyanides · molybdenum compounds · polymers · tin compounds · tungsten compounds

[1] U. Behrens, A. K. Brimah, T. M. Soliman, R. D. Fischer, D. C. Apperley, N. A. Davies, R. K. Harris, *Organometallics* **1992**, *11*, 1718, and references therein.
[2] U. Behrens, A. K. Brimah, K. Yunlu, R. D. Fischer, *Angew. Chem.* **1993**, *105*, 117; *Angew. Chem. Int. Ed. Engl.* **1993**, *32*, 82.
[3] A. K. Brimah, F. Siebel, R. D. Fischer, N. A. Davies, D. C. Apperley, R. K. Harris, *J. Organomet. Chem.* **1994**, *475*, 85.
[4] B. F. Abrahams, B. F. Hoskins, D. M. Michall, R. Robson, *Nature*, **1994**, *369*, 727; B. F. Abrahams, M. J. Hardie, B. F. Hoskins, R. Robson, E. E. Sutherland, *J. Chem. Soc. Chem. Commun.* **1994**, 1049; B. F. Hoskins, R. Robson, *J. Am. Chem. Soc.* **1990**, *112*, 1546; B. F. Abrahams, B. F. Hoskins, J. Liu, R. Robson, *J. Am. Chem. Soc.* **1991**, *113*, 3045.
[5] K. M. Park, T. Iwamoto, *J. Incl. Phenom.* **1991**, *11*, 397; S. Nishikiori, T. Hasegawa, T. Iwamoto, *ibid.* **1991**, *11*, 137.
[6] A. G. Sharpe in *Comprehensive Coordination Chemistry, Vol. 2* (Eds.: G. Wilkinson, R. D. Gillard, J. A. McCleverty), Pergamon Press, New York, **1987**, p. 11.
[7] K. F. Purcell, R. S. Drago, *J. Am. Chem. Soc.* **1966**, *88*, 919; D. F. Shriver, J. Posner, *ibid.* **1966**, *88*, 1672.
[8] **1**·2THF: $M = 1103.58$, space group $I\bar{4}22$, $a = 13.191(2)$, $c = 11.448(2)$ Å, $V = 1992.1(6)$ Å^3, $Z = 2$, $\rho_{calcd} = 1.84$ g cm^{-3}, $-50(2)$ °C, 823 reflections with $I > 3\sigma$, $R(F) = 0.0226$ and $R_w(F) = 0.0311$. The structure was solved by the direct-methods (software: SHELXS-86). All the atoms were refined anisotropically except the site attributed to the disordered THF molecule (software: CRYSTALS). **2**·2THF: $M = 1191.49$, space group $I\bar{4}22$, $a = 13.182(2)$, $c = 11.434(2)$ Å, $V = 1987.2(7)$ Å^3, $Z = 2$, $\rho_{calcd} = 1.99$ g cm^{-3}, $-50(2)$ C, 746 reflections with $I > 3\sigma$, $R(F) = 0.0386$ and $R_w(F) = 0.0372$. The structure was solved and refined in similar fashion to **1**. Further details of the crystal structure investigation may be obtained from the Director of the Cambridge Crystallographic Data Centre, 12 Union Road, GB-Cambridge CB2 1EZ (UK), on quoting the full journal citation.
[9] Elemental analysis: **1**·1.61THF calculated: C 29.52, H 4.55, N 10.42, Sn 44.18, Mo 8.93; found: C 29.48, H 4.57, N 10.40, Sn 43.9, Mo 8.91. **2**·1.08 THF calculated: C 25.95, H 3.97, N 9.96, Sn 42.2, W 16.4; found: C 25.90, H 3.91, N 9.72, Sn 41.8, W 16.0 (calculated based on oxygen analysis and by difference).
[10] J. L. Hoard, H. H. Nordsieck, *J. Am. Chem. Soc.* **1939**, *61*, 2853.

Te_8^{4+}: A Cubic Polycation in the Structure of $Te_8(VOCl_4)_2$

Johannes Beck* and Gunter Bock

Tellurium does not exhibit the allotropic diversity of the lighter homologues sulfur and selenium; under normal conditions, only one stable modification of tellurium is known. However, very recent discoveries have shown the existence of neutral, eight-membered tellurium rings in the polytelluride Cs_3Te_{22}.[1] In comparision to this structural paucity, polyanionic[2] and polycationic[3] forms of tellurium abound and exhibit an unusually rich and varied structural chemistry.

Polycations of tellurium can be obtained either through selective oxidation of the element itself, or through Lewis acid base reactions of suitable halide ion acceptors with the subhalides of tellurium. To date, the ions Te_4^{2+},[4] Te_6^{2+},[5] Te_6^{4+},[6] $[Te_7^{2+}]_n$,[7] and Te_8^{2+}[8] have been characterized. The halides and halide oxides of the elements in group 7, that is niobium and tantalum, have proven to be suitable Lewis acids; the weak basic character of anions obtained from these compounds suffices to stabilize the polycations of tellurium as for example in $Te_4^{2+}(Nb_2OCl_{10}^{2-})$,[9] $Te_4^{2+}(TaCl_6^-)_2$,[10] and $Te_7^{2+}(NbOX_4^-)(X^-)$ (X = Cl, Br).[11] We have extended these reactions to include the chloride oxide of pentavalent vanadium. The reaction of elemental tellurium with $VOCl_3$ in a temperature gradient of 190 to 170 °C leads to **1**, in the form of black, rodlike crystals.

$Te_8(VOCl_4)_2$ **1**

An X-ray structure analysis[12] shows that **1** contains one-dimensional polymeric $VOCl_4^{2-}$ chains and strands of Te_8^{4+} ions. The $VOCl_4^{2-}$ chains lie along a 4_1 screw axis and the cationic chains along a $\bar{4}$ inversion axis. The chains of cations and anions in the structure are arranged in the sense of a tetragonal rod-packing. Figure 1 shows the unit cell of **1**; the structure of the Te_8^{4+} polycations and a section of the polymeric $VOCl_4^{2-}$ chain are depicted in Figure 2. The $VOCl_4^{2-}$ chains contain square-pyramidal $VOCl_4$ units, which show an approximate C_{4v} symmetry and are linked together through shared oxygen atoms to give linear chains. The $VOCl_4$ units are eclipsed, similar to the

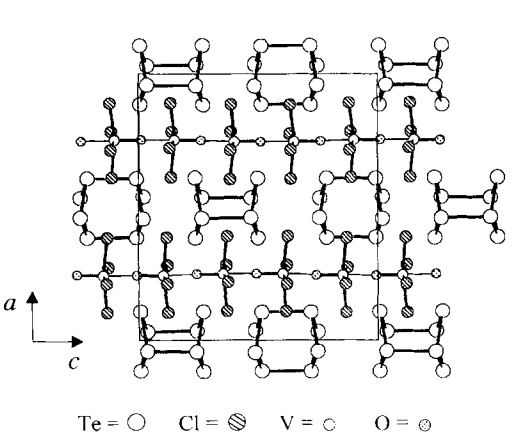

Fig. 1. A view of the unit cell of **1** along [010].

[*] Prof. Dr. J. Beck, Dr. G. Bock
Institut für Anorganische und Analytische Chemie der Universität
Heinrich-Buff-Ring 58, D-35392 Giessen (Germany)
Telefax: Int. code + (641)702-5661
e-mail: beck@beck.anorg.chemie.uni-giessen.de

[**] This work was supported by the Deutsche Forschungsgemeinschaft and the Fonds der Chemischen Industrie.

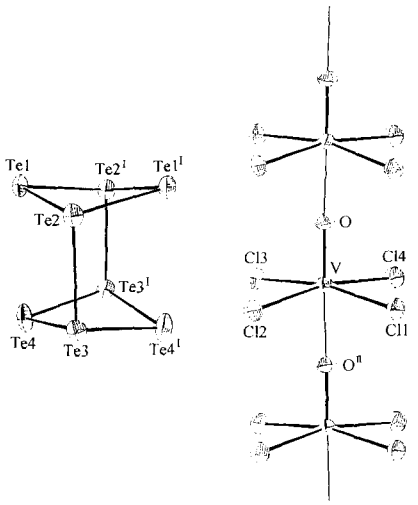

Fig. 2. The Te_8^{2+} polycation and a section of the polymeric $VOCl_4^{2-}$ chain in the structure of **1** (thermal ellipsoids drawn at the 70% probability level). Symmetry operations: I $= -x+1, -y+1/2, z$; II $= y+3/4, -x+3/4, z-1/4$; selected bond lengths [pm] and angles [°]: Te(1)–Te(2) 278.5(1), Te(1)–Te(2^{I}) 276.2(1), Te(2)–Te(3) 301.0(1), Te(3)–Te(4) 274.8(1), Te(3)–Te(4^{I}) 274.3(1); Te(2)-Te(1)-Te(2^{I}) 87.51(2), Te(1)-Te(2)-Te(1^{I}) 89.91(2), Te(1)-Te(2)-Te(3) 99.18(2), Te(3)-Te(4)-Te(3^{I}) 88.48(2), Te(4)-Te(3)-Te(4^{I}) 88.84(2), Te(2)-Te(3)-Te(4) 98.16(2); V-O 161.8(4), V-O^{II} 205.1(4), V-Cl(1) 239.9(2), V-Cl(2) 238.2(2), V-Cl(3) 238.1(2), V-Cl(4) 239.4(2); O-V-O^{II} 178.3(2), O-V-Cl 95.0(2) to 96.5(2).

situation found in the structure of $WOCl_4$.[13] The short V=O distance (162 pm) indicates the presence of a double bond, the long V···O^{II} distance (205 pm) a weak, coordinative bond. The V–Cl bond lengths differ only slightly; they lie between 238 and 240 pm. That the vanadium center in **1** is present in the + IV oxidation state was confirmed by a magnetic measurement, which delivered the paramagnetism expected from one unpaired electron per vanadium ion. The reciprocal susceptibility is a nearly linear function of the temperature between 76 and 295 K. The Curie–Weiss constant is + 5 K and the magnetic moment is 1.84 μ_B. Thus, **1** contains a polymeric $^{1}_{\infty}[VOCl_4^{2-}]$ dianion. This is confirmed by comparing the bond lengths in **1** with those in $[(C_6H_5)_4As][VOCl_4]$,[14] which contains a monomeric, square-pyramidal $VOCl_4^{-}$ anion with ideal C_{4v} symmetry; the vanadium is present in the + V oxidation state. The V=O bond length of 155 pm and the V–Cl distance of 226 pm are, as expected, considerably shorter than those for the polymeric $^{1}_{\infty}[VOCl_4^{2-}]$ ion of **1**.

The Te_8^{4+} ions in **1**, which deviate only slightly from cubic symmetry, are built up from two Te_4 rings that are linked together through two slightly elongated (301 pm) Te–Te bonds. The Te–Te distances (between 274 and 279 pm) in the four-membered rings lie in the range of Te–Te single bonds; the distances Te1–Te4 and Te1^{I}–Te4^{I} are 385 pm and lie on the upper limit of significant interactions. The four three-bonded, ψ-tetrahedrally coordinated Te atoms that connect the two four-membered rings each have a formal positive charge according to the Zintl–Klemm[15] concept.

The Te1 and Te1^{I} atoms are 359 pm apart as are the Te2 and Te2^{I} atoms in neighboring Te_8^{4+} ions. Single Te_8^{4+} ions are thus paired through weak interactions along the strand. These additional Te–Te interactions compensate the lengthening of the two bonds bridging the two four-memberd rings contained in a single Te_8^{4+} unit. A similar lengthening of the transannular bonds to 299 pm is observed in the bicyclic Te_8^{2+} ions found in **2**.[8] Further Te atoms become partially bonded to three centers

$Te_8(WCl_6)_2$ **2**

through the pairwise association of ions in the strands in **1** and through association into undulating chains in **2**, thus allowing the positive charge to be delocalized over several atoms in the polycations.

The typical chalcogen–halogen contacts in compounds containing chalcogen polycations and halogenometalate anions are also present in **1**. In fact, because of the high charge density present in Te_8^{4+} ions, an uncommonly large number of cation–anion interactions are found in **1**. Up to a limit of 370 pm, thus, a distance which lies well below the sum of the van der Waals radii of Te and Cl (400 pm),[16] 24 such contacts are found in the structure of **1**; however, only 14 such contacts are present in structure **2**.

The structure of this new Te_8^{4+} ion in **1** can be derived from already known structures of metals, or from structures of tellurium polycations (Fig. 3). The distorted cubic form of the Te_8^{4+} ion suggests that it is derived from the α-Po structure. If the

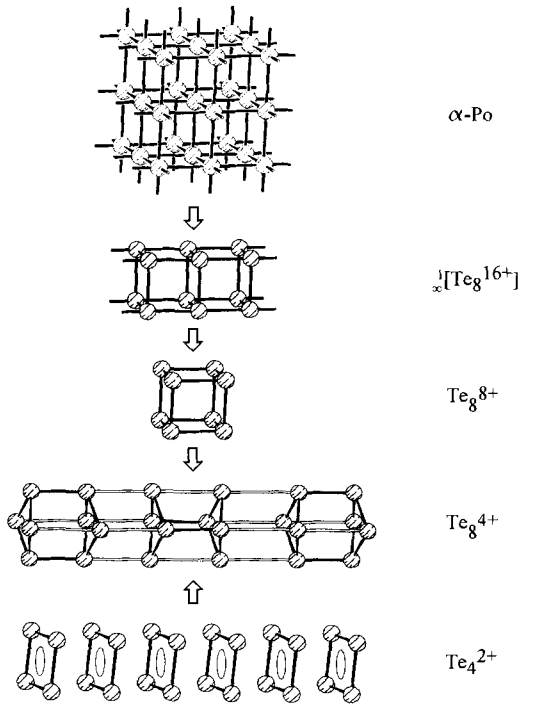

Fig. 3. The structure of the Te_8^{2+} polycation can be derived from the α-Po structure. Through systematic decreases in the number of bonds formed to Te, the Te_8^{4+} ion can be obtained via the hypothetical intermediate species $^{1}_{\infty}[Te_8^{16+}]$ and Te_8^{8+}. An alternative derivation assumes a stack of equidistant Te_4^{2+} ions, which are paired together in the sense of a Peierls distortion.

connectivity of the Te atoms in the three-dimensional network were to be decreased from six to four by removal of electrons, a hypothetical, one-dimensional polymeric $^{1}_{\infty}[Te^{16+}]$ ion would result in which each Te atom is four-bonded and carries a + 2 charge. The structure of this hypothetical polycation shows a considerable similarity to the strandlike structure of the Te_8^{4+} ions in **1**. The next step would then be to break Te–Te bonds by the introduction of pairs of electrons; thus leading to the as yet unknown monomeric Te_8^{8+} ion. This cubic ion is built up of eight three-bonded Te atoms, each carrying a single positive charge. If two opposite edges of the Te_8 cube are then stretched by addition of two pairs of electrons, the number of bonds per Te atom in the cube is further decreased and the Te_8^{4+} ion results, in which only four Te atoms are three-bonded. However, if the Te_8^{4+} ion is considered to be constructed of two four-membered

Te rings linked through two Te–Te bonds, an alternative possibility for the derivation of its structure exists. Pairing, in the sense of a Peierls distortion, occurs in strands of Te_4^{2+} ions arranged parallel and equidistant. The delocalized double bond character in the Te_4^{2+} ions is lost through the formation of inter-ion bonds, resulting in $(Te_4^{2+})_2$ pairs with localized bonding. Associated with this is the increase in the bond lengths in the four-membered rings from 267 pm in Te_4^{2+} to 274 pm in Te_8^{4+} and the loss of planarity. However, as yet, dimerization of Te_4^{2+} ions has not been observed.

Discrete Te_4^{2+} ions are found in conjunction with a multitude of counterions, however, not with one-dimensional polyanions. Undoubtedly, the formation of Te_8^{4+} ions is favored by the rigid framework provided by the polymeric $^1_\infty[VOCl_4^{2-}]$ counterion.

Experimental Procedure

A 15 cm-long glass ampoule with a diameter of 1.5 cm was freed from adsorbed moisture by heating in vacuo. The ampoule was then flushed with argon and filled with Te (0.65 g, 5.1 mmol). $VOCl_3$ (0.2 mL) was then added with a syringe. The ampoule was then cooled with liquid nitrogen, evacuated, and sealed, and subsequently heated for five hours at 200 °C in a horizontal tube furnace. During this heating process, green $VOCl_2$ powder and black crystals of Te_3Cl_2 were formed. These products were then melted together at 270 °C, and the ampoule was again placed in a horizontal position and a temperature gradient of 170 to 190 °C was applied. The melt was located at the warmer end of the temperature gradient. After a week, black, tetragonal, rodlike crystals of **1** were deposited at the cooler end of the ampoule. The yield was approximately 70%.

Received: July 14, 1995 [Z8212IE]
German version: *Angew. Chem.* **1995**, *107*, 2739–2741

Keywords: main group element clusters · polycations · solid-state structures tellurium compounds

[1] W. S. Sheldrick, M. Wachhold, *Angew. Chem.*, **1995**, *107*, 490; *Angew. Chem. Int. Ed. Engl.* **1995**, *34*, 450
[2] P. Böttcher, *Angew. Chem.* **1988**, *100*, 781; *Angew. Chem. Int. Ed. Engl.* **1988**, *27*, 759
[3] J. Beck, *Angew. Chem.* **1994**, *106*, 172; *Angew. Chem. Int. Ed. Engl.* **1994**, *33*, 163
[4] T. W. Couch, D. A. Lokken, J. D. Corbett, *Inorg. Chem.*, **1972**, *11*, 357
[5] J. Beck, *Chem. Ber.* **1995**, *128*, 23
[6] R. C. Burns, R. J. Gillespie, W. C. Luk, D. R. Slim, *Inorg. Chem.* **1979**, *18*, 3086
[7] J. Beck, *Angew. Chem.* **1991**, *103*, 1149; *Angew. Chem. Int. Ed. Engl.* **1991**, *30*, 1128
[8] J. Beck, *Angew. Chem.* **1990**, *102*, 301; *Angew. Chem. Int. Ed. Engl.* **1990**, *29*, 293
[9] M. J. Collins, R. J. Gillespie, J. W. Kolis, J. F. Sawyer, *Acta Crystallogr.* Sect. C, **1987**, *43*, 2033
[10] J. Beck, G. Bock, *Z. Naturforsch.*, **1995**, in press.
[11] J. Beck, G. Bock, *Z. Anorg. Allg. Chem.* **1994**, *620*, 1971.
[12] X-ray structure analysis of **1**: Crystal dimensions: $0.45 \times 0.05 \times 0.05$ mm^3, crystal system: tetragonal, $I4_1/a$, cell constants: $a = 1643.1(6)$, $c = 1467.1(4)$ pm, $V = 3960.8 \times 10^6$ pm^3, $\rho_{calcd} = 4.83$ g cm^{-3}, $2\theta max = 56°$, $Mo_{K\alpha}$ radiation, $\lambda = 71.073$ pm, STOE IPDS area detection diffractometer, $T = 298$ K, 17056 measured reflections, 2367 independent reflections, numerical absorption correction, $\mu = 128.2$ cm^{-1}, direct methods (SHELXS 86 [17]), least squares fit based on F^2 (SHELXL 93 [18]), 92 free parameters, $R(F) = 0.048$, $wR(F^2) = 0.115$, max./ min. residual electron density: $+1.7/-1.7$ e10^6 pm^3. Further details on the crystal structure can be obtained from the Fachinformationszentrum Karlsruhe, D-76344 Eggenstein-Leopoldshafen (Germany) on quoting the depository number CSD-4004030.
[13] H. Hess, H. Hartung, *Z. Anorg. Allg. Chem.* **1966**, *344*, 157
[14] G. Beindorf, J. Strähle, W. Liebelt, K. Dehnicke, *Z. Naturforsch. B* **1980**, *35*, 522
[15] H. G. von Schnering, *Angew. Chem.* **1981**, *93*, 44; *Angew. Chem. Int. Ed. Engl.* **1981**, *20*, 33
[16] L. Pauling, *The Nature of the Chemical Bond*, Cornell University Press, Ithaca, NY, USA, **1960**.
[17] G. M. Sheldrick, SHELXS86, A Program for Crystal Structure Determination, Universität Göttingen, **1986**.
[18] G. M. Sheldrick, SHELXL93, A Program for Crystal Structure Refinement, Universität Göttingen, **1993**.

Corrigendum

In the communication "Porous Solids by Design: $[Zn(4,4'\text{-bpy})_2(SiF_6)]_n \cdot x$DMF, a Single Framework Octahedral Coordination Polymer with Large Square Channels" by S. Subramanian and M. J. Zaworotko (*Angew. Chem. Int. Ed. Engl.* **1995**, *34*, 2127–2129), the German version of Scheme 1 was inadvertently printed. The correct English version is shown below.

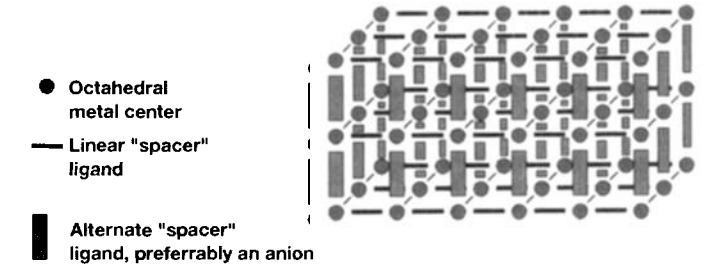

Scheme 1. Schematic illustration of how a three-dimensional coordination polymer might be generated by cross-linking of square grids.

 © VCH Verlagsgesellschaft mbH, D-69451 Weinheim, 1995 0570-0833/95/3422-2561 $ 10.00+.25/0

Chemistry Beyond the Molecule

Supramolecular Chemistry. Concepts and Perspectives. By *J.-M. Lehn*. VCH Verlagsgesellschaft, Weinheim, 1995. 271 pp., hardcover DM 128.00.—ISBN 3-527-29312-4; softcover DM 58.00.—ISBN 3-527-29311-6

The embryonic science of supramolecular chemistry existed before Jean-Marie Lehn, but he has given the field its name, an intellectual focus, and a vision for the future. Supramolecular chemistry is "chemistry beyond the molecule", and its goal is to gain control over the intermolecular noncovalent bond. It is, therefore, concerned with the organization and properties of ensembles of molecules held together by weak interactions rather than with the individual molecules themselves. Host-guest complexes, self-assembled objects, and spatially organized films can all be conjured out of small building blocks by the careful exploitation of hydrogen bonds, metal-ligand binding, $\pi-\pi$ interactions, and hydrophobic effects, and the resulting ensembles have potential as catalysts, sensors, or new materials. In one sense, of course, there is nothing new in all this: as Lehn himself points out early in this book, Werner's complexes have been known for a hundred years, and the hydrogen-bonded acetic acid dimer for over fifty. But the bringing together of such disparate elements to form an emerging, coherent discipline that crosses conventional boundaries is relatively new and is partly a result of Lehn's passionate advocacy over many years.

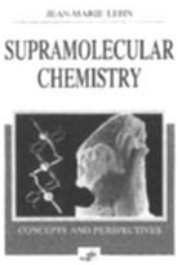

This book is an attempt to summarize Lehn's concepts of supramolecular chemistry. It is based on two sets of lectures; most of the discussion is centered around his own group's enormous contributions. The attraction of this personal approach is that enthusiasm and immediacy leap off the page as the author guides us through twenty years of his research. Starting with the recognition of simple metal ions by macrocycles, we move through chapters on anion recognition, receptors with multiple sites, supramolcular reactivity and catalysis, transport, devices, and self-assembly. Each chapter brings a new species into his "molecular bestiary" including coronands, spherands, and cryptophanes. There is also a whole new vocabulary of categories and topics: here are endoreceptors, nanostructures, semiophores, and chemionics in all their glory. At this stage in their development, many of these words may feel like unnecessary jargon, and some will undoubtedly wither into obscurity, but many of them will come to be essential as they provide the linguistic key for communicating the ideas they represent.

This is an excellent guide to the supramolecular efforts of Lehn and over 200 coworkers, bringing together hundreds of papers that are scattered through the literature of several disciplines. This approach, however, does not make an ideal text for teaching purposes. It assumes too much fundamental knowledge of kinetics, thermodynamics, intermolecular interaction, and synthesis to provide the basis for a satisfying teaching course except at a very high level. There is still room for a real textbook of supramolecular chemistry.

A final feature of the personal approach is that it enables Lehn to bring in connections with literature and sculpture, placing chemistry in a wider, philosophical context. He ends with an inspirational call to chemistry to invent, and above all, to *create*. The joy of chemistry in general, and of supramolecular chemistry in particular, is that we are not limited to the repertoire of reactions and receptors that Nature has provided or the natural products that have evolved over the millenia: we can create our own. And each of us can create a unique structure: whereas in most fields scientists are competing to clone the same receptor, solve the same equation, or make the same natural product, those of us in the supramolecular community can cooperate, each building block from each laboratory contributing its own unique features and personality. It is this combination of cooperativity, art, and science that makes supramolecular chemistry such fun, and it is a feeling that Jean-Marie Lehn has captured so well in this book.

Jeremy K. M. Sanders
Department of Chemistry
University of Cambridge (UK)

Container Molecules and Their Guests. By *D. J. Cram* and *J. M. Cram*. (Series: Monographs in Supramolecular Chemistry, Vol. 4). Royal Society of Chemistry, Cambridge, 1994. 223 pp., hardcover £ 49.50.—ISBN 0-85186-972-6

In this monograph devoted to supramolecular chemistry the authors review a subject that originates mainly from their own research into host-guest complexation chemistry, and include closely related results from other groups. The ten chapters of the book present topics covering the twenty-five year period from 1970, with a particular emphasis on the authors' work from 1987. As defined by D. J. Cram in his preface, this review is "essentially a chronicle of the more successful parts of the journey [his] research group took into the wilderness of complexation phenomena". It is indeed a fascinating and impressive presentation of a masterpiece of supramolecular chemistry. The design of synthetic molecular receptors is one of the main challenges facing organic chemists in the field of supramolecular chemistry. This book will familiarize the reader with new classes of molecular containers, i.e. new molecules large enough to trap and encapsulate ionic or neutral guests to form a supramolecular complex. There is a thorough dis-

This section contains book reviews and a list of new books received by the editor. Book reviews are written by invitation from the editor. Suggestions for books to be reviewed and for book reviewers are welcome. Publishers should send brochures or (better) books to Dr. Ralf Baumann, Redaktion Angewandte Chemie, Postfach 101161, D-69451 Weinheim, Federal Republic of Germany. The editor reserves the right of selecting which books will be reviewed. Uninvited books not chosen for review will not be returned.

cussion of the methods for achieving synthesis and structural recognition in complexation. The dependence of binding power on structure is discussed at length, as it depends on many factors including size and stereoelectronic complementarities, topology of the host, solvation effects, the nature and the number of binding sites, and preorganization of the partners involved.

In Chapter 1 the authors define the terms "host" and "guest", and the concept of host–guest complexation, terms which form the basis of the design of container molecules. The first section is concerned with fundamentals, namely the molecular receptors based on crown ether structures. Because of the importance of structural recognition in complexation, the authors discuss crystal structure and molecular modeling, including examination of CPK molecular models, as the necessary tools of the supramolecular chemist ("the crystal structures and molecular modeling connection").

Chapter 2 deals with synthesis, complexation, and molecular structures of spherands and their relatives. Spherands and hemispherands provide a series of preorganized hosts whose complexing properties are the basis of the principles of complementarity and preorganization, which respectively govern structural recognition and binding power. The wide-ranging importance of chiral recognition is emphasized by devoting a separate chapter to this topic. Chapter 3 provides a survey of the results in this field, extending from 2,2′-disubstituted-1,1′-binaphthyl corands as resolving agents for primary amine salts to the concepts of a "resolving machine" and chiral catalysis; this chapter is highly recommended for chirophiles. Chapter 4 ("Partial Enzyme Mimics") discusses the use of binaphthyl corands and preorganized hosts as organic catalysts. The authors describe their approach and results for a transacylase mimic based on their synthetic hosts. The different factors that influence the catalytic reaction are examined, and in this context the authors report on the effect of preorganization and on the design of more elaborate host molecules that could stabilize transition states. The introduction of cyclic urea units has been a further step in the design of such molecular receptors, and they have been applied in the approach to a serine protease mimic.

Chapters 5 and 6 introduce the reader to the concept of container molecules through the chemistry of *cavitands*. These are rigid hollow organic hosts containing an interior cavity large enough to form complexes (*caviplexes*) with organic guests. The tetraresorcinol cyclic oligomer is the building block of this widely developed chemistry. It forms the basis of the numerous molecular receptors that were obtained by substituting the phenol groups with bridging units leading to cavitands (bowl-shaped receptors described in Chapter 5) and other vases, kites, and velcrands (Chapter 6). All these molecular vessels have specific complexing properties that are related to their molecular size and the nature of the substituents that allow the formation of enforced cavities. These chapters are devoted to the synthesis, solid state structures, and formation of complexes.

The last four chapters are concerned with the most recent molecular containers, the *carcerands*, and their complexed forms, the *carceplexes*. Over a hundred pages are devoted to the molecular design and architecture of these structures. This new family of synthetic hosts is actually the most sophisticated one. It arose from the logical approach of the Cram group to the design of preorganized molecular systems with highly efficient complexing properties. The carcerands are essentially closed surface molecular spheres whose guest molecules are permanently encapsulated during synthesis to form carceplexes. The question regarding the properties of the inner part of the molecule has been examined, and a new phase of matter was proposed on the basis of the special status of the imprisoned guest. The authors report on the movements and the particular reactivity of the encapsulated guests. *Hemicarcerands* containing portals large enough for encapsulated guests to escape from their host are described. Complexation–decomplexation processes in these systems are temperature-dependent, and have been studied mainly by NMR spectroscopy.

The book is readily understandable and the numerous three-dimensional structures of molecules presented throughout the ten chapters make reading them even more enjoyable and instructive. This is not only a highly recommended reference book on container molecules, it is also an important contribution to modern organic chemistry which any chemist, even a newcomer to the field, would be well advised to own. As you leaf through this book, you will be impressed and fascinated by the beauty and the importance of the work and ideas that were developed by the Cram group. This monograph is recommended to all who are concerned with synthesis and applications of supermolecules, as well as advanced students and academic and industrial chemists interested in the progress of the chemical sciences.

Jean-Pierre Dutasta
CNRS
Ecole Normale Supérieure de Lyon
Lyon (France)

Kirk/Othmer Encyclopedia of Chemical Technology. 4th Edition. Series editor: *J. I. Kroschwitz*. Vols. 3–10. Wiley, Chichester, 1992–1994. 1050–1316 pp., hardcover, 195.00 £ per volume.—ISBN 0-471-52671-1, -52672-X, -52673-8, -52674-6, -52675-4, -52676-2, -52677-0, -52678-9

Since the first two volumes of the 4th Edition were reviewed a further eight have been published. Thus the publishers have kept to the timetable that was originally announced.

The numbers of individual contributions contained in Volumes 3–10 range from 21 in Volume 10 to 38 in Volume 4. In accordance with the usual practice followed in Kirk–Othmer, the volumes present the various articles in alphabetical order and describe products and classes of compounds (from antibiotics to fire retardants) together with the relevant manufacturing processes, basic chemical engineering operations (distillation, filtration, drying, etc.), analytical and measurement methods, computer-based techniques (CAD, expert systems, chemometrics, etc.), and other topic areas concerned with industrial production, such as availability of raw materials, energy management, and criteria for economic evaluation.

The choice of articles to be included has taken into account the most important advances in science and technology. Thus, for example, there are new chapters on biotechnology, biosensors, and carbon fibers. Topics that have declined in importance, such as benzidine, crotonaldehyde, and cork, are no longer covered by separate articles.

The marked upsurge in the importance of environmental protection since the third edition is reflected in the inclusion of a separate chapter on "Environmental Impact". Environmental and safety aspects are also treated in detail in the articles on the relevant types of substances (e.g. dyes). There are also separate articles on important environmental protection methods (e.g. combustion technology).

In general the articles are well written and clearly understandable. Attention is drawn to new developments in manufac-

 © VCH Verlagsgesellschaft mbH, D-69451 Weinheim, 1995 0044-8249/95/10722-2564 $ 10.00+.25/0

turing processes (e.g. the synthesis of ethylene from methane by oxidative coupling), to new product types (e.g. fullerenes), and to relevant developments in basic science and technology (e.g. the use of pervaporation as a separation method for the removal of alcohol from whisky).

The literature references and the data that are included are up-to-date. The few exceptions to this, for example in the chapter on "Azine Dyes" which includes no references later than 1987, and in that on energy management where the data on energy consumption by industry in the USA extend only up to 1988, only emphasize the general rule.

The illustrations (reaction schemes, diagrams, etc.) are clear and well presented. Where necessary for clarity, use has been made of three-dimensional illustrations (e.g. in descriptions of apparatus) or of color (e.g. in the chapter on color photography). In contrast to the previous two volumes, the use of abbreviations has been reduced to a sensible level, and those used are fully explained.

To summarize, after looking through the first ten volumes it is clear that the fourth edition of Kirk-Othmer is again a work of reference of world class, providing expert and comprehensive coverage of the field of chemical technology. Libraries concerned with science and technology are recommended to buy it.

Friedbert Nees
BASF Aktiengesellschaft
Ludwigshafen (Germany)

Inorganic Experiments. Edited by *J. D. Woollins*. VCH Verlagsgesellschaft, Weinheim, 1994. 286 pp., hardcover DM 148.00.—ISBN 3-527-29235-7

The editor of this book, J. D. Woollins, has succeeded in enlisting no less than 71 authors from throughout the world as contributors. The result is a collection of 64 laboratory recipes for preparations to be carried out in inorganic chemistry student practical sessions. The experiments are grouped into three categories, described as "introductory" (16), "intermediate" (23), and "advanced" (25). This classification is intended as a guide both to the learning content and to the need for specialized apparatus. Most of the descriptions follow a set pattern, consisting of a short introduction, sometimes with an explanation of the teaching objective, a paragraph (highlighted) on safety precautions and health risks, the actual experimental procedure, and relevant literature references. Some of the experiments are valuable new material in works of this kind, for example those on the preparations of siloxane polymers, of arsenium cations, and of liquid-crystalline metal complexes, and the magnetic studies on exchange coupling in bimetallic paramagnetic complexes. Highly topical experiments such as these cannot be found in standard works on preparative inorganic chemistry, such as *Brauers Handbuch* or *Inorganic Syntheses*. On the other hand, some other experiments are "old friends", such as the preparations of Fremy's salt, ferrocene, and potassium peroxochromate. In his preface the editor explains that he deliberately avoided trying to introduce a uniform style, so as not to lose the lessons that can be drawn from comparing the procedures in the various laboratories. Nevertheless, the book would have benefited from the imposition of a small degree of uniformity and editorial tidying-up. One occasionally encounters local peculiarities that are incomprehensible, as when a glass beaker is cleaned by using a "policeman", when "methylated spirits" is used as a solvent, and where one is continually instructed to proceed "carefully" or "cautiously" without a more specific explanation of what this means. The concentration of aqueous ammonia is specified in three different ways (in %, in vol, and as 0.880, the latter being presumably the density). Some of the experiments described could only be performed in a small number of laboratories, such as the preparation of metal carbonyls by reductive carbonylation in an autoclave under CO at high pressure. Some could not be carried out at all—for example, where one is instructed to condense 1.73 g of a gas from a pressurized vessel into a solution maintained in a frozen state by liquid nitrogen, without explaining how such a precise dosage is to be achieved. Some of the experiments lack safety recommendations, while for others there are no literature references.

However, the descriptions of most of the experiments are good. The introductions explaining the learning points, the exercise problems, and the notes on identification of the products (mainly by spectroscopy) are useful. Undoubtedly one of the book's particular strengths is the topicality of many of the experiments in the "advanced" part, many of which are very attractive for use in advanced practical sessions. The book is of interest to all college and university teachers and assistants responsible for practical classes in inorganic chemistry. Those interested in discovering what is being done in other laboratories, or who can benefit from a little gold-mine of ideas for new practical exercises, should certainly buy this book. However, many of the procedures need to be thoroughly checked before introducing them into one's course.

Johannes Beck
Institut für Anorganische
und Analytische Chemie
der Universität Giessen (Germany)

Palladium-Catalyzed Reactions of Propargylic Compounds in Organic Synthesis

Jiro Tsuji* and Tadakatsu Mandai

Palladium was used in organic synthesis for long time only as a heterogeneous catalyst for hydrogenating unsaturated compounds. But in recent years palladium compounds have found broad application as homogeneous catalysts. In the last decade, homogeneous catalysis relying on transition metal complexes has led to innovations in organic synthesis. Complexes of various transition metals are now used for organic synthesis, and each metal has its own characteristic features. Palladium complexes are the most versatile and used extensively in organic synthesis, particularly for carbon–carbon bond formation. Palladium-catalyzed reactions can be classified into several groups based on their substrates: organic halides, allylic compounds, conjugated dienes, alkenes, and alkynes. Propargylic compounds undergo a variety of palladium-catalyzed transformations and make up one important class of these reactions. It is well known that copper and silver salts promote or catalyze several reactions of propargylic compounds. However, palladium compounds, particularly Pd^0 complexes, show catalytic activities entirely different from those of silver and copper salts. Advances in the research on the palladium-catalyzed reactions of propargylic compounds in the last decade have made the scope of the reactions clear. The ready availability of numerous propargylic alcohols and their esters by the reaction of terminal alkynes with carbonyl compounds clearly enhances the synthetic utility of their reactions. Palladium complexes, in particular palladium phosphane complexes, are soluble in organic solvents and behave as active catalysts under homogeneous conditions.

Keywords: alkynes · carbonylations homogeneous catalysis · palladium compounds · propargylic compounds

1. Introduction

Many useful synthetic reactions catalyzed by homogeneous palladium catalysts are classified based on substrates.[1] As one important class of substrates, propargylic compounds undergo several types of transformations promoted by palladium catalysts. Propargylic compounds (2-alkynyl compounds) are derivatives of alkynes; however, palladium-catalyzed reactions of propargylic compounds, particularly their esters and halides, are clearly different mechanistically from those of simple alkynes except in a few cases. Therefore the palladium-catalyzed reactions of propargylic compounds should be treated independently of those of simple alkynes. Copper and silver-catalyzed and -promoted reactions of propargylic compounds are known,[2] but they differ distinctly from the palladium-catalyzed reactions.

Since the discovery of carbon–carbon bond formation by the reaction of π-allylpalladium complexes with carbon nucleophiles such as malonates and β-keto esters,[3] the chemistry of π-allylpalladium complexes has been studied extensively. Catalytic reactions, in particular, attract the attention of synthetic organic chemists, and many useful synthetic reactions based on π-allylpalladium compounds have been discovered.[4] Later, allylic carbonates were found to be more reactive sources of allyl ligands than allylic acetates, which were used under basic conditions; the former undergo several transformations under mild and neutral conditions not possible with corresponding acetates.[5] As an example, the reaction of allyl methyl carbonate (**1**) with malonate is outlined in Scheme 1. The key steps in the palladium-catalyzed reaction of allylic carbonates are the facile decarboxylation and the subsequent in situ generation of a methoxide ion, which acts as a base and abstracts a proton from

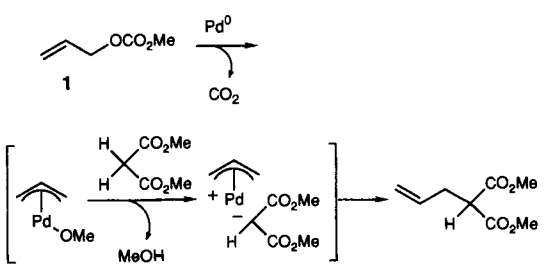

Scheme 1. Palladium-catalyzed allylation of malonate via a π-allylpalladium complex.

[*] Prof. Dr. J. Tsuji
Department of Applied Chemistry
Okayama University of Science, Ridai-cho, Okayama 700 (Japan)
Telefax: Int. code +(86) 252 6891
Prof. Dr. T. Mandai
Department of Chemical Technology
Kurashiki University of Science and the Arts
Tsurajima-cho, Kurashiki, Okayama 712 (Japan)

 © *VCH Verlagsgesellschaft mbH, D-69451 Weinheim, 1995* *0570-0833/95/3423-2589 $ 10.00+.25/0*

malonate. Thus the allylation of malonate can be carried out under neutral conditions without any added base. Carbonate is also the best leaving group in the palladium-catalyzed reactions of propargylic compounds.

In contrast to the extensive studies conducted on the palladium-catalyzed reactions of allylic compounds, studies on the analogous reactions of propargylic compounds were initiated much later and were less extensive. One reason is that propargylic compounds are less reactive toward palladium catalysts than allylic compounds. For example, the reaction of a mixture of allyl carbamate **2** and propargyl carbamate **3** with 5,5-dimethyl-1,3-cyclohexanedione (dimedone) (**4**) gave only the allylated product **5**. Propargyl carbamate **3** was recovered, showing that an allyl carbamate is more reactive than a propargyl carbamate (Scheme 2).[6]

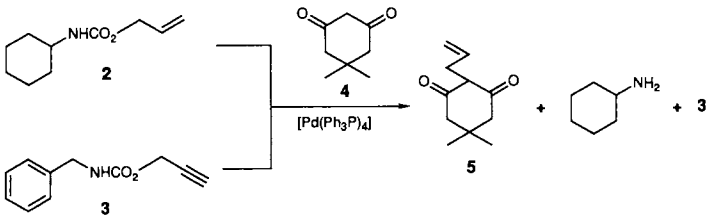

Scheme 2. Competition reaction between an allyl and a propargyl carbamate.

Allylic acetates also react smoothly with dimethyl malonate, whereas the reaction of malonate with the corresponding propargylic acetates does not occur under the same conditions. On the other hand, both allylic acetate **6** and propargylic acetate **7** react with phenylzinc chloride to afford **8** and **9** with comparable rates.[7]

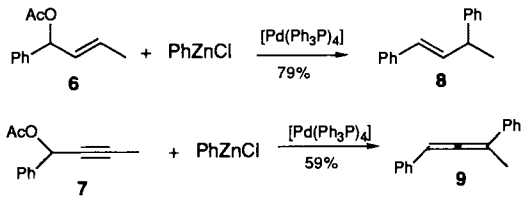

Another reason for the limited interest in the Pd-catalyzed reactions of propargylic compounds may be the instability of the reaction products. Allene derivatives are formed from propargylic compounds in many cases, and these highly unsaturated products frequently undergo further, sometimes complex Pd-catalyzed transformations. Thus the reaction conditions and isolation methods for the reactions of propargylic compounds must be chosen much more carefully than for the analogous reactions of allylic compounds.

In the last ten years, the scope of the palladium-catalyzed reactions of propargylic compounds has been defined through careful studies. Therefore it seems timely to summarize the behavior of propargylic compounds in the presence of palladium catalysts under various conditions. This review is intended to give an overview of the palladium-catalyzed reactions of propargylic compounds and their synthetic applications. Since propargylic alcohols **10** are easily prepared by the reaction of terminal alkynes with carbonyl compounds (Scheme 3), the palladium-catalyzed transformation of various propargylic compounds has high synthetic value.

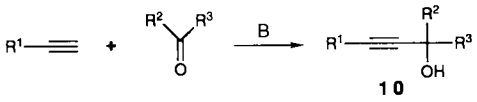

Scheme 3. R^1, R^2, R^3 = alkyl, aryl. B = base.

2. Classification of Catalytic Reactions Based on Mechanistic Considerations

Pd^0 complexes are active catalysts in most cases. The Pd^0-catalyzed reactions of propargylic compounds can be understood by the following mechanistic considerations. The first step of the catalytic reaction is the oxidative addition of a propargylic com-

Jiro Tsuji was born in 1927 in Shiga, Japan. He received his B.S. from Kyoto University, and his Ph.D. from Columbia University in 1960 for his work with G. Stork on natural product synthesis. After returning to Japan, he worked at Basic Research Laboratories, Toray Industries Inc., and moved in 1974 to the Tokyo Institute of Technology as a professor. In 1988 he moved to the Okayama University of Science, where he is now a professor. His major research interests include the development of new synthetic reactions catalyzed by transition metal complexes, particularly palladium complexes, and application of these new catalytic reactions to the total synthesis of natural products. His awards include the Japan Chemical Society award, the Synthetic Society of Japan award, and the Silver Medal with Purple Ribbon from the Japanese government.

J. Tsuji

T. Mandai

Tadakatsu Mandai was born in 1951 and received his doctorate in 1979 from the Tokyo Institute of Technology for research with J. Tsuji. In 1979 he joined the Okayama University of Science as an assistant professor, and in 1995 he was promoted to full professor. His major research interest is synthetic organic chemistry using sulfur compounds and palladium-catalyzed reactions; these synthetic methods are also applied to natural product synthesis. He received the Japan Chemical Society Award for Young Chemists in 1985.

pound to the Pd^0 species to form an intermediate complex.[8] In this step Pd^0 is oxidized to Pd^{II}. The intermediate Pd^{II} complex undergoes further reactions with other reactants. The stoichiometric reactions of propargylic chlorides **11** and **13** with tetrakis(triphenylphosphane)palladium $[Pd(Ph_3P)_4]$ were studied; the σ-allenylpalladium complex **12** and the propargylpalladium complex **14** were isolated as yellow powders.[9] The allenylpalladium chloride **12** is formed by the S_N2'-type displacement of the chlorine by Pd^0. Compound **14**, generated by direct oxidative addition, forms when a bulky group such as trimethylsilyl or *tert*-butyl is attached to the alkyne terminus. Propargylic acetate **15** is unreactive, but it can be converted to the allenylpalladium chloride **16** by reaction with $[Pd(Ph_3P)_4]$ in the presence of zinc chloride or lithium chloride. It is reasonable to expect that Pd^0-catalyzed reactions of propargylic compounds proceed via either intermediate **12** or **14**, which seem to be in equilibrium.

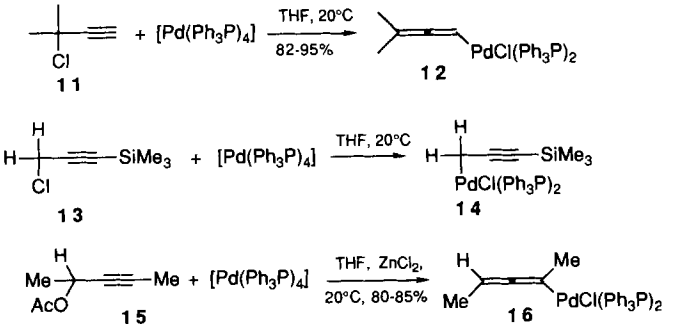

The known Pd^0-catalyzed reactions of propargylic compounds can be classified into four types (I, II, III, and IV) based on their mechanisms. The intermediate complex **17** can undergo three types of transformations depending on the reactants. Reactions of type I proceed by insertion of unsaturated bonds into the σ bond between palladium and the sp^2 carbon in **17** (Scheme 4).

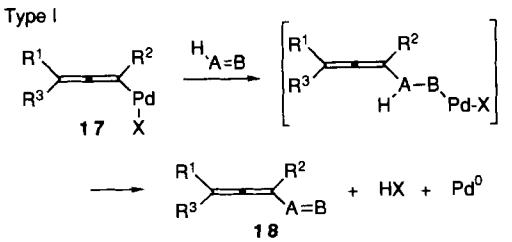

Scheme 4. Insertion reaction to allenylpalladium complexes **17**; R^1, R^2, R^3 = alkyl, aryl.

The reactivity of this σ bond is similar to that of the σ bond formed by the oxidative addition of alkenyl halides to Pd^0 in the Heck reaction. Therefore, intermediate **17** is expected to undergo reactions similar to those observed under the Heck conditions. Alkenes and carbon monoxide are known to insert into the palladium–carbon σ bond, and allene derivatives **18** result.

Reactions of type II proceed by transmetalation of complex **17**. Hard carbon nucleophiles MR (M = main group metals) such as Grignard reagents and metal hydrides MH undergo transmetalation with **17** to generate **19**. Subsequent reductive elimination gives the allene derivative **20** as the final product (Scheme 5).

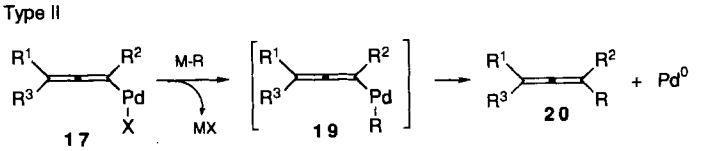

Scheme 5. Transmetalation of allenylpalladium complexes **17**; R^1, R^2, R^3 = alkyl, aryl.

In reactions of type III a nucleophile attacks at the central sp carbon of the allenyl system of complex **17**. Reactions of soft carbon nucleophiles derived from compounds with activated methylene groups, for example β-keto esters and malonates, as well as oxygen nucleophiles, belong to this type. The attack of the nucleophile generates intermediate **21**, which can be considered equivalent to the palladium–carbene complex **22**. Intermediate **21** abstracts a proton from the activated methylene group and the π-allylpalladium complex **23** is formed, which, as expected, undergoes further reaction with a nucleophile to give alkene **24** (Scheme 6).

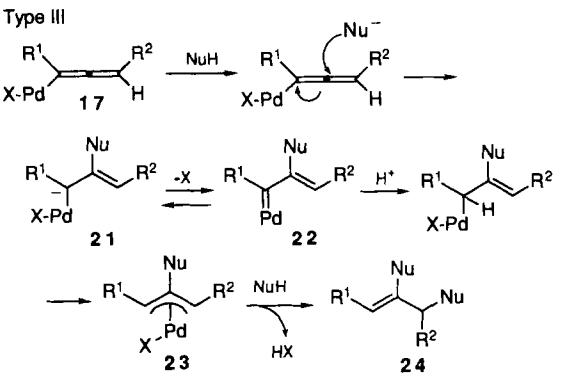

Scheme 6. Reaction of soft carbon nucleophiles with allenylpalladium complexes **17**; R^1, R^2 = alkyl, aryl.

Most of the known Pd^0-catalyzed reactions of propargylic compounds can be explained by the formation of allenylpalladium intermediates like **12** and are of types I, II, or III.

Two reactions are known, however, that are of type IV. They proceed via propargylpalladium complexes like **25**. Direct displacement of palladium in **25** with hydride to form alkynes **26** is one possibility (Scheme 7). Elimination of a Pd–H species from **25** to form enyne **27** is another (Scheme 8).

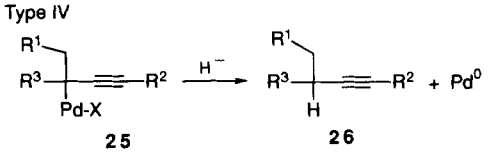

Scheme 7. Hydrogenolysis of propargylpalladium intermediates **25** to form alkynes **26**; R^1, R^2, R^3 = alkyl, aryl.

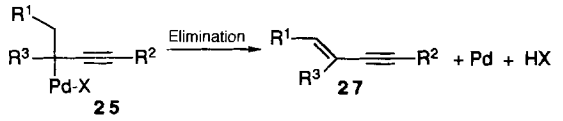

Scheme 8. Formation of enynes by elimination from propargylpalladium complexes **25**; R^1, R^2, R^3 = alkyl, aryl.

The selection of reaction conditions is crucial for the palladium-catalyzed reactions of propargylic compounds. The most essential factor is choosing the appropriate phosphane ligand (particularly monodentate and bidentate phosphanes) for a given reaction.

A number of propargylic derivatives can be used for the palladium-catalyzed reactions, but they have different reactivities. Propargylic halides are used with or without palladium catalysts in the presence of bases. Although propargylic alcohols are most easily available, they are less reactive substrates; however, their esters such as acetates, carbonates, and phosphates are reactive. Propargylic acetates are used in the presence of bases, but they are less reactive than the corresponding carbonates. Propargylic carbonates like **28** are highly reactive and undergo various palladium-catalyzed reactions smoothly, especially under neutral conditions, as observed with allylic carbonates.[5] In the facile irreversible oxidative addition of a propargylic carbonate carbon dioxide is evolved and an allenylpalladium methoxide such as **29** results (Scheme 9). The reaction can be carried out under

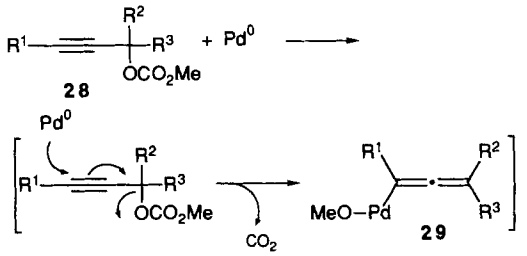

Scheme 9. Formation of an allenylpalladium methoxide **29** from a propargyl carbonate **28**; R^1, R^2, R^3 = alkyl, aryl.

neutral conditions because methoxide is generated. Therefore in most of the extensive studies on propargylic compounds propargylic carbonates were used as convenient substrates. Alkynyloxiranes **30** also undergo facile reactions with Pd^0 catalysts under neutral conditions via alkoxypalladium complexes **31** (Scheme 10).

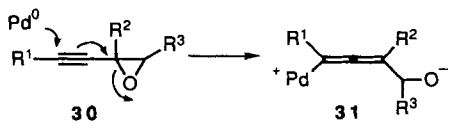

Scheme 10. Formation of allenylpalladium complex **31** from alkynyloxirane **30**; R^1, R^2, R^3 = alkyl, aryl.

In the next sections we will discuss the Pd^0-catalyzed reactions of propargylic compounds based on the above-mentioned classification. But first the syntheses of suitable Pd^0 catalysts need comment. The commercially available Pd^0 complexes $[Pd(Ph_3P)_4]$ and $[Pd_2(dba)_3]$ (dba = dibenzylideneacetone) or $[Pd(dba)_2]$ are used directly. In addition, some Pd^{II} salts can be used as precursors of Pd^0 species. $Pd(OAc)_2$ is used in many cases, because $Pd(OAc)_2$ is easily reduced to Pd^0 in situ with reducing agents such as CO,[10] alcohols, alkenes, and even aqueous KOH.[11] In the most convenient preparations Pd^0 species are generated by the reaction of $Pd(OAc)_2$ with phosphanes; Ph_3P is known to reduce $Pd(OAc)_2$ slowly.[12, 13] The reduction proceeds rapidly when $Pd(OAc)_2$ is mixed with nBu_3P in solution to form a very active Pd^0 catalyst and phosphane oxide **32**.[14]

$$Pd(OAc)_2 + n\text{-}Bu_3P \xrightarrow{H_2O} Pd^0 + n\text{-}Bu_3PO + AcOH$$
32

3. Type I Reactions: Insertion into the Pd–C_{sp^2} Bond

3.1. Reaction of Alkenes: Formation of 1,2,4-Trienes

The reaction of propargylic carbonates **33** with alkenes **34** provides a good synthetic approach to 1,2,4-trienes **36**. Smooth insertion of alkene **34** into the allenylpalladium bond generates **35**, and subsequent elimination of a β-hydrogen atom affords the 1,2,4-triene **36** (Scheme 11).[15] The reaction proceeds

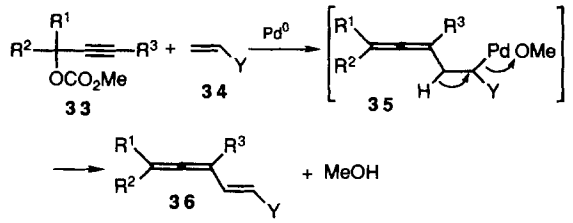

Scheme 11. Preparation of 1,2,4-alkatrienes **36**; R^1, R^2, R^3 = alkyl, aryl.

smoothly in dimethylformamide (DMF) at 70 °C with $Pd(OAc)_2/Ph_3P$ as the catalyst. The addition of potassium bromide and triethylamine is important. The reaction of methyl acrylate with **37** afforded 2,4,5-trienoate **38** in good yield. The reaction of allyl alcohol (**40**) as an olefin component with **39** gave the allenyl aldehyde **42** by the elimination of a β-hydrogen atom from the O-substituted carbon atom of intermediate **41** (Scheme 12).

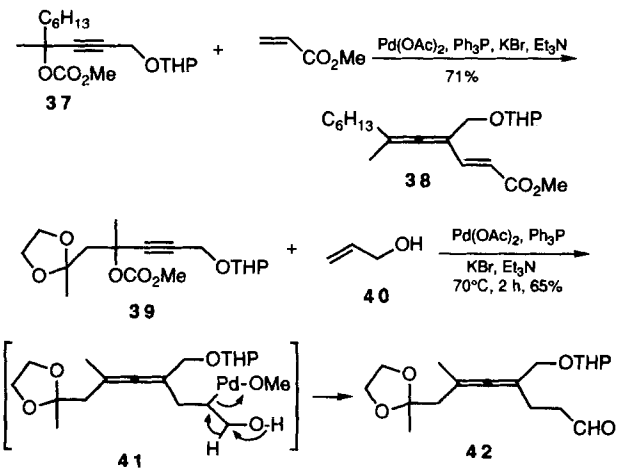

Scheme 12. Formation of triene **38** from **37** and methyl acrylate, and of aldehyde **42** from propargyl carbonate **39** and allyl alcohol (**40**).

3.2. Carbonylation

3.2.1. Reaction Features

Carbon monoxide also reacts with complex **17** by insertion. Propargylic compounds undergo facile palladium-catalyzed mono- and dicarbonylations, depending on reaction conditions.[16] The palladium-catalyzed carbonylation of propargylic compounds was first reported in 1966. In this first study the carbonylation of propargylic alcohols was carried out under fairly severe conditions to afford mainly dicarbonylation products.[17, 18] Later it was found that facile monocarbonylation proceeds under milder conditions when propargylic carbonates are used.[19] The mono- and dicarbonylations in an alcohol solvent can be explained by the following mechanism. In the first step, insertion of carbon monoxide into the allenylpalladium intermediate generates the acylpalladium complex **44**, which reacts with the alcohol to give the 2,3-dienoate **45**. Under certain conditions, **45** isomerizes to the 2,4-dienoate **46** (Scheme 13).

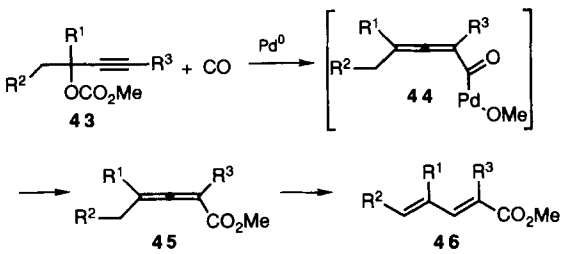

Scheme 13. Monocarbonylation of propargylic carbonates to give 2,3-dienoates; R^1, R^2, R^3 = alkyl, aryl.

Carbonylation of propargylic carbonates under mild conditions stops at this stage. Under high CO pressure or when the substrate has an activating group (e.g. $R^3 = CO_2R$), further attack of carbon monoxide at the central sp carbon of the allenyl intermediate **45** takes place to give the diester **47** (Scheme 14).

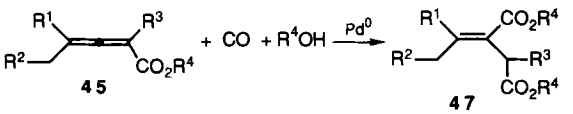

Scheme 14. Further carbonylation of 2,3-dienoates; R^1, R^2, R^3 = alkyl, aryl; R^4 = alkyl.

In the next sections the mono- and dicarbonylations of propargylic carbonates, alcohols, and halides will be treated. Then the extension of the carbonylation reactions to various derivatives of propargylic carbonates to yield cyclic compounds will be discussed.

3.2.2. Preparation of 2,3-Dienoates and Their Derivatives by Monocarbonylation

Similar to the facile decarboxylation–carbonylation of allylic carbonates to afford 3-alkenoates,[20] smooth decarboxylation–carbonylation of propargylic carbonates **43** occurs in alcohol solvents to afford 2,3-dienoates **45** under mild neutral conditions. The reaction offers a new preparative method for 2,3-dienoates **45**.[19] In this carbonylation, carbon monoxide is introduced at the γ position of propargylic carbonates. The reaction proceeds at 50 °C under 1–10 atm of carbon monoxide. The yield of 2,3-butadienoate **49**, the simplest 2,3-dienoate, from methyl propargyl carbonate (**48**) is somewhat low, because **49** is very reactive. In some cases, a mixture of 2,3- and 2,4-dienoates (**45** and **46**) is obtained. When the reaction is conducted in ether instead of in methanol and for a longer time, 2,4-dienoates **46** are formed by isomerization of 2,3-dienoates **45**. The facile carbonylation of propargylic carbonates shows that, as in the reaction of allylic carbonates, carbonate is an excellent leaving group under mild and neutral conditions. The terminal allenic ester **51** is prepared in good yield from **50**. The tertiary propargylic carbonate **52** with a terminal triple bond is very reactive and gives a high yield of the allenic ester **53**.

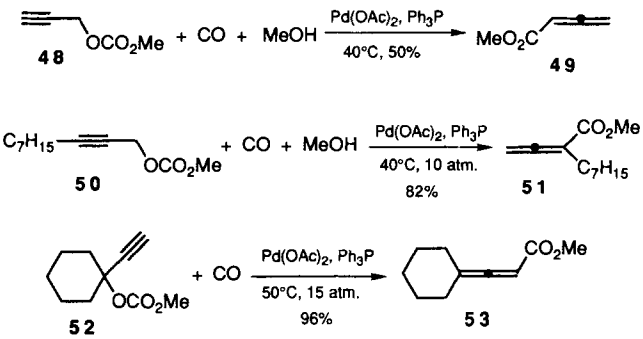

Carbonylation of propargylic acetates and phosphates proceeds in the presence of bases under somewhat more severe conditions (100 °C, 50 atm). Carbonylation of the optically active propargylic phosphate **54** gave the optically active 2,3-dienoate **55** with retention of configuration. The use of biden-

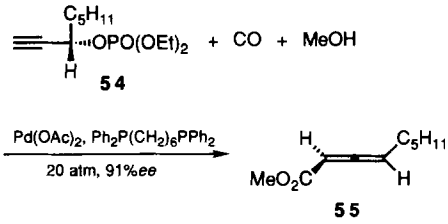

tate ligands such as 1,3-bis(diphenylphosphino)propane (dppp) and 1,6-bis(diphenylphosphino)hexane is important for complete chirality transfer.[21] Carbonylation of propargylic acetate **56** under mild conditions (1 atm, 55 °C) in a two-phase system of aqueous sodium hydroxide and 4-methyl-2-pentanone in the presence or absence of tetrabutylammonium bromide gave 2,3-pentadienoic acid **57**.[22] Carbonylation of propargyl bromide (**58**) in methanol in the presence of either

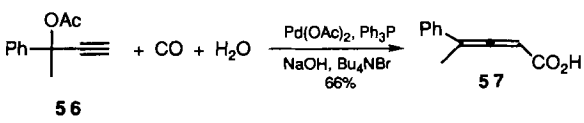

triethylamine or diethylamine under high pressure (20 bar) at 45 °C afforded methyl 2,3-butadienoate (**49**) in 85% yield.[23] 1-Bromo-3-*tert*-butyl-1,2-butadiene (**59**) was converted into 4-*tert*-butyl-2,3-pentadienoate (**60**) via an analogous allenylpalladium intermediate under similar conditions.

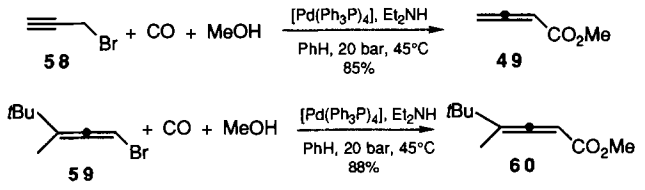

Propargylic alcohols are less reactive than their esters, and their carbonylation requires more severe conditions. Carbonylation of the tertiary propargylic alcohol **61** in THF using a cationic palladium complex as a catalyst gave the 2,3-dienoic acid **62** and the 2(5*H*)-furanone **63** in high yields in a ratio of 83:17 in one hour; **62** is easily converted into furanone **63** by treatment with *p*-toluenesulfonic acid.[24] Similarly, the carbonylation of the tertiary propargylic alcohol **64** at high pressure and temperature (20 atm, 150 °C) in dimethoxyethane (DME) under neutral conditions and with dppb as a ligand afforded the 2(5*H*)-furanone **65**. But a different mechanism not

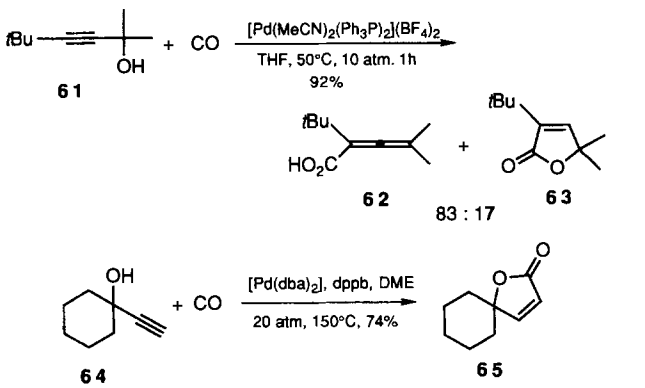

involving cleavage of the C–O bond in **64** was proposed for the formation of this furanone.[25] The 2,4-dienoate **67** was obtained when a cationic aqua(hydrido) complex and dppb were used for the carbonylation of 1-ethynylcyclooctanol (**66**); the presence of *p*-toluenesulfonic acid is essential for this reaction. Formation of **67** may be explained by the acid-catalyzed isomerization of the 2,3-dienoate formed initially.[26]

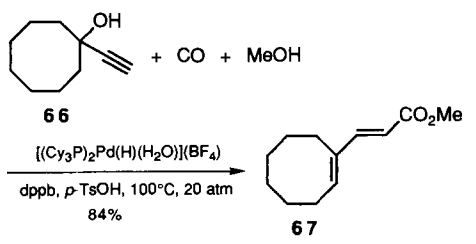

3.2.3. *Preparation of Triesters by Dicarbonylation*

Selective monocarbonylation takes place when the carbonylation is carried out under mild conditions, as described in Section 3.2.2. But dicarbonylation dominates when the triple bond of the propargylic carbonate bears an ester group. In the carbonylation of the 1-substituted 3-methoxycarbonyl-2-propynyl methyl carbonate **69**, vicinal dicarbonylation rather than the monocarbonylation occurs to afford triester **71**. This shows that the ester group has a strong activating effect (Scheme 15).[27]

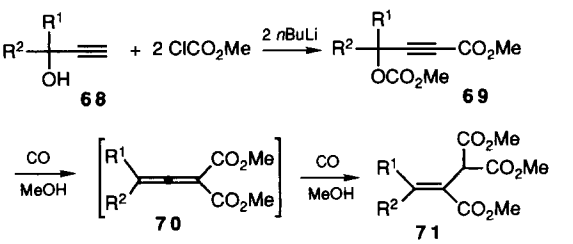

Scheme 15. Preparation of triesters **71** from propargylic alcohols by dicarbonylation; R^1, R^2 = alkyl, aryl.

The dicarbonylation proceeds at room temperature, and it is not possible to stop the reaction after the monocarbonylation forming **70**. Bidentate ligands such as dppp and 1,1′-bis(diphenylphosphino)ferrocene (dppf) are the most effective for the dicarbonylation. Triphenylphosphane is not a suitable ligand.

The carbonylation of tertiary carbonate **73** proceeds at room temperature under 1 atm of carbon monoxide to yield **74** (Scheme 16). But secondary carbonates are less reactive and

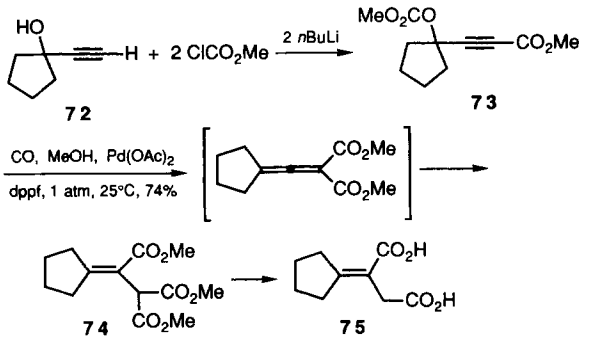

Scheme 16. Preparation of alkylidenesuccinic acid **75** from propargylic alcohol **72**.

their reaction proceeds only under 5 atm of carbon monoxide. Exclusive formation of (*E*) double bonds in the triesters **71** is observed. Acetylenic esters **69** and **73** can be prepared easily in one step by the treatment of propargylic alcohols **68** and **72** with two equivalents of *n*-butyllithium and reaction with two equivalents of methyl chloroformate. The dicarboxylic acid **75** (alkylidenesuccinic acid), obtained by hydrolysis and decarboxylation of triester **74**, resembles product **76** of the Stobbe condensation (Scheme 17).[28]

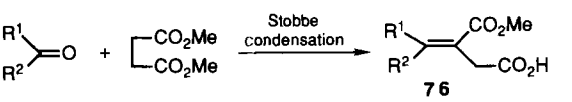

Scheme 17. R^1, R^2 = alkyl, aryl.

One possible mechanism is the following: The geminal allenyl diester **77**, which is not isolable, is expected to be susceptible to Michael-type addition of L_nPd^0 species to the allenyl sp carbon yielding palladacyclopropane **78**. Insertion of carbon monoxide and methanolysis affords the triester **79** (Scheme 18). The con-

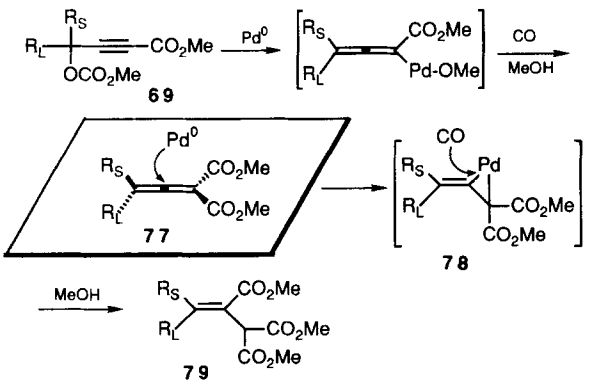

Scheme 18. Mechanism of stereoselective dicarbonylation; $R_L > R_S$; R = alkyl, aryl; L = large, S = small.

figuration of the double bond in product **79** is exclusively (*E*). The high stereoselectivity can be rationalized by assuming that the nucleophilic attack of the Pd^0 species to the allenyl sp carbon in **77** occurs from the less hindered side having the smaller alkyl substituent (R_S). Needless to say, in allene **77** the two ester groups and the substituents R_L and R_S are perpendicular.

3.2.4. Dicarbonylation of Propargylic Chlorides and Alcohols

Dicarbonylation occurs mainly when the carbonylation of propargylic halides and alcohols is carried out under high CO pressure. The carbonylation of propargyl bromide (**58**) at 20 bar affords 2,3-butadienoate (**49**) as described in Section 3.2.2. In contrast, carbonylation of propargyl chloride (**80**) in methanol at room temperature under high pressure (100 atm) catalyzed by $PdCl_2$ or Pd/charcoal affords methyl itaconate (**82**). The primary product seems to be 2,3-butadienoate (**81**≡**49**), which is carbonylated further.[17, 18] As supporting evidence, diethyl itaconate (**84**) is produced in 64% yield by the carbonylation of ethyl 2,3-butadienoate (**83**) at room temperature under high pressure.

Propargylic alcohols are less reactive than their esters, and their carbonylation requires somewhat severe conditions (100 °C, 100 atm).[17, 18] The carbonylation products under

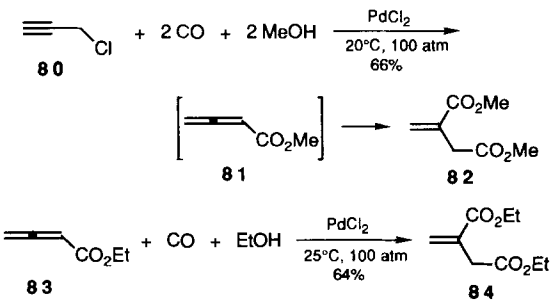

these conditions are different from those obtained by the carbonylation of the corresponding carbonates under milder conditions. Carbonylation of propargyl alcohol (**85**) in methanol without a phosphane ligand proceeds in the presence of hydrochloric acid to afford methyl itaconate (**82**) as a main product and methyl aconitate (**86**) as a minor product. In addition, a small amount of methyl 2-methoxymethacrylate (**87**) is formed. $PdCl_2$ and Pd/charcoal are active catalysts.[18]

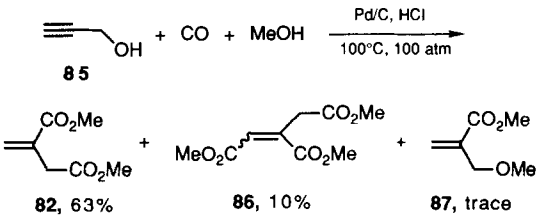

The formation of these products can be understood by assuming that two reaction pathways are possible for the carbonylation of propargyl alcohol under high pressure. One is the Pd^0-catalyzed carbonylation and the other is the Pd^{II}-catalyzed oxidative carbonylation. 2,3-Butadienoate **83** is a primary product of the Pd^0-catalyzed carbonylation, but further attack of carbon monoxide at the central sp carbon of **83** under high CO pressure yields itaconate **84** as the dicarbonylation product.

The formation of aconitate **86** is explained by the oxidative dicarbonylation of a triple bond with a Pd^{II} species, followed by Pd^0-catalyzed allylic carbonylation. As supporting evidence, methyl aconitate (**86**) was obtained selectively in 65% overall yield by the palladium-catalyzed two-step carbonylation of propargyl alcohol (**85**). The first step is the oxidative dicarbonylation of the triple bond using PdI_2 under oxygen atmosphere to give hydroxymethylfumarate (**88**). In the second step the allylic alcohol moiety of **88** is carbonylated further to give aconitate **86**. β-Lactone **90** was obtained when 2-methyl-3-butyn-2-ol (**89**) was carbonylated under similar conditions (Scheme 19).[29] It is known that fumarate and maleate are obtained by the oxidative dicarbonylation of acetylene using $PdCl_2$.[30]

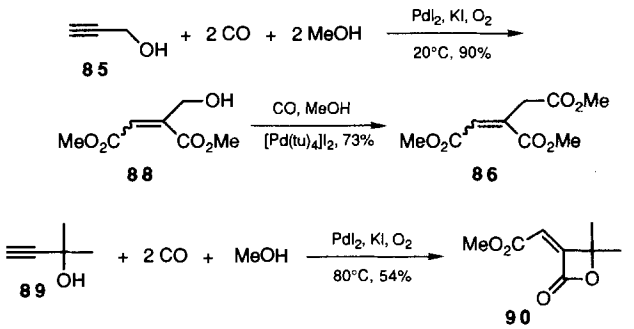

Scheme 19. tu = thiourea.

Carbonylation of 2,5-dimethyl-3-hexyne-2,5-diol (**91**) in ethanol containing hydrochloric acid (5%) affords diethyl diisopropylidenesuccinate (**94**). The reaction is explained by the Pd^0-catalyzed dicarbonylation to give **93**, and subsequent elimination of water to give **94**.[18]

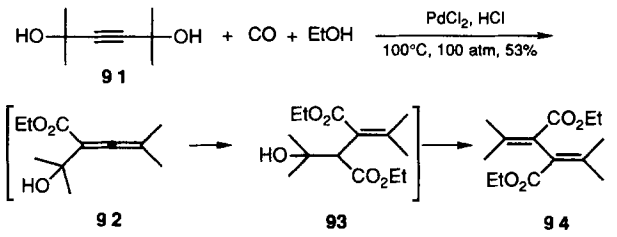

Dicarbonylations in aprotic solvents yield acid anhydrides and in some cases lactones by the Pd^0-catalyzed carbonylation and Pd^{II}-catalyzed oxidative carbonylation. Teraconic anhydride (**96**) is obtained by the Pd^0-catalyzed dicarbonylation of 2-methyl-3-butyn-2-ol (**89**) via **95** in benzene. Similarly, fulgide **98** (a derivative of dimethylenesuccinic anhydride) was obtained in 49% yield by the Pd^0-catalyzed dicarbonylation of 2,5-dimethyl-3-hexyne-2,5-diol (**97**≡**91**) in benzene; bis(1-hydroxy-1-methylethyl)fumaric acid dilactone (**99**) was obtained as a

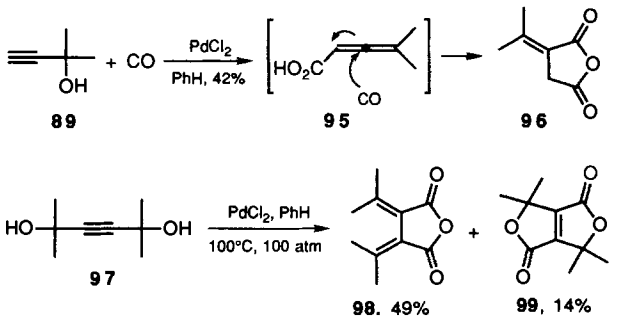

by-product (14%). This dilactone is a product of the oxidative dicarbonylation and bislactonization.[18] The fulgide-forming reaction was improved by using $Pd(OAc)_2$ as the catalyst with iodine ($Pd:I_2 = 1:1$) instead of hydrochloric acid. When [$PdCl_2(Ph_3P)_2$] was used as the catalyst, furanone **100** was obtained in 61% yield by monocarbonylation.[31] Fulgides are photochromic substances and this straightforward synthesis is useful.

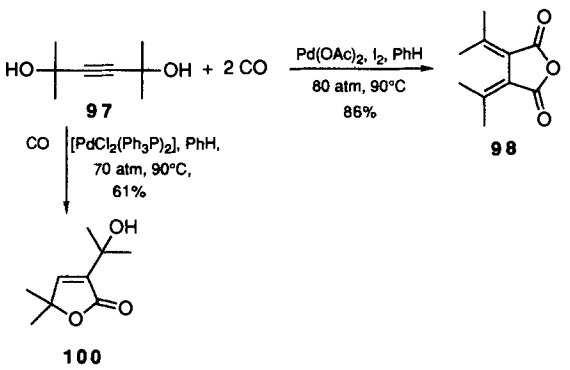

3.2.5. *Preparation of α-Alkenylidene-γ-lactones*

α-Alkenylidene-γ-lactones **102** are prepared in good yields by carbonylation of 5-hydroxy-2-alkynyl methyl carbonates **101** under mild conditions (Scheme 20).[32] The reaction proceeds at room temperature under 1–10 atm CO. Ph_3P is not a suitable

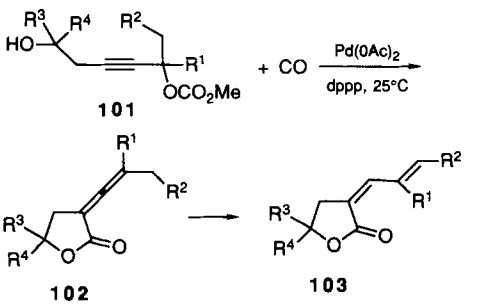

Scheme 20. Formation of α-alkenylidene-γ-lactones **102**; R^1, R^2, R^3, R^4 = alkyl, aryl.

ligand; bidentate ligands, particularly dppp and dppf, are the best ligands. Although α-alkenylidene-γ-lactone **102** is the main product, it isomerizes to form 1,3-diene **103** depending on the substrate, reaction time, and ligand. The isomerization is complete when dppp is used as a ligand or when a longer reaction time is chosen. No isomerization to give a triple bond was observed. As a typical example, carbonylation of **104** afforded products **105**–**107**, whose ratios depend on the reaction conditions.

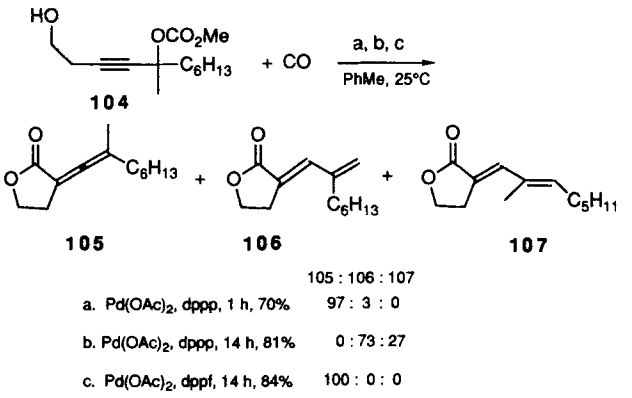

3.2.6. *Preparation of α-Alkenylidene-β-lactams*

In addition to alcohols, other nucleophiles can be used to trap the acylpalladium intermediates. Carbonylation in the presence of amines yields amides. α-Alkenylidene-β-lactams **109** are prepared by the carbonylation of 4-benzylamino-2-alkynyl methyl carbonates **108** (Scheme 21).[33] Selection of the ligand is crucial for the smooth formation of β-lactams. The best results are obtained with the cyclic phosphite 4-ethyl-2,6,7-trioxa-1-phos-

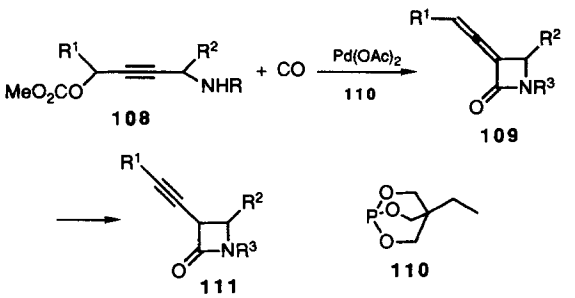

Scheme 21. Preparation of α-alkenylidene-β-lactams **109**; R^1, R^2, R^3 = alkyl, aryl.

phabicyclo[2.2.2]octane (**110**); triphenylphosphane and bidentate phosphanes give rather poor results. Another important factor is the selection of a protecting group for the amino function. Free amines cannot be used for the carbonylation. When the amino group is protected by benzylation, the reaction proceeds under neutral conditions and α-alkenylidene-β-lactams **109** are obtained. The carbonylation of *p*-tosylated amines must be carried out in the presence of potassium carbonate as a base, without which the yield is low. Under these conditions, the alkenylidenelactam isomerizes to the α-alkynyl-β-lactam **111**. For example, the α-alkynyl-β-lactam **113** is obtained as the sole product of the carbonylation of the *p*-tosyl amide **112**. In contrast, carbonylation of the benzylamine **114** affords the α-alkenylidene-β-lactam **115**. The carbonylation is carried out in THF or acetonitrile as the solvent at 50 °C under 1 – 10 atm CO. R^1 and R^2 in **108** can be any alkyl group. When R^1 = H, as in **116**, the α-vinylidene-β-lactam **117** is obtained.

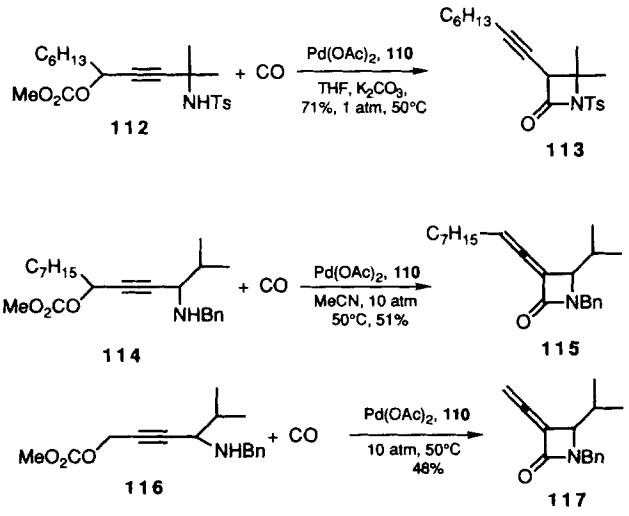

The α-alkenylidene-β-lactams **109** are known inhibitors of β-lactamases. Although several derivatives have been prepared by other methods,[34] the palladium-catalyzed carbonylation seems to offer the most convenient synthetic method for this type of β-lactam.

3.2.7. *Carbonylation in the Presence of Compounds with Activated Methylene and Methyne Groups*

Acylpalladium complexes, the intermediates in palladium-catalyzed carbonylations, can be trapped by nucleophiles other than alcohols. Compound **118**, which has an activated methylene group, can be used for trapping the acylpalladium complex (Scheme 22). Allenyl ketone **119** is formed by carbonylation in the presence of malonate, β-keto ester, or a β-diketone and a strong base; the methyl ester is not formed, showing that the carbanion formed from **118** by reaction with NaH is more reactive toward the acylpalladium intermediate than methoxide ion.[35] The triketone **121** is obtained by the reaction with cyclohexane-1,3-dione (**120**). The carbonylation proceeds under atmospheric pressure at 50 °C; triphenylphosphane is a suitable ligand.

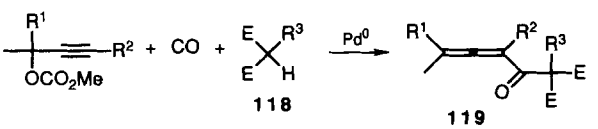

Scheme 22. Preparation of allenyl ketones **119** by reaction with compounds having activated methylene groups; E = electron-withdrawing group; R^1, R^2, R^3 = alkyl, aryl.

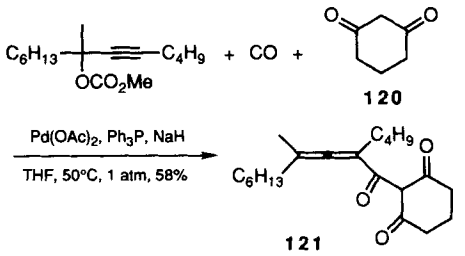

3.2.8. *Tandem Carbonylation and Diels–Alder Reaction*

The allenyl unit in conjugation with an ester group, which is formed by the carbonylation of propargylic carbonates, is highly reactive and reacts further when other double bonds are present in the molecule. As one example, the dienyne carbonate **122** undergoes smooth carbonylation, followed by intramolecular Diels–Alder reaction under mild conditions (Scheme 23).

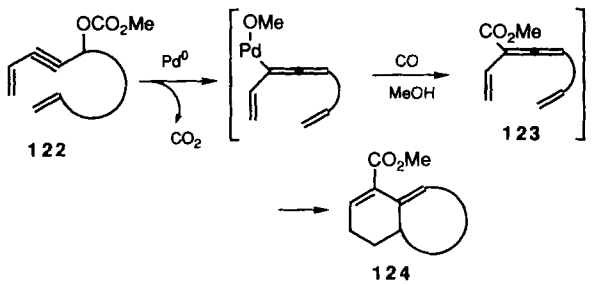

Scheme 23. Tandem carbonylation and Diels–Alder reaction.

The reaction proceeds smoothly in benzene at 50 °C under 1 atm CO and does not stop after formation of the allenyl ester **123**. The cyclized product **124** formed by an intramolecular Diels–Alder reaction is isolated in good yields (Scheme 23);[36] dppp is the most suitable ligand. This uncatalyzed intramolecular

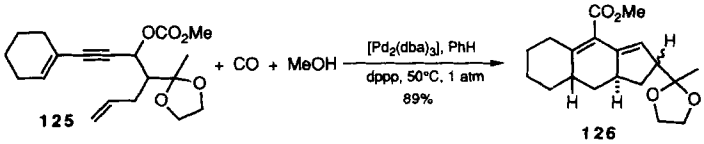

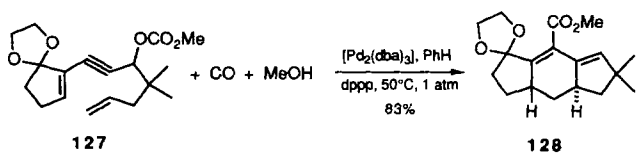

Diels–Alder reaction proceeds under surprisingly mild conditions, showing that the allenyl system is very reactive. Tricyclic compounds **126** and **128** are obtained in high yields by the carbonylation of **125** and **127**, respectively, at 50 °C under 1 atm.

The reaction proceeds even at room temperature when the dienophile has an electron-donating group. Carbonylation of the propargylic carbonate **129** at room temperature under 1 atm affords the cyclized products **131a** and **131b** in 70% total yield. Thus the Diels–Alder reaction of intermediate **130**, in which the diene has an electron-withdrawing group (CO_2Me) and the dienophile has an electron-donating group (OMe), proceeds at room temperature (Scheme 24).[37] This reaction provides access to the bicyclic skeleton of glycinoeclepin (**132**).

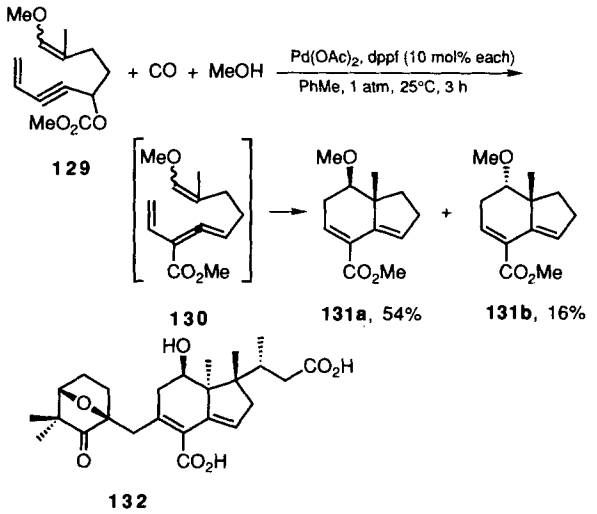

Scheme 24. Preparation of the bicyclic skeleton of glycinoeclepin (**132**).

Facile intramolecular Diels–Alder reaction of the related allenyldiene **134**, generated by the C–O → C–P rearrangement of **133**, yields **135** (Scheme 25).[38]

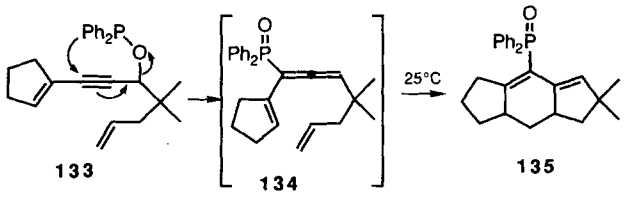

Scheme 25. Tandem C–O → C–P rearrangement and Diels–Alder reaction affording **135**.

3.2.9. *Tandem Carbonylation and Ene Reaction*

The allenyl esters formed by Pd-catalyzed carbonylation undergo an intramolecular ene reaction when a double bond is located at a suitable position. The cyclopentene derivative **138** was obtained in 77% yield by the carbonylation of dehydrolinalyl methyl carbonate (**136**) (Scheme 26).[19] The allenyl ester **137** is first formed and undergoes an intramolecular ene reaction to give **138**.

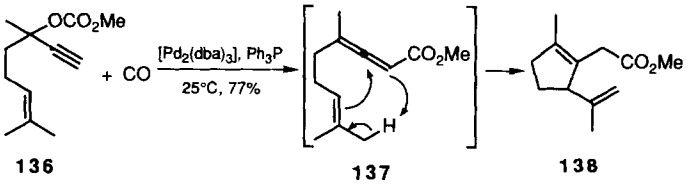

Scheme 26. Tandem carbonylation and ene reaction yielding **138**.

A particularly facile ene reaction is observed with propargyl carbonates having an ester group attached to the triple bond. The carbonylation and intramolecular ene reaction of methyl carbonates **139** and **143** afford cyclohexadiene **142** and cyclopentene **145** via the geminal allenyl diesters **140** and **144**, respectively (Schemes 27 and 28).[39] Further carbonylation of

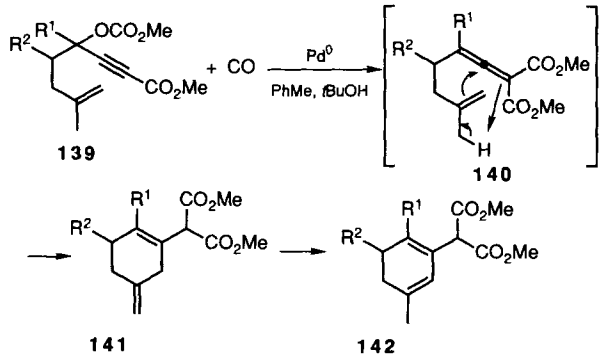

Scheme 27. Tandem carbonylation and ene reaction to give cyclohexadienes **142**; R^1, R^2 = alkyl, aryl.

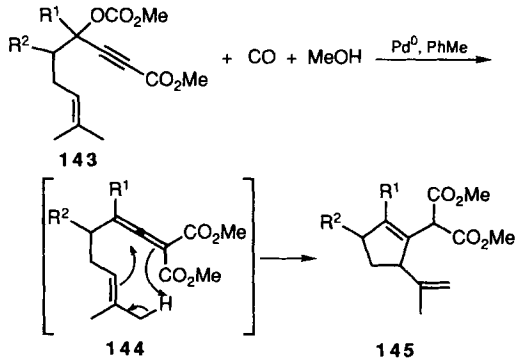

Scheme 28. Tandem carbonylation and ene reaction to form cyclopentenes **145**; R^1, R^2 = alkyl, aryl.

intermediates **140** and **144** to afford the corresponding triesters (cf. **71** in Scheme 15) does not occur. Instead, the sole reaction is the intramolecular ene reaction, which takes place smoothly at 50 °C under 1 atm CO and with $Pd(OAc)_2$/dppp or $Pd(OAc)_2$/dppf (1:2 ratio) as the catalyst.

Substrates **139** and **146**, which both bear an isopropenyl group, undergo palladium-catalyzed monocarbonylation followed by an ene reaction via intermediates like **140** to yield products containing six-membered rings. The ensuing thermodynamically controlled isomerization of the 1,4-dienes **141** and **147** affords the 1,3-cyclohexadienes **142** and **148**, respectively, in high yields (Scheme 27). In sharp contrast, carbonylation of the

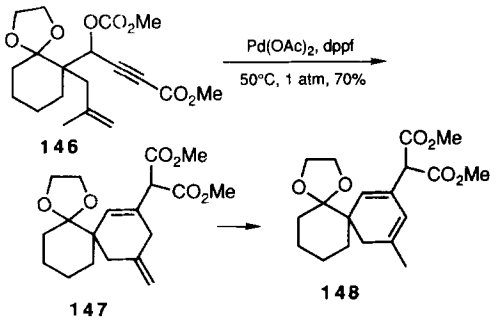

substrates **143** and **149**, which both have 2-methyl-1-propenyl groups, proceeds via intermediates like **144** and yields products **145** and **150** with five-membered rings and isopropenyl substituents (Scheme 28).

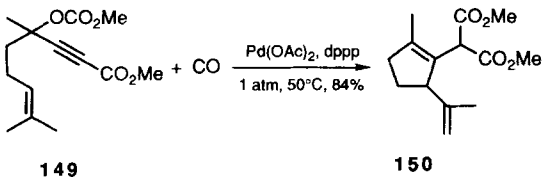

3.2.10. Preparation of Cyclopentenonecarboxylates

The tandem carbonylation and Diels–Alder reaction described in Section 3.2.8 proceeds only intramolecularly. Attempted carbonylation and intermolecular Diels–Alder reaction of conjugated 4-en-2-ynyl carbonates **151** (5 atm CO, room temperature) in the presence of various alkenes as dienophiles gave entirely different products. The 4-oxo-5-alkylidene-2-cyclopentenecarboxylates **152** are obtained unexpectedly by the incorporation of two molecules of carbon monoxide (Scheme 29). In a

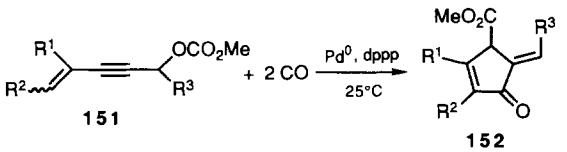

Scheme 29. One-step synthesis of cyclopentenonecarboxylates **152**; R^1, R^2, R^3 = alkyl, aryl.

specific case, cyclopentenone **154** was obtained in 82% yield by the reaction of **153** at 25 °C under 5 atm CO.[40] Bidentate ligands such as dppp or bis(diphenylphosphino)ethane (dppe) are required; triphenylphosphane is not effective.

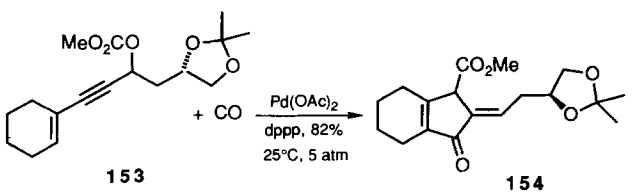

Results of the following experiments give important clues to the mechanism. Isolation of the expected intermediate, a trienecarboxylate ester, is not possible in most cases. As an exception, the trienecarboxylate **156** was isolated (64%) together with the cyclized product **157** (22%) from the reaction of **155** after 4 h. Intermediate **156** was converted into the cyclized product **157** on further exposure to the carbonylation conditions, showing that it is a precursor of **157**.

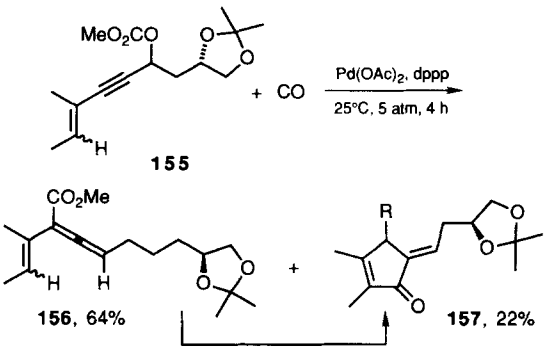

Also the carbonylation of the 1,4-enyne **158** gives only the allenecarboxylate **159**. Further carbonylation to give the cyclic ketones **160** or **161** is not observed (Scheme 30). In addition, the

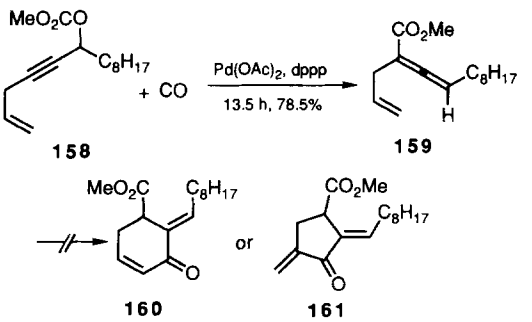

Scheme 30. Monocarbonylation of 1,4-enyne **158**.

1,3-diene ester **162** is recovered intact under the same carbonylation conditions and the cyclized product **163** is not obtained.

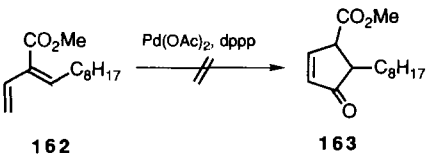

These results imply that the conjugated enallene ester system (1,2,4-triene-3-carboxylate) is required for incorporation of the second molecule of carbon monoxide, and the following mechanism has been proposed. Palladacyclopentene **165** is presumed to arise from **164** and is postulated as an intermediate in the formation of **168**. Insertion of CO into palladacycle **165** generates the acylpalladium complex **166**. Subsequent reductive elimination affords cyclopentenone **167**, which isomerizes to give cyclopentenone **168** as the final product (Scheme 31).

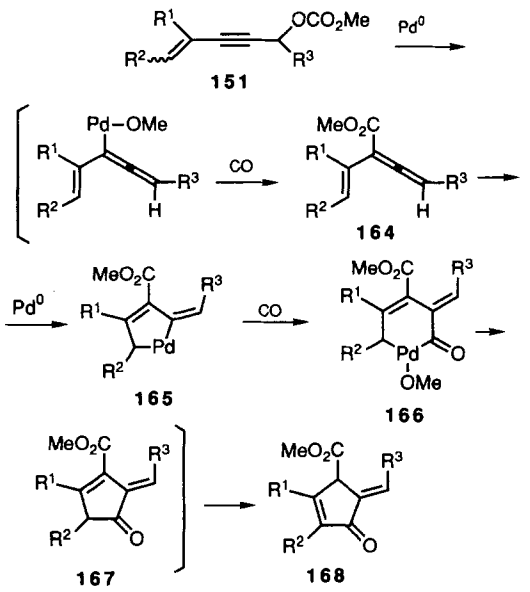

Scheme 31. Proposed mechanism for the formation of cyclopentenonecarboxylates **168**; R^1, R^2, R^3 = alkyl, aryl.

4. Type II Reactions: Transmetalations and Related Reactions

4.1. Reactions with Hard Carbon Nucleophiles

Pd^0-catalyzed reactions of propargylic compounds with hard carbon nucleophiles give different products than those with soft carbon nucleophiles. Propargylic halides, acetates, and phosphates react with hard carbon nucleophiles MR (M = main group elements such as Mg, Zn, B) to give allenyl derivatives. Octylmagnesium chloride reacts with 3-chloro-1-butyne (**169**) to give 2,3-dodecadiene (**170**).[41] Reaction of phenylzinc chloride with 3-acetoxy-3-methyl-1-butyne (**171**) affords 1-phenyl-3-methyl-1,2-butadiene (**174**) in high yield (Scheme 32).[7, 42, 43]

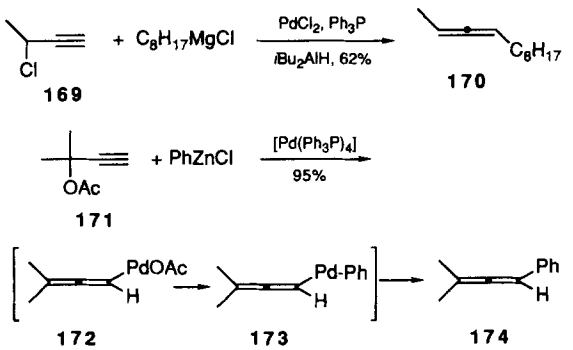

Scheme 32. Transmetalation reactions and mechanism of the reaction of phenylzinc chloride with propargyl acetate **171**.

The reaction can be explained by transmetalation of the allenylpalladium intermediate **172** with phenylzinc chloride to generate the allenyl(phenyl)palladium intermediate **173**, followed by reductive elimination to afford **174**.

anti Stereoselectivity was observed in the reaction of (*R*)-(−)-1-phenyl-1-trifluoroacetoxy-2-propyne (**175**) with phenylzinc chloride to produce the levorotatory allene (*R*)-**176**; the ratio of *anti* vs. *syn* 1,3-substitution was approximately 82:18. Also the reaction of the 17β propargylic ester **177** with phenylzinc chloride gave mainly the *anti* product **178** with high stereoselectivity. The observed *anti* stereoselectivity is explained by assuming that formation of the allenylpalladium intermediate involves configuration inversion; the transmetalation and reductive elimination proceed with retention of configuration.[43] It is well-established that the same stereoselectivity (overall inversion) is observed in the Pd^0-catalyzed substitution reaction of allylic esters with hard carbon nucleophiles.

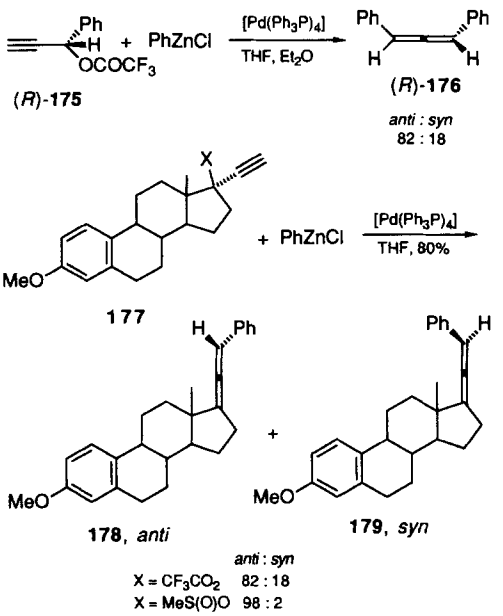

2-Alkynyloxiranes react smoothly with alkynyl-, alkenyl-, and arylzinc reagents. Reaction of 2-methyl-2-(1-propynyl)-oxirane (**181**) with vinylzinc chloride (**180**) yields 2,4-dimethyl-2,3,5-hexatrien-1-ol (**182**).[44]

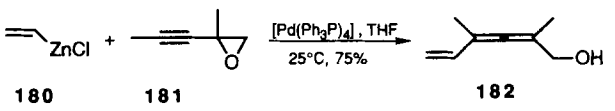

Organoboranes also react with propargylic carbonates. Usually, addition of a base is indispensable for palladium-catalyzed reactions of organoboranes with aryl, alkenyl, and allyl halides. But the reaction of organoboranes with methyl propargyl carbonates proceeds without added base, because methoxide is generated in situ from the carbonate. For example, 1,3,4-triene **185** is obtained from the reaction of alkenylborane **184** with propargylic carbonate **183** under neutral conditions.[45]

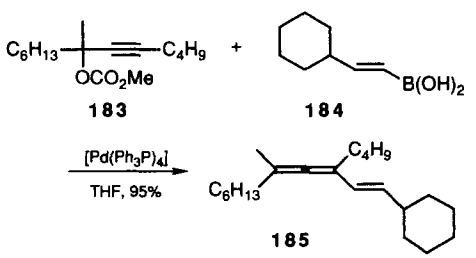

4.2. Reactions of Terminal Alkynes; Formation of 1,2-Dien-4-ynes

1,2-Dien-4-ynes **190** (allenylacetylenes) can be prepared in good yields by the palladium-catalyzed coupling of terminal alkynes **187** with propargylic compounds such as carbonates, acetates, and halides in the presence of the cocatalyst cuprous iodide (Scheme 33). Addition of cuprous iodide is not necessary

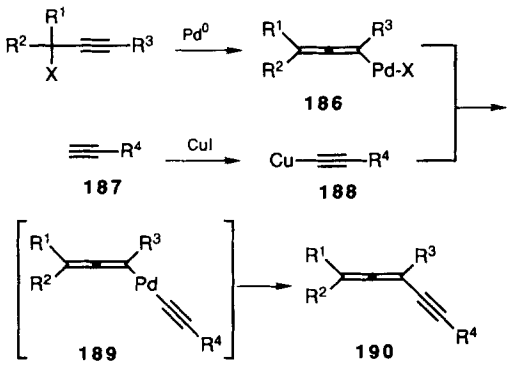

Scheme 33. Mechanism of the Pd/Cu-catalyzed coupling of propargylic compounds with terminal alkynes; X = OCO_2Me, OAc, Cl; R^1, R^2, R^3, R^4 = alkyl, aryl.

when metal acetylides are used. The Pd/Cu-catalyzed coupling of propargylic carbonates with terminal alkynes proceeds at room temperature rapidly within 30 min.[46] The addition of lithium chloride or potassium bromide and diethylamine rather than triethylamine gives better results. The allenylalkynes formed by the coupling are reactive and apparently undergo further palladium-catalyzed reactions—their yields tend to decrease for extended reaction times. Therefore the reaction must be stopped as soon as the coupling is complete. The reaction can be explained by the following mechanism (Scheme 33). Reaction of cuprous iodide with the terminal alkyne **187** affords the copper acetylide **188**, which undergoes transmetalation with **186** to form the allenyl(alkynyl)palladium intermediate **189**. Reductive elimination then gives the allenylacetylene **190**. The coupling of **191** with propargyl alcohol (**85**) gave rise to 1,2-dien-4-yne **192** at room temperature in 85% yield in 25 min.

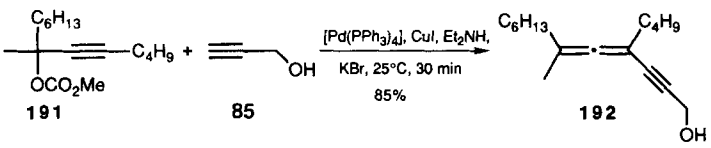

The cyclic carbonate **193** reacts with the terminal alkyne **194** under similar conditions to give the 2,3-alkadien-4-yn-1-ol derivative **195**.[47]

Propargylic chlorides also react with terminal alkynes in the presence of triethylamine or diisopropylamine. 5-Butyldodeca-3,4-dien-6-yne (**197**) was obtained in 91% yield from the reaction of 3-chloro-4-nonyne (**196**) with 1-heptyne in diisopropylamine. Coupling of the propargylic acetate **198** with 1-heptyne is possible in the presence of three equivalents of zinc chloride with or without cuprous iodide to give the 2,3-dien-5-yne **199**.[48]

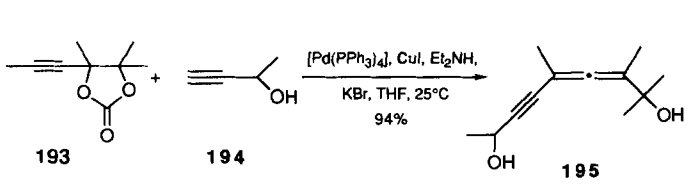

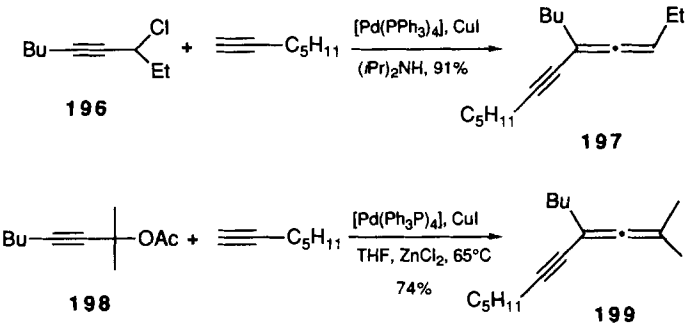

Various metal acetylides can be coupled smoothly with propargylic halides and acetates, and with 2-(1-alkynyl)oxiranes to give 2,3-dien-5-yn-1-ols.[42,44] In one synthetic application the unstable 2,3-octadiene-5,7-diyn-1-ol (**203**), a fungus metabolite, was prepared by coupling 4-trimethylsilylbutadiynylzinc chloride (**200**) with 2-ethynyloxirane (**201**) to give the allenyl alcohol **202**, which was then desilylated (Scheme 34).[44]

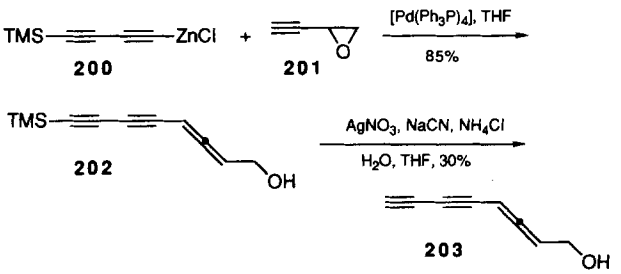

Scheme 34. Synthesis of 2,3-octadiene-5,7-diyn-1-ol (**203**), a fungus metabolite.

The unsaturated *exo*-enol lactone **207** was obtained by coupling the propargylic acetate **204** (≡**171**) with 4-pentynoic acid (**205**) in the presence of potassium bromide and with tri(2-furyl)phosphane (TFP) as the ligand. Oxypalladation of the triple bond of 4-pentynoic acid (**205**) with the allenylpalladium intermediate and the carboxylate (as shown in **206**) is the first step, and the subsequent reductive elimination affords lactone **207** (Scheme 35). The (*E*) double bond is formed because the oxypalladation is a *trans* addition.[49]

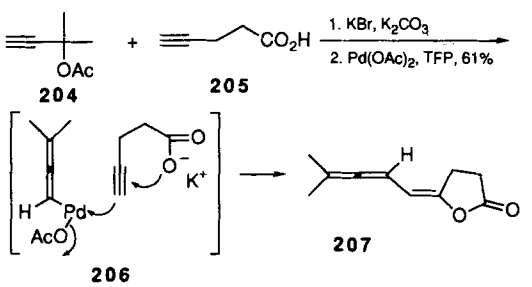

Scheme 35. Formation of the unsaturated *exo*-enol lactone **207** from 4-pentynoic acid (**205**).

4.3. Hydrogenolysis of Propargylic Compounds Having Terminal Triple Bonds with Formate and Other Hydrides to Give Allenes

The Pd-catalyzed reaction of the terminal allylic esters geranyl carbonate (**208a**) and acetate (**208b**) with ammonium formate or triethylammonium formate affords olefin **209**, which has a terminal double bond, regioselectively.[50] Hydrogenolysis with other hydrides affords the isomeric diene **210** with two

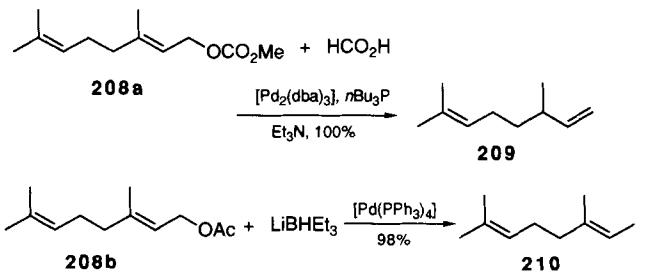

internal double bonds.[51] Formate is a special reducing agent since it gives the terminal alkene with high regioselectivity. Similarly, the facile hydrogenolysis of the terminal propargylic carbonate **211** at room temperature with ammonium formate using $[Pd_2(dba)_3]/nBu_3P$ in THF affords 1,2-undecadiene (**212**). The reaction of the isomeric carbonate **213** having an internal triple bond is slower and proceeds at 70 °C to give allene **212**.[52] In addition, alkyne **214** is formed as a by-product. Formation of

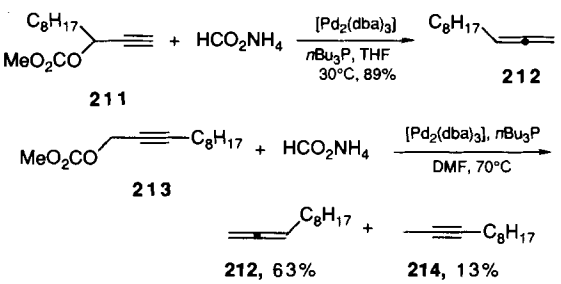

alkynes as the main product of the hydrogenolysis of propargylic esters will be discussed separately in Section 6.1, because it is a type IV reaction.[52] The selective, Pd^0-catalyzed formation of allenes by hydrogenolysis is a convenient means of preparing allenes from propargylic alcohols. Allenes are reduced further to 1-alkenes by treatment with an excess of ammonium formate at 65–100 °C. As an example, the 1-alkene **217** is obtained from **215** directly by reduction with five equivalents of ammonium formate at 100 °C in dioxane. Allene **216** is obtained by treatment of **215** with two equivalents of ammonium formate at room temperature in THF.

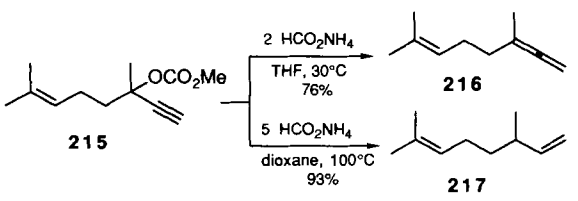

The formation of allenes from terminal propargylic esters proceeds much more cleanly when propargylic formates are used. Decarboxylation–hydrogenolysis giving allenes is then possible without ammonium formate. Allene **219** is obtained cleanly from the propargylic formate **218**; only a small amount of alkyne **220** is formed (MOM = methoxymethyl).

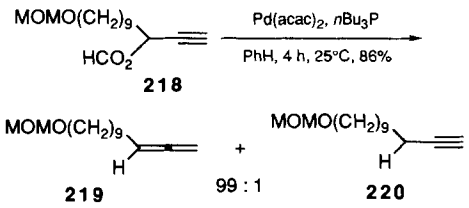

Preparation of an active Pd^0 catalyst is crucial for the clean formation of allenes. The catalyst generated in situ from $Pd(OAc)_2$ or $Pd(acac)_2$ and nBu_3P (1:1 ratio) is very active and particularly effective for this reaction.[14] The most satisfactory results with this catalyst are obtained with primary and secondary propargylic formates having terminal triple bonds. Tertiary propargylic formates cannot be prepared; in this case the corresponding carbonates are reduced by treatment with triethylammonium formate. Triethylammonium formate is more soluble than ammonium formate in organic solvents and thus gives better results. In addition, propargylic formates are superior to other esters, because the allenes produced are not reduced further to the corresponding alkenes. In particular, the reaction of terminal propargylic formates affords allenes smoothly.[53, 54]

Propargylic esters with internal triple bonds are converted into alkynes by the hydrogenolysis discussed in Section 6.1. In one exception, the primary propargylic formate **221** gives allene **222** as the main product and alkyne **223** as a minor product.

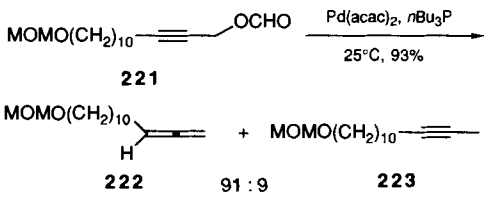

The hydrogenolysis of the 2-(1-alkynyl)oxirane **224** with triethylammonium formate is not selective. A mixture of 1-alkyn-4-ol **225** and the expected 1,2-dien-4-ol **226** was obtained in a ratio of 6:4.[52] However, the reaction of 2-(1-alkynyl)oxirane

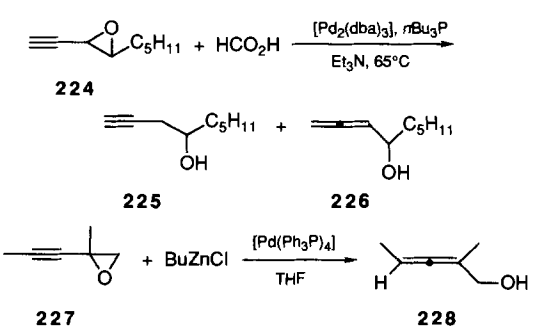

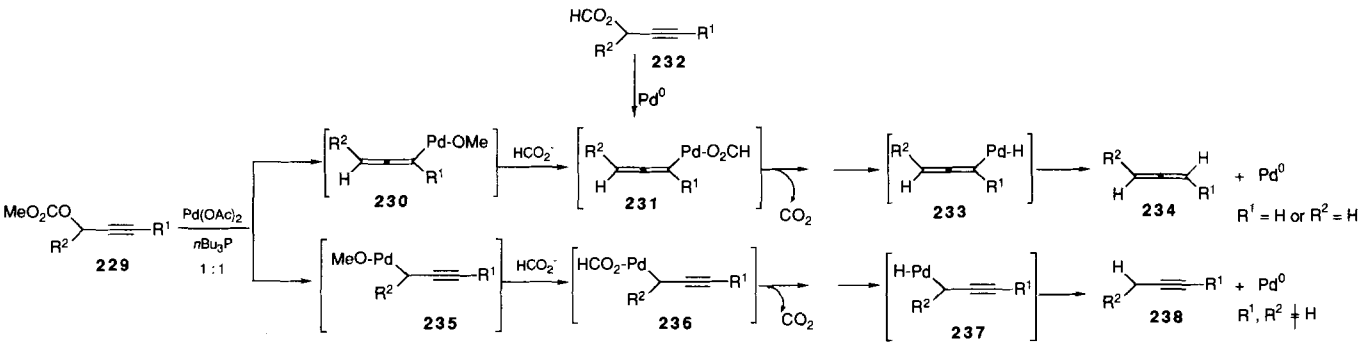

Scheme 36. Mechanism of the hydrogenolysis of propargylic esters **229** with formate.

227 (≡**181**) with *n*-butylzinc chloride afforded the expected 2,3-dien-1-ol **228** as the main product.[44]

The following mechanism has been proposed for the hydrogenolysis of propargylic carbonate **229** with ammonium formate (Scheme 36). Oxidative addition yields the allenylpalladium methoxide **230**, which reacts with ammonium formate to generate the allenylpalladium formate complex **231**. This intermediate is also formed directly by oxidative addition of the corresponding propargylic formate **232**. Decarboxylation of **231** gives the allenylpalladium hydride complex **233**, which finally undergoes reductive elimination to give allene **234** and the Pd^0 catalyst. The propargylic complex **235** may also be formed, depending on the substituent, and converted into propargylic formate **236**. Alkyne **238** is obtained from the propargylpalladium hydride comple **237**, which is considered to be in equilibrium with **233**.

Hydrogenolysis of the cyclic alkynyl carbonate **239** with triethylammonium formate afforded the α-allenyl alcohol **240** when dppe was used as a ligand. On the other hand, the homopropargylic alcohol **241** was obtained with nBu$_3$P.[55]

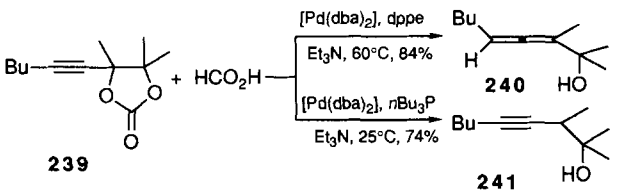

Terminal propargylic bromides, mesylates, and phosphates are hydrogenolyzed with $LiAlH_4$, $NaBH_4$, and $LiBHEt_3$, and the selectivity is dependent on the hydride species. Hydrogenolysis of the terminal propargylic bromide **242** with $LiBHEt_3$ gives allene **243** with high selectivity. Propargylic mesylates, bromides, and phosphates with internal triple bonds are converted into mixtures of allenes and alkynes with these metal hydrides. Treatment of the propargylic mesylate **244** with $LiBEt_3H$ gives allene **245** as the main product and alkyne **246** as a minor product. But a considerable amount of overreduction to alkene **247** is also observed.[56]

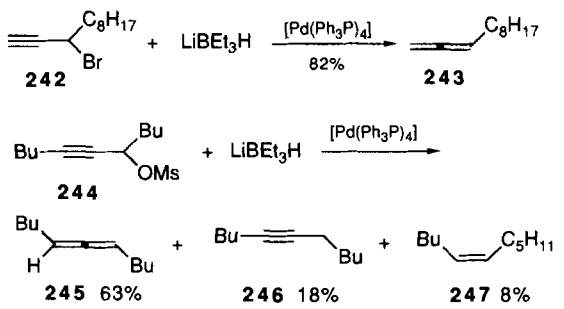

Propargylic acetates are not suitable for the hydrogenolysis with ammonium formate. At room temperature, almost no reaction of propargylic acetates with ammonium formate takes place, and a mixture of allene and 1-alkene is obtained at elevated temperatures. Thus propargylic formates and carbonates are the best substrates for the allene formation. The method offers a new and efficient preparative approach to allenes from easily available propargylic alcohols via their formates or carbonates.

Reduction of propargylic compounds with samarium diiodide is possible in the presence of palladium catalysts. Propargylic acetate **248** is converted mainly to allene **251** by the palladium-catalyzed reaction with samarium diiodide in the presence of a proton source. Propargylic phosphates react with samarium diiodide similarly.[57] In this reaction, the allenylpalladium complex **249** is reduced with bivalent samarium to give the allenyl anion **250**, which is protonated to afford the allene **251**. Alkyne **252** is formed as a by-product (Scheme 37). The reactive

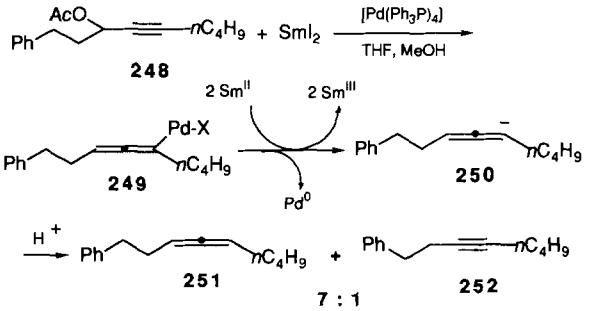

Scheme 37. Mechanism of the hydrogenolysis of propargylic acetate **248** with SmI_2.

intermediate 2,3-naphthoquinodimethane (**256**) can be generated by this reaction. Treatment of 1,2-di(1-acetoxypropynyl)benzene (**253**) with samarium diiodide affords 1,2-dipropadienylbenzene (**255**), which spontaneously cyclizes to give 2,3-naphthoquinodimethane (**256**). Then facile Diels–Alder reaction of **256** with fumarate (**254**) gives the tetrahydroanthracene derivative **257** (Scheme 38).[58] Similarly, compound

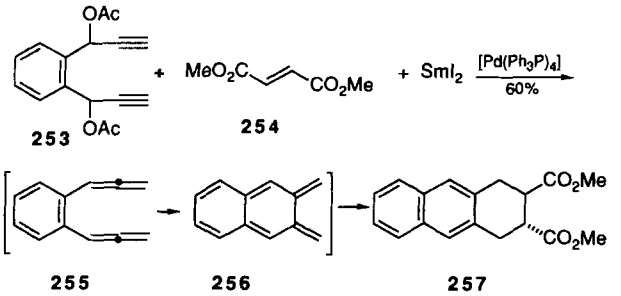

Scheme 38. Tandem hydrogenolysis of propargylic acetate **253** with SmI_2 and Diels–Alder reaction.

259, a synthetic equivalent of a propargylic anion, is generated by the reaction of propargylic acetate **258** with samarium diiodide; the anion attacks the ketone intramolecularly to give the homopropargyl cycloalkanol **260** (Scheme 39).[59a] The reaction was applied to the synthesis of the enyne A ring synthon of 1α-hydroxy vitamin D.[59b]

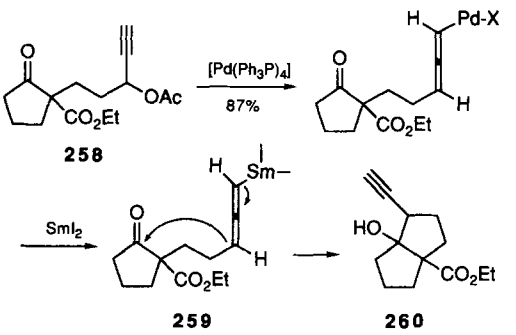

Scheme 39. Generation of intermediate **259**, a synthetic equivalent of a propargylic anion.

5. Type III Reactions: Reactions with Soft Carbon and Oxo Nucleophiles

5.1. Reactions with Soft Carbon Nucleophiles

Type III reactions proceed by attack of a nucleophile at the central sp carbon of the allenylpalladium complex. In contrast to allylic esters, which undergo facile Pd^0-catalyzed reactions with soft carbon nucleophiles via π-allylpalladium intermediates, propargylic esters are less reactive. Propargylic acetates do not react with soft carbon nucleophiles. But soft carbon nucleophiles such as β-keto esters and malonates react with propargylic carbonates under neutral conditions and with dppe as the Pd ligand.[60]

2-Propynyl carbonate (**48**) reacts with two equivalents of malonate **262** or methyl α-alkylacetoacetate **268** to give the 2,3-disubstituted propenes **266**, **267**, and **269** under neutral conditions in boiling THF (Scheme 40). The carbanion **262** attacks the central sp carbon of the allenylpalladium species **261** to generate **263**, which abstracts a proton from malonate to form the π-allylpalladium intermediate **265**. Intermediate **263** can be considered equivalent to the palladium carbene complex **264**. In the last step malonate anion attacks the π-allylpalladium intermediate **265**, as expected, to give **266**. Migration of the double bond in

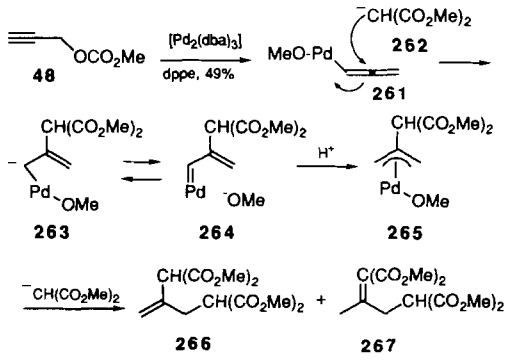

Scheme 40. Mechanism of the reaction of propargyl carbonate **48** with malonate **262**.

266 affords **267**. The reaction of α-alkylacetoacetate **268** gives **269**.[60,61] Thus the propargylic carbonate **48** has two sites for nucleophilic attack. The best ligand for the reaction is dppe; the reaction is slow when Ph_3P is used.

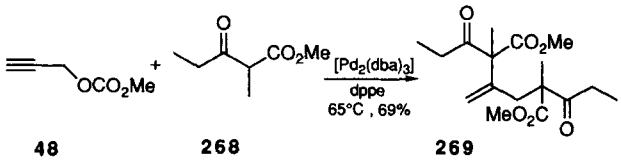

Acetoacetate **270**, bearing two activated hydrogen atoms, reacts with methyl propargyl carbonate (**48**) in a 1:1 ratio in THF under neutral conditions at room temperature to give an entirely different product. In the first step C-alkylation generates the π-allylpalladium intermediate **271** (Scheme 41). Intramolecular

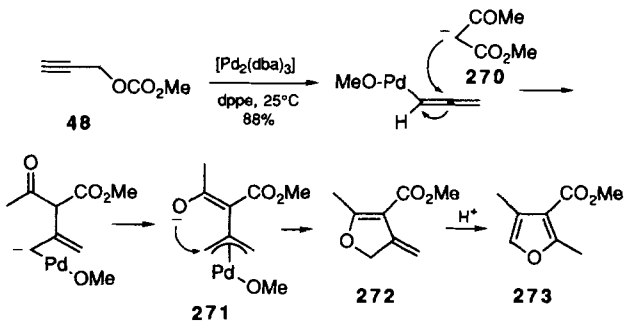

Scheme 41. Mechanism of furan formation by the Pd-catalyzed reaction of acetoacetate **270** with propargyl carbonate (**48**).

attack by the nucleophilic enolate oxygen then gives 4-(methoxycarbonyl)-5-methyl-3-methylene-2,3-dihydrofuran (**272**) in 88% yield. The methylenedihydrofuran **272** is unstable and isomerizes to the stable furan **273** quantitatively under slightly acidic conditions.[60,61] This type of C- and O-alkylation of propargylic carbonates provides a useful approach to furans. Acetylacetone (**274**) reacts analogously with **48** to give the corre-

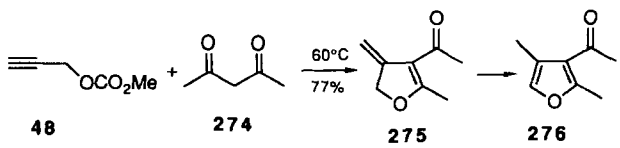

sponding dihydrofuran **275**, which isomerizes to **276**. Similarly, reactions of dimethyl 3-oxoglutarate (**277**) and 1,3-cyclohexanedione (**279**≡**120**) afford **278** and **280**, respectively, in good yields.

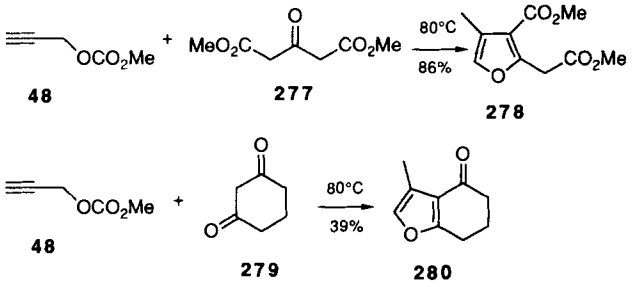

This method for the preparation of substituted furans has been applied to the synthesis of phenylthiomethyl-substituted furan **282** by the reaction of **48** with β-keto ester **281**; furan **282** was used for the syntheses of natural products such as neoliacine.[62]

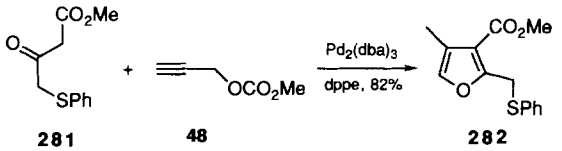

To study the mechanism of the furan formation, the reactions of methyl acetoacetate (**270**) with the isomeric 2-butynyl methyl carbonate (**283**) and 1-methylpropynyl methyl carbonate (**284**) were examined. Both give the product **285**, indicating that the furan formation from **283** and **284** proceeds via a common intermediate. However, reactions of **283** and **284** with methyl 2,2-bisdeuterioacetoacetate (**286**) gave products deuterated at different carbons. The 2-deuterio-3-hydrofuran **290** was obtained from **283** via **289** (Scheme 42), whereas reaction of **284** with **286** afforded furan **294** via **293** (Scheme 43). These results are explained by assuming that the attack of oxygen nucleophilic (O-allylation) occurs at the more substituted side of π-allylpalladium systems in **289** and **293**.

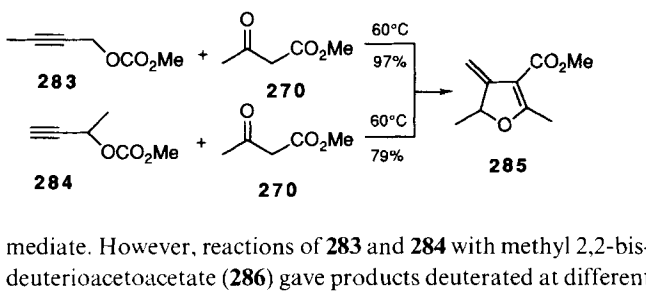

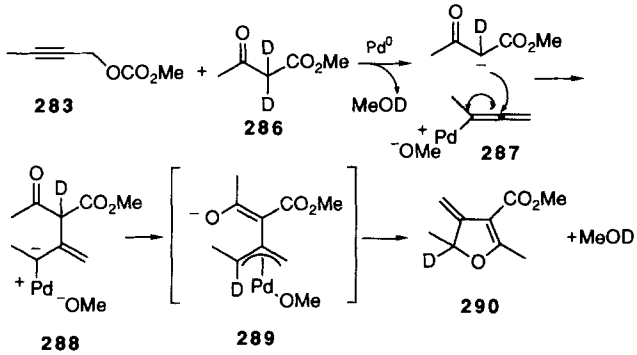

Scheme 42. Deuterium incorporation in a furan derivative formed by the reaction of deuterated acetoacetate **286** with **283**.

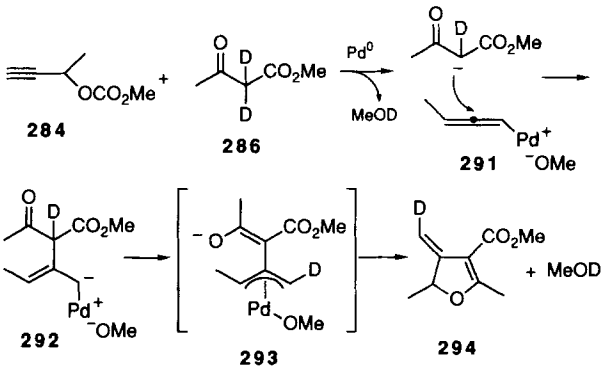

Scheme 43. Deuterium incorporation in a furan derivative formed by the reaction of deuterated acetoacetate **286** with **284**.

Formation of the labeled furans from **283** and **284** is explained by the following mechanism (Scheme 44). In the first step propargylic carbonate **283** (**284**) reacts with Pd^0 to give the allenylpalladium carbonate **295**, which is converted into the palladium methoxide complex **296**. The methoxide abstracts an acidic hydrogen (or deuterium) from acetoacetate **286** to give **297**. Then the enolate anion **297** attacks the central carbon of the allenyl moiety of **296** to generate **298**, and intramolecular deuterium transfer furnishes the π-allylpalladium complex **299** (**300**). This, intermediate undergoes intramolecular O-alkylation with the enolate oxygen to give the labeled *exo*-methylene furan **290** (**294**). The key conclusion is that the oxygen anion attacks the more substituted side of the π-allyl systems in **299** and **300**.

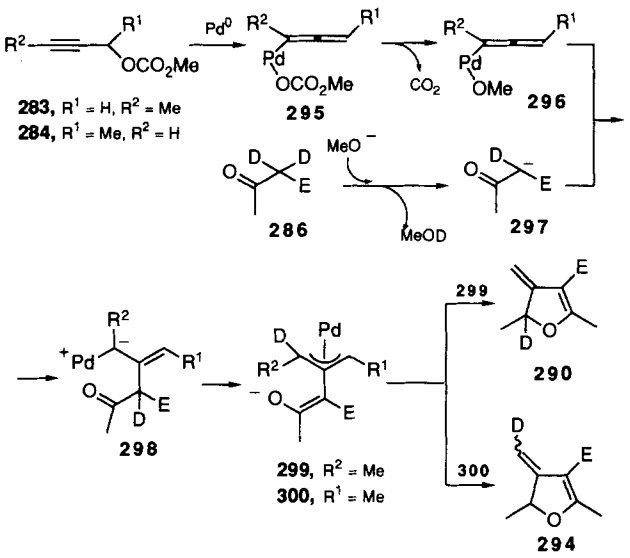

Scheme 44. Mechanism for the formation of the labeled furans **290** and **294**; E = CO_2Me.

The reaction of propargyl carbonate **48** with 2,5-hexanedione-3,4-dicarboxylate (**301**) catalyzed by $[Pd_2(dba)_3]$/dppe afforded after seven hours methylenecyclobutane **302** (double C-alkylation) and 3-methylenedihydropyran **303** (C- and O-alkylations) in 52 and 45% yield, respectively. Since cyclobutane **302** is a product of a reversible reaction, 33% of **302** could be converted into **303** by treatment with the same catalyst for seven hours.[63]

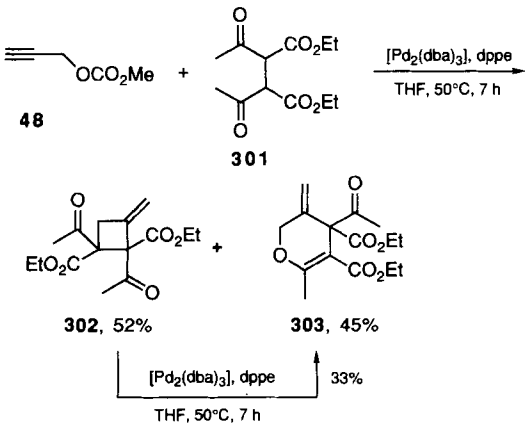

2-Alkynyloxiranes **304** undergo the palladium-catalyzed furan formation with soft nucleophiles by two cyclization paths to give either **308** or **309** as the primary product (Scheme 45). The

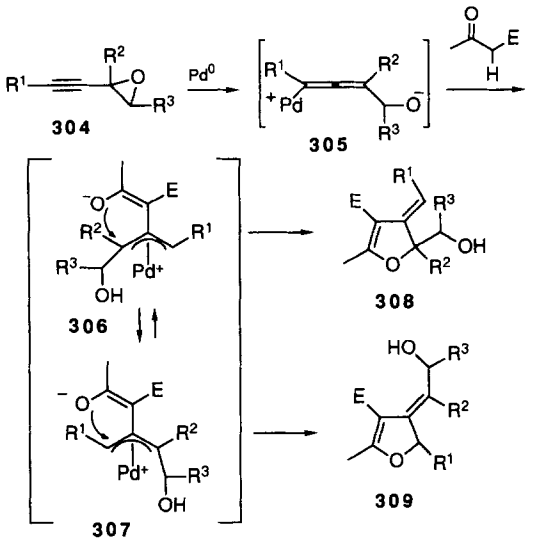

Scheme 45. Furan formation from 2-(1-alkynyl)oxiranes **304**; R^1, R^2, R^3 = alkyl, aryl.

dihydrofuran undergoes further transformations depending on its substituents.[61, 64] In the first step the allenylpalladium complex **305** is generated, which is converted into the two π-allylpalladium complexes **306** and **307**, from which two products are formed. When R^2 is not H, the enolate oxygen attacks the more substituted side to give furan **308**. Formation of **311** and **318** can be explained by evoking the π-allylpalladium complex **306** as an intermediate (Scheme 46). When R^2 is H, furan **309** is obtained.

The formation of furans **314** and **321** also belongs to this class of reactions (Scheme 47). Furthermore, the final products depend on the substitutents, as shown by the following examples.

Oxirane **310** reacted with methyl acetoacetate (**270**) in the presence of $[Pd_2(dba)_3]$ and dppe in dry THF at 60 °C to give

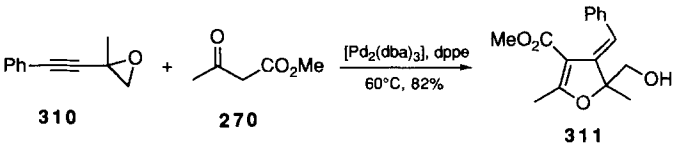

2,3-dihydrofuran-4-carboxylate **311** in 82% yield. The *exo* double bond in **311** has (*E*) configuration, since the reaction proceeds via π-allylpalladium intermediate **306**, in which R^1 (Ph) assumes the *syn* orientation preferentially for steric reasons. In addition, the fact that the furan **313**, formed from **312** and **270**, undergoes facile lactonization to form furolactone **314**

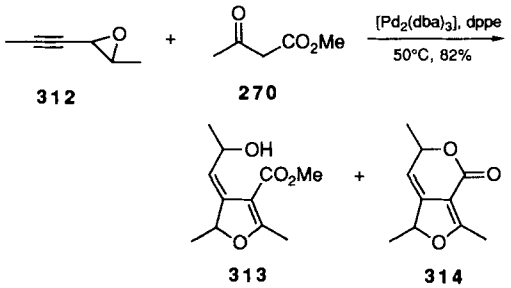

supports the (*E*) configuration of the *exo* double bond in **313**. The *exo*-methylenefuran **317**, formed from **315** via π-allylpalladium intermediate **316**, is a highly acid-sensitive compound. The dehydroxymethylation to give methyl 2,4,5-trimethylfuran-3-carboxylate (**318**) can be observed by NMR analysis in $CDCl_3$; the reaction also takes place quantitatively on treatment with acid (Scheme 46). On the other hand, benzylidenefuran **311**

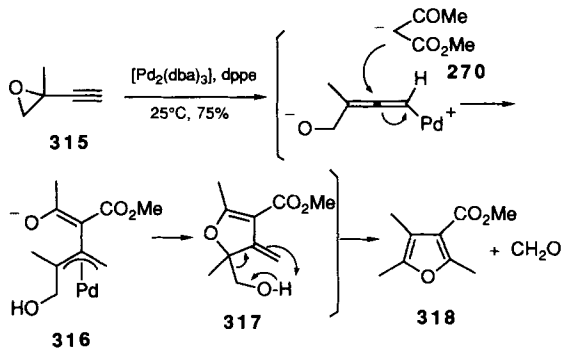

Scheme 46. Furan formation with elimination of formaldehyde.

does not undergo either dehydroxymethylation or dehydration under the same conditions. The 2-phenyldihydrofuran **320** formed from **319** undergoes facile dehydration to give **321**, rather than lactonization (Scheme 47).

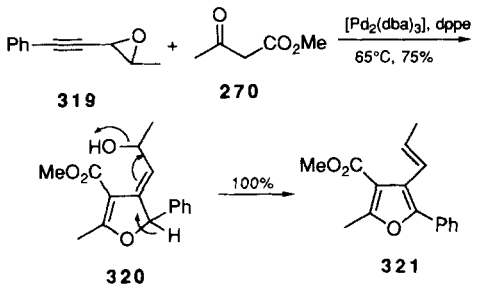

Scheme 47. Furan formation with dehydration.

In an intramolecular reaction of the malonate-type carbon nucleophile in **322**, the intermediate π-allylpalladium complex **323** undergoes β-hydride elimination to form the diene **324** (Scheme 48).[65]

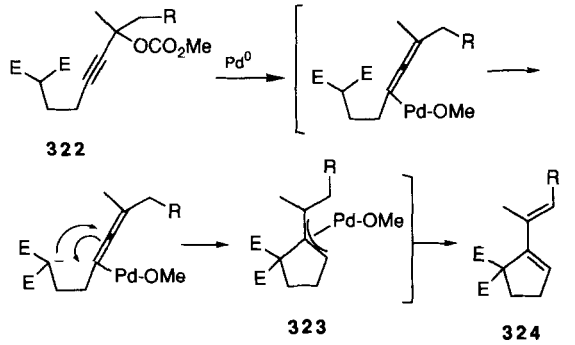

Scheme 48. Intramolecular attack of a malonate-type anion followed by elimination; E = CO_2R, R = alkyl.

Carbon–carbon bond formation can take place by the Pd^0-catalyzed reaction of propargylic carbonates with silyl enol ethers or by rearrangement of propargylic enol carbonates as masked carbon nucleophiles. Propargylic carbonates are expected to react with silyl enol ethers via allylpalladium enolates by transmetalation. In an attempted synthesis of unsaturated isoprenoid aldehydes, the reaction of 1-trimethylsiloxyisoprene (**326**) with 1,1-dimethylpropynyl methyl carbonate (**325**) gave the α,β-unsaturated isoprenoid allenyl aldehyde **328** and the unsaturated alkynyl aldehyde **329**, although the yield was low (30%). The allenylpalladium complex **327** is an intermediate of **328**, which is converted to dehydrocitral **330** (Scheme 49).[66] It is well-established that the corresponding allylic carbonates react with silyl enol ethers by transmetalation to afford allylated carbonyl compounds in good yields.[67]

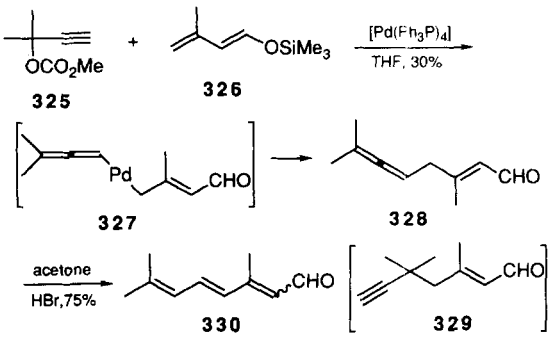

Scheme 49. Reaction of silyl enol ether **326** with propargylic carbonate **325** to give allenyl aldehyde **328**, and its conversion into triene aldehyde **330**.

α,β-Unsaturated isoprenoid allenyl aldehydes can be prepared in higher yields by rearrangement of mixed propargyl enol carbonates. Carbonate **332** was prepared from β-ionone (**331**) and allowed to undergo the palladium-catalyzed rearrangement to give the allenyl aldehyde **334** as an (*E*/*Z*) mixture and alkynyl aldehyde **335** in 54% combined yield, as well as an elimination product **336** (25%) (Scheme 50); trinaphthylphosphane was used as the ligand. The allenylpalladium complex **333** is an intermediate of the rearrangement and its reductive elimination affords **334**. Aldehyde **334** is reconjugated with hydrogen bromide, and the all-*trans* isomer of retinal (**337**) is obtained by a simple equilibration.[66] The reaction is applicable to syntheses of polyunsaturated aldehydes and ketones. The single product **339** was obtained in high yield by the palladium-catalyzed rearrangement of the propargylic enol carbonate **338**.[68] It should be added that the corresponding allyl enol carbonates undergo a similar rearrangement to give α-allyl aldehydes in high yields.[69]

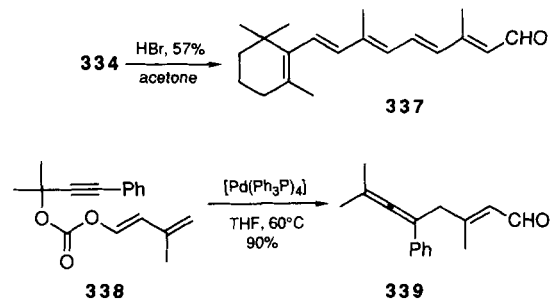

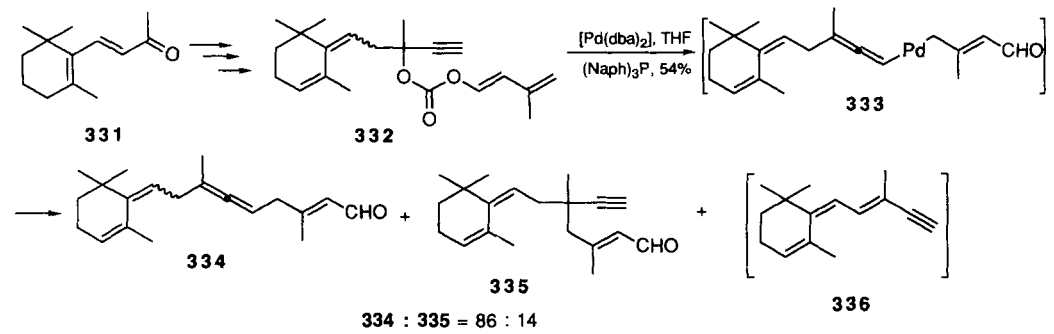

Scheme 50. Rearrangement of propargyl enol carbonate **332** to give allenyl aldehyde **334**.

5.2. Reactions with Oxo Nucleophiles

Propargylic carbonate **340** is cyclized by attack of the C-5 hydroxyl group at the central carbon of the initially formed allenyl system **341**. The intermediate σ-allylpalladium complex **342** undergoes β-hydride elimination to give the dienes **343** and **344**, which are converted into the more stable furan **345** as the final product (Scheme 51).[70] The reaction proceeds in the presence of diazabicycloundecane (DBU). The primary products **343** and **344** are isomerized easily to the furan **345** during column chromatography on silica gel. In a related example, propargylic carbonate **346** was converted into the furan **347** in

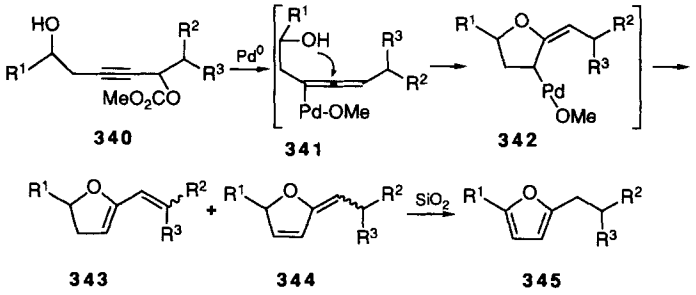

Scheme 51. Furan formation by intramolecular reaction of propargylic carbonates with OH groups; R^1, R^2, R^3 = alkyl, aryl.

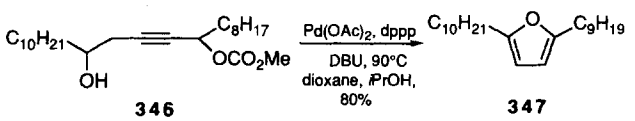

80% yield in refluxing dioxane and with dppp as the ligand. Similarly, dihydropyrans **350** and **351** are formed from 6-hydroxy carbonates **348** via intermediate **349** (Scheme 52). Formation of the dihydropyrans **353** and **354** from **352** is another example.

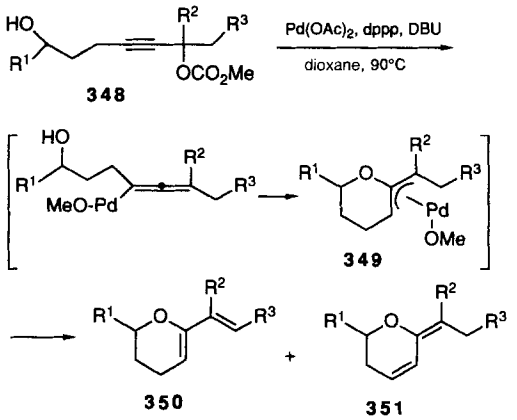

Scheme 52. Dihydropyran formation by intramolecular reaction of propargylic carbonates with OH groups; R^1, R^2, R^3 = alkyl, aryl.

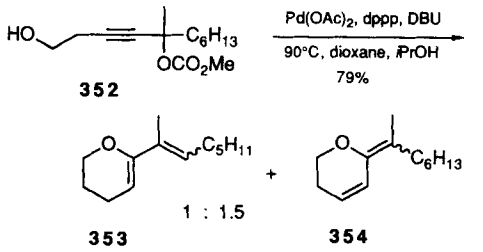

6. Type IV Reactions: Reactions via Propargylpalladium Intermediates

6.1. Hydrogenolysis of Propargylic Compounds Having an Internal Triple Bond with Formate and Other Hydrides

Palladium-catalyzed reactions via propargylic palladium intermediates like **356** are rather rare. One reaction that certainly proceeds via **356** is the decarboxylation–hydrogenolysis of propargylic formates **355**, which have an internal triple bond and can have various functional groups. Treatment of formate **355** with a Pd^0 catalyst in benzene or THF at room temperature gives the internal alkyne **357** almost exclusively and not allene **358** (Scheme 53).

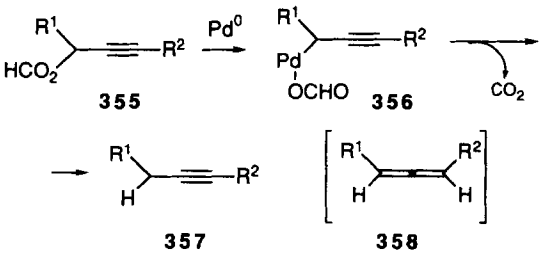

Scheme 53. Mechanism of the hydrogenolysis of propargylic formates to give alkynes; R^1, R^2 = alkyl, aryl.

The preparation of the catalyst is crucial to this reaction. A catalyst prepared by mixing Ph_3P or dppe with $[Pd_2(dba)_3]$ does not give **357** cleanly. The best catalyst is prepared by mixing $Pd(OAc)_2$ or $Pd(acac)_2$ with nBu_3P in a ratio of 1:1.[114] With this catalyst, the internal alkynes **360** and **362** were formed in high yields and with over 97% selectivity from the functionalized propargylic formates **359** and **361**, respectively; the corresponding allenes were not formed.

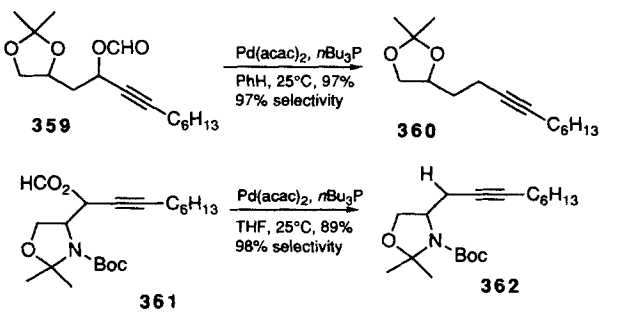

This reaction is useful for selective preparation of internal alkynes, particularly those with labile functional groups. It is not always easy to prepare disubstituted alkynes **364** by simple alkylation of terminal alkynes **363**. Propargylic alcohols **365** are

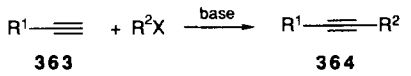

prepared more easily by reaction of terminal alkynes **363** with ketones or aldehydes, and internal alkynes **367** are prepared by the hydrogenolysis of their formates or carbonates **366** (formates of primary and secondary alcohols, and carbonates of tertiary alcohols) (Scheme 54).

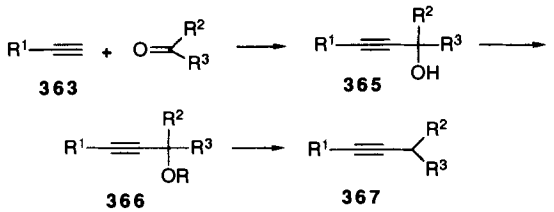

Scheme 54. Preparation of internal alkynes from terminal alkynes; R^1, R^3 = alkyl, aryl; when R^2 = H, R = CHO; when R^2 = alkyl, aryl, R = CO_2Me.

Internal propargylic halides and phosphates are reduced to internal alkynes with $LiAlH_4$, $NaBH_4$, and $LiAlEt_3H$ in the presence or absence of palladium catalysts. Selectivity is highly dependent on the hydride used.[56]

6.2. Eliminations: Formation of Conjugated Enynes

When the propargylic carbonate **368** is treated with a palladium catalyst in the absence of any other reactant, elimination of a β-hydrogen atom from the propargylpalladium intermediate **369** occurs to afford the conjugated enyne **370**. Formation of 1,2,3-triene **372** by elimination from the allenylpalladium intermediate **371** is not observed (Scheme 55).[54, 71] The elimination reaction proceeds with a variety of propargylic carbonates under mild and neutral conditions. Bidentate phosphanes, particularly dppf, are the best ligands for tertiary carbonates, and Ph_3P is used for secondary carbonates. The reaction with the tertiary

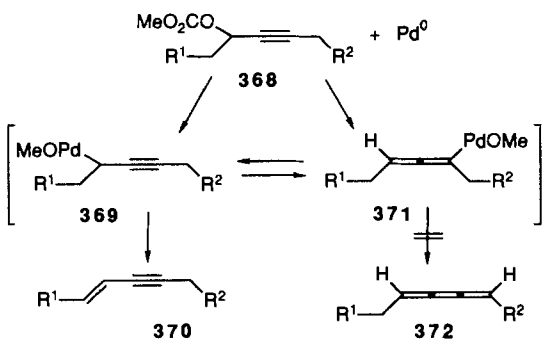

Scheme 55. Preparation of conjugated enyne **370** by elimination of propargylic carbonates; R^1, R^2 = alkyl, aryl.

propargylic carbonate **373** derived from cyclooctanone proceeds smoothly to give the conjugated enyne **374** in good yield. The reaction is applicable to a number of other cyclic ketones

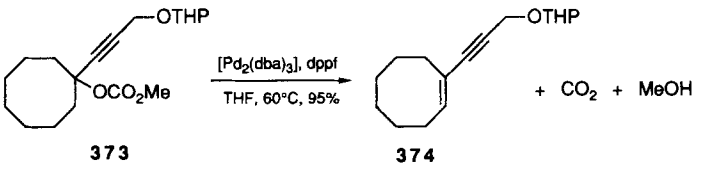

but not to cyclohexanone. The regioselectivity in the elimination of **375** is significantly affected by the catalytic species. When Ph_3P is used as the ligand, elimination from **375** gives mainly the disubstituted alkene **377**; with dppf the major product is enyne **376**.[54, 71]

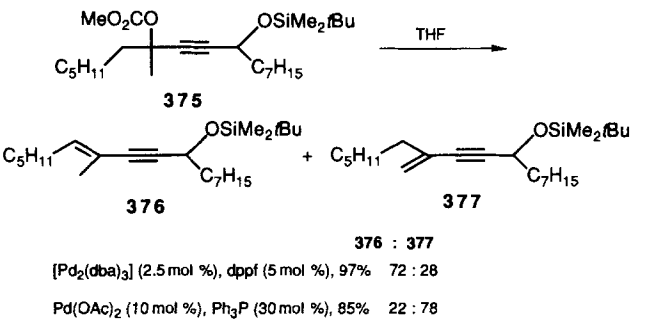

In another elimination reaction the propargylic alcohol **378** is dehydrated to give the conjugated enyne **379** in 1,3-dimethylimidazolidin-2-one (DMI) at 70 °C in the presence of a palladium catalyst and a stoichiometric amount of stannous chloride.[72]

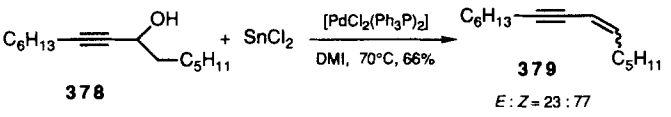

Another Pd-catalyzed reaction providing the conjugated enynes **382** is the coupling of alkenyl halides **381** with terminal alkynes **380** (≡**363**).[73] Although the method is useful, the preparation of alkenyl halides **381**, particularly those having a labile functional group, is not always easy. The present carbonate method can be carried out easily using carbonyl compounds as building blocks even in the presence of functional groups.

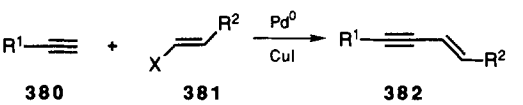

7. Miscellaneous Reactions

Some reactions of propargylic compounds that do not belong to the above-mentioned types are known. These reactions are surveyed in this section, although their mechanisms are not always clear.

Propargylic ester **383** undergoes an interesting oxidative rearrangement catalyzed by Pd^{II} salts under oxygen atmosphere to yield the α,β-unsaturated α-acyloxy aldehyde **386** in high yield (Scheme 56).[74] The reaction proceeds by intramolecular oxy-

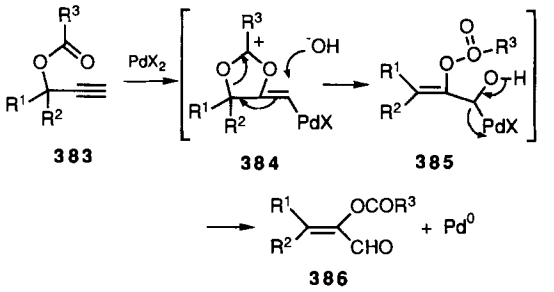

Scheme 56. Mechanism of formation of the α,β-unsaturated α-acyloxy aldehydes **386** from propargylic esters **383**; R^1, R^2, R^3 = alkyl, aryl.

palladation of the triple bond to generate **384**, followed by an attack of hydroxide to form **385**. Elimination of Pd^0 from **385** affords **386**. Somehow Pd^0 is reoxidized to Pd^{II} with oxygen and recycled. The propargylic ester **387** is oxidized to give **388** in

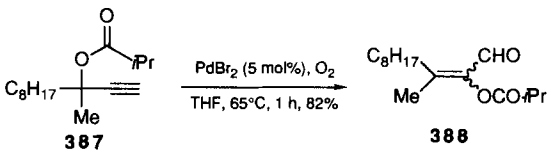

satisfactory yield by using 5 mol% of $PdBr_2$ under oxygen. This rearrangement was used to introduce the side chain in the corticosteroid **392** starting from the 17-keto steroid **389**. Preparation of propargylic ester **390** from **389** and its rearrangement gave **391** in 95% yield. The reaction proceeded with a catalytic amount of $PdBr_2$ in DME under oxygen atmosphere. Isobutyrate and benzoate gave better results than acetate for this reaction. Treatment of **391** with a base then gave **392**.[75]

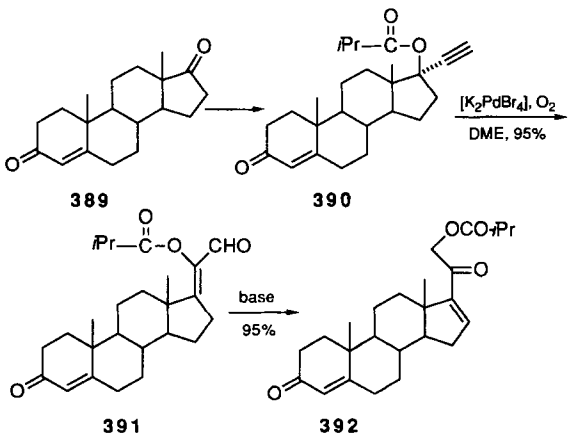

In a related reaction, oxidative conversion of the propargylic acetate **393** into the α,β-unsaturated α-acetoxyketone **394** takes place with a stoichiometric amount of $[PdCl_2(MeCN)_2]$ in aqueous THF. Hydrolysis of **394** gives rise to the α-diketone **395**.[76]

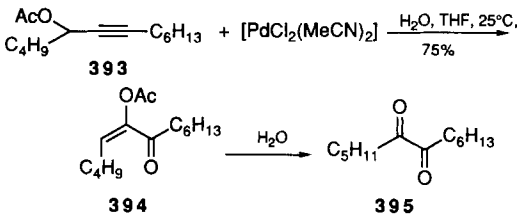

Propargylic acetates are less reactive than the corresponding carbonates toward Pd^0 and do not form allenylpalladium intermediates easily. Addition of acetic acid to the propargylic acetate **396** catalyzed by $[Pd_2(dba)_3]/Ph_3P$ affords the geminal allylic diacetate **397**. An intramolecular version of this reaction

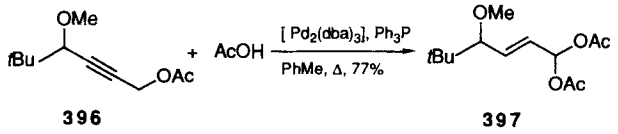

offers a good synthetic method for acetoxylactones. The 14-membered acetoxylactone **399** was obtained in refluxing benzene in 52% yield from **398**.[77]

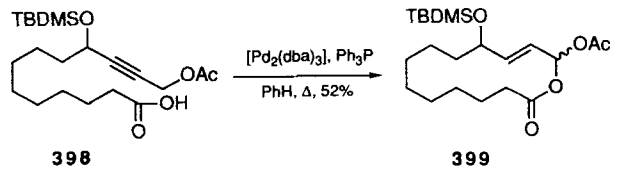

Propargylic acetates undergo facile transformations catalyzed by Pd^{II} salts. $[PdCl_2(MeCN)_2]$ is a good catalyst for some reactions involving transposition of the acetoxy group. The reaction of 1,1-dimethyl-2-propynyl acetate (**400**≡**171**) catalyzed by $[PdCl_2(MeCN)_2]$ furnished the interesting conjugated triene **401** as a homocoupling product in 20% yield along with several other minor products such as **402** and **403**. The conjugated diene **404** was obtained in 30% yield by the cross-coupling of **400** with 1-decene. These reactions proceed via a palladium–carbene intermediate.[78]

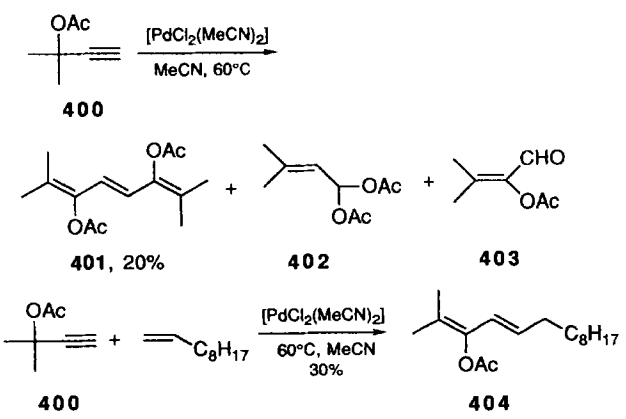

A variant of the Nazarov cyclization of 1-ethynyl-2-propenyl acetate derivatives giving cyclopentenones is possible with a Pd^{II} salt as the catalyst. 3-Acetoxy-4-methylene-1-decyne (**405**) was converted to 3-hexyl-2-cyclopentenone (**407**) in 63% yield in the presence of one equivalent of acetic acid. Formation of the acetoxycyclopentadiene **406** as a precursor of **407** was confirmed by trapping with *N*-phenylmaleimide. A palladium–carbene complex is assumed to be the intermediate of this reaction, too.[79]

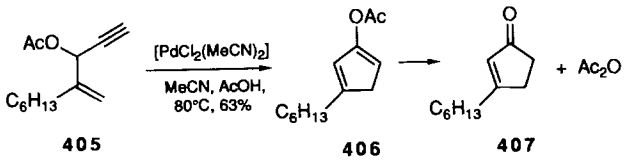

405 **406** **407**

8. Summary and Outlook

New synthetic approaches to allene derivatives have been uncovered by the palladium-catalyzed reactions of propargylic compounds. Since propargylic esters are readily available by the reaction of terminal alkynes with carbonyl compounds and subsequent esterification, applications of propargylic esters can be important in organic synthesis. A number of compounds containing interesting functional groups, which are difficult to synthesize by other means, can be prepared easily by the palladium-catalyzed reactions of propargylic compounds. Applications of the palladium-catalyzed reactions surveyed in this review have hardly been tapped. The synthesis of novel complex molecules, in particular, based on these transformations is open for further study. Because most of the products of the palladium-catalyzed reactions, including allenes, are chiral, asymmetric synthesis with these interesting compounds should be possible. But so far no studies have been reported on successful catalytic enantioselective reactions of propargylic compounds. In addition, since preparation of optically active propargylic alcohols is rather easy, chirality transfer in their palladium-catalyzed reactions is another interesting problem to be studied. Progress in this area would lead to interesting optically active compounds.

Research on the palladium-catalyzed reactions of propargylic carbonates has been carried out at both the Tokyo Institute of Technology and the Okayama University of Science. We thank our many collaborators in these two laboratories who are cited in the references.

Received: February 1, 1995
Revised version: May 2, 1995 [A 103 IE]
German version: *Angew. Chem.* **1995**, *107*, 2830–2854

[1] Books on palladium-catalyzed reactions: a) J. Tsuji, *Organic Synthesis with Palladium Compounds*, Springer, Berlin, **1980**; b) R. F. Heck, *Palladium Reagents in Organic Synthesis*, Academic Press, London, **1985**; c) J. Tsuji, *Palladium Reagents and Catalysts; Innovations in Organic Synthesis*, Wiley, Chichester, **1995**.

[2] A review on the reactions of propargyl and allenyl transition metal compounds: H. Yamamoto in *Comprehensive Organic Synthesis, Vol. 2* (Eds.: B. M. Trost, I. Fleming, C. H. Heathcock), Pergamon, Oxford, **1991**, p. 81.

[3] a) J. Tsuji, H. Takahashi, M. Morikawa, *Tetrahedron Lett.* **1965**, 4387; b) review: J. Tsuji, *Acc. Chem. Res.* **1969**, *2*, 144.

[4] Recent reviews on the reactions of allylic compounds via π-allylpalladium intermediates: a) J. Tsuji, *Tetrahedron* **1986**, *42*, 4361; b) B. M. Trost, T. R. Verhoeven in *Comprehensive Organometallic Chemistry, Vol. 8* (Eds.: G. Wilkinson, F. G. A. Stone, E. Abel), Pergamon, Oxford, **1982**, p. 799; c) S. Godleski in *Comprehensive Organic Synthesis, Vol. 4* (Eds.: B. M. Trost, I. Fleming, M. F. Semmelhack), Pergamon, Oxford, **1991**, p. 585; d) C. G. Frost, J. Howarth, J. M. J. Williams, *Tetrahedron Asymmetry* **1992**, *3*, 1089.

[5] a) J. Tsuji, I. Shimizu, I. Minami, Y. Ohashi, *Tetrahedron Lett.* **1982**, *23*, 4809; b) J. Tsuji, I. Minami, I. Shimizu, *Chem. Lett.* **1983**, 1325; c) *Tetrahedron Lett.* **1983**, *24*, 4713; d) *ibid.* **1984**, *25*, 5157; d) I. Minami, I. Shimizu, J. Tsuji, *J. Organomet. Chem.* **1985**, *296*, 269; e) J. Tsuji, I. Shimizu, I. Minami, Y. Ohashi, T. Sugiura, K. Takahashi, *J. Org. Chem.* **1985**, *50*, 1523.

[6] H. X. Zhang, F. Guibe, G. Balavoine, *Tetrahedron Lett.* **1988**, *29*, 623.

[7] E. Keinan, E. Bosch, *J. Org. Chem.* **1986**, *51*, 4006.

[8] The term "oxidative addition", which is somewhat confusing for organic chemists, is defined for organometallic chemistry in ref. [1c].

[9] a) C. J. Elsevier, H. Kleijn, K. Ruitenberg, P. Vermeer, *J. Chem. Soc. Chem. Commun.* **1983**, 1529; b) C. J. Elsevier, H. Kleijn, J. Boersma, P. Vermeer, *Organometallics* **1986**, *5*, 716.

[10] T. A. Stromnova, M. N. Vargaftik, I. I. Moiseev, *J. Organomet. Chem.* **1983**, *252*, 113.

[11] V. V. Grushin, H. Alper, *Organometallics* **1993**, *12*, 1890.

[12] C. Amatore, A. Jutand, M. A. M'Barki, *Organometallics* **1992**, *11*, 3009.

[13] a) F. Ozawa, A. Kubo, T. Hayashi, *Chem. Lett.* **1992**, 2177; b) *Pure Appl. Chem.* **1992**, *64*, 421.

[14] T. Mandai, T. Matsumoto, J. Tsuji, S. Saito, *Tetrahedron Lett.* **1993**, *34*, 2513.

[15] T. Mandai, M. Ogawa, H. Yamaoki, T. Nakata, H. Murayama, M. Kawada, J. Tsuji, *Tetrahedron Lett.* **1991**, *32*, 3397.

[16] Review: J. Tsuji, T. Mandai, *J. Organomet. Chem.* **1993**, *451*, 15.

[17] J. Tsuji, T. Nogi, *Tetrahedron Lett.* **1966**, 1801.

[18] T. Nogi, J. Tsuji, *Tetrahedron* **1969**, *25*, 4099.

[19] J. Tsuji, T. Sugiura, I. Minami, *Tetrahedron Lett.* **1986**, *27*, 731.

[20] a) J. Tsuji, K. Sato, H. Okumoto, *Tetrahedron Lett.* **1982**, *23*, 5189; b) *J. Org. Chem.* **1984**, *49*, 1341.

[21] S. Murahashi, Y. Imada, T. Mori, T. Kitamura, *Abstr. Jpn. Chem. Soc. Annu. Meet.* **1993**, Vol. II, p. 345.

[22] H. Arzoumanian, M. Choukrad, D. Nuel, *J. Mol. Catal.* **1993**, *85*, 287.

[23] N. D. Trieu, C. J. Elsevier, K. Vrieze, *J. Organomet. Chem.* **1987**, *325*, C23.

[24] K. Matsushita, T. Komori, S. Oi, Y. Inoue, *Tetrahedron Lett.* **1994**, *35*, 5889.

[25] K. T. Huh, A. Orita, H. Alper, *J. Org. Chem.* **1993**, *58*, 6956.

[26] E. Ali, H. Alper, *J. Org. Chem.* **1991**, *56*, 5357.

[27] T. Mandai, Y. Tsujiguchi, S. Matsuoka, J. Tsuji, S. Saito, *Tetrahedron Lett.* **1994**, *35*, 5697.

[28] W. S. Johnson, G. H. Daub, *Org. React.* **1951**, *6*, 1.

[29] a) B. Gabriele, M. Costa, G. Salerno, G. P. Chiusoli, *J. Chem. Soc. Chem. Commun.* **1992**, 1007; b) *ibid.* **1994**, 1429.

[30] J. Tsuji, M. Morikawa, N. Iwamoto, *J. Am. Chem. Soc.* **1964**, *86*, 2095.

[31] J. Kiji, H. Konishi, T. Okano, S. Kometani, A. Iwasa, *Chem. Lett.* **1987**, 313.

[32] T. Mandai, Y. Tsujiguchi, S. Matsuoka, S. Saito, J. Tsuji, *J. Organomet. Chem.* **1995**, *488*, 127.

[33] T. Mandai, K. Ryoden, M. Kawada, J. Tsuji, *Tetrahedron Lett.* **1991**, *32*, 7683.

[34] a) J. D. Buynak, J. Mathew, M. N. Rao, E. Haley, C. George, U. Siriwardane, *J. Chem. Soc. Chem. Commun.* **1987**, 735; b) J. D. Buynak, H. B. Borate, C. Husting, T. Hurd, J. Vallabh, J. Mathew, J. Lambert, U. Siriwardane, *Tetrahedron Lett.* **1988**, *29*, 5053.

[35] T. Mandai, H. Kunitomi, K. Higashi, M. Kawada, J. Tsuji, *Synlett* **1991**, 697.

[36] T. Mandai, S. Suzuki, A. Ikawa, T. Murkami, M. Kawada, J. Tsuji, *Tetrahedron Lett.* **1991**, *32*, 7687.

[37] T. Mandai, J. Tsuji, unpublished results.

[38] a) W. H. Okamura, *Acc. Chem. Res.* **1983**, *16*, 81; b) W. H. Okamura, M. L. Curtin, *Synlett* **1990**, 1.

[39] T. Mandai, Y. Tsujiguchi, J. Tsuji, S. Saito, *Tetrahedron Lett.* **1994**, *35*, 5701.

[40] T. Mandai, J. Tsuji, Y. Tsujiguchi, S. Saito, *J. Am. Chem. Soc.* **1993**, *115*, 5865.

[41] T. Jeffery Luong, G. Linstrumelle, *Tetrahedron Lett.* **1980**, *21*, 5019.

[42] a) K. Ruitenberg, H. Kleijn, C. J. Elsevier, J. Meijer, P. Vermeer, *Tetrahedron Lett.* **1981**, *22*, 1451; b) K. Ruitenberg, H. Kleijn, H. Westmijze, J. Meijer, P. Vermeer, *Recl. Trav. Chim. Pays-Bas* **1982**, *101*, 405.

[43] C. J. Elsevier, P. M. Stehouwer, H. Westmijze, *J. Org. Chem.* **1983**, *48*, 1103.

[44] H. Kleijn, I. Meijer, G. C. Overbeek, P. Vermeer, *Recl. Trav. Chim. Pays-Bas* **1982**, *101*, 97.

[45] T. Moriya, N. Miyaura, A. Suzuki, *Synlett* **1994**, 149.

[46] a) T. Mandai, T. Nakata, H. Murayama, H. Yamaoki, M. Ogawa, M. Kawada, J. Tsuji, *Tetrahedron Lett.* **1990**, *31*, 7179; b) *J. Organomet. Chem.* **1991**, *417*, 305.

[47] C. Darcel, C. Bruneau, P. H. Dixneuf, *J. Chem. Soc. Chem. Commun.* **1994**, 1845.

[48] S. Gueugnot, G. Linstrumelle, *Tetrahedron Lett.* **1993**, *34*, 3853.

[49] D. Bouyssi, J. Gore, G. Balme, D. Louis, J. Wallach, *Tetrahedron Lett.* **1993**, *34*, 3129.

[50] a) J. Tsuji, T. Yamakawa, *Tetrahedron Lett.* **1979**, 613; b) J. Tsuji, I. Shimizu, I. Minami, *Chem. Lett.* **1984**, 1017.

[51] R. O. Hutchins, K. Learn, *J. Org. Chem.* **1982**, *23*, 241.

[52] a) J. Tsuji, T. Sugiura, M. Yuhara, I. Minami, *J. Chem. Soc. Chem. Commun.* **1986**, 922; b) J. Tsuji, T. Sugiura, I. Minami, *Synthesis* **1987**, 603.
[53] T. Mandai, T. Matsumoto, M. Kawada, J. Tsuji, *Tetrahedron Lett.* **1993**, *34*, 2161.
[54] T. Mandai, T. Matsumoto, Y. Tsujiguchi, S. Matsuoka, J. Tsuji, *J. Organomet. Chem.* **1994**, *473*, 343.
[55] C. Darvel, S. Bartsch, C. Bruneau, P. H. Dixneuf, *Synlett* **1994**, 457.
[56] Y. Colas, B. Cazes, J. Gore, *Tetrahedron Lett.* **1984**, *25*, 845; *Bull. Soc. Chim. Fr.* **1986**, 165.
[57] a) T. Tabushi, J. Inanaga, M. Yamaguchi, *Tetrahedron Lett.* **1986**, *27*, 5237; b) A. Sugino, T. Hanamoto, J. Inanaga, *ibid.* **1995**, *36*, 907.
[58] J. Inanaga, Y. Sugimoto, T. Hanamoto, *Tetrahedron Lett.* **1992**, *33*, 7035.
[59] a) J. M. Aurrecoechea, R. F. Anton, *J. Org. Chem.* **1994**, *59*, 702; b) J. M. Aurrecoechea, W. H. Okamura, *Tetrahedron Lett.* **1987**, *28*, 4947.
[60] J. Tsuji, H. Watanabe, I. Minami, I. Shimizu, *J. Am. Chem. Soc.* **1985**, *107*, 2196.
[61] I. Minami, M. Yuhara, H. Watanabe, J. Tsuji, *J. Organomet. Chem.* **1987**, *334*, 225.
[62] N. Greeves, J. S. Torode, *Synthesis* **1993**, 1109.
[63] a) L. Geng, X. Lu, *Tetrahedron Lett.* **1990**, *31*, 111; b) *J. Chem. Soc. Perkin Trans. 1*, **1992**, 17.
[64] I. Minami, Y. Yuhara, J. Tsuji, *Tetrahedron Lett.* **1987**, *28*, 629.
[65] T. Mandai, J. Tsuji, unpublished results.
[66] H. Bienayme, *Tetrahedron Lett.* **1994**, *35*, 7383.
[67] J. Tsuji, I. Minami, I. Shimizu, *Chem. Lett.* **1983**, 1325.
[68] H. Bienayme, *Tetrahedron Lett.* **1994**, *35*, 7387.
[69] J. Tsuji, I. Minami, I. Shimizu, *Tetrahedron Lett.* **1983**, *24*, 1793.
[70] T. Mandai, J. Tsuji, unpublished results.
[71] T. Mandai, Y. Tsujiguchi, S. Matsuoka, J. Tsuji, *Tetrahedron Lett.* **1993**, *34*, 7615.
[72] Y. Masuyama, J. P. Takahara, K. Hashimoto, Y. Kurusu, *J. Chem. Soc. Chem. Commun.* **1993**, 1219.
[73] a) K. Sonogashira, Y. Tohda, N. Hagihara, *Tetrahedron Lett.* **1975**, 4467; b) for preparative applications, see: K. C. Nicolaou, W. M. Dai, *Angew. Chem.* **1991**, *103*, 1453; *Angew. Chem. Int. Ed. Engl.* **1991**, *30*, 1387.
[74] H. Kataoka, K. Watanabe, K. Goto, *Tetrahedron Lett.* **1990**, *31*, 4181.
[75] H. Kataoka, K. Watanabe, K. Miyazaki, S. Tahara, K. Ogu, R. Matsuoka, K. Goto, *Chem. Lett.* **1990**, 1705.
[76] R. Mahrwald, H. Schick, *Angew. Chem.* **1991**, *103*, 577; *Angew. Chem. Int. Ed. Engl.* **1991**, *30*, 593.
[77] B. M. Trost, W. Brieden, K. H. Baringhaus, *Angew. Chem.* **1992**, *104*, 1392; *Angew. Chem. Int. Ed. Engl.* **1992**, *31*, 1335.
[78] V. Rautenstrauch, *Tetrahedron Lett.* **1984**, *25*, 3845.
[79] V. Rautenstrauch, *J. Org. Chem.* **1984**, *49*, 950.

Computer-Assisted Planning of Organic Syntheses: The Second Generation of Programs**

Wolf-Dietrich Ihlenfeldt and Johann Gasteiger*

Dedicated to Professor Paul von Ragué Schleyer on the occasion of his 65th birthday

The planning of syntheses in organic chemistry has continuously been given more solid foundations during the last decades. Widely applicable rules have been formulated. Nearly parallel with the systematization of this field the potential for the automation of synthesis planning by the use of computers has been promulgated. However, after more than two decades of continuing efforts by a number of groups, computer-assisted synthesis planning, which relies on large libraries of synthons and transforms, has failed to establish itself firmly. This is in marked contrast to the acceptance of reaction databases. Their use has become routine within a surprisingly short time. Apparently the classical approaches to computer-assisted synthesis planning do not satisfy the needs of the preparative chemist. However, this lack of success does not yet mean the complete demise of the whole field. The conceptual shortcomings and problems of the first generation of programs are both of technical and psychological nature and need to be critically analyzed. Meanwhile, work has begun on systems of the second generation, which try to support the chemist in the synthesis laboratory with new methods in novel ways. Care is taken to mimic and support the typical planning style of the human chemist, who often on the spur of the moment switches direction in planning as well as his (sub) goals and methods. New tools that correspond better to the thinking patterns and working habits of chemists empower the user to plan syntheses of organic molecules in an interactive and innovative fashion. We feel that this field is far from dead and continue our research activities. In this article we introduce a system with a number of novel concepts and demonstrate its capabilities with some practical examples.

Keywords: computer chemistry · synthesis planning · WODCA

1. The First Generation

Amongst the most important progress in the concepts of organic chemistry during the last three decades is the systematization and categorization of organic synthesis. No chemists today finish their university education without learning the step-by-step planning of simple model syntheses with the aid of Corey's synthon concepts.[1–4] The clear and logical structure of this concept and alternative models has been a challenge for chemists and computer scientists since their development. The aim of computer-assisted design has been the implementation of these principles with computer programs to make the computer a tool in synthesis planning.[5] At the same time the laudable fact that about all relevant literature in chemistry has been abstracted in computer-readable form has motivated researchers to make this enormous treasure of experimental knowledge and experience searchable and retrievable. The ultimate goal here is to replace the traditional walk to the library in order to look for information on the feasibility of a planned reaction or synthesis step with more effective means of information retrieval, directly from the laboratory workplace.

1.1. Computer-Assisted Synthesis Planning

During the last decades two main classes of programs for organic synthesis-planning support in the broadest sense have emerged: One group comprises synthesis-planning systems based on the synthon and transform principles (or related concepts) or formal reaction generation. The second group are reaction databases, which make a large number of reactions that have already been performed in the laboratory searchable and retrievable. They inform the synthetic chemist about solutions of problems from related tasks. A third, smaller but nevertheless important class of programs predict reactions. They model chemical reactions and provide information about products and reaction conditions by interpolating within or extrapolating

[*] Prof. Dr. J. Gasteiger, Dr. W.-D. Ihlenfeldt
Computer-Chemie-Centrum, Institut für Organische Chemie
Universität Erlangen-Nürnberg
Nägelsbachstrasse 25, D-91052 Erlangen (Germany)
Telefax: Int. code +(9131) 856566
e-mail: gasteiger@eros.ccc.uni-erlangen.de

[**] A glossary of important acronyms used in this review is provided at the end of the text.

 © VCH Verlagsgesellschaft mbH, D-69451 Weinheim, 1995 0570-0833/95/3423-2613 $ 10.00+.25/0

beyond a training set of known reactions. Quantum chemical computations become increasingly important for the prediction and optimization of compound properties. In the field of reaction prediction, however, they have, almost without exception, not yet been very successful for practical systems. In the following two sections we try to give a short historical overview of the history of the classical systems.

1.2. Programs for Synthesis Planning and Reaction Prediction

The development of synthesis-planning and reaction-prediction programs is closely related to progress in both reaction systematization and the mind-boggling advances in computers and peripherals. Readers of historical papers tend to be utterly surprised at how limited the core memory was and how primitive I/O devices were with which the pioneers somehow managed, and at what ingenious tricks they used to code chemical structures in this environment. The total number of programs that are in some way related to synthesis planning is estimated to exceed 50.[5] The number of systems that handle the planning of organic syntheses in a more comprehensive manner is smaller. We estimate it to be around 10.

1.2.1. The Synthon Principle

Today the synthon principle is regarded as obvious and natural. But its introduction was a major, nearly iconoclastic change of paradigm. Syntheses were no longer viewed from the aspect of potential name reactions and single steps, but as the global transformation of the skeleton and the pattern of charges and polarities, decoupled from the nature of the substituent that is the origin of the charge pattern. A central point of such an analysis is consideration of reactions used in synthesis from the opposite direction (retrosynthetically). These reverse (retro) reactions are typically called transforms. Scheme 1 shows this idea for the aldol reaction.

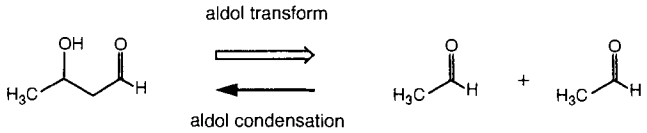

Scheme 1. The retrosynthetic point of view: the aldol condensation and the corresponding retrosynthetic transform.

A synthesis planned according to the textbook follows two steps:

a) The strategic bonds are defined and b) the specific transformations that connect or disconnect the strategic bonds in the desired fashion are formulated. A broken strategic bond yields (typically charged) fragments called *synthons*. They are converted by the addition or removal of atoms, ions, or chemical groups into specific molecules. These are precursors or starting materials (Scheme 2).

In the simplest case the reactions required are known from the literature. Other possibilities are generalizations from success-

J. Gasteiger

W.-D. Ihlenfeldt

Johann Gasteiger was born in Dachau, Germany, in 1941. After studying chemistry at the universities in Munich and Zürich, he obtained his doctorate under the supervision of Prof. Rolf Huisgen in 1971. He spent one year as postdoctoral fellow with Prof. A. Streitwieser, Jr., at the University of California in Berkeley, after which he accepted a post at the Technische Universität (TU) München and completed his habilitation there in 1979. In recognition of his contributions to computer chemistry he was awarded the 1991 Gmelin-Beilstein Medal of the GDCh. In 1994 he accepted a position as professor of Organic Chemistry at the Universität Erlangen–Nürnberg. Together with Prof. Dr. P. von Ragué Schleyer and Priv.-Doz.T. Clark he founded the Computer-Chemie-Centrum der Universität Erlangen–Nürnberg. His main research topics are the development of computer programs for synthesis planning, reaction prediction, and reactivity prediction, for the analysis and simulation of mass and infrared spectra, and for the discovery of lead structures with biological properties. The extraction of information from chemical databanks and the application of neural networks and genetic algorithms for chemical problems are further fields of interest.

Wolf-Dietrich Ihlenfeldt was born in Hamburg in 1963. He studied Chemistry in Hamburg, Heidelberg, and at the TU München, completing his doctorate with Professor Gasteiger on synthesis planning in 1991. He then worked as postdoctoral fellow at the Toyohashi University of Technology (Japan) until October 1994 on novel network-supported chemical information systems. At present he is working under commission of the Fachinformationszentrum Chemie, Berlin, on the evaluation of innovative information distribution and generation models in Chemistry. The focus of his interests is the linking of global computer networks and the dynamic, open techniques for data representation and manipulation with information data and processing specific to Chemistry, a field at the interface of Chemistry and Computer Science.

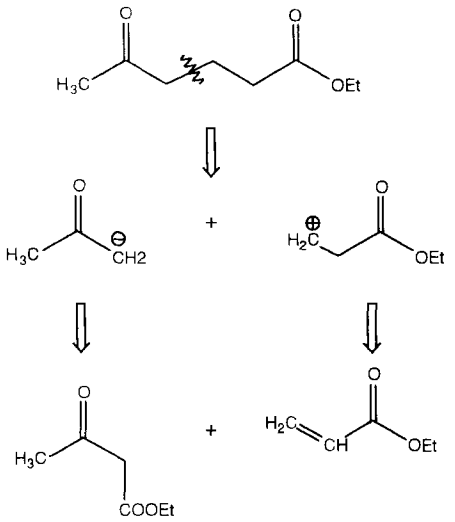

Scheme 2. Dissection of a target compound at a strategic bond yielding the (charged) synthons, followed by transformation to specific reagents.

fully applied reactions for molecules with a similar substituent pattern or even from purely formal, unprecedented bond rearrangements. This multilevel process provides some promising starting points for the development of algorithms. The simplest approach is the systematic application of reactions, described more abstractly as synthon schemes. However, because the number and variation of known reactions is enormous, some control and screening is mandatory. The selection of strategic bonds and the rating of a carefully selected subset of reactions is qualitatively much more difficult than simple, systematic structure transformation. The consecutive and parallel application of this approach results in an ever broadening scheme of steps and sequences of retroreactions. This plot is called the *synthesis tree* (Fig. 1).

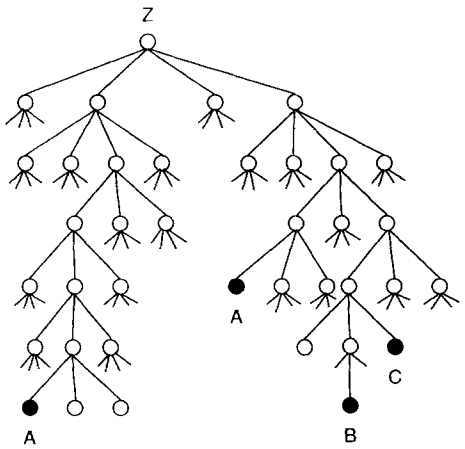

Fig. 1. A synthesis tree displayed as a sequence of retroreactions, which were obtained by systematic retrosynthetic analysis. A, B, and C are available starting materials; Z is the target molecule.

A synthesis tree easily becomes very large. Even if for each intermediate only ten alternative retroreactions are considered the tree already contains $10^3 = 1000$ reactions and precursors in the third level and after five levels more than $10^5 = 100000$ entries. All these entries have to be evaluated and compared, an immensely laborious task though a five-step synthesis is not lengthy. This example shows the problems inherent in a systematic retrosynthetic approach. An extremely careful evaluation of merit and a rigorous and early rejection of possible, but not very promising reaction sequences is mandatory. However, the price of not discovering potentially interesting syntheses has often to be paid if cuts in the synthesis tree are made too early or too deep.

1.2.2. Coding of Reactions

The classical programs for synthesis planning and reaction prediction[5] use comparatively few, simple models for the internal representation of their database. A core element is the description of the reaction center and the changes it undergoes during a reaction. This description consists of either a complete reaction including a full set of bond reordering instructions, or a set of half reactions (that is, a formal dissociation step followed by a separate recombination step), or a series of microsteps that describe single bond cuts and bond formations. Some programs store additional information such as details about interfering substituents, general considerations like an estimation of usability and synthetic merit of a reaction, or even physicochemical models of the reactivity of the bonds contained in the reaction center.

An important point is that only an isolated part of the data described in the literature is stored. The knowledge base of the classical synthesis-planning programs does not contain complete and detailed descriptions of single reactions with the relevant background information, but rather the distilled essence of many sources and practical experience. This raw information is concentrated and leads to either estimated or statistically validated parameters, depending on the specific philosophy of a system. In the more modern systems the knowledge base is kept outside the core system and can be edited and expanded; it therefore acquires some characteristics of a database. In contrast to reaction databases the raw information has been heavily processed. Every scheme, every reaction model is equivalent to the condensed essence of a normally large number of reactions taken from literature, while a plain reaction database contains isolated citations. The process of data compression and model building has not yet been reliably automated.

1.2.3. Representative Systems

LHASA,[6] the successor of OCSS[7] is generally considered to be the first synthon-based system. Its development still continues. Another important disconnection system is SECS[8] and its derivative CASP, which has been developed by a group of German and Swiss chemical companies. Some other representative examples are SYNCHEM,[9] SYNGEN,[10] SCANCHEM,[11] COMPASS,[12] SYNSUP-MB,[13] AIPHOS,[14] LILITH,[15] TRESOR,[16] and SYNTHON.[17] These classic systems either rely on a database of completely defined reactions including classical name reactions and, due to continuous literature survey, also a large number of exotic reactions, or they are based on more generally formulated synthon schemes or half-reactions.

The merit evaluation of a reaction in these programs is based on the analysis of the character of the substituents in and around

the reaction center, a scan for interfering functionality at other sites, and some general rules about usefulness. Every reaction or synthon scheme is coded manually (SYNCHEM and AIPHOS contain mechanisms for unsupervised learning from reaction databases, and for SECS add-ons are available for the same purpose[18]) and augmented with estimated parameters for the merit evaluation functions. Additional modules may allow a tighter control of the course of the program, for example, by the detection of strategic bonds by general, reaction-independent heuristics, the intentional, preferential application of reactions with large synthetic potential,[6c] or the use of global strategic concepts.[19]

A more formal approach was taken in the EROS system.[20] Reactions are coded in a way reminiscent of the mechanistic electron shifts with the curved arrows a chemist writes on paper to explain the mechanism of a reaction. With very few such shift patterns a large part of the stock of organic reactions can be covered. The central problem was then the development of methods that could decide which shift patterns to select and to which bonds in a given molecule they should be applied.

The selection of bonds to break and make during a reaction is based on quantitative estimations of electronic and energy effects on the atoms and bonds of the molecule.[20c] After performing a reaction a final merit evaluation takes place. Factors such as reaction enthalpy,[21] charge distribution,[22] inductive[23] and resonance effect,[22] as well as polarizability[24] are used. The direction of the reaction design (forward for reaction prediction, backward for synthesis planning) decides how these factors are combined to a final merit value.

Because of the strong emphasis on physicochemical rating of reactions, the further development of EROS quite naturally focused on reaction prediction. Continuous refinement of the merit evaluation procedures led to a point where it seemed no longer reasonable to treat both reaction prediction and synthesis planning in a single program system. Accordingly, these two problems are now handled by separate systems: EROS has been completely redesigned, and its use from version 6.0 onwards is essentially limited to reaction prediction.[25a] The merit evaluation functions for the different types of chemical reactions are kept separate from the core program in rule data files and can be easily modified and refined.[25b] The reaction models derived with these rules arise from careful statistical analyses[25b] or are represented by neural networks.[26] The generation of validation or reaction models for EROS 6 is demanding, but the models obtained are often very precise.[27]

For synthesis planning a radically different approach was adopted: The WODCA (*W*orkbench for the *O*rganization of *D*ata for *C*hemical *A*pplications) system combines a multitude of methods and tools that can be applied to the various problems of synthesis planning. This will be explained in detail in the following chapters.

A different approach for reaction prediction is taken by the CAMEO program.[28] Hundreds of estimated reactivity parameters cover a wide scope of reactions without relying on predefined bond rearrangement schemes. The reaction conditions and acceptable reaction classes are, however, selected by the user. The CAMEO parameters are more easily obtained than those in the EROS system (sometimes they are just estimated) but often lack fundamental statistical validation. This diminishes the reliability. Nevertheless, this system generates mostly correct predictions about major and minor products under the specified reaction conditions (but not about product ratios or kinetics) under a wide range of conditions. Classical organic chemistry is covered nearly completely, much more completely than, for example, in the EROS system, which has reaction models only for a few selected reaction classes at present.

A strong formal treatment of reactions is the basis of the Dugundji–Ugi matrix model of constitutional chemistry.[29] Building on this concept, a scheme for reaction classification was developed, which was implemented in a program designed for formal reaction generation called IGOR.[30] This program can generate a complete set of atom and bond mappings for a specific reaction scheme. A complementary program, RAIN, creates isomeric ensembles from a given molecular ensemble and can be used for the generation of structures and reactions.[31] In another operation mode, it formulates a network of reactions that connects two molecular ensembles.[31]

Both IGOR and RAIN rely exclusively on formal criteria such as allowed valence levels and number or structural characteristics of the intermediates specified by the user in their selection of structures and reaction. The advantage is that all conceivable structures and reactions are obtained, including unprecedented ones. Still, the task of selecting the reactions that can actually be carried out is left to the user, because no merit evaluation, for example, by physicochemical characteristics of structures and reactions or by comparison with known reactions or reaction types, is undertaken.[29]

Finally, one important program has characteristics difficult to assign to the program types introduced so far. CHIRON[32] is basically a system for the retrieval and analysis of molecular structures in which structures are mapped onto each other to detect common structural fragments, especially with respect to stereochemical relationships. CHIRON is no synthesis-planning or reaction-prediction system per se, and it does not implement many traditional database retrieval operations, but it is definitely useful for the discovery of starting materials with a stereochemical configuration appropriate for the target. A particular strength of CHIRON is its large, manualy compiled catalog with about 2000 compounds with well-defined stereochemical features. It does not only contain commercially available compounds, but also many from the literature, which can be synthesized in few steps from easily secured starting materials. This unique catalog can also be used by our new WODCA system as will be explained later.

1.3. Reaction Databases

Within this decade the number of accessible reaction databases has increased enormously.[33–38] While there seems to be no aggressively marketed synthesis-planning program outside the educational sector, numerous reaction-retrieval systems and reaction databases have been on offer for quite a while.

1.3.1. Principles and Availability

It was already mentioned that the information content of reaction databases is much more elementary than that of transform libraries. At the same time the raw information content is

much larger. Entries in a reaction database typically include complete literature citations with information on reaction conditions, yields, and references to the reactions of previous and subsequent steps in longer syntheses. If a clear connection between a planned reaction and a literature precedent can be established, the difficulties of the actual synthesis can be estimated rather easily. It must, however, be noted that the detection of such a connection is not always trivial. The focus of interest typically is the reaction center, that is, the atoms and bonds directly involved in the bond-rearrangement process. The presence or absence of potentially disturbing chemical groups can be established by simple substructure search. However, the automatic or manual identification of the reaction center is not unequivocally possible in every case. The bond-rearrangement process with the smallest number of discrete steps is not always the one occurring in reality. This is still an active research area, and progress is steady. Most of these systems have another criticized weakness: negative (that is, failed) reaction entries are missing.

Searches in reaction databases have become routine in many laboratories. Reaction databases are helpful only if the searcher has a rough idea of the kind of reaction required. Whereas the classical reaction-prediction and synthesis-planning programs can, at least in principle, employ their knowledge base systematically and exhaustively, the user of a reaction database must already have devised the general framework of the synthesis.

1.3.2. Reaction Database Application

The extent to which reactions are systematically abstracted from literature has increased enormously. Since the introduction of CASREACT,[34] ChemInform RX,[35] and ChemReact, a broad field is exhaustively covered and continuously updated. Classical, molecule-oriented databases such as Beilstein provide search facilities that indirectly lead to results comparable to the direct search in reaction-oriented databases.[39] Important data sets of basic reactions such as the catalogs of Theilheimer, CRDS (Chemical Reactions Documentation Service), JSM (Journal of Synthetic Methods), and from the *Organic Synthesis* book series are now also available.[40]

As far as companies with a large number of proprietary reaction data are concerned, reaction databases provide many advantages over the maintenance of transform systems. The most important benefit is that the systems operate exclusively with "hard", uninterpreted data, which can be input without any technical problems or even directly transferred from an electronic laboratory journal. In such a database every entered reaction is valuable, but for a transform or synthon record a single instance of a reaction is not sufficient. The generally accepted standpoint is that transforms that were compiled from too few instances of reactions or from too narrow an application are damaging, not beneficial, because they yield too many overrated results stemming from extrapolation beyond the area covered by the example data. Even if a carefully crafted new entry is important and beneficial in principle, it is difficult to balance the merit functions of the new entry against those of the old, especially if the team in charge comprises several chemists with divergent background and experience.

The automated extraction of transform libraries from reaction data is not yet well advanced. One of the main problems is the grouping of exemplary reactions into classes that form the basis for meaningful generalizations of reactions.[18,41] When these methods are sufficiently advanced and reliable to be able to work autonomously on large reaction databases, they should be able to automatically derive knowledge for reaction prediction and synthesis planning, which might foster the importance of reaction prediction, or maybe even the synthon/transform concept within synthesis-planning systems. In this context once again the very same problem as before arises: reactions which do *not* run as expected (negative examples) are hardly documented, either in literature or in reaction databases. The difficulties that had to be overcome before the reaction proceeded smoothly with an acceptable yield are also often lacking. This information would, however, be of prime importance to fence the area of applicability of a reaction or transform and evaluate its general usefulness. This problem also occurs during a simple reaction database query but is somewhat ameliorated by the auxiliary information attached to the retrieved entries.

The automatic classification of the contents of reaction databases or larger sets of hits from the queries on such databases will become mandatory in the long run anyway. Parallel to the increase of the number of database entries—some databases already contain more than a million reactions (for instance, CASREACT)[34]—the hit-lists grow longer. The number of answers a human chemist is willing to page through is limited. Here a hierarchical reaction classification (an additional step of computerized processing) must be inserted in order to sort the hits into a classified graph showing the hidden relationships between the reaction instances. Such a highly structured access to the voluminous factual material assists the user to perceive the gist of the database query results. Work has begun on these topics.[41]

1.4. The End of the Road for First Generation Programs

Computer-assisted synthesis planning has been met with utter scepticism, even hostility, from the majority of chemists. Now, after 25 years of development in this field by several teams of researchers not a single system has become widely accepted as a routine tool, and the generally very critical attitude toward this kind of system has been corroborated. Even those scientists who initially greeted computer-assisted synthesis planning with enthusiasm have lost their illusions. One of the major disappointments was certainly the suspension of development of the CASP system. Among all the transform-based systems CASP by far owns the largest collection of reaction types. The lack of truly convincing results gained from this monumental knowledge base, combined with the general lack of acceptance from synthetic chemists defines an endpoint in the evolution of this kind of system. This does not mean that CASP is not used anymore, but the extension of the transform database within the program framework has been recognized as too burdensome and no longer promising. The conceptual limits of this system have been reached. Attempts to generate transforms for this program automatically from reaction databases have also failed. The last large-scale project supported by a consortium of chemical com-

panies with plenty of financial funding is the Japanese AIPHOS system.[14] In the end this system also applies synthons and transforms on strategic bonds, so ultimately the same kind of problems are to be expected if innovative concepts are not integrated. Though new lines of research are being followed at the conceptual and early implementation level,[42] it is too early to comment on the possible impact of those approaches.

2. New Approaches

The success or demise of a program system is determined by the end-users, not the developers. The user statistics of the CAOS/CAMM Center[43] (Table 1) is a good reflection of the situation today, if users have complete freedom of choice among a multitude of system. The dominance of reaction databases becomes obvious from these figures alone. Furthermore, according to the author of the survey, the majority of the activations of the synthesis-planning systems are motivated by curiosity, because a significant, but not exactly known number of activations are explorations by first-time users, who do not come back again and should therefore be subtracted from the true user count. The statistics for ORAC include structure searches in the Fine Chemicals Directory (FCD), a comprehensive listing of commercially available chemicals. The majority of the CAMEO activations are thought to be pK_a evaluations, not reaction predictions. At least in tendency these numbers support the thesis that the average chemist-user does not know how to benefit from the current generation of synthesis-planning systems.

Table 1. User statistics of the CAOS/CAMM Center (January 1993–May 1993).

Program	N [a]	Program	N [a]
LHASA	ca. 25	ORAC	877
CAMEO	7	REACCS	103
CHIRON	12	SYNLIB	123
SYNGEN	8		

[a] N = number of activations.

2.1. Conceptual Problems of the Classical Systems

The numbers in Table 1 make clear that the currently available program systems are either grossly immature or are off-target, missing the needs of the synthetic chemists. The methods utilized by practicing chemists for synthesis-planning tasks vary, of course, with personal style and experience, but general trends can be formulated.

Chemists don't follow a rigid scheme when they plan syntheses. They consider individual reactions or even synthons often only at the very last stage. At the beginning of the development of a strategy larger structural fragments that might serve as building blocks for the target molecule are sought. This approach is augmented by the examination of functionality in the target structure and its distribution on the skeleton. These functionality patterns are not necessarily immediately categorized according to the synthon principle, because the arsenal of umpolung methods is now so extensive that a wrong polarity at some positions is no longer an insurmountable obstacle. Furthermore, very early in the planning procedure long-range relationships to potential starting materials and other, structurally related compounds are recognized. Only after a crude structural classification of possible intermediates and starting materials has been established are the remaining gaps filled with specific reactions or synthon schemes. During this final bridging and gap-filling procedure the precise structures of the intermediates and starting materials crystallize step by step and under continuous interplay with the modifications of the global plan. This is neither a classical bottom-up nor a top-down search, nor a simple bidirectional search, but rather a complex network consisting of the target molecule, possible starting materials, shadowy intermediates perceived as potentially useful by the chemist, and knowledge about usable reactions and available reagents. The search for synthetic pathways does not proceed in ordered small steps from one compound to the next, but rather in a random mixture of small and large jumps in both synthetic and retrosynthetic directions during which the structure of the linking intermediates and starting materials change continuously. This approach is demonstrated in Fig. 2 with the example of three published syntheses of the anti-malaria drug qinghaosu (**1**).[45a]

The first essential step during the development of a synthesis for **1** was the idea of constructing the unusual 1,2,4-trioxane

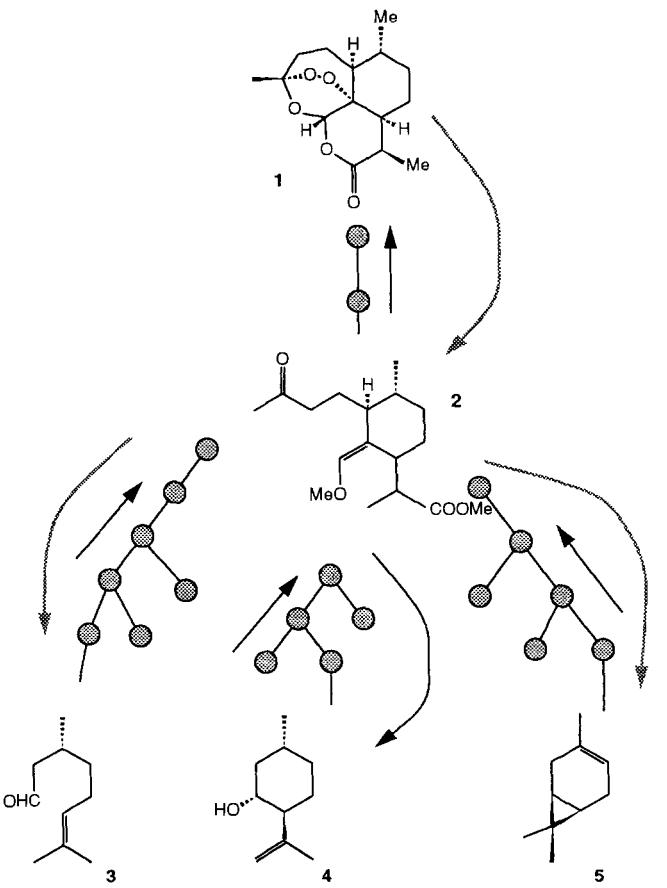

Fig. 2. Synthesis planning in reality: an array of different methods for search and planning, applied both in retrosynthetic and synthetic direction, is utilized in order to avoid tracking the entire synthesis tree. For details, see text.

ring by a photooxidation of the precursor **2**. The transformation of **2** to **1** could be accomplished with only two steps.[45b] After **2** was defined as a central intermediate and forward planning from **2** to target **1** revealed a promising route, the synthesis of **2** had to be designed. Three competing research groups looked for readily available starting materials that already contained important structural features of precursor **2**. *R*-(+)-citronellol (**3**),[45b] (−)-isopulegol (**4**),[45c] and (+)-car-3-ene (**5**)[45d] were somehow selected by the three groups. The three cited syntheses were developed in forward direction from the starting materials, always focusing on the agreed upon intermediate **2**. The combination of a retroanalysis to a central precursor, the development of a method to convert this precursor into the target, the detection of structural similarity between the precursor and readily obtainable starting materials, and the sometimes tedious pathfinding from the starting material to the central precursor was finally met with success in all three groups. None of them planned their synthesis by systematic, stepwise retrosynthetic analysis.

Another problem that is difficult to treat with the classical approaches to computer-assisted synthesis planning is the lack of a rigidly defined target structure. Especially in the pharmaceutical sector the target structure is sometimes defined as a hypothetical pharmacophore, and the precise structural definition of the synthesis target is the solution of an optimization problem tightly coupled to the synthesis-planning process. External parameters such as charge distribution and shape characteristics need to be included in the evolution of a lead structure to a specific synthesis target. The target becomes fuzzy, and an efficient synthesis yielding a compound that is functionally equivalent to a model structure, but only similar and not structurally identical to it, becomes an acceptable problem solution. This kind of problem is very difficult to treat with classical transform-based methods, because a specific target structure for systematic dissection is required.

During the fill-up step between the landmarks of a synthesis, reaction databases can be extremely useful. Full structure or substructure searches in catalogs of chemicals are very well suited to detecting specific starting materials. These mature technologies have been readily accepted by synthetic chemists. In comparison, classical synthesis-planning programs are far less useful. Systematic searches typically generate enormous synthesis trees with single-step reactions and precursors, which are extremely unwieldy and predominantly contain dead ends that an experienced chemist would have intuitively avoided. If the search is limited to short sequences, useful, but often obvious reactions are the result. Still, because of the nature of the underlying transform and synthon schemes, there is no guarantee that a precedence under comparable conditions exists. This needs to be checked by consulting a reaction database or the literature, and since the reaction sequence is short, this kind of verification can be performed directly without the aid of a synthesis-planning program. Furthermore, the nodes in the synthesis tree are completely defined compounds that are linked by completely defined reactions. Small variations in a target or subtarget require renewed program runs, or, if this variation was already generated in the original run, gives rise to an independent subtree and participates in inflating the synthesis tree to its intractable size.

2.2. New Methodology To Support Synthetic Chemists

The detection of long-range relationships and similarities between the target compound, commercially available starting materials, and potential precursors is one of the central issues of practical planning. The present systems fail to support the chemist in this essential task. A system that reveals potentially synthetically exploitable similarity between the target compound and the stock of commercially marketed compounds, which is too large for the human chemist to overview, will certainly be very helpful for synthesis design. The emphasis on *synthetically exploitable* similarity is intentional. This requirement is not very well covered by traditional similarity detection algorithms.[46]

The methods for the computation of a minimal chemical distance,[47] that is, the minimal set of bond rearrangements, subject to boundary conditions, between two molecules are valuable for the recognition of potential complex sequences of bond rearrangements. Because of the computational demands, these methods cannot yet be used for the systematic comparison of a target compound with thousands of potential starting materials. The current implementations are exclusively based on topological criteria, that is, reactivity criteria are not taken into account, and accordingly the chances for a practical implementation of a bond-rearrangement scheme is not assessed. The potential of these methods lies particularly in the recognition of rearrangement paths, and they will certainly become a tool for special cases but probably no remedy for all the various problems of recognizing similarity.

If no direct link between a target compound and a starting material can be found, mechanisms for the systematization of a synthesis study beyond the synthesis tree are needed. Manual or computer-assisted breakdown of a target compound at bonds recognized as strategic leads to central intermediates, which can be subjected to further search and planning operations such as similarity search, reaction planning, reaction prediction, and additional decomposition steps. The elements registered in such a study are no longer simple molecules but fragmentation groups, hit-lists from database queries, or reaction-prediction results. The chemist is given a set of tools that supports him in his quest and protocols the steps taken. He must be free to use any tool of his choice at any point he deems promising, so that he can switch freely between synthetic and retrosynthetic analysis. Human reasoning is superior to any synthesis-planning program if large uninteresting regions need to be excluded from a study. It does not mean that the big advantage of unbiased computation is lost. Paths not found because the chemist could not or would not perform a specific search exhaustively, should still be unlockable. If a chemist encounters troublesome areas in a study, or if some region of a study is not obvious or not resolved satisfactorily, the user can still instruct the computer to examine this problem systematically, as deeply as he chooses. The common opinion among users and experts is that the systematic application of thousands of transforms on multiple levels, which is the basic functionality of the classical systems, yields so much uninteresting data that a search for the golden needle in the haystack is not reasonable for the average user.

2.3. Structural Similarity

One of the most urgently needed methods is the detection of *synthetically exploitable similarity*. This term that has not yet been unequivocally defined. Similarity search procedures are applied with success in biological activity studies or QSAR (*Q*uantitative *S*tructure–*A*ctivity *R*elationships) models.[46] However, the similarity criteria in this kind of application are not necessarily compatible with the requirements of synthesis planning. A popular method, for example, is the counting of chemical groups and atoms in the molecules of the data set.[48] The counts of the structural elements are tied to a similarity rating, which often correlates well with physiological activity. The problem with this kind of similarity measure is the lack of sensitivity toward changes in the core skeleton and the overrating of changes in the reactive heteroatom centers. For physiological activity, often the addition or removal of a methyl group is quite irrelevant, but it can be a decisive factor for usability in a synthesis if the target is fixed, or this group influences a reaction center through reactivity or spatial effects. On the other hand the specific nature of a reactive heteroatom center is uninteresting for an intermediate in a synthesis as long as reactivity and propensity for selective attack are still maintained, and the reaction conditions can be adapted to these changes. The synthetic potential of a compound is dependent on many factors that are interrelated in complex ways specific to synthesis planning.

This rule generally applies to most similarity criteria from QSAR, and the extensive set of criteria from this field can be utilized for synthesis planning only in a very limited way. The classic substructure search methods from database applications are too inflexible. Queries become rather nonselective and inefficient if a carbon skeleton is input with the specification that all open valencies are hydrogen or any heteroatom. In addition, such search methods do not consider reactivity, for example, the influence of the environment on the reactivity of hydrogen atoms.

SST[49] is a pioneering system providing in a very elementary approach a relationship between a target compound and a catalog of starting materials. SST is not a synthesis-planning system but simply offers as query methods three degrees of abstraction for the substituents in the core carbon skeleton, which are searched on the database whose entries have been pretransformed with the same abstracting process. In our group we have developed a number of similarity definitions and methods that are specifically aimed at detection of structural similarities for synthetic problems.[50a–c] Some of these are based on extended common substructures such as ring systems and core carbon skeletons in the molecules to be compared. The majority of these methods though, rely on criteria that have been derived directly from generalized chemical reactions. It has been observed that these are the most powerful methods for synthesis-planning problems. Algorithms for these novel similarity criteria have been integrated into the WODCA system. This will be discussed in detail in the following sections of this paper.

3. The WODCA System

During the last six years the WODCA system has been developed in our group.[50] WODCA is an interactive, graphics-oriented support system for chemists working on synthetic problems. WODCA fulfills the requirements for a new generation of synthesis-planning programs outlined in the previous sections and implements novel ideas and algorithms for such systems. It serves as a test bed for the fundamental ideas and methods. As the name already intimates, the system is not only a synthesis-planning program but fulfills other purposes within our group. This paper will only describe the synthesis-planning aspects.

Among the highlights of the system are the implementation of novel similarity criteria for database queries, the use of a flexible system for the organization of studies, and the dynamic integration of modules that perform intelligent operations on and with molecules (for example, merit evaluations and the detection of strategic bonds). The application of a classical synthon- or transform-oriented knowledge base has been consistently avoided. A number of external programs can be used from within WODCA: the programs of the EROS series[20] for reaction prediction and reactivity estimation, PETRA for the computation of physicochemical properties of molecular structures,[21–24] and a number of auxiliary help and visualization applications such as structure and reaction displays, plan overviews, and a report generator. Classical database search methods such as full structure and substructure queries and some published similarity algorithms are an integral part of the system. Linking WODCA to reaction databases is one of the next goals and currently under way.

WODCA is an interactive system with strong graphics support. Figure 3 shows a typical example for the information transmitted graphically during a WODCA session. Modern window systems (here on a Sun workstation under SunView; ports to X11 and MS Windows are in progress) allow the concurrent display of the results of many analysis and search methods. This approach intentionally and specifically supports the lateral thinking of chemists who jump back and forth between different threads of thought and problem areas. In Figure 3 the results of a strategic bond determination, a query for starting materials suitable for the synthesis of the fragments obtained by cutting the bond, and the full catalog data and ordering information for one of the possible starting materials are simultaneously displayed.

This pictures also demonstrates how a user actively participates in a synthesis-planning study. He freely selects instruments from WODCA's toolbox, gets new ideas by scanning the results of the chosen search and retrieval methods, and quickly drives the study to ward those results that are most useful.

The collection of methods in WODCA are meant to supply the chemist with immediate answers to "what would happen if" questions in a continuous interactive exchange between the creativity of the experienced chemist and the speed, precision, and thoroughness of the computer. Speed of execution was an important design goal. Normally, a preliminary answer computed by a workstation should be available within seconds, and the user can always interrupt processing after only the first few answers of the full scan. The chemist is in charge of selecting the methods best suited to the task at hand. WODCA refrains from forcing the user to adhere to rigid rules concerning sequence and thoroughness of scans and operations, but rather relies on the experience and intelligence of the chemist. If the system

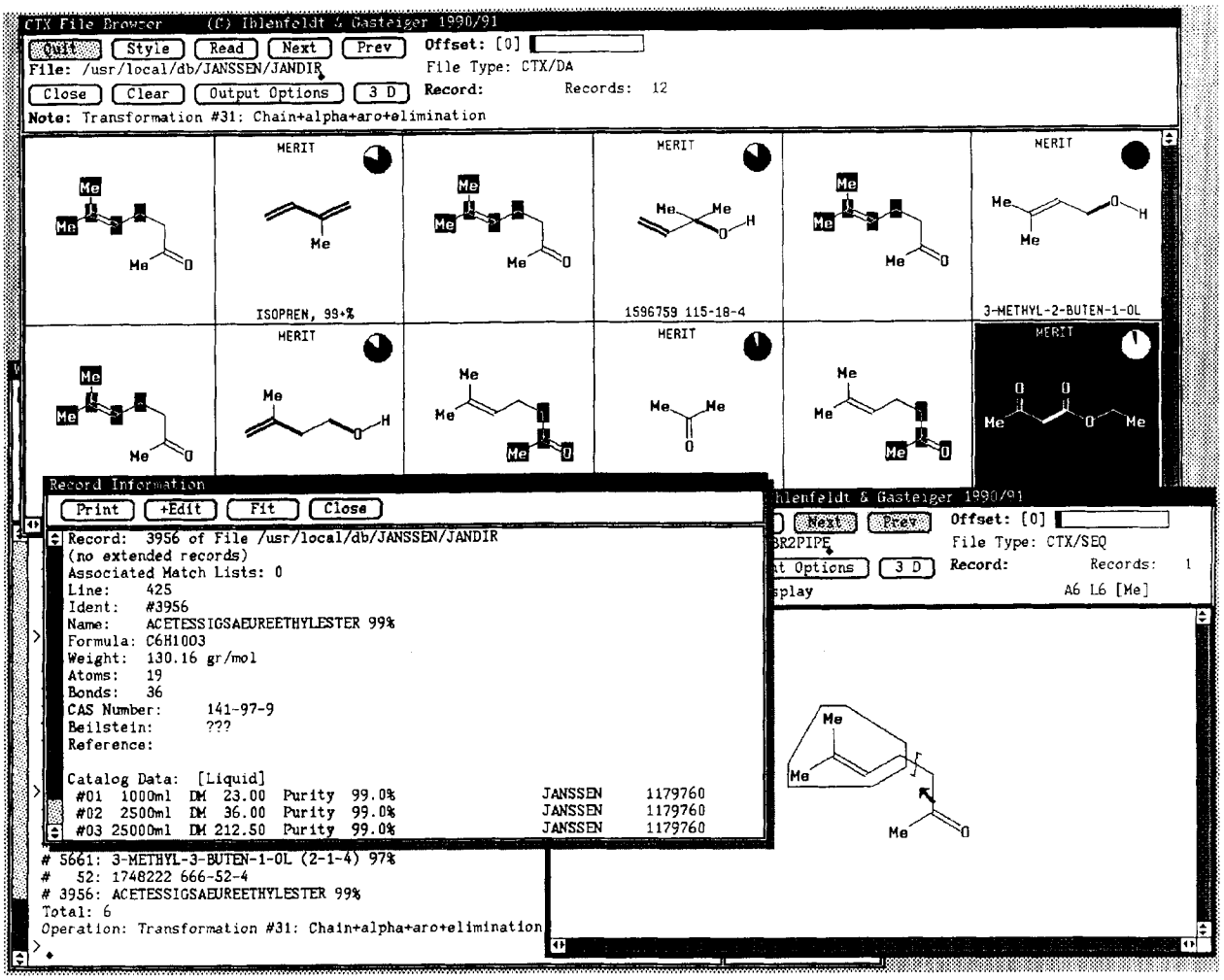

Fig. 3. Graphical user interface of WODCA: The window on the lower right-hand displays the target molecule. The strategic bond currently being worked on is marked. One of the fragments obtained from breaking this bond has been highlighted by a frame. The upper region of the screen copy shows compounds from a starting material catalog that were recognized as being related to either one of the two fragments. Left of each of the possible starting materials, is the formula of the target on which the coincidence with the embedded fragment is highlighted by black boxes. The calculated degree of structural similarity is visualized as a pie diagram in the upper right corner. The similarity criterion selected by the user (in bottom left corner: transformation no. 31: core carbon skeleton + α-hetero atoms + preserved arenes + elimination) requires correspondence of the preserved carbon skeleton and the heteroatoms of the α sphere. Arene rings must not be changed, but structural differences that can be removed by generic elimination-type reactions are allowed. The user has selected one of the proposed compounds (dark background) in order to retrieve further information from the starting material library. This auxiliary data such as name, structural formula, molar mass, CAS registry number, and pricing information is listed in the uppermost floating window.

generates proposals with which the user disagrees, a different proposal can be entered manually or the system's answer can be edited before this data is passed to another module. Examples of this kind of editing operation are automatically detected strategic bonds, where the user sometimes has a broader perspective than the system. Strategic bonds can be deleted, added, or their attribute set changed with a mouse click.

The whole arsenal of methods can be applied to any suitable object within a study, and thus the study can be expanded in any direction starting at arbitrary points. The system comprehensively records not only the results of the operations but also the selected operations themselves. These data are stored in logfiles and can be viewed immediately. Every step becomes a plan element, and the relationships between these plan elements are shown graphically. Important classes of plan elements are structures, sets of strategic bonds, fragments, results from database queries (match-lists), and results from reaction prediction. Studies can be interrupted and resumed at any time.

3.1. Core Operations of the System

The general course of actions during the study of a synthesis problem with WODCA is displayed in Figure 4. In the current program configuration three core operations can be identified:

- search for starting materials
- search for synthesis precursors
- prediction of reactions

The difference between a synthesis precursor and a starting material in this context is that a starting material is a fully specified molecule found in a catalog of chemicals while a synthesis precursor is a vaguely defined, compound, hovering somewhere between starting material and target. The gaps between these three species are bridged step by step.

The most important task in synthesis planning is the establishment of a relationship between the target and suitable starting materials. Therefore, databases with commercially marketed compounds figure prominently within the WODCA system.

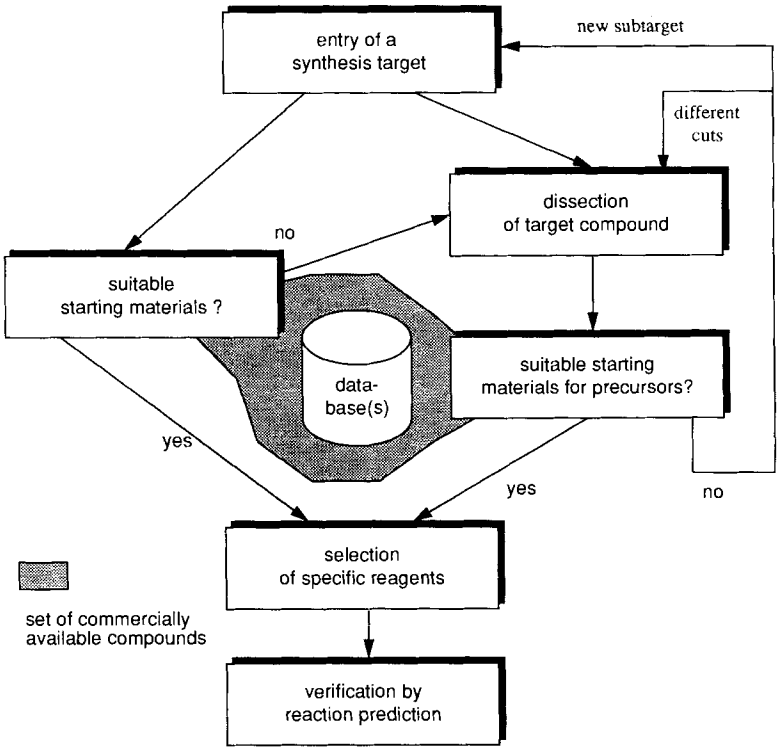

Fig. 4. Flowchart explaining the sequence of actions in a synthesis planning study with WODCA: an interplay of starting material search, determination of precursors, and verification by reaction prediction.

Many query methods (see Section 3.1.1 and Fig. 5) are provided for the retrieval of suitable starting materials for a synthesis (left-hand branch in Fig. 4). For more complex target compounds this will not be directly possible. The molecule therefore needs to be dissected into fragments at bonds perceived as strategic. These fragments are then submitted to the search for starting materials (right-hand branch of Fig. 4). The process of dissection and search for starting materials is repeated until all precursors can be linked to readily available starting materials. From the set of potential starting materials suitable reagents are selected, and with the aid of reaction prediction a verification step examines whether the reaction really proceeds in the intended direction (lower part of Fig. 4). Precursors and starting materials are entered into a planning tree, which coarsely resembles a synthesis tree but is far smaller than in a classical, retrosynthetic analysis. On the other hand, the information content and complexity (classification, history, relationships to other entries) is much higher.

3.1.1. Search for Starting Materials

One of the most important aspects of working with WODCA is the creation of relationships between a synthesis target or precursor and a starting material. A number of catalogs of chemicals are available in the system, including the lists of several manufacturers of fine chemicals, special hand-compiled catalogs, and the database of the CHIRON program.[32] Additional compound libraries can be added easily. All operations can function on any catalog, and the user is free to switch catalogs within a study.

WODCA provides classical retrieval methods such as full structure search (by a novel hashcoding procedure[51]), fragment-oriented similarity measures, and general-purpose database queries such as numerical and textual search on names and structure attributes. Additionally a number of methods were developed that focus on synthetically exploitable similarity. Two of the new methods are the following:

1. Transformation searches: A query structure is transformed by clearly defined principles, which correspond to generalized reaction types and emphasize certain structural elements. It is then compared to the similarly transformed molecules in the database. The new hashcoding algorithm[51] is applied here as well, and consequently, this type of search yields results extremely fast, typically in less than a seond.

2. Pathlength code searches: The substitution pattern and structure of the core skeleton of a pair of molecules are compared in a synthetically significant manner. Some applications are found in Sections 4.1 and 4.2. Figure 5 shows a general overview of the arsenal of methods in WODCA.

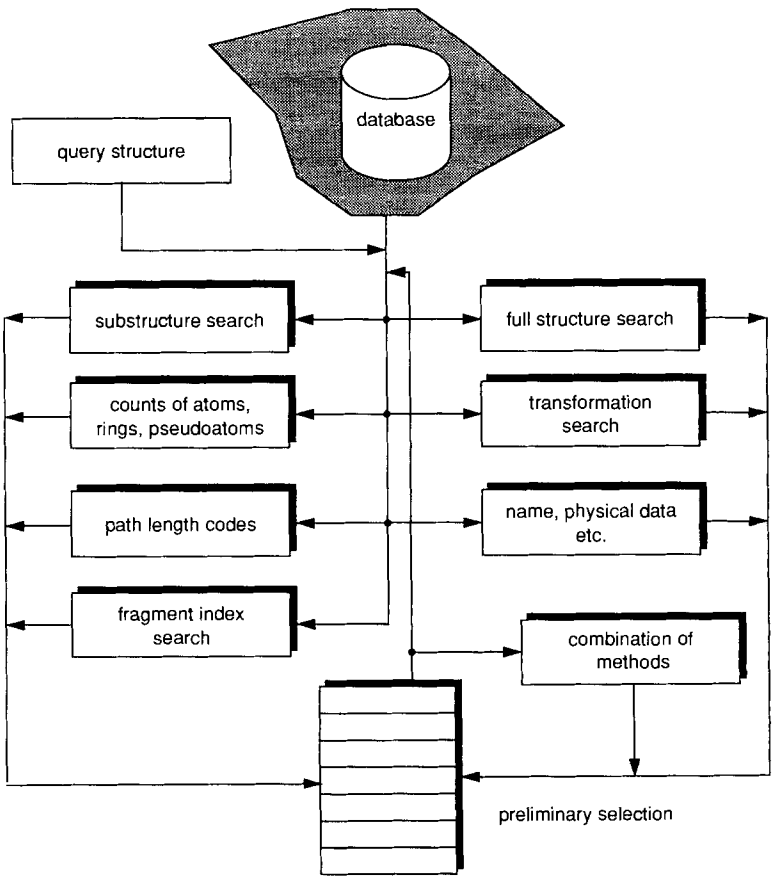

Fig. 5. Arsenal of available methods for preselection of starting materials.

Because transformation searches and pathlength code searches are extremely powerful in defining synthetically exploitable similarity, their use will be emphasized in this paper. A more detailed explanation of the transformation search principles, and examples that highlight their importance for synthesis planning have been published.[50a-c] Generally speaking, transformation searches can be classified into two groups: A class that detects similarity by important common substructures and another class that defines similarity of compounds by interconvertability through generalized reaction types such as substitution, hydrolysis, or oxidation. The boundaries between these two classes are sometimes not very sharp, because many transformations of the first class have been designed around core structure elements that remain constant during the course of reactions.

Figure 6 shows the result of a similarity search with 1,8-diazabicyclo[5.4.0]undec-7-ene (**12**) as query structure. This search

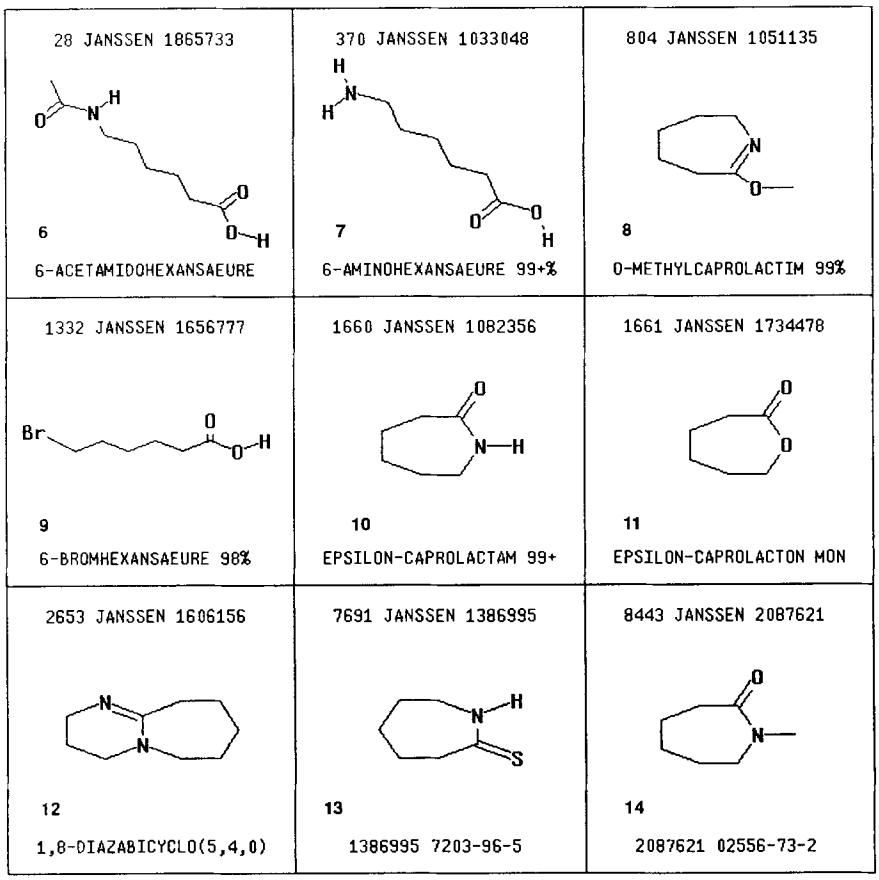

Fig. 6. Compounds similar to 1,8-diaza-bicyclo[5.4.0]undec-7-ene. They contain the same carbon skeleton and the same substitution pattern for heteroatoms.

employed, as most examples in this paper, the 1988 catalog of Janssen Chimica (now Acros Organica Division), which contains 8465 compounds. Of these compounds 7849 are structurally different, that is, they are not variations in purity, quality, preparation method, or isotope labeling. Stereoisomers are different compounds by this definition.

For this example, a similarity criterion based on a common substructure was selected. Molecules are perceived as similar if they contain the same carbon skeleton with the same substitution pattern of heteroatoms. Basically, all listed compounds are reduced by this transformation to structure **15**. If, like query molecule **12**, a molecule is broken into two fragments during a transformation, the procedure continues with only the single molecule containing the largest number of carbon atoms. In the current implementation it is assumed that the largest fragment has the most interesting functionality. This simplification certainly fails in some instances but serves well as a rule of thumb in the large majority of cases.

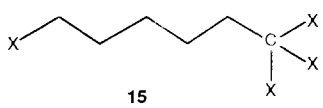

15

Confronted with this list of compounds it is easy for chemists to recall intermediates and reactions that might lead to a successful synthesis of **12**, proceeding most favorably via ε-caprolactam (**10**). Should any doubts remain about the feasibility of the transformation of **10** to **12** (reaction with acrylonitrile and hydrogenation with ring closure), similarity searches with the smaller structural fragment, tetrahydropyrimidine, would be initiated. Possible syntheses for ε-caprolactam (**10**) are obvious from the list of structures in Figure 6: ring closure reactions with **7** or with **6** after cleavage of the protecting group, and from **9** and **11** after treatment with ammonia. The other structures (**8**, **13**, and **14**) can also be synthesized from **10**.

This example demonstrates how the results of a similarity search can inspire chemists to creatively design a synthesis with their knowledge: chemist and program form a team for the efficient solution of synthetic problems. In the next example (Fig. 7) we introduce a similarity criterion based on a generalized reaction type: here, elimination. All compounds displayed in Figure 7 can be transformed into each other by an elimination and/or addition. Note that the Saytsev rule is observed. Such queries, which are oriented along reactivity patterns, are extremely difficult to specify by normal substructure search mechanisms. Once again the task to select reagents and reaction conditions for the practical implementation is left in the first phase to the chemist (how to achieve Markovnikov or anti-Markovnikov addition?). Chemists will need verification by a search in a reaction database only in nontrivial cases, and they decide on this themselves.

Another similarity definition combines compounds that can be interconverted by substitution reactions. It is easily understood that this similarity measure is more restrictive, because from the compounds in Figure 10 this criterion recognizes only structures **16**, **17**, and **19** as related and puts them into one

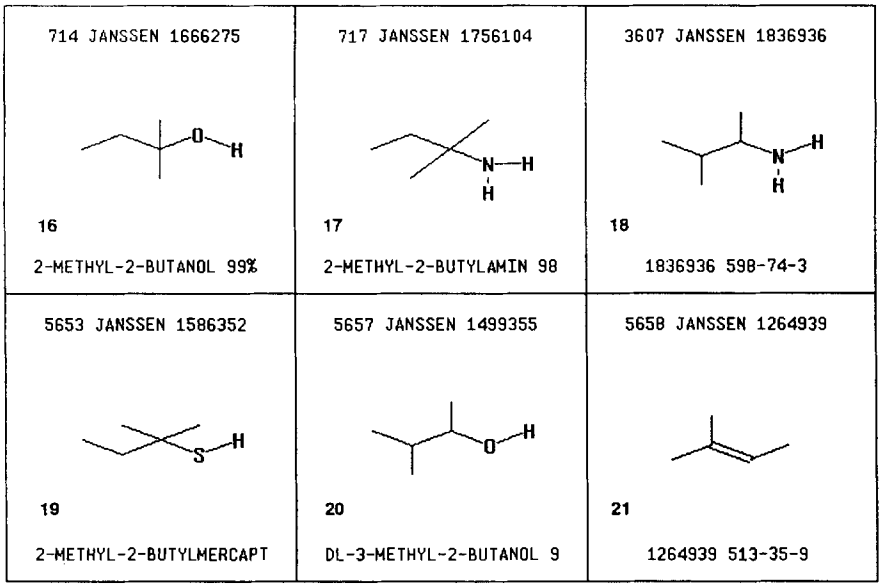

Fig. 7. Compounds detected as similar, because they can be converted by elimination into the same product.

group. Molecules **18** and **20** are put in a separate group. The direct relationship between **21** and the structures in the other two groups will be lost, together with possibility of transforming one group into the other via **21**. Some of the similarity definitions take into account the configuration of chiral centers and stereogenic bonds.

The similarity criteria that are based on structural transformations detect similarity and specify the structural changes or reaction classes that can exploit this structural identity, but do not give a quantitative measure of similarity. In order to define similarity quantitatively, another approach was taken: the computation of pathlength codes. The starting point has been an idea from Randic and Wilkins.[52] In a molecule all paths of length one (one bond or atom pair), two (a sequence of three linked atoms) etc. are counted. We have significantly extended this simple approach by including heteroatoms, rings, aromatic systems, multiple bonds, etc. Figure 8 shows the result of an example query with structure **22** and two molecules **23** and **24**

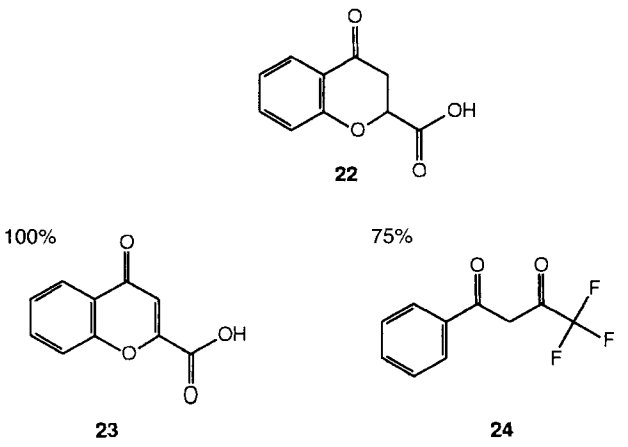

Fig. 8. A target molecule and two potential starting materials found by a pathlength code search. The similarity rating is normalized to 100%.

recognized as similar by pathlength coding. The percentage is the scaled numerical degree of similarity. Compound **23** with the highest similarity rating needs only reduction to be converted into the target structure **22**, while compound **24** requires more extensive structural modifications.

This example once again underscores the big advantage of similarity criteria defined by transformations: they often directly hint at reactions that can be employed to achieve the structural conversion. Measures based on pathlength codes detect similarity only by summing up substructural features without implicit reference to applicable reactions.

All these methods are used only for a quick preselection of candidate structures and are not expected to yield a final result. WODCA incorporates mechanisms to determine the degree of suitability of a compound as a starting material precisely and comprehensibly. One of the most powerful methods is the merit evaluation of good overlaps of starting material molecules and the target compound or intermediates. Factors like stereochemical compatibility, reactivity of the centers that need to be modified, and the possibility of selective attack on these modification sites are estimated. Accessibility and reactivity also influence the merit evaluation of the stereocenters requiring inversion, so this is not just a simple projection and count of necessary modifications. For the reactivity estimation WODCA uses the same physicochemical parameters that the EROS program series employs for reaction prediction,[20, 21, 25] where they have already proven their validity. An example for the power of these rating functions will be discussed in Section 4.3.

3.1.2. *The Search for Precursors*

Only in simple and propitious cases can a link between the target and a starting material be established directly. WODCA therefore includes mechanisms to dissect structures and subdivide the problem. To do this WODCA features functions that recognize and mark strategic bonds. Both topological and reactivity-oriented data, which are extracted from an analysis of the pattern of physicochemical properties of atoms and bonds, are procured and analyzed. This is not yet a final retrosynthetic analysis but only defines first locations for cuts. The atoms and groups that are ultimately used to generate specific precursors or reagents from the fragments (synthons) are not yet defined at this step or are present only as tendency markers (electron-withdrawing group).

Bonds between carbon atoms and heteroatoms are important locations for the dissection of a compound into smaller fragments. Strategic merit values are assigned to the bonds on the basis of the nature of the heteroatoms and their electronegativity, the resonance stabilization of charges generated after het-

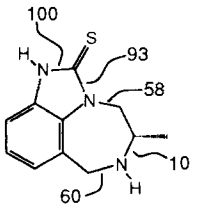

25

erolytic bond cleavage, the size of the rings etc. Compound **25** is an example in which the strategic bonds together with the respective merit values have been automatically determined.

The chemical intelligence contained in the automatic functions for strategic bond detection is illustrated with the tricyclic compound **25**. C–X bonds are correctly perceived as the primary focus of interest and breakable in retrosynthetic direction. In the imidazolthione ring the bonds from the nitrogen atoms to the thione groups receive excellent ratings, while the bonds from the nitrogen atoms leading to the aromatic ring are recognized as difficult to break retrosynthetically. For the evaluation the methods take into account that these bonds can only be formed by nucleophilic aromatic substitution. These kind of reactions typically require drastic reaction conditions and hence do not possess a high degree of synthetic versatility. The ratings of the two bonds to the third nitrogen atom have different values of 10 and 60, respectively. The low value of 10 arises because this bond leads to a chiral center. Since its formation (that is, in synthetic direction) requires a stereospecific reaction, it is much more preferable to have this bond in the starting material already and to form the bond between the nitrogen atom and the benzylic carbon atom. Consequently, this preferred bond is rated much higher (60).

Of course, methods that detect strategic carbon–carbon bonds are also available. Polar reactions play an important role in the construction of carbon skeletons in organic compounds. Accordingly, during the determination of strategic bonds in a synthetic target special regard is given to the distribution and stabilization of the formal charges generated by cutting these bonds. Resonance stabilization of the charges is especially important. Both heterolytic cuts of every relevant C–C bond are examined. Detection functions also exist for the rating of radical processes. Besides local stabilization issues, general topological factors such as the distance to the center of the molecule and inclusion of the bond in a ring influence the merit evaluation.

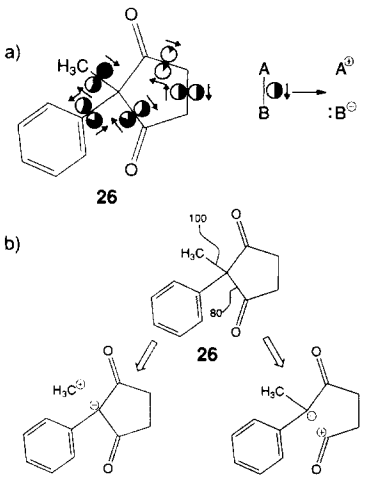

Fig. 9. a) Heterolytic cleavage of C–C bonds in 2-methyl-2-phenylcyclopentane-1,3-dione (**26**), and the amount of resonance stabilization estimated for the formal charges after bond cleavage. The arrow indicates the direction in which the electron pair from the broken bond moves. The shaded circles indicate the amount of resonance stabilization. b) Strategic bonds obtained by analysis of the resonance stabilization data in **26** and the synthons generated using this information.

Figure 9 presents the amount of resonance stabilization experienced by the formal charges generated by separate heterolytic cleavage of all C–C bonds (except those in the aromatic ring) in 2-methyl-2-phenylcyclopentane-1,3-dione (**26**). The more favorable heterolytic processes lead to cyclopentane-2,5-dion-1-ide. The detachment of the methyl cation is presumed to be more favorable than the generation of a phenyl cation. Furthermore, stabilization is expected to be relatively high for the dissection of the C1–C2 ring bond, which leads to an acyl cation and an enolate anion. Only very limited stabilization is anticipated for the other C–C ring bonds. These deliberations eventually point out and rate two strategic bonds as shown in Figure 9 b and their attached ratings. The disconnection of a phenyl cation is "penalized" by the system, so that this bond is no longer considered strategic. The target molecule can now be cut automatically at the strategic locations. The fragments are converted into precursors and can be subjected to similarity searches. The user may also add handpicked strategic bonds or exclude bonds from the automatically generated set, to steer the analysis into the desired direction. The relationship between the dissections, which can be extended across several levels, and the target compound is entered into the synthesis plan. All potential operations on the target compound can also be applied to these fragments. Thus a path that consists not of complete reactions, but of vaguely specified intermediates can be paved to the starting materials (see Fig. 4). The gaps between the stations are filled by reaction prediction (Section 3.1.3) or, in a future version, by reaction database queries until a reaction sequence is completed from starting material to target.

3.1.3. Reaction Prediction

WODCA cannot yet connect to a reaction database in order to extend plans stepwise in retrosynthetic direction with reactions from literature. Nevertheless, it is already possible to use the EROS system for reaction prediction and thus for verification of a proposed route in the forward direction. The latest version, EROS 6,[25] allows the automatic generation of reaction rules from reaction samples in a database. These rules have predictive power that extends beyond the training set. If a genuinely substantial training set is provided, and the reaction class under examination is not too erratically sensitive to peripheral influences such as temperature, ions and solvent, even absolute reaction rates and product ratios can be predicted to within a few percent.[25] Reaction simulation is always the method of choice if no strikingly similar reaction can be uncovered in literature. EROS can model the influence of substituents and generates predictions that are more reliable than those from database searches. The Diels–Alder reaction (including the hetero-Diels–Alder reaction) is an example of a reaction that can be modeled very well. The amide hydrolysis reaction showed that simulations by EROS can also predict absolute reaction rates reliably.[27] If an EROS reaction rule exists for a reaction class, it is possible to check immediately whether WODCA's fragmentation proposals or manually selected sets of strategic bonds lead to feasible syntheses. The simulation results are also added to the plan and can be analyzed later.

An example for a reaction prediction by EROS 6 initiated by WODCA is shown in Figure 10. Strategic bonds for a potential Diels–Alder reaction have been recognized automatically (small window left of center). Yet the character of the reagents is so unusual that the practical success of the reaction is doubtful. EROS predicts only one product with a scaled rating of more

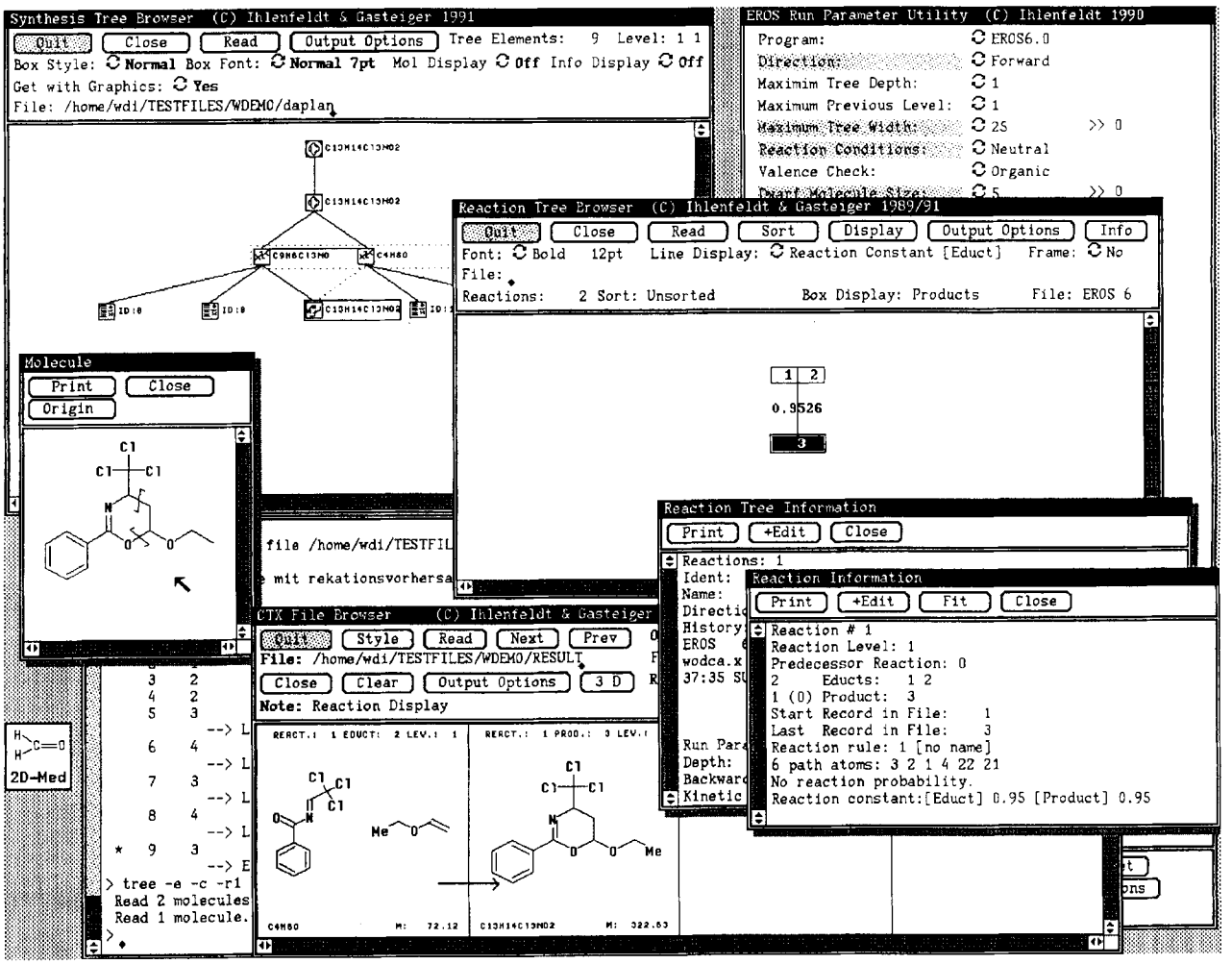

Fig. 10. Prediction of regioselectivity in a Diels–Alder reaction by the EROS program in the context of a verification of WODCA's strategic bond proposal. For a detailed explanation of the information displayed in the various windows, see text.

than 95% (central window, slightly to the right) and the required orientation (central bottom).[53] The prediction becomes part of the evolving plan (upper left).

3.2. System Design

The description as *program system* already implies that WODCA is not a single program but a set of cooperating programs. Most of the programs run in parallel and exchange data in real time. WODCA itself is the core system, which is surrounded by a shell of peripheral programs. The strict modularization has a number of advantages:

- smaller programs are more easily maintained
- memory consumption is relatively small, because the user selects only those subsystems needed for the work on a specific project
- parallel development of subsystems by teams of programmers is easier
- various tools with distinct user interfacing and interaction philosophy but providing similar functionality can be freely selected
- use of single tools is detached from the complete system for special tasks.

Peripheral programs, which run in parallel to the core system, are distinct from secondary programs, which are started from WODCA. Secondary programs are either called from within WODCA and continue to run independently or WODCA starts them and waits until they deliver their results. In contrast to the peripheral programs one cannot switch at will between them.

All functions representing the chemical intelligence of the system (merit evaluation of starting materials, search for strategic bonds, filter functions) are not hard-coded in the program but stored in external data files, which are read during the run. This mechanism can supply not only generally applicable functions but also specialized functions for specific cases, which are loaded when necessary. The user not only controls the general method suitable for a specific problem but also selects the particular variation of a method and how the results should be interpreted. Figure 11 displays the dataflow between the interactive program set. Unidirectional and bidirectional data streams are distinguished by the arrowheads attached to the channels.

To avoid waste of memory space, the WODCA system can be configurated to the task at hand. Before starting the system the user selects those tools that are necessary besides the core program. They are started together with the core program and shut

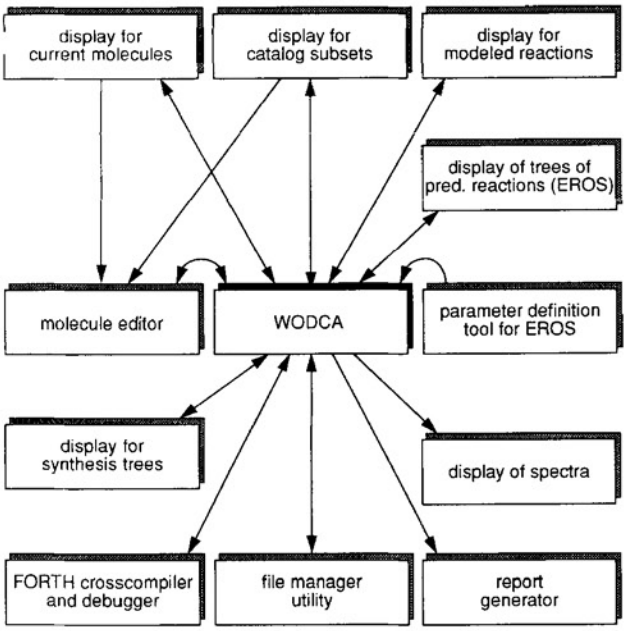

Fig. 11 Data flow in the WODCA system.

down when the core program exits. The set of programs is configured by clicking on the icon panel displayed in Figure 12. Currently, all peripheral programs to be used in a study must be chosen at start-up.

Although the system has been running in the described configuration for several years, it is a young system just emerging from development. Some efforts are still required to make the system even more user-friendly.

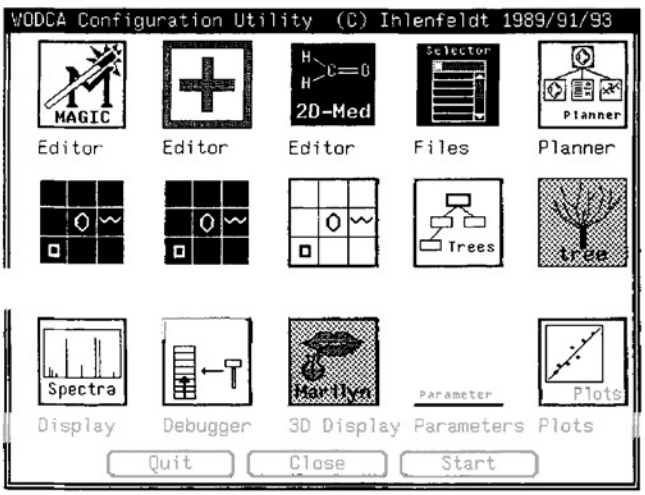

4. Examples for the Work with WODCA

The following three examples are intended to give a global and preferably untechnical overview of the practical work with WODCA. The examples have been chosen to demonstrate a large number of the basic operations of the system without undue repetition. Due to constraints in space and to maintain readability of this paper, the developed synthesis studies and plans are kept smaller than usual or incomplete. They are meant to serve as a guided tour through WODCA, not as comprehensive real-life studies.

4.1. Calicheamicin

The first example demonstrates in a general manner the setup of a plan and simple database queries to retrieve starting materials. It is somewhat limited and artificial, because the studied compound is only an intermediate in a larger synthesis and parts of the structure are protecting groups. The target compound **27** is an intermediate in a calicheamicin synthesis.[54]

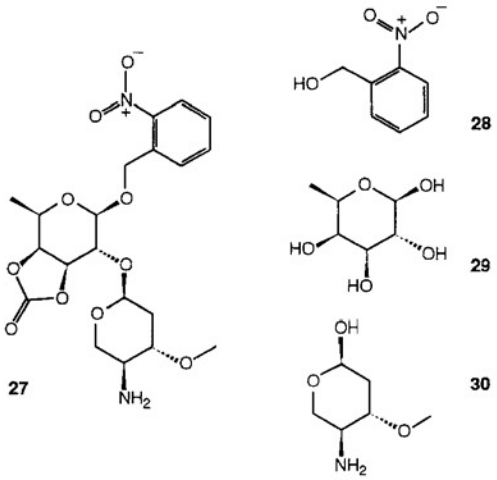

Structure **27** obviously can be dissected into three larger fragments **28**, **29**, and **30**, a process also carried out fully automatically by WODCA, based on perceived strategic bonds. The small ester protecting group is considered structurally uninteresting and is therefore discarded in the first coarse partitioning step. WODCA does not yet restrict the oxygen atoms at the cuts to any precursor. They are simply duplicated on each fragment where they serve as a space-holder for arbitrary functionality. This kind of bond cleavage is distinctly different from a transform-oriented retrosynthesis. Here no assumptions are made about the reactions that will link the fragments. Only structural fragments and their relationship to the whole target are isolated for separate processing later. The closing of the gap between the generalized precursors and the target is an altogether separate task.

The synthesis target, the set of (in this case automatically selected) bonds that are the cleavage points of the fragmentation, and finally the set of molecules that are generated after cutting these strategic bonds form the first building block of the emerging plan, which is shown in Figure 13. This plan uses only a single set of strategic bonds (in this example C–X bonds), which are converted by a single method into actual fragments. In more complicated studies several alternative sets of strategic bonds may be employed, which, for example, may have been found by different methods for strategic bond detection. Each of these sets can be cut with alternative methods. Adjustable parameters for bond cutting include, but are not limited to, the

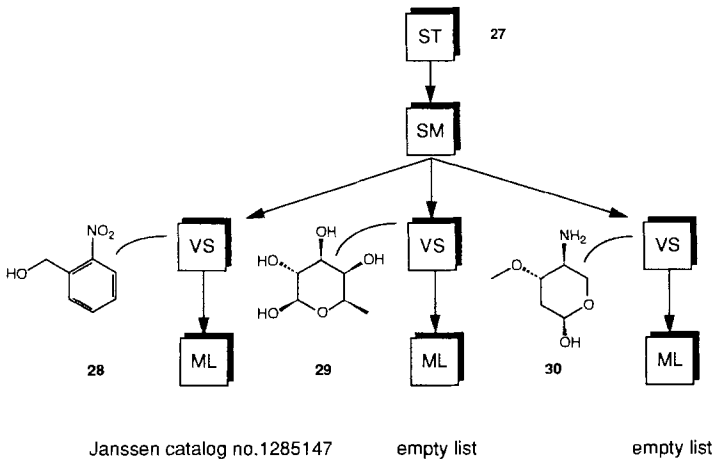

Fig. 13. First step of the synthesis plan for the calicheamicin precursor **27**. As a start a nonspecialized broad-range method is applied to determine the strategic bonds in the synthesis target (ST) automatically. This step yields the strategic molecule (SM) with attached strategic bond information. Cutting **27** at the strategic sites results in precursors **28**, **29** and **30**. Each of these compounds is submitted to a full structure search in the Janssen Chimica catalog but only 2-nitrobenzyl alcohol (**28**) is found to be directly available. The other two match lists (ML) remain empty (contain no structures).

maximum number of bonds cut in parallel and sequencing hints for these cuts, types of filler atoms to saturate the open valences, or directions for the elimination of atoms or ions in order to produce an uncharged precursor. In addition, after cutting the bonds or a bond subset, another detailed evaluation of the fragments and the remaining strategic bonds that were not yet cut can be inserted, because at this level the environment of the remaining strategic bonds has changed, and new insight for the evaluation of the merit of these bonds can be gained.

In the next step an attempt is made to find the precursors as full structures in a catalog of starting materials. The largest library presently accessible to WODCA is the catalog of Janssen Chimica with nearly 8000 compounds. The full structure search can be applied automatically in parallel for all precursors. The result of the query is protocoled and inserted as a logical link to its corresponding query structure in the plan, even if an empty hit-list shows that no corresponding starting material was found. This is done in order to log all steps undertaken during a study, so that it can be reproduced and reexamined in its entirety any time later. Only *o*-nitrobenzylalkohol **28** is found with this classical search method in the compound catalog. The search in the CHIRON catalog and in an extract of the Aldrich catalog also does not yield the remaining two compounds **29** and **30**.

After relaxing the match criteria a little by the application of a similarity search with a transformation hashcoding, which preserves the central carbon skeleton, the α-heteroatoms, and, of course, the stereochemistry, but ignores differences in the substituents of the second sphere onwards and does not distinguish between open-chain and cyclic forms, D-fucose (**31**) is found in the Aldrich catalog as matching compound for **29**.

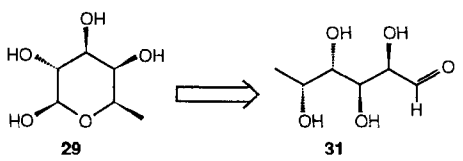

Only the third precursor, the 2′-deoxyaminosugar **30** remains without a direct link to a commerical product. This compound is not registered in open-chain or cyclic form in any of the catalogs accessible to WODCA. Searching with an even broader similarity definition is required. A search method that recognizes the substituent pattern on the core carbon skeleton, but ignores the nature of the substituent and stereochemistry, provides a list of eight structures from the CHIRON catalog (Fig. 14). The search on the 2211 entries of the CHIRON catalog took less than five seconds via pathlength codes, and the list represents those structures that exhibit a scaled similarity rating of more than 10%. The ratings are not yet a detailed merit evaluation. WODCA also provides methods for a more detailed examination of such a preselection, which will be explained in some of the examples in the next sections. Nevertheless, this first selection is surprisingly discriminating. Penta-1,4-dien-3-ol is probably not a very interesting compound, but some of the other compounds are certainly worth a second look. We refrain from disclosing a more in-depth analysis of these potential

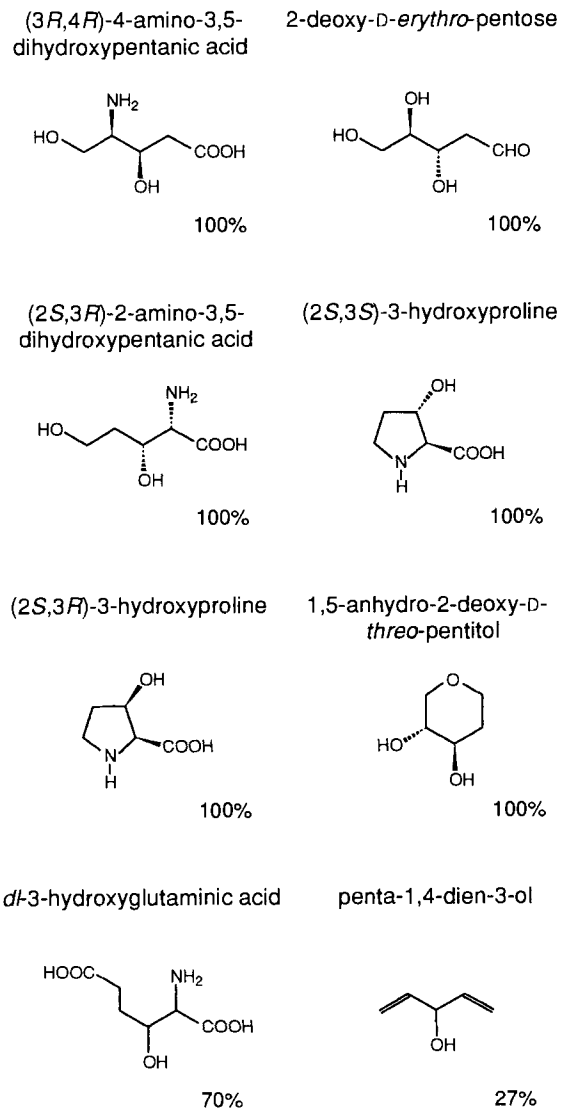

Fig. 14. Preselection of eight potential starting materials for the calicheamicin precursor **30**, selected by a pathlength code search. The percentages are the measure of similarity inherent in the search procedure; they do not include an estimate of synthetic usefulness or stereochemical factors.

precursors and the development of a sequence of reactions to synthesize **30**, because without experimental verification it remains speculative. Finally all fragments of **27** are now associated with starting materials. The next step would be the search for specific reactions to fill the gaps in the forward direction. This part of WODCA is still under construction.

The published synthesis actually uses *o*-nitrobenzyl-alcohol (**28**) and D-fucose (**31**). The third precursor was introduced into the reaction sequence as a protected fluoride. It was prepared from the hydrochloride of L-serine methyl ester in twelve steps with an accumulated yield of 14% up to the 9th step. Maybe some of the compounds in the list might lead in fewer steps and with a higher yield to the used precursor. Unfortunately, again this paper[54] does not provide any hints on how the starting materials and reagents were selected. This is a general problem in complex syntheses: the applied reactions are often very well documented with many literature references and were probably known to the authors when they devised their synthesis. On the other hand, starting materials are regarded as self-explanatory, and no more documentation on this aspect is provided besides sometimes a catalog number of the manufacturer. This is incompatible with our notion of the importance of the methods that lead to the selection of starting materials, an operation at the very heart of synthesis planning. In our opinion they should be documented much more carefully.

4.2. Sexual Hormones of the Green Stink Bug

The complex sexual hormones of the green stink bug (bisabolenes) were synthesized first by Nicolaou et al. in 1989.[55] The pheromones of this class differ in the stereochemistry of the attachment points of the alkyl groups. In this example we treat only a single compound: (+)-α-bisabolene (**32**).

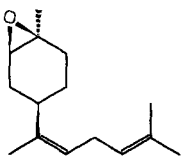

32

According to WODCA's automatic analysis, only two strategic C–C bonds are present: the double bonds. The central double bond is rated higher because of general tactical advantages (it is more central, and therefore the chances for a convergent synthesis are higher). If WODCA is allowed to proceed unguided, both possible dissections are entered into the plan (Fig. 15). The right-hand branch, which was evaluated lower by WODCA, leads to precursor **35** and a fragment with an isopropyl skeleton. It does not look very promising. The isopropyl fragment is of course available in hundreds of variations, but the larger fragment **35** cannot be connected by any substructure search or similarity transformation to a related compound in any of the catalogs available to WODCA.

For the analysis of the left-hand branch of the synthesis tree leading to precursors **33** and **34**, the CHIRON catalog is activated first in order to have the maximum choice among terpenoid structures with defined stereochemistry. A simple substructure search (a search for fragment **33** embedded in the catalog compounds), neglecting stereochemistry but with the constraint that the skeleton size of the catalog compounds must not exceed the skeleton size of the query structure by more than 25 percent and requiring at least one stereocenter with defined configuration

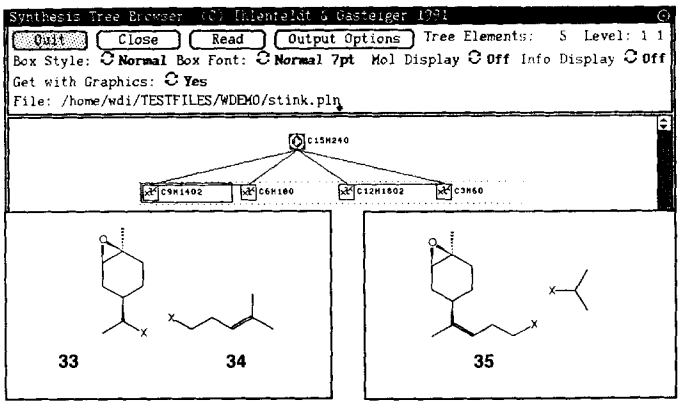

Fig. 15. First steps of the synthesis plan of (+)-α-bisabolene (**32**).

somewhere in the molecule, retrieved 24 potential precursors. Then the rating functions mentioned in the previous section are employed. All 24 candidates are superimposed on the query fragment **33**, and the complexity of the required transformations as well as the stereochemical complementarity are estimated. The candidates rated best by WODCA (**36**–**39**) cannot be ordered from a supplier because they were extracted for the CHIRON database from literature. Since the database includes the literature citations, they can be displayed with a mouse click and sent to a printer if desired. The common characteristic of these top rated structures is a defined configuration at the methyl-substituted ring atom.

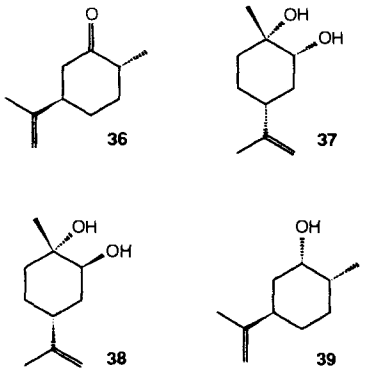

On the other hand, the top-rated commercially available compounds ((*R*)-limonene **40** and (*R*)-carvone, **41**) are reactive at this position (because of a double bond), but are not yet stereochemically differentiated at this site. The stereochemical merit evaluation function attempts to estimate to what extent the proximate groups might influence the stereochemical course of a reaction. For **40** and **41**, however, the potential for induction is regarded as rather small. Consequently, these compounds received a distinctly lower score than compounds **36**–**39**.

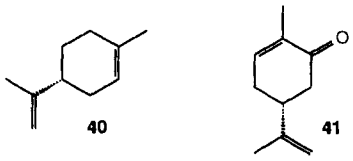

Remarkably, all compounds selected by WODCA contain a larger carbon skeleton than the required precursor **33**. The normal size (and typically also complexity) relationship between synthesis target and precursor has been inverted, and the starting materials contain one more carbon atom (and some exhibit more structural complexity) than the synthetic product. Classical inflexible methods, which expect the starting material to be a substructure of the target compound, can overcome this com-

plication only with difficulty; the search strategy from the WODCA toolbox employed here encounters no difficulties.

In the original paper[55] racemic, epoxidized limonene was ozonized, and the resulting racemate was resolved. Epoxidized limonene was bought in the original study but is not listed in the catalogs accessible to WODCA. For commercial compounds the complete catalog information is in the database and can be viewed. It is even possible to send selected candidate records to an external report generator, which can print summary tables or completed order forms.

After finding apparently quite suitable precursors for the synthesis of **33** in carvone and limonene, the second fragment **34** needs attention. At first glance it does not look very complicated. Surprisingly, not a single compound with the same carbon skeleton and substitution pattern as **34** exists in the diverse WODCA catalogs with altogether more than 10000 structures. Clearly, the substitution-pattern-oriented pathlength codes search is again required. One of the characteristics of this method, which has already been briefly mentioned in Section 3.1.1, is the identification of structures whose carbon skeletons are very similar to, but not necessarily absolutely identical to the query structure. At the same time, whereas the substituent pattern can be varied, it should be similar. The specific type of the substituents is ignored, and true substituents and carbon–carbon double bonds are also somewhat interchangeable. Even this type of search does not yield any clearly ideal starting material. However, a closer analysis of the hits reveals some interesting relationships, which probably would have been overlooked on paging through printed catalogs. Nine structures (**42**–**50**) taken from the condensed subset of the 30 top-rated compounds extracted from the catalog in a few seconds are shown in Figure 16.

None of the listed molecules can be used immediately. Nonetheless, this selection will indeed stimulate new ideas. The

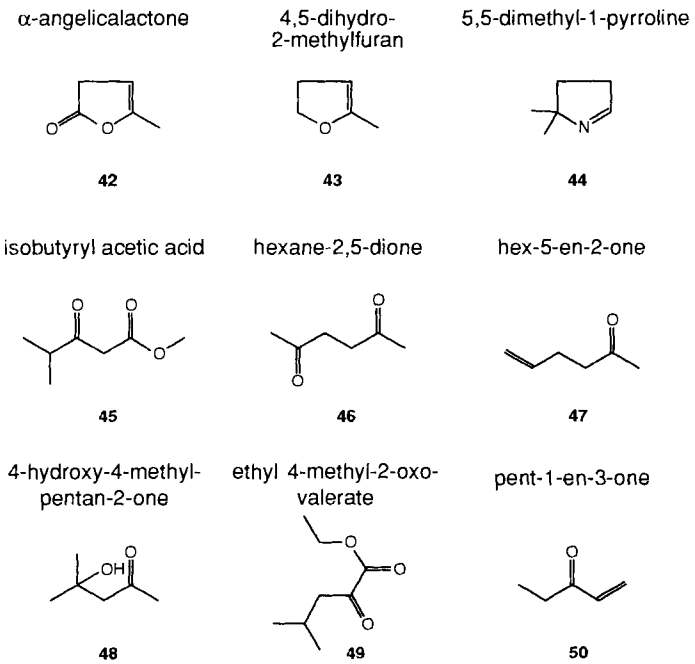

Fig. 16. Potential starting materials for the synthesis of **34**, obtained in a very broad-range search.

ring of the pyrroline **44** can certainly be opened, and functionality is present for the introduction of the double bond and the adjustment of the terminal group. After ring-opening, angelicalactone (**42**) and the dihydrofuran derivative (**43**) also possess functionality at the right place, but both require the introduction of a methyl group. In this case the compounds obtained high ratings because of the good fit of functionality in spite of an incomplete core carbon skeleton. Compounds such as hex-5-en-2-one (**47**) require a degradation (double bond cleavage) as well as a methylation of the skeleton in order to obtain the terminal functionality. Other candidates such as 4-hydroxy-4-methyl-pentan-2-one (**48**) have the basic structure including the central double bond, but the functionality needs to be shifted to the terminal atom. Some molecules that appear strange at first glance trigger a cascade of associations in the mind of the chemist on a more thorough examination. Of course, it is possible to dissect fragment **34** further. WODCA then finds unerringly 3-methyl-but-2-en-1-ol (**51**) and derivatives of 3,3-dimethylacrylic acid (**52**). These compounds were also perceived as similar in the original search but are placed rather low on the list sorted according to the similarity value because of the much reduced size of the carbon skeleton.

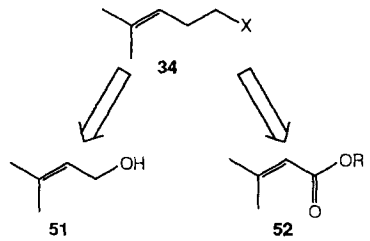

In the original synthesis[55] fragment **34** was assembled from tiny building blocks. In six steps three carbon-containing compounds (two C_1 fragments and a C_4 fragment) were attached to the limonene frame. Surely this cannot be called a convergent synthesis. If such tiny building blocks are assembled one can no longer speak of similarity and the recognizable relationship to the target molecule. It is not within the realm of WODCA during a first analysis to generate associations that lead to such tiny synthetic steps. Only if no suitable synthesis is suggested under a more global perspective is a second analysis initiated to cover the minute details of such kind of synthesis approach.

4.3. (+)-7,8-Epoxy-2-basmen-6-one

The last example is the search for starting materials for (+)-7,8-epoxy-2-basmen-6-one (**53**). This example was selected to demonstrate WODCA's ability to yield valuable starting points for synthesis planning across extreme synthesis distances.

Compound **53**, which occurs in nature in dried tobacco leaves, was prepared for the first time in 1991 by Paquette in a total synthesis. Search operations for this target with a rather complex stereochemistry were again based on the CHIRON catalog. The natural approach to such complicated compounds is to pass along as much stereochemistry as possible from starting materials. It appears the logical choice to start with a compound that already possesses one of the two five-membered rings. Consequently, the boundary con-

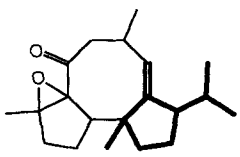

ditions for the first selection of starting material candidates were exactly one single five-membered ring, but no six-membered rings (in the SSSR—the *s*mallest *s*et of *s*mallest *r*ings[57]), plus at least one stereocenter with defined configuration. These filtering conditions yielded 84 candidates. Their merits were again estimated by the stereochemical fitness function of WODCA. The list, sorted according to the result of the merit evaluation, is presented to the user as a table as well as graphically with plots of the candidate structures.

It was not specified which one of the two five-membered rings should be the starting point. All of the compounds in the list were superimposed in all conceivable orientations[58] over both five-membered rings of the target and were also mapped onto the other structural regions. Especially good fits were evaluated in detail. The results are listed in Table 2 and Figure 17. The

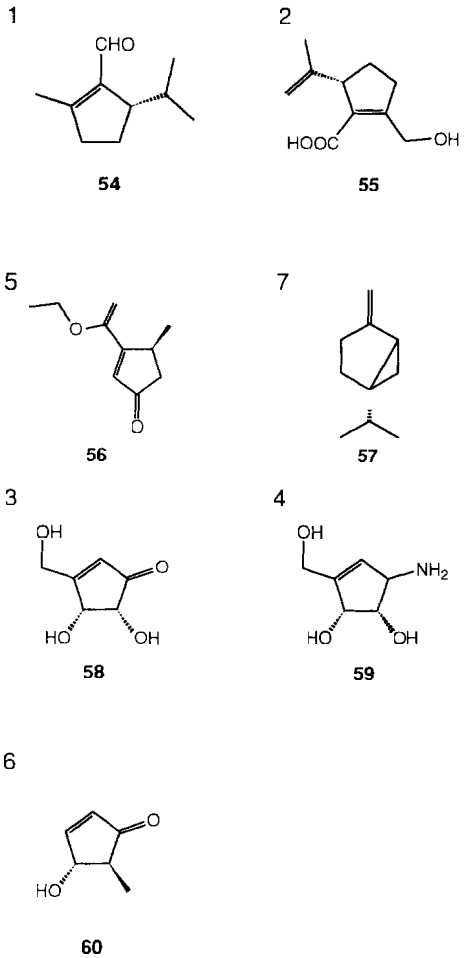

Fig. 17. Potential starting materials that include the right-hand (top two rows) and left-hand (bottom two rows) five-membered ring in (+)-7,8-epoxy-2-basmen-6-one **53**.

better candidates were found for the right-hand five-membered ring. Only for this ring were positive merit values for best fits computed at all. The best fit of the top-rated starting material **54** into target **53** is shown in Scheme 3.

This embedding appears to be obvious but it certainly is not the only orientation examined. The six best orientations for the top candidate, taken from several dozen mappings evaluated in detail for this compound alone, are displayed in Figure 18.

Table 2. Merit of basmenone precursors that include right-hand five-membered ring (fist four entries) and the left-hand five-membered ring (last three entries).

Rank	Merit	Compound
1	979	(5*S*)-5-isopropyl-2-methylcyclopentenecarboxaldehyde **54**
2	959	DL-2-hydroxymethyl-5-isopropenylcyclopent-1-enecarboxylic acid **55**
5	−148	ethyl (5*S*)-5-methylcyclopent-1-en-3-onecarboxylate **56**
7	−194	sabinene **57**
3	−56	(4*R*,5*R*)-4,5-dihydroxy-3-hydroxymethylcyclopent-2-enone **58**
4	−59	(3*R*,4*S*,5*R*)-3-amino-4,5-dihydroxy-1-(hydroxymethyl)-cyclopentene **59**
6	−173	(4*R*,5*S*)-*trans*-4-hydroxy-5-methylcyclopent-2-enone **60**

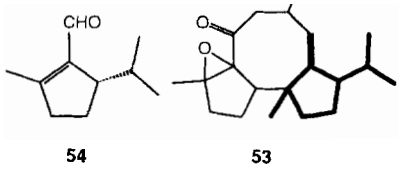

54 **53**

Scheme 3. Most promising starting material **54** and its fit into the target compound **53**.

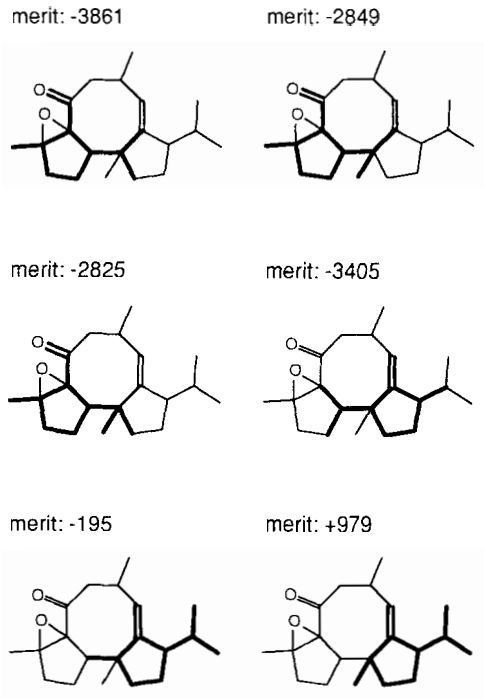

Fig. 18. Most important embeddings of **54** into the target compound **53**, together with their evaluated merits.

By comparison of the rating values and the corresponding fits it is possible to understand the factors influencing the rating procedure. Stereochemical complementarity weighted by the reactivity of the involved centers, reactivity of the connection points that need modification on the way to the target structure (compare the numbers for the embeddings on the lower right and lower left), and more general topological factors are the core elements of this algorithm. It is important to know that not only embeddings of the whole starting material, that is, of the

full carbon skeleton (of course with hydrogen atoms and heteroatoms) were computed. Dozens of alternatives where parts of the starting material carbon skeleton were no longer present in the target were examined as well. In this case (in contrast to the bisabolene example) they did not receive competitive ratings. The stereochemical complementarity of the second best candidate **55** is about as good as that of the top candidate, but more structural conversions are necessary, and thus the evaluation score is lower. The difference is rather small in this example, because the positions which need to undergo transformation in structure **55** are, in principle, quite accessible. On the other hand the enantiomer of the top candidate, which is also contained in the CHIRON database, receives a low score. Because the configuration of a difficult and rather unreactive center must be inverted, this compound does not appear in the top twenty of the 85 scanned library entries.

Some of the search compounds that included the left-hand five-membered ring of **53** provide better starting points for synthesis. The three best-rated candidates **58**–**60** of this type are depicted in Figure 17 (in the bottom two lines), and the best overlays of two of these compounds are shown in Figure 19.

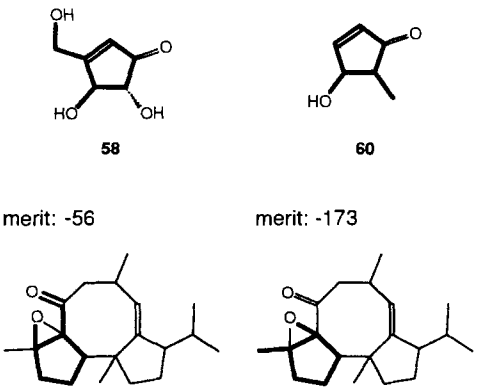

Fig. 19. Best merit values for the fit of **58** and **60** into the left-hand five-membered ring in (+)-7,8-epoxy-2-basmen-6-one (**53**).

The published synthesis[56] did in fact use (5*S*)-5-isopropyl-2-methylcyclopentenecarboxaldehyde (**54**) as starting material. WODCA's analysis is confirmed. The synthesis starting from this material required 28 or 30 steps, depending on the step counting method. Unfortunately, again no information about the way the starting material was selected was published. WODCA has proved in this example that it can perceive synthetically exploitable and convincing structural similarity over an enormous chemical distance. However, this computation cannot be executed any longer in a truly interactive manner. For the close evaluation of the 85 candidates, preselected in a few seconds, about 25 minutes of computer time were spent on a Sparc II workstation. In this time span some hundred thousand superpositions were generated and about 1000 were submitted for merit value computation. This time needs to be seen in comparison to the concentrated effort and limited thoroughness of a human chemist flipping through catalogs manually—it then seems negligible. Moreover, state-of-the-art computers used routinely nowadays for molecular modeling tasks have ten times more computing power, so that the interactive treatment even of such a complex problem is on the horizon.

5. Conclusion and Perspectives

WODCA is a prototype of a new generation of synthesis planning programs, which are oriented closer to the thought patterns of synthesis chemists. WODCA offers a broad spectrum of methods that support chemists in their self-guided search for syntheses of organic compounds. Some of the tools found to be of special importance for this task were custom developed for the field of synthesis planning and were collected, together with known search methodology, into a program. The program is now mature enough to provide ideas for real-world synthetic tasks. One can only hope that WODCA and other systems that shed the rigid synthon and transform schemes of the synthesis-planning programs of the first generation manage to achieve wide acceptance and become as common a planning tool as the library has been for hundreds of years and the reaction database has developed into during the last decade. It is too early to announce the requiem for computer-assisted synthesis planning. The design faults and shortcomings of the first generation of programs have been analyzed and understood. The second generation is now waiting for the signal to commence.

The development of the WODCA system has been made possible by a doctoral scholarship from Studienstiftung des deutschen Volkes for W.-D. Ihlenfeldt and through support from DFG project Ga 208/17-1. We express our thanks to Shell Forschung (now: Cyanamid Forschung) and in that team particularly to Prof. Dr. R. Mengel for helpful support. Prof. S. Hanessian, University of Montreal, generously provided the catalog of the CHIRON system. Janssen Chimica (now: Acros Organica Division) made their starting materials catalog available in computer-readable form. R. Fick created and ran some of the examples described in this review.

Received: May 10, 1995
Revised version: April 6, 1995 [A 65]
German version: *Angew. Chem.* **1995**, *107*, 2807

Glossary of Acronyms

AIPHOS: Artificial Intelligence for Planning and Handling Organic Synthesis
CASP: Computer Assisted Synthesis Planning
CAMEO: Computer Assisted Mechanistic Evaluation of Organic reactions
CHIRON: CHIral synthON (and name of the wisest of the centaurs)
COMPASS: COMPuter ASSisted organic synthesis
EROS: Evaluation of Reactions for Organic Synthesis
Hashcoding: A method of one-way data compression that loses information. A complex set of data is reduced to a single number, which has a high probability of being unique for the specific input data (see Ref. [51]).
IGOR: Interactive Generation of Organic Reactions
LHASA: Logics and Heuristics Applied to Synthetic Analysis
LILITH: no acronym, name of a demoness in spider shape
OCSS: Organic Chemistry Synthesis Strategies
RAIN: Reactions And Intermediates Network
SECS: Simulation and Evaluation of Chemical Synthesis
SSSR (Smallest Set of Smallest Rings): A set of elementary rings that forms the basis of all other rings (for instance, envelopes).
SST: Starting Material Strategies
SYNCHEM: SYNthetic CHEMistry
TRESOR: TRacing and Evaluation of Syntheses in Organic Reactions
WODCA: Workbench for the Organization of Data for Chemical Applications

[1] E. J. Corey, *Pure Appl. Chem.* **1969**, *14*, 19–37.

[2] E. J. Corey, *Angew. Chem.* **1991**, *103*, 469–479; *Angew. Chem. Int. Ed. Engl.* **1991**, *30*, 455–465.

[3] S. Warren, *Organic Synthesis – The Disconnection Approach*, Wiley, Chichester, **1981**.

[4] E. J. Corey, X.-M. Cheng, *The Logic of Chemical Synthesis*, Wiley, New York, **1989**.

[5] Overviews of computer-assisted synthesis planning: a) M. Bersohn, *Chem. Rev.* **1976**, *76*, 269–282; b) J. Gasteiger in *Computer in der Chemie* (Ed.: E. Ziegler), 2nd edition, Springer, Berlin, **1985**, pp. 207–257; c) R. Barone, M. Chanon in *Computer Aids to Chemistry* (Eds: G. Vermin, M. Chanon), Ellis Horwood, Chichester, **1986**, pp. 19–102; d) G. Loftus, *Chemical Information Systems – Beyond the Structure Diagram*, Ellis Horwood, New York, **1991**, pp. 222–262; e) M. A. Ott, J. H. Noordik, *Recl. Trav. Chim. Pays Bas* **1992**, *111*, 239–246. The journal *Recueil des Travaux Chimiques des Pays-Bas* published a special issue on this topic (June 1992, Vol. 111) and printed papers from ten research groups that develop program systems for computer-assisted synthesis planning. The first paper gives an introduction.

[6] a) E. J. Corey, G. A. Petersson, *J. Am. Chem. Soc.* **1972**, *94*, 460–465; b) E. J. Corey, W. J. Howe, H. W. Orf, D. A. Pensak, G. Petersson, *ibid.* **1975**, *97*, 6116–6124; c) E. J. Corey, A. K. Long, J. Mulzer, H. W. Orf, P. Johnson, A. P. W. Hewett, *J. Chem. Inf. Comput. Sci.* **1980**, *20*, 221–230; d) E. J. Corey, A. P. Johnson, A. K. Long, *J. Org. Chem.* **1980**, *45*, 2051–2057; e) E. J. Corey, A. K. Long, G. I. Lotto, S. D. Rubenstein, *Recl. Trav. Chim. Pays Bas* **1992**, *111*, 304–309; f) A. P. Johnson, C. Marshall, P. N. Hudson, *Recl. Trav. Chim. Pays Bas* **1992**, *111*, 310–316.

[7] E. J. Corey, W. T. Wipke, *Science* **1969**, *176*, 178–186.

[8] W. T. Wipke, G. I. Ouchi, S. Krishnan, *Artif. Intell.* **1978**, *11*, 173–193.

[9] H. L. Gelernter, A. F. Sanders, D. L. Larsen, K. K. Agarwal, R. H. Boivie, G. A. Spritzer, J. E. Searleman, *Science* **1977**, *197*, 1041–1049.

[10] J. B. Hendrickson, *Angew. Chem.* **1990**, *102*, 1328–1338; *Angew. Chem. Int. Ed. Engl.* **1990**, *29*, 1286–1296.

[11] Z. S. Hippe, G. Fic, M. Marcus, *Recl. Trav. Chim. Pays Bas* **1992**, *111*, 255–261.

[12] E. V. Gordeeva, D. E. Lushnikov, N. S. Zevirov, *Tetrahedron Comput. Methodol.* **1990**, *3*, 445–459.

[13] I. Dohgane, T. Takabatake, M. Bersohn, *Recl. Trav. Chim. Pays Bas* **1992**, *111*, 291–296.

[14] K. Funatsu, S. Sasaki, *Tetrahedron Comput. Methodol.* **1988**, *1*, 27–38; *AIPHOS kouyuuta ni yoru yuukigouseikeirotansaku*, Kyouritsushuppan, Tokio, **1994**.

[15] G. Sello, *J. Chem. Inf. Comput. Sci.* **1994**, *34*, 120–129.

[16] R. Moll, *J. Chem. Inf. Comput. Sci.* **1994**, *34*, 117–119.

[17] A. Weise, *J. Chem. Inf. Comput. Sci.* **1990**, *30*, 490–491.

[18] M. Yanaka, K. Nakamura, A. Kurumisawa, W. T. Wipke, *Tetrahedron Comput. Methodol.* **1990**, *3*, 359–375.

[19] E. S. Blurock, *Tetrahedron Comput. Methodol.* **1989**, *2*, 207–222.

[20] a) J. Gasteiger, C. Jochum, *Top. Curr. Chem.* **1978**, *74*, 93–128; b) J. Gasteiger, M. G. Hutchings, B. Christoph, L. Gann, C. Hiller, P. Löw, M. Marsili, H. Saller, K. Yuji, *ibid.* **1987**, *137*, 19–73; c) J. Gasteiger, M. Marsili, M. G. Hutchings, H. Saller, P. Löw, P. Röse, K. Rafeiner, *J. Chem. Inf. Comput. Sci.* **1990**, *30*, 467–476.

[21] J. Gasteiger, *Tetrahedron* **1979**, *35*, 1419–1426.

[22] a) J. Gasteiger, M. Marsili, *Tetrahedron* **1980**, *36*, 3219–3228; b) J. Gasteiger, H. Saller, *Angew. Chem.* **1985**, *97*, 699–701; *Angew. Chem. Int. Ed. Engl.* **1985**, *24*, 687–689.

[23] M. G. Hutchings, J. Gasteiger, *Tetrahedron Lett.* **1983**, *24*, 2541–2544.

[24] J. Gasteiger, M. G. Hutchings, *J. Chem. Soc. Perkin Trans. 2* **1984**, 559–564.

[25] a) P. Röse, J. Gasteiger, *Anal. Chim. Acta* **1990**, *235*, 163–168; b) in *Software-Development in Chemistry 4* (Ed: J. Gasteiger), Springer, Heidelberg, **1990**, pp. 275–288.

[26] V. Simon, J. Gasteiger, J. Zupan, *J. Am. Chem. Soc.* **1993**, *115*, 9148–9159.

[27] J. Gasteiger, U. Hondelmann, P. Röse, W. Witzenbichler, *J. Chem. Soc. Perkin Trans. 2* **1995**, 193–204.

[28] a) T. D. Salatin, W. L. Jorgensen, *J. Org. Chem.* **1980**, *45*, 2043–2051; b) W. L. Jorgensen, E. R. Laird, A. J. Gishorst, J. M. Fleischer, S. A. Gothe, H. E. Helson, G. D. Padres, S. Sinclair, *Pure Appl. Chem.* **1990**, *62*, 1921–1932; E. R. Laird, W. L. Jorgensen, *J. Chem. Inf. Comput. Sci.* **1990**, *30*, 458–466.

[29] a) J. Dugundji, I. Ugi, *Top. Curr. Chem.* **1973**, *39*, 19; b) I. Ugi, J. Bauer, K. Bley, A. Dengler, A. Dietz, E. Fontain, B. Gruber, R. Herges, M. Knauer, K. Reitsam, N. Stein, *Angew. Chem.* **1993**, *105*, 210–239; *Angew. Chem. Int. Ed. Engl.* **1993**, *32*, 201–227.

[30] a) J. Bauer, I. Ugi, *J. Chem. Res. Synop.* **1982**, 298; *J. Chem. Res. Miniprint* **1982**, 3101; b) J. Bauer, R. Herges, E. Fontain, I. Ugi, *Chimia* **1985**, *39*, 43–53; c) J. Bauer, *Tetrahedron Comput. Methodol.* **1989**, *2*, 269–293.

[31] a) E. Fontain, J. Bauer, I. Ugi, *Chem. Lett.* **1987**, 37; E. Fontain, J. Bauer, I. Ugi, *Z. Naturforsch. B* **1987**, *42*, 297; b) E. Fontain, *Tetrahedron Comput. Methodol.* **1990**, *3*, 469; E. Fontain, K. Reitsam, *J. Chem. Inf. Comput. Sci.* **1991**, 96–101.

[32] a) S. Hanessian, J. Franco, B. Larouche, *Pure Appl. Chem.* **1990**, *62*, 1887–1910; b) S. Hanessian, J. Franco, G. Gagnon, D. Laramée, B. Larouche, *J. Chem. Inf. Comput. Sci.* **1990**, *30*, 413–425.

[33] E. Zass, *J. Chem. Inf. Comput. Sci.* **1990**, *30*, 360–372.

[34] J. L. Blake, R. C. Dana, *J. Chem. Inf. Comput. Sci.* **1990**, *30*, 394–399.

[35] a) A. Parlow, C. Weiske, J. Gasteiger, *J. Chem. Inf. Comput. Sci.* **1990**, *30*, 400–402; b) J. Gasteiger, C. Weiske, *Nachr. Chem. Tech. Lab.* **1992**, *40*, 1114–1120.

[36] D. F. Chodosh, J. Hill, L. Shpilsky, W. L. Mendelson, *Recl. Trav. Chim. Pays Bas* **1992**, *111*, 247–254.

[37] G. A. Hopkinson, T. P. Cook, I. P. Buchan in *Chemical Information Systems – Beyond the Structure Diagram* (Eds: D. Bawden, E. Mitchell), Ellis Horwood, New York, **1990**, pp. 83–91.

[38] T. E. Moock, J. G. Nourse, D. Grier, W. D. Hounshell in *Chemical Structures: The International Language of Chemistry* (Ed.: W. A. Warr), Springer, Berlin, **1988**, pp. 303–313.

[39] C. Jochum, *J. Chem. Inf. Comput. Sci.* **1994**, *34*, 71–73.

[40] A. Barth, *J. Chem. Inf. Comput. Sci.* **1990**, *30*, 384–393.

[41] a) H. L. Gelernter, J. R. Rose, C. Chen, *J. Chem. Inf. Comput. Sci.* **1990**, *30*, 492–504; b) J. R. Rose, J. Gasteiger, *ibid.* **1994**, *34*, 74–90; c) E. S. Blurock, *ibid.* **1990**, *30*, 505–510; d) L. Chen, J. Gasteiger, J. R. Rose, *J. Org. Chem.*, in press.

[42] H. Satoh, K. Funatsu, *J. Chem. Inf. Comput. Sci.*, **1995**, *35*, 34–39.

[43] Summary of a couple of replies to a question about user experiences with synthesis-planning systems, posted on the *OSC Chemistry Mailing List* chemistry@osc.edu, July 26th, 1993. The original message that we cite originated from J. W. Boiten.

[44] One of the referees was of the opinion that this is not a valid comparison. He stated that often a reaction database query would be initiated just to check the feasibility of a reaction when a chemists does some manual planning. In our opinion this clearly is a significant symptom of a lack of acceptance of synthesis-planning programs. Ideally any plan should be developed in an integrated planning system, and the query should originate from such a system in order to verify the program's proposal.

[45] a) W. S. Zhou, X. X. Xu, *Acc. Chem. Res.* **1994**, *27*, 211–216; b) X. X. Xu, J. Zhu, D. Z. Huang, W. S. Zhou, *Tetrahedron* **1986**, *42*, 819; c) G. Schmid, W. Hofheinz, *J. Am. Chem. Soc.* **1983**, *105*, 624–625; d) T. Ravindranathan, M. A. Kumar, R. B. Memon, S. V. Hiremath, *Tetrahedron Lett.* **1990**, *31*, 755.

[46] a) P. Willett, *Similarity and Clustering in Chemical Information Systems*, Wiley, New York, **1987**; b) M. A. Johnson, G. M. Maggiora, *Concepts and Applications of Molecular Similarity*, Wiley, New York, **1990**.

[47] M. Wochner, J. Brandt, A. von Scholley, I. Ugi, *Chimia* **1988**, *42*, 217–225.

[48] P. Willet, V. Winterman, *Quant. Struct. Activ. Relat.* **1986**, *5*, 18–25.

[49] W. T. Wipke, D. Rogers, *J. Chem. Inf. Comput. Sci.* **1984**, *24*, 71–78.

[50] a) J. Gasteiger, W. D. Ihlenfeldt, *Software Dev. Chem. 4 Proc. Workshop Comput. Chem. 4th* **1990**, 57–65; b) W. D. Ihlenfeldt, J. Gasteiger, *Software Dev. Chem. 5 Proc. Workshop Comput. Chem. 5th* **1991**, 59–67; c) J. Gasteiger, W. D. Ihlenfeldt, R. Fick, J. R. Rose, *J. Chem. Inf. Comput. Sci.* **1992**, *32*, 700–712; d) J. Gasteiger, W. D. Ihlenfeldt, P. Röse, R. Wanke, *Anal. Chim. Acta* **1990**, *235*, 65–75; e) J. Gasteiger, W. D. Ihlenfeldt, P. Röse, *Recl. Trav. Chim. Pays Bas* **1992**, *111*, 270–290; f) R. Fick, W. D. Ihlenfeldt, J. Gasteiger, *Heterocycles* **1995**, *40*, 993–1007.

[51] W. D. Ihlenfeldt, J. Gasteiger, *J. Comput. Chem.* **1994**, *15*, 793–813.

[52] M. Randic, C. L. Wilkins, *J. Chem. Inf. Comput. Sci.* **1979**, *19*, 31–37.

[53] A. D. Sinitsa, B. S. Drach, *J. Org. Chem. USSR* **1973**, *9*, 706–709.

[54] a) K. C. Nicolaou, R. D. Groneberg, N. A. Stylianides, T. Miyazaki, *J. Chem. Soc. Chem. Commun.* **1990**, 1275–1277; b) K. C. Nicolaou, E. P. Schreiner, W. Stahl, *Angew. Chem.* **1991**, *103*, 566–568; *Angew. Chem. Int. Ed. Engl.* **1991**, *30*, 585–587.

[55] B. E. Marron, K. C. Nicolaou, *Synthesis* **1989**, *55*, 537–539.

[56] L. A. Paquette, H.-J. Kang, *J. Am. Chem. Soc.* **1991**, *113*, 2610–2621.

[57] Here, in the case of sabinene, the six-membered ring is an envelope. The elementary rings are the three- and five-membered rings. Therefore the six-membered ring is allowed and passes.

[58] This statement is not absolutely correct. The exhaustive mapping of two graphs in all possible orientations is computationally too demanding. Therefore WODCA uses some heuristics in order to reduce the number of mappings in a synthetically sound manner. The maximum common substructure is only among the examined mappings if at least some part of the border region between the embedded substructure and the compared compounds contains reactive centers.

X-ray Crystal Structures of Cytochrome c Oxidases from *Paracoccus denitrificans* and Bovine Heart and Their Implications for the Molecular Mechanism of Cell Respiration

Bernhard Kadenbach*

Thirty-four years ago, two years after the first high-resolution X-ray structure analysis of a protein (myoglobin) by Kendrew, crystals of cytochrome c oxidase (COX) from bovine heart were obtained by Yonetani.[1] But all efforts to determine the three-dimensional structure of the enzyme at the atomic level failed due to the poor quality of crystals.[2] Now high-resolution (2.8 Å) X-ray crystal structures of the oxidized COX from *Paracoccus denitrificans* and from bovine heart have been published almost simultaneously by Michel and co-workers,[3] and by Yoshikawa and co-workers,[4] respectively. In the two cases, however, different approaches were used. Michel et al. obtained crystals of COX from *Paracoccus* only after forming a complex with the variable fragment of a monoclonal antibody, whereas Yoshikawa et al. obtained crystals of COX from bovine heart only after addition of the detergent decylmaltoside during crystallization.

COX, the terminal enzyme of the respiratory chain of bacteria and mitochondria from all eucaryotes, is essential for life on earth, because it is the only enzyme that reduces oxygen to water without producing reactive intermediates and conserves the released energy. After its first description in 1925 by Warburg as "Atmungsferment" and 1925 by Keilin as cytochrome aa_3, the enzyme was intensively studied, but not until recently were all the metal atoms participating in the reduction of oxygen identified. The two membrane-bound oxidases from *Paracoccus* and bovine heart are almost identical in their catalytic properties. Both transfer electrons from cytochrome c to molecular oxygen accompanied by formation of an electrochemical proton gradient across the membrane. But they differ in their number of protein subunits. COX from *Paracoccus* has four different subunits, the enzyme from bovine heart and other mammals has thirteen.[5] The three largest subunits, which are homologous to those of the bacterial enzyme, are encoded on mitochondrial DNA, the other ten on nuclear DNA.

The reports of the X-ray structures emphasize different aspects. Whereas Michel et al. describe the catalytic centers and the structures of the four bacterial subunits in detail, Yoshikawa et al. concentrate on the metal centers and postpone the much more complicated description of the thirteen protein subunits to a later publication. The structures of both enzymes confirm many structural features previously concluded from biochemical studies. All four and thirteen subunits of the two enzyme complexes have been confirmed in equimolar ratios. Also, the pathway for electrons from cytochrome c to Cu_A in subunit II, via heme *a* and heme a_3-Cu_B in subunit I, and finally to O_2 is corroborated by both structures. Concerning the general structure, the "lopsided Y" deduced from electron microscopic studies on two-dimensional crystals[6] could not be verified. Interestingly the bovine heart enzyme crystallized as a dimer, as was previously found by electron microscopic studies on "membrane sheets".[6] In contrast, the bacterial COX, which is more lipophilic owing to the absence of the subunits coded by nuclear DNA, crystallized as a monomer only after complexation with the variable fragment of a monoclonal antibody. This type of cocrystallization could be useful for the crystallization of other hydrophobic proteins.

Until recently, in addition to the two heme *a* groups, only two copper ions (Cu_A and Cu_B) have been assumed to occur in the catalytic center of COX. The finding that the Cu_A site contains two copper atoms led for the first time to speculations on the occurrence of a Cu–Cu bond in a biomolecule.[7] The X-ray structures of both enzymes, however, revealed that the two copper atoms are in a plane with and coordinated to two cysteine S atoms. This structure corresponds to the [2Fe–2S] center of iron–sulfur proteins, which instead contain inorganic sulfur. The tetrahedral coordination environments of the two copper ions, each with a charge of +1.5, are completed by a histidine and methionine, and by a histidine and a peptide carbonyl group of glutamic acid, respectively, all within subunit II. Except for the peptide carbonyl group, all other ligands had been identified correctly by site-directed mutagenesis of bacterial COX.[8] The distances between the copper atoms were determined to be 2.6 Å (*Paracoccus*) and 2.7 Å (bovine heart).

Three further metal atoms of the catalytic center of COX, two iron atoms (in heme *a* and heme a_3) and Cu_B, are located within the periplasmic (*Paracoccus*) or cytoplasmic half (bovine heart) of the membrane domain of subunit I. Subunit I contains twelve transmembrane helices (TM), representing the center of the enzyme, which is almost identical in both enzymes. In principle, the twelve TM had already been deduced correctly from hydropathy plots, but the boundaries of the transmembrane re-

[*] Prof. Dr. B. Kadenbach
Fachbereich Chemie der Universität
Hans-Meerwein-Strasse, D-35032 Marburg (Germany)
Telefax: Int. code +(6421) 282191
e-mail: Kadenbac@ps1515.chemie.uni-marburg.de

 © VCH Verlagsgesellschaft mbH, D-69451 Weinheim, 1995 0570-0833/95/3423-2635 $ 10.00+.25/0

gions vary. The planes of heme *a* and heme a_3 are perpendicular to the membrane plane and form an angle of 108° (*Paracoccus*) and 104° (bovine heart). The fifth and sixth ligands of heme *a* Fe are imidazole groups located at TM-II and TM-X. The latter transmembrane also contains the fifth ligand of heme a_3 Fe, again an imidazole group of a conserved histidine. These ligands have also been identified previously by site-directed mutagenesis.[9] A sixth ligand of heme a_3 Fe was not found, but it could be a delocalized water molecule not detectable by X-ray diffraction.

The heme a_3–Cu_B binuclear center binds molecular oxygen, which is reduced to water by four electrons from cytochrome c and four protons from the cytoplasm (*Paracoccus*) or matrix space (bovine heart). In COX from *Paracoccus* a heme a_3 Fe–Cu_B distance of 5.2 Å was found, and in COX from bovine heart a distance of 4.5 Å was determined. The difference could be due to crystallization of the *Paracoccus* enzyme in the presence of azide, a ligand of the binuclear center. In EXAFS measurements (EXAFS = extended X-ray absorption fine structure) with the oxidized enzyme from bovine heart and from *Paracoccus* Powers et al. found a distance of only 3.75 Å and a sulfur atom (methionine or cysteine) as bridging ligand. But this repeatedly postulated bridging ligand was not found in either of the present structures.

Cu_B is complexed by a histidine in TM VI and two histidines of the loop region between TM VII and TM VIII. These histidine ligands of Cu_B were also identified earlier by site-directed mutagenesis in bacterial COX.[9] While in the enzyme from bovine heart all three histidine ligands of Cu_B were evident, in the *Paracoccus* enzyme the electron density of the side chain of His325 was lacking. This finding, indicating multiple conformations of the imidazole group, was the starting point for the development of a mechanism for proton translocation in COX by Michel et al. (vide infra).

The arrangement of the twelve transmembrane helices of subunit I within the membrane was surprising. Four helices together form a semicircle, which forms a pore with one helix of another semicircle. Thus the pores A (of TM III–VI with TM II), B (of TM VII–X with TM VI), and C (of TM XI, XII, I, II with TM X) are formed with threefold rotational symmetry (Fig. 1). Pore A contains mainly conserved aromatic amino acids, pore B contains the binuclear center heme a_3–Cu_B, and pore C contains heme *a*; in the latter a hydrophobic hydroxyethylfarnesyl side chain seals the pore to the cytoplasm. For the reduction of

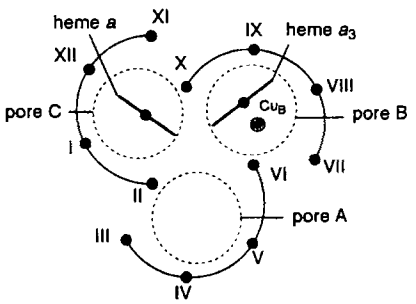

Fig. 1. Schematic representation of the transmembrane helices I–XII of subunit I in COX from *Paracoccus*. Sets of four helices are arranged together in semicircles and form pores (A, B, C) with one helix of an adjacent semicircle (taken from ref. [3] with permission).

an O_2 molecule four protons are taken up from the cytoplasmic (*Paracoccus*) or matrix space (bovine heart), while for the coupled proton translocation four further protons are transported from the cytoplasm (matrix) into the periplasmic (cytosolic) space.

Michel et al. postulate separate channels for the "chemical" and the translocated protons. The "chemical" protons could pass through pore B directly to the O_2-binding site (heme a_3–Cu_B). In fact, hydrophilic groups (Ser291, Lys354, Thr351, the hydroxyl group of heme a_3, and Tyr280) are located within this channel. This is unexpected, because normally only hydrophobic amino acids are found in transmembrane helices. The pumped protons could be translocated through the cytoplasmic half of pore A and the periplasmatic half of pore B. In the lower part of pore A hydrophilic amino acids are also found (Asp124, Thr203, Asn199, Asn113, and Asn131). Exchange of one of these amino acids by a hydrophobic one through site-directed mutagenesis resulted in inhibition of proton translocation but not of electron transport (H_2O formation)[11]. These latter results had led previously to the proposal of separate channels for "chemical" and translocated protons.

For proton pumping in COX Michel et al. developed a "histidine cycle/shuttle" mechanism, following the "histidine cycle" mechanism of Wikström et al.[12] In this mechanism His325 cycles through the imidazolate, imidazole, and imidazolium states and shuttles between two positions. Proton translocation is mainly based on protonation of the imidazole of His325 while it is bound to Cu_B, and its deprotonation in its second position as a ligand of the formyl side chain of heme a_3. This plausible mechanism, however, has not yet been proven. In their crystal structure Yoshikawa et al. found imidazole rings with the expected electron density for all three ligands of Cu_B (His240, His290, and His291) and thus obtained no indication of multiple conformations.

Michel et al. also describe subunit III, which contains seven transmembrane helices and contributes largely to the mass of the membrane-bound enzyme. It binds to subunit I at the side opposite to subunit II, but its function is unknown. Within subunit III of *Paracoccus* COX a phosphatidylcholine molecule with unknown function was found. The lipid cardiolipin, essential for the catalytic activity of COX, was not found in either the enzyme from *Paracoccus* or that from bovine heart.

In the paper of Yoshikawa et al. the position of a magnesium ion is described, which was already known as a stoichiometric COX component. It has distorted tetrahedral coordination to two ligands of subunit I (Asp369, His368), one ligand of subunit II (Glu198), and one water molecule. The conserved amino acids Asp and His were identified previously by site-directed mutagenesis in bacterial COX as ligands of manganese, which can be exchanged by magnesium.[13] The authors postulate that the magnesium center is not only important for the structure but also serves in the redox state dependent regulation of the electron transfer from Cu_A to Fe_a and from Fe_a to Fe_{a3}. In COX from bovine heart the position of a zinc ion was described, which is located in the nontransmembrane subunit Vb at the matrix side and complexed by four sulfur atoms (Cys60, Cys62, Cys82, and Cys85). The function of the zinc ion, which is absent in the bacterial enzyme, is so far unknown.

 © VCH Verlagsgesellschaft mbH, D-69451 Weinheim, 1995 0570-0833/95/3423-2636 $ 10.00+.25/0

The two X-ray crystal structures are milestones on the way to understanding the structure and function of COX. Surprisingly many previous results could be corroborated; others were proven wrong. A number of unsolved questions like the mechanisms of electron transport and of proton translocation will only be solved by parallel functional studies. This holds in particular for questions on the regulation of activity, which, due to the large number of additional subunits in the mammalian COX, appears to be particularly complex.

German version: *Angew. Chem.* **1995**, *107*, 2855–2857

Keywords: cell respiration · cytochrome c oxidases · proton transfer · structure elucidation

[1] T. Yonetani, *J. Biol. Chem.* **1961**, *236*, 1680.
[2] T. Ozawa, H. Suzuki, M. Tanaka, *Proc. Natl. Acad. Sci. USA* **1980**, *77*, 928; T. Ozawa, M. Tanaka, T. Wakabayashi, *ibid.* **1982**, *79*, 7175; S. Yoshikawa, S. Tera, Y. Takahashi, T. Tsukihara, W. S. Caughey, *ibid.* **1988**, *85*, 1354.
[3] S. Iwata, C. Ostermeier, B. Ludwig, H. Michel, *Nature* **1995**, *376*, 660.
[4] T. Tsukihara, H. Aoyama, E. Yamashita, T. Tomizaki, H. Yamaguchi, K. Shinzawa-Itoh, R. Nakashima, R. Yaono, S. Yoshikawa, *Science* **1995**, *269*, 1069.
[5] B. Kadenbach, *Angew. Chem.* **1983**, *95*, 273; *Angew. Chem. Int. Ed. Engl.* **1983**, *22*, 275; B. Kadenbach, *Trends Biochem. Sci.* **1983**, *8*, 398; B. Kadenbach, J. Jarausch, R. Hartmann, P. Merle, *Anal. Biochem.* **1983**, *129*, 517; B. Kadenbach, L. Kuhn-Nentwig, U. Büge, *Curr. Top. Bioenerg.* **1987**, *15*, 113.
[6] J. F. Deatherage, R. Henderson, R. A. Capaldi, *J. Mol. Biol.* **1982**, *158*, 501.
[7] H. Bertagnolli, W. Kaim, *Angew. Chem.* **1995**, *107*, 847; *Angew. Chem. Int. Ed. Engl.* **1995**, *34*, 770.
[8] M. Kelly, P. Lappalainen, G. Talbo, T. Haltia, J. van der Oost, M. Saraste, *J. Biol. Chem.* **1993**, *268*, 16781.
[9] J. P. Hosler, S. Ferguson-Miller, M. W. Calhoun, J. F. Thomas, J. Hill, L. Lemieux, J. Ma, C. Georgiou, J. Fetter, J. Shapleigh, M. M. J. Tecklenburg, G. T. Babcock, R. B. Gennis, *J. Bioenerg. Biomembr.* **1993**, *25*, 121; B. L. Trumpower, R. B. Gennis, *Annu. Rev. Biochem.* **1994**, *63*, 675.
[10] L. Powers, B. Chance, Y. Ching, P. Angiolillo, *Biophys. J.* **1981**, *34*, 465.
[11] J. W. Thomas, A. Puustinen, J. O. Alben, R. B. Gennis, M. Wikström, *Biochemistry* **1993**, *32*, 10923.
[12] J. E. Morgan, M. I. Verkhovsky, M. Wikström, *J. Bioenerg. Biomembr.* **1994**, *26*, 599; M. Wikström, A. Bogachev, M. Finel, J. E. Morgan, A. Puustinen, M. Raitio, M. Verkhovskaya, *Biochim. Biophys. Acta* **1995**, *1187*, 106.
[13] J. P. Hosler, M. P. Espe, Y. Zhen, G. T. Babcock, S. Ferguson-Miller, *Biochemistry* **1995**, *34*, 7586; M. P. Espe, J. P. Hosler, S. Ferguson-Miller, G. T. Babcock, J. McCracken, *ibid.* **1995**, *34*, 7593.

New Evidence Concerning the Structure of Amorphous Red Phosphorus

Hans Hartl*

One of the unsolved problems of the structural chemistry of elemental phosphorus is the structure of amorphous red phosphorus, a material found on nearly every matchbox for more than 150 years. Since an X-ray structural characterization of this material has not been possible, our knowledge derives from indirect evidence, which is providing more and more precise information about the structural principles of this phosphorus modification. Two important contributions in this respect are the recently published results of Böcker and Häser[1] as well as those of Pfitzner and Freudenthaler.[2] The combination of their results with the findings of earlier investigations allows a model of the structure of amorphous red phosphorus to be established that seems to be not far from reality.[3–5]

The trivalency of phosphorus atoms with slightly varying P–P bond lengths (ca. 220 pm) and P-P-P angles ranging from 60° to 120° permits a great variety of different types of atomic connectivities. Between the three basic types—white, red, and black phosphorus—a series of further allotropic forms of phosphorus are conceivable, ranging from small phosphorus clusters to phosphorus-rich oligomers as well as one-, two-, and three-dimensional polymers. Baudler and Glinka[4] as well as von Schnering and Hönle[5] emphasized in their brillant reviews about mono- and polycyclic phosphanes and phosphorus-rich polyphosphides, respectively, the diversity of atomic frameworks of phosphorus-rich compounds with P–P bonds. They pointed out that a close relationship exists between these compounds and unsubstituted, uncharged P_n clusters.

Baudler and Glinka proposed a set of rules for the construction of larger phosphorus frameworks by aggregation and/or condensation of small subunits. One of these rules (not to be taken as reaction mechanisms!) states that a larger framework with an additional five-membered ring can be built up by a formal [2+3]cycloaddition. The fact that five-membered rings are preferred and widespread structural units in polyphosphanes, polyphosphides, and also in Hittorf's phosphorus led to the statement that among isomeric structures those with the largest number of five-membered rings are favored.[4] These and other "Baudler rules" which have been verified by already known structures were recently refined and extended by Böcker and Häser.[1, 6] Based on these rules they introduced a very helpful symbolic notation[7] and a chemical heuristic for the systematic deduction of covalent phosphorus frameworks in polycyclic phosphanes, phosphorus-rich polyphosphides, and allotropes of phosphorus (with the exception of black phosphorus). The authors did not confine themselves to deducing experimentally established structural units but also designed hypothetical phosphorus structures not yet represented by already known structures. They discussed the existence of those structures only known on paper, including macromolecular forms of elemental phosphorus, on the basis of energetic stabilities calculated by ab initio techniques (SCF/SVP level; relative equilibrium energies given in kJ mol$(P_4)^{-1}$ as compared with molecular

[*] Prof. Dr. H. Hartl
Institut für Anorganische und Analytische Chemie der Freien Universität
Fabeckstrasse 34/36, D-14195 Berlin (Germany)
Telefax: Int. code +(30) 8382424

 © VCH Verlagsgesellschaft mbH, D-69451 Weinheim, 1995 0570-0833/95/3423-2637 $ 10.00+.25/0

phosphorus P_4).[1] The quality of calculation techniques employed was tested by comparing the theoretically calculated energies, bond lengths, and bond angles with the experimentally determined values for Hittorf's phosphorus. The agreement is so convincing that one can also expect that the analogous calculations of the energies of experimentally not yet established structures which could be possible modifications of red phosphorus should also be very reliable (relative stabilities: $E_{theor.} = -61\ kJ\,mol(P_4)^{-1}$; $E_{exp.} = -62\ kJ\,mol(P_4)^{-1}$). In Hittorf's

$^{2}_{\infty}\{]P2[P8]P2[P9]\}$ **1**

phosphorus **1** (notation of Böcker and Häser[1, 7]), P_8 and P_9 clusters are connected by P_2 units through formal [2+3]cycloaddition, forming tubular strands (Fig. 1a). These tubes are

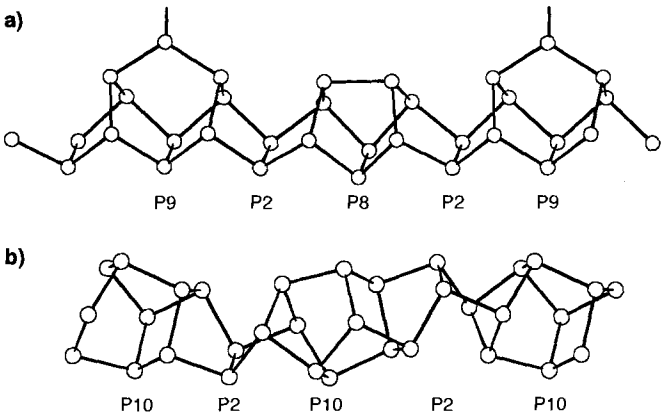

Fig. 1. Phosphorus strands $^{1}_{\infty}\{]P2[P8]P2[P9]\}$ (a) and $^{1}_{\infty}\{]P2[P10]\}$ (b). The notations P2, P8, P9, and P10 characterize phosphorus clusters (basic units) [7]. P_2 units connect P_8, P_9, and P_{10} clusters through formal [2+3]cycloaddition. Six- and predominantly five-membered rings exist in both types of chains.

oriented *perpendicular* to each other and cross-linked to the double layers of Hittorf's[3] phosphorus by the free valences of one of the phosphorus atoms of the P_9 units (according to Baudler and Glinka a formal condensation!).

Among the polymeric phosphorus structures with the highest calculated, relative stabilities are **2**, in which pairs of tubular strands of the same type as in Hittorf's phosphorus (Fig. 1a) are linked *parallel* ($E_{theor.} = -62\ kJ\,mol(P_4)^{-1}$), and **3**, in which P_{10} clusters are connected by P_2 units, once again through a formal [2+3]cycloaddition, forming polymeric helical tubes (Fig. 1b) without free valences suitable for further cross-links ($E_{theor.} = -61\ kJ\,mol(P_4)^{-1}$).

$^{1}_{\infty}\{(]P2[P8]P2[P9])_2\}$ **2**

$^{1}_{\infty}\{]P2[P10]\}$ **3**

The proposed structural unit **3** is a fascinating model for the structure of amorphous red phosphorus: calculated radial distribution functions agree very well with those derived from X-ray and neutron diffraction experiments on amorphous red phosphorus.[1, 3, 8] Furthermore, the existence of the chain **3** was established experimentally. Recently Pfitzner and Freudenthaler isolated the crystalline compound $(CuI)_3P_{12}$ in connection with attempts to synthesize new Cu^I ionic conductors.[2] Two nearly identical, crystallographically independent helical strands **3** are embedded into a matrix of CuI layers. Both chains differ mainly with respect to their Cu^I environments. The coordination of phosphorus to Cu^I apparently has no significant influence on the structure of the phosphorus framework and the P–P bond lengths. The Cu^I/I^- system builds up very flexible CuI frameworks, which serve not only as adaptable host lattices for uncharged molecules but also for anions, as long as there is an excess of Cu^I (for example $^{1}_{\infty}[P^{-}_{15}]$ in $Cu_3I_2P_{15}$[9]), and for cations with different shapes and sizes in case of excess I^-.[10, 11] The CuI host lattices in combination with Cu^I–P interactions promote the development of an ordered structure with helix **3** as a subunit, whereas unfavorable packing conditions seem to prevent the crystallization of a corresponding pure allotropic phosphorus modification. The CuI sublattice of $(CuI)_2P_3$ stabilizes chains of type **4**.[12] The structure of **4** contains not only five- and six-membered rings but also energetically unfavored four-membered rings. Accordingly, the ab initio calculations show a lower stability for this atomic arrangement than for those in structures **1**, **2**, and **3** with only five- and six-membered rings ($E_{theor.} = -48\ kJ\,mol(P_4)^{-1}$).[1]

$^{1}_{\infty}\{]P4(4)[P8]\}$ **4**

Missing steps to a definitive proof of the structure of amorphous red phosphorus are the synthesis of **3** by leaching CuI out of $(CuI)_3P_{12}$, the isolation of **3** from red phosphorus by reaction with CuI, and conclusive solid-state ^{31}P NMR spectroscopic investigations of the reaction products. If these experiments can be carried out successfully, the last sceptics should be convinced that $^{1}_{\infty}\{]P2[P10]\}$ strands are an essential component of amorphous red phosphorus.

German version: *Angew. Chem.* **1995**, *107*, 2857–2859

Keywords: ab initio calculations · allotropy · phosphorus · red phosphorus

[1] S. Böcker, M. Häser, *Z. Anorg. Allg. Chem.* **1995**, *621*, 258–286.
[2] A. Pfitzner, E. Freudenthaler, *Angew. Chem.* **1995**, *107*, 1784–1786; *Angew. Chem. Int. Ed. Engl.* **1995**, *34*, 1647–1649.
[3] H. Thurn, H. Krebs, *Acta Crystallogr. Sect. B* **1969**, *25*, 125–135.
[4] M. Baudler, K. Glinka, *Chem. Rev.* **1993**, *93*, 1623–1667.
[5] H. G. von Schnering, W. Hönle, *Chem. Rev.* **1988**, *88*, 243–273.
[6] M. Häser, *J. Am. Chem. Soc.* **1994**, *116*, 6925–6929.
[7] Comment on the nomenclature: P_n denotes a structural unit consisting of *n* phosphorus atoms (basic unit). The formation of oligomeric or polymeric structures by known basic units P_n [1, 4, 5] can be clearly described by the notation of Böcker and Häsler [1]. The notation P2[P8 stands for a phosphorus cluster in which a P_2 unit is connected with a P_8 basic unit to a larger structural cluster by formal [2 + 3] cycloaddition; in P8]P2[P9 a P_8 and a P_9 cluster are bridged by a P_2 group and so on (detailed explanations can be found in the original paper [1]).
[8] H. Krebs, H. U. Gruber, *Z. Naturforsch. A* **1967**, *22*, 96–102.
[9] A. Pfitzner, E. Freudenthaler, *Z. Kristallogr.* **1995**, *210*, 59.
[10] For example H. Hartl, F. Mahdjour-Hassan-Abadi, *Angew. Chem.* **1994**, *106*, 1929–1931; *Angew. Chem. Int. Ed. Engl.* **1994**, *33*, 1841–1842; M. Hoyer, H. Hartl, *Z. Anorg. Allg. Chem. 1992*, *612*, 45–50; *ibid.* **1991**, *598/599*, 151–162; D. Adam , B. Herrschaft, H. Hartl, *Z. Naturforsch. B* **1990**, *46*, 738–746.
[11] S. Jagner, G. Helegesson, *Adv. Inorg. Chem.* **1991**, *37*, 1–45.
[12] M. H. Möller, W. Jeitschko, *J. Solid State Chem.* **1986**, *65*, 178–189

 © VCH Verlagsgesellschaft mbH, D-69451 Weinheim, 1995 0570-0833/95/3423-2638 $ 10.00+.25/0

Regio- and Diastereoselective Synthesis of β-Amino Ketones by Addition of Imines to Iminium Salts**

Michael Arend and Nikolaus Risch*

β-Amino ketones (Mannich bases) and their derivatives have a wide range of applications, for example in drugs, crop protection agents, and as general synthetic building blocks.[2] However, the Mannich reaction, the classical method of synthesizing β-amino ketones is fraught with many serious disadvantages—drastic reaction conditions, formation of undesired side products, little or no stereo- or regioselectivity, etc.[2] Numerous attempts have been made to overcome these limitations owing to the importance of the products.[3] Therefore, methods of stereoselective aminomethylation[4] and aminoalkylation[1, 5] are currently active areas of research.

In addition to controlling stereoselectivity, directing regioselectivity is a central, frequently unsolved problem in modern chemistry. Many attempts have been made to improve the regioselectivity of aminomethylation[3, 6] and thus simultaneously provide a versatile method for the regioselective functionalization of ketones (generation of Michael acceptors; the amino group can also be substituted readily).[2] The most important regioselective variants of the Mannich reaction are the reactions of methylene iminium salts with ketones,[6a] enolates, and enol ethers.[6b] However, these reactions either require tedious procedures, or their applications and efficiency have only limited known scope.

In comparison, the reaction of preformed iminium salts **1**[7] with imines **2** (Scheme 1) has fundamental advantages. The starting materials can be prepared readily from economical reagents or, like the methylene iminium salt **1** (R^1 = H), are commercially available. The preliminary, laborious regioselective synthesis of enolates or enol ethers is not necessary. This is not only a simple and convenient method, it also has a wide range of applications. The Mannich bases are prepared under mild conditions and obtained generally in analytically pure form in good yields and with excellent regioselectivities. In contrast to all other approaches, our method can also be used for regioselective amino*alkyl*ation, which is highly diastereoselective as well (Table 1).

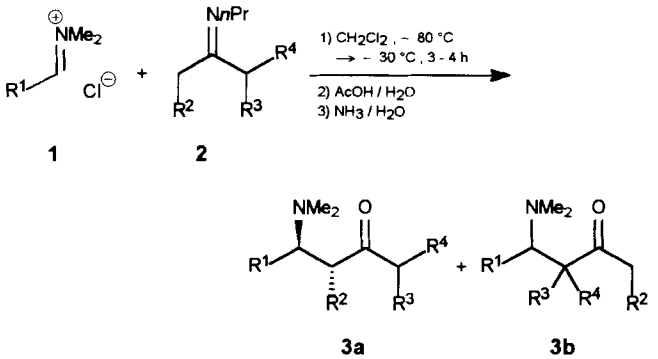

Scheme 1. Regio- and diastereoselective aminoalkylation of imines **2** with iminium salts **1**.

Table 1. Regio- and diastereoselective aminoalkylation of imines **2** with iminium salts **1**.

Entry	R^1	R^2	R^3	R^4	**3a**:**3b** [a]	Yield [%]
1	Ph	Me	Me	H		75
2	Ph	$(CH_2)_3$		H	-	69
3	H	$(CH_2)_3$		Me	≥99: ≤1	76 [b]
4	Ph	$(CH_2)_3$		Me	≥99: ≤1	68 [c]
5	H	Me	Me	Me	≥99: ≤1	76
6	Ph	Me	Me	Me	≥99: ≤1	69 [d]
7	H	Me	*i*Pr	H	94: 6	72
8	Ph	Me	*i*Pr	H	≥99: ≤1	62
9	H	Me	Et	H	73: 27	71
10	Ph	Me	Et	H	75: 25	69 [e]
11	H	Ph	Me	H	≥99: ≤1	78
12	Ph	Ph	Me	H	81: 19	68

[a] The ratios of regio- and diastereoisomers were determined by ^1H and ^{13}C NMR spectroscopy. Unless specified otherwise the products are diastereomerically pure (≥ 99% *ds*). [b] Two diastereomers (*cis*/*trans* diastereomers relative to the α and α′ centers) are obtained in a ratio of 63:37. The relative configurations of the diastereomers could not yet be determined. [c] Two diastereomers are obtained in a ratio of 7:3; these are presumably *cis*/*trans* diastereomers relative to the α and α′ centers (cf. footnote [b]). The relative configurations of the diastereomers could not yet be determined. [d] If the reaction is conducted at 25 °C (2 h), regioisomeric products are obtained with a ratio (**3a**:**3b**) of ≥99: ≤1 (59% yield). [e] If the reaction is conducted at 25 °C (2 h), regioisomeric products are obtained with a ratio (**3a**:**3b**) of 73:27 (62% yield). Similar results were obtained in THF (73:27, 61%) and MeCN (74:26, 60%), and when the iminium tetrachloroaluminate salt was used instead of the chloride salt (76:24, 59%).

In analogy to the mechanisms previously proposed for reactions of imines with other electrophiles,[8] we assume that not the imines but rather the corresponding tautomeric secondary enamines react with the iminium salts. This hypothesis is supported by the finding that identical products are obtained regardless of whether the benzylidene iminium salt **1** with R^1 = Ph is treated with imines **2** (Table 1, Entries 1,2) or with the corresponding tertiary enamines (pyrrolidine derivatives).[1] Typically the reaction of iminium salts **1** (R^1 = alkyl, aryl) with enamines yields exclusively the *anti* Mannich bases.[1] For this reason and also based on NMR spectroscopic data, we have assigned the *anti* configuration to all the β-amino ketones formed in the reaction of **1** (R^1 = Ph) with **2**.

This reaction differs from related reactions, for example the alkylation of imines with Michael acceptors[8] and the aminomethylation of ketones with methylene iminium salts,[6a] in a number of respects. Whereas in these other reactions the more highly substituted α-C atom is generally attacked, in our

[*] Prof. Dr. N. Risch, Dipl.-Chem. M. Arend
Fachbereich Chemie und Chemietechnik der Universität-Gesamthochschule Warburger Strasse 100, D-33098 Paderborn (Germany)
Telefax: Int. code +(5251)60-3245
e-mail: nr@chemie.uni-paderborn.de

[**] Stereoselective Synthesis of Mannich Bases, Part 3. This work was supported by the Deutsche Forschungsgemeinschaft and the Fonds der Chemischen Industrie. Part 2: ref. [1].

case the iminium salt attacks the sterically less hindered α position of the imine with high regioselectivity. Good regioselectivities are achieved even when the two α-C atoms are only marginally different (Table 1, cf. Entries 7 and 9, 8 and 10). Within the limits of our studies, the solvent, the counterion of the iminium salt, and the reaction temperature do not have a significant effect on the regio- and diastereoselectivity of the reaction (Table 1, footnotes [d] and [e]). The regioselectivity reversed, as expected, only when electronics dictate that the sterically more hindered tautomeric enamine is virtually the exclusive intermediate (Table 1, Entries 11, 12).

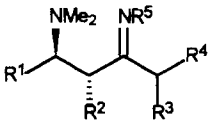

4

Besides these advantages the reaction of imines with iminium salts offers a list of notable prospects. The initially formed imines **4**, for example, are interesting synthetic building blocks, which may allow easy access to many valuable products (e.g. β-lactams and 1,3-diamines). Preliminary experiments also indicate that Mannich bases such as **5** can be obtained by bisaminomethylation with high regioselectivities and in good yields. Moreover, based on the excellent results achieved in the alkylation of chiral imines with Michael acceptors,[8] we expect our method to be suitable for the enantioselective synthesis of β-amino ketones.

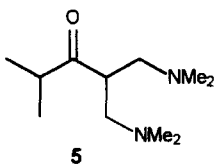

5

Experimental Procedure

3a: The reactions were conducted in water-free apparatus under argon. A solution of imine **2** (2.5 mmol) in anhydrous CH_2Cl_2 (2.5 mL) was cooled to −80 °C. The iminium salt **1** (2.5 mmol) was added in one portion and the reaction mixture was stirred for 3–4 h, during which the temperature increased to about −30 °C. To obtain good results in every case the reaction mixture should be stored for about 15 h at this temperature in a freezer before the workup. The reaction mixture was treated with aqueous AcOH solution (2 N, 5 mL) and Et_2O (50 mL), and stirred at 25 °C for 3–4 h. Then HCl (6 N, 5 mL) was added and the mixture stirred a further 10 min. The organic phase was decanted off and the aqueous phase washed with Et_2O (2 × 50 mL). The aqueous phase was finally treated with dilute NH_3 solution (25 mL, 25% NH_3:H_2O = 1:4) with vigorous stirring and extracted with Et_2O (3 × 50 mL, 1 min each). The combined organic phases were dried over Na_2SO_4 and the solvent removed on a rotary evaporator without heating.

Received: September 8, 1995 [Z8382IE]
German version: *Angew. Chem.* **1995**, *107*, 2861–2862

Keywords: aminoalkylations · asymmetric syntheses · imines · Mannich bases

[1] N. Risch, M. Arend, *Angew. Chem.* **1994**, *106*, 2531; *Angew. Chem. Int. Ed. Engl.* **1994**, *33*, 2422.
[2] M. Tramontini, *Synthesis* **1973**, 703; M. Tramontini, L. Angiolini, *Tetrahedron* **1990**, *46*, 1791.
[3] E. F. Kleinman in *Comprehensive Organic Synthesis, Vol. 2* (Eds.: B. M. Trost, C. H. Heathcock), Pergamon, Oxford, **1991**, p. 893; E. Winterfeldt, *J. Prakt. Chem.* **1994**, *336*, 91.
[4] N. Risch, A. Esser, *Liebigs Ann. Chem.* **1992**, 233.
[5] D. Seebach, M. Schiess, W. B. Schweizer, *Chimia* **1985**, *39*, 272; A. R. Katritzky, P. A. Harris, *Tetrahedron* **1990**, *46*, 987; E. G. Nolen, A. Allocco, M. Broody, A. Zuppa, *Tetrahedron Lett.* **1991**, *32*, 73; G. Oszbach, A. Neszmélyi, *Liebigs Ann. Chem.* **1990**, 211; M. R. Saidi, A. Heydari, J. Ipaktschi, *Chem. Ber.* **1994**, *127*, 1761.
[6] a) G. Kinast, L. F. Tietze, *Angew. Chem.* **1976**, *88*, 261; *Angew. Chem. Int. Ed. Engl.* **1976**, *15*, 239; Y. Jasor, M. Gaudry, M. J. Luche, A. Marquet, *Tetrahedron* **1977**, *33*, 295; b) J. Hooz, J. N. Bridson, *J. Am. Chem. Soc.* **1973**, *95*, 602; S. Danishefsky, M. Prisbylla, B. Lipisko, *Tetrahedron Lett.* **1980**, *21*, 805; S. Danishefsky, M. Kahn, M. Silvestri, *ibid.* **1982**, *23*, 1419; C. Rochin, O. Babot, J. Dunoguès, F. Duboudin, *Synthesis* **1986**, 667.
[7] N. Risch, M. Arend, *Methoden Org. Chem. (Houben-Weyl) 4th ed. 1952–, Vol. E21b* **1995**, p. 1925, and references therein.
[8] J. d'Angelo, D. Desmaële, F. Dumas, A. Guingant, *Tetrahedron Asymmetry* **1992**, *3*, 459; P. W. Hickmott in *The Chemistry of Enamines* (Ed.: Z. Rappoport), Wiley, Chichester, **1994**, p. 843, and references therein.

Asymmetric Sulfide Oxidation with Vanadium Catalysts and H_2O_2**

Carsten Bolm* and Frank Bienewald

The evaluation of asymmetric catalytic reactions often fails to consider practical criteria important for applications in large-scale reactions.[1] Generally, attention is focused on the enantioselectivity and not on the practicability of the reaction or the catalytic efficiency, which is measured as the turnover number per time. There are only few enantioselective catalytic reactions that meet the expectations of the users and are therefore employed in syntheses by people both outside and inside the research groups originally involved in their development.[2] We report herein a method for the asymmetric oxidation of sulfides,[3] which provides optically active sulfoxides with *ee* values up to 85%. Moreover, this method proceeds under very simple reaction conditions (room temperature, exclusion of air and humidity unnecessary) and can be performed with H_2O_2, a cheap and safe oxidizing agent, as well as with a readily accessible chiral vanadium catalyst (≤ 1 mol%) [Eq.(a)].

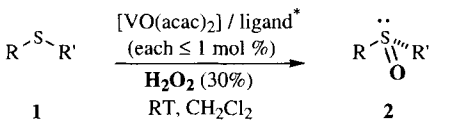

1 → **2** (a)

Enantioselective oxidations of aryl alkyl sulfides with vanadium complexes were reported by Fujita and co-workers as early as 1986. Using 10 mol% of the vanadium–salen catalyst **3** and cumyl hydroperoxide as the oxygen source, they obtained enantioselectivites of up to 40% *ee*.[4–6] The enantioselectivities reported by Fujita et al. are lower than those obtained when using

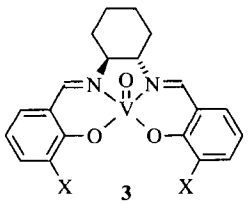

3

X = OMe, OEt, *t*Bu

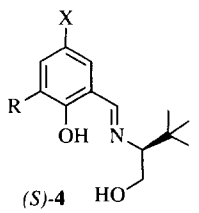

(S)-**4**

a: R = *t*Bu, X = NO_2
b: R = X = *t*Bu
c: R = $SiPh_2$*t*Bu, X = *t*Bu
d: R = H, X = NO_2

the modified Sharpless reagent [tartrate, $[Ti(OiPr)_4]$, H_2O, organic hydroperoxide],[7] which was introduced by Kagan et al. for the oxidation of sulfides. Nevertheless, the vanadium-catalyzed transformation has the advantage of requiring a smaller amount of the carrier of chiral information (metal and ligand).

We have now found that sulfides can be oxidized rapidly and efficiently into optically active sulfoxides (ee_{max} = 85%) by us-

[*] Prof. Dr. C. Bolm, Dipl.-Chem. F. Bienewald
Fachbereich Chemie der Universität
Hans-Meerwein-Strasse, D-35032 Marburg (Germany)
Telefax: Int. code +(6421)288917
e-mail: Bolm@Ps1515.chemie.uni-marburg.de

[**] This work was supported by the Deutsche Forschungsgemeinschaft (Schwerpunktprogramm: Sauerstofftransfer/Peroxidchemie, Graduierten-Kolleg). We thank the BASF for a doctoral stipend (F. B.) and the Degussa for the donation of chemicals.

ing a catalyst formed in situ from $[VO(acac)_2]$ (acac = acetylacetonate) and ligands of type **4**.[8, 9] This catalytic reaction is remarkable for the following reasons: 1) Aqueous H_2O_2 (30%, 1.1 equivalents) is the most efficient oxidizing agent. Other vanadium-catalyzed reactions have been reported, which use *tert*-butylhydroperoxide as the oxygen source. Those catalytic reactions, however, are often inhibited by the presence of water. 2) The reaction conditions are unusually simple. The oxidation maybe performed in open reaction vessels, since atmospheric oxygen and water do not affect the outcome. 3) The catalytic system is extremely efficient and catalyzes the sulfoxide formation in concentrations of 0.01 mol% of the complex. When 1 mol% of the catalyst is used, the reaction becomes very rapid and vigorous; for that reason, the oxidizing agent has to be added slowly, because an increase of the reaction temperature results in the formation of the respective sulfone. 4) The use of the very simple ligands readily available from salicylaldehydes and amino alcohols gives rise to relatively high *ee* values (Table 1). 5) The reaction is ligand-accelerated,[10] and the enantioselectivity is not or only slightly affected by the presence of achiral vanadium species (that is, excess $[VO(acac)_2]$). A ligand/vanadium ratio of 1:1 is therefore sufficient to obtain good asymmetric induction.

Table 1. Catalytic enantioselective oxidation of sulfides with H_2O_2 and 1 mol% of $[VO(acac)_2]$ as well as 1.5 mol% of the ligand.

No.	Ligand	Sulfide	Sulfoxide	Yield[%]	*ee*[%]	Config.[a]
1	**4a**	Ph-S-Me	**2a**	94	70	(*S*)-(−)
2	**4b**	Ph-S-Me	**2a**	73	59	(*S*)-(−)
3	**4c**	Ph-S-Me	**2a**	54	56	(*S*)-(−)
4	**4d**	Ph-S-Me	**2a**	88	50	(*S*)-(−)
5	**4a**	Ph-S-*i*Pr	**2b**	64	62	(*S*)-(−)
6	**4a**	Ph-S-*n*-$C_{10}H_{21}$	**2c**	77	53	(*S*)-(−)[b]
7	**4a**	*p*$NO_2C_6H_4$-S-Me	**2d**	55	63	(*S*)-(−)[b]
8	**4a**	*t*Bu-S-CH_2Ph	**2e**	91	65	(−)[b]
9	**4a**	**5**	**6**	77	76	(−)[b]
10	**4b**	**5**	**6**	84	85	(−)[b]
11	**4b**	**7**	**8**	65	57	(−)[b]

[a] The *ee* values were determined by HPLC on a chiral phase; the absolute configurations were obtained from optical rotations (**2a** in EtOH; **2b**, **6** in $CHCl_3$; **2c**–**e**, **8** in acetone) and by comparing the obtained data with the literature values. [b] The absolute configuration of the products was not determined unequivocally and is, in some cases, based on analogous systems.

The influence of the ligand structure on the product configuration and the obtained enantioselectivity has been thoroughly studied in the oxidation of methyl phenyl sulfide (**1a**) (Table 1). Both factors are primarily determined by the steric demand of the imino alcohol substituent and the stereoelectronic properties of the aryl substituent of the ligand. The highest enantioselectivities were obtained with ligands derived from *tert*-leucinol. The (*S*) enantiomer yielded the (*S*)-configurated product in excess. A sterically demanding substituent, such as the *tert*-butyl group, at C-6 of the aryl group generally enhanced the enantioselectivity. Ligands containing large silyl substituents or simply a hydrogen atom at the same position (**4c** and **4d**, respectively) furnished the corresponding sulfoxides with lower *ee* values. A significant improvement in the enantioselectivity was obtained with *p*-nitro-substituted ligands.

The chiral vanadium/H_2O_2 catalyst system oxidizes a variety of structurally different sulfides enantioselectively (Table 1). Aryl alkyl sulfides gave the corresponding sulfoxides in 53–70% *ee*. The best result was obtained in the case of thioacetal **5**. When ligand **4b** was used, the *trans*-sulfoxide **6** was formed exclusively in 85% *ee*, whereas the catalyst containing the nitro-substituted ligand **4a** resulted in a lower enantioselectivity (77% yield, 76% *ee*). Alkyl benzyl sulfides as well as functionalized sulfides (entries 8 and 11) can also be converted into optically active sulfoxides.

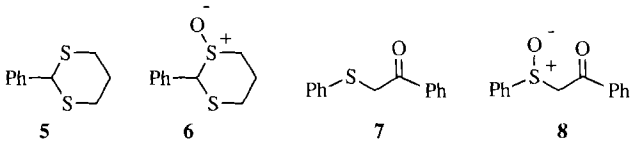

5 **6** **7** **8**

Sulfones are formed only in low quantities when using the vanadium complex described here.[11] From the reactivity difference between sulfide **1** and sulfoxide **2** it is deduced that the *ee* value of **2** does not arise from a selectivity enhancement caused by kinetic resolution of the chiral sulfoxide,[12] but is the direct result of the enantioselective oxidation.[13] This conclusion is further supported by the fact that the enantiomeric excess of **2a** does not change significantly during the reaction.

Since we did not observe chiral amplification,[14] we assume that the catalyst contains only one ligand in the configuration-determining step. ^{51}V NMR spectroscopic investigations of mixtures containing $[VO(acac)_2]$, the ligand, and H_2O_2 showed that several species of vanadium with higher oxidation states are formed. Consequently, vanadium(v) compounds such as $VOCl_3$ or V_2O_5 can also be used as catalyst precursors.[15] Attempts to replace vanadium by niobium in the oxidation of methyl phenyl sulfide (1 mol% of $NbCl_5$/**4b**, 1.1 equivalents of H_2O_2, room temperature, 20 h) resulted in the formation of the corresponding sulfoxide **2a** in a yield of 86% but in only 7% *ee*.

Investigations are currently underway to expand the scope of this reaction[16] and to determine which vanadium species[17, 18] is responsible for the obtained enantioselectivities and the reaction behavior.

Experimental Procedure

$[VO(acac)_2]$ (2.6 mg, 0.01 mmol) and the ligand (0.015 mmol) were dissolved in a test tube in dichloromethane (2 mL), and the solution was stirred for 5 min. After the additon of the sulfide (1 mmol) and the dropwise addition of 30% H_2O_2 (1.1 mmol), the mixture was stirred for 16 h at ambient temperature (approximately 200 r min^{-1}). The aqueous layer was separated off, and the solvent removed in vacuo from the remaining mixture. The crude product was purified by chromatography on silica gel and—if necessary—also by Kugelrohr distillation under high vacuum. The enantioselectivities were determined by chiral HPLC (Daicel UV detector (254 nm), flow rate 0.5 mL min^{-1}). Retention times [min]: (*R*)-**2a** 21.4, (*S*)-**2a** 26.5 (Chiralcel OD, hexane/2-propanol 9/1); (*R*)-**2b** 20.6, (*S*)-**2b** 24.7 (Chiralcel OD-H, hexane/2-propanol 96/4); (+)-**2c** (acetone) 13.5, (−)-**2c** 16.1 (Chiralcel OD-H, hexane/2-propanol 9/1); (+)-**2d** (acetone) 38.8, (−)-**2d** 44.9 (Chiralcel OJ, hexane/2-propanol 7/3); (−)-**2e** (acetone) 22.6, (+)-**2e** 31.4 (Chiralcel OD, hexane/2-propanol 9/1); (−)-**6** ($CHCl_3$) 15.0, (+)-**6** 34.5 (Chiralcel OD, hexane/2-propanol 7/3); (+)-**8** (acetone) 38.6, (−)-**8** 55.6 (Chiralcel OD, hexane/2-propanol 9/1).

Received: July 24, 1995 [Z8252IE]
German version: *Angew. Chem.* **1995**, *107*, 2883–2885

Keywords: asymmetric synthesis · catalysis · oxidations · sulfoxides · vanadium compounds

[1] Asymmetric catalysis in industry: a) G. W. Parshall, S. D. Ittel, *Homogeneous Catalysis*, Wiley, New York, **1992**; b) *Chirality in Industry* (Eds.: A. M. Collins, G. N. Shedrake, J. Crosby), Wiley, Chichester, **1992**; c) S. Kotha, *Tetrahedron* **1994**, *50*, 3639–3662; d) *Catalytic Asymmetric Synthesis* (Ed.: I. Ojima), VCH, New York, Weinheim, **1993**.

[2] For positive examples of metal-catalyzed asymmetric oxidations: a) R. A. Johnson, K. B. Sharpless in ref. [1d], pp. 227–272; b) H. C. Kolb, M. S. van Nieuwenhze, K. B. Sharpless, *Chem. Rev.* **1994**, *94*, 2483–2547; c) E. N. Jacobsen in ref. [1d], pp. 159–202.

[3] For excellent reviews see a) H. B. Kagan in ref. [1d], S. 203–226; b) H. B. Kagan, F. Rebière, *Synlett* **1990**, 643–650.

[4] a) K. Nakajima, K. Kojima, J. Fujita, *Chem. Lett.* **1986**, 1483–1486; b) K. Nakajima, K. Kojima, M. Kojima, T. Aoyama, J. Fujita, *Bull. Chem. Soc. Jpn.* **1990**, *63*, 2620–2630.

[5] Other chiral metal/Schiff base catalysts for the asymmetric sulfur oxidation: a) [Ti]: C. Sasaki, K. Nakajima, M. Kojima, J. Fujita, *Bull. Chem. Soc. Jpn.* **1991**, *64*, 1318–1324; b) [Ti]: S. Colonna, A. Manfredi, M. Spadoni, L. Casella, M. Gullotti, *J. Chem Soc. Perkin Trans 1*, **1987**, 71–73; c) [Ti]: A. Colombo, G. Marturano, A. Pasini, *Gazz. Chim. Ital.* **1986**, *116*, 35–40; d) [Mn]: M. Palucki, P. Hanson, E. N. Jacobsen, *Tetrahedron Lett.* **1992**, *33*, 7111–7114; e) [Mn]: K. Noda, N. Hosoay, R. Irie, Y. Yamashita, T. Katsuki, *Tetrahedron* **1994**, *50*, 9609–9618.

[6] The results of mechanistic studies indicate that the catalytic reaction proceeds through the intermediacy of highly oxidized vanadium species [4]. See also R. Curci, F. Di Furia, R. Testi, G. Modena, *J. Chem. Soc. Perkin Trans 2* **1974**, 752–757.

[7] a) P. Pitchen, E. Duñach, M. N. Deshmukh, H. B. Kagan, *J. Am. Chem. Soc.* **1984**, *106*, 8188–8193; b) S.-H. Zhao, O. Samuel, H. B. Kagan, *Tetrahedron* **1987**, *43*, 5135–5144; c) H. B. Kagan, E. Duñach, C. Nemecek, P. Pitchen, O. Samuel, S.-H. Zhao, *Pure Appl. Chem.* **1985**, *57*, 1911–1916; d) S.-H. Zhao, O. Samuel, H. B. Kagan, *Org. Synth.* **1989**, *68*, 49–54; e) F. Di Furia, G. Modena, R. Seraglia, *Synthesis* **1984**, 325–326.

[8] For applications of these ligands in other metal-catalyzed reactions, see a) [Cu]: T. Aratani, *Pure Appl. Chem.* **1985**, *57*, 1839–1844; b) [Ti]: M. Hayashi, Y. Miyamoto, T. Inoue, N. Oguni, *J. Org. Chem.* **1993**, *58*, 1515–1522; c) [Ti]: M. Hayashi, T. Inoue, Y. Miyamoto, N. Oguni, *Tetrahedron* **1994**, *50*, 4385–4398.

[9] Vanadium catalysts with structurally similar *N*-salicylidene amino acid ligands afford racemic sulfoxides [5b] or products with low *ee* values (4–14% *ee*); K. Nakajima, M. Kojima, K. Toriumi, K. Saito, J. Fujita, *Bull. Chem. Soc. Jpn.* **1989**, *62*, 760–767.

[10] D. J. Berrisford, C. Bolm, K. B. Sharpless, *Angew. Chem.* **1995**, *107*, 1159–1171; *Angew. Chem. Int. Ed. Engl.* **1995**, *34*, 1059–1070.

[11] The use of **3** also yielded the sulfone [4]. For the $[VO(acac)_2]$/*tert*-butyl hydroperoxide catalyst system, the oxidation ratio SBu_2:$OSBu_2$ was determined to be 100:1.7 [6].

[12] This behavior can be used to obtain sulfoxides with high *ee* values: a) N. Komatsu, M. Hashizume, T. Sugita, S. Uemura, *J. Org. Chem.* **1993**, *58*, 4529–4533; b) *ibid.* **1993**, *58*, 7624–7626.

[13] The difference in reactivity between the sulfide and the sulfoxide can be used to characterize the electronic nature of the oxygen transfer reagent: W. Adam, W. Haas, B. B. Lohray, *J. Am. Chem. Soc.* **1991**, *113*, 6202–6208.

[14] a) R. Noyori, M. Kitamura, *Angew. Chem.* **1991**, *103*, 34–55; *Angew. Chem. Int. Ed. Engl.* **1991**, *30*, 49–69; b) D. Guillaneux, S.-H. Zhao, O. Samuel, D. Rainford, H. B. Kagan, *J. Am. Chem. Soc.* **1994**, *116*, 9430–9439; c) C. Bolm in *Advanced Asymmetric Synthesis* (Ed.: G. R. Stephenson), Blackie, Glasgow, in press.

[15] The complex formation of V_2O_5 and the ligand is apparently very slow under the given reaction conditions.

[16] An asymmetric vanadium(IV)-catalyzed cycloaddition: A. Togni, G. Rist, G. Rihs, A. Schweiger, *J. Am. Chem. Soc.* **1993**, *115*, 1908–1915.

[17] Reviews on ligand design for oxidation catalysts: T. J. Collins, *Acc. Chem. Res.* **1994**, *27*, 279–285.

[18] Peroxo vanadium complexes: A. Butler, M. J. Clague, G. E. Meister, *Chem. Rev.* **1994**, *94*, 625–638.

The First μ(OH)-Bridged Model Complex for the Mixed-Valent $Fe^{II}Fe^{III}$ Form of Hemerythrin**

Ursula Bossek, Helga Hummel, Thomas Weyhermüller, Eckhard Bill, and Karl Wieghardt*

There is at least one mixed-valent $Fe^{II}Fe^{III}$ form known for the iron-containing metalloproteins hemerythrin, ribonucleotide reductase, purple acid phosphatase, and methanemonooxygenase.[1] The electronic structures of the active dimetallic centers have been well characterized with spectroscopic methods (UV/Vis, ESR and, to some extent, Mössbauer spectroscopy). In the case of hemerythrin three such species have been reported; they differ in the coordination at the two iron centers (Scheme 1).[2] Recent ENDOR and ESEEM studies (ENDOR = Electron Nuclear Double Resonance, ESEEM = Electron Spin Echo Envelope Modulation) on the mixed-valent forms of hemerythrin and methanemonooxygenase have detected the presence of a bridging OH group between the Fe^{II} and Fe^{III} ions.[3]

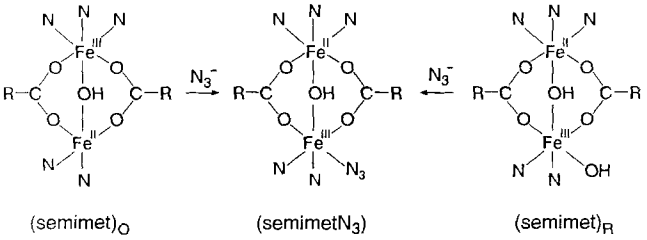

Scheme 1. Three mixed-valent species of semimethemerythrin (semimet).

Although there are good model complexes for the completely reduced Fe^{II}_2 and oxidized Fe^{III}_2 species containing these active dimetallic centers, no mixed-valent $Fe^{II}Fe^{III}$ complexes with a bridging OH group have been reported to date. On the other hand, $Fe^{II}Fe^{III}$ complexes with a bridging phenoxy group are well known.[4] In these *redox-stable* complexes the valences are frequently localized (class I or II; even at 300 K); this causes a weak, intramolecular antiferromagnetic coupling between the high-spin Fe^{II} (d^6) ion and the high-spin Fe^{III}(d^5) ion, which results in an ESR-active $S_t = 1/2$ ground state. A probably μ-oxo bridged $Fe^{II}Fe^{III}$ complex was characterized in solution by ESR spectroscopy.[5]

We have now discovered that the reaction of 1,4,7-trimethyl-1,4,7-triazacyclononane (L) with $Fe^{II}(ClO_4)_2 \cdot 6H_2O$ and pivalic acid (piv) gives a transparent, light green solution in acetone under argon. The color quickly turns blue-violet on controlled exposure to air. When kept for a prolonged period at $-18\,^{\circ}C$ we obtained blue-violet crystals of **1**-$(ClO_4)_2$. If a solution of **1** was purged with air, or oxidized by addition of H_2O_2, we obtained an orange solution from which orange crystals of **2**-$(ClO_4)_2$ were isolated.

$[LFe^{III}(\mu\text{-}OH)(\mu\text{-}piv)_2Fe^{II}L](ClO_4)_2$ **1**-$(ClO_4)_2$

$[L_2Fe^{III}_2(\mu\text{-}O)(\mu\text{-}piv)_2](ClO_4)_2$ **2**-$(ClO_4)_2$

[*] Prof. Dr. K. Wieghardt, U. Bossek, Dipl.-Chem. H. Hummel, Dr. T. Weyhermüller, Dr. E. Bill
Max-Planck-Institut für Strahlenchemie
Stiftstrasse 34–36, D-45470 Mülheim an der Ruhr (Germany)
Telefax: Int. code +(208)3063952

[**] We are grateful to the Fonds der Chemischen Industrie for support of this work.

The X-ray crystal structure analyses of **1** and **2**[6] prove the dinuclear nature of these complexes; both salts crystallize in the space group $P2_1/n$ with very similar unit cell dimensions; Figure 1 shows the structure of **1**. The corresponding Fe–X bond lengths in **1** at the two iron atoms, Fe(1) and Fe(2), differ only

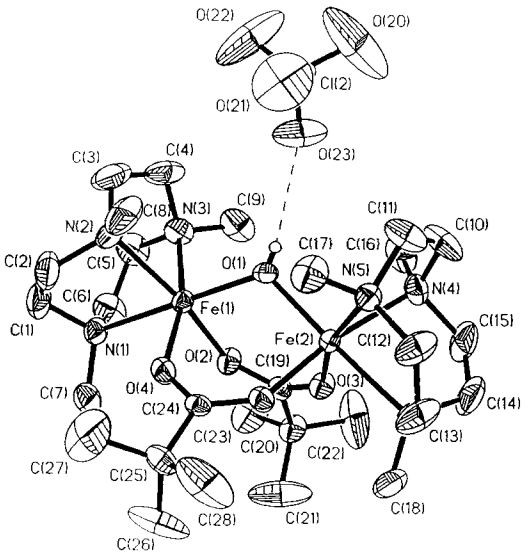

Fig. 1. Structure of **1** with one ClO_4^- counterion; the structure of **2** is very similar and is not represented. Selected distances [Å] and angles [°] (the corresponding values for **2** are given in parentheses): Fe(1)-N(1) 2.254(5) (2.269(7)), Fe(1)-N(2) 2.215(6) (2.188(9)), Fe(1)-N(3) 2.216(6) (2.204(9)), Fe(1)-O(1) 2.005(5) (1.800(5)), Fe(1)-O(2) 2.040(4) (2.025(6)), Fe(1)-O(4) 2.057(4) (2.026(6)), Fe(1)···Fe(2) 3.400(3) (3.123(2)), O(1)···O(23) 2.961(5) (4.097(7)), Fe(2)-N(4) 2.186(5) (2.177(7)), Fe(2)-N(5) 2.236(4) (2.212(7)), Fe(2)-N(6) 2.248(5) (2.281(8)), Fe(2)-O(1) 1.961(5) (1.788(6)), Fe(2)-O(3) 2.020(4) (2.033(6)), Fe(2)-O(5) 2.004(4) (2.021(6)); Fe(1)-O(1)-Fe(2) 118.1(2) (121.0(3)).

very slightly; in the cation of **2**, they are of equal length. The bent Fe^{II}-OH-Fe^{III} unit is not quite symmetrical: one $Fe-O_{hydroxo}$ distance is longer than the other. The valences of the Fe ions are almost localized in the solid state (class II according to Robin and Day): Fe(1) is Fe^{II} whilst Fe(2) is an Fe^{III} ion. One O atom of the ClO_4^- counterion forms a weak O–H···O hydrogen bond with the OH bridge of **1**; in **2** there is no such OH bridge. The structure of **2** is very similar to the analogous model complexes with a bent $Fe_2^{III}(\mu\text{-O})$ structural unit.[2]

The UV/Vis spectrum of **2** in acetonitrile exhibits a series of absorption maxima in the visible region typical for metazidohemerythrin and $Fe_2^{III}(\mu\text{-O})$ model complexes with bent Fe^{III}-O-Fe^{III} units.[2f] On the other hand, deoxyhemerythrin and its yellow model complex $[L_2Fe_2^{II}(\mu\text{-OH})(\mu\text{-ac})_2](ClO_4)\cdot H_2O$[5, 7] show d–d transitions of only very low intensity at 928 nm ($\varepsilon = 10\ L\,mol^{-1}\,cm^{-1}$) and 1100 nm (sh) ($7\ L\,mol^{-1}\,cm^{-1}$). The UV/Vis spectrum of **1** in anhydrous acetonitrile shows an intervalence band at 1350 nm ($138\ L\,mol^{-1}\,cm^{-1}$) along with a few bands of greater intensity in the visible region, which, in contrast to the μ-phenoxy-bridged $Fe^{II}Fe^{III}$ complexes, cannot be assigned to phenolate → Fe^{III} charge-transfer bands. In the spectrum of semimethemerythrin (N_3), two maxima in the NIR region were found at 910 and 1190 nm.[8] The latter was assigned to an intervalence band.

Measurements of the temperature dependence of the susceptibility[9] of solid samples of **2** showed a strong ($J = -111\ cm^{-1}$) intramolecular antiferromagnetic coupling (Fig. 2); this coupling is weaker for **1** ($J = -12.9\ cm^{-1}$). In good agreement with this, a coupling of $J \approx -15\ cm^{-1}$ was determined for

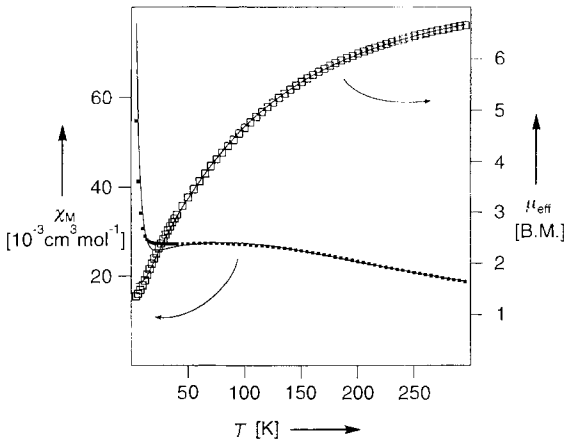

Fig. 2. Temperature dependence of the molar susceptibility and of the magnetic moment of solid **1**. The solid lines repesent the results of the fitting calculations [9].

semimethemerythrin (N_3),[10] whilst it is noticeably smaller for phenoxy-bridged complexes ($J \approx -3$ – $-7\ cm^{-1}$). Therefore, the ground state of complex **2** is diamagnetic with $S_t = 0$ and for complex **1** it is paramagnetic with $S_t = 1/2$.

The X-band ESR spectrum of the cation in **1** in acetonitrile at 10 K confirms the $S_t = 1/2$ ground state. The signal is rhombic with $g_1 = 1.95$, $g_2 = 1.52$, $g_3 = 1.43$ (from a simulation). Typically for mixed-valent forms of the metalloproteins and for all of the $Fe^{II}Fe^{III}$ model complexes known to date, g values are smaller than 2; in the spectrum of semimethemerythrin (N_3) the rhombic signal has g values of 1.92, 1.82, 1.50.[10]

The valences in **1** also appear to be essentially localized on the time scale of Mössbauer spectroscopy ($\approx 10^{-7}$ s). The zero-field spectrum at 300 K shows two quadrupole doublets of almost equal intensity with isomeric shifts relative to α-Fe at 25 °C of $\delta = 0.80(2)\ mm\,s^{-1}$ and $0.55(2)\ mm\,s^{-1}$ and corresponding quadrupole splittings of $\Delta E_Q = 1.12(1)\ mm\,s^{-1}$ and $0.68(1)\ mm\,s^{-1}$, respectively. The former is typical of a high-spin Fe^{II} ion in an octahedral environment, whilst the latter can be assigned to a high-spin Fe^{III} ion likewise in an octahedral environment. The Mössbauer spectrum of solid **2** at 4.2 K shows only one quadrupole doublet; values of $\delta = 0.48(1)\ mm\,s^{-1}$ and $\Delta E_Q = 1.54(1)\ mm\,s^{-1}$ were determined.

The natural form of hemerythrin consists of eight identical subunits, each of which contains an active diiron center (a total of 16 Fe). Wilkins et al.[1b] found that the forms of semimethemerythrin containing eight $Fe^{II}Fe^{III}$ subunits are unstable and disproportionate[10] to produce four homovalent Fe_2^{II} and four Fe_2^{III} subunits [Eq. (a)]. From the kinetic point of view, this is a first-order process.

$$[Fe^{II}Fe^{III}]_8 \longrightarrow [Fe_2^{II}]_4[Fe_2^{III}]_4 \qquad (a)$$

A striking feature is that O_2-free, blue-violet solutions of **1**-$(ClO_4)_2$ in anhydrous aceto- or butyronitrile are only stable for 10–30 min at 25 °C, they then suddenly change color to orange within 5 min. This process can be followed by spectrophotometry as a function of time (Fig. 3). At first the spectrum of **1** is observed, it remains practically unchanged for about 30 min. The final spectrum after about 50 min corresponds to pure **2**. Quantitative analysis of this spectrum shows that exactly half of the original **1** was transformed into **2**. The other half must then be present as the very pale yellow $[L_2Fe_2^{II}(\mu\text{-OH})(\mu\text{-piv})_2]^+$ ion. That this is, in fact, the case was proved by aerating the above reaction solution after the anaerobic color change; the position

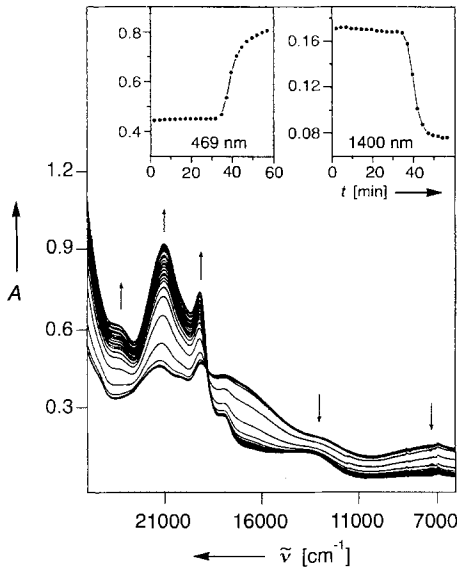

Fig. 3. Vis spectrum of **1** (1.1×10^{-3} M) in dry CH_3CN at 298 K and under Ar as a function of time (spectra were recorded every 2.5 min). The insets show the absorption at 469 nm and at 1400 nm as a function of time.

of the maxima in the spectrum did not change, but the intensity doubled. Thus anaerobic disproportionation of **1** and subsequent oxidation with O_2 yields **2** quantitatively.

The long induction period for the disproportionation of **1** under anaerobic conditions indicates that the reaction is autocatalytic. As shown in Scheme 2, **1** (**D** in Scheme 2) in solution

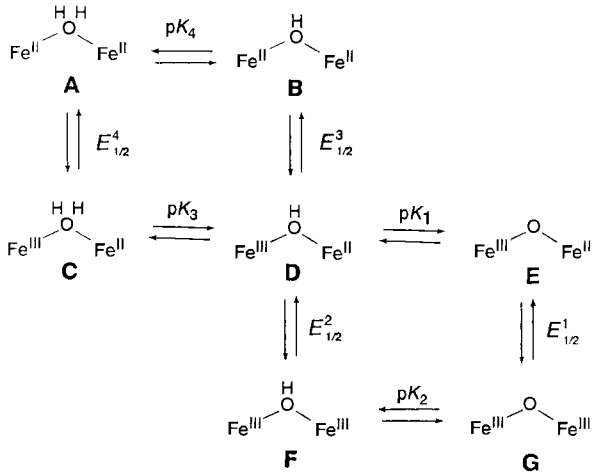

Scheme 2. Possible protonated and redox species of the diiron centers in hemerythrin and in the model complexes.

can be protonated on the OH-bridge to give the μ-aqua complex **C**, or it can be deprotonated to the μ-oxo form **E**.[11] There is a pH-dependent equilibrium between the complexes **C**, **D**, and **E**. The more protonated mixed-valent species is a stronger oxidizing agent than the less protonated species;[5] this results in intermolecular electron-transfer between the more or less highly protonated species as given in Equations (b)–(d).

$$\mathbf{D} + \mathbf{C} \longrightarrow \mathbf{F} + \mathbf{A} \quad \text{(b)}$$

$$\mathbf{E} + \mathbf{D} \longrightarrow \mathbf{G} + \mathbf{B} \quad \text{(c)}$$

$$\mathbf{C} + \mathbf{E} \longrightarrow \mathbf{A} + \mathbf{G} \quad \text{(d)}$$

Because both product **F** and **A** are strong acids, the protons that are thus set free during the course of the disproportionation can protonate **D**. In this way the relative concentration of **C** increases: Thus, the disproportionation is accelerated by autocatalysis. This mechanism is supported by the observation that not only the addition of acid ($HClO_4$) but also of base (triethylamine) to the CH_3CN solution of **1**-$(ClO_4)_2$ drastically shortens the period of induction. Futhermore, the orange solution containing 50% of **2** is obtained during dissolution of **1**-$(ClO_4)_2$ in protic solvents such as water, methanol, or ethanol.

Therefore, complex **1** is not only a good structural model for the mixed-valent active center in semimethemerythrin (N_3) as it has a very similar electronic structure, but it also shows similar redox reactivity. Thus, **1** is also a functional model. With complex **1**, along with $[L_2Fe^{II}_2(\mu\text{-OH})(\mu\text{-acetate})_2]^{+}$ [5, 7] and $[L_2Fe^{III}_2(\mu\text{-O})(\mu\text{-acetate})_2]^{2+}$ [5, 7], there is now a series of very good models available for all the redox states of hemerythrin. The extent to which the structural and electronic relationships in the active center of the metalloprotein is reproduced by these complexes is very gratifying.

Experimental Procedure

1-$(ClO_4)_2$: A light green solution of 1,4,7-trimethyl-1,4,7-triazacyclononane (L, 0.5 g), purged with argon, 0.4 g pivalic acid, and 1.0 g $Fe^{II}(ClO_4)_2 \cdot 6H_2O$ in 40 mL acetone at 25 °C was carefully purged with air for 5 min until the color changed to blue-violet. This solution was subsequently purged with argon until it was air-free and then stored in a sealed vessel at −18 °C for 2 d. Blue-violet crystals of **1**-$(ClO_4)_2$ were isolated in about 70% yield (0.85 g). Single crystals were obtained by slow evaporation of the reaction solution in a stream of argon. $C_{28}H_{61}Cl_2N_6O_{13}Fe_2$ (872.4 g mol^{-1}); elemental analysis: found C 38.3, H 7.3, N 9.6%; calcd. C 38.5, H 7.0, N 9.6%. UV/Vis (CH_3CN): λmax (ε) = 346 (3.0×10^3), 413(sh) (≈380), 472 (363), 496(sh) (342), 526 (404), 561 (417), ≈800(sh) (≈200), 1350 nm (138 L mol^{-1} cm^{-1}); MS(FAB): m/z = 772.3 $[M - (ClO_4)]^+$.

2-$(ClO_4)_2$: To a solution of 0.5 g L and 0.4 g pivalic acid in 40 mL acetone was added 1.0 g $Fe^{II}(ClO_4)_2 \cdot 6H_2O$. The mixture was vigorously stirred at 20 °C for 30 min in air (alternatively 30% H_2O_2 (2 mL) was added) until the solution became a transparent orange. On slow evaporation of the reaction mixture in a stream of air, orange crystals of **2**-$(ClO_4)_2$ were isolated in about 70% yield. Single crystals were obtained from a saturated acetone solution of **2**-$(ClO_4)_2$. $C_{28}H_{60}Cl_2N_6O_{13}Fe_2$ (871.4 g mol^{-1}); elemental analysis: found C 38.4, H 7.1, N 9.5%; calcd. C 38.6, H 6.9, N 9.6%. UV/Vis (CH_3CN) λ_{max} (ε) = 248 (15.9×10^3), 355 (7.7×10^3), 430(sh) (945), 475 (1406), 520 (1.1×10^3), 560(sh) (286), 729 nm (167 L mol^{-1} cm^{-1}); MS(FAB): m/z 771.2 $[M - (ClO_4)]^+$.

Received: July 14, 1995 [Z8213IE]
German version: *Angew. Chem.* **1995**, *107*, 2885–2888

Keywords: hemerythrin · iron compounds · magnetic properties · mixed-valent compounds · model complexes

[1] Hemerythrin: B. B. Muhoberac, D. C. Wharton, L. M. Babcock, P. C. Harrington, R. G. Wilkins, *Biochem. Biophys. Acta* **1980**, *626*, 337; L. M. Babcock, Z. Bradic, P. C. Harrington, R. G. Wilkins, G. S. Yoneda, *J. Am. Chem. Soc.* **1980**, *102*, 2849; ribonucleotide reductase: M. Atta, K. K. Andersson, R. Ingemarson, L. Thelander, A. Gräslund, *ibid.* **1994**, *116*, 6429; R. Davydov, S. Kuprin, A. Gräslund, A. Ehrenberg, *ibid.* **1994**, *116*, 11120; violet acid phosphatases and uteroferrin: E. P. Day, S. S. David, J. Peterson, W. R. Dunham, J. J. Bonvoisin, R. H. Sands, L. Que, Jr., *J. Biol. Chem.* **1988**, *263*, 15561; methanemonooxygenase: M. P. Woodland, D. S. Patil, R. Cammack, H. Dalton, *Biochem. Biophys. Acta* **1986**, *873*, 237; B. G. Fox, K. K. Surerus, E. Münck, J. D. Lipscomb, *J. Biol. Chem.* **1988**, *263*, 10553; M. P. Hendrich, B. G. Fox, K. K. Anderson, P. G. Debrunner, J. D. Lipscomb, *ibid.* **1992**, *267*, 261.

[2] Reviews: a) J. B. Vincent, G. L. Olivier-Lilley, B. A. Averill, *Chem. Rev.* **1990**, *90*, 1447; b) S. J. Lippard, *Angew. Chem.* **1988**, *100*, 353; *Angew. Chem. Int. Ed. Engl.* **1988**, *27*, 344; c) D. M. Kurtz, Jr., *Chem. Rev.* **1990**, *90*, 585; d) J. Sanders-Loehr, in *Iron Carriers and Iron Proteins, Physical Bioinorganic Chemistry Series* (Ed.: T. M. Loehr), VCH Publishers, New York, **1989**, p. 373; e) L. Que, Jr., A. E. True, *Prog. Inorg. Chem.* **1990**, *38*, 97; f) electronic structure of $Fe^{III}_2(\mu\text{-O})$ complexes: C. A. Brown, G. J. Remar, R. L. Musselman, E. I. Solomon, *Inorg. Chem.* **1995**, *34*, 688.

[3] a) V. J. DeRose, K. E. Liu, D. M. Kurtz, Jr., B. M. Hoffman, S. J. Lippard, *J. Am. Chem. Soc.* **1993**, *115*, 6440; b) H. Thomann, M. Bernardo, J. M. McCormick, S. Pulver, K. K. Anderson, J. D. Lipscomb, E. I. Solomon, *ibid.* **1993**, *115*, 8881.

[4] Structurally characterized triply bridged $Fe^{II}Fe^{III}$ complexes: a) A. S. Borovik, V. Papaefthymiou, L. F. Taylor, O. P. Anderson, L. Que, Jr., *J. Am. Chem. Soc.* **1989**, *111*, 6183; b) M. S. Mashuta, R. J. Webb, J. K. McCusker, E. A. Schmitt, K. J. Oberhausen, J. F. Richardson, R. M. Buchanan, D. N. Hendrickson, *ibid.* **1992**, *114*, 3815; c) K. Schepers, B. Bremer, B. Krebs, G. Henkel, E. Althaus, B. Mosel, W. Müller-Warmuth, *Angew. Chem.* **1990**, *102*, 582; *Angew. Chem. Int. Ed. Engl.* **1990**, *29*, 531; d) E. Bernard, W. Moneta, J. Langier, S. Chardon-Noblat, A. Deronzier, J.-P. Tuchagues, J.-M. Latour, *ibid.* **1994**, *106*, 914; *ibid.* **1994**, *33*, 887.

[5] J. A. R. Hartman, R. L. Rardin, P. Chaudhuri, K. Pohl, K. Wieghardt, B. Nuber, J. Weiss, G. C. Papaefthymiou, R. B. Frankel, S. J. Lippard, *J. Am. Chem. Soc.* **1987**, *109*, 7387.

[6] Crystallographic data (298 K) of **1** and, in parentheses, **2**: space group $P2_1/n$ ($P2_1/n$), $a = 11.851(2)$ (11.949(2)), $b = 16.162(3)$ (15.942(3)), $c = 21.391(4)$ (21.087(3)) Å, $\beta = 98.29(2)$ (96.89(1)), $Z = 4$ (4), four-circle diffractometer Siemens P4, $Mo_{K\alpha}$ radiation, graphite monochromator, ω scan, measured range $2\theta = 4.0$–55.0 (4.0–48.0), 8807 (3334) independent reflections, no absorption correction, $\mu(Mo_{K\alpha}) = 0.911$ (0.926) mm^{-1}. Crystal dimensions $0.42 \times 0.36 \times 0.54$ ($0.34 \times 0.42 \times 0.48$) mm^3, $\rho_{calcd} = 1.429$ (1.451) $g\,cm^{-3}$, calculation program: Siemens-SHELXTL-PLUS, PC version (G. M. Sheldrick, University of Göttingen). $R = 0.065$ (0.068), $R_w = 0.070$ (0.066). The position of the OH proton in **1** was localized and refined in the final difference Fourier synthesis; all the remaining H atoms in calculated positions. Residual electron density: 0.82 (0.66) e $Å^{-3}$. Further details of the crystal structure investigation may be obtained from the Fachinformationszentrum Karlsruhe, D-76344 Eggenstein-Leopoldshafen (Germany) on quoting the depository number CSD-59135.

[7] P. Chaudhuri, K. Wieghardt, B. Nuber, J. Weiss, *Angew. Chem.* **1985**, *97*, 774; *Angew. Chem. Int. Ed. Engl.* **1985**, *24*, 778.

[8] J. Sanders-Loehr, T. M. Loehr, A. G. Mauk, H. B. Gray, *J. Am. Chem. Soc.* **1980**, *102*, 6992.

[9] The temperature dependence of the molar magnetic susceptibility was measured with a SQUID-magnetometer (Quantum Design) in the range 2–300 K on solid samples of **1** and **2**. After diamagnetic correction of the raw data, fitting calculations were carried out using the isotropic Heisenberg-Dirac-van Vleck model ($H = -2JS_1 \cdot S_2$). The fitting shown in Figure 2 for **1** was obtained with the following parameters: $S_1 = 5/2$, $S_2 = 2$, $J = -12.9(\pm 0.5)\ cm^{-1}$, $g_1 = 2.0$ (fixed), $g_2 = 2.16$, and zero-field splitting parameters $D_1 = D_2 = 0$ (fixed); there was also a small paramagnetic impurity with $S = 5/2$ of 0.6%. For **2** ($S_1 = S_2 = 5/2$, $g_1 = g_2 = 2.0$, $D_1 = D_2 = 0$ (fixed)), these calculations gave a coupling constant of $J = -111(\pm 3)\ cm^{-1}$.

[10] a) M. J. Maroney, D. M. Kurtz, Jr., J. M. Noak, L. L. Pearce, L. Que, Jr., *J. Am. Chem. Soc.* **1986**, *108*, 6871; b) L. L. Pearce, D. M. Kurtz, Jr., Y.-M. Xia, P. G. Debrunner, *ibid.* **1987**, *109*, 7286.

[11] Interestingly, a model complex has been described and structurally characterized for both **A** and **F** (Scheme 2); there are no structural data reported for **C** and **E**. However, species **E** has been obtained by electrochemical one-electron reduction of $[L_2Fe_2^{III}(\mu\text{-}O)(\mu\text{-acetate})_2]^{2+}$ in anhydrous CH_2Cl_2 and has been characterized by ESR spectroscopy [5]. $[(HB(pz)_3)_2Fe_2^{III}(\mu\text{-}OH)(\mu\text{-acetat})_2]\text{-}ClO_4$: W. H. Armstrong, S. J. Lippard, *J. Am. Chem. Soc.* **1984**, *106*, 4632; P. N. Turowski, W. H. Armstrong, S. Liu, S. N. Brown, S. J. Lippard, *Inorg. Chem.* **1994**, *33*, 636; $[(tmen)_2Fe_2^{II}(\mu\text{-}H_2O)(\mu\text{-}O_2CC_6H_5)_4]$: K. S. Hagen, R. J. Lachicotte, *ibid.* **1992**, *114*, 8741.

[12] We would like to thank Dr. V. Schünemann and Prof. Dr. A. X. Trautwein (Medizinische Universität Lübeck) for the Mössbauer and ESR spectra.

Synthesis and Structures of Triamino- and Tetraaminosilanes**

Karsten Wraage, Antje Künzel, Mathias Noltemeyer, Hans-Georg Schmidt, and Herbert W. Roesky*

Dedicated to Professor Richard Neidlein on the occasion of his 65th birthday

In 1993 P. P. Power et al. described the first triaminosilane containing a carbon-bound organic substituent; this had the composition $RSi(NH_2)_3$ ($R = (C_6H_5)_3C_6H_2$).[1] To date further reactions of this compound have not been reported. In light of our experience with valence-isoelectronic silanetriols,[2, 3] we were interested in triamino- and tetraaminosilanes ($R_2NSi(NH_2)_3$, $ROSi(NH_2)_3$) with substituents bound through nitrogen and oxygen, respectively. These two systems have the advantage that the group containing organic substituents can be subsequently hydrolytically removed after reaction at the NH_2 groups, whereas this is not possible for the carbon-bound triaminosilanes under mild conditions.

The above-mentioned silanetriols[2, 3] show interesting reactivity. Among other applications, they can be used to make soluble zeolite precursors [4] and titanium-containing heterocubanes. We now report on the synthesis and reactivity of compounds of the form $RSi(NH_2)_3$.

The trichlorosilanes $RSiCl_3$, $R = iPr_2C_6H_3NSiMe_3$ or $R = tBu_3C_6H_2O$, react in liquid ammonia, with formation of ammonium chloride, to give **1a** and **1b**, respectively [Eq. (a)]. These compounds are very soluble in common organic solvents. Single crystals of the compounds were obtained from *n*-hexane.

$$RSiCl_3 + 6\ NH_3 \xrightarrow[-3\,NH_4Cl]{} RSi(NH_2)_3 \qquad \text{(a)}$$

1a: $R = iPr_2C_6H_3NSiMe_3$

1b: $R = tBu_3C_6H_2O$

Compound **1a** forms colorless needles that melt at 73 °C and are stable at room temperature under an inert atmosphere. The colorless crystals of **1b** melt at 170 °C. Characteristic broad singlets are observed for the amino protons in the ^1H NMR spectra ($\delta = 0.5$ (**1a**) and $\delta = 1.14$ (**1b**)). The IR spectra show three N–H bands in the region for valence vibrations (3345.4 to 3472.2 cm^{-1} (**1a**) and 3407.5 to 3502.6 cm^{-1} (**1b**)).

The Si–N bond lengths (168.7 to 172.0 pm) in **1a** and **1b** are similar to those in the known triaminosilane[1] (Figs. 1 and 2). The amino groups on silicon in **1a** and **1b** are arranged in a distorted tetrahedral manner with bond angles ranging from 101.10(12) to 123.3(3)°. In the solid state **1a** and **1b** show nitrogen–hydrogen bridges (**1a**: 241.4 pm and **1b**: 266.1 pm). In **1a** two amino groups form bridging interactions, while in **1b** only one N–H bridge forms. The latter is attributed to the more sterically demanding ligands in **1b**. In the unit cell of **1b** the molecules are rotated with respect to each other so as to maximize the distance between them. As a result, only two amino groups are capable of forming bridges.

[*] Prof. Dr. H. W. Roesky, K. Wraage, Dipl.-Chem. A. Künzel, Dr. M. Noltemeyer, H.-G. Schmidt
Institut für Anorganische Chemie der Universität
Tammannstrasse 4, D-37077 Göttingen (Germany)
Telefax: Int. code +(551)393373

[**] This work was supported by the Hoechst AG, the Volkswagen-Stiftung, and the Deutsche Forschungsgemeinschaft.

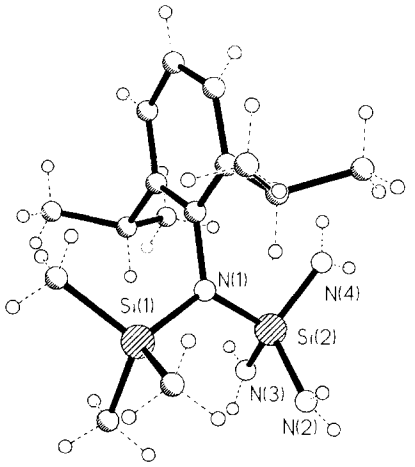

Fig. 1. Structure of **1a** in the crystal. Selected bond lengths [pm] and angles [°]: Si(2)-N(2) 171.4(2), Si(2)-N(3) 172.0(2), Si(2)-N(4) 169.3(2); N(2)-Si(2)-N(3) 101.10(12), N(4)-Si(2)-N(3) 105.80(11), N(4)-Si(2)-N(2) 121.36(12) [7].

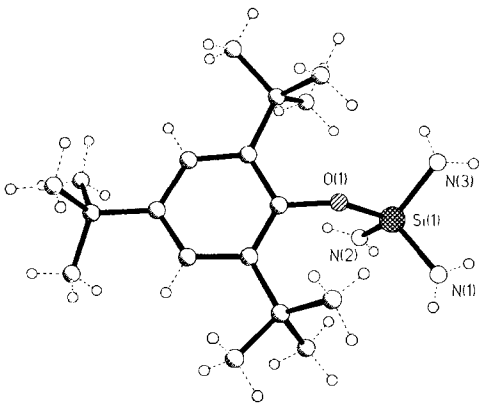

Fig. 2. Structure of **1b** in the crystal. Selected bond lengths [pm] and angles [°]: Si(1)-N(1) 168.8(6), Si(1)-N(2) 168.7(5), Si(1)-N(3) 170.3(6); N(2)-Si(1)-N(1) 108.1(3), N(2)-Si(1)-N(3) 123.3(3), N(1)-Si(1)-N(3) 100.9(3) [7].

Compound **2** is formed by the addition of a solution of **1a** to $[Cp^*TiMe_3]$[5] ($Cp^* = C_5Me_5$) in *n*-hexane at room temperature [Eq. (b)] and is soluble in common organic solvents. The ^1H NMR spectrum of **2** shows a singlet ($\delta = 0.34$) for the protons on the amino group; this signal is shifted to higher field in comparison to that for **1a** ($\Delta\delta = 0.5$).

$$\underset{\textbf{1a}}{RSi(NH_2)_3} + [Cp^*TiMe_3] \xrightarrow[-2\ MeH]{} \underset{\textbf{2}}{R{-}Si(NH)_2{-}Ti(Cp^*)(Me){-}NH} \qquad (b)$$

A comparison of the structure of **2** with **1a** shows similar Si–N bond lengths (169.8(3) to 173.9(2) pm) (Fig. 3). The Ti–N distances are 190.6 and 190.0 pm. The N(1)-Si(2)-N(2) bond angle (90.91(11)°) of the titanium-bound amino groups is about 20° smaller than that of the unbound amino groups. Compound **2** forms a distorted silicon-nitrogen-titanium heterocycle with some widely varying bond angles (N(1)-Ti(1)-N(2) 81.10(10)°, Si(2)-N(1)-Ti(1) 93.91°, Si(2)-N(2)-Ti(1) 93.89°).

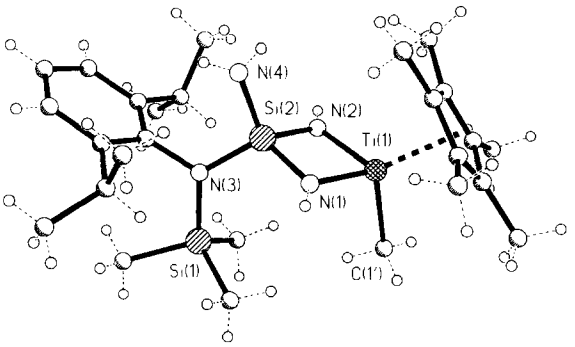

Fig. 3. Structure of **2** in the crystal. Selected bond lengths [pm] and angles [°]: Si(2)-N(1) 173.3(2), Si(2)-N(2) 173.9(2), Si(2)-N(4) 169.8(3), Ti(1)-N(1) 190.6(2), Ti(1)-N(2) 190.0(2); N(1)-Si(2)-N(2) 90.91(11), N(4)-Si(2)-N(2) 112.54(13), N(4)-Si(2)-N(1) 116.36(13), N(1)-Ti(1)-N(2) 81.10(10), Si(2)-N(1)-Ti(1) 93.91(11), Si(2)-N(2)-Ti(1) 93.89(11) [7].

Compound **3** is formed by the reaction of **1a** with Me_3SnCl (in excess) in boiling *n*-hexane [Eq. (c)]. It is soluble in common

$$\underset{\textbf{1a}}{RSi(NH_2)_3} + Me_3SnCl \xrightarrow[-HCl]{} \underset{\textbf{3}}{RSi(NH_2)_2(NHSnMe_3)} \qquad (c)$$

organic solvents and melts at 62 °C. The ^{119}Sn NMR spectrum shows a singlet ($\delta = 168.40$) for the tin atom in the $SnMe_3$ group. In addition, one N–H band disappears from the IR spectrum.

Compounds **2** and **3** show that selective substitutions of the amino groups can be achieved. Furthermore, compounds **1a** and **1b** are possible precursors for dendrimers and ceramics; they contain reactive hydrogen atoms ideal for these syntheses. The high hydrogen content favors the elimination of the organic group in the synthesis of ceramics.

Experimental Procedure

1a: $iPr_2C_6H_3NSiMe_3SiCl_3$ (1.2 g, 3.1 mmol) [2] was dissolved in liquid ammonia (25 g) at −78 °C and then heated at reflux for 4 h at −30 °C. Thereafter, the ammonia was evaporated off, the residue taken up in diethyl ether, and the ammonium chloride formed was removed by filtration. Removal of the solvent in vacuo left a colorless solid, which was recrystallized from *n*-hexane (5 mL). Yield 0.8 g (79%) **1a**. $C_{15}H_{32}N_4Si_2$ (M = 324.22 g mol^{-1}; m.p. 73 °C; ^1H NMR (200 MHz, C_6D_6, TMS): δ = 0.2 (s, 9 H, $SiMe_3$), 0.5 (s, 6 H, $Si(NH_2)_3$), 1.22 (d, ^3J(H,H) = 6.9 Hz, 6 H, $CH(CH_3)_2$), 1.25 (d, ^3J(H,H) = 6.9 Hz, 6 H, $CH(CH_3)_2$), 3.65 (sept, 2 H, $CH(CH_3)_2$), 7.05 (s, 3 H, H_{arom}); ^{29}Si NMR (49 MHz, C_6D_6, TMS): δ = 3.6 ($SiMe_3$), −41.0 ($Si(NH_2)_3$); IR (KBr, Nujol): 3345.4, 3392.4, 3472.2 cm^{-1}; MS (EI, 70 eV): 324 (M^+, 12%), 307 ($M^+ - NH_2$, 100%); correct elemental analysis [6].

1b: **1b** was prepared analogously to **1a**. Yield 1.5 g (80%) **1b**. $C_{18}H_{35}N_3OSi$ (M = 337.58 g mol^{-1}); m.p. 170 °C; ^1H NMR (200 MHz, $CDCl_3$, TMS): δ = 1.14 (bs, 6 H, NH_2), 1.30 (s, 9 H, *t*Bu), 1.49 (s, 18 H, 2 *t*Bu), 7.27 (s, 2 H, H_{arom}); ^{29}Si NMR (50 MHz, $CDCl_3$, TMS): δ = −50.05 ($Si(NH_2)_3$); IR (KBr, Nujol): 3407.5, 3481.2, 3502.6 cm^{-1}; MS (EI, 70 eV): 337 (M^+, 28%), 280 ($M^+ - t$Bu, 100%); correct elemental analysis [6].

2: A solution of **1a** (0.65 g, 2.0 mmol) in *n*-hexane (5 mL) was added dropwise at room temperature to $[Cp^*TiMe_3]$ (0.46 g, 2.0 mmol) [5] in *n*-hexane (8 mL). After the gas evolution had ceased, the solution was stirred for 1 h and then the solvent was removed in vacuo. The resulting solid was recrystallized from pentane (8 mL). Yield 0.92 g (91%) **2**. $C_{25}H_{44}N_4Si_2Ti$ (M = 522.30 g mol^{-1}); m.p. 148 °C (decomp.); ^1H NMR (200 MHz, C_6D_6, TMS): δ = 0.22 (s, 9 H, $SiMe_3$), 0.34 (s, 4 H, $Si(NH)_2NH_2$), 1.25 (m, 12 H, $CH(CH_3)_2$), 1.76 (m, 15 H, Cp^*), 2.08 (s, 3 H, $Ti\text{-}CH_3$), 3.72 (sept, 2 H, $CH(CH_3)_2$), 7.05 (m, 3 H, H_{arom}); ^{29}Si NMR (50 MHz, C_6D_6, TMS): δ = 3.22 ($SiMe_3$), −38.53 ($Si(NH)_2NH_2$); IR (KBr, Nujol): 3366.8, 3404.0, 3494.6 cm^{-1}; MS (EI, 70 eV): 505 ($M^+ - Me$, 100%); correct elemental analysis [6].

3: **1a** (2.0 g, 6.2 mmol) and Me_3SnCl (3.7 g, 18.6 mmol) were combined as solids and then heated at reflux in *n*-hexane (30 mL). Thereafter, the solution was allowed to cool to room temperature and the solvent was removed in vacuo. A colorless solid was obtained and recrystallized from *n*-hexane (10 mL). Yield 2.5 g (83%) **3**.

$C_{18}H_{40}N_4Si_2Sn$ (M = 487.43 gmol^{-1}); m.p. 62 C; ^{1}H NMR (200 MHz, $CDCl_3$, TMS): δ = 0.11 (s, 9 H, $SiMe_3$), 0.64 (s, 9 H, $SnMe_3$), 0.78 (s, 5 H, $Si(NH_2)_2NH$), 1.17 (d, ^3J(H,H) = 6.9 Hz, 6 H; $CH(CH_3)_2$), 1.21 (d, ^3J(H,H) = 6.9 Hz, 6 H, $CH(CH_3)_2$), 3.54 (sept, 2 H, $CH(CH_3)_2$), 7.04 (t, 3 H, H_{arom}); ^{29}Si NMR (50 MHz, $CDCl_3$, TMS): δ = 4.02 ($SiMe_3$), −40.29 ($Si(NH_2)_2NH$); ^{119}Sn NMR (93 MHz, $CDCl_3$, $SnMe_4$): δ = 168.40 ($SnMe_3$); IR (KBr, Nujol): 3413.0, 3499.4 cm^{-1}; MS (EI; 70 eV): 307 (M^+ − $SnMe_3$ − NH_2, 100%), 472 (M^+ − Me, 1.4%); correct elemental analysis [6].

Received: July 13, 1995 [Z81991E]
German version: *Angew. Chem.* **1995**, *107*, 2954–2956

Keywords: nitrogen compounds · silicon compounds · substitutions · titanium compounds

[1] K. Ruhlandt-Senge, R. A. Bartlett, M. M. Olmstead, P. P. Power, *Angew. Chem.* **1993**, *105*, 459–461; *Angew. Chem. Int. Ed. Engl.* **1993**, *32*, 425.

[2] N. Winkhofer, A. Voigt, H. Dorn, H. W. Roesky, A. Steiner, D. Stalke, A. Reller, *Angew. Chem.* **1994**, *106*, 1414–1416; *Angew. Chem. Int. Ed. Engl.* **1994**, *33*, 1352.

[3] N. Winkhofer, H. W. Roesky, M. Noltemeyer, W. T. Robinson, *Angew. Chem.* **1992**, *104*, 670–671; *Angew. Chem. Int. Ed. Engl.* **1992**, *31*, 599.

[4] G. Perego, G. Ballussi, C. Corno, M. Tamarasso, F. Buonomo, A. Esposito in *Studies in Surface Science and Catalysis: New Developments in Zeolite Science and Technology* (Eds.: Y. Murakami, A. Iijima, J. W. Word), Elsevier, Amsterdam, **1986**.

[5] M. Mena, P. Royo, R. Serrano, M. A. Pellinghelli, A. Tiripicchio, *Organometallics* **1989**, *8*, 476.

[6] Minor deviations in the elemental analysis data are due to the formation of silicon carbide and silicon nitride.

[7] a) Crystallographic data for **1a** at 153 K: space group $P2_1/n$, monoclinic, a = 828.98(10), b = 1448.6(2), c = 1641.5(2) pm, β = 98.822(10), V = 1.9480(4) nm^3, Z = 4, ρ_{calcd} = 1.107 Mgm^{-3}, $F(000)$ = 712, 2242 [$I > 2\sigma(I)$], R = 0.0371; b) crystallographic data for **1b** at 153 K: space group $Pca2_1$, orthorhombic, a = 1177(3), b = 1581.7(5), c = 1084.90(10) pm, V = 2.020(5) nm^3, Z = 4, ρ_{calcd} = 1.110 Mgm^{-3}, $F(000)$ = 744, 1702 [$I > 2\sigma(I)$], R = 0.0511; c) crystallographic data for **2** at 223 K: space group $P\bar{1}$, triclinic, a = 854.0(2), b = 1194.2(4), c = 1503.0(5) pm, α = 99.25(3), β = 91.53(3), γ = 90.01(3), V = 1.5123(8) nm^3, Z = 2, ρ_{calcd} = 1.144 Mgm^{-3}, $F(000)$ = 564, 6049 [$I > 2\sigma(I)$], R = 0.0543; Further details of the crystal structure investigation may be obtained from the Fachinformationszentrum Karlsruhe, D-76344 Eggenstein-Leopoldshafen (Germany), on quoting the depository number CSD-404264, 404265, and 404266.

Fivefold Deprotonated D-Mannose as Ligand in Homoleptic Dinuclear Metalates of Trivalent Iron, Vanadium, Chromium, Aluminum, and Gallium**

Joachim Burger, Claudia Gack, and Peter Klüfers*

The trivalent ions of the 3d metals as well as those of aluminum and its homologues form mononuclear aqua ions in aqueous solution only at low pH, but in the physiological pH range they are, to a large extent, condensed to isopolybases. The identification of low molecular weight "bioligands" that form complexes with the M^{III} ions in neutral aqueous solution, competing with the formation of networks of hydroxo and oxo bridges, is one of the basic aims of bioinorganic chemistry. A concrete example is the question of the constitution of the coordination spheres of the metals during transfer between macromolecules like transferrin and ferritin.[7a] In particular for iron(III), the investigations extend to carbohydrates, which are ubiquitous in organisms;[2a, b] because the crystallization of the target complexes is problematic,[2c] however, definite proposals for the structure are lacking. For iron(III) complexes, which have been studied by numerous methods, most structural suggestions concentrate around dinuclear hydroxo-iron cores surrounded by sugar ligands that are assumed to be up to doubly deprotonated.[2d, e, g] We now report on a series of isotypic sugar complexes of trivalent metals, that could be crystallized from weakly basic aqueous solution. The compounds $Ba_2[M^{III}_2(\beta\text{-D-Man}f\text{H}_{-5})_2]\cdot n\,H_2O$ (M = Fe (**1**), V (**2**), Cr (**3**), Al (**4**), Ga (**5**); Man$f$ = mannofuranose; $n \approx 13$) are each the first structurally characterized complex of the particular metal with a nonprotected monosaccharide.

Starting point for the study was a "barium ferri mannose" that was described by Traube, Kuhbier, and Härting in 1933 as the trihydrate $BaFeC_6H_7O_6\cdot 3\,H_2O$ with fivefold deprotonated D-mannose.[3] The compound forms from an aqueous solution of sodium hydroxide, D-mannose and iron(III) nitrate on precipitation with $BaCl_2$. This time we were successful in crystallizing Traube et al.'s mannose compound both with D-mannose and with D-fructose—as well as with D-glucose in low yield—from weakly alkaline solution (pH of the mother liquor at the end of the diffusion experiments was approximately 9) in the form of yellow rhombic prisms and in characterizing them structurally (Table 1).[4] Compound **1** contains a homoleptic sugar–iron complex as anion (Fig. 1), which despite the preparation from aqueous solution includes no hydroxo or oxo ligands. Instead all the protons of the five hydroxyl groups of mannose are split off to form a pentaanionic polyolato ligand. The polyolate is derived from the β-furanose form of the free mannose, which is insignificant in solution,[5] but is the only form with all the hydroxyl groups on one side of the ring. In the stable forms of D-mannose—the two anomeric pyranose forms with $^4C_1$ conformation—this bonding mode is just as inconceivable as with the two less favorable pyranoid anomers with $^1C_4$ conformation (Scheme 1). For all the other aldohexoses, only in one other case, the rare gulose, can there be a similar favorable arrangement of all hydroxyl groups. The isomerization to a sugar ligand with the highest possible denticity, observed here for D-fructose and D-glucose, has already been described for an oxomolybdenum(VI) complex: thus the formation of β-D-mannofuranose from the epimeric D-glucose corresponds entirely to an analogous transformation of the aldopentose D-xylose into the fourfold deprotonated β-D-lyxofuranose ligand.[6]

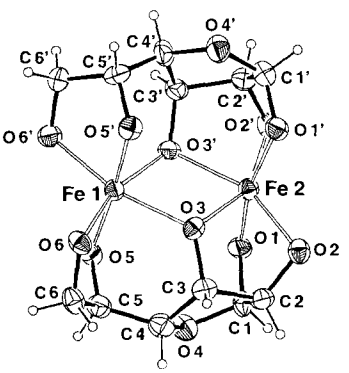

Fig. 1. The $[Fe_2(\beta\text{-D-Man}f\text{H}_{-5})_2]^{4-}$ ion in **1**; for distances and angles see Table 1. Average distances [pm] (standard deviation in the last decimal place on averaging): C O_{deprot} 141.2(15), C O_{Ring} 146.0(17), C C 154.1(22), Ba1 to the seven neighboring O 278.3(30), Ba2 to the six neighboring O 275.2(47); puckering parameters [9] of the furanose ring containing O4-C1...: Q_2 = 34.7(10) pm, ϕ_2 = 267.1(14)°, containing O4'-C1'...: Q_2 = 35.0(10) pm, ϕ_2 = 261.5(14)°.

[*] Prof. Dr. P. Klüfers, Dipl.-Chem. J. Burger, Dipl.-Chem. C. Gack
Institut für Anorganische Chemie der Universität
Engesserstrasse, Gebäude 30.45, D-76128 Karlsruhe (Germany)
Telefax: Int. code +(721)608-2135
e-mail: kluefers@achibm2.chemie.uni-karlsruhe.de

[**] Polyol Metal Complexes, Part 16. This work was supported by the Deutsche Forschungsgemeinschaft (Project Kl-624/4-1) and the Akzo AG, Wuppertal. Part 15: Ref. [1].

Table 1. Crystal structure data of **1**–**5**.

	1	**2**	**3**	**4**	**5**
M_r	970.79	960.98	963.09	913.06	998.53
Crystal dimensions [10^{-6} mm^3]	12 × 3 × 1	9 × 5 × 2	27 × 10 × 5	27 × 10 × 9	15 × 8 × 3
a [pm]	1089.7(3)	1085.4(3)	1086.4(2)	1077.1(3)	1084.6(1)
b [pm]	1498.7(2)	1491.3(3)	1491.7(2)	1492.0(2)	1497.1(2)
c [pm]	1794.5(3)	1788.7(3)	1785.8(2)	1770.2(3)	1789.4(3)
V [10^6 pm^3]	2930.8(10)	2895.3(11)	2894.0(7)	2844.8(10)	2905.6(7)
$\rho_{ber.}$ [g cm^{-3}]	2.2003(8)	2.2046(8)	2.2104(5)	2.1319(8)	2.2827(5)
$2\theta_{max}$ [°]	48	56	52	52	56
N_{hkl} (total, $I > 0$)	16637	13312	13092	13066	14706
R_{int}	0.074	0.036	0.020	0.032	0.041
N_{hkl} (asym., $I > 0$)	4599	6242	5370	5375	6540
$N_{hkl}(\|F_o\| \geq 4\sigma(F_o))$	3969	5773	5184	5264	6324
No. of parameters	431	431	424	419	425
$wR(F^2)$	0.079	0.076	0.082	0.082	0.083
$R(F)_{4\sigma}$	0.046	0.028	0.027	0.027	0.029
S	1.046	1.058	1.144	1.082	1.105
$\Delta\rho_{max}$ [10^{-6} e pm^{-3}]	0.564	1.110	0.916	0.909	1.400
M1-M2	329.75(19)	319.39(15)	309.97(12)	309.5(2)	322.90(9)
M1-O3	208.1(6)	205.1(3)	202.3(4)	196.5(4)	204.9(3)
M1-O5	200.9(6)	201.4(4)	198.3(4)	187.5(4)	195.0(3)
M1-O6	198.1(6)	197.3(4)	197.0(4)	188.8(4)	195.7(3)
M1-O3′	208.8(6)	205.2(4)	202.4(4)	197.3(4)	205.2(3)
M1-O5′	196.4(6)	198.8(4)	195.3(4)	185.8(4)	192.0(3)
M1-O6′	202.4(6)	199.7(3)	198.3(4)	191.7(4)	198.1(3)
M2-O1	199.8(6)	200.4(4)	198.2(4)	188.3(4)	195.4(3)
M2-O2	201.7(6)	202.0(3)	200.0(4)	190.8(4)	198.9(3)
M2-O3	205.4(6)	200.8(4)	198.7(4)	192.6(4)	201.0(3)
M2-O1′	199.8(6)	200.0(4)	197.9(4)	188.9(4)	195.5(3)
M2-O2′	200.9(6)	198.3(4)	200.2(4)	191.5(4)	197.7(3)
M2-O3′	208.0(6)	204.1(3)	200.6(4)	196.3(4)	205.2(3)
M-O3-M	105.8(3)	103.8(2)	101.2(2)	105.3(2)	105.37(14)
M-O3′-M	104.6(3)	102.61(15)	100.5(2)	103.6(2)	103.77(14)

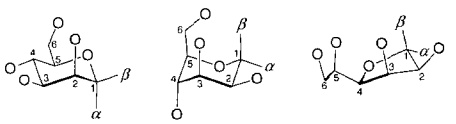

$^4C_1$ $^1C_4$ E_2

Scheme 1. Coordination possibilities for the chair conformations of D-mannopyranose and for the E_2 envelope conformation of D-mannofuranose (without H atoms and charges).

The environments of the two iron atoms in **1** are not equivalent. Fe1 forms five- and six-membered chelates with the open-chain part of the ligand, whereas Fe2 is surrounded by two oxolanetriolato fragments in a distorted E_2 conformation; this yields the α-D-erythrofuranose partial structure, which is also present in one of the anomers of each of D-ribo- and D-lyxo-, as well as D-talo- and D-allofuranose. In the envelope conformation with C2 as flap, the O1 and O3 atoms are closest together. As is usual for polyolato complexes of other metals, in **1** the alkoxide functions are also either bound to cations (here 6+1- and 7+1-fold coordinated barium), or they are acceptors in a hydrogen-bonding system constructed from water molecules in which the donors are distributed over extended cooperative sequences, or both.

Green prisms of **2** and **3**, as well as colorless crystals of **4** and **5** were obtained analogously if instead of iron nitrate vanadium(III), chromium(III), aluminum(III), or gallium(III) salts are employed.

The structure analyses demonstrate that monosaccharides can also be multiply deprotonated in the presence of metal ions as was shown for the sugar alcohols recently with D-sorbitol.[1] The mentioned M^{III} ions are converted into small anionic complexes in weakly alkaline aqueous solution with the hexoses common in organisms.[7] Charge and binding modes of the ligand in **1**–**5** now reveal that species of a different kind than previously assumed are possible in solution.

For the imminent study of equilibria in solution it is particularly advantageous that the complexes contain central metals that can be well studied by spectroscopy (V^{III}: visible spectroscopy as described in reference [8], but without limitations by slow ligand exchange as in Cr^{III} or by weak absorption because of a spin-forbidden d–d transition as in Fe^{III}; Al and Ga: NMR spectroscopy).

Received: June 21, 1995
Revised version: September 29, 1995 [Z 8119 IE]
German version: *Angew. Chem.* **1995**, *107*, 2950–2951

Keywords: carbohydrates · chelate ligands · complexes with oxygen ligands · iron compounds · polyols

[1] P. Klüfers, J. Schuhmacher, *Angew. Chem.* **1995**, *107*, 2290–2292; *Angew. Chem. Int. Ed. Engl.* **1995**, *34*, 2119–2122.

[2] a) D. M. Whitfield, S. Stojkovski, B. Sarkar, *Coord. Chem. Rev.* **1993**, *122*, 171–225; b) ref. [2f], pp. 236–283; c) ref. [2f], p. 252; d) ref. [2f], p. 255ff., p. 265ff; e) K. Geetha, M. S. S. Raghavan, S. K. Kulshreshtha, R. Sasikala, C. P. Rao, *Carbohydr. Res.* **1995**, *271*, 163–175; f) K. Burger, L. Nagy in *Bioco-ordination Chemistry* (Ed.: K. Burger), Ellis Horwood, Chichester, **1990**. g) For an inositolato-Fe^{III} complex see K. Hegetschweiler, L. Hausherr-Primo, W. H. Koppenol, V. Gramlich, L. Odier, W. Meyer, H. Winkler, A. X. Trautwein, *Angew. Chem.* **1995**, *107*, 2421–2423; *Angew. Chem. Int. Ed. Engl.* **1995**, *34*, 2242–2243.

[3] W. Traube, F. Kuhbier, H. Härtling, *Ber. Dtsch. Chem. Ges.* **1933**, *66*, 1545–1556.

[4] **1**: Pale yellow crystal from a solution of NaOH, D-fructose, and $Fe(NO_3)_3 \cdot 9H_2O$ (molar ratio 6:2:1, $c(Fe^{III}) = 0.04$ mol L^{-1}) into which $BaCl_2$ had been diffused over 5 d. Isotypical crystals were obtained with D-mannose and D-glucose; the rhombic prisms (prism axis [010]) show anomalous double refraction (cf. B. Kahr, J. M. McBride, *Angew. Chem.* **1992**, *104*, 1–28; *Angew. Chem.* **1992**, *31*, 1–26). The growth of larger crystals is currently under way to be able to study an optically uniform sector. $C_{12}H_{14}Ba_2Fe_2O_{12} \cdot 13H_2O$, orthorhombic, $P2_12_12_1$, $Z = 4$, room temperature; Lorentz and polarization cor-

rection, no absorption correction (μ_{max}(**5**) = 4.6 mm^{-1}), H atoms on C refined in calculated positions with common U, water-H atoms with identical O-H and H···H distances for all H_2O molecules (in total 31 restraints); besides the ten fully occupied H_2O sites, other residual maxima were refined as partially occupied oxygen sites; these take their place as acceptors in the hydrogen-bonding system; the given water content of 13 H_2O corresponds to the crystallographically obtained value for **2** that was determined with a low-temperature data set. Stoe-IPDS area detector, $Mo_{K\alpha}$ radiation, graphite monochromator, λ = 71.069 pm, for **1**, **2**, and **4** Siemens rotating anode with 4.5 kW power, direct methods (SHELXS), refinement with full matrix against F^2 (SHELXL), no absorption correction, processing and representation with PLATON and ORTEP (50% probability ellipsoids). **2**-**5**: Preparation and investigation of the crystals as described for **1**, for **2** under inert gas (N_2), diffraction experiment at 220 K. Further details of the crystal structure investigations may be obtained from the Fachinformationszentrum Karlsruhe, D-76344 Eggenstein-Leopoldshafen (Germany) on quoting the depository numbers CSD-401934 (**1**), CSD-404413 (**2**), CSD-404414 (**3**), CSD-404415 (**4**), and CSD-404416 (**5**).

[5] D. J. Wilbur, C. Williams, A. Allerhand (*J. Am. Chem. Soc.* **1977**, *99*, 5450–5452) reported that the proportion of β-furanose form was 0.3% (aqueous solution, 36 °C, mannose 4 M); the stabilization of the β-furanose form does not require binding to a polyolato complex; β-D-mannofuranose is also present in the polyol complex [$CaCl_2$·β-D-mannose]·4H_2O; M. L. Dheu-Andries, S. Pérez, *Carbohydr. Res.* **1983**, *124*, 324–332.

[6] G. E. Taylor, J. M. Waters, *Tetrahedron Lett.* **1981**, *22*, 1277–1278; review on metal-mediated epimerization of sugars: S. Yano, *Coord. Chem. Rev.* **1988**, *92*, 113–156.

[7] Biochemical significance: a) small iron-containing transfer complexes: B. F. Matzanke, R. Böhnke, E. Bill, A. X. Trautwein, H. Winkler, *J. Inorg. Biochem.* **1995**, *59*, 111; B. F. Matzanke, *Encyclopedia of Inorganic Chemistry, Vol. 4* (Ed.: R. B. King), Wiley, New York, **1994**, pp. 1915–1932; b) toxicity of mobilized Al^{3+} ions: R. B. Martin, *Acc. Chem. Res.* **1994**, *27*, 204–210; M. Tonković, H. Bilinski, M. E. Smith, *Polyhedron* **1995**, *14*, 1025–1030; c) nutritional significance of sugar-bound chromium(III): Ž. T. Petrović, M. L. Mandić, J. Grgić, Z. Grgić, *Z. Lebensm. Unters. Forsch.* **1994**, *198*, 36–39; d) use of Ga^{III} as Fe^{III}-mimicking central ion: A. R. Barron, A. N. MacInnes, *Encyclopedia of Inorganic Chemistry, Vol. 3* (Ed.: R. B. King), Wiley, New York, **1994**, pp. 1249–1269. Oxovanadium(III) species have only been described in organisms in acidic solution: R. Meier, M. Boddin, S. Mitzenheim, K. Kanamori in *Metal Ions in Biological Systems* (Ed.: H. Sigel, A. Sigel), M. Dekker, New York, **1995**, pp. 45–88.

[8] W. Burchard, N. Habermann, P. Klüfers, B. Seger, U. Wilhelm, *Angew. Chem.* **1994**, *106*, 936–939; *Angew. Chem. Int. Ed. Engl.* **1994**, *33*, 884–887.

[9] D. Cremer, J. A. Pople, *J. Am. Chem. Soc.* **1975**, *97*, 1354–1358.

dad Compounds of Niobium and Tantalum: Examples of the Structural Flexibility of dad Ligands**

Bodo Richter, Joachim Scholz, Joachim Sieler, and Karl-Heinz Thiele*

Lately the number of structurally characterized dad complexes of the early transition metals and lanthanides has increased substantially. Because of the stability of the high oxidation states of the metal ions, the dad ligands have been reduced to the dianion (enediamide) in most of these complexes.[1] In addition, irrespective of the type of complex and the kind of coligands, the N-heterodienes are bound to the metal as chelate in all cases. This structural uniformity is surprising in the light of the electron and steric diversity of dad ligands, and is in contrast to the large range of structures of dad complexes with late transition metals.[2] Versatile applications for dad complexes of the early transition metals can be expected only if different dad–metal interactions can be realized.[3] We report here novel dad complexes of niobium and tantalum, which demonstrate that a variety of coordination types is possible for the dad ligand with the early transition metals. A particularly good example is the dinuclear niobium complex **3**, in which the dad ligands are coordinated to the metal atoms in three different ways.

In the reaction of $NbCl_5$ or $TaCl_5$ with the di-*tert*-butyl-substituted dad derivative **1** in a 1:3 molar ratio in diethyl ether, the compounds **2a** and **2b** are formed (Scheme 1) as yellow,

$[Li\{M(tBu\text{-}dad)_3\}]$ M = Nb (**2a**), Ta (**2b**)

air- and moisture-sensitive crystals. Surprisingly, they are very soluble not only in polar solvents like diethyl ether or THF, but also in *n*-pentane. This property and the lack of coordinated

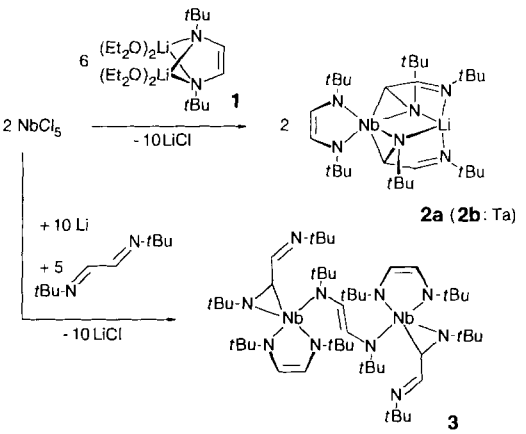

Scheme 1. Synthesis of **2a**, **b** and **3**.

solvent molecules (NMR evidence) suggest that both the transition metal atom and the lithium atom are coordinatively saturated within one ligand shell formed by the three dad ligands, and that this feature masks the ionic character of these complexes. A crystal structure analysis of **2a** confirms this supposition.[4] The unit cell contains two crystallographically independent molecules; however, their interatomic distances and bond angles do not differ significantly. One of the two molecules is shown in Figure 1.

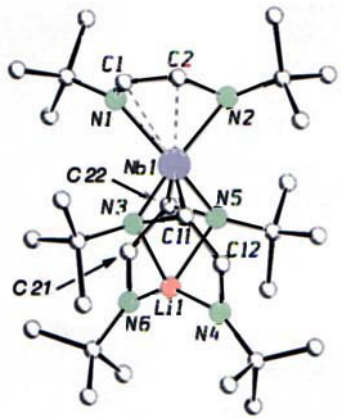

Fig. 1. Crystal structure of **2a**. The figure shows one of the two crystallographically independent molecules. Selected bond lengths [Å] and angles [°]: Nb1-N1 2.072(7), Nb1-N2 2.069(7), Nb1-N3 1.993(6), Nb1-N5 2.004(6), Nb1-C1 2.443(14), Nb1-C2 2.43(2), Nb1-C11 2.245(10), Nb1-C21 2.263(10), Nb1-Li1 2.82(2), Li1-N3 2.12(2), Li1-N4 2.07(2), Li1-N5 2.20(2), Li1-N6 1.98(2), N1-C1 1.44(2), N2-C2 1.49(2), C1-C2 1.32(2), N3-C11 1.44(1), N4-C12 1.30(1), C11-C12 1.42(1), N5-C21 1.41(1), N6-C22 1.27(1), C21-C22 1.45(1); N1-Nb1-N2 84.1(3), N3-Nb1-C11 39.1(3), N5-Nb1-C21 37.9(3), N3-Li1-N4 87.2(6), N5-Li1-N6 86.7(7), Nb1-N3-Li1 86.7(6), Nb1-N5-Li1 84.3(6); N3-C11-C12-N4 16.9(11); N5-C22-C21-N6 9.3(11); [N1-Nb1-N2][N1-C1-C2-N2] 67.2.

[*] Prof. Dr. K.-H. Thiele, Dr. J. Scholz, Dr. B. Richter
Institut für Anorganische Chemie der Universität Halle-Wittenberg
Geuser Strasse, D-06217 Merseburg (Germany)
Telefax: Int. code +(3461)462370
Prof. Dr. J. Sieler
Institut für Anorganische Chemie der Universität Leipzig (German)

[**] This work was supported by the Fonds der Chemischen Industrie and the Deutsche Forschungsgemeinschaft. dad = 1,4-diaza-1,3-butadiene; *t*Bu-dad = *N*,*N*′-bis(*tert*-butyl)-1,4-diaza-1,3-butadiene.

The Nb atom is surrounded by three dad ligands. Only one is coordinated to the metal as *cis*-configured dad dianion and forms a folded Nb–N–C=C–N five-membered ring (envelope structure[5]). The other two dad ligands are each η^2-coordinated to the Nb atom through an N=C group. Consequently, the N=C bond lengths are substantially lengthened and are hardly distinguishable from usual N–C single-bond distances (N5–C21 1.408(12), N3–C11 1.437(12) Å.[6] Since the Nb–N and Nb–C distances resemble those of known Nb–N and Nb–C single bonds[7] (Nb1–N3 1.993(6), Nb1–C11 2.245(10), Nb1–N5 2.004(6), Nb1–C21 2.263(10) Å), the bonding in **2a** is similar to that in other azametallacyclopropane rings.[8] In addition, the two N atoms of these Nb,N,C three-membered rings act as a bridge between the Nb atom and the Li^+ ion. The remaining positions of the slightly distorted coordination tetrahedron around the Li^+ ion are occupied by the still intact imine groups of the dad ligands coordinated in an η^2 fashion to the Nb atom. In this way the lithium ion is surrounded in a stable fashion and without solvent molecules by the ligand molecules of the complex.

Temperature-independent NMR spectra, which are analogous for **2a** and **2b** to a large extent, indicate that in solution the structure of both compounds resemble that of **2a** in the solid state (Table 1). For instance, the signal for the imine hydrogen atoms of the dad ligand that coordinates as chelate to the transition metal center is, as expected, observed in the typical range for olefinic protons (**2a**: δ = 5.72, 5.69; **2b**: δ = 5.74, 5.62). In contrast, a distinct charge differentiation can be seen for the imine-H protons of the two η^2-coordinated dad ligands. Whereas the signals of the H atoms of the azametallacyclopropane rings are shifted to higher field than those of the chelating dad ligand (**2a**: δ = 3.09, 2.25; **2b**: δ = 2.77, 2.03), those of the imine groups bound to the lithium ion are shifted strongly downfield (**2a**: δ = 8.44, 8.05; **2b**: δ = 8.48, 8.14). This charge differentiation is more pronounced in the ^{13}C NMR spectra (Table 1). Thus, within these two dad ligands there is a difference in function of the C=N groups: one acts exclusively as σ donor at the lithium ion and the other exclusively as π acceptor at the transition metal center.

Table 1. Physical and NMR spectroscopic data of **2a,b** and **3** [a].

2a: yellow crystals; m.p. 188 °C; ^1H NMR: δ = 8.44, 8.05 (d, ^3J(H,H) = 2.4 Hz, 1H: N=C*H*), 5.72, 5.69 (d, ^3J(H,H) = 3.2 Hz, 1H; =C*H*-N), 3.09, 2.25 (d, ^3J(H,H) = 2.5 Hz, 1H: NbC*H*), 1.40, 1.37, 1.35, 1.21, 1.17, 0.96 (s, 9H; NCMe_3). ^{13}C NMR: δ = 176.9 (dd, ^1J(C,H) = 146.6, ^2J(C,H) = 8.3 Hz; N=*C*H), 175.5 (dd, ^1J(C,H) = 146.0, ^2J(C,H) = 8.5 Hz; N=*C*H), 108.0 (dd, ^1J(C,H) = 164.0, ^2J(C,H) = 10.8 Hz; =*C*H-N), 102.9 (dd, ^1J(C,H) = 170.6, ^2J(C,H) = 9.5 Hz; =CH-N), 60.9 (dd, ^1J(C,H) = 156.9, ^2J(C,H) = 14.3 Hz; NbCH), 57.5 (dd, ^1J(C,H) = 157.7, ^2J(C,H) = 14.0 Hz; NbCH), 62.7, 62.0, 57.4, 55.0, 54.7 (s; N*C*Me$_3$), 33.1, 32.5, 31.7, 31.6, 31.5, 31.4 (q; NCMe_3)

2b: yellow crystals; m.p. 192 °C; ^1H NMR: δ = 8.48 (d, ^3J(H,H) = 1.8 Hz, 1H; N=C*H*), 8.14 (d, ^3J(H,H) = 2.2 Hz, 1H; N=C*H*), 5.74, 5.62 (d, ^3J(H,H) = 3.2 Hz, 1H; =C*H*-N), 2.77 (d, ^3J(H,H) = 2.6 Hz, 1H; TaC*H*), 2.03 (d, ^3J(H,H) = 3.1 Hz, 1H; TaC*H*), 1.35 (s, 18H; NCMe_3), 1.38, 1.21, 1.18, 0.96 (s, 9H; NCMe_3), ^{13}C NMR: δ = 177.6 (dd, ^1J(C,H) = 146.4, ^2J(C,H) = 7.7 Hz; N=*C*H), 176.1 (dd, ^1J(C,H) = 144.9, ^2J(C,H) = 7.6 Hz; N=*C*H), 105.5 (dd, ^1J(C,H) = 165.7, ^2J(C,H) = 11.0 Hz; =*C*H-N), 101.6 (dd, ^1J(C,H) = 171.8, ^2J(C,H) = 9.2 Hz; =*C*H-N), 62.6 (dd, ^1J(C,H) = 155.4, ^2J(C,H) = 14.0 Hz; Ta*C*H), 58.9 (dd, ^1J(C,H) = 155.8, ^2J(C,H) = 13.8 Hz; Ta*C*H), 62.2, 60.9, 58.5, 57.4, 54.9, 54.6 (s; N*C*Me$_3$), 33.1, 32.6, 31.8, 31.7, 31.6 (q; NCMe_3)

3: orange crystals; m.p. 174 °C; ^1H NMR: δ = 7.08 (d, ^3J(H,H) = 8.0 Hz, 2H; N=C*H*), 6.56 (d, ^3J(H,H) = 2.8 Hz, 2H; =C*H*-N), 6.20 (d, ^3J(H,H) = 2.6 Hz, 2H; =C*H*-N), 5.41 (s, 2H; =C*H*-N), 3.79 (d, ^3J(H,H) = 8.0 Hz, 2H; NbC*H*), 1.42, 1.39, 1.32, 1.05, 1.02 (s, 18H, NCMe_3), ^{13}C NMR: δ = 167.2 (dd, ^1J(C,H) = 146.0, ^2J(C,H) = 6.1 Hz; N=*C*H), 121.6 (dd, ^1J(C,H) = 157.8, ^2J(C,H) = 2.9 Hz; N=*C*H), 112.4 (dd, ^1J(C,H) = 167.8, ^2J(C,H) = 10.3 Hz; =CH-N), 100.7 (dd, ^1J(C,H) = 171.3, ^2J(C,H) = 11.5 Hz; =*C*H-N), 75.0 (dd, ^1J(C,H) = 160.3, ^2J(C,H) = 10.3 Hz; NbCH), 63.0, 61.3, 60.1, 58.5, 55.4 (s; N*C*Me$_3$), 32.2, 31.3, 30.8, 30.3, 29.8 (q; NCMe_3)

[a] ^1H NMR: 300 MHz ([D$_8$]THF, 25 °C); ^{13}C NMR: 75 MHz ([D$_8$]THF, 25 °C).

The dinuclear niobium complex **3** in which a dad dianion links two niobium atoms arises when $NbCl_5$, Li, and *t*Bu-dad in a 2:10:5 molar ratio are allowed to react in diethyl ether. Compound **3** crystallizes from diethyl ether as orange prisms and can be handled in air for short periods.

The crystal structure analysis of **3**[4] (Fig. 2) shows that this dinuclear niobium complex contains five dad ligands in three different bonding modes. The coordination geometry at the two niobium atoms is virtually identical. One dad ligand binds as *cis*-configured enediamide dianion to each metal center; in this way two five-membered rings folded along the N,N axis are formed. Another two dad ligands are coordinated only through one imine function in a η^2 fashion. As in **2a**, they form azametallacyclopropane rings with relatively short Nb–N and

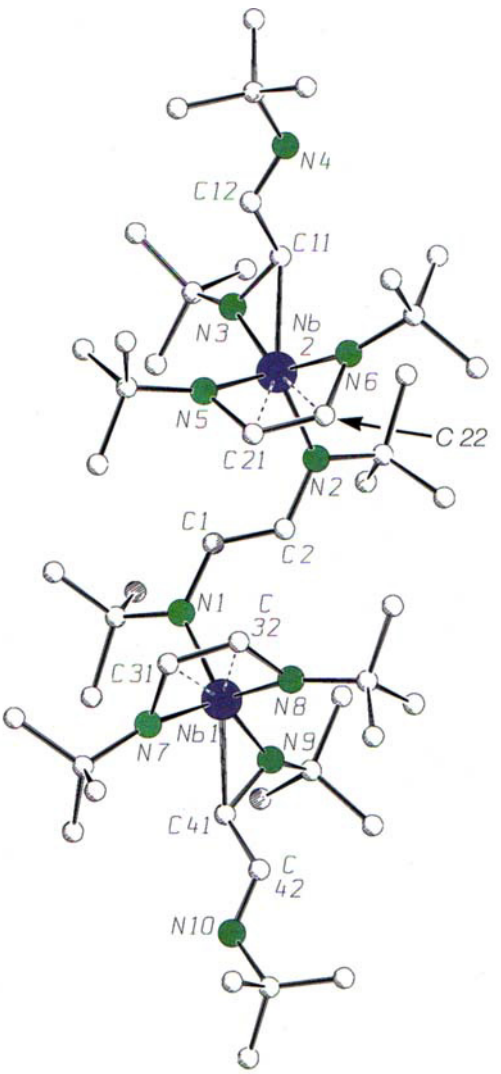

Fig. 2. Crystal structure of **3**. Selected bond lengths [Å] and angles [°]: Nb1-N1 2.050(3), Nb1-N7 2.034(3), Nb1-N8 1.988(3), Nb1-N9 1.946(3), Nb1-C31 2.498(3), Nb1-C32 2.473(3), Nb1-C41 2.223(3), Nb2-N2 2.036(3), Nb2-N5 1.975(3), Nb2-N6 2.045(3), Nb2-N3 1.943(3), Nb2-C21 2.452(3), Nb2-C22 2.485(3), Nb2-C11 2.217(3), N1-C1 1.409(4), N2-C2 1.406(4), C1-C2 1.323(5), N3-C11 1.424(4), N4-C12 1.270(4), C11-C12 1.457(5), N9-C41 1.433(4), N10-C42 1.266(5), C41-C42 1.454(5), N5-C21 1.395(4), N6-C22 1.379(4), C21-C22 1.355(5), N7-C31 1.385(4), N8-C32 1.392(4); N7-Nb1-N8 86.1(1), N5-Nb2-N6 86.3(1), N9-Nb1-C41 39.5(1), N3-Nb2-C11 39.3(1); N1-C1-C2-N2 177.1(4), N3-C11-C12-N4 −162.8(3), N9-C41-C42-N10 −153.6(4); [N7-Nb1-N8][N7-C31-C32-N8] 54.4, [N5-Nb2-N6][N5-C21-C22-N6] 53.3.

 © VCH Verlagsgesellschaft mbH, D-69451 Weinheim, 1995 0570-0833/95/3423-2650 $ 10.00+.25/0

Nb–C contacts[7] (Nb1–N9 1.946(3), Nb2–N3 1.943(3), Nb1–C41 2.223(3), Nb2–C11 2.217(3) Å) and N–C single bonds (N3–C11 1.424(4), N9–C41 1.433(4) Å).[6] The bonding mode of the fifth dad ligand has not previously been observed in complexes between dad and transition metals: this ligand is a *trans*-configured enediamide dianion (N1–C1–C2–N2 177.1(4)°) bridging the two Nb atoms. A similar *trans* structure in a dad ligand is present in the dinuclear Pt complex $[\{PtCl_2(PBu_3)\}_2(t\text{Bu-dad})]$.[9] In contrast to **3**, however, in this complex the only transition metal complex with a μ-η^1,η^1-dad bridge that has yet been structurally characterized, the *t*Bu-dad ligand is bound as neutral bidentate σ donor.

From the temperature-independent ^{1}H NMR spectra of **3** it may be deduced that the exceptional molecular structure persists in solution. In accord with the three coordination modes of the dad ligands, three complete sets of signals are observed, which could be unequivocally assigned on the basis of the crystal structure. So, for instance, the imine-H signals at $\delta = 6.56$ and 6.20 are attributable to the two dad ligands that form enediamide chelates as in **2a** and **2b**. The imine-H resonance of the C=N groups coordinated in an η^2 fashion to the Nb atoms is strongly shifted to higher field as expected ($\delta = 3.79$), whereas the chemical shift of the CH=N group of the noncoordinated half of the ligand hardly differs from that of the free dad ligand ($\delta = 7.08$).[10] The singlet at $\delta = 5.41$ is attributable to the imine-H atom of the μ-η^1,η^1-bound dad bridging ligand.

The unusual structures of **2a** and **3** show that although the dad ligands in these complexes are all bound as dianions to the metal centers, other types of coordination are viable than the chelate that was the exclusive structure known till now. Accordingly the steric flexibility of dad ligands is also preserved in their dianionic form, which opens the way to similar applications of dad chemistry for the early transition metals as for the late transition metals.

Experimental Procedure

2a: A solution of **1**, prepared from *t*Bu-dad (3.73 g, 22.2 mmol) and lithium (0.30 g, 44.4 mmol) in diethyl ether (50 mL) was added dropwise to a suspension of $NbCl_5$ (2.0 g, 7.40 mmol) in diethyl ether (50 mL) at -78 °C. The orange-brown reaction mixture was stirred for a further 8 h at room temperature and then filtered. After concentration and storage at -20 °C, yellow crystals separate from the filtrate. These were recrystallized from diethyl ether/*n*-pentane (10/1). Yield: 2.1 g (48%); correct C, H, N analysis.

2b: The synthesis is analogous to that of **2a**. From the reaction of $TaCl_5$ (2.6 g, 7.40 mmol) and **1** (22.2 mmol) yellow crystals of **2b** were isolated (2.8 g, 54%). Correct C, H, N analysis.

3: $NbCl_5$ (5.34 g, 19.8 mmol) and lithium (0.69 g, 99.4 mmol) was added at room temperature to a solution of *t*Bu-dad (10 g, 59.4 mmol) in diethyl ether (100 mL). The color of the reaction mixture changed immediately to red-brown. The mixture was stirred overnight, and the LiCl formed was then filtered off. From the filtrate, which was concentrated to half its volume and cooled to -20 °C, orange prisms of **3** separated. Repeated concentration and cooling yielded more of **3**. The crystals were recrystallized from a mixture of diethyl ether and *n*-pentane. Overall yield: 8.9 g (43%); correct C, H, N analysis.

Received: June 14, 1995 [Z 8095 IE]
German version: *Angew. Chem.* **1995**, *107*, 2865–2867

Keywords: diazadiene complexes · heterodiene compounds · niobium compounds · tantalum compounds

[1] a) S. L. Latesky, A. K. McMullen, G. P. Niccolai, I. P. Rothwell, J. C. Huffman, *Organometallics* **1985**, *4*, 1896–1898; b) F. G. N. Cloke, H. C. de Lemos, A. A. Sameh, *J. Chem. Soc. Chem. Commun.* **1986**, 1344–1345; c) B. Hessen, J. E. Bol, J. L. de Boer, A. Meetsma, J. Teuben, *J. Chem. Soc. Chem. Commun.* **1989**, 1276–1277; d) J. Scholz, M. Dlikan, D. Ströhl, A. Dietrich, H. Schumann, K.-H. Thiele, *Chem. Ber.* **1990**, *123*, 2279–2285; e) H. tom Dieck, H. J. Rieger, G. Fendesak, *Inorg. Chim. Acta* **1990**, *177*, 191–197; f) C. Woitha, U. Behrens, V. Vergopoulos, D. Rehder, *J. Organomet. Chem.* **1990**, *393*, 97–109; g) J. Scholz, A. Dietrich, H. Schumann, K.-H. Thiele, *Chem. Ber.* **1991**, *124*, 1035–1039; h) W. A. Herrmann, M. Denk, W. Scherer, F.-R. Klingan, *J. Organomet. Chem.* **1993**, *444*, C21–C24; i) L. G. Hubert-Pfalzgraf, A. Zaki, L. Toupet, *Acta Crystallogr. Sect. C* **1993**, *49*, 1609–1611; j) R. Goddard, C. Krüger, G. A. Hadi, K.-H. Thiele, J. Scholz, *Z. Naturforsch. B* **1994**, *49*, 519–528; k) A. A. Trifonov, L. N. Zakharov, M. M. Bochkarev, Y. T. Struchkov, *Izv. Akad. Nauk SSSR, Ser. Khim.* **1994**, 148–151; l) B. Richter, Dissertation, Martin-Luther-Universität Halle-Wittenberg, **1995**; m) H. Görls, B. Neumüller, A. Scholz, J. Scholz, *Angew. Chem.* **1995**, *107*, 732–735; *Angew. Chem. Int. Ed. Engl.* **1995**, *34*, 673–676.

[2] a) K. Vrieze, G. van Koten, *Adv. Organomet. Chem.* **1982**, *21*, 151–239; b) K. Vrieze, *J. Organomet. Chem.* **1986**, *300*, 307–326.

[3] Examples for the applications of dad complexes of the late transition metals: H. tom Dieck, C. Munz, J. Ehlers in *Organometallics in Organic Synthesis, Vol. 2* (Eds.: H. Werner, G. Erker), Springer, Heidelberg, **1989**, pp. 21–43.

[4] Crystal structure analysis of **2a**: $C_{30}H_{60}LiN_6Nb$, $M_r = 604.6$ g mol^{-1}, space group *Cc* (No. 9), $Z = 8$, $a = 22.914(3)$, $b = 17.545(4)$, $c = 18.953(3)$ Å, $\beta = 113.77(2)°$, $V = 6973(2)$ Å^3, $\rho_{calcd} = 1.152$ g cm^{-3}, $F(000) = 2608$, $\lambda = 0.71069$ Å, $T = 163$ K, $\mu(Mo_{K\alpha}) = 0.371$ mm^{-1}, Stoe STADI-4 diffractometer, crystal dimensions: $0.24 \times 0.21 \times 0.18$ mm, $\omega - \theta$ scans, $3° \leq 2\theta \leq 52°$; 12766 measured, 12756 symmetry-independent reflections ($R_{int} = 0.0145$), empirical absorption correction (ψ scans), structure solution possible only with DIRDIF [11], refinement with full matrix according to the method of least squares, 707 parameters, all atoms anisotropic, H atoms isotropic in calculated positions, program used SHELXL 93 [12], *R* values: for $[I > 2\sigma(I)]$ $R_1 = 0.0587$, $wR_2 = 0.1435$, all data: $R_1 = 0.1348$, $wR_2 = 0.1660$. Crystal structure analysis of **3**: $C_{50}H_{100}N_{10}Nb_2$, $M_r = 1027.2$ g mol^{-1}, space group $P2_1/n$ (No. 15), $Z = 4$, $a = 21.761(4)$, $b = 12.387(2)$, $c = 21.933(4)$ Å, $\beta = 94.71(2)°$, $V = 5892(2)$ Å^3, $\rho_{calcd} = 1.158$ g cm^{-3}, $F(000) = 2208$, $\lambda = 0.71069$ Å, $T = 163$ K, $\mu(Mo_{K\alpha}) = 0.427$ mm^{-1}, Stoe STADI-4 diffractometer, crystal dimensions: $0.32 \times 0.24 \times 0.18$ mm, $\omega - \theta$ scans, $3° \leq 2\theta \leq 50°$; 10656 measured, 10337 symmetry-independent reflections ($R_{int} = 0.0904$), structure solution with Patterson methods, refinement with full matrix according to the method of least squares, 561 parameters, all atoms anisotropic, H atoms isotropic, program used SHELXL 93 [12], *R* values: for $[I > 2\sigma(I)]$ $R_1 = 0.0366$, $wR_2 = 0.0899$, all data: $R_1 = 0.0694$, $wR_2 = 0.1031$. Representation of the structures of **2a** and **3** with SCHAKAL 88B/V16 (E. Keller, Univerisity of Freiburg, **1990**). Further details of the crystal structure investigation may be obtained from the Fachinformationszentrum Karlsruhe, D-76344 Eggenstein-Leopoldshafen (Germany) on quoting the depository numbers CSD-401153 (**2a**) and 404151 (**3**).

[5] a) All the dad complexes reported in Ref. [1] display a folding of the 1,3-diaza-2-metallacyclopent-4-ene ring M(NC=CN) along the N,N′ axis (σ^2,π bond). This folding is electronically favored, but it is easy to influence how pronounced the effect is (cf. Ref. [5b]: P. Hofmann, M. Frede, P. Stauffert, W. Lasser, U. Thewalt, *Angew. Chem.* **1985**, *97*, 693–694; *Angew. Chem. Int. Ed. Eng.* **1985**, *24*, 712–713); b) in Ta(dad) complex $[(PhO)_3Ta\{N(R)C(R')=C(R')NR\}]$, dad as enediamide dianion forms a planar five-membered ring with the Ta atom probably for steric reasons: L. R. Chamberlain, L. D. Durfee, P. E. Fanwick, L. M. Kobriger, S. L. Latesky, A. K. McMullen, B. D. Steffey, I. P. Rothwell, K. Folting, J. C. Huffman, *J. Am. Chem. Soc.* **1987**, *109*, 6068–6076.

[6] C_{sp^3}-N_{sp^3}: 1.469 Å; F. H. Allen, O. Kennard, D. G. Watson, L. Brammer, A. G. Orpen, R. Taylor, *J. Chem. Soc. Perkin Trans. 2* **1987**, 1–19.

[7] a) Nb-C: 2.32 Å; A. G. Orpen, L. Brammer, F. H. Allen, O. Kennard, D. G. Watson, R. Taylor, *J. Chem. Soc. Dalton Trans.* **1989**, 1–83; other examples: b) $[Cp_2Nb(\eta^2\text{-}C_2H_4)CH_2CH_3]$: 2.316(8), 2.277(9), 2.320(9) Å; L. J. Guggenberger, P. Meakin, F. N. Tebbe, *J. Am. Chem. Soc.* **1974**, *96*, 5420–5427; c) $[Cp_2Nb(Cl)CH_2SiMe_3][PF_6]$: 2.208(8) Å; J. Arnold, T. D. Tilley, A. L. Rheingold, S. J. Geib, *Organometallics* **1987**, *6*, 473–479; d) $[CpNb(NAr)(CH_2CMe_3)_2]$: 2.215(3), 2.174(3) Å; A. D. Poole, D. N. Williams, A. M. Kenwright, V. C. Gibson, W. Clegg, D. C. R. Hockless, P. A. O'Neil, *Organometallics* **1993**, *12*, 2549–2555; e) Nb-N: $[Nb(OC_6H_2\text{-}t\text{Bu}_2\text{-}6\text{-}Ph)_2(NMe_2)_3]$: the Nb–N lengths vary depending on the extent of the π-bonding component in the Nb–N bond: 1.940(3), 2.032(3), 2.036(3) Å; V. M. Visciglio, P. E. Fanwick, I. P. Rothwell, *Inorg. Chim. Acta* **1993**, *211*, 203–209.

[8] Selected structural and NMR data from azametallacyclopropane complexes: a) $[Cp^*Ta\{\eta^2\text{-}N(C_6H_3\text{-}2,6\text{-}Me_2)CMe_2\}Me_2]$: Ta-N 1.930(4), Ta-C 2.209(6), C-N 1.467(7) Å, ^{13}C NMR (C_6D_6, 25 °C): $\delta_{\eta^2\text{-}C=N} = 82.9$; M. V. Galakhov, M. Gomez, G. Jimenez, P. Royo, M. A. Pellinghelli, A. Tiripicchio, *Organometallics* **1995**, *14*, 1901–1910; b) $[(ArO)_2Ti\{\eta^2\text{-}N(t\text{Bu})C(CH_2Ph)_2\}(py)]$: Ti-N 1.855(2), Ti-C 2.150(2), C-N 1.421(7) Å, ^{13}C NMR (C_6D_6, 30 °C): $\delta_{\eta^2\text{-}C=N} = 96.3$; C. L. D. Durfee, J. E. Hill, P. E. Fanwick, I. P. Rothwell, *Organometallics* **1990**, *9*, 75–80.

[9] $[\{PtCl_2(PBu_3)\}_2(\mu\text{-}\eta^1,\eta^1\text{-}t\text{Bu-dad})]$: C=N 1.27(3), C-C 1.48(2) Å; H. van der Poel, G. van Koten, K. Vrieze, M. Kokkes, C. H. Stam, *Inorg. Chim. Acta* **1980**, *39*, 197–205.

[10] a) C=N 1.267(2) Å, C-C 1.467(2) Å, N-C-C 120.1(1)°; C. J. M. Huige, A. L. Spek, J. L. de Boer, *Acta Crystallogr. Sect. C* **1985**, *41*, 113–116; b) ^{1}H NMR (300 MHz, $[D_8]$THF, 20 °C): $\delta = 7.83$ (s, 2H; N=CH), 1.20 (s, 18H, CMe_3); ^{13}C NMR (75 MHz, $[D_8]$THF, 25 °C): $\delta = 158.14$ (dd, $^1J(C,H) = 161.1$, $^2J(C,H) = 10.6$ Hz; N=CH), 58.40 (s; CMe_3), 29.72 (q, $^1J(C,H) = 125.8$ Hz; CMe_3).

[11] P. T. Beurskens, DIRDIF, Nijmegen, **1992**.

[12] G. M. Sheldrick, SHELXL 93, Göttingen, **1993**.

Zeolite Encaged Cu(Histidine) Complexes as Mimics of Natural Cu Enzymes **

Bert M. Weckhuysen,* An A. Verberckmoes, Ina P. Vannijvel, Josephina A. Pelgrims, Philip L. Buskens, Pierre A. Jacobs, and Robert A. Schoonheydt

The most abundant, active, and selective catalysts in nature are enzymes. Their operational domain is, however, relatively narrow as far as temperature and solvent are concerned. Enzyme mimicking is the building of the active center of enzymes (or an analogy of it) into a matrix which allows a larger operational temperature domain and a broader spectrum of solvents. In the case of inorganic matrices, zeolites are the obvious choice because the pore diameters and pore geometry introduce shape selectivity in the reactions. Up to now, the active center of the enzyme has been mimicked by construction of robust, rigid, and stable transition metal ion complexes in zeolite cavities and channels.[1, 2] The most prominent examples are phthalocyanine and bipyridine complexes.[3, 4] However, these complexes can only be synthesized in situ and this procedure is time-consuming. Moreover, the turnover numbers in catalytic oxidations are relatively low.

Here, we report for the first time on the immobilization of Cu(histidine) complexes in zeolites by a simple ion exchange procedure. Amino acids, like histidine, are the key building units of natural enzymes; therefore, the obtained inorganic enzyme has an active center, very close to that of its natural enzyme counterparts. In addition, the complexes are built in by a simple ion exchange procedure. Cu^{2+} was chosen as the transition metal ion, because its complexes are stable[5] and easily characterized by electron spin resonance (ESR) and diffuse reflectance spectroscopy (DRS) in the UV/VIS/NIR region.[6] Furthermore, copper proteins play a key role in both plant and animal physiology, for example hemocyanin is the oxygen-carrying protein in the hemolymph of molluscs and arthropods; ascorbate oxidase catalyzes the oxidation of L-ascorbate and galactose oxidase, which catalyzes the oxidation of galactose and many other substrates, like aliphatic and aromatic alcohols.[7–11]

Cu(histidine) complexes are typically prepared in bidistilled water with a histidine:Cu^{2+} ratio of 5:1. By using an increasing amount of preformed $[Cu(His)_2]^+$ complex at pH 7.3 in bidistilled water[12] together with a zeolite Na-Y, we have measured the amount of released Na^+, together with the amount of Cu^{2+} taken up by the zeolite material. The results are presented in Figure 1. Although there is a considerable spread of points, the data show unambiguously that ion exchange is operative. The slope of the straight line ($7Na^+/Cu^{2+}$) indicates that besides $[Cu(His)_2]^+$, His^+ is exchanged too. Chemical analysis indeed confirms that the histidine:Cu^{2+} ratio on the solid is 6:1. Thus at the low exchange levels investigated,[13] for each $[Cu(His)_2]^+$ exchanged, four His^+ cations are co-exchanged. The fact that on the average seven Na^+ ions are released and not six is indicative for charge compensation by H^+; thus some residual acidity is expected on the solids.

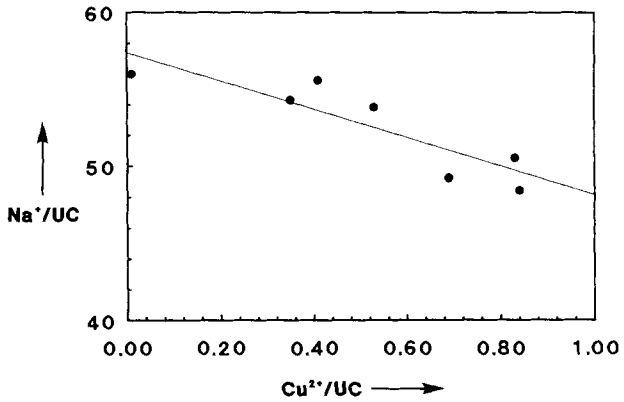

Fig. 1. The amount of released Na^+ and immobilized Cu^{2+} complex in zeolite Y for increasing concentration of Cu(histidine) complex in the ion exchange solution. UC = unit cell.

The hydrated light blue samples are characterized by an absorption band around 15600 cm^{-1} in the diffuse reflectance spectrum and a typical axially symmetric ESR spectrum with hyperfine splitting (hfs) with values for $g_\parallel$, $g_\perp$, and $A_\parallel$ of around 2.27, 2.06, and 170 G, respectively, and a seven-line superhyperfine structure (shfs) with an $A_{N\perp}$ value of 12.3 G (Fig. 2). These spectroscopic features are due to the presence of

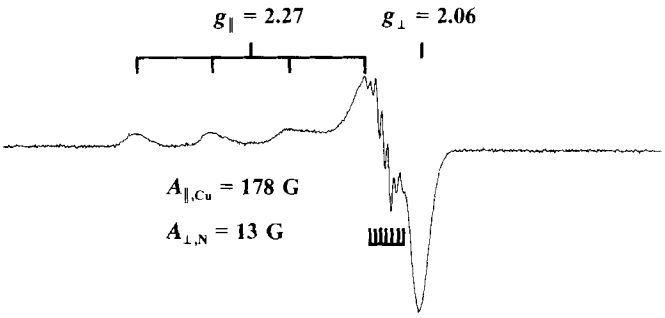

Fig. 2. ESR spectrum of a $[Cu(His)_2]^+$ complex in zeolite Y.

three nitrogen atoms ($2 \times I_N \times n_N + 1 = 7$) in the first coordination sphere of the Cu^{2+} ion. Comparable spectroscopic parameters are observed for copper proteins (e.g. galactose oxidase with an absorption at 15900 cm^{-1} and ESR parameters:[8] $g_\parallel = 2.24$; $g_\perp = 2.06$; $A_\parallel = 175$ G (hfs); $A_\perp < 0.5$ G with shfs : $A_{N\perp} = 15.1$ G) with an NNNO coordination around the Cu^{2+} ion. The intensity of the d–d absorption band in the diffuse reflectance spectrum and the amount of Cu^{2+}, as determined by quantitative ESR measurements, are given in Figure 3 for increasing Cu(histidine) loading in zeolite Y. The d–d absorption band of Cu^{2+} linearly increases with increasing Cu loading. The same holds for the intensity of the ESR signal, suggesting the presence of only one type of occluded Cu(histidine) complex. In addition, the amount of ESR-visible Cu^{2+} equals the amount determined by chemical analysis, confirming the absence of uncomplexed Cu^{2+}.

The occluded $[Cu(His)_2]^+$ can be envisaged as a complex with a Cu^{2+} center surrounded by three nitrogen atoms and one oxygen atom by ligation of two histidine molecules, one coordinating by two N ligands, the other only by one O and N atom. The fourth ligand is thus an oxygen atom of the carboxy group of histidine. A possible representation of this Cu complex is shown in Figure 4. Molecular modeling shows that the

[*] Dr. B. Weckhuysen, A. A. Verberckmoes, I. P. Vannijvel, J. A. Pelgrims, Dr. P. L. Buskens, Prof. P. A. Jacobs, Prof. R. A. Schoonheydt
Centrum voor Oppervlaktechemie en Katalyse
Katholieke Universiteit Leuven
Kardinaal Mercierlaan 92, B-3001 Heverlee (Belgium)
Telefax: Int. code +(16)32 19 98
e-mail: Bert.Weckhuysen@agr.kuleuven.ac.be

[**] This work was supported by the Belgian Government in the frame of a Interuniversity Attraction Pole (IUAP). We are indebted to N. F. W. O. (B. M. W.) and I. W. T. (A.A.V.) for fellowships as research assistants.

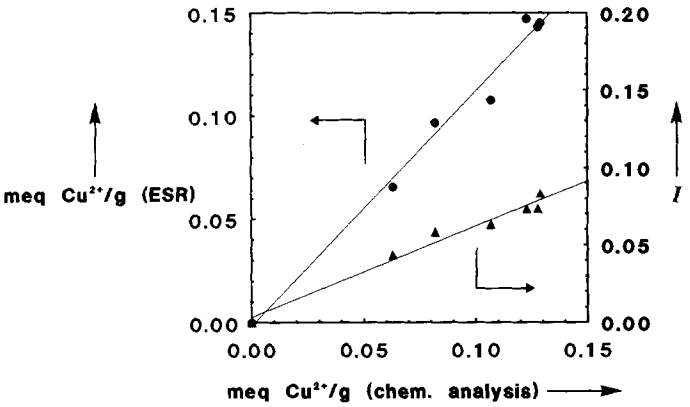

Fig. 3. Intensities of the Cu^{2+} signals in the diffuse reflectance spectrum (I) and ESR spectrum as function of the loading of the [Cu(His)] complex in zeolite Y. meq = milliequivalents.

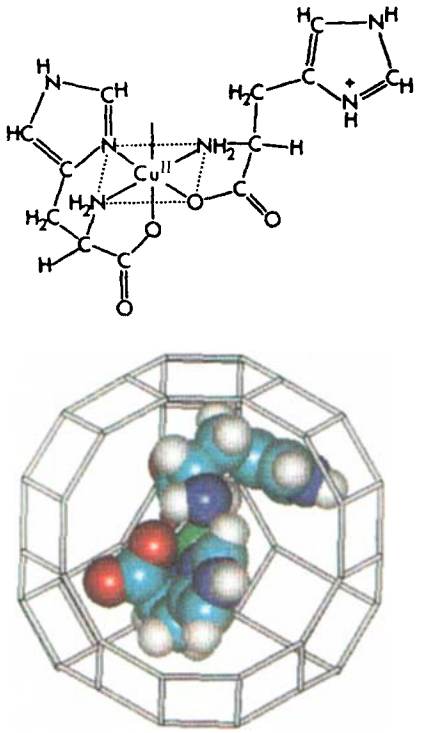

Fig. 4. Representation of $[Cu(His)_2]^+$ occluded in the supercage of zeolite Y. Top: schematic representation of the $[Cu(His)_2]^+$ complex; Bottom: space-filling molecular model, as generated by Hyperchem (light blue, carbon; black, hydrogen; green, copper; red, oxygen; dark blue, nitrogen).

$[Cu(His)_2]^+$ complex is occluded in the zeolite supercage without distortion.

Drying of the samples results in the removal of water and only a slight shift in the absorption in the diffuse reflectance spectrum (15700 cm^{-1}) and ESR parameters ($g_{\|}$, $g_{\perp}$, and $A_{\|}$ values are 2.26, 2.07, and 175 G,respectively). Furthermore, the occluded $[Cu(His)_2]^+$ complexes are thermally stable up to 100 °C. Admission of ammonia onto the sample dried at room temperature results in the formation of a $Cu(His)_2(NH_3)_x$ complex with an absorption at 16000 cm^{-1} and $g_{\|}$, $g_{\perp}$, and $A_{\|}$ values of 2.26, 2.07, and 160 G, respectively. The absence of the superhyperfine splitting in the ESR spectrum is due to a distortion of the complex. Removal of the ammonia in vacuo at 50 °C leads to the initial Cu^{2+} state and this process is totally reversible. Thus, by simple evacuation a free coordination site is produced.

The presence of such a coordination site gives catalytic potential to these materials. The oxidation of alcohols and alkenes with *tert*-butyl hydroperoxide, an environmentally friendly and cheap oxidant,[14] in the presence of $[Cu(His)_2]^+$-Y has been studied at 60 °C in batch-type reactors. The catalytic performances of $[Cu(His)_2]^+$-Y with 0.75 Cu/UC are summarized in Table 1. 1-Pentanol is oxidized to pentanoic acid with a selectivity of 100%, while the oxidation of benzyl alcohol gives both benzaldehyde and benzoic acid in a ratio of about 2:1. Similar oxidation reactions are catalyzed by galactose oxidase, which has a broad substrate specificity.[15] Excellent catalytic results were, however, obtained for the epoxidation of cyclohexene. At a turnover of 3230, the major reaction product is 1,2-cyclohexanediol. This product is formed from the hydrolysis of cyclohexenoxide, on some acid sites of zeolite Y. A minor allylic oxidation is also observed, indicative of only traces of free copper. After reaction, no free Cu ions were detected in the reaction mixture and combined DRS and ESR measurements show also that the $[Cu(His)_2]^+$ complexes were maintained inside the cages of zeolite Y. This strong encapsulation can be explained by the positive charge of the complex. Furthermore, after repeated regeneration (three times), no changes in catalytic and spectroscopic properties were observed. Thus, a new stable and selective oxidation catalyst has been designed.

Table 1. Catalytic performances of $[Cu(His)_2]$ complexes encaged in zeolite Y at 60 °C [a].

Substrate [a]	Time [h]	Conversion [%]	TON [b]	Selectivity [mol%]
1-pentanol	24	12	1425	pentanoic acid [100]
benzylalcohol	24	56	2421	benzoic acid [33], benzaldehyde [66]
cyclohexene	24	28	3230	cyclohexenoxide [9], 1,2-cyclohexanediol [89], cyclohex-2-en-1-ol [0.3] and cyclohex-2-en-1-one [1.7]

[a] 100 mmol substrate, 150 mmol *tert*-butyl hydroperoxide; no Cu leaching during reaction, as determined by AAS; no catalytic activity was observed for zeolite Y and histidine exchanged zeolite Y, while Cu/zeolite Y only decomposes the peroxide. [b] TON = turnover number.

In conclusion, we have discovered that $[Cu(His)_2]^+$ complexes can be immobilized in the cages of zeolite Y by a simple ion exchange method, which results in the formation of a typical coordination geometry frequently encountered in biological Cu proteins. The presence of a free coordination site opens the way for oxidation catalysis at relatively low temperatures in the presence of peroxides, especially olefin epoxidations and alcohol oxidations. To our knowledge, this system is the first example of immobilized transition metal ion (amino acids) complexes in zeolites. Further studies on the mechanism of the oxidations and the extension to other transition metal ions, amino acids, and inorganic oxides are in progress and should increase our understanding of these occluded complexes.

Experimental Procedure

The Cu(histidine)/Y samples were prepared starting from Na-Y from Ventron (Si:Al ratio of 2.49 and cation exchange capacity of 4.32 meq g^{-1}) after the zeolite had been put in its Na^+ form by two successive exchanges with 1 M NaCl solutions, followed by washing until free from Cl^- ions, and drying in air at room temperature overnight. The zeolites obtained were then ion exchanged with a solution of Cu(histidine) in bidistilled water at a fixed pH. After ion exchange, the samples were separated from the solution by centrifugation, washed, and dried at 60 °C overnight in air. The amounts of Na^+ and Cu^{2+} were determined by atomic absorption

spectroscopy (AAS) after dissolution of known quantities of the zeolites materials in HF/H_2SO_4. AAS measurements were performed with an Instrumentation Laboratory Inc. apparatus with a nitrous oxide/acetylene flame. Scanning electron micrographs (SEM) were obtained by using a Jeol Superprobe 733 instrument, while diffuse reflectance spectroscopy (DRS) was performed on a Varian Cary 5 UV/VIS/NIR spectrophotometer at room temperature. The diffuse reflectance spectra were recorded against a halon white reflectance standard in the range 2200–200 nm. The computer processing of the spectra consisted of the following steps: 1) subtraction of the baseline, 2) conversion to wavenumber, and 3) calculation of the Kubelka-Munk (KM) function. For ESR spectroscopy, a Bruker ESP300E spectrometer at X-band (ca. 9.5 GHz) was used. Quantitative ESR results were obtained by comparison with Cu(acetylacetonate)/KCl reference samples (spin density : 10^{16}–10^{20} $Cu^{2+}\,g^{-1}$). The molecular models were generated by the commercial software package Hyperchem™ of Autodesk.

Received: March 7, 1995
Revised version: May 3, 1995 [Z 7769 IE]
German version: *Angew. Chem.* **1995**, *107*, 2868–2870

Keywords: amino acids · catalysis · copper compounds · enzyme mimetics · zeolites

[1] W. J. Mortier, R. A. Schoonheydt, *Prog. Solid State Chem.* **1985**, *16*, 1.
[2] D. E. De Vos, P. P. Knops-Gerrits, R. F. Parton, B. M. Weckhuysen, P. A. Jacobs, R. A. Schoonheydt, *J. Inclus. Phen. Mol. Recogn. Chem.* **1995**, *21*, 185.
[3] B. V. Romanovskii, *Proc. 5th Int. Symp. Rel. Homog. Heterog. Catal.*, VNU Science Press, **1986**, p. 343; R. F. Parton, L. Uytterhoeven, P. A. Jacobs, *Stud. Surf. Sci. Catal.* **1991**, *59*, 395.
[4] W. De Wilde, J. H. Lunsford, *Inorg. Chim. Acta* **1979**, *34*, L229; K. Mizuno, J. H. Lunsford, *Inorg. Chem.* **1983**, *22*, 3484.
[5] D. R. Williams, *The Metals of Life : The Solution Chemistry of Metal Ions in Biological Systems*, Van Nostrand Reinhold Company, New York, **1971**, p.49.
[6] R. A. Schoonheydt, *Catal. Rev. Sci. Eng.* **1993**, *35* (1), 129.
[7] P. M. Colman, H. C. Freeman, J. M. Guss, M. Murata, V. A. Norris, J. A. M. Ramshaw, M. P. Venkatappa, *Nature* **1978**, *272*, 319; D. J. Cookson, M. T. Hayes, P. E. Wright, *ibid.* **1980**, *283*, 682.
[8] R. Lontie, *Copper Proteins and Copper Enzymes, Vol.1–3*, CRC Press, Boca Raton, FL, USA, **1984**.
[9] R. Lontie, R. Witters in *Inorganic Biochemistry, Vol. 1* (Ed. G. L. Eichhorn), Elsevier, Amsterdam, **1973**, p. 344.
[10] P. L. Lovett-Janison, J. M. Nelson, *J. Am. Chem. Soc.* **1940**, *62*, 1409.
[11] W. E. Blumberg, B. L. Horecker, F. Kelly-Falcoz, J. Peisach, *Biochim. Biophys. Acta* **1965**, *96*, 336.
[12] T. P. Kruck, B. Sarkar, *Can. J. Chem.* **1973**, *51*, 3563.
[13] A. Cremers in *Molecular Sieves II* (Ed.: J. R. Katzer) *A. C. S. Symp. Ser.* **1977**, *40*, 179.
[14] K. B. Sharpless, T. R. Verhoeven, *Aldrichimica Acta* **1979**, *12*, 63.
[15] P. Tressel, *PhD Thesis*, State University of New York, Buffalo, **1980**.

Self-Assembly of 1,3,5-Benzenetricarboxylic Acids (Trimesic Acids) and Several Analogues in the Solid State**

Sergei V. Kolotuchin, Edward E. Fenlon, Scott R. Wilson, Colin J. Loweth, and Steven C. Zimmerman*

The design of organic compounds that crystallize in a predictable way remains a contemporary challenge to chemists.[1] Particular attention has recently focused on the rational design of clathrates that may be useful in separations or catalysis.[2] Hydrogen bonding can be useful in this regard[3] because it is a moderately directional intermolecular interaction that may control short-range packing. Ideally, each functional group or set of groups would form a single hydrogen bonding motif. Unfortunately, however, the complex interplay of crystal packing forces makes this less likely to occur. For example, carboxylic acids are well-known to form centrosymmetric dimers (Scheme 1, **A**), but

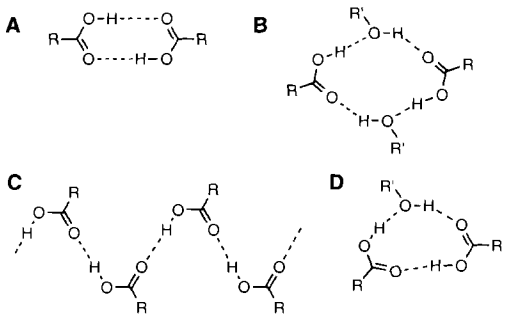

Scheme 1. Four hydrogen bonding motifs for carboxylic acids. **A**: symmetrical dimer, **B**: doubly bridged dimer, **C**: catemer, **D**: singly bridged dimer.

other motifs exist.[4] These alternate motifs are nonetheless rare and the reported high frequency of dimer formation suggests that carboxylic acids are attractive candidates for controlling short-range crystal packing.[1a]

Longer range packing might be controlled through compounds containing two or more such functional groups in a defined spatial arrangement. Two paradimatic examples of this approach to engineering hydrogen bonded networks are adamantanetetracarboxylic acid (**1**) and 1,3,5-benzenetricarboxylic acid (trimesic acid, **2**), which form diamondoid[5] and

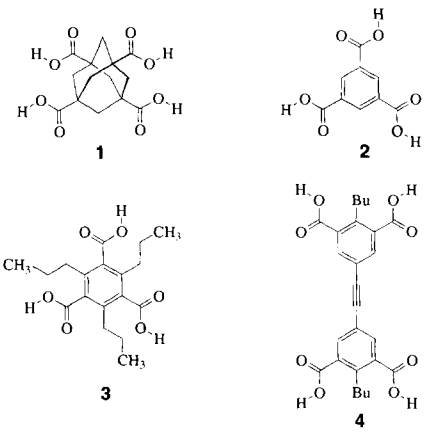

hexagonal[6] networks, respectively. However, channels or cavities are not present as a result of extensive interpenentration. In the case of **2**, the "chicken-wire" networks of trimesic acid molecules are pleated and the 14 Å holes are filled by a mutual triple catenation. Herein we describe the results from three different approaches to break the interpenetration of the trimesic acid lattice to give cavity clathrates. The results bear on the issue of whether the hydrogen bonding of carboxylic acids, and by extension, related functional groups can be used to reliably control the structure of crystals.

The first approach to break interpenetration involved crystallization of trimesic acid in the presence of a guest that might pack efficiently within the 14 Å channels. Partial success using this approach was reported by Herbstein et al. in 1987.[7] How-

[*] Prof. S. C. Zimmerman, S. V. Kolotuchin, E. E. Fenlon, Dr. S. R. Wilson, C. J. Loweth
Department of Chemistry, University of Illinois
600 S. Mathews Ave., Urbana, IL 61801 (USA)
Telefax: Int. code + (217)244-9919

[**] This work was supported by the National Institutes of Health (GM 39782).

ever, the incorporated guests such as *n*-octane and isooctane were highly disordered, and the goal to construct long channels by aligning the chicken-wire networks was not achieved. With *n*-octane and isooctane as guest molecules, the number of stacked two-dimensional networks was only two and three, respectively.

We reasoned that a larger and less flexible guest molecule (e.g. a polycyclic aromatic compound) would produce a more ordered structure(s) which would, hopefully, retain the stacked chicken-wire networks. Of the many aromatic guests tried, pyrene readily formed a cocrystal by slow evaporation from ether/ethanol that was suitable for single-crystal X-ray diffraction (Fig. 1).[8a] The lattice was found to be monoclinic with a

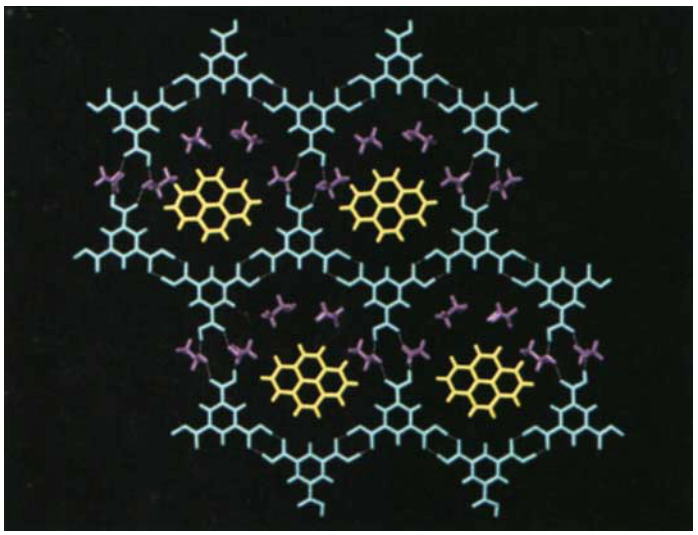

Fig. 1. Section from one layer of the crystal lattice of [2**2** · pyrene · 2 EtOH]. Light blue: **2**; yellow: pyrene; purple: EtOH.

large unit cell that contained 16 molecules of trimesic acid, 8 of pyrene, and 16 of ethanol. The structure consists of stacked layers of noninterpenetrated hydrogen bonded networks that superficially resemble the chicken-wire motif found in trimesic acid. In actuality the hydrogen bonded network is expanded. Thus, "infinite" ribbons are found wherein each trimesic acid is linked to two other trimesic acids by standard carboxylic acid dimers. The layers are formed by linking the remaining carboxylic acids with two ethanol molecules in a 12-membered hydrogen bonded ring (Scheme 1, **B**). The holes created by these "expanded" carboxylic acid dimers reside within one layer and are filled by one pyrene molecule and the ethyl groups of two ethanol molecules from an adjacent layer.

The second approach to disrupt interpenetration involved functionalizing the trimesic acid core.[9] Molecular modeling indicated that the chicken-wire networks derived from 2,4,6-tri-*n*-propyltrimesic acid (**3**) would have cylindrical holes with a diameter of approximately 6 Å. However, it remained to be seen whether the highly hindered carboxylic acids could form dimers, whether such dimers would result in hexagonal networks, and whether the layers would stack to form channels or cavities. For example, dimer formation is disfavored in 2,6-disubstituted benzoic acids.[10] The synthesis of **3** began with 1,3,5-trichlorobenzene, which was coupled with *n*-propylmagnesium bromide and [Ni(dppe)Cl_2] (dppe = ethane-1,2-diylbis(diphenylphosphane)) to give 1,3,5-tripropylbenzene in 64% yield.[11] Exhaustive bromination (62% yield) was followed by treatment with cuprous cyanide to give 2,4,6-tricyano-1,3,5-tri-*n*-propylbenzene in 80% yield. Hydrolysis to give the tricarboxylic acid occurred through the intermediacy of the triamide (80% w/w aq H_2SO_4, 155 °C), which was treated directly with sodium nitrite (95 °C) to give **3**. Compound **3** was best purified *in* the form of its trimethyl ester (CH_2N_2, 41% yield from nitrile); chromatography removed compounds containing unreacted nitrile or amide functions. The triester was converted into **3** in 64% yield by heating with a solution of hydrogen bromide in acetic acid.

Crystals of the acid were grown by slow evaporation from acetone and from aqueous ethanol, both giving the same X-ray structure (Fig. 2).[8b] All the carboxylic acid groups in the structure are nearly perpendicular to the plane of the benzene ring, yet two from each molecule form standard carboxylic acid dimers. These contacts produce an infinite ribbon similar to that found in isophthalic acid[12] and the trimesic acid inclusion complex described above. Rather than engaging in normal carboxylic acid dimers, which would produce the hexagonal networks found in trimesic acid, the third set of carboxylic acid groups form hydrogen bonded chains of type **C** (Scheme 1, Fig. 2). There is precedent for this nonstandard hydrogen bonding motif, known as the "catemer" motif, but it has been considered rare.[4] In the present structure this motif allows the third set of carboxylic acids in each stack of ribbons to be linked to those in two adjacent stacks. Close packing results with retention of the linear hydrogen bonds between the carboxylic acid groups.

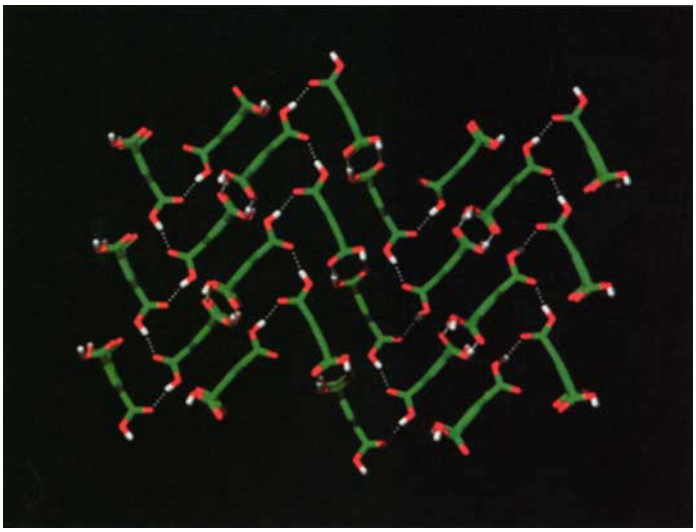

Fig. 2. View of the X-ray crystal structure of **3** along the *b* axis. The region $3a \times 2b \times 2c$ is shown. The propyl groups are removed for clarity.

The Cambridge Crystallographic Data File (CCDF, version 5.09) was searched to evaluate the number of examples containing the hydrogen bonding motifs **B**–**D** relative to those with the standard carboxylic acid dimer.[13] With the criterion that the intermolecular H···O distance in O–H···O interactions be < 2.8 Å and with an angle of > 90°,[14] 709 cases (90%) contained the standard dimer motif **A**, 31 (4%) the catemer

motif **C**, 39 (5%) the doubly bridged dimer **B**, and 9 (1%) the singly bridged dimer **D**. Although the 90% abundance of motif **A** indicates a degree of reliability, this figure is an upper limit because other packing motifs that occur were not considered. It is clear that carboxylic acid groups have a strong tendency to form centrosymmetric dimers, but several other motifs are possible.

A common feature that emerges in the structures of [2**2**·pyrene·2EtOH], **3**, and isophthalic acid[12] is the linking of benzene-1,3-dicarboxylic acid groups by carboxylic acid dimers to form ribbons. In the two structures described herein, the nonstandard carboxylic acid contacts occurred between the third carboxylic acid groups which link ribbons. This observation suggested the replacement of this putative carboxylic acid dimer by a covalent linkage that would unambigously hold the two isophthalic acid units in the desired orientation. For this reason **4** was synthesized[11] by palladium-mediated coupling of *tert*-butyl 5-bromo-2-butylbenzene-1,3-dicarboxylate and *tert*-butyl 5-ethynyl-2-butyl-benzene-1,3-dicarboxylate (30% yield) followed by deprotection with a mixture of formic and trifluoroacetic acid (90% yield).

Crystals of tetracarboxylic acid **4** were obtained by slow evaporation from tetrahydrofuran. Its structure, determined by X-ray analysis, showed the predicted hydrogen bonded network (Fig. 3),[8e] in which two layers stack with a slight offset along

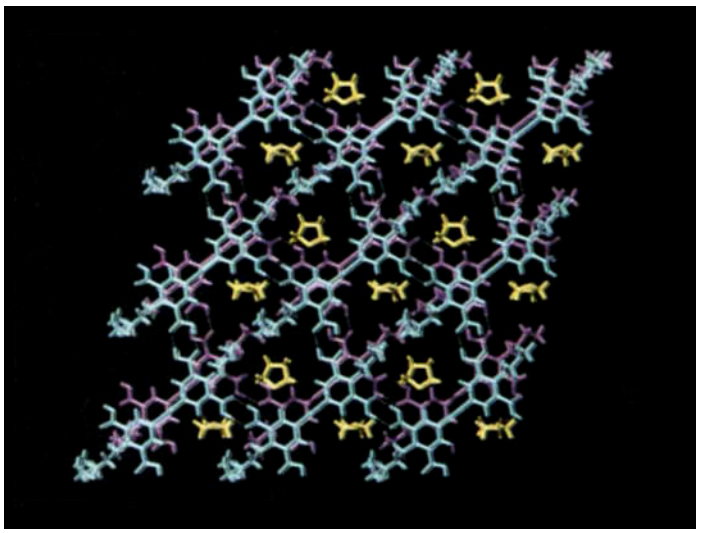

Fig. 3. View of the X-ray crystal structure of **4**·2THF along the *c* axis. The region $2a \times 2b \times 0.5c$ is shown.

the axis of the acetylene groups. Four butyl groups project into each of the resultant holes, partitioning them into two cavities, each of which is occupied by a THF molecule. The next two pairs of layers are identically stacked, but offset relative to the first pair to enclose the THF molecules in cavities. Two of the eight butyl groups of **5** in the unit cell are disordered in their methyl group positions.

The crystal packing of carboxylic acids has been studied extensively by Leiserowitz,[4] Etter,[10b] and others.[10a, 15] Our results with **2**–**4** and the CCDF searches described above indicate an even greater diversity of packing motifs for carboxylic acids, including dimers expanded by incorporation of one or two hydroxyl groups. Although there is a clear preference for formation of standard carboxylic acid dimers in the solid state, the reliability of this motif is perhaps less than previously thought. This lack of "geometrical persistence" presumably occurs because these alternative motifs allow for more favorable overall packing energies. We further suggest that nonstandard motifs are more common when the desired hydrogen bonded lattice is porous and thus in conflict with the demands of close packing. The design of **4**, which successfully crystallized as a clathrate, took into account the longer range packing preference that isophthalic acid exhibits in forming ribbons. We are currently testing the generality of this design strategy.

Received: May 13, 1995 [Z79831E]
German version: *Angew. Chem.* **1995**, *107*, 2873–2876

Keywords: carboxylic acids · clathrates · crystal engineering hydrogen bonds

[1] a) G. R. Desiraju, *Crystal Engineering*, Elsevier, New York, **1989**; b) C. B. Aakeröy, K. R. Seddon, *Chem. Soc. Rev.* **1993**, *22*, 397–407; c) J. C. MacDonald, G. M. Whitesides, *Chem. Rev.* **1994**, *94*, 2383–2420; d) M. J. Zaworotko, *Chem. Soc. Rev.* **1994**, *23*, 283–288; e) G. R. Desiraju, *Angew. Chem.* **1995**, *107*, 2541–2558; *Angew. Chem. Int. Ed. Engl.* **1995**, *107*.

[2] a) D. D. MacNicol, J. J. McKendrick, D. R. Wilson, *Chem. Soc. Rev.* **1978**, *7*, 65–87; b) H. Hart, L.-T. W. Lin, D. L. Ward, *J. Am. Chem. Soc.* **1984**, *106*, 4043–4045; c) E. Weber, W. Seichter, I. Goldberg, *Chem. Ber.* **1990**, *123*, 811–820.

[3] a) M. Simard, D. Su, J. D. Wuest, *J. Am. Chem. Soc.* **1991**, *113*, 4696–4698; b) M. R. Ghadiri, J. R. Granja, R. A. Milligan, D. E. McRee, N. Khazanovich, *Nature (London)* **1993**, *366*, 324–327; c) K. Kobayashi, K. Endo, Y. Aoyama, H. Masuda, *Tetrahedron Lett.* **1993**, 7929–7932; d) J. S. Moore, S. Lee, *Chem. Ind.* **1994**, *5*, 556–560.

[4] L. Leiserowitz, *Acta Crystallogr. Sect. B* **1976**, *32*, 775–802.

[5] O. Ermer, *J. Am. Chem. Soc.* **1988**, *110*, 3747–3754.

[6] D. J. Duchamp, R. E. Marsh, *Acta Crystallogr. Sect. B* **1969**, *25*, 5–19.

[7] F. H. Herbstein, M. Kapon, G. M. Reisner, *J. Inclusion Phenom.* **1987**, *5*, 211–214.

[8] a) [2**2**·pyrene·2EtOH]: crystal dimensions $0.2 \times 0.8 \times 0.8$ mm, monoclinic, space group $C2/c$, $Z = 40$, $a = 28.128(5)$, $b = 16.550(3)$, $c = 14.725(4)$ Å, $\beta = 95.13(2)^\circ$, $V = 6827(11)$ Å^3, $\rho_{calcd} = 1.391$ g cm^{-3}, $1.0^\circ < \theta < 25.0^\circ$, $Mo_{K\alpha}$ ($\lambda = 0.71073$ Å), 9455 reflections measured, 6003 independent, $R = 0.053$ (3425 reflections with $I > 2.58\sigma(I)$), $R_w = 0.063$. Structure solved by direct methods (SHELXS-86), 497 variables, with heavy atoms refined anisotropically. Carboxyl and hydroxyl H atoms were located and refined but appeared disordered; idealized positions used for contributions of remaining H atoms, full matrix refinement on $|F|$ (SHELX-76), residual electron density 0.56/−0.44. b) **3**: Crystal dimensions $0.65 \times 0.55 \times 0.52$ mm, orthorhombic, space group *Pnma*, $Z = 4$, $a = 7.082(2)$, $b = 16.381(4)$, $c = 15.853(3)$ Å, $V = 1839.1(8)$ Å^3, $\rho_{calcd} = 1.215$ g cm^{-3}, $3.58^\circ < \theta < 26.96^\circ$, $Mo_{K\alpha}$ ($\lambda = 0.71073$ Å), 2160 reflections measured, 2050 independent, $R1 = 0.0468$ (1599 reflections with $I > 2\sigma(I)$), $wR2 = 0.1168$. Structure solved by direct methods (SHELXS-86), 175 parameters, with heavy atoms refined anisotropically. Hydrogen atom positions, including disordered H-3 and H-4, were refined from idealized locations, full matrix refinement on $|F^2|$ (SHELX-93), residual electron density 0.295/−0.204. c) **4**: Crystal dimensions $0.45 \times 0.24 \times 0.16$ mm, triclinic, space group $P\bar{1}$, $Z = 4$, $a = 13.937(5)$, $b = 13.971(5)$, $c = 14.967(6)$ Å, $\alpha = 86.47(3)$, $\beta = 79.94(3)$, $\gamma = 76.32(3)^\circ$, $V = 2787(2)$ Å^3, $\rho_{calcd} = 1.283$ g cm^{-3}, $1.52 < \theta < 23.47^\circ$, $Mo_{K\alpha}$ ($\lambda = 0.71073$ Å), 8631 reflections measured, 8238 independent, $R = 0.0883$ (3111 reflections with $I > 2\sigma(I)$), $wR2 = 0.1844$. Structure solved by direct methods (SHELXS-86), 721 parameters, with heavy atoms refined anisotropically. C25 was disordered with relative site occupancy converging at 0.55(2). H atoms were included as fixed idealized contributors, full matrix refinement on $|F^2|$ (SHELX-93), residual electron density 0.478/−0.395. Further details of the crystal structure investigations are available on request from the Director of the Cambridge Crystallographic Data Centre, 12 Union Road, GB-Cambridge CB2 1EZ (UK), on quoting the full journal citation.

[9] Ermer and Lindenberg showed that substitution of **1** reduced the degree of interpenetration and resulted in clathration: O. Ermer, L. Lindenberg, *Helv. Chim. Acta* **1991**, *74*, 825–877.

[10] a) G. R. Desiraju, B. N. Murty, K. V. R. Kishan, *Chem. Mater.* **1990**, *2*, 447–449; b) G. M. Frankenbach, M. C. Etter, *ibid.* **1992**, *4*, 272–278.
[11] All new compounds gave correct elemental analyses and had spectral data in accord with their structures. Full details of the syntheses will be published in a full paper.
[12] J. L. Derissen *Acta Crystallogr. Sect. B* **1974**, *30*, 2764–2765.
[13] For references to encoding and decoding hydrogen bonding patterns see: M. C. Etter, *Acc. Chem. Res.* **1990**, *23*, 120–126; M. C. Etter, *J. Phys. Chem.* **1991**, *95*, 4601–4610; M. C. Etter, J. C. MacDonald, J. Bernstein, *Acta Crystallogr. Sect. B* **1990**, *46*, 256–262.
[14] For a discussion of this distance criterion see: G. A. Jeffrey, W. Saenger, *Hydrogen Bonding in Biological Structures*, Springer, Berlin, **1991**; T. Steiner, W. Saenger *Acta Crystallogr. Sect. B* **1994**, *50*, 348–357.
[15] R. S. Miller, D. Y. Curtin, I. C. Paul, *J. Am. Chem. Soc.* **1974**, *96*, 6340–6349.

Synthesis and Structure of the Nanodimensional Multicyclophane "Kuratowski Cyclophane", an Achiral Molecule with Nonplanar $K_{3,3}$ Topology**

Chao-Tsen Chen, Peter Gantzel, Jay S. Siegel,* Kim K. Baldridge,* Robin B. English, and Douglas M. Ho

As chemists strive to synthesize polycyclic molecules with nanometer dimensions, problems of molecular entwinement become more prevalent,[1] and the general task of achieving topological stereocontrol arises.[2] The synthesis of molecules having the form of Möbius ladders,[3] trefoil knots,[4] and catenanes[5] exemplify topological stereocontrol in the construction of macrocycles (Fig. 1).[6] Möbius ladders belong to a family of

Fig. 1. Topologically defined synthetic targets. Möbius ladder (left), trefoil knot (middle), catenane (right).

structures with a nonplanar graph as their topological stereoelement.[7] The stereoelement of the Möbius-[3]ladder contains two sets of three points (atoms), where each point in one set is connected to every point in the other set; this element is called $K_{3,3}$.[8, 9] In general, topological stereoelements have symmetry as well as connectivity characteristics, and in the case of the Möbius-[3]ladder, the $K_{3,3}$ element is chiral. Directed construction of an achiral $K_{3,3}$ stereoelement is unrepresented in macrocyclophane synthesis.[10, 11] To address this issue, we present the molecular design, synthesis, and structure elucidation of an achiral (D_{2d}) macrocyclophane belonging to the $K_{3,3}$ nonplanar molecular graph family.

Kuratowski cyclophane **1**,[12] a polycyclic macrocyclophane, comprises a prolate spicular core of eight benzene rings (**2**) with the flanking rings connected pairwise across the equator by four 2,7-dihydroxynaphthalene units. The $K_{3,3}$ subgraph embeds on the molecular skeleton such that the vertices of the two independent three-point sets are one terminal benzene ring and the two flanking benzene rings of the opposite terphenyl crescent (Fig. 2).[13] The maximal symmetry is D_{2d} with achiral subsymmetries of C_{2v}, S_4, and C_s.

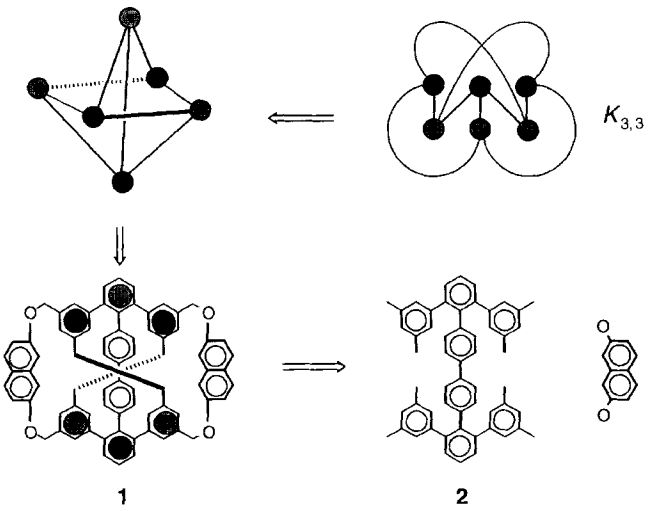

Fig. 2. Relationship between the $K_{3,3}$ graph and the structure of **1**, and dissection of **1** into its components.

The strategy for the synthesis of **1** was first to prepare the core and then perform a multifold macrocyclic ring closure to form eight bonds and four cycles in one step. The symmetric octaphenyl core could be prepared convergently from two different dissections: one divides the core into two quaterphenyl moities, whereas the other requires the capping of biphenyl with two terphenyl crescents (Fig. 3). Such *m*-terphenyl units can be

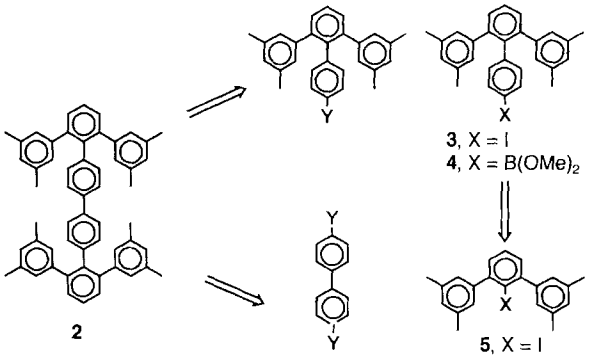

Fig. 3. Retrosynthetic analysis of the octaphenyl core **2**.

[*] Prof. J. S. Siegel, C.-T. Chen, Dr. P. Gantzel
Department of Chemistry
University of California at San Diego
La Jolla, CA 92093-0358 (USA)
Telefax: Int. code +(619) 534-5383
e-mail: jss@chem.ucsd.edu
Dr. K. K. Baldridge
San Diego Supercomputer Center
P.O. Box 85608, San Diego, CA 92186 (USA)
Telefax: Int. code +(619) 534-5149
e-mail: kimb@sdsc.edu
Prof. R. B. English (deceased)
Department of Chemistry, Rhodes University
Box 94, Grahamstown 6140 (South Africa)
Dr. D. M. Ho
Department of Chemistry, Princeton University
Princeton, NJ 08544 (USA)

[**] This work was supported by the National Science Foundation (CHE-9307582; ACS-8902827) and the Alfred P. Sloan Foundation.

readily synthesized via benzyne intermediates by the action of an excess of an aryl Grignard reagent on 1,3-dichloro-2-iodobenzene (Hart reaction).[14]

Application of the Hart reaction of 3,5-dimethylphenylmagnesium bromide with 1,3-dichloro-2-iodobenzene followed by quenching with iodine, and alternatively trimethoxyborate, gave direct access to the terphenyl crescents **3** and **4**, respectively (Scheme 1). Ullmann coupling of **3** with 4-iodonitrobenzene followed by reduction of the nitro group with iron and Sandmeyer substitution ($NH_2 \rightarrow I$) produced quaterphenyl **5**, the sample of which was partitioned in two.[15] One part was converted to the boronic acid and then coupled with the other portion (Suzuki reaction) to yield the octamethyloctaphenyl core **2** (Table 1). Alternatively, direct Suzuki coupling of **4** with 4,4′-diiodobiphenyl gave **2** in one step. Conversion of the eight methyl groups of **2** into bromomethyl groups proceeded in four steps (oxidation with permanganate/pyridine, formation of the methyl ester, reduction with lithium aluminum hydride, and bromination with phosphorus tribromide/benzene) to give **6** in 50% overall yield (Table 1). Macrocyclization of **6** with four equivalents of 2,7-dihydroxynaphthalene formed macrocyclophanes **7** and **1**, which were separated by flash chromatography, in yields of 10 and 15%, respectively (Table 1). The two products showed the same molecular weight, and number and type of ^1H and ^{13}C NMR signals, indicating that both the D_{2h} and D_{2d} modes of cyclization occurred.

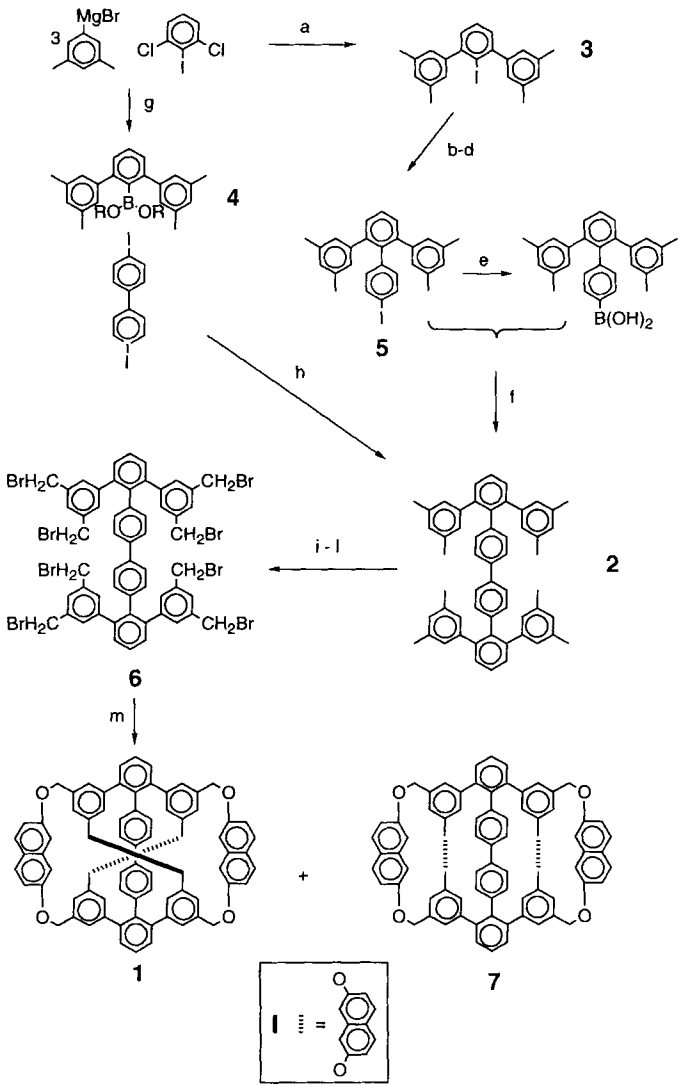

Scheme 1. a) I_2; b) 4-iodonitrobenzene, Cu(bronze); c) Fe, HCl; d) $NaNO_2$, HCl, KI/H_2O; e) BuLi, $B(OMe)_3$, 5% HCl; f) $[Pd(PPh_3)_4]$; g) $B(OMe)_3$; h) $[Pd(PPh_3)_4]$; i) $KMnO_4$, pyridine/water; j) thionyl chloride, methanol; k) $LiAlH_4$, THF, reflux; l) PBr_3, benzene (pyridine); m) 2,7-dihydroxynaphthalene, Cs_2CO_3, *N,N*-dimethylacetamide.

Table 1. Physical data for compounds **1**, **2**, **6**, and **7**.

1: M.p. >300 °C (decomp); ^1H NMR (500 MHz, $CDCl_3$): δ = 4.86 (d, J = 13 Hz, 8H), 4.93 (d, J = 8 Hz, 4H), 5.14 (d, J = 13 Hz, 8H), 5.39 (d, J = 8 Hz, 4H), 6.74 (d, J = 2 Hz, 8H), 6.89 (dd, J = 9, 2 Hz, 8H), 6.97 (br.s, 8H), 7.14 (s, 4H), 7.35–7.45 (m, 6H), 7.68 (d, J = 9 Hz, 8H); $^{13}C\{^1H\}$ NMR (125 MHz, $CDCl_3$): δ = 69.7, 106.7, 117.3, 121.5, 124.6, 125.7, 127.3, 127.5, 127.8, 129.2, 131.2, 135.9, 137.4, 138.7, 139.9, 140.6, 141.4, 141.9, 157.4; IR (KBr): $\tilde{\nu}$ = 1620, 1590, 1500, 1380, 1200 cm^{-1}; FAB-MS (low resolution): m/z: 1347, 1191, 1035, 721

2: ^1H NMR (360 MHz, $CDCl_3$): δ = 2.13 (s, 24H), 6.70 (s, 8H), 6.76 (s, 4H), 6.83 (d, J=7.9 Hz, 4H), 7.15 (d, J=7.9 Hz, 4H), 7.41 (s, 6H); $^{13}C\{^1H\}$ NMR (125 MHz, $CDCl_3$): δ = 21.1, 125.1, 127.1, 127.6, 127.9, 129.3, 131.8, 136.8, 138.0, 138.6, 138.7, 141.8, 142.0; IR(KBr): $\tilde{\nu}$ = 1600, 1570, 1500, 1450, 1060 cm^{-1}; FAB-MS (high resolution): m/z: 722.3890 (M^+, $C_{56}H_{52}$, calcd 722.39125); Anal. calcd for $C_{56}H_{52}$: C 92.77, H 7.23; found: C 91.15, H 6.99

6: M.p. >300 °C (decomp); ^1H NMR (360 MHz, $CDCl_3$): δ = 4.29 (s, 16H), 6.76 (d, J=7.9 Hz, 4H), 7.04 (d, J = 1.03 Hz, 8H), 7.15 (d, J=7.9 Hz, 4H), 7.16 (d, J = 1.03 Hz, 4H), 7.45–7.50 (m, 6H); $^{13}C\{^1H\}$ NMR (125 MHz, [D_6]benzene): δ = 32.7, 126.5, 127.7, 128.3, 129.99, 130.03, 131.8, 137.8, 138.1, 139.0, 139.2, 140.9, 143.0; IR (KBr): $\tilde{\nu}$ = 1600, 1500, 1440, 1210 cm^{-1}; FAB-MS (high resolution): m/z: 1354.98 (M^+, $C_{56}H_{42}Br_8$, calcd 1354.78)

7: M.p. >300 °C (decomp); ^1H NMR (500 MHz, $CDCl_3$): δ = 4.92 (d, J = 13 Hz, 8H), 5.01 (d, J = 13 Hz, 8H), 5.79 (d, J = 8 Hz, 4H), 6.19 (d, J = 8 Hz, 4H), 6.82 (d, J = 2 Hz, 8H), 6.85 (br.s, 8H), 7.11 (dd, J = 9, 2 Hz, 8H), 7.50 (t, J=7 Hz, 2H), 7.52 (s, 4H), 7.55 (d, J=7 Hz, 4H), 7.63 (d, J = 9 Hz, 8H); IR (KBr): $\tilde{\nu}$ = 1630, 1605, 1510, 1250 cm^{-1}; FAB-MS (low resolution): m/z: 1347

Semiempirical computations give energy-minimized structures for **7** and **1** with D_2 and S_4 symmetry, respectively.[16] The energy of **7** is 2.3 kcal mol^{-1} higher than that of **1** as gauged by the AM1 Hamiltonian. The ideal D_{2d} structure of **1** is a stationary point roughly 14 kcal mol^{-1} higher in energy than the S_4 conformation. Although the S_4 conformer is the most stable, dynamically a whole manifold of conformational minima are accessible. This dynamic behavior is responsible for the fluxional symmetry deduced from the degeneracy of the NMR signals.

Crystals of **1** and **7** were grown from benzene/hexane and subjected to X-ray diffraction analysis.[19] Diffraction data for **7** was consistent with the space group of *Pbcn* with four molecules in the unit cell. The direct-methods solution revealed **7** to be the "D_{2h}"-symmetric isomer. The data for **1** was collected assuming a $P\bar{1}$ space group with four molecules in the unit cell. A solution in line with the "D_{2d}"-symmetric isomer was proposed.[20] This solution refined to an R factor of 0.148. A disorder model using the chemically reasonable geometry from the AM1 calculations refined to a similar R factor. Neither isomer **7** nor **1** adopts its idealized symmetry in the crystal; **7** sits on a twofold axis and **1** in a C_1 general position. From the molecular geometry the structure of **1** is approximately S_4-symmetric, consistent with the calculations (Fig. 4). Each of the isomers crystallized with two benzenes of solvation per macrocyclophane included in the unit cell. In the case of **7**, the benzenes of solvation are trapped in specific clefts of the host molecule (Fig. 5) and are situated such that attractive polar/π interactions are maximized.[21] In the case of **1**, the benzenes of solvation form a herringbone channel filling the space between host molecules.[22]

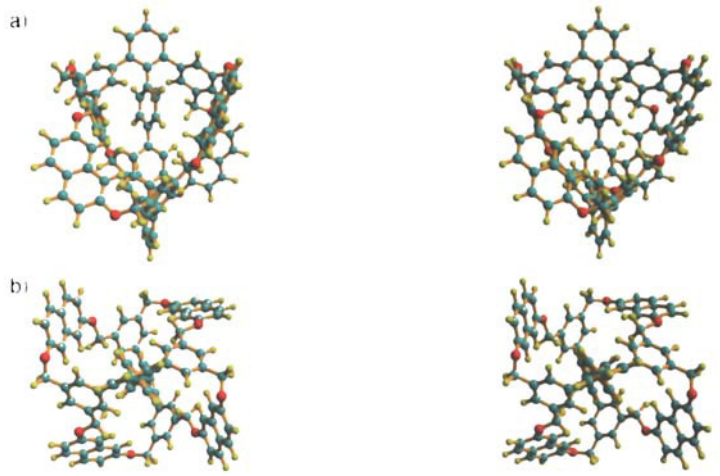

Fig. 4. Stereoview of **1** a) perpendicular to and b) down the long molecular axis (AM1 structure).

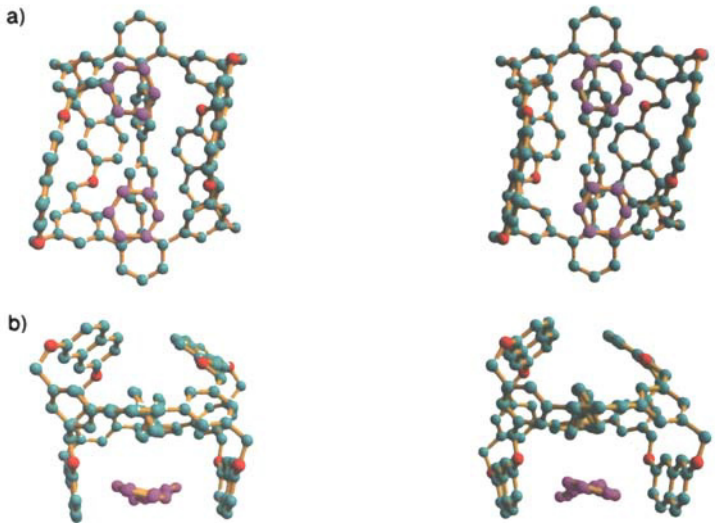

Fig. 5. Stereoview of **7** a) perpendicular to and b) down the long molecular axis (X-ray structure analysis).

The dimensions of these intricately entwined macrocyclophanes are nanometers in terms of length and kilodaltons in terms of mass, yet they can be prepared rapidly with clearly defined relative molecular masses, modeled accurately by a variety of computational algorithms, and characterized to atomic resolution by modern X-ray diffraction methods. The octaphenyl core of **1** can serve as a building block for the design of 10 kDa molecules that extend 100 Å. Thus, this study of a fundamental frontier of stereochemistry will expand to the development of molecules of novel dimensions and architectures.

Received: May 2, 1995 [Z 7962 IE]
German version: *Angew. Chem.* **1995**, *107*, 2870–2873

Keywords: cyclophanes · macrocycles · supramolecular chemistry

[1] a) J.-M. Lehn, *Pure Appl. Chem.* **1994**, *66*, 1961; b) *Angew. Chem.* **1990**, *102*, 1347; *Angew. Chem. Int. Ed. Engl.* **1990**, *29*, 1304; c) G. M. Whitesides, E. E. Simanek, J. P. Mathais, C. T. Seto, *Acc. Chem. Res.* **1995**, *28*, 37; d) G. M. Whitesides, J. P. Mathais, C. T. Seto, *Science* **1991**, *254*, 1312; e) J.-M. Lehn, *Supramolecular Chemistry*, VCH, Weinheim, **1995**; f) *NATO-ASI Ser. C* **1995**, 473.

[2] a) J.-P. Sauvage, *Acc. Chem. Res.* **1990**, *23*, 319; b) N. Van Gulick, *New J. Chem.* **1993**, *17*, 619; c) V. I. Sokolov, *Russ. Chem. Rev. (Engl. Transl.)* **1973**, *42*, 452.

[3] a) D. M. Walba, R. M. Richards, S. P. Sherwood, R. C. Haltiwanger, *J. Am. Chem. Soc.* **1981**, *103*, 6213; b) D. M. Walba, R. M. Richards, R. C. Haltiwanger, *ibid.* **1982**, *104*, 3219.

[4] a) C. O. Dietrich-Buchecker, J.-P. Sauvage, *Angew. Chem.* **1989**, *101*, 192; *Angew. Chem. Int. Ed. Engl.* **1989**, *28*, 189; b) C. O. Dietrich-Buchecker, J. Guilhem, C. Pascard, J.-P. Sauvage, *ibid.* **1990**, *102*, 1202 and **1990**, *29*, 1154; c) C. O. Dietrich-Buchecker, J.-P. Sauvage, A. de Cian, J. Fisher, *J. Chem. Soc. Chem. Commun.* **1994**, 2231.

[5] From a field replete with elegant syntheses we highlight here: a) olympiadane ([5]catenane): D. B. Amabilino, P. R. Ashton, A. S. Reder, N. Spencer, J. F. Stoddart, *Angew. Chem.* **1994**, *106*, 1316; *Angew. Chem. Int. Ed. Engl.* **1994**, *33*, 1286; b) a double interlocked [2]catenane: J.-F. Nierengarten, C. O. Dietrich-Buchecker, J.-P. Sauvage, *J. Am. Chem. Soc.* **1994**, *116*, 375; c) hydrogen bond templated [2]catenanes: C. A. Hunter, *J. Am. Chem. Soc.* **1992**, *114*, 5303; F. Vögtle, S. Meier, R. Hoss, *Angew. Chem.* **1992**, *104*, 1628; *Angew. Chem. Int. Ed. Engl.* **1992**, *31*, 1619.

[6] It is important that the reader and practitioner in the area of topological stereochemistry understand that a structure's "topology" is strongly dependent on definitions of connectivity (bonding), which in turn are dependent upon the context of the structural discussion. Indeed, in a trivial sense, crystalline sodium chloride is rich with topological networks, if each coulombic interaction is viewed as a connection. Thus, without novel structural design, chemical synthesis, and/or molecular properties as motivation, the chemical significance of such investigations loses context.

[7] D. M. Walba, *Tetrahedron* **1985**, *41*, 3161.

[8] Within mathematical graph theory there are two fundamental nonplanar graphs, the graph of five points maximally connected to one another (K_5) [9], and the graph of two sets of three points maximally cross connected ($K_{3,3}$). See: F. Harary, *Graph Theory*, Addison-Wesley, Reading, MS, USA, **1969**.

[9] For molecules described by K_5 graphs see a) chiral: H. E. Simmons, III, J. E. Maggio, *Tetrahedron Lett.* **1981**, *22*, 287; S. A. Benner, J. E. Maggio, H. E. Simmons, III, *J. Am. Chem. Soc.* **1981**, *103*, 1581; b) achiral: D. Kuck, A. Schuster, *Angew. Chem.* **1988**, *100*, 1222; *Angew. Chem. Int. Ed. Engl.* **1988**, *27*, 1192.

[10] Liang and Mislow have surveyed structures including those of coordination compounds and iron–sulfur clusters and have found alternative achiral $K_{3,3}$ molecules, which they discuss in the context of the classification of topological molecules, see: C. Liang, K. Mislow, *J. Math. Chem.* **1994**, *15*, 245.

[11] For a discussion of the complete molecular graph and its ramifications on discussions of chemical connectivity and topology. See: K. Mislow, *Bull. Soc. Chim. Belg.* **1977**, *86*, 595.

[12] Compound **1** was named after the mathematician Casimir Kuratowski, who first proved that K_5 and $K_{3,3}$ are the fundamental nonplanar graphs and that every nonplanar graph must contain one or both of these fundamental graphs. See: C. Kuratowski, *Fund. Math.* **1930**, *15*, 271.

[13] Identifying the vertices of the graph with entire benzene nuclei, as we have in Fig. 2, yields a representation that is contractible only to $K_{3,3}$. Liang and Mislow have chosen to view our structure with specific atoms as vertices; the added cyclic paths lead to a graph connectivity that can be contracted to either K_5 or $K_{3,3}$ [10]. The possibility of graphs having both K_5 and $K_{3,3}$ subgraphs is an instructive demonstration. See: R. J. Trudeau, *Dots and Lines*, Kent State University Press, **1976**, p. 91.

[14] C.-J. F. Du, H. Hart, K.-K. D. Ng, *J. Org. Chem.* **1986**, *51*, 3162.

[15] a) N. Miyaura, T. Yanagi, A. Suzuki, *Synth. Commun.* **1981**, *11*, 513; b) R. B. Miller, S. Dugar, *Organometallics* **1984**, *3*, 1261; c) M. J. Sharp, W. Cheng, V. Snieckus, *Tetrahedron Lett.* **1987**, *28*, 5093.

[16] The molecular structures considered in this work were calculated using the semiempirical numerical gradient techniques in GAMESS [17], which are based on concepts in MOPAC6.0 [18]. We have employed the AM1 [18c] Hamiltonian, which has been shown to provide reasonable structural results for compounds similar to those considered here.

[17] a) M. W. Schmidt, K. K. Baldridge, J. A. Boatz, J. H. Jensen, S. Koseki, M. S. Gordon, K. A. Nguyen, T. L. Windus, S. T. Elbert, *QCPE Bull.* **1990**, *10*, 52; b) M. W. Schmidt, K. K. Baldridge, J. A. Boatz, S. T. Elbert, M. S. Gordon, J. H. Jensen, S. Koseki, N. Matsunaga, K. A. Nguyen, S. Su, T. L. Windus, M. Dupuis, J. A. Montgomery, Jr., *J. Comput. Chem.* **1993**, *14*, 1347.

[18] a) J. J. P. Stewart, *MOPAC* 6.0 Program 455, QCPE, Bloomington, IN; b) *J. Comput.-Aided Mol. Design* **1990**, *4*, 1; c) M. J. S. Dewar, E. G. Zoebisch, E. F. Healy, J. J. P. Stewart, *J. Am. Chem. Soc.* **1985**, *107*, 3902.

[19] a) **1** ($C_{96}H_{66}O_8 \cdot 2C_6H_6$): Colorless crystal ($0.4 \times 0.4 \times 0.4$ mm); triclinic ($P\bar{1}$); $a = 20.308(8)$, $b = 20.805(2)$, $c = 23.033(5)$ Å, $\alpha = 91.25(4)$, $\beta = 93.56(3)$, $\gamma = 112.81(3)°$, $V = 8942(7)$ Å^3; $Z = 4$; $\rho_{calcd} = 1.099$ Mg m^{-3}. Data collected on a Siemens R3m diffractometer ($4.0 < 2\theta < 50.0$); unique reflections = 23360 ($R_{int} = 0.0207$), observed reflections = 10444 ($F > 4.0\sigma(F)$), parameters = 578. Solution by direct methods; $R = 0.15$ ($Rw = 0.19$); max./min. residual electron density 0.95 and -0.80 e Å^{-3}, respectively; GooF = 3.31. b) **7** ($C_{96}H_{66}O_8 \cdot 2C_6H_6$): Colorless plate ($0.12 \times 0.12 \times 0.38$ mm); orthorhombic ($Pbcn$); $a = 24.640(8)$, $b = 12.463(2)$, $c = 25.802(5)$ Å, $V = 7924(3)$ Å^3; $Z = 4$; $\rho_{calcd} = 1.261$ g cm^{-3}. Data collected on a Siemens P4 diffractometer ($4.0 < 2\theta < 50.0$); unique reflections = 7020 ($R_{int} = 0.0244$), observed reflections; 1395 ($F > 3.0\sigma(F)$), parameters = 253.

Solution by direct methods (XS:TREF); $R(R_w) = 0.0659$ (0.0649); max./min. residual electron density 0.23 and -0.25 e Å^{-3}, respectively; GooF = 0.79. c) Further details of the crystal structure investigations may be obtained from the Director of the Cambridge Crystallographic Data Centre, 12 Union Road, GB-Cambridge CB2 1EZ (UK), on quoting the full journal citation.

[20] After many attempts in many laboratories, we sent our diffraction data to George Sheldrick, Göttingen (Germany), who, using an experimental version of his direct methods software, proposed a solution that refined to an *R* factor of less than 0.20. This allowed us to develop a disordered model using computational geometries.

[21] a) M. Nishio, M. Hirota, *Tetrahedron* **1989**, *45*, 7201; b) F. Cozzi, J. S. Siegel, *Pure Appl. Chem.* **1995**, *67*, 683.

[22] For a similar solvent packing, see M. D. Radcliffe, A. Cutierrez, J. F. Blount, K. Mislow, *J. Am. Chem. Soc.* **1984**, *106*, 682.

Homeomorphic Isomerism in a Peptidic Macrobicycle**

Richard S. Wareham, Jeremy D. Kilburn,*
David L. Turner, Nicholas H. Rees,
and Duncan S. Holmes

Bicyclic molecules with sp^3-hybridized carbon bridgehead atoms exhibit an unusual form of isomerism, since such molecules can exist as *in–in* (**1**), *out-out* (**2**), or *in-out* isomers (**3** and **4**) (Scheme 1).[1] In principle, isomers (atropisomers) **1** and **2** can interconvert when one of the chains slips through the center of the ring it bridges, effectively turning the molecule inside out—a process referred to as homeomorphic isomerization.[2] A similar homeomorphic isomerization is also possible for the *in–out* isomers **3** and **4**, although these two structures are degenerate unless one of the chains is appropriately labeled, since the sense of each bridgehead is simply exchanged. Although a number of possible isomers of bicyclic systems with sp^3-hybridized carbon bridgehead atoms have been prepared,[3] interconversion of such compounds by homeomorphic isomerization has rarely been reported.[4] *In–out* homeomorphic isomerism was first observed for large bicyclic polyethers,[5] based on changes in the NMR spectra of these compounds at low temperature, and more recently *in–in* to *out–out* homeomorphic isomerism of bicyclo[6.5.1]tetradecane has been described,[3c] again based on NMR studies of the equilibrium mixture.

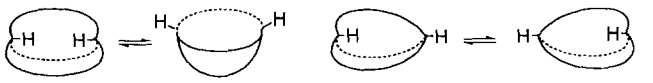

Scheme 1. Diagrammatic representation of homeomorphic isomerization.

[*] Dr. J. D. Kilburn, Dr. R. S. Wareham, Dr. D. L. Turner, Dr. N. H. Rees
Department of Chemistry, University of Southampton
Highfield, GB-Southampton, SO17 1BJ (UK)
Telefax: Int. code +(1703) 593781
e-mail: JDK1@soton.ac.uk

Dr. D. S. Holmes
Department of Biomolecular Structure
Glaxo Research and Development Ltd., Greenford (UK)

[**] We would like to thank Glaxo Research and Development and the SERC for a CASE award to R. S. W., and Dr. Graham Calder, Rowett Research Institute, Aberdeen (UK), for the amino acid analysis.

In our own work we have synthesized a series of macrobicyclic molecules, designed to serve as receptors for peptide derivatives by combining binding sites for the carboxylic acid terminus of a peptidic guest with additional amide functionalities to bind to the backbone of such a guest.[6] Thus we have reported the synthesis of the racemic C_2-symmetric (L-Glu, L-Glu) macrobicycle **5**, which was prepared along with the diastereomeric (L-Glu, D-Glu) macrobicycle **6**.[6b] Determination of the solution conformation of **5** revealed that it exists as the *out–out* isomer, with no trace of the corresponding *in–in* isomer. The diastereomeric macrobicycle **6** can be viewed as an *in–out* isomer, but homeomorphic isomerization of this compound (L-Glu-*out*,D-Glu-*in* ↔ L-Glu-*in*,D-Glu-*out*) merely leads to the mirror-image structure. In this paper we describe a related macrobicycle, which has been isolated as two distinct *in–out* atropoisomers and which, in solution in DMSO at room temperature, interconvert with a half-life of the order of several days.

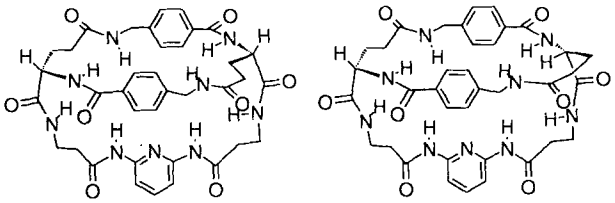

5 (L-Glu-*out*, L-Glu-*out*)

6 (L-Glu-*out*, D-Glu-*in*)

Our original studies[6b] on the solution conformation of macrobicycle **5** revealed that the amidopyridine unit is inverted and sandwiched between the aromatic units of the two other chains, in a conformation that is not predisposed to bind peptides as we had planned. In addition **5** is soluble only in polar solvents such as DMSO, which tends to preclude strong hydrogen bonding interactions in host–guest complexes. To improve the solubility of related compounds we undertook the synthesis of the closely related macrobicycle **10**, which simply required the replacement of β-alanine in the original structure **5** with the more lipophilic benzyl ester of aspartic acid. The synthesis of **10** (Scheme 2) parallels the original synthesis of **5**, and, as before, racemization of the glutamic acid centers in the course of the synthesis led to the isolation of diastereomeric macrobicycles, including the desired C_2-symmetric (L-Glu, L-Asp, L-Asp, L-Glu) macrobicycle **10** and the C_2-symmetric (D-Glu, L-Asp, L-Asp, D-Glu) macrobicycle **11**.[7]

In addition we isolated two other macrobicyclic structures, **12** and **13**, with different R_f values and whose NMR spectra (Fig. 1) indicate that they are not C_2 symmetric. On standing in a solution of DMSO at room temperature, however, both of these initially pure compounds converted over several days to a mixture of the two. Three pairs of amide proton resonances (NH_a, NH_b, and NH_c, Scheme 2) were monitored during equilibration by NMR spectra measured at 20 °C, starting from a pure sample of the minor form. The changes in the integrals of these signals over time yielded a half-life of 158 h ($k_{20} = 1.22 \times 10^{-6}$ s^{-1}) for the major component; the final ratio of isomers of 62:38 corresponds to a difference in energy of 1.16 kJ mol^{-1}. Monitoring the later stage of equilibration at 50 °C gave a half-life of 4 h ($k_{50} = 4.84 \times 10^{-5}$ s^{-1}) and an approximate activation energy of 95 kJ mol^{-1}. Subsequent amino acid analysis of the two separate compounds indicated that they were both derived from L-aspartic acid and a 50:50 mixture of

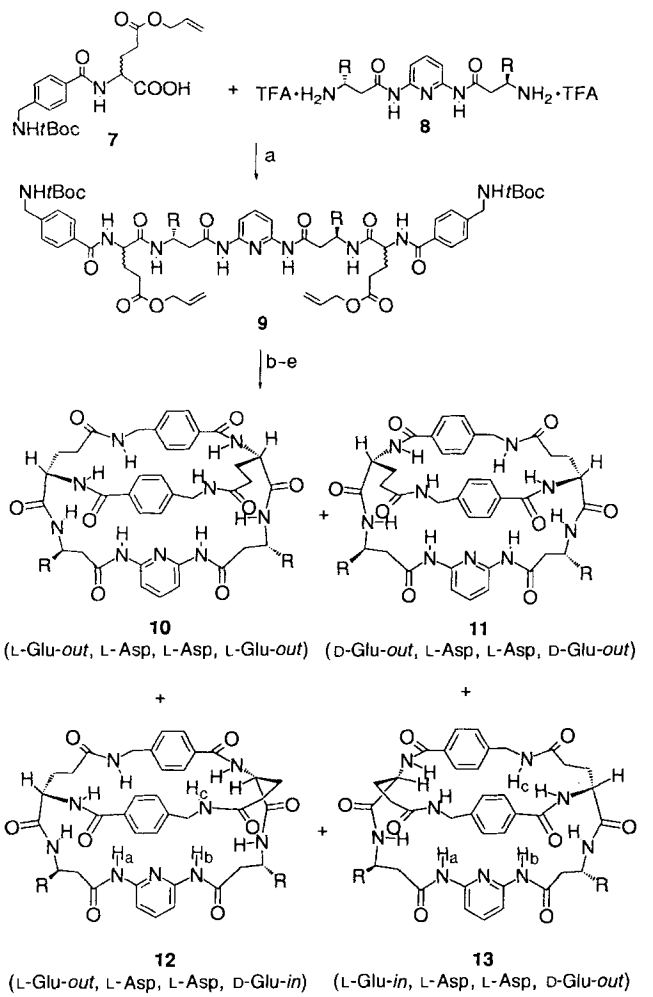

Scheme 2. Synthesis of macrobicycles **10**–**13**, R = CO_2Bn. a) PyBOP, DIPEA, DMF (57%); b) 5 mol% $[Pd(PPh_3)_4]$, 12.5 mol% Ph_3P, pyrrolidine, CH_2Cl_2 (100%); c) C_6F_5OH, DCC, THF; d) 25% TFA in CH_2Cl_2; e) syringe pump addition of bis(TFA) salt in DMF to a solution of DIPEA (6.0 equiv) in CH_3CN at 30 °C, 5 mM final concentration (30% combined yield of **10**–**13** over three steps). PyBOP = benzotriazol-1-yloxytripyrrolidinophosphonium hexafluorophosphate; DIEA = diisopropylethylamine; DCC = dicyclohexylcarbodiimide; TFA = trifluoroacetic acid.

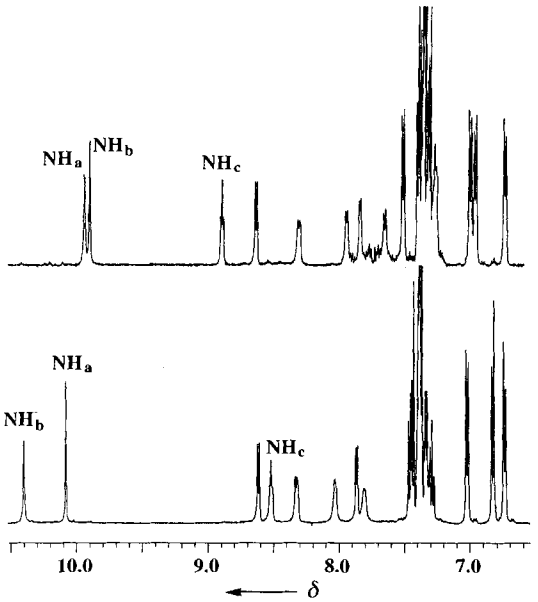

Fig. 1. 500 MHz ^1H NMR spectra of the minor (top) and major (bottom) forms of the macrobicyclic isomers **13** and **12**, respectively.

L- and D-glutamic acid.[8] Furthermore, the interproton distances across the peptide linkages (based on self-consistent distance constraints obtained from ROESY spectra of each form; vide infra) showed unequivocally that the amide bonds are all *trans* in both compounds. This rules out the possibility that the two compounds result from *cis*–*trans* configurational isomerism of one of the amide bonds. We therefore concluded that the interconversion of the two compounds is due to conformational (homeomorphic) isomerism of the two atropoisomers of the (L-Glu, L-Asp, L-Asp, D-Glu) macrobicycle, namely, the (L-Glu-*in*, L-Asp, L-Asp, D-Glu-*out*) isomer **12** and the (L-Glu-*out*, L-Asp, L-Asp, D-Glu-*in*) isomer **13**, which are distinguishable by virtue of the stereocenters in the aspartic acid residues.

Interconversion of **12** and **13** requires one of the chains to slip through the ring it bridges. To establish the most likely mechanism for this process we have determined the conformations of both **12** and **13** in DMSO solution by means of distance geometry calculations[9] with self-consistent distance constraints[10] based on the ROESY spectra. The NMR spectra of both forms were fully assigned using ROESY, TOCSY, and COSY spectra obtained at 500 MHz, as described previously.[6b] Self-consistent distance constraints were obtained from the ROESY spectra of each form by using a model with bridgehead carbons having D and L configurations but with the absolute configurations of the carbons bearing the benzyl ester substituents unspecified. Stereochemical assignment of the methylene protons in the chains with phenyl groups proved straightforward. Also, although the phenylene groups rotate rapidly in both forms, with the assumption of 180° ring flips,[6b] several crosspeaks could be assigned specifically to one side or the other of each phenylene ring. The orientation of one phenylene ring was more clearly defined than the other, indicating that it occupies a central position in the structure. The conformations obtained for the two forms (excluding the benzyl ester substituents) were well defined and almost exact mirror images, even though the limited time allowed for data acquisition (before appreciable isomerization had occurred) meant that interproton distances were defined for the minor form with an accuracy of only 0.45 nm and only 0.40 nm for the major form. The similarity between the two conformations is consistent with the similar patterns of NMR coupling constants and the observation that the chemical shifts of individual protons change by no more than 0.5 ppm between the two forms. However, the absolute configurations at the sites of benzyl ester attachment are not clear cut as a result of a lack of constraints, partially due to signal overlap. This uncertainty is not surprising in view of the small energy difference between the conformers, which implies that the ester groups are sterically unconstrained in both forms, and the absence of cross peaks to the benzyl ester methylene protons. However, the minor form (Fig. 2) fits structure **13** slightly better.

The solution conformations clearly indicate that the isomers isolated are indeed the two atropoisomers **12** and **13** of the (L-Glu, L-Asp, L-Asp, D-Glu) macrobicycle. Furthermore, whereas in the solution conformation of the *out*–*out* macrobicycle **5**[6b] the amidopyridine unit is inverted and sandwiched between the aromatic units of the two other chains, in the solution conformations of the *in*–*out* macrobicycles **12** and **13** the amidopyridine unit is folded around the outside, effectively sandwiching one of the two phenylene groups between the amidopyridine unit and the other phenylene. These conformations suggest that in a likely mechanism of isomerization the central chain, incorporating the sandwiched phenylene group, moves through the ring it bridges. The measured activation energy for interconversion (95 kJ mol^{-1}) is sufficiently high for the transition state to involve nonplanar peptide links, and ex-

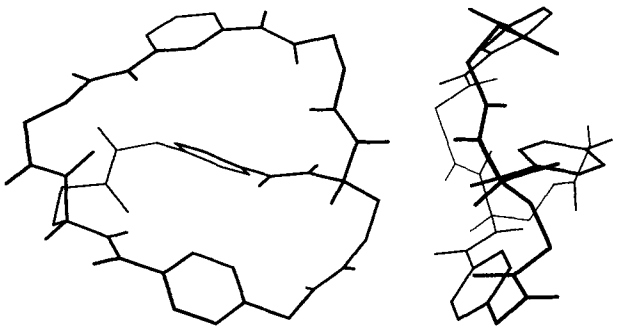

Fig. 2. Views of the solution conformation of the minor atropisomer, excluding hydrogen atoms (except NH and the two bridgehead protons) and the benzyl ester substituents. All protons were assigned except for those on the chain containing the amidopyridine unit. The distance geometry calculations included 68 upper and 60 lower limit distance constraints, none of which were violated by more than 0.5 Å. This form probably corresponds to **13** (see text).

amination of CPK models suggests that interconversion may indeed require substantial twisting of amide bonds. Examination of CPK models also indicates that the alternative mechanism, slippage of the diamidopyridine chain through the center of the structure, is sterically improbable.

In conclusion, two interconverting atropoisomers of an *in–out* bicyclic compound with sp^3-hybridized bridgehead carbon atoms have been isolated for the first time. The solution conformations of these isomers have been determined and a likely mechanism for the interconversion (homeomorphic isomerism) has been identified.

Received: June 26, 1995 [Z 8132 IE]
German version: *Angew. Chem.* **1995**, *107*, 2902–2904

Keywords: atropisomerism · isomerizations · macrocycles

[1] The *in–in/out–out* nomenclature is commonly used and is readily understood, but it is not strictly unambiguous; see refs. [4, 5b].

[2] a) C. H. Parks, H. E. Simmons, *J. Am. Chem. Soc.* **1968**, *90*, 2431; b) *ibid.* **1972**, *94*, 7184.

[3] Selected references: a) J. D. Winkler, E. A. Gretler, P. G. Willard, *J. Org. Chem.* **1993**, *58*, 1973, and references therein; b) R. S. Macomber, D. E. Rardon, T. J. Emge, *ibid.* **1992**, *57*, 433, and references therein; c) M. Saunders, N. Krause, *J. Am. Chem. Soc.* **1990**, *112*, 1791, and references therein.

[4] Bicyclic systems with nitrogen bridgehead atoms can also exhibit *in–in*, *out–out*, or *in–out* isomers, and have been studied in detail: see R. W. Alder, E. Heilbronner, E. Honegger, A. B. McEwen, R. E. Moss, E. Olefirowicz, P. A. Petillo, R. B. Sessions, G. R. Weisman, J. M. White, Z.-Z. Yang, *J. Am. Chem. Soc.* **1993**, *115*, 6580, and references therein. However, intercoversion between the various isomeric forms can occur by inversion of the nitrogen atom, which is not homeomorphic isomerism.

[5] a) B. J. Gregory, A. H. Haines, P. Karntiang, *J. Chem. Soc. Chem. Commun.* **1977**, 918; b) A. H. Haines, P. Karntiang, *J. Chem. Soc. Perkin Trans. 1* **1979**, 2577.

[6] a) G. J. Pernia, J. D. Kilburn, M. Rowley, *J. Chem. Soc. Chem. Commun.* **1995**, 305; b) R. S. Wareham, J. D. Kilburn, N. H. Rees, D. L. Turner, A. R. Leach, D. S. Holmes, *Tetrahedron Lett.* **1995**, *36*, 3047; c) C. P. Waymark, J. D. Kilburn, I. Gillies, *ibid.* **1995**, *36*, 3051.

[7] Close similarities between the 1D ^{1}H NMR and ROESY spectra of **5**, and of **10** and **11**, indicate that the latter two are also *out–out* isomers, and also probably have the pyridine inverted as described for **5**. No compounds that might correspond to the *in–in* isomers were isolated in these studies.

[8] Amino acid analysis was performed by complete hydrolysis of **12** and **13** and conversion of the resulting amino acids into their methyl ester *N*-pentafluoropropionyl derivatives. The D and L isomers were separated on a Chirasil-L-Val capillary column.

[9] P. Güntert, W. Braun, K. Wüthrich, *J. Mol. Biol.* **1991**, *217*, 517.

[10] D. L. Turner, *J. Magn. Reson.* **1994**, *A107*, 239.

Synthesis and Structure of $[Li(thf)_4]_2(Ph_2P)_{10}Cd_4]$ Containing a Dianion with a Cd_4P_{10} Adamantanoid Core**

Michael A. Beswick, Paul R. Raithby, Christopher A. Russell, Alexander Steiner, Kerry L. Verhorevoort, Gregory N. Ward, and Dominic S. Wright*

In the past twenty years there has been considerable interest in "single-source" precursors, in particular those containing elements of Groups 13 and 15 in well-defined stoichiometries, for vapor-phase deposition of semiconducting thin films such as [GaAs] and [InP].[1–3] The use of such precursors has considerable advantages over more traditional two-component deposition, for example GaAs from $[GaMe_3]$ and $[AsH_3]$, because their stoichiometry is easier to control and they are easier to purify, less toxic, and less pyrophoric. In contrast, single-source materials containing mixtures of elements from Groups 12/15 and Groups 12/16 have been studied far less extensively, despite the potential applications of these materials to a number of technologically important phases such as [CdS][4] and $[Zn_3P_2]$.[5] We have recently reported the syntheses and structures of a number of molecular zinc phosphide complexes generated from metalation of secondary phosphanes R_2PH with $ZnEt_2$.[6] These complexes, containing various Zn:P ratios, are potential single-source materials for the deposition of Zn/P phases. However, possibly owing to the lack of a commercially available organometallic source of Cd and partly as a result of the lack of a general method of synthesis, very few Cd/P complexes have been investigated. The monomer $[Cd\{P(SiPh_3)_2\}_2]$[7] and the dimer $[\{(Me_3Si)_2PCd[\mu\text{-}P(SiMe_3)_2]\}_2]$[8] are prepared by deprotonating $(R_3Si)_2PH$ (R = Ph, Me) with $[Cd\{N(SiMe_3)_2\}_2]$. These complexes, along with the trimer $[\{MeCd(\mu\text{-}PtBu_2)\}_3]$, which is prepared by the ligand transfer reaction of Me_2Cd with $[Ga(PtBu_2)_3]$,[9] are among the few simple phosphido complexes that have been structurally characterized. With respect to the lack of generality of synthetic routes to these complexes, it is noteworthy that desilylation reactions of phosphide anions result in mixed-ligand (phosphide/halide) aggregates, as is observed in the synthesis of $[Cd_4Cl_4(PPh_2)_4(PnPr_3)_2]$ from the reaction of Ph_2PSiMe_3 and $CdCl_2$ in the presence of $PnPr_3$.[10]

We report here the high-yielding synthesis of complex **1** from the nucleophilic substitution reaction of $[Cd\{N(SiMe_3)_2\}_2]$ with $[LiPPh_2]$ (mol ratio 1:2) in THF (Scheme 1). The complex con-

$[Li(thf)_4]_4[(Ph_2P)_{10}Cd_4]$ **1**

tains an adamantane-like $[(Ph_2P)_{10}Cd_4]^{2-}$ anion, the first polynuclear, organometallic, anionic cadmium phosphide to be structurally characterized. The product of the reaction of $[Cd\{N(SiMe_3)_2\}_2]$ with phosphide anions appears to be dictated by the organic groups R present in the alkali metal diorganophosphide $LiPR_2$. In contrast to the synthesis of **1**, the reaction of $[Cd\{N(SiMe_3)_2\}_2]$ with $[LiP(cy)_2]$ (cy = cyclohexyl, C_6H_{11}) results in the formation of $(cy_2P)_2$ **2**[11] as a consequence of a

[*] Dr. D. S. Wright, Dr. M. A. Beswick, Dr. P. R. Raithby, C. A. Russell, Dr. A. Steiner, K. L. Verhorevoort, G. N. Ward
University Chemical Laboratory
Lensfield Road, GB-Cambridge CB2 1EW (UK)
Telefax: Int. code +(1223) 336-362

[**] We gratefully acknowledge the EPSRC (M. A. B., P. R. R., C. A. R., K. L. V., D. S. W.), the Royal Society (D. S. W., P. R. R.), the Associated Octel Co., Ltd., Ellesmere Port, UK (D. S. W., K. L. V.), the Commitee of Vice-Chancellors and Principles (ORS award for G. N. W.), the CCT (bursary for G. N. W.) and the European Community (fellowship for A. S.) for financial support.

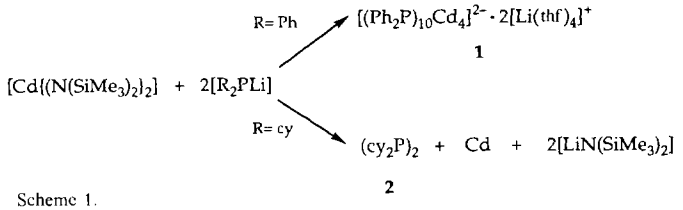

Scheme 1.

coupling reaction (see Experimental Procedure). This observation presumably reflects the relative stability of the intermediate Group 12 metal phosphide complexes initially formed and may be attributed to the lack of conjugative stabilization in the cyclohexylphosphide anion.

An X-ray crystallographic study of **1** shows that the complex is an ion-separated species (Fig. 1).[12] In addition, 5.5 molecules of THF as lattice solvent are present per asymmetric unit.

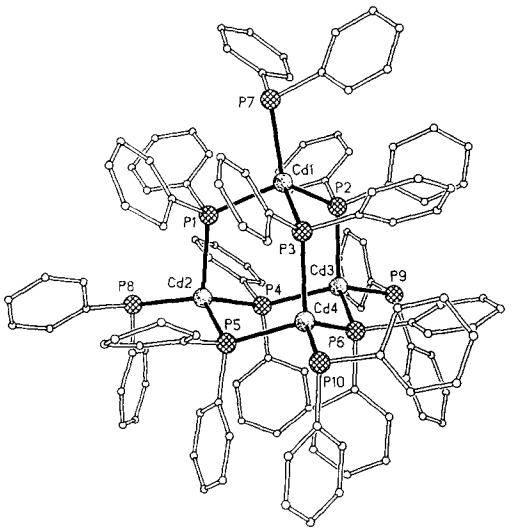

Fig. 1. Molecular structure of the dianion in **1**. Lattice-bound THF molecules and hydrogen atoms have been omitted for clarity. Selected bond lengths [Å] and angles [°]: Cd(1)-P(1) 2.647, Cd(1)-P(2) 2.646(3), Cd(1)-P(3) 2.661(3), Cd(1)-P(7) 2.596(3), Cd(2)-P(1) 2.683(3), Cd(2)-P(4) 2.684(3), Cd(2)-P(5) 2.635(3), Cd(2)-P(8) 2.624(3), Cd(3)-P(2) 2.651(3), Cd(3)-P(4) 2.649(3), Cd(3)-P(6) 2.635(3), Cd(3)-P(9) 2.604(3), Cd(4)-P(3) 2.687(3), Cd(4)-P(5) 2.674(3), Cd(4)-P(6) 2.635(3), Cd(4)-P(10) 2.612(3); P(1)-Cd(1)-P(2) 109.07(8), P(1)-Cd(1)-P(3) 99.11(8), P(1)-Cd(1)-P(7) 106.76(9), P(2)-Cd(1)-P(3) 104.53(8), P(2)-Cd(1)-P(7) 121.40(9), P(3)-Cd(1)-P(7) 113.69(9), P(1)-Cd(2)-P(4) 101.94(8), P(1)-Cd(2)-P(5) 106.52(8), P(1)-Cd(2)-P(8) 105.20(9), P(4)-Cd(2)-P(5) 106.59(8), P(4)-Cd(2)-P(8) 107.83(9), P(5)-Cd(2)-P(8) 126.24(8), P(2)-Cd(3)-P(4) 105.71(8), P(2)-Cd(3)-P(6) 106.01(8), P(2)-Cd(3)-P(9) 106.54(9), P(4)-Cd(3)-P(6) 103.62(9), P(4)-Cd(3)-P(9) 121.54(9), P(6)-Cd(3)-P(9) 112.34(10), P(3)-Cd(4)-P(5) 104.98(8), P(3)-Cd(4)-P(6) 102.72(8), P(3)-Cd(4)-P(10) 109.43(9), P(5)-Cd(4)-P(6) 103.58(8), P(5)-Cd(4)-P(10) 110.36(9), P(6)-Cd(4)-P(10) 124.07(9), Cd(1)-P(1)-Cd(2) 119.34(10), Cd(1)-P(2)-Cd(3) 115.97(9), Cd(1)-P(3)-Cd(4) 121.62(9), Cd(2)-P(4)-Cd(3) 118.48(10), Cd(2)-P(5)-Cd(4) 116.24(9), Cd(3)-P(6)-Cd(4) 119.78(10).

The $[(Ph_2P)_{10}Cd_4]^{2-}$ ion of **1** contains a Cd_4P_6 core with the adamantanoid structural motif of three interlocking six-membered rings containing μ-PPh_2 ligands. Each cadmium center is also bonded to a terminal PPh_2 phosphido moiety. The Cd-μ-P bonds are longer than those made with the terminal phosphido ligands, (av Cd-μ-P 2.66 Å, cf. 2.54 Å in $[Cd_4Cl_4(PPh_2)_4(PnPr_3)_2]$;[10] av $Cd-P_{terminal}$ 2.63 Å). Presumably as a consequence of the steric requirements of the phenyl rings, the cadmium centers have distorted tetrahedral coordination environments (μ-P-Cd-$P_{terminal}$ angles range 105.20(9)–126.24(8)°, μ-P-Cd-μ-P angles range 99.11(8)–109.43(9)°). In contrast, the Cd-P-Cd bond angles within the cage are more uniform (range 115.97(9)–121.62(9)°).

Adamantanoid cores have also been observed in the structures of a few cadmium sulfides: $(NMe_4)_2[(\mu\text{-}SC_6H_5)_6Cd_4Br_4]$,[14] $(Et_3NH)_2[(\mu\text{-}SC_6H_5)_6Cd_4(SC_6H_5)_4]$,[15] $(NEt_4)_2[(\mu\text{-}SiPr)_6Cd_4Br_4]$,[16] and $[(\mu\text{-}SiPr)_6(CdPPh_3)_2(CdOClO_3)_2]\cdot EtOH$.[17] Although $[Cd_4Cl_4(PPh_2)_4(PnPr_3)_2]$ contains a neutral adamantanoid core, **1** contains the first structurally characterized homolyptic cadmium phosphide adamantanoid fragment. The exclusion of the halide is of importance in the anion of **1** because of its potential application as a single-source precursor for semiconducting Cd/P phases.

The ^{31}P NMR spectrum of **1** in solution exhibits a single resonance at room temperature ($\delta = -41.5$). As the temperature is decreased, splitting of the signal is observed (<213 K). The low temperature required for this resolution corresponds to the low activation energy of a process such as intramolecular interconversion of the terminal and bridging PPh_2 ligands of the anion. In addition, at lower temperatures satellites are also observed, corresponding to the $^{31}P-^{111/113}Cd$ coupling of roughly 100 Hz.

In conclusion, complex **1** is a rare example of a structurally characterized organometallic cadmium phosphide, which not only has an interesting structure but is also a potential single-source precursor for the formation of a Cd/P semiconducting phase.

Experimental Procedure

1: BuLi (3.13 mL of 1.6 M solution in hexanes, 5.0 mmol; Aldrich) was added to a solution of diphenylphosphane (0.87 mL, 5.0 mmol; Strem) in 10 mL of THF. $[Cd\{N(SiMe_3)_2\}_2]$ [18] (1.0 mL, 2.5 mmol) was added to the red solution formed. The reaction mixture was stirred at room temperature for 5 min. The resulting yellow precipitate was dissolved by the addition of a further 30 mL of THF and heated to reflux. The yellow solution was allowed to stand for 12 h at room temperature, and air-sensitive, yellow crystals of **1** formed in 70% yield (1.00 g, first batch). During isolation the lattice-bound THF was removed under vacuum (10^{-2} atm, 10 min), resulting in an amorphous yellow powder, which was used in the following analyses: decomposition to a black solid above 200 °C; ^1H NMR (+25 °C, 250 MHz, 0.2 mol L^{-3}, $[D_8]$THF): $\delta = 7.41-7.26$ (overlapping multiplets, 100 H, Ph), 3.60 (m, 32 H, THF), 1.75 (m, 32 H, THF); ^{31}P NMR (+25 °C, 101.2 MHz, 0.2 mol L^{-3}, $[D_8]$THF, referenced to 85% H_3PO_4 at $\delta = 0$): $\delta = -41.5$; Anal. calcd C 63.0, H 5.7, P 10.7; found C 62.4, H 5.7, P 10.4.

2: BuLi (3.13 mL of 1.6 M solution in hexanes, 5.0 mmol; Aldrich) was added to a solution of cy_2PH (1.1 mL, 5.0 mmol; Strem) in 10 mL of THF. $[Cd\{N(SiMe_3)_2\}_2]$ [18] (1.0 mL, 2.5 mmol) was added to the yellow solution produced and the mixture was brought to reflux for 5 min. The reaction mixture was filtered (Celite, porosity 3) to produce a yellow solution. The solution was reduced in vacuo to 7 mL and 2 mL of hexane was added. Subsequent storage for 24 h at room temperature yielded air-sensitive, colorless crystals of **2** in 35% yield (0.35 g, first batch). Physical properties of **2** are in agreement with the literature data [11, 19]. M.p. 173 °C; ^1H NMR (+25 °C, 250 MHz, 0.2 mol L^{-3}, $[D_8]$THF): $\delta = 2.04-1.22$ (overlapping multiplets, 44 H, cy); ^{31}P NMR (+25 °C, 101.2 MHz, 0.2 mol L^{-3}, $[D_8]$THF, referenced to 85% H_3PO_4 at $\delta = 0$): $\delta = -22.2$ (s); Anal. calcd C 73.0, H 11.2, P 15.7; found C 72.4, H 11.0, P 15.0.

Received: August 2, 1995 [Z 8273 IE]
German version: *Angew. Chem.* **1995**, *107*, 2891–2892

Keywords: adamantanoid compounds · cadmium compounds · complexes with phosphorus ligands

[1] A. H. Cowley, R. A. Jones, *Angew. Chem.* **1989**, *101*, 1235; *Angew. Chem. Int. Ed. Engl.* **1989**, *28*, 1208.
[2] R. L. Wells, *Coord. Chem. Rev.* **1992**, 273.
[3] M. A. Paver, C. A. Russell, D. S. Wright, *Comprehensive Organometallic Chemistry, Vol. II* (Eds.: F. G. A. Stone, G. Wilkinson, E. W. Abel), Pergamon, Oxford, **1995**.
[4] M. Bochmann, K. Webb, M. Harman, M. B. Hursthouse, *Angew. Chem.* **1990**, *102*, 703; *Angew. Chem. Int. Ed. Engl.* **1990**, *29*, 638.
[5] S. C. Goel, M. Y. Chiang, D. J. Rauscher, W. E. Buhro, *J. Am. Chem. Soc.* **1990**, *112*, 5636.

 © VCH Verlagsgesellschaft mbH, D-69451 Weinheim, 1995 0570-0833/95/3423-2663 $ 10.00+.25/0

[6] M. G. Davidson, A. J. Edwards, M. A. Paver, P. R. Raithby, C. A. Russell, A. Steiner, K. L. Verhorevoort, D. S. Wright, *J. Chem. Soc. Chem. Commun.* **1995**, 1989.
[7] M. A. Matchett, M. Y. Chiang, W. E. Buhro, *Inorg. Chem.* **1994**, *33*, 1109.
[8] S. C. Goel, M. Y. Chiang, D. J. Rauscher, W. E. Buhro, *J. Am. Chem. Soc.* **1993**, *115*, 160.
[9] B. L. Benac, A. H. Cowley, R. A. Jones, C. M. Nunn, T. C. Wright, *J. Am. Chem. Soc.* **1989**, *111*, 4986.
[10] A. Eichöfer, J. Eisenmann, D. Fenske, F. Simon, *Z. Anorg. Allg. Chem.* **1993**, *619*, 1360.
[11] K. Issleib, G. Döll, *Chem. Ber.* **1963**, *96*, 1544.
[12] Crystal data for **1**: $C_{152}H_{164}Cd_4Li_2O_8P_{10}\cdot 5.5\,THF$, $M = 3288.58$, triclinic, space group $P\bar{1}$, $a = 17.261(6)$, $b = 17.996(6)$, $c = 29.470(13)$ Å, $\alpha = 88.89(3)$, $\beta = 89.14(2)$, $\gamma = 61.85(2)°$, $V = 8070(5)$ Å^3, $Z = 2$, $\rho_{calc} = 1.353$ Mgm^{-3}, $\lambda = 0.71073$ Å, $T = 153$ K, $\mu(Mo_{K\alpha}) = 0.679$ mm^{-1}. Data was collected on a Siemens-Stoe AED diffractometer using an oil-coated, rapidly cooled crystal of dimensions $0.4 \times 0.3 \times 0.3$ mm mounted directly from solution [13]; θ/ω method ($5° \le 2\theta \le 45°$). The data were corrected for absorption by a semiempirical method based upon Ψ-scan data with maximum and minimum transmission of 0.908 and 0.775, respectively. Of 21 897 reflections collected, 21 131 were independent. The structure was solved by direct methods (SHELXTL PLUS) and refined by full matrix least squares on F^2; $R1$ [$F > 4\sigma(F)$] and $wR2$ (all data) to 0.0729 and 0.1656, respectively (SHELXL-93, Göttingen, **1993**). All the non-hydrogen atoms in the anion of **1** were refined with anisotropic displacement parameters. One of the $[Li(thf)_4]^+$ cations and 3.5 of the 5.5 independent noncoordinated THF molecules are disordered on two positions, half of them on the inversion center. All five non-hydrogen atoms of each THF molecule in the unit cell were refined with the same isotropic parameters and distance restraints. Hydrogen atoms were set geometrically. Maximum and minimum residual electron density in the final difference map, 2.018 and -1.103 e Å^{-3}, respectively. Further details of the crystal structure investigation may be obtained from the Director of the Cambridge Crystallographic Data Centre, 12 Union Road, GB-Cambridge CB2 1EZ (UK), on quoting the full journal citation.
[13] T. Kottke, D. Stalke, *J. Appl. Crystallogr.* **1993**, *26*, 615.
[14] P. A. W. Dean, J. J. Vittal, N. C. Payne, *Inorg. Chem.* **1987**, *26*, 1683.
[15] J. L. Hencher, M. A. Khan, F. F. Said, D. G. Tuck, *Polyhedron* **1985**, *4*, 1263.
[16] P. A. W. Dean, J. J. Vittal, Y. Wu, *Can. J. Chem.* **1992**, *70*, 779.
[17] P. A. W. Dean, N. C. Payne, J. J. Vittal, Y. Wu, *Inorg. Chem.* **1993**, *32*, 4632.
[18] H. Bürger, W. Sawdony, U. Wannagat, *J. Organomet. Chem.* **1965**, *3*, 113.
[19] R. Richter, J. Kaiser, J. Sieler, H. Hartung, C. Peter, *Acta Crystallogr. Sect. B* **1977**, *33*, 1887.

Luminescence Stimulated by Electron Transfer: Fluorescent Donor/Acceptor-Substituted Stilbenes Containing Pyrenoid and Heteroaromatic Subunits**

Andreas Knorr and Jörg Daub*

Dedicated to Professor Paul von Ragué Schleyer on the occasion of his 65th birthday

The donor/acceptor concept has gained fundamental meaning for the chemistry and the physics of dyes because it describes both the absorption and the nonlinear optical (NLO) effects (e.g. molecular hyperpolarization) of compounds with auxochromic and antiauxochromic groups.[1] Donor and acceptor subunits not only lead to the polarization of conjugated π-electron systems, they can also participate in the exchange of electrons, resulting in the formation of radical cations and radical anions. In the broadest sense, this structural principle is responsible for the basic process of artificial and natural photosynthesis (photochemically induced charge separation)[2] and also serves as a basis for developing model compounds.[3] The energy stored in radical anion/radical cation pairs can also lead to the emission of electromagnetic radiation, a process that occurs in solution as electrochemically generated luminescence (ECL).[4] This process is at present under intensive investigation in view of the application of polymeric and oligomeric compounds in light-emitting devices.[5] We report here on specially designed donor/acceptor-substituted stilbenes. The "optoelectronic" multifunctionality of these compounds is determined by the electron transfer active donor/acceptor subunits and by the luminescent substructure. These stilbenes have been studied in detail by using electrochemical and optoelectrochemical methods to clarify the relation of electron transfer, electronic structure, and molecular structure. The long-range goal is to develop substances and materials for the conversion of electrochemical energy into photonic energy.[6]

Stilbenes **1**–**4** contain the pyrene chromophore as an acceptor group and phenothiazine, thianthrene, dibenzodioxine, or phenoxathiin building blocks as donor groups. These combined units

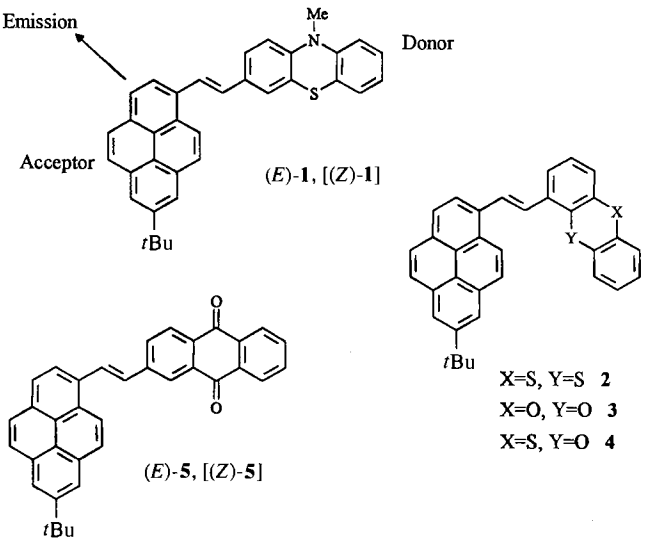

are expected to give rise to an adequate emission.[7] For comparison, pyrenyl vinyl anthraquinone **5** is included in the investigations.

Compounds **1**–**5** were synthesized by Wittig reactions of suitable precursors. The (*E*)/(*Z*) isomers were separated by conventional column chromatography on silica gel.[8]

Cyclic voltammetry shows that it is not the heterocyclic but rather the pyrene subunit that is responsible for the formation of the radical cations of **2**–**4** by oxidation; the radical cations are formed at a potential typical of pyrenes and the process is irreversible. The oxidation of the anthraquinone derivatives (*Z*)-**5** and (*E*)-**5** is also irreversible. In the case of the phenothiazine derivative **1**, the reversible oxidations observed are typical of phenothiazines. In compounds **1**–**4**, the electron transfer in the reduction region is determined by the pyrene substructure, as expected. On the other hand, the anthraquinone derivatives (*Z*)-**5** and (*E*)-**5** show three reversible reduction waves in the cyclic voltammogram: the first two electron transfers can be assigned to the anthraquinone and the third electron transfer to the pyrene (Table 1).

Generally, in all electrochemical processes of **1**–**5** one observes a shift of the $|E|$ values of the electron transfer processes to

[*] Prof. Dr. J. Daub, Dr. A. Knorr
Institut für Organische Chemie der Universität
Universitätsstrasse 31, D-93040 Regensburg (Germany)
Telefax: Int. code + (941) 943-4984
e-mail: joerg.daub@chemie.uni-regensburg.de

[**] A. K. is grateful to the Stiftung Stipendien-Fonds des Verbandes der Chemischen Industrie, Frankfurt, for a doctoral fellowship. This project was supported by the Bundesministerium für Forschung und Technologie (grant number 03N1004C6) and the Bayerische Staatsregierung (Sonderprogramm für Infrastrukturmassnahmen).

Table 1. Selected electrochemical data for compounds **1**–**5** obtained by cyclic voltammetry. FOC = ferrocene.

	E/mV vs FOC	E_{pc}	E_{pa}	$E_{1/2}$
(*Z*)-**1** [a]	Ox. 1	235	326	280
	Ox. 2	573	686	630
	Red. 1	−2339	−2241	−2290
	Red. 2	−2570	−2525, −695	–
(*E*)-**1** [a]	Ox. 1	223	287	255
	Ox. 2	569	686	625
	Red. 1	−2306	−2238	−2270
	Red. 2	−2585	−2530, −481	–
(*Z*)-**5** [a]	Ox.	546	840	–
	Red. 1	−1320	−1250	−1285
	Red. 2	−1905	−1826	−1865
	Red. 3	−2466	−2408	−2435
(*E*)-**5** [a]	Ox.	530	755	–
	Red. 1	−1297	−1236	−1265
	Red. 2	−1844	−1783	−1815
	Red. 3	−2462	−2381	−2420
2 [a]	Ox.	–	705	–
	Red. 1	−2176	−2113	−2145
	Red. 2	−2450	−2347	–
3 [a]	Ox.	595	680	–
	Red. 1	−2215	−2154	−2185
	Red. 2	−2510, −2600	−2530, −495	–
4 [a]	Ox.	605	685	–
	Red. 1	−2235	−2176	−2205
	Red. 2	−2605	−2535, −2440, −710, −505	–

[a] Half-wave potentials $E_{1/2}$ [mV] of the parent compounds: pyrene: Red. −2535, Ox. (E_{pa}) 910; *N*-methylphenothiazine: Ox. 325; 9,10-anthraquinone: Red. 1 −1320, Red. 2 −1920; thianthrene: Ox. 835; dioxine: Ox. 995; phenoxathiin: Ox. 800.

lower potentials in comparison to those of the unsubstituted electrophores. This indicates that the energy of the highest occupied molecular orbital increases and/or the energy of the lowest unoccupied molecular orbitals decreases in comparison to those of the parent structures (Table 1).

This observation is again confirmed by spectroelectrochemical studies. Reversible processes on the time scale of electrochemistry are found for the oxidation of (*E*)-**1** to its radical cation as well as for the reduction of **2**–**5** to their radical anions. In all cases both the wavelength of the absorption bands and the structure of the spectra are remarkably different from those from the spectra of the unsubstituted electrophores (Table 2). In particular, the longest wavelength absorptions of **1**–**5** are significantly red-shifted with respect to those of the unsubstituted subunits (Table 2). This indicates that the optical properties are not determined by substructures but by the whole chromophore. However, in case of (*Z*)-**5** similarities with the unsubstituted anthraquinone are apparent, indicating a localized anthraquinone/semiquinone spectrum, which can be explained by a nonplanar structure and pronounced twisting between the substructures.

Table 2. UV/Vis/NIR data of the radical ions and UV/Vis data of the neutral compounds from spectroelectrochemical experiments. Isosb. pt. = isosbestic point.

Process [a]	Neutral cmpd. λ [nm] (log ε) [b]	Radical ion λ [nm] [c]	Isosb. pt. λ [nm] [c]
SN → SN$^{\cdot+}$	/	846	331
(*E*)-**1** → (*E*)-**1**$^{\cdot+}$	398 (4.5), 358 (sh), 287 (4.4), 236 (4.6)	1115	443
An → An$^{\cdot-}$	/	980	337
(*Z*)-**5** → (*Z*)-**5**$^{\cdot-}$	425 (3.6), 343 (4.3), 327 (sh), 275 (sh), 265 (4.6), 241 (4.7)	1025	444
(*E*)-**5** → (*E*)-**5**$^{\cdot-}$	436 (4.4), 370 (4.6), 295 (sh), 278 (sh), 235 (4.8)	1111	504
P → P$^{\cdot-}$	/	1030	339
2 → **2**$^{\cdot-}$	375 (4.4), 283 (4.3), 235 (4.6)	1305	418
3 → **3**$^{\cdot-}$	375 (4.6), 286 (4.4), 233 (4.7)	1325	416
4 → **4**$^{\cdot-}$	375 (4.6), 285 (4.4), 233 (4.8)	1345	420

[a] For comparison, the data of the unsubstituted electrophores are also given: SN = *N*-methylphenothiazine, An = 9,10-anthraquinone, P = pyrene. [b] Measurements in acetonitrile; sh = shoulder; not listed in the table: (*Z*)-**1** UV/Vis: λ [nm] [log ε]: 386 (sh), 342 (4.2), 326 (sh), 274 (4.4), 267 (4.4), 242 (4.5). [c] Only the long wavelength absorptions and the isosbestic points of the radical ions are listed.

The *cis*-stilbenes (*Z*)-**1** and (*Z*)-**5** show a photochemical "one-way" isomerization:[9] irradiation of the (*Z*) compounds in solution (cyclohexane and acetonitrile) leads exclusively to the (*E*) isomers, as proven by a comparison with the spectra of the pure (*E*) isomers. In contrast, irradiation of the (*E*) isomers has no effect on the UV spectra. The spectroelectrochemical studies of these cisoid stilbenes indicate that the oxidation of (*Z*)-**1** is accompanied by a *cis*/*trans* isomerization at the stage of the radical cation. After one oxidation/reduction cycle the UV spectrum of the neutral form of (*E*)-**1** is obtained (Scheme 1). The two-step reduction/reoxidation of (*Z*)-**5** via the dianion leads to the UV spectrum of (*E*)-**5**, indicating (*Z*)/(*E*) isomerization of the dianion $\mathbf{5}^{2-}$. At the end of the spectroelectrochemical experiment, the UV absorptions of (*Z*)-**5** are found. In contrast, the radical anion of (*Z*)-**5** is configurationally stable. Thus, one can conclude that the "one-way" isomerization may be effected not only photochemically but also by both reductive and oxidative electron transfer processes.

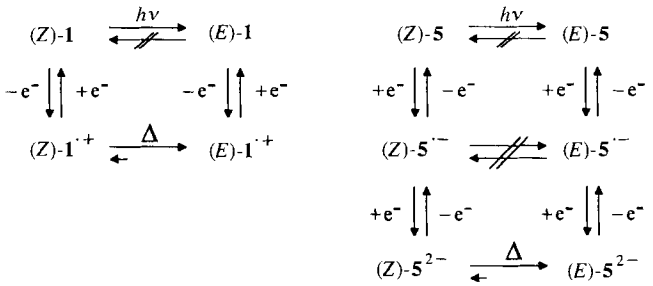

Scheme 1. Isomerization of (*Z*)-**1** and (*Z*)-**5** during irradiation and electron transfer.

In addition to the electrochemical and spectroelectrochemical behavior of these compounds, their fluorescent properties are of interest. (Experimental optical data: Table 3; for conditions see Experimental Procedure.)

Table 3. Data from emission and ECL measurements; see also Fig. 1.

λ_{em} [nm]	Emission	Excimer [a]	ECL
(*E*)-**1**	593 [b]	620	600
2	455, 555 (sh)	550	525
3	433, 447	545	510
4	439 (sh), 456, 525 (sh)	541	523

[a] The values given are approximate. [b] Uncorrected; the corrected emission maximum is located slightly above 600 nm.

In almost all of the concentration-dependent measurements made in various solvents (cyclohexane, methylene chloride, and acetonitrile) an excimer emission could be observed in addition to the normal emission band, a phenomenon not uncommon for pyrenoid compounds.[10]

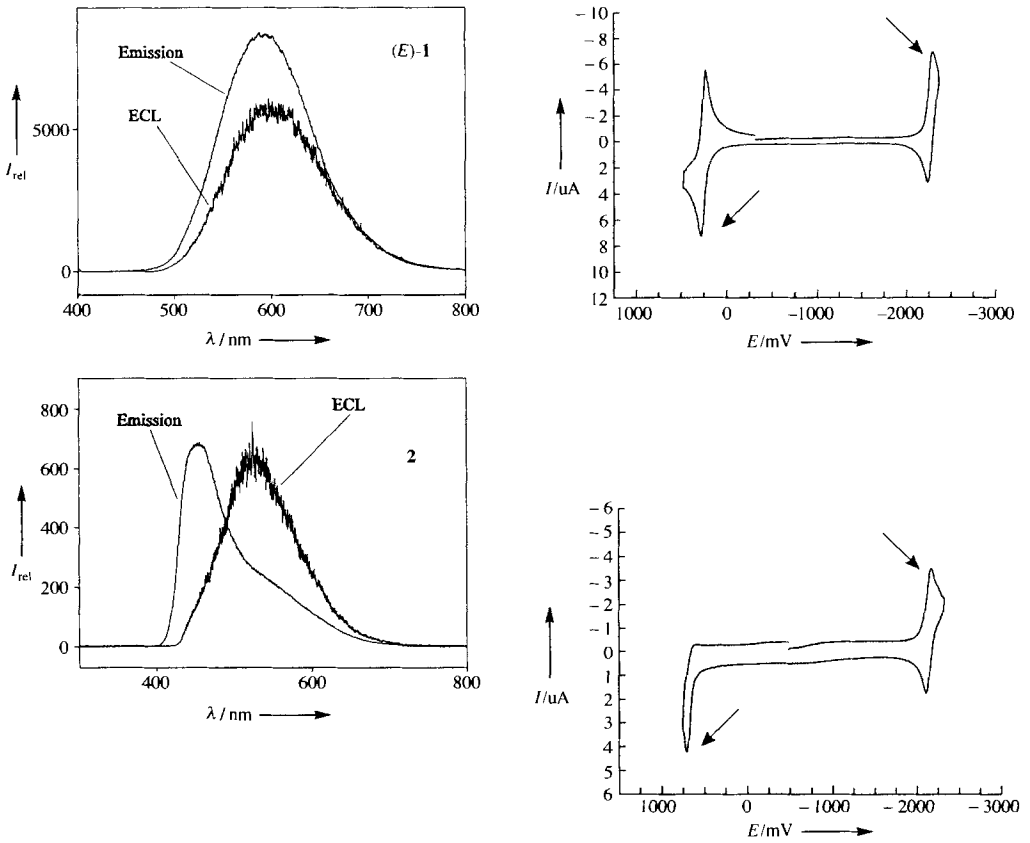

Fig. 1. Left: Comparison of the ECL and emission spectra of (*E*)-**1** and **2**; for conditions see Experimental Procedure. Right: Corresponding cyclic voltammograms with the switching potentials indicated by arrows.

It is also remarkable that in all cases except **5**, which is non-emissive in acetonitrile, the generation of radical cation/radical anion pairs electrochemically is followed by the formation of an electronically excited state and subsequent emission. However, whereas the ECL curve of (*E*)-**1** is compatible with the photoemission spectrum, this is not the case for the compounds **2**–**4**. A comparison of the electrochemical and photochemical experiments suggests that the electrochemically generated emission is essentially based on the formation of an excimer (Table 3, Fig. 1), especially since the energy brought into the system electrochemically would not be sufficient to populate directly the S_1 state of the monomeric species. Furthermore the encounter complex preceding an electron transfer is certainly structurally similar to that of an excimer.

Experimental Procedure

Cyclic voltammetry: Solvent acetonitrile; potentials in [mV] versus ferrocene (FOC); reversible half-wave potential $E_{1/2}$, anodic and cathodic peak potentials E_{pa} and E_{pc}. Experimental conditions: room temperature, scan rate: 250 mVs^{-1}, working electrode: platinum disc electrode, pseudo reference electrode: Ag/AgCl, counter electrode: platinum spiral electrode; supporting electrolyte: tetrabutylammonium hexafluorophosphate (TBAHFP).

Optical spectra: If not indicated otherwise, the emission spectra are true spectra. All measurements were carried out in acetonitrile at concentrations between 5×10^{-5} and 5×10^{-6} M, excitation wavelength: (*E*)-**1**: 398 nm; **2**–**4**: 375 nm (these excitation wavelengths were also used for recording the excimer emission). Due to low solubility only an approximate wavelength of the excimer emission can be given, since this band appears as a shoulder of the normal emission. The determination was made by means of measurements at different concentrations.

ECL: The ECL measurements were carried out with an unstirred solution ($c = 1 \times 10^{-3}$ to 1×10^{-4} M; supporting electrolyte: 0.1 M TBHFP) in an electrochemical cell specially constructed for this purpose [11]. The applied potential was switched with alternation between the oxidation and reduction potentials determined by cyclic voltammetry at time intervals of 20 ms.

Received: May 12, 1995
Revised version: August 22, 1995 [Z 7979 IE]
German version: *Angew. Chem.* **1995**, *107*, 2925–2927

Keywords: electron transfer · isomerizations · luminescence pyrenes · stilbenoids

[1] H. Zollinger, *Color Chemistry – Syntheses, Properties and Applications of Organic Dyes and Pigments*, 2nd ed., VCH, Weinheim, **1991**.
[2] Primary Events in Photosynthesis (*Isr. J. Chem.* **1992**, *32*, 369–518).
[3] M. R. Wasielewski, M. P. O'Neil, D. Gosztola, M. P. Niemczyk, W. A. Svec, *Pure Appl. Chem.* **1992**, *64*, 1319–1325; D. Gust, T. A. Moore, *Adv. Photochem.* **1991**, *16*, 1–65; L. Sung, I. von Gersdorff, D. Niethammer, P. Tian, H. Kurreck, *Angew. Chem.* **1994**, *106*, 2396–2399; *Angew. Chem. Int. Ed. Engl.* **1994**, *33*, 2318–2320.
[4] T. Kuwana, *Electroanal. Chem.* **1966**, *1*, 197–240; D. M. Hercules, *Acc. Chem. Res.* **1969**, *2*, 301–307; L. R. Faulkner, *Int. Rev. Sci. Phys. Chem. Ser. Two 1975–1976* **1975**, *9*, 213–263; F. Pragst, *Z. Chem.* **1978**, *18*, 41–50; L. R. Faulkner, A. J. Bard, *Electroanal. Chem.* **1977**, *10*, 1–95.
[5] J. H. Burroughes, D. D. C. Bradley, A. R. Brown, R. N. Marks, K. Mackay, R. H. Friend, P. L. Burns, A. B. Holmes, *Nature* **1990**, *347*, 539–541.
[6] J. Pommerehne, H. Vestweber, W. Guss, R. F. Mahrt, H. Bässler, M. Porsch, J. Daub, *Adv. Mater.* **1995**, *7*, 551–554.
[7] B. M. Krasovitskii, B. M. Bolotin, *Organic Luminescent Materials*, VCH, Weinheim, **1988**.
[8] A. Knorr, Dissertation, Universität Regensburg, **1995**.
[9] G. Bartocci, U. Mazzucato, A. Spalletti, G. Orlandi, G. Poggi, *J. Chem. Soc. Faraday Trans.* **1992**, *88*, 3139–3144; T. Arai, T. Karatsu, H. Misawa, Y. Kuriyama, H. Okamoto, T. Hiresaki, H. Furuuchi, H. Zeng, H. Sakuragi, K. Tokumaru, *Pure Appl. Chem.* **1988**, *60*, 989–998.
[10] T. Förster, *Angew. Chem.* **1969**, *81*, 364–374; *Angew. Chem. Int. Ed. Engl.* **1969**, *8*, 333; T. J. Maloy, A. J. Bard, *J. Am. Chem. Soc.* **1971**, *93*, 5968–5981.
[11] S. Hien, Dissertation, Universität Regensburg, **1995**.

 © *VCH Verlagsgesellschaft mbH, D-69451 Weinheim, 1995* *0570-0833/95/3423-2666 $ 10.00+.25/0*

Glc-PC, a New Type of Glucosidic Phospholipid**

Michael Mickeleit, Thomas Wieder, Klaus Buchner, Christoph Geilen, Johann Mulzer,* and Werner Reutter*

Dedicated to Professor Richard R. Schmidt on the occasion of his 60th birthday

Phospholipids such as phosphatidyl choline (PC) are fundamental structural components of biological membranes. In addition to their structural role, they are also important in cellular signal transduction[1] and as regulators of enzyme activity.[2] It has been known for some time that 2-*O*-alkyl and 2-*O*-acyl derivatives of 2-lysophosphatidylcholine display both cytotoxic and growth-promoting activities,[3] and this has led to the development of dermatological agents, for instance for the treatment of skin metastases.[4] Until now, it was not possible to suppress the cytotoxic effects of these compounds without decreasing their ability to inhibit cell proliferation. With the synthesis of a new type of glyceroglycophospholipid (Glc-PC **1**, Scheme 1), we have now found a solution to this problem. The starting material, (*R*)-isopropylideneglyceraldehyde (**2**),[5] was converted into the α,β-unsaturated ester **3** to better differentiate between the quasi-enantiotopic end groups. The primary advantage of this unusual "protective group" is that it minimizes steric hindrance in the later 2-glycosidation and can be removed under extremely mild conditions (ozonolysis/reduction) without the danger of a 1,3-acyl migration. After acidic hydrolysis of the acetonide ring in **3** to give the diol **4**, ester **5** was synthesized by a highly chemoselective monoacylation of the primary OH function and then converted into a mixture of anomers **7** ($\alpha:\beta = 9:1$) by treatment with glucosylfluoride **6**.[7]

Before the phosphate could be introduced as the final glycerol substituent, the olefinic unit generated early in the synthesis was oxidized to produce the aldehyde **8**, and this was reduced to the alcohol **9**. Selective reduction of **8** without endangering the stearoyl ester was achieved with zinc borohydride in ether as the reducing agent.[9] The alcohol was esterified with phosphorylchloride, and the dichloro ester was treated immediately with choline tosylate to produce the phosphocholine **10**.[10, 11]

Since the stearoyl group is labile under hydrogenolytic conditions, it was not entirely surprising that removal of the protective benzyl group presented considerable problems. After careful optimization, however, the reaction gave good yields (Scheme 1). Compound **1** was obtained in gram quantities in eight reaction steps with an overall yield of 22% (for spectroscopic data see Table 1). It should be possible to introduce many different acyl and glycosyl residues.

The biological test of cytotoxicity was performed in a serum-free cell culture system. Figure 1 B shows that Glc-PC **1** is non-

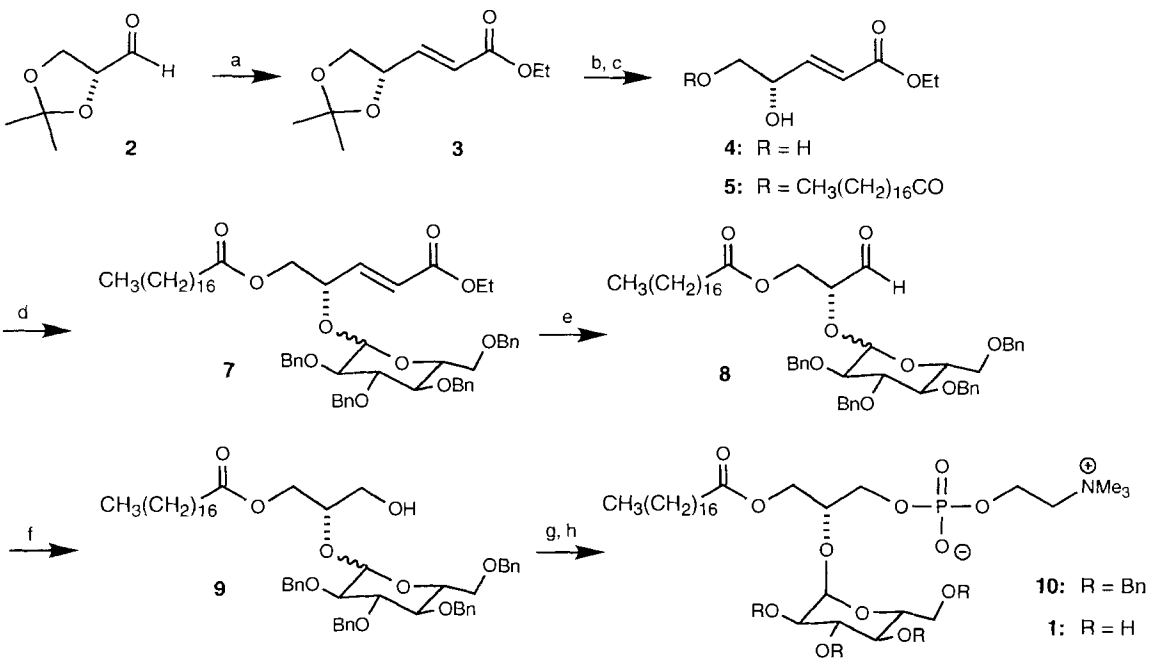

Scheme 1. Synthesis of **1** and **10**. a) Triethylphosphonoacetate, NaH, THF, −20 °C (84%); b) $AcOH/H_2O$ (60/40) (81%); c) $CH_3(CH_2)_{16}COCl$, DMAP, py, 0 °C (75%); d) 2,3,4,6-tetra-*O*-benzyl-β-D-glucopyranosylfluoride (**6**), $AgClO_4$, $SnCl_2$, 4 Å mol. sieves, Et_2O, −15 °C (89%); e) 1. O_3, CH_2Cl_2, −78 °C; 2. Ph_3P (89%); f) $Zn(BH_4)_2$, Et_2O, 0 °C (75%); g) 1. $POCl_3$, Et_3N, $CHCl_3$, 0 °C; 2. choline tosylate, py, 0 °C (67%); h) H_2 (2 atm.), Pd/C (5%), CH_3OH, 12 d (81%). DMAP = 4-(dimethylamino)pyridine, py = pyridine.

[*] Prof. Dr. J. Mulzer, Dr. M. Mickeleit
Institut für Organische Chemie der Universität
Marie-Curie-Strasse 11, D-60439 Frankfurt am Main (Germany)
Telefax: Int. code +(69) 798-29464

Prof. Dr. W. Reutter, Dr. T. Wieder, Dr. C. Geilen
Institut für Molekularbiologie und Biochemie der Freien Universität
Arnimallee 22, D-14195 Berlin-Dahlem (Germany)
Telefax: Int. code +(30) 838-2141

Dr. K. Buchner
Institut für Biochemie der Freien Universität Berlin (Germany)

[**] This research was supported by the Fonds der Chemischen Industrie and the Sonnenfeld-Stiftung.

toxic up to a concentration of 10 $\mu mol\,L^{-1}$ (cell viability >95%). The protected intermediate **10** (Bn-PC) showed only low toxicity even at 1000 $\mu mol\,L^{-1}$ (Fig. 1 A), and it inhibited cell proliferation only at relatively high concentrations, namely, greater than 100 $\mu mol\,L^{-1}$; this effect is probably due to unspecific cell damage (Fig. 1 A). In nontoxic concentrations, **1** inhibits the proliferation of HaCaT cells; thus, at 10 $\mu mol\,L^{-1}$ cell proliferation was inhibited by 80% (Fig. 1 B).

Since, as a group, various isoenzymes of protein kinase C (PKC) play an essential role in the control of cell proliferation,[12] we tested the effect of **1** on this enzyme. As already

Table 1. Selected physical properties and spectroscopic data of **10** and **1**.

10: colorless oil; $[\alpha]_D^{20} = +53.7$ ($c = 1.35$ in $CHCl_3$); ^1H NMR (500 MHz, $CDCl_3$): $\delta = 0.88$ (t, $J = 6.25$ Hz, 3H), 1.18–1.30 (m, 28H), 1.53 (m_c, 2H), 2.23 (t, $J = 6.25$ Hz, 2H), 3.18 (s, 9H), 3.44–3.54 (m, 2H), 3.56 (dd, $J = 10.0$, 3.75 Hz, 1H), 3.61–3.64 (m_c, 1H), 3.64–3.69 (dd, $J = 10.0$ Hz, 1H), 3.71–3.75 (dd, $J = 10.0$, 3.75 Hz, 1H), 3.89–3.94 (dd, $J = 10.0$ Hz, 1H), 3.96–4.03 (m, 3H), 4.09–4.14 (m, 1H), 4.14–4.21 (m, 3H), 4.30 (dd, $J = 10.0$, 3.75 Hz, 1H), 4.42–4.93 (m, 8H), 5.21 (d, $J = 3.75$ Hz, 1H), 7.12–7.40 (m, 20H); IR (KBr): $\tilde{\nu} = 2925$, 2853, 1731, 1456, 1453, 1249, 1091, 1069 cm^{-1}; MS (FAB^+): *m/z* (%): 1047 (0.7), 524 (3.2), 224 (4.8), 91 (100)

1: colorless amorphous solid; M.p. 185 °C; $[\alpha]_D^{20} = +61.3$ ($c = 1$ in CH_3OH); ^1H NMR (500 MHz, CD_3OD): $\delta = 0.90$ (t, $J = 6.25$ Hz, 3H), 1.23–1.36 (m, 28H), 1.60 (m_c, 2H), 2.36 (t, $J = 6.25$ Hz, 2H), 3.23 (s, 9H), 3.30 (m_c, 1H), 3.32 (dd, $J = 8.75$ Hz, 1H), 3.38 (dd, $J = 10.0$, 3.75 Hz, 1H), 3.59–3.65 (m, 3H), 3.67–3.78 (m, 2H), 3.97–4.04 (m, 2H), 4.08 (m_c, 1H), 4.21–4.33 (m, 4H), 5.04 (d, $J = 3.75$ Hz, 1H); IR (KBr, Pl): $\tilde{\nu} = 3387$, 2922, 1794, 1645, 1467, 1229, 1086, 1053 cm^{-1}; MS (FAB^+): *m/z* (%): 686 (8.5), 524 (4.9), 420 (4.6), 241 (5.2), 224 (19.1), 184 (74.0), 166 (20.7), 86 (54.9)

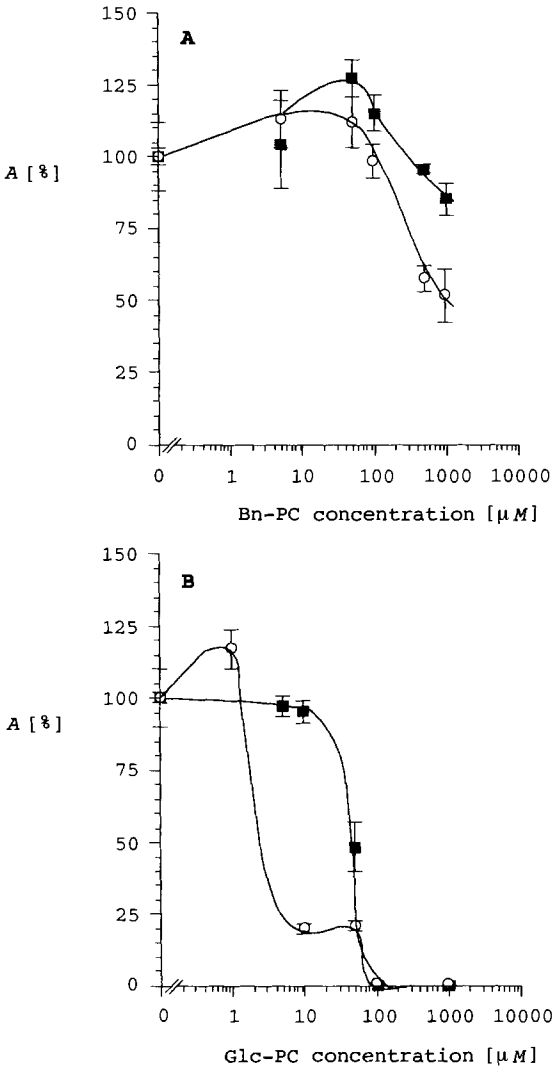

Fig. 1. Influence of **1** and **10** on the viability (■) and proliferation (○) of HaCaT cells. Confluent HaCaT cells were treated for 3 h with different concentrations of Bn-PC **10** (A) or Glc-PC **1** (B). The controls contained DMSO (A) or no further additions (B). After incubation, cell viability was determined as described in the Experimental Procedure (■). Values *A* refer to the activity [%] relative to the control experiment. HaCaT cells (20000 cells cm^{-2}) were treated for 24 h with different concentrations of **10** (A) or **1** (B). The controls contained DMSO (A) or no further additions (B). After incubation the cell count was determined by the crystal violet method (○). Values *A* refer to the activity [%] relative to the control experiment.

shown for 2-lysophosphatidylcholine,[13] the PKC activity at low concentrations of **1** was increased by up to 70%. At higher concentrations of **1** this activation decreased (Fig. 2). In contrast to 2-lysophosphatidylcholine, however, even high, toxic concentrations of **1** do not inhibit PKC activity in vitro. Compound **1** also had no effect on basal activity.[14]

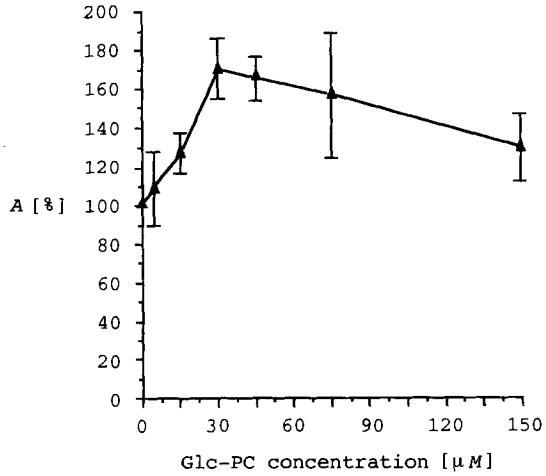

Fig. 2. Influence of **1** on the activity of protein kinase C. The activity of PKC was determined in the presence of different concentrations of Glc-PC **1** as a percentage of the activity *A* under control conditions. Up to concentrations of 100 mg L^{-1}, **1** caused an increase of PKC activity; a maximal activation of about 1.7 times the control value was observed at 20–30 mg L^{-1}. Each point is derived from the results of four to six experiments.

Compound **1** is therefore a noncytotoxic inhibitor of cell proliferation, whose inhibitory action is not mediated by protein kinase C. Further 2-glycosidic derivatives must now be synthesized to determine whether this unusual property is due to the glucoside residue.

Experimental Procedure

Cell culture: HaCaT cells [15] were maintained in liquid culture medium [16]. Confluent cells were released from the plate with 0.1% trypsin/0.02% EDTA solution, then passaged. For the duration of the experiment, the cells were kept in serum-free keratinocyte growth medium. Compound **10** was first dissolved in DMSO (85 mmol L^{-1}) then added to keratinocyte growth medium to obtain the required concentration. Compound **1** was dissolved directly in keratinocyte growth medium.

Cytotoxicity test: The cytotoxicity of **10** and **1** against HaCaT cells was determined by the trypan blue exclusion method. Confluently grown HaCaT cells were incubated for 3 h with different concentrations of the two synthesized lipids. The media were removed by aspiration, and the cells were washed with phosphate-buffered saline (PBS). Trypan blue solution (0.1% in PBS) was then added, and the blue (dead) and colorless (live) cells counted under a diavert microscope. At least 200 cells were counted for each determination. As an additional control of the cytotoxicity of **10** and **1**, the alkaline phosphatase activity of the treated HaCaT cells was determined [17].

Measurement of cell proliferation: The influence of **10** and **1** on the proliferation of HaCaT cells was determined by the crystal violet method [18]. HaCaT cells were sown at a density of about 20000 cells cm^{-2}. The cells were allowed to adhere then incubated for 24 h with different concentrations of **10** and **1**. The medium was removed by aspiration and the cells washed with PBS. Finally, cell numbers were determined after staining with 0.1% crystal violet solution [19].

Measurement of protein kinase C activity: Protein kinase C was purified from bovine brain [20]. Enzyme activity was determined in a reaction mixture (total volume 50 μL) containing 20 mM triethanolamine (pH 7.4), 4 mM magnesium acetate, 0.1 mM $CaCl_2$, 50 mM mercaptoethanol, 0.1 g L^{-1} histone III S, 50 g L^{-1} phosphatidylserine, 5 g L^{-1} diolein, and 20 mM ATP supplement with [γ-^{32}P]ATP (total radioactivity 2×10^5 cpm). Phosphatidylserine, diolein, and **1** were dissolved in methanol/chloroform (1:1). Before addition to the reaction mixture, the solvent was removed under nitrogen and the residue suspended in a suitable volume of 20 mM triethanolamine by ultrasonic treatment. The reaction was started by addition of enzyme (10–20 ng). After 2 min incubation at 30 °C, an aliquot (40 μL) of

 © VCH Verlagsgesellschaft mbH, D-69451 Weinheim, 1995 0570-0833/95/3423-2668 $ 10.00+.25/0

the reaction mixture was transferred to a Whatman P81 filter. The filter was washed three times in 0.5% phosphoric acid, and the radioactivity determined by measurement of the Cerenkov radiation in water [21, 22].

Received: June 9, 1995 [Z 8079 IE]
German version: *Angew. Chem.* **1995**, *107*, 2879–2881

Keywords: glyceraldehyde · glycosidations · phospholipids · proliferation inhibitors · protein kinase C

[1] D. E. Vance, *Biochem. Cell Biol.* **1990**, *68*, 1151–1165; J. H. Exton, *J. Biol. Chem.* **1990**, *265*, 1–4; S. H. Zeisel, *FASEB J.* **1993**, *7*, 551–557.
[2] P. C. Choy, D. E. Vance, *J. Biol. Chem.* **1978**, *253*, 5163–5167; K. Oishi, R. L. Raynor, P. A. Charp, J. F. Kuo, *ibid.* **1988**, *263*(14), 6865–6871; C. C. Geilen, T. Wieder, W. Reutter, *ibid.* **1992**, *267*, 6719–6724; M. Mosior, R. M. Epand, *Biochemistry* **1993**, *32*, 66–75; C. C. Geilen, A. Haase, T. Wieder, D. Arndt, R. Zeisig, W. Reutter, *J. Lipid Res.* **1994**, *35*, 625–632.
[3] H. U. Weltzien, O. Westphal, *Liebigs Ann. Chem.* **1967**, *709*, 240–243; R. Andreesen, M. Modolell, H. U. Weltzien, H. Eibl, H. H. Common, G. W. Lör, P. G. Munder, *Cancer Res.* **1978**, *38*, 3894–3899; W. E. Berdel, W. R. E. Bausert, V. Fink, J. Rastetter, P. G. Munder, *Anticancer Res.* **1981**, *1*, 345–352; C. C. Geilen, R. Haase, K. Buchner, T. Wieder, F. Hucho, W. Reutter, *Eur. J. Cancer* **1991**, *27*, 1650–1653.
[4] C. Unger, H. Eibl, H. W. von Heyden, M. Peukert, H. Sindermann, G. A. Nagel, *Onkologie* **1990**, *13*, 56.
[5] J. Mulzer, A. Angermann, *Tetrahedron Lett.* **1983**, *24*, 2843–2846; J. Jurczak, S. Pikul, T. Bauer, *ibid.* **1986**, *42*, 447–488; J. Mann, N. K. Partlett, A. Thomas, *J. Chem. Res.* **1987**, 369.
[6] T. Mukaiyama, Y. Murai, S. Shoda, *Chem. Lett.* **1981**, 431–432.
[7] G. H. Posner, S. H. Haines, *Tetrahedron Lett.* **1985**, *26*, 5–8.
[8] The use of benzyl protective groups is essential. The acetates, which are commonly used in sugar chemistry, give only small yields.
[9] B. C. Ranu, *Synlett* **1993**, 885–892; W. J. Gensler, F. A. Johnson, A. D. B. Sloan, *J. Am. Chem. Soc.* **1960**, *82*, 6074–6079.
[10] G. Hirth, H. Saroka, W. Bannwarth, R. Barner, *Helv. Chim. Acta* **1983**, *66*, 1210–1240.
[11] At this stage, the anomers produced in the glycosidation can be separated by HPLC ($MeOH/CH_2Cl_2$, 4:1). The final product is the pure α-anomer.
[12] M. J. Clemens, I. Trayner, J. Menaya, *J. Cell Sci.* **1992**, *103*, 881–887; Y. Nishizuka, *Science* **1992**, *258*, 607–614.
[13] K. Oishi, R. L. Raynor, P. A. Charp, J. F. Kuo, *J. Biol. Chem.* **1988**, *263*(14), 6865–6871.
[14] The basal activity was measured without addition of phosphatidylserin/diolein.
[15] P. Boukamp, R. T. Petrussevska, D. Breitkreutz, J. Hornung, A. Markham, N. E. Fusenig, *J. Cell Biol.* **1988**, *106*, 761–771.
[16] The spontaneously immortalized human keratinocyte cell line HaCaT ([14]) was kindly provided by Dr. N. E. Fusenig (DKFZ Heidelberg, Germany).
[17] J. G. Culvenor, A. W. Harris, T. E. Mandel, A. Whitelaw, E. Ferber, *J. Immunol.* **1981**, *126*, 1974–1977.
[18] R. J. Gillies, N. Didier, M. Denton, *Anal. Biochem.* **1986**, *159*, 109–113.
[19] C. C. Geilen, R. Haase, K. Buchner, T. Wieder, F. Hucho, W. Reutter, *Eur. J. Cancer* **1991**, *27*, 1650–1653.
[20] H. Krüger, W. Schröder, K. Buchner, F. Hucho, *J. Protein Chem.* **1990**, *9*, 467–473.
[21] Since the substrate is histone, the measured activity is due predominantly to the "classical" isoforms of protein kinase C (α, β, γ). The test system consists of purified components only and contains no other enzymes besides PKS. A role for Glc-PC as a prodrug with respect to 2-lysophosphatidylcholine (LPC) can thus be ruled out.
[22] M. Liyanage, D. Frith, E. Livneh, S. Stabels, *Biochem. J.* **1992**, *283*, 781–787.

A New Dimension in Radical Chain Group Transfer Reaction by Photosensitized Electron Transfer (PET) Reductive Activation of $PhSeSiR_3$**

Ganesh Pandey* and K. S. Sesha Poleshwar Rao

Dedicated to Professor U. R. Ghatak on the occasion of his 65th birthday

Despite the drawbacks[1] associated with tin hydrides, most of the recent applications of radical reactions in organic synthesis[2] are based on the use of this reagent. While alternative approaches involving the silyl radical,[3] which is a better halophile than its tin radical counterpart,[4] have partially overcome the limitations of the tin reagent, the high cost of its precursor tris(trimethylsilyl)silane (TMSS) and the loss of functionality during the last chain propagation step has limited its popularity among organic chemists. To circumvent the known limitations of these two reagents, and the necessity for a better reagent for radical chain reactions in organic synthesis, we introduce here $PhSeSiR_3$ **1**[5, 6] ($R_3 = Ph_2tBu$), which under PET (photosensitized electron transfer) reductive reaction conditions initiates radical chain group transfer reactions (Scheme 1).

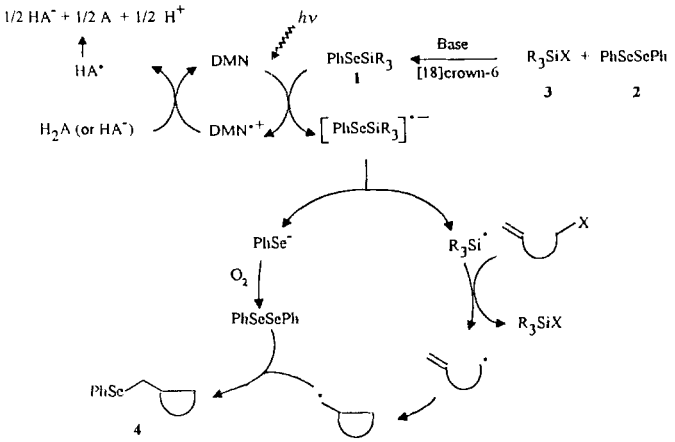

Scheme 1. Mechanism of the PET-driven reduction of **1** and the radical chain sequences. DMN = 1,5-dimethoxynaphthalene; H_2A = ascorbic acid; HA^- = ascorbate; A = dehydroascorbic acid, $PhSeSiR_3$ = $PhSeSiPh_2tBu$.

The potential of **1** to initiate the radical chain sequences shown in Scheme 1 was envisaged by considering the expected dissociation of the radical anion $\mathbf{1}^{\bullet-}$ into the silyl radical, useful for chain initiation, and PhSeSePh (**2**). The latter was formed after the oxidative dimerization of the corresponding $PhSe^-$ anion and participates in the termination step.[7] The generation of $\mathbf{1}^{\bullet-}$ was envisioned through one-electron PET reductive processes involving 1,5-dimethoxynaphthalene (DMN) as a light harvesting (> 300 nm) electron donor and ascorbic acid (H_2A) as co-reductant.[8] The thermodynamic feasibility of electron

[*] Dr. G. Pandey, K. S. S. P. Rao
Division of Organic Chemistry (Synthesis)
National Chemical Laboratory
Pune 411 008 (India)
Telefax: Int. code +(212) 330233
e-mail: pandey@ncl.ernet.in

[**] This work was supported by the Department of Atomic Energy (Dr. K. S. Krishnan Fellowship to K. S. S. P. R.) and partly by the Department of Science and Technology, New Delhi. We are grateful to Dr. K. Vijay Mohan and M. P. Vinod for measuring reduction potentials of **1** and H_2A.

transfer (ET) between DMN* and **1** was established by estimating the ΔG_{et} value ($-210\ kJ\,mol^{-1}$)[13] by using the Weller equation.[9, 10] Further evidence for the ET phenomenon between DMN* and **1** was obtained by evaluating the rate constant of the diffusion-controlled ($1.09\times10^{10}\ M^{-1}s^{-1}$) fluorescence quenching ($\lambda_{exc}=300$ nm, $\lambda_{em}=344$ nm) of DMN at varying concentrations of **1**. Ground state association between **1** and DMN was ruled out since the absorption spectroscopic properties did not change. The exciplex emission was not detected either in polar or in nonpolar solvents and therefore the charge-transfer (CT) stabilized intermediate between ^{1}DMN* and **1** could be implicated to explain the observed photophysical observations. Similarly, the feasibility of ET between $DMN^{\cdot+}$ and H_2A was evaluated by estimating the Gibbs free energy change ($\Delta G_{et}=-18\ kJ\,mol^{-1}$).[12, 13] The transformation of the ascorbate ion (HA^-) to the dehydroascorbic acid (A) and a proton shown in Scheme 1 is known.[14]

Preparative photolysis (>300 nm, light absorbed by DMN only) of a mixture of DMN (0.1 mmol), **1** (0.3 mmol), and H_2A (0.3 mmol) in CH_3CN, without the removal of the dissolved oxygen, led to the rapid disappearance ($\phi_{disapp}=0.0423$)[15] of **1** and the formation of **2** and the disilane $(R_3Si)_2$. DMN remained quantitatively unchanged after the reaction. The formation of these products was rationalized by implicating heterolytic cleavage of the primary product $\mathbf{1}^{\cdot-}$ and subsequent dimerization of the resultant phenylselenyl anion and silyl radical species.

The correlation between the observed photophysical processes and the photochemical cleavage of **1** could be quantified by a double reciprocal plot (ϕ^{-1} vs. $[Q]^{-1}$) of ϕ_{disapp} and the concentration of DMN. Within the limits of experimental error this plot showed a linear relationship and gave an identical $Kq\tau$ value ($0.993\times10^{10}\ M^{-1}s^{-1}$, intercept/slope) to that obtained from fluorescence quenching measurements ($1.023\times10^{10}\ M^{-1}s^{-1}$). The limiting quantum yield ($\phi_{lim}=1$/intercept) was also estimated to be 0.034.

The efficient generation of $R_3Si^{\cdot}$ and **2** by the cleavage of $\mathbf{1}^{\cdot-}$ provided us with an unique opportunity to use **1** for radical chain initiation and group transfer reactions. These expectations were confirmed by the smooth cyclization of **5** to **6** (81% yield) by photolyzing **5** in the presence of DMN, H_2A, and **1** for 7 h. Additional reactions reveal the efficiency and generality of the method (Table 1, Scheme 2). The regio- and stereochemistry of the cyclization products (Table 1) are in accord with standard Beckwith rules.[16] Radical chain processes could be initiated with both -C-Cl (**7a**, **11a**, **15**) and -C-Br compounds; however, the rate of the reaction with -C-Br compounds was slightly higher. Photolysis under conditions where **1** absorbed light (254 nm) failed to initiate radical chain reactions; a very complicated uncharacterizable reaction mixture ensued.

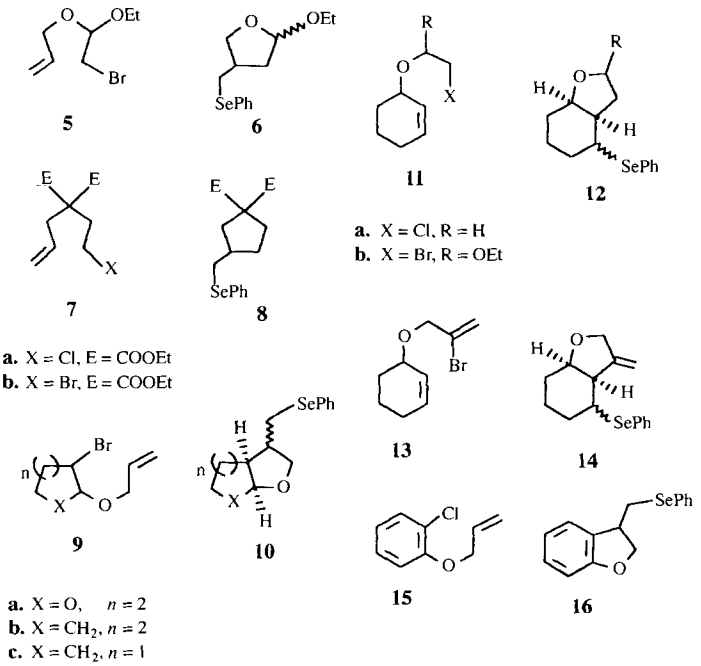

Scheme 2. Formulae of the compounds given in Table 1.

The conceptually new strategy for radical chain group transfer reactions presented here circumvents the limitations of earlier methodologies. Further applications of this approach for intermolecular reactions are in progress and the results will be disclosed in a full paper.

Table 1. Radical chain group transfer reactions.

Substrate [a]	Product(s) [b, c]	*cis/trans* ratio [d]	Yield [%] [e]	*exo/endo* ratio [d]
5	**6**	16/84	81	–
7a	**8a**	–	68	95/5
7b	**8b**	–	77	94/6
9a	**10a**	73/27	87	94/6
9b	**10b**	81/19	82	95/5
9c	**10c**	82/18	77	–
11a	**12a**	77/23	72	97/3
11b	**12b**	88/12	84	–
13	**14**	–	63	–
15	**16**	–	55	–

[a] Irradiated until 70% consumption of substrates. [b] Characterized by ^{1}H and ^{13}C NMR spectroscopy and mass spectrometry. [c] Irradiation time varies from 7–12 h. [d] Ratios measured by using ^{1}H NMR and HPLC analysis. [e] Yields not optimized: calculated based on consumption of substrates.

Experimental Procedure

A solution of **5** (0.261 g, 1.25 mmol), **1** (0.55 g, 1.4 mmol), DMN (0.094 g, 0.5 mmol), and H_2A (0.246 g, 1.4 mmol) in CH_3CN (250 mL) was irradiated, without removing dissolved oxygen from the solution, with a Pyrex-jacketed 450 W Hanovia medium-pressure mercury vapor lamp at room temperature. The progress of the reaction was monitored by HPLC analysis. After irradiation for 7 h (consumption of **5**, 70%), the photolysis was stopped and the solvent was removed under reduced pressure. The crude photolysate was chromatographed on silica gel to afford **6** (0.201 g) in 81% yield as a pale yellow liquid. DMN was recovered (99%) as such. The product **6** was characterized by ^{1}H and ^{13}C NMR spectroscopy and mass spectrometry.

Received: April 25, 1995
Revised version: August 28, 1995 [Z 7930 IE]
German version: *Angew. Chem.* **1995**, *107*, 2934–2935

Keywords: electron transfer · naphthalene derivatives · photochemistry · radicals · selenium compounds

[1] S. Z. Zard, J. Boivin, J. Camara, *J. Am. Chem. Soc.* **1992**, *114*, 7909–7910, and references therein.
[2] A. L. J. Beckwith, S. W. Westwood, *Tetrahedron* **1989**, *45*, 5269–5282; D. P. Curran, *Synthesis* **1988**, 417–439, *ibid.* **1988**, 489–513; B. Giese, *Radicals in Organic Synthesis: Formation of Carbon-Carbon Bonds*, Pergamon, Oxford, **1986**; M. Ramaiah, *Tetrahedron* **1987**, *43*, 3541.
[3] C. Chatgilialoglu, *Acc. Chem. Res.* **1992**, *25*, 188–194; C. Chatgilialoglu, K. U. Ingold, J. C. Scaiano, *J. Am. Chem. Soc.* **1982**, *104*, 5123–5127.
[4] C. Chatgilialoglu, D. Griller, M. Lesage, *J. Org. Chem.* **1988**, *53*, 3641–3642; C. Chatgilialoglu, J. Dickhaut, B. Giese, *ibid.* **1991**, *56*, 6399–6403.
[5] Compound **1** was synthesized in 82% yield by following a modified procedure [M. R. Detty, M. D. Seidler, *J. Org. Chem.* **1981**, *46*, 1283–1292] in the presence of [18]crown-6.

[6] Several compounds of the type $PhSeSiR_3$ ($R_3 = Me_3$, Et_3, Me_2Ph, Me_2tBu, Ph_2tBu) were screened for this purpose; however, compound **1** was best suited for the radical chain group transfer reaction because of its stability to hydrolysis [4].
[7] M. Newcomb, D. J. Marquardt, M. U. Kumar, *Tetrahedron* **1990**, *46*, 2345–2352; J. H. Byers, T. G. Gleason, K. S. Knight, *J. Chem. Soc. Chem. Commun.* **1991**, 354–356.
[8] T. Hamada, A. Nishida, O. Yonemitsu, *J. Am. Chem. Soc.* **1986**, *108*, 140–145; T. Hamada, A. Nishida, O. Yonemitsu, *ibid.* **1980**, *102*, 3978–3980.
[9] D. Rehm, A. Weller, *Isr. J. Chem.* **1970**, *8*, 259.
[10] The oxidation potential ($E_{1/2}^{[ox]} = 1.28$ eV/SCE) and energy of excitation ($E_{0,0} = 367.37$ kJ) values for DMN were taken from ref. [8], whereas the $E_{1/2}^{[red]}$ of **1** was determined by cyclic voltametry [11].
[11] $E_{1/2}^{[red]}$ of **1** and $E_{1/2}^{[ox]}$ of H_2A were determined by cyclic voltammetry, by using a PAR 173 potentiostat coupled with a PAR 175 universal programmer, and the data were recorded on a RE0091 X-Y recorder; Pt UME (Ultra micro electrode) working electrode, Pt foil counter electrode; tetrabutylammonium hexafluoroborate ($TBABF_6$) in dry CH_3CN as supporting electrolyte. The CH_3CN solution was degassed by argon bubbling for 10 min before measurement. The scan rate was 500 mVs^{-1} and values are relative to SCE.
[12] The Gibbs free energy was determined with the equation $\Delta G_{et} = E_{1/2}^{[ox]} - E_{1/2}^{[red]}$, in which the $E_{1/2}^{[ox]}$ value of H_2A estimated by cyclic voltammetry [10] was 1.084 eV/SCE and the $E_{1/2}^{[red]}$ value for $DMN^{\cdot+}$ was 1.28 eV/SCE [8].
[13] Since the reduction potentials are quasireversible, the ΔG_{et} values obtained are only approximate; however, they generally agree quite well with the experimental values.
[14] G. M. Brown, B. S. Brunschwig, C. Creutz, J. F. Endicott, N. Sutin, *J. Am. Chem. Soc.* **1979**, *101*, 1298–1300; B. H. J. Bielski, D. A. Comstock, R. A. Bowen, *ibid.* **1971**, *93*, 5624–5629.
[15] Quantum yields were determined with an instrument from Applied Photophysics; light intensities were estimated by using uranyl oxalate as a chemical actinometer. Quantum disappearance of **1** was measured by HPLC (Perkin Elmer 135C, Diode-Array detector, C_8 reverse-phase column).
[16] A. L. J. Beckwith, C. J. Easton, A. K. Serelis, *J. Chem. Soc. Chem. Commun.* **1980**, 482–483; A. L. J. Beckwith, T. Lawrence, A. K. Serelis, *ibid.* **1980**, 484–485.

A Highly Reactive and Catalytically Active Model System for Intradiol-Cleaving Catechol Dioxygenases: Structure and Reactivity of Iron(III) Catecholate Complexes of *N,N'*- Dimethyl-2,11-diaza[3.3](2,6)pyridinophane**

Welf O. Koch and Hans-Jörg Krüger*

In memory of Professor Nobumasa Kitajima

Intradiol-cleaving catechol dioxygenase[1] represents a class of bacterial enzymes that catalyzes the oxidative cleavage of the *intradiol*-C–C bond of various catechol derivatives with molecular oxygen, yielding the corresponding muconic acid [Eq. (a)].

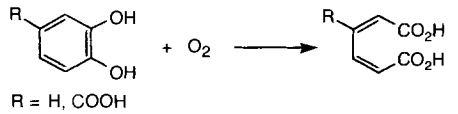

R = H, COOH (a)

In its resting state, the active site of the enzyme comprises a high-spin iron(III) ion coordinated by two histidines, two tyrosinates, and a water molecule or a hydroxide ion in a trigonal-bipyramidal geometry.[2] Probably the most unusual property of this enzyme is that the trivalent oxidation state of the iron center is retained during the entire catalytic cycle. Through the prominent work of L. Que and co-workers,[1] a mechanism was proposed which is displayed in Scheme 1. After the initial coordination of the substrate, the resulting catecholate complex reacts with the oxygen molecule to form an intermediary peroxo complex. Only now the C–C bond cleavage occurs to yield the muconic anhydride which is subsequently hydrolyzed. The unusual reactivity of an iron(III) complex with oxygen is explained by the partial transfer of electron density from the bound catecholate ligand to the metal ion, thereby furnishing the coordinated catecholate with partial semiquinone character and partially reducing the trivalent metal ion.

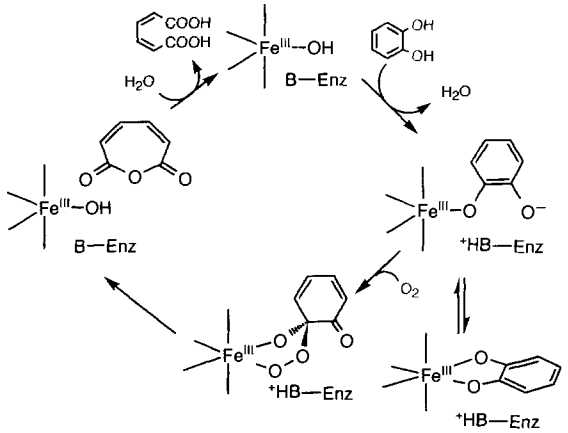

Scheme 1. Postulated mechanism of the intradiol-cleaving catechol dioxygenase [1].

A study[3] on biomimetic model complexes revealed that two easily accessible *cis* coordination sites are needed for coordination of the catecholate ligand and its subsequent reaction with molecular oxygen. In a series of complexes containing different tripodal ligands, it was shown that the order of reactivity of the coordinated 3,5-di-*tert*-butylcatecholate ligand (dbc^{2-})[4] in the complexes $[Fe(tpa)(dbc)]^+ > [Fe(bpg)(dbc)] > [Fe(pda)(dbc)]^- > [Fe(nta)(dbc)]^{2-}$ is correlated to the Lewis acidity of the iron(III) ion. This result was interpreted to mean that increasing the Lewis acidity of the metal ion enhances the previously mentioned partial transfer of electron density from the coordinated catecholate ligand to the metal ion. Accordingly, a correlation was observed between the reactivity and the energy of the LMCT band in the visible region of the electronic absorption spectrum as well as the chemical shifts of the ^1H NMR signals of the coordinated catecholate. Of all the complexes mentioned above, only the $[Fe(nta)(dbc)]^{2-}$ complex has been reported[3c] to catalyze the conversion of $dbcH_2$ to 3,5-di-*tert*-butyl-5-carboxymethyl-2-furanone (**1**)[5] with small amounts of 3,5-di-*tert*-butyl-1,2-benzoquinone (**2**) as by-product. However, the reaction proceeds very slowly and needs several days for completion. In addition, a borate buffer is needed to prevent the oxidation of the catechol derivative by air itself to **2**. Further, and most noteworthy, the product distribution has been questioned, since instead of the oxidative-cleavage product **1**, the *o*-quinone **2** was found to be the major product in this reaction.[6] Here we report on the synthesis of two iron(III) catecholate complexes and their reactivity with oxygen. For the first time, a highly reactive and catalytically active compound is presented that models the reactivity of intradiol-cleaving catechol dioxygenase; its use in catalytic reactions yields muconic anhydride as the main product.

[*] Dr. H.-J. Krüger, W. O. Koch
Institut für Anorganische und Angewandte Chemie der Universität
Martin-Luther-King-Platz 6, D-20146 Hamburg (Germany)
Telefax: Int. code + (40) 4123-2893

[**] This work was supported by the Deutsche Forschungsgemeinschaft.

The reaction of the tetraazamacrocyclic ligand L-N_4Me_2 with iron(III) chloride in an alcoholic solution followed by addition of catecholate anions (cat^{2-} or dbc^{2-}) results in the formation of intense purple-colored solutions of the ions **3** and **4**, respectively. Metathesis with lithium tetraphenylborate affords both compounds as microcrystalline materials in good yields. The visible regions of the electronic absorption spectra of solutions of the complexes **3** and **4** in acetonitrile are dominated by two intense LMCT bands at 501 and 734 nm and at 553 and 784 nm, respectively. The similarity of the electronic absorption spectra to those spectra of solid samples of the compounds implies that the modes of coordination of the catecholate ligands prevail also to the largest extent in solution.

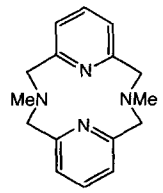

L-N_4Me_2

$[(L\text{-}N_4Me_2)Fe(cat)]^+$ **3**

$[(L\text{-}N_4Me_2)Fe(dbc)]^+$ **4**

A structure determination was carried out on complex **3**.[7] A perspective view of the complex cation is shown in Figure 1.

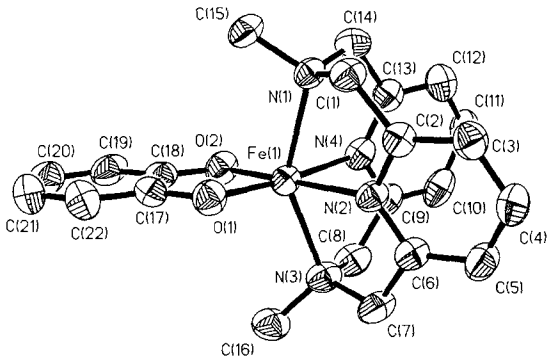

Fig. 1. Crystal structure of **3** showing thermal ellipsoids at 50% probability and the atom numbering scheme. Selected distances [Å] and angles [°]: Fe(1)-O(1) 1.903(3), Fe(1)-O(2) 1.915(3), Fe(1)-N(1) 2.222(3), Fe(1)-N(2) 2.105(3), Fe(1)-N(3) 2.223(3), Fe(1)-N(4) 2.106(3), O(1)-C(17) 1.353(5), O(2)-C(18) 1.329(5); O(1)-Fe(1)-O(2) 85.6(1), O(1)-Fe(1)-N(1) 97.7(1), O(1)-Fe(1)-N(2) 100.4(1), O(1)-Fe(1)-N(3) 107.3(1), O(1)-Fe(1)-N(4) 174.7(1), O(2)-Fe(1)-N(1) 103.7(1), O(2)-Fe(1)-N(2) 173.7(1), O(2)-Fe(1)-N(3) 99.0(1), O(2)-Fe(1)-N(4) 93.0(1), N(1)-Fe(1)-N(2) 77.4(1), N(1)-Fe(1)-N(3) 147.3(1), N(1)-Fe(1)-N(4) 77.6(1), N(2)-Fe(1)-N(3) 77.6(1), N(2)-Fe(1)-N(4) 81.1(1), N(3)-Fe(1)-N(4) 77.9(1).

Due to the small cavity of the twelve-membered macrocyclic ring, a distorted *cis* octahedral coordination geometry is found around the iron ion.[8] The ligand is folded along the N_{amine}-N_{amine} axis, and the metal ion protrudes to some extent out of the cavity as manifested by the deviation of the N_{amine}-Fe-N_{amine} angle (147.3°) from the ideal value of 180°. The Fe-N_{py} and Fe-N_{amine} distances of 2.106 and 2.223 Å, respectively, are within the range commonly observed for these bonds in high-spin iron(III) complexes with this ligand.[8] The catecholate ligand is bound to the *cis* coordination sites in the equatorial plane of the complex. As expected for a molecule with approximate C_{2v} symmetry, both Fe-O bond lengths are almost the same (deviation: 0.012 Å). The Fe-O bond length of 1.909 Å and the average C-O bond length of 1.341 ± 0.012 Å show no manifestation of a partial semiquinone character. A preliminary X-ray structure determination assigns an analogous structure to complex **4** with Fe-O bond lengths of 1.899 ± 0.012 Å and C-O bond lengths of 1.351 ± 0.003 Å. Similar Fe-O bond lengths have been observed for $[Fe(tpa)dbc]^+$ ions.[3a]

Both complexes react with oxygen as indicated by the disappearance of the purple color of the solutions. The progress of the oxygenation reaction, for example of complex **4** in acetonitrile, can be monitored by the decrease of intensity of the charge-transfer (CT) bands in the electronic absorption spectrum over time (Fig. 2). Analysis of the reaction products reveals that the coordinated dbc^{2-} ion in complex **4** is nearly quantitatively converted to the intradiol cleavage products 3,5-di-*tert*-butylmuconic anhydride (**5**) (47%) and the γ-lactone **1** (48%).[9] Preliminary kinetic evaluations of the disappearance of the lowest energy CT bands indicate pseudo-first order kinetics for the reactions of the catecholate complexes in acetonitrile solutions. The reaction velocity constants for complexes **3**[10] and **4** at room temperature were determined to be $2.77 \times 10^{-3}\ M^{-1}s^{-1}$ and $3.77 \times 10^{-1}\ M^{-1}s^{-1}$, respectively ($[O_2] = 8.1$ mM in acetonitrile,[11] pressure 1 atm). The increase of the reaction velocity by a factor of 100 for complex **4** is paralleled by a red shift of the LMCT absorption bands of the complex by 50 nm. This correlation agrees with the previously discussed dependence of the reactivity on the extent of partial transfer of electron density from the catecholate moiety to the metal ion. It is noteworthy that here, for the first time, ring opening has been demonstrated for the reaction of oxygen with coordinated catecholate,[10] the true substrate of intradiol-cleaving catechol dioxygenase, although the reaction velocity is considerably lower than that observed for the enzyme ($2.5 \times 10^5\ M^{-1}s^{-1}$).[12] The reactivity of complex **4** lies between those of the $[Fe(tpa)(dbc)]^+$ and [Fe(bpg)(dbc)] complexes. Dei and co-workers,[13] who observed no reaction for the $[Fe(cyclam)(dbc)]^+$ ion with oxygen despite the rather low energy of the LMCT band (833 nm), deduced that in addition to the two *cis* coordination sites for the catecholate, a third one is needed for the attack of the oxygen onto the metal. While the inertness towards partial substitution may be questioned for tripodal ligands,[14] from our experience

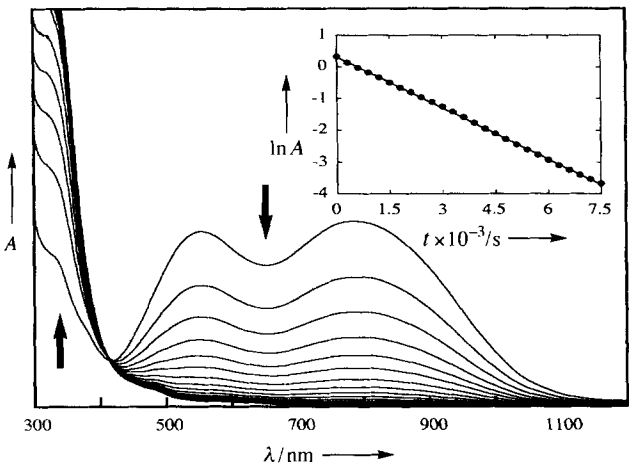

Fig. 2. Progress of the reaction of **4** with air in MeCN at room temperature as monitored by electronic absorption spectroscopy in 10 min intervals. The arrows indicate how the intensities of absorption bands change over time. Inset: plot of ln *A* vs. time *t*. *A* = absorption.

of the NMR properties of diamagnetic complexes with the L-N_4Me_2 ligand, we are quite certain that because of its pronounced rigidity, the ligand, once coordinated, remains bound through all nitrogen donor atoms to the metal ion at all times. This inertness to substitution can be extended to the iron(III) catecholate complexes under current discussion. Therefore the attack of the oxygen molecule must occur either directly onto the catecholate ligand coordinated in a bidentate fashion to the iron(III), or, an equilibrium must be inferred to exist in solution between a bi- and a monodentate coordination mode of the catecholate ligand in order that the reaction of the oxygen can take place with a five-coordinate iron intermediate.

A prerequisite for any catalytic activity is that the iron catecholate complex has to be stable in the presence of a large excess of unbound catecholate. By UV/Vis spectroscopy it was shown that even a 100fold excess of dbc^{2-} ions was not able to expel the tetraazamacrocyclic ligand from the coordination sphere of the iron(III) ion to yield the corresponding triscatecholatoferrate(III) complex. Addition of a tenfold excess of dbc^{2-} ions to a solution containing stoichiometric amounts of iron(III) perchlorate and L-N_4Me_2 in DMF, followed by the exposure of the resulting purple mixture to air resulted, in contrast to the stoichiometric reaction, in the persistence of the initial intensity of the absorption band at 780 nm for about 13 h after which the CT band disappeared. The absorption band could be recovered with its original intensity by the addition of another tenfold excess of dbc^{2-} ions and vanished again after a further 13 h of exposure to air. This finding is clear evidence that **4** is a catalyst for the oxidative cleavage of catechol.

In a typical catalytic reaction, a mixture of iron(III) perchlorate (0.1 mmol) and L-N_4Me_2 (0.1 mmol) in DMF (10 mL) was treated under anaerobic conditions with a solution of $dbcH_2$ (1 mmol) and triethylamine (0.2 mmol) in DMF (10 mL) and then exposed to an atmosphere of pure oxygen. In addition to the change of color from purple to yellow, the progress of the reaction can be monitored by ^1H NMR spectroscopy (Fig. 3). The decrease in the intensities of the NMR signals of unbound catechol (δ = 6.83, 6.76, 1.38, and 1.22) over time is accompanied by the appearance of signals corresponding to the major product muconic anhydride **5** (δ = 6.74, 6.29, 1.28, and 1.18) and the minor product *o*-benzoquinone **2** (δ = 7.08, 6.15, 1.25, and 1.23). The reaction is essentially finished after 3 h. Workup afforded 70% of **5** and 13% of **2**. Based on the NMR signals between δ = 0.97 and 1.16, the residual products are attributed to some not yet identified derivatives of **1** and, therefore, the yield of oxidative-cleavage products is even higher than 70%. In this study, the direct observation of the products' composition over time during catalytic turnovers allows the conclusion that muconic anhydride is indeed the direct product of the oxygenation reaction. The products' evolution over time definitely excludes any involvement of benzoquinone as an intermediate in the oxygenation reaction.[15] Since the amounts of the minor product **2** increase in the catalytic reaction compared to the stoichiometric reaction and, since catechol itself is susceptible to oxidation by oxygen in basic solutions, the formation of **2** is thought to be not mediated by the iron complex **4**. For the catalytic reaction, only two equivalents of a base are needed per iron(III) ion. With 1% of the iron(III) catalyst, yields of 54% of **5** and 17% of **2** were obtained after a reaction time of 30 h. In contrast to the previous study with $[Fe(nta)(dbc)]^{2-}$ ions,[3c] no borate buffer was needed to protect $dbcH_2$ from oxygen and the reaction proceeded in considerably less time. The investigation of this very efficient catalytic cycle with turnover numbers of 54 is summarized in Scheme 2.

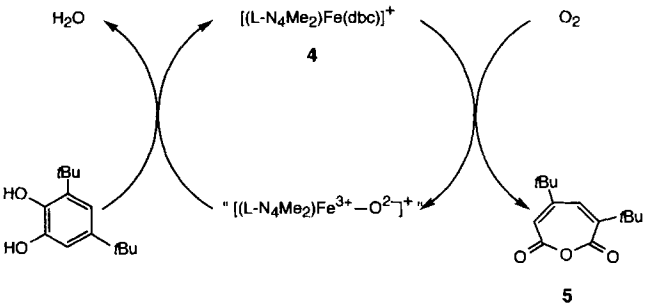

Scheme 2. Catalytic cycle of the oxygenation with **4**.

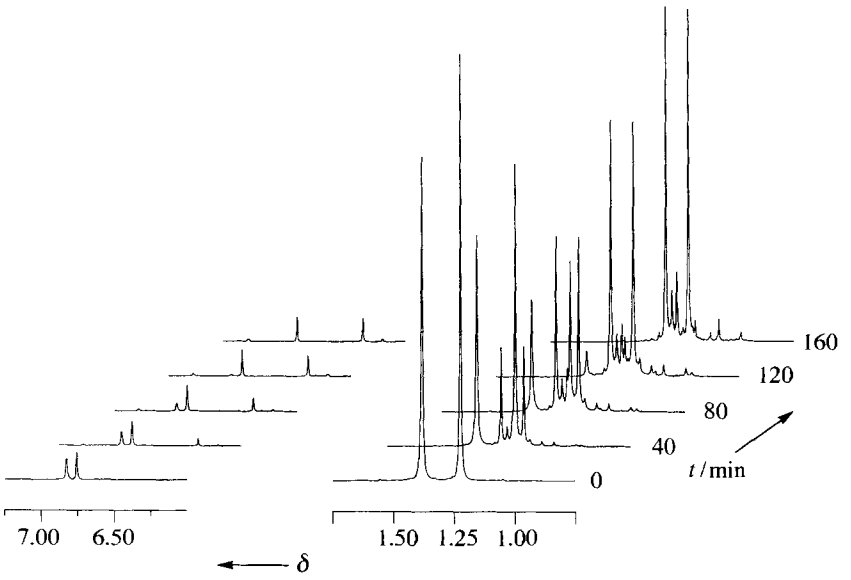

Fig. 3. Catalytic oxidation of $dbcH_2$ in $[D_7]$DMF as monitored by ^1H NMR spectroscopy (oxygen pressure 1 atm, room temperature, initial ratio of $dbcH_2$:$[D_{15}]NEt_3$:$[Fe(L\text{-}N_4Me_2)(DMF)_2]^{3+}$ = 10:2:1).

The exact identity of the putative "$[(L\text{-}N_4Me_2)Fe^{3+}\text{-}O^{2-}]^+$" intermediate is not yet known. In contrast to the $[Fe(tpa)(dbc)]^+$ complex,[3a] the products of the stoichiometric reaction of **4** with oxygen display none of the characteristic CT transitions of a μ-oxo-μ-furanoneacetato-bridged diiron(III) complex in the electronic absorption spectrum. However, the considerably less paramagnetically shifted ^1H NMR signals of the coordinated ligand and the substantial decrease of magnetic susceptibility of the products indicate formation of an antiferromagnetically coupled μ-oxo bridged diiron(III) species. The detection of the cleavage products **1** and **5** in a ratio of approximately 1:1 agrees well with reaction (b). Whether in the catalytic reaction a basic mononuclear iron(III) or a μ-oxo-bridged diiron(III) species reacts with $dbcH_2$, cannot be elucidated at the moment and therefore any preference would only be speculative.

 © VCH Verlagsgesellschaft mbH, D-69451 Weinheim, 1995 0570-0833/95/3423-2673 $ 10.00+.25/0

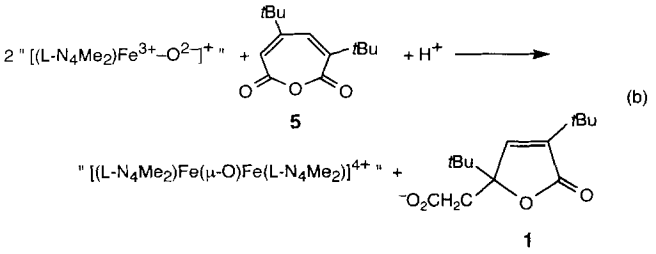

Herein we have reported a well-defined stoichiometrically functioning and catalytically highly active biomimetic model system for the reactivity of intradiol-cleaving catechol dioxygenases. Even though the coordination environment of the iron centers in complexes **3** and **4** does not match that of the enzyme, a detailed study on the mechanistic aspects of the reaction of these complexes with oxygen promises to contribute to the elucidation of the intimate mechanism of the enzyme, where questions regarding the C–C cleavage step and the actual attack of the iron(III) catecholate complex by an oxygen molecule still remain open. These mechanistic studies and the description of the electronic properties of reactive iron(III) catecholate complexes such as **3** and **4** will be reported elsewhere.

Experimental Procedure

Preparation of [(L-N_4Me_2)Fe(dbc)](BPh_4) (**4**): Under strictly oxygen-free conditions, a solution of $FeCl_3 \cdot 6H_2O$ (135 mg, 0.5 mmol) in methanol (10 mL) was added to solution of L-N_4Me_2 (134 mg, 0.5 mmol) in methanol (20 mL). After the reaction mixture was heated shortly to reflux temperature and then allowed to cool again to room temperature, it was treated with a solution containing $dbcH_2$ (111 mg, 0.5 mmol) and triethylamine (210 μL, 1.5 mmol) in methanol (10 mL). An immediate color change from orange-yellow to purple occurred. After filtration and metathesis with 10 mL of a methanolic solution of tris(ethylenglycoldimethylether)lithium tetraphenylborate (300 mg, 0.5 mmol), the resulting crystalline purple material was isolated by filtration, washed twice with small amounts of methanol and dried in vacuo to afford 387 mg of analytically pure product (90% yield). Anal. calcd. for $C_{54}H_{60}BFeN_4O_2$: C 75.09, H 7.00, N 6.49; found: C 74.50, H 6.75, N 6.46. Absorption spectrum (acetonitrile): λ_{max} (ε_M) = 553 (2640), 784 (2780) nm.

Preparation of [(L-N_4Me_2)Fe(cat)](BPh_4) (**3**): Accordingly, in an only slightly modified procedure using 96% ethanol as solvent and catechol as ligand, [(L-N_4Me_2)Fe(cat)](BPh_4) was prepared in 81% yield as a dark blue crystalline material. Anal. calcd. for $C_{46}H_{44}BFeN_4O_2$: C 73.52, H 5.90, N 7.45; found: C 73.66, H 5.82, N 7.56. Absorption spectrum (acetonitrile): λ_{max} (ε_M) = 501 (2580), 734 (2920) nm.

Received: April 29, 1995 [Z 7945 IE]
German version: *Angew. Chem.* **1995**, *107*, 2928–2931

Keywords: catechol dioxygenases · enzyme catalysis · iron compounds · oxygenations

[1] L. Que, Jr. in *Iron Carriers and Iron Proteins* (Ed.: T. M. Loehr), VCH, New York, **1989**, p. 467.
[2] a) D. H. Ohlendorf, J. D. Lipscomb, P. C. Weber, *Nature* **1988**, *336*, 403; b) D. H. Ohlendorf, A. M. Orville, J. D. Lipscomb, *J. Mol. Biol.* **1994**, *244*, 586.
[3] a) H. G. Jang, D. D. Cox, L. Que, Jr., *J. Am. Chem. Soc.* **1991**, *113*, 9200; b) D. D. Cox, L. Que, Jr., *ibid.* **1988**, *110*, 8085; c) M. G. Weller, U. Weser, *ibid.* **1982**, *104*, 3752.
[4] $dbcH_2$ = 3,5-di-*tert*-butylcatechol; tpa = tris(2-pyridylmethyl)amine; bpgH = *N*,*N*-bis(2-pyridylmethyl)glycine; $pdaH_2$ = *N*-(carboxymethyl)-*N*-(2-pyridylmethyl)glycine; $ntaH_3$ = *N*,*N*-bis(carboxymethyl)glycine; L-N_4Me_2 = *N*,*N*′-dimethyl-2,11-diaza[3.3](2,6)pyridinophane; $catH_2$ = catechol; cyclam = 1,4,8,11-tetraazacyclotetradecane.
[5] The γ-lactone of the 3,5-di-*tert*-butylmuconic acid, 3,5-di-*tert*-butyl-5-carboxymethyl-2-furanone (**1**), is also an intradiol cleavage product.
[6] a) T. Funabiki, T. Konishi, S. Kobayashi, A. Mizoguchi, M. Takano, S. Yoshida, *Chem. Lett.* **1987**, 719. b) Similar results with **2** as the main product were also obtained in our laboratory.
[7] Crystallographical data of [Fe(L-N_4Me_2)(cat)](BPh_4) · 2.5 MeCN: crystal size 0.1 × 0.3 × 0.5 mm, crystal system triclinic, space group $P\bar{1}$, a = 13.206(2), b = 14.214(2), c = 15.037(2) Å, α = 99.04(1), β = 107.22(1), γ = 113.70(1)°, V = 2342.4(6) Å^3, Z = 2, ρ_{calcd} = 1.21 g cm^{-3}; $2\Theta_{max}$ = 153.14°, λ = 1.54178 Å, scan method ω-2Θ, temperature 153 K, 10097 collected reflections; 9540 unique reflections (7778 reflections with $F_o > 4\sigma(F_o)$), $\mu(Cu_{K\alpha})$ = 29.36 cm^{-1}, Enraf-Nonius-CAD4-diffractometer; graphite monochromatized $Cu_{K\alpha}$ radiation, structure solution and refinement: direct methods (SHELXS-86) and full-matrix least-squares on F^2 (SHELXL-93); 609 parameters; anisotropic refinement of all non-hydrogen atoms (with the exception of one highly disordered solvent molecule), isotropic refinement of calculated hydrogens; R = 0.0781 ($F_o > 4\sigma(F_o)$); R_w = 0.1983, extinction coefficient = 0.0028(4), largest difference peak and hole = 0.887 and −0.614 e Å^{-3}. Further details of the crystal structure investigation are available on request from the Fachinformationszentrum Karlsruhe, D-76344 Eggenstein-Leopoldshafen (Germany), on quoting the depository number CSD-401747.
[8] a) H.-J. Krüger, *Chem. Ber.* **1995**, *128*, 531; b) H.-J. Krüger, unpublished results.
[9] 3,5-Di-*tert*-butyl-1,2-benzoquinone **2** was only produced in minor amounts (< 1%).
[10] Here, the analysis of reaction products is much more difficult due to the instability and reactivity of muconic anhydride or the acid itself in the presence of a Lewis acid like Fe^{III}. In the oxidation of **3** in MeOH in the presence of thiocyanate, in addition to a few not yet identified products, the methyl ester of the γ-lactone could be identified as one of the products, indicating that at least to some extent intradiol cleavage did occur.
[11] D. T. Sawyer, *Oxygen Chemistry*, Oxford University Press, New York, **1991**, p. 21.
[12] T. A. Walsh, D. P. Ballou, R. Mayer, L. Que, Jr., *J. Biol. Chem.* **1983**, *258*, 14422.
[13] A. Dei, D. Gatteschi, L. Pardi, *Inorg. Chem.* **1993**, *32*, 1389.
[14] R. R. Jacobson, Z. Tyeklar, A. Farooq, K. D. Karlin, S. Liu, J. Zubieta, *J. Am. Chem. Soc.* **1988**, *110*, 3690–3692.
[15] a) M. Matsumoto, K. Kuroda, *J. Am. Chem. Soc.* **1982**, *104*, 1433; b) M. M. Rogic, T. R. Demmin, *ibid.* **1978**, *100*, 5473.

Assessing Similarity and Diversity of Combinatorial Libraries by Spatial Autocorrelation Functions and Neural Networks**

Jens Sadowski, Markus Wagener, and Johann Gasteiger*

Dedicated to Professor Ivar Ugi on the occasion of his 65th birthday

The recent availability of high throughput techniques to find new lead structures by random screening has increased the need for a continuous supply of novel compounds. One way of fulfilling this need is by preparation of chemical libraries through combinatorial chemistry:[1] The repetitive and systematic application of a synthesis principle to a number of chemical building blocks can produce large populations of different structures. Thus, a library of 20^4 = 160000 compounds can be built by systematically connecting twenty building blocks in four reaction steps. By changing some of the building blocks or the reactions used, a nearly unlimited number of different libraries can be realized. Therefore, efficient means for comparing libraries and for assessing the diversity of the compounds contained in them are needed. We present here a new approach for the analysis of chemical libraries, which is based on spatial autocorrela-

[*] Prof. Dr. J. Gasteiger, Dr. J. Sadowski, Dr. M. Wagener
Computer-Chemie-Centrum
Institut für Organische Chemie der Universität Erlangen-Nürnberg
Nägelsbachstrasse 25, D-91052 Erlangen (Germany)
Telefax: Int. code +(9131) 85-6566
e-mail: Gasteiger@EROS.CCC.Uni-Erlangen.DE

[**] This work was supported by the Bundesministerium für Bildung, Wissenschaft, Forschung und Technologie (BMBF), Germany.

tion functions and neural networks. Using this method several chemical libraries are compared, and an estimation of their similarity and diversity is given. This analysis leads to recommendations for the proper selection of libraries for further investigations.

Recently we introduced autocorrelation vectors as 3D-QSAR descriptors that combine the spatial positions of points on a molecular surface with property values (for example, the electrostatic potential) at these points.[2] To determine this descriptor the distances between randomly chosen surface points are sorted into intervals with preset lower and upper bounds, d_l and d_u. An autocorrelation coefficient $A(d_l, d_u)$ can then be obtained from Equation (a). The variables p_i and p_j are the property

$$A(d_l, d_u) = 1/L \sum_{ij} p_i p_j \qquad (d_l \le d_{ij} < d_u) \qquad \text{(a)}$$

values at surface points i and j, respectively, and L is the total number of distances in the interval $[d_l, d_u[$. For a series of distance intervals with different lower and upper bounds, a low-dimensional vector of autocorrelation coefficients is obtained. It represents a condensed description—a fingerprint—of the distribution of the property p over the molecule. Since only distances are used in Equation (a), the 3D-structures do not need to be aligned in 3D-space. This descriptor was successfully used for modeling the biological activity of two different classes of compounds.[2] It can be determined in a way efficient enough to cope with the enormous number of compounds commonly contained in combinatorial libraries.

In order to outline the computational methods and to demonstrate their merits for handling combinatorial libraries we have chosen an example from the literature. Rebek et al. recently reported on the synthesis and screening of libraries of semirigid compounds in solution for finding potent trypsin inhibitors.[3] The libraries were obtained by combining rigid central molecules like the xanthene derivative **1** or the cubane derivative **2** with a mixture of 19 L-amino acids.[4]

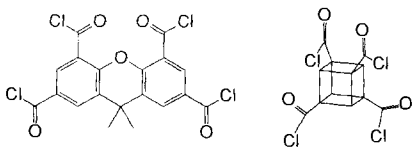

1

2

Combination of **1** and the 19 building blocks theoretically yields 65 341 different structures. Due to its higher symmetry, **2** combines with the same set of building blocks to form only 11 191 compounds. The libraries obtained were screened on a trypsin assay and subsequently broken down into sublibraries. Finally a new potent lead was identified.[3b]

Compounds based on xanthene **1** should adopt a disklike shape, whereas derivatives of cubane **2** should give molecules with a more spherical shape. Thus, a 3D-descriptor for handling this type of combinatorial libraries seems to be crucial.

To prepare for the computational study, we first generated the 3D-autocorrelation descriptors for all compounds of the two libraries in five distinct steps: 1) 3D-models of the central molecules **1** or **2** and the 19 L-amino acids were obtained by the 3D-structure generator Corina.[5] 2) These fragments were fed into a structure generator that fully exploded them into 3D-structures of all possible combinations. 3) Atomic charges were calculated by fast empirical methods.[6] 4) The electrostatic potential at randomly distributed points on the van der Waals surface with a point density of 1 point per Å^2 was calculated by a classical Coulomb approach. 5) The distances between points were split into twelve equally spaced intervals between 2 and 20 Å. Autocorrelation coefficients were then calculated according to Equation (a) by using the electrostatic potential values, yielding a total of 12 autocorrelation coefficients for each molecule. For the 65 341 compounds of the xanthene library this required about 49 hours on a Sun Sparc 10/512 workstation and took about 4 MB disk space for the descriptors—rather moderate resources.

The question is now: How can one extract useful information about the nature of the xanthene and cubane libraries from this sea of numbers (65 341 × 12 descriptors for the xanthene library only)? We used a Kohonen network[7] to visualize the chemical diversity of the library compounds. The Kohonen procedure is an unsupervised learning method, which is able to project information from a high-dimensional descriptor space into a two-dimensional map retaining the topology of the information.[8] Thus, neighboring points in the descriptor space occupy neighboring neurons in the map. Figure 1 illustrates this process.

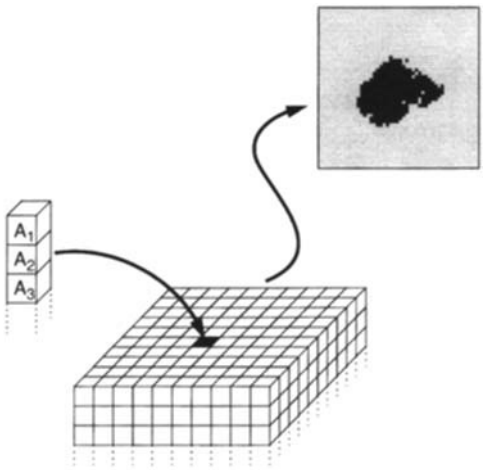

Fig. 1. Projection of the xanthene and cubane libraries onto a Kohonen map. Twelve-dimensional input vectors, $\mathbf{A}_1, \mathbf{A}_2, \ldots, \mathbf{A}_{12}$ are used to train the Kohonen net. After the training the neurons can be colored according to the core molecule: xanthene gray and cubane black.

The twelve-dimensional autocorrelation vectors **A** describing the xanthene and cubane library compounds obtained from the structure generator (step 2) were used to train a 50 × 50 network. This required about twelve minutes on a Sun Sparc 10/512 workstation. After training was finished each compound corresponded to one distinct neuron of the network. The core molecule of the library compounds was used to visualize the xanthene (gray) and the cubane (black) derivatives in a two-dimensional map (see Fig. 2a). The total chemical space spanned by the two libraries corresponds to the 50 × 50 map. All 2500 neurons are occupied. The cubane derivatives (black) form a discrete cluster surrounded by the compounds of the xanthene library. Only a small number of xanthene and cubane derivatives occupy the same neuron (2649 compounds or 3%). Thus, the network was able to separate the two libraries completely. The conclusion drawn from this result is that the two libraries are diverse enough that both warrant synthesis and testing, since they occupy different parts of the chemical space.

In order to show that our method can also be used to determine the similarity of libraries we defined a third, hypothetical library that was assumed to be closely related to the cubane

 © VCH Verlagsgesellschaft mbH, D-69451 Weinheim, 1995 0570-0833/95/3423-2675 $ 10.00+.25/0

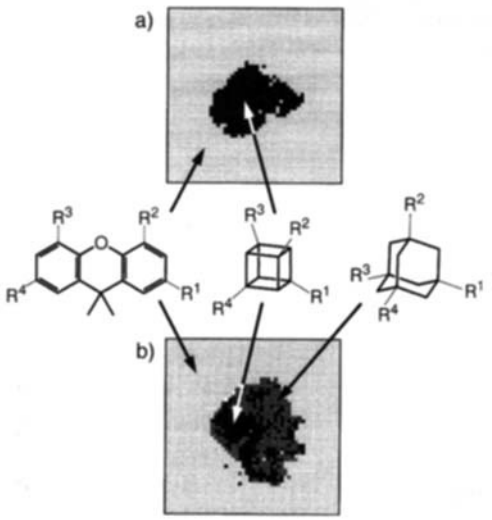

Fig. 2. a) Kohonen projection of the xanthene and the cubane libraries onto a two-dimensional map. b) Kohonen projection of all three libraries—xanthene, cubane, and adamantane—onto a two-dimensional map. In both cases the same color scheme is used: xanthene light gray, adamantane dark gray, and cubane black.

library. We chose adamantane functionalized at the four bridgehead atoms as the central building block, because the amino acids have directions comparable to those in the cubane derivatives. The same number of compounds as for the cubane library (11191) were generated. Figure 2b shows the Kohonen map trained with the data of the three libraries, where each neuron was colored according to the most frequent core molecule. Again, a sharp border between the xanthene derivatives and the other compounds is observed. However, the network was unable to distinguish between the cubane and the adamantane libraries, as they form a single cluster in Figure 2b. In this cluster 92% of the cubane and adamantane derivatives are grouped together into common neurons, making the cluster even more homogeneous than indicated by Figure 2b.

To put this visual impression onto a quantitative basis we looked for equivalent compounds in the three libraries, that is, those compounds having the same substitution pattern (for example, Ala, Gly, Leu, Pro). Their distance in the Kohonen map in the form of the median number of neurons between them should give a quantitative measure for the similarity of the libraries: xanthenes–cubanes 19 neurons; xanthenes–adamantanes 19 neurons; cubanes–adamantanes 4 neurons. Thus, the cubane and the adamantane libraries are close together and occupy almost the same part of the chemical space. They should be able to replace each other. It is therefore only worth the effort to synthesize the xanthene library and one of the other two libraries.

Rebek et al.[3] found that only the xanthene library showed significant trypsin inhibition. Thus, they decided next to deconvolute the xanthene library into sublibraries for subsequent testing. From the original set of 19 amino acids[4] cysteine was omitted. The remaining 18 amino acids were split into six groups, each containing three amino acids with similar side chains. Groups 1 and 2 contained alkyl amino acids, group 3 basic amino acids, group 4 hydroxy- and methylthio-functionalized amino acids, group 5 aromatic amino acids, and group 6 amino acids bearing a second acid or an amide function.[9] Each sublibrary was obtained by omitting the three amino acids of one group from the full set. Thus, six sublibraries built from xanthene **1** and fifteen amino acids resulting in 25425 compounds per library were obtained. The overlap between these sublibraries is rather high: Each sublibrary has 10440 compounds (41%) in common with any other sublibrary, and each compound is contained in at least two sublibraries.

For the computer analysis of this partitioning again a Kohonen map was used. First, the network was trained with the data of the 65341 compounds of the complete xanthene library. This gave a map defining the total chemical space spanned by the xanthene library. Then, the trained network was used for the subsequent visualization of the neurons occupied by single sublibraries. Figure 3 shows these maps and the numbers of unoccupied neurons.

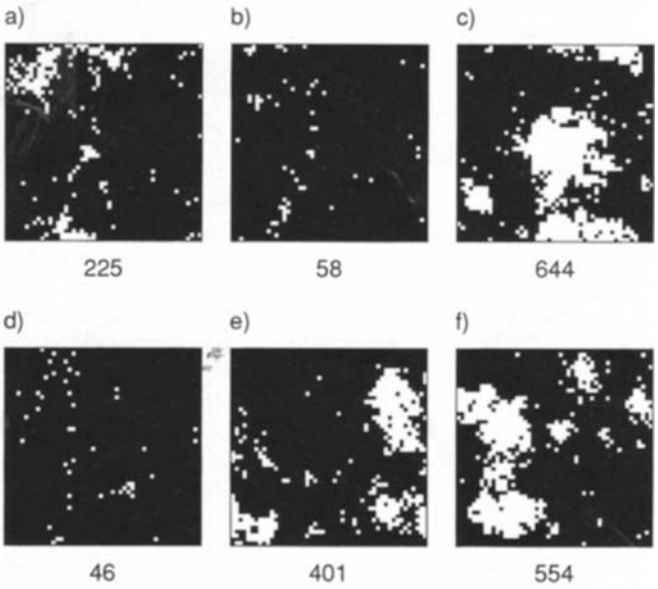

Fig. 3. Visualization of the six xanthene sublibraries in a map trained with the complete xanthene library. The number of unoccupied neurons is given below each map. In a) and b) alkyl amino acids were omitted, in c) basic amino acids, in d) the hydroxyl- and methylthio-functionalized amino acids, in e) aromatic amino acids, and in f) amino acids bearing a second acid or an amide function [9].

The visual inspection of white areas in the maps, that is, those neurons with no corresponding structures, gives an impression of how diverse the individual sublibraries are. The more unoccupied neurons there are, the smaller the diversity of the sublibrary. Despite the high redundancy in the sublibraries (vide supra), the maps show remarkable differences. Sublibraries 2 and 4 (Fig. 3b, d) fill almost the complete map. Thus, the omission of the larger alkyl amino acids (group 2) or the hydroxy- and methylthio-substituted amino acids (group 4) does not seem to result in a loss of diversity. The other sublibraries show large white areas in the maps—parts of the chemical space not covered by them. The largest number of unoccupied neurons can be found for sublibrary 3 (Fig. 3c). Therefore, the basic amino acids (group 3) omitted in this sublibrary seem to have some qualities that cannot be covered by any other building block.

In order to show which compounds were considered similar by the Kohonen network, the contents of one arbitrarily chosen single neuron of the complete xanthene map are given in Scheme 1. Four pairs of structures (**3** and **4**, **5** and **6**, **7** and **8**, **9** and **10**) differ only by one amino acid—a chemist would group them together, too. On the other hand, the similarities between these four pairs are not as evident. Only the analysis with the Kohonen network revealed their similar distribution of the electrostatic potential on the molecular surface—a finding that cannot easily be derived from the structure diagrams.

 © VCH Verlagsgesellschaft mbH, D-69451 Weinheim, 1995 0570-0833/95/3423-2676 $ 10.00+.25/0

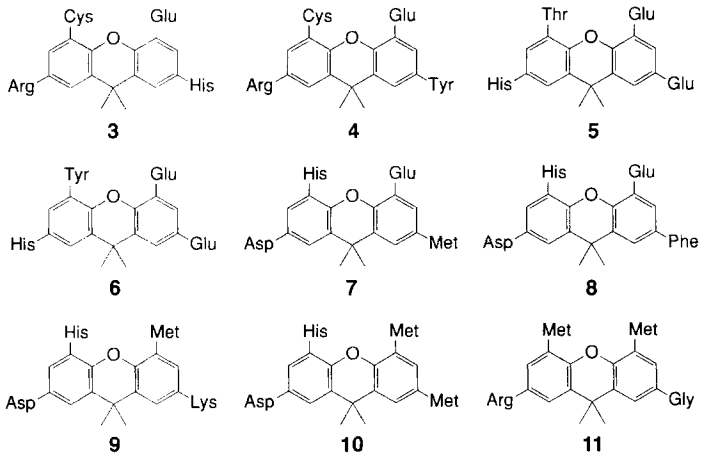

Scheme 1. Nine xanthene derivatives that were grouped together into neuron (6, 13) of the Kohonen map trained with the complete xanthene library.

It would be interesting to compare the result of this kind of similarity analysis with activity data as well. Unfortunately only for two of the xanthene library compounds[3b] is the exact activity known. We have found that 41 compounds were grouped together with the most potent trypsin inhibitor into one neuron of the Kohonen net. In our opinion, these 41 compounds would be worthwhile targets for further testing.

Received: July 17, 1995 [Z 8217 IE]
German version: *Angew. Chem.* **1995**, *107*, 2892–2895

Keywords: autocorrelation · compound libraries · computer chemistry · neural networks

[1] M. A. Gallop, R. W. Barrett, W. J. Dower, S. P. A. Fodor, E. M. Gordon, *J. Med. Chem.* **1994**, *37*, 1233–1251; E. M. Gordon, R. W. Barrett, W. J. Dower, S. P. A. Fodor, M. A. Gallop, *ibid.* **1994**, *37*, 1385–1401.

[2] M. Wagener, J. Sadowski, J. Gasteiger, *J. Am. Chem. Soc.* **1995**, *117*, 7769–7775.

[3] a) T. Carell, E. A. Wintner, A. Bashir-Hashemi, J. Rebek, Jr., *Angew. Chem.* **1994**, *106*, 2159–2162; *Angew. Chem. Int. Ed. Engl.* **1994**, *33*, 2059; b) T. Carell, E. A. Wintner, J. Rebek, Jr., *ibid.* **1994**, *106*, 2162–2165 bzw. **1994**, *33*, 2062; T. Carell, E. A. Wintner, A. J. Sutherland, J. Rebek, Jr., Y. M. Dunayevskiy, P. Vouros, *Chem. Biol.* **1995**, *2*, 171–183.

[4] Three-letter abbreviations of the 19 amino acids used as building blocks: Gly, Ala, Val, Leu, Ile, Pro, Arg, Lys, His, Ser, Thr, Met, Phe, Tyr, Trp, Glu, Asp, Asn, Cys.

[5] J. Gasteiger, C. Rudolph, J. Sadowski, *Tetrahedron Comput. Methodol.* **1990**, *3*, 537–547; J. Sadowski, J. Gasteiger, *Chem. Rev.* **1993**, *93*, 2567–2581; J. Sadowski, J. Gasteiger, G. Klebe, *J. Chem. Inf. Comput. Sci.* **1994**, *34*, 1000–1008.

[6] J. Gasteiger, M. Marsili, *Tetrahedron* **1980**, *36*, 3219–3228; J. Gasteiger, H. Saller, *Angew. Chem.* **1985**, *97*, 699–701; *Angew. Chem. Int. Ed. Engl.* **1985**, *24*, 687–689.

[7] T. Kohonen, *Self-Organization and Associative Memory*, 3rd ed., Springer, Berlin, **1989**.

[8] J. Zupan, J. Gasteiger, *Neural Networks for Chemists – An Introduction*, VCH, Weinheim, **1993**.

[9] The six groups generated from the 18 amino acids: 1) Gly, Ala, Val, 2) Leu, Ile, Pro, 3) Arg, Lys, His, 4) Ser, Thr, Met, 5) Phe, Tyr, Trp, 6) Glu, Asp, Asn.

Synthesis of a Cationic 1,3-Diphospha-2,4-dipallada(II)tricyclo[1.1.1]pentane Derivative: The First Structurally Characterized Pyramidal μ_2-Phosphinidene**

Yves Canac, Antoine Baceiredo, Heinz Gornitzka, Dietmar Stalke, and Guy Bertrand*

Dedicated to Professor Herbert Roesky on the occasion of his 60th birthday

The phosphinidene fragment can give rise to six different types of complex **A**–**F**[1] (Scheme 1). Recently, a few examples of stable η^1(bent)[1a–c, 2] and η^1(linear)-phosphinidene complexes (types **A** and **B**, respectively)[3] have been reported. The μ_3- and μ_4-phosphinidenes have been extensively used as building blocks for transition metal clusters (types **C** and **D**, respectively).[1e, f] Dinuclear phosphinidene compounds of type **E** in

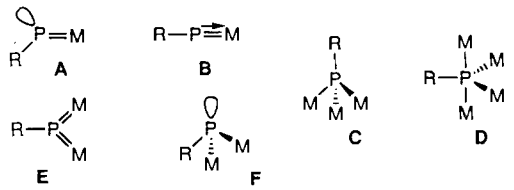

Scheme 1.

which an RP entity, by virtue of its two lone pairs, forms two donor bonds to two coordinatively unsaturated transition metal centers are well known.[1d–f] Since there is no lone pair left at the phosphorus center, there is no reason for pyramidalization around phosphorus and hence the three-center–four π-electron system **E** is trigonal planar. Phosphinidine complexes of type **F** can merely be considered as phosphanes with organometallic moieties on substituents, but very surprisingly only one example of a pyramidal μ_2-phosphinidene of this type has been reported and it has only been characterized by IR spectroscopy.[4] Here we report the synthesis and structure of the title compound, which features two nonplanar μ_2-phosphinidene units.

Palladium tetrakis(triphenylphosphane)[5] cleanly reacts at $-40\,^{\circ}C$ with one equivalent of diphosphacyclopropenium ion **1**[6] to yield the 1-pallada(II)-2σ^4,4σ^2-diphosphacyclobutene **2**. Very surprisingly, when a solution of complex **2** in dichloromethane was refluxed overnight in the presence of the three-membered heterocycle **1** (0.5 equiv) a new complex **3a** was formed (Scheme 2); no other species were detected by ^{31}P NMR spectroscopy. After workup, **3a** was isolated as a yellow powder (in 25% yield based on **2**; m.p. 175–176 °C).[7] Note that **3a** can also be directly obtained by heating **1** with 0.75 equivalents of the palladium(0) complex (Scheme 2). The low solubility of **3a** in nonpolar solvents was strong evidence of its ionic nature, which was confirmed by the presence of a sharp singlet for BF_4^-

[*] Dr. G. Bertrand, Y. Canac, Dr. A. Baceiredo
Laboratoire de Chimie de Coordination du CNRS
205, route de Narbonne, F-31077 Toulouse Cédex (France)
Telefax: Int. code +61 55 30 03
e-mail: gbertran@lcctoul.lcc-toulouse.fr
Dr. D. Stalke, Dr. H. Gornitzka
Institut für Anorganische Chemie der Universität
Tammannstrasse 4, D-37077 Göttingen (Germany)

[**] Thanks are due to the CNRS, the Deutsche Forschungsgemeinschaft, and the Fonds der Chemischen Industrie for financial support of this work. According to IUPAC rules RP: should be named phosphanediyl; however in agreement with usual conventions the term phosphinidene is used in this article.

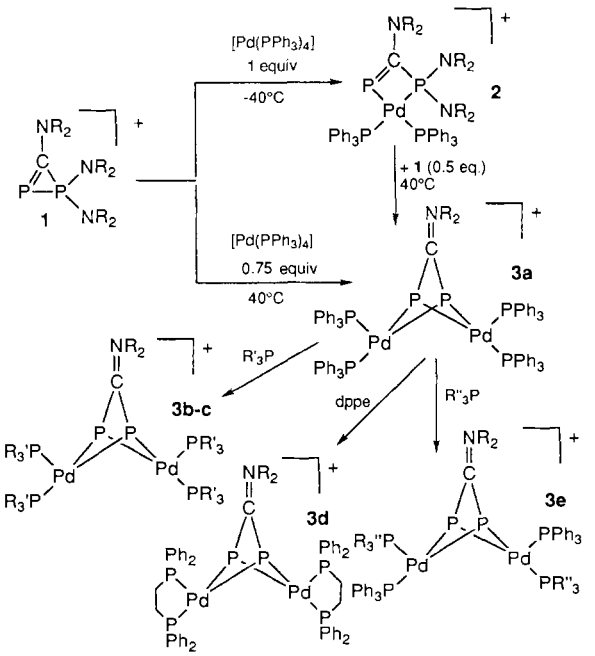

Scheme 2. R = iPr$_2$N, counterion BF_4^-. R'$_3$P = Me$_3$P (**3b**), Ph$_2$MeP (**3c**); R"$_3$P = (c-Hex)$_3$P. dppe = bis(diphenylphosphino)ethane.

at $\delta = 0$ in the ^{11}B NMR spectrum. According to ^{1}H and ^{13}C NMR spectroscopy, only one diisopropylamino group, not directly bonded to phosphorus, and four triphenylphosphane ligands were present in the molecule. The ^{31}P{^{1}H} NMR spectrum showed a triplet at $\delta = +17.7$ and a quintet at $\delta = +66.0$ (J(P,P) = 16.8 Hz), demonstrating the presence of two and four magnetically equivalent phosphorus atoms.

Since no obvious structure could be deduced from the spectroscopic data and the stoichiometry of the reaction, and since all attempts to obtain crystals of **3a** suitable for an X-ray diffraction study failed, we carried out exchange reactions with a variety of phosphanes (Scheme 2). Using trimethylphosphane, diphenylmethylphosphane, and 1,2-bis(diphenylphosphino)ethane, the four triphenylphosphane ligands of **3a** were exchanged giving **3b–d**, while with tricyclohexylphosphane only two of these ligands were replaced affording **3e**.[7] According to the spectroscopic data, the basic skeletons of complexes **3a–e** were identical; for **3e**, careful ^{13}C NMR ^{31}P coupled and decoupled experiments revealed the presence of one carbon directly bonded to two equivalent phosphorus atoms ($\delta = 234.1$, t, J(P,C) = 89.6 Hz).

The exact structure of complex **3e** (m.p. 178–180 °C) was determined by a single-crystal X-ray diffraction analysis[8] (Fig. 1). The C1–N1 bond length (1.325(10) Å) is in the range expected for a C–N double bond, implying that the positive charge is more or less localized at nitrogen. The palladium centers have a slightly distorted square-planar geometry and can be considered as Pd^{II}. At a first glance, this compound can be regarded either as a [1.1.1]propellane **3**,[9] which possesses bridgehead phosphorus atoms having an inverted tetrahedral geometry (Scheme 3), or alternatively as a tricyclo[1.1.1]pentane (asterane) **3** in which the P–P bond is broken. The P1 $\cdots$ P2 distance (2.681(3) Å) is much shorter than that observed in the 1,3-diphospha-2,4-disila-5-platinabicyclo[1.1.1]pentane (3.063 Å)[10] and related P_2B_3, P_2B_2Si, and P_2B_2Ge derivatives (2.86–3.07 Å),[11] but longer than normal P–P single bonds (2.20–2.35 Å).[12] The P1-Pd-P2 and P1-C1-P2 bond angles (69.17(8), 69.48(8), and 96.4(4)°, respectively) resemble those observed in the four-membered ring **2** (70.23 and 96.2°, respectively); however, the P1-C1-P2 bond angle is much larger than that in the three-membered ring **1** (73.9°). Therefore, complex **3** has an asterane structure with two strongly pyramidalized bridgehead phosphorus atoms (sum of angles = 254.0 and 251.7°).

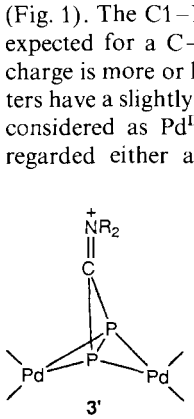

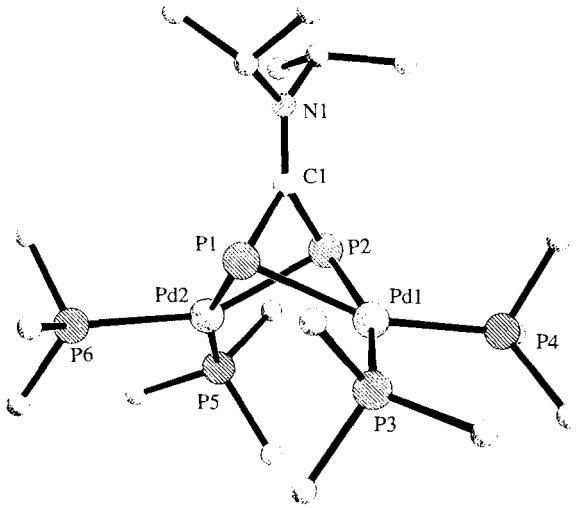

Fig. 1. Crystal structure of **3e**. For clarity only the C$_\alpha$ atoms of the cyclohexyl groups on the P3 and P5 and the C(ipso) atoms of the phenyl groups on the P4 and P6 atoms are shown. Selected bond lengths [Å] and angles [°]: Pd1-P1 2.358 (2), Pd1-P2 2.365 (2), Pd1-P3 2.394 (2), Pd1-P4 2.369 (2), Pd2-P1 2.336 (2), Pd2-P2 2.368 (2), Pd2-P5 2.392 (2), Pd2-P6 2.379 (2), P1-C1 1.794 (8), P2-C1 1.803 (4), C1-N1 1.325 (10); P1-Pd1-P2 69.17 (8), P1-Pd1-P3 90.88 (8), P3-Pd1-P4 106.77 (8), P2-Pd1-P4 93.44 (8), P1-Pd2-P2 69.48 (8), P1-Pd2-P6 91.74 (8), P5-Pd2-P6 106.68 (8), P2-Pd2-P5 94.28 (8), P1-C1-P2 96.4 (4), C1-P1-Pd1 81.6 (3), C1-P1-Pd2 84.4 (3), Pd2-P1-Pd1 88.01 (8), C1-P2-Pd1 81.3 (3), C1-P2-Pd2 83.3 (3), Pd2-P2-Pd1 87.11 (8).

Although the stoichiometry of the reaction, the cleavage of the diisopropylamino groups, and the mechanism as a whole for the reaction leading to **3a** is still obscure and deserves further study, this type of complex is unique in several respects: it features two pyramidalized μ_2-phosphinidene units, it contains metal atoms from Group 10, and can be considered as a 2,4-dimetallatricyclo[1.1.1]pentane and as an asterane possessing a trigonal carbon atom.

Received: July 24, 1995 [Z 8247 IE]
German version: *Angew. Chem.* **1995**, *107*, 2904–2906

Keywords: asteranes · palladium compounds · phosphorus compounds · polycycles

[1] Reviews: a) F. Mathey, *Angew. Chem.* **1987**, *99*, 285–296; *Angew. Chem. Int. Ed. Engl.* **1987**, *26*, 275–286; b) A. H. Cowley, A. R. Barron, *Acc. Chem. Res.* **1988**, *21*, 81–87; c) F. Mathey in *Multiple Bonds and Low Coordination in Phosphorus Chemistry* (Eds.: M. Regitz, O. J. Scherer), Thieme, Stuttgart, **1990**, p. 33; d) G. Huttner in *Multiple Bonds and Low Coordination in Phosphorus Chemistry* (Eds.: M. Regitz, O. J. Scherer), Thieme, Stuttgart, **1990**, S. 48; e) G. Huttner, K. Evertz, *Acc. Chem. Res.* **1986**, *19*, 406–413; f) G. Huttner, K. Knoll, *Angew. Chem.* **1987**, *99*, 765–782; *Angew. Chem. Int. Ed. Engl.* **1987**, *26*, 743–760.

[2] P. B. Hitchcock, M. F. Lappert, W.-P. Leung, *J. Chem. Soc. Chem. Commun.* **1987**, 1282–1283.

[3] a) A. H. Cowley, B. Pellerin, J. L. Atwood, S. G. Bott, *J. Am. Chem. Soc.* **1990**, *112*, 6734–6735; b) C. C. Cummins, R. R. Schrock, W. M. Davis, *Angew. Chem.* **1993**, *105*, 758–761; *Angew. Chem. Int. Ed. Engl.* **1993**, *32*, 756–759; c) P. P. Power, *ibid.* **1993**, *105*, 893–894 bzw. **1993**, *32*, 850–851.

[4] J. C. Burt, G. Schmid, *J. Chem. Soc. Dalton Trans* **1978**, 1385–1387.

[5] Y. Canac, M. Soleilhavoup, L. Ricard, A. Baceiredo, G. Bertrand, *Organometallics* **1995**, *14*, 3614–3616.
[6] F. Castan, A. Baceiredo, J. Fischer, A. De Cian, G. Commenges, G. Bertrand, *J. Am. Chem. Soc.* **1991**, *113*, 8160–8161.
[7] **3a**-BF_4: To a solution of **1**-BF_4 (0.46 g, 1 mmol) in dichloromethane (5 mL) at −50 °C was added palladium tetrakis(triphenylphosphane) (0.86 g, 0.75 mmol). After stirring for 18 h at 40 °C, the solvent was removed in vacuo, and the residue was washed several times with toluene and ether to give **3a**-BF_4 as a yellow powder (25% yield); m.p. 175–176 °C; ^{31}P NMR ($CDCl_3$): $\delta = +17.7$ (t, ^2J(P,P) = 16.8 Hz, Ph_3P), +66.0 (q, ^2J(P,P) = 16.8 Hz, Pd-P-C); ^{1}H NMR ($CDCl_3$): $\delta = 1.08$ (d, ^3J(H,H) = 6.8 Hz, 12H, CH_3), 4.07 (sept., ^3J(H,H) = 6.8 Hz, 2H, CH), 7.00–7.28 (m, 60H, H_{arom}); ^{13}C NMR ($CDCl_3$): $\delta = 19.1$ (s, CH_3), 52.7 (s, CH), 127.8 (s, C_m), 129.5 (s, C_p), 132.7 (m, C_i), 133.5 (s, C_o), the signal of PCP was not observed; MS (FAB/NPOE, CH_2Cl_2): 1174 [$M^+ - Ph_3P$].

3b–**e** (as BF_4 salts): To a solution of **3a**-BF_4 in dichloromethane at room temperature was added 4 equiv of phosphane [(trimethylphosphane) (**3b**), (diphenylmethylphosphane) (**3c**), (tricyclohexylphosphane) (**3e**)], or 2 equiv of 1,2-bis(diphenylphosphino)ethane (**3d**). After 30 min at room temperature, the solvent was removed in vacuo, and the residue was washed several times with toluene and ether to eliminate the excess of phosphane. Complexes **3b**–**e** (as BF_4 salts) were obtained in near quantitative yield **3b**-BF_4: red oil; ^{31}P NMR ($CDCl_3$): $\delta = -28.0$ (t, ^2J(P,P) = 20.3 Hz, Me_3P), +65.8 (m, Pd-P-C); **3c**-BF_4: red oil; ^{31}P NMR (C_6D_6): $\delta = -1.7$ (t, ^2J(P,P) = 18.1 Hz, Ph_2PMe), +73.0 (q, ^2J(P,P) = 18.1 Hz, Pd-P-C); **3d**-BF_4: red oil; ^{31}P NMR (C_6D_6): $\delta = 31.5$ (t, ^2J(P,P) = 14.7 Hz, Ph_2PCH_2), +75.9 (m, Pd-P-C); **3e**-BF_4: orange crystals; m.p. 178–180 °C; ^{31}P NMR ($CDCl_3$): $\delta = +14.2$ (m, *c*-Hex_3P), +21.4 (m, Ph_3P), +65.1 (m, Pd-P-C).
[8] Crystal data of **3e**-BF_4: $C_{107}H_{166}BF_4NO_2P_6Pd_2$ were grown from a THF/ether solution, $M = 2064.85$, triclinic, space group $P\bar{1}$, $a = 1445.2(3)$, $b = 1655.9(3)$, $c = 2354.1(5)$ pm, $\alpha = 97.51(3)$, $\beta = 104.52(3)$, $\gamma = 95.77(3)°$; $V = 5.355(2)$ nm^3; $Z = 2$; $\rho_{calcd} = 1.281$ Mg m^{-3}, $F(000) = 2190$, $\lambda = 71.073$ pm, $T = 153$ K, $\mu(Mo_{K\alpha}) = 0.485$ mm^{-1}, data were collected on a Stoe-Siemens-AED diffractometer. Intensities of a 0.3 × 0.3 × 0.2 mm rapidly cooled crystal in an oil drop [13] were collected by the $2\theta/\omega$ method in the range of $8 \le 2\theta \le 45°$. Of a total of 14777 reflections, 14002 were independent, and after empirical absorption correction 13994 reflections were used to refine 1431 parameters. largest difference peak and hole: 0.539 and −0.548 e Å^{-3}, $R1(F > 2\sigma(F)) = 0.069$ and $wR2 = 0.169$ (all data) with $R1 = \sum||F_o| - |F_c||/\sum|F_o|$ and $wR2 = (\sum w(F_o^2 - F_c^2)^2/\sum w(F_o^2)^2)^{0.5}$. The structure was solved with direct methods (SHELXS-92) [14] and refined by full-matrix least-squares on F^2 (SHELXL-93) [15]. A riding model was applied to refine the hydrogen atom positions. The uncoordinated disordered THF molecules were refined by applying 1-2- and 1-3-similarity restraints. Further details of the crystal structure investigations are available on request from the Director of the Cambridge Crystallographic Data Centre, 12 Union Road, GB-Cambridge CB2 1EZ (UK), on quoting the full journal citation.
[9] a) K. B. Wiberg, *Acc. Chem. Res.* **1984**, *17*, 379–386; b) K. B. Wiberg, S. T. Waddell, *J. Am. Chem. Soc.* **1990**, *112*, 2194–2216; c) N. V. Riggs, U. Zoller, M. T. Nguyen, L. Radom, *ibid.* **1992**, *114*, 4354–4356; d) L. R. Sita, I. Kinoshita, *ibid.* **1990**, *112*, 8839–8843; e) H. Yoshida, Y. Takahara, T. Erata, W. Ando, *ibid.* **1992**, *114*, 1098–1100.
[10] a) M. Driess, A. D. Fanta, D. R. Powell, R. West, *Angew. Chem.* **1989**, *101*, 1087–1089; *Angew. Chem. Int. Ed. Engl.* **1989**, *28*, 1038–1040; b) A. D. Fanta, M. Driess, D. R. Powell, R. West, *J. Am. Chem. Soc.* **1991**, *113*, 7806–7808.
[11] R. T. Paine, H. Nöth, *Chem. Rev.* **1995**, *95*, 343–379.
[12] a) A. H. Cowley, *Chem. Rev.* **1965**, *65*, 617–634; b) J. R. Durig, L. A. Carreira, J. D. Odom, *J. Am. Chem. Soc.* **1974**, *96*, 2688–2693; c) *CRC Handbook of Chemistry and Physics* (Hrsg.: D. R. Lide), CRC, Boca Raton, FL, **1992**, S. 9-1.
[13] T. Kottke, D. Stalke, *J. Appl. Crystallogr.* **1993**, *26*, 615.
[14] G. M. Sheldrick, *Acta Crystallogr. Sect. A* **1990**, *46*, 467.
[15] G. M. Sheldrick, SHELXL-93, programm for crystal structure refinement, Göttingen, **1993**.

Two Diorganopotassates: Crystal Structure of $[K(C_6H_6)][K\{C(SiMe_3)_2(SiMe_2Ph)\}_2]$**

Colin Eaborn, Peter B. Hitchcock, Keith Izod, and J. David Smith*

Salts **1a**–**1c** containing the diorganolithate anion $[LiR_2]^-$, R = $C(SiMe_3)_3$ (Scheme 1), were isolated between 1983 and 1986[1] and the first dialkylsodate, **2**, was described recently.[2]

$M[Li\{C(SiMe_3)_3\}_2]$ **1a**, M = $[Li(thf)_4]$
1b, M = $[Li(tmen)_2]$
1c, M = [(pmdeta)Li(μ-Cl)Li(pmdeta)]

$[Na(tmen)_2(OEt_2)][Na\{C(SiMe_3)_3\}_2]$ **2**

$[K(C_6H_6)][K\{C(SiMe_3)_2(SiMe_2Ph)\}_2]$ **3**

$[K(OSiMe_2)_7][K\{C(SiMe_3)_2[SiMe_2(HC{=}CH_2)]\}_2]$ **4**

Scheme 1. tmen = *N*,*N*,*N*′,*N*′-Tetramethylethylenediamine, pmdeta = *N*,*N*,*N*′,*N*″-pentamethyldiethylenetriamine.

Reactions between the methyl derivatives of the heavier alkali metals[3] and $HC(SiMe_3)_3$ gave solvent-free compounds $M[C(SiMe_3)_3]$ which, in the solid state, formed chains of alternate cations M^+ and planar anions $[C(SiMe_3)_3]^-$ (M = K,[4] Rb[5]) or ion pairs separated by coordinated benzene (M = Cs).[5] The analogous compounds $M[C(SiMe_2Ph)_3]$, M = Na,[2] K,[4] Cs,[6] all crystallized as yellow solids which were rather insoluble in organic solvents. In crystals alternate anions and cations were linked by coordination between alkali metal and phenyl groups from the anion periphery.

The different structures adopted by the compounds $M[C(SiMe_3)_3]$ and $M[C(SiMe_2Ph)_3]$ suggested that it might be rewarding to synthesize the compound $K[C(SiMe_3)_2(SiMe_2Ph)]$. This was readily achieved by metalation of $HC(SiMe_3)_2(SiMe_2Ph)$ with methylpotassium, and crystals suitable for an X-ray diffraction study were obtained from benzene. The structure[7] (Fig. 1) consists of chains of alternate K^+ ions and $[C(SiMe_3)_2(SiMe_2Ph)]^-$ ions, but as there are two distinct environments for potassium it is best described as a potassium dialkylpotassate (**3**) (Scheme 1). The cation K1 lies on a twofold

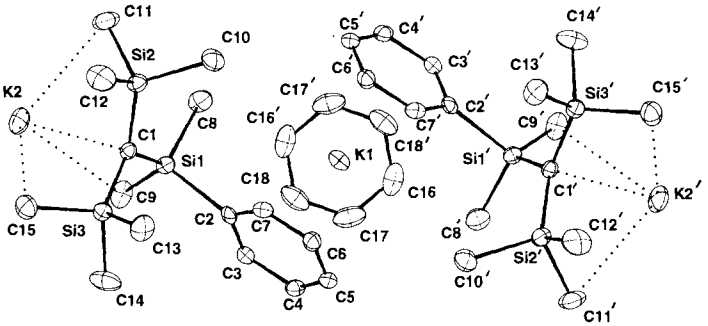

Fig. 1. Crystal structure of **3**. Important distances [pm] and angles [°]: K1–Ph* 287, K1–C_6H_6* 297, K2–C1 291.4(5), K2–C9 344.8(5), K2–C11 329.4(6), K2–C15 333.5(6), Si–C1 180.7(5)*, Si-Me 188.6(6)*, Si-C(2) 191.9(5), Ph-K-C_6H_6* 118.8, Si1-C1-Si3 117.2, Si1-C1-Si2 119.6, Si3-C1-Si2 120.0, Me-Si-Me 103.6*. Values marked with * refer to centroids of Ph or C_6H_6; mean values are marked with*.

[*] Dr. J. D. Smith, Prof. C. Eaborn, Dr. P. B. Hitchcock, Dr. K. Izod
School of Chemistry and Molecular Sciences
University of Sussex
Brighton BN1 9QJ (UK)
Telefax: Int. code + (1273)677196

[**] This work was supported by the Engineering and Physical Sciences Research Council.

axis and is bound to two phenyl groups from the neighboring anions and a molecule of benzene. Interactions between alkali metals and benzene or phenyl groups have been identified in a wide range of organometallic compounds.[8, 9] In contrast to the benzene molecule in $Cs[C(SiMe_2Ph)_3]\cdot 3C_6H_6$[5] that in **3** is held tenaciously: it is not removed by pumping under vacuum for several hours at 10^{-3} Torr. The tight bonding is reflected in the K–C(C_6H_6) bond lengths (mean 3.28(1) Å) which are comparable with the values of 3.33 to 3.43 Å in various liquid clathrates.[9c–f] The K–C(Ph) distances (3.155(4)–3.190(5) Å) are similar to those in [KCPh$_3$·thf·pmdeta].[9a] and $K_2[Ph_2CCH{=}CHCPh_2]\cdot 2Et_2O$.[9b] The second potassium ion in **3**, K2, lies at a crystallographic center of symmetry and is bound to the two central carbon atoms from adjacent $C(SiMe_3)_2(SiMe_2Ph)$ groups and, more weakly, to six methyl groups. The fact that all the K2–C distances are significantly shorter than those in $K[C(SiMe_3)_3]$ is consistent with the description of the compound as a potassium potassate. A polymeric compound $[K(thf)]_n[K\{C_3N_3Ph_2nButBu\}_2]_n$ containing substituted dihydrotriazine residues has recently been described[10] but, as far as we are aware, **3** is the first dialkylpotassate to be isolated.

Metalation of $HC(SiMe_3)_2(SiMe_2(CH{=}CH_2))$ with methylpotassium likewise gave an organopotassium derivative, and NMR data suggested that this was $K[C(SiMe_3)_2(SiMe_2(CH{=}CH_2))]$. The fine crystals obtained from methylcyclohexane/Et_2O, which were too fragile for an X-ray structure determination, were allowed to stand in the mother liquor for four weeks, during which larger crystals appeared. These were shown to consist of the potassate **4**, but because of disorder in the anion the data are not sufficiently accurate to justify a detailed discussion.[11] The cation in **4** has been reported previously;[12] as in our work it was formed by the adventitious reaction between an organometallic compound and a hydrocarbon solution containing a trace of silicone grease. Since in our experiments the Schlenk tube was at all times kept upright the grease must have dissolved as solvent distilled slowly on to the stopper and ran back into the solution.

Experimental Procedure

3: $HC(SiMe_3)_2(SiMe_2Ph)$ (5.0 g, 17 mmol) was added to a cold (−10 °C) suspension of MeK (27 mmol) in Et_2O (50 mL). The mixture was stirred for 1 h at −10 °C and then for a further 16 h during which time it was allowed to warm to room temperature. Solvent was removed under vacuum, the sticky residue was extracted into warm benzene/THF (1:1, 70 mL), the extract filtered and solvent evaporated. The solid obtained was washed with light petroleum (b. p. 40–60 °C) and recrystallized from hot benzene to give orange crystals of **3**. The compound was too air- and moisture-sensitive for satisfactory C and H analysis; ^{1}H NMR ([D$_8$]THF, chemical shifts relative to SiMe$_4$, 25 °C): $\delta = -0.11$ (s, 18H, Me_3Si), 0.12 (s, 6H, Me_2Si), 6.96 (m, 1H, *p*-H), 7.05 (m, 2H, *m*-H), 7.30 (s, 3H, C_6H_6), 7.68 (m, 2H, *o*-H); ^{13}C NMR: $\delta = 0.2$ (CSi_3), 7.3 ($SiMe_2$), 8.4 ($SiMe_3$), 125.9, 126.5, 135.1, 154.4 (Ph), 128.9 (C_6H_6); ^{29}Si NMR: $\delta = -9.6$ ($SiMe_2$), −7.5 ($SiMe_3$).

4: $HC(SiMe_3)_2(SiMe_2(CH{=}CH_2))$ (1.3 g, 5.35 mmol) was added to a suspension of KMe (6.21 mmol) in Et_2O at −10 °C. The mixture was allowed to warm slowly with stirring to room temperature. Solvent was removed, the residue extracted into benzene, and the extract was filtered and concentrated. The crystals which separated were washed with light petroleum. ^{1}H NMR (C_6D_6, 25 °C): $\delta = 0.34$ (s, 18H, Me_3Si), 0.47 (s, 6H, Me_2Si), 5.46 (dd, 1H), 5.62 (dd, 1H), and 6.64 (dd, 1H) ($H_2C{=}CH$); ^{13}C NMR: $\delta = 5.3$ (CSi_3), 5.4 (Me_2Si), 8.5 (Me_3Si), 124.2, 154.5 (C=C); ^{29}Si NMR: $\delta = -14.5$ (Me_2Si), −10.4 (Me_3Si). Fine crystals were obtained from methylcyclohexane/Et_2O. After four weeks larger crystals were formed and these were shown by X-ray diffraction to be **4**; ^{1}H NMR ([D$_8$]THF, 25 °C): $\delta = -0.06$ (s, 18H, Me_3Si), −0.01 (s, 6H, Me_2Si), 0.08 (s, 21H, Me_2SiO), 5.42 (dd, 1H), 5.54 (dd 1H), 6.42 (dd, 1H) and ($H_2C{=}CH$).

Received: July 24, 1995 [Z 8251 IE]
German version: *Angew. Chem.* **1995**, *107*, 2936–2937

Keywords: potassium compounds · silicon compounds · structure elucidation

[1] For a review see C. Eaborn, K. Izod, J. D. Smith, *J. Organomet. Chem.* **1995**, *500*, 89.
[2] S. S. Al-Juaid, C. Eaborn, P. B. Hitchcock, K. Izod, M. Mallien, J. D. Smith, *Angew. Chem.* **1994**, *106*, 1336; *Angew Chem. Int. Ed. Engl.* **1994**, *33*, 1268.
[3] E. Weiss, *Angew. Chem.* **1993**, *105*, 1565; *Angew. Chem. Int. Ed. Engl.* **1993**, *32*, 1501.
[4] C. Eaborn, P. B. Hitchcock, K. Izod, J. D. Smith, *Organometallics* **1994**, *13*, 753.
[5] C. Eaborn, P. B. Hitchcock, K. Izod, J. D. Smith, *Angew. Chem.* **1995**, *107*, 756; *Angew Chem. Int. Ed. Engl.* **1995**, *34*, 687.
[6] C. Eaborn, P. B. Hitchcock, K. Izod, J. D. Smith, unpublished.
[7] Crystal data for **3**: $M_r = 371.8$, monoclinic, space group $C2/c$, $a = 15.535(5)$, $b = 9.448(2)$, $c = 30.444(9)$ Å, $\beta = 102.53(3)°$, $V = 4362(2)$ Å^3, $Mo_{K\alpha}$ radiation, $\lambda = 0.71073$ Å, $Z = 8$, $\rho = 1.13$ Mgm^{-3}, $F(000) = 1608$, $\mu(Mo_{K\alpha}) = 0.41$ mm^{-1}, $T = 173(2)$ K. 3028 unique reflections measured and all used. No absorption or decay correction. Structure analysis by direct methods with SHELXLS-86. Full matrix least squares refinement on F^2 with SHELXL-93, non-hydrogen atoms anisotropic and H at calculated positions with common U_{iso} for phenyl and methyl which refined to 0.050(6) and 0.087(4) Å^2 respectively. Final $R1 = 0.058$ for 1928 reflections with $I > 2\sigma(I)$, $wR2 = 0.109$ for all reflections. Further details of the crystal structure investigation may be obtained from the Director of the Cambridge Crystallographic Data Centre, 12 Union Road, Cambridge CB2 1EZ (UK), on quoting the full journal citation.
[8] H. Bock, K. Ruppert, C. Näther, Z. Havlas, H.-F. Herrmann, C. Arad, I. Göbel, A. John, J. Meuret, S. Nick, A. Rauschenbach, W. Seitz, T. Vaupel, B. Solouki, *Angew. Chem.* **1992**, *104*, 564; *Angew Chem. Int. Ed. Engl.* **1992**, *31*, 550.
[9] a) D. Hoffmann, W. Bauer, P. von R. Schleyer, U. Pieper, D. Stalke, *Organometallics* **1993**, *12*, 1193; b) H. Bock, C. Näther, K. Ruppert, *J. Chem. Soc. Chem. Commun.* **1992**, 765; c) J. L. Atwood, K. D. Crissinger, R. D. Rogers, *J. Organomet. Chem.* **1978**, *155*, 1; d) J. L. Atwood, D. C. Hrnčíř, R. D. Priester, R. D. Rogers, *Organometallics* **1983**, *2*, 985; e) J. L. Atwood, D. C. Hrnčíř, R. D. Rogers, *J. Inclusion Phenom* **1983**, *1*, 199; f) J. L. Atwood, W. E. Hunter, R. D. Rogers, J. A. Weeks, *J. Inclusion Phenom* **1985**, *3*, 113.
[10] W. Clegg, L. Horsburgh, R. E. Mulvey, M. J. Ross, *J. Chem. Soc. Chem. Commun.* **1994**, 2393.
[11] Crystal data for **4**: $M_r = 1084.5$, monoclinic, space group $C2/c$, $a = 15.149(7)$, $b = 19.194(5)$, $c = 24.100(8)$ Å, $\beta = 100.60(3)°$, $V = 6888(4)$ Å^3, $Mo_{K\alpha}$ radiation $\lambda = 0.71073$ Å, $Z = 4$.
[12] M. R. Churchill, C. H. Lake, S.-H. L. Chao, O. T. Beachley, *J. Chem. Soc. Chem. Commun.* **1993**, 1577.

Structure-Determining C–H···O–Si Hydrogen Bonds in Cobaltocenium Fluoride Nonasil**

Peter Behrens,* Gianpietro van de Goor, and Clemens C. Freyhardt

The formation of zeolite-type solids by hydrothermal treatment of silica gels or solutions in the presence of organic molecules is currently under intensive investigation.[1] Organic molecules like amines, alkylammonium ions, or cyclic ethers are incorporated in the voids of the crystallizing framework and influence the type of structure that is formed. However, there are no clear host–guest relations in the sense of a real template effect. In accordance with this, in most of the cases the guest molecules exhibit orientational or rotational disorder at room temperature.[1] Nevertheless, there is at least some control of the reaction product, which could lead to a design of solid-state structures[2] (structure-directed synthesis of solids). The size and shape of the structure-directing molecules were recognized

[*] Prof. Dr. P. Behrens, Dipl.-Chem. G. van de Goor
Institut für Anorganische Chemie der Universität
Meiserstrasse 1, D-80333 München (Germany)
Telefax: Int. code + (89)5902-578
e-mail: pbe@anorg.chemie.uni-muenchen.de
Dr. C. C. Freyhardt
Fakultät für Chemie, Universität Konstanz (Germany)

[**] This work was carried out in the group of Prof. J. Felsche at the University of Konstanz. We thank him, the Deutsche Forschungsgemeinschaft (Be1664/1-2), and the Fonds der Chemischen Industrie for support.

as the most important parameters. These determine the size and the shape of the voids in the tetrahedral network of the host.[3] Details of the interaction between the organic guest molecules and the host framework, however, are known only in a few cases.

Currently, there is considerable interest in using organometallic complexes as components for the construction of solid inorganic compounds.[4] Metallocene complexes have been intercalated into layered sulfides[4a-c] and inserted into zeolites.[4d,e] These reactions often yield products with ill-defined stoichiometries, the structures of which are difficult to characterize. In contrast, self-assembly from solution gives stoichiometric products, often as single crystals, as presented recently by Schwarz et al.[4f] They investigated the reaction of cobaltocenium cations, hexacyanoferrate(II) anions, and trimethyltin chloride which leads to a channel-type inclusion compound with a three-dimensional framework structure.

Recently, it was shown that organometallic complexes can also act as structure-directors in the hydrothermal synthesis of zeolite-type compounds.[5-7] We[6] found that the cobaltocenium cation $[Co(C_5H_5)_2]^+$, $[CoCp_2]^+$, directs the formation of stoichiometrically well-defined clathrasils[8a] of the nonasil, the octadecasil, and the dodecasil 1H type (abbreviated as NON, AST, and DOH, respectively;[8b] the topology of the nonasil structure is shown in Fig. 1a). With increasing temperature, structures with increasingly larger cages are formed.[9] Of special interest here is the nonasil $[CoCp_2]^+F^-[SiO_2]_{22}$ **1**, prepared

$$[CoCp]^+F^-[SiO_2]_{22} \triangleq [CoCp_2]F\text{-NON} \quad \mathbf{1}$$

by the fluoride method,[10] which is the compound that crystallizes in the lowest temperature regime (between 420–440 K). The single-crystal X-ray structural analysis of this product (performed at 220 K) reveals some extraordinary features.[6]

The similarity of the shape of the largest void of the nonasil structure, the $[5^86^{12}]$ cage, and of the sandwich complex (Fig. 1b and 1c respectively), suggested that the organometallic cation occupies this void. Indeed, we found the cobaltocenium cation

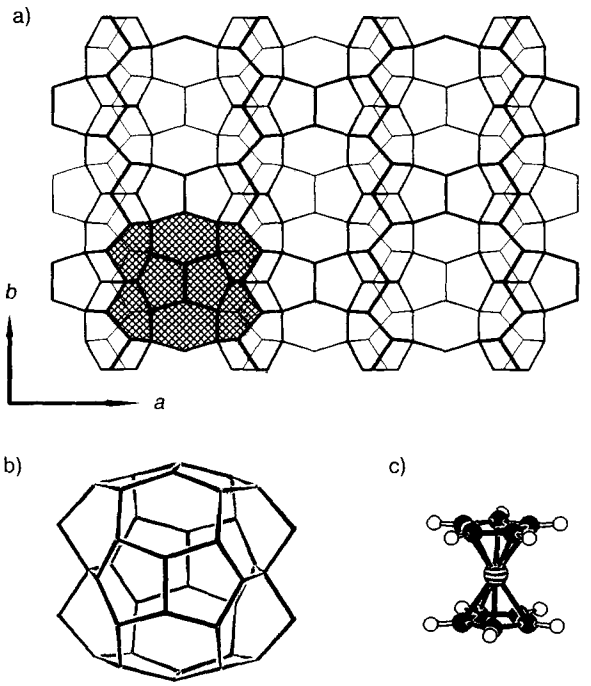

Fig. 1. a) Topology of the nonasil structure (oxygen atoms omitted); b) the $[5^86^{12}]$ cage of the nonasil structure; its shape resembles that of the cobaltocenium cation (c).

in the expected orientation in a staggered conformation which conforms to the symmetry of the inversion center in the center of the cage (at the position of the Co atom). The cation is fixed and does not show rotational disorder with regard to its fivefold axis (Fig. 2a). This result was unexpected, because sandwich complexes with unsubstituted cyclopentadienyl ligands often exhibit such disorder also in simple salts; in the case of a zeolite-type host–guest compound, where the guest species usually are disordered at room temperature, the absence of disorder is even more unexpected. A reversible phase transition, which is associated with the onset of rotation of the $[CoCp_2]^+$ ions, was observed at $T_c = 485$ K by microcalorimetry (DSC).[6]

The detailed description of the C–H···O–Si contacts as derived from the X-ray structural analysis[11] reveals the type of the unusual strong host–guest interactions which are responsible for the absence of disorder. Figures 2b and 2c depict the

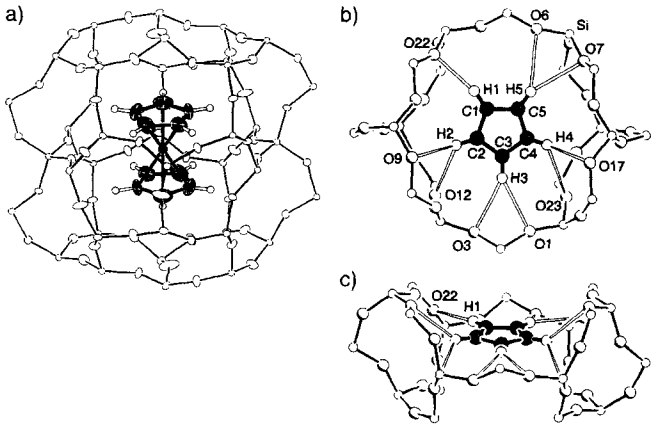

Fig. 2. Crystal structure of **1** [11]: a) ORTEP drawing of the $[5^86^{12}]$ cage containing the cobaltocenium cation; b) and c): SCHAKAL plots showing the C–H···O–Si interactions between the cobaltocenium cation and the SiO_2 framework. Important bond lengths and angles (d(H···O) in Å, d(C···O) in Å, ∢ C–H···O in °): C1–H1···O22: 2.309, 3.369, 166.7; C2–H2···O9: 2.645, 3.527, 138.5; C2–H2···O12: 2.846, 3.527, 121.1; C3–H3···O1: 2.604, 3.591, 151.6; C3–H3···O3: 2.700, 3.677, 150.3; C4–H4···O17: 2.699, 3.544, 134.8; C4–H4···O23: 2.884, 3.554, 120.4; C5–H5···O6: 2.765, 3.704, 145.3; C5–H5···O7: 2.644, 3.649, 154.5.

arrangement of a cyclopentadienyl ring with regard to the surrounding oxygen atoms of the framework (due to the inversion center at the site of the Co atom the situation is the same for the opposing five-ring of the CoCp cation). Four of the five hydrogen atoms (H2 to H5) of a Cp ring have C–H···O–Si contacts with distances in the range of d(H···O) = 2.60–2.88 Å or d(C···O) = 3.53–3.70 Å (∢ C–H···O = 120–155°); for each hydrogen atom, two framework oxygen atoms are in this distance range. The fifth hydrogen atom of a Cp ring (H1) exhibits only one C–H···O–Si contact, which, however, is considerably shorter: d(H1···O) = 2.31 Å or d(C1···O) = 3.37 Å (∢ C–H1···O = 167°).

In the last few years, it has become apparent that C–H···O interactions exist in organic crystals[13,14] and that they influence the packing of molecules in crystals,[14] disorder phenomena,[15] and thermal parameters of neighboring atoms.[16] On the basis of these results, criteria were developed with regard to the occurrence of C–H···O hydrogen bonds in organic compounds.[17,18] Steiner's criteria[18] are: d(H···O) < 2.8 Å and ∢ C–H···O > 90°.

The bifurcated C–H···O interactions of H atoms H2 to H5 are thus located on the border between van der Waals contacts[19] and hydrogen bonds. Such C–H···O–Si interactions probably occur in many porosils[8a] that contain organic guest

molecules, although only a few quantitative investigations have been carried out to date. In trioxane silica sodalite, for example, each trioxane molecule is involved in a total of eighteen C–H···O–Si interactions of this kind (d(O-H): 9 × 2.72 Å and 9 × 2.93 Å). In spite of these interactions the trioxane molecules are disordered over four equivalent sites at room temperature.[20] Therefore, we believe that also in the case of $[CoCp_2]$F-NON **1** the longer C–H···O–Si contacts alone are not sufficient to fix the $[CoCp_2]^+$ ions. In our opinion, the absence of rotational disorder is due to the short C–H1···O–Si interactions, which clearly must be classified as hydrogen bonds. Interestingly, in this context, Steiner et al.[15] have recently attributed the absence of (expected) disorder in a β-cyclodextrin complex of pentane-1,5-diol to a C–H···O hydrogen bond.

The IR spectrum of **1** exhibits a splitting of the C–H valence bands, corresponding to the different strengths of the C–H bonds which vary due to the different C–H···O–Si interactions (Fig. 3). In comparison to the C–H bands of cobaltocenium hexafluorophosphate (ν_{C-H} = 3128 cm^{-1}) and of the cobaltocenium clathrasil of the DOH type (ν_{C-H} = 3120 cm^{-1}),[21] an additional signal appears in the nonasil **1** at ν_{C-H} = 3100 cm^{-1}, which we assign to the C–H valence vibration of the H1 atom. The splitting decreases with increasing temperature, especially above T_c.[22] The IR spectrum of the DOH clathrasil shows no indications of a similarly strong C–H···O–Si interaction and, on the basis of this and the results of other investigations,[21] we assume that in this case the complex is rotationally disordered at room temperature. Since the complex cation occupies a considerably larger void in the DOH compound (430 Å^3 compared to 290 Å^3 in NON), one can assume that the extraordinarily strong interaction in nonasil **1** is due to steric reasons rather than being caused by specific properties of the $[CoCp_2]^+$ ion: The geometry of the sandwich complex fits perfectly to that of the $[5^86^{12}]$ cage of the NON framework (Figs. 1b, c, Fig. 2a), and this perfect fit may well be the driving force for the formation of the strong C–H···O–Si interactions. A further indication for this is the fact that the temperature region, in which **1** crystallizes (420–440 K), has a rather low upper limit. Evidently, above this limit, the space requirement of the complex cations in the synthesis gel increases too strongly because of their dynamical movements, and thus a structure with a larger cage is formed (AST type, volume of the largest cage: 360 Å^3).

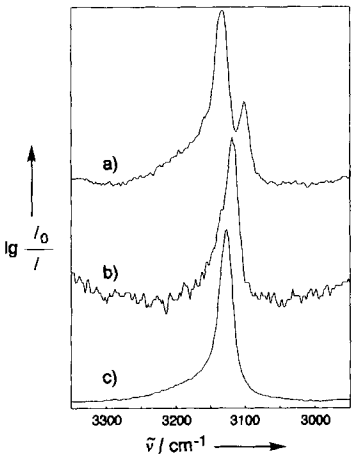

Fig. 3. IR spectra: Region of C–H valence vibrations of the cobaltocenium cation in the fluoride nonasil **1** (a), in the dodecasil 1H (b), and in the hexafluorophosphate (c).

This work provides the first direct proof of strong C–H···O–Si hydrogen bonds between a guest molecule and a zeolite-type host framework. We suppose that the C–H···O–Si interactions found in the crystal may also play a role during nucleation in the synthesis gel within the temperature regime of 420–440 K. This idea is supported by the fact that the phase transition temperature T_c, which marks the onset the rotational disorder,[6] lies well above the synthesis temperature (485 K versus 420–440 K). Our results are not only of importance with regard to the synthesis of zeolite-type phases. The proof that strong C–H···O–Si bonds are possible is of general importance for the interactions of organic or organometallic molecules with solid surfaces. Such interactions also play a role in heterogeneous catalysis and in biomineralization.

Received: April 20, 1995
Revised version: June 23, 1995 [Z 7907 IE]
German version: *Angew. Chem.* **1995**, *107*, 2895–2898

Keywords: clathrasils · cobalt compounds · hydrogen bonds · silicon dioxide · zeolites

[1] M. E. Davis, R. F. Lobo, *Chem. Mater.* **1992**, *4*, 756.
[2] M. E. Davis, *CHEMTECH* **1994**, 22.
[3] H. Gies in *Inclusion Compounds, Vol. 5* (Eds.: J. L. Atwood, J. E. D. Davies, D. D. MacNicol), Oxford University Press, Oxford, **1991**, p. 1; H. Gies, B. Marler, *Zeolites* **1992**, *12*, 42.
[4] a) D. G. Clerc, D. A. Cleary, *Chem. Mater.* **1992**, *4*, 1344; *J. Phys. Chem. Solids* **1995**, *56*, 69; b) L. Hernán, J. Morales, L. Sánchez, J. L. Tirado, A. R. González-Elipe, *J. Chem. Soc. Chem. Commun.* **1994**, 1081; c) D. O'Hare, J. S. O. Evans, P. J. Wiseman, C. K. Prout, *Angew. Chem.* **1991**, *103*, 1175, *Angew. Chem. Int. Ed. Engl.* **1991**, *30*, 1156; d) G. A. Ozin, C. Gil, *Chem. Rev.* **1989**, *89*, 1749; e) M. Endregard, D. G. Nicholson, M. Stöker, B. Beagley, *J. Mater. Chem.* **1995**, *4*, 485; f) P. Schwarz, E. Siebel, R. D. Fischer, D. C. Apperley, N. A. Davies, R. K. Harris, *Angew. Chem.*, **1995**, *107*, 1311, *Angew. Chem. Int. Ed. Engl.* **1995**, *34*, 1197.
[5] K. J. Balkus, S. Shepelev, *Microporous Mater.* **1993**, *1*, 383.
[6] G. van de Goor, C. C. Freyhardt, P. Behrens, *Z. Anorg. Allg. Chem.* **1995**, *621*, 311.
[7] G. van de Goor, B. Lindlar, J. Felsche, P. Behrens, *J. Chem. Soc. Chem. Commun.*, in press.
[8] For the nomenclature of zeolite-type phases see a) F. Liebau, H. Gies, R. P. Gunawardane, B. Marler, *Zeolites* **1986**, *6*, 373; b) W. M. Meier, D. H. Olson, *Atlas of Zeolite Structure Types*, 3rd ed., Butterworth-Heinemann, London, **1992**.
[9] Similar changes of products with increasing reaction temperatures have been observed before [3].
[10] H. Kessler, *Stud. Surf. Sci. Cat.* **1989**, *52*, 17, and references therein.
[11] The crystal structure investigation, which was performed at 220 K, has been described in ref. [6]. Further details of the crystal structure investigation may be obtained from the Fachinformationszentrum Karlsruhe, D-76344 Eggenstein-Leopoldshafen, on quoting the depository number CSD-58258. For the results described here, it is of importance that the positions of all H atoms were constructed geometrically and refined fixed to the respective carbon atom (riding mode). The typical value of C–H bond lengths in arenes (0.97 Å), as obtained from X-ray diffraction analyses [12], was used for the refinement. For the calculation of interatomic $H_{guest}\cdots O_{host}$ distances, an approximate correction of the well-known systematic error of X-ray methods was applied. The lengths of the C–H bonds in the arene rings were set to the standard value of 1.08 Å [12]. Thus, the H–O distances of the C–H···O–Si contacts discussed here were not determined directly from the experiment. However, regarding the rigid geometry of the $[CoCp_2]^+$ ions, the true positions of the H atoms cannot deviate significantly from the positions used here.
[12] F. H. Allen, *Acta Crystallogr. Sect. B* **1986**, *42*, 515.
[13] R. Taylor, O. Kennard, *J. Am. Chem. Soc.* **1982**, *104*, 5063.
[14] G. R. Desijaru, *Acc. Chem. Res.* **1991**, *24*, 290.
[15] T. Steiner, G. Koellner, K. Gessler, W. Saenger, *J. Chem. Soc. Chem. Commun.* **1995**, 511.
[16] T. Steiner, *J. Chem. Soc. Chem. Commun.* **1994**, 101.
[17] V. R. Pedireddi, G. R. Desiraju, *J. Chem. Soc. Chem. Commun.* **1992**, 988.
[18] T. Steiner, *J. Chem. Soc. Chem. Commun.* **1994**, 2341.
[19] Based on the work of A. Bondi (*J. Phys. Chem.* **1964**, *68*, 441) and A. I. Kitaigorodsky (*Molecular Crystals and Molecules*, Academic Press, London, **1973**), a van der Waals distance of 2.70 Å results from the addition of the van der Waals radii of the hydrogen atom (1.20 Å) and the oxygen atom (1.50 Å). See also the discussion in ref. [13].
[20] P. Behrens, G. van de Goor, M. Wiebcke, C. Braunbarth, A. M. Schneider, J. Felsche, G. Engelhardt, P. Fischer, K. Fütterer, W. Depmeier, Poster on the 8th International Symposium on Molecular Recognition and Inclusion, Ottawa, 31.7.–5. 8.1994.
[21] Using the fluoride method, $[CoCp_2]$F-DOH is formed only as a by-product at high synthesis temperatures [6]. Pure, single-phase $[CoCp_2]$OH-DOH is obtained in the classical basic hydrothermal synthesis. Rietveld refinement of X-ray powder diffraction data, refinement of a single-crystal diffraction data set (both measured at 298 K), the occurrence of a phase transition at 228 K as well as the IR spectrum shown in Figure 3 indicate that the $[CoCp_2]^+$ ions in $[CoCp_2]$OH-DOH are rotationally disordered at room temperature (B. Lindlar, G. van de Goor, A. M. Schneider, P. Behrens, J. Felsche, unpublished results).
[22] G. van de Goor, K. Hoffmann, F. Marlow, S. Kallus, P. Behrens, F. Schüth, *Adv. Mater.*, **1996**, *8*, in press.

Cascade Radical Reactions of Isonitriles: A Second-Generation Synthesis of (20*S*)-Camptothecin, Topotecan, Irinotecan, and GI-147211C**

Dennis P. Curran,* Sung-Bo Ko, and Hubert Josien

The camptothecin family of molecules has recently moved to the forefront of research in the treatment of solid tumors by chemotherapy.[1] The parent of this family, (20*S*)-camptothecin (**1a**), is highly active, and it is thought to operate by interfering with the unwinding of DNA by the enzyme topoisomerase I.[2] Camptothecin's clinical use has been limited by its insolubility, but extensive structure–activity studies have identified many analogs of camptothecin with equal or better antitumor activity and with better solubility properties.[3] Generally speaking, substitution at C7 and C9–C11 is permitted, while substitution at other positions tends to decrease or completely eliminate activity. Several analogs of camptothecin with improved solubility in water, including topotecan (**1b**),[1] irinotecan (**1c**),[1] and GI-147211C (**1d**),[4] are now in various stages of clinical trials around the world.

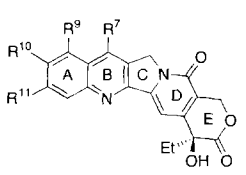

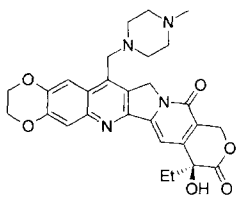

1a, camptothecin, R^7-R^{11} = H
1b, topotecan, R^7,R^{11} = H, R^9 = CH_2NMe_2, R^{10} = OH
1c, irinotecan, R^7 = Et, R^9,R^{11} = H, R^{10} = OCON
1d, GI-147211C

The synthesis of camptothecin was an active area of research about 20 years ago,[5] and the medicinal importance of this family has now rekindled interest. A number of new syntheses and significant improvements to existing syntheses have recently been reported.[6] In late 1992, we described a formal synthesis of racemic camptothecin that featured a new radical cascade reaction.[7] Reaction of phenyl isonitrile (**2**) with the readily available bromopyridone **3** provided the well-known "Danishefsky tetracycle" **4**.[8] Though very short (8 steps) and efficient, this synthesis suffered from two major problems: 1) the final products were racemic; and 2) the introduction of the E-ring lactone by hydroxymethylation of **4** occurred in poor yield, and the conditions were not tolerant of substituents on the A and B rings.[7d]

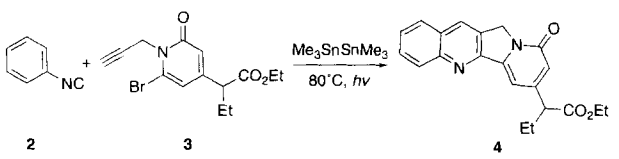

2 **3** **4**

Because the cascade radical reaction should tolerate all kinds of A- and B-ring substituents, we reformulated the synthetic plan to proceed via the key pyridone lactone **5** [Eq. (a)]. Variation of the propargyl substituent R^7 in **6** (X = I, Br) and the aryl substituents of isonitrile **7** should then allow access to camptothecin as well as known and new analogs. We now report a highly convergent second-generation synthesis of (20*S*)-camptothecin (**1a**). The synthesis is well suited to preparing A- and B-ring analogs of camptothecin, and to demonstrate this we have also synthesized GI-147211C (**1d**) and the immediate precursors of topotecan (**1b**) and irinotecan (**1c**).

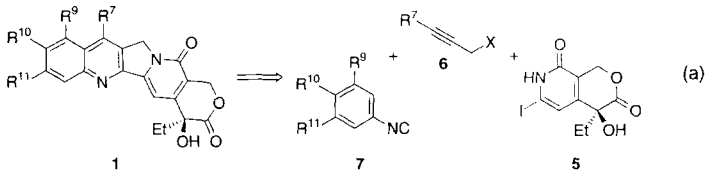

1 **7** **5** (a)

The synthesis of lactone **5** is summarized in Scheme 1. Metalation of 2-bromo-6-methoxypyridine and quenching with TMSCl provided **8**. This was then converted in one step to iodoaldehyde **9** by following the procedure of Comins.[9] The E ring was then introduced by a sequence of reductive etherification[10] to form **10** and subsequent Heck reaction[11] to give enol ether **11**.[12] The Sharpless asymmetric dihydroxylation[13] of **11** followed from a model study,[14] and **12** was obtained in 85% yield and 94% *ee* after oxidation of the intermediate α-hydroxy lactol.[12] Exchange of the TMS group in **12** for iodine occurred upon exposure to ICl.[5] At about 50% conversion of **12** the reaction rate slowed dramatically. When the reaction was stopped at this point, iodide **13** was isolated in 47% yield and **12** was recovered in 45% yield. Demethylation of **13** then provided **5**.

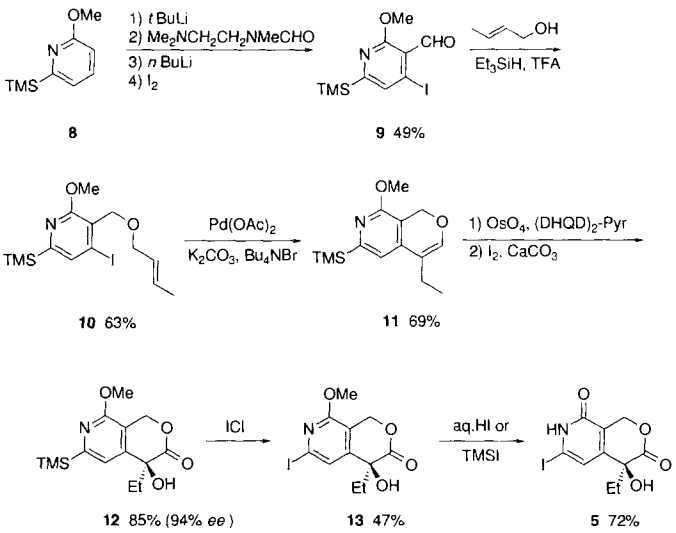

8 **9** 49% **10** 63% **11** 69% **12** 85% (94% *ee*) **13** 47% **5** 72%

Scheme 1. Synthesis of intermediate **5**. TMS = trimethylsilyl, TFA = trifluoroacetic acid.

N-Propargylation of **5** under optimized conditions[16] with **14a** provided **15a** in 88% yield. In the key radical cascade,[17] a solution of **15a**, phenyl isonitrile (**2**), and hexamethyldistannane (1.5 equiv) in benzene was warmed to 70 °C and irradiated with

[*] Prof. D. P. Curran, S.-B. Ko, Dr. H. Josien
Department of Chemistry, University of Pittsburgh
Pittsburgh, PA 15260 (USA)
Telefax: Int. code + (412)624-9861
e-mail: curran+@pitt.edu

[**] We thank the National Institutes of Health for funding this work. Financial support for H. J. from the Association Française pour la Recherche Thérapeutique is gratefully acknowledged. We thank Prof. K. B. Sharpless, Scripps Institute, San Diego, CA (USA), for a generous gift of *O*,*O*'-(2,5-diphenylpyrimidine-4,6-diyl)bis(dihydroquinidine), $(DHQD)_2$-Pyr.

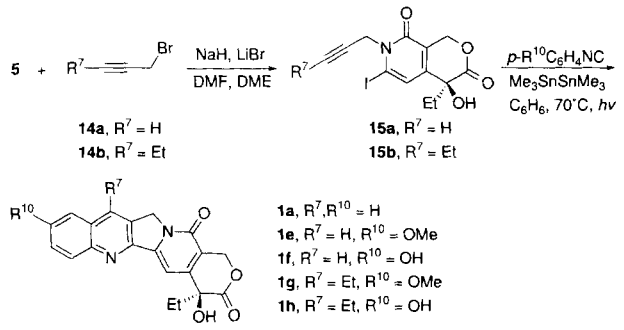

1a, R^7,R^{10} = H
1e, R^7 = H, R^{10} = OMe
1f, R^7 = H, R^{10} = OH
1g, R^7 = Et, R^{10} = OMe
1h, R^7 = Et, R^{10} = OH

a sunlamp. Highly enantiomerically enriched (20*S*)-camptothecin (95% *ee*) crystallized from the reaction mixture and was isolated in 63% yield by simple filtration and washing with ether. Camptothecin (**1a**) could also be produced by substituting hexamethyldisilane for the distannane (52%) or by using *t*-butyl alcohol as the solvent (45%). Reaction of **15a** with *p*-methoxyphenylisonitrile provided **1e** in 51% yield, and subsequent demethylation with HBr provided 10-hydroxycamptothecin (**1f**).[18] This highly active natural product is the precursor of topotecan (**1b**).[19]

To prepare irinotecan (**1c**), lactone **5** was N-propargylated with **14b**, and the resulting product **15b** was treated with *p*-methoxyphenylisonitrile under the standard conditions. Demethylation of the product **1g** with HBr then gave 7-ethyl-10-hydroxycamptothecin (**1h**),[18] which is both a synthetic precursor of irinotecan (**1c**)[20] and the active antitumor agent produced in vivo when irinotecan is metabolized.[21]

The synthesis of GI-147211C (**1d**) starts with N-propargylation of **5** with **16** followed by addition of *N*-methylpiperazine to provide lactone **17**. Reaction of this lactone with 3,4-ethylene-

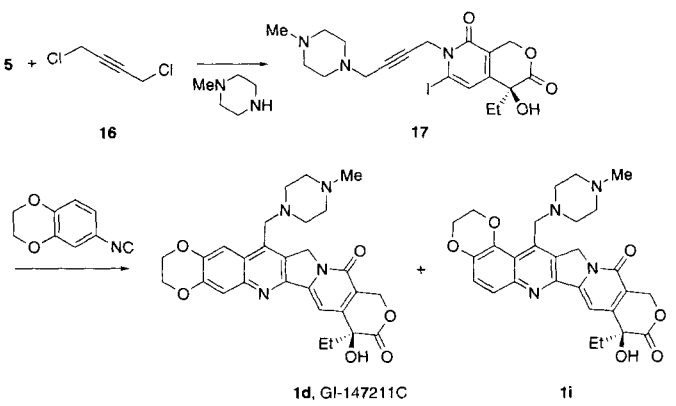

dioxyphenylisonitrile then provided an inseparable 3:2 mixture of GI-147211C (**1d**) and its regioisomer **1i** in 57% yield. This reaction illustrates a frequent regiochemical problem that occurs when *meta*-substituted isonitriles are used in radical cascade reactions.[17] A strategic solution to this problem has recently been developed and this will be reported separately.

This synthesis of camptothecin and its analogs provides a graphic demonstration of the power of cascade radical reactions. The approach is short and efficient, and it may be useful for preparing larger quantities of these compounds. Perhaps more importantly, the modular "mix-and-match" strategy [Eq. (a)] implemented in the radical cascade is ideally suited to the known structure–activity relationship of the camptothecin family. Lactone **5** is an invariant module that can be combined in as few as two steps with two variable modules—propargyl bromide **6** and aryl isonitrile **7**—to give a member of the camptothecin family. Because the radical reaction tolerates functional groups, the strategy promises to be useful in preparing a large assortment of both known and new analogs of camptothecin.

Received: August 10, 1995 [Z8298IE]
German version: *Angew. Chem.* **1995**, *107*, 2948–2950

Keywords: camptothecin · cascade reactions · isonitriles radicals

[1] *Camptothecins: New Anticancer Agents* (Eds.: M. Potmesil, H. Pinedo), CRC, Boca Raton, FL, **1995**.
[2] a) Y. H. Hsiang, R. P. Hertzberg, S. Hecht, L. F. Liu, *J. Biol. Chem.* **1985**, *260*, 14873; b) Y. H. Hsiang, L. F. Liu, *Cancer Res.* **1988**, *48*, 1722; c) C. D. Lima, J. C. Wang, A. Mondragon, *Nature* **1994**, *367*, 138.
[3] Leading references: a) M. Sugimori, A. Ejima, S. Ohsuki, K. Matsumoto, Y. Kawato, M. Yasuoka, H. Tagawa, H. Terasawa, *Heterocycles* **1994**, *38*, 81; b) K. H. Lee, L. Sun, H. K. Wang, *J. Chin. Chem. Soc. (Taipei)* **1994**, *41*, 371; c) T. Yaegashi, S. Sawada, H. Nagata, T. Furuta, T. Yokokura, T. Miyasaka, *Chem. Pharm. Bull.* **1994**, *12*, 2518; d) H.-K. Wang, S.-Y. Liu, K.-M. Hwang, G. Taylor, K.-H. Lee, *Bioorg. Med. Chem.* **1994**, *2*, 1397; e) M. Sugimori, A. Ejima, S. Ohsuki, K. Uoto, I. Mitsui, K. Matsumoto, Y. Kawato, M. Yasuoka, K. Sato, H. Tagawa, H. Terasawa, *J. Med. Chem.* **1994**, *37*, 3033; f) D. E. Uehling, S. S. Nanthakumar, D. Croom, D. L. Emerson, P. P. Leitner, M. J. Luzzio, G. McIntyre, B. Morton, S. Profeta, J. M. Sisco, D. D. Sternbach, W.-Q. Tong, A. Vuong, J. M. Besterman, *ibid.* **1995**, *38*, 1106; g) L. Snyder, W. Shen, W. G. Bornmann, S. J. Danishefsky, *J. Org. Chem.* **1994**, *59*, 7033.
[4] M. J. Luzzio, J. M. Besterman, D. L. Emerson, M. G. Evans, K. Lackey, P. L. Leitner, G. McIntyre, B. Morton, P. L. Myers, M. Peel, J. M. Sisco, D. D. Sternbach, W.-Q. Tong, A. Truesdale, D. E. Uehling, A. Vuong, J. Yates, *J. Med. Chem.* **1995**, *38*, 395.
[5] A. G. Schultz, *Chem. Rev.* **1973**, *73*, 385.
[6] a) D. L. Comins, M. F. Baevsky, H. Hong, *J. Am. Chem. Soc.* **1992**, *114*, 10971; b) W. Shen; C. A. Coburn, W. G. Bornmann, S. J. Danishefsky, *J. Org. Chem.* **1993**, *58*, 611; c) D. L. Comins, H. Hong, G. Jianhua, *Tetrahedron Lett.* **1994**, *35*, 5331; d) D. L. Comins, H. Hong, J. K. Saha, G. Jianhua, *J. Org. Chem.* **1994**, *59*, 5120; e) F. G. Fang, S. Xie, M. W. Lowery, *ibid.* **1994**, *59*, 6142; f) A. V. R. Rao, J. S. Yadav, V. Muralikrishna, *Tetrahedron Lett.* **1994**, *35*, 3613; g) S.-S. Jew, K.-D. Ok, H.-J. Kim, M. G. Kim, J. M. Kim, J. M. Hah, Y.-S. Cho, *Tetrahedron: Asymmetry* **1995**, *6*, 1245.
[7] a) D. P. Curran, H. Liu, *J. Am. Chem. Soc.* **1992**, *114*, 5863; b) D. P. Curran, *J. Chin. Chem. Soc. (Taipei)* **1993**, *40*, 1; c) D. P. Curran, J. Sisko, P. E. Yeske, H. Liu, *Pure Appl. Chem.* **1993**, *65*, 1153; d) H. Liu, Dissertation, University of Pittsburgh, **1994**.
[8] a) S. Danishefsky, R. Volkmann, *Tetrahedron Lett.* **1973**, 2521; b) R. Volkmann, S. Danishefsky, J. Eggler, D. M. Soloman, *J. Am. Chem. Soc.* **1971**, *93*, 5576.
[9] D. L. Comins, *Synlett* **1992**, 615. See also ref. [6a].
[10] M. P. Doyle, D. J. DeBruyn, D. A. Kooistra, *J. Am. Chem. Soc.* **1972**, *94*, 3659.
[11] R. Grigg, V. Sridharan, P. Stevenson, S. Sukirthalingam, T. Worakun, *Tetrahedron* **1990**, *46*, 4003.
[12] A similar sequence was developed independently at Glaxo [6e].
[13] H. C. Kolb, M. S. VanNieuwenhze, K. B. Sharpless, *Chem. Rev.* **1994**, *94*, 2483.
[14] D. P. Curran, S.-B. Ko, *J. Org. Chem.* **1994**, *59*, 6139.
[15] S.-S. P. Chou, H. L. Kuo, C. J. Wang, C. Y. Tsai, C. M. Sun, *J. Org. Chem.* **1989**, *54*, 860.
[16] D. P. Curran, H. Liu, S.-B. Ko, H. Josien, *Tetrahedron Lett.*, in press.
[17] D. P. Curran, H. Liu, *J. Am. Chem. Soc.* **1991**, *113*, 2127.
[18] S. Sawada, S.-I. Matsuoka, K.-I. Nokata, H. Nagata, T. Furuta, T. Yukokura, T. Miyasaka, *Chem. Pharm. Bull.* **1991**, *39*, 3183.
[19] W. D. Kingsbury, J. C. Boehm, D. R. Jakas, K. G. Holden, S. M. Hecht, G. Gallagher, M. J. Caranfa, F. L. McCabe, L. F. Faucette, R. K. Johnson, R. P. Hertzberg, *J. Med. Chem.* **1991**, *34*, 98.
[20] S. Sawada, S. Okajima, R. Aiyama, K.-I. Nokata, T. Furuta, T. Yokokura, E. Sugino, K. Yamaguchi, T. Miyasaka, *Chem. Pharm. Bull.* **1991**, *39*, 1446.
[21] a) N. Kaneda, H. Nagata, T. Furuta, Y. Yokotura, *Cancer Res.* **1990**, *50*, 1715; b) Y. Kawato, M. Aonuma, Y. Hirota, H. Kuga, K. Sato, *ibid.* **1991**, *51*, 4187.

The Formal Potentials of Solid Metal Hexacyanometalates**

Fritz Scholz* and Aleš Dostal

We report here on the first formal potentials of a series of solid metal hexacyanometalates $(M^+)_nM'[M''(CN)_6]$ (M^+ = Li^+, K^+, Na^+, Rb^+, Cs^+; M' = Ag, Al, Cd, Co, Cr, Cu, Fe, Ga, In, Mn, Ni, Pb; M'' = Cr, Fe, Mn), as determined by solid-state voltammetric experiments. The experimental data can be understood both in terms of the polarizing effect (ionic potential) of the nitrogen-bonded M'^{n+} ions and also in terms of the free energy of hydration of the cations M^+, which are inserted into the channels and holes of the zeolitic structure of the solid compounds during reduction of the $[M''(CN)_6]^{m-}$ units of the solid compounds. The results of this study support the assumption that M''→C π back bonding increases as the acid–base interaction on the nitrogen end of the cyanide ions increases.

Recently, increasing attention has focused not only on electrochemical reactions with solid electrolytes,[1] but also on electrochemical reactions in which electron transfer is coupled with an ion transfer between the electrolyte solution and the solid compound. Typical examples are topotactic electrochemical reactions with ion insertion (or intercalation in the case of layer structures),[2] for instance the reactions of Prussian blue and other metal hexacyanometalates.[3–5]

If "Ox" denotes the oxidized form and "Red" the reduced form of a metal ion in the solid compound, and if M^+ is the cation inserted into the solid compound during reduction, the electrode reaction with the potential $E^\circ_{s,f}$ can be formulated according to Equation (a). Here $E^\circ_{s,f}$ is the formal potential of

$$\{Ox\}_s + e^- + M^+ \rightleftharpoons \{RedM\}_s \quad (a)$$

this electrode reaction (the subscript s indicates that the entire redox couple is confined to the solid phase). The electrode reaction can be separated into two independent equilibria [Eq. (b) (standard potential: E°_s) and Eq. (c) (equilibrium constant K)]. Equilibrium (c) is itself an electrochemical reaction because it describes the distribution of a charged particle between two phases. For equilibrium (b) we can formulate the Nernst equation in Equation (d), where E°_s is the standard

$$\{Ox\}_s + e^- \rightleftharpoons \{Red\}_s^- \quad (b)$$

$$\{RedM\}_s \rightleftharpoons \{Red\}_s^- + M^+ \quad (c)$$

$$E = E^\circ_s + RT/nF\ln(f_{Ox}/f_{Red}) + RT/nF\ln(c_{Ox}/c_{Red}) \quad (d)$$

potential of the redox system in the solid matrix. Equilibrium (c) can be described by the constant defined in Equation (e). The combination of Equations (d) and (e) yields Equation (f), where

$$K = (a_{Red}a_M)/a_{RedM} = (f_{Red}c_{Red}a_M)/(f_{RedM}c_{RedM}) \quad (e)$$

$$E = E^\circ_s + RT/nF\ln(f_{Ox}/f_{Red}) - RT/nF\ln(K/f_{Red}) + RT/nF\ln(c_{Ox}/c_{RedM}) + RT/nF\ln a_M \quad (f)$$

the first three terms can be regarded as the formal potential $E^\circ_{s,f}$ of reaction (a). Unfortunately, a separate experimental determination of E°_s and K is not possible.

Previously the determination of the formal potentials of metal hexacyanometalates was possible only when these compounds could be precipitated on metal electrodes. In some cases the metal hexacyanometalates were chemically bonded to the electrode surface or they were incorporated into graphite oil pastes.[6] Of course, these techniques do not yield the formal potentials of pure solid metal hexacyanometalates.

Recently, we introduced a new electrode technique that enables direct electrochemical measurements on pure solid materials.[7, 8] Here the solid compound is immobilized as microcrystalline particles on a suitable electrode. This technique was applied for the study of insoluble organometallic compounds[9, 10] and also for the determination of thermodynamic data of insoluble compounds.[11, 12] This technique combined with cyclic voltammetry can also be used to determine the formal potentials $E^\circ_{s,f}$ of reaction (a) of metal hexacyanometalates. The cyclic voltammograms of the hexacyanometalate ions indicate that the electrochemical reaction is diffusion controlled. At a given concentration of K^+, the formal potential is calculated as $E_f = (E_{p,a} + E_{p,c})/2$, where $E_{p,a}$ and $E_{p,c}$ are the anodic and cathodic peak potentials, respectively. The formal potential $E^\circ_{s,f}$ is determined by extrapolating the E_f values to $a_{K^+} = 1$. Activities for potassium ions in dilute solutions were calculated by the simple Debye–Hückel approximation. Table 1 shows the formal potentials of the solid metal hexacyanometalates for the insertion of potassium ions. These values are compared to the standard potentials of the hexacyanometalate ions in aqueous solution. Table 2 gives the formal potentials $E_{s,f}$ (these values refer to $c_{K^+} = 0.1$ mol L^{-1}) of some hexacyanoferrates for the insertion reaction with different alkali metal ions.

Table 1. Formal potentials $E^\circ_{s,f}$ of metal hexacyanometalates on potassium ion insertion as well as the difference ΔE between the standard potentials E°_{aq} of the hexametalate ions [a] in aqueous solution and $E^\circ_{s,f}$.

Solid Cmpd [b]	$E^\circ_{s,f}$ [c] [V vs. SHE]	$\Delta E = E^\circ_{aq} - E^\circ_{s,f}$ [V]
$Cr^{3+}[Fe(CN)_6]$	1.005	− 0.650
$Cd^{2+}[Fe(CN)_6]$	0.858	− 0.504
$Cu^{2+}[Fe(CN)_6]$	0.982	− 0.527
$Ni^{2+}[Fe(CN)_6]$	0.857	− 0.502
$Pb^{2+}[Fe(CN)_6]$	0.976	− 0.621
$Fe^{3+}[Fe(CN)_6]$	1.168	− 0.813
$Co^{2+}[Fe(CN)_6]$	0.966	− 0.611
$In^{3+}[Fe(CN)_6]$	1.006	− 0.651
$Ag^{+}[Fe(CN)_6]$	0.880	− 0.525
$Ga^{3+}[Fe(CN)_6]$	1.173	− 0.818
$Al^{3+}[Fe(CN)_6]$	1.151	− 0.796
$Mn^{2+}[Fe(CN)_6]$	0.811	− 0.456
$Cr^{2+}[Cr(CN)_6]$	− 0.562	− 0.578
$Mn^{2+}[Cr(CN)_6]$	− 0.804	− 0.336
$Fe^{2+}[Cr(CN)_6]$	− 0.860	− 0.280
$Mn^{2+}[Mn^{1+/2+}(CN)_6]$	− 0.712	− 0.338
$Mn^{2+}[Mn^{2+/3+}(CN)_6]$	0.052	− 0.292
$Fe^{2+}[Mn^{2+/3+}(CN)_6]$	0.075	− 0.315
$Cr^{3+}[Mn^{2+/3+}(CN)_6]$	0.352	− 0.592

[a] The following standard potentials for the hexacyanometalate ions in aqueous solution were used: $[Fe(CN)_6]^{3/4-}$: + 0.355 V, $[Cr(CN)_6]^{3/4-}$: − 1.140 V, $[Mn(CN)_6]^{4/5-}$: − 1.050 V, $[Mn(CN)_6]^{3/4-}$: − 0.240 V (all vs. SHE) [15]. [b] The formulas M'[M''(CN)$_6$] indicate only the metal M' coordinated to nitrogen and the metal M'' coordinated to carbon. Depending on the oxidation state of M'' the charge is compensated by the alkali metal ions inserted from the solution, which are not given in the formulas. [c] The formal potentials were determined by cyclic voltammetry with a scan rate of 0.1 Vs^{-1} at 22 °C. For experimental details, see refs. [5, 8].

Table 1 indicates that hexacyanometalate (hcm) ions in the solid state are generally much stronger oxidants than in aqueous solution. If ΔG°_{aq} is the standard free energy of the electrochemical oxidation of hcm ions dissolved in water and ΔG°_s is the standard free energy of the electrochemical oxidation of the

[*] Prof. Dr. F. Scholz, Dipl.-Chem. A. Dostal
Institut für Chemie der Humboldt-Universität
Hessische Strasse 1–2, D-10115 Berlin (Germany)
Telefax: Int. code + (30) 28 468 685

[**] This work was supported by the Deutsche Forschungsgemeinschaft and the Fonds der Chemischen Industrie. SHE = standard hydrogen electrode

Table 2. Formal potentials $E_f = (E_{p,a} + E_{p,c})/2$ of metal hexacyanometalates immobilized on a graphite electrode and immersed in 0.1 M solutions of alkali metal chlorides (scan rate 0.1 Vs^{-1}). ΔG_h is the standard free energy of hydration of the alkali metal ions [17].

	$Cu[Fe(CN)_6]$	$Ni[Fe(CN)_6]$ E_f [V vs. SHE]	$Cd[Fe(CN)_6]$	ΔG_h [kJ mol^{-1}]
Li^+	0.848	0.693	0.664	−114.6
Na^+	0.808	0.602	0.673	− 89.7
K^+	0.888	0.768	0.768	− 73.5
Rb^+	1.008	0.773	1.002	− 67.5
Cs^+	0.775 [a]	0.533	0.923	− 60.8

[a] The voltammetric system was poorly developed.

same hcm ions when they are bonded to M′ in a solid compound, we can write Equation (g). Here, ΔG°_{it} denotes the

$$\Delta G^\circ_s = \Delta G^\circ_{aq} + \Delta G^\circ_{intr} + \Delta G^\circ_{it} \quad (g)$$

standard free energy of the ion transfer of M^+ ions, and ΔG°_{intr} is the intrinsic change in the standard free energy caused by the bonding of the nitrogen atoms of the cyanide ions to M′ instead of to water. ΔG°_{it} cannot be determined separately ($\Delta G^\circ_{it} = -RT\ln K$), because the difference between E°_{aq} and E°_s is not known. It can be supposed that ΔG°_{intr} is determined by the strengths of the bond between M′ and the nitrogen atoms of the cyanide ions. For a series of hexacyanoferrates with the same inserting cation (e.g. K^+), it was assumed that ΔG°_{it} is almost constant and $E^\circ_{s,f}$ can be correlated with the polarization power of M′. The plot of $E^\circ_{s,f}$ versus the ionic potential Φ ($\Phi = z/r_{eff}$; z = charge, r = effective radius) of the Me^I ions has a statistically significant ($p > 0.99$) correlation ($r_{corr} = 0.74$, $n = 12$) (Fig. 1a). The effective radii of the M′ ions are those of the hexacoordinated high-spin ions because the ligand field of the nitrogen-coordi nated cyanide ions is rather weak. The stronger the polarizing effect is, the weaker the σ bond between the iron atom and the cyanide ions is, which is accompanied by an increase in π back

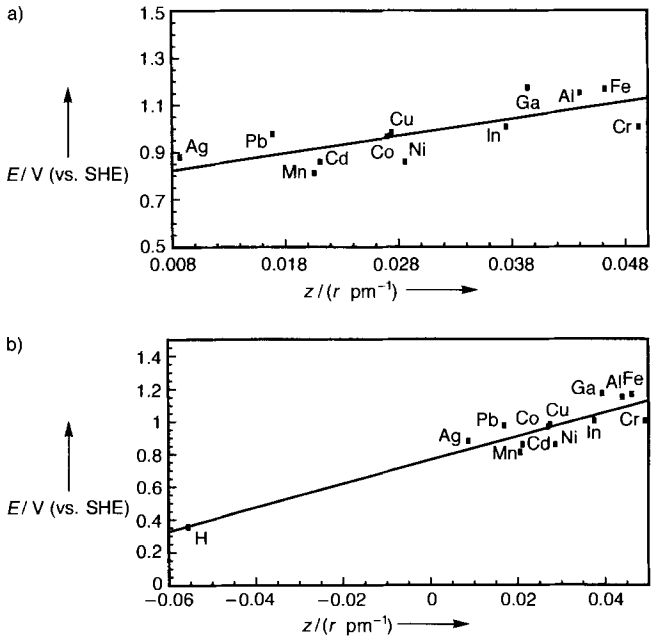

Fig. 1. a) Plot of $E^\circ_{s,f}$ of solid metal hexacyanoferrates M′[M″(CN)$_6$] versus the ratio z/r of the effective charge and radius of the metal ions M′. b) The same plot as in Fig. 1a but with the standard potential E°_{aq} of the hexacyanoferrate ions in water as well as the ratio z/r for protons.

bonding. According to Shriver[19] this leads to a decrease in the absolute energy of the fully filled t^6_{2g} orbitals (low-spin Fe^{2+} ions). This favors the +2 oxidation state of the iron centers and shifts the oxidation potentials towards more positive values. Figure 1b shows the same function as Figure 1a, but the bridging proton of a H_2O molecule is included, for which the effective radius is −18 pm (coordination number 2).[16] The corresponding ionic potential of the proton is the standard potential of the hexacyanoferrate ions in water. The inclusion of the proton in the correlation is justified because in aqueous solution the hexacyanoferrate ions are coordinated to water, in other words bound to protons, rather than to monovalent metal ions. It is very remarkable that the coordinates of the proton lie on the line of the formal potentials of solid metal hexacyanoferrates. This implies that ΔG°_{intr} is much more important for $E^\circ_{s,f}$ than ΔG°_{it} is. In fact, the plot in Figure 1b bridges the solution and solid-state chemistry of the hexacyanoferrates, which has not been shown earlier. The interpretation of the plot given in Figure 1a is strongly supported by Mössbauer spectra of these compounds, which show that the increasing polarizing effect of M′ decreases the electron density at the iron ion.[20] This is also supported by infrared data for cyanide.[19]

It is evident from Table 2 that the $E^\circ_{s,f}$ values also depend to some extent on the nature of the M^+ ions. ΔG°_{it} can be taken as the difference between ΔG°_{stab}, which is the free energy of the "solvation" of M^+ ions in the metal hexacyanometalate host lattice, and ΔG°_h, which is the free energy of hydration of M^+ ions in water. Our values in Table 2 and also those reported earlier for thin films of nickel hexacyanoferrate on nickel[18] show that the transfer of the alkali metal cations from the aqueous phase to the metal hexacyanometalate phase is generally easier the bigger the alkali metal ions are. The channel diameter of the solid hexacyanometalates is nearly constant (ca. 320 pm) for different metal M′ hexacyanometalates.[14] The diameters of the naked cations are: Li^+ 148, Na^+ 204, K^+ 276, Rb^+ 298, and Cs^+ 340 pm.[13] When the cations enter the channel, the hydration sphere is disassemblied by the orifice and the channel, and hydration is possible, if at all, only along the axis of the channel. Since the number of water molecules in the solvation sphere decreases from lithium to cesium, and hence the free energy of solvation decreases in the same way, it is much easier to transfer the higher alkali metal ions than lithium ions. Rubidium is the largest alkali metal ion that can be electrochemically inserted into the holes of the hcm. Presumably cesium ions are attached only to the surface of the solid, which explains why Cs^+ does not usually fit the general trend in potentials from Li to Rb.

Figure 2 shows a plot of the lattice constants of solid metal hexacyanometalates versus the formal potentials $E^\circ_{s,f}$ of the hexa-

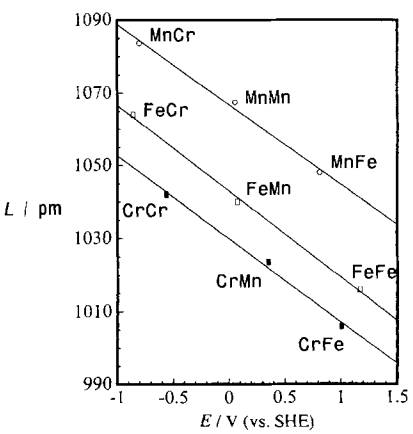

Fig. 2. Plot of the lattice constants L of solid metal hexacyanometalates M′[M″(CN)$_6$] versus the formal potentials $E^\circ_{s,f}$ of the hexacyanometalate ions [M″(CN)$_6$]. The compounds are indicated as M′M″. The lattice constants were taken from refs. [21–24].

cyanometalate ions in the solid compounds. It is very interesting that the formal potentials of the hexacyanoferrates, hexacyanochromates, and hexacyanomanganates change in the same way when they are coordinated to manganese, iron, and chromium ions. The order of formal potentials is the same for the solid compounds as it is for the hexacyanometalate ions dissolved in water (see footnote [a] of Table 1). The reason for the linear correlation in the plot in Figure 2 is the fact that the strength of π back bonding increases from chromium to iron in the hexacyanometalate ions. This is accompanied by a decrease in lattice constants and by an increase of formal potentials.

Received: June 8, 1995
Revised version: September 6, 1995 [Z 8069 IE]
German version: *Angew. Chem.* **1995**, *107*, 2876–2878

Keywords: hexacyanoferrates · hexacyanometalates · solid-state electrochemistry · voltammetry

[1] H. Schmalzried, *Chemical Kinetics of Solids*, VCH, Weinheim, **1995**.
[2] M. Schöllhorn, *Angew. Chem.* **1980**, *92*, 1015–1035; *Angew. Chem. Int. Ed. Engl.* **1980**, *19*, 983–1003.
[3] K. Itaya, I. Uchida, V. D. Neff, *Acc. Chem. Res.* **1986**, *19*, 162–168.
[4] A. Dostal, U. Schröder, F. Scholz, *Inorg. Chem* **1995**, *34*, 1711–1717.
[5] A. Dostal, B. Meyer, F. Scholz, U. Schröder, A. M. Bond, F. Marken, S. J. Shaw, *J. Phys. Chem.* **1995**, *99*, 2096–2103.
[6] L. T. Kubota, Y. Gushkiem, *J. Electroanal. Chem.* **1993**, *362*, 219–225.
[7] F. Scholz, L. Nitschke, G. Henrion, *Naturwissenschaften* **1989**, *76*, 71.
[8] F. Scholz, B. Meyer, *Chem. Soc. Rev.* **1994**, *23*, 341–347.
[9] A. M. Bond, R. Colton, F. Daniels, D. R. Fernando, F. Marken, Y. Nagaosa, R. F. M. Van Steveninck, J. N. Walter, *J. Am. Chem. Soc.* **1993**, *115*, 9556–9562.
[10] A. M. Bond, F. Marken, *J. Electroanal. Chem.* **1994**, *372*, 125–135.
[11] A. M. Bond, F. Scholz, *J. Phys. Chem.* **1991**, *95*, 7460–7465.
[12] B. Lange, F. Scholz, H.-J. Bautsch, F. Damaschun, G. Wappler, *Phys. Chem. Minerals* **1993**, *19*, 486–491.
[13] *Encyclopedia of Inorganic Chemistry*, *Vol. 1*, (Ed.: R. B. King), Wiley, Chichester, **1994**, p. 38.
[14] G. Seyfer, *Zh. Neorg. Khim.* **1962**, *7*, 1208–1209.
[15] S. Kotrlý, L. Šůcha, *Handbook of Chemical Equilibria in Analytical Chemistry*, Wiley, New York, **1985**.
[16] J. E. Huheey, *Inorganic Chemistry, Principles of Structure and Reactivity*, Harper & Row, New York, **1972**, p. 74.
[17] K. Schwabe, *Physikalische Chemie, Elektrochemie*, Akademie-Verlag, Berlin, **1974**, p. 106.
[18] S. Sinha, B. D. Humphrey, A. B. Bocarsly, *Inorg. Chem.* **1984**, *23*, 203–212.
[19] D. F. Shriver, *Struct. Bonding (Berlin)* **1966**, *1*, 32–58.
[20] B. V. Borshagovskii, V. I. Goldanskii, G. B. Seifer, R. A. Stukan, *Izvest. Akad. Nauk S. S. S. R. Ser. Khim.* **1968**, 87–91.
[21] A. Ferrari, M. E. Tani, *Acta Crystallogr.* **1962**, *15*, 90; *ibid.* **1964**, *17*, 311.
[22] D. B. Brown, D. F. Shriver, L. H. Schwartz, *Inorg. Chem.* **1968**, *7*, 77–83.
[23] D. B. Brown, D. F. Shriver, *Inorg. Chem.* **1969**, *8*, 37–42.
[24] A. Ludi, H. U. Güdel, *Struct. Bonding (Berlin)* **1973**, *14*, 1–22.

Palladium Complex Catalyzed Asymmetric Allylic Substitutions with Nitromethane: Enantioselectivities Exceeding 99.9% *ee***

Heiko Rieck and Günter Helmchen*

The reaction of allylic acetates or carbonates with stabilized, soft carbanions such as malonates is among the most important methods for C–C bond formation in asymmetric synthesis.[1] In reactions of this type the use of palladium complexes of 4,5-dihydrooxazoles **1**, chiral ligands introduced by us and others,

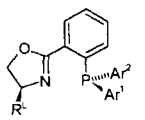

1

	R^L	Ar^1	Ar^2
1a	*i*Pr	Ph	Ph
1b	Ph	Ph	Ph
1c	*t*Bu	Ph	Ph
1d	(*i*BuSCH$_2$)Me$_2$C	Ph	Ph
1e	*i*Pr	1-($C_{10}H_7$)	Ph
1f	*i*Pr	Ph	1-($C_{10}H_7$)
1g	*i*Pr	1-($C_{10}H_7$)	1-($C_{10}H_7$)

gave enantioselectivities of over 98% *ee* for several cases.[2] The stereochemical course of this substitution can be generally described by a transition state in which the nucleophile attacks at the carbon atom of the allylic moiety in *trans* position relative to the phosphorus atom of the *exo* isomer (Fig. 1).[3]

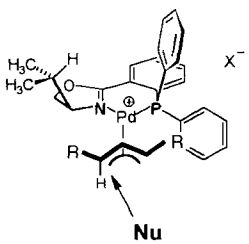

Fig. 1. Postulated transition state for the reaction of a nucleophile Nu with an allyl palladium complex of the ligand **1a**.

We have now used nitronates derived from nitromethane as nucleophiles, which were not extensively studied previously because of multiple alkylation and formation of side products. Nitronates are of interest as nucleophiles,[4] because the resultant products can be further transformed into a variety of synthetically important compounds. Despite this, reactions with chiral catalysts were studied for only one particular intramolecular reaction, which gave at best 70% *ee* with Pd complexes of classical C_2-symmetric diphosphanes.[5]

Carbonates **2a**–**2c** served as representative allylic compounds (Schemes 1 and 2). The comparatively complicated reaction mixtures were analyzed by chromatography (see Experimental Procedure). O-Alkylation of nitronates, typical for the uncatalyzed reaction, was not observed with palladium complexes of dihydrooxazoles **1** as catalysts. With analogous N,S and N,Se ligands[3] very low turnover was observed at best.

With the alkylated substrates **2a** and **2b** only monosubstitution products **3a** and **3b**, respectively, are formed in very high yield (Table 1). In case of the aryl-substituted substrate **2c** rates of the mono- and the disubstitution are similar (Table 2). The disubstitution products include diastereomers *meso*-**4**, which

[*] Prof. Dr. G. Helmchen, H. Rieck
Organisch-chemisches Institut der Universität
Im Neuenheimer Feld 270, D-69120 Heidelberg (Germany)
Telefax: Int. code + (6221) 564205
e-mail: en 4@ix.urz.uni-heidelberg.de

[**] This work was supported by the Deutsche Forschungsgemeinschaft (Sonderforschungsbereich 247) and the Fonds der Chemischen Industrie. Essential results were already presented in poster A-8 at the Ninth International Symposium on Homogeneous Catalysis, Jerusalem, August 21–26, 1994.

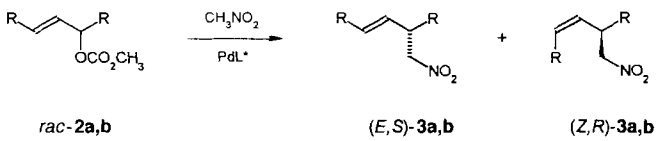

2a,3a : R = Me; **2b,3b** : R = Et

Scheme 1. Monoallylation of nitromethane (L* = **1a,c,d**).

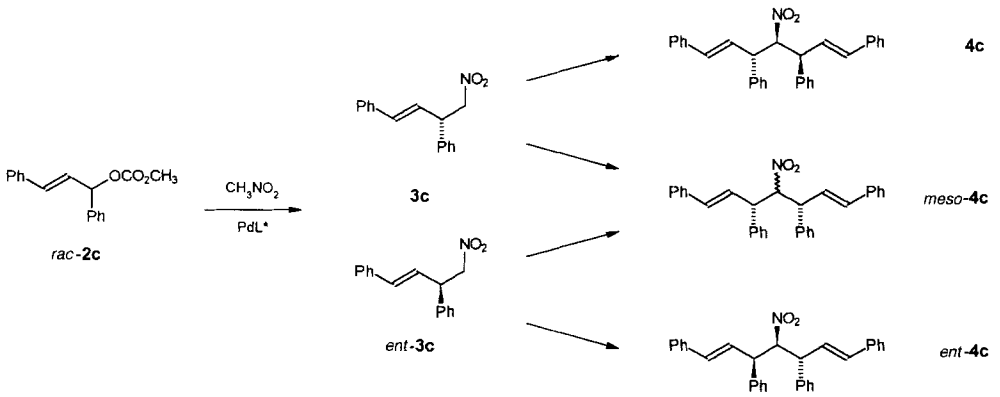

Scheme 2. Mono- and disubstitution with (1,3-diphenylallyl)methylcarbonate (L* = **1a–g**).

Table 1. Dependence of the enantioselectivity on the allylic system [a].

Substrate	Ligand	CH_3NO_2:**2**	Ratio (*E*)-**3**:(*Z*)-**3**	Yield [%]	*ee* [%] (*E*)-**3**	(*Z*)-**3**
2a	**1a**	5	60:40	89	61	47
2a	**1c**	5	63:37	91	72	56
2a	*ent*-**1d**	0.5	30:70	87	78	28
2a	*ent*-**1d**	5	57:43	85	80	57
2a	*ent*-**1d**	20	74:26	85	76	57
2b	**1a**	5	59:41	89	74	55
2b	**1a**	10	73:27	96	75	57
2b	**1c**	5	64:36	81	76	70
2b	**1c**	10	74:26	90	77	70
2b	*ent*-**1d**	5	59:41	96	84	73
2b	*ent*-**1d**	70 [b]	92:8	83	71	n.d. [d]
2c	**1a**	100	[c]	89	96.7	
2c	**1c**	100	[c]	90	98.5	
2c	*ent*-**1d**	100	[c]	87	>99	

[a] For the reaction conditions and analysis of the enantiomers, see Experimental Procedure. [b] Nitromethane was used as solvent. [c] The (*Z*) isomer was not detected. [d] n.d. = not determined.

Table 2. Dependence of the chemo- and enantioselectivity on the chiral ligand **1** [a].

Entry	Ligand	Reaction time [h]	Molar ratio **3c**:**4c**	Yield [%] **3c** + **4c**	*ee* [%] **3c**	**4c**
1	PPh_3	20	44:56 [b]	95		
2	$Ph_2P(CH_2)_2PPh_2$	5	30:70 [b]	96		
3	**1a**	16	47:53	>98	96.7	99.9
4	*ent*-**1b**	3	59:41	93	97.1	99.9
5	**1c**	4	64:36	95	98.5	>99.9
6	**1e**	480	73:27	68	97.0	99.7
7	**1f**	480	72:28	84	92.9	99.3
8	**1g**	480	82:18	70	97.1	99.8
9 [c]	**1a**	24	1:99	96 [d]	n.d. [e]	>99.9

[a] As in Table 1; molar ratio CH_3NO_2: **2c** = 5:1 for entries 1–8. [b] (**4** + *ent*-**4**):*meso*-**4** = 47:53. [c] Molar ratio CH_3NO_2: **2c** = 5:1. [d] Yield of **4c**. [e] n.d. = not determined.

have a pseudoasymmetric carbon atom, in addition to enantiomers **4** and *ent*-**4**. The composition of the product mixture can be controlled by adjusting the molar ratio of nitromethane and allylic compound **2**. Figure 2 demonstrates that the disubstitution product **4** can be obtained almost exclusively when a stoichiometric ratio of reactants is employed. For example, the reaction with the molar ratios **2c**:CH_3NO_2 = 2:1 and 1:100 yields mixtures of products with the ratios **3c**:**4c** = 1:99 and 94:6, respectively. Entries 6–8 of Table 2 show that when the ligand has a bulkier diarylphosphanyl group, the reactivity decreases and the monoallylation product dominates (cf. entries 3 and 8).

The enantioselectivity of the monosubstitution (see Table 1) depends on the steric situation in the complex, and is slightly higher with nitronates as the nucleophile than with malonates[2] or amines.[6] The substituent R^L in the dihydrooxazole ring of ligand **1** is particularly important for the small substrates

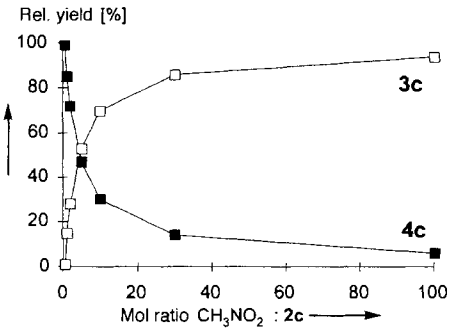

Fig. 2. Relative yields of **3c** and **4c** versus the molar ratio of nitromethane to **2c** (ligand **1a**; reaction conditions described in the Experimental Procedure).

2a and **2b**: the larger the substituent, the higher the enantioselectivity. Similarly, increasing the steric bulk of the substituent on the allyl moiety enhances the enantioselectivity. With the new ligand **1d**, easily available from penicillamine, reactions with 80% *ee* were possible with substrate **2a**, which is a distinct advance over the previous highest value of 60% *ee*.

For compounds with R = Ph, obtained from substrate **2c**, only substitution products with (*E*) configuration were formed, as anticipated; however, in the case of the alkyl-substituted compounds **2b** and **2c** (*Z*)-configurated products were obtained in up to 70% yield (Table 1). This is very surprising because reactions of these substrates with amines[6] and malonates[2] gave (*Z*) isomers in less than 5% yield. Equally interesting is the (*R*) configuration of the (*Z*) product and the possibility of controlling the (*E*)/(*Z*) ratio by adjusting the ratio of nitromethane to substrate. We assume that the (*E*,*S*) products are formed by the pathway mentioned in the introduction, but that the (*Z*) products arise by a yet unknown reaction path leading to **3a,b** with (*Z*,*R*) configuration.[7]

For substrates with R = Ph we were able to determine precisely the enantioselectivities of the mono- (**3c**) as well as the

disubstitution products (**4c**) (Table 2). Interestingly, the disubstitution products were invariably formed with higher enantiomeric purity than the monosubstitution products. When ligand **1c** was used, an enantioselectivity exceeding 99.9% *ee* was obtained. This can be rationalized by assuming that the selectivity of the substitution reaction is independent of the nucleophile. Thus, in the first step **3c** and *ent*-**3c** are formed in a ratio of roughly 100:1. In the subsequent step **4c** is formed preferentially from **3c** with approximately equal selectivity and in a configuratively analogous manner, but *ent*-**3c** leads to one of the diastereomers *meso*-**4c**; this causes a decrease of the relative amount of *ent*-**4c** and an increase of the ratio **4c**:*ent*-**4c** to a value of approximately 10000:1.[8]

When ligands with opposite configurations, **1** and *ent*-**1**, are used for the mono- and the bisallylation, the *meso* compounds *meso*-**4** are expected to be favored. These products can indeed be prepared in a controlled way, however, only as mixtures of pseudoasymmetric diastereomers, which equilibrate under the reaction conditions because of epimerization of the stereogenic center carrying the NO_2 group.[9] Thus, the reaction of nitromethane with the carbonate **2c** catalyzed by the Pd complex of the ligand **1c** first yields (+)-**3c**; its further reaction with **2c** catalyzed by the Pd complex of the ligand *ent*-**1b** affords a 1:1 mixture of the diastereomers *meso*-**4c** in 98% yield.

These results demonstrate that under appropriate conditions nitronates are well suited as nucleophiles for Pd-catalyzed allylic substitutions. Of particular general interest is the new reaction channel. Currently, further experiments are being carried out to elucidate the reaction mechanism.

Experimental Procedure

3a: Under an inert atmosphere at ca. 25 °C, $Pd_2dba_3 \cdot CHCl_3$ [10] (25.9 mg, 50 μmol with respect to Pd) and **1d** (27.5 mg, 60 μmol) were dissolved in 12 mL of dry THF to give a dark red solution. After 20 min the resulting yellow-orange solution was treated with **2a** (721 mg, 5.0 mmol) and nitromethane (6.1 g, 0.1 mol). After 4 d the solvent was removed in vacuo and the residue dissolved in ether. The solution was extracted with NH_4Cl and NaCl solution, the organic phase concentrated to dryness, and the residue purified by chromatography (50 g silica gel, *n*-hexane/ethyl acetate (20/1)). Yield of **3a**: 85%; (*E*)-**3a**:(*Z*)-**3a** = 74:26; GC: Chrompack CP Chirasil DEX CB, 75 °C, t_R[(*E*)-**3a**] = 17.4/18.4 min, t_R[(*Z*)-**3a**] = 17.2/21.3 min.

3b: In analogy to the preparation of **3a**, carbonate **2b** (172 mg, 1.0 mmol) was treated with $Pd_2dba_3 \cdot CHCl_3$ (12.8 mg, 25 μmol with respect to Pd), **1d** (14.0 mg, 30 μmol), and nitromethane (305 mg, 5.0 mmol) in 5 mL of dry THF. Yield of **3b**: 96%; (*E*)-**3b**:(*Z*)-**3b** = 59:41; GC: Macherey-Nagel FS-Lipodex E, 90 °C, t_R[(*E*)-**3b**] = 18.8/19.3 min, t_R[(*Z*)-**3b**] = 20.6/21.0 min.

3c: In analogy to the preparation of **3a**, carbonate **2c** (536 mg, 2.0 mmol) was treated with $Pd_2dba_3 \cdot CHCl_3$ (15.0 mg, 30 μmol with respect to Pd), **1a** (22.5 mg, 60 μmol), and nitromethane (12.2 g, 0.2 mol) in 10 mL of dry THF. After 16 h, 449 mg of **3c** (89%) was obtained with enantiomeric purity of 96.7% *ee* (HPLC, Daicel Chiralcel OD H, *n*-hexane/*i*PrOH (4/1)).

4c: In analogy to the preparation of **3a**, carbonate **2c** (2.0 mmol) was treated with $Pd_2dba_3 \cdot CHCl_3$ (15.0 mg, 30 μmol with respect to Pd), **1a** (22.5 mg, 60 μmol), and nitromethane (61.0 mg, 1.0 mmol) in 10 mL of dry THF (reaction time: 1 d). Yield of **4c**: 94%; enantiomeric purity of **4c**: >99.9% *ee* (HPLC, Daicel Chiralcel OD H, *n*-hexane/EtOH (250/1)). The minor enantiomer was determined precisely with the help of standard solutions.

Received: June 23, 1995
Revised version: September 5, 1995 [Z8125IE]
German version: *Angew. Chem.* **1995**, *107*, 2881–2883

Keywords: asymmetric syntheses · catalysis · nitro compounds · palladium compounds · substitutions

[1] T. Hayashi in *Catalytic Asymmetric Synthesis* (Ed.: I. Ojima), VCH, Weinheim, **1993**, p. 325–365.

[2] J. Sprinz, G. Helmchen, *Tetrahedron Lett.* **1993**, *34*, 1769–1772; P. von Matt, A. Pfaltz, *Angew. Chem.* **1993**, *105*, 614–615; *Angew. Chem. Int. Ed. Engl.* **1993**, *32*, 566–568; G. J. Dawson, C. G. Frost, J. M. J. Williams, S. J. Coote, *Tetrahedron Lett.* **1993**, *34*, 3149–3150.

[3] J. Sprinz, M. Kiefer, G. Helmchen, M. Reggelin, G. Huttner, O. Walter, L. Zsolnai, *Tetrahedron Lett.* **1994**, *35*, 1523–1526.

[4] P. Aleksandrowicz, H. Piotrowska, W. Sas, *Tetrahedron* **1982**, *38*, 1321–1327; P. A. Wade, S. D. Morrow, S. A. Hardinger, *J. Org. Chem.* **1982**, *47*, 365–367; J. E. Bäckvall, S. E. Byström, J. E. Nyström, *ibid.* **1992**, *57*, 1588–1591; D. R. Deardorff, M. J. Shulman, J. E. Sheppeck, *Tetrahedron Lett.* **1989**, *30*, 6625–6628; M. R. Peel, D. D. Sternbach, M. R. Johnson, *J. Org. Chem.* **1991**, *56*, 4990–4993; B. M. Trost, L. Li, S. D. Guile, *J. Am. Chem. Soc.* **1992**, *114*, 8745–8747.

[5] J. P. Genet, S. Grisoni, *Tetrahedron Lett.* **1988**, *36*, 4543–4546.

[6] P. von Matt, O. Loiseleur, G. Koch, A. Pfaltz, C. Lefeber, T. Feucht, G. Helmchen, *Tetrahedron: Asymmetry* **1994**, *5*, 573.

[7] The absolute configuration of the monosubstituted products was determined for compound (*E*)-**3a** by reduction (H_2/Raney Ni, MeOH) to the known (+)-(*R*)-2-methylpentylamine (P. A. Levene, R. E. Marker, *J. Biol. Chem.* **1932**, *98*, 1–7). (*Z*) and (*E*) isomers were correlated by light-induced (*Z*)–(*E*) isomerization ($Ph_2S/\lambda > 300$ nm, benzene).

[8] For other examples of double asymmetric induction, see: S. Masamune, W. Choy, J. S. Petersen, L. R. Sita, *Angew. Chem.* **1985**, *97*, 1–31; *Angew. Chem. Int. Ed. Engl.* **1985**, *24*, 1–30.

[9] Because of this facile epimerization the simple diastereoselectivity of the allylic alkylation of nitro compounds RCH_2NO_2 is probably small.

[10] dba = 1,5-Diphenyl-1,4-pentadien-3-one.

Transition Metal Complexes as Both Host and Guest: Second-Sphere Coordination between a Pt-Azacrown Ether Host and a Pt-NH_3 Guest**

Beth R. Cameron, Sonia S. Corrent, and Stephen J. Loeb*

A transition metal complex containing hydrogen-bond donor groups on its periphery (for example M-NH_3) can act as a guest, binding to a hydrogen-bond receptor through second-sphere coordination. This phenomenon has been discussed in a review by Stoddart et al.;[1] the majority of the adducts of this type are those between crown ethers or benzocrown ethers and transition metal complexes containing aqua or ammine ligands. Alternatively, transition metal complexes with peripheral hydrogen-bond acceptor groups have recently been used as hosts to bind neutral, cationic, and anionic guests. This form of host is often referred to as a *metalloreceptor*.[2–5]

We describe herein the preparation of a new class of metalloreceptor based on covalently linking azacrown ethers to a phosphaneplatinum(II) unit, the use of ^{31}P NMR spectroscopy as a probe for measuring host–guest association constants, and the structure elucidation of the first host–guest complex in which *both* the host and guest are transition metal compounds.

The reaction of equimolar amounts of *trans*-[$PtCl_2(PEt_3)(NH_3)$] and azacrown ethers such as [12]NO_3, [15]NO_4, and [18]NO_5[6] in chloroform, results in substitution of the ammine ligand at Pt^{II} by the secondary nitrogen atom of the azacrown ether and formation of complexes of the type [$PtCl_2(PEt_3)$(azacrown)] (Scheme 1). Also, if two equivalents of *trans*-[$PtCl_2(PEt_3)(NH_3)$] are treated with one equivalent of [18]N_2O_4, a dinuclear complex [$\{PtCl_2(PEt_3)\}_2$([18]N_2O_4)], similar to the known complex[7] [$\{Rh(nbd)(NH_3)\}_2$([18]N_2O_4)], is formed with the loss of two equivalents of ammonia.

[*] Prof. Dr. S. J. Loeb, Dr. B. R. Cameron, S. S. Corrent
Department of Chemistry and Biochemistry
University of Windsor, Windsor, Ontario N9B 3P4 (Canada)
Telefax: Int. code + (519)973-7098
e-mail: loeb@uwindsor.ca

[**] This work was supported by the Natural Science and Engineering Research Council of Canada and the Petroleum Research Fund administered by the American Chemical Society.

 © VCH Verlagsgesellschaft mbH, D-69451 Weinheim, 1995 0570-0833/95/3423-2689 $ 10.00+.25/0

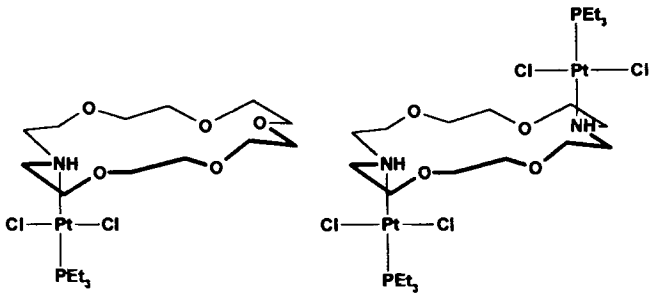

Scheme 1.

The X-ray structure analysis[8] of $[PtCl_2(PEt_3)([18]NO_5)]$ (Fig. 1) demonstrates that these complexes are square-planar species in which the P-Pt-N vector is perpendicular to the crown

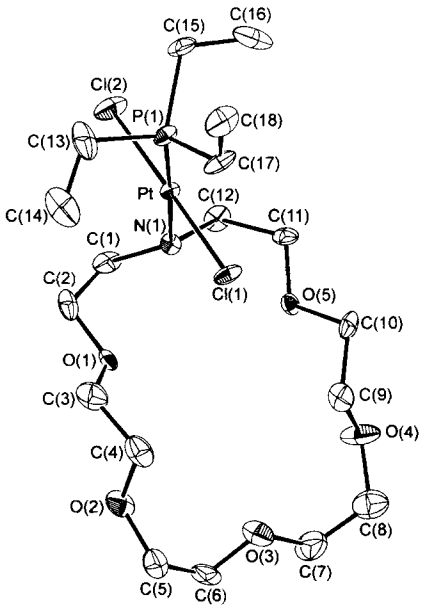

Fig. 1. Crystal structure of the host $[PtCl_2(PEt_3)([18]NO_5)]$ (ORTEP drawing). Selected distances [Å] and angles [°]: Pt–P(1) 2.231(6), Pt–Cl(1) 2.282(5), Pt–Cl(2) 2.316(6), Pt–N(1) 2.10(2); P(1)-Pt-Cl(1) 92.9(2), P(1)-Pt-Cl(2) 89.7(2), P(1)-Pt-N(1) 177.9(5), Cl(1)-Pt-Cl(2) 177.4(2), Cl(1)-Pt-N(1) 87.7(4), Cl(2)-Pt-N(1) 89.7(4).

ether ring. The azacrown ether complex has alternating oxygen atoms O(1), O(3), and O(5) available for hydrogen bonding to an appropriate guest molecule such as an ammonium ion which contains a complementary, triangular array of hydrogen atoms and leads to adducts of type **A**.

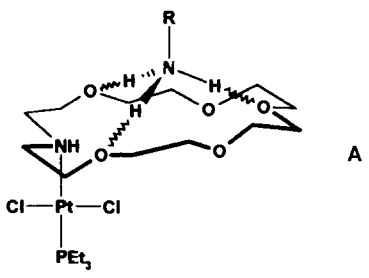

A

In derivatizing these azacrown ethers with a $Pt-PEt_3$ unit, it was reasoned that the host properties of the parent azacrown ether would largely be retained, while the ability to measure binding by ^{31}P NMR spectroscopy would be introduced. Initial host–guest experiments employing $[PtCl_2(PEt_3)([18]NO_5)]$ involved binding to the cations NH_4^+, $tBuNH_3^+$ (as BPh_4^- salts) and the neutral species *trans*-$[PtCl_2(PEt_3)(NH_3)]$.[9] In the $^{31}P\{^1H\}$ NMR spectra of the host–guest complexes, only a singlet with ^{195}Pt-satellites is observed for the single ^{31}P nucleus of the host; an exception is *trans*-$[PtCl_2(PEt_3)(NH_3)]$ as a guest for which a further set of ^{31}P resonances were observed. The downfield shift of this easily detectable resonance with increasing guest concentration was used to determine association constants in $[D_6]$acetone for the supramolecular species $\{(NH_4)\cdot[PtCl_2(PEt_3)([18]NO_5)]\}^+$ ($170 \pm 28\ M^{-1}$) and $\{(tBuNH_3)\cdot[PtCl_2(PEt_3)([18]NO_5)]\}^+$ ($45 \pm 7\ M^{-1}$).[9] However, when *trans*-$[PtCl_2(PEt_3)(NH_3)]$ was employed as guest, accurate determination of a binding constant could not be made since saturation of host with guest, in $CDCl_3$, resulted in too small a change in chemical shift for a reliable analysis.

An X-ray structural analysis (Fig. 2) of the second-sphere adduct $\{[PtCl_2(PEt_3)(NH_3)]\cdot[PtCl_2(PEt_3)([18]NO_5)]\}$ verifies the nature of the hydrogen-bonding interaction inferred for the host–guest interactions described above. This adduct is the first

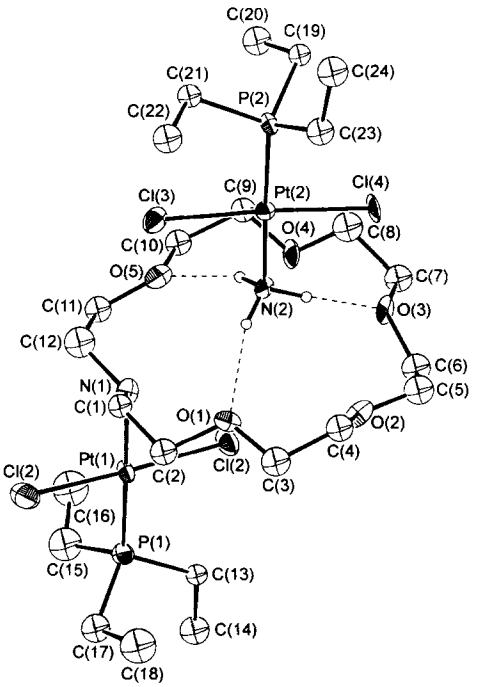

Fig. 2. Crystal structure of the supramolecular, host–guest complex $\{[PtCl_2(PEt_3)(NH_3)]\cdot[PtCl_2(PEt_3)([18]NO_5)]\}$ (ORTEP drawing). Selected distances [Å] and angles [°]: Pt(1)-P(1) 2.21(1), Pt(1)-Cl(1) 2.27(1), Pt(1)-Cl(2) 2.29(1), Pt(1)-N(1) 2.14(3), Pt(2)-P(2) 2.23(1), Pt(2)-Cl(3) 2.30(1), Pt(2)-Cl(4) 2.28(1), Pt(2)-N(2) 2.21(2); P(1)-Pt(1)-Cl(1) 94.6(4), P(1)-Pt(1)-Cl(2) 89.3(4), P(1)-Pt(1)-N(1) 179(1), Cl(1)-Pt(1)-Cl(2) 176.1(3), Cl(1)-Pt(1)-N(1) 86.1(9), Cl(2)-Pt(1)-N(1) 90.9(9), P(2)-Pt(2)-Cl(3) 96.1(4), P(2)-Pt(2)-Cl(4) 88.0(4), P(2)-Pt(2)-N(2) 174.8(8), Cl(3)-Pt(2)-Cl(4) 175.7(3), Cl(3)-Pt(2)-N(2) 86.9(8), Cl(4)-Pt-N(2) 90.0(8).

example of a host–guest complex in which *both* host and guest are transition metal compounds. The interaction of host and guest occurs through hydrogen bonding of the Pt-bound NH_3 group of the $[PtCl_2(PEt_3)(NH_3)]$ guest to alternating ether oxygen atoms on the $[PtCl_2(PEt_3)([18]NO_5)]$ host. The macrocycle adopts the familiar all-*gauche* conformation characteristic of RNH_3^+, BX_3NH_3, and $[PtCl_2(PMe_3)(NH_3)]$ binding to [18]crown-6 derivatives.[1] The guest perches over the crown ether ring on the side of the ring opposite the $Pt-PEt_3$ unit of the host. Each of the hydrogen atoms of the ammine ligand is involved in a linear hydrogen bond to alternating O atoms of the crown ether moiety: N···O distances [Å]: N(2)···O(1) 3.13(3), N(2)···O(3) 3.19(4), N(2)···O(5) 2.98(3); H···O distances [Å]:

H(N2A)···O(1) 2.21, H(N2C)·····O(3) 2.27, H(N2B)···O(5) 2.06; N-H···O angles [°]: N(2)-H(N2A)···O(1) 164, N(2)-H(N2C)···O(3) 160, N(2)-H(N2B)···O(5) 161.

Derivatization of an azacrown ether with a Pt–PEt_3 unit results in a simple crown ether type host containing a lariat ether type, peripheral appendage. The phoshorus atom of the Pt complex fragment serves as a NMR spectroscopic marker and allows a straightforward determination of host–guest association constants. The X-ray structure determination of the first host–guest complex in which *both* the host and guest are transition metal complexes provides detailed solid-state evidence for the hydrogen-bonding nature of the noncovalent interaction.

Experimental Procedure

$[PtCl_2(PEt_3)([18]NO_5)]$: *trans*-$[PtCl_2(PEt_3)(NH_3)]$ [10] (50.0 mg, 0.125 mmol) was added with stirring to a solution (1 mL) containing aza[18]crown-6 (33.0 mg, 0.125 mmol) in chloroform, and the mixture stirred for three hours. The solvent was removed to give a yellow solid which was recrystallized from chloroform and diethyl ether. Yield of yellow crystals: 73 mg (90%). ^1H NMR ([D$_6$]acetone): $\delta = 4.15$ (br. s, 2H, OCH_2), 3.74–3.52 (m, 18H, OCH_2), 3.29 (br. s, 2H, NCH_2), 2.90 (br. s, 2H, NCH_2), 1.86 (m, 6H, PCH_2), 1.17 (m, 9H CH_3). $^{31}P\{^1H\}$ NMR 3.17 (^1J(P,Pt) = 3373 Hz).

$\{[PtCl_2(PEt_3)(NH_3)]\cdot[PtCl_2(PEt_3)([18]NO_5)]\}$: A solution containing equimolar amounts of *trans*-$[PtCl_2(PEt_3)(NH_3)]$ and $[PtCl_2(PEt_3)([18]NO_5)]$ in chloroform was allowed to slowly evaporate in a fumehood. After four days, yellow crystals suitable for X-ray crystallography were isolated by filtration; yield 42%. ^1H NMR ($CDCl_3$): $\delta = 4.24$ (t, 4H, OCH_2), 3.84 (m, 4H, OCH_2), 3.73 (m, 4H, OCH_2), 3.62 (m, 4H, OCH_2), 3.34 (t, 4H, OCH_2), 2.93 (m, 4H, NCH_2), 2.73 (s, br, 1H, N H), 2.02 (s, br, 3H, NH_3), 1.83 (m, 12H, PCH_2), 1.16 (m, 18H CH_3); $^{31}P\{^1H\}$ NMR ([D$_6$]acetone) 3.36, (^1J(P,Pt) = 3376 Hz), 1.41, (^1J(P,Pt) = 3461 Hz).

Received: August 10, 1995 [Z 8299 IE]
German version: *Angew. Chem.* **1995**, *107*, 2900–2902

Keywords: crown ethers · host–guest chemistry · platinum compounds · second-sphere coordination · supramolecular chemistry

[1] H. M. Colquhoun, J. F. Stoddart, D. J. Williams, *Angew. Chem.* **1986**, *98*, 483; *Angew. Chem. Int. Ed. Engl.* **1986**, *25*, 487; J. F. Stoddart, R. Zarzycki, *Cation Binding by Macrocycles*; (Eds.: Y. Inoue, G. W. Gokel), Marcel Dekker, New York, **1990**, p. 631 and references therein.

[2] D. M. Rudkevich, J. D. Mercer-Chalmers, W. Verboom, R. Ungaro, F. de Jong, D. N. Reinhoudt, *J. Am. Chem. Soc.* **1995**, *117*, 6124 and references therein; F. C. J. M. van Veggel, W. Verboom, D. N. Reinhoudt, *Chem. Rev.* **1994**, *94*, 279; A. R. van Doorn, D. J. Rushton, W. F. van Straaten-Nijenhuis, W. Verboom, D. N. Reinhoudt, *Recl. Trav. Chim. Pays-Bas* **1992**, *111*, 421; M. T. Reetz, C. M. Niemeyer, M. Hermes, M. Goddard, *Angew. Chem.* **1992**, *104*, 1053; *Angew. Chem. Int. Ed. Engl.* **1992**, *31*, 1017.

[3] Y. Aoyama, A. Yamagishi, M. Asagawa, H. Toi; H. Ogoshi, *J. Am. Chem. Soc.* **1988**, *110*, 4076; T. Mizutani, T. Ema, T. Yoshida, Y. Kurado, H. Ogoshi, H. *Inorg. Chem.* **1993**, *32*, 2072.

[4] M. Shionoya, E. Kimura, S. Shiro, *J. Am. Chem. Soc.* **1993**, *115*, 6730; M. Shionoya, T. Ikeda, E. Kimura, S. Shiro, *ibid* **1994**, *116*, 3848.

[5] J. E. Kickham, S. J. Loeb, S. L. Murphy, *J. Am. Chem. Soc.* **1993**, *115*, 7031; J. E. Kickham, S. J. Loeb, *J. Chem. Soc. Chem. Commun.* **1993**, 1848; J. E. Kickham, S. J. Loeb, *Inorg. Chem.* **1994**, *33*, 4351.

[6] Abbreviations used: $[12]NO_3$, aza[12]crown-4; $[15]NO_4$, aza[15]crown-5; $[18]NO_5$, aza[18]crown-6; $[18]N_2O_4$, 4,13-diaza[18]crown-6, nbd, norbornadiene.

[7] H. M. Colquhoun, S. M. Doughty, A. M. Z. Slawin, J. F. Stoddart, D. J. Williams, *Angew. Chem.* **1985**, *97*, 124; *Angew. Chem. Int. Ed. Engl.* **1985**, *24*, 135.

[8] Crystal data for $[PtCl_2(PEt_3)([18]NO_5)]$: $C_{18}H_{40}Cl_2NO_5PPt$, monoclinic, $P2_1/c$, $a = 14.072(8)$, $b = 11.960(4)$, $c = 15.434(3)$ Å, $\beta = 97.65(3)°$, $V = 2574(2)$ Å^3, $Z = 4$, $\rho_{calcd} = 1.67$ g cm^{-3}, $\mu(Mo_{K\alpha}) = 58.02$ cm^{-1}. Rigaku AFC6S diffractometer, 1948 unique reflections with $F_o^2 > 3\sigma(F_o^2)$, $R = 0.0445$ and $R_w = 0.0544$. Crystal data for $\{[PtCl_2(PEt_3)(NH_3)]\cdot[PtCl_2(PEt_3)([18]NO_5)]\}$: $C_{24}H_{58}Cl_4N_2O_5P_2Pt_2$, monoclinic, $P2_1/n$, $a = 7.980(8)$, $b = 42.004(9)$, $c = 11.623(4)$ Å, $\beta = 97.17(5)°$, $V = 3865(3)$ Å^3, $Z = 4$, $\rho_{calcd} = 1.80$ g cm^{-3}, $\mu(Mo_{K\alpha}) = 75.92$ cm^{-1}. Rigaku AFC6S diffractometer, 2074 unique reflections with $F_o^2 > 3\sigma(F_o^2)$, $R = 0.0577$ and $R_w = 0.0676$. Empirical absorption corrections were applied to the data sets and the solutions of the structures obtained by using standard Patterson and difference Fourier methods. All atoms were refined with anistropic thermal parameters except the carbon atoms of $\{[PtCl_2(PEt_3)(NH_3)]\cdot[PtCl_2(PEt_3)([18]NO_5)]\}$ [11–15].

[9] The program EQNMR was employed to evaluate NMR titration data. M. J. Hynes, *J. Chem. Soc. Dalton Trans.* **1993**, 311. To date, no attempts have been made to measure binding constants for $[PtCl_2(PEt_3)([15]NO_4)]$ or $[PtCl_2(PEt_3)([12]NO_3)]$.

[10] R. G. Gunther, D. S. Martin, Jr., *Inorg. Chim. Acta* **1972**, *6*, 81.

[11] TEXSAN-TEXRAY Structure Analysis Package, Molecular Structure Corp., The Woodlands, TX, **1985**.

[12] D. T. Cromer, J. T. Waber, *International Tables for X-ray Crystallography*, *Vol. IV*, Kynoch Press, Birmingham, **1974**, Table 2.2A.

[13] J. A. Ibers, H. A. Hamilton, *Acta Crystallogr.* **1974**, *17*, 781.

[14] D. T. Cromer, *International Tables for X-ray Crystallography*, *Vol. IV*, Kynoch Press, Birmingham, **1974**, Table 2.3.1.

[15] Further details of the crystal structure investigations may be obtained from the Director of the Cambridge Crystallographic Data Centre, University Chemical Laboratory, Lensfield Road, GB-Cambridge CB2 1EW (UK), on quoting the full journal citation.

A Study on Rhodium–Vinylallene Complexes Leading to a New Reaction, Rhodium-Catalyzed Carbonylative [4 + 1]Cycloaddition

Masahiro Murakami,* Kenichiro Itami, and Yoshihiko Ito*

The coordination of unsaturated organic molecules to transition metals has been studied intensively both experimentally and theoretically; η^4 complexes of 1,3-dienes constitute an important class.[1] Conjugated dienes that are extended with a cumulated double bond, like vinylketenes (**1**, X = O), also form η^4 complexes having interesting structures and reactivities.[2] Although vinylallenes (**2**, X = CR_2) also belong to this class of cumulated diene systems, their η^4 complexes have been rare; examples have been limited to iron carbonyl complexes prepared directly from a vinylallene[3] and a phenylallene,[4] or indirectly via η^4-vinylketene complexes.[5] In the course of our studies,[6] we became interested in why η^4-vinylallene complexes are so uncommon. We report here on the synthesis of (vinylallene)rhodium(I) complexes with two different coordination modes, η^2 coordination and η^4 coordination, and a reaction proceeding via the latter type of complex, the rhodium(I)-catalyzed carbonylative [4 + 1]cycloaddition of vinylallenes. The insight into the fundamental properties of (vinylallene)rhodium(I) complexes has opened a pathway to a new catalytic carbonylation.

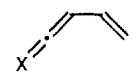

1 X = O
2 X = CR_2

In the first experiment vinylallene **2a**, which has no substituents at the terminal allenic carbon, was treated with $[RhCl(PPh_3)_3]$ in benzene at room temperature. In analogy to the related reaction of a simple allene,[7] **2a** displaced one PPh_3 ligand from the rhodium to afford **3** in 78% isolated yield (Scheme 1). The molecular structure, determined by an X-ray crystallographic analysis, indicates η^2 coordination at the terminal allenic π bond (Fig. 1).[8] The rhodium center has a square-planar coordination geometry, the less hindered side of the allenyl group is *trans* to the chlorine atom, and the axis of the

[*] Prof. M. Murakami, Prof. Y. Ito, K. Itami
Department of Synthetic Chemistry and Biological Chemistry
Kyoto University, Yoshida, Kyoto 606-01 (Japan)
Telefax: Int. code + (75)753-5668

 © VCH Verlagsgesellschaft mbH, D-69451 Weinheim, 1995 0570-0833/95/3423-2691 $ 10.00+.25/0

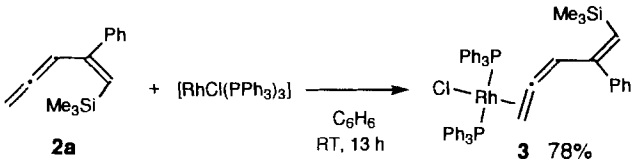

Scheme 1. Synthesis of the η^2-(vinylallene)rhodium complex **3**. RT = room temperature.

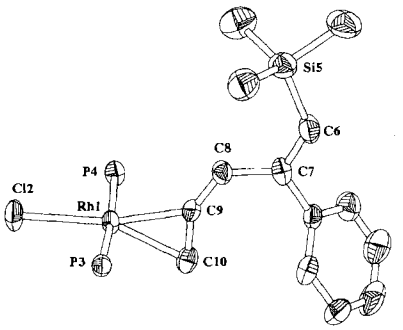

Fig. 1. Molecular structure of **3** in the crystal; the phenyl groups on the phosphorus atom and the hydrogen atoms are omitted for clarity (thermal ellipsoids at 40% probability) [8].

η^2-coordinated bond lies perpendicular to the RhP_2Cl plane. As a consequence of the η^2 coordination, the allenyl group is distorted from linearity (C8-C9-C10 149.6(9)°). As was observed previously,[7, 9] the distance from the rhodium atom to the central allenic carbon atom C9 (2.015(9) Å) is less than that to the terminal allenic carbon C10 (2.115(10) Å), probably reflecting the higher s character in the hybrid orbital on C9.

Next, vinylallene **2b**, which has two methyl groups at the allenic terminal, was treated with $[RhCl(PPh_3)_3]$. In marked contrast to the reaction of **2a**, two PPh_3 ligands were displaced to yield (η^4-vinylallene)rhodium(I) complex **4** as a mixture of *endo* and *exo* isomers isolated in 44 and 19% yield, respectively (Scheme 2). The structure of *endo*-**4** was determined by X-ray

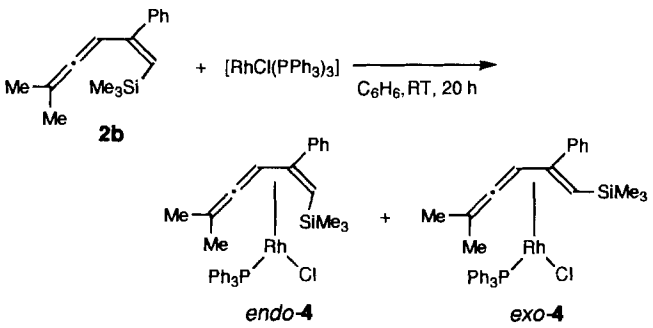

Scheme 2. Synthesis of the η^4-(vinylallene)rhodium complexes *endo*-**4** and *exo*-**4**.

crystallography (Fig. 2 left).[8] The rhodium(I) atom has a distorted square-planar coordination environment. The two *cis* sites are occupied by the internal allenic π bond and the vinylic π bond; the chlorine atom is *trans* to the former π bond. The η^4-coordinated skeleton is in a cisoid, planar form. The silicon atom in *endo* position deviates from this plane, away from the metal, with a torsion angle Si4-C5-C6-C7 of 52.7°. The Rh1–C8 bond is shorter than those to the other coordinated carbon atoms, presumably due to the difference in hybridization.

The X-ray structure analysis of *exo*-**4** confirms an *exo* orientation of the trimethylsilyl group (Fig. 2 right).[8] Interestingly,

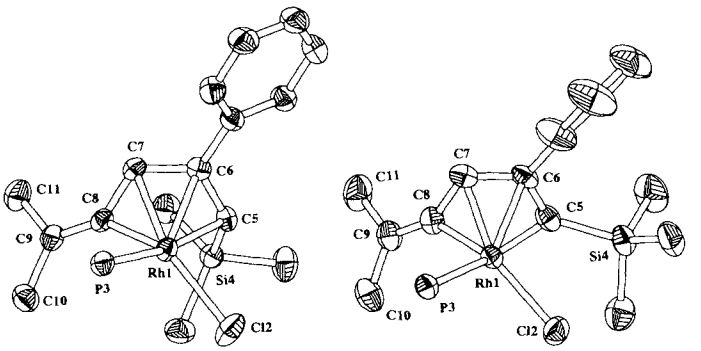

Fig. 2. Molecular structures of *endo*-**4** (left) and *exo*-**4** (right); the phenyl groups on the phosphorus atoms and the hydrogen atoms are omitted for clarity (thermal ellipsoids at 40% probability) [8].

the C5–Si4 bond is approximately coplanar with the η^4-coordinated skeleton, or rather, slightly bent toward the metal center (torsion angle Si4-C5-C6-C7 170.3°).

It is instructive to compare the reactivity of butadiene **5**, which has the same substitution pattern as **2** but lacks the cumulated double bond. When **5** was treated with a stoichiometric amount of $[RhCl(PPh_3)_3]$ under conditions similar to those used for the synthesis of **4**, no ligand exchange was evident in the ^1H NMR spectrum. This result underlines the facility of vinylallenes for ligand exchange. The preferred η^4 coordination of ligand **2b** can be ascribed to spatial interactions between the allenic substituents and phosphane ligands, which would disfavor the sterically more demanding η^2 coordination of the terminal allenic π bond. Although this steric effect controlling the coordination mode of vinylallenes may be amplified in the present case with $[RhCl(PPh_3)_3]$, which has bulky phosphane ligands, it is reasonable to assume that a similar determinant operates generally in ligand substitution reactions with vinylallenes.

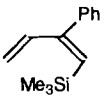

5

Notably, isolated *endo*-**4** in C_6D_6 underwent gradual isomerization to *exo*-**4** on standing at 70 °C ($t_{1/2}$ = 22.5 h). In contrast, *exo*-**4** did not isomerize. A plausible mechanism for this thermal *endo*–*exo* isomerization is based on the rhodacyclo-3-pentene intermediate **6** (Scheme 3).[10] Decomplexation of the double

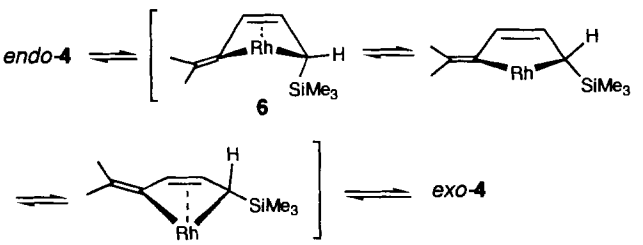

Scheme 3. The thermal flip-envelope isomerization of *endo*-**4** to give *exo*-**4**.

bond of **6** and a subsequent flip of the rhodacycle envelope lead back to the η^4 complex with *exo* orientation. It is likely that in the reaction of **2b** with $[RhCl(PPh_3)_3]$, simple ligand substitution results in the initial formation of *endo*-**4** with retention of the original orientation of the silyl group. A "flip-envelope" isomerization subsequently occurs to furnish a mixture of the two forms.

The observed isomerization of *endo*-**4** suggests considerable contribution from the rhodacyclo-3-pentene form. One impor-

tant ramification is that incorporation of carbon monoxide into the conjugated diene skeleton may be possible by coordination and insertion of carbon monoxide into the C–Rh σ bond of the rhodacyclo-3-pentene. This would result in a [4 + 1] assembly. Moreover, η^4 coordination of a vinylallene to rhodium through straightforward ligand exchange is particularly attractive because it would offer access to a catalytic cycle. Thus, we next examined the reaction of the rhodium(I) complex *endo*-**4** with carbon monoxide (Scheme 4). A solution of *endo*-**4** in

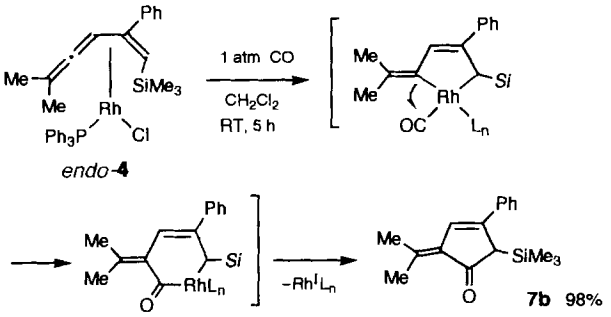

Scheme 4. [4 + 1]Cycloaddition of the η^4-(vinylallene)rhodium complex *endo*-**4** with CO.

CH_2Cl_2 was stirred at room temperature under CO at atmospheric pressure. A [4 + 1]cycloaddition reaction proceeded cleanly to furnish 2-(alkylidene)cyclopentenone **7b** in 98% yield. A plausible mechanism is shown in Scheme 4. Carbon monoxide is introduced into the coordination sphere of the metal to give a (vinylallene)(carbonyl)rhodium, which also acquires the contribution of a rhodacyclo-3-pentene resonance form in solution. Migratory insertion of the carbonyl group into the Rh–C_{sp^2} (or Rh–C_{sp^3}) σ bond of the rhodacyclo-3-pentene and the subsequent reductive elimination of Rh^I produce **7b**. In contrast, the η^2 complex **3** afforded no cycloaddition product under analogous conditions, indicating that η^4 coordination is requisite for the carbonylative [4 + 1]cycloaddition.

Our efforts were then directed at establishing a catalytic system. A free vinylallene was treated with a catalytic quantity of a variety of rhodium(I) complexes under carbon monoxide (1 atm). Whereas little activity was observed with [RhCl(PPh$_3$)$_3$], cationic rhodium complexes like [Rh(cod)(MeCN)$_2$]PF$_6$ and [Rh(cod)(dppb)]BF$_4$ (cod = cyclooctadiene, dppb = bis(diphenylphosphino)butane) were found to efficiently catalyze the carbonylative [4 + 1]cycloaddition of vinylallenes (Table 1). The corresponding 2-alkylidene-3-cyclopentenone **7** was obtained together with 2-alkylidene-4-cyclopentenone **7′** in good yield. The ratio **7′**:**7** increased as the reaction proceeded, suggesting that **7′** forms by transposition of the C^3–C^4 double bond of the primary product **7** through double-bond isomerization and/or protodesilylation. The trimethylsilyl groups of the primary products from **2b** and **2d** are located α to both the carbonyl group and the C–C double bond, and hence, these trimethylsilyl groups are extremely labile toward hydrolysis. It is likely that the trimethylsilyl group reacts with water in the reaction mixture and is cleaved as trimethylsilanol.

It is reasonable to assume that the catalytic cycle is analogous to the reaction shown in Scheme 4 followed by coordination of a new vinylallene molecule to the rhodium(I) center. Vinylallenes **2d** and **2e**, in which the allenyl group is not symmetrically substituted, gave only one stereoisomer with regards to the exocyclic C=C bond. This stereoselectivity can be accounted for by assuming face-selective η^4 coordination from the less-hindered

Table 1. Rh^I-catalyzed [4 + 1]cycloaddition of vinylallenes with CO [a]. dppe = Bis(diphenylphosphino)ethane, dppb = bis(diphenylphosphino)butane, dppp = bis(diphenylphosphino)pentane, cod = cyclooctadiene.

2	Catalyst/ conditions	7, 7′ [b] (Yield [%]) [c]	Total yield [%] [c]
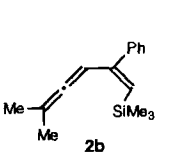	[Rh(cod)-(MeCN)$_2$]PF$_6$ CH_2Cl_2 reflux 21 h	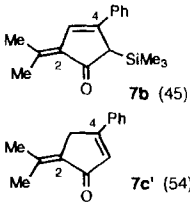 **7b** (45) **7c′** (54)	99
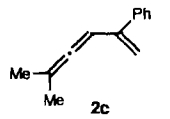	[Rh(cod)$_2$]PF$_6$/ dppe toluene [d] 80 °C 20 h	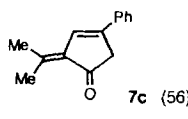 **7c** (56) **7c′** (26)	82
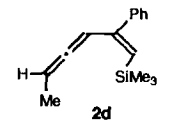	[Rh(cod)$_2$]PF$_6$/ dppe toluene 80 °C 2 h	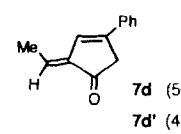 **7d** (50) **7d′** (47)	97
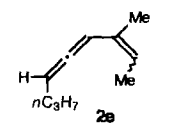	[Rh(cod)-dppb]BF$_4$ toluene 80 °C 6 d	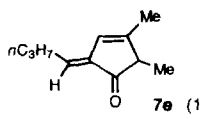 **7e** (17) **7e′** (61)	78
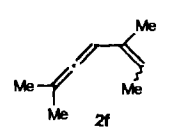	[Rh(cod)$_2$]PF$_6$/ dppe toluene 80 °C 24 h	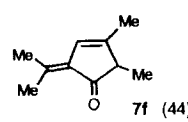 **7f** (44) **7f′** (47)	91
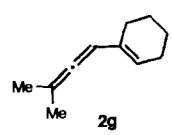	[Rh(cod)$_2$]PF$_6$ /dppp toluene 80 °C 60 h	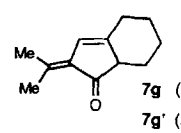 **7g** (42) **7g′** (53)	95

[a] The reaction was carried out with 2–10 mol% of the Rh^I complex under CO (1 atm) unless otherwise noted. [b] Compound numbers with a prime designate 2-(alkylidene)-4-cyclopentenone forms. [c] Yield of isolated product. [d] The reaction was carried out in an autoclave under 15 atm CO.

side of the vinylallene and subsequent specific disrotatory ring closure to give a rhodacyclo-3-pentene intermediate. In contrast to the vinylallenes listed in Table 1, which have substituents at the allenyl terminal, the vinylallene **2a** failed to undergo catalytic cycloaddition. This result can be explained in terms of the steric preference of η^4 over η^2 coordination.

Although the [4 + 1]cycloaddition is a potential method for the construction of five-membered carbocycles,[11] there have been no reports on the transition metal catalyzed carbonylation of 1,3-dienes without cumulated double bonds.[12] Two examples reported make use of bisallene[13] and 4-en-2-ynyl carbonate.[14] Indeed, similar Rh^I-catalyzed carbonylation reactions failed to proceed with 1,3-dienes like 2,3-dimethyl-1,3-butadiene, 2,3-diphenyl-1,3-butadiene, and 1,4-diphenyl-1,3-butadiene. The pronounced reactivity of vinylallenes can be ascribed to both the substantial facility for ligand exchange and

the significant contribution from a metallacyclo-3-pentene resonance form in the resultant η^4 complex. We are currently examining further utilization of the potential of vinylallenes in reactions with transition metal catalysts proceeding through η^4 complexes.

Experimental Procedure

3: To a solution of (*E*)-4-phenyl-5-(trimethylsilyl)-1,2,4-pentatriene (**2a**, 25 mg, 0.12 mmol) in benzene (3 mL) at room temperature was added $[RhCl(PPh_3)_3]$ (129 mg, 0.139 mmol). After the mixture was stirred for 13 h, the solvent was removed under vacuum. The residue was subjected to column chromatography (silica gel, CH_2Cl_2:hexane = 3:1) to afford **3** (80 mg, 78%) as a yellow powder.

4: To a solution of (*E*)-5-methyl-2-phenyl-1-(trimethylsilyl)-1,3,4-hexatriene (**2b**, 40 mg, 0.165 mmol) in benzene (4 mL) at room temperature was added $[RhCl(PPh_3)_3]$ (153 mg, 0.165 mmol). After the mixture was stirred for 20 h, the solvent was removed under vacuum. The residue was subjected to preparative thin-layer chromatography (silica gel, CH_2Cl_2:hexane = 3:1) to afford *endo*-**4** (47 mg, 44%, orange powder) and *exo*-**4** (20 mg, 19%, yellow powder).

7c, **7c'**: A mixture of $[Rh(cod)_2]PF_6$ (10.9 mg, 23.5 μmol), dppe (11.2 mg, 28.1 μmol), and **2c** (200 mg, 1.17 mmol) in toluene (2 mL) was stirred at 80 °C for 20 h under 15 atm of CO in an autoclave. After the mixture was cooled, the solvent was removed under vacuum. The residue was subjected to column chromatography (silica gel, ether:hexane = 1:10) to afford **7c** (130 mg, 56%) and **7c'** (60.0 mg, 26%) as colorless solids.

Received: July 3, 1995
Revised version: September 26, 1995 [Z8164/8165IE]
German version: *Angew. Chem.* **1995**, *107*, 2943–2946

Keywords: carbonylations · coordination · cycloadditions · rhodium complexes · vinylallenes

[1] a) D. M. P. Mingos in *Comprehensive Organometallic Chemistry, Vol. 3* (Eds.: G. W. Wilkinson, F. G. A. Stone, K. W. Abel), Pergamon, Oxford, **1982**, Chapter 19; b) J. P. Collman, L. S. Hegedus, J. R. Norton, R. G. Finke, *Principles and Applications of Organotransition Metal Chemistry*, University Science Books, Mill Nalley, CA, USA, **1989**, Chapter 17.

[2] A. C. Reduto dos Reis, L. S. Hegedus, *Organomeallics* **1995**, *14*, 1586, and references therein.

[3] P. Areces, S. Jeganathan, W. H. Okamura, *Anal. Quim.* **1993**, *89*, 101.

[4] L. S. Trifonov, A. S. Orahovats, R. Trewo, H. Heimgartner, *Helv. Chim. Acta* **1988**, *71*, 551.

[5] S. P. Saberi, S. E. Thomas, *J. Chem. Soc. Perkin Trans. 1* **1992**, 259.

[6] a) M. Murakami, H. Amii, N. Takizawa, Y. Ito, *Organometallics* **1993**, *12*, 4223; b) M. Murakami, H. Amii, K. Itami, Y. Ito, *Angew. Chem.* **1995**, *107*, 1649; *Angew. Chem. Int. Ed. Engl.* **1995**, *34*, 1476.

[7] a) S. Otsuka, A. Nakamura, *Adv. Organomet. Chem.* **1976**, *14*, 245; b) T. Kashiwagi, N. Yasuoka, N. Kasai, M. Kukudo, *J. Chem. Soc. Chem. Commun.* **1969**, 317.

[8] Further details of the crystal structure investigations may be obtained from the Director of the Cambridge Crystallographic Data Centre, 12 Union Road, GB-Cambridge CB21EZ (UK), on quoting the full journal citation.

[9] a) H. Werner, P. Schwab, N. Mahr, J. Wolf, *Chem. Ber.* **1992**, *125*, 2641; b) H. Werner, D. Schneider, M. Schulz, *J. Organomet. Chem.* **1993**, *451*, 175.

[10] a) J. W. Faller, A. M. Rosan, *J. Am. Chem. Soc.* **1977**, *99*, 4858; b) B. Eaton, J. A. King, Jr., K. P. C. Vollhardt, *ibid.* **1986**, *108*, 1359.

[11] a) L. S. Liebeskind, R. Chidambaram, *J. Am. Chem. Soc.* **1987**, *109*, 5025; b) D. P. Curran, H. Liu, *ibid.* **1991**, *113*, 2127.

[12] For the transition metal catalyzed [4 + 1]cycloaddition of heteroconjugated systems such as allenyl ketones and allenyl imines to give five-membered heterocycles, see: a) M. S. Sigman, C. E. Kerr, B. E. Eaton, *J. Am. Chem. Soc.* **1993**, *115*, 7545; b) M. S. Sigman, B. E. Eaton, *J. Org. Chem.* **1994**, *59*, 7488.

[13] B. E. Eaton, B. Rollman, J. A. Kaduk, *J. Am. Chem. Soc.* **1992**, *114*, 6245.

[14] a) J. Tsuji, T. Mandai, *J. Organomet. Chem.* **1993**, *451*, 15; b) T. Mandai, J. Tsuji, Y. Tsujiguchi, *J. Am. Chem. Soc.* **1993**, *115*, 5865.

Distinguishing the Silanol Groups in the Mesoporous Molecular Sieve MCM-41**

Jiesheng Chen,* Qinghua Li, Ruren Xu, and Fengshou Xiao

The successful synthesis of M41S materials,[1,2] a new family of novel silicates with uniform mesopores, opened a vast range of applications[3–7] in catalysis, sorption, molecular recognition, electronics, and photochemistry. One of the members of this family of materials is MCM-41, which contains a hexagonal array of mesopores with a pore diameter of 20–100 Å depending on the conditions of its synthesis. It is postulated[2] that the inorganic walls around the mesopores of MCM-41 are constructed of disordered SiO_4 tetrahedral units, as is also the case for amorphous silicates. NMR studies[2,8] reveal that MCM-41 contains many silanol groups both before and after the template molecules have been removed. These silanols may act as functional groups in chemical reactions or can be utilized to attach molecules having other functional groups. Although the structure and stability of the pores are well understood, little is known about the nature of the silanol groups in MCM-41. To shed some light on this, we monitored the IR absorptions of the silanol groups in template-free MCM-41 as a function of evacuation temperature before and after silylation by chlorotrimethylsilane (CTMS) and chlorotriphenylsilane (CTPS).

Figure 1 shows the IR spectra between 4000 and 2400 cm^{-1} of template-free MCM-41 evacuated (1×10^{-3} mbar) at various temperatures. At room temperature the spectrum exhibits a broad featureless band between 3700 and 3200 cm^{-1} with the maximum at around 3525 cm^{-1}, and a less distinct shoulder absorption at about 3740 cm^{-1}. A small band (not shown in Fig. 1) is also observed at about 1685 cm^{-1}, which is due to

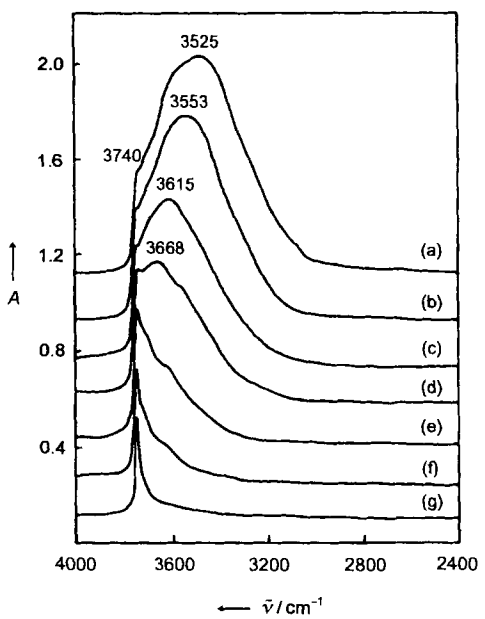

Fig. 1. IR spectra of template-free MCM-41 evacuated at a) ca. 25 °C, b) 100 °C, c) 150 °C, d) 200 °C, e) 250 °C, f) 300 °C, g) 350 °C, and h) 450 °C.

[*] Prof. J. Chen, Q. Li, Prof. R. Xu, Dr. F. Xiao
Department of Chemistry, Jilin University
Changchun 130023 (China)
Telefax: Int. code + (431)892-3907

[**] This work was supported by the National Natural Science Foundation of China and the Key Laboratory of Inorganic Hydrothermal Synthesis, Jilin University.

adsorbed water. Upon evacuation at 100 °C, this absorption disappears, indicating removal of the adsorbed water. At the same time the band between 3700 and 3200 cm^{-1} becomes narrower and its maximum shifts towards higher frequency to about 3553 cm^{-1}. The absorption at 3740 cm^{-1}, which was also observed[9] previously for a MCM-41 sample calcined in vacuum, is attributed to isolated silanol groups, whereas that at 3553 cm^{-1} is associated with hydrogen-bonded silanols.[10, 11] Since the internal surface area of MCM-41 is much greater than the external, it is assumed that the majority of the silanol groups are located on the internal surface. At higher temperatures the low-frequency side of the broad band disappears, indicating condensation of the H-bonded silanol groups. At 450 °C only the absorption at 3740 cm^{-1} remains and its intensity is more or less the same as that at room temperature. Apparently the isolated silanol groups in MCM-41 are much more resistant to high-temperature evacuation than the hydrogen-bonded species. It is almost impossible to distinguish between these H-bonded silanols in MCM-41 since they interact with one another to give a broad IR band.

When MCM-41 is silylated with chlorotrimethylsilane (CTMS), the IR spectra change (Fig. 2). All the spectra show a

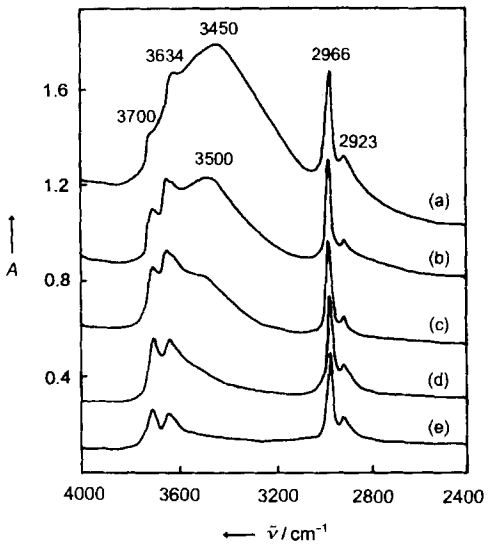

Fig. 2. IR spectra of CTMS-silylated MCM-41 evacuated at a) ca. 25 °C, b) 100 °C, c) 200 °C, d) 300 °C, and e) 450 °C.

sharp peak at 2966 cm^{-1} and a weak absorption at 2923 cm^{-1} characteristic of the trimethylsilyl groups. The absence of the band at 3740 cm^{-1} suggests that all the isolated silanol groups are highly accessible and have reacted with CTMS to form Si-O-$Si(CH_3)_3$ bonds. It has been shown[2] that silylation with CTMS results in a distinct decrease in the pore size of MCM-41, indicating that the silylation occurs inside the mesoporous channels. At room temperature a broad band with shoulders at 3700 and 3634 cm^{-1}, which are not observed for the nonsilylated sample, appears between 3600 and 3200 cm^{-1}. The absorption at 1685 cm^{-1} confirms that the sample contains adsorbed water molecules. As is the case for the nonsilylated material, when the evacuation temperature is increased, the adsorbed water molecules are removed and the broad band becomes narrower. In contrast, the two absorptions at 3700 and 3634 cm^{-1} remain even at 450 °C, although their intensities are greatly reduced.

A similar change occurs in the spectrum of the CTPS-silylated MCM-41 when the temperature is increased (Fig. 3). The small

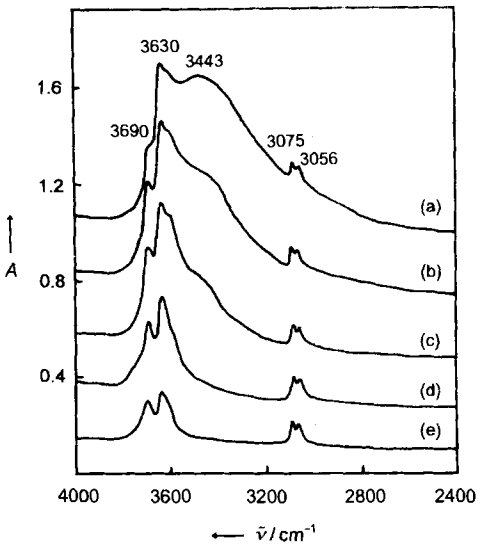

Fig. 3. IR spectra of CTPS-silylated MCM-41 evacuated at a) ca. 25 °C, b) 100 °C, c) 200 °C, d) 300 °C, and e) 450 °C.

absorption peaks at 3075 and 3056 cm^{-1} are assigned to the triphenylsilyl moieties. A peak at 3740 cm^{-1} is not evident, but when the sample is evacuated at elevated temperatures two bands at 3690 and 3630 cm^{-1} appear. The presence of triphenylsilyl moieties and the absence of isolated silanol groups strongly suggest that in spite of their bulk CTPS molecules react with the isolated hydroxyl groups present in the nonsilylated MCM-41 to form Si-O-$SiPh_3$ bonds.

By comparing the spectra for the nonsilylated and silylated MCM-41 materials, it can be concluded that there are at least four types of silanol groups in template-free MCM-41: 1) isolated silanol groups corresponding to the 3740 cm^{-1} absorption, 2) silanol groups associated with the band at 3690–3700 cm^{-1}, 3) silanol groups responsible for the 3620–3640 cm^{-1} band, and 4) silanol groups with IR absorptions at lower frequencies (3600–3450 cm^{-1}). The latter three types of silanol groups are believed to be involved in hydrogen bonding, but the strength of the hydrogen bonds differ from type to type. On the basis of the literature,[10–12] we assign the silanol groups of types 2–4 as follows (Fig. 4): Type 2 silanols are those in which the O atom forms a hydrogen bond with a H atom of an adjacent silanol. Type 3 silanols correspond to hydroxyl groups in which a H atom forms a hydrogen bond with the O atom of an adjacent silanol. Type 4 species are probably chains of hydroxyl groups[12] that contain more than one pair of mutually hydrogen-bonded OH groups.

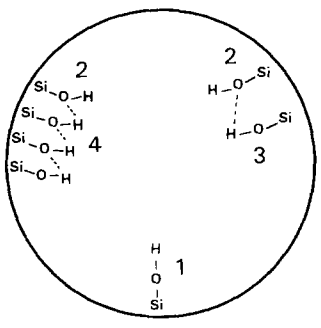

Fig. 4. Representation of the four types of silanol groups in a channel of MCM-41; for an explanation see discussion in text.

In the original nonsilylated MCM-41, interactions not only within each type of silanol group but also among all four types are evident. As a result, silanol groups of types 2–4 are not distinguishable even when a considerable amount of the OH groups have been removed by evacuation at elevated temperatures. However, when the sample is silylated, some of the hydrogen-bonded species are converted to siloxanes, which prevent

interactions. As some of the OH groups condense at elevated temperatures, the remaining species give more distinct IR signals. Moreover, these siloxane barriers impede the movement of protons on the surface of MCM-41, rendering the hydrogen-bonded silanols much more difficult to remove by evacuation than those in the nonsilylated material. This is reflected by the fact that the signals of all the H-bonded silanol groups for the nonsilylated MCM-41 disappear at 450 °C, whereas silanol groups of type 2 and 3 are still evident in the two silylated MCM-41 samples at this temperature. It seems that silylation with CTPS yields a more effective barrier than that with CTMS, probably due to the bulk of the triphenylsilyl group; the IR intensities of type 2 and type 3 OH groups in CTPS-silylated MCM-41 are distinctly stronger than those in the CTMS-silylated MCM-41 at a given temperature (cf. Figs. 2 and 3).

Experimental Procedure

The MCM-41 sample was prepared hydrothermally by following the procedure described elsewhere [2]. The silicate gel used had a molar composition of $0.35\,TMAOH:SiO_2:0.7\,CTABr:25.0\,H_2O$ (TMAOH = tetramethylammonium hydroxide, CTABr = cetyltrimethylammonium bromide as template). X-ray powder diffraction (XRD) indicated that the sample corresponded to MCM-41 with high crystallinity. The template molecules were removed by calcination at 550 °C in air for 10 h. Silylation was conducted by stirring the template-free sample, which was preheated at 100 °C to remove most of the adsorbed water, with a solution of chlorotrimethylsilane or chlorotriphenylsilane in toluene at 80 °C for 48 h. The solid was recovered by centrifuging, then washed with refluxing toluene and acetone, and dried at ambient temperature. The IR spectra were recorded on a Nicolet 5DX FTIR spectrometer. Samples were pressed into pellets (each wafer was 10 mg in weight and 12 mm in diameter) and mounted in a quartz cell with CaF_2 windows. XRD proved the wafers to be as crystalline as the unpressed powder samples. Prior to measurement, each sample was evacuated at a particular temperature for about 1 h then allowed to cool to room temperature. The resolution for the spectra was 4 cm^{-1}.

Received: June 30, 1995 [Z8149IE]
German version: *Angew. Chem.* **1995**, *107*, 2898–2900

Keywords: IR spectroscopy · mesoporous materials · silicon compounds

[1] C. T. Kresge, M. E. Leonowicz, W. J. Roth, J. C. Vartuli, J. S. Beck, *Nature* **1992**, *359*, 710.
[2] J. S. Beck, J. C. Vartuli, W. J. Roth, M. E. Leonowicz, C. T. Kresge, K. D. Schmitt, C. T-W. Chu, D. H. Olson, E. W. Sheppard, S. B. McCullen, J. B. Higgins, J. L. Schlenker, *J. Am. Chem. Soc.* **1992**, *114*, 10834.
[3] J. M. Thomas, *Nature* **1994**, *368*, 289.
[4] P. T. Tanev, M. Chibwe, T. J. Pinnavaia, *Nature* **1994**, *368*, 322.
[5] R. Schmidt, M. Stocker, E. Hansen, D. Akporiaye, O. H. Ellestad, *Microporous Mater.* **1995**, *3*, 443.
[6] C. G. Wu, T. Bein, *Chem. Mater.* **1994**, *6*, 1109; C. G. Wu, T. Bein, *Science* **1994**, *264*, 1757.
[7] A. Corma, V. Fornes, H. Garcia, M. A. Miranda, M. J. Sabater, *J. Am. Chem. Soc.* **1994**, *116*, 9767.
[8] C. Y. Chen, H. X. Li, M. E. Davis, *Microporous Mater.* **1993**, *2*, 17.
[9] A. Corma, V. Fornes, M. T. Navarro, J. Perez-Pariente, *J. Catal.* **1994**, *148*, 569.
[10] R. K. Iler, *The Chemistry of Silica*, Wiley, New York, **1979**, pp. 622–729.
[11] B. A. Morrow, A. J. McFarlan, *Langmuir*, **1991**, *7*, 1695.
[12] A. Zecchina, S. Bordiga, G. Spoto, L. Marchese, G. Petrini, G. Leofanti, M. Padovan, *J. Phys. Chem.* **1992**, *96*, 4991, and references therein.

Fluorophosphazenate Ions: A Route to Complexation of Fluoride Ions**

Enno Lork, Dieter Böhler, and Rüdiger Mews*

Dedicated to Professor Herbert W. Roesky on the occasion of his 60th birthday

The incorporation of anions into molecular hosts is a very topical area of research in inorganic as well as organic chemistry.[1–3] Attempts at the complexation of fluoride ions, however, have been relatively unsuccessful so far.[4] We are endeavoring to achieve this goal by using multifunctional sulfur and phosphorus compounds. Sulfanuric fluoride (1,3,5-trifluoro-1,3,5-trioxo-1λ^6,3λ^6,5λ^6,2,4,6-trithiatriazine), $(NS(O)F)_3$[5] and the isoelectronic cyclofluorophosphazenes $(NPF_2)_n$ (n = 3–17[6]) appear to us to be ideal host molecules, and we have chosen $(Me_2N)_3S^+Me_3SiF_2^-$ (TAS-fluoride)[7] as the fluoride ion donor because of its high solubility in organic solvents. Structural investigations on $TAS^+S_3N_3O_3F_4^-$[8] show that in the anion, one of the axial fluoro substituents of the pentacoordinate sulfur center is three-coordinate[8] (1 + 2), as a result of strong, nonbonding interactions with both of the remaining two sulfur atoms. $P_3N_3F_7^-$, the phosphazenate analogue of $S_3N_3O_3F_4^-$, undergoes further reaction, even at −40 °C (with formation of $P_3N_3F_5NPF_2NPF_2NPF_5^{2-}$[9]). Nevertheless, the fluoride ion addition products of the larger rings, $(NPF_2)_n$ (n = 4–6), have proved to be isolable, as reported herein.

Salt **1** was isolated in quantitative yield as a colorless solid (m.p. 79 °C) from the reaction of TASF with $P_4N_4F_8$ in CH_3CN at −30 °C [Eq. (a)]. After removal of the volatile products and

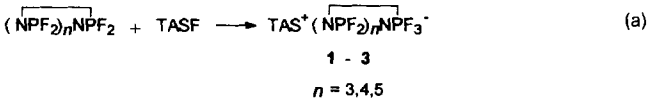

(a)

solvent, **2** and **3** remained behind in almost analytically pure form as viscous, pale yellow residues; the melting points of both compounds lie below 0 °C.

The products were unambiguously characterized by NMR spectroscopy and X-ray crystal structure analysis (for **1** and **3**). Only one resonance was observed in both the ^{19}F and ^{31}P NMR spectra of the cyclic anions at all temperatures down to the freezing point of the solvent used (CD_3CN), indicating that all fluorine and phosphorus nuclei are magnetically equivalent due to a rapid exchange process. The observed splitting of the signals (Table 1) suggests an intramolecular exchange of fluoro substituents between each of the phosphorus centers.

The structure of the $P_4N_4F_9^-$ ion in **1** is shown in Figure 1.[10] Addition of a fluoride ion to one of the tetracoordinate phosphorus centers of $P_4N_4F_8$ leads to the transformation of the saddle conformation[11] into a boat conformation. F(1) draws closer to the other three ring-phosphorus atoms (F(1)–P(2) 275.3, F(1)–P(4) 276.5, and F(1)–P(3) 305.9 pm) as a result of

[*] Prof. Dr. R. Mews, Dr. E. Lork
Institut für Anorganische und Physikalische Chemie der Universität
Leobener Strasse NW2, Postfach 33 04 40, D-28334 Bremen (Germany)
Telefax: Int. code +(421)218 4267
Dr. D. Böhler
Institut für Anorganische Chemie der Universität Göttingen (Germany)

[**] This work was supported by the Fonds der Chemischen Industrie. We thank Dr. P. G. Watson for helpful discussions.

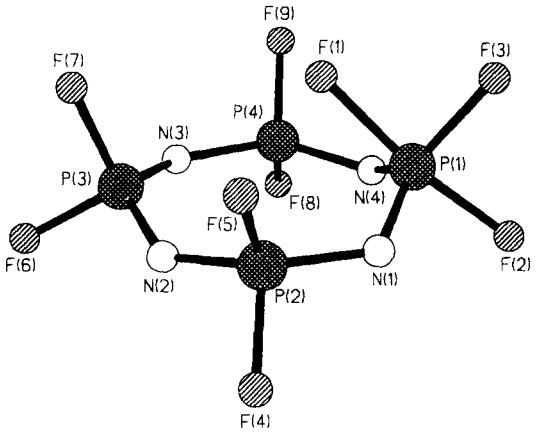

Fig. 1. Structure of the $P_4N_4F_9^-$ ion in the crystal. Selected bond lengths [pm] and angles [°]: P(1)-F(1) 171.4(1), P(1)-F(3) 162.8(1), P(1)-N(1) 160.6(2), P(1)-N(4) 160.8(2), P(1)-F(3) 156.4(1), N(1)-P(2) 153.2(2), N(4)-P(4) 153.5(2), P-N 152.3(2)-155.6(2), P-F 152.7(2)-153.9(2); F(1)-P(1)-F(2) 171.26(8), F(1)-P(1)-F(3) 84.68(8), F(1)-P(1)-N(1) 92.81(8), F(1)-P(1)-N(4) 92.24(9), F(2)-P(1)-N(1) 91.65(8), F(2)-P(1)-N(4) 91.45(9), F(3)-P(1)-N(1) 117.59(9), F(3)-P(1)-N(4) 118.08(9), N(1)-P(1)-N(4) 124.33(11), F(2)-P(1)-F(3) 86.59(8), P(1)-N(1)-P(2) 127.10(11), P(1)-N(4)-P(4) 130.40(12), P-N-P 138.0(2)-140.7(2), N-P-N 123.74(11)-125.67(11).

Table 1. ^{19}F and ^{31}P NMR data for the cyclophosphazenate ions (CD_3CN solution, -40 °C) [a].

Anion	$\delta^{31}P$	$\delta^{19}F$	J(P,F)
$P_3N_3F_7^-$	-5 (oct)	-46 (quar)	258
$P_4N_4F_9^-$	-17.8 (dec)	-53.43 (quin)	185.3
$P_5N_5F_{11}^-$	-23.77 (dod)	-54.7 (sex)	157.2
$P_6N_6F_{13}^-$	-21.4 (tede)	-52.9 (sep)	136

[a] quar = quartet, quin = quintet, sex = sextet, sep = septet, dec = decet, dod = dodecaplet, tede = tetradecaplet.

the large *syn*-leaning of the F(1)-P(1)-F(2) axis. These distances are considerably shorter than the sum of the van der Waals radii of P and F (325 pm); F(1) forms the apex of a heavily distorted square pyramid and may be described as tetracoordinate (1 + 3). These strong interactions explain the rapid, intramolecular fluoride exchange in solution.

$P_5N_5F_{11}^-$ could only be detected by NMR spectroscopy (Table 1). The rapid fluorine exchange in solution and the flexibility of the PN backbone[12] suggest that in the solid state one of the fluorine centers probably interacts with all five phosphorus atoms.

A side-on view of the structure of the s-shaped $P_6N_6F_{13}^-$ ion in **3** is presented in Figure 2.[13,14] All P-N (152.6(4) pm) and P-F (152.1(3) pm) bond lengths to the tetracoordinate phosphorus centers are identical within the limits of error. The bonding situation at the pentacoordinate phosphorus center is comparable to that of P(1) in $P_4N_4F_9^-$. In the $P_6N_6F_{13}^-$ ion, the atoms P(2), N(2), P(3), P(5), N(5), and P(6) form a central plane from which the atoms deviate very little (max. 7.4 pm). P(1) sits 163 pm above and P(4) 167 pm below this plane. The position of F(1) is remarkable, as it can be considered as the center of this anion. F(1) sits only 54 pm above the central plane; it is unable to come any closer due to repellent interactions to N(5) and N(2) (nonbonding distances 288.9 and 290.4 pm, respectively, sum of the van der Waals radii of N and F is 290 pm). The distances from F(1) to the phosphorus atoms P(2) (272.0 pm), P(3) (288.3 pm), P(5) (291.9 pm), and P(6) (270.4 pm) in the plane are all significantly shorter than the sum of the van der Waals

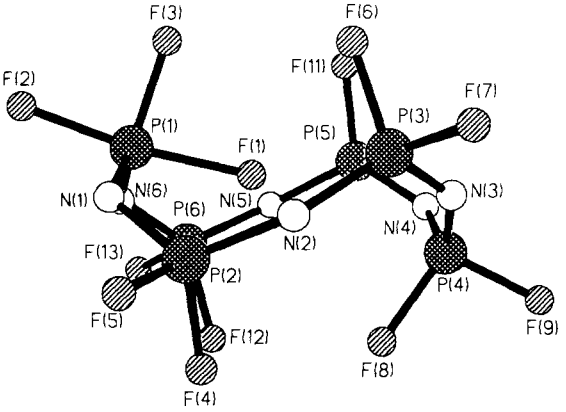

Fig. 2. Structure of the $P_6N_6F_{13}^-$ ion in the crystal. Selected bond lengths [pm] and angles [°]: P(1)-F(1) 172.1(7), P(1)-F(2) 161.9(7), P(1)-F(3) 155.6(7), P(1)-N(1) 159.5(10), P(1)-N(6) 160.8(10), N(1)-P(2) 156.3(9), N(6)-P(6) 149.3(10), P-N 152.0(11)-153.9(10), P-F 149.9(7)-154.1(9); F(1)-P(1)-F(2) 172.2(4), F(1)-P(1)-F(3) 84.6(4), F(1)-P(1)-N(1) 92.9(4), F(1)-P(1)-N(6) 91.0(4), F(2)-P(1)-N(1) 90.4(4), F(2)-P(1)-N(6) 92.9(5), F(3)-P(1)-N(1) 117.3(5), F(3)-P(1)-N(6) 117.8(4), N(1)-P(1)-N(6) 124.9(5), F(2)-P(1)-F(3) 87.7(4), P(1)-N(1)-P(2) 129.2(6), P(1)-N(6)-P(6) 131.8(7), P-N-P 142.3(8)-144.6(7), N-P-N 122.2(6)-126.3(6)

radii of P and F, and the distance from F(1) to P(4) on the other side of the ring is 294.7 pm, only marginally longer than these. The interactions of the six phosphorus atoms of the ring system results in a distorted octahedral coordination for F(1), in which the "coronate" $P_6N_6F_{12}$ ligand wraps around the central fluoride ion in three dimensions. The coordination sphere of the central fluoride ion is illustrated in Figure 3. Remarkably, none of the

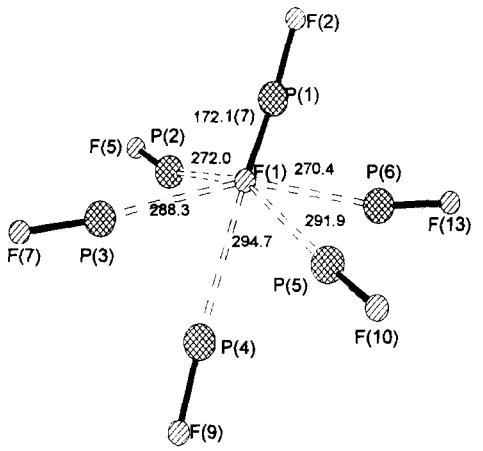

Fig. 3. Coordination of the central fluoride ion in the $P_6N_6F_{13}^-$ ion.

F···P-F angles deviate significantly from 180°. Theoretical studies should show whether this is due to purely electrostatic effects or if multicenter bonding is a more appropriate description. Besides the development of a bonding model for these intramolecular interactions, it is also of interest in the field of fluorophosphazenate ions whether higher coordination for the fluoride ion can be achieved by using larger ring systems, whether multiple fluoride ion addition is possible, and by which reaction pathways the intramolecular fluoride exchanges take place.

Experimental Procedure

1: $(NPF_2)_4$ (0.8 g, 2.66 mmol) was condensed into a λ-shaped Schlenk vessel with a Teflon valve, containing $(Me_2N)_3S^+Me_3SiF_2^-$ (0.6 g, 2.18 mmol) in CH_3CN (5 mL), at -196 °C. The vessel was placed in an ethanol bath (-35 °C) and the

 © VCH Verlagsgesellschaft mbH, D-69451 Weinheim, 1995 0570-0833/95/3423-2697 $ 10.00+.25/0

reaction mixture allowed to stir at this temperature. After 15 minutes, diethyl ether (10 mL) was condensed onto the mixture, and **1** precipitated as a colorless solid. The liquid was decanted into the second arm of the Schlenk vessel, the volatiles were pumped off under dynamic vacuum at −30 °C, and the solid was then allowed to warm slowly to room temperature.

2, **3**: After addition of the ether at −35 °C a second phase was formed which was decanted into the second arm of the reaction vessel. The workup of the residue was carried out as described for **1**.

Received: June 21, 1995
Revised version: August 11, 1995 [Z8118IE]
German version: *Angew. Chem.* **1995**, *107*, 2915–2917

Keywords: fluorine compounds · heterocycles · host–guest chemistry · nitrogen compounds · phosphazenes

[1] F. P. Schmidtchen, *Nachr. Chem. Tech. Lab.* **1988**, *36*, 8.
[2] B. Dietrich, *Pure Appl. Chem.* **1993**, *65*, 1457.
[3] D. E. Kaufmann, A. Otten, *Angew. Chem.* **1994**, *106*, 1917; *Angew. Chem. Int. Ed. Engl.* **1994**, *33*, 1832.
[4] Fluoride ions have been added to perfluorinated crown ethers: R. Lagow, T.-Y. Lin, H. W. Roesky, W. D. Clark, W.-H. Lin, J. S. Brodbelt, S. D. Maleknia, C. C. Liou in *Inorganic Fluorine Chemistry: Toward the 21st Century* (Eds.: J. S. Thrasher, S. H. Strauss) (ACS Symp. Ser. **1994**, *555*, 216).
[5] F. Seel, G. Simon, *Z. Naturforsch.B* **1964**, *19*, 354.
[6] A. C. Chapman, N. L. Paddock, D. H. Paine, H. T. Searle, D. R. Smith, *J. Chem. Soc.* **1960**, 3608.
[7] W. J. Middleton, (du Pont) US-A 3940402 **1976**; *Org. Synth.* **1985**, *64*, 221.
[8] E. Lork, R. Mews, *J. Chem. Soc. Chem. Commun.*, **1995**, 1113.
[9] E. Lork, P. G. Watson, R. Mews, *J. Chem. Soc. Chem. Commun.* **1995**, 1717.
[10] X-ray crystal structure analysis of **1** ($C_6H_{18}F_9N_7P_4S$). $M = 515.21$; crystal dimensions $0.8 \times 0.6 \times 0.5$ mm^3; monoclinic, space group $P2_1/c$, $a = 787.6(2)$, $b = 1797.7(4)$, $c = 1393.9(8)$ pm, $\beta = 95.22(3)°$, $V = 1.9654(8)$ nm^3, $Z = 4$, $\rho_{calcd} = 1.741$ Mg m^{-3}, $\mu = 0.581$ mm^{-1}. A crystal suitable for X-ray analysis was fixed to a glass fiber with Kel-F oil and measured on a Siemens P4 four-circle diffractometer at −100 °C (graphite monochromator, $Mo_{K\alpha}$ radiation, $\omega/2\theta$ scan). Of the 5901 measured reflections ($2.6° < \theta < 27.9°$), 4491 independent reflections remained after averaging. The structure was solved by direct methods. The refinement calculations converged at $wR_2 = 0.1090$ (refined against F^2) for all 4491 reflections and 252 variables [$R_1 = 0.0406$ for 3592 reflections with $I > 2\sigma(I)$]; heavy atoms were assigned individual anisotropic deflection parameters. Hydrogen atoms were calculated with common isotropic temperature factors. A difference Fourier synthesis indicated no residual electron density beyond +511 e nm^{-3} and −366 e nm^{-3}. The structure solution and preparation of the drawings were performed with the SHELXTL programme package [15], the refinements with the program SHELXL-93 [16,17].
[11] From our own studies and the unpublished results of B. Krebs and G. Henkel and from H. Oberhammer and G. Haist it was observed that $P_4N_4F_8$ has a nonplanar saddle structure (D_{2d} symmetry), in both the solid state and gas phase, in which the four phosphorus atoms form a plane.
[12] The structure of one of the structurally characterized conformers of $P_5N_6F_{10}$ (J. G. Hartsuiker, A. J. Wagner, *J. Chem. Soc. Dalton Trans.* **1978**, 1425) corresponds to the P(1)N(1)P(2)N(2)P(3)P(5)N(5)P(6)N(6) fragment of the $P_6N_6F_{13}^-$ ion.
[13] X-ray crystal structure analysis of **3** ($C_6H_{18}F_{13}N_9P_6S$). $M = 681.17$; crystal dimensions $0.4 \times 0.3 \times 0.2$ mm^3; orthorhombic, space group $P2_12_12_1$, $a = 798.4(2)$, $b = 1416.0(3)$, $c = 2197.2(4)$ pm, $V = 2.4840(9)$ nm^3, $Z = 4$, $\rho_{calcd} = 1.821$ Mg m^{-3}, $\mu = 0.631$ mm^{-1}. A crystal suitable for X-ray analysis was fixed to a glass fiber with Kel-F oil and measured on a Siemens P4 four-circle diffractometer at −100 °C (graphite monochromator, $Mo_{K\alpha}$ radiation, $\omega/2\theta$ scan). Of the 4650 measured reflections ($2.7° < \theta < 23.8°$), 3534 independent reflections remained after averaging. The structure was solved by direct methods. The refinement calculations converged at $wR_2 = 0.0904$ (refined against F^2) for all 3534 reflections and 323 variables [$R_1 = 0.0584$ for 1438 reflections with $I > 2\sigma(I)$]; heavy atoms were assigned individual anisotropic deflection parameters. Hydrogen atoms were calculated with common isotropic temperature factors. A difference Fourier synthesis indicated no residual electron density beyond +327 e nm^{-3} and −319 e nm^{-3}. The structure solution and preparation of the drawings were performed with the SHELXTL programme package [15], the refinements with the program SHELXL-93 [16,17].
[14] The PN backbone of the only structurally characterized, twelve-membered cyclophosphazene, $(NPMe_2)_6$, has a "double-tub" conformation: R. T. Oakley, N. L. Paddock, S. J. Rettig, J. Trotter, *Can. J. Chem.*, **1977**, *55*, 3118.
[15] Siemens SHELXTL-Plus: Release for Siemens R3 Crystallographic Research Systems, Siemens Analytical X-Ray Instruments Inc. Madison, WI, **1989**.
[16] G. M. Sheldrick, SHELXL-93, Universität Göttingen, **1993**.
[17] Further details of the crystal structure investigations may be obtained from the Director of the Cambridge Crystallographic Data Centre, 12 Union Road, GB-Cambridge CB2 1EZ, on quoting the full journal citation.

A Novel Class of Versatile Solvents for Two-Phase Catalysis: Hydrogenation, Isomerization, and Hydroformylation of Alkenes Catalyzed by Rhodium Complexes in Liquid 1,3-Dialkylimidazolium Salts**

Yves Chauvin,* Lothar Mussmann, and Hélène Olivier

The decisive advantages of homogeneous over heterogeneous catalysis with respect to activity and selectivity are well documented,[1] but the problems associated with the separation of products from the catalyst constitute major drawbacks for industrial applications. Possible solutions to this problem include "heterogenizing" a homogeneous catalyst, either by anchoring the catalyst on a support, or by using a liquid–liquid two-phase system. Aqueous/organic systems have been applied to the hydrogenation and hydroformylation of unsaturated substrates catalyzed by rhodium and ruthenium complexes.[2] Nevertheless, in spite of many advantages, the use of these systems suffers from low reaction rates, due to the poor ability of water to dissolve organic substrates. On the other hand, water is a strongly coordinating protic solvent that limits the application to ligands and catalysts that are stable in water. Nonpolar perfluorohydrocarbons have recently been proposed as a nonaqueous phase for the two-phase catalytic hydroformylation of olefins; however, to solubilize rhodium complexes in the "fluorous" phase, special fluorinated ligands have to be designed.[3]

Our new approach reported herein, involves the use of room temperature ionic liquids based on 1-*n*-butyl-3-methylimidazolium (BMI^+) salts[4] as nonaqueous solvents for Rh-catalyzed two-phase hydrogenation, isomerization, and hydroformylation of unsaturated substrates (Scheme 1). In these solvents, catalysts

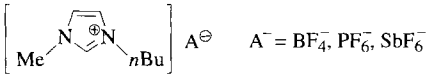

Scheme 1. BMI^+ salts used.

can be "immobilized" either because of their ionic character or by using polar modified ligands. From the wide range of ionic liquids, we have selected those based on nonnucleophilic PF_6^-, SbF_6^-, BF_4^-, and $CuCl_2^-$ ions, since they are easy to prepare and handle, and are also stable in air and water.[5] As these media are known to dissolve charged species, we first applied them to the hydrogenation of pent-1-ene using the Osborn complex **1** as the cationic catalyst precursor.[6]

$[Rh(nbd)(PPh_3)_2]^+PF_6^-$ **1** (nbd = norbornadiene)

As illustrated in Table 1, remarkable solvent effects are observed. When the $BMI^+SbF_6^-$ salt was used, hydrogenation rates were nearly five times higher (Table 1, entry 2) than for the comparable homogeneous reaction in acetone (Table 1, entry 1), in spite of the expected limited solubilities of reactants in the polar phase. A plot of the product distribution as a function of time shows that there is a competitive fast isomerization of pent-1-ene. However, the formation of pent-2-ene did not significantly detract the hydrogenation rate (Fig. 1).

[*] Dr. Y. Chauvin, Dr. L. Mussmann, H. Olivier
Institut Français du Pétrole
Boîte Postale 311, F-92506 Rueil-Malmaison (France)
Telefax: Int. code + (1) 47 52 60 55
e-mail: chauvin@irvax1.ifp.fr

[**] We thank Aurore Calmels for assistance.

Table 1. Rh-catalyzed hydrogenation of pent-1-ene [a].

Entry	Solvent	Conversion [%] pent-1-ene	Yield [%] pentane	Yield [%] pent-2-ene	TOF [min^{-1}] [b]
1 [c]	acetone	99	38	61	0.55
2	$BMI^+SbF_6^-$	96	83	13	2.54
3	$BMI^+PF_6^-$	97	56	41	1.72
4	$BMI^+BF_4^-$	10	5	5	0.15
5 [d]	BMI^+Cl^-:CuCl	18	0	18 (98% *cis*)	0
6 [e]	$BMI^+PF_6^-$	99	25	74	0.73

[a] **1**: 0.05 mmol; pent-1-ene: 18.4 mmol; solvent: 4 mL; $T = 30\,^{\circ}C$; $p(H_2) = 0.1$ MPa; $t = 2$ h. [b] Turnover frequency (TOF) defined as mol(pentane) per mol(rhodium) per min. [c] Acetone: 10 mL; pent-1-ene: 9.2 mmol. [d] Molten salt prepared by reacting 1.5 equiv of CuCl with 1 equiv of BMI^+Cl^-. [e] Acetone (2 mL) added.

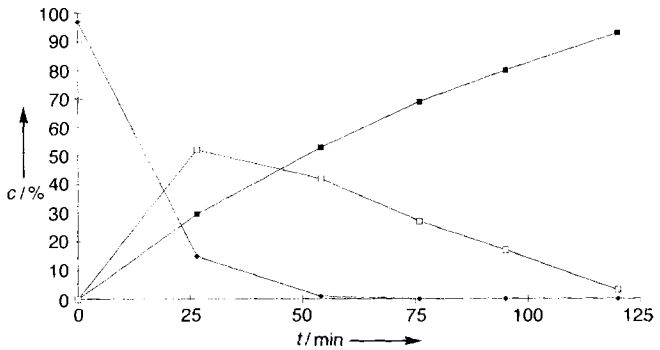

Fig. 1. A plot of the product distribution as a function of time for hydrogenation and isomerization of pent-1-ene catalyzed by **1** in the $BMI^+SbF_6^-$ salt; (•) pent-1-ene, (□) *cis*/*trans* pent-2-ene, (■) pentane.

When the $BMI^+PF_6^-$ salt was used (Table 1, entry 3), lower turnover frequencies were observed. This effect is not easy to understand. On the one hand, it is well known that the nature of anion associated with cationic Rh catalysts does not affect the rate of hydrogenation.[6] On the other hand, preliminary experiments indicate that the solubility of pent-1-ene is two times higher in the SbF_6^- based salt than in the PF_6^- salt. In the case of the $BMI^+BF_4^-$ salt, which is water-miscible and which cannot be properly purified, the lower activity can be ascribed to the presence of trace amounts of the strongly coordinating chloride ion in the salt (Table 1, entry 4).

When ionic liquids prepared from BMI^+Cl^- and CuCl (1:1.5) were used only isomerization to *cis*-pent-2-ene was observed with a selectivity of 98% (Table 1, entry 5), in sharp contrast to the previous results. This demonstrates that selectivity can be strongly influenced by the nature of the anion. The addition of small amounts of a coordinating solvent (acetone, Table 1, entry 6) to the $BMI^+PF_6^-$ salt leads to a decrease of the reaction rate.

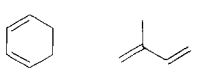

2 **3**

Conjugated diolefins such as cyclohexa-1,3-diene (**2**) and 2-methylbuta-1,3-diene (**3**) can also be hydrogenated. This is all the more interesting since diolefins are more soluble in ionic liquids than the corresponding monoalkenes (e.g. **2** is five times more soluble than cyclohexene in the $BMI^+SbF_6^-$ salt). This can improve potentially the selectivity of the hydrogenation. When complex **1** was used as the catalyst precursor in the $BMI^+SbF_6^-$ salt under the reaction conditions given in Table 1, **2** gave cyclohexene with 98% selectivity at 96% conversion. The reaction activity (TOF = 3.2 min^{-1}) was comparable to that observed in organic solvents. Substitution of the triphenylphosphane ligand in complex **1** by the chelating 1,2-bis(diphenylphosphino)ethane (dppe) ligand provides the $[Rh(nbd)dppe]PF_6$ catalyst precursor which catalyzes the hydrogenation of **3** (TOF = 3.1 min^{-1}). As in the homogeneous reaction, a mixture of 2-methylbut-1-ene (22%), 3-methylbut-1-ene (10%), and 2-methylbut-2-ene (23%) is obtained.[7]

In all these experiments, the ionic solutions containing the catalyst can be reused. Only a negligible loss of rhodium was observed (less than 0.02%; under the detection limit). In comparison to the recently described aqueous two-phase system, no formation of stable emulsions occurred.[2d]

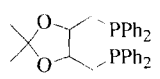

= diop

As an extension, the chiral cationic $[Rh(cod)\{(-)\text{-diop}\}]PF_6$ (cod = cycloocta-1,3-diene) complex (0.03 mmol), dissolved in the $BMI^+SbF_6^-$ salt (4 mL), catalyzed the asymmetric hydrogenation of α-acetamidocinnamic acid (3 mmol in 8 mL of *i*PrOH) to (*S*)-phenylalanine in 64% *ee*. The product could be separated quantitatively and the recovered ionic liquid can be reused.

By analogy to homogeneous catalysis, we first supposed the existence of an equilibrium between a cationic Rh-dihydrido complex, which would be responsible for the hydrogenation, and a noncharged monohydrido complex, which would be responsible for both the hydrogenation and isomerization reactions [Eq. (a)]. Surprisingly, addition of two equivalents of the

$$[H_2Rh(PPh_3)_2(Solv.)_n]^+ \rightleftharpoons[-H^+] [HRh(PPh_3)_2(Solv.)_n] \qquad (a)$$

acid HPF_6 (60% in water) to the active Rh catalyst in the $BMI^+SbF_6^-$ salt, neither suppresses isomerization by shifting the equilibrium to the dihydrido cationic complex, nor decreases the hydrogenation activity. Direct characterization of the active species in these media is not easy. Upon activation by molecular hydrogen, the orange complex **1** gives a brown solution. Norbornane is detected in the organic phase by GC. The ^{31}P NMR spectrum of the $BMI^+SbF_6^-$ salt displays a doublet at $\delta = 40.6$ [$^1J_{Rh,P} = 103$ Hz] suggesting the formation of a symmetrical Rh-hydride.

Thus, as ionic liquids are known to stabilize preferably cationic species and do not solvate the Rh complex, we assume that the prevailing active catalyst is a cationic unsolvated Rh-dihydrido complex which has two free coordination sites (see the detrimental effect of acetone: Table 1, entry 6). To our knowledge, this is the first example of two-phase hydrogenation reactions in which an active rhodium catalyst is "immobilized" in a polar phase without special ligand design.

Two-phase pent-1-ene hydroformylation can also be achieved, as hexanals are poorly soluble in ionic liquids. Preliminary experiments using the $[Rh(CO)_2(acac)/PPh_3]$ uncharged molecular system as catalyst precursor, show high catalytic activity in the $BMI^+PF_6^-$ salt (TOF = 333 h^{-1}; Table 2, entry 2).

Table 2. Rh-catalyzed hydroformylation of pent-1-ene [a].

Entry	Solvent	Ligand	Rh/P	Yield [%]	*n*/*i* [b]	TOF [h^{-1}] [c]
1	toluene	PPh_3	0.106	95	2	297
2	$BMI^+PF_6^-$	PPh_3	0.106	99	3	333
3 [d]	$BMI^+PF_6^-$	tppms	0.106	16	3.9	59
4 [e]	$EMI^+BF_4^-$	tppts	0.33	33	2.8	103

[a] $[Rh(CO)_2(acac)]$: 0.075 mmol; pent-1-ene: 68 mmol; solvent: 4 mL; $T = 80\,^{\circ}C$; $p(H_2/CO\ 1/1) = 2$ MPa; $t = 2$ h; 2 mL heptane. [b] *n*/*i* = *n*-aldehyde/*i*-aldehyde. [c] Turnover frequency (TOF) defined as mol(converted pent-1-ene) per mol(rhodium) per hour. [d] THF (1 mL) added. [e] $p(H_2/CO\ 1/1) = 4$ MPa, 5 mL heptane, 0.2 mL H_2O, EMI^+ = 1-ethyl-3-methylimidazolium.

After removal of the organic products, the ionic phase can also be reused and gives quite similar activity. However, a small part of the active Rh catalyst is extracted into the organic phase. Thus, in contrast to the hydrogenation reactions, the uncharged $[Rh(CO)_2(acac)]$ catalyst precursor has to be immobilized in the salt by a polar ligand. For this purpose, the sodium salts of monosulfonated- (tppms) and trisulfonated- (tppts) triphenylphosphane ligands have been used. In this way, extraction of the Rh catalyst could be completely avoided. Although catalytic reaction rates are lower when the $[Rh(CO)_2(acac)]$/tppms or $[Rh(CO)_2(acac)]$/tppts systems are used in the $BMI^+PF_6^-$ or $BMI^+BF_4^-$ salts, reasonable TOF are still obtained (Table 2, entries 3 and 4).

Investigations on modified phosphites, which are not stable in an aqueous two-phase system[9], but seem to be promising ligands in these nonaqueous ionic liquids, are currently under way. In summary, this paper describes a few examples illustrating the advantages of using BMI^+ molten salts as novel solvents for two-phase Rh-catalyzed reactions. In view of the existing limitations of the present liquid–liquid systems, these nonaqueous solvents could be a potentially valuable medium for further developments of two-phase catalysis.

Experimental Procedure

Hydrogenation: **1** (0.05 mmol) dissolved in $BMI^+SbF_6^-$ molten salt (4 mL) was transferred under argon, into a 70 mL Fischer-Porter glass flask, equipped with a magnetic stirring bar. After the evacuation of argon , the hydrogen pressure was adjusted to 0.1 MPa and the catalyst was activated with stirring for 10 min. The reactor was depressurized and pent-1-ene (18.4 mmol) was injected through a septum. The hydrogen pressure was again adjusted to 0.1 MPa, and the reaction was monitored by GC (PONA, 50 m × 0.2 mm). For further experiments with the same molten salt, the remaining upper organic phase was removed, the molten salt evacuated (15–20 min, 30 °C), the reactor was flushed twice with H_2 (0.1 MPa) and pent-1-ene (18.4 mmol) was added and the reaction was started again.

Asymmetric hydrogenation: The reactions were conducted as previously described except that the starting material (α-acetamidocinnamic acid) was dissolved in *i*PrOH (5 mL). At the end of the reaction, the upper organic phase was evaporated to dryness and the product workup was carried out as described in ref. [9].

Hydroformylation: A 100 mL stainless steel autoclave, equipped with a glass lining, was charged with a mixture of $[Rh(CO)_2(acac)]$ (0.075 mmol) and 3 to 10 equivalents of the phosphorus ligand dissolved in 4 mL of the ionic liquid. The autoclave was purged with CO/H_2 (1/1) and pent-1-ene (68 mmol) with heptane (2 mL; internal standard) was added. The temperature was raised to 80 °C, the pressure (CO/H_2) was adjusted to 2 MPa, and the mixture was then stirred. The product distribution was determined by GC.

Received: August 18, 1995 [Z 8325 IE]
German version: *Angew. Chem.* **1995**, *107*, 2941–2943

Keywords: hydroformylations · hydrogenations · ionic liquids · two-phase catalysis

[1] G. W. Parshall, S. D. Ittel in *Homogeneous Catalysis*, 2nd ed., Wiley, New York, **1992**.
[2] a) G. E. Kuntz, *CHEMTECH* **1987**, 570; b) W. A. Herrmann, C. W. Kohlpaintner, *Angew. Chem.* **1993**, *105*, 1588–1609; *Angew. Chem. Int. Ed. Engl.* **1993**, *32*, 1524–1544, and references therein; c) E. Wiebus, B. Cornils, *Chem. Ing. Tech.* **1994**, *66*, 916; d) E. Renaud, R. B. Russell, S. Fortier, S. J. Brown, M. C. Baird, *J. Organomet. Chem.* **1991**, *419*, 403; e) W. A. Herrmann, C. W. Kohlpaintner, H. Bahrmann, W. Konkol, *J. Mol. Catal.* **1992**, *73*, 191; f) H. Ding, B. E. Hanson, T. Bartik, B. Bartik, *Organometallics* **1994**, *13*, 3761; g) R. T. Smith, R. K. Ungar, L. J. Sanderson, M. C. Baird, *ibid.* **1983**, *2*, 1138; h) B. Cornils, *Angew. Chem.* **1995**, *107*, 1709–1711; *Angew. Chem. Int. Ed. Engl.* **1995**, *34*, 1575–1577.
[3] I. T. Horváth, J. Rábai, *Science* **1994**, *266*, 72.
[4] a) Y. Chauvin, H. Olivier, *CHEMTECH* **1995**, No. 26; b) Y. Chauvin, S. Einloft, H. Olivier, *Ind. Eng. Chem. Res.* **1995**, *34*, 1149.
[5] J. Fuller, R. T. Carlin, H. C. De Long, D. Haworth, *J. Chem. Soc. Chem. Commun.* **1994**, 229.
[6] R. R. Schrock, J. A. Osborn, *J. Am. Chem. Soc.* **1976**, *98*, 2134.
[7] R. R. Schrock, J. A. Osborn, *J. Am. Chem. Soc.* **1976**, *98*, 4450.
[8] B. Fell, G. Papadogianakis, W. Konkol, J. Weber, H. Bahrmann, *J. Prakt. Chem.* **1993**, *335*, 75.
[9] R. Glaser, S. Geresh, J. Blumenfeld, *J. Organomet. Chem.* **1976**, *112*, 355.

Synthesis and Coordination Chemistry of *ortho*-Functionalized Dimercaptobenzene: Building Blocks for Tripodal Hexathiol Ligands**

F. Ekkehardt Hahn* and Wolfram W. Seidel

Tripodal tricatechol ligands with six oxygen atoms of type H_6-**1**[1] have been investigated thoroughly, because they have a high affinity for various metal ions and are model substances for the siderophore enterobactin.[2] Tripodal ligands with three *ortho*-phenylenediamine groups[3] have also been described, whereas hexathiol ligands of type H_6-**2** derived from dimercaptobenzene are still unknown. Polythiol ligands that contain aliphatic[4] or aromatic thiol groups[5] as well as both thioether and thiol groups[6] as donor functions are well established, but the bridging of dimercaptobenzene units to give a poly(dithiolene) ligand has not been achieved so far. Being aware of the interesting coordination chemistry of dithiols for different oxidation states of the metal atom,[7] we expected to find in complexes with ligands of type H_6-**2** not only the stabilization of metal ions in unusual oxidation states but also—caused by the tripodal backbone—the formation of coordination polyhedra that do not form with unbridged dimercaptobenzene ligands. In this paper we report a method for the preparation of *o*-functionalized dimercaptobenzene that will allow for the first time the synthesis of tripodal tris(dithiol) ligands such as H_6-**2**, as well as initial investigations concerning the coordination chemistry of H_6-**2**.

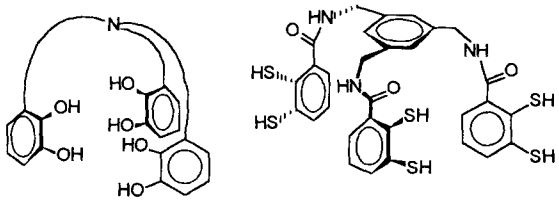

H_6-**1** H_6-**2**

The synthesis of H_6-**2** is best achieved by the reaction of 2,3-dimercaptobenzoyl chloride with 1,3,5-tris(aminomethyl)-benzene under formation of three amide bonds, a strategy that has been proved successful for the preparation of various tripodal tri(carboxamidocatechol) ligands.[8] The starting point for our work was the synthesis of *ortho*-mercaptobenzoic acid from thiophenol, published in 1989.[9]

The reaction of *ortho*-dimercaptobenzene (**3**)[10] with three equivalents of *n*BuLi and dry CO_2 yields after hydrolysis with H_2O/HCl (Scheme 1) a mixture of the benzoic acid derivative **4a** and the terephthalic acid derivative **4b**.[11] Attempts to separate the components of this mixture were not successful. To facilitate this separation on the one hand and to make the next step to the amide possible without interference by acidic groups on the other, the thiol functions were protected by the reaction with isopropyl bromide/sodium methanolate. The resulting derivatives **5a**/**5b** could then be separated by column chromatography. This way we obtained **5a** analytically pure as crystals and confirmed its identity by X-ray crystallography (Fig. 1).[12]

[*] Prof. Dr. F. E. Hahn, Dipl.-Chem. W. W. Seidel
Institut für Anorganische und Analytische Chemie der Freien Universität
Fabeckstrasse 34–36, D-14195 Berlin (Germany)
Telefax: Int. code +(30)838-2424.

[**] This work was supported by the Deutsche Forschungsgemeinschaft and the Fonds der Chemischen Industrie.

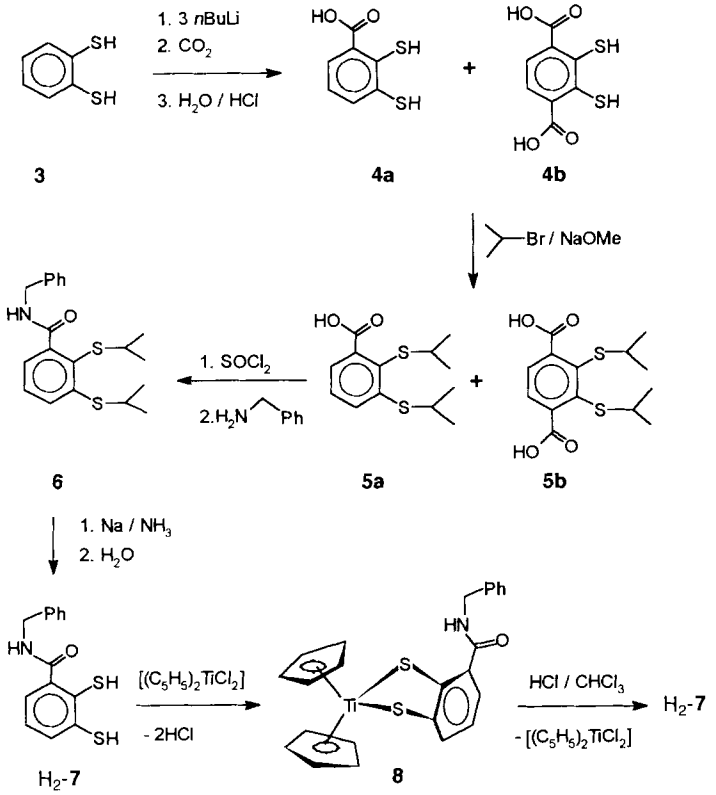

Scheme 1. Synthesis and reactions of 2,3-dimercaptobenzoic acid.

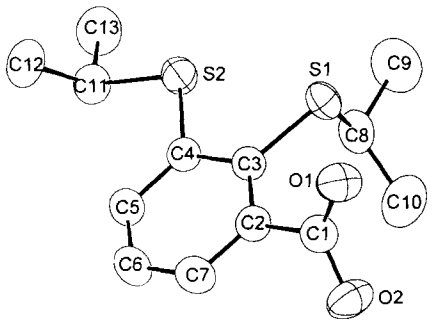

Fig. 1. ORTEP plot of **5a** in the crystal. Selected bond lengths [Å] and angles [°]: S1–C3 1.771(2), S1–C8 1.827(3), S2–C4 1.761(2), S2–C11 1.815(3), C1–C2 1.498(3), C1–O1 1.237(3), C1–O2 1.279(3); C3-S1-C8 100.2(1), C4-S2-C11 105.8(1), O1-C1-O2 123.4(2), O1-C1-C2 120.7(2), O2-C1-C2 115.9(2).

Derivative **5a** crystallizes without intermolecular oxygen–oxygen contacts shorter than 2.6 Å. Apparently the formation of intermolecular hydrogen bonds is prevented by the bulky substituents on the sulfur atoms. The $S-C_{sp^2}$ distances are, as expected, approximately 0.05 Å shorter than the $S-C_{sp^3}$ distances. The atoms of the aromatic ring form a plane that also contains the atoms S1, S2, and C1 (maximum deviation 0.08 Å for S1). The typical lengthening of the (S)C–C(S) bond in the ring observed in coordinated *ortho*-dimercaptobenzene (which can be explained by the resonance of coordinated dithiolate and dithioketone[17b–d]) was not observed in **5a**.

After treatment with $SOCl_2$, **5a** can be converted into the amide **6** by the reaction with benzylamine (Scheme 1).[11] We found that the protection groups in **6** can be removed easily by reaction with sodium in ammonia[13] (Scheme 1).[11] The formation of cyclohexadienes or side reactions at the amide group were not observed. The bidentate dithiol ligand H_2-**7** was obtained as an impure white solid.

The purification of the dithiol H_2-**7** turned out to be extremely difficult because of its facile oxidation by atmospheric oxygen. Purification by formation and controlled decomposition of a metal complex provides a simple alternative. For that purpose we treated impure H_2-**7** with $[(C_5H_5)_2TiCl_2]$ and isolated the blue-green complex $[(C_5H_5)_2Ti(7)]$ **8**.[11] Unlike H_2-**7**, this complex is air-stable and can be purified very easily by chromatography. The X-ray structure analysis confirmed the identity of **8** (Fig. 2).[12]

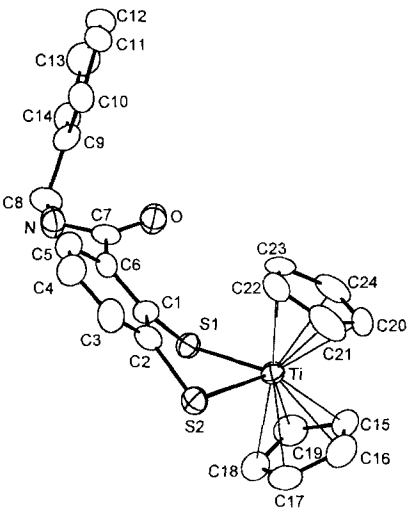

Fig. 2. ORTEP plot of **8** in the crystal. Selected bond lengths [Å] and angles [°] (Cp1 and Cp2 are the centroids of the cyclopentadienyl rings): Ti–S1 2.389(3), Ti–S2 2.418(3), Ti–Cp1 2.035, Ti–Cp2 2.073, S–C1 1.76(1), S2–C2 1.76(1); S1-Ti-Cp1 104.6, S1-Ti-Cp2 110.7, S1-Ti-S2 81.4(1), S2-Ti-Cp1 108.0, S2-Ti-Cp2 108.5, Cp1-Ti-Cp2 132.0, Ti-S1-C1 97.4(4), Ti-S2-C2 95.9(4).

Bond lengths and bond angles of the $(C_5H_5)_2Ti(S_2C_6)$ unit in **8** differ only slightly from those in $[(C_5H_5)_2Ti(S_2C_6H_4)]$.[14] Only one Ti–S bond in **8** is slightly shorter than the corresponding bond in $[(C_5H_5)_2Ti(S_2C_6H_4)]$. The substitution of the dithiol by a bulky amide in *ortho* position has no consequences for the binding to the titanium atom. Thus it can be predicted that no steric factors hinder the coordination of poly(dithiols) bridged over amide groups in *ortho* position. Ligand **7** in complex **8** adopts the envelope conformation in which the five-membered chelate ring is folded along the S–S axis [the angle between the TiS_2 and C_6 planes is 42.7(4)°]. This folding leads to remarkably short Ti–C1 [3.14(1) Å] and Ti–C2 [3.13(1) Å] distances. Also remarkable are the large torsion angles for C5-C6-C7-N [– 45.3°] and C5-C6-C7-O [131.0°], which show clearly how the amide function is twisted out of the plane of the aromatic dithiolate system (Fig. 2).

As a consequence of the folding of the chelate ring around the S–S axis, the cyclopentadienyl ligands do not have the same environment. However, at increased temperature in solution (313 K) a flip around the S–S axis is observed,[15] which leads to the observation of only one slightly broadened signal for the cyclopentadienyl protons in the ^{1}H NMR spectrum.[11] Both conformational isomers can be observed at low temperature, which is illustrated by two signals for the cyclopentadienyl protons together with two signals for the diastereotypical benzyl protons.[11] The difference in the chemical shift for the cyclopentadienyl protons of **8** at 233 K ($\Delta\nu$ = 165 Hz) is far greater than was observed for the similarly built complex with an

unsubstituted dimercaptobenzene.[16] However, owing to the different coalescence temperatures, the estimated activation energy of 55 kJ mol^{-1} for the flip falls in the range described for $[(C_5H_5)_2Ti(S_2C_6H_4)]$ (53 kJ mol^{-1}).[16]

The recovery of pure H_2-**7** from **8** is complete within seconds by reaction with HCl in $CHCl_3$ with formation of the deep red $[(C_5H_5)_2TiCl_2]$. Syntheses and characterization of compounds **5**–**7** clearly showed that the preparation of tripodal tris(dithiol) ligands such as H_6-**2** by bridging three dimercaptobenzoic acid units through a tripodal triamine should be possible. We therefore attempted the synthesis of H_6-**2** according to Scheme 2.

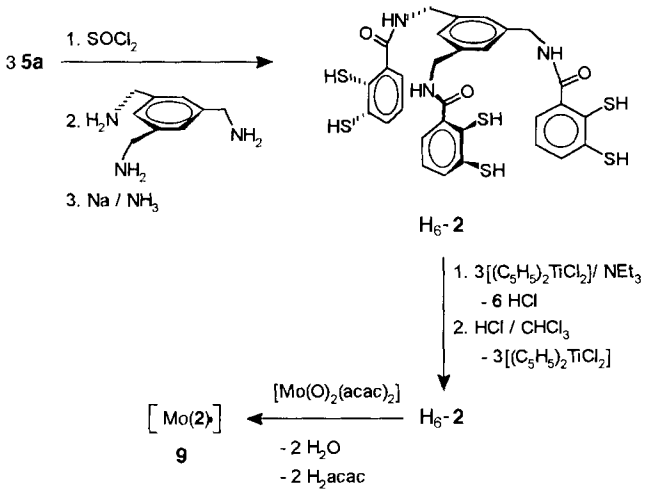

Scheme 2. Synthesis and reactions of the tris(dithiol) ligand H_6-**2**.

The reaction of three equivalents of **5a** with the tripodal triamine 1,3,5-tris(aminomethyl)benzene[8e] yielded the tripodal hexathioether. The removal of the protection groups was achieved as for H_2-**7**. Through reaction with three equivalents of $[(C_5H_5)_2TiCl_2]$, the impure ligand H_6-**2** was transformed into the trinuclear complex $[\{(C_5H_5)_2Ti\}_3$(**2**)], which, in turn, was purified very easily by chromatography. Reaction of $[\{(C_5H_5)_2Ti\}_3$(**2**)] with HCl in $CHCl_3$ led to $[(C_5H_5)_2TiCl_2]$ (soluble in $CHCl_3$) and H_6-**2**, which precipitated from the chloroform solution as a white, analytically pure powder.[17] In a first experiment H_6-**2** was suspended in methanol and mixed with a colorless methanolic solution of $[Mo(O)_2(acac)_2]$. Within an hour the deep green color typical for molybdenum tris(dithiolate) complexes appeared (Scheme 2).[18] The complex [Mo(**2**)] (**9**) can be purified by chromatography on SiO_2 (eluent CH_2Cl_2/MeOH). UV/Vis and mass spectra prove the formation of a mononuclear Mo^{VI} tris(dithiolate) complex. Further investigations on the molecular structures and properties of complexes with the described tris(dithiolene) ligands are in progress.

Received: July 13, 1995 [Z 8200 IE]
German version: *Angew. Chem.* **1995**, *107*, 2938–2941

Keywords: chelate ligands · molybdenum compounds · thiols · tripodal ligands

[1] a) A. R. Bulls, C. G. Pippin, F. E. Hahn, K. N. Raymond, *J. Am. Chem. Soc.* **1990**, *112*, 2627; b) T. M. Garrett, T. J. McMurry, M. W. Hosseini, Z. E. Reyes, F. E. Hahn, K. N. Raymond, *J. Am. Chem. Soc.* **1991**, *113*, 2965; c) F. E. Hahn, S. Rupprecht, K. H. Moock, *J. Chem. Soc. Chem. Commun.* **1991**, 224.

[2] T. B. Karpishin, K. N. Raymond, *Angew. Chem.* **1992**, *104*, 486; *Angew. Chem. Int. Ed. Engl.* **1992**, *31*, 466.

[3] F. E. Hahn, A. Dittler-Klingemann, *Z. Naturforsch. B* **1991**, *46*, 779.

[4] a) P. J. Blower, J. R. Dilworth, J. P. Hutchinson, T. Nicholson, J. Zubieta, *J. Chem. Soc. Dalton Trans.* **1986**, 1339; b) H. Spies, M. Glaser, H.-J. Pietzsch, F. E. Hahn, O. Kintzel, T. Lügger, *Angew. Chem.* **1994**, *106*, 1416; *Angew. Chem. Int. Ed. Engl.* **1994**, *33*, 1354.

[5] N. de Vries, J. Cook, A. G. Jones, A. Davison, *Inorg. Chem.* **1991**, *30*, 2662.

[6] a) D. Sellmann, S. Fünfgelder, G. Pöhlmann, F. Knoch, M. Moll, *Inorg. Chem.* **1990**, *29*, 4772; b) D. Sellmann, W. Soglowek, F. Knoch, G. Ritter, J. Dengler, *Inorg. Chem.* **1992**, *31*, 3711.

[7] a) E. I. Stiefel, R. Eisenberg, R. C. Rosenberg, H. B. Gray, *J. Am. Chem. Soc.* **1966**, *88*, 2956; b) M. Cowie, M. J. Bennett, *Inorg. Chem.* **1976**, *15*, 1584; c) *ibid.* **1976**, *15*, 1589; d) *ibid.* **1976**, *15*, 1595; e) G. Henkel, K. Greiwe, B. Krebs, *Angew. Chem.* **1985**, *97*, 113; *Angew. Chem. Int. Ed. Engl.* **1985**, *24*, 117.

[8] a) F. L. Weitl, K. N. Raymond, *J. Am. Chem. Soc.* **1979**, *101*, 2728; b) S. J. Rodgers, C.-W. Lee, C. Y. Ng, K. N. Raymond, *Inorg. Chem.* **1987**, *26*, 1622; c) M. S. Mitchell, D.-L. Walker, J. Whelan, B. Bosnich, *Inorg. Chem.* **1987**, *26*, 396.

[9] G. D. Figuly, C. K. Loop, J. C. Martin, *J. Am. Chem. Soc.* **1989**, *111*, 654.

[10] D. M. Giolando, K. Kirschbaum, *Synthesis* **1992**, 451.

[11] Correct elemental analyses for **5a**, **5b**, **6**, and **8**. For the synthesis of a mixture of **4a** and **4b**, compound **3** (4.0 mL, 34.8 mmol) dissolved in cyclohexane (10 mL) was added dropwise to a solution of *n*BuLi (174 mmol) and *N*,*N*,*N*′,*N*′-tetramethylethylenediamine (174 mmol) in cyclohexane (90 mL). The resulting yellowish suspension was stirred for 4 days under argon at room temperature. Thereafter, CO_2 (dried over P_4O_{10}) was bubbled through the ice-cooled reaction mixture for 30 min. After hydrolysis with H_2O/HCl the mixture was extracted with diethyl ether. The product mixture **4a**/**4b** contains up to 30% of **3**. To separate the products the mixture **4a**/**4b**/**3** was added to a solution of sodium (3.2 g, 140 mmol) in methanol (100 mL). To this was added isopropyl bromide (13.2 mL, 140 mmol), and the reaction solution was heated at reflux for 24 h. After removal of the solvent the reaction mixture was hydrolyzed with water/HCl, extracted with diethyl ether, and the resulting product mixture separated chromatographically (SiO_2, diethyl ether/petroleum ether, 1/2; v/v). Yield 3.2 g (11.8 mmol, 34%) **5a** and 1.5 g (4.7 mmol, 13%) **5b**. Selected spectroscopic data for **5a**: IR (KBr): $\tilde{\nu}$ [cm^{-1}] = 1701 (s, CO); ^{1}H NMR (250 MHz, $CDCl_3$): δ = 8.00 (m, 1H; Ar-H), 7.40 (m, 2H; Ar-H), 3.40 (m, 1H; SCH), 3.35 (m, 1H; SCH), 1.42 (d, 6H; $CH(CH_3)_2$), 1.31 (d, 6H; $CH(CH_3)_2$); LRMS (70 eV): m/z = 270 ([M^+], 100%), 228 ([M^+] − C_3H_6, 9%). For **5b**: IR (KBr): $\tilde{\nu}$ [cm^{-1}] = 1704 (s, CO); ^{1}H NMR (250 MHz, $CDCl_3$): δ = 8.05 (s, 2H; Ar-H), 3.55 (sept, 2H; SCH), 1.35 (d, 12H; $CH(CH_3)_2$); LR-MS (70 eV): m/z 314 ([M^+], 76%), 229 ([M^+ − C_3H_6 − C_3H_7], 100%). For **6**: IR (KBr): $\tilde{\nu}$ [cm^{-1}] = 1637, 1538 (s, CO); ^{1}H NMR (250 MHz, $CDCl_3$): δ = 7.45–7.25 (m, 8H; Ar-H), 7.12 (t, 1H; N-H), 4.65 (d, 2H; CH_2), 3.50–3.35 (m, 2H; SCH), 1.40 (d, 6H; $CH(CH_3)_2$), 1.15 (d, 6H; $CH(CH_3)_2$); LR-MS (70 eV): m/z 359 ([M^+], 91%). For the removal of the protection groups, **6** (dissolved in THF) was added dropwise to a solution of ammonia and sodium (stoichiometric excess of Na). The reaction was complete after 30 min, and the ligand H_2-**7** was obtained after removal of the NH_3, hydrolysis with H_2O/HCl, and extraction with ether as a colorless, not yet analytically pure, oxidation-sensitive powder. The pure compound was obtained by the synthesis of **8** from H_2-**7** and $[(C_5H_5)_2TiCl_2]$ in THF in the presence of triethylamine. Complex **8** was obtained as blue-green plates in 70% yield (based on **6**). **8**: IR (KBr): $\tilde{\nu}$ [cm^{-1}] = 1664, 1499 (s, CO); ^{1}H NMR (300 MHz, $CDCl_3$, T = 313 K): δ = 7.75 (dd, 1H; Ar-H), 7.56 (dd, 1H; Ar-H), 7.51 (s, br, 1H; N-H), 7.40–7.17 (m, 6H; Ar-H), 6.06 (s, br, 10H; C_5H_5), 4.69 (d, 2H, CH_2); (T = 233 K): N-H and Ar-H signals are almost unchanged, 6.42 (s, 5H; C_5H_5), 5.87 (s, 5H; C_5H_5), 4.82 (dd, 1H; CH_2), 4.64 (dd, 1H; CH_2). The liberation of H_2-**7** from **8** takes place within a few seconds by treatment of **8** with $CHCl_3$/HCl to form $[(C_5H_5)_2TiCl_2]$. H_2-**7**: ^{1}H NMR (270 MHz, $CDCl_3$): δ = 7.45–7.23 (m, 7H; Ar-H), 7.04 (t, 1H; Ar-H), 6.35 (s, br, 1H; N-H), 5.62 (s, 1H; S-H), 4.60 (d, 2H; CH_2), 3.81 (s, 1H; S-H).

[12] Crystal structure analyses: Crystals of **8** crystallized from benzene are systematically twinned. Data sets for both individuals of one crystal were recorded. The data for the larger individual were used for the structure determination and refinement. From the two orientation matrices and the scan range 216 overlapping reflexes were identified, of which 83 were suppressed in the following least-squares refinement. Structure parameters: **5a** [**8**]: $C_{13}H_{18}O_2S_2$ [$C_{24}H_{21}ONS_2Ti$], triclinic [triclinic], space group $P\bar{1}$ [$P\bar{1}$], a = 7.952(3) [8.186(4)], b = 9.420(5) [11.417(7)], c = 10.671(4) [12.445(7)] Å, α = 105.21(4) [67.48(4)], β = 91.79 [71.35(4)], γ = 111.80(3) [85.54(4)]°, V = 708.8(13) [1016.7(12)] Å^3, Z = 2 [2], ρ_{exp} = 1.28 [1.46], ρ_{calcd} = 1.267 [1.475] g cm^{-3}, $Mo_{K\alpha}$ radiation (λ = 0.71073 Å), $\mu(Mo_{K\alpha})$ = 3.15 [6.28] cm^{-1}. 2847 [2658] symmetry-independent data measured at 20(2) [20(2)] °C in the 2θ-range [°] 4–48 [2–45]. Structure determination with direct methods, refinement of the positional parameters of all non-hydrogen atoms with anisotropic thermal parameters, hydrogen atoms on calculated positions [d(C-H) = 0.95 Å, d(N-H) = 0.87 Å] with U_H = 0.081 Å^2 (for **5a**), B_H = 1.3 $B_{eq(C)}$ (for **8**), respectively, position of the carboxylate hydrogen atom in **5a** was not determined. R = 3.88 [6.75], R_w = 3.74 [9.71] for 2087 [1630] structure factors $I \geq 2\sigma(I)$ [$F_o^2 \geq 3\sigma(F_o^2)$] and 155 [262] variables. Further details of the crystal structure investigations may be obtained from the Fachinformationszentrum Karlsruhe, D-76344 Eggenstein-Leopoldshafen, on quoting the depository number CSD-59134.

[13] a) E. Block in *The Chemistry of Ethers, Crown Ethers, Hydroxyl Groups and Their Sulfur Analogues* (Ed.: S. Patai), Wiley, New York, **1980**, Supplement E, p. 587ff. and references therein; b) A. Ferretti, *Org. Synth.* **1962**, *42*, 54.
[14] A. Kotoglu, *Z. Anorg. Allg. Chem.* **1972**, *390*, 195.
[15] H. Köpf, *Angew. Chem.* **1971**, *83*, 146; *Angew. Chem. Int. Ed. Engl.* **1971**, *10*, 134.
[16] H. Köpf, T. Klapötke, *J. Chem. Soc. Chem. Commun.* **1986**, 1192.
[17] Correct elemental analyses for H_6-**2**, $[\{(C_5H_5)_2Ti\}_3(\mathbf{2})]$, **9**. Selected spectroscopic data for $[\{(C_5H_5)_2Ti\}_3(\mathbf{2})]$: IR (KBr): $\tilde{\nu}$ [cm^{-1}] = 1647, 1517 (s, CO); ^{1}H NMR (250 MHz, $CDCl_3$): δ = 7.91 (t, 3H; NH), 7.65 (d, 3H; Ar-H), 7.52 (d, 3H; Ar-H), 7.37 (s, 3H; Ar-H), 7.20 (t, 3H; Ar-H), 6.05 (s, br, 30H; C_5H_5), 4.60 (d, 6H; CH_2); FAB-MS (negative ions): 1196 [$(M - H)^-$], 955 [$(M - (C_5H_5)_2TiS_2)^-$]. For H_6-**2**: IR (KBr): $\tilde{\nu}$ [cm^{-1}] = 2526 (m, SH), 1636, 1522 (s, CO); ^{1}H NMR (250 MHz, [D$_6$]DMSO): δ = 9.22 (t, 3H; NH), 7.51 (d, 3H; Ar-H), 7.35 (d, 3H; Ar-H), 7.25 (s, 3H; Ar-H), 7.02 (t, 3H; Ar-H), 5.7 (s, br, 6H; SH), 4.46 (d, 6H; CH_2). For **9**: FAB-MS (negative ions): 760 [$(M - H)^-$], experimentally measured isotope distribution corresponds to the calculated distribution; UV/Vis (CH_3OH, % T): $\tilde{\nu}$ [cm^{-1}] = 14800 (42), 24000 (13), compare with $[Mo(S_2C_2H_6)_3]$ $\tilde{\nu}$ [cm^{-1}] = 14640 and 22990 [18].
[18] M. Kawashima, M. Koyama, T. Fujinaga, *J. Inorg. Nucl. Chem.* **1976**, *38*, 801.

$Ta_5(S,Te)_2$: Microporous Tantalum with Chalcogen-Coated Inner Surfaces**

Thomas Degen and Bernd Harbrecht*

The structural chemistry of tantalum-rich chalcogenides is dominated by the competition between two basic building principles. On one hand, chalcogenides are known that fragmentarily contain the body-centered cubic (bcc) arrangement of the metal components. The prototype is Ta_2Se.[1] This layered structure, which is symmetry related to bcc tantalum, consists of two-dimensional bcc-Ta fragments. The remaining valences on the surfaces of each sheet are saturated with selenium. The mixed sulfide selenides, $Ta_2(S,Se)$[2] (Ta_2Se-type), $Ta_5(S,Se)_2$[4] (isostructural with $(Nb,Ta)_5S_2$[3]), and $Ta_9(S,Se)_4$,[4] the latter of which results from a chemical intergrowth of the 2:1 and 5:2 phases, form similar layered-type, bcc-related structures. Binary pendants of the metal-rich 5:2 and 9:4 phases do not seem to exist. The sulfides meet this building principle only if tantalum is partly replaced, for example by niobium. $(Nb,Ta)_nS_4$ (n = 11, 12)[5] and the quaternary sulfide telluride $(Nb,Ta)_9(S,Te)_5$[6] are typical representatives of structures resulting from a three-dimensional cross-linking of columnar bcc fragments.

On the other hand, there are tantalum-rich chalcogenides that contain centered, distorted, Ta_{13} icosahedra as a uniform structural motif. The metal icosahedra interpenetrate along a pseudo-fivefold rotation axis, thus forming pentagonal-antiprismatic chains. Ta_6S (dimorphic),[7] Ta_2S,[8] Ta_3S_2,[9] and the substitution phases of the type $M_xTa_{6-x}S$ (M = V, Cr)[10] comprise such chains. The recently characterized telluride Ta_6Te_5[11] exhibits the same feature.

[*] Prof. Dr. B. Harbrecht,[+] Dipl.-Chem. T. Degen
Institut für Anorganische Chemie der Universität
Gerhard-Domagk-Strasse 1, D-53121 Bonn (Germany)
[+] New address:
Fachbereich Chemie der Universität
D-35032 Marburg (Germany)
Telefax: Int. code +(6421)-28-8917

[**] This work was supported by the Deutsche Forschungsgemeinschaft, the Fonds der Chemischen Industrie, and the Ministerium für Wissenschaft und Technologie des Landes Nordrhein-Westfalen. We thank Dr. M. Nieger for the measurement of the single-crystal data.

The surprising result that the telluride is structurally related to the tantalum-rich sulfides, but not to the tantalum-rich selenides, has led us to preparatively explore the tantalum-rich region of the system Ta-S-Te for the existence of additional phases with complex structures. As part of these investigations we uncovered two new phases, $Ta_5(S,Te)_2$ and $Ta_{61}(S,Te)_{30}$.[12] Herein we report on the 5:2 phase $Ta_5(S,Te)_2$ (**1**).[13] It has the same composition as the sulfide selenide richest in tantalum; its structure, however, is not composed of bcc fragments, but results from the meandered penetration of three chemically independent, centered, icosahedral clusters.

Coarse crystals of **1** (up to 4 mm) were prepared by reduction of an equimolar mixture of the dichalcogenides with tantalum in the presence of iodine as a transport agent at about 1800 K within one day. The reactions were performed in tantalum ampoules. The rod-shaped crystals preferentially grew fascicularly on the interior wall of the tantalum ampoule. Similar reactions performed without iodine yielded **1** as a nearly pure, microcrystalline product. The phase composition of the samples was controlled by X-ray powder diffractometry and Rietveld refinements[14] (Fig. 1). The tellurium-rich compounds additionally

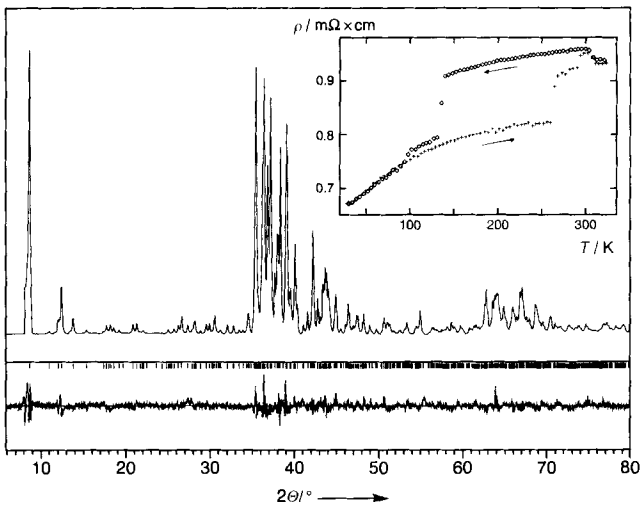

Fig. 1. Rietveld refinement of an X-ray powder pattern of $Ta_5(S,Te)_2$ **1**. Top: measured (dotted) and calculated profile; middle: calculated Bragg positions; bottom: difference between calculated and measured intensity; insert: electrical resistivity of a single crystal of $Ta_5(S,Te)_2$ as a function of the temperature; (◇ = cooling, + = heating; crystal dimensions: 2.65 × 0.15 × 0.12 mm^3, current: 1 mA, contacted with epoxy silver paste).

contained at least one more phase which has not yet been fully characterized. In samples richer in sulfur the sulfide telluride **1** forms together with Ta_6S or Ta_2S. Energy dispersive microanalyses (EDX) point to a narrow homogeneity range ($Ta_5S_{1.0(1)}Te_{1.0(1)}$). The differences between the lattice parameters[15] (< 4 pm) of phases at both stability boundaries are correspondingly small.

$Ta_5(S,Te)_2$ exhibits an unexpected microporous tantalum partial structure for such a metal-rich compound. Figure 2 shows a polyhedral representation[16] of the metal framework as a projection along the c axis. Large channels with a free width of more than 0.6 nm run through the structure that results from the interpenetration of three distinct clusters. The metal atoms of the clusters are grouped around the icosahedrally coordinated atoms Ta1, Ta4, and Ta8. As can be seen from Figure 3, only Ta4 is exclusively coordinated by tantalum atoms. The metal coordination about Ta1 corresponds to an *arachno*-Ta_{11}, that

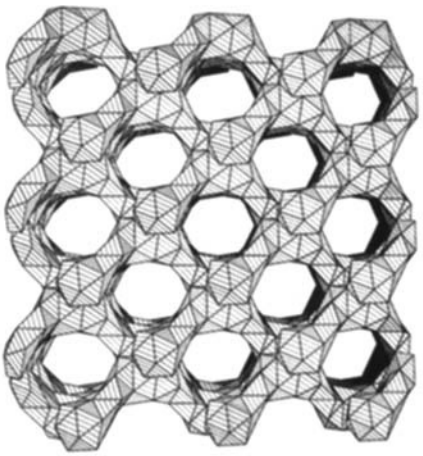

Fig. 2. Polyhedral representation of a section of the metal partial structure of **1** (projection along the *c* axis).

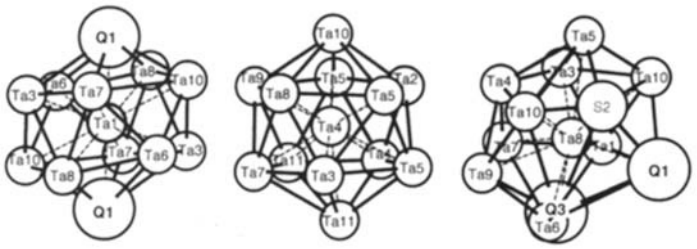

Fig. 3. Polyhedra about the three distorted icosahedrally coordinated atoms: Ta1(295.9), Ta4(290.4), and Ta8(296.8) (values in parentheses correspond to mean distances [pm] for the coordination number 12).

about Ta8 to a *hypho*-Ta_{10} icosahedral fragment. Q1 (mixed occupied site: 96% Te, 4% S) completes the Ta_{11} fragment, Q3 (34% Te, 66% S) and S2 complete the Ta_{10} fragment to give closed deltahedra. The three clusters interpenetrate to form meandered chains running along the *a* axis (Fig. 4). The specific

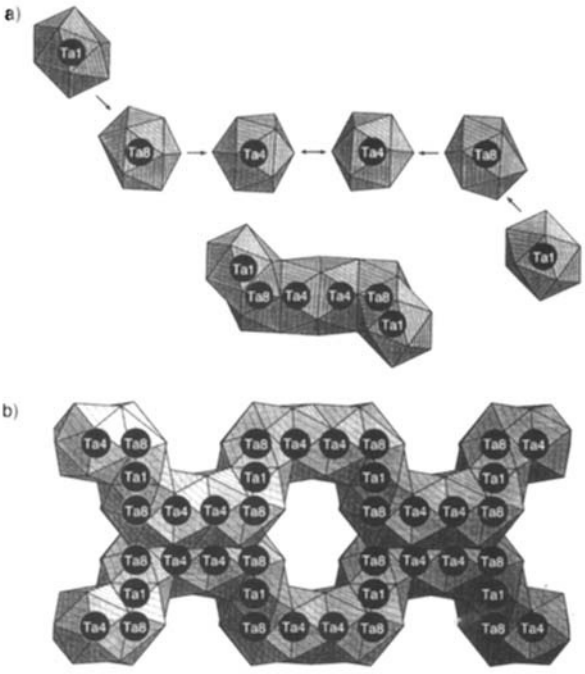

Fig. 4. a) Mutual penetration of the three icosahedral clusters around Ta1, Ta4, and Ta8 to form a meandered chain; b) linkage of two such chains depicted as a projection along the *c* axis.

mutual orientation of the chains that are three-dimensionally linked by common edges (2 × Ta5) and apices (Ta10), leads to pores which are limited by 16 icosahedral groupings in the projection plane. The chalcogen atoms contributing to the icosahedral coordinations of Ta1 and Ta8, namely Q1, Q3, and S2, are located at the pore walls. The remaining atoms S1 and Q2 (92% Te, 8% S) cover the rest of the interior metal surfaces. In accord with the surface-covering function, the chalcogen atoms are always one-sided fourfold (Q2,Q3), fivefold (Q1,S1), or sixfold (S2) surrounded by Ta. The five coordination polyhedra of seemingly arbitrary shape (Fig. 5) are more or less open frag-

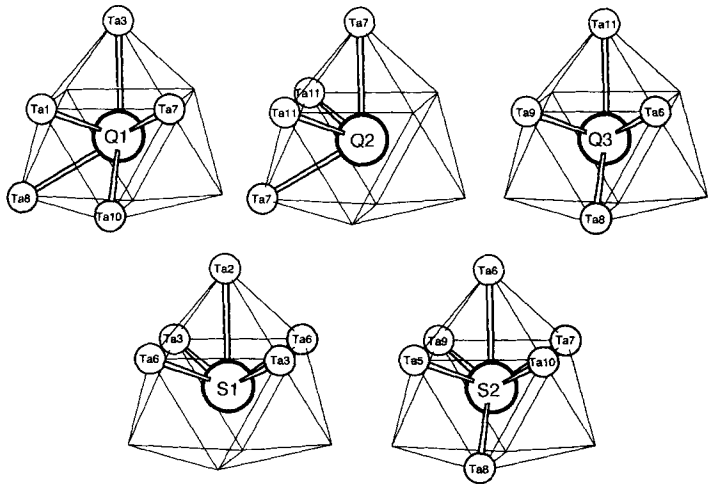

Fig. 5. Coordination polyhedra around the five distinct chalcogen atoms, Q1(294.3), Q2(291.4), Q3(270.4), S1(249.8), and S2(254.6), schematically depicted as fragments of an imaginary triangulated tetrakaidecahedron (values in parentheses represent mean Q,S–Ta distances [pm] for the respective coordination number).

ments of an imaginary QTa_9 polyhedron, a tetrakaidecahedron confined by 14 triangular planes. S1 and S2 cover the surface in areas of larger, Q1, Q2, and Q3 in areas of lesser pore curvature. Some of the neighboring chalcogen atoms are in close contact (Q1–S1 = 325.7 pm, Q1–Q3 = 332.7 pm). Q2, located in the center of the area of lower flexure, is—similar to the case of layered-type chalcogenides—sixfold surrounded by S2, Q1, and Q3. These atoms are in van the Waals contact (349.6–374.5 pm). Four further distant Q1 and Q3 centers (389.7 and 390.7 pm) are situated at the opposite pore wall. The chalcogen atoms that are segregated at the inner surface of the microporous tantalum partial structure themselves sheathe empty channel-like hollows, which potentially could serve as receptors for small metal atoms.

Ta–Ta and Ta–Q bonds contribute in different ways to the stability of $Ta_5(S,Te)_2$ **1**: in regions deviating away from the pore walls the cohesion is solely maintained by three-dimensionally extended, Ta–Ta interactions. Strong metal–metal bonds are reflected in numerous short Ta–Ta contacts (270.5–337.5 pm). The bonds between Ta and the chalcogen atoms can barely compensate the high cohesive energy of the 5d metal, upon which this complex metal partial structure is based. They afford an additional stabilization through the formation of heteronuclear bonding regions (246.7–306.2 pm) that are uncoupled from the metal cores. These bonds are confined to areas near the pore walls. Thus, the hierarchy of the bonding interactions explains why the structure of this tantalum-rich chalcogenide is not shaped by the dispersion of the minor components (S, Te) in the metal but by the spatial segregation of the metal and non-

metal components. The spatial confinement of the metallic bonding regions associated with the pores might give rise to quantum size effects for this clusterlike compound. The electrical resistivity of single crystals measured by a four-point-direct current method[17] (Fig. 1) confirms that the title compound is a metallic conductor. The resistivity lies in the mΩ cm range and is nearly two orders of magnitude larger than that of elemental tantalum. Anomalies in the temperature dependence of the resistivity—in accordance with the large hysteresis—point to a first-order phase transition.

Received: July 13, 1995 [Z 8207 IE]
German version: *Angew. Chem.* **1995**, *107*, 2888–2890

Keywords: solid-state structures · sulfides · tantalum compounds · tellurides

[1] B. Harbrecht, *Angew. Chem.* **1989**, *101*, 1696–1697; *Angew. Chem. Int. Ed. Engl.* **1989**, *28*, 1660–1662.
[2] K. S. Nanjundaswamy, T. Hughbanks, *J. Solid State Chem.* **1992**, *98*, 278–290.
[3] X. Yao, H. F. Franzen, *J. Am. Chem. Soc.* **1991**, *113*, 1426–1427.
[4] $Ta_5(S,Se)_2$ together with another metal-rich phase, $Ta_9(S,Se)_4$, has been part of a conference contribution: B. Harbrecht, T. Degen, *7. Tagung Festkörperanalytik* (GdCh), (Chemnitz, Germany) **1993**, 136; data (X-ray powder pattern, Rietveld refinement): $Ta_5S_{1.5}Se_{0.5}$: space group *I4/mmm*, $Z = 2$, $a = 333.37(7)$, $c = 2190.38(7)$ pm, $R_P = 0.051$, $R_{B(I)} = 0.034$; $Ta_9S_{2.9}Se_{1.1}$: space group *I4/mmm*, $Z = 2$, $a = 333.84(1)$, $c = 4053.6(3)$ pm, $R_P = 0.058$, $R_{B(I)} = 0.044$.
[5] a) X. Yao, H. F. Franzen, *J. Solid State Chem.* **1990**, *86*, 88–93; b) X. Yao, H. F. Franzen, *Z. Anorg. Allg. Chem.* **1991**, *598/599*, 353–362.
[6] T. Degen, B. Harbrecht, *Angew. Chem.* **1995**, *107*, 1226–1228, *Angew. Chem. Int. Ed. Engl.* **1995**, *34*, 1089–1090.
[7] a) H. F. Franzen, J. G. Smeggil, *Acta Crystallogr. Sect. B* **1970**, *26*, 125–129; b) B. Harbrecht, *J. Less-Common Met.* **1988**, *138*, 225–234; c) H. Nozaki, H. Wada, S. Takekawa, *J. Phys. Soc. Jpn.* **1991**, *60*, 3510–3515.
[8] H. F. Franzen, J. G. Smeggil, *Acta Crystallogr. Sect. B* **1969**, *25*, 1736–1741.
[9] a) H. Wada, M. Onoda, *Mater. Res. Bull.* **1989**, *24*, 191–196; b) S. J. Kim, K. S. Nanjundaswamy, T. Hughbanks, *Inorg. Chem.* **1991**, *30*, 159–164; c) K. Ahn, T. Hughbanks, *J. Solid State Chem.* **1993**, *102*, 446–454; d) T. Degen, B. Harbrecht, *Acta Crystallogr. Sect. C*, in press.
[10] B. Harbrecht, H. F. Franzen, *Z. Anorg. Allg. Chem.* **1987**, *551*, 74–84.
[11] M. Conrad, B. Harbrecht, *IVth Euro. Conf. on Solid State Chem.* (Dresden, Germany) **1992**, 324.
[12] Crystallographic data for $Ta_{61}(S,Te)_{30}$ **1**: space group *C2/m*, $Z = 2$, $a = 1962.9(13)$, $b = 1817.9(2)$, $c = 1294.2(7)$ pm, $\beta = 124.77(4)°$, $R(F_o) = 0.062$, composition as determined by X-ray single crystal structure analysis: $Ta_{61}S_{15.1}Te_{14.9}$.
[13] Crystal structure analysis of $Ta_5(S,Te)_2$: $Mo_{K\alpha}$ radiation, CAD4 diffractometer, SDP Plus (Enraf Nonius), crystal dimensions: $0.40 \times 0.03 \times 0.02$ mm^3, space group: *C2/c*, $Z = 16$, $a = 1547.5(6)$, $b = 1421.3(4)$, $c = 1041.1(4)$ pm, $\beta = 108.65(3)°$, ω-2θ scans, $\theta_{max} = 32°$, 6745 reflections, 1927 unique reflections with $I_o > 3(I_o)$, absorption correction (psi-scans), $R_{int}(F) = 0.047$, 134 variables, $R(F_o)/R_w(F_o) = 0.045/0.052$, composition as determined by X-ray crystal structure analysis: $Ta_5S_{1.12}Te_{0.88(2)}$. Further details of the crystal structure investigation may be obtained from the Fachinformationszentrum Karlsruhe, D-76344 Eggenstein-Leopoldshafen (Germany), on quoting the depository number CSD-59131.
[14] C. J. Howard, R. J. Hill, Rietveld-program *LHPM*, (AAEC Report No. M112) **1986**; V. Wagner, T. Degen, program package DIFFRAKT (V 1.0), Institut für Anorganische Chemie der Universität Bonn, **1995**.
[15] Maximum (1) and minimum (2) lattice parameters from Rietveld refinements of X-ray powder patterns: (1) $a = 1546.89(7)$, $b = 1422.35(6)$, $c = 1039.62(5)$ pm, $\beta = 108.592(3)°$; (2) $a = 1544.84(21)$, $b = 1418.99(18)$, $c = 1038.59(13)$ pm, $\beta = 108.677(8)°$.
[16] K. Brandenburg, G. Bergerhoff, Graphics-program package DIAMOND (V. 1.0), Institut für Anorganische Chemie der Universität Bonn, **1995**.
[17] K. L. Horovitz, V. A. Johnson, *Methods of Experimental Physics, Vol. 6, Part B*, Academic Press, New York, **1959**, pp. 33–37.

Towards the Development of Molecular Wires: Electron Localization, Exchange, and Transfer in Alkyne-Bridged Multinuclear Complexes**

Vincent Grosshenny, Anthony Harriman,* and Raymond Ziessel*

Stepwise assembly of preformed molecular modules around a metal center provides an attractive means for constructing multicomponent arrays capable of information storage and transport.[1] To ensure fast and quantitative exchange of information within the array, the bridge must facilitate strong electronic communication between the components. This situation is realized, at least for through-bond electron transfer, when the energy level of the bridge slightly exceeds that of the reactants.[2] Thus, alkenes[3–5] and alkynes[6–9] appear to be promising bridges, and the latter is ideal for construction of rigid, rodlike arrays.[10, 11] The efficacy of alkynes for promoting long-range electronic coupling has not been explored extensively, although several systems have been studied because of their nonlinear optical properties.[12–15] Here, we describe the processes that occur upon excitation of multinuclear complexes assembled from ruthenium(II) bis(terpyridyl) subunits covalently attached to a free terpyridyl ligand by ethynediyl or butynediyl bridges.[9] If a second metal cation is included in this complex,[16, 17] a linear, photoactive array results, in which ruthenium(II) units are termini (Scheme 1) and the central cation (M) controls the photochemistry.

It is important to recall that the parent compound $[Ru^{II}(terpy)_2]^{2+}$ is a poor sensitizer at ambient temperature.[18] This is partly because a relatively low-lying metal-centered (MC) excited state promotes nonradiative deactivation of the lowest energy triplet excited state, which has metal-to-ligand charge-transfer (MLCT) character, to the ground state. Incorporation of an alkyne group into one of the terpyridyl ligands, however, decreases the energy of this MLCT triplet state, thereby minimizing the extent of its mixing with the higher energy MC state.[9] Thus, excitation into the MLCT absorption transition localized on the $[Ru^{II}(terpy)_2]^{2+}$ subunits of the Zn^{II}-containing complexes **Ru_2Zn(1)** and **Ru_2Zn(2)** in acetonitrile at 20 °C results in luminescence. The emission maxima (λ_P) of these compounds are red-shifted and the luminescence quantum yields (Φ_L) are significantly enhanced relative to the weakly emissive parent (Table 1). The triplet lifetimes (τ_T) of the trinuclear complexes, measured in deoxygenated acetonitrile, are much longer than that of $[Ru^{II}(terpy)_2]^{2+}$ (Table 1) and of other mononuclear derivatives having comparable triplet energies.[18–20] In contrast, the half-wave potentials for one-electron oxidation of the Ru^{II} center ($E^{ox}_{1/2}$) are similar to that of the parent,[21] as might be expected for derivatives with a weakly electron-withdrawing substituent.[19] Since the redox potentials for one-electron reduction of the terpyridyl ligand ($E^{red}_{1/2}$) are slightly less negative for the alkyne-substituted ligands than for the parent (Table 1), the decreased triplet energy noted for **Ru_2Zn(1)** and **Ru_2Zn(2)** might arise, in part, from an electronic effect. It is also important to note that in the complexes with the

[*] Dr. R. Ziessel, V. Grosshenny
Laboratoire de Chimie, d'Electronique et de Photonique Moléculaires
Ecole Européenne Chimie, Polymère, Matériaux
IPCMS, UMR 46, 1, rue Blaise Pascal, F-67008 Strasbourg (France)
Telefax: Int. code +88416825
Prof. A. Harriman
Center for Fast Kinetics Research
The University of Texas at Austin, Austin, TX 78712 (USA)
Telefax: Int. code +(512)471-6095

[**] This work was supported by the NIH and the CNRS.

 © VCH Verlagsgesellschaft mbH, D-69451 Weinheim, 1995 0570-0833/95/3423-2705 $ 10.00+.25/0

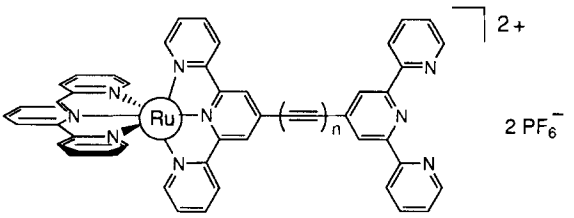

Ru(1) n=1
Ru(2) n=2

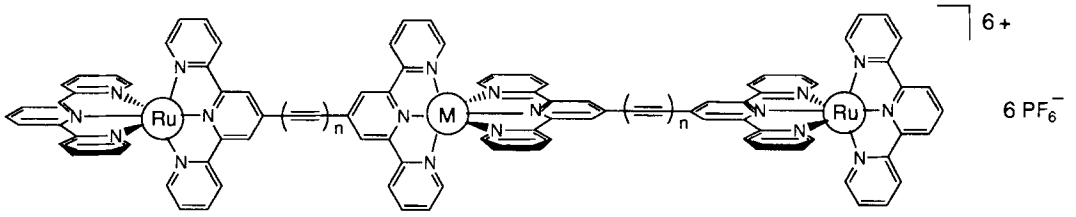

$Ru_2Zn(1)$ n=1
$Ru_2Zn(2)$ n=2
$Ru_2Fe(1)$ n=1
$Ru_2Fe(2)$ n=2
$Ru_2Co(1)$ n=1
$Ru_2Co(2)$ n=2

Scheme 1. Molecular structures of the metal complexes studied in this investigation.

butynediyl bridge, oxidation of the Ru^{II} center occurs at much higher potential for the Fe^{II}- and Co^{II}-containing trinuclear complexes, in which the central metal (M) has a lower oxidation potential (Table 1). This behavior is suggestive of electronic coupling between the metal centers.

The enhanced triplet lifetimes of the two Zn^{II}-containing complexes relative to that of the parent compound might arise from decoupling of the MC and MLCT excited states. To isolate this effect from any additional stabilization phenomena due to the alkyne group, luminescence studies were conducted in ethanol at 77 K. Under these conditions the emission maxima are blue-shifted and the triplet lifetimes of the parent and Zn^{II}-containing complexes increase dramatically (Table 1). At 77 K the triplet lifetimes of **$Ru_2Zn(1)$** and **$Ru_2Zn(2)$** are similar to that of the parent, despite their significantly lower triplet energy; the "energy-gap law" demands that the rates of nonradiative transitions increase with decreasing triplet energy.[22] By comparing the triplet lifetimes (τ_T) measured for **$Ru_2Zn(1)$** and **$Ru_2Zn(2)$** with those expected for a $[Ru^{II}(terpy)_2]^{2+}$ derivative having the same triplet energy (τ_O),[18–20] one can estimate the stabilizing effect of the ethynyl groups. This property is reflected by the ratio of triplet lifetimes[23] measured at 77 K and corresponds to an approximate fivefold increase in the lifetime of the triplet state. The origin of this "stabilization effect" may be vibronic and/or electronic in nature but a full quantum mechanical explanation is not yet available.

Irradiation into the MLCT absorption transition of these asymmetrical $[Ru^{II}(terpy)_2]^{2+}$ derivatives promotes a d electron from the Ru^{II} center to the alkyne-substituted terpyridyl ligand. The electron is localized on this ligand but, because of increased conjugation, it resides in an extended π^* orbital that includes the alkyne bridge and the bridging terpyridyl ligands.[9] Laser flash photolysis studies in deoxygenated acetonitrile at 20 °C indicate that, in addition to bleaching of the ground-state MLCT band ($\lambda = 497$ nm), an intense absorption band appears at longer wavelength ($\lambda \approx 640$ nm), which is not seen for the parent complex (Fig. 1a). Similar bands can be observed for the alkyne-substituted mononuclear $[Ru^{II}(terpy)_2]^{2+}$ derivatives **Ru(1)** and **Ru(2)**; the photophysical properties of these complexes are similar to those of **$Ru_2Zn(1)$** and **$Ru_2Zn(2)$** (Table 1). These absorption bands, which exhibit maxima at roughly 600 nm (**$Ru_2Zn(1)$**) and 640 nm (**$Ru_2Zn(2)$**), are likely due to the π radical anion of the alkyne-substituted terpyridyl ligands, although they are much more intense than those reported for mononuclear $[Ru^{II}(terpy)_2]^{2+}$ derivatives.[20]

The iron(II)-containing complexes **$Ru_2Fe(1)$** and **$Ru_2Fe(2)$** are nonemissive, but MLCT absorption transitions associated with $[Ru^{II}(terpy)_2]^{2+}$ ($\lambda_{max} \approx 500$ nm) and $[Fe^{II}(terpy)_2]^{2+}$ ($\lambda_{max} \approx 595$ nm) subunits are well resolved. Irradiation in acetonitrile solution into the $[Fe^{II}(terpy)_2]^{2+}$ absorption band generates the triplet state localized on the Fe^{II} unit, which has a lifetime of 2.6 ± 0.4 ns (**$Ru_2Fe(1)$**) and 3.9 ± 0.5 ns (**$Ru_2Fe(2)$**). Similarly, excitation into the $[Ru^{II}(terpy)_2]^{2+}$ absorption band leads to the triplet state of that chromophore with a lifetime of 12 ± 2 ps (**$Ru_2Fe(1)$**) and (16 ± 3) ps (**$Ru_2Fe(2)$**). This deactiva-

Table 1. Photophysical and electrochemical properties recorded for the ruthenium(II) bis(terpyridyl) subunits of the mononuclear and trinuclear complexes studied in acetonitrile solution at 273 K or an ethanol glass at 77 K [a].

Cmpd	Acetonitrile at 273 K					Ethanol at 77 K		
	λ_p/nm[b]	τ_T/ns[c]	Φ_L[d]	$E^{ox}_{1/2}$[e]	$E^{red}_{1/2}$[e]	λ_p/nm[b]	τ_T/μs[c]	τ_T/τ_0[f]
$[Ru^{II}(terpy)_2]^{2+}$	640	0.62	<0.0002	1.34	−1.21	610	11.0	1.0
Ru(1)	690	50	0.0003	1.37	−1.11	675	14.0	4.5
Ru(2)	710	165	0.0006	1.36	−0.98	685	13.6	5.2
$Ru_2Zn(1)$	700	180	0.0008	1.41	−1.04	680	12.8	4.6
$Ru_2Zn(2)$	715	190	0.0008	1.32	−1.00	690	12.7	5.3
$Ru_2Fe(1)$	nd	0.012	nd	1.46[g]	−1.10	nd	-	na
$Ru_2Fe(2)$	nd	0.016	nd	1.47[g]	−1.05	nd	-	na
$Ru_2Co(1)$	nd	0.006	nd	1.47[g]	−1.00	nd	-	na
$Ru_2Co(2)$	nd	0.008	nd	1.49[g]	−0.95	nd	-	na

[a] nd: not detectable; na: not applicable. [b] ±5 nm. [c] ±10%. [d] ±30%. [e] ±20 mV. [f] See ref. [23]. [g] Waves at lower potential are assigned to oxidation of the central metal (M).

 © VCH Verlagsgesellschaft mbH, D-69451 Weinheim, 1995 0570-0833/95/3423-2706 $ 10.00+.25/0

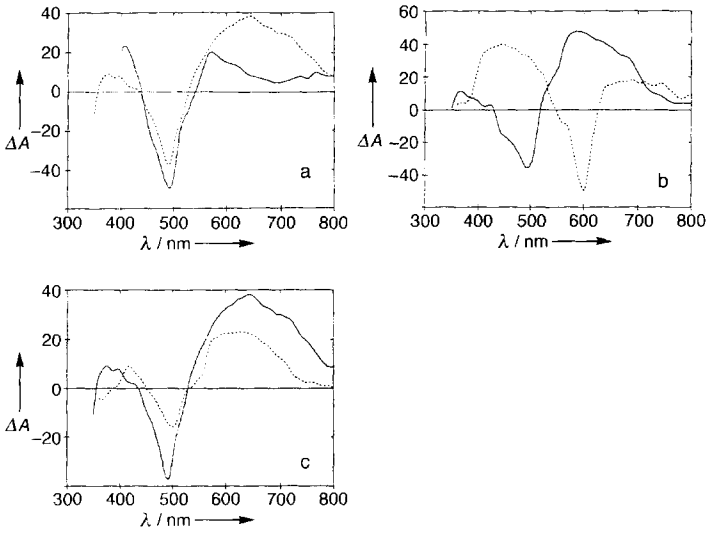

Fig. 1. Transient differential absorption spectra a) of $[Ru^{II}(terpy)_2]^{2+}$ (—) and **$Ru_2Zn(2)$** (- - -) recorded in deoxygenated acetonitrile at 20 °C immediately after excitation at 532 nm with a 30-ps laser pulse, b) of **$Ru_2Fe(1)$** recorded 1 ps (—) and 100 ps (- - -) after laser excitation of with a subpicosecond laser pulse at 440 nm, c) of **$Ru_2Co(2)$** recorded 1 ps (—) and 30 ps (- - -) after laser excitation at 440 nm. The absorbance scale is given in units of optical density divided by 1000.

tion is accompanied by bleaching of the MLCT transition associated with the $[Fe^{II}(terpy)_2]^{2+}$ subunits (Fig. 1b), the rate of which matches the rate of restoration of the ground state of the $[Ru^{II}(terpy)_2]^{2+}$ chromophore. This situation is ascribed to intramolecular energy transfer between the triplet states,[10, 18] which most probably occurs by way of electron exchange since the overlap integral for dipole-dipole transfer is rather small. Electron exchange corresponds to concerted transfer of an electron and a positive hole through orbitals localized on the alkyne bridge. Electron transfer may be facilitated by selective population of the orbitals of the bridging ligand followed by electron delocalization over an extended π^* orbital that encompasses the terpyridyl ligand and part of the alkyne bridge. Conversely, hole transfer involves d orbitals localized on each metal center. The fast rate of energy transfer, occurring over distances of 15.2 Å (**$Ru_2Fe(1)$**) and 17.7 Å (**$Ru_2Fe(2)$**) indicates that the subunits are in good electronic communication. A schematic description of the overall process in shown in Scheme 2.

Luminescence could not be detected for the Co^{II}-containing trinuclear complexes **$Ru_2Co(1)$** and **$Ru_2Co(2)$**; however, excitation at 440 nm generates the triplet state of the $[Ru^{II}(terpy)_2]^{2+}$ chromophore, which has a lifetime of 6 ± 2 ps and 8 ± 2 ps, respectively. A longer-lived transient species persisted after decay of the triplet (Fig. 1c), which was identified[24] as containing a $[Co^{III}(terpy)_2]^{3+}$ unit and the reduced form of the $[Ru^{II}(terpy)_2]^{2+}$ unit generated by intramolecular one-electron transfer ($\Delta G^0 \approx -0.37$ eV). This species has a lifetime of 125 ± 25 ps (**$Ru_2Co(1)$**) and 140 ± 20 ps (**$Ru_2Co(2)$**) before charge recombination occurs to restore the ground state ($\Delta G^0 \approx -1.75$ eV). The forward (light-induced) step involves long-range (over 15–18 Å) hole transfer from Ru^{III} to Co^{II}, occurring through HOMOs on the bridging ligand. Subsequent restoration of the ground state occurs through electron transfer from the alkyne-substituted terpyridyl π radical anion to the Co^{III} center. The rates of both forward and reverse steps are only weakly dependent on the length of the bridge, but the forward reaction is at least ten times faster than the reverse process, possibly due to the large amount of vibrational energy that must be dissipated during charge recombination. In fact, our results can be explained by assuming that the forward reaction occurs close to the apex of a Marcus-type bell-shaped curve (for the plot of rate vs energy gap), while charge recombination occurs well within the inverted region of the curve. This situation, in turn, demands that the total reorganization energy accompanying electron tranfer is in the region of about 0.5 eV. A schematic description of the overall process in shown in Scheme 3.

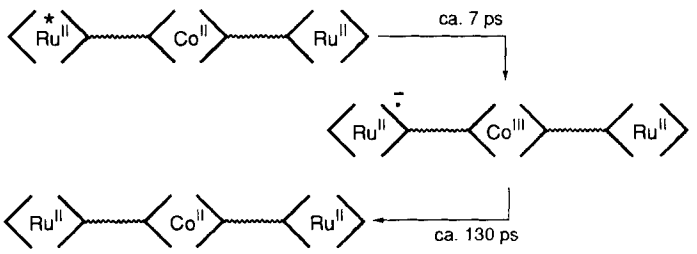

Scheme 3. Activation and deactivation of complexes **$Ru_2Co(1)$** and **$Ru_2Co(2)$**.

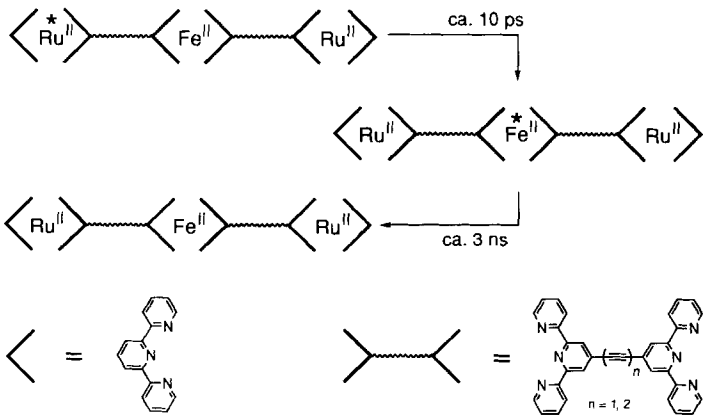

Scheme 2. Activation and deactivation of complexes **$Ru_2Fe(1)$** and **$Ru_2Fe(2)$**.

It is interesting to consider the requirements for the spacer group in such multicomponent systems and to see how well the alkyne group fares. First, the spacer must function as a molecular scaffold, providing spatial rigidity and integrity, and should inhibit incoherent migration of individual subunits. The alkyne bridge, especially in conjunction with terpyridyl ligands, acts as a rigid, photochemically inactive girder separating the metal centers by well-defined distances, which increase incrementally by roughly 2.5 Å per ethynyl group. Second, the spacer group must provide a means of directionality corresponding to vectorial transfer of information. Integration of an alkyne group into one of the terpyridyl ligands renders the complex sufficiently asymmetric that the electron in the MLCT triplet state is completely localized on the alkyne-containing ligand. This propensity for electron capture, together with subsequent delocalization of the electron over an extended π^* orbital, provides the directive for propagation of energy or electron transfer along the bridge. Third, the spacer must actively promote, not simply mediate, the transfer while inhibiting reverse processes that restore the ground state. In particular, the primary step should be quantitative so as to avoid undesired side reactions. The alkyne substituent group increases the triplet lifetime of $[Ru^{II}(terpy)_2]^{2+}$ at room temperature, thereby facilitating reactions that might not otherwise compete with nonradiative deactivation of the excited state. Intramolecular electron exchange (for **$Ru_2Fe(1)$** and **$Ru_2Fe(2)$**) and electron transfer (for **$Ru_2Co(1)$**

and $\mathbf{Ru_2Co(2)}$) proceed rapidly but the products survive for reasonably long times. These processes are quantitative and unidirectional.

The observation of fast energy and electron transfer in these systems and electron delocalization in the Zn^{II}-containing trinuclear complexes indicates efficient electronic coupling between the terminal $[Ru^{II}(terpy)_2]^{2+}$ subunit and the alkyne bridge. The rate of through-bond electron or hole transfer in these systems is only slightly attenuated. Rough estimates[10] for the attenuation factor (β) for hole tunneling ($\beta \approx 0.12 \pm 0.06$ Å^{-1}) and for electron tunneling ($\beta \approx 0.04 \pm 0.02$ Å^{-1}) are available from the kinetic results obtained with the Co^{II}-containing trinuclear complexes. Despite the large error limits, it seems probable that hole transfer is more attenuated than electron transfer, whilst the attenuation factor for triplet energy transfer[10] ($\beta \approx 0.17 \pm 0.05$ Å^{-1}) corresponds to the sum of factors derived for electron and hole transfer.[23] The energy of the bridge presumably decreases with increasing length, due to conjugation, which might offset the effect of increasing the length of the bridge. In this way, individual ethynyl groups exert a positive cooperative effect for promoting through-bond electron and/or hole transfer and form bridges having excellent potential as molecular wires.

Experimental Procedure

Photophysical measurements were made with a variety of laser excitation sources. In most cases the compounds were excited at 532 nm with a 30-ps laser pulse. The $[Fe^{II}(terpy)_2]^{2+}$ subunit in $\mathbf{Ru_2Fe(1)}$ and $\mathbf{Ru_2Fe(2)}$ was excited at 595 nm with a 0.3-ps laser pulse, while the $[Ru^{II}(terpy)_2]^{2+}$ chromophore in these compounds and in the corresponding Co^{II}-containing materials was excited at 440 nm. Redox potentials were measured by cyclic voltammetry with a silver reference electrode and tetrabutylammonium hexafluorophosphate as supporting electrolyte. All photophysical and electrochemical studies were made in acetonitrile, which had been deoxygenated by bubbling with N_2.

Synthesis: To an argon deoxygenated solution of complexes **Ru(1)** or **Ru(2)** (10 mg) in 7 mL of CH_3CN/H_2O 1/1 (for Fe), CH_3CN/CH_3OH 1/1 (for Co), or CH_3OH (for Zn) was added solid $FeSO_4 \cdot 7H_2O$, $CoCl_2 \cdot 6H_2O$, or $Zn(CH_3COO)_2 \cdot 2H_2O$ in threefold excess. Ten minutes exposure to ultrasound (35 kHz, 800 W, room temperature) resulted in marked and characteristic color changes due to metal complexation. The solution was stirred overnight at room temperature before NH_4PF_6 (5 equiv) in H_2O (10 mL) was added. Slow evaporation of the organic solvent resulted in precipitation of a dark solid. This precipitate was washed by centrifugation with water (3 × 10 mL) and diethyl ether (3 × 20 mL), dried under high vacuum, and recrystallized by slow evaporation of acetone from acetone/hexane solution to give analytically pure complexes.

Characterization of the complexes:

$Ru_2Zn(1)$: 87% yield; $R_f = 0.81$ (alumina, eluent CH_2Cl_2/MeOH (8/2)); Electrospray MS (in H_2O/CH_3CN (1/1), grammicidin as internal standard): *m/z*: 285.5 [$(M - 6PF_6)/6$, calcd 285.2], 500.6 [$(M - 4PF_6)/4$, calcd 500.3], 715.5 [$(M - 3PF_6)/3$, calcd 715.3], 1145.8 [$(M - 2PF_6)/2$, calcd 1145.5]; UV/Vis (CH_3CN): λ_{max} (ε [$M^{-1}cm^{-1}$]) = 498.2 nm (45000); Anal. calcd. for $C_{94}H_{62}F_{36}N_{18}P_6Ru_2Zn$ (M_r = 2580.968): C 43.75, H 2.42, N 9.77; found: C 43.53, H 2.28, N 9.49.

$Ru_2Zn(2)$: 77% yield; $R_f = 0.79$; Electrospray MS: *m/z*: 293.8 [$(M - 6PF_6)/6$, calcd 293.2], 512.9 [$(M - 4PF_6)/4$, calcd 512.3], 731.9 [$(M - 3PF_6)/3$, calcd 731.4], 1170.1 [$(M - 2PF_6)/2$, calcd 1169.5]; UV/Vis (CH_3CN): λ_{max} (ε [$M^{-1}cm^{-1}$]) = 496.6 nm (34300); Anal. calcd. for $C_{98}H_{62}F_{36}N_{18}P_6Ru_2Zn$ (M_r = 2629.012): C 44.77, H 2.38, N 9.59; found: C 44.49, H 2.17, N 9.36.

$Ru_2Fe(1)$: 91% yield; $R_f = 0.32$; Electrospray MS: *m/z*: 284.5 [$(M - 6PF_6)/6$, calcd 283.6], 498.3 [$(M - 4PF_6)/4$, calcd 497.9], 712.0 [$(M - 3PF_6)/3$, calcd 712.2], 1140.2 [$(M - 2PF_6)/2$, calcd 1140.7]; UV/Vis (CH_3CN): λ_{max} (ε [$M^{-1}cm^{-1}$]) = 596 (57500), 497 nm (43200); Anal. calcd. for $C_{94}H_{62}F_{36}N_{18}P_6Ru_2Fe + CH_3COCH_3$ (M_r = 2571.434 + 58.081): C 44.31, H 2.61, N 9.59; found: C 43.95, H 2.54, N 9.23.

$Ru_2Fe(2)$: 90% yield; $R_f = 0.10$; Electrospray MS: *m/z*: 292.4 [$(M - 6PF_6)/6$, calcd 291.6], 510.5 [$(M - 4PF_6)/4$, calcd 509.9], UV/Vis (CH_3CN): λ_{max} (ε [$M^{-1}cm^{-1}$]) = 596 (59300), 499 nm (48600); Anal. calcd. for $C_{98}H_{62}F_{36}N_{18}P_6Ru_2Fe + CH_3COCH_3$ (M_r = 2619.479 + 58.081): C 45.31, H 2.56, N 9.42; found: C 44.98, H 2.41, N 9.09.

$Ru_2Co(1)$: 94% yield; $R_f = 0.66$; Electrospray MS: *m/z*: 284.6 [$(M - 6PF_6)/6$, calcd 284.1], 499.1 [$(M - 4PF_6)/4$, calcd 498.6], 713.7 [$(M - 3PF_6)/3$, calcd 713.2], 1142.8 [$(M - 2PF_6)/2$, calcd 1142.3]; UV/Vis (CH_3CN): λ_{max} (ε [$M^{-1}cm^{-1}$]) = 503.4 nm (55600); Anal. calcd. for $C_{94}H_{62}F_{36}N_{18}P_6Ru_2Co$ (M_r = 2574.21): C 43.85, H 2.43, N 9.79; found: C 43.39, H 2.18, N 9.43.

$Ru_2Co(2)$: 94% yield; $R_f = 0.72$; Electrospray MS: *m/z*: 292.7 [$(M - 6PF_6)/6$, calcd 292.1], 511.3 [$(M - 4PF_6)/4$, calcd 510.7], 729.8 [$(M - 3PF_6)/3$, calcd 729.2]; UV/Vis (CH_3CN): λ_{max} (ε [$M^{-1}cm^{-1}$]) = 501.2 nm (51300); Anal. calcd. for $C_{98}H_{62}F_{36}N_{18}P_6Ru_2Co$ (M_r = 2622.565): C 44.88, H 2.38, N 9.61; found: C 44.42, H 2.07, N 9.29.

Received: July 13, 1995 [Z8206IE]
German version: *Angew. Chem.* **1995**, *107*, 2921–2925

Keywords: electron transfer · molecular wires · organic conductors · ruthenium compounds

[1] F. Odobel, J. P. Sauvage, *New J. Chem.* **1994**, *18*, 1139.
[2] H. M. McConnell, *J. Chem. Phys.* **1961**, *35*, 508.
[3] M. R. Wasielewski, D. G. Johnson, W. A. Svec, K. M. Kersey, D. E. Cragg, D. W. Minsek in *Photochemical Energy Conversion* (Eds.: J. R. Norris, D. Meisel) Elsevier, New York, **1989**, p. 135.
[4] A. Slama-Schwok, M. Blanchard-Desce, J. M. Lehn, *J. Phys. Chem.* **1990**, *94*, 3894.
[5] A. C. Benniston, V. Goulle, A. Harriman, J. M. Lehn, B. Marczinke, *J. Phys. Chem.* **1994**, *98*, 7798.
[6] A. E. Stiegman, V. M. Miskowski, J. W. Perry, D. R. Coulter, *J. Am. Chem. Soc.* **1987**, *109*, 5884.
[7] L. R. Khundkar, A. E. Stiegman, J. W. Perry, *J. Phys. Chem.* **1990**, *94*, 1224.
[8] F. Vögtle, M. Frank, M. Nieger, P. Belser, A. von Zelewsky, V. Balzani, F. Barigelletti, L. De Cola, L. Flamigni, *Angew. Chem.* **1993**, *105*, 1706; *Angew. Chem. Int. Ed. Engl.* **1993**, *32*, 1643.
[9] A. C. Benniston, V. Grosshenny, A. Harriman, R. Ziessel, *Angew. Chem.* **1994**, *106*, 1956; *Angew. Chem. Int. Ed. Engl.* **1994**, *33*, 1884.
[10] V. Grosshenny, A. Harriman, R. Ziessel, *Angew. Chem.* **1995**, *107*, 1211; *Angew. Chem. Int. Ed. Engl.* **1995**, *34*, 1100.
[11] R. W. Wagner, J. S. Lindsey, *J. Am. Chem. Soc.* **1994**, *116*, 9759.
[12] A. E. Stiegman, E. Graham, K. J. Perry, L. R. Khundkar, L. T. Cheng, J. W. Perry, *J. Am. Chem. Soc.* **1991**, *113*, 7658.
[13] F. Meyers, J. L. Brédas, J. Zyss, *J. Am. Chem. Soc.* **1992**, *114*, 2914.
[14] C. Dehu, F. Meyers, J. L. Brédas, *J. Am. Chem. Soc.* **1993**, *115*, 6198.
[15] H. L. Anderson, S. J. Martin, D. D. C. Bradley, *Angew. Chem.* **1994**, *106*, 711; *Angew. Chem. Int. Ed. Engl.* **1994**, *33*, 655.
[16] V. Grosshenny, R. Ziessel, *J. Organomet. Chem.* **1993**, *453*, C19.
[17] E. C. Constable, A. M. W. Cargill-Thompson, *J. Chem. Soc. Dalton Trans.* **1995**, 1615.
[18] J. P. Sauvage, J. P. Collin, J. C. Chambron, S. Guillerez, C. Coudret, V. Balzani, F. Barigelletti, L. De Cola, L. Flamigni, *Chem. Rev.* **1994**, *94*, 993.
[19] E. C. Constable, A. M. W. Cargill-Thompson, N. Armaroli, V. Balzani, M. Maestri, *Polyhedron* **1992**, *11*, 2707.
[20] E. Amouyal, M. Mouallem-Bahout, G. Calzaferri, *J. Phys. Chem.* **1991**, *95*, 7641.
[21] D. E. Morris, K. W. Hanck, M. K. DeArmond, *J. Electroanal. Chem.* **1983**, *149*, 115.
[22] R. Englman, J. Jortner, *Mol. Phys.* **1970**, *18*, 145.
[23] A reasonably linear plot was obtained for the logarithm of the inverse of the triplet lifetime versus the triplet energy for nonalkyne-substituted $[Ru^{II}(terpy)_2]^{2+}$ complexes, in accordance with the energy-gap law. The gradient of this plot was used to estimate the expected triplet lifetime (τ_O) of a nonalkyne-substituted compound having a given triplet energy. Subsequently, the magnitude of the stabilization effect (τ_T/τ_O) was derived by comparing this extrapolated lifetime with that obtained for an alkyne-substituted compound having an identical triplet energy (τ_T).
[24] Spectral characterization was accomplished by spectroelectrochemistry for $[Co^{II/III}(terpy)_2]^{2+}$ and by one-electron pulse radiolytic reduction of **Ru(1)** and **Ru(2)**.

 © VCH Verlagsgesellschaft mbH, D-69451 Weinheim, 1995 0570-0833/95/3423-2708 $ 10.00+.25/0

Butatrienes by Cumuhomologation of Propadienes

Rolf. W. Saalfrank*, Andreas Welch, and Martin Haubner

In the series of butatrienes only a few derivatives that exhibit functionality are known.[1-4] In particular, fewer than half a dozen papers have been published on formyl/acyl-[2] and acyloxy-substituted[3,4] butatrienes. Established methods for the synthesis of butatrienes[5] do not work for acyloxy-substituted butatrienes. In contrast, a strategy to generate butatrienic carboxylates by elimination from suitable substituted allenic precursors turned out to be extremely successful.[4]

Transallenation of 1,3-bis(dialkylamino)-1,3-diethoxyallenes with disubstituted malonyl chlorides yielded allene-1,1-dicarboxamides.[6-8] In addition we synthesized new *N*-phenylallenecarboxanilides starting from the reaction of 1,1-disubstituted propargylic ethers with diphenylcarbamoyl chloride and followed by reactions with sulfinyl chlorides, sulfenyl chlorides, diethoxy- and diphenylchlorophosphane, or orthoesters, and subsequent [2,3] and [3,3] sigmatropic rearrangements.[7] However, our efforts to expand this transallenation reaction to a cumuhomologation reaction failed. Thus, reaction of 1,3-bis(dialkylamino)-1,3-diethoxyallene with alkylidenemalonyl chloride yielded only the vinylacetylene isomer of the expected butatriene.[8,9]

We therefore developed a new method. Starting from alcohol **1** and potassium hypobromite we synthesized bromoalkynol **2**.[10] Reaction of **2** with the orthoesters **3** generates the bromoalkynyl vinyl ether intermediates **4**, which undergo spontaneous [3,3] sigmatropic rearrangements under the reaction conditions applied to yield bromoallenes **5**.[11] Elimination of hydrogen bromide from the allene **5a** with sodium ethanolate in ethanol gives butatriene **6**. In contrast, elimination of hydrogen bromide from the allene **5b** to give butatriene **7a** is accomplished by sodium bis(trimethylsilyl)amide, whereas **5c** is dehydrohalogenated to **7b** by use of sodium bis(trimethylsilyl)amide in combination with silver acetate. The cumuhomologation[12] reaction of the propadienes **5** to give butatrienes **6** and **7** is impressive in its simplicity and in the high yields obtained.

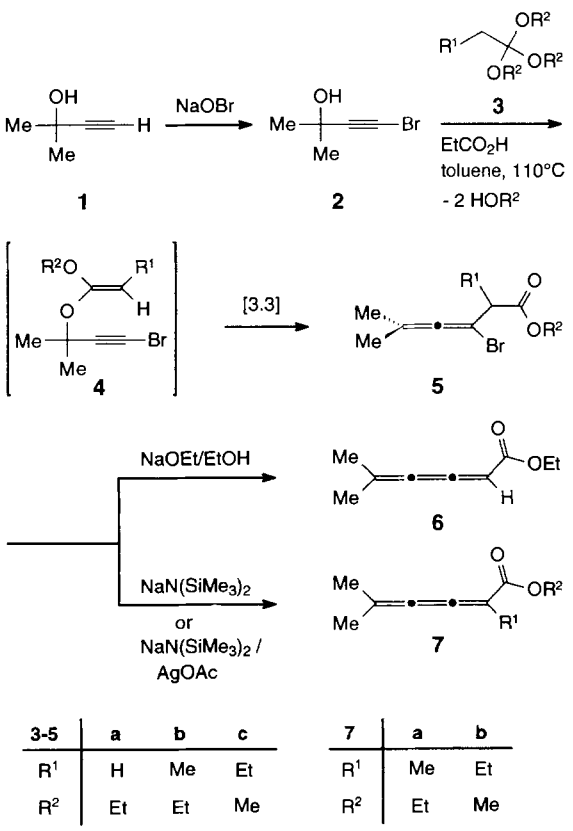

3-5	a	b	c
R^1	H	Me	Et
R^2	Et	Et	Me

7	a	b
R^1	Me	Et
R^2	Et	Me

Experimental Procedure

5: General procedure: To a solution of bromoalkynol **2** (7.8 g, 48 mmol) in dry toluene (20 mL) were added orthoester **3** (144 mmol) and five drops of propionic acid, and the reaction mixture was heated for 3 h at 105–110 °C while the generated alcohol was removed continuously in a gentle flow of nitrogen. The solvent was removed under reduced pressure, the excess of orthoester subsequently distilled off at 65–70 C/0.5 Torr over a Vigreux column, and the residue dissolved in diethyl ether (20 mL). The organic layer was washed with hydrochloric acid (50 mL, 5%) and saturated sodium bicarbonate solution (50 mL), and then dried over magnesium sulfate. The solvent was removed under reduced pressure, and the product purified by vacuum distillation. Yields: 60–85%. **5a**: colorless liquid, b.p. 83 °C (2.5 Torr); IR (NaCl): $\tilde{\nu}$ = 1970 (C=C=C), 1740 cm^{-1} (C=O); ^1H NMR ($CDCl_3$): δ = 1.28 (t, J = 7.3 Hz, 3H, CH_3); 1.82 (s, 6H, 2 CH_3); 3.41 (s, 2H, CH_2); 4.19 (q, J = 7.3 Hz, 2H, CH_2); ^{13}C NMR ($CDCl_3$): δ = 14.16, 20.51 ($3CH_3$); 44.51 (CH_2); 61.09 (OCH_2); 81.32, 105.76 (2 =C); 169.25 (C=O); 198.74 (=C=); EI-MS (70 eV): m/z (%): 232 (41) [M^+ − H].

6: Under exclusion of air and moisture, sodium ethanolate (0.3 g, 4.5 mmol) diluted in dry ethanol (10 mL) was added to a solution of bromoallene **5a** (1.0 g, 4.3 mmol) in dry ethanol (50 mL) at − 50 °C. The colorless solution turned deep yellow. The solution was allowed to warm to 20 °C within 2 h, and the solvent removed under reduced pressure. The residue was dissolved in hexane (40 mL), and after 5 min of stirring, the solvent was removed under reduced pressure. Yield: 95–98% [13], yellow liquid; IR (NaCl): $\tilde{\nu}$ = 2040 (=C=C=), 1710 cm $^{-1}$(C=O); ^1H NMR (400 MHz, $CDCl_3$): δ = 1.30 (t, J = 7.1 Hz, 3H, CH_3), 2.07, 2.13 (s, 3H, CH_3), 4.20 (q, J = 7.1 Hz, 2H, CH_2), 5.58 (s, 1H, =CH); ^{13}C NMR (100.5 MHz, $CDCl_3$): δ = 14.29, 25.23, 25.85 ($3CH_3$), 60.66 (CH_2), 93.03 (=CH), 132.20, 154.33, 165.62, 171.52 (3 =C, C=O); EI-MS (70 eV) m/z (%): 152 (100) [M^+].

7: To a solution of bromoallene **5b** [11] (1.0 g, 4 mmol) or bromoallene **5c** [11] (1.0 g, 4 mmol) in dry acetonitrile (80 mL) under exclusion of air and moisture was added sodium bis(trimethylsilyl)amide (0.75 g, 4.1 mmol) at − 40 °C [and for **7b** additionally silver acetate (1.34 g, 8 mmol)]. The solution was allowed to warm to 20 °C within 2 h, the solvent was removed under reduced pressure, the residue was dissolved in hexane (40 mL), and after 5 min of stirring the solvent was removed under reduced pressure. **7a**: Yield: 95–98% [13], yellow liquid; IR (NaCl): $\tilde{\nu}$ = 2050 cm^{-1} (=C=C=), 1710 (C=O); ^1H NMR (400 MHz, $CDCl_3$): δ = 1.30 (t, J = 7.1 Hz, 3H, CH_3), 2.04 (s, 6H, 2 CH_3), 2.07 (s, 3H, CH_3), 4.19 (q, J = 7.1 Hz, 2H, CH_2); ^{13}C NMR (100.5 MHz, $CDCl_3$): δ = 14.20, 18.01, 24.80, 25.19 ($4CH_3$), 60.74 (CH_2), 101.79, 125.69, 153.18, 166.24, 166.71 (4 =C, C=O); EI-MS (70 eV) m/z (%): 166 (100) [M^+]. **7b**: Yield: 95–98% [13], yellow liquid; IR (NaCl): $\tilde{\nu}$ = 2060 cm $^{-1}$ (=C=C=), 1700 (C=O); ^1H NMR (400 MHz, $CDCl_3$): δ = 1.10 (t, J = 7.3 Hz, 3H, CH_3), 2.05, 2.07 (s, 3H, CH_3), 2.40 (q, J = 7.3 Hz, 2H, CH_2), 3.74 (s, 3H, OCH_3); ^{13}C NMR (100.5 MHz, $CDCl_3$): δ = 12.61, 25.08, 25.23 ($3CH_3$), 24.61 (CH_2), 52.00 (OCH_3), 108.25, 125.84, 154.91, 165.59, 166.80 (4 =C, C=O); EI-MS (70 eV) m/z (%): 166 (100) [M^+].

Received: August 16, 1995 [Z8312IE]
German version: *Angew. Chem.* **1995**, *107*, 2937–2938

Keywords: butatrienes · cumulenes · propadiene

[*] Prof. Dr. R. W. Saalfrank, Dr. A. Welch, Dipl. Chem. M. Haubner
Institut für Organische Chemie der Universität Erlangen-Nürnberg
Henkestrasse 42, D-91054 Erlangen (Germany)
Telefax: Int. code + (9131)85-6864

[**] Cumulenes, Part 8. This work was supported by the Deutsche Forschungsgemeinschaft and the Fonds der Chemischen Industrie. A. W. thanks the Freistaat Bayern for a scholarship. Part 7: Ref. [8].

[1] A. Roedig, G. Zaby, *Tetrahedron Lett.* **1977**, *18*, 1771–1772; R. G. Visser, H. J. T. Bos, L. Brandsma, *Recl. Trav. Chim. Pays-Bas* **1981**, *100*, 34–36; R. W. Saalfrank, *Methoden Org. Chemie* (Houben-Weyl), 4th ed. 1952–, Vol. E15/Part 3, **1993**, p. 3108.

[2] E. M. Kosower, T. S. Sorensen, *J. Org. Chem.* **1963**, *28*, 687–692; M. Bertrand, C. Rouvier, *Bull. Soc. Chim. Fr.* **1968**, 2537–2541; H. Hopf, in *The Chemistry of Ketenes, Allenes and Related Compounds, Vol. 2* (Ed.: S. Patai), Wiley, Chichester, **1980**, p. 872; P. Battioni, L. Vo-Quang, Y. Vo-Quang, *Tetrahedron Lett.* **1972**, *13*, 4803–4806.

[3] R. Gompper, U. Wolff, *Tetrahedron Lett.* **1978**, *19*, 4263–4264.

[4] F. W. Nader, C.-D. Wacker, *Angew. Chem.* **1985**, *97*, 876–877; *Angew. Chem. Int. Ed. Engl.* **1985**, *24*, 851–852.

[5] M. Murray, *Methoden Org. Chemie* (Houben-Weyl), 4th ed., Vol. V/2a, (Ed.: E. Müller), **1977**, p. 967; P. Cadiot, W. Chodkiewicz, J. Rauss-Godineau, *Bull. Soc. Chim. Fr.* **1961**, 2176–2193; H. Hopf in *The Chemistry of Ketenes, Allenes and Related Compounds, Vol. 2 (Ed.: S. Patai)*, Wiley, Chichester **1980**, p. 779.
[6] R. W. Saalfrank, F. Schütz, U. Moenius, *Synthesis* **1985**, 1062–1067; R. W. Saalfrank, W. Rost, F. Schütz, U. Röß, *Angew. Chem.* **1984**, *96*, 597–599; *Angew. Chem. Int. Ed. Engl.* **1984**, *23*, 637–638.
[7] R. W. Saalfrank, U. Bauer, K. Hilbig, A. Welch, *Chem. Ber.* **1993**, *126*, 823–835.
[8] R. W. Saalfrank, K. Hilbig, F. Schütz, K. Peters, H. G. von Schnering, *Chem. Ber.* **1988**, *121*, 1291–1297.
[9] R. W. Saalfrank, F. Schütz, H.-U. Hummel, *Z. Naturforsch.* **1987**, *42b*, 97–100.
[10] F. Strauss, L. Kollek, W. Heyn, *Chem. Ber.* **1930**, *63*, 1868–1885.
[11] R. W. Saalfrank, A. Welch, U. Bauer, M. Haubner, *Liebigs Ann. Chem.* **1996**, in press.
[12] See also M. Parmantier, J. Galloy, M. van Meerssche, H. G. Viehe, *Angew. Chem.* **1975**, *87*, 33–34; *Angew. Chem. Int. Ed. Engl.* **1975**, *14*, 53.
[13] According to the spectra the compound was pure. Chromatography or distillation led to decomposition.

New Fluorescent Water-Soluble Taxol Derivatives**

André A. Souto, A. Ulises Acuña, José M. Andreu, Isabel Barasoain, Miguel Abal, and Francisco Amat-Guerri*

Paclitaxel (taxol, **1**), a natural diterpenoid found in the stem bark of the pacific yew *Taxus brevifolia*,[1] is one of the most promising anticancer agents for a variety of tumors,[2] due to its unique ability to inhibit cell division as well as other interphase processes by stabilizing microtubules.[3] This has stimulated an intense and detailed study in many laboratories of the chemistry and the biochemistry of this exciting antitumor agent. Reports describing the total synthesis of taxol,[4] its chemical modification and structural analysis,[5] and the search for new taxoids with improved pharmacological properties[6] have been published. The basic mechanism of the biological action of taxol is also a research topic of relevance for the development of practical therapies with this drug.[7] We have described the low-resolution solution structures of taxoid-induced microtubules,[8] the assembly of purified GDP-tubulin in the presence of taxoids, and the link between the taxoid binding and microtubule assembly reactions.[9] In the course of these investigations we realized that a fluorescent and water-soluble taxol derivative would be an enormous help, because a) it would allow the direct in vivo study of the target microtubules in tumour cell cultures by fluorescence microscopy, and b) it would provide an extremely useful tool for the study of the molecular mechanisms of taxoid-induced microtubule assembly, as well as for the discovery of other putative taxol targets and clinical diagnostic assays.

The synthesis of fluorescent taxol analogues has been attempted before but with limited success. Thus, Kingston et al.[5a] mentioned a fluorescent taxol derivative with a low-absorbance dansyl group linked through a β-alanyl amino spacer to the 7-position; the bioactivity of this compound has, however, yet to be demonstrated. Another emitting taxoid with a *meta*-amino group at the 2-benzoyl substituent, but less active than the parent drug, has also been briefly reported.[10] Somewhat related to our purpose is the synthesis of photoactivatable taxoids with an azido substituent at the 3′-benzoylamino group,[11] which are useful as photoaffinity labels in the mapping of the taxoid binding site in tubulin.

Here we report the synthesis and the characterization of two new bioactive fluorescent taxol derivatives, one of which is much more water-soluble than taxol itself, and provide an example of their use in the first direct visualization of the taxol-microtubule system in cultured cells. As it has been established that modifications at the 7-hydroxyl group do not appreciably affect the biological activity of taxol,[5b, c, 12] we selected this position for the linking of two fluorescent dyes through a spacer containing a free amino group. The synthesis of the 7-ester of taxol with L-alanine (**2**) has been previously described by Mathew et al.[13]

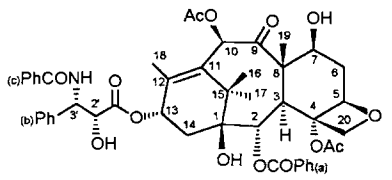

1

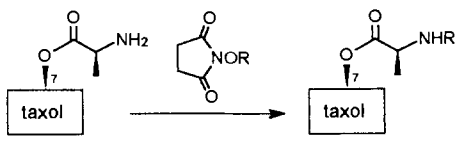

2 **3, 4**

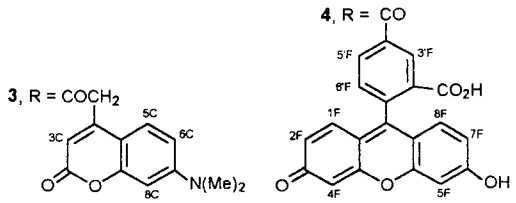

during their search for water-soluble taxoids. Starting from taxol (**1**), this synthesis comprises three steps: 1) esterification of both the 7- and 2′-OH groups of the taxol molecule with the NH_2-protected amino acid *N*-(*tert*-butyloxycarbonyl)-L-alanine (BOC-alanine), yielding 2′,7-di(BOC-L-alanyl)taxol; 2) deprotection with formic acid of both amino groups, producing 2′,7-di(L-alanyl)taxol; and 3) selective aqueous hydrolysis of the 2′-ester group, eventually yielding 7-(L-alanyl)taxol (**2**).[14] Amino acid esters of taxol deprotected at the NH_2 group are difficult to purify, because they degrade easily through epimerization and side-chain cleavage during the workup.[13] However, we have found that the crude product **2** can readily react through the free amino group with amine-reactive fluorescent dyes such as the succinimidyl esters of 7-dimethylaminocoumarin-4-acetic acid[15] or of 4′-fluoresceincarboxylic acid, to produce the corresponding conjugates **3** and **4** in good yields. The proper selection of solvent for this reaction is crucial, particularly for compound **4**. The structure of each compound was confirmed by MS-FAB$^+$ and ^{1}H NMR spectroscopy.[16] These two fluorophors were preferred, because they show spectroscopic and photophysical

[*] Dr. F. Amat-Guerri, A. A. Souto
Instituto de Química Orgánica, C. S. I. C.
Juan de la Cierva 3, E-28006 Madrid (Spain)
Telefax: Int. code +(1) 564-4853
Dr. A. U. Acuña
Instituto de Química Física Rocasolano, C. S. I. C., Madrid
Dr. J. M. Andreu, Dr. I. Barasoain, M. Abal
Centro de Investigaciones Biológicas, C. S. I. C., Madrid

[**] This work was supported by the Dirección General de Investigación Científica y Técnica of Spain (Projects PB93-0126 and PB92-0007) and by Acción Especial C. S. I. C. Taxol was provided by Bristol-Myers Squibb, the owner of the registered trade name. A. A. S. acknowledges a fellowship from CNPq (Brazil). We thank J. Evangelio for the HPLC analysis.

properties that are optimal for our purposes: large absorption coefficients at wavelengths well separated from the protein's intrinsic absorption and matching available laser excitation sources, as well as large emission yield and anisotropy. The synthetic method reported here is of general applicability for the introduction of fluorophors into the taxol molecule and can be used to generate a family of new fluorescent taxol derivatives.

An important limitation in the clinical use of taxol is its low solubility in water (5 μM),[17] and therefore it is not surprising that much effort is aimed at the synthesis of soluble taxol derivatives. This has been achieved by introducing polar or ionic substituents at the 2′ and/or 7-hydroxyl groups, in many cases linked through spacers.[18] In this way water solubilities as high as 0.01 M[18e–e] and, in the case of a derivative with a 7-(polyethylene glycol) chain, 0.1 M[18f] have been demonstrated, although in many cases the biological activity of these drugs, when tested in whole cells, was seriously impaired relative to that of the parent compound **1**. In the case of the fluorescent derivatives **3** and **4**, although the water solubility of the former (approximately 1 μM) is less than that of taxol, that of the bioactive fluorescein taxoid **4** is about two orders of magnitude higher (0.3 mM) than that of the natural drug.

The biochemical and cell biological properties of compound **4** are being compared with those of taxol. Interestingly, preliminary results indicate that compound **4** retains essentially the activity of the parent drug, and that it is able to induce the assembly of otherwise inactive GDP-tubulin into microtubules, a unique characteristic of active taxoids.[9] When this probe is tested in epithelial PtK2 cultured cells, the microtubule system can readily be seen under the fluorescence microscope (Fig. 1).

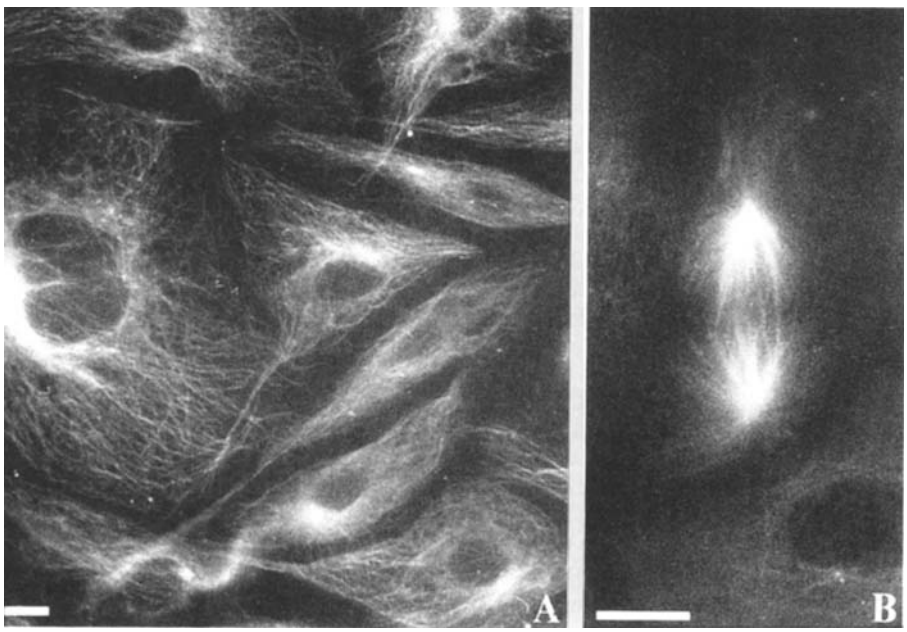

Fig. 1. Image of microtubules in epithelial PtK2 cultured cells with the fluoresceinated taxol derivative **4** [19]. A: A representative view of interphase cells. B: Enlargement of a bright mitotic spindle in a dividing cell. The bar corresponds to 10 μm.

Experimental Procedure

3: To a solution of crude 7-(L-alanyl)taxol **2** (10 mg, 10.8 mmol) and Et_3N (15 μL, 108 mmol) in dioxane (1 mL) was added another solution of succinimidyl 7-dimethylaminocoumarin-4-acetate (5.6 mg, 16.2 μmol) in dioxane (0.5 mL). After stirring for 24 h at room temperature in the dark, the solvent was removed. The crude product **3** was purified by preparative TLC (silicagel, 1:1 ethyl acetate-dichloromethane). Yield 9.5 mg (77%). M.p. 182–185 °C. HPLC purity >96% (C-4 column, 20 to 80% acetonitrile in water as eluent). FAB$^+$-MS (*m*-NBA, *m/z*: 1176.50 ($M + Na^+$), 1154.50 (MH^+, calculated for $C_{63}H_{67}N_3O_{18}$ 1153.44); UV/Vis (MeOH): λ_{max} (ε) = 376 nm (20200 $M^{-1}\,cm^{-1}$); emission (excitation at 376 nm): λ_{max} 462 nm; ^1H NMR (500 MHz, $CDCl_3$, 30 °C, TMS): δ = 8.10 (d, J = 7.3 Hz, 2H, *o*-H of Ph(a)), 7.75 (d, J = 7.3 Hz, 2H, *o*-H of Ph(c)), 7.61 (t, J = 7.5 Hz, 1H, *p*-H of Ph(a)), 7.50 (m, 6H, H-5C, *m*-H of Ph(a), *o*-H of Ph(b), *p*-H of Ph(c)), 7.41 (m, 4H, *m*-H of Ph(b), *m*-H of Ph(c)), 7.35 (t, J = 7.3 Hz, 1H, *p*-H of Ph(b)), 6.98 (d, J = 9.0 Hz, 1H, 3′-N*H*), 6.67 (d, J = 8.9 Hz, 1H, NH of Ala), 6.59 (dd, J = 2.4, 8.9 Hz, 1H, H-6C), 6.48 (d, J = 2.4 Hz, 1H, H-8C), 6.17 (t, J = 8.5 Hz, 1H, H-13), 6.12 (s, 1H, H-3C), 6.09 (s, 1H, H-10), 5.78 (dd, J = 2.4, 9.0 Hz, 1H, H-3′), 5.65 (d, J = 6.7 Hz, 1H, H-2), 5.60 (dd, J = 7.3, 10.4 Hz, 1H, H-7), 4.89 (d, J = 8.9 Hz, 1H, H-5), 4.78 (dd, J = 2.4, 5.1 Hz, 1H, H-2′), 4.68 (m, 1H, CH of Ala), 4.30 (d, J = 8.3 Hz, 1H, H-20a), 4.16 (d, J = 8.3 Hz, 1H, H-20b), 3.88 (d, J = 6.7 Hz, 1H, H-3), 3.65 (s, 2H, CH_2CONH), 3.56 (d, J = 5.1 Hz, 1H, 2′-O*H*), 3.03 (s, 6H, $N(CH_3)_2$), 2.47 (m, 1H, H-6a), 2.36 (s, 3H, 4-CH_3CO), 2.32 (m, 2H, H-14), 2.10 (s, 3H, 10-CH_3CO), 1.84 (m, 1H, H-6β), 1.79 (s, 3H, H-18), 1.76 (s, 3H, H-19), 1.73 (s, 1H, 1-O*H*), 1.19 (s, 3H, H-17), 1.13 (overlapped d, 3H, CH_3 of Ala), 1.12 (s, 3H, H-16).

4: To a solution of crude **2** (10 mg, 10.8 mmol) in DMF (1 mL) and aqueous pH 9 carbonate/bicarbonate buffer (1 mL) was added another solution of succinimidyl fluorescein-4′-carboxylate (7.7 mg, 16.2 mmol) in the same solvent mixture (1 mL). After stirring for 2 h, the solvent was removed, and the crude product **4** was purified by preparative TLC (silica gel, 1:4 ethyl acetate–dichloromethane). Yield 8.0 mg (60%). M.p. >300 °C. HPLC purity >92% (C-18 column, 20 to 80% acetonitrile in water as eluent). FAB$^+$-MS (*m*-NBA), *m/z*: 1305.50 [$M + Na^+$], 1283.50 (MH^+, calculated for $C_{71}H_{66}N_2O_{21}$ 1282.42); UV/Vis (water): λ_{max} 494 nm; (basic MeOH) λ_{max} 499 nm (ε 70000 $M^{-1}\,cm^{-1}$); emission (in water, excitation at 494 nm): λ_{max} 520 nm; ^1H NMR (500 MHz, D_2O, 40 °C, ref. H_2O at δ = 4.61): δ = 8.20 (s, 1H, H-3′F), 8.00 (d, J = 8.0 Hz, 3H, *o*-H of Ph(a), H-5′F), 7.81 (d, J = 7.9 Hz, 2H, *o*-H of Ph(c)), 7.68 (t, J = 8.0 Hz, 1H, *p*-H of Ph(a)), 7.63 (t, J = 7.9 Hz, 1H, *p*-H of Ph(c)), 7.58 (t, J = 8.0 Hz, 2H, *m*-H of Ph(a)), 7.54 (t, J = 7.9 Hz, 2H, *m*-H of Ph(c)), 7.50 (overlapped d, 2H, H-1F, H-8F), 7.49 (s, 2H, H-4F, H-5F), 7.31 (m, 1H, *p*-H of Ph(b)), 7.13 (m, 2H, *m*-H of Ph(b)), 6.69 (d, J = 8.0 Hz, 4H, H-2F, H-7F, *o*-H of Ph(b)), 6.62 (d, J = 8.4 Hz, 1H, H-6′F), 6.34 (s, 1H, H-10), 6.10 (t, J = 9.0 Hz, 1H, H-13), 5.64 (d, J = 7.7 Hz, 1H, H-2), 5.52 (m, 1H, H-7), 5.46 (d, J = 7.1 Hz, 1H, H-3′), 5.04 (m, 1H, H-5), 4.85 (d, J = 7.1 Hz, 1H, H-2′), 4.73 (q, J = 7.5 Hz, 1H, CH of Ala), 4.24 (m, 2H, H-20), 3.79 (d, J = 7.7 Hz, 1H, H-3), 2.64 (m, 1H, H-6a), 2.29 (s, 3H, 4-CH_3CO), 2.19 (s, 3H, 10-CH_3CO), 1.91 (m, 2H, H-6b, H-14a), 1.86 (s, 3H, H-19), 1.78 (s, 3H, H-18), 1.74 (m, 1H, H-14b), 1.45 (d, J = 7.5 Hz, 3H, CH_3 of Ala), 1.16 (s, 6H, H-16, H-17).

Received: July 18, 1995 [Z 8224 IE]
German version: *Angew. Chem.* **1995**, *107*, 2910–2912

Keywords: drugs · fluorescence markers · taxol

[1] M. C. Wani, H. L. Taylor, M. E. Wall, P. Coggon, A. T. McPhail, *J. Am. Chem. Soc.* **1971**, *93*, 2325–2327.

[2] Recent reviews on the taxol therapy: a) K. Gelmon, *The Lancet* **1994**, *344*, 1267–1272; b) E. K. Rowinsky, R. C. Donehower, *New Engl. J. Med.* **1995**, *332*, 1004–1014.

[3] a) P. B. Schiff, J. Fant, S. B. Horwitz, *Nature* **1979**, *277*, 665–667; b) P. B. Schiff, S. B. Horwitz, *Proc. Natl. Acad. Sci. USA* **1980**, *77*, 1561–1565.

[4] The total synthesis of taxol has been reported independently by the groups of Nicolaou and Holton: a) K. C. Nicolaou, Z. Yang, J. J. Liu, H. Ueno, P. G. Nantermet, R. K. Guy, C. F. Clairborne, J. Renaud, E. A. Couladouros, K. Paulvannan, E. J. Sorensen, *Nature* **1994**, *367*, 630–634; K. C. Nicolaou, P. G. Nantermet, H. Ueno, R. K. Guy, E. A. Couladouros, E. J. Sorensen, *J. Am. Chem. Soc.* **1995**, *117*, 624–633; K. C. Nicolaou, J.-J. Liu, Z. Yang, H. Ueno, E. J. Sorensen, C. F. Clairborne, R. K. Guy, C.-K. Hwang, M. Nakada, P. G. Nantermet, *ibid.* **1995**, *117*, 634–644; K. C. Nicolaou, Z. Yang, J.-J. Liu, P. G. Nantermet, C. F. Clairborne, J. Renaud, R. K. Guy, K. Shibayama, *ibid.* **1995**, *117*, 645–652; K. C. Nicolaou, H. Ueno, J.-J. Liu, P. G. Nantermet, Z. Yang, J. Renaud, K. Paulvannan, R. Chadha, *ibid.* **1995**, *117*, 653–659; see also K. C. Nicolaou, R. K. Guy, *Angew. Chem.* **1995**, *107*, 2247; *Angew. Chem. Int. Ed. Engl.* **1995**, *34*, 2079–2090; b) R. A. Holton, C. Somoza, H.-B. Kim, F. Liang, R. J. Biediger, P. D. Boatman, M. Shindo, C. C. Smith, S. Kim, H. Nadizadeh, Y. Suzuki, C. Tao, P. Vu, S. Tang, P. Zhang, K. K. Murthi, L. N.

Gentile, J. H. Liu, *J. Am. Chem. Soc.* **1994**, *116*, 1597–1598; R. A. Holton, H.-B. Kim, C. Somoza, F. Liang, R. J. Biediger, P. D. Boatman, M. Shindo, C. C. Smith, S. Kim, H. Nadizadeh, Y. Suzuki, C. Tao, P. Vu, S. Tang, P. Zhang, K. K. Murthi, L. N. Gentile, J. H. Liu, *ibid.* **1994**, *116*, 1599–1600. c) For a commented history of both synthetic achievements see: L. Wessjohann, *Angew. Chem.* **1994**, *106*, 1011; *Angew. Chem. Int. Ed. Engl.* **1994**, *33*, 959–961; S. B. Horwitz, *Nature* **1994**, *367*, 593–594.

[5] Selected reviews on the chemistry and biology of taxol: a) D. G. I. Kingston, *Pharmacol. Ther.* **1991**, *52*, 1–34; b) *Trends Biotechnol.* **1994**, *12*, 222–227; c) K. C. Nicolaou, W.-M. Dai, R. K. Guy, *Angew. Chem.* **1994**, *106*, 38; *Angew. Chem. Int. Ed. Engl.* **1994**, *33*, 15–44. The conformation of taxol in several organic solvents has been studied: S. V. Balasubramanian, J. L. Alderfer, R. M. Straubinger, *J. Pharm. Sci.* **1994**, *83*, 1470–1476.

[6] a) F. Guéritte-Voegelein, D. Guénard, F. Lavelle, M.-T. Le Goff, L. Mangatal, P. Potier, *J. Med. Chem.* **1991**, *34*, 992–998; b) C. S. Swindell, N. E. Krauss, S. B. Horwitz, I. Ringel, *ibid.* **1991**, *34*, 1176–1184; c) G. Appendino, H. C. Ozen, P. Gariboldi, B. Gabetta, E. Bombardelli, *Fitoterapia* **1993**, *64*, 47–81; d) A. N. Boa, P. R. Jenkins, N. J. Lawrence, *Contemp. Org. Synth.* **1994**, *1*, 47–75.

[7] a) W. D. Howard, S. N. Timasheff, *J. Biol. Chem.* **1988**, *263*, 1342–1346; b) S. B. Horwitz, *Trends Pharmacol. Sci.* **1992**, *13*, 134–136; c) R. B. Dye, S. P. Fink, R. C. Williams, Jr., *J. Biol. Chem.* **1993**, *268*, 6874–6850; d) M. A. Jordan, R. J. Toso, H. Thrower, L. Wilson, *Proc. Natl. Acad. Sci. USA* **1993**, *90*, 9552–9556; e) E. Nogales, S. G. Wolf, I. A. Khan, R. F. Ludueña, K. H. Downing, *Nature* **1995**, *375*, 424–427.

[8] a) J. M. Andreu, J. Bordas, J. F. Díaz, J. García de Ancos, R. Gil, F. J. Medrano, E. Nogales, E. Pantos, E. Towns-Andrews, *J. Mol. Biol.* **1992**, *226*, 169–184; b) J. M. Andreu, J. F. Díaz, R. Gil, J. M. de Pereda, M. García de Lacoba, V. Peyrot, C. Briand, E. Towns-Andrews, J. Bordas, *J. Biol. Chem.* **1994**, *269*, 31785–31792.

[9] a) J. F. Díaz, J. M. Andreu, *Biochemistry* **1993**, *32*, 2747–2755; b) J. F. Díaz, M. Menendez, J. M. Andreu, *ibid.* **1993**, *32*, 10067–10077.

[10] Y. Han, A. G. Chaudhary, M. D. Chordia, D. L. Sackett, D. G. I. Kingston, S. B. Hastie, *Mol. Biol. Cell* **1994**, *5*, 284a.

[11] a) G. I. Georg, T. C. Boge, H. Park, R. H. Himes, *Bioorg. Med. Chem. Lett.* **1995**, *5*, 615–620; b) C. Combeau, A. Commerçon, C. Mioskowski, B. Rousseau, F. Aubert, M. Goeldner, *Biochemistry* **1994**, *33*, 6676–6683; c) S. Rao, N. E. Krauss, J. M. Heerding, C. S. Swindell, I. Ringel, G. A. Orr, S. B. Horwitz, *J. Biol. Chem.* **1994**, *269*, 3132–3134; d) C. S. Swindell, J. M. Heerding, N. E. Krauss, S. B. Horwitz, S. Rao, I. Ringel, *J. Med. Chem.* **1994**, *37*, 1446–1449; e) D. Dasgupta, H. Park, G. C. Harriman, G. I. Georg, R. H. Himes, *ibid.* **1994**, *37*, 2976–2980. The ester 7-[(*m*-azido-*o*-nitro)benzoyl]taxol has been also used as a photoaffinity analog: J. M. Carboni, V. Farina, S. Rao, S. I. Hauck, S. B. Horwitz, I. Ringel, *J. Med. Chem.* **1993**, *36*, 513–515.

[12] W. Mellado, N. F. Magri, D. G. I. Kingston, R. Garcia Arenas, G. A. Orr, S. B. Horwitz, *Biochem. Biophys. Res. Commun.* **1984**, *124*, 329–336.

[13] A. E. Mathew, M. R. Mejillano, J. P. Nath, R. H. Himes, V. J. Stella, *J. Med. Chem.* **1992**, *35*, 145–151.

[14] Our total yield of ester **2** was about 70%.

[15] Direct esterification of the 7-hydroxyl in 2′-[(2,2,2-trichloroethyl)oxycarbonyl]taxol (N. F. Magri, D. G. I. Kingston, *J. Org. Chem.* **1986**, *51*, 797–802) with 7-dimethylaminocoumarin-4-acetic acid under different experimental conditions was unsuccessful, probably due to a severe steric hindrance, as molecular models suggest.

[16] ROESY experiments showed that in $CDCl_3$ solution the coumarin group in compound **3** must be close to protons H-3 and H-7 of the taxol moiety, because measurable NOE effects were observed with proton H-3C in the coumarin group. Cross peaks between the aromatic signals in the taxol moiety were not found, which supports the assumption that the corresponding rings are not close (absence of clustering), as expected in this nonpolar solvent (D. G. Vander Velde, G. I. Georg, G. L. Grunewald, C. W. Gunn, L. A. Mitscher, *J. Am. Chem. Soc.* **1993**, *115*, 11650–11651).

[17] K. C. Nicolaou, C. Riemer, M. A. Kerr, D. Rideout, W. Wrasidio, *Nature* **1993**, *364*, 464–466.

[18] a) H. M. Deutsch, J. A. Glinski, M. Hernandez, R. D. Haugwitz, V. L. Narayanan, M. Suffness, L. H. Zalkow, *J. Med. Chem.* **1989**, *32*, 788–792; b) Z. Zhao, D. G. I. Kingston, A. R. Crosswell, *J. Nat. Prod.* **1991**, *54*, 1607–1611; c) K. C. Nicolaou, R. K. Guy, E. N. Pitsinos, W. Wrasidlo, *Angew. Chem.* **1994**, *106*, 1672; *Angew. Chem. Int. Ed. Engl.* **1994**, *33*, 1583–1587; d) L. G. Paloma, R. K. Guy, W. Wrasidlo, K. C. Nicolaou, *Chem. Biol.* **1994**, *1*, 107–112; e) K. C. Nicolaou, J. Renaud, P. G. Nantermet, E. A. Couladouros, R. K. Guy, W. Wrasidlo, *J. Am. Chem. Soc.* **1995**, *117*, 2409–2420; f) R. B. Greenwald, A. Pendri, D. Bolikal, *J. Org. Chem.* **1995**, *60*, 331–336; g) Y. Ueda, J. D. Matiskella, A. B. Mikkilineni, V. Farina, J. O. Knipe, W. C. Rose, A. M. Casazza, D. M. Vyas, *Bioorg. Med. Chem. Lett.* **1995**, *5*, 247–252.

[19] PtK2 cells attached to a coverslip were cultured overnight with the taxol derivative **4** (1 μM), washed twice with phosphate buffered saline, mounted without fixation in 0.13 M glycine buffer pH 8.6, 0.20 M NaCl, 70% glycerol, and observed. The cells were cultured and photographed as described: C. de Inés, D. Leynadier, I. Barasoain, V. Peyrot, P. Garcia, C. Briand, G. A. Renner, C. Temple, *Cancer Res.* **1994**, *54*, 75–84.

Saccharide–Peptide Hybrids as Novel Oligosaccharide Mimetics**

Hans Peter Wessel,* Catherine M. Mitchell, Cinta Maria Lobato, and Gérard Schmid

The important role of carbohydrates in physiological processes has been increasingly recognized in recent years. The establishment of "glycobiology" as a new area of research has evoked growing interest in carbohydrate mimetics. Examples of monosaccharide mimetics are hydroxylated piperidine derivatives, which have been investigated particularly in their role as glycosidase inhibitors.[1] Oligosaccharides have been mimicked by C-disaccharides[2] or C,C-trisaccharides[3] in which the interglycosidic oxygen atom is replaced by a methylene group. In other disaccharide analogues, pyranose rings are coupled directly,[4] through substituted methylene groups,[5] or also through more extended units.[6] We present here novel oligosaccharide mimetics consisting of peptide-linked monomers.

Carbohydrate amino acids such as muramic acid[7] are well known in nature and have also been prepared synthetically, for example to induce defined peptide conformations.[8] Carbohydrate amino acids of type **1** not only contain an intact carbohydrate epitope, but can also undergo reaction to form amide linkages. This procedure has the advantage over oligomerization through glycosidic linkages that no stereoisomers are formed; in addition, methods for the oligomerization of amino acids in solution or on solid phase are well established. The oligomerization of identical or different carbohydrate amino acids, and thus the formation of novel compound libraries, should be feasible. The approach is exemplified[9] here by the synthesis of a tetramer containing normuramic acid (**2**)[10] as a building block.

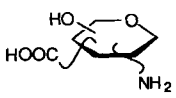

1

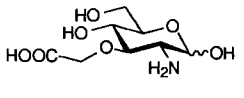

2

This building block is characterized by the free anomeric center, which provides the option of introducing a hydrophobic group to increase protein binding;[11] in the present example we have employed benzyl glycosides. Normuramic acid derivatives suited for oligomerization can be prepared in very good yield; reaction of the known[12] glucopyranoside **3** with a bromoacetic acid ester results in **4**, which can be deblocked to furnish the free acid **5** or, alternatively, amine **6** (Scheme 1).

Coupling to give dimers has been carried out by the diester method (Scheme 2); the known[13] benzyl glucopyranoside **7** was chosen as a terminal building block. The benzylidene protective groups were removed at the dimer level, since the cleavage from higher oligomers proved to be troublesome. The activating reagent of our choice for the highly polar acid derivative **9** was 2-chloro-4,6-dimethoxy-1,3,5-triazine (CDMT);[14] the coupling could be carried out in DMF as a solvent.

[*] Dr. H. P. Wessel, C. M. Mitchell,[+] Dr. C. M. Lobato,[+] Dr. G. Schmid
Pharma Division, Preclinical Research
F. Hoffmann-La Roche Ltd
CH-4002 Basel (Switzerland)
Telefax: Int. code +(61)688-6459
E-mail: hans_p.wessel@roche.com

[+] Post-doctoral fellow (1993) from the University of Barcelona, Spain. Present address: Institute of Organic Chemistry, University of Basel

[+] Summer student 1993 from the University of Basel, Switzerland. Present address: Institute of Organic Chemistry, University of Würzburg (Germany)

[**] We wish to thank Roland Keller for technical assistance.

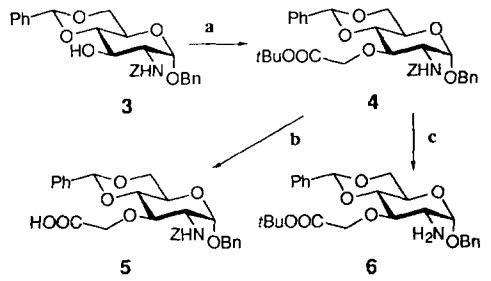

Scheme 1. a) $BrCH_2COOtBu$, KOH, dioxane, 55 °C, 2 h, 91%; b) $KOCMe_3$, THF, H_2O, 0 °C, 2 min, 95%; c) H_2, Pd/C, MeOH/THF, 20 °C, 1.5 h, 96% (Z = benzyloxycarbonyl).

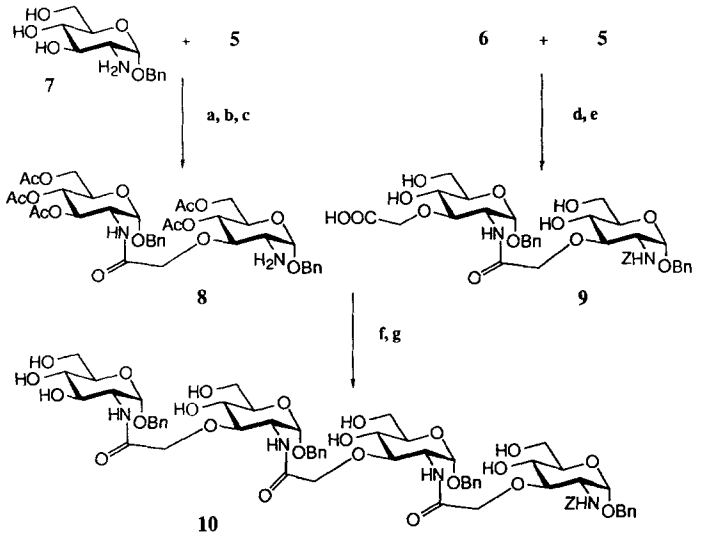

Scheme 2. a) $ClCOOiBu$, NEt3, THF/MeCN, 20 °C, 12 h; Ac_2O, Py, 87%; b) AcOH 80%, 80 °C, 1.5 h; Ac_2O, Py, 20 °C, 18 h, 90%; c) H_2, Pd/C (10%), dioxane/H_2O, 20 °C, 1.5 h, 95%; d) $ClCOOiBu$, NEt_3, THF/MeCN, 20 °C, 30h, 84%; e) AcOH 80%, 80 °C, 1.5 h; 0.3 M NaOMe, dioxane/MeOH, 20 °C, 10 h, 85%; f) CDMT, *N*-methylmorpholine, DMF, 50 °C, 18h; Ac_2O, Py 40%; g) 0.3 M NaOMe, dioxane/methanol, 20 °C, 2.5 h, 81%.

This block synthesis of tetramer **10**[15] demonstrates the comparatively efficient access to a novel class of oligosaccharide mimetics comprising peptide–saccharide hybrids.

Experimental Procedure

To a suspension of **9** (771 mg) in DMF (3 mL), activated with CDMT (176 mg) in the presence of *N*-methylmorpholine (121 µL) for 1.5 h, is added a solution of **8** (789 mg) in DMF (2 mL). After stirring for 18 h at 50 °C the reaction mixture is concentrated and acetylated with Ac_2O/pyridine. The solvent is removed, and the residue chromatographed over silica gel (eluent: ethyl acetate/hexane). Pure product fractions (684 mg, 40%) are deacetylated in a mixture of methanol (6 mL) and dioxane (4 mL) containing 0.3 M sodium methanolate solution in methanol (1 mL). Neutralization with ion exchange resin (Amberlite IR120 H^+) and chromatography over silica gel (ethyl acetate/methanol/water 85/10/5) affords pure amorphous **10** (81%).

Received: July 18, 1995 [Z 8225 IE]
German version: *Angew. Chem.* **1995**, *107*, 2920–2921

Keywords: carbohydrate amino acids · compound libraries · normuramic acid · oligosaccharide mimetics

[1] a) E. Truscheit, W. Frommer, B. Junge, L. Müller, D. D. Schmidt, W. Wingender, *Angew. Chem.* **1981**, *93*, 738; *Angew. Chem. Int. Ed. Engl.* **1981**, *20*, 744; b) L. E. Fellows, *Chem. Brit.* **1987**, *23*, 847; c) N. M. Carpenter, G. W. Fleet, I. Cenci di Bello, B. Winchester, L. E. Fellows, R. J. Nash, *Tetrahedron Lett.* **1989**, *30*, 7261; d) M. L. Sinott, *Chem. Rev.* **1990**, *90*, 1171; e) G. Legler, *Adv. Carbohydr. Chem. Biochem.* **1990**, *48*, 319; f) H. Paulsen, M. Matzke, B. Orthen, R. Nuck, W. Reutter, *Liebigs Ann. Chem.* **1990**, 953; g) G. Papandreou, M. K. Tong, B. Ganem, *J. Am. Chem. Soc.* **1993**, *115*, 11682.

[2] a) D. Rouzaud, P. Sinaÿ, *J. Chem. Soc. Chem. Commun.* **1983**, 1353; b) B. Giese, T. Witzel, *Angew. Chem.* **1986**, *98*, 459; *Angew. Chem. Int. Ed. Engl.* **1986**, *25*, 450; c) O. R. Martin, F. Xie, R. Kakarla, R. Benhamza, *Synlett* **1993**, 165; d) B. Vauzeilles, D. Cravo, J.-M. Mallet, P. Sinaÿ, *ibid.* **1993**, 522; e) A. Wei, Y. Kishi, *J. Org. Chem.* **1994**, *59*, 88; f) L. Lay, F. Nicotra, C. Pangrazio, L. Panza, G. Russo, *J. Chem. Soc. Perkin Trans. 1* **1994**, 333; g) H. Dietrich, R. R. Schmidt, *Liebigs Ann. Chem.* **1994**, 975; h) R. Ferritto, P. Vogel, *Tetrahedron Asymm.* **1994**, *5*, 2077.

[3] T. Haneda, P. G. Goekjian, S. H. Kim, Y. Kishi, *J. Org. Chem.* **1992**, *57*, 490.

[4] a) R. J. Ferrier, N. Prasad, *J. Chem. Soc. C* **1969**, 581; b) J. Jurczak, T. Bauer, S. Jarosz, *Tetrahedron Lett.* **1984**, *25*, 4809; c) B. Giese, B. Rückert, K. S. Gröninger, R. Muhn, H. J. Lindner, *Liebigs Ann. Chem.* **1988**, 997; d) R. W. Armstrong, B. R. Teegarden, *J. Org. Chem.* **1992**, *57*, 915; e) H. P. Wessel, G. Englert, *J. Carbohydr. Chem.* **1995**, *14*, 179.

[5] a) B. Aebischer, J. H. Bieri, R. Prewo, A. Vasella, *Helv. Chim. Acta* **1982**, *65*, 2251; b) J. M. Beau, P. Sinaÿ, *Tetrahedron Lett.* **1985**, *26*, 6189, 6193; c) S. J. Danishefsky, W. H. Pearson, F. D. Harvey, C. J. Maring, J. P. Springer, *J. Am. Chem. Soc.* **1985**, *107*, 1256; d) I. M. Dawson, T. Johnson, R. M. Paton, R. A. C. Rennie, *J. Chem. Soc. Chem. Commun.* **1988**, 1339; e) W. B. Motherwell, B. K. Ross, M. J. Tozer, *Synlett* **1989**, 68; f) A. de Raadt, A. E. Stütz, *Carbohydr. Res.* **1991**, *220*, 101; g) R. R. Schmidt, A. Beyerbach, *Liebigs Ann. Chem.* **1992**, 983; h) H. M. Binch, A. M. Griffin, S. Schmidetzki, M. V. J. Ramsey, T. Gallagher, F. W. Lichtenthaler, *J. Chem. Soc. Chem. Commun.* **1995**, 967.

[6] a) S. Jarosz, D. Mootoo, B. Fraser-Reid, *Carbohydr. Res.* **1986**, *147*, 59; b) S. M. Daly, R. W. Armstrong, *Tetrahedron Lett.* **1989**, *30*, 5713; c) J. Alzeer, A. Vasella, *Helv. Chim. Acta* **1995**, *78*, 177.

[7] Muramic acid (= (*R*)-2-amino-3-*O*-(1-carboxyethyl)-2-deoxy-D-glucose) is found in the bacterial cell wall.

[8] E. Graf von Roedern, H. Kessler, *Angew. Chem.* **1994**, *106*, 684; *Angew. Chem. Int. Ed. Engl.* **1994**, *33*, 687.

[9] A similar approach has been mentioned in the context of nucleoside mimetics synthesis: K. C. Nicolaou, H. Flörke, M. G. Egan, T. Barth, V. A. Estevez, *Tetrahedron Lett.* **1995**, *36*, 1775.

[10] a) R. Gigg, P. M. Carroll, *Nature* **1961**, *191*, 495; b) T. Miyazaki, Y. Matsushima, *Bull. Chem. Soc. Jpn.* **1968**, *41*, 2723.

[11] Dissociation constants of carbohydrate–protein complexes are generally in the upper micromolar range, as hydrogen bonding dominates, and strong hydrophobic interactions are missing; cf. C.-H. Wong, R. L. Halcomb, Y. Ichikawa, T. Kajimoto, *Angew. Chem.* **1995**, *1067*, 569; *Angew. Chem. Int. Ed. Engl.* **1995**, *34*, 521.

[12] P. C. Wyss, J. Kiss, *Helv. Chim. Acta* **1979**, *58*, 1833.

[13] W. Meyer zu Reckendorf, B. Radatus, E. Bischof, R. Weber, *Chem. Ber.* **1974**, *107*, 869. We have prepared **7** from the *N*-Z-protected precursor (H. P. Wessel, *J. Carbohydr. Chem.* **1988**, *7*, 263).

[14] Z. J. Kaminski, *Synthesis* **1987**, 419.

[15] Physical data of **10**: $[\alpha]_D^{20} = +125$ ($c = 0.2$ in methanol); MS (laser desorption) m/z 1353 (90%, $[M+Na]^+$); ^1H NMR (400 MHz, $[D_6]$DMSO, TMS): δ = 8.20 (d, 1H, J = 8.7 Hz, NH), 8.15 (d, 1H, J = 8.6 Hz, NH), 7.94 (d, 1H, J = 8.6 Hz, NH), 7.76 (br. d, 1H, $J \approx 7.2$ Hz, NH).

Synthesis and X-ray Structure of a Shape-Persistent Macrocyclic Amphiphile

Sigurd Höger* and Volker Enkelmann

The study of shape-persistent, structurally defined macrocycles capable of binding guest molecules within their cavities has attracted a great deal of interest during the last few years.[1] For example, naturally occuring cyclodextrins and their derivatives are able to bind organic substrates through hydrophobic interactions and are also capable of catalyzing chemical reactions of certain substrates.[2] Host molecules having a hydrophobic exterior and a hydrophilic interior have also been synthesized and studied in detail as models for enzymes.[3] A great

[*] Dr. S. Höger, Dr. V. Enkelmann
Max-Planck-Institut für Polymerforschung
Ackermannweg 10, D-55128 Mainz (Germany)
Telefax: Int. code +(6131)379100

deal of effort has been directed recently towards the preparation of macrocycles with cavities having nanometer dimensions.[4] In addition to their ability to complex large guest molecules, large macrocycles may play an important role in the design of organic zeolites.[5]

Here we describe the synthesis and X-ray structure of **1**, an interesting example of a macrocyclic amphiphile, which has a shape-persistent molecular backbone and hydrophilic and hydrophobic substituents. Our research has been directed towards the synthesis of molecules of defined shape, size, and functionality,[6] in which the polarity of the interior depends on the polarity of the surrounding solvent and/or confined guest molecules.

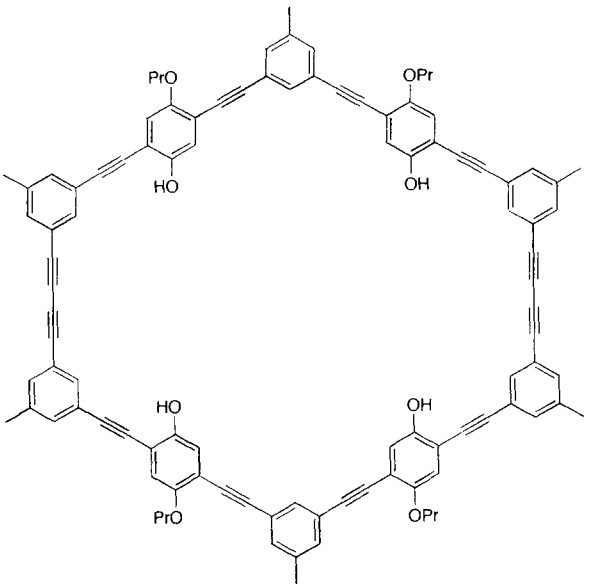

1

The preparation of large amounts of the macrocycle **1** described here depended on an efficient route to monoprotected diynes of type **2**. Preliminary attempts to obtain the trimethylsilyl (TMS) analogue of **2**, starting from the corresponding diyne, by deprotonation with EtMgBr and trapping of the acetylide with TMSCl led to a statistical mixture of starting material and mono- and bis-TMS-protected compounds. We were not able to separate larger amounts of these materials because of their similar R_f values. Therefore, it was necessary to find an alternative way to **2** (Scheme 1). The key steps in this approach are the selective coupling of a terminal alkyne with an aryl iodide in the presence of an aryl bromide[7] and the site-selective removal of the TMS group in the presence of the triisopropylsilyl (TIPS) group.[8]

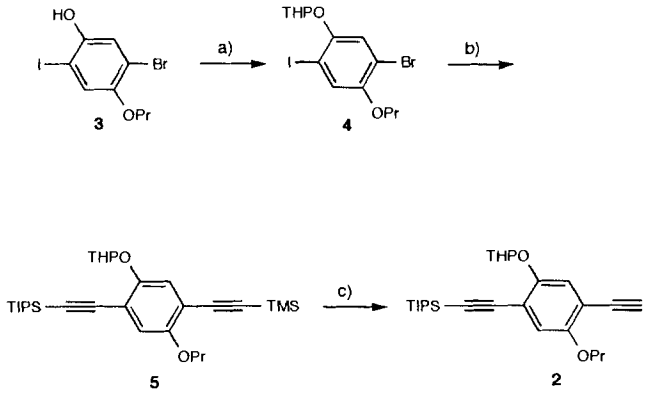

Scheme 1. a) 3,4-Dihydro-2*H*-pyran, CH_2Cl_2, H^+, 0 °C 1 h, room temperature (RT), 1 h (90%); b) 1. 1.1 equiv TIPS-acetylene, 4 mol% $[PdCl_2(PPh_3)_2]$, 2 mol% CuI, piperidine, 55 °C, 4 d; 2. 2 equiv TMS-acetylene, 4 d (82%); c) 1 N NaOH, MeOH/THF (1/1), RT, 30 min (96%).

Phenol **3**[9] was first converted into the tetrahydro-(2*H*)-pyranyl (THP) ether **4**, which was coupled successively in a one-pot Pd-catalyzed reaction with 1.1 equivalents of TIPS-acetylene for four days at 55 °C and then two equivalents of TMS-acetylene for an additional four days at the same temperature to yield **5**. Selective removal of the TMS group was accomplished by stirring a solution of **5** in MeOH/THF (1/1) in the presence of a small amount of 1 N aqueous NaOH. This method can be used to prepare **2** in 20–30 g quantities.

Palladium-catalyzed coupling of **2** with 3,5-diiodotoluene, followed by removal of the TIPS protecting group, yielded tetrayne **6** (Scheme 2). Coupling of **6** with 3-bromo-5-iodotoluene gave the dibromide **7**. The much higher reactivity of aryl iodides over aryl bromides prevents, in this case, formation of oligomeric side products. Coupling of **7** with TMS-acetylene, followed by removal of the TMS group, generated the bisacetylene **8**. The

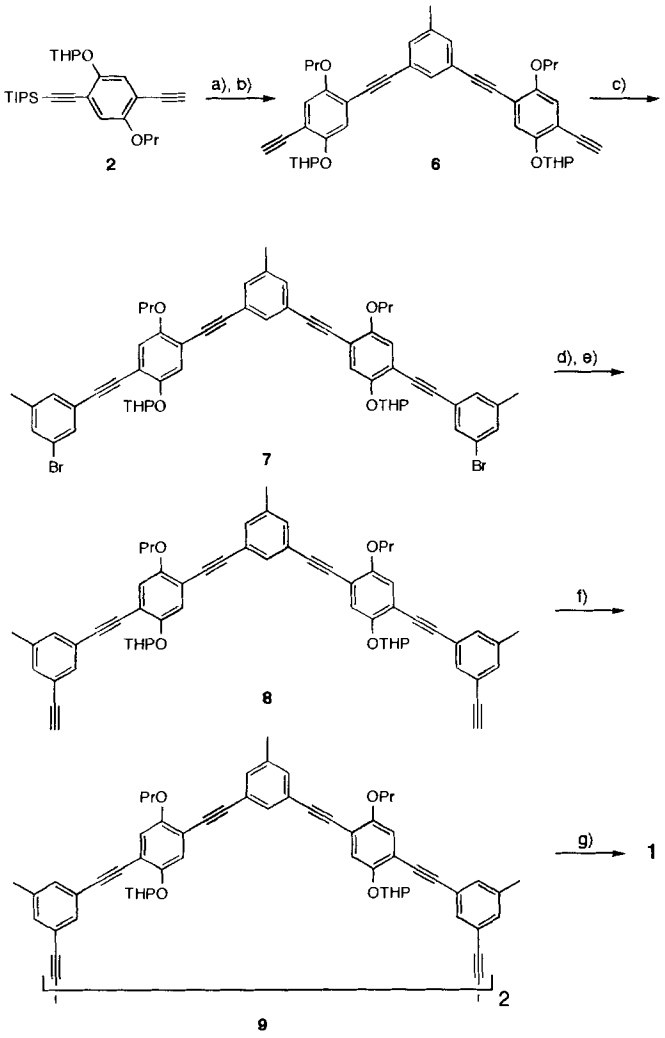

Scheme 2. a) 3,5-diiodotoluene, 4 mol% $[PdCl_2(PPh_3)_2]$, 2 mol% CuI, piperidine, 55 °C, 14 h; b) Bu_4NF, THF, RT, 2 h (88%); c) 3-bromo-5-iodotoluene, 4 mol% $[PdCl_2(PPh_3)_2]$, 2 mol% CuI, piperidine, 55 °C, 14 h (84%); d) TMS-acetylene, 4 mol% $[PdCl_2(PPh_3)_2]$, 2 mol% CuI, piperidine, 55 °C, 4 d; e) 1 N NaOH, MeOH/THF (1/1), RT, 3 h (70%); f) CuCl/$CuCl_2$, pyridine, RT (60–65%); g) CH_2Cl_2/MeOH (2/1), H^+, 1 d (quantitative).

THP-protected macrocycle **9** was obtained by a modified Eglington–Glaser coupling[10] of **8** under high-dilution conditions.[11] The crude product was recrystallized from CH_2Cl_2 to give **9** in 45% yield as slightly yellow crystals, which were unstable when removed from the mother liquor.[12] Acid-catalyzed deprotection of **9** produced compound **1** in nearly quantitative yield.[13] All synthetic procedures outlined can be scaled up such that this new amphiphile is available in gram quantities.

In its synthesis macrocycle **1** is formed as a slightly yellow precipitate, which darkens in the presence of air but is stable under an inert atmosphere. The compound is marginally soluble in most organic solvents but readily soluble in THF, pyridine, pyridine–water mixtures (with only limited amounts of water) at room temperature and in tetrachloroethane at elevated temperatures. Single crystals suitable for X-ray analysis were obtained by recrystallization from pyridine. Like crystals of **9**, these also decompose, although more slowly, when removed from the mother liquor due to loss of solvent. A suitable crystal was therefore embedded in Inertoil and the data collection was performed at 165 K.[14] Under these conditions the crystal was stable for several weeks and a good-quality X-ray structure of **1** was obtained (Figs. 1 and 2). The *R*-value after anisotropic refinement was 0.063.[15]

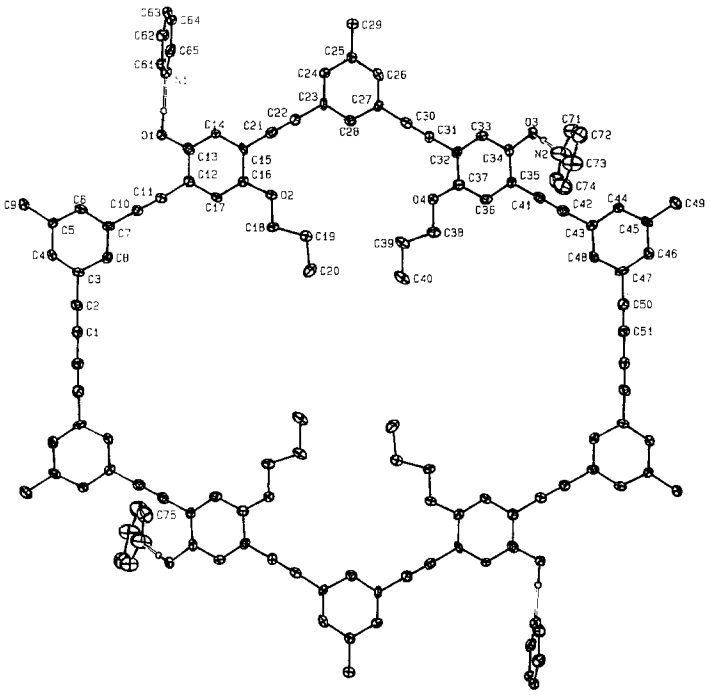

Fig. 1. Crystal structure of **1**; top view of the macrocycle. For clarity only the hydrogen bonded pyridine molecules are shown.

The nonbonding distances of C51–C51′ (2.400(1) nm) and C28–C28′ (2.009(1) nm) give an idea of the size of the interior of the macrocycle. In its crystal structure **1** has a center of symmetry. For each macrocycle eight molecules of pyridine were localized. Four of them form hydrogen bonds (distances: O3···N2: 2.85 Å, O1···N1: 2.72 Å) with the phenolic OH groups on the outside of the ring. The remaining pyridines pack within the crystal lattice without specific interactions with the macrocycle. One of them is localized at the center of symmetry, which leads to orientational disorder. In this case the N and one C atom occupy the same position with a probability of 50%. The macrocycle itself is not planar; the torsion angle around the

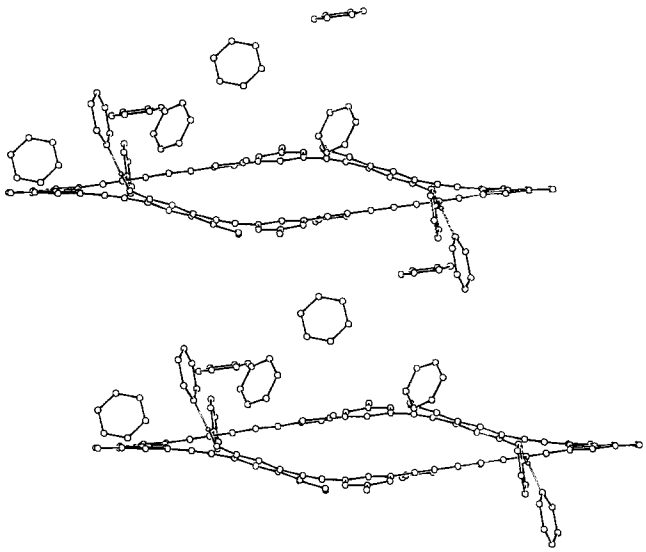

Fig. 2. Crystal structure of **1**; view perpendicular to the stacking axis.

diyne bridge is 6.7°. It is interesting to note that the deformation of the macrocycle is not symmetrical. The section ring(C3...8)/ring(C12...17)/ring(C23...28) is nearly linear, whereas the rest (C30...47) shows a strong bending (C27-C30-C31 173.3(10)°, C30-C31-C32 175.4(10)° deviate significantly from linearity). As a result of this torsion and deformation the arene units C23... C28 and C23′... C28′ are separated by a vertical distance of 3.4 Å within the macrocycle. ^{1}H NMR data at room temperature and above show that in solution the macrocycle is either symmetric or, more probable, in several, rapidly interconverting conformations. It is still unclear whether the propyloxy groups, which are coplanar with their aromatic rings in the crystal structure, prefer to be on the inside of the ring in solution.

Compound **1** is the first example of an amphiphilic shape-persistent macrocycle, in which free rotation about diphenyl acetylene units in the molecule should result in either a more hydrophilic or a more hydrophobic interior. Current studies of **1**, derivatives of **1**, and amphiphilic macrocycles of other size and structure are addressing this issue.

Received: July 21, 1995 [Z8231IE]
German version: *Angew. Chem.* **1995**, *107*, 2917–2919

Keywords: amphiphiles · macrocycles · nanostructures · supramolecular chemistry

[1] Recent examples: a) H. L. Anderson, A. Bashall, K. Hendrick, M. McPartlin, J. K. M. Sanders, *Angew. Chem.* **1994**, *106*, 445; *Angew. Chem. Int. Ed. Engl.* **1994**, *33*, 429, and references therein; b) M. R. Ghadiri, K. Kobayashi, J. R. Granja, R. K. Chadha, D. E. McRee, *ibid.* **1995**, *107*, 76 and **1995**, *34*, 93; c) D. J. Cram, *Nature* **1992**, *356*, 29; d) J. M. Lehn, *Science* **1993**, *260*, 1762; e) F. Diederich, *Nature* **1994**, *369*, 199.

[2] a) G. Wenz, *Angew. Chem.* **1994**, *106*, 851; *Angew. Chem. Int. Ed. Engl.* **1994**, *33*, 803; b) W. Saenger, *ibid.* **1980**, *92*, 343 and **1980**, *19*, 344.

[3] a) Y. H. Kim, O. W. Webster, *J. Am. Chem. Soc.* **1990**, *112*, 4592; b) F. Diederich, K. Dick, D. Griebel, *ibid.* **1986**, *108*, 2273, and references therein.

[4] a) J. S. Moore, J. Zhang, *Angew. Chem.* **1992**, *104*, 873; *Angew. Chem. Int. Ed. Engl.* **1992**, *31*, 922; b) P. Timmermann, W. Verboom, F. C. J. M. van Veggel, W. P. van Hoorn, D. N. Reinhoudt, *ibid.* **1994**, *106*, 1313 and **1994**, *33*, 1292; c) A. M. Boldi, F. Diederich, *ibid.* **1994**, *106*, 482 and **1994**, *33*, 486; d) A. de Meijere, S. Kozhushkov, C. Puls, T. Haumann, R. Boese, M. J. Cooney, L. T. Scott, *ibid.* **1994**, *106*, 934 and **1994**, *33*, 869; A. de Meijere, S. Kozhushkov, T. Haumann, R. Boese, C. Puls, M. J. Cooney, L. T. Scott, *Chem. Eur. J.* **1995**, *1*, 124.

[5] Z. Wu, J. S. Moore, *Polym. Prepr. (Am. Chem. Soc. Div. Polym. Chem.)* **1993**, *34*(1), 122.

[6] M. Antonietti, S. Heinz, *Nachr. Chem. Techn. Lab.* **1992**, *40*, 310.

[7] a) K. Sonogashira, Y. Tohda, N. Hagihara, *Tetrahedron Lett.* **1975**, 4467; b) Y. Tohda, K. Sonogashira, N. Hagihara, *Synthesis* **1977**, 777.
[8] P. Fitton, A. E. Rick, *J. Organomet. Chem.* **1971**, *93*, 254.
[9] S. Höger, unpublished.
[10] D. O'Krongly, S. R. Denmade, M. Y. Chiang, R. Breslow, *J. Am. Chem. Soc.* **1985**, *107*, 5544.
[11] The cyclization was performed by the dropwise addition of a pyridine solution of **8** with a syringe pump over 96 hours to a slurry of CuCl and $CuCl_2$ in pyridine at room temperature. After workup no signals attributable to alkyne protons were found in the ^1H NMR spectrum. The yield of **9** by determined by HPLC was 60–65%; no starting material was evident.
[12] Macrocycles with analogous behavior have been described by others, e.g. a) J. S. Moore, *Polym. Prepr. (Am. Chem. Soc. Div. Polym. Chem.)*, **1993**, *34*(1), 170; b) A. de Meijere, F. Jaekel, A. Simon, H. Borrmann, J. Köhler, D. Johnels, L. T. Scott, *J. Am. Chem. Soc.* **1991**, *113*, 3935.
[13] Selected spectroscopic data of **1**: ^1H NMR (300 MHz, [D$_5$]pyridine, 50° C): $\delta = 1.11$ (t, $J = 7.4$ Hz, 12H), 1.87 (m, 8H), 2.14 (s, 6H), 2.15 (s, 12H), 4.09 (t, $J = 6.5$ Hz, 8H), 4.60 (br. s, OH), 7.29 (m, 4H), 7.31 (m, 8H), 7.46 (s, 4H), 7.69 (s, 4H), 7.80 (s, 2H). Characteristic ^{13}C NMR signals (75 MHz, [D$_5$]pyridine, 50 °C): $\delta = 74.8$, 81.9, 87.4, 88.7, 94.1, 94.6.
[14] Crystal structure data for **1**: $C_{102}H_{72}O_8 \cdot 8C_5H_5N$, triclinic, space group $P\bar{1}$, $a = 12.297(2)$, $b = 13.963(5)$, $c = 17.454(6)$ Å; $\alpha = 85.642(31)$, $\beta = 80.644(22)$, $\gamma = 68.344(23)$°, $V = 2887$ Å^3, $Z = 2$, $\rho_{calcd} = 1.184$ g cm^{-3}, $\mu = 5.435$ cm^{-1}, $T = 165$ K. A crystal with the dimensions $0.4 \times 0.2 \times 0.1$ mm was placed in Inertoil (Type RS 3000, Riedel de Haen). Nonius CAD4 diffractometer, graphite-monochromated $Cu_{K\alpha}$ radiation, $\lambda = 1.5418$ Å, $\theta_{max} = 62°$, $\theta/2\theta$ scans, 9473 independent reflections, of which 4280 were observed ($I > 3\sigma(I)$), empirical absorption correction. The structure was solved by direct methods. Refinement was done by full-matrix least squares analysis with anisotropic temperature factors for C, H, and O. Hydrogen atoms were refined with fixed isotropic temperature factors in the riding mode. The refinement converged at $R = 0.063$ and $R_w = 0.067$. Difference Fourier analysis showed no peaks beyond $+0.35$ or -0.27 e Å^{-3}. Further details on the crystal structure investigation may be obtained from the Director of the Cambridge Crystallographic Data Centre, 12 Union Road, GB-Cambridge CB2 1EZ (UK), on quoting the full journal citation.
[15] X-ray data of other shape-persistent macrocycles having cavities of nanometer dimensions: a) D. Venkataraman, S. Lee, J. Zhang, J. S. Moore, *Nature* **1994**, *371*, 591; b) H. L. Anderson, A. Bashall, K. Henrick, M. McPartlin, J. K. M. Sanders, *Angew. Chem.* **1994**, *106*, 445; *Angew. Chem. Int. Ed. Engl.* **1992**, *31*, 429; c) S. Anderson, H. L. Anderson, A. Bashall, M. McPartlin, J. K. M. Sanders, *ibid.* **1995**, *107*, 1196 and **1995**, *34*, 1096.

Structure and Magnetic Properties of a Decanuclear Oxoiron(III) Cluster: A Further Step to Understanding Iron Aggregation Processes**

Andrea Caneschi, Andrea Cornia, Antonio C. Fabretti, and Dante Gatteschi*

The hydrolysis of iron salts can be controlled by organic ligands so as to yield soluble molecular aggregates with nanometer dimensions, which can often be isolated in crystalline form and structurally characterized.[1–3] Though some work has been carried out directly in aqueous environments, the use of nonaqueous media with a low water content has led to the synthesis of an unexpected variety of polynuclear clusters.

[*] Prof. D. Gatteschi, Dr. A. Caneschi
Dipartimento di Chimica, Università degli Studi di Firenze
I-50144 Florence (Italy)
Telefax: Int. code +(55)354845
e-mail: gattesch@chimat1.chim1.unifi.it
Dr. A. Cornia, Prof. A. C. Fabretti
Dipartimento di Chimica, Università degli Studi di Modena (Italy)

[**] This work was supported by the Italian Ministero dell'Università e della Ricerca Scientifica e Tecnologica. The authors acknowledge the Centro Interdipartimentale di Calcolo Automatico e Informatica Applicata of Modena University for computer facilities.

Our group has isolated cyclic hexairon(III) complexes of general formula **1** (M = Li, Na; HL = Hdbm, Hpmdbm[5]).[1, 4]

$[MFe_6(OCH_3)_{12}L_6]^+$ **1**

These compounds are reliable structural models of OH-bridged polynuclear complexes believed to exist in aqueous solution. In the course of this study Fe_2,[4] Fe_3,[6] and Fe_4[4] complexes were also isolated. Though these complexes contain CH_3O and L ligands, they are structurally reminiscent of the infinite lattices of iron oxides and hydroxides.[6] Here we report the synthesis, crystal structure, and magnetic properties of the novel decairon(III) cluster $\mathbf{2} \cdot x CHCl_3$, which extends the previously

$[Fe_{10}O_4(OCH_3)_{16}(dbm)_6] \cdot x CHCl_3$ $\mathbf{2} \cdot x CHCl_3$

mentioned series of polynuclear compounds and has an inorganic core arising from hydrolysis.

The crystal lattice[7] of $\mathbf{2} \cdot x CHCl_3$ contains decairon clusters **2** and highly disordered chloroform molecules. The structure of **2** is shown in Figure 1. A view of the iron–oxygen core is presented in Figure 2. Cluster **2** can be formally broken down into two pentanuclear subunits related by an inversion center, which are assigned primed and unprimed atom labels in Figures 1 and 2. The iron(III) ions in each subunit are found to lie on a plane (max. deviation 0.08 Å). The intralayer Fe–Fe separations are

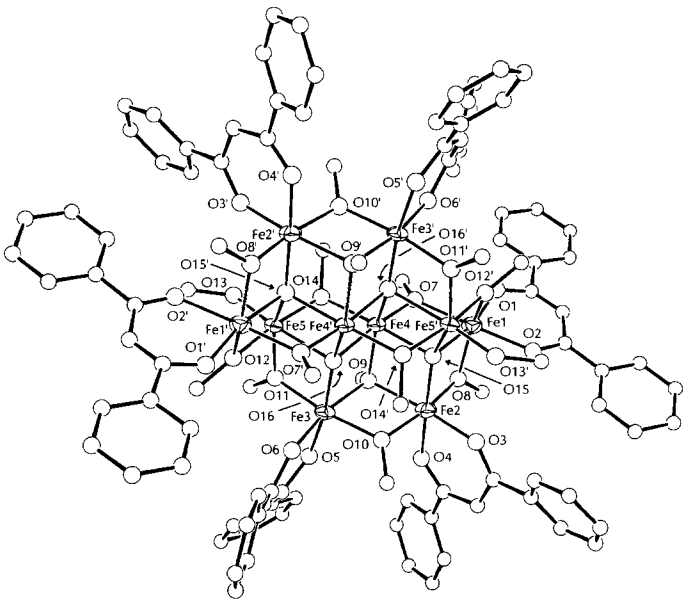

Fig. 1. Structure of **2** (ORTEP representation with atom labels). Hydrogen atoms have been omitted for clarity. An inversion center relates the primed atoms to the unprimed ones. Thermal ellipsoids for iron atoms enclose 35% probability. All the remaining atoms are represented by spheres of arbitrary radius. Relevant distances [Å] and angles [°]: O1-Fe1 2.07(3), O2-Fe1 2.06(3), O7-Fe1 2.00(3), O8-Fe1 2.05(2), O15-Fe1 2.07(3), O12'-Fe1 1.97(3), O3-Fe2 1.98(3), O4-Fe2 2.07(2), O8-Fe2 2.00(3), O9-Fe2 2.15(2), O10-Fe2 2.02(3), O15-Fe2 1.96(2), O5-Fe3 2.00(2), O6-Fe3 2.00(3), O9-Fe3 2.15(3), O10-Fe3 1.99(3), O11-Fe3 2.00(3), O16-Fe3 1.89(2), O7-Fe4 1.94(3), O9-Fe4 2.17(2), O14-Fe4 1.98(2), O15-Fe4 2.04(2), O16-Fe4 2.09(3), O16'-Fe(4) 2.00(3), O16-Fe5 2.20(3), O11-Fe5 1.97(2), O12-Fe(5) 2.05(3), O13-Fe5 1.90(3), O14-Fe5 2.03(3), O15'-Fe5 2.04(2); Fe2-O15-Fe1 99(1), Fe2-O15-Fe5' 148(1), Fe4-O15-Fe5' 99(1), Fe1-O15-Fe5' 100(1), Fe4-O15-Fe1 98(1), Fe4-O15-Fe2 103.7(9), Fe4-O16-Fe3 105(1), Fe4'-O16-Fe3 155(2), Fe4'-O16-Fe4 94(1), Fe4'-O16-Fe5 95(1), Fe3-O16-Fe5 100(1), Fe4-O16-Fe5 96(1), O12'-Fe1-O8 152(1), O16'-Fe4-O9 157(1).

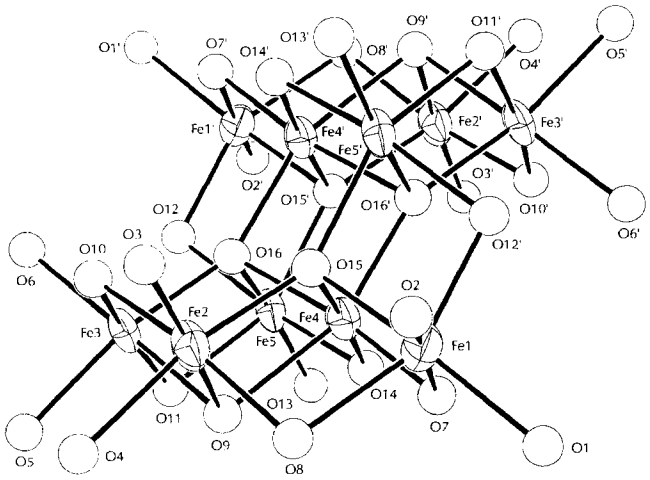

Fig. 2. ORTEP view of the iron–oxygen core of **2**. See legend to Figure 1 for details.

in the range 3.07–3.20 Å, but the shortest Fe–Fe contact occurs between metal ions belonging to different layers (Fe4–Fe4′ 2.99 Å). μ_2-OCH_3, μ_3-OCH_3, and μ_4-O ligands interconnect the iron(III) ions and are key structural elements in the architecture of the core. Notably, the iron atoms Fe4 and Fe5 are bound to CH_3O and O ligands only. The two subunits are connected through O12, O15, O16, and their symmetry equivalents. As a result, severe distortions affect the binding geometry of the μ_4-O ligands and the coordination spheres of Fe1 and Fe4.

It can be easily seen in Figure 2 that the oxygen atoms in each pentanuclear fragment form two layers on each side of the Fe_5 moiety. Planes *a* (O1, O4, O5, O7, O8, O9, O11, O13, O14) and *b* (O2, O3, O6, O10, O12, O15, O16) form a dihedral angle of 7° and are parallel to the best plane through the Fe centers (deviation 5°). The O–O separations within planes *a* and *b* average 3.0(2) and 3.1(2) Å, respectively.

The whole architecture of the iron–oxygen core can be rationalized in a straightforward manner by referring to an idealized overall cubic closest packing (ccp) of oxygen atoms (Fig. 3).[8] The O atoms belonging to planes *b* and *b*′ are thus in the same plane $b + b'$, which now comprises 14 atoms. The iron ions occupy the octahedral holes between plane $b + b'$ and planes *a* and *a*′.

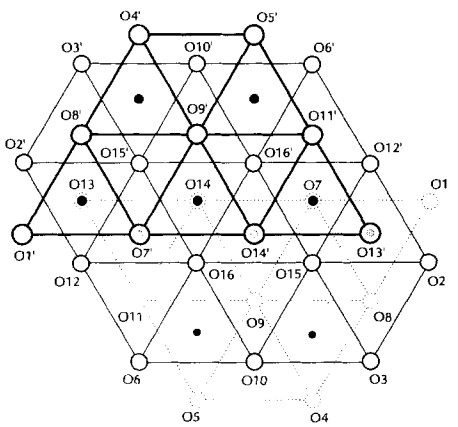

Fig. 3. The arrangement of the oxygen atoms in the core of **2**. Bold, normal, and dotted lines denote the upper (*a*′), middle ($b + b'$), and lower (*a*) layers, respectively. The iron atoms are represented by filled circles. An inversion center relates primed atoms to unprimed ones. Three iron atoms are hidden under O13′, O14′, and O7′.

Two well-defined layers of closest packed oxygen atoms have been identified in a number of alkoxoiron(III) clusters with β-diketonate ligands.[1, 4, 6] The cores of the clusters $[Fe_{17}O_4(OH)_{16}(heidi)_8(H_2O)_{12}]^{3+}$ and $[Fe_{19}O_6(OH)_{14}(heidi)_{10}(H_2O)_{12}]^{+}$,[3, 5] which assemble in water/pyridine, are characterized by an analogous double layer of closest packed oxygen atoms from hydroxo ligands. More than two layers of oxygen atoms displaying cubic closest packing similar to that in **2** are apparent in few polyiron(III) aggregates such as the octahedral clusters $[N(CH_3)_4]_2[Fe_6O(thme)_6]\cdot 4CH_3OH$ and $Na_2[Fe_6O(OCH_3)_{18}]\cdot 6CH_3OH$,[5, 9] and in two mixed-valent dodecairon clusters.[4, 10] Structurally, these compounds resemble the solid-state structures of iron oxides and hydroxides such as FeO (wüstite), and γ-FeOOH (lepidocrocite).[6] The structure of α-FeOOH (göthite) is based on a hexagonal closest packing (hcp) of oxygen atoms. Among the products arising from the methanolysis of Fe^{II}/Fe^{III} in the presence of β-diketonates, complex **2** is unique in that its core contains O ligands of hydrolytic origin.[11] The isolation and characterization of **2** can be of particular relevance to the study of iron(III) aggregation processes. The presence of two layers of metal atoms suggests that formation of **2** may be a result of water-promoted condensation of two pentanuclear clusters having the tentative formula $[Fe_5(OCH_3)_{11}(dbm)_4]$ [Eq. (a)] and the same layered CdI_2-type

$$2[Fe_5(OCH_3)_{11}(dbm)_4] + 4H_2O \longrightarrow [Fe_{10}O_4(OCH_3)_{16}(dbm)_6] + 6CH_3OH + 2Hdbm \quad (a)$$

structure found in triiron(III), tetrairon(III) and hexairon(III) species with the same ligands.

The temperature dependence of the magnetic susceptibility of **2** in an applied field of 1 T has been investigated. χ increases continuously as the temperature is lowered. χT decreases smoothly from 18.8 emu K mol^{-1} at 260 K to 9.0 emu K mol^{-1} at 60 K. Below about 60 K the decrease becomes steeper and χT reaches 1.2 emu K mol^{-1} at 2.7 K. The χT value at 260 K is substantially lower than that calculated for ten uncoupled $S = 5/2$ spins (43.8 emu K mol^{-1}, $g = 2.00$). The Curie–Weiss law is roughly followed for $T > 150$ K ($C = 33.90$ emu K mol^{-1}, $\theta = -210.5$ K). The overall magnetic behavior is therefore indicative of the presence of rather strong antiferromagnetic interactions between the $S = 5/2$ iron(III) centers, with a low value of S in the ground state, probably $S = 0$. Intercluster interactions must play a minor role, since an analysis of the crystal packing revealed no magnetically significant contact between clusters. Given the complexity of the network of possible exchange–coupling interactions, it is not possible at this stage to give any explanation of the nature of the ground state. The fact that no maximum in the susceptibility is observed seems to be indicative of spin frustration effects, in agreement with the numerous triangles present in the spin topology. Some further hints on the nature of the lowest lying spin states can be obtained from the field dependence of the magnetization at 4.2 K. In the range 0–7 T the magnetization increases continuously and almost linearly, with no tendency toward saturation at the highest fields. This points to the presence of a ladder of closely spaced spin states near the ground state, in other words, a solid-state behavior that is presumably related to the compact structure of the core.[12]

Experimental Procedure

Iron(III) chloride (1.622 g, 10 mmol) was allowed to react with Hdbm (2.243 g, 10 mmol, 1 equiv) and 4 equiv of sodium methoxide in 150 mL of methanol (distilled over Mg/I_2 shortly before use). The resulting yellow solid is soluble in organic solvents; prolonged diffusion of methanol vapors in a chloroform solution led to

 © VCH Verlagsgesellschaft mbH, D-69451 Weinheim, 1995 0570-0833/95/3423-2717 $ 10.00+.25/0

yellow-orange block-shaped crystals in very low yield (5–10%). After removal of the lattice chloroform molecules in vacuo, the compound analyzed (C, H, Fe) satisfactorily as $[Fe_{10}O_4(OCH_3)_{16}(dbm)_6]$. The crystals are *extremely* air-sensitive; one large individual was sealed in a thin-walled capillary tube containing the mother liquor and was used for an X-ray diffraction experiment.

Received: July 21, 1995 [Z 8236 IE]
German version: *Angew. Chem.* **1995**, *107*, 2862–2864

Keywords: aggregation processes · complexes with oxygen ligands · iron compounds · magnetic properties

[1] A. Caneschi, A. Cornia, S. J. Lippard, *Angew. Chem.* **1995**, *107*, 511; *Angew. Chem. Int. Ed. Engl.* **1995**, *34*, 467, and references therein.
[2] V. S. Nair, K. S. Hagen, *Inorg. Chem.* **1994**, *33*, 185; J.-M. Vincent, S. Ménage, J.-M. Latour, A. Bousseksou, J.-P. Tuchagues, A. Decian, M. Fontecave, *Angew. Chem.* **1995**, *107*, 199; *Angew. Chem. Int. Ed. Engl.* **1995**, *34*, 205.
[3] A. K. Powell, S. L. Heath, D. Gatteschi, L. Pardi, R. Sessoli, G. Spina, F. Del Giallo, F. Pieralli, *J. Am. Chem. Soc.* **1995**, *117*, 2491.
[4] A. Caneschi, A. Cornia, A. C. Fabretti, D. Gatteschi, S. J. Lippard, W. Malavasi, R. Grandi, L. Schenetti, R. Sessoli, unpublished results.
[5] Abbreviations used: Hdbm = dibenzoylmethane (1,3-diphenyl-1,3-propanedione); Hpmdbm = 1,3-di(*p*-methoxyphenyl)-1,3-propanedione; Hdpm = dipivaloylmethane (2,2,6,6-tetramethyl-3,5-heptanedione); H_3thme = 1,1,1-tris(hydroxymethyl)ethane; H_3heidi = $N(CH_2COOH)_2(CH_2CH_2OH)$.
[6] A. Caneschi, A. Cornia, A. C. Fabretti, D. Gatteschi, W. Malavasi, *Inorg. Chem.* **1995**, *34*, 4660.
[7] Crystal data for **2** ($x = 1$): $Fe_{10}C_{107}H_{115}O_{32}Cl_3$, $M_r = 2577.9$, crystal size $0.2 \times 0.3 \times 0.4$ mm, $Mo_{K\alpha}$ radiation, $\lambda = 0.71069$ Å, triclinic, space group $P\bar{1}$, $a = 15.072(2)$, $b = 18.047(3)$, $c = 29.105(4)$ Å, $\alpha = 91.02(1)$, $\beta = 94.72(1)$, $\gamma = 112.77(1)°$, $Z = 2$, $V = 7264(3)$ Å^3, $T = 298$ K, $5° < 2\theta < 40°$, $\omega - 2\theta$ scan mode, $\rho_{calcd} = 1.18$ g cm^{-3}, $\mu = 10.2$ cm^{-1}, 9740 reflections collected, 9520 independent (4028 with $I > 4\sigma(I)$); Lorentz polarization but no absorption correction applied; direct methods (SHELX86); for 742 parameters $R(F_o) = 0.121$ and $R_w(F_o) = 0.128$; anisotropic thermal parameters for metal and chlorine atoms only; hydrogen atoms treated as fixed contributors in calculated positions with $B(H) = 1.2\ B(C)$. Two centrosymmetric clusters are located around inversion centers at (0, 0.5, 0.5) and (0.5, 0, 0). The metrical parameters of the two clusters show insignificant differences. The relatively high R values reflect the bad diffracting quality of the crystals and the high degree of disorder of the lattice chloroform. One disordered chloroform molecule per cluster was clearly located, but several low-intensity peaks (< 1.2 e Å^{-3}) were still present in the final ΔF map. The given formula weight and the calculated density, which is quite low for this kind of compound, must therefore be taken as lower limits. Further details of the crystal structure investigation may be obtained from the Director of the Cambridge Crystallographic Data Centre, 12 Union Road, GB-Cambridge CB21EZ (UK), on quoting the full journal citation.
[8] A. F. Wells, *Structural Inorganic Chemistry*, 5th ed., Clarendon Press, Oxford, **1984**, p. 258.
[9] K. Hegetschweiler, H. W. Schmalle, H. M. Streit, W. Schneider, *Inorg. Chem.* **1990**, *29*, 3625; K. Hegetschweiler, H. W. Schmalle, H. M. Streit, V. Gramlich, H.-U. Hund, I. Erni, *ibid.* **1992**, *31*, 1299.
[10] K. L. Taft, G. C. Papaefthymiou, S. J. Lippard, *Inorg. Chem.* **1994**, *33*, 1510; K. L. Taft, G. C. Papaefthymiou, S. J. Lippard, *Science* **1993**, *259*, 1302.
[11] After distillation over Mg/I_2, the methanol used contained about 0.01% of water, which is likely to represent the source of oxide ions for the formation of the core.
[12] W. Micklitz, V. McKee, R. L. Rardin, L. E. Pence, G. C. Papaefthymiou, S. G. Bott, S. J. Lippard, *J. Am. Chem. Soc.* **1994**, *116*, 8061.

"Fast Amide Cleavage" or Reproducible, Concentration- and Time-Dependent Aggregation of Anionic and Cationic Surfactants?

Wilmer K. Fife* and Shanghao Liu

A recent report by Menger and Fei in this journal[1] announced unprecedented, rapid hydrolysis ($t_{1/2} \approx 3$ min, pH 8, 25 °C) of the activated amide **1a**, within aggregates that contained 1.0 equivalent of hexadecanoate ion. We have reinvestigated this experiment in connection with our on-going study of synthetic, enzyme-like, acyl transfer catalysts. We find that the process reported previously as amide hydrolysis [Eq. (a)] is a time-dependent, concentration-dependent aggrega-

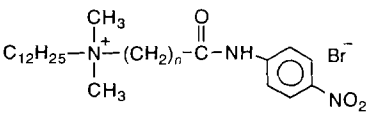

1a, $n = 1$
1b, $n = 3$

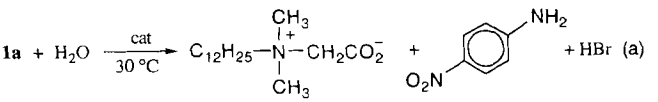

tion of amide substrate **1**, a cationic surfactant, with hexadecanoate ion, an anionic surfactant. Anion–cation surfactant pairs are known to form molecular aggregates such as bilayer membranes or vesicles at concentrations well below the CMC values (CMC = critical micelle concentrations) of the individual surfactants.[2–4]

Surfactant-enhanced hydrolysis of lipophilic substrates, especially *p*-nitrophenyl esters, has received much attention.[1, 5, 6] The reactivity of carboxamides, however, is widely known to be quite different from that of related *p*-nitrophenyl esters,[1, 7] so discovery of rapid hydrolysis of an amide under mild conditions commands attention.

Reinvestigation of the Menger–Fei experiment in our laboratory with **1a** (2×10^{-5} M) and hexadecanoate (1×10^{-5} and 2×10^{-5} M) gave results similar to theirs (Fig. 1 and Table 1). For example, researchers in both laboratories obtained the value 0.12 min^{-1} for k_{obs} at 1×10^{-5} M hexadecanoate and observed an approximate doubling of the values of k_{obs} and ΔA_{390} (the difference between absorbance values of the reaction mixture at 390 nm for $t = 0$ and ∞) when the hexadecanoate concentration was increased to 2×10^{-5} M. However, we found that no further increases in k_{obs} and ΔA_{390} accompany increases in concentration of both **1a** and hexadecanoate to 3×10^{-5} or 4×10^{-5} M. Additional experiments with dodecyl sulfate or hexadecane sulfonate as the anionic surfactant or replacement of **1a** with the unactivated amide **1b** as the cationic surfactant produced time-dependent increases in A_{390} similar to those described above. Menger and Fei[1] reported no "reaction" for mixtures of **1b** and hexadecanoate ion. Thus, they failed to observe the absorbance increases we repeatedly obtained at

[*] Prof. W. K. Fife, Dr. S. Liu
Department of Chemistry, Indiana University-Purdue University
402 N. Blackford Street
Indianapolis, IN 46202 (USA)
Telefax: Int. code +(317)274-4701
e-mail: fife@chem.iupui.edu

[**] This work was supported by the Office of Naval Research. We greatly appreciate the discussions with Professor F. M. Menger who encouraged us to pursue these experiments. We thank Professors E. W. Kaler and D. Jaeger for helpful discussion and suggestions.

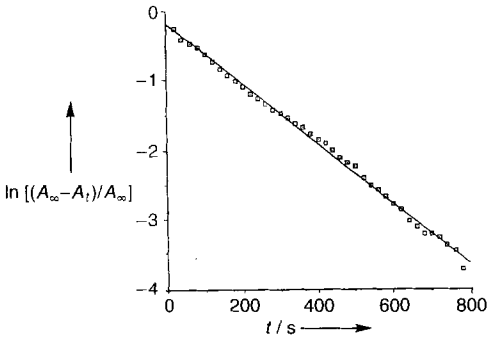

Fig. 1. Plot of $\ln[(A_\infty - A_t)/A_\infty]$ ($\lambda = 390$ nm) vs. time t [s] for an equimolar mixture of **1a** and hexadecanoate (2×10^{-5} M) at pH 8, 30 °C in water. Fitted line: $y = -0.18898 - 4.3126 \times 10^{-3} x$; $R^2 = 0.997$.

Table 1. Kinetic data from A_{390} vs. time plots for amides **1** in water at 30.0 °C [a].

Cationic "substrate"	Anionic "catalyst"	["Catalyst"] [mol L^{-1}]	k_{obs} [min^{-1}]	ΔA_{390} [b]
1a	–	–	$-(1.3 \times 10^{-6})$ [c]	
1a	hexadecanoate	1×10^{-5}	0.12 (0.12) [c]	0.061
1a	hexadecanoate	2×10^{-5}	0.26 (0.22) [c]	0.135
1a	hexadecanoate	4×10^{-5}	0.24	0.100
1a [d]	hexadecanoate	3×10^{-5}	0.28	0.160
1a [e]	hexadecanoate	4×10^{-5}	0.27	0.220
1a	tetradecanoate	2×10^{-5}	0.08	0.026
1a	dodecyl sulfate	1×10^{-5}	0.17	0.025
1a	dodecyl sulfate	2×10^{-5}	0.30	0.105
1a	hexadecanesulfonate	1×10^{-5}	0.51	0.036
1a	hexadecanesulfonate	2×10^{-5}	1.09	0.089
1b	hexadecanoate	2×10^{-5}	0.14	0.124
1b	dodecyl sulfate	2×10^{-5}	0.3	0.17
1b	hexadecansulfonate	2×10^{-5}	0.47	0.109
2	hexadecanoate	2×10^{-5}	–	<0.01
2	dodecyl sulfate	2×10^{-5}	–	<0.01

[a] The reaction medium was 2×10^{-5} M in cationic surfactant amide, and buffered at pH 8 (0.05 M in $H_2PO_4^-$/ HPO_4^{2-}). [b] $\Delta A_{390} = A_{390}(t_x) - A_{390}(t_0)$. [c] Value taken from ref. [1]. The "reaction" temperature was 25.0 °C. [d] Concentration: 3×10^{-5} M. [e] Concentration: 4×10^{-5} M.

390 nm with various anion–cation surfactant mixtures (see Table 1). We have no explanation for these differences in results. In contrast to the experiments with **1a** and **1b**, equimolar mixtures of **2**, the *N*-methyl analog of **1a**, and hexadecanoate or dodecyl sulfate give *no increase* in A_{390} over time.

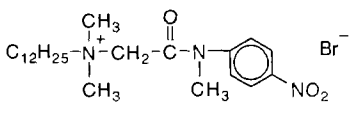

2

Full spectral scans (200–800 nm) of the various surfactant mixtures at different times after mixing yielded significant results (Fig. 2). The mixture of **1a** and hexadecanoate in pH 8 buffer clearly showed a time-dependent, progressive increase in absorbance at 390 nm *and throughout the UV/VIS spectrum* (Fig. 2, scans a → d); however, λ_{max} remained at 310 nm. Addition of concentrated aqueous sodium hydroxide to make the mixture 1.0 M in hydroxide ion caused almost immediate restoration of the original base line; that is, loss of turbidity, disappearance of the absorption band at 310 nm, and appearance of a new band at 360 nm. The band at 360 nm gave way to another at 380 nm ($\varepsilon = 1.4 \times 10^4$ M^{-1}) over several hours. This latter band, (Fig. 2, scan e) is identical to that reported for

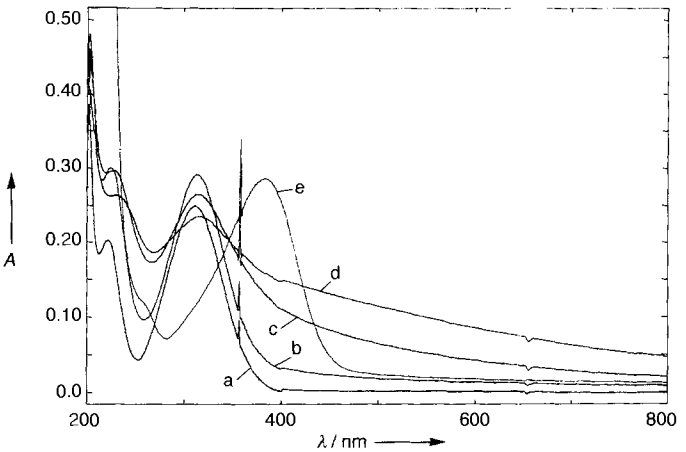

Fig. 2. Scans of A_{390} vs. wavelength [nm] for mixtures equimolar in **1a** and hexadecanoate (2×10^{-5} M) at pH 8, 30 °C in water: a) For **1a** alone; b) within 10 s, c) 3.5 min, d) 40 min after adding hexadecanoate; and e) 7 h after adding NaOH to make mixture 1.0 M in hydroxide ion. The spikes at 360 nm are instrument artifacts.

p-nitroaniline[8] and is stable over the pH range 8 to 14. When a fresh mixture of **1a** and hexadecanoate ion was quickly scanned at pH > 12, only one band at $\lambda_{max} = 354$ nm ($\varepsilon = 1.06 \times 10^4$ M^{-1}) was observed. Immediately after acidification of the mixture with hydrochloric acid to pH < 9, a spectrum identical to that in Figure 2a, was obtained. If the mixture of **1a** and hexadecanoate ion is maintained at pH > 12 for several days, its spectrum becomes identical to that in Figure 2e. These observations are consistent with rapid, reversible deprotonation–protonation of **1a** [Eq. (b)], and very slow hydrolysis of it at high

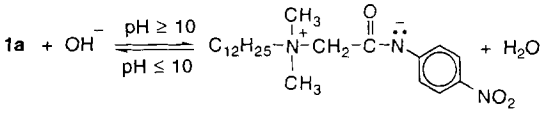

(b)

3

pH. The pK_a value of **1a** in water is 10.42 as determined by spectrometric titration of **1a** ($\lambda_{max} = 310$ nm) and its conjugate base **3** ($\lambda_{max} = 354$ nm). Similar results were obtained with **1b** whose pK_a value is 12.82 with absorption maxima at 310 nm for **1b** and 365 nm for its conjugate base. Results from analogous experiments with **2** show that it not only fails to undergo rapid hydrolysis but it also does not exhibit the acid–base chemistry of amides **1**.

An accurate explanation for the observed behavior of the anion–cation surfactant pairs is complicated by the overlapping spectral bands of *p*-nitroaniline, the expected hydrolysis product of **1a** and **1b**, and zwitterion **3**, the conjugate base of **1a**, as well as time-dependent absorbance increases of the solutions of the anion–cation surfactant pairs themselves. All of these processes, chemical and physical, are marked by increases in absorbance in the 350–400 nm region of the UV/Vis spectrum.

Enzymes remain supreme as catalysts and chemists remain unable to replace them with simple, inexpensive surfactants such as hexadecanoate. However, the present study and the earlier report of Menger and Fei[1] document for the first time the reproducible nature of *a kinetically slow* anionic–cationic surfactant aggregation process. The time and concentration dependence of the process closely resembles that of a true chemical reaction. Finally, we must point out that two rapid stages of surfactant aggregation equilibria are well-known and have received intensive study over the past 20 years.[9]

Experimental Procedure

Amides **1** were synthesized by the reaction sequence: $Br(CH_2)_nCOCl \rightarrow Br(CH_2)_nCONHPhNO_2 \rightarrow [C_{12}H_{25}N^+(CH_3)_2(CH_2)_nCONHPhNO_2]\,Br^-$. After recrystallization from EtOAc/CH_3CN **1a** had a melting point of 208–209 °C and **1b** melted at 156–157 °C. Cationic substrate **2** was obtained as a gel-like, yellow solid from *N*-methyl-*p*-nitroaniline according to the Scheme for **1** above. All compounds had ^1H and ^{13}C NMR spectra and elemental analysis consistent with given formulae. Kinetic data were obtained by following the absorbance of reaction mixtures containing surfactant components at 390 nm (Table 1). All UV/Vis data were obtained with a Hewlett-Packard Model 8450 spectrophotometer. Mixture components were added to the cuvet by pipet and shaken vigorously by hand for 2–3 s. The results were not influenced by the order of addition of mixture components.

Received: August 7, 1995 [Z8285IE]
German version: *Angew. Chem.* **1995**, *107*, 2946–2948

Keywords: amide hydrolysis · anion–cation surfactant aggregation · enzyme mimetics

[1] F. M. Menger, Z. X. Fei, *Angew. Chem.* **1994**, *106*, 329; *Angew. Chem. Int. Ed. Engl.* **1994**, *33*, 346.
[2] P. Jokela, B. Jönsson, A. Khan, *J. Phys. Chem.* **1987**, *91*, 3291.
[3] E. W. Kaler, A. K. Murthy, B. E. Rodriguez, J. A. N. Zasadzinski, *Science* **1989**, *245*, 1371; E. W. Kaler, K. L. Herrington, A. K. Murthy, J. A. N. Zasadzinski, *J. Phys. Chem.* **1992**, *96*, 6698.
[4] H. Fukuda, K. Kawata, H. Okuda, S. L. Regen, *J. Am. Chem. Soc.* **1990**, *112*, 1635; K. Hirano, H. Fukuda, S. L. Regen, *Langmuir* **1991**, *7*, 1045.
[5] A. Ochoa-Solano, G. Romero, C. Gitler, *Science* **1967**, *156*, 1243; C. Gitler, A. Ochoa-Solano, *J. Am. Chem. Soc.* **1968**, *90*, 5004.
[6] R. G. Shorenstein, C. S. Pratt, C. J. Hsu, T. E. Wagner, *J. Am. Chem. Soc.* **1968**, *90*, 6199.
[7] F. M. Menger, M. Ladika, *J. Am. Chem. Soc.* **1987**, *109*, 3145.
[8] The values of $\lambda_{max} = 381$ nm and $\varepsilon_{max} = 1.35 \times 10^4\ M^{-1}$ for *p*-nitroaniline are given in R. M. Silverstein, G. C. Bassler, T. C. Morill, *Spectrophotometric Identification of Organic Compounds*, 5th ed., Wiley, New York, **1991**, p. 309.
[9] E. A. G. Aniansson, H. Hoffmann, R. Zana, *J. Phys. Chem.* **1976**, *80*, 905; M. Frindi, B. Michels, R. Zana, *ibid.* **1994**, *98*, 6607.

A Strategy of "Random Glycosylation" for the Production of Oligosaccharide Libraries**

Osamu Kanie, Frank Barresi, Yili Ding, Jill Labbe, Albin Otter, L. Scott Forsberg, Beat Ernst, and Ole Hindsgaul*

The use of combinatorial chemistry for the rapid, simultaneous synthesis of individual molecules, or mixtures containing a large number of molecules, is considered one of the new frontiers in organic chemistry useful in drug discovery. Tremendous successes were achieved initially in the area of oligopeptides and oligonucleic acids and their analogs, and more recently in the area of small organic molecules.[1]

[*] Prof. O. Hindsgaul, O. Kanie, F. Barresi, Y. Ding, J. Labbe, A. Otter
Department of Chemistry
University of Alberta, Edmonton, AB T6G 2G2 (Canada)
Telefax: Int. code +(403)-492-7705
L. S. Forsberg
Complex Carbohydrate Research Center
University of Georgia, Athens, GA 30602-7229 (USA)
Dr. B. Ernst
Ciba, Central Research Laboratories, CH-4002 Basel (Switzerland)

[**] This work was initiated through a Steacie Fellowship Award to OH by the Natural Sciences and Engineering Research Council of Canada and supported financially by Ciba-CANADA. We thank Ms. Y. Kanie for assistance with the HPLC separations.

Despite their potential importance[2] both for the discovery of carbohydrate-binding receptors and for the identification of new lead compounds (for example, cell-adhesion inhibitors) the generation of oligosaccharide libraries remains unexplored. This is most probably because of the serious logistical difficulties that would be encountered when currently available glycosylation and protecting-group technologies are applied to the conversion of polyvalent monosaccharide residues into useful mixtures of oligosaccharides.

We report here the first results obtained with a new strategy of "random glycosylation" for the production of oligosaccharide libraries. The objective is to produce mixtures of products (typically trisaccharides) that contain all of the possible desired oligosaccharide products and to evaluate the mixture itself in a biological assay. The random-glycosylation strategy is illustrated in Figure 1, where it is contrasted with the classical multistep synthesis[3] of a systematic series of trisaccharides. In this hypothetical example the objective is to prepare all six α-fucosylated βGal(1 → 3)βGlcNAc sequences, some of which are known blood-group antigens[2] that react with antibodies, enzymes, and receptors. The conventional multistep synthesis approach would produce the individual fucosylated trisaccharides as shown. Starting from the unprotected disaccharide acceptor **1** having six free OH-groups, at least 12–15 protecting-group manipulation steps would be required to produce individual acceptors for six independent α-fucosylation reactions. The final removal of protecting groups would require several steps for each trisaccharide, depending on the number of protecting groups used. The protecting-group manipulations would have to be different for every new disaccharide acceptor. For example, if the terminal sugar in **1** is changed from Gal to Glc, the protection schemes would get significantly longer. Chromatographic purification would have to be performed at almost every step in this approach.

In contrast, in the random-glycosylation strategy (Fig. 1) the unprotected disaccharide **1** is directly α-fucosylated with an appropriate donor at low conversion (approximately 30%) to produce predominantly trisaccharides in a single step. These would be separated from unchanged **1** and over-fucosylated tetrasac-

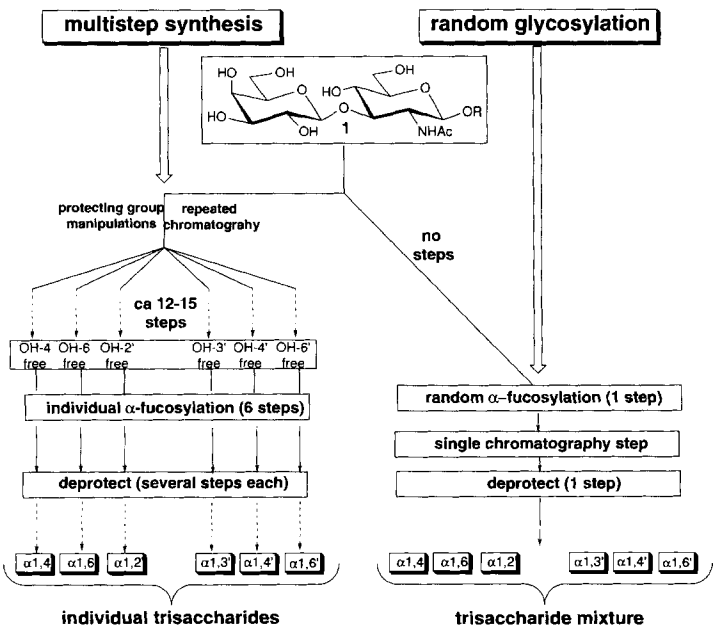

Fig. 1. The contrast between the preparation of the six possible α-fucosides that can be formed from **1** using systematic multistep synthesis and random glycosylation.

charides in one chromatographic step, and only one step would be sufficient for removal of the protecting groups, which are present only on the donor. Thus, only two chemical steps would be required to produce the same six trisaccharides as in the multistep approach, but these would be present as a mixture. If the oligosaccharide mixture produced by this method showed activity in a biological assay (for example, as an enzyme substrate or as an inhibitor of carbohydrate–protein recognition in cell adhesion), the active component would have to be identified through a classical deconvolution strategy: either through affinity or conventional chromatography followed by structural elucidation or through the systematic multistep synthesis of individual members of the mixture.

If it could be implemented, the random-glycosylation strategy could tremendously accelerate the initial phases of the search for new ligands. For this strategy to be useful, however, at least two criteria must be met: firstly, random-glycosylation reactions must produce mixtures that contain all the possible target oligosaccharides, ideally in nearly equal amounts. Secondly, for the generation of a true library rather than just a mixture of a small number of oligosaccharides, sequential, random glycosylation reactions should be feasible. In this paper, we present the first results demonstrating that the first criterion can indeed be fulfilled, since conditions for α-fucosylation were developed that proceed with near complete lack of regiospecificity.

Random glycosylation of unprotected oligosaccharides requires a polar solvent to dissolve the polyhydroxylated acceptor. DMF or DMF–acetonitrile mixtures were found to be interchangeable. Fucose residues are present only in the α-L configuration in mammalian oligosaccharides, so 2,3,4-tri-*O*-benzyl-activated fucopyranose derivatives were examined as the glycosyl donors. Fucosyl bromide, fluoride, thioglycosides, xanthates, pentenyl glycoside, phosphites, and trichloroacetimidate were evaluated with many of the commonly used activating agents.[3] Only the trichloroacetimidate method developed by Schmidt[3f] reproducibly gave clean reaction products with either BF_3-Et_2O or trimethylsilyl triflate (TMSOTf) as the promoters.

Hydrophobic 8-*p*-methoxyphenoxyoctyl glycosides[4] were used as the disaccharide acceptors for both convenience of isolation[5] and detection by UV absorption. Thus, reaction of βGal(1 → *n*)βGlcNAc-OR (*n* = 3, 4, or 6, R = $(CH_2)_8OC_6H_4pOCH_3$; Scheme 1) with tri-*O*-benzylfucopyranosyl trichloroacetimidate[4f] (2.0 equiv) in the presence of BF_3-Et_2O (0.2 equiv) in DMF (room temperature, 3 h) gave the sought-after complex mixtures in which about 30% of the starting disaccharide acceptors were fucosylated. Separation of acceptors having no benzyl groups from trisaccharides (having three benzyl groups) and tetrasaccharides (having six benzyl groups) could be conveniently accomplished with a step gradient in reverse phase chromatography.[6] Hydrogenolysis of the resulting trisaccharide fraction then gave the product mixture, which was adsorbed onto C-18 resin[5] and then washed with water to remove by-products formed by the degradation of the fucosyl donor. The trisaccharides were then eluted with methanol.

The ^1H NMR spectra of the three trisaccharide mixtures thus obtained are shown in Figure 2. The starting disaccharides contained only β-linkages, so the new doublets (J = 3–4 Hz) appearing in the region δ = 4.7–5.3 are from the 1-H atoms of the added α-fucose residue. The fast atom bombardment (FAB) mass spectra confirmed that the products were the expected trisaccharides with minor contamination by difucosylated tetrasaccharides (due to column overloading). Minor signals from these are also seen in the ^1H NMR spectra. Integration of the 1-H signals revealed that mixtures A and B contained

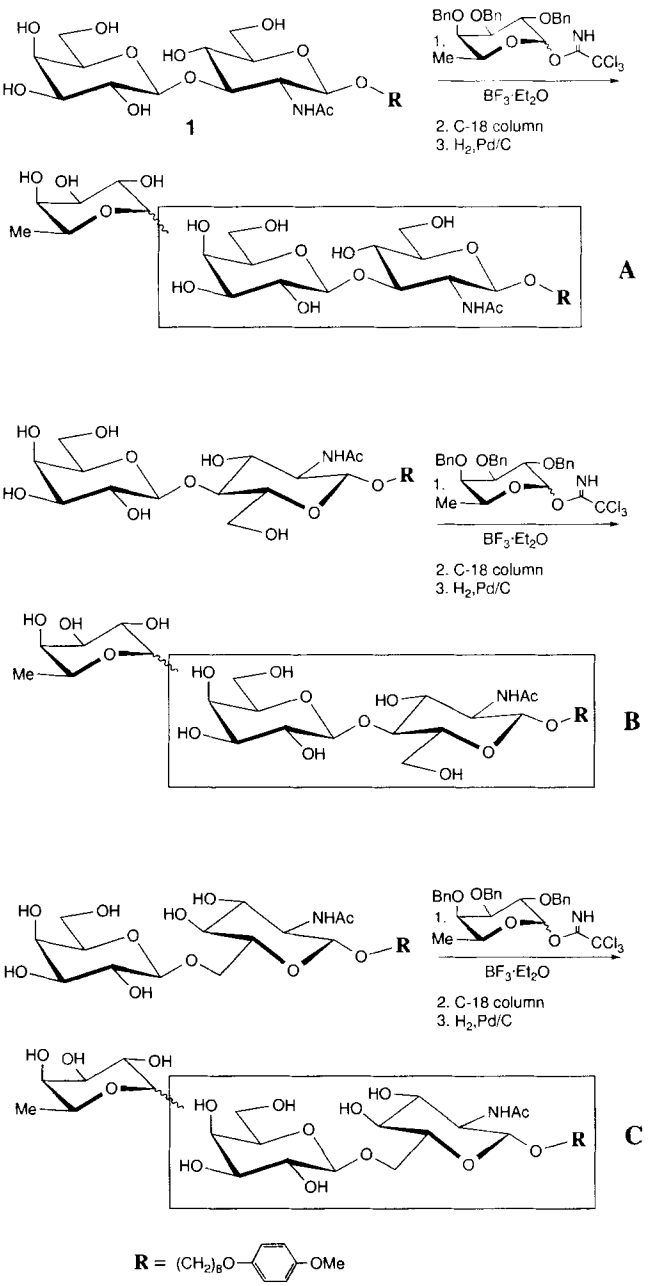

Scheme 1. Random fucosylation of βGal(1 → *n*)βGlcNAc-OR (*n* = 3, 4, or 6) to produce trisaccharide mixtures A, B, and C. R = $(CH_2)_8OC_6H_4pOCH_3$

about 20% of β-linked fucose, while mixture C contained nearly 5%.

Only mixture A, produced by random fucosylation of βGal(1 → 3)βGlcNAc-OR, was analyzed in detail through separation of the individual isomers by repeated chromatography[7] at both the protected and deprotected stages, followed by ^1H NMR analysis to determine the anomeric configuration of the sugar residues. Methylation analysis[8] was used for assigning the position of attachment of the new fucosyl units.[9] The distribution of the α-fucosylation on disaccharide **1** was thus shown to be 12% α(1 → 4), 22% α(1 → 6), 19% α(1 → 2′), 23% α(1 → 3′), 8% α(1 → 4′) and 16% α(1 → 6′). The statistical distribution would be 17% of each isomer. Figure 2a also shows the presence of the characteristic[10] downfield-shifted quartet ($\delta \approx 4.8$) for 5-H of fucose α-linked to 4-O of the GlcNAc

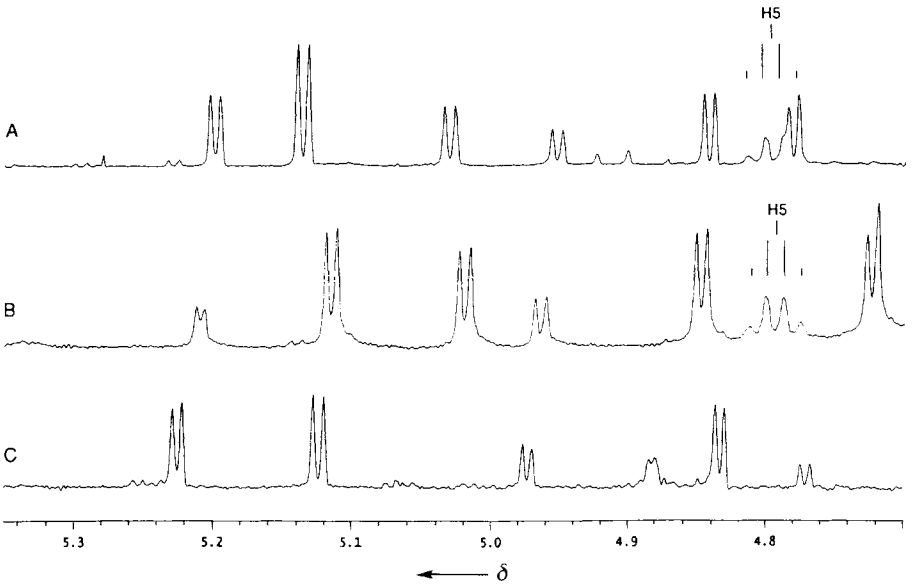

Fig. 2. ^{1}H NMR spectra (500 MHz, 45 °C, CD_3OD) of the α-anomeric region of the mixtures of trisaccharides obtained by random fucosylation of βGal(1 → 3)βGlcNAc-OR (A), βGal(1 → 4)βGlcNAc-OR (B), or βGal(1 → 6)βGlcNAc-OR (C).

residue in the Lewis^a blood group trisaccharide βGal(1 → 3)-[αFuc(1 → 4]βGlcNAc-OR that had formed as 12% of the product mixture.

Mixture B, produced by random fucosylation of βGal(1 → 4)βGlcNAc-OR and processed in the same way, gave a strikingly similar pattern in the ^{1}H NMR spectrum. The identity of the individual isomers was not established, but since only six α-fucosylated trisaccharides are possible, and six α-doublets are seen, they are all present in the mixture in comparable amount. The characteristic[10] 5-H quartet of the α-linked fucose residue in the blood-group Lewis^x structure βGal(1 → 4)-[αFuc(1 → 3)]βGlcNAc-OR is also seen near $\delta = 4.8$. Finally, the ^{1}H NMR spectrum of mixture C, produced by random fucosylation of βGal(1 → 6)βGlcNAc-OR, again confirmed the presence of all six possible α-linked fuco-trisaccharides, none of which has an unusually shifted signal for 5-H of fucose.

Chemical intuition, based on numerous literature precedents[3] demonstrating highly varying hydroxyl-group reactivities, would have predicted that the major products in the above fucosylation reactions would be those formed by glycosylation of the least hindered primary alcohols, 6-OH or 6′-OH. This was clearly not the case in any of the three examples. The greatest difference between the major and the minor α-fucoside, based on integration of the anomeric signals, is only 3:1 and all isomers are present in at least half the expected statistical amount. The mixtures produced were confirmed to contain the kinetic product distribution, since running the reactions at much lower conversion (10%) to trisaccharides, or leaving the reaction for much longer (16 h) yielded the same distribution of products. It is astonishing that all of the OH groups on the acceptor disaccharides showed such a similar reactivity. The explanation is undoubtedly complex but will include the fact that since no protecting groups are used, no added steric hindrance prevents access of the glycosyl donor to any of the OH groups. In addition, the reaction is taking place in DMF, a very polar hydrogen-bond-accepting solvent, and the reacting molecules are very likely involved in very complex arrays of inter- and intramolecular hydrogen bonds.

Further investigations on the random glycosylation of unprotected acceptor oligosaccharides are in progress to evaluate the generality of the method for the production of oligosaccharide libraries. Clearly, sugars other than fucose must be demonstrated to be capable of nonregiospecific glycosylations,[11] and methods for biasing the anomeric configurations of the newly formed linkages must also be developed, so that β-glycosides can be made to dominate if so desired. Meanwhile, even in the present primitive formulation, the random glycosylation strategy successfully generated all 18 possible αFuc(1 → *m*)-[βGal(1 → *n*)βGlcNAc] trisaccharides (*n* = 3, 4, or 6, $n \neq m$) from their unprotected disaccharide precursors[12] in the simplest and fastest manner possible.

Received: August 14, 1994 [Z8305IE]
German version: *Angew. Chem.* **1995**, *107*, 2912–2915

Keywords: combinatorial chemistry · glycosylations · oligosaccharides

[1] Recent comprehensive reviews: a) M. A. Gallop, R. W. Barrett, W. J. Dower, S. P. A. Fodor, E. M. Gordon, *J. Med. Chem.* **1994**, *37*, 1233–1251; b) E. M. Gordon, R. W. Barrett, W. J. Dower, S. P. A. Fodor, M. A. Gallop, *ibid.* **1994**, *37*, 1385–1401.

[2] A. Varki, *Glycobiology* **1993**, *3*, 97–130.

[3] a) H. Paulsen, *Angew. Chem.* **1982**, *94*, 184–201; *Angew. Chem. Int. Ed. Eng.* **1982**, *21*, 155–173; b) R. R. Schmidt, *ibid.* **1986**, *98*, 213–236 and **1986**, *25*, 212–235; c) H. Paulsen, *ibid.* **1990**, *102*, 851–867 and **1990**, *29*, 823–839; d) O. Kanie, O. Hindsgaul, *Curr. Opin. Struct. Biol.* **1992**, *2*, 674–681; e) K. Toshima, K. Tatsuta, *Chem. Rev.* **1993**, *93*, 1503–1531; f) R. R. Schmidt, W. Kinzy, *Adv. Carbohydr. Chem. Biochem.* **1994**, *50*, 21–124. Comprehensive review of the oligosaccharides synthesized in 1994 and the methods used: g) "Glycosylation Methods in Oligosaccharide Synthesis": F. Barresi, O. Hindsgaul in *Modern Synthetic Methods, Vol. 7* (Eds.: B. Ernst, C. Leuman), Helvetica Chimica Acta, Basel, **1995**, pp. 281–330; h) *J. Carbohydr. Chem.* **1995**, *14*, 1043–1087. Example of highly regioselective glycosylation of a partially acceptor disaccharide containing four free OH groups: i) S. J. Danishefsky, J. Gervay, J. M. Peterson, F. E. McDonald, K. Koseki, T. Oriyama, D. A. Girffith, C. H. Wong, D. P. Dumas, *J. Am. Chem. Soc.* **1992**, *114*, 8329–8331.

[4] B. Ernst, B. Wagner, *Helv. Chim. Acta* **1989**, *7*, 165–171.

[5] M. M. Palcic, L. D. Heerze, M. Pierce, O. Hindsgaul, *Glycoconjugate J.* **1988**, *5*, 49–63.

[6] The trisaccharides were eluted from C-18 reverse phase columns in MeOH/H_2O (82/18), whereas the minor tetrasaccharides require MeOH/H_2O (90/10).

[7] The initial benzylated oligosaccharide mixture was partially resolved by silica gel chromatography using a step gradient from MeOH/CH_2Cl_2 (3/97) to CH_2Cl_2/MeOH/H_2O (60/35/6) and, after debenzylation, further fractionated by HPLC on Whatman PAC columns (CH_3CN/H_2O 91/9).

[8] Methylation analysis (B. Lindberg, J. Lonngren, *Methods Enzymol.* **1978**, *50*, 3–33) was performed by the Complex Carbohydrate Research Center, University of Georgia.

[9] The methylation analyses also confirmed that all six α-fucosylated trisaccharides contained a 3-O-substituted GlcNAc and a nonsubstituted Fuc residue.

[10] R. U. Lemieux, K. Bock, L. T. J. Delbaere, S. Koto, V. S. Rao, *Can. J. Chem.* **1980**, *58*, 631–653.

[11] In initial experiments, tetra-*O*-benzyl-D-galactopyranosyl trichloroacetimidate reacted with **1** to give all six possible α-galactosylated trisaccharides in ratios similar to those found in mixtures **A**, **B**, and **C**.

[12] βGal(1 → *n*)βGlcNAc-O$(CH_2)_8OC_6H_4$-*p*-OMe (*n* = 3, 4, and 6) were prepared on gram scale by multistep synthesis and fully characterized: Y. Ding, J. Labbe, O. Kanie, O. Hindsgaul, *Bioorg. Biomed. Chem.*, in press.

A New Nickel-Catalyzed Cross-Coupling Reaction between sp^3 Carbon Centers**

Arokiasamy Devasagayaraj, Thomas Stüdemann, and Paul Knochel*

The cross-coupling between sp^3-hybridized C centers is an important method for forming carbon–carbon bonds.[1] The severe limitations of the classical Wurtz reaction led to the development of transition metal catalyzed methods. Copper(I)-catalyzed coupling reactions of organomagnesium halides and organocuprate-mediated substitutions have proven to be especially useful.[2] Yet the drawbacks of these methods such as the necessity of using organomagnesium or organolithium compounds having few functional groups[2, 3] and the need of stoichiometric amounts of copper salts for the formation of cuprates make alternative approaches still desirable. Nickel and palladium catalysts have been used with great success for cross-coupling reactions[4] between unsaturated halides and organotin reagents, but coupling between two sp^3 C centers is almost unknown.[5] Herein, we report a new nickel-catalyzed cross-coupling reaction between sp^3 C centers allowing the synthesis of polyfunctional products.

In the course of studies on radical cyclizations using Et_2Zn,[6] we observed that the unsaturated alkyl bromides **1a** and **1b** undergo a fast coupling reaction with Et_2Zn in the presence of catalytic amounts of $[Ni(acac)_2]$ (7.5 mol%) and LiI (20 mol%) in THF (−35 °C, 4 h for **1a**, 18 h for **1b**) to afford the ethylated products **2a** and **2b**, respectively (81–82% yield; Scheme 1).

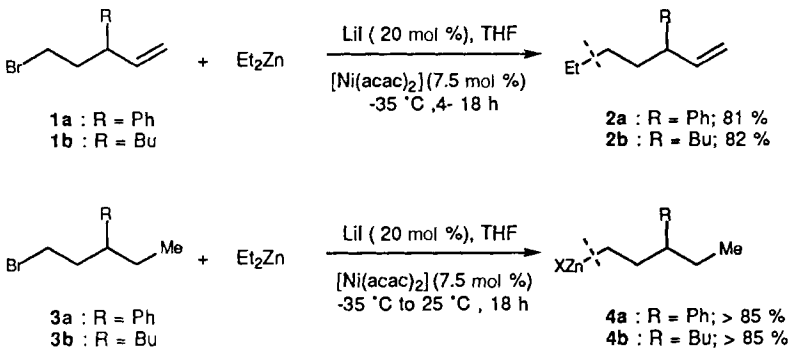

Scheme 1.

This behavior was unusual[5, 6] and led us to suspect that the presence of the double bond in the alkyl iodide was responsible for the easy coupling of **1a**,**b**.[7] To test this assumption we prepared the corresponding saturated bromoalkanes **3a** and **3b** and submitted them to the same reaction conditions. No coupling reaction was observed at −35 °C, but when the reaction mixture was allowed to warm to room temperature, a nickel-catalyzed bromine–zinc exchange took place leading to the zinc reagents **4a** and **4b** in over 85% yield as shown by iodolysis experiments.[8] The absence of cross-coupling products shows clearly the importance of the double bond in the alkyl iodide for this reaction pathway. Based on the pioneering work of Yamamoto and Sustmann,[7] a reasonable mechanism was proposed (Scheme 2).

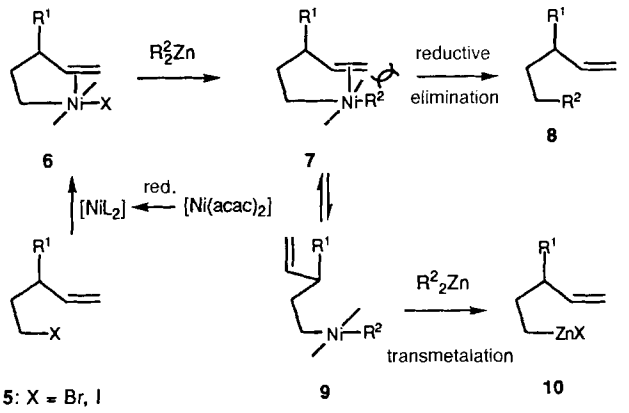

Scheme 2.

The catalytically active species $[L_2Ni^0]$, obtained by the in situ reduction of $[Ni(acac)_2]$, undergoes oxidative addition to the alkyl halide **5** producing a nickel(II) complex **6**, in which the double bond is complexed to the metal center. After ligand exchange with the dialkylzinc compound R^2_2Zn, the new complex **7** is obtained. The coordination of the double bond by nickel removes electron density from the metal and favors therefore the reductive elimination affording the coupling product **8**. However, if the alkyl group R^2 is too large or if the double bond is only weakly coordinated to nickel due to steric interactions with the carbon backbone, then dissociation may occur leading to the nickel(II) complex **9**. Dialkylnickel and -palladium complexes are known to have a low tendency for reductive elimination and prefer to undergo transmetalation with the dialkylzinc compound R^2_2Zn leading to the organozinc derivative **10**.[6a, 8] Low temperatures (−35 °C) favors the cross-coupling reaction, whereas higher temperatures, which promotes the dissociation of the double bond in **7**, lead to mixtures of the cross-coupling product **8** and halogen–zinc exchange product **10**. Also under the reaction conditions described in Scheme 1, a more bulky zinc reagent like dipentylzinc reacts with alkyl bromides leading to mixtures of products **8** and **10**. This may be explained by the steric bulk of the pentyl group in complex **7** or to the lower reactivity of an alkyl bromide in the coupling reaction.

Interestingly, replacing the $[Ni(acac)_2]$ catalyst by $[PdCl_2(CH_3CN)_2]$ or related palladium(II) complexes leads only to the bromine–zinc exchange products—an indication that nickel complexes are better catalysts for the cross-coupling reaction.

The mechanistic picture shown in Scheme 2 was very useful for improving the synthetic scope of the reaction. After much experimentation we found reaction conditions for the efficient cross-coupling of a wide range of diorganozinc compounds with primary unsaturated alkyl iodides (Schemes 3, 4 and Table 1). Thus the reaction of dialkylzinc **11**, prepared either by iodine–zinc exchange[9] or by boron–zinc exchange,[10] with an unsaturated alkyl iodide **12** bearing a double bond either in position 4 or 5 in the presence of $[Ni(acac)_2]$ (7–10 mol%) in THF/NMP

[*] Prof. Dr. P. Knochel, Dr. A. Devasagayaraj, Dipl.-Chem. T. Stüdemann
Fachbereich Chemie der Universität
Hans-Meerwein-Strasse, D-35032 Marburg (Germany)
Telefax: Int. code +(6421)282189

[**] This work was supported by the Fonds der Chemischen Industrie and the Deutsche Forschungsgemeinschaft (SFB 260). A. D. thanks the Alexander-von-Humboldt-Stiftung for a fellowship. We thank BASF AG, Witco, Schering AG, Bayer AG, Sipsy SA, and Chemetall GmbH for gifts of chemicals.

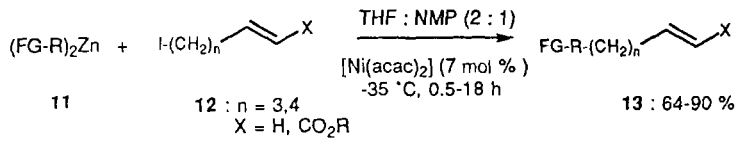

Scheme 3. FG-R = functionalized alkyl group, NMP = *N*-methylpyrrolidinone.

Table 1. Products **13a–j** obtained by the nickel-catalyzed cross-coupling of dialkylzinc compounds **11** and alkyl iodides **12a–d** in THF/NMP.

Entry	Alkyl iodide **12**	Diorganozinc **11** [a]	Prod. **13**	Yield [%]
1	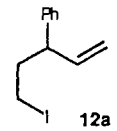 **12a**	$Pent_2Zn$	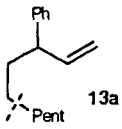 **13a**	80 (73) [c]
2	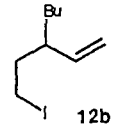 **12b**	$Pent_2Zn$	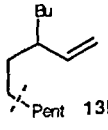 **13b**	72
3	**12a**	$(PivO(CH_2)_3)_2Zn$	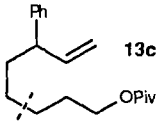 **13c**	90 (77) [c]
4	**12b**	$(PivO(CH_2)_3)_2Zn$	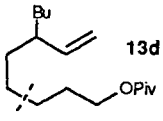 **13d**	70 (32) [c]
5	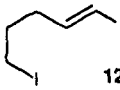 **12c**	$Pent_2Zn$	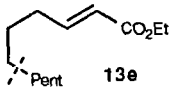 **13e**	83
6	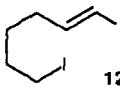 **12d**	Et_2Zn	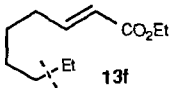 **13f**	84
7	**12c**	$(PivO(CH_2)_3)_2Zn$	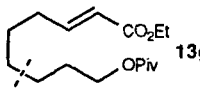 **13g**	79
8	**12d**	$(AcO(CH_2)_5)_2Zn$	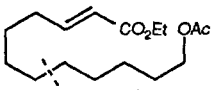 **13h**	78
9	**12d**	$(PivO(CH_2)_6)_2Zn$	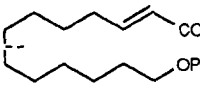 **13i**	73
10	**12c**	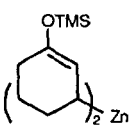	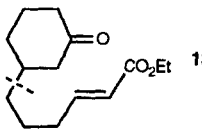 **13j**	65

[a] Pent = pentyl, Piv = pivaloyl, TMS = trimethylsilyl. [b] Yield of analytically pure products. [c] Yield for the reaction conducted in THF in parentheses.

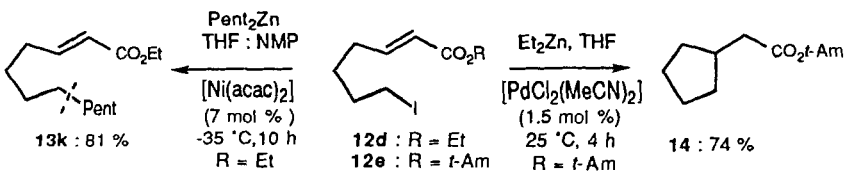

Scheme 4. *t*-Am = *t*-amyl = $C(CH_3)C_2H_5$, Pent = $(CH_2)_4CH_3$.

(2/1) at −35 °C provides a range of polyfunctional cross-coupling products **13** in good yields (65–90%). The use of NMP as cosolvent dramatically accelerates the reaction (3 h reaction time instead of 24 h in THF for the formation of **13a**) and improves the yields (entries 1, 3, and 4 of Table 1). The presence of an electron-withdrawing substituent like an ester group at the double bond also has a beneficial effect, since it strengthens the nickel–olefin bond (entries 5–10). The structure of the nickel-olefin complex is also important, and the alkyl iodides **12a–c** ($n = 3$) react faster than the corresponding alkyl iodide **12d**, in which the double bond is at a more remote position ($n = 4$). It is remarkable that the coupling reaction[11] proceeds at temperatures as low as −35 °C, since the related Negishi coupling reaction[4c, d, 12] of alkylzinc halides with alkenyl and aryl iodides in the presence of a palladium catalyst occurs only at or above room temperature. The difference in chemoselectivity between the nickel and palladium complexes is best shown in Scheme 5. Thus the reaction of **12d** with $Pent_2Zn$ in the presence of $[Ni(acac)_2]$ in THF/NMP (2/1) furnishes the coupling product **13k**, whereas in the presence of $[PdCl_2(CH_3CN)_2]$ as catalyst (1.5 mol%) and Et_2Zn in THF, the cyclization product **14** is obtained as sole product in 74% yield.

We have shown that the presence of a remote double bond in a primary alkyl iodide enables the first selective nickel-catalyzed cross-coupling reactions between sp^3 C centers, because the intramolecular complexation of the double bond on the nickel center favors the reductive elimination. Further studies to determine the synthetic scope of the method and other extensions of the chemistry of nickel–olefin complexes are currently underway in our laboratories.

Experimental Procedure

General procedure: Preparation of **13h** (entry 8 of Table 1): A 50 mL two-necked flask equipped with an argon inlet and a rubber septum was charged with $[Ni(acac)_2]$ (116 mg, 0.45 mmol, 7.5 mol%). After the flask was cooled to −40 °C, THF (2.5 mL), NMP (1.5 mL), and **12d** (1.69 g, 6 mmol, 1.0 equiv) were added successively by syringe. The reaction mixture was cooled to −78 °C. Then a solution of bis(5-acetoxypentyl)zinc [9] (3.88 g, 12 mmol, 2 equiv) in THF (2 mL) prepared from 5-iodopentyl acetate (6.14 g, 24 mmol) and Et_2Zn by an iodine–zinc exchange reaction was slowly added. The reaction mixture was allowed to warm up to −35 °C and was stirred for 15 h at this temperature. Excess dialkylzinc was quenched with saturated aqueous NH_4Cl solution. After the usual workup the resulting crude oil obtained after evaporation of the solvents was purified by chromatography (hexanes/ether 20/1 to 5/1) affording **13h** (1.33 g, 4.7 mmol, 78% yield) as a colorless oil.

Received: July 25, 1995 [Z 8257 IE]
German version: *Angew. Chem.* **1995**, *107*, 2952–2954

Keywords: alkene complexes · catalysis · cross-coupling · nickel compounds · zinc compounds

[1] D. C. Billington, *Comprehensive Organic Synthesis, Vol 3* (Eds.: B. M. Trost, I. Fleming), Pergamon Press, Oxford **1991**, pp. 413–434.
[2] B. H. Lipshutz, S. Sengupta, *Organic Reactions* **1992**, *41*, 135–631.
[3] For the cross-coupling of alkylzinc/copper reagents with alkyl iodides leading to polyfunctional products, see: C. E. Tucker, P. Knochel, *J. Org. Chem.* **1993**, *58*, 4781–4782.
[4] a) K. Tamao, M. Kumada, *The Chemistry of the Metal–Carbon Bond*, Vol. 4, (Ed.: F. R. Hartley), Wiley, New York, **1987**, pp. 819–887; b) R. J. P. Corriu, J. P. Masse, *J. Chem. Soc. Chem. Commun.*, **1972**, 144; c) E. Negishi, L. F. Valente, M. Kobayashi, *J. Am. Chem. Soc.* **1980**, *102*, 3298–3299; d) E. Erdik, *Tetrahedron*, **1992**, *48*, 9577–9648.
[5] a) P. L. Castle, D. A. Widdowson, *Tetrahedron Lett.* **1986**, *27*, 6013–6016; b) K. Yuan, W. J. Scott, *ibid.* **1989**, *30*, 4779–4782; c) K. Yuan, W. J. Scott, *J. Org. Chem.* **1990**, *55*, 6188–6194.
[6] a) H. Stadtmüller, R. Lentz, C. E. Tucker, T. Stüdemann, W. Dörner, P. Knochel, *J. Am. Chem. Soc.* **1993**, *115*, 7027–7028; b) P. Knochel, *Synlett*, **1995**, 393–403.

[7] a) T. Yamamoto, A. Yamamoto, S. Ikeda, *J. Am. Chem. Soc.* **1971**, *93*, 3350–3359; b) R. Sustmann, J. Lau, M. Zipp, *Tetrahedron Lett.* **1986**, *27*, 5207–5210; c) R. Sustmann, J. Lau, *Chem. Ber.* **1986**, *119*, 2531–2541; d) R. Sustmann, J. Lau, M. Zipp, *Recl. Trav. Chim. Pays-Bas* **1986**, *105*, 356–359; e) R. Sustmann, P. Hopp, P. Holl, *Tetrahedron Lett.* **1989**, *30*, 689–692; F) R. van Asselt, C. J. Elsevier, *Tetrahedron* **1994**, *50*, 323–334.

[8] The nickel-catalyzed bromine–zinc exchange reaction has been studied extensively in our laboratories: a) A. Vaupel, P. Knochel, *Tetrahedron Lett.* **1994**, *35*, 8349–8352; b) I. Klement, P. Knochel, K. Chau, G. Cahiez, *ibid.* **1994**, *35*, 1177–1180; c) S. Vettel, A. Vaupel, P. Knochel, *ibid.* **1995**, *36*, 1023–1026.

[9] M. J. Rozema, S. AchyuthaRao, P. Knochel, *J. Org. Chem.* **1992**, *57*, 1956–1958.

[10] F. Langer, A. Devasagayaraj, P.-Y. Chavant, P. Knochel, *Synlett* **1994**, 410–412.

[11] The oxidative addition of nickel or palladium(0) complexes to alkyl iodides may proceed by a radical mechanism: a) A. V. Kramer, J. A. Labinger, J. S. Bradley, J. A. Osborn, *J. Am. Chem. Soc.* **1974**, *96*, 7145–7147. b) A. V. Kramer, J. A. Osborn, *ibid.* **1974**, *96*, 7832–7833; c) M. Chanon, *Bull. Soc. Chim. Fr.* **1982**, II, 197–238.

[12] E. Negishi, *Acc. Chem. Res.* **1982**, *15*, 340–348.

Water-Soluble Dendritic Iron Porphyrins: Synthetic Models of Globular Heme Proteins**

Peter J. Dandliker, François Diederich,* Jean-Paul Gisselbrecht, Alain Louati, and Maurice Gross*

Current interest in dendritic polymers stems from their unique structural properties and potential utility. Through judicious choice of branched building blocks and functional group chemistry, one can precisely control their shape, dimensions, density, polarity, flexibility, and solubility.[1] Dendrimers with functional components located on the exterior surface,[2] within the dendritic branches,[3] and at the interior core[4] are of particular interest since they exploit dendritic topology to modify the physical and chemical behavior of those components, giving rise to new materials with desirable properties.[5]

Functional dendrimers could also serve as synthetic models of globular enzymes. Dendritic mimics of heme-containing proteins such as cytochrome c are particularly intriguing targets, since their study could help clarify the reasons for the large changes in redox potential of the Fe^{III}/Fe^{II} couple observed in the biological systems.[6, 7] To systematically investigate the influence of peptide-like superstructure on iron porphyrin redox potentials in a purely synthetic system, we designed and synthesized the first and second generation dendrimers **1·FeCl** and **2·FeCl**, which contain an iron porphyrin core unit, and studied their redox behavior in both CH_2Cl_2 and aqueous solution. We found that as the dendritic structure progresses from being relatively open in **1·FeCl** to densely packed in **2·FeCl**, the redox potential for the Fe^{III}/Fe^{II} couple, measured in water, becomes 420 mV more positive. We attribute this substantial potential shift to the structured hydrophobic microenvironment created by the dendritic branches around the core iron porphyrin of the higher generation.

The dendritic iron porphyrins **1·FeCl** and **2·FeCl** were synthesized from the zinc derivatives **3** and **4**, respectively.[8] Activation of the carboxylic acid end groups in **3** and **4** with *N*,*N*′-dicyclohexylcarbodiimide (DCC) and 1-hydroxybenzotriazole (HOBT) in triethyleneglycol monomethyl ether as solvent, followed by preparative gel permeation chromatography (GPC), yielded **1·Zn** and **2·Zn** in 92 and 89% yield, respectively (Schemes 1 and 2, Table 1).

Table 1. Selected physical and spectroscopic data of compounds **1·FeCl**, **2·Zn**, **2·H_2**, and **2·FeCl** [a].

1·FeCl: Viscous brown oil. FT-IR ($CHCl_3$): $\tilde{\nu}$ = 1728, 1615 (C=O) cm^{-1}; ^1H NMR (300 MHz, $CDCl_3$, 298 K): δ = −0.8–5.9 (br. signals, about 280 H), 13.13 (bs, 4H, β_2-H), 15.24 (bs, 4H, β_1-H); porphyrin *meso* H (2H) and aryl H (6H) not visible; UV/Vis ($CHCl_3$): λ_{max} (ε) = 375 (sh, 57500), 409 (107000), 460 (sh, 11000), 504 (13200), 572 (5500), 644 (4400); FAB-MS: *m/z* (%): 3955.2 (100, $[M-Cl]^+$, $^{12}C_{182}{}^{13}C_2H_{296}FeN_8O_{80}$ requires 3955.9).

2·Zn: Viscous red oil. FT-IR ($CHCl_3$): $\tilde{\nu}$ = 1733, 1668 (C=O) cm^{-1}; ^1H NMR (300 MHz, $CDCl_3$, 298 K): δ = 1.12–1.42 (br.m, 8H, $OCH_2CH_2CH_2CH_2$), 1.71–1.83 (br.m, 8H, $OCH_2CH_2CH_2CH_2$), 2.45 (br.s, 24H, OCH_2CH_2, first generation), 2.44–2.60 (br.m, 72H, OCH_2CH_2, second generation), 3.24–3.75 (m, 660H, dendritic ether and triethyleneglycol monomethyl ether protons), 3.80 (br.s, 8H, $OCH_2CH_2CH_2$), 4.14 (br.s, 72H, $CO_2CH_2CH_2$), 6.14–6.26 (br.s, 16H, NH), 7.06 (δ, J = 7.5 Hz, 4H, *m*-aryl H), 7.69 (t, J = 7.5 Hz, 2H, *p*-aryl H), 8.94 (d, J = 3.9 Hz, 4H, β_2-H), 9.26 (d, J = 3.9 Hz, 4H, β_1-H), 10.07 (s, 2H, *meso* H); ^{13}C NMR (125 MHz, $CDCl_3$, 298 K): δ = 23.8, 31.8, 34.6, 36.8, 58.7, 59.6 (2×), 63.4, 66.5 (2×), 67.3, 68.8 (2×), 68.9, 70.2, 70.3 (2×), 71.6, 104.5, 105.1, 111.6, 120.7, 129.8, 131.0, 131.5, 148.7, 150.2, 159.5, 170.9, 171.3, 172.0; UV/Vis ($CHCl_3$): λ_{max} (ε) = 394 (sh, 34700), 415 (468000), 545 (16200); MALDI-TOF-MS (positive ion, linear mode): *m/z*: 11330 ($[M+Na]^+$, $^{12}C_{502}{}^{13}C_6H_{884}N_{20}O_{248}{}^{66}Zn$ + Na requires 11329), and fragments for loss of $C[CH_2OCH_2CH_2CO_2(CH_2CH_2O)_3CH_3]_3$.

2·H_2: Viscous dark purple oil. FT-IR ($CHCl_3$): $\tilde{\nu}$ = 1733, 1667 (C=O) cm^{-1}; ^1H NMR (300 MHz, $CDCl_3$, 298 K): δ = −3.13 (br.s, 2H, pyrrole NH), 1.23–1.46 (br.m, 8H, $OCH_2CH_2CH_2CH_2$), 1.68–1.85 (br.m, 8H, $OCH_2CH_2CH_2CH_2$), 2.35 (br.s, 24H, OCH_2CH_2, first generation), 2.49 (br.s, 72H, OCH_2CH_2, second generation), 3.20–3.70 (m, 660H, dendritic ether and triethyleneglycol monomethyl ether protons), 3.79 (br.s, 8H, $OCH_2CH_2CH_2CH_2$), 4.14 (br.s, 72H, $CO_2CH_2CH_2$), 6.06–6.18 (br.s, 16H, amide NH), 7.05 (d, J = 8.0 Hz, 4H, *m*-aryl H), 7.68 (t, J = 8.0 Hz, 2H, *p*-aryl H), 8.92 (d, J = 4.5 Hz, 4H, β_2-H), 9.25 (d, J = 4.5 Hz, 4H, β_1-H), 10.12 (s, 2H, *meso*-H); ^{13}C NMR (75 MHz, $CDCl_3$, 298 K): δ = 23.6, 31.8, 34.7, 37.0, 58.9, 59.7 (2×), 63.5, 66.6 (2×), 67.4, 68.9 (2×), 69.0, 70.4 (3×), 71.8, 104.1, 105.3, 111.5, 118.9, 130.5, 131.1 (2×), 144.7, 147.5, 159.5, 170.9, 171.4, 172.1; UV/Vis ($CHCl_3$): λ_{max} (ε) = 391 (sh, 67600), 410 (331000), 504 (11500), 540 (5400), 577 (5000), 630 (500); MALDI-TOF-MS (positive ion, linear mode): *m/z*: 11260 ($[M+Na]^+$, $^{12}C_{502}{}^{13}C_6H_{886}N_{20}O_{248}$ + Na requires 11265), and fragments for successive loss of $C[CH_2OCH_2CH_2CO_2(CH_2CH_2O)_3CH_3]_3$.

2·FeCl: Viscous brown oil. FT-IR ($CHCl_3$): $\tilde{\nu}$ = 1738, 1667 (C=O) cm^{-1}; ^1H NMR (300 MHz, $CDCl_3$, 298 K): extremely broad spectrum with aliphatic signals between $\delta \approx$ 1.7 and 4.5, 13.22 (br.s, 4H, β_2-H), 15.25 (br.s, 4H, β_1-H); porphyrin *meso* H (2H) and aryl H (6H) not visible; UV/Vis ($CHCl_3$): λ_{max} (ε) = 375 (sh, 69200), 415 (95500), 461 (sh, 11700), 505 (10700), 551 (7100), 645 (3100); MALDI-TOF-MS (positive ion, linear mode): *m/z*: 11299 ($[M-Cl]^+$, $^{12}C_{502}{}^{13}C_6H_{884}FeN_{20}O_{248}$ requires 11296), and fragments for successive loss of $C[CH_2OCH_2CH_2CO_2(CH_2CH_2O)_3CH_3]_3$.

[a] The matrices for FAB-and MALDI-TOF-MS were 3-nitrobenzyl alcohol and 2,4,6-trihydroxyacetophenone, respectively.

Demetalation of **1·Zn** and **2·Zn** with HCl in $CHCl_3$ gave the corresponding dendritic free-base porphyrins **1·H_2** and **2·H_2** in 93 and 88% yield, respectively. The Zn–H exchange was confirmed by the appearance of ^1H NMR signals at about δ = −3.13 (pyrrole NH), the appearance of four bands in the visible absorption spectrum characteristic of metal-free porphyrin, and correct mass spectral data (Table 1). Heating **1·H_2** or **2·H_2** at reflux in THF with $FeCl_2$ followed by removal of the solvent, re-dissolution in $CHCl_3$, and extensive washing with water provided **1·FeCl** and **2·FeCl** in 85 and 80% yield, respectively. The successful introduction of the metal ion was con-

[*] Prof. F. Diederich, Dr. P. J. Dandliker
Laboratorium für Organische Chemie, ETH Zentrum
Universitätstrasse 16, CH-8092 Zürich (Switzerland)
Telefax: Int. code + (1)632-1109
e-mail: Diederich@org.chem.ethz.ch
Prof. M. Gross, Dr. A. Louati, Dr. J.-P. Gisselbrecht
Laboratoire d'Electrochimie et de Chimie Physique du Corps Solide
U. R. A. au C. N. R. S. no 405
Faculté de Chimie, Université Louis Pasteur
1 et 4, rue Blaise Pascal, F-67008 Strasbourg Cedex (France)

[**] This work was supported by a grant from the research council of the ETH Zürich and the U. S. Office of Naval Research.

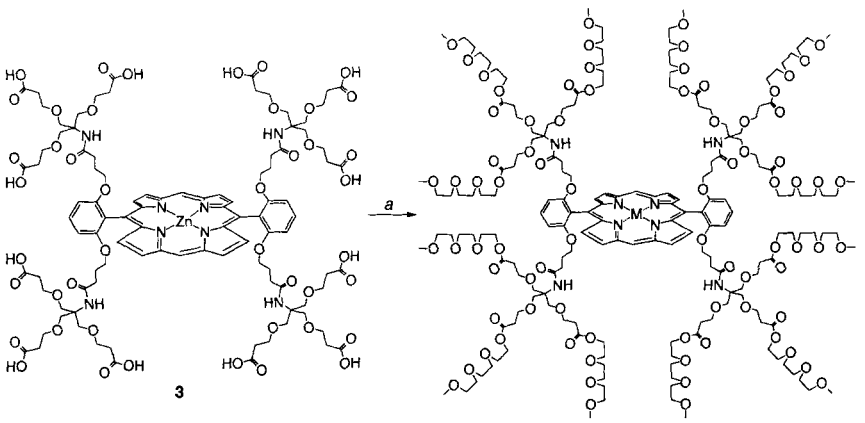

Scheme 1. Synthesis of dendritic porphyrins **1·Zn**, **1·H$_2$**, and **1·FeCl**. a) DCC, HOBT, collidine, triethyleneglycol monomethyl ether, 0 °C to 20 °C, 2 days, 92%. b) 0.4 M aq. HCl, $CHCl_3$, 20 °C, 5 min, 93%. c) $FeCl_2$, THF, reflux, 1 h, 85%.

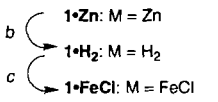

in organic solvents.[8, 10] In particular, Momenteau and co-workers synthesized bridged "basket-handle" iron porphyrins in which the bridging chains, containing ether or amide groups, were linked directly over the metalloporphyrin's π-faces.[10] The amide-containing chains sterically hindered the approach of solvent and counterions to the porphyrin and also exerted a marked through-space electrostatic effect, thus shifting the half-wave potential of the Fe^{III}/Fe^{II} couple to more positive values. Given the steric bulk of the dendritic shell and the high local density of polar amide groups near the porphyrin ring in **1·FeCl** and **2·FeCl**, we expected similar effects to operate in these systems.

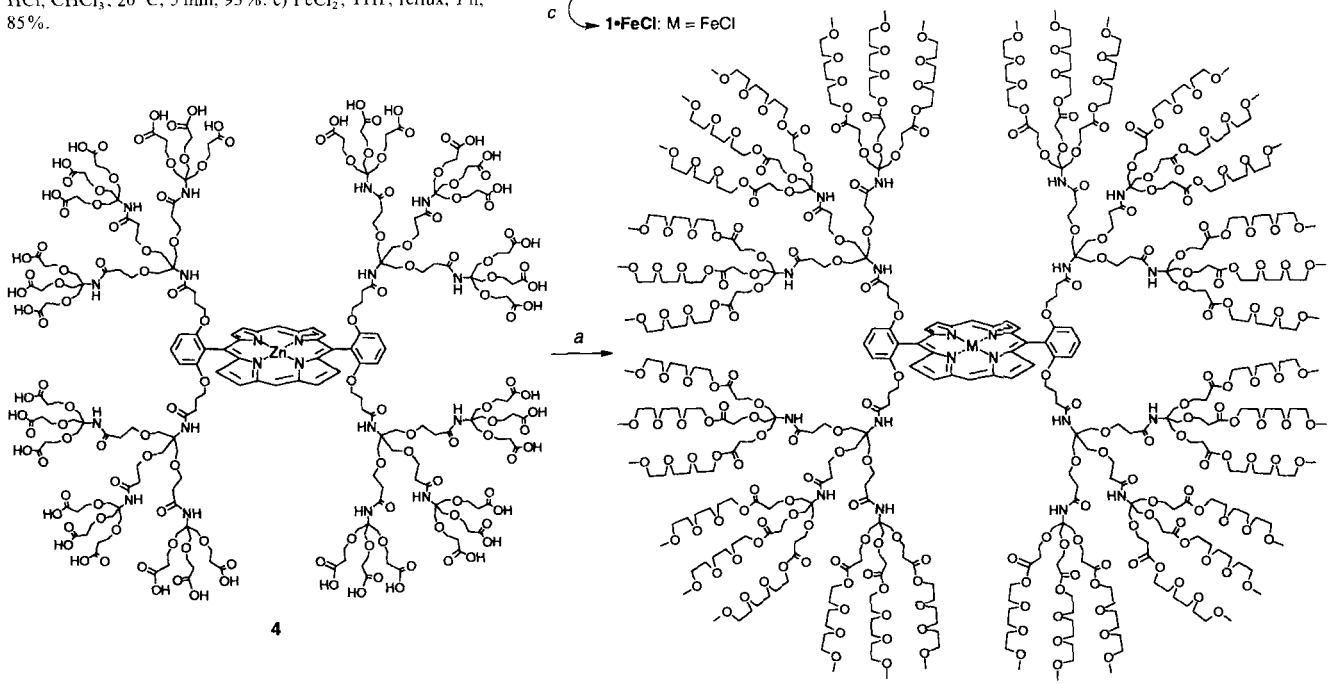

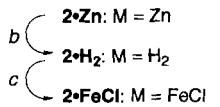

Scheme 2. Synthesis of dendritic porphyrins **2·Zn**, **2·H$_2$**, and **2·FeCl**. a) DCC, HOBT, collidine, triethyleneglycol monomethyl ether, 0 °C to 20 °C, 2 days, 89%. b) 0.4 M aq. HCl, $CHCl_3$, 20 °C, 5 min, 88%. c) $FeCl_2$, THF, reflux, 1 h, 80%.

firmed by the characteristic UV/Vis spectrum for iron(III) porphyrins, ^{1}H NMR signals for the β-pyrrole protons at about $\delta = 13.2$ and 15.2, and the expected mass spectral data (Table 1). All dendritic porphyrins **1** and **2** are viscous oils that dissolve remarkably well in solvents in the polarity range between water ($E_T(30) = 63.1$) and *p*-xylene ($E_T(30) = 33.1$).[9] Control compound **6·FeCl** without dendritic branches was synthesized from the free-base porphyrin **5** in a similar manner.

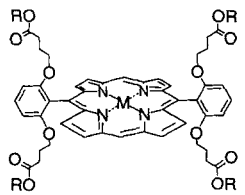

5: R = H, M = H_2

6·FeCl: R = $CH_2(CH_2OCH_2)_2CH_2OCH_3$, M = FeCl

The effects of bulky superstructure on the electrochemical properties of porphyrins have been studied extensively

Cyclic voltammetry in CH_2Cl_2 (glassy carbon electrode, 0.1 M Bu_4NPF_6 as supporting electrolyte) showed irreversible waves for the Fe^{III}/Fe^{II} couple in **6·FeCl**, typical of Fe^{III} porphyrin chlorides, and consistent with equilibrated dissociation of the chloride counterion from the metal ion during electroreduction.[11] In contrast, both **1·FeCl** and **2·FeCl** showed reversible waves for the Fe^{III}/Fe^{II} couple at -10 and $+70$ mV vs. the standard calomel electrode (SCE), respectively (Table 2).

Both **6·FeCl** and **1·FeCl** showed waves for one-electron oxidation at $+1.06$ V, and waves for one-electron reduction from Fe^{II} to Fe^{I} at -1.29 and -1.27 V, respectively, typical values for iron porphyrins (Table 2). The potential difference between the oxidation at $+1.06$ V and reduction to Fe^{I} was within the normal value of 2.25 ± 0.15 V reported for other metalloporphyrin complexes.[12] Compound **2·FeCl** underwent reduction from

Table 2. Half-wave potentials of the dendritic iron porphyrins in CH_2Cl_2 [a].

Porphyrin	$E^{1/2}(Fe^{II}/Fe^{I})$	$E^{1/2}(Fe^{III}/Fe^{II})$	$E^{1/2}_{ox}$
6·FeCl	− 1.29 [b]	− 0.59 [c, d] + 0.12 [c, e]	+ 1.06 [b]
1·FeCl	− 1.27 [c]	− 0.01 [f]	+ 1.06 [b]
2·FeCl	− 1.46 [c]	+ 0.07 [f]	–

[a] Redox potentials in CH_2Cl_2 determined by cyclic voltammetry (CV): $E^{1/2}$ (approximated by $(E^a_p + E^c_p)/2$) in V vs. SCE; supporting electrolyte 0.1 M Bu_4NPF_6; glassy carbon working electrode, scan rate = 0.1 Vs^{-1}, T = 293 K. [b] Quasi-reversible transfer. [c] Irreversible transfer, peak potential from CV. [d] Cathodic peak potential. [e] Anodic peak potential. [f] Reversible transfer.

Fe^{II} to Fe^{I} at −1.46 V, that is, at a 170 mV more negative potential than the reference compound **6·FeCl**.

In order to assign the observed cyclic voltammetric signals to particular redox reactions of the core iron porphyrin, spectroelectrochemical studies were performed at a platinum grid working electrode in CH_2Cl_2 with 0.1 M Bu_4NPF_6 as supporting electrolyte. Compound **1·FeCl** exhibited well-defined isosbestic points on the first reduction step, and the absorption spectrum remained characteristic of an iron porphyrin with only small changes in the position of the Soret and Q bands. Following the second reduction step, the spectrum remained typical for the metalloporphyrin, displaying red shifts of 20 nm for the Soret band and 16 nm for the Q band. This behavior is characteristic of successive metal-centered reductions from Fe^{III} to Fe^{II} and Fe^{I} porphyrins, respectively. Compound **2·FeCl** exhibited analogous behavior, which confirmed that the first reduction step corresponded to the Fe^{III}/Fe^{II} couple. The presumed generation of an Fe^{I} species during the second reduction step at −1.46 V vs. SCE could not be monitored, since it occurred too close to the accessible cathodic potential limit of the solvent.

To compare the redox behavior of the dendritic iron porphyrins to that of heme proteins more directly, cyclic voltammetric studies in water with 0.1 M Et_4NClO_4 as the supporting electrolyte were carried out. For solubility reasons, only compounds **1·FeCl** and **2·FeCl** could be studied in aqueous solution. They both exhibited irreversible one-electron oxidation waves at the glassy carbon electrode at + 0.97 and + 1.09 V vs. SCE, respectively (Table 3). Compounds **1·FeCl** and **2·FeCl** also exhibited two reductions, the second of which was irreversible and occurred at the same potential of −1.26 V vs. SCE. In contrast, the increased density of the dendritic superstructure in **2·FeCl** relative to **1·FeCl** caused the potential of the fully reversible Fe^{III}/Fe^{II} couple of **2·FeCl** to shift from −0.23 V to + 0.19 V and thus to become 420 mV more positive.

Table 3. Half-wave potentials of the dendritic iron porphyrins in H_2O [a].

Porphyrin	$E^{1/2}(Fe^{II}/Fe^{I})$	$E^{1/2}(Fe^{III}/Fe^{II})$	$E^{1/2}_{ox}$
1·FeCl	− 1.26 [b]	− 0.23 [c]	+ 0.97 [b]
2·FeCl	− 1.26 [b]	+ 0.19 [c]	+ 1.09 [b]

[a] Redox potentials in H_2O determined by cyclic voltammetry (CV): $E^{1/2}$ (approximated by $(E^a_p + E^c_p)/2$) in V vs. SCE; supporting electrolyte 0.1 M Et_4NClO_4; glassy carbon working electrode, scan rate = 0.1 Vs^{-1}, T = 293 K. [b] Irreversible transfer, peak potential from CV. [c] Reversible transfer.

These results show that environmental polarity strongly influences the redox potential of electrochemical reactions that occur at the heme metal center. In CH_2Cl_2, the iron porphyrins in both the more open **1·FeCl** and the more densely packed **2·FeCl** experience similar microenvironments; hence similar potentials for the Fe^{III}/Fe^{II} couple are measured. In water, the relatively open dendritic branches of **1·FeCl** do not impede aqueous solvation of the iron porphyrin, whereas the densely packed dendritic superstructure of **2·FeCl** significantly reduces contact between the heme and external solvent, destabilizing the oxidized, more charged state and shifting the redox potential to a more positive value.

The remarkable potential difference between **2·FeCl** and **1·FeCl** is similar to that (about 300 mV) found between cytochrome c and a similarly ligated, more solvent-exposed cytochrome c heme octapeptide.[13] Despite resemblance in globular shape and dimensions between **2·FeCl** and cytochrome c,[14] as suggested by computer modeling, further analogies between dendritic and biological system are currently limited by the difference in axial ligation to the heme iron. Whereas the protein uses a histidine-N atom and a methionine-S atom, the nature of the axial ligands of the dendrimer in water is different but remains to be determined. By covalently inserting the natural N- and S-ligands into dendritic iron porphyrins, their model character for cytochrome c could be further extended in future work.

Received: July 12, 1995 [Z 8198 IE]
German version: *Angew. Chem.* **1995**, *107*, 2906–2909

Keywords: dendrimers · electrochemistry · heme-protein mimics · iron compounds · porphyrinoids

[1] a) D. A. Tomalia, A. M. Naylor, W. A. Goddard, III, *Angew. Chem.* **1990**, *102*, 119–157; *Angew. Chem. Int. Ed. Engl.* **1990**, *29*, 138–175; b) H. B. Mekelburger, W. Jaworek, F. Vögtle, *ibid.* **1992**, *104*, 1609–1614 and **1992**, *31*, 1571–1576; c) D. A. Tomalia, *Adv. Mater.* **1994**, *6*, 529–539.

[2] a) Y.-H. Liao, J. R. Moss, *Organometallics* **1995**, *14*, 2130–2132; b) C. J. Hawker, J. M. J. Fréchet, *J. Chem. Soc. Perkin Trans. 1* **1992**, 2459–2469; c) K. L. Wooley, C. J. Hawker, J. M. J. Fréchet, *ibid.* **1991**, 1059–1076; d) F. Moulines, L. Djakovitch, R. Boese, B. Gloaguen, W. Thiel, J.-L. Fillaut, M.-H. Delville, D. Astruc, *Angew. Chem.* **1993**, *105*, 1132–1133; *Angew. Chem. Int. Ed. Engl.* **1993**, *32*, 1075–1077; e) M. R. Bryce, W. Devonport, A. J. Moore, *ibid.* **1994**, *106*, 1862–1864 and **1994**, *33*, 1761–1763; f) R. Roy, D. Zanini, S. J. Meunier, A. Romanowska, *J. Chem. Soc. Chem. Commun.* **1993**, 1869–1872; g) P. Singh, F. Moll, S. H. Lin, C. Ferzli, K. S. Yu, R. K. Koski, R. G. Saul, P. Cronin, *Clin. Chem.* **1994**, *40*, 1845–1849.

[3] a) T. Nagasaki, M. Ukon, S. Arimori, S. Shinkai, *J. Chem. Soc. Chem. Commun.* **1992**, 608–610; b) G. R. Newkome, F. Cardullo, E. C. Constable, C. N. Moorefield, A. M. W. C. Thompson, *ibid.* **1993**, 925–927; c) S. Achar, R. J. Puddephatt, *Angew. Chem.* **1994**, *106*, 895–897; *Angew. Chem. Int. Ed. Engl.* **1994**, *33*, 847–849; d) G. R. Newkome, C. N. Moorefield, J. M. Keith, G. R. Baker, G. H. Escamilla, *ibid.* **1994**, *106*, 701–703 and **1994**, *33*, 666–668; e) S. Serroni, G. Denti, S. Campagna, A. Juris, M. Ciano, V. Balzani, *ibid.* **1992**, *104*, 1540–1542 and **1992**, *31*, 1493–1495.

[4] a) R.-H. Jin, T. Aida, S. Inoue, *J. Chem. Soc. Chem. Commun.* **1993**, 1260–1262; b) C. J. Hawker, K. L. Wooley, J. M. J. Fréchet, *J. Am. Chem. Soc.* **1993**, *115*, 4375–4376; c) K. L. Wooley, C. J. Hawker, J. M. J. Fréchet, F. Wudl, G. Srdanov, S. Shi, C. Li, M. Kao, *ibid.* **1993**, *115*, 9836–9837; d) S. Serroni, S. Campagna, A. Juris, M. Venturi, V. Balzani, *Gazz. Chim. Ital.* **1994**, *124*, 423–427.

[5] a) J. Issberner, R. Moors, F. Vögtle, *Angew. Chem.* **1994**, *106*, 2507–2514; *Angew. Chem. Int. Ed. Engl.* **1994**, *33*, 2413–2420; b) J. F. G. A. Jansen, R. A. J. Janssen, E. M. M. de Brabander-van den Berg, E. W. Meijer, *Adv. Mater.* **1995**, *7*, 561–564.

[6] a) G. R. Moore, G. W. Pettigrew, *Cytochromes-c: Evolutionary, Structural, and Physicochemical Aspects*, Springer, Berlin, **1990**, pp. 309–362; b) S. Komar-Panicucci, J. Bixler, G. Bakker, F. Sherman, G. McLendon, *J. Am. Chem. Soc.* **1992**, *114*, 5443–5445; c) K. L. Bren, H. B. Gray, *ibid.* **1993**, *115*, 10382–10383; d) V. T. Taniguchi, W. R. Ellis, Jr., V. Cammarata, J. Webb, F. C. Anson, H. B. Gray, *Adv. Chem. Ser.* **1982**, *201*, 51–68; e) T. Daido, T. Akaike, *J. Electrounal. Chem.* **1993**, *344*, 91–106; f) P. K. Warme, L. P. Hager, *Biochemistry* **1970**, *9*, 1606–1614.

[7] a) H. X. Zhou, *J. Am. Chem. Soc.* **1994**, *116*, 10362–10375; b) A. M. Bond, *Inorg. Chim. Acta* **1994**, *226*, 293–340; c) T. Yagi, *Meth. Enzym.* **1994**, *243*, 104–118; d) F. Malatesta, G. Antonini, P. Sarti, M. Brunori, *Biophys. Chem.* **1995**, *54*, 1–33.

[8] P. J. Dandliker, F. Diederich, M. Gross, C. B. Knobler, A. Louati, E. M. Sanford, *Angew. Chem.* **1994**, *106*, 1821–1825; *Angew. Chem. Int. Ed. Engl.* **1994**, *33*, 1739–1742.

[9] C. Reichardt, *Solvents and Solvent Effects in Organic Chemistry*, 2nd ed., VCH, Weinheim, **1988**.
[10] a) D. Lexa, M. Momenteau, P. Rentien, G. Rytz, J.-M. Savéant, F. Xu, *J. Am. Chem. Soc.* **1984**, *106*, 4755–4765; b) C. Gueutin, D. Lexa, M. Momenteau, J.-M. Savéant, F. Xu, *Inorg. Chem.* **1986**, *25*, 4294–4307; c) P. Maillard, C. Schaeffer, C. Huel, J. M. Lhoste, M. Momenteau, *J. Chem. Soc. Perkin Trans 1* **1988**, 3285–3296.
[11] K. M. Kadish, L. A. Bottomley, *Inorg. Chem.* **1981**, *20*, 1348–1357.
[12] J.-H. Fuhrhop, K. M. Kadish, D. G. Davis, *J. Am. Chem. Soc.* **1973**, *95*, 5140–5147.
[13] R. J. Kassner, *J. Am. Chem. Soc.* **1973**, *95*, 2674–2677.
[14] a) N. Tanaka, Y. Yamane, T. Tsukihara, T. Ashida, M. Kaduko, *J. Biochem. (Tokyo)* **1975**, *77*, 147–161; b) T. Takano, R. E. Dickerson, *J. Mol. Biol.* **1981**, *153*, 79–94.

A New Strategy in Heterogeneous Catalysis: The Design of Cortex Catalysts

Manfred T. Reetz,* Stefan A. Quaiser, Rolf Breinbauer, and Bernd Tesche

The majority of chemical transformations in industry are catalytic processes, more than 75% of which are carried out using heterogeneous catalysts.[1] A large group of heterogeneous catalysts are the impregnation catalysts, prepared by impregnating solid supports with metal salts followed by calcination and reduction at high temperatures.[1, 2] More recently, solvated metal atoms[3] as well as certain molecular metal complexes and metal clusters have been immobilized on commercial solid metal oxides.[4] Another current approach concerns surface organometallic chemistry according to which discrete catalytically active species are anchored on solid supports.[5] Although many of these catalysts have been characterized by a variety of techniques such as transmission electron microscopy (TEM), energy dispersive X-ray analysis (EDX), and X-ray photoelectron spectroscopy (XPS),[1–6] the precise location of the metal particles or ligated metals on the support remains unclear. Generally, it is desirable to achieve metal dispersion preferably on the outer surface of the support, because this minimizes diffusion problems. This is the reason why shell catalysts, especially those of the eggshell type, are often preferred. Accordingly, mm-sized pellets are treated in special impregnation procedures during which a metal-containing outer region several hundred μm thick is formed. However, it is likely that in this macroscopically visible region the metal particles are not exclusively fixed on the outer surface in a microscopic sense, but are also distributed deep in the pores of the solid support. In order to prevent this, we have now immobilized preformed and size-selectively prepared metal clusters on solid supports. By considering pore diameter and cluster size, it is possible to design catalysts in which metal particles of a specified size are found solely on the outer surface of the support.

Recently we described an electrochemical process for the production of nanostructured transition metal clusters (e.g. Ni, Pd, Pt, Co, Rh, Ru)[7] and dimetallic clusters (e.g. Ni/Pd, Fe/Co, Fe/Ni, Pt/Sn)[8, 9] stabilized by tetraalkylammonium salts. The diameter of the particles ranges between 1 and 10 nm and can be controlled by adjusting the current density. The spherical clusters are surrounded by tetraalkylammonium salts that function as a stabilizing mantle; the visualization of this protective monomolecular layer is possible through a combination of transmission electron and scanning tunneling microscopy (TEM/STM).[10] The solubility of these stabilized clusters is dependent on the ammonium salt; thus, those with $(C_{18}H_{37})_4N^+Br^-$ are soluble in nonpolar solvents such as pentane and those with betains such as $C_{12}H_{25}$-$(CH_3)_2N^+CH_2CH_2CH_2SO_3^-$ are soluble in water.[8]

Upon stirring solutions of these preformed clusters at room temperature in the presence of solid supports such as SiO_2 or Al_2O_3 in the form of powders or pellets, immobilization occurs without any change in cluster size.[8, 11] This means that metal crystallites of a defined size and elemental composition can be specifically placed on such supports. In the case of pellets, shell catalysts[1, 2] are easily produced without the need for special preparation techniques necessary in conventional impregnation processes such as pretreatment of the solid support with certain salts, use of viscous solvents or additives, or special drying procedures. For example, impregnation of Al_2O_3 pellets (Johnson Matthey 11838) with a 0.5M THF solution of 3 nm sized (by TEM) $(C_8H_{17})_4N^+Br^-$-stabilized Pd clusters leads to rapid immobilization. Eggshell catalysts are obtained within 1–4 s, as shown by photographs of pellet cross sections (Fig. 1a, b). The

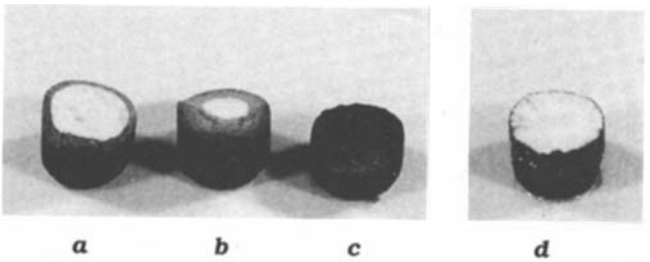

Fig. 1. Cross sections of Al_2O_3 pellets (diameter 3.2 mm). a) After penetration with a 0.5M tetrahydrofuran solution of $(C_8H_{17})_4N^+Br^-$-stabilized Pd clusters for 1 second. b) For 4 seconds. c) For 10 seconds. d) After penetration with an aqueous 0.5M solution of betain-stabilized Pd clusters for 5 h.

extent of the uniform macroscopic penetration is time-dependent; the penetration is complete after 10 s (Fig. 1c). In sharp contrast, interaction of the same pellets with a 0.5M aqueous solution of betain-stabilized Pd clusters (3 nm by TEM) affords only eggshell-type catalysts (penetration < 100 μm), even after prolonged periods of interaction. For example, gentle shaking of such a black-colored solution of the cluster with the above Al_2O_3 pellets for 5 h results in complete immobilization of the cluster (Fig. 1d). Following decantation, the water is completely colorless and contains about 70% of the original betain stabilizer. If so desired, further washing can remove up to 95% of the stabilizer.

The dramatic difference in the rate and depth of penetration in going from $(C_8H_{17})_4N^+Br^-$ to $C_{12}H_{25}$-$(CH_3)_2N^+CH_2CH_2CH_2SO_3^-$ can be explained on the basis of different degrees of interaction of the stabilizer with the support. In the case of the $(C_8H_{17})_4N^+Br^-$ stabilizer which has four lipophilic *n*-octyl chains at nitrogen, the interaction with the hydrophilic surface of Al_2O_3 is relatively weak, and rapid macroscopic penetration occurs as the cluster-containing solvent moves into the pellet. In the case of the betain-stabilized clusters, strong interaction between the polar substituents of the stabilizer and the Al_2O_3 surface lowers the rate and degree of

[*] Prof. Dr. M. T. Reetz, Dr. S. A. Quaiser, Dipl.-Ing. R. Breinbauer, Dr. B. Tesche
Max-Planck-Institut für Kohlenforschung
Kaiser-Wilhelm-Platz 1, D-45470 Mülheim an der Ruhr (Germany)
Telefax: Int. code +(208) 306 2985

 © VCH Verlagsgesellschaft mbH, D-69451 Weinheim, 1995 0570-0833/95/3423-2728 $ 10.00+.25/0

penetration. The use of aqueous solutions of betain-stabilized clusters is noteworthy, because such a procedure is economically and ecologically attractive. In comparison, conventional impregnation of the same Al_2O_3 pellets with a 0.5 M aqueous solution of $Pd(OAc)_2$ for one minute without special precautions results in fully penetrated pellets (characterized following calcination/reduction).

Methods for the controlled positioning of metal particles on a *microscopic* level are even more important because catalytically active components far inside small pores are not readily accessible during catalytic reactions. Furthermore, catalysts having the dispersed metals mainly on the outer surface can be expected to be more selective in industrially important reactions such as selective hydrogenation or partial oxidation because of short contact times. We have discovered that the use of the preformed ammonium-stabilized metal clusters described here allows for such a control. Indeed, the metal crystallites can be positioned precisely on the outer surface of the support without deep penetration into the pores.

For example, using a commercially available alumina (Aldrich 19997-4) with an average pore size of 5.8 nm, $(C_4H_9)_4N^+Br^-$-stabilized Pd clusters with an inner metal core diameter of 3.5 nm (by TEM) and an outer diameter of 4.9 nm (by STM) were immobilized in the usual way. Following the removal of the solvent the solid material was washed several times with ethanol to remove the stabilizer. The concentration and amount of Pd clusters were varied so that materials containing 1% and 5% palladium were obtained. Conventional TEM analyses showed that in both cases materials with particles with an average diameter of 3.5 nm are obtained, again demonstrating that undesired agglomeration does not occur. However, such conventional studies provide only limited characterization because they do not reveal where the clusters are actually located, since by nature the transmission electron micrographs are only two-dimensional projections of three-dimensional materials.[6]

To solve this analytical problem, we have applied a technique well known in biology, medicine, and materials science, but seldom used in heterogeneous catalysis, namely ultramicrotometry in combination with TEM.[12] Accordingly, particles of the two Pd-containing Al_2O_3 powders (1% and 5% metal loading) were first embedded in an epoxy resin. Slices of ultramicrotometrically cut materials were then studied by TEM. Figure 2a shows the TEM image of such a cross section. Clearly, most of the metal particles are located on the outer surface of the Al_2O_3 particles. This means that the preformed clusters have not entered the pores of the Al_2O_3 support to any significant extent (less than 10 nm penetration). In contrast, samples of a commercial Pd catalyst on Al_2O_3, prepared by conventional impregnation/calcination/reduction, have completely different morphological features. The corresponding TEM image in Figure 2b shows that in this case the metal is distributed more or less evenly throughout the three-dimensional network of the support. Evidently, impregnation of Al_2O_3 by palladium salts results in uncontrolled migration into the pores of the solid matrix before the corresponding Pd^0 particles are formed in the final reduction step. Capillary forces operating in the pores induce this type of salt penetration on a microscopic level, a process which does not occur as readily with the relatively large-sized preformed metal clusters.

Using supports such as Al_2O_3, we have applied our approach successfully to Pd clusters of different sizes (e.g., 1.4 and 4.8 nm-sized samples), to Ni clusters, and to Pt/Sn dimetallic clusters. It remains to be seen whether such morphologically well-defined materials, which we call *cortex* catalysts (to distinguish them from the usual shell catalysts), have significant advantages over heterogeneous catalysts prepared by conventional procedures. In preliminary experiments involving the hydrogenation of cyclooctene, a palladium cortex catalyst (5% Pd on Al_2O_3; see Fig. 2a) turned out to be about three times more active than a comparable commercially available industrial catalyst (5% Pd on Al_2O_3; Aldrich 37148-3).

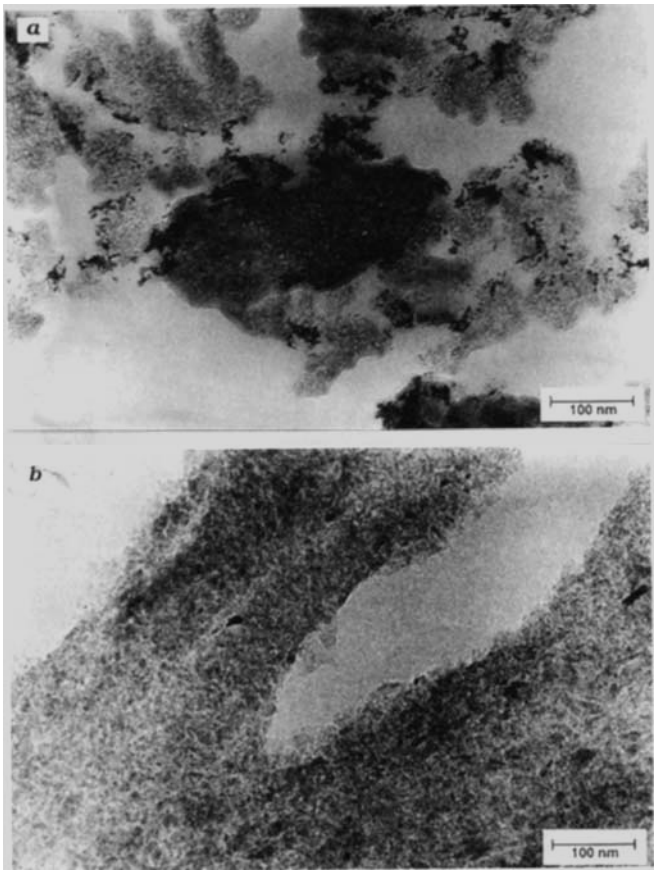

Fig. 2. TEM images of ultramicrotometrically cut alumina powders. a) After penetration with a 0.5 M solution of $(C_4H_9)_4N^+Br^-$-stabilized Pd clusters. b) Conventionally prepared impregnation catalyst (Aldrich 37148-3).

The present findings together with the fact that ammonium-stabilized homo- and dimetallic clusters are accessible in a size-selective manner and defined composition allow for the design of heterogeneous catalysts with well-defined compositional and structural features on a macroscopic and microscopic level. Due to the simplicity of the method of preparation, these cortex catalysts may be industrially viable.

Received: October 26, 1995 [Z 8502 IE]
German version: *Angew. Chem.* **1995**, *107*, 2956–2958

Keywords: catalysis · clusters · immobilization · surface chemistry

[1] E. F. Gallei, H.-P. Neumann, *Chem. Ing. Tech.* **1994**, *66*, 924.
[2] J. M. Thomas, *Angew. Chem.* **1994**, *106*, 963; *Angew. Chem. Int. Ed. Engl.* **1994**, *33*, 913; E. Iglesia, S. L. Soled, J. E. Baumgartner, S. C. Reyes, *J. Catal.* **1995**, *153*, 108; K. Foger, in *Catalysis—Science and Technology, Vol. 6* (Eds.: J. R. Anderson, M. Boudart), Springer, Berlin, **1984**, p. 227; M. A. M. Luengo, P. A. Sermon, K. S. W. Sing, in *Preparation of Catalysts IV* (Eds.: B. Delmon, P. Grange, P. A. Jacobs, G. Poncelet), Elsevier, Amsterdam, **1987**, p. 29; T. Fujiyama, M. Otsuka, H. Tsuiki, A. Ueno, *J. Catal.* **1987**, *104*, 323; M. S. Heise, J. A. Schwarz, *Stud. Surf. Sci. Catal.* **1987**, *31*, 1.
[3] K. J. Klabunde, Y.-X. Li, B.-J. Tan, *Chem. Mater.* **1991**, *3*, 30.

[4] G. Schmid, M. Harms, J.-O. Malm, J.-O. Bovin, J. van Ruitenbeck, H. W. Zandbergen, W. T. Fu, *J. Am. Chem. Soc.* **1993**, *115*, 2046; C. Binet, A. Jadi, J.-C. Lavalley, M. Boutonnet-Kizling, *J. Chem. Soc. Faraday Trans.* **1992**, *88*, 2079.

[5] "Surface Organometallic Chemistry: Molecular Approaches to Surface Catalysis": *NATO ASI Ser. Ser. C* **1988**, *231*; B. C. Gates, *Chem. Rev.* **1995**, *95*, 511.

[6] M. José-Yacamán, G. Díáz, A. Gómez, *Catal. Today* **1995**, *23*, 161.

[7] Clusters stabilized by tetraalkylammonium salts have been known for some time: J. Kiwi, M. Grätzel, *J. Am. Chem. Soc.* **1979**, *101*, 7214; J. Blum, Y. Sasson, A. Zoran, *J. Mol. Catal.* **1981**, *11*, 293; M. Boutonnet, J. Kizling, P. Stenius, G. Maire, *Colloids Surf.* **1982**, *5*, 209; N. Toshima, T. Takahashi, H. Hirai, *Chem. Lett.* **1985**, 1245; M. Boutonnet, J. Kizling, R. Touroude, G. Maire, P. Stenius, *Appl. Catal.* **1986**, *20*, 163; K. Meguro, M. Toriyuka, K. Esumi, *Bull. Chem. Soc. Jpn.* **1988**, *61*, 341; J. Wiesner, A. Wokaun, H. Hoffmann, *Prog. Coll. Polym. Sci.* **1988**, *76*, 271; N. Satoh, K. Kimura, *Bull. Chem. Soc. Jpn.* **1989**, *62*, 1758; H. Bönnemann, W. Brijoux, R. Brinkmann, E. Dinjus, T. Joussen, B. Korall, *Angew. Chem.* **1991**, *103*, 1344; *Angew. Chem. Int. Ed. Engl.* **1991**, *30*, 1312; N. Toshima, T. Takahashi, *Bull. Chem. Soc. Jpn.* **1992**, *65*, 400; M. T. Reetz, W. Helbig, S. A. Quaiser in *Active Metals—Preparation, Characterization, Applications* (Ed. A. Fürstner), VCH, Weinheim, **1995**, p. 279.

[8] M. T. Reetz, W. Helbig, *J. Am. Chem. Soc.* **1994**, *116*, 7401; M. T. Reetz, W. Helbig, S. A. Quaiser, patent application, **1994**; M. T. Reetz, S. A. Quaiser, *Angew. Chem.* **1995**, *107*, 2461; *Angew. Chem., Int. Ed. Engl.* **1995**, *34*, 2240.

[9] J. A. Becker, R. Schäfer, R. Festag, W. Ruland, J. H. Wendorff, J. Pebler, S. A. Quaiser, W. Helbig, M. T. Reetz, *J. Chem. Phys.* **1995**, *103*, 2520; M. T. Reetz, W. Helbig, S. A. Quaiser, *Chem. Mater.* **1995**, in press.

[10] M. T. Reetz, W. Helbig, S. A. Quaiser, U. Stimming, N. Breuer, R. Vogel, *Science* **1995**, *267*, 367.

[11] Immobilization of $R_4N^+X^-$-stabilized clusters on charcoal: H. Bönnemann, W. Brijoux, R. Brinkmann, R. Fretzen, T. Joussen, R. Köppler, B. Korall, P. Neiteler, J. Richter, *J. Mol. Catal.* **1994**, *86*, 129.

[12] *Procedures in Electron Microscopy* (Eds.: A. W. Robards, A. J. Wilson), Wiley, Chichester, **1994**; *Catalyst Characterization* (Eds.: B. Imelik, J. C. Vedrine), Plenum, New York, **1993**.

1-Phenyl-1,2-cyclooctadiene Dimerizes in an Unusual Manner**

Manfred Christl,* Marcus Rudolph, Eva-Maria Peters, Karl Peters, and Hans Georg von Schnering

As has been demonstrated recently,[1] the dimerization of the seven-membered cycloallene **1** proceeds in the usual manner[2,3] to yield the C_2 symmetric 1,2-bismethylenecyclobutane derivative **2**.[1] On thermolysis, **2** is converted into the isomers **3** (configuration unknown) and **4**. Finally, **3** rearranges to **4** as well. According to the present knowledge,[4] a tetramethyleneethane diradical has to be assumed as the intermediate for both the formation of **2** and its isomerization. En route to **4**, this diradical closes a six-membered ring by attack of one allyl radical terminus at the phenyl group of the second phenylallyl radical subunit. With the allene **6**, we have now synthesized a compound for which this elementary process is kinetically preferred, furnishing the unusual dimer **7**.

1-*tert*-Butyl-1,2-cyclooctadiene is the only eight-membered cycloallene stable at 20 °C.[5] The parent compound[6,7] and its 1-methyl derivative [2] can be observed; however, they dimerize

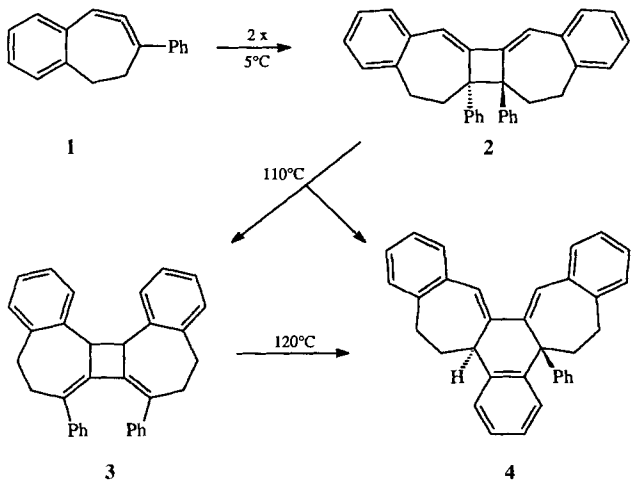

rather rapidly even at 20 °C to give the usual products, namely the C_2 symmetric 1,2-bismethylenecyclobutane derivatives.[6,7] These reactions were investigated in detail recently by application of the Doering–Moore–Skattebøl method for the preparation of these allenes.[7] Using this procedure, we also generated **6**; the dibromocarbene adduct **5**[8] of 1-phenylcycloheptene was treated with methyllithium in ether at −40 °C. After work up at this temperature, **6** could not be detected by low-temperature ^{13}C NMR spectroscopy. Only signals of the methylene-1,3-cyclohexadiene derivative **7** were present, which was isolated in 50–60% yield and structurally elucidated by X-ray diffraction[9] (Fig. 1).

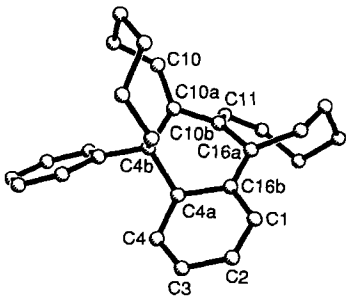

Fig. 1. Crystal structure of **7** [9]. The C4a–C4b bond is particularly long (160.9 pm), probably due to steric overcrowding. Whereas the ethene subunits C4–C3, C2–C1, and C16b–C16a are almost coplanar (torsional angles −1.8 and −178.2°), the torsional angle for C16b–C16a and C10b–C11 is −127°; however, this does not prevent a long-wavelength absorption in the UV spectrum (see Table 1). The ethene subunits are strongly twisted against each other (−51.0°) also in the 1,3-butadiene system C10-C10a-C10b-C11.

Unlike the precursor to **4**, which is analogous to **7**, compound **7** did not aromatize on heating, but rearranged to give a symmetric dimer of **6** (6 d, 20 °C, CH_2Cl_2 or 4 h, 70 °C, C_6H_6, 50%). The addition product from this dimer and tetracyanoethylene (TCNE) is symmetric as well, which is why the C_s symmetric formulas **12** and **8** have to be ascribed to this adduct and the precursor diene, respectively. The configuration of **8** was confirmed by an X-ray structure analysis[9] (Fig. 2). 1,2-Cyclononadiene does form a C_s symmetric dimer,[10]

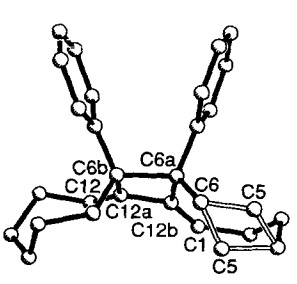

Fig. 2. Crystal structure of **8** [9]. In one of the two eight-membered rings, the second CH_2 group (C5) next to the phenyl-substituted bridgehead is disordered. As a result of severe steric overcrowding, the C6a–C6b bond is unusually long (165.0 pm) and is thus similar to the corresponding bonds in **2** [1] and another sterically highly encumbered 1,2-bismethylenecyclobutane [11]. The 1,3-butadiene system C1-C12b-C12a-C12 deviates only slightly from the planar arrangement (torsional angle −11.2°).

[*] Prof. Dr. M. Christl, Dipl.-Chem. M. Rudolph
Institut für Organische Chemie der Universität
Am Hubland, D-97074 Würzburg (Germany)
Telefax: Int. code + (931)888-4606
E.-M. Peters, Dr. K. Peters, Prof. Dr. H. G. von Schnering
Max-Planck-Institut für Festkörperforschung, Stuttgart (Germany)

[**] Cycloallenes, Part. 10. This work was supported by the Fonds der Chemischen Industrie and by CHEMETALL GmbH. Part 9: M. Christl, M. Braun, E. Wolz, W. Wagner, *Chem. Ber.* **1994**, *127*, 1137–1142.

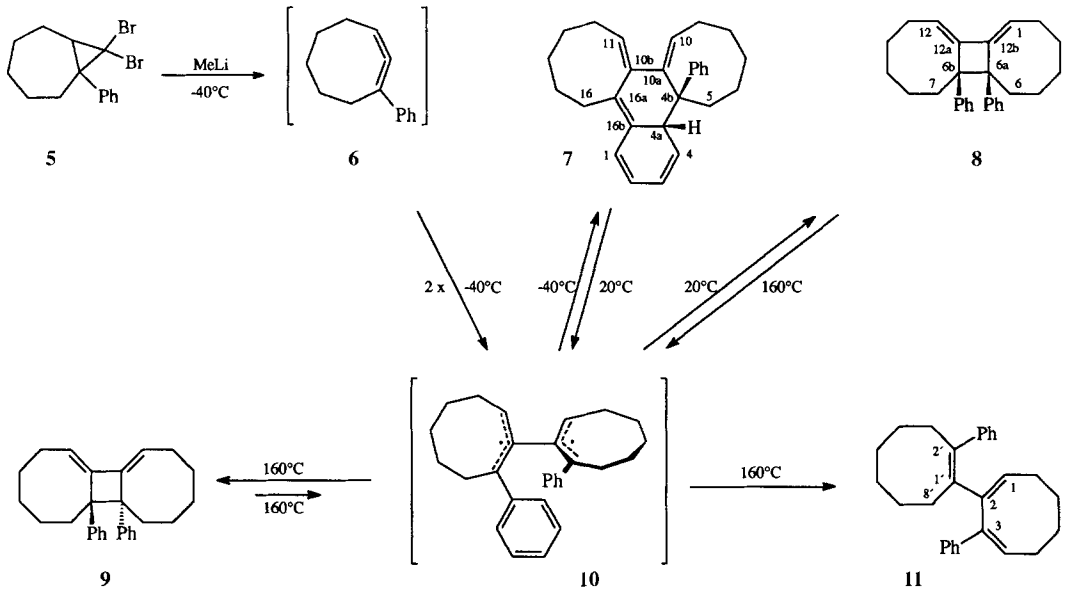

5 6 7 8

9 10 11

symmetric dimer,[10] however, such a product is as yet unknown from a cycloallene with an eight-membered or a smaller ring.

The bismethylenecyclobutane **8** was not the final product of the thermolysis; upon heating at 160 °C (24 h, C_6H_6), **8** was converted into the cyclooctenylcyclooctadiene **11** (90%), the structure of which was determined by NMR spectroscopic studies (2D-INADEQUATE). At intermediate stages of the thermolysis, the NMR spectra of the solution indicated further components. The most important one, as far as quantity is concerned, reached a proportion of 25% prior to the formation of larger amounts of **11** (after 4 h at 160 °C). A fraction strongly enriched in that compound could be obtained by chromatography. Based on the similarity to those of **8**, its NMR spectra support the structure of the *trans*-annulated 1,2-bismethylenecyclobutane **9**.

Although **7** is formally the product of a Diels–Alder reaction of two molecules of **6**, all the above processes should be mediated by the tetramethyleneethane diradical **10**, the formation of which has to be expected on dimerization of **6**.[4] The fast collapse of **10** to give the new six-membered ring of **7** is probably caused by the conformation of the eight-membered rings placing the reaction centers in favorable positions. This prerequisite is obviously absent in the less flexible diradical originating analogously from **1**, since it selects the closure of a six-membered ring only as the route for final stabilization.

Dimer **7** seems to be in equilibrium with **10** in solution even at 20 °C; the latter then collapses to give **8**. As shown by the relatively high concentration of **9** on thermolysis of **8**, the thermodynamic stability of **9** should resemble that of **8**. However, the kinetic barrier to formation of **9** from **10** must be much higher than that of **8**. This is astounding because the least-motion process of **10** providing a bismethylenecyclobutane (conrotation) would just furnish **9**. En route to **8**, both the allyl radical subunits of **10** would have to arrange in a common plane and then form the bond by disrotation. Possibly, instead of **10**, its diastereomer with *one* 3-phenylcyclooct-*trans*-2-en-1-yl moiety is involved, the least-motion ring closure of which would lead to **8**. Both alternatives appear to be costly in terms of the energy demand. The comparison with the route to **2** indicates that the conformation of the eight-membered rings of **10** should be the reason for the much higher barrier separating **10** from **9**. The conversion of **8** and **9** into **11** should proceed via **10** as well, in which a hydrogen atom has to be transferred from one eight-membered ring to the other. Albeit intermolecular, such disproportionations are well-known elementary reactions of radicals.

The addition of TCNE to cycloallene dimers has been employed repeatedly for the structure elucidation of such dienes.[3,7,12] As mentioned above, the reaction of **8** with TCNE (24 h, 20 °C, C_6H_6) gave rise to the tetracycle **12** (31%). Akin to

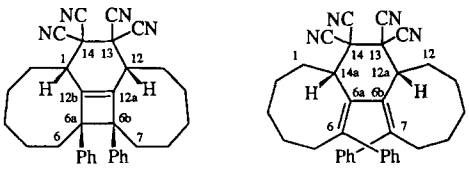

12 13

other 3,4-diphenylcyclobutenes,[13] **12** underwent opening of the four-membered ring under mild conditions (slowly at 20 °C and rapidly at 80 °C in C_6H_6). As revealed by an X-ray structure analysis (Fig. 3), formula **13** has to be ascribed to the product (28% from **8**). Hence, contrary the rules regarding the conservation of orbital symmetry, a disrotatory motion governed the isomerization. The rigid helical arrangement of the *Z*,*Z*-1,4-diphenyl-1,3-butadiene subunit is responsible for the missing symmetry of **13** indicated by the NMR spectra (Table 1).

We achieved the aromatization by treating **7** with *p*-toluenesulfonic acid (4 h, 20 °C, CH_2Cl_2, 50%). NOE measurements support structure **14** by proving the proximity of the olefinic proton (16-H) to one proton of the annulated benzene moiety (1-H).

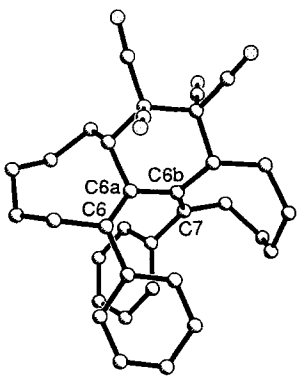

Fig. 3. Crystal structure of **13** [9]. The 1,3-butadiene system C6-C6a-C6b-C7 deviates strongly from the planar arrangement (torsional angle 74.8°), which is why the UV spectrum shows short-wavelength absorptions (see Table 1) only.

Table 1. Selected physical data of 7–**9** and **11**–**14**; ^{1}H and ^{13}C NMR spectra (600 and 151 MHz, respectively, measured in $CDCl_3$, except where stated otherwise); in so far as specified, the assignments of the NMR signals are supported by DEPT, ^{1}H,^{1}H-COSY, and 2D-INADEQUATE spectra as well as NOE measurements.

7: M.p. 113 °C (from pentane); ^{1}H NMR (250 MHz): δ = 1.15-2.00 (m; 15H), 2.21 (br. ddd, J = 15, 10, 5 Hz; 1H), 2.34-2.64 (m; 3H), 2.74 (ddt, J = 16.9, 9.5, 3.2 Hz; 1H), 3.15 (br. s; H4a), 5.19 (br. dd, J(3,4) = 9.8, J(4,4a) = 4.7 Hz; H4), 5.71 (≈ t, J = 8.9 Hz), 6.06 (dd, J = 6.9, 4.8 Hz) (H10,11), 5.77 (br. dd, J = 9.7, 5.7 Hz), 5.99 (dddd, J = 9.7, 5.7, 2.2, 0.8 Hz) (H2,3), 6.50 (dq, J = 9.6, 0.8 Hz; H1), 7.19 (*p*-H), 7.29 (*m*-H), 7.36 (*o*-H); ^{13}C NMR (63 MHz): δ = 22.4, 23.4, 23.7, 25.7, 25.8, 28.5, 28.7, 29.9, 30.4, 34.7 (C5-9,12-16), 52.5 (C4b), 53.5 (C4a), 120.7, 124.7 (C2,3), 122.5 (C1), 129.9 (C4), 123.4, 125.2 (C10,11), 125.4 (*p*-C), 127.5 (*o*-C), 127.6 (*m*-C), 129.5, 135.3, 142.8, 146.1, 148.0 (C10a,10b,16a,16b, *i*-C); UV (CH_3CN): λ_{max} (lg ε) = 357 nm (4.772).

8: M.p. 123–125 °C (from pentane); ^{1}H NMR (250 MHz): δ = 1.05–2.10 (m; 8H), 2.18 (br. dd, J = 14.0, 9.7 Hz; 1H), 2.34 (br. dd, J = 14.0, 6.7 Hz; 1H), 6.05 (dd, J(1,2) = 7.7, 6.3 Hz; H1), 6.70 (br.; 1 aromat. H), 6.78-6.98 (br.; 4 aromat. H); ^{13}C NMR (63 MHz): δ = 23.8, 26.2, 27.3, 28.8, 35.6 (C2-6), 63.1 (C6a), 118.1 (C1), 124.6 (*p*-C), 126.7, 126.9, 127.2, 129.5 (br., *o*-,*m*-C), 143.3, 143.7 (C12a, *i*-C); UV (CH_3CN): λ_{max} (lg ε) = 264 nm (4.152).

9: ^{1}H NMR (250 MHz): δ = 0.60–2.20 (m; 10H), 5.95 (dd, J(1,2) = 9.3, 7.2 Hz; H1), 7.00–7.30 (m; 4 aromat. H), 7.47 (m; 1 *o*-H); ^{13}C NMR (63 MHz): δ = 22.1, 26.1, 27.2, 28.0, 40.6 (C2-6), 61.2 (C6a), 117.8 (C1), 125.7, 126.3, 127.2, 127.9, 131.4 (*o*-,*m*-,*p*-C), 141.3, 144.2 (C12a, *i*-C).

11: Oil (glass), b.p. 250–300 °C (bath)/10 $^{-3}$ Torr; ^{1}H NMR: δ = 0.84–1.09 (m; 2H), 1.19–1.89 (m; 12H), 1.89–2.39 (m; 6H), 5.54 (dd, J = 9.2, 7.3 Hz), 5.91 (dd, J = 8.8, 7.6 Hz) (H1,4), 6.89 (m; 2 *o*-H), 6.94 (m; 2 *o*-H), 6.97–7.19 (m; 4 *m*-H, 2 *p*-H); ^{13}C NMR: δ = 23.2 (C6), 23.6 (C7), 26.7 (C5′), 26.8 (C6′), 28.1 (2 signals; C8,4′), 29.0 (C5), 30.7 (C7′), 32.7 (C8′), 35.2 (C3′), 125.5 (*p*′-C), 126.2 (*p*-C), 126.8 (*m*′-C), 127.4 (2 signals; *o*-,*m*-C), 129.0 (*o*′-C), 130.8 (C4), 132.8 (C1), 135.9 (C1′), 138.9 (C2′), 139.2 (2 signals; C2,3), 141.5 (*i*-C), 144.8 (*i*′-C); UV (CH_3CN): λ_{max} (lg ε) = 236 nm (4.313).

12: M.p. 182–183 °C (from petroleum ether/ethyl acetate); ^{1}H NMR: δ = 1.17–1.25 (m; 2H), 1.39 (m;1H), 1.71–1.85 (m; 4H), 2.03–2.12 (m; 2H), 2.75 (br. d, J ≈ 15 Hz; 1H), 3.55 (br. t, J ≈ 9 Hz; 1H), 6.75 (m; 1 *o*-H), 6.85 (m; 1 aromat. H), 6.90-6.94 (m; 2 aromat. H), 6.96 (m; 1 *o*-H); ^{13}C NMR: δ = 22.2, 22.7, 26.4, 27.7, 32.7 (C2-6), 40.7 (C1), 45.5 (C13), 66.3 (C6a), 110.5, 112.0 (2 CN), 125.9, 127.3 (2 signals), 127.6, 129.3 (*o*-,*m*-,*p*-C), 141.0, 144.7 (C12a, *i*-C).

13: M.p. 219–220 °C (from petroleum ether/ethyl acetate); ^{1}H NMR: δ = 0.41 (br.; 1H), 1.12-1.23 (m; 2H), 1.38 (m; 1H), 1.42–1.53 (m; 3H), 1.59 (m; 1H), 1.78 (br.; 1H), 1.90 (m; 1H), 1.97 (m; 1H), 2.04–2.17 (m; 3H), 2.27 (m; 1H), 2.42–2.51 (m; 2H), 2.59 (m; 1H), 2.77 (m; 1H), 3.42 (m; 1H), 3.57 (m; 1H), 3.74 (m; 1H), 6.32 (br.; 2 *o*-H), 7.08 (m; 2 *m*-H), 7.16 (m; 1 *p*-H), 7.18 (m; 2 *o*-H), 7.36-7.43 (m; 2 *m*-H, 1 *p*-H); ^{13}C NMR: δ = 23.4, 24.0, 25.9, 26.0, 26.7, 29.2, 31.6, 31.9, 35.4, 36.1 (C1-5,8-12), 46.8 (C13 or C14), 47.1 (2 signals; C12a or 14a, C14 or C13), 51.1 (C14a or C12a), 110.5, 111.1, 111.6, 112.2 (4 CN), 124.6, 129.3 (C6,7), 126.8 (*p*-C), 127.2 (*o*-C), 127.5 (*m*-C), 128.0 (*p*-C), 128.1 (*m*-C), 128.3 (*o*-C), 143.5, 144.0, 144.4, 147.2 (C6a,6b, 2 *i*-C); UV (CH_3CN): λ_{max} (lg ε) = 255 nm (4.048 sh), 236 (4.165).

14: M.p. 124–125 °C (from pentane); ^{1}H NMR (C_6D_6): δ = 1.14–1.22 (m; 2H), 1.30–1.42 (m; 6H), 1.45–1.51 (m; 2H), 1.61–1.67 (m; 2H), 1.69–1.75 (m; 2H), 2.08–2.50 (m; 4H), 2.39 (t, J = 7.0 Hz; 2H), 2.42 (m; 15-H_2), 6.24 (t, J = 8.4 Hz; 16-H), 7.06 (m; *o*-H), 7.08 (m; *p*-H), 7.14 (m; *m*-H), 7.20 (td, J(1,2)= J(2,3) = 7.6, J(2,4) = 1.3 Hz; H2), 7.24 (td, J(3,4) = 7.6, J(1,3) = 1.6 Hz; H3), 7.57 (dd; H4), 7.58 (dd; H1); ^{13}C NMR: δ = 24.3 (3 signals), 25.8, 26.6, 28.3, 30.3, 31.6 (2 signals), 38.4 (2 signals) (C5-15), 46.9 (C4b), 124.5, 124.9 (C1,4), 125.58, 125.64, 126.2 (C2,3, *p*-C), 125.8 (C16), 127.6 (*o*-C), 130.3 (*m*-C), 133.3, 138.4, 139.1, 141.0, 144.1, 147.4 (C4a,10a,10b,16a,16b, *i*-C); UV (hexane): λ_{max} (lg ε) = 270 nm (4.074).

Correct elemental analyses have been obtained from all isolated products except **11**, the empirical formula of which is supported by a high-resolution mass spectrum. Selected data of the compounds **7**–**9** and **11**–**14** are collected in Table 1.

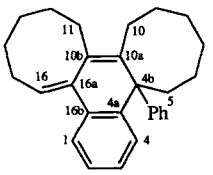

14

Received: August 14, 1995 [Z8307IE]
German version: *Angew. Chem.* **1995**, *107*, 2931–2934

Keywords: 1,2-bismethylenecyclobutanes · cycloallenes · dimerizations · diradicals

[1] H. Jelinek-Fink, M. Christl, E.-M. Peters, K. Peters, H. G. von Schnering, *Chem. Ber.* **1991**, *124*, 2569–2575.
[2] R. P. Johnson, *Chem. Rev.* **1989**, *89*, 1111–1124.
[3] Y. K. Yildiz, H. Seçen, M. Krawiec, W. H. Watson, M. Balci, *J. Org. Chem.* **1993**, *58*, 5355–5359.
[4] H. Hopf in *The Chemistry of Allenes, Vol. 2* (Ed.: R. S. Landor), Academic Press, London, **1982**, p. 525.
[5] J. D. Price, R. P. Johnson, *Tetrahedron Lett.* **1986**, *27*, 4679–4682.
[6] E. T. Marquis, P. D. Gardner, *Tetrahedron Lett.* **1966**, 2793–2798.
[7] J. Pietruszka, W. A. König, H. Maelger, J. Kopf, *Chem. Ber.* **1993**, *126*, 159–166.
[8] O. M. Nefedov, E. S. Agavelyan, *Izv. Akad. Nauk SSSR, Ser. Khim.* **1973**, 2045–2051; *Chem. Abstr.* **1974**, *80*, 59120u.
[9] $Mo_{K\alpha}$ radiation, graphite monochromator, $2\theta_{max.}$ = 55°, ω scan; the structure was solved by direct methods and refined by using the Siemens-SHELXTL-Plus program system. **7**: $C_{28}H_{32}$, M = 368.56, monoclinic, space group $P2_1/a$, a = 1734.4(8), b = 930.8(3), c = 1327.8(6) pm, β = 96.49(4)°, V = 2130(2) × 10^6 pm^3, Z = 4, ρ_{calcd} = 1.149 g cm^{-3}; 4880 independent reflections, 2419 independent reflections with $F > 3\sigma(F)$, F_o/parameter ratio = 9.52; R = 0.069, R_w = 0.053. **8**: $C_{28}H_{32}$, M = 368.56, monoclinic, space group $C2_1/c$, a = 1700.3(9), b = 932.8(6), c = 2728(1) pm, β = 95.06(2)°, V = 4311(6) × 10^6 pm^3, Z = 8, ρ_{calcd} = 1.136 g cm^{-3}; 4966 independent reflections, 2040 independent reflections with $F > 3\sigma(F)$, F_o/parameter ratio = 7.76; R = 0.126, R_w = 0.081. **13**: $C_{34}H_{32}N_4$, M = 496.65, orthorhombic, space group $Pca2_1$, a = 1562.5(3), b = 1345.7(1), c = 1302.9(2) pm, V = 2739.6(6) × 10^6 pm^3, Z = 4, ρ_{calcd} = 1.204 g cm^{-3}; 3568 independent reflections, 3198 independent reflections with $F > 3\sigma(F)$, F_o/parameter ratio = 9.35; R = 0.048, R_w = 0.047. Further details of the crystal structure investigations may be obtained from the Fachinformationszentrum Karlsruhe, D-76344 Eggenstein-Leopoldshafen (Germany) on quoting the depository numbers CSD-401984 (**8**), 401985 (**7**), and 404222 (**13**).
[10] W. R. Moore, R. D. Bach, T. M. Ozretich, *J. Am. Chem. Soc.* **1969**, *91*, 5918–5919.
[11] E. Weber, W. Seichter, I. Goldberg, G. Will, H.-J. Dasting, *J. Incl. Phenom.* **1991**, *10*, 267-282.
[12] G. Wittig, H.-L. Dorsch, J. Meske-Schüller, *Liebigs Ann. Chem.* **1968**, *711*, 55–64; G. Wittig, J. Meske-Schüller, *ibid.* **1968**, *711*, 76–81; G. Wittig, P. Fritze, *ibid.* **1968**, *711*, 82–87.
[13] H. H. Freedman, G. A. Doorakian, V. R. Sandel, *J. Am. Chem. Soc.* **1965**, *87*, 3019–3020; J. I. Brauman, W. C. Archie, Jr., *Tetrahedron* **1971**, *27*, 1275–1280.

The editorial staff and publishers express their thanks to all readers, authors, referees, and advertisers for their continued interest and support over the past year and wish them a prosperous 1996.

New Gmelin Volumes:
Gmelin Handbook of Inorganic and Organometallic Chemistry. 8th Ed.

Os, Organoosmium Compounds. Ergänzungsband b, Part 3. Edited by **J. Füssel, K. Behrends.** Springer, Berlin, **1994.** 282 pp., hardcover, DM 1.790.00.—ISBN 3-540-93697

Os, Organoosmium Compounds. Ergänzungsband b, Part 5. Edited by **J. Füssel et al.** Springer, Berlin, **1994.** 389 pp., hardcover, DM 2.290.00.—ISBN 3-540-93698-X

Mn, History. Occurrence. Teil A/3, Part b. Minerals (Oxides of Type M_3O_4). Edited by **R. Ditz, W. Töpper.** Springer, Berlin, **1994.** 271 pp., hardcover, DM 1.690.00. ISBN 3-540-93699-8

Mn, History. Occurrence. Teil A Lieferung 4. Minerals (Oxides of Type M_2O_3). Edited by **B. Sarbas, W. Töpper.** Springer, Berlin, **1994.** 220 pp., hardcover, DM 1.370.00. ISBN 3-540-93700-5

Mo, Molybdän. Molybdenum. Supplement A-B. Part B. The Compounds. Delivery 8. Edited by **H. Katscher, B. Mohsin.** Springer, Berlin. **1995.** 308 pp., hardcover, DM 1.950.00.—ISBN 3-540-93705-6

Supramolecular Chemistry. Concepts and Perspectives. By **J.-M. Lehn.** VCH, Weinheim, **1995.** 271 pp., softcover, DM 58.00/$ 39.95.—ISBN 3-527-23911-6

Der Kongreß. Vorbereitung und Durchführung wissenschaftlicher Tagungen. 3rd extended edition. By **V. Neuhoff.** VCH, Weinheim, **1995.** 277 pp., hardcover, DM 78.00/$ 49.95. ISBN 3-527-29287-X

Analytische Chemie. By **M. Otto.** VCH, Weinheim, **1995.** 668 pp., softcover, DM 68.00.—ISBN 3-527-28691-8

Theorie elektrischer Maschinen. By **G. Müller.** VCH, Weinheim, **1995.** 607 pp., softcover, DM 88.00. ISBN 3-527-28392-7

Organische Synthese mit Übergangsmetallen. By **L. S. Hegedus.** VCH, Weinheim, **1995.** 313 pp., softcover, DM 58.00. ISBN 3-527-29255-1

Electron Transfer and Radical Processes in Transition-Metal Chemistry. By **D. Astruc.** VCH, New York, **1995.** 630 pp. hardcover, DM 225.00/$ 140.00.—ISBN 1-56081-642-2

Inorganic Experiments. Edited by **J. D. Woollins.** VCH, Weinheim, **1994.** 286 pp., softcover, DM 58.00/$ 39.95. ISBN 3-527-29253-5

Grundkurs Chemie II. Organische Chemie. By **A. Arni.** VCH, Weinheim, **1995.** 196 pp., softcover, DM 42.00.—ISBN 3-527-29229-2

Extremophile. Mikroorganismen in ausgefallenen Lebensräumen. 2nd edition. Edited by **K. Hausmann, B. P. Kremer.** VCH, Weinheim, **1995.** 422 pp., hardcover, DM 49.00. ISBN 3-527-30068-6

Surface Electron Transfer Processes. By **R. J. D. Miller et al.** VCH, New York, **1995.** 370 pp., hardcover, DM 128.00/$ 79.95. ISBN 1-56081-036-X

Conformational Behavior of Six-Membered Rings. Analysis, Dynamics, and Stereoelectronic Effects. Edited by **E. Juarist.** VCH, New York, **1995.** 306 pp., hardcover. DM 160.00/$ 100.00.—ISBN 1-56081-683-X

Encyclopedia of Applied Physics. Vol. 12. Nuclear Waste Management to Optics, Underwater. Edited by **G. L. Trigg.** VCH, Weinheim/New York, **1995.** 608 pp., hardcover, DM 450.00/$ 295.00.—ISBN 3-527-28134-7/ISBN 1-56081-071-8

Frontiers in Analytical Spectroscopy. Edited by **D. L. Andrews, A. M. C. Davies.** Royal Society of Chemsitry, Cambridge, **1995.** 248 pp., hardcover, £ 62.50.—ISBN 0-85404-730-1

Food Macromolecules and Colloids. Edited by **E. Dickinson, D. Lorient.** Royal Society of Chemistry, Cambridge, **1995.** 586 pp., hardcover, £ 92.50.—ISBN 0-85404-700-X

Magnetic Resonance in Food Science. Edited by **P. S. Belton et al.** Royal Society of Chemistry, Cambridge, **1995.** 292 pp., hardcover, £ 55.00.—ISBN 0-85404-725-5

Chemometrics in Analytical Spectroscopy. By **M. J. Adams.** Royal Society of Chemistry, Cambridge, **1995.** 216 pp., hardcover, £ 39.50.—ISBN 0-85404-555-4

Ultrafast Processes in Chemistry and Photobiology. Edited by **M. A. El-Sayed et al.** Blackwell Science, **1995.** 306 pp., hardcover, £ 59.50.—ISBN 0-86542-893-X

Fractal Concepts in Surface Growth. By **A.-L. Barabási, H. E. Stanley.** Cambridge University Press, Cambridge, **1995.** 366 pp., paperback, £ 16.95.—ISBN 0-521-48318-2

Excipients and Delivery Systems for Pharmaceutical Formulations. Edited by **D. R. Karsa, R. A. Stephenson.** Royal Society of Chemistry, Cambridge, **1994.** 192 pp., hardcover, £ 39.50.—ISBN 0-85404-715-8

Chemical Aspects of Biosynthesis. (Oxford Chemistry Primers). By **J. Mann.** Oxford University Press, Oxford, **1994.** 92 pp., paperback, £ 4.99.—ISBN 0-19-855676-4

Inorganic Materials Chemistry. (Oxford Chemistry Primers). By **M. T. Weller.** Oxford University Press, Oxford, **1995.** 92 pp., paperback, £ 4.99.—ISBN 0-19-855798-1

Microbiological Control for Foods and Agricultural Products. Edited by **C. M. Bourgeois, J. Y. Leveau.** VCH, New York, **1995.** 542 pp., hardcover, DM 228.00/$ 145.00 ISBN 1-56081-673-2

Vom Wasser. Vol. 84, 1995. Edited by **Fachgruppe Wasserchemie in der GDCh.** VCH, Weinheim, **1995.** 446 pp., hardcover, DM 278.00.—ISBN 3-527-28677-2 (ISSN 0083-6915)

The Biological Chemistry of Magnesium. Edited by **J. A. Cowan.** VCH, New York, **1995.** 254 pp., hardcover, DM 98.00/$ 59.95.—ISBN 1-56081-627-9

Organocopper Reagents. A Practical Approach. Edited by **R. J. K. Taylor, L. M. Harwood, C. J. Moody.** Oxford University Press, Oxford, **1995.** 362 pp., paperback, £ 25.00.—ISBN 0-19-855758-2

Optical Polarization of Molecules. By **M. Auzinsh, R. Ferber.** Cambridge University Press, Cambridge, **1995.** 306 pp., hardcover, £ 50.00.—ISBN 0-521-44346-6

Official and Standardized Methods of Analysis. Third Edition. Edited by **C. Watson.** Royal Society of Chemistry, Cambridge, **1994.** 778 pp., hardcover, £ 110.00.—ISBN 0-85186-441-4

Alkaloids: Chemical & Biological Perspectives. Vol. 9. Edited by **S. W. Pelletier.** Pergamon (Elsevier Science Ltd.), Oxford, **1995.** 286 pp., hardcover, £ 78.00. ISBN 0-08-042089-3

Organic Reactivity: Physical and Biological Aspects. Edited by **B. T. Golding, R. J. Griffin, H. Maskill.** Royal Society of Chemistry, Cambridge, **1995.** 453 pp., hardcover, £ 69.50.—ISBN 0-85404-710-7

Multidimensional Solid-State NMR and Polymers. By **K. Schmidt-Rohr, H. W. Spiess.** Academic Press, London, **1994.** 478 pp., hardcover, £ 65.00.—ISBN 0-12-626630-1

An Atlas of Fullerenes. By **P. W. Fowler, D. E. Manolopoulos.** Oxford University Press, Oxford, **1995.** 392 pp., hardcover, £ 65.00.—ISBN 0-19-855787-6

Handbook of Food Additives. Compiled by **M. and I. Ash.** Gower, Hampshire, **1995.** 1040 pp., hardcover, £ 175.00. ISBN 0-566-07592-X

Special Trends in Thermal Analysis. By **F. Paulik.** Wiley, Chichester, **1995.** 459 pp., hardcover, £ 90.00.—ISBN 0-471-95769-0

Advances in Photochemistry, Vol. 19. Edited by **D. C. Neckers, D. H. Volman, G. von Bünau.** Wiley, Chichester, **1995.** 325 pp., hardcover, £ 96.00. ISBN 0-471-04912-3

Spectra of Atoms and Molecules. By **P. F. Bernath.** Oxford University Press, Oxford, **1995.** 400 pp., hardcover, £ 37.50.—ISBN 0-19-507598-6

Advances in Mass Spectrometry, Vol. 13. Proceedings of the 13th International Mass Spectrometry Conference. Edited by **I. Cornides, G. Horváth, K. Vékey.** Wiley, Chichester, **1995.** 645 pp., hardcover, £ 120.00.—ISBN 0-471-95323-7

Chemical Principles of Synthetic Fibre Dyeing. By **S. M. Burkinshaw.** Blackie Academic, London. **1995.** 223 pp., hardcover, £ 55.00.—ISBN 0-7514-0043-3

Spectroscopy in Environmental Science. Advances in Spectroscopy, Vol. 24. Edited by **R. J. H. Clark, R. E. Hester.** Wiley, Chichester, **1995.** 462 pp., hardcover, £ 130.00.—ISBN 0-471-95370-9

Macromolecular Reactions. Peculiarities, Theory and Experimental Approaches. By **N. A. Platé, A. D. Litmanovich, O. V. Noah.** Wiley, Chichester, **1995.** 438 pp., hardcover, £ 80.00.—ISBN 0-471-94392-4

Organomagnesium Methods in Organic Synthesis. By **B. J. Wakefield.** Academic Press, London, **1995.** 249 pp., hardcover, £ 50.00.—ISBN 0-12-730945-4

Surfactant-Enhanced Subsurface Remediation: Emerging Technologies. Edited by **D. A. Sabatini, R. C. Knox, J. H. Harwell.** American Chemical Society, Washington, **1995.** 312 pp., hardcover, $ 84.95.—ISBN 0-8412-3225-3

Röntgenfluoreszenzanalytische Methoden. Grundlagen und praktische Anwendung in den Geo-, Material- und Umweltwissen-schaften. By **P. Hahn-Weinheimer, A. Hirner, K. Weber-Diefenbach.** Vieweg, Wiesbaden, **1995.** 283 pp., hardcover, DM 98.00.—ISBN 3-528-06579-6

Destillation, Absorption, Extraktion. By **E.-U. Schlünder, F. Thurner.** Vieweg, Wiesbaden, **1995.** 215 pp., paperback, DM 49.50.—ISBN 3-528-06678-4

Immunoanalysis of Agrochemicals: Emerging Technologies. ACS Symposium Series No. 586. Edited by **A. E. Karu, J. O. Nelson, R. B. Wong.** American Chemical Society, Washington. **1995.** 380 pp., hardcover, $ 99.95.—ISBN 0-8412-3149-4

Reduction of Nitrogen Oxide Emissions. ACS Symposium Series No. 587. Edited by **U. S. Ozkan, S. K. Agarwal, G. Marcelin.** American Chemical Society, Washington, **1995.** 248 pp., hardcover, $ 79.95. ISBN 0-8412-3150-8

Modern Countercurrent Chromatography. ACS Symposium Series No. 593. Edited by **W. D. Conway, R. J. Petroski.** American Chemical Society, Washington, **1995.** 248 pp., hardcover. $ 69.95.—ISBN 0-8412-3167-2

Fruit Flavors: Biogenesis, Characterization, and Authentication. ACS Symposium Series No. 596. Edited by **R. L. Rouseff, M. M. Leahy.** American Chemical Society, Washington, **1995.** 304 pp., hardcover, $ 84.95.—ISBN 0-8412-3227-X

Flow-Induced Structure in Polymers. ACS Symposium Series No. 597. Edited by **A. I. Nakatani, M. D. Dadmun.** American Chemical Society, Washington, **1995.** 378 pp., hardcover, $ 99.95.—ISBN 0-8412-3230-X

AUTHOR INDEX [*Angew. Chem. Int. Ed. Engl.* 1995, *34*]

The page numbers in square brackets refer to the German edition [*Angew. Chem.* **1995**, *107*] of Angewandte Chemie. Page numbers in round brackets indicate errata.

à Brassard, L. 898 [984]
Abal, M. 2710 [2910]
Abiko, A. 793 [869]
Ablelom, T. 1340 [1476]
Achiba, Y. 1094, 2139 [1228, 2303]
Acuña, A. U. 2710 [2910]
Adachi, T. 319 [351]
Adam, W. 107, 2156 [91, 2326]
Adams, D. M. 1481 [1580]
Adams, H. 2535 [2749]
Ahrens, B. 2538 [2763]
Ajito, K. 576 [614]
Akasaka, T. 2139 [2303]
Akimoto, J. 1199 [1313]
Al-Ahmad, S. 1357 [1479]
Alaimo, C. A. 452 [495]
Albanese, G. P. 811 [893]
Albert, K. 641, 1014 [699, 1102]
Albinati, A. 2507 [2711]
Albrecht, M. 2134 [2285]
Albritton-Thomas, J. 68 [117]
Alcaraz, G. 1246 [1358]
Alfaro, J. 186 [207]
Allen, L. C. 2003 [2157]
Allwohn, J. 657 [728]
Als-Nielsen, J. 649 [707]
Altmann, M. 569 [603]
Amabilino, D. B. 2378 [2569]
Amat-Guerri, F. 2710 [2910]
Ames, F. 814 [891]
Amigó, J. M. 55 [99]
Amii, H. 1476 [1649]
Amoroso, A. J. 1443 [1577]
Amrein, W. 805 [898]
Andersen, O. K. 103 [81]
Andersen, R. A. 791 [877]
Anderson, H. L. 1096 [1196]
Anderson, M. W. 1003 [1115]
Anderson, S. 1096, 1596 [1196, 1722]
Andreu, J. M. 2710 [2910]
Anke, T. 196 [255]
Annunziata, R. 1019 [1092]
Antonelli, D. M. 2014 [2202]
Apfel, T. 186 [207]
Apperley, D. C. 1197 [1311]
Arana, C. R. 1122 [1191]
Aranyos, A. 2551 [2767]
Arend, M. 2639 [2861]
Armstrong, D. R. 478 [514]
Arnold, F. H. 905 [994]
Arnold, F. P. 1887 [2029]
Arslan, F. 183 [205]
Artus, G. R. J. 2371 [2602]
Aschi, M. 1589 [1719]
Ashe III, A. J. 1357 [1479]
Ashton, P. R. 571, 1862, 1865, 1869, 2378 [607, 1994, 1997, 2001, 2569]
Attinà, M. 654, 1589 [754, 1719]
Aubin, S. M. J. 887 [969]
Avarvari, N. 590 [623]
Ayalon, A. 816 [888]
Ayougou, K. 343 [370]
Baak, M. 595 [634]
Baceiredo, A. 1246, 2677 [1358, 2904]
Bach, T. 2271 [2455]
Bäckvall, J.-E. 2551 [2767]
Bahl, A. 1485 [1587]
Bahrmann, H. 811 [893]
Bailey, N. A. 2535 [2749]
Baker, R. T. 1336 [1451]
Bakos, J. 1645 [1728]
Balaban, T. S. 330 [360]
Balch, A. L. 194, 2252 [220, 2467]
Baldes, R. 321 [380]
Baldridge, K. K. 1454, 2657 [1575, 2870]
Ball, S. C. 921 [1002]
Ballmaier, D. 2156 [2326]
Balzani, V. 595 [634]
Banert, K. 1627 [1776]
Banfi, L. 2393 [2613]
Banner, D. W. 1739 [1874]
Barasoain, I. 2710 [2910]
Bardet, M. 588 [625]
Barnham, K. J. 1874 [2040]
Barr, D. 1012 [1088]
Barresi, F. 2720 [2912]
Barrett, A. G. M. 2020 [2173]
Barron, A. R. 1201 [1315]
Barth, S. 484 [485]
Bartl, J. 490 [519]
Bartnik, E. 990 [1104]
Bartoli, G. 2046 [2163]
Barton, L. 1641 [1744]
Bartos, M. J. 1216 (1649) [1345]
Bashall, A. 1096 [1196]
Bats, J. W. 2383 [2597]
Batten, S. R. 820 [884]
Battersby, A. R. 383 [421]
Bauer, W. 1319, 1594 [1446, 1766]
Bäuerle, P. 303, 781 [335, 859]
Baumeister, F. 555 [640]
Beatrix, B. 2398 [2573]
Beau, J.-M. 909 [990]
Becher, J. 2524 [2719]
Beck, J. 2559 [2739]
Beck, W. 1449, 2489 [1570, 2695]
Becker, P. 1849 [2012]
Beckers, H.-G. 1325 [1464]
Beckhaus, R. 688 [738]
Beelen, T. P. M. 73 [122]
Behrendt, M. 183 [205]
Behrens, P. 2680 [2895]
Behrens, U. 443 [516]
Beifuss, U. 647 [705]
Bell, T. W. 2163 [2321]
Beller, M. 1316, 1844, 1848 [1436, 1989, 1992]
Belser, P. 595 [634]
Belshaw, P. J. 2129 [2313]
Benhamu, B. 1483 [1644]
Bergemann, K. 1330 [1481]
Berger, S. 657 [728]
Bergman, R. G. 2266 [2423]
Bergsträsser, U. 484 [485]
Berkessel, A. 2247 [2418]
Bernadou, J. 746 [819]
Bernard, E. 588 [625]
Bernardinelli, G. 582, 2161 [618, 2305]
Berndt, A. 327, 657, 1111, 1340 [368, 728, 1194, 1476]
Berners-Price, S. J. 1874 [2040]
Berno, P. 822, 2264 [871, 2457]
Bernstein, J. 1555 [1689]
Bernstein, P. R. 1117 [1218]
Berrisford, D. J. 178, 1059, 1717 [192, 1159, 1862 (2214)]
Bertagnolli, H. 771 [847]
Bertrand, G. 1246, 2677 [1358, 2904]
Bestmann, H. J. 2017 [2186]
Beswick, M. A. 2662 [2891]
Bettray, W. 455 [527]
Bickelhaupt, F. 2553 [2728]
Bidlingmeier, B. 303 [335]
Bienewald, F. 2640 [2883]
Bill, E. 343, 669, 2642 [370, 744, 2885]
Binger, P. 81, 484, 2227 [114, 485, 2411]
Blake, A. J. 2374 [2563]
Blanche, F. 383 [421]
Blechert, S. 1900, 2137 [2025, 2317]
Blixt, J. 2264 [2457]
Blum, O. 229 [210]
Boche, G. 487, 2158 [509, 2328]
Bock, G. 2559 [2739]
Bock, H. 76, 1353, 1355 [120, 1439, 1441]
Bocquet, B. 582 [618]
Boese, R. 781, 1478 [859, 1630]
Bogdanovic, S. 112 [63]
Bögge, H. 779, 2122 [857, 2293]
Bohanon, T. M. 58 [102]
Böhler, D. 2696 [2915]
Böhm, D. 198 [251]
Böhmer, J. 1435 [1603]
Böhmer, V. 713 [785]
Boland, W. 1600, 1602 [1715, 1717]
Bolli, M. 694 [740]
Bolm, C. 1059, 1717, 2640 [1159, 1862 (2214), 2883]
Born, M. 309 [342]
Borovik, A. S. 1359 [1473]
Borzyk, O. 1001 [1094]
Bossek, U. 2642 [2885]
Bothner, B. 2053 [2209]
Bott, S. G. 1201 [1315]
Böttcher, F. 567 [647]
Boudon, C. 805 [898]
Bould, J. 1641 [1744]
Bourhill, G. 1485 [1587]
Bousseksou, A. 205, 588 [199, 625]
Bouwman, W. G. 649 [707]
Brandherm, M.-T. 1578 [1712]
Bras, W. 73 [122]
Bräse, S. 2545 [2741]
Bräuchle, C. 1485 [1587]
Braumann, U. 1014 [1102]
Braun, T. P. 567 [647]
Braunschweig, H. 825 [904]
Braunstein, P. 1010 [1090]
Braxmeier, T. 2497 [2746]
Breinbauer, R. 2728 [2956]
Breit, B. 2386 [2577]

Brenner, T. 439 [481]
Breuer, K. 1021 [1119]
Brintzinger, H.-H. 791, 1143 (1368) [877, 1255 (1652)]
Brockunier, L. 222 [254]
Brode, S. 1021 [1119]
Broger, C. 2280 [2452]
Bronger, W. 898 [984]
Bröring, M. 2511, 2515 [2705, 2709]
Brossmer, C. 1844, 1848 [1989, 1992]
Bruckmann, J. 2227 [2411]
Brzozka, Z. 2124 [2300]
Bu, X. 1745 [1911]
Bubenitschek, P. 661, 685, 2367, 2502 [752, 742, 2592, 2743]
Bublitz, F. 1600 [1715]
Buchner, K. 2667 [2879]
Buchwald, S. L. 1348, 1760 [1456, 1877]
Buckel, W. 1502, 2398 [1595, 2573]
Buhr, W. 1366 [1485]
Bunz, U. H. F. 569 [603]
Burak, R. 993 [1085]
Burdett, J. K. 2003 [2157]
Burger, J. 2647 [2950]
Burgess, K. 907 [975]
Bürgi, H.-B. 1454 [1575]
Burgstaller, P. 1189 [1303]
Burkard, M. 2402 [2608]
Burkhardt, A. 103 [81]
Burrell, A. K. 900 [986]
Burth, D. 800 [881]
Buschmann, J. 914 [988]
Buse, G. 1488 [1615]
Bushaw, B. A. 181 [202]
Buskens, P. L. 2652 [2868]

Cacace, F. 654, 1589 [754, 1719]
Cadet, J. 107 [91]
Cainelli, G. 2150 [2336]
Cameron, B. 383 [421]
Cameron, B. R. 2689 [2900]
Cammenga, H. K. 1171 [1284]
Campbell, P. J. 1865 [1997]
Camps, P. 912 [1011]
Canac, Y. 2677 [2904]
Caneschi, A. 467, 2716 [511, 2862]
Cao, W. 1091 [1206]
Cardoso Gil, R. H. 103 [81]
Cardullo, F. 2023 [2159]
Carell, T. 2491 [2697]
Carlucci, L. 1895 [2037]
Carmona, E. 231 [242]
Carpenter, G. B. 2540 [2734]
Carpentier, J.-F. 1474 [1608]
Castanet, Y. 1474, 2269 [1608, 2450]
Castaño, A. M. 2551 [2767]
Casutt, M. 2391 [2582]
Catalán, J. 105 [86]
Catlin, K. K. 585, 2147 [616, 2330]
Chadha, R. K. 93 [76]
Chan, K. W. K. 2511 [2705]
Chang, N.-L. 1555 [1689]
Chardon-Noblat, S. 588 [625]
Charnock, J. M. 343 [370]
Charpin, P. 2381 [2567]
Charrier, C. 590 [623]
Chauvin, Y. 2698 [2941]
Chelucci, G. 78 [104]
Chen, C.-T. 2657 [2870]
Chen, H. 1514 [1590]
Chen, J. 2515, 2694 [2709, 2898]
Chen, J. K. 953 [1041]
Chen, L. 1877 [2050]
Chen, Q. 223 [229]
Chiesi-Villa, A. 1092, 1510 [1200, 1621]
Chin, J. 472, 2412 [529, 2594]
Chisholm, M. H. 110, 891 [61, 977]
Chivers, T. 2549 [2756]
Chmielewski, P. J. 2252 [2467]
Choudhary, V. R. 665 [721]
Christl, M. 2730 [2931]
Christoffers, J. 2266 [2423]
Christou, G. 887, 889 [969, 971]
Chrystal, E. J. T. 1865, 1869 [1997, 2001]
Ciani, G. 1895 [2037]
Cinquini, M. 1019 [1092]
Cirujeda, J. 55 [99]
Claessens, C. G. 1862 [1994]
Clark, G. C. 1216 (1649) [1345]
Clearfield, A. 1508 [1650]
Clegg, W. 1233, 2389 [1353, 2580]
Cohen, Y. 816 [888]
Coleman, A. W. 2381 [2567]
Collins, T. J. 1216 (1649) [1345]
Comba, P. 1883 [2047]
Cook, S. N. 1629 [1736]
Cooper, J. M. 91, 2409 [84, 2610]
Corbett, J. D. 233, 2262 [234, 2463]
Cordier, G. 1761 [1879]
Cornia, A. 467, 2716 [511, 2862]
Cornils, B. 1575 [1709]
Cornish, V. W. 621 [677]
Coronado, E. 1460 [1601]
Corrent, S. S. 2689 [2900]
Corval, A. 2530 [2753]
Costa, D. A. 194 [220]
Cottaz, S. 1239 [1361]
Cotton, F. A. 1877 [2050]
Cowley, A. H. 332 [378]
Cozzi, F. 1019 [1092]
Crabtree, R. H. 2507 [2711]
Cragg-Hine, I. 921 [1002]
Crasnier, F. 578 [610]
Cremer, D. 929 [999]
Crouzet, J. 383 [421]
Cummins, C. C. 2042 [2181]
Cuny, G. D. 1760 [1877]
Curran, D. P. 2683 [2948]

Dahan, F. 916, 1246 [1005, 1358]
Dahan, M. 1587 [1740]
Dähne, L. 690 [735]
Dall'Acqua, F. 107 [91]
Dance, I. 201 (1032), 314 [215, 366]
Dandliker, P. J. 2725 [2906]
Danishefsky, S. J. 452, 1721, 1723 [495, 1883, 1886]
Danley, L. E. 1629 [1736]
Dann, S. E. 2414 [2606]
Dapprich, S. 354 [383]
Daub, J. 2664 [2925]
Davidson, M. G. 478, 921 [514, 1002]
Davies, N. A. 1197 [1311]
Davies, R. P. 921 [1002]
Davis, R. E. 1555 [1689]
Davis, W. M. 2042, 2044 [2181, 2184]
De Angelis, S. 1092 [1200]
de Brabander-Van den Berg, E. M. M. 1206 [1321]
de Bruin, B. 2132 [2288]
De Cian, A. 205, 1115, 2530 [199, 1204, 2753]
De Clercq, P. J. 1749 [1898]
De Cola, L. 595 [634]
de Jong, J. C. 348 [346]
de Kanter, F. J. J. 2553 [2728]
de Lange, B. 348 [346]
de Meijere, A. 781, 1492, 2545 [859, 1642, 2741]
de Rango, C. 2381 [2567]
De Vos, D. E. 560 [637]
de Wolf, W. H. 2553 [2728]
Dean, P. A. W. 314 [366]
Debaecker, N. 588, 2535 [625, 2749]
Debussche, L. 383 [421]
Decker, H. 1107 [1214]
Dedecke, T. 71 [97]
Dedieu, A. 1742 [1905]
Deegan, M. D. 1209, 1212 [1324, 1327]
Deforth, T. 681 [748]
Degen, T. 1089, 2703 [1226, 2888]
Dehnicke, K. 1235, 1362 [1349, 1469]
Deissenberger, R. 814 [891]
Denninger, U. 592 [631]
Denzinger, S. 58 [102]
Dérer, T. 84 [66]
Desiraju, G. R. 2328 [2541]
Detellier, C. 2264 [2457]
Detzel, M. 1321 [1454]
Devasagayaraj, A. 2723 [2952]
Diederich, F. 805, 1466, 1596, 1739, 2725 [898, 1636, 1722, 1874, 2906]
Diederich, M. 1026 [1095]
Diemann, E. 2122 [2293]
Diercks, H. 186 [207]
Dillinger, S. 2122, 2311 [2293, 2505]
Ding, H. 1645 [1728]
Ding, Y. 2720 [2912]
Dixon, R. P. 1237 [1343 (1786)]
Dodt, J. 867 [948]
Dokter, W. H. 73 [122]
Dombrowski, E. 1008 [1098]
Dömling, A. 2238 [2465]
Donath, J. 1600 [1715]
Dorhout, P. K. 2509 [2737]
Dorigo, A. E. 115, 476 [108, 492]
Dostal, A. 2685 [2876]
Dötz, K. H. 1856 [2023]
Dreisbach, C. 2005 [2165]
Dreos, R. 2245 [2414]
Driess, M. 316, 1614 [354, 1746]
Driguez, H. 1239 [1361]
Dronskowski, R. 1126 [1230]
Du Bois, J. 1359 [1473]
Dücker-Benfer, C. 2245 [2414]
Dullaghan, C. A. 2540 [2734]
Durbin, M. K. 1497 [1646]
Durkin, J. 484 [485]
Dürr, H. 1005 [1112]
Dutta, P. 1497 [1646]
Dux, R. 595 [634]
Dyker, G. 2223, 2502 [2407, 2743]

Eaborn, C. 687, 2679 [756, 2936]
Eaton, P. E. 2030 [2206]
Ebel, K. 1021 [1119]
Eberhardt, K. 814 [891]
Eberson, L. 2268 [2417]
Eberstadt, M. 1671 [1813]
Echegoyen, L. 2023 [2159]
Edelmann, F. T. 981, 2466 [1071, 2647]
Edgar, R. 649 [707]
Edwards, A. J. 921, 1012 [1002, 1088]
Effing, J. J. 88 [88]
Egan, M. G. 576 [614]
Egerer-Sieber, C. 2017 [2186]

Ehlenz, R. 1856 [2023]
Eichen, Y. 2530 [2753]
Eiermann, M. 1591 [1733]
Eisenstein, O. 110, 2507 [61, 2711]
Ejiri†, S. 2154 [2338]
Elguero, J. 105 [86]
Elison, M. 2371 [2602]
Ellern, A. 1586 [1772]
Elling, L. 1748 [1881]
Ellis, J. E. 2489 [2695]
Ellman, J. A. 1629 [1736]
Elsegood, M. R. J. 2389 [2580]
Enders, D. 455, 1021, 1219, 2278 [527, 1119, 1332, 2442]
Enemark, E. J. 996 [1082]
Engehausen, R. 2273 [2469]
Engel, J. 238 [195]
Englert, U. 1010, 2236 [1090, 2435]
English, R. B. 2657 [2870]
Enkelmann, V. 1583, 2713 [1751, 2917]
Epe, B. 107, 2156 [91, 2326]
Epple, M. 1171 [1284]
Erden, I. 1091 [1206]
Erdmann, N. 814 [891]
Erker, G. 1755 [1867]
Ernst, B. 1841, 2720 [2034, 2912]
Ernst, L. 1881 [2010]
Ernst, W. 183 [205]
Estournès, C. 1115 [1204]
Etienne, M. 916 [1005]
Etzkorn, M. 1016 [1109]
Evans, D. A. 798 [864]
Eyrisch, O. 1639 [1738]

Fabretti, A. C. 2716 [2862]
Facey, G. A. 2264 [2457]
Famulok, M. 1189 [1303]
Fath, A. 1883 [2047]
Fau, S. 327, 1340 [368, 1476]
Faucher, J.-P. 578 [610]
Faust, R. 1429 [1559]
Fawcett, W. R. 194 [220]
Fedurco, M. 194 [220]
Feiner, F. 1485 [1587]
Feng, P. 1745 [1911]
Fenlon, E. E. 2654 [2873]
Fenske, D. 307, 1122 [340, 1191]
Fenton, D. E. 2535 [2749]
Ferguson, R. 1510 [1621]
Feringa, B. L. 348, 1512 [346, 1610]
Ferreira, A. 1003 [1115]
Fessner, W.-D. 1639 [1738]
Festag, R. 1631 [1780]
Fettinger, J. C. 112 [63]
Fey, O. 2500 [2717]
Fiedler, A. 2282, 2517 [2430, 2714]
Fife, W. K. 2718 [2946]
Filippini, G. 76 [120]
Filippou, A. C. 924 [1007]
Filla, S. A. 793 [869]
Finckh, E. 183 [205]
Fink, J. 2511 [2705]
Fink, R. 58 [102]
Finney, N. S. 676 [750]
Fischer, A. 307 [340]
Fischer, D. 1143 (1368) [1255 (1652)]
Fischer, H. (Eindhoven) 795 [879]
Fischer, H. (Frankfurt) 1844, 1848 [1989, 1992]
Fischer, J. 1115, 2371, 2530 [1204, 2602, 2753]
Fischer, K. 1472 [1606]
Fischer, R. D. 1197 [1311]
Fischer, T. 303 [335]
Fish, R. H. 1514 [1590]
Fisher, K. 201 (1032), 314 [215, 366]
Fleischer, R. 1492 [1642]
Floriani, C. 1092, 1446, 1510 [1200, 1565, 1621]
Flörke, U. 1325 [1464]
Folkerts, H. 1362 [1469]
Folting, K. 887 [969]
Folting-Streib, K. 110 [61]
Font-Bardia, M. 912 [1011]
Fontecave, M. 203, 205 [198, 199]
Fornarini, S. 654 [754]
Forsberg, L. S. 2720 [2912]
Fortin, J. B. 2507 [2711]
France, M. B. 2039 [2179]
Franck, B. 1795 [1941]
Frank, N. L. 1454 [1575]
Frank, W. 2416 [2572]
Freeman, P. K. 337 [332]
Freeman, W. P. 1887 [2029]
Fremy, G. 1474, 2269 [1608, 2450]
Frenkiel, T. A. 1874 [2040]
Frenking, G. 327, 354, 1340, 1362 [368, 383, 1476, 1469]
Freudenthaler, E. 1647 [1784]
Frey, O. 2026 [2194]
Frey, U. 1874 [2040]
Freyhardt, C. C. 2680 [2895]
Friedrich, G. 1321 [1454]
Fröhlich, R. 189, 1755, 2007 [218, 1867, 2188]
Froment, G. F. 2528 [2726]
Fu, G. 1499 [1582]
Fuchs, A. 555 [640]
Fujita, K. 1621 [1783]
Fujiwara, H. 1222 [1340]
Fukazawa, Y. 1345 [1443]
Fukuzumi, S. 1225 [1351]
Funasaka, H. 2139 [2303]
Funk, H. 814 [891]
Fürstner, A. 678 [725]
Fyfe, C. A. 1499 [1582]

Gabor, B. 81, 2227 [114, 2411]
Gabrielson, K. D. 2091 [2260]
Gack, C. 2647 [2950]
Gade, L. H. 547 [595]
Galán-Mascarós, J. R. 1460 [1601]
Galanski, M. 1103 [1220]
Gallo, E. 1446 [1565]
Gallop, M. A. 60 [94]
Galloway, C. P. 1890 [2027]
Gambarotta, S. 822, 2141, 2264 [871, 2319, 2457]
Gantzel, P. 1454, 2657 [1575, 2870]
Gantzel, P. K. 1887 [2029]
Gao, X. 2549 [2756]
García-Ruano, J. L. 1351 [1452]
Garner, C. D. 343 [370]
Gasteiger, J. 2613, 2674 [2807, 2892]
Gates, D. P. 1506 [1633]
Gatteschi, D. 2716 [2862]
Gavezzotti, A. 76 [120]
Gehm, H. 647 [705]
Geilen, C. 2667 [2879]
Geissler, B. 484 [485]
Gemmecker, G. 1671 [1813]
Genet, M. J. 560 [637]
Gennari, C. 1763, 1765 [1892, 1894]
George, R. 2115 [2311]
Gericke, K.-H. 885 [967]
Gerle, M. 1472 [1606]
Gerlitz, M. 1617 [1757]
Germanas, J. P. 1622 [1773]
Gescheidt, G. 1016 [1109]
Geus, J. W. 457 [500]
Geyer, A. 2520 [2730]
Ghadiri, M. R. 93, 95 [76, 79]
Ghosh, A. 1028 [1117]
Ghosh, S. S. 795 [879]
Giacomini, D. 2150 [2336]
Gies, H. 63 [125]
Giffels, G. 2005 [2165]
Gill, M. S. 1612, 2495 [1778, 2701]
Gilman, A. G. 1406 [1533]
Giménez-Saiz, C. 1460 [1601]
Gisselbrecht, J.-P. 805, 2725 [898, 2906]
Glaser, G. 81 [114]
Gleason, M. M. 350 [356]
Gleiter, R. 789, 1001 [867, 1094]
Glink, P. T. 1865, 1869 [1997, 2001]
Gloe, K. 481 [523]
Gobbato, K. I. 2244 [2433]
Goddard, R. 678, 1030 [725, 1107]
Godínez, L. A. 235 [236]
Goebel, M. 1104 [1208]
Goeldner, M. 1296 [1391]
Gokel, G. W. 235 [236]
Goldberg, N. 213 [225]
Goldfuss, B. 337 [332]
Golding, B. T. 2389, 2398 [2580, 2573]
Gómez-García, C. J. 1460 [1601]
Gomez-Paloma, L. 576 [614]
Gompper, R. 464 [531]
González, A. M. 1351 [1452]
Goodgame, D. M. L. 574 [605]
Gordon-Wylie, S. W. 1216 (1649) [1345]
Görls, H. 325, 673, 1860 [386, 732, 2022]
Gornitzka, H. 2677 [2904]
Gorny, R. 2007 [2188]
Goto, K. 1124 [1202]
Goto, S. 787 [862]
Gould, R. O. 2374 [2563]
Gräber, P. 2056 [2168]
Graf, E. 1115 [1204]
Graffeuil, M. 578 [610]
Grahn, W. 1485 [1587]
Gramlich, V. 805, 1596, 1739, 2242 [898, 1722, 1874, 2421]
Graness, G. 67 [116]
Granja, J. R. 93, 95 [76, 79]
Greb, G. 183 [205]
Grehl, M. 189 [218]
Greiving, H. 685 [742]
Griesbeck, A. G. 474 [498]
Grimm, G. N. 2156 [2326]
Grin, Y. 1204 [1318]
Grissom, J. W. 2037 [2196]
Grohmann, A. 2107 [2279]
Grohol, D. 1508 [1650]
Gross, J. 481 [523]
Gross, M. 805, 2725 [898, 2906]
Gross, U. 1858 [2019]
Grösser, T. 1343, 2257 [1462, 2473]
Grosshenny, V. 1100, 2705 [1211, 2921]
Groves, P. 1483 [1644]
Grubbs, R. H. 2039 [2179]
Gruber, K. 84 [66]
Grubmayr, K. 1733 [1896]
Grün, K. 2500 [2717]
Grützmacher, H. 295 [323]
Guanti, G. 2393 [2613]

Gubernator, K. 2280 [2452]
Gumbmann, F. 183 [205]
Gunale, A. 1111 [1194]
Gunaratne, H. Q. N. 1728 [1889]
Guram, A. S. 1348 [1456]
Gürtler, C. F. 1900 [2025]
Güther, R. 2023 [2159]
Guy, R. K. 2079 [2247]

Haag, R. 1492 [1642]
Haag, S. 1107 [1214]
Haarer, D. 2530 [2753]
Häberlen, O. D. 1353 [1439]
Habib-Jiwan, J.-L. 1728 [1889]
Haddon, R. C. 1591 [1733]
Hafenbradl, D. 1898 [2015]
Hafner, K. 330 [360]
Hagedorn, A. 1085 [1187]
Hahn, F. E. 2700 [2938]
Halcomb, R. L. 412, 521 [453, 569]
Halcrow, M. A. 889, 1193 [971, 1307]
Haller, M. 183 [205]
Hambley, T. W. 1883 [2047]
Hamilton, A. D. 1237 [1343 (1786)]
Häming, L. 919 [1015]
Hampel, F. 439, 441, 993, 1319, 2017 [481, 483 (1016), 1085, 1446, 2186]
Hamprecht, D. 1469 [1639]
Han, P. 1890 [2027]
Hanan, G. S. 1122 [1191]
Händel, H. 1014 [1102]
Hansen, K. B. 676 [750]
Hanson, B. E. 1645 [1728]
Hao, L. 346 [349]
Harbrecht, B. 1089, 2703 [1226, 2888]
Hardcastle, K. 1454 [1575]
Harder, G. 481 [523]
Harlan, C. J. 1201 [1315]
Harms, K. 487, 2158 [509, 2328]
Harriman, A. 1005, 1100, 2705 [1112, 1211, 2921]
Harris, R. K. 1197 [1311]
Harrison, W. T. A. 2557 [2759]
Hartl, H. 2637 [2857]
Hartmann, K. 464 [531]
Hartshorn, M. P. 2268 [2417]
Hashmi, A. S. K. 1581 [1749]
Haubner, M. 2709 [2937]
Hauck, T. 1353 [1439]
Haucke, G. 67 [116]
Haumann, T. 781 [859]
Haupt, H.-J. 1325 [1464]
Haushalter, R. C. 223 [229]
Hausherr-Primo, L. 2242 [2421]
Häussermann, C. 1462 [1593]
Havlas, Z. 76, 1355 [120, 1441]
Hawker, C. J. 1456 [1623]
Hawthorne, M. F. 1332 [1470]
Hayes, W. 1862 [1994]
He, Z. 916 [1005]
Hecht, J. 2271 [2455]
Heckel, M. 557, 989 [628, 1122]
Hegde, V. R. 2143 [2333]
Hegetschweiler, K. 2242 [2421]
Heinemann, C. 213 [225]
Heinemann, O. 592 [631]
Heiney, P. A. 795 [879]
Heinze, J. 1016 [1109]
Heller, W. 312 [376]
Helmchen, G. 2687 [2881]
Henderson, K. W. 1117 [1218]
Hendrickson, D. N. 887, 1481 [969, 1580]
Hendrix, C. 1338 (2165) [1483]
Henke, H. 2402 [2608]
Henkel, G. 1488 [1615]
Henz, A. 474 [498]
Herberhold, M. 656, 1837 [716, 1985]
Herberich, G. E. 1010 [1090]
Herbst-Irmer, R. 919 [1015]
Herdewijn, P. 1338 (2165) [1483]
Herdtweck, E. 557, 924 [628, 1007]
Herges, R. 51, 1016 [57, 1109]
Herker, M. 1362 [1469]
Herrmann, E. 1355 [1441]
Herrmann, G. 181, 814, 1713 [202, 891, 1857]
Herrmann, W. A. 112, 811, 1844, 1848, 2187, 2371, 2517 [63, 893, 1989, 1992, 2371, 2602, 2714]
Hertkorn, N. 312 [376]
Herwig, P. 1609 [1768]
Hiemstra, H. 457, 2391 [500, 2582]
Higuchi, N. 1222 [1340]
Hildebrandt, F. 1631 [1780]
Hildebrandt, P. 669 [744]
Hilf, C. 487 [509]
Hilgard, P. 238 [195]
Hiller, W. 989, 1362 [1122, 1469]
Hindsgaul, O. 2720 [2912]
Hintermann, L. 931 [996]
Hinz, D. J. 71 [97]
Hiroya, K. 2287 [2445]
Hirsch, A. 1343, 1607, 2257 [1462, 1755, 2473]
Hirth, U.-A. 2500 [2717]
Hitchcock, P. B. 484, 492, 687, 2679 [485, 522, 756, 2936]
Ho, D. M. 2657 [2870]
Hoffman, B. M. 2020 [2173]
Hoffmann, H. M. R. 100 [73]
Hoffmann, M. 2026 [2194]
Hofmann, M. 484, 657 [485, 728]
Hofmann, S. 183 [205]
Hogan, T. 68 [117]
Höger, S. 2713 [2917]
Hollnagel, H. 2538 [2763]
Holm, R. H. 226 [248]
Holmes, D. S. 2660 [2902]
Holst, O. 2000 [2154]
Holthausen, M. C. 2282 [2430]
Hönle, W. 103 [81]
Hopf, H. 685, 2367 [742, 2592]
Hopke, J. 1600 [1715]
Hoppe, D. 323, 2158 [344, 2328]
Hoppe, I. 2158 [2328]
Horsburgh, L. 1233 [1353]
Horváth, I. T. 791 [877]
Hoskins, B. F. 820, 1203 [884, 1317]
Hosmane, N. S. 332 [378]
Hosseini, M. W. 1115 [1204]
Hou, Z. 2163 [2321]
Houk, K. N. 2511, 2515 [2705, 2709]
Hovemeier, K. 779 [857]
Hövermann, K. 789 [867]
Howdle, S. M. 1275 [1409]
Huang, D. 2037 [2196]
Huber, M. 849 [929]
Huber, N. W. 2187 [2371]
Hucho, F. 39 [23]
Huck, N. P. M. 348 [346]
Huffman, J. C. 889 [971]
Hüls, C. 990 [1104]
Hummel, H. 2642 [2885]
Hunter, C. A. 1079 [1181]
Hutschka, F. 1742 [1905]
Huttner, G. 316 [354]

Ibers, J. A. 1879 [2044]
Ibrom, K. 1881 [2010]
Ichikawa, Y. 412, 521 [453, 569]
Ihlenfeldt, W.-D. 2613 [2807]
Ikeda, T. 663 [711]
Inazu, T. 1364 [1459]
Inokuchi, F. 1364 [1459]
Inoue, K. 927 [973]
Isaacs, L. 1466 [1636]
Isaacs, R. C. A. 452 [495]
Itami, K. 1476, 2691 [1649, 2943]
Ito, Y. 1476, 2691 [1649, 2943]
Iwamura, H. 927 [973]
Izod, K. 687, 2679 [756, 2936]

Jack, W. E. 1629 [1736]
Jacobs, P. A. 560, 2528, 2652 [637, 2726, 2868]
Jacobsen, E. N. 676 [750]
Jacobson, A. J. 2557 [2759]
Jaeschke, G. 2395 [2605]
Jager, W. F. 348 [346]
Jagerovic, N. 105 [86]
Jahnke, W. 469 [536]
Jakubke, H.-D. 175 [189]
Janda, K. D. 2275 [2448]
Janoschek, R. 1614 [1746]
Jansen, J. F. G. A. 1206 [1321]
Janssen, M. D. 219 [239]
Jastrzebski, J. T. B. H. 219 [239]
Jeffery, J. C. 1443 [1577]
Jeger, P. 2161 [2305]
Jendrny, J. 2515 [2709]
Jenkins, H. 2264 [2457]
Jennissen, H. P. 2495 [2701]
Jiang, L. 2409 [2610]
Jiang, W. 1332 [1470]
Jiang, Z.-H. 2520 [2730]
Jiao, H. 334, 337 [329, 332]
Jin, G.-X. 656 [716]
Jochem, G. 1853 [2006]
Jödicke, K. 2271 [2455]
Johnson, J. R. 1760 [1877]
Johnston, A. G. 1209, 1212 [1324, 1327]
Jonczyk, A. 2056 [2168]
Jones, C. 492 [522]
Jones, P. G. 448, 661, 685, 1485, 2367, 2502, 2538 [489, 752, 742, 1587, 2592, 2743, 2763]
Jones, P. L. 1443 [1577]
Joselevich, E. 1005 [1112]
Josien, H. 2683 [2948]
Jubian, V. 1237 [1343 (1786)]
Jung, D. K. 452 [495]
Jungblut, T. P. 312 [376]
Jüstel, T. 669 [744]

Kadenbach, B. 2635 [2855]
Kador, L. 2365 [2561]
Kaifer, A. E. 235 [236]
Kaim, W. 771 [847]
Kaiser, B. 323 [344]
Kajimoto, T. 412, 521 [453, 569]
Kajiwara, K. 1472 [1606]
Kaminsky, W. 2273 [2469]
Kampa, J. J. 1241 [1334]
Kampf, J. W. 1357 [1479]
Kanatzidis, M. G. 68, 2109 [117, 2281]

Kanda, W. 588, 2535 [625, 2749]
Kanie, O. 2720 [2912]
Kannewurf, C. R. 68 [117]
Kapfer, I. 1296 [1391]
Karl, J. 1755 [1867]
Karl, R. M. 1104 [1208]
Karsch, H. H. 557 [628]
Karschnick, R. 183 [205]
Kather, K. 2271 [2455]
Kato, T. 1094, 2139 [1228, 2303]
Katopodis, A. 1841 [2034]
Katz, E. 1604 [1730]
Kauffmann, K. E. 1216 (1649) [1345]
Kaupp, M. 986 [1076]
Kawachi, A. 818 [886]
Kayyem, J. F. 352 [358]
Kazarian, S. G. 1275 [1409]
Kazmaier, U. 2012 [2213]
Keeffe, J. R. 1091 [1206]
Keese, R. 1502 [1595]
Keller, M. 1898 [2015]
Kellner, R. 464 [531]
Kelly, P. F. 1758 [1903]
Keppler, B. K. 1103 [1220]
Keshavaraja, A. 2143 [2333]
Kessler, H. 469, 1671, 2026 [536, 1813, 2194]
Kettrup, A. 1735 [1865]
Khenkin, A. M. 1587 [1740]
Kido, M. 2254 [2459]
Kidwell, C. 1216 (1649) [1345]
Kikuchi, K. 1094, 2139 [1228, 2303]
Kilburn, J. D. 2660 [2902]
Kim, J. 2048 [2191]
Kim, K. 2396 [2587]
Kimura, E. 663 [711]
King, J. F. 1612, 2495 [1778, 2701]
Kirchmeier, R. L. 586 [645]
Kisielowski, L. 2017 [2186]
Kiyozumi, Y. 1199 [1313]
Kjaer, K. 649 [707]
Klaffke, W. 1748 [1881]
Klapdor, M. F. 2244 [2433]
Klapötke, T. M. 213, 511 [225, 559]
Klaus, E. 667 [713]
Klein, M. 183 [205]
Kleppinger, R. 1631, 1637 [1780, 1762]
Klessinger, M. 549 [597]
Klettke, T. 1860 [2022]
Klinkhammer, K. W. 1334 [1448]
Klösel, R. 1104 [1208]
Klostermeyer, D. 196 [255]
Klotz-Berendes, B. 189 [218]
Klüfers, P. 2119, 2647 [2290, 2950]
Kluge, H.-J. 181, 814 [202, 891]
Klumpp, G. W. 2152 [2324]
Knauer, M. 2389 [2580]
Kniep, R. 1761 [1879]
Knieriem, B. 781 [859]
Knight, B. 1591 [1733]
Knobler, C. B. 1332 [1470]
Knoch, F. 198 [251]
Knöchel, A. 186 [207]
Knochel, P. 2723 [2952]
Knölker, H.-J. 2497 [2746]
Knoll, W. 2056 [2168]
Knopf, N. 316 [354]
Knopp, M. 2278 [2442]
Knorr, A. 2664 [2925]
Ko, S.-B. 2683 [2948]
Kobayashi, Kaoru 1094, 2139 [1228, 2303]
Kobayashi, Kenji 93, 95 [76, 79]
Kobuke, Y. 693 [717]
Koch, M. 989 [1122]
Koch, W. 2282 [2430]
Koch, W. O. 2671 [2928]
Köcher, C. 2371 [2602]
Koert, U. 298, 773 [326, 849]
Koetzle, T. F. 2507 [2711]
Koga, T. 1621 [1783]
Köhler, B. 2389 [2580]
Köhler, J. 2113 [2307]
Köhler, S. 814 [891]
Kokotailo, G. T. 1499 [1582]
Kolotuchin, S. V. 2654 [2873]
Kolter, T. 2362 [2559]
Komatsu, H. 576 [614]
König, B. 661, 2538 [752, 2763]
König, W. A. 1635 [1771]
Kooijman, H. 2132 [2288]
Kopf, J. 2273 [2469]
Kopp, R. 2056 [2168]
Koppenol, W. H. 2242 [2421]
Körning, J. 2502 [2743]
Kotila, S. 1755, 2134 [1867, 2285]
Kottke, T. 1517 [1612]
Kotzyba-Hibert, F. 1296 [1391]
Kozhushkov, S. 781 [859]
Krack, G. 1014 [1102]
Kragl, U. 2005 [2165]
Krahn, E. 1071 [1172]
Kramer, K. S. 891 [977]
Kratky, C. 84 [66]
Krauth-Siegel, R. L. 141 [153]
Kräutler, B. 84, 87 [66, 69]
Krautscheid, H. 2035 [2166]
Krebs, A. 2012 [2213]
Kreitmeier, P. 2230 [2439]
Křen, V. 893 [979]
Kretschmer, W. 183 [205]
Kretzschmar, G. 990 [1104]
Kreuder, R. 1023 [1099]
Krickemeyer, E. 779, 2122 [857, 2293]
Krier, G. 103 [81]
Kroll, F. K. 2398 [2573]
Krotz, A. H. 2406 [2584]
Krüger, C. 592, 678, 1030, 2227 [631, 725, 1107, 2411]
Krüger, H.-J. 2671 [2928]
Krüger, P. 1330 [1481]
Krumm, B. 586 [645]
Kubik, S. W. 1885 [2031]
Kula, M.-R. 1748 [1881]
Kumar, P. 2143 [2333]
Kummer, S. 198 [251]
Kunath, A. 2028 [2201]
Kündig, E. P. 2161 [2305]
Kunz, H. 803, 990 [901, 1104]
Künzel, A. 2645 [2954]
Kurihara, Y. 2287 [2445]
Kurreck, H. 849 [929]
Kusch, D. 784 [874]
Kustos, M. 1330 [1481]
Kutscher, B. 238 [195]
Kuwatani, Y. 1892 [2017]
Kwak, J. C. T. 88 [88]
Kwan, W.-S. 2404 [2589]
Kyritsakas, N. 1115 [1204]

Labarre, J.-F. 578 [610]
Labarre, M.-C. 578 [610]
Labbe, J. 2720 [2912]
Lagow, R. J. 1241, 1517 [1334, 1612]
Lahana, R. 578 [610]
Lahav, M. 649 [707]
Lambert, J. B. 98 [106]
Lamparth, I. 1607, 2257 [1755, 2473]
Lampe, D. 1933 [2085]
Landry, C. C. 1201 [1315]
Lange, S. J. 2020 [2173]
Lange, T. 805 [898]
Langer, M. 1464 [1585]
Langhals, H. 2234 [2436]
Lantzsch, J. 181 [202]
Laplaza, C. E. 2042 [2181]
Lappe, P. 811 [893]
Larbig, M. 460 [505]
Larka, E. 2048 [2191]
Lash, T. D. 683, 2533 [723, 2703]
Latos-Grażyński, L. 2252 [2467]
Latour, J.-M. 205, 588, 2535 [199, 625, 2749]
Laugier, J. 588 [625]
Laynez, J. L. 105 [86]
Lebuis, A.-M. 2412 [2594]
Lee, J. C., Jr. 2507 [2711]
Leeper, F. J. 383 [421]
Lehn, J.-M. 209, 1119, 1122, 2530 [244, 1188, 1191, 2753]
Lehnhoff, S. 1104 [1208]
Leigh, D. A. 1209, 1212 [1324, 1327]
Leininger, S. 2227 [2411]
Leiserowitz, L. 649 [707]
Leitner, W. 1742, 2207 [1905, 2391]
Leize, E. 209 [244]
Lemoigno, F. 110 [61]
Lengen, M. 669 [744]
Lenoir, D. 1735 [1865]
Lentmaier, J. 993 [1085]
Lentz, D. 914 [988]
Lerner, R. A. 2275 [2448]
Leumann, C. 694 [740]
Lex, J. 2511, 2515 [2705, 2709]
Li, B. 1481 [1580]
Li, G. 207 [232]
Li, Q. 2694 [2898]
Li, Q. C. 1591 [1733]
Li, Tianhu 576 [614]
Li, Tingyu 2275 [2448]
Li, Z.-T. 2524 [2719]
Lillya, C. P. 1637 [1762]
Lin, Weiping 1497 [1646]
Lin, Wenbin 1497 [1646]
Lin, Z. 1003 [1115]
Lincke, A. 784 [874]
Link, J. T. 1723 [1886]
Linkletter, B. 472 [529]
Linthicum, D. S. 907 [975]
Lion-Dagan, M. 1604 [1730]
Lippard, S. J. 467 [511]
Liu, F.-Q. 1872 [2004]
Liu, K.-Q. 2129 [2313]
Liu, P. 84 [66]
Liu, S. 2718 [2946]
Lloyd-Jones, G. C. 462 [534]
Lo, L.-C. 2275 [2448]
Lobato, C. M. 2712 [2920]
Loeb, S. J. 2689 [2900]
Lohrenz, J. C. W. 487 [509]
Long, J. R. 226 [248]
Long, N. J. 21 (826) [37 (905)]
López-Solera, I. 921, 1351 [1002, 1452]
Lork, E. 443, 2376, 2696 [516, 2565, 2915]
Louati, A. 2725 [2906]
Lough, A. J. 998, 1506 [1079, 1633]
Löw, N. 993 [1085]

Loweth, C. J. 2654 [2873]
Lu, J. 2557 [2759]
Lu, T. 235 [236]
Lubben, M. 1512 [1610]
Lucchini, V. 1343 [1462]
Ludwig, M. 1761 [1879]
Luftmann, H. 1755, 2023 [1867, 2159]
Luger, P. 914 [988]
Luitjes, H. 2152 [2324]
Lulei, M. 2262 [2463]
Lund, K. H. 2524 [2719]
Lungwitz, B. 924 [1007]
Lüning, U. 2555 [2723]
Lunsford, J. H. 970 [1059]

Maatta, E. A. 2547 [2751]
McCleverty, J. A. 1443 [1577]
McCoy, C. P. 1728 [1889]
McDonald, F. E. 350 [356]
MacDonald, M.-A. 1230 [1337]
Machinek, R. 565 [643]
Mackiol, J. 183 [205]
McMahon, R. J. 2009 [2198]
McNeil, C. J. 2409 [2610]
McPartlin, M. 1096 [1196]
McRee, D. E. 93 [76]
Maeda, K. 1199 [1313]
Maestre, M. F. 1514 [1590]
Maggini, M. 1591 [1733]
Magnani, J. L. 1841 [2034]
Maguire, J. A. 332 [378]
Mahler, R. 902 [1012]
Mai, H.-J. 1235 [1349]
Maichle-Mössmer, C. 1607 [1755]
Maier, G. 1439 [1627]
Maier, I. 1602 [1717]
Maigrot, N. 590 [623]
Majewski, J. 649 [707]
Malik, A. 1497 [1646]
Malisch, W. 2500 [2717]
Maliszewskyj, N. C. 795 [879]
Mandai, T. 2589 [2830]
Mandon, D. 343 [370]
Manetsberger, R. B. 811 [893]
Manners, I. 998, 1506 [1079, 1633]
Marcantoni, E. 2046 [2163]
Marder, T. B. 1336 [1451]
Märkl, G. 2230 [2439]
Marks, T. J. 155, 1497 [167, 1646]
Marsch, M. 487, 2158 [509, 2328]
Martens, J. A. 2528 [2726]
Martin, J. D. 233 [234]
Martín, N. 1591 [1733]
Maruta, J. 1225 [1351]
Maruyama, Y. 1094 [1228]
Marx-Tibbon, S. 1005, 1604 [1112, 1730]
Masaguer, J. R. 1351 [1452]
Masamune, S. 793 [869]
Massa, W. 327, 657, 1235, 1340 [368, 728, 1349, 1476]
Masters, J. J. 452, 1723 [495, 1886]
Mathey, F. 590 [623]
Mathieu, R. 916 [1005]
Matsumoto, N. 1446 [1565]
Mattausch, H. 1633, 2113 [1764, 2307]
Matzger, A. J. 1478 [1630]
Mauermann-Düll, H. 1583 [1751]
Maynollo, J. 87 [69]
Mayr, H. 490, 1225, 2250 [519, 1351, 2428]
Mazéas, D. 909 [990]
Mead, P. J. 2414 [2606]
Meade, T. J. 352 [358]
Meetsma, A. 348, 1512 [346, 1610]
Meggers, E. 2137 [2317]
Megges, R. 282 [308]
Mehle, S. 327, 657 [368, 728]
Meier, H. 1437 [1598]
Meijer, E. W. 1206 [1321]
Meisel, R. 1856 [2023]
Melder, J.-P. 1021 [1119]
Melzer, K. 895 [981]
Ménage, S. 203, 205 [198, 199]
Mendel, D. 621 [677]
Menger, F. M. 585, 2091, 2147 [616, 2260, 2330]
Menke, C. 2122 [2293]
Menzel, M. 327, 657, 1340 [368, 728, 1476]
Menzer, S. 100, 574, 1862, 1865, 1869, 1894 [73, 605, 1994, 1997, 2001, 2045]
Metzger, J. O. 902 [1012]
Metzger, J. W. 312 [376]
Meunier, B. 746 [819]
Mews, R. 443, 2376, 2696 [516, 2565, 2915]
Meyer, G. 71 [97]
Meyer, J. 2122 [2293]
Meyer, W. 2242 [2421]
Meyer zu Köcker, R. 1235 [1349]
Mickeleit, M. 2667 [2879]
Micura, R. 1733 [1896]
Mierke, D. F. 1671 [1813]
Miller, S. J. 798 [864]
Milstein, D. 229 [210]
Mingos, D. M. P. 1894 [2045]
Mirkin, C. A. 1624 [1725]
Misaki, Y. 1222 [1340]
Mitchell, C. 2712 [2920]
Miyahara, Y. 1364 [1459]
Miyasaka, H. 1446 [1565]
Mizukami, F. 1199 [1313]
Mohler, D. L. 563, 1478 [601, 1630]
Möhr, S. 634 [691]
Moldes, I. 916 [1005]
Moncrieff, D. 478 [514]
Moneta, W. 588 [625]
Monflier, E. 1474, 2269 [1608, 2450]
Montero, M. L. 2504 [2761]
Montforts, F.-P. 784 [874]
Monz, L. 181 [202]
Moolenaar, M. J. 2391 [2582]
Moorefield, C. N. 2023 [2159]
Mootz, D. 2244 [2433]
Moreira da Silva, A. M. 1452 [1573]
Morgan, H. 91 [84]
Morgenroth, G. 183 [205]
Mori, H. 1222 [1340]
Mori, T. 1222 [1340]
Moriya, O. 793 [869]
Morrison, K. L. 2129 [2313]
Mortimer, M. D. 1332 [1470]
Mortreux, A. 1474, 2269 [1608, 2450]
Motherwell, W. B. 2031 [2207]
Mühlecker, W. 84 [66]
Mukaiyama, T. 2145 [2309]
Mülhaupt, R. 1143 (1368) [1255 (1652)]
Mulla, S. A. R. 665 [721]
Müllen, K. 1323, 1583, 1609 [1487, 1751, 1768]
Müller, Achim 779, 1071, 2122, 2311 [857, 1172, 2293, 2505]
Müller, Arnd 1488 [1615]
Müller, H. 325 [386]
Müller, J. 1452 [1573]
Müller, J. G. 141 [153]
Müller, K. 1437 [1598]
Müller, M. 1583 [1751]
Müller, T. 1328 [1467]
Müller-Buschbaum, H. 634 [691]
Mulvey, R. E. 1233 [1353]
Mulzer, J. 895, 2667 [981, 2879]
Münck, E. 1216 (1649) [1345]
Murahashi, S.-I. 2443 [2670]
Murakami, M. 1476, 2691 [1649, 2943]
Murer, P. 2116 [2297]
Murry, J. A. 798 [864]
Mussmann, L. 2698 [2941]
Musso, F. 1510 [1621]
Mynott, R. 81, 2227 [114, 2411]

Nagase, S. 1094, 2139 [1228, 2303]
Nagata, T. 2145 [2309]
Nägele, E. 2259 [2425]
Nail, J. W. 1241 [1334]
Nakamura, E. 2154 [2338]
Nakao, Y. 1094 [1228]
Nakatani, Y. 1898 [2015]
Nass, K. 1735 [1865]
Nasu, K. 1621 [1783]
Näther, C. 76, 1353 [120, 1439]
Naumann, R. 2056 [2168]
Navarro-Ranninger, C. 1351 [1452]
Neibecker, D. 916 [1005]
Neidlein, U. 1596 [1722]
Nendel, M. 2511, 2515 [2705, 2709]
Nesper, R. 1462 [1593]
Nestler, H. P. 1763, 1765 [1892, 1894]
Neumann, H. 1016 [1109]
Neumann, R. 1587 [1740]
Neumüller, B. 673 [732]
Neuschütz, M. 1010 [1090]
Newkome, G. R. 2023 [2159]
Nezhat, L. 1212 [1327]
Nguyen, P. 1336 [1451]
Ni, Y. 998 [1079]
Nicolaou, K. C. 576, 2079, 2289 [614, 2247, 2476]
Nicolis, I. 2381 [2567]
Niecke, E. 460, 555, 1849, 2369 [505, 640, 2012, 2600]
Nieger, M. 460, 555, 1849, 2369 [505, 640, 2012, 2600]
Niess, S. 181 [202]
Nishimi, T. 585 [616]
Nixon, J. F. 484, 492 [485, 522]
Nogami, Y. 1621 [1783]
Nolte, R. J. M. 2132 [2288]
Noltemeyer, M. 647, 2645 [705, 2954]
Nolting, H.-F. 1488 [1615]
Nonn, A. 1795 [1941]
Nonnenbruch, F. 2122 [2293]
Norcross, R. D. 798 [864]
Noren, C. J. 1629 [1736]
Nössner, G. 238 [195]
Nöth, H. 1853, 2230 [2006, 2439]
Nova, M. P. 2289 [2476]
Novak, B. H. 683 [723]
Nubbemeyer, U. 1026 [1095]
Nuber, B. 789, 1103, 1435, 2257 [867, 1220, 1603, 2473]
Nunnemann, M. 814 [891]
Nüske, J. 1600 [1715]

Oberhammer, H. 586, 2244 [645, 2433]
Obst, U. 1739 [1874]
Ochando, L. E. 55 [99]
O'Connor, D. 1005 [1112]

Odier, L. 2242 [2421]
Oechsner, H. P. 2017 [2186]
Öfele, K. 1844, 1848 [1989, 1992]
Officer, D. L. 900 [986]
Ogasawara, K. 2287 [2445]
Ohno, T. 1591 [1733]
Ohta, K. 1621 [1783]
Okawa, H. 1446, 2535 [1565, 2749]
Okazaki, R. 1124 [1202]
Olah, G. A. 1393 [1519]
Olivier, H. 2698 [2941]
Olmstead, M. M. 1514, 2252 [1590, 2467]
Onitsuka, K. 319 [351]
Oppermann, H. 2113 [2307]
Örlygsson, G. 2398 [2573]
Otera, J. 2254 [2459]
Otte, A. R. 100 [73]
Otten, E. W. 181 [202]
Otter, A. 2720 [2912]
Ottosson, C.-H. 929 [999]
Ouahab, L. 1460 [1601]
Ourisson, G. 1898 [2015]

Paasch, K. 2369 [2600]
Pacholska, E. 2252 [2467]
Pack, D. W. 905 [994]
Pacl, H. 1439 [1627]
Pagels, C. 183 [205]
Paleos, C. M. 1696 [1839]
Pandey, B. 2143 [2333]
Pandey, G. 2669 [2934]
Parandoosh, Z. 2289 [2476]
Park, C.-W. 1879 [2044]
Park, T. K. 452 [495]
Parks, D. J. 809, 1230 [895, 1337]
Parsons, S. 2374 [2563]
Parton, R. 2528 [2726]
Parvez, M. 2549 [2756]
Passler, G. 814 [891]
Patz, M. 490, 1225 [519, 1351]
Pauling, A. 1464 [1585]
Paulsen, H. 1432 [1562]
Paulus, W. 58 [102]
Paver, M. A. 1012, 1545 [1088, 1679]
Payre, N. 1239 [1361]
Peerlings, H. W. I. 1206 [1321]
Pelgrims, J. A. 2652 [2868]
Pérez, F. 912 [1011]
Pérez, P. J. 231 [242]
Pérez-Cordero, E. 2023 [2159]
Pérez-García, L. 571, 2378 [607, 2569]
Peris, E. 2507 [2711]
Perpetuo, G. 914 [988]
Persson, O. 2268 [2417]
Peschel, S. 1442 [1568]
Peseke, K. 1856 [2023]
Peters, E.-M. 474, 993, 2730 [498, 1085, 2931]
Peters, F. 2122 [2293]
Peters, K. 191, 474, 993, 1085, 2730 [213 (1364), 498, 1085, 1187, 2931]
Peters, T. 1841 [2034]
Peukert, S. 2386 [2577]
Pfaltz, A. 462 [534]
Pfitzner, A. 1647 [1784]
Pflug, J. L. 98 [106]
Philippou, A. 1003 [1115]
Philp, D. 1865 [1997]
Piers, W. E. 809, 1230 [895, 1337]
Piguet, C. 582 [618]
Plass, W. 2122 [2293]
Plasseraud, L. 916 [1005]
Plattner, D. A. 2511, 2515 [2705, 2709]
Plenio, H. 800 [881]
Plesnivy, T. 795 [879]
Podlech, J. 471 [507]
Poetsch, E. 2391 [2582]
Pohnert, G. 1602 [1717]
Polborn, K. 464, 1449, 1469 [531, 1570, 1639]
Poli, R. 112 [63]
Poliakoff, M. 1275 [1409]
Poll, W. 2244 [2433]
Pomrehn, B. 1319 [1446]
Ponzini, F. 1019 [1092]
Poojary, D. M. 1508 [1650]
Popovitz-Biro, R. 649 [707]
Potter, B. V. L. 1933 [2085]
Poveda, M. L. 231 [242]
Prasanna de Silva, A. 1728 [1889]
Prato, M. 1343, 1591 [1462, 1733]
Pratviel, G. 746 [819]
Priermeier, T. 112, 1737, 1844 [63, 1870, 1989]
Prinzbach, H. 1016 [1109]
Pritchard, D. J. 91 [84]
Pritchard, R. J. 1209 [1324]
Pritzkow, H. 316, 681, 1111, 1614 [354, 748, 1194, 1746]
Proserpio, D. M. 1895 [2037]
Ptock, A. 678 [725]
Puchberger, M. 84 [66]
Puddephatt, R. J. 346 [349]
Pudelski, J. K. 1506 [1633]

Quaiser, S. A. 2240, 2728 [2461, 2956]
Quante, H. 1323 [1487]
Que, L., Jr. 203, 1512, 2048 [198, 1610, 2191]

Raabe, G. 1021, 2278 [1119, 2442]
Rabe, J. P. 303, 1609 [335, 1768]
Radek, C. 2374 [2563]
Rademacher, O. 2113 [2307]
Rafalko, P. W. 222 [254]
Raithby, P. R. 921, 1012, 1351, 2662 [1002, 1088, 1452, 2891]
Ramadan, N. A. 1030 [1107]
Ramaiah, D. 107 [91]
Ramaswamy, A. V. 2143 [2333]
Ramig, K. 222 [254]
Randerath, M. 2122 [2293]
Rao, K. S. S. P. 2669 [2934]
Rath, N. P. 1641 [1744]
Ratner, M. A. 155 [167]
Rauchfuss, T. B. 1890 [2027]
Rauschenbach, A. 76 [120]
Ravikumar, V. T. 2406 [2584]
Ravindranathan, T. 2143 [2333]
Raymond, C. C. 2509 [2737]
Raymond, K. N. 1359 [1473]
Re, N. 1446 [1565]
Rebek, J., Jr. 446, 1885 [503, 2031]
Rechinger, M. 441 [483 (1016)]
Reck, G. 690 [735]
Reddy, A. C. 1495 [1619]
Rees, N. H. 2660 [2902]
Reetz, M. T. 301, 2240, 2728 [373, 2461, 2956]
Regitz, M. 484 [485]
Reichelt, W. 2113 [2307]
Reid, D. C. W. 900 [986]
Reihs, S. 993 [1085]
Rein, T. 1023 [1099]
Reinaud, O. M. 2051 [2171]
Reinhold, U. 1219 [1332]
Reinhoudt, D. N. 2124 [2300]
Reisenauer, H. P. 1439 [1627]
Reiser, O. 1023 [1099]
Reisinger, C.-P. 1844 [1989]
Reisner, A. 1485 [1587]
Reiss, G. J. 2416 [2572]
Reiss, M. 2230 [2439]
Rell, S. 1614 [1746]
Rennels, R. A. 1348 [1456]
Rennie, M.-A. 1012 [1088]
Repke, K. R. H. 282 [308]
Rétey, J. 652, 1464, 2389 [719, 1585, 2580]
Rettig, S. J. 1230 [1337]
Reuter, H. 1578, 2311 [1712, 2505]
Reutter, W. 2667 [2879]
Reymond, J.-L. 2285 [2471]
Rheingold, A. L. 656, 998, 1887, 1890, 2051, 2507 [716, 1079, 2029, 2027, 2171, 2711]
Ricci, J. S. 2507 [2711]
Rice, T. E. 1728 [1889]
Richardson, T. I. 1227 [1355]
Richens, D. T. 1883 [2047]
Richter, A. G. 1497 [1646]
Richter, B. 2649 [2865]
Rieck, H. 2687 [2881]
Riegel, J. 814 [891]
Rieger, A. L. 2540 [2734]
Rieger, B. 1143 (1368) [1255 (1652)]
Rieger, P. H. 2540 [2734]
Ries, R. 1472 [1606]
Ringsdorf, H. 58, 795, 2056 [102, 879, 2168]
Risch, N. 2639 [2861]
Ritter, A. 1030 [1107]
Ritter, H. 309 [342]
Ritter, J. 789 [867]
Rius, J. 55 [99]
Rizzoli, C. 1092, 1510 [1200, 1621]
Robson, R. 820, 1203 [884, 1317]
Rocha, J. 1003 [1115]
Rodbell, M. 1420 [1549]
Rödel, M. 661 [752]
Rodríguez, J. H. 1351 [1452]
Roesky, H. W. 919, 1872, 2504, 2645 [1015, 2004, 2761, 2954]
Röhr, C. 2115 [2311]
Rohr, J. 565, 881, 1107, 1617 [643, 963, 1214, 1757]
Röhrig, C. 63 [125]
Rösch, N. 1353 [1439]
Rosen, D. 2511 [2705]
Rosenblum, J. S. 2275 [2448]
Ross, H. 2555 [2723]
Ross, M. J. 1233 [1353]
Roth, M. 2250 [2428]
Röttele, H. 652 [719]
Rouxhet, P. G. 560 [637]
Rovira, C. 55 [99]
Rowan, A. E. 2132 [2288]
Rozov, L. A. 222 [254]
Ruban, A. V. 460 [505]
Rück, K. 433 [475]
Rudkevich, D. M. 2124 [2300]
Rudolph, M. 2730 [2931]
Rulkens, R. 1506 [1633]
Runsink, J. 1021, 2278 [1119, 2442]
Runte, O. 2187 [2371]
Ruppert, R. 1115 [1204]

Russell, C. A. 1012, 1545, 2662 [1088, 1679, 2891]
Russell, K. C. 209 [244]
Rychnovsky, S. D. 1227 [1355]

Saalfrank, R. W. 993, 2709 [1085, 2937]
Saba, A. 78 [104]
Sadler, P. J. 1874 [2040]
Sadowski, J. 2674 [2892]
Saenger, W. 1452 [1573]
Saha-Möller, C. R. 107, 2156 [91, 2326]
Saiz, J. L. 105 [86]
Sakamoto, Y. 1345 [1443]
Sakiyama, H. 2535 [2749]
Salm, R. J. 1879 [2044]
Salom, B. 1763, 1765 [1892, 1894]
Sambri, L. 2046 [2163]
Sander, W. 929 [999]
Sandermann, H., Jr. 312 [376]
Sanders, J. K. M. 217, 1096 [223, 1196]
Sandhoff, K. 2362 [2559]
Sasaki, D. Y. 905 [994]
Sastry, G. N. 1495 [1619]
Sato, T. 2254 [2459]
Saxena, A. K. 332 [378]
Scarlett, N. V. Y. 1203 [1317]
Schäfer, H. J. 189, 2007 [218, 2188]
Schäfer, M. 191 [213 (1364)]
Schakel, M. 2152 [2324]
Schardt, S. 330 [360]
Scharn, D. 914 [988]
Schaub, M. 340 [363]
Scheer, M. 1997 [2151]
Scheerer, F. 814 [891]
Scheffler, K. 1841 [2034]
Scheib, S. 781 [859]
Schenk, W. A. 1008 [1098]
Schenning, A. P. H. J. 2132 [2288]
Scherer, O. J. 1321 [1454]
Scherl, M. 2530 [2753]
Schiavo, C. 1869 [2001]
Schick, G. 2257 [2473]
Schick, H. 2028 [2201]
Schindler, J. L. 68 [117]
Schirmer, R. H. 141 [153]
Schlechtingen, G. 2497 [2746]
Schleicher, M. 183 [205]
Schleyer, P. von R. 115, 334, 337, 476, 484, 657, 1594 [108, 329, 332, 492, 485, 728, 1766]
Schlotterbeck, G. 1014 [1102]
Schmalz, H.-G. 1833, 2383 [1981, 2597]
Schmeusser, M. 2500 [2717]
Schmickler, H. 2511, 2515 [2705, 2709]
Schmid, G. 1442, 2712 [1568, 2920]
Schmidpeter, A. 1853 [2006]
Schmidt, G. 2402 [2608]
Schmidt, H.-G. 647, 2645 [705, 2954]
Schmidt, M. 1472 [1606]
Schmidt, P. C. 1761 [1879]
Schmidt, R. R. 1328, 2520 [1467, 2730]
Schmidt, U. 198 [251]
Schmidtchen, F. P. 65 [71]
Schmitz, R. F. 2152 [2324]
Schneider, A. 557 [628]
Schneider, H.-J. 321 [380]
Schneider, J. 2416 [2572]
Schneider, J. J. 592 [631]
Schnitzler, J.-P. 312 [376]
Schnyder, A. 931 [996]
Schödel, H. 1355 [1441]
Schoeller, W. W. 555, 1849 [640, 2012]
Schoepfer, J. G. 2129 [2313]
Scholz, A. 673 [732]
Scholz, F. 2685 [2876]
Scholz, J. 673, 2649 [732, 2865]
Schön, J. C. 1081, 2004 [1183, 2158]
Schön, R. 282 [308]
Schoonheydt, R. A. 2652 [2868]
Schoop, T. 919 [1015]
Schrader, T. 917 [1001]
Schreiber, S. L. 953, 2129 [1041, 2313]
Schrock, R. R. 2044 [2184]
Schrödel, H.-P. 1853 [2006]
Schröder, D. 1973, 2517 [2126, 2714]
Schröder, M. 2374 [2563]
Schröter, J. A. 1631 [1780]
Schubert, C. 652 [719]
Schuhmacher, J. 2119 [2290]
Schultz, P. G. 621, 1629 [677, 1736]
Schulz, S. 919 [1015]
Schünke, C. 1731 [1901]
Schwab, P. 2039 [2179]
Schwalbach, R. 181 [202]
Schwarz, H. 213, 1973, 2033, 2282, 2517 [225, 2126, 2176, 2430, 2714]
Schwarz, M. 181 [202]
Schwarz, P. 1197 [1311]
Schwarz, W. 1334 [1448]
Schweikart, D. 327 [368]
Schwieger, W. 1499 [1582]
Sczakiel, G. 643 [701]
Searle, M. S. 1483 [1644]
Sebald, A. 667 [713]
Seburg, R. A. 2009 [2198]
Seebach, D. 471, 553, 2116, 2395 [507, 622, 2297, 2605]
Seidel, W. 325 [386]
Seidel, W. W. 2700 [2938]
Seiler, M. 1005 [1112]
Seiler, P. 1466 [1636]
Seitz, M. 795 [879]
Seitz, O. 803 [901]
Selg, P. 791 [877]
Sen Gupta, R. 186 [207]
Senyei, A. 2289 [2476]
Seppelt, K. 1586, 1858 [1772, 2019]
Seufert, M. 340 [363]
Severin, K. 1449 [1570]
Seyferth, D. 2236 [2435]
Shaik, S. 1495 [1619]
Shair, M. D. 1721 [1883]
Sharman, G. J. 1483 [1644]
Sharpless, K. B. 1059 [1159]
Sheldrick, W. S. 450 [490]
Shimada, H. 1621 [1783]
Shimoni, L. 1555 [1689]
Shin, H. 907 [975]
Shing, T. K. M. 1643 [1742]
Shinkai, S. 1364 [1459]
Shionoya, M. 663 [711]
Shiro, M. 663 [711]
Shivanyuk, A. N. 2124 [2300]
Shnek, D. R. 905 [994]
Shreeve, J. M. 586 [645]
Sibert, J. W. 2020 [2173]
Siebel, E. 1197 [1311]
Siebert, W. 681, 1111 [748, 1194]
Siegel, J. S. 1019, 1454, 2657 [1092, 1575, 2870]
Siegel, S. 2383 [2597]
Sieler, J. 2649 [2865]
Simon, A. 567, 1633, 2113 [647, 1764, 2307]
Simon, J. D. 1481 [1580]
Simpelkamp, J. 301 [373]
Singewald, E. T. 1624 [1725]
Singh, S. K. 60 [94]
Sini, G. 2507 [2711]
Sironi, A. 1895 [2037]
Siuzdak, G. 2053 [2209]
Skiebe, A. 2257 [2473]
Skrydstrup, T. 909 [990]
Slany, M. 484 [485]
Slawin, A. M. Z. 1758 [1903]
Smart, J. P. 1212 [1327]
Smit, B. 2543 [2765]
Smith, A. M. 574 [605]
Smith, B. M. 576 [614]
Smith, D. P. 1514 [1590]
Smith, J. D. 687, 2679 [756, 2936]
Snaith, R. 921 [1002]
Snyder, J. P. 80, 986 [112, 1076]
Snyder, L. B. 452, 1723 [495, 1886]
Soghomonian, V. 223 [229]
Söhnel, T. 2113 [2307]
Sokabe, M. 693 [717]
Solans, X. 912 [1011]
Solari, E. 1092, 1510 [1200, 1621]
Sommerfeld, T. L. 553 [622]
Song, J.-I. 2141 [2319]
Sonogashira, K. 319 [351]
Sorger, K. 1594 [1766]
Soulimane, T. 1488 [1615]
Soumillion, J.-P. 1728 [1889]
Sournies, F. 578 [610]
Souto, A. A. 2710 [2910]
Souverijns, W. 2528 [2726]
Speckamp, W. N. 457, 2391 [500, 2582]
Speiser, B. 1086 [1222]
Spek, A. L. 219, 2132 [239, 2288]
Spence, R. E. von H. 809, 1230 [895, 1337]
Spencer, N. 1865 [1997]
Spitz, U. P. 1885, 2030 [2031, 2206]
Spraul, M. 652, 1014 [719, 1102]
Sprengard, U. 990 [1104]
Squire, R. C. 887 [969]
Stabel, A. 303, 1609 [335, 1768]
Stachel, H.-D. 993 [1085]
Stack, T. D. P. 996 [1082]
Stadler, S. 1485 [1587]
Stahl, D. 1761 [1879]
Stahl, H. 1086 [1222]
Stalke, D. 1492, 1594, 1752, 1849, 1872, 2677 [1642, 1766, 1908, 2012, 2004, 2904]
Stannek, J. 2227 [2411]
Stark, J. L. 2547 [2751]
Starnecker, M. 2238 [2465]
Staufer, M. 1353 [1439]
Steckhan, E. 1900, 2137 [2025, 2317]
Steenken, S. 490 [519]
Steffan, B. 196 [255]
Steffens, G. C. M. 1488 [1615]
Steglich, W. 196, 1449, 1469 [255, 1570, 1639]
Stein, A. 1748 [1881]
Stein, P. C. 2524 [2719]
Steiner, A. 919, 1752, 2662 [1015, 1908, 2891]
Steiner, D. 327, 1111, 1340 [368, 1194, 1476]
Steiner, T. 1452 [1573]
Stekar, J. 238 [195]
Stenner, J. 181 [202]
Stephan, H. 481 [523]

Stern, C. L. 98, 1624, 2020 [106, 1725, 2173]
Stetter, K. O. 1898 [2015]
Steudel, R. 1313, 1330 [1433, 1481]
Stevens, R. A. 2509 [2737]
Still, W. C. 1763, 1765 [1892, 1894]
Stoddart, J. F. 571, 1862, 1865, 1869, 2378 [607, 1994, 1997, 2001, 2569]
Straub, W. 1856 [2023]
Strauss, I. 688 [738]
Streib, W. E. 887, 891 [969, 977]
Streubel, R. 436 [478]
Stucky, G. D. 1745 [1911]
Stüdemann, T. 2723 [2952]
Sturm, V. 330 [360]
Subramanian, S. 2127 (2561) [2295]
Sulikowski, G. A. 2396 [2587]
Sun, S. 2540 [2734]
Sung, K. 1517 [1612]
Suzuki, T. 1094, 1591, 2139 [1228, 1733, 2303]
Svenstrup, N. 2524 [2719]
Sweigart, D. A. 2540 [2734]
Szabó, K. J. 2551 [2767]
Szczepura, L. F. 1890 [2027]
Szymczak, W. 312 [376]

Takahashi, Takashi 1345 [1443]
Takahashi, Takeshi 2139 [2303]
Tamao, K. 818 [886]
Tamaru, Y. 787 [862]
Tamburini, M. 2046 [2163]
Tanaka, A. 787 [862]
Tanaka, Shigeaki 319 [351]
Tanaka, Shoji 1222 [1340]
Tanaka, Shuji 787 [862]
Tanaka, Y. 693 [717]
Tasker, P. A. 1865, 1869 [1997, 2001]
Taulelle, F. 1115 [1204]
Teichert, M. 2504 [2761]
Teixeira-Dias, J. J. C. 1452 [1573]
Teles, J. H. 1021 [1119]
Teller, G. 1898 [2015]
Temme, B. 1755 [1867]
Tesche, B. 2728 [2956]
Thauer, R. K. 2247 [2418]
Theopold, K. H. 2051 [2171]
Thibaut, D. 383 [421]
Thiel, W. R. 1737 [1870]
Thiele, K.-H. 2649 [2865]
Thiem, J. 893 [979]
Thiessen, P. A. 2163 [2321]
Thornton, P. 1443 [1577]
Tiedtke, D. B. 110 [61]
Tietze, L. F. 1366, 1731 [1485, 1901]
Tilley, T. D. 1887 [2029]
Tödter, K. 186 [207]
Togni, A. 931 [996]
Tokitoh, N. 1124 [1202]
Töllner, E. 784 [874]
Tornieporth-Oetting, I. C. 213, 511 [225, 559]
Toth, C. 1627 [1776]
Trautmann, N. 181, 814 [202, 891]
Trautwein, A. X. 343, 669, 2242 [370, 744, 2421]
Triki, S. 1460 [1601]
Trojandt, G. 1449 [1570]
Trommer, M. 929 [999]
Trommsdorff, H. P. 2530 [2753]
Trost, B. M. 259, 2386 [285, 2577]
Tschierske, C. 1631 [1780]
Tsiourvas, D. 1696 [1839]
Tsivgoulis, G. M. 1119 [1188]
Tsuji, J. 2589 [2830]
Tuchagues, J.-P. 205 [199]
Tumelty, D. 60 [94]
Turner, D. L. 2660 [2902]

Udvarnoki, G. 565, 1107, 1617 [643, 1214, 1757]
Ueda, I. 1892 [2017]
Ueno, F. 567 [647]
Ugi, I. 1104, 2238 [1208, 2465]
Uhl, W. 989 [1122]
Ulic, S. E. 2244 [2433]
Unverzagt, M. 657 [728]
Uphade, B. S. 665 [721]
Urakawa, H. 1472 [1606]
Urban, F.-J. 814 [891]
Urland, W. 71 [97]
Usón, I. 2504 [2761]
Usui, S. 1345 [1443]

Valdés, C. 1885 [2031]
Van Aerschot, A. 1338 (2165) [1483]
van Benthem, R. A. T. M. 457 [500]
van de Goor, G. 2680 [2895]
Van Dorsselaer, A. 209 [244]
van Eldik, R. 2245 [2414]
van Es, D. S. 2553 [2728]
van Esch, J. 2056 [2168]
van Garderen, H. F. 73 [122]
van Hooff, J. H. C. 2543 [2765]
van Koten, E. M. 219 [239]
van Koten, G. 219 [239]
van Leeuwen, P. W. N. M. 457 [500]
van Santen, R. A. 73, 2543 [122, 2765]
van Well, W. J. M. 2543 [2765]
Vannijvel, I. P. 2652 [2868]
Vanoppen, D. L. 560 [637]
Vázquez, S. 912 [1011]
Veciana, J. 55 [99]
Verberckmoes, A. A. 2652 [2868]
Verboom, W. 2124 [2300]
Verheggen, I. 1338 (2165) [1483]
Verhorevoort, K. L. 2662 [2891]
Veronese, A. 1237 [1343 (1786)]
Verrelst, W. 2528 [2726]
Verseck, S. 1748 [1881]
Vetter, D. 60 [94]
Vidakovic, M. 1622 [1773]
Vielsack, F. 2035 [2166]
Vij, A. 586 [645]
Vincent, J.-M. 205 [199]
Vittal, J. J. 346 [349]
Vogel, E. 2511, 2515 [2705, 2709]
Vögtle, F. 481 [523]
Voigt, A. 2504 [2761]
Vollhardt, K. P. C. 563, 1478 [601, 1630]
von der Gönna, V. 460 [505]
von Matt, P. 798 [864]
von Schnering, H. G. 103, 191, 474, 986, 993, 1085, 1204, 2730 [81, 213 (1364), 498, 1076, 1085, 1187, 1318, 2931]
von Unold, P. 2234 [2436]
von Zezschwitz, P. 1023 [1099]
Vuilhorgne, M. 383 [421]
Vyboishchikov, S. F. 1362 [1469]

Wachhold, M. 450 [490]
Wagener, M. 2674 [2892]
Wagner, C. 565 [643]
Wagner, M. 1583 [1751]
Wagner, T. 688, 825 [738, 904]
Wahl, H. 455 [527]
Wahnon, D. 2412 [2594]
Waldmann, H. 2005, 2259, 2402 [2165, 2425, 2608]
Wallbaum, S. 2280 [2452]
Walter, C. J. 217 [223]
Walter, K. 181 [202]
Walther, D. 1860 [2022]
Walzl, M. 2150 [2336]
Wan, L. H. 1643 [1742]
Wandrey, C. 2005 [2165]
Wang, J. 1749 [1898]
Wang, W. T. 1841 [2034]
Wang, Y. M. 2395 [2605]
Wanner, J. 476 [492]
Wanninger, K. M. A. 924 [1007]
Ward, G. N. 2662 [2891]
Ward, M. D. 1443 [1577]
Wareham, R. S. 2660 [2902]
Wataoka, I. 1472 [1606]
Waymouth, R. M. 1143 (1368) [1255 (1652)]
Weber, L. 1739, 2280 [1874, 2452]
Weck, M. 58 [102]
Wecker, U. 1246 [1358]
Weckhuysen, B. M. 2652 [2868]
Wedig, U. 1204 [1318]
Wedler, C. 2028 [2201]
Wegner, G. 340 [363]
Weidenbruch, M. 1085 [1187]
Weigerding, M. 2005 [2165]
Weiland, J. 282 [308]
Weinmann, H. 448 [489]
Weintraub, S. T. 1216 (1649) [1345]
Weintritt, H. 678 [725]
Weis, U. 2500 [2717]
Weisemann, R. 1841 [2034]
Weiss, Raymond 343 [370]
Weiss, Robert 439, 441, 1319 [481, 483 (1016), 1446]
Weissgräber, S. 1488 [1615]
Welch, A. 2709 [2937]
Weller, M. T. 2414 [2606]
Wendorff, J. H. 1631 [1780]
Wendt, K. 181 [202]
Wenz, G. 340 [363]
Werle, A. 196 [255]
Werner, C. 2367 [2592]
Werner, H. 191, 1244 [213 (1364), 1359]
Weseloh, G. 1635 [1771]
Wesemann, L. 2236 [2435]
Wesendrup, R. 2033 [2176]
Wessel, H. P. 2712 [2920]
Wessel, Jens 443, 2376 [516, 2565]
Wessel, Jeremy 2507 [2711]
Westcott, S. A. 1336 [1451]
Weyhermüller, T. 669, 2642 [744, 2885]
Wheeler, P. 2406 [2584]
White, A. J. P. 571, 1862 [607, 1994]
Wieczorek, C. 657 [728]
Wiedemann, R. 1244 [1359]
Wieder, T. 2667 [2879]
Wieghardt, K. 669, 1435, 2642 [744, 1603, 2885]
Wijkens, P. 219 [239]
Wilde, A. 100 [73]
Wilkinson, E. C. 203, 1512, 2048 [198, 1610, 2191]
Willemsen, S. 914 [988]
Willett, G. 201 (1032) [215]
Williams, A. F. 582 [618]

Williams, A. S. 2031 [2207]
Williams, D. H. 1483 [1644]
Williams, D. J. 100, 571, 574, 1862, 1865, 1869, 1894 [73, 607, 605, 1994, 1997, 2001, 2045]
Williamson, A. S. 226 [248]
Williard, P. G. 1117 [1218]
Willner, H. 2244 [2433]
Willner, I. 1005, 1604 [1112, 1730]
Wilson, S. R. 1890, 2654 [2027, 2873]
Winkler, H. 343, 2242 [370, 2421]
Winkler, H.-J. 327, 657, 1340 [368, 728, 1476]
Winkler, U. 1614 [1746]
Winterfeldt, E. 448 [489]
Wintermantel, M. 1472 [1606]
Wirth, T. 1726 [1872]
Witt, E. 557 [628]
Wocadlo, S. 1235 [1349]
Wojtczak, W. A. 1877 [2050]
Wolf, C. 1635 [1771]
Wolf, J. 191, 1244 [213 (1364), 1359]
Wolff, J. J. 2225 [2409]
Wolff, S. 563 [601]
Wollenweber, M. 1016 [1109]
Wolmershäuser, G. 1321 [1454]
Wolski, A. 439, 441 [481, 483 (1016)]
Wolthuizen, J. P. 2543 [2765]
Wong, C.-H. 412, 521 [453, 569]
Wong, G. K. 1497 [1646]
Worm, K. 65 [71]
Wraage, K. 2645 [2954]
Wright, D. S. 1012, 1545, 2662 [1088, 1679, 2891]
Wu, Y.-D. 2511, 2515 [2705, 2709]
Wudl, F. 1343, 1591 [1462, 1733]
Wulff, C. 1023 [1099]
Wulff, G. 1812 [1958]
Würthner, F. 446 [503]

Xiao, F. 2694 [2898]
Xiao, J. 346 [349]
Xiao, X.-Y. 2289 [2476]
Xiong, X. 1629 [1736]
Xu, R. 2694 [2898]

Yaghi, O. M. 207 [232]
Yamabe, T. 1222 [1340]
Yamada, H. 1345 [1443]
Yamada, S. 1113 [1224]
Yamada, T. 2145 [2309]
Yamago, S. 2154 [2338]
Yamamoto, K. 2139 [2303]
Yamasaki, Y. 585 [616]
Yang, C. 1637 [1762]
Yap, G. P. A. 2051, 2507 [2171, 2711]
Yasui, K. 787 [862]
Yau, J. 1894 [2045]
Ying, J. Y. 2014 [2202]
Yitzchaik, S. 1497 [1646]
Yoon, T.-Y. 1721 [1883]
Yorozu, K. 2145 [2309]
Yoshida, T. 319 [351]
Young, V. G., Jr. 2547 [2751]
Young, W. B. 452, 1723 [495, 1886]

Zahavy, E. 1005 [1112]
Zambrano, J. 2386 [2577]
Zander, L. 2515 [2709]
Zanetti, N. C. 2044 [2184]
Zapf, S. 196 [255]
Zaworotko, M. J. 1230, 2127 (2561) [1337, 2295]
Zelder, O. 2398 [2573]
Zenneck, U. 53, 198 [59, 251]
Zhang, H. 332 [378]
Zhang, L. 235 [236]
Zhang, Xiang 68 [117]
Zhang, Xiongzhi 1858 [2019]
Zheng, Y. 1890 [2027]
Ziessel, R. 1100, 2705 [1211, 2921]
Ziller, J. 1454 [1575]
Ziller, J. W. 2039, 2386 [2179, 2577]
Zimmer, K. 181 [202]
Zimmerman, S. C. 2163, 2404, 2654 [2321, 2589, 2873]
Zonta, A. 301 [373]
Zsolnai, L. 316 [354]
Zubieta, J. 223 [229]

INDEX OF AUTHORS AND REVIEWERS OF BOOKS

This index lists separately the names of Authors/Editors and Reviewers, respectively, of books reviewed in *Angew. Chem. Int. Ed. Engl.* **1995**, *34*.

Bookauthors

Albert, W. H. 243
Aldersey-Williams, H. 1769
Atherton, N. M. 1033
Atkins, P. W. 599
Baneyx, F. 697
Behr, J.-P. 2293
Bertini, I. 1036
Bogdanov, A. A. 1521
Breggin, G. R. 1250
Breggin, P. R. 1250
Briggs, D. 2059
Brown, B. R. 1249
Buback, M. 120
Buchachenko, A. L. 936
Carlson, R. M. K. 1903
Charushin, V. N. 2419
Chupakhin, O. N. 2419
Cintas, P. 121
Cram, D. J. 2563
Cram, J. M. 2563
Cramer, F. 1771
Craver, C. D. 601
Croasmun, W. R. 1903
Daintith, J. 2167
Daniel, H.-D. 359
Dettmann, J. 1769
DiTrocchio, F. 1370
Djerassi, C. 241
Emsley, J. 2059
Feltz, A. 242
Frankevitch, E. L. 936
Gjertsen, D. 2167
Glusker, J. P. 2060
González-Morega, G. 121
Gray, H. B. 1036
Griesbeck, A. 1770
Hampden-Smith, M. J. 1651
Haslam, E. 361
Hassner, A. 935
Hayashi, T. 1904
Hegedus, L. S. 1035
Hirsch, A. 1904
Ho, T.-L. 1369
Huisgen, R. 1129
Kavarnos, G. J. 495
Kennewell, P. D. 828
Klabunde, K. J. 1252
Kleinpeter, E. 1251
Knight, D. 1034
Kocienski, P. J. 1370
Kodas, T. T. 1651
Kosuge, K. 1033
Kroschwitz, J. I. 2564
Kyriacou, D. 1521
Laidler, K. J. 360
Langford, C. H. 599
Lappin, A. G. 1249
Laue, T. 935
Lehn, J.-M. 2563
Lewis, M. 2060
Lippard, S. J. 1036
Lucotte, G. 697
Lunn, G. 1037
Masseyeff, R. F. 243
Mattay, J. 1770
Mezey, P. G. 361
Mitchell, S. 2167
Möckel, K. 1769
Niemantsverdriet, J. W. 495
Nógrádi, M. 1372
Papp, R. B. 935
Patai, R. 2419
Patai, S. 1251
Pepperrell, C. 359
Perkins, M. J. 1771
Pihlaja, K. 1251
Plagens, A. 935
Pollard, B. D. 935
Porter, R. 2168
Quin, L. D. 1651
Rappoport, Z. 1251
Rhodes, G. 496
Roesky, H. W. 1769
Rossi, M. 2060
Sansone, E. B. 1037
Schmid, G. 122
Seah, M. P. 2059
Shabarova, Z. A. 1521
Shriver, D. F. 599
Splitter, J. S. 497
Staines, N. A. 243
Stoltzenberg, D. 119
Stumer, C. 935
Suppan, P. 599

Talsky, G. 1522
Taylor, J. B. 828
Taylor, L. R. 935
Thomas, E. L. 600
Togni, A. 1904
Tootill, E. 2167
Tsukerblat, B. S. 1772
Tureček, F. 497
Urban, M. U. 601
Valentine, J. S. 1036
van der Plas, H. C. 2419
van Gunsteren, W. F. 1034
Verkade, J. G. 1651
Vögele, H. P. 120
Wagnière, G. H. 827
Weiner, P. K. 1034
Whitesides, G. M. 1523
Wilkinson, A. J. 1034
Wong, C.-H. 1523
Woolins, J. D. 2565
Zollinger, H. 1653

Reviewers

Anslyn, E. V. 2293
Bach, T. 1369
Bain, C. D. 827
Beck, J. 2565
Braun, N. 935
Bubert, H. 2059
Butenschön, H. 935
Calado, J. C. G. 1771
Cornils, B. 119
Dinse, K.-P. 1033
Dutasta, J.-P. 2563
Effenberger, F. 1653
Ernst, L. 1251
Famulok, M. 697
Fischer, R. A. 1651
Gade, L. H. 121, 122
Gerischer†, H. 360
Giannis, A. 828
Glüsenkamp, K.-H. 243
Goez, M. 936
Gügel, A. 1769
Haase, D. 1772
Heilbronner, E. 2167
Heise, H. M. 1522
Heitele, H. 495
Hoffmann, R. W. 1129
Hopf, H. 241, 1370
Kauffman, G. B. 1250, 2059, 2168, 2419
Kauffman, L. M. 2059
Knochel, P. 121
Koert, U. 1370
Kräutler, B. 1904
Laszlo, P. 1034
Lauterwein, J. 1903
Luftmann, H. 497
Lüning, U. 1771
Mahnig, M. 359
Maier, J. 1033
Mąkosza, M. 2419
Meier, C. 1521
Merz, A. 1037
Metz, P. 1035
Müller, G. 2060
Nees, F. 2564
Nilges, M. 1034
Plagens, A. 241
Plenio, H. 1904
Raschke, D. 1769
Reuter, H. 242
Rohr, J. 361
Rouvray, D. H. 359, 361
Rück, K. 1372
Saenger, W. 496
Sander, W. 120
Sanders, J. K. M. 2563
Schick, H. 1523
Schneider, J. J. 1252
Seifert, K. 1521
Strasdeit, H. 1036
Streubel, R. 1651
van Eldik, R. 1249
Virgil, S. 1770
von Schnering, H. G. 1769
Wandelt, K. 495
Wenig, W. 600, 601
Wenschuh, E. 1251
Wimmer, F. L. 599
Wöhrle, D. 599
Würthwein, E.-U. 1249

SUBJECT INDEX [*Angew. Chem. Int. Ed. Engl.* 1995, *34*]

(A second page number to an entry indicates an erratum to the corresponding article.)

(R) = Review Article (H) = Highlight (C) = Short Communication (B) = Book Review (L) = Correspondence

Ab initio calculations
- An Ab Initio Investigation of the Rh^{I}-Catalyzed Hydroboration of C=C Bonds: Evidence for Hydrogen Migration in the Key Step (C) 115
- A P_2C_2 Four-Membered Ring with Unusual Bonding—Synthesis, Structure, and Ring Opening of a 1,3-Diphosphacyclobutane-2,4-diyl (C) 555
- Aromaticity and Antiaromaticity in Five-Membered C_4H_4X Ring Systems: "Classical" and "Magnetic" Concepts May Not Be "Orthogonal" (C) 337
- 4c/3e Radical Cations with Cage-Directed Configurations (C) 1016
- Compounds with Planar Tetracoordinate Boron Atoms: Anti van't Hoff/Le Bel Geometries without Metal Centers (C) 327
- Computational Evidence for the Existence of Cu^{III} Intermediates in Addition and Substitution Reactions with Dialkylcuprates (C) 476
- Conical Intersections and the Mechanism of Singlet Photoreactions (H) 549
- Coordination of Dioxygen in Three Representative Transition Metal Cations: FeO_2^+, CrO_2^+, and $[CH_3Re(O_2)_2O]^+$ (C) 2517
- Covalent Inorganic Azides (R) 511
- Diborylcarbenes as Reactive Intermediates in Double 1,2-Rearrangements with Low Activation Enthalpies (C) 1340
- Distinguishing Copper d^8 and d^{10} Configurations in a Highly Ionic Complex; A Nonformal Metal Oxidation State (C) 986
- Electrochemistry and Ab Initio Study of the Dimetallofullerene $La_2@C_{80}$ (C) 1094
- Electron Transfer and Polar Reactions of Cyclizable Anion Radicals: Structural Consequences of Orbital Selection Rules and Chain-Length Constraints (C) 1495
- Elusiveness of Cu^{III} Complexation; Preference for Trifluoromethyl Oxidation in the Formation of $[Cu^{I}(CF_3)_4]^-$ Salts (C) 80
- Fluorocarbonate, $[FCO_2]^-$: Preparation and Structure (C) 1858
- Formal Oxidation State versus Partial Charge—A Comment (C) 986
- Formation and Structures of New Metallo- and Metallapolysulfanes, $[MS_y]^+$ (y = 2–16) (C) 201 (1032)
- Mechanism of the Fe^+ Mediated C–C and C–H Bond Activations in Ethane from a Theoretical Viewpoint (C) 2282
- σ Metathesis as a Critical Step for the Transition Metal Catalyzed Formation of Formic Acid from CO_2 and H_2? An Ab Initio Investigation (C) 1742
- N-Confused Porphyrins and Singlet Carbenes: Is There a Connection? (C) 1028
- New Evidence Concerning the Structure of Amorphous Red Phosphorus (H) 2637
- Reaction of 1,1-Dimethylsilene with Formaldehyde (C) 929
- $S(NPMe_3)_4^{2+}$: The First Structure Determination of a Dication of Hexavalent Sulfur (C) 1362
- Structure and Bonding of Transition Metal Dihydrogen Complexes $[M(CO)_5(H_2)]$ (M = Cr, Mo, W) (C) 354
- Tetraphosphatricyclo[4.2.0.$0^{2,5}$]octadienes; New Phosphaalkyne Cyclotetramers Derived from $\lambda^3\sigma^2$-Diphosphetes (C) 484
- The Cope Rearrangement Transition Structure Is Not Diradicaloid, but Is It Aromatic? (C) 334
- The First Unambiguous Characterization of a Neutral Phosphorus Ylide–Lithium Complex: Isolation, Structure, and Ab Initio Investigations of $[(PhCH_2)_2NLi{\cdot}CH_2PPh_3]_2$ (C) 478

Acepentalenes
- Dilithium Acepentalenediide: An Unusual Dimer of Contact Ion Triplets with Bowl-Shaped Dianions (C) 1492

Acetylcholine receptor
- Toxins as Tools in Neurochemistry (R) 39

Acetylene complexes
- A Li_2Ti_2-Substituted Acetylene Formed from Ethylene by Reaction with (*meso*-Octaethylporphyrinogen)titanium (C) 1092

Actinides
- First Determination of the Ionization Potential of Americium and Curium (C) 814

Activated metals
- Activated Metals in Organic Synthesis (B) 121

Acyl anions
- α-Ethoxyvinyllithium: An Unexpected Polymeric Structure—Tetrameric Subunits Linked by Li–C π Interactions (C) 1594

Acylations
- Crystal Structure of the Dimeric (4-*tert*-Butylthiazolato)(glyme)lithium: Carbene Character of a Formyl Anion Equivalent (C) 487

Acyliminium ions
- Synthesis of D-(+)-Biotin through Selective Ring Closure of *N*-Acyliminium Silyl Enol Ethers (C) 2391

Acyloin condensation
- Peripherally Substituted Cobaloximes; X-Ray Crystal Structure Analysis of σ-Hexylbis[1,8-di(*N*-morpholino)octane-4,5-dioximato]pyridinecobalt(III) (C) 2389

Adamantanoid compounds
- Synthesis and Structure of $[Li(thf)_4]_2[Ph_2P)_{10}Cd_4]$ Containing; a Dianionic with a Cd_4P_{10} Adamantanoid Core (C) 2662

Adducts
- Stable 1:1 Adducts from Iodoacetylenes and Iodide Ions: Ion Pair Strain as an Additional Driving Force? (C) 441
- The Consequences of an Electrostatic "Forced Marriage" between Two Electron-Rich Particles: Strained Ion Pairs (C) 439

Adenylate cyclases
- G Proteins and Regulation of Adenylate Cyclase (Nobel Lecture) (R) 1406

Aggregation
- $(C_5Me_5)TiF_2$—A Versatile Building Block for Generating Large Soluble Dimetallic Aggregates (C) 1872
- Structure and Magnetic Properties of a Decanuclear Oxoiron(III) Cluster: A Further Step to Understanding Iron Aggregation Processes (C) 2716

Agostic interactions
- Unprecedented Mode of Bonding for Olefins on Bimetallic Complexes: An Agostic Interaction of a sp^2 C–H Bond with a Ruthenium Center in Addition to a π bond to a Rhenium Center (C) 916

Aldehydes
- A Highly Stereoselective Synthesis of 1,2-*trans*-C-Glycoside via Glycosyl Samarium(III) Compounds (C) 909

Aldolases
- Disaccharide Mimetics by Enzymatic Tandem Aldol Additions (C) 1639
- (*S*)-Selective Retroaldol Reaction and (*R*)-Selective β-Elimination with an Aldolase Catalytic Antibody (C) 2285

Aldol reactions
- (*S*)-Selective Retroaldol Reaction and (*R*)-Selective β-Elimination with an Aldolase Catalytic Antibody (C) 2285
- Synthesis and Characterization of the First Mixed Alkali Metal Enolate Containing Amine Ligands: A Novel "Open-Stack" Structure and its Implications for Aldol Addition (C) 1117

Alkali metal compounds
- Alkali Metallocene Anions: Syntheses and Structures (C) 2376
- Binding of Boron and Alkali Metal Cations by a Pseudocryptand (C) 1115
- "Cation-π Interactions" Detected by Mass Spectrometry; Selective Recognition of Alkali Metal Cations by a π-Basic Molecular Cavity (C) 1364
- Discrete Crown-Shaped Te_8 Rings in Cs_3Te_{22} (C) 450
- Synthesis and Characterization of the First Mixed Alkali Metal Enolate Containing Amine Ligands: A Novel "Open-Stack" Structure and its Implications for Aldol Addition (C) 1117
- The First Unambiguous Characterization of a Neutral Phosphorus Ylide–Lithium Complex: Isolation, Structure, and Ab Initio Investigations of $[(PhCH_2)_2NLi{\cdot}CH_2PPh_3]_2$ (C) 478
- The Stabilization of the Rb^- Ion in $Na_{16}Rb_7Sb_7 = Na_{16}(RbRb_6)Sb_7$ (C) 103
- The Synthesis and Crystal Structures of $RbC(SiMe_3)_3$ and $CsC(SiMe_3)_3{\cdot}3.5C_6H_6$: A One-Dimensional Ionic Solid and an Ionic Solid with a Molecular Structure (C) 687

Alkaline earth metal compounds
- Coordination of CO to the Alkaline Earth Metallocene $[(Me_5C_5)_2Ca]$ (C) 791

Alkanes
- Commensurate Freezing of *n*-Alkanes in Silicalite (C) 2543
- Selective Isomerization of Hydrocarbon Chains on External Surfaces of Zeolite Crystals (C) 2528

Alkene complexes
- A New Nickel-Catalyzed Cross-Coupling Reaction between sp^3 Carbon Centers (C) 2723
- Does the Facile Inter- and Intramolecular C–H Bond Activation by Tp*–Rh Complexes Proceed via Rh^{I} or Rh^{III} Intermediates? (C) 231
- New Findings in the Electrophilic Addition of Halogens to Olefins (H) 51

- Synthesis and Structure of 1-Aza- and 1-Phospha-2-titanacyclobut-4-enes (C) 688

Alkenes
- Cerium(III) Chloride Promoted Nucleophilic Addition of Organolithium Reagents to α-Alkyl-β-Ketophosphine Oxides: A New Protocol for the Synthesis of Stereochemically Defined Trisubstituted Olefins (C) 2046
- Control of the Reactivity of Double Bonds through Their Fixed Geometrical Arrangement (H) 2225
- Reaction of (Butadiene)zirconocene with Tris(pentafluorophenyl)borane—A Novel Way of Generating Methylalumoxane-Free Homogeneous Ziegler-Type Catalysts (C) 1755
- Rhodium-Catalyzed Hydroformylation of Internal Alkynes to α,β-Unsaturated Aldehydes (C) 1760
- Stereospecific Olefin Polymerization with Chiral Metallocene Catalysts (R) 1143 (1368)
- Synthesis, Chemical Trapping, and Dimerization of 3,7-Dimethyltricyclo-[3.3.0.0^{3,7}]oct-1(5)-ene: [2+2] Retrocycloaddition of the Cyclobutane Dimer (C) 912

Alkoxo clusters
- A Hexadecanuclear Polyolatometalate of Copper(II) Ions and Multideprotonated D-Sorbitol (C) 2119

Alkylations
- A Camouflaged Icosahedral Carborane: Dodecamethyl-1,12-dicarbo-*closo*-dodecaborane(12) and Related Compounds (C) 1332
- A New Platform for Designing Ligands for Asymmetric Induction in Allylic Alkylations (C) 2386
- Asymmetric Alkylation of Amide Enolates with Pseudoephedrine and Ephedrine as Chiral Auxiliaries—Unexpected Influence of Additives? (H) 433
- Benzopyranoisoxazolidines as Chiral Auxiliaries for Asymmetric Synthesis (C) 793
- Cerium(III) Chloride Promoted Nucleophilic Addition of Organolithium Reagents to α-Alkyl-β-Ketophosphine Oxides: A New Protocol for the Synthesis of Stereochemically Defined Trisubstituted Olefins (C) 2046
- Chiral Phosphanodihydrooxazoles in Asymmetric Catalysis: Tungsten-Catalyzed Allylic Substitution (C) 462
- The Crafts–Friedel Reaction: Aromatic Alkylation within the Complex Formed upon Addition of a Gaseous Arenium Ion to an Olefin (C) 1589

Alkyne complexes
- New Findings in the Electrophilic Addition of Halogens to Olefins (H) 51
- $[Ni_3(alkyne)_4]$—The First Homoleptic Alkyne–Metal Oligomer (Alkyne: 2,5,5-Trimethylhex-3-yn-2-ol) (C) 1860

Alkynes
- Novel "π-Boat" Cage Compounds as Potential Cryptands (C) 789
- Palladium-Catalyzed Resactions of Propargylic Compounds in Organic Synthesis (R) 2589
- Rhodium-Catalyzed Hydroformylation of Internal Alkynes to α,β-Unsaturated Aldehydes (C) 1760
- The Reactivity of 1,3-Butadiyne Moieties in the "Exploding" [*n*]Rotanes—A Crown of Thiophenes (C) 781

Alkynetrimerization
- A Rhodium-Mediated, Stepwise Trimerization of an Alkyne That Does Not Lead to a Benzene but Selectively to a Hexadienyne Derivative (C) 191

Allenes
- Transition Metal Catalyzed Dimerization of Allenyl Ketones (C) 1581

Allosterism
- Complexes from Polyazacyclophanes, Fluorescence Indicators, and Metal Cations—An Example of Allosterism through Ring Contraction (C) 321

Allotropy
- New Evidence Concerning the Structure of Amorphous Red Phosphorus (H) 2637

Allylation
- Highly Stereoselective Allylation of Benzaldehyde: Generation of a Stereochemically Defined Allylzinc Species from a π-Allylpalladium Intermediate and Diethylzinc (C) 787

Allyl complexes
- C–C Coupling Reactions as a Novel Synthetic Route to π-Allyl- and π-Butadienylrhodium Complexes (C) 1244

Allylsilanes
- Intramolecular Allylsilane Addition to Chiral Alkylidene-1,3-dicarbonyl Compounds for the Synthesis of Enantiomerically Pure *trans*-1,2-Disubstituted Cyclopentanes and Cyclohexanes (C) 1731

Altrose
- β-Cycloaltrin: A Cyclooligosaccharide Consisting of Seven α(1→4)-Linked Altropyranoses (C) 1621

Aluminum compounds
- AlMepO-α: A Novel Open-Framework Aluminum Methylphosphonate with Organo-Lined Unidimensional Channels (C) 1199
- Al,Ti Avoidance in the Microporous Titanoaluminosilicate ETAS-10 (C) 1003
- Cobalt-Containing Molecular Sieves as Catalysts for the Low Conversion Autoxidation of Pure Cyclohexane (C) 560
- Galloxane and Alumoxane Hydroxides: $[Ga_{12}tBu_{12}(\mu_3\text{-}O)_8(\mu\text{-}O)_2(\mu\text{-}OH)_4]$ and $[Al_6tBu_6(\mu_3\text{-}O)_4(\mu\text{-}OH)_4]$ (C) 1201
- Soluble Aluminosilicates with Frameworks of Minerals (C) 2504
- Structure Organization of Aluminosilicate Polyanions with Surfactants: Optimization of Al Incorporation in Aluminosilicate Mesostructural Materials (C) 1499
- Synthesis and Structure of Organometallic Compounds with $(Al_2Si)_2$ and Al_3Sb_2 Frameworks (C) 919
- The "Submetalate" $Ba_{17}Al_3O_7$: The First Member of a New Class of Compounds (C) 2115

Americium
- First Determination of the Ionization Potential of Americium and Curium (C) 814

Amide hydrolysis
- "Fast Amide Cleavage" or Reproducible, Concentration- and Time-Dependent Aggregation of Anionic and Cationic Surfactants? (C) 2718

Amides
- Relationship between C(O)–N Twist Angles and ^{17}O NMR Chemical Shifts in a Series of Twisted Amides (C) 1113
- The First Unambiguous Characterization of a Neutral Phosphorus Ylide–Lithium Complex: Isolation, Structure, and Ab Initio Investigations of $[(PhCH_2)_2NLi\cdot CH_2PPh_3]_2$ (C) 478

Aminations
- Palladium-Catalyzed Amination of Aryl Halides—Catalysts on New Routes to Known Targets (H) 1316

Amino acids
- Asymmetric Pictet–Spengler Reactions Employing *N,N*-Phthaloyl Amino Acids as Chiral Auxiliary Groups (C) 2402
- Enantioselective Synthesis of β-Amino Acids: TMS-SAMP as a Chiral Ammonia Equivalent for the Aza Analogous Michael Addition to α,β-Unsaturated Esters (C) 455
- Photo Electron Transfer Induced Macrocyclization of *N*-Phthaloyl-ω-aminocarboxylic Acids (C) 474
- Probing Protein Structure and Function with an Expanded Genetic Code (R) 621
- Recent Trends in Photoaffinity Labeling (R) 1296
- Synthesis of Chiral γ,δ-Unsaturated Amino Acids by Asymmetric Ester Enolate Claisen Rearrangement (C) 2012
- The Arndt–Eistert Reaction in Peptide Chemistry: A Facile Access to Homopeptides (C) 471

Amino alcohols
- Diastereo- and Enantioselective Synthesis of 1,2-Amino Alcohols from Glycol Aldehyde Hydrazones; Asymmetric Synthesis of (*R,R*)-Statin (C) 1219

Amino aldehydes
- First Dynamic Kinetic Resolution of Racemic α-Amino Aldehydes (C) 1023

Aminoalkylations
- Regio- and Diastereoselective Synthesis of β-Amino Ketones by Addition of Imines to Iminium Salts (C) 2639

Amino compounds
- Zeolite Encaged Cu(Histidine) Complexes as a Mimic of Natural Cu Enzymes (C) 2652

Aminocyclopentadienes
- Aminocyclopentadienes, Aminoferrocenes, and Aminocobaltocenes (C) 800

Aminosugars
- Enantiospecific Syntheses of Valiolamine and Its (1*R*), (2*R*), (1*R*,2*R*) Diastereomers from (−)-Quinic Acid (C) 1643

Amorphous inorganic materials
- Amorphous Inorganic Materials and Glasses (B) 242

Amphiphiles
- Mesogenic Properties of Amphiphilic Liquid Crystals with an Unusual Head-Group Topology (C) 1631
- Synthesis and X-ray Structure of a Shape-Persistent Macrocyclic Amphiphile (C) 2713

α-Amylase assay
- Chemoenzymatic Synthesis of a Modified Pentasaccharide as a Specific Substrate for a Sensitive Assay of α-Amylase by Fluorescence Quenching (C) 1239

Analytical methods
- Basic Principles of Thermoanalytical Techniques and Their Applications in Preparative Chemistry (R) 1171
- Instrumental Methods for Determining Elements (B) 935
- Methods of Immunological Analysis, Vols. 1–3 (B) 243
- Vibrational Spectroscopy in Supercritical Fluids: From Analysis and Hydrogen Bonding to Polymers and Synthesis (R) 1275

Anhydrides
- Highly Enantioselective Opening of Cyclic *meso*-Anhydrides to Isopropyl Hemiesters with Diisopropoxytitanium TADDOLates (C) 2395

Anilines
- Complexation of [*N,N'*-Bis(salicylidene)-ethylenediiminato]cobalt(III)$^+$ by Anilines in Dimethylformamide (C) 1086

Anion complexation
- Molecular Recognition of Anions by Zwitterionic Host Molecules in Water (C) 65

Anion–cation surfactant aggregation
- "Fast Amide Cleavage" or Reproducible, Concentration- and Time-Dependent Aggregation of Anionic and Cationic Surfactants? (C) 2718

Annulation
- Sequential Transformation of Benzothiopyrylium Salts to Diastereoselectively Annulated Benzothiopyranones (C) 647

Annulenes
- Novel Structures from Tris(benzocyclobutadieno)cyclohexatriene: Triscyclopropanation and Trisoxacyclopropanation to the First [2.1.2.1.2.1]Hexaannulanes (C) 563
- Synthesis of Belt Cyclophanes (C) 1437

Anthraquinones
- Total Synthesis of (±)-Dynemicin A (C) 1721

Antiaromaticity
- C_3-Symmetric Hexakis(trimethylsilyl)[7]-phenylene ["Tris(biphenylenocyclobutadieno)cyclohexatriene"], a Polycyclic Benzenoid Hydrocarbon with Slightly Curved Topology (C) 1478

Antibiotics
- Biosyntheses of Novel Emycins from the Mutant Strain *Streptomyces cellulosae* ssp. *griseoincarnatus* 1114-2 (C) 1617
- Efficient Total Synthesis of the Pharmacophore of the Anticancer Antibiotic CC-1065 by Zirconocene- and Palladium-Initiated Cyclizations (C) 1366
- Estramycins: A New Diyl Precursor Family Derived from Estradiol (C) 1749
- 9-Methoxystrobilurins—A Link Between Strobilurins and Oudemansins (C) 196
- Relative and Absolute Configuration of Filipin III (C) 1227
- Total Synthesis of Natural (+)-SF2315A and Determination of the Absolute Configuration (C) 2396

Antibodies
- Micron-Scale Patterning of Biological Molecules (C) 91

Antidepressants
- Talking Back to Prozac: What Doctors Aren't Telling You about Today's Most Controversial Drug (B) 1250

Antimony compounds
- Cage Expansion of $[\{(cyNLi)_3Sb\}_2]$; Synthesis and Structure of the Trimetallic Complex $[\{(cyNLi)_3Sb\}_2(t\text{BuOK})_3 \cdot x C_6H_5CH_3]$ (C) 1012
- Structure and Bonding in Organometallic Anions of Heavy Group 14 and 15 Elements (R) 1545
- Synthesis and Structure of Organometallic Compounds with $(Al_2Si)_2$ and Al_3Sb_2 Frameworks (C) 919
- The First Distibabutadiene: Synthesis and Structure of *trans*-1,4-Bis(trimethylsiloxy)-1,4-bis(2,4,6-tri-*tert*-butylphenyl)-2,3-distibabutadiene (C) 492
- The Stabilization of the Rb^- Ion in $Na_{16}Rb_7Sb_7 = Na_{16}(RbRb_6)Sb_7$ (C) 103

Antisense systems
- 1,5-Anhydrohexitol Nucleic Acids, a New Promising Antisense Construct (C) 1338 (2165)
- Phosphorothioates: β-Fragmentation versus β-Silicon Effect (C) 2406

Antitumor agents
- Efficient Total Synthesis of the Pharmacophore of the Anticancer Antibiotic CC-1065 by Zirconocene- and Palladium-Initiated Cyclizations (C) 1366
- Estramycins: A New Diyl Precursor Family Derived from Estradiol (C) 1749
- Lactendiynes: A New Class of Triggered Cyclic Enediynes (C) 2393
- Platination Pathways for Reactions of Cisplatin with GG Single-Stranded and Double-Stranded Decanucleotides (C) 1874
- Synthesis, Antitumor Activity, and Tolerability of Phospholipids with Nitrogen Homologues (C) 238

Anti van't Hoff/Le Bel geometries
- Compounds with Planar Tetracoordinate Boron Atoms: Anti van't Hoff/Le Bel Geometries without Metal Centers (C) 327

Aqua complexes
- The Nonaaquabismuth(III) Cation (C) 2416

Archaea bacteria
- On the Mechanism of Catalysis by a Metal-Free Hydrogenase from Methanogenic Archaea: Enzymatic Transformation of H_2 without a Metal and Its Analogy to the Chemistry of Alkanes in Superacidic Solution (C) 2247

Arene anions
- Self-Diffusion of Charged Polycyclic Systems and Their Parent Compounds: A PGSE NMR Study (C) 816

Arene complexes
- Additions of Carbanions to a Cationic Cyclopentadienyl(naphthalene)iron Complex (C) 2161
- Aromatic Gallium Heterocycles: Synthesis of the First Gallatabenzene (C) 1357
- Hydrocarbon Activation with Metal Halides: Catalysis of the Jacobsen Rearrangement by $(ZrCl_4)_n$ in the Presence of Aromatic Hydrocarbons (C) 1510
- Mononuclear Tris(arene)–Metal Complexes (H) 53
- Radical Additions to (η^6-Arene)-(tricarbonyl)chromium Complexes: Diastereoselective Synthesis of Hydrophenalene and Hydrobenzindene Derivatives by Samarium(II) Iodide Induced Cyclization (C) 2383
- Synthesis and Structure of Bimetallic η^4,η^6-Naphthalene Complexes Containing a Mn–Mn Moiety Bonded in a *Syn*-Facial Manner: A General Route to Homo- and Heteronuclear Bimetallic Complexes of Polyarenes (C) 2540
- [Bis{(η^5-pentamethylcyclopentadienyl)-cobalt}-μ-(η^4:η^4-arene)]: Synthesis, Structure, and Unusual Reactivity of a New Type of Triple-Decker with Bridging Arene Ligands (C) 592
- $[R_3Si-\text{arene}]^+$ σ Complexes in the Gas Phase (C) 654

Arene oxidation
- Catalytic Photoinduced Charge-Transfer Osmylation: A Novel Pathway from Arenes to Cyclitol Derivatives (C) 2031

Arenes
- Diodelike Current–Voltage Curves for a Single Molecule—Tunneling Spectroscopy with Submolecular Resolution of an Alkylated, *peri*-Condensed Hexabenzocoronene (C) 1609
- First-Ever Per(onio) Substitution of Benzene: The Role of the Counterion (C) 1319
- Fullerene Model Compounds: Bowl-Shaped Aromatic Hydrocarbons and Cyclophane-Based Cage Molecules (H) 1429
- Quaterrylenebis(dicarboximides) (C) 1323
- Reactions of Neopentyl 2,2,-Trifluoroethanesulfonate (Neopentyl Tresylate) with Nucleophiles: A Model Study for the Coupling of Nucleophiles with Tresyl Agarose (C) 2495
- Self-Diffusion of Charged Polycyclic Systems and Their Parent Compounds: A PGSE NMR Study (C) 816

Arndt–Eistert reactions
- The Arndt–Eistert Reaction in Peptide Chemistry: A Facile Access to Homopeptides (C) 471

Aromaticity
- Aromaticity and Antiaromaticity in Five-Membered C_4H_4X Ring Systems: "Classical" and "Magnetic" Concepts May Not Be "Orthogonal" (C) 337
- Five-Membered Aromatic and Anti-aromatic Rings with Gallium, Germanium, and Bismuth Centers: A Short March through the Periodic Table (H) 295
- Novel Porphyrinoids for Chemistry and Medicine by Biomimetic Syntheses (R) 1795
- Oxybenziporphyrin, a Fully Aromatic Semiquinone Porphyrin Analog with Pathways for 18π-Electron Delocalization (C) 2533
- Synthesis and Structure of a Free Germacyclopentadienide Ion: $[Li([12]crown-4)_2][C_4Me_4GeSi(SiMe_3)_3]$ (C) 1887
- 1,3,5,7-Tetra-*tert*-butyl-4-aza- and 1,3,5,7-Tetra-*tert*-butyl-4-phospha-*s*-indacene (C) 330

Aromatic substitutions
- Nucleophilic Aromatic Substitution of Hydrogen (B) 2419
- The Crafts–Friedel Reaction: Aromatic Alkylation within the Complex Formed upon Addition of a Gaseous Arenium Ion to an Olefin (C) 1589

Arsenic compounds
- η^5:η^2 Coordination of a *cyclo*-E_5 Ligand, E = P, As (C) 1321
- Diphosphanyl- and Diarsanyl-Substituted Carbene Homologues: Germanediyls, Stannanediyls, and Plumbanediyls with Remarkable Electronic Structures (C) 1614

Arylamines
- A Simple Catalytic Method for the Conversion of Aryl Bromides to Arylamines (C) 1348
- Palladium-Catalyzed Amination of Aryl Halides—Catalysts on New Routes to Known Targets (H) 1316

Arynes
- Single-Crystal X-Ray Structure of the Metastable Aryne Precursor Tetrafluorophenyllithium and of 1,2,3,4-Tetrafluorobenzene (C) 1517

Asteranes
- Synthesis of a Cationic 1,3-Diphospha-2,4-dipallada(II)tricyclo[1.1.1]pentane Derivative: The First Structurally Characterized Pyramidal μ_2-Phosphinidene (C) 2677

Asymmetric syntheses
- A Chiral Cyanohydrin Phosphate for Carbonyl Umpolung—Stereoselective Synthesis of Tertiary Cyanohydrins (C) 917
- Acyclic 1,4-Diastereoselectivity in γ-Substituted α-Enones: Transmission of Chiral Information through Conjugation (C) 2254
- A Highly Stereoselective Synthesis of 1,2-*trans*-C-Glycoside via Glycosyl Samarium(III) Compounds (C) 909
- A New Platform for Designing Ligands for Asymmetric Induction in Allylic Alkylations (C) 2386
- A Simple, Chirogenic, Enantioselective Synthesis of Chlorins and Isobacteriochlorins (C) 784

- Asymmetric Alkylation of Amide Enolates with Pseudoephedrine and Ephedrine as Chiral Auxiliaries—Unexpected Influence of Additives? (H) 433
- Asymmetric Allylic Substitution with Nitromethane Catalyzed by a Pd Complex: Enantioselectivities Exceeding 99.9% ee (C) 2687
- Asymmetric Pictet–Spengler Reactions Employing *N,N*-Phthaloyl Amino Acids as Chiral Auxiliary Groups (C) 2402
- Asymmetric Reaction of Arylalkenes with Diselenides (C) 1726
- Asymmetric Sulfide Oxidation with Vanadium Catalysts and H_2O_2 (C) 2640
- Asymmetric Syntheses of Stavudine (d4T) and Cordycepin by Cycloisomerization of Alkynyl Alcohols to Endocyclic Enol Ethers (C) 350
- Asymmetrization of *meso* 1,4-Enediol Ethers by Isomerization with a Chiral binap–Rh^I Catalyst (C) 2287
- Benzopyranoisoxazolidines as Chiral Auxiliaries for Asymmetric Synthesis (C) 793
- Carbenoid Transfer to Imines: A New Asymmetric Catalytic Synthesis of Aziridines (C) 676
- Catalytic Asymmetric Carbonyl–Ene Reactions (H) 1717
- Catalytic Asymmetric C–C Bond Formation: New Enolato- and Organolithium Chemistry (H) 178
- Cerium(III) Chloride Promoted Nucleophilic Addition of Organolithium Reagents to α-Alkyl-β-Ketophosphine Oxides: A New Protocol for the Synthesis of Stereochemically Defined Trisubstituted Olefins (C) 2046
- Chiral Phosphanodihydrooxazoles in Asymmetric Catalysis: Tungsten-Catalyzed Allylic Substitution (C) 462
- Chiral Titanium Alkoxides as Catalysts for the Enantioselective Reduction of Ketones with Boranes (C) 2005
- Diastereo- and Enantioselective Synthesis of 1,2-Amino Alcohols from Glycol Aldehyde Hydrazones; Asymmetric Synthesis of (*R,R*)-Statin (C) 1219
- Diastereo- and Enantioselective Synthesis of Polyfunctional Ketones with Adjacent Quaternary and Tertiary Centers by Asymmetric Carroll Rearrangement (C) 2278
- Diastereoselective Coupling of Anodically Produced Radicals Bearing Chiral Amide Groups (C) 189
- Discrimination between Enantiotopic Groups in a Diels–Alder Reaction (C) 448
- Enantioselective Reduction of Ketones with Sodium Borohydride, Catalyzed by Optically Active (β-Oxoaldiminato)-cobalt(II) Complexes (C) 2145
- Enantioselective Synthesis of β-Amino Acids: TMS-SAMP as a Chiral Ammonia Equivalent for the Aza Analogous Michael Addition to α,β-Unsaturated Esters (C) 455
- Enantiospecific Syntheses of Valiolamine and Its (1*R*), (2*R*), (1*R*,2*R*) Diastereomers from (−)-Quinic Acid (C) 1643
- Facial Diastereoselectivity in the Paternò–Büchi Reaction of Chiral Silyl Enol Ethers (C) 2271
- First Dynamic Kinetic Resolution of Racemic α-Amino Aldehydes (C) 1023
- Generation of Enantiomerically Enriched Lithium Indenides by Means of (−)-Sparteine: Structure, Stereoselective Substitution, and Solvent Effects (C) 2158
- Highly Enantioselective Opening of Cyclic *meso*-Anhydrides to Isopropyl Hemiesters with Diisopropoxytitanium TADDOLates (C) 2395
- Intramolecular Allylsilane Addition to Chiral Alkylidene-1,3-dicarbonyl Compounds for the Synthesis of Enantiomerically Pure *trans*-1,2-Disubstituted Cyclopentanes and Cyclohexanes (C) 1731
- Ligand-Accelerated Catalysis (R) 1059
- Preparation of a Surface-Active Chiral Diphosphane and Its Use in the Hydrogenation of Prochiral Olefins (C) 1645
- Regio- and Diastereoselective Synthesis of β-Amino Ketones by Addition of Imines to Iminium Salts (C) 2639
- Stereoselective Syntheses of Peptide Derivatives with 2-Acetamido-3,4,6-tri-*O*-acetyl-1-amino-2-deoxy-β-D-glucopyranose by Four-Component Condensation (C) 1104
- Stereoselective Synthesis (B) 1372
- Strong Electronic Effects on Enantioselectivity in Rhodium-Catalyzed Hydroborations with Novel Pyrazole-Containing Ferrocenyl Ligands (C) 931
- C_2-Symmetric Cationic Copper(II) Complexes as Chiral Lewis Acids: Counterion Effects in the Enantioselective Diels–Alder Reaction** (C) 798
- Synthesis and Properties of First to Third Generation Dendrimers with Doubly and Triply Branched Chiral Building Blocks (C) 2116
- Synthesis and Structural Characterization of a Stereospecific Dinuclear Gallium Triple Helix: Use of the *trans*-Influence in Metal-Assisted Self-Assembly (C) 996
- Synthesis of Chiral γ,δ-Unsaturated Amino Acids by Asymmetric Ester Enolate Claisen Rearrangement (C) 2012

Atmospheric chemistry
- Sulfuric Acid, from Sulfur Trioxide and Water—A Surprisingly Complex Reaction (H) 1313

ATP
- Octacationic Cyclophanes: Binding of ATP and Other Anionic Guests in Water (C) 2147

ATPase
- Incorporation of Membrane Proteins in Solid-Supported Lipid Layers (C) 2056

Atropisomerism
- A New Application of Capillary Zone Electrophoresis: Determination of Energy Barriers of Configurationally Labile Chiral Compounds (C) 1635
- Homeomorphic Isomerism in a Peptidic Macrobicycle (C) 2660

Aurophilicity
- A Gold(I) [2]Catenane (C) 1894
- Gold in Chains: Self-Assembly of a Gold(I) Catenane (H) 2107

Autocorrelation
- Assessing Similarity and Diversity of Combinatorial Libraries by Spatial Autocorrelation Functions and Neural Networks (C) 2674

Automerizations
- Automerizations and Isomerizations in Propynylidene (HCCCH), Propadienylidene (H_2CCC), and Cyclopropenylidene (c-C_3H_2) (C) 2009
- Fluxionality Induced by High Pressure: [9-D]9-Homocubyl Triflate, a Pressure-Sensing Molecule (C) 2030

Autoxidation
- Cobalt-Containing Molecular Sieves as Catalysts for the Low Conversion Autoxidation of Pure Cyclohexane (C) 560

Aza-Claisen reaction
- Synthesis of Optically Active Nine-Membered Ring Lactams by a Zwitterionic Aza-Claisen Reaction (C) 1026

Azacyclophanes
- Complexes from Polyazacyclophanes, Fluorescence Indicators, and Metal Cations—An Example of Allosterism through Ring Contraction (C) 321

Azepines
- First Synthesis of 2*H*-Azepine (C) 1469

Azetidinones
- Lactendiynes: A New Class of Triggered Cyclic Enediynes (C) 2393

Azides
- Covalent Inorganic Azides (R) 511
- Ring Expansion of the Fullerene Core by Highly Regioselective Formation of Diazafulleroids (C) 1343

Aziridines
- Carbenoid Transfer to Imines: A New Asymmetric Catalytic Synthesis of Aziridines (C) 676

Azo compounds
- Photoswitchable Phase Separation in Hydrophobically Modified Poly(acrylamide)/Surfactant Systems (C) 88

Azolides
- Tris(dimethylamino)sulfoniumcyclopentadienide $[TAS]^+[C_5H_5]^-$ and Tris(dimethylamino)sulfoniumpyrrolide $[TAS]^+[C_4H_4N]^-$: Two Isostructural Salts with "Naked" Anions A^- and the "Inverse" Sandwich-Cations $[\{(Me_2N)_3S\}_2A]^+$ (A = $C_5H_5^-$, $C_4H_4N^-$) (C) 443

Azomethine ylides
- Design of Novel, Nonpeptidic Thrombin Inhibitors and Structure of a Thrombin–Inhibitor Complex (C) 1739

Azoninones
- Synthesis of Optically Active Nine-Membered Ring Lactams by a Zwitterionic Aza-Claisen Reaction (C) 1026

Baccatin III
- A Novel Intramolecular Heck Reaction: Synthesis of a Cholesterol–Baccatin III Hybrid (C) 452
- A Total Synthesis of Taxol (C) 1723

Barbituric acid
- Barbituric Acid/2,4,6-Triaminopyrimidine Aggregates in Water and Their Competitive Interaction with Monolayers of Barbituric Acid Lipids at the Gas–Water Interface (C) 58

Barium compounds
- The Lipophilically Wrapped Polyion Aggregate $\{[Ba_6Li_3O_2]^{11+}[^-OC(CH_3)_3]_{11}(OC_4H_8)_3\}$, a Face-Sharing (Octahedron + Prismane) $Ba_6Li_3O_2$ Polyhedron in a Hydrocarbon Ellipsoid: Preparation, Single Crystal Structure Analysis, and Density Functional Calculations (C) 1353
- The "Submetalate" $Ba_{17}Al_3O_7$: The First Member of a New Class of Compounds (C) 2115

Benzodiphospholes
- A Facile Access to $1\lambda^5,3\lambda^5$-Benzodiphospholes (C) 2017

Biaryls
- Activation of Macrocyclic Biaryl-Enediynes by Metal Ion Coordination (C) 2538
- A New Family of Chiral Binaphthyl-Derived Cyclophane Receptors: Complexation of Pyranosides (C) 1596

Bicyclonucleotides
- Triple-Helix Formation of Oligodeoxynucleotides Containing [(3′*S*,5′*R*)-2′-Deoxy-3′,5′-ethano-β-D-ribofuranosyl]nucleosides ("Bicyclo-deoxynucleosides") (C) 694

Bicyclopentanes
- Heteroatom-Substituted Bicyclo[1.1.1]-pentanes with Two Boron Atoms as Electron-Deficient Centers (C) 657

Binuclear complexes
- Unprecedented Mode of Bonding for Olefins on Bimetallic Complexes: An Agostic Interaction of a sp^2 C–H Bond with a Ruthenium Center in Addition to a π bond to a Rhenium Center (C) 916

Biochemistry
- Chaos and Order. The Complex Structure of Living Systems (B) 1771
- Computer Simulations of Biomolecular Systems. Theoretical and Experimental Applications. Vol. 2 (B) 1034
- Crystallography Made Crystal Clear. A Guide for Users of Macromolecular Models (B) 496
- Direct Electrochemical Coupling of Components of the Biological Electron Transfer Chain to Modified Surfaces: Molecular Recognition between Cytochrome c Peroxidase and Cytochrome c (C) 2409
- One-Electron Redox Reactions of CoASH Esters in Anaerobic Bacteria—A Mechanistic Proposal (C) 1502
- Photochemically Initiated Protein Splicing (C) 1629
- Synthesis of an RGD-Sialyl-Lewis^X Glycoconjugate: A New Highly Active Ligand for P-Selectin (C) 990
- The Bourbaki Gambit (B) 241
- The Three-Dimensional Structure of Hammerhead Ribozymes (H) 643

Biographies
- Fritz Haber—Chemiker, Nobelpreisträger, Deutscher, Jude (B) 119
- The Adventure Playground of Mechanisms and Novel Reactions (B) 1129

Bioinorganic chemistry
- Bioinorganic Chemistry (B) 1036
- Electron Transfer through DNA: Site-Specific Modification of Duplex DNA with Ruthenium Donors and Acceptors (C) 352
- Octadecanuclearity in Manganese Carboxylate Chemistry: $K_4[Mn_{18}O_{16}(O_2CPh)_{22}(phth)_2(H_2O)_4]$ ($phthH_2$ = phthalic acid) (C) 887
- On the Synthesis of the FeMo Cofactor of Nitrogenase: Gene-Controlled in Nature versus Laboratory-Produced by Man (R) 1071
- Rapid Hydrolysis of RNA with a Cu^{II} Complex (C) 472
- The Structure of the *D. gigas* [NiFe] Hydrogenase and the Nature of the Hydrogenase Nickel Complex (H) 1193

Biomembranes
- Barbituric Acid/2,4,6-Triaminopyrimidine Aggregates in Water and Their Competitive Interaction with Monolayers of Barbituric Acid Lipids at the Gas–Water Interface (C) 58
- Toxins as Tools in Neurochemistry (R) 39

Biomimetic syntheses
- Novel Porphyrinoids for Chemistry and Medicine by Biomimetic Syntheses (R) 1795

Bioorganic chemistry
- Advanced Organic Chemistry of Nucleic Acids (B) 1521
- Synthesis of the Palmitoylated and Farnesylated C-Terminal Lipohexapeptide of the Human N-*Ras* Protein by Employing an Enzymatically Removable Urethane Protecting Group (C) 2259
- Vitamin B_{12}: How the Problem of Its Biosynthesis Was Solved (R) 383

Biosyntheses
- Biosyntheses of Novel Emycins from the Mutant Strain *Streptomyces cellulosae* ssp. *griseoincarnatus* 1114-2 (C) 1617
- Biosynthetic Origin of the Oxygen Atoms of Tetracenomycin C (C) 565
- Combinatorial Biosynthesis—An Approach in the Near Future? (H) 881
- Novel Genetically Engineered Tetracenomycins (C) 1107
- On the Synthesis of the FeMo Cofactor of Nitrogenase: Gene-Controlled in Nature versus Laboratory-Produced by Man (R) 1071
- Oxidative Polycyclization versus the "Polyepoxide Cascade": New Pathways in Polyether (Bio)synthesis? (H) 298
- Pericyclic Reactions in Nature: Spontaneous Cope Rearrangement Inactivates Algae Pheromones (C) 1602
- Vitamin B_{12}: How the Problem of Its Biosynthesis Was Solved (R) 383

Biotechnology
- Synthesis of dTDP-6-Deoxy-4-ketoglucose and Analogues with Native and Recombinant dTDP-Glucose-4,6-dehydratase (C) 1748

Biotin
- Synthesis of D-(+)-Biotin through Selective Ring Closure of *N*-Acyliminium Silyl Enol Ethers (C) 2391

Biphasic catalysis
- Enhancement of Catalytic Activity for Hydroformylation of Methyl Acrylate by Using Biphasic and "Supported Aqueous Phase" Systems (C) 1474

Biphenyls
- A New Application of Capillary Zone Electrophoresis: Determination of Energy Barriers of Configurationally Labile Chiral Compounds (C) 1635

1,2-Bismethylenecyclobutanes
- 1-Phenyl-1,2-cyclooctadiene Dimerizes in an Unusual Manner (C) 2730

Bismuth compounds
- Five-Membered Aromatic and Antiaromatic Rings with Gallium, Germanium, and Bismuth Centers: A Short March through the Periodic Table (H) 295
- Structure and Bonding in Organometallic Anions of Heavy Group 14 and 15 Elements (R) 1545
- The Nonaaquabismuth(III) Cation (C) 2416

Bleomycin
- Carbon–Hydrogen Bonds of DNA Sugar Units as Targets for Chemical Nucleases and Drugs (R) 746

Blood clotting
- Anticoagulatory Substances of Blood-sucking Animals: From Hirudin to Hirudin Mimetics (R) 867

Bolaamphiphiles
- Structure Determination in the Twilight Region Between Monolayers and 3-D Crystals; a Grazing Incidence X-Ray Diffraction Study of Nanocrystalline Aggregates of α,ω-Docosanediol at the Air–Water Interface (C) 649

Bond activation
- C–H and C–C Bond Activation by Bare Transition-Metal Oxide Cations in the Gas Phase (R) 1973
- Mechanism of the Fe^+ Mediated C–C and C–H Bond Activations in Ethane from a Theoretical Viewpoint (C) 2282

Bond length alternation
- X-Ray Diffraction Evidence for a Cyclohexatriene Motif in the Molecular Structure of Tris(bicyclo[2.1.1]hexeno)benzene: Bond Alternation after the Refutation of the Mills–Nixon Theory (C) 1454

Bond theory
- Does the Death Knell Toll for the Metallic Bond? (H) 1081
- The Metallic Bond—Dead or Alive? A Comment and a Reply (C) 2003

Borole ligands
- The First Mixed-Metal Borole Cluster; Stabilization of Formally 14e Pd Centers in the Re_2Pd_2 Electron-Deficient $[\{[(\eta^5\text{-}C_4H_4BPh)(CO)_3Re]Pd\}_2]$ Cluster (C) 1010

Boron compounds
- A Camouflaged Icosahedral Carborane: Dodecamethyl-1,12-dicarbo-*closo*-dodecaborane(12) and Related Compounds (C) 1332
- A μ-η^6:η^6-1,3,5-Triboratabenzenebis(cyclopentadienylcobalt) Triple-Decker Complex (C) 681
- Binding of Boron and Alkali Metal Cations by a Pseudocryptand (C) 1115
- Bis(pentafluorophenyl)borane: Synthesis, Properties, and Hydroboration Chemistry of a Highly Electrophilic Borane Reagent (C) 809
- Bromides of Rare Earth Metal Boride Carbides—A System of Building Blocks (C) 1633
- Competing Pathways in the Reaction of Bis(pentafluorophenyl)borane with Bis(η^5-cyclopentadienyl)dimethylzirconium: Methane Elimination versus Methyl–Hydride Exchange and an Example of Pentacoordinate Carbon (C) 1230
- Compounds with Planar Tetracoordinate Boron Atoms: Anti van't Hoff/Le Bel Geometries without Metal Centers (C) 327
- Diborylcarbenes as Reactive Intermediates in Double 1,2-Rearrangements with Low Activation Enthalpies (C) 1340
- Dicobalt and Diplatinum Complexes of Diborylcarbenes (C) 1111
- First Reaction of 1,2-Dimethyl-*o*-silaborane: Nucleophilic Degradation (C) 2236
- Heteroatom-Substituted Bicyclo[1.1.1]-pentanes with Two Boron Atoms as Electron-Deficient Centers (C) 657
- Synthesis and Structure of the First Transition Metal Borylene Complexes (C) 825
- Transition Metal Catalyzed Diboration of Vinylarenes (C) 1336
- *closo*-$[B_5H_4PPh_3\{Fe(CO)_3\}\{Ir(CO)_2PPh_3\}]$: The First Structurally Characterized *closo*-Heterobimetallaheptaborane System (C) 1641

Brain lipids
- New Brain Lipids that Induce Sleep (H) 2362

Bridging ligands
- A Li_2Ti_2-Substituted Acetylene Formed from Ethylene by Reaction with (*meso*-Octaethylporphyrinogen)titanium (C) 1092
- Oligomethylene-Bridged Vitamin B_{12} Dimers (C) 84

Bromine compounds
- Bromides of Rare Earth Metal Boride Carbides—A System of Building Blocks (C) 1633
- Synthesis, Structure, and Decay of In_4Br_7 (C) 1126

Butatrienes
- Butatrienes by Cumuhomologation of Propadienes (C) 2709

Cadmium compounds
- Self-Assembled Helicates of Zinc and Cadmium Cyanides, $[M_x(CN)_{2x+1}]^-$, $x \leq 27$ (C) 314

- Synthesis and Structure of Tetra- and Octanuclear Chelate Complexes—Exohedral Guest Exchange in Tetrahemispheraplexes (C) 993
- Synthesis and Structure of $[Li(thf)_4]_2[Ph_2P)_{10}Cd_4]$ Containing; a Dianionic with a Cd_4P_{10} Adamantanoid Core (C) 2662

Cage compounds
- Cage Expansion of $[\{(cyNLi)_3Sb\}_2]$; Synthesis and Structure of the Trimetallic Complex $[\{(cyNLi)_3Sb\}_2(tBuOK)_3 \cdot xC_6H_5CH_3]$ (C) 1012
- Crystal Structure of Dilithioacetylacetone: A Twenty-Four Vertex Li-O Cage Molecule with Limited Li–C(terminal) Bonding and Selective THF Solvation (C) 1233
- Fullerene Model Compounds: Bowl-Shaped Aromatic Hydrocarbons and Cyclophane-Based Cage Molecules (H) 1429
- Galloxane and Alumoxane Hydroxides: $[Ga_{12}tBu_{12}(\mu_3\text{-}O)_8(\mu\text{-}O)_2(\mu\text{-}OH)_4]$ and $[Al_6tBu_6(\mu_3\text{-}O)_4(\mu\text{-}OH)_4]$ (C) 1201
- Modeling the Remote-Controlled Organization of Particles in a Nanodimensional Cavity: Synthesis and Properties of $(Et_3NH)_3(tBuNH_3)_2Na_2[(H_2O)_2,N_3^-\subset V_{14}O_{22}(OH)_4(PhPO_3)_8]\cdot 6\,H_2O\cdot 2$ DMF (C) 779
- Novel "π-Boat" Cage Compounds as Potential Cryptands (C) 789
- Synthesis, Chemical Trapping, and Dimerization of 3,7-Dimethyltricyclo-[3.3.0.0^{3,7}]oct-1(5)-ene: [2+2] Retrocycloaddition of the Cyclobutane Dimer (C) 912
- *meso*-Tetrakis[4-(diphenylphosphino)-phenyl]porphyrin and a Water-Soluble Octakis(phosphonium salt) Porphyrin Double-Decker with a Cage Structure. (C) 2230

Calcium compounds
- New Surprises in Metal Carbonyl Chemistry (H) 2489

Calixarenes
- Calixarenes, Macrocycles with (Almost) Unlimited Possibilities (R) 713
- "Cation-π Interactions" Detected by Mass Spectrometry; Selective Recognition of Alkali Metal Cations by a π-Basic Molecular Cavity (C) 1364
- Concave Reagents Based on Calixarenes (C) 2555
- Molecular Recognition at an Interface: Binding of Monolayer-Anchored Ferrocenyl Groups by an Amphiphilic Calixarene Host (C) 235
- Silicon-Bridged Macrocycles—Synthesis of Sila-Calixarenes (C) 661

Calonyctin A
- The Macrolidic Glycolipid Calonyctin A, a Plant Growth Regulator: Synthesis, Structural Assignment, and Conformational Analysis in Micellar Solution (C) 2520

Camptothecin
- Cascade Radical Reactions of Isonitriles: A Second-Generation Synthesis of (20*S*)-Camptothecin, Topotecan, Irinotecan, and GI-147211C (C) 2683

Capillary zone electrophoresis
- A New Application of Capillary Zone Electrophoresis: Determination of Energy Barriers of Configurationally Labile Chiral Compounds (C) 1635
- Direct On-Line Coupling of Capillary Electrophoresis and ^1H NMR Spectroscopy (H) 641

Carbene analogues
- Diphosphanyl- and Diarsanyl-Substituted Carbene Homologues: Germanediyls, Stannanediyls, and Plumbanediyls with Remarkable Electronic Structures (C) 1614

Carbene complexes
- A Series of Well-Defined Metathesis Catalysts—Synthesis of $[RuCl_2(=CHR')(PR_3)_2]$ and Its Reactions (C) 2039
- Carbene Complex Functionalized Sugars (C) 1856
- Catalytic Ring-Closing Metathesis: A New, Powerful Technique for Carbon–Carbon Coupling in Organic Synthesis (H) 1833
- Dicobalt and Diplatinum Complexes of Diborylcarbenes (C) 1111

Carbene reactions
- (*S*)-(+)- and (*R*)-(−)-1,5-Dimethyl-4-phenyl-1,5-dihydro-2*H*-pyrrol-2-ones by Carbene Ring Contraction and Decarboxylation of (2*R*,3*S*)-(−)- and (2*S*,3*R*)-(+)-6-Diazo-3,4-dimethyl-2-phenyloxazepane-5,7-diones (C) 78

Carbenes
- Automerizations and Isomerizations in Propynylidene (HCCCH), Propadienylidene (H_2CCC), and Cyclopropenylidene ($c\text{-}C_3H_2$) (C) 2009
- Crystal Structure of the Dimeric (4-*tert*-Butylthiazolato)(glyme)lithium: Carbene Character of a Formyl Anion Equivalent (C) 487
- Diborylcarbenes as Reactive Intermediates in Double 1,2-Rearrangements with Low Activation Enthalpies (C) 1340
- Metal Complexes of N-Heterocyclic Carbenes—A New Structural Principle for Catalysts in Homogeneous Catalysis (C) 2371
- N-Confused Porphyrins and Singlet Carbenes: Is There a Connection? (C) 1028
- Preparation, Structure, and Reactivity of 1,3,4-Triphenyl-4,5-dihydro-1*H*-1,2,4-triazol-5-ylidene, a New Stable Carbene (C) 1021
- Reaction of 1,1-Dimethylsilene with Formaldehyde (C) 929
- Synthesis of a 2*H*-Azirine by [1+2] Cycloaddition of a Phosphinocarbene with a Nitrile and Its Ring-Expansion to a 1,2λ^5-Azaphosphete (C) 1246

Carbenoids
- Carbenoid or Lithium Complex of a Carbanion? Synthesis and Structure of $(Me_3Si)_2C{=}P(aryl){=}C(Cl)Li(thf)_3$ and LiCl Elimination To Give the Phosphirene (C) 1849
- α-Ethoxyvinyllithium: An Unexpected Polymeric Structure—Tetrameric Subunits Linked by Li–C π Interactions (C) 1594

Carbides
- Bromides of Rare Earth Metal Boride Carbides—A System of Building Blocks (C) 1633

Carbocations
- 4c/3e Radical Cations with Cage-Directed Configurations (C) 1016
- Common Origin of Enthalpic and Entropic Substituent Effects in Reactions of Benzhydryl Cations with Nucleophiles (C) 490
- Fluxionality Induced by High Pressure: [9-D]9-Homocubyl Triflate, a Pressure-Sensing Molecule (C) 2030
- My Search for Carbocations and Their Role in Chemistry (Nobel Lecture) (R) 1393
- On the Mechanism of Catalysis by a Metal-Free Hydrogenase from Methanogenic Archaea: Enzymatic Transformation of H_2 without a Metal and Its Analogy to the Chemistry of Alkanes in Superacidic Solution (C) 2247
- Reactions of Carbocations with π Nucleophiles: Polar Mechanism and No Outer Sphere Electron Transfer Processes (C) 1225
- The Coexistence of the Reactivity–Selectivity Principle and of Linear Free Energy Relationships: A Diffusion Clock for Determining Carbocation Reactivities (C) 2250

Carbocycles
- Transition Metal Catalyzed Synthesis of Seven-Membered Carbocyclic Rings (H) 2223

Carbohydrate amino acids
- Saccharide–Peptide Hybrids as Novel Oligosaccharide Mimetics (C) 2712

Carbohydrates
- A New Family of Chiral Binaphthyl-Derived Cyclophane Receptors: Complexation of Pyranosides (C) 1596
- Carbene Complex Functionalized Sugars (C) 1856
- Disaccharide Mimetics by Enzymatic Tandem Aldol Additions (C) 1639
- Enzymes in Organic Synthesis: Application to the Problems of Carbohydrate Recognition (Part 1) (R) 412
- Enzymes in Organic Synthesis: Application to the Problems of Carbohydrate Recognition (Part 2) (R) 521
- Fivefold Deprotonated D-Mannose as Ligand in Homoleptic Dinuclear Metalates of Trivalent Iron, Vanadium, Chromium, Aluminum, and Gallium (C) 2647
- Mesogenic Properties of Amphiphilic Liquid Crystals with an Unusual Head-Group Topology (C) 1631
- Palladacycles as Structurally Defined Catalysts for the Heck Olefination of Chloro- and Bromoarenes (C) 1844
- Reactions of Neopentyl 2,2,2-Trifluoroethanesulfonate (Tresylate) with Nucleophiles: A Model Study for the Coupling of Nucleophiles with Tresyl Agarose (C) 1612
- Thymidine Diphospho-6-deoxy-α-D-*ribo*-3-hexulose—Synthesis of a Central Intermediate in the Biosynthesis of Di- and Trideoxysugars (C) 1328

Carbon allotropes
- Solubilized Derivatives of C_{195} and C_{260}: The First Members of a New Class of Carbon Allotropes $C_{n(60+5)}$ (C) 1466

Carbon dioxide
- Carbon Dioxide as a Raw Material: The Synthesis of Formic Acid and Its Derivatives from CO_2 (R) 2207
- Fluorocarbonate, $[FCO_2]^-$: Preparation and Structure (C) 1858
- σ Metathesis as a Critical Step for the Transition Metal Catalyzed Formation of Formic Acid from CO_2 and H_2? An Ab Initio Investigation (C) 1742
- Tantalum-Mediated Coupling of Methane and Carbon Dioxide in the Gas Phase (C) 2033

Carbonylations
- Palladium-Catalyzed Resactions of Propargylic Compounds in Organic Synthesis (R) 2589
- Rhodium–Vinylallene Complexes and a New Reaction, Rhodium-Catalyzed Carbonylative [4+1]Cycloaddition (C) 2691

Carbonyl complexes
- Coordination of CO to the Alkaline Earth Metallocene $[(Me_5C_5)_2Ca]$ (C) 791

- New Surprises in Metal Carbonyl Chemistry (H) 2489

Carbonyl–ene reactions
- Catalytic Asymmetric Carbonyl–Ene Reactions (H) 1717

Carbon–carbon coupling
- Atom Economy—A Challenge for Organic Synthesis: Homogeneous Catalysis Leads the Way (R) 259
- C–C Coupling Reactions as a Novel Synthetic Route to π-Allyl- and π-Butadienylrhodium Complexes (C) 1244

Carboranes
- A Camouflaged Icosahedral Carborane: Dodecamethyl-1,12-dicarbo-*closo*-dodecaborane(12) and Related Compounds (C) 1332
- Surprising Formation of a Carborane-Substituted Digallane (C) 332

Carboximides
- Quaterrylenebis(dicarboximides) (C) 1323

Carboxylic acids
- Self-Assembly of 1,3,5-Benzenetricarboxylic Acids (Trimesic Acids) and Their Analogues in the Solid State (C) 2654

Carbyne complexes
- Aminocarbyne Complexes of Chromium in a High Oxidation State—Synthesis, Structure, and Reactivity (C) 924

Cascade reactions
- Cascade Radical Reactions of Isonitriles: A Second-Generation Synthesis of (20*S*)-Camptothecin, Topotecan, Irinotecan, and GI-147211C (C) 2683
- Sequential Transformation of Benzothiopyrylium Salts to Diastereoselectively Annulated Benzothiopyranones (C) 647
- Unprecedented Intra- and Intermolecular Palladium-Catalyzed Coupling Reactions with Methylenecyclopropane Type Tetrasubstituted Alkenes (C) 2545

Catalysis
- An Ab Initio Investigation of the Rh^I-Catalyzed Hydroboration of C=C Bonds: Evidence for Hydrogen Migration in the Key Step (C) 115
- A New Method for the Preparation of Nanostructured Metal Clusters (C) 2240
- A New Nickel-Catalyzed Cross-Coupling Reaction between sp^3 Carbon Centers (C) 2723
- A New Strategy in Heterogeneous Catalysis: The Design of Cortex Catalysts (C) 2728
- A Simple Catalytic Method for the Conversion of Aryl Bromides to Arylamines (C) 1348
- Asymmetric Allylic Substitution with Nitromethane Catalyzed by a Pd Complex: Enantioselectivities Exceeding 99.9% ee (C) 2687
- Asymmetric Sulfide Oxidation with Vanadium Catalysts and H_2O_2 (C) 2640
- Asymmetrization of *meso* 1,4-Enediol Ethers by Isomerization with a Chiral binap–Rh^I Catalyst (C) 2287
- A Tailor-Made Metallocene for the Copolymerization of Ethene with Bulky Cycloalkenes (C) 2273
- Atom Economy—A Challenge for Organic Synthesis: Homogeneous Catalysis Leads the Way (R) 259
- Catalytic Asymmetric Carbonyl–Ene Reactions (H) 1717
- Catalytic Asymmetric C–C Bond Formation: New Enolato- and Organolithium Chemistry (H) 178
- Catalytic Ring-Closing Metathesis: A New, Powerful Technique for Carbon–Carbon Coupling in Organic Synthesis (H) 1833
- Chiral Phosphanodihydrooxazoles in Asymmetric Catalysis: Tungsten-Catalyzed Allylic Substitution (C) 462
- Chiral Titanium Alkoxides as Catalysts for the Enantioselective Reduction of Ketones with Boranes (C) 2005
- Cobalt-Containing Molecular Sieves as Catalysts for the Low Conversion Autoxidation of Pure Cyclohexane (C) 560
- Commensurate Freezing of *n*-Alkanes in Silicalite (C) 2543
- Competing Pathways in the Reaction of Bis(pentafluorophenyl)borane with Bis(η^5-cyclopentadienyl)dimethylzirconium: Methane Elimination versus Methyl–Hydride Exchange and an Example of Pentacoordinate Carbon (C) 1230
- Enantioselective Reduction of Ketones with Sodium Borohydride, Catalyzed by Optically Active (β-Oxoaldiminato)-cobalt(II) Complexes (C) 2145
- Enhancement of Catalytic Activity for Hydroformylation of Methyl Acrylate by Using Biphasic and "Supported Aqueous Phase" Systems (C) 1474
- Exciting Results from the Field of Homogeneous Two-Phase Catalysis (H) 1575
- Ligand-Accelerated Catalysis (R) 1059
- Metal Complexes of N-Heterocyclic Carbenes—A New Structural Principle for Catalysts in Homogeneous Catalysis (C) 2371
- σ Metathesis as a Critical Step for the Transition Metal Catalyzed Formation of Formic Acid from CO_2 and H_2? An Ab Initio Investigation (C) 1742
- Models for Bimetallic Catalysts: Multiple Oxidation States in Pt_3Re Cluster Cations (C) 346
- Molecular Imprinting in Cross-Linked Materials with the Aid of Molecular Templates—A Way towards Artificial Antibodies (R) 1812
- New Process for the Sulfonation of Phosphane Ligands for Catalysts (C) 811
- Palladacycles as Efficient Catalysts for Aryl Coupling Reactions (C) 1848
- Palladium-Catalyzed Amination of Aryl Halides—Catalysts on New Routes to Known Targets (H) 1316
- Preparation of a Surface-Active Chiral Diphosphane and Its Use in the Hydrogenation of Prochiral Olefins (C) 1645
- Rhodium-Catalyzed Hydroformylation of Internal Alkynes to α,β-Unsaturated Aldehydes (C) 1760
- Selective Isomerization of Hydrocarbon Chains on External Surfaces of Zeolite Crystals (C) 2528
- Stereospecific Olefin Polymerization with Chiral Metallocene Catalysts (R) 1143 (1368)
- Sulfoxide-Stabilized Giant Palladium Clusters in Catalyzed Oxidations (C) 457
- Synthetic Aspects of Metal-Catalyzed Oxidations of Amines and Related Reactions (R) 2443
- Synthetic Ribozymes and the First Deoxyribozyme (H) 1189
- The Catalytic Oxidative Coupling of Methane (R) 970
- The First Clusters with a Y-Shaped Arrangement of Ligands at Three-Coordinate Rh^I Atoms in the Solid State: $[M^1M^2\{\mu\text{-}P(C_6H_{11})_2\}(CO)_8Rh(PPh_3)]$ (M^1, M^2 = Mn, Re) (C) 1325
- The First Olefin-Substituted Peroxomolybdenum Complex: Insight into a New Mechanism for the Molybdenum-Catalyzed Epoxidation of Olefins (C) 1737
- Transition Metal Catalyzed Diboration of Vinylarenes (C) 1336
- Transition Metal Catalyzed Synthesis of Seven-Membered Carbocyclic Rings (H) 2223
- Zeolite Encaged Cu(Histidine) Complexes as a Mimic of Natural Cu Enzymes (C) 2652

Catalytic antibodies
- Antibody-Catalyzed Phosphate Triester Hydrolysis (C) 2275
- Peptide Ligases—Tools for Peptide Synthesis (H) 175
- (*S*)-Selective Retroaldol Reaction and (*R*)-Selective β-Elimination with an Aldolase Catalytic Antibody (C) 2285

Catechol
- Formation of a "*meso*-Helicate" by Self-Assembly of Three Bis(catecholate) Ligands and Two Titanium(IV) Ions (C) 2134

Catechol dioxygenases
- A Highly Reactive and Catalytically Active Model System for Intradiol-Cleaving Catechol Dioxygenases: Structure and Reactivity of Iron(III) Catecholate Complexes of *N*,*N*′-Dimethyl-2,11-diaza[3,3](2,6)pyridinophane (C) 2671

Catenanes
- A Gold(I) [2]Catenane (C) 1894
- Controlling Translational Isomerism in [2]Catenanes (C) 571
- Facile Synthesis and Solid-State Structure of a Benzylic Amide [2]Catenane (C) 1209
- Gold in Chains: Self-Assembly of a Gold(I) Catenane (H) 2107
- Kinetic Selection in the Template-Directed Self-Assembly of [2]Catenanes (C) 2378
- Structurally Diverse and Dynamically Versatile Benzylic Amide [2]Catenanes Assembled Directly from Commercially Available Precursors (C) 1212
- Synthesis of Novel Tetrathiafulvalene-(TTF)-Based [3]Pseudocatenanes by Self-Assembly; Prevention of *trans*/*cis* Isomerization (C) 2524
- $[Mn(C_{18}H_{16}N_2O_2)_3](ClO_4)_2$: A Polymeric 34- and 68-Membered Metallacyclic Network Forming a Novel Woven Polycatenated Structure (C) 574

Catenates
- Formation of the First Isomeric [2]Catenates by Self-Assembly about Two Different Metal Ions (C) 582

cyclo-C_n compounds
- Solubilized Derivatives of C_{195} and C_{260}: The First Members of a New Class of Carbon Allotropes $C_{n(60+5)}$ (C) 1466

Cell respiration
- X-ray Crystal Structures of Cytochrome c Oxidases from *Paracoccus denitrificans* and Bovine Heart and Their Implications for the Molecular Mechanism of Cell Respiration (H) 2635

Cellulose derivatives
- Topochemical Aspects of the Formation of Networks in Layered Langmuir–Blodgett (LB) Assemblies (C) 340

Cerium compounds
- Cerium(III) Chloride Promoted Nucleophilic Addition of Organolithium Reagents to α-Alkyl-β-Ketophosphine Oxides: A New Protocol for the Synthesis of Stereochemically Defined Trisubstituted Olefins (C) 2046

C-glycosides
- A Highly Stereoselective Synthesis of 1,2-*trans*-C-Glycoside via Glycosyl Samarium(III) Compounds (C) 909
- Stereoselective Syntheses of Retro-Isomers of *N*-Glucoasparagine (C) 2026

Chalcogen compounds
- From *cyclo*-Te_8 to Te_x^{n-} Sheets: Are Non-classical Polytellurides More Classical than We Thought? (H) 2109
- $(Nb,Ta)_9(S,Te)_5$, a Metal-Rich Chalcogenide with a Microporous Metal Substructure (C) 1089

Channel structures
- AlMepO-α: A Novel Open-Framework Aluminum Methylphosphonate with Organo-Lined Unidimensional Channels (C) 1199

Chaos theory
- Chaos and Order. The Complex Structure of Living Systems (B) 1771

Charge transfer complexes
- Electronic Energy Transfer in a Supramolecular Species Containing the $[Ru(bpy)_3]^{2+}$, $[Os(bpy)_3]^{2+}$, and Anthracene Chromophoric Units (C) 595

Chelate ligands
- A Novel Hexanuclear Fe^{III}-*cis*-Inositolato Complex as a Model for Fe^{III}–Polyol Interactions in Aqueous Solution (C) 2242
- Fivefold Deprotonated D-Mannose as Ligand in Homoleptic Dinuclear Metalates of Trivalent Iron, Vanadium, Chromium, Aluminum, and Gallium (C) 2647
- Metal Oxo Cation Receptors: Multimode Coordination to the Dioxoosmium(VI) Cation (C) 1359
- Stereoselective Synthesis of Chiral Zirconocenes from Doubly Substituted, Donor Functionalized Cyclopentadienes via Helical Chelate Complexes (C) 2266
- C_2-Symmetric Cationic Copper(II) Complexes as Chiral Lewis Acids: Counterion Effects in the Enantioselective Diels–Alder Reaction** (C) 798
- Synthesis and Coordination Chemistry of *ortho*-Functionalized Dimercaptobenzene: Building Blocks for Tripodal Hexathiol Ligands (C) 2700
- Synthesis and Structure of Tetra- and Octanuclear Chelate Complexes—Exohedral Guest Exchange in Tetrahemispheraplexes (C) 993
- The Formation of a Mixed Organolithium Aggregate $Li_4R_2nBu_2$ (R = 2,6-$(CH_2NMe_2)_2$-3,5-$Me_2C_6HCH_2$) during the Heteroatom-Assisted Lithiation of 1,3-Bis(dimethylaminomethyl)-2,4,6-trimethylbenzene (C) 219

Chemicals of everyday life
- The Consumer's Good Chemical Guide. A Jargon-free Guide to the Chemicals of Everyday Life (B) 2059

Chemoenzymatic syntheses
- Chemoenzymatic Synthesis of a Modified Pentasaccharide as a Specific Substrate for a Sensitive Assay of α-Amylase by Fluorescence Quenching (C) 1239

Chiral auxiliaries
- A New Platform for Designing Ligands for Asymmetric Induction in Allylic Alkylations (C) 2386
- Asymmetric Pictet–Spengler Reactions Employing *N,N*-Phthaloyl Amino Acids as Chiral Auxiliary Groups (C) 2402
- Benzopyranoisoxazolidines as Chiral Auxiliaries for Asymmetric Synthesis (C) 793
- Carbenoid Transfer to Imines: A New Asymmetric Catalytic Synthesis of Aziridines (C) 676
- Catalytic Asymmetric Carbonyl–Ene Reactions (H) 1717
- Chiral Titanium Alkoxides as Catalysts for the Enantioselective Reduction of Ketones with Boranes (C) 2005
- Diastereoselective Coupling of Anodically Produced Radicals Bearing Chiral Amide Groups (C) 189
- Enantioselective Reduction of Ketones with Sodium Borohydride, Catalyzed by Optically Active (β-Oxoaldiminato)-cobalt(II) Complexes (C) 2145
- Enantioselective Synthesis of β-Amino Acids: TMS-SAMP as a Chiral Ammonia Equivalent for the Aza Analogous Michael Addition to α,β-Unsaturated Esters (C) 455
- First Dynamic Kinetic Resolution of Racemic α-Amino Aldehydes (C) 1023
- Generation of Enantiomerically Enriched Lithium Indenides by Means of (−)-Sparteine: Structure, Stereoselective Substitution, and Solvent Effects (C) 2158
- Preparation of a Surface-Active Chiral Diphosphane and Its Use in the Hydrogenation of Prochiral Olefins (C) 1645
- Stereoselective Syntheses of Peptide Derivatives with 2-Acetamido-3,4,6-tri-*O*-acetyl-1-amino-2-deoxy-β-D-glucopyranose by Four-Component Condensation (C) 1104
- Synthesis of Chiral γ,δ-Unsaturated Amino Acids by Asymmetric Ester Enolate Claisen Rearrangement (C) 2012

Chiral dendrimers
- Synthesis and Properties of First to Third Generation Dendrimers with Doubly and Triply Branched Chiral Building Blocks (C) 2116

Chiral diselenides
- Asymmetric Reaction of Arylalkenes with Diselenides (C) 1726

Chirality
- A New Application of Capillary Zone Electrophoresis: Determination of Energy Barriers of Configurationally Labile Chiral Compounds (C) 1635
- Optical Activity of Chiral Dendritic Surfaces (C) 1206
- Preparation and Detection of Enantiomerically Enriched and Configurationally Stable α-Thioalkyllithium Compounds (C) 323
- Stereoselective Synthesis of Chiral Zirconocenes from Doubly Substituted, Donor Functionalized Cyclopentadienes via Helical Chelate Complexes (C) 2266

Chirality transfer
- Synthesis of Optically Active Nine-Membered Ring Lactams by a Zwitterionic Aza-Claisen Reaction (C) 1026

Chiroptical studies
- Optical Activity of Chiral Dendritic Surfaces (C) 1206

2-Chlorocarboxylic acids
- Unexpected Course of the Darzens Reaction of Phenyl Esters of α-Chlorocarboxylic Acids with Carbonyl Compounds—A Novel One-Step Synthesis of α-Chloro-β-lactones (C) 2028

α-Chloro-β-lactones
- Unexpected Course of the Darzens Reaction of Phenyl Esters of α-Chlorocarboxylic Acids with Carbonyl Compounds—A Novel One-Step Synthesis of α-Chloro-β-lactones (C) 2028

Chromatography
- Structure Determination of Vitamin A Acetate Isomers through Coupled HPLC and ^1H NMR Spectroscopy (C) 1014
- Synthesis of dTDP-6-Deoxy-4-ketoglucose and Analogues with Native and Recombinant dTDP-Glucose-4,6-dehydratase (C) 1748
- Trace Analysis of the Radionuclides ^{90}Sr and ^{89}Sr in Environmental Samples III: Development of a Fast Analytical Method (C) 186

Chromium compounds
- Aminocarbyne Complexes of Chromium in a High Oxidation State—Synthesis, Structure, and Reactivity (C) 924
- Radical Additions to (η^6-Arene)-(tricarbonyl)chromium Complexes: Diastereoselective Synthesis of Hydrophenalene and Hydrobenzindene Derivatives by Samarium(II) Iodide Induced Cyclization (C) 2383
- Synthesis, Structural Investigation, and Ligand Properties of Isocyanoacetonitrile (C) 914

Circular dichroism
- Optical Activity of Chiral Dendritic Surfaces (C) 1206
- Synthesis and Properties of First to Third Generation Dendrimers with Doubly and Triply Branched Chiral Building Blocks (C) 2116

Clathrasils
- Structure-Determining C-H · · · O-Si Hydrogen Bonds in Cobaltocenium Fluoride Nonasil (C) 2680

Clathrates
- Self-Assembly of 1,3,5-Benzenetricarboxylic Acids (Trimesic Acids) and Their Analogues in the Solid State (C) 2654
- Supramolecular Synthons in Crystal Engineering—A New Organic Synthesis (R) 2328

Clusters
- A New Method for the Preparation of Nanostructured Metal Clusters (C) 2240
- A New Strategy in Heterogeneous Catalysis: The Design of Cortex Catalysts (C) 2728
- $ATh_{12}N_6X_{29}$ (A = Li...Rb; X = Cl, Br): A New Type of Thorium Cluster with a $Th_{12}N_6$ Core (C) 567
- Cluster Chemistry (B) 121
- Clusters and Colloids. From Theory to Applications (B) 122
- Condensed $RuSn_6$ Octahedra in $Ru_3Sn_{15}O_{14}$ (C) 2113
- Dimensional Reduction of $Re_6Se_8Cl_2$: Sheets, Chains, and Discrete Clusters Composed of Chloride-Terminated $[Re_6Q_8]^{2+}$ (Q = S, Se) Cores (C) 226
- First Steps Towards Ordered Monolayers of Ligand-Stabilized Gold Clusters (C) 1442
- Free Atoms, Clusters and Nanoscale Particles (B) 1252
- Models for Bimetallic Catalysts: Multiple Oxidation States in Pt_3Re Cluster Cations (C) 346
- $Na_2Ti_2Cl_8$: From Isolated Ti^{2+} Ions to $[Ti_3]^{6+}$ Clusters (C) 71
- New Selenolato-Bridged Clusters of Iron and Nickel; the Structures of $[Fe_{12}(SePh)_{24}]$ and $[Na_2(POPh_3)_6]$-$[Ni_{20}Se_{12}(SeMe)_{10}]$ (C) 307
- Novel Alkali Metal Phosphanide Aggregates (C) 316
- $(Sr_6N)[Ga_5]$ and $(Ba_6N)[Ga_5]$: Compounds with Discrete (M_6N) Octahedra and $[Ga_5]$ Clusters (C) 1761
- Sulfoxide-Stabilized Giant Palladium Clusters in Catalyzed Oxidations (C) 457
- Supramolecular Synthons in Crystal Engineering—A New Organic Synthesis (R) 2328
- The First Clusters with a Y-Shaped Arrangement of Ligands at Three-Coordinate Rh^I Atoms in the Solid State: $[M^1M^2\{\mu\text{-}P(C_6H_{11})_2\}(CO)_8Rh(PPh_3)]$ (M^1, M^2 = Mn, Re) (C) 1325

- The $[Zr_6X_{18}H_5]^{3-}$ Ions with X = Cl, Br, and Related Species (C) 1877
- $[Mo_{154}(NO)_{14}O_{420}(OH)_{28}(H_2O)_{70}]^{(25\pm5)-}$: A Water-Soluble Big Wheel with More than 700 Atoms and a Relative Molecular Mass of About 24000 (C) 2122

Cobaloxime
- Peripherally Substituted Cobaloximes; X-Ray Crystal Structure Analysis of σ-Hexylbis[1,8-di(*N*-morpholino)octane-4,5-dioximato]pyridinecobalt(III) (C) 2389

Cobalt compounds
- A Co_3 Complex Containing a Bent Trimetal Chain, and Other 1,1′-Ferrocenedithiolato Complexes (C) 656
- A μ-η^6:η^6-1,3,5-Triboratabenzenebis(cyclopentadienylcobalt) Triple-Decker Complex (C) 681
- Complexation of [*N*,*N*′-Bis(salicylidene)ethylenediiminato]cobalt(III)$^+$ by Anilines in Dimethylformamide (C) 1086
- Dicobalt and Diplatinum Complexes of Diborylcarbenes (C) 1111
- Enantioselective Reduction of Ketones with Sodium Borohydride, Catalyzed by Optically Active (β-Oxoaldiminato)cobalt(II) Complexes (C) 2145
- Hydrolysis of a Phosphate Diester Doubly Coordinated to a Dinuclear Cobalt(III) Complex: A Novel Mechanism (C) 2412
- Novel Binuclear Cobalt Dioxygen Complex—A Step on the Path to Dioxygen Activation (C) 2051
- Oligomethylene-Bridged Vitamin B_{12} Dimers (C) 84
- Phosphorane Iminato Complexes of Manganese and Cobalt with Heterocubane Structure (C) 1235
- Photoinduced Valence Tautomerism in Cobalt Complexes Containing Semiquinone Anion as Ligand: Dynamics of the High-Spin $[Co^{II}(3,5\text{-dtbsq})_2]$ to Low-Spin $[Co^{III}(3,5\text{-dtbsq})(3,5\text{-dtbcat})]$ Interconversion (C) 1481
- Polymers with Complexed Cyclobutadiene Units in the Main Chain: The First Example of a Thermotropic, Liquid Crystalline Organometallic Polymer (C) 569
- Structure-Determining C-H···O-Si Hydrogen Bonds in Cobaltocenium Fluoride Nonasil (C) 2680
- [Bis{(η^5-pentamethylcyclopentadienyl)cobalt}-μ-(η^4:η^4-arene)]: Synthesis, Structure, and Unusual Reactivity of a New Type of Triple-Decker with Bridging Arene Ligands (C) 592
- $_\infty^3$[$(CoCp_2)_2$⊂Fe(μ-CNSnMe$_3$NC)$_3$]: A Purely Organometallic Channel Inclusion Compound (C) 1197

Coenzymes
- Evidence for a Mechanism Involving Transient Fragmentation in Carbon Skeleton Rearrangements Dependent on Coenzyme B_{12} (C) 2398
- One-Electron Redox Reactions of CoASH Esters in Anaerobic Bacteria—A Mechanistic Proposal (C) 1502

Colloids
- Clusters and Colloids. From Theory to Applications (B) 122

Combinatorial chemistry
- A Strategy of "Random Glycosylation" for the Production of Oligosaccharide Libraries (C) 2720
- Combinatorial Synthesis and Multidimensional NMR Spectroscopy: An Approach to Understanding Protein–Ligand Interactions (R) 953
- Optimization of the Biological Activity of Combinatorial Compound Libraries by a Genetic Algorithm (C) 2280
- Radiofrequency Encoded Combinatorial Chemistry (C) 2289
- Solid-Phase Synthesis of Vinylogous Sulfonyl Peptides (C) 1763
- Synthetic Receptors Based on Vinylogous Sulfonyl Peptides (C) 1765

Complexes with arsenic ligands
- η^5:η^2 Coordination of a *cyclo*-E_5 Ligand, E = P, As (C) 1321

Complexes with boron ligands
- Synthesis and Structure of the First Transition Metal Borylene Complexes (C) 825

Complexes with carbon ligands
- A Rhodium-Mediated, Stepwise Trimerization of an Alkyne That Does Not Lead to a Benzene but Selectively to a Hexadienyne Derivative (C) 191
- Nucleophilic Addition to (π-Allyl)-palladium Complexes: Control of the Attack at the Central or Terminal Carbon Atom by Ligands (C) 2551
- Synthesis and Structure of Bimetallic η^4,η^6-Naphthalene Complexes Containing a Mn–Mn Moiety Bonded in a *Syn*-Facial Manner: A General Route to Homo- and Heteronuclear Bimetallic Complexes of Polyarenes (C) 2540
- Synthesis, Structural Investigation, and Ligand Properties of Isocyanoacctonitrile (C) 914
- $[Fe(2,4,6\text{-}tBu_3C_6H_2)_2]$, a Monomeric Diaryl Complex with Two-Coordinate Iron(II) (C) 325
- $[\{Ti(\mu\text{-}CH_3)_5(\mu\text{-}CH_2)\}\{(tmeda)Li\}_3]\cdot$ THF: An Unusual and Highly Fluxional Titanium Organometallic Compound (C) 2264

Complexes with carboxylato ligands
- Octadecanuclearity in Manganese Carboxylate Chemistry: $K_4[Mn_{18}O_{16}(O_2CPh)_{22}(phth)_2(H_2O)_4]$ ($phthH_2$ = phthalic acid) (C) 887

Complexes with chalcogen ligands
- Models for Bimetallic Catalysts: Multiple Oxidation States in Pt_3Re Cluster Cations (C) 346

Complexes with elements of group 15
- Terminal E_1 Ligands from Elements of Group 15 (H) 1997

Complexes with ferrocenyl ligands
- A Functionalized Polyoxometalate Bearing a Ferrocenylimido Ligand: Preparation and Structure of $[(FcN)Mo_6O_{18}]^{2-}$ (C) 2547

Complexes with hydrido ligands
- Reaction of a Vanadium(III) Amide with H_2: Isolation and Characterization of a Polynuclear Mixed-Valence Polyhydrido–Nitrido Complex (C) 822

Complexes with macrocyclic ligands
- Double Helical Dinuclear Copper(I) Complexes of Macrocyclic Bis(dithiadiimine) Ligands (C) 1883
- The First Dinuclear Low-Valent Samarium Complex with a Short Sm–Sm Contact (C) 2141

Complexes with nitrido ligands
- Reaction of a Vanadium(III) Amide with H_2: Isolation and Characterization of a Polynuclear Mixed-Valence Polyhydrido–Nitrido Complex (C) 822

Complexes with nitrogen ligands
- A Dinuclear (μ-Carboxylato)manganese(II) Complex Derived from a Macrocyclic Ligand: A Structural Model for Active Sites in Natural Systems (C) 2535
- A Model of Semimet Hemerythrin; NMR Spectroscopic Evidence of Valence Localization in Bis(μ-carboxylato)(μ-phenolato)diiron(II,III) in Solution (C) 588
- A Nickel(II) Azide Cubane Characterization of the Magnetic Exchange Interactions Mediated by a Triply Bridging Azide Group Bound End-On (C) 889
- Lanthanoid Complexes with [(dad)Li]Ligands—New Starting Materials for Organolanthanoid Chemistry (C) 673
- Metal Oxo Cation Receptors: Multimode Coordination to the Dioxoosmium(VI) Cation (C) 1359
- Molecular Recognition of Terephthalic Acid by Supramolecular Self-Assembly of an Acridine-Pendant Cyclen–Zn^{II} Complex (C) 663
- Mutually Interpenetrating Sheets and Channels in the Extended Structure of [Cu(4,4′-bpy)Cl] (C) 207
- μ-Nitridodiiron Complexes with Asymmetric $[Fe^{IV}\equiv N\text{–}Fe^{III}]^{4+}$ and Symmetric $[Fe^{IV}=N=Fe^{IV}]^{5+}$ Structural Elements (C) 669
- Novel Networks of Unusually Coordinated Silver(I) Cations: The Wafer-Like Structure of $[Ag(pyz)_2][Ag_2(pyz)_5](PF_6)_3\cdot 2G$ and the Simple Cubic Frame of $[Ag(pyz)_3](SbF_6)$ (C) 1895
- Self-Assembly of a Ferromagnetically Coupled Manganese(II) Tetramer (C) 1443
- Synthesis, Structure, and Properties of Dinuclear and Trinuclear Rack-Type Ru^{II} Complexes (C) 1122
- The pH-Dependent Synthesis and Structural Study of Dimeric and Cyclic Trimeric Complexes of 9-Methyl- or 9-Ethylhypoxanthine Nucleobases with (η^5-Pentamethylcyclopentadienyl)rhodium Aqua Complexes (C) 1514
- 2,4,6-Tri(4-pyridyl)-1,3,5-triazine as a 3-Connecting Building Block for Infinite Nets (C) 820
- [WL(NO)(O)(CH_3)]—An Unusual Nitrosyltungsten Complex (C) 1435

Complexes with oxygen ligands
- A Cyclic Hexairon(III) Complex with an Octahedrally Coordinated Sodium Ion at the Center, an Example of the [12]Metallacrown-6 Structure Type (C) 467
- A Model of Semimet Hemerythrin: NMR Spectroscopic Evidence of Valence Localization in Bis(μ-carboxylato)(μ-phenolato)diiron(II,III) in Solution (C) 588
- A New Type of Trinuclear Oxoiron(III) Cluster (C) 205
- A Nickel(II) Azide Cubane: Characterization of the Magnetic Exchange Interactions Mediated by a Triply Bridging Azide Group Bound End-On (C) 889
- A Novel Hexanuclear Fe^{III}-*cis*-Inositolato Complex as a Model for Fe^{III}–Polyol Interactions in Aqueous Solution (C) 2242
- A Stable Aquairon(III) Complex with S = 1: Structure and Spectroscopic Properties (C) 1216 (1649)
- Complexes with Polar W–W Multiple Bonds: $[W_2(OiPr)_4L(dmpe)_2]$ (L = $(H)_2$, CO) and $[W_2(O)_4(\mu\text{-}O)\{W(CO)(dmpe)_2\}_2]$ (C) 891
- Fivefold Deprotonated D-Mannose as Ligand in Homoleptic Dinuclear Metalates of Trivalent Iron, Vanadium, Chromium, Aluminum, and Gallium (C) 2647
- Formation of an Alkylperoxoiron(III) Complex during Oxidations Catalyzed by μ-Oxodiiron(III) Complexes (C) 203

- Solid-State and Solution Structures of $[\{NW(OC(CH_3)_2CF_3)_3\}_3]$ and Factors Favoring the Metathesis of C–N and N–W Triple Bonds in Reactions Involving Organic Nitriles and Ditungsten Hexaalkoxides (C) 110
- Structure and Magnetic Properties of a Decanuclear Oxoiron(III) Cluster: A Further Step to Understanding Iron Aggregation Processes (C) 2716
- $[Mn(C_{18}H_{16}N_2O_2)_3](ClO_4)_2$: A Polymeric 34- and 68-Membered Metallacyclic Network Forming a Novel Woven Polycatenated Structure (C) 574
- $[Mo_{154}(NO)_{14}O_{420}(OH)_{28}(H_2O)_{70}]^{(25\pm5)-}$: A Water-Soluble Big Wheel with More than 700 Atoms and a Relative Molecular Mass of About 24000 (C) 2122
- $[WL(NO)(O)(CH_3)]$—An Unusual Nitrosyltungsten Complex (C) 1435

Complexes with phosphorus ligands
- A Molybdenum–Phosphorus Triple Bond: Synthesis, Structure, and Reactivity of the Terminal Phosphido (P^{3-}) Complex $[Mo(P)(NRAr)_3]$ (C) 2042
- A Redox-Switchable Hemilabile Ligand: Electrochemical Control of the Coordination Environment of a Rh^I Complex (C) 1624
- Complexes with Polar W–W Multiple Bonds: $[W_2(O\mathit{i}Pr)_4L(dmpe)_2]$ (L = $(H)_2$, CO) and $[W_2(O)_4(\mu\text{-}O)\{W(CO)(dmpe)_2\}_2]$ (C) 891
- $\eta^5{:}\eta^2$ Coordination of a *cyclo*-E_5 Ligand, E = P, As (C) 1321
- 2,4-Di-*tert*-butyl-1λ^3,3λ^3-diphosphinines: Targeted Synthesis at Iron(0) Centers and Oxidative Release (C) 198
- Monomeric Molybdenum and Tungsten Complexes That Contain a Metal–Phosphorus Triple Bond (C) 2044
- ^{31}P CP/MAS NMR Spectroscopy of Transition Metal Phosphane Complexes: "*J*-Recoupling" between Chemically Equivalent ^{31}P Nuclei in Polycrystalline Compounds of the Type *trans*-$[(PR_3)_2MX_2]$, M = Pd, Pt (C) 667
- P–H-Functionalized Phosphenium Complexes $[C_5R_5(OC)_2W{=}P(H)R']$ (R' = *t*Bu, sMes): Synthesis, Isomerization, and Transformation into Hydrido Complexes Containing a *t*BuP(H)OH Ligand (C) 2500
- Synthesis and Structure of $[Li(thf)_4]_2[Ph_2P)_{10}Cd_4]$ Containing; a Dianionic with a Cd_4P_{10} Adamantanoid Core (C) 2662

Complexes with P,N ligands
- Strong Electronic Effects on Enantioselectivity in Rhodium-Catalyzed Hydroborations with Novel Pyrazole-Containing Ferrocenyl Ligands (C) 931

Complexes with selenium ligands
- New Selenolato-Bridged Clusters of Iron and Nickel; the Structures of $[Fe_{12}(SePh)_{24}]$ and $[Na_2(POPh_3)_6]$-$[Ni_{20}Se_{12}(SeMe)_{10}]$ (C) 307

Complexes with semiquinone ligands
- Photoinduced Valence Tautomerism in Cobalt Complexes Containing Semiquinone Anion as Ligand: Dynamics of the High-Spin $[Co^{II}(3,5\text{-dtbsq})_2]$ to Low-Spin $[Co^{III}(3,5\text{-dtbsq})(3,5\text{-dtbcat})]$ Interconversion (C) 1481

Complexes with sulfur ligands
- A Co_3 Complex Containing a Bent Trimetal Chain, and Other 1,1'-Ferrocenedithiolato Complexes (C) 656
- *Enantiomerically Pure Palladacycles Derived from β-Ketosulfoxides (C) 1351*
- $[Cp^*(Me_3P)_2Ru(\eta^2\text{-}O{=}SO_2)]PF_6$, the First Complex between a Transition Metal and Sulfur Trioxide (C) 1008

Composites
- A Molecular Composite Containing Organic and Inorganic Components—A Complex from β-Cyclodextrin and Hydrated Magnesium Chloride (C) 2381

Compound libraries
- Assessing Similarity and Diversity of Combinatorial Libraries by Spatial Autocorrelation Functions and Neural Networks (C) 2674
- Optimization of the Biological Activity of Combinatorial Compound Libraries by a Genetic Algorithm (C) 2280
- Saccharide–Peptide Hybrids as Novel Oligosaccharide Mimetics (C) 2712

Computer chemistry
- Assessing Similarity and Diversity of Combinatorial Libraries by Spatial Autocorrelation Functions and Neural Networks (C) 2674
- Computer-Assisted Planning of Organic Syntheses: The Second Generation of Programm (R) 2613

Concave reagents
- Concave Reagents Based on Calixarenes (C) 2555

Conduritols
- Catalytic Photoinduced Charge-Transfer Osmylation: A Novel Pathway from Arenes to Cyclitol Derivatives (C) 2031

Configuration determination
- Carbon–Carbon Bond Cleavage with Inversion of Configuration: Conversion of (*R*)-(+)-1-Methoxytetrafluoropropionic Acid to (*S*)-(−)-1,2,2,2-Tetrafluoroethyl Methyl Ether (C) 222

Conformation
- Activation of Macrocyclic Biaryl-Enediynes by Metal Ion Coordination (C) 2538

Conical intersection
- Conical Intersections and the Mechanism of Singlet Photoreactions (H) 549

Coordination
- Galloxane and Alumoxane Hydroxides: $[Ga_{12}t\mathrm{Bu}_{12}(\mu_3\text{-}O)_8(\mu\text{-}O)_2(\mu\text{-}OH)_4]$ and $[Al_6t\mathrm{Bu}_6(\mu_3\text{-}O)_4(\mu\text{-}OH)_4]$ (C) 1201
- Octathioporphyrazine Crown Ethers: An Octanuclear Ag^I Complex with Coordination in the *meso* Pocket (C) 2020
- Rhodium–Vinylallene Complexes and a New Reaction, Rhodium-Catalyzed Carbonylative [4+1]Cycloaddition (C) 2691
- Structure and Bonding of Transition Metal Dihydrogen Complexes $[M(CO)_5(H_2)]$ (M = Cr, Mo, W) (C) 354
- The First Clusters with a Y-Shaped Arrangement of Ligands at Three-Coordinate Rh^I Atoms in the Solid State: $[M^1M^2\{\mu\text{-}P(C_6H_{11})_2\}(CO)_8Rh(PPh_3)]$ (M^1, M^2 = Mn, Re) (C) 1325
- The pH-Dependent Synthesis and Structural Study of Dimeric and Cyclic Trimeric Complexes of 9-Methyl- or 9-Ethylhypoxanthine Nucleobases with (η^5-Pentamethylcyclopentadienyl)rhodium Aqua Complexes (C) 1514
- Volatile Metal Alkoxides According to the Concept of Donor Functionalization (R) 2187

Coordination polymers
- Novel Networks of Unusually Coordinated Silver(I) Cations: The Wafer-Like Structure of $[Ag(pyz)_2][Ag_2(pyz)_5](PF_6)_3\cdot 2G$ and the Simple Cubic Frame of $[Ag(pyz)_3](SbF_6)$ (C) 1895

Cope rearrangements
- Pericyclic Reactions in Nature: Spontaneous Cope Rearrangement Inactivates Algae Pheromones (C) 1602
- The Cope Rearrangement Transition Structure Is Not Diradicaloid, but Is It Aromatic? (C) 334

Copolymerizations
- A Tailor-Made Metallocene for the Copolymerization of Ethene with Bulky Cycloalkenes (C) 2273

Copper compounds
- A Hexadecanuclear Polyolatometalate of Copper(II) Ions and Multideprotonated D-Sorbitol (C) 2119
- C_2-Symmetric Cationic Copper(II) Complexes as Chiral Lewis Acids: Counterion Effects in the Enantioselective Diels–Alder Reaction** (C) 798
- Carbenoid Transfer to Imines: A New Asymmetric Catalytic Synthesis of Aziridines (C) 676
- Computational Evidence for the Existence of Cu^{III} Intermediates in Addition and Substitution Reactions with Dialkylcuprates (C) 476
- $(CuI)_3P_{12}$: A Solid Containing a New Polymer of Phosphorus Predicted by Theory (C) 1647
- Distinguishing Copper d^8 and d^{10} Configurations in a Highly Ionic Complex; A Nonformal Metal Oxidation State (C) 986
- Double Helical Dinuclear Copper(I) Complexes of Macrocyclic Bis(dithiadiimine) Ligands (C) 1883
- Elusiveness of Cu^{III} Complexation; Preference for Trifluoromethyl Oxidation in the Formation of $[Cu^I(CF_3)_4]^-$ Salts (C) 80
- Formal Oxidation State versus Partial Charge—A Comment (C) 986
- Mutually Interpenetrating Sheets and Channels in the Extended Structure of [Cu(4,4'-bpy)Cl] (C) 207
- Novel Biological Copper Proteins through Anion Addition to the Mutant Met121Gly of *Pseudomonas aeruginosa* Azurin (C) 1622
- Rapid Hydrolysis of RNA with a Cu^{II} Complex (C) 472
- The Metallic Bond—Dead or Alive? A Comment and a Reply (C) 2003
- Zeolite Encaged Cu(Histidine) Complexes as a Mimic of Natural Cu Enzymes (C) 2652

Correspondences
- Distinguishing Copper d^8 and d^{10} Configurations in a Highly Ionic Complex; A Nonformal Metal Oxidation State (C) 986
- Formal Oxidation State versus Partial Charge—A Comment (C) 986
- Reactions of Neopentyl 2,2,-Trifluoroethanesulfonate (Neopentyl Tresylate) with Nucleophiles: A Model Study for the Coupling of Nucleophiles with Tresyl Agarose (C) 2495
- The Metallic Bond—Dead or Alive? A Comment and a Reply (Comment) (C) 2003

Corrigenda 240, 826, 1032, 1368, 1649, 2165, 2561

Cosensitization
- Radical C–C Bond Formation by Photoinduced Electron Transfer Addition of α-Silyl Carbamates to Acceptor-Substituted Alkenes (C) 2137

Cracking
- Coupling of Endothermic Thermal Cracking with Exothermic Oxidative Dehydrogenation of Ethane to Ethylene Using a Diluted SrO/La_2O_3 Catalyst (C) 665

Cross-coupling
- A New Nickel-Catalyzed Cross-Coupling Reaction between sp^3 Carbon Centers (C) 2723

Crown compounds
- Controlling Translational Isomerism in [2]Catenanes (C) 571
- Dialkylammonium Ion/Crown Ether Complexes: The Forerunners of a New Family of Interlocked Molecules (C) 1865
- Doubly Encircled and Double-Stranded Pseudorotaxanes (C) 1869
- Investigation of Self-Assembled Supramolecular Species in Solution by IL-ESMS, a New Mass Spectrometric Technique (C) 209
- Octathioporphyrazine Crown Ethers: An Octanuclear Ag^I Complex with Coordination in the *meso* Pocket (C) 2020
- Self-Assembly of Polyanions at a Metal Cation Template: Syntheses and Structures of $[\{Ag([18]aneS_6)\}I_7]_n$ and $[Ag([18]aneS_6)]I_3$ (C) 2374
- Strong Binding of Paraquat and Polymeric Paraquat Derivatives by Basket-Shaped Hosts (C) 2132
- Synthesis of Novel Tetrathiafulvalene-(TTF)-Based [3]Pseudocatenanes by Self-Assembly; Prevention of *trans/cis* Isomerization (C) 2524
- The Reactivity of 1,3-Butadiyne Moieties in the "Exploding" [*n*]Rotanes—A Crown of Thiophenes (C) 781
- Transition Metal Complexes as Both Host and Guest: Second-Sphere Coordination between a Pt-Azacrown Ether Host and a $Pt\text{-}NH_3$ Guest (C) 2689

Cryptands
- Binding of Boron and Alkali Metal Cations by a Pseudocryptand (C) 1115

Crystal engineering
- Porous Solids by Design: $[Zn(4,4'\text{-}bpy)_2(SiF_6)]_n \cdot x$DMF, a Single Framework Octahedral Coordination Polymer with Large Square Channels (C) 2127 (2561)
- Self-Assembly of 1,3,5-Benzenetricarboxylic Acids (Trimesic Acids) and Their Analogues in the Solid State (C) 2654
- Supramolecular Inorganic Chemistry: Small Guests in Small and Large Hosts (R) 2311

Crystallization
- Homogeneous versus Heterogeneous Zeolite Nucleation (C) 73

Crystallography
- Crystallography Made Crystal Clear. A Guide for Users of Macromolecular Models (B) 496
- Crystal Structure Analysis for Chemists and Biologists (B) 2060

Cumulenes
- *para*- and *ortho*-Quinodimethanes Intermediates with Cumulative Double Bonds (C) 2367
- Butatrienes by Cumuhomologation of Propadienes (C) 2709

Cuprates
- Computational Evidence for the Existence of Cu^{III} Intermediates in Addition and Substitution Reactions with Dialkylcuprates (C) 476
- Distinguishing Copper d^8 and d^{10} Configurations in a Highly Ionic Complex; A Nonformal Metal Oxidation State (C) 986
- Elusiveness of Cu^{III} Complexation; Preference for Trifluoromethyl Oxidation in the Formation of $[Cu^I(CF_3)_4]^-$ Salts (C) 80
- Formal Oxidation State versus Partial Charge—A Comment (C) 986

Curium
- First Determination of the Ionization Potential of Americium and Curium (C) 814

Curtin-Hammett principle
- Kinetic Selection in the Template-Directed Self-Assembly of [2]Catenanes (C) 2378

CVD precursors
- Volatile Metal Alkoxides According to the Concept of Donor Functionalization (R) 2187

CVD techniques
- The Chemistry of Metal CVD (B) 1651

Cyanides
- Self-Assembled Helicates of Zinc and Cadmium Cyanides, $[M_x(CN)_{2x+1}]^-$, $x \leq 27$ (C) 314
- Synthesis and Structure of the Three-Dimensional Coordination Polymers $[(Me_3Sn)_4M(CN)_8]$ (M = Mo, W) (C) 2557

Cyano complexes
- Six Interpenetrating Quartz-Like Nets in the Structure of $ZnAu_2(CN)_4$ (C) 1203

Cyanohydrins
- A Chiral Cyanohydrin Phosphate for Carbonyl Umpolung—Stereoselective Synthesis of Tertiary Cyanohydrins (C) 917

Cyclic voltammetry
- 4c/3e Radical Cations with Cage-Directed Configurations (C) 1016
- Molecular Recognition at an Interface: Binding of Monolayer-Anchored Ferrocenyl Groups by an Amphiphilic Calixarene Host (C) 235
- Oligothiophenes—Yet Longer? Synthesis, Characterization, and STM Images of Homologous, Isomerically Pure Oligo(alkylthiophene)s (C) 303

Cyclizations
- A P_2C_2 Four-Membered Ring with Unusual Bonding—Synthesis, Structure, and Ring Opening of a 1,3-Diphosphacyclobutane-2,4-diyl (C) 555
- Asymmetric Syntheses of Stavudine (d4T) and Cordycepin by Cycloisomerization of Alkynyl Alcohols to Endocyclic Enol Ethers (C) 350
- Catalytic Ring-Closing Metathesis: A New, Powerful Technique for Carbon–Carbon Coupling in Organic Synthesis (H) 1833
- Diastereoselective Cathodic Cyclization of 1-(4- and 1-(3-Oxoalkyl)pyridinium Salts to Quinolizidine and Indolizidine Derivatives (C) 2007
- Efficient Total Synthesis of the Pharmacophore of the Anticancer Antibiotic CC-1065 by Zirconocene- and Palladium-Initiated Cyclizations (C) 1366
- Intramolecular Allylsilane Addition to Chiral Alkylidene-1,3-dicarbonyl Compounds for the Synthesis of Enantiomerically Pure *trans*-1,2-Disubstituted Cyclopentanes and Cyclohexanes (C) 1731
- Low-Temperature Tandem Enyne Allene Radical Cyclizations: Efficient Synthesis of 2,3-Dihydroindenes from Simple Enediynes (C) 2037
- Oxidative Polycyclization versus the "Polyepoxide Cascade": New Pathways in Polyether (Bio)synthesis? (H) 298
- Photo Electron Transfer Induced Macrocyclization of *N*-Phthaloyl-ω-aminocarboxylic Acids (C) 474
- Radical Additions to (η^6-Arene)-(tricarbonyl)chromium Complexes: Diastereoselective Synthesis of Hydrophenalene and Hydrobenzindene Derivatives by Samarium(II) Iodide Induced Cyclization (C) 2383
- Radical Cation [4+2] Cycloadditions with 2-Vinylindoles (C) 1900
- Synthesis of D-(+)-Biotin through Selective Ring Closure of *N*-Acyliminium Silyl Enol Ethers (C) 2391
- 1,3,5,7-Tetraphosphabarrelene: A New Cyclic Phosphaalkyne Tetramer (C) 81

Cycloadditions
- A Concise Synthetic Route to Cyclopentenes by [3+2] Cycloaddition of Dipolar Trimethylenemethane to Alkynes (C) 2154
- A Cycloaddition–Cyclodehydrogenation Route from Stilbenoids to Extended Aromatic Hydrocarbons (C) 1583
- Atom Economy—A Challenge for Organic Synthesis: Homogeneous Catalysis Leads the Way (R) 259
- Control of the Reactivity of Double Bonds through Their Fixed Geometrical Arrangement (H) 2225
- Design of Novel, Nonpeptidic Thrombin Inhibitors and Structure of a Thrombin–Inhibitor Complex (C) 1739
- Facial Diastereoselectivity in the Paternò–Büchi Reaction of Chiral Silyl Enol Ethers (C) 2271
- Preparation, Structure, and Reactivity of 1,3,4-Triphenyl-4,5-dihydro-1*H*-1,2,4-triazol-5-ylidene, a New Stable Carbene (C) 1021
- Rhodium–Vinylallene Complexes and a New Reaction, Rhodium-Catalyzed Carbonylative [4+1]Cycloaddition (C) 2691
- Synthesis of a 2*H*-Azirine by [1+2] Cycloaddition of a Phosphinocarbene with a Nitrile and Its Ring-Expansion to a $1,2\lambda^5$-Azaphosphete (C) 1246
- The Dimerization of (*E*)-1,3-Diphenyl-1,3-butadiene Proceeds Suprafacially with Respect to Both Components: Evidence for a Concerted [4+2] Cycloaddition (C) 895
- Transition Metal Catalyzed Synthesis of Seven-Membered Carbocyclic Rings (H) 2223

Cycloalkynes
- Automerizations and Isomerizations in Propynylidene (HCCCH), Propadienylidene (H_2CCC), and Cyclopropenylidene ($c\text{-}C_3H_2$) (C) 2009

Cycloallenes
- 1-Phenyl-1,2-cyclooctadiene Dimerizes in an Unusual Manner (C) 2730

β-Cycloaltrin
- β-Cycloaltrin: A Cyclooligosaccharide Consisting of Seven α(1→4)-Linked Altropyranoses (C) 1621

Cycloaromatizations
- Lactendiynes: A New Class of Triggered Cyclic Enediynes (C) 2393

Cyclobutadienes
- A P_2C_2 Four-Membered Ring with Unusual Bonding—Synthesis, Structure, and Ring Opening of a 1,3-Diphosphacyclobutane-2,4-diyl (C) 555
- Polymers with Complexed Cyclobutadiene Units in the Main Chain: The First Example of a Thermotropic, Liquid Crystalline Organometallic Polymer (C) 569
- [Bis{(η^5-pentamethylcyclopentadienyl)-cobalt}-μ-(η^4:η^4-arene)]: Synthesis, Structure, and Unusual Reactivity of a New Type of Triple-Decker with Bridging Arene Ligands (C) 592

Cyclobutenes
- A Remarkable Effect of Silyl Substitution on Electrocyclization of Vinylallenes (C) 1476
Cyclodehydrogenations
- A Cycloaddition–Cyclodehydrogenation Route from Stilbenoids to Extended Aromatic Hydrocarbons (C) 1583
Cyclodextrins
- A Molecular Composite Containing Organic and Inorganic Components—A Complex from β-Cyclodextrin and Hydrated Magnesium Chloride (C) 2381
- A New Application of Capillary Zone Electrophoresis: Determination of Energy Barriers of Configurationally Labile Chiral Compounds (C) 1635
- β-Cycloaltrin: A Cyclooligosaccharide Consisting of Seven α(1 → 4)-Linked Altropyranoses (C) 1621
- Molecular Recognition between Chemically Modified β-Cyclodextrin and Dec-1-ene: New Prospects for Biphasic Hydroformylation of Water-Insoluble Olefins (C) 2269
- Rapid Water Diffusion in a Cage-Type Crystal Lattice: β-Cyclodextrin Dodecahydrate (C) 1452
- Side-Chain Polyrotaxanes with a Tandem Structure Based on Cyclodextrins and a Polymethacrylate Main Chain (C) 309
Cyclohexanes
- Intramolecular Allylsilane Addition to Chiral Alkylidene-1,3-dicarbonyl Compounds for the Synthesis of Enantiomerically Pure *trans*-1,2-Disubstituted Cyclopentanes and Cyclohexanes (C) 1731
Cyclohexatriene
- X-Ray Diffraction Evidence for a Cyclohexatriene Motif in the Molecular Structure of Tris(bicyclo[2.1.1]hexeno)benzene: Bond Alternation after the Refutation of the Mills–Nixon Theory (C) 1454
Cyclooctatetraene complexes
- Cyclopentadienyl-Free Organolanthanide Chemistry (R) 2466
Cycloolefin copolymers
- A Tailor-Made Metallocene for the Copolymerization of Ethene with Bulky Cycloalkenes (C) 2273
Cyclooligomerizations
- Selective Syntheses of 1,3-Diphosphacyclobutadiene, Dewar-1,3,5-triphosphabenzene, 1,3,5-Triphosphabenzene, and 1,3,5,7-Tetraphosphabarrelene by Cyclooligomerization of Phosphaalkynes (C) 2227
Cyclopentadiene analogues
- Lanthanoid Complexes with [(dad)Li]Ligands—New Starting Materials for Organolanthanoid Chemistry (C) 673
Cyclopentadienes
- Aminocyclopentadienes, Aminoferrocenes, and Aminocobaltocenes (C) 800
- Stereoselective Synthesis of Chiral Zirconocenes from Doubly Substituted, Donor Functionalized Cyclopentadienes via Helical Chelate Complexes (C) 2266
Cyclopentadienides
- Five-Membered Aromatic and Anti-aromatic Rings with Gallium, Germanium, and Bismuth Centers: A Short March through the Periodic Table (H) 295
Cyclopentadienyl complexes
- Aggregation of Nitrido–Metal Complexes: The Example of $[(\eta^5\text{-}C_5Me_5)\text{-}Mo(N)Cl_2]$ (C) 112
- Macrobicyclic Titanium(IV) Complexes with C_3-Symmetric Synthetic Peptides (C) 1449
- Tris(dimethylamino)sulfoniumcyclopentadienide $[TAS]^+[C_5H_5]^-$ and Tris(dimethylamino)sulfoniumpyrrolide $[TAS]^+[C_4H_4N]^-$: Two Isostructural Salts with "Naked" Anions A^- and the "Inverse" Sandwich-Cations $[\{(Me_2N)_3S\}_2A]^+$ (A = $C_5H_5^-$, $C_4H_4N^-$) (C) 443
Cyclopentanes
- Intramolecular Allylsilane Addition to Chiral Alkylidene-1,3-dicarbonyl Compounds for the Synthesis of Enantiomerically Pure *trans*-1,2-Disubstituted Cyclopentanes and Cyclohexanes (C) 1731
Cyclopentenes
- A Concise Synthetic Route to Cyclopentenes by [3+2] Cycloaddition of Dipolar Trimethylenemethane to Alkynes (C) 2154
Cyclophanes
- *para*- and *ortho*-Quinodimethanes Intermediates with Cumulative Double Bonds (C) 2367
- A New Family of Chiral Binaphthyl-Derived Cyclophane Receptors: Complexation of Pyranosides (C) 1596
- A New Quantitative Description of the Distance Dependence of Through-Space $^{19}F,^{19}F$ Spin–Spin Coupling (C) 1881
- "Cation-π Interactions" Detected by Mass Spectrometry; Selective Recognition of Alkali Metal Cations by a π-Basic Molecular Cavity (C) 1364
- Fullerene Model Compounds: Bowl-Shaped Aromatic Hydrocarbons and Cyclophane-Based Cage Molecules (H) 1429
- Octacationic Cyclophanes: Binding of ATP and Other Anionic Guests in Water (C) 2147
- Synthesis and Structure of the Nanodimensional Multicyclophane "Kuratowski Cyclophane", an Achiral Molecule with Nonplanar $K_{3,3}$ Topology (C) 2657
- Synthesis of a Stable Arenesulfenic Acid Bearing a Bowl-Shaped Macrobicyclic Cyclophane Skeleton (C) 1124
- Synthesis of Belt Cyclophanes (C) 1437
- Topochemical Reaction Control in Solution (C) 685
- 6,7-Bis(methoxycarbonyl)-2,3-dimethyl [5](1,4)naphthalenophane; the First Benzoannelated [5]Paracyclophane (C) 2553
Cyclophilin
- Rational Design of Orthogonal Receptor–Ligand Combinations (C) 2129
Cyclopropanations
- Isolation and X-Ray Crystal Structure of a Palladacyclobutane: Insight into the Mechanism of Cyclopropanation (C) 100
- Novel Structures from Tris(benzocyclobutadieno)cyclohexatriene: Triscyclopropanation and Trisoxacyclopropanation to the First [2.1.2.1.2.1]Hexaannulanes (C) 563
- Reversible Template-Directed Activation of Equatorial Double Bonds of the Fullerene Framework: Regioselective Direct Synthesis, Crystal Structure, and Aromatic Properties of $T_h\text{-}C_{66}(COOEt)_{12}$ (C) 1607
Cyclopropanes
- Formation of Nitronic Acids by Ring Opening of Nitrocyclopropanes by a Concerted, Acid-Catalyzed Mechanism (C) 1091
- Unprecedented Intra- and Intermolecular Palladium-Catalyzed Coupling Reactions with Methylenecyclopropane Type Tetrasubstituted Alkenes (C) 2545
Cyclopropenylium compounds
- Stable 1:1 Adducts from Iodoacetylenes and Iodide Ions: Ion Pair Strain as an Additional Driving Force? (C) 441
- The Consequences of an Electrostatic "Forced Marriage" between Two Electron-Rich Particles: Strained Ion Pairs (C) 439
Cyclosporin
- Rational Design of Orthogonal Receptor–Ligand Combinations (C) 2129
Cyclotetramers
- Tetraphosphatricyclo[4.2.0.0^{2,5}]octadienes; New Phosphaalkyne Cyclotetramers Derived from $\lambda^3\sigma^2$-Diphosphetes (C) 484
Cystine
- X-Ray Structure of a Self-Assembled Gelating Fiber (C) 585
Cytochrome c peroxidase
- Direct Electrochemical Coupling of Components of the Biological Electron Transfer Chain to Modified Surfaces: Molecular Recognition between Cytochrome c Peroxidase and Cytochrome c (C) 2409
Cytochrome c oxidase
- The Active Sites of the Native Cytochrome-c Oxidase from Bovine Heart Mitochondria: EXAFS-Spectroscopic Characterization of a Novel Homobinuclear Copper Center (Cu_A) and of the Heterobinuclear $Fe_{a3}\text{-}Cu_B$ Center (C) 1488
- The Dinuclear Cu_A Center in Cytochrome *c* Oxidase and N_2O Reductase—A Metal–Metal Bond in Biology? (H) 771
- X-ray Crystal Structures of Cytochrome c Oxidases from *Paracoccus denitrificans* and Bovine Heart and Their Implications for the Molecular Mechanism of Cell Respiration (H) 2635
Cytomimetic chemistry
- Cytomimetic Organic Chemistry: Early Developments (R) 2091
C–H activation
- An Alkylperoxoiron(III) Intermediate and Its Role in the Oxidation of Aliphatic C–H Bonds (C) 2048
- Does the Facile Inter- and Intramolecular C–H Bond Activation by Tp*–Rh Complexes Proceed via Rh^I or Rh^{III} Intermediates? (C) 231
- Unprecedented Mode of Bonding for Olefins on Bimetallic Complexes: An Agostic Interaction of a sp^2 C–H Bond with a Ruthenium Center in Addition to a π bond to a Rhenium Center (C) 916

Darzens reaction
- Unexpected Course of the Darzens Reaction of Phenyl Esters of α-Chlorocarboxylic Acids with Carbonyl Compounds—A Novel One-Step Synthesis of α-Chloro-β-lactones (C) 2028
Dehydratases
- Synthesis of dTDP-6-Deoxy-4-ketoglucose and Analogues with Native and Recombinant dTDP-Glucose-4,6-dehydratase (C) 1748
Dehydroalanine
- The Role of Dehydroalanine in Catalysis by Histidine Ammonia Lyase (C) 1464
Dehydroannulenes
- Synthesis of New Sworski-Type Dehydroannulenes: 3,4-Benz-1,2,5,6,8,9,12,13-octadehydro[14]annulenes (C) 1892
Dehydrogenations
- Coupling of Endothermic Thermal Cracking with Exothermic Oxidative Dehydrogenation of Ethane to Ethylene Using a Diluted SrO/La_2O_3 Catalyst (C) 665
Dendralenes
- Unprecedented Intra- and Intermolecular Palladium-Catalyzed Coupling Reactions with Methylenecyclopropane Type Tetrasubstituted Alkenes (C) 2545

Dendrimers
- Optical Activity of Chiral Dendritic Surfaces (C) 1206
- Routes to Dendritic Networks: Bis-Dendrimers by Coupling of Cascade Macromolecules through Metal Centers (C) 2023
- Spherical Cyclophosphazene Dendrimers to the Fifth Generation (C) 578
- Synthesis and Properties of First to Third Generation Dendrimers with Doubly and Triply Branched Chiral Building Blocks (C) 2116
- Synthesis and Structure of a Dendritic Polysilane (C) 98
- Water-Soluble Dendritic Iron Porphyrins: Synthetic Models of Globular Heme Proteins (C) 2725

De novo design
- Design of Novel, Nonpeptidic Thrombin Inhibitors and Structure of a Thrombin–Inhibitor Complex (C) 1739

Density functional calculations
- Mechanism of the Fe^+ Mediated C–C and C–H Bond Activations in Ethane from a Theoretical Viewpoint (C) 2282
- N-Confused Porphyrins and Singlet Carbenes: Is There a Connection? (C) 1028
- Self-Assembled Helicates of Zinc and Cadmium Cyanides, $[M_x(CN)_{2x+1}]^-$, $x \leq 27$ (C) 314
- The Lipophilically Wrapped Polyion Aggregate $\{[Ba_6Li_3O_2]^{11+}[^-OC(CH_3)_3]_{11}(OC_4H_8)_3\}$, a Face-Sharing (Octahedron + Prismane) $Ba_6Li_3O_2$ Polyhedron in a Hydrocarbon Ellipsoid: Preparation, Single Crystal Structure Analysis, and Density Functional Calculations (C) 1353

Deoxycarbohydrates
- Synthesis of dTDP-6-Deoxy-4-ketoglucose and Analogues with Native and Recombinant dTDP-Glucose-4,6-dehydratase (C) 1748

Deoxysugars
- Thymidine Diphospho-6-deoxy-α-D-*ribo*-3-hexulose Synthesis of a Central Intermediate in the Biosynthesis of Di- and Trideoxysugars (C) 1328

Dewar naphthalene
- 6,7-Bis(methoxycarbonyl)-2,3-dimethyl [5](1,4)naphthalenophane; the First Benzoannelated [5]Paracyclophane (C) 2553

Dialuminoxane
- Tetrakis[bis(trimethylsilyl)methyl]dialuminoxane with a Linear Al-O-Al Group (C) 989

Diazadiene complexes
- DAD Compounds of Niobium and Tantalum: Examples of the Structural Flexibility of DAD Ligands (C) 2649

Diazo compounds
- (*S*)-(+)- and (*R*)-(−)-1,5-Dimethyl-4-phenyl-1,5-dihydro-2*H*-pyrrol-2-ones by Carbene Ring Contraction and Decarboxylation of (2*R*,3*S*)-(−)- and (2*S*,3*R*)-(+)-6-Diazo-3,4-dimethyl-2-phenyloxazepane-5,7-diones (C) 78
- A Series of Well-Defined Metathesis Catalysts Synthesis of $[RuCl_2(=CHR')(PR_3)_2]$ and Its Reactions (C) 2039
- Diazo Chemistry I (B) 1653

Diborations
- Transition Metal Catalyzed Diboration of Vinylarenes (C) 1336

Di-*tert*-butyl dicarbonate
- Reactions of Neopentyl 2,2,-Trifluoroethanesulfonate (Neopentyl Tresylate) with Nucleophiles: A Model Study for the Coupling of Nucleophiles with Tresyl Agarose (C) 2495

Diels–Alder reactions
- A Cycloaddition–Cyclodehydrogenation Route from Stilbenoids to Extended Aromatic Hydrocarbons (C) 1583
- A Highly Symmetric Sixfold Cycloaddition Product of Fullerene C_{60} (C) 87
- An Yttrium-Based Strong Lewis Acid for the Heterogeneous Catalysis of the Diels–Alder Reaction (C) 2143
- C_2-Symmetric Cationic Copper(II) Complexes as Chiral Lewis Acids: Counterion Effects in the Enantioselective Diels–Alder Reaction** (C) 798
- Discrimination between Enantiotopic Groups in a Diels–Alder Reaction (C) 448
- First Synthesis of 2*H*-Azepine (C) 1469
- Free-Energy Profile for a Host-Accelerated Diels–Alder Reaction: The Sources of *exo* Selectivity (C) 217
- Synthesis, Chemical Trapping, and Dimerization of 3,7-Dimethyltricyclo-[3.3.0.$0^{3,7}$]oct-1(5)-ene: [2+2] Retrocycloaddition of the Cyclobutane Dimer (C) 912
- Total Synthesis of Natural (+)-SF 2315A and Determination of the Absolute Configuration (C) 2396
- Transition Metal Catalyzed Synthesis of Seven-Membered Carbocyclic Rings (H) 2223

Dienynes
- A Rhodium-Mediated, Stepwise Trimerization of an Alkyne That Does Not Lead to a Benzene but Selectively to a Hexadienyne Derivative (C) 191

Diffusion
- Rapid Water Diffusion in a Cage-Type Crystal Lattice: β-Cyclodextrin Dodecahydrate (C) 1452
- Self-Diffusion of Charged Polycyclic Systems and Their Parent Compounds: A PGSE NMR Study (C) 816

Digallanes
- Surprising Formation of a Carborane-Substituted Digallane (C) 332

Digitalis
- Digitalis Research in Berlin–Buch—Retrospective and Perspective Views (R) 282

Dihydroindenes
- Low-Temperature Tandem Enyne Allene Radical Cyclizations: Efficient Synthesis of 2,3-Dihydroindenes from Simple Enediynes (C) 2037

Dihydrooxazinones
- The Arndt–Eistert Reaction in Peptide Chemistry: A Facile Access to Homopeptides (C) 471

Dihydrooxazoles
- Chiral Phosphanodihydrooxazoles in Asymmetric Catalysis: Tungsten-Catalyzed Allylic Substitution (C) 462

Dihydroxylations
- Enantiospecific Syntheses of Valiolamine and Its (1*R*), (2*R*), (1*R*,2*R*) Diastereomers from (−)-Quinic Acid (C) 1643
- Ligand-Accelerated Catalysis (R) 1059

Dimerizations
- 1-Phenyl-1,2-cyclooctadiene Dimerizes in an Unusual Manner (C) 2730
- Synthesis of Belt Cyclophanes (C) 1437
- The Dimerization of (*E*)-1,3-Diphenyl-1,3-butadiene Proceeds Suprafacially with Respect to Both Components: Evidence for a Concerted [4+2] Cycloaddition (C) 895

Dioxygen complexes
- Novel Binuclear Cobalt Dioxygen Complex—A Step on the Path to Dioxygen Activation (C) 2051

Diphosphaallylic cations
- A Facile Access to $1\lambda^5,3\lambda^5$-Benzodiphospholes (C) 2017

Diphosphacyclopentenes
- Synthesis of 1,2-Diphospholide Ions (C) 590

Diphosphete derivatives
- Tetraphosphatricyclo[4.2.0.$0^{2,5}$]octadienes; New Phosphaalkyne Cyclotetramers Derived from $\lambda^3\sigma^2$-Diphosphetes (C) 484

Diphospholides
- Synthesis of 1,2-Diphospholide Ions (C) 590

Diradicaloids
- Conical Intersections and the Mechanism of Singlet Photoreactions (H) 549

Diradicals
- Estramycins: A New Diyl Precursor Family Derived from Estradiol (C) 1749
- 1-Phenyl-1,2-cyclooctadiene Dimerizes in an Unusual Manner (C) 2730
- The Dimerization of (*E*)-1,3-Diphenyl-1,3-butadiene Proceeds Suprafacially with Respect to Both Components: Evidence for a Concerted [4+2] Cycloaddition (C) 895

Disaccharide mimetics
- Disaccharide Mimetics by Enzymatic Tandem Aldol Additions (C) 1639

Distannenes
- Bis(hypersilyl)tin and Bis(hypersilyl)lead, Two Electron-Rich Carbene Homologs (C) 1334

Distellenes
- Synthesis of Rodlike Distellenes (C) 1001

DNA
- 1,5-Anhydrohexitol Nucleic Acids, a New Promising Antisense Construct (C) 1338 (2165)
- Platination Pathways for Reactions of Cisplatin with GG Single-Stranded and Double-Stranded Decanucleotides (C) 1874
- Triple-Helix Formation of Oligodeoxynucleotides Containing [(3′*S*,5′*R*)-2′-Deoxy-3′,5′-ethano-β-D-ribofuranosyl]nucleosides ("Bicyclo-deoxynucleosides") (C) 694

DNA-binding molecules
- DNA–Carbohydrate Recognition: Design and Synthesis of an Eight-Base Sequence-Specific DNA-Binding Oligosaccharide (C) 576

DNA cleavage
- Carbon–Hydrogen Bonds of DNA Sugar Units as Targets for Chemical Nucleases and Drugs (R) 746
- DNA–Carbohydrate Recognition: Design and Synthesis of an Eight-Base Sequence-Specific DNA-Binding Oligosaccharide (C) 576

DNA enzymes
- Synthetic Ribozymes and the First Deoxyribozyme (H) 1189

DNA oxidation
- *N*-Hydroxypyridinethiones as Photochemical Hydroxyl Radical Sources for Oxidative DNA Damage (C) 2156
- Photosensitized Formation of 8-Hydroxy-2′-deoxyguanosine in Salmon Testes DNA by Furocoumarin Hydroperoxides: A Novel, Intercalating "Photo-Fenton" Reagent for Oxidative DNA Damage (C) 107

DNA repair
- Sunlight-Damaged DNA Repaired with Sunlight (H) 2491

Donor functionalization
- Volatile Metal Alkoxides According to the Concept of Donor Functionalization (R) 2187

Donor–acceptor systems
- A Functionalized Polyoxometalate Bearing a Ferrocenylimido Ligand: Preparation and Structure of $[(FcN)Mo_6O_{18}]^{2-}$ (C) 2547

Drugs
- A Chiral Cyanohydrin Phosphate for Carbonyl Umpolung—Stereoselective Synthesis of Tertiary Cyanohydrins (C) 917
- Digitalis Research in Berlin–Buch—Retrospective and Perspective Views (R) 282
- Disulfide-Reductase Inhibitors as Chemotherapeutic Agents: The Design of Drugs for Trypanosomiasis and Malaria (R) 141
- Endotoxin Antagonists: Possible Candidates for the Treatment of Gram-Negative Sepsis (H) 2000
- New Fluorescent Water-Soluble Taxol Derivatives (C) 2710
- Three-Dimensional Chemical Similarity Searching (B) 359

Dyes
- Bis(dicyanomethylene) and Bis(cyanoimino) Derivatives of Indigo and Thioindigo (C) 464
- Deformation of Polymethine Structures by Intermolecular Interactions (C) 690
- Novel Porphyrinoids for Chemistry and Medicine by Biomimetic Syntheses (R) 1795
- Quaterrylenebis(dicarboximides) (C) 1323

Dynemicins
- Synthesis of a Dynemicin A Analogue and Its Bergman-Type Cycloaromatization (C) 1345
- Total Synthesis of (±)-Dynemicin A (C) 1721

Electrochemistry
- A New Method for the Preparation of Nanostructured Metal Clusters (C) 2240
- A Redox-Switchable Hemilabile Ligand: Electrochemical Control of the Coordination Environment of a Rh^I Complex (C) 1624
- Diastereoselective Cathodic Cyclization of 1-(4- and 1-(3-Oxoalkyl)pyridinium Salts to Quinolizidine and Indolizidine Derivatives (C) 2007
- Electrochemical Evidence for Through-Space Orbital Interactions in Spiromethanofullerenes (C) 1591
- Electrochemical Synthesis of a Redox-Active Polymer Based on Buckminsterfullerene Epoxide (C) 194
- Electrochemistry and Ab Initio Study of the Dimetallofullerene $La_2@C_{80}$ (C) 1094
- Incorporation of Membrane Proteins in Solid-Supported Lipid Layers (C) 2056
- Modern Electroorganic Chemistry (B) 1521
- Photoswitchable Electrical Communication of Glucose Oxidase and Glutathione Reductase with Electrode Surfaces through Photoisomerizable Redox Mediators (C) 1604
- Radical Cation [4+2] Cycloadditions with 2-Vinylindoles (C) 1900
- Routes to Dendritic Networks: Bis-Dendrimers by Coupling of Cascade Macromolecules through Metal Centers (C) 2023
- Water-Soluble Dendritic Iron Porphyrins: Synthetic Models of Globular Heme Proteins (C) 2725

Electrocyclic reactions
- A Remarkable Effect of Silyl Substitution on Electrocyclization of Vinylallenes (C) 1476

Electron-deficient compounds
- Diborylcarbenes as Reactive Intermediates in Double 1,2-Rearrangements with Low Activation Enthalpies (C) 1340
- The First Mixed-Metal Borole Cluster; Stabilization of Formally 14e Pd Centers in the Re_2Pd_2 Electron-Deficient $[\{[(\eta^5\text{-}C_4H_4BPh)(CO)_3Re]Pd\}_2]$ Cluster (C) 1010

Electron diffraction
- Bis(trifluoromethyl)trioxide: First Structure of a Straight-Chain Trioxide (C) 2244
- Hexakis(trifluoromethyl)tetrazane (C) 586

Electronic energy transfer
- Electronic Energy Transfer Across Ethynyl-Bridged Ru^{II}/Os^{II} Terpyridyl Complexes (C) 1100

Electronic structure
- A P_2C_2 Four-Membered Ring with Unusual Bonding—Synthesis, Structure, and Ring Opening of a 1,3-Diphosphacyclobutane-2,4-diyl (C) 555
- A Stable Aquairon(III) Complex with $S = 1$: Structure and Spectroscopic Properties (C) 1216 (1649)
- Distinguishing Copper d^8 and d^{10} Configurations in a Highly Ionic Complex; A Nonformal Metal Oxidation State (C) 986
- Elusiveness of Cu^{III} Complexation; Preference for Trifluoromethyl Oxidation in the Formation of $[Cu^I(CF_3)_4]^-$ Salts (C) 80
- Formal Oxidation State versus Partial Charge—A Comment (C) 986
- Structure Determination from Powder X-Ray Diffraction Data of a Hydrogen-Bonded Molecular Solid with Competing Ferromagnetic and Antiferromagnetic Interactions: The 2-(3,4-Dihydroxyphenyl)-α-Nitronyl Nitroxide Radical (C) 55

Electron localization
- Hyperbolic Lone Pair Structure in $RhBi_4$ (C) 1204
- μ-Nitridodiiron Complexes with Asymmetric $[Fe^{IV}\equiv N-Fe^{III}]^{4+}$ and Symmetric $[Fe^{IV}=N=Fe^{IV}]^{5+}$ Structural Elements (C) 669
- The Stabilization of the Rb^- Ion in $Na_{16}Rb_7Sb_7 = Na_{16}(RbRb_6)Sb_7$ (C) 103

Electron polarization
- Deformation of Polymethine Structures by Intermolecular Interactions (C) 690

Electron transfer
- A New Dimension in Radical Chain Group Transfer Reaction by Photosensitized Electron Transfer (PET) Reductive Activation of $PhSeSiR_3$ (C) 2669
- Catalytic Photoinduced Charge-Transfer Osmylation: A Novel Pathway from Arenes to Cyclitol Derivatives (C) 2031
- Direct Electrochemical Coupling of Components of the Biological Electron Transfer Chain to Modified Surfaces: Molecular Recognition between Cytochrome c Peroxidase and Cytochrome c (C) 2409
- Effective Charge Separation in Intermolecular Complexes of an Electron Donor and a Doubly Branched Triad Assembly: A Model System for Environmental Effects Controlling Electron Transfer (C) 1005
- Electron Transfer and Polar Reactions of Cyclizable Anion Radicals: Structural Consequences of Orbital Selection Rules and Chain-Length Constraints (C) 1495
- Electron Transfer through DNA: Site-Specific Modification of Duplex DNA with Ruthenium Donors and Acceptors (C) 352
- Fundamentals of Photoinduced Electron Transfer (B) 495
- Luminescence Stimulated by Electron Transfer: Fluorescent Donor/Acceptor-Substituted Stilbenes Containing Pyrenoid and Heteroaromatic Subunits (C) 2664
- Model Reactions for Photosynthesis—Photoinduced Charge and Energy Transfer between Covalently Linked Porphyrin and Quinone Units (R) 849
- New Fluorescent Model Compounds for the Study of Photoinduced Electron Transfer: The Influence of a Molecular Electric Field in the Excited State (C) 1728
- Photoinduced Valence Tautomerism in Cobalt Complexes Containing Semiquinone Anion as Ligand: Dynamics of the High-Spin $[Co^{II}(3,5\text{-dtbsq})_2]$ to Low-Spin $[Co^{III}(3,5\text{-dtbsq})(3,5\text{-dtbcat})]$ Interconversion (C) 1481
- Radical Additions of Activated Haloalkanes to Alkenes Initiated by Electron Transfer from Copper in Solvent-Free Systems (C) 902
- Radical Cation [4+2] Cycloadditions with 2-Vinylindoles (C) 1900
- Reactions of Carbocations with π Nucleophiles: Polar Mechanism and No Outer Sphere Electron Transfer Processes (C) 1225
- Redox Mechanisms in Inorganic Chemistry (B) 1249
- Sunlight-Damaged DNA Repaired with Sunlight (H) 2491
- Towards the Development of Molecular Wires: Electron Localization, Exchange, and Transfer in Alkyne-Bridged Multinuclear Complexes (C) 2705

Electrophilic additions
- New Findings in the Electrophilic Addition of Halogens to Olefins (H) 51
- Reactions of Carbocations with π Nucleophiles: Polar Mechanism and No Outer Sphere Electron Transfer Processes (C) 1225

Electrophilic substitutions
- A Camouflaged Icosahedral Carborane: Dodecamethyl-1,12-dicarbo-*closo*-dodecaborane(12) and Related Compounds (C) 1332
- Lithium Intermediates during the α-Lithiation and Subsequent α-Substitution of Heterocyclic Amines in the Presence of CO_2 (C) 921

Electrostatic interactions
- Antibody-Catalyzed Phosphate Triester Hydrolysis (C) 2275
- Burial of Hydrocarbon Causes Cooperative Enhancement of Electrostatic Binding (C) 1483

Electrostriction
- Fluxionality Induced by High Pressure: [9-D]9-Homocubyl Triflate, a Pressure-Sensing Molecule (C) 2030

Element 110
- Two at One Blow: The New Chemical Elements 110 and 111 (H) 1713

Element 111
- Two at One Blow: The New Chemical Elements 110 and 111 (H) 1713

Eliminations
- Peripherally Substituted Cobaloximes; X-Ray Crystal Structure Analysis of σ-Hexylbis[1,8-di(*N*-morpholino)octane-4,5-dioximato]pyridinecobalt(III) (C) 2389

Enantiomeric resolution
- First Dynamic Kinetic Resolution of Racemic α-Amino Aldehydes (C) 1023

- Molecular Imprinting in Cross-Linked Materials with the Aid of Molecular Templates—A Way towards Artificial Antibodies (R) 1812
- Reactions of Hexa-*tert*-butylcyclotrigermane: Isolation of an Enantiomerically Pure 1,3-Diiodotrigermane (C) 1085

Encyclopedia
- Biographical Encyclopedia of Scientists (B) 2167
- Kirk/Othmer Encyclopedia of Chemical Technology (B) 2564
- The Biographical Dictionary of Scientists (B) 2168

Endotoxins
- Endotoxin Antagonists: Possible Candidates for the Treatment of Gram-Negative Sepsis (H) 2000

Enediols
- First Isolation of an Enol of a Carboxylic Acid by Complexation to an (Ethane-1,2-diamine)platinum(II) Fragment (C) 1103

Enediynes
- Activation of Macrocyclic Biaryl-Enediynes by Metal Ion Coordination (C) 2538
- Carbon–Hydrogen Bonds of DNA Sugar Units as Targets for Chemical Nucleases and Drugs (R) 746
- Estramycins: A New Diyl Precursor Family Derived from Estradiol (C) 1749
- Lactendiynes: A New Class of Triggered Cyclic Enediynes (C) 2393
- Synthesis of a Dynemicin A Analogue and Its Bergman-Type Cycloaromatization (C) 1345
- Synthesis of New Sworski-Type Dehydroannulenes: 3,4-Benz-1,2,5,6,8,9,12,13-octadehydro[14]annulenes (C) 1892
- Total Synthesis of (±)-Dynemicin A (C) 1721

Energy transfer
- Electronic Energy Transfer in a Supramolecular Species Containing the $[Ru(bpy)_3]^{2+}$, $[Os(bpy)_3]^{2+}$, and Anthracene Chromophoric Units (C) 595
- Model Reactions for Photosynthesis—Photoinduced Charge and Energy Transfer between Covalently Linked Porphyrin and Quinone Units (R) 849
- Sunlight-Damaged DNA Repaired with Sunlight (H) 2491

Enolates
- Crystal Structure of Dilithioacetylacetone: A Twenty-Four Vertex Li-O Cage Molecule with Limited Li–C(terminal) Bonding and Selective THF Solvation (C) 1233
- Synthesis and Characterization of the First Mixed Alkali Metal Enolate Containing Amine Ligands: A Novel "Open-Stack" Structure and its Implications for Aldol Addition (C) 1117
- Synthesis of Chiral γ,δ-Unsaturated Amino Acids by Asymmetric Ester Enolate Claisen Rearrangement (C) 2012

Enones
- Acyclic 1,4-Diastereoselectivity in γ-Substituted α-Enones: Transmission of Chiral Information through Conjugation (C) 2254

Enyne allenes
- Low-Temperature Tandem Enyne Allene Radical Cyclizations: Efficient Synthesis of 2,3-Dihydroindenes from Simple Enediynes (C) 2037

Enzymatic catalysis
- A Highly Reactive and Catalytically Active Model System for Intradiol-Cleaving Catechol Dioxygenases: Structure and Reactivity of Iron(III) Catecholate Complexes of *N,N'*-Dimethyl-2,11-diaza[3,3](2,6)pyridinophane (C) 2671
- A Multienzyme System for a One-Pot Synthesis of Sialyl T-Antigen (C) 893
- Efficient Heterogeneous Biocatalysts by Entrapment of Lipases in Hydrophobic Sol–Gel Materials (C) 301
- Evidence for a Mechanism Involving Transient Fragmentation in Carbon Skeleton Rearrangements Dependent on Coenzyme B_{12} (C) 2398
- The Role of Dehydroalanine in Catalysis by Histidine Ammonia Lyase (C) 1464

Enzyme inhibitors
- Design of Novel, Nonpeptidic Thrombin Inhibitors and Structure of a Thrombin–Inhibitor Complex (C) 1739
- Disulfide-Reductase Inhibitors as Chemotherapeutic Agents: The Design of Drugs for Trypanosomiasis and Malaria (R) 141
- Optimization of the Biological Activity of Combinatorial Compound Libraries by a Genetic Algorithm (C) 2280

Enzyme mechanisms
- On the Mechanism of Action of Urocanase: Observation of the Enzyme-Bound NAD^+–Inhibitor Adduct by ^{13}C NMR Spectroscopy (C) 652

Enzyme mimetics
- "Fast Amide Cleavage" or Reproducible, Concentration- and Time-Dependent Aggregation of Anionic and Cationic Surfactants? (C) 2718
- Zeolite Encaged Cu(Histidine) Complexes as a Mimic of Natural Cu Enzymes (C) 2652

Enzyme models
- Acceleration of a Phosphate Diester Transesterification Reaction by Bis(alkylguanidinium) Receptors Containing an Appended General Base (C) 1237
- A Phycocyanobilin Seryliminoester as a New Model for the Chromophore–Protein Interaction in Phytochrome (C) 1733
- Formation of an Alkylperoxoiron(III) Complex during Oxidations Catalyzed by μ-Oxodiiron(III) Complexes (C) 203
- Free-Energy Profile for a Host-Accelerated Diels–Alder Reaction: The Sources of *exo* Selectivity (C) 217
- Hydrolysis of a Phosphate Diester Doubly Coordinated to a Dinuclear Cobalt(III) Complex: A Novel Mechanism (C) 2412

Enzymes
- A Dinuclear (μ-Carboxylato)manganese(II) Complex Derived from a Macrocyclic Ligand: A Structural Model for Active Sites in Natural Systems (C) 2535
- Chemoenzymatic Synthesis of a Modified Pentasaccharide as a Specific Substrate for a Sensitive Assay of α-Amylase by Fluorescence Quenching (C) 1239
- Enzymes in Organic Synthesis: Application to the Problems of Carbohydrate Recognition (Part 1) (R) 412
- Enzymes in Organic Synthesis: Application to the Problems of Carbohydrate Recognition (Part 2) (R) 521
- Enzymes in Synthetic Organic Chemistry (B) 1523
- Incorporation of Membrane Proteins in Solid-Supported Lipid Layers (C) 2056
- On the Mechanism of Catalysis by a Metal-Free Hydrogenase from Methanogenic Archaea: Enzymatic Transformation of H_2 without a Metal and Its Analogy to the Chemistry of Alkanes in Superacidic Solution (C) 2247
- Photoswitchable Electrical Communication of Glucose Oxidase and Glutathione Reductase with Electrode Surfaces through Photoisomerizable Redox Mediators (C) 1604
- Synthesis of dTDP-6-Deoxy-4-ketoglucose and Analogues with Native and Recombinant dTDP-Glucose-4,6-dehydratase (C) 1748
- Synthesis of the Palmitoylated and Farnesylated C-Terminal Lipohexapeptide of the Human N-*Ras* Protein by Employing an Enzymatically Removable Urethane Protecting Group (C) 2259

Ephedrine
- (*S*)-(+)- and (*R*)-(−)-1,5-Dimethyl-4-phenyl-1,5-dihydro-2*H*-pyrrol-2-ones by Carbene Ring Contraction and Decarboxylation of (2*R*,3*S*)-(−)- and (2*S*,3*R*)-(+)-6-Diazo-3,4-dimethyl-2-phenyloxazepane-5,7-diones (C) 78

Epoxidations
- Ligand-Accelerated Catalysis (R) 1059
- Novel Structures from Tris(benzocyclobutadieno)cyclohexatriene: Triscyclopropanation and Trisoxacyclopropanation to the First [2.1.2.1.2.1]Hexaannulanes (C) 563
- The First Olefin-Substituted Peroxomolybdenum Complex: Insight into a New Mechanism for the Molybdenum-Catalyzed Epoxidation of Olefins (C) 1737

EPR spectroscopy
- A New Type of Trinuclear Oxoiron(III) Cluster (C) 205
- 4c/3e Radical Cations with Cage-Directed Configurations (C) 1016
- Characterization of an Oxo(porphyrinato)manganese(IV) Complex by X-ray Absorption Spectroscopy (C) 343
- Novel Biological Copper Proteins through Anion Addition to the Mutant Met121Gly of *Pseudomonas aeruginosa* Azurin (C) 1622
- Principles of Electron Spin Resonance (B) 1033

Estrogens
- Estramycins: A New Diyl Precursor Family Derived from Estradiol (C) 1749

Ethane
- Coupling of Endothermic Thermal Cracking with Exothermic Oxidative Dehydrogenation of Ethane to Ethylene Using a Diluted SrO/La_2O_3 Catalyst (C) 665

Ethylene
- Coupling of Endothermic Thermal Cracking with Exothermic Oxidative Dehydrogenation of Ethane to Ethylene Using a Diluted SrO/La_2O_3 Catalyst (C) 665

Evaporative cooling
- Aligning and Trapping Molecules with Light (H) 2365

EXAFS spectroscopy
- Characterization of an Oxo(porphyrinato)manganese(IV) Complex by X-ray Absorption Spectroscopy (C) 343
- The Dinuclear Cu_A Center in Cytochrome *c* Oxidase and N_2O Reductase—A Metal–Metal Bond in Biology? (H) 771

Ferrocenyl ligands
- Strong Electronic Effects on Enantioselectivity in Rhodium-Catalyzed Hydroborations with Novel Pyrazole-Containing Ferrocenyl Ligands (C) 931

Filipin
- Relative and Absolute Configuration of Filipin III (C) 1227

Five-coordinate carbon
- Competing Pathways in the Reaction of Bis(pentafluorophenyl)borane with Bis(η^5-cyclopentadienyl)dimethylzirconium: Methane Elimination versus Methyl–Hydride Exchange and an Example of Pentacoordinate Carbon (C) 1230

Flash pyrolysis
- Silacyclopropene: Generation by High-Vacuum Flash Pyrolysis and Matrix-Spectroscopic Identification (C) 1439

Fluorescence
- Chemoenzymatic Synthesis of a Modified Pentasaccharide as a Specific Substrate for a Sensitive Assay of α-Amylase by Fluorescence Quenching (C) 1239
- Photonic Molecular Devices: Reversibly Photoswitchable Fluorophores for Nondestructive Readout for Optical Memory (C) 1119
- Tetracarboxylic Bisimide–Lactam Ring Contraction: A Novel Type of Rearrangement (C) 2234

Fluorescence markers
- New Fluorescent Water-Soluble Taxol Derivatives (C) 2710

Fluorescence quenching
- New Fluorescent Model Compounds for the Study of Photoinduced Electron Transfer: The Influence of a Molecular Electric Field in the Excited State (C) 1728

Fluorescence spectroscopy
- Direct Spectroscopic Evidence for a Hitherto Elusive "Zwitterionic" Excited State (H) 547

Fluorescent sensors
- Complexes from Polyazacyclophanes, Fluorescence Indicators, and Metal Cations—An Example of Allosterism through Ring Contraction (C) 321
- Metal-Induced Dispersion of Lipid Aggregates: A Simple, Selective, and Sensitive Fluorescent Metal Ion Sensor (C) 905

Fluorine compounds
- $(C_5Me_5)TiF_2$—A Versatile Building Block for Generating Large Soluble Dimetallic Aggregates (C) 1872
- Fluorocarbonate, $[FCO_2]^-$: Preparation and Structure (C) 1858
- Fluorophosphazenate Ions: A Route to Complexation of Fluoride Ions (C) 2696
- Polar Interactions between Stacked π Systems in Fluorinated 1,8-Diarylnaphthalenes: Importance of Quadrupole Moments in Molecular Recognition (C) 1019
- The Synthesis of Tris(perfluoroalkyl)-phosphanes (C) 1241
- $XeOF_5^-$, an Anion with Pentagonal-Pyramidal Structure (C) 1586

Fluoroarenes
- A New Quantitative Description of the Distance Dependence of Through-Space $^{19}F,^{19}F$ Spin–Spin Coupling (C) 1881
- Single-Crystal X-Ray Structure of the Metastable Aryne Precursor Tetrafluorophenyllithium and of 1,2,3,4-Tetrafluorobenzene (C) 1517

Fluorocarbonate
- Fluorocarbonate, $[FCO_2]^-$: Preparation and Structure (C) 1858

Fluorohydrocarbons
- Carbon–Carbon Bond Cleavage with Inversion of Configuration: Conversion of (*R*)-(+)-1-Methoxytetrafluoropropionic Acid to (*S*)-(−)-1,2,2,2-Tetrafluoroethyl Methyl Ether (C) 222
- Gas-Phase Activation of Fluorocarbons by "Bare" and "Coordinated" Praseodymium Cations (C) 213

Fluvirucin
- Catalytic Ring-Closing Metathesis: A New, Powerful Technique for Carbon–Carbon Coupling in Organic Synthesis (H) 1833

Fluxionality
- Fluxionality Induced by High Pressure: [9-D]9-Homocubyl Triflate, a Pressure-Sensing Molecule (C) 2030

Formic acid
- Carbon Dioxide as a Raw Material: The Synthesis of Formic Acid and Its Derivatives from CO_2 (R) 2207

Formyl anion equivalent
- Crystal Structure of the Dimeric (4-*tert*-Butylthiazolato)(glyme)lithium: Carbene Character of a Formyl Anion Equivalent (C) 487

Four-component reactions
- Stereoselective Syntheses of Peptide Derivatives with 2-Acetamido-3,4,6-tri-*O*-acetyl-1-amino-2-deoxy-β-D-glucopyranose by Four-Component Condensation (C) 1104

Fraud in science
- Der große Schwindel (B) 1370

Fullerenes
- A Highly Symmetric Sixfold Cycloaddition Product of Fullerene C_{60} (C) 87
- $C_{59}N^+$ and $C_{69}N^+$: Isoelectronic Heteroanalogues of C_{60} and C_{70} (C) 2257
- Dilithium Acepentalenediide: An Unusual Dimer of Contact Ion Triplets with Bowl-Shaped Dianions (C) 1492
- Electrochemical Evidence for Through-Space Orbital Interactions in Spiromethanofullerenes (C) 1591
- Electrochemical Synthesis of a Redox-Active Polymer Based on Buckminsterfullerene Epoxide (C) 194
- Filled Buckyballs: Recent Developments from the Endohedral Metallofullerenes of Lanthanides (H) 981
- Fullerene – die Bucky-Balls erobern die Chemie (B) 1769
- Fullerene Model Compounds: Bowl-Shaped Aromatic Hydrocarbons and Cyclophane-Based Cage Molecules (H) 1429
- Reversible Template-Directed Activation of Equatorial Double Bonds of the Fullerene Framework: Regioselective Direct Synthesis, Crystal Structure, and Aromatic Properties of T_h-$C_{66}(COOEt)_{12}$ (C) 1607
- Ring Expansion of the Fullerene Core by Highly Regioselective Formation of Diazafulleroids (C) 1343
- Solubilized Derivatives of C_{195} and C_{260}: The First Members of a New Class of Carbon Allotropes $C_{n(60+5)}$ (C) 1466
- Synthesis of the First Adducts of the Dimetallofullerenes $La_2@C_{80}$ and $Sc_2@C_{84}$ by Addition of a Disilirane (C) 2139
- The Chemistry of the Fullerenes (B) 1904
- The Colors of C_{60} Solutions (C) 105
- The Most Beautiful Molecule. An Adventure in Chemistry (B) 1769

Fulvalenes
- A Novel Chainlike Heteropolyanion Formed by Keggin Units: Synthesis and Structure of $(ET)_{8n}[PMnW_{11}O_{39}]_n \cdot 2nH_2O$ (C) 1460

Fungicides
- 9-Methoxystrobilurins—A Link Between Strobilurins and Oudemansins (C) 196

Furans
- Transition Metal Catalyzed Dimerization of Allenyl Ketones (C) 1581

Furocoumarins
- Photosensitized Formation of 8-Hydroxy-2′-deoxyguanosine in Salmon Testes DNA by Furocoumarin Hydroperoxides: A Novel, Intercalating "Photo-Fenton" Reagent for Oxidative DNA Damage (C) 107

β-Galactosidase
- A Multienzyme System for a One-Pot Synthesis of Sialyl T-Antigen (C) 893

Gallium compounds
- A Framework Containing Ga-O-Ga Links: The Synthesis and Structure of Gallobicchulite $Ca_8(Ga_2SiO_6)_4(OH)_8$ (C) 2414
- Aromatic Gallium Heterocycles: Synthesis of the First Gallatabenzene (C) 1357
- Five-Membered Aromatic and Anti-aromatic Rings with Gallium, Germanium, and Bismuth Centers: A Short March through the Periodic Table (H) 295
- Galloxane and Alumoxane Hydroxides: $[Ga_{12}tBu_{12}(\mu_3\text{-}O)_8(\mu\text{-}O)_2(\mu\text{-}OH)_4]$ and $[Al_6tBu_6(\mu_3\text{-}O)_4(\mu\text{-}OH)_4]$ (C) 1201
- New Tellurometalates of Gallium and Indium: $K[K([18]crown\text{-}6)]_2[GaTe_3] \cdot 2CH_3CN$ and $[(NEt_4)_5][In_3Te_7] \cdot 0.5\,Et_2O$ (C) 1879
- $(Sr_6N)[Ga_5]$ and $(Ba_6N)[Ga_5]$: Compounds with Discrete (M_6N) Octahedra and $[Ga_5]$ Clusters (C) 1761
- Surprising Formation of a Carborane-Substituted Digallane (C) 332
- Synthesis and Structural Characterization of a Stereospecific Dinuclear Gallium Triple Helix: Use of the *trans*-Influence in Metal-Assisted Self-Assembly (C) 996

Gas-phase chemistry
- C–H and C–C Bond Activation by Bare Transition-Metal Oxide Cations in the Gas Phase (R) 1973
- The Crafts–Friedel Reaction: Aromatic Alkylation within the Complex Formed upon Addition of a Gaseous Arenium Ion to an Olefin (C) 1589
- $[R_3Si-arene]^+$ σ Complexes in the Gas Phase (C) 654

Gels
- X-Ray Structure of a Self-Assembled Gelating Fiber (C) 585

Gene technology
- Combinatorial Biosynthesis—An Approach in the Near Future? (H) 881
- Introduction to Molecular Cloning Techniques (B) 697
- Novel Genetically Engineered Tetracenomycins (C) 1107

Genetic algorithm
- Optimization of the Biological Activity of Combinatorial Compound Libraries by a Genetic Algorithm (C) 2280

Geometrical reaction control
- Control of the Reactivity of Double Bonds through Their Fixed Geometrical Arrangement (H) 2225

Germacyclopentadienide
- Synthesis and Structure of a Free Germacyclopentadienide Ion: $[Li([12]crown\text{-}4)_2][C_4Me_4GeSi(SiMe_3)_3]$ (C) 1887

Germanium compounds
- Five-Membered Aromatic and Anti-aromatic Rings with Gallium, Germanium, and Bismuth Centers: A Short March through the Periodic Table (H) 295
- Reactions of Hexa-*tert*-butylcyclotrigermane: Isolation of an Enantiomerically Pure 1,3-Diiodotrigermane (C) 1085

Glyceraldehyde
- Glc-PC, a New Type of Glucosidic Phospholipid (C) 2667

Glycolipids
- The Macrolidic Glycolipid Calonyctin A, a Plant Growth Regulator: Synthesis, Structural Assignment, and Conformational Analysis in Micellar Solution (C) 2520
Glycopeptides
- A Novel Allylic Anchor for Solid-Phase Synthesis: Synthesis of Protected and Unprotected O-Glycosylated Mucin-Type Glycopeptides (C) 803
- A Versatile Solid-Phase Synthesis of N-Linked Glycopeptides (C) 60
- Synthesis of an RGD-Sialyl-Lewis^X Glycoconjugate: A New Highly Active Ligand for P-Selectin (C) 990
Glycoproteins
- Palladacycles as Structurally Defined Catalysts for the Heck Olefination of Chloro- and Bromoarenes (C) 1844
Glycosidations
- Glc-PC, a New Type of Glucosidic Phospholipid (C) 2667
Glycoside syntheses
- The Macrolidic Glycolipid Calonyctin A, a Plant Growth Regulator: Synthesis, Structural Assignment, and Conformational Analysis in Micellar Solution (C) 2520
Glycosylated amino acids
- Stereoselective Syntheses of Retro-Isomers of *N*-Glucoasparagine (C) 2026
Glycosylations
- A Strategy of "Random Glycosylation" for the Production of Oligosaccharide Libraries (C) 2720
Glycosyl fluorides
- Progress in Oligosaccharide Synthesis through a New, Orthogonal Glycosylation Strategy (H) 1432
Gold compounds
- A Gold(I) [2]Catenane (C) 1894
- First Steps Towards Ordered Monolayers of Ligand-Stabilized Gold Clusters (C) 1442
- Gold in Chains: Self-Assembly of a Gold(I) Catenane (H) 2107
- Six Interpenetrating Quartz-Like Nets in the Structure of $ZnAu_2(CN)_4$ (C) 1203
- Transition Metal Catalyzed Diboration of Vinylarenes (C) 1336
G proteins
- G Proteins and Regulation of Adenylate Cyclase (Nobel Lecture) (R) 1406
- Signal Transduction: Evolution of an Idea (Nobel Lecture) (R) 1420
Graft polymers
- Architectural Control in "Living" Free Radical Polymerizations: Preparation of Star and Graft Polymers (C) 1456
Graphitic sections
- A Cycloaddition–Cyclodehydrogenation Route from Stilbenoids to Extended Aromatic Hydrocarbons (C) 1583
Grignard compounds
- Silicon Analogues of Grignard Compounds: Synthesis and Structure of Amine-Stabilized Trimethylsilylmagnesium Halides (C) 1030
Group theory
- Group Theory in Chemistry and Spectroscopy. A Simple Guide to Advanced Usage (B) 1772
Guanidines
- Acceleration of a Phosphate Diester Transesterification Reaction by Bis(alkylguanidinium) Receptors Containing an Appended General Base (C) 1237

H/D exchange
- Rapid Water Diffusion in a Cage-Type Crystal Lattice: β-Cyclodextrin Dodecahydrate (C) 1452
Haber, Fritz
- Fritz Haber—Chemiker, Nobelpreisträger, Deutscher, Jude (B) 119
Hafnium compounds
- Selective Syntheses of 1,3-Diphosphacyclobutadiene, Dewar-1,3,5-triphosphabenzene, 1,3,5-Triphosphabenzene, and 1,3,5,7-Tetraphosphabarrelene by Cyclooligomerization of Phosphaalkynes (C) 2227
Halogen compounds
- $CsPr_9NbBr_{15}N_6$: A New Type of Interstitially Stabilized Cluster Compound (C) 2262
- LaI: An Unprecedented Binary Rare Earth Metal Monohalide with a NiAs-Type Structure (C) 233
- Stable 1:1 Adducts from Iodoacetylenes and Iodide Ions: Ion Pair Strain as an Additional Driving Force? (C) 441
- The Consequences of an Electrostatic "Forced Marriage" between Two Electron-Rich Particles: Strained Ion Pairs (C) 439
Hammerhead ribozymes
- The Three-Dimensional Structure of Hammerhead Ribozymes (H) 643
Haptotropic rearrangements
- Additions of Carbanions to a Cationic Cyclopentadienyl(naphthalene)iron Complex (C) 2161
Hazardous chemicals
- Destruction of Hazardous Chemicals in the Laboratory (B) 1037
H_2 complexes
- Structure and Bonding of Transition Metal Dihydrogen Complexes $[M(CO)_5(H_2)]$ (M = Cr, Mo, W) (C) 354
Heck reactions
- A Novel Intramolecular Heck Reaction: Synthesis of a Cholesterol–Baccatin III Hybrid (C) 452
- A Total Synthesis of Taxol (C) 1723
- Efficient Total Synthesis of the Pharmacophore of the Anticancer Antibiotic CC-1065 by Zirconocene- and Palladium-Initiated Cyclizations (C) 1366
- Metal Complexes of N-Heterocyclic Carbenes—A New Structural Principle for Catalysts in Homogeneous Catalysis (C) 2371
- Palladacycles as Efficient Catalysts for Aryl Coupling Reactions (C) 1848
- Palladium-Catalyzed Amination of Aryl Halides—Catalysts on New Routes to Known Targets (H) 1316
Helical structures
- A Highly Stereoselective Optical Switching Process Based on Donor–Acceptor Substituted Dissymmetric Alkenes (C) 348
- Double Helical Dinuclear Copper(I) Complexes of Macrocyclic Bis(dithiadiimine) Ligands (C) 1883
- Formation of the First Isomeric [2]Catenates by Self-Assembly about Two Different Metal Ions (C) 582
- Self-Assembled Helicates of Zinc and Cadmium Cyanides, $[M_x(CN)_{2x+1}]^-$, $x \leq 27$ (C) 314
- Stereoselective Synthesis of Chiral Zirconocenes from Doubly Substituted, Donor Functionalized Cyclopentadienes via Helical Chelate Complexes (C) 2266
- Synthesis and Structural Characterization of a Stereospecific Dinuclear Gallium Triple Helix: Use of the *trans*-Influence in Metal-Assisted Self-Assembly (C) 996
Heme-protein mimics
- Water-Soluble Dendritic Iron Porphyrins: Synthetic Models of Globular Heme Proteins (C) 2725
Hemerythrin
- A Model of Semimet Hemerythrin: NMR Spectroscopic Evidence of Valence Localization in Bis(μ-carboxylato)(μ-phenolato)diiron(II,III) in Solution (C) 588
- The First μ(OH)-Bridged Model Complex for the Mixed-Valent $Fe^{II}Fe^{III}$ Form of Hemerythrin (C) 2642
Hemiesters
- Highly Enantioselective Opening of Cyclic *meso*-Anhydrides to Isopropyl Hemiesters with Diisopropoxytitanium TADDOLates (C) 2395
Heptonamides
- Stereoselective Syntheses of Retro-Isomers of *N*-Glucoasparagine (C) 2026
Heteroallyl anions
- A Simple Route to the 1-Aza-3-Phosphaallyl System: Structure of a Dimeric Lithium Complex and Protonation To Give the First NH_2-Substituted Phosphaalkene (C) 2369
Heteroarenes
- A μ-η^6:η^6-1,3,5-Triboratabenzenebis(cyclopentadienylcobalt) Triple-Decker Complex (C) 681
- 2,4-Di-*tert*-butyl-1λ^3,3λ^3-diphosphinines: Targeted Synthesis at Iron(0) Centers and Oxidative Release (C) 198
Heterobutadienes
- The First Distibabutadiene: Synthesis and Structure of *trans*-1,4-Bis(trimethylsiloxy)-1,4-bis(2,4,6-tri-*tert*-butylphenyl)-2,3-distibabutadiene (C) 492
Heterocubanes
- A Nickel(II) Azide Cubane: Characterization of the Magnetic Exchange Interactions Mediated by a Triply Bridging Azide Group Bound End-On (C) 889
- Phosphorane Iminato Complexes of Manganese and Cobalt with Heterocubane Structure (C) 1235
Heterocycles
- (*S*)-(+)- and (*R*)-(−)-1,5-Dimethyl-4-phenyl-1,5-dihydro-2*H*-pyrrol-2-ones by Carbene Ring Contraction and Decarboxylation of (2*R*,3*S*)-(−)- and (2*S*,3*R*)-(+)-6-Diazo-3,4-dimethyl-2-phenyloxazepane-5,7-diones (C) 78
- A Comparison of Enthalpies of Formation in Solution and Enthalpies for HPLC Retention for Hydrogen-Bonded Host–Guest Complexes (C) 2404
- A New Method for the Synthesis of Amphipolar Phosphorus-Containing Heterocycles (C) 557
- Aromatic Gallium Heterocycles: Synthesis of the First Gallatabenzene (C) 1357
- Aromaticity and Antiaromaticity in Five-Membered C_4H_4X Ring Systems: "Classical" and "Magnetic" Concepts May Not Be "Orthogonal" (C) 337
- A $Te_2N_6Li_4$ Cage Containing the Tris(*tert*-butylimido)tellurite Dianion (C) 2549
- Diastereoselective Cathodic Cyclization of 1-(4- and 1-(3-Oxoalkyl)pyridinium Salts to Quinolizidine and Indolizidine Derivatives (C) 2007
- First Synthesis of 2*H*-Azepine (C) 1469
- Fluorophosphazenate Ions: A Route to Complexation of Fluoride Ions (C) 2696
- Lithium Intermediates during the α-Lithiation and Subsequent α-Substitution of Heterocyclic Amines in the Presence of CO_2 (C) 921

- Preparation, Structure, and Reactivity of 1,3,4-Triphenyl-4,5-dihydro-1*H*-1,2,4-triazol-5-ylidene, a New Stable Carbene (C) 1021
- Selective Syntheses of 1,3-Diphosphacyclobutadiene, Dewar-1,3,5-triphosphabenzene, 1,3,5-Triphosphabenzene, and 1,3,5,7-Tetraphosphabarrelene by Cyclooligomerization of Phosphaalkynes (C) 2227
- Synthesis and Structure of a Free Germacyclopentadienide Ion: $[Li([12]crown-4)_2][C_4Me_4GeSi(SiMe_3)_3]$ (C) 1887
- Synthesis of a 2*H*-Azirine by [1+2] Cycloaddition of a Phosphinocarbene with a Nitrile and Its Ring-Expansion to a $1,2\lambda^5$-Azaphosphete (C) 1246
- Synthesis of 1,2-Diphospholide Ions (C) 590
- The First Sulfur(VI)–Nitrogen–Phosphorus Macrocycles (C) 998
- The Preparation of Salts of $[Pd_2(\mu\text{-}Se_2N_2)Cl_6]^{2-}$, the First Adducts of Diselenium Dinitride (C) 1758
- Unexpected Course of the Darzens Reaction of Phenyl Esters of α-Chlorocarboxylic Acids with Carbonyl Compounds—A Novel One-Step Synthesis of α-Chloro-β-lactones (C) 2028
- Ylidediyl Halophosphane Oligomers, $(Ph_3PCPX)_n$—A Structurally Diverse Class of Compounds (C) 1853

Heterodiene complexes
- DAD Compounds of Niobium and Tantalum: Examples of the Structural Flexibility of DAD Ligands (C) 2649
- Lanthanoid Complexes with [(dad)Li]Ligands—New Starting Materials for Organolanthanoid Chemistry (C) 673

Heterofullerenes
- $C_{59}N^+$ and $C_{69}N^+$: Isoelectronic Heteroanalogues of C_{60} and C_{70} (C) 2257

Heterogeneous catalysis
- An Yttrium-Based Strong Lewis Acid for the Heterogeneous Catalysis of the Diels–Alder Reaction (C) 2143
- Coupling of Endothermic Thermal Cracking with Exothermic Oxidative Dehydrogenation of Ethane to Ethylene Using a Diluted SrO/La_2O_3 Catalyst (C) 665
- Spectroscopy in Catalysis. An Introduction (B) 495

Hexacyanometalates
- The Formal Potentials of Solid Metal Hexacyanometalates (C) 2685

Hexafluoropropanol
- Detection and Reactions of Radical Cations Generated by Photolysis of Aromatic Compounds with Tetranitromethane in 1,1,1,3,3,3-Hexafluoro-2-propanol at Room Temperature (C) 2268

Hexakis(trifluoromethyl)tetrazane
- Hexakis(trifluoromethyl)tetrazane (C) 586

High-pressure chemistry
- Coordination of CO to the Alkaline Earth Metallocene $[(Me_5C_5)_2Ca]$ (C) 791
- Fluxionality Induced by High Pressure: [9-D]9-Homocubyl Triflate, a Pressure-Sensing Molecule (C) 2030

High temperature particles
- Free Atoms, Clusters and Nanoscale Particles (B) 1252

High-temperature reactions
- Preparative Solid-State Chemistry with High-Power CO_2 Lasers (R) 634

Hirudin
- Anticoagulatory Substances of Blood-sucking Animals: From Hirudin to Hirudin Mimetics (R) 867

Histidine
- The Role of Dehydroalanine in Catalysis by Histidine Ammonia Lyase (C) 1464

History of chemistry
- Fritz Haber—Chemiker, Nobelpreisträger, Deutscher, Jude (B) 119
- Ideas in Chemistry. A History of the Science (B) 1034
- The Jewish Alchemists. A History and Source Book (B) 2419
- The World of Physical Chemistry (B) 360

History of science
- Biographical Encyclopedia of Scientists (B) 2167
- Der große Schwindel (B) 1370
- The Biographical Dictionary of Scientists (B) 2168

Homobenzenes
- Novel Structures from Tris(benzocyclobutadieno)cyclohexatriene: Triscyclopropanation and Trisoxacyclopropanation to the First [2.1.2.1.2.1]Hexaannulanes (C) 563

Homogeneous catalysis
- Carbon Dioxide as a Raw Material: The Synthesis of Formic Acid and Its Derivatives from CO_2 (R) 2207
- Cyclopentadienyl-Free Organolanthanide Chemistry (R) 2466
- Ferrocenes. Homogeneous Catalysis. Organic Synthesis. Materials Science (B) 1904
- Palladium-Catalyzed Resactions of Propargylic Compounds in Organic Synthesis (R) 2589

Homopeptides
- The Arndt–Eistert Reaction in Peptide Chemistry: A Facile Access to Homopeptides (C) 471

Horner–Wadsworth–Emmons reactions
- First Dynamic Kinetic Resolution of Racemic α-Amino Aldehydes (C) 1023

Horner–Wittig reactions
- Cerium(III) Chloride Promoted Nucleophilic Addition of Organolithium Reagents to α-Alkyl-β-Ketophosphine Oxides: A New Protocol for the Synthesis of Stereochemically Defined Trisubstituted Olefins (C) 2046

Host–guest chemistry
- A Cyclic Hexairon(III) Complex with an Octahedrally Coordinated Sodium Ion at the Center, an Example of the [12]Metallacrown-6 Structure Type (C) 467
- Assembly and Crystal Structure of a Photoactive Array of Five Porphyrins (C) 1096
- Calixarenes, Macrocycles with (Almost) Unlimited Possibilities (R) 713
- "Cation-π Interactions" Detected by Mass Spectrometry; Selective Recognition of Alkali Metal Cations by a π-Basic Molecular Cavity (C) 1364
- $C_{60}H_{60}$ and $C_{54}H_{48}$: Silver Ion Extraction with New Concave Hydrocarbons (C) 481
- Complexes from Polyazacyclophanes, Fluorescence Indicators, and Metal Cations—An Example of Allosterism through Ring Contraction (C) 321
- Fluorophosphazenate Ions: A Route to Complexation of Fluoride Ions (C) 2696
- Free-Energy Profile for a Host-Accelerated Diels–Alder Reaction: The Sources of *exo* Selectivity (C) 217
- Molecular Mosaics Formed by a Square Cyclophane and Its Inclusion Complex with Ferrocene (C) 1862
- Molecular Recognition of Anions by Zwitterionic Host Molecules in Water (C) 65
- Pseudo-Spherical Host Molecules: Synthesis, Dimerization, and Nucleation Effects (C) 1885
- Synthesis and Structure of Tetra- and Octanuclear Chelate Complexes—Exohedral Guest Exchange in Tetrahemispheraplexes (C) 993
- Transition Metal Complexes as Both Host and Guest: Second-Sphere Coordination between a Pt-Azacrown Ether Host and a $Pt\text{-}NH_3$ Guest (C) 2689
- $^3_\infty[(CoCp_2)\subset Fe(\mu\text{-}CNSnMe_3NC)_3]$: A Purely Organometallic Channel Inclusion Compound (C) 1197

HPLC
- A Comparison of Enthalpies of Formation in Solution and Enthalpies for HPLC Retention for Hydrogen-Bonded Host–Guest Complexes (C) 2404

HPLC–^{1}H NMR coupling
- Structure Determination of Vitamin A Acetate Isomers through Coupled HPLC and ^{1}H NMR Spectroscopy (C) 1014

Hückel rules
- 1,3,5,7-Tetra-*tert*-butyl-4-aza- and 1,3,5,7-Tetra-*tert*-butyl-4-phospha-*s*-indacene (C) 330

Huisgen, Rolf
- The Adventure Playground of Mechanisms and Novel Reactions (B) 1129

Hydrazones
- Diastereo- and Enantioselective Synthesis of 1,2-Amino Alcohols from Glycol Aldehyde Hydrazones; Asymmetric Synthesis of (*R,R*)-Statin (C) 1219

Hydrides
- An Unconventional Intermolecular Three-Center $N\text{–}H\cdots H_2Re$ Hydrogen Bond in Crystalline $[ReH_5(PPh_3)_3]\cdot$ indole$\cdot C_6H_6$ (C) 2507
- $Li_5Pt_2H_9$, a Complex Hydride Containing Isolated $[Pt_2H_9]^{5-}$ Ions (C) 898
- The $[Zr_6X_{18}H_5]^{3-}$ Ions with X = Cl, Br, and Related Species (C) 1877

Hydroborations
- An Ab Initio Investigation of the Rh^I-Catalyzed Hydroboration of C=C Bonds: Evidence for Hydrogen Migration in the Key Step (C) 115
- Bis(pentafluorophenyl)borane: Synthesis, Properties, and Hydroboration Chemistry of a Highly Electrophilic Borane Reagent (C) 809
- Strong Electronic Effects on Enantioselectivity in Rhodium-Catalyzed Hydroborations with Novel Pyrazole-Containing Ferrocenyl Ligands (C) 931

Hydrocarbons
- $C_{60}H_{60}$ and $C_{54}H_{48}$: Silver Ion Extraction with New Concave Hydrocarbons (C) 481
- Hexakis(trimethylsilylethynyl)[3]radialene: A Carbon-Rich Chromophore with Unusual Electronic Properties (C) 805
- Hydrocarbon Activation with Metal Halides: Catalysis of the Jacobsen Rearrangement by $(ZrCl_4)_n$ in the Presence of Aromatic Hydrocarbons (C) 1510
- My Search for Carbocations and Their Role in Chemistry (Nobel Lecture) (R) 1393
- Synthesis, Chemical Trapping, and Dimerization of 3,7-Dimethyltricyclo-$[3.3.0.0^{3,7}]$oct-1(5)-ene: [2+2] Retrocycloaddition of the Cyclobutane Dimer (C) 912
- Synthesis of Rodlike Distellenes (C) 1001

Hydroformylations
- A Novel Class of Versatile Solvents for Two-Phase Catalysis: Hydrogenation, Isomerization, and Hydroformylation of Alkenes Catalyzed by Rhodium Complexes in Liquid 1,3-Dialkylimidazolium Salts (C) 2698
- Enhancement of Catalytic Activity for Hydroformylation of Methyl Acrylate by Using Biphasic and "Supported Aqueous Phase" Systems (C) 1474
- Exciting Results from the Field of Homogeneous Two-Phase Catalysis (H) 1575
- Molecular Recognition between Chemically Modified β-Cyclodextrin and Dec-1-ene: New Prospects for Biphasic Hydroformylation of Water-Insoluble Olefins (C) 2269
- Rhodium-Catalyzed Hydroformylation of Internal Alkynes to α,β-Unsaturated Aldehydes (C) 1760

Hydrogenases
- On the Mechanism of Catalysis by a Metal-Free Hydrogenase from Methanogenic Archaea: Enzymatic Transformation of H_2 without a Metal and Its Analogy to the Chemistry of Alkanes in Superacidic Solution (C) 2247
- The Structure of the *D. gigas* [NiFe] Hydrogenase and the Nature of the Hydrogenase Nickel Complex (H) 1193

Hydrogenations
- A Novel Class of Versatile Solvents for Two-Phase Catalysis: Hydrogenation, Isomerization, and Hydroformylation of Alkenes Catalyzed by Rhodium Complexes in Liquid 1,3-Dialkylimidazolium Salts (C) 2698
- Exciting Results from the Field of Homogeneous Two-Phase Catalysis (H) 1575
- σ Metathesis as a Critical Step for the Transition Metal Catalyzed Formation of Formic Acid from CO_2 and H_2? An Ab Initio Investigation (C) 1742
- Preparation of a Surface-Active Chiral Diphosphane and Its Use in the Hydrogenation of Prochiral Olefins (C) 1645

Hydrogen bonds
- A Comparison of Enthalpies of Formation in Solution and Enthalpies for HPLC Retention for Hydrogen-Bonded Host–Guest Complexes (C) 2404
- A Molecular Composite Containing Organic and Inorganic Components—A Complex from β-Cyclodextrin and Hydrated Magnesium Chloride (C) 2381
- A New Family of Chiral Binaphthyl-Derived Cyclophane Receptors: Complexation of Pyranosides (C) 1596
- An Unconventional Intermolecular Three-Center N–H···H_2Re Hydrogen Bond in Crystalline $[ReH_5(PPh_3)_3]\cdot$indole·C_6H_6 (C) 2507
- A Self-Assembled Bifunctional Receptor (C) 2124
- Designed Assemblies in Open Framework Materials Synthesis: An Interrupted Sodalite and An Expanded Sodalite (C) 1745
- Dialkylammonium Ion/Crown Ether Complexes: The Forerunners of a New Family of Interlocked Molecules (C) 1865
- Highly Effective Hydrogen-Bonding Receptors for Guanine Derivatives (C) 2163
- Mesogenic Properties of Amphiphilic Liquid Crystals with an Unusual Head-Group Topology (C) 1631
- Metal Oxo Cation Receptors: Multimode Coordination to the Dioxoosmium(VI) Cation (C) 1359
- Patterns in Hydrogen Bonding: Functionality and Graph Set Analysis in Crystals (R) 1555
- Porous Solids by Design: $[Zn(4,4'\text{-bpy})_2(SiF_6)]_n\cdot x$DMF, a Single Framework Octahedral Coordination Polymer with Large Square Channels (C) 2127 (2561)
- Self-Assembling Discotic Mesogens (C) 1637
- Self-Assembly of 1,3,5-Benzenetricarboxylic Acids (Trimesic Acids) and Their Analogues in the Solid State (C) 2654
- Structure-Determining C-H···O-Si Hydrogen Bonds in Cobaltocenium Fluoride Nonasil (C) 2680
- Sulfuric Acid from Sulfur Trioxide and Water—A Surprisingly Complex Reaction (H) 1313
- Supramolecular Inorganic Chemistry: Small Guests in Small and Large Hosts (R) 2311
- The Consequences of an Electrostatic "Forced Marriage" between Two Electron-Rich Particles: Strained Ion Pairs (C) 439
- The Nonaaquabismuth(III) Cation (C) 2416
- Thermotropic Liquid Crystals Formed by Intermolecular Hydrogen Bonding Interactions (R) 1696
- $[WL(NO)(O)(CH_3)]$—An Unusual Nitrosyltungsten Complex (C) 1435

Hydrolyses
- Antibody-Catalyzed Phosphate Triester Hydrolysis (C) 2275
- Hydrolysis of a Phosphate Diester Doubly Coordinated to a Dinuclear Cobalt(III) Complex: A Novel Mechanism (C) 2412

Hydroperoxides
- Nonheme Iron Centers in Oxygen Activation: Characterization of an Iron(III) Hydroperoxide Intermediate (C) 1512
- Photosensitized Formation of 8-Hydroxy-2′-deoxyguanosine in Salmon Testes DNA by Furocoumarin Hydroperoxides: A Novel, Intercalating "Photo-Fenton" Reagent for Oxidative DNA Damage (C) 107

Hydrophobic effect
- Burial of Hydrocarbon Causes Cooperative Enhancement of Electrostatic Binding (C) 1483

Hydrothermal syntheses
- Hydrothermal Synthesis of a Novel Se_{12} Ring in $[\{(NH_4)_2[Mo_3S_{11.72}Se_{1.28}]\}_2\cdot[Se_{12}]]$ (C) 2509
- Investigations into the Targeted Design of Solids: Hydrothermal Synthesis and Structures of One-, Two-, and Three-Dimensional Phases of the Oxovanadium–Organodiphosphonato System (C) 223

Hydroxamic acids
- Formation of Nitronic Acids by Ring Opening of Nitrocyclopropanes by a Concerted, Acid-Catalyzed Mechanism (C) 1091

Hydroxyaldehydes
- Temperature and Solvent Effect on the Nucleophilic Addition of *n*-Butyllithium to the *N*-(Trimethylsilyl)imine of (2*S*)-Lactal (C) 2150

8-Hydroxy-2′-deoxyguanosine
- Photosensitized Formation of 8-Hydroxy-2′-deoxyguanosine in Salmon Testes DNA by Furocoumarin Hydroperoxides: A Novel, Intercalating "Photo-Fenton" Reagent for Oxidative DNA Damage (C) 107

Hydroxyl radicals
- *N*-Hydroxypyridinethiones as Photochemical Hydroxyl Radical Sources for Oxidative DNA Damage (C) 2156
- Photosensitized Formation of 8-Hydroxy-2′-deoxyguanosine in Salmon Testes DNA by Furocoumarin Hydroperoxides: A Novel, Intercalating "Photo-Fenton" Reagent for Oxidative DNA Damage (C) 107

N-hydroxypyridinethione
- *N*-Hydroxypyridinethiones as Photochemical Hydroxyl Radical Sources for Oxidative DNA Damage (C) 2156

Hyperconjugation
- Heteroatom-Substituted Bicyclo[1.1.1]-pentanes with Two Boron Atoms as Electron-Deficient Centers (C) 657

Hypersilyl derivatives
- Bis(hypersilyl)tin and Bis(hypersilyl)lead, Two Electron-Rich Carbene Homologs (C) 1334

Hypervalent compounds
- Stable 1:1 Adducts from Iodoacetylenes and Iodide Ions: Ion Pair Strain as an Additional Driving Force? (C) 441

ICR spectroscopy
- The Crafts–Friedel Reaction: Aromatic Alkylation within the Complex Formed upon Addition of a Gaseous Arenium Ion to an Olefin (C) 1589

Imides
- Tetracarboxylic Bisimide–Lactam Ring Contraction: A Novel Type of Rearrangement (C) 2234

Imines
- Regio- and Diastereoselective Synthesis of β-Amino Ketones by Addition of Imines to Iminium Salts (C) 2639
- $S(NPMe_3)_4^{2+}$: The First Structure Determination of a Dication of Hexavalent Sulfur (C) 1362
- Temperature and Solvent Effect on the Nucleophilic Addition of *n*-Butyllithium to the *N*-(Trimethylsilyl)imine of (2*S*)-Lactal (C) 2150

Iminophosphoranes
- Substituent-Controlled Reactions of Iminophosphoranes with Methyllithium (C) 1752

Immobilization
- A New Strategy in Heterogeneous Catalysis: The Design of Cortex Catalysts (C) 2728
- Direct Electrochemical Coupling of Components of the Biological Electron Transfer Chain to Modified Surfaces: Molecular Recognition between Cytochrome c Peroxidase and Cytochrome c (C) 2409
- Efficient Heterogeneous Biocatalysts by Entrapment of Lipases in Hydrophobic Sol–Gel Materials (C) 301
- Micron-Scale Patterning of Biological Molecules (C) 91

Immunological analysis
- Methods of Immunological Analysis, Vols. 1–3 (B) 243

Immunophilins
- Rational Design of Orthogonal Receptor–Ligand Combinations (C) 2129

Immunosensors
- Micron-Scale Patterning of Biological Molecules (C) 91

Imprinting
- Molecular Imprinting in Cross-Linked Materials with the Aid of Molecular Templates—A Way towards Artificial Antibodies (R) 1812

Inclusion compounds
- Dialkylammonium Ion/Crown Ether Complexes: The Forerunners of a New Family of Interlocked Molecules (C) 1865

- $^3_\infty[(CoCp_2)\subset Fe(\mu\text{-}CNSnMe_3NC)_3]$: A Purely Organometallic Channel Inclusion Compound (C) 1197

Indacenes
- 1,3,5,7-Tetra-*tert*-butyl-4-aza- and 1,3,5,7-Tetra-*tert*-butyl-4-phospha-*s*-indacene (C) 330

Indenes
- Generation of Enantiomerically Enriched Lithium Indenides by Means of (−)-Sparteine: Structure, Stereoselective Substitution, and Solvent Effects (C) 2158

Indigo
- Thermal Isomerization of Indigo (C) 67

Indigo derivatives
- Bis(dicyanomethylene) and Bis(cyanoimino) Derivatives of Indigo and Thioindigo (C) 464

Indium compounds
- New Tellurometalates of Gallium and Indium: $K[K([18]crown\text{-}6)]_2[GaTe_3]\cdot 2CH_3CN$ and $[(NEt_4)_5][In_3Te_7]\cdot 0.5\,Et_2O$ (C) 1879
- Synthesis, Structure, and Decay of In_4Br_7 (C) 1126

Indoles
- An Unconventional Intermolecular Three-Center $N-H\cdots H_2Re$ Hydrogen Bond in Crystalline $[ReH_5(PPh_3)_3]\cdot indole\cdot C_6H_6$ (C) 2507
- A Simple Catalytic Method for the Conversion of Aryl Bromides to Arylamines (C) 1348
- Titanium-Induced Zipper Reactions (C) 678

Indolizidines
- Diastereoselective Cathodic Cyclization of 1-(4- and 1-(3-Oxoalkyl)pyridinium Salts to Quinolizidine and Indolizidine Derivatives (C) 2007

Induced volatiles
- Jasmonic Acid and Coronatin Induce Odor Production in Plants (C) 1600

Inhalational anesthetics
- Carbon–Carbon Bond Cleavage with Inversion of Configuration: Conversion of (*R*)-(+)-1-Methoxytetrafluoropropionic Acid to (*S*)-(−)-1,2,2,2-Tetrafluoroethyl Methyl Ether (C) 222

Inorganic chemistry
- Inorganic Chemistry (B) 599
- Inorganic Experiments (B) 2565
- Redox Mechanisms in Inorganic Chemistry (B) 1249

Inositol phosphates
- Chemistry of Inositol Lipid Mediated Cellular Signaling (R) 1933

Inositols
- Catalytic Photoinduced Charge-Transfer Osmylation: A Novel Pathway from Arenes to Cyclitol Derivatives (C) 2031

Insertions
- Preparation, Structure, and Reactivity of 1,3,4-Triphenyl-4,5-dihydro-1*H*-1,2,4-triazol-5-ylidene, a New Stable Carbene (C) 1021

π–π Interactions
- Novel, Blue-Transparent Frequency Doublers Based on 1,8-Di(hetero)arylnaphthalenes (C) 1485

π Interactions
- Tetrakis[bis(trimethylsilyl)methyl]dialuminoxane with a Linear Al-O-Al Group (C) 989

Intermetallic phases
- Hyperbolic Lone Pair Structure in $RhBi_4$ (C) 1204

In vitro selection
- Synthetic Ribozymes and the First Deoxyribozyme (H) 1189

Iodine compounds
- $[Pb_{18}I_{44}]^{8-}$—An Iodoplumbate with an Unusual Structure (C) 2035

Ion channels
- A Non-Peptidic Ion Channel with K^+ Selectivity (C) 693
- Toxins as Tools in Neurochemistry (R) 39

Ion chromatography
- Trace Analysis of the Radionuclides ^{90}Sr and ^{89}Sr in Environmental Samples III: Development of a Fast Analytical Method (C) 186

Ionic liquids
- A Novel Class of Versatile Solvents for Two-Phase Catalysis: Hydrogenation, Isomerization, and Hydroformylation of Alkenes Catalyzed by Rhodium Complexes in Liquid 1,3-Dialkylimidazolium Salts (C) 2698

Ionization potentials
- First Determination of the Ionization Potential of Americium and Curium (C) 814

Ion pairs
- Deformation of Polymethine Structures by Intermolecular Interactions (C) 690
- The Consequences of an Electrostatic "Forced Marriage" between Two Electron-Rich Particles: Strained Ion Pairs (C) 439

Ion–molecule reactions
- Control of Ion–Molecule Reactions in the Gas Phase (H) 885

Iridium compounds
- A Co_3 Complex Containing a Bent Trimetal Chain, and Other 1,1′-Ferrocenedithiolato Complexes (C) 656
- Direct Observation of O–H Reductive Elimination from Ir^{III} Complexes (C) 229
- *closo*-$[B_5H_4PPh_3\{Fe(CO)_3\}\{Ir(CO)_2PPh_3\}]$: The First Structurally Characterized *closo*-Heterobimetallaheptaborane System (C) 1641

Iron compounds
- A Cyclic Hexairon(III) Complex with an Octahedrally Coordinated Sodium Ion at the Center, an Example of the [12]Metallacrown-6 Structure Type (C) 467
- Additions of Carbanions to a Cationic Cyclopentadienyl(naphthalene)iron Complex (C) 2161
- A Highly Reactive and Catalytically Active Model System for Intradiol-Cleaving Catechol Dioxygenases: Structure and Reactivity of Iron(III) Catecholate Complexes of *N*,*N*′-Dimethyl-2,11-diaza[3,3](2,6)pyridinophane (C) 2671
- A Model of Semimet Hemerythrin; NMR Spectroscopic Evidence of Valence Localization in Bis(μ-carboxylato)(μ-phenolato)diiron(II,III) in Solution (C) 588
- An Alkylperoxoiron(III) Intermediate and Its Role in the Oxidation of Aliphatic C–H Bonds (C) 2048
- A New Type of Trinuclear Oxoiron(III) Cluster (C) 205
- A Novel Hexanuclear Fe^{III}-*cis*-Inositolato Complex as a Model for Fe^{III}–Polyol Interactions in Aqueous Solution (C) 2242
- A One-Step Synthesis of Squalene from Farnesol under Prebiotic Conditions (C) 1898
- A Stable Aquairon(III) Complex with $S = 1$: Structure and Spectroscopic Properties (C) 1216 (1649)
- Distorted Sandwich Compounds: [1]Ferrocenophanes and [2]Ruthenocenophanes (H) 1837
- Ferrocenes. Homogeneous Catalysis. Organic Synthesis. Materials Science (B) 1904
- Fivefold Deprotonated D-Mannose as Ligand in Homoleptic Dinuclear Metalates of Trivalent Iron, Vanadium, Chromium, Aluminum, and Gallium (C) 2647
- Formation of an Alkylperoxoiron(III) Complex during Oxidations Catalyzed by μ-Oxodiiron(III) Complexes (C) 203
- Formation of the First Isomeric [2]Catenates by Self-Assembly about Two Different Metal Ions (C) 582
- New Selenolato-Bridged Clusters of Iron and Nickel; the Structures of $[Fe_{12}(SePh)_{24}]$ and $[Na_2(POPh_3)_6][Ni_{20}Se_{12}(SeMe)_{10}]$ (C) 307
- μ-Nitridodiiron Complexes with Asymmetric $[Fe^{IV}\equiv N-Fe^{III}]^{4+}$ and Symmetric $[Fe^{IV}=N=Fe^{IV}]^{5+}$ Structural Elements (C) 669
- Structure and Magnetic Properties of a Decanuclear Oxoiron(III) Cluster: A Further Step to Understanding Iron Aggregation Processes (C) 2716
- The First μ(OH)-Bridged Model Complex for the Mixed-Valent $Fe^{II}Fe^{III}$ Form of Hemerythrin (C) 2642
- Water-Soluble Dendritic Iron Porphyrins: Synthetic Models of Globular Heme Proteins (C) 2725
- *closo*-$[B_5H_4PPh_3\{Fe(CO)_3\}\{Ir(CO)_2PPh_3\}]$: The First Structurally Characterized *closo*-Heterobimetallaheptaborane System (C) 1641
- $^3_\infty[(CoCp_2)\subset Fe(\mu\text{-}CNSnMe_3NC)_3]$: A Purely Organometallic Channel Inclusion Compound (C) 1197
- $[Fe(2,4,6\text{-}tBu_3C_6H_2)_2]$, a Monomeric Diaryl Complex with Two-Coordinate Iron(II) (C) 325

Iron–molybdenum cofactor
- On the Synthesis of the FeMo Cofactor of Nitrogenase: Gene-Controlled in Nature versus Laboratory-Produced by Man (R) 1071

Iron–sulfur cluster
- On the Synthesis of the FeMo Cofactor of Nitrogenase: Gene-Controlled in Nature versus Laboratory-Produced by Man (R) 1071

IR spectroscopy
- Barbituric Acid/2,4,6-Triaminopyrimidine Aggregates in Water and Their Competitive Interaction with Monolayers of Barbituric Acid Lipids at the Gas–Water Interface (C) 58
- Distinguishing the Silanol Groups in the Mesoporous Molecular Sieve MCM-41 (C) 2694
- FT-NIR Atlas (B) 120
- Reaction of 1,1-Dimethylsilene with Formaldehyde (C) 929
- Vibrational Spectroscopy in Supercritical Fluids: From Analysis and Hydrogen Bonding to Polymers and Synthesis (R) 1275

Isocyanides
- Cascade Radical Reactions of Isonitriles: A Second-Generation Synthesis of (20*S*)-Camptothecin, Topotecan, Irinotecan, and GI-147211C (C) 2683
- Synthesis and Reactions of Vinyl Isoselenocyanates (C) 1627
- Synthesis, Structural Investigation, and Ligand Properties of Isocyanoacetonitrile (C) 914

Isomerism
- Reversible Template-Directed Activation of Equatorial Double Bonds of the Fullerene Framework: Regioselective Direct Synthesis, Crystal Structure, and Aromatic Properties of T_h-$C_{66}(COOEt)_{12}$ (C) 1607

Isomerizations
- Asymmetrization of *meso* 1,4-Enediol Ethers by Isomerization with a Chiral binap–Rh^I Catalyst (C) 2287
- C–C Coupling Reactions as a Novel Synthetic Route to π-Allyl- and π-Butadienylrhodium Complexes (C) 1244
- Homcomorphic Isomerism in a Peptidic Macrobicycle (C) 2660
- Hydrocarbon Activation with Metal Halides: Catalysis of the Jacobsen Rearrangement by $(ZrCl_4)_n$ in the Presence of Aromatic Hydrocarbons (C) 1510
- Light-Switchable Catalysis in Synthetic Receptors (C) 446
- Luminescence Stimulated by Electron Transfer: Fluorescent Donor/Acceptor-Substituted Stilbenes Containing Pyrenoid and Heteroaromatic Subunits (C) 2664
- Photoswitchable Phase Separation in Hydrophobically Modified Poly(acrylamide)/Surfactant Systems (C) 88
- Selective Isomerization of Hydrocarbon Chains on External Surfaces of Zeolite Crystals (C) 2528
- Thermal Isomerization of Indigo (C) 67

Isoselenocyanates
- Synthesis and Reactions of Vinyl Isoselenocyanates (C) 1627

Isoxazolidines
- Benzopyranoisoxazolidines as Chiral Auxiliaries for Asymmetric Synthesis (C) 793

Jacobsen rearrangement
- Hydrocarbon Activation with Metal Halides: Catalysis of the Jacobsen Rearrangement by $(ZrCl_4)_n$ in the Presence of Aromatic Hydrocarbons (C) 1510

Jahn–Teller distortion
- Synthesis, Structure, and Decay of In_4Br_7 (C) 1126

Jasmonic acid
- Jasmonic Acid and Coronatin Induce Odor Production in Plants (C) 1600

Keggin anions
- A Novel Chainlike Heteropolyanion Formed by Keggin Units: Synthesis and Structure of $(ET)_{8n}[PMnW_{11}O_{39}]_n \cdot 2nH_2O$ (C) 1460

Ketones
- A Highly Stereoselective Synthesis of 1,2-*trans*-C-Glycoside via Glycosyl Samarium(III) Compounds (C) 909
- Diastereo- and Enantioselective Synthesis of Polyfunctional Ketones with Adjacent Quaternary and Tertiary Centers by Asymmetric Carroll Rearrangement (C) 2278

Ketosugars
- Thymidine Diphospho-6-deoxy-α-D-*ribo*-3-hexulose—Synthesis of a Central Intermediate in the Biosynthesis of Di- and Trideoxysugars (C) 1328

Keto–enol tautomerism
- First Isolation of an Enol of a Carboxylic Acid by Complexation to an (Ethane-1,2-diamine)platinum(II) Fragment (C) 1103
- Oxybenziporphyrin, a Fully Aromatic Semiquinone Porphyrin Analog with Pathways for 18π-Electron Delocalization (C) 2533

Ketyl radicals
- Radical Additions to (η^6-Arene)-(tricarbonyl)chromium Complexes: Diastereoselective Synthesis of Hydrophenalene and Hydrobenzindene Derivatives by Samarium(II) Iodide Induced Cyclization (C) 2383

Kinetics
- Basic Principles of Thermoanalytical Techniques and Their Applications in Preparative Chemistry (R) 1171
- Control of Ion–Molecule Reactions in the Gas Phase (H) 885
- C–H and C–C Bond Activation by Bare Transition-Metal Oxide Cations in the Gas Phase (R) 1973
- Electronically Tuned *trans* Labilization Controls the Substitution Behavior of Rhodoximes (C) 2245
- Free-Energy Profile for a Host-Accelerated Diels–Alder Reaction: The Sources of *exo* Selectivity (C) 217
- Synthesis of a Stable Arenesulfenic Acid Bearing a Bowl-Shaped Macrobicyclic Cyclophane Skeleton (C) 1124
- The Coexistence of the Reactivity–Selectivity Principle and of Linear Free Energy Relationships: A Diffusion Clock for Determining Carbocation Reactivities (C) 2250
- The Crafts–Friedel Reaction: Aromatic Alkylation within the Complex Formed upon Addition of a Gaseous Arenium Ion to an Olefin (C) 1589

Kirk–Othmer
- Kirk/Othmer Encyclopedia of Chemical Technology (B) 2564

Kolbe electrolysis
- Diastereoselective Coupling of Anodically Produced Radicals Bearing Chiral Amide Groups (C) 189

Laboratory guidebooks
- Chemische Kabinettstücke (B) 1769
- Inorganic Experiments (B) 2565
- Introduction to Molecular Cloning Techniques (B) 697
- Tactics of Organic Synthesis (B) 1369

Lactams
- Synthesis of Optically Active Nine-Membered Ring Lactams by a Zwitterionic Aza-Claisen Reaction (C) 1026
- Tetracarboxylic Bisimide–Lactam Ring Contraction: A Novel Type of Rearrangement (C) 2234
- The β-Lactam-Nucleoside Chimera (C) 2238

β-Lactones
- Unexpected Course of the Darzens Reaction of Phenyl Esters of α-Chlorocarboxylic Acids with Carbonyl Compounds—A Novel One-Step Synthesis of α-Chloro-β-lactones (C) 2028

Lanthanide compounds
- A Silicon Strand of More than 7 Å in Diameter in $Ba_2Eu_3Si_7$ (C) 1462
- Bromides of Rare Earth Metal Boride Carbides—A System of Building Blocks (C) 1633
- $CsPr_9NbBr_{15}N_6$: A New Type of Interstitially Stabilized Cluster Compound (C) 2262
- Cyclopentadienyl-Free Organolanthanide Chemistry (R) 2466
- Electrochemistry and Ab Initio Study of the Dimetallofullerene $La_2@C_{80}$ (C) 1094
- Filled Buckyballs: Recent Developments from the Endohedral Metallofullerenes of Lanthanides (H) 981
- Gas-Phase Activation of Fluorocarbons by "Bare" and "Coordinated" Praseodymium Cations (C) 213
- LaI: An Unprecedented Binary Rare Earth Metal Monohalide with a NiAs-Type Structure (C) 233
- Lanthanoid Complexes with [(dad)Li]Ligands—New Starting Materials for Organolanthanoid Chemistry (C) 673
- Synthesis of the First Adducts of the Dimetallofullerenes $La_2@C_{80}$ and $Sc_2@C_{84}$ by Addition of a Disilirane (C) 2139

Laser ablation
- Formation and Structures of New Metallo- and Metallapolysulfanes, $[MS_y]^+$ (y = 2–16) (C) 201 (1032)

Laser chemistry
- Aligning and Trapping Molecules with Light (H) 2365
- Preparative Solid-State Chemistry with High-Power CO_2 Lasers (R) 634

Layer compounds
- Supramolecular Synthons in Crystal Engineering—A New Organic Synthesis (R) 2328

Lead compounds
- Structure and Bonding in Organometallic Anions of Heavy Group 14 and 15 Elements (R) 1545
- $[Pb_{18}I_{44}]^{8-}$—An Iodoplumbate with an Unusual Structure (C) 2035

Lewis acids
- An Yttrium-Based Strong Lewis Acid for the Heterogeneous Catalysis of the Diels–Alder Reaction (C) 2143
- C_2-Symmetric Cationic Copper(II) Complexes as Chiral Lewis Acids: Counterion Effects in the Enantioselective Diels–Alder Reaction** (C) 798

Ligand effects
- Nucleophilic Addition to (π-Allyl)-palladium Complexes: Control of the Attack at the Central or Terminal Carbon Atom by Ligands (C) 2551

Ligand transfer
- S_7NH and S_7NCH_3 as Novel Chelating Ligands in $[(\eta^5\text{-}C_5H_5)_2Ti]$ Complexes: Synthesis of Medium-Sized Sulfur–Nitrogen Rings by Ligand Transfer (C) 1330

Ligases
- Peptide Ligases—Tools for Peptide Synthesis (H) 175

Linear free energy relationships
- Common Origin of Enthalpic and Entropic Substituent Effects in Reactions of Benzhydryl Cations with Nucleophiles (C) 490
- Reactions of Carbocations with π Nucleophiles: Polar Mechanism and No Outer Sphere Electron Transfer Processes (C) 1225
- The Coexistence of the Reactivity–Selectivity Principle and of Linear Free Energy Relationships: A Diffusion Clock for Determining Carbocation Reactivities (C) 2250

Lipases
- Efficient Heterogeneous Biocatalysts by Entrapment of Lipases in Hydrophobic Sol–Gel Materials (C) 301

Lipids
- Incorporation of Membrane Proteins in Solid-Supported Lipid Layers (C) 2056
- Metal-Induced Dispersion of Lipid Aggregates: A Simple, Selective, and Sensitive Fluorescent Metal Ion Sensor (C) 905

Lipopolysaccharides
- Endotoxin Antagonists: Possible Candidates for the Treatment of Gram-Negative Sepsis (H) 2000

Liquid crystals
- Formation of a Hexagonal Columnar Mesophase by N-Acylated Poly(ethylenimine) (C) 795
- Lyotropic Phases Formed by "Molecular Bottlebrushes" (C) 1472

- Mesogenic Properties of Amphiphilic Liquid Crystals with an Unusual Head-Group Topology (C) 1631
- Polymers with Complexed Cyclobutadiene Units in the Main Chain: The First Example of a Thermotropic, Liquid Crystalline Organometallic Polymer (C) 569
- Self-Assembling Discotic Mesogens (C) 1637
- Synthesis of Belt Cyclophanes (C) 1437
- Thermotropic Liquid Crystals Formed by Intermolecular Hydrogen Bonding Interactions (R) 1696

Lithium compounds
- A Simple Route to the 1-Aza-3-Phosphaallyl System: Structure of a Dimeric Lithium Complex and Protonation To Give the First NH_2-Substituted Phosphaalkene (C) 2369
- A $Te_2N_6Li_4$ Cage Containing the Tris(*tert*-butylimido)tellurite Dianion (C) 2549
- Cage Expansion of $[\{(cyNLi)_3Sb\}_2]$; Synthesis and Structure of the Trimetallic Complex $[\{(cyNLi)_3Sb\}_2(t BuOK)_3 \cdot x C_6H_5CH_3]$ (C) 1012
- Carbenoid or Lithium Complex of a Carbanion? Synthesis and Structure of $(Me_3Si)_2C=P(aryl)=C(Cl)Li(thf)_3$ and LiCl Elimination To Give the Phosphirene (C) 1849
- Catalytic Asymmetric C–C Bond Formation: New Enolato- and Organolithium Chemistry (H) 178
- Crystal Structure of Dilithioacetylacetone: A Twenty-Four Vertex Li-O Cage Molecule with Limited Li–C(terminal) Bonding and Selective THF Solvation (C) 1233
- α-Ethoxyvinyllithium: An Unexpected Polymeric Structure—Tetrameric Subunits Linked by Li–C π Interactions (C) 1594
- Generation of Enantiomerically Enriched Lithium Indenides by Means of (−)-Sparteine: Structure, Stereoselective Substitution, and Solvent Effects (C) 2158
- Influence of Lewis Base Complexation and the Degree of Aggregation of Alkyllithium Compounds on the Ratio in Which They Form Addition Products and Enolates with Ketones (C) 2152
- $Li_5Pt_2H_9$, a Complex Hydride Containing Isolated $[Pt_2H_9]^{5-}$ Ions (C) 898
- Lithium Intermediates during the α-Lithiation and Subsequent α-Substitution of Heterocyclic Amines in the Presence of CO_2 (C) 921
- Novel Alkali Metal Phosphanide Aggregates (C) 316
- Preparation and Detection of Enantiomerically Enriched and Configurationally Stable α-Thioalkyllithium Compounds (C) 323
- Single-Crystal X-Ray Structure of the Metastable Aryne Precursor Tetrafluorophenyllithium and of 1,2,3,4-Tetrafluorobenzene (C) 1517
- Substituent-Controlled Reactions of Iminophosphoranes with Methyllithium (C) 1752
- The Formation of a Mixed Organolithium Aggregate $Li_4R_2nBu_2$ (R = 2,6-$(CH_2NMe_2)_2$-3,5-$Me_2C_6HCH_2$) during the Heteroatom-Assisted Lithiation of 1,3-Bis(dimethylaminomethyl)-2,4,6-trimethylbenzene (C) 219
- The Lipophilically Wrapped Polyion Aggregate $\{[Ba_6Li_3O_2]^{11+}[^-OC(CH_3)_3]_{11}(OC_4H_8)_3\}$, a Face-Sharing (Octahedron + Prismane) $Ba_6Li_3O_2$ Polyhedron in a Hydrocarbon Ellipsoid: Preparation, Single Crystal Structure Analysis, and Density Functional Calculations (C) 1353

Lock and key principle
- The Lock and Key Principle. The State of the Art—100 Years on (B) 2293

Low-valent compounds
- A New Method for the Synthesis of Amphipolar Phosphorus-Containing Heterocycles (C) 557

Luminescence
- Effective Charge Separation in Intermolecular Complexes of an Electron Donor and a Doubly Branched Triad Assembly: A Model System for Environmental Effects Controlling Electron Transfer (C) 1005
- Luminescence Stimulated by Electron Transfer: Fluorescent Donor/Acceptor-Substituted Stilbenes Containing Pyrenoid and Heteroaromatic Subunits (C) 2664

McMurry reactions
- Titanium-Induced Zipper Reactions (C) 678

Macrocycles
- Activation of Macrocyclic Biaryl-Enediynes by Metal Ion Coordination (C) 2538
- A Stable Aquairon(III) Complex with $S = 1$: Structure and Spectroscopic Properties (C) 1216 (1649)
- Binding of Boron and Alkali Metal Cations by a Pseudocryptand (C) 1115
- Concave Reagents Based on Calixarenes (C) 2555
- Facile Synthesis and Solid-State Structure of a Benzylic Amide [2]Catenane (C) 1209
- From Porphyrin Isomers to Octapyrrolic "Figure Eight" Macrocycles (C) 2511
- Homeomorphic Isomerism in a Peptidic Macrobicycle (C) 2660
- Macrobicyclic Titanium(IV) Complexes with C_3-Symmetric Synthetic Peptides (C) 1449
- Octacationic Cyclophanes: Binding of ATP and Other Anionic Guests in Water (C) 2147
- Octaphyrin-(1.0.1.0.1.0.1.0) (C) 2515
- Photo Electron Transfer Induced Macrocyclization of *N*-Phthaloyl-ω-aminocarboxylic Acids (C) 474
- Self-Assembly of Polyanions at a Metal Cation Template: Syntheses and Structures of $[\{Ag([18]aneS_6)\}I_7]_n$ and $[Ag([18]aneS_6)]I_3$ (C) 2374
- Silicon-Bridged Macrocycles—Synthesis of Sila-Calixarenes (C) 661
- Structurally Diverse and Dynamically Versatile Benzylic Amide [2]Catenanes Assembled Directly from Commercially Available Precursors (C) 1212
- Synthesis and Structure of the Nanodimensional Multicyclophane "Kuratowski Cyclophane", an Achiral Molecule with Nonplanar $K_{3,3}$ Topology (C) 2657
- Synthesis and X-ray Structure of a Shape-Persistent Macrocyclic Amphiphile (C) 2713
- *meso*-Tetrakis[4-(diphenylphosphino)-phenyl]porphyrin and a Water-Soluble Octakis(phosphonium salt) Porphyrin Double-Decker with a Cage Structure. (C) 2230
- The Reactivity of 1,3-Butadiyne Moieties in the "Exploding" [*n*]Rotanes—A Crown of Thiophenes (C) 781

Macrolides
- Relative and Absolute Configuration of Filipin III (C) 1227
- The Macrolidic Glycolipid Calonyctin A, a Plant Growth Regulator: Synthesis, Structural Assignment, and Conformational Analysis in Micellar Solution (C) 2520

Macromolecules
- Routes to Dendritic Networks: Bis-Dendrimers by Coupling of Cascade Macromolecules through Metal Centers (C) 2023

Magnesium compounds
- Silicon Analogues of Grignard Compounds: Synthesis and Structure of Amine-Stabilized Trimethylsilylmagnesium Halides (C) 1030

Magnetic properties
- A Cyclic Hexairon(III) Complex with an Octahedrally Coordinated Sodium Ion at the Center, an Example of the [12]Metallacrown-6 Structure Type (C) 467
- A New Type of Trinuclear Oxoiron(III) Cluster (C) 205
- A Nickel(II) Azide Cubane: Characterization of the Magnetic Exchange Interactions Mediated by a Triply Bridging Azide Group Bound End-On (C) 889
- $Na_2Ti_3Cl_8$: From Isolated Ti^{2+} Ions to $[Ti_3]^{6+}$ Clusters (C) 71
- Octadecanuclearity in Manganese Carboxylate Chemistry: $K_4[Mn_{18}O_{16}(O_2CPh)_{22}(phth)_2(H_2O)_4]$ ($phthH_2$ = phthalic acid) (C) 887
- Self-Assembly of a Ferromagnetically Coupled Manganese(II) Tetramer (C) 1443
- Structure and Magnetic Properties of a Decanuclear Oxoiron(III) Cluster: A Further Step to Understanding Iron Aggregation Processes (C) 2716
- Structure Determination from Powder X-Ray Diffraction Data of a Hydrogen-Bonded Molecular Solid with Competing Ferromagnetic and Antiferromagnetic Interactions: The 2-(3,4-Dihydroxyphenyl)-α-Nitronyl Nitroxide Radical (C) 55
- The First μ(OH)-Bridged Model Complex for the Mixed-Valent $Fe^{II}Fe^{III}$ Form of Hemerythrin (C) 2642
- The Two-Dimensional Network Structure and Metamagnetic Properties of the 2:1 Complex of $[Mn(3\text{-}MeOsalen)(H_2O)]ClO_4$ and $K_3[Fe(CN)_6]$ (C) 1446
- 2-[*p*-(*N*-*tert*-butyl-*N*-oxyamino)phenyl]-4,4,5,5-tetramethyl-4,5-dihydroimidazol-3-oxide-1-oxyl, a Stable Diradical with a Triplet Ground State (C) 927

Main group elements
- Synthesis and Structure of Organometallic Compounds with $(Al_2Si)_2$ and Al_3Sb_2 Frameworks (C) 919
- Te_8^{4+}: A Cubic Polycation in the Structure of $Te_8(VOCl_4)_2$ (C) 2559

Manganese compounds
- A Dinuclear (μ-Carboxylato)manganese(II) Complex Derived from a Macrocyclic Ligand: A Structural Model for Active Sites in Natural Systems (C) 2535
- Aromatic Gallium Heterocycles: Synthesis of the First Gallatabenzene (C) 1357
- Characterization of an Oxo(porphyrinato)manganese(IV) Complex by X-ray Absorption Spectroscopy (C) 343
- Octadecanuclearity in Manganese Carboxylate Chemistry: $K_4[Mn_{18}O_{16}(O_2CPh)_{22}(phth)_2(H_2O)_4]$ ($phthH_2$ = phthalic acid) (C) 887
- Phosphorane Iminato Complexes of Manganese and Cobalt with Heterocubane Structure (C) 1235

- Self-Assembly of a Ferromagnetically Coupled Manganese(II) Tetramer (C) 1443
- Synthesis and Structure of Bimetallic η^3,η^6-Naphthalene Complexes Containing a Mn–Mn Moiety Bonded in a *Syn*-Facial Manner: A General Route to Homo- and Heteronuclear Bimetallic Complexes of Polyarenes (C) 2540
- Synthesis and Structure of the First Transition Metal Borylene Complexes (C) 825
- The Two-Dimensional Network Structure and Metamagnetic Properties of the 2:1 Complex of $[Mn(3\text{-}MeOsalen)(H_2O)]\text{-}ClO_4$ and $K_3[Fe(CN)_6]$ (C) 1446
- $[Mn(C_{18}H_{16}N_2O_2)_3](ClO_4)_2$: A Polymeric 34- and 68-Membered Metallacyclic Network Forming a Novel Woven Polycatenated Structure (C) 574

Mannich bases
- Regio- and Diastereoselective Synthesis of β-Amino Ketones by Addition of Imines to Iminium Salts (C) 2639

Mass spectrometry
- An Alkylperoxoiron(III) Intermediate and Its Role in the Oxidation of Aliphatic C–H Bonds (C) 2048
- Applications of Mass Spectrometry to Organic Stereochemistry (B) 497
- "Cation-π Interactions" Detected by Mass Spectrometry; Selective Recognition of Alkali Metal Cations by a π-Basic Molecular Cavity (C) 1364
- $C_{59}N^+$ and $C_{69}N^+$: Isoelectronic Heteroanalogues of C_{60} and C_{70} (C) 2257
- Coordination of Dioxygen in Three Representative Transition Metal Cations: FeO_2^+, CrO_2^+, and $[CH_3Re(O_2)_2O]^+$ (C) 2517
- C–H and C–C Bond Activation by Bare Transition-Metal Oxide Cations in the Gas Phase (R) 1973
- Formation and Structures of New Metallo- and Metallapolysulfanes, $[MS_y]^+$ (y = 2–16) (C) 201 (1032)
- Gas-Phase Activation of Fluorocarbons by "Bare" and "Coordinated" Praseodymium Cations (C) 213
- Gas-Phase Micelles (C) 2053
- Investigation of Self-Assembled Supramolecular Species in Solution by IL-ESMS, a New Mass Spectrometric Technique (C) 209
- Nonheme Iron Centers in Oxygen Activation: Characterization of an Iron(III) Hydroperoxide Intermediate (C) 1512
- Synthesis and Properties of First to Third Generation Dendrimers with Doubly and Triply Branched Chiral Building Blocks (C) 2116
- Tantalum-Mediated Coupling of Methane and Carbon Dioxide in the Gas Phase (C) 2033
- The Synthesis of Tris(perfluoroalkyl)-phosphanes (C) 1241
- Trace Analysis of the Radionuclides ^{90}Sr and ^{89}Sr in Environmental Samples II: Accelerator Mass Spectrometry (AMS) (C) 183
- Trace Analysis of the Radionuclides ^{90}Sr and ^{89}Sr in Environmental Samples I: Laser Mass Spectrometry (C) 181
- $[R_3Si-arene]^+$ σ Complexes in the Gas Phase (C) 654

Matrix isolation
- Reaction of 1,1-Dimethylsilene with Formaldehyde (C) 929

Medicinal chemistry
- Digitalis Research in Berlin–Buch—Retrospective and Perspective Views (R) 282
- Endotoxin Antagonists: Possible Candidates for the Treatment of Gram-Negative Sepsis (H) 2000
- Modern Medicinal Chemistry (B) 828
- Talking Back to Prozac: What Doctors Aren't Telling You about Today's Most Controversial Drug (B) 1250

Membrane models
- A Non-Peptidic Ion Channel with K^+ Selectivity (C) 693

Membrane proteins
- Incorporation of Membrane Proteins in Solid-Supported Lipid Layers (C) 2056

Mercury compounds
- 2,4,6-Tri(4-pyridyl)-1,3,5-triazine as a 3-Connecting Building Block for Infinite Nets (C) 820

Mesophases
- Structure Organization of Aluminosilicate Polyanions with Surfactants: Optimization of Al Incorporation in Aluminosilicate Mesostructural Materials (C) 1499

Mesoporous materials
- Distinguishing the Silanol Groups in the Mesoporous Molecular Sieve MCM-41 (C) 2694
- Synthesis of Hexagonally-Packed Mesoporous TiO_2 by a Modified Sol–Gel Method (C) 2014

Metabolism
- Shikimic Acid (B) 361

Metacyclophanes
- Calixarenes, Macrocycles with (Almost) Unlimited Possibilities (R) 713

Metalates
- Mononuclear Tris(arene)–Metal Complexes (H) 53
- New Tellurometalates of Gallium and Indium: $K[K([18]crown\text{-}6)]_2[GaTe_3]\cdot 2CH_3CN$ and $[(NEt_4)_5][In_3Te_7]\cdot 0.5\,Et_2O$ (C) 1879

Metalations
- Asymmetric Alkylation of Amide Enolates with Pseudoephedrine and Ephedrine as Chiral Auxiliaries—Unexpected Influence of Additives? (H) 433
- Enantiomerically Pure Palladacycles Derived from β-Ketosulfoxides (C) 1351
- The Formation of a Mixed Organolithium Aggregate $Li_4R_2nBu_2$ (R = 2,6-$(CH_2NMe_2)_2$-3,5-$Me_2C_6HCH_2$) during the Heteroatom-Assisted Lithiation of 1,3-Bis(dimethylaminomethyl)-2,4,6-trimethylbenzene (C) 219
- The Synthesis and Crystal Structures of $RbC(SiMe_3)_3$ and $CsC(SiMe_3)_3\cdot 3.5\,C_6H_6$: A One-Dimensional Ionic Solid and an Ionic Solid with a Molecular Structure (C) 687

Metal ion analysis
- Metal-Induced Dispersion of Lipid Aggregates: A Simple, Selective, and Sensitive Fluorescent Metal Ion Sensor (C) 905

Metallabenzenes
- Solid-State and Solution Structures of $[\{NW(OC(CH_3)_2CF_3)_3\}_3]$ and Factors Favoring the Metathesis of C–N and N–W Triple Bonds in Reactions Involving Organic Nitriles and Ditungsten Hexaalkoxides (C) 110

Metallaboranes
- *closo*-$[B_5H_4PPh_3\{Fe(CO)_3\}\{Ir(CO)_2PPh_3\}]$: The First Structurally Characterized *closo*-Heterobimetallaheptaborane System (C) 1641

Metallacycles
- Synthesis and Structure of 1-Aza- and 1-Phospha-2-titanacyclobut-4-enes (C) 688
- $[Mn(C_{18}H_{16}N_2O_2)_3](ClO_4)_2$: A Polymeric 34- and 68-Membered Metallacyclic Network Forming a Novel Woven Polycatenated Structure (C) 574

Metallapolysulfanes
- Formation and Structures of New Metallo- and Metallapolysulfanes, $[MS_y]^+$ (y = 2–16) (C) 201 (1032)

Metallic bond
- Does the Death Knell Toll for the Metallic Bond? (H) 1081
- The Metallic Bond–Dead or Alive? A Comment and a Reply (C) 2003

Metallic conductors
- LaI: An Unprecedented Binary Rare Earth Metal Monohalide with a NiAs-Type Structure (C) 233

Metallocene anions
- Alkali Metallocene Anions: Syntheses and Structures (C) 2376

Metallocenophanes
- Distorted Sandwich Compounds: [1]Ferrocenophanes and [2]Ruthenocenophanes (H) 1837
- Synthesis and Structure of the First Sulfur-Bridged [1]Ferrocenophane (C) 1506

Metalloenzymes
- Synthetic Ribozymes and the First Deoxyribozyme (H) 1189
- The Active Sites of the Native Cytochrome-c Oxidase from Bovine Heart Mitochondria: EXAFS-Spectroscopic Characterization of a Novel Homobinuclear Copper Center (Cu_A) and of the Heterobinuclear Fe_{a3}-Cu_B Center (C) 1488
- The Three-Dimensional Structure of Hammerhead Ribozymes (H) 643

Metallofullerenes
- Filled Buckyballs: Recent Developments from the Endohedral Metallofullerenes of Lanthanides (H) 981

Metalloporphyrins
- Characterization of an Oxo(porphyrinato)manganese(IV) Complex by X-ray Absorption Spectroscopy (C) 343

Metalloproteins
- Novel Biological Copper Proteins through Anion Addition to the Mutant Met121Gly of *Pseudomonas aeruginosa* Azurin (C) 1622
- The Dinuclear Cu_A Center in Cytochrome *c* Oxidase and N_2O Reductase—A Metal–Metal Bond in Biology? (H) 771

Metal-modified sugars
- Carbene Complex Functionalized Sugars (C) 1856

Metal salt effect
- Asymmetric Alkylation of Amide Enolates with Pseudoephedrine and Ephedrine as Chiral Auxiliaries—Unexpected Influence of Additives? (H) 433

Metal salts
- A New Method for the Preparation of Nanostructured Metal Clusters (C) 2240
- Volatile Metal Alkoxides According to the Concept of Donor Functionalization (R) 2187

Metal–metal interactions
- Complexes with Polar W–W Multiple Bonds: $[W_2(OiPr)_4L(dmpe)_2]$ (L = $(H)_2$, CO) and $[W_2(O)_4(\mu\text{-}O)\{W(CO)(dmpe)_2\}_2]$ (C) 891
- Direct Spectroscopic Evidence for a Hitherto Elusive "Zwitterionic" Excited State (H) 547
- Synthesis and Structure of Bimetallic η^3,η^6-Naphthalene Complexes Containing a Mn–Mn Moiety Bonded in a *Syn*-Facial Manner: A General Route to Homo- and Heteronuclear Bimetallic Complexes of Polyarenes (C) 2540

- The First Dinuclear Low-Valent Samarium Complex with a Short Sm–Sm Contact (C) 2141
- The Novel Copper Polytelluride Salts $NaBa_6Cu_3Te_{14}$ and $(K_{0.60}Ba_{0.40})Ba_6Cu_{2.58}Te_{14}$: Discrete Clusters or Extended Solids? (C) 68

Metastable compounds
- Preparative Solid-State Chemistry with High-Power CO_2 Lasers (R) 634

Metathesis
- A Series of Well-Defined Metathesis Catalysts—Synthesis of $[RuCl_2(=CHR')(PR_3)_2]$ and Its Reactions (C) 2039
- Catalytic Ring-Closing Metathesis: A New, Powerful Technique for Carbon–Carbon Coupling in Organic Synthesis (H) 1833
- Solid-State and Solution Structures of $[\{NW(OC(CH_3)_2CF_3)_3\}_3]$ and Factors Favoring the Metathesis of C–N and N–W Triple Bonds in Reactions Involving Organic Nitriles and Ditungsten Hexaalkoxides (C) 110

Methane activation
- Tantalum-Mediated Coupling of Methane and Carbon Dioxide in the Gas Phase (C) 2033
- The Catalytic Oxidative Coupling of Methane (R) 970

Methyl acrylate
- Enhancement of Catalytic Activity for Hydroformylation of Methyl Acrylate by Using Biphasic and "Supported Aqueous Phase" Systems (C) 1474

Methyleneboranes
- Compounds with Planar Tetracoordinate Boron Atoms: Anti van't Hoff/Le Bel Geometries without Metal Centers (C) 327

Methylenecyclopropane
- A Concise Synthetic Route to Cyclopentenes by [3+2] Cycloaddition of Dipolar Trimethylenemethane to Alkynes (C) 2154

Micelles
- Gas-Phase Micelles (C) 2053

Michael additions
- Enantioselective Synthesis of β-Amino Acids: TMS-SAMP as a Chiral Ammonia Equivalent for the Aza Analogous Michael Addition to α,β-Unsaturated Esters (C) 455

Microporosity
- Al,Ti Avoidance in the Microporous Titanoaluminosilicate ETAS-10 (C) 1003
- Structure Organization of Aluminosilicate Polyanions with Surfactants: Optimization of Al Incorporation in Aluminosilicate Mesostructural Materials (C) 1499
- Synthesis and X-Ray Powder Structure of a Novel Porous Uranyl Phenylphosphonate Containing Unidimensional Channels Flanked by Hydrophobic Regions (C) 1508

Microreactors
- Radiofrequency Encoded Combinatorial Chemistry (C) 2289

Microscopy
- Cytomimetic Organic Chemistry: Early Developments (R) 2091

Microwaves
- Chemical Generation and Reception of Radio- and Microwaves (B) 936

Mills–Nixon effect
- X-Ray Diffraction Evidence for a Cyclohexatriene Motif in the Molecular Structure of Tris(bicyclo[2.1.1]hexeno)benzene: Bond Alternation after the Refutation of the Mills–Nixon Theory (C) 1454

Mixed-valent compounds
- The First μ(OH)-Bridged Model Complex for the Mixed-Valent $Fe^{II}Fe^{III}$ Form of Hemerythrin (C) 2642

Model complexes
- The First μ(OH)-Bridged Model Complex for the Mixed-Valent $Fe^{II}Fe^{III}$ Form of Hemerythrin (C) 2642

Molecular dynamics simulations
- Computer Simulations of Biomolecular Systems. Theoretical and Experimental Applications. Vol. 2 (B) 1034
- The Macrolidic Glycolipid Calonyctin A, a Plant Growth Regulator: Synthesis, Structural Assignment, and Conformational Analysis in Micellar Solution (C) 2520

Molecular modeling
- Double Helical Dinuclear Copper(I) Complexes of Macrocyclic Bis(dithiadiimine) Ligands (C) 1883

Molecular recognition
- A New Family of Chiral Binaphthyl-Derived Cyclophane Receptors: Complexation of Pyranosides (C) 1596
- A Self-Assembled Bifunctional Receptor (C) 2124
- Barbituric Acid/2,4,6-Triaminopyrimidine Aggregates in Water and Their Competitive Interaction with Monolayers of Barbituric Acid Lipids at the Gas–Water Interface (C) 58
- Binding of Boron and Alkali Metal Cations by a Pseudocryptand (C) 1115
- Burial of Hydrocarbon Causes Cooperative Enhancement of Electrostatic Binding (C) 1483
- Combinatorial Synthesis and Multidimensional NMR Spectroscopy: An Approach to Understanding Protein–Ligand Interactions (R) 953
- DNA–Carbohydrate Recognition: Design and Synthesis of an Eight-Base Sequence-Specific DNA-Binding Oligosaccharide (C) 576
- Doubly Encircled and Double-Stranded Pseudorotaxanes (C) 1869
- Highly Effective Hydrogen-Bonding Receptors for Guanine Derivatives (C) 2163
- Kinetic Selection in the Template-Directed Self-Assembly of [2]Catenanes (C) 2378
- Molecular Imprinting in Cross-Linked Materials with the Aid of Molecular Templates—A Way towards Artificial Antibodies (R) 1812
- Molecular Recognition of Anions by Zwitterionic Host Molecules in Water (C) 65
- Molecular Recognition of Terephthalic Acid by Supramolecular Self-Assembly of an Acridine-Pendant Cyclen–Zn^{II} Complex (C) 663
- Polar Interactions between Stacked π Systems in Fluorinated 1,8-Diarylnaphthalenes: Importance of Quadrupole Moments in Molecular Recognition (C) 1019
- Self-Assembly of Molecular-Sized Boxes (H) 1079
- Supramolecular Inorganic Chemistry: Small Guests in Small and Large Hosts (R) 2311
- The Lock and Key Principle. The State of the Art—100 Years on (B) 2293

Molecular shape
- Shape in Chemistry. An Introduction to Molecular Shape and Topology (B) 361

Molecular sieves
- Synthesis of Hexagonally-Packed Mesoporous TiO_2 by a Modified Sol–Gel Method (C) 2014

Molecular switches
- A Highly Stereoselective Optical Switching Process Based on Donor–Acceptor Substituted Dissymmetric Alkenes (C) 348
- Photonic Molecular Devices: Reversibly Photoswitchable Fluorophores for Nondestructive Readout for Optical Memory (C) 1119

Molecular wires
- Towards the Development of Molecular Wires: Electron Localization, Exchange, and Transfer in Alkyne-Bridged Multinuclear Complexes (C) 2705

Molybdenum compounds
- A Functionalized Polyoxometalate Bearing a Ferrocenylimido Ligand: Preparation and Structure of $[(FcN)Mo_6O_{18}]^{2-}$ (C) 2547
- Aggregation of Nitrido–Metal Complexes: The Example of $[(\eta^5\text{-}C_5Me_5)Mo(N)Cl_2]$ (C) 112
- A Molybdenum–Phosphorus Triple Bond: Synthesis, Structure, and Reactivity of the Terminal Phosphido (P^{3-}) Complex $[Mo(P)(NRAr)_3]$ (C) 2042
- Hydrothermal Synthesis of a Novel Se_{12} Ring in $[\{(NH_4)_2[Mo_3S_{11.72}Se_{1.28}]\}_2\text{-}[Se_{12}]]$ (C) 2509
- Monomeric Molybdenum and Tungsten Complexes That Contain a Metal–Phosphorus Triple Bond (C) 2044
- Synthesis and Coordination Chemistry of *ortho*-Functionalized Dimercaptobenzene: Building Blocks for Tripodal Hexathiol Ligands (C) 2700
- Synthesis and Structure of the Three-Dimensional Coordination Polymers $[(Me_3Sn)_4M(CN)_8]$ (M = Mo, W) (C) 2557
- Terminal E_1 Ligands from Elements of Group 15 (H) 1997
- The First Olefin-Substituted Peroxomolybdenum Complex: Insight into a New Mechanism for the Molybdenum-Catalyzed Epoxidation of Olefins (C) 1737
- $[Mo_{154}(NO)_{14}O_{420}(OH)_{28}(H_2O)_{70}]^{(25\pm5)-}$: A Water-Soluble Big Wheel with More than 700 Atoms and a Relative Molecular Mass of About 24000 (C) 2122

Monolayers
- First Steps Towards Ordered Monolayers of Ligand-Stabilized Gold Clusters (C) 1442

Mössbauer spectroscopy
- A New Type of Trinuclear Oxoiron(III) Cluster (C) 205
- μ-Nitridodiiron Complexes with Asymmetric $[Fe^{IV}\equiv N\text{–}Fe^{III}]^{4+}$ and Symmetric $[Fe^{IV}=N=Fe^{IV}]^{5+}$ Structural Elements (C) 669

Multicomponent reactions
- Optimization of the Biological Activity of Combinatorial Compound Libraries by a Genetic Algorithm (C) 2280
- The β-Lactam-Nucleoside Chimera (C) 2238

Multiple bonds
- A Molybdenum–Phosphorus Triple Bond: Synthesis, Structure, and Reactivity of the Terminal Phosphido (P^{3-}) Complex $[Mo(P)(NRAr)_3]$ (C) 2042
- Monomeric Molybdenum and Tungsten Complexes That Contain a Metal–Phosphorus Triple Bond (C) 2044
- Terminal E_1 Ligands from Elements of Group 15 (H) 1997
- The First Distibabutadiene: Synthesis and Structure of *trans*-1,4-Bis(trimethylsiloxy)-1,4-bis(2,4,6-tri-*tert*-butylphenyl)-2,3-distibabutadiene (C) 492

Mutagenesis
- Novel Biological Copper Proteins through Anion Addition to the Mutant Met121Gly of *Pseudomonas aeruginosa* Azurin (C) 1622
- Probing Protein Structure and Function with an Expanded Genetic Code (R) 621

Name reactions
- Namen- und Schlagwortreaktionen der Organischen Chemie (B) 935
- Organic Syntheses Based on Name Reactions and Unnamed Reactions (B) 935

Nanostructures
- First Steps Towards Ordered Monolayers of Ligand-Stabilized Gold Clusters (C) 1442
- New Dimensions in the Sol–Gel Process (H) 1578
- Synthesis and X-ray Structure of a Shape-Persistent Macrocyclic Amphiphile (C) 2713
- The Structural and Thermodynamic Basis for the Formation of Self-Assembled Peptide Nanotubes (C) 93

Nanotubes
- Filled Buckyballs: Recent Developments from the Endohedral Metallofullerenes of Lanthanides (H) 981
- Molecular Mosaics Formed by a Square Cyclophane and Its Inclusion Complex with Ferrocene (C) 1862

Naphthalenes
- A New Dimension in Radical Chain Group Transfer Reaction by Photosensitized Electron Transfer (PET) Reductive Activation of $PhSeSiR_3$ (C) 2669
- Novel, Blue-Transparent Frequency Doublers Based on 1,8-Di(hetero)arylnaphthalenes (C) 1485
- Synthesis and Structure of Bimetallic η^4,η^6-Naphthalene Complexes Containing a Mn–Mn Moiety Bonded in a *Syn*-Facial Manner: A General Route to Homo- and Heteronuclear Bimetallic Complexes of Polyarenes (C) 2540

Natural products
- A Novel Intramolecular Heck Reaction: Synthesis of a Cholesterol–Baccatin III Hybrid (C) 452
- Biosynthetic Origin of the Oxygen Atoms of Tetracenomycin C (C) 565
- Structures of UV-B Induced Sunscreen Pigments of Scots Pine (*Pinus sylvestris* L.) (C) 312
- The Conquest of Taxol (R) 2079
- Total Syntheses of Zaragozic Acid (H) 773
- Total Synthesis of Natural (+)-SF 2315A and Determination of the Absolute Configuration (C) 2396

Neighboring-group effects
- Phosphorothioates: β-Fragmentation versus β-Silicon Effect (C) 2406

Neural networks
- Assessing Similarity and Diversity of Combinatorial Libraries by Spatial Autocorrelation Functions and Neural Networks (C) 2674

Neurotoxins
- Toxins as Tools in Neurochemistry (R) 39

Neurotransmitters
- New Brain Lipids that Induce Sleep (H) 2362

Neutron diffraction
- A Framework Containing Ga-O-Ga Links: The Synthesis and Structure of Gallobicchulite $Ca_8(Ga_2SiO_6)_4(OH)_8$ (C) 2414
- $Li_5Pt_2H_9$, a Complex Hydride Containing Isolated $[Pt_2H_9]^{5-}$ Ions (C) 898

Nickel compounds
- A New Nickel-Catalyzed Cross-Coupling Reaction between sp^3 Carbon Centers (C) 2723
- A Nickel(II) Azide Cubane: Characterization of the Magnetic Exchange Interactions Mediated by a Triply Bridging Azide Group Bound End-On (C) 889
- New Selenolato-Bridged Clusters of Iron and Nickel; the Structures of $[Fe_{12}(SePh)_{24}]$ and $[Na_2(POPh_3)_6][Ni_{20}Se_{12}(SeMe)_{10}]$ (C) 307
- The Structure of the *D. gigas* [NiFe] Hydrogenase and the Nature of the Hydrogenase Nickel Complex (H) 1193
- $[Ni_3(alkyne)_4]$—The First Homoleptic Alkyne–Metal Oligomer (Alkyne: 2,5,5-Trimethylhex-3-yn-2-ol) (C) 1860

Niobium compounds
- $CsPr_9NbBr_{15}N_6$: A New Type of Interstitially Stabilized Cluster Compound (C) 2262
- DAD Compounds of Niobium and Tantalum: Examples of the Structural Flexibility of DAD Ligands (C) 2649
- $(Nb,Ta)_9(S,Te)_5$, a Metal-Rich Chalcogenide with a Microporous Metal Substructure (C) 1089

NIR atlas
- FT-NIR Atlas (B) 120

Nitrides
- $CsPr_9NbBr_{15}N_6$: A New Type of Interstitially Stabilized Cluster Compound (C) 2262
- The Preparation of Salts of $[Pd_2(\mu\text{-}Se_2N_2)Cl_6]^{2-}$, the First Adducts of Diselenium Dinitride (C) 1758

Nitrido complexes
- Aggregation of Nitrido–Metal Complexes: The Example of $[(\eta^5\text{-}C_5Me_5)Mo(N)Cl_2]$ (C) 112
- Solid-State and Solution Structures of $[\{NW(OC(CH_3)_2CF_3)_3\}_3]$ and Factors Favoring the Metathesis of C–N and N–W Triple Bonds in Reactions Involving Organic Nitriles and Ditungsten Hexaalkoxides (C) 110

Nitriles
- Synthesis and Structure of 1-Aza- and 1-Phospha-2-titanacyclobut-4-enes (C) 688
- Synthesis, Structural Investigation, and Ligand Properties of Isocyanoacetonitrile (C) 914

Nitro compounds
- Asymmetric Allylic Substitution with Nitromethane Catalyzed by a Pd Complex: Enantioselectivities Exceeding 99.9% ee (C) 2687
- Dependent on Photochromism Crystal Packing: Photoinduced and Thermal Proton-Transfer Processes in Single Crystals f 6-(2,4-Dinitrobenzyl)-2,2′-Bipyridine (C) 2530
- Detection and Reactions of Radical Cations Generated by Photolysis of Aromatic Compounds with Tetranitromethane in 1,1,1,3,3,3-Hexafluoro-2-propanol at Room Temperature (C) 2268

Nitrogenases
- On the Synthesis of the FeMo Cofactor of Nitrogenase: Gene-Controlled in Nature versus Laboratory-Produced by Man (R) 1071

Nitrogen compounds
- A $Te_2N_6Li_4$ Cage Containing the Tris(*tert*-butylimido)tellurite Dianion (C) 2549
- Covalent Inorganic Azides (R) 511
- Fluorophosphazenate Ions: A Route to Complexation of Fluoride Ions (C) 2696
- Ring Expansion of the Fullerene Core by Highly Regioselective Formation of Diazafulleroids (C) 1343
- S_7NH and S_7NCH_3 as Novel Chelating Ligands in $[(\eta^5\text{-}C_5H_5)_2Ti]$ Complexes: Synthesis of Medium-Sized Sulfur–Nitrogen Rings by Ligand Transfer (C) 1330
- $(Sr_6N)[Ga_5]$ and $(Ba_6N)[Ga_5]$: Compounds with Discrete (M_6N) Octahedra and $[Ga_5]$ Clusters (C) 1761
- Synthesis and Structure of Triamino- and Tetraaminosilanes (C) 2645
- Synthesis, Structure, and Reactivity of an Imido- and an Oxo(imido)phosphorane $R\text{–}P(=X)=NR$ (X = NH, O; $R = tBu_3C_6H_2$) (C) 460
- The First Sulfur(VI)–Nitrogen–Phosphorus Macrocycles (C) 998
- The Organic Chemistry of Aliphatic Nitrogen Compounds (B) 1249

Nitrogen fixation
- On the Synthesis of the FeMo Cofactor of Nitrogenase: Gene-Controlled in Nature versus Laboratory-Produced by Man (R) 1071

Nitrogen–fluorine compounds
- Hexakis(trifluoromethyl)tetrazane (C) 586

Nitronic acids
- Formation of Nitronic Acids by Ring Opening of Nitrocyclopropanes by a Concerted, Acid-Catalyzed Mechanism (C) 1091

Nitroxides
- Structure Determination from Powder X-Ray Diffraction Data of a Hydrogen-Bonded Molecular Solid with Competing Ferromagnetic and Antiferromagnetic Interactions: The 2-(3,4-Dihydroxyphenyl)-α-Nitronyl Nitroxide Radical (C) 55
- 2-[*p*-(*N*-*tert*-butyl-*N*-oxyamino)phenyl]-4,4,5,5-tetramethyl-4,5-dihydroimidazol-3-oxide-1-oxyl, a Stable Diradical with a Triplet Ground State (C) 927

NLO materials
- Design, Synthesis, and Properties of Molecule-Based Assemblies with Large Second-Order Optical Nonlinearities (R) 155
- New Nonlinear Optical Materials: Expedient Topotactic Self-Assembly of Acentric Chromophoric Superlattices (C) 1497
- Organometallic Compounds for Nonlinear Optics—The Search for En-light-enment! (R) 21 (826)

NMR spectroscopy
- A Framework Containing Ga-O-Ga Links: The Synthesis and Structure of Gallobicchulite $Ca_8(Ga_2SiO_6)_4(OH)_8$ (C) 2414
- A New Quantitative Description of the Distance Dependence of Through-Space $^{19}F,^{19}F$ Spin–Spin Coupling (C) 1881
- Carbon-13 NMR Chemical Shifts in Structural and Stereochemical Analysis (B) 1251
- Combinatorial Synthesis and Multidimensional NMR Spectroscopy: An Approach to Understanding Protein–Ligand Interactions (R) 953
- Direct On-Line Coupling of Capillary Electrophoresis and ^1H NMR Spectroscopy (H) 641
- Modified Triple Resonance NMR Experiments with Optimized Sensitivity for Rapidly Exchanging Protons (C) 469
- On the Mechanism of Action of Urocanase: Observation of the Enzyme-Bound NAD^+–Inhibitor Adduct by ^{13}C NMR Spectroscopy (C) 652
- Palladacycles as Structurally Defined Catalysts for the Heck Olefination of Chloro- and Bromoarenes (C) 1844

- ^{31}P CP/MAS NMR Spectroscopy of Transition Metal Phosphane Complexes: "*J*-Recoupling" between Chemically Equivalent ^{31}P Nuclei in Polycrystalline Compounds of the Type *trans*-[$(PR_3)_2MX_2$], M = Pd, Pt (C) 667
- Phosphorus-31 NMR Spectral Properties in Compound Characterization and Structural Analysis (B) 1651
- Platination Pathways for Reactions of Cisplatin with GG Single-Stranded and Double-Stranded Decanucleotides (C) 1874
- Relationship between C(O)–N Twist Angles and ^{17}O NMR Chemical Shifts in a Series of Twisted Amides (C) 1113
- Scalar Coupling Constants—Their Analysis and Their Application for the Elucidation of Structures (R) 1671
- Self-Diffusion of Charged Polycyclic Systems and Their Parent Compounds: A PGSE NMR Study (C) 816
- Structure Determination of Vitamin A Acetate Isomers through Coupled HPLC and ^{1}H NMR Spectroscopy (C) 1014
- Substituent-Controlled Reactions of Iminophosphoranes with Methyllithium (C) 1752
- The Synthesis of Tris(perfluoroalkyl)-phosphanes (C) 1241
- Two-Dimensional NMR Spectroscopy. Applications for Chemists and Biochemists (B) 1903
- Ylidediyl Halophosphane Oligomers, $(Ph_3PCPX)_n$—A Structurally Diverse Class of Compounds (C) 1853

Nobel lectures
- G Proteins and Regulation of Adenylate Cyclase (Nobel Lecture) (R) 1406
- My Search for Carbocations and Their Role in Chemistry (Nobel Lecture) (R) 1393
- Signal Transduction: Evolution of an Idea (Nobel Lecture) (R) 1420

Noncovalent interactions
- Self-Assembly of Molecular-Sized Boxes (H) 1079

Nonheme iron compounds
- Nonheme Iron Centers in Oxygen Activation: Characterization of an Iron(III) Hydroperoxide Intermediate (C) 1512

Nonlinear optics
- Design, Synthesis, and Properties of Molecule-Based Assemblies with Large Second-Order Optical Nonlinearities (R) 155
- Linear and Nonlinear Optical Properties of Molecules (B) 827
- New Nonlinear Optical Materials: Expedient Topotactic Self-Assembly of Acentric Chromophoric Superlattices (C) 1497
- Novel, Blue-Transparent Frequency Doublers Based on 1,8-Di(hetero)arylnaphthalenes (C) 1485

Nonmetal chemistry
- Fluorocarbonate, $[FCO_2]^-$: Preparation and Structure (C) 1858

Non-stoichiometric compounds
- Chemistry of Non-Stoichiometric Compounds (B) 1033

N_2O reductase
- The Dinuclear Cu_A Center in Cytochrome *c* Oxidase and N_2O Reductase—A Metal–Metal Bond in Biology? (H) 771

Normuramic acid
- Saccharide–Peptide Hybrids as Novel Oligosaccharide Mimetics (C) 2712

Nuclear stability
- Two at One Blow: The New Chemical Elements 110 and 111 (H) 1713

Nucleic acids
- Advanced Organic Chemistry of Nucleic Acids (B) 1521
- 1,5-Anhydrohexitol Nucleic Acids, a New Promising Antisense Construct (C) 1338 (2165)
- Rapid Hydrolysis of RNA with a Cu^{II} Complex (C) 472

Nucleobases
- The pH-Dependent Synthesis and Structural Study of Dimeric and Cyclic Trimeric Complexes of 9-Methyl- or 9-Ethylhypoxanthine Nucleobases with (η^5-Pentamethylcyclopentadienyl)rhodium Aqua Complexes (C) 1514

Nucleophilic additions
- Acyclic 1,4-Diastereoselectivity in γ-Substituted α-Enones: Transmission of Chiral Information through Conjugation (C) 2254
- Additions of Carbanions to a Cationic Cyclopentadienyl(naphthalene)iron Complex (C) 2161
- Diastereo- and Enantioselective Synthesis of 1,2-Amino Alcohols from Glycol Aldehyde Hydrazones; Asymmetric Synthesis of (*R,R*)-Statin (C) 1219
- Nucleophilic Addition to (π-Allyl)-palladium Complexes: Control of the Attack at the Central or Terminal Carbon Atom by Ligands (C) 2551
- Temperature and Solvent Effect on the Nucleophilic Addition of *n*-Butyllithium to the *N*-(Trimethylsilyl)imine of (2*S*)-Lactal (C) 2150

Nucleophilic aromatic substitutions
- First-Ever Per(onio) Substitution of Benzene: The Role of the Counterion (C) 1319

Nucleoside analogues
- The β-Lactam-Nucleoside Chimera (C) 2238

Nucleoside diphosphate sugars
- Thymidine Diphospho-6-deoxy-α-D-*ribo*-3-hexulose—Synthesis of a Central Intermediate in the Biosynthesis of Di- and Trideoxysugars (C) 1328

Nucleosides
- Asymmetric Syntheses of Stavudine (d4T) and Cordycepin by Cycloisomerization of Alkynyl Alcohols to Endocyclic Enol Ethers (C) 350
- Highly Effective Hydrogen-Bonding Receptors for Guanine Derivatives (C) 2163

Nucleotides
- Phosphorothioates: β-Fragmentation versus β-Silicon Effect (C) 2406
- Platination Pathways for Reactions of Cisplatin with GG Single-Stranded and Double-Stranded Decanucleotides (C) 1874

O_2 activation
- Coordination of Dioxygen in Three Representative Transition Metal Cations: FeO_2^+, CrO_2^+, and $[CH_3Re(O_2)_2O]^+$ (C) 2517
- Hydroxylation of Alkanes with Molecular Oxygen Catalyzed by a New Ruthenium-Substituted Polyoxometalate, $[WZnRu^{III}_2(OH)(H_2O)(ZnW_9O_{34})_2]^{11-}$ (C) 1587
- Nonheme Iron Centers in Oxygen Activation: Characterization of an Iron(III) Hydroperoxide Intermediate (C) 1512
- Reactions of 1,1′-Ferrocenediylbis{chloro-[(1,2,5,6-η)-1,5-cyclooctadiene]}-diplatinum with Triarylphosphane and Molecular Oxygen (C) 319

Octaphyrin
- Octaphyrin-(1.0.1.0.1.0.1.0) (C) 2515

Octapyrroles
- From Porphyrin Isomers to Octapyrrolic "Figure Eight" Macrocycles (C) 2511

Oligomers
- $[Ni_3(alkyne)_4]$—The First Homoleptic Alkyne–Metal Oligomer (Alkyne: 2,5,5-Trimethylhex-3-yn-2-ol) (C) 1860
- 1,3,5,7-Tetraphosphabarrelene: A New Cyclic Phosphaalkyne Tetramer (C) 81

Oligonucleotides
- Electron Transfer through DNA: Site-Specific Modification of Duplex DNA with Ruthenium Donors and Acceptors (C) 352
- Triple-Helix Formation of Oligodeoxynucleotides Containing [(3′*S*,5′*R*)-2′-Deoxy-3′,5′-ethano-β-D-ribofuranosyl]nucleosides ("Bicyclo-deoxynucleosides") (C) 694

Oligophenylenes
- C_3-Symmetric Hexakis(trimethylsilyl)[7]-phenylene ["Tris(biphenylenocyclobutadieno)cyclohexatriene"], a Polycyclic Benzenoid Hydrocarbon with Slightly Curved Topology (C) 1478

Oligosaccharide mimetics
- Saccharide–Peptide Hybrids as Novel Oligosaccharide Mimetics (C) 2712

Oligosaccharides
- A Multienzyme System for a One-Pot Synthesis of Sialyl T-Antigen (C) 893
- A Strategy of "Random Glycosylation" for the Production of Oligosaccharide Libraries (C) 2720
- Chemoenzymatic Synthesis of a Modified Pentasaccharide as a Specific Substrate for a Sensitive Assay of α-Amylase by Fluorescence Quenching (C) 1239
- β-Cycloaltrin: A Cyclooligosaccharide Consisting of Seven $\alpha(1\rightarrow4)$-Linked Altropyranoses (C) 1621
- DNA–Carbohydrate Recognition: Design and Synthesis of an Eight-Base Sequence-Specific DNA-Binding Oligosaccharide (C) 576
- Progress in Oligosaccharide Synthesis through a New, Orthogonal Glycosylation Strategy (H) 1432

Oligothiophenes
- Oligothiophenes—Yet Longer? Synthesis, Characterization, and STM Images of Homologous, Isomerically Pure Oligo(alkylthiophene)s (C) 303

On-line detectors
- Trace Analysis of the Radionuclides ^{90}Sr and ^{89}Sr in Environmental Samples III: Development of a Fast Analytical Method (C) 186

Optical data storage
- A Highly Stereoselective Optical Switching Process Based on Donor–Acceptor Substituted Dissymmetric Alkenes (C) 348

Optically active carbene complexes
- Carbene Complex Functionalized Sugars (C) 1856

Optical readout
- Photonic Molecular Devices: Reversibly Photoswitchable Fluorophores for Nondestructive Readout for Optical Memory (C) 1119

Organic chemistry
- The Organic Chemistry of Aliphatic Nitrogen Compounds (B) 1249

Organic conductors
- $(DTEDT)[Au(CN)_2]_{0.4}$: An Organic Superconductor Based on the Novel π-Electron Framework of Vinylogous Bis-Fused Tetrathiafulvalene (C) 1222
- Electrochemical Synthesis of a Redox-Active Polymer Based on Buckminsterfullerene Epoxide (C) 194

- Towards the Development of Molecular Wires: Electron Localization, Exchange, and Transfer in Alkyne-Bridged Multinuclear Complexes (C) 2705

Organic solids
- Orthorhombic and Monoclinic 2,3,7,8-Tetramethoxythianthrene: Small Structural Difference—Large Lattice Change (C) 76

Organolanthanide compounds
- Cyclopentadienyl-Free Organolanthanide Chemistry (R) 2466

Organometallic polymers
- Polymers with Complexed Cyclobutadiene Units in the Main Chain: The First Example of a Thermotropic, Liquid Crystalline Organometallic Polymer (C) 569

Osmium compounds
- Electronic Energy Transfer Across Ethynyl-Bridged Ru^{II}/Os^{II} Terpyridyl Complexes (C) 1100
- Metal Oxo Cation Receptors: Multimode Coordination to the Dioxoosmium(VI) Cation (C) 1359

Osmylation
- Catalytic Photoinduced Charge-Transfer Osmylation: A Novel Pathway from Arenes to Cyclitol Derivatives (C) 2031

Oudemansins
- 9-Methoxystrobilurins—A Link Between Strobilurins and Oudemansins (C) 196

Oxetanes
- Facial Diastereoselectivity in the Paternò–Büchi Reaction of Chiral Silyl Enol Ethers (C) 2271

Oxidations
- Alteration of the Reactivity of a Tellurophene Within a Core-Modified Porphyrin Environment: Preparation and Oxidation of 21-Telluraporphyrin (C) 2252
- Aminocarbyne Complexes of Chromium in a High Oxidation State—Synthesis, Structure, and Reactivity (C) 924
- A Stable Aquairon(III) Complex with $S = 1$: Structure and Spectroscopic Properties (C) 1216 (1649)
- Asymmetric Sulfide Oxidation with Vanadium Catalysts and H_2O_2 (C) 2640
- Coupling of Endothermic Thermal Cracking with Exothermic Oxidative Dehydrogenation of Ethane to Ethylene Using a Diluted SrO/La_2O_3 Catalyst (C) 665
- Formation of an Alkylperoxoiron(III) Complex during Oxidations Catalyzed by μ-Oxodiiron(III) Complexes (C) 203
- Oxidative Polycyclization versus the "Polyepoxide Cascade": New Pathways in Polyether (Bio)synthesis? (H) 298
- Oxidative Transformations of a Pyrimidalized 1,5-Diene (C) 2502
- Sulfoxide-Stabilized Giant Palladium Clusters in Catalyzed Oxidations (C) 457
- Synthetic Aspects of Metal-Catalyzed Oxidations of Amines and Related Reactions (R) 2443
- The Catalytic Oxidative Coupling of Methane (R) 970

Oxidative coupling
- A New Method for the Synthesis of Amphipolar Phosphorus-Containing Heterocycles (C) 557

Oxidative fragmentations
- Radical C–C Bond Formation by Photoinduced Electron Transfer Addition of α-Silyl Carbamates to Acceptor-Substituted Alkenes (C) 2137

Oxidoreductases
- Biosyntheses of Novel Emycins from the Mutant Strain *Streptomyces cellulosae* ssp. *griseoincarnatus* 1114-2 (C) 1617

Oxygenations
- A Highly Reactive and Catalytically Active Model System for Intradiol-Cleaving Catechol Dioxygenases: Structure and Reactivity of Iron(III) Catecholate Complexes of *N,N'*-Dimethyl-2,11-diaza[3,3](2,6)pyridinophane (C) 2671
- Complexation of [*N,N'*-Bis(salicylidene)ethylenediiminato]cobalt(III)$^+$ by Anilines in Dimethylformamide (C) 1086

Oxygen compounds
- Bis(trifluoromethyl)trioxide: First Structure of a Straight-Chain Trioxide (C) 2244

O–H bond formation
- Direct Observation of O–H Reductive Elimination from Ir^{III} Complexes (C) 229

Pagodanes
- 4c/3e Radical Cations with Cage-Directed Configurations (C) 1016

Palladium compounds
- A New Platform for Designing Ligands for Asymmetric Induction in Allylic Alkylations (C) 2386
- A Simple Catalytic Method for the Conversion of Aryl Bromides to Arylamines (C) 1348
- Asymmetric Allylic Substitution with Nitromethane Catalyzed by a Pd Complex: Enantioselectivities Exceeding 99.9% ee (C) 2687
- Enantiomerically Pure Palladacycles Derived from β-Ketosulfoxides (C) 1351
- Highly Stereoselective Allylation of Benzaldehyde: Generation of a Stereochemically Defined Allylzinc Species from a π-Allylpalladium Intermediate and Diethylzinc (C) 787
- Isolation and X-Ray Crystal Structure of a Palladacyclobutane: Insight into the Mechanism of Cyclopropanation (C) 100
- Metal Complexes of N-Heterocyclic Carbenes—A New Structural Principle for Catalysts in Homogeneous Catalysis (C) 2371
- Nucleophilic Addition to (π-Allyl)-palladium Complexes: Control of the Attack at the Central or Terminal Carbon Atom by Ligands (C) 2551
- Palladacycles as Efficient Catalysts for Aryl Coupling Reactions (C) 1848
- Palladium-Catalyzed Resactions of Propargylic Compounds in Organic Synthesis (R) 2589
- Sulfoxide-Stabilized Giant Palladium Clusters in Catalyzed Oxidations (C) 457
- Synthesis of a Cationic 1,3-Diphospha-2,4-dipallada(II)tricyclo[1.1.1]pentane Derivative: The First Structurally Characterized Pyramidal μ_2-Phosphinidene (C) 2677
- The First Mixed-Metal Borole Cluster; Stabilization of Formally 14e Pd Centers in the Re_2Pd_2 Electron-Deficient [{[(η^5-C_4H_4BPh)($CO)_3$Re]Pd}$_2$] Cluster (C) 1010
- Transition Metal Catalyzed Dimerization of Allenyl Ketones (C) 1581
- Unprecedented Intra- and Intermolecular Palladium-Catalyzed Coupling Reactions with Methylenecyclopropane Type Tetrasubstituted Alkenes (C) 2545

Paraquat
- Strong Binding of Paraquat and Polymeric Paraquat Derivatives by Basket-Shaped Hosts (C) 2132

Paternò–Büchi reactions
- Facial Diastereoselectivity in the Paternò–Büchi Reaction of Chiral Silyl Enol Ethers (C) 2271

Peer Review
- Guardians of Science. Fairness and Reliability of Peer Review (B) 359

Pentalenes
- Dilithium Acepentalenediide: An Unusual Dimer of Contact Ion Triplets with Bowl-Shaped Dianions (C) 1492

Peptide analogues
- Macrobicyclic Titanium(IV) Complexes with C_3-Symmetric Synthetic Peptides (C) 1449
- Synthetic Receptors Based on Vinylogous Sulfonyl Peptides (C) 1765
- The Arndt–Eistert Reaction in Peptide Chemistry: A Facile Access to Homopeptides (C) 471

Peptide isosters
- Synthesis of $\Psi[SCH_2]$-, $\Psi[SOCH_2]$-, and $\Psi[SO_2CH_2]$-Peptide Isosters (C) 553

Peptides
- A Novel Allylic Anchor for Solid-Phase Synthesis—Synthesis of Protected and Unprotected O-Glycosylated Mucin-Type Glycopeptides (C) 803
- A Versatile Solid-Phase Synthesis of N-Linked Glycopeptides (C) 60
- Burial of Hydrocarbon Causes Cooperative Enhancement of Electrostatic Binding (C) 1483
- Peptide Ligases—Tools for Peptide Synthesis (H) 175
- Radiofrequency Encoded Combinatorial Chemistry (C) 2289
- β-Sheet Peptide Architecture: Measuring the Relative Stability of Parallel vs. Antiparallel β-Sheets (C) 95
- Solid-Phase Synthesis of Vinylogous Sulfonyl Peptides (C) 1763
- Stereoselective Syntheses of Peptide Derivatives with 2-Acetamido-3,4,6-tri-*O*-acetyl-1-amino-2-deoxy-β-D-glucopyranose by Four-Component Condensation (C) 1104
- The Structural and Thermodynamic Basis for the Formation of Self-Assembled Peptide Nanotubes (C) 93

Pericyclic reactions
- Conical Intersections and the Mechanism of Singlet Photoreactions (H) 549
- Pericyclic Reactions in Nature: Spontaneous Cope Rearrangement Inactivates Algae Pheromones (C) 1602

Periodic nodal surfaces
- Hyperbolic Lone Pair Structure in $RhBi_4$ (C) 1204

Peroxo complexes
- An Alkylperoxoiron(III) Intermediate and Its Role in the Oxidation of Aliphatic C–H Bonds (C) 2048

Perylenes
- Quaterrylenebis(dicarboximides) (C) 1323

Phanes
- Novel "π-Boat" Cage Compounds as Potential Cryptands (C) 789
- Topochemical Reaction Control in Solution (C) 685

Pharmaceuticals
- Anticoagulatory Substances of Blood-sucking Animals: From Hirudin to Hirudin Mimetics (R) 867
- Digitalis Research in Berlin–Buch—Retrospective and Perspective Views (R) 282

Phase separation
- Photoswitchable Phase Separation in Hydrophobically Modified Poly(acrylamide)/Surfactant Systems (C) 88

Phase transfer catalysis
- Molecular Recognition between Chemically Modified β-Cyclodextrin and Dec-1-ene: New Prospects for Biphasic Hydroformylation of Water-Insoluble Olefins (C) 2269

Phase transformations
- Basic Principles of Thermoanalytical Techniques and Their Applications in Preparative Chemistry (R) 1171
Phenanthridinones
- Self-Assembling Discotic Mesogens (C) 1637
Pheromones
- Pericyclic Reactions in Nature: Spontaneous Cope Rearrangement Inactivates Algae Pheromones (C) 1602
Phosphaalkenes
- A Simple Route to the 1-Aza-3-Phosphaallyl System: Structure of a Dimeric Lithium Complex and Protonation To Give the First NH_2-Substituted Phosphaalkene (C) 2369
Phosphaalkynes
- 2,4-Di-*tert*-butyl-1λ^3,3λ^3-diphosphinines: Targeted Synthesis at Iron(0) Centers and Oxidative Release (C) 198
- Phosphaalkyne Cyclooligomers: From Dimers to Hexamers—First Steps on the Way to Phosphorus–Carbon Cage Compounds (H) 436
- Selective Syntheses of 1,3-Diphosphacyclobutadiene, Dewar-1,3,5-triphosphabenzene, 1,3,5-Triphosphabenzene, and 1,3,5,7-Tetraphosphabarrelene by Cyclooligomerization of Phosphaalkynes (C) 2227
- Synthesis and Structure of 1-Aza- and 1-Phospha-2-titanacyclobut-4-enes (C) 688
- 1,3,5,7-Tetraphosphabarrelene: A New Cyclic Phosphaalkyne Tetramer (C) 81
- Tetraphosphatricyclo[4.2.0.0^{2,5}]octadienes; New Phosphaalkyne Cyclotetramers Derived from $\lambda^3\sigma^2$-Diphosphetes (C) 484
Phosphane ligands
- New Process for the Sulfonation of Phosphane Ligands for Catalysts (C) 811
Phosphanes
- Reactions of 1,1′-Ferrocenediylbis{chloro-[(1,2,5,6-η)-1,5-cyclooctadiene]}-diplatinum with Triarylphosphane and Molecular Oxygen (C) 319
- Substituent-Controlled Reactions of Iminophosphoranes with Methyllithium (C) 1752
Phosphates
- Antibody-Catalyzed Phosphate Triester Hydrolysis (C) 2275
Phosphazenes
- Fluorophosphazenate Ions: A Route to Complexation of Fluoride Ions (C) 2696
- The First Sulfur(VI)–Nitrogen–Phosphorus Macrocycles (C) 998
Phosphenium complexes
- P–H-Functionalized Phosphenium Complexes $[C_5R_5(OC)_2W{=}P(H)R']$ (R′ = *t*Bu, sMes): Synthesis, Isomerization, and Transformation into Hydrido Complexes Containing a *t*BuP(H)OH Ligand (C) 2500
Phosphinomethanide
- A New Method for the Synthesis of Amphipolar Phosphorus-Containing Heterocycles (C) 557
Phospholipids
- Glc-PC, a New Type of Glucosidic Phospholipid (C) 2667
- Synthesis, Antitumor Activity, and Tolerability of Phospholipids with Nitrogen Homologues (C) 238
Phosphonates
- Synthesis and X-Ray Powder Structure of a Novel Porous Uranyl Phenylphosphonate Containing Unidimensional Channels Flanked by Hydrophobic Regions (C) 1508
Phosphorane iminato complexes
- Phosphorane Iminato Complexes of Manganese and Cobalt with Heterocubane Structure (C) 1235
Phosphoranes
- Synthesis, Structure, and Reactivity of an Imido- and an Oxo(imido)phosphorane R–P(=X)=NR (X = NH, O; R = tBu$_3$C$_6$H$_2$) (C) 460
Phosphorus
- New Evidence Concerning the Structure of Amorphous Red Phosphorus (H) 2637
Phosphorus compounds
- A Facile Access to 1λ^5,3λ^5-Benzodiphospholes (C) 2017
- A Molybdenum–Phosphorus Triple Bond: Synthesis, Structure, and Reactivity of the Terminal Phosphido (P^{3-}) Complex $[Mo(P)(NRAr)_3]$ (C) 2042
- A P_2C_2 Four-Membered Ring with Unusual Bonding—Synthesis, Structure, and Ring Opening of a 1,3-Diphosphacyclobutane-2,4-diyl (C) 555
- A Simple Route to the 1-Aza-3-Phosphaallyl System: Structure of a Dimeric Lithium Complex and Protonation To Give the First NH_2-Substituted Phosphaalkene (C) 2369
- Carbenoid or Lithium Complex of a Carbanion? Synthesis and Structure of $(Me_3Si)_2C{=}P(aryl){=}C(Cl)Li(thf)_3$ and LiCl Elimination To Give the Phosphirene (C) 1849
- η^5:η^2 Coordination of a *cyclo*-E_5 Ligand, E = P, As (C) 1321
- $(CuI)_3P_{12}$: A Solid Containing a New Polymer of Phosphorus Predicted by Theory (C) 1647
- Diphosphanyl- and Diarsanyl-Substituted Carbene Homologues: Germanediyls, Stannanediyls, and Plumbanediyls with Remarkable Electronic Structures (C) 1614
- Hydrolysis of a Phosphate Diester Doubly Coordinated to a Dinuclear Cobalt(III) Complex: A Novel Mechanism (C) 2412
- Monomeric Molybdenum and Tungsten Complexes That Contain a Metal–Phosphorus Triple Bond (C) 2044
- Novel Alkali Metal Phosphanide Aggregates (C) 316
- Phosphorothioates: β-Fragmentation versus β-Silicon Effect (C) 2406
- Selective Syntheses of 1,3-Diphosphacyclobutadiene, Dewar-1,3,5-triphosphabenzene, 1,3,5-Triphosphabenzene, and 1,3,5,7-Tetraphosphabarrelene by Cyclooligomerization of Phosphaalkynes (C) 2227
- $S(NPMe_3)_4^{2+}$: The First Structure Determination of a Dication of Hexavalent Sulfur (C) 1362
- Spherical Cyclophosphazene Dendrimers to the Fifth Generation (C) 578
- Synthesis of a 2*H*-Azirine by [1+2] Cycloaddition of a Phosphinocarbene with a Nitrile and Its Ring-Expansion to a 1,2λ^5-Azaphosphete (C) 1246
- Synthesis of a Cationic 1,3-Diphospha-2,4-dipallada(II)tricyclo[1.1.1]pentane Derivative: The First Structurally Characterized Pyramidal μ_2-Phosphinidene (C) 2677
- Synthesis of 1,2-Diphospholide Ions (C) 590
- Synthesis, Structure, and Reactivity of an Imido- and an Oxo(imido)phosphorane R–P(=X)=NR (X = NH, O; R = tBu$_3$C$_6$H$_2$) (C) 460
- Terminal E_1 Ligands from Elements of Group 15 (H) 1997
- *meso*-Tetrakis[4-(diphenylphosphino)-phenyl]porphyrin and a Water-Soluble Octakis(phosphonium salt) Porphyrin Double-Decker with a Cage Structure. (C) 2230
- The First Sulfur(VI)–Nitrogen–Phosphorus Macrocycles (C) 998
- The Synthesis of Tris(perfluoroalkyl)-phosphanes (C) 1241
- Ylidediyl Halophosphane Oligomers, $(Ph_3PCPX)_n$—A Structurally Diverse Class of Compounds (C) 1853
Phosphorus heterocycles
- Phosphaalkyne Cyclooligomers: From Dimers to Hexamers—First Steps on the Way to Phosphorus–Carbon Cage Compounds (H) 436
- Tetraphosphatricyclo[4.2.0.0^{2,5}]octadienes; New Phosphaalkyne Cyclotetramers Derived from $\lambda^3\sigma^2$-Diphosphetes (C) 484
Phosphorus ylides
- A New Method for the Synthesis of Amphipolar Phosphorus-Containing Heterocycles (C) 557
- The First Unambiguous Characterization of a Neutral Phosphorus Ylide–Lithium Complex: Isolation, Structure, and Ab Initio Investigations of $[(PhCH_2)_2NLi{\cdot}CH_2PPh_3]_2$ (C) 478
Phosphorus–carbon cage compounds
- Phosphaalkyne Cyclooligomers: From Dimers to Hexamers—First Steps on the Way to Phosphorus–Carbon Cage Compounds (H) 436
- Tetraphosphatricyclo[4.2.0.0^{2,5}]octadienes; New Phosphaalkyne Cyclotetramers Derived from $\lambda^3\sigma^2$-Diphosphetes (C) 484
Photoaffinity labeling
- Recent Trends in Photoaffinity Labeling (R) 1296
Photochemistry
- A New Dimension in Radical Chain Group Transfer Reaction by Photosensitized Electron Transfer (PET) Reductive Activation of $PhSeSiR_3$ (C) 2669
- Automerizations and Isomerizations in Propynylidene (HCCCH), Propadienylidene (H_2CCC), and Cyclopropenylidene (c-C_3H_2) (C) 2009
- Chemistry and Light (B) 599
- Conical Intersections and the Mechanism of Singlet Photoreactions (H) 549
- Detection and Reactions of Radical Cations Generated by Photolysis of Aromatic Compounds with Tetranitromethane in 1,1,1,3,3,3-Hexafluoro-2-propanol at Room Temperature (C) 2268
- Direct Spectroscopic Evidence for a Hitherto Elusive "Zwitterionic" Excited State (H) 547
- Effective Charge Separation in Intermolecular Complexes of an Electron Donor and a Doubly Branched Triad Assembly: A Model System for Environmental Effects Controlling Electron Transfer (C) 1005
- Electronic Energy Transfer Across Ethynyl-Bridged Ru^{II}/Os^{II} Terpyridyl Complexes (C) 1100
- Electronic Energy Transfer in a Supramolecular Species Containing the $[Ru(bpy)_3]^{2+}$, $[Os(bpy)_3]^{2+}$, and Anthracene Chromophoric Units (C) 595
- Facial Diastereoselectivity in the Paternò–Büchi Reaction of Chiral Silyl Enol Ethers (C) 2271
- Fundamentals of Photoinduced Electron Transfer (B) 495
- Light-Switchable Catalysis in Synthetic Receptors (C) 446

- Photochemical Key Steps in Organic Synthesis—An Experimental Coursebook (B) 1770
- Photo Electron Transfer Induced Macrocyclization of *N*-Phthaloyl-ω-aminocarboxylic Acids (C) 474
- Photoswitchable Electrical Communication of Glucose Oxidase and Glutathione Reductase with Electrode Surfaces through Photoisomerizable Redox Mediators (C) 1604
- Silacyclopropene: Generation by High-Vacuum Flash Pyrolysis and Matrix-Spectroscopic Identification (C) 1439
- Synthesis of Belt Cyclophanes (C) 1437
- Topochemical Reaction Control in Solution (C) 685
- Vibrational Spectroscopy in Supercritical Fluids: From Analysis and Hydrogen Bonding to Polymers and Synthesis (R) 1275
- 6,7-Bis(methoxycarbonyl)-2,3-dimethyl [5](1,4)naphthalenophane; the First Benzoannelated [5]Paracyclophane (C) 2553

Photochromism
- Dependent on Photochromism Crystal Packing: Photoinduced and Thermal Proton-Transfer Processes in Single Crystals f 6-(2,4-Dinitrobenzyl)-2,2'-Bipyridine (C) 2530
- Photonic Molecular Devices: Reversibly Photoswitchable Fluorophores for Nondestructive Readout for Optical Memory (C) 1119

Photoelectron spectroscopy
- Practical Surface Analysis. A2, Vol. 1. Auger and X-Ray Photoelectron Spectroscopy (B) 2059

Photoelectron transfer
- Radical C–C Bond Formation by Photoinduced Electron Transfer Addition of α-Silyl Carbamates to Acceptor-Substituted Alkenes (C) 2137

Photolithography
- Micron-Scale Patterning of Biological Molecules (C) 91

Photolyases
- Sunlight-Damaged DNA Repaired with Sunlight (H) 2491

Photolysis
- Photochemically Initiated Protein Splicing (C) 1629

Photosynthesis
- Aldehyde-Appended Tetraphenylporphyrin: A New Building Block for Porphyrin Arrays (C) 900
- Assembly and Crystal Structure of a Photoactive Array of Five Porphyrins (C) 1096
- Model Reactions for Photosynthesis—Photoinduced Charge and Energy Transfer between Covalently Linked Porphyrin and Quinone Units (R) 849

Phycocyanobilin
- A Phycocyanobilin Seryliminoester as a New Model for the Chromophore–Protein Interaction in Phytochrome (C) 1733

Physical chemistry
- The World of Physical Chemistry (B) 360

Phytochrome
- A Phycocyanobilin Seryliminoester as a New Model for the Chromophore–Protein Interaction in Phytochrome (C) 1733

Phytohormones
- Jasmonic Acid and Coronatin Induce Odor Production in Plants (C) 1600

Pictet–Spengler reactions
- Asymmetric Pictet–Spengler Reactions Employing *N,N*-Phthaloyl Amino Acids as Chiral Auxiliary Groups (C) 2402

Pinacol coupling
- Synthesis of New Sworski-Type Dehydroannulenes: 3,4-Benz-1,2,5,6,8,9,12,13-octadehydro[14]annulenes (C) 1892

Platinum compounds
- A μ-η^6:η^6-1,3,5-Triboratabenzenebis(cyclopentadienylcobalt) Triple-Decker Complex (C) 681
- Dicobalt and Diplatinum Complexes of Diborylcarbenes (C) 1111
- First Isolation of an Enol of a Carboxylic Acid by Complexation to an (Ethane-1,2-diamine)platinum(II) Fragment (C) 1103
- $Li_5Pt_2H_9$, a Complex Hydride Containing Isolated $[Pt_2H_9]^{5-}$ Ions (C) 898
- Models for Bimetallic Catalysts: Multiple Oxidation States in Pt_3Re Cluster Cations (C) 346
- Platination Pathways for Reactions of Cisplatin with GG Single-Stranded and Double-Stranded Decanucleotides (C) 1874
- Reactions of 1,1'-Ferrocenediylbis{chloro-[(1,2,5,6-η)-1,5-cyclooctadiene]}diplatinum with Triarylphosphane and Molecular Oxygen (C) 319
- Transition Metal Complexes as Both Host and Guest: Second-Sphere Coordination between a Pt-Azacrown Ether Host and a Pt-NH_3 Guest (C) 2689

Plumbylenes
- Bis(hypersilyl)tin and Bis(hypersilyl)lead, Two Electron-Rich Carbene Homologs (C) 1334

Polarizability
- Aligning and Trapping Molecules with Light (H) 2365

Polyacetylenes
- Organometallic Compounds for Nonlinear Optics—The Search for En-light-enment! (R) 21 (826)

Poly(acrylamide)s
- Photoswitchable Phase Separation in Hydrophobically Modified Poly(acrylamide)/Surfactant Systems (C) 88

Polyalcohols
- 1,5-Anhydrohexitol Nucleic Acids, a New Promising Antisense Construct (C) 1338 (2165)

Polycations
- First-Ever Per(onio) Substitution of Benzene: The Role of the Counterion (C) 1319
- Te_8^{4+}: A Cubic Polycation in the Structure of $Te_8(VOCl_4)_2$ (C) 2559

Polychalcogenides
- From *cyclo*-Te_8 to Te_x^{n-} Sheets: Are Nonclassical Polytellurides More Classical than We Thought? (H) 2109

Polycycles
- A Cycloaddition–Cyclodehydrogenation Route from Stilbenoids to Extended Aromatic Hydrocarbons (C) 1583
- Calculation of the Thermodynamic Properties of Polycyclic Aromatic Hydrocarbons by an Incremental Procedure (C) 1735
- Synthesis of a Cationic 1,3-Diphospha-2,4-dipallada(II)tricyclo[1.1.1]pentane Derivative: The First Structurally Characterized Pyramidal μ_2-Phosphinidene (C) 2677
- Tetraphosphatricyclo[4.2.0.0^{2,5}]octadienes; New Phosphaalkyne Cyclotetramers Derived from $\lambda^3\sigma^2$-Diphosphetes (C) 484

Polyenes
- Relative and Absolute Configuration of Filipin III (C) 1227

Polyethers
- Oxidative Polycyclization versus the "Polyepoxide Cascade": New Pathways in Polyether (Bio)synthesis? (H) 298

Poly(ethylenimine)s
- Formation of a Hexagonal Columnar Mesophase by N-Acylated Poly(ethylenimine) (C) 795

Polyhedral nets
- Hyperbolic Lone Pair Structure in $RhBi_4$ (C) 1204

Polyiodides
- Self-Assembly of Polyanions at a Metal Cation Template: Syntheses and Structures of $[\{Ag([18]aneS_6)\}I_7]_n$ and $[Ag([18]aneS_6)]I_3$ (C) 2374

Polyion aggregates
- The Lipophilically Wrapped Polyion Aggregate $\{H_{120}C_{144}O_{24}(OP)_2N^-Na_6^+\}$, a Hexameric Sodium Tetraphenyl Imidodiphosphate Containing an $[Na_6O_{12}]$ Core in a Hydrocarbon Ellipsoid (C) 1355
- The Lipophilically Wrapped Polyion Aggregate $\{[Ba_6Li_3O_2]^{11+}[^-OC(CH_3)_3]_{11}\cdot(OC_4H_8)_3\}$, a Face-Sharing (Octahedron + Prismane) $Ba_6Li_3O_2$ Polyhedron in a Hydrocarbon Ellipsoid: Preparation, Single Crystal Structure Analysis, and Density Functional Calculations (C) 1353

Polyketides
- Biosyntheses of Novel Emycins from the Mutant Strain *Streptomyces cellulosae* ssp. *griseoincarnatus* 1114-2 (C) 1617
- Combinatorial Biosynthesis—An Approach in the Near Future? (H) 881
- Novel Genetically Engineered Tetracenomycins (C) 1107

Polymacromonomers
- Lyotropic Phases Formed by "Molecular Bottlebrushes" (C) 1472

Polymerizations
- Distorted Sandwich Compounds: [1]Ferrocenophanes and [2]Ruthenocenophanes (H) 1837
- Reaction of (Butadiene)zirconocene with Tris(pentafluorophenyl)borane—A Novel Way of Generating Methylalumoxane-Free Homogeneous Ziegler-Type Catalysts (C) 1755
- Stereospecific Olefin Polymerization with Chiral Metallocene Catalysts (R) 1143 (1368)
- Synthesis and Structure of the First Sulfur-Bridged [1]Ferrocenophane (C) 1506

Polymers
- Architectural Control in "Living" Free Radical Polymerizations: Preparation of Star and Graft Polymers (C) 1456
- $C_4S_6^{2-}$: A Bridging Bis(dithiolato) Ligand for the Preparation of Semiconducting Inorganic Polymers (C) 1890
- Design, Synthesis, and Properties of Molecule-Based Assemblies with Large Second-Order Optical Nonlinearities (R) 155
- Electrochemical Synthesis of a Redox-Active Polymer Based on Buckminsterfullerene Epoxide (C) 194
- Formation of a Hexagonal Columnar Mesophase by N-Acylated Poly(ethylenimine) (C) 795
- Lyotropic Phases Formed by "Molecular Bottlebrushes" (C) 1472
- Molecular Imprinting in Cross-Linked Materials with the Aid of Molecular Templates—A Way towards Artificial Antibodies (R) 1812
- Structure and Properties of Polymers (B) 600
- Structure – Property Relations in Polymers. Spectroscopy and Performance (B) 601

- Synthesis and Structure of the Three-Dimensional Coordination Polymers $[(Me_3Sn)_4M(CN)_8]$ (M = Mo, W) (C) 2557
- $[Mn(C_{18}H_{16}N_2O_2)_3](ClO_4)_2$: A Polymeric 34- and 68-Membered Metallacyclic Network Forming a Novel Woven Polycatenated Structure (C) 574

Poly(metallocene)s
- Synthesis and Structure of the First Sulfur-Bridged [1]Ferrocenophane (C) 1506

Polymethacrylate
- Side-Chain Polyrotaxanes with a Tandem Structure Based on Cyclodextrins and a Polymethacrylate Main Chain (C) 309

Polymethines
- Deformation of Polymethine Structures by Intermolecular Interactions (C) 690

Polymorphism
- Orthorhombic and Monoclinic 2,3,7,8-Tetramethoxythianthrene: Small Structural Difference—Large Lattice Change (C) 76

Polyolato complexes
- A Hexadecanuclear Polyolatometalate of Copper(II) Ions and Multideprotonated D-Sorbitol (C) 2119

Polyols
- A Novel Hexanuclear Fe^{III}-*cis*-Inositolato Complex as a Model for Fe^{III}–Polyol Interactions in Aqueous Solution (C) 2242
- Fivefold Deprotonated D-Mannose as Ligand in Homoleptic Dinuclear Metalates of Trivalent Iron, Vanadium, Chromium, Aluminum, and Gallium (C) 2647

Polyoxometalates
- A Functionalized Polyoxometalate Bearing a Ferrocenylimido Ligand: Preparation and Structure of $[(FcN)Mo_6O_{18}]^{2-}$ (C) 2547
- A Novel Chainlike Heteropolyanion Formed by Keggin Units: Synthesis and Structure of $(ET)_{8n}[PMnW_{11}O_{39}]_n \cdot 2nH_2O$ (C) 1460
- Hydroxylation of Alkanes with Molecular Oxygen Catalyzed by a New Ruthenium-Substituted Polyoxometalate, $[WZnRu^{III}_2(OH)(H_2O)(ZnW_9O_{34})_2]^{11-}$ (C) 1587
- Investigations into the Targeted Design of Solids: Hydrothermal Synthesis and Structures of One-, Two-, and Three-Dimensional Phases of the Oxovanadium–Organodiphosphonato System (C) 223
- Supramolecular Synthons in Crystal Engineering—A New Organic Synthesis (R) 2328
- $[Mo_{154}(NO)_{14}O_{420}(OH)_{28}(H_2O)_{70}]^{(25\pm5)-}$: A Water-Soluble Big Wheel with More than 700 Atoms and a Relative Molecular Mass of About 24000 (C) 2122

Polyrotaxanes
- Side-Chain Polyrotaxanes with a Tandem Structure Based on Cyclodextrins and a Polymethacrylate Main Chain (C) 309

Polyselenides
- Hydrothermal Synthesis of a Novel Se_{12} Ring in $[\{(NH_4)_2[Mo_3S_{11.72}Se_{1.28}]\}_2\text{-}[Se_{12}]]$ (C) 2509

Polysilanes
- Synthesis and Structure of a Dendritic Polysilane (C) 98

Polysulfides
- Hydrothermal Synthesis of a Novel Se_{12} Ring in $[\{(NH_4)_2[Mo_3S_{11.72}Se_{1.28}]\}_2\text{-}[Se_{12}]]$ (C) 2509

Porous materials
- Porous Solids by Design: $[Zn(4,4'\text{-bpy})_2(SiF_6)]_n \cdot x$DMF, a Single Framework Octahedral Coordination Polymer with Large Square Channels (C) 2127 (2561)

Porphyrazines
- Octathioporphyrazine Crown Ethers: An Octanuclear Ag^I Complex with Coordination in the *meso* Pocket (C) 2020

Porphyrinoids
- Aldehyde-Appended Tetraphenylporphyrin: A New Building Block for Porphyrin Arrays (C) 900
- A Li_2Ti_2-Substituted Acetylene Formed from Ethylene by Reaction with (*meso*-Octaethylporphyrinogen)titanium (C) 1092
- Alteration of the Reactivity of a Tellurophene Within a Core-Modified Porphyrin Environment: Preparation and Oxidation of 21-Telluraporphyrin (C) 2252
- A Simple, Chirogenic, Enantioselective Synthesis of Chlorins and Isobacteriochlorins (C) 784
- Assembly and Crystal Structure of a Photoactive Array of Five Porphyrins (C) 1096
- Characterization of an Oxo(porphyrinato)manganese(IV) Complex by X-ray Absorption Spectroscopy (C) 343
- Free-Energy Profile for a Host-Accelerated Diels–Alder Reaction: The Sources of *exo* Selectivity (C) 217
- From Porphyrin Isomers to Octapyrrolic "Figure Eight" Macrocycles (C) 2511
- Model Reactions for Photosynthesis—Photoinduced Charge and Energy Transfer between Covalently Linked Porphyrin and Quinone Units (R) 849
- N-Confused Porphyrins and Singlet Carbenes: Is There a Connection? (C) 1028
- Novel Porphyrinoids for Chemistry and Medicine by Biomimetic Syntheses (R) 1795
- Octaphyrin-(1.0.1.0.1.0.1.0) (C) 2515
- Oxybenziporphyrin, a Fully Aromatic Semiquinone Porphyrin Analog with Pathways for 18π-Electron Delocalization (C) 2533
- *meso*-Tetrakis[4-(diphenylphosphino)-phenyl]porphyrin and a Water-Soluble Octakis(phosphonium salt) Porphyrin Double-Decker with a Cage Structure. (C) 2230
- Tetraphenanthro[9,10-*b*:9,10-*g*:9,10-*l*:9,10-*q*]porphyrin, a New Highly Conjugated Porphyrin System (C) 683
- The First Dinuclear Low-Valent Samarium Complex with a Short Sm–Sm Contact (C) 2141
- Water-Soluble Dendritic Iron Porphyrins: Synthetic Models of Globular Heme Proteins (C) 2725

Potassium compounds
- Cage Expansion of $[\{(cyNLi)_3Sb\}_2]$; Synthesis and Structure of the Trimetallic Complex $[\{(cyNLi)_3Sb\}_2(t\text{BuOK})_3 \cdot xC_6H_5CH_3]$ (C) 1012
- Two Diorganopotassates: Crystal Structure of $[K(C_6H_6)][K\{C(SiMe_3)_2(SiMe_2Ph)\}_2]$ (C) 2679

Prebiotic syntheses
- A One-Step Synthesis of Squalene from Farnesol under Prebiotic Conditions (C) 1898

Product selectivity
- Control of Ion–Molecule Reactions in the Gas Phase (H) 885

Proliferation inhibitors
- Glc-PC, a New Type of Glucosidic Phospholipid (C) 2667

Propadiene
- Butatrienes by Cumuhomologation of Propadienes (C) 2709

Propargylic compounds
- Palladium-Catalyzed Resactions of Propargylic Compounds in Organic Synthesis (R) 2589

Propellanes
- Oxidative Transformations of a Pyrimidalized 1,5-Diene (C) 2502

Protecting groups
- Protecting Groups (B) 1370
- Synthesis of the Palmitoylated and Farnesylated C-Terminal Lipohexapeptide of the Human N-*Ras* Protein by Employing an Enzymatically Removable Urethane Protecting Group (C) 2259

Protein dimerization
- Rational Design of Orthogonal Receptor–Ligand Combinations (C) 2129

Protein kinase C
- Glc-PC, a New Type of Glucosidic Phospholipid (C) 2667

Protein mimics
- A Model of Semimet Hemerythrin; NMR Spectroscopic Evidence of Valence Localization in Bis(μ-carboxylato)(μ-phenolato)diiron(II,III) in Solution (C) 588

Proteins
- Combinatorial Synthesis and Multidimensional NMR Spectroscopy: An Approach to Understanding Protein–Ligand Interactions (R) 953
- Crystal Structure Analysis for Chemists and Biologists (B) 2060
- Modified Triple Resonance NMR Experiments with Optimized Sensitivity for Rapidly Exchanging Protons (C) 469
- Photochemically Initiated Protein Splicing (C) 1629
- Probing Protein Structure and Function with an Expanded Genetic Code (R) 621
- Recent Trends in Photoaffinity Labeling (R) 1296

Ras proteins
- Synthesis of the Palmitoylated and Farnesylated C-Terminal Lipohexapeptide of the Human N-*Ras* Protein by Employing an Enzymatically Removable Urethane Protecting Group (C) 2259

Proton transfer
- Dependent on Photochromism Crystal Packing: Photoinduced and Thermal Proton-Transfer Processes in Single Crystals f 6-(2,4-Dinitrobenzyl)-2,2'-Bipyridine (C) 2530
- X-ray Crystal Structures of Cytochrome c Oxidases from *Paracoccus denitrificans* and Bovine Heart and Their Implications for the Molecular Mechanism of Cell Respiration (H) 2635

Prozac
- Talking Back to Prozac: What Doctors Aren't Telling You about Today's Most Controversial Drug (B) 1250

Prussian blue
- The Two-Dimensional Network Structure and Metamagnetic Properties of the 2:1 Complex of $[Mn(3\text{-MeOsalen})(H_2O)]\text{-}ClO_4$ and $K_3[Fe(CN)_6]$ (C) 1446

Pseudodimers
- Pseudo-Spherical Host Molecules: Synthesis, Dimerization, and Nucleation Effects (C) 1885

Pyramidalized alkenes
- Oxidative Transformations of a Pyrimidalized 1,5-Diene (C) 2502

Pyrenes
- Luminescence Stimulated by Electron Transfer: Fluorescent Donor/Acceptor-Substituted Stilbenes Containing Pyrenoid and Heteroaromatic Subunits (C) 2664

Quinic acid
- Enantiospecific Syntheses of Valiolamine and Its (1*R*), (2*R*), (1*R*,2*R*) Diastereomers from (−)-Quinic Acid (C) 1643

Quinodimethanes
- *para*- and *ortho*-Quinodimethanes Intermediates with Cumulative Double Bonds (C) 2367

Quinolizines
- Diastereoselective Cathodic Cyclization of 1-(4- and 1-(3-Oxoalkyl)pyridinium Salts to Quinolizidine and Indolizidine Derivatives (C) 2007

Quinones
- Model Reactions for Photosynthesis—Photoinduced Charge and Energy Transfer between Covalently Linked Porphyrin and Quinone Units (R) 849

Radialenes
- Hexakis(trimethylsilylethynyl)[3]radialene: A Carbon-Rich Chromophore with Unusual Electronic Properties (C) 805

Radical cations
- Detection and Reactions of Radical Cations Generated by Photolysis of Aromatic Compounds with Tetranitromethane in 1,1,1,3,3,3-Hexafluoro-2-propanol at Room Temperature (C) 2268
- Radical Cation [4+2] Cycloadditions with 2-Vinylindoles (C) 1900

Radical polymerization
- Architectural Control in "Living" Free Radical Polymerizations: Preparation of Star and Graft Polymers (C) 1456

Radicals
- A New Dimension in Radical Chain Group Transfer Reaction by Photosensitized Electron Transfer (PET) Reductive Activation of $PhSeSiR_3$ (C) 2669
- A Second-Generation Synthesis of (20*S*)-Camptothecin, Topotecan, Irinotecan, and GI-147211C (C) 2683
- Diastereoselective Coupling of Anodically Produced Radicals Bearing Chiral Amide Groups (C) 189
- Low-Temperature Tandem Enyne Allene Radical Cyclizations: Efficient Synthesis of 2,3-Dihydroindenes from Simple Enediynes (C) 2037
- Radical Additions of Activated Haloalkanes to Alkenes Initiated by Electron Transfer from Copper in Solvent-Free Systems (C) 902
- Radical Chemistry (B) 1771
- Radical C–C Bond Formation by Photoinduced Electron Transfer Addition of α-Silyl Carbamates to Acceptor-Substituted Alkenes (C) 2137
- Structure Determination from Powder X-Ray Diffraction Data of a Hydrogen-Bonded Molecular Solid with Competing Ferromagnetic and Antiferromagnetic Interactions: The 2-(3,4-Dihydroxyphenyl)-α-Nitronyl Nitroxide Radical (C) 55
- The Catalytic Oxidative Coupling of Methane (R) 970
- 2-[*p*-(*N*-*tert*-butyl-*N*-oxyamino)phenyl]-4,4,5,5-tetramethyl-4,5-dihydroimidazol-3-oxide-1-oxyl, a Stable Diradical with a Triplet Ground State (C) 927

Radionuclides
- Trace Analysis of the Radionuclides ^{90}Sr and ^{89}Sr in Environmental Samples II: Accelerator Mass Spectrometry (AMS) (C) 183
- Trace Analysis of the Radionuclides ^{90}Sr and ^{89}Sr in Environmental Samples III: Development of a Fast Analytical Method (C) 186
- Trace Analysis of the Radionuclides ^{90}Sr and ^{89}Sr in Environmental Samples I: Laser Mass Spectrometry (C) 181

Raman spectroscopy
- Novel Biological Copper Proteins through Anion Addition to the Mutant Met121Gly of *Pseudomonas aeruginosa* Azurin (C) 1622
- Rapid Water Diffusion in a Cage-Type Crystal Lattice: β-Cyclodextrin Dodecahydrate (C) 1452
- Vibrational Spectroscopy in Supercritical Fluids: From Analysis and Hydrogen Bonding to Polymers and Synthesis (R) 1275

Reaction mechanisms
- Common Origin of Enthalpic and Entropic Substituent Effects in Reactions of Benzhydryl Cations with Nucleophiles (C) 490
- Electronically Tuned *trans* Labilization Controls the Substitution Behavior of Rhodoximes (C) 2245
- Formation of Nitronic Acids by Ring Opening of Nitrocyclopropanes by a Concerted, Acid-Catalyzed Mechanism (C) 1091
- Influence of Lewis Base Complexation and the Degree of Aggregation of Alkyllithium Compounds on the Ratio in Which They Form Addition Products and Enolates with Ketones (C) 2152
- New Findings in the Electrophilic Addition of Halogens to Olefins (H) 51
- One-Electron Redox Reactions of CoASH Esters in Anaerobic Bacteria—A Mechanistic Proposal (C) 1502
- Reactions of Carbocations with π Nucleophiles: Polar Mechanism and No Outer Sphere Electron Transfer Processes (C) 1225
- The Catalytic Oxidative Coupling of Methane (R) 970
- The Cope Rearrangement Transition Structure Is Not Diradicaloid, but Is It Aromatic? (C) 334
- The Role of Dehydroalanine in Catalysis by Histidine Ammonia Lyase (C) 1464

Reactive intermediates
- My Search for Carbocations and Their Role in Chemistry (Nobel Lecture) (R) 1393
- Recent Trends in Photoaffinity Labeling (R) 1296

Reactivity–selectivity principle
- The Coexistence of the Reactivity–Selectivity Principle and of Linear Free Energy Relationships: A Diffusion Clock for Determining Carbocation Reactivities (C) 2250

Rearrangements
- A Facile Access to $1\lambda^5,3\lambda^5$-Benzodiphospholes (C) 2017
- Biosyntheses of Novel Emycins from the Mutant Strain *Streptomyces cellulosae* ssp. *griseoincarnatus* 1114-2 (C) 1617
- Diastereo- and Enantioselective Synthesis of Polyfunctional Ketones with Adjacent Quaternary and Tertiary Centers by Asymmetric Carroll Rearrangement (C) 2278
- Diborylcarbenes as Reactive Intermediates in Double 1,2-Rearrangements with Low Activation Enthalpies (C) 1340
- Evidence for a Mechanism Involving Transient Fragmentation in Carbon Skeleton Rearrangements Dependent on Coenzyme B_{12} (C) 2398
- Oxidative Transformations of a Pyrimidalized 1,5-Diene (C) 2502
- Phosphorothioates: β-Fragmentation versus β-Silicon Effect (C) 2406
- Synthesis and Reactions of Vinyl Isoselenocyanates (C) 1627
- Synthesis of Chiral γ,δ-Unsaturated Amino Acids by Asymmetric Ester Enolate Claisen Rearrangement (C) 2012
- Tetracarboxylic Bisimide–Lactam Ring Contraction: A Novel Type of Rearrangement (C) 2234

Receptors
- Synthetic Receptors Based on Vinylogous Sulfonyl Peptides (C) 1765

Redox reactions
- One-Electron Redox Reactions of CoASH Esters in Anaerobic Bacteria—A Mechanistic Proposal (C) 1502

Red phosphorus
- New Evidence Concerning the Structure of Amorphous Red Phosphorus (H) 2637

Reductions
- Acyclic 1,4-Diastereoselectivity in γ-Substituted α-Enones: Transmission of Chiral Information through Conjugation (C) 2254
- Carbon Dioxide as a Raw Material: The Synthesis of Formic Acid and Its Derivatives from CO_2 (R) 2207
- Chiral Titanium Alkoxides as Catalysts for the Enantioselective Reduction of Ketones with Boranes (C) 2005
- Enantioselective Reduction of Ketones with Sodium Borohydride, Catalyzed by Optically Active (β-Oxoaldiminato)-cobalt(II) Complexes (C) 2145

Reductive elimination
- Direct Observation of O–H Reductive Elimination from Ir^{III} Complexes (C) 229

Resorcarenes
- Calixarenes, Macrocycles with (Almost) Unlimited Possibilities (R) 713

Resorcinol
- A Non-Peptidic Ion Channel with K^+ Selectivity (C) 693

Rhenium compounds
- An Unconventional Intermolecular Three-Center N–H···H_2Re Hydrogen Bond in Crystalline $[ReH_5(PPh_3)_3]\cdot$indole$\cdot C_6H_6$ (C) 2507
- Dimensional Reduction of $Re_6Se_8Cl_2$: Sheets, Chains, and Discrete Clusters Composed of Chloride-Terminated $[Re_6Q_8]^{2+}$ (Q = S, Se) Cores (C) 226
- Models for Bimetallic Catalysts: Multiple Oxidation States in Pt_3Re Cluster Cations (C) 346
- The First Mixed-Metal Borole Cluster; Stabilization of Formally 14e Pd Centers in the Re_2Pd_2 Electron-Deficient $[\{[(\eta^5\text{-}C_4H_4BPh)(CO)_3Re]Pd\}_2]$ Cluster (C) 1010
- Unprecedented Mode of Bonding for Olefins on Bimetallic Complexes: An Agostic Interaction of a sp^2 C–H Bond with a Ruthenium Center in Addition to a π bond to a Rhenium Center (C) 916

Rhodium compounds
- A Co_3 Complex Containing a Bent Trimetal Chain, and Other 1,1′-Ferrocenedithiolato Complexes (C) 656
- An Ab Initio Investigation of the Rh^I-Catalyzed Hydroboration of C=C Bonds: Evidence for Hydrogen Migration in the Key Step (C) 115

- A Redox-Switchable Hemilabile Ligand: Electrochemical Control of the Coordination Environment of a Rh^{I} Complex (C) 1624
- A Rhodium-Mediated, Stepwise Trimerization of an Alkyne That Does Not Lead to a Benzene but Selectively to a Hexadienyne Derivative (C) 191
- Asymmetrization of *meso* 1,4-Enediol Ethers by Isomerization with a Chiral binap-Rh^{I} Catalyst (C) 2287
- Does the Facile Inter- and Intramolecular C–H Bond Activation by Tp*–Rh Complexes Proceed via Rh^{I} or Rh^{III} Intermediates? (C) 231
- Electronically Tuned *trans* Labilization Controls the Substitution Behavior of Rhodoximes (C) 2245
- Enhancement of Catalytic Activity for Hydroformylation of Methyl Acrylate by Using Biphasic and "Supported Aqueous Phase" Systems (C) 1474
- σ Metathesis as a Critical Step for the Transition Metal Catalyzed Formation of Formic Acid from CO_2 and H_2? An Ab Initio Investigation (C) 1742
- Molecular Recognition between Chemically Modified β-Cyclodextrin and Dec-1-ene: New Prospects for Biphasic Hydroformylation of Water-Insoluble Olefins (C) 2269
- Rhodium-Catalyzed Hydroformylation of Internal Alkynes to α,β-Unsaturated Aldehydes (C) 1760
- Rhodium–Vinylallene Complexes and a New Reaction, Rhodium-Catalyzed Carbonylative [4+1]Cycloaddition (C) 2691
- The First Clusters with a Y-Shaped Arrangement of Ligands at Three-Coordinate Rh^{I} Atoms in the Solid State: $[M^1M^2\{\mu\text{-}P(C_6H_{11})_2\}(CO)_8Rh(PPh_3)]$ (M^1, M^2 = Mn, Re) (C) 1325
- The pH-Dependent Synthesis and Structural Study of Dimeric and Cyclic Trimeric Complexes of 9-Methyl- or 9-Ethylhypoxanthine Nucleobases with (η^5-Pentamethylcyclopentadienyl)rhodium Aqua Complexes (C) 1514
- Transition Metal Catalyzed Synthesis of Seven-Membered Carbocyclic Rings (H) 2223

Ribozymes
- Synthetic Ribozymes and the First Deoxyribozyme (H) 1189

Ring-opening polymerization
- Synthesis and Structure of the First Sulfur-Bridged [1]Ferrocenophane (C) 1506

RNA
- 1,5-Anhydrohexitol Nucleic Acids, a New Promising Antisense Construct (C) 1338 (2165)
- The Three-Dimensional Structure of Hammerhead Ribozymes (H) 643
- Triple-Helix Formation of Oligodeoxynucleotides Containing [(3′*S*,5′*R*)-2′-Deoxy-3′,5′-ethano-β-D-ribofuranosyl]nucleosides ("Bicyclo-deoxynucleosides") (C) 694

RNA cleavage
- Rapid Hydrolysis of RNA with a Cu^{II} Complex (C) 472

RNase A
- Peptide Ligases—Tools for Peptide Synthesis (H) 175

Rotanes
- The Reactivity of 1,3-Butadiyne Moieties in the "Exploding" [*n*]Rotanes—A Crown of Thiophenes (C) 781

Rotaxanes
- Dialkylammonium Ion/Crown Ether Complexes: The Forerunners of a New Family of Interlocked Molecules (C) 1865
- Doubly Encircled and Double-Stranded Pseudorotaxanes (C) 1869

Ruthenium compounds
- A Series of Well-Defined Metathesis Catalysts—Synthesis of $[RuCl_2(=CHR')(PR_3)_2]$ and Its Reactions (C) 2039
- Condensed $RuSn_6$ Octahedra in $Ru_3Sn_{15}O_{14}$ (C) 2113
- Distorted Sandwich Compounds: [1]Ferrocenophanes and [2]Ruthenocenophanes (H) 1837
- Effective Charge Separation in Intermolecular Complexes of an Electron Donor and a Doubly Branched Triad Assembly: A Model System for Environmental Effects Controlling Electron Transfer (C) 1005
- Electronic Energy Transfer Across Ethynyl-Bridged Ru^{II}/Os^{II} Terpyridyl Complexes (C) 1100
- Electron Transfer through DNA: Site-Specific Modification of Duplex DNA with Ruthenium Donors and Acceptors (C) 352
- Hydroxylation of Alkanes with Molecular Oxygen Catalyzed by a New Ruthenium-Substituted Polyoxometalate, $[WZnRu_2^{III}(OH)(H_2O)(ZnW_9O_{34})_2]^{11-}$ (C) 1587
- Routes to Dendritic Networks: Bis-Dendrimers by Coupling of Cascade Macromolecules through Metal Centers (C) 2023
- Synthesis, Structure, and Properties of Dinuclear and Trinuclear Rack-Type Ru^{II} Complexes (C) 1122
- Towards the Development of Molecular Wires: Electron Localization, Exchange, and Transfer in Alkyne-Bridged Multinuclear Complexes (C) 2705
- Unprecedented Mode of Bonding for Olefins on Bimetallic Complexes: An Agostic Interaction of a sp^2 C–H Bond with a Ruthenium Center in Addition to a π bond to a Rhenium Center (C) 916
- $[Cp^*(Me_3P)_2Ru(\eta^2\text{-}O=SO_2)]PF_6$, the First Complex between a Transition Metal and Sulfur Trioxide (C) 1008

Salen complexes
- The Two-Dimensional Network Structure and Metamagnetic Properties of the 2:1 Complex of $[Mn(3\text{-}MeOsalen)(H_2O)]ClO_4$ and $K_3[Fe(CN)_6]$ (C) 1446

Samarium compounds
- A Highly Stereoselective Synthesis of 1,2-*trans*-C-Glycoside via Glycosyl Samarium(III) Compounds (C) 909
- Radical Additions to (η^6-Arene)-(tricarbonyl)chromium Complexes: Diastereoselective Synthesis of Hydrophenalene and Hydrobenzindene Derivatives by Samarium(II) Iodide Induced Cyclization (C) 2383
- The First Dinuclear Low-Valent Samarium Complex with a Short Sm–Sm Contact (C) 2141

SAMP hydrazones
- Diastereo- and Enantioselective Synthesis of Polyfunctional Ketones with Adjacent Quaternary and Tertiary Centers by Asymmetric Carroll Rearrangement (C) 2278

Sandwich complexes
- A Co_3 Complex Containing a Bent Trimetal Chain, and Other 1,1′-Ferrocenedithiolato Complexes (C) 656
- Alkali Metallocene Anions: Syntheses and Structures (C) 2376
- Aminocyclopentadienes, Aminoferrocenes, and Aminocobaltocenes (C) 800
- A Tailor-Made Metallocene for the Copolymerization of Ethene with Bulky Cycloalkenes (C) 2273
- Competing Pathways in the Reaction of Bis(pentafluorophenyl)borane with Bis(η^5-cyclopentadienyl)dimethylzirconium: Methane Elimination versus Methyl–Hydride Exchange and an Example of Pentacoordinate Carbon (C) 1230
- η^5:η^2 Coordination of a *cyclo*-E_5 Ligand, E = P, As (C) 1321
- Coordination of CO to the Alkaline Earth Metallocene $[(Me_5C_5)_2Ca]$ (C) 791
- Distorted Sandwich Compounds: [1]Ferrocenophanes and [2]Ruthenocenophanes (H) 1837
- Ferrocenes. Homogeneous Catalysis. Organic Synthesis. Materials Science (B) 1904
- Molecular Mosaics Formed by a Square Cyclophane and Its Inclusion Complex with Ferrocene (C) 1862
- Molecular Recognition at an Interface: Binding of Monolayer-Anchored Ferrocenyl Groups by an Amphiphilic Calixarene Host (C) 235
- Organometallic Compounds for Nonlinear Optics—The Search for En-light-enment! (R) 21 (826)
- Reaction of (Butadiene)zirconocene with Tris(pentafluorophenyl)borane—A Novel Way of Generating Methylalumoxane-Free Homogeneous Ziegler-Type Catalysts (C) 1755
- Reactions of 1,1′-Ferrocenediylbis{chloro-[(1,2,5,6-η)-1,5-cyclooctadiene]}-diplatinum with Triarylphosphane and Molecular Oxygen (C) 319
- Stereospecific Olefin Polymerization with Chiral Metallocene Catalysts (R) 1143 (1368)
- Synthesis and Structure of the Firs Sulfur-Bridged [1]Ferrocenophane (C) 1506
- Synthesis of 1,2-Diphospholide Ions (C) 590
- Tris(dimethylamino)sulfoniumcyclopentadienide $[TAS]^+[C_5H_5]^-$ and Tris(dimethylamino)sulfoniumpyrrolide $[TAS]^+[C_4H_4N]^-$: Two Isostructural Salts with "Naked" Anions A^- and the "Inverse" Sandwich-Cations $[\{(Me_2N)_3S\}_2A]^+$ (A = $C_5H_5^-$, $C_4H_4N^-$) (C) 443
- [Bis{(η^5-pentamethylcyclopentadienyl)-cobalt}-μ-(η^4:η^4-arene)]: Synthesis, Structure, and Unusual Reactivity of a New Type of Triple-Decker with Bridging Arene Ligands (C) 592

Scandium compounds
- Synthesis of the First Adducts of the Dimetallofullerenes $La_2@C_{80}$ and $Sc_2@C_{84}$ by Addition of a Disilirane (C) 2139

Scanning tunneling microscopy
- Diodelike Current–Voltage Curves for a Single Molecule—Tunneling Spectroscopy with Submolecular Resolution of an Alkylated, *peri*-Condensed Hexabenzocoronene (C) 1609
- Oligothiophenes—Yet Longer? Synthesis, Characterization, and STM Images of Homologous, Isomerically Pure Oligo(alkylthiophene)s (C) 303

Schiff base complexes
- Complexation of [*N*,*N*′-Bis(salicylidene)-ethylenediiminato]cobalt(III)$^+$ by Anilines in Dimethylformamide (C) 1086

Second messengers
- Chemistry of Inositol Lipid Mediated Cellular Signaling (R) 1933

Second-sphere coordination
- Transition Metal Complexes as Both Host and Guest: Second-Sphere Coordination between a Pt-Azacrown Ether Host and a Pt-NH_3 Guest (C) 2689

Selectins
- Palladacycles as Structurally Defined Catalysts for the Heck Olefination of Chloro- and Bromoarenes (C) 1844
- Synthesis of an RGD-Sialyl-Lewis^x Glycoconjugate: A New Highly Active Ligand for P-Selectin (C) 990

Selenium compounds
- A New Dimension in Radical Chain Group Transfer Reaction by Photosensitized Electron Transfer (PET) Reductive Activation of $PhSeSiR_3$ (C) 2669
- Asymmetric Reaction of Arylalkenes with Diselenides (C) 1726
- Hydrothermal Synthesis of a Novel Se_{12} Ring in $[\{(NH_4)_2[Mo_3S_{11.72}Se_{1.28}]\}_2\text{-}[Se_{12}]]$ (C) 2509
- Synthesis and Reactions of Vinyl Isoselenocyanates (C) 1627
- The Preparation of Salts of $[Pd_2(\mu\text{-}Se_2N_2)Cl_6]^{2-}$, the First Adducts of Diselenium Dinitride (C) 1758

Self-assembly
- A Gold(I) [2]Catenane (C) 1894
- A Self-Assembled Bifunctional Receptor (C) 2124
- Controlling Translational Isomerism in [2]Catenanes (C) 571
- Design, Synthesis, and Properties of Molecule-Based Assemblies with Large Second-Order Optical Nonlinearities (R) 155
- Dialkylammonium Ion/Crown Ether Complexes: The Forerunners of a New Family of Interlocked Molecules (C) 1865
- Doubly Encircled and Double-Stranded Pseudorotaxanes (C) 1869
- Formation of a "*meso*-Helicate" by Self-Assembly of Three Bis(catecholate) Ligands and Two Titanium(IV) Ions (C) 2134
- Formation of the First Isomeric [2]Catenates by Self-Assembly about Two Different Metal Ions (C) 582
- Gold in Chains: Self-Assembly of a Gold(I) Catenane (H) 2107
- Kinetic Selection in the Template-Directed Self-Assembly of [2]Catenanes (C) 2378
- Molecular Mosaics Formed by a Square Cyclophane and Its Inclusion Complex with Ferrocene (C) 1862
- New Nonlinear Optical Materials: Expedient Topotactic Self-Assembly of Acentric Chromophoric Superlattices (C) 1497
- Patterns in Hydrogen Bonding: Functionality and Graph Set Analysis in Crystals (R) 1555
- Pseudo-Spherical Host Molecules: Synthesis, Dimerization, and Nucleation Effects (C) 1885
- Self-Assembling Discotic Mesogens (C) 1637
- Self-Assembly of a Ferromagnetically Coupled Manganese(II) Tetramer (C) 1443
- Self-Assembly of Molecular-Sized Boxes (H) 1079
- Self-Assembly of Polyanions at a Metal Cation Template: Syntheses and Structures of $[\{Ag([18]aneS_6)\}I_7]_n$ and $[Ag([18]aneS_6)]I_3$ (C) 2374
- β-Sheet Peptide Architecture: Measuring the Relative Stability of Parallel vs. Antiparallel β-Sheets (C) 95
- Structurally Diverse and Dynamically Versatile Benzylic Amide [2]Catenanes Assembled Directly from Commercially Available Precursors (C) 1212
- Synthesis and Structural Characterization of a Stereospecific Dinuclear Gallium Triple Helix: Use of the *trans*-Influence in Metal-Assisted Self-Assembly (C) 996
- Synthesis and Structure of Tetra- and Octanuclear Chelate Complexes—Exohedral Guest Exchange in Tetrahemispheraplexes (C) 993
- Synthesis of Novel Tetrathiafulvalene-(TTF)-Based [3]Pseudocatenanes by Self-Assembly; Prevention of *trans/cis* Isomerization (C) 2524
- Synthesis, Structure, and Properties of Dinuclear and Trinuclear Rack-Type Ru^{II} Complexes (C) 1122
- The Structural and Thermodynamic Basis for the Formation of Self-Assembled Peptide Nanotubes (C) 93
- X-Ray Structure of a Self-Assembled Gelating Fiber (C) 585

Semiconductors
- $C_4S_6^{2-}$: A Bridging Bis(dithiolato) Ligand for the Preparation of Semiconducting Inorganic Polymers (C) 1890
- The Novel Copper Polytelluride Salts $NaBa_6Cu_3Te_{14}$ and $(K_{0.60}Ba_{0.40})Ba_6Cu_{2.58}Te_{14}$: Discrete Clusters or Extended Solids? (C) 68

Semiempirical calculations
- LaI: An Unprecedented Binary Rare Earth Metal Monohalide with a NiAs-Type Structure (C) 233
- Synthesis of a Dynemicin A Analogue and Its Bergman-Type Cycloaromatization (C) 1345
- Thermal Isomerization of Indigo (C) 67

Sensitization
- Radical C–C Bond Formation by Photoinduced Electron Transfer Addition of α-Silyl Carbamates to Acceptor-Substituted Alkenes (C) 2137

Sensors
- New Fluorescent Model Compounds for the Study of Photoinduced Electron Transfer: The Influence of a Molecular Electric Field in the Excited State (C) 1728

Shape selectivity
- Selective Isomerization of Hydrocarbon Chains on External Surfaces of Zeolite Crystals (C) 2528

β-Sheet structures
- β-Sheet Peptide Architecture: Measuring the Relative Stability of Parallel vs. Antiparallel β-Sheets (C) 95

Shikimic Acid
- Shikimic Acid (B) 361

Sialyl Lewis^x
- Palladacycles as Structurally Defined Catalysts for the Heck Olefination of Chloro- and Bromoarenes (C) 1844
- Synthesis of an RGD-Sialyl-Lewis^x Glycoconjugate: A New Highly Active Ligand for P-Selectin (C) 990

Sialyltransferase
- A Multienzyme System for a One-Pot Synthesis of Sialyl T-Antigen (C) 893

Signal transduction
- Chemistry of Inositol Lipid Mediated Cellular Signaling (R) 1933
- Signal Transduction: Evolution of an Idea (Nobel Lecture) (R) 1420

Silaboranes
- First Reaction of 1,2-Dimethyl-*o*-silaborane: Nucleophilic Degradation (C) 2236

Silacyclopentadienide
- Synthesis and Structure of a Free Germacyclopentadienide Ion: $[Li([12]crown\text{-}4)_2][C_4Me_4GeSi(SiMe_3)_3]$ (C) 1887

Silanetriols
- Soluble Aluminosilicates with Frameworks of Minerals (C) 2504

Silenes
- Reaction of 1,1-Dimethylsilene with Formaldehyde (C) 929

Silicon compounds
- A Framework Containing Ga-O-Ga Links: The Synthesis and Structure of Gallobicchulite $Ca_8(Ga_2SiO_6)_4(OH)_8$ (C) 2414
- Al,Ti Avoidance in the Microporous Titanoaluminosilicate ETAS-10 (C) 1003
- A New Zincosilicate Zeolite with Nine-Ring Channels (C) 63
- A Silicon Strand of More than 7 Å in Diameter in $Ba_2Eu_3Si_7$ (C) 1462
- Distinguishing the Silanol Groups in the Mesoporous Molecular Sieve MCM-41 (C) 2694
- First Reaction of 1,2-Dimethyl-*o*-silaborane: Nucleophilic Degradation (C) 2236
- Homogeneous versus Heterogeneous Zeolite Nucleation (C) 73
- New Surprises in Metal Carbonyl Chemistry (H) 2489
- Silacyclopropene: Generation by High-Vacuum Flash Pyrolysis and Matrix-Spectroscopic Identification (C) 1439
- Silicon Analogues of Grignard Compounds: Synthesis and Structure of Amine-Stabilized Trimethylsilylmagnesium Halides (C) 1030
- Silicon-Bridged Macrocycles—Synthesis of Sila-Calixarenes (C) 661
- Structure-Determining C-H $\cdots$ O-Si Hydrogen Bonds in Cobaltocenium Fluoride Nonasil (C) 2680
- Structure Organization of Aluminosilicate Polyanions with Surfactants: Optimization of Al Incorporation in Aluminosilicate Mesostructural Materials (C) 1499
- Synthesis and Structure of a Dendritic Polysilane (C) 98
- Synthesis and Structure of Organometallic Compounds with $(Al_2Si)_2$ and Al_3Sb_2 Frameworks (C) 919
- Synthesis and Structure of Triamino- and Tetraaminosilanes (C) 2645
- The Chemistry of Silylenoids: Preparation and Reactivity of (Alkoxysilyl)-lithium Compounds (C) 818
- Two Diorganopotassates: Crystal Structure of $[K(C_6H_6)][K\{C(SiMe_3)_2\text{-}(SiMe_2Ph)\}_2]$ (C) 2679

Silver compounds
- $C_{60}H_{60}$ and $C_{54}H_{48}$: Silver Ion Extraction with New Concave Hydrocarbons (C) 481
- Formation of the First Isomeric [2]Catenates by Self-Assembly about Two Different Metal Ions (C) 582
- Novel Networks of Unusually Coordinated Silver(I) Cations: The Wafer-Like Structure of $[Ag(pyz)_2][Ag_2(pyz)_5]\text{-}(PF_6)_3\cdot 2G$ and the Simple Cubic Frame of $[Ag(pyz)_3](SbF_6)$ (C) 1895
- Octathioporphyrazine Crown Ethers: An Octanuclear Ag^I Complex with Coordination in the *meso* Pocket (C) 2020

- Self-Assembly of Polyanions at a Metal Cation Template: Syntheses and Structures of $[\{Ag([18]aneS_6)\}I_7]_n$ and $[Ag([18]aneS_6)]I_3$ (C) 2374

Silyl cations
- $[R_3Si-arene]^+$ σ Complexes in the Gas Phase (C) 654

Silyl effect
- A Remarkable Effect of Silyl Substitution on Electrocyclization of Vinylallenes (C) 1476

Silylenoids
- The Chemistry of Silylenoids: Preparation and Reactivity of (Alkoxysilyl)-lithium Compounds (C) 818

Silyl enol ethers
- Synthesis of D-(+)-Biotin through Selective Ring Closure of *N*-Acyliminium Silyl Enol Ethers (C) 2391

Single molecule spectroscopy
- Diodelike Current–Voltage Curves for a Single Molecule—Tunneling Spectroscopy with Submolecular Resolution of an Alkylated, *peri*-Condensed Hexabenzocoronene (C) 1609

Sodalites
- A Framework Containing Ga-O-Ga Links: The Synthesis and Structure of Gallobicchulite $Ca_8(Ga_2SiO_6)_4(OH)_8$ (C) 2414
- Designed Assemblies in Open Framework Materials Synthesis: An Interrupted Sodalite and An Expanded Sodalite (C) 1745

Sodium compounds
- $Na_2Ti_3Cl_8$: From Isolated Ti^{2+} Ions to $[Ti_3]^{6+}$ Clusters (C) 71
- The Lipophilically Wrapped Polyion Aggregate $\{H_{120}C_{144}O_{24}(OP)_2N^-Na_6^+\}$, a Hexameric Sodium Tetraphenyl Imidodiphosphate Containing an $[Na_6O_{12}]$ Core in a Hydrocarbon Ellipsoid (C) 1355

Solid-phase syntheses
- A Novel Allylic Anchor for Solid-Phase Synthesis—Synthesis of Protected and Unprotected O-Glycosylated Mucin-Type Glycopeptides (C) 803
- A Versatile Solid-Phase Synthesis of N-Linked Glycopeptides (C) 60
- Solid-Phase Syntheses of Unnatural Biopolymers Containing Repeating Urea Units (C) 907
- Solid-Phase Synthesis of Vinylogous Sulfonyl Peptides (C) 1763

Solids
- Novel Networks of Unusually Coordinated Silver(I) Cations: The Wafer-Like Structure of $[Ag(pyz)_2][Ag_2(pyz)_5](PF_6)_3 \cdot 2G$ and the Simple Cubic Frame of $[Ag(pyz)_3](SbF_6)$ (C) 1895

Solid-state chemistry
- $ATh_{12}N_6X_{29}$ (A = Li...Rb; X = Cl, Br): A New Type of Thorium Cluster with a $Th_{12}N_6$ Core (C) 567
- Chemistry of Non-Stoichiometric Compounds (B) 1033
- Dimensional Reduction of $Re_6Se_8Cl_2$: Sheets, Chains, and Discrete Clusters Composed of Chloride-Terminated $[Re_6Q_8]^{2+}$ (Q = S, Se) Cores (C) 226
- Does the Death Knell Toll for the Metallic Bond? (H) 1081
- Preparative Solid-State Chemistry with High-Power CO_2 Lasers (R) 634
- The Metallic Bond—Dead or Alive? A Comment and a Reply (Comment) (C) 2003

Solid-state electrochemistry
- The Formal Potentials of Solid Metal Hexacyanometalates (C) 2685

Solid-state structures
- A Novel Chainlike Heteropolyanion Formed by Keggin Units: Synthesis and Structure of $(ET)_{8n}[PMnW_{11}O_{39}]_n \cdot 2nH_2O$ (C) 1460
- A Silicon Strand of More than 7 Å in Diameter in $Ba_2Eu_3Si_7$ (C) 1462
- Bromides of Rare Earth Metal Boride Carbides—A System of Building Blocks (C) 1633
- Condensed $RuSn_6$ Octahedra in $Ru_3Sn_{15}O_{14}$ (C) 2113
- $CsPr_9NbBr_{15}N_6$: A New Type of Interstitially Stabilized Cluster Compound (C) 2262
- $(CuI)_3P_{12}$: A Solid Containing a New Polymer of Phosphorus Predicted by Theory (C) 1647
- Dependent on Photochromism Crystal Packing: Photoinduced and Thermal Proton-Transfer Processes in Single Crystals f 6-(2,4-Dinitrobenzyl)-2,2′-Bipyridine (C) 2530
- Designed Assemblies in Open Framework Materials Synthesis: An Interrupted Sodalite and An Expanded Sodalite (C) 1745
- Discrete Crown-Shaped Te_8 Rings in Cs_3Te_{22} (C) 450
- Investigations into the Targeted Design of Solids: Hydrothermal Synthesis and Structures of One-, Two-, and Three-Dimensional Phases of the Oxovanadium–Organodiphosphonato System (C) 223
- LaI: An Unprecedented Binary Rare Earth Metal Monohalide with a NiAs-Type Structure (C) 233
- $(Nb,Ta)_9(S,Te)_5$, a Metal-Rich Chalcogenide with a Microporous Metal Substructure (C) 1089
- Patterns in Hydrogen Bonding: Functionality and Graph Set Analysis in Crystals (R) 1555
- Rapid Water Diffusion in a Cage-Type Crystal Lattice: β-Cyclodextrin Dodecahydrate (C) 1452
- Six Interpenetrating Quartz-Like Nets in the Structure of $ZnAu_2(CN)_4$ (C) 1203
- $(Sr_6N)[Ga_5]$ and $(Ba_6N)[Ga_5]$: Compounds with Discrete (M_6N) Octahedra and $[Ga_5]$ Clusters (C) 1761
- Stable 1:1 Adducts from Iodoacetylenes and Iodide Ions: Ion Pair Strain as an Additional Driving Force? (C) 441
- Substituent-Controlled Reactions of Iminophosphoranes with Methyllithium (C) 1752
- Synthesis, Structure, and Decay of In_4Br_7 (C) 1126
- $Ta_5(S,Te)_2$: Microporous Tantalum with Chalcogen-Coated Inner Surfaces (C) 2703
- The Synthesis and Crystal Structures of $RbC(SiMe_3)_3$ and $CsC(SiMe_3)_3 \cdot 3.5C_6H_6$: A One-Dimensional Ionic Solid and an Ionic Solid with a Molecular Structure (C) 687
- 2,4,6-Tri(4-pyridyl)-1,3,5-triazine as a 3-Connecting Building Block for Infinite Nets (C) 820

Solvent effects
- The Colors of C_{60} Solutions (C) 105

Solvent-free conversions
- Radical Additions of Activated Haloalkanes to Alkenes Initiated by Electron Transfer from Copper in Solvent-Free Systems (C) 902

Sol–gel processes
- Efficient Heterogeneous Biocatalysts by Entrapment of Lipases in Hydrophobic Sol–Gel Materials (C) 301
- New Dimensions in the Sol–Gel Process (H) 1578
- Synthesis of Hexagonally-Packed Mesoporous TiO_2 by a Modified Sol–Gel Method (C) 2014

D-Sorbitol
- A Hexadecanuclear Polyolatometalate of Copper(II) Ions and Multideprotonated D-Sorbitol (C) 2119

Spectroelectrochemistry
- Hexakis(trimethylsilylethynyl)[3]radialene: A Carbon-Rich Chromophore with Unusual Electronic Properties (C) 805

Spectrophotometry
- Derivative Spectrophotometry. Low and Higher Order (B) 1522

Spectroscopy
- Spectroscopy in Catalysis. An Introduction (B) 495
- Thermal Isomerization of Indigo (C) 67

Spherands
- $C_{60}H_{60}$ and $C_{54}H_{48}$: Silver Ion Extraction with New Concave Hydrocarbons (C) 481

Sphingosines
- New Brain Lipids that Induce Sleep (H) 2362

Spin chemistry
- Chemical Generation and Reception of Radio- and Microwaves (B) 936

Spin crossover
- Photoinduced Valence Tautomerism in Cobalt Complexes Containing Semiquinone Anion as Ligand: Dynamics of the High-Spin $[Co^{II}(3,5\text{-dtbsq})_2]$ to Low-Spin $[Co^{III}(3,5\text{-dtbsq})(3,5\text{-dtbcat})]$ Interconversion (C) 1481

Splicing
- Photochemically Initiated Protein Splicing (C) 1629

Squalene
- A One-Step Synthesis of Squalene from Farnesol under Prebiotic Conditions (C) 1898

Squalestatins
- Total Syntheses of Zaragozic Acid (H) 773

Stacking interactions
- Polar Interactions between Stacked π Systems in Fluorinated 1,8-Diarylnaphthalenes: Importance of Quadrupole Moments in Molecular Recognition (C) 1019

Stannylenes
- Bis(hypersilyl)tin and Bis(hypersilyl)lead, Two Electron-Rich Carbene Homologs (C) 1334

Star polymers
- Architectural Control in "Living" Free Radical Polymerizations: Preparation of Star and Graft Polymers (C) 1456

Statins
- Diastereo- and Enantioselective Synthesis of 1,2-Amino Alcohols from Glycol Aldehyde Hydrazones; Asymmetric Synthesis of (*R*,*R*)-Statin (C) 1219

Stereochemistry
- Optical Activity of Chiral Dendritic Surfaces (C) 1206

Steric shielding
- Tetrakis[bis(trimethylsilyl)methyl]dialuminoxane with a Linear Al-O-Al Group (C) 989

Steroids
- Digitalis Research in Berlin–Buch—Retrospective and Perspective Views (R) 282

Stilbenoids
- Luminescence Stimulated by Electron Transfer: Fluorescent Donor/Acceptor-Substituted Stilbenes Containing Pyrenoid and Heteroaromatic Subunits (C) 2664

Strained rings
- Formation of Nitronic Acids by Ring Opening of Nitrocyclopropanes by a Concerted, Acid-Catalyzed Mechanism (C) 1091

- Novel Structures from Tris(benzocyclobutadieno)cyclohexatriene: Triscyclopropanation and Trisoxacyclopropanation to the First [2.1.2.1.2.1]Hexaannulanes (C) 563
- Silacyclopropene: Generation by High-Vacuum Flash Pyrolysis and Matrix-Spectroscopic Identification (C) 1439
- C_3-Symmetric Hexakis(trimethylsilyl)[7]-phenylene ["Tris(biphenylenocyclobutadieno)cyclohexatriene"], a Polycyclic Benzenoid Hydrocarbon with Slightly Curved Topology (C) 1478
- 6,7-Bis(methoxycarbonyl)-2,3-dimethyl [5](1,4)naphthalenophane; the First Benzoannelated [5]Paracyclophane (C) 2553

Strobilurins
- 9-Methoxystrobilurins—A Link Between Strobilurins and Oudemansins (C) 196

Strontium
- Trace Analysis of the Radionuclides ^{90}Sr and ^{89}Sr in Environmental Samples II: Accelerator Mass Spectrometry (AMS) (C) 183
- Trace Analysis of the Radionuclides ^{90}Sr and ^{89}Sr in Environmental Samples III: Development of a Fast Analytical Method (C) 186
- Trace Analysis of the Radionuclides ^{90}Sr and ^{89}Sr in Environmental Samples I: Laser Mass Spectrometry (C) 181

Structure elucidation
- A Molecular Composite Containing Organic and Inorganic Components—A Complex from β-Cyclodextrin and Hydrated Magnesium Chloride (C) 2381
- A New Zincosilicate Zeolite with Nine-Ring Channels (C) 63
- Applications of Mass Spectrometry to Organic Stereochemistry (B) 497
- Bis(trifluoromethyl)trioxide: First Structure of a Straight-Chain Trioxide (C) 2244
- Carbenoid or Lithium Complex of a Carbanion? Synthesis and Structure of $(Me_3Si)_2C=P(aryl)=C(Cl)Li(thf)_3$ and LiCl Elimination To Give the Phosphirene (C) 1849
- $(C_5Me_5)TiF_2$—A Versatile Building Block for Generating Large Soluble Dimetallic Aggregates (C) 1872
- Crystallography Made Crystal Clear. A Guide for Users of Macromolecular Models (B) 496
- Crystal Structure Analysis for Chemists and Biologists (B) 2060
- Crystal Structure of Dilithioacetylacetone: A Twenty-Four Vertex Li-O Cage Molecule with Limited Li–C(terminal) Bonding and Selective THF Solvation (C) 1233
- Dilithium Acepentalenediide: An Unusual Dimer of Contact Ion Triplets with Bowl-Shaped Dianions (C) 1492
- Facile Synthesis and Solid-State Structure of a Benzylic Amide [2]Catenane (C) 1209
- Homogeneous versus Heterogeneous Zeolite Nucleation (C) 73
- Modified Triple Resonance NMR Experiments with Optimized Sensitivity for Rapidly Exchanging Protons (C) 469
- $Na_2Ti_3Cl_8$: From Isolated Ti^{2+} Ions to $[Ti_3]^{6+}$ Clusters (C) 71
- Orthorhombic and Monoclinic 2,3,7,8-Tetramethoxythianthrene: Small Structural Difference—Large Lattice Change (C) 76
- Recent Trends in Photoaffinity Labeling (R) 1296
- Relationship between C(O)–N Twist Angles and ^{17}O NMR Chemical Shifts in a Series of Twisted Amides (C) 1113
- Relative and Absolute Configuration of Filipin III (C) 1227
- Scalar Coupling Constants—Their Analysis and Their Application for the Elucidation of Structures (R) 1671
- Self-Assembly of a Ferromagnetically Coupled Manganese(II) Tetramer (C) 1443
- Silicon Analogues of Grignard Compounds: Synthesis and Structure of Amine-Stabilized Trimethylsilylmagnesium Halides (C) 1030
- Single-Crystal X-Ray Structure of the Metastable Aryne Precursor Tetrafluorophenyllithium and of 1,2,3,4-Tetrafluorobenzene (C) 1517
- Structure Determination in the Twilight Region Between Monolayers and 3-D Crystals; a Grazing Incidence X-Ray Diffraction Study of Nanocrystalline Aggregates of α,ω-Docosanediol at the Air–Water Interface (C) 649
- Structures of UV-B Induced Sunscreen Pigments of Scots Pine (*Pinus sylvestris* L.) (C) 312
- Sulfuric Acid from Sulfur Trioxide and Water—A Surprisingly Complex Reaction (H) 1313
- Synthesis and X-Ray Powder Structure of a Novel Porous Uranyl Phenylphosphonate Containing Unidimensional Channels Flanked by Hydrophobic Regions (C) 1508
- The Lipophilically Wrapped Polyion Aggregate $\{H_{120}C_{144}O_{24}(OP)_2N^-Na_6^+\}$, a Hexameric Sodium Tetraphenyl Imidodiphosphate Containing an $[Na_6O_{12}]$ Core in a Hydrocarbon Ellipsoid (C) 1355
- The Lipophilically Wrapped Polyion Aggregate $\{[Ba_6Li_3O_2]^{11+}[^-OC(CH_3)_3]_{11}\cdot(OC_4H_8)_3\}$, a Face-Sharing (Octahedron + Prismane) $Ba_6Li_3O_2$ Polyhedron in a Hydrocarbon Ellipsoid: Preparation, Single Crystal Structure Analysis, and Density Functional Calculations (C) 1353
- The Three-Dimensional Structure of Hammerhead Ribozymes (H) 643
- The $[Zr_6X_{18}H_5]^{3-}$ Ions with X = Cl, Br, and Related Species (C) 1877
- Three-Dimensional Chemical Similarity Searching (B) 359
- Two Diorganopotassates: Crystal Structure of $[K(C_6H_6)][K\{C(SiMe_3)_2(SiMe_2Ph)\}_2]$ (C) 2679
- X-ray Crystal Structures of Cytochrome c Oxidases from *Paracoccus denitrificans* and Bovine Heart and Their Implications for the Molecular Mechanism of Cell Respiration (H) 2635
- X-Ray Structure of a Self-Assembled Gelating Fiber (C) 585
- $[Fe(2,4,6\text{-}tBu_3C_6H_2)_2]$, a Monomeric Diaryl Complex with Two-Coordinate Iron(II) (C) 325
- $[Pb_{18}I_{44}]^{8-}$—An Iodoplumbate with an Unusual Structure (C) 2035

Structure relations
- Structure – Property Relations in Polymers. Spectroscopy and Performance (B) 601

Subnitrides
- The "Submetalate" $Ba_{17}Al_3O_7$: The First Member of a New Class of Compounds (C) 2115

Suboxides
- The "Submetalate" $Ba_{17}Al_3O_7$: The First Member of a New Class of Compounds (C) 2115

Substituent effects
- Common Origin of Enthalpic and Entropic Substituent Effects in Reactions of Benzhydryl Cations with Nucleophiles (C) 490

Substitutions
- Asymmetric Allylic Substitution with Nitromethane Catalyzed by a Pd Complex: Enantioselectivities Exceeding 99.9% ee (C) 2687
- Electronically Tuned *trans* Labilization Controls the Substitution Behavior of Rhodoximes (C) 2245
- Electron Transfer and Polar Reactions of Cyclizable Anion Radicals: Structural Consequences of Orbital Selection Rules and Chain-Length Constraints (C) 1495
- Reactions of Neopentyl 2,2,2-Trifluoroethanesulfonate (Tresylate) with Nucleophiles: A Model Study for the Coupling of Nucleophiles with Tresyl Agarose (C) 1612
- Synthesis and Structure of Triamino- and Tetraaminosilanes (C) 2645

Subtilisin
- Peptide Ligases—Tools for Peptide Synthesis (H) 175

Subvalent compounds
- Diphosphanyl- and Diarsanyl-Substituted Carbene Homologues: Germanediyls, Stannanediyls, and Plumbanediyls with Remarkable Electronic Structures (C) 1614

Sulfenic acids
- Synthesis of a Stable Arenesulfenic Acid Bearing a Bowl-Shaped Macrobicyclic Cyclophane Skeleton (C) 1124

Sulfides
- $Ta_5(S,Te)_2$: Microporous Tantalum with Chalcogen-Coated Inner Surfaces (C) 2703

Sulfonamides
- Solid-Phase Synthesis of Vinylogous Sulfonyl Peptides (C) 1763

Sulfonations
- New Process for the Sulfonation of Phosphane Ligands for Catalysts (C) 811
- Preparation of a Surface-Active Chiral Diphosphane and Its Use in the Hydrogenation of Prochiral Olefins (C) 1645

Sulfonic acids
- Reactions of Neopentyl 2,2,2-Trifluoroethanesulfonate (Tresylate) with Nucleophiles: A Model Study for the Coupling of Nucleophiles with Tresyl Agarose (C) 1612

Sulfonium salts
- Tris(dimethylamino)sulfoniumcyclopentadienide $[TAS]^+[C_5H_5]^-$ and Tris(dimethylamino)sulfoniumpyrrolide $[TAS]^+[C_4H_4N]^-$: Two Isostructural Salts with "Naked" Anions A^- and the "Inverse" Sandwich-Cations $[\{(Me_2N)_3S\}_2A]^+$ (A = $C_5H_5^-$, $C_4H_4N^-$) (C) 443

Sulfoxides
- Asymmetric Sulfide Oxidation with Vanadium Catalysts and H_2O_2 (C) 2640
- Enantiomerically Pure Palladacycles Derived from β-Ketosulfoxides (C) 1351

Sulfur compounds
- $C_4S_6^{2-}$: A Bridging Bis(dithiolato) Ligand for the Preparation of Semiconducting Inorganic Polymers (C) 1890
- Sequential Transformation of Benzothiopyrylium Salts to Diastereoselectively Annulated Benzothiopyranones (C) 647
- S_7NH and S_7NCH_3 as Novel Chelating Ligands in $[(\eta^5\text{-}C_5H_5)_2Ti]$ Complexes: Synthesis of Medium-Sized Sulfur–Nitrogen Rings by Ligand Transfer (C) 1330
- $S(NPMe_3)_4^{2+}$: The First Structure Determination of a Dication of Hexavalent Sulfur (C) 1362

- Sulfuric Acid from Sulfur Trioxide and Water– A Surprisingly Complex Reaction (H) 1313
- Synthesis of Sulphones, Sulphoxides and Cyclic Sulphides (B) 1251
- Synthesis of Ψ[SCH_2]-, Ψ[$SOCH_2$]-, and Ψ[SO_2CH_2]-Peptide Isosters (C) 553
- The First Sulfur(VI)–Nitrogen–Phosphorus Macrocycles (C) 998
- [$Cp^*(Me_3P)_2Ru(\eta^2\text{-}O=SO_2)$]$PF_6$, the First Complex between a Transition Metal and Sulfur Trioxide (C) 1008

Sulfuric acid
- Sulfuric Acid from Sulfur Trioxide and Water—A Surprisingly Complex Reaction (H) 1313

Sulfur trioxide
- [$Cp^*(Me_3P)_2Ru(\eta^2\text{-}O=SO_2)$]$PF_6$, the First Complex between a Transition Metal and Sulfur Trioxide (C) 1008

Sunscreen pigments
- Structures of UV-B Induced Sunscreen Pigments of Scots Pine (*Pinus sylvestris* L.) (C) 312

Superconductors
- (DTEDT)[$Au(CN)_2]_{0.4}$: An Organic Superconductor Based on the Novel π-Electron Framework of Vinylogous Bis-Fused Tetrathiafulvalene (C) 1222

Supercritical fluids
- Vibrational Spectroscopy in Supercritical Fluids: From Analysis and Hydrogen Bonding to Polymers and Synthesis (R) 1275

Superexchange
- A Hexadecanuclear Polyolatometalate of Copper(II) Ions and Multideprotonated D-Sorbitol (C) 2119

Suppressor tRNA
- Photochemically Initiated Protein Splicing (C) 1629

Supramolecular chemistry
- A Comparison of Enthalpies of Formation in Solution and Enthalpies for HPLC Retention for Hydrogen-Bonded Host–Guest Complexes (C) 2404
- Activation of Macrocyclic Biaryl-Enediynes by Metal Ion Coordination (C) 2538
- Calixarenes, Macrocycles with (Almost) Unlimited Possibilities (R) 713
- Concave Reagents Based on Calixarenes (C) 2555
- Container Molecules and Their Guests (B) 2563
- Cytomimetic Organic Chemistry: Early Developments (R) 2091
- Double Helical Dinuclear Copper(I) Complexes of Macrocyclic Bis(dithiadiimine) Ligands (C) 1883
- Electronic Energy Transfer in a Supramolecular Species Containing the $[Ru(bpy)_3]^{2+}$, $[Os(bpy)_3]^{2+}$, and Anthracene Chromophoric Units (C) 595
- Gold in Chains: Self-Assembly of a Gold(I) Catenane (H) 2107
- Investigation of Self-Assembled Supramolecular Species in Solution by IL-ESMS, a New Mass Spectrometric Technique (C) 209
- Modeling the Remote-Controlled Organization of Particles in a Nanodimensional Cavity: Synthesis and Properties of $(Et_3NH)_3(t\text{BuNH}_3)_2Na_2[(H_2O)_2,N_3^-\subset V_{14}O_{22}(OH)_4(PhPO_3)_8]\cdot 6\,H_2O\cdot 2\,DMF$ (C) 779
- Molecular Recognition at an Interface: Binding of Monolayer-Anchored Ferrocenyl Groups by an Amphiphilic Calixarene Host (C) 235
- Molecular Recognition of Terephthalic Acid by Supramolecular Self-Assembly of an Acridine-Pendant Cyclen–Zn^{II} Complex (C) 663
- Octacationic Cyclophanes: Binding of ATP and Other Anionic Guests in Water (C) 2147
- Photoswitchable Electrical Communication of Glucose Oxidase and Glutathione Reductase with Electrode Surfaces through Photoisomerizable Redox Mediators (C) 1604
- Side-Chain Polyrotaxanes with a Tandem Structure Based on Cyclodextrins and a Polymethacrylate Main Chain (C) 309
- Silicon-Bridged Macrocycles—Synthesis of Sila-Calixarenes (C) 661
- Strong Binding of Paraquat and Polymeric Paraquat Derivatives by Basket-Shaped Hosts (C) 2132
- Supramolecular Chemistry. Concepts and Perspectives (B) 2563
- Supramolecular Inorganic Chemistry: Small Guests in Small and Large Hosts (R) 2311
- Supramolecular Synthons in Crystal Engineering—A New Organic Synthesis (R) 2328
- Synthesis and Structural Characterization of a Stereospecific Dinuclear Gallium Triple Helix: Use of the *trans*-Influence in Metal-Assisted Self-Assembly (C) 996
- Synthesis and Structure of the Nanodimensional Multicyclophane "Kuratowski Cyclophane", an Achiral Molecule with Nonplanar $K_{3,3}$ Topology (C) 2657
- Synthesis and X-ray Structure of a Shape-Persistent Macrocyclic Amphiphile (C) 2713
- Synthesis, Structure, and Properties of Dinuclear and Trinuclear Rack-Type Ru^{II} Complexes (C) 1122
- Synthetic Receptors Based on Vinylogous Sulfonyl Peptides (C) 1765
- Thermotropic Liquid Crystals Formed by Intermolecular Hydrogen Bonding Interactions (R) 1696
- Topochemical Aspects of the Formation of Networks in Layered Langmuir–Blodgett (LB) Assemblies (C) 340
- Transition Metal Complexes as Both Host and Guest: Second-Sphere Coordination between a Pt-Azacrown Ether Host and a Pt-NH_3 Guest (C) 2689

Surface analysis
- Practical Surface Analysis. A2, Vol. 1. Auger and X-Ray Photoelectron Spectroscopy (B) 2059

Surface chemistry
- A New Strategy in Heterogeneous Catalysis: The Design of Cortex Catalysts (C) 2728
- The Chemistry of Metal CVD (B) 1651

Surfactants
- Photoswitchable Phase Separation in Hydrophobically Modified Poly(acrylamide)/Surfactant Systems (C) 88
- Structure Organization of Aluminosilicate Polyanions with Surfactants: Optimization of Al Incorporation in Aluminosilicate Mesostructural Materials (C) 1499

Suzuki coupling
- Novel, Blue-Transparent Frequency Doublers Based on 1,8-Di(hetero)arylnaphthalenes (C) 1485
- Palladacycles as Efficient Catalysts for Aryl Coupling Reactions (C) 1848

Synthesis planning
- Computer-Assisted Planning of Organic Syntheses: The Second Generation of Programm (R) 2613

Synthetic methods
- Activated Metals in Organic Synthesis (B) 121
- Atom Economy—A Challenge for Organic Synthesis: Homogeneous Catalysis Leads the Way (R) 259
- Diazo Chemistry I (B) 1653
- Enzymes in Organic Synthesis: Application to the Problems of Carbohydrate Recognition (Part 1) (R) 412
- Enzymes in Organic Synthesis: Application to the Problems of Carbohydrate Recognition (Part 2) (R) 521
- Enzymes in Synthetic Organic Chemistry (B) 1523
- Modern Electroorganic Chemistry (B) 1521
- Nucleophilic Aromatic Substitution of Hydrogen (B) 2419
- Photochemical Key Steps in Organic Synthesis—An Experimental Coursebook (B) 1770
- Protecting Groups (B) 1370
- Supramolecular Inorganic Chemistry: Small Guests in Small and Large Hosts (R) 2311
- Synthesis of Sulphones, Sulphoxides and Cyclic Sulphides (B) 1251
- Synthetic Aspects of Metal-Catalyzed Oxidations of Amines and Related Reactions (R) 2443
- Tactics of Organic Synthesis (B) 1369
- Transition Metals in the Synthesis of Complex Organic Molecules (B) 1035

TADDOL
- Highly Enantioselective Opening of Cyclic *meso*-Anhydrides to Isopropyl Hemiesters with Diisopropoxytitanium TADDOLates (C) 2395

Tandem reactions
- Disaccharide Mimetics by Enzymatic Tandem Aldol Additions (C) 1639

Tantalum compounds
- DAD Compounds of Niobium and Tantalum: Examples of the Structural Flexibility of DAD Ligands (C) 2649
- $(Nb,Ta)_9(S,Te)_5$, a Metal-Rich Chalcogenide with a Microporous Metal Substructure (C) 1089
- Tantalum-Mediated Coupling of Methane and Carbon Dioxide in the Gas Phase (C) 2033
- $Ta_5(S,Te)_2$: Microporous Tantalum with Chalcogen-Coated Inner Surfaces (C) 2703

T-antigen
- A Multienzyme System for a One-Pot Synthesis of Sialyl T-Antigen (C) 893

Tautomerism
- Dependent on Photochromism Crystal Packing: Photoinduced and Thermal Proton-Transfer Processes in Single Crystals f 6-(2,4-Dinitrobenzyl)-2,2′-Bipyridine (C) 2530
- Photoinduced Valence Tautomerism in Cobalt Complexes Containing Semiquinone Anion as Ligand: Dynamics of the High-Spin $[Co^{II}(3,5\text{-dtbsq})_2]$ to Low-Spin $[Co^{III}(3,5\text{-dtbsq})(3,5\text{-dtbcat})]$ Interconversion (C) 1481

Taxol
- A Novel Intramolecular Heck Reaction: Synthesis of a Cholesterol–Baccatin III Hybrid (C) 452
- A Total Synthesis of Taxol (C) 1723
- New Fluorescent Water-Soluble Taxol Derivatives (C) 2710
- The Conquest of Taxol (R) 2079

Tellurium compounds
- Alteration of the Reactivity of a Tellurophene Within a Core-Modified Porphyrin Environment: Preparation and Oxidation of 21-Telluraporphyrin (C) 2252
- A $Te_2N_6Li_4$ Cage Containing the Tris(*tert*-butylimido)tellurite Dianion (C) 2549
- Discrete Crown-Shaped Te_8 Rings in Cs_3Te_{22} (C) 450
- From *cyclo*-Te_8 to Te_x^{n-} Sheets: Are Nonclassical Polytellurides More Classical than We Thought? (H) 2109
- New Tellurometalates of Gallium and Indium: $K[K([18]crown\text{-}6)]_2[GaTe_3]\cdot 2CH_3CN$ and $[(NEt_4)_5][In_3Te_7]\cdot 0.5\,Et_2O$ (C) 1879
- $Ta_5(S,Te)_2$: Microporous Tantalum with Chalcogen-Coated Inner Surfaces (C) 2703
- Te_8^{4+}: A Cubic Polycation in the Structure of $Te_8(VOCl_4)_2$ (C) 2559
- The Novel Copper Polytelluride Salts $NaBa_6Cu_3Te_{14}$ and $(K_{0.60}Ba_{0.40})Ba_6Cu_{2.58}Te_{14}$: Discrete Clusters or Extended Solids? (C) 68

Template syntheses
- Controlling Translational Isomerism in [2]Catenanes (C) 571
- Designed Assemblies in Open Framework Materials Synthesis: An Interrupted Sodalite and An Expanded Sodalite (C) 1745
- Kinetic Selection in the Template-Directed Self-Assembly of [2]Catenanes (C) 2378
- Light-Switchable Catalysis in Synthetic Receptors (C) 446

Terpenoids
- A One-Step Synthesis of Squalene from Farnesol under Prebiotic Conditions (C) 1898

Tetracenomycins
- Biosynthetic Origin of the Oxygen Atoms of Tetracenomycin C (C) 565
- Novel Genetically Engineered Tetracenomycins (C) 1107

Tetrahydrocarbolines
- Asymmetric Pictet–Spengler Reactions Employing *N,N*-Phthaloyl Amino Acids as Chiral Auxiliary Groups (C) 2402

2,3,7,8-Tetramethoxythianthrene
- Orthorhombic and Monoclinic 2,3,7,8-Tetramethoxythianthrene: Small Structural Difference – Large Lattice Change (C) 76

Tetranitromethane
- Detection and Reactions of Radical Cations Generated by Photolysis of Aromatic Compounds with Tetranitromethane in 1,1,1,3,3,3-Hexafluoro-2-propanol at Room Temperature (C) 2268

Tetraphenanthroporphyrins
- Tetraphenanthro[9,10-*b*:9,10-*g*:9,10-*l*:9,10-*q*]porphyrin, a New Highly Conjugated Porphyrin System (C) 683

Tetraphosphabarrelene
- 1,3,5,7-Tetraphosphabarrelene: A New Cyclic Phosphaalkyne Tetramer (C) 81

Tetrathiafulvalenes
- (DTEDT)$[Au(CN)_2]_{0.4}$: An Organic Superconductor Based on the Novel π-Electron Framework of Vinylogous Bis-Fused Tetrathiafulvalene (C) 1222
- Synthesis of Novel Tetrathiafulvalene-(TTF)-Based [3]Pseudocatenanes by Self-Assembly; Prevention of *trans*/*cis* Isomerization (C) 2524

Tetrazanes
- Hexakis(trifluoromethyl)tetrazane (C) 586

Textbooks
- Bioinorganic Chemistry (B) 1036
- Chemistry and Light (B) 599
- Cluster Chemistry (B) 121
- Fundamentals of Photoinduced Electron Transfer (B) 495
- Inorganic Chemistry (B) 599
- Introduction to Molecular Cloning Techniques (B) 697
- Modern Medicinal Chemistry (B) 828
- Namen- und Schlagwortreaktionen der Organischen Chemie (B) 935
- Organic Syntheses Based on Name Reactions and Unnamed Reactions (B) 935
- Radical Chemistry (B) 1771

Thallium compounds
- Structure and Bonding in Organometallic Anions of Heavy Group 14 and 15 Elements (R) 1545

The Bourbaki Gambit
- The Bourbaki Gambit (B) 241

Theoretical chemistry
- Group Theory in Chemistry and Spectroscopy. A Simple Guide to Advanced Usage (B) 1772
- Shape in Chemistry. An Introduction to Molecular Shape and Topology (B) 361

Thermal analysis
- Basic Principles of Thermoanalytical Techniques and Their Applications in Preparative Chemistry (R) 1171

Thermochemistry
- Commensurate Freezing of *n*-Alkanes in Silicalite (C) 2543

Thermodynamics
- A Comparison of Enthalpies of Formation in Solution and Enthalpies for HPLC Retention for Hydrogen-Bonded Host–Guest Complexes (C) 2404

Thin films
- Design, Synthesis, and Properties of Molecule-Based Assemblies with Large Second-Order Optical Nonlinearities (R) 155
- Molecular Recognition at an Interface: Binding of Monolayer-Anchored Ferrocenyl Groups by an Amphiphilic Calixarene Host (C) 235
- New Dimensions in the Sol–Gel Process (H) 1578
- New Nonlinear Optical Materials: Expedient Topotactic Self-Assembly of Acentric Chromophoric Superlattices (C) 1497
- Structure Determination in the Twilight Region Between Monolayers and 3-D Crystals; a Grazing Incidence X-Ray Diffraction Study of Nanocrystalline Aggregates of α,ω-Docosanediol at the Air–Water Interface (C) 649
- Topochemical Aspects of the Formation of Networks in Layered Langmuir–Blodgett (LB) Assemblies (C) 340

Thioethers
- Preparation and Detection of Enantiomerically Enriched and Configurationally Stable α-Thioalkyllithium Compounds (C) 323

Thioglycosides
- Progress in Oligosaccharide Synthesis through a New, Orthogonal Glycosylation Strategy (H) 1432

Thioindigo derivatives
- Bis(dicyanomethylene) and Bis(cyanoimino) Derivatives of Indigo and Thioindigo (C) 464

Thiols
- Synthesis and Coordination Chemistry of *ortho*-Functionalized Dimercaptobenzene: Building Blocks for Tripodal Hexathiol Ligands (C) 2700

Thiones
- $C_4S_6^{2-}$: A Bridging Bis(dithiolato) Ligand for the Preparation of Semiconducting Inorganic Polymers (C) 1890
- Relationship between C(O)–N Twist Angles and ^{17}O NMR Chemical Shifts in a Series of Twisted Amides (C) 1113

Thiophenes
- Oligothiophenes—Yet Longer? Synthesis, Characterization, and STM Images of Homologous, Isomerically Pure Oligo(alkylthiophene)s (C) 303
- The Reactivity of 1,3-Butadiyne Moieties in the "Exploding" [*n*]Rotanes—A Crown of Thiophenes (C) 781

Thioxanthenes
- A Highly Stereoselective Optical Switching Process Based on Donor–Acceptor Substituted Dissymmetric Alkenes (C) 348

Thorium compounds
- $ATh_{12}N_6X_{29}$ (A = Li...Rb; X = Cl, Br): A New Type of Thorium Cluster with a $Th_{12}N_6$ Core (C) 567

Thrombin
- Anticoagulatory Substances of Blood-sucking Animals: From Hirudin to Hirudin Mimetics (R) 867
- Design of Novel, Nonpeptidic Thrombin Inhibitors and Structure of a Thrombin–Inhibitor Complex (C) 1739

Through-bond interactions
- Synthesis of Rodlike Distellenes (C) 1001

Through-space interactions
- Electrochemical Evidence for Through-Space Orbital Interactions in Spiromethanofullerenes (C) 1591

Tin compounds
- Condensed $RuSn_6$ Octahedra in $Ru_3Sn_{15}O_{14}$ (C) 2113
- Structure and Bonding in Organometallic Anions of Heavy Group 14 and 15 Elements (R) 1545
- Synthesis and Structure of the Three-Dimensional Coordination Polymers $[(Me_3Sn)_4M(CN)_8]$ (M = Mo, W) (C) 2557

Titanium compounds
- A Li_2Ti_2-Substituted Acetylene Formed from Ethylene by Reaction with (*meso*-Octaethylporphyrinogen)titanium (C) 1092
- Al,Ti Avoidance in the Microporous Titanoaluminosilicate ETAS-10 (C) 1003
- Catalytic Asymmetric Carbonyl–Ene Reactions (H) 1717
- $(C_5Me_5)TiF_2$—A Versatile Building Block for Generating Large Soluble Dimetallic Aggregates (C) 1872
- Formation of a "*meso*-Helicate" by Self-Assembly of Three Bis(catecholate) Ligands and Two Titanium(IV) Ions (C) 2134
- Highly Enantioselective Opening of Cyclic *meso*-Anhydrides to Isopropyl Hemiesters with Diisopropoxytitanium TADDOLates (C) 2395
- Ligand-Accelerated Catalysis (R) 1059
- Macrobicyclic Titanium(IV) Complexes with C_3-Symmetric Synthetic Peptides (C) 1449
- Mononuclear Tris(arene)–Metal Complexes (H) 53
- $Na_2Ti_3Cl_8$: From Isolated Ti^{2+} Ions to $[Ti_3]^{6+}$ Clusters (C) 71
- S_7NH and S_7NCH_3 as Novel Chelating Ligands in $[(\eta^5\text{-}C_5H_5)_2Ti]$ Complexes: Synthesis of Medium-Sized Sulfur–Nitrogen Rings by Ligand Transfer (C) 1330
- Synthesis and Structure of 1-Aza- and 1-Phospha-2-titanacyclobut-4-enes (C) 688

- Synthesis and Structure of Triamino- and Tetraaminosilanes (C) 2645
- Synthesis of Hexagonally-Packed Mesoporous TiO_2 by a Modified Sol–Gel Method (C) 2014
- Titanium-Induced Zipper Reactions (C) 678
- $[\{Ti(\mu\text{-}CH_3)_5(\mu\text{-}CH_2)\}\{(tmeda)Li\}_3]\cdot$ THF: An Unusual and Highly Fluxional Titanium Organometallic Compound (C) 2264

Topochemistry
- Control of the Reactivity of Double Bonds through Their Fixed Geometrical Arrangement (H) 2225
- Topochemical Aspects of the Formation of Networks in Layered Langmuir–Blodgett (LB) Assemblies (C) 340
- Topochemical Reaction Control in Solution (C) 685

Total syntheses
- A Total Synthesis of Taxol (C) 1723
- Synthesis of D-(+)-Biotin through Selective Ring Closure of *N*-Acyliminium Silyl Enol Ethers (C) 2391
- The Conquest of Taxol (R) 2079
- Total Syntheses of Zaragozic Acid (H) 773
- Total Synthesis of (±)-Dynemicin A (C) 1721
- Total Synthesis of Natural (+)-SF 2315A and Determination of the Absolute Configuration (C) 2396

Transesterifications
- Acceleration of a Phosphate Diester Transesterification Reaction by Bis(alkylguanidinium) Receptors Containing an Appended General Base (C) 1237

Transition metals
- Carbon Dioxide as a Raw Material: The Synthesis of Formic Acid and Its Derivatives from CO_2 (R) 2207
- Carbon–Hydrogen Bonds of DNA Sugar Units as Targets for Chemical Nucleases and Drugs (R) 746
- Cluster Chemistry (B) 121
- Coordination of Dioxygen in Three Representative Transition Metal Cations: FeO_2^+, CrO_2^+, and $[CH_3Re(O_2)_2O]^+$ (C) 2517
- C–H and C–C Bond Activation by Bare Transition-Metal Oxide Cations in the Gas Phase (R) 1973
- Electronic Energy Transfer in a Supramolecular Species Containing the $[Ru(bpy)_3]^{2+}$, $[Os(bpy)_3]^{2+}$, and Anthracene Chromophoric Units (C) 595
- Transition Metals in the Synthesis of Complex Organic Molecules (B) 1035

Transition states
- Antibody-Catalyzed Phosphate Triester Hydrolysis (C) 2275
- Electron Transfer and Polar Reactions of Cyclizable Anion Radicals: Structural Consequences of Orbital Selection Rules and Chain-Length Constraints (C) 1495

Translational isomerism
- Controlling Translational Isomerism in [2]Catenanes (C) 571

Transmission electron microscopy
- A New Method for the Preparation of Nanostructured Metal Clusters (C) 2240
- Sulfoxide-Stabilized Giant Palladium Clusters in Catalyzed Oxidations (C) 457

Transuranium elements
- Two at One Blow: The New Chemical Elements 110 and 111 (H) 1713

Triaminopyrimidine aggregates
- Barbituric Acid/2,4,6-Triaminopyrimidine Aggregates in Water and Their Competitive Interaction with Monolayers of Barbituric Acid Lipids at the Gas–Water Interface (C) 58

Triazines
- 2,4,6-Tri(4-pyridyl)-1,3,5-triazine as a 3-Connecting Building Block for Infinite Nets (C) 820

Trigermanes
- Reactions of Hexa-*tert*-butylcyclotrigermane: Isolation of an Enantiomerically Pure 1,3-Diiodotrigermane (C) 1085

Trimethylenemethane
- A Concise Synthetic Route to Cyclopentenes by [3+2] Cycloaddition of Dipolar Trimethylenemethane to Alkynes (C) 2154

Trioxides
- Bis(trifluoromethyl)trioxide: First Structure of a Straight-Chain Trioxide (C) 2244

Triple-decker complexes
- A μ-η^6:η^6-1,3,5-Triboratabenzenebis(cyclopentadienylcobalt) Triple-Decker Complex (C) 681
- [Bis{(η^5-pentamethylcyclopentadienyl)cobalt}-μ-(η^4:η^4-arene)]: Synthesis, Structure, and Unusual Reactivity of a New Type of Triple-Decker with Bridging Arene Ligands (C) 592

Tripodal ligands
- Synthesis and Coordination Chemistry of *ortho*-Functionalized Dimercaptobenzene: Building Blocks for Tripodal Hexathiol Ligands (C) 2700

Tris(*tert*-butylimido)tellurite
- A $Te_2N_6Li_4$ Cage Containing the Tris(*tert*-butylimido)tellurite Dianion (C) 2549

Tris(pyrazolyl)borates
- Novel Binuclear Cobalt Dioxygen Complex—A Step on the Path to Dioxygen Activation (C) 2051

Tumor therapy
- Novel Porphyrinoids for Chemistry and Medicine by Biomimetic Syntheses (R) 1795

Tungsten compounds
- Chiral Phosphanodihydrooxazoles in Asymmetric Catalysis: Tungsten-Catalyzed Allylic Substitution (C) 462
- Complexes with Polar W–W Multiple Bonds: $[W_2(O\mathit{i}Pr)_4L(dmpe)_2]$ (L = $(H)_2$, CO) and $[W_2(O)_4(\mu\text{-}O)\{W(CO)(dmpe)_2\}_2]$ (C) 891
- Monomeric Molybdenum and Tungsten Complexes That Contain a Metal–Phosphorus Triple Bond (C) 2044
- P–H-Functionalized Phosphenium Complexes $[C_5R_5(OC)_2W{=}P(H)R']$ (R′ = *t*Bu, sMes): Synthesis, Isomerization, and Transformation into Hydrido Complexes Containing a *t*BuP(H)OH Ligand (C) 2500
- Solid-State and Solution Structures of $[\{NW(OC(CH_3)_2CF_3)_3\}_3]$ and Factors Favoring the Metathesis of C–N and N–W Triple Bonds in Reactions Involving Organic Nitriles and Ditungsten Hexaalkoxides (C) 110
- Synthesis and Structure of the Three-Dimensional Coordination Polymers $[(Me_3Sn)_4M(CN)_8]$ (M = Mo, W) (C) 2557
- Synthesis, Structural Investigation, and Ligand Properties of Isocyanoacetonitrile (C) 914
- Terminal E_1 Ligands from Elements of Group 15 (H) 1997
- *meso*-Tetrakis[4-(diphenylphosphino)-phenyl]porphyrin and a Water-Soluble Octakis(phosphonium salt) Porphyrin Double-Decker with a Cage Structure. (C) 2230
- [WL(NO)(O)(CH_3)]—An Unusual Nitrosyltungsten Complex (C) 1435

Two-phase catalysis
- A Novel Class of Versatile Solvents for Two-Phase Catalysis: Hydrogenation, Isomerization, and Hydroformylation of Alkenes Catalyzed by Rhodium Complexes in Liquid 1,3-Dialkylimidazolium Salts (C) 2698
- Exciting Results from the Field of Homogeneous Two-Phase Catalysis (H) 1575

Umpolung
- A Chiral Cyanohydrin Phosphate for Carbonyl Umpolung—Stereoselective Synthesis of Tertiary Cyanohydrins (C) 917
- Highly Stereoselective Allylation of Benzaldehyde: Generation of a Stereochemically Defined Allylzinc Species from a π-Allylpalladium Intermediate and Diethylzinc (C) 787

Uranium compounds
- New Surprises in Metal Carbonyl Chemistry (H) 2489

Uranyl phenylphosphonates
- Synthesis and X-Ray Powder Structure of a Novel Porous Uranyl Phenylphosphonate Containing Unidimensional Channels Flanked by Hydrophobic Regions (C) 1508

Urea
- Solid-Phase Syntheses of Unnatural Biopolymers Containing Repeating Urea Units (C) 907

Urocanase
- On the Mechanism of Action of Urocanase: Observation of the Enzyme-Bound NAD^+–Inhibitor Adduct by ^{13}C NMR Spectroscopy (C) 652

UV/Vis spectroscopy
- Barbituric Acid/2,4,6-Triaminopyrimidine Aggregates in Water and Their Competitive Interaction with Monolayers of Barbituric Acid Lipids at the Gas–Water Interface (C) 58
- Quaterrylenebis(dicarboximides) (C) 1323
- The Colors of C_{60} Solutions (C) 105

Vacuum traps
- Aligning and Trapping Molecules with Light (H) 2365

Valiolamine
- Enantiospecific Syntheses of Valiolamine and Its (1*R*), (2*R*), (1*R*,2*R*) Diastereomers from (−)-Quinic Acid (C) 1643

Vanadium compounds
- Asymmetric Sulfide Oxidation with Vanadium Catalysts and H_2O_2 (C) 2640
- Investigations into the Targeted Design of Solids: Hydrothermal Synthesis and Structures of One-, Two-, and Three-Dimensional Phases of the Oxovanadium–Organodiphosphonato System (C) 223
- Modeling the Remote-Controlled Organization of Particles in a Nanodimensional Cavity: Synthesis and Properties of $(Et_3NH)_3(\mathit{t}BuNH_3)_2Na_2[(H_2O)_2,N_3^-\subset V_{14}O_{22}(OH)_4(PhPO_3)_8]\cdot 6\,H_2O\cdot 2\,DMF$ (C) 779
- Reaction of a Vanadium(III) Amide with H_2: Isolation and Characterization of a Polynuclear Mixed-Valence Polyhydrido–Nitrido Complex (C) 822

Vapor pressure
- Calculation of the Thermodynamic Properties of Polycyclic Aromatic Hydrocarbons by an Incremental Procedure (C) 1735

Vesicles
- Cytomimetic Organic Chemistry: Early Developments (R) 2091
- Metal-Induced Dispersion of Lipid Aggregates: A Simple, Selective, and Sensitive Fluorescent Metal Ion Sensor (C) 905

Vinylallenes
- A Remarkable Effect of Silyl Substitution on Electrocyclization of Vinylallenes (C) 1476
- Rhodium–Vinylallene Complexes and a New Reaction, Rhodium-Catalyzed Carbonylative [4 + 1]Cycloaddition (C) 2691

Vinylidene complexes
- C–C Coupling Reactions as a Novel Synthetic Route to π-Allyl- and π-Butadienylrhodium Complexes (C) 1244

Vitamin A
- Structure Determination of Vitamin A Acetate Isomers through Coupled HPLC and ^{1}H NMR Spectroscopy (C) 1014

Vitamin B_{12}
- Oligomethylene-Bridged Vitamin B_{12} Dimers (C) 84
- Peripherally Substituted Cobaloximes; X-Ray Crystal Structure Analysis of σ-Hexylbis[1,8-di(*N*-morpholino)octane-4,5-dioximato]pyridinecobalt(III) (C) 2389
- Vitamin B_{12}: How the Problem of Its Biosynthesis Was Solved (R) 383

Voltammetry
- The Formal Potentials of Solid Metal Hexacyanometalates (C) 2685

Wacker oxidation
- Molecular Recognition between Chemically Modified β-Cyclodextrin and Dec-1-ene: New Prospects for Biphasic Hydroformylation of Water-Insoluble Olefins (C) 2269

WODCA
- Computer-Assisted Planning of Organic Syntheses: The Second Generation of Programm (R) 2613

Xenon compounds
- $XeOF_5^-$, an Anion with Pentagonal-Pyramidal Structure (C) 1586

X-ray absorption spectroscopy
- The Active Sites of the Native Cytochrome-c Oxidase from Bovine Heart Mitochondria: EXAFS-Spectroscopic Characterization of a Novel Homobinuclear Copper Center (Cu_A) and of the Heterobinuclear Fe_{a3}-Cu_B Center (C) 1488

X-ray scattering
- Lyotropic Phases Formed by "Molecular Bottlebrushes" (C) 1472

D-Xylose isomerase
- A Dinuclear (μ-Carboxylato)manganese(II) Complex Derived from a Macrocyclic Ligand: A Structural Model for Active Sites in Natural Systems (C) 2535

Ylides
- Ylidediyl Halophosphane Oligomers, $(Ph_3PCPX)_n$—A Structurally Diverse Class of Compounds (C) 1853

Yttrium compounds
- An Yttrium-Based Strong Lewis Acid for the Heterogeneous Catalysis of the Diels–Alder Reaction (C) 2143

Zaragozic acids
- Total Syntheses of Zaragozic Acid (H) 773

Zeolite analogues
- AlMepO-α: A Novel Open-Framework Aluminum Methylphosphonate with Organo-Lined Unidimensional Channels (C) 1199
- Mutually Interpenetrating Sheets and Channels in the Extended Structure of [Cu(4,4′-bpy)Cl] (C) 207

Zeolites
- Al,Ti Avoidance in the Microporous Titanoaluminosilicate ETAS-10 (C) 1003
- A New Zincosilicate Zeolite with Nine-Ring Channels (C) 63
- Cobalt-Containing Molecular Sieves as Catalysts for the Low Conversion Autoxidation of Pure Cyclohexane (C) 560
- Commensurate Freezing of *n*-Alkanes in Silicalite (C) 2543
- Designed Assemblies in Open Framework Materials Synthesis: An Interrupted Sodalite and An Expanded Sodalite (C) 1745
- Homogeneous versus Heterogeneous Zeolite Nucleation (C) 73
- Selective Isomerization of Hydrocarbon Chains on External Surfaces of Zeolite Crystals (C) 2528
- Soluble Aluminosilicates with Frameworks of Minerals (C) 2504
- Structure-Determining C-H · · · O-Si Hydrogen Bonds in Cobaltocenium Fluoride Nonasil (C) 2680
- Zeolite Encaged Cu(Histidine) Complexes as a Mimic of Natural Cu Enzymes (C) 2652
- $_\infty^3[(CoCp_2)\subset Fe(\mu\text{-}CNSnMe_3NC)_3]$: A Purely Organometallic Channel Inclusion Compound (C) 1197

Ziegler catalysts
- Reaction of (Butadiene)zirconocene with Tris(pentafluorophenyl)borane—A Novel Way of Generating Methylalumoxane-Free Homogeneous Ziegler-Type Catalysts (C) 1755

Zinc compounds
- A New Nickel-Catalyzed Cross-Coupling Reaction between sp^3 Carbon Centers (C) 2723
- A New Zincosilicate Zeolite with Nine-Ring Channels (C) 63
- Highly Stereoselective Allylation of Benzaldehyde: Generation of a Stereochemically Defined Allylzinc Species from a π-Allylpalladium Intermediate and Diethylzinc (C) 787
- Molecular Recognition of Terephthalic Acid by Supramolecular Self-Assembly of an Acridine-Pendant Cyclen–Zn^{II} Complex (C) 663
- Porous Solids by Design: $[Zn(4,4'\text{-}bpy)_2(SiF_6)]_n \cdot x$DMF, a Single Framework Octahedral Coordination Polymer with Large Square Channels (C) 2127 (2561)
- Self-Assembled Helicates of Zinc and Cadmium Cyanides, $[M_x(CN)_{2x+1}]^-$, $x \leq 27$ (C) 314
- Six Interpenetrating Quartz-Like Nets in the Structure of $ZnAu_2(CN)_4$ (C) 1203

Zintl anions
- A Silicon Strand of More than 7 Å in Diameter in $Ba_2Eu_3Si_7$ (C) 1462

Zintl phases
- New Tellurometalates of Gallium and Indium: $K[K([18]crown\text{-}6)]_2[GaTe_3] \cdot 2CH_3CN$ and $[(NEt_4)_5][In_3Te_7] \cdot 0.5\,Et_2O$ (C) 1879
- The Stabilization of the Rb^- Ion in $Na_{16}Rb_7Sb_7 = Na_{16}(RbRb_6)Sb_7$ (C) 103

Zirconium compounds
- Competing Pathways in the Reaction of Bis(pentafluorophenyl)borane with Bis(η^5-cyclopentadienyl)dimethylzirconium: Methane Elimination versus Methyl–Hydride Exchange and an Example of Pentacoordinate Carbon (C) 1230
- Efficient Total Synthesis of the Pharmacophore of the Anticancer Antibiotic CC-1065 by Zirconocene- and Palladium-Initiated Cyclizations (C) 1366
- Hydrocarbon Activation with Metal Halides: Catalysis of the Jacobsen Rearrangement by $(ZrCl_4)_n$ in the Presence of Aromatic Hydrocarbons (C) 1510
- Mononuclear Tris(arene)–Metal Complexes (H) 53
- Reaction of (Butadiene)zirconocene with Tris(pentafluorophenyl)boranc—A Novel Way of Generating Methylalumoxane-Free Homogeneous Ziegler-Type Catalysts (C) 1755
- Stereoselective Synthesis of Chiral Zirconocenes from Doubly Substituted, Donor Functionalized Cyclopentadienes via Helical Chelate Complexes (C) 2266
- 1,3,5,7-Tetraphosphabarrelene: A New Cyclic Phosphaalkyne Tetramer (C) 81
- The $[Zr_6X_{18}H_5]^{3-}$ Ions with X = Cl, Br, and Related Species (C) 1877

ZSM-22
- Selective Isomerization of Hydrocarbon Chains on External Surfaces of Zeolite Crystals (C) 2528

Zwitterionic states
- Direct Spectroscopic Evidence for a Hitherto Elusive "Zwitterionic" Excited State (H) 547